Can. J. Chem. Downloaded from www.nrcresearchpress.com by 210.87.254.5 on 09/05/12
For personal use only.

Canadian Journal of Chemistry

Published by
THE NATIONAL RESEARCH COUNCIL OF CANADA

Journal canadien de chimie

Publié par
LE CONSEIL NATIONAL DE RECHERCHES DU CANADA

Volume 51 Number 1 January 1, 1973

Volume 51 numéro 1 le 1 janvier 1973

The Transformations of Dimeric Tri-*O*-acetyl-2-deoxy-2-nitroso-α-D-hexopyranosyl Chlorides in Dimethylformamide[1]

R. U. LEMIEUX, T. L. NAGABHUSHAN,[2] AND K. JAMES[3]

Department of Chemistry, University of Alberta, Edmonton, Alberta

Received June 2, 1972

The dimeric nitrosyl chloride adducts of tri-*O*-acetyl-1,5-anhydro-2-deoxy-D-*arabino*-hex-1- and D-*lyxo*-hex-1- enitols (glycals) dissociate in dimethylformamide to the monomeric forms which rapidly isomerize to the corresponding tri-*O*-acetyl-2-oximino-α-D-hexopyranosyl chlorides. Evidence is provided for the dehydrochlorination of these latter compounds to highly reactive tri-*O*-acetyl-1,5-anhydro-2-deoxy-2-nitroso-D-hex-1-enitols.

Les adduits entre le chlorure de nitrosyle dimère et les tri-*O*-acétyl anhydro-1,5 déoxy-2 D-*arabino* et D-*lyxo*-hexenitols-1 (glycals) se dissocient dans le diméthylformamide en formes monomères qui s'isomèrisent rapidement en chlorures de tri-*O*-acétyl oximino-2-α-D, hexopyranosyles. La déhydrochloration de ces derniers composés en tri-*O*-acétyl-anhydro-1,5 deoxy-2-nitroso-D-hexenitols-1 hautement réactifs a été mise en évidence. [Traduit par le journal]

Can. J. Chem., **51**, 1 (1973)

Previous communications (1–3) have shown that nitrosyl chloride adds readily to the acetylated 1,5-anhydro-2-deoxy-D-hex-1-enitols of the *arabino*- and *lyxo*-configurations and 1,5-anhydro-2-deoxy-D-*threo*-pent-1-enitol (acetylated glycals) to give acetylated 2-deoxy-2-nitroso-α-D-glycopyranosyl chlorides of the *gluco*-, *galacto*-, and *xylo*-configurations, respectively. The compounds crystallize as the dimers (1). Tri-*O*-acetyl-2-deoxy-2-nitroso-α-D-glucopyranosyl chloride dimer (**1**) was shown to react with alcohols in dimethylformamide to form alkyl tri-*O*-acetyl-2-oximino-α-D-*arabino*-hexopyranosides in high yield and with a high degree of stereoselectivity for the *Z*- (4) and α-D-configurations (5–7). Furthermore, it was shown that the oximinoglycosides of the *arabino*-configuration can be reduced to 2-amino-2-deoxy-α-D-gluco and 2-amino-2-deoxy-α-D-mannopyranosides (8). Also, deoximation of the acetylated 2-oximino-α-D-*arabino*-hexopyranosides followed by reduction with sodium borohydride was shown to provide α-D-glucopyranosides in good yield (6, 7, 9). Further accounts of these reactions are presented in the accompanying publications (10–14). The purpose of this communication is to report a study of the chemical properties of the dimeric nitrosyl chloride adducts of the triacetates of D-glucal (**1**) and D-galactal (**5**) as reflected by dissolution in anhydrous dimethylformamide (DMF) (see Scheme 1).

Freshly prepared solutions (0.05 *M*) of either dimeric tri-*O*-acetyl-2-deoxy-2-nitroso-α-D-glucopyranosyl chloride (**1**) or dimeric tri-*O*-acetyl-2-deoxy-2-nitroso-α-D-galactopyranosyl chloride (**5**) in DMF are virtually colorless but mutarota-

[1]Presented in part at the 161st National American Chemical Society Meeting, Los Angeles, California, March 28, 1971.

[2]Professional Research Associate, 1970–1972.

[3]University of Alberta, Postdoctoral Fellow, 1970-1972.

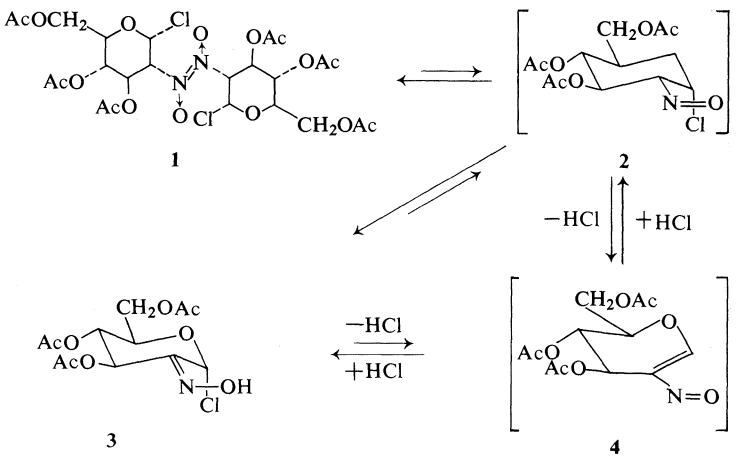

SCHEME 1

TABLE 1. First order velocity constants* for the formation of tri-*O*-acetyl-2-oximino-α-D-hexopyranosyl chlorides from dimeric tri-*O*-acetyl-2-deoxy-2-nitroso-α-D-glycopyranosyl chlorides

Configuration	Initial concentration of the dimer (*M*)	Method†	$k \times 10^3$ min^{-1}
arabino (**1**)	0.05	Polarimetric	11.8
arabino (**1**)	0.4	Polarimetric	11.6
arabino (**1**)	0.4	N.m.r.	12.0
2-Deuterio-	0.4	Polarimetric	11.4
arabino (**1**)	0.4	N.m.r.	12.6
lyxo (**5**)	0.05	Polarimetric	7.2
lyxo (**5**)	0.4	Polarimetric	7.8
lyxo (**5**)	0.4	N.m.r.	9.6

*At 25° in anhydrous dimethylformamide.
†The experimental error was estimated to be about ±2% for the polarimetric rates and about ±5% for those determined using n.m.r. by following the change in the relative intensities of the signals for the anomeric protons of **1** and **3**.

tion occurs: for **1**, $[\alpha]_D^{25}$ + 172° → +248° (8 h); for **5**, $[\alpha]_D^{25}$ + 137° → +238° (9.5 h). At this concentration, the final rotations are highly stable with little change being observed over a period of 3 days. Log plots of the changes in rotation indicated first order processes; $t_{1/2}$ = 59 min for **1** and $t_{1/2}$ = 96 min for **5** (see Table 1). It was desired to study the course of the reaction using n.m.r. and for this purpose (see below) 0.4 *M* solutions in DMF were used. At this higher concentration, the same maximum specific rotations were reached but these decayed with extended periods of time (greater than 8 h for **1** and 10 h for **5**). This change is attributed to slow decomposition of the product. By taking the observed α_{max} as equal to α_∞, velocity constants were calculated and found to be in good agreement with those determined for the mutarotation for 0.05 *M* solutions (Table 1).

In order to establish the cause of the mutarotation, the changes in n.m.r. spectra accompanying the mutarotation for 0.4 *M* solutions were determined. The spectra for the freshly prepared solutions and the solutions at maximum rotation using DMF-d_7 as solvent are presented in Fig. 1. At all intermediate reaction times, the spectra

Can. J. Chem. Downloaded from www.nrcresearchpress.com by 210.87.254.5 on 09/05/12
For personal use only.

Can. J. Chem. Downloaded from www.nrcresearchpress.com by 210.87.254.5 on 09/05/12
For personal use only.

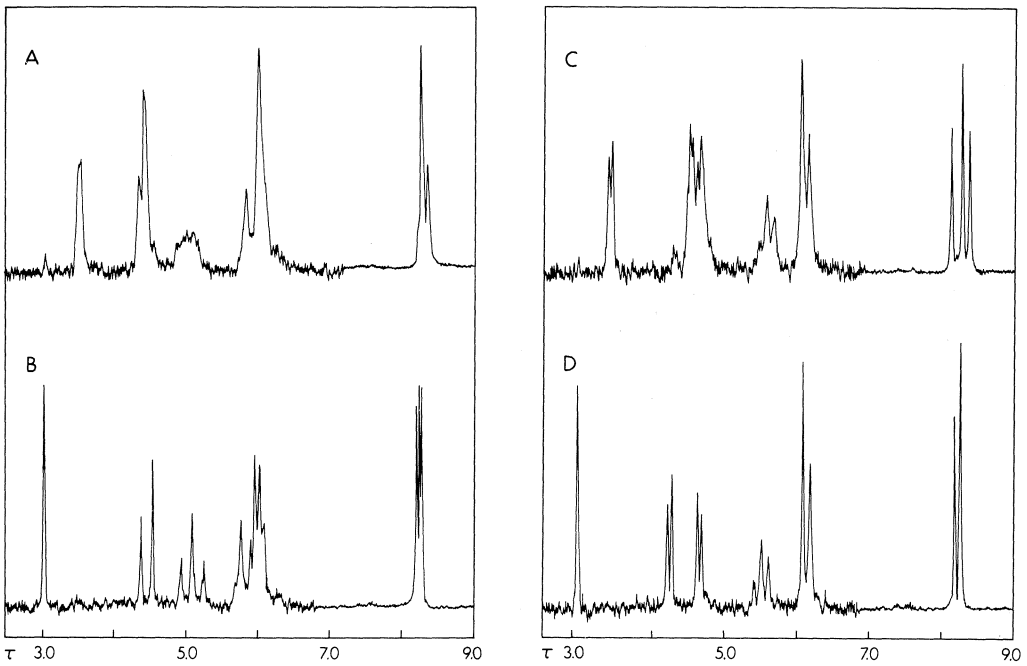

FIG. 1. P.m.r. spectra in DMF-d_7 at 60 MHz. (A) Dimeric tri-*O*-acetyl-2-deoxy-2-nitroso-α-D-glucopyranosyl chloride (**1**). (B) Tri-*O*-acetyl-2-oximino-α-D-*arabino*-hexopyranosyl chloride (**3**). (C) Dimeric tri-*O*-acetyl-2-deoxy-2-nitroso-α-D-galactopyranosyl chloride (**5**). (D) Tri-*O*-acetyl-2-oximino-α-D-*lyxo*-hexopyranosyl chloride (**6**).

TABLE 2. N.m.r. parameters for tri-*O*-acetyl-2-oximino-α-D-hexopyranosyl chlorides

		Chemical shifts (τ)				Spacings (Hz)	
Configuration	Solvent	H-1	H-3	H-4	Oxime hydroxyl proton	$J_{3,4}$	$J_{4,5}$
arabino (**3**)	DMF-d_7	3.05	4.46	5.11	−2.5*	9.75	9.25
	$CDCl_3$	2.83	4.10	4.74	−1.19†	9.75	9.0
lyxo (**6**)	DMF-d_7	2.96	4.24	4.66	−2.31*	3.25	3.75
	$CDCl_3$	2.75	3.99	4.45	−1.21†	3.25	3.50

*Broad peak.
†Sharp singlet.

were those of the starting material superimposed on that of the product. Examination of the signals and their integration clearly required the formation in each case of only one observable product. No intermediates were detected.[4] The rates of the reactions were calculated from the n.m.r. data and the first order velocity constants were found to be in close agreement (see Table 1) with those determined polarimetrically.

The products **3** and **6** proved to be highly labile and neither was obtained in crystalline form. Nevertheless, preparations of greater than 90% purity could be obtained by removal of the DMF in high vacuum. The n.m.r. parameters are compared for solutions in DMF-d_7 and $CDCl_3$ in Table 2 where it is seen (as in Fig. 1) that the products are assigned the tri-*O*-acetyl-2-oximino-α-D-*arabino*- (**3**) and tri-*O*-acetyl-2-oximino-α-D-*lyxo*-hexopyranosyl chloride (**6**) structures. These assignments are required by the singlets for the anomeric hydrogens and the presence in each

[4]In early experiments, there was an appearance of a singlet at τ 4.11 during the mutarotation of **1** which disappeared with prolonged reaction time. This phenomenon was traced to the presence of small amounts of water leading to 3,4,6-tri-*O*-acetyl-2-oximino-D-glucose which subsequently was consumed by condensation with the excess glycosyl chloride.

Can. J. Chem. Downloaded from www.nrcresearchpress.com by 210.87.254.5 on 09/05/12
For personal use only.

case of signals for oxime hydroxyl groups (see Table 2). The positions of the anomeric signals at lower field than those of the starting material, the high dextrorotations, and theoretical considerations (5) leave no doubt that the anomeric configurations are α-D in both cases. The rearrangement of dimeric nitrosyl chloride adducts of alkenes to α-chlorooximes is well known (15).

Since the monitoring of the reactions by n.m.r. did not reveal intermediate compounds, it was apparent that the rate-determining step for the overall reactions in both cases was the dissociation of the dimeric starting material. This was confirmed for the *gluco*-compound **1** by a kinetic investigation of the 2-deuterio derivative. The compound was prepared in the normal manner starting from 2-deuterio-D-glucose pentaacetate which in turn was prepared from isopropyl 2-deuterio-α-D-glucopyranoside (6). Two distinctly different routes (16, 17) can be envisaged for the conversion of **1** to **3**. One route would involve a prototropic shift involving H-2 of the monomeric nitrosochloride **2** to yield **3**. The other route would involve dehydrochlorination of **2** to the nitrosoglycal **4** which subsequently undergoes 1,4-addition of the hydrogen chloride to form **3**. Both of these reaction routes are expected to display primary kinetic isotope effects since in both cases cleavage of the C_2—H_2 bond occurs in the rate-controlling stage. Since the 2-deuterated **1** underwent conversion to **3** at about the same rate, within experimental error, as did **1** (see Table 1), it is further apparent that dissociation of **1** to **2** is indeed the rate-controlling step. Thus, the slower transformation of the *lyxo*-dimer (**5**) appears related to an inherently greater stability of this dimer rather than shielding of H-2 by the axial acetoxy group at C-4 affecting the rate of the isomerization of the monomeric form.

The formation of α-oximinoglycoside on reacting **1** with an alcohol in DMF is considered to proceed by way of the nitrosoglycal **4** (10). Glycoside formation also takes place starting from the oximinochloride **3** (10) and **4** is a plausible intermediate in this reaction as well. Indeed, the possibility existed that, starting with **1** in the presence of an alcohol, the formation of oximinochloride **3** is effectively the first stage of the reaction and that oximinoglycoside formation then follows. An accompanying paper (10) establishes this to be essentially the route of reaction.

The postulation of the nitrosoglycal **4** as an intermediate in oximinoglycoside formation was previously based on the appearance of a faintly blue coloration for concentrated solutions of **1** in methylene chloride buttressed by theoretical considerations (5). We now wish to report direct observation of this intermediate.

It is known that solutions of cyclic α,β-unsaturated monomeric nitroso compounds are blue and show absorption maxima in the neighborhood of 700 mμ (15). A 0.2 *M* solution of **1** in chloroform was faintly blue and showed a weak absorption maximum at 680 mμ with a shoulder at 620 mμ. On addition of triethylamine, the blue coloration became intense and the intensity of the peak at 680 mμ was greatly enhanced. Oximinochloride (**3**) formation is a very slow process with chloroform as solvent in spite of nitrosoglycal formation being evident. Thus, both 0.2 and 0.425 *M* solutions in $CDCl_3$ showed essentially no change in their n.m.r. spectra over 4 days at 25°. It is reasonable to assign the shoulder at 620 mμ to monomer **2**. Although the dimer **1** does not absorb in the visible, it shows an absorption maximum at 300 mμ (ε 10 000) which is characteristic of dimeric α-chloronitroso structures (16). It is apparent then that, in chloroform, **1** reversibly dissociates to **2** which dehydrochlorinates to **4** and that the latter process is reversed by highly preferential 1,2-addition of the hydrogen chloride. This may also be the case with DMF as solvent but the relative rates of the various reactions do not allow investigation of this matter. It is likely that in chloroform, as in DMF, the oximinochloride **3** is the stable reaction product but its rate of formation is extremely slow. Lemieux *et al.* (5) demonstrated the preparation of oximinoglycosides by reaction of **1** with an alcohol in refluxing methylene chloride. Under these conditions, the hydrogen chloride is continuously removed from the reaction mixture by volatilization. Thus, reaction of **4** with the alcohol is promoted.

Both freshly prepared 0.4 *M* solutions of **1** and solutions of **3** in DMF are colorless. However, addition of triethylamine to either solution rapidly leads to a deep blue coloration which disappears in a few minutes. The maximum coloration was greater starting from the oximinochloride **3** and this is in line with the requirement that the dimer **1** must first dissociate before dehydrochlorination to nitrosoglycal **4** can occur. When a 0.4 *M* solution of **1** was treated with 0.5 equiv of triethylamine, the deep blue solution

Can. J. Chem. Downloaded from www.nrcresearchpress.com by 210.87.254.5 on 09/05/12
For personal use only.

rapidly filtered free of precipitated triethylamine hydrochloride, and the n.m.r. spectrum was determined within 2 min, the intensity of the signal for anomeric hydrogen of **1** was decreased to half its original intensity and there appeared a sharp singlet at τ 0.3. This signal decayed rapidly at about the same rate as the blue coloration as judged by visual inspection. Further addition of triethylamine deepened the blue coloration, and completely eliminated the doublet at τ 3.61 but slightly increased the intensity of the signal at τ 0.3 before it vanished completely with the disappearance of the blue color. The latter signal is assigned to H-1 of tri-*O*-acetyl-2-nitroso-D-glucal (**4**). The nitroso group is expected (5) to strongly deshield H-1 especially in the *syn*-configuration. The signal for H-1 of tri-*O*-acetyl-2-nitro-D-glucal is at τ 1.67 (2).

The discoloration of the blue color of solutions of 1-nitrosocyclohexene has been attributed to polymerization (15). Addition of 1 equiv of triethylamine to a freshly prepared 0.022 *M* solution of **1** in DMF led to a deep blue solution with an absorption maximum at 645 mμ. The decrease in the intensity of the absorption with time was followed. A clear yellow solution resulted after 7 h. At higher (0.5 *M*) initial concentrations of **1**, the blue coloration disappeared more rapidly. The product is an amorphous solid with the composition and average molecular weight (osmometric) corresponding to about a tetramer of **4**.

The reaction properties of **5** were not examined in as much detail as those of **1** but cursory tests indicated very similar properties.

In conclusion, the present results indicate that the dimeric nitrosyl chloride adducts of acetylated glycals have very similar properties to those described by Pritzkow and coworkers (15, 16) for α-chloronitrosoalkanes. Because of activation by the ring oxygen in the development of positive charge at the anomeric center, the glycosyl chlorides are much more reactive. Further details on the reaction properties of these compounds in the presence of alcohols are presented in an accompanying paper (10).

Experimental

Absorption spectra were obtained with a Cary Recording Spectrophotometer Model 14 M using a 1 cm cell. N.m.r. spectra were recorded at 60 MHz on a Varian A 56–60 instrument at 25 ± 0.5° using tetramethylsilane as the external standard. Optical rotations were determined in a Perkin–Elmer Model 141 automatic recording polarimeter at 25 ± 0.5°.

Tri-*O*-acetyl-2-deoxy-2-nitroso-α-D-glucopyranosyl chloride dimer (**1**) and its *galacto*-isomer **5** were prepared as previously described (2, 7), recrystallized twice from chloroform – *n*-hexane, and dried *in vacuo* over phosphorus pentoxide and stored at 4°. Before each experiment, the compounds were redried and the purity of the materials checked by t.l.c. (ethyl acetate – *n*-hexane (1:1)) and m.p.

Reagent grade dimethylformamide and dimethylformamide-d_7 (Merck, Sharp and Dohme of Canada Ltd., Montreal) were distilled from phosphorus pentoxide.

2-Deuterio-β-D-glucopyranose pentaacetate (Raylo Chemicals Ltd., Edmonton, Alberta) was converted to 2-deuterio-D-glucal triacetate using standard procedure (18). The structure of the compound was confirmed by n.m.r. in deuteriochloroform at 100 MHz using tetramethylsilane as the internal standard (τ 3.54, H-1, $J_{1,3}$ = 1.5 Hz (deuterium decoupled at 15.351 MHz); 4.66, H-3, $J_{3,4}$ = 6.0 Hz; 4.80, H-4, $J_{4,5}$ = 7 Hz). The dimeric nitrosyl chloride adduct of 2-deuterio-D-glucal triacetate was prepared as previously described for the non-deuterated analog (2, 7).

We wish to thank the National Research Council of Canada for support of this work through a grant-in-aid of research (A-172) to R.U.L., and Mr. W. Merlo and Miss P. Nayar for technical assistance. Thanks are also expressed to R.N. Swindlehurst, J. Hoyle, and Mrs. D. Formanski for measurements of n.m.r. spectra.

1. R. U. Lemieux, T. L. Nagabhushan, and I. K. O'Neill. Tetrahedron Lett. 1909 (1964).
2. R. U. Lemieux, T. L. Nagabhushan, and I. K. O'Neill. Can. J. Chem. **46**, 413 (1968).
3. W. J. Serfontein, J. H. Jordaan, and J. White. Tetrahedron Lett. 1069 (1964).
4. R. U. Lemieux, R. A. Earl, K. James, and T. L. Nagabhushan. Can. J. Chem. **51**, 19 (1973).
5. R. U. Lemieux, T. L. Nagabhushan, and S. W. Gunner. Can. J. Chem. **46**, 405 (1968).
6. R. U. Lemieux, R. Suemitsu, and S. W. Gunner. Can. J. Chem. **46**, 1060 (1968).
7. R. U. Lemieux and T. L. Nagabhushan. Methods in carbohydrate chemistry. Vol. VI. Editors, R. L. Whistler and J. N. BeMiller. Academic Press, New York. 1972. p. 487.
8. R. U. Lemieux and S. W. Gunner. Can. J. Chem. **46**, 397 (1968).
9. T. L. Nagabhushan. Can. J. Chem. **48**, 257 (1970).
10. R. U. Lemieux, Y. Ito, K. James, and T. L. Nagabhushan. Can. J. Chem. **51**, 7 (1973).
11. R. U. Lemieux, K. James, and T. L. Nagabhushan. Can. J. Chem. **51**, 27 (1973).
12. R. U. Lemieux, K. James, T. L. Nagabhushan, and Y. Ito. Can. J. Chem. **51**, 33 (1973).
13. R. U. Lemieux, K. James, and T. L. Nagabhushan. Can. J. Chem. **51**, 42 (1973).
14. R. U. Lemieux, K. James, and T. L. Nagabhushan. Can. J. Chem. **51**, 48 (1973).

15. W. PRITZKOW, H. SCHAEFER, P. PABST, A. EBENROTH, and J. BEGER. J. Prakt. Chem. **29**, 123 (1965).
16. G. COLLIN, R. HÖHN, H. G. HAUTHAL, H. HÜBNER, W. PRITZKOW, W. ROLLE, H. SCHAEFER, and M. WAHREN. Ann. **702**, 55 (1967).
17. A. DORNOW and H. D. JORDAN. Chem. Ber. **94**, 76 (1961).
18. F. SHAFIZADEH and M. STACEY. J. Chem. Soc. 3608 (1952).

Can. J. Chem. Downloaded from www.nrcresearchpress.com by 210.87.254.5 on 09/05/12
For personal use only.

The Reaction of Dimeric Tri-*O*-acetyl-2-deoxy-2-nitroso-α-D-hexopyranosyl Chlorides with Alcohols[1]

R. U. LEMIEUX, Y. ITO,[2] K. JAMES,[3] AND T. L. NAGABHUSHAN[4]

Department of Chemistry, University of Alberta, Edmonton, Alberta

Received June 2, 1972

The kinetics of the reactions of dimeric tri-*O*-acetyl-2-deoxy-2-nitroso-α-D-glucopyranosyl chloride (**1**) with simple aliphatic alcohols (4 mol equiv) in dimethylformamide to form alkyl tri-*O*-acetyl-2-oximino-α-D-*arabino*-hexopyranosides (**5**) were investigated by n.m.r. and optical rotation. It is concluded that the conversion of **1** to **5** proceeds basically by way of three successively formed intermediates, namely, the monomeric form (**2**) of **1**, the tri-*O*-acetyl-2-oximino-α-D-*arabino*-hexopyranosyl chloride (**3**), and the tri-*O*-acetyl-1,5-anhydro-2-deoxy-2-nitroso-D-*arabino*-hex-1-enitol (**4**). Direct evidence was obtained only for the intermediacy of **3** and the transient existence at low concentration of an uncharacterized intermediate which may be the β-anomer of **5**. The intermediate **4** could form directly from **2** and thereby provide a mechanism for the formation of **5** which by-passes **3**. However, the kinetic investigations showed this route to be of very minor, if any, importance. In all cases, the rate of the disappearance of **1** was virtually the same and within experimental error the same as for the isomerization of **1** to **3** in the absence of the alcohol for which the rate-controlling stage is dissociation of **1** to **2**. Methanol reacts with **4** only about 5 times faster than does *t*-butanol.

The utility of the reaction for the preparation of oximinoglycosidic structures related to disaccharides is illustrated by glycosidations of 1,2;3,4-di-*O*-isopropylidene-α-D-galactopyranose, 1,2;5,6-di-*O*-isopropylidene-α-D-glucofuranose both by **1** and by the dimeric tri-*O*-acetyl-2-deoxy-2-nitroso-α-D-galactopyranosyl chloride (**6**) and of 2,3;5,6-di-*O*-isopropylidene-α-D-mannofuranose by **1**. The reaction of **6** with 1,2;3,4-di-*O*-isopropylidene-α-D-galactopyranose provided an 8.7% yield of the β-oximinoglycoside along with an 80% yield of the α-anomer.

Les cinétiques de réaction entre le chlorure de tri-*O*-acétyl déoxy-2 nitroso-2-α-D-glucopyranosyle dimère (**1**) et les alcools aliphatiques simples (4 mol equiv) dans le diméthylformamide pour conduire aux alkyles tri-*O*-acétyl oximino-2-α-D-*arabino*-hexopyranosides (**5**) ont été étudiées par r.m.n. et rotation optique. On a conclu que la conversion de **1** à **5** procède surtout par la formation successive de trois intermédiaires à savoir, la forme monomère (**2**) de **1**, le chlorure de tri-*O*-acétyl oximino-2-α-D-*arabino*-hexopyranosyle (**3**) et le tri-*O*-acétyl anhydro-1,5 deoxy-2 nitroso-2-D-*arabino*-hexenitol (**4**). Une preuve directe a été obtenue seulement pour l'intermédiaire **3** de même que l'existence transitoire, à faible concentration, d'un intermédiaire non caractérisé qui pourrait être l'anomère β de **5**. L'intermédiaire **4** peut se former directement à partir de **2** et de ce fait, fournit un mécanisme pour la formation de **5** sans passer par **3**. Les études cinétiques montrent que cette voi est cependant d'importance mineure. Dans tous les cas, la vitesse de disparition de **1** reste virtuellement la même; de même que pour l'isomèrisation de **1** en **3**, dans les limites de l'erreur expérimentale, en l'absence d'alcool pour laquelle l'étape déterminante est la dissociation de **1** en **2**. Le méthanol réagit avec **4** environ 5 fois plus vite que le *t*-butanol.

L'utilité de cette réaction dans la préparation de structures oximinoglycosidiques apparentées aux disaccharides est illustrée par les glycosidations du di-*O*-isopropylidène-1,2,3,4-α-D-galactopyranose, du di-*O*-isopropylidène-1,2,5,6-α-D-glucofuranose par **1** et par le chlorure de tri-*O*-acétyl-deoxy-2 nitroso-2-α-D-galactopyranosyle (**6**) et du di-*O*-isopropylidène-2,3,5,6-α-D-mannofuranose par **1**. La réaction de **6** avec le di-*O*-isopropylidène-1,2,3,4-α-D-galactopyranose conduit à 8.7% de β-oximinoglycoside et 80% d'anomère α. [Traduit par le journal]

Can. J. Chem., **51**, 7 (1973)

The reaction of dimeric tri-*O*-acetyl-2-deoxy-2-nitroso-α-D-glucopyranosyl chloride (**1**) with simple alcohols in dimethylformamide (DMF) was reported to yield tri-*O*-acetyl-2-oximino-α-D-*arabino*-hexopyranosides in high yield (1). The synthetic usefulness of this reaction was reported in previous (2–6) and accompanying communications (7–11) where it is shown that the α-oximinoglycosides are excellent precursors of α-glucopyranosides and α-glucopyranosaminides. In view of this, we have examined in some detail the reaction of **1** with simple alcohols and ex-

[1]Presented in part at the 161st National American Chemical Society Meeting, Los Angeles, California, March 28, 1971.

[2]University of Alberta Postdoctoral Fellow, 1965. Present address: Microbial Chemistry Research Laboratory, Tanabe Seiyaku Co. Ltd., Toda-Shi, Saitama-ken, Japan.

[3]University of Alberta Postdoctoral Fellow, 1970–1972.

[4]Professional Research Associate, 1970–1972.

Can. J. Chem. Downloaded from www.nrcresearchpress.com by 210.87.254.5 on 09/05/12
For personal use only.

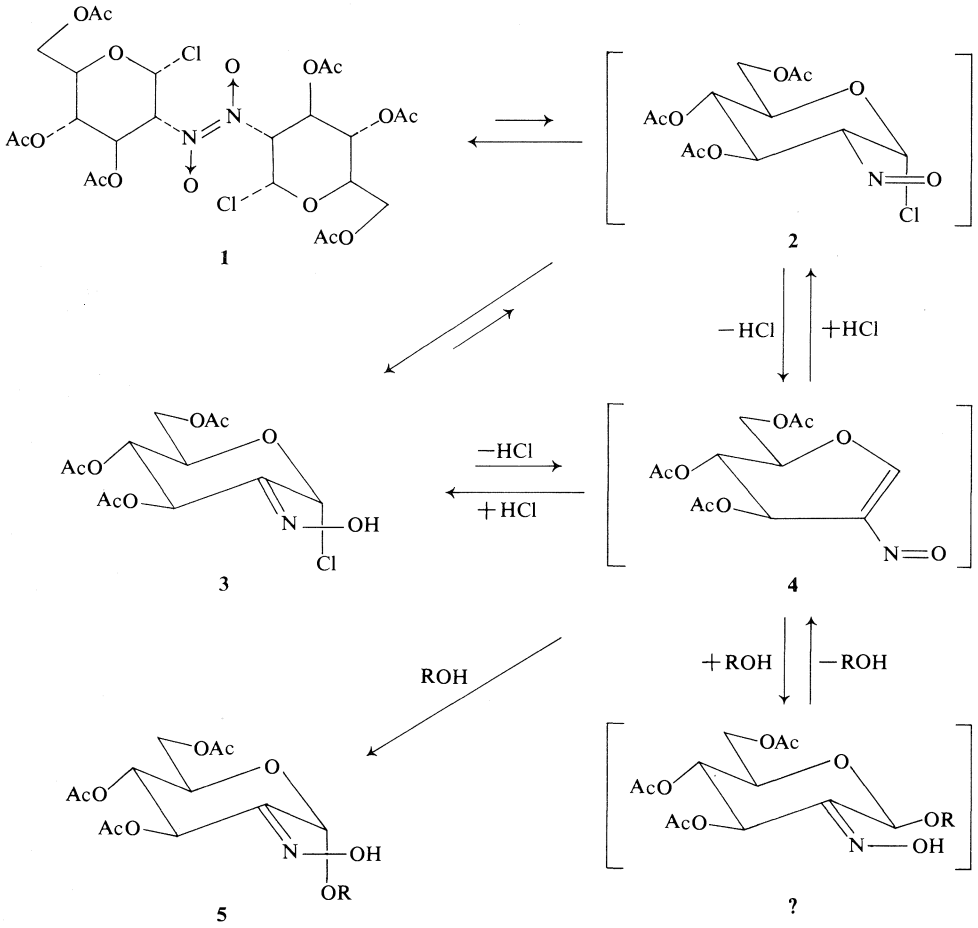

tended it to the preparation of tri-*O*-acetyl-2-oximino-α-D-*arabino*- (and α-D-*lyxo*-) hexopyranosyl derivatives of suitably protected monosaccharides (see Scheme 1).

When the course of the reaction of either tri-*O*-acetyl-2-deoxy-2-nitroso-α-D-glucopyranosyl chloride dimer (**1**) or its *galacto*-isomer **6** with an alcohol in DMF is followed polarimetrically, an initial upward mutarotation of the solution occurs which is soon followed by a downward change. Typical mutarotation curves obtained for reactions of **1** with 4 mol equiv (2 mol equiv per mol of monomeric form) of alcohols in dry DMF at 25° are shown in Fig. 1. It was established in the previous paper (12) of this series that compounds **1** and **6** isomerize in dimethylformamide to the more dextrorotatory oximinochlorides **3** and **7**, respectively. Therefore, the initial increases in rotation observed for the reactions of **1** and **6** with alcohols in DMF were expected to be related to the appearance of compounds **3** and **7**, respectively, as reaction intermediates. Indeed, when the reactions were followed by p.m.r. using DMF-d_7 as solvent, compounds **3** and **7** were clearly apparent as the main reaction intermediates.

The formation of the oximinoglycosides (**5**) is not expected to occur with direct involvement of the oximinochloride precursor. The reactions of α-chlorooximes appear generally to proceed first by dehydrochlorination to highly reactive nitrosoalkene intermediates which subsequently undergo nucleophilic attack to form the α-substituted oximes (13). The formation of tri-*O*-acetyl-1,5-anhydro-2-deoxy-2-nitroso-D-*arabino*-hex-1-enitol (**4**) from the oximinochloride (**3**) was demonstrated (12) by the addition of triethylamine in order to render the rate of its formation more

Can. J. Chem. Downloaded from www.nrcresearchpress.com by 210.87.254.5 on 09/05/12
For personal use only.

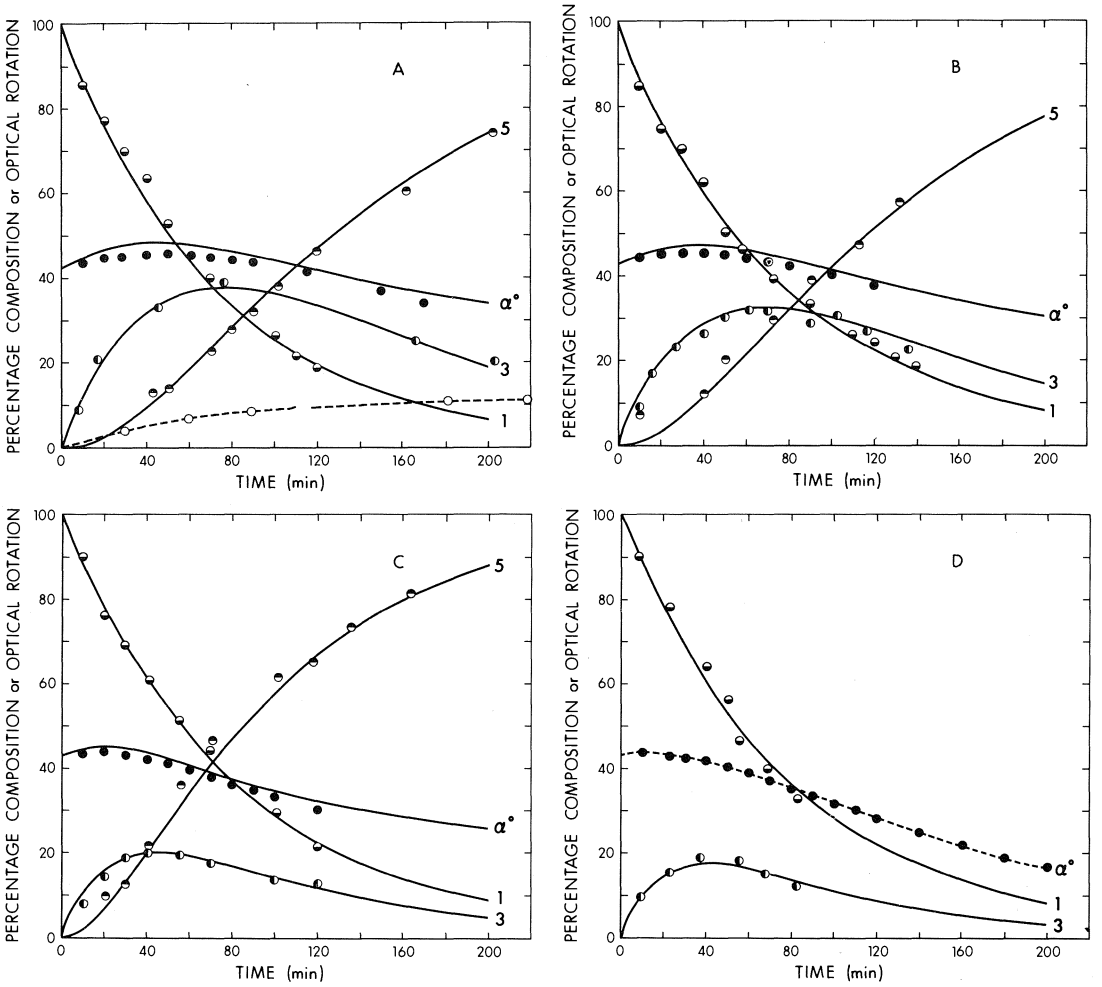

FIG. 1. Experimental values for the concentrations of dimeric tri-*O*-acetyl-2-deoxy-2-nitroso-α-D-glucopyranosyl chloride (**1**), ◒; tri-*O*-acetyl-2-oximino-α-D-*arabino*-hexopyranosyl chloride (**3**), ◐; and alkyl tri-*O*-acetyl-2-oximino-α-D-*arabino*-hexopyranoside (**5**), ◓; plus an apparent glycocidic intermediate. The approximate concentration of the intermediate is represented by the dotted line, ○, in part A. All measurements involved reaction of 0.4 *M* **1** with the hydroxy compound (1.6 *M*) in DMF at 25°. The alcohol was *t*-butanol in A, isopropanol in B, and methanol in C. Part D is for the reaction using deuterium oxide. These values were estimated by n.m.r. The solid lines are the result of calculations assuming that only **3** and **5** were formed. The points represented by ● are the observed rotations of the reaction mixtures. The solid α° lines in A, B, and C are the observed rotations expected with only **3** and **5** as products of the reaction. The dotted α° line in D represents the observed rotations.

rapid than its rate of disappearance through polymer formation.

For the above-stated reasons, the course of events on mixing the dimer **1** with an alcohol (ROH) in DMF is considered to first involve reversible dissociation of **1** to a very low near steady-state concentration of the monomer **2**. The formation of the oximinochloride **3** could occur by loss of hydrogen chloride (**2** → **4**) followed by addition of hydrogen chloride (**4** → **3**). However, the direct conversion of **2** to **3** by simple prototropic shift may be considered the predominant route since, as will be seen below, no evidence was obtained for the formation of **5** without the intervening formation of **3**. The oximinochloride (**3**) is expected to be particularly prone to dehydrochlorination (15) to the intermediate **4** and this reversible reaction is expected to be promoted by the weakly basic polar solvent DMF. That the acidity of the oximino group pro-

Can. J. Chem. Downloaded from www.nrcresearchpress.com by 210.87.254.5 on 09/05/12
For personal use only.

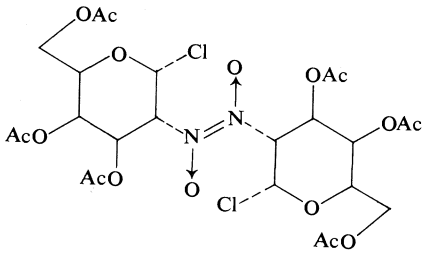

6

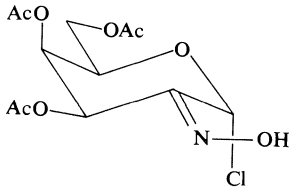

7

vides a facile mechanism for the dehydrochlorination is supported by the observation that the *O*-acetyl derivative of **3** (2-acetoximino-tri-*O*-acetyl-α-D-*arabino*-hexopyranosyl chloride) did not react with isopropanol in DMF. However, neither the rate of the formation of **3** from **1** nor the formation of **5** from **3** is appreciably affected by the presence of hydrogen chloride. This was evident from the observation that the presence of hydrogen chloride (0.4 *M*) at the beginning of the reactions had no effect on the mutarotation observed and reported in Fig. 1. Furthermore, in the case of the reaction with methanol, the reaction in the presence of the added hydrogen chloride was followed by n.m.r. The values for k_1 and k_2 estimated were, within experimental error, the same as those reported in Table 1.

Hydrogen chloride is expected to depress the concentration of **4** but to catalyze the reaction of **4** with ROH to form oximinoglycosides. In the absence of alcohol or hydrogen chloride **4** can polymerize (12). When the reaction of **1** with isopropanol in DMF was kept weakly basic throughout the course of reaction by the presence initially of an equimolar amount of *sym*-collidine, the initial rise in optical rotation was not observed and the yield of α-oximinoglycoside was low (about 50%). Thus, we do not recommend basic reaction conditions for the preparation of α-oximinoglycosides (16). As will be seen below, the possibility exists that α-oximinoglycoside formation may involve to some extent anomerization of initially formed β-oximinoglycoside.

A study was made of oximinoglycoside formation from the oximinochloride (**3**). In view of the uncertainty in the purity of the starting material, the results can only be considered semi-quantitative. A 0.4 *M* solution of **1** in DMF was first allowed to isomerize to **3** and then 2 equiv of either methanol or *t*-butanol were added. Reaction began immediately to form eventually the corresponding alkyl tri-*O*-acetyl-2-oximino-α-D-*arabino*-hexopyranoside (**5**) in greater than 85% yield. Since these alkyl groups provide singlet n.m.r. signals and the chemical shifts of the glycosidic alkyl groups were to lower field than those of the alcoholic alkyl groups, it was possible to estimate the rates of glycoside formation by measuring, after various reaction times, the intensities of these signals relative to the group of signals arising from the acetoxy groups. Analysis showed the rates of appearance of oximinoglycoside (**5**) to be first-order as were the changes in optical rotation during the course of the reactions. The velocity constant thus determined for methanol was 0.025 min^{-1} by n.m.r. and 0.028 min^{-1} by polarimetry. For *t*-butanol, the velocity constant was estimated to be 0.012 min^{-1} by n.m.r. and 0.018 min^{-1} by polarimetry. These first-order changes together with the observation that an electrophilic reaction with methanol is only about twice as fast as for *t*-butanol indicated that the overall rate of reaction was controlled by the rate of the conversion of **3** to the nitrosoglycal **4**. Since the solutions remained colorless and **4** is a deeply blue-colored compound (12), the concentration of **4** must remain extremely small throughout the course of reaction. When the product formed from a 0.4 *M* solution of **1** in DMF containing 1 mol equiv of both methanol and *t*-butanol was analyzed by n.m.r., the ratio of the methyl to *t*-butyl oximinoglycosides was near 5 after 10 h and this ratio remained constant within experimental error up to 48 h. Thus, the nitrosoglycal **4** shows little discrimination between the two alcohols as may be expected for a highly reactive species. The *t*-butyl oximinoglycoside was dissolved in DMF at 25° which was 0.8 *M* both in methanol and in hydrogen chloride to afford a 0.8 *M* concentration of the oxime. There was no change in the n.m.r. spectrum of the solution after 5 h and no appearance of the

Can. J. Chem. Downloaded from www.nrcresearchpress.com by 210.87.254.5 on 09/05/12
For personal use only.

TABLE 1. Reactions of dimeric tri-*O*-acetyl-2-deoxy-2-nitroso-α-D-glucopyranosyl chloride (**1**) (0.4 *M*) with alcohols and deuterium oxide (1.6 *M*) in *N*,*N*-dimethylformamide at 25°

	α_{max}°*		$k_1 \times 10^3$, min^{-1}		t_{max}, min†		C_{max}, %‡		$k_2 \times 10^3$, min^{-1}§	
	Found	Calcd.	Found	Calcd.	Found	Calcd.	Found	Calcd.	Found	Calcd.
Deuterium oxide	43.4 (16)	—	12.0	12.6	40	40	19	17	—	44
Methanol	43.8 (16)	45.2 (19)	12.6	12.6	45	45	22	20	28 (25)	36
Isopropanol	45.6 (31)	47.1 (37)	13.8	12.6	70	70	34	32	—	16
t-Butanol	45.6 (47)	48.4 (48)	12.6	13.6	85	80	39	42	18 (12)	13

*The maximum observed rotation achieved with, in parentheses, the reaction time (min) elapsed.
†Reaction time for maximum accumulation of **3**.
‡Maximum concentration of **3**, achieved as percentage of the original concentration of **1**.
§Calculated values by curve fitting (see Fig. 1) assuming two consecutive first-order processes $\mathbf{1} \xrightarrow{k_1} \mathbf{3} \xrightarrow{k_2} \mathbf{5}$. The found values are from the polarimetric rates starting with **3**. The values in parentheses were determined by following the reaction by n.m.r. These constants must be considered as very approximate.

methyl glycoside after 2 days at 25°. However, some decomposition (about 10%) of the *t*-butyl glycoside had occurred. Thus, the formation of the α-oximinoglycosides (**5**) is essentially irreversible under these reaction conditions. For these reasons, as will be seen below, an effort was made to rationalize the reactions of **1** with methanol, isopropanol, and *t*-butanol on the basis of two irreversible consecutive first-order reactions, namely,

$$\mathbf{1} \xrightarrow{k_1} \mathbf{3} \xrightarrow{k_2} \mathbf{5}$$

The reactions of **1** with deuterium oxide, methanol, isopropanol, and *t*-butanol were followed both polarimetrically and by n.m.r. under the conditions described in Table 1. The data accumulated are plotted in Fig. 1. The n.m.r. measurements were complicated by the movement of a wide band attributed to signal from exchangeable hydrogen across the τ 3–4 region (where the signals for the anomeric hydrogens of **1**, **3**, and **5** occur) as reaction proceeded. As a result, it was not possible to estimate the relative concentrations of **1** and **3** to an acceptable degree of accuracy at some of the reaction times. The extent of glycoside formation was best assessed when methanol and *t*-butanol were the reagents since in these experiments it was possible to measure the intensity of the signal arising from the alkyl group of the glycoside relative to that arising from the three acetyl groups. In both cases, two signals for the glycosidic alkyl group were present shortly after the beginning of the reaction. The less intense signal reached a maximum somewhat later than did the oximinochloride intermediate (**3**) and was not present at the end of the reaction (about one day). When reaction mixtures containing the two signals were worked-up by solvent removal, the product showed only one signal. Thus, isomerization of this labile intermediate to the *Z*-α-oximinoglycoside (**5**) (14) appears to occur during the work-up. This phenomenon could not be traced to oxime hydrochloride formation. It could conceivably arise through transient formation of either *Z*- or *E*-β-oximinoglycoside (17) or *E*-α-oximinoglycoside in their acetylated forms.

The intermediate was also observed when **3** was the starting material and its formation appears to be promoted by dilution of the mixture. Thus, when *t*-butanol (4 mol equiv) was reacted with **1** at initial concentrations of **1** of 0.4, 0.2, and 0.1 *M*, the reaction mixtures after 26 h, as measured by n.m.r., contained ~0, 11, and 19% of the reactive intermediate. After 48 h, the 0.2 *M* solution was free of the signal for the intermediate and that for the 0.1 *M* solution was reduced to 12%.

The extent of the formation of this intermediate could only be estimated quantitatively for *t*-butyl glycoside formation and only very approximately since the two singlets were partially overlapped. These data are plotted in Fig. 1A where it is seen that the maximum accumulation was about 11% under the conditions described.

The structure of this intermediate is under investigation. That it may be the β-anomer of **5** is possible since direct evidence for the formation of β-oximinoglycoside in low yield was obtained by the isolation of 6-*O*-(tri-*O*-acetyl-2-oximino-β-D-*lyxo*-hexopyranosyl)-1,2;3,4-di-*O*-isopropylidene-α-D-galactopyranose (**10**) in 8.7% yield. It is believed that the β-anomer of compound **8** was also formed but this product was not characterized as such. Thus, it may prove that to a degree

Can. J. Chem. Downloaded from www.nrcresearchpress.com by 210.87.254.5 on 09/05/12
For personal use only.

Can. J. Chem. Downloaded from www.nrcresearchpress.com by 210.87.254.5 on 09/05/12
For personal use only.

β-oximinoglycoside formation precedes formation of the α-anomer but is anomerized by way of **4**.

In an attempt to gain insight on the nature of the unknown intermediate, an examination was made of whether or not the polarimetric and n.m.r. rates were compatible by assuming only the presence of compounds **1**, **3**, and **5** during the course of reaction. As seen in Fig. 1 and Table 1 treatment of the data as resulting from two consecutive first-order reactions allowed fairly good fits of theoretical curves.[5] As seen from Table 1, this was accomplished with $k_1 = 0.0126$ min^{-1} for deuterium oxide, methanol, and isopropanol. The determination of k_1 in the absence of alcohol was previously reported (12). The slightly higher value, $k_1 = 0.0136$ min^{-1} was required for an equally good fit for the data using *t*-butanol. Using these calculated values and the observed rotations of **1** (42.5°), **3** (67.0°), and of the appropriate glycoside, methyl (12.2°), isopropyl (22.3°), and *t*-butyl (24.5°), measured in 0.8 *M* hydrogen chloride in DMF at 25°, the expected polarimetric curves were calculated and shown in Fig. 1. Considering the rather large experimental uncertainties involved, the fit is considered to be remarkably good in all instances and it must be concluded that the overall process is largely **1** → **3** → **5**. It is noteworthy, however, that for the three alcohols the measured upward change in rotation was slightly less than that expected by calculation. This result would be in line with the formation of a labile intermediate of lower optical rotation than the *Z*-α-oximinoglycoside (**5**) such as would be the case for its *Z*-β-anomer.

The main objective of this investigation was to establish practical means for the synthesis of α-linked oligosaccharide structures. In order to assess the method for this purpose, the reactions of the dimeric nitrosochlorides **1** and **6** with the well known di-*O*-isopropylidene derivatives of D-galactopyranose, D-glucofuranose, and D-mannofuranose were examined. Thus, experience was gained with the glycosidation of a primary hydroxyl group, a hindered secondary hydroxyl group, and an hemiacetal hydroxyl group. In each case, the desired α-oximinoglycoside was obtained in crystalline condition in good to excellent yield (see **8**, **9**, **11**, **12**, and **13**). The compositions and n.m.r. spectra (see Table 2) were in agreement with the assigned structures and the anomeric configurations of the oximinoglycosyl units were firmly established by conversion of compounds **8**, **9**, **11**, and **12** to α-glycosides (10). A consideration of the n.m.r. data presented in Table 2 leaves no doubt on this matter and the data also infer like configurations for the oximino groups since much greater changes in chemical shifts for the hydrogens of the oximinoglycosyl units, especially H-1′ and -3′, would be expected should any of the oximes not be in the *Z*-configuration (14).

To date, all our syntheses of oximinoglycosides using the nitrosyl chloride adducts **1** and **6** have led to the α-anomer as the major glycosidic product of reaction. However, evidence for the formation of the β-anomer was obtained for both the reactions of **1** and **6** with the primary hydroxyl group of 1,2;3,4-di-*O*-isopropylidene-α-D-galactopyranose. In the case of the crude product from the reaction of **1**, thin layer chromatographic examination showed the presence of a minor component with an R_f value very close to that of the major product (**8**) which gave a positive ferric chloride – ferricyanide reaction for oxime. This product could not be isolated in pure condition for characterization but its behavior was very similar to a minor product isolated in 8.7% yield in crystalline condition from the reaction of **6** with the diisopropylidene galactose. In an experiment prior to our achieving crystalline **8**, a crude preparation of **8** was reduced with lithium aluminum hydride and the *N*-2,4-dinitrophenyl derivative of the products were chromatographed on a silicic acid column. A chromatographic fraction containing a minor component was acetylated and the two products separated by preparative t.l.c. The composition and n.m.r. spectrum of one of the components were consistent with those expected for 6-*O*-[tri-*O*-acetyl-2-deoxy-(2,4-dinitroanilino)-β-D-mannopyranosyl]-1,2;3,4-di-*O*-isopropylidene-α-D-galactopyranose.

Reaction of **6** with 1,2;3,4-di-*O*-isopropylidene-α-D-galactopyranose provided the above-mentioned minor product and the major product (**9**) isolated in 80% yield. The minor product appeared to be the β-D-*lyxo*-isomer (**10**) of compound **9** since their compositions and n.m.r. spectra required the compounds to be isomers. The possibility that compound **10** was the *anti*-form of the major product did not appear compatible with the chemical shift of the anomeric

[5]The authors are indebted to Dr. R. E. D. McClung of this Department for his generous offer to provide the analog computer simulations shown in Fig. 1, which enabled us to obtain the calculated values listed in Table 1.

Can. J. Chem. Downloaded from www.nrcresearchpress.com by 210.87.254.5 on 09/05/12
For personal use only.

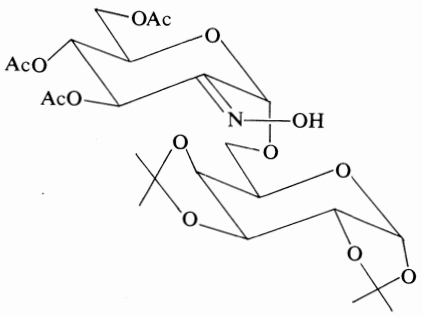

8 (67%)

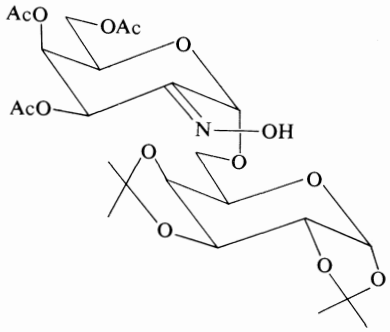

9 (80%)

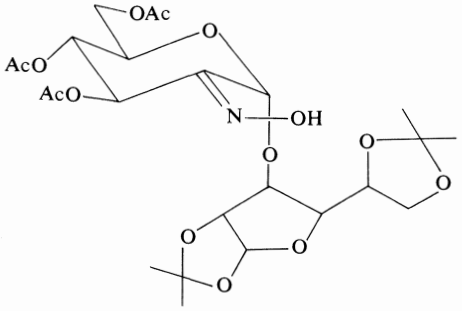

11 (59%)

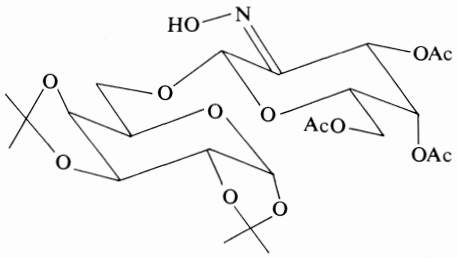

10 (8.7%)

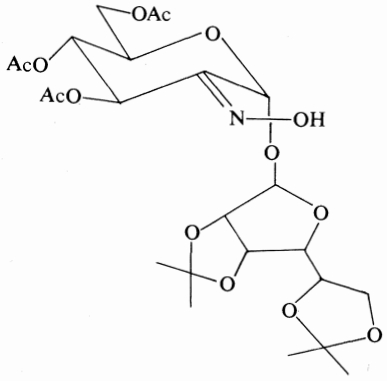

13 (41%)

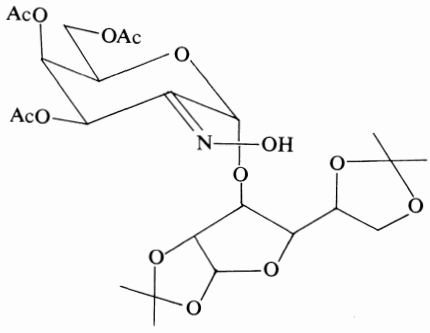

12 (53%)

hydrogen of the oximinoglycosyl unit since the signal was only 0.28 τ values to higher field than that of the major product. A shift of near 0.9 τ-value would be expected (14). Furthermore, the chemical shift of H-3′ was near that for the isomer (**9**). The compound (**10**) was deoximated and the product reduced with sodium borohydride to provide a single product which on acid hydrolysis liberated only D-talose and D-galactose (7). The specific rotation of the intermediate 1,2;3,4-di-*O*-isopropylidene-6-*O*-(β-D-talopyranosyl)-α-D-galactopyranose, was $-24.6°$ as compared to $+10°$ for 1,2,3,4-di-*O*-isopropylidene-6-*O*-(α-D-talopyranosyl)-α-D-galactopyranose (10). Thus, the β-

Can. J. Chem. Downloaded from www.nrcresearchpress.com by 210.87.254.5 on 09/05/12
For personal use only.

TABLE 2. N.m.r. parameters (60 MHz) for tri-*O*-acetyl-2-oximino-α-D-*arabino*- and α-D-*lyxo*-hexopyranosides and their oximeacetates in deuteriochloroform

	Oximinoglycosyl unit							Aglycon unit		
	Chemical shift (τ-values)					Spacings (Hz)		Chemical shift (τ-values)		Spacings (Hz)
Compound	H-1′	H-3′	H-4′	Acetyl	Oxime OH	$J_{3',4'}$	$J_{4',5'}$	H-1	Isopropylidene	$J_{1,2}$
6-O-(Tri-O-acetyl-α-D-hexopyranosyl)-1,2;3,4-di-O-isopropylidene-α-D-galactopyranose										
2-Oximino-*arabino*- **(8)**	3.98	4.25	4.84	7.93, 7.93, 7.93	0.56	10.0	9.75	4.50	8.48, 8.59, 8.68, 8.68	5.0
2-Acetoximino-*arabino*-	4.07	4.18	4.72	7.85, 7.90, 7.95, 7.95	—	11.0	—	4.50	8.46, 8.57, 8.68, 8.68	5.0
2-Oximino-*lyxo*- **(9)**	3.92	4.15	4.50	7.87, 7.93, 7.93	0.57	3.0	4.0	4.50	8.47, 8.56, 8.67, 8.67	4.0
2-Acetoximino-*lyxo*-	3.96	4.38	4.49	7.81, 7.88, 7.88, 7.95	—	3.50	—	4.49	8.45, 8.57, 8.67, 8.68	5.0
3-O-(Tri-O-acetyl-α-D-hexopyranosyl)-1,2;5,6-di-O-isopropylidene-α-D-glucopyranose										
2-Oximino-*arabino*- **(11)**	3.70	4.17	4.81	7.87, 7.91, 7.91	0.75	10.0	10.0	4.03	8.46, 8.56, 8.65, 8.65	3.50
2-Acetoximino-*arabino*-	3.84	4.17	4.78	7.83, 7.88, 7.92, 7.92	—	10.0	10.0	4.13	8.52, 8.60, 8.68, 8.68	3.50
2-Oximino-*lyxo*- **(12)**	3.70	4.17	4.51	7.89, 7.90, 7.94	0.54	3.50	—	4.11	8.50, 8.60, 8.67, 8.67	4.0
2-Acetoximino-*lyxo*-	3.71	4.04	4.42	7.78, 7.85, 7.87, 7.90	—	—	3.75	4.04*	8.39, 8.57, 8.66, 8.66	—
1-O-(Tri-O-acetyl-α-D-hexopyranosyl)-2,3;5,6-di-O-isopropylidene-α-D-mannofuranose										
2-Oximino-*arabino*- **(13)**	3.56	4.21	—	7.91, 7.91, 7.94	0.78	9.75	—	4.68	8.52, 8.57, 8.63, 8.63	0
2-Acetoximino-*arabino*-	3.77	4.19	4.72	7.83, 7.88, 7.94, 7.94	—	9.75	9.50	4.72	8.53, 8.57, 8.67	0

*Center of a pair of doublets due to superimposition of the anomeric signal of the glucofuranosyl unit on the H-3 signal of the oximinoglycosyl unit.

Can. J. Chem. Downloaded from www.nrcresearchpress.com by 210.87.254.5 on 09/05/12
For personal use only.

configuration was required. The 100 MHz n.m.r. spectra of the latter two compounds in deuterium oxide were virtually superimposable and could readily be taken as identical. However, the compounds were clearly different since they were readily separated by t.l.c.

Condensation of **1** with 1,2;5,6-di-*O*-isopropylidene-α-D-glucofuranose afforded crystalline 3-*O*-(tri-*O*-acetyl-2-oximino-α-D-*arabino*-hexopyranosyl)-1,2;5,6-di-*O*-isopropylidene-α-D-glucofuranose (**11**) in 59% yield. Similarly, the *lyxo*-isomer **12** was obtained in crystalline form from **6** in 53% yield. The n.m.r. spectra (Table 2) indicated that the oximinoglycosyl portion of compounds **11** and **12** possessed the α-configuration and this conclusion was confirmed by conversion to α-D-glycopyranosides (9).

The α-configuration of the oximinoglycosyl unit of 1-*O*-(tri-*O*-acetyl-2-oximino-α-D-*arabino*-hexopyranosyl)-2,3;5,6-di-*O*-isopropylidene-α-D-mannofuranose was indicated by the n.m.r. spectrum (Table 2) and confirmed by the n.m.r. spectrum of the 1-*O*-(α-D-glucopyranosyl)-2,3;5,6-di-*O*-isopropylidene-α-D-mannofuranose (18). The α-configuration is assigned to the mannofuranosyl portion of these compounds since in both cases the anomeric proton of this structural unit was a sharp singlet as found for the starting material, 2,3;5,6-di-*O*-isopropylidene-α-D-mannofuranose and expected only for vicinal hydrogens in *trans*-relationship on a furanose ring. Thin layer chromatograms of the crude reaction product showed the presence of a second major component. The structure of this compound was not established but presumably is the β-D-*manno*-isomer of **13** which formed as the result of anomerization of the starting material during the course of the reaction.

Experimental

Optical rotations were measured in a 1 dm tube with a Perkin–Elmer model 141 polarimeter. Mutarotations were recorded automatically at 25 ± 0.5°. N.m.r. spectra were taken on a Varian A60 spectrometer.

The column chromatograms employed silicic acid (CC7, 100–200 mesh, Mallinckrodt Chemical Works, St. Louis, Mo.) using 10 g per gram of reaction product with ether – Skellysolve B (3:2) as the developing solvent unless otherwise stated. T.l.c. on silica gel G (E. Merck A.G., Darmstadt) was performed using 20 cm^2 plates with ether – Skellysolve B (4:1) as the developing solvent. The spots were visualized by spraying the plates with a solution of chlorosulfonic acid (10% v/v) in glacial acetic acid and then heating in an oven at 120°.

Dimethylformamide (DMF) was dried over barium oxide and then distilled from phosphorus pentoxide and stored under strictly anhydrous conditions. All solvent removals were carried out *in vacuo* (water aspirator or oil pump).

1,2;5,6-Di-*O*-isopropylidene-α-D-glucofuranose and 1,2;3,4-di-*O*-isopropylidene-α-D-galactopyranose were purchased from Raylo Chemicals Ltd., Edmonton, Alberta.

Kinetic Studies

Solutions (3.2 *M*) of deuterium oxide, methanol, isopropanol, and *t*-butanol in dry DMF were prepared. At 0 time, a 5 ml aliquot of the solution (16 mmol) was added at 25° to 4 mmol (2.70 g) of the dimeric compound **1**. The solution was rapidly made up to 10 ml using dry DMF while maintaining the temperature at 25°. A sample was transferred to an n.m.r. tube for examination at 60 MHz at 25 ± 1°. The changes in composition with time were estimated by comparing integrations of the signals for anomeric hydrogen at τ 3.16 (singlet for compound **3**), 3.64 (doublet for compound **1**), and 8.1–8.3 (the acetyl group signals used as internal reference). After about 1 h reaction time, a broad band of exchangeable hydrogens moved downfield across the τ 3–4 region and interfered with the integration of the signals for the anomeric hydrogens. This phenomenon appears related to the liberation of signal for the oxime hydroxyl at low field since it was not observed in reactions starting with the oximino chloride **3**. The signals at τ 6.83 were used to estimate the total amount of glycoside with R = CH_3 and those at τ 9.02 to estimate the total amount of glycoside with R = $C(CH_3)_3$. The relative intensities of the signals after a given reaction time could be reproduced well within 5%. The glycoside contents using methanol and *t*-butanol were estimated from the relative intensities of the alkyl group and acetyl group signals. Both the glycosidic methyl and *t*-butyl groups appeared as two signals, τ 6.83 and 6.84 for methyl and 9.01 and 9.04 for *t*-butyl. The lower field signal is that due to oximinoglycoside **5**. The higher field signal must be assigned to uncharacterized intermediate. In both cases, the amount of this product was about the same as of the glycoside **5** in the very early (less than 5 min) stage of the reaction. Because of the small shift difference, the relative amounts could not be estimated in the case of methanol. For *t*-butanol, the amount of the intermediate could be roughly estimated (see Fig. 1A).

In the case of isopropanol, the amount of glycoside formation was estimated by comparing the intensities of the signals for the anomeric protons of **1** and **3** to the intensity of the signals for acetyl groups and attributing the loss of signal for these anomeric hydrogens to glycoside formation.

The polarimetric rates were determined on a sample of the solution used for the n.m.r. study. The observed rotation of the dimer **1** (0.4 *M*) in DMF was estimated to be 42.5° by extrapolation to 0 time and that of the oximinochloride **3** (0.8 *M*) to be 67.0°, the maximum rotation achieved in the transformation of the 0.4 *M* solution of **1** to **3**. The observed rotations of the oximinoglycosides were 12.2 (R = CH_3), 22.3 (R = $CH(CH_3)_2$) and 24.5° (R = $C(CH_3)_3$) as 0.8 *M* solutions in DMF. The rotations were not appreciably changed by the presence of hydrogen chloride (0.8 *M*).

Can. J. Chem. Downloaded from www.nrcresearchpress.com by 210.87.254.5 on 09/05/12
For personal use only.

The n.m.r. spectrum of the above solution using *t*-butanol showed no signal for the by-product after 26 h. However, when the initial concentrations of the reactants were decreased to one-half, the yield of the by-product after 26 h was 11%. At one-half this concentration, the yield of by-product was 19%. The solutions were evaporated to dryness *in vacuo* at about 40° (water bath). The n.m.r. spectra of the residue in DMF were measured. The product prepared from the 0.2 *M* solution of **1** now showed no evidence of the by-product. That from the 0.1 *M* solution of **1** still contained about 14% of the uncharacterized compound. The products were purified by chromatography on silicic acid. The yields of pure crystalline oximinoglycoside (**5**, R = *t*-butyl) were, within experimental error, the same at 66%. The actual yields were estimated to be about 90% from the n.m.r. spectra of the solutions prior to the chromatograms.

In order to estimate the rate of reaction of the oximino chloride **3** with methanol and *t*-butanol, a 0.59 *M* solution of **1** in DMF was prepared and its transformation to **3** followed both by polarimetry and n.m.r. When the reaction appeared complete, 6.77 ml of the solution was brought to 25° and 2.5 ml of a 6.4 *M* solution of the alcohol in DMF was added. The resulting solution was then rapidly made up to 10 ml by the addition of DMF and kept at 25°. A portion of the solution was used to follow the change in optical rotation with time and another portion to follow the change in its n.m.r. spectrum.

2-Acetoximino-tri-O-acetyl-α-D-arabino-hexopyranosyl Chloride

A solution of dimeric tri-*O*-acetyl-2-deoxy-2-nitroso-α-D-glucopyranosyl chloride (10.13 g, 15 mmol) in acetyl chloride (70 ml) was cooled to 5°. Triethylamine (3.03 g, 30 mmol) was then added, dropwise, with stirring. The reaction mixture was allowed to reach room temperature after which time the thick slurry was shaken at room temperature for 18 h. T.l.c. (ethyl acetate – Skellysolve B (2:1)) showed the presence of no starting material but a single spot for the product. Anhydrous ether (100 ml) was then added and the mixture stirred for 15 min. The precipitated triethylamine hydrochloride was removed by filtration and the filtrate was evaporated to an oil (10.54 g, 92%). The n.m.r. spectrum of the product in deuteriochloroform at 60 MHz showed a singlet at τ 2.95 (H-1), a doublet at 3.95 (H-2, $J_{2,3}$ = 10.0 Hz), a triplet at 5.40 (H-3, $J_{3,4}$ = 9.50 Hz). The acetyl signals appeared at τ 7.78, 7.85, and 7.90 in the ratio of 1:1:2. The spectrum required the compound to be greater than 95% pure.

The optical rotation, $[\alpha]_D^{25}$ +184°, of a 0.8 *M* solution of a freshly prepared sample of 2-acetoximino-tri-*O*-acetyl-α-D-*arabino*-hexopyranosyl chloride in DMF containing 2 equiv of isopropanol at 25° was unchanged over a period of 12 h. T.l.c. examination of the solution (ethyl acetate – *n*-hexane (1:1)) showed a single spot with the same R_f value as that of the starting material which could be separated from isopropyl 2-acetoximino-tri-*O*-acetyl-α-D-*arabino*-hexopyranoside (1).

*6-O-(Tri-O-acetyl-2-oximino-α-D-arabino-hexopyranosyl)-1,2;3,4-di-O-isopropylidene-α-D-galactopyranose (**8**)*

The product obtained from the reaction of 1,2;3,4-di-*O*-isopropylidene-α-D-galactopyranose (8.0 g) with dimeric tri-*O*-acetyl-2-deoxy-2-nitroso-α-D-glucopyranosyl chloride (**1**) (3) (13.0 g) in DMF (210 ml) for 36 h at room temperature was isolated and purified by column chromatography on silicic acid. Crystallization of the main fraction from ethyl acetate – Skellysolve B provided the pure material (11.5 g, 67%) m.p. 137–138°, $[\alpha]_D^{27}$ +9.2° (*c*, 1.8 in chloroform).

Anal. Calcd. for $C_{24}H_{35}NO_{14}$: C, 51.33; H, 6.28; N, 2.49. Found: C, 51.13; H, 6.26; N, 2.40.

Evidence for the formation of the β-oxime as a minor product in the reaction of **1** with 1,2;3,4-di-*O*-isopropylidene-α-D-galactopyranose was obtained in an experiment involving the lithium aluminum hydride reduction of an oxime preparation, $[\alpha]_D^{25}$ −1.05°, obtained in 73% yield by chromatographic purification of the crude reaction product on a silicic acid column using ethylene chloride – ethyl acetate (2:1) as the eluent. This product was reduced in ether following the procedure described in an accompanying paper (8). The 2,4-dinitrophenyl derivative (19) of the crude ninhydrin-positive product (obtained in 55% yield) (8) was chromatographed on a silicic acid column using chloroform – benzyl alcohol – acetic acid (24:10:1). Two main fractions were isolated. The faster moving material was characterized as 6-*O*-[2-deoxy-2-(2,4-dinitroanilino)-α-D-glucopyranosyl]-1,2;3,4-di-*O*-isopropylidene-α-D-galactopyranose (8). The slower moving component proved to be the *manno*-isomer. A fraction was collected between the two bands but close to the glucosaminide fraction which was acetylated with acetic anhydride in pyridine. The product, 100 mg, was subjected to t.l.c. on silica gel using benzene–methanol (20:1). Two components were detected. The faster moving material was isolated (51 mg) and established to be 6-*O*-[3,4,6-tri-*O*-acetyl-2-deoxy-2-(2′,4′-dinitroanilino)-α-D-glucopyranosyl]-1,2;3,4-di-*O*-isopropylidene-α-D-galactopyranose, $[\alpha]_D^{30}$ −29° (*c*, 0.4 in chloroform) (8). The slower moving component (28 mg) had $[\alpha]_D^{25}$ −128° (*c*, 0.4 in chloroform). The 100 MHz spectrum in deuteriochloroform required a high degree of purity and established the compound to be 6-*O*-[3,4,6-tri-*O*-acetyl-2-deoxy-2-(2,4-dinitroanilino)-β-D-mannopyranosyl]-1,2;3,4-di-*O*-isopropylidene-α-D-galactopyranose. The expected signals for the acetyl and *C*-methyl groups were present. The chemical shifts and approximate coupling constants for the hydrogens on the pyranose ring of amino-sugar residue were established and confirmed by appropriate spin-decoupling experiments. The chemical shifts for H-1′, -2′, -3′, -4′, and -5′ were τ 5.06, 5.39, 4.82, 4.65, and 6.25, respectively. The approximate coupling constants observed were $J_{1',2'}$ = 1.25, $J_{2',3'}$ = 4.0, $J_{3',4'}$ = 9.0, and $J_{4',5'}$ = 9.5 Hz. The magnitude of $J_{2',3'}$ requires the *manno*-configuration. The doublet signal for the amide hydrogen was at τ 0.97 with a spacing of 9.0 Hz. For both the α-*manno*- and α-*gluco*-isomers, the chemical shift of H-5′ was to lower field, τ 5.92, as is expected in view of the deshielding effect of the axial O-1′ on the *syn*-axial H-5′ (20).

6-O-(2-Acetoximino-tri-O-acetyl-α-D-arabino-hexopyranosyl)-1,2;3,4-di-O-isopropylidene-α-D-galactopyranose

Acetylation of the oxime **8** with acetic anhydride in

Can. J. Chem. Downloaded from www.nrcresearchpress.com by 210.87.254.5 on 09/05/12
For personal use only.

pyridine yielded an oil, $[\alpha]_D^{23}$ +0.65° (*c*, 2.6 in chloroform).

Anal. Calcd. for $C_{26}H_{37}NO_{15}$: C, 51.74; H, 6.18; N, 2.32. Found: C, 51.59; H, 6.08; N, 2.48.

*6-O-(Tri-O-acetyl-2-oximino-α-D-lyxo-hexopyranosyl)-1,2;3,4-di-O-isopropylidene-α-D-galactopyranose (**9**) and the β-Anomer (**10**)*

A solution of dimeric tri-*O*-acetyl-2-deoxy-2-nitroso-α-D-galactopyranosyl chloride (**6**) (13.0 g) (21) and 1,2;3,4-di-*O*-isopropylidene-α-D-galactopyranose (8.0 g) in DMF (210 ml) was kept at room temperature for 36 h. The resulting pale yellow solution was concentrated at a bath temperature of less than 50° to an oil which was dissolved in ether (500 ml). The ethereal solution was washed four times with water (300 ml). Evaporation of the ether left an oil which crystallized spontaneously on the addition of ethanol. Recrystallization from ethyl acetate – Skellysolve B gave the α-anomer (13.8 g, 80%); m.p. 171–172°; $[\alpha]_D^{23}$ +14° (*c*, 3.0 in chloroform).

Anal. Calcd. for $C_{24}H_{35}NO_{14}$: C, 51.33; H, 6.28; N, 2.49. Found: C, 51.08; H, 6.05; N, 2.38.

Evaporation of the alcoholic mother liquors left an oil which crystallized on the addition of ether. Recrystallization from ethanol yielded the β-anomer (**10**) (0.3 g, 1.7%); m.p. 90–92°; $[\alpha]_D^{23}$ −94° (*c*, 2.6 in chloroform).

Anal. Calcd. for $C_{24}H_{35}NO_{14}$: C, 51.33; H, 6.28; N, 2.49. Found: C, 51.13; H, 6.46; N, 2.59.

In a larger scale experiment this compound was obtained in 8.7% yield.

A solution of the oxime (**10**) (1.5 g) in acetonitrile (5 ml), hydrochloric acid (4 ml of 1 *N*) and acetaldehyde (1.5 ml) was kept at room temperature for 4 h. The product was isolated and reduced with sodium borohydride (10). Complete deacetylation of the product with triethylamine (0.5 ml) in aqueous methanol for 12 h at 0° yielded, on work-up, an oil which only showed one component on t.l.c. analysis using the upper phase of an ethyl acetate – dioxane–water (2:2:1) system as the developing solvent. Chromatography on Dowex 1-X2 (200–400 mesh OH^- form) gave an amorphous powder, $[\alpha]_D^{21}$ − 24.6° (*c*, 2 in DMF). Hydrolysis with dilute hydrochloric acid produced only talose and galactose. The compound was clearly different from 6-*O*-(α-D-talopyranosyl)-1,2;3,4-di-*O*-isopropylidene-α-D-galactopyranose on the basis of t.l.c. comparisons. This evidence together with the n.m.r. data indicated that the compound was 6-*O*-(β-D-talopyranosyl)-1,2;3,4-di-*O*-isopropylidene-α-D-galactopyranose.

6-O-(2-Acetoximino-tri-O-acetyl-α-D-lyxo-hexopyranosyl)-1,2;3,4-di-O-isopropylidene-α-D-galactopyranose

A solution of 6-*O*-(tri-*O*-acetyl-2-oximino-α-D-*lyxo*-hexopyranosyl)-1,2;3,4-di-*O*-isopropylidene-α-D-galactopyranose (6.0 g) (**9**) in pyridine (18.0 ml) was cooled to 0° and acetic anhydride (3.0 ml) added. This solution was kept at 0° for 12 h and then concentrated to an oil which was dissolved in dichloromethane. The resulting solution was washed sequentially with water, dilute hydrochloric acid, water, saturated aqueous sodium bicarbonate solution, water and then evaporated to afford an oil (6.4 g); $[\alpha]_D^{23}$ +6.1° (*c*, 3.8 in chloroform).

Anal. Calcd. for $C_{26}H_{37}NO_{15}$: C, 51.74; H, 6.18; N, 2.32. Found: C, 51.52; H, 6.00; N, 2.49.

*3-O-(Tri-O-acetyl-2-oximino-α-D-arabino-hexopyranosyl)-1,2;5,6-di-O-isopropylidene-α-D-glucofuranose (**11**)*

The product from the reaction of 1,2;5,6-di-*O*-isopropylidene-α-D-glucofuranose (8.0 g) and dimeric tri-*O*-acetyl-2-deoxy-2-nitroso-α-D-glucopyranosyl chloride (**1**) (13.0 g) (3) in DMF (210 ml) at room temperature for 36 h was chromatographed on silicic acid. The main component crystallized from ethyl acetate – Skellysolve B (10.2 g, 59%), m.p. 160–161°, $[\alpha]_D^{27}$ +66° (*c*, 1.1 in chloroform).

Anal. Calcd. for $C_{24}H_{35}NO_{14}$: C, 51.33; H, 6.28; N, 2.49. Found: C, 51.14; H, 6.03; N, 2.31.

3-O-(2-Acetoximino-tri-O-acetyl-α-D-arabino-hexopyranosyl)-1,2;5,6-di-O-isopropylidene-α-D-glucofuranose

The appropriate oxime **11** (4.0 g) was acetylated with acetic anhydride in pyridine and the product isolated as an oil. Crystallization from ether – Skellysolve B yielded the title compound (3.7 g, 86.6%), m.p. 102–104°, $[\alpha]_D^{23}$ +46° (*c*, 4 in chloroform).

Anal. Calcd. for $C_{26}H_{37}NO_{15}$: C, 51.74; H, 6.18; N, 2.32. Found: C, 51.21; H, 6.20; N, 2.65.

*3-O-(Tri-O-acetyl-2-oximino-α-D-lyxo-hexopyranosyl)-1,2;5,6-di-O-isopropylidene-α-D-glucofuranose (**12**)*

A solution of 1,2;5,6-di-*O*-isopropylidene-α-D-glucofuranose (8.0 g) and dimeric tri-*O*-acetyl-2-deoxy-2-nitroso-α-D-galactopyranosyl chloride (**6**) (13.0 g) in DMF (210 ml) was kept at ambient temperature for 36 h. The product was isolated as an oil (22.0 g). Column chromatography on silicic acid yielded an oil which crystallized in 53% yield from ethyl acetate – Skellysolve B, m.p. 149–150°, $[\alpha]_D^{23}$ +62° (*c*, 1 in chloroform).

Anal. Calcd. for $C_{24}H_{35}NO_{14}$: C, 51.74; H, 6.18; N, 2.32. Found: C, 51.01; H, 6.12; N, 2.26.

*3-O-(2-Acetoximino-tri-O-acetyl-α-D-lyxo-hexopyranosyl)-1,2;5,6-di-O-isopropylidene-α-D-glucofuranose (**17**)*

The oxime precursor (**12**) (4.09 g) was acetylated and the product was isolated as an oil which crystallized from ethyl acetate – Skellysolve B, (4.39 g), m.p. 134–135°, $[\alpha]_D^{23}$ +44.2° (*c*, 3.8 in chloroform).

Anal. Calcd. for $C_{26}H_{37}NO_{15}$: C, 51.74; H, 6.18; N, 2.32. Found: C, 51.30; H, 5.99; N, 2.68.

*(Tri-O-acetyl-2-oximino-α-D-arabino-hexopyranosyl)-2,3;5,6-di-O-isopropylidene-α-D-mannofuranoside (**13**)*

The crude product isolated from the reaction of 2,3;5,6-di-*O*-isopropylidene-α-D-mannofuranose (8.0 g) with dimeric tri-*O*-acetyl-2-deoxy-2-nitroso-α-D-glucopyranosyl chloride (**1**) (13.0 g) in DMF (210 ml) was purified by column chromatography on silicic acid. The appropriate column fractions were combined and crystallized from ethanol, (7.0 g, 41%), m.p. 86–87°, $[\alpha]_D^{32}$ +87.9° (*c*, 1.0 in chloroform).

Anal. Calcd. for $C_{24}H_{35}NO_{14}$: C, 51.33; H, 6.28; N, 2.49. Found: C, 51.06; H, 6.21; N, 2.44.

(2-Acetoximino-tri-O-acetyl-α-D-arabino-hexopyranosyl)-2,3;5,6-di-O-isopropylidene-α-mannofuranoside (23)

(Tri-*O*-acetyl-2-oximino-α-D-*arabino*-hexopyranosyl)-2,3;5,6-di-*O*-isopropylidene-α-D-mannofuranoside **(13)** (6.2 g) was acetylated to provide an oil (6.5 g), $[\alpha]_D^{23}$ +99° (*c*, 3.3 in chloroform).

Anal. Calcd. for $C_{26}H_{37}NO_{15}$: C, 51.74; H, 6.18; N, 2.32. Found: C, 51.71; H, 6.22; N, 2.57.

The research was supported by a grant (A-172) to R.U.L. from the National Research Council of Canada. Technical assistance was provided by the spectroscopy and microanalytical service laboratories of this Department and by Miss P. Nayar and W. Merlo.

1. R. U. LEMIEUX, T. L. NAGABHUSHAN, and S. W. GUNNER. Can. J. Chem. **46**, 405 (1968).
2. R. U. LEMIEUX, R. SUEMITSU, and S. W. GUNNER. Can. J. Chem. **46**, 1040 (1968).
3. R. U. LEMIEUX and T. L. NAGABHUSHAN. Methods in carbohydrate chemistry. Vol. VI. Editors, R. L. Whistler and J. N. BeMiller. Academic Press, N.Y. 1972. p. 487.
4. T. L. NAGABHUSHAN. Can. J. Chem. **48**, 383 (1970).
5. T. L. NAGABHUSHAN and C. G. CHIN. Can. J. Chem. **48**, 3097 (1970).
6. R. U. LEMIEUX and S. W. GUNNER. Can. J. Chem. **46**, 397 (1968).
7. R. U. LEMIEUX, K. JAMES, and T. L. NAGABHUSHAN. Can. J. Chem. **51**, 27 (1973).
8. R. U. LEMIEUX, K. JAMES, T. L. NAGABHUSHAN, and Y. ITO. Can. J. Chem. **51**, 33 (1973).
9. R. U. LEMIEUX, K. JAMES, and T. L. NAGABHUSHAN. Can. J. Chem., **51**, 42 (1973).
10. R. U. LEMIEUX, K. JAMES, T. L. NAGABHUSHAN. Can. J. Chem., **51**, 48 (1973).
11. R. U. LEMIEUX, T. L. NAGABHUSHAN, K. J. CLEMETSON, and L. C. N. TUCKER. Can. J. Chem. **51**, 53 (1973).
12. R. U. LEMIEUX, T. L. NAGABHUSHAN, and K. JAMES. Can. J. Chem., **51**, 1 (1973).
13. W. PRITZKOW, H. SCHAEFER, P. PABST, A. EBENROTH, J. BEGER. J. Prakt. Chem. **29**, 123 (1965).
14. R. U. LEMIEUX, R. A. EARL, K. JAMES, and T. L. NAGABHUSHAN. Can. J. Chem. **51**, 19 (1973).
15. R. U. LEMIEUX and D. R. LINEBACK. Can. J. Chem. **43**, 94 (1965).
16. K. MIYAI and R. W. JEANLOZ. Carbohydr. Res. **21**, 45 (1972).
17. J. E. BLACKWOOD, C. L. GLADYS, K. L. LOENING, A. E. PETRARCA, and J. E. RUSH. J. Am. Chem. Soc. **90**, 509 (1968).
18. R. U. LEMIEUX, K. JAMES, and T. L. NAGABHUSHAN. In preparation.
19. P. F. LLOYD and G. P. ROBERTS. J. Chem. Soc. 6910, (1965).
20. R. U. LEMIEUX and J. D. STEVENS. Can. J. Chem. **43**, 2059 (1965).
21. R. U. LEMIEUX, T. L. NAGABHUSHAN, and I. K. O'NEIL. Can. J. Chem. **46**, 413 (1968).

Can. J. Chem. Downloaded from www.nrcresearchpress.com by 210.87.254.5 on 09/05/12
For personal use only.

Isopropyl Tri-*O*-acetyl-α-D-hexopyranosulosides. The Configurations of the Parent Oximes[1]

R. U. LEMIEUX, R. A. EARL,[2] K. JAMES,[3] AND T. L. NAGABHUSHAN[4]

Department of Chemistry, University of Alberta, Edmonton, Alberta

Received June 2, 1972

A variety of methods are described for the deoximation of isopropyl tri-*O*-acetyl-2-oximino-α-D-*arabino*-hexopyranoside (**1**) to isopropyl tri-*O*-acetyl-α-D-*arabino*-hexopyranosuloside (**3**). Using acetaldehyde in acetonitrile and hydrochloric acid, both **3** and its *lyxo*-isomer (**4**), from the corresponding oxime (**2**), were obtained in crystalline form. Comparisons of the chemical shifts of the anomeric hydrogens of the ulosides with those of the corresponding oximes require the oximes to possess the C-1/OH *syn*- or *Z*-configuration.

Diverses méthodes de déoximation de l'isopropyl tri-*O*-acétyl-oximino-2-α-D-*arabino*-hexopyranoside (**1**) en isopropyl tri-*O*-acétyl-α-D-*arabino*-hexopyranosuloside (**3**) sont décrites. En utilisant l'acétaldéhyde dans l'acétonitrile et l'acide chlorhydrique, **3** et son isomère *lyxo* (**4**) sont tous deux obtenus sous forme cristalline à partir de l'oxime correspondante **2**. Les comparaisons des déplacements chimiques des hydrogènes anomères des ulosides avec ceux d'oximes correspondantes impliquent une configuration C-1/OH *syn* ou *Z* pour les oximes. [Traduit par le journal]

Can. J. Chem. **51**, 19 (1973)

The reduction of tri-*O*-acetyl-α-D-hexopyranosulosides, which are obtained by deoximation of the readily prepared tri-*O*-acetyl-2-oximino-α-D-hexopyranosides (1, 2) promises to become a generally useful method for the preparation of a number of α-D-hexopyranosides (3–5). We wish to provide a proof of the configuration of the oximes obtained as intermediates and to describe methods for their deoximation to the ulosides.

The classical deoximation procedure utilizes a transoximation reaction in which a ketoxime or an aldoxime is treated with an excess of a hydroxylamine acceptor in the form of an aldehyde or ketone in the presence of a mineral acid. Hershberg (6) has recommended aqueous pyruvic acid buffered with sodium acetate as the reagent. DePuy and Ponder (7) have reported that excess levulinic acid in the presence of mineral acid is a highly satisfactory reagent and, in some cases, superior to pyruvic acid. Levulinic acid was used in our initial experiments (3) but, because of the problems associated with the separation of this compound from the product, a variety of other carbonyl compounds were examined including acetone, acetylacetone, pentane-2,4-dione, hexane-2,5-dione, benzaldehyde, and acetaldehyde.[5] Deoximation occurred in all cases and for obvious reasons of convenience attention was concentrated on the two simple aldehydes. Although complete deoximation could be effected with either compound, the reaction with acetaldehyde was much more rapid and has become our method of choice when the strongly acidic conditions are allowed. By using 1.3 equiv of acetaldehyde in acetonitrile containing 1 equiv of hydrochloric acid, the reaction is complete within 3 h at room temperature. Thus, the oxime **1** was converted to the uloside **3** isolated in the hydrated form in near quantitative yield. Dehydration and recrystallization provided **3** in 77% yield. The experience in converting **2** to **4** was similar. Since compounds **3** and **4** are the first examples of crystalline acetylated ulosides, their n.m.r. spectra are reproduced in Fig. 1. It is seen that the spectra are in complete accord with the structures assigned.

Recently, Timms and Wildsmith (8) reported a mild deoximation procedure involving reduction of oximes with trivalent titanium followed by hydrolysis of the resulting imine. Accordingly,

[1]Presented in part at the 161st National American Chemical Society Meeting, Los Angeles, California, March 28 – April 2, 1971 and at the 172nd Meeting of the Japan Antibiotic Association, Tokyo, April 4, 1970.

[2]Part of this research was presented in a thesis by R. A. Earl in partial fulfillment of the requirements for the Ph.D. degree, 1970. Present address: Department of Chemistry, University of Utah, Salt Lake City, Utah.

[3]University of Alberta Postdoctoral Fellow, 1970–1972.

[4]Professional Research Associate, 1970–1972.

[5]These tests were conducted by L.C.N. Tucker.

Can. J. Chem. Downloaded from www.nrcresearchpress.com by 210.87.254.105 on 09/05/12
For personal use only.

Can. J. Chem. Downloaded from www.nrcresearchpress.com by 210.87.254.105 on 09/05/12
For personal use only.

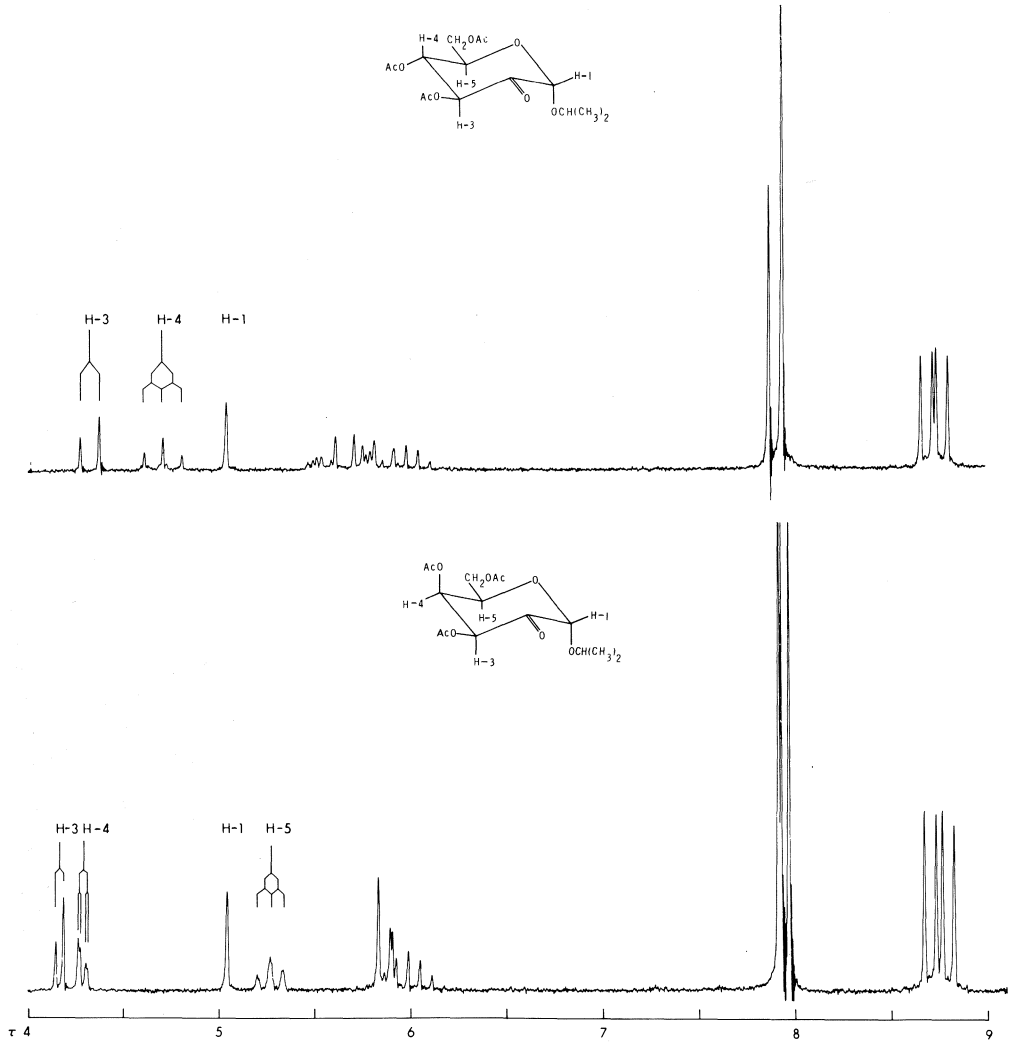

FIG. 1. The 100 MHz spectra of isopropyl tri-*O*-acetyl-α-D-*arabino*-hexopyranosuloside (**3**) ($J_{3,4} = J_{4,5} = 10$ Hz) and isopropyl tri-*O*-acetyl-α-D-*lyxo*-hexopyranosuloside (**4**) ($J_{3,4} = 5.5$, $J_{4,5} = 1.5$ Hz) in deuteriochloroform.

the oximinoglycoside **1** was treated with 6 equiv of 20% aqueous titanium trichloride solution in dioxane containing ammonium acetate. Crude uloside (**3**) was isolated in the same yield (90%) as using acetaldehyde and the purity was similar (t.l.c. and n.m.r.).

Deoximation of **1** by nitrous acid under the conditions reported by Wolfrom (9) for deoximation of acetylated *aldehydo*-sugar oximes was also examined. Although the crude uloside product (**3**) was of a high degree of purity, the yield was only 55%. This low yield was probably mainly related to problems of isolation from the aqueous acetic acid.

Reduction of the crude uloside preparations mentioned above using sodium borohydride in aqueous dioxane followed by deacetylation and purification by passing down a resin column in the hydroxide form (10) gave pure isopropyl α-D-glucopyranoside in 78, 75, and 71% yields using the acetaldehyde, titanium trichloride, and nitrous acid methods, respectively. It was found that isopropyl α-D-glucopyranoside could be recovered from the resin column in only 90% yield.

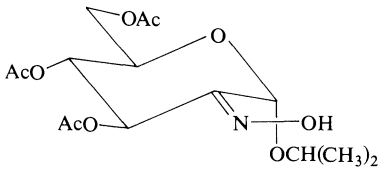

1

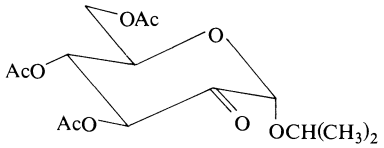

3

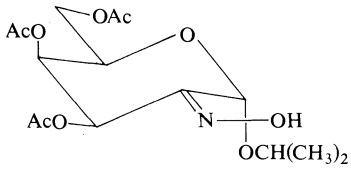

2

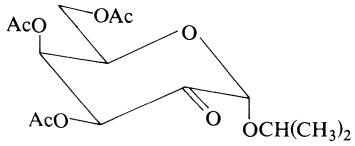

4

Thus, the actual yields of the glucoside from the reductions of the crude ulosides were 87, 84, and 79%, respectively. Using either the levulinic acid or acetaldehyde methods for deoximation and subsequent reduction of the crude uloside followed by acetylation, isopropyl tetra-*O*-acetyl-α-D-glucopyranoside was obtained in approximately 80% yield. Although chromatography on the basic resin appears wasteful in product, the quality of the separations achieved, especially for complex structures (11), strongly commends the method. The essentially neutral conditions present in deoximations using titanium trichloride have proven useful for preparing complex ulosides which possess highly acid-labile *O*-isopropylidene groups (5).

The oximinoglycosides **1** and **2** are shown in the C-1/OH *syn*-form which corresponds to the *Z*-form using the recently proposed nomenclature (12). This configuration was previously surmised (1) on theoretical grounds because of the stereoselectivity of the reaction and the fact that only one of the two possible forms was detected in the crude reaction products. Recent studies (13) of the conformational properties of 2-substituted cyclohexanone oximes have provided results in accordance with the predictions made. It was intended to obtain evidence by X-ray crystallography but a publication by Trager and Huitric (14) provided the basis for a simple n.m.r. proof of structure. It was pointed out that, when both the isomeric *syn*- and *anti*-forms of a six-membered cyclic oxime are available, the deshielding of an equatorially oriented vicinal hydrogen by the opposing oxime hydroxyl allows an assignment of configuration. This deshielding effect has been observed in other laboratories (13, 15, 16) and is similar to the deshielding of an axial hydrogen by a *syn*-axial oxygen atom (17). Thus, for example, Trager and Huitric found the equatorial hydrogens at the 2- and 6-positions of 4-*t*-butylcyclohexanone oxime to be chemically shifted by 0.91 τ-values. It occurred to us that, when only one form of an oxime is available, a decision could be reached by comparing the chemical shift of a vicinal equatorial hydrogen in the parent ketone with its shift in the oxime derivative. Thus, in the case of 4-*t*-butylcyclohexanone and its oxime, one of the vicinal hydrogens in the oxime produces its signal only 0.28 τ-values to lower field than H-2 (or H-6) of the ketone whereas the other is 1.19 τ-values to lower field. It seemed desirable to test this hypothesis by the comparison of a number of suitable model compounds.

Reaction of a mixture of the *cis*- and *trans*-4-*t*-butylcyclohexene oxides with benzyl alcohol in the presence of boron trifluoride occurred predominantly by axial attack to produce a mixture of the compounds **5** and **6** which were readily separated by fractional crystallization. Hydrogenolysis of both compounds gave the known *trans*-2-hydroxy-*cis*-4-*t*-butylcyclohexanol (18). The position of the benzyl group was established by first replacing the hydroxyl group of **6** by chlorine using phosphorus trichloride, then removing the benzyl group by hydrogenolysis and oxidizing the product to chloroketone. Finally, hydrogenolysis of the chloroketone produced 3-*t*-butylcyclohexanone.

O-Methylation of **5** followed by hydrogenolysis of the benzyl group produced *cis*-4-*t*-butyl-*trans*-

Can. J. Chem. Downloaded from www.nrcresearchpress.com by 210.87.254.105 on 09/05/12
For personal use only.

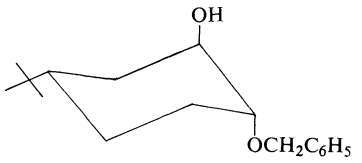

5

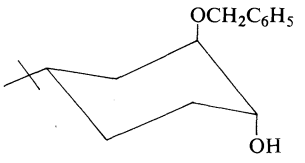

6

2-methoxycyclohexanol which was oxidized to the ketone **7**. Oxidation of **5** to *cis*-2-benzyloxy-5-*t*-butylcyclohexanone and reduction with sodium borohydride provided *cis*-2-benzyloxy-*cis*-5-*t*-butylcyclohexanol which was *O*-methylated. Removal of the benzyl group by hydrogenolysis followed by oxidation provided the ketone **10**. Oxidation of **7** provided both the isomeric oximes **8** and **9** but only the *E*-oxime **9** was obtained pure. Only the oxime **11** was detected in the product from **10**.

The chemical shifts for H-2 and -6 in equatorial orientations are presented as τ-values for compounds **7** to **11** alongside the symbols for these hydrogens in the formulas. The chemical shift shown for H-2 of the *Z*-oxime **8** was obtained from the n.m.r. spectrum of the crude reaction product. Consideration of these chemical shifts shows H-2 of **8** to be deshielded by 1.4 τ-values from the value for the parent ketone **7**. On the other hand, relatively little effect was observed on the chemical shift of H-6. It is seen that the reverse was found for the isomeric oxime **9**. In this case, it is H-6 that was strongly deshielded (about 0.9 τ-values) on oximation. The chemical shift of H-2 was decreased by only 0.3 τ-values. In contrast to the oximation of **7**, the ketone **10** provided only one detectable oxime, the expected (1, 13) *Z*-oxime **11**. The configuration of this oxime was evident from the fact that the oximation had a strong deshielding effect (0.9 τ-value) on the chemical shift of the equatorial H-6. It is seen that there was little effect on the chemical shift of the axial H-2.

In view of the above data, it can be concluded that the oximinoglycosides **1** and **2** possess the C-1/OH *syn*(*Z*)-configuration. This follows since the chemical shift of the equatorial anomeric hydrogen of **1** is 1.14 τ-values to lower field than that of the parent uloside **3** and that of the oximinoglycoside **2** is 1.34 τ-values to lower field than that of the parent uloside **4**. Furthermore, treatment of the uloside **3** with hydroxylamine under buffered conditions provided **1** in high yield. As previously pointed out (1), the steric requirements for C-1/OH *syn*-oxime formation is likely an important component of the driving force responsible for the high stereoselectivity of α-oximinoglycoside formation.

It may be noted that a number of other 2-substituted 4-*t*-butylcyclohexanones and their oximes were prepared (19) and all provided n.m.r. spectra in accord with expectations based on the above findings.

Experimental

Deoximation Reactions

Except for the reaction using titanium trichloride, the course of the reaction was followed by t.l.c. on silica gel G with ether – Skellysolve B (3:2) as the developing solvent and the product isolated after the presence of the oxime could not be detected. In all cases, the n.m.r. spectrum of the crude product required a high degree (> 90%) of purity.

(a) Using Levulinic Acid

The oxime (**1**) (1) (1.08 g) was dissolved in acetic acid (2 ml), levulinic acid (1.74 g) and 1 *N* hydrochloric acid (3 ml) were added. The solution was maintained at room temperature. The reaction was complete after 3 h. The solution was diluted with methylene chloride and the organic layer washed free of acid with water and then sodium bicarbonate solution. The solution was dried and evaporated to an oil (0.94 g, 90%).

(b) Using Acetaldehyde

A solution of **1** (2.00 g) in acetonitrile (6 ml) and 1 *N* hydrochloric acid (4.8 ml) containing acetaldehyde (0.4 ml) was kept at room temperature for 3 h after which time the reaction was complete. The resulting solution was diluted with ethyl acetate (15 ml) and the aqueous layer was extracted with a further portion of ethyl acetate (15 ml). The combined ethyl acetate extracts were washed once with water (10 ml), dried, and evaporated to yield a clear oil (1.80 g, 94%).

(c) Using Titanium Trichloride

Ammonium acetate (4.0 g) was added to a stirred solution of (**1**) (2.0 g) in dioxane (20 ml). Nitrogen was bubbled through the solution to maintain a nitrogen atmosphere and a 20% aqueous solution of titanium trichloride (10 g) was added dropwise. After 3 h, further portions of dioxane (20 ml), ammonium acetate (4.0 g), and titanium trichloride (10 g) were added. The suspension was stirred for a further 2 h prior to extraction with methylene chloride (160 ml). The methylene chloride

Can. J. Chem. Downloaded from www.nrcresearchpress.com by 210.87.254.105 on 09/05/12
For personal use only.

Can. J. Chem. Downloaded from www.nrcresearchpress.com by 210.87.254.105 on 09/05/12
For personal use only.

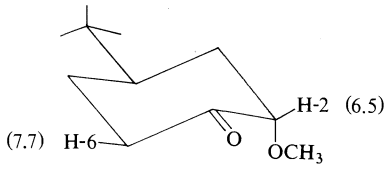

7

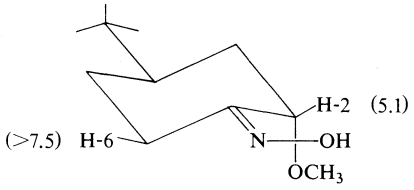

8

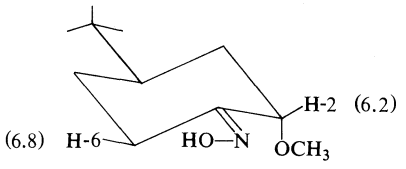

9

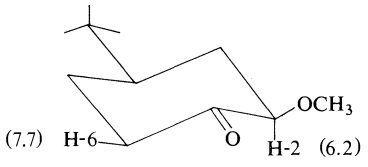

10

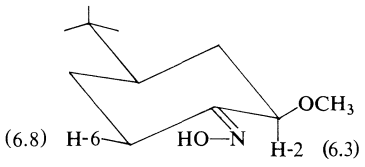

11

Can. J. Chem. Downloaded from www.nrcresearchpress.com by 210.87.254.105 on 09/05/12
For personal use only.

layer was successively washed with water, sodium bicarbonate solution, water, and dried. Solvent removal left a clear oil (1.8 g, 94%).

(d) Using Nitrous Acid

The oxime **1** (2.00 g) was dissolved in glacial acetic acid (38 ml) and a solution of sodium nitrite (7.7 g) in water (15 ml) was added dropwise over 10 min. After 2 h, this addition of sodium nitrite solution was repeated and the stirring continued for a further 1 h. Deoximation was then complete (t.l.c.) and methylene chloride (150 ml) was added. The organic layer was washed successively with water, sodium bicarbonate solution, water, and dried. Solvent removal left a clear oil (1.10 g, 57%).

The above described crude preparations of the uloside **3** were examined as follows.

(i) Conversion to Isopropyl Tetra-O-acetyl-α-D-glucopyranoside

The crude uloside (**3**) was dissolved in a 1:1 mixture of dioxane and water (5 ml/g) and an ice-cold solution of sodium borohydride in the same solvent (1 g/4 ml) was added dropwise to the stirred solution kept below 5°. After standing in an ice-water bath for 0.5 h, the solution was left at room temperature for 2 h. The excess borohydride was decomposed with acetone and the solution deionized with Amberlite MB3. The residue obtained on solvent removal was acetylated with acetic anhydride in pyridine in the usual manner. The crude uloside (**3**) obtained by using levulinic acid provided an 80% overall yield of pure isopropyl tetra-*O*-acetyl-α-D-glucopyranoside (3). The acetaldehyde procedure gave an 81% overall yield.

(ii) Conversion to Isopropyl α-D-Glucopyranoside

The sodium borohydride reduction was performed as described above and the deionized solution was added to a Dowex 1-X2 (200–400 mesh, OH^- form) column (30 in. × 1 in.) and eluted with water. The overall yields using the acetaldehyde, titanium trichloride, and nitrous acid procedures were 73, 70, and 40%, respectively. The yields from crude uloside were 78, 75, and 71%, respectively.

Pure isopropyl α-D-glucopyranoside (1.24 g) was added to the basic resin column and recovered in 90% yield.

Isopropyl Tri-O-acetyl-α-D-arabino-hexopyranosuloside (3)

A solution of isopropyl tri-*O*-acetyl-2-oximino-α-D-*arabino*-hexopyranoside (**1**) (20 g) in acetonitrile (60 ml) and 1 *N* hydrochloric acid (48 ml) containing acetaldehyde (4 ml) was stored at room temperature for 3 h. The resulting solution was diluted with ethyl acetate (150 ml), and the aqueous layer was extracted with a further portion of ethyl acetate (50 ml). The combined ethyl acetate extracts were washed once with water (100 ml) and evaporated to yield a clear oil (16 g, essentially pure as shown by t.l.c.). The oil was dehydrated by azeotropic distillation using 200 ml of benzene for 4 h. Solvent removal left an oil which crystallized on storage. Recrystallization from ether – Skellysolve B provided a slightly sticky precipitate (14.8 g, 77%). The analytical sample, m.p. 88.5–89.5°, $[\alpha]_D^{28}$ +40.5° (*c*, 1.3 in chloroform), was obtained by recrystallization from ether at −25°. The n.m.r. spectrum is shown in Fig. 1.

Anal. Calcd. for $C_{15}H_{21}O_9$: C, 52.17; H, 6.13. Found: C, 52.24; H, 6.30.

Isopropyl Tri-O-acetyl-α-D-lyxo-hexopyranosuloside (4)

A solution of isopropyl tri-*O*-acetyl-2-oximino-α-D-*lyxo*-hexopyranoside (**2**) (8.5 g) in acetonitrile (25 ml) and 1 *N* hydrochloric acid (20 ml) containing acetaldehyde (1.75 ml) was kept at room temperature for 3 h. The product was isolated and dehydrated as described above to afford an oil (7.5 g) (highly pure by n.m.r. and t.l.c.) which crystallized from ether to yield the pure ketone (3.0 g), m.p. 97.5–98.5°, $[\alpha]_D^{28}$ +89.5° (*c*, 0.79 in chloroform).

Anal. Calcd. for $C_{15}H_{21}O_9$: C, 52.17; H, 6.13. Found: C, 51.94; H, 6.15.

Oximation Reactions

The p*H* of a solution of sodium acetate (1 g) and hydroxylamine hydrochloride (0.5 g) in water (5 ml) was adjusted to 4.5 using glacial acetic acid. Isopropyl tri-*O*-acetyl-α-D-*arabino*-hexopyranosuloside (**3**) (0.40 g) was then added and the solution was kept at room temperature for 1 h. Dichloromethane (10 ml) was added and the organic layer was washed sequentially with water, saturated aqueous sodium bicarbonate solution, and water. Evaporation left an oil (0.40 g) which crystallized from isopropanol. The product (0.35 g, 84%) was indistinguishable from an authentic sample of **1** (1).

Starting with isopropyl tri-*O*-acetyl-α-D-*lyxo*-hexopyranosuloside (**4**) and using the above procedure, the oxime **2** was isolated in 80% yield. The syrupy compound was identical with an authentic sample of **2** (1).

trans-2-Benzyloxy-trans-5-t-butylcyclohexanol and trans-2-Benzyloxy-cis-4-t-butylcyclohexanol

The procedure of Jones and coworkers (20) was used to prepare a mixture of the *cis*- and *trans*-4-*t*-butylcyclohexene oxides except that methylene chloride was used as the solvent with a 30% excess of peracetic acid. The yield of the mixture was 83%.

The mixture (210 g, 1.4 mol) was added dropwise during 40 min to a cold stirred solution of boron trifluoride etherate (3.5 ml) in freshly distilled benzyl alcohol (800 ml, 7.7 mol). The temperature was maintained in the range 7–13°. After the addition was complete, the somewhat viscous mixture was stirred for a further 10 min at room temperature, and then 6 *N* aqueous ammonia (15 ml) and 1 l of ether were added. The solution was washed with water (100 ml), saturated sodium chloride solution (30 ml), and concentrated. The residue was fractionally distilled to a product (319.2 g, 90%), b.p. 128–139°/0.08–0.12 mm, which crystallized. Analysis by g.c. on a 5 ft × 0.25 in. column of 15% ethylene glycol succinate on non-acid washed Chromosorb W (30–60 mesh) at 205° gave two overlapping peaks with retention times of 27.0 and 28.6 min, respectively, in the ratio of 3:2.

The crystalline material was separated into its components by fractional crystallization from Skellysolve B. The more abundant and faster moving (g.c.) isomer crystallized out first. Two recrystallizations yielded pure *trans*-2-benzyloxy-*cis*-4-*t*-butylcyclohexanol, m.p. 61–64°. The n.m.r. spectrum showed 1H multiplets at τ 6.16 (half-band width 7.5 Hz) and 6.44 (half-band width 7.5 Hz) that are assigned to the hydrogens geminal to the benzyl-

Can. J. Chem. Downloaded from www.nrcresearchpress.com by 210.87.254.105 on 09/05/12
For personal use only.

oxy and hydroxy groups. The small half-band widths require that both of these hydrogens be equatorial.

Anal. Calcd. for $C_{17}H_{26}O_2$: C, 77.82; H, 9.99. Found: C, 77.63; H, 9.71.

The isomeric *trans*-2-benzyloxy-*trans*-5-*t*-butylcyclohexanol crystallized, on concentrating the mother liquor, in the form of a voluminous precipitate. Five recrystallizations were required to achieve purity, m.p. 79.5–81.7°. The n.m.r. spectrum showed 1H multiplets at τ 6.01 (half-band width 10 Hz) snd 6.6 (half-band width 8 Hz) that are attributed to equatorial hydrogens geminal to the benzyloxy and hydroxy groups.

Anal. Calcd. for $C_{17}H_{26}O_2$: C, 77.82; H, 9.99. Found: C, 78.01; H, 9.79.

A suspension of *trans*-2-benzyloxy-*cis*-4-*t*-butylcyclohexanol (300 mg, 1.15 mmol) (**6**), 5% palladium-on-carbon (100 mg), and concentrated hydrochloric acid (0.1 ml, 1.2 mmol) in 90% ethanol (10 ml) was hydrogenated for 18 h. The reaction mixture was filtered through Celite, and the filtrate concentrated to a solid material (197 mg, 100%) which was crystallized twice from acetone – Skellysolve B. The white platelets (150 mg) melted at 143.5–146° (lit. (17), m.p. 141–142°).

De-*O*-benzylation of *trans*-2-benzyloxy-*trans*-5-*t*-butylcyclohexanol (**5**) as described above produced a product, m.p. 144–146°, identical to the product obtained from **6**.

Proof of the Structure of trans-2-Benzyloxy-cis-4-t-butylcyclohexanol (6)

(a) trans-2-Benzyloxy-cis-4-t-butylcyclohexyl Chloride

Trans-2-benzyloxy-*cis*-4-*t*-butylcyclohexanol (**6**) was chlorinated using the procedure of Bridgewater and Shoppee (21). A solution of **6** (4 g, 15.3 mmol) in dry Skellysolve B (10 ml) was added, dropwise during 25 min, to a cold (0°) stirred suspension of phosphorus pentachloride (7 g, 33.6 mmol) and anhydrous calcium carbonate (5 g) in Skellysolve B (30 ml). After addition, the mixture was stirred for 1.6 h at room temperature and then washed with ice-water. The organic layer was separated and the aqueous layer extracted twice with Skellysolve B (2 × 10 ml). The extracts were combined and washed with saturated aqueous sodium bicarbonate solution and then concentrated. Distillation of the residue yielded a colorless chlorine-containing oil (3.57 g, 86%), b.p. 105–106°/0.05 mm. The n.m.r. spectrum showed narrow 1H multiplets at τ 6.03 and 6.5 attributed to the hydrogens geminal to the benzyloxy and chloro groups. The half-band width (7 Hz) of these signals indicated that both of these hydrogens were equatorial.

Anal. Calcd. for $C_{17}H_{25}ClO$: C, 72.70; H, 8.97. Found: C, 72.63; H, 8.87.

(b) trans-5-t-Butyl-trans-2-chlorocyclohexanol

A suspension of *trans*-2-benzyloxy-*cis*-4-*t*-butylcyclohexyl chloride (3.02 g, 10.6 mmol), anhydrous sodium acetate (1.64 g, 20 mmol), and 5% palladium-on-carbon (300 mg) in glacial acetic acid (15 ml) was hydrogenated for 18 h. The reaction mixture was filtered through Celite and then partitioned between water (100 ml) and methylene chloride (3 × 20 ml). The methylene chloride extracts were combined, washed with water, and concentrated to a crystalline residue. Recrystallization from Skellysolve B gave 1.67 g (80%) of material, m.p. 76–78.5°. A sample was recrystallized twice from Skellysolve B to give colorless crystals, m.p. 78.5–80° (lit. (22), m.p. 74–76°). The 60 MHz n.m.r. spectrum in carbon tetrachloride was in agreement with the published data (22) and the compound contained chlorine.

Anal. Calcd. for $C_{10}H_{18}ClO$: C, 63.31; H, 9.56. Found: C, 63.19; H, 10.09.

(c) cis-5-t-Butyl-2-chlorocyclohexanone

A solution of *trans*-5-*t*-butyl-*trans*-2-chlorocyclohexanol (1.0 g, 5.2 mmol) in acetone (5.9 ml) was cooled to 0° and chromic acid (2 ml of a 3 *M* aqueous solution) was added dropwise with stirring. After 10 min, the reaction mixture was partitioned between cold water (10 ml) and Skellysolve B (10 ml). The organic layer was washed twice with water followed by saturated sodium bicarbonate solution and then concentrated to a clear oil (0.99 g). The i.r. spectrum showed a sharp carbonyl absorption at 1725 cm^{-1}, but no absorption for hydroxyl group. This compound was used without further characterization.

(d) 3-t-Butylcyclohexanone

A suspension of the α-chloroketone obtained above (0.99 g, 5.2 mmol), anhydrous sodium acetate (0.434 g, 5.3 mmol), and 5% palladium-on-carbon (0.25 g) in anhydrous methanol (10 ml) was stirred under an atmosphere of hydrogen until it absorbed 80 ml and the solids were then removed by filtration through Celite. The filtrate was concentrated to 3 ml, diluted with methylene chloride (10 ml), and washed once with saturated sodium bicarbonate solution and then evaporated to an oil. Short path distillation of the residue yielded ketonic material (0.51 g, 64%) (carbonyl absorption at 1718 cm^{-1}). The 2,4-dinitrophenyl hydrazone derivative melted at 164–166° (lit. (23), m.p. 161–162.5°), the semicarbazone at 207–208° (dec.) (lit. (24), m.p. 205–206°).

trans-4-t-Butyl-2-methoxycyclohexanone (7)

Trans-2-benzyloxy-*trans*-5-*t*-butylcyclohexanol (**5**) was methylated using the procedure of Eades and coworkers (25). A near quantitative yield of a clear oil (b.p. 80–85°/0.05 mm) was obtained.

Anal. Calcd. for $C_{18}H_{28}O_2$: C, 78.21; H, 10.21. Found: C, 78.50; H, 10.28.

The oil, 9.11 g, was dissolved in 250 ml of 95% ethanol containing 2 ml of concentrated hydrochloric acid and the stirred solution subjected to 1 atm of hydrogen in the presence of 0.6 g of 5% palladium-on-charcoal for 17 h. The usual work-up provided 5.75 g (88%) of an oil (b.p. 55–63°/0.06 mm). The n.m.r. spectrum agreed with that expected for *cis*-4-*t*-butyl-*trans*-2-methoxycyclohexanol and provided a phenylurethane derivative, m.p. 152–153°.

Oxidation of 5.0 g of the above alcohol under the conditions described above for the oxidation of *trans*-5-*t*-butyl-*trans*-2-chlorocyclohexanol provided 4.73 g (96%) of liquid, b.p. 90–100°/15–20 mm.

Anal. Calcd. for $C_{11}H_{20}O_2$: C, 71.69; H, 10.94. Found: C, 71.49; H, 11.16.

The i.r. spectrum showed a sharp carbonyl absorption at 1726 cm^{-1}. The n.m.r. spectrum showed the expected signals for the methoxy and *t*-butyl groups at τ 6.75 and 9.15, respectively. The 1H multiplet, half-band width 7 Hz, at τ 6.53 was assigned to the equatorial H-2. A multiplet centered at about τ 7.7 was assigned to the equatorial H-6.

trans-4-t-Butyl-2-methoxycyclohexanone oxime (E-) (9)

Standard oximation procedure provided a near

quantitative yield of crude oxime as gummy solid. Sublimation at 50°/0.02 mm gave a crystalline solid which had the large melting point range, 64–81°, after recrystallization from methanol water. The n.m.r. spectrum and composition were consistent with that expected for a mixture of the *syn-* (*Z-*) (**8**) and *anti-* (*E-*) (**9**) oximes. Narrow multiplets (half-band widths of 7 Hz) were present at τ 5.10 and 6.18 which were assigned to the equatorial H-2 atoms of **8** and **9**, respectively. Resublimation and recrystallization provided a 55% overall yield of a solid, m.p. 66–73° which appeared (n.m.r.) to be about 85% pure **9**. A broad near 1H multiplet centered at about τ 6.8 which was superimposed on the methoxy group signal was assigned to the equatorial H-6 of **9**.

Anal. Calcd. for $C_{11}H_{21}NO_2$: C, 66.29; H, 10.62; N, 7.03. Found: C, 66.41; H, 10.82; N, 7.31.

*cis-4-t-Butyl-2-methoxycyclohexanone (**10**)*

Oxidation of *trans*-2-benzyloxy-*trans*-5-*t*-butylcyclohexanol (**6**) with chromic acid as described above gave *cis*-2-benzyloxy-5-*t*-butylcyclohexanone (b.p. 85–90°/0.07 mm) in near quantitative yield. Reduction of this ketone with sodium borohydride in aqueous tetrahydrofuran under the usual conditions provided an oil which appeared to be about a 1:5 mixture of isomers. The major component crystallized on cooling and after three recrystallizations from Skellysolve B there resulted *cis*-2-benzyloxy-*cis*-5-*t*-butylcyclohexanol of high purity, m.p. 55.5–58°.

Anal. Calcd. for $C_{17}H_{26}O_2$: C, 77.82; H, 9.99. Found: C, 78.08; H, 9.96.

The n.m.r. spectrum was in complete accord with the assigned structure and configuration.

Methylation of the above alcohol using methyl iodide and sodium hydride in tetrahydrofuran (25) gave a near quantitative yield of a liquid, b.p. 65–70°/0.02 mm, which was hydrogenated under the conditions described above for the preparation of the isomeric *cis*-4-*t*-butyl-*trans*-2-methoxycyclohexanol. The overall yield was near quantitative of a liquid with a sweet odor, b.p. 60°/0.06 mm. The n.m.r. spectrum showed signals for a methoxy group (τ 6.63), an hydroxy group (τ 7.64) and a *t*-butyl group (τ 9.17) as expected for *cis*-4-*t*-butyl-*cis*-2-methoxycyclohexanol.

Anal. Calcd. for $C_{11}H_{22}O_2$: C, 70.92; H, 11.90. Found: C, 70.73; H, 11.61.

Chromic acid oxidation (26) provided the title compound (**10**).

Anal. Calcd. for $C_{11}H_{20}O_2$: C, 71.69; H, 10.94. Found: C, 71.64; H, 10.99.

The i.r. spectrum possessed the expected sharp carbonyl absorption at 1726 cm^{-1} and t.l.c. showed the ketone to be free of the parent alcohol. The n.m.r. spectrum was in complete accord with the expected structure. The half-band width of 20 Hz observed for the signal of H-2 at τ 6.22 is in accord with the assigned configuration.

*cis-4-t-Butyl-2-methoxycyclohexanone oxime (E-) (**11**)*

The crystalline oxime was readily obtained and appeared pure after two recrystallizations from methanol–water and a sublimation at 80°/0.04 mm. The yield was 66% of material melting at 166–168°.

Anal. Calcd. for $C_{11}H_{21}NO_2$: C, 66.29; H, 10.62; N, 7.03. Found: C, 66.47; H, 10.48; N, 7.29.

The n.m.r. spectrum was in support of the assigned structure. The 1H quartet at τ 6.28 had spacings, 5 and 9 Hz in accord with an axial H-2. A narrow (half-band width 7 Hz) multiplet at τ 6.84 was assigned to the equatorial H-6.

The financial support of the National Research Council of Canada through a grant-in-aid of research (A-172) to R.U.L. is gratefully acknowledged. The microanalyses and n.m.r. spectra were carried out by the analytical and spectral services laboratories of this department.

1. R. U. Lemieux, T. L. Nagabhushan, and S. W. Gunner. Can. J. Chem. **46**, 405 (1968).
2. R. U. Lemieux, K. James, and T. L. Nagabhushan. Can. J. Chem., **51**, 27 (1973).
3. R. U. Lemieux, R. Suemitsu, and S. W. Gunner. Can. J. Chem. **46**, 1040 (1968).
4. R. U. Lemieux and T. L. Nagabhushan. Methods in carbohydrate chemistry. Vol. VI. Editors, R. L. Whistler and J. N. BeMiller. Academic Press, New York. 1972. p. 487.
5. R. U. Lemieux, K. James, and T. L. Nagabhushan. Can. J. Chem., **51**, 42 (1973).
6. E. B. Hershberg. J. Org. Chem. **13**, 542 (1948).
7. C. H. DePuy and B. W. Ponder. J. Am. Chem. Soc. **81**, 4629 (1959).
8. G. H. Timms and E. Wildsmith. Tetrahedron Lett. 195 (1971).
9. M. L. Wolfrom. J. Am. Chem. Soc. **56**, 1794 (1934).
10. P. W. Austin, F. E. Hardy, J. G. Buchanan, and J. Baddiley. J. Chem. Soc. 5350 (1963).
11. R. U. Lemieux, T. L. Nagabhushan, K. J. Clemetson, and L. C. N. Tucker. Can. J. Chem. **51**, 53 (1973).
12. J. E. Blackwood, C. L. Gladys, K.L. Loening, A. E. Petrarca, and J. E. Rush. J. Am. Chem. Soc. **90**, 509 (1968).
13. H. Saito, I. Terasawa, M. Ohno, and K. Nukada. J. Am. Chem. Soc. **91**, 6696 (1969).
14. W. F. Trager and A. C. Huitric. Tetrahedron Lett. 825 (1966).
15. G. Janzsó, F. Kállay, I. Koczor, and L. Radics. Tetrahedron, **23**, 3699 (1967).
16. A. Daniel and A. A. Pavia. Tetrahedron Lett. 1145 (1967).
17. R. U. Lemieux and J. D. Stevens. Can. J. Chem. **44**, 249 (1966).
18. N. A. LeBel and R. F. Czaja. J. Org. Chem. **26**, 4768 (1961).
19. R. A. Earl. Ph.D. Thesis. University of Alberta, Edmonton, Alberta, 1970.
20. W. M. Jones, T. G. Squires, and M. Lynn. J. Am. Chem. Soc. **89**, 318 (1967).
21. R. J. Bridgewater and C. W. Shoppee. J. Chem. Soc. 1709 (1953).
22. A. B. Devine and R. E. Lack. J. Chem. Soc. C, 1902 (1966).
23. C. Djerassi, E. J. Warawa, R. E. Wolff, and E. J. Eisenbraun. J. Org. Chem. **25**, 917 (1960).
24. L. Schmerling. J. Am. Chem. Soc. **69**, 1121 (1947).
25. E. D. M. Eades, D. H . Ball, and L. Long, Jr. J. Org. Chem. **30**, 3949 (1965).
26. A. S. Hussey and R. M. Baker. J. Org. Chem. **25**, 1434 (1960).

Can. J. Chem. Downloaded from www.nrcresearchpress.com by 210.87.254.105 on 09/05/12
For personal use only.

Reduction of α-D-Hexopyranosulosides[1]

R. U. LEMIEUX, K. JAMES,[2] AND T. L. NAGABHUSHAN[3]
Department of Chemistry, University of Alberta, Edmonton, Alberta
Received June 2, 1972

Reduction of isopropyl tri-*O*-acetyl-α-D-*arabino*-hexopyranosuloside with sodium borohydride or diborane leads almost exclusively to the *gluco*-configuration. Catalytic reductions, on the other hand, provide an epimeric mixture with the *manno*-configuration predominating in ratios of about 2:1. The reduction of isopropyl tri-*O*-acetyl-α-D-*lyxo*-hexopyranosuloside with either sodium borohydride or diborane is less stereoselective than in the case of the *arabino*-isomer and leads to compounds of the *galacto*- and *talo*-configurations in the ratio of 3:2. The latter is formed highly stereoselectively when the lyxosuloside derivative is hydrogenated catalytically.

2-*O*-(α-D-Mannopyranosyl)-glycerol and the *gluco*-isomer are synthesized.

La réduction de l'isopropyl tri-*O*-acétyl-α-D-*arabino*-hexopyranosuloside par le borohydrure de sodium ou le diborane conduit presqu'exclusivement à la configuration *gluco*. Les réductions catalytiques donnent d'autre part, un mélange d'épimères avec la configuration *manno* prédominante dans des rapports de 2:1 environ. La réduction de l'isopropyl tri-*O*-acétyl-α-D-*lyxo*-hexopyranosuloside soit avec le borohydrure de sodium soit avec le diborane est moins stéréosélective que dans le cas de l'isomère *arabino* et conduit aux composés de configuration *galacto* et *talo* dans le rapport 3:2. Ce dernier est formé de façon hautement stéréosélective lorsque le dérivé lyxosuloside est hydrogéné catalytiquement.

Le *O*-(α-D-mannopyranosyl)-2 glycérol et l'isomère *gluco* ont été synthétisés.

[Traduit par le journal]

Can. J. Chem., **51**, 27 (1973)

Can. J. Chem. Downloaded from www.nrcresearchpress.com by 210.87.254.5 on 09/05/12
For personal use only.

In a previous publication (1), we reported the facile deoximations of isopropyl tri-*O*-acetyl-2-oximino-α-D-*arabino*-hexopyranoside and its *lyxo*-isomer to the corresponding keto-sugars **1** and **2**, respectively, which were characterized as crystalline compounds. Reductions of these ulosides to glycosides under a variety of conditions have now been examined. The promise of this approach for the synthesis of α-glucopyranosides was reported in a preliminary communication (2) where it was shown that the reduction of crude isopropyl tri-*O*-acetyl-α-D-*arabino*-hexopyranosuloside (**1**) by sodium borohydride followed by *O*-acetylation led to isopropyl tetra-*O*-acetyl-α-D-glucopyranoside in an overall yield of 80% from the oxime precursor.

The purpose of this paper is to report details of this work and to extend the method to preparations of α-D-mannopyranosides, α-D-galactopyranosides, and α-D-talopyranosides.

As previously reported (2, 3), reduction of **1** with sodium borohydride gave isopropyl α-D-glucopyranoside, isolated as the tetraacetate, in high yield (see Table 1). The *manno*-isomer was formed only in about 4% yield. Reduction of **1** with diborane in tetrahydrofuran was equally stereoselective but, in practice, the use of sodium borohydride is more convenient. The high stereoselectivity for the *gluco*-configuration has permitted convenient syntheses of a number of α-linked disaccharides (4) and kanamycin analogs (5).

The synthesis of α-D-mannopyranosides (6) is of considerable interest in view of the widespread natural occurrence of the α-D-mannopyranosyl units. In addition to their presence in a variety of mannans such as yeast mannan (7, 8) and ivory nut mannan (9), and the red algae *furcellario fastigiata* (10), the α-D-mannopyranosyl groups are found in a number of glycolipids (11) and teichoic acids of bacterial cell walls (12). Recently another naturally occurring antibiotic was shown to contain an α-D-mannopyranosyl unit (13), namely, 2-amino-2-deoxy-α-D-glucopyranosyl α-D-mannopyranoside (14), an epimer of the antibiotic trehalosamine.

Acid-catalyzed alcoholysis of D-mannose provides α-D-mannopyranosides but is virtually limited to simple alcohols that can be used as

[1]Presented in part at the 161st National American Chemical Society Meeting, Los Angeles, California, March 28 – April 2, 1971.
[2]University of Alberta Postdoctoral Fellow, 1970–1972.
[3]Professional Research Associate, 1970–1972.

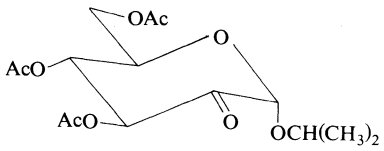

1

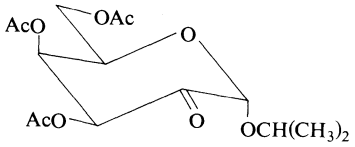

2

TABLE 1. Reduction of isopropyl tri-*O*-acetyl-α-D-hexopyranosulosides

	Ratio (%)*			
	arabino		*lyxo*	
Reducing agent	*gluco*	*manno*	*galacto*	*talo*
$NaBH_4$ in aqueous dioxane	96	4	60	40
B_2H_6 in tetrahydrofuran	94	6	60	40
H_2/5% Pd-on-carbon†	32	68	9	91
H_2/5% Ru-on-alumina†	40	60	20	80
H_2/5% Rh-on-carbon†	20	80	15	85
H_2/PtO_2†	75	25	13	87
H_2/Raney nickel†	60	40	17	83

*Estimated by g.c.
†At 60 p.s.i. in 95% aqueous ethanol at room temperature.

solvents (15). Since the tetra-*O*-acyl-D-mannopyranosyl halides are only available in the α-configuration and the C_2-acyloxy group is well disposed for participation in the replacement of the *trans*-axial-1-halogen atoms, the so-called acylhalogenomannoses are highly prone to orthoester formation (6, 16). However, the presence of non-participating *O*-substituents at the 2-position has provided a useful synthesis of β-D-mannopyranosides (17). Efforts in this laboratory (18) to obtain α-D-mannopyranosides from the corresponding 1,2-orthoacetyl derivatives have not succeeded under conditions which were partially successful with 1,2-orthoacetyl derivatives of D-glucopyranose (19). However, a recent publication by Franks and Montgomery (20) reports acid-catalyzed rearrangement of tri-*O*-benzyl-β-D-mannopyranose 1,2-(alkyl orthoacetates) to the α-D-mannopyranoside derivatives in yields ranging between 74–79%. Yet another method for the synthesis of α-D-mannopyranosides was demonstrated by Ferrier and Prasad (21). These authors synthesized, although in low overall yield, 6-*O*-α-D-mannopyranosyl-α-D-galactose by reaction of 1,2:3,4-di-*O*-isopropylidene-α-D-galactose with tri-*O*-acetyl-2-deoxy-1,5-anhydro-D-*arabino*-hex-1-enitol (tri-*O*-acetyl-D-glucal) in the presence of boron trifluoride dietherate followed by *cis*-hydroxylation of the resulting 2,3-unsaturated glycoside with aqueous permanganate and then removal of the protecting groups.

It was anticipated that catalytic hydrogenation of **1** may tend to favor formation of the axial alcohol. As seen in Table 1, this was the case for reductions using palladium, ruthenium, and rhodium catalysts. Although the synthesis of an α-D-mannopyranoside by this procedure will require the separation of the epimers, it can provide a useful approach. This is illustrated by the preparation of 2-*O*-(α-D-mannopyranosyl) glycerol (**3**), a compound previously prepared by Charlson and coworkers (7) by degradation of 2-*O*-(α-D-mannopyranosyl)-D-mannose.

The 2-*O*-(tri-*O*-acetyl-2-oximino-α-D-*arabino*-hexopyranosyl)-1,3-di-*O*-benzoyl glycerol was obtained in 71% yield. Deoximation followed by hydrogenation over palladium-on-carbon gave a product which was deacylated. The n.m.r. spectrum showed two glycosidic components in the ratio 1.7:1 with doublet signals for anomeric hydrogens τ 4.83 (spacing 1.75 Hz) and 4.77 (spacing 3.75 Hz), respectively. The product was chromatographed on a Dowex 1-X2 column in the hydroxide form (22) to provide a 42% yield of the major product which liberated mannose and glycerol on acid hydrolysis. The product from

Can. J. Chem. Downloaded from www.nrcresearchpress.com by 210.87.254.5 on 09/05/12
For personal use only.

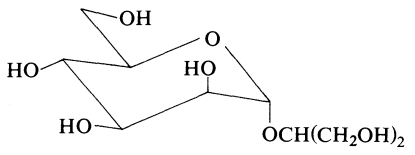

3

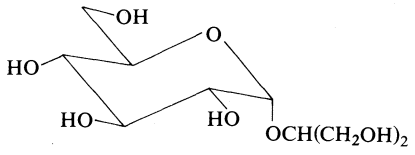

4

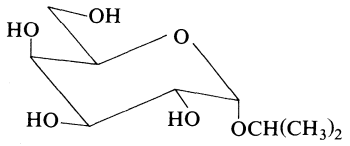

5

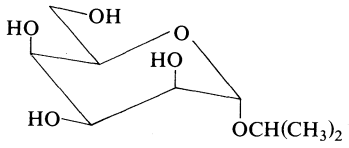

6

periodate oxidation of this component liberated glycerol on acid hydrolysis and the compound is therefore assigned the structure 2-*O*-(α-D-mannopyranosyl)-glycerol (**3**). The specific rotation, 75°, was substantially higher than that, 51°, previously reported (7) for this compound. The hydrolysis and periodate oxidation – hydrolysis data for the other glycosidic component which was obtained in 20% yield allowed assignment of the structure to be 2-*O*-(α-D-glucopyranosyl)-glycerol (**4**). The specific rotation, 122°, was in good agreement with that, 121°, previously reported (7).

The products of the hydrogenation of **1** were isolated as their 3,4,6-tri-*O*-acetyl derivatives by column chromatography. The n.m.r. spectra required high purity and the free hydroxyl is expected to be at the 2-position for both compounds in view of the mode of preparation. The glucose derivative possessed the same n.m.r. spectrum as an authentic sample prepared by treating tri-*O*-acetyl-α-D-glucopyranose 1,2-(ethyl orthoacetate) with isopropanol in methylene chloride containing toluenesulfonic acid (19).

α-D-Galactopyranosyl units are found as building blocks of the capsular substances of pneumococci (23) and the blood group B substances (24). For these reasons, a practical synthesis of α-D-galactopyranosides is becoming of increasing importance and the reduction of α-D-*lyxo*-hexopyranosulosides was examined in this regard.

The reduction of an α-*lyxo*-hexosuloside either with sodium borohydride or diborane proved much less stereoselective than the similar reductions of the *arabino*-isomer. For example, starting from **2**, a mixture of the galacto- (**5**) and talopyranoside (**6**) in about 3:2 ratio, respectively, was obtained (see Table 1). Undoubtedly, this result is related to a hindrance by the axial 4-substituent in **2** to axial attack by the hydride to provide equatorial C_2-hydroxyl. Nevertheless, when combined with the powerful means for separation available by chromatography, especially on resin columns (22, 25), the method is considered to provide a synthetic route to α-D-galactopyranosides of high utility.

Although α-talosides are not widely distributed in nature, the α-D-talopyranosyl group is linked to the *N*-methyldeoxystreptamine residue in the antibiotic hygromycin B_2 (26). In view of this, an α-taloside synthesis by way of reduction of tri-*O*-acetyl-α-D-*lyxo*-hexopyranosulosides could be of synthetic importance. As seen in Table 1, catalytic hydrogenation of isopropyl tri-*O*-acetyl-α-D-*lyxo*-hexopyranosuloside can increase the ratio of *talo*- (**6**) to *galacto*- (**5**) isomer to as high as 4:1.

The above described hexosides were characterized by hydrolysis to the hexoses and by n.m.r. Table 2 reports n.m.r. parameters for the four isopropyl tetra-*O*-acetyl-α-D-hexopyranosides. The assignments of the signals for compounds **5** and **6** were made possible by reduction of **2** with sodium borodeuteride to produce the 2-deuterio derivatives.

Experimental

Melting points were determined in capillary tubes and are uncorrected. Optical rotations were measured in a 1 dm tube with a Perkin–Elmer Model 141 polarimeter. N.m.r. spectra were taken on Varian HA100 spectrometer. Chemical shifts are given in τ-values and refer to spectra measured either in deuteriochloroform using tetramethylsilane (TMS) as the internal standard or in deuterium

Can. J. Chem. Downloaded from www.nrcresearchpress.com by 210.87.254.5 on 09/05/12
For personal use only.

TABLE 2. N.m.r. parameters for isopropyl tetra-*O*-acetyl-α-D-hexopyranosides in deuteriochloroform at 100 MHz

	Chemical shifts, τ-values (spacings, Hz)					Isopropyl	
Configuration	H-1($J_{1,2}$)	H-2($J_{2,3}$)	H-3($J_{3,4}$)	H-4($J_{4,5}$)	OAc	C*H*	$(CH_3)_2$
gluco	4.82(3.75)	5.21(10)	4.53(9.5)	4.97(9.5)	7.95, 7.97 7.99, 8.00	5.89(6.0)	8.76, 8.89
manno	5.13(1.75)	—	—	—	7.90, 7.96 8.00, 8.06	6.12(6.0)	8.79, 8.85
galacto	4.78(3.65)	4.94(10.4)	4.67(3.75)	4.55(1.25)	7.84, 7.91 7.94, 7.99	6.12(6.0)	8.72, 8.83
talo	5.06	5.02	4.73	4.73	7.90, 7.90 8.01, 8.04	6.11(6.0)	8.80, 8.86

oxide using the same reference compound as the external standard.

G.c. was carried out with an F and M Model 500 gas chromatograph using a 6 ft column packed with LP 45 (ethylene glycol adipate 1.5%) on acid washed chromosorb W, 60–80 mesh at 175° (27). Although the actual yields of the glycosides prepared under the various conditions reported in Table 1 were not determined, separations of synthetic mixtures of pure samples established the reliability of the ratios measured. The starting materials (**1** and **2**) survived the g.c. and were not present in the chromatograms of the products of hydrogenation. In all cases, t.l.c. examination of the acetylated reduced products gave no indication of components other than the acetylated glycosides.

Column chromatography was performed on silicic acid, CC7, 100–200 mesh (Mallinckrodt Chemical Works, St. Louis, Mo.), using 10 g per gram of compound and t.l.c. on Silica Gel G (E. Merck A.G., Darmstadt) using 20 cm^2 plates. The spots were visualized by spraying the plates with a solution of chlorosulfonic acid (10%, v/v) in glacial acetic acid and then heating in an oven at 120°. The descending paper chromatograms on Whatman No. 1 paper were developed with *n*-butanol – pyridine–water – acetic acid (6:4:3:1), and visualized by spraying with alkaline silver nitrate. The R_f values for glucose, mannose, galactose, and talose were 0.4, 0.48, 0.35, and 0.58, respectively.

Solutions were dried over magnesium sulfate and all solvent removals were carried out *in vacuo* using a rotary evaporator.

The hydrogenation catalysts were purchased from Engelhardt Industries, Newark, New Jersey. Diborane in THF was bought from Alfa Inorganics, Beverly, Massachusetts.

*Reduction of Isopropyl Tri-O-acetyl-α-D-arabino-hexopyranosuloside(**1**)*

(a) By Sodium Borohydride

A solution of **1** (1) (0.5 g) in dioxane (8 ml) and water (1 ml) was cooled to 0° and sodium borohydride (50 mg) was then added in small portions, while maintaining the temperature at 0°. The resulting solution, after being stirred for 30 min at 0° and then for 3 h at room temperature, was cooled to 0° and neutralized with glacial acetic acid. Evaporation of the solution yielded a white solid which was acetylated with acetic anhydride in pyridine (10 ml of a 1:1 mixture) at 0°. Isolation of the product by standard procedures yielded an oil which crystallized on storage. G.c. analysis of the crude acetylated mixture is reported in Table 1. Recrystallization from 95% ethanol afforded pure isopropyl tetra-*O*-acetyl-α-D-glucopyranoside, m.p. 86–87°, $[\alpha]_D^{24}$ +145° (*c*, 1.6 in chloroform) in 85% yield (lit. (28), m.p. 86–88° (corr.), $[\alpha]_D$ +145° (*c*, 2 in chloroform)). The n.m.r. spectrum of the crystalline compound (Table 2) was identical with that of an authentic sample and the melting point of an admixture of the two was not depressed.

(b) By Diborane

A solution of **1** (3.4 g) was dissolved in tetrahydrofuran (15 ml) and cooled to 0°. Diborane (40 ml of a molar solution in tetrahydrofuran) was then added at such a rate as to maintain the temperature at 0°. On completion of the addition, the temperature of the solution was allowed to rise to room temperature and the mixture was then set aside for 24 h. The solution was again cooled to 0° and excess methanol was added with caution. The solution was concentrated to dryness, dissolved in methanol, and re-evaporated in order to remove methyl borate. This procedure was repeated three more times. The residual oil was dried and acetylated with acetic anhydride in pyridine (20 ml of a 1:1 mixture) at 0°. Isolation of the product by normal procedures afforded a pale yellow oil which was crystallized from ether – Skellysolve B. G.c. analysis of the crude product is reported in Table 1. Recrystallization from 95% ethanol gave pure isopropyl tetra-*O*-acetyl-α-D-glucopyranoside, m.p. 86–87° and $[\alpha]_D^{24}$ +144° (*c*, 1.65 in chloroform), in 85% yield.

(c) By Catalytic Hydrogenation

A solution of **1** (2.0 g) in 95% ethanol (40 ml) was hydrogenated in the presence of 5% by weight of catalyst (Table 1) at 60 p.s.i. and room temperature for 24 h. The catalyst was removed by filtration through a Celite bed and the filtrate concentrated to a mobile oil (1.77 g). T.l.c. examination of the oil using ether – Skellysolve B (3:2) as the developing solvent showed the presence of two components, the one with lower mobility being the major component.

A 50-mg portion of the above oil was acetylated with pyridine and acetic anhydride (1 ml of 1:1 mixture). The crude product isolated in the usual manner was

Can. J. Chem. Downloaded from www.nrcresearchpress.com by 210.87.254.5 on 09/05/12
For personal use only.

Can. J. Chem. Downloaded from www.nrcresearchpress.com by 210.87.254.5 on 09/05/12
For personal use only.

examined by t.l.c. and analyzed by g.c. The results are presented in Table 1.

The remaining portion of the oil (1.72 g) was chromatographed on silicic acid using ether – Skellysolve B (3:2) as the developing solvent on a column of 2.5 cm diameter and the eluate was monitored by t.l.c. using the same solvent system. The two compounds were isolated as syrups by removal of the solvents. The faster moving compound, $[\alpha]_D^{28}$ +142° (*c*, 1.86 in chloroform) had an n.m.r. spectrum identical to an authentic sample of isopropyl 3,4,6-tri-*O*-acetyl-α-D-glucopyranoside (19) and was converted by acetylation to crystalline isopropyl tetra-*O*-acetyl-α-D-glucopyranoside characterized as mentioned above.

The slower moving compound, $[\alpha]_D^{28}$ +83° (*c*, 1.23 in chloroform) possessed an n.m.r. spectrum consistent with that expected for isopropyl 3,4,6-tri-*O*-acetyl-α-D-mannopyranoside.

Anal. Calcd. for $C_{15}H_{24}O_9$: C, 51.72; H, 6.90. Found: C, 52.23; H, 7.12.

The above crude reduction product was deacetylated and chromatographed on ion-exchange resin (Dowex 1-X2 200–400 mesh) in the hydroxide form to yield isopropyl α-D-mannopyranoside (0.6 g, 47%) which crystallized from isopropanol to yield material m.p. 113–114°, $[\alpha]_D^{21}$ +83° (*c*, 1.02 in water).

Anal. Calcd. for $C_{10}H_{18}O_6$: C, 48.65; H, 8.11. Found: C, 48.38; H, 8.15.

Hydrolysis by aqueous acid liberated mannose as determined by paper chromatography. The n.m.r. spectrum in D_2O showed a doublet for the anomeric hydrogen at τ 4.88 with a spacing of 1.6 Hz. The spectrum of the tetra-*O*-acetyl derivative is reported in Table 2.

Isopropyl Tetra-O-acetyl-α-D-galacto- and α-D-talopyranosides

Isopropyl tri-*O*-acetyl-α-D-*lyxo*-hexopyranosuloside (**2**) (1) (2.0 g) was reduced with sodium borohydride and the reduction product acetylated with acetic anhydride in pyridine by the procedure described above. The fully acetylated material was subjected to column chromatography using ether – Skellysolve B (4:6) as the developing solvent. The first major fraction was crystallized from methanol and then recrystallized from 95% ethanol to afford pure isopropyl tetra-*O*-acetyl-α-D-galactopyranoside (1.2 g, 51%), m.p. 109–110°, $[\alpha]_D^{27}$ +152.5° (*c*, 0.74 in chloroform). The n.m.r. spectrum is reported in Table 2.

Anal. Calcd. for $C_{17}H_{26}O_{10}$: C, 52.30; H, 6.71. Found: C, 52.26; H, 6.62.

A sample of the above compound (0.05 g) was deacetylated as mentioned above and the n.m.r. spectrum of the product in D_2O showed the anomeric hydrogen at τ 4.8 as a doublet with a spacing of 2.5 Hz.

The second major fraction from the chromatogram crystallized from methanol. Recrystallization from aqueous ethanol gave a pure compound (0.6 g, 26%), m.p. 67–68°, $[\alpha]_D^{27}$ +73° (*c*, 0.57 in chloroform) characterized as isopropyl tetra-*O*-acetyl-α-D-talopyranoside. The n.m.r. spectrum (see Table 2) was fully in accord with this structure.

Anal. Calcd. for $C_{17}H_{26}O_{11}$: C, 52.40; H, 6.45. Found: C, 52.47; H, 6.44.

The preparation was repeated under similar conditions except that sodium borodeuteride was used as reducing agent. The n.m.r. spectra in $CDCl_3$ of these acetylated 2-deuterio-α-D-galacto- and 2-deuterio-α-D-talopyranosides showed that signals at τ 4.94 and 5.02, respectively, had disappeared when compared to spectra of the natural compounds and are assigned to H-2 for these compounds.

The chemical shifts of H-1 (singlet), -3 (doublet), and -4 (quartet) for isopropyl tetra-*O*-acetyl 2-deuterio-α-D-galactopyranoside were at τ 4.78, 4.67, and 4.55, respectively. In the case of the corresponding taloside, the deuteration gave rise to a narrow multiplet with an intensity for two hydrogens at τ 4.73 and sharp singlet for one hydrogen at τ 5.06. The latter signal is assigned to the anomeric hydrogen because of the close correspondence of its chemical shift with that for this signal for isopropyl tetra-*O*-acetyl-α-D-mannopyranoside, namely τ 5.13. The multiplet to lower field was assigned to H-3 and -4.

A sample of isopropyl tetra-*O*-acetyl-α-D-talopyranoside (0.1 g) was deacetylated as mentioned above and the n.m.r. spectrum of the product in D_2O showed the anomeric hydrogen at τ 4.73 with a spacing of 1.2 Hz.

1,3-Di-O-benzoylglycerol

A solution of glycerol (10.0 g) in pyridine (100 ml) was cooled to 0° and benzoyl chloride (34.5 g) was added dropwise with stirring. The resulting solution was kept at ambient temperature for 12 h and then poured into an ice-water mixture. After standing for 12 h the aqueous layer was decanted and the residual semi-crystalline material dissolved in ether. The ether layer was washed sequentially with water, dilute hydrochloric acid, and water and then concentrated to a mobile oil (31.0 g). Column chromatography of this oil using benzene as the developing solvent yielded the tri-*O*-benzoyl glycerol (0.5 g) which was crystallized from ether – Skellysolve B, m.p. 71–72°. The n.m.r. in $CDCl_3$ was that expected with the multiplet signal for H-2 at τ 4.2 and the doublet for the two methylene groups centered at τ 5.3. Subsequent elution of the column with dichloromethane afforded 1,3-di-*O*-benzoyl glycerol (20 g, 61%) which was crystallized from ether – Skellysolve B, m.p. 50–51°.

Anal. Calcd. for $C_{17}H_{16}O_5$: C, 67.99; H, 5.37. Found: C, 68.05; H, 5.20.

The n.m.r. spectrum in $CDCl_3$ showed a doublet for the hydroxyl hydrogen at τ 6.5 (spacing 4 Hz). The five other hydrogens of the glycerol residue appeared as a band in the region τ 5.35–5.7. The doublet for the O*H* and lack of signal for H-2 to lower field require the assigned structure.

2-O-(Tri-O-acetyl-2-oximino-α-D-arabino-hexopyranosyl)-1,3-di-O-benzoylglycerol

A solution of 1,3-di-*O*-benzoylglucerol (2.75 g) and dimeric tri-*O*-acetyl-2-deoxy-2-nitroso-α-D-glycopyranosyl chloride (4.5 g) in dry dimethylformamide (20 ml) was kept at ambient temperature for 72 h. The resulting highly colored solution was concentrated and the residual oil dissolved in dichloromethane and the solution washed with water (3 × 100 ml) and then concentrated to yield an oil (6.3 g). Column chromatography of this material using ether – Skellysolve B (3:2) as the developing solvent afforded the title compound as an oil (3.75 g, 71%), $[\alpha]_D^{23}$ +42° (*c*, 3.4 in chloroform).

Anal. Calcd. for $C_{29}H_{31}NO_{13}$: C, 57.90; H, 5.19; N, 2.33. Found C, 57.90; H, 5.16; N, 2.30.

*2-O-(α-D-Gluco- and Mannopyranosyl)-glycerol (**3** and **4**)*

A solution of 2-*O*-(tri-*O*-acetyl-2-oximino-α-D-*arabino*-hexopyranosyl)-1,3-di-*O*-benzoylglycerol (5.0 g) in acetonitrile (12 ml) and dilute hydrochloric acid (10 ml) containing acetaldehyde (2 ml) was kept at ambient temperature for 3 h. This solution was diluted with ethyl acetate (150 ml) and the aqueous layer extracted with a further portion of ethyl acetate (50 ml). The combined ethyl acetate extracts were washed once with water and evaporated to a thick oil (4.0 g). Column chromatography of this oil using ether – Skellysolve B (3:2) as the developing solvent afforded 2-*O*-(tri-*O*-acetyl-α-D-*arabino*-hexopyranosulosyl)-1,3-di-*O*-benzoylglycerol (3.6 g). This material (3.0 g) was dissolved in 95% ethanol and hydrogenated using Pd/C (5%) for 24 h at 60 p.s.i. The catalyst was removed by filtration and the solution evaporated to an oil which was deacylated with sodium methoxide in methanol for 3 h. The solution was neutralized with ion-exchange resin (Dowex 50W-X8 H^+ form) and evaporated to an oil. This oil was partitioned between dichloromethane and water. Evaporation of the aqueous layer yielded an oil (1.3 g) which was chromatographed on ion-exchange resin (Dowex 1X2, 200–400 mesh, OH^- form) to yield 2-*O*-(α-D-mannopyranosyl)-glycerol (**3**) (0.54 g, 42%), $[\alpha]_D^{21}$ +75° (*c*, 0.56 in water), (lit. (7), $[\alpha]_D$ +51° (water)) followed by 2-*O*-(α-D-glucopyranosyl)-glycerol (**4**) (0.26 g, 20%), $[\alpha]_D^{21}$ +122° (*c*, 0.92 in water), (lit. (7), $[\alpha]_D$ +121° (water)).

*Periodate Oxidation of 2-O-(α-D-Glucopyranosyl) and 2-O-(α-D-Mannopyranosyl)-glycerol (**4** and **3**)*

To a solution of 0.054 mmol each of **4**, **3**, and isopropyl α-D-glucopyranoside in 0.5 ml water was added sodium metaperiodate (0.04 g) and the mixture was set aside in the dark for 18 h. Excess periodate was destroyed by the addition of sodium bisulfite (0.021 g) and to the resulting solution was added 2 *N* hydrochloric acid (1 ml). The mixture was heated for 1 h at 100° and then concentrated down before spotting on a t.l.c. plate. Simultaneously, a solution of glycerol (3.75 mg) in 2 *N* hydrochloric acid (1 ml) was heated for 1 h at 100°, concentrated down to a low volume, and chromatographed for comparison on the same plate using the upper phase of ether acetate – dioxane–water (2:2:1) as the solvent. The spots were visualized by heating this with sulfuric acid. Only **3** and **4** showed the presence of glycerol (R_f 0.14) thus confirming the assigned structures.

The financial support of the National Research Council of Canada through a grant-in-aid of research (A-172) to R.U.L. is gratefully acknowledged. The microanalyses and n.m.r. spectra were carried out by the analytical and spectral services laboratories of this department.

1. R. U. LEMIEUX, R. A. EARL, K. JAMES, and T. L. NAGABHUSHAN. Can. J. Chem. **51**, 19 (1973).
2. R. U. LEMIEUX, R. SUEMITSU, and S. W. GUNNER. Can. J. Chem. **46**, 1040 (1968).
3. R. U. LEMIEUX and T. L. NAGABHUSHAN. Methods in carbohydrate chemistry. Vol. VI. Editors, R. L. Whistler and J. N. BeMiller. Academic Press, New York. 1972. p. 487.
4. R. U. LEMIEUX, K. JAMES, and T. L. NAGABHUSHAN. Can. J. Chem. **51**, 42 (1973).
5. R. U. LEMIEUX, T. L. NAGABHUSHAN, K. J. CLEMETSON, and L. C. N. TUCKER. Can. J. Chem. **51**, 53 (1973).
6. P. A. J. GORIN and A. S. PERLIN. Can. J. Chem. **37**, 1930 (1959).
7. A. J. CHARLSON, P. A. J. GORIN, and A. S. PERLIN. Can. J. Chem. **34**, 1811 (1956).
8. Y. C. LEE and C. E. BALLOU. Biochem. **4**, 257 (1965).
9. G. O. ASPINALL, R. B. RASHBROOK, and G. KESSLER. J. Chem. Soc. 215 (1958)
10. B. LINDBERG. Acta Chem. Scand. **9**, 1093 (1955).
11. E. LEDERER. Adv. Carbohydr. Chem. **16**, 207 (1961).
12. A. R. ARCHIBALD and J. BADDILEY. Adv. Carbohydr. Chem. **21**, 323 (1966).
13. J. FRIED and H. E. STAVELY. J. Am. Chem. Soc. **74**, 5461 (1952).
14. M. URAMATO, N. OTAKE, H. YONEHARA. J. Antibiot. (Jap.) Ser. A, **20**, 236, 1967.
15. V. SMIRNYAGIN and C. T. BISHOP. Can. J. Chem. **46**, 3085 (1968).
16. H. L. FRUSH and H. S. ISBELL. J. Res. Natl. Bur. Stand. **27**, 413 (1941).
17. P. A. J. GORIN and A. S. PERLIN. Can. J. Chem. **39**, 2474 (1961).
18. M. POMPIPOM. Ph.D. Thesis. University of Alberta, Edmonton, Alberta.
19. R. U. LEMIEUX and A. R. MORGAN. IUPAC Symposium on the Chemistry of Natural Products, Kyoto, Japan, April 12–18, 1964.
20. N. E. FRANKS and R. MONTGOMERY. Carbohydr. Res. **6**, 286 (1968).
21. R. J. FERRIER and N. PRASAD. Chem. Commun. 476 (1968).
22. P. W. AUSTIN, F. E. HARDY, J. G. BUCHANAN, and J. BADDILEY. J. Chem. Soc. 5350 (1963).
23. P. A. REBERS and M. HEIDELBERGER. J. Am. Chem. Soc. **83**, 3056 (1961).
24. R. D. MARSHALL and A. NEUBERGER. Adv. Carbohydr. Chem. **25**, 407 (1970).
25. R. M. SAUNDERS. Carbohydr. Res. **7**, 76 (1968).
26. P. F. WILEY, M. V. SIGAL, JR., and O. WEAVER. J. Org. Chem. **27**, 2793 (1962).
27. S. J. ANGYAL and K. JAMES. Carbohydr. Res. **12**, 147 (1970).
28. E. PACSU, J. JANSON, and B. LINDBERG. Methods in carbohydrate chemistry. Vol. II. Editors, R. L. Whistler and M. L. Wolfrom. Academic Press, New York. 1963. p. 376.

Can. J. Chem. Downloaded from www.nrcresearchpress.com by 210.87.254.5 on 09/05/12
For personal use only.

Reduction of Isopropyl Tri-*O*-acetyl-2-oximino-α-D-hexopyranosides[1]

R. U. LEMIEUX, K. JAMES,[2] T. L. NAGABHUSHAN,[3] AND Y. ITO[4]

Department of Chemistry, University of Alberta, Edmonton, Alberta

Received June 2, 1972

Hydrogenation of 2-oximino-α-D-*arabino*-hexopyranosides in the presence of palladium and hydrazine provided high stereoselectivity for the formation of 2-amino-2-deoxy-α-D-glucopyranosides including disaccharide structures. Similar yields of *gluco*-isomer were normally obtained on reduction by borane of 2-acetoximino-tri-*O*-acetyl-α-D-*arabino*-hexopyranosides in tetrahydrofuran. However, reduction of 2-*O*-(2-acetoximino-tri-*O*-acetyl-α-D-*arabino*-hexopyranosyl)-1,3-dibenzoylglycerol provided a ratio of about 3:2 of the *gluco*- to *manno*-isomers. Reductions with lithium aluminum hydride were not appreciably stereoselective. Treatment of isopropyl 2-oximino-α-D-*arabino*-hexopyranoside with hydrazine in the presence of palladium catalyst gave isopropyl 2-deoxy-α-D-*arabino*-hexopyranoside in a novel room-temperature Wolff–Kishner type reaction.

Reduction of isopropyl tri-*O*-acetyl 2-oximino-α-D-*lyxo*-hexopyranoside both with borane and lithium aluminum hydride proceeded with slight stereoselectivity for the *galacto*-isomer.

L'hydrogénation des oximino-2-α-D-*arabino*-hexopyranosides en présence de palladium et d'hydrazine conduit à la formation d'amino-2 déoxy-2-α-D-glucopyranosides incluant des structures disaccharides, avec une haute stéréoselectivité. Des rendements similaires en isomère *gluco* ont été normalement obtenus par réduction avec le diborane d'acétoximino-2- tri-*O*-acétyl-α-D-*arabino*-hexopyranosides dans le tétrahydrofurane. La réduction de l'*O*-(acétoximino-2 tri-*O*-acétyl-α-D-*arabino*-hexopyranosyl)-2 dibenzoyl-1,3 glycérol conduit cependant aux isomères *gluco* et *manno* dans un rapport d'environ 3:2. Les réductions par l'hydrure de lithium et d'aluminium ne sont pas stéréosélectives de façon appréciable. Le traitement de l'isopropyl oximino-2-α-D-*arabino*-hexopyranoside par l'hydrazine en présence de palladium fournit le déoxy-2-α-D-*arabino*-hexopyranoside selon un nouveau type de Wolff-Kishner à température ambiante.

La réduction de l'isopropyl tri-*O*-acétyl oximino-2-α-D-*lyxo*-hexopyranoside par le borane et l'hydrure de lithium et d'aluminium se fait avec une stéréosélectivité faible en faveur de l'isomère *galacto*.

[Traduit par le journal]

Can. J. Chem., **51**, 33 (1973)

Several methods based on Koenigs–Knorr type reactions have provided synthetic approaches to 2-amino-2-deoxy-α-D-glucopyranosides. These include reactions using the *N*-4-methoxybenzylidene (1, 2), *N*-2,4-dinitrophenyl (3–5), and *N*-diphenyl phosphoryl (6) derivatives of 3,4,6-tri-*O*-acetyl-2-amino-2-deoxy-α-D-glucopyranosyl bromide. The reactions are not highly selective for the synthesis of the α-linkage and the yields are generally low. Nevertheless, for example, using tri-*O*-acetyl-2-(2,4-dinitroanilino)-2-deoxy-α-D-glucopyranosyl bromide as reagent, it was possible to achieve isolable yields of paromamine (7) and an isomer (8). Trehalosamine was synthesized using tri-*O*-acetyl-2-amino-2-deoxy-*N*-(4′-methoxybenzylidene)-α-D-glucopyranosyl bromide (9). 2-Amino-2-deoxy-α-glycopyranosyl residues are not only found in numerous antibiotics (10) but are also widely distributed in nature in bacterial cell walls (11), mucopolysaccharides (12) such as heparin and glycoproteins and the blood group substances (13). The ease of preparation and the attractive yields obtained for tri-*O*-acetyl-2-oximino-α-D-*arabino*-(**1**) and *lyxo*-hexopyranosides (**2**) (14) prompted the investigation of the reduction of these oximes to amines. In principle, stereoselective reductions would allow these compounds to serve as precursors to 2-amino-2-deoxy-α-D-glucopyranosides (**3**), 2-amino-2-deoxy-α-D-mannopyranosides (**4**),

[1]Presented in part at the 154th National American Chemical Society Meeting, Chicago, Illinois, September 11, 1967 and at the 161st National American Chemical Society Meeting, Los Angeles, California, March 28, 1971.

[2]University of Alberta Postdoctorate Fellow 1970–1972.

[3]Professional Research Associate, 1970–1972.

[4]University of Alberta Postdoctorate Fellow, 1965. Present address: Microbial Chemistry Research Laboratory, Tanabe Seiyaku Co. Ltd., Toda-Shi, Saitama-ken, Japan.

Can. J. Chem. Downloaded from www.nrcresearchpress.com by 210.87.254.105 on 09/05/12
For personal use only.

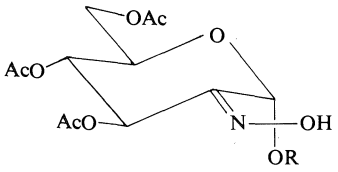

1

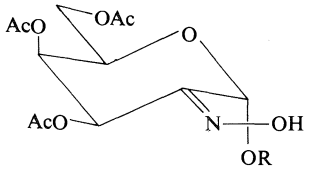

2

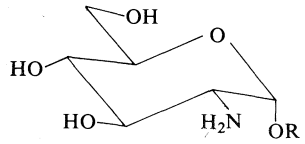

3

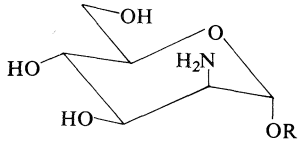

4

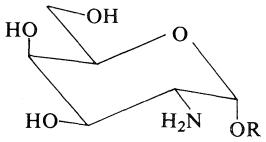

5

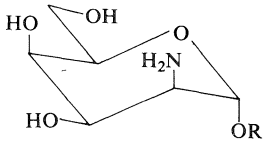

6

2-amino-2-deoxy-α-D-galactopyranosides (**5**), and 2-amino-2-deoxy-α-D-talopyranosides (**6**).

The purpose of this publication is to report that conditions were established for the reduction of **1** with a high degree of stereoselectivity to the *gluco*-product **3** and with moderate stereoselectivity to the *manno*- (**4**) and *talo*- (**6**) products. Stereoselective reduction to the *galacto*-configuration (**5**) was not accomplished, the best yields being 60%. An accompanying paper (15) describes the utilization of these reactions for the preparation of six 2-acetamido-2-deoxy-α-D-hexopyranosyl derivatives of hexoses.

The stereochemical result of catalytic hydrogenation of alkyl 2-oximino-α-D-*arabino*-hexopyranosides and methyl 6-*O*-(2-oximino-α-D-*arabino*-hexopyranosyl)-β-D-glucoypranoside over palladium-on-carbon in the presence of hydrochloric acid was discussed in a previous publication (16). The fraction of the *gluco*-isomer formed in each case varied substantially with the nature of the aglycon group; *viz.*, methyl 71%; ethyl or *n*-propyl 62%, isopropyl 80%, and methyl 6-*C*-β-D-glucopyranosidyl 50%. Attempts to hydrogenate the oximes in neutral, weakly acidic or weakly basic media using a variety of catalysts and pressures led to generally slow reactions without marked stereoselectivity. In view of the high yields of aminodeoxyalditols obtained on hydrogenation of sugars in the presence of hydrazine (17), the hydrogenation of the oxime (**7**) in the presence of hydrazine was examined (see Scheme 1). It was anticipated that exchange from oxime (**7**) to hydrazone (**9**) would occur and that the hydrazone would reduce efficiently to amine. Although Paulsen and Stoye (18, 19) have recently reported a number of carbohydrate hydrazones which displayed little tendency for azine formation, experiments aimed at preparing pure hydrazone (**9**) did not succeed. However, the formation of **9** was demonstrated by the addition of hydrazine to the uloside **10** followed by hydrogenation of the mixture. Isopropyl 2-amino-2-deoxy-α-D-glucopyranoside was isolated as its tetraacetyl derivative in 30% yield. When the oxime **7** was used as starting material, the compound was reclaimed unchanged on hydrogenation in the absence of the hydrazine; however, in the presence of hydrazine, the aminoglucoside **11** was formed in nearly quantitative yield. Formation of the hydrazone from the oxime was also indicated by the discovery of a novel Wolff–Kishner type reaction to form deoxyglucoside to be discussed below. The transformation of the oxime to

Can. J. Chem. Downloaded from www.nrcresearchpress.com by 210.87.254.105 on 09/05/12
For personal use only.

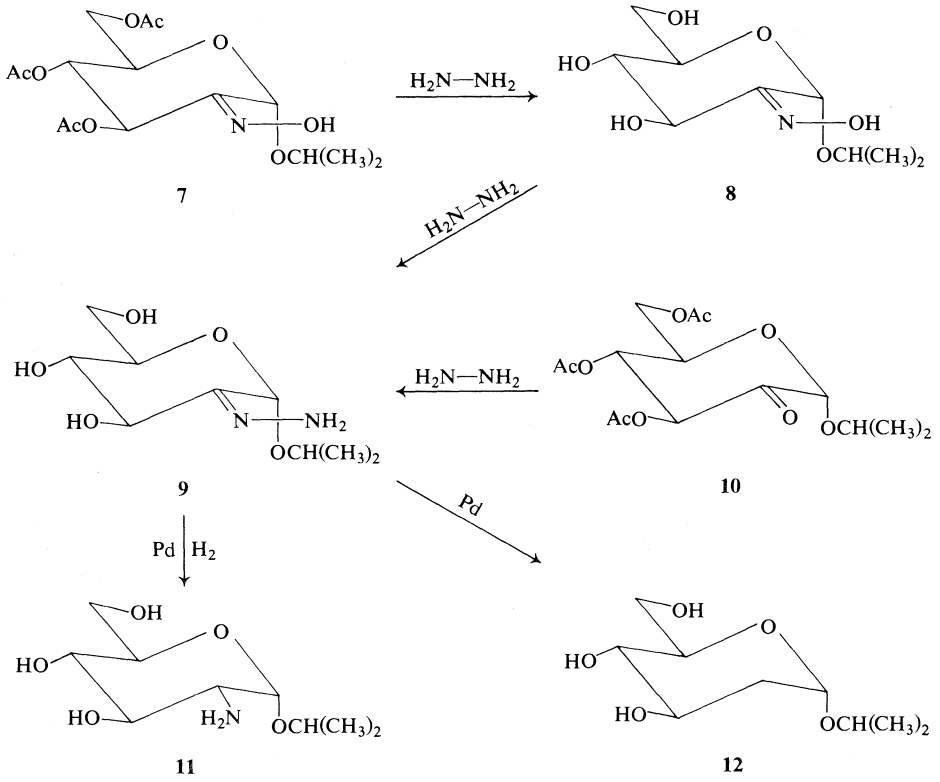

SCHEME 1

hydrazone appears either to be slow or the equilibrium to strongly favor the oxime. The first stage of the reaction involves de-*O*-acetylation. Thus after treating compound **7** in 90% aqueous ethanol with a tenfold molar excess of hydrazine for 2 h at room temperature, acetyl hydrazine and an acetyl-group free product (**8**) were formed. The latter substance gave a positive ferric chloride – ferricyanide test for oxime and, on acetylation, provided isopropyl 2-acetoximo-tri-*O*-acetyl-α-D-*arabino*-hexopyranoside (**17**) in a highly pure form.

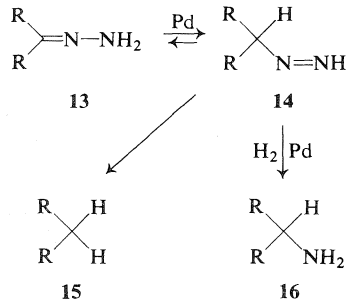

SCHEME 2

The reductive aminations of isopropyl tri-*O*-acetyl-2-oximino-α-D-*arabino*-hexopyranoside (**7**), 6-*O*-(tri-*O*-acetyl-2-oximino-α-D-*arabino*-hexopyranosyl)-1,2;3,4-di-*O*-isopropylidene-α-D-galactopyranose, and 3-*O*-(tri-*O*-acetyl-2-oximino-α-D-*arabino*-hexopyranosyl)-1,2;5,6-di-*O*-isopropylidene-α-D-glucofuranose in 90% aqueous ethanol by hydrogenation catalyzed by palladium-on-carbon in the presence of hydrazine were found to provide the *gluco*-configuration (equatorial amine) in excellent yield (better than 90%). However, the reaction was found to be erratic and the high yields not always reproducible. A study of this matter led to the discovery that reaction occurred on stirring the mixture of the oxime **7**, hydrazine, and palladium catalyst in 90% aqueous ethanol at room temperature in the *absence* of hydrogen to provide isopropyl 2-deoxy-α-D-*arabino*-hexopyranoside (**12**). When the palladium catalyst was not included, no trace of the latter compound could be detected in the product. Thus, it is apparent that palladium can catalyze the isomerization of a hydrazone (**13**) to the diimide structure (**14**) which readily decomposes,

Can. J. Chem. Downloaded from www.nrcresearchpress.com by 210.87.254.105 on 09/05/12
For personal use only.

Can. J. Chem. Downloaded from www.nrcresearchpress.com by 210.87.254.105 on 09/05/12
For personal use only.

under the influence of the base to hydrocarbon (**15**) following the usually accepted mechanism for Wolff–Kishner reduction on treating a hydrazone with base (20) (see Scheme 2). The generality of this reduction has not been examined but could provide a route to the synthesis of 2-deoxyglycosides (21) under reaction conditions which are much milder than those normally required for Wolff–Kishner reduction (19). Clearly, the existence of this mode of reaction implies hydrazone formation from the oxime. Apparently, when the catalyst is saturated with hydrogen, hydrogenation to amine (**16**) takes precedence over decomposition of the diimide intermediate. The formation of the diimide intermediate as a reversible reaction can be expected to be subject to thermodynamic control. Thus, hydrogenation of the diimide group in the equatorial orientation would explain the high stereoselectivity found for this reaction.

Attempts to apply the hydrogenation–hydrazine procedure to isopropyl tri-*O*-acetyl-α-D-*lyxo*-hexopyranoside failed to yield a characterizable product. It is possible that, because of the axial C_4-substituent, the intermediate uloside is too prone to β-elimination. This matter will receive further examination.

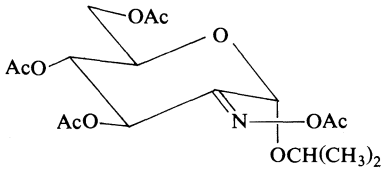

17

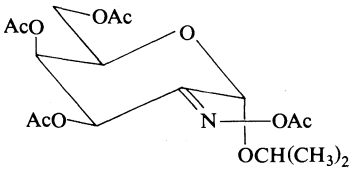

18

The reductions of oxime acetates and oxime tosylates (22) as well as oxime ethers (23) by borane in tetrahydrofuran, wherein the reagent is the complex between the borane (Lewis acid) and the tetrahydrofuran, are reported to provide the amine. Thus, it was of interest to examine the reductions of the *O*-acetyl derivatives of **7** and its *lyxo*-isomer, namely compounds **17** and **18**. Indeed, the yields of amine were excellent. In the case of compound **17**, the yield of the equatorial amine **3** (R = isopropyl) was over 90% by g.c. analysis (see Table 1). Isopropyl 2-amino-2-deoxy-α-D-glucopyranoside was isolated as its crystalline hydrochloride directly from the crude product in 73% yield. The tetraacetyl derivative was formed in 80% yield from the crude product. The reduction of **18** however showed little stereoselectivity. These results are reminiscent of the stereochemical results obtained on reducing the ulosides prepared from these oximes both by sodium borohydride in aqueous dioxane and by borane in tetrahydrofuran (24). Thus, the reactions appear to proceed by axially directed nucleophilic attack by the borane complex at C-2 and the presence of an axial substituent at C-4, as is present in the acetoxime **18**, renders this approach less favorable than was found for the reduction of **17**. Application of this reduction to more complex acetoximes of the *lyxo* configuration was found (15) to be even less favorable for the formation of the equatorial amine.

It was to be expected (23) that borane reduction of the oximinoglycosides would provide the 2-amino-2-deoxy-*N*-hydroxy glycosides. However, this appeared not to be the case, the only products isolated being glycosaminides (see below).

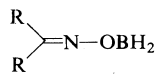

19

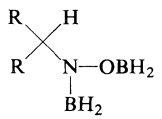

20

It is not possible to predict with certainty the mode of the initial attack of an oxime by borane. However, the ease with which borane reduces carboxylic acids suggests that the first stage involves attack of the hydroxyl group of the oxime to form a product of type **19**. Thus, the nucleophilic attack at the unsaturated carbon would be on **19** to form **20** and this product was proposed by Feuer and coworkers (23) as the precursor of the hydroxylamines they obtained on hydrolysis. However, they envisaged attack of the nitrogen by the borane in the first stage of the hydroboration of the double bond. As mentioned above, nucleophilic attack at the carbon center would seem more in accord with our present results. Although Feuer and coworkers generally obtained good to excellent yields of hydroxylamines especially when the product was subjected to

TABLE 1. Reductions of 2-oximino and 2-acetoximino hexopyranosides

Starting compound*	Reducing conditions	Relative amounts of epimers in product	
		gluco†	*manno*†
2-Oximino-α-D-*arabino* (**1**)	H_2, Pd, N_2H_4	92	8
	BH_3, THF	70	30
	$LiAlH_4$, THF	40	60
2-Acetoximino-α-D-*arabino*	BH_3, THF	95	5
		galacto‡	*talo*‡
2-Oximino-α-D-*lyxo* (**2**)	BH_3, THF	57	43
	$LiAlH_4$, ether	60	40
	$LiAlH_4$, THF	69	31
2-Acetoximino-α-D-*lyxo*	BH_3, THF	53	47

*Derivatives of isopropyl tri-*O*-acetylhexopyranoside.
†Estimated by g.c. analysis.
‡Estimated by column chromatography.

acid hydrolysis, it is noteworthy that basic hydrolysis caused a dismutation of the hydroxylamine to form amine and oxime in the case of an α-aryl aldoxime and an aryl ketoxime. The possibility therefore exists that the amines obtained on borane reduction of our oximes are artifacts of the mode of the decomposition of the reaction mixture and isolation (treatment in methanol with a strongly basic ion exchange resin). However, the yield of amine obtained on borane reduction of the oximes **1** and **2** with R = isopropyl were 48 and 78%, respectively. These yields are too high for production of amine by dismutation of the hydroxylamine only. Evidently, neighboring groups can influence the extent of the borane reduction of an oxime. Many possibilities exist including anchimeric assistance to further reduction of the nitrogen by neighboring borohydride complexes and increased ease of elimination of a species such as $HOBH_2$ from an intermediate such as **20** to an imine structure which is subsequently reduced to hydroborated amine.

Lithium aluminum hydride is well known to reduce oximes to amines (25). Reduction of the oximinoglycoside **1** with this reagent was examined with ether, tetrahydrofuran, and ethylene glycol dimethyl ether as the solvents. The axial amine was formed to a greater extent in most cases but never surpassed in stereoselectivity the 1:1.5 ratio for *gluco*- to *manno*-isomers obtained on reducing **1** (R = isopropyl). A 2.2:1 ratio for *galacto*- to *talo*-isomers was obtained on reducing **2** (R = isopropyl) using tetrahydrofuran as solvent. This ratio was 1.5:1 when ether was the solvent. The lithium aluminum hydride reductions of 6-*O*-(tri-*O*-acetyl-2-oximino-α-D-*arabino*-hexopyranosyl)-1,2;3,4-di-*O*-isopropylidene-α-D-galactopyranose and 3-*O*-(tri-*O*-acetyl-2-oximino-α-D-*arabino*-hexopyranosyl)-1,2;5,6-di-*O*-isopropylidene-α-D-glucofuranose gave (14) in each case about 1:1 mixtures of the *gluco*- to *manno*-isomers. In contrast, the hydrogenation of these compounds in the presence of hydrazine gave the glucosaminide products in near quantitative yields. The reductions of these oximinodisaccharides by borane are reserved for a separate publication (15).

The reduction of 2-(2-acetoximino-tri-*O*-acetyl-α-D-*arabino*-hexopyranosyl)-1,3-di-*O*-benzoylglycerol with borane in tetrahydrofuran provided, after chromatographic separation, a 36% yield of 3-*O*-(2-amino-2-deoxy-α-D-glucopyranosyl)-glycerol, a compound previously synthesized by Hardy (2) in an effort to characterize a degradation product of the intracellular teichoic acid of *Staphylococcus aureus*. A 21% yield of 2-*O*-(2-amino-2-deoxy-α-D-mannopyranosyl)-glycerol was also obtained. This high *manno* to *gluco* ratio (about 3:2) for a borane reduction indicates that the stereochemical route of reduction can be influenced by groups neighboring to the oximino group. The catalytic hydrogenation of 2-(2-oximino-tri-*O*-acetyl-α-D-*arabino*-hexopyranosyl)-1,3-di-*O*-benzoylglycerol in the presence of hydrazine was examined. However, in the one attempt made, a complex product was obtained which was not further characterized. Thus, the scope of this mode of reduction may also be limited. The product will be further investigated.

Can. J. Chem. Downloaded from www.nrcresearchpress.com by 210.87.254.105 on 09/05/12
For personal use only.

Can. J. Chem. Downloaded from www.nrcresearchpress.com by 210.87.254.105 on 09/05/12
For personal use only.

Experimental

The measurements of optical rotations, n.m.r. spectra, and the techniques of chromatography are the same as those presented in related work (26). The g.c. analyses reported in Table 1 were made using a 6 ft (1/4 in. o.d.) column packed with LP45 (ethylene glycol adipate, 1.5%) (Wilkens Instrument and Research, Inc.) on acid-washed Chromosorb W, 60–80 mesh (Johns–Manville Products Corp.) at 175°. The chromatograms were made with the peracetylated derivatives. These conditions failed to separate isopropyl 2-acetamido-tri-*O*-acetyl-2-deoxy-α-D-galactopyranoside from its *talo*-isomer. The ratios of these isomers in the various products (see Table 1) were estimated from the weights in the fractions from the chromatographic separation of the de-*O*-acetylated mixture on a Dowex 1-X2 (200–400 mesh, hydroxide form) ion-exchange resin and using water as the developing solvent (27).

Methods for Reduction

(a) Hydrogenation in the Presence of Hydrazine

The oxime (5 mmol) was dissolved in 90% aqueous ethanol (25 ml) containing 85% aqueous hydrazine (2.0 g). The solution was kept at room temperature for 2 h prior to hydrogenation at 60 p.s.i. over 5% palladium-on-carbon (3.0 g) for 24 h. Catalyst removal and concentration in the usual manner left a residue which was further processed as described under the preparation of the following compounds.

(b) Reduction with Diborane

A solution of the oxime or the acetoxime (10 mmol) in tetrahydrofuran (20 ml) was cooled to −5° under an atmosphere of nitrogen. A 1 *M* solution of borane (50 ml) in tetrahydrofuran was added with stirring at a rate that maintained the temperature at −5°. After the addition was complete, the solution was allowed to warm to room temperature and left for 24 h in the case of an oxime but only 3 h for an acetoxime. Methanol was then added to destroy the excess borane. Solvent removal left a foam which was dissolved in methanol for treatment with ion-exchange resin (Dowex 1-X8, hydroxide form). Removal of the solvent by evaporation *in vacuo* left a solid which was processed as described below when this procedure was used.

(c) Reduction with Lithium Aluminum Hydride

The oxime (4 mmol) was dissolved in the solvent specified (25 ml). Solid lithium aluminum hydride (0.95 g, 28 mmol) was then added in portions and the resulting mixture was stirred under reflux in a nitrogen atmosphere for about 3 h. The excess hydride was then destroyed by the careful addition of ethyl acetate. The addition of a 50% aqueous methanol (100 ml) caused a precipitation. The precipitate was collected and thoroughly washed with water. The filtrates were combined and the p*H* adjusted to 4.5 with hydrochloric acid. Solvent removal *in vacuo* left a residue which was further processed as described below.

Derivatives of Isopropyl 2-Amino-2-deoxy-α-D-glucopyranoside

The reduction products of isopropyl tri-*O*-acetyl-2-oximino-α-D-*arabino*-hexopyranoside (**7**) (28) were further processed as follows.

The product from the catalytic hydrogenation of **7** in the presence of hydrazine was stirred with tetrahydrofuran (15 ml) for 1 h. The solids were gathered by filtration and dissolved in methanol. The resulting solution was acidified with hydrogen chloride in ether and on evaporation a spontaneous crystallization of material occurred. Recrystallization from ethyl alcohol – ethyl acetate mixture provided a 55% yield of isopropyl 2-amino-2-deoxy-α-D-glucopyranoside as the hydrochloride salt, m.p. 202° (dec.) identical to an authentic sample (16).

Peracetylation of a sample of the crude product followed by g.c. analysis showed an 11.5:1 ratio of the *gluco*- to *manno*-isomers (see Table 1).

The product from the reduction of the oxime **7** with diborane was acetylated with acetic anhydride in pyridine in the usual manner. G.c. analysis of the product showed a 7:3 ratio of the *gluco*- to *manno*-isomers (see Table 1). Chromatography on a silicic acid column using ether – Skellysolve B (4:1) gave a major fraction which was crystallized from ethyl acetate – Skellysolve B. The product was isopropyl 2-acetamido-tri-*O*-acetyl-2-deoxy-α-D-glucopyranoside (48% yield), m.p. 149–150°, $[\alpha]_D^{28}$ 94° (*c*, 1.4 in chloroform) identified by comparison with product obtained in acetylation of isopropyl 2-amino-2-deoxy-α-D-glucopyranoside hydrochloride.

The product from the reduction with diborane of the *O*-acetyl derivative of **7** (the acetoxime **17**) on g.c. analysis showed a 19:1 ratio for the *gluco*- and *manno*-isomers (see Table 1). When the deionized methanolic solution was acidified with hydrogen chloride in ether and the resulting solution was concentrated, isopropyl 2-amino-2-deoxy-α-D-glucopyranoside crystallized as its hydrochloride salt. The yield was 73%, m.p. 202° (dec.), after recrystallization from ethanol – ethyl acetate.

The crude product from the lithium aluminum hydride reduction of **7** in tetrahydrofuran was acetylated with pyridine (15 ml) and acetic anhydride (6 ml) and work-up in the usual manner afforded a sirupy product (90%). G.c. analysis of the oil indicated a 1:1.5 ratio of the *gluco*- and *manno*-isomers. Hydrolysis of a sample by treatment with 4 *N* hydrochloric acid at 100° for 1 h liberated two ninhydrin-positive sugars with migrations on paper electrophoresis (29) corresponding to mannosamine and glucosamine. On standing for 3 days at room temperature, the crude syrupy product deposited crystals which were isolated by trituration with ether (28% yield) and identified by m.p. and 60 MHz n.m.r. to be isopropyl 2-acetamido-tri-*O*-acetyl-2-deoxy-α-D-glucopyranoside (described above).

Derivatives of Isopropyl 2-Amino-2-deoxy-α-D-galactopyranoside and its talo-Isomer

Attempts to hydrogenate isopropyl tri-*O*-acetyl-2-oximino-α-D-*lyxo*-hexopyranoside (28) in the presence of hydrazine failed to yield a characterizable product.

The product from the reduction of the oxime with diborane was estimated by chromatography on the ion-exchange resin to comprise a ratio of about 3:2 of the *galacto*- and *talo*-isomers (see Table 1) and was not examined further.

The product from the reduction with diborane of the *O*-acetyl derivative of the oxime (the acetoxime **18**) was *N*-acetylated and found by the ion-exchange chromatography to comprise a mixture of the *galacto*- and *talo*-

Can. J. Chem. Downloaded from www.nrcresearchpress.com by 210.87.254.105 on 09/05/12
For personal use only.

isomers in a ratio of about 1:1. The crude reduction product was dissolved in ethanol and the solution was acidified with hydrogen chloride in ether. On concentration, a syrup was obtained which crystallized from ethanol – ethyl acetate. The yield was 18% of isopropyl 2-amino-2-deoxy-α-D-galactopyranoside as the hydrochloride salt, m.p. 160–164°, $[\alpha]_D^{23}$ + 138° (*c*, 1.5 in water).

Anal. Calcd. for $C_9H_{20}NO_5Cl$: C, 41.94; H, 7.82; N, 5.44; Cl, 13.76. Found: C, 41.94; H, 7.55; N, 5.51; Cl, 13.84.

The n.m.r. spectrum of this salt in deuterium oxide was in agreement with the structure assigned.

The salt was acetylated with acetic anhydride in pyridine in the usual manner to provide crystalline isopropyl 2-acetamido-tri-*O*-acetyl-2-deoxy-α-D-galactopyranoside which was recrystallized from ether – Skellysolve B. The yield was 93%, m.p. 139–140°, $[\alpha]_D^{23}$ + 110° (*c*, 1.35 in chloroform).

Anal. Calcd. for $C_{17}H_{27}NO_9$: C, 52.43; H, 6.99; N, 3.60. Found: C, 52.48; H, 7.23; N, 3.78.

The hydrochloride salt was reacted with 1-fluoro-2,4-dinitrobenzene in aqueous bicarbonate–acetone solution and the product acetylated with acetic anhydride and pyridine to provide a yellow solid which was recrystallized from ethanol to yield isopropyl tri-*O*-acetyl-2-deoxy-2-(2′,4′-dinitroanilino)-α-D-galactopyranoside, m.p. 172–173°, $[\alpha]_D^{23}$ −21.5° (*c*, 1 in chloroform).

Anal. Calcd. for $C_{21}H_{27}N_3O_{12}$: C, 49.12; H, 5.30; N, 8.18. Found: C, 48.91; H, 4.98; N, 7.94.

A product obtained by the diborane reduction of the acetoxime (**18**) (2.30 g) was dissolved in 50% aqueous methanol (10 ml) and acetic anhydride (4 ml) was added. The syrup obtained on solvent removal was added to a 40 in. × 3/4 in. column of Dowex 1-X2 (200–400 mesh, hydroxide form) and the column was eluted with water at a flow rate of 1 ml/min. The elution was followed by t.l.c. on silica gel using the upper phase of an ethyl acetate – dioxane–water (2:2:1) system as developing phase. Combination of the appropriate fractions provided solutions of two major components.

Evaporation of the solution of the faster moving compound readily provided crystalline isopropyl 2-acetamido-2-deoxy-α-D-galactopyranoside in 41% yield. Recrystallization from ethyl acetate gave a pure product, m.p. 191–192°, $[\alpha]_D^{23}$ +192° (*c*, 0.8 in dimethylformamide).

Anal. Calcd. for $C_{11}H_{21}NO_6$: C, 50.18; H, 8.04; N, 5.32. Found: C, 49.97; H, 7.83; N, 5.17.

The slower moving product was obtained as an oil, $[\alpha]_D^{21}$ +49° (*c*, 1.7 in dimethylformamide), 37% yield. and assigned the structure isopropyl 2-acetamido-2-deoxy-α-D-talopyranoside on the basis of its composition and n.m.r. spectrum.

Anal. Calcd. for $C_{11}H_{21}NO_6$: C, 50.18; H, 8.04; N, 5.32. Found: C, 49.88; H, 7.98; N, 5.38.

Reduction of the oxime with lithium aluminum hydride in tetrahydrofuran and acetylation of the crude product as before gave a syrupy product in near quantitative yield. Trituration with ether gave crystalline isopropyl 2-acetamido-tri-*O*-acetyl-2-deoxy-α-D-galactopyranoside identical to the product obtained from the diborane reduction of the acetyl derivative of **2** in an overall yield of 40%.

A sample of the crude acetylated reduction product (0.1 g) was *O*-deacetylated with triethylamine (0.5 ml) in 50% aqueous methanol (5 ml) and after removal of the solvents, the residue was freeze-dried from deuterium oxide. Examination of the residue by n.m.r. at 60 MHz showed the presence of a doublet at τ 5.0 (H-1, *galacto*-isomer, $J_{1,2}$ = 3.5 Hz) and a singlet at 5.06 (H-1, *talo*-isomer) in the ratio of about 2.2:1. Furthermore, when the crude *O*-deacetylated product was chromatographed on the basic column as described above, two main fractions were obtained. Hydrolysis of the first fraction that was eluted from the column with 4 *N* hydrochloric acid for 1.5 h liberated galactosamine as indicated by paper electrophoresis (29). The other fraction liberated talosamine. The 60 MHz n.m.r. spectra of the compounds were indistinguishable from those obtained for isopropyl 2-acetamido-2-deoxy-α-D-galactopyranoside and the *talo*-isomer prepared by reduction of **2** with diborane. Judging from the weights of the fractions, the isomers were formed in the ratio of 2.2:1 (*galacto*:*talo*). This ratio was 1.5:1 when ether was used as the solvent for the reduction.

2-O-(2-Amino-2-deoxy-α-D-gluco- and manno-pyranosyl)-glycerol Hydrochlorides

2-*O*-(Tri-*O*-acetyl-2-oximino-α-D-*arabino*-hexopyranosyl)-1,3-di-*O*-benzoylglycerol (5.0 g) (24) was acetylated with acetic anhydride (4.0 ml) in pyridine (20 ml) for 2 h at 0°. The 2-acetoximino derivative was isolated as an oil (5.0 g) and reduced with 1 *M* borane in tetrahydrofuran (50 ml). The crude reduction product was isolated as a foam using the procedure described above. Ion-exchange chromatography of this material on Dowex 1-X2 (200–400 mesh, hydroxide form) yielded first 2-*O*-(2-amino-2-deoxy-α-D-glucopyranosyl)-glycerol, characterized as its hydrochloride salt (0.85 g, 36%), $[\alpha]_D^{23}$ + 113° (*c*, 1.3 in water) which in our hands resisted crystallization. Hardy (2) reported a crystalline preparation, m.p. 160–162°, $[\alpha]_D$ +117° (water). The n.m.r. spectrum in deuterium oxide showed a one-hydrogen doublet at τ 4.65 with a spacing of 4.0 Hz which was assigned to the anomeric hydrogen.

Further elution of the column produced a product which was converted to the hydrochloride salt (0.40, 21%), $[\alpha]_D^{23}$ −17.6° (*c*, 1.07 in water). The compound liberated mannosamine on acid hydrolysis and produced a doublet signal assigned to anomeric proton at τ 4.90 with spacing of 1.6 Hz.

Anal. Calcd. for $C_9H_{20}NO_7Cl$: C, 37.31; H, 6.96; N, 4.84; Cl, 12.24. Found: C, 37.18; H, 6.86; N, 4.83; Cl, 12.32.

Derivatives of 6-O-(2-Amino-2-deoxy-α-D-glucopyranosyl)-1,2;3,4-di-O-isopropylidene-α-D-galactopyranose and 6-O-(2-Amino-2-deoxy-α-D-mannopyranosyl)-1,2;3,4-di-O-isopropylidene-α-D-galactopyranose

Catalytic hydrogenation of 6-*O*-(3,4,6-tri-*O*-acetyl-2-oximino-α-D-*arabino*-hexopyranosyl)-1,2;3,4-di-*O*-isopropylidene-α-D-galactopyranose (**21**) (14) in the presence of hydrazine gave a product which was acetylated using acetic anhydride in pyridine. The n.m.r. spectrum at 100 MHz of the crude product required that 6-*O*-(2-acetamido-3,4,6-tri-*O*-acetyl-2-deoxy-α-D-glucopyranosyl)-1,2;3,4-di-*O*-isopropylidene-α-D-galactopyranose was formed in near quantitative yield. The compound crystallized from

Can. J. Chem. Downloaded from www.nrcresearchpress.com by 210.87.254.105 on 09/05/12
For personal use only.

ethyl acetate – *n*-hexane in 56% yield, m.p. 125–127°, $[\alpha]_D^{25}$ +25° (*c*, 1 in chloroform).

Anal. Calcd. for $C_{26}H_{39}NO_{14}$: C, 52.96; H, 6.67; N, 2.38. Found: C, 52.89; H, 6.44; N, 2.03.

The n.m.r. spectrum was in accord with the assigned structure.

The product from the reduction of **21** with lithium aluminum hydride in tetrahydrofuran gave an n.m.r. spectrum consistent with a 1:1.2 mixture of the *gluco*- and *manno*-isomers, respectively. This ratio was near 1:1 when ethylene glycol dimethyl ether was used as solvent. With ether as solvent, the ratio was 1:1.5.

The product from the reduction in ether was made to react with 1-fluoro-2,4-dinitrobenzene in aqueous sodium bicarbonate – acetone solution in the usual manner. The crude yield of the *N*-dinitrophenyl derivatives was near quantitative. A sample (373 mg) of the mixture was subjected to preparative t.l.c. on silica gel using benzene–pyridine (4:1) as developing phase. Elution of the slower moving yellow band provided a solid sample which, on hydrolysis at 100° in 3 *N* hydrochloric acid for 1 h, liberated a yellow substance with the same R_f value by t.l.c. on silica gel using *n*-butanol – ethanol–water (3:1:1), as an authentic sample of 2-deoxy-2-(2′,4′-dinitrophenylamino)-glucose. The remainder was treated with acetic anhydride and pyridine. The crude acetylated product appeared homogeneous on t.l.c. (benzene–methanol, 20:1) and provided an n.m.r. spectrum at 100 MHz compatible with a high degree of chemical homogeneity. Recrystallization from ethyl acetate – *n*-hexane gave fine needles (107 mg), m.p. 200–202°, $[\alpha]_D^{23}$ −29° (*c*, 0.44 in chloroform).

Anal. Calcd. for $C_{30}H_{39}N_3O_{17}$: C, 50.49; H, 5.51; N, 5.89. Found: C, 50.47; H, 5.29; N, 5.83.

The 100 MHz n.m.r. spectrum of the above compound in deuteriochloroform showed a doublet at τ 5.00 with a spacing of 4.0 Hz which was assigned to H-1 of the amino-sugar residue. On this basis, together with the fact that the spectrum in all other respects was in accord with that expected, the compound was assigned the structure 6-*O*-[3,4,6-tri-*O*-acetyl-2-deoxy-2-(2,4-dinitroanalino)-α-D-glucopyranosyl]-1,2;3,4-di-*O*-isopropylidene-α-D-galactopyranose.

The product isolated from the faster moving yellow band in the above-mentioned preparative thin layer chromatogram was acetylated and the crude product (152 mg) recrystallized from benzene and *n*-hexane. The material, $[\alpha]_D^{30}$ −86° (*c*, 0.42 in chloroform), sintered at 92° and melted in the range 149–151°. The 100 MHz n.m.r. spectrum in deuteriochloroform showed a one-hydrogen doublet at τ 5.03 with a spacing of 1.5 Hz. In view of this observation and the fact that the n.m.r. spectrum in all other regards was consistent with the expected structure, the compound was assigned as 6-*O*-[3,4,6-tri-*O*-acetyl-2-deoxy-2-(2,4-dinitroanilino)-α-D-mannopyranosyl)-1,2;3,4-di-*O*-isopropylidene-α-D-galactopyranose.

Anal. Calcd. for $C_{30}H_{39}N_3O_{17}$: C, 50.49; H, 5.51; N, 5.89. Found: C, 50.52; H, 5.28; N, 5.85.

Derivatives of 3-O-(2-Amino-2-deoxy-α-D-glucopyranosyl)-1,2;5,6-di-O-isopropylidene-α-D-glucofuranose and 3-O-(2-Amino-2-deoxy-α-D-mannopyranosyl)-1,2;5,6-di-O-isopropylidene-α-D-glucofuranose

Catalytic hydrogenation of 3-*O*-(3,4,6-tri-*O*-acetyl-2-oximino-α-D-*arabino*-hexopyranosyl)-1,2;5,6-di-*O*-isopropylidene-α-D-glucofuranose (**22**) (14) in the presence of hydrazine provided a product which was reacted with 1-fluoro-2,4-dinitrobenzene prior to acetylation with acetic anhydride and pyridine. The yield of crude crystalline material was 88%. Recrystallization from ethyl acetate and *n*-hexane gave a product, m.p. 211–212°, $[\alpha]_D$ +12° (*c*, 0.5 in chloroform).

Anal. Calcd. for $C_{30}H_{39}N_3O_{17}$: C, 50.49; H, 5.51; N, 5.89. Found: C, 50.31; H, 5.33; N, 5.84.

The n.m.r. spectrum at 100 MHz in deuteriochloroform allowed assignment of the structure 3-*O*-[3,4,6-tri-*O*-acetyl-2-deoxy-2-(2,4-dinitroanalino)-α-D-glucopyranosyl]-1,2;5,6-di-*O*-isopropylidene-α-D-glucofuranose. A one-hydrogen doublet at τ 5.32 with a spacing of 4.5 Hz was assigned to H-1 of the glucosamine residue.

Reduction of the oxime **22** with lithium aluminum hydride in ethylene glycol dimethyl ether provided a ninhydrin-positive product which was converted to the *N*-2,4-dinitrophenyl derivative. The product showed two yellow major components on t.l.c. with benzene–pyridine (4:1) as solvent. Preparative t.l.c. under the same conditions gave two products which were acetylated with acetic anhydride and pyridine.

The material originating from the slower moving band crystallized readily and was identical in every respect to the product described above and obtained by way of hydrogenation.

The material from the slower moving band also crystallized readily. The relative amounts of the two crude products were 1.2:1 from the slower and faster moving zones, respectively. Recrystallization from ethyl acetate and *n*-hexane mixture gave a product, $[\alpha]_D^{25}$ −76° (*c*, 0.4 in chloroform) which melted in the range 93–105°. However, the n.m.r. spectrum at 100 MHz in deuteriochloroform allowed the conclusion that the product was highly pure and to be 3-*O*-[3,4,6-tri-*O*-acetyl-2-deoxy-2-(2,4-dinitroanalino)-α-D-mannopyranosyl]-1,2;5,6-di-*O*-isopropylidene-α-D-glucofuranose. The one-hydrogen doublet at τ 5.15 with a spacing of 2.0 Hz and assigned to H-1′ is consistent with the α-configuration.

*Isopropyl 2-Deoxy-α-D-arabino-hexopyranoside (**12**)*

A solution of isopropyl tri-*O*-acetyl-2-oximino-α-D-*arabino*-hexopyranoside (5.0 g) (7) in 90% aqueous ethanol (75 ml) containing 85% hydrazine hydrate (10 g) was kept at ambient temperature for 2 h. Palladium-on-carbon (5 g of 5% containing approximately 60% water) was then added and the suspension was stirred for 72 h open to the atmosphere (vigorous initial evolution of a gas occurred). The catalyst was removed and the filtrate was concentrated *in vacuo* to an oil (4.0 g) which was chromatographed on an ion-exchange resin (Dowex 1-X2 (200–400 mesh) hydroxide form). The major fraction (1.4 g, 51%) was a chromatographically pure oil which crystallized on storage. Recrystallization from ethyl acetate gave material, m.p. 103–104°, $[\alpha]_D^{21}$ +128° (*c*, 1.4 in water).

Anal. Calcd. for $C_9H_{18}O_5$: C, 52.41; H, 8.80. Found: C, 52.62; H, 8.82.

The n.m.r. spectrum was that expected (30) for 2-deoxy-α-D-glucopyranosides. The chemical shifts for H-1, -2_{ax}, -2_{eq}, and the two methyl groups were τ 4.39, 7.66, 8.03, 8.51, and 8.57, respectively. The spacings required coupling constants of about $J_{1,2_{eq}} = 1.5$, $J_{1,2_{ax}} = 3.5$, $J_{2_{eq},2_{ax}} = 13$, $J_{2_{eq},3} = 5.5$, $J_{2_{ax},3} = 11.5$ Hz.

Acetylation provided isopropyl tri-*O*-acetyl-2-deoxy-

α-D-*arabino*-hexopyranoside, m.p. 73–74°, $[\alpha]_D^{23}$ +127° (*c*, 1.0 in chloroform) in near quantitative yield.

Anal. Calcd. for $C_{15}H_{24}O_8$: C, 54.21; H, 7.28. Found: C, 54.04; H, 7.16.

The n.m.r. spectrum was in complete accord with assigned structure: $J_{1,2_{eq}} = \sim 1.5$, $J_{1,2_{ax}} = \sim 3.5$, $J_{2_{eq},3} = 5.5$, $J_{2_{ax},3} = 11.0$, and $J_{3,4} = J_{4,5} = 9.5$ Hz (as derived by measuring the spacings).

When the above experiment was repeated except that the palladium catalyst was omitted, t.l.c. examination of the crude reaction product showed no evidence for isopropyl 2-deoxy-α-D-*arabino*-hexopyranoside. The t.l.c. was made on silica gel using the upper phase of an ethyl acetate – dioxane–water (2:2:1) system and developed with 10% chlorosulfonic acid in glacial acetic acid, a reagent which provided an intense black spot on heating at 120° and which detects trace amounts of 2-deoxyglycosides.

Crude isopropyl tri-*O*-acetyl-α-D-*arabino*-hexopyranosuloside obtained from the oxime precursor (5 g) (24) was treated as described above. The product from the ion-exchange chromatogram was an oil (1.4 g) which resisted crystallization. The material was acetylated with acetic anhydride in pyridine and the product was chromatographed on a silicic acid column using ether – Skellysolve B (2:3) as developing solvent. The product obtained was identical with the above-mentioned isopropyl tri-*O*-acetyl-2-deoxy-α-D-*arabino*-hexopyranoside.

When the crude uloside obtained from isopropyl tri-*O*-acetyl-2-oximino-α-D-*arabino*-hexopyranoside (7) (5 g) was treated under the hydrogenation conditions in the presence of hydrazine, a product was obtained which was acetylated as above. Column chromatography on silicic acid using ethyl acetate – Skellysolve B (3:2) resulted in the isolation of 1.6 g (30% yield) of isopropyl 2-acetamido-tri-*O*-acetyl-2-deoxy-α-D-glucopyranoside.

The financial support of the National Research Council of Canada through a grant-in-aid of research (A-172) to R.U.L. is gratefully acknowledged. The microanalyses and n.m.r. spectra were determined by the analytical and spectral services of this Department.

1. F. E. Hardy, J. G. Buchanan, and J. Baddiley. J. Chem. Soc. 3360 (1963).
2. F. E. Hardy. J. Chem. Soc. 375 (1965).
3. P. F. Lloyd and M. Stacey. Tetrahedron, **9**, 116 (1960).
4. P. F. Lloyd and G. P. Roberts. J. Chem. Soc. 6910 (1965).
5. P. F. Lloyd, B. Evans, and R. J. Fiedler. Carbohydr. Res. **22**, 111 (1972).
6. K. Heyns, R. Harrison, K. Propp, and H. Paulsen. Chem. Commun. 671 (1966).
7. S. Umezawa and S. Koto. Bull. Chem. Soc. Jap. **39**, 2014 (1966).
8. S. Umezawa and S. Koto. J. Antibiot. Ser. A, **17**, 186 (1964).
9. S. Umezawa, K. Tatsuta, and R. Muto. J. Antibiot. Ser. A, **20**, 388 (1967).
10. K. L. Rinehart, Jr., J. Infect. Dis. **119**, 345 (1969).
11. N. Sharon. Ann. Rev. Biochem. **35**, 485 (1966).
12. J. F. Kennedy. Carbohydr. Chem. Vol. 4, The Chemical Society, London. p. 178.
13. R. D. Marshall and A. Neuberger. Adv. Carbohydr. Chem. Biochem. **25**, 407 (1970).
14. R. U. Lemieux, Y. Ito, K. James, and T. L. Nagabhushan. Can. J. Chem. **51**, 7 (1973).
15. R. U. Lemieux, K. James, and T. L. Nagabhushan. Can. J. Chem. **51**, 48 (1973).
16. R. U. Lemieux and S. W. Gunner. Can. J. Chem. **46**, 397 (1968).
17. R. U. Lemieux. U.S. Pat. 2 830 983. Chem. Abstr. **52**, 14668 (1958).
18. H. Paulsen and D. Stoye. Chem. Ber. **102**, 834 (1969).
19. H. Paulsen and D. Stoye. Chem. Ber. **102**, 3824 (1969).
20. D. J. Cram and J. S. Bradshaw. J. Am. Chem. Soc. **85**, 1108 (1962).
21. R. U. Lemieux and A. R. Morgan. Can. J. Chem. **43**, 2190 (1965).
22. A. Harsnev and P. Catsoulacos. Chem. Commun. 590 (1967).
23. H. Feuer, B. F. Vincent, Jr., and R. S. Bartlett. J. Org. Chem. 2877 (1965).
24. R. U. Lemieux, K. James, and T. L. Nagabhushan. Can. J. Chem. **51**, 27 (1973).
25. H. Felkin. C. R. **230**, 304 (1950).
26. R. U. Lemieux, K. James, and T. L. Nagabhushan. Can. J. Chem. **51**, 42 (1973).
27. P. W. Austin, F. E. Hardy, J. G. Buchanan, and J. Baddiley. J. Chem. Soc. 5350 (1963).
28. R. U. Lemieux, T. L. Nagabhushan, and S. W. Gunner. Can. J. Chem. **46**, 405 (1968).
29. R. U. Lemieux and T. L. Nagabhushan. Can. J. Chem. **46**, 401 (1968).
30. R. U. Lemieux and S. Levine. Can. J. Chem. **42**, 1473 (1964).

Can. J. Chem. Downloaded from www.nrcresearchpress.com by 210.87.254.105 on 09/05/12
For personal use only.

Chemical Syntheses of α-Linked Disaccharides[1]

R. U. LEMIEUX, K. JAMES,[2] AND T. L. NAGABHUSHAN[3]
Department of Chemistry, University of Alberta, Edmonton, Alberta
Received June 2, 1972

Chemical syntheses of six α-linked disaccharides are described, namely, 6-*O*-(α-D-glucopyranosyl)-D-galactose (**1**), 6-*O*-(α-D-galactopyranosyl)-D-galactose (**2**), 6-*O*-(α-D-talopyranosyl)-D-galactose (**3**), 3-*O*-(α-D-glucopyranosyl)-D-glucose (nigerose) (**4**), 3-*O*-(α-D-galactopyranosyl)-D-glucose (**5**), and 3-*O*-(α-D-talopyranosyl)-D-glucose (**6**).

Les synthèses chimiques de six disaccharides branchés en α sont décrites, à savoir le *O*-[α-D-glucopyranosyl]-6-D-galactose [**1**], le *O*-[α-D-galactopyranosyl]-6-D-galactose (**2**), le *O*-[α-D-talopyranosyl]-6-D-galactose (**3**), le *O*-[α-D-glucopyranosyl]-3-D-glucose (nigérose) (**4**), le *O*-[α-D-galactopyranosyl]-3-D-glucose (**5**), et le *O*-[α-D-talopyranosyl]-3-D-glucose (**6**).

[Traduit par le journal]

Can. J. Chem., **51**, 42 (1973)

Can. J. Chem. Downloaded from www.nrcresearchpress.com by 210.87.254.40 on 09/05/12
For personal use only.

This paper presents syntheses of the six α-linked disaccharides (**1** to **6**) from previously reported (1) oximino-disaccharide structures; namely, the tri-*O*-acetyl-2-oximino-α-D-*arabino*-hexopyranosyl and tri-*O*-acetyl-2-oximino-α-D-*lyxo*-hexopyranosyl derivatives of 1,2;5,6-di-*O*-isopropylidene-α-D-glucofuranose and of 1,2;3,4-di-*O*-isopropylidene-α-D-galactopyranose. The latter compounds were deoximated (2) and the resulting ketonic substances were reduced with sodium borohydride (3) without prior purification. In the preparation of compounds **4**, **5**, and **6**, the use of acetaldehyde in acetonitrile–hydrochloric acid reagent (2) for deoximation caused substantial loss of the acid labile 5,6-*O*-isopropylidene protecting group. However, in the preparation of compounds **1**, **2**, and **3**, deoximation under similar conditions caused only small losses of the *O*-isopropylidene groups. Treatment of the crude ketones in these cases with 2,2-dimethoxypropane and *p*-toluenesulfonic acid monohydrate re-introduced these groups in near quantitative yields. This was not the case in the preparation of compounds **4**, **5**, and **6**. Therefore, for the synthesis of these compounds deoximation under neutral conditions with titanium trichloride (3, 4) was used. Reduction followed by *O*-acetylation enabled compounds **1** to **4** to be isolated as the *O*-(tetra-*O*-acetyl-α-D-hexopyranosyl)-di-*O*-isopropylidene-D-hexoses.

In view of the high degree of stereoselectivity observed in the reductions to α-D-glucopyranosides (3), the preparations of compounds **1** and **4** proceeded with little difficulty in 54 and 67% yields, respectively. Although both the intermediate 6-*O*-(α-D-glucopyranosyl)-1,2;3,4-di-*O*-isopropylidene-α-D-galactopyranose and its tetraacetate failed to crystallize, both 3-*O*-(α-D-glucopyranosyl)-1,2;5,6-di-*O*-isopropylidene-α-D-glucofuranose and its tetraacetate were obtained in crystalline condition.

As previously reported (3), the reduction of a tri-*O*-acetyl-α-D-*lyxo*-hexosuloside with sodium borohydride leads to a mixture of galactosides and talosides. 6-*O*-(Tetra-*O*-acetyl-α-D-galactopyranosyl)-1,2;3,4-di-*O*-isopropylidene-α-D-galactopyranose was obtained crystalline in 51% yield and was readily separated from 6-*O*-(tetra-*O*-acetyl-α-D-talopyranosyl)-1,2;3,4-di-*O*-isopropylidene-α-D-galactopyranose (30% yield as a syrup) by column chromatography on silicic acid. Column chromatography on a resin in the hydroxide form (5) was used to separate 3-*O*-(α-D-galactopyranosyl)-1,2;5,6-di-*O*-isopropylidene-α-D-glucofuranose from the *talo*-isomer. Both compounds were obtained crystalline.

The disaccharides (**1** to **6**) were prepared from the di-*O*-isopropylidene derivatives by hydrolysis of the isopropylidene groups using aqueous trifluoroacetic acid (6) followed by chromatographic purification using an ion-exchange resin in the potassium salt from (7). Although none of the disaccharides was obtained crystalline, all provided the expected hexoses (or hexose) on acid

[1]Presented at the 161st National American Chemical Society Meeting, Los Angeles, California, March 28, 1971.
[2]University of Alberta Postdoctoral Fellow, 1970–1972.
[3]Professional Research Associate, 1970–1972.

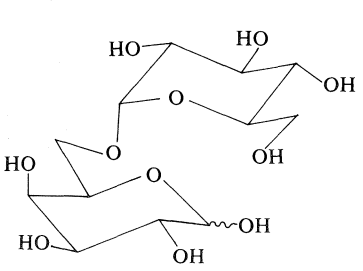

α-D-Glc*p*-(1 → 6)-D-Gal

1

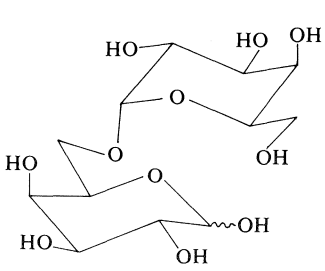

α-D-Gal*p*-(1 → 6)-D-Gal

2

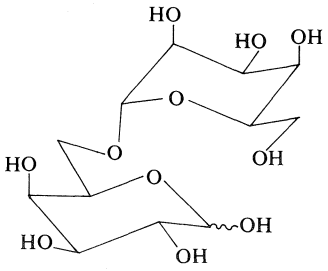

α-D-Tal*p*-(1 → 6)-D-Gal

3

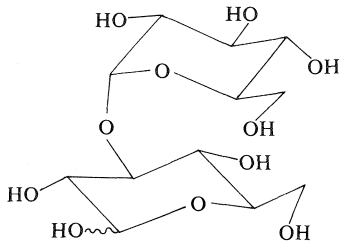

α-D-Glc*p*-(1 → 3)-D-Glc

4

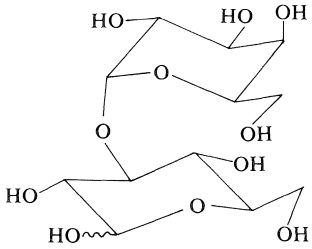

α-D-Gal*p*-(1 → 3)-D-Glc

5

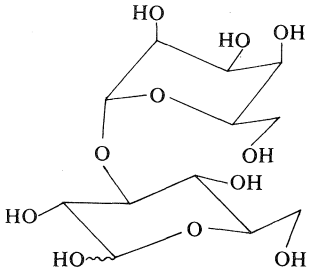

α-D-Tal*p*-(1 → 3)-D-Glc

6

hydrolysis and possessed n.m.r. spectra in accordance with the assigned structures. The chemical shifts and spacings for the signals of the anomeric hydrogens for mutarotated solutions in deuterium oxide are reported in Table 1. The R_f values relative to maltose on Whatman No. 1 paper using *n*-butanol – pyridine–water – acetic acid (6:4:3:1) are also reported in Table 1.

The above-described results offer a solution to the long-standing problem of carbohydrate chemistry, namely, the controlled synthesis of α-linked oligosaccharide structures in good yield. The key to the method is the high stereoselectivity for 2-oximino-α-glycoside formation (1). Whether or not the preferential formation of the α-linkage will remain essentially independent of the structural features of the alcohol remains to be thoroughly tested. To date, 2-oximino-β-glycoside formation has only been definitely observed in one instance (1) (about 9% yield).

The first preparation of an α-D-glucopyranosyl disaccharide was by anomerization of gentiobiose to isomaltose by Lindberg in 1949 (8). Goldstein and Whelan (9) applied this method to convert synthetic 6-*O*-(β-D-glucopyranosyl)-D-galactose to the α-anomer, compound **1** of the present research, which appears (10) to be liberated on partial hydrolysis of polysaccharides from *Salmonella senftenberg* and *S. typhimurium*.

The first syntheses of α-D-glucopyranosyl disaccharides were those of maltose and sucrose employing tri-*O*-acetyl-1,2-anhydro-α-D-glucopyranose as reagent (11, 12). Haq and Whelan (13) synthesized nigerose, compound **4** of this paper, by a chemically related route. The modification of the Koenigs–Knorr reaction involving the use of mercuric cyanide as condensing agent, introduced by Zemplén and Gerecs (14) and used by Matsuda (15) for the synthesis of α-D-glucopyranosides, failed (9) to provide **1** but did provide nigerose (15, 16). The chemical nature of this approach to the synthesis of α-D-glucopyranosides remains obscure (17) but it has provided syntheses of a number of complex α-D-glucopyranosides in low yield (18–20). Nigerose is liberated on partial hydrolysis of nigeran, a polysaccharide isolated from *Aspergillus niger* (21) and may be a minor structural unit of amylopectin (22). Lemieux, James, and Hendriks (23) have synthesized 3-*O*-(tetra-*O*-benzyl-α-D-glucopyranosyl)-1,2;5,6-di-*O*-isopropylidene-α-D-glucofuranose in 42% yield by their so-called halide-ion

Can. J. Chem. Downloaded from www.nrcresearchpress.com by 210.87.254.40 on 09/05/12
For personal use only.

TABLE 1. Characterizations of the disaccharides

Compound	Temperature (°C)	Chemical shifts of the anomeric hydrogens, τ-values (spacings, Hz)* Non-reducing unit	Reducing unit	Paper chromatographic mobilities (cm)†
α-D-Glc*p*-(1 → 4)-D-Glc (maltose)	15	4.37 (3.50)	4.56 (3.50), 5.13 (8.00)	6.7
α-D-Glc*p*-(1 → 6)-D-Gal (**1**)	22	4.83 (3.37)	4.52 (2.87), 5.18 (7.25)	2.7
α-D-Gal*p*-(1 → 6)-D-Gal (**2**)	15	4.82 (2.50)	4.53 (3.00), 5.25 (7.50)	1.9
α-D-Tal*p*-(1 → 6)-D-Gal (**3**)	15	4.79 (0)	4.54 (3.00), 5.22 (7.25)	5.5
α-D-Glc*p*-(1 → 3)-D-Glc (**4**) (nigerose)	15	4.42 (3.50)	4.55 (3.50), 5.12 (8.00)	7.5
α-D-Gal*p*-(1 → 3)-D-Glc (**5**)	33	4.46 (2.50)	4.60 (3.50), 5.16 (8.00)	9.0
α-D-Tal*p*-(1 → 3)-D-Glc (**6**)	15	4.43 (0)	4.56 (3.50), 5.12 (8.00)	9.6

*The n.m.r. spectra were measured at 100 MHz in deuterium oxide (c = 12.5%). In all cases the β to α anomeric ratio of the reducing sugar unit was near 1.5.
†Whatman No. 1 paper using butanol – pyridine–water – acetic acid (6:4:3:1) for 36 h.

catalyzed synthesis of α-glucopyranosides. The yield of 6-*O*-(tetra-*O*-benzyl-α-D-glucopyranosyl)-1,2;3,4-di-*O*-isopropylidene-α-D-galactopyranose was 65%. The key step in these syntheses was the reaction of tetra-*O*-benzyl-α-D-glucopyranosyl bromide with the di-*O*-isopropylidene-hexose in methylene chloride and in the presence of tetraethylammonium bromide and ethyldiisopropylamine. This promising alternative approach to the synthesis of α-D-hexopyranosides is under further investigation and details will be published in the near future. Recent publications (24, 25) from other laboratories report related research. 6-*O*-(α-D-Galactopyranosyl)-D-galactose (**2**) has been obtained both by acid reversion (26) and by enzymic polymerization (27) of D-galactose. The present report appears to be the first controlled synthesis of this compound. 3-*O*-(α-D-Galactopyranosyl)-D-glucose (**4**) has not been previously characterized. It is noteworthy that Rebers and Heidelberger (28) have provided evidence that this disaccharide is a building unit of the specific polysaccharide of type VI pneumococcus. The talosides **3** and **6** were isolated as by-products; these are not known to have direct biological significance.

Experimental

Descending paper chromatography was performed on Whatman No. 1 paper using *n*-butanol – pyridine–water – acetic acid (6:4:3:1) as the developing solvent and the components visualized by spraying with alkaline silver nitrate (30). The thin layer chromatograms were developed on silica gel G (E. Merck A.G., Darmstadt) using 20 cm² plates and in the solvent specified. The adsorption chromatograms were conducted on silicic acid, CC7, 100–200 mesh (Mallinckrodt Chemical Works, St. Louis, Mo.) using a 3:2 mixture of ether and Skellysolve B. The chromatograms on ion exchange resin in the hydroxide form were performed using Dowex 1-X2 (200–400 mesh) supplied by Sigma Chemicals Co., St. Louis, Mo. and eluted with water. The chromatograms on resin in the potassium form were developed with water and used ion exchange resin CGC 241 (200–400 mesh) supplied in the sodium form by J. T. Baker Chemical Co., Phillipsburg, N.J. The eluants for the column chromatograms were collected in 10 ml fractions. The presence of material in a given fraction was established and the nature and purity of the material assessed by either t.l.c. or paper chromatography prior to pooling. All deionizations employed Amberlite MB-3 (20–50 mesh) supplied by Mallinckrodt.

All the products described were examined by 100 MHz n.m.r. and the spectra obtained were in accord with the structures assigned. The chemical shifts and spacings observed for the disaccharides are reported in Table 1. The disaccharides were further characterized by hydrolysis using 1 *N* hydrochloric acid at 100° for 1 h followed by comparison of the hydrolysis products by paper chromatography with authentic samples of the hexoses.

*6-O-(α-D-Glucopyranosyl)-D-galactose (**1**)*

A solution of 6-*O*-(tri-*O*-acetyl-2-oximino-α-D-*arabino*-hexopyranosyl)-1,2;3,4-di-*O*-isopropylidene-α-D-galactopyranose (4.40 g) (1) in acetonitrile (13.5 ml), 1 *N* hydrochloric acid (11.5 ml), and acetaldehyde (4.0 ml) was kept at room temperature for 4 h. The solution was then diluted with ethyl acetate (50 ml) and the organic layer was washed once with water (20 ml). Concentration of this solution afforded a syrup which was dissolved in 2,2-dimethoxypropane (25 ml) containing *p*-toluenesulfonic acid monohydrate (25 mg). The resulting solution was left for 12 h st 5°, diluted with ethyl acetate, and subsequently washed with saturated aqueous sodium bicarbonate solution. Evaporation left an oil which was dissolved in dioxane (25 ml) and water (20 ml). The solution was cooled to 0° with stirring and sodium borohydride (0.30 g) was added in small aliquot portions. On completion of the addition, the solution was maintained at ambient temperature for 3 h. Excess sodium borohydride was then destroyed by the addition of acetone and the resulting solution concentrated to a semi-crystalline mass which was extracted with ethyl acetate to remove inorganic material. Evaporation left an oily residue which was de-

Can. J. Chem. Downloaded from www.nrcresearchpress.com by 210.87.254.40 on 09/05/12
For personal use only.

Can. J. Chem. Downloaded from www.nrcresearchpress.com by 210.87.254.40 on 09/05/12
For personal use only.

acetylated by treatment with triethylamine (5 ml) in 50% aqueous methanol (20 ml) for 12 h at 4°. Solvent removal left a residue (3.42 g) which was dissolved in 90% aqueous trifluoroacetic acid (34 ml). The solution was kept at about 25° for 15 min and then concentrated *in vacuo* (below 40°) to a syrup which turned to an amorphous powder (2.9 g) on trituration with ether. Paper chromatography indicated that the major portion of this material was a reducing disaccharide. Purification was achieved by chromatographing 1.0 g portions, at a flow rate of 1 ml/min, on a 48 in. × 1.5 in. ion-exchange column in the potassium form. The appropriate fractions were combined and concentrated to yield the title compound (1.45 g, 54%); $[\alpha]_D^{22}$ +127° (*c*, 0.69 in water) (lit. (29) $[\alpha]_D$ +125 → 138° (water)).

A number of the intermediates were characterized as follows.

(a) 6-O-(Tetra-O-acetyl-α-D-glucopyranosyl)-1,2;3,4-di-O-isopropylidene-α-D-galactopyranose

The above described crude product from the sodium borohydride reduction (0.50 g) was acetylated with acetic anhydride (4 ml) in pyridine (5 ml). After isolation of the product by normal procedures followed by column chromatography on silicic acid using ether – Skellysolve B (6:4) as the developing solvent, the title compound was obtained as an oil (0.35 g), $[\alpha]_D^{25}$ +47° (*c*, 3.3 in chloroform).

Anal. Calcd. for $C_{26}H_{38}O_{15}$: C, 52.87; H, 6.49. Found: C, 52.91; H, 6.44.

(b) 6-O-(α-D-Glucopyranosyl)-1,2;3,4-di-O-isopropylidene-α-D-galactopyranose

The above described compound (0.50 g) was deacetylated with triethylamine (2 ml) in 50% aqueous methanol (10 ml) at 4°. Evaporation of the solution left the title compound as an oil (0.34 g), $[\alpha]_D^{25}$ +29.2° (*c*, 0.92 in chloroform).

Anal. Calcd. for $C_{18}H_{30}O_{11}$: C, 51.18; H, 7.16. Found: C, 51.01; H, 7.00.

6-O-(Tetra-O-acetyl-α-D-galactopyranosyl)- and 6-O-(Tetra-O-acetyl-α-D-talopyranosyl)-1,2;3,4-di-O-isopropylidene-α-D-galactopyranose

A solution of 6-*O*-(tri-*O*-acetyl-2-oximino-α-D-*lyxo*-hexopyranosyl)-1,2;3,4-di-*O*-isopropylidene-α-D-galactopyranose (6.50 g) (1) in acetonitrile (20 ml), 1 *N* hydrochloric acid (16.2 ml), and acetaldehyde (6 ml) was kept at room temperature for 4 h. The ketone obtained from the reaction was isolated, treated with 2,2-dimethoxypropane (25 ml), and then reduced with sodium borohydride as described above. The material obtained from the borohydride reduction was acetylated with acetic anhydride (15 ml) in pyridine (20 ml) for 48 h at room temperature and the product isolated as an oil (6.5 g) by normal procedures. Analysis of this material by t.l.c. using ether – Skellysolve B (4:1) as the developing solvent indicated the presence of two main components. Column chromatography on silicic acid yielded 6-*O*-(tetra-*O*-acetyl-α-D-galactopyranosyl)-1,2;3,4 di-*O*-isopropylidene α-D-galactopyranose (3.5 g, 51%) which crystallized from ethyl acetate – Skellysolve B, m.p. 87–89°, $[\alpha]_D^{23}$ +54.5° (*c*, 2 in chloroform).

Anal. Calcd. for $C_{26}H_{38}O_{15}$: C, 52.87; H, 6.49. Found: C, 52.57; H, 6.46.

Further elution provided a second major fraction, 6-*O*-(tetra-*O*-acetyl-α-D-talopyranosyl)-1,2;3,4-di-*O*-isopropylidene-α-D-galactopyranose (2.0 g; 30%) as an oil, $[\alpha]_D^{23}$ +13° (*c*, 1.3 in chloroform).

Anal. Calcd. for $C_{26}H_{38}O_{15}$: C, 52.88; H, 6.49. Found: C, 53.08; H, 6.15.

6-O-(α-D-Galactopyranosyl)-1,2;3,4-di-O-isopropylidene-α-D-galactopyranose

6-*O*-(Tetra-*O*-acetyl-α-D-galactopyranosyl)-1,2;3,4-di-*O*-isopropylidene-α-D-galactopyranose (2.0 g) was deacetylated with triethylamine (4 ml) in 50% aqueous methanol (20 ml) for 12 h at 4°. Evaporation of the solution afforded an oil, $[\alpha]_D^{23}$ +55.4° (*c*, 1.7 in DMF).

Anal. Calcd. for $C_{18}H_{30}O_{11}$: C, 51.18; H, 7.16. Found: C, 50.98; H, 7.27.

6-*O*-(α-D-Talopyranosyl)-1,2;3,4-di-*O*-isopropylidene-α-D-galactopyranose was obtained as a syrup from its tetra-*O*-acetyl derivative by deacetylation as described above, $[\alpha]_D^{23}$ +10° (*c*, 0.5 in DMF).

Anal. Calcd. for $C_{18}H_{30}O_{11}$: C, 51.18; H, 7.16. Found: C, 51.15; H, 7.22.

6-O-(α-D-Galactopyranosyl)-D-galactose (2)

A solution of 6-*O*-(α-D-galactopyranosyl)-1,2;3,4-di-*O*-isopropylidene-α-D-galactopyranose (1.40 g) in 90% aqueous trifluoroacetic acid (14 ml) was kept at room temperature for 15 min and then concentrated *in vacuo* to an oil. Trituration of this material with ether gave an amorphous powder which was purified by chromatography as described above in the preparation of **1**. The product (0.75 g, 66.1%), was an amorphous powder, $[\alpha]_D^{22}$ +149° (*c*, 0.36 in water) (lit. (26) $[\alpha]_D$ +149° (water)).

6-O-(α-D-Talopyranosyl)-D-galactose (3)

The compound was prepared from 6-*O*-(α-D-talopyranosyl)-1,2;3,4-di-*O*-isopropylidene-α-D-galactopyranose (0.50 g) and the product purified by the procedures described above for the preparation and purification of **2** to give an amorphous powder (0.30 g, 74%), $[\alpha]_D^{22}$ +101° (*c*, 0.64 in water).

3-O-(Tetra-O-acetyl-α-D-glucopyranosyl)-1,2;5,6-di-O-isopropylidene-α-D-glucofuranose

A solution of 3-*O*-(tri-*O*-acetyl-2-oximino-α-D-*arabino*-hexopyranosyl)-1,2;5,6-di-*O*-isopropylidene-α-D-glucofuranose (3.25 g) in dioxane was reduced with titanium trichloride and the product (3.10 g) isolated as an oil by the procedures to be described below for the deoximation of the *lyxo*-isomer. Without further purification the material was reduced with sodium borohydride (0.15 g) in 60% aqueous dioxane (25 ml). After 3 h this solution was de-ionized with the mixed-bed resin and then concentrated to yield an oil which was subsequently acetylated with acetic anhydride in pyridine. Isolation of the peracetylated material by normal procedures followed by crystallization from ethyl acetate – Skellysolve B yielded the title compound (2.5 g, 73%), m.p. 139–140°, $[\alpha]_D^{21}$ +75.3° (*c*, 1.48 in chloroform).

Anal. Calcd. for $C_{26}H_{37}O_{15}$: C, 52.97; H, 6.33. Found: C, 52.80; H, 6.50.

3-O-(α-D-Glucopyranosyl)-1,2;5,6-di-O-isopropylidene-α-D-glucofuranose

3-*O*-(Tetra-*O*-acetyl-α-D-glucopyranosyl)-1,2;5,6-di-*O*-isopropylidene-α-D-glucofuranose (0.70 g) was deacetyl-

ated with triethylamine (1.0 ml) in 50% aqueous methanol (10 ml) for 12 h at 0°. The solution was then concentrated and the residual oil chromatographed on ion-exchange resin in the hydroxide form using a 36 in. × 3/4 in. column to give the title compound (0.50 g, 79%) which crystallized from ethyl acetate – Skellysolve B, m.p. 174–175°, $[\alpha]_D^{22}$ +74.6° (*c*, 1.02 in DMF).

Anal. Calcd. for $C_{18}H_{30}O_{11}$: C, 51.18; H, 7.16. Found: C, 51.47; H, 6.83.

3-O-(α-D-Glucopyranosyl)-D-glucose (4)

3-*O*-(α-D-Glucopyranosyl)-1,2;5,6-di-*O*-isopropylidene-α-D-glucofuranose (0.70 g) was hydrolyzed with 90% aqueous trifluoroacetic acid and the product purified by the general procedure described above to yield an amorphous material (0.38 g, 67%), $[\alpha]_D^{20}$ +136° (*c*, 0.45 in water) (lit. (29), $[\alpha]_D$ 125 → 138° (water)).

3-O-α-D-Galactopyranosyl- and 3-O-α-D-Talopyranosyl Derivatives of 1,2;5,6-Di-O-isopropylidene-α-D-glucofuranose

A 20% aqueous solution of titanium trichloride (30.0 g) was added dropwise with stirring under an atmosphere of nitrogen to a solution of 3-*O*-(tri-*O*-acetyl-2-oximino-α-D-*lyxo*-hexopyranosyl)-1,2;5,6-di-*O*-isopropylidene-α-D-glucofuranose (6.50 g) and ammonium acetate (12.0 g) in dioxane (60 ml). Stirring was continued for 3 h after the addition was complete, following which ammonium acetate (12.0 g) and dioxane (60 ml) were added and then titanium trichloride (30.0 g) added dropwise. The resulting suspension was stirred for a further 2 h and then extracted with dichloromethane (500 ml). The organic extract was washed first with saturated aqueous sodium bicarbonate solution and then water. Evaporation yielded an oil which partially crystallized on storage. Recrystallization from ethyl acetate – Skellysolve B afforded material (2.10 g) which is considered to be the hydrated ketone (n.m.r. spectrum). An oil (3.80 g) was isolated from the mother liquor.

The crystalline material (1.90 g) was reduced with sodium borohydride (0.20 g) in 60% aqueous dioxane (15 ml) for 3 h and the resulting solution was then deionized with the mixed-bed resin. Subsequent evaporation of the solution left an oil which was deacetylated with triethylamine (2 ml) in 60% aqueous methanol for 12 h at 4°. Concentration of this solution gave an oil (1.66 g) which was shown, by t.l.c. using the upper phase of an ethyl acetate – dioxane – water (2:2:1) system as the developing solvent, to be a two component mixture. Ion-exchange chromatography of this material on a 36 in. × 3/4 in. column of resin in hydroxide form yielded 3-*O*-(α-D-galactopyranosyl)-1,2;5,6-di-*O*-isopropylidene-α-D-glucofuranose (0.48 g) which crystallized from ethyl acetate – Skellysolve B, m.p. 154–156°, $[\alpha]_D^{23}$ +94.4° (*c*, 0.89 in DMF).

Anal. Calcd. for $C_{18}H_{30}O_{11}$: C, 51.18; H, 7.16. Found: C, 51.23; H, 7.00.

Further elution with water afforded 3-*O*-(α-D-talopyranosyl)-1,2;5,6-di-*O*-isopropylidene-α-D-glucofuranose (0.57 g) which crystallized from ethyl acetate – Skellysolve B, m.p. 144–145°, $[\alpha]_D^{23}$ +51.4° (*c*, 1.1 in DMF).

Anal. Calcd. for $C_{18}H_{30}O_{11}$: C, 51.18; H, 7.16. Found: C, 51.00; H, 7.17.

Similar treatment of the above-described oil (3.80 g) yielded 3-*O*-(α-D-talopyranosyl)-1,2;5,6-di-*O*-isopropylidene-α-D-glucofuranose (0.82 g), and 3-*O*-(α-D-galactopyranosyl)-1,2;5,6-di-*O*-isopropylidene-α-D-glucofuranose (0.66 g). The compounds were identical to the products described above and obtained from the hydrated uloside intermediate.

3-O-(α-D-Galactopyranosyl)-D-glucose (5)

A solution of 3-*O*-(α-D-galactopyranosyl)-1,2;5,6-di-*O*-isopropylidene-α-D-glucofuranose (0.70 g) in 90% aqueous trifluoroacetic acid (7.0 ml) was kept at room temperature for 15 min and then concentrated *in vacuo*. Trituration of the residue with ether yielded an amorphous powder which was chromatographed on a 48 in. × 1.5 in. column of ion-exchange resin in the potassium form to yield a pure disaccharide as an amorphous solid (0.40 g, 71%), $[\alpha]_D^{22}$ +159° (*c*, 1.06 in water).

3-O-(α-D-Talopyranosyl)-D-glucose (6)

3-*O*-(α-D-*Talopyranosyl*)-1,2;5,6-di-*O*-isopropylidene-α-D-glucofuranose (1.1 g) was hydrolyzed with 90% trifluoroacetic acid (11.0 ml) and the product purified as described above to yield an amorphous powder (0.65 g, 73%), $[\alpha]_D^{22}$ +115° (*c*, 0.65 in water).

The financial support of the National Research Council of Canada through a grant-in-aid of research (A-172) to R.U.L. is gratefully acknowledged. The microanalyses and n.m.r. spectra were carried out by the analytical and spectral services laboratories of this department.

1. R. U. Lemieux, Y. Ito, K. James, and T. L. Nagabhushan. Can. J. Chem. **51**, 7 (1973).
2. R. U. Lemieux, R. A. Earl, K. James, and T. L. Nagabhushan. Can. J. Chem. **51**, 19 (1973).
3. R. U. Lemieux, K. James, and T. L. Nagabhushan. Can. J. Chem. **51**, 27 (1973).
4. G. H. Timms and E. Wildsmith. Tetrahedron Lett. 195 (1971).
5. P. W. Austin, F. E. Hardy, J. G. Buchanan, and J. Baddiley. J. Chem. Soc. 5350 (1963).
6. J. E. Christensen and L. Goodman. Carbohydr. Res. **7**, 510 (1968).
7. R. M. Saunders. Carbohydr. Res. **7**, 76 (1968).
8. B. Lindberg. Acta Chem. Scand. **3**, 1355 (1949).
9. I. J. Goldstein and W. J. Whelan. J. Chem. Soc. 4264 (1963).
10. B. A. D. Stocker, A. M. Staub, R. Tinelli, and B. Kopacka. Ann. Inst. **98**, 505 (1960).
11. R. U. Lemieux. Can. J. Chem. **31**, 949 (1953).
12. R. U. Lemieux and G. Huber. J. Am. Chem. Soc. **78**, 4117 (1956).
13. S. Haq and W. J. Whelan. J. Chem. Soc. 1342 (1958).
14. G. Zemplén and A. Gerecs. Ber. 2720 (1930).
15. K. Matsuda. Chem. and Ind. 1627 (1958).
16. K. Matsuda and T. Sekiguchi. Nippon Nageikagaku Kaishi, **33**, 309 (1959).
17. R. U. Lemieux and T. L. Nagabhushan. Methods in carbohydrate chemistry. Vol. VI. Editors, R. L. Whistler and J. N. BeMiller. Academic Press, New York. 1972. p. 487.
18. S. Umezawa, S. Koto, K. Tatsuta, and T. Tsumura. Bull. Chem. Soc. Jap. **42**, 529 (1969).

Can. J. Chem. Downloaded from www.nrcresearchpress.com by 210.87.254.40 on 09/05/12
For personal use only.

19. S. UMEZAWA, K. TATSUTA, and S. KOTO. Bull. Chem. Soc. Jap. **42**, 533 (1969).
20. S. UMEZAWA, S. KOTO, K. TATANTA, H. HINONO, Y. NISHIMURA, and T. TSUMURA. Bull. Chem. Soc. Jap. **42**, 537 (1969).
21. S. A. BARKER, E. J. BOURNE, and M. STACEY. J. Chem. Soc. 3084 (1953).
22. M. L. WOLFROM and A. THOMPSON. J. Am. Chem. Soc. **77**, 6403 (1955).
23. R. U. LEMIEUX, K. JAMES, and K. B. HENDRIKS. To be published.
24. T. ISHIKAWA and H. G. FLETCHER, JR. J. Org. Chem. **34**, 563 (1969).
25. J. M. FRECHET and C. SCHUERCH. J. Am. Chem. Soc. **94**, 604 (1972).
26. C. N. TURTON, A. BEBBINGTON, S. DIXON, and E. PACSU. J. Am. Chem. Soc. **77**, 2565 (1965).
27. M. J. CLARREY and W. J. WHELAN. Biochem. J. **76**, 22P (1960).
28. P. A. REBERS and M. HEIDELBERGER. J. Am. Chem. Soc. **81**, 3056 (1961).
29. F. YAMANCHI and K. MATSUDA. Nature, **204**, 1088 (1964).
30. W. G. TREVELYAN, D. P. PROCTOR, and J. S. HARRISON. Nature **166**, 444 (1950).

Can. J. Chem. Downloaded from www.nrcresearchpress.com by 210.87.254.40 on 09/05/12
For personal use only.

Chemical Synthesis of α-Linked 2′-Amino-2′-deoxydisaccharides

R. U. LEMIEUX, K. JAMES,[1] AND T. L. NAGABHUSHAN[2]

Department of Chemistry, University of Alberta, Edmonton, Alberta

Received June 2, 1972

The reduction by borane in tetrahydrofuran of the 2-acetoximino-tri-*O*-acetyl-α-D-*arabino*-hexopyranosyl derivatives of 1,2;3,4-di-*O*-isopropylidene-α-D-galactopyranose and 1,2;5,6-di-*O*-isopropylidene-α-D-glucofuranose (**1** and **4**, respectively) proceeds with a high degree of stereoselectivity for the α-D-*gluco*-configuration and affords a convenient route to 2-amino-2-deoxy-α-D-glucopyranosides. The reduction of the corresponding 2-acetoximino-tri-*O*-acetyl-α-D-*lyxo*-hexopyranosyl derivatives (**7** and **12**) proceeds with slight stereoselectivity favoring the α-D-*talo*-configuration. Chromatographic separation was required to provide the *N*-acetyl derivatives of 2-amino-2-deoxy-α-D-galactopyranosides and 2-amino-2-deoxy-α-D-talopyranosides.

La réduction par le borane dans le tétrahydrofurane des dérivés de l'acétoximino-2-tri-*O*-acétyl-α-D-*arabino*-hexopyranosyle du di-*O*-isopropylidène-1,2;3,4-α-D-galactopyranose et di-*O*-isopropylidène-1,2;5,6-α-D-glucofuranose (**1** et **4**, respectivement) se fait avec un haut degré de stéréosélectivité en faveur de la configuration α-D-*gluco* et fournit une voie d'accès commode aux amino-2 déoxy-2-α-D-glucopyranosides. La réduction des dérivés acétoximino-2-tri-*O*-acétyl-α-D-*lyxo*-hexopyranosyles correspondants (**7** et **12**) se fait avec une stéréosélectivité faible en faveur de la configuration α-D-*talo*. La séparation chromatographique a été nécessaire pour obtenir les dérivés *N*-acétylés des amino-2-déoxy-2-α-D-galactopyranosides et des amino-2-déoxy-2-α-D-talopyranosides. [Traduit par le journal]

Can. J. Chem., **51**, 48 (1973)

Umezawa has recently offered the opinion that "the preparation of α-glycopyranosides in high yields still remains the most important problem of carbohydrate chemistry" (1). This challenge also applies to the related problem of the synthesis of α-linked 2-amino-2-deoxyglycopyranosides (2, 3). In this paper, we report by way of the preparation of six 2-acetamido-2-deoxy-α-D-glycopyranosyl-D-hexopyranoses (compounds **3**, **6**, **10**, **11**, **15**, and **16**) a synthetic approach which offers a solution to this problem. The *N*-acetyl compounds were prepared primarily for reasons of convenience; the method provides ready access to the free aminoglycosides. 2-Amino-2-deoxy-α-D-glucopyranosides are obtained in high yield but 2-amino-2-deoxy-α-D-galactopyranosides are only available as the minor component of a mixture with the *talo*-isomer.

A previous publication (4) described the preparation of the acetoximes **1**, **4**, **7**, and **12**. In another paper (3), methods were developed for the reduction of these compounds and the parent oximes to 2-amino-2-deoxyglycopyranosides mainly through a study of model 2-oximinoglycopyranosides. The reduction of the above-mentioned acetoximes with borane in tetrahydrofuran and characterization of the products leading to the disaccharide structures **3**, **6**, **10**, **11**, **15**, and **16** was reserved for this paper.

The reduction of the 2-acetoximino-α-D-*arabino*-hexopyranosides **1** and **4** provided the 2-amino-2-deoxy-α-D-glucopyranosides **2** and **5** in near quantitative yield. These latter products were characterized as the *N*-acetyl derivatives which, on hydrolysis to remove the isopropylidene groups, provided the disaccharide structures **3** and **6**.

In contrast to the high degree of stereoselectivity achieved in the reductions of compounds **1** and **4** by borane, the reductions of the 2-acetoximino-α-D-*lyxo*-hexopyranosides **7** and **12** gave mixtures of the epimeric *galacto*- and *talo*- products. This result appears related to hindrance by the C_4-substituent to axial approach to the reacting center (3, 5). The ratio of compounds **8** (*galacto*) and **9** (*talo*) isolated by chromatography of their *N*-acetyl derivatives was 1:2. This ratio was 3:4 for compounds **13** (*galacto*) and **14** (*talo*). The *N*-acetyl derivatives of compounds **8**, **9**, **13**, and **14** were isolated in pure crystalline condition. The characterizations were by n.m.r. and hydrol-

[1]University of Alberta Postdoctorate Fellow, 1970–1972.

[2]Professional Research Associate, 1970–1972.

Can. J. Chem. Downloaded from www.nrcresearchpress.com by 210.87.254.5 on 09/05/12
For personal use only.

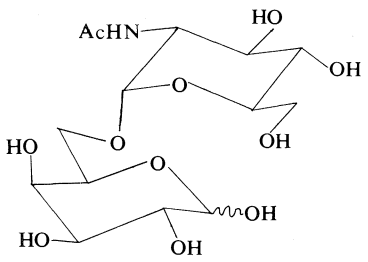

α-D-GlcNAc*p*-(1→6)-D-Gal

3

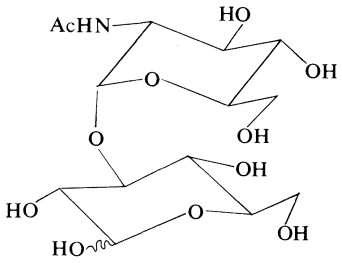

α-D-GlcNAc*p*-(1→3)-D-Glc

6

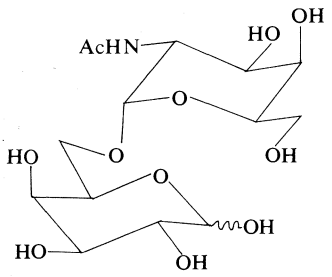

α-D-GalNAc*p*-(1→6)-D-Gal

10

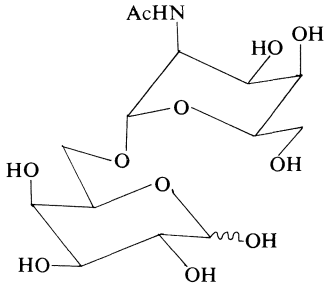

α-D-TalNAc*p*-(1→6)-D-Gal

11

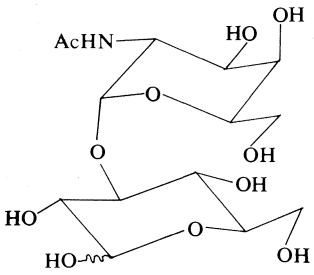

α-D-GalNAc*p*-(1→3)-D-Glc

15

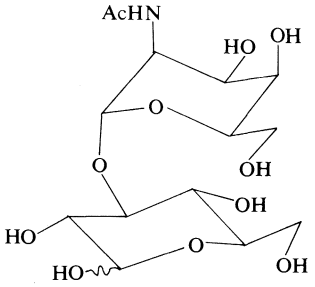

α-D-TalNAc*p*-(1→3)-D-Glc

16

ysis to the component monosaccharides. Hydrolytic removal of the isopropylidene groups in 90% aqueous trifluoroacetic acid provided the disaccharide structures **10**, **11**, **15**, and **16** (see Table 1).

In summary, this research has led to a synthetic method which promises to offer means for the synthesis in good overall yield of 2-amino-2-deoxy-α-glucopyranosides with complex aglycons as are found in many important antibiotics (6, 7). The research was to an important degree motivated by the occurrence of a 2-acetamido-2-deoxy-α-D-galactopyranosyl residue in the antigenic determinant of blood group substance A (8). Although the method has allowed the synthesis of 3-*O*-(2-acetamido-2-deoxy-α-D-galactopyranosyl)-D-galactose (9), the yield of the *galacto*-configuration in the borane reduction was low as

Can. J. Chem. Downloaded from www.nrcresearchpress.com by 210.87.254.5 on 09/05/12
For personal use only.

TABLE 1. Characterizations of the α-linked 2′-acetamido-2′-deoxydisaccharides

Compound	Temperature (°C)	Chemical shifts of the anomeric hydrogens, τ-values (spacings, Hz)* Non-reducing unit	Reducing unit	Paper chromatographic mobilities (cm)†
α-D-GlcNAc*p*-(1 → 6)-D-Gal (**3**)	24	4.89 (3.5)	4.53 (2.5), 5.21 (7.5)	7.6
α-D-GlcNAc*p*-(1 → 3)-D-Glc (**6**)	15	4.52 (3.5)	4.57 (3.5), 5.14 (8.0)	14.3
α-D-GalNAc*p*-(1 → 6)-D-Gal (**10**)	33	4.90 (3.5)	4.57 (3.0), 5.26 (7.5)	7.0
α-D-TalNAc*p*-(1 → 6)-D-Gal (**11**)	33	4.95 (0)	4.58 (3.0), 5.26 (7.5)	12.5
α-D-GalNAc*p*-(1 → 3)-D-Glc (**15**)	33	4.53 (3.5)	4.55 (3.5), 5.18 (8.0)‡	12.5
α-D-TalNAc*p*-(1 → 3)-D-Glc (**16**)	8	4.54§	4.63 (3.5), 5.18 (8.0)	22.3

*The n.m.r. spectra were measured at 100 MHz in deuterium oxide (c = 12.5%). In all cases the β to α anomeric ratio of the reducing sugar unit was near 1.5.
†Whatman No. 1 paper using butanol–pyridine–water – acetic acid (6:4:3:1) for 36 h.
‡From spectrum taken at +10°.
§Broad singlet.

Can. J. Chem. Downloaded from www.nrcresearchpress.com by 210.87.254.5 on 09/05/12
For personal use only.

experienced in the preparations of compounds **8** and **13**. The challenge then remains to establish means for the stereoselective reduction of 2-oximino-α-D-*lyxo*-hexopyranosides to 2-amino-2-deoxy-α-D-galactopyranosides. This matter is under investigation.

Experimental

The experimental procedures were the same as those previously reported (3, 10). The elution chromatograms on microcrystalline cellulose (Avicel, FMC Corporation, Newark, Delaware) (11) employed 100 g per gram of crude mixture using *n*-butanol – pyridine – water – acetic acid (6:4:3:1) as the developing phase. The conditions for the ion-exchange and thin layer chromatograms were reported in an accompanying paper (10).

The 100 MHz spectra were measured for all the products reported herein. In each case, the spectrum required high purity and was in complete accord with that expected for the assigned structure

Reductions with Diborane

The acetoxime, compound **1**, **4**, **7**, or **12** (10 mmol) was dissolved in 45 ml of tetrahydrofuran (THF) and the solution was cooled to −5° under an atmosphere of nitrogen. A molar solution of borane in THF (45 ml) was then added at such a rate as to maintain the temperature near −5°. The resulting solution was left at room temperature for 3 h. Methanol (100 ml) was then added dropwise and the solution evaporated to a solid residue. The residue was taken up in methanol (150 ml) and the solution stirred briefly with ion-exchange resin (Dowex 1-X8 in the hydroxide form) (50 ml). Removal of the resin and evaporation provided a solid foam which was further processed as described below depending on the compound reduced.

Hydrolysis of the Isopropylidene Groups

The compound (approximately 10 mmol) was dissolved in 50 ml of 90% trifluoroacetic acid and the solution kept at room temperature for 15 min (12). The solution was then evaporated, *in vacuo* below 40°, to an oil which, on trituration with ether, provided an amorphous powder.

Acetylations

Direct *N*-acetylations were performed by dissolving the amine (10 mmol) in 50% aqueous methanol (20 ml) and adding acetic anhydride (10 ml). After 2 h at room temperature, the solution was evaporated to dryness *in vacuo*.

Peracetylations were carried out by dissolving the compound (10 mmol) in acetic anhydride – pyridine (1:2) and maintaining the solution at 4° for 12 h. The product was isolated by first removing the solvents *in vacuo*, adding water, and isolating the product by extraction with chloroform in the usual manner.

De-*O*-acetylations were performed by dissolving the compound (10 mmol) in 50% aqueous methanol (50 ml) and adding 2 ml of triethylamine. The solution was kept refrigerated for 12 h and then evaporated to yield the crude product.

N-2,4-Dinitrophenylation

The amine, about 1 mmol, was dissolved in water (10 ml) containing sodium bicarbonate (0.21 g). A solution of 1-fluoro-2,4-dinitrobenzene (0.25 g) in acetone (5 ml) was then added. After stirring for 24 h, the solution was taken to dryness and the residue acetylated.

Hydrolyses

Hydrolysis of the 2′-acetamido-2′-deoxydisaccharides was effected by heating a solution in 4 *N* hydrochloric acid at 100° for 1 h. The amino-sugar liberated was identified by paper electrophoresis (13).

The aglycon-sugars were best identified by paper chromatography (10) after hydrolyzing the disaccharide in 1 *N* hydrochloric acid at 100° for 1 h.

6-O-(2-Acetamido-tri-O-acetyl-2-deoxy-α-D-glucopyranosyl)-1,2;3,4-di-O-isopropylidene-α-D-galactopyranose

The crude product (**2**) obtained by reduction of **1** was acetylated to yield material which appeared to be homogeneous on t.l.c. examination. Crystallization from ethanol

Can. J. Chem. Downloaded from www.nrcresearchpress.com by 210.87.254.5 on 09/05/12
For personal use only.

yielded the title compound (77%), m.p. 128–129°, $[\alpha]_D^{28}$ +23° (*c*, 1.7 in chloroform).

Anal. Calcd. for $C_{26}H_{39}NO_{14}$: C, 52.96; H, 6.67; N, 2.38. Found: C, 53.13; H, 6.74; N, 2.23.

6-O-(2-Acetamido-2-deoxy-α-D-glucopyranosyl)-D-galactopyranose (3)

The above compound was de-*O*-acetylated in quantitative yield to a single product (t.l.c.) which was not further characterized. Hydrolysis of the isopropylidene groups gave a powder which was taken up in methanol and reprecipitated by adding ether. The yield was 62% of a white powder, $[\alpha]_D^{23}$ +126° (*c*, 0.65 in water). The n.m.r. spectrum and paper chromatographic behavior were consistent with the assigned structure in a high degree of purity (see Table 1).

Anal. Calcd. for $C_{14}H_{25}NO_{11}$: C, 43.86; H, 6.57; N, 3.65. Found: C, 44.04; H, 6.83; N, 3.92.

6-O-[Tri-O-acetyl-2-deoxy-2-(2,4-dinitroanilino)-α-D-glucopyranosyl]-1,2;3,4-di-O-isopropylidene-α-D-galactopyranose

A sample of the crude reduction product of **1** was converted to the *N*-2,4-dinitrophenyl derivative and then acetylated. The product crystallized readily and was recrystallized from ethanol, m.p. 201–202° (sintering 185–190°), $[\alpha]_D^{28}$ −28° (*c*, 1.2 in chloroform).

Anal. Calcd. for $C_{30}H_{39}N_3O_{17}$: C, 50.49; H, 5.51; N, 5.89. Found: C, 50.20; H, 5.30; N, 5.93.

3-O-(2-Acetamido-tri-O-acetyl-2-deoxy-α-D-glucopyranosyl)-1,2;5,6-di-O-isopropylidene-α-D-glucofuranose

The product (impure **5**) from the reduction of **4** was acetylated. The product crystallized readily and was recrystallized from ethyl acetate – Skellysolve B in 75% yield, m.p. 168–170°, $[\alpha]_D^{23}$ +32° (*c*, 1.2 in chloroform).

Anal. Calcd. for $C_{26}H_{39}NO_{14}$: C, 52.96; H, 6.67; N, 2.38. Found: C, 52.51; H, 6.72; N, 2.48.

3-O-(2-Acetamido-2-deoxy-α-D-glucopyranosyl)-1,2;5,6-di-O-isopropylidene-α-D-glucofuranose

De-*O*-acetylation of the above compound gave a crystalline product which was recrystallized from ethanol (90% yield), m.p. 228–229°, $[\alpha]_D^{23}$ +80° (*c*, 1.8 in DMF).

Anal. Calcd. for $C_{20}H_{33}NO_{11}$: C, 51.82; H, 7.19; N, 3.02. Found: C, 52.10; H, 7.23; N, 3.24.

3-O-[Tri-O-acetyl-2-deoxy-2-(2,4-dinitroanilino)-α-D-glucopyranosyl]-1,2;5,6-di-O-isopropylidene-α-D-glucofuranose

This compound was prepared from crude **5**. After recrystallization from ethanol, the product melted at 216–218°, $[\alpha]_D^{28}$ +15° (*c*, 1.7 in chloroform).

Anal. Calcd. for $C_{30}H_{39}N_3O_{17}$: C, 50.49; H, 5.51; N, 5.89. Found: C, 50.31; H, 5.57; N, 5.86.

3-O-(2-Acetamido-2-deoxy-α-D-glucopyranosyl)-D-glucopyranose (6)

The above-described 3-*O*-(2-acetamido-2-deoxy-α-D-glucopyranosyl)-1,2;5,6-di-*O*-isopropylidene-α-D-glucofuranose was hydrolyzed to remove the isopropylidene groups to provide an amorphous material. The product crystallized from ethanol in 45% yield, m.p. 212–215°, $[\alpha]_D^{21}$ +182.2 → 157.8° (*c*, 0.92 in water).

Anal. Calcd. for $C_{14}H_{25}NO_{11}$: C, 43.86; H, 6.57; N, 3.65. Found: C, 44.18; H, 6.44; N, 3.51.

6-O-(2-Acetamido-2-deoxy-α-D-galactopyranosyl)-1,2;3,4-di-O-isopropylidene-α-D-galactopyranose and 6-O-(2-Acetamido-2-deoxy-α-D-talopyranosyl)-1,2;3,4-di-O-isopropylidene-α-D-galactopyranose

N-Acetylation of the reduction product (crude mixture of **8** and **9**) of compound **7** gave an amorphous powder which was chromatographed on ion-exchange resin (Dowex 1, 200–400 mesh, hydroxide form) to yield first, 6-*O*-(2-acetamido-2-deoxy-α-D-galactopyranosyl)-1,2;3,4-di-*O*-isopropylidene-α-D-galactopyranose (1.39 g; 29%) which crystallized from ethyl acetate – Skellysolve B, m.p. 151–153°, $[\alpha]_D^{23}$ +69° (*c*, 1 in DMF).

Anal. Calcd. for $C_{20}H_{33}NO_{11}$: C, 51.82; H, 7.19; N, 3.02. Found: C, 51.43; H, 7.12; N, 3.24.

The *talo*-isomer followed (2.79 g, 59%) which crystallized from water, m.p. 119–121°, $[\alpha]_D^{23}$ −9.7° (*c*, 1.5 in DMF).

Anal. Calcd. for $C_{20}H_{33}NO_{11}$: C, 51.82; H, 7.19; N, 3.02. Found: C, 51.52; H, 7.38; N, 2.89.

6-O-(2-Acetamido-2-deoxy-α-D-galactopyranosyl)-D-galactose (10) and 6-O-(2-Acetamido-2-deoxy-α-D-talopyranosyl)-D-galactose (11)

The crude product from the reduction of the acetoxime **7** was *N*-acetylated, the *O*-isopropylidene groups removed, and the product chromatographed on a column of microcrystalline cellulose. The first fraction was compound **11** (*talo*-isomer) isolated in 48% yield, $[\alpha]_D^{21}$ +65° (*c*, 3.2 in water). This compound liberated talosamine and galactose on acid hydrolysis and was identical to the product formed on hydrolysis of the above-described di-*O*-isopropylidene derivative.

Anal. Calcd. for $C_{14}H_{25}NO_{11}$: C, 43.86; H, 6.57; N, 3.65. Found: C, 43.62; H, 6.55; N, 3.57.

Further elution afforded 6-*O*-(2-acetamido-2-deoxy-α-D-galactopyranosyl)-D-galactose (**10**) in 25% yield, $[\alpha]_D^{25}$ +137° (*c*, 0.6 in water); (lit. (14), $[\alpha]_D$ +142° (water)).

Anal. Calcd. for $C_{14}H_{25}NO_{11}$: C, 43.86; H, 6.57; N, 3.65. Found: C, 43.77; H, 6.58; N, 4.14.

This compound was also obtained on removal of the isopropylidene groups of the above described *N*-acetyl derivative of **8**.

3-O-(2-Acetamido-2-deoxy-α-D-galactopyranosyl)-1,2;5,6-di-O-isopropylidene-α-D-glucofuranose and 3-O-(2-Acetamido-2-deoxy-α-D-talopyranosyl)-1,2;5,6-di-O-isopropylidene-α-D-glucofuranose

N-Acetylation of the reduction product (crude mixture of **13** and **14**) of compound **12** gave an amorphous powder which was chromatographed on ion-exchange resin (Dowex 1, 200–400 mesh in the hydroxide form). The first fraction, 35% yield, crystallized spontaneously and was recrystallized from ethyl acetate, m.p. 223–224°, $[\alpha]_D^{23}$ +95° (*c*, 0.6 in DMF).

Anal. Calcd. for $C_{20}H_{33}NO_{11}$: C, 51.82; H, 7.19; N, 3.02. Found: C, 51.63; H, 7.36; N, 3.15.

The corresponding *talo*-isomer was then obtained from the chromatogram as an oil in 47% yield which crystallized from ethyl acetate – Skellysolve B, m.p. 163–165°, $[\alpha]_D^{23}$ +27.3° (*c*, 0.52 in DMF).

Anal. Calcd. for $C_{20}H_{33}NO_{11}$: C, 51.83; H, 7.13; N, 3.02. Found: C, 51.79; H, 6.95; N, 3.30.

3-O-(2-Acetamido-2-deoxy-α-D-galactopyranosyl)-D-glucose (15)

Hydrolysis of the above-described *N*-acetyl derivative of **13** provided a product which crystallized from ethanol, m.p. 212–215°, $[\alpha]_D^{21}$ +177→ 187° (*c*, 0.9 in water) (see Table 1).

Anal. Calcd. for $C_{14}H_{25}NO_{11}$: C, 43.86; H, 6.57; N, 3.65. Found: C, 44.18; H, 6.44; N, 3.63.

3-O-(Acetamido-2-deoxy-α-D-talopyranosyl)-D-glucose (16)

Hydrolysis of the above-described *N*-acetyl derivative of **14** provided a product which crystallized from ethanol, m.p. 190–195°, $[\alpha]_D^{23}$ +82 → 70° (*c*, 0.5 in water) (see Table 1).

Anal. Calcd. for $C_{14}H_{25}NO_{11}$: C, 43.86; H, 6.57; N, 3.65. Found: C, 43.65; H, 6.83; N, 3.43.

The financial assistance of the National Research Council of Canada through a grant-in-aid of research (A-172) to R.U.L. is gratefully acknowledged as are the important contributions by the analytical and spectral service laboratories of this Department under the supervision of R. N. Swindlehurst.

1. S. Umezawa, S. Koto, K. Tatsuta, and T. Tsumura. Bull. Chem. Soc. Jap. **42**, 529 (1969).
2. S. Umezawa and S. Koto. Bull. Chem. Soc. Jap. **39**, 2014 (1966).
3. R. U. Lemieux, K. James, T. L. Nagabhushan, and Y. Ito. Can. J. Chem. **51**, 33 (1973).
4. R. U. Lemieux, Y. Ito, K. James, and T. L. Nagabhushan. Can. J. Chem. **51**, 7 (1973).
5. R. U. Lemieux, K. James, and T. L. Nagabhushan. Can. J. Chem. **51**, 27 (1973).
6. R. U. Lemieux, T. L. Nagabhushan, K. J. Clemetson, and L. C. N. Tucker. Can. J. Chem. **51**, 53 (1973).
7. K. L. Rinehart, Jr. J. Infect. Dis. **119**, 345 (1969).
8. R. D. Marshall and A. Neuberger. Adv. Carbohydr. Chem. Biochem. **25**, 407 (1970).
9. R. U. Lemieux and R. V. Stick. In preparation.
10. R. U. Lemieux, K. James, and T. L. Nagabhushan. Can. J. Chem. **51**, 42 (1973).
11. M. L. Wolfrom, D. H. Busek, R. M. De Lederkremer, S. C. Vergez, and J. R. Vercellotti. J. Chromatogr. **18**, 42 (1965).
12. J. E. Christensen and L. Goodman. Carbohydr. Res. **7**, 510 (1968).
13. R. U. Lemieux and T. L. Nagabhushan. Can. J. Chem. **46**, 401 (1967).
14. W. M. Watkins. Nature **181**, 117 (1958).

Can. J. Chem. Downloaded from www.nrcresearchpress.com by 210.87.254.5 on 09/05/12
For personal use only.

The Synthesis of Kanamycin Analogs I. α-D-Glucopyranosyl Derivatives of Deoxystreptamine[1]

R. U. LEMIEUX, T. L. NAGABHUSHAN,[2] K. J. CLEMETSON,[3] AND L. C. N. TUCKER[4]

Department of Chemistry, University of Alberta, Edmonton, Alberta

Received June 2, 1972

The procedure developed in this laboratory for the synthesis of α-D-glucopyranosides based on the reaction of dimeric tri-*O*-acetyl-2-deoxy-2-nitroso-α-D-glucopyranosyl chloride with alcohols was employed to synthesize the three α-D-glucopyranosyl deoxystreptamines and 4,6-di-*O*-α-D-glucopyranosyl deoxystreptamine. Effects of p*H* change on the n.m.r. spectra of kanamycins A and B and of the above synthetic compounds are interpreted in terms of a conformational change.

Le procédé développé au laboratoire pour la synthèse des α-D-glucopyranosides à partir de la réaction entre le chlorure de tri-*O*-acétyl-déoxy-2 nitroso-2-α-D-glucopyranosyle dimère et les alcools, a été utilisé pour obtenir les trois α-D-glucopyranosyl déoxystreptamines et le di-*O*-α-D-glucopyranosyl-4,6-déoxystreptamine. Les effets du p*H* sur les spectres r.m.n. des kanamycines A et B des composés synthétiques ci dessus sont interprétés par rapport au changement conformationnel.

[Traduit par le journal]

Can. J. Chem., **51**, 53 (1973)

The widespread distribution of α-glycosidic bonds in naturally occurring antibiotics (1) has strongly motivated an interest in improved methodology for the stereoselecive synthesis of α-glycosides in high yield. Such developments are of interest not only for the possible total synthesis of therapeutically useful antibiotics, but also, by making available synthetic analogs, for improving our knowledge of structure-activity relationships.

The so-called aminocyclitol group of antibiotics (1) provide a most interesting subject for synthetic investigations in view of the large and ever increasing number of the members of this family which have deoxystreptamine (1,3-diamino-1,2,3-trideoxy-*myo*-inositol) as a building unit. The deoxystreptamine antibiotics include the kanamycins A, B, and C, the neomycins A, B, and C, the paromomycins I and II, the gentamycins, hygromycin B_2, the nebramycins (see ref. 1 for a review of the foregoing antibiotics), butyrosins (2), destomycin A (3), and sisomycin (4). In many of these antibiotics at least one of the glycosidic bonds to the deoxystreptamine residue involves an α-D-*gluco*-linkage with or without an amino group at the 2-position. Thus, in order to effectively synthesize such structures, the stereoselective synthesis of α-D-glucopyranosides in good yield is a basic requirement. For this reason, research was initiated in this laboratory several years ago toward the development of improved methodology to cope with this classical problem of carbohydrate chemistry. As a result, a method was established (5–8) based on the nitrosyl chloride adduct of D-glucal triacetate (tri-*O*-acetyl-1,5-anhydro-2-deoxy-D-*arabino* hex-1-enitol) (9, 10) as the glycosylating reagent. A main purpose of the present research was to test the effectiveness of this approach for the synthesis of α-D-glucopyranosides of deoxystreptamine. It has already been demonstrated (11) that the method can be used for the preparation of simple glycosides of 6-amino-6-deoxy-D-glucose, a building unit of kanamycin. A second purpose of the research was to obtain model compounds for the study of the chemical shifts which occur for the two anomeric hydrogens of kanamycin A, since such studies may provide information on the conformation of kanamycin A in aqueous solution.

A number of total syntheses of aminocyclitol antibiotics have appeared since the advent of this research program. All these syntheses were

[1]Presented in part at the 172nd Meetimg of the Japan Antibiotic Research Association, Tokyo, April 4, 1970 and at the Joint Meeting of the American Chemical Society and Chemical Institute of Canada, Toronto, Ontario, 1970.

[2]Research Associate, 1970–1972.

[3]University of Alberta Postdoctorate Fellow, 1968–1970.

[4]University of Alberta Postdoctorate Fellow, 1967–1969. Present address: Department of Chemistry, University of Dundee, Scotland.

Can. J. Chem. Downloaded from www.nrcresearchpress.com by 210.87.254.105 on 09/05/12
For personal use only.

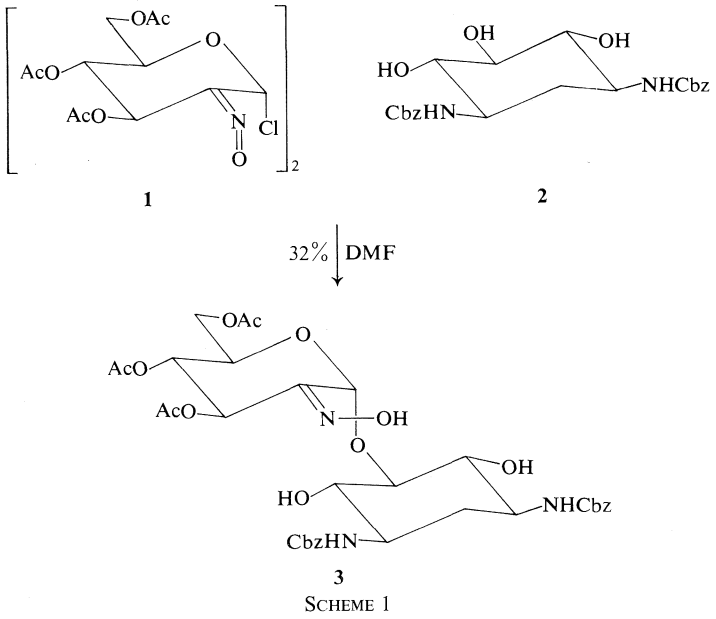

SCHEME 1

modelled on more classical approaches to the synthesis of α-D-glycosidic linkages and include the syntheses of kanamycin A (12, 13), kanamycin B (14), kanamycin C (15), paromamine (16), and neomycin A (neamine) (17). The nitrosyl chloride adduct of a glycal structure was employed in an ingenious preparation of the cyclitol antibiotic kasugamycin by Umezawa and coworkers (18). This antibiotic possesses a 2,3,4,6-tetradeoxy-α-D-*arabino*-hexopyranosyl building unit. Our approach to the synthesis of α-D-glucopyranosides of deoxystreptamine proceeds by way of 2-oximino-α-D-*arabino*-hexopyranosides. These intermediates can also be reduced to 2-amino-2-deoxy-α-D-glucopyranosyl derivatives of deoxystreptamine, the structural units of which are found in the aminocyclitol antibiotics, for example, kanamycin C, paromomycin, and streptomycin.

Syntheses of Mono-O-α-D-glucopyranosyl Derivatives of Deoxystreptamine

The 1,3-di-*N*-benzyloxycarbonyl derivative of deoxystreptamine (**2**) has been reported (19) to be a suitable derivative of deoxystreptamine for the synthesis of a variety of its *O*-glycosides. The good solubility of **2** in dimethylformamide and the ease of removal of the protecting groups by catalytic hydrogenation appeared in our hands also to be superior to other possible derivatives. Since Umezawa and Ito (19) reported a good yield of the di-*O*-(tetra-*O*-acetyl-β-D-glucopyranosyl)-1,3-di-*N*-benzyloxycarbonyldeoxystreptamine by reaction of **2** (without further blocking) with tetra-*O*-acetyl-α-D-glucopyranosyl bromide in the presence of mercuric cyanide, it was thought that it should be possible to prepare kanamycin A analogs similarly. However, when **2** was reacted with an equivalent amount of the nitrosyl chloride adduct **1** (10), the main product formed (32% yield) was characterized as 5-*O*-(tri-*O*-acetyl-2-oximino-α-D-*arabino*-hexopyranosyl)-1,3-di-*N*-benzyloxycarbonyldeoxystreptamine (**3**) (see Scheme 1). The crude glycosidic products were obtained in 83% yield (calculated as pure **3**) and 11% of **2** was reclaimed. The crude material was separated into three fractions by column chromatography. Comparison of these materials with samples of 4,6-di-*O*-(tri-*O*-acetyl-2-oximino-α-D-*arabino*-hexopyranosyl)-1,3-di-*N*-benzyloxycarbonyldeoxystreptamine (**17**, to be described below) and the mixture of the diastereoisomeric 4- and 6-*O*-(tri-*O*-acetyl-2-oximino-α-D-*arabino*-hexopyranosyl)-1,3-di-*N*-benzyloxycarbonyldeoxystreptamine (**11** and **12**, also to be described below) were made by t.l.c. The substance which moved fastest was different to the latter three compounds. The second fraction from the column chromatogram had the same R_f value as the dioximinoglycoside **17** and the third had the same R_f value

Can. J. Chem. Downloaded from www.nrcresearchpress.com by 210.87.254.105 on 09/05/12
For personal use only.

Can. J. Chem. Downloaded from www.nrcresearchpress.com by 210.87.254.105 on 09/05/12
For personal use only.

as the above-mentioned mixture of monooximinoglycosides, **11** and **12**, the components of which could not be separated. These latter two fractions were not further characterized.

The first substance to appear in the eluate of the above chromatogram was found to be the 5-*O*-monooximinoglycosyl derivative (**3**) of 1,3-di-*N*-benzyloxycarbonyldeoxystreptamine as follows. The substance was deoximated and then reduced with borohydride. Acetylation provided a crystalline product **4** (see Scheme 2). The protecting groups of **4** were removed to give a basic, dextrorotatory material **5** which was purified by chromatography on Dowex-1-X2 in the hydroxide form in 88% yield from **4**, corresponding to an overall yield of 23% from **2**. The pure but amorphous compound was obtained in the crystalline form after rechromatographing until its optical rotation was constant (two chromatographs). The overall yield of the crystalline material **5**, m.p. 191–192° with decomposition beginning at 180°, $[\alpha]_D^{25}$ +107.5°, was 14% from 1,3-di-*N*-benzyloxycarbonyldeoxystreptamine (**2**). The n.m.r. spectrum showed a doublet at τ 4.70 with a spacing of 3.0 Hz, the approximate position and structure of which is characteristic of the signal for the anomeric hydrogen of α-D-glucopyranosides. Both paper electrophoresis and paper chromatography indicated the compound to be homogeneous. Furthermore, acid hydrolysis cleaved it to only D-glucose and deoxystreptamine as identified by paper chromatography. The position of attachment of the α-D-glucopyranosyl group was established to be the 5-position of the deoxystreptamine residue by periodate oxidation of the 1,3-di-*N*-acetyl derivative **6**. As expected from this structure, the deoxystreptamine residue survived the oxidation. This was not the case, as will be seen below, for the isomers **15** and **16** which have the α-D-glucopyranosyl group at the 6- and the 4-position, respectively, of the 1,3-di-*N*-acetyldeoxystreptamine. On the basis of these results it is concluded that the rate of reaction of **1** with **2** occurs substantially more rapidly at the 5-position of **2** than at either positions **4** or **6**, a remarkable finding in view of the opposite situation in the case of β-D-glucopyranoside formation (19).

In order to synthesize 4-*O*-α-D-glucopyranosyldeoxystreptamine (**14**) and the diastereoisomer **13** which has the glucose residue at the 6-position, it was necessary to block the 5-position of **2**. A suitable derivative appeared to be the racemic mixture of 4,5- and 5,6-*O*-isopropylidene-1,3-di-*N*-benzyloxycarbonyldeoxystreptamine (**7** and **8**) described by Nakajima and coworkers (20). Condensation of **1** with this compound in dimethylformamide at room temperature for 5 days afforded a mixture of products from which the desired diastereoisomeric mixture of 4-*O*- and 6-*O*-(tri-*O*-acetyl-2-oximino-α-D-*arabino*-hexopyranosyl)-*O*-isopropylidene-1,3-di-*N*-benzyloxycarbonyldeoxystreptamine was isolated in 53% yield (from compound **2**) by column chromatography (see Scheme 3). This mixture, $[\alpha]_D^{24}$ +30°, gave an n.m.r. spectrum, τ 8.60 (isopropylidene group), 7.96 (*O*-acetyl groups), 3.86 (H-1, singlet), 4.92 and 2.71 (benzyloxy groups), which was in agreement with the expected structures. Some cleavage of the acid-labile *trans*-*O*-isopropylidene groups occurred during the condensation.

Deoximation of the mixture in the presence of hydrochloric acid led to simultaneous hydrolysis of the isopropylidene groups (see Scheme 4). Reduction of the crude ketone with sodium borohydride followed by *O*-acetylation afforded hexa-*O*-acetyl-α-D-glucopyranosyl-1,3-di-*N*-benzyloxycarbonyldeoxystreptamine as a mixture of isomers. After removal of the *O*- and *N*-protecting groups, the two main components, which showed signals for anomeric hydrogens in the n.m.r. spectrum at τ 4.92 and 4.72 were separated by chromatography on a Dowex-1-X2 (hydroxide form) column. The compounds (**13** and **14**) were indistinguishable by both paper electrophoresis and chromatography. However, the substance which was eluted from the column first possessed an n.m.r. spectrum showing a single anomeric signal at τ 4.91 with a spacing of 3.5 Hz. On rechromatographing the product four times, until its rotation was constant, the compound crystallized, m.p. 264–265° with decomposition beginning at 240°, $[\alpha]_D^{25}$ +86.5°, $[\alpha]_{436}^{24}$ +170° (water), $\Delta[M]_{TACu}$ −720° (21, 22). In a subsequent preparation of this compound, it could be isolated directly from the crude mixture in the crystalline form by seeding.

The other compound had an n.m.r. spectrum showing the H-1 signal at τ 4.71 with a spacing of 3.5 Hz. Although this product was obtained in a very high state of purity by chromatographing several times until its rotation was constant, the product has failed to crystallize. The amorphous white solid had $[\alpha]_D^{25}$ +98°, $[\alpha]_{436}^{24}$ +159.5° water and $\Delta[M]_{TACu}$ +746° (21, 22).

Can. J. Chem. Downloaded from www.nrcresearchpress.com by 210.87.254.105 on 09/05/12
For personal use only.

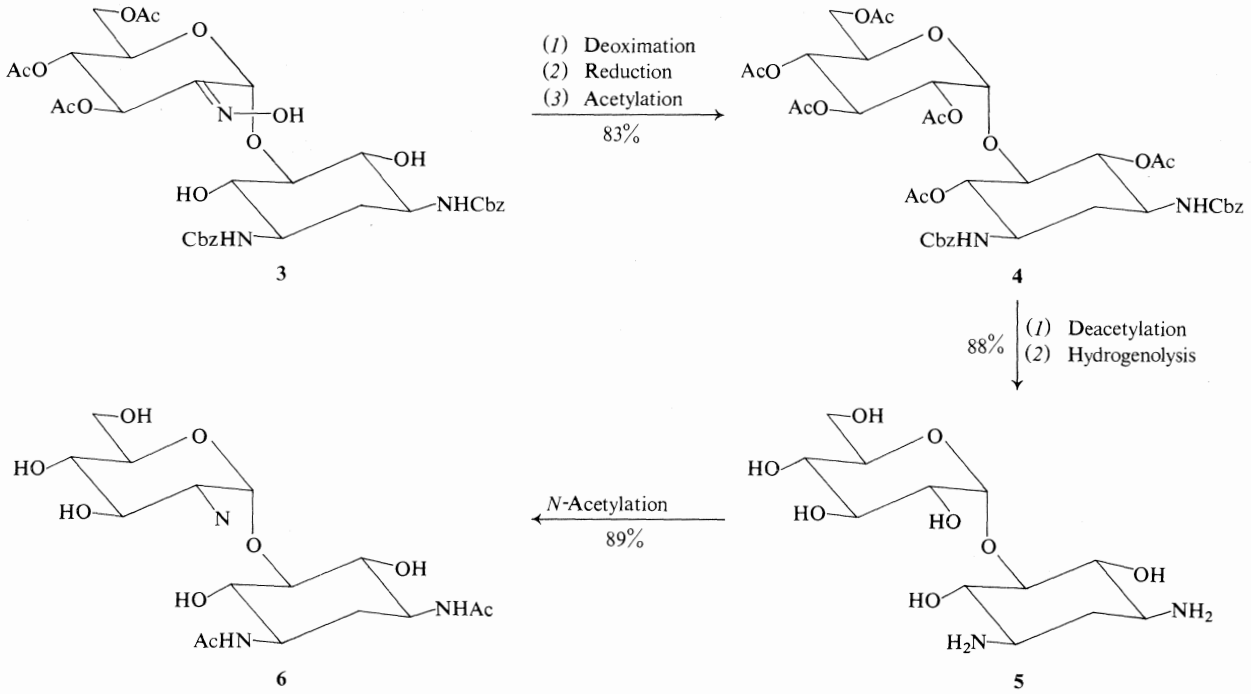

SCHEME 2

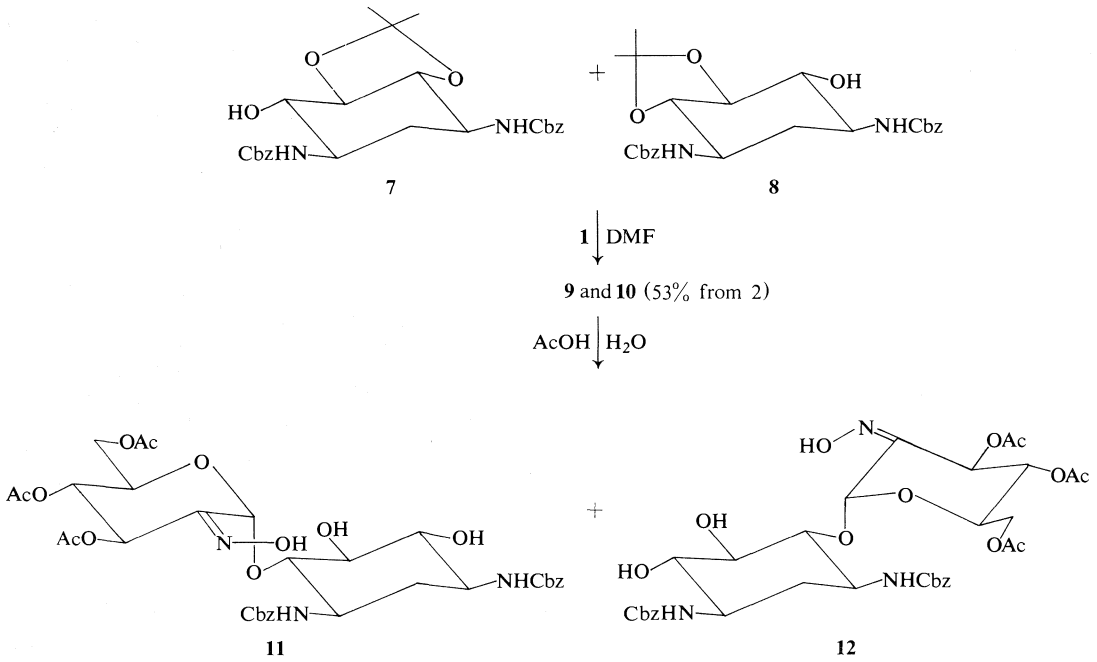

SCHEME 3

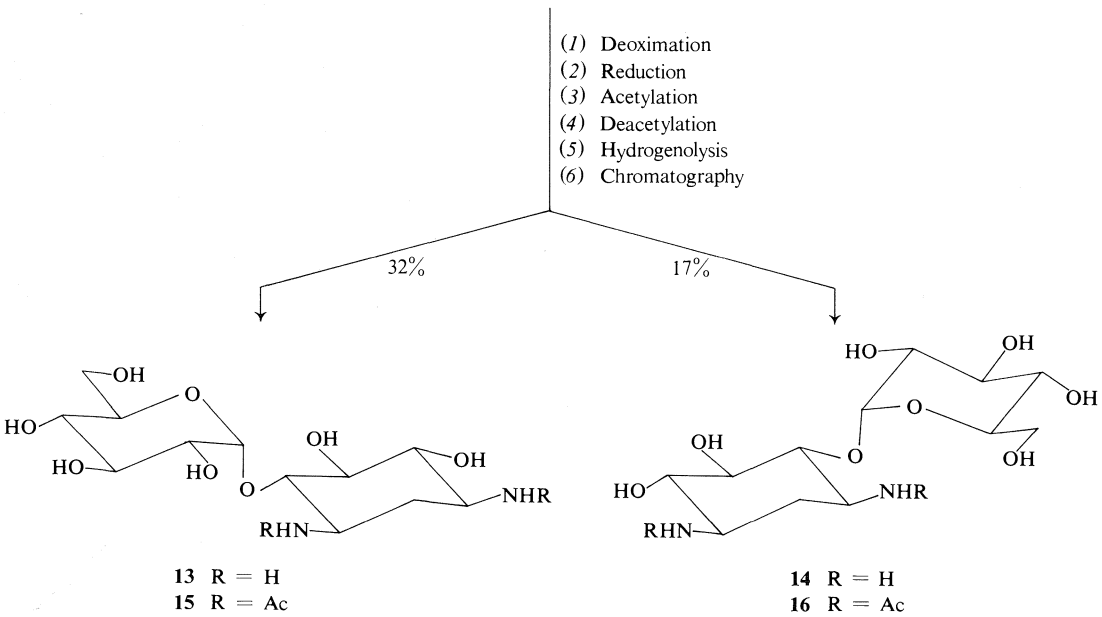

SCHEME 4

Can. J. Chem. Downloaded from www.nrcresearchpress.com by 210.87.254.105 on 09/05/12
For personal use only.

Can. J. Chem. Downloaded from www.nrcresearchpress.com by 210.87.254.105 on 09/05/12
For personal use only.

From n.m.r. and optical rotary data it was evident that the compounds **13** and **14** were α-D-glucopyranosyl derivatives of deoxystreptamine. The positions of linkages to deoxystreptamine were established to be O-6 and O-4, respectively, since periodate oxidation of both **13** and **14** and their respective *N*-acetyl derivatives **15** and **16** destroyed the deoxystreptamine molecule completely as ascertained by acid hydrolysis of the oxidized products followed by their analysis by paper electrophoresis. The observed positive $\Delta[M]_{TACu}$ for compound **14** required (21, 22) it to be the 4-isomer. Similarly, the negative $\Delta[M]_{TACu}$ shown by **13** indicates that it is the 6-isomer.

During the preparation of this manuscript Nishimura *et al.* (23) reported the preparation of **13** and **14** from 1,3-diethoxycarbonyldeoxystreptamine by a modified Koenigs–Knorr reaction. It is noteworthy that while the overall yield of **13** and **14** by their procedure is 6.3 and 0.5%, respectively, the yields by the method described in this paper are 17 and 9%. The $\Delta[M]_{TACu}$ values of $-720°$ for compound **13** and $+746°$ for **14** found in this laboratory are in close agreement with those, $-730°$ and $+735°$, reported for the same compounds by the above authors.

Synthesis of 4,6-Di-O-α-D-glucopyranosyl-deoxystreptamine (18)

For the synthesis of a kanamycin A analog, 4,6-di-*O*-α-D-glucopyranosyl-deoxystreptamine (**18**), it was felt that condensation of the diastereoisomeric mixture of 4- and 6-*O*-(tri-*O*-acetyl-2-oximino-α-D-*arabino*-hexopyranosyl)-1,3-di-*N*-benzyloxycarbonyldeoxystreptamine (**11** and **12**) with the nitrosyl chloride adduct **1** should give mainly 4,6-di-*O*-(tri-*O*-acetyl-2-oximino-α-D-*arabino*-hexopyranosyl)-1,3-di-*N*-benzyloxycarbonyldeoxystreptamine (**17**) (see Scheme 5). This reasoning was based on the fact that attempted condensation of **3** with excess **1** did not yield an appreciable amount of either the 4,5- or the 5,6-diglycoside. Thus, the introduction of a glycosidic linkage strongly hinders further glycosidation at a neighboring position. Further evidence in this regard was by our observation (24) that reaction of a mixture of 4- and 6-*O*-acetyl-1,3-di-*N*-benzyloxycarbonyldeoxystreptamine (prepared from **7** and **8** by *O*-acetylation followed by removal of the *O*-isopropylidene group) with a large excess of **1** gave only very low yields of the 4,5- and 5,6-dioximinoglycoside. Similar results were obtained by Nakajima and coworkers (12) in the condensation of 4-*O*-(6-acetamido-tri-*O*-benzyl-6-deoxy-α-D-glucopyranosyl)-1,3-di-*N*-benzyloxycarbonyldeoxystreptamine with 3-acetamido-tri-*O*-benzyl-3-deoxy-α-D-glucopyranosyl chloride. Whereas the 4,6-derivative was formed in 41% yield at 30°, the 4,5-isomer was formed in only 5% yield. Indeed, when the mixture of compounds **9** and **10** was hydrolyzed to remove the isopropylidene groups and the product (mixture of **11** and **12**) was condensed with a slight excess of **1**, 4,6-di-*O*-(tri-*O*-acetyl-2-oximino-α-D-*arabino*-hexopyranosyl)-1,3-di-*N*-benzyloxycarbonyldeoxystreptamine (**17**) was formed in good yield. Deoximation of this product followed by borohydride reduction and removal of the protecting groups as before gave pure 4,6-di-*O*-α-D-glucopyranosyldeoxystreptamine (**18**) after column chromatography on Dowex 1-X2 hydroxide form ion-exchange resin in an overall yield of 26% from 1,3-di-*N*-benzyloxycarbonyl deoxystreptamine (**2**). The white solid thus obtained was homogeneous when examined by paper chromatography and paper electrophoresis. The structure of the compound was established as follows. Acid hydrolysis gave only D-glucose and deoxystreptamine as identified by paper chromatography. The n.m.r. spectrum showed two anomeric signals at τ 4.64 and 4.83 each with a spacing of 3.5 Hz indicating the α-*gluco*-configuration. This conclusion was substantiated by the close agreement between the specific rotation of the compound, $+130°$ in water and that of kanamycin A free base, $+130.5°$ in water. The rotation of the corresponding β,β-anomeric structure is reported to be $-4.69°$ (19).

The points of attachment of the glucose residues in **18** were established by demonstrating that, whereas both deoxystreptamine and 5-*O*-α-D-glucopyranosyldeoxystreptamine (**5**) underwent oxidation by periodic acid with destruction of the aminocyclitol ring, the deoxystreptamine residue of both kanamycin A and compound **18** survived the oxidation in high yield. This data together with the n.m.r. data to be presented later on can leave no doubt that **18** indeed has the structure expected from the mode of synthesis. For unknown reasons, the deoxystreptamine residue did not survive oxidation when kanamy-

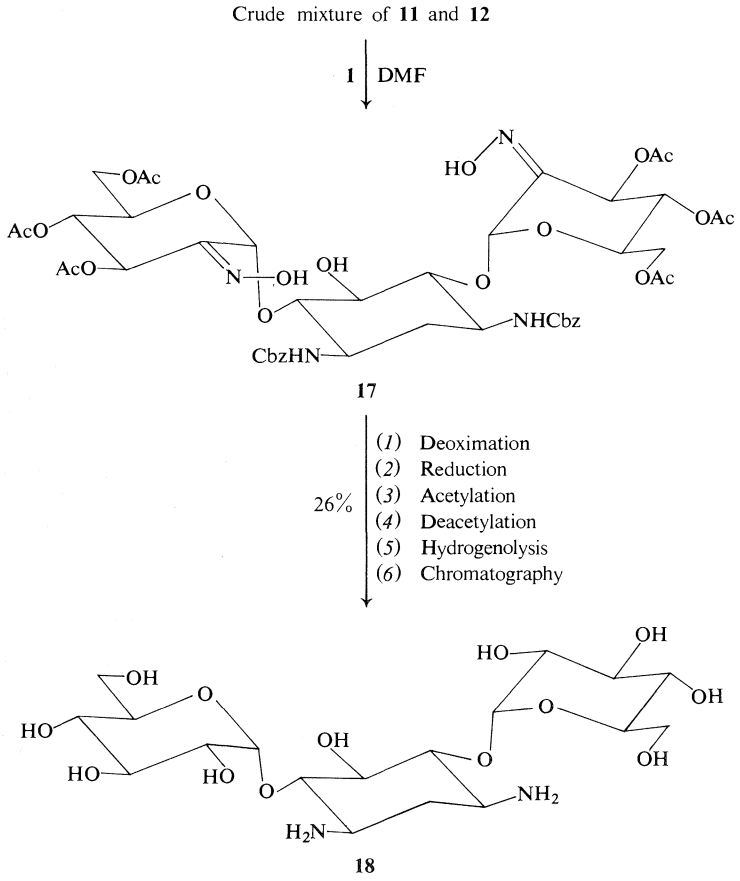

SCHEME 5

cin A and the analog **18** were oxidized at higher p*H* using sodium metaperiodate.

The Conformations of α-D-*Glucopyranosyl Derivatives of Deoxystreptamine and Kanamycin A in Solution*

The absolute configuration of kanamycin A was first established by chemical means (25–27) and the conclusions substantiated recently by X-ray crystallography (28). It is noteworthy that although the numbering of the positions in kanamycin A has consistently been made following the proposal by Hichens and Rinehart, Jr. (25), the basis for this proposal has not, to our knowledge, been presented. However, examination of the configurations of the 4- and 6-positions in terms of the Cahn–Ingold–Prelog sequence rule shows these centres to possess the R- and S-configurations, respectively. Thus, following the convention of giving R preference over S, the currently used numbering of the carbon atoms of deoxystreptamine is in accord with this procedure. In order to specify positions in the hexose residues, the carbons of the residue at the 4-position of the deoxystreptamine are assigned primed numbers, for example, 6′-amino-6′-deoxy-α-D-glucopyranosyl, and those at the 6-position are assigned double primed numbers, for example, 3′′-amino-3′′-deoxy-α-D-glucopyranosyl. These conventions for nomenclature are those used in the following discussions.

The n.m.r. spectrum of kanamycin A free base is shown in Fig. 1 and the spacings of the signals for H′ and H′′ clearly establish the α-linkage for both the amino-sugar units. The substantial chemical shift difference of τ 0.29 (see also Table 1) for these two anomeric hydrogens must arise from their different environments in the aqueous (D_2O) solution. These differences would presumably arise, in part, from differences in the

Can. J. Chem. Downloaded from www.nrcresearchpress.com by 210.87.254.105 on 09/05/12
For personal use only.

Can. J. Chem. Downloaded from www.nrcresearchpress.com by 210.87.254.105 on 09/05/12
For personal use only.

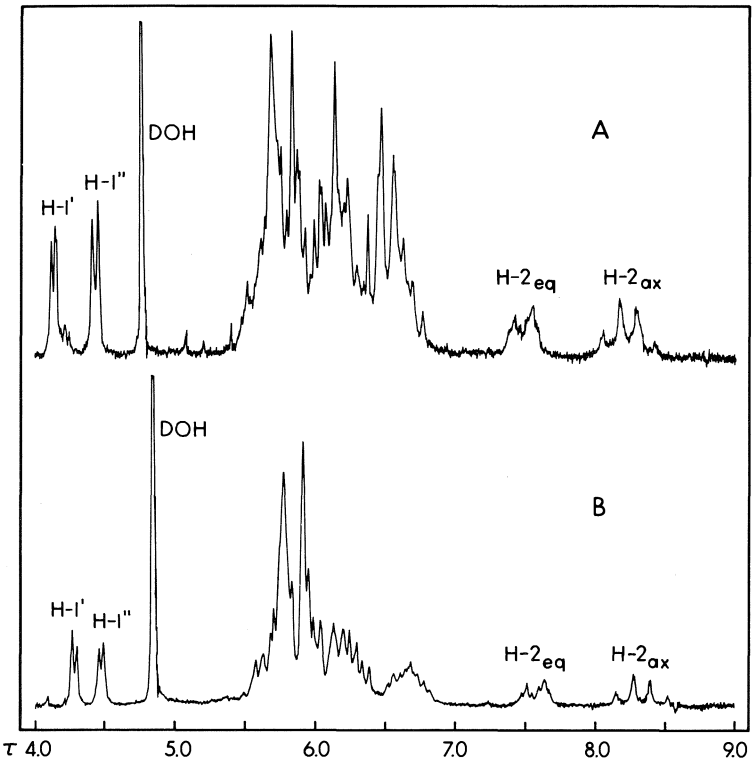

FIG. 1. The 100 MHz n.m.r. spectra in deuterium oxide of kanamycin A (spectrum A) and the synthetic 4,6-di-*O*-α-D-glucopyranosyl-deoxystreptamine (spectrum B) using pure tetramethylsilane as external reference.

structures of the amino-sugar units. However, the influence of the deoxystreptamine portion on the immediate environment of the two anomeric hydrogens could be expected to be different and perhaps dominating. It was of interest, therefore, to examine the n.m.r. spectral properties of 4,6-di-*O*-(α-D-glucopyranosyl)-deoxystreptamine (**18**) to assess these possibilities. The spectrum of this kanamycin analog (Fig. 1) shows that, as for kanamycin A, a substantial chemical shift difference exists between the two anomeric protons. Therefore, it is concluded that the main influence on the relative shielding of these two hydrogens arises from the deoxystreptamine unit.

The chemical shift difference, 0.29 p.p.m., for the anomeric protons of kanamycin A free base is larger than that, 0.19 p.p.m., for the diglucoside **18**. However, the chemical shift difference is increased for both compounds on converting the free base to salts either with acetic acid or hydrochloric acid. These differences are 0.43 and 0.41 p.p.m., respectively, for kanamycin A and 0.26 and 0.31 p.p.m., respectively, for **18**. It is to be noted, however, that this change arises in each case largely by a downfield shift of one of the protons. The signal for anomeric proton at the higher field which has a chemical shift virtually independent of p*H* is assigned to hexose residue at position 6 for two reasons. First of all, as seen in Table 1, the signal for the anomeric proton of 6-*O*-α-D-glucopyranosyl deoxystreptamine (**13**) is 0.16 p.p.m. to higher field than its 4-isomer (**14**) and its chemical shift is essentially p*H* independent. On the other hand, as expected from the behavior of kanamycin A and **18**, the signal for the anomeric proton (H-1′) of 4-*O*-α-D-glucopyranosyl deoxystreptamine moved to lower field for the salt forms. Secondly, it is known that the 2′,6′-diamino-2′,6′-dideoxy-α-D-glucopyranosyl group of kanamycin B is at the 4-position. It would be expected that conversion of kanamycin B to a salt form would lead to strong deshielding of H-1′ since salt formation is at the adjacent 2-position and, if the above assignment is correct, the chemical shift for H-1″ would be little affected. Indeed, as seen in Table 1, on conversion

TABLE 1. Chemical shifts* (τ-values) for the anomeric hydrogens of kanamycin A and related compounds in D_2O

	Free base		Acetate salt		Hydrochloride salt		*N*-Acetyl derivative	
	H-1′	H-1″	H-1′	H-1″	H-1′	H-1″	H-1′	H-1″
Kanamycin A	4.67	4.96	4.47	4.90	4.41	4.82	4.67	4.90
Kanamycin B	4.70	4.97	4.12	4.90	4.02	4.85	—	—
4,6-Di-*O*-α-D-Glucopyranosyl-deoxystreptamine (**18**)	4.64	4.83	4.52	4.78	4.49	4.80	4.66	4.92
4-*O*-α-D-Glucopyranosyl-deoxystreptamine (**14**)	4.76	—	4.63	—	4.52	—	4.68	—
6-*O*-α-D-Glucopyranosyl-deoxystreptamine (**13**)	4.92	—	4.96	—	4.94	—	4.94	—
5-*O*-α-D-Glucopyranosyl-deoxystreptamine (**5**)	4.70	—	4.63	—	4.63	—	4.69	—
6-*O*-3″-Amino-3″-deoxy-α-D-glucopyranosyl-deoxystreptamine	—	—	4.88	—	—	—	4.90	—

*Measured at 60 MHz with 5% tetramethylsilane in chloroform as external reference.

of kanamycin B to either salt, the higher field signal has very nearly the same chemical shift as the corresponding signal in the salts of kanamycin A but the lower field signal is substantially to lower field than in the corresponding salts of kanamycin A. These assignments are in agreement with those made by Nakajima and coworkers (12, 29) on the basis of the chemical shifts of *N*-acetyl derivatives of kanamycin A and related structures. The n.m.r. data for the *N*-acetyl derivatives listed in Table 1 further confirm these assignments. It is therefore concluded that it is the anomeric hydrogen (H-1′) of the 6′-amino-6′-deoxy-α-D-glucopyranosyl residue which has a chemical shift highly sensitive to protonation of the amino groups of the deoxystreptamine residue.

Both because of the *exo*-anomeric effect and ordinary steric considerations (30), it is to be expected that both C-4 and -6 will project between the anomeric hydrogen and ring oxygen of the adjacent glucosyl residue as depicted in formula **19**. The torsional angle defined with the anomeric hydrogen may be very small, for example, only about 10° for the 1 → 4′ α-D-glucosidic linkage of crystalline methyl β-maltoside (31). Indeed, the X-ray crystallographic structures of kanamycin A both as the monosulfate and the monoselenate salts in the monohydrate forms conform to this prediction. Therefore, it seems necessary to conclude that in kanamycin A, H-1′ will project toward O-5 and H-1″ will project toward N-1. This conclusion is supported by the fact that H-1′ of 5-*O*-α-D-glucopyranosyl deoxystreptamine (**5**) must project toward an oxygen atom of the deoxystreptamine residue and, indeed, its chemical shift is near those of H-1′ of both kanamycin A and **18** and the shift is not highly sensitive to change in p*H*.

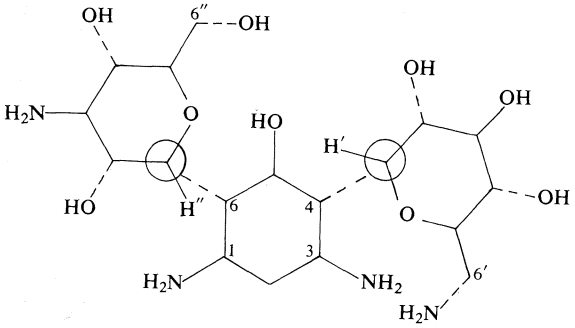

19

It may have been expected that H-1″ would be the anomeric hydrogen of either kanamycin A or **18** with a chemical shift sensitive to protonation rather than H-1′ which is relatively remote from amino groups. Since the reverse is the case, it seems likely that protonation of N-3 brings about a change in the chemical shift of H-1′ through a change in conformation about the glycosidic bond system for the 6′-amino-6′-deoxy-α-D-glucopyranosyl group which exposes H-1′ more to the applied magnetic field. A possible explanation is that protonation of N-3 leads to hydrogen bonding of N-3 with the ring

Can. J. Chem. Downloaded from www.nrcresearchpress.com by 210.87.254.105 on 09/05/12
For personal use only.

Can. J. Chem. Downloaded from www.nrcresearchpress.com by 210.87.254.105 on 09/05/12
For personal use only.

oxygen O-5′. These considerations are likely of importance since kanamycin A must be extensively protonated under physiological conditions. That the presence of the amino groups and their relative distributions in space is of critical importance to the antibiotic activities of kanamycin A is evidenced by the fact that the diglucoside **18** is virtually devoid of antibiotic activity.

In conclusion, we contend that the above-described syntheses of α-D-glucopyranosidic linkages in kanamycin-like structures exhibit substantial advantage over the relatively sterically uncontrolled methods based in Koenigs–Knorr type reactions and augur well for the ability of the synthetic organic chemist to provide complex glycosidic structures of interest to medicinal chemistry. It is planned to examine the reductions of the oximinoglycosidic structures **3**, **9**, **10**, and **17** to provide the corresponding 2-amino-2-deoxy-α-D-glucopyranosides.

Experimental

Methods

Melting points were determined on a heating stage and are uncorrected. Optical rotations were measured with a Perkin–Elmer Model 141 polarimeter. N.m.r. spectra were taken with Varian A60 and Varian HA100 spectrometers.

Paper electrophoresis was carried out using a Gilson Medical Electronics Model D high voltage electrophorator at 2 kV, 200 mA with pyridine – acetic acid – water, 10:1:89 (p*H* 6.0) buffer on Whatman No. 3MM paper. T.l.c. was carried out on Silica Gel G (E. Merck A. G., Darmstadt) using 25% sulfuric acid as the visualizer. Paper chromatography was carried out on Whatman No. 1 paper, using *n*-butanol – pyridine – water – acetic acid, 6:4:3:1 or *n*-propanol – pyridine – water – acetic acid, 15:10:12:3 as developer. Amino-sugars were detected using ninhydrin spray reagent (32) and other reducing sugars by silver nitrate – sodium hydroxide spray reagents (33). *N*-Acetyl derivatives of deoxystreptamine were detected by periodate–permanganate spray reagent (34).

Unless otherwise stated, dry column chromatography (35) was carried out using Silica Gel PF254 (E. Merck A.G., Darmstadt). Wet column chromatography was carried out using SilicAr CC-7, 100–200 mesh (Mallinckrodt Chemical Works, St. Louis, Mo.). All ion-exchange chromatograms were carried out with Dowex 1-X2 (OH^- form), 200–400 mesh resin using water as eluant (36).

Hydrogenations were carried out at 60 p.s.i. using 5% palladium-on-charcoal (Engelhardt Industries, Newark, New Jersey) as catalyst.

Solutions were dried over anhydrous sodium sulfate and all solvent removals were carried out *in vacuo* using rotary evaporator. Dimethylformamide was removed at 45° using the vacuum from an oil pump.

Determination of Points of Glucosidic Attachment to Deoxystreptamine

(1) By Chemical Degradation

(a) Control Experiments

(i) Determination of time required by periodic acid to oxidize deoxystreptamine

The time required for periodic acid to oxidize deoxystreptamine completely was determined as follows: A 1 mg sample of deoxystreptamine was dissolved in 1 ml water along with 10 mg periodic acid. The solution was set aside in the dark. Aliquots of 0.3 ml were withdrawn after 24, 48, and 72 h, respectively and treated with 0.03 ml ethylene glycol to destroy excess periodic acid. After 2 h, concentrated hydrochloric acid was added to the solution to make it approximately 4 *N* and heated on a steam bath for 1 h. The hydrolyzate thus obtained was analyzed both by paper electrophoresis and paper chromatography as described above. The intensity of the spot was compared with that of deoxystreptamine which had been similarly treated in a simultaneous experiment except for periodic acid which was omitted. Deoxystreptamine was still detected in samples which had been treated with periodic acid for 24 and 48 h, but was completely absent in the sample treated for 72 h. Hence in all the cases where periodic acid oxidations were performed, the samples were oxidized for 72 h.

(ii) Periodic acid oxidation of kanamycin A

A 1 mg sample of kanamycin A was dissolved in 1 ml water together with 10 mg periodic acid.The solution was left in the dark at room temperature for 72 h. Excess periodic acid was destroyed by addition of 0.1 ml ethylene glycol. After 2 h concentrated hydrochloric acid was added to the solution to make it approximately 4 *N* and the mixture was heated on a steam bath for 1 h. The resulting hydrolyzate was analyzed by paper chromatography and paper electrophoresis as described above. The hydrolyzate showed the presence of deoxystreptamine but no 6-amino-6-deoxy-D-glucose or 3-amino-3-deoxy-D-glucose indicating that both the amino-sugar residues were oxidized by periodic acid. In order to further confirm that the amino-sugars were not oxidized after hydrolytic cleavage of the glycosidic bonds, a concurrent experiment was carried out in which a solution of 10 mg periodic acid in 1 ml was set aside 72 h in the dark and then treated with 0.1 ml ethylene glycol for 2 h. Kanamycin A (1 mg) was now introduced followed by concentrated hydrochloric acid as above. The mixture was heated on a steam bath for 1 h and the hydrolyzate analyzed as above. Kanamycin A was also hydrolyzed similarly with 4 *N* hydrochloric acid and comparison of the two hydrolyzates clearly showed the presence of both the amino-sugars in the former thus confirming that the method could be used to determine the position of glycosidic attachment to deoxystreptamine unambiguously.

(b) Determination of the Position of Attachment in α-D-Glucopyranosyl Derivatives of Deoxystreptamine

A 1 mg sample of the glycoside, the position of attachment to deoxystreptamine of which was to be determined and its *N*-acetyl derivative were oxidized by periodic acid, hydrolyzed, and analyzed in the manner similar to that described above for kanamycin A. Authentic samples were

Can. J. Chem. Downloaded from www.nrcresearchpress.com by 210.87.254.105 on 09/05/12
For personal use only.

used to identify spots on paper chromatograms and paper electrophoretograms. Kanamycin A, deoxystreptamine, their *N*-acetyl derivatives, and glucose were used as controls for the periodic acid oxidations. Positive tests for the presence of deoxystreptamine in the hydrolyzates were obtained for kanamycin A, tetra-*N*-acetyl kanamycin A, the monoglucoside **5**, the diglucosyl compound **18**, and its di-*N*-acetyl derivative **20**. Deoxystreptamine was not however found in the hydrolyzates from the monoglucosides **13**–**16**. A positive test for 3-amino-3-deoxy-D-glucose was obtained for tetra-*N*-acetylkanamycin A but not for kanamycin A. 6-Amino-6-deoxy-D-glucose was not present in these hydrolyzates. Glucose was not detected in the hydrolyzates from compounds **5**, **6**, **13**, **14**, **15**, **16**, **18**, and **20**.

(2) By Optical Rotation

The tetramine copper(II) sulfate, $Cu(NH_3)_4SO_4 \cdot H_2O$-(TACu) was prepared according to the method of Horn and Taylor (37) and the $\Delta[M]_{TACu}$ values determined as described by Umezawa *et al.* (21). The weighed sample of the compound (~0.02 mmol) was dissolved in 2 ml of 3.95% w/v TACu solution and the rotation measured at 436 mμ. An aqueous solution of the same compound was prepared at the same time and its rotation at 436 mμ also measured. The $\Delta[M]_{TACu}$ value was then obtained from the expression

$$\Delta[M]_{TACu} = ([\alpha]_{436}TACu - [\alpha]_{436}\,water) \times mol \cdot wt/100$$

as suggested by Umezawa *et al.* (21).

Nuclear Magnetic Resonance Spectra of Derivatives of Deoxystreptamine and Kanamycin A

The n.m.r. spectra were measured at 60 MHz at a concentration of 20% in carbon dioxide free deuterium oxide with the instrument operating at 33 ± 1°. The samples were prepared by freeze drying three times from solution of deuterium oxide. Chemical shifts are given in τ values and refer to spectra measured with 5% tetramethylsilane in chloroform as the external standard. The spectra of kanamycin A and **18** shown in Fig. 1 were obtained at 100 MHz at 33°.

*5-O-α-D-Glucopyranosyl-deoxystreptamine (**5**)*

1,3-Di-*N*-benzyloxycarbonyldeoxystreptamine (**2**) (19) (1 g, 2.32 mmol) and tri-*O*-acetyl-2-deoxy-2-nitroso-α-D-glucopyranosyl chloride dimer (**1**) (10) (0.9 g, 1.33 mmol, 0.34 mequiv excess) were dissolved in 20 ml of dry dimethylformamide. The solution was left in the dark at room temperature until the t.l.c. (acetone – *n*-hexane 1:1) indicated completion of reaction (120 h). The solution was then concentrated to a thin syrup which was dissolved in chloroform for washing with water. In the course of the two water washes a precipitate appeared which was collected by filtration and identified (i.r) as the starting material **2**. The amount recovered was 110 mg (11%). The clarified chloroform solution was dried and concentrated to a light yellow solution (~10 ml) which was poured with stirring into 500 ml of *n*-hexane. The solid precipitate was collected by filtration, washed with *n*-hexane, and dried. The yield was 1.4 g (83%). Inspection by t.l.c. as above showed the substance to contain one major component (R_f 0.53), two minor components (R_f 0.46 and 0.29), a trace amount of **2**, and traces of very minor components.

A dry column of silica gel (22 cm × 4 cm in diameter) was prepared and the product was added to the top of the column as a solution in 10 ml of 1:1 mixture of acetone – *n*-hexane. The column was eluted with a mixture of acetone – *n*-hexane 3:7. Ten-milliliter fractions of the eluate were collected and examined for purity by t.l.c. Three main fractions were separated and only those portions were pooled which appeared homogeneous by t.l.c. In this manner, products A (535 mg), B (124 mg), and C (212 mg) were obtained. A total of 220 mg of interzone material was also isolated. Product B is considered to be a mixture of di-*O*-(tri-*O*-acetyl-2-oximino-α-D-*arabino*-hexopyranosyl)-derivatives of **2** since its R_f value was in close correspondence with that observed on the same t.l.c. for authentic sample of this compound (see below). Furthermore, the relative intensities of the signals for acetyl (τ, 7.9–8.1) and phenyl group (τ, 2.68) protons in the n.m.r. spectrum were consistent with this structural assignment. Fractions A and C both appeared to be monoglycosyl derivatives of **2** as judged from the relative intensities of the signals for acetyl (τ 7.95, 8.01, and 8.05) and phenyl group (τ, 2.68) protons in their n.m.r. spectra.

Fraction A, $[\alpha]_D^{24}$ +65.5° (*c* 2 in chloroform), was an amorphous white solid (32% yield).

Anal. Calcd. for $C_{34}H_{41}O_{15}N_3$: C, 55.81; H, 5.65; N, 5.74. Found: C, 55.82; H, 5.60; N, 5.89.

Fraction C possessed the same R_f value on t.l.c. as the mixture of the 4- and 6-*O*-(tri-*O*-acetyl-2-oximino-α-D-*arabino* hexopyranosyl)-1,3-di-*N*-benzyloxycarbonyldeoxystreptamine (**13** and **14**).

Fraction A, assigned structure **3** (0.535 g), was dissolved in a mixture of acetonitrile (4 ml) and 1 *N* hydrochloric acid (1 ml) and acetaldehyde (4 ml) was added. After stirring for 3 h, the acetaldehyde was removed by partial evaporation and the mixture partitioned between ethyl acetate and water. The water layer was extracted with ethyl acetate and the combined ethyl acetate fractions were washed with saturated aqueous sodium bicarbonate solution. The extract was dried and concentrated to a yellow syrup. The syrup was dissolved in dichloromethane (5 ml) and added with stirring to 200 ml *n*-hexane. The precipitate was isolated, washed with *n*-hexane and dried. Yield 0.473 g, 88%. $[\alpha]_D^{24}$ +67° (*c*, 2 in $CHCl_3$). N.m.r. τ, 8.08, 8.11 (3 *O*-acetyl groups), 5.05 (2 CH_2 groups of the benzyloxy group).

Anal. Calcd. for $C_{34}H_{40}N_2O_{15} \cdot (H_2O)$: C, 55.58; H, 5.76; N, 3.81. Found: C, 55.48; H, 5.55; N, 3.55.

The above product (0.473 g) was dissolved in 10 ml of dioxane and 5 ml of water. The solution was cooled to 0° and sodium borohydride (200 mg) dissolved in 7.5 ml of dioxane–water (2:1) was added dropwise with stirring. The mixture was stirred at 0° for 0.5 h and then at room temperature for 1.5 h. The solution was then acidified with acetic acid and taken to dryness. The boric acid was was removed as methyl borate by co-distillation with methanol three times. The residue was acetylated overnight using 10 ml of pyridine and 2 ml of acetic anhydride at room temperature. The product, 0.513 g (94% yield from the above ketone) was isolated in the usual manner and 5-*O*-(tetra-*O*-acetyl-α-D-glucopyranosyl)-4,6-di-*O*-acetyl-1,3-di-*N*-benzyloxycarbonyldeoxystreptamine (**4**) was obtained in the form of a white fibrous crystalline solid (from benzene – *n*-hexane), m.p. 111–112°, $[\alpha]_D$

+66.5° (*c*, 2 in $CHCl_3$). The n.m.r. spectrum at 60 MHz showed the following features; six acetyl singlets at τ 8.13, 8.08, 8.02, 7.98, 7.93, 7.86; two phenyl groups at 2.70, and two methylene protons of the benzyloxycarbonyl group at 4.91.

Anal. Calcd. for $C_{40}H_{48}N_2O_{18}$: C, 56.87; H, 5.73; N, 3.32. Found: C, 56.71; H, 5.78; N, 3.15.

The above compound (0.513 g) was dissolved in a mixture of methanol (15 ml) and water (3 ml) and triethylamine (1.5 ml) was added. The resulting solution was left overnight at room temperature prior to solvent removal. The syrupy residue was dissolved in a mixture of dioxane (5 ml), water (2.5 ml), and acetic acid (0.3 ml) and hydrogenated for 8 h in the presence of 100 mg of catalyst. The solids were removed by filtration through a bed of Celite and the filtrate was concentrated to a pale brown syrup. The syrup was taken up in 5 ml of water for transfer to the ion-exchange resin column, 100 cm × 1.5 cm in diameter. Examination of fractions for purity by paper electrophoresis led to the pooling of fractions which, on freeze drying, provided 170 mg of a white amorphous powder. This corresponds to an overall yield of 23% from **2**. The n.m r spectrum at 100 MHz showed the following features: τ 4.76 (H-1, doublet, $J_{1,2}$ = 3.5 Hz); 7.8–9.1 (methylene protons of deoxystreptamine).

Anal. Calcd. for $C_{12}H_{24}O_8N_2$: C, 44.44; H, 7.46; N, 8.64. Found: C, 44.14; H, 7.47; N, 8.22.

A sample of the above compound (0.125 g) was rechromatographed as above on a 2.5 cm × 100 cm column until its rotation was constant (required twice rechromatographing). The product was crystallized from aqueous ethanol to give 0.077 g (14% overall yield from **2**), m.p. 191–192° with decomposition beginning at 180°, $[\alpha]_D^{24}$ +107.5° (*c*, 2 in water).

Anal. Calcd. for $C_{12}H_{24}O_8N_2$: C, 44.44; H, 7.46; N, 8.64. Found: C, 44.28; H, 7.39; N, 8.52.

5-O-α-D-Glucopyranosyl-1,3-di-N-acetyldeoxystreptamine (6)

Acetic anhydride (0.08 g) was added to a solution of **5** (0.108 g) in water (0.7 ml) and methanol (0.3 ml). The clear solution was set aside 1 h after which time 1 ml of Amberlite IRA 400 (OH^- form) was added and the mixture stirred for additional 1 h. The resin was removed and the solution concentrated to dryness. The residual solid was dried, dissolved in hot anhydrous methanol, and after cooling to room temperature precipitated with ether. The white precipitate was isolated by filtration, washed with ether and dried. The yield of **6**, $[\alpha]_D^{25}$ +65.5° (*c*, 0.3 in water) was 89%. The n.m.r. spectrum of the compound showed the anomeric signal at τ 4.69 with a spacing of 3.5 Hz and the *N*-acetyl protons appeared at τ 7.99 as a sharp singlet.

Anal. Calcd. for $C_{16}H_{28}N_2O_{10}$: C, 47.05; H, 6.91; N, 6.86. Found: C, 46.80; H, 6.86; N, 6.56.

6-O-α-D-Glucopyranosyl-deoxystreptamine (13) and 4-O-α-D-Glucopyranosyl-deoxystreptamine (14)

A mixture of 4,5- and 5,6-di-*O*-isopropylidene-1,3-di-*N*-benzyloxycarbonyldeoxystreptamine (**7** and **8**) (20) (19.75 g, 42 mmol) and tri-*O*-acetyl-2-deoxy-2-nitroso-α-D-glucopyranosyl chloride (**1**) (15.8 g, 46.5 mmol) was dissolved in dimethylformamide (200 ml) and left for 120 h in the dark at room temperature. The solution was concentrated to ~50 ml and diluted with 150 ml of dichloromethane. Some precipitate separated which was collected by filtration (0.5 g yield) and shown by i.r. spectroscopy to be 1,3-di-*N*-benzyloxycarbonyldeoxystreptamine (**2**). The clear filtrate was washed with water three times, then with saturated sodium chloride solution, dried, and concentrated to a brown foam. Yield 34.0 g (still contained some dimethylformamide).

Examination by t.l.c. (acetone – *n*-hexane, 1:1) showed one major fast-moving component R_f 0.73 and three minor components R_f 0.53, 0.46, and 0.29. The above mixture was transferred to the top of a silica gel column (120 cm × 4 cm) as a saturated solution in acetone – *n*-hexane 3:7 and eluted with the same solvent system. Twenty-milliliter fractions were collected and examined by t.l.c. Those containing pure, faster moving component were pooled and concentrated to give a brownish sticky foam which resisted crystallization. The yield of **9** and **10** was 17.2 g (53%), $[\alpha]_D^{24}$ +30° (*c*, 2 in $CHCl_3$). The n.m.r. spectrum of the material showed the isopropylidene signals at τ 8.59 (6-protons), the *O*-acetyl signals at 7.98 (9-protons), the methylene signals of the benzyloxycarbonyl group at 4.89 (4-protons), and the phenyl signal at 2.64 (10-protons).

Anal. Calcd. for $C_{37}H_{45}N_3O_{15}$: C, 57.58; H, 5.88; N, 5.45. Found: C, 57.16; H, 5.80; N, 5.28.

The crude material (10 g, 13 mmol) was dissolved in acetonitrile (100 ml) and 1 *N* hydrochloric acid (10 ml) and acetaldehyde (20 ml) were added. After stirring for 5 h, the acetaldehyde was removed by partial evaporation and the mixture partitioned between ethyl acetate (100 ml) and water (100 ml). The water was extracted with ethyl acetate (50 ml) and the combined ethyl acetate fractions were washed with sodium bicarbonate solution, dried, and concentrated to 9.5 g of residue. N.m.r. data: τ 8.02, 7.98, and 7.92 (three *O*-acetyl groups); 4.93 (four-methylene protons of the benzyloxycarbonyl group), 2.62 (ten aromatic hydrogens).

Anal. Calcd. for $C_{34}H_{40}N_2O_{15} \cdot H_2O$: C, 55.58; H, 5.76; N, 3.81. Found: C, 55.51; H, 5.45; N, 3.99.

The above material (9.0 g) was dissolved in dioxane (140 ml) and water (70 ml). The solution was cooled to 0° and sodium borohydride (2.5 g) dissolved in 30 ml of dioxane–water (2:1) was added dropwise with stirring. The mixture was stirred at 0° for 0.5 h and then at room temperature for 2.5 h. The solution was then acidified with acetic acid and taken to dryness. The boric acid was removed as methyl borate by codistillation with methanol three times. The residue was acetylated overnight using 30 ml of pyridine and 5 ml of acetic anhydride. The product, 5.63 g (51% from **9** and **10**), was isolated in the usual manner.

The above material (4.5 g, 5.34 mmol) was dissolved in 300 ml of ethanol–water (2:1) and triethylamine (5 ml) added. The mixture was left overnight at room temperature. The solution was concentrated and the residue dissolved in 100 ml of dioxane–water (2:1). Acetic acid (5 ml) and catalyst (1.0 g) were added to the solution and the mixture hydrogenated for 24 h. The solids were removed by filtration through a bed of Celite and the filtrate concentrated to a pale brown syrup (5.1 g). The syrup was taken up in 20 ml of water and transferred to the ion-exchange resin column (100 cm × 2.5 cm) for chromatography. Ten-milliliter fractions were collected and examined by paper electrophoresis. Two major

Can. J. Chem. Downloaded from www.nrcresearchpress.com by [illegible]
For personal use only.

Can. J. Chem. Downloaded from www.nrcresearchpress.com by 210.87.254.105 on 09/05/12
For personal use only.

products, with identical mobilities on paper electrophoresis, but moving at different rates on the ion-exchange resin were obtained from the pooled fractions. Fraction I (32% yield from **9** and **10**), $[\alpha]_D^{24}$ +70.1° (*c*, 2.2 in water) showed an n.m.r. spectrum which had the anomeric signal at τ 4.92 with a spacing of 3.5 Hz. A sample of this fraction (0.6 g) was rechromatographed as above until its rotation was constant (required four chromatographs) and crystallized from aqueous methanol to give 0.1 g of pure **13**, m.p. 264–265° (with decomposition beginning at 240°), $[\alpha]_D^{24}$ +83.5° (*c*, 2.2 in water), $[\alpha]_{436}^{24}$ +170° (*c*, 0.3 in water), $[\alpha]_{436}^{24}$ −52.4° (*c*, 0.26 in TACu), $\Delta[M]_{TACu}$ −721° (lit. (23); m.p. 231–232° (dec.), $[\alpha]_D^{15}$ +102° (*c*, 1 in water), $[\alpha]_{436}^{15}$ +186° (*c*, 0.1 in water), $[\alpha]_{436}^{15}$ −40° (*c*, 0.1 in TACu), $\Delta[M]_{TACu}$ −730°). In a subsequent experiment it was found that crystalline **13** could be directly obtained from fraction I by seeding in an overall yield of 21% from **2**. The n.m.r. spectrum of crystalline **13** in deuterium oxide showed the anomeric signal at τ 4.92.

Anal. Calcd. for $C_{12}H_{24}O_8N_2$: C, 44.44; H, 7.46; N, 8.64. Found: C, 44.12; H, 7.19; N, 8.53.

Fraction II (17% yield from **9** and **10**), $[\alpha]_D^{24}$ +92.5° (*c*, 2.2 in water) showed an n.m.r. spectrum which had the anomeric signal at τ 4.72 with a spacing of 3.5 Hz. This fraction was rechromatographed twice as above (until its rotation was constant) to obtain pure **14** in an overall yield of 11% from **2**. The product had $[\alpha]_D^{24}$ +95° (*c*, 2 in water), $[\alpha]_{436}^{24}$ +159.5° (*c*, 0.42 in water), $[\alpha]_{436}^{24}$ +390° (*c*, 0.26 in TACu), $\Delta[M]_{TACu}$ +747° (lit. (23); $[\alpha]_D^{15}$ +127° (*c*, 0.15 in water), $[\alpha]_{436}^{15}$ +238° (*c*, 0.15 in water), $[\alpha]_{436}^{15}$ +465° (*c*, 0.15 TACu), $\Delta[M]_{TACu}$ +735°). The n.m.r. spectrum of pure **14** showed the anomeric signal at τ 4.76 with a spacing of 3.5 Hz.

Anal. Calcd. for $C_{12}H_{28}N_2O_8$: C, 44.44; H, 7.41; N, 8.64. Found: C, 44.64; H, 7.33; N, 8.29.

*6-O-α-D-Glucopyranosyl-1,3-di-N-acetyldeoxystreptamine (**15**)*

This compound was prepared from **13** (0.2 g) in a manner similar to that described above for the preparation of **6** from **5**. The yield of **15**, $[\alpha]_D^{25}$ +61.5° (*c*, 0.5 in water) was 85%. The n.m.r spectrum of the compound showed the anomeric hydrogen at τ 4.94 as a doublet with a spacing of 3.5 Hz.

Anal. Calcd. for $C_{16}H_{28}N_2O_{10}$: C, 47.05; H, 6.91; N, 6.86. Found: C, 46.74; H, 6.71; N, 7.11.

*4-O-α-D-Glucopyranosyl-1,3-di-N-acetyldeoxystreptamine (**16**)*

This compound was prepared from **14** (0.2 g) in a manner similar to that described above for the preparation of **6** from **5**. The yield of **16**, $[\alpha]_D^{25}$ +73.4° (*c*, 0.7 in water), was 85%. The n.m.r. spectra of the compound in deuterium oxide showed the anomeric proton at τ 4.68 as a doublet with a spacing of 3.5 Hz. The *N*-acetyl protons gave a signal at τ 8.01.

Anal. Calcd. for $C_{16}H_{28}N_2O_{10}$: C, 47.05; H, 6.91; N, 6.86. Found: C, 47.15; H, 6.95; N, 6.66.

*4,6-Di-O-(α-D-glucopyranosyl)-deoxystreptamine (**18**)*

The above described mixture of the 4- and 6-*O*-(tri-*O*-acetyl-2-oximino-α-D-*arabino*-hexopyranosyl)-*O*-isopropylidene-1,3-di-*N*-benzyloxycarbonyldeoxystreptamine (**9** and **10**) (3.9 g, 8.3 mmol) was dissolved in 80% acetic acid (30 ml) and set aside 18 h. The solution was concentrated and partitioned between methylene chloride (200 ml) and water (100 ml). The methylene chloride layer was dried, concentrated to ~50 ml, and poured into *n*-hexane (500 ml) with stirring. The precipitate was collected by filtration, washed with *n*-hexane, and dried. The crude product (3.5 g) (mixture of **11** and **12**) was dissolved with tri-*O*-acetyl-2-deoxy-2-nitroso-α-D-glucopyranosyl chloride dimer ((**1**) (10), 1.78 g, 2.65 mmol (0.50 mequiv excess)) in 50 ml of dry dimethylformamide. The solution was left at room temperature in the dark for 96 h. After this reaction time, t.l.c. using acetone–*n*-hexane 1:1 indicated completion of reaction as noted by the disappearance of **1**. The solution was concentrated to 20 ml, the residue was dissolved in 200 ml of chloroform, and the solution washed three times with water. After drying, the solution was concentrated to about 50 ml and poured with stirring into 500 ml of *n*-hexane. The precipitate was collected, washed with *n*-hexane, and dried to give 5.10 g of a light yellow powder, $[\alpha]_D^{24}$ +30.7° (*c*, 2 in chloroform). The n.m.r. spectrum showed bands for acetyl groups (τ 8.00) and benzyloxycarbonyl groups (τ 2.67 and 4.92) about the relative intensities expected for di-*O*-(tri-*O*-acetyl-2-oximino-α-D-*arabino*-hexopyranosyl-deoxystreptamine (**17**).

The above crude product, 5.10 g, was dissolved in a mixture of acetic acid (60 ml), levulinic acid (4.5 ml), and 1 *N* hydrochloric acid (4.1 ml) and the solution was left at room temperature overnight. The solution was diluted with methylene chloride (50 ml) and washed with water and then with saturated aqueous sodium bicarbonate until neutral. After drying, the solvent was removed to leave 3.8 g of syrupy material which was not characterized. The syrup was dissolved in dioxane (40 ml) and water (10 ml). A solution of sodium borohydride (0.6 g) in dioxane (10 ml) and water (5 ml) was then added dropwise in the range 0–5°. The solution was then left at room temperature for 1.5 h before adding acetic acid to destroy the excess borohydride. The solution was then concentrated to a syrupy residue which was taken up in methanol and the methanol removed by distillation to remove the boric acid as trimethyl borate. The residual solvent was removed and the product acetylated with pyridine (40 ml) and acetic anhydride (7 ml). Work-up in the usual manner afforded a syrup which was dissolved in 50 ml methylene chloride and the solution poured with stirring into 1 l of *n*-hexane. The resulting precipitate was collected, washed with *n*-hexane, and dried to give 3.7 g of a light brown powder. Integration of the n.m.r. spectrum indicated the presence of about 4.5 acetyl groups per benzyloxycarbonyl group as required for a di-*O*-(tetra-*O*-acetyl-α-D-glucopyranosyl)-5-*O*-acetyl-1,3-di-*N*-benzyloxycarbonyldeoxystreptamine.

The above material (500 mg) was dissolved in methanol (20 ml), water (5 ml) and triethylamine (2.5 ml) and the solution left overnight at room temperature. Solvent removal left 342 mg of a solid which was dissolved in dioxane (4 ml), water (2.5 ml), and acetic acid (0.3 ml). This solution was hydrogenated for 8 h in the presence of 100 mg of catalyst. Catalyst removal followed by solvent removal left 233 mg of a brown syrup which was applied in aqueous solution to the top of a 100 cm × 1.5 cm ion-exchange resin column and chromatographed. Examination of the fractions (10 ml) containing nin-

hydrin-positive material by electrophoresis allowed the pooling of fractions containing only material of the same mobility (R_f 0.54 as compared to deoxystreptamine and 0.66 as compared to kanamycin A). Removal of most of the water followed by freeze-drying left 155 mg (26% overall from **9** and **10**) of a white solid, $[\alpha]_D^{24}$ +130° (*c*, 2 in water).

The n.m.r. spectrum (Fig. 1) at 100 MHz showed the following features: τ 4.64, H-1′ (doublet, $J_{1',2'}$ = 3.5 Hz); 4.83, H-1″ (doublet $J_{1'',2''}$ = 3.5 Hz); 7.9–9.1 (methylene protons of deoxystreptamine).

Anal. Calcd. for $C_{18}H_{34}N_2O_{13}$: C, 44.44; H, 7.05; N, 5.76. Found: C, 44.14; H, 7.22; N, 5.42.

*4,6-Di-O-(α-D-glucopyranosyl)-1,3-di-N-acetyldeoxystreptamine (**20**)*

The free base **18** (0.2 g) was *N*-acetylated following the procedure described for the preparation of **6**. The product was isolated in near quantitative yield. The n.m.r. spectrum of the compound in deuterium oxide showed two doublets at τ 4.66 and 4.92 for the two anomeric signals each with a spacing of 3.5 Hz. The *N*-acetyl protons appeared at τ 8.04.

Anal. Calcd. for $C_{22}H_{38}N_2O_{15}$: C, 46.31; H, 6.71; N, 4.91. Found: C, 46.11; H, 6.49; N, 4.77.

The authors wish to thank Mr. W. Merlo for excellent technical assistance. The financial support of the National Research Council of Canada is gratefully acknowledged (A-172).

1. K. L. Rinehart, Jr., J. Infect. Dis. **119**, 345 (1969).
2. P. W. K. Woo, H. W. Dion, and Q. R. Bartz. Tetrahedron Lett. 2625 (1971).
3. S. Kondo, E. Akita, and M. Koike. J. Antibiot. A**19**, 139 (1966). (Ger. 1 914 527).
4. D. J. Cooper, R. S. Jaret, and H. Reimann. Chem. Commun. 285 (1971).
5. R. U. Lemieux, T. L. Nagabhushan, and S. W. Gunner. Can. J. Chem. **46**, 405 (1968).
6. R. U. Lemieux, R. Suemitsu, and S. W. Gunner. Can. J. Chem. **46**, 1040 (1968).
7. R. U. Lemieux, K. James, and T. L. Nagabhushan. Can. J. Chem. **51**, 27 (1973).
8. R. U. Lemieux and S. W. Gunner. Can. J. Chem. **46**, 397 (1968).
9. W. J. Serfontein, J. H. Jordaan, and J. White. Tetrahedron Lett. **18**, 1069 (1964).
10. R. U. Lemieux, T. L. Nagabhushan, and I. K. O'Neill. Can. J. Chem. **46**, 413 (1968).
11. T. L. Nagabhushan. Can. J. Chem. **48**, 257 (1970).
12. A. Hasegawa, N. Kurihara, D. Nishimura, and M. Nakajima. Arg. Biol. Chem. **32**, 1130 (1968).
13. S. Umezawa, K. Tatsuta, and S. Koto. Bull. Chem. Soc. Jap. **42**, 533 (1969).
14. S. Umezawa, S. Koto, K. Tatsuta, H. Hineno, Y. Nishimura, and T. Tsumura. Bull. Chem. Soc. Jap. **42**, 537 (1969).
15. S. Umezawa, S. Koto, K. Tatsuta, and T. Tsumura. Bull. Chem. Soc. Jap. **42**, 529 (1969).
16. S. Umezawa and S. Koto. Bull. Chem. Soc. Jap. **39**, 2014 (1966).
17. K. Tatsuta, E. Kitazawa, and S. Umezawa. Bull. Chem. Soc. Jap. **40**, 2371 (1967).
18. Y. Suhara, F. Sasaki, K. Maeda, H. Umezawa, and M. Ohno. J. Am. Chem. Soc. **90**, 6559 (1968).
19. S. Umezawa and Y. Ito. Bull. Chem. Soc. Jap. **34**, 1540 (1961).
20. A. Hasegawa, N. Kurihara, D. Nishimura, and M. Nakajima. Agric. Biol. Chem. Jap. **32**, 1123 (1968).
21. S. Umezawa, T. Tsuchiya, and K. Tatsuta. Bull. Chem. Soc. Jap. **39**, 1235 (1966).
22. S. Umezawa, K. Tatsuta, and T. Tsuchiya. Bull. Chem. Soc. Jap. **39**, 1244 (1966).
23. Y. Nishimura, T. Tsuchiya, and S. Umezawa. Bull. Chem. Soc. Jap. **43**, 2960 (1970).
24. R. U. Lemieux, T. L. Nagabhushan, and K. James. Unpublished results.
25. M. Hichens and K. L. Rinehart, Jr. J. Am. Chem. Soc. **85**, 1547 (1963).
26. S. Tatsuoka, S. Horii, K. L. Rinehart, Jr., and T. Nakabayashi. J. Antibiot. Jap. Ser. A. **17**, 88 (1964).
27. R. J. Cushley. Ph.D. Thesis. University of Alberta, Edmonton, Alberta, 1965.
28. G. Koyama, Y. Titaka, K. Maeda, and H. Umezawa. Tetrahedron Lett. 1975 (1968).
29. M. Nakajima, A. Hasegawa, N. Kurihara, H. Shibata, T. Ueno, and D. Nishimura. Tetrahedron Lett. 623 (1968).
30. R. U. Lemieux, A. A. Pavia, J. C. Martin, and K. A. Watanabe. Can. J. Chem. **47**, 4427 (1969).
31. Calculated by M. N. G. James, Department of Biochemistry of this University from a publication by S. S. C. Chu and G. A. Jeffrey. Alta. Crystallogr. **23**, 1038 (1967).
32. J. F. Thompson, R. M. Zacharius, and F. C. Steward. Plant Physiol. **26**, 375, 421 (1951).
33. W. G. Trevelyan, D. P. Procter, and J. S. Harrison. Nature. **166**, 444 (1950).
34. R. U. Lemieux and H. F. Bauer. Anal. Chem. **26**, 920 (1954).
35. B. Loev and M. M. Goodman. Chem. Ind. 2026 (1967).
36. P. W. Austin, F. E. Hardy, J. G. Buchanan, and J. Baddiley. J. Chem. Soc. 5350 (1963).
37. D. W. Horn and E. E. Taylor. J. Am. Chem. Soc. **32**, 253 (1904).

Can. J. Chem. Downloaded from www.nrcresearchpress.com by 210.87.254.105 on 09/05/12
For personal use only.

Kinetics of Reactions of Hexa(dimethylsulfoxide)nickel(II) Ion with Dithiocarbamate Ligands

R. R. SCHARFE, V. S. SASTRI, C. L. CHAKRABARTI,[1] AND C. H. LANGFORD

Department of Chemistry, Carleton University, Ottawa, Canada K1S 5B6

Received June 1, 1972

The kinetics of complex formation $Ni(DMSO)_6^{2+}$ with dithiocarbamate ligands at 25 °C in DMSO is reported. The reactions display the apparent "anomaly" in the direction of slow reaction reported earlier for some other complex formation reactions of $Ni(DMSO)_6^{2+}$ in DMSO.

Les cinétiques de formation du complexe $Ni(DMSO)_6^{2+}$ avec les ligands dithiocarbamates, à 25 °C, dans le DMSO sont rapportées. Les réactions manifestent une "anomalie" apparente dans le sens d'une réaction lente précédemment rapportée pour quelques autres réactions de formation de complexe de $Ni(DMSO)_6^{2+}$ dans le DMSO. [Traduit par le journal]

Can. J. Chem., **51**, 67 (1973)

Can. J. Chem. Downloaded from www.nrcresearchpress.com by 210.87.254.5 on 09/05/12
For personal use only.

This paper concerns complex formation kinetics in the reaction of $Ni(DMSO)_6^{2+}$ (1–5) (DMSO = dimethylsulfoxide) with several dithiocarbamate ions (DTC). Commonly, such kinetics have been interpreted via the Eigen mechanism (3) shown in reaction 1.

$$Ni(DMSO)_6^{2+} + L^- \overset{K_E}{\rightleftharpoons} Ni(DMSO)_6^{2+}, L^- \quad [1]$$

$$Ni(DMSO)_6^{2+}, L^- \underset{k_{-1}}{\overset{k_1}{\rightleftharpoons}} Ni(DMSO)_4L^+ + 2DMSO$$

In most cases, including that of the present study, observed complex formation kinetics are second order (1) and the mechanism of reaction 1 has been tested as follows. The experimental rate constant for complex formation is assumed to be equal to the equilibrium constant for outer sphere complex formation (first step of reaction 1) multiplied by the first order rate constant for entry into the inner sphere. If we define k_f as the *experimental* rate constant for complex formation, $k_f = K_E k_1$. k_1 is determined as k_f/K_E after theoretical calculation of K_E from an electrostatic model (6, 7). This procedure involves an approximate theoretical calculation but a superior approach to mechanistic analysis is not generally available.

The experimental methods here are essentially those described in ref. 1. Kinetics were obtained from stopped flow measurements. The sodium dithiocarbamate salts are characterized in ref. 8. Reactions were followed at 390 nm where $Ni(DTC)^+$ complexes absorb strongly with confirmation from some runs at 340, 350, and 365 nm. Figure 1 shows the spectrum of the diethyldithiocarbamate complex of Ni(II) in DMSO at a concentration of $2.5 \times 10^{-5} M$. In all experiments, Ni(II) was in excess to ensure that the observed kinetics were pseudo first order and that only mono complexes, $Ni(DTC)^+$, would be formed.

In these circumstances (1), a plot of the pseudo first order rate constants (evaluated as the average of at least triplicate determinations) against the concentration of the excess reagent, Ni^{2+}, should give a straight line with a slope equal to k_f and an intercept equal to the rate constant for dissociation of the $Ni(DTC)^+$ complex in s^{-1}. The success of this treatment is illustrated in Fig. 2 for the case of the di-isopropyldithiocarbamate

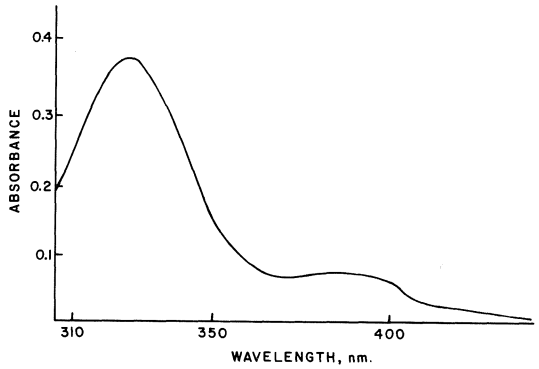

FIG. 1. Spectrum of $2.5 \times 10^{-5} M$ $NiEt_2DTC^+$ in DMSO; concentration of DTC was $2.5 \times 10^{-5} M$; concentration of Ni^{2+} was $50 \times 10^{-5} M$ (1 cm cell).

[1]To whom correspondence should be addressed.

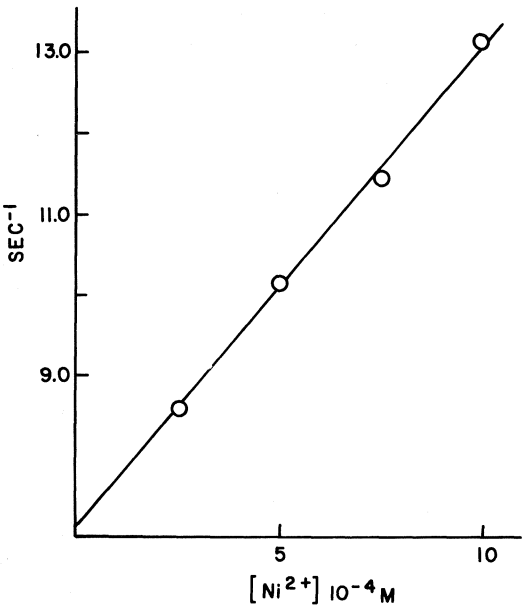

FIG. 2. Apparent rate constant for formation of Ni(*i*-pr$_2$DTC)$^+$ in DMSO at 25 °C as a function of concentration of Ni^{2+}; the initial concentration of DTC was 2.50×10^{-5} *M*; the initial concentration of Ni^{2+} was from 10 to 40 times that of DTC.

reaction. A summary of results for various dithiocarbamates appears in Table 1.

The interpretation of k_f values in Table 1 according to the mechanism in reaction 1 requires the theoretical evaluation of K_E, an "ion pairing" constant, so that k_1 may be calculated. This evaluation is carried out using the Fuoss–Eigen equation (1, 6, 7) based on an electrostatic model. There is one crucial adjustable parameter, the distance of closest approach between the two ions of the outer sphere complex. In Table 2, values of k_1 are collected and computed from Fuoss–Eigen K_E values for both a lower (5 Å) and upper (7 Å) value for the distance of closest approach.

TABLE 1. Rates of formation in DMSO: slope and intercept of plot of apparent rate as a function of Ni^{2+} concentration at 25 °C; Ni^{2+} from $2–10 \times 10^{-4}$ *M*; DTC = 2.5×10^{-5} *M*

Ligand*	Slope ($l\ mol^{-1}\ s^{-1}$) (k_f)	Intercept (s^{-1})
Me_2DTC	1.5×10^4	19
Et_2DTC	1.6×10^4	11
n-pr$_2$DTC	2.7×10^4	7.9
i-pr$_2$DTC	0.59×10^4	7.1
Pyrr DTC	2.4×10^4	11
PipDTC	2.0×10^4	10
HexaDTC	2.5×10^4	9.0

*Me = CH_3—, Et = CH_3CH_2—, *n*-pr and *i*-pr = normal and isopropyl, pyrr = pyrrolidine, pip = piperidine, and hexa = hexamethylene. These abbreviations will be repeated in the next table.

We now come to the significance of the results. The k_1 values in Table 2 range from 10 to 50 times smaller than the rate of solvent exchange of $Ni(DMSO)_6^{2+}$ in DMSO, which recent studies evaluate between 4 and $9 \times 10^3\ s^{-1}$ (9). The usual "dissociative interchange" (3) interpretation of the mechanism of eq. 1 does not *easily* accommodate this difference. That mechanism requires that complex formation rates should fall below solvent exchange rates by *only* a statistical factor for the number of outer sphere sites (1, 3). This has been estimated to be a matter of a factor of 5–10. We are inclined, therefore, to conclude that complex formation reactions of $Ni(DMSO)_6^{2+}$ with dithiocarbamate ions are "anomalously" slow. This conclusion has been reached by Bennetto and Caldin (4) with respect to

TABLE 2. Values of k_1 with K_E calculated for 5 Å and 7 Å distance of closest approach

Ligand	$k_E K_1$ ($l\ mol^{-1}\ s^{-1}$)	k_1 (s^{-1}) K_E = 5 Å	k_1 (s^{-1}) K_E = 7 Å	p*k**
Me_2DTC	1.5×10^4	3×10^2	5×10^2	3.22
Et_2DTC	1.6×10^4	3×10^2	5×10^2	3.38
n-pr$_2$DTC	2.7×10^4	5×10^2	9×10^2	3.47
i-pr$_2$DTC	0.6×10^4	1×10^4	2×10^2	4.3
PyrrDTC	2.4×10^4	5×10^2	8×10^2	3.30
PipDTC	2.0×10^4	4×10^2	7×10^2	3.21
HexaDTC	2.5×10^4	5×10^2	9×10^2	3.29

*This column records the logarithm of the acidity constant of the DTC as reported in ref. 8.

Can. J. Chem. Downloaded from www.nrcresearchpress.com by 210.87.254.5 on 09/05/12
For personal use only.

reactions with bipyridine, and by Langford and Tsiang (1) with respect to reactions with murexide and thiocyanate ions. (Recently, Hoffman and co-worker (5) have challenged the conclusion for SCN^-.) The "anomaly" may reflect a new mechanism or failure of the simplistic Fuoss–Eigen equation. This cannot be decided by kinetic studies alone (10).

1. C. H. LANGFORD and H. G. TSIANG. Inorg. Chem. **9**, 2346 (1970).
2. L. S. FRANKEL. Inorg. Chem. **10**, 814 (1971).
3. C. H. LANGFORD and H. B. GRAY. Ligand substitution processes. W. A. Benjamin, New York. 1966. Chapt. 1; C. H. LANGFORD and V. S. SASTRI. MTP International review of science. Inorganic Chemistry Series One. Vol. 9. Butterworths, London. 1972. Chapt. 6.
4. H. P. BENNETTO and E. F. CALDIN. Chem. Commun. 599 (1969).
5. F. DICKERT and H. HOFFMAN. Ber. Bunsenges. **75**, 1320 (1971).
6. R. M. FUOSS. J. Am. Chem. Soc. **80**, 5059 (1958).
7. M. EIGEN. Z. Phys. Chem. (Frankfurt am Main), **1**, 176 (1954).
8. K. I. ASPILA, C. L. CHAKRABARTI, and V. S. SASTRI. Anal. Chem. In press.
9. S. BLACKSTAFFE and R. A. DWEK. Mol. Phys. **15**, 279 (1968); N. S. ANGERMAN and R. B. JORDAN. Inorg. Chem. **8**, 2579 (1969).
10. A. FANELLI and S. PETRUCCI. J. Phys. Chem. **75**, 2649 (1971).

Can. J. Chem. Downloaded from www.nrcresearchpress.com by 210.87.254.5 on 09/05/12
For personal use only.

Refinement of the Crystal Structure of Synthetic Chervetite, $Pb_2V_2O_7$

ROBERT D. SHANNON[1] AND CRISPIN CALVO

Institute for Materials Research, McMaster University, Hamilton, Ontario

Received July 20, 1972

The structure of synthetic chervetite has been refined by full matrix least-squares to a $\omega_R = 0.029$ using 1105 reflections. Unit cell dimensions are $a = 13.3689(7)$, $b = 7.1607(4)$, $c = 7.1027(4)$ Å, $\beta = 105935(5)°$, and the space group is $P2_1/a$. The structure, originally solved by Kawahara, is a dichromate-type structure with a $V_2O_7^{4-}$ group eclipsed to within $11 \pm 5°$. The Pb^{2+} ions are irregularly coordinated to 8 or 9 oxygens with distances from 2.40 to 3.20 Å. The distortion of the Pb–O distances is considerably greater than the corresponding distortions of the Sr–O distances in the similar β-$Sr_2V_2O_7$ structure and is related to the tendency of Pb^{2+} to form directional covalent bonds. The V–O distances range from 1.665 to 1.720 Å for terminal oxygens and are 1.812 and 1.821 Å for the bridging oxygens. The V–O distances are consistent with the strengths of the Pb—O bonds.

Nous avons raffiné la structure de la chervétite synthétique par moindres carrés de matrice pleine, au moyen de 1105 réflexions, jusqu'à une valeur finale de $\omega_R = 0.029$. Les dimensions de la maille sont $a = 13.3689(7)$, $b = 7.1607(4)$, $c = 7.1027(4)$ Å, $\beta = 105.935(5)$, et le groupe spatial est $P2_1/a$. La structure résolue pour la première fois par Kawahara, est du type dichromate avec un groupe $V_2O_7^{4-}$ éclipsé de $11 \pm 5°$. Les ions Pb^{2+} sont coordonnés de façon irrégulière à 8 ou 9 oxygènes, à des distances de 2.40 à 3.20 Å. La distorsion des distances Pb–O est considérablement plus grande que celle qu'on remarque pour les liaisons Sr—O, dans la structure semblable présentée par le β-$Sr_2V_2O_7$ et tend de façon semblable à Pb^{2+}, à former des liens covalents directionnels. Les distances V–O varient de 1.665 à 1.720 Å, pour les oxygènes terminaux et vont de 1.812 et 1.821 Å pour les oxygènes de ponts. Les distances V–O sont compatibles avec la force des liaisons Pb—O.

[Traduit par le journal]

Can. J. Chem., **51**, 70 (1973)

Introduction

The structure of natural chervetite was solved by Kawahara (1). The structure contains pyrovanadate groups in the eclipsed configuration which is typical of dichromates and some diphosphates (2). We were interested in comparing the average V—O distances in this compound with average distances in other vanadates containing more electropositive cations because there was some indication of a correlation between average electronegativity of cations and bond distances (Noll (3), Brown and Gibbs (4), and Shannon (5)).

Kawahara's results were obtained from a mineral specimen using visually estimated Weissenberg data. In this paper we report the results of a refinement of the crystal structure of synthetic $Pb_2V_2O_7$ using counter data collected on a four circle diffractometer.

Experiments

Stoichiometric quantities of reagent grade PbO and V_2O_5 were melted together in a Pt crucible at 760 °C. Crystals were grown on the end of a Pt wire dipped into the melt. The resultant light tan boule was not a single crystal; however, mono-crystalline fragments approximately 1 mm in size were obtained upon fracturing the boule. These fragments were ground into spheres. X-Ray powder diffraction patterns were taken using a Hägg–Guinier camera and a KCl internal standard according to a procedure described earlier (6). The cell dimensions obtained from a least-squares refinement with KCl as an internal standard of these data are: $a = 13.3689(7)$, $b = 7.1607(4)$, $c = 7.1027(4)$ Å, and $\beta = 105.935(5)°$ at 20 °C with these errors indicating the precision indicated by the refinement. Other crystal data are: Space group = $P2_1/a$, formula weight = 628.30, $V = 653.8$ Å^3, $D_x = 6.381$ g/cc, $Z = 4$, and $\mu = 535.2$ cm^{-1}.

A sphere of radius 0.138 mm ($\mu_r = 7.39$) was chosen for data collection. The average and maximum deviation from the mean radius was about 2 and 5%, respectively. Intensity data were collected on a Syntex automatic diffractometer using MoKα radiation, 4° take-off angle, a graphite monochromator ($2\theta = 12°$) and a scintillation detector. Reflections were scanned at variable rates from 2.0 to 24.0°/min, depending on the peak count, through an angle of 2° plus the α_1–α_2 separation. Background counts were made at the extreme of each scan for times equal to the peak count. A total of 2300 reflections were measured out to $2\theta = 50.0°$. After averaging of equivalent reflections, there were 1105 reflections of which 863 were considered to be observed. Intensities with less than 3 times the standard deviation of the background were considered to be unobserved. The intensities were corrected for Lorentz and polarization factors and absorp-

[1]On leave of absence from Central Research Department, E. I. du Pont de Nemours, Wilmington, Delaware.

Can. J. Chem. Downloaded from www.nrcresearchpress.com by 210.87.254.5 on 09/05/12
For personal use only.

Can. J. Chem. Downloaded from www.nrcresearchpress.com by 210.87.254.5 on 09/05/12
For personal use only.

TABLE 1. Atom parameters for $Pb_2V_2O_7$

Atom	x	y	z	U(Å)	U_{11}†(Å²)	U_{22}(Å²)	U_{33}(Å²)	U_{12}(Å²)	U_{13}(Å²)	U_{23}(Å²)
Pb(1)	−0.13290(5)	0.40884(9)	0.05433(9)	—	0.0600(3)	0.0162(4)	0.0109(4)	−0.0001(3)	0.0011(3)	0.0017(3)
Pb(2)	0.15435(5)	0.19265(9)	0.33445(9)	—	0.0114(4)	0.0199(4)	0.0095(4)	0.0019(3)	0.0029(3)	0.0012(3)
V(1)	0.1087(2)	0.0591(4)	−0.2015(4)	—	0.0070(12)	0.0094(13)	0.0063(12)	−0.0025(10)	−0.0000(9)	0.0000(9)
V(2)	−0.0850(2)	0.3229(4)	−0.3843(4)	—	0.0056(12)	0.0087(12)	0.0062(12)	−0.0003(10)	−0.0010(9)	0.0003(10)
O(1)	0.4621(8)	0.3757(15)	0.1531(15)	0.0141(23)						
O(2)	0.1587(9)	0.1946(16)	−0.0015(16)	0.0176(24)						
O(3)	0.2900(9)	0.4761(16)	0.2691(16)	0.0170(24)						
O(4)	0.4679(9)	0.7014(16)	0.4001(16)	0.0165(23)						
O(5)	0.0488(8)	0.5002(16)	0.2156(14)	0.0113(21)						
O(6)	0.1598(9)	0.8236(17)	0.3002(17)	0.0203(25)						
O(7)	0.3463(8)	0.0854(15)	0.3980(15)	0.0127(22)						

*Standard deviations are given in parentheses.
†Calculated from $\beta_{ij} = 2\pi^2 b_i b_j U_{ij}$ where $T = \exp -(\beta_{11}h^2 + \ldots + 2\beta_{12}hk + \ldots)$ is the temperature factor appearing in the structure factor equation and b_i's are the reciprocal lattice vectors.

tion using the X-ray 67 Program System for X-ray Crystallography written by J. M. Stewart, University of Maryland, and adapted to the CDC 6400 computer by H. D. Grundy. Secondary extinction coefficients were calculated for each reflection according to Zachariasen (7).

The initial parameters used for refinement were those of Kawahara (1). Several cycles of refinement using the full-matrix least squares program CUDLS (8) reduced

$$\omega R = \left\{\frac{\sum \omega||F_o| - |F_c|^2}{\sum \omega|F_o|^2}\right\}^{1/2} \text{ to } 0.053$$

using isotropic temperature factors and weights

$$\omega = \left\{86.86 - 1.095|F_o| + 0.00368|F_o|^2 + 4072\left|\frac{\sigma(F_o)}{|F_o|}\right|^2\right\}^{-1}$$

This weighting scheme was chosen to make the variation in $\omega||F_o| - |F_c||^2$ independent of the variation in F_o. Further refinement using anisotropic temperature factors for Pb and V and varying the secondary extinction parameters according to the method of Larson (9), with $\beta(2\theta)$ ranging from 18.7 to 2.1, lowered ω_R to 0.029, and R to 0.040. The standard deviation, S, of an observation of unit weight was 1.03. Several cycles of refinement using anisotropic temperature factors for the oxygen atoms had no effect on ω_R and the temperature factors for O(1) and O(3) become non-positive definite. Scattering factors for Pb^0, V^0, and O^0 were taken from Cromer and Waber (10) and anomalous dispersion corrections were taken from Cromer (11). The final positional and thermal parameters for the model using anisotropic Pb and V and isotropic O temperature factors are listed in Table 1 and observed and calculated structure factors are listed in Table 2.[2] Table 3 lists the pertinent bond distances and angles.

Results and Discussion

The basic structure of $Pb_2V_2O_7$ as reported by Kawahara (1) is correct. However, Kawahara noted that the distance between V(1) and the terminal oxygen O(3) was unreasonably long (1.88 Å) and the Pb(2)—O(7) distance was too short (2.24 Å). The refinement reported here using 3-dimensional data has produced significant shifts in the oxygen parameters and thus results in changes in the detailed geometry of the $V_2O_7^{4-}$ ion.

Figures 1 and 2 show a perspective view looking down the *b* axis showing only the Pb—O bonds and V—O bonds, respectively. All the

[2]Table 2 is available, at a nominal charge, from the Depository of Unpublished Data, National Science Library, National Research Council of Canada, Ottawa, Canada K1A 0S2.

TABLE 3

(*a*) Bond distances in $Pb_2V_2O_7$

Bond	Distance (Å)
V(1)—O(1)	1.707(11)
—O(2)	1.698(11)
—O(3)	1.665(12)
—O(4)	1.813(10)
⟨V(1)—O⟩ =	1.721
V(2)—O(4)	1.821(12)
—O(5)	1.718(10)
—O(6)	1.668(10)
—O(7)	1.699(10)
⟨V(2)—O⟩ =	1.726
Pb(1)—O(1)	2.402(10)
—O(2*b*)	2.873(11)
—O(2*c*)	2.803(11)
—O(3)	2.778(9)
—O(5)	2.473(9)
—O(5*b*)	2.559(11)
—O(6)	2.958(12)
—O(7)	2.532(11)
⟨Pb(1)—O⟩ =	2.672
Pb(2)—O(1*c*)	2.586(10)
—O(2)	2.403(12)
—O(3)	2.844(11)
—O(3*a*)	3.121(10)
—O(4*a*)	2.814(12)
—O(5)	2.627(10)
—O(6)	2.656(12)
—O(6*a*)	3.201(10)
—O(7)	2.597(10)
⟨Pb(2)—O⟩ =	2.761

(*b*) Bond angles in $Pb_2V_2O_7$

Bond	Angle (deg)
O(1*a*)—V(1)—O(2)	112.5(6)
—O(3*a*)	108.9(6)
—O(4*a*)	113.3(5)
O(2)— —O(3*d*)	106.3(6)
—O(4*a*)	109.8(6)
O(3*a*)— —O(4*a*)	107.9(6)
O(7*c*)—V(2)—O(4*a*)	112.8(6)
—O(5*b*)	109.1(6)
—O(6*b*)	110.0(6)
O(4*a*)— —O(5*b*)	108.3(5)
—O(6*b*)	109.4(6)
O(5*b*)— —O(6*b*)	107.2(6)
O(1*c*)—Pb(1)—O(2*c*)	104.0(4)
—O(5*b*)	97.4(4)
—O(6*b*)	72.7(4)
—O(7*c*)	85.5(4)
—O(2*b*)	155.8(4)
—O(3*b*)	135.4(4)
—O(5)	73.5(4)

Can. J. Chem. Downloaded from www.nrcresearchpress.com by 210.87.254.5 on 09/05/12
For personal use only.

Can. J. Chem. Downloaded from www.nrcresearchpress.com by 210.87.254.5 on 09/05/12
For personal use only.

TABLE 3 (*Concluded*)

(*b*) Bond angles in $Pb_2V_2O_7$

Bond		Angle (deg)
O(2*c*)—	—O(5*b*)	125.8(4)
	—O(6*b*)	81.2(4)
	—O(7*c*)	76.9(4)
	—O(2*b*)	99.4(4)
	—O(3*b*)	57.6(4)
	—O(5)	161.3(4)
O(5*b*)—	—O(6*b*)	58.7(4)
	—O(7*c*)	154.9(4)
	—O(2*b*)	73.3(4)
	—O(3*b*)	72.1(4)
	—O(5)	72.7(4)
O(6*b*)—Pb(1)—	O(7*c*)	144.2(4)
	—O(2*b*)	117.6(4)
	—O(3*b*)	64.9(4)
	—O(5)	144.7(4)
O(7*c*)—	—O(2*b*)	93.9(4)
	—O(3*b*)	122.3(4)
O(2*b*)—	—O(5)	84.4(4)
	—O(3*b*)	64.1(4)
	—O(5)	82.3(4)
O(3*b*)—	—O(5)	136.7(4)
O(1*c*)—Pb(2)—	O(2)	78.4(4)
	—O(3)	130.2(4)
	—O(5)	79.3(4)
	—O(7)	146.2(4)
	—O(4*a*)	69.9(4)
	—O(5)	68.1(4)
O(2)—	—O(3)	69.1(4)
	—O(6)	84.6(4)
	—O(7)	83.2(4)
	—O(4*a*)	147.4(4)
	—O(5)	80.4(4)
O(3)—	—O(6)	131.4(4)
	—O(7)	66.1(4)
	—O(4*a*)	127.4(4)
	—O(5)	70.1(4)
O(6)—	—O(7)	70.8(4)
	—O(4*a*)	96.8(4)
	—O(5)	146.2(4)
O(7)—	—O(4*a*)	128.2(4)
	—O(5)	136.2(4)
O(4*a*)—	—O(5)	56.3(4)

cations lie in layers approximately parallel to $(10\bar{1})$. Pb(1) is surrounded by 8 oxygen atoms at distances of 2.40 to 2.96 Å with a mean value of 2.67 Å and Pb(2) is surrounded by 9 oxygens at distances of 2.40 to 3.20 Å with a mean value of 2.76(1) Å. Each Pb(1) polyhedron shares O(1) and O(5) with Pb(2) in its layer and is linked to two other Pb(2) polyhedra in the adjacent layer by O(2) and O(7) and by O(3) and O(6). Adjacent Pb(1) atoms in the layer share O(2) atoms whereas Pb(1) atoms in different layers share O(5).

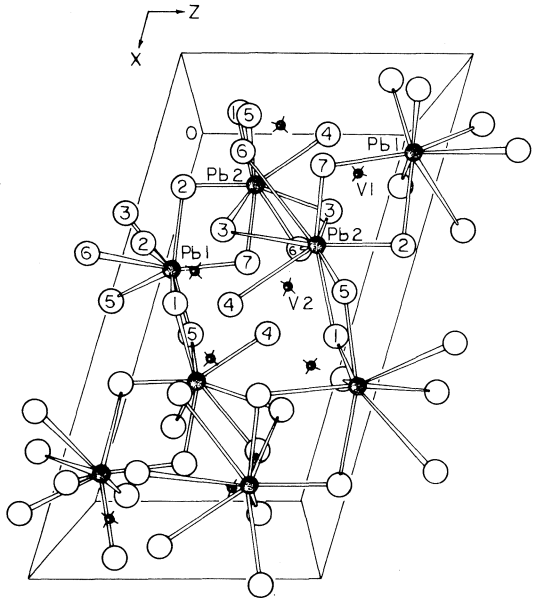

FIG. 1. An *ac* projection of $Pb_2V_2O_7$ showing only Pb—O bonds.

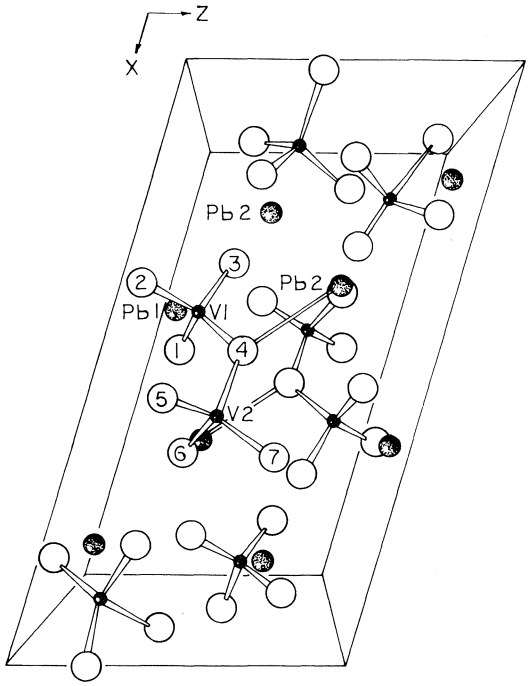

FIG. 2. An *ac* projection of $Pb_2V_2O_7$ showing the configuration of the pyrovanadate ion and the Pb—O bond to the bridging oxygen.

TABLE 4. Comparison of Pb—O distances and angles in PbO with the four shortest distances in $Pb_2V_2O_7$

	Bond	Distance (Å)	Bonds	Angle (deg)
PbO	Pb—O(1)	2.214	O(1)—Pb—(O)2	90.4
	Pb—O(2)	2.223	O(3)—Pb—(O)3′	147.5
	2(Pb—O3)	2.987	O(1)—Pb—(O)3 × 2	79.8
			O(2)—Pb—(O)3 × 2	79.0
$Pb_2V_2O_7$	Pb(1)—O(1)	2.402	O(1)—Pb(1)—O(5)	73.5
	Pb(1)—O(5)	2.473	O(1)— —O(5*b*)	97.4
	Pb(1)—O(7)	2.532	O(1)— —O(7)	85.5
	Pb(1)—O(5*b*)	2.559	O(5)— —O(5*b*)	72.7
			O(5)— —O(7)	84.4
			O(7)— —O(5*b*)	154.9
	Pb(2)—O(2)	2.403	O(1*c*)—Pb(2)—O(2)	78.4
	—O(1)	2.586	—O(5)	68.1
	O(7)	2.597	O(7)	146.5
	O(5)	2.627	O(2)—Pb(2)—O(5)	80.4
			—O(7)	83.2
			O(5)— —O(7)	136.2

TABLE 5. Comparison of observed and predicted V—O distances $Pb_2V_2O_7$ and β-$Sr_2V_2O_7$

Compound	Bond	p_0	Δp	d_{obs}	d_{pred}*	Δd
$Pb_2V_2O_7$	V(1)—O(1)	1.72	−0.37	1.707	1.66	−0.05
	O(2)	1.97	−0.12	1.698	1.70	+0.00
	O(3)	1.94	−0.15	1.665	1.70	+0.03
	O(4)	2.72	+0.63	1.813	1.82	+0.01
	Mean	2.09		1.721		
	V(2)—O(4)	2.72	+0.63	1.821	1.82	+0.00
	O(5)	1.97	−0.12	1.718	1.70	−0.02
	O(6)	1.94	−0.15	1.668	1.70	+0.03
	O(7)	1.72	−0.37	1.699	1.66	−0.04
	Mean	2.09		1.726		
β-$Sr_2V_2O_7$	V(1)—O(1)	1.94	−0.15	1.72	1.70	−0.02
	O(2)	1.97	−0.12	1.70	1.70	0.00
	O(3)	1.72	−0.37	1.63	1.66	+0.03
	O(4)	2.75	+0.66	1.80	1.82	+0.02
	Mean	2.09				
	V(2)—O(4)	2.75	+0.67	1.82	1.82	0.00
	O(5)	1.69	−0.39	1.67	1.66	−0.01
	O(6)	1.94	−0.14	1.76	1.70	−0.06
	O(7)	1.94	−0.14	1.65	1.70	+0.05
	Mean	2.08				
	V(3)—O(8)	1.72	−0.37	1.69	1.66	−0.03
	O(9)	1.97	−0.12	1.70	1.70	0.00
	O(10)	1.97	−0.12	1.71	1.70	−0.01
	O(11)	2.72	+0.63	1.80	1.82	+0.02
	Mean	2.09				
	V(4)—O(11)	2.72	+0.63	1.81	1.82	+0.01
	O(12)	1.97	−0.12	1.67	1.70	+0.03
	O(13)	1.94	−0.15	1.77	1.70	−0.07
	O(14)	1.72	−0.37	1.69	1.66	−0.02
	Mean	2.09				

*$d_{pred} = 1.721 + 0.1602\ (\Delta p_0)$.

Can. J. Chem. Downloaded from www.nrcresearchpress.com by 210.87.254.5 on 09/05/12
For personal use only.

Can. J. Chem. Downloaded from www.nrcresearchpress.com by 210.87.254.5 on 09/05/12
For personal use only.

There is a weak link between adjacent Pb(2) atoms in the layer via O(3) at 3.12 Å and O(6) at 3.20 Å.

A comparison of the cation environments in β-$Sr_2V_2O_7$ (12) and $Pb_2V_2O_7$ reflects the formation of four strong Pb—O and four weaker bonds about both Pb(1) and Pb(2). In β-$Sr_2V_2O_7$, Sr(1) and Sr(9) which are bonded to pyrovanadate bridging oxygens and thus correspond to Pb(2) in $Pb_2V_2O_7$, have 8 or 9 oxygen neighbors at distances of 2.53–3.04 Å, respectively. Thus Sr(1) and Sr(4) have a smaller range of distances than Pb(2). Furthermore, in spite of the fact that the ionic radius (13) of Sr^{2+} (1.25 Å) is smaller than that of Pb^{2+} (1.29 Å), Sr(1) and Sr(4) have larger minimum contact distances. This tendency to form directional bonds is of course most pronounced in PbO (14, 15) where Pb^{2+} is at the apex of a square pyramid with oxygen atoms at the corners of the base. A comparison of the four smallest Pb—O bond distances and the pertinent O—Pb—O angles in PbO and $Pb_2V_2O_7$ in Table 4 shows that some degree of Pb—O covalent bonding is probably present in $Pb_2V_2O_7$. In both compounds the shorter Pb—O bond lengths all lie on one side of the ion. Pb(2), however, shows an additional short interaction to O(6) which has distorted the angles somewhat.

The pyrovanadate ion has an approximately eclipsed configuration typical of the alkali dichromate structures (2). The average angle of twist from the V1–V2 axis is 11 ± 5°. The geometry of the $V_2O_7^{4-}$ ion is almost identical to the pyrovanadate ion in β-$Sr_2V_2O_7$. Figure 3 shows a comparison of the pyrovanadate ion in $Pb_2V_2O_7$ with the two corresponding groups in β-$Sr_2V_2O_7$. Table 5 compares the observed V—O distances with those calculated according to Baur's scheme (16) assuming a CN of 8 for Pb(1), Sr(1), and Sr(3) and 9 for Pb(2), Sr(2), and Sr(4) but using $d(V—O) = 1.721 + 0.1602(\Delta p_0)$ (17, 18). The agreement is not satisfactory and, as in the case of $Cu_3V_2O_8$ (19) is a consequence of the distorted nature of the M—O polyhedron. Figure 3*A* shows that longer V—O distances are associated with more and shorter M—O bonds (M = Sr or Pb) and conversely shorter V—O distances are associated with fewer and long M—O bonds. For example d(V(1)–O(2)) > d(V(1)–O(3)) because the sum of the Pb—O(2) distances is less than the sum of the Pb—O(3) distances. These principles have been systematized by Brown and Shannon (20) for the

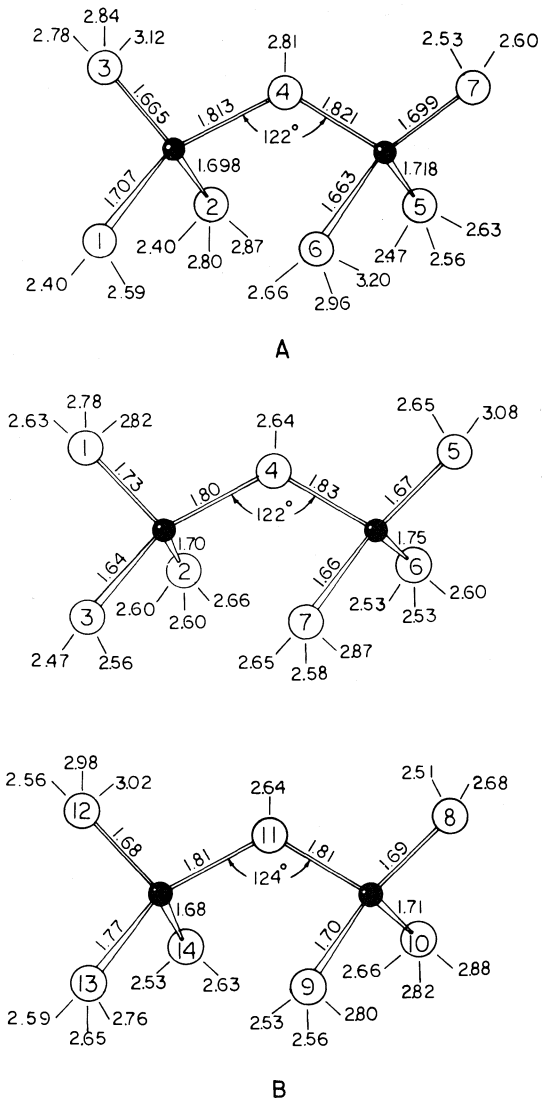

FIG. 3. The pyrovanadate ions in (*A*) $Pb_2V_2O_7$ and (*B*) β-$Sr_2V_2O_7$, showing V—O bonds and distances of neighboring Pb or Sr ions from the oxygen ions.

first three rows of the periodic table. Although a Sr—O bond strength – bond length curve is not available and the e.s.d.'s on the V—O bonds in β-$Sr_2V_2O_7$ are quite large (0.03 Å), it is possible using just qualitative bond strength considerations mentioned above for $Pb_2V_2O_7$ to make some estimates of the validity of the distances assuming the Sr—O distances are not in error by more than 0.03 Å. Most of V—O bonds are consistent with the number and distances of Sr neighbors but several deviate; thus, the following relationships should hold:

V(1)—O(1) < V(1)—O(2)
V(1)—O(1) < V(2)—O(9)
V(1)—O(2) > V(2)—O(10)
V(1)—O(2) > V(2)—O(13)
$\Big\}$ $d_{pred} = 1.70$[3]

V(1)—O(3) > V(1)—O(5)
V(1)—O(3) > V(2)—O(8)
V(1)—O(3) > V(2)—O(14)
$\Big\}$ $d_{pred} = 1.66$[3]

V(1)—O(6) > V(2)—O(13) $d_{pred} = 1.70$[3]

Several of these deviations are as large as 0.04–0.07 Å. It should be noted that all of these pairs according to Baur's predictions based on average coordination number of Sr should be equal. A more accurate structure refinement of β-$Sr_2V_2O_7$ will be necessary to resolve these inconsistencies.

The mean V—O distances within the two tetrahedra are 1.721 and 1.726 Å and agree well with the grand mean value of 1.721 ± 0.012 Å determined from 22 accurately refined vanadate structures (18). The effective ionic radius of V^{5+} in $Pb_2V_2O_7$, obtained by subtracting the appropriate oxygen radius (5) (0.351) is intermediate between that in $Cu_3V_2O_8$ (0.365) (19) or $Cu_5V_2O_{10}$ (0.364) (21) and Li_3VO_4 (0.337) (18), $Na_3VO_4 \cdot 12H_2O$ (0.321) (22), Ca_2VO_4Cl (0.327) (23), and $Ca_3V_2O_8$ (0.335) (24). This behavior, discussed in more detail in refs. 5 and 18, is associated with the bond strength (as determined by electronegativity or electrostatic bond strength criteria) of the M—O bonds where M = Cu^{2+}, Pb^{2+}, Li^+, Na^+, or Ca^{2+}. Stronger bonds such as Cu^{2+}—O and Pb^{2+} result in longer average V^{5+}—O bonds than weaker bonds such as Li^+—O, Na^+—O, or Ca^{2+}—O.

[3] $d_{pred} = 1.721 + 0.1602(\Delta p_0)$.

We would like to thank Mrs. S. Leung for preparing the crystals of $Pb_2V_2O_7$, R. Faggiani for assistance with intensity measurements, and Dr. J. F. Whitney and Mrs. C. F. Foris of the Central Research Laboratory, E. I. duPont de Nemours and Co. for the Guinier photographs. This research was supported by the National Research Council of Canada.

1. A. Kawahara. Bull. Soc. Fr. Mineral. Crystallogr. **90**, 279 (1967).
2. I. D. Brown and C. Calvo. J. Solid State Chem. **1**, 173 (1970).
3. W. Noll, Angew. Chem. Int. Educ. **2**, 73 (1963).
4. G. E. Brown and G. V. Gibbs. Am. Min. **55**, 1587 (1970).
5. R. D. Shannon. Chem. Commun. 881 (1971).
6. D. B. Rogers, R. D. Shannon, A. W. Sleight, and J. L. Gillson. Inorg. Chem. **8**, 841 (1969).
7. W. H. Zachariasen. Acta Cryst. **16**, 1139 (1963).
8. J. S. Stephens. Unpublished results.
9. A. C. Larson. Acta Cryst. **23**, 664 (1967).
10. D. T. Cromer and J. T. Waber. Acta Cryst. **18**, 104 (1965).
11. D. T. Cromer. Acta Cryst. **18**, 17 (1965).
12. J. A. Baglio and J. N. Dann. J. Solid State Chem. **4**, 87 (1972).
13. R. D. Shannon and C. T. Prewitt. Acta Cryst. **B25**, 725 (1969).
14. M. I. Kay. Acta Cryst. **14**, 80 (1961).
15. B. Dickens. J. Inorg. Nucl. Chem. **27**, 1495 (1965).
16. W. Baur. Trans. Am. Cryst. Assoc. **6**, 129 (1970); Am. Min. **56**, 1573 (1971).
17. R. Gopal. Ph.D. Thesis. McMaster University, Hamilton, Ontario. 1972.
18. R. D. Shannon and C. Calvo. J. Solid State Chem. To be published.
19. R. D. Shannon and C. Calvo. To be published.
20. I. D. Brown and R. D. Shannon. To be published.
21. R. D. Shannon and C. Calvo. To be published.
22. E. Tillmanns and W. H. Baur. Acta Cryst. **B27**, 2124 (1970).
23. E. Banks, M. Greenblatt, and B. Post. Inorg. Chem. **9**, 2259 (1970).
24. R. Gopal and C. Calvo. Z. Krist. To be published.

Can. J. Chem. Downloaded from www.nrcresearchpress.com by 210.87.254.5 on 09/05/12
For personal use only.

Rearrangements in the Diterpenoid Series. I. The Solvolysis of Methyl 15β-tosyloxy-13-isopropyl-17-noratis-13-en-18-oate

WILLIAM A. AYER AND PANDURANG D. DESHPANDE[1]

Chemistry Department, University of Alberta, Edmonton, Alberta

Received July 5, 1972

The synthesis of methyl 15β-hydroxy-13-isopropyl-17-noratis-13-en-18-oate (**14***b*) is described. Compound **14***b* was prepared from the ketone **12***b*, in turn derived from the Diels–Alder adduct formed between levopimaric acid (**7**) and α-acetoxyacrylonitrile. Solvolysis of the tosylate of **14***b* proceeds predominantly with rearrangement and elimination to give methyl 16-isopropylidene-7,17-secoacon-8(15)-en-18-oate (**16***a*). This rearrangement serves as a model for the proposed biosynthetic transformation of atisine-type alkaloids into alkaloids of the aconitine series. The degradation of **16***a* into the unsaturated ketone **19**, which contains the 19 carbons of the aconane skeleton, is described. The Diels–Alder addition of methyl vinyl ketone to levopimaric acid is reported and the adduct is shown to possess structure **8**.

La synthèse du β-hydroxy-15 isopropyl-13 nor-17 atisène-13 oate-18 de méthyle (**14***b*) est décrite. Le composé **14***b* a été préparé à partir de la cétone **12***b*, qui dérive à son tour de l'adduit entre l'acide levopimarique (**7**) et l'α-acétoxyacrylonitrile, selon une réaction de Diels–Alder. La solvolyse du tosylate de **14***b* procède de façon prédominante par réarrangement et élimination pour conduire à l'isopropylidène-16 secoacon-7,17 ène-8(15) oate-18 de méthyle (**16***a*). Ce réarrangement sert de modèle pour la transformation biosynthétique proposée pour les alcaloides de type atisine en alcaloides de la série aconitine. La dégradation de **16***a* en cétone insaturée **19**, qui contient les 19 carbones du squelette aconane, est donnée. L'addition, selon Diels–Alder, de la méthylvinylcétone sur l'acide lévopimarique est rapportée; l'adduit résultant possède la structure **8**. [Traduit par le journal]

Can. J. Chem., **51**, 77 (1973)

Can. J. Chem. Downloaded from www.nrcresearchpress.com by 210.87.254.42 on 09/05/12
For personal use only.

In 1956 the simple relationship between the atisane (**1**)[2] and the 7,17-secoaconane (**2**) skeleton was noted (1, 2). At that time it was pointed out

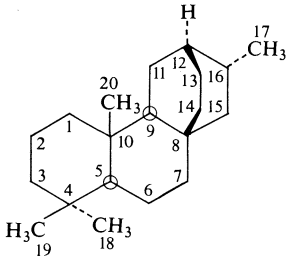

1

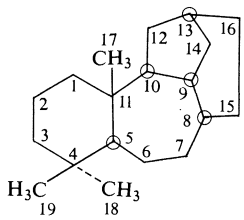

2

that rearrangement (Scheme 1) (1) of an atisine-type intermediate **3**, coupled with demethylation (loss of C-17, atisane numbering), would lead to an intermediate **4** which on closure of the C_7—C_{17} (aconane numbering) bond would furnish the lycoctonine–aconitine skeleton **5**. Since it appeared that compounds of the type **6***a*, where X is a suitable leaving group, would be readily available by Diels–Alder addition of the appropriate dienophile (3) to levopimaric acid (**7**, R = H), we decided to investigate the solvolytic reactions of compounds of type **6***a* as a model for the atisine–aconitine skeletal rearrangement. Attempts to execute this rearrangement on derivatives of atisine itself have met with limited success. Pelletier and Ichihara (4) observed only migration of the C-13,14 bridge on solvolysis of appropriate derivatives, whereas Johnston and Overton (5) observed both this migration (solvolytic conditions) and the desired rearrangement (pyrolytic conditions). This paper describes the preparation and rearrangement of the tosylate **6***b*. A later paper will describe the preparation and deamination of the amine **6***c*.

The simplest route to compounds of type **6***a* with an oxygen function at C-15 appeared to be the Diels–Alder addition of vinyl acetate to levopimaric acid. We were, however, unable to effect this addition. Addition of methyl vinyl ketone to levopimaric acid proceeded smoothly in refluxing benzene to give the keto acid **8**

[1]Taken in part from the Ph.D. thesis of P. D. Deshpande, University of Alberta, Edmonton, Alberta, 1967.

[2]Nomenclature is based on "The Common and Systematic Nomenclature of Cyclic Diterpenes", third revision with addenda and corrigenda, February 1969, available from Dr. J. W. Rowe, U.S. Forest Products Laboratory, Madison, Wisconsin 43705.

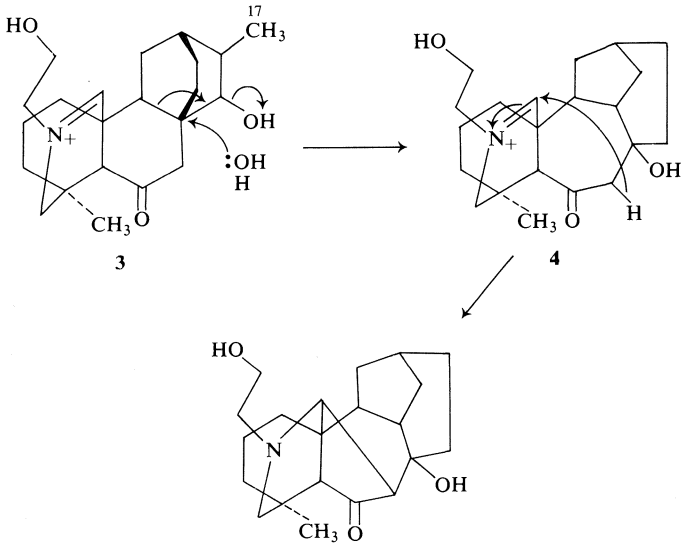

SCHEME I

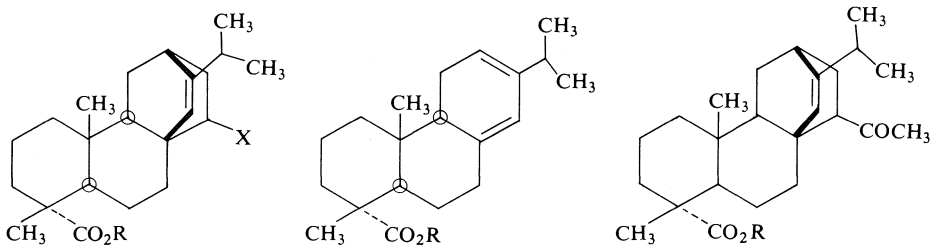

a
b R = CH_3; X = OTs
c R = CH_3; X = NH_2

(R = H), isolated as its cyclohexylamine salt in 70% yield. Decomposition of the salt with dilute phosphoric acid gave the crystalline acid **8** (R = H) which on treatment with diazomethane gave the keto ester **8** (R = CH_3). The i.r. and n.m.r. spectra of the acid and its ester are consistent with the assigned structure. In particular, the chemical shift of the C-10 methyl group (τ 9.38) indicates (6) that addition has occurred from the α-face and the unusually high chemical shift of the acetyl methyl (τ 8.07) is indicative of its *endo* orientation, in which the methyl protons are shielded by the C_{13}—C_{14} double bond. By analogy with the reaction of other monosubstituted dienophiles with levopimaric acid (3) it was expected that addition would occur in such a way as to give the 15-acetyl compound **8** rather than the 16-acetyl compound. In order to confirm the position and orientation of the acetyl group the adduct was treated with sodium hypobromite. After the crude product of this reaction was esterified with diazomethane and subjected to chromatography over alumina the isopropylidene lactone **9** of known constitution (3, 7, 8) was obtained in 11% yield, establishing that the acetyl group is located at C-15 and supporting the *endo* assignment of configuration.

Alkyl methyl ketones when subjected to Baeyer–Villiger oxidation usually afford alkyl acetates of retained configuration (9). Ordinarily a carbon–carbon double bond is more reactive than a ketone towards peracids. In this case approach

Can. J. Chem. Downloaded from www.nrcresearchpress.com by 210.87.254.42 on 09/05/12
For personal use only.

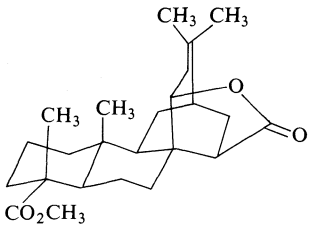

9

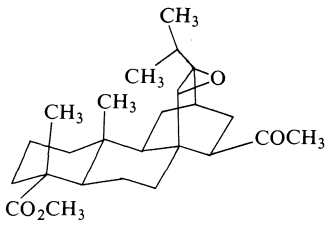

10

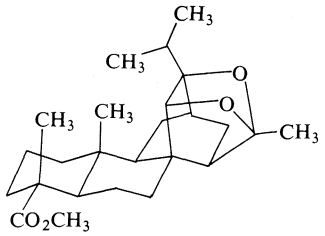

11

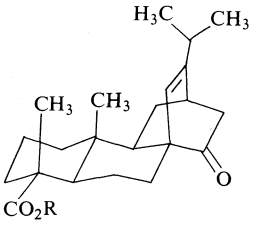

12

a R=H
b R=CH_3

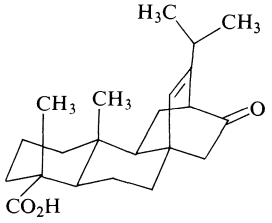

13

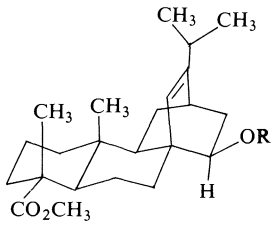

14

a R=Ac
b R=H
c R=Ts

to the double bond is hindered (10) and it was hoped that a selective reaction could be induced at the ketonic carbonyl of the ester **8** (R = CH_3). However, treatment of ester **8** (R = CH_3) with either *m*-chloroperbenzoic acid in benzene or monoperphthalic acid in ether gave the epoxide **10**. None of the desired Baeyer–Villiger product could be detected. The i.r. spectrum of **10** showed ketonic carbonyl absorption at 1700 cm^{-1} and the n.m.r. spectrum showed a one-proton singlet at τ 6.90 attributable to the proton on C-14, as well as a three-proton singlet at τ 7.98 due to the acetyl methyl. The remaining features on the n.m.r. spectrum were similar to those reported (10, 11) for the epoxide of methyl maleopimarate. The epoxide **10** was obtained as an amorphous solid which could not be isolated in pure form. The material crystallized after contact with chloroform, but the properties of the crystalline material were markedly different from those of the crude epoxide **10**. The crystalline material proved to be a compound $C_{25}H_{38}O_4$, isomeric with the epoxide **10**, to which we tentatively assign the ketal structure **11**. The i.r. spectrum of the crystalline material shows a single band in the carbonyl region at 1720 cm^{-1} attributable to the carbomethoxyl group. In the n.m.r. spectrum of **11** there is no signal in the τ 7.8–8.1 region due to an acetyl group but there is a signal (3H) at τ 8.50 due to the methyl attached to the ketal carbon.[3] The signal which appears at τ 6.90 in the spectrum of **10** is replaced by a singlet at τ 5.73 in the spectrum of **11**, a shift which is as expected for the change from an oxirane proton to an α-proton of a tetrahydrofuran system (12).

The epoxide oxygen in **10** is ideally situated for acid-catalyzed ketal formation with the carbonyl group (Scheme 2), a reaction for which there are numerous precedents (13). Examination of models indicates that the non-bonded interaction between the C-13 isopropyl and the C-10 methyl is, at least in part, relieved in the transformation of **10** into **11**. This may help to explain the facility with which this reaction occurs and the fact that the ketal **11** is recovered unchanged from attempted acid hydrolysis.

The desired alcohol **6***a* (X = OH) was obtained

[3]The methyl attached to the acetal carbon of acetaldehyde diethyl acetal appears at τ 8.68 (23).

Can. J. Chem. Downloaded from www.nrcresearchpress.com by 210.87.254.42 on 09/05/12
For personal use only.

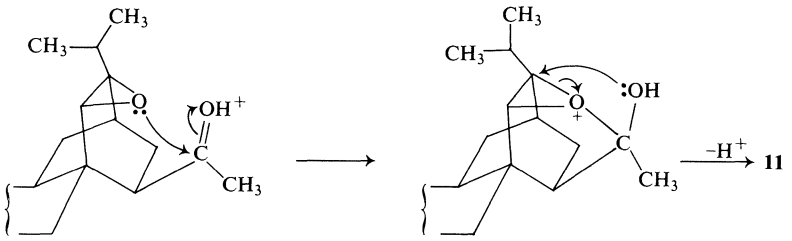

SCHEME 2

in the following manner. Addition of α-acetoxyacrylonitrile to levopimaric acid (**7**, R = H) was effected in refluxing toluene. The reaction mixture was extracted with dilute alkali. The crude acidic product thus obtained did not show nitrile absorption in the i.r., but did show intense absorption in the carbonyl region as well as a band at 1410 cm^{-1} (scissoring vibration of an active methylene) suggestive of a ketone. It was inferred that the Diels–Alder reaction had taken place and that the acetoxycyano compound(s) thus formed had been hydrolyzed to the ketone(s) **12***a* and/or **13** during the work-up. Isolation of the ketoacid **12***a*, obtained in 35% yield, was facilitated by the use of Girard's T reagent. Further quantities of **12***a* were obtained by alkaline hydrolysis of the neutral portion of the addition product which apparently contained the mixed anhydride of the desired acid and acetic acid. The i.r., n.m.r., and mass spectra of the acid **12***a* and its methyl ester **12***b* were consistent (see Experimental) with the assigned structure. In particular, the signal for the C-10 methyl group appeared at high field (τ 9.25) indicating α-addition (see above), and the base peak in the mass spectrum of the methyl ester **12***b* appeared at $M^+ - 42$ (loss of ketene via retro-Diels–Alder). These spectra however did not serve to distinguish **12***a* from **13**. This distinction may be made on the basis of optical rotatory dispersion measurements (14). A strongly positive Cotton effect is predicted (14) for **12***a* and a strongly negative Cotton effect is predicted for **13**. The ketoacid shows a strongly positive Cotton effect ($a = +523$) indicating that it has structure **12***a*.

The ketoacid **12***a* was reduced with sodium borohydride in dimethoxyethane. The crude product was esterified with diazomethane and then acetylated to give a mixture of acetoxyesters **14***a* and **15***a*. The n.m.r. spectrum of the mixture shows signals at τ 8.08 and 7.94 (ratio about 3:4) attributable to the C-15 acetoxyl groups. Since it seemed reasonable to assign the signal at τ 8.08 to the *endo* acetoxy compound **14***a* (acetoxyl methyl shielded by the C_{13}—C_{14} double bond) it appeared that the desired alcohol **14***b* was the minor product of the borohydride reduction. Reduction with lithium–ammonia–methanol, which should favor the production of the thermodynamically more stable alcohol, gave the same two alcohols in a ratio of about 4:3, this time the *endo* alcohol **14***b* predominating. Attempts to separate the mixture of alcohols **14***b* and **15***b* met with limited success, however, the corresponding acetyl derivatives **14***a* and **15***a* were readily separable by chromatography over alumina. The *exo* acetoxy compound **15***a* was eluted first. The n.m.r. spectrum showed the acetoxyl methyl signal at τ 7.94 and a doublet ($J = 9$ and 3 Hz) at τ 5.84 for the proton geminal to the acetoxyl group. In the *endo* compound **14***a* this latter signal appeared as a doublet ($J = 8$ and 3 Hz) at τ 5.44, in keeping with the observation (15) that the *endo* proton in a bicyclo[2.2.2]octene system appears at higher field than the corresponding *exo* proton. Hydrolysis (methanolic KOH) of the acetoxy compounds **14***a* and **15***a* gave the alcohols **14***b* and **15***b*, respectively. In support of the assigned structures, alcohol **14***b* shows an intramolecularly hydrogen-bonded (OH to π) hydroxyl absorption in the i.r. (16) whereas **15***b* shows only free hydroxyl absorption.

It has been shown (17) that solvolysis of *endo*-bicyclo[2.2.2]oct-5-en-2-yl *p*-toluenesulfonate gives mainly rearranged bicyclo[3.2.1]octene derivatives. In order to study the solvolysis in this case, the alcohol **14***b*, a readily purified, crystalline solid was transformed to the tosylate **14***c* by treatment with *p*-toluenesulfonyl chloride in pyridine. Tosylate **14***c* was obtained as an amorphous solid which could not be induced to crystallize. The spectroscopic properties (see Experimental) of the product were, however, in complete accord with structure **14***c*. In an attempt

Can. J. Chem. Downloaded from www.nrcresearchpress.com by 210.87.254.42 on 09/05/12
For personal use only.

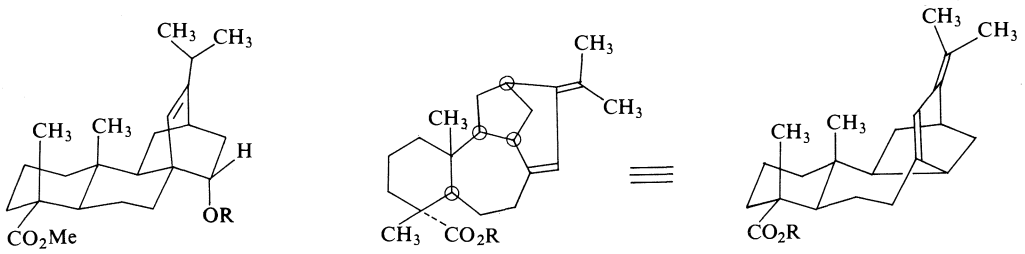

15
a R = Ac
b R = H

16
a R = CH_3
b R = H

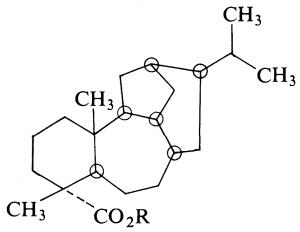

17
a R = CH_3
b R = H

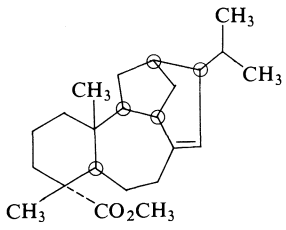

18

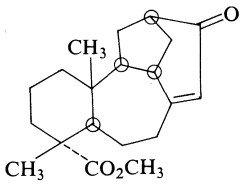

19

Can. J. Chem. Downloaded from www.nrcresearchpress.com by 210.87.254.42 on 09/05/12
For personal use only.

to purify the tosylate the crude product was subjected to chromatography over silica gel. As soon as the colorless benzene solution of the tosylate was transferred to the column the top portion of the adsorbent became deep purple. Elution of the column with benzene gave the diene **16***a* in 70% yield. Further elution gave the alcohol **14***b* in 15–20% yield.

The structure of diene **16***a* is assigned on the following basis. The i.r. spectrum does not show absorption attributable to a tosyloxy group, but does show ester carbonyl (1720 cm^{-1}) and conjugated olefin (1635, 1620) absorption. The conjugated diene system gives rise to an absorption maximum in the u.v. at 258 nm (ε 18 000). The n.m.r. spectrum reveals the presence of only two methyl groups attached to saturated carbon. The signal at τ 9.13 is assigned to the C-11 methyl and that at τ 8.78 to the C-4 methyl. The methyl groups of the isopropylidene group appear at τ 8.28 and 8.34. The olefinic proton gives rise to a singlet at τ 4.15. The ester group at C-4 proved difficult to saponify, however hydrolysis was achieved using potassium *t*-butoxide – dimethylsulfoxide (18) to give the acid **16***b*. The acid, like the ester, was unstable in air and attempted recrystallization led to decomposition.

Catalytic hydrogenation of the ester **16***a* over Adams' catalyst gave the tetrahydro compound **17***a* (stereochemistry at C-8 and -16 assigned on the assumption that the catalyst would approach from the less hindered side). Treatment of **17***a* with potassium *t*-butoxide-dimethylsulfoxide gave the stable, crystalline acid **17***b*. The n.m.r. spectrum shows no olefinic absorption and the methyls of the isopropyl group gave rise to a pair of doublets centered at τ 9.11 and 9.14. When the hydrogenation of **16***a* was carried out for a short time in the presence of palladium–charcoal the dihydro derivative **18** was obtained. The n.m.r. spectrum clearly shows that the double bond of the isopropylidene group has been hydrogenated, since an isopropyl methyl doublet (6H, $J \simeq 6$ Hz) is apparent at τ 9.15 and an olefinic proton signal is evident as a broadened singlet at τ 4.93.

Since it appeared that the tetrasubstituted double bond was more reactive (accessible) than the trisubstituted double bond we decided for two reasons to attempt a selective cleavage of this double bond. Firstly, the spectral properties of the α,β-unsaturated ketone **19** would serve to further confirm the structure of the diene and secondly, the ketone **19** contains the 19 carbon atoms of the aconane skeleton and might

Can. J. Chem. Downloaded from www.nrcresearchpress.com by 210.87.254.42 on 09/05/12
For personal use only.

possibly serve as a useful synthetic intermediate in the construction of compounds related to the aconite alkaloids. Accordingly, the diene **16***a* was treated with a limited amount of ozone in methylene chloride (19) at $-70°$. Chromatography of the neutral portion of the product over silica gel gave the ketone **19** in about 10% yield. The presence of the conjugated keto grouping was indicated by i.r. absorption at 1670 and 1630 cm^{-1} and by u.v. absorption at 243 nm (ε 11 000). The n.m.r. spectrum of **19** shows the presence of only two C-methyl groups (singlets at τ 9.18 (C-10 methyl) and 8.77 (C-4 methyl)). The olefinic proton gives rise to a singlet at τ 4.38. Ketone **19** has also been obtained by the action of nitrous acid on the amine **6***c* (7).

To determine whether the rearrangement of tosylate **14***c* to diene **16***a* is specifically brought about on the surface of silica gel, or whether it is of more general nature, the crude tosylate was subjected to solvolysis in hot acetic acid containing sodium acetate. The product consisted mainly of diene **16***a* and *endo* acetate **14***a* as judged from the n.m.r. spectrum. Chromatography of the solvolysis product over alumina furnished the diene **16***a* in *ca.* 40% yield and **14***a* in *ca.* 12% yield. The n.m.r. spectra of intermediate fractions indicated the presence of minor amounts of at least two other acetates, but these were not isolated in pure form. It thus appears that a carbonium ion, most economically represented as **20**, is formed during the solvolysis and that this reacts further either by elimination of a proton to give the rearranged diene **16***a* (path *a*) or by attack of solvent at C-15 to give the *endo* acetate **14***a* (path *b*) (see Scheme 3).

Attempts to prepare the tosylate of the alcohol **15***b* have so far been unsuccessful. Treatment of **15***b* with *p*-toluenesulfonyl chloride in pyridine results in the formation of a mixture of products free of both hydroxyl and tosyloxyl absorption in the i.r. The products of this reaction have not as yet been identified. It is apparent, however, that the diene **16***a* is not formed, at least to any great extent in this reaction.

The ease with which the desired rearrangement (*i.e.*, **14***c* → **16***a*) occurs in this case contrasts with that observed (4, 5) in the case of derivatives of atisine itself. It appears, not unexpectedly (20), that the presence of the C_{13}—C_{14} unsaturation greatly facilitates the rearrangement. Attempts to hydrogenate the hindered olefinic linkage in **14***b*, and thereafter to compare the reactivity of the saturated with the unsaturated compound, were unsuccessful.

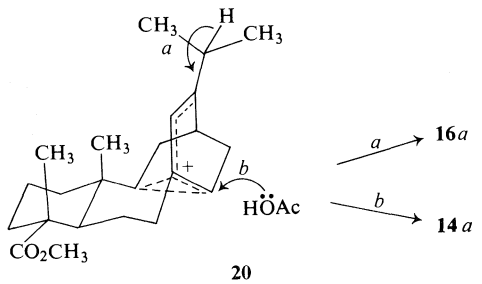

20

SCHEME 3

Experimental Section[4]

*Preparation of 15β-Acetyl-13-isopropyl-17-noratis-13-en-18-oic Acid (**8**, R = H)*

A solution of levopimaric acid (12 g) (21), methyl vinyl ketone (20 ml), and hydroquinone (0.2 g) in benzene (50 ml) was heated on the steam bath for 8 h. Excess methyl vinyl ketone and solvent were removed under reduced pressure, the residue dissolved in benzene (100 ml), washed with water, dried ($MgSO_4$), and concentrated to a white foam (14 g). This was dissolved in cold acetone (100 ml), cyclohexylamine (6 ml) added, and the resulting precipitate filtered and washed with cold acetone to give the cyclohexylamine salt of **8** (R = H) (13 g). The salt was suspended in ether (200 ml) and shaken with 10% phosphoric acid (50 ml). The ether layer was washed with water, dried ($MgSO_4$), and concentrated to a colorless foam (10.5 g) which was crystallized from acetonitrile to give the acid **8** (R = H) (8 g): m.p. 135–136°; i.r. ($CHCl_3$) 3200–2400 (carboxyl OH), 1700 cm^{-1} (C=O of acid and ketone); n.m.r. τ 9.38 (s, 3, C-10 methyl), 8.95 (d, 6, J = 6.5 Hz, isopropyl methyls), 8.86 (s, 3, C-4 methyl), 8.07 (s, 3, acetyl methyl), 4.58 (s, 1, H-14), −0.75 (s, 1, COOH).

Anal. Calcd. for $C_{24}H_{36}O$ (mol. wt. 372.2665): C, 77.38; H, 9.74. Found (372.2669 (h.r.m.s.)): C, 77.30, 77.09; H, 9.75, 9.84.

Treatment of the acid with ethereal diazomethane gave the oily methyl ester **8** (R = CH_3), which was purified by evaporative distillation: i.r. 1730 (ester), 1700 cm^{-1} (ketone); n.m.r. τ 9.40 (s, 3, C-10 methyl), 8.95 (d, 6,

[4]Melting points were determined on a hot-stage and are uncorrected. Unless otherwise stated i.r. spectra were determined in carbon tetrachloride, u.v. spectra in 95% ethanol, and n.m.r. spectra in deuteriochloroform with tetramethylsilane as internal standard. Mass spectra were determined on an A.E.I. MS-2H or A.E.I. MS-9 mass spectrometer. High resolution measurements (h.r.m.s.) were performed on the latter instrument. Alumina, unless otherwise specified, means basic alumina of activity II–III (Brockmann scale). Skellysolve B refers to Skelly Oil Company light petroleum, b.p. 62–70°. Microanalyses were performed by G. Gygli, Toronto, Ontario, and D. Mahlow of this Department.

Can. J. Chem. Downloaded from www.nrcresearchpress.com by 210.87.254.42 on 09/05/12
For personal use only.

J = 6.5 Hz), 8.87 (s, 3, C-4 methyl), 8.08 (s, 3, acetyl methyl), 6.36 (s, 3, methoxyl), 4.55 (s, 1, H-14); mass spectrum (70 eV) *m/e* (relative intensity) 386 (3), 316 (39), 301 (38), 43 (100).

Treatment of **8** *(R = H) with Sodium Hypobromite*

The adduct **8** (R = H) (157 mg) was added in small portions to an ice-cold stirred solution of bromine (0.36 g) and sodium hydroxide (1.86 g) in water (8 ml). The solution was kept at room temperature overnight then excess bromine destroyed with sodium sulfite. The solution was acidified (concentrated HCl) and extracted with chloroform to give an amorphous material (0.16 g) which was treated with ethereal diazomethane. A portion (0.14 g) of the product was chromatographed over neutral alumina (7 g, activity II). Elution with benzene (90 ml) gave 58 mg of unidentified material. Further elution with benzene (90 ml) gave the lactone **9** (15 mg), m.p. 191–192° (lit. (8) m.p. 196–197°), identical with a sample prepared by methylation of the corresponding acid (3). Elution with benzene–ether gave further crystalline material which has not been identified.

Peracid Oxidation of Ester **8** *(R = CH_3)*

(a) With m-Chloroperbenzoic Acid

A solution of the ketoester **8** (R = CH_3) (105 mg) and *m*-chloroperbenzoic acid (69 mg) in benzene (15 ml) was kept at room temperature for 12 days (t.l.c. at this point indicated complete disappearance of starting material). The reaction mixture was diluted with ether and washed with dilute sodium sulfite and then dilute sodium bicarbonate, dried ($MgSO_4$), and concentrated to an amorphous solid (95 mg), believed on the basis of the following spectroscopic data to consist mainly of the expoxide **10**: i.r. 1735 (ester), 1700 cm^{-1} (ketone); n.m.r. τ 9.28 (d, 3, J = 7 Hz, nonequivalent methyl of isopropyl), 9.19 (s, 3, C-10 methyl), 8.94 (d, 3, J = 7 Hz, nonequivalent methyl of isopropyl), 8.85 (s, 3, C-4 methyl), 7.98 (s, 3, acetyl methyl), 6.9 (br.s, 1, H-14), 6.37 (s, 3, methoxyl). The solution used to measure the n.m.r. spectrum was concentrated to a glassy solid which slowly solidified. Trituration with Skellysolve B left the ketal **11**, m.p. 149–150°: i.r. ($CHCl_3$) 1720 cm^{-1} (ester); n.m.r. τ 9.06 (d, 6, J = 7 Hz, isopropyl methyls), 9.04 (s, 3, C-10 methyl), 8.84 (s, 3, C-4 methyl), 8.50 (s, 3, ketal methyl), 6.37 (s, 3, methoxyl), 5.90 (br. s, 1, H-14); mass spectrum (70 eV *m/e* (relative intensity) 402 (69), 387 (20), 359 (61), 343 (59), 342 (54), 331 (45), 317 (76), 316 (69), 43 (100).

Mol. Wt. Calcd. for $C_{25}H_{38}O_4$: 402.2770. Found: 402.2767.

Ketal **11** in aqueous acetone was heated under reflux for 6 h in the presence of *p*-toluenesulfonic acid. Work-up in the usual manner gave unchanged ketal **11** as indicated by i.r. spectroscopy.

(b) With Monoperphthalic Acid

A solution of ketoester **8** (R = CH_3) (0.41 g) in ether (10 ml) was added to an ice-cold solution of monoperphthalic acid (0.8 g) in ether (20 ml) and the resulting solution kept at 0–5° for 3 weeks. The solution was then washed with dilute sodium sulfite, dilute sodium bicarbonate, dried ($MgSO_4$), and concentrated. The product thus obtained possessed spectral properties (i.r. and n.m.r.) identical with those displayed by the product obtained when *m*-chloroperbenzoic acid was used.

*Preparation of 13-Isopropyl-15-oxo-17-noratis-13-en-18-oic Acid (***12***a)*

A solution of levopimaric acid (2.5 g), α-acetoxyacrylonitrile (5 g, (22)), and hydroquinone (0.14 g) in toluene was heated under reflux for 8 h, then kept overnight at room temperature. Ether (100 ml) was added and the solution washed several times with water to remove hydroquinone. The organic layer was then extracted with aqueous sodium hydroxide (5%, 3 × 50 ml), washed with water, dried ($MgSO_4$), and concentrated to give neutral material (0.44 g), which showed i.r. absorption at 1800 and 1750 cm^{-1}.

The alkaline extract was acidified with concentrated HCl and extracted with ether to give 2.68 g of acidic material. This was combined with a further 1.1 g from another experiment and crystallized from acetonitrile to give keto acid **12***a* (1.25 g), m.p. 195–196°: i.r. ($CHCl_3$) 3200–2400, 1700–1715 (carbonyl of carboxyl and ketone), 1410 cm^{-1} (active methylene); n.m.r. τ 9.25 (s, 3, C-10 methyl), 8.97 (d, 6, J = 6.5 Hz, isopropyl methyls), 8.83 (s, 3, C-4 methyl), 4.72 (s, 1, H-14), −1.3 (s, 1, COO*H*); r.d. in methanol (*c*, 0.038): $[\alpha]_{500}$ +210, $[\alpha]_{400}$ +525, $[\alpha]_{319}$ +7350 (peak), $[\alpha]_{279}$ −7900° (trough).

Anal. Calcd. for $C_{22}H_{32}O_3$: C, 76.70; H, 9.38. Found: C, 76.58; H, 8.92.

Further keto acid **12***a* was obtained in the following manner. The acetonitrile mother liquors from several preparations were combined and concentrated. A solution of the noncrystalline residue (4.7 g) and Girard T reagent (2.35 g) in ethanol (45 ml) containing acetic acid (5 ml) was heated on the steam bath for 2 h. The cooled solution was then added to a mixture of ether (225 ml) and water (225 ml) containing sodium chloride (10 ml of saturated solution). The aqueous layer was separated, concentrated HCl (11 ml) added, and the solution heated on the steam bath for 45 min. The cooled solution was extracted with ether to give a colorless foam (1.68 g), which on crystallization from acetonitrile gave ketoacid **12***a* (1.1 g). The neutral material (0.44 g) obtained from the Diels–Alder reaction was heated under reflux with 10% methanolic sodium hydroxide (30 ml) for 3 h. Work-up in the usual way gave a colorless foam (0.35 g) which on crystallization from acetonitrile gave ketoacid **12***a* (0.2 g), m.p. 192–194°.

Esterification of **12***a* with ethereal diazomethane gave the methyl ester **12***b*, m.p. 83–84° (from Skellysolve B): i.r. ($CHCl_3$) 1720 (ester and ketone), 1415 cm^{-1} (active methylene); mass spectrum (70 eV) *m/e* (relative intensity) 358 (25), 316 (100), 299 (28), 239 (25), 146 (55), 134 (30), 133 (33), 121 (40), 105 (27), 101 (30).

Mol. Wt. Calcd. for $C_{23}H_{34}O_3$: 358.2508. Found (h.r.m.s.): 358.2511.

Reduction of Ketoacid **12***a*

(a) With Sodium Borohydride

Sodium borohydride (55 mg) was added to a solution of ketoacid **12***a* (110 mg) in dimethoxyethane (20 ml) and the resulting solution was stirred at room temperature for 5 h, then more sodium borohydride (55 mg) was added, and stirring continued overnight. The solution was concentrated, diluted with water, and acidified with phosphoric acid. Extraction with ether gave an amorphous solid (105 mg) which consisted mainly of two components as determined by t.l.c. The mixture was esterified (diazomethane) and acetylated (acetic anhy-

Can. J. Chem. Downloaded from www.nrcresearchpress.com by 210.87.254.42 on 09/05/12
For personal use only.

dride – pyridine). The ratio of *endo*-acetate **14***a* to *exo*-acetate **15***a*, as determined from the relative intensities of the signals at τ 8.08 and 7.94 in the n.m.r. was 3:4. The separation and characterization of the components is described below.

(b) With Lithium–Ammonia–Methanol

A solution of ketoacid **12***a* (1.0 g) in ether (25 ml) was added to liquid ammonia (100 ml) containing methanol (15 ml). Lithium (1.5 g) was added in small portions, with stirring, over 70 min. More methanol (5 ml) was then added and the stirring continued for 40 min, then ammonium chloride (15 g) was added and the ammonia was allowed to evaporate. The residue was diluted with water, acidified with phosphoric acid, and extracted with chloroform. The crude product (1.0 g) was esterified and acetylated as in section *a*. N.m.r. analysis indicated that **14***a* and **15***a* were present in a ratio of 4:3.

*Isolation of **14**a and **15**a*

The mixture of acetates **14***a* and **15***a* obtained above (1.1 g) was chromatographed over alumina (55 g). Elution with Skellysolve B (400 ml) gave unidentified material (25 mg). Elution with Skellysolve B – benzene (1.2 l of 1:1) gave the oily *exo*-acetate **15***a* (0.36 g) which was purified by evaporative distillation (125°/0.05 mm): i.r. ($CHCl_3$) 1720 (ester carbonyls), 1650 (w, C=C); n.m.r. τ 9.37 (s, 3, C-10 methyl), 9.02 (d, 6, J = 6 Hz, isopropyl methyls), 8.86 (s, 3H, C-4 methyl), 7.94 (s, 3, $OCOCH_3$), 6.36 (s, 3, methoxyl), 5.84 (q, 1, J = 9 and 3 Hz, H-15), 4.72 (s, 1, $w_{1/2}$ = 4 Hz, H-14). Continued elution with Skellysolve B – benzene (200 ml of 1:1) and benzene (100 ml) gave a mixture of **14***a* and **15***a* (24 mg). Elution with benzene (1.3 l) gave the oily *endo*-acetate **14***a* (0.475 g), characterized as the alcohol **14***b* (see below). The acetate **14***a* showed the following properties: i.r. ($CHCl_3$) 1720 (ester carbonyls), 1640 cm^{-1} (v.w., C=C); n.m.r. τ 9.37 (s, 3, C-10 methyl), 8.93 (d, J = 7 Hz, isopropyl methyls), 8.86 (s, 3, C-4 methyl), 8.08 (s, 3, $OCOCH_3$), 6.38 (s, 3, methoxyl), 5.44 (q, 1, J = 8 and 3 Hz, H-15), 4.72 (s, 1, $w_{1/2}$ = 3.5 Hz, H-14).

*Methyl 15β-Hydroxy-13-isopropyl-17-noratis-13-en-18-oate (**14**b)*

The acetate **14***a* (0.30 g) was heated on the steam bath with 10% potassium hydroxide in methanol (30 ml) for 3 h. The solution was concentrated on a rotary evaporator and the residue diluted with water and acidified with concentrated HCl. Extraction with chloroform gave the crude *endo*-alcohol **14***b* (0.25 g). Since the i.r. spectrum indicated the presence of some C-4 acid, the crude product was treated with ethereal diazomethane. Crystallization from Skellysolve B gave pure **14***b*, m.p. 92–93°: i.r. ($CHCl_3$) 3570 (concentration independent, intramolecular hydrogen-bonded OH), 1720 (ester), 1635 cm^{-1} (C=C); n.m.r. τ 9.38 (s, 3, C-10 methyl), 8.97 (d, J = 6.5 Hz, isopropyl methyls), 8.86 (s, 3, C-4 methyl), 6.64 (q, 1, J = 8 and 3 Hz, H-15), 6.38 (s, 3, methoxyl), 4.75 (s, 1, H-14).

Anal. Calcd. for $C_{23}H_{36}O_3$: C, 76.62; H, 10.00. Found: C, 76.77; H, 9.91.

*Methyl 16-Isopropylidene-7,17-secoacon-8(15)-en-18-oate (**16**a)*

A solution of alcohol **14***b* (234 mg) and *p*-toluenesulfonyl chloride (185 mg) in pyridine (2 ml) was kept at room temperature for 3.5 days. Water (50 ml) and ether (100 ml) were added and then the ether layer was separated and washed successively with dilute sulfuric acid, water, saturated sodium bicarbonate, and water. The dried ($MgSO_4$) ether solution was concentrated to a pale green amorphous solid (0.32 g). The crude tosylate **14***c* showed the following properties: i.r. ($CHCl_3$) 1720 (ester), 1645 (C=C), 1600 (aromatic), 1350 and 1175 (tosyloxy), 910 and 890 cm^{-1}; n.m.r. τ 9.42 (s, 3, C-10 methyl), 9.02 (d, 6, J = 7 Hz, isopropyl methyls), 8.88 (s, 3, C-4 methyl), 7.60 (s, 3, aromatic methyl), 6.38 (s, 3, methoxyl), 5.66 (d of d, 1, J's 8 and 2.5 Hz, H-14), 4.78 (s, 1, H-15), 2.73 (d, 1, J = 8 Hz, aromatic) and 2.33 (d, 1, J = 8 Hz, aromatic).

A benzene solution of tosylate **14***c* (0.24 g) was adsorbed on a column of silica gel (6 g, BDH, 60–120 mesh for chromatography). The top portion of the column immediately turned deep purple on introduction of the solution. After 2 h the column was eluted with benzene (200 ml) to give the oily diene **16***a* (0.11 g), purified by evaporative distillation (130°/0.05 mm): i.r. ($CHCl_3$) 1720 (ester), 1635 and 1620 (conjugated olefin); u.v. (95% EtOH) 258 nm (ε 18 000); n.m.r. τ 9.13 (s, 3, C-11 methyl), 8.78 (s, 3, C-4 methyl), 8.34 and 8.28 (three-proton singlets, olefinic methyls), 6.36 (s, methoxyl), 4.15 (s, 1, $w_{1/2}$ = 3 Hz, H-15); mass spectrum (70 eV) *m/e* (relative intensity) 342 (46), 327 (17), 107 (100).

The diene was somewhat unstable in air and was analyzed by h.r.m.s.

Mol. Wt. Calcd. for $C_{23}H_{34}O_2$: 342.2559. Found (h.r.m.s.): 342.2564.

Elution of the silica gel column with ether (150 ml) gave the alcohol **14***b* (36 mg).

The diene **16***a* was also prepared by solvolysis of the tosylate **14***c* in acetic acid as follows: a solution of the tosylate **14***c* (166 mg) in glacial acetic acid (15 ml) containing sodium acetate (123 mg) was heated under reflux for 5 h. The cooled solution was diluted with ether (100 ml) and the resulting solution was washed successively with water, 10% sodium carbonate, and water. The dried ($MgSO_4$) ether solution was concentrated and the residue (125 mg) was subjected to chromatography over alumina (6.25 g). Elution with Skellysolve B (180 ml) and Skellysolve B – benzene (270 ml of 9:1) gave diene **16***a* (47 mg). Elution with Skellysolve B – benzene (300 ml) and benzene (90 ml) gave unidentified material (14 mg). Further elution with benzene (135 ml) gave the *endo*-acetate **14***a* (16 mg), identical in i.r. spectrum and t.l.c. behavior with an authentic sample. Further elution with ether, chloroform, and chloroform–methanol (9:1) gave intractable material (25 mg).

*Hydrolysis of **16**a*

The diene **16***a* (0.11 g) was added to a solution of potassium *t*-butoxide (0.4 g) in anhydrous dimethyl sulfoxide (6 ml) and the resulting solution was heated on the steam bath for 1 1/2 h, then diluted with water (60 ml), acidified (concentrated HCl), and extracted with ether. The ethereal extract was washed with water, dried ($MgSO_4$), and concentrated. The residue (0.10 g) crystallized from acetonitrile to give round clusters (0.06 g) of the acid **16***b*: i.r. ($CHCl_3$) 3200–2400 (carboxyl OH), 1725 sh (monomeric carboxyl), 1685 (dimeric carboxyl), 1630 and 1620 cm^{-1} (conjugated olefin); n.m.r. τ 9.12

Can. J. Chem. Downloaded from www.nrcresearchpress.com by 210.87.254.42 on 09/05/12
For personal use only.

(s, 3, C-11 methyl), 8.77 (s, 3, C-4 methyl), 8.32 and 8.28 (three-proton singlets, isopropylidene methyls), 4.11 (s, 1, H-15); mass spectrum (70 eV) *m/e* (relative intensity) 328 (26), 313 (11), 107 (100), 106 (66), 91 (20).

Attempted recrystallization of **16***b* from acetonitrile resulted in the formation of an intractable dark material.

Catalytic Hydrogenation of Diene **16***a*

(a) Over Platinum

The diene **16***a* (57 mg) was dissolved in ethanol (20 ml) and the solution hydrogenated over Adams' catalyst (26 mg) at room temperature and atmospheric pressure for 3.5 h. Removal of the catalyst and solvent left the oily ester **17***a* (57 mg), purified by evaporative distillation (125°/0.05 mm); i.r. ($CHCl_3$) 1715 cm^{-1}; n.m.r. τ 9.13 (br.d, 6, $J \simeq 6$ Hz, isopropyl methyls), 8.92 (s, 3, C-11 methyl), 8.79 (s, 3, C-4 methyl), 6.38 (s, 3, methoxyl); mass spectrum (70 eV) *m/e* (relative intensity) 346 (66), 303 (21), 218 (86), 217 (93), 121 (59), 107 (53), 95 (79), 93 (58), 91 (48), 81 (85), 55 (100).

Hydrolysis of the ester using potassium *t*-butoxide – dimethylsulfoxide as above gave the acid **17***b*, m.p. 128–132° (from acetonitrile): i.r. ($CHCl_3$) 3200–2400 (carboxyl OH), 1730 sh (monomeric carboxyl), 1690 cm^{-1} (dimeric carboxyl); n.m.r. τ 9.14 and 9.11 (two three-proton doublets, non-equivalent methyls of isopropyl), 8.88 (s, 3, C-11 methyl), 8.76 (s, 3, C-4 methyl), −0.4 (broad, 1, COO*H*).

Mol. Wt. Calcd. for $C_{22}H_{36}O_2$: 332.2715. Found (h.r.m.s.): 332.2718.

(b) Over Palladium–Charcoal

Diene **16***a* (70 mg) in ethanol (20 ml) was hydrogenated over 5% palladium-on-charcoal at room temperature and atmospheric pressure. After an uptake of hydrogen (5 ml) during the first 20 min no further absorption was noticeable and the hydrogenation was discontinued. Removal of the catalyst and solvent gave the dihydro compound **18** as a glass: i.r. ($CHCl_3$) 1715 (ester), 1655 (C=C); n.m.r. τ 9.15 (d, 6, $J = 6$ Hz, isopropyl methyls), 9.02 (s, 3, C-11 methyl), 8.80 (s, 3, C-4 methyl), 6.36 (s, 3, methoxyl), 4.93 (s, 1, H-15); mass spectrum (70 eV) *m/e* (relative intensity) 344 (21), 329 (26), 301 (39), 121 (52), 91 (100).

*Methyl 13-Oxo-7,17-secoacon-8(15)-en-13-on-18-oate (**19**)*

A solution of diene **16***a* (48 mg) in methylene chloride was cooled to −70° and a saturated solution of ozone in methylene chloride (6 ml (19)) at −70° was added. The blue color of the ozone solution soon disappeared. After 0.5 h at −70° the solution was allowed to warm to room temperature, the solvent removed at the pump, and the residue treated with water (10 ml) and 30% hydrogen peroxide (0.8 ml) on the steam bath for 0.5 h. The reaction mixture was extracted with chloroform. The chloroform solution was washed with 5% sodium carbonate, water, and concentrated to give neutral material (37 mg), which was chromatographed over silica gel (4 g). Elution with benzene (160 ml) gave unidentified material (8 mg). Elution with benzene–ether (60 ml of 32:1 and 100 ml of 9:1) gave material (15 mg) rich in ketone **19** as judged by i.r. In another experiment conducted in the same manner 62 mg of diene **16***a* gave 17 mg of material rich in ketone **19**. The ketone-rich fractions were combined (32 mg) and chromatographed over alumina (2.5 g). Fractions eluted with benzene (120 ml) and benzene–ether (100 ml of 19:1) gave crystalline ketone **19** (14 mg), m.p. 132–133° (from Skellysolve B): i.r. 1720 (ester), 1670 (ketone), 1625 (conjugated C=C); n.m.r. τ 9.18 (s, 3, C-11 methyl), 8.77 (s, 3, C-4 methyl), 6.33 (s, 3, methoxyl), 4.38 (s, 1, H-15); u.v. (EtOH) 243 nm (ε 11 000); mass spectrum (70 eV) *m/e* (relative intensity) 316 (100), 301 (12), 257 (43), 181 (15), 136 (85), 121 (78), 91 (34).

A recrystallized sample which showed a single spot on t.l.c. (alumina and silica gel) was used for analysis.

Mol. Wt. Calcd. for $C_{20}H_{28}O_3$: 316.2040. Found: 316.2044.

*Methyl 15α-Hydroxy-13-isopropyl-17-noratis-13-en-18-oate (**15***b*)*

The *exo*-acetate **15***a* (0.65 g) was hydrolyzed on the steam bath with 10% potassium hydroxide in methanol. Work-up in the usual manner gave the alcohol **15***b* (0.58 g) which after crystallization from Skellysolve B melted at 116–119°: i.r. ($CHCl_3$) 3610 (OH), 1720 (ester), 1640 (C=C): mass spectrum (70 eV) *m/e* (relative intensity) 360 (3), 316 (100), 187 (27), 146 (57), 134 (27), 133 (27), 123 (20), 121 (41), 105 (20), 101 (25).

Anal. Calcd. for $C_{23}H_{36}O_3$ (mol. wt. 360.2665): C, 76.62; H, 10.06. Found (360.2667 (h.r.m.s.)): C, 77.48; H, 9.92.

We wish to thank the National Research Council of Canada for financial support, the University of Alberta for a dissertation fellowship (to P.D.D.), and Dr. J. Hooz for helpful discussion. The authors gratefully acknowledge the help of Dr. A. M. Hogg, Mr. R. N. Swindlehurst, and Mr. G. Bigam in the determination of the n.m.r., i.r., and mass spectra.

1. Z. Valenta and K. Wiesner. Chem. and Ind. (London), 354 (1956).
2. R. C. Cookson and M. E. Trevett. J. Chem. Soc. 3121 (1956).
3. N. J. Halbrook, R. V. Lawrence, R. L. Dressler, R. C. Blackstone, and W. Herz. J. Org. Chem. **29**, 1017 (1964).
4. S. W. Pelletier and A. Ichihara. Chem. and Ind. (London), 2149 (1967).
5. J. P. Johnston and K. H. Overton. Chem. Commun. 329 (1969).
6. W. A. Ayer, C. E. McDonald, and J. B. Stothers. Can. J. Chem. **41**, 1113 (1963).
7. W. A. Ayer and P. D. Deshpande. In preparation.
8. W. Herz, R. N. Mirrington, H. Young, and Y. Y. Lin. J. Org. Chem. **33**, 4210 (1968).
9. J. A. Berson and S. Suzuki. J. Am. Chem. Soc. **81**, 4088 (1959).
10. L. H. Zalkow, M. V. Kulkarni, and N. N. Girotra. J. Org. Chem. **30**, 1679 (1965). See, however, W. Herz and R. C. Blackstone. J. Org. Chem. **34**, 1257 (1969).
11. N. Langlois and B. Gastambide. Bull. soc. chim. Fr. 2966 (1965).
12. L. M. Jackman. Applications of nuclear magnetic resonance spectroscopy in organic chemistry. Pergamon Press, New York. 1959. p. 55.

13. A. ROSOWSKY. *In* Heterocyclic compounds with three- and four-membered rings. *Edited by* A. Weissberger. Interscience Publishers, New York. 1964. pp. 456–457.
14. A. MOSCOWITZ, K. MISLOW, M. A. W. GLASS, and C. DJERASSI. J. Am. Chem. Soc. **84**, 1945 (1962).
15. K. TORI, Y. TOKANO, and K. KITAHONOKI. Chem. Ber. **97**, 2798 (1964).
16. P. VON R. SCHLEYER, D. S. TRIFAN, and R. BAESKOI. J. Am. Chem. Soc. **80**, 6691 (1958).
17. H. L. GOERING, R. W. GREINER, and M. F. SLOAN. J. Am. Chem. Soc. **83**, 1391 (1961).
18. F. C. CHANG and N. F. WOOD. Tetrahedron Lett. 2969 (1964).
19. W. L. MEYER, D. D. CAMERON, and W. S. JOHNSON. J. Org. Chem. **27**, 1130 (1962).
20. H. L. GOERING and M. F. SLOAN. J. Am. Chem. Soc. **83**, 1992 (1961).
21. W. D. LLOYD and G. W. HEDRICK. Org. Syn. **45**, 64 (1965).
22. J. SMRT and F. SORM. Chem. Listy. **48**, 217 (1954).
23. Varian spectra catalog. Varian Associates, Palo Alta, California. Spectrum 143.

Can. J. Chem. Downloaded from www.nrcresearchpress.com by 210.87.254.42 on 09/05/12
For personal use only.

Crystal Structure of 1-Cyanotetracyclo[3.3.1.1^{3,7}.0^{3,7}]decane

CYRIL S. GIBBONS AND JAMES TROTTER

Department of Chemistry, University of British Columbia, Vancouver 8, British Columbia

Received June 29, 1972

Crystals of 1-cyanotetracyclo[3.3.1.1^{3,7}.0^{3,7}]decane, $C_{11}H_{13}N$, are monoclinic, a = 6.442(2), b = 11.739(2), c = 11.965(4) Å, β = 98.14(9)°, Z = 4, space group $P2_1/c$. The structure was determined with CuKα scintillation counter data by direct methods, and refined by full-matrix least-squares techniques to R 0.048 for 690 observed reflexions. C(3) and C(7) have all four bonds directed to one side of the atoms, and the central bond distance is 1.643 Å. Other bond lengths and angles are normal.

Le composé cyano-1 tétracyclo[3.3.1.1^{3,7}.0^{3,7}]décane, $C_{11}H_{13}N$, cristallise dans le système monoclinique aux caractéristiques suivantes: a = 6.442(2) Å, b = 11.739(2) Å, c = 11.965(4) Å, β = 98.14 (9)°, Z = 4, groupe d'espace $P2_1/c$. La structure a été déterminée à partir des mesures de diffraction, obtenues par comptage de scintillations (radiation Kα du cuivre), et a été affinée par la méthode de moindres carrés (matrice complète) jusqu'à un facteur de reliabilité R = 0.048 pour 690 réflexions. Toutes les quatre liaisons des carbones C(3) et C(7) se dirigent vers un côté de l'atome, et la longueur de la liaison central est 1.643 Å. Les autres longueurs de liaison et les angles sont normaux.

Can. J. Chem., **51**, 87 (1973)

Can. J. Chem. Downloaded from www.nrcresearchpress.com by 210.87.254.6 on 09/05/12
For personal use only.

Introduction

The preparation of a 1,3-dehydro derivative of adamantane has been reported (1), with the suggestion that the bridgehead atoms have all four bonds extended from one side of the atoms, as in tricyclo [3.2.1.0^{1,5}]octane (2). A single crystal X-ray analysis of a cyano-derivative of 1,3-dehydro-adamantane has now been carried out to provide details of the unusual geometry at the "inverted" bridgehead carbon atoms.

Experimental

Crystals of 1-cyanotetracyclo[3.3.1.1^{3,7}.0^{3,7}]decane are colorless prisms elongated along a. The unit cell parameters and space group were determined from precession photographs and diffractometer data, the unit cell parameters being refined by a least-squares procedure applied to the $\sin^2\theta$ values of 20 reflexions measured on the diffractometer with CuKα radiation. Crystal data are:

$C_{11}H_{13}N$ f.w. = 159.32

Monoclinic, a = 6.442(2), b = 11.739(2), c = 11.965(4) Å, β = 98.14(9)°, V = 895.8 Å^3, Z = 4, ρ_c = 1.18, $F(000)$ = 344 (20 °C; CuKα, λ = 1.5418 Å, μ = 5.3 cm^{-1}). Space group $P2_1/c$ from systematic absences. The density was not measured due to the extreme reactivity of the compound.

The intensities of all reflexions with 2θ(CuKα) ≤ 100° (minimum interplanar spacing, 1.01 Å) were measured on a Datex automated General Electric XRD 6 spectrogoniometer with a scintillation counter, approximately monochromatic CuKα radiation (Ni-filter and pulse-height analyzer), and a θ–2θ scan of 4° min^{-1} in 2θ. Background counts were made at the beginning and end of each scan. As the crystals were observed to decompose quickly in the X-ray beam, a new crystal was selected for the data collection from a freshly sublimed sample, and sealed inside a glass capillary. A check reflexion was measured periodically, showing the steady decomposition of the crystal, and the scale was adjusted accordingly.

The crystal used for data collection was a prism with dimensions 0.6 × 0.25 × 0.25 mm, and was mounted with a^* parallel to the φ axis of the goniostat. No absorption correction was made. Lorentz and polarization factors were applied and the structure amplitudes derived. Of the 919 reflexions, 690 (75%) had intensities greater than 3σ(I) above background, where $\sigma^2(I) = S + B + (0.05S)^2$, where S = scan count and B = background count. The remaining 229 reflexions were classified as unobserved.

Structure Analysis

The structure was solved by a direct sign-determining procedure (3), which uses a reiterative application of Sayre relationships (4). The carbon and nitrogen positions were determined from an E-map, and a structure factor calculation carried out with scattering factors from ref. 5, and isotropic temperature factors B = 4.0 Å^2, gave R = 0.30. After two cycles of full-matrix least-squares refinement with $\sqrt{w} = |F_o|/6.0$ when $|F_o| < 6.0$, $\sqrt{w} = 6.0/|F_o|$ when $|F_o| \geq 6.0$, $\sqrt{w}$(unobs) = 0.25, R was 0.16, and a difference electron-density map revealed the positions of the hydrogen atoms. These were included in the refinement with scattering factors from ref. 6, and isotropic B = 4.0 Å^2, and after two cycles of refinement R was 0.11. The carbon and nitrogen atoms were then assigned anisotropic thermal parameters and after several cycles of refinement, the final R value was 0.048. The 002, 020, 110, and 11$\bar{2}$ reflexions were given zero weight in the final cycles because of suspected extinction errors. The maximum parameter shift in the final cycle was 0.11σ, and a final difference map showed maximum fluctuations of ±0.16 e Å^{-3}.

Final positional and thermal parameters are listed in

Can. J. Chem. Downloaded from www.nrcresearchpress.com by 210.87.254.6 on 09/05/12
For personal use only.

TABLE 1. Final positional (fractional × 10^4) and thermal (Å^2 for isotropic; Å^2 × 10^2 for anisotropic) parameters, with standard deviations in parentheses, t.f. = exp $-10^{-2} \times 2\pi^2(h^2a^{*2}U_{11} + \ldots + 2hka^*b^*U_{12} + \ldots)$

Atom	*X*	*Y*	*Z*
C(1)	768(4)	3091(3)	4157(2)
C(2)	534(6)	3124(3)	5419(3)
C(3)	2556(5)	2524(3)	5887(2)
C(4)	2394(8)	1250(4)	5799(3)
C(5)	2679(6)	1193(4)	4572(3)
C(6)	4758(6)	1800(4)	4576(3)
C(7)	4237(5)	2928(3)	5053(3)
C(8)	2925(5)	3664(4)	4186(3)
C(9)	929(7)	1816(3)	3812(3)
C(10)	4540(6)	3153(4)	6278(3)
C(11)	−914(6)	3665(3)	3405(3)
N	−2207(5)	4119(3)	2824(3)

Atom	*X*	*Y*	*Z*	*B*
H(2)	451(46)	3920(31)	5678(25)	6.42(77)
H(2′)	−635(42)	2697(24)	5610(22)	5.21(69)
H(4)	1130(50)	995(28)	5912(25)	6.15(93)
H(4′)	3425(54)	865(29)	6286(29)	6.92(86)
H(5)	2647(59)	392(47)	4265(37)	11.34(132)
H(6)	5871(55)	1405(33)	5076(30)	8.34(89)
H(6′)	5144(50)	1856(30)	3817(30)	7.93(88)
H(8)	3451(43)	3664(27)	3433(27)	6.72(74)
H(8′)	2873(51)	4387(40)	4415(30)	8.04(108)
H(9)	−339(52)	1465(28)	3838(24)	5.97(80)
H(9′)	1247(50)	1813(31)	3018(33)	8.46(96)
H(10)	4394(48)	3919(31)	6491(26)	6.64(86)
H(10′)	5661(48)	2707(30)	6789(28)	6.94(76)

Atom	U_{11}	U_{22}	U_{33}	U_{12}	U_{13}	U_{23}
C(1)	7.04(20)	6.62(21)	5.57(18)	−0.22(16)	0.18(13)	0.31(14)
C(2)	7.49(23)	7.33(25)	6.76(21)	0.06(20)	1.41(15)	−0.42(17)
C(3)	8.25(23)	7.84(25)	5.24(18)	0.91(18)	1.25(15)	−0.07(15)
C(4)	9.45(33)	8.48(30)	8.72(30)	0.35(25)	0.13(23)	0.20(21)
C(5)	10.63(31)	8.53(28)	8.86(28)	0.86(24)	0.35(20)	0.76(21)
C(6)	8.23(27)	10.64(30)	7.34(25)	2.35(23)	1.49(20)	0.25(21)
C(7)	8.09(22)	8.43(24)	7.22(22)	1.38(19)	−0.01(17)	−0.26(18)
C(8)	8.41(25)	7.88(28)	6.68(24)	−0.69(19)	1.19(17)	0.96(19)
C(9)	8.70(27)	6.92(25)	7.06(24)	−0.63(21)	0.66(19)	−0.77(17)
C(10)	9.33(27)	8.66(31)	7.73(25)	0.42(23)	0.12(19)	−0.30(21)
C(11)	8.33(23)	7.26(22)	7.17(21)	−0.19(19)	−0.20(18)	−0.27(18)
N	10.25(24)	9.67(22)	10.08(24)	0.82(18)	−1.94(19)	0.72(18)

Table 1, and interatomic distances and angles in Table 2. Figure 1 shows a general view of the molecule, and Fig. 2 shows the packing of the molecules in the unit cell.

Measured and calculated structure factors are in the Depository of Unpublished Data.[1]

[1]Table of measured and calculated structure factors is available, at a nominal charge, from the Depository of Unpublished Data, National Science Library, National Research Council of Canada, Ottawa, Canada K1A 0S2.

Discussion

The crystal analysis has shown the present compound to be related to adamantane by the formation of the bond C(3)—C(7) with corresponding loss of hydrogen (in the adamantane numbering system, this corresponds to 1,3-dehydrogenation), and has given details of the geometry of the tetracyclic ring system and the "inverted" bridgehead carbon atoms.

Can. J. Chem. Downloaded from www.nrcresearchpress.com by 210.87.254.6 on 09/05/12
For personal use only.

TABLE 2

(*a*) Interatomic distances*

Bond	Distance (Å)	Bond	Distance (Å)
C(1)—C(2)	1.539(4)	C(2)—H(2)	0.99(4)
C(1)—C(8)	1.540(4)	C(2)—H(2′)	0.96(3)
C(1)—C(9)	1.560(5)	C(4)—H(4)	0.90(3)
C(1)—C(11)	1.471(5)	C(4)—H(4′)	0.94(4)
C(2)—C(3)	1.517(4)	C(5)—H(5)	1.01(5)
C(3)—C(4)	1.502(5)	C(6)—H(6)	0.98(4)
C(3)—C(7)	1.643(4)	C(6)—H(6′)	0.98(3)
C(3)—C(10)	1.493(5)	C(8)—H(8)	1.01(3)
C(4)—C(5)	1.507(5)	C(8)—H(8′)	0.89(4)
C(5)—C(6)	1.517(5)	C(9)—H(9)	0.92(3)
C(5)—C(9)	1.531(5)	C(9)—H(9′)	1.00(4)
C(6)—C(7)	1.499(5)	C(10)—H(10)	0.94(3)
C(7)—C(8)	1.513(5)	C(10)—H(10′)	1.02(3)
C(7)—C(10)	1.476(5)		
C(11)—N	1.139(4)		

*Standard deviations in parentheses.

(*b*) Bond angles*

Bonds	Angle (deg)	Bonds	Angle (deg)
C(11)—C(1)—C(2)	115.0(3)	C(5)—C(6)—H(6)	110(2)
C(11)—C(1)—C(8)	113.5(3)	C(5)—C(6)—H(6′)	112(2)
C(11)—C(1)—C(9)	110.4(2)	C(7)—C(6)—H(6)	112(2)
C(9)—C(1)—C(2)	107.7(3)	C(7)—C(6)—H(6′)	113(2)
C(9)—C(1)—C(8)	109.4(3)	H(6)—C(6)—H(6′)	110(3)
C(8)—C(1)—C(2)	100.4(3)	C(6)—C(7)—C(8)	112.2(3)
C(1)—C(2)—C(3)	98.7(2)	C(6)—C(7)—C(3)	100.3(3)
C(1)—C(2)—H(2)	110(2)	C(6)—C(7)—C(10)	122.1(3)
C(1)—C(2)—H(2′)	114(2)	C(8)—C(7)—C(3)	103.2(2)
C(3)—C(2)—H(2)	114(2)	C(8)—C(7)—C(10)	124.2(3)
C(3)—C(2)—H(2′)	109(2)	C(10)—C(7)—C(3)	56.9(2)
H(2)—C(2)—H(2′)	110(2)	C(7)—C(8)—C(1)	100.4(3)
C(2)—C(3)—C(4)	112.9(3)	C(7)—C(8)—H(8)	113(2)
C(2)—C(3)—C(7)	104.3(2)	C(7)—C(8)—H(8′)	112(2)
C(2)—C(3)—C(10)	122.6(3)	C(1)—C(8)—H(8)	113(2)
C(4)—C(3)—C(7)	106.8(3)	C(1)—C(8)—H(8′)	110(2)
C(4)—C(3)—C(10)	124.2(4)	H(8)—C(8)—H(8′)	108(3)
C(7)—C(3)—C(10)	55.9(2)	C(1)—C(9)—C(5)	111.8(3)
C(3)—C(4)—C(5)	95.5(3)	C(1)—C(9)—H(9)	109(2)
C(3)—C(4)—H(4)	112(2)	C(1)—C(9)—H(9′)	107(2)
C(3)—C(4)—H(4′)	114(2)	C(5)—C(9)—H(9)	110(2)
C(5)—C(4)—H(4)	112(2)	C(5)—C(9)—H(9′)	109(2)
C(5)—C(4)—H(4′)	114(2)	H(9)—C(9)—H(9′)	110(3)
H(4)—C(4)—H(4′)	109(3)	C(3)—C(10)—C(7)	67.2(2)
C(4)—C(5)—C(6)	101.8(3)	C(3)—C(10)—H(10)	116(2)
C(4)—C(5)—C(9)	112.1(4)	C(3)—C(10)—H(10′)	116(2)
C(4)—C(5)—H(5)	113(3)	C(7)—C(10)—H(10)	116(2)
C(6)—C(5)—H(5)	114(2)	C(7)—C(10)—H(10′)	119(2)
C(6)—C(5)—C(9)	110.7(4)	H(10)—C(10)—H(10′)	115(3)
C(9)—C(5)—H(5)	105(2)	C(1)—C(11)—N	179.3(3)
C(5)—C(6)—C(7)	99.8(3)		

*Standard deviations in parentheses.

TABLE 3. Equations of mean planes, in the form $lX' + mY + nZ' = p$, where X', Y, and Z' are coordinates in Å referred to orthogonal axes, a, b, and c^*, with deviations from the planes in Å

Atoms	l	m	n	p	Displacement of C(3)	Displacement of C(7)
2,4,10	0.3855	0.0101	−0.9227	−6.1062	−0.047	+1.342
6,8,10	0.8936	0.4249	−0.1445	2.1610	−1.330	+0.109

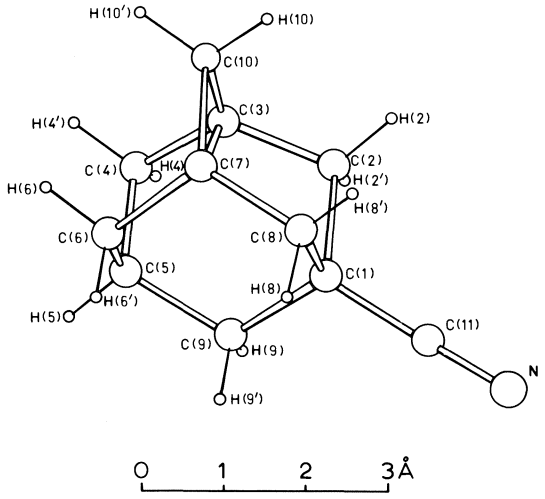

FIG. 1. Molecular diagram showing the numbering system used.

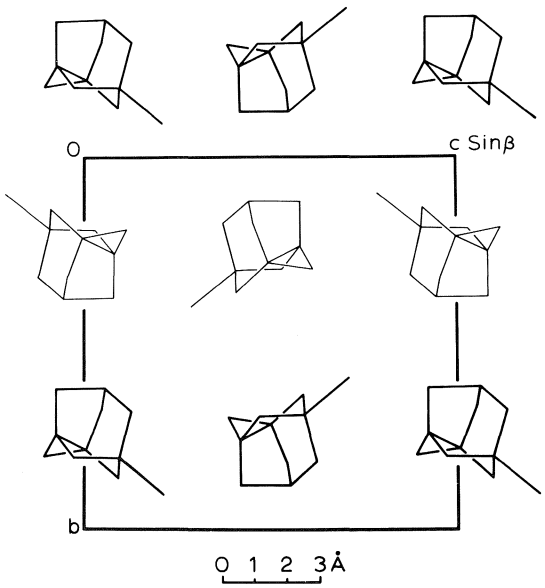

FIG. 2. Packing of the molecules in the unit cell (heavy lines indicate molecules in the top part of the cell).

Planes calculated through atoms C(2), C(4), C(10), and C(6), C(8), C(10) are given in detail in Table 3, and the bridgehead atoms C(3) and C(7) lie on the opposite sides of these planes from the rest of the molecule. Thus, these atoms are "inverted", in the sense that all four bonds are directed to one side of the atoms. It has been shown theoretically for tricyclo[1.1.1.$0^{1,3}$]pentane (7) that the energy minimum is obtained for a central bond length of 1.60 Å, and a side bond of 1.53 Å. The central bond length determined for the present compound agrees well with this at 1.643 Å, but the side bonds (1.476–1.517 Å) appear to be somewhat shorter than the theoretical value, or the observed value for cyclopropane (8, 9), although these differences are small, and the comparison may not be valid. The side bonds correspond closely with the value expected for C(sp^2)—C(sp^3) bonds, 1.515 Å, giving some support for the assumption of sp^2 hybridization at the bridgehead, with pσ overlap for the central bond.

Apart from the "inverted" carbon atom geometry, the bond lengths and angles are normal (9) with a mean C—C distance of 1.532, and a C≡N distance of 1.139 Å. The average C–H distance is 0.96 Å.

Intermolecular contacts correspond to van der Waals interactions, the shortest C...N and C...C distances being 3.72 and 3.87 Å, respectively.

We thank Dr. R. E. Pincock for crystals and discussion, the University of British Columbia Computing Centre for assistance, and the National Research Council of Canada for financial support.

1. R. E. PINCOCK and E. J. TORUPKA. J. Am. Chem. Soc. **91**, 4593 (1969).
2. K. B. WIBERG, G. J. BURGMAIER, K.-W. SHEN, S. J. LAPLACA, W. C. HAMILTON, and M. D. NEWTON. J. Am. Chem. Soc. **94**, 7402 (1972).
3. R. E. LONG. Ph. D. Thesis. University of California, Los Angeles, California. 1965.

Can. J. Chem. Downloaded from www.nrcresearchpress.com by 210.87.254.6 on 09/05/12
For personal use only.

4. D. SAYRE. Acta Cryst. **5**, 60 (1952).
5. International tables for X-ray crystallography. Vol. III. Kynoch Press, Birmingham. 1962.
6. R. F. STEWART, E. R. DAVIDSON, and W. F. SIMPSON. J. Chem. Phys. **22**, 235 (1965).
7. M. D. NEWTON and J. M. SCHULMAN. J. Am. Chem. Soc. **94**, 773 (1972).
8. O. BASTIANSEN, F. N. FRITSCH, and K. HEDBERG. Acta Cryst. **17**, 538 (1964); A. HARTMAN and F. L. HIRSHFELD. Acta Cryst. **20**, 80 (1966).
9. Chem. Soc. Spec. Publ. No. 11 (1958) and No. 18 (1965).

Can. J. Chem. Downloaded from www.nrcresearchpress.com by 210.87.254.6 on 09/05/12
For personal use only.

Halogenoammine Complexes of Osmium(III)

A. D. Allen and J. R. Stevens

Lash Miller Chemical Laboratories, University of Toronto, Toronto 5, Ontario

Received July 13, 1972

The complexes $[Os(NH_3)_5X]X_2$, *cis*-$[Os(NH_3)_4X_2]X$, and *trans*-$[Os(NH_3)_4X_2]X$ (X = Cl, Br, I) have been prepared and their infrared spectra measured between 4000–150 cm^{-1}. Assignments have been made for the observed absorption bands. The electronic spectra of the complexes were measured and compared with those of the analogous ruthenium(III) species.

Nous avons préparé les complexes $[Os(NH_3)_5X]X_2$, *cis*-$[Os(NH_3)_4X_2]X$, et le *trans*-$[Os(NH_3)_4X_2]X$ (où X = Cl, Br, I) et mesuré leurs spectres infrarouge entre 4000–150 cm^{-1}. Nous avons assigné les bandes d'absorption observées. Les spectres électroniques de complexes ont été mesurés et comparés à ceux de complexes analogues du ruthénium(III). [Traduit par le journal]

Can. J. Chem., **51**, 92 (1973)

Can. J. Chem. Downloaded from www.nrcresearchpress.com by 210.87.254.6 on 09/05/12
For personal use only.

Introduction

Little work has been done previously on the ammine complexes of trivalent osmium. This neglect has probably stemmed from the poor synthetic routes so far developed. The first complex of this type prepared was $K_2[OsCl_5(NH_3)]$ (1) although for many years this was thought to be $K_2[OsCl_5(NH_2)]$ (2). Dwyer and Hogarth (3) isolated $[Os(NH_3)_5Br]Br_2 \cdot H_2O$ and $[Os(NH_3)_5Cl]Cl_2 \cdot \frac{1}{2}H_2O$ from the reaction of $(NH_4)_2[OsBr_6]$ and $(NH_4)_2[OsCl_6]$, respectively, with ammonia under pressure. Later they identified $[Os(NH_3)_6]^{3+}$ as a more soluble product from the same reaction (4). This reaction was investigated in more detail by Watt and Vaska (5), who determined that for the bromo complex the two major products were $[Br(NH_3)_4OsNOs(NH_3)_4Br]Br_3$ and $[Os(NH_3)_6][OsBr_6]$. These authors, and Belova and Syrkin (6), who were working about the same time, both reported that the reactions were extremely sensitive to the conditions under which they were performed.

The only reported spectroscopic studies of osmium(III) ammines are infrared measurements of $[Os(NH_3)_6]Br_3$ (7) and $[Os(NH_3)_6][OsBr_6]$ (8). In contrast trivalent ruthenium ammine complexes have been studied in some detail (8–10). This report describes a convenient synthetic route to the complexes $[Os(NH_3)_5X]X_2$, *cis*-$[Os(NH_3)_4X_2]X$, and *trans*-$[Os(NH_3)_4X_2]X$ (X = Cl, Br, I) and their characterization by infrared and electronic spectroscopy.

Experimental

The infrared spectra were recorded on a Perkin–Elmer 180 Spectrophotometer as Nujol mulls between KBr plates or polyethylene sheets. The electronic spectra were recorded on either a Bausch and Lomb 505 Spectrophotometer or a Unicam SP 800A Ultraviolet Spectrophotometer in 1 cm quartz cells using distilled water. Microanalyses were performed by A. B. Gygli, Toronto, Ontario and halides were determined by potentiometric titration at 0° with silver nitrate. $[Os(NH_3)_5(N_2)]Cl_2$ was prepared in the usual manner (11) and *cis*-$[Os(NH_3)_4(N_2)_2]Br_2$ by the published procedure (12). All other chemicals were reagent grade and used without further purification.

Preparation of the Complexes

Iodopentaammineosmium (III) Iodide, $[Os(NH_3)_5I]I_2$

Nitrogenpentaammineosmium(II) chloride (1 g) was slurried with 50 ml of water and 10 ml of concentrated hydriodic acid. Excess iodine (0.5 g) was added and the mixture refluxed vigorously for 4 h. The excess iodine was expelled from the solution by strong heating and the solution was then cooled to ice temperature. The orange product was collected, washed with 95% ethanol and diethyl ether and air-dried. It was recrystallized from very dilute hot hydriodic acid as orange crystals. Yield 1.5 g (90%). Microanalyses for this and other complexes reported in this work are listed in Table 1.

Chloropentaammineosmium(III) Chloride, $[Os(NH_3)_5Cl]Cl_2$

Iodopentaammineosmium(III) iodide (0.5 g) was dissolved in hot dilute hydrochloric acid (50 ml) and the chloride concentration made as large as possible without precipitating any of the complex, by the addition of concentrated hydrochloric acid. The solution was refluxed for 48 h until it became almost colorless. On cooling and adding more concentrated hydrochloric acid, a lemon-yellow precipitate came down. The product was collected, washed with 95% ethanol and diethyl ether, and air-dried. Yield 0.2 g (70%).

The alternative direct preparation via atmospheric oxidation of $[Os(NH_3)_5(N_2)]Cl_2$ in hydrochloric acid is less satisfactory because a second species believed to be $[OsO_2(NH_3)_4]Cl_2$ is also formed.

Bromopentaammineosmium(III) Bromide, $[Os(NH_3)_5Br]Br_2$

Iodopentaammineosmium(III) iodide (0.5 g) was dissolved in hot dilute hydrobromic acid (75 ml) and the

TABLE 1. Analytical results

Complex	% N		% H		% Halide	
	Calculated	Found	Calculated	Found	Calculated	Found
$[Os(NH_3)_5Cl]Cl_2$	18.35	18.32	3.94	3.81	18.6	18.4
$[Os(NH_3)_5Br]Br_2$	13.59	13.66	2.91	2.78	31.1	31.0
$[Os(NH_3)_5I]I_2$	10.67	10.85	2.29	2.60	38.7	38.2
cis-$[Os(NH_3)_4Cl_2]Cl\cdot H_2O$	14.64	14.87	3.66	3.67	9.3	10.1
cis-$[Os(NH_3)_4Br_2]Br\cdot\frac{1}{4}C_2H_5OH$*	10.99	10.85	2.65	2.63	15.7	16.2
cis-$[Os(NH_3)_4I_2]I$	8.76	8.88	1.88	2.42	19.9	19.9
trans-$[Os(NH_3)_4Cl_2]Cl\cdot H_2O$	14.64	15.35	3.66	3.51	9.3	10.0
trans-$[Os(NH_3)_4Br_2]Br$	11.24	11.40	2.41	2.74	16.1	15.8
trans-$[Os(NH_3)_4I_2]I$	8.76	8.73	1.88	2.02		

* % C calcd. 1.18; found 1.53.

bromide concentration increased, without causing precipitation, by the addition of concentrated hydrobromic acid. The solution was then refluxed for 24 h or until the 407 nm absorption, characteristic of $[Os(NH_3)_5I]^{2+}$, had disappeared. On cooling and adding concentrated hydrobromic acid, a bright yellow powder was obtained. This was recrystallized from hot dilute hydrobromic acid. Yield 0.3 g (75%).

cis-Dichlorotetraammineosmium(III) Chloride Hydrate, cis-[Os(NH$_3$)$_4$Cl$_2$]Cl·H$_2$O

cis-Bisnitrogentetraammineosmium(II) bromide (0.25 g) was slurried with 20 ml of 3 *M* hydrochloric acid in a flask. The mixture was heated at 60° for 15 h and then refluxed for 5 h. The resulting yellow solution was filtered to remove a little yellow precipitate and 5 ml of concentrated hydrochloric acid and 25 ml of 95% ethanol were added to the filtrate. Upon standing at −20° for 24 h a flocculent yellow precipitate was obtained. This was collected, washed with 95% ethanol and diethyl ether then dried at 65% under vacuum in the presence of P_4O_{10}.

cis-Dibromotetraammineosmium(III) Bromide Tetroethanolate, cis-[Os(NH$_3$)$_4$Br$_2$]Br·¼C$_2$H$_5$OH

cis-Bisnitrogentetraammineosmium(II) bromide (0.2 g) was mixed with 5 ml of concentrated hydrobromic acid and 15 ml of water. The resulting off-white slurry was heated gently for 10 h or until all of the starting material had reacted and the solution had become clear and yellow. After cooling to ice temperature, 5 ml of concentrated hydrobromic acid and 20 ml of 95% ethanol were added and the solution cooled to −20°. A flocculent orange precipitate was obtained. This was collected, washed with 95% ethanol and diethyl ether, then dried for 24 h at 78° under vacuum in the presence of P_4O_{10}. Yield 0.15 g (72%).

cis-Diiodotetraammineosmium(III) Iodide, cis-[Os(NH$_3$)$_4$I$_2$]I

cis-Bisnitrogentetraammineosmium(II) bromide (0.12 g) was slurried with 40 ml of 1:4 hydriodic acid. The mixture was refluxed gently for 15 h during which time a clear orange-red solution formed. A flocculent orange-red precipitate was obtained by adding 5 ml of concentrated hydriodic acid and 25 ml of 95% ethanol and then cooling the solution to −20°. The product was recrystallized from hot dilute hydriodic acid as long, very deep red, leaflets. Yield 0.14 g (85%).

trans-Dichlorotetraammineosmium(III) Chloride Hydrate, trans-[Os(NH$_3$)$_4$Cl$_2$]Cl·H$_2$O

cis-Dibromotetraammineosmium(III) bromide (0.15 g) was dissolved in 10 ml of water and 10 ml of concentrated hydrochloric acid added. The solution was refluxed under nitrogen for 3 days during which time it became a lighter shade of yellow. On cooling and adding 5 ml of concentrated hydrochloric acid a bright yellow precipitate was obtained. This was collected, washed with 95% ethanol and diethyl ether, then dried at 78° under vacuum for 24 h. Yield 0.06 g (55%).

trans-Dibromotetraammineosmium(III) Bromide, trans-[Os(NH$_3$)$_4$Br$_2$]Br

The procedure was identical to that used for *trans*-$[Os(NH_3)_4Cl_2]Cl$ except hydrobromic acid replaced hydrochloric acid. Yield 0.08 g (53%).

trans-Diiodotetraammineosmium(III) Iodide, trans-[Os(NH$_3$)$_4$I$_2$]I

trans-Dichlorotetraammineosmium(III) chloride hydrate (0.1 g) was added to 20 ml of 1:4 hydriodic acid and the solution was refluxed under nitrogen for 24 h. After cooling to 0° to ensure complete precipitation, the product was collected and washed with 95% ethanol and diethyl ether. It was recrystallized from very dilute hot hydriodic acid as dark red shiny needles. Yield 0.08 g (50%).

Results and Discussion

As was reported previously (13), iodine oxidation of $[Os(NH_3)_5(N_2)]^{2+}$ results in a convenient, rapid synthesis of $[Os(NH_3)_5I]^{2+}$. Chatt *et al.* (14) noted the presence of a species having an infrared absorption at 2130 cm^{-1} in the unstable mixture produced by I_2 oxidation of $[Os(NH_3)_5(N_2)](BPh_4)_2$ in ethanol. This is probably the unstable $[Os(NH_3)_5(N_2)]^{3+}$ ion detected by Elson *et al.* (15) and suggests that in the preparation of $[Os(NH_3)_5I]^{2+}$, the first step is an oxidation and this is followed by a substitution.

$$[1]\quad 2[Os(NH_3)_5(N_2)]^{2+} + I_2 \rightarrow 2[Os(NH_3)_5(N_2)]^{3+} + 2I^- \rightarrow 2[Os(NH_3)_5I]^{2+} + 2N_2$$

Can. J. Chem. Downloaded from www.nrcresearchpress.com by 210.87.254.6 on 09/05/12
For personal use only.

Can. J. Chem. Downloaded from www.nrcresearchpress.com by 210.87.254.6 on 09/05/12
For personal use only.

Atmospheric oxygen was also found to be a suitable oxidizing agent, but the simultaneous formation of $[OsO_2(NH_3)_4]^{2+}$ reduced the yield, and made this method less desirable. Interconversion of the halides by refluxing in the appropriate hydrohalic acid was slow but efficient. An intermediate aqua complex was not detected.

The yellow color of $[Os(NH_3)_5Cl]Cl_2$ and $[Os(NH_3)_5Br]Br_2$ is not in accord with the data of Dwyer and Hogarth (3), Watt and Vaska (5), or Sutton (16). This may be accounted for by different crystal sizes but our compounds were yellow even in powdered form. Neither osmium nor total bromine analysis will distinguish $[Os(NH_3)_5Br]Br_2 \cdot H_2O$ from $[Os(NH_3)_6]Br_3$ or $[Os(NH_3)_5(H_2O)]Br_3$. The low nitrogen analyses reported in refs. 3 and 5 eliminate $[Os(NH_3)_6]Br_3$ from consideration but the lighter color reported for the monohydrate suggests, by analogy with the corresponding ruthenium(III) complexes, that the water is coordinated. Sutton (16) found $[Os(NH_3)_5I]I_2$ to be chocolate brown in color but the cation gave light orange solutions in water as does our orange compound. He found the light brown bromo complex to be a 2:1 electrolyte in methanol and reported that the bromide ligand was very labile in aqueous solution. Dwyer and Hogarth had earlier remarked on the lability of the coordinated chloride in $[Os(NH_3)_5Cl]^{2+}$. By contrast we find that all three halogens are tightly bound to the metal and are very inert to substitution. In fact the ionic halides may be titrated with silver nitrate at 0° without interference from the coordinated halide.

The *cis*-$[Os(NH_3)_4(N_2)_2]^{2+}$ ion provided a convenient starting material for the preparation of the previously unreported *cis*-$[Os(NH_3)_4X_2]X$ complexes (X = Cl, Br, I). The diiodo complex can be prepared at refluxing temperatures in good yield. The dichloro and dibromo complexes must be prepared at lower temperatures and the formation of side products reduces the yields. If the bisnitrogen complex is treated with hydrohalic acid under nitrogen or argon in the absence of I_2, a disproportionation occurs. The stoichiometry is inferred from the observed products.

$$[2]\quad 3\ cis\text{-}[Os(NH_3)_4(N_2)_2]^{2+} + 4HX \rightarrow 2\ cis\text{-}[Os(NH_3)_4X_2]^{+} + Os + 4NH_4^{+}$$

When *cis*-$[Os(NH_3)_4X_2]^{+}$ (X = Cl, Br) is refluxed in hydrobromic acid under nitrogen for several days, isomerization occurs and *trans*-$[Os(NH_3)_4Br_2]^{+}$ is formed. With hydrochloric acid a similar isomerization occurs to produce *trans*-$[Os(NH_3)_4Cl_2]^{+}$

$$[3]\quad cis\text{-}[Os(NH_3)_4X_2]^{+} + 2HBr \xrightarrow[3\ days]{reflux} trans\text{-}[Os(NH_3)_4Br_2]^{+} + 2HX\ (X = Cl, Br)$$

but with hydriodic acid only substitution occurs.

$$[4]\quad cis\text{-}[Os(NH_3)_4X_2]^{+} + 2HI \xrightarrow[3\ days]{reflux} cis\text{-}[Os(NH_3)_4I_2]^{+} + 2HX\ (X = Cl, Br, I)$$

The *trans*-$[Os(NH_3)_4I_2]^{+}$ ion could be prepared by starting with a *trans* isomer.

$$[5]\quad trans\text{-}[Os(NH_3)_4X_2]^{+} + 2HI \xrightarrow[24\ hr]{reflux} trans\text{-}[Os(NH_3)_4I_2]^{+} + 2HX\ (X = Cl, Br)$$

The principal side product formed during the preparation of *cis*-$[Os(NH_3)_4Cl_2]Cl$ was identified by electronic spectroscopy as *trans*-$[Os(NH_3)_4Cl_2]Cl$. Great care must be exercised during the preparation of *cis*-$[Os(NH_3)_4Cl_2]Cl$ and to a lesser extent, *cis*-$[Os(NH_3)_4Br_2]Br$, not to overheat the solutions or isomerization will occur. The tendency for the stereochemical change, *cis* → *trans*, to occur, decreases markedly in the order Cl > Br > I. No evidence of isomerization of either iodo species was obtained after several days at refluxing temperatures.

The infrared spectral data for the complexes is listed in Table 2. The ammine vibrations were assigned in the usual manner by comparison with other ammine complexes (17).

The far infrared region, 520–160 cm^{-1}, contains the skeletal modes of the complex ions. The bands between 446 and 504 cm^{-1} are assigned to the osmium–nitrogen stretching vibrations (18). For the pentaammine series (C_{4v} symmetry) there are four infrared-active metal–ligand stretching modes ($3A_1 + E$). One A_1 mode is the osmium–halogen stretching mode which leaves three $\nu(Os—NH_3)$ modes. All three are observed in the spectra of the chloro and bromo complexes and two are visible in the spectrum of the iodo complex, (see Fig. 1). The E mode is split in all three complexes and appears as a well-defined doublet. The osmium–halogen stretching vibrations are easily identified since they exhibit the greatest variation on changing the halogen. The osmium–nitrogen deformation modes occur as strong bands about 240 cm^{-1}.

TABLE 2. Infrared vibrational frequencies and band assignments for haloammineosmium (III) complexes*

	Frequency, cm^{-1}								
	$[Os(NH_3)_5X]X_2$, X =			*cis*-$[Os(NH_3)_4X_2]X$, X =			*trans*-$[Os(NH_3)_4X_2]X$, X =		
Assignment	Cl	Br	I	Cl	Br	I	Cl	Br	I
ν(N—H)	3260 vs 3160 vs	3260 vs 3160 s	3250 vs 3160 s	3250 s 3175 s,b	3270 s,b 3170 s,b	3225 s 3145 s	3290 vs 3200 s 3180 s 3130 m	3270 vs 3170 vs	3255 sh 3212 s 3155 s
$\delta(NH_3)$deg	1630 m	1628 m	1615 m	1644 m	1630 s	1608 m	1617 m	1608 m	1611 m
$\delta(NH_3)$sym	1326 vs 1290 m	1326 vs 1297 m	1327 vs 1304 w	1361 m 1332 s	1353 s 1326 vs	1353 m 1330 s 1311 vs 1307 vs	1330 s 1320 s	1335 s 1331 s 1307 s	1330 vs 1321 vs 1303 vs
$\rho(NH_3)$	847 sh 827 s	819 s	807 s	845 m 817 m	833 m 814 m	800 m	821 sh 815 s	809 m	771 w
ν(Os—NH_3)	504 w 488 vw 468 w 457 w	499 w 484 vs 464 w 452 w	492 w 457 w 446 w	496 vvw 476 vw 456 w	492 vw 469 w 453 w	499 vw 469 vw 456 w	455 w 447 w	461 w	458 w
ν(Os—X)	302 s	200 s	160 m	305 sh 298 s 256 m	205 s	167 m 160 m 240 m	317 s 258 m	222 m 245 m	180 m 235 m
δ(N—Os—N)	245 s	240 s	240 s	245 m 225 m	258 s 237 s	211 w	244 m		
Other bands					3445 w 1530 sh 1074 vw 1043 w 788 sh		3485 s 3420 m 1650 b 555 w		292 w

*s = strong; m = medium; w = weak; v = very; b = broad; sh = shoulder.

TABLE 3. Electronic spectra (cm^{-1}) of halogenoammine complexes of ruthenium(III) and osmium(III)

Complex ion	Ligand field bands		Charge-transfer bands	
$[Ru(NH_3)_5Cl]^{2+}$†	44 200(75)*	38 450(145)	30 480(1.93×10^3)	
$[Ru(NH_3)_5Br]^{2+}$†	40 500(90)	30 290(185)	25 120(1.92×10^3)	
$[Ru(NH_3)_5I]^{2+}$†		27 170(210)	18 500(2.05×10^3)	
trans-$[Ru(NH_3)_4Cl_2]^+$‡	40 500(125)	34 130(245)	30 200(4.75×10^3)	
trans-$[Ru(NH_3)_4Br_2]^+$‡	42 550(55)	30 400(220)	25 000(4.95×10^3)	
cis-$[Ru(NH_3)_4Cl_2]^+$‡	39 160(92)		32 250(1.38×10^3)	28 400(1.64×10^3)
cis-$[Ru(NH_3)_4Br_2]^+$‡	34 470(35)		27 020(1.37×10^3)	22 620(1.67×10^3)
$[Os(NH_3)_5Cl]^{2+}$		40 980(200)	37 450(2.01×10^3)	
$[Os(NH_3)_5Br]^{2+}$		38 170(67)	31 850(1.87×10^3)	
$[Os(NH_3)_5I]^{2+}$	36 900	33 330	24 570(1.97×10^3)	
trans-$[Os(NH_3)_4Cl_2]^+$	47 200(1610)	40 800(1290)	36 900(4.81×10^3)	
trans-$[Os(NH_3)_4Br_2]^+$		35 700(870)	31 500(4.69×10^3)	
trans-$[Os(NH_3)_4I_2]^+$	32 500(245)	27 200(860)	23 900(4.92×10^3)	
cis-$[Os(NH_3)_4Cl_2]^+$			39 220(2.03×10^3)	35 200(1.68×10^3)
cis-$[Os(NH_3)_4Br_2)^+$	41 320(380)		33 560(1.60×10^3)	29 070(1.62×10^3)
cis-$[Os(NH_3)_4I_2]^+$	34 840(530)	29 590(370)	26 460(1.68×10^3)	21 280(2.07×10^3)

*Molar extinction coefficients in brackets.
†Reference 9.
‡Reference 10.

Can. J. Chem. Downloaded from www.nrcresearchpress.com by 210.87.254.6 on 09/05/12
For personal use only.

Can. J. Chem. Downloaded from www.nrcresearchpress.com by 210.87.254.6 on 09/05/12
For personal use only.

For the *trans*-tetraammine series (D_{4h} symmetry), there are only two infrared-active metal–ligand stretching modes ($A_{2u} + E_u$). The A_{2u} mode is the asymmetric osmium–halogen stretching vibration and the E_u mode is the similar vibration of the osmium–nitrogen bonds. The latter is readily assigned to the 458 cm^{-1} band in the iodo species, the 461 cm^{-1} band is the bromo species, and to the doublet at 455 and 447 cm^{-1} in the chloro species (see Fig. 2). The osmium–halogen stretching modes are assigned to the bands at 180, 222, and 317 cm^{-1} in the iodo, bromo, and chloro salts, respectively.

For the C_{2v} symmetry *cis*-tetraammine complexes, there are six infrared-active stretching fundamentals ($3A_1 + 2B_1 + B_2$). These represent symmetric and asymmetric motions of the three pairs of similar ligands. (The ammonia ligands are differentiated by the nature of the ligand in the *trans* position). Unfortunately only three of the ν(Os—NH_3) frequencies are observed (Fig. 3) and only in the spectrum of the iodo complex are the two osmium–halogen frequencies resolved. However, the ν(Os—Cl) and ν(Os—Br) absorptions are broader in the *cis*-tetraammines than in the pentaammines.

As can be seen in Table 3 the electronic spectra of the complexes $[M(NH_3)_{6-a}X_a]^{(3-a)+}$ (M = Ru, Os; X = Cl, Br, I; a = 1, 2) are characterized by one or two moderately intense absorptions with one or two weaker absorptions at higher energy. More specifically it can be noted that the pentaammines exhibit one intense band, the *cis*-tetraammines two bands, and the *trans*-tetraammines one, but it is considerably more intense than in the other complexes. Jørgensen has classified these bands as $\pi \rightarrow \gamma_5$ or ligand $\pi \rightarrow$ metal $d\pi$ charge transfer bands (19).

The relevant energy levels are depicted schematically in Fig. 4. The observed charge-transfer transitions from the ligand π-orbitals to the metal d-orbitals are indicated. The occurrence of the transition at approximately the same energy for both pentaammine and *trans*-tetraammine complexes suggests that there is very little π interaction between the halide $p\pi$ orbitals and the metal $d\pi$ orbitals. That this is not the case is shown by the significant splitting observed in the *cis*-tetraammine complexes. The origin of this splitting is shown (Fig. 4) to be a result of two types of ligand π-orbitals. There is no metal π-orbital of b_1 symmetry and the $3b_1$ ligand

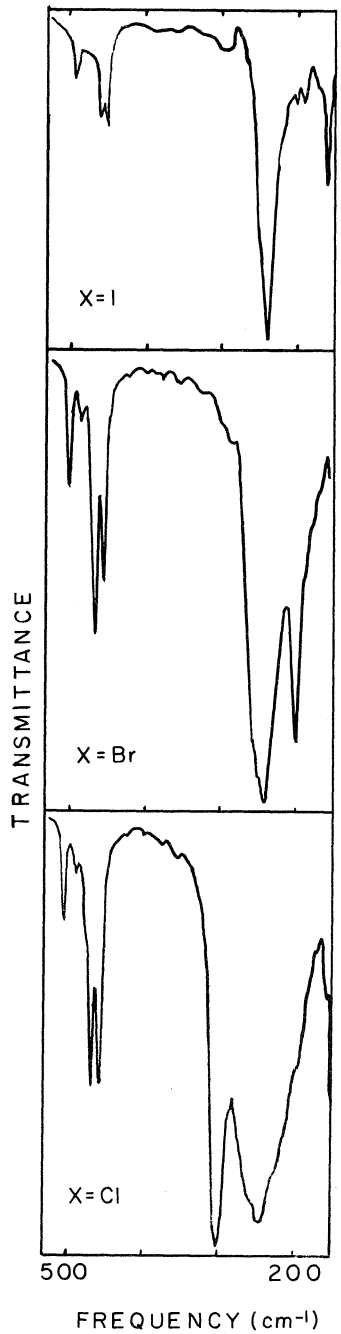

FIG. 1. Far infrared spectra (520–150 cm^{-1}) of $[Os(NH_3)_5X]X_2$ complex salts (X = I, Br, Cl).

Can. J. Chem. Downloaded from www.nrcresearchpress.com by 210.87.254.6 on 09/05/12
For personal use only.

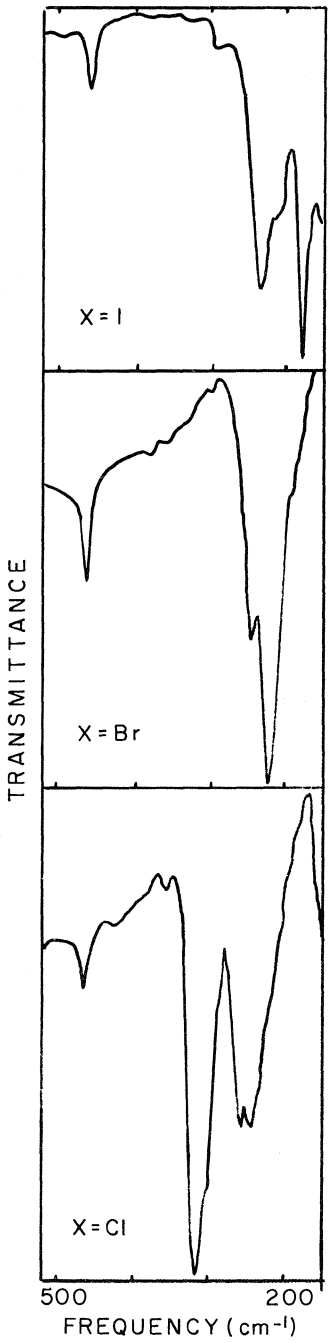

FIG. 2. Far infrared spectra (520–150 cm^{-1}) of *trans*-$[Os(NH_3)_4X_2]X$ complex salts (X = I, Br, Cl). The chloride salt contains water of crystallization.

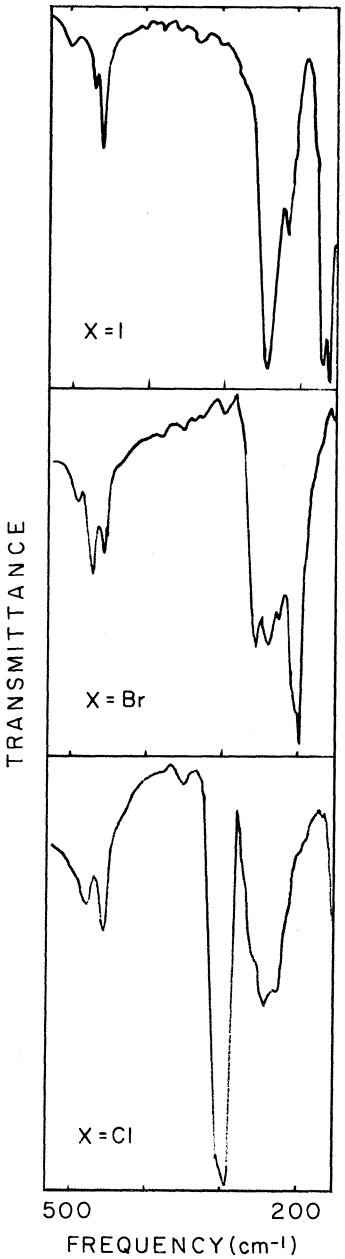

FIG. 3. Far infrared spectra (520–150 cm^{-1}) of *cis*-$[Os(NH_3)_4X_2]X$ complex salts (X = I, Br, Cl). The bromide salt contains ethanol of crystallization.

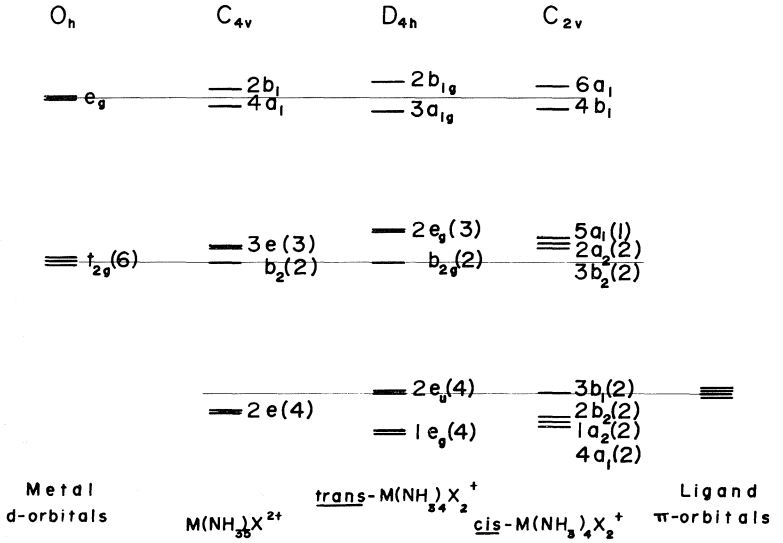

FIG. 4. Schematic energy level diagram (not to scale) of metal d-orbitals and ligand π-orbitals for ruthenium(III) and osmium(III) halogenoammine complexes.

π-orbital remains non-bonding. The other three ligand π-orbitals all interact to some degree with the metal orbital of the appropriate symmetry resulting in a stabilization of the ligand π-orbitals and a destabilization of the metal dπ-orbitals. Thus the similarity of the band positions of the pentaammines and *trans*-tetraammines results from the destabilization of the $3e_g$ level in the D_{4h} complexes being about equal to the stabilization of the $2e$ plus the destabilization of the $3e$ levels in the C_{4v} complexes.

The weaker bands observed at higher energy than the ligand-to-metal charge-transfer bands are undoubtedly ligand field transitions. No assignments are possible because there are a large number of excited states for low-spin d^5 systems and yet no more than two transitions are ever observed. Furthermore there is also the possibility that one or more ligand field bands occur at lower energy and are thus obscured by the charge-transfer bands.

The similarity of the spectra of the analogous complexes of ruthenium and osmium is readily apparent. The charge transfer bands of the osmium complexes lie at higher energy than those of their ruthenium counterparts. It is thus more difficult to reduce trivalent osmium than trivalent ruthenium. In the *cis*-tetraammines the splitting of the charge-transfer bands is relatively independent of the metal atom but slightly dependent on the halide.

We thank the National Research Council of Canada for financial support.

1. W. P. GRIFFITH. J. Chem. Soc. (A), 899 (1966).
2. L. BRIZARD. Ann. Chim. Phys. **21**, 375 (1900).
3. F. P. DWYER and J. W. HOGARTH. J. Roy. Soc. N.S.W. **84**, 117 (1951).
4. F. P. DWYER and J. W. HOGARTH. J. Roy. Soc. N.S.W. **85**, 113 (1951).
5. G. W. WATT and L. VASKA. J. Inorg. Nucl. Chem. **5**, 308 (1958); **6**, 246 (1958).
6. V. I. BELOVA and YA. K. SYRKIN. Russ. J. Inorg. Chem. **3**, 2016 (1958).
7. J. W. PALMER and F. BASOLO. J. Inorg. Nucl. Chem. **15**, 279 (1960).
8. A. D. ALLEN and C. V. SENOFF. Can. J. Chem. **45**, 1337 (1967).
9. H. HARTMANN and C. BUSHBECK. Z. Phys. Chem. **11**, 120 (1957).
10. T. ELIADES. Ph.D. Dissertation. University of Toronto, Toronto, Ontario. 1968.
11. A. D. ALLEN and J. R. STEVENS. Can. J. Chem. **50**, 3093 (1972).
12. H. A. SCHEIDEGGER, J. N. ARMOR, and H. TAUBE. J. Am. Chem. Soc. **90**, 3263 (1968).
13. A. D. ALLEN and J. R. STEVENS. Chem. Commun. 1147 (1967).
14. J. CHATT, J. R. DILWORTH, H. P. GUNZ, G. J. LEIGH, and J. R. SANDERS. Chem. Commun. 90 (1970).
15. C. M. ELSON, J. GULENS, I. J. ITZKOVITCH, and J. A. PAGE. Chem. Commun. 875 (1970).
16. G. J. SUTTON. Aust. J. Chem. **14**, 33 (1961).
17. K. NAKAMOTO. Infrared spectra of inorganic and coordination compounds. 2nd ed. Wiley–Interscience. 1970.
18. D. M. ADAMS. Metal–ligand and related vibrations. Arnold, London. 1967. p. 275.
19. C. K. JØRGENSEN. Mol. Phys. **2**, 309 (1959).

Can. J. Chem. Downloaded from www.nrcresearchpress.com by 210.87.254.6 on 09/05/12
For personal use only.

Urea – Boron Trihalide Adducts. II. Enhancement of Barriers to Rotation in *sym*- and *unsym*-Dialkylureas on BF_3 Complexation

J. S. HARTMAN[1] AND G. J. SCHROBILGEN[2]

Department of Chemistry, Brock University, St. Catharines, Ontario

Received May 4, 1972

N.m.r. evidence is presented for restricted rotation and oxygen donation in dialkylurea – boron trihalide adducts. Conformer populations in *sym*-dimethylurea.BF_3 are not the same as in the previously reported *sym*-dialkylurea–$SbCl_5$ adducts.

Une preuve par r.m.n. est présentée pour la rotation restreinte et pour la complexation sur l'oxygène dans les complexes dialkylurée–trihalogénure de bore. Les populations des conformations des complexes *sym*-diméthylurée–BF_3 ne sont pas les mêmes que pour le *sym*-dialkylurée–$SbCl_5$ précédemment rapportées. [Traduit par le journal]

Can. J. Chem., **51**, 99 (1973)

Can. J. Chem. Downloaded from www.nrcresearchpress.com by 210.87.254.40 on 09/05/12
For personal use only.

Introduction

Both nitrogen and oxygen are potential donor sites in ureas. From a number of different lines of evidence we have proposed that oxygen is the donor site in the 1:1 adduct of tetramethylurea (TMU) and boron trifluoride (1). We now report n.m.r. studies of the BF_3 adducts of *sym*- and *unsym*-dialkylureas ($(RNH)_2CO$ and $R_2NC(O)NH_2$, respectively, R = Me and Et) which show that hindered rotation about the central C—N bonds occurs in these adducts. By analogy with amide adducts (2), this supports oxygen donation. In the course of this work reports have appeared of restricted rotation in *sym*-dialkylureas complexed to antimony pentachloride (3) and in alkylthioureas complexed to cobalt(II) and zinc(II) (4).

Experimental

Materials were handled under anhydrous conditions on a vacuum line or in a dry box. Boron trifluoride and methylene chloride were purified as described previously (1). The dialkylureas (Aldrich) were dried overnight as fine powders under high vacuum before use. Nitromethane was dried overnight over magnesium sulfate. Deuterated *sym*-dimethylurea was prepared by dissolving *sym*-dimethylurea in deuterium oxide and evaporating to dryness. This procedure was repeated four times, giving a 99% *N*-deuterated product. The final product was twice recrystallized from anhydrous diethyl ether, powdered, and dried overnight under high vacuum.

Solutions of the BF_3 adducts were prepared by standard high-vacuum techniques. Methylene chloride – nitromethane mixed solvent (50:50, v/v) was used when solubility in methylene chloride alone was insufficient. Known amounts of BF_3 were condensed from a calibrated volume directly into 5 mm tubes containing degassed solutions of the ureas. Proton and ^{19}F spectra were referenced by condensing in small quantities of tetramethylsilane and trichlorofluoromethane. The samples were sealed off with the contents still at liquid nitrogen temperature, then warmed to room temperature.

The n.m.r. instrumentation has been described (1).

Results

60 MHz ^1H spectra of uncomplexed *sym*- and *unsym*-dimethylureas (DMU's) in methylene chloride solution showed only one methyl environment at temperatures down to $-80°$, rather than separate signals corresponding to methyls *cis* and *trans* to the carbonyl group as are observed in amides (2). The NH and NH_2 peaks were broad and not easily visible due to ^{14}N quadrupole relaxation, but the methyl protons couple to the NH proton in the *sym* compound to give a methyl doublet ($J_{H-C-N-H}$ = 5.0 Hz (3)). This doublet collapsed on addition of a trace of HF or BF_3 to the solution. Complexation with BF_3 shifted the methyl resonances to low field (Table 1). At room temperature a single methyl peak was observed for the BF_3 adduct of *unsym*-DMU; the methyl resonance of the *sym* adduct was split into a doublet ($J_{H-C-N-H}$ = 5.0 Hz) by coupling to the NH proton. When excess urea was present, separate methyl resonances were observed for the free urea and the 1:1 BF_3 adduct. The methyl doublet of uncomplexed *sym*-DMU was collapsed to a singlet when adduct was present, but the doublet survived in the adduct.

[1]To whom correspondence should be addressed.

[2]Present address: Department of Chemistry, McMaster University, Hamilton, Ontario.

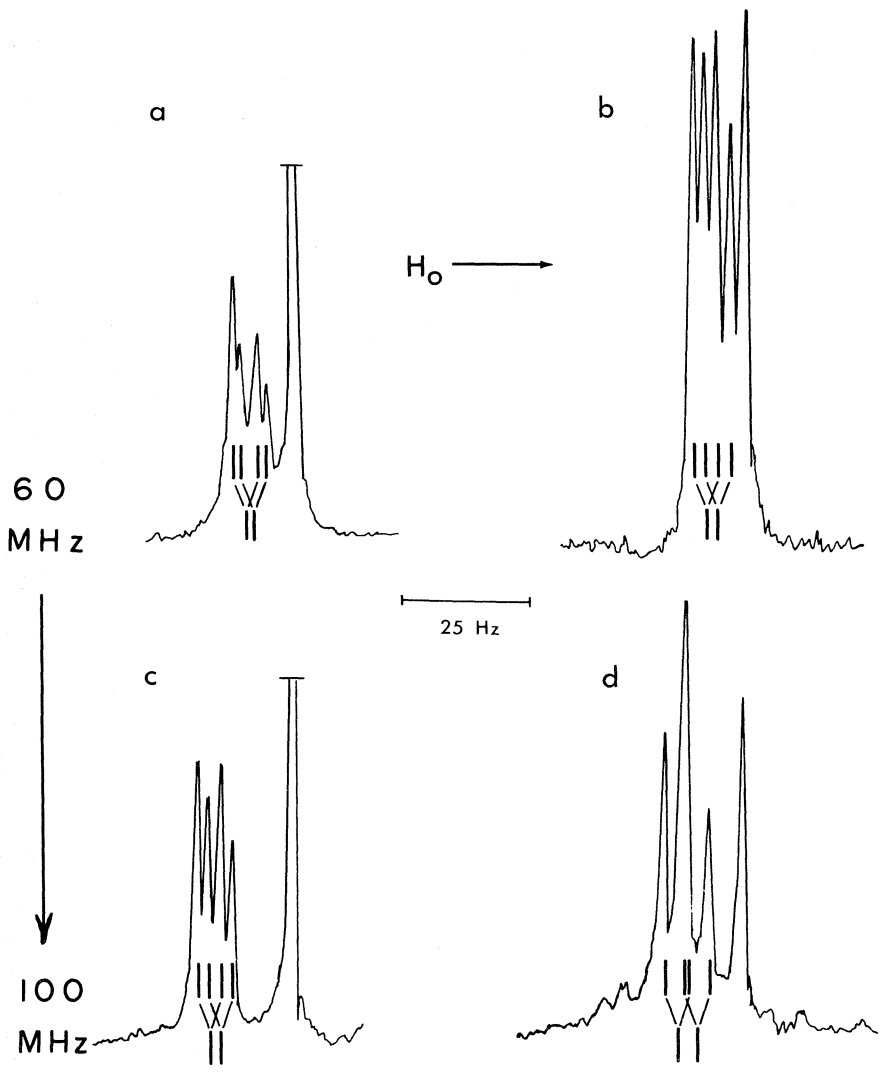

FIG. 1. The $-20°$ ^1H spectra of *sym*-DMU/BF_3 systems for $[BF_3]/[sym\text{-DMU}] = 0.50$ (*a*, *c*) and 0.75 (*b*, *d*) at 60 MHz (*a*, *b*) and 100 MHz (*c*, *d*). Splittings due to J_{HCNH} are shown schematically. The increase in magnetic field strength causes the small methyl chemical shift difference to become comparable to J_{HCNH}.

Cooling caused splitting of the adduct methyl resonances to give two singlets for *unsym*-DMU.BF_3, two doublets ($J_{H-C-N-H} = 5.0$ Hz) for *sym*-DMU.BF_3, and two sets of triplets for each of the DEU adducts. Coalescence temperatures are given in Table 1; $-20°$ 60 MHz and 100 MHz ^1H spectra of solutions of *sym*-DMU and BF_3, with *sym*-DMU present in excess, are shown in Fig. 1. Only the methyl peaks are shown. The high-field singlet arises from uncomplexed *sym*-DMU. The change in magnetic field strength shows that the four adduct peaks are made up of two 1:1 spin–spin doublets of unequal intensity (low field : high field = 61:39). The origin of the splittings was confirmed by studies of the BF_3 adduct of the *N*-deuterated compound, $(MeND)_2CO$, which gave two broadened *singlets* of unequal intensity at low temperatures since the much smaller splittings due to H—C—N—D coupling were not resolved. Peak separations at $-20°$ were somewhat dependent on sample composition, probably as a result of varying degrees of intermolecular association of adduct and free urea.

The BF_3 adducts of the *sym*- and *unsym*-diethylureas (DEU's) gave more complex spectra

Can. J. Chem. Downloaded from www.nrcresearchpress.com by 210.87.254.40 on 09/05/12
For personal use only.

TABLE 1. Nuclear magnetic resonance data

Compound	^{1}H chemical shifts* Free urea CH_3	Free urea CH_2	BF_3 adduct CH_3	BF_3 adduct CH_2	Separation of adduct methyl peaks at −20 °C† Hz (at 60 MHz)	p.p.m.	Adduct ^{19}F chemical shifts‡	Coalescence temperature of adduct methyl resonances§
sym-DMU	2.72	—	2.90	—	1.7	0.028	149.0	+15°
sym-DMU-d_2	2.72	—	2.90	—	2.0	0.033	—	+14°
unsym-DMU	2.89	—	3.08	—	1.2	0.020	148.9	+3°
sym-DEU	1.08	3.17‖	1.23	3.36‖	3.6	0.060	148.2	+14°
unsym-DEU	1.12	3.24¶	1.22	3.38¶	3.2	0.053	147.9	+14°
TMU**	2.75	—	3.02	—	—	—	149.2	< −95°

*37 °C; p.p.m. to low field of tetramethylsilane; somewhat dependent on sample composition.
†Dependent on the BF_3–urea ratio; values given are for a 1:1 ratio.
‡26 °C; p.p.m. to high field of $CFCl_3$.
§1:1 ratio of BF_3 to urea; 0.5 *M* in CH_2Cl_2/CH_3NO_2 mixed solvent (50:50, v/v).
‖$J_{H-C-N-H}$ = 5.8 Hz, $J_{H-C-C-H}$ = 7.0 Hz in *sym*-DEU and its BF_3 adduct.
¶$J_{H-C-C-H}$ = 7.1 Hz in *unsym*-DEU and its BF_3 adduct.
**Reference 1.

because of spin–spin coupling within the ethyl groups. As in the DMU adducts, cooling caused a doubling of the adduct signals due to "freezing out" of the exchange process. The adduct CH_2 signals were complex, but the two overlapping methyl triplets of each of the adducts were easily observed at −20°. In both the *sym*- and *unsym*-DEU adducts the two triplets were of near-equal intensity (low field:high field ratio: *sym*-DEU, 0.47:0.53; *unsym*-DEU, 0.52:0.48; estimated experimental error, ±0.05).

^{19}F chemical shifts of the four dialkylurea adducts are very similar and very close to the value for the tetramethylurea adduct (Table 1). As with TMU.BF_3 (1), at low temperatures the ^{19}F peak is split by a ^{10}B–^{11}B isotope shift.

As in the TMU–BF_3 system (1), traces of the protonated ureas were present as their BF_4^- salts. Thus in the absence of an excess of the urea the ^{1}H spectra of *sym*-DMU.BF_3 solutions contained a small additional peak in the adduct methyl region (2.89 δ), which is assigned to the methyl resonance of *sym*-DMU.H^+. Since this peak was removed by coalescence with the higher-field free-urea peak when free *sym*-DMU was present, relative areas of the adduct peaks could be obtained without interference. The coalescence pattern of the adduct peaks is apparently little affected by the presence of the impurity peak.

Discussion

Donor Site

Our data are consistent with oxygen donation (**1**) but not with nitrogen donation (**2**). In the *sym*-dialkylureas nitrogen donation would give two *equally* populated alkyl environments: (*a*) the

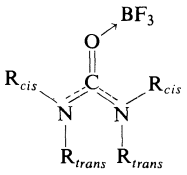

1

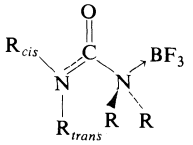

2

alkyl bonded to the donor nitrogen and (*b*) the alkyl far removed from the donor nitrogen. Interconversion of the two alkyl environments would require breaking of the donor–acceptor bond from one nitrogen and formation of an equivalent bond with the second nitrogen, which is unlikely; *inter*molecular exchange of BF_3 is slow and hence the donor–acceptor bonds are not easily broken. Thus both the unequal populations of the alkyl environments and the ease of interconversion of the two environments exclude nitrogen donation in *sym*-DMU.BF_3.

In the *sym*-dialkylureas the distribution of alkyl groups between positions *cis* and *trans* to the carbonyl should be dependent on steric effects, as in *N*-alkylamides (2). Thus the alkyl environments *cis* and *trans* to the carbonyl are likely to be unequally populated if oxygen is the donor. Formation of an adduct by oxygen donation should enhance the multiple bond character in the central C—N bonds, as in amides (5), and hence should decrease the rate of rotation about the central C—N bonds. In addition the relative populations of the *cis* and *trans* alkyl positions should change. By both of these criteria oxygen donation accounts for the spectra of the *sym*-dialkylurea adducts, if the two alkyl environments detectable by n.m.r. are indeed alkyl groups *cis*

Can. J. Chem. Downloaded from www.nrcresearchpress.com by 210.87.254.40 on 09/05/12
For personal use only.

Can. J. Chem. Downloaded from www.nrcresearchpress.com by 210.87.254.40 on 09/05/12
For personal use only.

and *trans* to the carbonyl. Although recent n.m.r. studies have shown restricted rotation in ureas (3, 6, 7) and thio- and selenoureas (4, 7, 8), the separate peaks coalesce at much lower temperatures in the free ureas than in their adducts.

In the *unsym*-dialkylurea adducts two equally populated alkyl environments would result from donation by either oxygen or the NH_2 nitrogen. Donation from either of these sites would leave an amide-like $C(O)NR_2$ fragment in which the central C—N bond would still have some double-bond character. However, oxygen donation would enhance the π-bonding in the central C—N bonds and hence the barrier to rotation, while donation from the NH_2 nitrogen would be unlikely to have much effect on the π-bonding or barrier to rotation in the C—NMe_2 bond. The observation of distinct alkyl environments in the BF_3 adducts but not in the free bases thus strongly supports oxygen donation.

Evidence from both the *sym*- and *unsym*-dialkylurea adducts supports oxygen donation. The similar coalescence temperatures for the *sym* and *unsym* adducts confirm that coordination to BF_3 has similar effects on both series and thus that the coordination site is the same in both series. The similarity of the ^{19}F chemical shifts of the dialkylurea adducts to that of the tetramethylurea adduct (Table 1) is further evidence that the coordination site is the same in all of these adducts. Further evidence for oxygen donation has recently been provided by a study of ^{15}N–^{1}H couplings in the BF_3 and $SbCl_5$ adducts of ^{15}N-labelled *sym*-DMU (9). Thus our previous conclusions (1), based on indirect evidence, are confirmed.

Conformer Populations and Interconversion

Only one conformation, with the methyl environments *cis* and *trans* to the carbonyl equally populated, is possible in the *unsym*-dialkylureas. Unless chemical shift degeneracy occurs, the observation of a single methyl resonance in *unsym*-DMU shows that rotation about the central C—N bond of the NMe_2 group occurs rapidly. Chemical shift degeneracy seems unlikely since addition of aromatic solvents, which cause very different solvent-induced shifts for *cis* and *trans* methyls in amides (10), does not split the single low-temperature peak. *Sym*-dialkylureas have three possible conformations, **3**–**5**. Calculations on *sym*-DMU indicate that **3** is much more stable than **5** (11), and an infrared study

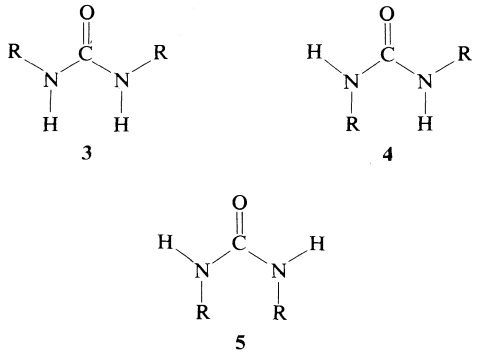

3 **4** **5**

has been interpreted as indicating that *sym*-DMU takes up conformation **3** exclusively in chloroform solution (11). If this is the case all methyl groups are in the same environment and rapid rotation need not be invoked to explain the single methyl peak. However, *sym*-DMU has been reported to give two ^{1}H methyl resonances of unequal intensity at temperatures below −120° in methanol solution (7), showing that two different environments are populated and that interconversion of conformers is rapid on the n.m.r. time scale above −120°. These studies can be reconciled if conformer populations are dependent on solvent. It seems clear that interconversion of conformers occurs in both *sym*- and *unsym*-dialkylureas and is rapid on the n.m.r. time scale at ordinary temperatures.

Formation of the BF_3 adduct by oxygen donation would give a single conformation from each of **3** and **5**, but two possible conformations,

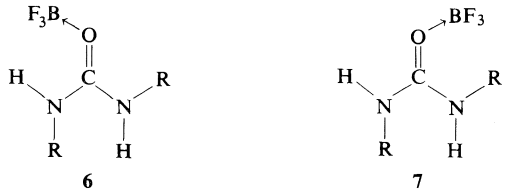

6 **7**

6 and **7**, from **4**. In their study of the $SbCl_5$ adducts of *sym*-dialkylureas Stilbs and co-workers (3) concluded that only the $SbCl_5$ analog of **6** was present and that the collapse of n.m.r. peaks was due to a concerted exchange of all three of the substituents of the central carbon:

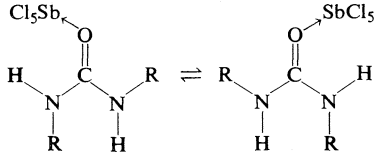

Can. J. Chem. Downloaded from www.nrcresearchpress.com by 210.87.254.40 on 09/05/12
For personal use only.

Evidence supporting this was obtained from studies of *sym*-dialkylurea–$SbCl_5$ adducts in which the two alkyl groups were different (3). Conformation **6** requires equal populations of alkyl groups *cis* and *trans* to the carbonyl. Since we have found that the two alkyl environments of *sym*-DMU.BF_3 are *unequally* populated, conformation **6** cannot be the only one present in this adduct.

The two methyl peaks of unequal intensities which are observed at low temperatures in the ^1H spectra of *sym*-DMU (7) and its BF_3 adduct probably arise from methyls *cis* and *trans* to the carbonyl group, as in *N*-alkylamides (2). Since only two peaks are observed, it seems that the two NHMe groups in the molecule are quasi-independent in their chemical shift behavior, *i.e.*, the conformation of the second NHMe group in the molecule has little effect on the chemical shift of the first NHMe group. Likewise the possible *cis–trans* orientation of the BF_3 fragment about the carbonyl group does not give rise to additional peaks at $-20°$; *cis–trans* isomerism of BF_3 about a carbonyl group has been detected by n.m.r. only below $-120°$ (12). The large anisotropy effect of the carbonyl group (2) apparently outweighs other effects in determining chemical shift differences.

In dialkylamides the *N*-alkyl absorptions at higher and lower field most frequently arise from the alkyl groups *cis* and *trans* to the carbonyl, respectively (2, 13). A similar assignment best accounts for the changes in relative peak areas of *sym*-DMU on complexation. Thus conformation **3** is favored in free *sym*-DMU (7), as expected (11), but in the BF_3 adduct the methyl groups tend to be forced into positions *trans* to the carbonyl by repulsion from BF_3. As in the $SbCl_5$ adducts, **6** is a likely major conformer. However, by the above assignment 61% rather than 50% of the methyls of *sym*-DMU.BF_3 are in positions *trans* to the carbonyl, implying an appreciable population of the BF_3 adduct of **5**, in spite of the methyl–methyl repulsion involved. With the greater ethyl–ethyl repulsions in *sym*-DEU.BF_3 this conformation apparently becomes negligible, and the pattern becomes consistent with that reported for the *sym*-dialkylurea–$SbCl_5$ adducts (3). We do not feel, however, that a concerted conformational exchange process (3) is the only one which can account for this pattern; small amounts of other conformations might still be present, acting as intermediates in the interconversion of the major conformers.

In an earlier study (1) it was not possible to observe separate methyl resonances for methyls *cis* and *trans* to the carbonyl group in the tetramethylurea.BF_3 adduct. This was attributed to the destabilization of the planar $C_2NC(O)NC_2$ skeleton due to steric hindrance (14). In the dialkylurea–BF_3 adducts steric hindrance is much less important.

We thank the National Research Council of Canada for financial assistance, Dr. P. Bickart and Dr. J. M. Miller for helpful discussions, and Mr. M. J. Bula for assistance with the experimental work.

1. J. S. Hartman and G. J. Schrobilgen. Can. J. Chem. **50**, 713 (1972).
2. W. E. Stewart and T. H. Siddall, III. Chem. Rev. **70**, 517 (1970).
3. G. Olofsson, P. Stilbs, T. Drakensberg, and S. Forsén. Tetrahedron, **27**, 4583 (1971).
4. D. R. Eaton and K. Zaw. Can. J. Chem. **49**, 3315 (1971); A. M. Giuliani. J. Chem. Soc. Dalton, 497 (1972).
5. E. S. Gore, D. J. Blears, and S. S. Danyluk. Can. J. Chem. **43**, 2135 (1965).
6. P. Stilbs and S. Forsén. J. Phys. Chem. **75**, 1901 (1972).
7. M.-L. Filleux-Blanchard and A. Durand. Org. Mag. Res. **3**, 187 (1971).
8. A. S. Tompa, R. D. Barefoot, and E. Pryce. J. Phys. Chem. **73**, 435 (1969); L. W. Reeves, R. C. Shaddick, and K. N. Shaw. J. Phys. Chem. **75**, 3372 (1971); M.-L. Filleux-Blanchard and A. Durand. C. R. **273**, 1770 (1971).
9. P. Stilbs. Tetrahedron Lett. 227 (1972).
10. L. L. Graham and M. R. Miller. Org. Mag. Res. **4**, 327 (1972).
11. C. N. R. Rao, K. G. Rao, A. Goel, and D. Balasubramanian. J. Chem. Soc. **A**, 3077 (1971).
12. U. Henriksson and S. Forsén. Chem. Commun. 1229 (1970).
13. L. R. Isbrandt and M. T. Rogers. Chem. Commun. 1378 (1971).
14. R. L. Middaugh, R. S. Drago, and R. J. Niedzielski. J. Am. Chem. Soc. **86**, 388 (1964).

Phosphonic Acid Analogs of Carbohydrate Metabolites. IV. Synthesis of DL-Glyceraldehyde-3-phosphonic Acid[1]

ERICH BAER AND RANGA ROBINSON

Banting and Best Department of Medical Research, University of Toronto, Toronto, Ontario

Received July 19, 1972

A chemical synthesis of DL-glyceraldehyde-3-phosphonic acid, the phosphonic acid analog of DL-glyceraldehyde-3-phosphoric acid, is reported. It was obtained from dimer DL-glyceraldehyde by two procedures differing solely in their protective groups via the following intermediates. *Procedure 1*: 2,5-diiodomethyl-3,6-dimethoxy-1,4-dioxane → 2,5-bis(methylphosphonic acid diethyl ester)-3,6-dimethoxy-1,4-dioxane → 2,5-bis(methylphosphonic acid)-3,6-dimethoxy-1,4-dioxane → DL-glyceraldehyde-3-phosphonic acid. *Procedure 2*: 2,5-bis(*p*-toluenesulfonyloxymethyl)-3,6-dibenzoxy-1,4-dioxane → 2,5-diiodomethyl-3,6-dibenzoxy-1,4-dioxane → 2,5-bis(methylphosphonic acid diethyl ester)-3,6-dibenzoxy-1,4-dioxane → 2,5-bis(methylphosphonic acid)-3,6-dibenzoxy-1,4-dioxane → DL-glyceraldehyde-3-phosphonic acid.

La synthèse chimique de l'acide DL-glycéraldehyde phosphonique-3, analogue de l'acide DL-glyceraldehyde phosphorique-3, est décrite. Cet acide a été obtenu à partir du dimère du DL-glyceraldéhyde selon deux voies différant seulement par les groupes protecteurs engagés, via les intermédaires suivants. *Voie 1*: diiodométhyl-2,5 diméthoxy-3,6 dioxane-1,4 → acide bis(méthylphosphonique)-2,5 diméthoxy-3,6 dioxane-1,4 → acide DL-glycéraldéhyde phosphonique-3. *Voie 2*: bis[*p*-toluenesulfonyloxyméthyl]-2,5 dibenzoxy-3,6 dioxane-1,4 → diiodométhyl-2,5 dibenzoxy-3,6 dioxane-1,4 → diethylester de l'acide bis-(méthylphosphonique)-2,5 dibenzoxy-3,6 dioxane-1,4 → acide bis(méthylphosphonique)-2,5 dibenzoxy-3,6 dioxane-1,4 → acide DL-glycéraldéhyde phosphonique-3. [Traduit par le journal]

Can. J. Chem., **51**, 104 (1973)

In 1929, Mendel (1) made the discovery that DL-glyceraldehyde inhibits *in vitro* the glycolysis of *Jensen* sarcoma.[2] The inhibitory effect according to Needham and Lehman (2) is caused by the L-isomer. One year earlier, Meyerhof *et al.* (3) had shown that the enzyme aldolase condenses dihydroxyacetone-phosphate with D- and L-glyceraldehyde yielding D-fructose-1-phosphate and L-sorbose-1-phosphate, respectively. The latter, according to Lardy *et al.* (4), inhibits hexokinase, thus providing a possible explanation for the inhibition of glycolysis by L-glyceraldehyde. Attempts by Schoeller[3] to effect a cure of cancer by intravenous injections of aqueous solutions of glyceraldehyde were unsuccessful. The aldehyde apparently was metabolized before reaching the tumor. More recently, however, Warburg *et al.* (5) reported that they had succeeded in curing Ehrlich's mouse-ascite tumor with both D- and L-glyceraldehyde by injecting sub-toxic doses of these compounds into the abdominal cavity. No spontaneous recurrences were observed. Neither ingestion nor subcutaneous or intravenous application of glyceraldehyde had any retarding effect on the growth of the ascite tumors. Thus, the feasibility of effecting a cancer cure by destroying the tumor cells through inhibition of their glycolytic process with a compound closely related to a carbohydrate metabolite has been demonstrated, at least for one specific type of tumor. Other types calling for subcutaneous or intravenous application of the cytostatica to reach the tumor site obviously require that they be less prone than glyceraldehyde to inactivation by body fluids. It occurred to us that phosphonic acid analogs of carbohydrate metabolites, in particular of glyceraldehyde-3-phosphoric acid (**A**) may possess the cytostatic activity of glyceraldehyde combined with greater biological stability. Hence the synthesis of glyceraldehyde-3-phosphonic acid (**B**) was undertaken. It is the third in a series of phosphonic acid analogs of carbohydrate metabolites that have been synthesized in

[1]Synonyms: DL-lactic acid aldehyde-3-phosphonic acid, DL-2-hydroxy-3-phosphonopropionaldehyde, DL-1-al-2-hydroxypropyl-3-phosphonic acid.

[2]The initial experiments were carried out with DL-glyceraldehyde provided by one of the present authors (E.B.).

[3]See ref. 5

Can. J. Chem. Downloaded from www.nrcresearchpress.com by 210.87.254.105 on 09/05/12
For personal use only.

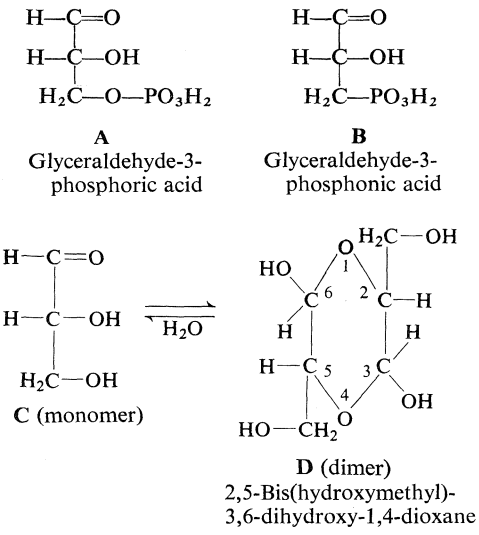

this laboratory. The others are L-α-glycerophosphonic acid (6) and 2,3-diphosphono-DL-glyceric acid (7).

Methods

Glyceraldehyde can exist in both a monomer and dimer form (formulae **C** and **D**, respectively). Derivatives of both forms are known. Thus far, however, only DL-glyceraldehyde has been obtained in crystalline form. D- and L-glyceraldehyde, both highly viscous glasses, when mixed in equimolecular proportions, readily form crystalline DL-glyceraldehyde (8). The dimer glyceraldehyde (formula **D**) can be regarded as a derivative of 1,4-dioxane. It is formed by the intermolecular condensation of the carbonyl groups of 2 mol of monomer glyceraldehyde (**C**) with their secondary hydroxyl groups (reaction **C** → **D**). As long as the hydroxyls of the two hemiacetal groups thus formed are unsubstituted, the reaction is reversible in water (reaction **D** → **C**). On replacing the hydrogen atoms of the hemiacetal-hydroxyl groups by methyl or benzyl radicals, the dioxane structure of dimer glyceraldehyde is stabilized. The use of dimer glyceraldehyde has the advantage that its derivatives are solids and that the carbonyl and secondary hydroxyl functions, in form of the hemiacetal, can be blocked by one protective group. The use of the methyl radical as protective group offers the advantage that it can be removed by a simple chemical operation, *i.e.* acid hydrolysis. This requires, however, that the hydrolysis product is acid-stable. Since we expected DL-glyceraldehyde-3-phosphonic acid to be an acid-stable compound, because of its C—P bond, we attempted its synthesis by using first the methyl radical as protective group. The procedure is outlined by pathway 1 of Scheme 1. Compound **6**, 2,5-bis(*p*-toluenesulfonyloxymethyl)-3,6-dimethoxy-1,4-dioxane, prepared by known methods, was treated with sodium iodide and the reaction product, 2,5-diiodomethyl-3,6-dimethoxy-1,4-dioxane (**7**), was condensed with triethyl phosphite yielding 2,5-bis(methylphosphonic acid diethyl ester)-3,6-dimethoxy-1,4-dioxane (**8**). Hydrolysis of the ester groups of **8** with chlorotrimethylsilane followed by hydrolysis of the methyl cycloacetal groups with 2 *N* hydrochloric acid at 80° for 20 h yielded 2,5-bis(methylphosphonic acid)-3,6-dimethoxy-1,4-dioxane (**9**), and DL-glyceraldehyde-3-phosphonic acid (**10**), respectively. The latter, on treatment in the *cold* with a solution of 2,4-dinitrophenylhydrazine in 2 *N* hydrochloric acid, gave immediately an orange colored precipitate consisting of a mixture of the dinitrophenylhydrazone and dinitrophenylosazone of glyceraldehyde-3-phosphonic acid. Since glyceraldehyde-3-phosphoric acid under the same conditions yields exclusively the dinitrophenylhydrazone (9), we entertained some doubts as to the homogeneity of compound **10** obtained by acid hydrolysis. To determine whether the facile formation in the cold of the dinitrophenylosazone is a typical reaction of glyceraldehyde-3-phosphonic acid caused by a rapid oxidation of its secondary hydroxyl group by hydrazine, or due to the presence of an oxidation product of glyceraldehyde-3-phosphonic acid formed during hydrolysis of its cyclomethyl acetal, we repeated the synthesis of glyceraldehyde-3-phosphonic acid using benzyl as protective group (pathway 2). It has the advantage that it can be removed under mild conditions in a reducing atmosphere.

Experimental

Materials

DL-Glyceraldehyde was washed several times with anhydrous acetone and dried *in vacuo* at 56°, m.p. 138°. Commercial triethyl phosphite was purified by fractional distillation, and the fraction boiling from 156–157° at 756 mm Hg was used. The palladium black catalyst was prepared by the reduction of palladium chloride with formic acid as described by Tausz and Putnoky (10), except that the catalyst, after washing thoroughly with water, was suspended several times in fresh portions of

Can. J. Chem. Downloaded from www.nrcresearchpress.com by 210.87.254.105 on 09/05/12
For personal use only.

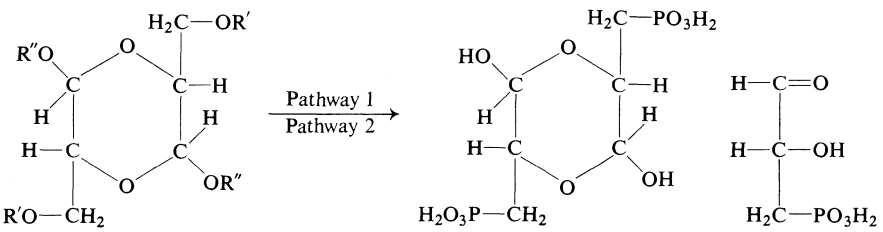

1 (dimer) DL-Glyceraldehyde

10 (dimer) **11** (monomer) DL-Glyceraldehyde-3-phosphonic acid

Pathway 1:

1 R′, R″ = H
2 R′, R″ = OC—CH_3
3 R′ = OC—CH_3; OR″ = Br
4 R′ = OC—CH_3; R″ = CH_3
5 R′ = H; R″ = CH_3
6 R′ = $SO_2C_6H_4CH_3$-*p*; R″ = CH_3
7 OR′ = I; R″ = CH_3
8 OR′ = $P(O)(OC_2H_5)_2$; R″ = CH_3
9 OR′ = PO_3H_2; R″ = CH_3
10 OR′ = PO_3H_2; R″ = H

Pathway 2:

1 R′, R″ = H
2 R′, R″ = OC—CH_3
3 R′ = OC—CH_3; OR″ = Br
12 R′ = OC—CH_3; R″ = $CH_2C_6H_5$
13 R′ = H; R″ = $CH_2C_6H_5$
14 R′ = $SO_2C_6H_4CH_3$-*p*; R″ = $CH_2C_6H_5$
15 OR′ = I; R″ = $CH_2C_6H_5$
16 OR′ = $P(O)(OC_2H_5)_2$; R″ = $CH_2C_6H_5$
17 OR′ = PO_3H_2; R″ = $CH_2C_6H_5$
10 OR′ = PO_3H_2; R″ = H

SCHEME 1. Synthesis of DL-glyceraldehyde-3-phosphonic acid.

glacial acetic acid. By avoiding drying, a much more active palladium catalyst is obtained. Glacial acetic acid for catalytic purposes was refluxed for 6 h with chromic acid anhydride and distilled twice under anhydrous conditions.

Pathway 1

2,5-Bis(acetoxymethyl)-3,6-bis(acetoxymethyl)-1,4-dioxane (**2**)(11,12), 2,5-bis(acetoxymethyl)-3,6-dibromo-1,4-dioxane (**3**) (13), 2,5-bis(acetoxymethyl)-3,6-dimethoxy-1,4-dioxane (**4**) (13), 2,5-bis(hydroxymethyl)-3,6-dimethoxy-1,4-dioxane (**5**) (13), and 2,5-bis(*p*-toluenesulfonyloxymethyl)-3,6-dimethoxy-1,4-dioxane (**6**) (14) were prepared as described in the literature.

2,5-Diiodomethyl-3,6-dimethoxy-1,4-dioxane (7)

A mixture of 5.16 g (10.0 mmol) of 2,5-bis(*p*-toluenesulfonyloxymethyl)-3,6-dimethoxy-1,4-dioxane (**6**) and 8.9 g (60 mmol) of anhydrous sodium iodide in 60 ml of dry methyl ethyl ketone was refluxed for 8 h (bath temperature 100°). The mixture was filtered with suction, the sodium *p*-toluenesulfonate was washed thoroughly with methyl ethyl ketone, and the combined filtrates were evaporated to dryness under reduced pressure (10–12 mm Hg) at a bath temperature of 30–35°. The residue was taken up in 30 ml of water and 100 ml of ether, the layers were separated, and the ether layer was washed successively with three 25 ml portions of 0.1 *N* sodium thiosulfate, three 10 ml portions of water, and finally was dried with anhydrous sodium sulfate. Removal of the ether by distillation under reduced pressure and drying the residue at 56° (boiling acetone) for 4 h at a pressure of 0.05 mm Hg gave 3.63 g (84.9% of theoretical yield) of 2,5-diiodomethyl-3,6-dimethoxy-1,4-dioxane, m.p. 138–139°. The compound was obtained in centimeter-long prisms by recrystallization from 80 ml of low-boiling petroleum ether, m.p. 138–139°, R_f 0.53 on silica gel H (solvent mixture: petroleum ether (b.p. 30–60°) and ether, 85:15, v/v). At room temperature, the compound is soluble in ether, sparingly soluble in petroleum ether (b.p. 30–60°) and insoluble in water, 99% ethanol or methanol.

Anal. Calcd. for $C_8H_{14}O_4I_2$ (mol. wt. 428): C, 22.45; H, 3.30; I, 59.30. Found: C, 22.43; H, 3.35; I, 59.60.

2,5-Bis(methylphosphonic acid diethyl ester)-3,6-dimethoxy-1,4-dioxane (8)

Into a two-necked 250 ml round flask equipped with a Liebig condenser and a gas-inlet tube were placed 8.56 g (20.0 mmol) of 2,5-diiodomethyl-3,6-dimethoxy-1,4-dioxane (**7**) and 83 g (0.5 mol) of triethyl phosphite, and the mixture was kept for 44 h at 140–145° (oil bath temperature). To facilitate the removal of ethyl iodide, a slow stream of nitrogen was passed through the apparatus and the temperature of the condenser was kept at 55° (±5°). The excess of triethyl phosphite was removed by distillation under reduced pressure (10–12 mm Hg) at a bath temperature ranging from 60–70°, and the residue was kept at room temperature for 4 h at a pressure of 0.01 mm Hg. The remaining viscous material was triturated with 60 ml of petroleum ether, and the mixture was set aside for crystallization. On standing overnight at room temperature, a crystalline material formed which was filtered off with suction, washed on the filter with 10 ml of petroleum ether, and dried for 4 h at 56° over phosphorus pentoxide at a pressure of 0.01 mm Hg. The 2,5-bis(methylphosphonic acid diethyl ester)-3,6-dimethoxy-1,4-dioxane weighed 8.08 g (90.1 % of theoretical yield), m.p. 62-63°. The melting point remained unchanged

Can. J. Chem. Downloaded from www.nrcresearchpress.com by 210.87.254.105 on 09/05/12
For personal use only.

Can. J. Chem. Downloaded from www.nrcresearchpress.com by 210.87.254.105 on 09/05/12
For personal use only.

on recrystallization of the substance from 250 ml of a boiling mixture of ether – petroleum ether (4:1, v/v); R_f 0.36 on silica gel G (chloroform–methanol, 95:5, v/v).

Anal. Calcd. for $C_{16}H_{34}O_{10}P_2$ (mol. wt. 448.4): C, 42.85; H, 7.64; P, 13.82. Found: C, 42.90; H, 7.59; P, 13.61.

*2,5-Bis(methylphosphonic acid)-3,6-dimethoxy-1,4-dioxane (**9**)*

(a) Hydrolysis

A mixture of 2.24 g (5.0 mmol) of 2,5-bis(methylphosphonic acid diethyl ester)-3,6-dimethoxy-1,4-dioxane (**8**) and 90 ml of chlorotrimethylsilane, in a pressure bottle, was kept at a temperature of 70–75° for 3 days. The excess of chlorotrimethylsilane was distilled off under reduced pressure at a bath temperature of 30–32°, the residue was dissolved in 100 ml of water, and the water-insoluble material was removed by extraction with three 45 ml portions of chloroform. The aqueous solution was kept for 3 days at a temperature of 45°, freed by filtration of any solid material which may have formed (*; see also Direct Procedure below) and concentrated under reduced pressure to a volume of about 30 ml.

(b) Dicyclohexylammonium salt

To the aqueous solution was added dropwise cyclohexylamine until it was slightly alkaline, approximately 2.6 ml of the base were required, and the solution was further concentrated under reduced pressure to a volume of about 10 ml. To the concentrate were added 20 ml of 99% ethanol and the mixture was kept overnight at −6°. The crystalline material was filtered off with suction, washed on the filter with 10 ml of anhydrous ether, and was dried for 4 h at 100° over phosphorus pentoxide at a pressure of 0.01 mm Hg. The dicyclohexylammonium salt weighed 2.36 g (88.4% of theoretical yield).

Anal. Calcd. for $[C_8H_{18}O_{10}P_2][C_6H_{13}N]_2$ (mol. wt. 534.5): C, 44.94; H, 8.30; N, 5.24; P, 11.59. Found[4]: C, 44.38; H, 8.17; N, 5.32; P, 12.10 and C, 44.50; H, 8.07; N, 5.70; P, 11.21.

(c) Removal of cyclohexylamine

A solution of 2.67 g (5.0 mmol) of the dicyclohexylammonium salt of compound **9** in 60 ml of distilled water was stirred for 1 h with 45 ml of Amberlite® IR-120 (H^+ form). The Amberlite was filtered off, washed with water, and the combined filtrates were evaporated to dryness under reduced pressure (10–12 mm Hg) at a bath temperature of 30–35°. The solid material remaining was dried at 80° over phosphorus pentoxide at 0.01 mm Hg for 3 h. The 2,5-bis(methylphosphonic acid)-3,6-dimethoxy-1,4-dioxane weighed 1.49 g (88.8% of theoretical yield), m.p. 149–150° (slight sintering at 146°).

Anal. Calcd. for $C_8H_{18}O_{10}P_2$ (mol. wt. 336.2): C, 28.58; H, 5.39; P, 18.43. Found: C, 28.11; H, 5.46; P, 18.47.

*2,5-Bis(methylphosphonic acid)-3,6-dimethoxy-1,4-dioxane (**9**) (Direct Procedure)*

The hydrolysis of 2.24 g (5.0 mmol) of **8** with chlorotrimethylsilane was carried out as described above (section *a*) following the procedure to the asterisk. The aqueous solution was evaporated to dryness under reduced pressure at a bath temperature of 30–35°, and the remaining hygroscopic material was triturated with 50 ml of anhydrous ether. The ether was distilled off under reduced pressure and the addition of ether and its removal by distillation was repeated twice more. After a final addition of 50 ml of ether, the mixture was kept for 2 days at −6°. The solid material was filtered off, washed with a small volume of ether, and dried for 3 h at 80° over phosphorus pentoxide at a pressure of 0.01 mm Hg. The 2,5-bis(methylphosphonic acid)-3,6-dimethoxy-1,4-dioxane weighed 1.43 g (85.2% of theoretical yield), m.p. 149–150°.

Anal. Calcd. for $C_8H_{18}O_{10}P_2$ (mol. wt. 336.2): P, 18.43. Found: P, 18.28.

*DL-Glyceraldehyde-3-phosphonic Acid (**10**, **11**).*

A solution of 0.370 g (1.10 mmol) of 2,5-bis(methylphosphonic acid)-3,6-dimethoxy-1,4-dioxane in 30 ml of 2.5 *N* hydrochloric acid in a 100 ml two-necked round flask, equipped with a condenser and gas-inlet tube, was kept at 80° for 24 h, while passing a slow stream of nitrogen through the apparatus. The solution was evaporated under reduced pressure (8–10 mm Hg) at a bath temperature of 30–32°. The residue was dissolved in 3 ml of distilled water, and the water was removed by distillation under reduced pressure as described above. This operation was repeated once more. To ensure a complete removal of hydrochloric acid and water, the material was kept for 7 days in a desiccator over sodium hydroxide powder and calcium chloride at a pressure of 0.01 mm Hg, renewing occasionally both reagents. The glyceraldehyde-3-phosphonic acid, a glass-like mass, weighed 0.317 g (93.9% of theoretical yield).

Anal. Calcd. for $C_3H_7O_5P$ (mol. wt. 154.1): C, 23.39; H, 4.58; P, 20.11. Found: C, 22 96; H, 5.03; P, 20.00.

DL-Glyceraldehyde-3-phosphonic Acid 2,4-Dinitrophenylosazone

To 10 ml of an aqueous solution containing 60 mg of glyceraldehyde-3-phosphonic acid were added 20 ml of 2 *N* hydrochloric acid and 310 mg of 2,4-dinitrophenyl hydrazine, and the mixture was boiled under reflux for 1 h. The dark orange–red osazone was collected by centrifugation, washed with two 6 ml portions of 2 *N* hydrochloric acid, and was dried at room temperature over sodium hydroxide powder and phosphorus pentoxide for 5 h at a pressure of 0.05 mm Hg. The glyceraldehyde-3-phosphonic acid dinitrophenylosazone weighed 188.0 mg (94.3% of theoretical yield).

Anal. Calcd. for $C_{15}H_{13}O_{11}N_8P$ (mol. wt. 512.3): N, 21.87; P, 6.04. Found: N, 22.02; P, 5.98.

Calcium DL-Glyceraldehyde-3-phosphonate

To an ice-cold solution of 154.1 mg (1.0 mmol) of DL-glyceraldehyde-3-phosphonic acid and 264 mg (1.5 mmol) of calcium acetate (1 mol of water) in 2.8 ml of water were added dropwise 3.5 ml of 95% ethanol over a period of 30 min, and the mixture was kept in ice for a further 30 min. The precipitate was collected by centrifugation, washed with two 2 ml portions of a mixture of ethanol and water (4:6, v/v), and was dried for 4 days over calcium chloride and Drierite® at a pressure of 0.01 mm Hg. The calcium salt, weighing 150.7 mg (87.2% of theoretical yield), contained 1 atom of calcium per 2 mol of glyceraldehyde-3-phosphonic acid.

Anal. Calcd. for $[C_3H_6O_5P]_2Ca$ (mol. wt. 346.2): C, 20.81; H, 3.49; P, 17.89; Ca, 11.57. Found: C, 20.67; H, 3.59; P, 17.67; Ca, 11.72.

[4]Analytical values of two independent preparations of the cyclohexylammonium salt.

Can. J. Chem. Downloaded from www.nrcresearchpress.com by 210.87.254.105 on 09/05/12
For personal use only.

Stability of the C—P Bond of Glyceraldehyde-3-phosphonic Acid Towards Alkali and Acid

Alkali

To a solution containing 7.52 mg of glyceraldehyde-3-phosphonic acid in 1.0 ml of water were added 5.0 ml of 0.1 *N* sodium hydroxide, and the solution was kept at room temperature (23°) for 1 h. At the end of this period, the contents of inorganic phosphorus in the solution (*a*), and in a blank (*b*) consisting of 5.0 ml of 0.1 *N* sodium hydroxide, were determined colorimetrically by the method of King.

Calcd.: Inorg. P, 1.512 mg (for 100% of liberation of organic P). Found: Inorg. P, 0.006 mg; (*a*) = 0.003 mg, (*b*) = 0.003 mg or 0.2% P.

Acid

A solution of 7.52 mg of glyceraldehyde-3-phosphonic acid in 10.0 ml of 0.1 *N* hydrochloric acid was boiled under reflux for 1 h, and the inorganic phosphorus in an aliquot of 5.0 ml was determined as above.

Calcd.: Inorg. P, 0.756 mg (for 100% liberation of org. P). Found: Inorg. P, 0.022 mg or 2.9% of theory.

Pathway 2

2,5-Bis(acetoxymethyl)-3,6-dibenzoxy-1,4-dioxane (**12**) (15) and 2,5-bis(hydroxymethyl)-3,6-dibenzoxy-1,4-dioxane (**13**) (15) were prepared as described in the literature.

*2,5-Bis(p-toluenesulfonyloxymethyl)-3,6-dibenzoxy-1,4-dioxane (**14**)*

To a solution of 7.21 g (20.0 mmol) of 2,5-bis(hydroxymethyl)-3,6-dibenzoxy-1,4-dioxane (**13**) in a mixture of 8.0 ml (0.1 mol) of anhydrous pyridine and 80 ml of ethanol-free chloroform were added 7.62 g (40 mmol) of *p*-toluenesulfonyl chloride, and the mixture was kept under anhydrous conditions at a temperature of 38–40° for 2 days. At the end of this period, a small amount of ice and 55 ml of 0.1 *N* sulfuric acid were added, and the chloroform solution and the aqueous suspension of the toluenesulfonate were separated. The aqueous suspension was filtered with suction, and the material on the filter was washed with water until the filtrate was neutral. The chloroform solution, after washing several times with water, was dried with anhydrous sodium sulfate and the solvent was removed by distillation under reduced pressure at a bath temperature of 25–30°. The combined solids were triturated three times with 150 ml of water and dried at room temperature over calcium chloride at a pressure of 0.01 mm Hg for 20 h. The already fairly pure toluenesulfonate (m.p. 165–166°) weighed 12.38 g (92.5% of theoretical yield). Dissolving the substance with warming in 360 ml of chloroform, keeping the solution overnight at 6° and drying the precipitate for 4 h over phosphorus pentoxide at 56° (boiling acetone) and a pressure of 0.01 mm Hg, gave 10.06 g (75.2% of theory) of pure 2,5-bis(*p*-toluenesulfonyloxymethyl)-3,6-dibenzoxy-1,4-dioxane, m.p. 169–170° (dec.). T.l.c. on silica gel H with a solvent mixture of ether and low-boiling petroleum ether (80:20, v/v) gave one spot with an R_f value of 0.79. At room temperature, the compound is moderately soluble in chloroform, and sparingly soluble in ether, acetone, methanol, and ethanol (99%).

Anal. Calcd. for $C_{34}H_{36}O_{10}S_2$ (mol. wt. 668.8): C, 61.06; H, 5.42; S, 9.59. Found: C, 61.38; H, 5.11; S, 9.50.

*2,5-Diiodomethyl-3,6-dibenzoxy-1,4-dioxane (**15**)*

To 80 ml of dry methyl ethyl ketone were added 7.70 g (11.5 mmol) of 2,5-bis(*p*-toluenesulfonylhydroxymethyl)-3,6-dibenzoxy-1,4-dioxane (**14**) and 10.4 g (69.4 mmol, three-fold excess) of anhydrous sodium iodide, and the mixture was refluxed under anhydrous conditions for 20 h (temperature of oil bath 90–95°). The reaction mixture then was cooled to room temperature, filtered with suction, and the solid material was washed on the filter with 100 ml of methyl ethyl ketone. The combined filtrates were evaporated to dryness under reduced pressure (8–12 mm Hg), and the solid residue together with the earlier precipitate were suspended with stirring in 200 ml of water. The mixture was filtered with suction, and the material was washed on the filter with 50 ml of 0.1 *N* sodium thiosulfate followed by 200 ml of water. On drying at room temperature over calcium chloride at a pressure of 0.01 mm Hg, the already fairly pure iodo-compound weighed 6.39 g (95.8% of theory), m.p. 127–129°. It was further purified by dissolving it in 500 ml of a warm mixture of ether and low boiling petroleum ether (4:1, v/v), filtering the warm solution if necessary, and keeping the filtrate overnight at room temperature. The 2,5-diiodomethyl-3,6-dibenzoxy-1,4-dioxane, which separated in the form of centimeter-long narrow prisms, was dried as described above. The pure iodo-compound weighed 5.44 g (81.4% of theory), m.p. 129–130°. T.l.c. on silica gel H with a solvent mixture of petroleum ether (30–60°) and ether (85:15, v/v) gave a single spot with an R_f value of 0.57. At room temperature, the iodo-compound is readily soluble in acetone, ether, and chloroform, sparingly soluble or insoluble in dry methanol and ethanol.

Anal. Calcd. for $C_{20}H_{22}O_4I_2$ (mol. wt. 580.2): C, 41.40; H, 3.82; I, 43.75. Found: C, 41.70; H, 3.77; I, 43.92.

*2,5-Bis(methylphosphonic acid diethyl ester)-3,6-dibenzoxy-1,4-dioxane (**16**)*

Into a two-necked 250 ml round-bottomed flask equipped with a Liebig condenser and a gas-inlet tube were placed 4.79 g (8.26 mmol) of 2,5-diiodomethyl-3,6-dibenzoxy-1,4-dioxane (**15**) and 50 g (0.3 mol) of triethyl phosphite, and the mixture was kept at 140–145° (oil bath) for 48 h. To facilitate the removal of ethyl iodide a slow stream of nitrogen was passed through the apparatus and the condenser water was kept at 55° (±5°). At the end of this period, the excess of triethyl phosphite was distilled off under reduced pressure (10 mm Hg) at a bath temperature of 75–80°. To remove the last traces of triethyl phosphite, the highly viscous, pale yellow residue was kept for 4 h at 45–50° and a pressure of 0.01 mm Hg. The remaining material, which solidified on triturating with 25 ml of low boiling petroleum ether, was filtered off with suction, washed with 10 ml of petroleum ether, and was dried for 4 h at room temperature over calcium chloride at a pressure of 0.01 mm Hg. The material, weighing 4.62 g (93.1% of theory), and melting from 70–72°, on crystallization from 100 ml of a mixture of ether and low-boiling petroleum ether (9:1, v/v), and drying as described above, gave 4.60 g (92.7% of theory) of pure 2,5-bis(methylphosphonic acid diethyl ester)-3,6-dibenzoxy-1,4-dioxane, m.p. 74–74.5°. The melting point remained unchanged on further crystallization. T.l.c. on silica Gel H with chloroform and methanol (95:5, v/v) gave a single spot with an R_f value of 0.46. The com-

Can. J. Chem. Downloaded from www.nrcresearchpress.com by 210.87.254.105 on 09/05/12
For personal use only.

pound is readily soluble in methanol, ethanol, acetone, chloroform, ethyl acetate, and ether, and in warm petroleum ether (b.p. 30–60°).

Anal. Calcd. for $C_{28}H_{42}O_{10}P_2$ (mol. wt. 600.6): C, 55.99; H, 7.05; P, 10.31. Found: C, 55.70; H, 7.24; P, 10.49.

*2,5-Bis(methylphosphonic acid)-3,6-dibenzoxy-1,4-dioxane (**17**)*

A mixture of 600 mg (1.0 mmol) of 2,5-bis(methylphosphonic acid diethyl ester)-3,6-dibenzoxy-1,4-dioxane and 35 ml of trimethylchlorosilane was kept in a pressure vessel for 3 days at a temperature of 70–75° At the end of this period, the excess of chlorotrimethylsilane was distilled off under reduced pressure at a bath temperature of 30–32°. The residue was dissolved in 200 ml of distilled water and the solution was kept for 4 days at a temperature of 40–42°. The aqueous solution, after extracting with two 25 ml portions of chloroform, was evaporated to dryness under reduced pressure at a bath temperature of 30–32°. The material remaining was dissolved in 15 ml of ethanol (95%), and the solvent was distilled off under reduced pressure. The operation was repeated once more with 15 ml of ethanol. The residue was triturated with 10 ml of dry ether, and the ether was removed by distillation. The crude product after drying weighed 433.4 mg (88.3% of theory). For further purification, it was dissolved with warming in 45 ml of ethanol (95%), the solution was decolorized with a small amount of charcoal (Norit A, acid-washed) and filtered while still warm. The filtrate was kept overnight at −6°. The precipitate was filtered off with suction and was dried for 4 h over phosphorus pentoxide at 80° (boiling benzene) and a pressure of 0.01 mm Hg. The 2,5-bis(methylphosphonic acid)-3,6-dibenzoxy-1,4-dioxane weighing 330 mg was obtained in a yield of 67.5% of theory, m.p. 160–161°. At room temperature (22°), the compound is readily soluble in methanol and ethanol, sparingly soluble in water, and insoluble in acetone, ethyl acetate, ether, petroleum ether, chloroform, or benzene.

Anal. Calcd. for $C_{20}H_{26}O_{10}P_2$ (mol. wt. 488.4): C, 49.18; H, 5.37; P, 12.69. Found: C, 48.79; H, 5.71; P, 12.75.

*DL-Glyceraldehyde-3-phosphonic Acid (**10**, **11**)*

2,5-Bis(methylphosphonic acid)-3,6-dibenzoxy-1,4-dioxane (**17**) (652 mg), 400 mg of palladium black, and 100 ml of glacial acetic acid were placed in an all-glass reduction vessel of 500 ml capacity, and the mixture was shaken vigorously in an atmosphere of pure hydrogen at an initial pressure of 40 cm of water until the absorption of hydrogen ceased. After replacing the hydrogen by nitrogen, the catalyst was removed by filtration, and washed with three 20 ml portions of acetic acid. The combined filtrates were cleared by centrifugation, and the acetic acid was distilled off under reduced pressure (8–10 mm Hg) at a bath temperature of 30–32°. The residue was dissolved in 10 ml of distilled water, the solution, if necessary, was freed of insoluble material and the water was removed by distillation under reduced pressure and a bath temperature of 35°. This operation was repeated once more in 10 ml of water. The remaining, colorless and highly viscous material was freed of last traces of water and acetic acid by keeping it for 3 days over calcium chloride and sodium hydroxide (powder) at a pressure of 0.02 mm Hg, occasionally changing the drying agents. The DL-glyceraldehyde-3-phosphonic acid, a glass-like material, weighed 394 mg (95.8% of theoretical yield).

Anal. Calcd. for $C_3H_7O_5P$ (mol. wt. 154.1): C, 23.39; H, 4.58; P, 20.11. Found: C, 23.86; H, 5.09; P, 19.94.

Glyceraldehyde-3-phosphonic Acid 2,4-Dinitrophenylosazone

Treating a solution of 37.6 mg of glyceraldehyde-3-phosphonic acid in 5 ml of water with 2,4-dinitrophenylhydrazine in 2 *N* hydrochloric acid, as described above, gave 115.8 mg (92.6% of theory) of glyceraldehyde-3-phosphonic acid 2,4-dinitrophenylosazone.

Anal. Calcd. for $C_{15}H_{13}O_{11}N_8P$ (mol. wt. 512.3): P, 6.04. Found: P, 6.11.

Calcium DL-Glyceraldehyde-3-phosphonate

The calcium salt was prepared as described above and was obtained in a yield of 89.9% of theory.

Anal. Calcd. for $[C_3H_6O_5P]_2Ca$ (mol. wt. 346.2): C, 20.81; H, 3.49; P, 17.89. Found: C, 20.57; H, 3.89; P, 17.79.

Discussion

Having obtained DL-glyceraldehyde-3-phosphonic acid (GLA-3-PnA) by catalytic reduction of its benzyl cycloacetal (pathway 2), it was found that at 0° it also readily forms a mixture of 2,4-dinitrophenylhydrazone and 2,4-dinitrophenylosazone of GLA-3-PnA. It thus behaves towards 2,4-dinitrophenylhydrazine hydrochloride in the same manner as GLA-3-PnA prepared by acid hydrolysis of its methyl cycloacetal (Pathway 1). The formation of the dinitrophenylosazone of GLA-3-PnA at 0°, hence is not caused by an oxidation product of GLA-3-PnA, formed during acid hydrolysis of the methyl cycloacetal, but is a result of the oxidation of the secondary hydroxyl-group of GLA-3-PnA by dinitrophenylhydrazine. The fact that GLA-3-PnA, in contrast to glyceraldehyde-3-phosphoric acid (GLA-3-PA) does not yield a pure dinitrophenylhydrazone at 0°, is an indication that its secondary hydroxyl-group is more readily oxidized than that of GLA-3-PA. The triose-phosphonate, because of its chemically highly stable C—P bond differs from GLA-3-PA also in several other respects. Unlike GLA-3-PA, it neither forms methylglyoxal or lactic acid on treatment with acid or alkali, respectively, nor does it lose its phosphonic acid on forming a dinitrophenylhydrazone or dinitrophenylosazone. GLA-3-PnA and GLA-3-PA thus are readily distinguishable from each other by chemical means. The triose-phosphonate further differs from GLA-3-PA in that under identical experimental conditions it yields a calcium salt which contains only 1 atom of calcium per 2 mol of GLA-3-PnA.

The support of this work by grants from the J. P. Bickell Foundation, the Medical Research Council of Canada (MT-684), and the National Heart and Lung Institute (HL-08780-08), United States Public Health Service, is gratefully acknowledged.

1. B. MENDEL. Klin. Wschr. **8**, 169 (1929).
2. J. NEEDHAM and H. LEHMANN. Biochem. J. **31**, 1913 (1937).
3. O. MEYERHOF, K. LOHMAN, and P. SCHUSTER. Biochem. Z. **286**, 319 (1936).
4. H. A. LARDY, K. D. WIEBELHAUS, and K. M. MANN. J. Biol. Chem. **187**, 325 (1950).
5. O. WARBURG, K. GAWEHN, A. W. GEISSLER, and S. LORENZ. Z. Klin. Chem. **1**, 175 (1963).
6. E. BAER and H. BASU. Can. J. Biochem. **47**, 955 (1969).
7. E. BAER and R. ROBINSON. Can. J. Biochem. **49**, 300 (1971).
8. E. BAER and H. O. L. FISCHER. J. Am. Chem. Soc. **61**, 761 (1939).
9. H. O. L. FISCHER and E. BAER. Ber. Deut. Chem. Ges. **65**, 337 (1932).
10. J. TAUSZ and N. v. PUTNOCKY. Ber. Deut. Chem. Ges. **52**, 1573 (1919).
11. H. O. L. FISCHER, C. TAUBE, and E. BAER. Ber. Deut. Chem. Ges. **60**, 479 (1927).
12. E. BAER. Inaugural-dissertation, Friedrich–Wilhelms Universität, Berlin, Germany. 1927. p. 28.
13. H. O. L. FISCHER and C. TAUBE. Ber. Deut. Chem. Ges. **60**, 1704 (1927).
14. H. O. L. FISCHER and E. BAER. Ber. Deut. Chem. Ges. **63**, 1744 (1930).
15. H. O. L. FISCHER and E. BAER. Ber. Deut. Chem. Ges. **65**, 337 (1932).

Can. J. Chem. Downloaded from www.nrcresearchpress.com by 210.87.254.105 on 09/05/12
For personal use only.

Termolecular Recombination Rate Constant and Triple Collision Cross-section[1]

W. H. Wong and G. Burns

Lash Miller Chemical Laboratories, University of Toronto, Toronto 181, Ontario

Received June 1, 1972

The concept of triple collisions cross-section in termolecular recombination reaction was investigated. The hard-sphere model was tested against experimental data, and it was found to predict, in disagreement with experiments, a positive temperature dependence for the recombination rate constants. Average cross-sections were obtained from experimental rate data. Two empirical functions widely used for summarizing experimental rate data were inverted through an inverse Laplace transform to give the triple collision cross-section.

Nous avons étudié le phénomène de surface de triple collision dans les réactions de recombinaison termoléculaire. Le modèle de la sphère rigide a été vérifié à partir des données expérimentales; nous constatons qu'il prédit, contrairement à ce qui découle de l'expérience, une dépendance positive de la température sur les constantes de vitesse de recombinaison. Les surfaces moyennes sont tirées des données expérimentales de vitesse. Deux fonctions empiriques largement utilisées dans l'expression des résultats de vitesse expérimentale, ont été interverties au moyen d'une transformée inverse de Laplace, pour obtenir la surface de triple collision. [Traduit par le journal]

Can. J. Chem., **51**, 111 (1973)

Introduction

Recent advances in experimental techniques in studying gas phase reaction are beginning to yield data that are more fundamental than the overall rate coefficient. These data, in conjunction with the modern collision theory, will eventually reveal the microscopic properties of the species involved. In collision theory, the basic quantity is the S-matrix, the modulus square of its elements is a measure of the probability of state transformation. The formal expression relating this quantity to the phenonomenological rate coefficient has been obtained by Smith (1). Even though this S-matrix embodies all the dynamical properties of a microscopic process, it is not the physical quantity that is directly observed in experiments. Rather, it is the cross-section which is a ratio of the flux into a specific final channel to the incident flux that is directly observable.

The concept of collision cross-section has been most fruitfully pursued in the study of elementary bimolecular reaction. From the experimental side, various beam experiments directly determine this quantity (see, for example, ref. 2). The theoretical calculations of reaction cross-section by quantum scattering theory (see, for example, ref. 3), by classical mechanics (4), and by some form of statistical theory (5, 6) have been one of the focal points in modern kinetics. The connection between this bimolecular cross-section and the rate coefficient is very well known (7, 8), and the possibility of extracting the former from the rate data has also been studied by several authors (9, 10). Also with the aid of the concept of reaction cross-section, the validity of the conventional formulation of the activated complex theory is being tested (11), and the modern version of this theory is being developed (12). From all these theoretical and experimental efforts, the general features of different categories of bimolecular reaction cross-section have emerged.

The situation in termolecular recombination reaction is much less favorable. In fact, the concept of triple collision cross-section and its relation to the recombination rate coefficient was only recently introduced by Smith (1, 13, 14). Furthermore, the triple collision cross-section suffers from the disadvantage of being less amenable to elementary physical interpretation. In a binary collision, the dimension of the reaction cross-section is length squared per molecule (cm^2/molecule), and it could be interpreted physically as an effective target area of the species undergoing the specified transformation. In triple collision, however, there are a total of six co-ordinates in the

[1]Research sponsored, in part, by the Air Force Office of Scientific Research, Air Force Systems Command, USAF, under grant No. AFOSR-71-2016A. The United States Government is entitled to reproduce and distribute reprints for Government purposes notwithstanding any copyright notation hereon.

Can. J. Chem. Downloaded from www.nrcresearchpress.com by 210.87.254.40 on 09/05/12
For personal use only.

Can. J. Chem. Downloaded from www.nrcresearchpress.com by 210.87.254.40 on 09/05/12
For personal use only.

center-of-mass system. After singling out one as progress variable with respect to reaction, there are still five orthogonal co-ordinates that describe the "cross-section" in this 6-dimensional hyperspace. But the fact that the dimension of a triple collision cross-section is $cm^5/molecule^2$ should not obscure the significance of this quantity which, like its counterpart in bimolecular collision, is a measure of the ratio of the flux into the product channel to that from the incident channel. Presently, we further explored Smith's formulation (1, 13–15) which established the formal relationship between the termolecular rate coefficient and the triple collision cross-section. First, recombination rate constants were constructed from the triple collision reactive cross-section obtained from a 3-body hard-sphere model which was suggested by Smith (15) as a standard reference. The trends emerged from this model were discussed in light of experimental observations. Then the experimental rate data obtained over a fairly wide temperature range were converted to approximate triple collision cross-sections and their main features noted. Finally, attempts were made to extract the cross-section function from recombination rate constants.

Triple Collision Cross-section and Atomic Recombination Rate Constant

Completely analogous to bimolecular collision, the reactive cross-section in a triple collision σ_3 can be defined as

$$[1]\quad Z = N_A N_B N_C \int\int\int v_3 \sigma_3(v_3) f_A(\boldsymbol{v}_A) \times f_B(\boldsymbol{v}_B) f_C(\boldsymbol{v}_C) d^3\boldsymbol{v}_A d^3\boldsymbol{v}_B d^3\boldsymbol{v}_C$$

in which Z is the number of reactive triple collision per unit time per unit volume, N_i is the number density of the ith species with a normalized velocity distribution $f_i(\boldsymbol{v}_i)$, and v_3 is the velocity of approach in the 3-body center-of-mass system. (Throughout this paper, the subscript 3 emphasizes the quantity pertinent to a triple collision.) Confining to collisions that lead to recombination, one can write the rate coefficient of the process as

$$[2]\quad k_r(T) = \int\int\int v_3 \sigma_3(v_3) f_A(\boldsymbol{v}_A) f_B(\boldsymbol{v}_B) \times f_C(\boldsymbol{v}_C) d^3\boldsymbol{v}_A d^3\boldsymbol{v}_B d^3\boldsymbol{v}_C$$

In a Boltzmann ensemble, Smith (1, 14, 15) was able to reduce the above expression to

$$[3]\quad k_r(T) = (2\mu_3)^{-1/2}(kT)^{-3} \times \int_0^\infty \exp\left(\frac{-E_3}{kT}\right)\sigma_3(E_3){E_3}^{5/2} dE_3$$

in which k is the Boltzmann constant, μ_3 is the reduced mass in the 3-body system that diagonalizes the kinetic energy and is given by

$$[4]\quad \mu_3 = \frac{\prod m_i}{\left(\sum_i m_i\right)^{1/2}} \qquad i = A, B, C$$

where m_i is the mass of species i. The kinetic energy E_3 in the 3-body system is then

$$[5]\quad E_3 = \frac{1}{2}\mu_3 {v_3}^2$$

It follows from eq. 3 that the recombination rate coefficient is proportional to the Laplace transform of ${E_3}^{5/2}\sigma_3(E_3)$. Similar to the treatment in bimolecular collision, one could in principle extract the cross-section through an inverse Laplace transform

$$[6]\quad \sigma_3(E_3) = (2\mu_3)^{1/2}{E_3}^{-5/2} \times \frac{1}{2\pi i}\int_{c-i\infty}^{c+i\infty} \beta^{-3} k_r(\beta) e^{\beta E_3} d\beta$$

where

$$\beta = 1/kT$$

If $k_r(T)$ and hence $k_r(\beta)$ is formulated by some form of statistical theory, the inversion can either be obtained in closed form or can be evaluated approximately by the method of steepest descent. Similar procedure was employed by Eu, Morokuma, and Karplus (11) and by Lin and Eyring (9) in testing the bimolecular activated complex theory by extracting the 2-body cross-section from the rate coefficient expressed as a ratio of partition functions. Similar principles were used in the work of Marcus and co-worker (6, 12) who developed the statistical–dynamical model of bimolecular reaction cross-section within the framework of the microcannonical activated complex theory. If the $k_r(T)$ is known experimentally over a sufficiently wide temperature range and if it is fitted into a functional form in terms of T, similar procedure could also be applied in the present case. But if the $k_r(T)$ is known only within a limited range of temperature, a more drastic approximation has to be introduced. In the latter case, eq. 3 can be rewritten as

Can. J. Chem. Downloaded from www.nrcresearchpress.com by 210.87.254.40 on 09/05/12
For personal use only.

[7] $$k_r(T) = \langle v_3 \rangle \langle \sigma_3 \rangle$$

where

[8] $$\langle v_3 \rangle = (2\mu_3)^{-1/2}(kT)^{-3} \times \int_0^\infty E_3^{5/2} \exp \frac{-E_3}{kT}\, dE_3 = \frac{15\pi}{8}\left(\frac{kT}{2\pi\mu_3}\right)^{1/2}$$

and

[9] $$\langle \sigma_3 \rangle = \frac{\int_0^\infty E_3^{5/2}\sigma_3(E_3) \exp\left(\frac{-E_3}{kT}\right) dE_3}{\int_0^\infty E_3^{5/2} \exp\left(\frac{-E_3}{kT}\right) dE_3}$$

Thus the quantities $\langle v_3 \rangle$ and $\langle \sigma_3 \rangle$ are just velocity and cross-section averaged over the entire ensemble at a specified temperature. The dimension of σ_3 is cm^5 molecule^{-2} in eq. 7, since $k_r(T)$ is in units of cm^6 molecule^{-2} s^{-1}. As discussed by Smith (15), the average velocity of approach in a 3-body system as given by eq. 8 is different from the corresponding quantity in bimolecular collision at the same temperature ($\langle v_2 \rangle = (8kT/\pi\mu_2)^{1/2}$). The resulting energy of approach in these two modes of collision will also be different. In fact the ratio E_3/E_2 is about 2.17. It is interesting to note that if $\sigma_3(E_3)$ in eq. 3 is independent of energy, one could rigorously write

[10] $$k_r(T) = \langle v_3 \rangle \sigma_3^0$$

It is the parallelism between this expression and its counterpart in bimolecular collision that led Smith (15) to suggest a 3-body hard-sphere model for triple collision as a standard for comparison. In this model the radius of the hard-sphere is determined by the geometric mean of impact distance between each pair of colliding species. If the collision radius of the species i is r_i, the normalized distance between each pair of colliding particles is (13, 15)

[11] $$R_{AB} = (r_A + r_B) \times \left[\frac{m_A m_B (m_A + m_B + m_C)}{m_C (m_A + m_B)^2}\right]^{1/4}$$

The hard-sphere radius is then given by the symmetric formula

[12] $$R_0 = (R_{AB}R_{BC}R_{CA})^{1/3}$$

and the cross-section in this 6-dimensional hypersphere is

[13] $$\sigma_3^0 = \frac{8\pi^2}{15} R_0^5$$

When the above expression is substituted into eq. 10, the "hard-sphere" recombination constant is obtained.

Calculation and Discussion

(A) Recombination Rate Constant from a 3-Body Hard-Sphere Model

The rate constants for the recombination of iodine and of bromine in inert gas (Xe, Ar, He) were calculated from the 3-body hard-sphere model as depicted by eqs. 8–11. The main difficulty encountered here was the choice of relevant collision radius of each species in a triple collision. It is not at all clear whether the covalent atomic radius or the van der Waals' radius is appropriate for this purpose. Furthermore, the triple collision cross-section (and hence the rate constant) is even more sensitive to the collision radii of the species involved than its counterpart in a binary collision, because in a triple collision the cross-section is proportional to the fifth power of the radius while in a binary collision it is proportional to the square of the radius. However, our chief objective in this work is to map out the main features of this model; we employed the covalent radii which were summarized in Table 1.

The calculated recombination rate constants for bromine and for iodine as well as the corresponding experimental data (16) are presented in Figs. 1 and 2, respectively. From these plots, it is obvious that the hard-sphere model not only fails to predict the magnitude of the observed rate data, but it also reveals the reverse trend with respect to temperature variation. The discrepancy between the absolute values of the calculated data and the experimental data is not the most damaging since it may just reflect the inappro-

TABLE 1. Atomic radii*

Atom	Radius (Å)
I	1.333
Br	1.142
Xe	2.18
Ar	1.92
He	1.53

*Data from ref. 24.

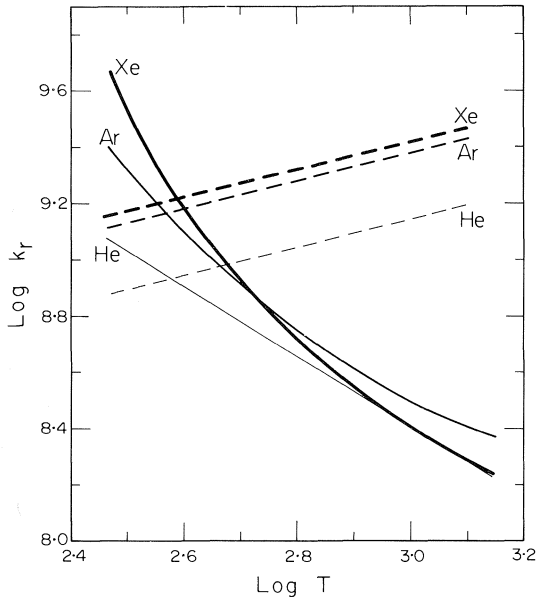

FIG. 1. Recombination rate constants (l^2 mol^{-2} s^{-1}) of bromine in different inert gases (Xe, Ar, He): solid lines indicate experimental data of ref. 16; dashed lines are results from the hard-sphere model.

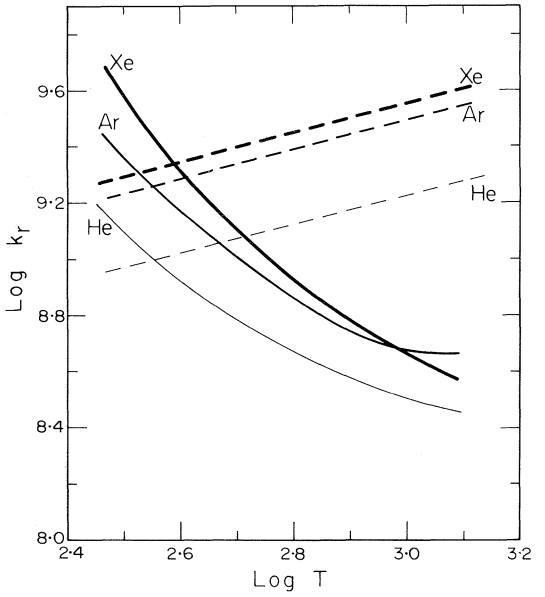

FIG. 2. Recombination rate constants (l^2 mol^{-2} s^{-1}) of iodine in different inert gases (Xe, Ar, He): solid lines indicate experimental data of ref. 16; dashed lines are results from the hard-sphere model.

priate choice of collision radius of each species. However, the fact that the recombination rate constant predicted by this model increases with increasing temperature while the reverse trend was observed experimentally does indicate that the difficulty of this model is fundamental.

The result that the hard-sphere rate constant increases with temperature is not at all surprising since eqs. 8 and 10 clearly show that the rate constant should increase monotonically with temperature ($\sim T^{1/2}$), provided that the cross-section is independent of energy.

(B) Approximate Triple Collision Cross-section from Recombination Rate Data

The average triple collision cross-sections in the recombination of bromine and of iodine in inert gas (Xe, Ar, He) were calculated from the experimental data of Burns and co-workers (16). These experimental data cover a fairly wide temperature range (298 to 1300 °K), which permits us to obtain the average cross-section within a range of energy. The recombination dynamics in these systems has also been studied by classical trajectory calculations (17).

The computation of the average cross-section is based on eqs. 7 to 9. The average energy of the system at a specified temperature is defined as (eqs. 4, 5, and 8).

$$\langle E_3 \rangle = \tfrac{1}{2}\mu_3 \langle v_3 \rangle^2 \approx 2.67kT$$

The plots of $\langle \sigma_3 \rangle$ against $\langle E_3 \rangle$ for the recombination of bromine and of iodine are shown in Figs. 3 and 4, respectively. One novel feature of these plots is that unlike the familiar bimolecular (neutral–neutral) reaction cross-section which usually shows a threshold energy below which the reaction cross-section is negligible, the cross-section in a triple (reactive) collision has no such threshold. This is reasonable since in termolecular recombination, there is no energy barrier for the system to surmount. However, the exceedingly steep rise of the cross-section at low energy, particularly in systems with heavy inert gas (Xe, Ar) as third body, certainly reflects the dominance of the mechanism involving bound intermediates (for example, IXe and BrXe complexes held together by van der Waals' attraction). Once the mechanism involving bound intermediates becomes predominant, the rate-controlling elementary process is essentially a binary encounter, and the formulation entirely based on triple collisions will not be appropriate.

Can. J. Chem. Downloaded from www.nrcresearchpress.com by 210.87.254.40 on 09/05/12
For personal use only.

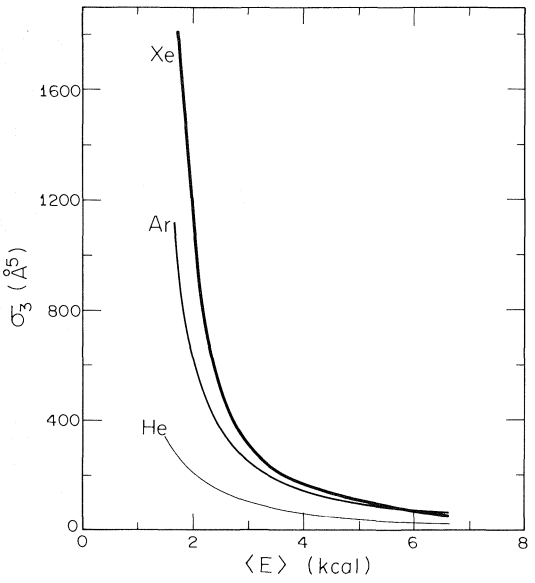

FIG. 3. Average triple collision cross-section (σ_3) extracted from the rate data of bromine recombination.

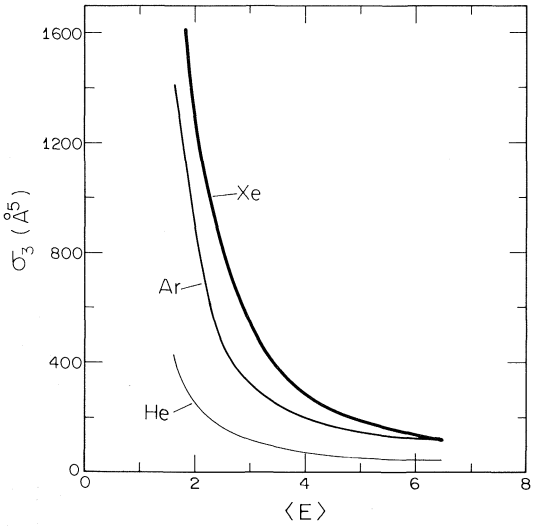

FIG. 4. Average triple collision cross-section (σ_3) extracted from the rate data of iodine recombination.

Trajectory studies performed on these systems (17) did reveal that at low temperature and with heavy inert gas, the mechanism involving bound intermediates was indeed predominant.

Another interesting feature revealed in these calculations is that the cross-section decreases asymptotically within our studied energy range, which is in contrast to the asymptotic increase in the post-threshold region of the corresponding quantity in bimolecular (neutral–neutral) reaction. It is certain though that the triple collision cross-section, just like its counterpart in binary collision (4), should ultimately taper off simply because of the inadequate interaction time at very high energy.

(C) Extraction of Triple Collision Cross-section from Rate Coefficients Expressed as a Function of Temperature

In this section, we attempt to extract the triple collision cross-section from two simple functions which are widely used to summarize observed recombination rate constants which decrease with increasing temperature.

(1) The empirical function is a polynomial of inverse power of T, namely,

$$k_r(T) = \sum_n \frac{A_n'}{T^n}$$

where A_n' is the coefficient of the nth term and n is a positive integer including zero. When k_r is expressed as a function of β ($\beta = 1/kT$), it takes the form

$$k_r(\beta) = \sum_n A_n \beta^n$$

in which

$$A_n = A_n' k^n$$

Then eq. 6 can be rewritten as

$$[14] \quad \sigma_3(E_3) = (2\mu_3)^{1/2} E_3^{-5/2} \times \frac{1}{2\pi i} \int_{c-i\infty}^{c+i\infty} \left(\sum_n A_n \beta^{n-3} \right) e^{\beta E_3} d\beta$$

Quite often only a few terms of the polynomial are needed to fit the data. For example, if only three terms are used (*i.e.* $n = 0, 1, 2$), the solution to eq. 14. is simply

$$[15] \quad \sigma_3(E_3) = (2\mu_3)^{1/2} E_3^{-5/2} \times \left[\sum_{n=0}^{2} \frac{A_n}{(2-n)!} E_3^{2-n} \right]$$

It may be pointed out that the polynomial of inverse power of T, presently employed, can only predict the features of the cross-section within a relatively narrow range of energy because the contour integral involved in the inverse Laplace transformation truncates the series.

(2) The empirical relationship is a logarithmic function (16) such as

$$[16] \quad \ln k_r(T) = A + B(\ln aT) + C(\ln aT)^2$$

Can. J. Chem. Downloaded from www.nrcresearchpress.com by 210.87.254.40 on 09/05/12
For personal use only.

in which A, B, C, and a are constants. When expressed in terms of β, the above expression assumes the form

$$[17] \quad \ln k_r(\beta) = A + B(\ln D\beta^{-1}) + C(\ln D\beta^{-1})^2$$

in which the constant D is related to a in eq. 16 by

$$D = a/k$$

Equation 6 can then be written as

$$[18] \quad \sigma_3(E_3) = (2\mu_3)^{1/2}E_3^{-5/2} \times \frac{1}{2\pi i}\int_{c-i\infty}^{c+i\infty} \exp[F(\beta)]d\beta$$

where

$$[19] \quad F(\beta) = \ln k_r(\beta) - 3\ln\beta + \beta F_3 = A + B\ln(D\beta^{-1}) + C\ln^2(D\beta^{-1}) - 3\ln\beta + \beta E_3$$

We employed the method of steepest descent to evaluate the above integral (18). The saddle point (β*) can be located by setting

$$\partial F(\beta)/\partial\beta = 0$$

which gives

$$E_3 = \frac{3}{\beta^*} - \frac{\partial \ln k_r(\beta^*)}{\partial\beta^*}$$

The exponent $F(\beta)$ of the integrand in eq. 18 was then expanded in the vicinity of β* in the imaginary direction ($\beta = \beta_1 + i\beta_2$) of the complex β plane to give

$$[20] \quad F(\beta) = \sum_{n=0}^{\infty}(n!)^{-1}\left.\frac{\partial^n F(\beta)}{\partial\beta^n}\right|_{\beta^*}(i\beta_2)^n = F(\beta^*) + \sum_{n=2}^{\infty}(n!)^{-1}\left.\frac{\partial^n F(\beta)}{\partial\beta^n}\right|_{\beta^*}(i\beta_2)^n$$

In this expression, the first partial derivative vanishes because the expansion is around the saddle point. With this expansion we can rewrite eq. 18 as

$$[21] \quad \sigma_3(E_3) = (2\mu_3)^{1/2}E_3^{-5/2}\left\{F(\beta^*) + \frac{1}{2\pi}\int_{-\infty}^{+\infty}\exp\left[\sum_{n=2}^{\infty}(n!)^{-1}\left.\frac{\partial^n F(\beta)}{\partial\beta^n}\right|_{\beta^*}\beta_2{}^n(-1)^{n-1}\right]d\beta_2\right\}$$

in which we have chosen the path of integration as a straight line passing through the saddle point and running parallel to the imaginary axis. In the first-order approximation, we have

$$[22] \quad \sigma_3(E_3) = (2\mu_3)^{1/2}E_3^{-5/2}\left\{F(\beta^*) + \frac{1}{2\pi}\int_{-\infty}^{+\infty}\exp\left[-\frac{1}{2}\left.\frac{\partial^2 F(\beta)}{\partial\beta^2}\right|_{\beta^*}\beta_2{}^2\right]d\beta_2\right\}$$
$$= (2\mu_3)^{1/2}E_3^{-5/2}\left\{F(\beta^*) + \left[2\pi\left.\frac{\partial^2 F(\beta)}{\partial\beta^2}\right|_{\beta^*}\right]^{-1/2}\right\}$$

where $F(\beta)$ is given by eq. 19 and

$$[23] \quad \frac{\partial^2 F(\beta)}{\partial\beta^2} = \frac{3}{\beta^2} + \frac{k_r(\beta)}{\beta}\left[\left(B + 2C\ln\frac{D}{\beta}\right)^2 + B + 2C\left(1 + \ln\frac{D}{\beta}\right)\right]$$

Finally, by combining eqs. 18, 22, and 23, one obtains

$$[24a] \quad \sigma_3(E_3) = (2\mu)^{1/2}E_3^{-5/2}\left[\ln\frac{k_r(\beta^*)}{\beta^{*3}} + E_3\beta^* + \frac{\beta^*}{(2\pi)^{1/2}}H\right]$$

in which

$$[24b] \quad H = 3 + k_r(\beta^*)\left[\left(B + 2C\ln\frac{D}{\beta^*}\right)^2 + B + 2C\left(1 + \ln\frac{D}{\beta^*}\right)\right]^{-1/2}$$

Can. J. Chem. Downloaded from www.nrcresearchpress.com by 210.87.254.40 on 09/05/12
For personal use only.

Can. J. Chem. Downloaded from www.nrcresearchpress.com by 210.87.254.40 on 09/05/12
For personal use only.

As remarked in previous section, this inversion procedure would be particularly useful if the rate constant could be formulated theoretically. However, care should be taken in selecting a realistic theoretical model. For example, the activated complex theory cannot be meaningfully applied to termolecular atomic recombination reactions. This is because it is difficult to make an unambiguous choice of a meaningful structure for the activated complex. Eyring, Sun, and Gershinowitz (19) have applied the activated complex theory to such reactions; their work is now commonly quoted (20). As can be seen from ref. 20, eq. 15, $k_r \approx T^{-3/2}$ if the H factor is independent (20) of T, and if vibrations of the complex are neglected. However, if vibrations are included, as has been suggested previously (20, 21), then $k_r \approx T^{3/2}$. Recently, it was shown unambiguously (17*b*, 22, 23) that vibrations are strongly coupled to rotations in the "activated complex", and for this reason, use of the activated complex theory would predict $k_r \approx T^{3/2}$, in obvious disagreement with experiment.

Summary

The qualitative features of (reactive) triple collision cross-section relevant to atomic recombination reaction have been investigated. It was found that the recombination rate constant predicted by the hard-sphere model failed to yield the temperature characteristics of the experimental data. This failure led us to conclude that the hard-sphere model, despite its simplicity, had little to offer in explaining recombination reaction.

The approximate triple cross-sections relevant to the recombination of bromine and of iodine in inert gas were deduced from the experimental rate data. These cross-sections decrease asymptotically with increasing energy within the temperature range used, a feature which is in marked contrast to that of the corresponding quantity in bimolecular (neutral–neutral) reaction. An inversion procedure employing the method of steepest descent to obtain the cross-section from recombination rate constants, expressed as simple functions of temperature, was also investigated.

We would like to acknowledge the support of the Air Force Office of Scientific Research and the donors of the Petroleum Research Fund, administered by the American Chemical Society. This work was also supported in part by the National Research Council of Canada and by the Defence Research Board of Canada, Grant No. 9530–54.

1. F. T. SMITH. J. Chem. Phys. **36**, 248 (1962).
2. D. R. HERSCHBACH. Adv. Chem. Phys. **10**, 319 (1966).
3. J. C. LIGHT. Adv. Chem. Phys. **20**, 1 (1971).
4. M. KARPLUS, R. N. PORTER, and R. D. SHARMA. J. Chem. Phys. **43**, 3259 (1965). P. J. KUNTZ, E. M. NEMETH, J. C. POLANYI, and W. H. WONG. J. Chem. Phys. **52**, 4654 (1970).
5. J. C. LIGHT. Discuss. Faraday Soc. **44**, 14 (1967).
6. R. A. MARCUS. J. Chem. Phys. **45**, 2630 (1966); **46**, 959 (1967).
7. M. A. ELIASON and J. O. HIRSCHFELDER. J. Chem. Phys. **30**, 1426 (1959).
8. (*a*) M. MENZINGER and R. WOLFGANG. Angew. Chem. **8**, 438 (1969). (*b*) R. L. LEROY. J. Phys. Chem. **73**, 4338 (1969).
9. S. H. LIN and H. EYRING. Proc. Nat. Acad. Sci. **68**, 402 (1971). S. H. LIN and H. EYRING. J. Chem. Phys. **55**, 5657 (1971).
10. L. A. MELTON and R. G. GORDON. J. Chem. Phys. **51**, 5449 (1969).
11. (*a*) K. MOROKUMA, B. C. EU, and M. KARPLUS. J. Chem. Phys. **51**, 5193 (1969). (*b*) K. MOROKUMA and M. KARPLUS. J. Chem. Phys. **55**, 63 (1971).
12. (*a*) R. A. MARCUS. J. Chem. Phys. **45**, 2138 (1966). (*b*) W. H. WONG and R. A. MARCUS. J. Chem. Phys. **55**, 5625 (1971).
13. F. T. SMITH. Discuss. Faraday Soc. **33**, 183 (1962).
14. F. T. SMITH. Phys. Rev. **120**, 1058 (1960).
15. F. T. SMITH. *In* Kinetic processes in gases and plasma. *Edited by* A. R. Hochstim. Academic Press, New York. 1969. Chap. 9.
16. (*a*) J. K. K. IP and G. BURNS. J. Chem. Phys. **51**, 3414 (1969). (*b*) S. K. CHANG, A. G. CLARKE, and G. BURNS. J. Chem. Phys. **54**, 1836 (1971). (*c*) J. K. K. IP and G. BURNS. J. Chem. Phys. **56**, 3155 (1972).
17. (*a*) A. G. CLARKE and G. BURNS. J. Chem. Phys. **55**, 4717 (1971). (*b*) A. G. CLARKE and G. BURNS. J. Chem. Phys. **56**, 4636 (1972). (*c*) W. H. WONG and G. BURNS. To be published.
18. R. KUBO. Statistical mechanics. North-Holland, Amsterdam. 1965. p. 102.
19. H. EYRING, C. E. SUN, and H. GERSHINOWITZ. J. Chem. Phys. **3**, 786 (1935).
20. S. GLASSTONE, K. J. LAIDLER, and H. EYRING. The theory of rate processes. McGraw-Hill Book Company. New York and London. 1941. p. 217.
21. I. AMDUR. J. Am. Chem. Soc. **57**, 856 (1935).
22. A. GELB, R. KAPRAL, and G. BURNS. J. Chem. Phys. **56**, 4631 (1972).
23. A. G. CLARKE and G. BURNS. J. Chem. Phys. In press.
24. Tables of Interatomic Distances, Special Publication. No. 11. Chemical Society, London. 1958.

Raman and Infrared Studies of Hexa-, Tetra-, and Dihydrates of Crystalline Magnesium Nitrate[1]

TIEN-CHUNG GODFREY CHANG AND DONALD E. IRISH[2]

Chemistry Department, University of Waterloo, Waterloo, Ontario

Received June 30, 1972

Raman and infrared spectra of $Mg(NO_3)_2 \cdot 6H_2O$, $Mg(NO_3)_2 \cdot 6D_2O$ and partially dehydrated products have been obtained and assigned. As the water content is reduced a different set of lines appears and maximizes at the composition $Mg(NO_3)_2 \cdot 4H_2O$. On further dehydration a third set of lines characteristic of $Mg(NO_3)_2 \cdot 2H_2O$ appears. The existence of the metastable tetrahydrate had not been confirmed since it was reported in 1932. The spectra suggest that four equatorial sites aroung Mg^{2+} in the tetrahydrate are occupied by four water molecules and two axial sites by nitrate ions, oriented in monodentate fashion. The spectra suggest that in the dihydrate approximately octahedral coordination is maintained by having two nitrate ions oriented in bidentate fashion and two water molecules *trans* to each other on the remaining sites.

Nous avons obtenu et assigné les spectres Raman et infrarouge de $Mg(NO_3)_2 \cdot 6H_2O$, $Mg(NO_3)_2 \cdot 6D_2O$ et de leurs dérivés partiellement déshydratés. Si la teneur en eau diminue, un ensemble différent de bandes apparait et devient maxium à la conjonction $Mg(NO_3)_2 \cdot 4H_2O$. Si la molécule est déshydratée un peu plus un troisième groupe de bandes, caractéristiques de $Mg(NO_3)_2 \cdot 2H_2O$ apparait. L'existence du composé tétrahydraté métastable n'a pas été confirmée depuis sa découverte en 1932. Les spectres suggèrent que les quatre sites équatoriaux, autour de Mg^{2+}, dans le tétrahydrate, sont occupés par quatre molécules d'eau et les deux sites axiaux par des ions nitrates, orientés de façon monodentée. On tire aussi des spectres que dans le dihydrate, une coordination approximativement octaédrique est maintenue au moyen de deux ions nitrates orientés de façon bidentée, et de deux molécules d'eau, *trans* une par rapport à l'autre sur les sites restants. [Traduit par le journal]

Can. J. Chem., **51**, 118 (1973)

Introduction

The commonly accepted compositions of hydrated magnesium nitrate crystals are: $Mg(NO_3)_2 \cdot 9H_2O$ (*ca.* 30 °C), $Mg(NO_3)_2 \cdot 6H_2O$, and $Mg(NO_3)_2 \cdot 2H_2O$. Sieverts and Petzold (1) reported the existence of a metastable tetrahydrate which has a small field of existence between 50 and 58 °C in the vicinity of an apparent eutectic point which occurs at a composition of 4 moles water per mole salt. Ewing *et al.* (2) were not able to confirm the existence of this hydrate. In this study we report confirmation of the tetrahydrate and report its Raman and infrared spectra. The spectra of the hexa- and dihydrates are also reported. Spectra of the hexahydrate have been, in part, interpreted in terms of the space group determined in X-ray studies by Braibanti *et al.* (3). For the tetra- and dihydrates inferences, based on the spectral changes, are made concerning the coordination sphere around Mg^{2+}.

[1]Contribution to the XIV International Conference on Coordination Chemistry, Toronto, Ontario, June 22–28, 1972.

[2]To whom correspondence should be addressed.

Experimental

$Mg(NO_3)_2 \cdot 6H_2O$ was obtained by twice recrystallizing the magnesium nitrate provided by Fisher Scientific Co. $Mg(NO_3)_2 \cdot 6D_2O$ was prepared as follows. Partially dehydrated magnesium nitrate was dissolved in excess D_2O. The solution was placed under vacuum at 30 °C till dried. The resulting solid substance was partially dehydrated, and again dissolved in excess D_2O. This solution was concentrated until crystals were obtained. The water content was determined by Karl–Fisher titration, which yielded results consistent with the formula. Infrared and Raman spectra indicated that only a trace of H_2O was present in the product. Samples of $Mg(NO_3)_2 \cdot nH_2O$ ($n < 6$) were obtained from the hexahydrate by placing the solid under vacuum at 30–40 °C. The partially dehydrated solids were melted to insure homogeneity and then cooled. The water contents of the resulting polycrystalline powders were determined by Karl–Fisher titrations.

Raman spectra of the powders, contained in sealed Pyrex glass tubes of 3 mm i.d., were obtained with a modified Cary 81 Raman spectrometer. Either the 488.0 or the 514.5 nm line of a Coherent Radiation Model 54 argon-ion laser was directed onto the tube, and the Raman radiation was focused by a cylindrical lens directly onto the slits of the monochromator. The laser beam, sample, lens, and slits were arranged in the same horizontal plane and thus the conventional foreoptics of the Cary 81 were not used. Infrared spectra were recorded

Can. J. Chem. Downloaded from www.nrcresearchpress.com by 210.87.254.40 on 09/05/12
For personal use only.

Can. J. Chem. Downloaded from www.nrcresearchpress.com by 210.87.254.40 on 09/05/12
For personal use only.

using the multiple internal reflectance (MIR) technique (4). A sample was placed against a KRS-5 prism with face angle of either 45° or 60°. The Wilks Model 9 MIR accessory was used in conjunction with a Beckman IR-9 spectrophotometer. Debye–Scherrer X-ray diffraction photographs of the powders were taken with a powder camera (PW 1020) with a diameter of 114.83 mm. A Philips PW 1010 X-ray generator equipped with a fine focus X-ray diffraction tube with copper target (Cu-Kα, 1.541 Å) was used.

Results

Raman spectra of the powders $Mg(NO_3)_2 \cdot nH_2O$ ($n < 6$) can be understood as the superposition of spectra of three different polycrystalline hydrates *viz.* $\cdot 6H_2O$, $\cdot 4H_2O$, and $\cdot 2H_2O$. Consider first the symmetric stretching spectral region of NO_3^-. The hexahydrates (either $\cdot 6H_2O$ or $\cdot 6D_2O$) generate a single line at 1060 cm^{-1}. Samples with a smaller average water content exhibit two new lines at 1050 and 1070 cm^{-1} (Fig. 1). On reduction of the water:magnesium nitrate ratio the 1050 cm^{-1} line grows at the expense of the 1060 cm^{-1} line and attains maximum intensity when n is 4 (Fig. 2). The 1070 cm^{-1} line grows at the expense of the 1050 cm^{-1} line and is the only line present when n is 2. The three nondegenerate modes of vibration are therefore assigned to the three different hydrates. The complementary infrared spectra (Fig. 3) support this interpretation.

Analogous changes are observed in other spectral regions. The 1100–1700 cm^{-1} region is illustrated in Figs. 4 and 5, the low frequency region in Fig. 6 and the 3000–3800 cm^{-1} region (the H_2O stretching region) in Fig. 7. Data, sorted according to crystal type, are presented in Table 1.

The X-ray powder photographs clearly showed that the three crystal types have different structures. The lines are narrow and well defined; the possibility of the samples being glasses after melting is ruled out. Data for the $\cdot 6H_2O$ and $\cdot 6D_2O$ are identical. The data are on file with the National Science Library.[3]

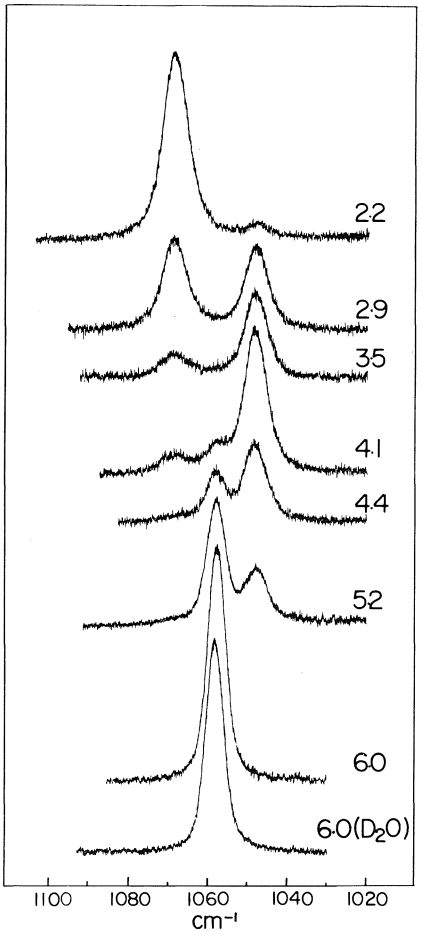

FIG. 1. Raman spectra for $Mg(NO_3)_2 \cdot nH_2O$ crystals in the 1050 cm^{-1} region. Values of n are shown on the contours.

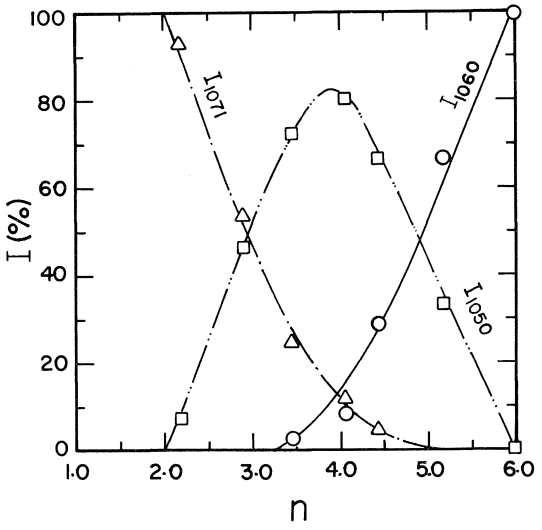

FIG. 2. The percentage of the total intensity generated by the 1060, 1050, and 1071 cm^{-1} bands of hydrated magnesium nitrate *vs.* molar ratio of water to magnesium nitrate, n.

[3]Photocopies of material on deposit are available, at a nominal charge, from the Depository of Unpublished Data, National Science Library, National Research Council of Canada, Ottawa, Canada, K1A 0S2.

Can. J. Chem. Downloaded from www.nrcresearchpress.com by 210.87.254.40 on 09/05/12
For personal use only.

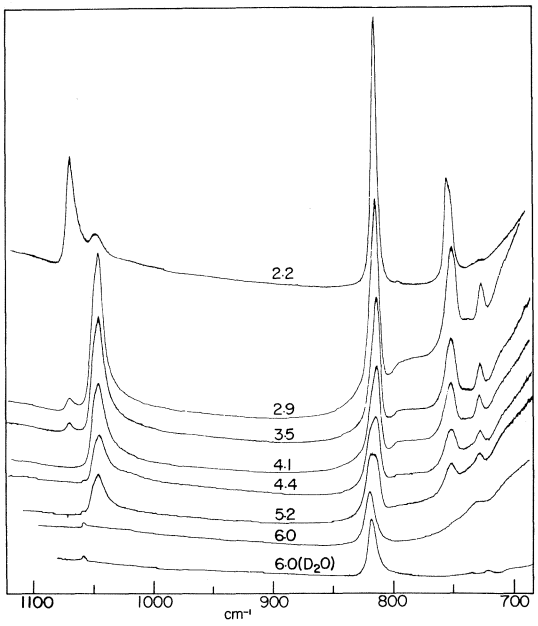

FIG. 3. MIR spectra of $Mg(NO_3)_2 \cdot nH_2O$ and $Mg(NO_3)_2 \cdot 6D_2O$ crystals in the 700–1100 cm^{-1} region.

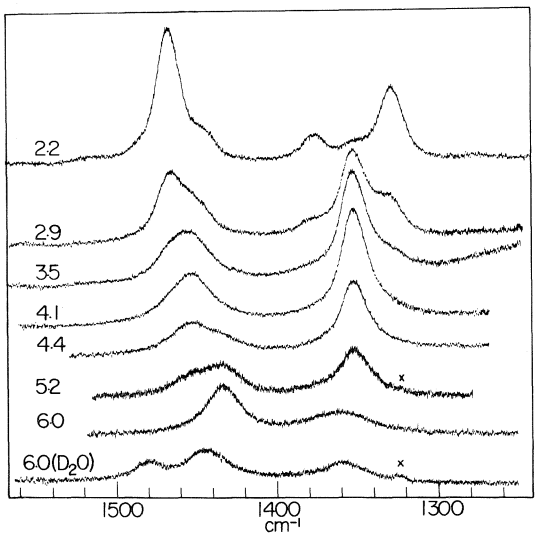

FIG. 4. Raman spectra of $Mg(NO_3)_2 \cdot nH_2O$ and $Mg(NO_3)_2 \cdot 6D_2O$ crystals in the 1250–1550 cm^{-1} region. The crosses denote a plasma line.

Discussion

$Mg(NO_3)_2 \cdot 6H_2O$ and $Mg(NO_3)_2 \cdot 6D_2O$

Braibanti *et al.* (3) reported that $Mg(NO_3)_2 \cdot 6H_2O$ crystals are monoclinic, space group $P2_1/c$ (C_{2h}^5, No. 14), with 2 molecules per unit cell. The $Mg(H_2O)_6^{2+}$ is a distorted octahedron with the Mg—OH_2 distances 2.053, 2.061, and 2.063 Å; the unique H_2O—Mg—OH_2 angles are 91.3, 90.7, and 90.4°. The nitrate ion is also distorted. The N—O bond lengths are 1.20, 1.25, and 1.26 Å and the four atoms are not exactly coplanar. The similarity of the powder patterns indicates that $Mg(NO_3)_2 \cdot 6D_2O$ and $Mg(NO_3)_2 \cdot 6H_2O$ are isomorphic.

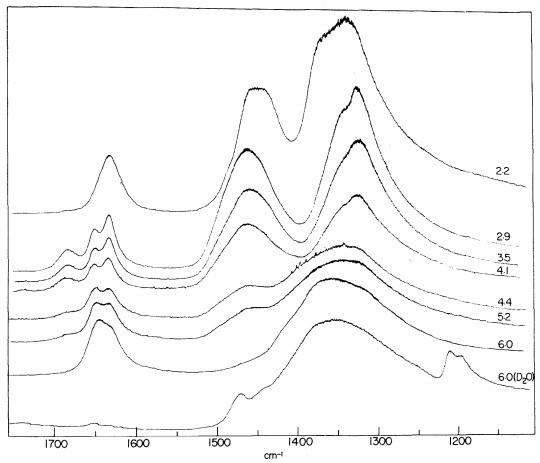

FIG. 5. MIR spectra of $Mg(NO_3)_2 \cdot nH_2O$ and $Mg(NO_3)_2 \cdot 6D_2O$ crystals in the 1100–1700 cm^{-1} region.

The four nitrate ions occupy C_1 sites in the Bravais cell and the correlation field effects may be interpreted in terms of the factor group C_{2h}. The correlation from the symmetry of the undistorted ion, D_{3h}, is as follows:

	D_{3h}	C_1	C_{2h}
ν_1	A_1'(R)		A_g(R)
ν_2	A_2''(i.r.)	A(i.r.,R)	B_g(R)
ν_3, ν_4	E'(i.r.,R)		A_u(i.r.)
			B_u(i.r.)

Since there are two E' modes, if correlation field splitting is detectable there will be twelve Raman active and twelve noncoincident infrared active modes in the spectrum. Under the conditions of the experiment (room temperature powders) these were not all observed. It is noteworthy that the correlation field effects are more pronounced for $Mg(NO_3)_2 \cdot 6D_2O$ than for $Mg(NO_3)_2 \cdot 6H_2O$; especially note the ν_4 region. (*cf.* with $Zn(NO_3)_2 \cdot 6D_2O$ (5).) The assignments are presented in Table 2. The consequences of the perturbation of the nitrate ion by its environment are not large. Low intensities of the infrared component at

www.nrcresearchpress.com by 210.87.254.40 on 09/05/12
For personal use only.

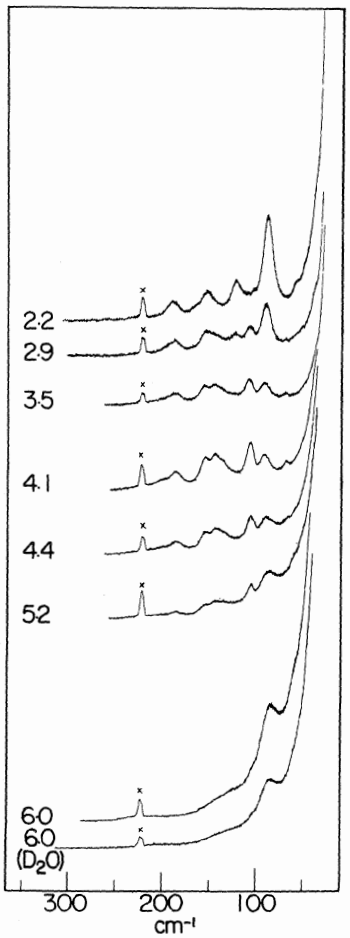

FIG. 6. Raman spectra of $Mg(NO_3)_2 \cdot nH_2O$ and $Mg(NO_3)_2 \cdot 6D_2O$ crystals in the 30–300 cm^{-1} region.

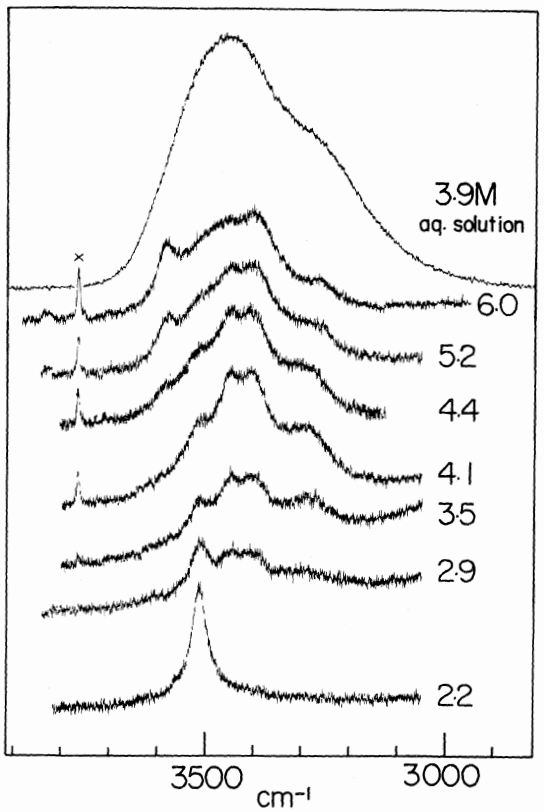

FIG. 7. Raman spectra of $Mg(NO_3)_2 \cdot nH_2O$ in the 3000–3800 cm^{-1} region. The cross denotes a plasma line.

1059 cm^{-1} and the Raman component at 824 or 826 cm^{-1} and the lack of observable site splitting of $\nu_4(E')$ in the case of the $Mg(NO_3)_2 \cdot 6H_2O$ may be attributed to the reduction of polarizing power of Mg^{2+} cation by the coordinated water molecules. Distortions of the nitrate ion of the magnitude indicated by Braibanti *et al.* (3) might be expected to generate more pronounced changes in the vibration spectrum; the structural parameters they report have a relatively large uncertainty ($R = 0.156$). Thus the spectral data probably provide a more accurate indication of the symmetry.

A complete analysis of the rotatory and translatory motions would account for 99 optical modes. The data do not warrant such a detailed interpretation. We will consider the vibrations which can clearly be assigned to the $Mg(H_2O)_6^{2+}$ unit. The remaining vibrations which occur in the low frequency region are lattice modes, reported for completeness but unassigned.

The X-ray data suggest a distorted octahedral arrangement of water molecules about Mg^{2+}. If O_h symmetry is adopted and the hydrogen atoms are ignored the unit would generate three low frequency Raman lines.

$$\Gamma_{VIB} = A_{1_g}(R) + E_g(R) + F_{2_g}(R) + 2F_{1u}(\text{i.r.}) + F_{2u}(\text{inactive})$$

Lines at 362, 312, and 222 cm^{-1} can be assigned to the A_{1_g}, E_g, and F_{2_g} modes, respectively. These assignments are consistent with the interpretation for solutions (6, 7). They show appropriate shifts to 344, 300, and 208 cm^{-1} when H_2O is replaced by D_2O (6). However, the calculations of Ananthanarayanan (8) suggest different assignments for the $Mg(H_2O)_6^{2+}$ complex. The 362 cm^{-1} band is still assigned to an A_{1g} mode but the broad, relatively intense 222 cm^{-1} line would be

TABLE 1. Vibrational frequencies for $Mg(NO_3)_2 \cdot 6D_2O$, $Mg(NO_3)_2 \cdot 6H_2O$, $Mg(NO_3)_2 \cdot 4H_2O$, and $Mg(NO_3)_2 \cdot 2H_2O$ crystals*

$Mg(NO_3)_2 \cdot 6D_2O$		$Mg(NO_3)_2 \cdot 6H_2O$		$Mg(NO_3)_2 \cdot 4H_2O$		$Mg(NO_3)_2 \cdot 2H_2O$	
Raman	i.r.	Raman	i.r.	Raman	i.r.	Raman	i.r.
60vw		60vw		67w		60w	
84m		85m		91w		89s	
				106m			
136w		135w		134sh		122m	
				144m			
				155m		154m	
						170sh	
				185w		190m	
208vw		222vw		~220vw		226vw	
300vw		312vw		300vw			
344vw		362vw		350vw		340vw	
			~550w		~580w		~575w
			~630w				~650w
		690vw	700w	690vw	690w	690vw	690w
720w	721vw						727vvw
736w	734vw	731w	730w	729w	727vw	733w	733vvw
				748w	750w	749w	750sh
							755m
					814s		815vs
	818s		819s	~820vvw		~818vvw	
~824vvw		~826vvw					
					1045s		
				1050vs			
1060vs	1059vvw	1060vs	1059vvw				
						1071vs	1070s
1196vvw	1195m						
1210vvw	1210m						
					1322vs		
				1352m	1340sh	1330m	1334vs
1360vw	1350s	1360vw	~1360s,br				
						1376w	1368sh
1446w	1445sh	1434w	~1420sh			~1450w,sh	1440sh
				1453w	1460s	1466m	1460s
1480w	1470w						
			1632m		1632m		
		1640sh,w		1637w		1632w	1632m,br
1648w			1647m		1650m		
		1656w					
					1683w		
2400sh	2390w	3265sh	3242w				
				3285sh	3288m,br		
			3352m,br				
					3387m		
2500m	2470m	3405m		3405m			
2540m	2540sh	3450m		3445m	3443sh		
		3500sh	3520sh	3515sh	3510sh	3515m	3510m
							3550sh
2650w	2640w	3580m	3580sh				

*Low frequency region (< 500 cm^{-1}) was not investigated in infrared spectra.

attributed to both the E_g and F_{2g} components in his scheme and the 312 cm^{-1} line must then be a lattice mode despite the shift on deuteration. The unit occupies a C_i site in the crystal and thus a lifting of the degeneracy of the E_g and F_{2g} modes could occur; however, no manifestation of site or coupling effects was apparent.

Two additional Raman lines are expected if

Can. J. Chem. Downloaded from www.nrcresearchpress.com by 210.87.254.40 on 09/05/12
For personal use only.

TABLE 2. Assignment of the modes associated with the nitrate ion

Free ion D_{3h} notation	Factor group assignment	$Mg(NO_3)_2 \cdot 6D_2O$ Raman	$Mg(NO_3)_2 \cdot 6D_2O$ i.r.	$Mg(NO_3)_2 \cdot 6H_2O$ Raman	$Mg(NO_3)_2 \cdot 6H_2O$ i.r.
$2\nu_2$		1648		1656, 1640	
$\nu_3(E')$	A_g, B_g	1446, 1480		1434	
	A_u, B_u		1445, 1470		~1420
	A_g, B_g	1360		1360	
	A_u, B_u		~1350		~1360
$\nu_1(A_1')$	A_g, B_g	1060.3		1059.8	
	A_u, B_u		1059		1059
$\nu_2(A_2'')$	A_g, B_g	824		826	
	A_u, B_u		818		819
$\nu_4(E')$	A_g, B_g	736		731	
	A_u, B_u		734		730
	A_g, B_g	720			
	A_u, B_u		721		

the symmetry is lowered to D_{4h}:

$$\Gamma_{VIB} = 2A_{1g}(R) + B_{1g}(R) + B_{2g}(R) + E_g(R) + 2A_{2u}(i.r.) + B_{2u}(\text{inactive}) + 3E_u(i.r.)$$

Although the lines are broad and may envelope components, the number of observed lines does not provide strong support for a large distortion. The presence of at least two different Mg—OH_2 distances is revealed by the spectra of the deformation (1600 cm^{-1}) and stretching regions (3400 cm^{-1}), however. The distances 2.061 and 2.063 Å and the angles 90.4° and 90.7° are virtually equivalent and thus the X-ray data also suggest two significantly different types of water in the crystal. Consistent with this, the deformation mode is a doublet (1632 and 1647 cm^{-1}). The stretching region is a multiplet which can be understood in terms of different O—H vibrations from the two types of water molecules and additional splitting arising from coupling, probably enhanced by hydrogen bonding. Manifestations of coupling are generally most apparent in the antisymmetric stretching region.

$Mg(NO_3)_2 \cdot 4H_2O$

The nitrate bands attributed to $Mg(NO_3)_2 \cdot 4H_2O$ are listed in Table 1. The lifting of the degeneracy of the $\nu_4(E')$ mode is apparent. The high frequency component is at 748 cm^{-1} (Raman) and 750 cm^{-1} (i.r.), which suggests direct contact between NO_3^- and the Mg^{2+} cation (9). There is evidence that a coordination number of six is retained in the tetrahydrate with four water molecules and two NO_3^- ions in the first coordination sphere. The $\nu_1(A_1')$ and $\nu_2(A_2'')$ modes appear as single bands: $\nu_1(A_1')$: 1050 cm^{-1} (R), 1045 cm^{-1} (i.r.); and $\nu_2(A_2'')$: *ca.* 820 cm^{-1} (R), 814 cm^{-1} (i.r.). The lack of infrared–Raman coincidence is obvious for all the spectral bands, and strongly suggests a center

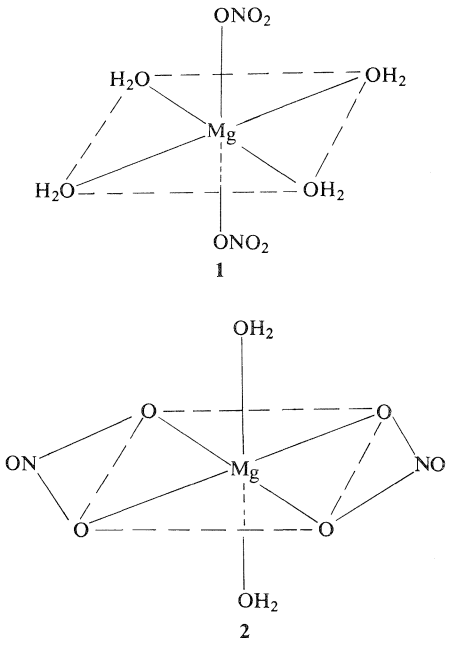

FIG. 8. Models to illustrate the coordination spheres of the magnesium ions in $Mg(NO_3)_2 \cdot 4H_2O$ (**1**) and $Mg(NO_3)_2 \cdot 2H_2O$ (**2**).

Can. J. Chem. Downloaded from www.nrcresearchpress.com by 210.87.254.40 on 09/05/12
For personal use only.

Can. J. Chem. Downloaded from www.nrcresearchpress.com by 210.87.254.40 on 09/05/12
For personal use only.

of symmetry. Thus we infer that the two nitrate ions coordinated to Mg^{2+} are equivalent and *trans* to each other as in Fig. 8. The Raman spectrum shows that in the $\nu_3(E')$ region, the low frequency component, 1352 cm^{-1}, is much more intense than the high frequency component, 1453 cm^{-1}, and an intensity reversal is observed in the infrared spectrum. It is a general rule that, in this region, a polarized Raman band of *A* symmetry has a higher intensity than a depolarized Raman band of *B* symmetry and an intensity reversal occurs in the infrared spectrum. Therefore, it is very likely that the 1352 cm^{-1} band is polarized and the 1453 cm^{-1} band depolarized as observed for very concentrated solutions of $Mg(NO_3)_2$ (10). The implication is that the NO_3^- ions are coordinated to the Mg^{2+} ions in a monodentate fashion (11–13).

The number of low frequency bands is almost double that of $Mg(NO_3)_2 \cdot 6H_2O$ crystal (Table 1, Fig. 6). The complicated situation prevents reliable assignments for all bands. Hester and Krishnan (14, 15) observed no Raman bands in the 200–400 cm^{-1} region of the $Mg(NO_3)_2$–MNO_3 (M = alkali metal) melts. By comparison with the $Mg(NO_3)_2 \cdot 6H_2O$ spectrum, the 350, 300, and 200 cm^{-1} bands can be assigned to Mg^{2+}—OH_2 vibrations. Their frequencies are lower than their counterparts in the $Mg(NO_3)_2 \cdot 6H_2O$ crystal, which probably is due to the weakening of the Mg^{2+}—OH_2 bonds by the introduction of the NO_3^- ions to the first coordination sphere around Mg^{2+} ion and to the change in symmetry.

The infrared spectrum (Fig. 5) shows that there are three bands, 1632, 1650, and 1683 cm^{-1}, for the water bending mode. Of these the 1683 cm^{-1} band has the largest linewidth, which probably implies that there are two bands under the enveloping curve. This leads us to suspect that the four Mg^{2+}—OH_2 bonds are of different lengths. The four pronounced features in the 3400 cm^{-1} region can also be interpreted in this manner. The breadths of the lines suggest extensive hydrogen bonding.

$Mg(NO_3)_2 \cdot 2H_2O$

The $\nu_1(A_1')$ and $\nu_2(A_2'')$ modes are single bands in the Raman or infrared spectra: $\nu_1(A_1')$: 1071 (R), 1070 (i.r.); $\nu_2(A_2'')$: 818 (R), 815 (i.r.). These facts indicate that the nitrate ions are equivalent in the dihydrate crystals. The lifting of degeneracy of the two E' modes of nitrate ions is apparent. In the $\nu_4(E')$ region there are two bands at 733 and 749 cm^{-1} in the Raman spectrum, but four bands, 727, 733, 750, and 755 cm^{-1} in the infrared spectrum. Four bands are found in the $\nu_3(E')$ region in both Raman and infrared spectra. The further splitting of the E' mode from two to four components can be ascribed to correlation field splitting, but it is not interpretable without knowledge of the space group. The Raman spectrum in the $\nu_3(E')$ region shows two distinct features. First, the high frequency band at 1466 cm^{-1} is much more intense than the low frequency band at 1330 cm^{-1}; the opposite intensity ratio was observed for the tetrahydrate. Secondly, the separation between the 1466 and 1330 cm^{-1} bands is 136 cm^{-1}, which is larger than the corresponding separation for the tetrahydrate. These observations suggest that the nitrate ions are oriented in bidentate fashion around magnesium ions (10–13) as shown in Fig. 8. The symmetric model is preferred to one in which nitrate ions are adjacent. It provides for greater negative charge separation and probably more efficient packing. Although the i.r. and Raman lines are virtually noncoincident, implying a centre of symmetry, the evidence is not decisive and proof must await an X-ray structure determination.

The 340 and 226 cm^{-1} bands are assigned to Mg—OH_2 vibrations. The lowering of the frequency of the 340 cm^{-1} band (*cf.* 362 cm^{-1} for hexahydrate, and 350 cm^{-1} for tetrahydrate) is probably due to the influence of the neighboring negatively charged nitrate ions.

Only one infrared band, 1632 cm^{-1} can be attributed to the water bending mode. This band is broad compared with those in other hydrates (Fig. 5). These data suggest that the two Mg—OH_2 bonds are equivalent, or very similar. This is consistent with the proposed model shown in Fig. 8. The Raman and infrared spectra in the 3400 cm^{-1} region are much simpler than those of tetra- and hexahydrates. Hydrogen bonding is much less extensive; the water molecules can be almost considered as isolated discrete units in the inorganic matrix, oriented by the cations. The very low Raman intensity of the 3550 cm^{-1} ν_3 asymmetric stretching frequency is noteworthy.

This work was supported by the National Research Council of Canada. The assistance of Dr. D. J. Lockwood is gratefully acknowledged.

1. A. SIEVERTS and W. PETZOLD. Z. anorg. allgem. Chem. **205**, 113 (1932).
2. W. W. EWING, J. D. BRANDNER, C. B. SLICHTER, and W. K. GRIESINGER. J. Am. Chem. Soc. **55**, 4822 (1933).
3. A. BRAIBANTI, A. TRIRIPICCHIO, A. M. M. LANFREDI, and F. BIGOLI. Acta Cryst. **B25**, 354 (1969).
4. M. H. BROOKER and D. E. IRISH. Spectrochim. Acta, **28A**, 701 (1972).
5. M. H. BROOKER and D. E. IRISH. Can. J. Chem. **49**, 1510 (1971).
6. A. DA SILVEIRA, M. A. MARQUES, and N. M. MARQUES. Mol. Phys. **9**, 271 (1965).
7. D. E. IRISH. *In* Ionic interactions. Vol. 2. *Edited by* S. Petrucci. Academic Press, New York. 1971. Chap. 9. p. 221.
8. V. ANANTHANARAYANAN. J. Chem. Phys. **52**, 3844 (1970).
9. D. E. IRISH, T. G. CHANG, and D. L. NELSON. Inorg. Chem. **9**, 425 (1970).
10. T. G. CHANG and D. E. IRISH. J. Phys. Chem. In press.
11. C. C. ADDISON, N. LOGAN, S. C. WALLWORK, and C. D. GARNER. Q. Rev. **25**, 289 (1971).
12. H. BRINTZINGER and R. E. HESTER. Inorg. Chem. **5**, 980 (1966).
13. R. E. HESTER and W. E. GROSSMAN. Inorg. Chem. **5**, 1308 (1966).
14. R. E. HESTER and K. KRISHNAN. J. Chem. Phys. **47**, 1747 (1967).
15. R. E. HESTER and K. KRISHNAN. J. Chem. Soc. (A), 1955 (1968).

Can. J. Chem. Downloaded from www.nrcresearchpress.com by 210.87.254.40 on 09/05/12
For personal use only.

The Crystal Structure of the Platinum Acetylenic Complex, $K[Pt((C_2H_5)_2C(OH)C{\equiv}CC(OH)(C_2H_5)_2)Cl_3]$

A. L. Beauchamp, Fernande D. Rochon,[1] and T. Theophanides

Département de Chimie, Université de Montréal, Montréal, Québec

Received July 7, 1972

The complex salt $K[Pt((C_2H_5)_2C(OH)C{\equiv}CC(OH)(C_2H_5)_2)Cl_3]$ forms monoclinic crystals, a = 10.841(5), b = 9.796(4), c = 17.414(6) Å, β = 100.44(2)°, Z = 4, space group $P2_1/c$. Positional and anisotropic thermal parameters were refined to R = 0.069 and R_w = 0.064 by using 1662 independent reflections.

The coordination around platinum is planar, and the triple bond of the acetylenic ligand is approximately perpendicular to the coordination plane. The triple bond is 1.18(3) Å and the C≡C—C angles (≃160°) show a deformation of the ligand in a direction away from the platinum atom with the two hydroxyl groups in *cis* configuration, above and below the plane of the $PtCl_3$ group. The *cis* Pt—Cl bonds are of normal length, but the *trans* Pt—Cl bond seems to be shorter. The K^+ ion is surrounded by four chlorine atoms and two oxygen atoms at relatively short distances. The oxygen–potassium attraction seems to be the predominant direct interaction of the —OH groups with the rest of the crystal.

Le sel complexe $K[Pt((C_2H_5)_2C(OH)C{\equiv}CC(OH)(C_2H_5)_2)Cl_3]$ cristallise dans le système monoclinique, a = 10.841(5), b = 9.796(4), c = 17.414(6) Å, β = 100.44(2)°, Z = 4, groupe spatial $P2_1/c$. Les coordonnées et les facteurs thermiques anisotropes ont été affinés au moyen de 1662 réflexions indépendantes jusqu'à R = 0.069 et R_w = 0.064.

Une coordination plane est observée autour du platine et la triple liaison du ligand acétylénique est à peu près perpendiculaire au plan de coordination. La longueur de la triple liaison est de 1.18(3) Å et les angles C≡C—C (≃160°) indiquent que le ligand subit une déformation dans le sens opposé à celui du platine. Les groupes hydroxyles, situés de part et d'autre du plan de coordination, adoptent une configuration *cis*. Les liaison Pt—Cl *cis* sont de longueur normale, mais la liaison Pt—Cl *trans* paraît plus courte. L'ion K^+ est entouré de quatre atomes de chlore et de deux atomes d'oxygène à des distances relativement courtes. Les attractions oxygène–potassium semblent le principal mode d'interaction directe des groupes —OH avec le reste du cristal.

Can. J. Chem., **51**, 126 (1973)

Introduction

Platinum(II) forms compounds of the types $K[Pt(ac)Cl_3]$ and *trans*-$[Pt(ac)Cl_2(amine)]$ with several acetylenic ligands (ac). X-Ray diffraction work on the neutral complex *trans*-$[PtCl_2(Bu^tC{\equiv}CBu^t)(p\text{-toluidine})]$ showed that the triple bond is nearly perpendicular to the coordination plane with the acetylenic carbon atoms above and below the plane (1). The structure is similar to that of Zeise's salt as determined by Owston and co-workers (2). It is generally admitted that the $K[Pt(ac)Cl_3]$ compounds involve the same type of bonding as the olefinic analogs.

A variety of $K[Pt(ac)Cl_3]$ complexes with acetylenic ligands were investigated by Chatt and co-workers (3–5). It was noticed that particularly stable compounds are obtained with α,α′-dihydroxy acetylenic derivatives. The hydroxyl groups were assumed to be involved in the stabilization of the compounds (4–7). It was felt that any important interaction of the hydroxyl groups would force them into a preferred orientation. The crystal structure of the complex salt $K[Pt((C_2H_5)_2C(OH)C{\equiv}CC(OH)(C_2H_5)_2)Cl_3]$ was therefore studied in order to locate the hydroxyl groups. A ligand without methyl groups on the tertiary carbon atoms was selected to facilitate the unambiguous identification of the hydroxyl groups in the structure.

Crystal Data

$KPtCl_3C_{12}H_{22}O_2$ *f.w.* = 542.86

Monoclinic, $P2_1/c$, a = 10.841(5), b = 9.796(4), c = 17.414(6) Å, β = 100.44°(2), V = 1818.7Å^3, Z = 4, ρ_c = 1.982, ρ_o = 1.98 (flotation), $\lambda CuK\bar{\alpha}$ = 1.5418 Å, $\lambda CuK\beta$ = 1.3922 Å.

Experimental

The compound was prepared as previously described (7) and recrystallized from an acetone–ether mixture. A yellow plate with dimensions 0.025 × 0.24 × 0.06 mm was found suitable for X-ray work. The $P2_1/c$ space group

[1]Present address: Département de Chimie, Université du Québec à Montréal, Montréal, Québec.

Can. J. Chem. Downloaded from www.nrcresearchpress.com by 210.87.254.40 on 09/05/12
For personal use only.

TABLE 1. Final parameters (e.s.d.'s) × 10^4; $\pm|x, y, z; x, \frac{1}{2}-y, \frac{1}{2}+z|$; $T.F. = \exp[-(\beta_{11}h^2 + \beta_{22}k^2 + \beta_{33}l^2 + 2\beta_{12}hk + 2\beta_{13}hl + 2\beta_{23}kl)]$

Atom	x	y	z	β_{11}	β_{22}	β_{33}	β_{12}	β_{13}	β_{23}
Pt	397.2(.9)	2714.7(.8)	3573.6(.6)	100.6(1.2)	57.8(1.2)	38.1(.5)	−5.3(1.)	33.3(.5)	−6.4(.6)
Cl(1)	−761(5)	4037(6)	2587(4)	99(7)	125(8)	44(3)	18(6)	14(3)	−14(4)
Cl(2)	1526(6)	1355(5)	4558(3)	186(9)	97(7)	45(3)	1(6)	41(4)	17(4)
Cl(3)	−1402(6)	1609(6)	3694(4)	140(8)	93(7)	110(5)	−15(6)	81(5)	−15(5)
K	239(5)	3682(5)	981(3)	185(8)	75(6)	59(3)	−1(5)	51(4)	16(3)
C(11)	1866(15)	4203(19)	3724(12)	16(18)	86(28)	43(11)	−23(18)	12(11)	14(14)
C(21)	1890(20)	5558(20)	4138(14)	104(29)	63(26)	56(13)	−35(23)	28(16)	−27(15)
C(31)	1963(24)	5296(20)	5012(14)	250(44)	86(30)	50(13)	−95(29)	98(20)	−36(16)
C(41)	3028(21)	6347(21)	3970(11)	161(33)	141(33)	14(9)	−22(27)	18(14)	−12(14)
C(51)	3141(27)	4685(26)	5501(14)	243(48)	199(46)	40(13)	47(37)	−33(20)	44(19)
C(61)	3224(22)	7804(20)	4331(13)	183(35)	99(30)	50(12)	33(17)	33(17)	−34(16)
C(12)	2083(20)	3328(20)	3299(12)	105(27)	65(26)	47(12)	−44(22)	26(15)	−35(14)
C(22)	2753(22)	2546(21)	2732(14)	134(32)	99(32)	52(13)	−20(27)	9(17)	−6(17)
C(32)	3684(22)	3672(22)	2487(14)	149(33)	119(33)	60(13)	−56(27)	47(17)	−26(17)
C(42)	3536(22)	1364(19)	3181(14)	171(35)	61(26)	61(13)	36(25)	69(18)	−3(15)
C(52)	4488(26)	3056(26)	1903(17)	242(46)	207(44)	112(19)	−103(36)	140(26)	−67(24)
C(62)	4597(20)	1655(29)	3923(13)	86(28)	324(55)	54(13)	39(32)	−27(16)	−90(22)
O(1)	765(13)	6292(13)	3765(8)	111(19)	91(18)	58(8)	55(16)	−5(10)	−26(10)
O(2)	1900(13)	2116(12)	2027(8)	120(17)	88(17)	32(6)	4(15)	27(9)	−13(9)

was established from a set of Weissenberg and precession photographs.

The intensity data were collected on a manually operated Picker FACS-1 diffractometer, using Ni-filtered CuKα radiation. Prior to data collection, all axial reflections with appreciable intensity were centered in the counter aperture through a search with the angles of the instrument. The refined cell constants so obtained were used to calculate the settings for data collection. Towards the end of the work, a fully automatic FACS-1 system became available and the cell constants were redetermined from 12 automatically centered Kβ peaks. The parameters obtained by the latter method are reported here and do not differ appreciably from those originally determined.

The integrated intensities of 2021 independent reflections (hkl, $hk\bar{l}$) within a sphere of $2\theta \leqslant 105°$ were measured by the $\theta/2\theta$ scan technique. Each peak was scanned at a rate of 1° (2θ)/min over a range of 2° (2θ). Stationary background counts of 20 s were taken at each limit of the scan. Periodic check of the standard reflections 006 and 1 10 0 did not indicate any significant variation. Reflections (359) with net intensities less than 3 times the total count σ were rejected. An absorption correction based on the equations of the crystal faces was applied to the 1662 observed reflections, which were finally corrected for the polarization and Lorentz effects.

The platinum atom was located from the Patterson map. The positions of all other atoms except hydrogens were obtained by structure factor and Fourier map calculations. The parameters were refined by the conventional full-matrix least-squares method. The form factors used were those of Cromer and Waber and the anomalous dispersion contribution $\Delta f'$ and $\Delta f''$ for Pt, K, and Cl were included in the calculations (8). At the latest stages of the refinement, each reflection was assigned an individual weight based on the equations: $\sigma = \sigma_a(1 + b(F_o - c))^{\frac{1}{2}}$ if $F_o > c$, $\sigma = \sigma_a$ if $c > F_o > d$ and $\sigma = \sigma_a(1 + f(F_o - d))^{\frac{1}{2}}$ if $d > F_o$, where $b = 0.15$, $c = 95$, $d = 45$, $f = 0.02$, and σ_a = total count standard deviation. These constants were adjusted to obtain a uniform distribution of the average weighted residual as a function of F_o and sin θ/λ. The hydrogen atoms of the methylene groups were fixed at the calculated positions, while those of the methyl and hydroxyl groups were neglected. The refinement of the scale factor, the coordinates and anisotropic temperature factors of all atoms except hydrogens yielded a residual $R = \Sigma(|F_o| - |F_c|)/\Sigma|F_o|$ of 0.069 and a weighted residual $R_w = [\Sigma w(|F_o| - |F_c|)^2/\Sigma w|F_o|^2]^{\frac{1}{2}}$ of 0.064. The final difference Fourier map using all observed reflections showed no significant peak, except for one peak of ±0.9 e/Å^3 at less than 1 Å from the platinum atom.[2] The refined parameters are given in Table 1.

The calculations were performed with a CDC 6600 computer. The following programs were used: F.R. Ahmed, NRC-1 (diffractometer settings); F.R. Ahmed and C.P. Huber, NRC-2 (data reduction); F.R. Ahmed and P. Singh, NRC-3 (absorption correction); C.T. Prewitt, SFLS5 (full matrix least-squares); A. Zalkin, FORDAP (Patterson and Fourier maps); C.K. Johnson, ORTEP (drawings); M.E. Pippy and F.R. Ahmed, NRC-12 (bond distances and angles); J.S. Wood, MGEOM (molecular geometry); R.E. Elder, PUBTAB (structure factor table).

Description of the Structure and Discussion

The structure of the $[Pt(ac)Cl_3]^-$ complex ion is shown in Fig. 1 and the list of bond lengths and

[2]The structure factor table is available at a nominal charge from the Depository of Unpublished Data, National Science Library, National Research Council of Canada, Ottawa, Canada, KIA 0S2.

Can. J. Chem. Downloaded from www.nrcresearchpress.com by 210.87.254.40 on 09/05/12
For personal use only.

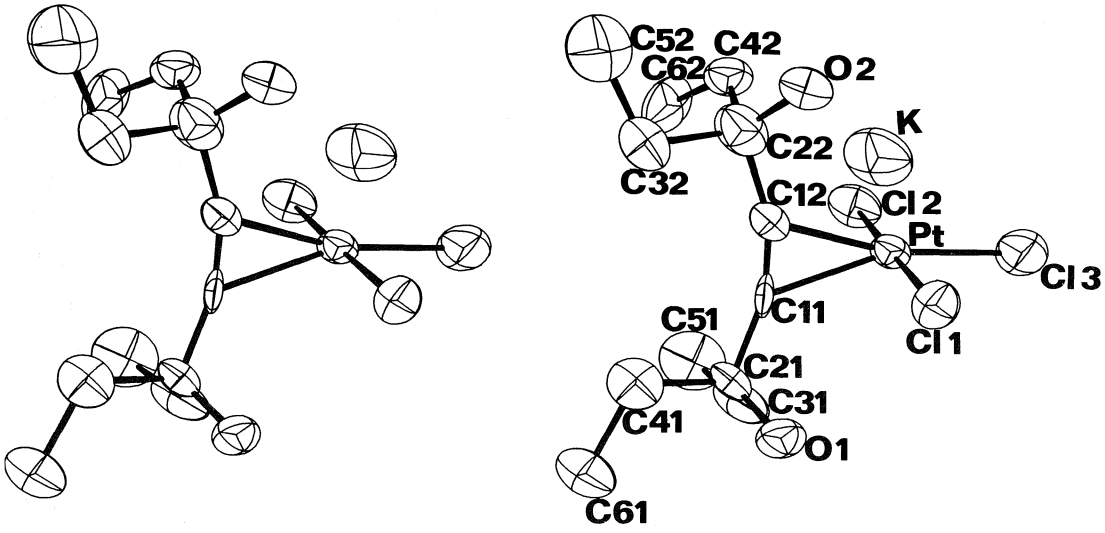

FIG. 1. Structure of $K[Pt((C_2H_5)_2C(OH)C{\equiv}CC(OH)(C_2H_5)_2)Cl_3]$

angles is given in Table 2. Three chlorine atoms and the mid-point X of the C(11)—C(12) triple bond achieve the square planar coordination expected for Pt(II) complexes. The weighted best plane was calculated through the platinum and chlorine atoms. The deviations from this plane are: Pt, 0.001; Cl(1), −0.008; Cl(2), −0.007; and Cl(3), 0.007 Å. The mid-point X of the triple bond is ~ 0.1 Å above the plane. The Cl—Pt—Cl angles are all close to the ideal values of 90° or 180°. The triple bond is nearly perpendicular (∠Pt—X—C(11), 93.8°) to the line joining the mid-point X to the platinum atom, and it is also rotated by ~3° around that line.

In Zeise's salt, the geometry of the ethylene molecule is modified upon complexation: the C=C double bond seems to be longer (1.37(3) and 1.354(15) Å) and the hydrogens are not in the plane of the double bond (2, 9). In the present case, the C(11)—C(12) bond length (1.18(3) Å) is not significantly different from a normal triple bond (1.202(5) Å) (10). However, the C(21)—C(11)—C(12)—C(22) segment of the coordinated ligand is not linear. The C(21) and C(22) atoms are displaced, producing a *cis* deformation in the direction opposite to the platinum atom, the C—C≡C angles averaging 160°. A similar non-linearity of the coordinated acetylenic ligand has been reported for the neutral complex $[PtCl_2(Bu^tC{\equiv}CBu^t)(p\text{-toluidine})]$ (1). The ligand conformation in both of these compounds is closely related. In the neutral compound, the main chain of six carbon atoms is roughly C-shaped and occupies a crystallographic mirror plane which also contains the platinum atom and the *trans* nitrogen atom. In the present case, the chain has two more carbon atoms and it is also C-shaped. Eight of the twelve carbon atoms, the platinum atom, and the *trans* chlorine atom are nearly in the same plane. Both hydroxyl groups are found on the same side of the planar chain, the two remaining ethyl groups being on the opposite side. Consequently, the complex ion approximates a C_s point group symmetry with a mirror plane through the coordination plane.

Platinum forms two equal *cis* bonds with Cl(1), 2.334 Å, and Cl(2), 2.339 Å, but the Pt—Cl(3) bond *trans* to the acetylenic ligand appears significantly shorter (2.287 Å). At the moment, there is no definite agreement as to how and by what amount a bond distance should be perturbed when the *trans* position is occupied by a ligand with a high *trans* influence. The crystallographic data on olefinic complexes generally failed to show any significant systematic lengthening or contraction of the *trans* bond (2, 9, 11). To our knowledge, this is the first crystal structure work on a $[Pt(ac)Cl_3]^-$ salt. Even if the difference between the *trans* and the *cis* Pt—Cl bonds corresponds to 4 times the sum of their respective e.s.d.'s, we feel that shorter *trans* Pt—Cl bonds should first be observed with other similar compounds before an interpretation is attempted. We may reasonably believe that in the crystal, the

Can. J. Chem. Downloaded from www.nrcresearchpress.com by 210.87.254.40 on 09/05/12
For personal use only.

TABLE 2. Interatomic distances and bond angles

Bond*	Distance (Å)	Bonds	Angle (deg)
Pt—Cl(1)	2.334(6)	Cl(1)—Pt—Cl(2)	178.8(2)
Pt—Cl(2)	2.339(6)	Cl(1)—Pt—Cl(3)	88.3(2)
Pt—Cl(3)	2.287(6)	Cl(1)—Pt—C(11)	90.4(5)
Pt—C(11)	2.148(18)	Cl(1)—Pt—C(12)	93.1(6)
Pt—C(12)	2.075(22)	Cl(1)—Pt—X	91.8(6)
Pt—X	2.026(20)	Cl(2)—Pt—X	89.3(6)
C(11)—C(12)	1.184(28)	Cl(2)—Pt—Cl(3)	90.6(2)
C(11)—C(21)	1.508(28)	Cl(2)—Pt—C(11)	90.8(5)
C(12)—C(22)	1.537(32)	Cl(2)—Pt—C(12)	87.8(6)
C(21)—C(31)	1.534(33)	Cl(3)—Pt—C(11)	161.0(5)
C(22)—C(32)	1.609(32)	Cl(3)—Pt—C(12)	166.5(6)
C(21)—C(41)	1.536(31)	Pt—C(11)—C(12)	70.3(13)
C(22)—C(42)	1.562(31)	Pt—C(12)—C(11)	77.2(14)
C(31)—C(51)	1.530(37)	Pt—X—C(11)	93.8(27)
C(32)—C(52)	1.579(37)	Pt—X—C(12)	86.3(28)
C(41)—C(61)	1.559(29)	C(11)—Pt—C(12)	32.5(8)
C(42)—C(62)	1.598(33)	Cl(1)—O(1)—C(21)	103.8(11)
C(21)—O(1)	1.470(26)	C(11)—C(12)—C(22)	159.4(22)
C(22)—O(2)	1.464(27)	C(12)—C(11)—C(21)	161.3(21)
Pt—O(1)	3.536(13)	C(22)—O(2)—Pt	67.4(10)
Pt—O(2)	3.451(13)	C(21)—O(1)—Pt	68.2(10)
Cl(1)—K	3.203(8)	C(21)—O(1)—O(2)^b	165.6(12)
Cl(1)—O(1)	3.261(15)	C(22)—O(2)—O(1)^a	148.7(12)
Cl(1)—O(2)	3.751(15)	C(21)—O(1)—Cl(1)^b	124.1(11)
K—O(2)	2.788(14)	C(22)—O(2)—Cl(1)^a	107.0(11)
Cl(1)—O(1)^a	3.575(14)		
Cl(1)—O(2)^b	3.375(13)		
K—Cl(2)^c	3.066(8)		
K—Cl(2)^b	3.286(8)		
K—Cl(3)^b	3.145(8)		
K—O(1)^a	2.656(14)		
O(1)—O(2)^b	3.095(20)		

*Coordinates x, y, z except a, $x, y - \frac{1}{2}, \frac{1}{2} - z$; b, $\bar{x}, \frac{1}{2} + y, \frac{1}{2} - z$; c, $x, \frac{1}{2} - y, z - \frac{1}{2}$.

trans effect might be partially obscured or even reversed by other factors related either to the crystal itself (packing around the cation for example) or to the technique and interpretation of the data (absorption correction, weighting scheme).

Various intramolecular interactions involving the hydroxyl groups have been proposed to explain the stability of the platinum complexes with acetylenic glycols. A direct interaction of the Pt atom with either the oxygen or the hydrogen of the hydroxyl group was first suggested, but subsequently abandoned by Chatt *et al.* (4, 5). If there were such interaction, the —OH groups would be carried inside the molecule, above and below the platinum atom, by a rotation of the tertiary groups around the single bonds. In the present compound, the ligand shows a different conformation. The *cis* conformation of the tertiary carbons towards the outside of the molecule results in large Pt—O distances of 3.54 and 3.45 Å, and unfavorable C—O—Pt angles of 67.4 and 68.2°, which would make the above proposed interactions rather unlikely. Intramolecular hydrogen bonding to one or both of the *cis* chlorine atoms was suggested (4). The oxygen–chlorine contacts given in Table 2 do not suggest strong hydrogen bonding in the crystal. The O(1)—Cl(1) distance (3.26 Å) is just within the range 2.9–3.3 Å suggested for hydrogen bonds of this type (12). A hydrogen atom on the O(1) . . . Cl(1) line would define a C—O—H angle of 104°. This could imply a weak intramolecular hydrogen bonding. The intermolecular oxygen–chlorine contact between O(2) and Cl(1) is 3.37 Å and the angle C—O—H would be 107°. The oxygen–oxygen contacts are all well outside the hydrogen bonding range of 2.4–2.9 Å (12) and the angles are also unfavorable (Table 2). Consequently, although some weak hydrogen bonds might contribute to the stabilization of the compound, it is doubtful that their influence is predominant.

Can. J. Chem. Downloaded from www.nrcresearchpress.com by 210.87.254.40 on 09/05/12
For personal use only.

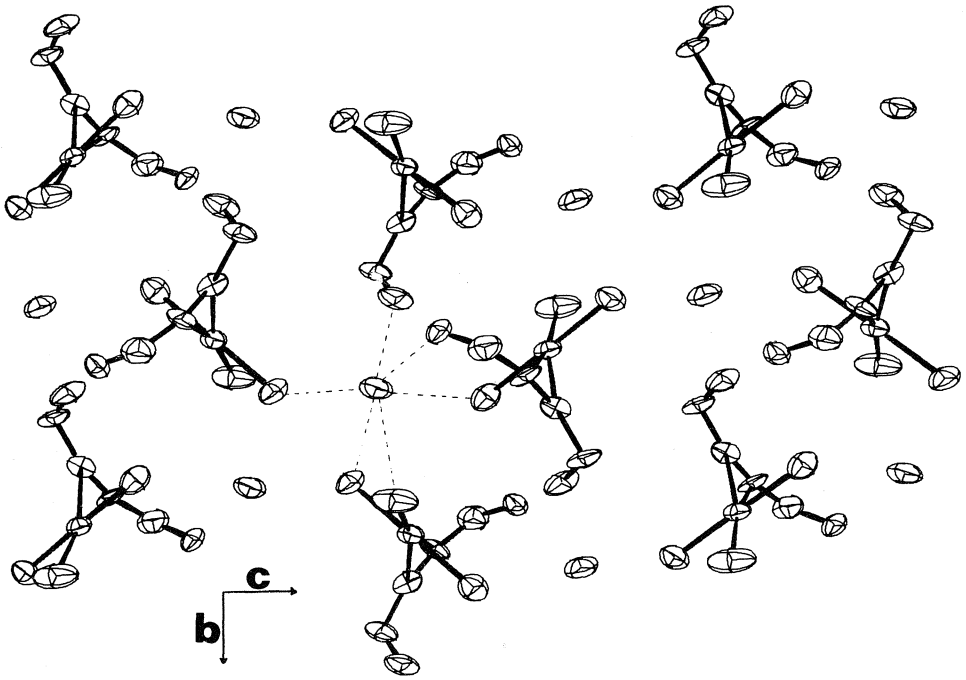

FIG. 2. Packing in the crystal of $K[Pt((C_2H_5)_2C(OH)C{\equiv}CC(OH)(C_2H_5)_2)Cl_3]$ (the ethyl groups have been removed for simplicity reasons).

The infrared spectra of the solid complex (15) show that the OH stretching frequency is lowered from 3610 cm^{-1} (CCl_4) in the free ligand to 3505 and 3475 cm^{-1} in the complex salt (KBr). The slight splitting of the band into two components may be explained by the presence of two hydroxyl groups in different crystallographic environments. Although the lowering of the frequency is usually interpreted in terms of hydrogen bonding, it may also be due to other factors, such as the ligand perturbation by the metal and the potassium–oxygen attraction in the crystal.

For a solid compound, the packing energy may be an important stabilizing factor and its contribution should not be overlooked in the case of the complex salts, where the cation might have a determining influence. Chatt *et al.* (4) mentioned that the Na $[Pt(ac)Cl_3]$ salts are usually less stable than the corresponding K salts, whereas salts with $[NH(C_2H_5)_3]^+$ were isolated while the corresponding K salts could not be isolated (13). In the present case, the K^+ ion is surrounded by four chlorine atoms at 3.07, 3.14, 3.20, and 3.29 Å and two oxygen atoms at 2.79 and 2.66 Å, defining a distorted trigonal prismatic geometry (Fig. 2). The interesting point is that both hydroxyl groups are part of the close environment of the K^+ ion with short K—O contacts similar to those found in carboxylates (2.6–3.0 Å) (14). In a $K[Pt(ac)Cl_3]$ complex with an acetylenic hydrocarbon, the replacement of the —OH groups by methyl groups, for example, would leave only three chlorine atoms per complex ion to fulfill the packing requirements around the cation, not more than two of which could effectively be found near a given cation. This would presumably result in a certain crowding of the complex ions around the cations. Consequently, the chances that the structure of the free complex ion is preserved in the crystals would certainly be better when 5 electronegative atoms or groups are available (glycol complexes) than when only 3 chlorine atoms (hydrocarbon complexes) can fulfill the packing requirements around the cation. It seems therefore that the oxygen–potassium attraction is the predominant direct interaction of the —OH groups with the rest of the crystal. Chatt *et al.* (4) have shown that the stability of the platinum complexes with $R_1—C{\equiv}C—R_2$ hydrocarbons increases with the increasing positive indictive effect of the R_1 and R_2 groups. The above K—O attraction might explain the

Can. J. Chem. Downloaded from www.nrcresearchpress.com by 210.87.254.40 on 09/05/12
For personal use only.

stabilization of the platinum glycol salt, in spite of the negative inductive effect of the two —OH groups.

Grateful acknowledgment is made to the National Research Council of Canada for financial support and to Johnson Matthey and Mallory Ltd. for the loan of platinum metal.

1. G. R. DAVIES, W. HEWERTSON, R. H. B. MAIS, and P. G. OWSTON. Chem. Commun. 423 (1967); G. R. DAVIES, W. HEWERTSON, R. H. B. MAIS, P. G. OWSTON, and C. G. PATEL. J. Chem. Soc. 1873 (1970).
2. J. A. J. JARVIS, B. T. KILBOURN, and P. G. OWSTON. Acta Cryst. B**27**, 366 (1971).
3. J. CHATT, R. G. GUY, and L. A. DUNCANSON. J. Chem. Soc. 827 (1961).
4. J. CHATT, R. G. GUY, L. A. DUNCANSON, and D. T. THOMPSON. J. Chem. Soc. 5170 (1963).
5. J. CHATT, L. A. DUNCANSON, and R. G. GUY. Nature, **184**, 526 (1959).
6. A. D. ALLEN and T. THEOPHANIDES. Can. J. Chem. **44**, 2703 (1966); **43**, 290 (1965).
7. T. THEOPHANIDES. Ph.D. Thesis. University of Toronto, Toronto, Ontario. 1963.
8. D. T. CROMER and J. T. WABER. Acta Cryst. **18**, 104 (1965); D. T. CROMER. Acta Cryst. **18**, 17 (1965).
9. W. C. HAMILTON, K. A. KLANDERMAN, and R. SPARTLEY. Acta Cryst. A**25**, S172 (1969).
10. Chemical Society of London. Table of Interatomic Distances and Configurations in Molecules and Ions. Special Publ. No. 18 (1965).
11. M. COLAPIETRO and L. ZAMBONELLI. Acta Cryst. B**27**, 734 (1971).
12. G. C. PIMENTEL and A. L. MCCLELLAN. The hydrogen bond. Freeman Co., San Francisco. 1960.
13. S. V. BUKHOVETS and N. K. PUKHOVA. Zhur. Neorg. Khim. **3**, 1714 (1958).
14. R. W. G. WYCKOFF. Crystal structures. Vol. 5 (1966) and Vol. 6 (1969). Interscience Publishers, New York.
15. F. D. ROCHON. Ph.D. Thesis. Université de Montréal, Montréal, Québec. 1970.

Can. J. Chem. Downloaded from www.nrcresearchpress.com by 210.87.254.40 on 09/05/12
For personal use only.

The Mass Spectra of Imidoyl Halides and Bromoiminium Bromides

J. GAL,[1] B. A. PHILLIPS,[2] AND R. SMITH

Chemistry Department, West Virginia University, Morgantown, West Virginia 26506

Received July 4, 1972

The mass spectra of imidoyl halides **1–6** and bromoiminium bromides **7–9** have been studied and their fragmentation pattern discussed. Loss of halogen atom from the molecular ion of imidoyl halides to form a *N*-alkylnitrilium ion is a major process. When the *N*-alkyl group is larger than methyl the fragmentation of *N*-alkylnitrilium ions with hydrogen rearrangement to give the $[PhC{\equiv}NH]^+$ ion becomes important. Thermolysis of bromoiminium bromides in the inlet system of the mass spectrometer produces imidoyl bromides via dealkylation (or dehydrobromination) and α,α-dibromobenzylamines via addition of bromide to the C=N bond.

Nous avons étudié le spectre de masse des halogénures d'imidoyl **1–6** et des bromures de bromoiminium **7–9** et étudié leur patron de fragmentation. La perte d'un atome d'halogène de l'ion moléculaire des halogénures d'imidoyl pour former un ion *N*-alkylnitrilium constitue un processus important. Lorsque le groupe *N*-alkyl est plus gros que le méthyle, la fragmentation des ions *N*-alkylnitrilium avec un réarrangement d'hydrogène pour donner l'ion $[PhC{\equiv}NH]^+$, devient importante. La thermolyse des bromures de bromoiminium dans le système d'entrée du spectromètre de masse produit des bromures d'imidoyl via la déalkylation (ou la déhydrobrominature) et des α,α-dibromobenzylamines via l'addition de bromure au lien C=N. [Traduit par le journal]

Can. J. Chem., **51**, 132 (1973)

Can. J. Chem. Downloaded from www.nrcresearchpress.com by 210.87.254.40 on 09/05/12
For personal use only.

Imidoyl chlorides (**I**, X = Cl) and chloroiminium chlorides (**II**, X = Cl) have been known for over half a century (1, 2). These compounds provide useful intermediates for the synthesis of numerous nitrogen-containing derivatives, and also play an important role in mechanistic organic chemistry. For example, chloroiminium chlorides and/or imidoyl chlorides have been shown to be intermediates in such classical name reactions as the Vilsmeier–Haack aldehyde synthesis, the von Braun amide degradation, and the Beckmann rearrangement. Recently there has been a marked awakening of interest in these compounds, especially in 1,3-dipolar addition reactions, and in imidoyl fluorides (I, X = F), which had escaped study in earlier years. These and other aspects of the chemistry of imidoyl halides and haloiminium halides have been the subject of several extensive reviews (3). However, no mass-spectral fragmentation study of these compounds has been published.

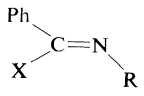

I

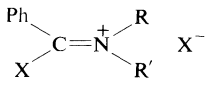

II

	R	X
1	CH_3	Cl
2	CH_3	Br
3	CH_3CH_2	Cl
4	CH_3CH_2	Br
5	n-C_4H_9	Cl
6	$Br(CH_2)_5$	Br

	R	R′	X
7	H	n-C_4H_9	Br
8	CH_3	CH_3	Br
9	—$(CH_2)_5$—		Br

In connection with our investigation (4, 5) of the mechanism of the von Braun amide degradation a number of imidoyl halides (**1–6**) and bromoiminium bromides (**7–9**) were prepared and their low-resolution mass spectra determined.

Results and Discussion

The results are given in Figs. 1–5 and in Table 1. It was found that imidoyl chlorides **1** and **3** show a weak molecular ion, whereas the imidoyl bromides (**2**, **4**, **6**) and imidoyl chloride **5** show no molecular ion. However, several ions containing the imidoyl chloride functionality were detected in the spectrum of *N*-*n*-butylbenzimidoyl chloride (**5**, Fig. 1). As shown in Scheme 1, β-fission of the *N*-alkyl group leads to the ion at *m*/*e* 152, while γ-fission gives an ion of *m*/*e* 166. The latter ion is probably in the cyclic aziridinium form indicated

[1]To whom inquiries should be addressed at the Department of Pharmaceutical Chemistry, School of Pharmacy, University of California, San Francisco, Calif. 94122.

[2]ACS–PRF Fellow, 1970–1972.

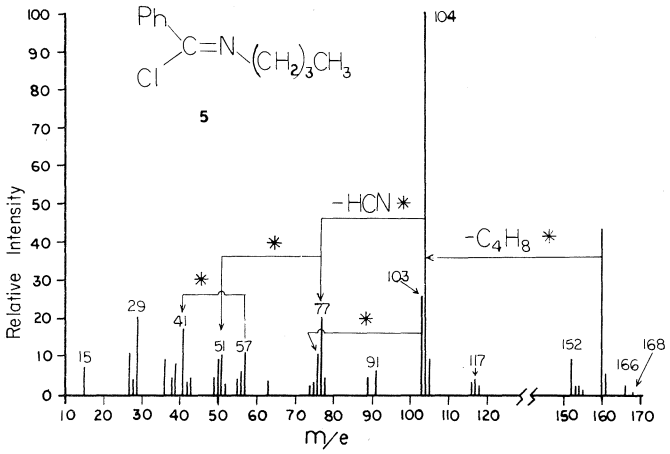

FIG. 1. The mass spectrum of *N*-*n*-butylbenzimidoyl chloride (**5**).

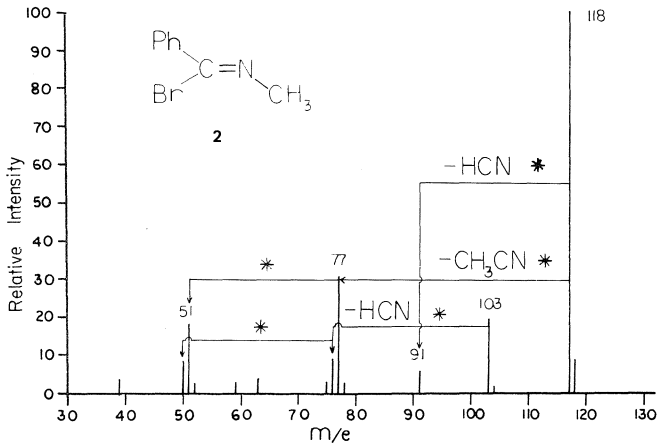

FIG. 2. The mass spectrum of *N*-methylbenzimidoyl bromide (**2**).

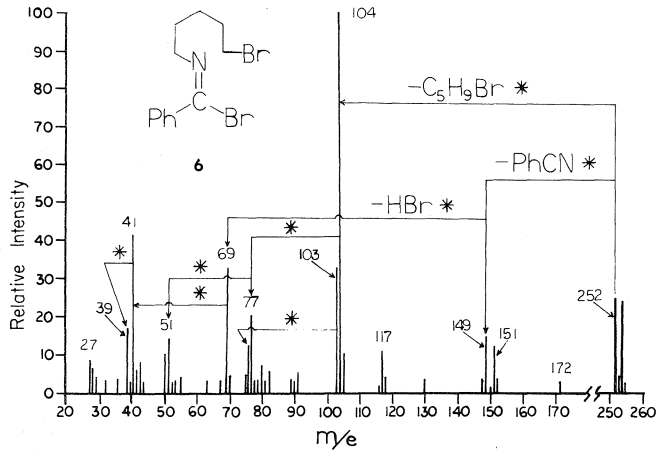

FIG. 3. The mass spectrum of *N*-5-bromopentylbenzimidoyl bromide (**6**).

Can. J. Chem. Downloaded from www.nrcresearchpress.com by 210.87.254.40 on 09/05/12
For personal use only.

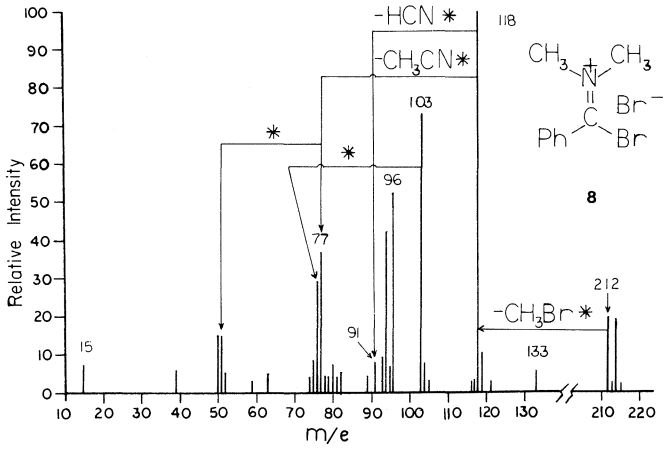

FIG. 4. The mass spectrum of *N*,*N*-dimethyl-α-bromobenziminium bromide (**8**).

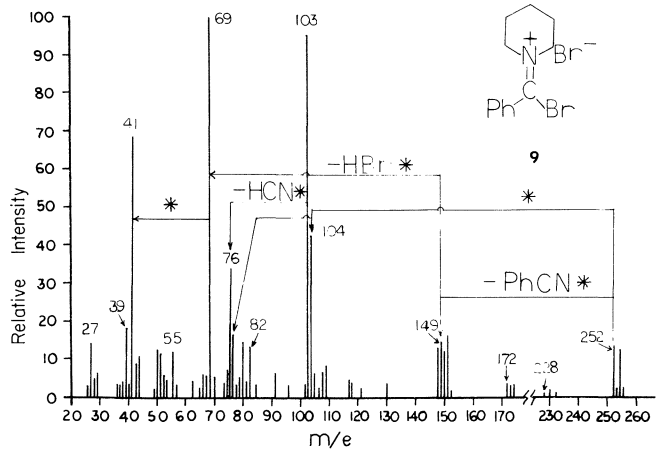

FIG. 5. The mass spectrum of *N*,*N*-pentamethylene-α-bromobenziminium bromide (**9**).

in Scheme 1. Similar *N*-alkylideneaziridinium ions are frequently encountered in the spectra of *N*-alkylaziridines (6).

An important process in the fragmentation of all of the imidoyl halides studied is the loss of a halogen atom to give the stable *N*-alkylnitrilium ion (eq. 1). This process is analogous to the loss

[1] 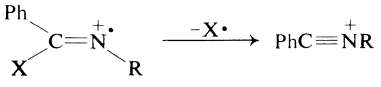

of halogen from the molecular ion of benzoyl halides (7) to give the corresponding stable acylium ion. The nitrilium ion (*a*) at *m*/*e* 118 (Scheme 2) is the base peak in the spectra of *N*-methylbenzimidoyl halides **1** and **2** (Table 1 and Fig. 2). The ion of *m*/*e* 103 (*b*) most likely arises by loss of the elements of methyl halide from the parent ion. This process is reminiscent of the electron-impact-induced loss of H_2O and H_2S from the imide form of benzamide and thiobenzamide, respectively (8). The alternative formation of (*b*), loss of a methyl radical from the even electron ion (*a*), is unfavored. The benzonitrile ion (*b*) then loses HCN to give $[C_6H_4]^{+\cdot}$ (*m*/*e* 76) and also, to a lesser extent, $H_2CH^{\cdot}$ to give $[C_6H_3]^+$ (*m*/*e* 75). The latter two ions are also observed in the mass spectrum of benzonitrile (9). The nitrilium ion (*a*) may lose either CH_3CN to give the phenyl ion (*m*/*e* 77) or HCN to give the $[C_7H_7]^+$ (most likely tropylium) ion at *m*/*e* 91.

The spectra of imidoyl halides having an *N*-

Can. J. Chem. Downloaded from www.nrcresearchpress.com by 210.87.254.40 on 09/05/12
For personal use only.

Can. J. Chem. Downloaded from www.nrcresearchpress.com by 210.87.254.40 on 09/05/12
For personal use only.

TABLE 1. Mass spectra of compounds **1–9**

	Relative intensity (%)								
m/e	**1**	**2**	**3**	**4**	**5**	**6**	**7**	**8**	**9**
255	—	—	—	—	—	3	—	—	2
254	—	—	—	—	—	24	—	—	13
253	—	—	—	—	—	5	—	—	2
252	—	—	—	—	—	25	—	—	14
232	—	—	—	—	—	—	—	—	1
230	—	—	—	—	—	—	—	—	2
228	—	—	—	—	—	—	—	—	1
215	—	—	—	—	—	—	—	2	—
214	—	—	—	—	—	—	—	19	—
213	—	—	—	—	—	—	—	2	—
212	—	—	—	—	—	—	—	20	—
174	—	—	—	—	—	—	—	—	3
173	—	—	—	—	—	—	—	—	3
172	—	—	—	—	—	—	—	—	4
169	—	—	2	—	—	3	—	—	—
168	—	—	—	—	1	—	—	—	—
167	—	—	6	—	—	—	—	—	—
166	—	—	—	—	2	—	—	—	—
161	—	—	—	—	6	—	7	—	—
160	—	—	—	—	43	—	45	—	—
155	1	—	—	—	2	—	—	—	—
154	—	—	—	—	3	—	—	—	—
153	3	—	—	—	3	—	—	—	—
152	—	—	—	—	9	4	—	—	2
151	—	—	—	—	—	13	—	—	16
150	—	—	—	—	—	2	—	—	12
149	—	—	—	—	—	15	—	—	15
148	—	—	—	—	—	4	—	—	13
133	—	—	10	10	—	—	—	6	—
132	—	—	80	75	—	—	—	—	—
130	—	—	—	—	—	4	—	—	4
121	—	—	—	—	—	—	—	3	2
119	10	9	—	—	—	—	—	11	—
118	100	100	3	—	2	5	—	100	3
117	—	—	—	—	4	12	7	3	5
116	—	—	—	—	3	3	—	2	—
109	—	—	—	—	—	—	—	—	8
107	—	—	—	—	—	—	—	—	7
106	—	—	—	—	—	—	—	—	2
105	—	—	10	11	10	11	11	4	6
104	3	2	100	100	100	100	100	8	43
103	23	19	24	49	26	33	22	74	95
102	—	—	—	—	—	—	—	—	3
96	—	—	—	—	—	—	—	53	—
95	—	—	—	—	—	—	—	7	3
94	—	—	—	—	—	—	—	43	—
93	—	—	—	—	—	—	—	10	—
91	6	5	3	5	7	6	3	8	6
89	4	—	4	—	4	4	3	4	—
84	—	—	—	—	—	—	—	—	3
82	—	—	—	—	—	6	15	6	13
81	—	—	—	—	—	3	5	4	4
80	—	—	—	—	—	8	11	7	14
79	—	—	—	—	—	4	6	4	5
78	4	3	5	5	4	4	—	5	3
77	37	31	28	37	20	21	15	37	17
76	14	9	17	25	11	13	9	29	34

TABLE 1. (*Concluded*)

	Relative intensity (%)								
m/e	**1**	**2**	**3**	**4**	**5**	**6**	**7**	**8**	**9**
75	5	3	5	7	3	5	—	8	7
74	3	—	3	6	2	—	—	4	4
70	—	—	—	—	—	5	—	—	6
69	—	—	—	—	—	34	—	—	100
68	—	—	—	—	—	—	—	—	6
67	—	—	—	—	—	4	—	—	6
64	—	—	2	3	—	—	—	—	—
63	4	3	3	7	4	4	—	5	4
62	3	—	3	5	—	—	—	—	—
59	3	3	—	—	—	—	—	3	—
57	—	—	—	—	11	—	5	—	—
56	—	—	—	—	6	—	—	—	3
55	—	—	—	—	4	5	—	—	12
53	—	—	—	—	—	4	—	—	4
52	3	2	4	8	3	—	—	5	6
51	17	18	17	30	11	15	6	16	12
50	11	8	9	19	9	12	3	16	13
49	—	—	3	—	5	—	—	—	2
44	—	—	—	—	—	3	—	—	—
43	—	—	—	—	5	9	—	—	12
42	—	—	—	—	4	6	—	—	9
41	—	—	—	—	18	42	6	—	59
40	—	—	—	—	—	3	—	—	4
39	4	4	5	8	8	18	4	6	19
38	—	—	4	4	4	—	—	—	4
37	—	—	—	—	—	—	—	—	3
36	—	—	11	—	10	4	—	—	4
32	—	—	—	—	—	4	—	—	—
29	—	—	11	9	21	5	6	—	6
28	—	—	3	3	4	7	3	—	15
27	—	—	12	12	11	10	—	—	—
26	—	—	4	4	—	—	—	—	3
15	—	—	—	—	7	—	—	7	—

alkyl group larger than methyl (**3–6**) show the nitrilium ion $[PhC{\equiv}NH]^+$ (*c*) at *m/e* 104 as the base peak. This ion arises from the *N*-alkylnitrilium ion via rearrangement of a hydrogen from the *N*-alkyl group, as shown in eq. 2. Metastables found for this transition are listed in Table 2. This

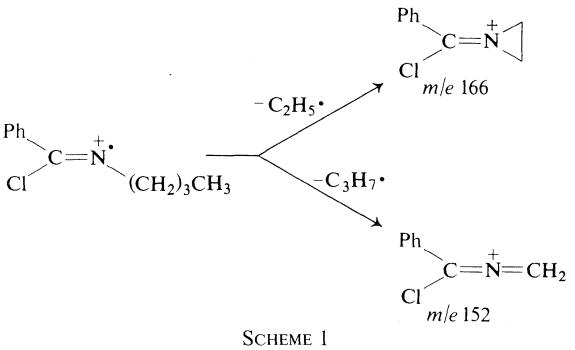

SCHEME 1

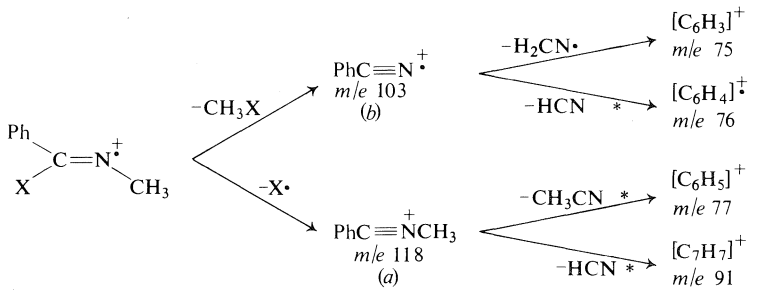

SCHEME 2

TABLE 2. Metastables for transition of PhC≡NR to PhC≡NH

Compound	R	*m*(Calcd.)	*m*(Found)
3	C_2H_5	81.9	82.1
4	C_2H_5	81.9	82.0
5	*n*-C_4H_9	67.6	67.7
6	$(CH_2)_5Br$	42.9	42.9
		42.6	42.7
7	*n*-C_4H_9	67.6	67.5

[2] 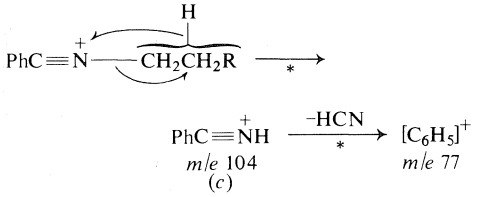

rearrangement has previously been observed in the spectra of *N*-alkyl azomethines (10), amines (11), and ethers (12). Fisher and Djerassi have suggested (10) that the migrating hydrogen may originate from the α, β, γ, or δ carbon atom. The low intensity of (*c*) in the spectra of the *N*-methylbenzimidoyl halides **1** (3%) and **2** (2%) indicate that when the α-carbon is primary, hydrogen rearrangement, as would be expected (13), is not an important process. The $[PhC{\equiv}NH]^+$ ion (*c*) then generates the $[C_6H_5]^+$ ion at *m/e* 77 via loss of HCN as indicated by the appropriate metastable in the spectra of **3**–**6** (found: 57.0; calcd.: 57.0).

The nitrilium ion (*d*) at *m/e* 252 in the spectrum of *N*-5-bromopentylbenzimidoyl bromide (**6**) loses benzonitrile to give the bromine-containing ion at *m/e* 149 (eq. 3). The latter then yields the ion at *m/e* 69.

Heating non-volatile salts in the inlet of a mass spectrometer first leads to the formation of neutral species which are then vaporized (14). Upon

[3] 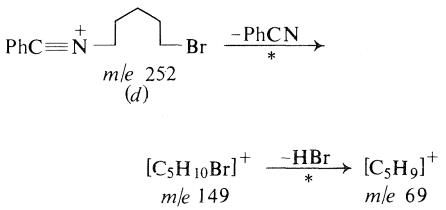

heating to 80° in the inlet system *N*-*n*-butylbenzimidoyl bromide hydrobromide (**7**, Table 1) liberates hydrogen bromide. The spectrum of the free base shows, as expected, no molecular ion. Loss of bromine atom gives the nitrilium ion at *m/e* 160, which then fragments with hydrogen rearrangement (eq. 2, Table 2). Interestingly, fragmentations analogous to the processes shown in Scheme 1 for the corresponding imidoyl chloride **5** are not seen in the spectrum of **7**. This is probably due to the greater ease of loss of a bromine atom from the molecular ion.

The thermal decomposition of *N*,*N*-dimethyl-α-bromobenziminium bromide (**8**, Fig. 4) in the mass spectrometer occurs in two ways. Nucleophilic dealkylation, commonly observed in the mass spectra of ammonium salts (14), leads to methyl bromide (*m/e* 94) and *N*-methylbenzimidoyl bromide (**2**, Scheme 3). In fact, this reaction has been shown to proceed by isolation of **2** in 75% yield from refluxing **8** in dibromomethane (5). Comparing Figs. 2 and 4 it can be seen that **2** formed thermally from **8** at 140° generates ions similar to those found in the spectrum of independently synthesized **2**. At this inlet temperature partial decomposition of **2** to benzonitrile and methyl bromide occurs. In the case of imidoyl chlorides this thermal decomposition is well known from the von Braun amide degradation (15) (eq. 4). Such formation of benzonitrile explains the greater relative intensity of the ions at *m/e* 103 (74%) and *m/e* 76 (29%) in the spectrum

Can. J. Chem. Downloaded from www.nrcresearchpress.com by 210.87.254.40 on 09/05/12
For personal use only.

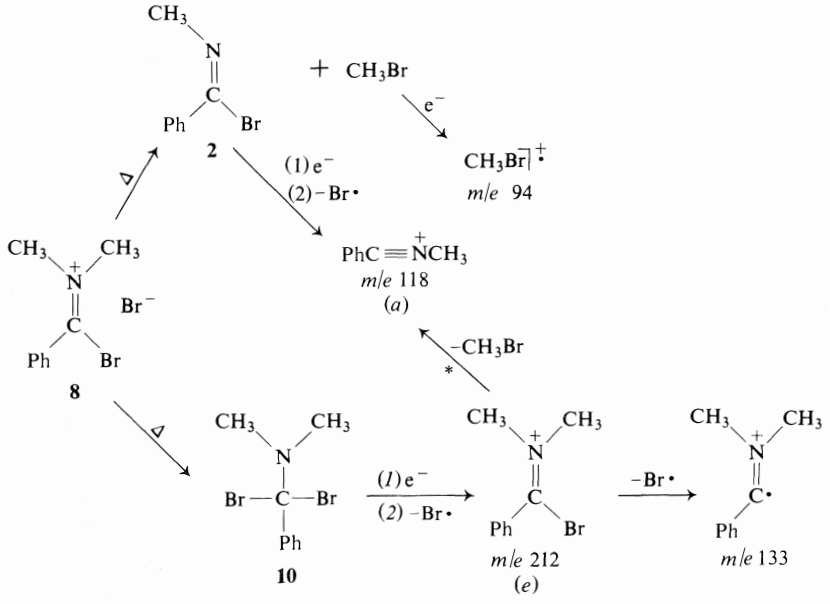

SCHEME 3

[4] 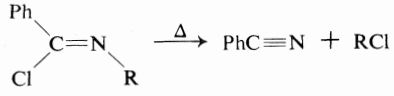

of **8** (Fig. 4) as compared to 19 and 9%, respectively, in the spectrum of **2** (Fig. 2).

The second thermal neutralization process for **8** is formation of *N*-α,α-dibromobenzyldimethyl amine (**10**) via attack of bromide ion on the sp^2 carbon bonded to nitrogen. Evidence suggesting the existence of *gem*-dihalides such as **10** has been offered in the literature. Namanworth (16) found that chloroformiminium chloride (**11**) is in equilibrium with its *gem*-dichloro isomer (**12**) in chloroform or thionyl chloride solution (eq. 5). Furthermore, the facile exchange of covalent halide in haloiminium salts of type **II** has been suggested (17) to proceed via a *gem*-dihalo intermediate. It is also well established (18) that fluoroiminium fluorides, which are stable, distillable liquids, exist entirely in the covalent *gem*-difluoro form **13**. Volatilization of **10** is followed by ionization, and loss of a bromine atom to give (*e*) at *m/e* 212 (Scheme 3). This ion then loses methyl bromide in a one step process, as indicated by the appropriate metastable (found: 65.5 broad; calcd.: 65.0 and 65.7), to contribute to the intensity of the nitrilium ion (*a*). The ion at *m/e* 133 probably arises via loss of bromine atom from (*e*).

[5] 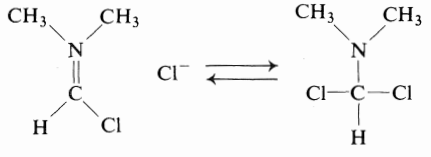

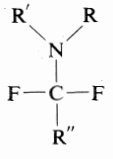

In a manner analogous to **8** the thermolysis of *N*,*N*-pentamethylene-α-bromobenziminium bromide (**9**) gives *N*-5-bromopentylbenzimidoyl bromide (**6**) as shown in Scheme 4. With an inlet temperature of 300° the imidoyl bromide **6** undergoes partial von Braun degradation to benzonitrile and 1,5-dibromopentane (*m/e* 228). These von Braun products account for the greater relative intensity of the ions at *m/e* 148, 103, 76, 69, and 41 in Fig. 5, as compared to Fig. 3. The thermal formation of *N*-α,α-dibromobenzylpiperidine (**14**) followed by ionization and loss of a bromine atom from the molecular ion would give an ion (*f*) indistinguishable from the *N*-5-bromopentylnitrilium ion (*d*) at *m/e* 252. However, based

Can. J. Chem. Downloaded from www.nrcresearchpress.com by 210.87.254.40 on 09/05/12
For personal use only.

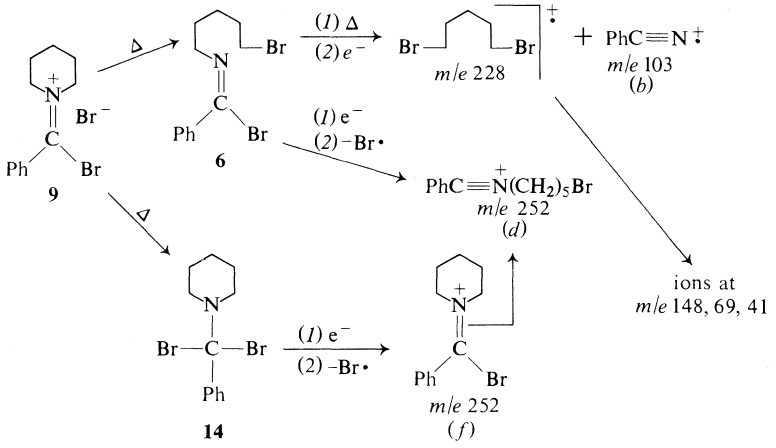

SCHEME 4

on analogy to the fragmentation of **8** (Scheme 3), the process **9** → **14** → (*f*) → (*d*) most likely contributes to the intensity of the *m/e* 252 peak.

Experimental

The mass spectra were obtained on a Nuclide 12-90-G instrument, operated at 70 eV ionizing energy. The imidoyl halides were introduced by the direct insertion technique at a source temperature of 60°. A heated direct-inlet system was used for the iminium salts, with source temperatures as indicated in the text.

Imidoyl chlorides **1**, **3**, and **5** were prepared as described in the literature (19). The synthesis of imidoyl bromides and bromoiminium bromides are described (4, 5) or are to be described (20) in other papers in this series.

Acknowledgment is made to the donors of The Petroleum Research Fund, administered by the American Chemical Society, for support of this work. One of us (J. G.) wished to thank Research Corporation for financial support. The authors would also like to thank Professor G. Fodor for his interest and encouragement. Help with the preparation of the diagrams by Mr. B. Heitke is gratefully acknowledged.

1. H. VON PECHMANN. Ber. **33**, 611 (1900).
2. J. VON BRAUN. Ber. **37**, 2678 (1904).
3. (*a*) H. ULRICH. *In* The chemistry of imidoyl halides. Plenum Press, New York. 1968; (*b*) R. BONNETT. *In* The chemistry of the carbon–nitrogen double bond. *Edited by* S. Patai. Interscience Publishers, New York. 1970. p. 597; (*c*) H. EILINGSFELD, M. SEEFELDER, and H. WEIDINGER. Angew. Chem. **72**, **836** (1960).
4. G. FODOR and B. A. PHILLIPS. Abstracts. 162nd National Meeting of the American Chemical Society. Washington, D.C., No. ORGN 19.
5. B. A. PHILLIPS, J. GAL, and G. FODOR. Proceedings of the West Virginia Academy of Science. 1972. In press.
6. Q. N. PORTER and R. J. SPEAR. Org. Mass Spectrom. **3**, 1259 (1970).
7. (*a*) R. H. SHAPIRO and J. W. SERUM. Org. Mass Spectrom. **2**, 533 (1969); (*b*) *In* Index of mass spectral data. ASTM Committee E-14 on Mass Spectrometry. Ser. No. GCC 22. p. 39.
8. J. L. HOLMES and F. BENOIT. Org. Mass Spectrom. **5**, 525 (1971).
9. *In* Index of mass spectral data. ASTM Committee E-14 on Mass Spectrometry. Ser. No. API 509. p. 17.
10. M. FISHER and C. DJERASSI. Chem. Ber. **99**, 1541 (1966).
11. C. DJERASSI and C. FENSELAU. J. Am. Chem. Soc. **87**, 5752 (1965).
12. C. DJERASSI and C. FENSELAU. J. Am. Chem. Soc. **87**, 5747 (1965).
13. H. BUDZIKIEWICZ, C. FENSELAU, and C. DJERASSI. Tetrahedron, **22**, 1391 (1966).
14. H. J. VEITH and M. HESSE. Helv. Chim. Acta, **52**, 2004 (1969).
15. J. VON BRAUN. Ber. **37**, 2915 (1904).
16. E. NAMANWORTH. Ph.D. Thesis. Yale University, New Haven, Connecticut, 1965.
17. R. BONNET. *In* The chemistry of the carbon–nitrogen double bond. *Edited by* S. Patai. Interscience Publishers, New York. 1970. p. 628.
18. R. BONNET. *In* The chemistry of the carbon–nitrogen double bond. *Edited by* S. Patai. Interscience Publishers, New York. 1970. p. 615.
19. I. UGI, F. BECK, and U. FETZER. Ber. **95**, 126 (1962).
20. G. FODOR, J. J. RYAN, J. GAL, and B. A. PHILLIPS. J. Am. Chem. Soc. Submitted.

Can. J. Chem. Downloaded from www.nrcresearchpress.com by 210.87.254.40 on 09/05/12
For personal use only.

Theoretical Evidence for a Stable form of Cyclic Ozone, and its Chemical Consequences

JAMES S. WRIGHT

Department of Chemistry, Carleton University, Ottawa, Canada K1S 5B6

Received June 30, 1972

The total energy of the symmetrical, bent O_3 molecule is studied as a function of internuclear angle and internuclear distance. The method used is an *ab initio* molecular orbital calculation with a minimum basis set of Slater-type orbitals, plus limited configuration interaction. Best single configuration energies show the existence of *two* stable minima: a cyclic (60°) structure and a bent (115°) structure. The cyclic structure is preferred by 48 kcal/mol, contrary to experiment (116° 48′). Configuration interaction results with two low lying orbitals show the cyclic form still preferred by 6 kcal/mol. A transition state for the bent-cyclic pathway lies 26 kcal/mol (or less) above the bent form. Based on these results, a possible low energy path via the cyclic form is proposed for the thermal decomposition of ozone. It is also proposed that cyclic ozone may have been observed in the pulse radiolysis of oxygen.

L'énergie totale de la molécule O_3, symétrique et recourbée, a été étudiée en fonction de l'angle et de la distance internucléaires. La méthode utiliséé est celle du calcul *ab initio* des orbitales moléculaires avec unsystème minimal d'orbitales de base de type Slater plus une interaction limitée de configuration. Les meilleures énergies pour une configuration simple montrent l'existence de deux minima stables = une structure cyclique (60°) et une structure recourbée (115°). La structure cyclique est plus favorisée de 48 kcal/mol, contrairement à l'expérience (116° 48′). Les résultats de l'interaction de configuration avec deux orbitales basses montrent encore une préférence pour la forme cyclique de 6 kcal/mol. Un état de transition par le chemin réactionnel "cyclique-courbé" se situe à 26 kcal/mol (ou moins) au dessus de la forme courbe. Ces résultats montrent l'existence d'une voie réactionnelle possible de basse énergie, via la forme cyclique, pour la décomposition thermique de l'ozone. L'ozone cyclique a pu être observé lors de la radiolyse pulsée de l'oxygène, comme cela à été proposé. [Traduit par le journal]

Can. J. Chem., **51**, 139 (1973)

Can. J. Chem. Downloaded from www.nrcresearchpress.com by 210.87.254.5 on 09/05/12
For personal use only.

Introduction

The structure determination of the ozone molecule has an interesting history, with much discussion revolving around the interpretation of the gas-phase infrared spectrum. A review by Mulliken (1) in 1942 strongly supported the analysis of the i.r. spectrum by Hettner *et al.* (2), stating that ozone has an acute-angled structure (an isosceles triangle), with the unique internuclear angle $\theta = 39°$.

In 1943 an electron diffraction result (3) showed a symmetrical bent structure with $\theta = 127°$.

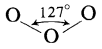

Herzberg (4) in 1945 criticized the acute-angled model and vibrational assignment of Hettner *et al.* (2) as leading to an abnormally high force constant between the two closer O-atoms; however, he also pointed to difficulties if the ozone spectrum were assigned to a symmetrical, bent obtuse-angled structure. The spectral difficulties were apparently resolved when Wilson and Badger (5) discovered a previously hidden vibrational peak at 1110 cm^{-1} and assigned the three fundamental frequencies as arising from a symmetrical bent structure, with $\nu_1 = 1110\ cm^{-1}$ (symmetric stretch), $\nu_2 = 705\ cm^{-1}$ (symmetric bend), and $\nu_3 = 1043\ cm^{-1}$ (antisymmetric stretch). Precise microwave studies by Trambarulo *et al.* (6), Kaplan *et al.* (7), and Hughes (8), who assumed the frequencies of Badger and Wilson (5), gave a bent structure with $R = 1.278 \pm 0.002$ Å, $\theta = 116° 45′ \pm 30′$. This was confirmed by an analysis of the far-i.r. spectrum by Danti and Lord (9), and is considered to be the definitive result for the ozone structure. An *ab initio* molecular orbital calculation by Peyerimhoff and Buenker (ref. 10, hereafter referred to as P–B) gave $\theta = 118.5°$, in good agreement with the previous experimental result. Thus theory and experiment agree that ozone possesses a symmetrical, bent structure.

However, the chemistry of ozone is quite puzzling when one assumes this structure. This

Can. J. Chem. Downloaded from www.nrcresearchpress.com by 210.87.254.5 on 09/05/12
For personal use only.

can be seen by considering the bond energies for ozone and molecular oxygen, and by the activation energies for $O_3 \rightarrow O_2 + O$ and the reverse reaction. The *mean thermochemical bond energy* of ozone can be derived from the following thermocycle (11):

$$\begin{aligned} O_2(g) + \tfrac{1}{2}O_2(g) &\rightarrow O_3(g) & \Delta H_f^0 &= 34 \text{ kcal/mol} \\ 2O &\rightarrow O_2(g) & \Delta H^0 &= -118 \text{ kcal/mol} \\ O &\rightarrow \tfrac{1}{2}O_2(g) & \Delta H^0 &= -59 \text{ kcal/mol} \\ O + O + O &\rightarrow O_3(g) & \Delta H^0 &= -143 \text{ kcal/mol} \end{aligned}$$

Since the bent ozone structure has two bonds, the mean thermochemical bond energy is 71.5 kcal/mol per bond. However, the *bond dissociation energy* of ozone is quite different

$$O_3 \rightarrow O_2 + O \quad \Delta H^0 = -34 + 59 = +25 \text{ kcal/mol}$$

The bond dissociation energy of 25 kcal/mol, defined as the energy necessary to break the first bond, is far less than the mean thermochemical value of 71.5 kcal/mol. Writing resonance structures for ozone as

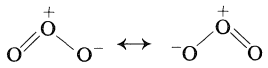

suggests that the bond is intermediate between single and double. Using Pauling's figures (11) of 33 kcal/mol for O—O and 96 kcal/mol for O=O (based on the energy of the $^1\Delta_g$ state) leads to an approximate bond energy of 65 kcal/mol; this is reasonably consistent with the mean thermochemical bond energy but gives no clue as to why the bond dissociation energy should be so low.

The kinetics of the gas phase thermal decomposition of ozone were studied by Benson and Axworthy (12) at temperatures near 100 °C. Assuming the mechanism

$$M + O_3 \underset{k_2}{\overset{k_3}{\rightleftharpoons}} M + O_2 + O$$

$$O_3 + O \xrightarrow{k_3} 2O_2 \quad M = O_3, O_2, N_2, \text{etc.}$$

they obtained

$$k_1 = 4.61 \times 10^{12} \exp(-24\,000/RT) \text{ l/mol s}$$

$$k_2 = 6.00 \times 10^{7} \exp(+600/RT) \text{ l}^2/\text{mol}^2 \text{ s}$$

$$k_3 = 2.96 \times 10^{10} (-6\,000/RT) \text{ l/mol s}$$

The activation energy is thus 24 kcal/mol for the ozone decomposition and negative (0.6 kcal/mol) for its formation. The bond dissociation energy and the activation energy are essentially identical.

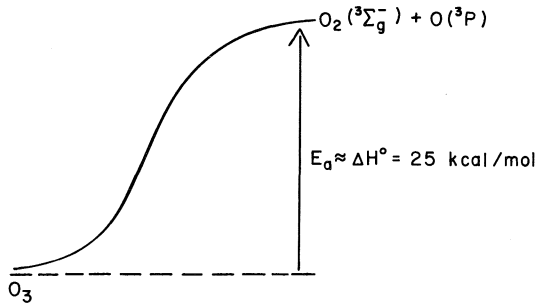

FIG. 1. Thermal activation barrier for $O_3 \rightarrow O_2 (^3\Sigma_g^-) + O (^3P)$.

These energy relationships are diagrammed in Fig. 1.

The activation barrier is seen to be simply the thermochemical energy difference between O_3 and $O_2 + O$. Now the remarkable thing about this barrier is that it is so small; much below the bond energy for bent ozone. This fact would be more understandable if ozone had an acute-angled structure such as

with one relatively intact O_2 molecule and a more distant oxygen atom, weakly held by two equivalent bonds. Indeed, this was pointed out by Herzberg (4) in 1945. Another structure which would be possible is the asymmetric bent structure

with one short and one long bond. Although both the acute-angled and asymmetric structures could be used to explain the infrared spectrum (4), they were excluded on the basis of the electron diffraction result (3) (symmetrical, bent, $\theta = 127°$, $R = 1.26$ Å) and microwave studies (6–8) (symmetrical, bent, $\theta = 116° 45'$, $R = 1.278$). The very low dissociation energy of ozone is therefore difficult to understand.

Another interesting aspect of ozone chemistry which is not well understood is the formation of an ozone "precursor" in the pulse radiolysis of oxygen at atmospheric pressure. According to Riley and Cahill (13), a transient species identified by previous workers (14) as vibrationally excited ozone is incorrect, and they find an ozone precursor with an ultraviolet spectrum distinct from ozone itself. The identity of this precursor was not established, but it was thought to be a distinct chemical species.

Can. J. Chem. Downloaded from www.nrcresearchpress.com by 210.87.254.5 on 09/05/12
For personal use only.

It is now proposed that the low bond dissociation energy, and possibly the ozone precursor, can be explained in terms of a new structure: *cyclic ozone.*

A structure in which the oxygen atoms form an equilateral triangle has been discussed by Pauling (ref. 11, p. 87) as a possible ozone geometry; he discards this structure as being unfavored in bond energy (33 kcal/mol per single bond = 99 kcal/mol total) relative to the observed value of 143 kcal/mol. However the calculations of Pererimhoff and Buenker (10) showed a secondary minimum near $\theta = 70°$ (primary minimum at 118.5°) of almost the same energy as the favored bent configuration, the difference between the two minima being about 10 kcal/mol.[1] Because the calculations of P–B focused on the energy variation as a function of internuclear angle θ, and assumed a fixed bond distance of 2.50 a.u. (1.323 Å), it was not clear whether this distance would favor the cyclic or bent structure. Therefore this study was undertaken to examine the variation of energy as a function of internuclear angle and internuclear distance, assuming a symmetric (C_{2v}) structure. As will be shown, closed-shell single configuration minima were found at two angles: 60° (the cyclic structure) and 115° (the experimental structure). The fact that the cyclic structure is energetically *preferred* in these calculations is a startling result, and suggests that the thermal decomposition may proceed through the following path

$$O_3(115°) \xrightarrow{\text{(slow)}} O_3(60°) \xrightarrow{\text{(fast)}} O_2 + O$$

Method

The Roothaan self-consistent field equations (15) are solved using a minimum basis set of Slater-type orbitals. The *ab initio* molecular orbital program used was written by Stevens, and has been described elsewhere (16).[2] All calculations use Clementi's (17) "best atom" exponents for the basis orbitals: $1s_0 = 7.658$, $2s_0 = 2.2458$, $2p_0 = 2.2266$. A check on the program was made by recalculating the minimum basis set result for ozone of Petrongolo *et al.* (18); the two calculations gave identical results. For a given choice of θ, the O—O—O angle, three values of R_{O-O} were used so that an optimum bond distance is established at each angle θ. C_{2v} symmetry was assumed throughout, with the same coordinate axes and symmetry orbitals as used by P–B.

TABLE 1. MO notation and orbital occupancy (C_{2v}) for various closed-shell configurations

Configuration wavefunction	P–B notation	Orbital occupancy (filled)			
		a_1	a_2	b_1	b_2
ψ_1	$\{2b_1^2\}$	6	1	1	4
ψ_2	$\{6a_1^2\}$	5	1	2	4
ψ_3	$\{4b_2^2\}$	6	1	2	3
ψ_4	$\{1a_2^2\}$	6	0	2	4
ψ_5		7	0	2	3

Semilocalized Orbitals and Electron Configuration

To discuss the various possible electronic configurations, the notation of P–B is adopted. Table 1 shows the relevant closed shell electronic configurations. The first column gives a wave function designation by which the configuration may be identified, the second column shows the symbol of P–B used for this wave function, and succeeding columns show the orbital occupancy of each symmetry type in C_{2v} symmetry. The configuration ψ_5 was thought to be important by Mulliken (1) for the acute-angled ozone; this is included along with the configurations $\psi_1 - \psi_4$ studied by P–B.

As shown in Fig. 4 (*a*) of P–B, as θ is closed from 180° to 60° there is a change of ground state configuration from ψ_1 to ψ_3 which occurs near 90°. In this region there is an orbital crossing between the $4b_2$ and $2b_1$ molecular orbitals. Put more simply, two electrons from the π-bond in bent ozone (2 σ-, 1 π-bond) are transferred to a σ-bond in cyclic ozone (3 σ-bonds). The orbitals which are involved here and in the discussion to follow may conveniently be referred to in terms of semi-localized symmetry orbitals.[3] Assuming cyclic ozone to be sp^3 hybridized and bent (~120°) ozone to be sp^2 hybridized (20), the orbitals are shown and classified according to their C_{2v} symmetry type in Figs. 2 and 3. The

[1]Estimated from Fig. 4, P–B.

[2]All calculations on ozone assumed C_{2v} symmetry. Since the program uses molecular symmetry to reduce integral evaluation times, a typical calculation required 5 min of IBM 360/65 CPU time.

[3]See ref. 19 for a similar treatment for cyclobutane.

Can. J. Chem. Downloaded from www.nrcresearchpress.com by 210.87.254.5 on 09/05/12
For personal use only.

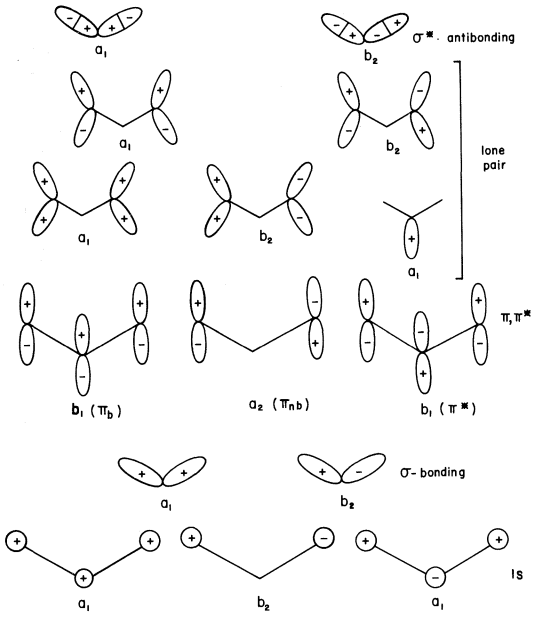

FIG. 2. Semilocalized orbitals for bent (120°) ozone (sp^2, p-hybridization is assumed, with σ, lone pair, and σ* orbitals in the molecular plane, and π, π* orbitals perpendicular to it).

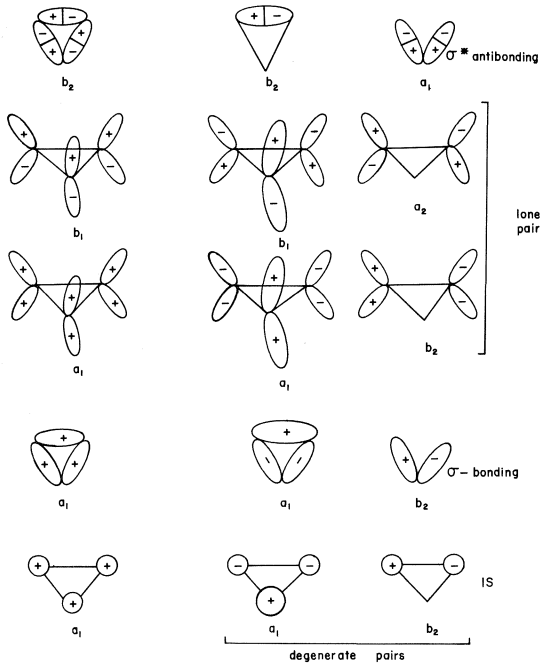

FIG. 3. Semilocalized orbitals for cyclic (60°) ozone (sp^3-hybridization assumed).

orbitals are also identified at the right by their common names. (A less familiar notation is introduced in Fig. 2, where the π-nonbonding orbitals are distinguished by the subscripts nb, π_{nb}.) In Fig. 2, all orbitals except the π π* lie in the plane of the molecule. The σ-bonding orbitals, for example, are formed by the bonding overlap of sp^2 hybrids:

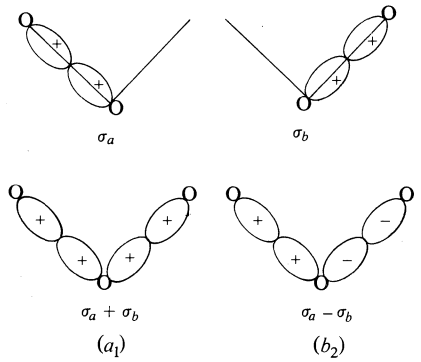

The lone pair symmetry orbitals (Fig. 2) are derived as symmetric (a_1) and antisymmetric (b_2) combinations of the lone pair sp^2-hybridized basis orbitals. In Fig. 3 the lone-pair orbitals lie outside the plane of the ring, with the other orbitals (1s, σ, σ*) lying in plane. At 60° the C_{2v} group becomes D_{3h}, and the orbitals which actually represent degenerate pairs are grouped together.

The electronic configurations of the bent and cyclic forms can now be guessed by inspection of the semilocalized orbitals. Ozone has 24 electrons, so in the bent structure (Fig. 2) all orbitals will be doubly occupied except the π* and σ*, which are empty. The configuration is therefore $(6a_1)^2(1a_2)^2(1b_1)^2(4b_2)^2$. The $1a_2$ orbital (π_{nb}) is expected to be the highest occupied, and $2b_1$ orbital (π*) the lowest vacant orbital. In cyclic ozone the three antibonding σ* orbitals will be vacant, and the others filled. The configuration of cyclic ozone is thus $(6a_1)^2(1a_2)^2(2b_1)^2(3b_2)^2$ which is different from that of bent ozone. Nodal properties indicate that the $1a_2$ lone pair (or its degenerate equivalent $2b_1$) should be the highest occupied, and the unique b_2 σ* the lowest vacant orbital. We shall see that these results are borne out by the MO calculations.

Results and Discussion

Table 2 shows the variation in the total energy as a function of θ and R. In this table, ψ denotes the electronic configuration referred to in Table 1,

TABLE 2. Energy variation as a function of internuclear angle (optimum R)

θ (deg.)	ψ	E_0 (a.u.)	R_0 (a.u.)	E (a.u.)	R (a.u.)
40	ψ_3	−223.3903	3.1*	−223.4274	3.1
	ψ_5	−223.1935	3.1*	−223.2638	3.1
55	ψ_3	−223.5480	2.760	−223.5958	2.795
60	ψ_3	−223.5568	2.677	−223.5999	2.710
65	ψ_3	−223.5494	2.624	−223.6001	2.669
70	ψ_3	−223.5307	2.588	−223.5957	2.658
75	ψ_3	−223.5058	2.566	−223.5872	2.654
85	ψ_1	−223.3906	2.585	−223.5127	2.595
	ψ_3	−223.4520	2.564	−223.5661	2.636
90	ψ_1	−223.4211	2.548	−223.5428	2.567
	ψ_3	−223.4267	2.572	−223.5548	2.632
95	ψ_1	−223.4437	2.516	−223.5639	2.543
	ψ_3	−223.4043	2.585	−223.5432	2.624
110	ψ_1	−223.4768	2.454	−223.5903	2.493
	ψ_3	−223.3518	2.631		
115	ψ_1	−223.4793	2.444	−223.5904	2.482
	ψ_3	−223.3337	2.647	−223.4949	2.600
120	ψ_1	−223.4785	2.436	−223.5871	2.475
	ψ_3	−223.3242	2.660	−223.4815	2.595
125	ψ_1	−223.4750	2.432	−223.5810	2.468
	ψ_3	−223.3115	2.675	−223.4676	2.587

*At θ = 40° only a single data point was taken, where R = 3.1 a.u.

R_0 is the optimum distance and E_0 the optimum energy for this (single) configuration. E represents the energy obtained on doing a 3 × 3 configuration interaction calculation based on ψ and its virtual orbitals, and R is the distance which optimizes the CI energy (the CI treatment will be discussed following the analysis of single-configuration energies and molecular orbitals). Except for one calculation at 40° which includes ψ_5, data are given only for configurations ψ_1 and ψ_3 (for configurations ψ_2 and ψ_4 refer to P–B), since these are relevant to a study of the ground state of ozone.

The results in Table 2 are shown graphically in Fig. 4. The dashed lines show the single configuration energies ψ_1 and ψ_3 as a function of θ with R optimized. There is a clear minimum for ψ_1 at θ = 115°, R = 2.444 a.u. (1.291 Å), E_0 = −233.4793 a.u. This is in good agreement with the experimental result (8) of θ = 116° 45′, R = 1.278 Å. However, a much deeper minimum occurs for ψ_3 at θ = 60°, R = 2.677 a.u. (1.417 Å), E_0 = −223.5568 a.u. The cyclic configuration is seen to be a true equilateral triangle (θ = 60°) and its energy is below that of the bent (115°) structure by a remarkable 48 kcal/mole! When one considers that *ab initio* minimum basis set calculations are quite reliable for predictions of molecular geometry (22), this result is indeed surprising. It suggests, on the one hand, that minimum basis set calculations even for comparisons among closed shell molecules can be unreliable by an amount of the order of 2 eV. On the other hand, it also suggests that cyclic ozone should exist as a stable secondary minimum.

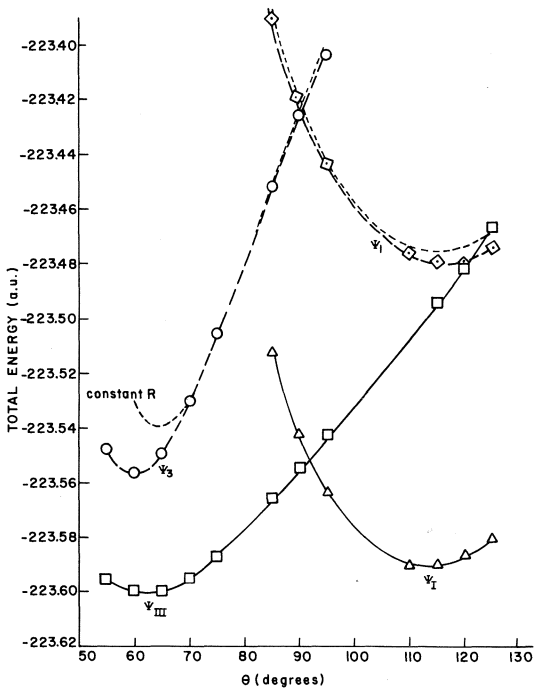

FIG. 4. Variation of the total SCF energy as a function of θ, with R optimized at each angle.

Can. J. Chem. Downloaded from www.nrcresearchpress.com by 210.87.254.5 on 09/05/12
For personal use only.

TABLE 3. Orbital energies for configurations ψ_1 and ψ_3 near their energy minima

ψ_1			ψ_3		
Symmetry type	Orbital energy (a.u.)	Chemical type	Symmetry type	Orbital energy (a.u.)	Chemical type
$1a_1$	−20.9586	1s	$1a_1$	−20.7739	1s
$1b_2$	−20.6760	1s	$1b_2$	−20.7739	1s
$2a_1$	−20.6759	1s	$2a_1$	−20.7737	1s
$3a_1$	− 1.6662		$3a_1$	− 1.6541	σ-bond†
$2b_2$	− 1.3317		$4a_1$	− 1.1670	σ-bond
$4a_1$	− 1.0085		$2b_2$	− 1.1670	σ-bond
$5a_1$	− 0.7093		$1b_1$	− 0.7071	lone pair
$1b_1$	− 0.6782	π_b	$5a_1$	− 0.6251	lone pair
$3b_2$	− 0.6709		$6a_1$	− 0.5466	lone pair
$4b_2$	− 0.4381		$3b_2$	− 0.5466	lone pair
$6a_1$	− 0.4214		$1a_2$	− 0.4464	lone pair
$1a_2$	− 0.3482	π_{nb}	$2b_1$	− 0.4464	lone pair
$2b_1$	+ 0.0749	π^*	$4b_2$	+ 0.2554	σ*
$7a_1$	+ 0.4836	σ*	$7a_1$	+ 0.3868	σ*
$5b_2$	+ 0.5798	σ*	$5b_2$	+ 0.3868	σ*

†Considerable mixing occurs between chemical types of symmetry a_1 and b_2.

The importance of including bond distance R as a variable in the calculations is seen by inspection of Table 2, where the optimized R_0's vary from 2.760 a.u. (1.461 Å) for ψ_3 at 55° to 2.432 a.u. (1.287 Å) for ψ_1 at $\theta = 125°$. Since P–B used only a single distance of $R = 2.50$ a.u. for their calculations, the minimum basis set result at $R = 2.50$ a.u. has been included in Fig. 4 (dotted line) for comparison with the result at optimum R (dashed line). Although the fixed-R calculation correctly predicts a minimum at $\theta = 115°$, it incorrectly shifts the energy minimum for the cyclic configuration to $\theta = 65°$. This is because the ring has not been allowed to expand as it closes.

A single data point at $\theta = 40°$, $R = 3.1$ a.u. was calculated to test the prediction of Mulliken (1) that an acute-angled ozone of these approximate dimensions would have electron configuration ψ_5. As shown in Table 2, however, ψ_5 lies far above ψ_3 in energy so calculations using ψ_5 and acute-angled geometries ($\theta < 55°$) were not pursued.

The molecular orbital energies and orbital types for configurations ψ_1 and ψ_3 near their respective minima are listed in Table 3. For ψ_1 the smallest energy gap occurs for the $1a_2$–$2b_1$ (π-π^*) transition, followed by $6a_1$–$2b_1$ and $4b_2$–$2b_1$. The low lying excited states so formed will be of B_2, B_1, and A_2 symmetry, the latter resulting from a forbidden transition. The π–π^* transition is allowed and should be relatively intense. For ψ_3 low lying transitions will be from the degenerate pair ($1a_2$,$2b_1$) to the vacant orbital $4b_2$. These will not give rise to intense absorption. However, the transitions from the pair ($6a_1$,$3b_2$) to $4b_2$ are strongly allowed. It is possible that the u.v. spectrum of the "ozone precursor" is due to this transition, the distinctive u.v. transition being due to the cyclic rather than the bent form of ozone.

The difference in energy between cyclic and bent structures is considerably ameliorated by the introduction of configuration interaction. Figure 4 shows the CI state energies (solid line) for states formed from ψ_1 (labelled ψ_I) and ψ_3 (labelled ψ_{III}) by introducing a 3 × 3 CI in the following way. The virtual orbitals chosen for the CI calculation were those which interact strongly with the ground state. For the double excitation $(\phi_i)^2 \rightarrow (\phi_j)^2$, where two electrons are promoted from occupied molecular orbital ϕ_i to vacant molecular orbital ϕ_j, the interaction was considered important if the energy gap $(E_j - E_i)$ was small and the exchange integral K_{ij} was large. This led to the following CI scheme:

Can. J. Chem. Downloaded from www.nrcresearchpress.com by 210.87.254.5 on 09/05/12
For personal use only.

TABLE 4. Calculated values of θ, R, and E

Structure	θ (deg.)	R (a.u.)	E (kcal/mol)
Cyclic	62.5	2.690	0
Transition state	92	~2.60	31
Bent	112.5	2.487	6

That is, in the bent configuration there is a strong π_{nb}–π^* interaction as well as the π_b–π^* interaction and the CI is very important. Interaction is weaker, but still significant in the cyclic system, where the double excitation now promotes electrons from lone pair (non-bonding) oxygen orbitals to an antibonding σ* orbital. The bent structure is strongly stabilized by an amount 0.1117 a.u. (70.0 kcal/mol) and its energy minimum is slightly shifted (θ = 112.5°, R = 2.487 a.u.). The cyclic structure is stabilized by an amount 0.0437 a.u. (27.4 kcal/mol) with its energy minimum also slightly shifted (θ = 62.5°, R = 2.690 a.u.). The cyclic configuration is now favored by 223.6005 − 223.5910 = 0.0095 a.u. or 6.0 kcal/mol. Since the bent structure has more low-lying orbitals available to it than the cyclic (see discussion to follow, or Fig. 4 or P–B), further introduction of CI should favor the bent structure relative to the cyclic. The correlation correction thus introduced would then be expected to lead to agreement with the experimental results,[4] with the bent structure becoming the most stable.

An indication of the activation energy for the bent-cyclic interconversion is seen by following the variation of ψ_I and ψ_{III} in Fig. 4. The states ψ_I and ψ_{III} have the same energy E = −223.551 a.u. at θ = 92°. Since ψ_1 and ψ_3 are both closed-shell configurations they are both totally symmetric and thus the CI calculation based on ψ_1 and ψ_3 should show an avoided crossing. This is not taken into account in the limited CI actually performed, which shows a genuine crossing of ψ_I and ψ_{III}. The two configurations ψ_1 and ψ_3 differ in the occupancy of the orbitals $2b_1$ and $4b_2$, so if the CI had included the $2b_1$–$4b_2$ excitation the crossing of ψ_I and ψ_{III} should become avoided. However, the difference in spatial properties of the $2b_1$ (a π* type) and $4b_2$ (a σ* type) orbitals leads to a very small exchange integral between the two (about 0.01 a.u., compared to K_{ij} = 0.20 a.u. for $1a_2 \rightarrow 2b_1$) so that the actual crossing point shown for ψ_I and ψ_{III} should be near to, and slightly above, the energy of the true avoided crossing. The crossing point of ψ_I and ψ_{III} thus gives an estimate of the energy of the transition state for the bent-cyclic interconversion. Ignoring zero-point energy differences, the results derived from these calculations, where relative energies are indicated, are listed in Table 4. These results indicate that the cyclic and bent forms of ozone are of comparable stability, with a transition state for interconversion between the two lying 25–30 kcal/mol above.

Since this is close to the observed energy for the thermal decomposition of ozone, it suggests the possible reaction scheme

$$O_3(\text{bent}) \xrightarrow{\text{slow}} O_3(\text{cyclic}) \xrightarrow{\text{fast}} O_2 + O$$

The cyclic ozone should decompose more easily than the bent ozone because it contains three single bonds. A normal mode leading to O_2 + O would then be the degenerate bending vibration[5]

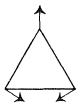

The exploration of this decomposition pathway would be quite interesting. A complete potential surface for the $O_3 \rightarrow O_2$ + O reaction should therefore include the region around the cyclic

[4]The program used is capable of dealing with extended basis sets of Slater-type orbitals. A double-ξ calculation would be interesting as an approximation to the H–F limit for cyclic and bent ozone. This was seriously considered but eventually rejected as too expensive. See, however, an important paper which appeared when this manuscript was completed, which deals with this question also (21).

[5]It has been pointed out (21) that if ozone were an equilateral triangle (D_{3h}) it would decompose into the excited state products $O(^1D) + O_2(^2\Delta_g)$. However, if ozone has C_{2v} symmetry (θ ≠ 60°) the decomposition to $O(^3P) + O_2(^3\Sigma_g^-)$ is allowed. Since it is not certain whether the cyclic molecule has θ = 60°, the correlation with products is uncertain. Also, if ozone has symmetry D_{3h} the degenerate bending vibration is i.r.-active but the ring breathing vibration is not (4). If cyclic ozone were indeed of comparable stability to bent ozone, the bending peak should be present in the ozone i.r. spectrum.

Can. J. Chem. Downloaded from www.nrcresearchpress.com by 210.87.254.5 on 09/05/12
For personal use only.

structure as well as the region around the bent structure, in searching for the lowest energy transition state leading to the observed products.

The author would like to thank Dr. Alain Devaquet for useful discussions and communication of results prior to publication.

1. R. S. MULLIKEN. Rev. Mod. Phys. **14**, 204 (1942).
2. G. HETTNER, R. POHLMAN, and H. J. SCHUMACHER. Zeits. Phys. **91**, 372 (1934).
3. W. SHAND, JR., and R. A. SPURR. J. Am. Chem. Soc. **65**, 179 (1943).
4. G. HERZBERG. Molecular spectra and molecular structure. II. Infrared and raman spectra of polyatomic molecules. D. Van Nostrand Co., Inc., New Jersey. 1945. pp. 285–287.
5. M. K. WILSON and R. M. BADGER. J. Chem. Phys. **16**, 741 (1948); R. M. BADGER and M. K. WILSON. J. Chem. Phys. **18**, 998 (1950).
6. R. TRAMBARULO, S. N. GHOSH, C. A. BURRUS, JR., and W. GORDY. J. Chem. Phys. **21**, 851 (1953).
7. L. D. KAPLAN, M. V. MIGEOTTE, and L. NEVEN. J. Chem. Phys. **24**, 1183 (1956).
8. R. HUGHES. J. Chem. Phys. **24**, 131 (1956).
9. A. DANTI and R. C. LORD. J. Chem. Phys. **30**, 1310 (1959).
10. S. D. PEYERIMHOFF and R. J. BUENKER. J. Chem. Phys. **47**, 1953 (1967).
11. L. PAULING. The nature of the chemical bond. 3rd ed. Cornell University Press, Ithaca, N. Y. pp. 85, 189.
12. S. W. BENSON and A. E. AXWORTHY, JR. J. Chem. Phys. **26**, 1718 (1957).
13. J. F. RILEY and R. W. CAHILL. J. Chem. Phys. **52**, 3297 (1970).
14. C. H. HOCHANADEL, J. A. GHORMLEY, and J. W. BOYLE. J. Chem. Phys. **48**, 2416 (1968).
15. C. C. J. ROOTHAAN. Rev. Mod. Phys. **23**, 161 (1951).
16. R. M. STEVENS. J. Chem. Phys. **52**, 1397 (1970).
17. E. CLEMENTI and D. L. RAIMONDI. J. Chem. Phys. **38**, 2686 (1963).
18. C. PETRONGOLO, E. SCROCCO, and J. TOMASI. J. Chem. Phys. **48**, 407 (1968).
19. L. SALEM and J. S. WRIGHT. J. Am. Chem. Soc. **91**, 5947 (1969).
20. R. HOFFMANN. J. Am. Chem. Soc. **90**, 1475 (1968).
21. P. J. HAY and W. A. GODDARD. Chem. Phys. Lett. **14**, 46 (1972).
22. M. D. NEWTON, W. A. LATHAN, W. J. HEHRE, and J. A. POPLE. J. Chem. Phys. **52**, 4064 (1970).

Can. J. Chem. Downloaded from www.nrcresearchpress.com by 210.87.254.5 on 09/05/12
For personal use only.

Can. J. Chem. Downloaded from www.nrcresearchpress.com by 210.87.254.6 on 09/05/12
For personal use only.

Pressure Dependence of Product Yields in the Direct Photolysis of Methanol Vapor at 1849 Å

O. Sonia Herasymowych[1] and Arthur R. Knight

Departments of Chemistry and Chemical Engineering, University of Saskatchewan, Saskatoon, Saskatchewan

Received September 6, 1972

Hydrogen and methane yields from the 1849 Å photolysis of methanol vapor in an all-quartz system have been investigated as a function of exposure time and pressure of CH_3OH and added CO_2.

Product yields are decreased by the inert addend, and by the substrate itself at high pressures, in contrast to the collision-induced quantum yield enhancement reported to be occurring in this system.

La quantité libérée d'hydrogène et de méthane, lors de la photolyse du méthanol gaseux à 1849 Å dans un système en quartz, a été étudiée en fonction du temps d'exposition et de la pression du méthanol et de CO_2 ajouté.

Les rendements en produits sont diminués par l'addition du composé inerte et par le substrat lui-même à des pressions élevées au contraire de l'augmentation du rendement quantique, induite par des collisions, qui est rapporté se presenter dans ce système. [Traduit par le journal]

Can. J. Chem., **51**, 147 (1973)

It has been reported (1–3) that in the photolysis of methanol vapor in a Pyrex system at 1849 Å a quantum yield enhancement, ascribed to collision-induced predissociation, results from increasing substrate pressure or inert addend pressure. A recent investigation (4) of the photolysis of 2-propanol vapor at 1800–2000 Å carried out in this laboratory, however, indicated that product yields decrease with increasing addend pressure, suggesting a fundamental difference in the two systems. Because the methanol system represents the only reported case of collision-induced predissociation in a polyatomic system, and the possibility that the investigation of CH_3OH may be complicated by the formation of trimethyl borate when methanol vapor is in contact with boron containing glass (5), we have reinvestigated the direct photolysis of methanol vapor at 1849 Å in an all quartz, mercury free system.

Fisher reagent methanol was distilled from sodium into a quartz storage vessel and photolyzed at 25 °C in a 20 cm × 4.5 cm o.d. Supracil cell using a Hanovia LO 735A-7 low pressure Hg resonance lamp. Products non-condensable at −196 °C, H_2, and CH_4, were removed through a liquid nitrogen trap to an auxiliary system where they were measured in a gas burette and subsequently analyzed by g.c. Over the range 5–60 min, the yields of hydrogen and methane were found to vary linearly with exposure time.

Figure 1 shows the observed dependence of $R(H_2)$ and $R(CH_4)$ on methanol pressure. Both rates behave in the same manner, increasing up to

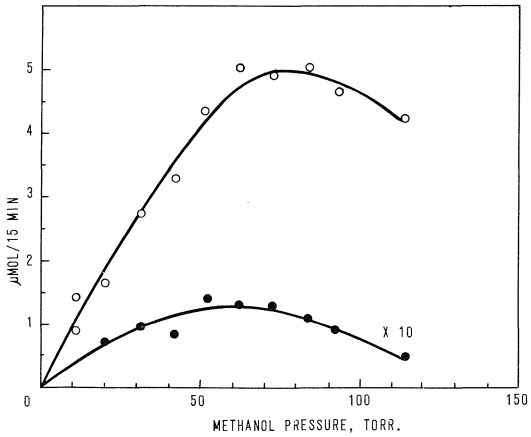

FIG. 1. Rate of formation of hydrogen, ○, and methane, ●, (× 10) in the 1849 Å photolysis of methanol vapor at 25 °C, as a function of CH_3OH pressure, for an exposure time of 15 min.

[1]Present address, Department of Chemistry, University of Alberta, Edmonton, Alberta.

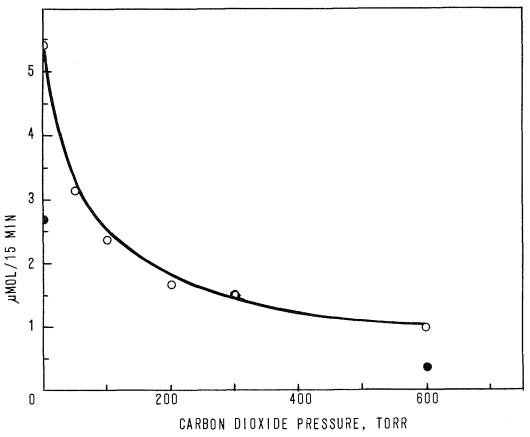

FIG. 2. Rate of formation of hydrogen in the 1849 Å photolysis of methanol vapor at 25 °C and a pressure of 84 Torr, ○, and 31 Torr, ●, as a function of pressure of added carbon dioxide.

$P(CH_3OH) \simeq 60$–70 Torr and thereafter showing a decrease. The proportion of hydrogen and methane formed is consistent with the observations of Porter and Noyes (6) who suggested that *ca.* 5% of the primary process results in the formation of CH_3 radicals. Both Hagege *et al.* (3) and Porter and Noyes (6) have reported that $R(H_2)$ increases continuously up to about 100 Torr methanol. In the latter investigation, however, such an increase is to be expected since a monochromatic light source was not employed. The increase in yields in the low pressure region observed in the present investigation can be ascribed, at least in part, to increased absorption in the reaction cell. A Beer's law calculation indicates that at 1849 Å absorption should be complete at $P(CH_3OH) = 10$ Torr, but unless a perfectly collimated and focused light beam were employed higher pressures might be required.[2]

[2]For example, only 87% absorption was found at 1849 Å at $P(CH_3OH) = 12$ Torr in the cell using a Zeiss PMQ II spectrophotometer with the photolysis lamp as light source. Such measurements determine the absorption through only a small fraction of the total cross section of the light beam.

Wall recombination of hydrogen atoms may also be important since Hagege *et al.* (3) report a dependence of yields on cell geometry.

The rate of hydrogen formation was determined in a series of experiments carried out with up to 600 Torr of CO_2 at methanol pressures of 84 and 31 Torr. The results are given in Fig. 2 and show a very definite decline as the pressure of addend is increased at both substrate pressures. Carbon dioxide was chosen for investigation since this inert addend was reported (2, 3) to be the most efficient in promoting the observed increase in hydrogen quantum yields.

On the basis of the results reported here it would appear that the methanol photolysis at 1849 Å proceeds, at least in part, via an excited state of sufficient longevity to be susceptible to collisional deactivation by either an inert addend or by the substrate itself. The deactivational process is manifested by observed decreases in $R(H_2)$ when the addend is present and at high pressures of the substrate.

Thus when the methanol system is investigated under conditions where the formation of trimethyl borate is not possible, its behavior closely parallels that of 2-propanol and no evidence is obtained for collision induced predissociation.

The authors acknowledge the financial support of the National Research Council of Canada for this work and a special grant from the University of Saskatchewan.

1. J. HAGEGE, S. LEACH, and C. VERMEIL. J. chim. phys. **62**, 736 (1965).
2. J. HAGEGE, P. C. ROBERGE, and C. VERMEIL. J. chim. phys. **65**, 641 (1968).
3. J. HAGEGE, P. C. ROBERGE, and C. VERMEIL. Trans. Faraday Soc. **64**, 3288 (1968).
4. O. S. HERASYMOWYCH and A. R. KNIGHT. Can. J. Chem. **50**, 2217 (1972).
5. R. P. PORTER. J. Phys. Chem. **61**, 1260 (1957).
6. R. P. PORTER and W. A. NOYES, JR. J. Am. Chem. Soc. **81**, 2308 (1959).

Can. J. Chem. Downloaded from www.nrcresearchpress.com by 210.87.254.6 on 09/05/12
For personal use only.

Charge Scavenging by Benzene in γ-Irradiated Liquid Cyclohexane

MICHAEL G. KENNEDY AND JOHN A. STONE
Chemistry Department, Queen's University, Kingston, Ontario

Received September 20, 1972

The effect of benzene on the yield of propane formed by H_2 transfer to cyclopropane in γ-irradiated liquid cyclohexane has been used to determine the efficiency of cation scavenging by benzene. The reduction of the hydrogen yield from cyclohexane by the addition of low concentrations of benzene may be accounted for by a combination of cation and H atom scavenging. G(benzene in polymer) found in previous studies correlates well with G(H atoms scavenged).

L'effet du benzène sur le rendement en propane, découlant du transfert d'hydrogène sur le cyclopropane dans le cyclohexane liquide γ-irradié, a été utilisé pour déterminer l'efficacité du piègeage du cation par le benzène. La baisse du rendement en hydrogène à partir du cyclohexane par addition de faibles concentrations en benzène, peut être attribuée à la combinaison du cation et de l'atome d'hydrogène piégé. Le G(pour le benzène dans le polymère) tiré des études antérieures est en bonne corrélation avec le G(pour les atomes d'hydrogène piégés). [Traduit par le journal]

Can. J. Chem., **51**, 149 (1973)

Can. J. Chem. Downloaded from www.nrcresearchpress.com by 210.87.254.6 on 09/05/12
For personal use only.

The non-linear relationship between the reduction of the hydrogen yield from irradiated liquid cyclohexane and the concentration of added benzene was one of the earliest phenomena studied in radiation chemistry (1, 2). Many mechanistic explanations have been advanced including "excitation" transfer, H atom scavenging, charge transfer, and combinations of all three. (A discussion of published results and suggested mechanisms is given in ref. 3.) Recent pulse radiolysis studies have suggested that benzene is a positive ion scavenger in cyclohexane (4) and that it is also a somewhat inefficient H atom scavenger (5). We have confirmed the positive ion scavenging and have investigated its contribution to the overall decrease in hydrogen yield by measuring the effect of benzene on the propane formed by H_2 transfer to cyclopropane from the cyclohexane molecular ion (6).

[1] $\text{cyclo-}C_6H_{12}^+ + \text{cyclo-}C_3H_6 \rightarrow \text{cyclo-}C_6H_{10}^+ + C_3H_8$

Propane yields in the presence and absence of 0.09 M benzene are shown in Fig. 1. The experimental points have been fitted by the expression developed by Warman, Asmus, and Schuler (6). In the absence of benzene

$$G(\text{propane}) = 0.63\left[G_{fi} + \frac{G_{gi}\sqrt{\alpha_1[\Delta]}}{1+\sqrt{\alpha_1[\Delta]}}\right]$$

while in the presence of benzene

$$G(\text{propane}) = 0.63\left[G_{fi} + \frac{G_{gi}\sqrt{\alpha_1[\Delta]+\alpha_2[B]}}{1+\sqrt{\alpha_1[\Delta]+\alpha_2[B]}}\right]\left[\frac{\alpha_1[\Delta]}{\alpha_1[\Delta]+\alpha_2[B]}\right]$$

Where Δ and B are cyclopropane and benzene, respectively, G_{fi} is the yield of free ions = 0.15 (7), G_{gi} is the yield of geminate ions = 3.8 (6), and α_1 and α_2 are constants which are measures of the relative rates of electron-geminate ion combination and positive charge scavenging by cyclopropane and benzene, respectively. The correction factor 0.63 is used since only 63% of the ion scavenging by cyclopropane occurs via reaction 1 to yield propane (8). The curves are drawn with $\alpha_1 = 0.40\ M^{-1}$ and $\alpha_2 = 1.20\ M^{-1}$. Benzene is therefore three times as efficient a cation scavenger as is cyclopropane and is also slightly more efficient than ND_3 ($\alpha = 0.85\ M^{-1}$ (9)). The above interpretation assumes that the low concentration of benzene does not significantly change the spatial distribution of the electrons at thermalization and that propane is formed solely by the H_2 transfer reaction (reaction 1).

The extent of ion scavenging by benzene in irradiated solutions of benzene in cyclohexane may now be calculated from

$$G(\text{ions scavenged}) = 0.15 + \frac{3.8\sqrt{\alpha_2[B]}}{1+\sqrt{\alpha_2[B]}}$$

TABLE 1. Calculated and experimental reductions in $G(H_2)$ for dilute solutions of benzene in cyclohexane

Benzene (M)	G(ions scavenged)	$G(H\cdot)$	$G(H\cdot$ scavenged)	$\Delta G(H_2)$ Calcd.	$\Delta G(H_2)$ Expt.
1.00×10^{-3}	0.27	1.40	0.005	0.28	0.19
5.00×10^{-3}	0.41	1.37	0.025	0.43	0.33
1.00×10^{-2}	0.51	1.35	0.049	0.56	0.47
5.00×10^{-2}	0.87	1.26	0.20	1.07	1.07
1.00×10^{-1}	1.10	1.21	0.33	1.43	1.42
2.00×10^{-1}	1.26	1.18	0.51	1.87	1.87
3.00×10^{-1}	1.53	1.12	0.60	2.13	2.23

The value of this function is shown in column 2 of Table 1. Since a negligible amount of hydrogen arises from benzene at this concentration (10) G(ions scavenged) may be equated to the reduction in hydrogen yield due to ion scavenging. The measured reduction exceeds this at benzene concentrations greater than 1.00×10^{-2} M (Table 1, column 6). $G(H) = 1.46$ in cyclohexane, 61% of this having ionic precursors (11). Positive ion scavenging will reduce the yield of H atoms and this reduced yield is calculated and presented in column 3. $k_{H+C_6H_6}/k_{H+cyclo-C_6H_{12}} = 35$ (5) is used to determine the number of H atoms scavenged by benzene (column 4). The total calculated reduction in $G(H_2)$ (columns 2 plus 4) appears in column 5.

The agreement between columns 5 and 6 is far greater than is warranted by the experimental uncertainty of at least ± 0.10 in the measured values of $G(H_2)$ and the stated uncertainty in the ratio of rate constants ($\pm 40\%$). Within the limitations imposed by these uncertainties the results show that the reduction in hydrogen yields by benzene *over the concentration range studied* may be completely ascribed to a combination of positive ion and H atom scavenging.

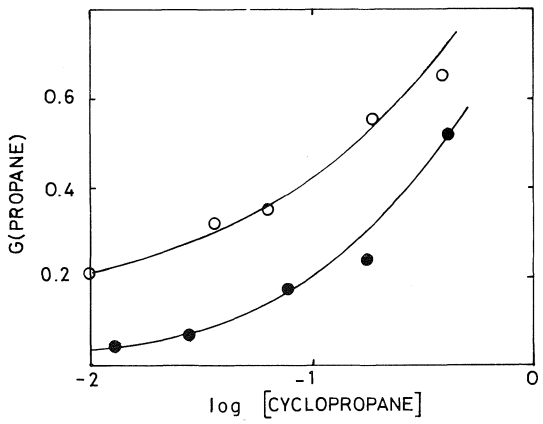

FIG. 1. Propane yields from cyclopropane in cyclohexane in the absence ○ and presence ● of benzene. The curves are calculated as described in the text.

TABLE 2. Propane yield from cyclo-C_6H_{12}/cyclopropane (1.6×10^{-2} M)/carbon tetrachloride (0.26 M) solutions

Benzene (M)	G(Propane)
0	0.78
0.001	0.57
0.012	0.50
0.059	0.33
0.093	0.29
0.10	0.26
0.23	0.14

As a final check on the cation scavenging ability of benzene, propane yields were measured for solutions 1.6×10^{-1} M in cyclopropane and 0.26 M in CCl_4. The presence of the latter will extend the lifetime of the charge separated state leading to an increased propane yield and will eliminate the possibility of electron scavenging by benzene. The results in Table 2 confirm the occurrence of cation scavenging by benzene.

In the cyclohexane/benzene system G(benzene) is approximately 0.3 at 0.1 M benzene (10). The only benzene containing products found are phenylcyclohexane in very low yield ($G \sim 0.1$) (10) and a benzene containing polymer (12). At 1.0, 2.0, and 3.0×10^{-1} M benzene $G(-$benzene in polymer$) = 0.31$, 0.47, and 0.63, respectively (12), which are to be compared with G(H atoms scavenged) of 0.33, 0.51, and 0.60. This comparison strongly suggests that polymer formation is initiated by H atom addition to benzene and that charge transfer does not lead to the disappear-

Can. J. Chem. Downloaded from www.nrcresearchpress.com by 210.87.254.6 on 09/05/12
For personal use only.

ance of benzene. Thomas and Mani (4) suggest that neutralization of the benzene cation leads to a diradical which can either decay to the ground state of benzene or give products. The above correlation favors the former mechanism.

Experimental

Conventional radiation chemical techniques were used for sample preparation and radiolysis (10). The samples containing propane were irradiated in Pyrex tubes with gas space no greater than 10% of the liquid volume. The propane yield was determined by gas solid chromatography using an F1 alumina column at 75 °C and the cyclopropane present as an internal standard. The dose rate in the ^{60}Co γ-source was 5.6×10^{17} eV ml^{-1} min^{-1} in cyclohexane and total doses of 1.1×10^{19} eV ml^{-1} were employed.

The authors thank the Defence Research Board and the National Research Council of Canada for financial assistance.

1. C. S. SCHOEPPFLE and C. H. FELLOWS. Ind. Eng. Chem. **23**, 1396 (1931).
2. J. P. MANION and M. BURTON. J. Phys. Chem. **56**, 560 (1952).
3. W. A. CRAMER. *In* Aspects of hydrocarbon chemistry. *Edited by* T. Gäumann and J. Hoigné. Academic Press. 1968. p. 153.
4. J. K. THOMAS and I. MANI. J. Chem. Phys. **51**, 1834 (1969).
5. MYRAN C. SAUER, JR. and INDER MANI. J. Phys. Chem. **72**, 3856 (1968).
6. JOHN M. WARMAN, K.-D. ASMUS, and ROBERT H. SCHULER. J. Phys. Chem. **73**, 931 (1969).
7. WERNER F. SCHMIDT and A. O. ALLEN. Science, **160**, 301 (1968).
8. STEFAN J. RZAD, ROBERT H. SCHULER, and ANDRIES HUMMEL. J. Chem. Phys. **51**, 1369 (1969).
9. K.-D. ASMUS. Int. J. Radiat. Phys. Chem. **3**, 419 (1971).
10. J. A. STONE and P. J. DYNE. Radiat. Res. **17**, 353 (1962).
11. K-D. ASMUS, JOHN M. WARMAN, and ROBERT H. SCHULER. J. Phys. Chem. **74**, 246 (1970).
12. J. A. STONE, P. J. DYNE, and M. G. BAILEY. Can. J. Chem. **42**, 963 (1964).

Can. J. Chem. Downloaded from www.nrcresearchpress.com by 210.87.254.6 on 09/05/12
For personal use only.

Can. J. Chem. Downloaded from www.nrcresearchpress.com by 210.87.254.5 on 09/05/12
For personal use only.

Canadian Journal of Chemistry

Published by
THE NATIONAL RESEARCH COUNCIL OF CANADA

Journal canadien de chimie

Publié par
LE CONSEIL NATIONAL DE RECHERCHES DU CANADA

Volume 51 Number 2 January 15, 1973

Volume 51 numéro 2 15 janvier 1973

A Synthetic Route to Dihydrojasmone; Sulfuric Acid as Dethioacetalization Agent

TSE-LOK HO,[1] HONOR C. HO, AND C. M. WONG

Department of Chemistry, University of Manitoba, Winnipeg, Manitoba R3T 2N2

Received August 11, 1972

Dihydrojasmone has been synthesized in three steps from the dithiane **2**. Hydrolysis of vinylic chloride and a dithioacetal group was achieved simultaneously using sulfuric acid. The scope of this dethioacetalization procedure has been explored.

La dihydrojasmone a été synthétisée en trois étapes à partir du dithiane **2**. Utilisant de l'acide sulfurique, l'hydrolyse du chlorure vinylique se fait simultanément avec celle du groupe acétal. Les possibilités de ce procédé de déthioacétalisation ont été explorées.

[Traduit par le journal]

Can. J. Chem., **51**, 153 (1973)

Organic chemists have long been fascinated with *cis*-jasmone (**1***a*) and dihydrojasmone (**1***b*)(1), the odoriferous constituents of the *Jasminum* family, and these molecules are still popular synthetic goals even though the pioneering work of Treff and Werner (2) was nearly forty years ago.[2]

These cyclopentenone derivatives, though of simple stuctures, continue to inspire the design of synthetic methods. Whenever there is a discovery of new synthon related to γ-diketones or cyclopentenones, chemists can hardly resist the temptation of applying it to the synthesis of these natural molecules. In particular, regiospecific hydration of γ-ketoacetylenes (3), Barton's nitrite photolysis of functionalizing a γ-position (4), pyrolytic rearrangement of cyclopropyl ketoesters (5), fragmentation of acylcyclopropanol derivatives (6), cleavage of cyclobutan-1,2-diols (secured in three steps from photocyclization of pentan-2,3-dione) (7), ynamine addition (8), decarbonylative ring contraction (9) of a cyclohexan-1,3-dione, internal Friedel–Crafts acylation of γ-lactones (10) with polyphosphoric acid, and numerous ancillary methods such as titanium-(III)-promoted generation of carbonyl from a

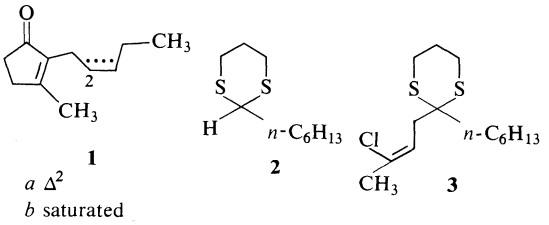

1
a Δ^2
b saturated

2

3

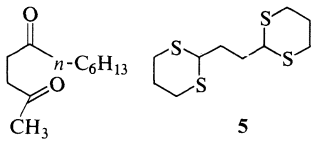

4

5

[1]To whom inquiries may be addressed.

[2]Clarification of the side-chain stereochemistry (*cis* double bond) of *cis*-jasmone was first reported by Crombie and Harper (25).

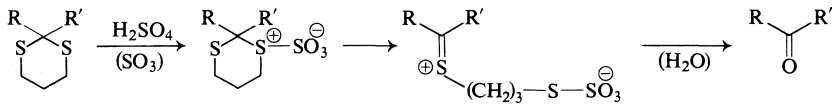

SCHEME 1

nitro group (11), Lindlar hydrogenation (5, 9, 11, 12), ceric ammonium nitrate dethioacetalization (1*a*), and Corey's methyl ketone synthesis (13) using dimsyl sodium, have been either developed specially or further extended in their utility, for this purpose.

We have for some time entertained the idea of synthesizing dihydrojasmone *via* a convenient route outlined as **2**→**3**→**4**→**1***b*. The dithiane **2** (14) is readily available from acid-catalyzed condensation between *n*-heptanal and 1,3-propanedithiol. Its metallation with *n*-butyllithium followed by alkylation with 1,3-dichlorobut-2-ene should present no unforeseen problems, as this type of reaction is now well-documented (15). And since cyclization of **4** → **1***b* is already known (1*a*), the only uncertainty remaining in the whole sequence would be the step **3**→**4**.

At the outset of our research utilizing this dithiane approach, we recognized the requisite of incorporating at C-2 a four-carbon segment with the proviso of subsequently transforming the γ-atom into a carbonyl group. Of the several precursors of this fragment which may be envisaged, 4-bromobut-1-yne, 1-bromobutan-3-one acetal, and thioacetal derivatives suffer, in one way or another, from the drawbacks of instability, low reactivity, and difficult availability, while 1,3-dichlorobut-2-ene does not have any of the above disadvantages.

As the hydrolysis of vinylic chloride is generally done by admixture with concentrated sulfuric acid (Wichterle reaction) (16), we were concerned about the survival of the dithioacetal group in **3** under such drastic conditions. However, it was imagined also, to the advantage of our synthetic strategy, that regeneration of the ketone from the dithiane protecting group could be accomplished during the same treatment. The rationale behind this conjecture lies in the fact that concentrated sulfuric acid is also a very strong oxidizing agent, capable of inducing a reaction such as that proposed in Scheme 1.

The feasibility of this novel procedure for dethioacetalization has been scrutinized, the results of which gratifyingly bear out our expectations. We were, in fact, greatly surprised and encouraged by the excellent yields (Table 1) obtained from this reaction, in comparison with those from known methods (15, 17, 18) and our other experiences with ceric ammonium nitrate (19), thallic trifluoroacetate (20), and methyl fluorosulfonate (21) mediated hydrolysis.

TABLE 1. Dethioacetalization with concentrated sulfuric acid

	Aldehyde or ketone	Yield % of parent compound	B.p. (m.p.) (°C)
1,3-Dithiolanes	Acetophenone	92	199–202
	Benzophenone	98	(237–239)†
	Benzil*	93	(92–94)
	Benzaldehyde	70	178–180
1,3-Dithianes	Phenylacetone	91	214–217
	Cycloheptanone	95	177–181

*Mono(dithiolane) of benzil.
†2,4-Dinitriphenylhydrazone.

In the synthesis of dihydrojasmone, the diketone **4** was obtained directly from **3** in 32% yield after standing in sulfuric acid for 20 min with subsequent quenching by ice-water. Optimization of this reaction has not been attempted, and the low yield must have been caused in part by inefficient dispersion of the sulfuric acid solution during the quenching process. Careful investigation by Marshall and Schaeffer (16) on this facet of the Wichterle reaction has led to yields of approximately 50%.

With the obtention of **4**, the synthesis of dihydrojasmone is formally completed. Recently there appeared a pertinent report (22) of *cis*-jasmone and dihydrojasmone syntheses via successive alkylation of the ethano-bisdithiane **5** (23) with methyl iodide and pentyl or pentenyl bromide.

Experimental

I.r. spectra were determined on a Perkin–Elmer 710 spectrophotometer. N.m.r. spectra were obtained on a Varian A56/60A spectrometer with TMS as internal standard. Analytical t.l.c. was performed using Eastman silica-coated sheets. Elemental analysis was done by

Can. J. Chem. Downloaded from www.nrcresearchpress.com by 210.87.254.5 on 09/05/12
For personal use only.

Can. J. Chem. Downloaded from www.nrcresearchpress.com by 210.87.254.5 on 09/05/12
For personal use only.

Dornis u. Kolbe Mikroanalytisches Laboratorium, Mülheim, Germany.

2-(n-Hexyl)-1,3-dithiane

A solution of *n*-heptanal (12.3 g, 0.11 mol) and 1,3-propanedithiol (12 ml) in chloroform (250 ml) was stirred for 1 h at room temperature. After addition of boron trifluoride etherate (5 ml) in one portion, the mixture was stored in the refrigerator for 16 h, washed with dilute alkali, dried over magnesium sulfate, and concentrated in a rotary evaporator. The residual oil was distilled to provide dithiane **1** (17.4 g, 87%), b.p. 122–126° (1.5 Torr); i.r. (CH_2Cl_2) 900 cm^{-1}; n.m.r. (CCl_4) τ 6.06 (1H, t, J = 6 Hz), 7.0–7.4 (4H, m), 9.11 (3H, t, J = 5 Hz).

Alkylation of Dithiane 2

A solution of *n*-butyllithium (2.3 *M* in hexane, Alfa Chemical Co., 4.8 ml, 11.0 mmol) was injected dropwise via a syringe into a stirred solution of dithiane **2** (2.0 g, *ca.* 10 mmol) in anhydrous tetrahydrofuran (15 ml) cooled to −35° under nitrogen. The mixture was kept at −35 to −25° for 3.5 h, and 1,3-dichlorobut-2-ene (1.30 g, 10.4 mmol) was then introduced slowly. The colorless solution turned orange, brown, then green and finally faded to light yellow during the addition. After 2 h at −20°, it was allowed to warm up gradually to room temperature overnight, poured into water, and extracted twice with ether. The combined ether extracts were dried ($MgSO_4$), and concentrated in a rotary evaporator. The residue was distilled to give the dithiane **3** (2.40 g, 82%), b.p. 150–152° (1.5 Torr); i.r. (CH_2Cl_2) 1660 cm^{-1}; n.m.r. (CCl_4) τ 4.47 (1H, txq, J = 6.5, J' = 1.5 Hz), 7.0–7.4 (6H, m), 7.88 (3H, m), 9.10 (3H, t, J = 5 Hz).

Anal. Calcd. for $C_{14}H_{25}ClS_2$: C, 57.34; H, 8.60. Found: C, 57.26; H, 8.65.

Undecan-2,5-dione

Admixture of dithiane **3** (190 mg, 0.65 mmol) with concentrated sulfuric acid (1 ml) at room temperature resulted in a thick, red solution. After standing for 20 min, it was added to a stirred mixture of ice and water. The turbid mixture was extracted with ether, and the extracts were dried ($MgSO_4$) and evaporated to yield an oil which was not resolvable on t.l.c. Therefore it was treated with Girard reagent T (200 mg) in methanol (5 ml, containing 0.2 ml glacial acetic acid) under reflux for 2 h. Standard work-up (24) afforded undecan-2,5-dione (38 mg, 32%), identical with (i.r., n.m.r., t.l.c.) an authentic sample (1*a*).

General Procedure for Hydrolysis of Dithioacetals

The dithioacetal (1 mmol) was homogenized with ice cold concentrated sulfuric acid (1 ml) and allowed to stand at room temperature for 10 min. The solution was then added to a vigorously stirred ice-water mixture and extracted with benzene. Solvent was removed from the dried extracts and the residue was processed by evaporative distillation, recrystallization from an appropriate solvent, or derivatized into the 2,4-dinitrophenylhydrazone. Identification of the product was performed by comparison (i.r., n.m.r.) with authentic specimen.

This work was supported in part by the National Research Council of Canada.

1. (*a*) H. C. Ho, T. L. Ho, and C. M. Wong. Can. J. Chem. **50**, 2718 (1972) and refs. cited therein; (*b*) P. A. Grieco. J. Org. Chem. **37**, 2363 (1972).
2. W. Treff and H. Werner. Ber. **66**, 1521 (1933); **68**, 640 (1935).
3. G. Stork and R. Borch. J. Am. Chem. Soc. **86**, 936 (1964).
4. M. Fétizon and J. Schalbar. La France et ses Parfums, **12**, 330 (1969).
5. W. F. Berkowitz. J. Org. Chem. **37**, 341 (1972).
6. (*a*) J. E. McMurry and T. E. Glass. Tetrahedron Lett. 2575 (1971); (*b*) E. Wenkert, A. Mueller, E. J. Reardon, Jr., S. S. Sathe, D. J. Scharf, and G. Tosi. J. Am. Chem. Soc. **92**, 7428 (1970).
7. S. M. Weinreb and R. J. Cvetovich. Tetrahedron Lett. 1233 (1972).
8. J. Ficini, J. D'Angelo, J. P. Genêt, and J. Noiré. Tetrahedron Lett. 1569 (1971).
9. G. Büchi and B. Egger. J. Org. Chem. **36**, 2021 (1971).
10. (*a*) C. Rai and S. Dev. J. Indian Chem. Soc. **34**, 178 (1957) and refs. cited therein; (*b*) P. E. Eaton, G. F. Cooper, R. C. Johnson, and R. H. Mueller. J. Org. Chem. **37**, 1947 (1972).
11. J. E. McMurry and J. Melton. J. Am. Chem. Soc. **93**, 5309 (1971).
12. K. Shishido and Y. Kawashima. Japan (Patent) 7 014 779; Chem. Abstr. **73**, 120181*p* (1970).
13. A. Takeda, H. Hosisima, and S. Torii. Bull. Chem. Soc. Japan, **39**, 1354 (1966).
14. E. Vedejs and P. L. Fuchs. J. Org. Chem. **36**, 366 (1971).
15. D. Seebach. Syn. 17 (1969).
16. J. A. Marshall and D. J. Schaeffer. J. Org. Chem. **30**, 3642 (1965) and refs. cited therein.
17. W. F. J. Huurdeman, H. Wynberg, and D. W. Emerson. Tetrahedron Lett. 3449 (1971) and refs. therein.
18. (*a*) M. Fetizon and M. Jurion. Chem. Commun. 382 (1972); (*b*) T. Oishi, K. Kamemoto, and Y. Ban. Tetrahedron Lett. 1085 (1972); (*c*) H.-L. W. Chang. Tetrahedron Lett. 1989 (1972).
19. T.-L. Ho, H. C. Ho, and C. M. Wong. Chem. Commun. 791 (1972).
20. T.-L. Ho and C. M. Wong. Can. J. Chem. **50**, 3740 (1972).
21. T.-L. Ho and C. M. Wong. Syn. 561 (1972).
22. R. A. Ellison and W. D. Woessner. Chem. Commun. 529 (1972).
23. D. Seebach, N. R. Jones, and E. J. Corey. J. Org. Chem. **33**, 300 (1967).
24. A. I. Vogel. A text-book of practical organic chemistry. 3rd ed. Longmans, London. 1962. p. 976.
25. L. Crombie and S. H. Harper. J. Chem. Soc. 869 (1952).

Mass Spectra of Some Sulfinate Esters and Sulfones

W. H. BAARSCHERS AND B. W. KRUPAY

Department of Chemistry, Lakehead University, Thunder Bay, Ontario

Received June 14, 1972

The mass spectra of some alkyl arenesulfinates were found to be distinctly different from the spectra of the isomeric aryl alkanesulfinates. Both classes of compounds in turn could easily be distinguished mass spectroscopically from the sulfones with which they are isomeric. The preparation of a new aryl alkanesulfinate, $CH_3S(O)OC_6H_4CH_3$, is described.

Il a été trouvé que les spectres de masse de quelques arènesulfinates d'alkyle sont distinctivement différents des alcanes sulfinates d'aryle isomères. Chaque classe de composé peut par ailleurs être facilement distingué par spectrométrie de masse des sulfones isomères. La préparation d'un nouvel alcane sulfinate d'aryle, $CH_3S(O)OC_6H_4CH_3$ est décrite. [Traduit par le journal]

Can. J. Chem., **51**, 156 (1973)

Can. J. Chem. Downloaded from www.nrcresearchpress.com by 210.87.254.42 on 09/05/12
For personal use only.

Introduction

The mass spectra of diaryl sulfones (1) and alkyl aryl sulfones (2) have been interpreted partly in terms of a rearrangement in which an aryl group migrates from sulfur to oxygen. In some cases there is evidence for the migration of alkyl groups (3). These migrations lead to the formation of sulfinate esters as intermediates in the fragmentation process. However, the mass spectra of sulfinate esters have, to our knowledge, not been reported in the literature before. The characterization of some novel diarylsulfones, recently prepared in this laboratory, led to the question as to whether, in view of these arrangements, mass spectrometry could be used to distinguish between these sulfones and the isomeric sulfinate esters.

Therefore, a number of suitable model compounds were studied. The spectra of the aryl methyl sulfones **1** and **4** were compared with those of the corresponding *alkyl* arenesulfinates **2** and **5** and of the *aryl* alkanesulfinates **3** and **6**.

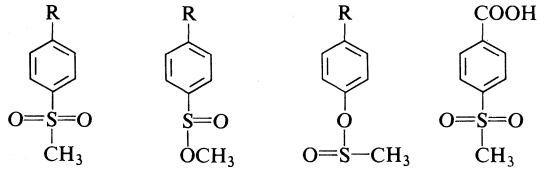

1 R = H **2** R = H **3** R = H **7**
4 R = CH_3 **5** R = CH_3 **6** R = CH_3

The preparation of *p*-tolyl methanesulfinate has not been reported in the literature before.

In view of the rearrangements of diarylsulfones to aryl arenesulfinates under electron impact, it was also of interest to study the mass spectra of aryl arenesulfinate esters. However, attempts to prepare *p*-tolyl benzenesulfinate were unsuccessful.

Since the spectra of the sulfones **1** and **4** seemed to indicate that hydrogen migration from the methyl group to oxygen is subject to a substituent effect, the spectrum of the methyl aryl sulfone **7** was used to gain information on the influence of an electron withdrawing substituent on this hydrogen migration.

Experimental

Apparatus

Mass spectra were recorded with a Hitachi–Perkin–Elmer model RMU-7 double focussing mass spectrometer. Unless otherwise stated samples were introduced through an all glass liquid inlet, and subjected to an ionizing potential of approximately 70 eV. The n.m.r. measurements were made with a Varian model A60-A spectrometer for deuteriochloroform or carbon tetrachloride solutions with tetramethylsilane as an internal reference at τ 10.00. The i.r. spectra were recorded with a Beckman IR 12 spectrophotometer.

Sulfones

Methyl *p*-tolyl sulfone (**4**) and 4-(methylsulfonyl)-benzoic acid (**7**) were commercial specimens supplied by Aldrich Chemical Co. Inc., and were used directly. The latter, **7**, was introduced into the mass spectrometer via the direct inlet. Methyl phenyl sulfone (**1**) was prepared by Friedel–Craft sulfonylation of benzene according to the method of Truce and Vriesen (4). The product of this reaction had m.p. 84–85° (lit. 84–85° (4)).

Anal. Calcd. for $C_7H_8O_2S$: C, 53.83; H, 5.16. Found: C, 53.61; H, 5.11.

Deuterium Exchange Reactions

The sulfones (50–100 mg samples) were added to a solution of sodium (10–20 mg) in deuteriomethanol (MeOD, 10 ml) in dry nitrogen. The mixtures were kept

Can. J. Chem. Downloaded from www.nrcresearchpress.com by 210.87.254.42 on 09/05/12
For personal use only.

at room temperature overnight, neutralized with a solution of PCl_5 in D_2O, and extracted with ether. The purity of the deuterated products was confirmed by t.l.c.

Methanesulfinyl Chloride

The acid chloride was prepared from dimethyl disulfide according to Douglas and Poole (5). The product, obtained as a clear yellow oil, gave rise to a single peak in its n.m.r. spectrum at τ 6.62 and was characterized as its anilide **9**, which had m.p. 86–87°, (lit. (6) 86–88°).

Anal. Calcd. for C_7H_9NOS: C, 54.16; H, 5.85; N, 9.02. Found: C, 54.22; H, 5.98; N, 9.08.

Phenyl Methanesulfinate[1]

Phenol (2.65 g) was added to methanesulfinyl chloride (2.40 g) at room temperature in nitrogen. Stirring of the mixture initiated the evolution of hydrogen chloride and the development of an orange color. The reaction vessel was connected to a flash evaporator and kept at 0–5° for 2 h. The resulting light yellow oil (4.57 g) was dissolved in methylene chloride and *p*-toluidine (0.25 g) was added. After 5 min the mixture was filtered and the precipitate washed with methylene chloride (3 × 5 ml). This procedure was repeated with 0.1 g of *p*-toluidine. The combined methylene dichloride solutions were washed with cold water (10 ml), 2 *N* aqueous hydrochloric acid (12 ml), and again with water (3 × 10 ml). Removal of the solvent from the dried organic layer yielded a yellow oil (2.3 g) which was immediately[2] chromatographed on silica gel (60 g). Elution with petroleum ether–ether (3:1) gave phenyl methanesulfinate (**3**) as a colorless oil, which had ν_{max} (SO) 1148 cm^{-1}. The n.m.r. spectrum (CCl_4) contained the S—CH_3 signal at τ 7.24 and the aromatic proton signals at τ 2.50–3.00.

Mass Spec. Calcd. for $C_7H_8O_2S$: M^+, 156.021. Found: M^+, 156.025.

Many chromatography fractions were contaminated with varying amounts of phenol, evident from OH absorption at ν_{max} 3400 cm^{-1}. It was therefore difficult to establish the yield of pure phenyl methanesulfinate (see comments on yield of *p*-tolyl methanesulfinate below).

p-Tolyl Methanesulfinate

p-Cresol (6.91 g) was added to methanesulfinyl chloride (5.28 g) and the mixture was treated as above. The crude product (7.48 g) which was a deep red oil, on chromatography yielded *p*-tolyl methanesulfinate (**6**) as a pale yellow oil. A fraction which did not show any impurities in its n.m.r. spectrum (in CCl_4, τ 7.67 (3H, aromatic CH_3), 7.28 (3H, S—CH_3), and 2.96 (4H)) had ν_{max} (SO) 1120 cm^{-1}. A weak i.r. absorption at ν_{max} 3400 cm^{-1} indicated the possible presence of a small amount of *p*-cresol.

Mass Spec. Calcd. for $C_8H_{10}O_2S$: M^+, 170.040. Found: M^+, 170.043.

The n.m.r. spectrum of the crude product contains the methyl signal of *p*-cresol at τ 7.82. Thus, in this case, the relative intensities of the two aromatic methyl group signals allowed a calculation of the yield of *p*-tolyl methanesulfinate which was found to be 60%.

Attempted Preparation of p-Tolyl Benzenesulfinate

Benzenesulfinyl chloride was prepared by chlorination of thiophenol according to Douglas (8). Its identity was confirmed by its reaction with methanol to give methyl benzenesulfinate (**2**) which was identical in all respects with an authentic specimen.[3] However, several attempts to prepare *p*-tolyl benzenesulfinate by reaction of this acid chloride with *p*-cresol were unsuccessful.

Results and Discussion

Methyl phenyl sulfone (**1**) has been studied before and our results agree with those of Bowie *et al.* (2). The major fragmentation paths (Scheme 1) are reproduced here for comparison.[4] The spectrum[4] of methyl benzenesulfinate (**2**)[3] contains the molecular ion at *m/e* 156 and the loss of the methoxy group leads to the base peak at *m/e* 125 (ion **a** in Scheme 1). Further loss of SO then leads to **b** at *m/e* 77. A corresponding direct cleavage pattern of the sulfone **1** involves loss of the methyl group to give **c**, resulting in a peak at *m/e* 141. Further loss of SO_2 then leads to the ion **b**, to which the base peak of this spectrum at *m/e* 77 may be assigned (Table 1).

Although these direct fragmentations are sufficiently different to be considered characteristic, some fragments arising from rearrangements are even more distinctive. Whereas the sulfone **1** rearranges to the sulfinate ester ion **d** which has been suggested (2) to lead directly to the ionized phenol (**e**, *m/e* 94), the sulfinate ester **2** apparently undergoes a rearrangement similar to that observed for sulfoxides (9) which leads to the thiapyrrylium ion **f** at *m/e* 97.

Phenyl methanesulfinate (**3**) only gives a molecular ion when the ionizing voltage is decreased to approximately 14 eV. The rather simple spectrum[4] obtained in this way indicates that the only significant fragmentation for this ester involves S—O cleavage and hydrogen transfer leading again to the ionized phenol **e** at *m/e* 94 (Scheme 1). It was

[1]This compound was first reported by Engberts and Zuidema. The authors gratefully acknowledge the cooperation of Professor Engberts in supplying the experimental details used in his preparation of this ester (7).

[2]When this product was kept under refrigeration for 5 days, it became dark yellow and was no longer soluble in most organic solvents indicating extensive decomposition.

[3]The authors wish to express their appreciation to Dr. I. B. Douglas, Department of Chemistry, University of Maine, for a gift of samples of methyl benzenesulfinate (**2**) and methyl *p*-toluenesulfinate (**5**).

[4]The mass spectra of the compounds described herein have been lodged in the Depository of Unpublished Data, National Science Library, National Research Council of Canada, Ottawa, Canada K1A 0S2. Table 1 summarizes the major peaks in these spectra.

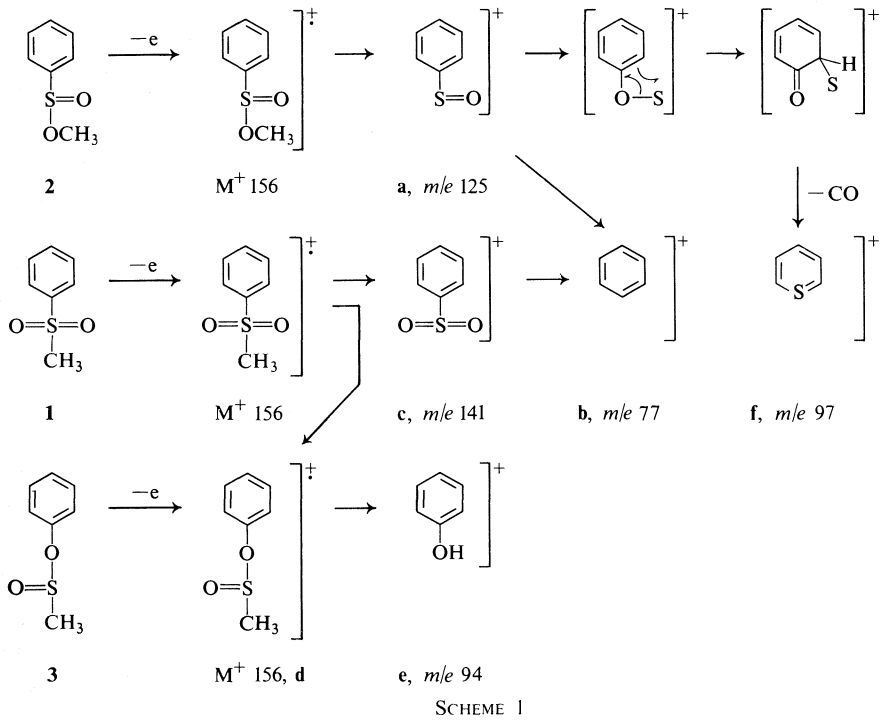

SCHEME 1

TABLE 1. *m/e* of major peaks (relative intensity, %)

No.	Compound	M^+	M^+-CH_3	M^+-OCH_3	Ar	Other
1	$Ar—SO_2—CH_3$	156(28%)	141(27%)	—	77(100%)	(**e**),94(31%)*
2	$Ar—SO—OCH_3$	156(84%)	141(15%)	125(100%)	77(84%)	(**f**),97(26%)
3	$ArO—SO—CH_3$	156(15%)	—	—	—	(**e**),94(100%)
4	$Ar—SO_2—CH_3$	170(33%)	155(36%)	139(2%)	91(100%)	(**l**),107(27%)
5	$Ar—SO—OCH_3$	170(49%)	155(3%)	139(100%)	91(39%)	(**m**),111(6%)
6	$ArO—SO—CH_3$	170(31%)	—	—	—	(**l**),107(100%)
7	$HOOC—Ar—SO_2—CH_3$	200(37%)	185(36%)	—	—	(**p**),138(88%); (**q**)121(100%); (**r**)93(10%)

*Letters in parentheses refer to ions as indicated in Schemes 1, 2, and 3.

found that repeated chromatography of this ester leads to increasing decomposition without yielding a completely phenol-free product. Since the presence of even small amounts of phenol affects the intensity of the base peak, the relative intensities in table 1 for compound (**3**) are not representative of a pure specimen. However, that at least part of the ion current at *m/e* 94 is due to this fragmentation follows from the observation of a metastable peak at *m/e* 56.6.

A consideration of the toluene homologues **4**, **5**, and **6** leads to an overall picture summarized in Scheme 2 consistent with the above results. Thus, methyl *p*-tolyl sulfone (**4**) not only decomposes with the consecutive loss of CH_3 (**i**, *m/e* 155) and SO_2 (**h**, *m/e* 91) but also loses CH_3SO in a one-step process to give *m/e* 107 ($C_7H_7O^+$).[4] This latter signal which does not shift after deuteration of the methyl group, may be assigned the structure **l** arising from the rearranged molecular ion **k**. The observation that in this case no hydrogen migration from the methyl group takes place is further discussed below.

The loss of CH_3SO from the ion **k** to give **l**, (*m/e* 107) is the major fragmentation observed in the spectrum of *p*-tolyl methanesulfinate **6**.[4] Slight

Can. J. Chem. Downloaded from www.nrcresearchpress.com by 210.87.254.42 on 09/05/12
For personal use only.

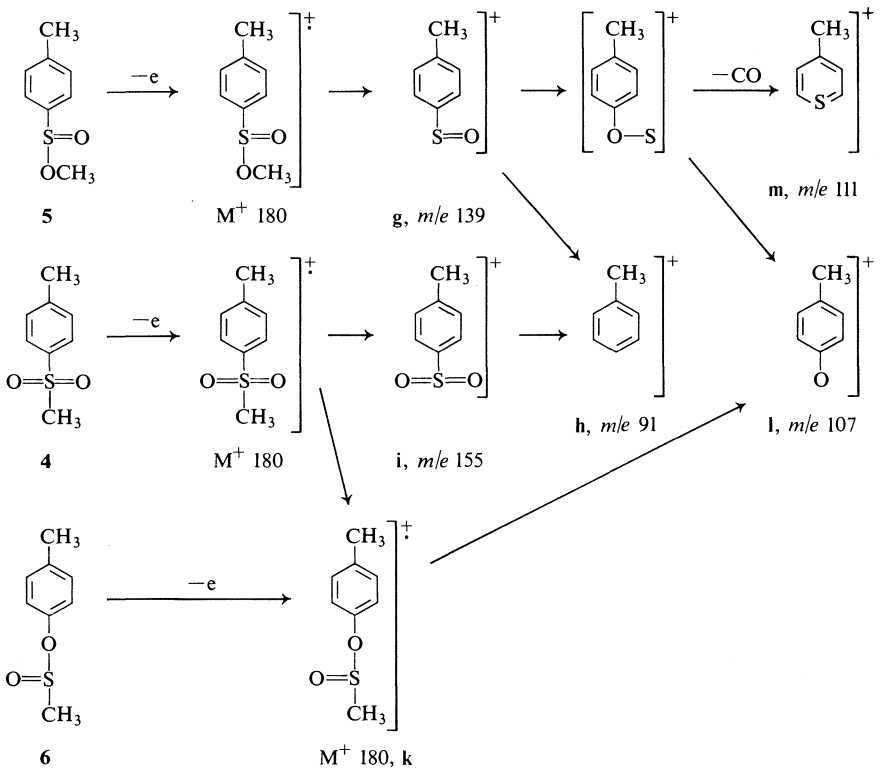

SCHEME 2

contamination of this sample with free *p*-cresol, which is responsible for the ion current at *m/e* 108, in this case does not affect the base peak of the spectrum.

Also, methyl *p*-toluenesulfinate **5**[4] undergoes cleavages similar to the corresponding phenylsulfinate. Thus it is suggested that the base peak at *m/e* 139 represents the ion **g**, which is formed by loss of the methoxy group. Subsequent loss of SO then leads to **h** which gives rise to the peak at *m/e* 91. The rearrangement of **g** to give the methyl thiapyrrylium ion **m** at *m/e* 111 is less pronounced in this case, but is nevertheless evident from the presence of a metastable peak at *m/e* 88.4.

In order to compare in a similar fashion the mass spectra of diaryl sulfones with those of the isomeric aryl arenesulfinates, attempts were made to synthesize *p*-tolyl benzenesulfinate from benzenesulfinyl chloride and *p*-cresol. These attempts, however, were wholly unsuccessful. Examination of the various reaction mixtures suggested that this ester, if at all formed, rapidly decomposed. Sulfinate esters of this kind have, to our knowledge, not been reported in the literature before.

The results discussed so far show that, quite apart from differences in chemical behavior, mass spectrometry is sufficiently characteristic to distinguish alkyl aryl sulfones from the stable sulfinate esters with which they are isomeric.

An anomaly was noted concerning the migration of hydrogen from the methyl group, which in the case of methyl phenyl sulfone (**1**) leads to the formation of ionized phenol (**e**, Scheme 1). Such a hydrogen transfer is distinctly absent from the spectrum of methyl *p*-tolyl sulfone (**4**) which contains **l** at *m/e* 107 rather than ionized *p*-cresol at *m/e* 108. Assuming that the electron donating methyl group inhibits this hydrogen transfer in the latter case, it is of interest to study the effect of an electron withdrawing substituent, particularly since it was found (3) that the *p*-nitro group in 2-chloro-ethyl *p*-nitrophenyl sulfone (**8**) appears to prevent migration of the aryl group to oxygen.

The spectrum[4] of 4-(methylsulfonyl)-benzoic

Can. J. Chem. Downloaded from www.nrcresearchpress.com by 210.87.254.42 on 09/05/12
For personal use only.

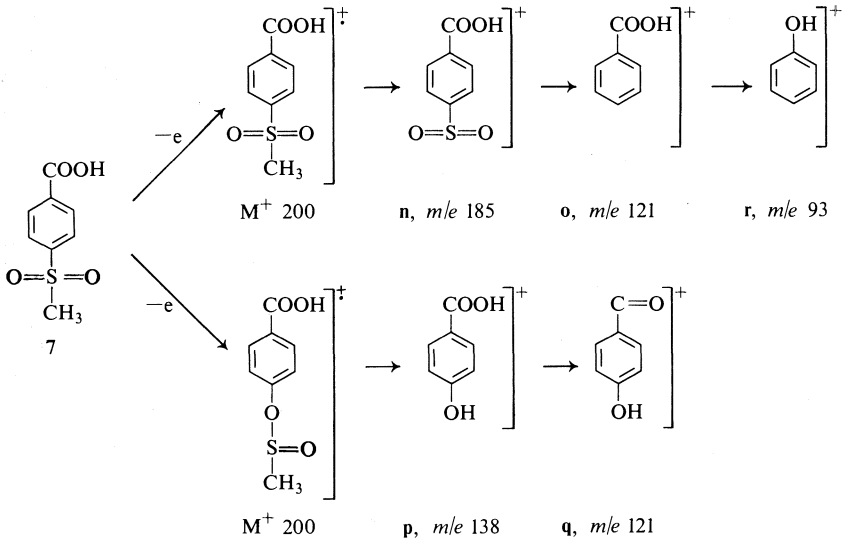

SCHEME 3

acid (**7**) contains a strong peak at *m/e* 138. This peak, which shifts to *m/e* 139 after deuteration of the methyl group may be attributed to the ion (**p**, Scheme 3) as derived from the rearranged molecular ion. Thus the carboxyl group, while preserving the low electron density on the aromatic ring required for hydrogen migration, is not a strong enough electron withdrawing group to prevent the migration of the aryl group to oxygen.

The base peak of this spectrum, which is found at *m/e* 121, originates from two different fragmentation processes, as indicated by the observation of metastable peaks. Firstly, the ion **n** at *m/e* 185 loses SO_2 (*m** 79.2) to give **o** at *m/e* 121, and secondly, the ion **p**, after loss of 17 mass units (*m** − 106.2) also leads to a fragment at *m/e* 121, for which structure **q** is proposed. That the first process (*i.e.* **n** → **o**) makes the largest contribution to the base peak follows from the observation that in the spectrum of the deuterated sulfone, the base peak is still found at *m/e* 121, while only a weak signal (~15%) is observed at *m/e* 122 (*i.e.* monodeuterated **q**). Also, although both **o** and **q** may lead to ionized phenol **r** at *m/e* 93, no peak is observed at *m/e* 94 after deuteration.

Finally, it is of interest to note that the migration of hydrogen from the methyl group is not restricted to sulfones and aryl alkanesulfinates. Methanesulfinanilide (**9**) obtained from the characterization of methanesulfinyl chloride gave a mass spectrum in which the base peak is found

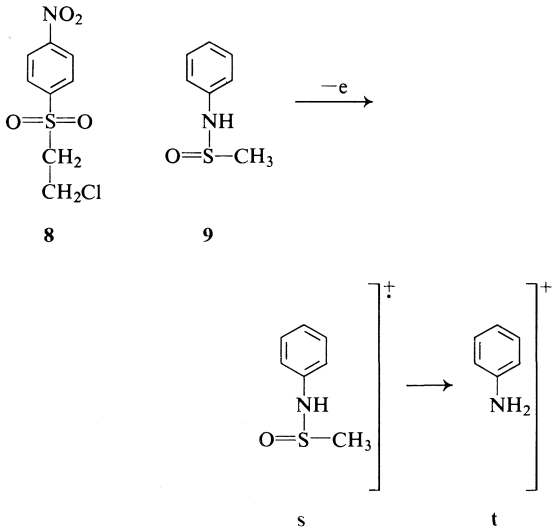

at *m/e* 93, and it is reasonable to suggest that this peak represents the ion **t**, formed according to the sequence **9** → **s** → **t**.

The authors gratefully acknowledge financial support from the National Research Council of Canada (Grant no. A 5422) and from Lakehead University.

1. S. MEYERSON, H. DREWS, and E. K. FIELDS. Anal. Chem. **36**, 1294 (1964).
2. J. H. BOWIE, D. H. WILLIAMS, S. O. LAVESSON, J. O. MADSEN, C. NOLDE, and G. SCHROLL. Tetrahedron, **22**, 3515 (1966).

Can. J. Chem. Downloaded from www.nrcresearchpress.com by 210.87.254.42 on 09/05/12
For personal use only.

3. R. J. SOOTHILL and L. R. WILLIAMS. Org. Mass Spectrom. **6**, 141 (1972).
4. W. E. TRUCE and C. W. VRIESEN. J. Am. Chem. Soc. **75**, 5032 (1953).
5. I. B. DOUGLAS and D. R. POOLE. J. Org. Chem. **22**, 536 (1957).
6. I. B. DOUGLAS and B. S. FARAH. J. Org. Chem. **23**, 805 (1958).
7. J. B. F. N. ENGBERTS and G. ZUIDEMA. Rec. Trav. **89**, 1202 (1970).
8. I. B. DOUGLAS. J. Org. Chem. **30**, 633 (1964).
9. G. BUDZIKIEWICZ, C. DJERASSI, and D. H. WILLIAMS. Mass spectrometry of organic compounds. Holden-Day Inc., San Francisco. 1967. p. 555.

Can. J. Chem. Downloaded from www.nrcresearchpress.com by 210.87.254.42 on 09/05/12
For personal use only.

Conformations of Bridged Diphenyls. IV. Diphenyl Ether Conformations and Proton Chemical Shifts

J. J. BERGMAN,[1] E. A. H. GRIFFITH, B. E. ROBERTSON, AND W. D. CHANDLER[2]

Division of Natural Sciences and Mathematics, University of Saskatchewan, Regina, Saskatchewan S4S 0A2

Received June 2, 1972

The conformationally dependent chemical shifts for the ring protons of some diphenyl ethers can be explained approximately by the ring-current model for benzene magnetic anisotropy. Although the model underestimates the shielding in the region above the plane of the ring it is the best of the models investigated for this purpose.

Les déplacements chimiques, en fonction de la conformation des protons du cycle de quelques diphénylethers peuvent être expliqués de façon approximative par le modèle du courant de cycle pour l'anisotropie magnétique du benzène. Bien que ce modèle sous estime le blindage de la région au dessus du plan de cycle, c'est le meilleur étudié jusqu'ici dans ce but. [Traduit par le journal]

Can. J. Chem., **51**, 162 (1973)

Introduction

Using a series of triply ortho-substituted diphenyl ethers, **1**, and the corresponding anisoles, **2**, we have shown previously how a double-difference p.m.r. analysis could be applied to obtain information about diphenyl ether conformations in solution (1). From the derived equations, that part of the chemical shift arising in relative "other-ring" shielding $\delta_{\omega}{}^{j} - \delta_{\omega H}{}^{j}$ was estimated to be -0.396, -0.140, and 0.135 p.p.m. for j = a, b, and c respectively. $\delta_{\omega}{}^{j}$ and $\delta_{\omega H}{}^{j}$ represent the contribution to the chemical shift of the jth ring proton from the conformation-dependent "other-ring" shielding in the diphenyl ethers with X ≠ H and X = H.[3]

At the same time it was shown that it is possible to calculate the "other-ring" shielding expected at each proton for a particular conformation defined by the three angular parameters θ, ϕ, and ψ where θ is the COC bond angle, ϕ the rotation of the X-substituted ring from the COC plane, and

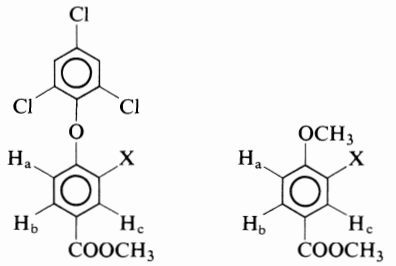

1 **2**

X=NO_2, NH_2, I, Cl, H, OCH_3, CN

ψ the rotation of the trichlorophenyl ring from a plane perpendicular to the COC plane (Fig. 1). These calculations made use of the ring-current model of magnetic anisotropy elaborated by Johnson and Bovey (2). A comparison of the experimental shieldings and those calculated for a number of conformations suggested that θ must have a value near 120° while the ethers librate about an equilibrium H-inside conformation (Fig. 1) by angles up to 20° (ϕ = 0 ± 20°, ψ = 0 ± 20°).

There are three areas in which the previous work could be questioned: (*i*) as a result of the

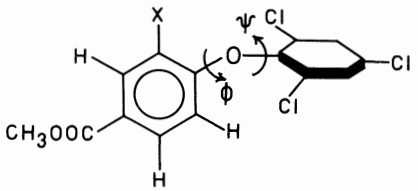

FIG. 1. H-Inside conformation of ethers in series **1**.

[1]Present address: Department of Chemistry, Saint Francis Xavier University, Antigonish, Nova Scotia.

[2]Author to whom correspondence should be addressed.

[3]For all of the diphenyl ethers, rotation of the trichlorophenyl ring through 180° produces an identical, mirror-image conformer. In addition, when X = H in series **1** there must be two identical, average conformations, generated by rotation of the X-substituted ring through 180°, to account for the p.m.r. equivalence of the two ortho-protons and the equivalence of the two meta-protons. The resulting AA′BB′ spectral pattern is dependent on the temperature and the nature of the substituents on the other ring (1, 3).

Can. J. Chem. Downloaded from www.nrcresearchpress.com by 210.87.254.5 on 09/05/12
For personal use only.

TABLE 1. $\delta_{DX}{}^{j} - \delta_{AX}{}^{j}$ for series **1** and **2***

X	$\delta_{DX}{}^{a} - \delta_{AX}{}^{a}$ (p.p.m.)	$\delta_{DX}{}^{b} - \delta_{AX}{}^{b}$ (p.p.m.)	$\delta_{DX}{}^{c} - \delta_{AX}{}^{c}$ (p.p.m.)
NO_2	−0.485†	−0.103	0.168
NH_2	−0.475	−0.163	0.121
I	−0.465	−0.137	0.100
Cl	−0.468	−0.128	0.115
OCH_3	−0.448	−0.140	0.135
CN	−0.442	−0.107	0.132

*In solution in chloroform-*d*.
†The δ values were measured relative to tetramethylsilane so as to increase as the applied magnetic field decreases. The negative sign indicates that H_a and H_b are more shielded in the diphenyl ether than in the anisole.

TABLE 2. $\delta_{DX}{}^{j} - \delta_{AX}{}^{j}$ for series **3** and **4***

X	$\delta_{DX}{}^{a} - \delta_{AX}{}^{a}$ (p.p.m.)	$\delta_{DX}{}^{b} - \delta_{AX}{}^{b}$ (p.p.m.)	$\delta_{DX}{}^{c} - \delta_{AX}{}^{c}$ (p.p.m.)
NO_2	−0.476†	−0.127	0.155
NH_2	−0.501	−0.175	0.102
I	−0.524	−0.110	0.167
Cl	−0.501	−0.106	0.164
H	−0.520	−0.127	0.150
OCH_3	−0.505	−0.132	0.117
CN	−0.486	−0.110	0.155

*In solution in chloroform-*d*.
†The δ values were measured relative to tetramethylsilane so as to increase as the applied magnetic field decreases. The negative sign indicates that H_a and H_b are more shielded in the diphenyl ether than in the anisole.

several assumptions and simplifications inherent in the double-difference method, the experimental "other-ring" shielding values could be somewhat in error; (*ii*) in using the ring-current model of magnetic anisotropy for these ethers certain structural parameters had to be assumed; (*iii*) the ring-current model itself is a simplified, classical model.

In this paper new p.m.r. results will be presented that strengthen the case made previously for the double-difference method. In addition, "other-ring" shielding, calculated for structures suggested by recent X-ray diffraction data, will be shown to indicate that, while the ring-current model is better than others, it is not entirely adequate.

Results and Discussion

Experimental Values of "Other-ring" Shielding Chemical Shifts

Additional evidence in support of the double-difference method of obtaining "other-ring" shielding values comes from a comparison of p.m.r. spectra of similarly-substituted compounds in the series **3** and **4**, isomeric with **1** and **2**.

It is reasonable to expect the conformation of the two series, **1** and **3** to be basically the same since the same 2,4-disubstitution pattern occurs in both, and H_a is observed to be shielded by about the same amount, relative to the anisole, for corresponding ethers in both series (Tables 1 and 2).

Series **3** has an advantage over **1** in that the variable substituent X is not ortho to the ether oxygen and should not affect the conformation

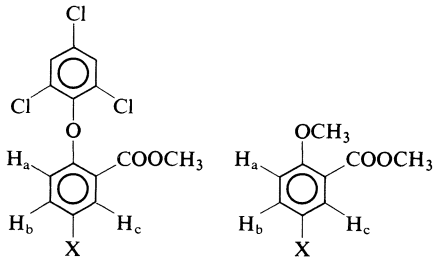

3

a X = NO_2
b X = NH_2
c X = I
d X = Cl

4

e X = H
f X = OCH_3
g X = CN

Can. J. Chem. Downloaded from www.nrcresearchpress.com by 210.87.254.5 on 09/05/12
For personal use only.

Can. J. Chem. Downloaded from www.nrcresearchpress.com by 210.87.254.5 on 09/05/12
For personal use only.

by direct steric interference. As a result, the assumption that the conformation is substituent independent is even more valid in this case. However, the double-difference method cannot be applied since **3***e*, the ether having X = H, must have the same conformation as the other six. Nonetheless, if the method of chemical shift dissection has merit (1), for j = b and c,

$$[1]\quad \delta_{DX}{}^{b} - \delta_{AX}{}^{b} = (\delta_{D}{}^{b} - \delta_{A}{}^{b}) + I_{X}{}^{b}(I_{D}{}^{b} - I_{A}{}^{b}) + \delta_{\omega}{}^{b}$$

$$[2]\quad \delta_{DX}{}^{c} - \delta_{AX}{}^{c} = (\delta_{D}{}^{c} - \delta_{A}{}^{c}) + I_{X}{}^{c}(I_{D}{}^{c} - I_{A}{}^{c}) + \delta_{\omega}{}^{c}$$

$\delta_{DX}{}^{j}$ and $\delta_{AX}{}^{j}$ are the chemical shifts of the jth proton in the diphenyl ether and corresponding anisole respectively. $\delta_{D}{}^{j}$ and $\delta_{A}{}^{j}$ are the contributions to the chemical shift from the molecule exclusive of the substituent X. The $I_{Z}{}^{j}$ parameters are interaction contributions and $\delta_{\omega}{}^{j}$ is the "other-ring" shielding.

Since for **3** and **4** both H_b and H_c are meta to the ether oxygen and ortho to the substituent X, $\delta_{D}{}^{b} - \delta_{A}{}^{b} \simeq \delta_{D}{}^{c} - \delta_{A}{}^{c}$, $I_{X}{}^{c} = I_{X}{}^{c}$ and $I_{D}{}^{b} - I_{A}{}^{b} \simeq I_{D}{}^{c} - I_{A}{}^{c}$. The difference between [1] and [2] should then be a constant independent of the substituent X.

$$[3]\quad (\delta_{DX}{}^{b} - \delta_{AX}{}^{b}) - (\delta_{DX}{}^{c} - \delta_{AX}{}^{c}) = \delta_{\omega}{}^{b} - \delta_{\omega}{}^{c}$$

Table 3 shows that the experimental data for these series support this conclusion reasonably well; the average value of $(\delta_{DX}{}^{b} - \delta_{AX}{}^{b}) - (\delta_{DX}{}^{c} - \delta_{AX}{}^{c})$ is −0.270 p.p.m. with the deviations of all but X = OCH_3 falling within the estimated experimental error. There is probably a larger steric interaction between OCH_3 and the ring protons than occurs with other substituents and the single interaction parameters $I_{Z}{}^{j}$ cannot accommodate steric and electronic effects of any size simultaneously.

TABLE 3. Values of $(\delta_{DX}{}^{b} - \delta_{AX}{}^{b}) - (\delta_{DX}{}^{c} - \delta_{AX}{}^{c})$ for series **3** and **4**

X	$(\delta_{DX}{}^{b} - \delta_{AX}{}^{b}) - (\delta_{DX}{}^{c} - \delta_{AX}{}^{c})$ (p.p.m.)
NO_2	−0.282
NH_2	−0.276
I	−0.276
Cl	−0.270
H	−0.276
OCH_3	−0.248
CN	−0.264

In addition to being substituent independent, the values in Table 3 are exactly what would be expected if the diphenyl ethers of series **1** and **3** *did* adopt the same conformation. From the previous work for series **1** $\delta_{\omega}{}^{b} - \delta_{\omega H}{}^{b} = -0.140$ and $\delta_{\omega}{}^{c} - \delta_{\omega H}{}^{c} = 0.135$ p.p.m. Since, as noted in footnote 3, $\delta_{\omega H}{}^{b} = \delta_{\omega H}{}^{c}$

$$[4]\quad (\delta_{\omega}{}^{b} - \delta_{\omega H}{}^{b}) - (\delta_{\omega}{}^{c} - \delta_{\omega H}{}^{c}) = \delta_{\omega}{}^{b} - \delta_{\omega}{}^{c} = -0.275 \text{ p.p.m.}$$

One would conclude then that the double-difference technique does have considerable justification in spite of what appear to be overly-simple assumptions, and that the conformationally-dependent, "other-ring" shielding, $\delta_{\omega}{}^{j} - \delta_{\omega H}{}^{j}$, can be taken with confidence to be −0.40, −0.14, and 0.14 p.p.m. for j = a, b, and c respectively in series **1**.[4,5]

It should be noted that the experimental values provided by the double-difference analysis are actually sums of *two terms* and do not represent a single $\delta_{\omega}{}^{j}$ (1). Montaudo *et al.* (4, 5), using a single-difference method (diphenyl ether and corresponding anisole), estimated the shielding $\delta_{\omega}{}^{a}$ for H_a in some 2,4-disubstituted ethers to be between −0.30 and −0.57 p.p.m. However, the single difference includes terms other than $\delta_{\omega}{}^{j}$ unless they happen to be vanishingly small (1). The wide range of values quoted by Montaudo for ethers of similar structure suggests that allowance has to be made for substituent effects in some way and the double-difference approach does that.

Calculations of "Other-ring" Shielding Based on Conformations in the Solid State

Until recently there have been no reliable studies made of the bond lengths and angles in diphenyl ethers. The previous paper on the double-difference technique (1) used a value of 1.28 Å for the C—O bond length as proposed by Toussaint (6) although this seemed rather low. Since then, in parts I, II, and III of this series

[4]It has been pointed out previously that the fact that $\delta_{\omega}{}^{b} - \delta_{\omega H}{}^{b}$ and $\delta_{\omega}{}^{c} - \delta_{\omega H}{}^{c}$ have the same value, within experimental error, can be taken as a justification for the double-difference technique; based on the assumptions used they should be identical except for sign.

[5]The terms $\delta_{\omega}{}^{j} - \delta_{\omega H}{}^{j}$ have validity as experimental "other-ring" shielding values only for series **1** although the values would presumably be the same for series **3** and other similarly-substituted ethers if they could be obtained for the latter by the double-difference method.

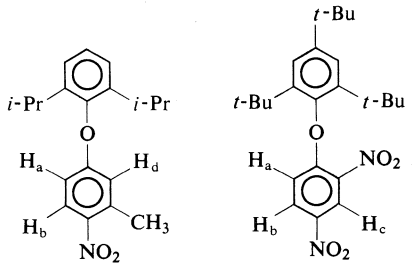

5 6

(7–9), we have reported the crystal structures of ethers **5**, **6**, and ***3a***, and several other authors have published similar structures (10–12).

Our X-ray diffraction studies, besides giving accurate bond lengths and ring angles, have shown that in the solid state (*i*) the conformations are close to the average H-inside conformation predicted from solution p.m.r. work (Table 4), (*ii*) the COC bond angle, θ, is very nearly 120° as predicted, and (*iii*) the ring which is close to being in the COC plane (the ring whose rotation is described by ϕ and the ring to which H_a, H_b, and H_c belong) is deformed somewhat so that H_a and H_b are positioned differently relative to the other ring than would be predicted on the basis of a perfectly hexagonal ring. Figure 2 is a representation of this distortion for the ether **5**.

Using the structural parameters[6] obtained by X-ray diffraction it was possible to calculate the cylindrical coordinates, ρ and *z*, for each ring proton relative to the center of the other ring.[7] With these coordinates and the equations developed by Johnson and Bovey (2) the "other-ring" shielding, δ_ω^j, has been calculated for each proton and is given in Table 5. Since none of the three ethers studied has four ring protons, an imaginary proton had to be placed at C-2′ for ***3a*** and **6**, and at C-3′ for **5**. The proton was placed so that the carbon–proton distance was equal to the average of all similar distances in the molecule. The shielding for this proton was calculated as well and appears in Table 5.

TABLE 4. Angular parameters defining the conformation in the solid state

Compound	ϕ(°)	ψ(°)	θ(°)
3a	8.8*	14.0	119.3
	4.6	0.3	117.9
5	5.7*	12.8	119.7
	2.1	10.5	120.0
6	3.2	2.5	116.8

*There are two different molecules in the unit cell. Differences have been discussed previously (7, 9).

Since for the ether with X = H in series **1**

$$[5] \qquad \delta_{\omega H}{}^a = (\delta_\omega{}^a + \delta_\omega{}^d)/2$$

$$[6] \qquad \delta_{\omega H}{}^b = (\delta_\omega{}^b + \delta_\omega{}^c)/2$$

where H_d is the other ortho-hydrogen, then the calculated values for the "other-ring" shielding will be given by

$$[7] \qquad \delta_\omega{}^a - \delta_{\omega H}{}^a = (\delta_\omega{}^a - \delta_\omega{}^d)/2$$

and

$$[8] \qquad \delta_\omega{}^b - \delta_{\omega H}{}^b = (\delta_\omega{}^b - \delta_\omega{}^c)/2$$

These values, which are to be compared with the experimental ones determined by means of the double-difference technique, have been derived from the data of Table 5 and are shown in Table 6 (see footnote 5).

These data indicate that $\delta_\omega{}^a$ is higher than Montaudo had estimated from his single-difference analysis (4, 5). At the same time $(\delta_\omega{}^a - \delta_\omega{}^d)/2$ for ***3a*** is 7 and 48% higher than our experimental value of −0.40 p.p.m., depending on which of the two different molecules in the crystal is chosen for comparison. The difference could be attributed to the fact that the values in Tables 5 and 6 are calculated using crystal conformations that do not allow for librations in ϕ and ψ which would lower the experimental "other-ring" shielding values obtained for molecules in solution. However, librations would also lower the values of $(\delta_\omega{}^b - \delta_\omega{}^c)/2$ which are already considerably lower than the experimental −0.14 p.p.m. There is an inconsistency in this result in that the predicted value of $(\delta_\omega{}^a - \delta_\omega{}^d)/2$ seems quite reasonable while the predicted value for $(\delta_\omega{}^b - \delta_\omega{}^c)/2$

[6]The scattering factor used for the hydrogen atoms in the X-ray studies was that given by Stewart *et al.* (20) for a bonded hydrogen atom which is part of a hydrogen molecule. These authors have compared the C—H bond lengths obtained using this scattering factor with bond lengths determined by other techniques and have concluded that those obtained by X-ray diffraction, using their factor, are short by 0.07 Å. For this reason, the position of the proton associated with each of H_a, H_b, and H_c has been assumed to be 0.07 Å further from the carbon atom than the center of electron density as determined by X-ray analysis.

[7]The phrase *center of the ring* is somewhat ambiguous since none of the rings has a perfectly hexagonal shape. The center was taken as the point of intersection of two diagonals.

Can. J. Chem. Downloaded from www.nrcresearchpress.com by 210.87.254.5 on 09/05/12
For personal use only.

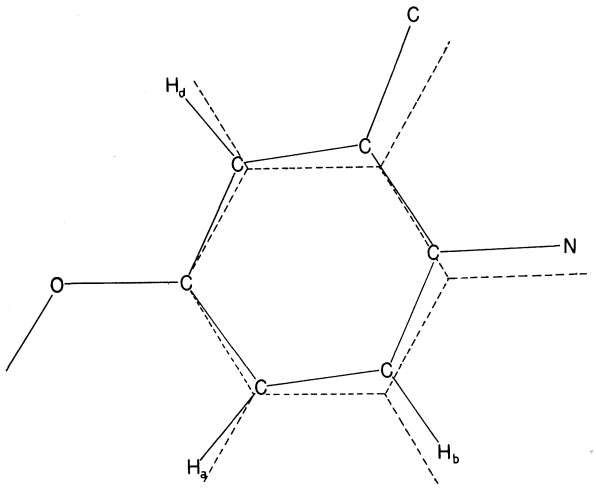

FIG. 2. Shape of phenyl ring to which H_a is bonded in **5** as determined by X-ray diffraction. Dashed figure is a perfectly hexagonal ring.

TABLE 5. $\delta_\omega{}^j$ values calculated using solid state geometry

Compound	$\delta_\omega{}^a$ (p.p.m.)	$\delta_\omega{}^b$ (p.p.m.)	$\delta_\omega{}^c$ (p.p.m.)	$\delta_\omega{}^d$ (p.p.m.)
3a	−0.682*	−0.111	0.071	0.176†
	−1.005	−0.185	0.055	0.178†
5	−0.699*	−0.122	0.068†	0.190
	−1.006	−0.143	0.050†	0.206
6	−1.355	−0.253	0.031	0.080†

*There are two different molecules in the unit cell.
†Calculated for an imaginary proton.

TABLE 6. "Other-ring" shielding values calculated using solid state geometry

Compound	$(\delta_\omega{}^a - \delta_\omega{}^d)/2$ (p.p.m.)	$(\delta_\omega{}^b - \delta_\omega{}^c)/2$ (p.p.m.)
3a	−0.429*	−0.091
	−0.591	−0.120
5	−0.444*	−0.095
	−0.606	−0.097
6	−0.717	−0.143

*There are two different molecules in the unit cell.

appears to be too low for the fixed crystal conformation and would be even lower for a more mobile system.

There are two possible explanations for the discrepancy between the experimental $\delta_\omega{}^j - \delta_{\omega H}{}^j$ and the calculated values of Table 6 for ether *3a*: (*i*) the nitro-substituted ring, although nearly in the COC plane, is deformed within that plane as in Fig. 2 and it is possible that the deformation does not occur to the same extent in solution; (*ii*) the ring-current model may not give a completely adequate three-dimensional representation of the associated magnetic field.

If the first explanation were correct, the change in deformation on going from solid to dilute solution would have to have a relatively greater effect on H_b and H_c than on H_a and H_d. Such is not the case. The $\delta_\omega{}^j$ values for *3a* were recalculated using the same angular parameters and average bond lengths found in the solid but having all ring angles of 120°. These new values are given in Table 7. On going from the deformed to perfectly hexagonal ring $(\delta_\omega{}^a - \delta_\omega{}^d)/2$ increases by about 28% for both molecules, while $(\delta_\omega{}^b - \delta_\omega{}^c)/2$ increases by only 15%.

Moreover, there are indications that the crystal and solution conformations are qualitatively the same. Tables 5 and 6 indicate the larger shielding calculated for **6** than for *3a* at both H_a and H_b. The differences in $\delta_\omega{}^a$ and $\delta_\omega{}^b$ between **6** and one

Can. J. Chem. Downloaded from www.nrcresearchpress.com by 210.87.254.5 on 09/05/12
For personal use only.

TABLE. 7. δ_ω^j values for **3***a* calculated using perfectly hexagonal ring

δ_ω^a (p.p.m.)	δ_ω^b (p.p.m.)	δ_ω^c (p.p.m.)	δ_ω^d (p.p.m.)
−0.933*	−0.166	0.050	0.173†
−1.340	−0.218	0.048	0.173†

*There are two different molecules in the unit cell.
†Calculated for an imaginary proton.

molecule of **3***a* are 0.350 and 0.069 p.p.m. respectively. A similar observation is made for a solution p.m.r. comparison of **6** and the corresponding mesityl ether **7**. H_a is more shielded in the tri-*t*-butyl ether by 0.317 p.p.m. and H_b is more shielded by 0.050 p.p.m. Because the two diphenyl ethers are so similar in structure this difference must be a function of conformation

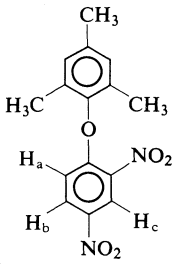

7

exclusively, making it remarkably close to the calculated difference noted above. In solution, librations in ϕ and ψ would be expected to be somewhat less with the bulky *t*-butyl groups substituted in the ortho positions. The average shielding at H_a and H_b would be greater as the conformation more nearly approaches the H-inside conformation ($\phi = \psi = 0$). The X-ray data of Table 3 indicate that the angles ϕ and ψ are smaller in **6** than in the others for the solid state so that one would conclude that the solution conformations are qualitatively the same as the crystal conformations, and that changes in ring deformations from one phase to the other are not responsible for discrepancies between experimental and calculated values of the "other-ring" shielding.

It would appear that the simple, ring-current theory, although giving an approximate three-dimensional representation of the magnetic field, is not entirely adequate. If, as Haigh and Mallion (21) suggest, it underestimates the shielding of protons above the plane of the ring, it is a greater failure for those protons, like H_b, further away from the ring than H_a.

The fault may arise in three areas: (*i*) no account is taken of the effect of substituents such as the three chlorines in **1** and **3**; (*ii*) the use of two separated π-currents is questionable, and (*iii*) the trichloro-substituted ring has been shown to be deformed slightly in the crystal so that calculations based on loops of cylindrical symmetry may be quite in error (9). However, other models fare even worse in predicting the magnetic field in the region of interest. For example, if one uses the model proposed recently by Haigh and Mallion (21) the calculated "other-ring" shielding values for **3***a*, **5**, and **6** are only 40% of those shown in Tables 5, 6, and 7 for *all* the ring protons. Not only are these values far too small to be taken seriously in comparison with the experimental values, the model has made no improvement in the relative, three-dimensional shielding picture. The double torroidal-shell model of Farnum and Wilcox (22) is no better because it *increases all* δ_ω^j by 13%.

Although the ring-current model of benzene ring, magnetic anisotropy has some inadequacies it is the best one for explaining the results presented for diphenyl ethers.

Experimental

The p.m.r. experimental procedure including concentrations, spectral analysis and estimation of errors has been given previously (1).

Melting points were determined on a Kofler, micro hot-stage apparatus and are reported uncorrected.

The preparation and properties of the following have been described previously (3, 13, 14): 2-(2′-carbomethoxy-4′-nitrophenoxy)-1,3,5-trichlorobenzene (**3***a*); 2-(3′-methyl-4′-nitrophenoxy)-1,3-diisopropylbenzene (**5**); 2-(2′,4′-dinitrophenoxy)-1,3,5-tri-*t*-butylbenzene (**6**); 2-(2′,4′-dinitrophenoxy)-1,3,5-trimethylbenzene (**7**). Methyl 2-methoxybenzoate (**4***e*) was purchased from Eastman and was used without further purification.

2-(2′-Carbomethoxy-4′-aminophenoxy)-1,3,5-trichlorobenzene (3b)

2-(2′-Carbomethoxy-4′-nitrophenoxy)-1,3,5-trichlorobenzene (2.8 g) was dissolved in 95% ethanol (300 ml) and about 2 g of W-2 Raney nickel added. The hot solution was hydrogenated for 3 h at a pressure of 45 lb/in.^{2} using a Parr shaker apparatus. Sufficient acetone was added to dissolve the precipitate before the catalyst was removed by filtration. The colorless filtrate was evaporated to yield 2.47 g (94%) of white crystals, m.p. 106–108°. Further recrystallizations from 95% ethanol gave the analytical sample, m.p. 107–108.5°.

Anal. Calcd. for $C_{14}H_{10}NO_3Cl_3$: C, 48.51; H, 2.91; N, 4.04; Cl, 30.69. Found: C, 48.43, 48.44; H, 2.78, 2.71; N, 4.35, 4.16; Cl, 30.36, 30.28.

Can. J. Chem. Downloaded from www.nrcresearchpress.com by 210.87.254.5 on 09/05/12
For personal use only.

Can. J. Chem. Downloaded from www.nrcresearchpress.com by 210.87.254.5 on 09/05/12
For personal use only.

2-(2′-Carbomethoxy-4′-iodophenoxy)-1,3,5-trichlorobenzene (3c)

2-(2′-Carbomethoxy-4′-aminophenoxy)-1,3,5-trichlorobenzene (12.0 g) was dissolved in a mixture of concentrated sulfuric acid (125 ml) and glacial acetic acid (125 ml). A solution of sodium nitrite (3.2 g) in a mixture of sulfuric acid (61 ml) and glacial acetic acid (61 ml) was prepared and added slowly, over a period of 2.5 h, to the solution of the amine kept at 5°. After stirring for an additional 1 h, the mixture was poured into a beaker containing water (600 ml), chloroform (250 ml), potassium iodide (39 g), iodine (39 g), and urea (12 g). The contents of the beaker were stirred for 15 h after which the organic layer was separated and washed with a saturated aqueous solution of sodium bisulfite. Evaporation of the chloroform gave a red oil which recrystallized from ethanol–water as brownish crystals (12.6 g). An additional recrystallization from ethanol–water gave 10.1 g (64%) of yellow crystals, m.p. 109–110°, a portion of which was sublimed to give the analytical sample, m.p. 110.5–111.5°.

Anal. Calcd. for $C_{14}H_8Cl_3IO_3$: C, 36.77; H, 1.76; Cl, 23.25; I, 27.74. Found: C, 36.75; H, 1.72; Cl, 23.11; I, 25.82.

2-(2′-Carbomethoxy-4′-chlorophenoxy)-1,3,5-trichlorobenzene (3d)

2-(2′-Carbomethoxy-4′-iodophenoxy)-1,3,5-trichlorobenzene (5 g) was dissolved in dimethylformamide (40 ml) and cuprous chloride (5.1 g) was added. The mixture was heated with stirring at 140° for 18 h and then poured into a beaker containing 6 *N* hydrochloric acid (200 ml) and ferric chloride (10 g). After cooling a brown gum formed which was crystallized from methanol as brown crystals (3.5 g). Since the p.m.r. spectrum of this material showed evidence of the presence of considerable starting material the product was subjected to the same reaction conditions again. This time 2.3 g (58%) of brown crystals were obtained, m.p. 105–110°. Sublimation did not improve the melting point and the p.m.r. spectrum showed the presence of about 5% of the starting iodo compound. The impurity could not be reduced by recrystallization or sublimation so the product was used as it was for p.m.r. analysis.

2-(2′-Carbomethoxyphenoxy)-1,3,5-trichlorobenzene (3e)

Diazotization of 2-(2′-carbomethoxy-4′-aminophenoxy)-1,3,5-trichlorobenzene (4.9 g) was carried out as described in the synthesis of 2-(2′-carbomethoxy-4′-iodophenoxy)-1,3,5-trichlorobenzene. The cold diazonium salt solution was poured into a beaker containing crushed ice (500 g), and 50% hypophosphorous acid (100 ml) with stirring. After being left for 18 h, chloroform (150 ml) was added and the mixture stirred for 15 min. The organic layer was separated and the chloroform evaporated to give 4.2 g (90%) of an orange solid. After two recrystallizations from 95% ethanol and one from ligroin the resulting yellow crystals were sublimed to yield a white product, m.p. 70–71°.

Anal. Calcd. $C_{14}H_9Cl_3O_3$: C, 50.71; H, 2.74; Cl, 32.08. Found: C, 50.50; H, 2.68; Cl, 31.70.

2-(2′-Carbomethoxy-4′-methoxyphenoxy)-1,3,5-trichlorobenzene (3f)

2-(2′-Carbomethoxy-4′-aminophenoxy)-1,3,5-trichlorobenzene (4.9 g) was dissolved in 70% aqueous sulfuric acid (30 ml) and the solution cooled to 5°. A solution of sodium nitrite (1.15 g) in concentrated sulfuric acid (20 ml) was prepared, cooled to 5°, and added to the amine solution over a period of 2 min. The resulting purple solution was allowed to stand at 5° for 45 min and then was added rapidly to boiling 55% aqueous, sulfuric acid (55 ml). After boiling for 15 min and cooling a grey precipitate formed which was collected (4.3 g), m.p. 203–227°. The solid was dissolved in dilute, sodium bicarbonate solution, filtered and the filtrate acidified with dilute HCl to give 3.9 g (79%) of tan crystals, m.p. 221–228°.

All of this crude 2-(2′-carboxy-4′-hydroxyphenoxy)-1,3,5-trichlorobenzene was added to ethereal diazomethane and the ether was evaporated in a fume hood. Of the resulting 3.6 g of white crystals 1.9 g was dissolved in 15% aqueous sodium hydroxide (15 ml) and dimethyl sulfate (20 ml) was added in small portions with stirring and the alternate addition of enough base to maintain a basic solution. Finally, dimethyl sulfate (10 ml) and sodium hydroxide (10 g) were added and the solution was refluxed overnight. Acidification with HCl and filtration of the precipitate produced 1.6 g of 2-(2′-carboxy-4′-methoxyphenoxy)-1,3,5-trichlorobenzene, m.p. 173–177°. The crude acid was treated with ethereal diazomethane and the ether evaporated to give a brown oil (1.5 g). One recrystallization from methanol and a sublimation yielded the analytical sample as white prisms, m.p. 93–93.5°.

Anal. Calcd. for $C_{15}H_{11}Cl_3O_4$: C, 49.82; H, 3.07; Cl, 29.41. Found: C, 50.00; H, 2.95; Cl, 29.25.

2-(2′-Carbomethoxy-4′-cyanophenoxy)-1,3,5-trichlorobenzene (3g)

2-(2′-Carbomethoxy-4′-iodophenoxy)-1,3,5-trichlorobenzene (6 g) was dissolved in dimethylformamide (60 ml) and cuprous cyanide (1.95 g) was added. The dark mixture was refluxed gently for 4 h with stirring and then poured into a beaker containing ferric chloride (15 g) and 6 *N* hydrochloric acid (200 ml). A dark oil formed but solidified on cooling. The aqueous solution was filtered and the filtrate extracted with chloroform (150 ml). The extract was combined with the solid and the chloroform was evaporated. The residue was crystallized from 95% ethanol as tan crystals (4.3 g, 93%), m.p. 151–153°. Two additional recrystallizations from 95% ethanol gave the analytical sample, m.p. 152–153°.

Anal. Calcd. for $C_{15}H_8Cl_3NO_3$: C, 50.52; H, 2.26; N, 3.93; Cl, 29.83. Found: C, 50.23; H, 2.24; N, 3.83; Cl, 29.50.

Methyl 2-Methoxy-5-nitrobenzoate (4a)

2-Methoxybenzoic acid (40 g) was nitrated according to the method of Simonsen and Rau (15). The desired 2-methoxy-5-nitrobenzoic acid was separated from its 3-nitro isomer according to the scheme of Hirwe and Patel (16) and was obtained in pure form after recrystallization from water (18.7 g, 36%) m.p. 161–164°. Esterification followed the general procedure of Clinton and Laskowski (17). Evaporation of the dichloroethane gave a white residue which was recrystallized from 95% ethanol to yield 16.2 g, m.p. 100–101°. The literature m.p. is 99–100° (17).

Methyl 2-Methoxy-5-aminobenzoate (4b)

Methyl 2-methoxy-5-nitrobenzoate (25 g) was dis-

Can. J. Chem. Downloaded from www.nrcresearchpress.com by 210.87.254.5 on 09/05/12
For personal use only.

solved in hot, 95% ethanol (300 ml) and about 2 g of W-2 Raney nickel was added. The mixture was hydrogenated using a Parr shaker apparatus at a pressure of 45 lb/in.^{2} until the uptake of hydrogen ceased (3.5 h). The catalyst was removed by filtration and the ethanol evaporated under reduced pressure to yield 23.4 g of a green liquid. This was distilled to give 17.6 g (88%) of a yellow oil, b.p. 140–141°/0.02 mm Hg. The product appeared to decompose slowly on standing. Although initial attempts to induce crystallization failed, the oil did crystallize after several months. However, the crystals decomposed readily. The compound was concluded to be the named product from its p.m.r. and i.r. spectra and by its reaction to produce the cyano anisole (**4***g*). Attempts to prepare a benzoyl derivative appeared to produce a mixture of products.

*Methyl 2-Methoxy-5-iodobenzoate (**4***c*)

5-Iodosalicylic acid (52.8 g), sodium hydroxide (16 g), and water (450 ml) were placed in a flask and dimethyl sulfate (20 ml) was added slowly with stirring to the warm solution. After addition was complete, the mixture was left for 1 h and then a further 15 ml of dimethyl sulfate were added. At all times the reaction mixture was kept basic by the addition of sufficient sodium hydroxide. After standing overnight, the white product was collected and acidified with aqueous HCl to give a white solid (34.9 g, 63%), m.p. 197–199°. The literature m.p. for 2-methoxy-5-iodobenzoic acid is 197° (18).

Some of the acid (4.1 g) and potassium carbonate (2.2 g) were added to a solution of methyl iodide (3 ml) in 50% aqueous ethanol (160 ml). The mixture was refluxed overnight and then diluted with water (200 ml) to produce a white solid. Recrystallization of the solid from water–ethanol gave white needles (2.35 g, 55%), m.p. 57.5–59°. A further recrystallization from the same solvent gave the analytical sample, m.p. 59–59.5°.

Anal. Calcd. for $C_9H_9IO_3$: C, 37.01; H, 3.10; I, 43.45. Found: 37.07; H, 3.05; I, 43.03.

*Methyl 2-Methoxy-5-chlorobenzoate (**4***d*)

5-Chlorosalicylic acid (30 g) was treated with dimethyl sulfate (70 ml) and sodium hydroxide as described in the synthesis of methyl 2-methoxy-5-iodobenzoate. Acidification of the reaction mixture gave 20.0 g (62%) of 2-methoxy-5-chlorobenzoic acid. This was esterified according to the method of Clinton and Laskowski (17) and the resulting yellow oil was distilled to give a colorless liquid (13.8 g, 65%), b.p. 113°/0.03 mm Hg. The reported b.p. is 235–240°/760 mm Hg (19).

*Methyl 2,5-Dimethoxybenzoate (**4***f*)

2,5-Dihydroxybenzoic acid (30 g) was treated with dimethyl sulfate (70 ml) and sodium hydroxide as in the synthesis of methyl 2-methoxy-5-iodobenzoate. Acidification of the reaction mixture with aqueous HCl caused a liquid to separate but this soon solidified. The dimethoxybenzoic acid was collected (20.6 g, 59%) and esterified according to the method of Clinton and Laskowski (17). The yellow oil that resulted was distilled to yield 18.7 g (84%) of a colorless liquid, b.p. 110°/0.05 mm Hg.

Anal. Calcd. for $C_{10}H_{12}O_4$: C, 61.22; H, 6.17. Found: C, 61.22; H, 6.19.

*Methyl 2-Methoxy-5-cyanobenzoate (**4***g*)

Methyl 2-methoxy-5-aminobenzoate (21 g) was dissolved in dilute sulfuric acid (50 ml) and sodium nitrite (8.0 g) was added until an immediate positive test was obtained with starch–iodide paper. The temperature of the mixture was kept at 5° during and after the addition. The solution thus obtained was neutralized with excess sodium bicarbonate before being poured into a beaker containing a solution of cuprous cyanide (14 g) in water (100 ml) with sufficient sodium cyanide added to effect solution. Toluene (250 ml) was added and the two phase mixture allowed to reach room temperature. The mixture was filtered, the toluene layer separated and the toluene evaporated to give a black residue. The tar was extracted with ether (400 ml) and the ether evaporated to yield 13 g of a semi-crystalline material. Distillation gave 4.8 g (46%) of a light orange liquid which soon solidified, b.p. 140–144°/0.03 mm Hg. Two recrystallizations from 95% ethanol gave the analytical sample of white crystals, m.p. 103–104°.

Anal. Calcd. for $C_{10}H_9NO_3$: C, 62.82; H, 4.74; N, 7.33. Found: C, 62.63; H, 4.72; N, 7.31.

The authors wish to acknowledge the support of the National Research Council of Canada for grants in aid of research and for a bursary to one of us (J.J.B.).

1. J. J. Bergman, W. D. Chandler, and R. Y. Moir. Can. J. Chem. **49**, 225 (1971).
2. C. E. Johnson and F. A. Bovey. J. Chem. Phys. **29**, 1012 (1958).
3. J. J. Bergman and W. D. Chandler. Can. J. Chem. **50**, 353 (1972).
4. G. Montaudo, P. Finocchiaro, E. Trivellone, F. Bottino, and P. Maravigna. Tetrahedron, **27**, 2125 (1971).
5. G. Montaudo, P. Finocchiaro, F. Bottino, S. Caccamese, P. Maravigna, and E. Trivellone. Proc. XXIII Int. Cong. Pure and Appl. Chem. **II**, 1169 (1971).
6. O. J. Toussaint. Bull. Soc. Roy. Sci. Liège, **15**, 86 (1946).
7. E. A. H. Griffith, W. D. Chandler, and B. E. Robertson. Can. J. Chem. **50**, 2963 (1972).
8. E. A. H. Griffith, W. D. Chandler, and B. E. Robertson. Can. J. Chem. **50**, 2972 (1972).
9. E. A. H. Griffith, W. D. Chandler, and B. E. Robertson. Can. J. Chem. **50**, 2979 (1972).
10. P. A. Lehmann and E. Shefter. Rev. Latinoamer. Quím. In press.
11. V. Cody, W. L. Duax, and D. A. Norton. Chem. Commun. 683 (1971).
12. N. Camerman and A. Camerman. Science, **175**, 764 (1972).
13. W. D. Chandler, J. J. Bergman, and G. H. Haas. Can. J. Chem. **49**, 583 (1971).
14. J. Wright and E. C. Jorgensen. J. Org. Chem. **33**, 1245 (1968).
15. J. L. Simonsen and M. G. Rau. J. Chem. Soc. **111**, 220 (1917).
16. N. W. Hirwe and B. V. Patel. Proc. Ind. Acad. Sci. **5A**, 321 (1937); Chem. Abstr. **31**, 6216 (1937).

17. R. O. CLINTON and S. C. LASKOWSKI. J. Am. Chem. Soc. **70**, 3135 (1948).
18. Dictionary of organic compounds. Vol. 3. 4th ed. Eyre and Spottiswoode, London. 1703. 1965.
19. Beilsteins handbuch der organischen chemie. Vol. 10. *Edited by* Hans-G. Bart. Springer-Verlag, Berlin. 1920. **10**, Part II. p. 62.
20. R. F. STEWART, E. R. DAVIDSON, and W. T. SIMPSON. J. Chem. Phys. **42**, 3175 (1965).
21. C. W. HAIGH and R. B. MALLION. Org. Mag. Res. **4**, 203 (1972).
22. D. G. FARNUM and C. F. WILCOX. J. Am. Chem. Soc. **89**, 5379 (1967).

Can. J. Chem. Downloaded from www.nrcresearchpress.com by 210.87.254.5 on 09/05/12
For personal use only.

Preparation and Stereochemistry of *N*-Methyl-*N*-phenacylpiperidinium Salts

ROBERT V. SMITH[1]

Division of Medicinal Chemistry, College of Pharmacy, University of Iowa, Iowa City, Iowa 52240

AND

FREDERICK W. BENZ[2] AND JOHN P. LONG

Department of Pharmacology, College of Medicine, University of Iowa, Iowa City, Iowa 52240

Received July 18, 1972

The *N*-methyl-*N*-phenacylquaternary salts of 2-, 3-, and 4-methylpiperidines have been prepared and characterized. N.m.r. spectroscopy was employed in analyzing the proportion of diastereomers formed following reciprocal alkylations with methyl iodide and phenacyl halides. Preferential axial attack was observed with *N*-methylation while *N*-phenacylation primarily proceeded by equatorial atatck.

Nous avons préparé et caractérisé les sels *N*-méthyl-*N*-phénacyl quaternaires des dérivés 2-, 3-, et 4-méthylpipéridines. La r.m.n. a été utilisée pour analyser la proportion de diastéréoisomères formés, à la suite des alkylations réciproques avec l'iodure de méthyl et les halogénures de phénacyl. Nous observons une attaque axiale préférentielle avec la *N*-méthylation, tandis que la *N*-phénacylation se produit à la suite d'une attaque équatoriale [Traduit par le journal]

Can. J. Chem., **51**, 171 (1973)

Introduction

The hemicholinium-3 analog, **1**, exerts interesting effects on the autonomic nervous system (1–4). Attempts to compare the structure–biological activity relationships of **1** to its saturated analogs (**2***a–c*) were hampered by a lack of information on the course of quaternization involving phenacyl type alkylating agents and 2-, 3-, and 4-methylpiperidines (2).

Numerous reports have appeared on the stereochemistry resulting from quaternization of relatively rigid *N*-alkylpiperidines with methyl (5–17, 19), ethyl (5–7, 10, 11, 13, 17, 18), *n*- or *i*-propyl (6–8, 10, 11), and benzyl (5–7, 9–11, 13–15) alkylating agents; the stereochemistry of piperidine quaternizations in general has recently been reviewed (20, 21). There is, however, a paucity of literature relative to the *N*-phenacylation of such systems or, indeed, to the methylation of *N*-phenacylpiperidines (2). The work reported herein was designed to investigate the synthesis and resulting stereochemistry of compounds **3–6**, which would serve as models for the bis-quaternary systems (**2***a–c*).

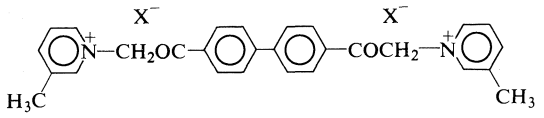

1

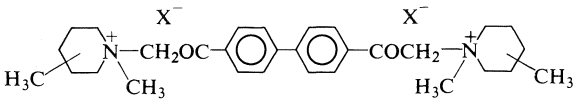

2

a 2-CH_3
b 3-CH_3
c 4-CH_3

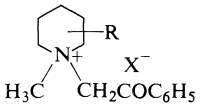

3 R = H (*a*, X = Br; *b*, X = Cl; *c*, X = I)
4 R = 2-CH_3 (*a*, X = Br; *b*, X = Cl; *c*, X = I)
5 R = 3-CH_3 (*a*, X = Br; *b*, X = Cl; *c*, X = I)
6 R = 4-CH_3 (*a*, X = Br; *b*, X = Cl; *c*, X = I)

Experimental

N-Methylpiperidines

A literature procedure (22) was employed in preparing 1-methyl-, 1,2-dimethyl-, 1,3-dimethyl-, and 1,4-dimethylpiperidines; yields were 60–70%.

N-Phenacylpiperidine Hydrobromides

α-Chloroacetophenone was reacted with an excess of piperidine, 2-methyl-, 3-methyl-, or 4-methylpiperidine in ethanol at 60–70° C for 12 h. Following treatment with 5% sodium hydroxide, the amines were extracted into ether. Dried ether extracts were treated with gaseous hydrobromic acid. The hydrobromides were recrystallized twice from *n*-propanol; yields were 60–80%.

[1]To whom all inquiries should be addressed.

[2]Present address: National Institute for Medical Research, The Ridgeway, Mill Hill, London NW7, England.

Can. J. Chem. Downloaded from www.nrcresearchpress.com by 210.87.254.40 on 09/05/12
For personal use only.

TABLE 1. Characterization of piperidines

Compound	M.p. or b.p.* (°C)	Analyses (%)† Calcd. C	H	N	Found C	H	N
N-Methylpiperidine	107‡						
1,2-Dimethylpiperidine	125–126§						
1,3-Dimethylpiperidine	123–124¶						
1,4-Dimethylpiperidine	122–123‖						
1-Phenacylpiperidine HBr	243–244	54.95	6.34	4.93	54.91	6.55	4.91
1-Phenacyl-2-methylpiperidine HBr	201–202	56.39	6.71	4.70	56.60	7.01	4.59
1-Phenacyl-3-methylpiperidine HBr	212–213	56.39	6.71	4.70	56.51	6.98	4.64
1-Phenacyl-4-methylpiperidine HBr	248–250	56.39	6.71	4.70	56.60	7.00	4.64
3*a*	184–186	56.39	6.71	4.70	56.69	6.83	4.64
3*b*	171–172	66.27	7.89	5.52	66.50	8.01	5.53
3*c*	180–182	48.71	5.80	4.06	48.44	5.94	4.11
4*a*	135–137	57.71	7.05	4.49	57.65	7.18	4.44
4*b*	161–163	67.29	8.22	5.23	67.26	8.33	5.21
4*c*	153–156	50.15	6.13	3.90	50.24	6.01	3.93
5*a*	192–193	57.71	7.05	4.49	57.80	6.87	4.46
5*b*	184–186	67.29	8.22	5.23	67.30	8.34	5.31
5*c*	135–137	50.15	6.13	3.90	50.25	6.21	3.80
6*a*	178–180	57.71	7.05	4.49	58.00	7.20	4.46
6*b*	190–192	67.29	8.22	5.23	67.48	8.38	5.29
6*c*	161–163	50.15	6.13	3.90	50.25	6.01	3.80

*Boiling points at 760 mm; compounds **4–6** are mixtures of diastereomers prepared by procedures I*a* and I*b*.
†Compounds **3***a–c* show i.r. carbonyl absorption between 1677–1682 cm^{-1} (Nujol mull).
‡Literature 107 °C (23).
§Literature 127.9 °C (23).
¶Literature 124–126 °C (23).
‖Literature 125 °C (24).

Phenacylation (Quaternization) of N-Methylpiperidines (Procedure Ia)

α-Bromoacetophenone or α-chloroacetophenone (25 mmol) and *N*-methylpiperidines (25 mmol) were dissolved in acetonitrile and allowed to react at room temperature for 1 week. The quaternary ammonium compounds were collected after removal of solvent *in vacuo* and were washed with ether; yields were 89–99%.

Methylation (Quaternization) of N-Phenacylpiperidines (Procedure Ib)

Methyl iodide (25 mmol) and *N*-phenacylpiperidines (25 mmole) generated from hydrobromide salts, were dissolved in acetonitrile (100 ml) and allowed to react at room temperature for 1 week. After removal of the solvent *in vacuo* and washing with ether, the quaternary ammonium iodides were collected; yields were 72–88%.

Alternative Quaternization Method (Procedure II)

N-Methyl or *N*-phenacylpiperidines (25 mmol) were reacted with α-bromo (α-chloro) acetophenone or methyl iodide (25 mmol) in acetonitrile or ether (100 ml) at 30 °C for 72 h. Products were isolated following solvent evaporation at 30 °C *in vacuo* and were subjected to n.m.r. analysis.

All boiling and melting points are uncorrected. The n.m.r. spectra were recorded at 60 MHz using Varian A-60 and T-60 spectrometers. Solvents used were $CDCl_6$ or D_2O. Microanalyses were obtained with a Hewlett-Packard model 185 CHN analyzer. Characterizing data for all compounds are indicated in Table 1.

Results and Discussion

The course of alkylation of *N*-substituted piperidines can be affected by two conformational equilibria, *viz.* nitrogen inversion and ring inversion. The effect of these equilibria on the preparation of **3***a–c* cannot be evaluated because of the apparently rapid ring inversion in the latter materials (*vide infra*). In reactions leading to compounds **4–6** piperidine starting materials with equatorial *C*-methyl groups should predominate by about 20:1 (25–27). Thus, the course of alkylation can be related to the preferential axial or equatorial attack on *either* structures **7***a* or *b*.

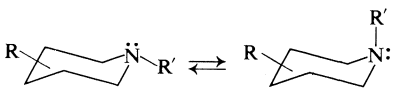

7*a* 7*b*

R = 2-, 3-, or 4-CH_3 (equatorial)
R′ = CH_3 or $CH_2COC_6H_5$

Can. J. Chem. Downloaded from www.nrcresearchpress.com by 210.87.254.40 on 09/05/12
For personal use only.

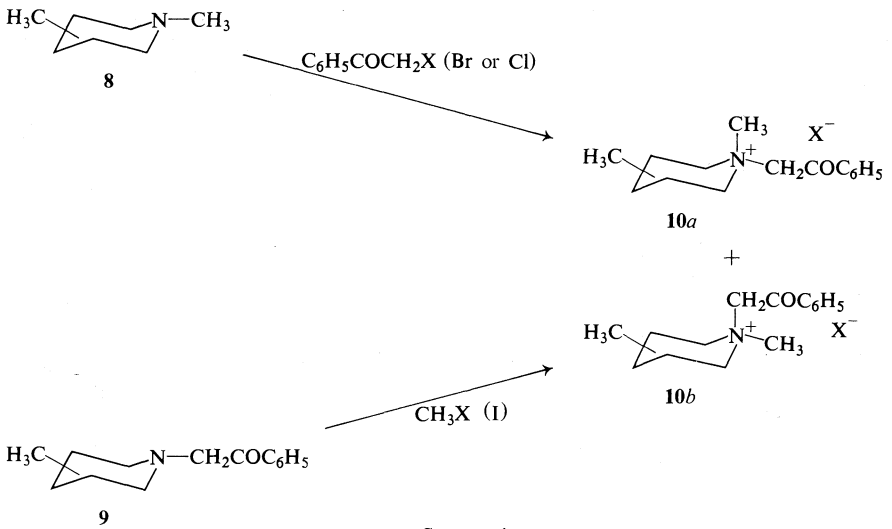

SCHEME 1

TABLE 2. Chemical shifts of *N*-methyl and *N*-phenacylmethylene protons of piperidinium salts*

Compound	$C_6H_5COCH_2$—N—+		CH_3—N—+					
3a	5.87		3.57					
3b	5.89		3.55					
3c	5.77		3.60					
					D_2O†		$\Delta_{CDCl_3-D_2}$(p.p.m.)	
	Equatorial	Axial	Equatorial	Axial	Equatorial	Axial	Equatorial	Axial
4a	5.80‡	5.50‡	3.69	3.45	3.45	3.25	0.24	0.20
4b	5.81‡	5.52‡	3.67	3.43	3.48	3.28	0.19	0.15
4c	5.68‡	5.34‡	3.68	3.45	3.38	3.18	0.30	0.27
5a	5.99	5.62	3.63	3.57	3.42		—	—
5b	6.02	5.65	3.62	3.55	3.40		—	—
5c	5.85	5.50	3.62	3.57	3.40		—	—
6a	6.00	5.65	3.62	3.52	3.38		—	—
6b	6.03	5.68	3.62	3.49	3.40		—	—
6c	5.84	5.50	3.61	3.51	3.32		—	—

*All chemical shifts were measured in $CDCl_3$ with respect to internal TMS (δ-values), unless indicated otherwise. All resonances are singlets except where indicated otherwise.

†Chemical shifts were measured in D_2O with respect to internal DSS. *N*-Phenacylmethylene protons were not observed in D_2O. These protons are relatively acidic due to their location between carbonyl and quaternary nitrogen groups; thus, they exchange with the deuterium of the solvent.

‡AB quartets centered at the δ-values quoted; J = 18 Hz ($J_{\delta H_A - H_B}$ = 18 Hz).

In each case, reciprocal alkylations were studied; that is, the appropriate *N*-alkylated derivatives of *C*-methylpiperidines were reacted to form qualitatively similar mixtures of piperidinium salts (Scheme 1).

N.m.r. spectroscopy was utilized in studying product compositions. Chemical shift and coupling constant data for all quaternary salts investigated appear in Table 2. The spectra of **3***a–c* revealed single resonances for their *N*-methyl and *N*-methylene protons. This is believed to be due to rapid ring inversion leading to averaged resonances for these protons, since the δ-values for these averaged resonances lie between the δ-values for the axial and equatorial resonances observed in the corresponding salts in **6**, where the *C*-methyl group is too far removed to substantially influence the *N*-methyl and *N*-methylene

Can. J. Chem. Downloaded from www.nrcresearchpress.com by 210.87.254.40 on 09/05/12
For personal use only.

TABLE 3. Diastereomer ratios* of *N*-methyl-*N*-phenacylpiperidinium salts

Reactants		Product	Diastereomer ratio, axial methyl/equatorial methyl	
			Procedures I*a* and I*b*†	Procedure II†
Phenacyl bromide	1,2-DMP‡	**4***a*	4.2 (1.7¶)	4.3
Phenacyl chloride	1,2-DMP	**4***b*	4.5 (20.3¶)	3.8
Methyl iodide	1-Ph-2-MP§	**4***c*	1.6	1.5
Phenacyl bromide	1,3-DMP	**5***a*	1.5	1.5 (1.0‖)
Phenacyl chloride	1,3-DMP	**5***b*	1.7 (2.9¶)	1.6
Methyl iodide	1-Ph-3-MP	**5***c*	2.1	2.0 (3.4‖)
Phenacyl bromide	1,4-DMP	**6***a*	1.6	1.7
Phenacyl chloride	1,4-DMP	**6***b*	1.7	1.5
Methyl iodide	1-Ph-4-MP	**6***c*	1.8	1.7

*Determined in $CDCl_3$ by integration of n.m.r. *N*-Methyl and/or *N*-phenacylmethylene signals; RSD's < ±3%.
†Prepared in acetonitrile.
‡DMP = Dimethylpiperidine.
§Ph = Phenacyl; MP = methylpiperidine.
¶Ratio resulting after washing the diastereomer mixture with acetone.
‖Prepared in ether.

shifts. Compounds **4–6** revealed two singlets between 3.43–3.69 p.p.m. for their *N*-methyl groups. Assignment of the upfield singlets to the axial methyl groups and the lower field resonances to equatorial methyl protons was based on data in the literature for such systems (5–7, 9–11, 13–18).[3] The assignment of the lower field absorptions to equatorial *N*-methyl groups was corroborated by n.m.r. experiments involving solvent-induced shifts. Piperidyl *N*-methyl resonances shift to higher fileds when going from $CDCl_3$ to D_2O. The shifts noted are proportionately greater for equatorial methyl protons (29). In compounds **4***a–c*, the lower field *N*-methyl signal shows the greater shift when spectra taken in $CDCl_3$ and D_2O are compared (Table 2). When the diastereomers, **5** and **6** were examined in D_2O, unresolved singlets were observed for their *N*-methyl protons. These singlets, however, appeared at positions upfield from the higher field *N*-methyl protons of **5** and **6** in $CDCl_3$ (Table 2). This effect is indicative of the lower field resonances undergoing the greater shift and further confirms the assignment of the downfield absorptions (in $CDCl_3$) to equatorial *N*-methyl protons (29).

N-Methylene protons in compounds **5** and **6** showed two singlets between 5.50–6.03 p.p.m. In compounds **4***a–c* these protons exhibited an AB quartet for each diastereomer. Similar AB patterns have been observed for the methylene protons in α-methyl-*N*-benzylpiperidines and their salts (13, 30–33). It has been shown that this non-equivalence is only observed when the α-methyl substituent is in the equatorial position (32, 33). If this relationship holds for the methyl quaternary salts of such systems, then the observation of an AB quartet for the methylene protons in compounds **4***a–c* furnishes spectral evidence for the equatorial disposition of the *C*-methyl group. AB patterns are not usually observed for β-methyl substituted piperidines because the chiral center is too far removed (30–33). Chemical shift data for phenacylmethylene resonances in piperidyl systems have not been reported but the same axial–equatorial relationship (*i.e.* axial signals upfield of equatorial signals) is indicated from work with electronically and/or sterically similar groups (5, 9–11, 13) and because this assignment is the one internally consistent with the *N*-methyl assignments with respect to diastereomer product ratios.

The *C*-methyl resonances for compounds **5** and **6** were doublets with splittings of **6** and **5** Hz, respectively. The α-*C*-methyl resonances for compounds **4***a–c* were triplets resulting from the overlap of two apparent doublets with splittings of 7 Hz (16, 34). The estimated intensity ratio of the upfield "doublet" to the lower field "doublet" for each salt is the same as the diastereomer ratio shown in Table 3. Thus, the upfield "doublet" is assigned to the equatorial α-*C*-methyl group adjacent to the axial *N*-methyl diastereomer and the downfield "doublet" to the equatorial α-*C*-methyl group adjacent to the equatorial *N*-methyl diastereomer.

Diastereomer ratios were obtained by integra-

[3]Delpeuch and Deschamps (28) consider the opposite assignment to be valid for certain tertiary amines in acid solvents unless the amine is α-substituted.

Can. J. Chem. Downloaded from www.nrcresearchpress.com by 210.87.254.40 on 09/05/12
For personal use only.

Can. J. Chem. Downloaded from www.nrcresearchpress.com by 210.87.254.40 on 09/05/12
For personal use only.

tion of the *N*-methyl and/or *N*-methylene n.m.r. signals and are listed in Table 3. The ratios listed under procedure II should reflect the stereochemical course of the quaternization reactions since these ratios were obtained on products, (*a*) from thermostatted (30 °C) reactions, reportedly limiting any drift toward equilibrium by product interconversion which is known to occur in refluxing solvents (10, 14, 35), and (*b*) unwashed and unrecrystallized so as to avoid product fractionation. However, independent, alternate syntheses of these products (procedures I*a* and I*b*), which incorporated an ether wash to remove starting materials and solvent before C, H, and N analyses, showed virtually identical product ratios (Table 3). Thus, washing with ether is a useful method of purifying such products without introducing fractionation. Washing with acetone instead of ether, however, caused significant changes in certain product ratios (Table 3).

The product ratios in Table 3 indicate that the diastereomers bearing axial *N*-methyl groups predominate in all reactions. That is, whether structures **8** or **9** are alkylated, the proportion of **10***a* is greater than **10***b*. This finding leads to the conclusion that *N*-phenacylation proceeds by preferential equatorial attack while *N*-methylation occurs predominantly *via* axial attack. Preferred axial attack during *N*-methylation is expected and has been observed in many similar systems (5–7, 9–17, 19). While there is less concensus of opinion on the stereochemical approach in alkylation of *N*-methylpiperidines, a number of workers have observed enhanced equatorial attack with alkylating agents which are more sterically demanding than methyl (5, 10, 11, 13, 14, 36). In addition, it has been shown that the more reactive triethyloxonium fluoroborate (18) shows marked tendencies to alkylate equatorially. It seems quite reasonable, therefore, that the reactive and bulky α-halo phenacyl ketones (15, 37) used in this study should also alkylate equatorially.[4] In spite of this, it was initially surprising to find that *N*-phenacylation of 1,2-dimethylpiperidine yields the product ratios indicated for **4***a* and *b*, thereby showing higher stereoselectivity than the reciprocal alkylation yielding product **4***c* (Table 3). Kawazoe and Tsuda have shown (17) that α-substituents affect the stability of the reaction intermediates at the transition state in these quaternizations such that the axial approach of the alkylating agent becomes more difficult than the equatorial approach and that this is more so for larger alkylating agents than for methyl halides. Thus, they found greater selectivity in the equatorial ethylation of 1-methyl-2-ethylpiperidine than in the axial methylation of this amine. A similar rationalization can be used to explain the greater apparent equatorial phenacylation leading to **4***a* and *b*. Lyle *et al.* (39) also report a higher incidence of equatorial attack (during quaternization) of 1-methyl-2-alkylated piperidines, relative to their 3- and 4-substituted analogs.[5]

A change in product ratios was obtained when **5***a* and *c* were prepared in ether as compared to acetonitrile (Table 3). Bottini and O'Rell (9) point out that an increase in equatorial alkylation occurs when going from a more polar to a less polar solvent. The opposite of this was observed with **5***a* and *c*, but this result concurs with the findings of Kawazoe and Tsuda (17). In general, solvent effects on quaternization ratios seem to be difficult to predict (15, 20).

[4]Duke *et al.* (38) have recently shown by X-ray crystallography that 1-ethyl-4-phenylpiperidine and 1-isopropyl-4-phenylpiperidine undergo equatorial *N*-benzylation, which supports this conclusion.

[5]One referee has suggested that the following mechanism might be invoked to explain the preferred equatorial *N*-phenacylation leading to **4***a–b*, **5***a–b*, and **6***a–b*.

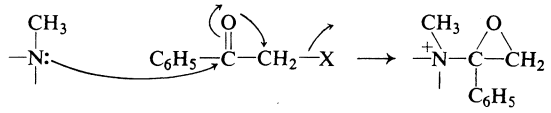

11

The epoxammonium salt (**11**), however, can be eliminated as a structure for compounds noted, based on the following: (*1*) compounds **3***a–***6***c* show i.r. carbonyl absorption (see Table 1) at frequencies expected for structures **10***a* and *b*; (*2*) the chemical shifts and multiplicities of phenacyl methylene protons of **3***a–***6***c* are in accord with structures **10***a* and *b* (5) while the oxirane–methylene protons of **11** would likely appear at higher fields (40) and would display splitting patterns (40) which were not observed in the n.m.r. spectra of **3***a–***6***c*; (3) the rapid exchange of the phenacylmethylene protons of **3***a–***6***c* in deuterium oxide is expected for compounds with structures such as **10***a* and *b* (5) but would not be predicted for the oxirane–methylene protons of **11**. The intermediacy of **11** in equatorial *N*-phenacylation is not as easily disproven; however, this proposal requires ultimate collapse of **11** accompanied by migration of a phenyl-ring. This suggestion seems unlikely without further evidence.

The authors are grateful to Professor A. T. Bottini, University of California, Davis, Calif. for a number of helpful suggestions during the initial stages of this investigation. This work was supported in part by USPHS Grant NS-4431 and USPHS Training Grant 5-TO1 GM 00141-15.

1. J. P. LONG and F. W. SCHUELER. J. Am. Pharm. Assoc. Sci. Ed. **43**, 79 (1954).
2. F. W. BENZ and J. P. LONG. J. Pharmacol. Exp. Ther. **166**, 225 (1969).
3. F. W. BENZ and J. P. LONG. J. Pharmacol. Exp. Ther. **168**, 315 (1969).
4. F. W. BENZ and J. P. LONG. J. Pharm. Pharmacol. **22**, 20 (1970).
5. H. O. HOUSE, B. A. TEFERTILLER, and C. G. PITT. J. Org. Chem. **31**, 1073 (1966).
6. J. MCKENNA, J. M. MCKENNA, A. TULLEY, and J. WHITE. J. Chem. Soc. 1711 (1965).
7. J. K. BECCONSALL, R. A. Y. JONES, and J. MCKENNA. J. Chem. Soc. 1726 (1965).
8. J. L. IMBACH, A. R. KATRITZKY, and R. A. KOLINSKI. J. Chem. Soc. B, 556 (1966).
9. A. T. BOTTINI and M. K. O'RELL. Tetrahedron Lett. 423 (1967).
10. D. R. BROWN, R. LYGO, J. MCKENNA, J. M. MCKENNA, and B. G. HUTLEY. J. Chem. Soc. B, 1184 (1967).
11. M. A. IORIO and S. CHIAVARELLI. Tetrahedron, **25**, 5235 (1969).
12. R. BRETTLE, D. R. BROWN, J. MCKENNA, and R. MASON. Chem. Commun. 339 (1969).
13. D. R. BROWN, B. G. HUTLEY, J. MCKENNA, and J. M. MCKENNA. Chem. Commun. 719 (1966).
14. D. R. BROWN, J. MCKENNA, J. M. MCKENNA, and J. M. STUART. Chem. Commun. 380 (1967).
15. R. A. Y. JONES, A. R. KATRITZKY, and P. G. MENTE. J. Chem. Soc. B, 1210 (1970).
16. Y. KAWAZOE, M. TSUDA, and M. OHNISHI. Chem. Pharm. Bull. (Tokyo), **15**, 51 (1967).
17. Y. KAWAZOE and M. TSUDA. Chem. Pharm. Bull. (Tokyo), **15**, 1405 (1967).
18. D. R. BROWN, J. MCKENNA, and J. M. MCKENNA. Chem. Commun. 186 (1969).
19. W. FEDELI, F. MAZZA, and A. VACIAGO. J. Chem. Soc. B, 1218 (1970).
20. J. MCKENNA. Topics in stereochemistry. Vol. 5. *Edited by* N. L. Allinger and E. L. Eliel. Wiley Interscience, New York. 1970. p. 275.
21. J. MCKENNA. Organic chemistry monograph series. Conformational analysis. Vol. 21. *Edited by* G. Chiurdoglu. Academic Press, New York. 1971. p. 165.
22. H. T. CLARKE, H. B. GILLESPIE, and S. Z. WEISSHAUS. J. Am. Chem. Soc. **55**, 4571 (1933).
23. Handbook of chemistry and physics. 52nd ed. The Chemical Rubber Co., Cleveland, Ohio. 1971. pp. C435–436.
24. D. D. LIBMAN, D. L. PAIN, and R. SLACK. J. Chem. Soc. 2305 (1952).
25. M. L. STEIN, R. OTTINGER, J. REISSE, and G. CHIURDOGLU. Tetrahedron Lett. 1521 (1968).
26. H. BOOTH and J. H. LITTLE. Tetrahedron, **23**, 291 (1967).
27. J. MCKENNA and J. M. MCKENNA. J. Chem. Soc. B, 644 (1969).
28. J. J. DELPEUCH and M. N. DESCHAMPS. Tetrahedron, **26**, 2723 (1970).
29. A. T. BOTTINI and M. K. O'RELL. Tetrahedron Lett. 429 (1967).
30. R. K. HILL and T. H. CHAN. Tetrahedron, **21**, 2015 (1965).
31. D. R. BROWN, J. MCKENNA, and J. M. MCKENNA. J. Chem. Soc. B, 1195 (1967).
32. R. E. LYLE and J. J. THOMAS. Tetrahedron Lett. 897 (1969).
33. R. E. LYLE, J. J. THOMAS, and D. A. WALSH. Organic chemistry monograph series. Conformational analysis. Vol. 21. *Edited by* G. Chiurdoglu. Academic Press, New York. 1970. p. 157.
34. A. F. CASY. PMR Spectroscopy in medicinal and biological chemistry. Academic Press, New York. 1971. pp. 153–154.
35. J. MCKENNA, J. M. MCKENNA, and J. WHITE. J. Chem. Soc. 1733 (1966).
36. A. F. CASY, A. H. BECKETT, and M. A. IORIO. Tetrahedron, **22**, 2751 (1966).
37. H. DORN, A. R. KATRITZKY, and M. R. NESBIT. J. Chem. Soc. B, 501 (1967).
38. R. P. DUKE, R. A. Y. JONES, and A. R. KATRITZKY. Chem. Commun. 455 (1972).
39. R. E. LYLE, E. W. SOUTHWICK, and J. J. KAMINSKI. J. Am. Chem. Soc. **94**, 1413 (1972).
40. H. A. SZYMANSKI and R. E. YELIN. NMR band handbook. Plenum, New York. 1968. pp. 194–195.

Can. J. Chem. Downloaded from www.nrcresearchpress.com by 210.87.254.40 on 09/05/12
For personal use only.

Paramagnetic Ring Current in Cyclooctatetraene: Evidence from ^{1}H Nuclear Magnetic Resonance Shifts of Fused Benzo Derivatives

G. W. BUCHANAN AND A. R. MCCARVILLE

Department of Chemistry, Carleton University, Ottawa, Canada K1S 5B6

Received June 27, 1972

The ^{1}H n.m.r. aromatic spectral regions of benzocyclooctatetraene and several related compounds have been analyzed using the LAOCOON 3 program. Assignments are based on the analysis of the ^{13}C satellite spectrum of the parent compound. Results are interpreted in terms of appreciable π-electron delocalization in the 8π-electron eight-membered rings giving rise to measurable paramagnetic anisotropic effects.

Les régions aromatiques des spectres r.m.n. du benzocyclooctatetraène et de plusieurs composés similaires ont été analysées utilisant un programme de LAOCOON 3. Les attributions sont basées sur l'analyse des satellites ^{13}C du spectre du composé fondamental. Les résultats sont interprétés en terme d'une délocalisation appréciable des huit électrons-π du cycle à huit donnant lieu à des effets paramagnétiques anisotropiques mesurables. [Traduit par le journal]

Can. J. Chem., **51**, 177 (1973)

Can. J. Chem. Downloaded from www.nrcresearchpress.com by 210.87.254.5 on 09/05/12
For personal use only.

Introduction

The presence or absence of a ring current in cyclooctatetraene has been the subject of considerable discussion in the literature in recent years. As a [4*n*] π-electron annulene, cyclooctatetraene would be expected to show a strong paramagnetic ring current if it were planar (1). Such a geometry is likely in the transition state for ring inversion of the molecule. Recently experimental evidence for the anti-aromaticity of planar 8π-electron systems has been reported using ring inversion results for substituted tetraphenylene (2) and benzocyclooctatetraene (3).

In its "tub"-like ground state conformation however, cyclooctatetraene is expected to exhibit little if any ring current because of the less effective overlap of 2pπ atomic orbitals. Dauben *et al.* (4), on the basis of diamagnetic susceptibility exhaltation measurements, concluded that no ring current was present. The reliability of these results for molecules exhibiting relatively small ring currents has been questioned by Anet and Schenck (5) in the light of ^{1}H n.m.r. solvent effect results using a series of hydrocarbons, from which the presence of a weak paramagnetic ring current in cyclooctatetraene has been suggested.

We present the results of a ^{1}H n.m.r. spectral examination of benzocyclooctatetraene, two isomeric benzocyclooctatrienes, and 1,2,5,6-dibenzocyclooctatetraene. These data and those for the related 1,2,4,5-dicyclooctatetraenobenzene are interpreted in terms of modest paramagnetic ring currents in the *non planar* eight-membered rings of the tetraenes.

Results and Discussion

Designations of protons in compounds **1**–**5** are shown below.

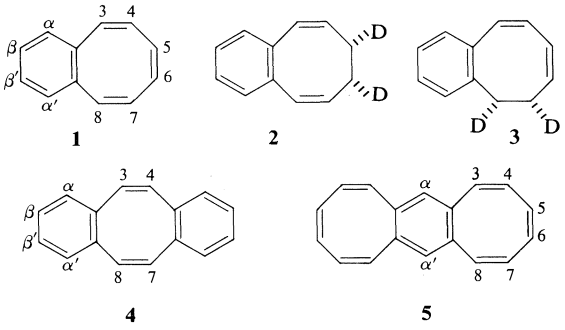

1 **2** **3**

4 **5**

To aid discussion of trends, the benzenoid proton data are presented in Tables 1 and 2. Those for the eight-membered ring protons are collected in Table 3.

(a) Benzenoid Protons

For compounds **1**, **2**, and **4**, the data in Tables 1 and 2 were obtained by iterative analysis of the AA′BB′ spin system due to the aromatic hydrogens using the LAOCOON 3 program. The shift in compound **5** is taken from the literature (6). The benzenoid region of the spectrum of compound **3** is almost identical to that of compound **2**, although the four benzenoid protons of **3** con-

TABLE 1. ^{1}H n.m.r. data for aromatic protons (CS_2 solutions)

Compound	Shift (Hz from TMS) ± 0.07*		Couplings (Hz) ± 0.07			
	H_α	H_β	$J_{\alpha\beta}$	$J_{\alpha\beta'}$	$J_{\alpha\alpha'}$	$J_{\beta\beta'}$
1†	678.34	703.66	7.67	1.29	0.41	7.24
1‡	678.96	704.28	7.67	1.29	0.41	7.24
2†	696.33	705.67	7.88	1.35	0.62	7.78
2‡	696.82	706.16	7.88	1.35	0.62	7.78
3†	(701.0)					
3‡	(701.5)					
4†	687.36	698.64	7.71	1.26	0.53	7.28
4‡	688.16	699.44	7.71	1.26	0.53	7.28

*At 100 MHz.
†0.2 *M* solution.
‡0.01 *M* solution.

TABLE 2. ^{1}H n.m.r. data for aromatic protons ($CDCl_3$ solutions)

Compound	Shift (Hz from TMS) ± 0.07*		Couplings (Hz) ± 0.07			
	H_α	H_β	$J_{\alpha\beta}$	$J_{\alpha\beta'}$	$J_{\alpha\alpha'}$	$J_{\beta\beta'}$
1†	690.84	715.16	7.65	1.28	0.42	7.20
1‡	686.74	711.06	7.65	1.28	0.42	7.20
2†	711.78	720.22	7.74	1.30	0.56	7.62
2‡	710.61	719.05	7.74	1.30	0.56	7.62
3†	(716.0)					
3‡	(714.0)					
4†	703.63	712.36	7.77	1.37	0.56	7.31
4‡	702.15	710.88	7.77	1.37	0.56	7.31
5§	659.0					

*At 100 MHz.
†0.2 *M* solution.
‡0.01 *M* solution.
§Unspecified concentration (6).

stitute an ABCD spin system. Since unambiguous assignments for this region of the spectrum of **3** are not possible, a detailed analysis was not performed.

For benzocyclooctatetraene **1**, a brief description of the 60 MHz ^{1}H spectrum has been published (7). No attempt, however, was made to assign *specifically* the benzenoid protons. In the present work, this has been accomplished using ^{13}C satellite spectral analysis (8) on a 0.2 *M* solution in CS_2. The α protons of **1** will give rise to a ^{13}C satellite spectrum showing *one* large coupling (to β) of 7.67 Hz, a smaller coupling (to β′) of 1.29 Hz and a ^5J coupling of 0.41 Hz (to α′). The β protons, however, will exhibit a pattern with *two* large couplings of 7.67 (to α) and 7.24 Hz (to β′). A further splitting of 1.29 Hz due to ^4J coupling with α′ will arise. Due to overlap with the resonances of the eight-membered ring protons, the low field ^{13}C satellite spectrum centered at δ 7.7 was recorded. The spectrum showed a quartet at higher field with couplings of 7.7 and 1.3 Hz. At lower field, the spectrum shown in Fig. 1 was recorded (81 scans using a C-1024 computer). Clearly this is due to the β proton, the observed pattern arising from two large and nearly equal couplings of *ca.* 7.5 Hz and one smaller coupling of *ca.* 1.3 Hz.

Thus in **1**, the aromatic protons *nearest* to the periphery of the eight-membered ring resonate at 0.25 p.p.m. *higher* field than the more distant β protons.

The ^{13}C satellite spectrum of **2** was uninterpretable due to overlap of the α and β satellite signals, since the shift difference between these protons is decreased relative to **1**. It is assumed that the higher field aromatic peaks are due to H_α and the lower field ones to H_β and assignments are made accordingly.

It is well known that proton shifts are influenced by (*a*) local diamagnetic effects, (*b*) solute–solvent interactions, (*c*) solute–solute association, (*d*)

Can. J. Chem. Downloaded from www.nrcresearchpress.com by 210.87.254.5 on 09/05/12
For personal use only.

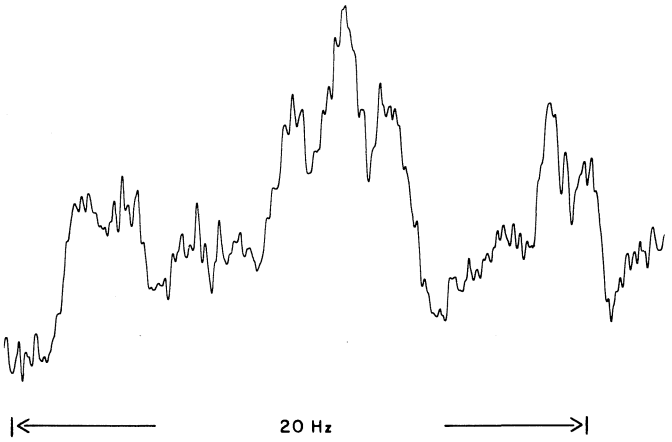

FIG. 1. ^{13}C satellite spectrum of low field aromatic protons of benzocyclooctatetraene (81 scans, 0.2 *M* in CS_2).

temperature, (*e*) other atom effects, and (*f*) ring current contributions. Effects from (*a*) are not likely to be significant in the molecules studied. To minimize the influence of (*b*) two relatively inert media, CS_2 and $CDCl_3$, have been employed. Spectra were obtained at concentrations of 0.2 and 0.01 *M* respectively to evaluate contributions from (*c*). A constant probe temperature was present throughout.

On examination of the benzenoid proton data in Tables 1 and 2, two main features are evident. Firstly, in all cases the centers of the aromatic spectral region for **2** and **3** are at lower field than in **1** by at least 0.1 p.p.m. Secondly, the shift differences between H_α and H_β in **2** are decreased to *ca.* 0.1 p.p.m., compared with *ca.* 0.25 p.p.m. in **1**. In CS_2 the α proton resonance of **2** shifts downfield by 18 Hz relative to **1** whereas the more remote β proton shifts only 2 Hz. In $CDCl_3$ these values are 21 and 5 Hz respectively for 0.2 *M* solutions. Although small concentration effects are observed, it is apparent that contributions from effects (*b*) and (*c*) are not dominant. Analyses of the aromatic proton resonances of **3** were not carried out but it is interesting to note that the center of the aromatic proton resonances is almost identical to that of **2** in all cases, and the spectra closely resemble those obtained for **2**.

We interpret these findings for compounds **1**, **2**, and **3** in terms of the presence of a small, but significant, paramagnetic ring current in the eight-membered ring of **1**. Using this model it is expected that the α benzenoid protons nearest the periphery of the 8π-electron ring of **1** will resonate at appreciably higher field than the more distant β protons (1). On reduction to either **2** or **3**, the 8π-electron character of the eight-membered ring is removed and cyclic delocalization of electrons can no longer exist in this system. As a result, the paramagnetic anisotropy of the eight-membered ring is lost and both H_α and H_β resonances move to lower field in **2** than in **1**. Due to the R^{-3} dependence of the anisotropy (9), the α protons nearer to the periphery of the eight-membered ring are affected to a much greater extent than the β hydrogens. The similarity in the spectra for **2** and **3** indicate that changes in the aromatic proton shifts on reduction of **1** are due to a change in the *overall* anisotropy of the eight-membered ring, rather than to a specific long-range anisotropy effect of a double bond.[1]

When two cyclooctatetraene moieties are fused to the benzene ring in compound **5**, the upfield shift of the benzenoid proton is even more pronounced. Relative to compound **1**, the additional cyclooctatetraene ring causes a shielding of *ca.* 0.30 p.p.m. in the α aromatic proton resonance.

For dibenzocyclooctatetraene (**4**) experimental and computer calculated spectra of the benzenoid

[1]A referee has suggested that the effects of the 5,6 and 7,8 double bonds may be equal due to a cancellation of the R^{-3} and cos $^2\theta$ terms in the anisotropy expression. From ring inversion results (3) it is deemed that the eight-membered ring of **2** has a tub-like ground state geometry and that of **3** is probably similar. Nearly identical J_{45} values for **1** and **3** support this conclusion. On this basis and from examination of molecular models a cancellation of R^{-3} and cos $^2\theta$ terms appears to be unlikely.

Can. J. Chem. Downloaded from www.nrcresearchpress.com by 210.87.254.5 on 09/05/12
For personal use only.

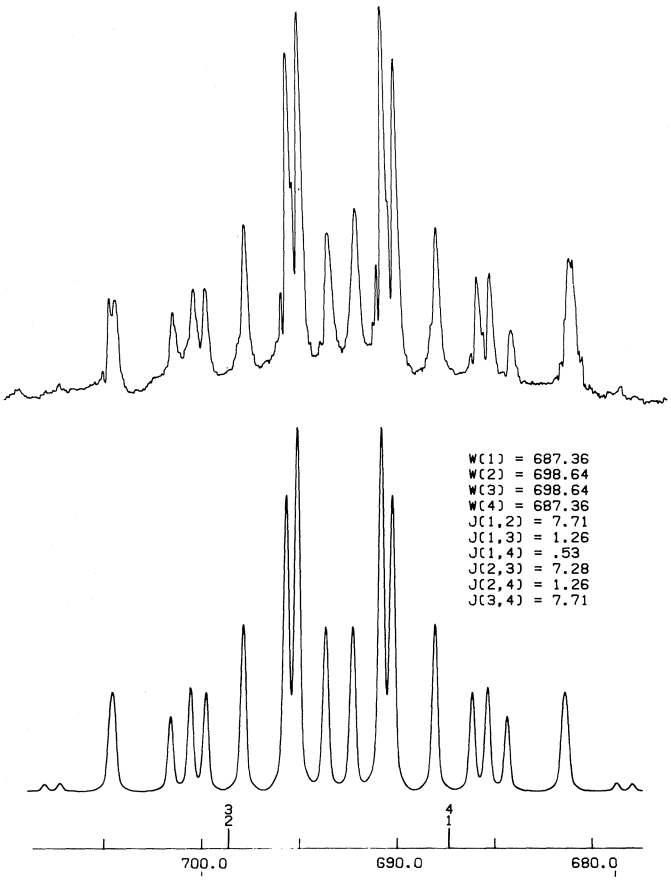

FIG. 2. Experimental and computer calculated spectrum of aromatic protons of 1,2,5,6-dibenzocyclooctatetraene (0.2 *M* in CS_2).

protons are shown in Fig. 2. Relative to benzocyclooctatetraene (**1**) the chemical shift difference between the α and β protons is decreased to *ca.* 0.1 p.p.m. and the α proton resonance is *deshielded* by *ca.* 0.1 p.p.m. These findings indicate that there has been a decrease in the paramagnetic anisotropy of the eight-membered ring on fusion of the second benzene function. Recently Figeys and Dralants (2) calculated the effect of successive addition of fused benzene rings on the intensity of the paramagnetic ring current in a *planar* 8π-electron ring of the complete series of benzocyclooctatetraenes. Benzene, with a diamagnetic ring current, was calculated to have a relative ring current intensity of +1.0; cyclooctatetraene, −0.88; benzocyclooctatetraene, −0.33; and *sym*-dibenzocyclooctatetraene was −0.16. Although the eight-membered rings are clearly not planar in their ground state conformation, the results of these molecular orbital calculations are consistent with our observed trends.

Finally, it is useful to compare the ^1H n.m.r. data herein with those for biphenylene (**6**) in which the existence of an induced paramagnetic ring current in the four-membered ring has been postulated by Figeys (10). Jones and Grant (11) have used Figeys' model to help explain ^{13}C shifts in this molecule. In biphenylene the α protons

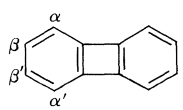

6

resonate at δ 6.70 and the β protons at δ 6.80. Both are considerably upfield from the benzene value of δ 7.27. Although quantitative comparisons are difficult, the α proton shift in biphenylene is comparable to those in **1**, **4**, and **5** and

Can. J. Chem. Downloaded from www.nrcresearchpress.com by 210.87.254.5 on 09/05/12
For personal use only.

TABLE 3. ^{1}H n.m.r. data for eight-membered ring protons

Compound	Solvent	Chemical shift (p.p.m. from TMS) ± 0.01						Couplings (Hz) ± 0.1			
		H_3	H_4	H_5	H_6	H_7	H_8	3,4	4,5	6,7	7,8
1	CS_2*	6.36	5.86	5.76	5.76	5.86	6.36	11.5	1.0	1.0	11.5
	CS_2†	6.37	5.87	5.77	5.77	5.87	6.37	11.5	1.0	1.0	11.5
	$CDCl_3$*	6.51	5.98	5.86	5.86	5.98	6.51	11.5	1.0	1.0	11.5
	$CDCl_3$†	6.47	5.94	5.82	5.82	5.94	6.47	11.5	1.0	1.0	11.5
2	CS_2*	6.38	5.78	2.26	2.26	5.78	6.38	11.5	5.1	5.1	11.5
	CS_2†	6.39	5.80	2.28	2.28	5.80	6.39	11.5	5.1	5.1	11.5
	$CDCl_3$*	6.52	5.91	2.30	2.30	5.91	6.52	11.9	5.2	5.2	11.9
	$CDCl_3$†	6.50	5.89	2.28	2.28	5.89	6.50	11.9	5.2	5.2	11.9
3	CS_2*	6.27	5.89	5.58	5.55	2.51	2.78	12.0	1.4		
	CS_2†	6.29	5.90	5.59	5.56	2.52	2.79	12.0	1.4		
	$CDCl_3$*	6.43	6.02	5.69	5.66	2.55	2.84	12.0	1.4		
	$CDCl_3$†	6.40	6.00	5.67	5.63	2.54	2.82	12.0	1.4		
4	CS_2*	6.59	6.59			6.59	6.59				
	CS_2†	6.60	6.60			6.60	6.60				
	$CDCl_3$*	6.74	6.74			6.74	6.74				
	$CDCl_3$†	6.71	6.71			6.71	6.71				
5	$CDCl_3$‡	6.49	6.03	5.84	5.84	6.03	6.49	12.0	1.0	1.0	12.0

*0.2 *M* solutions.
†0.01 *M* solutions.
‡Unspecified concentration (6).

support for the concept of an appreciable induced paramagnetic ring current in the eight-membered rings of these molecules is gained.

(b) Eight-membered Ring Protons

These data were obtained from a first order analysis of the spectra and are presented in Table 3. The *cis*-deuterated compounds **2** and **3** were employed since they were available from a previous study of ring inversion parameters (3). Small deuterium isotope effects on the ^{1}H shifts of **2** and **3** are no doubt present (12), but these will be omitted from the present considerations. A standard AB spectral analysis was carried out for H_3 and H_4 of compounds **1**, **2**, **3**, and **5**, and for H_7 and H_8 of compounds **1**, **2**, and **5**.

The chemical shift trends in **2** and **3** relative to **1** are as expected when a double bond is reduced. Olefinic protons closest to the site of reduction experience upfield shifts. In compound **4** the downfield shift for $H_{3,4,7,8}$ relative to H_3 and H_8 of **1** is interesting. If, as suggested earlier, there is a decreased paramagnetic ring current in the eight-membered ring of **4** compared to **1**, the "outer" protons of **4** will experience a smaller upfield shift than those of **1**. As these protons are closer to the periphery of the eight-membered ring than the benzenoid protons, the effects are more pronounced.

The main feature of the coupling constants worthy of note is the small magnitude of the J_{45} coupling in compounds **1**, **3**, and **5**. This is evidence that the eight-membered rings of the molecules are non planar. Similar conclusions for **1** and **5** have been drawn from u.v. spectral data (6).

Conclusions

The aromatic proton shieldings in compounds **1–5** are deemed indicative of appreciable electron delocalization in the 8π-electron eight-membered rings of compounds **1**, **4**, and **5**. Addition of fused benzene rings to cyclooctatetraene decreases the magnitude of the paramagnetic ring current. This finding for non planar systems parallels the results of LCAO MO calculations for planar cyclooctatetraene (2). Data for eight-membered ring protons are less useful for studying the anisotropy of the cyclooctatetraene moiety. A comparison of shifts in compounds **1** and **4**, however, supports conclusions based on benzenoid proton chemical shifts.

The feasibility of using ^{13}C shieldings as a probe for paramagnetic ring currents in these molecules is under investigation.

Experimental

Spectra

All proton spectra were recorded on a Varian XL-100-12 n.m.r. spectrometer at a probe temperature of

Can. J. Chem. Downloaded from www.nrcresearchpress.com by 210.87.254.5 on 09/05/12
For personal use only.

32.5 °C, using TMS as an internal standard. For the ^{13}C satellite spectra and the 0.01 *M* solutions, a Varian C-1024 time-averaging computer was employed.

Spectral analyses of the benzenoid protons were accomplished using the LAOCOON 3 program of Bothner-By and Castellano on the Carleton University XDS SIGMA 6 computer. Comparisons of observed spectra with those calculated were performed using a plotting routine in conjunction with a Cal-Comp plotter. The precision of the chemical shifts and coupling constants is judged to be ± 0.07 Hz. The spectra were fitted with an overall r.m.s. error of 0.066.

For the protons of the eight-membered rings, a first order analysis was employed. Shifts here are deemed accurate to ± 0.01 p.p.m. and couplings to ± 0.1 Hz.

Materials

Benzocyclooctatetraene was prepared by direct photolysis of benzobarrelene according to the published procedure (7).

A 40% yield of a mixture of 1,2-benzo-*cis*-7,8-dideuterio-1,3,5-cyclooctatriene (**3**) and 1,2-benzo-*cis*-5,6-dideuterio-1,3,7-cyclooctatriene (**2**) was obtained from the tetraene using deuterio diimide in methanol-*d*. The diimide was generated by dropwise addition of a solution of potassium ferricyanide in D_2O to hydrazine hydrate-d_6 over a period of 90 min. The products were separated from starting material by column chromatography (alumina, impregnated with 5% by weight $AgNO_3$ in H_2O) using 30–60° petroleum ether as solvent.

The 7,8-dideuterio triene was eluted first, as a colorless oil, n_D^{20} 1.5957, and low resolution mass spectral parent ion at *m/e* 158. Reported for the protio compound, n_D^{20} 1.5963 (13).

Further elution gave the isomeric 1,2-benzo-*cis*-5,6-dideuterio-1,3,7-cyclooctatriene, *m/e* 158, n_D^{20} 1.5991; reported for the protio analog, n_D^{20} 1.5987 (14).

The 1,2,5,6-dibenzocyclooctatetraene was purchased from the K&K Laboratories Inc., Plainsview, N.Y., and used without further purification.

We thank Dr. A. Fruchier for assistance with the LAOCOON 3 program and Professor F. A. L. Anet for a helpful discussion. The financial support of the National Research Council of Canada is gratefully recognized.

1. J. A. Pople and K. G. Untch. J. Am. Chem. Soc. **88**, 4811 (1966).
2. H. P. Figeys and A. Dralants. Tetrahedron Lett. 3901 (1971).
3. G. W. Buchanan. Tetrahedron Lett. 665 (1972).
4. H. J. Dauben, Jr., J. D. Wilson, and J. L. Laity. J. Am. Chem. Soc. **91**, 1991 (1969).
5. F. A. L. Anet and G. E. Schenck. J. Am. Chem. Soc. **93**, 556 (1971).
6. J. A. Elix, M. V. Sargent, and F. Sondheimer. J. Am. Chem. Soc. **92**, 962 (1970).
7. H. E. Zimmerman, R. S. Givens, and R. M. Pagni. J. Am. Chem. Soc. **90**, 6096 (1968).
8. L. M. Jackman and S. Sternhell. Applications of nuclear magnetic resonance spectroscopy in organic chemistry. 2nd Ed. Pergamon Press. 1969. p. 140.
9. J. A. Pople. J. Chem. Phys. **24**, 1111 (1956).
10. H. P. Figeys. Chem. Commun. 495 (1967); Angew. Chem. Int. Ed. **7**, 642 (1968).
11. A. J. Jones and D. M. Grant. Chem. Commun. 1670 (1968).
12. G. V. D. Tiers. J. Chem. Phys. **29**, 963 (1958).
13. G. Eglinton, W. McCrae, R. A. Raphael, and J. A. Zabkiewicz. J. Chem. Soc. C, 474 (1969).
14. G. Wittig, H. Eggers, and P. Duffner. Justus Liebigs Ann. **619**, 10 (1958).

Can. J. Chem. Downloaded from www.nrcresearchpress.com by 210.87.254.5 on 09/05/12
For personal use only.

A Study of the Decomposition of Sodium Azide using Differential Thermal Analysis

H. Potvin and M. H. Back

Chemistry Department, University of Ottawa, Ottawa, Canada K1N 6N5

Received June 27, 1972

Differential thermal analysis and thermogravimetric analysis of sodium azide diluted with sodium chloride both show one major peak followed by a second minor one. This is interpreted as indicating the occurrence of two distinct decomposition processes. The activation energy of the first, major process was 36 kcal/mol, which agrees with values reported previously from measurements of the rate of nitrogen evolution. Differential thermal analysis of sodium azide mixed with alumina was complicated by the presence of variable amounts of water adsorbed on the alumina. The presence of water was shown to have an inhibiting effect on the decomposition.

L'analyse thermique différentielle et l'analyse thermogravimétrique de l'azoture de sodium dilué dans du chlorure de sodium montrent toutes deux un pic majeur suivi d'un second pic mineur. Ceci a été interprété par l'existence de deux processus distincts de décomposition. L'énergie d'activation du premier processus majeur, est de 36 kcal/mol en accord avec les valeurs précédemment rapportées à partir des mesures sur la vitesse de dégagement de l'azote. L'analyse thermique différentielle de l'azoture de sodium mélangé à de l'alumine s'est vu compliquer par la présence de quantités variables d'eau adsorbée qui a un effet inhibiteur sur la décomposition. [Traduit par le journal]

Can. J. Chem., **51**, 183 (1973)

Can. J. Chem. Downloaded from www.nrcresearchpress.com by 210.87.254.6 on 09/05/12
For personal use only.

The kinetics of the thermal decomposition of metallic azides have been followed by measurements of the pressure change (1–4), by analysis of the products by mass spectrometry (5), and by measurement of light emission from the product nitrogen (6) and of chemi-electron emission (7). The reactions are complex and cannot be described by simple laws. A slow period of nucleation is followed by a rapid reaction as the metallic nuclei catalyze the decomposition. The rate-determining step in the decomposition is believed to be the transfer of an electron from the azide ion followed by combination of the azide radicals to give the product nitrogen and formation of neutral metal atoms (8).

In several studies of the decomposition of sodium azide reference has been made to the existence of two distinct decomposition processes. Mattler (9) and Lormeau (10) observed two activation energies from their measurements of the light emission from decomposing sodium azide. Secco (2) and Walker *et al.* (5) observed a white residue remaining after decomposition below 345 °C which was chemically identical to the original compound and which decomposed on heating to a higher temperature. In order to provide additional information which might relate to this phenomenon the decomposition of sodium azide was studied by differential thermal analysis (DTA) and by thermogravimetric analysis (TGA).

Reagent grade sodium azide (100–140 mesh[1]) was mixed with diluent, alumina or sodium chloride, in the proportion 1:10. Preliminary experiments were performed on a Fisher Differential Thermalyzer Model 260 using platinel thermocouples. Samples (100 mg) were weighed directly into quartz crucibles. A nitrogen flow of about 50 cc/min was passed over the sample holder. Most of the experiments were performed on a DuPont 900 Differential Thermal Analyzer using both the high temperature DuPont Cell and the standard DuPont Cell. A flow of nitrogen of about 1 l/min was maintained and the sample size was normally about 10 mg. The thermogravimetric analyses were obtained with a Cahn RH electrobalance. Pellets containing about 10 mg of sodium azide and about 500 mg of reference material were placed in the platinum crucible and the apparatus was evacuated.

With both diluents DTA gave a sharp exothermic peak followed by a small second peak which in some cases appeared as a tail on the larger peak. The difference in temperature between the two peaks was about 5°. Typical DTA curves are shown in Fig. 1. No indication of a phase transition occurring before decomposition was observed in any of the experiments. Use of

[1]A determination of the surface area by the BET method using nitrogen adsorption gave a value of 0.3 m^2/g.

TABLE 1. Temperature of the maximum rate of decomposition

DTA NaN_3:Al_2O_3			DTA NaN_3:NaCl		TGA NaN_3:NaCl		
						T_m (°C)	
Heating rate (°/min)	T_m (°C)	Peak height (arbitrary units)	Heating Rate (°/min)	T_m (°C)	Heating rate (°/min)	(*1*)	(*2*)
1	417	4.84	1	363	2	360	
3	419	4.92	2	370	5	372	379
3	388	1.00	2.5	373	5	370	376
5	393	1.00	3	366	10	386	403
5	380	0.90	3	370	10	388	403
5	398	1.70	5	398	20	414	
5	421	5.40	8	395			
5	426	7.20	10	392			
10	424	9.50	10	394			
10	424	8.6	10	388			
10	421	5.6	20	412			
10	402	2.4	20	420			
10	407	2.2					
10	389	1.70					
10	431	15.0					
20	435	off scale					
20	425	7.8					
20	421	4.8					
20	414	4.3					

helium or hydrogen instead of nitrogen gave similar results.

A series of experiments with different heating rates was performed with the DuPont apparatus. The results are summarized in Table 1. Sample sizes between 10 and 50 mg gave identical results. According to the method developed by Kissinger (11) the temperature at the maximum point of deflection will be a function of the heating rate for a reaction which has a finite activation energy. Following this method, log (Φ/T_m^2) was plotted against $1/T_m$, where Φ is the heating rate and T_m is the temperature at the maximum deflection, for the experiments using sodium chloride as diluent. From the slope of this curve a value of 36 ± 2 kcal/mol was calculated for the activation energy. A summary of values obtained previously is given in Table 2. It may be concluded that the rate measured by DTA corresponds to the rate measured by nitrogen evolution during the accelerated region and by chemiluminescence. Furthermore, the method for obtaining an activation energy from DTA appears to be valid even for a complex decomposition process involving an induction period.

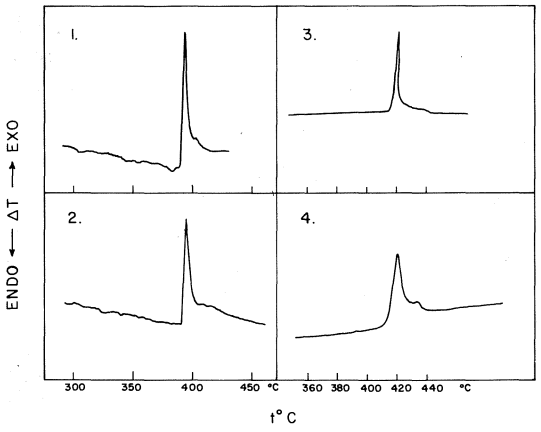

FIG. 1. Typical DTA curves for sodium azide: *1*, *2*, NaN_3:NaCl, 1:10; *3*, *4*, NaN_3:Al_2O_3, 1:10.

In the experiments using alumina as diluent the temperature of maximum deflection was quite independent of the heating rate. Instead the temperature at the maximum appeared to be a function of the peak height, increasing with increasing peak height. The explanation for this behavior was provided by the TGA of the alumina by itself which showed a gradual weight loss over the temperature range 70–370 °C. This can only indicate the gradual desorption of water, in spite of the fact that the alumina had been heated at

Can. J. Chem. Downloaded from www.nrcresearchpress.com by 210.87.254.6 on 09/05/12
For personal use only.

TABLE 2. Activation energies for the decomposition of sodium azide

Temperature range (°C)	E (kcal/mol)	Method	Reference
240–275	34	N_2 evolution	1
280–390	39	N_2 evolution	3
330–370	36.6	N_2 evolution	4
345–365	50	N_2 evolution (slow stage)	2
340–405	36	Luminescence	7
315–362	50	Luminescence	10
362–402	28		
	36	DTA	This work

1000 °C for 6 h and stored in a desiccator. A comparison of the TGA of alumina itself and of the alumina–azide mixtures showed that decomposition of the azide did not occur until practically all the water was desorbed from the alumina. It is known that water inhibits the decomposition of the azide by impeding the formation of nuclei of metallic sodium (4). Thus variation in the temperature of the maximum deflection may be the result of varying amounts of water which may be taken up by the alumina during the process of preparing the sample. This accounts for the observation that the temperature of decomposition was not dependent on the heating rate.

Furthermore, some experiments were performed in which the temperature was held constant after reaching a certain value in the range 350–400 °C. Decomposition was never observed during the period of constant temperature although the sample was maintained at a temperature as high as 400 °C for 2 h. When the temperature was subsequently raised decomposition occurred at the usual temperature. These results show the strongly inhibiting effect of water.

Experiments using TGA were performed at heating rates of 2, 5, 10, and 20°/min. At heating rates of 5 and 10°/min the curves of weight loss against temperature suggest the occurrence of two processes. Figure 2 shows the weight loss as a function of temperature for a heating rate of 10°/min and the differential weight loss calculated from it. Duplicate determinations showed good reproducibility. The separation between the peaks was 6° at a heating rate of 5°/min and 16° for a heating rate of 10°/min. At heating rates of 2 and 20°/min only one maximum in the rate was observed. At 2°/min the rate of weight loss was so fast that the differential curve could not be measured whereas at 20°/min the differential curve was a broad peak.

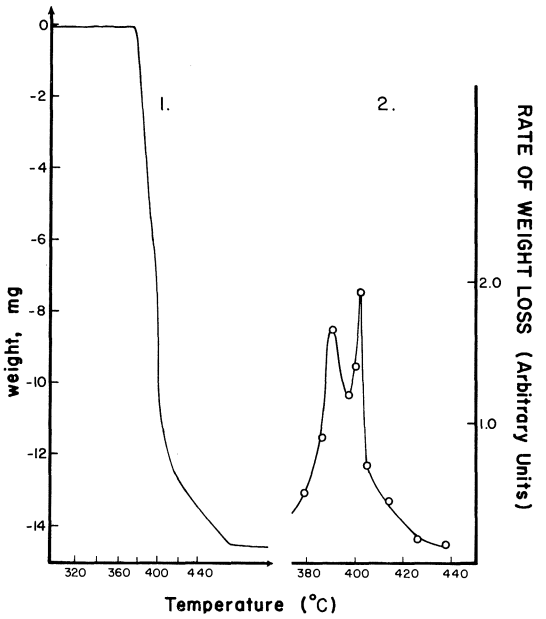

FIG. 2. Typical TGA of NaN_3:NaCl mixture: (*1*) weight as a function of temperature; (*2*) rate of weight loss as a function of temperature.

The results of both the DTA and TGA suggest the occurrence of two processes during the decomposition. The differential curves, however, do not show identical characteristics. In the DTA the first peak is large and sharp and the second small and broad while in the TGA the first peak is the smaller. The separation of the peaks did not change significantly with heating rate in the DTA while a large change was observed with the TGA. In spite of these differences it seems reasonable to conclude that the first peaks of each analysis are a measure of the same process. In each case the first peak corresponds to over

Can. J. Chem. Downloaded from www.nrcresearchpress.com by 210.87.254.6 on 09/05/12
For personal use only.

half the loss of the sample and the second peak is a minor process. The relative rates of the two processes need not correspond exactly since one analysis measures heat released while the reaction takes place in an atmosphere of nitrogen and the other measures weight loss under vacuum. In summary, the present results provide some new evidence for the possibility of the occurrence of two distinct processes in the decomposition of sodium azide.

The authors would like to thank Dr. V. S. Ramachandran of the National Research Council of Canada for the use of his DuPont 900 Differential Thermal Analyzer and for many helpful discussions. Thanks are also due to Mr. G. M. Polomark for his capable assistance with the experiments and to Mr. R. Myers for his measurement of the surface area of the sodium azide.

1. W. E. Garner and D. J. B. Marke. J. Chem. Soc. 657 (1936).
2. E. A. Secco. J. Phys. Chem. Solids, **24**, 469 (1963).
3. P. W. M. Jacobs and A. R. Tariq Kureishy. J. Chem. Soc. 4718 (1964).
4. K. Torkar, O. Heiss, A. Isenberg, and G. Herzog. Int. Symp. React. Solids, Munich, 1964. (1965). p. 519.
5. R. F. Walker, N. Gane, and F. P. Bowden. Proc. Royal Soc. **A294**, 417 (1966).
6. R. Audubert and G. Calmar. J. Chim. Phys. **54**, 324 (1957).
7. G. D. Singer and H. J. Mueller. Nature, **207**, 1073 (1965).
8. P. Gray. Q. Rev. **17**, 441 (1963).
9. J. Mattler. J. Chim. Phys. **35**, 277 (1938).
10. S. Lormeau. C. R. **226**, 247 (1948).
11. H. E. Kissinger. Anal. Chem. **29**, 1702 (1957).

Can. J. Chem. Downloaded from www.nrcresearchpress.com by 210.87.254.6 on 09/05/12
For personal use only.

Volumes and Heat Capacities of Transfer of Tetraalkylammonium Bromides from Water to Aqueous Urea Solutions at 25 °C

P. R. PHILIP, J. E. DESNOYERS,[1] AND A. HADE

Department of Chemistry, Université de Sherbrooke, Sherbrooke, and Department of Chemistry, Université du Québec, Montréal, Québec

Received July 13, 1972

The apparent molal volumes and heat capacities of tetraalkylammonium bromides were measured in urea–water mixtures at 25 °C. The volumes and heat capacities of transfer from water to urea–water mixtures indicate that structural hydration effects are smaller in urea–water mixtures than in water. Also a comparison with the corresponding transfer functions from H_2O to D_2O suggests that urea–water mixtures are less structured than pure water.

Les capacités calorifiques et volumes apparents molaires des bromures de tetraalkylammonium ont été mesurés dans des mélanges eau–urée à 25 °C. Les volumes et capacités calorifiques de transfert de l'eau aux mélanges eau–urée indiquent que les effets structuraux d'hydratation sont moins prononcés dans les mélanges eau–urée que dans l'eau. Egalement, une comparaison avec les fonctions de transfert correspondantes de H_2O à D_2O suggère que les mélanges eau–urée sont moins structurés que l'eau pure.

Can. J. Chem., **51**, 187 (1973)

Can. J. Chem. Downloaded from www.nrcresearchpress.com by 210.87.254.105 on 09/05/12
For personal use only.

Introduction

The importance of urea as a denaturant has led to numerous studies of its aqueous solutions; as a result, most of its physicochemical properties are now known: solubility (1), dielectric constants (2), densities (3), compressibilities (4), viscosities (5), diffusion (6–8), ultrasonic velocity and absorption (9), i.r. (10) and raman (11) spectra, n.m.r. (12), activity and osmotic coefficients (13, 14), heats of solution (15), heat capacities (16), and heats of dilution (17). The ternary systems, where an electrolyte or nonelectrolyte is added to the aqueous urea solution, have also been investigated thoroughly (18–25). Despite all these studies, the nature of the interactions between urea and water is still not fully understood. While urea usually appears as an overall structure breaker in ternary systems, there are some cases where the structural contribution is not clear; for example, the solubility of methane decreases in 7 *M* urea while that of ethane, propane, and butane is found to increase in the presence of urea (18).

The models suggested to explain the behavior of aqueous urea can be classified in four broad groups; urea is considered a structure breaker in a way similar to that of ions (26, 11), it is assumed to associate in water (27), Frank and Franks (28) prefer to say that it dissolves preferentially in the unbonded fraction of water molecules, thus shifting the equilibrium of water from bonded to unbonded molecules as a statistical structure breaker, and Abu-Hamdiyyah (29) suggests the formation of mixed clusters between urea and water. None of these models appears at the moment entirely satisfactory (30) and often all of these models can account qualitatively for the experimental observations.

It was shown recently that the heat capacities (31) and volumes (32) of transfer of tetraalkylammonium bromides from H_2O to D_2O were sensitive functions for the study of overall structural hydration effects. Since the net structural influence of tetraalkylammonium bromides on water is now well-established (31, 33, 34), it was felt that a similar study of the heat capacities and volumes of transfer of these salts from water to aqueous urea might indirectly throw some light on the nature of the urea–water interactions.

Experimental

The tetraalkylammonium bromides (Eastman Kodak) were purified as described elsewhere (35), and urea (Fisher Certified) was used as such after drying under vacuum at 60 °C for 48 h. All solutions were prepared by weight with water redistilled from an alkaline permanganate solution. The solutions were prepared fresh and used the same day to prevent any decomposition. All salt concentrations were expressed in aquamolalities (*m*), *i.e.* in number of

[1]To whom correspondence should be addressed.

Can. J. Chem. Downloaded from www.nrcresearchpress.com by 210.87.254.105 on 09/05/12
For personal use only.

moles of salt per 55.51 moles of mixed solvent (urea + water). The urea concentration is expressed in molalities (*m*).

The densities were measured with an Anton Paar digital Densitymeter (Model DMA02C) and the heat capacities with a flow microcalorimeter (16). A comparison with densities obtained in pure water by a buoyancy method (36) indicates that the present densities are reliable to $\pm 10^{-5}$ g cm^{-3} or better. Differences in heat capacities are measured to $\pm 0.5\%$ and the overall sensitivity of the flow microcalorimeter is 7×10^{-5} J K^{-1} g^{-1}.

Results

The densities and heat capacities were determined[2] at 25 °C for the following systems: *1*, Me_4NBr and nBu_4NBr in the concentration range 0.04 to 0.5 *m* at a fixed urea concentration of 2.955 *m*; *2*, Me_4NBr and nBu_4NBr at a fixed aquamolality of 0.05 *m* in a variable urea concentration (0.1 to 3 *m*); *3*, Et_4NBr and nPr_4NBr at 0.1 *m* salt concentration and 2.952 *m* urea concentration.

The apparent molal volumes and heat capacities were calculated from the relations:

$$[1] \qquad \phi_v = \frac{M}{d} + \frac{W_{55.51}(d_0 - d)}{dd_0m}$$

$$[2] \qquad \phi_c = Mc_p - \frac{W_{55.51}(c_{p0} - c_p)}{m}$$

where M is the salt molecular weight, $W_{55.51}$ is the weight of 55.51 moles of mixed solvent, m the salt aquamolality, c_{p0}, c_p, d_0, and d, the heat capacities (J K^{-1} g^{-1}) and densities (g cm^{-3}) of the mixed solvent and ternary solutions. The ϕ_c and ϕ_v of Me_4NBr and nBu_4NBr in pure water (16, 36) and in 2.955 *m* urea are plotted against the salt aquamolality in Figs. 1 to 3. The transfer functions $\Delta\phi_{ctr} = \phi_c$ (H_2O + urea) $- \phi_c(H_2O)$ and $\Delta\phi_{vtr} = \phi_v(H_2O$ + urea$) - \phi_v(H_2O)$ were plotted for Me_4NBr and nBu_4NBr at 0.05 *m* against the urea concentration in Figs. 4 and 5. Finally the $\Delta\phi_{ctr}$ and $\Delta\phi_{vtr}$ of the four tetraalkylammonium bromides at 0.1 *m* salt concentration and 2.95 urea concentration were plotted against the number of carbon atoms per chain on Fig. 6.

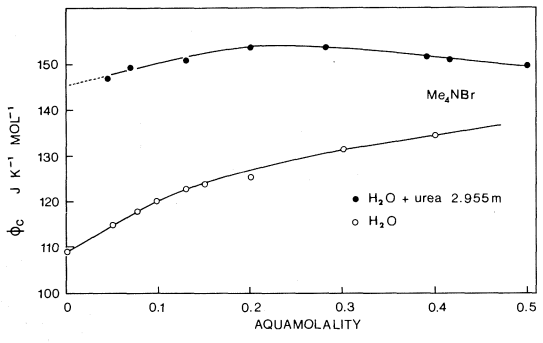

FIG. 1. Apparent molal heat capacities of Me_4NBr in water and mixtures (2.955 *m*) at 25 °C.

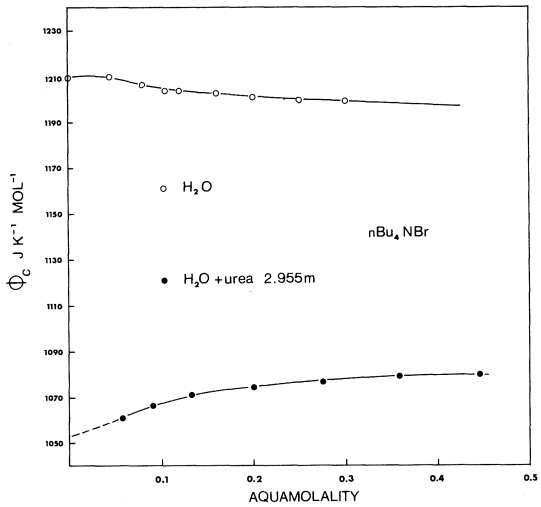

FIG. 2. Apparent molal heat capacities of nBu_4NBr in water and in urea–water mixtures (2.955 *m*) at 25 °C.

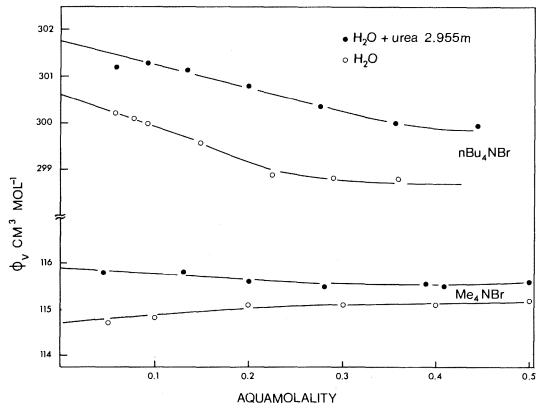

FIG. 3. Apparent molal volumes of Me_4NBr and nBu_4NBr in water and in urea–water mixtures (2.955 *m*) at 25 °C.

Discussion

The dielectric properties of water (37) and of aqueous urea solutions (2) are quite similar; although the dipole moments of water and urea

[2]Complete set of actual data is available, at a nominal charge, from the Depository of Unpublished Data, National Science Library, National Research Council of Canada, Ottawa, Canada, K1A 0S2.

Can. J. Chem. Downloaded from www.nrcresearchpress.com by 210.87.254.105 on 09/05/12
For personal use only.

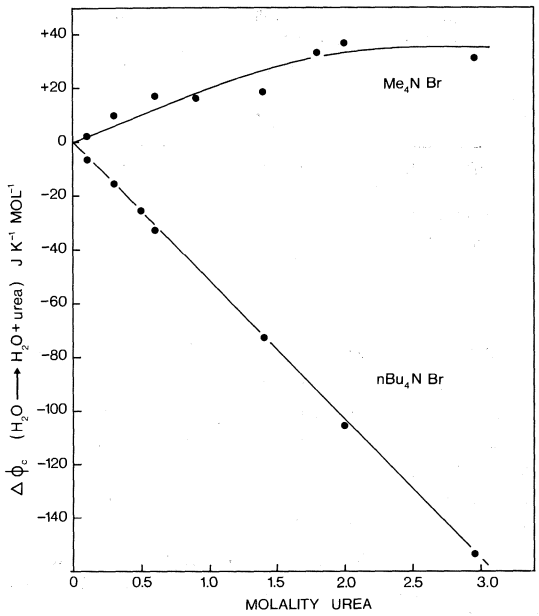

FIG. 4. Apparent molal heat capacities of transfer of 0.05 *m* Me_4NBr and *n*Bu_4NBr from water to urea–water mixtures at 25 °C.

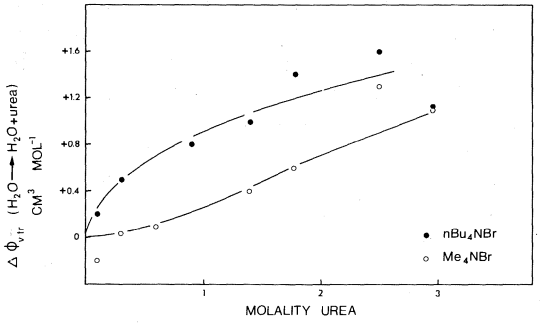

FIG. 5. Apparent molal volumes of transfer of 0.05 *m* Me_4NBr and *n*Bu_4NBr from water to urea–water mixtures at 25 °C.

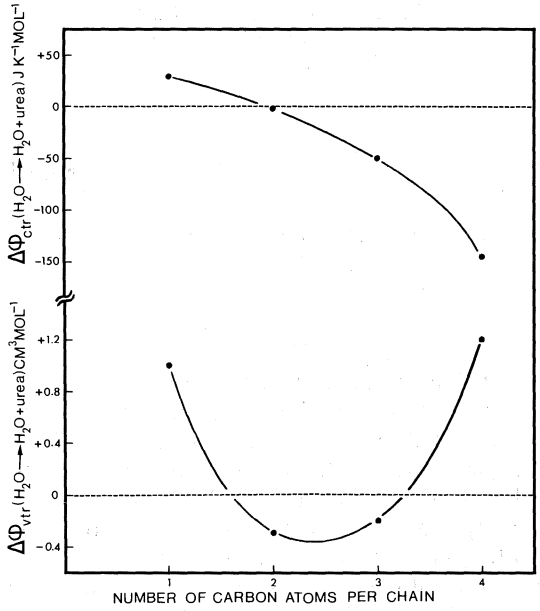

FIG. 6. Apparent molal volumes and heat capacities of transfer of 0.1 *m* tetraalkylammonium bromides from water to urea–water mixtures (2.95 *m*) at 25 °C.

are respectively 1.83 and 4.56 Debyes, with large ions like the tetraalkylammonium and the bromide ions, the electrostatic effects are sufficiently weak that we can probably ignore any specific (coulombic) solvation effects in urea water mixtures. Therefore, as a first approximation, we can assume that all electrostatic ion–solvent interactions would be equal in both water and mixed solvent, and that the transfer functions primarily reflect structural changes.

Heat Capacities

Me_4NBr and *n*Bu_4NBr are usually assumed to be respectively an overall structure breaker and a structure maker in water (33, 34). Also, an abnormally large ϕ_c in comparison with the intrinsic heat capacity is associated with structure making and a small ϕ_c with structure breaking (31). The values of ϕ_c in urea 2.955 *m* for Me_4NBr (Fig. 1) and *n*Bu_4NBr (Fig. 2) are closer to the intrinsic heat capacities of the solutes than the corresponding ϕ_c in water, indicating that the structural changes caused by the salts are less important in urea–water mixtures than in pure water. Further evidence for this comes from a comparison with the $\Delta\phi_{ctr}{}^0(H_2O \rightarrow D_2O)$ of the same salts as shown in Table 1.

There seems to be a direct relationship between the degree of structure of the medium and the importance of the structural interactions. For example, D_2O appears to be more structured than H_2O and structural changes caused by solutes are more pronounced in D_2O (*cf.* ref. 31). If this is correct, it is justified to claim that, since $\Delta\phi_{ctr}{}^0(H_2O \rightarrow H_2O$ + urea 2.955 *m*) is opposite that of $\Delta\phi_{ctr}{}^0(H_2O \rightarrow D_2O)$, the urea solution is less structured than pure water.

The present heat capacity data are in agreement with the excess enthalpies and entropies of Me_4NBr and *n*Bu_4NBr in urea–water mixtures (21). The $\Delta H_{tr}{}^0(H_2O \rightarrow H_2O$ + urea) and $\Delta S_{tr}{}^0$-$(H_2O \rightarrow H_2O$ + urea) are opposite in sign to

TABLE 1. Comparison of the standard volumes and heat capacities of transfer of Me_4NBr and nBu_4NBr from H_2O to D_2O and H_2O + urea 2.955 *m* at 25 °C

	$\Delta\phi_{vtr}^0$ ($cm^3\ mol^{-1}$)		$\Delta\phi_{ctr}^0$ ($J\ K^{-1}\ mol^{-1}$)	
	Me_4NBr	nBu_4NBr	Me_4NBr	nBu_4NBr
$H_2O \rightarrow D_2O$	−0.21*	+1.31*	−14†	+37†
$H_2O \rightarrow H_2O$ + urea (2.955 *m*)	+1.5	+1.1	+37	−153

*Reference 32.
†Reference 31.

those of $\Delta\phi_{ctr}(H_2O \rightarrow H_2O$ + urea) as we would expect from structural interaction models (38).

The effect of changing the urea concentration is illustrated in Fig. 4; $\Delta\phi_{ctr}(H_2O \rightarrow H_2O$ + urea) increases continuously in absolute magnitude and Sarma and Ahluwalia (25) have shown recently that the observed linearity in the case of nBu_4NBr extends to 10 *m* in urea, indicating that it is still possible to promote some structure even in these highly concentrated urea solutions. On the other hand, it seems from Fig. 4 that in the case of Me_4NBr $\Delta\phi_{ctr}(H_2O \rightarrow H_2O$ + urea) levels off at the higher urea concentrations. This could be interpreted in terms of a saturation effect; beyond a certain urea concentration Me_4NBr has no more structure to break.

The dependence of $\Delta\phi_{ctr}(H_2O \rightarrow H_2O$ + urea 2.95 *m*) at 0.1 aquamolality of salt, on the cation chain length of the tetraalkylammonium bromides (Fig. 6) can be compared with $\Delta\phi_{ctr}^0(H_2O \rightarrow D_2O)$ (31, 32) since the concentration dependence of $\Delta\phi_{ctr}(H_2O \rightarrow H_2O$ + urea 2.95 *m*) is small (*cf.* Figs. 1 and 2). As with the $H_2O \rightarrow D_2O$ transfer, Et_4NBr is a borderline case indicating that this salt is close to having no overall structural influence in aqueous media.

Volumes

The standard partial or apparent molal volumes of ions in water can be considered to arise from four main contributions

$$\phi_v^0 = \bar{V}(\text{in}) + \bar{V}(\text{el}) + \bar{V}(\text{struct}) + \bar{V}(\text{cav})$$

The intrinsic volume $\bar{V}$(in) disappears when transfer functions are considered. The electrostatic contribution $\bar{V}$(el), which gives rise to electrostriction, is probably small with R_4N^+ and Br^- ions and negligible when the transfer functions are considered. The structural contribution $\bar{V}$(struct) will be negative in the presence of structure breakers (Me_4N^+, Br^-) and positive with structure makers (nBu_4N^+) (38). However, the cavity effect $\bar{V}$(cav), which is intimately related to hydrophobic hydration, is negative since hydrophobic molecules or groups tend to be fitted, at least partially, in water cavities or cage-like structures (quasichlathrate environment) (34, 39, 40). There is a compensation between $\bar{V}$(cav) and $\bar{V}$(struct), but $\bar{V}$(cav) is usually assumed to be the leading term responsible for the large negative apparent molal compressibility ϕ_K and the large positive apparent molal expansitivity ϕ_E of nBu_4NBr (38); ϕ_K and ϕ_E reflect mostly the pressure and temperature dependence of the two terms $\bar{V}$(struct) + $\bar{V}$(cav) in the case of hydrophobic solutes. Going from a more structured medium (H_2O) to a less structured medium (H_2O + urea) is equivalent qualitatively to the effect of increasing the temperature on ϕ_v^0. Therefore, as expected from the sign of expansitivities, $\Delta\phi_{vtr}$ of Me_4NBr is positive ($\bar{V}$(struct) <0 and $\bar{V}$(cav) $\simeq 0$) and $\Delta\phi_{vtr}$ of nBu_4NBr is also positive ($\bar{V}$(cav) < 0) as shown in Figs. 3 and 5. The intermediate salts, Et_4NBr and nPr_4NBr pass through a minimum (Fig. 6) which would be close to zero if standard $\Delta\phi_{vtr}^0$ were plotted. However, if the $\Delta\phi_{vtr}(H_2O \rightarrow H_2O$ + urea) can be so explained, then the $\Delta\phi_{vtr}^0(H_2O \rightarrow D_2O)$ appears anomalous since its sign changes when going from Me_4NBr to nBu_4NBr. The explanation offered for this (31) was that, although $\bar{V}$(cav) was probably larger than $\bar{V}$(struct) in both H_2O and D_2O, it was probably about the same in both solvents. Thus, in this particular case, the transfer functions reflect mostly $\bar{V}$(struct).

The present results for $\Delta\phi_{vtr}(H_2O \rightarrow H_2O$ + urea) and $\Delta\phi_{ctr}(H_2O \rightarrow H_2O$ + urea) indicate that the water–urea mixture is less structured than pure water in so far as structural changes caused by solutes are smaller in urea–water mixtures than in water. In addition, the sign and magnitude of $\Delta\phi_{ctr}$ and $\Delta\phi_{vtr}$ of nBu_4NBr indicate that urea participates with, or at least affects significantly,

Can. J. Chem. Downloaded from www.nrcresearchpress.com by 210.87.254.105 on 09/05/12
For personal use only.

the chlathrate-type hydration near the hydrophobic ions. However, we cannot draw much information on the discrete nature of the urea–water interactions or on the origin of the structural interactions in urea–water mixtures. Still, the present data should be useful as a further piece of evidence that must be accommodated in any successful model for urea–water mixtures.

Excess Heat Capacities and Volumes

The value of the Debye-Hückel limiting slope for electrolytes in urea–water mixture is not known for ϕ_v or ϕ_c. Therefore, a discussion of structural solute–solute interactions (41) is more difficult. However, since the dielectric properties of urea solution are close to those of water (37), we can assume that, as a first approximation, the limiting Debye–Hückel slopes are about equal and that a comparison of the concentration dependence of ϕ_c and ϕ_v for electrolytes in water and urea–water mixtures will reflect primarily the structural ion–ion interactions. It was shown that structural solute–solute interactions are larger in D_2O than in H_2O (31); for the same reasons they should be smaller in urea–water mixtures. The concentration dependences on Figs. 1, 2, and 3 indicate a negative $\Delta\phi_{ctr}^{ex}(Me_4NBr)$, a positive $\Delta\phi_{ctr}^{ex}(nBu_4NBr)$, a negative $\Delta\phi_{vtr}^{ex}(Me_4NBr)$, and a positive $\Delta\phi_{vtr}^{ex}(nBu_4NBr)$ from H_2O to H_2O + urea mixtures in good agreement with the predictions of structural models (31, 38, 41).

We would like to thank the Defence Research Board of Canada (Grant No. 5405) and the National Research Council of Canada for its financial support.

1. F. W. Miller and H. R. Dittmar. J. Am. Chem. Soc. **56**, 848 (1934).
2. J. Wyman. J. Am. Chem. Soc. **55**, 4116 (1933).
3. F. T. Gucker, F. W. Gage, and C. E. Moser. J. Am. Chem. Soc. **60**, 2582 (1938).
4. E. P. Perman and W. D. Urry. Proc. Roy. Soc. London, **A126**, 44 (1929).
5. G. Jones and S. K. Talley. J. Am. Chem. Soc. **55**, 604 (1933).
6. L. J. Gostings and D. F. Akeley. J. Am. Chem. Soc. **74**, 2058 (1952).
7. I. V. Matyash, A. I. Toryanik, and V. V. Kisel'nik. J. Struct. Chem. **8**, 371 (1967).
8. J. G. Albright and R. Mills. J. Phys. Chem. **69**, 3120 (1965).
9. D. V. Beauregard and R. E. Barrett. J. Chem. Phys. **49**, 5241 (1968).
10. G. Barone, E. Rizzo, and V. Vitagliano. J. Phys. Chem. **74**, 2230 (1970).
11. G. E. Walrafen. J. Chem. Phys. **44**, 3726 (1966).
12. S. Subramanian, D. Balasubramanian, and J. C. Ahluwalia. J. Phys. Chem. **73**, 266 (1969); R. L. Vold, E. S. Daniel, and S. O. Chan. J. Am. Chem. Soc. **92**, 6771 (1970).
13. V. E. Bower and R. A. Robinson. J. Phys. Chem. **67**, 1524 (1963).
14. O. D. Bonner and W. H. Breazeale. J. Chem. Eng. D, **10**, 325 (1965).
15. S. Subramanian, T. S. Sarma, D. Balasubramanian, and J. C. Ahluwalia. J. Phys. Chem. **75**, 815 (1971).
16. P. Picker, P.-A. Leduc, P. R. Philip, and J. E. Desnoyers. J. Chem. Thermodyn. **3**, 631 (1971).
17. E. P. Egan and B. B. Luff. J. Chem. Eng. D, **11**, 192 (1966).
18. D. B. Wetlaufer, S. K. Malik, L. Stoller, and R. L. Coffin. J. Am. Chem. Soc. **86**, 508 (1964).
19. J. H. Stern and J. D. Kulluk. J. Phys. Chem. **73**, 2795 (1969).
20. W.-Y. Wen and C. L. Chen. J. Phys. Chem. **73**, 3249 (1969).
21. R. B. Cassel and W.-Y. Wen. J. Phys. Chem. **76**, 1369 (1972).
22. W. A. Hargraves and G. C. Kresheck. J. Phys. Chem. **73**, 3249 (1969).
23. G. A. Vidulich, J. R. Andrade, P. P. Blanchette, and T. J. Gilligan. J. Phys. Chem. **73**, 1621 (1969).
24. J. C. MacDonald and J. J. Guerrera. J. Chem. Eng. D, **15**, 546 (1970).
25. T. S. Sarma and J. C. Ahluwalia. J. Phys. Chem. **76**, 1366 (1972).
26. J. A. Rupley. J. Phys. Chem. **68**, 2002 (1964).
27. G. C. Kresheck and H. A. Scheraga. J. Phys. Chem. **69**, 1704 (1965).
28. H. S. Frank and F. Franks. J. Chem. Phys. **48**, 4746 (1968).
29. M. Abu-Hamdiyyah. J. Phys. Chem. **69**, 2720 (1965).
30. A. Holtzer and M. F. Emerson. J. Phys. Chem. **73**, 26 (1969).
31. P. R. Philip and J. E. Desnoyers. J. Solution Chem. In press.
32. B. E. Conway and L. H. Laliberté. Trans. Faraday Soc. **66**, 3032 (1970).
33. J. E. Desnoyers and G. Perron. J. Solution Chem. **1**, 199 (1972).
34. W.-Y. Wen. *In* Water and aqueous solutions. *Edited by* R. A. Horne. Wiley, New York. 1972. Chap. 15.
35. B. E. Conway, R. E. Verrall, and J. E. Desnoyers. Trans. Faraday Soc. **62**, 2738 (1966).
36. G. Perron and J. E. Desnoyers. J. Chem. Eng. D, **17**, 136 (1972).
37. C. G. Malmberg and A. A. Maryott. J. Res. Natl. Bur. Std. **56**, 1 (1956); C. G. Malmberg. J. Res. Natl. Bur. Std. **60**, 609 (1958).
38. J. E. Desnoyers. *In* Electrostatic interactions and the structure of water. XVè Conseil International de Chimie Solvay, Brussels. 1972. In press.
39. J. E. Desnoyers and M. Arel. Can. J. Chem. **45**, 359 (1967).
40. M. E. Friedman and H. A. Scheraga. J. Phys. Chem. **69**, 3795 (1965).
41. J. E. Desnoyers, M. Arel, G. Perron, and C. Jolicoeur. J. Phys. Chem. **73**, 3346 (1969).

Can. J. Chem. Downloaded from www.nrcresearchpress.com by 210.87.254.105 on 09/05/12
For personal use only.

1-Propanethiol as a Radical Scavenger in the γ-Radiolysis of Liquid Cyclohexane

JOSEPH ESSER AND JOHN A. STONE

Department of Chemistry, Queen's University, Kingston, Ontario

Received August 12, 1971[1]

1-Propanethiol is an excellent H atom and alkyl radical scavenger in the γ-radiolysis of liquid cyclohexane. The total radical yield (5.2) is measured by twice the yield of propyldisulfide which appears to be invariant with propanethiol concentration. 1-Propanethiol-*d* is about as efficient an H atom scavenger as ethylene. $C_3H_7S\cdot$ radicals add reversibly to cyclohexene.

Le 1-propanethiol est un excellent piège pour les atomes d'hydrogène et les radicaux alkyl dans la radiolyse-γ du cyclohexane liquide. Le rendement total en radical (5.2) est déterminé comme étant le double du rendement de disulfure de propyl, qui ne semble pas varier avec la concentration de propanethiol. L'atome de H est à peu près aussi efficacement piégé par le 1-propanethiol-*d* qu'il l'est par l'éthylène. Les radicaux $C_3H_7S\cdot$ se combinent réversiblement au cyclohexène.

[Traduit par le journal]

Can. J. Chem., **51**, 192 (1973)

Introduction

The sulfhydryl group, —SH, is of interest in radiation chemistry because of its ability to repair radiation damage by transfer of the H atom to a free radical (1). It is present in molecules of biological interest which have been extensively studied in irradiated aqueous solution. However its scavenging properties in irradiated liquid alkanes have received little attention.

Nevitt and Remsberg (2) briefly studied the scavenging of alkyl radicals by 1-butanethiol in cyclohexane. Hardwick (3) stated that 2-ethyl-2-propanethiol and other simple mercaptans are relatively inert towards H atoms in *n*-hexane when judged by the total hydrogen yield. Our isotopic experiments show that this yield is a poor measure of the reactivity. Bergdolt and Schulte-Frohlinde interpreted the hydrogen yields in cyclohexane–thiophenol-*d* (4) and 2,2,4-trimethylpentane–hexanethiol-1 (5) mixtures in terms of positive charge transfer, H atom scavenging, and electron scavenging. No liquid product yields were measured.

The present study was undertaken to determine the scavenging ability of an alkanethiol in an irradiated alkane. For experimental convenience 1-propanethiol was chosen since it is an easily handled liquid while cyclohexane was used as solvent since its major radiolytic products are few in number (6, 7) and their mode of formation appears to be reasonably well understood (8).

Experimental

Cyclohexane (Phillips Pure Grade) contained little cyclohexene ($<10^{-5}$ *M*) and was used as received. 1-Propanethiol (Baker) was fractionally distilled, a middle cut being taken which contained $\sim 10^{-5}$ *M* propyldisulfide. 1-Propanethiol-*d* (Merck, Sharp and Dohme) was subjected to the same distillation procedure.

The 2.5 ml liquid samples were irradiated under vacuum at 24 ± 2 °C in Pyrex tubes in a ^{60}Co γ source (Gammacell 220) at a dose rate of $\sim 1.0 \times 10^{19}$ eV l^{-1} s^{-1} in the Fricke dosimeter.

The disappearance of propanethiol was measured spectrophotometrically by the Ellman method (9) and the formation of H_2S by the methylene blue procedure (10). Hydrogen was measured volumetrically and its isotopic composition was determined by mass spectrometry. All other products were determined by g.l.c.; cyclohexene on a 7.5 ft, 20% β,β′-oxydipropionitrile column at 30 °C, bicyclohexyl, cyclohexylpropylsulfide, and propyldisulfide on a 6 ft, 10% SE-30 column at 105 °C, and propane on a 4 ft Chromosorb 102 column at 40 °C.

Results

The yields of all major products formed in liquid cyclohexane containing up to 0.16 *M* propanethiol are shown in Figs. 1 and 2. The dose was 1.5×10^{19} eV g^{-1} except where noted. The yields of all products are linear with dose up to this value except at low concentrations of propanethiol when there are significant changes in its concentration during radiolysis. Even under

[1]Revision received September 18, 1972.

Can. J. Chem. Downloaded from www.nrcresearchpress.com by 210.87.254.6 on 09/05/12
For personal use only.

TABLE 1. Sulfur balance in cyclohexane–propanethiol mixtures (1.5×10^{19} eV g^{-1})

Propanethiol (M)	$2G(C_3H_7SSC_3H_7) + G(c\text{-}C_6H_{11}SC_3H_7)$	$G(-C_3H_7SH)$
4.6×10^{-3}	4.5 ± 0.4	4.8 ± 0.3
2.3×10^{-3}	4.5 ± 0.2	4.9 ± 0.3

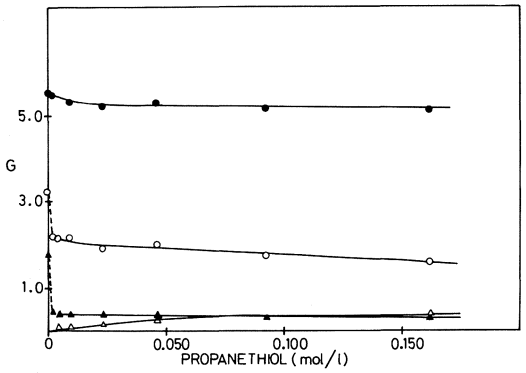

FIG. 1. Product yields in the radiolysis of cyclohexane–propanethiol mixtures (1.5×10^{19} eV g^{-1}). ●, Hydrogen; ○, cyclohexene; ▲, bicyclohexyl; △, hydrogen sulfide.

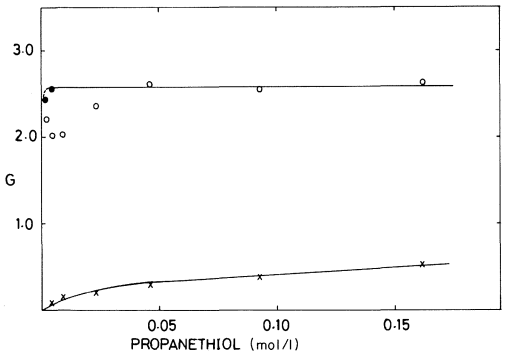

FIG. 2. The yields of propyldisulfide and cyclohexylpropylsulfide in cyclohexane–propanethiol mixtures ○,x, 1.5×10^{19} eV g^{-1}; ●, 3.6×10^{18} eV g^{-1}.

these circumstances it is only the disulfide yield that is markedly affected.

The disappearance of propanethiol was measured at 4.6 and 2.3×10^{-3} M and a good sulfur balance was obtained. $G(-C_3H_7SH)$ is compared with the yields of products containing sulfur in Table 1. The H_2S yield was too small to measure. Propyldisulfide constitutes more than 95% of these products. At the dose used (1.5×10^{19} eV g^{-1}) up to 50% of the propanethiol had disappeared at the conclusion of the irradiation of the solution containing the lower thiol concentration. Some of the disulfide formed will have disappeared by secondary reaction since at the lower dose of 3.6×10^{18} eV g^{-1} the yield is higher. Work now in progress on scavenging by disulfide shows that about half the disulfide which disappears leads neither to the formation of thiol nor to the production of cyclohexylpropylsulfide and cannot at present be accounted for (11).

Propanethiol-d (C_3H_7SD) produced a substantial yield of HD and a much smaller yield of D_2 (Fig. 3). $G(H_2 + HD + D_2)$ was equal at all propanethiol concentrations to $G(H_2)$ in the absence of this solute. The experimental points for HD are fitted by an equation describing H atom scavenging (see later). Sulfur hexafluoride and carbon tetrachloride, both excellent electron scavengers, reduced the yields of all hydrogen isotopes, the D_2 yield being most affected (Table 2).

In addition to the above results the following observations were made. (*i*) 4×10^{-2} M ethylene had no effect on $G(H_2S)$ at 8.8×10^{-2} M propanethiol but the electron scavengers CCl_4 and SF_6 reduced it considerable (Table 3). (*ii*) A small yield of propane was found. At 9.2×10^{-3} and 9.2×10^{-2} M propanethiol $G(C_3H_8)$ was 0.18

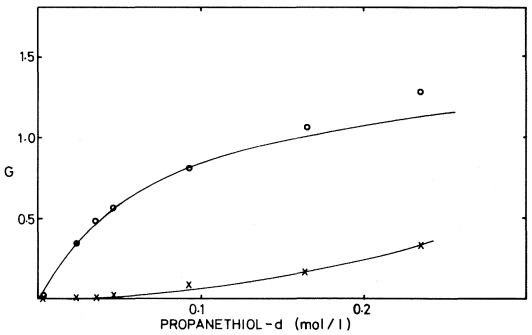

FIG. 3. HD (○) and D_2 (x) yields from cyclohexane–propanethiol-d mixtures (1.5×10^{19} eV g^{-1}). The curve drawn through the HD points is calculated as described in the text.

Can. J. Chem. Downloaded from www.nrcresearchpress.com by 210.87.254.6 on 09/05/12
For personal use only.

TABLE 2. Isotopic hydrogen yields in the presence of electron scavengers (0.035 M C_3H_7SD, 1.5×10^{19} eV g^{-1})

Scavenger	Concentration (M)	$G(H_2)$	$G(HD)$	$G(D_2)$
—	0	4.60	0.48	0.009
SF_6	0.00088	4.48	0.39	0.007
SF_6	0.0022	4.36	0.38	0.007
SF_6	0.022	3.79	0.25	0.003
SF_6	0.036	3.45	0.19	<0.002
SF_6	0.074	3.11	0.20	<0.002
CCl_4	0.015	3.68	0.41	0.011
CCl_4	0.061	3.18	0.15	<0.002
CCl_4	0.26	2.23	0.05	<0.002
CCl_4*	0.26	2.10	0.27	0.004

*C_3H_7SD = 0.14 M.

TABLE 3. H_2S yields in the presence of electron scavengers (0.09 M C_3H_7SH)

Scavenger	Concentration (M)	$G(H_2S)$
—	0	0.33
CCl_4	0.0317	0.23
CCl_4	0.0518	0.17
CCl_4	0.093	0.18
SF_6	0.0385	0.14
SF_6	0.167	0.15
SF_6	0.243	0.08

and 0.35 respectively when $G(H_2S)$ was 0.11 and 0.33. (*iii*) Cyclohexene, 9.9×10^{-4} M, increased $G(c\text{-}C_6H_{11}SC_3H_7)$ from 0.29 to 0.73 in cyclohexane containing 4.64×10^{-2} M propanethiol. However with 4.65×10^{-3} M propanethiol the same concentration of olefin increased the value only from 0.08 to 0.13. (*iv*) Propanethiol, 0.1 M, reduced $G(N_2)$ from a 0.04 M solution of N_2O in cyclohexane by ~4%. There was no measureable reduction at lower concentrations.

Discussion

The yields of the major liquid radiolysis products, cyclohexene and bicyclohexyl, from cyclohexane are efficiently reduced by propanethiol while the hydrogen yield is decreased only slightly (Fig. 1). This is consistent with a simple free radical scavenging mechanism.

[1] $c\text{-}C_6H_{12} \rightsquigarrow c\text{-}C_6H_{10}, H_2, c\text{-}C_6H_{11}\cdot, H\cdot$

[2] $H\cdot + c\text{-}C_6H_{12} \rightarrow H_2 + c\text{-}C_6H_{11}\cdot$

[3] $2c\text{-}C_6H_{11}\cdot \rightarrow (c\text{-}C_6H_{11})_2$
$\rightarrow c\text{-}C_6H_{10} + c\text{-}C_6H_{12}$

[4] $c\text{-}C_6H_{11}\cdot + C_3H_7SH \rightarrow c\text{-}C_6H_{12} + C_3H_7S\cdot$

[5] $H\cdot + C_3H_7SH \rightarrow H_2 + C_3H_7S\cdot$

[6] $2C_3H_7S\cdot \rightarrow C_3H_7SSC_3H_7$

The net result is the sacrificial protection of cyclohexane by propanethiol. Even at the lowest propanethiol concentration reaction 3 is superceded by 4 for all freely diffusing $c\text{-}C_6H_{11}\cdot$ radicals. The non-scavengeable yields of cyclohexene (2.2) and bicyclohexyl (0.4) are in good agreement with the values of 2.42 and 0.4 estimated by Bansal and Schuler (8). If a value of 10^9 l m^{-1} s^{-1} is taken for k_3, the rate constant for reaction 3 (12, 13), then k_4 must have a minimum value of 10^5 l m^{-1} s^{-1}. This is consistent with the values of 3.9×10^5 and 2.9×10^6 l m^{-1} s^{-1} for $c\text{-}C_6H_{11}\cdot + c\text{-}C_6H_{11}SH$ and $C_3H_7\cdot + C_3H_7SH$ respectively (12).

$G(C_3H_7SSC_3H_7)$ does not vary with propanethiol concentration from 0.05 to 0.16 M at a dose of 1.5×10^{19} eV g^{-1}. At 0.05 M at the completion of the irradiation 2% of the propanethiol has disappeared. At lower concentrations and for the same dose the disulfide yield is lower presumably due to secondary reaction (Fig. 2). With 4.6×10^{-3} M thiol and a dose of 3.6×10^{18} eV g^{-1} 5% of the thiol has disappeared to yield disulfide, the G value for which is 5.2. Since the radical scavenging efficiencies of propanethiol and propyldisulfide are approximately the same (11) it appears that the initial disulfide yield is independent of thiol concentration up to at least 0.16 M.

Twice $G(C_3H_7SSC_3H_7)$ represents the total yield of scavengeable radicals. Hydrogen atom scavenging will be negligible at the lowest propanethiol concentration and therefore 5.2 is the yield of scavengeable aklyl radicals. These must be essentially all cyclohexyl radicals since $\Delta G(c\text{-}C_6H_{10} + (c\text{-}C_6H_{11})_2) = 5.0$ (obtained by linear extrapolation to zero thiol concentration of the linear portions of the yield curves at high propanethiol concentrations in Fig. 1). Using low concentrations of radioactive iodine and a dose approximately ten times less than ours, Bansal and Schuler (8) obtain $G(c\text{-}C_6H_{11}) = 5.3 - 5.4$. However after theoretical corrections for H atom and ion scavenging their value is raised to 5.7. No such correction is required for H atom scavenging in the present work since the same yield of $C_3H_7S\cdot$ is obtained by reactions 2 and 4 as by reaction 5. Ion scavenging, if it indeed occurs, is not efficient and must also lead to disulfide since the yield of the latter remains constant. We therefore fail to

Can. J. Chem. Downloaded from www.nrcresearchpress.com by 210.87.254.6 on 09/05/12
For personal use only.

Can. J. Chem. Downloaded from www.nrcresearchpress.com by 210.87.254.6 on 09/05/12
For personal use only.

understand the discrepancy of 0.5 G between the two results. It might be argued that H atom abstraction by alkyl radicals from other than the SH group in propanethiol is occurring but there is no experimental evidence that this is of significance in the gas or liquid phases and even if it did occur the radical formed, $\cdot C_3H_6SH$, would surely abstract from the —SH group.

[7] $\cdot C_3H_6SH + C_3H_7SH \rightarrow C_3H_7SH + C_3H_7S\cdot$

and the net result would be the same as if reaction 4 only occurred.

We believe that the use of a simple thiol such as propanethiol provides an excellent method for measuring the total radical yield in an irradiated liquid alkane. Although the disulfide yield is a little difficult to obtain accurately at very low thiol concentrations it appears to remain constant with increasing concentration.

The slight decrease in $G(H_2)$ in Fig. 1 is matched by a small yield of H_2S and, within experimental error, $G(H_2 + H_2S)$ remains constant. Also $G(C_3H_8)$ is approximately equal to $G(H_2S)$. Since ethylene has no effect on $G(H_2S)$, reaction 8,

[8] $H\cdot + C_3H_7SH \rightarrow H_2S + C_3H_7\cdot$

may be ruled out. The reduction in $G(H_2S)$ caused by the addition of SF_6 or CCl_4 (Table 3) shows that the main precursors of H_2S are ionic. Two possible mechanisms for H_2S formation, one involving proton transfer and the other electron capture, are

[9] $c\text{-}C_6H_{12}^+ + C_3H_7SH \rightarrow c\text{-}C_6H_{11}\cdot + C_3H_7SH_2^+$

[10] $C_3H_7SH_2^+ + e \rightarrow C_3H_7\cdot + H_2S$ (or $C_3H_8 + \cdot SH$)

and

[11] $e + C_3H_7SH \rightarrow C_3H_7SH^-$

[12] $C_3H_7SH^- + c\text{-}C_6H_{12}^+ \rightarrow C_3H_7\cdot + H_2S + c\text{-}C_6H_{11}\cdot$

Both reactions fit the above experimental facts and in both cases $G(C_3H_7SSC_3H_7)$ will remain constant since the total number of radicals reacting to produce $C_3H_7S\cdot$ radicals is unchanged. The very small reduction in $G(N_2)$ from an N_2O solution may be an indication that electron scavenging is occurring but due to our lack of knowledge of the complete reaction scheme for the production of N_2 the evidence cannot be regarded as conclusive. Reaction 11 is endothermic in the gas phase (14) but solvation by other propanethiol molecules may aid its occurrence in cyclohexane just as was suggested in the case of deuterium sulfide (15).

The large HD yields from propanethiol-*d* solutions (Fig. 3) suggest the occurrence of efficient H atom scavenging (reaction 5). On the assumption that all the HD arises in this manner, the experimental points in Fig. 3 have been fitted by the curve calculated from an equation describing competition between reactions 2 and 5

$$G(HD) = \frac{G^0(H)}{1 + \frac{k_2}{k_5}\frac{[c\text{-}C_6H_{12}]}{[C_3H_7SD]}}$$

$G^\circ(H)$, the yield of H atoms in pure $c\text{-}C_6H_{12}$, is taken as 1.46 (16). A best fit is obtained with $k_2/k_5 \sim 0.008$. This means that propanethiol-*d* is only slightly less efficient an H atom scavenger than ethylene for which the corresponding ratio is 0.00475 (16). This is consistent with gas phase data which show roughly equal efficiencies for H atom scavenging by alkanethiols and C_2H_4 (17, 18). The value for k_2/k_5 will be a lower limit since ionic reactions which are not present in pure cyclohexane may contribute to the HD yield. The extent of this can be deduced by the effect of added electron scavengers (Table 3). SF_6 reduces $G(HD)$ to ~40% of its initial yield while $G(D_2)$ is reduced to a much greater extent. Most of the D_2 must therefore be formed as a consequence of an ionic reaction *e.g.* proton transfer.

[13] $c\text{-}C_6H_{12}^+ + C_3H_7SD \rightarrow c\text{-}C_6H_{11}\cdot + C_3H_7SDH^+$

[14*a*] $e + C_3H_7SDH^+ \rightarrow D\cdot + C_3H_7SH$

[14*b*] $e + C_3H_7SDH^+ \rightarrow H\cdot + C_3H_7SD$

[15*a*] $D\cdot + C_3H_7SD \rightarrow D_2 + C_3H_7S\cdot$

[15*b*] $H\cdot + C_3H_7SD \rightarrow HD + C_3H_7S\cdot$

[16] $D\cdot + c\text{-}C_6H_{12} \rightarrow HD + c\text{-}C_6H_{11}\cdot$

The small D_2 yields at the C_3H_7SD concentrations used suggest that this reaction sequence is not of great importance. The analogous sequence involving ethanol-*d* is highly efficient (19), the much lower efficiency of propanethiol-*d* is consistent with its being a much softer base (20).

A correction may be made to the HD yield for such a reaction sequence. If y is the yield of hydrogen atoms in reaction 14 and if isotope effects are neglected then $y/2$ H and $y/2$ D atoms are produced. Let the fraction of these atoms scavenged by C_3H_7SD ([15*a*] and [15*b*]) be f then $G(D_2) =$

Can. J. Chem. Downloaded from www.nrcresearchpress.com by 210.87.254.6 on 09/05/12
For personal use only.

$y/2 = f$; G(HD) via [14a] and [16] $= y/2(1 - f)$; G(HD) via [14b] and [15b] $= yf/2$. The net yield of HD from the reaction sequence [13]–[16] is $y/2$ which is equal to $G(D_2)/f$. An approximation for f is $G(HD)/G°(H)$. If $G°(H)$ is taken as ~1.5 then the maximum correction to be applied to the HD yields (7%) occurs at 9.36×10^{-2} M C_3H_7SD. The value for k_2/k_5 which best fits the points still remains at 0.008 but $G°(H)$ is reduced by ~0.2 G.

The residual HD yields in the presence of SF_6 and in the presence of CCl_4 at the higher propanethiol concentration show that 30–40% of the HD is formed via a non-ionic mechanism at the low concentrations of propanethiol that we employ. Asmus *et al* (16) estimate that 39% of all H atoms in irradiated c-C_6H_{12} have non-ionic precursors. Therefore it does appear that most of the HD formed arises from the scavenging of thermalized H atoms with little contribution from other sources. The reduction of G(HD) by CCl_4 in high concentration is consistent with the proposed H atom and electron scavenging properties of this solute (16, 21), the relative rates of which are not known.

There is poor agreement between our result for k_2/k_5 (0.008) and those of Pryor and coworkers (22, 23) who find 0.062, 0.068, and 0.093 for scavenging of photolytically generated hydrogen atoms by *t*-butanethiol, thiophenol, and propanethiol, respectively in cyclohexane. In the gas phase $k_{H+C_3H_7SH}/k_{H+C_2H_4} \approx 2$ (18). A ratio of the order of unity is obtained for the rate of H atom addition to ethylene relative to reaction with compounds containing the —SH group in aqueous solution (24, 25). Citing these similarities of ratios for different phases one would expect that the ratio $k_{H+C_3H_7SH}/k_{H+C_2H_4}$ would be about the same in the gas phase and in liquid cyclohexane. This argument would favor our value for k_2/k_5. We have however no explanation for the large discrepancy between the two values. If there is any contribution from ion–molecule reactions to the HD yield in the present work then k_2/k_5 will be increased while a contribution from hot D atoms in the photolytic work would decrease the ratio. It may in fact be that the two values are upper and lower limits to the true one.

The remaining product which has not been discussed is the monosulfide, c-$C_6H_{11}SC_3H_7$. It cannot be formed by combination of c-C_6H_{11}· and C_3H_7S· radicals since its yield increases with increasing thiol concentration whereas the steady state concentration of c-C_6H_{11}· must be decreasing. $G((c\text{-}C_6H_{11})_2)$ remains practically constant with increasing propanethiol concentration which means that the gradual decrease in $G(c\text{-}C_6H_{10})$ is not due to radical scavenging in spurs. However $G(c\text{-}C_6H_{10}) + G(c\text{-}C_6H_{11}SC_3H_7)$ remains constant suggesting that the sulfide arises in a secondary reaction involving the olefin. This was confirmed by the addition of cyclohexene prior to irradiation. The absolute concentration of cyclohexene changes only slowly at the higher propanethiol concentrations and it is to be expected that the steady state concentration of C_3H_7S· radicals will also show little change so that an almost constant yield of sulfide would be expected via the addition reaction

[17] $$C_3H_7S· + c\text{-}C_6H_{10} \rightarrow c\text{-}\dot{C}_6H_{10}SC_3H_7$$

However such an addition is reversible in both gas and liquid phases (26) and it is only at the higher propanethiol concentrations, as was shown, that the raection

[18] $$c\text{-}\dot{C}_6H_{10}SC_3H_7 + C_3H_7SH \rightarrow c\text{-}C_6H_{11}SC_3H_7 + C_3H_7S·$$

can compete with the reverse of reaction 17 and lead to a significant yield of sulfide. Again the reaction sequence leading to sulfide formation does not alter the number of C_3H_7S· radicals which dimerize to form disulfide.

The authors thank the Defence Research Board, the National Research Council of Canada, and Atomic Energy of Canada Ltd., Commercial Products, for financial assistance.

1. G. E. Adams, G. S. McNaughton, and B. D. Michael. Trans. Faraday Soc. **64**, 902 (1968).
2. T. D. Nevitt and L. P. Remsberg. J. Phys. Chem. **64**, 969 (1960).
3. T. J. Hardwick. J. Phys. Chem. **66**, 117 (1962).
4. A. Bergdolt and D. Schulte-Frohlinde. Z. Naturforsch. **22b**, 270 (1967).
5. A. Bergdolt and D. Schulte-Frohlinde. Z. phys. Chem. Neue Folge, **56**, 254 (1967).
6. P. J. Dyne and J. A. Stone. Can. J. Chem. **39**, 2381 (1961).
7. S. K. Ho and G. R. Freeman. J. Phys. Chem. **68**, 2189 (1964).
8. K. M. Bansal and R. H. Schuler. J. Phys. Chem. **74**, 3924 (1970).
9. E. Bentler, A. Duron, and B. M. Kelly. J. Lab. Clin. Med. **61**, 882 (1963).
10. J. K. Fogo and M. Popowsky. Anal. Chem. **21**, 732 (1949).
11. J. Esser and J. A. Stone. Unpublished results.
12. R. D. Burkhart. J. Phys. Chem. **73**, 2703 (1969).

13. B. SMALLER, J. R. REMKO, and E. C. AVERY. J. Chem. Phys. **48**, 5174 (1968).
14. K. JÄGER and A. HENGLEIN. Z. Naturforsch. **21a**, 1251 (1966).
15. J. A. STONE and P. T. HOLLAND. Can. J. Chem. **48**, 3282 (1970).
16. K.-D. ASMUS, J. M. WARMAN, and R. H. SCHULER. J. Phys. Chem. **74**, 246 (1970).
17. R. P. STEER and A. R. KNIGHT. Can. J. Chem. **47**, 1335 (1969).
18. R. R. KUNTZ. J. Phys. Chem. **71**, 3343 (1967).
19. J. W. BUCHANAN and F. WILLIAMS. J. Chem. Phys. **44**, 4377 (1966).
20. R. G. PEARSON. J. Chem. Ed. **45**, 581 (1968).
21. J. A. STONE and P. J. DYNE. Can. J. Chem. **42**, 669 (1964).
22. W. A. PRYOR and M. G. GRIFFITH. J. Am. Chem. Soc. **93**, 1408 (1971).
23. W. A. PRYOR and J. P. STANLEY. J. Am. Chem. Soc. **93**, 1412 (1971).
24. P. NETA, R. W. FESSENDEN, and R. H. SCHULER. J. Phys. Chem. **75**, 1654 (1971).
25. P. NETA and ROBERT SCHULER. Rad. Res. **47**, 612 (1971).
26. R. M. KELLOG. *In* Methods in free radical chemistry. Vol. 2. *Edited by* E. S. Huyser. Marcel Dekker, New York. 1969. p. 1.

Can. J. Chem. Downloaded from www.nrcresearchpress.com by 210.87.254.6 on 09/05/12
For personal use only.

The Structure of the Capsular Polysaccharide from Klebsiella K-Type 21[1]

Y. M. Choy and G. G. A. Dutton

Department of Chemistry, University of British Columbia, Vancouver, British Columbia

Received July 27, 1972

Methylation, periodate oxidation, and partial hydrolysis studies on the capsular polysaccharide, and on the carboxyl reduced polymer, of *Klebsiella* K21 show the structure to consist of a repeating unit.

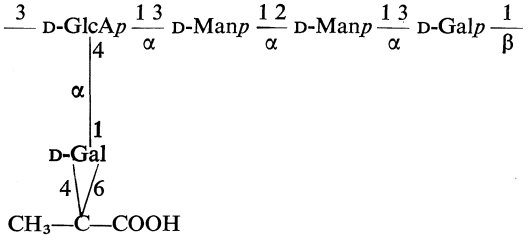

The anomeric linkages were determined by p.m.r. spectroscopy of isolated oligosaccharides and, in part, by specific enzymes. P.m.r. spectroscopy of the original polysaccharide in methyl sulfoxide-d_6 showed clearly a ratio of one pyruvic acid ketal (CH_3, τ 8.5) to five anomeric protons (τ 4.65–5.40).

Les méthodes de méthylation, oxydation periodique et hydrolyse partielle portées au polysaccharide capsulaire, et au polymère avec le groupe carboxyle réduit, de *Klebsiella* K21 ont démontré que la structure se compose d'une unité qui se répéte.

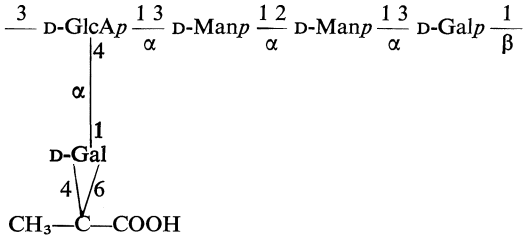

Les liaisons anomères ont été distinguées par la spectroscopie r.m.n. des oligosaccharides isolés et, en partie, par des enzymes spécifiques. La spectroscopie r.m.n. du polysaccharide original dans le méthyl sulfoxide-d_6 a établi le rapport un à cinq entre le cétal de l'acide pyruvique (CH_3, τ 8.5) et les protons anomères (τ 4.65–5.40).

Can. J. Chem., **51**, 198 (1973)

Qualitative analyses of the capsular polysaccharides of the 80 serotypes of *Klebsiella* bacteria have been provided by Nimmich (1, 2) who has shown that the great majority contain glucuronic acid in combination with hexose and deoxyhexose sugars. Approximately one half of the polysaccharides also contain pyruvic acid (3) covalently bound (1-carboxyethylidene ketals). Despite the amount of qualitative information available on *Klebsiella* polysaccharides detailed structures are only known for those capsular materials from types K2 (ref. 4), K5 (ref. 5), K8 (ref. 6), K9 (ref. 7), K20 (ref. 8), K54 (refs. 9–11), and three related but untyped species of *Aerobacter aerogenes* (12–14). The structure of the capsular polysaccharide from *Klebsiella* K21 is now reported. A preliminary report has appeared (15) which also gives other background references.

The acidic capsular polysaccharide from *Klebsiella* K21 was purified by one precipitation with Cetavlon and had $[\alpha]_D$ +130°. Gel filtration and electrophoresis showed the material to be homogeneous. In work with other *Klebsiella*

[1]Presented in part at the 55th Canadian Chemical Conference of the Chemical Institute of Canada, Quebec City, Quebec, June, 1972 and at the 6th International Carbohydrate Symposium, Madison, Wisconsin, August, 1972.

Can. J. Chem. Downloaded from www.nrcresearchpress.com by 210.87.254.6 on 09/05/12
For personal use only.

Can. J. Chem. Downloaded from www.nrcresearchpress.com by 210.87.254.6 on 09/05/12
For personal use only.

capsular polysaccharides it has been found that there is an approximate, inverse relationship between the equivalent weight of the polysaccharide and the distance of migration. One may predict that the polysaccharide from *Klebsiella* K62 will have an equivalent weight about 580 (Fig. 1).

The p.m.r. spectrum of a 2% solution of the polysaccharide in D_2O showed a sharp singlet at τ 8.5 indicative of a pyruvic acid ketal (16, 17). Determination of the pyruvic acid:sugar ratio was hampered by the presence of the HOD signal even after several exchanges with D_2O. The HOD peak was shifted downfield by the addition of trifluoroacetic acid or upfield by running the spectrum at 95–100° on the polysaccharide in methyl sulfoxide-d_6. In the latter case integration of the signals due to the anomeric protons and that of the methyl at τ 8.5 showed there was one pyruvic acid ketal to five sugar residues (Fig. 2).

Partial assignment of the anomeric signals may be made using the data of Table 1, which are based on examination of the oligosaccharides obtained in subsequent experiments, and similar data given by Conrad and coworkers (4) and others. These enable one to predict that of the five glycosidic bonds (per repeating unit) only one is of the β-D-configuration (shown subsequently to be β-D-galactose). In later work with other *Klebsiella* capsular polysaccharides (K20, K24) excellent spectra have been obtained by using the sodium salt of the polysaccharide in D_2O at 95° and dispensing with the use of methyl sulfoxide.

Acidic hydrolysis of the polysaccharide showed,

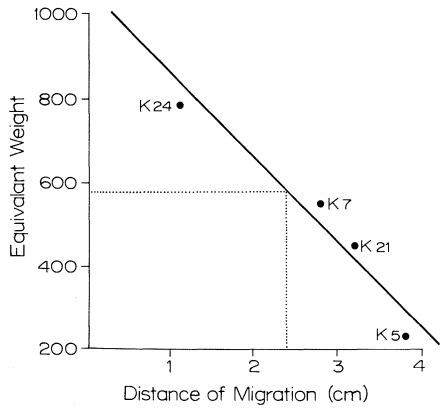

FIG. 1. *Klebsiella* capsular polysaccharides; electrophoresis on cellulose acetate at 300 V for 30 min (p*H* 8.8, veronal–tris buffer). Distance of migration *vs.* equivalent weight. K62 migrates 2.4 cm indicating an equivalent weight of 580.

by paper chromatography, the presence of D-mannose, D-galactose, D-glucuronic acid, lactone, and an aldobiouronic acid. Separation of the hydrolyzate into neutral and acidic fractions and g.l.c. of the former, both as trimethylsilyl derivatives and as alditol acetates, gave a ratio of D-mannose to D-galactose of 1:1.2. Collection of the alditol acetates permitted characterization of D-mannitol hexaacetate m.p. 118–121° and galactitol hexaacetate, m.p. 162°. The aldobiouronic acid was separated from the acidic fraction by paper chromatography and reduction of the carboxyl function followed by hydrolysis gave D-glucose and D-mannose, further characterized as their alditol acetates. The configuration of D-galactose was established by D-galactose oxidase, D-glucuronic acid as D-glucose by D-glucose oxidase, and D-mannose by the circular dichroism curve of D-mannitol hexaacetate (18).

Autohydrolysis of the polysaccharide gave pyruvic acid (19) characterized as the 2,4-dinitrophenylhydrazone (20). It was considered significant that the aqueous solution showed the presence of D-galactose as the only monosaccharide together with traces of oligosaccharides. The residual polysaccharide, obtained by dialysis and lyophilization of the aqueous hydrolyzate, was saved for subsequent methylation studies discussed later.

A sample of pure capsular polysaccharide was methylated (10, 21) and hydrolyzed to yield a neutral and an acidic fraction after separation on ion-exchange resins. Table 2 (A) gives the neutral sugars obtained which were identified as discussed in the experimental. These results show that D-mannose occurs in the polysaccharide linked in two ways; substituted at position 2 and at position 3. The ratio of 3,4,6-tri-*O*-methyl-D-mannose to the 2,4,6-isomer was 1.7:1, consistent with the concept that part of the mannose remained bound to the uronic acid. Isolation of 2,4,6-tri-*O*-methyl-D-galactose indicates that this unit represents a 3-substituted sugar in the chain. The 2,3-di-*O*-methyl-D-galactose cannot represent a branch point since no corresponding quantity of terminal units was found. The pyruvic acid must therefore be linked to D-galactose as a 4,6-ketal. The acidic fraction of the hydrolyzate was converted to the methyl ester glycoside, reduced and hydrolyzed to give 2,4,6-tri-*O*-methyl-D-mannose and 2-*O*-methyl-D-glucose, Table 2 (B). These results show that the aldobiouronic acid is 3-*O*-(glucopyranosyluronic acid)-D-mannose and that

TABLE 1. P.m.r. data on *Klebsiella* K21 capsular polysaccharide and derived oligosaccharides

Repeating unit or compound	Solvent, temperature (°)	τ-Value* (coupling constant, Hz)	Ratio of integrals	Proton assignment (all sugars have D-configuration)
Original polysaccharide	Me_2SO-d_6 100			
—Gal $\frac{1\,3}{\beta}$ GlcA $\frac{1\,3}{\alpha}$ Man $\frac{1\,2}{\alpha}$ Man $\frac{1\,3}{\alpha}$ Gal—		4.65	1	α-GlcA $\frac{1\,3}{}$ Man
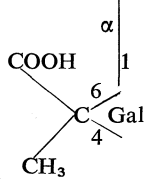		4.90+4.95	2	α-Man $\frac{1\,3}{}$ Gal α-Gal $\frac{1\,4}{}$ GlcA
		5.05	1	α-Man $\frac{1\,2}{}$ Man
		5.40	1	β-Gal $\frac{1\,3}{}$ GlcA
Aldotetrauronic acid	D_2O 95			
GlcA $\frac{1\,3}{\alpha}$ Man $\frac{1\,2}{\alpha}$ Man $\frac{1\,3}{\alpha}$ Gal—OH		4.75+4.80	2.5	α-GlcA $\frac{1\,3}{}$ Man α-Man $\frac{1\,3}{}$ Gal α-Gal—OH
		5.00	1	α-Man $\frac{1\,2}{}$ Man
		5.47 (8)	0.5	β-Gal—OH
Oligosaccharide from Smith degradation	D_2O 95			
Gal $\frac{1\,3}{\beta}$ GlcA $\frac{1\,3}{\alpha}$ Man $\frac{1}{\alpha}$ 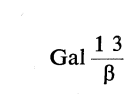		4.75	0.9	α-GlcA $\frac{1\,3}{}$ Man
		4.95	1.2	α-Man $\frac{1}{}$ 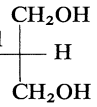
		5.47 (8)	1	β-Gal $\frac{1\,3}{}$ GlcA

*External tetramethylsilane standard for aqueous solutions, internal for methyl sulfoxide.

the D-glucuronic acid is a branch point in the chain. In the absence of tetramethylhexose as terminal groups the side chain attached to the glucuronic acid must be the 4,6-*O*-(1-carboxyethylidene)-D-galactose units. These methylation data permit the drawing of partial structures such as **A** and **B** but do not distinguish between them nor do they establish the position of attachment of the side chains nor the mode of linkage of the glucuronic acid in the main chain.

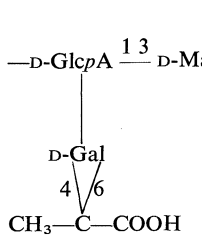

$\frac{1\,2}{}$ D-Man*p* $\frac{1\,3}{}$ D-Gal*p*— **A**

or

$\frac{1\,3}{}$ D-Gal*p* $\frac{1\,2}{}$ D-Man*p*— **B**

The residual polysaccharide recovered from the

Can. J. Chem. Downloaded from www.nrcresearchpress.com by 210.87.254.6 on 09/05/12
For personal use only.

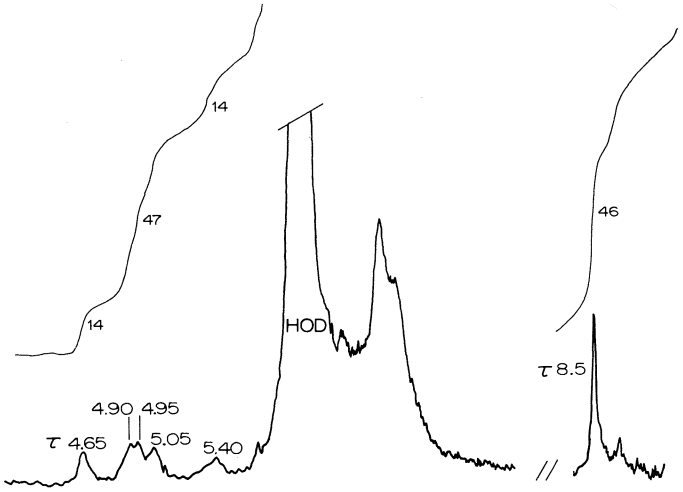

FIG. 2. P.m.r. spectrum of *Klebsiella* K21 capsular polysaccharide in methyl sulfoxide-d_6 at 100°. Tetramethylsilane internal standard (τ 10), 100 MHz.

TABLE 2. Methyl ethers from the hydrolysates of methylated *Klebsiella* K21 polysaccharides

Sugars	Sample*				
	A†	B	C	D	E
2,3,4,6-Tetra-*O*-methyl-D-galactose			3		
2,3,4,6-Tetra-*O*-methyl-D-mannose			1		
2,4,6-Tri-*O*-methyl-D-galactose	1.0		23		0.8
2,4,6-Tri-*O*-methyl-D-mannose	0.6	+	24	+	1.0
3,4,6-Tri-*O*-methyl-D-mannose	1.0		27		1.1
2,3-Di-*O*-methyl-D-galactose	1.0		2		1.0
2,4-Di-*O*-methyl-D-glucose				+	
2,6-Di-*O*-methyl-D-glucose					1.0
2-*O*-Methyl-D-glucose		+			

*A, neutral sugars from methylated original K21 polysaccharide; B, reduced aldobiouronic acid fraction from methylated original K21 polysaccharide; C, neutral sugars from methylated residual polysaccharide after autohydrolysis; D, reduced aldobiouronic acid from methylated residual polysaccharide after autohydrolysis; E, neutral sugars from methylated reduced K21 polysaccharide.

†Approximate molar ratios; (+) signifies present in about equimolecular amounts.

autohydrolysis described above was methylated and hydrolyzed to yield, after separation on ion-exchange columns, neutral and acidic fractions. The composition of the former is shown in Table 2 (C) and the significant feature is the virtually complete disappearance of 2,3-di-*O*-methyl-D-galactose and, incidentally, the very small amounts of tetramethyl sugar produced. Paper chromatography of the acidic fraction showed two components in apparently equal quantities with mobilities corresponding to partially methylated uronic acid (R_f 0.16) and aldobiouronic acid (R_f 0.23). Reduction and hydrolysis of this mixture yielded 2,4,6-tri-*O*-methyl-D-mannose and 2,4-di-*O*-methyl-D-glucose, Table 2 (D). The disappearance of 2,3-di-*O*-methyl-D-galactose in the neutral fraction and the appearance in the acid fraction of 2,4-di-*O*-methyl-D-glucuronic acid is convincing evidence that the 4,6-*O*-(1-carboxyethylidene)-D-galactose units are attached to position 4 of D-glucuronic acid which in turn must be linked through position 3 in the main chain.

The information thus far obtained was confirmed, and more accurate quantitative data were obtained, by examination of the carboxyl-reduced polysaccharide. This was prepared exactly as described for sapote gum using lithium boro-

Can. J. Chem. Downloaded from www.nrcresearchpress.com by 210.87.254.6 on 09/05/12
For personal use only.

Can. J. Chem. Downloaded from www.nrcresearchpress.com by 210.87.254.6 on 09/05/12
For personal use only.

hydride in tetrahydrofuran (22). This method has given virtually quantitative reduction with this and several related polysaccharides and is now our preferred method of achieving such a conversion.

It should also be noted that this reduced polysaccharide and the methylated polymer described above each showed a characteristic sharp singlet (τ *ca.* 8.6) for the methyl group of the corresponding pyruvic acid derivative. This signal thus affords not only a method for the quantitative estimation of 1-carboxyethylidene ketals but also for checking that the related hydroxyisopropylidene and 1-carbomethoxyethylidene groups survive subsequent chemical transformations. In the polysaccharide only small changes in chemical shift were detected in these methyl signals (16). Hydrolysis of the reduced polysaccharide gave D-mannose, D-galactose, and D-glucose in the ratio of 1:1:0.6 (as alditol acetates).

The reduced polysaccharide was methylated and gave on hydrolysis the sugars in the proportions shown in Table 2 (E). The formation of 2,6-di-*O*-methyl-D-glucose arises from the reduced D-glucuronic acid moiety and the quantitative data are consistent with the proposed partial structure.

A portion of the original capsular polysaccharide was autohydrolyzed at 95° for 3 days (initial p*H* 2.3) using the apparatus described by Galanos *et al.* (23) which circulates the polysaccharide solution through stages of heating, cooling, and dialysis and recycles unhydrolyzed material. This apparatus is a modern improvement on the ideas of Painter (24) and of Perila and Bishop (25) but because of the close control that can be exercized high yields of oligosaccharides may be obtained. As previously noted little, except D-galactose and pyruvic acid, is liberated on autohydrolysis; therefore the polysaccharide solution was made up to 0.125 *M* sulfuric acid and dialyzed against acid of the same concentration. Hydrolysis was continued for a further 3 days at 95°. The dialyzate was neutralized with barium carbonate and separated into neutral and acidic fractions. The latter was separated on paper to give, as the main component, an aldotetrauronic acid with lesser amounts of aldotri- and aldobiouronic acids. Table 1 gives the structure of the aldotetrauronic acid based on the evidence presented in the Experimental. The salient points are that partial hydrolysis of the aldotetrauronic acid gave D-galactose as the main monosaccharide and, similarly, hydrolysis after sodium borohydride reduction yielded galactitol. The other products of the partial hydrolysis corresponded to the aldotri- and aldobiouronic acids isolated. The aldobiouronic acid was resistant to the action of β-D-glucuronidase and gave D-mannose on hydrolysis. Identification of the aldotetrauronic acid enables a decision to be made in favor of structure **A**. The aldobiouronic acid 3-*O*-(α-D-glucopyranosyluronic acid)-D-mannose has been isolated previously from *Serratia marcescens* (26), Klebsiella K2 (ref. 4), and from *Pseudomonas aeruginosa* (27).

Confirmation of structure **A** was sought by periodate oxidation of the original capsular polysaccharide. Periodate consumption of 0.36 mol per hexose unit was constant after 3 days and the derived polyalcohol was hydrolyzed by heating an aqueous solution, initial p*H* 2.2, at 95° for 1 h. A separate paper has discussed the wide variety of conditions which has been applied in the hydrolysis step of Smith degradations and has noted that other authors have experienced difficulty in obtaining cleavage of acetal linkages in polymers containing uronic acids (28). Hydrolyses have commonly been carried out with acid strengths of 0.05–0.5 *M* although two groups have recently reported good results with 0.01 *M* acid (13, 29). Johnson and Percival (30) have utilized the acidity of sulfated polysaccharides to effect autohydrolysis of the polyalcohol but the present work appears to be the first instance where the acidity of the uronic acid has been used to achieve hydrolysis of the polyalcohol in a Smith degradation.

Paper chromatographic examination (solvent *A*) of the hydrolyzate showed the presence of (*a*) pyruvic acid, (*b*) glycerol, (*c*) D-threitol, (*d*) D-galactose (traces only), and (*e*) an oligosaccharide which had a mobility (in solvent *E*) intermediate between the aldobi- and aldotriouronic acids previously isolated. The ratio of glycerol to D-threitol was 1.2:1 by g.l.c. of the acetates.

It is pertinent to note here that even under these mild conditions of autohydrolysis the pyruvic acid ketal was hydrolyzed. Similarly, no conditions of partial hydrolysis of the original polysaccharide could be found which would permit the isolation of 4,6-*O*-(1-carboxyethylidene)-D-galactose. Furthermore, an attempt to achieve this by the use of α-galactosidase was unsuccessful since the enzyme was without action on the original polysaccharide. This acid lability

Can. J. Chem. Downloaded from www.nrcresearchpress.com by 210.87.254.6 on 09/05/12
For personal use only.

of the pyruvic acid ketal is in direct contrast to the result of Gorin and Ishikawa (16) who were able to hydrolyze the glycoside methyl 4,6-*O*-(1-carboxyethylidene)-α-D-galactoside without cleavage of the ketal. The difference in stability may be accounted for by the conformation of the ketal or by the proximity of the D-glucuronic acid moiety, but no information is as yet available on these points.

The oligosaccharide obtained in the Smith degradation was of sufficient molecular weight to be precipitated when the aqueous solution was poured into ethanol. The p.m.r. spectrum of the reduced oligosaccharide showed the presence of one β-D-linkage per three anomeric protons and incubation of the original oligosaccharide with β-galactosidase yielded D-galactose. When the reduced oligosaccharide was methylated and hydrolyzed examination by paper chromatography in solvent *D* showed 2,3,4,6-tetra-*O*-methyl-D-galactose to be the major neutral sugar with traces of 2,4,6-tri-*O*-methyl-D-mannose. This result was confirmed by g.l.c. Examination in solvent *E* showed also the presence of two acidic components with mobilities identical to 2,4-di-*O*-methyl-D-glucuronic acid and the partially methylated aldobiouronic acid isolated previously from the methylated residual polysaccharide. In neither case was the di-*O*-methylglycerol sought.

The sum of these results firmly establishes structure **A** as representing the repeating unit of the capsular polysaccharide of *Klebsiella* K21 and demonstrates for the first time the mode of attachment of the pyruvic acid in this genus. The structure found for K21 is similar to those previously reported for K2, K8, K9, K54 (refs. 4, 6, 7, 11) in that they each have a repeating unit of four or five sugars including a single unit side chain. That this is not an invariant rule for *Klebsiella* polysaccharides is shown by the structure of K5 (ref. 5) which has a repeat of three sugars and no side chain and of K20 (ref. 8) which has a repeat of four sugars including a two unit side chain. Full details of these other structures will be published in due course.

Experimental

General Methods

Paper chromatography was carried out by the descending method using Whatman No. 1 paper and the following solvent systems (v/v): (*A*) ethyl acetate – acetic acid – formic acid – water (18:3:1:4); (*B*) ethyl acetate – pyridine – water (4:1:1); (*C*) 1-butanol – acetic acid – water (2:1:1); (*D*) butanone saturated with 1% aqueous ammonia; (*E*) 1-butanol–ethanol–water (4:1:5). Chromatograms were developed with *p*-anisidine trichloroacetate spray (31) or with silver nitrate (32). The clarity of the colors on chromatograms of methylated sugars developed with the former spray is greatly improved by washing the paper under running hot water after heating the chromatogram at 100–110° in the normal manner.

G.l.c. was carried out on an F and M model 720 dual column instrument fitted with thermal conductivity detectors. The helium flow was 60–80 ml/min with the following columns: (*a*) 3% ECNSS-M on Chromosorb W (8 ft × 0.25 in.); (*b*) 5% butanediol succinate on Diatoport S (4 ft × 0.25 in.); (*c*) 8% SE-52 on Diatoport S (8 ft × 0.25 in.).

Circular dichroism spectra were run on a Jasco J-20 automatic recording spectropolarimeter using a quartz cell with path length 0.1 cm. Optical rotations were measured at 23 ± 2° on a Perkin–Elmer model 141 polarimeter. P.m.r. spectra were run on Varian T60 or XL100 instruments. Samples were prepared by dissolving in D_2O and freeze drying 3 or 4 times before dissolving in D_2O or methyl sulfoxide-d_6. Tetramethylsilane was used as a standard, externally for D_2O solutions and internally for methyl sulfoxide-d_6.

Mass spectra, obtained on individual fractions collected (33) from the gas chromatograph, were run on an MS 902 instrument at 70 eV. The position of methoxyl substitution was determined using the data of Lindberg and coworkers (34) and, where possible, by comparison of mass spectra with those of authentic compounds.

Methylations on polysaccharides and oligosaccharides were carried out by the method of Hakomori (9, 21). Partially methylated alditol acetates were demethylated by reaction with boron trichloride (35). All solutions were concentrated on a rotary evaporator *in vacuo* at a bath temperature of 40°.

D-Glucostat and D-Galactostat reagents were obtained from the Worthington Biochemical Corporation, β-D-galactosidase from Koch-Light, and β-D-glucuronidase from Sigma Chemical Company. α-D-Galactosidase was prepared from green coffee beans by the procedure of Clarke *et al.* (36). Sagavac 6F is a product of Seravac Laboratories, Cape Town.

Preparation and Properties of K21 Capsular Polysaccharide

A culture of *Klebsiella* K21 (1702/49) was obtained from Dr. Ørskov, Copenhagen, as an agar slant and was grown on the following medium for 3 days at 25°: 8 g NaCl, 4 g K_2HPO_4, 1 g $MgSO_4 \cdot 7H_2O$, 2 g $CaCO_3$, 120 g sucrose, and 8 g Bacto yeast extract in 4 l of water. Cells were harvested after 3 days, diluted with water containing 1% phenol, and centrifuged at 19 000 g. Capsular polysaccharide was obtained by concentrating the aqueous solution, pouring it into ethanol, and purifying the crude material by Cetavlon precipitation. A sample of the supernatant was shown to contain very little material and therefore this was not further examined. The yield of polysaccharide was approximately 2 g per 4 l of medium. Three batches were pooled and used for the structural studies of the polysaccharide.

Purified polysaccharide (2 g) was dissolved in distilled water (2 l), deionized with Amberlite IR 120 resin, dialyzed, and freeze-dried. The product had $[\alpha]_D$ +130°

Can. J. Chem. Downloaded from www.nrcresearchpress.com by 210.87.254.6 on 09/05/12
For personal use only.

(*c* 0.38, water), ash 0.8%, N 0.3%. The equivalent weight of the polysaccharide, determined by titration with 0.01 *M* sodium hydroxide was 455 (calcd. 447). The average molecular weight was *ca.* 4×10^5 as determined by gel permeation chromatography on Sagavac 6F through the courtesy of Dr. S. C. Churms. Electrophoresis at p*H* 3 and 8.8 showed the polysaccharide moved as a single component (migration 3.2 cm in 30 min at 300 V at p*H* 8.8; by courtesy of Dr. P. E. Reid and Miss C. Poder).

The p.m.r. spectrum of a 2% solution of D_2O showed a sharp singlet at τ 8.5 due to the CH_3 of the pyruvic acid ketal group. The relative amount of pyruvic acid was initially obtained by running the spectrum on a sample dissolved in 3 *M* trifluoroacetic acid in D_2O. Integration gave 17–18 units for the CH_3 signal at τ 8.5 and 146 units for the ring protons, excluding anomeric ones. The ratio was confirmed by running the spectrum of a 2% solution of the polysaccharide in methyl sulfoxide-d_6 at 100°. In this case the HOD peak was shifted upfield so that the anomeric proton signals were clear. These were at τ 4.65 (1H); 4.90, 4.95, 5.05 (3H); 5.40 (1H). The ratio of anomeric protons to pyruvate CH_3 was 5:3.

Hydrolysis of the Polysaccharide

Polysaccharide (0.1 g) was hydrolyzed with 0.5 *M* sulfuric acid at 100° for 8 h. Neutralization ($BaCO_3$) followed by paper chromatography (solvents *A* and *B*) showed D-mannose and D-galactose, D-glucuronolactone, D-glucuronic acid, and an aldobiouronic acid. The hydrolyzate was separated into neutral and acidic fractions using ion-exchange resins (Amberlite IR 120 and Duolite A4). The neutral fraction contained D-mannose and D-galactose in approximately equal amounts (1:1.2) as determined by g.l.c. of the trimethylsilyl derivatives (column *c*) and of the alditol acetates (column *a*). G.l.c. of the acetates permitted recovery of the individual compounds and identification of D-mannitol hexaacetate, m.p. and mixed m.p. 118–121°, and galactitol hexaacetate, m.p. 162° (37). A portion of the neutral fraction of the hydrolyzate was tested with D-Galactostat reagent and a positive response confirmed the D-configuration of galactose. Part of the mannitol hexaacetate collected by g.l.c. was recrystallized and dissolved in acetonitrile. A positive circular dichroism curve, identical to that given by a standard sample, confirmed the D-configuration of mannose (18).

The acidic fraction was separated into two parts by paper chromatography (solvent *A*). The slower migrating, major portion had the mobility of an aldobiouronic acid (R_{Gal} 0.39) and was converted into the ester glycoside by refluxing overnight with 3% methanolic hydrogen chloride. The product was dissolved in tetrahydrofuran and reduced by boiling under reflux overnight with lithium aluminum hydride. Hydrolysis of the neutral disaccharide gave approximately equimolar amounts of D-glucose and D-mannose as determined by g.l.c. of the alditol acetates. The configuration of the glucose was confirmed by the D-Glucostat reagent.

A separate portion (1.5 g) of the polysaccharide was dissolved in water (initial p*H* 2–2.3) and heated for 8 h at 95°. Paper chromatography (solvent *A*) of the concentrated solution showed a fast moving spot, chromatographically identical with pyruvic acid (R_f 0.74) and having the same characteristic fluorescence as a standard when sprayed with *o*-phenylenediamine and examined by u.v. (19). The chromatogram also showed D-galactose as the only monosaccharide and traces of slow moving oligomers. The aqueous solution was extracted with ether and the ether extract was treated with 2,4-dinitrophenylhydrazine to yield the derivative of pyruvic acid, m.p. 214–216°, undepressed by an authentic sample (20). The autohydrolysis solution was concentrated to 50 ml and dialyzed against distilled water (2 l). The non-dialyzable material (0.65 g) was recovered by freeze-drying and kept for methylation studies.

Methylation Analysis

Capsular polysaccharide (0.5 g) was methylated to give a product having a methoxyl content of 38.5% and showing no hydroxyl absorption in the i.r. The methoxyl content was not increased by two further treatments with silver oxide and methyl iodide. The fully methylated polysaccharide was dissolved in cold 72% sulfuric acid and after 1 h the solution was diluted to 1 *M* and hydrolyzed at 100° for 8 h. After neutralization and evaporation, the syrupy product was separated into neutral and acidic fractions by ion-exchange resins. The neutral portion was fractionated by cellulose column chromatography (38) using butanone–water azeotrope and the partially methylated sugars were characterized as follows:

Fraction I (80 mg) was shown by paper chromatography, (solvent *D*) to contain two components having R_f 0.57 and 0.55; the faster moving one (I*a*) gave a brownish yellow spot when sprayed with *p*-anisidine while the slower one (I*b*) gave a pink color. On demethylation, fraction I was shown by paper chromatography (solvents *A* and *B*) to contain only D-mannose. Fraction I (20 mg) was reduced by sodium borohydride and, after removal of the borate, the product was acetylated in a sealed tube by using pyridine and acetic anhydride (1:1, 2 ml, 100°, 20 min). After evaporation of the solvents, the alditol acetates were dissolved in a small volume of ethyl acetate and analyzed by g.l.c. on column *b* programmed from 150–200° at 2°/min; two peaks were observed.

The component eluted first had a retention time of 17.2 min and mass spectrometry showed it to be a 3,4,6-tri-*O*-methyl hexitol acetate. On demethylation and acetylation, D-mannitol hexaacetate was obtained (g.l.c., m.p., and mixed m.p. 118–121°). The second component had a retention time (19.6 min) identical to that of authentic 2,4,6-tri-*O*-methyl-D-mannitol triacetate. A sample collected from the gas chromatograph had m.p. 65–67° undepressed by authentic material (39) and the identity was further confirmed by the mass spectrum. The ratio of the amount of 3,4,6-isomer to that of the 2,4,6-compound was 1:0.6.

Fraction II (30 mg) was shown by paper chromatography to be a single compound (R_f 0.37, solvent *D*) and on demethylation, D-galactose was obtained. Crystallization of the syrupy sugar from ether gave 2,4,6-tri-*O*-methyl-D-galactose m.p. 103–105° (lit. (40) m.p. 102–105°). The derived alditol acetate had a retention time of 21 min (column *a*) and the mass spectrum was consistent with a 2,4,6-tri-*O*-methyl hexitol acetate.

Fraction III (35 mg) was shown by paper chromatography to be a single compound and to correspond to 2,3-di-*O*-methyl-D-galactose (R_f 0.18, solvent *D*). This assignment was confirmed by the mass spectrum of the

Can. J. Chem. Downloaded from www.nrcresearchpress.com by 210.87.254.6 on 09/05/12
For personal use only.

alditol acetate which on demethylation and acetylation gave galactitol hexaacetate, m.p. and mixed m.p. 162°.

The acidic fraction was heated under reflux overnight with 2% methanolic hydrogen chloride to give the ester glycoside which was reduced by boiling overnight with lithium borohydride in tetrahydrofuran. The product (20 mg) was hydrolyzed with 0.5 *M* sulfuric acid for 4 h. Paper chromatography showed the presence of 2,4,6-tri-*O*-methyl-D-mannose (R_f 0.5, solvent *D*; 0.80 solvent *E*) and 2-*O*-methyl-D-glucose (R_f 0.07, 0.24). The identities of both partially methylated sugars were confirmed by g.l.c. and mass spectrometry of the alditol acetates. The mannitol derivative crystallized, m.p. 64–66°, and the glucitol derivative was demethylated and acetylated to give glucitol hexaacetate m.p. 92–95°. 2-*O*-Methyl-D-glucitol pentaacetate has been isolated subsequently from *Klebsiella* K7 methylated polysaccharide and has m.p. 56–57°.

Methylation of Degraded Polysaccharide

Degraded polysaccharide (0.5 g), recovered from the autohydrolysis, was methylated, the product was dissolved in 5 ml of 72% sulfuric acid at 0° and then the solution was diluted to 1 *M* and hydrolyzed at 100° for 8 h. After neutralization the hydrolyzate was separated into acidic and neutral fractions. The latter was shown by paper chromatography (solvent *D*) and by g.l.c. of the alditol acetates (column *b*, 160–210° at 2°/min) to contain the sugars listed in Table 2 (C) which also gives their approximate molar ratios.

Paper chromatography of the acidic fraction (solvent *E*) showed two components with R_f 0.16 and 0.23 and in approximately equal amounts. When sprayed with *p*-anisidine trichloroacetate the slower gave the bright red color of a methylated uronic acid and the faster gave a reddish-brown color and was judged to be a partially methylated aldobiouronic acid. A portion of the mixture (20 mg) was converted to the ester glycosides and reduced with lithium borohydride in tetrahydrofuran. Paper chromatography, after acid hydrolysis, showed the presence of 2,4-di-*O*-methyl-D-glucose (R_f 0.18, solvent *D*) as the major component together with 2,4,6-tri-*O*-methyl-D-mannose. The identity of the former was confirmed by g.l.c. – mass spectrometry of the alditol acetate and that of the latter by the crystalline alditol acetate m.p. 64–66°.

Reduction of the Capsular Polysaccharide

Capsular polysaccharide (0.4 g) was converted into the methyl ester propionate and reduced with lithium borohydride as previously described (22) to give the reduced polysaccharide (0.3 g), $[\alpha]_D$ +115° (*c* 0.42, water). The reduced polysaccharide (0.1 g) was hydrolyzed with 0.5 *M* sulfuric acid at 100° for 8 h to give D-mannose, D-glucose, and D-galactose (paper chromatography, solvent *B*). The identities of the sugars were confirmed by g.l.c. of the alditol acetates and collection of the individual fractions afforded D-mannitol hexaacetate m.p. and mixed m.p. 118–120°, galactitol hexaacetate m.p. and mixed m.p. 160–162°, and D-glucitol hexaacetate m.p. and mixed m.p. 92–95°. The ratio of D-mannitol, galactitol, and D-glucitol hexaacetates was 1:1:0.6. The p.m.r. spectrum of reduced K21 polysaccharide in D_2O was shown to contain four anomeric signals at τ 4.54, 4.80, 5.00, and 5.15 in the ratio of 1:2:1:1. All the signals showed small coupling constants except that at τ 5.15 (7 Hz).

The remainder of the reduced polysaccharide (0.2 g) was methylated and hydrolyzed. Table 2 (E) shows the nature and proportion of the methylated sugars found and, in addition to those previously obtained from the methylated original polysaccharide, now included 2,6-di-*O*-methyl-D-glucose which was characterized by g.l.c. – mass spectrometry of its alditol acetate.

Partial Hydrolysis of Polysaccharide

K21 polysaccharide (1 g) was partially hydrolyzed at p*H* 2.3 at 95° for 3 days using an apparatus similar to that described by Galanos and coworkers (23). Since only D-galactose and pyruvic acid were found in the dialyzate the solution was made 0.125 *M* with sulfuric acid and hydrolyzed at 95° for a further 3 days. The dialyzate was neutralized ($BaCO_3$), evaporated, and separated by ion-exchange resins into acidic and neutral fractions. On paper chromatography (solvent *C*) the acidic fraction was shown to contain an aldotetrauronic acid (R_{Gal} 0.2) as the major component together with small amounts of aldobiouronic acid (R_{Gal} 0.70), aldotriouronic acid (R_{Gal} 0.42), and traces of higher oligomers. The acids were separated by paper chromatography (solvent *C*) and analyzed as follows.

The aldotetrauronic acid (50 mg) had an equivalent weight of 660 (NaOH titration, calcd. 680) and $[\alpha]_D$ +117° (*c* 1.2, water) indicating α-linkages. This was confirmed by the p.m.r. spectrum of a 4% solution in D_2O run at 95° (see Table 1). The aldotetrauronic acid (2 mg) was hydrolyzed with 0.5 *M* trifluoroacetic acid at 100° for 1 h. Paper chromatography (solvent *C*) showed the presence of D-galactose as the principle monosaccharide with traces of D-mannose and a series of aldobiouronic, aldotriouronic, and aldotetrauronic acids which had the same mobilities as the components of the original mixture. The aldotetrauronic acid (4 mg) was reduced with sodium borohydride and, after removal of borate, the product was hydrolyzed with 2 *M* trifluoroacetic acid for 2 h. On paper chromatography (solvents *A* and *B*), the neutral compounds found were D-mannose and galactitol. G.l.c. of the alditol acetates of the neutral compounds showed the ratio of galactitol and D-mannitol to be 1:1.3 and permitted characterization of each compound. The acidic sugars were D-glucuronic acid and the aldobiouronic acid.

The aldotetrauronic acid (11 mg) was methylated and then hydrolyzed by 2 *M* trifluoroacetic acid for 2 h. Paper chromatography (solvents *D* and *E*) showed the following partially methylated sugars to be present 3,4,6-tri-*O*-methyl-D-mannose (R_f 0.58, solvent *D*), 2,4,6-tri-*O*-methyl-D-mannose (R_f 0.55), 2,4,6-tri-*O*-methyl-D-galactose (R_f 0.40), 2,3,4-tri-*O*-methyl-D-glucuronic acid (R_f 0.22, solvent *E*), and traces of partially methylated aldobiouronic acid (R_f 0.28, solvent *E*). The identities of the neutral sugars were further characterized as the alditol acetates and the ratio was found to be approximately 1:1:1.

The aldotriouronic acid (R_{Gal} 0.42) had the same mobility on paper as a component obtained by partial hydrolysis of the tetrauronic acid and was not further examined.

Can. J. Chem. Downloaded from www.nrcresearchpress.com by 210.87.254.6 on 09/05/12
For personal use only.

The aldobiouronic acid (12 mg) had $[\alpha]_D$ +40° (*c* 0.62, water). A sample (2 mg) was hydrolyzed with 3 *M* hydrochloric acid for 2 h. The only neutral sugar found on paper chromatography (solvent *B*) was D-mannose. A negative result was obtained when the aldobiouronic acid (4 mg) was incubated with β-D-glucuronidase (3 mg) at p*H* 4.8 at 38° overnight. Under the same conditions the enzyme hydrolyzed 3-*O*-(β-D-glucopyranosyluronic acid)-D-galactose (from *Klebsiella* K20, ref. 8) and 6-*O*-(β-D-glucopyranosyluronic acid)-D-galactose.

When a portion (5 mg) of the aldobiouronic acid was methylated and then hydrolyzed by 3.5 *M* hydrochloric acid at 95° for 3 h paper chromatography showed the presence of 2,4,6-tri-*O*-methyl-D-mannose and 2,3,4-tri-*O*-methyl-D-glucuronic acid which had the same mobility as a standard (R_f 0.22, solvent *E*). The mannose derivative was further characterized as the alditol acetate, m.p. and mixed m.p. 64–65°.

Periodate Oxidation

The polysaccharide (0.25 g) was dissolved in aqueous sodium metaperiodate (100 ml, 0.025 *M*) and 0.36 mol of periodate per hexose unit was consumed after 3 days. Sodium borohydride (1 g) was added and the solution was left overnight. The solution was deionized with Amberlite IR 120, freeze-dried, and the product was distilled with several portions of methanol. The polyalcohol was dissolved in water (3 ml) to give a solution of p*H* 2.2 which was heated at 95° for 1 h. On paper chromatography (solvent *A*) the following compounds were identified by comparison with standards: (*a*) pyruvic acid (R_f 0.74), (*b*) glycerol (R_f 0.44), (*c*) D-threitol (R_f 0.30) (erythritol had R_f 0.32), (*d*) D-galactose (in traces only), and (*e*) an oligosaccharide which had a mobility intermediate between the aldobiouronic and the aldotriouronic acids in solvent *E*. The ratio of glycerol to D-threitol was found to be 1.2:1 by acetylation of part of the mixture and g.l.c. (column *b*, 150–180° at 2°/min). A control reaction showed that erythritol tetraacetate crystallized very easily while D-threitol tetraacetate remained as a syrup; both acetates had distinctly different retention times (13.5 and 15 min, respectively).

The oligosaccharide was obtained by precipitation into ethanol, yield 0.1 g. The product was reduced with sodium borohydride and, after removal of borate, the p.m.r. spectrum was run in D_2O (20 mg/5 ml) at 95°. One β-D- and two α-D-linkages were observed (Table 1). The signal at τ 5.47 was a doublet with a coupling constant of 8 Hz. The reduced oligosaccharide (10 ml) was dissolved in 0.5 *M* phosphate buffer (3 ml, p*H* 7.0), β-D-galactosidase (5 mg) was added, and the solution was incubated at 38° overnight. The monosaccharide liberated was D-galactose which was confirmed by g.l.c. of the alditol acetate, m.p. and mixed m.p. 160–162°.

The reduced oligosaccharide (50 mg) was methylated followed by hydrolysis with 2 *M* trifluoroacetic acid for 2 h. Paper chromatography (solvent *D*) showed, by comparison with a standard, that 2,3,4,6-tetra-*O*-methyl-D-galactose (R_f 0.68) was the major neutral sugar with traces of 2,4,6-tri-*O*-methyl-D-mannose. The tetramethylgalactitol acetate also had the same retention time as authentic material (11 min, column *a* at 200°). In solvent *E* the acidic components had the same mobilities as 2,4-di-*O*-methyl-D-glucuronic acid (R_f 0.16) and 3-*O*-(2,4-di-*O*-methyl-α-D-glucopyranosyluronic acid)-2,4,6-tri-*O*-methyl-D-mannose (R_f 0.23) previously isolated from the methylated degraded polysaccharide.

We are indebted to Dr. I. Ørskov, Copenhagen, for the gift of an authentic culture (1702/49) of *Klebsiella* K21, to Dr. P. J. Salisbury of this Department for growing the bacteria, and to Dr. G. H. N. Towers of the Department of Botany, University of British Columbia, for the use of his centrifuge. Gel filtration measurements were kindly made by Dr. S. C. Churms (Cape Town) and electrophoresis was carried out by Dr. P. E. Reid and Miss C. Poder of the Department of Pathology, University of British Columbia. P.m.r. spectra were determined by Miss P. Watson and Mr. A. Brooke of this Department.

The financial support of the National Research Council of Canada, and the award of a Killam Fellowship to Y.M.C. are gratefully acknowledged.

1. W. NIMMICH. Z. Med. Mikrobiol. Immunol. **154**, 117 (1968).
2. W. NIMMICH. Acta Biol. Med. Ger. **26**, 397 (1971).
3. W. NIMMICH. Personal communication.
4. L. C. GAHAN, P. A. SANDFORD, and H. E. CONRAD. Biochem. **6**, 2755 (1967).
5. G. G. S. DUTTON and M. T. YANG. Can. J. Chem. **50**, 2382 (1972).
6. I. W. SUTHERLAND. Biochem. **9**, 2180 (1970).
7. B. LINDBERG, J. LÖNNGREN, W. NIMMICH, and J. L. THOMPSON. Carbohydr. Res. In press.
8. Y. M. CHOY and G. G. S. DUTTON. J. Bacteriol. **112**, 635 (1972).
9. I. W. SUTHERLAND and J. F. WILKINSON. Biochem. J. **110**, 749 (1968).
10. P. A. SANDFORD and H. E. CONRAD. Biochem. **5**, 1508 (1966).
11. H. E. CONRAD, J. R. BAMBURG, J. D. EPLEY, and T. J. KINDT. Biochem. **5**, 2808 (1966).
12. D. E. KOELTZOW and H. E. CONRAD. Biochem. **10**, 214 (1971).
13. E. C. YUREWICZ, M. A. GHALAMBOV, and H. C. HEATH. J. Biol. Chem. **246**, 5596 (1971).
14. M. P. VENIAMIN. J. Chromatogr. Sci. **8**, 173 (1970).
15. G. G. S. DUTTON and Y. M. CHOY. Carbohydr. Res. **21**, 169 (1972).
16. P. A. J. GORIN and T. ISHIKAWA. Can. J. Chem. **45**, 521 (1967).
17. C. J. LAWSON, C. W. MCCLEARY, H. I. NAKADA, D. A. REES, I. W. SUTHERLAND, and J. F. WILKINSON. Biochem. J. **115**, 935 (1969).
18. G. M. BEBAULT, J. M. BERRY, Y. M. CHOY, G. G. S. DUTTON, N. FUNNELL, L. D. HAYWARD, and A. M. STEPHEN. Can. J. Chem. **51**, 324 (1973).
19. M. DUCKWORTH and W. YAPHE. Chem. Ind. (London), 747 (1970).
20. H. T. OPENSHAW. Qualitative organic analysis. Cambridge, 1946.
21. S. HAKOMORI. J. Biochem. (Tokyo), **55**, 205 (1964).
22. G. G. S. DUTTON and S. KABIR. Anal. Lett. **4**, 95 (1971).
23. C. GALANOS, O. LÜDERITZ, and K. HIMMELSPACH. Eur. J. Biochem. **8**, 332 (1969).
24. T. J. PAINTER. Chem. Ind. (London), 1214 (1960).

25. O. PERILA and C. T. BISHOP. Can. J. Chem. **39**, 815 (1961).
26. G. A. ADAMS and R. YOUNG. Can. J. Chem. **43**, 2940 (1965).
27. H. O. BOUVENG, I. BREMNER, and B. LINDBERG. Acta Chem. Scand. **19**, 1003 (1965).
28. G. G. S. DUTTON and K. B. GIBNEY. Carbohydr. Res. In press.
29. P. A. J. GORIN, J. F. T. SPENCER, and S. S. BHATTACHARJEE. Can. J. Chem. **47**, 1499 (1969) and refs. therein.
30. P. G. JOHNSON and E. PERCIVAL. J. Chem. Soc. C, 906 (1969).
31. L. HOUGH, J. K. N. JONES, and W. H. WADMAN. J. Chem. Soc. 1702 (1950).
32. W. E. TREVELYAN, D. P. PROCTOR, and J. S. HARRISON. Nature, **166**, 444 (1950).
33. G. G. S. DUTTON and K. B. GIBNEY. J. Chromatogr. **72**, 179 (1972).
34. H. BJÖRNDAL, C. G. HELLERQVIST, B. LINDBERG, and S. SVENSSON. Angew. Chem. Int. Ed. **9**, 610 (1970).
35. S. ALLEN, T. G. BONNER, E. J. BOURNE, and N. M. SAVILLE. Chem. Ind. (London), 630 (1958).
36. J. T. R. CLARKE, L. S. WOLFE, and A. S. PERLIN. J. Biol. Chem. **246**, 5563 (1971).
37. L. HOUGH and A. C. RICHARDSON. *In* Rodd's Chemistry of carbon compounds. 2nd ed. Vol. IF. Elsevier, Amsterdam. 1967. p. 22.
38. J. D. GEERDES, B. A. LEWIS, R. MONTGOMERY, and F. SMITH. Anal. Chem. **26**, 264 (1954).
39. Y. M. CHOY and A. M. UNRAU. Carbohydr. Res. **17**, 439 (1971).
40. D. J. BELL and S. WILLIAMSON. J. Chem. Soc. 1136 (1938).

Can. J. Chem. Downloaded from www.nrcresearchpress.com by 210.87.254.6 on 09/05/12
For personal use only.

The 2,2,2-Trichloroethyl Group for Carboxyl Protection During Peptide Synthesis[1]

BERNARD MARINIER,[2] YOON C. KIM, AND JEAN-MARIE NAVARRE
Research Laboratories, Frank W. Horner Limited, Montréal, Québec

Received July 14, 1972

The 2,2,2-trichloroethyl esters of several *N*-carbobenzoxy-amino acids were prepared by reacting the corresponding acid chlorides with trichloroethanol and the carbobenzoxy groups were selectively removed by HBr–AcOH. The resulting esters were then coupled with various *N*-carbobenzoxy-amino acids or peptides using dicyclohexylcarbodiimide in acetonitrile to give *N*-carbobenzoxy-peptide trichloroethyl esters. The selective removal of the trichloroethyl protecting group was effected by reduction using zinc in acetic acid. The optical activity of the *N*-carbobenzoxy-peptides so obtained agreed well with the values reported in the literature. The overall results suggest that the 2,2,2-trichloroethyl group could be useful for carboxyl protection during peptide synthesis.

Divers chlorures d'acides *N*-carbobenzoxy-aminés furent traités par le trichloroéthanol et ainsi transformés en esters trichloroéthyliques correspondants. L'enlèvement sélectif des groupes carbobenzoxy par HBr–AcOH suivi de la condensation, au moyen de la dicyclohexylcarbodiimide dans l'acétonitrile, des esters obtenus avec des acides aminés ou peptides protégés par des groupes carbobenzoxy donna les esters trichloroéthyliques de *N*-carbobenzoxy-peptides. Le groupe protecteur trichloroéthylique fut à son tour enlevé sélectivement par réduction avec le zinc dans l'acide acétique. Les indices de rotation des *N*-carbobenzoxy-peptides ainsi obtenus concordent avec les valeurs trouvées dans la littérature. Ces résultats indiquent que le groupe trichloro-2,2,2 éthylique pourrait être utilisé efficacement pour la protection des groupes carboxyliques dans les synthèses peptidiques.

Can. J. Chem., **51**, 208 (1973)

In recent years, several new methods for protecting the carboxyl group of amino acids in peptide synthesis have been introduced (1–4). Despite the ingenuity and usefulness of these methods, they suffer from certain disadvantages and the wide application of them has yet to be demonstrated. This prompted us to seek for an alternative method which hopefully could be employed more practically.

It has been shown (5) that the 2,2,2-trichloroethyl group is removed from its esters by treating them with zinc powder in acetic acid under mild conditions. This property has been used for the protection of the carboxyl group (5), the phosphate group (6), and indirectly the amino group (7) in organic synthesis. We have studied the possibility of using the 2,2,2-trichloroethyl group as a carboxyl protecting group in our peptide syntheses and the results are presented here.

Among several different methods tried for trichloroethylation of the carboxyl of amino acids,[3] the most satisfactory one appeared to be the acid chloride method which involves the treatment of the carbobenzoxy amino acids with $POCl_3$ or PCl_5 and then the reaction of the resulting acid chlorides *in situ* with an excess of 2,2,2-trichloroethanol in the presence of triethylamine. The trichloroethyl esters of general formula Z-A-OCH_2CCl_3[4] were all thick oils.

In an attempt to purify some of these esters by distillation under high vacuum, carbobenzoxy-proline trichloroethyl ester was obtained in good yield (83%) but the yield of the corresponding glycine derivative was extremely poor (3%). Since there was no compelling necessity to purify these esters, the crude oils were treated directly with hydrogen bromide in acetic acid to obtain, in most cases, the crystalline hydrobromides of esters, HBr·A-OCH_2CCl_3. Some of the hydrobromides were converted to the corresponding hydrochlorides, HCl·A-OCH_2CCl_3.

The yield of the ester hydrobromides ranged from 56 to 70% after two steps from the carbobenzoxy-amino acids. For the leucine derivative, the yield was 38%, calculated from unsubstituted

[1]Preliminary results were presented at the 38th ACFAS Congress, October 16, 1970, Québec, Québec.

[2]Present address: Université du Québec, 300, avenue des Ursulines, Rimouski, Québec.

[3]All amino acids used in the present work are the L-isomers.

[4]Abbreviations used: Z = $C_6H_5CH_2OCO$; A = amino acid.

Can. J. Chem. Downloaded from www.nrcresearchpress.com by 210.87.254.40 on 09/05/12
For personal use only.

TABLE 1. Hydrohalides of 2,2,2-trichloroethyl esters of amino acids, $HX \cdot A\text{-}OCH_2CCl_3$

Compound						Analysis[d]				
A	X	M.p. (°C)[a]	Yield (%)[b]	$[\alpha]_D$[c]	I.r.(CO) (cm^{-1}, ester)	C	H	Br	Cl	N
Gly	Br	242–244[e]	70		1767[f]	17.01 (16.72)	2.20 (2.46)	28.02 (27.81)	37.24 (37.01)	5.13 (4.87)
Ala	Br	240–243[e]	66	−1.8 (5.73)	1771	19.71 (19.92)	3.26 (3.01)	26.31 (26.51)	35.42 (35.29)	4.60 (4.65)
Phe	Br	194–196	63	0.0[g] (0.88)	1760	34.89 (35.00)	3.31 (3.47)	20.91 (21.17)	28.02 (28.18)	3.60 (3.71)
Val	Br	182–183	56	+3.93 (1.34)	1763	25.42 (25.51)	3.85 (3.98)	24.56 (24.26)	32.02 (32.29)	4.11 (4.25)
Leu	Br	190–193[h]	38[i]		1768					
Asp	Br	182–183	56[j]	0.0[g] (1.82)	1783 1763	20.40 (20.15)	2.04 (2.11)	17.01 (16.76)	44.91 (44.62)	3.14 (2.94)
Gly	Cl	217–220[e,k]	52[l]		1776					
Ala	Cl	188–190[e]	59[l]		1791	23.28 (23.37)	3.35 (3.53)		54.71 (55.19)	5.55 (5.45)
Leu	Cl	222–224	58[l]	+2.44[m] (2.16)	1771	32.25 (32.13)	5.04 (5.06)		47.20 (47.43)	4.48 (4.68)
Asp	Cl	166–168	87[l]		1778 1762	22.00 (22.22)	2.55 (2.33)		57.29 (57.40)	3.36 (3.24)

[a]As recrystallized from ethanol–ether. Uncorrected.
[b]Based on two-step reaction from the corresponding *N*-carbobenzoxy-amino acid unless otherwise stated.
[c]Read in dimethylformamide. Concentration of material in parentheses.
[d]Calculated values in parentheses.
[e]Decomposed.
[f]For n.m.r., see Experimental.
[g]Not necessarily racemic.
[h]Difficult to purify. The corresponding hydrochloride was more easily purified.
[i]Based on a three-step reaction from leucine.
[j]Diester.
[k]Literature value: 210–212° (9).
[l]From the corresponding hydrobromide.
[m]0.0 in methanol.

leucine instead of carbobenzoxy-leucine. The products were characterized by elemental analysis, i.r. spectra and, in some cases, n.m.r. spectra. The high-frequency carbonyl absorption in i.r. (1755–1775 cm^{-1}) and the low-field methylene resonance peak in n.m.r. (τ 4.95–5.30) were found to be characteristic of the $—COOCH_2CCl_3$ group (8). The crystalline ester hydrobromides and some of their physical data are presented in Table 1. Unfortunately, two amino acids, namely proline and isoleucine, gave oily ester hydrohalides, and some dipeptides containing these amino acids were also obtained as oils. The identity of these noncrystalline compounds was confirmed by converting them to the *p*-nitrobenzyl or the acetyl derivatives which were then characterized as shown in Table 2.

To prepare the 2,2,2-trichloroethyl ester of a polypeptide, a carbobenzoxy-amino acid or carbobenzoxy-peptide was condensed to the 2,2,2-trichloroethyl ester of a second amino acid or peptide. *N,N'*-Dicyclohexylcarbodiimide (DCC) was found to be an excellent condensing agent for this purpose when the reaction was carried out in acetonitrile, a solvent which is known to suppress the formation of undesirable *N*-acylurea (12). When the reactants were not sufficiently soluble in acetonitrile, a minimum amount of dimethylformamide was added to effect a satisfactory solution. The acid chloride method using $POCl_3$ or PCl_5 tended to result in tar which was difficult to work-up, although it worked fairly well for the preparation of carbobenzoxy-glycyl-glycine trichloroethyl ester. The polypeptides prepared are summarized in Table 3.

The removal of the 2,2,2-trichloroethyl protecting group was effected by dissolving the compound in 90% acetic acid and treating it with an excess (3–6 mol) of zinc powder for 1.5–2 h, while stirring and cooling in an ice bath. The

Can. J. Chem. Downloaded from www.nrcresearchpress.com by 210.87.254.40 on 09/05/12
For personal use only.

TABLE 2. 2,2,2-Trichloroethyl esters of miscellaneous acylamino acids and acyldipeptides

Compound[a]	M.p. (°C)[b]	Yield (%)[c]	$[\alpha]_D$[d]	I.r.(CO) (cm^{-1}, ester)	Analysis[e] C	H	Cl	N
*p*NBz-Pro-OR[f]	100–102	11 (4)	−44.9 (1.05)	1776[g] 1762	42.25 (42.50)	3.10 (3.31)	26.42 (26.89)	6.73 (7.08)
*p*NBz-Ile-OR[h]	92–93	16 (4)	+14.7 (1.43)	1761	44.04 (43.76)	4.36 (4.16)	26.05 (25.84)	7.06 (6.81)
*p*NBz-Pro-Gly-OR[i]	145–147	67 (3)	−69.9 (1.05)	1780 1770	42.83 (42.45)	3.69 (3.56)	23.26 (23.50)	9.39 (9.28)
*p*NBz-Gly-Leu-OR[j]	165–168	(6)	0.0 (1.21)	1765	43.84 (43.56)	4.51 (4.30)	22.57 (22.69)	9.09 (8.96)
*p*NBz-Gly-Ile-OR[h]	152–154	4 (6)	−11.3 (0.93)	1757	43.81 (43.56)	4.36 (4.30)	22.89 (22.69)	8.97 (8.96)
Ac-Pro-OR[f]	75–77	57 (4)	−67.0 (1.41)	1780 1775	37.80 (37.46)	4.27 (4.19)	36.60 (36.86)	4.81 (4.85)

[a]R = CH_2CCl_3; *p*NBz = *p*-nitrobenzyl; Ac = acetyl.
[b]As recrystallized from ethanol or methanol; uncorrected.
[c]The figure in parentheses is the number of steps involved.
[d]Read in DMF solution. Concentration of material in parentheses.
[e]Calculated values in parentheses.
[f]From proline.
[g]N.m.r. in $CDCl_3$: τ 7.82 (m, 4H, C-3 and -4 protons); 6.40 (m, 2H, C-5 protons); 5.27 (m, 1H, C-2 proton); 5.20 and 5.10 (two singlets of about equal intensity, 2H, $COOCH_2CCl_3$); 2.24 and 1.70 (in A_2B_2 pattern, 4H, aromatic); The two singlets for CH_2CCl_3 are probably due to the rotamers resulting from the restricted rotation along the N—CO bond (10, 11).
[h]From isoleucine
[i]From HBr·Gly-OCH_2CCl_3.
[j]From leucine; yield not calculated.

ester was thus selectively removed without affecting the carbobenzoxy group. The yields in general were good to fair (63–83%) except in the case of Z-Leu-Ala-Gly-OCH_2CCl_3 which gave only 31% of the corresponding carbobenzoxy–tripeptide acid. It must be pointed out, however, that the reaction conditions and yields reported are not necessarily optimal. The unreacted ester recovered during the work-up process (Z-Asn-Ala-OCH_2CCl_3, for example) was treated again with fresh zinc powder to enhance the yield. As expected, the high-frequency carbonyl absorption in i.r. and the low-field resonance peak in n.m.r. ascribed to the —$COOCH_2$-CCl_3 moiety were no longer observed in the detrichloroethylated products and the Beilstein test confirmed the absence of chlorine.

A relatively more thorough study was done on the removal of the trichloroethyl protecting group from carbobenzoxy-glycylglycine trichloroethyl ester. The reaction carried out in 70% acetic acid at room temperature for 1 h gave 80% yield as compared to 41% obtained from the reaction carried out in 90% acetic acid at ice bath temperature for 1.5 h. When the reaction was performed in glacial acetic acid at room temperature for 4 h, the completely deprotected glycylglycine was the only isolable product in 32% yield; not only the trichloroethyl group but also the carbobenzoxy group was removed.[5] On the other hand, no reaction took place in 60% acetic acid at room temperature for 2–3 h and the starting material was recovered. Certainly the yield can be improved by adjusting the conditions to the optimum, but as it stands now, it can be safely stated that the 2,2,2-trichloroethyl protecting group can be selectively removed without affecting the second protecting group. The carbobenzoxy-peptides thus prepared are listed in Table 4. The only racemization study performed during this work consisted in the comparison of the optical activity of several carbobenzoxy-peptides with literature values, when available. As shown in Table 4, all measured values except one (Z-Leu-Ala-Gly-Val-OH) agreed well with those already reported. This indicates only that if there is racemization at any stage of the reaction course (introduction or removal of the protecting group or peptide forma-

[5]Under the same conditions, Z-Gly-OH was practically unaffected (90% recovery). Apparently, the carbobenzoxy moiety of Z-Gly-OH is more resistant to Zn–AcOH treatment than that of Z-Gly-Gly-OCH_2CCl_3 for which we are unable to offer a reasonable explanation.

Can. J. Chem. Downloaded from www.nrcresearchpress.com by 210.87.254.40 on 09/05/12
For personal use only.

TABLE 3. 2,2,2-Trichloroethyl esters of some peptides

Compound[a]	M.p.(°C)[b] Solvents[c]	Yield %	$[\alpha]_D$[d]	I.r.(CO) (cm^{-1} ester)	Analysis[e] C	H	Cl	N
Z-Gly-Gly-OR[f]	96–98[g]	88		1778[i]	41.96	4.05	26.55	7.15
	M–W	68[h]		1770	(42.28)	(3.80)	(26.75)	(7.05)
Z-Gly-Ala-OR[f]	94–97							
	E–W	92	−30.7	1762	44.03	4.27	26.20	6.61
			(1.03)		(43.76)	(4.16)	(25.84)	(6.81)
Z-Pro-Leu-OR[f]	124–126	64	−35.3	1765	51.25	5.80	21.24	5.87
	E–W		(1.19)		(51.07)	(5.51)	(21.54)	(5.67)
Z-Phe-Gly-OR[f]	113–115	49	−20.1	1762	51.63	4.14	21.63	5.68
	E		(1.05)		(51.71)	(4.34)	(21.81)	(5.74)
Z-Asn-Leu-OR[f]	135–137[j]	72	−20.4[k]	1762	47.03	5.11	20.73	8.43
	EA–PE		(1.03)		(47.02)	(5.13)	(20.82)	(8.23)
	E–W							
Z-Leu-Ala-OR[f]	oil	98		1765	[l]			
HBr·Gly-Gly-OR[m]	220–223[n]	98		1766	20.93	3.03	30.69	8.24
	E				(20.92)	(2.93)	(30.88)	(8.14)
HBr·Gly-Ala-OR[m]	220–223[n]	86	−55.6	1755	23.12	3.19	29.41	8.00
	E		(0.85)		(23.45)	(3.38)	(29.67)	(7.82)
HBr·Gly-Val-OR[m]	163–165	66		1753	[l]			
	E–Eth							
Z-Pro-Gly-Gly-OR[o]	109–111	65	−27.9	1768	46.01	4.40	21.20	8.66
	MC–PE		(1.89)		(46.12)	(4.48)	(21.50)	(8.49)
Z-Pro-Val-Leu-OR[o]	153–155	78	−39.7	1763	52.83	5.90	17.60	7.00
	E		(1.19)		(52.66)	(6.12)	(17.94)	(7.09)
Z-Pro-Ile-Leu-OR[o]	159–161	40	−43.9	1765	53.63	6.11	17.35	6.85
	E		(1.32)		(53.43)	(6.31)	(17.53)	(6.92)
Z-Gly-Asn-Leu-OR[p]	156–158	80	−20.5	1763	46.78	5.35	18.75	10.14
	AA–W		(0.77)		(46.53)	(5.15)	(18.73)	(9.87)
Z-Asp-$(Gly\text{-}OR)_2$[f]	124–126	68	−4.95	1765	37.26	2.99	33.27	6.38
	E		(1.06)		(37.29)	(3.29)	(33.03)	(6.52)
Z-Leu-Ala-Gly-Val-OR[q]	135–138	66	−39.8[r]	1762	50.27	5.80	17.07	9.25
	EA–PE		(1.19)		(50.04)	(5.98)	(17.05)	(8.98)
Z-Glu-$(Gly\text{-}OR)_2$[f]	110–115	61		1767	[s]			
	EA–PE							
Z-Val-Glu-$(Gly\text{-}OR)_2$[t]	150–153	56	−25.0	1767	41.49	4.50	27.82	7.61
	EA–PE[j]		(1.05)		(41.23)	(4.26)	(28.09)	(7.40)
	E–W							

[a] R = CH_2CCl_3. All couplings were achieved by DCC in acetonitrile except one (see footnote *h*).
[b] Uncorrected.
[c] M = methanol; E = ethanol; W = water; EA = ethyl acetate; PE = petroleum ether (30–60°); Eth = diethyl ether; MC = methylene chloride; AA = acetic acid.
[d] Read in DMF solution; concentration in parentheses.
[e] Calculated values in parentheses.
[f] From the corresponding Z-A′-OH and HX·A″-OR.
[g] Dimorphism: m.p. 108–110° in ethanol.
[h] Obtained by PCl_5 in THF.
[i] For n.m.r., see Experimental.
[j] Recrystallized from EA–PE first and then from E–W.
[k] Read in ethanol solution.
[l] Not analyzed but used to prepare a tetrapeptide giving a good analysis (footnote *q*).
[m] From the corresponding Z-A′-A″-OR.
[n] Decomposed.
[o] From Z-Pro-OH and the appropriate HBr·A′-A″-OR.
[p] From Z-Gly-OH and HBr-Asn-Leu-OR.
[q] From Z-Leu-Ala-OH and HBr·Gly-Val-OR.
[r] Read in methanol solution.
[s] Not analyzed but used to prepare a tetrapeptide giving a good analysis (footnote *t*).
[t] From Z-Val-OH and HBr·Glu-$(Gly\text{-}OR)_2$.

Can. J. Chem. Downloaded from www.nrcresearchpress.com by 210.87.254.40 on 09/05/12
For personal use only.

TABLE 4. *N*-Carbobenzoxy-peptides obtained by removal of the 2,2,2-trichloroethyl protecting group

Compound	M.p.(°C)[a] solvents[b]	Yield %	$[\alpha]_D$[c]	I.r.(CO) (cm^{-1})(COOH)	Literature values M.p.(°C)	Literature values $[\alpha]_D$	Literature values Reference
Z-Gly-Gly-OH	176–178 E–W	83		1738	178		13
Z-Gly-Ala-OH	180–181 E–W	69	−9.5[d] (1.4)	1725	182–184	−10.0[d] (0.5)	14
Z-Pro-Leu-OH	114–115[e] EA–PE	81	−62.5[f] (4.97)	1730	136.5–139.5	−63.0[f] (5.0)	15
					118.5–119.5	−62.5[f] (5.0)	16
Z-Phe-Gly-OH	150–151 EA–PE	77	−9.9[g] (3.2)	1745	154	−10.2[g] (4.2)	17
Z-Asn-Leu-OH	174–176 DMF–W	61	−5.5[h] (1.4)	1725	178–180	+5.0[h,i] (1.0)	18
Z-Leu-Ala-OH	147–149 EA–PE	55	[j]	1722	151–152	−25.7 (2.6)	19
Z-Leu-Ala-Gly-Val-OH[k]	195–198 E–W	64	−35.2[f] (1.05) −29.4[d] (1.25)	1706	199–200	−23.8[d] (2.0)	20

[a]Uncorrected.
[b]For explanation, see footnote *c*, Table 3.
[c]Concentration in parentheses.
[d]Read in ethanol.
[e]Dimorphism (15, 16)
[f]Read in methanol.
[g]Read in acetic acid.
[h]Read in dimethylformamide.
[i]For the peptide prepared from D-amino acids.
[j]Not measured.
[k]Anal. Calcd. for $C_{24}H_{36}N_4O_7$: C, 58.52; H, 7.37; N, 11.38. Found: C, 58.66; H, 7.35; N, 11.14.

tion), its magnitude is not very great and the undesired isomer is finally easily removed.

The results of the present study, limited as they may be, indicate that the 2,2,2-trichloroethyl group is reasonably well introduced and selectively removed, permits the selective removal of the carbobenzoxy group and does not seem to induce more racemization than the other carboxyl protecting groups. Even if the complete absence of racemization remains to be proved and although the reaction conditions and yields are yet to be improved, this protecting group should find a good use, general or specific, in peptide synthesis. It might be useful, for example, in protecting the carboxyl group of asparagine and glutamine because, as is well known, the methyl or ethyl esters of these two amino acids give a certain amount of their respective iso-compound upon saponification (21, 22). By virtue of requiring no base for their removal, the corresponding trichloroethyl esters should avoid the formation of these secondary products during the deprotection step.

Experimental

Melting points are uncorrected and were determined in an electrical apparatus. Elemental analyses were effected by Dr. C. Daesslé, Organic Microanalysis, 5757, Decelles St., Montréal. Samples were dried at 80–100° under 0.1 mm of mercury during at least 18 h before analysis.

Preparation of 2,2,2-Trichloroethyl Esters of N-Carbobenzoxy-amino Acids

In a typical procedure, 2.5 ml (0.027 mol) of $POCl_3$ was added to a cooled (0°) and stirred solution of Z-Gly-OH (4.18 g, 0.02 mol) in 80–100 ml of tetrahydrofuran. The mixture was allowed to stir for an additional 2 h and then the solvent was removed by evaporation under vacuum at room temperature. The residue was dissolved in fresh tetrahydrofuran (30–50 ml) followed by removal of the solvent as before; the same procedure was repeated 2–3 times. The residue was finally dissolved in tetrahydrofuran (100 ml) and 7.45 g (0.05 mol) of CCl_3-CH_2OH was added. The mixture was made alkaline by adding 10–15 ml of triethylamine and stirred overnight. The precipitate was filtered and washed on the filter with tetrahydrofuran and the filtrate was concentrated under vacuum. The residue was taken in ether and washed with water, dilute HCl, dilute $NaHCO_3$, and water. The ether layer was dried over Na_2SO_4 and concentrated under vacuum to give a crude yellow or orange oil which was then treated with 3 *N* HBr–AcOH as described below.

Can. J. Chem. Downloaded from www.nrcresearchpress.com by 210.87.254.40 on 09/05/12
For personal use only.

Can. J. Chem. Downloaded from www.nrcresearchpress.com by 210.87.254.40 on 09/05/12
For personal use only.

Preparation of Hydrobromides of 2,2,2-Trichloroethyl Esters of Amino Acids

In a typical procedure, the unpurified oily Z-Gly-OCH_2CCl_3 described above was treated with 20 ml (0.06 mol) of 3 *N* HBr in acetic acid for 2 h at room temperature during which time a vigorous evolution of gas occurred. Dry ether was added to precipitate out the hydrobromide which was then filtered and recrystallized from ethanol–ether to yield 4.1 g (71%) of crystals, m.p. 238–240°. An analytical sample obtained by an additional recrystallization melted with decomposition at 242–244°. N.m.r. in DMSO-d_6: τ 5.93 (s, NCH_2CO), 4.96 (s, $COOCH_2CCl_3$), 1.46 (s, washed away with D_2O, NH_3^+). No coupling between the protons appearing at τ 5.93 and 1.46 was observed.

Preparation of 2,2,2-Trichloroethyl Esters of Polypeptides: 2,2,2-Trichloroethyl N-Carbobenzoxyglycylglycinate

Method A

To a cooled (ice bath) and stirred solution of 4.18 g (0.02 mol) of Z-Gly-OH in 80 ml of acetonitrile, there was added 4.08 g (0.02 mol) of dicyclohexylcarbodiimide dissolved in 40 ml of the same solvent followed by a suspension of 6.89 g (0.024 mol) of $HBr \cdot Gly\text{-}OCH_2CCl_3$ in 80 ml of acetonitrile containing 3.5 ml of triethylamine. The mixture protected from the atmospheric moisture was stirred for 1 h in the ice bath and then overnight at room temperature. The precipitated dicyclohexylurea (3.95 g) was filtered off and washed with CH_3CN and water. The filtrate and washes were combined and concentrated under vacuum, the residue was taken up in ether and washed with water, dilute HCl, dilute $NaHCO_3$, and water. Drying and evaporation of the solvent gave a solid which was crystallized in methanol–water yielding 6.96 g (87.7%) of crystals, m.p. 95–97°.

Method B

Tetrahydrofuran (200 ml) dried over $NaBH_4$ was distilled into a mixture of 4.1 g (0.0147 mol) of $HBr \cdot Gly\text{-}OCH_2CCl_3$ and 3 g (0.0147 mol) of Z-Gly-OH. While stirring and cooling in an ice-salt bath, the mixture was treated with 3.1 g (0.0147 mol) of PCl_5 for 1 h. Triethylamine (15 ml, 1 mol) was added and the mixture was stirred for 1 h in the ice bath and overnight at room temperature. The solvent was removed under vacuum and 150 ml of water was added to the oily residue which solidified when cooling in ice. The solid was filtered and recrystallized from ethanol–water, giving 4.1 g (70.2%) of crystals, m.p. 95–97°.

This compound exhibits dimorphism. When it was dissolved in boiling ethanol, filtered, and cooled, high-melting crystals were obtained, m.p. 108–110°. When it was dissolved in methanol at room temperature (1 g in 50–100 ml), filtered, and diluted with an equal volume of water, low-melting crystals were obtained, m.p. 96–98°. The i.r. spectra taken in Nujol mull showed distinct differences. In the amino and carbonyl region, the high-melting compound exhibited absorption bands at 3355, 3345, 3275, 3115, 1778 (w), 1763 (s), 1712, and 1680 cm^{-1} while the low-melting compound absorbed at 3350, 3290, 1778 (s), 1770 (s), 1714, 1697, and 1677 cm^{-1}. However, the spectra taken in chloroform solutions were identical with amino and carbonyl absorptions appearing at 3440, 3320, 1773, and 1730–1687 cm^{-1}. The n.m.r. spectra in chloroform for both compounds were the same: τ 6.13 (d, J = 6 Hz, $CH_2COOCH_2CCl_3$), 5.91 (d, J = 6 Hz, CH_2CONH), 5.27 (s, OCH_2CCl_3), 4.94 (s, $OCH_2C_6H_5$), 4.01 (t, J = 6 Hz, $NHCH_2COOCH_2CCl_3$), 2.78 (t, J = 6 Hz, $NHCH_2CONH$), 2.70 (s, C_6H_5). Furthermore, both substances, when treated with HBr–AcOH, yielded almost quantitatively the same hydrobromide of 2,2,2-trichloroethyl glycylglycinate, m.p. 220–223° (dec.) having i.r. absorptions in Nujol at 3283, 3208, 3054, 1766, 1690, and 1182 cm^{-1}.

Removal of the Trichloroethyl Group: Preparation of Carbobenzoxyleucylalanylglycylvaline

In a typical experiment, a solution of 0.5 g (0.8 mmol) of Z-Leu-Ala-Gly-Val-OCH_2CCl_3 in 25 ml of 90% acetic acid was treated under cooling with 2 g of zinc powder in three portions at 5 min intervals and the mixture was stirred for 1.5 h. The mixture was filtered and the unreacted zinc was washed with 90% acetic acid. The filtrate was concentrated under vacuum, the residue dissolved in 80 ml of dilute HCl and extracted with two 80-ml portions of ethyl acetate. The combined extracts were washed with 100 ml of saturated $NaHCO_3$ solution, this solution acidified with dilute HCl and the peptide reextracted with three 80-ml portions of AcOEt (or AcOEt–Et_2O mixture). The organic extracts were concentrated to give 0.25 g (63.5%) of crystals, m.p. 193–195°, having i.r. absorption in Nujol at 3275 (NH), 1706 (CO of COOH) and 1693 cm^{-1} (CO of amide). The analytical sample melts at 195–198° (EtOH–H_2O); (lit. (20), 199–200°).

Removal of the Trichloroethyl Group from 2,2,2-Trichloroethyl N-Carbobenzoxyglycylglycinate

Method 1

A solution of 0.92 g (2.32 mmol) of the peptide ester in 10 ml of 70% acetic acid was treated with 0.5 g of zinc powder for 1 h. The reaction mixture was diluted with water, filtered, and the filtrate extracted with ethyl acetate. The organic extract worked-up as described above gave 0.51 g (82.5%) of carbobenzoxyglycylglycine, m.p. 170–173° (ethanol–water), having a mixed m.p. 174–175° with an authentic sample (13).

Method 2

A solution of 0.8 g (2 mmol) of the peptide ester in 25 ml of 90% acetic acid was treated with 0.65 g of zinc powder and worked-up as described above for the tetrapeptide ester. A 41% yield (0.22 g) of carbobenzoxyglycylglycine, m.p. 176–178° was obtained.

Method 3

When 0.5 g (1.26 mmol) of Z-Gly-Gly-OCH_2CCl_3 was treated with 0.5 g of zinc powder in glacial acetic acid (5 ml) for 4 h, the only product isolated after work-up was 0.09 g of glycylglycine, m.p. 224–228° (dec.) (lit. 216–222° (dec.) (23)).

We thank the National Research Council of Canada for financial help and Dr. F. L. Chubb, Director of Chemical Research, for his understanding and encouragement throughout this work.

1. M. BODANSZKY and M. A. ONDETTI. Peptide synthesis. Interscience Publishers, New York. 1966. p.
2. A. KAPOOR. J. Pharm. Sci. **59**, 1 (1970).
3. A. E. GREENE, V. E. MARTYNOV, and M. I. TITOV. Zh. Obshch. Khim. **38**, 664 (1968); Chem. Abstr. **69**, 97143*j* (1968).
4. M. J. S. A. AMARAL. J. Chem. Soc. C, 2495 (1969).
5. R. B. WOODWARD, K. HEUSLER, S. GOSTELI, D. NAEGELI, W. OPPOLZER, R. RAMAGE, S. RANGANATHAN, and H. VORBRÜGEN. J. Am. Chem. Soc. **88**, 852 (1966).
6. F. ECKSTEIN. Angew. Chem. Int. Ed. **4**, 876 (1965).
7. T. B. WINDHOLZ and D. B. R. JOHNSON. Tetrahedron Lett. 2555 (1967).
8. E. D. EVANS, R. L. S. PATTERSON, and D. WOODCOCK. Tetrahedron Lett. 555 (1969).
9. E. S. GRANATEK and A. P. GRANATEK. S. Afr. 67 07 666, July 23, 1968.
10. G. H. COOPER. Chem. Ind. 1304 (1969).
11. R. GARNER and W. B. WATKINS. J. Chem. Soc. D, 386 (1969).
12. J. C. SHEEHAN, M. GOODMAN, and G. P. HESS. J. Am. Chem. Soc. **78**, 1367 (1956).
13. F. MICHEEL and W. MECKSTROTH. Ber. **92**, 1675 (1959).
14. G. LOSSE and E. DEMUTH. Ber. **94**, 1762 (1961).
15. W. D. CASH. J. Org. Chem. **26**, 2136 (1961).
16. G. W. ANDERSON and F. M. CALLAHAN. J. Am. Chem. Soc. **82**, 3359 (1960).
17. D. W. CLAYTON, J. A. FARRINGTON, G. W. KENNER, and J. M. TURNER. J. Chem. Soc. 1398 (1957).
18. E. NICOLAIDES, H. DEWALD, R. WESTLAND, M. LIPNIK, and J. POSLER. J. Med. Chem. **11**, 74 (1968).
19. H. D. JAKUBKE. Ann. **682**, 244 (1965).
20. R. B. MERRIFIELD. J. Am. Chem. Soc. **85**, 2149 (1963).
21. E. SONDHEIMER and R. W. HOLLEY. J. Am. Chem. Soc. **76**, 2467 (1954).
22. E. SONDHEIMER and R. W. HOLLEY. J. Am. Chem. Soc. **79**, 3767 (1957).
23. H. SCHWARZ and K. ARAKAWA. J. Am. Chem. Soc. **81**, 5691 (1959).

Can. J. Chem. Downloaded from www.nrcresearchpress.com by 210.87.254.40 on 09/05/12
For personal use only.

The Radiochemistry of Organoiron Compounds. III. $Fe(CO)_5$–Cyclopentadiene Solutions

W. KANELLAKOPULOS-DROSSOPULOS AND D. R. WILES

Institut für Heisse Chemie, Kernforschungzentrum Karlsruhe, Germany

and

Department of Chemistry, Carleton University, Ottawa, Canada K1S 5B6

Received July 13, 1972

Nucleogenesis of ^{59}Fe gives iron atoms which react with monomeric cyclopentadiene to produce $^{59}FeCp_2$, either in liquid or solid solutions, but do not react appreciably with dimeric cyclopentadiene. This is taken as showing that local thermal effects of the nuclear reactions are ineffective in causing the dissociation $(C_5H_6)_2 \rightarrow 2C_5H_6$. The concentration dependence of the yield of $^{59}FeCp_2$ indicates that the ^{59}Fe atom reacts primarily at its point of genesis rather than after diffusion.

La nucléogénèse du ^{59}Fe libère des atomes de fer qui réagissent avec du cyclopentadiène monomérique pour produire du $^{59}FeCp_2$, en solution liquide ou solide, mais ne réagissent pas d'une manière appréciable avec du cyclopentadiène dimérique. Ceci démontre que les effets thermiques locaux des réactions nucléaires ne sont pas efficaces pour causer la dissociation $(C_5H_6)_2 \rightarrow 2C_5H_6$. La dépendance du rendement du $^{59}FeCp_2$ sur la concentration montre que l'atome ^{59}Fe réagit principalement lors de sa génèse plutôt qu'après diffusion. [Traduit par le journal]

Can. J. Chem., **51**, 215 (1973)

Recent radiochemical studies of organoiron (1, 2) and organomanganese (3, 4) compounds have been directed toward identifying the nature and the times of chemical reactions which follow nuclear reactions and lead to the observed identifiable radioactive products. These reactions are caused by some manifestation of the nuclear excitation energy: physical recoil at energies of some hundreds of eV, or strong rapid ionization (up to +10 or +15) following the emission of Auger electrons, or some intermediate combination of these two extremes. It is not at present known whether it is the nuclear de-excitation which governs the ensuing chemical reactions or whether the reactions are more characteristic of the (damaged) matrix irrespective of the mode of generation of the radioactive atom. In particular, the time of the reaction has been under study: whether the reaction occurs immediately after the nuclear event, whether it occurs by subsequent thermal processes, or whether, in fact, some critical bonds remain intact during and after the nuclear transformation.

A recent study (2) using ^{58}Fe-depleted ferrocene ($FeCp_2$) has shown that $^{59}FeCp_2$ can be formed in good yield from ^{59}Fe atoms never before bonded to cyclopentadiene but which come rather from the reaction

$$[1] \qquad {}^{58}Fe(CO)_5\ (n,\gamma)\ {}^{59}Fe + \ldots$$

and which appear to exchange or otherwise react thermally with $FeCp_2$ molecules. On the other hand, a study of $[CpFe(CO)_2]_2$ activated by neutrons (1) showed that, while Fe—CO bonds can be formed subsequently to the nuclear reaction by thermal processes, there was no evidence to suggest that Fe—Cp bonds could be formed other than instantaneously. There appears thus to be an

$$[2] \qquad [CpFe(CO)_2]_2 \xrightarrow{(n,\gamma)} {}^{59}FeCp_2 + {}^{59}Fe(CO)_5 + [Cp^{59}Fe(CO)_2]_2 + \ldots$$

inconsistency in the behavior of the iron atoms. In the one case the Fe—Cp bond is formed by an apparently thermal reaction while in the other case the Fe—Cp bond formation seems to be exclusively epithermal.

It is often observed (2, 5, 6) that, when compounds are neutron irradiated in solution, the yield of the radioactive parent compound ("retention") is markedly lower. There are, however, some cases in which this is not so, notably instances in which the solvent is a potential reactant. For example, when $AsCl_3$ is neutron irradiated in benzene solution, various phenylarsenic compounds are formed (7). Ruthenium—Cp bonds are formed in high yield when ruthenium atoms are produced by nucleogenesis in solutions of monomeric cyclopentadiene, but not in solutions of the dimer (8). Furthermore, when

U_3O_8 and $FeCp_2$ are neutron-irradiated together as a mixture of the powdered solids, a large fraction of the fission-product ^{105}Ru is found (9) as $RuCp_2$, after the Fe—Cp bonds are somehow broken.

In an attempt to resolve the apparent contradiction in the behavior of iron atoms toward cyclopentadiene, we have studied the formation of $^{59}FeCp_2$ in solutions (both solid and liquid) composed of $Fe(CO)_5$, cyclopentadiene and benzene. The objective of the study was to learn whether the newly-generated ^{59}Fe atom is able to react with nearby (or distant) free $(Cp)_1$ and perhaps $(Cp)_2$ molecules or whether reaction must involve bonded Cp ligands.[1]

Experimental

Reagents used were the purest available, purified further by sublimation or distillation *in vacuo* or under nitrogen. Monomeric cyclopentadiene was produced by thermal cracking of the dimer and distillation at 40°, and preserved at liquid nitrogen temperature until use.

Samples for neutron irradiation were prepared under nitrogen, degassed, rapidly frozen, and sealed *in vacuo*. Those solutions which were to be irradiated at low temperatures were stored under liquid nitrogen, both before and after the irradiation, up to the time of the separation.

Neutron irradiation was done for 24 h in the thermal column of the FR-2 research reactor in Karlsruhe, where the reported thermal neutron flux is 3×10^{11} cm^{-2} s^{-1} and the temperature about 40°.

Separation of the components of the samples was done after adding 30 mg $FeCp_2$ carrier. Cyclopentadiene and $Fe(CO)_5$ were removed under vacuum at room temperature. The $FeCp_2$ was purified by column chromatography on silica gel, followed by sublimation under nitrogen. An experiment done without added carrier showed that no detectable quantity of $FeCp_2$ (*i.e.*, $\lesssim 0.1\%$ of the theoretical maximum) was produced either during long (5 days) standing of the samples at room temperature, or during 24-h neutron bombardment of the samples at 40°. All operations were carried out in subdued light to avoid the effects of possible photolysis.

Radioactivity measurements were made using a well-type sodium iodide scintillation counter. Correction was made for losses in chemical recovery. Only the yield of $^{59}FeCp_2$ was measured. This is reported as that fraction of the total ^{59}Fe radioactivity which appears as $^{59}FeCp_2$.

Results and Discussion

The results of neutron irradiation of solutions containing either monomeric $(Cp)_1$ or dimeric $(Cp)_2$ cyclopentadiene are given in Table 1.

TABLE 1. Yields of $^{59}FeCp_2$ from neutron irradiated solutions of $Fe(CO)_5$, benzene, and Cp_1 or Cp_2; volume ratio, 2:1:1.

Conditions*		$^{59}FeCp_2$ yields†	
		Observed	Corrected‡
−78 °C,	$(Cp)_2$	0.57±0.02$_5$§	0.0
−78 °C,	$(Cp)_1$	13.6 ±0.2	13.0
40 °C,	$(Cp)_2$	1.55±0.09	1.0
40 °C,	$(Cp)_1$	7.5 ±0.1	6.9

*Approximate irradiation temperatures and nominal Cp constitution.
†Yield based on the total ^{59}Fe produced.
‡Correct for exchange, see text.
§Error limits are standard deviations of the mean values, based on eight independent experiments for Cp_2 and four for Cp_1, each experiment done in duplicate.

Before discussing these data, possible sources of spurious effects must be examined. The simplest of these is the possibility of an exchange reaction occurring between the carrier ferrocene and some non-molecular form of the radioactive iron during the chemical separation[2]

[3] $$^{59}Fe + FeCp_2 \rightleftharpoons {}^{59}FeCp_2 + Fe$$

No detailed information on this reaction is available, although upper limits can be set. The value of 0.57% for the ^{59}Fe found as $FeCp_2$ in frozen $(Cp)_2$ solutions (see Table 1) and the value of 0.5% given in ref. 2 are supported by the results of direct measurements[3] made during the course of this work which gave from four determinations $0.64 \pm 0.16\%$ exchange during the separation procedure. We thus adopt the figure 0.6% as representing the extent of formation of ^{59}Fe by reactions such as that in reaction 3, during the chemical workup. Data corrected for this exchange are given in Table 1.

A second spurious effect could come from bulk radiolytic production of ferrocene, as in reaction 4

[4] $$Fe(CO)_5 + (Cp)_1, (Cp)_2 \xrightarrow{\gamma} FeCp_2 + CO + \ldots$$

As was shown above, it is clear that this bulk reaction must be minimal if it occurs at all.

We note the possibility of segregation of the

[1]We use the following notation for the various forms of cyclopentadiene: $(Cp)_2$ = dimeric $(C_5H_6)_2$; $(Cp)_1$ = monomeric C_5H_6; Cp = cyclopentadiene as ligand; ·Cp = cyclopentadiene radical or temporarily dissociation neutral ligand.

[2]The symbols ^{59}Fe and Fe are *not* intended to signify *atomic* iron, since we do not know the state of the iron at that stage.

[3]This was done by irradiating 2:1 $Fe(CO)_5$–benzene solutions with thermal neutrons and, after adding inactive $FeCp_2$ carrier, comparing the total radioactivity with that of the separated and purified $FeCp_2$. Clearly this exchange reaction could not have occurred during the neutron irradiation, since no $FeCp_2$ was present.

components in the frozen targets, as was suggested for the $FeCp_2$–$Fe(CO)_5$ system. We have no direct evidence on this question, except to point out that, at least in the case of the $(Cp)_1$ monomer, the yield in frozen targets is much higher than could be the case if crystal segregation were at all important. Moreover, the parallel between the $-78°$ and 40° data suggests that no such segregation has occurred to a significant extent.

Finally, there is the possibility that at 40° the dimer may partially monomerize, and *vice versa*. From published thermal data (10) we estimate the equilibrium constant for the dimerization to be about 2×10^4. Hence for our conditions, the equilibrium concentration of $(Cp)_1$ monomer in our dimer solutions is of the order of 0.01 mol l^{-1}, or 0.5% that of the dimer. While this is not a sufficient concentration to influence a hot reaction, it could well influence the fate of a diffusing reactive atom.

The question of dimerization of the monomer is one of the rate, rather than of the equilibrium position. Activation data in the literature (10) show a significant solvent dependence and are not available for the solutions used in this work. Using the data for benzene solutions of $(Cp)_1$, the rate constant for the dimerization in our solution is estimated to be about 0.02 l mol^{-1} h^{-1}, from which it is calculated that about 35% of the monomer remains after 24 h at 40°. The mean concentration is about 2.2 *M* over the 24-h period.

The dependence of the reaction on $(Cp)_1$ concentration is given in Fig. 1, where the yield of the $^{59}FeCp_2$ is shown for 24-h 40° experiments as a function of the initial concentration of the $(Cp)_1$ monomer.

The data presented here show clearly that, in accord with conclusions of Zahn and Harbottle (8), Fe—Cp bonds can be formed in both solid and liquid solutions containing monomeric cyclopentadiene. It is also clear that, when correction is made for reaction induced during separation and for dissociation of the dimer, the dimeric $(Cp)_2$ reacts little, if at all. The solid state results are particularly striking. The yield of 13.7% of $^{59}FeCp_2$ shows that a considerable portion of the (n,γ) events produce an iron atom which is chemically reactive toward $(Cp)_1$ molecules, and which is either unbound or only loosely bound to its former carbonyl ligands. This is in distinction from the results of the $Fe(CO)_5$–$^{56}FeCp_2$–C_6H_6 frozen solutions, where low yields of $^{59}FeCp_2$

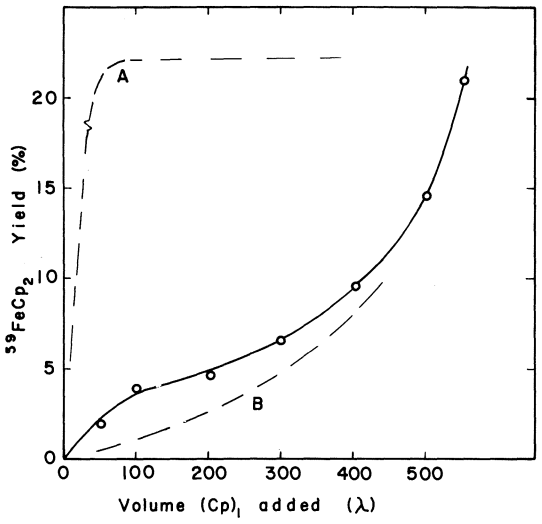

FIG. 1. Variation of the $^{59}FeCp_2$ yield with changes in the initial Cp_1 concentration. The total volume of the solutions was 1.05 ml, assuming no volume change on mixing. For description of curves A and B, see text.

were found and were tentatively interpreted as showing crystalline segregation of the components. By the same token, the present solutions evidently do not segregate on being frozen.

The data for dimeric $(Cp)_2$ solutions are significant in that they show that $(Cp)_2$ is not reactive toward the newly-produced ^{59}Fe atom. While the solid state yield could be explained by segregation on freezing, the above mentioned conclusion regarding the frozen monomeric $(Cp)_1$ solutions suggests that this is unlikely. The liquid solution data also show a very low yield which could perhaps result from the presence of the small amount ($\leqslant 1\%$) of monomer formed by thermal dissociation. This is qualitatively supported by an extrapolation of the data of Fig. 1.

The significant deduction from these results is that local heating from the nuclear reaction is not able to cause thermal dissociation of $(Cp)_2$. This could be for a variety of reasons, but most likely it is that the heated region is too short lived to effect molecular rearrangement. The only estimates published (and these for more tightly bound solids) suggest (11) that about 10^{-11} s is the maximum duration of such a "hot zone". Even if the molecule were to dissociate during this time, it is unlikely that the moieties could become separated and remain apart. If this reasoning is correct, it is apparent that the observed chemical

reactions result from something other than nuclear *recoil.*

The *time* of the reactions is a question which remains. The form of the curve in Fig. 1 may be enlightening in this respect.[4] The strong but slow increase in $^{59}FeCp_2$ yield as the $(Cp)_1$ concentration increases indicates that the Fe atom is essentially unable to react after even a short diffusion path. Curve A shows what one expects for good scavenging of Fe by some form of cyclopentadiene, such as by the exchange reaction shown in reaction 3. Curve B shows, on the other hand, what would be expected if the ^{59}Fe were to react only in its immediate neighborhood. (It is to be emphasized that curves A and B show only qualitative behavior. Quantitative behavior could be assessed only with the help of detailed information on competitive reaction rates, concentrations of competitive reactants, diffusion rates, and so on, which are at present not known.) One infers from the comparison of the data with curves A and B that the reaction is mostly with nearest neighbors. The small deviation from the form of curve B may indicate that a fraction of the ^{59}Fe atoms may react after diffusion. The data are not sufficiently extensive for one to be confident of this point, however.

This behavior is to be contrasted with the observation (12) that in $Ni(CO)_4$–hexane solutions the yield of $^{65}Ni(CO)_4$ remains high on progressive dilution with hexane, even when the target $Ni(CO)_4$ is diluted down to 2%. This observation is moreover in accord with the results for $[CpFe(CO)_2]_2$ in suggesting that the reaction Fe + Cp → Fe—Cp is very fast if it is to occur at all. The apparent conflict with the results of the $^{56}FeCp_2$–$^{58}Fe(CO)_5$ study (2) may suggest that the cyclopentadiene in ferrocene is somehow more reactive toward iron atoms than is $(Cp)_1$. One notes a difference between this reaction and that of $CH_3CpMn(CO)_3$ neutron bombarded in 2,2,4-trimethylpentane solutions (13). Here the $^{56}Mn(CO)_5$ radical is able to react effectively with radiolytically produced methyl groups so that the yield of $CH_3{}^{56}Mn(CO)_5$ increases ten-fold on dilution of the $CH_3CpMn(CO)_3$ sample (before neutron irradiation) with 2,2,4-trimethylpentane. It is interesting to recall that the further addition (also before neutron irradiation) of a small amount of $Fe(CO)_5$ entirely quenched the formation of $CH_3{}^{56}Mn(CO)_5$.

In summary, it is shown in this work that the reaction

$$[5] \qquad Fe(CO)_5 + (Cp)_1 \xrightarrow{(n,\gamma)} {}^{59}FeCp_2 + \ldots$$

occurs to a considerable extent between the newly-generated ^{59}Fe atom and adjacent monomeric $(Cp)_1$ molecules, but that neither reaction with dimeric $(Cp)_2$ nor reaction following short diffusion is effective. From this work and the previous study (2) on solutions of $FeCp_2$ in $Fe(CO)_5$, it appears that the order of reactivity of the cyclopentadiene with "hot" iron atoms is $FeCp_2 > (Cp)_1 \gg (Cp)_2$ in the reaction

$$[6] \quad {}^{59}Fe + \begin{cases} FeCp_2 \\ (Cp)_1 \\ (Cp)_2 \end{cases} \rightarrow {}^{59}FeCp_2 + \begin{cases} Fe, FeCp \\ H + \ldots \\ H \end{cases}$$

The next question, not answered in this work, is whether failure to react after diffusion is the result of loss of thermal or electronic excitation or whether it comes rather from competitive reaction with accidental (or radiolytic) scavengers.

We are pleased to express our gratitude to Professor dr. F. Baumgärtner for his support and criticism. Mrs. E. Rauch gave able experimental assistance.

1. W. Kanellakopulos-Drossopulos and D. R. Wiles. Can. J. Chem. **49**, 2977 (1971).
2. W. Kanellakopulos-Drossopulos and D. R. Wiles. Radiochim. Acta, **16**, 179 (1971).
3. I. G. de Jong, S. C. Srinivasan, and D. R. Wiles. Can. J. Chem. **47**, 1324 (1969).
4. I. G. de Jong, S. C. Srinivasan, and D. R. Wiles. J. Organometal. Chem. **26**, 119 (1971).
5. U. Zahn. Radiochim. Acta, **7**, 170 (1967).
6. I. C. Yang and D. R. Wiles. Can. J. Chem. **45**, 1357 (1967).
7. K. E. Siekierska, A. Sokolowska, and I. G. Campbell. J. Inorg. Nucl. Chem. **12**, 18 (1954).
8. U. Zahn and G. Harbottle. J. Inorg. Nucl. Chem. **28**, 925 (1966).
9. F. Baumgärtner and P. Reichold. Z. Naturforsch. **16a**, 374 (1961).
10. A. Wassermann. Diels–Alder reactions. Elsevier, London. 1965.
11. G. Harbottle and N. Sutin. J. Phys. Chem. **62**, 1344 (1958).
12. O. H. Wheeler, J. E. Trabal, and D. R. Wiles. Can. J. Chem. **48**, 3609 (1970).
13. I. G. de Jong, S. C. Srinivasan, and D. R. Wiles. Can. J. Chem. **47**, 1327 (1969).

[4]The trend of results in Fig. 1 could not be produced by radiolysis effects in $Fe(CO)_5$, since the iron carbonyl concentration was held constant for these experiments.

Complexes d'hematoporphyrine IX avec le platine(II)[1]: synthese, intermediaires, spectres, interet biologique

J. P. MACQUET ET T. THEOPHANIDES

Université de Montréal, Département de Chimie, Montréal 101, Québec

Reçu le 14 juillet, 1972

La métalloporphyrine HP.Pt a été préparée à partir de l'hématoporphyrine IX (HPH_2) et du platine(II). Un intermédiaire de réaction a été isolé correspondant à la formule $HPH_2.PtCl_2$. Les spectres u.v., visibles, et infrarouges de ces complexes font l'objet de cette présente étude. L'intermédiaire $HPH_2.PtCl_2$ portera la dénomination: "complexe coiffé" caractérisant ainsi la position du groupement $PtCl_2$ sur la porphyrine. Une application biologique de cet intermédiaire dans le traitement de certaines tumeurs est entrevue.

The platinum–porphyrin (HP.Pt) complex was prepared from hematoporphyrin IX (HPH_2) and potassium chloroplatinate(II). An intermediate complex was isolated corresponding to the formula $HPH_2.PtCl_2$. U.v., visible, and i.r. spectra of the complexes are obtained and are discussed. The complex $HPH_2.PtCl_2$ is the first intermediate identified in these reactions. A biological application of this intermediate for the treatment of tumors is sought.

Can. J. Chem., **51**, 219 (1973)

Introduction

L'étude des métalloporphyrines a déjà fait l'objet de maints travaux (1, 2), dûs à l'intérêt biologique qu'elles suscitent, autant dans le métabolisme que dans la photosynthèse. Les métaux les plus couramment rencontrés sont: le fer dans l'hémoglobine, le magnésium dans la chlorophylle, le cobalt dans la vitamine B_{12}, le manganèse dans les plantes et aussi dans le sang (3).

Notre choix s'est porté sur l'hématoporphyrine IX (fig. 1) qui a été trouvée s'accumulant sélectivement dans certaines tumeurs et dans des tissus se développant rapidement (4–6). Le rôle que certaines porphyrines pourraient avoir dans le dépistage de certaines tumeurs semble se concrétiser (7).

Le platine a été choisi pour deux raisons: tout d'abord pour sa forte tendance à former des complexes plan-carrés, stables, donc susceptible d'imposer son hybridation dsp^2 à la porphyrine. L'étude spectrale devrait nous confirmer la grande stabilité de cette métalloporphyrine (1*a*). La seconde raison est d'ordre biologique: certains sels de platine ont déjà montré leur efficacité dans le traitement de tumeurs (8–10).

Lors de la préparation de la métalloporphyrine HP.Pt, il nous a été possible d'isoler et d'identifier un intermédiaire correspondant à la formule $HPH_2.PtCl_2$. A notre connaissance, c'est la première fois qu'un tel intermédiaire est caractérisé de cette façon.

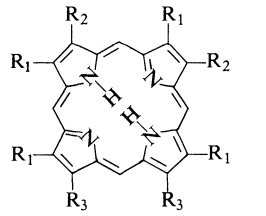

$R_1 = -CH_3$;
$R_2 = -CHOH-CH_3$;
$R_3 = -CH_2-CH_2-C(=O)-OH$

FIG. 1. Représentation structurale de l'hématoporphyrine IX.

Partie expérimentale

Préparation de la métalloporphyrine

La métalloporphyrine HP.Pt a été préparée de la façon suivante: l'hématoporphyrine neutre HPH_2 est dissoute dans de l'acide acétique glacial (1.7×10^{-3} *M*), puis portée à une température de 85 °C. Une solution de K_2PtCl_4 dans l'eau (2.1×10^{-3} *M*), est alors ajoutée à la même température. Les proportions utilisées sont stoechiométriques. Pour faciliter l'incorporation du platine dans la porphyrine, la réaction a lieu en présence d'acétate de sodium, le mélange tampon acide acétique – acétate de sodium s'avérant très efficace lors de la synthèse des métalloporphyrines (1*b*). Le temps de réaction est de 24 h; une partie du complexe reste en solution, la grosse majorité précipite. Le solvant est évaporé, on lave à l'acide acétique puis à l'eau, jusqu'à disparition de la bande Soret (1*c*) de l'hématoporphyrine. Le complexe est recristallisé dans un mélange

[1]Une communication préliminaire de cet article a été présentée au 55e congrès du CIC, Université Laval, 4–7 juin 1972, Québec.

Can. J. Chem. Downloaded from www.nrcresearchpress.com by 210.87.254.5 on 09/05/12
For personal use only.

Can. J. Chem. Downloaded from www.nrcresearchpress.com by 210.87.254.5 on 09/05/12
For personal use only.

DMF/H_2O; il est alors séché sous vide en présence d'anhydride phosphorique. Le rendement de la réaction est supérieur à 80%.

Préparation de l'intermédiaire

Le "complexe coiffé" $HPH_2.PtCl_2$ a été isolé en milieu acétique à 60 °C en utilisant les mêmes concentrations. Le temps de réaction est de 24 h. La purification de cet intermédiaire s'effectue de façon identique à celle de la métalloporphyrine correspondante. La recristallisation de ce complexe montrant une légère dégradation, il a été étudié après purification. Le rendement est de l'ordre de 60%.

L'acide acétique glacial de qualité "Reagent" a été distillé. Les solvants étaient tous de qualité "Reagent" ou "Spectrograde" suivant le cas. L'eau utilisée était distillée. L'hématoporphyrine neutre et le dichlorure provenaient de la compagnie Nutritional Biochemicals Corporation (NBC) et le sel de platine de la compagnie British Drug Houses (BDH).

Les composés préparés ne conduisent pas le courant donc ne présentent aucun caractère ionique. Dans le DMF à 10 °C, la conductivité molaire de $HPH_2.PtCl_2$ est égale à 7.2 et celle de HP.Pt à 2.9 $ohm^{-1}\ cm^2\ mol^{-1}$.

L'étude conductimétrique a été menée avec un "Konductoskop E 365 B", la cellule de verre étant du modèle EA 608.

Analyses

Anal. calc. pour $HPH_2.PtCl_2$: C, 47.22; H, 4.42; Pt, 22.56; Cl, 8.20. Trouvée: C, 47.20; H, 3.71; Pt, 22.14; Cl, 8.58.

Anal. calc. pour HP.Pt: C, 51.57; H, 4.58; Pt, 24.63. Trouvée: C, 51.45; H, 4.54; Pt, 24.14.

Les analyses du carbone et de l'hydrogène ont été effectuées par le laboratoire du Dr Daesslé à Montréal et par Chemalytics Inc., Tempe (Arizona), celles du platine et du chlore par nos soins.

Le pourcentage de platine a été trouvé par calcination du complexe (20 mg) dans un four Linberg Heavy-Duty à 850 °C pendant 45 min. Le dosage du chlore a été effectué avec un "Potentiograph E 336 A" couplé à un "Metrohm Herisav E 436 E", l'électrode utilisée étant une électrode combinée à un fil de platine.

Les spectres u.v., visibles ont été enregistrés sur un spectrophotomètre Cary 14, avec des cellules de quartz de 1 cm de largeur. Les spectres sont reproductibles avec une précision de 1 mμ.

L'étude infrarouge a été conduite avec un spectrophotomètre "Perkin–Elmer IR 621". Chaque complexe (2 mg) a été intimement mélangé à 150 mg de bromure de potassium; ce mélange comprimé sous forme de pastille a servi à l'obtention des spectres. La précision des spectres est de 4 cm^{-1} dans la région 4000–2000 cm^{-1} et de 2 cm^{-1} entre 2000 et 300 cm^{-1}. Un film de polystyrène a été utilisé pour la calibration de l'appareil.

Discussion

Etude visible

Les spectres d'absorption des porphyrines en visible sont interprétés comme étant le résultat de la superposition des vibrations de deux transitions électroniques (1*d*). La première transition s'effectue entre 450 et 700 mμ, elle comporte 4 bandes dont les intensités varient en fonction des substituants périphériques et correspond à la transition $a_{2u} \rightarrow e_g^*$ (π). La seconde a lieu entre 400 et 450 mμ, c'est la bande Soret qui correspond à la transition $a_{1u} \rightarrow e_g^*$ (π). La transformation porphyrine → métalloporphyrine conduit à une simplification du spectre. Les 4 bandes de la première transition sont alors réduites à 2 bandes que l'on appelle α et β (β pour les plus petites longueurs d'onde). Le même spectre est obtenu lors du passage porphyrine neutre → porphyrine diacide, les 4 atomes d'azote portant chacun un H et l'ensemble portant deux charges positives. Cette simplification du spectre a été attribuée à une augmentation de symétrie de la porphyrine (voir fig. ci-dessous).

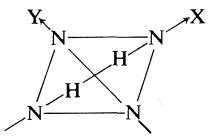

Porphyrine neutre
symétrie D_{2h}
(les axes X et Y ne
sont pas équivalents)

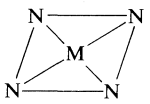

Métalloporphyrine
symétrie D_{4h}
(les axes X et Y
sont équivalents)

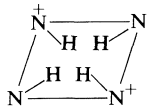

Porphyrine diacide
symétrie D_{4h} ou S_4
(les axes X et Y
sont équivalents)

Dans les solvants organiques, l'hématoporphyrine présente un spectre du type *aetio* (fig. 2): intensité bande IV > III > II > I; en milieu acétique glacial, son spectre se réduit à trois bandes avec deux forts épaulements (fig. 2), et en milieu acétique +1% HCl concentré, son spectre ne présente plus que deux bandes caractéristiques du dication (fig. 2).

La métalloporphyrine HP.Pt présente un spectre à deux bandes (fig. 3) dont le rapport des intensités bande α/β est supérieur à 1 (tableau 1); de plus, la bande Soret subit un déplacement hypsochrome de 13 mμ. Ces deux caractéristiques nous permettent d'avancer l'hypothèse d'une très grande stabilité de cette métalloporphyrine (1*a*).

Le spectre visible du "complexe coiffé" $HPH_2.PtCl_2$ possède la même allure que celui de

Can. J. Chem. Downloaded from www.nrcresearchpress.com by 210.87.254.5 on 09/05/12
For personal use only.

l'hématoporphyrine IX, mais est déplacé vers le rouge (tableau 1). On peut attribuer ce déplacement à l'influence polarisante du platine sur les atomes d'azote. La symétrie de la molécule n'ayant pas été affectée de façon notable, il est normal d'obtenir un spectre similaire. En milieu acétique glacial, les spectres des 3 composés: hématoporphyrine neutre HPH_2, du "complexe coiffé" $HPH_2.PtCl_2$ et de la métalloporphyrine HP.Pt sont différents (figs. 2, 4 (bande 1) et fig. 3). Afin de confirmer l'existence du "complexe coiffé" comme intermédiaire, il est possible de suivre la transformation $HPH_2.PtCl_2 \rightarrow HP.Pt + 2\ HCl$ (fig. 4) en milieu acétique glacial. L'évolution du spectre en fonction du temps montre le passage de l'intermédiaire (fig. 4, bande 1) à la métalloporphyrine finale (fig. 4, bande 2).

De nombreuses hypothèses ont été avancées quant à la nature du ou des composés obtenus par dissolution des porphyrines en milieu acétique. L'hématoporphyrine neutre et le dichlorure ont des spectres très différents en milieu acétique glacial. En milieu acétique dilué, dans le cas de l'hématoporphyrine neutre, on observe l'apparition d'une deuxième bande dans la région Soret vers les plus petites longueurs d'onde (fig. 5); cela n'est pas observé dans le cas du dichlorure. En milieu acétique +1% HCl, les spectres des deux composés sont identiques. De ces résultats, il ressort que si l'espèce diprotonée existe en milieu acétique glacial, elle se trouve en très faible quantité. Corwin *et al.* (11) ont résolu le problème en dissolvant l'ester dans un mélange acide acétique 60%, acétone 40%. L'isolation du monocation est à l'étude.

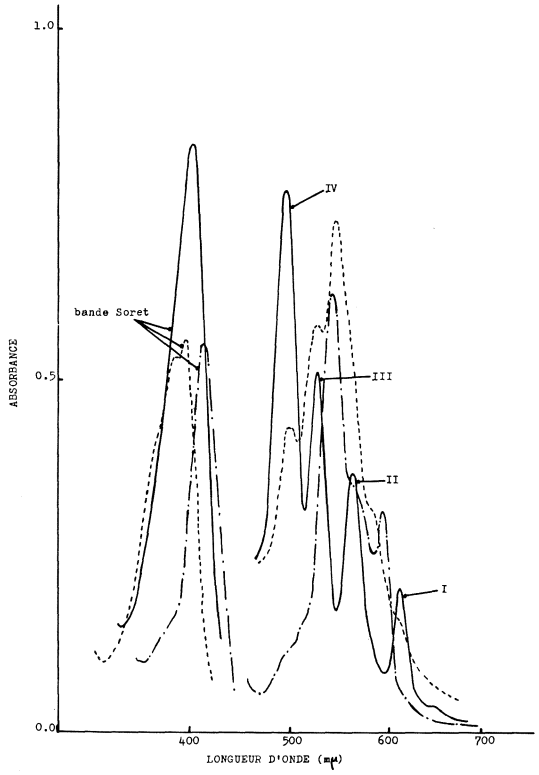

FIG. 2. (1) Spectres de l'hématoporphyrine IX dans (*a*) le DMF (—), concentration: région visible $C = 6.68 \times 10^{-5}\ M$, bande Soret $C/10$; (*b*) l'acide acétique glacial (---), concentration: région visible $C = 10^{-4}\ M$, bande Soret $C/20$; (2) Spectre du dichlorure d'hématoporphyrine dans l'acide acétique glacial (·····), concentration: région visible $C = 5.06 \times 10^{-5}\ M$, bande Soret $C/40$.

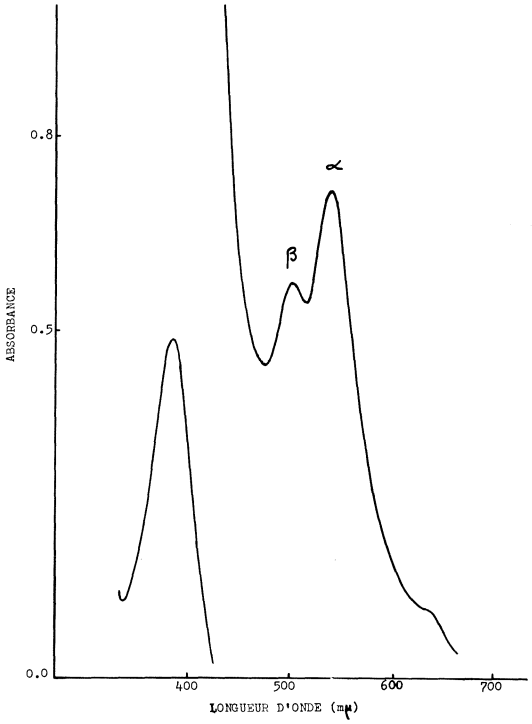

FIG. 3. Spectre de la platino-hématoporphyrine dans le DMF. Concentration: région visible, $C = 9.09 \times 10^{-5}\ M$; bande Soret, $C/10$.

Etude infrarouge

En comparant les spectres de l'hématoporphyrine IX et du "complexe coiffé" $HPH_2.PtCl_2$ avec celui de la métalloporphyrine HP.Pt (fig. 6 et tableau 2), on se rend compte d'une simplification spectrale dûe à l'augmentation de symétrie.

TABLEAU 1. Etude visible des composés préparés (λ en mμ et ε en 1 mol^{-1} cm^{-1})

Composés*		Bande Soret		Visible				
		Epaulement	Maximum	IV	III	II	I*a*	I
HPH_2	λ	378.5	401	501.5	535	572		623
dans DMF	$\varepsilon \times 10^{-3}$		116.8	10.7	7.1	5.0		2.8
HPH_2.2HCl	λ	377	400	498	531.5	568.5	595	622.5
dans DMF	$\varepsilon \times 10^{-3}$	87.5	164.7	13.9	8.8	6.4	1.5	4.2
$HPH_2.PtCl_2$	λ	381	406	507	542.5	577		632
dans DMF	$\varepsilon \times 10^{-3}$	40.1	53.8	5.9	4.4	3.35		1.6
			Bande		β	α	ép.	α/β
HP.Pt	λ		388		506	541.5	625	1.30–1.35
dans DMF	$\varepsilon \times 10^{-3}$		22.9		3.1	4.1	0.8	
HPH_2.2HCl dans	λ			412	554	597.5		0.35–0.40
acide acétique glacial	$\varepsilon \times 10^{-3}$			222.7	12.7	4.9		
HPH_2 dans acide	λ	381	393	402.5	505	536.5	558	
acétique glacial		(ép.)	(max.)	(ép.)				
	$\varepsilon \times 10^{-3}$		104.4		4.0	5.4	6.8	
HPH_2 dans acide	λ	376.5		404			554	590
acétique 50%		(bande)		(bande)				(ép.)
	$\varepsilon \times 10^{-3}$	87.3		133.3			7.9	3.4

*HPH_2: hématoporphyrine neutre; HPH_2.2HCl: dichlorure d'hématoporphyrine; $HPH_2.PtCl_2$: "complexe coiffé"; HP.Pt: platino-hématoporphyrine.

Comme Boucher et Katz (12), nous avons remarqué que les spectres étaient peu résolus sous 600 cm^{-1} pour HPH_2 et HP.Pt. Dans le cas de $HPH_2.PtCl_2$, la région 300–350 cm^{-1} est particulièrement révélatrice des vibrations Pt—Cl.

La première bande qui apparaît vers 3400 cm^{-1} est le massif intense caractéristique des ν_{OH}. Cette bande large et déplacée par rapport aux ν_{OH} libres (13) indique une liaison hydrogène.

Vibrations N—H

Dans l'hématoporphyrine neutre, la vibration de valence ν_{N-H} se trouve à 3308 cm^{-1}. On remarque un faible déplacement de cette bande vers les plus basses énergies en passant au "complexe coiffé" $HPH_2.PtCl_2$ (3308 $\rightarrow$ 3300 cm^{-1}). La vibration de déformation dans le plan δ_{N-H} a été identifiée par Boucher et Katz (12) à 1107 cm^{-1}. A 740 et 679 cm^{-1}, on trouve les déformations hors-plan γ_{N-H}. Il est à remarquer que l'intensité relative de ces bandes varie en passant de la porphyrine neutre au "complexe coiffé": la bande à 673 cm^{-1} dans l'intermédiaire a gagné en intensité par rapport à celle se trouvant à 740 cm^{-1}. De plus ces bandes sont déplacées vers des énergies plus basses comme en témoigne le tableau 2. On pourrait relier ce déplacement avec le déplacement bathochrome des bandes du spectre visible (tableau 1). Les vibrations N—H disparaissent dans la métalloporphyrine HP.Pt, dû au remplacement des 2 atomes d'hydrogène par le platine.

Vibrations C—H

Dans la région 3000–2800 cm^{-1}, on retrouve les vibrations de valence symétriques et antisymétriques des C—H des groupements alkyles (12, 14). Les bandes à 1445 et à 1378 cm^{-1} ont été attribuées à des déformations antisymétriques et symétriques des groupements —CH_2 et —CH_3 (14, 15).

Rimington *et al.* (16) et Ogoshi *et al.* (17) ont montré que la bande se trouvant à 1228 cm^{-1} était due à un mode de déformation C—H dans le plan. Par deutériation avec D_2O–D_2SO_4, Ogoshi et Yoshida (14, 17) ont montré que les bandes à 1220 et à 836 cm^{-1} dans l'octaéthyleporphyrine de zinc correspondaient aux déformations dans le plan et hors plan des C—H en position meso (C—H méthène). Par substitution du métal, ils ont relié le déplacement de ces bandes vers les plus fortes énergies au déplacement hypsochrome des bandes du visible. On remarque ce même déplacement en passant de HPH_2 à HP.Pt: 1228 $\rightarrow$ 1245 cm^{-1} pour δ_{C-H} et 834 $\rightarrow$ 839 cm^{-1} pour γ_{C-H} (tableau 2) et

Can. J. Chem. Downloaded from www.nrcresearchpress.com by 210.87.254.5 on 09/05/12
For personal use only.

401 → 388 mμ pour la bande Soret en proche-u.v. (tableau 1).

La vibration $\nu_{C=O}$ se situe à 1715 cm^{-1} dans l'hématoporphyrine et ne subit aucun déplacement dans les différents complexes.

Bandes sensibles au métal

Dans la région 1500–1700 cm^{-1}, on trouve les mouvements dans le plan des vibrations C=C et C=N des cycles tétrapyrroliques (14, 18). Cette région est sensible au remplacement des deux atomes d'hydrogène par la platine. Ogoshi *et al.* (14) ont montré que les bandes aux alentours de 1000 cm^{-1} étaient sensibles au métal; les bandes à 1070 et 1035 cm^{-1} semblent être associées avec la déformation dans le plan du noyau porphyrinique (14). Boucher et Katz (12) ont remarqué une augmentation de l'intensité de la bande à 1070 cm^{-1} en passant de la protoporphyrine à l'hématoporphyrine, ils ont suggéré une vibration de valence ν_{C-O} du groupement hydroxyéthyle.

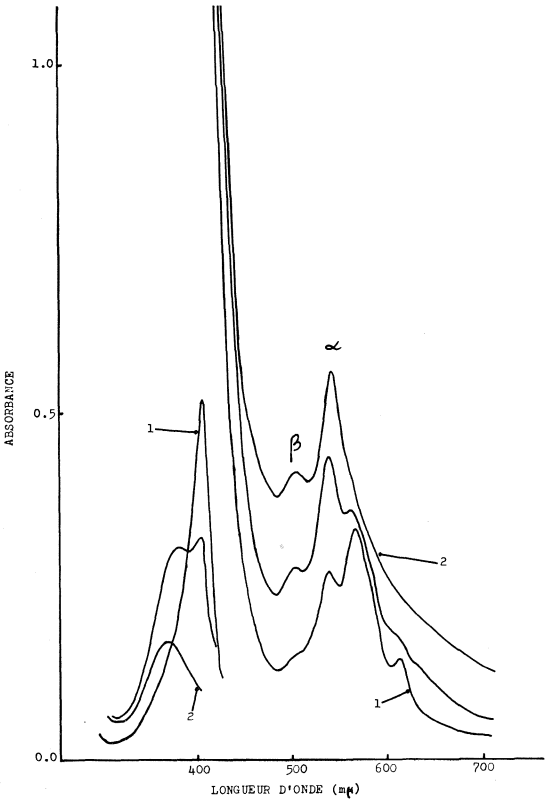

FIG. 4. Transformation du "complexe coiffé" $HPH_2.PtCl_2$ en métalloporphyrine HP.Pt dans l'acide acétique glacial. (*1*) Début de la réaction; (*2*) fin de la réaction. Concentration: région visible, $C = 5.55 \times 10^{-5}$ *M*; bande Soret, *C*/10.

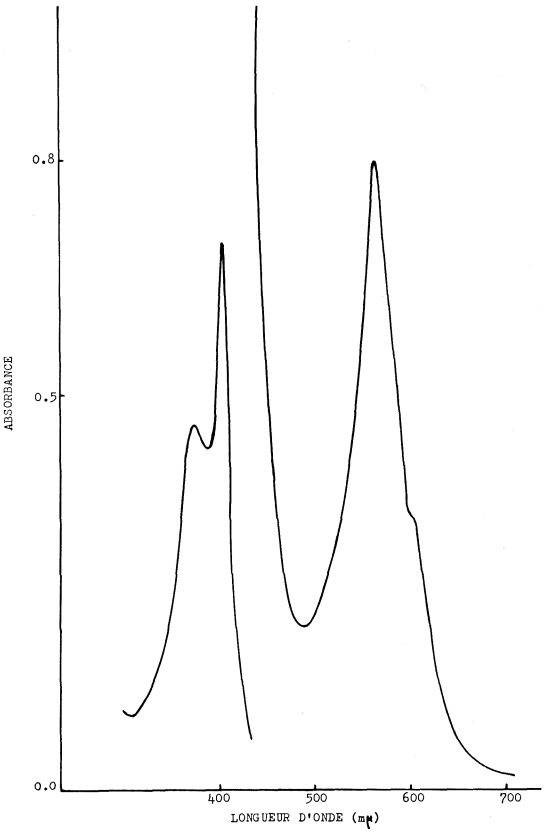

FIG. 5. Spectre de l'hématoporphyrine neutre dans l'acide acétique 50%. Concentration: région visible, $C = 9.68 \times 10^{-5}$ *M*; bande Soret, *C*/20.

Les bandes se trouvant dans la région 500–300 cm^{-1} ont été attribuées à des bandes de déformation du noyau tétrapyrrolique (12, 15). A 460 cm^{-1}, on remarque l'apparition d'une nouvelle bande intense que l'on pourrait attribuer à la vibration de valence ν_{N-Pt}. Le spectre du "complexe coiffé" $HPH_2.PtCl_2$ présente deux bandes à 332 et à 323 cm^{-1} d'intensité moyenne que l'on attribue aux vibrations de valence ν_{Pt-Cl}. Ces deux bandes indiquent une position *cis* des atomes de chlore sur le platine.

En 1960, Fleischer et Wang (19) ont détecté un intermédiaire de réaction entre la protoporphyrine et le chlorure ferrique dans le chloroforme. Le spectre de cet intermédiaire appelé "sitting-atop complex" ressemble étrangement au spectre du diacide (2). Par la suite, la structure cristalline d'un "S.A.T. complex" (20) montrait

Can. J. Chem. Downloaded from www.nrcresearchpress.com by 210.87.254.5 on 09/05/12
For personal use only.

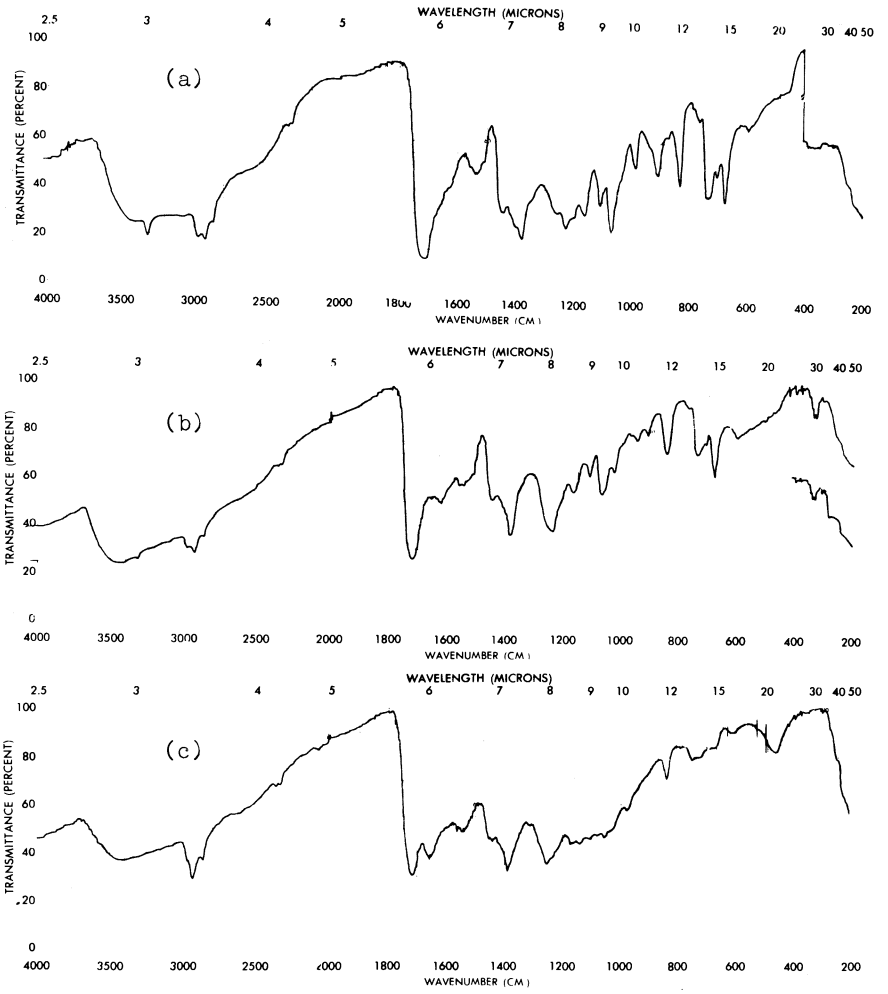

FIG. 6. Spectres infrarouges (pris à l'état solide dans le KBr) des composés suivants: (*a*) hématoporphyrine HPH_2; (*b*) "complexe coiffé" $HPH_2.PtCl_2$; (*c*) platino–hématoporphyrine HP.Pt.

que le composé isolé correspondait à la formule $[PH_4^{2+}Cl^-(FeCl_4^-)]$. D'autres intermédiaires ont été entrevus (21–26) se référant aux résultats de Fleischer et Wang, mais jamais caractérisés de façon systématique. A notre connaissance, c'est la première fois qu'un tel intermédiaire est isolé et étudié de cette façon. Les spectres visible et infrarouge indiquent que le platine ne s'est pas inséré entre les 4 atomes d'azote: les deux atomes d'hydrogène liés aux azotes sont présents. Les déplacements observés pour les vibrations N—H en infrarouge et des bandes du visible vers de plus faibles énergies nous amènent à penser à une coordination entre les deux atomes d'azote possédent un doublet électronique libre avec le platine, cette liaison étant du type donneur–accepteur. Le balancement des noyaux pyrroles en solution en milieu acétique (20) favorise l'attaque du platine sur les doublets libres des atomes d'azote. La coordination azote–platine peut s'effectuer soit sur deux atomes d'azote opposés, soit sur deux atomes d'azote adjacents. Dans le premier cas, la distance calculée d'après les rayons X sur la porphine (27), pour la liaison N—Pt est trop longue (supérieure à 2.7 Å) pour être considérée comme normale (28); dans le second cas, on trouve une distance tout-à-fait raisonnable comprise entre 2.0 et 2.1 Å, le platine gardant son hybridation dsp^2. La structure que nous proposons pour le "complexe coiffé" est celle représentée à la fig. 7.

Les résultats spectroscopiques, la stabilité de

Can. J. Chem. Downloaded from www.nrcresearchpress.com by 210.87.254.5 on 09/05/12
For personal use only.

Can. J. Chem. Downloaded from www.nrcresearchpress.com by 210.87.254.5 on 09/05/12
For personal use only.

TABLEAU 2. Vibrations caractéristiques des composés préparés et du ligand en infrarouge

HPH_2	$HPH_2.PtCl_2$	HP.Pt	Attribution
3400 M*	3450 M	3415 M	ν_{O-H}
3308 F	3300 m		ν_{N-H}
3089 Tf			
2967 F	2966 F	2954 F	
2918 F	2918 F	2920 F	ν_{C-H}
2863 F	2857 F	2857 F	
2355 f	2355 f	2355 f	
2334 f	2329 f	2325 f	
	2080 Tf	2080 Tf	
1715 TF	1715 TF	1714 TF	$\nu_{C=O}$
	1650 f	1650 M	
1625 ép.	1625 Mf		$\nu_{C=C} + \nu_{C=N}$
1540 Mf	1540 Mf	1540 Mm	
1509 ép.			
1445 m	1441 m	1440 m	$\delta_{a\ CH_2}$
1400 ép.			
1378 F	1379 F	1381 F	$\delta_{s\ CH_2}$
1345 ép.			
1262 ép.	1268 ép.		
1228 m	1228 F	1245 F	$\delta_{C-H\ (meso)}$
1200 ép.	1204 ép.		
1163 m	1161 f	1165 Tf	
		1135 Tf	
1107 m	1106 f		
		1098 Tf	δ_{N-H}
1070 F	1065 m		
		1046 Tf	
1035 ép.	1020 f	1020 Tf	
988 m	989 ép.	965 f	
950 ép.	945 Tf		
		930 ép.	
910 m	907 Tf		
877 Tf			
834 F	837 F	839 F	$\gamma_{C-H\ (meso)}$
788 ép.	788 ép.		
765 Tf	768 Tf		
		749 Mf	
740 F	733 m		γ_{N-H}
704 Tf	702 Tf	719 Mf	
679 m	673 F		γ_{N-H}
		665 Tf	
600 Tf	598 m	610 Tf	
501 Tf	499 Tf		
458 Tf		460 m	ν_{N-Pt}
	417 Tf	416 Tf	
393 Tf	395 Tf	390 Tf	
381 Tf	382 Tf		
371 Tf	375 Tf		
		350 Tf	
	332 m		
323 Tf	323 m		ν_{Pt-Cl}
	300 Tf		

*M, massif; m, moyen; TF, très fort; Tf, très faible; F, fort; f, faible; ép., épaulement; ν, vibration de valence; δ, vibration de déformation dans le plan; γ, vibration de déformation hors-plan; a, asymétrique; s, symétrique.

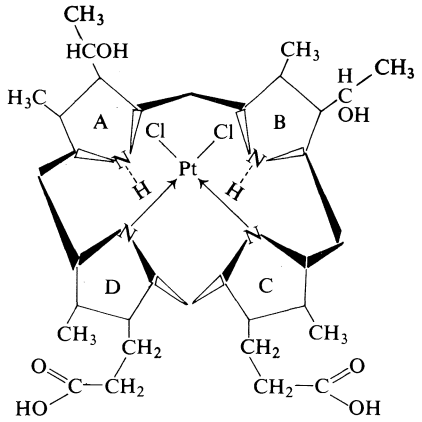

FIG. 7. Structure proposée du "complexe coiffé" $HPH_2.PtCl_2$. Les pyrroles A et B sont inclinés vers le bas, C et D vers le haut.

la métalloporphyrine vis-à-vis des acides forts nous conduisent à placer le platine entre les 4 atomes d'azote et ainsi à stabiliser la porphyrine.

Tout récemment, un complexe ionique a été isolé (identique à celui de Fleischer) correspondant à la formule $HPH_4^{2+}.PtCl_4^{2-}$, identifié par ses analyses C, H, N, Pt, Cl, par son spectre infrarouge et par sa conductivité. Ce complexe a été obtenu en changeant les conditions de la réaction (température = 25 °C, concentration: $HPH_2 = 5.5 \times 10^{-3}$ *M*, $K_2PtCl_4 = 3.3 \times 10^{-2}$ *M*), il est présentement à l'étude et fera l'objet d'une publication à venir.

Lors de la dissolution du K_2PtCl_4 dans l'eau, les espèces $PtCl_4^{2-}$, $PtCl_3(H_2O)^-$, et $PtCl_2(H_2O)_2$ sont en présence (29); l'espèce $PtCl_4^{2-}$ se trouve stabilisée par l'énorme cation HPH_4^{2+} pour donner le premier intermédiaire $HPH_4^{2+}.PtCl_4^{2-}$. A 60 °C, le départ de deux molécules d'HCl donne lieu à la formation du "complexe coiffé" $HPH_2.PtCl_2$ qui représente le second intermédiaire de réaction. Enfin, à 85 °C, le "complexe coiffé" se transforme en métalloporphyrine HP.Pt.

L'interaction hématoporphyrine–Platine en milieu acétique peut donc se résumer comme suit:

$$\underset{\text{dans AcOH}}{HPH_2} + \underset{\text{dans } H_2O}{PtCl_4^{2-}} \xrightarrow{25\ ^\circ C} \underset{\mathbf{1}}{HPH_4^{2+}.PtCl_4^{2-}}$$

$$\mathbf{1} \xrightarrow{60\ ^\circ C} \underset{\mathbf{2}}{HPH_2.PtCl_2} + 2HCl$$

$$\mathbf{2} \xrightarrow[-2HCl]{85\ ^\circ C} \underset{\mathbf{3}}{HP.Pt}$$

Schéma des trois étapes de la réaction conduisant à la formation de la platino-hématoporphyrine: **1**, premier intermédiaire, complexe ionique (marron-foncé); **2**, second intermédiaire, "complexe coiffé" (noir-bleuâtre); **3**, composé final, platino-hématoporphyrine (noir).

Il semblerait d'après ces résultats que la première interaction soit electrostatique (complexe ionique **1**), la seconde étape fixant le métal sur la porphyrine ("complexe coiffé" **2**) et enfin la dernière étape résultant d'une substitution des atomes d'hydrogène fixés sur les azotes, par le métal, conduisant à la métalloporphyrine (**3**) dans laquelle le métal est placé entre les 4 atomes d'azote dans le plan de la molécule.

Il y a quelques années, l'hématoporphyrine IX était utilisée en chirurgie, pour délimiter les tumeurs cancéreuses (30). En effet, on a remarqué que cette porphyrine s'accumulait préférentiellement dans les zones où se développaient des tissus de façon anormale et grâce à sa fluorescence, il était très aisé en travaillant sous lampe u.v. d'extraire ces tumeurs. L'activité antitumorale des sels de platine *cis*, a déjà prouvée (8–10). Le "complexe coiffé" $HPH_2.PtCl_2$ présente donc deux qualités remarquables pour le traitement des tumeurs: c'est un complexe de platine *cis* et c'est une porphyrine qui fluoresce, donc possibilité de suivre l'évolution du composé, dans l'organisme, et par conséquent du platine, s'il n'y a pas dégradation.

Les résultats obtenus dans cette présente étude nous conduisent à faire la cinétique d'incorporation du platine dans l'hématoporphyrine IX, à étudier l'interaction du "complexe coiffé" avec d'autres métaux, ainsi qu'à vérifier son activité anti-tumorale.

Tous nos remerciements au Conseil National de Recherches du Canada et au Ministère de l'Education du Québec pour le support financier qu'ils nous ont accordé.

1. J. E. FALK. Porphyrins and metalloporphyrins. Elsevier Publishing Co., New York. 1964. (*a*), pp. 34, 75; (*b*), p. 141; (*c*), p. 73; (*d*), p. 89.
2. P. HAMBRIGHT. Coord. Chem. Rev. **6**, 247 (1971).
3. D. C. BORG et G. C. COTZIAS. Nature, **182**, 1677 (1958).
4. F. H. J. FIGGE, G. S. WEILAND, et L. O. J. MANGARIELLO. Proc. Soc. Exp. Biol. Med. **67**, 640 (1948).
5. R. L. LIQSON, E. J. BALDES, et A. M. OLSEN. J. Natl. Cancer Inst. **26**, 1 (1961).
6. J. WINKELMAN. J. Natl. Cancer Inst. **27**, 1369 (1961).
7. D. A. RASMUSSEN TAXDEL, G. E. WARD, et F. H. J. FIGGE. Cancer, **8**, 78 (1955).
8. B. ROSENBERG, L. VAN CAMP, J. E. TROSKO, et V. H. MANSOUR. Nature, **222**, 385 (1969).
9. B. ROSENBERG. Platinum Met. Rev. **15**, 42 (1971).
10. R. J. BROMFIELD, R. H. DAINTY, R. D. GILLIARD, et B. T. HEATON. Nature, **223**, 735 (1969).
11. A. H. CORWIN, A. B. CHIVVIS, R. H. POOR, D. G. WHITTEN, et E. W. BAKER. J. Am. Chem. Soc. **90**, 6577 (1968).
12. L. J. BOUCHER et J. J. KATZ. J. Am. Chem. Soc. **89**, 1340 (1967).
13. K. UENO et A. E. MARTELL. J. Phys. Chem. **59**, 998 (1955).
14. H. OGOSHI, N. MASAI, Z. I. YOSHIDA, J. TAKEMOTO, et K. NAKAMOTO. Bull. Chem. Soc. Jap. **44**, 49 (1971).
15. L. J. BOUCHER. J. Am. Chem. Soc. **90**, 6640 (1968).
16. C. RIMINGTON, S. F. MASON, et O. KENNARD. Spectrochim. Acta, **12**, 65 (1958).
17. H. OGOSHI et Z. I. YOSHIDA. Bull. Chem. Soc. Jap. **44**, 1722 (1971).
18. D. W. THOMAS et A. E. MARTELL. J. Am. Chem. Soc. **78**, 1338 (1956).
19. E. B. FLEISCHER et J. H. WANG. J. Am. Chem. Soc. **82**, 3498 (1960).
20. A. L. STONE et E. B. FLEISCHER. J. Am. Chem. Soc. **90**, 2735 (1968).
21. D. A. BRISBIN et R. J. BALAHURA. Can. J. Chem. **44**, 2157 (1966).
22. D. G. DAVIS et J. G. MONTALVO, JR. Anal. Chem. **41**, 1195 (1969).
23. E. B. FLEISCHER, E. I. CHOI, P. HAMBRIGHT, et A. L. STONE. Inorg. Chem. **3**, 1284 (1964).
24. B. D. BEREZIN et G. I. SMIRNOVA. Russ. J. Phys. Chem. **41**, 702 (1967).
25. B. D. BEREZIN et A. N. DROBYSHEVA. Russ. J. Phys. Chem. **42**, 1500 (1968).
26. B. F. BURNHAM et J. J. ZUCKERMAN. J. Am. Chem. Soc. **92**, 1547 (1970).
27. L. E. WEBB et E. B. FLEISCHER. J. Chem. Phys. **43**, 3100 (1965).
28. J. M. ROBERTSON et I. WOODWARD. J. Chem. Soc. 36 (1940).
29. L. I. ELDING et I. LEDEN. Acta Chem. Scand. **20**, 706 (1966).
30. G. S. PECK, H. PATTERSON MACK, et F. H. J. FIGGE. Bull. Sch. of Med., Univ. of Maryland, **38**, 124 (1953).

Can. J. Chem. Downloaded from www.nrcresearchpress.com by 210.87.254.5 on 09/05/12
For personal use only.

Crystal and Molecular Structure of Hexaaquocobalt(II)–Hexafluorosilicate(IV), $[Co(H_2O)_6][SiF_6]$

H. LYNTON AND P-Y. SIEW

Department of Chemistry, University of New Brunswick, Fredericton, New Brunswick

Received June 19, 1972

The structure of hexaaquocobalt(II)-hexafluorosilicate(IV) has been determined by the heavy atom method. The compound crystallizes in the space group $R\bar{3}$, with three molecules in the hexagonal unit cell of dimensions $a = 9.358(16)$, $c = 9.712(14)$ Å. The atomic parameters were refined by block diagonal least squares using anisotropic thermal parameters. The hydrogen atom positions were established but the parameters were not refined. The final agreement residual for 151 observed reflections is $R = 0.043$.

The structure consists of discrete $Co(H_2O)_6^{2+}$ and $(SiF_6)^{2-}$ octahedra joined systematically by O---H'--F hydrogen bonds into chains parallel to the $\bar{3}$ axis.

La structure de l'hexaaquocobalt(II) hexafluorosilicate(IV) a été déterminée par la méthode de l'atome lourd. Le composé cristallise dans le groupe $R\bar{3}$ avec trois molécules par unité hexagonale de dimensions $a = 9.358(16)$Å, $c = 9.712(14)$ Å. Les paramètres atomiques ont été raffinés par la méthode des moindres carrés appliquée aux matrices diagonales qui utilise les paramètres d'anisotropie thermique. Les positions des atomes d'hydrogène ont été établies mais les paramètres n'ont pas été raffinés. L'accord final après 151 reflexions observées est $R = 0.043$.

La structure consiste en octaèdre discret de $Co(H_2O)_6^{2+}$ et $(SiF_6)^{2-}$ relié systématiquement par des liaisons hydrogène O---H---F, en chaînes parallèles aux axes $\bar{3}$.

[Traduit par le journal]

Can. J. Chem., **51**, 227 (1973)

Introduction

Cobalt fluorosilicate was prepared by the action of hydrofluorosilicic acid, H_2SiF_6, on cobalt carbonate, $CoCO_3$, and was found to have the formula $CoSiF_6.6H_2O$(1). The cell dimensions as given in the Powder line file (2) are $a = 9.370$ Å and $c = 9.732$ Å in space group $R3m$, No. 160, ref. 5. It had been reported that in compounds of the type $MSiF_6.xH_2O$, the $(SiF_6)^{2-}$ species was discrete and formed chains with the $M(H_2O)_x^{2+}$ species either through F—M coordination, as in $CuSiF_6.4H_2O$ (3), or F---O hydrogen bonding as in $[Fe(H_2O)_6][SiF_6]$ (4). An X-ray diffraction analysis was undertaken to determine the type of arrangement in $CoSiF_6.6H_2O$.

Experimental

The crystal data are as follows:

$[Co(H_2O)_6][SiF_6]$ f.w. = 308.98

Trigonal, $a = 9.358(16)$, $c = 9.712(14)$ Å, $v = 736.6$ Å^3, $\rho_o = 2.09(2)$, $z = 3$, $\rho_c = 2.089$ (20 °C, MoKα, $\lambda = 0.71069$ Å).

The unit cell dimensions and their estimated standard deviations (in parentheses) were obtained from a least squares evaluation of the positions of 12 independent reflections. The space group is $R\bar{3}$ (C_{3i}^2) No. 148 in ref. 5.

The crystals were pink, ditrigonal prisms, elongated in the c direction. They were air sensitive and slowly decomposed on prolonged air exposure.

A small crystal of size $0.6 \times 0.4 \times 0.3$ mm^3 was mounted, sealed inside a thin-walled Lindermann capillary, with the c axis parallel to the ϕ direction of the diffractometer. Intensity data were collected on a Picker, computer-controlled, four-angle diffractometer with β-filtered MoKα radiation and scintillation detector using a $\theta/2\theta$ scan. Two octants hkl and $hk\bar{l}$ were explored to a 2θ maximum of 40°. There were 189 accessible reflections in this region of which 151 were considered observed. The threshold was taken as 20 counts; a scan speed of 1°/min was used with a scan range of 1.5°, corrected for dispersion. The background was taken for 20 s at each end of the range. Data was also corrected against a standard reflection taken at intervals of 20 readings. The linear absorption coefficient for MoKα radiation is 19.6 cm^{-1}. No corrections were made for absorption or extinction.

Structure Analysis

The cobalt and silicon atoms were located from a three dimensional Patterson synthesis and are found to be in special positions 3*a* and 3*b* respectively. A Fourier synthesis established coordinates for the oxygen and fluorine atoms in general positions 18*f*.

Refinement was carried out by block-diagonal least squares, using 3×3 matrices for atomic coordinates and 6×6 matrices for anisotropic thermal parameters for each of the atoms. The quantity minimized was $\sum w(|F_o| - |F_c|)^2$.

Can. J. Chem. Downloaded from www.nrcresearchpress.com by 210.87.254.42 on 09/05/12
For personal use only.

TABLE 1. Final parameters (estimated standard deviations) $x, y, z \times 10^4$, $u_{ij} \times 10^3$
t.f. = exp $[-2\pi^2(a^{*2}h^2u_{11} + ... + 2b^*c^*klu_{23} + ...)]$

Atom	x	y	z	u_{11} (or u)	u_{22}	u_{33}	u_{23}	u_{13}	u_{12}
Co^{2+}	0	0	0	52(3)	52(3)	38(2)	0	0	26(2)
Si	0	0	5000	46(6)	46(6)	44(4)	0	0	23(3)
$F^{1/3-}$†	4958(5)	7626(4)	664(4)	78(5)	325(10)	63(5)	6(6)	15(4)	−10(6)
O	5196(5)	6790(6)	5418(4)	71(5)	124(6)	63(5)	−13(4)	6(4)	44(5)
H(1)	5021	6470	4473	35					
H(2)	6408	7644	5527	35					

†To attain charge neutrality the fluorine atom was assigned a charge of $1/3^-$ and the values for its scattering factor curve were obtained from interpolating those for F^0 and F^-.

Successive cycles gave an agreement residual, $R = \sum(||F_o| - |F_c||)/\sum|F_o|$, of 0.049 for the observed reflections for all atoms except the hydrogens. The weighting scheme used was $w = 1/\{1 + [(|F_o| - P_2)/P_1]^4\}$ with $P_1 = 35$ and $P_2 = 45$.

Scattering factor curves used were those given in ref. 6. The Co^{2+} and Si were corrected for anomalous dispersion.

A difference synthesis showed, in the vicinity of the oxygen positions, peaks of height around 0.5 e $Å^{-3}$. They grouped into two sets of general positions, 18*f*. These were taken to be the hydrogens. No other peaks with height greater than 0.3 e $Å^{-3}$ were present. The hydrogen coordinates were included in the least squares calculation and assigned an isotropic temperature parameter equal to that of the oxygen. The parameters for the hydrogens were not refined. The final agreement residual for all atoms was $R = 0.043$.

A table of structure factors for the final parameters as listed in Table 1 has been placed in the Depository of Unpublished Data.[1]

Discussion

The decrease in the residual R obtained by inclusion of the hydrogen atoms is significant by Hamilton's test (7) at the 0.025 (2.5%) level. These hydrogen positions are consistent with presence of hydrogen bonding in the structure.

The structure consists of discrete $Co(H_2O)_6^{2+}$ and $(SiF_6)^{2-}$ octahedra which are systematically joined by O—H---F hydrogen bonds into chains parallel to the $\bar{3}$ axis. The O—H---F distances 2.785(6) Å within, and 2.711(8) Å between chains are reasonable for such bonds (8). The discrete $Co(H_2O)_6^{2+}$ and $(SiF_6)^{2-}$ ions are rotated by 27.4(3)° with respect to each other about the $\bar{3}$ axis. Both are distorted such that the O—O(1) and F—F(1) distances are shorter than those of the O—O(2) and F—F(2). Similar distortion is found in the $Fe(H_2O)_6^{2+}$ ion of $[Fe(H_2O)_6][SiF_6]$. The bond distances and angles are listed in Tables 2 and 3.

Figure 1 gives a projection of the structure along the *b* axis. Hydrogen atoms are included to illustrate the bonding. Each of the fluorine atoms is involved in two hydrogen bonds.

Table 2 also compares $[Co(H_2O)_6][SiF_6]$ with the related $[Fe(H_2O)_6][SiF_6]$ structure. The bond lengths and bond angles for the two structures are close except for a longer O—F(2) distance of 2.785(6) Å and a correspondingly shorter Si—F

TABLE 2. Structural data for $[Co(H_2O)_6][SiF_6]$ and $[Fe(H_2O)_6][SiF_6]$*

	Distance (Å)	
Bond	$Co(H_2O)_6SiF_6$	$Fe(H_2O)_6SiF_6$
M—O	2.079(6)	2.146(12)
Si—F	1.643(5)	1.706(9)
O—F(2)	2.785(6)	2.681(13)
O—F(3)	2.711(8)	2.720(13)
O—O(1)	2.924(9)	2.991(19)
O—O(2)	2.955(6)	3.063(21)
F—F(1)	2.292(9)	2.390(15)
F—F(2)	2.355(6)	2.396(14)
	Angle (deg)	
Bonds	$Co(H_2O)_6SiF_6$	$Fe(H_2O)_6SiF_6$
O—M—O(1)	89.4(2)	88.6(3)
O—M—O(2)	90.6(2)	91.4(3)
F—Si—F(1)	88.5(3)	89.8(4)
F—Si—F(2)	91.6(3)	90.2(4)

*Estimated standard deviations in parentheses.

[1]Complete set of tabular data is available, at a nominal charge, from the Depository of Unpublished Data, National Science Library, National Research Council of Canada, Ottawa, Canada. K1A OS2.

Can. J. Chem. Downloaded from www.nrcresearchpress.com by 210.87.254.42 on 09/05/12
For personal use only.

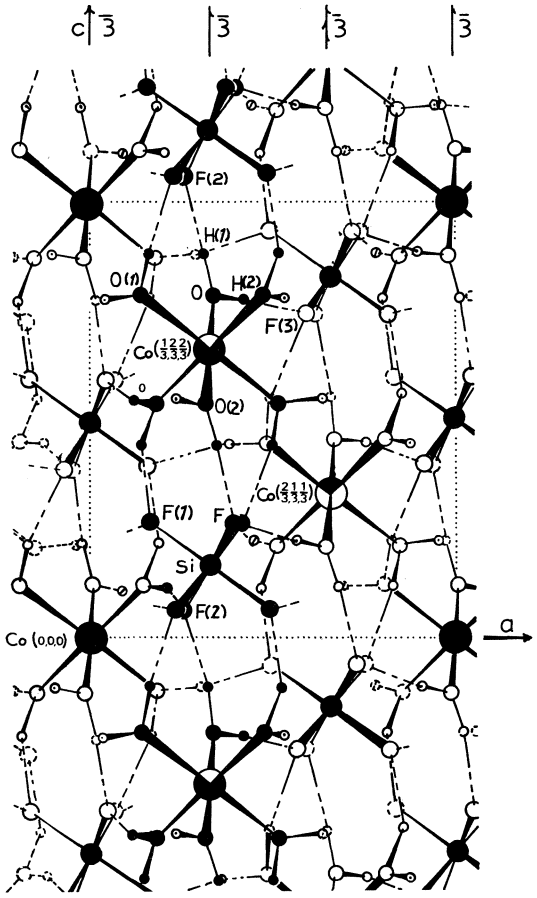

FIG. 1. $[Co(H_2O)_6][SiF_6]$: projection along the *b* axis.

distance of 1.643(5) Å for the $[Co(H_2O)_6][SiF_6]$ structure. The F—F distances are also different for the two compounds.

TABLE 3. Bonds involving hydrogen in $[Co(H_2O)_6][SiF_6]$

Bond*	Distance (Å)
O—H(1)	0.954
O—H(2)	1.015
H(1)—F(intra)	1.851
H(2)—F(inter)	1.705
O—H(1)—F(intra)	2.785(6)
O—H(2)—F(inter)	2.711(8)

Bonds	Angle (deg)
H(1)—O—H(2)	107.2
O—H(1)—F(intra)	165.9
O—H(2)—F(inter)	170.2

*Intra, bonds connecting atoms of same chain; inter, bonds connecting atoms of adjacent chains.

We wish to thank Dr. M. J. R. Clark for the cobalt fluorosilicate crystals and the National Research Council of Canada for their financial support. We also thank Dr. F. R. Ahmed of the Biochemistry Laboratory, National Research Council of Canada for use of his computer programs.

1. M. J. R. CLARK. Ph.D. Thesis. University of New Brunswick, Fredericton, New Brunswick, 1971.
2. National Bureau of Standards (U.S.) Monograph 25, Section 3 (1963).
3. M. J. R. CLARK, J. E. FLEMING, and H. LYNTON. Can. J. Chem. **47**, (20) 3959 (1969).
4. W. C. HAMILTON. Acta Cryst. **15**, 353 (1962).
5. International tables for X-ray crystallography. Vol. I. The Kynoch Press, Birmingham, England. 1965.
6. International tables for X-ray crystallography. Vol. III. The Kynoch Press, Birmingham, England. 1962.
7. W. C. HAMILTON. Acta Cryst. **18**, 502 (1965).
8. W. C. HAMILTON and J. A. IBERS. Hydrogen bonding in solids. W. A. Benjamin, Inc. N.Y. 1968.

Can. J. Chem. Downloaded from www.nrcresearchpress.com by 210.87.254.42 on 09/05/12
For personal use only.

Double Layer Structure at the Mercury/Acetonitrile Interface

W. R. FAWCETT[1] AND R. O. LOUTFY
Department of Chemistry, University of Guelph, Guelph, Ontario
Received July 21, 1972

The results of a study of double layer capacity at the mercury/acetonitrile interface in the presence of alkali metal and tetraalkylammonium perchlorates are presented. It is shown that the Li^+, Na^+, tetraethylammonium, and perchlorate ions are not significantly adsorbed over most of the polarizable range of the electrode, whereas the K^+ and Cs^+ ions are adsorbed at more cathodic potentials. Inner layer capacity data are presented and discussed in terms of the specific effects of ions on interfacial structure.

Nous présentons les résultats d'une étude de capacité de double couche, à l'interface d'un système mercure acétonitrile, en présence d'un alcalin et de perchlorates de tétraalkylammonium. Nous démontrons que les ions Li^+, Na^+, tétraéthylammonium, et perchlorate ne sont pas adsorbés de façon significative sur tout le domaine de polarisation de l'électrode, alors que K^+ et Cs^+ sont adsorbés à la plupart des potentiels cathodiques. Nous présentons les résultats de capacité de la couche interne et en discutons en termes d'effets spécifiques des ions sur la structure de l'interface.

[Traduit par le journal]

Can. J. Chem., **51**, 230 (1973)

Can. J. Chem. Downloaded from www.nrcresearchpress.com by 210.87.254.105 on 09/05/12
For personal use only.

Introduction

Acetonitrile (AN) is widely used as an aprotic solvent in studies of organic electrode reactions involving free radical intermediates (1, 2). In this regard, tetraalkylammonium (TAA) salts are commonly employed as background electrolytes because they dissolve easily in AN and permit the working electrode to be polarized to far cathodic potentials (3). Alkali metal salts, on the other hand, are either sparingly soluble (K^+, Rb^+, and Cs^+) (4), or they cause complications in the electrode process resulting from ion-pair formation (Li^+ and Na^+) (5). TAA cations are strongly adsorbed on mercury from aqueous solution but there is some experimental evidence that they are not significantly adsorbed from several non-aqueous solvents (6, 7).

Very few studies of the properties of the mercury/AN interface have been reported. Minc *et al.* (8) and Payne (9) measured the differential capacity of the interface in solutions of LiBr, CsI, and KPF_6. In contrast to other non-aqueous systems (6), no capacity hump was observed. Champion (10) obtained interfacial capacity data in $NaClO_4$ solutions of varying concentration, and concluded that neither the Na^+ cation nor the ClO_4^- anion was adsorbed over the available potential range. More recently, Crumm (11) examined the qualitative effects of a series of electrolytes on capacity-potential curves in AN, but the experimental technique employed was not sufficiently sensitive to permit the data to be analyzed quantitatively.

A knowledge of double layer structure at the electrode/solution interface is essential in interpreting the kinetics of electrode reactions and would be particularly useful in studies of the kinetics of the simple process of radical anion formation by one electron transfer to the parent molecule. In the present paper an investigation of the mercury/solution interface with the alkali metal and TAA perchlorates in AN is reported. In addition, the data necessary for correcting for double layer effects in electrode kinetics are presented and discussed.

Experimental

The differential capacity of the mercury/solution interface was determined by measuring the in- and out-of-phase components of the interfacial admittance using a phase sensitive detector as outlined previously (12). The cell, dropping mercury electrode, and Pt counter electrode have also been described. The dropping electrode performed satisfactorily for long periods without siliconization. The reference electrode (//0.05 *M* tetraethylammonium perchlorate in AN/AgCl/Ag) was connected to the working solution through a fine fritted glass disc of small diameter; the change in liquid junction potential with electrolyte concentration was determined by observing the change in half-wave potential of a reversible reduction reaction with change in electrolyte concentration. It should be noted that the electrolyte solution in the reference electrode contains some dissolved AgCl mainly as Ag^+ and $AgCl_2^-$ ions (13). Although the concentration of the potential determining ion is small (13),

[1]To whom correspondence should be addressed.

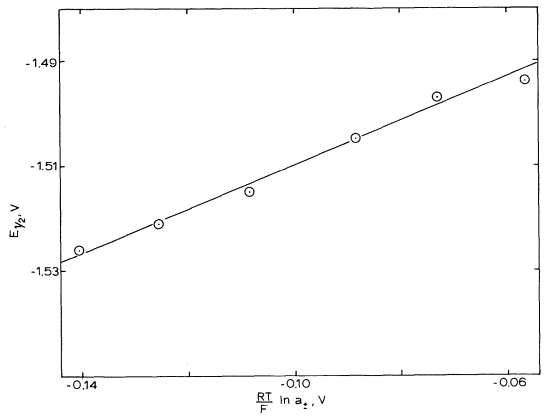

FIG. 1. Plot of the halfwave potential for the electroreduction of benzofurazan at Hg *vs.* $RT \ln a_\pm/F$ where $a_\pm$ is the mean activity of tetraethylammonium perchlorate in acetonitrile. The reduction reaction was reversible and not complicated by either adsorption on the electrode or ion-pairing of the resultant anion radical (13).

half-wave potentials measured with respect to different electrodes over a period of a year were reproduced to ± 1 mV indicating that the reference electrode is both stable and reproducible. TAA perchlorates (tetramethylammonium (TMAP), tetraethylammonium (TEAP), and tetra-*n*-butylammonium perchlorate (TBAP) were purified by multiple recrystallization from water and dried at 60 °C. The absence of water of crystallization was ascertained by examining the polarization characteristics of a Pt electrode in a solution of the salt in AN (14). Purification procedures for the alkali metal perchlorates, AN, and Hg have been described previously (14, 15). The experiments were carried out in a dry box under a nitrogen atmosphere which was purified by circulation over a copper catalyst at 150 °C to remove oxygen (BASF R3-11), and over P_2O_5 to remove water (Aquasorb, Mallinckrodt). The working solutions were degassed with purified nitrogen pre-saturated with AN vapor prior to the experiments. Other details of the experimental procedure have been given previously (12).

Method of Data Analysis

The capacity-potential data were integrated numerically from the point of zero charge (p.z.c.) using Stirling's rule to obtain charge–potential data. The integration was carried out so that data were tabulated for equal increments in charge, the corresponding potentials being calculated by the Newton–Raphson method.

Since activity coefficient data for perchlorate salts were not available, they were estimated from extended Debye–Hückel theory using the relationship

$$[1] \qquad \log \gamma_\pm = -1.594\, c^{1/2}/(1 + 0.481 a c^{1/2})$$

where $\gamma_\pm$ is the molar mean activity coefficient, c, the molar concentration of the given 1–1 electrolyte, and a, the ion size parameter set equal to the Bjerrum distance for ion pair formation in AN (7.64 Å) (16, 17). The above relationship ignores any difference in the rational and molar activity coefficient scales. It is easily shown that errors in $\gamma_\pm$ will not be important in calculated values of $\ln a_\pm/f$ where $a_\pm$ is the mean electrolyte activity, and $f = F/RT$; in fact, an error as high as 20% in $\gamma_\pm$ will result in a 1% error in $\ln a_\pm/f$.

The potential scale was converted to one of thermodynamic significance by evaluating the difference in the potentials of the Hg electrode in a cell with a reference electrode reversible to the anion of the electrolyte and no liquid junction,

$$[2] \qquad \text{Hg}/x\text{M MX/AgX/Ag} \qquad E_-$$

and the cell used in the experiments.

$$[3] \qquad \text{Hg}/x\text{M MX//0.05 } M \text{ TEAP/AgCl/Ag} \qquad E_x$$

The change in the liquid junction potential with electrolyte concentration in the latter cell was determined by observing the corresponding change in half-wave potential for electroreduction of benzofurazan (Fig. 1) (14). The slope of the plot of $E_{1/2}$ *vs.* $\ln a_\pm/f$ was 0.41; thus the relationship between E_- and E_x is (18)

$$[4] \qquad E_- = E_x + 0.59 n a_\pm/f + \text{constant}$$

Results and Discussion

Capacity–potential data for TEAP solutions in the concentration range 0.005 to 0.2 M are shown in Fig. 2. It is noted that the shape of the capacity curves is similar to that observed previously (8–11) and that a diffuse layer minimum is apparent on the curves for the more dilute solutions suggesting that specific adsorption is absent in that potential region. The two tests were carried out to determine whether specific adsorption is significant over any portion of the polarizable range of the Hg electrode. The first, applicable only in the vicinity of the p.z.c., involved plotting the reciprocal of the experimental capacity $1/C$ *vs.* the reciprocal of the diffuse layer capacity $1/C_d$ as estimated by Gouy–Chapman theory for constant electrode charge density q and varying electrolyte concentration (19). According to the Grahame model, the double layer can be represented as a series combination of two capacities, namely, that of the inner layer C_i and that of the diffuse layer C_d. Thus, the slope of the above plots should be unity provided that C_i does not change with electrolyte concentration. The resulting plots for the $LiClO_4$ and TEAP systems are shown in Fig. 3. In the first case the slope of the plots is unity for electrode charge densities in the range -5 to 5 $\mu C\ cm^{-2}$ indicating that ionic specific adsorption is absent. In the case of TEAP solutions, the plots have unit slope for positive electrode charge densities but the slope of the plots increases rapidly with decrease in electrode

Can. J. Chem. Downloaded from www.nrcresearchpress.com by 210.87.254.105 on 09/05/12
For personal use only.

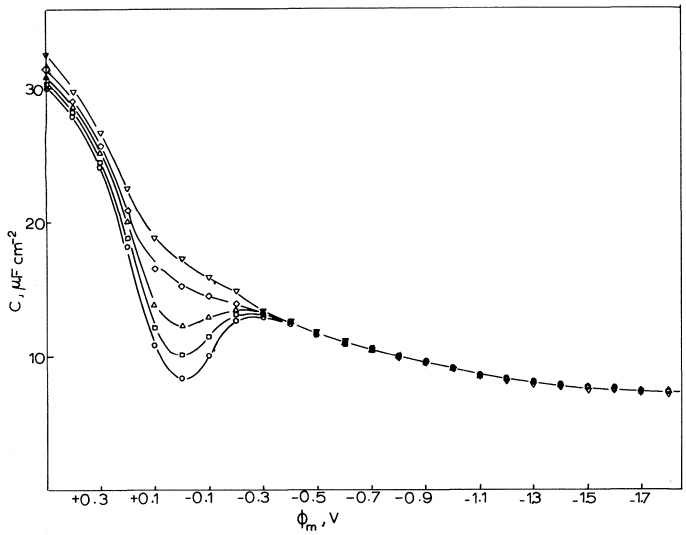

FIG. 2. Differential capacity of the mercury/solution interface for tetraethylammonium perchlorate solutions in acetonitrile at 25 °C *vs.* the electrode potential with respect to that at the point of zero charge (rational potential scale). Concentrations of TEAP: (○), 0.005; (□), 0.01; (△), 0.02; (◇), 0.05; and (▽), 0.10 *M*.

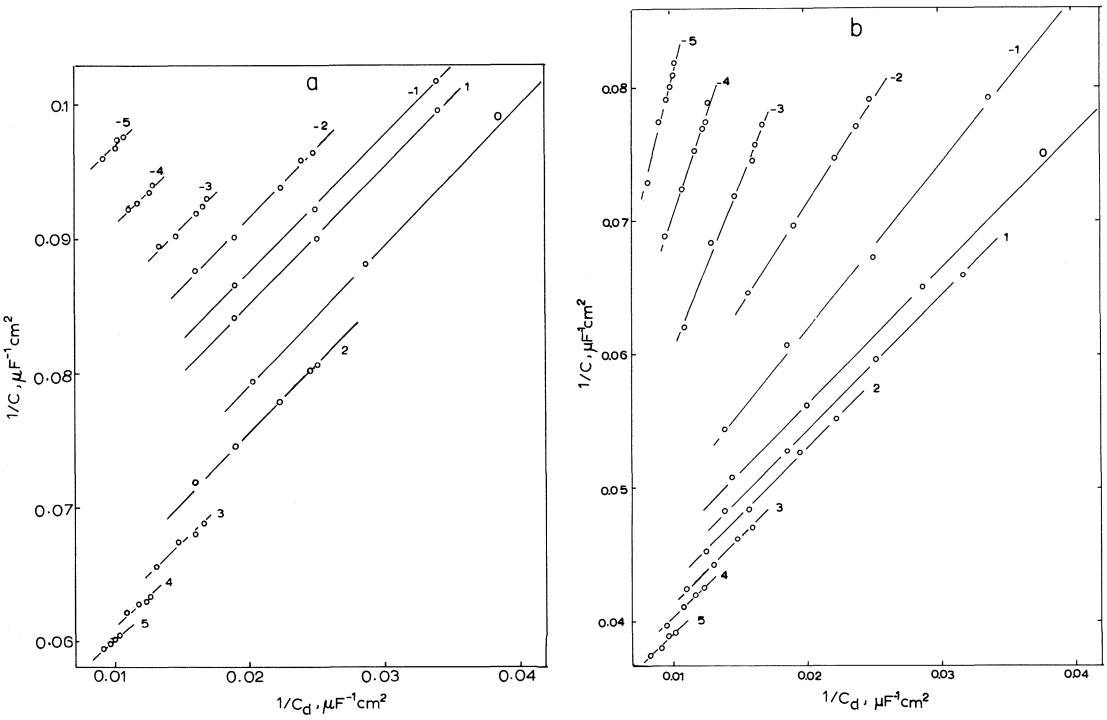

FIG. 3. Reciprocal of the differential capacity at constant electrode charge density *vs.* the reciprocal of the diffuse layer capacity calculated by the Gouy–Chapman theory for varying electrolyte concentration ($LiClO_4$, *a* and TEAP, *b*). The integers adjacent to each line indicate the electrode charge density in $\mu C\ cm^{-2}$. Plots for positive charge densities in the case of $LiClO_4$ have been shifted vertically by 0.02 $cm^2\ \mu F^{-1}$.

Can. J. Chem. Downloaded from www.nrcresearchpress.com by 210.87.254.105 on 09/05/12
For personal use only.

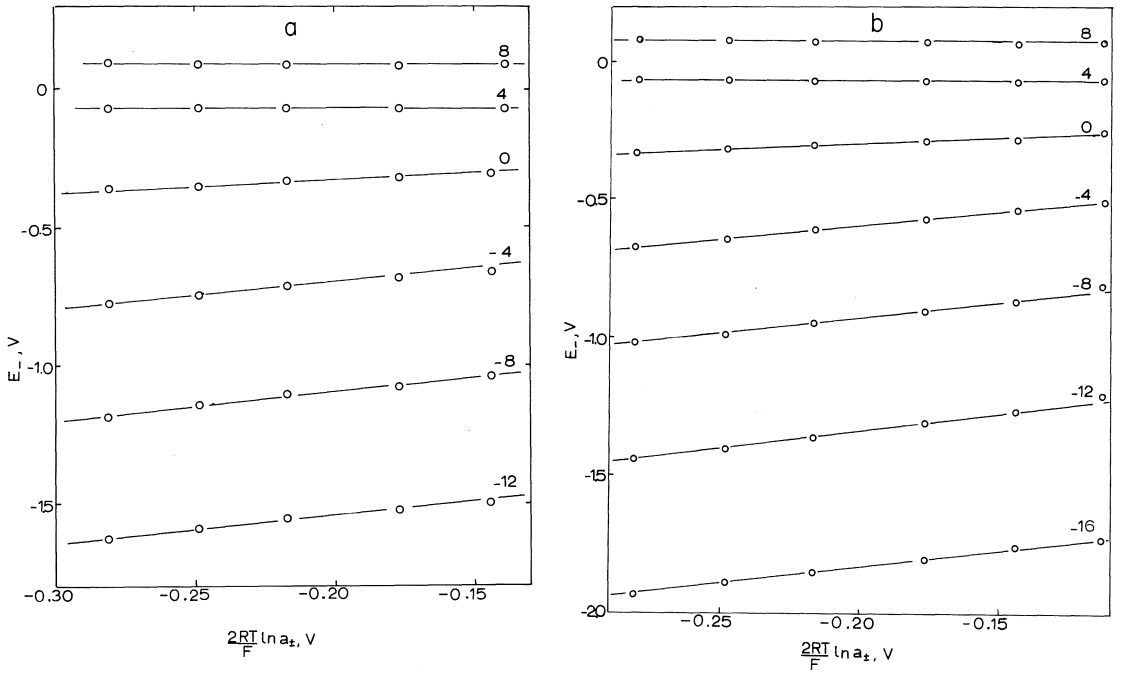

FIG. 4. Electrode potential with respect to an electrode reversible to the anion, E_- at constant electrode charge density *vs.* the change in chemical potential of the electrolyte, $2 \ln a_\pm/f$ for $LiClO_4$ (*a*) and TEAP (*b*). The integers adjacent to each line indicate the electrode charge density in $\mu C\ cm^{-2}$.

charge density at cathodic potentials. This indicates either that TEA cations are adsorbed in the inner layer at cathodic potentials or that the nature of the dielectric in the inner layer changes with change in electrolyte concentration.

The second test involved constructing Esin and Markov plots (20), in this case, plots of E_- *vs.* $2 \ln a_\pm/f$ at constant electrode charge density (Figs. 5, 6). In the absence of specific adsorption the slope of these plots should be zero at higher positive charge densities, one-half at the p.z.c., and one at higher negative charge densities. According to the Gouy–Chapman theory, the limiting slopes at higher charge densities obtain when $q^2 \gg 2RT\varepsilon c/\pi$ where ε is the dielectric constant of pure AN (3.7 at 25 °C). In the present case, this condition is met at the most dilute concentration for $|q| \geqslant 2\ \mu C\ cm^{-2}$ and at the most concentrated, for $|q| \geqslant 11\ \mu C\ cm^{-2}$. From Fig. 4, it is apparent that the $LiClO_4$ and TEAP data follow the predictions of the Gouy–Chapman theory over the entire polarizable range; thus, it is concluded that ionic specific adsorption is not significant in these systems. This conclusion is confirmed qualitatively by the presence of the diffuse layer minimum in the vicinity of the p.z.c. and by the coincidence of the capacity curves at far cathodic potentials.

According to the above analysis, the dielectric properties of the inner layer at cathodic potentials in TEAP solutions depend on electrolyte concentration even though specific adsorption is absent. As the charge on the electrode becomes more negative the concentration of TEA^+ ions at the outer Helmholtz plane (OHP) increases; considering the size of this ion, this process is undoubtedly accompanied by a decrease in the number of solvent molecules in the inner layer, the solvent molecules being replaced by the ethyl groups of the TEA^+ ion. Thus, the dielectric properties of the inner layer depend both on the field in the inner layer and the number of TEA^+ ions at the OHP. The same process does not occur in the case of Li^+ since this small monoatomic ion is strongly solvated by AN molecules. If the above explanation is correct, the inner layer capacity in the TEAP system should depend on electrolyte concentration only at those charge densities where the cation concentration at the OHP is significant and dependent on electrolyte concentration. By the

Can. J. Chem. Downloaded from www.nrcresearchpress.com by 210.87.254.105 on 09/05/12
For personal use only.

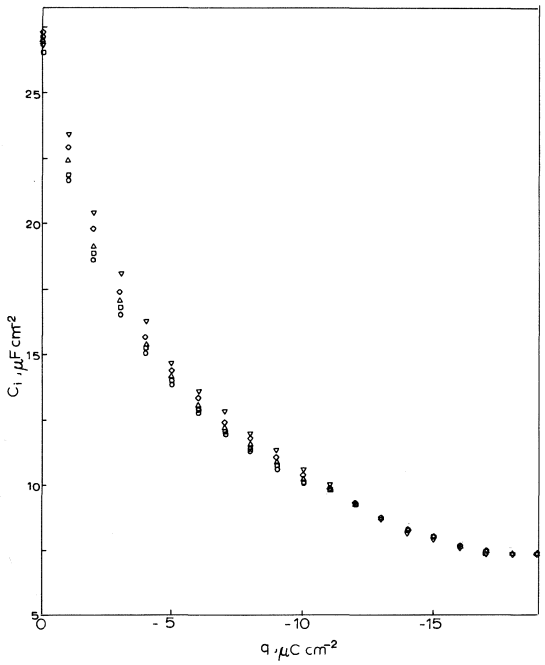

FIG. 5. Differential capacity of the inner layer for tetraethylammonium perchlorate at cathodic potentials *vs.* the electrode charge density. Concentrations of TEAP: (○), 0.005; (□), 0.01; (△), 0.02; (◇), 0.05; and (▽), 0.10 *M*.

Gouy–Chapman theory, the cation concentration at the OHP is given by

$$[5] \quad c_+(\mathrm{OHP}) = c\left(\frac{|q|}{2A} + \left(\frac{q^2}{4A^2} + 1\right)^{1/2}\right)^2 - c$$

where $A = (RT\varepsilon c/8\pi)^{1/2}$. In the limit that $q^2 \gg 4A^2$, this concentration is given by

$$[6] \quad c_+(\mathrm{OHP}) = \pi q^2/2RT\varepsilon$$

that is, it is independent of base electrolyte concentration. By the arguments presented above, this condition is met in the present case for $q \leqslant -11$ μC cm^{-2}. Inner layer capacities calculated from the TEAP data at cathodic potentials are presented in Fig. 5. It is apparent that C_i depends on electrolyte concentration in the range $0 \geqslant q \geqslant -11$ μC cm^{-2}, confirming the above explanation.

The effect of the nature of the alkali metal cation on capacity–potential curves in AN is shown in Fig. 6. At far cathodic potentials the capacity increases with increase in cation atomic number. The same ordering has been observed in water (21), methanol (22), and ethylene carbonate (23) whereas the opposite ordering has been found in formamide (24, 25), *N*-methylformamide (12, 26), *N*-methylacetamide (27), and dimethylsulfoxide (28). In the present case, the ordering can be attributed to a decrease in solvated ion size, which results in an increase in inner layer capacity, with increase in cation atomic number. This trend in solvated ion size has been confirmed for the alkali metal cations from measurements of Stoke's law radii in several solvents including AN (29). In the case of the amides and dimethyl sulfoxide, the observed ordering has been ascribed to a dependence of both the dielectric properties and the thickness of the inner layer on the nature of the cation at the OHP (12). Crumm (11) has attributed the cation effect at more cathodic potentials to cation specific adsorption, the extent of which increases in the order $Li^+ < Na^+ < K^+ < Cs^+$. As stated above no significant specific adsorption of Li^+ could be detected at cathodic potentials. On applying the same tests to data for Na^+, K^+, and $CsClO_4$ solutions, it was shown that specific adsorption of Na^+ was not significant over the whole cathodic range, and that of K^+ and Cs^+, for electrode charge densities greater than -12 μC cm^{-2}. Unfortunately the specific adsorption of K^+ and Cs^+ could not be investigated quantitatively due to the limited solubility of their salts in AN (<0.02 *M*). From the shape of the capacity curves obtained at 0.01 *M* it is apparent that Cs^+ is more strongly adsorbed than K^+. Average inner layer capacities calculated for at least three different electrolyte concentrations are reported in Table 1 for the range of cathodic

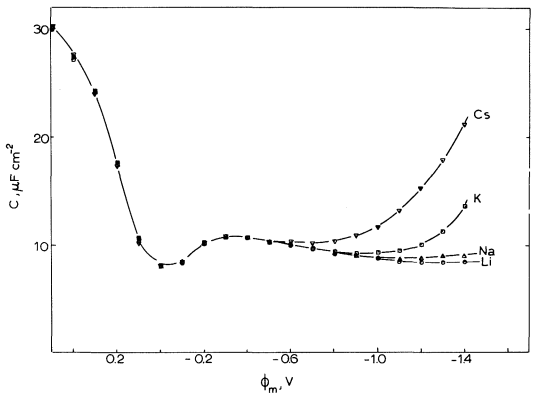

FIG. 6. Differential capacity of the mercury/solution interface *vs.* the rational potential for 0.01 *M* solutions of alkali metal perchlorates in acetonitrile.

Can. J. Chem. Downloaded from www.nrcresearchpress.com by 210.87.254.105 on 09/05/12
For personal use only.

Can. J. Chem. Downloaded from www.nrcresearchpress.com by 210.87.254.105 on 09/05/12
For personal use only.

TABLE 1. Differential capacity of the inner layer as a function of electrode charge density at cathodic potentials for the alkali metal perchlorates and for 0.1 *M* tetraethylammonium perchlorate in acetonitrile at 25 °C

Electrode charge density q, $\mu C\ cm^{-2}$	Differential capacity of the inner layer* C_i, $\mu F\ cm^{-2}$				
	$LiClO_4$	$NaClO_4$	$KClO_4$	$CsClO_4$	0.1 *M* TEAP
0	15.96	15.96	15.97	15.86	26.81
−1	15.13	15.39	15.59	15.53	23.67
−2	14.31	14.18	14.34	14.21	20.47
−3	13.16	13.14	13.22	13.06	18.06
−4	12.17	12.25	12.24	12.18	16.27
−5	11.40	11.38	11.39	11.51	14.69
−6	10.60	10.60	10.74	11.06	13.60
−7	10.15	9.90	10.20	10.82	12.78
−8	9.70	9.58	9.87	11.03	11.86
−9	9.27	9.27	9.70	11.26	11.31
−10	9.00	9.06	9.73	11.87	10.66
−11	8.83	9.12	10.14	12.94	10.00
−12	8.76	9.40	11.12	14.30	9.38
−14					8.30
−16					7.76
−18					7.42
−20					7.41

*The precision of the above data is better than ±1%.

charge densities over which cation specific adsorption is not significant. It is apparent from these data that the cation effect cannot be attributed entirely to cation specific adsorption as proposed by Crumm (11). Values of C_i for 0.1 *M* TEAP in AN are included in Table 1 for comparison.

The effect of ionic size on double layer properties was also investigated by obtaining capacity data for three TAA perchlorates in AN (Fig. 7). At far cathodic potentials the capacity decreases in the order $C(TMA^+) > C(TEA^+) > C(TBA^+)$, that is, with increase in ionic size. At very far cathodic potentials the capacity in the TBAP system increases, almost reaching that in the TEAP system, suggesting that the TBA^+ cation is adsorbed in this potential region. In the vicinity of the p.z.c., the ordering of capacities is reversed indicating that the effect of the cation on the dielectric properties of the inner layer is more important in determining inner layer properties at low electrode charge densities. As the size of the cation increases, more solvent molecules are replaced in the inner layer and the dielectric constant of this region increases. Apparently when the inner layer is mainly filled with alkyl groups at more cathodic potentials,

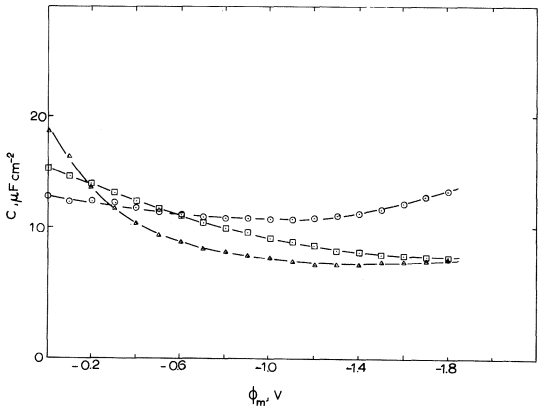

FIG. 7. Differential capacity of the mercury/solution interface versus the rational potential for 0.05 *M* solutions of tetraalkylammonium perchlorates in AN: (○), tetramethylammonium; (□), tetraethylammonium; (△), tetra-*n*-butylammonium.

the thickness of the inner layer is more important in determining its capacity.

It is interesting to note that no evidence for specific adsorption of perchlorate anion was obtained by the tests employed above. This conclusion was confirmed by calculating the inner layer capacity for the $LiClO_4$ and TEAP systems at anodic potentials assuming no ionic specific adsorption. Calculated values were found to be constant within experimental error for values of $q \leqslant 10\ \mu C\ cm^{-2}$ (Table 2). Perchlorate anion is weakly adsorbed on Hg from aqueous solutions (30), the adsorption being attributed to weak solvation of the anion in water and to its structure breaking properties (31). Coetzee and Campion (32) showed that perchlorate anion behaves unusually in AN, specifically, that it is more strongly solvated in this solvent than in water. This is indeed difficult to understand since anions are, in general, poorly solvated in aprotic solvents (33). Nevertheless, the stronger solvation of perchlorate in AN undoubtedly accounts for its not being significantly adsorbed on Hg from this solvent.

As pointed out above, no hump is apparent on the capacity–potential curves in AN for the electrolytes considered. There was some evidence that perchlorate anion was adsorbed on Hg at charge densities anodic of $10\ \mu C\ cm^{-2}$; this conclusion was based on the fact that inner layer capacities calculated assuming adsorption to be absent increased slightly with increase in electrolyte concentration. The onset of adsorption at

TABLE 2. Differential capacity of the inner layer as a function of electrode charge density at anodic potentials for the alkali metal perchlorates and tetraethylammonium perchlorate in acetonitrile at 25 °C

Electrode charge density q, μC cm^{-2}	Differential capacity of the inner layer C_i, μF cm^{-2}	
	$MClO_4$	TEAP
0	16.0	27.0
1	21.0	29.0
2	27.6	30.7
3	30.7	32.4
4	32.6	33.4
5	33.5	34.2
6	34.3	34.9
7	34.5	35.3
8	35.0	35.6
9	35.6	35.9
10	35.8	36.2

more anodic potentials would obscure a hump and result in measured capacities being higher than in the absence of adsorption. If the sharp increase in capacity at potentials just anodic of the p.z.c. is attributed to solvent reorientation, then it may be concluded that AN is strongly adsorbed on Hg with the positive end of its dipole towards the metal. In this regard, AN is similar to most other aprotic solvents (6).

Finally, the data recorded in Tables 1 and 2 may be used to calculate values of q and ϕ_2, the potential drop across the diffuse layer, as functions of electrode potential and electrolyte concentration according to the procedure outlined previously (15). A knowledge of ϕ_2 is essential in correcting for double layer effects in electrode kinetics. Since the inner layer capacity varies with electrolyte concentration for the TEAP system in AN, the data presented may only be used to calculate q and ϕ_2 for an electrolyte concentration of 0.1 M; however, this concentration is the one most often used in kinetic studies.

The financial support of the National Research Council of Canada and Defense Research Board of Canada is gratefully acknowledged.

1. YA. P. STRADYN' and R. A. GAVAR. Progress in the electrochemistry of organic compounds. Vol. 1. *Edited by* A. N. Frumkin and A. B. Ershler. 1969. p. 1.
2. C. K. MANN and K. K. BARNES. Electrochemical reactions in non-aqueous systems. Marcel Dekker, New York. 1970.
3. C. K. MANN. Electroanalytical Chemistry. Vol. 3. *Edited by* A. J. Bard. Dekker, New York. 1969. p. 57.
4. T. PAVLOPOULOS and H. STREHLOW. Z. physik. Chem. **202**, 474 (1954).
5. M. E. PEOVER. Electroanalytical Chemistry. Vol. 2. *Edited by* A. J. Bard. Dekker, New York. 1967. p. 1.
6. R. PAYNE. Advances in Electrochemistry and Electrochemical Engineering. Vol. 7. *Edited by* P. Delahay. Wiley–Interscience, New York. 1970. p. 1.
7. R. DIETZ and M. E. PEOVER. Discuss. Faraday. Soc. **45**, 154 (1968).
8. S. MINC, J. JASTRZEBSKA, and M. BRZOSTOWSKA. J. Electrochem. Soc. **108**, 1160 (1961).
9. R. PAYNE. J. Phys. Chem. **71**, 1548 (1967).
10. P. CHAMPION. C. R. (Paris), **272C**, 1090 (1971).
11. T. E. CRUMM. Doctoral Dissertation.University of Massachusetts, 1971; Diss. Abs. B, **32**, 3222-B, (1971/72).
12. W. R. FAWCETT and R. O. LOUTFY. J. Electroanal. Chem. **39**, 185 (1972).
13. D. C. LUEHRS, R. T. IWAMOTO, and J. KLEINBERG. Inorg. Chem. **5**, 201 (1966).
14. W. R. FAWCETT, P. A. FORTE, R. O. LOUTFY, and J. M. PROKIPCAK. Can. J. Chem. **50**, 263 (1972).
15. W. R. FAWCETT and M. D. MACKEY. J. Electroanal. Chem. **27**, 219 (1970).
16. B. CASE, N. S. HUSH, R. PARSONS, and M. E. PEOVER. J. Electroanal. Chem. **10**, 360 (1965).
17. J. F. COETZEE and J. J. CAMPION. J. Am. Chem. Soc. **89**, 2513 (1967).
18. P. DELAHAY. Double layer and electrode kinetics. Wiley–Interscience, New York. 1965. Chapt. 4.
19. R. PARSONS and F. G. R. ZOBEL. J. Electroanal. Chem. **9**, 333 (1965).
20. R. PARSONS. Proc. 2nd Int. Congr. Surf. Act. **3**, 38 (1957).
21. D. C. GRAHAME. J. Electrochem. Soc. **98**, 343 (1951).
22. S. MINC and M. BRZOSTOWSKA. Rocz. Chem. **34**, 1109 (1960).
23. W. R. FAWCETT and M. D. MACKEY. J. Chem. Soc. Far.Trans. I. In press.
24. B. B. DAMASKIN, R. V. IVANOVA, and A. A. SURVILA. Elektrokhimiya, **1**, 767 (1965).
25. G. H. NANCOLLAS, D. S. REID, and C. A. VINCENT. J. Phys. Chem. **70**, 3300 (1966).
26. B. B. DAMASKIN and YU.M. POVAROV. Dokl. Akad. Nauk SSSR, **140**, 394 (1961).
27. R. PAYNE. J. Phys. Chem. **73**, 3598 (1969).
28. R. PAYNE. J. Am. Chem. Soc. **89**, 48 (1967).
29. M. DELLA MONICA and L. SENATORE. J. Phys. Chem. **74**, 205 (1970).
30. R. PAYNE. J. Phys. Chem. **70**, 204 (1966).
31. R. PARSONS. Rev. Pure Appl. Chem. **18**, 91 (1968).
32. J. F. COETZEE and J. J. CAMPION. J. Am. Chem. Soc. **89**, 2517 (1967).
33. A. J. PARKER. Chem. Rev. **69**, 1 (1969).

Can. J. Chem. Downloaded from www.nrcresearchpress.com by 210.87.254.105 on 09/05/12
For personal use only.

The Master Equation for the Dissociation of a Dilute Diatomic Gas. VIII. The Rotational Contribution to Dissociation and Recombination

TOM ASHTON, D. L. S. MCELWAIN, AND H. O. PRITCHARD

Centre for Research in Experimental Space Science, York University, Downsview, Ontario

Received March 23, 1972

Can. J. Chem. Downloaded from www.nrcresearchpress.com by 210.87.254.42 on 09/05/12
For personal use only.

The dissociation of the $J = 21$ state of H_2, and the recombination of atoms into that state, have been examined in detail. The $J = 21$ state of H_2 has two quasi-bound levels, one long-lived and the other short-lived, but the rate constants for dissociation or recombination involving this state are almost completely independent of the tunnelling rates into and out of the quasi-bound levels, and are in fact determined by bottleneck effects occurring lower down the vibrational ladder. Direct integration of the relaxation equations shows that, either excluding or including tunnelling, the dissociation and recombination rate constants obey the rate-quotient law, and that in the latter case the lowest eigenvalue of the relaxation matrix properly reflects the pressure dependence of the dissociation rate constant. Less extensive examination of the dissociation properties of other rotational states indicates that these conclusions are general, except that there is no strong bottleneck effect for very high rotational states ($J \geqslant 30$).

It is shown that if full rotational equilibration is assumed, the sum, weighted over all J, of the individual dissociation rate constants leads to an overall dissociation rate constant which is much too high, suggesting strongly that rotational equilibration cannot occur amongst the very high J states.

A factored form of the master equation is then examined in which either only T–V or only T–R processes take place, over the temperature range 1500–5000 °K. It is found that in this approximation the upper rotational states are very strongly depleted, and that the Arrhenius temperature coefficients of the dissociation rate constants are between 92 and 94 kcal mol^{-1}, depending upon the choice of rotational transition probabilities. The calculation suggests that one contributory cause of "low activation energies" in dissociation reactions is strong rotational depopulation of the very high rotational states, and its importance in relation to other possible causes is discussed.

The smallest eigenvalues of the 177th order matrix representing the dissociation of para-H_2 and of the 172nd order matrix representing the dissociation of ortho-H_2 confirm that the factored model gives an acceptable representation of the dissociation rate of H_2 in this temperature range; hence the conclusions of the factored model in respect of strong rotational depopulation are probably valid. Finally, it is shown that the second smallest eigenvalue of the full relaxation matrix changes by a factor of three at 1500 °K or by a factor of ten at 5000 °K when *only* rotational transition probabilities are varied, thus identifying the relaxation which immediately precedes the dissociation reaction in a shock wave as a T–VR rather than a T–V relaxation.

An exploratory series of calculations for deuterium was carried out for the range of temperatures 700–5000 °K, using the latter model which includes full coupling between rotation, vibration, and dissociation, *i.e.*, using matrices of order 348 and 355 for ortho- and para-deuterium, respectively. These calculations predict that there should be a reversal in the isotope effect for both dissociation and recombination of hydrogen and deuterium as follows: (*i*) with helium as third body, deuterium should dissociate faster than hydrogen at high temperatures, but below about 2000 °K, the dissociation of deuterium will become the slower of the two processes; (*ii*) with argon as third body, deuterium should recombine faster than hydrogen at high temperatures, but below about 1000 °K, the recombination of deuterium will become the slower of the two processes; (*iii*) the rate constants for the recombination of hydrogen by hydrogen and for the recombination of deuterium by deuterium will probably cross over near 1000 °K, indicating a need for experiments in this region of temperature.

Nous avons étudié en détail la dissociation de l'état $J = 21$ de H_2 et la recombinaison des atomes dans cet état. L'état $J = 21$ de H_2 possède deux niveaux quasi-liés, un stable et l'autre instable, mais les constantes de vitesse de dissociation ou de recombinaison, impliquant cet état, sont presque complètement indépendantes des vitesses d'effet tunnel dans et à l'extérieur des niveaux quasi-liés; elles sont déterminées, en fait, par les effets de "goulot de bouteille" se produisant au bas de l'échelle vibrationnelle. L'intégration directe des équations de relaxation montre que, si on inclut ou exclut l'effet tunnel, les constantes de vitesse de dissociation et de recombinaison obéissent à la loi du quotient de vitesse, et que dans le dernier cas, la plus petite valeur fondamentale de la matrice de relaxation démontre clairement l'influence de la pression sur la constante de vitesse de dissociation. Un examen moins approfondi des propriétés de dissociation des autres états rotationnels indique la gérénalité de ces conclusions, à l'exception d'un faible effet de "goulot de bouteille" dans les états rotationnels très élevés ($J \geqslant 30$).

Nous démontrons que, étant supposé un équilibre rotationnel complet, la somme, pondérée sur tous les J, des constantes de vitesse de dissociation individuelle, amène à une constante de vitesse de dissociation totale beaucoup trop élevée, laissant supposer fortement que l'équilibre de rotation ne peut se produire dans les états J très élevés. Nous examinons alors l'équation principale sous forme de facteurs, où seuls apparaissent des processus T–V ou T–R, dans un domaine de température de 1500–5000 °K. Nous trouvons au moyen de cette approximation, que les niveaux rotationnels supérieurs sont très fortement affaiblis et que les coefficients de température d'Arrhénius des constantes de vitesse de dissociation se situent entre 92 et 94 kcal mole^{-1}, selon le choix des probabilités de transition rotationnelle. Le calcul suggère qu'une cause contribuant aux "basses énergies d'activation" dans les réactions de dissociation pourrait être une importante dépopulation rotationnelle des états rotationnels de très grande énergie, et nous discutons de son importance par rapport aus autres causes possibles.

Les plus petites valeurs fondamentales de la matrice d'ordre 177 représentant la dissociation de H_2-para et de la matrice d'ordre 172 représentant la dissociation de H_2-ortho confirment que le modèle sous forme de facteurs représente de façon acceptable la vitesse de dissociation de H_2 dans ce domaine de température; à partir de cela, les conclusions tirées du modèle sous forme de facteurs, concernant une forte dépopulation rotationnelle, sont probablement valides. Nous démontrons finalement que la deuxième plus petite valeur fondamentale de la matrice de relaxation globale change par un facteur de trois à 1500 °K, ou par un facteur de dix à 5000 °K, seulement lorsque les probabilités de transition rotationnelle varient, identifiant ainsi la relaxation qui précède immédiatement la réaction de dissociation dans une onde de choc telle que T–VR plutôt qu'une relaxation T–V.

Nous avons entrepris une série de calculs d'exploration pour le deutérium, dans un domaine de température de 700–5000 °K, au moyen du dernier modèle, qui inclut un couplage complet entre la rotation, la vibration et la dissociation, utilisant des matrices d'ordre 348 et 355 pour l'ortho et le para-deutérium respectivement. Ces calculs prédisent un renversement de l'effet isotopique pour la dissociation et la recombinaison de l'hydrogène et du deutérium, comme suit: (*i*) avec l'hélium comme troisième atome en présence, le deutérium doit se dissocier plus vite que l'hydrogène, à température élevée, mais au-dessous de 2000 °K, la dissociation du deutérium devient le plus lent des deux processus; (*ii*) l'argon étant le troisième atome en présence, le deutérium doit se recombiner plus vite que l'hydrogène à température élevée, mais au-dessous de 1000 °K, la recombinaison du deutérium devient le plus lent des deux processus; (*iii*) les constantes de vitesse de recombinaison de l'hydrogène par l'hydrogène et de la recombinaison du deutérium par le deutérium se croisent probablement près de 1000 °K, indiquant le besoin d'expérimenter dans ce domaine de température.

Can. J. Chem. Downloaded from www.nrcresearchpress.com by 210.87.254.42 on 09/05/12
For personal use only.

Introduction

It has been recognized since the early days of chemical reaction rate theory that rotational degrees of freedom may make important contributions to the rate of a dissociation reaction (1, 2). However, because of the sheer enormity of the problem of including explicit representation of individual rotational states into reaction rate theory, together with an almost complete lack of knowledge of transition probabilities for rotational energy changes, little real progress has been made in understanding these contributions. Consideration of such effects has usually been deferred because it has been rationalized that (except for very light molecules where tunnelling through the rotational pseudo-potential barrier is possible) a rotational contribution essentially increases the energy that is required to cause dissociation to take place (3–5), or is really in fact only of minor importance (1, 6), or else semi-classical simulations of the rotational pseudo-potential barrier have been invoked (2, 7). In this paper we attempt to give a correct description of the way in which a rotational barrier affects the nature of the dissociation process for a single rotational state of a molecule, and thereafter, how the overall dissociation (or recombination) rate is made up out of contributions from these individual processes.

Dissociation of the $J = 21$ State of H_2

The energy levels of the H_2 molecule have been calculated by Waech and Bernstein (8) and by LeRoy (9) from the theoretical internuclear potential of Kolos and Wolniewicz. The $J=21$ state was chosen as being representative of the general case, having two quasi-bound levels, one of which is, according to the calculations of Roberts (10), very long-lived ($\tau \approx 5 \times 10^{-4}$ s) and the other quite short-lived ($\tau \approx 10^{-13}$ s); the pseudo-potential curve and the disposition of the energy levels for this state are shown in Fig. 1. The heights $\varepsilon_{max}(J)$ of the effective rotational barriers are also available in these papers.

We remind the reader that this paper, as were others in this series (11–13), is concerned only with the properties of what is known as the

Can. J. Chem. Downloaded from www.nrcresearchpress.com by 210.87.254.42 on 09/05/12
For personal use only.

"energy-transfer" mechanism at infinite dilution: it is assumed that we are considering the dissociation of 3.5×10^{16} molecules cm^{-3} of H_2 diluted in 3.5×10^{19} atoms cm^{-3} of helium at constant volume and temperature and that (*i*) the He/H_2 dilution ratio is sufficiently great that H_2–H_2 collisions can be neglected; (*ii*) the He–H intermolecular attraction is so small that reactions cannot take place via HeH complexes; those two assumptions were discussed in detail in Part I of this series (11). Thus, modifying our earlier notation somewhat, the master equation with tunnelling for the $J = 21$ state of H_2 can be written as follows

$$[1]\quad \frac{dn_i}{dt} = \sum_{j=0}^{n-1} Z[M]\{(P_{ij}n_j - P_{ji}n_i) + (\bar{P}_{in}n_n^2 - \bar{P}_{ni}n_i)\} + [\bar{k}_{in}n_n^2 - \bar{k}_{ni}n_i] \qquad i = 0, 1, \ldots, (n-1)$$

$$[2]\quad \frac{dn_n}{dt} = \sum_{j=0}^{n-1} \{Z[M](\bar{P}_{nj}n_j - \bar{P}_{jn}n_n^2) + [\bar{k}_{nj}n_j - \bar{k}_{jn}n_n^2]\}$$

where n_i is the number of molecules per cc in the *i*th vibrational state of $J = 21$, P_{ji} is the probability per collision with M that a transition from state (i,J) to state (j,J) will occur, Z is the collision number, n_n is the number of dissociated molecules ($\equiv \frac{1}{2}[H]$), $\bar{P}_{ni}$ is the probability per collision of a direct dissociation, and $\bar{k}_{ni}$ is the rate constant for predissociation (or tunnelling) from the state (i,J) *if* state (i,J) is a quasi-bound level; $\bar{k}_{ni} = \bar{k}_{in} = 0$ for true bound states and the rate expressions in square brackets drop out. Again, following our earlier procedure, forward and backward rates can be related through the equilibrium population distributions, denoted by $\tilde{n}_i$, etc., *viz.*

$$[3a]\quad P_{ji}\tilde{n}_i = P_{ij}\tilde{n}_j$$

$$[3b]\quad \bar{P}_{ni}\tilde{n}_i = \bar{P}_{in}\tilde{n}_n^2$$

$$[3c]\quad \bar{k}_{ni}\tilde{n}_i = \bar{k}_{in}\tilde{n}_n^2$$

so that it is only necessary to assign the activation probabilities P_{ji} and the *dissociation* probabilities $\bar{P}_{ni}$ and $\bar{k}_{ni}$ on the left-hand sides of [3*a*], [3*b*], and [3*c*]; the deactivation and recombination probabilities follow from detailed balancing. It has been shown recently (14) that, as we have argued qualitatively in the past (3), the T–V transition probabilities for a Morse oscillator are relatively insensitive to the rotational energy of the diatom. Thus it is reasonable to make the very simple assumption that, whatever the rotational quantum number of the state, the probability of a pure increase in vibrational energy can be represented by our recipe III(1) which describes the calculated values for the $J = 0$ state in the form of a function of T, the temperature and Δ_{ij}, the difference in vibrational energy between the two levels.[1] Likewise, following our earlier procedures, the dissociation probabilities $\bar{P}_{ni}$ in [3*b*] are also represented by this formula, except that unlike the $J = 0$ state, the energy separation between the state (i,J) and the free atoms has to be taken as

$$[4]\quad \bar{\Delta}_{ni} = \varepsilon_{max}(J) - \varepsilon_i(J)$$

Finally, the $\bar{k}_{ni}$ of [3*c*] follow directly from the resonance widths Γ_i of the quasi-bound states calculated in the work of the Wisconsin group (8–10) via the relation

$$[5]\quad \bar{k}_{ni} = 2\pi c\Gamma_i$$

where c is the velocity of light and Γ_i is in cm^{-1}.

Using our eigenvalue method, described in Part III of this series (13), it is not necessary to know the $\bar{P}_{in}$ and $\bar{k}_{in}$ of equations [3*b*] and [3*c*], *cf.* equations III(4) and III(5) which define the matrix A_{00} whose smallest eigenvalue d_{n-1} is related to the rate constant. All that is necessary is that the diagonal elements of the relaxation matrix A_{00} be augmented by the extra predissociation term; thus the definition of the elements of A_{00} given in III(5) needs to be changed to

$$[6]\quad [A_{ij}] = (1 - \delta_{ij})Q_{ji} - \delta_{ij} \times \left[\bar{Q}_{ni} + \bar{k}_{ni} + \sum_{k=0}^{n-1}(1 - \delta_{ki})Q_{ki}\right]$$

where $Q_{ij} = [M]ZP_{ij}$; note that $\bar{k}_{ni}$ is a term which is independent of $[M]Z$, and hence the specific overall rate will be dependent on the H_2/He mixture ratio. In order to make a thorough test of the transcription of III(5) into [6], we first of all checked the consistency of the new eigenvalue formulation with the results of the direct integration of eqs. 1 and 2, and for this purpose one needs to know the recombination rate coefficients $\bar{P}_{in}$ and $\bar{k}_{in}$; as will be shown in the next

[1]Equations and tables taken from other papers in this series and used in the present paper are prefixed with the part numbers in Roman numerals.

TABLE 1. Comparison of rate constants obtained by direct integration of [1] and [2], or by solution of [6], for the $J = 21$ state of H_2 at 2000 °K: [M] = 3.5×10^{19} atoms cm^{-3}; $K(J) = 9.24719 \times 10^6$ molecule cm^{-3}

Parameter	Value: Without tunnelling	Value: With tunnelling	Units
$[M]^{-1}d_{n-1}(J)$	8.77788×10^{-16}	9.04962×10^{-16}	cm^3 molecule^{-1} s^{-1}
$k_d(J)$, eq. [8]	8.77788×10^{-16}	9.04962×10^{-16}	cm^3 molecule^{-1} s^{-1}
$[K(J)]^{-1}[M]^{-1}d_{n-1}(J)$	9.4925×10^{-23}	9.79×10^{-23}	cm^6 molecule^{-2} s^{-1}
$k_r(J)$, eq. [9]	9.4928×10^{-23}	9.84×10^{-23}	cm^6 molecule^{-2} s^{-1}

paragraph, the choice of these recombination coefficients is not unique.

Since we are basically interested in the partial contribution that the $J = 21$ state makes to the total dissociation process, we should consider for the direct integration a number of molecules initially in $v = 0, J = 21$ given by the ratio of the molecular partition functions $pf(J)/pf_{total}$ times the total number of 3.5×10^{16} molecules cm^{-3}. This will ensure that during the dissociation process, the populations of the various vibrational levels of the state J will be of the same order of magnitude as they would be in the complete dissociation, provided that the atoms considered to be in equilibrium with the $J = 21$ state are similarly partitioned. Thus we have the following definitions

$$[7] \qquad K = [H]^2/[H_2]$$
$$[H_2(J)] = pf(J)[H_2]/pf_{total}$$
$$[H(J)] = pf(J)[H]/pf_{total}$$
$$K(J) = [H(J)]^2/[H_2(J)] = pf(J)K/pf_{total}$$

The equilibrium constant K, and thence $K(J)$, can be calculated from the known rotation–vibration energy levels (9) by standard methods (15), and the values of K come out to be very close indeed to those given in the JANAF Tables (16). It should be understood that the partitioning of the H atoms into H(J), *i.e.* that fraction considered to be in equilibrium with $H_2(J)$, is only (at this stage) a computational convenience. If one started with *all* the H_2 molecules in $v = 0, J = 21$ instead of only the small fraction $pf(J)/pf_{total}$ of that number, the integration would have to follow the flow of all these molecules through the $J = 21$ state out into the atoms before the normal equilibrium vibrational distribution of the $J = 21$ state was achieved; this would be a lengthier calculation and for most of the time the populations of the $J = 21$ state would be far in excess of what they would be in the real process. On the other hand, if one started with the correct initial population of $H_2(v = 0, J = 21)$ but did not partition the atoms likewise, the final distribution would contain too few $J = 21$ H_2 molecules. The partitioning is also a convenience in that it enables each complete J-state to be treated in isolation from all others if there is full rotational equilibrium amongst complete J-states. To do this, one has to assume that any transfers into individual vibrational sublevels of the J-state in question from any other J-state are balanced by an equal number of transfers out; such artificial restrictions will be relaxated later in the paper when proper rotational–vibrational disequilibrium is considered.

With these constraints, the ten simultaneous equations [1] and [2] were solved for both dissociation and recombination by standard Runge–Kutta procedures, both with the predissociation rates $\bar{k}_{ni}$ set equal to zero, or having their correct values according to [5], with the surprising result that the very high tunnelling rate of the $v = 8$, $J = 21$ state makes only a few percent difference to the rate constant for dissociation of the $J = 21$ state. The rate constants for dissociation $k_d(J)$ and for recombination $k_r(J)$ are defined from the respective fluxes to be consistent with definition [7] as follows

$$[8] \qquad -R_{H_2(J)} = [M]k_d(J)\{[H_2(J)] - [K(J)]^{-1}[H(J)]^2\}$$

and

$$[9] \qquad R_{H_2(J)} = [M]k_r(J)\{[H(J)]^2 - K(J)[H_2(J)]\}$$

where, as is shown to be correct in Table 1, the rate quotient law

$$[10] \qquad k_d(J)/k_r(J) = K(J)$$

is assumed to hold. Table 1 shows the comparisons between the various rate constants for a

Can. J. Chem. Downloaded from www.nrcresearchpress.com by 210.87.254.42 on 09/05/12
For personal use only.

Can. J. Chem. Downloaded from www.nrcresearchpress.com by 210.87.254.42 on 09/05/12
For personal use only.

temperature of 2000 °K obtained by direct integration through the application of [8] and [9] after the induction period was over (12, 13), and also the same rate constants calculated from the lowest eigenvalue of the relaxation matrix [6] through equation III(21), *viz.*

$$[11] \qquad k_d(J) = -[M]^{-1} d_{n-1}(J)$$

Thus, direct integration and the eigenvalue of the modified relaxation matrix give the same answers, both with and without the contribution from predissociation. There is a slight discrepancy in the tunnelling case between the recombination rate constant obtained by direct integration and that found using the rate quotient law, *i.e.* [10] and [11]. This is because recombination integrations seem to be inherently less stable than dissociation integrations and this, taken together with the fact that the parasitic eigenvalues with tunnelling are very large indeed ($\sim 10^{13}\ s^{-1}$, *i.e.*, about 100 times bigger than those arising from purely collisional processes which are $\sim 10^{11}\ s^{-1}$ at 1 atm total pressure), makes this particular recombination calculation very time consuming; hence we did not explore step-length variations in enough detail to be able to present a very accurate value in this case, although there seems no reason to doubt that such agreement could be obtained.

The reason why the inclusion of tunnelling makes so little difference to the rate constant is revealed by an examination of typical pairs of population distributions, as is done in Table 2 for both dissociation and recombination. In dissociation, the reaction without tunnelling is very slightly less advanced than the one with tunnelling, and so there is a tendency for the n_i to be slightly higher and for n_n to be slightly less: this can be seen either by comparing the n_i directly, or the ξ_i. The only real difference between the two distributions is that the very high predissociation rate ($\bar{k}_{ni} = 9.1 \times 10^{12}\ s^{-1}$) of the $v = 8$, $J = 21$ state causes its population to be reduced by a factor of about three. To put it crudely, referring to Fig. 1, all that has happened by giving the $v = 8$ state this large tunnelling rate is that the top of the rotational pseudo-potential barrier has been cut off, and now the molecule only needs an energy $[\varepsilon_8(J) - \varepsilon_0(J)]$ to dissociate rather than $[\varepsilon_{max}(J) - \varepsilon_0(J)]$. Thus, the rate will be increased by roughly exp $[\varepsilon_{max}(J) - \varepsilon_8(J)]/kT$, which is virtually the ratio of the two values of $k_d(J)$ observed in Table 1, leaving the rate constant for

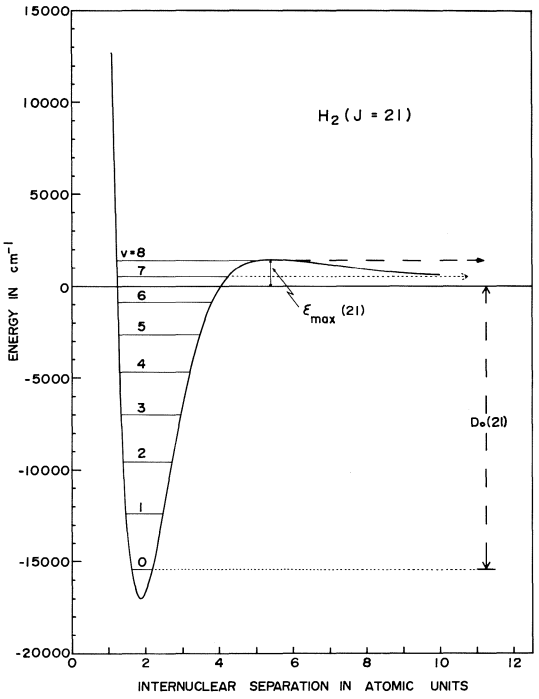

FIG. 1. Energy-level diagram for the $J = 21$ state of H_2.

dissociation (and therefore recombination) to be determined by cooperative bottleneck phenomena (17) lower down the vibrational ladder. The tunnelling rates into and out of $v = 8$ (4.005×10^{16} and 4.058×10^{16} molecules s^{-1}, respectively, at this time) are enormous when compared with individual collision transfer rates which for $v = 8$ do not exceed 4.7×10^{14} molecules s^{-1}. However, the net tunnelling rate for $v = 8$, *i.e.* the difference of the two rates, is only 5.34×10^{14} molecules s^{-1}, almost exactly the value for the rate of formation of $v = 8$ by the sum of all collision processes. Thus, these fluxes demonstrate clearly that, as is postulated by Roberts, Bernstein, and Curtiss (18), the wide quasi-bound resonances can be considered to be in very close equilibrium with the atoms, which is the same thing as saying that the top of the potential barrier is removed. As far as predissociation is concerned, the penultimate quasi-bound level is relatively unimportant: total collision rates into and out of this state exceed 10^{15} molecules s^{-1}, but with a net change of the order of 10^{10} molecules s^{-1}, of which about 1% is due to tunnelling.

In recombination, likewise, tunnelling has a negligible effect. With tunnelling, the reaction is

Can. J. Chem. Downloaded from www.nrcresearchpress.com by 210.87.254.42 on 09/05/12
For personal use only.

TABLE 2. Comparison of population distributions during dissociation of and recombination into the $J = 21$ state of H_2 at 2000 °K: total number of molecules = 3.36865×10^{10} per cc; all originally present in $v = 0$, $J = 21$ for dissociation, or as atoms for recombination; $t = 5 \times 10^{-8}$ s

		Dissociation				Recombination			
	Equilibrium population	Without tunnelling		With tunnelling		Without tunnelling		With tunnelling	
State	$\tilde{n}_i$	n_i	$\xi_i = n_i/\tilde{n}_i$	n_i	$\xi_i = n_i/\tilde{n}_i$	n_i	$\xi_i = n_i/\tilde{n}_i$	n_i	$\xi_i = n_i/\tilde{n}_i$
$v = 0$	2.9545×10^{10}	2.9758×10^{10}	1.00721	2.9757×10^{10}	1.00718	2.8300×10^{10}	0.9579	2.8341×10^{10}	0.9593
$v = 1$	3.3339×10^{9}	3.3558×10^{9}	1.00658	3.3556×10^{9}	1.00653	3.2517×10^{9}	0.9754	3.2548×10^{9}	0.9763
$v = 2$	4.4299×10^{8}	4.4438×10^{8}	1.00313	4.4431×10^{8}	1.00298	4.7641×10^{8}	1.0714	4.7386×10^{8}	1.0697
$v = 3$	6.9701×10^{7}	6.8910×10^{7}	0.9887	6.8870×10^{7}	0.9881	1.0273×10^{8}	1.474	1.0185×10^{8}	1.461
$v = 4$	1.3105×10^{7}	1.2310×10^{7}	0.9393	1.2283×10^{7}	0.9373	3.7287×10^{7}	2.845	3.6635×10^{7}	2.796
$v = 5$	2.9877×10^{6}	2.4078×10^{6}	0.8059	2.3901×10^{6}	0.8000	1.9585×10^{7}	6.555	1.9136×10^{7}	6.405
$v = 6$	8.4532×10^{5}	4.5368×10^{5}	0.5367	4.4303×10^{5}	0.5229	1.1869×10^{7}	14.040	1.1570×10^{7}	13.687
$v = 7$	3.0909×10^{5}	6.6819×10^{4}	0.2162	5.9669×10^{4}	0.1931	7.0944×10^{6}	22.952	6.9105×10^{6}	22.357
$v = 8$	1.6229×10^{5}	1.3430×10^{4}	0.0828	4.4647×10^{3}	0.0275	4.3268×10^{6}	26.662	4.3343×10^{6}	26.708
Dissociated molecules	2.7791×10^{8}	4.4414×10^{7}	0.1598	4.5792×10^{7}	0.1648	1.4772×10^{9}	5.315	1.4365×10^{9}	5.169

Can. J. Chem. Downloaded from www.nrcresearchpress.com by 210.87.254.42 on 09/05/12
For personal use only.

slightly more advanced, which means that the n_i or ξ_i for very low i will be slightly larger, and for high i will be slightly lower than the without-tunnelling case, which is true except for the wide quasi-bound level; this is slightly better coupled to the atom population than it would be if there were no preassociation, so its population is very slightly enhanced. Because it is important to understand the contribution which the quasi-bound resonance makes to the recombination process, we will try to analyze the population fluxes in the region of that level; tunnelling into the lower of the two quasi-bound levels can again be ignored. First, with the population distributions listed in Table 2, the predissociation rate is 3.9403×10^{19} and the preassociation rate 3.9418×10^{19}, with a net preassociation rate of 1.5×10^{16} molecules s^{-1}. Collisional dissociation from all states (principally from $v = 6$, 7, and 8) amounts to 2.63×10^{17} molecules s^{-1}, and three-body recombination into those states is 2.76×10^{17} molecules s^{-1}, with a net rate of collisional recombination of 1.3×10^{16} molecules s^{-1}. Hence, the total rate of recombination is 2.8×10^{16} molecules s^{-1}, which is consistent with the net flux calculated by [9] using the value of $k_r(J)$ from Table 1 and the concentrations from Table 2. The fates of those molecules passing through the quasi-bound level are as follows. The total collisional deactivation rate of $v = 8$ into $v = 7$, 6, 5, and below is 7.2×10^{16} molecules s^{-1}, and the total repopulation of $v = 8$ from below is 5.7×10^{16} molecules s^{-1}, corresponding to a net deactivation rate for the quasi-bound state of 1.5×10^{16} molecules s^{-1}. Collisional dissociation of $v = 8$ and three-body recombination into $v = 8$ balance almost exactly at about 2.1×10^{17} molecules s^{-1}, with a net recombination flux into $v = 8$ of a little under 10^{14} molecules s^{-1}; that this quantity is so small is a result of the enhanced degree of equilibration between the atoms and $v = 8$, resulting from the very high tunnelling rates for that level. Hence, the overall picture of the recombination flux is that it is made up approximately equally out of preassociation into $v = 8$ and out of three-body recombination into $v = 7$ and $v = 6$: that of the total of 4.15×10^{19} pairs of atoms per second which recombine by both mechanisms into $v = 8$, only 7.2×10^{16} per second are deactivated and of those, 5.7×10^{16} come back up to $v = 8$; and that this difference between depopulation and repopulation rates for $v = 8$ is almost exactly balanced by the net flux into $v = 8$ from atoms.

The Pressure Dependence of the Rate Constant $k_d(J)$

According to [1], the rate of dissociation of H_2 ($J = 21$) is made up from two kinds of contribution, those which are second order in [M] and n_i, and those which are first order in n_i only. At low pressures, the predissociating states will be very depleted if the tunnelling rate is high. However, as [M] increases, the collisional activation will tend to maintain n_i nearer its non-tunnelling pseudo-steady value, and as [M] $\rightarrow \infty$, the rate constant for dissociation will become truly second order. This is analogous to the fall-off of unimolecular rate constants from their high pressure limits, but is *not* the same effect that has been seen in the dissociation of I_2 at high pressure (19). A series of calculations in which $[H_2(J)]$ was held constant but [M] was varied from 3.5×10^7 to 3.5×10^{30} atoms cm^{-3} showed that for [M] > $[H_2]$, one would find a pseudo-bimolecular rate constant of the form

$$[12] \quad \text{“}k_d(J = 21)\text{”} = -[M]^{-1} d_{n-1}(J = 21) = k_d^0(J = 21) + [M]^{-1} k_t(J = 21)$$

where $k_d^0(J = 21) = 8.77788 \times 10^{-16}$ cm^3 molecule^{-1} s^{-1} (the without-tunnelling rate constant in Table 1) and an effective tunnelling rate constant $k_t(J = 21) = 951$ s^{-1}, the second term becoming negligible for [M] greater than about 10^{25} particles cm^{-3}. Equation 12 does not hold for low [M] because the collision rate cannot sustain the pseudo-steady state required for the first order decay process to be independent of pressure. Every state from $J = 4$ to $J = 38$ exhibits this kind of behavior, each with its own individual values of $k_d^0(J)$ and $k_t(J)$, but we believe that at the present time, this kind of pressure dependence is of secondary importance to the understanding of diatomic dissociation processes, and have not examined the matter further for the time being.

A “Δv or ΔJ” Factored Model

In describing the dissociation of a diatomic gas in a shock wave, it is usual to assume that, except at very high temperatures, rotational and vibrational equilibration precede dissociation. We have shown (12) that the assumption of vibrational equilibration is a reasonable one, except in respect

Can. J. Chem. Downloaded from www.nrcresearchpress.com by 210.87.254.42 on 09/05/12
For personal use only.

of some of the topmost vibrational states; (even in such a rapid dissociation as we see for the $J = 21$ state above, the lowest three states are very closely in equilibrium with each other, and the lowest six states may be considered as being reasonably equilibrated, with $1.01 \geqslant \xi_i \geqslant 0.8$). That the molecules will be rotationally equilibrated seems even more obvious, since rotational relaxation times are considerably shorter than vibrational ones. Hence, by solving each of the 39 vibration–dissociation master equations to find the 39 values of $d_{n-1}(J)$, given full rotational equilibration, it follows (20) from [7], [8], and [9] that

$$[13] \quad -R_{H_2(J)} = -\frac{d_{n-1}(J)pf(J)}{pf_{total}} \times \{[H_2] - K^{-1}[H]^2\}$$

whence the total rate of dissociation of H_2 would be

$$[14] \quad -\sum_J R_{H_2(J)} = -\sum_J \frac{d_{n-1}(J)pf(J)}{pf_{total}} \times \{[H_2] - K^{-1}[H]^2\}$$

which identifies the overall rate constant for dissociation with rotational equilibration as

$$[15] \quad \tilde{k}_{d,M} = -[M]^{-1} \sum_J \frac{d_{n-1}(J)pf(J)}{pf_{total}}$$

Table 3 lists the calculated values of $d_{n-1}(J)$ for all J, both with and without tunnelling, showing the individual contributions to [15], assuming a constant value of Z for all states, v and J. The following properties of these numbers are worth noting. First, the $d_{n-1}(J)$ increase monotonically with J, principally due to the change in the Boltzmann factor $\exp[-D_0(J)/kT]$. Second, when $J \geqslant 4$, the numerical magnitude of $d_{n-1}(J)$ is always greater with tunnelling than without, although sometimes the difference is insignificant as some of the lifetimes of quasi-bound levels with respect to predissociation are extremely long (18, 21); the first really significant difference occurs at $J = 30$. Third, if rotational equilibration is assumed, and if there were no tunnelling, there would be a significant contribution to the dissociation from all rotational states, with $J = 0$ and $J = 38$ being among the weakest contributors, the former because of its unfavorable statistical weight ($2J + 1 = 1$), and the latter because, despite its high statistical weight ($2J + 1 = 77$), the energy requirement is too high (the contributions from odd states of high J are about three times as large as for even J as expected). When tunnelling is included, however, there is a marginal increase in the sum up as far as $J = 36$, but the contributions from $J = 37$ and $J = 38$ become equal to all the rest put together, approximately doubling the total rate. The predicted rate constants are respectively about 1.7×10^{-20} and 3.5×10^{-20} cm^3 molecule^{-1} s^{-1}; the simple collision theory rate constant, assuming full contribution of rotational energy to the decomposition path would be 2.1×10^{-20} cm^3 molecule^{-1} s^{-1}. The one result is lower as a cumulative result of all the small departures from vibrational equilibrium, such as we have tabulated previously (12, 13) or shown in Table 2; the other is higher principally because the four topmost states $J = 35$, 36, 37, and 38 have only one level, and to assume that these levels are equilibrated automatically makes a large (first order) predissociation contribution to the total rate.

These results, especially the one including tunnelling, are unsatisfactory when it is remembered that they are based on a constant collision number Z which was chosen to be that of He atom and a ground-state H_2 molecule: if we had allowed for the fact that the excited states have very much larger effective cross-sections (18), then very significantly higher rate constants would have resulted. In comparison, experimental values of the rate constants are usually close to or a little less than the collision theory rate with a gas-kinetic value of Z: we have just shown that the cumulative effect of vibrational underpopulation (in the no-tunnelling case) is a depression of approximately 20% in the rate below the collision-theory value, and therefore one has to conclude that either the assumed vibrational transition probabilities are all much too large, or else one cannot assume rotational equilibration. Since there is at least some theoretical basis for the T–V transition probabilities that have been assumed (3, 13), it is obviously necessary to examine the assumption of rotational equilibration.

To do this, we now depart from our long-held philosophy (5) that our calculations have regarded H_2 simply as a model for a diatomic molecule, and we will now make use of the special feature of H_2 that the odd and the even J states do not mix, in order to reduce the magnitude of the computation. Even so, to extend our normal-mode approach to the calculation of the T–VR dissociation relaxation of either ortho- or para-H_2, and to

TABLE 3. Individual contributions to the total rate of dissociation assuming rotational equilibration: $T = 2000$ °K; [M] $= 3.5 \times 10^{19}$ atoms cm^{-3}

		Without tunnelling		With tunnelling	
J	$pf(J)$	$-d_{n-1}(J)$	$\frac{-pf(J)d_{n-1}(J)}{pf_{\text{total}}}$	$-d_{n-1}(J)$	$\frac{-pf(J)d_{n-1}(J)}{pf_{\text{total}}}$
0	1.053	4.37×10^{-2}	8.84×10^{-4}	4.37×10^{-2}	8.84×10^{-4}
1	8.707	4.76×10^{-2}	7.96×10^{-3}	4.76×10^{-2}	7.96×10^{-3}
2	4.084	5.64×10^{-2}	4.42×10^{-3}	5.64×10^{-2}	4.42×10^{-3}
3	13.333	7.25×10^{-2}	1.86×10^{-2}	7.25×10^{-2}	1.86×10^{-2}
4	4.098	1.00×10^{-1}	7.87×10^{-3}	1.00×10^{-1}	7.88×10^{-3}
5	9.974	1.49×10^{-1}	2.86×10^{-2}	1.54×10^{-1}	2.95×10^{-2}
6	2.421	2.16×10^{-1}	1.00×10^{-2}	2.16×10^{-1}	1.00×10^{-2}
7	4.816	3.73×10^{-1}	3.45×10^{-2}	3.73×10^{-1}	3.45×10^{-2}
8	0.979	6.83×10^{-1}	1.28×10^{-2}	7.05×10^{-1}	1.33×10^{-2}
9	1.661	1.17	3.74×10^{-2}	1.17	3.74×10^{-2}
10	0.293	2.43	1.37×10^{-2}	2.43	1.37×10^{-2}
11	0.437	5.23	4.39×10^{-2}	5.42	4.54×10^{-2}
12	6.8×10^{-2}	10.28	1.35×10^{-2}	10.28	1.35×10^{-2}
13	9.2×10^{-2}	24.32	4.31×10^{-2}	24.34	4.32×10^{-2}
14	1.3×10^{-2}	58.36	1.48×10^{-2}	60.36	1.54×10^{-2}
15	1.6×10^{-2}	1.26×10^{2}	4.00×10^{-2}	1.26×10^{2}	4.00×10^{-2}
16	2.2×10^{-3}	3.24×10^{2}	1.37×10^{-2}	3.38×10^{2}	1.43×10^{-2}
17	2.6×10^{-3}	7.21×10^{2}	3.58×10^{-2}	7.21×10^{2}	3.58×10^{-2}
18	3.3×10^{-4}	1.92×10^{3}	1.21×10^{-2}	1.99×10^{3}	1.26×10^{-2}
19	3.7×10^{-4}	4.26×10^{3}	3.03×10^{-2}	4.26×10^{3}	3.03×10^{-2}
20	4.6×10^{-5}	1.17×10^{4}	1.03×10^{-2}	1.20×10^{4}	1.05×10^{-2}
21	5.0×10^{-5}	3.07×10^{4}	2.96×10^{-2}	3.17×10^{4}	3.05×10^{-2}
22	6.1×10^{-6}	7.12×10^{4}	8.30×10^{-3}	7.27×10^{4}	8.48×10^{-3}
23	6.6×10^{-6}	1.85×10^{5}	2.35×10^{-2}	1.92×10^{5}	2.43×10^{-2}
24	8.0×10^{-7}	4.19×10^{5}	6.42×10^{-3}	4.30×10^{5}	6.58×10^{-3}
25	8.7×10^{-7}	1.07×10^{6}	1.79×10^{-2}	1.11×10^{6}	1.85×10^{-2}
26	1.1×10^{-7}	2.34×10^{6}	4.76×10^{-3}	2.42×10^{6}	4.92×10^{-3}
27	1.2×10^{-7}	5.80×10^{6}	1.31×10^{-2}	6.04×10^{6}	1.36×10^{-2}
28	1.5×10^{-8}	1.22×10^{7}	3.42×10^{-3}	1.28×10^{7}	3.59×10^{-3}
29	1.7×10^{-8}	2.95×10^{7}	9.46×10^{-3}	3.09×10^{7}	9.89×10^{-3}
30	2.1×10^{-9}	5.97×10^{7}	2.46×10^{-3}	1.43×10^{8}	5.88×10^{-3}
31	2.5×10^{-9}	1.44×10^{8}	7.07×10^{-3}	1.53×10^{8}	7.47×10^{-3}
32	3.4×10^{-10}	2.80×10^{8}	1.80×10^{-3}	3.13×10^{8}	2.02×10^{-3}
33	4.2×10^{-10}	7.22×10^{8}	5.85×10^{-3}	7.83×10^{8}	6.34×10^{-3}
34	5.5×10^{-11}	1.40×10^{9}	1.47×10^{-3}	1.65×10^{9}	1.73×10^{-3}
35	7.3×10^{-11}	4.02×10^{9}	5.62×10^{-3}	4.77×10^{9}	6.66×10^{-3}
36	7.7×10^{-12}	7.14×10^{9}	1.06×10^{-3}	9.76×10^{9}	1.44×10^{-3}
37	1.1×10^{-11}	2.24×10^{10}	4.64×10^{-3}	3.43×10^{11}	7.11×10^{-2}
38	1.8×10^{-12}	4.88×10^{10}	1.68×10^{-3}	1.59×10^{13}	5.50×10^{-1}
Total	52.052		0.5824		1.2121

calculate the population distribution would have required more fast core computer storage and more computer time than was available to us; we therefore investigated a rough factorized model in which we considered rotational relaxation amongst either the odd- or the even-J states, each J state having an effective T–V dissociation rate constant determined from the eigenvalue $d_{n-1}(J)$ given in Table 3. As will be shown later in this paper, we were able to find eigenvalues (but not eigenvectors) for the full T–VR dissociation calculation, in good agreement with the results of this factored model, so that the conclusions of this calculation in respect of population distributions should be reasonably reliable.

The first problem is to assign a reasonable set of T–R transition probabilities. Recent years have seen enormous activity in the theoretical calculation of translation–rotation transition probabilities, which it would be far beyond the scope of this paper for us to review: it suffices to say that the state of knowledge is still far from complete, and it is as yet impossible to write down transition probabilities for H_2/He collisions for any value of

Can. J. Chem. Downloaded from www.nrcresearchpress.com by 210.87.254.42 on 09/05/12
For personal use only.

Can. J. Chem. Downloaded from www.nrcresearchpress.com by 210.87.254.42 on 09/05/12
For personal use only.

ΔJ at any arbitrary temperature T. Based on two intuitive considerations: (*i*) that transition probabilities for the transfer of an amount of energy Δ_{ij} from translation to rotation will be subject to the same kinds of factors as those which determine how translation to vibration transition probabilities change with Δ_{ij} and with T; (*ii*) that there may be an extra penalty if ΔJ is not small; we chose the following empirical general form for endothermic T–VR transition probabilities

$$[16] \qquad P_{ij} = f(T,\Delta_{ij})e^{-\Delta_{ij}/kT}e^{-2.5|\Delta J|}$$

when $f(T,\Delta_{ij})$ is defined by equation III(1) and the corresponding deactivation probabilities follow from the detailed balancing equations [3*a*] and [3*b*] (remembering that if $\Delta J \neq 0$, statistical weight terms $(2J + 1)$ are involved). Equation 16 has the following properties. If $\Delta J = 2$, it gives a deactivation probability for $H_2(J = 2 \rightarrow J = 0)$ of about one in 250 collisions at room temperature, and the deactivation probabilities decrease slowly with increasing Δ_{ij} and with decreasing T: to this extent they crudely follow existing experimental observations (22–24). The exponent in $|\Delta J|$ represents an arbitrary penalty in ΔJ, the effect of which will be demonstrated later. The advantage of [16] is that if $\Delta v = 0$ its behavior is not unlike a realistic set of T–R transition probabilities (25), and if $\Delta J = 0$ it reduces to the T–V transition probabilities that we have used throughout this series: hence, it would appear to be a suitable vehicle for the subsequent comparison, later in this paper, of the present factored method with a full T–VR–dissociation relaxation; furthermore, for D_2, it yields a deactivation probability for $J = 2 \rightarrow J = 0$ of about 1 in 210 collisions at $T = 300$ °K, again closely mimicking existing experimental data (22).

The factored "Δv or ΔJ" calculation begins with all molecules in the $J = 0$ state, and at the temperature in question the relaxation towards equilibrium is governed by the T–R transition probabilities [16] and effective mean dissociation rate constants $k_d(J) = -[M]^{-1}d_{n-1}(J)$ determined from Table 3. Thus, the *effective* rotational master equation to be solved is (for even J)

$$[17] \quad \frac{dn_r}{dt} = \sum_{s=0,2,4\ldots}^{38} Z[M](P_{rs}n_s - P_{sr}n_r) + [M](k_r(r)n_n^2 - k_d(r)n_r) \qquad r = 0, 2, 4, \ldots, 38$$

$$[18] \quad \frac{dn_n}{dt} = \sum_{r=0,2,4\ldots}^{38} [M](k_d(r)n_r - k_r(r)n_n^2)$$

where n_r is the population of the rotational state r in molecules cm^{-3} and n_n is the number of dissociated molecules per cc, as usual. The combination rate constants $k_r(J)$ occurring in these two equations now refer, not to a subset of the free atoms partitioned by $pf(J)/pf_{total}$, but to a subset of the free atoms partitioned by $pf(\text{even})/pf_{total}$. As mentioned earlier, this partitioning facilitates the generation of representative population distributions, but is not necessary for the calculation of the rate constant by the eigenvalue method. Implicit in writing [17] and [18] are the following assumptions. One, that in using [16] to calculate P_{rs} between two states $J = s$ and $J = r$, the energy gap Δ_{rs} has to be a mean or effective value: we originally chose the mean vibrational energy of the particular rotational state as the reference point with respect to which to define Δ_{rs}; however, it is simpler and has little effect on the rate of dissociation (compare Tables 5 and 6 below) if other reference points *e.g.* $v = 0$, $J = s$ and $v = 0$, $J = r$ are used. Two, that the calculated overall rate of dissociation will be that corresponding to a product population distribution function, *i.e.* a product of the individual vibrational distributions for each J, such as those shown in Table 2, with the rotational distribution n_r, etc., resulting from the solution of [17] and [18]. Thus, each individual population $n(v,J)$ is not free to vary as it should in the real calculation, and the same kind of inflexibilities will arise as occur when product wave functions are used instead of fully variational ones to describe, for example, the helium atom (26).

Table 4 shows how the presence of tunnelling changes the populations of the rotational states in ortho-H_2, both in dissociation and in recombination, according to this approximate model. In the dissociation, the levels $J = 1$ to 19 come essentially into equilibrium with each other, but there is a very well defined bottleneck effect at about $J = 27$ or 29 with the very high rotational states being very markedly underpopulated; inclusion of tunnelling in these calculations has very little effect either upon the populations or the rate constant. In recombination, again there is a very marked bottleneck effect with states from $J = 27$ and above being in very close equilibrium indeed with each other and with the atoms: the lower J states are very much underpopulated at this early

TABLE 4. Comparison of rotational population distributions $\xi_r = n_r/\tilde{n}_r$ for ortho-H_2 at 2000 °K, for dissociation at $t = 7.5 \times 10^{-6}$ s and recombination at $t = 10^{-6}$ s: total number of H_2 molecules = 3.5×10^{16} cm^{-3}, *i.e.*, total number used in the ortho-H_2 partition = 8.75×10^{15} molecules cm^{-3}*

State J	Equilibrium distribution $\tilde{n}_r$	Dissociation		Recombination	
		Without tunnelling	With tunnelling	Without tunnelling	With tunnelling
1	1.535×10^{15}	1.0083	1.0083	4.023×10^{-3}	4.055×10^{-3}
3	3.020×10^{15}	1.0083	1.0083	4.046×10^{-3}	4.078×10^{-3}
5	2.391×10^{15}	1.0083	1.0083	4.202×10^{-3}	4.236×10^{-3}
7	1.182×10^{15}	1.0083	1.0083	5.072×10^{-3}	5.115×10^{-3}
9	4.118×10^{14}	1.0083	1.0083	9.701×10^{-3}	9.796×10^{-3}
11	1.087×10^{14}	1.0083	1.0083	3.668×10^{-2}	3.714×10^{-2}
13	2.299×10^{13}	1.0083	1.0083	2.089×10^{-1}	2.107×10^{-1}
15	4.086×10^{12}	1.0082	1.0082	1.380	1.394
17	6.367×10^{11}	1.0077	1.0077	9.090	9.207
19	9.034×10^{10}	1.0043	1.0042	57.258	58.276
21	1.206×10^{10}	0.9850	0.9843	3.342×10^{2}	3.430×10^{2}
23	1.561×10^{9}	0.8989	0.8960	1.567×10^{3}	1.608×10^{3}
25	2.009×10^{8}	0.6329	0.6249	5.379×10^{3}	5.492×10^{3}
27	2.632×10^{7}	0.2247	0.2165	1.123×10^{4}	1.135×10^{4}
29	3.588×10^{6}	0.0257	0.0238	1.408×10^{4}	1.411×10^{4}
31	5.195×10^{5}	8.14×10^{-4}	7.17×10^{-4}	1.444×10^{4}	1.444×10^{4}
33	8.170×10^{4}	1.05×10^{-5}	8.88×10^{-6}	1.445×10^{4}	1.445×10^{4}
35	1.436×10^{4}	4.03×10^{-7}	3.68×10^{-7}	1.445×10^{4}	1.445×10^{4}
37	2.968×10^{3}	2.24×10^{-7}	2.27×10^{-7}	1.445×10^{4}	1.445×10^{4}
atoms	7.218×10^{13}	4.71×10^{-4}	4.76×10^{-4}	1.202×10^{2}	1.202×10^{2}

*Rate constants determined from the fluxes: without tunnelling, $k_d = 1.59697 \times 10^{-20}$ cm^3 molecule^{-1} s^{-1}, $k_r = 6.64900 \times 10^{-33}$ cm^6 molecule^{-2} s^{-1}, $k_d/k_r = 2.40183 \times 10^{12}$ molecule cm^{-3}; with tunnelling, $k_d = 1.61484 \times 10^{-20}$ cm^3 molecule^{-1} s^{-1}, $k_r = 6.72343 \times 10^{-33}$ cm^6 molecule^{-2} s^{-1}, $k_d/k_r = 2.40181 \times 10^{12}$ molecule cm^{-3}; effective equilibrium constant $K(J = \text{odd}) = 2.40188 \times 10^{12}$ molecule cm^{-3}.

time in the reaction, but as expected, they are more-or-less in equilibrium amongst themselves also. Again, the effect of tunnelling is minimal; it facilitates the equilibration between the atoms and the upper J states somewhat, and causes a marginal increase in the rate. Note also that the rate constants quoted at the foot of Table 4, which are calculated from the transition fluxes by the analogs of equations [8] and [9], obey the rate quotient law quite accurately and are the same as those determined by the eigenvalue method to the number of decimal places quoted. Likewise, for para-H_2, with even J states, the bottleneck is in about the same place, near $J = 26$ or 28. Furthermore, the rotational bottleneck effect appears to be much more well-defined than the vibrational bottleneck which we have described on previous occasions (12, 13, 17, 27). For example, at 5000 °K, it is not immediately apparent from the vibrational population distributions (*e.g.* Table III(3)) that a bottleneck is present, and its existence was established by indirect evidence, such as is presented in Tables III(5) and V(1); however, in the rotational calculation at 5000 °K, the changeover from over- to under-population remains just as marked as is shown in Table 4, and at about the same J levels, both in dissociation and in recombination. It is not transparently obvious that the bottleneck should be so persistent and its position so stable, but clearly it is the result of progressively increasing rotational spacings, in contrast to progressively decreasing vibrational spacings.

Table 2 gives what may be roughly regarded in this approximation as a steady-state vibrational distribution during the dissociation process, and in principle, although we haven't reproduced the figures, such a distribution can be generated for every other J state (for $J = 0$, see Tables II(3) or III(3)). Thus, in the product approximation, a reasonable picture of the overall rotation–vibration distribution will be obtained by scaling each pseudo-steady vibrational distribution with the ξ_r of Table 4. This means that in dissociation, for example, low J and low v levels will all be in equilibrium with each other, high J and low v or low J and high v will be depleted to varying degrees, and high J and high v will be more

Can. J. Chem. Downloaded from www.nrcresearchpress.com by 210.87.254.42 on 09/05/12
For personal use only.

TABLE 5. Comparison of rate constants for dissociation of ortho-H_2 and para-H_2, with and without tunnelling, in units of cm^{-3} molecule $^{-1}$ s^{-1}, in the factored "Δv or ΔJ" approximation,* determined by the eigenvalue method

	para-H_2		ortho-H_2	
T (°K)	Without tunnelling	With tunnelling	Without tunnelling	With tunnelling
1500	2.93×10^{-24}	3.01×10^{-24}	3.87×10^{-24}	3.94×10^{-24}
2000	1.27×10^{-20}	1.29×10^{-20}	1.60×10^{-20}	1.61×10^{-20}
3000	4.08×10^{-17}	4.13×10^{-17}	4.81×10^{-17}	4.83×10^{-17}
4000	1.82×10^{-15}	1.84×10^{-15}	2.06×10^{-15}	2.07×10^{-15}
5000	1.63×10^{-14}	1.64×10^{-14}	1.80×10^{-14}	1.81×10^{-14}

*Δ_{rs} calculated between $v = 0$ levels of states $J = s$ and $J = r$.

TABLE 6. Comparison of the rate constants for dissociation of para-H_2 with various restrictions upon the assumed rotational transition probabilities: the calculations are for the factored "Δv or ΔJ" model,* with tunnelling, and the rate constants are in units of cm^3 molecule^{-1} s^{-1}

	Equation 16		Equation 16 or 16*a*	Equation 16*a*	
T (°K)	ΔJ unrestricted	$\Delta J = \pm 2, 4$ only	$\Delta J = \pm 2$ only	$\Delta J = \pm 2, 4$ only	ΔJ unrestricted
1500	2.89×10^{-24}	2.89×10^{-24}	2.89×10^{-24}	2.90×10^{-24}	2.90×10^{-24}
2000	1.22×10^{-20}	1.22×10^{-20}	1.22×10^{-20}	1.22×10^{-20}	1.22×10^{-20}
3000	3.90×10^{-17}	3.90×10^{-17}	3.90×10^{-17}	3.91×10^{-17}	3.91×10^{-17}
4000	1.75×10^{-15}	1.75×10^{-15}	1.75×10^{-15}	1.78×10^{-15}	1.78×10^{-15}
5000	1.58×10^{-14}	1.58×10^{-14}	1.58×10^{-14}	1.65×10^{-14}	1.66×10^{-14}

*Δ_{rs} calculated as between the mean vibrational energies of states $J = s$ and $J = r$.

severely depleted: the depletion however is a much more severe function of J than of v.

Table 5 compares for para-H_2 (even J) and for ortho-H_2 (odd J) the rate constants for dissociation from 1500 to 5000 °K, calculated according to [16], [17], and [18], both with and without tunnelling. It is obvious immediately that the inclusion of tunnelling from the predissociating levels makes only a negligible difference in this temperature range, this being particularly the case at high temperatures. Referring again to Table 3, this means that states above $J = 30$ must be severely depopulated at all temperatures, and therefore, make very much less contribution to the total rate than they would if there was rotational equilibration; this conclusion is borne out by all the population distributions we have calculated, *i.e.* those presented in Table 4 for ortho-H_2 at 2000 °K, and the ones cited for 5000 °K. The data in Table 3 show that with full equilibration, we could expect at 2000 °K a dissociation rate constant without tunnelling of about 1.7×10^{-20} cm^3 molecule^{-1} s^{-1} and with tunnelling, almost exactly twice that figure. The value found in Table 5 is somewhat less than the 1.7×10^{-20} figure, either for ortho- or para-H_2 with or without tunnelling; this could only be the case because in the relaxing system, the very high specific decomposition rates associated with the high J levels essentially kill their contribution since they have to be populated by rather large rotational energy jumps. Another point of considerable interest is that the Arrhenius temperature coefficients of the rates shown in Table 5 between 2000 and 5000 °K either with or without tunnelling are as follows: para-H_2, 93.2 kcal; ortho-H_2, 92.3 kcal. The experimental Arrhenius coefficient is about 92.6 kcal mol^{-1} (28); we will return to a discussion of the temperature coefficients later in the paper.

In Table 6, we explore several possible variations in respect of the chosen rotational transition probabilities in this factored approximation (using the same set of effective rotational spacings Δ_{rs} in all cases). Since there is so little difference between the inclusion or the exclusion of predissociation, only the rate constants for dissociation with tunnelling are listed. Furthermore, since ortho- and para-H_2 dissociation rates behave identically

Can. J. Chem. Downloaded from www.nrcresearchpress.com by 210.87.254.42 on 09/05/12
For personal use only.

Can. J. Chem. Downloaded from www.nrcresearchpress.com by 210.87.254.42 on 09/05/12
For personal use only.

under these changes, only the results for para-H_2 are quoted; fuller listings will be made available elsewhere (20). The first column shows the standard set of rate constants calculated according to [16] as listed in Table 5. The next two columns list rate constants calculated using [16] for the transition probabilities, but restricting changes in J to either ($\Delta J = \pm 2$ only), or ($\Delta J = \pm 2$ and ± 4 only); the rate constants change in the fourth or fifth decimal place under these restrictions, indicating very strongly indeed that with this set of transition probabilities, once the initial transients have passed the reaction proceeds to all intents and purposes by single step (*i.e.* $\Delta J = \pm 2$) transitions only (*cf.* ref. 12 for a fuller discussion of this effect for vibrational dissociation). The fourth and fifth columns of data in Table 6 repeat the calculations listed in the first and second columns except that the exp $(-2.5\,|\Delta J\,|)$ term in [16] is replaced by e^{-5} if $|\Delta J\,| > 2$ (denoted by [16*a*]). This has the effect of leaving the $\Delta J = \pm 2$ transition probabilities unchanged, but removes the penalty on larger changes in ΔJ; the ($\Delta J = \pm 2$ only) calculation is the same with either [16] or [16*a*]. The effect of removing the arbitrary $|\Delta J\,|$ penalty is negligible at low temperatures, but increases to about 5% at 5000 °K; also, using [16*a*] instead of [16], $\Delta J = \pm 4$ changes have some effect, as evidenced by the fact that the ($\Delta J = \pm 2$ and ± 4 only) rates resemble more nearly the unrestricted ΔJ rather than the ($\Delta J = \pm 2$ only) results. These small differences between the results from [16] and [16*a*] should not be misinterpreted, however, to mean that it does not matter whether or not large changes in ΔJ can occur, it only does not matter in the "Δv or ΔJ only" approximation.

Solution of the Full Set of Equations

The rotation–vibration spectrum of H_2 consists of 172 levels having odd J, and 177 levels having even J, according to the calculations of LeRoy (9). At the beginning of this research, it was not clear to us that we would be able to solve matrices of order 172 or 177 to find the eigenvalue of *smallest* numerical magnitude, *i.e.* the rate constant; further, if population distributions were required, the computer storage requirements would be beyond the capacity of our machine. Our aim in this section was therefore to attempt some solutions of the full eigenvalue problem and compare the rate constants with those obtained in the preceding section; subsequently, it emerged that we could find meaningful values of d_{n-1} at all temperatures from 1500–5000 °K for matrices of order 172 and 177, although at 1500 °K, the third decimal place was not too significant. However, because such eigenvalue calculations were at least twenty times more costly in computing time, only a limited number of experiments was performed, just sufficient to confirm the essential correctness of the conclusions found using the factored method above, and to investigate one or two aspects of the dissociation problem which are meaningless in the context of the factored model.

Equation 16 was taken as the standard set of transition probabilities with which to describe now simultaneous changes in v and J: thus, if $\Delta J = 0$, the probabilities are the Δv probabilities used in the T–V calculations, and if $\Delta v = 0$, they are the ΔJ probabilities used in the T–R calculations of the preceding section. Matrices of order either 172 or 177 were set up according to [6] using these probabilities and solved for the two smallest eigenvalues d_{n-1} and d_{n-2}, both with and without predissociation. The results for the dissociation rate constants obtained from the d_{n-1} are compared with each other in Table 7, where it can be seen that as we have now come to expect, the effect of tunnelling is very small indeed; again, we find, as in the factored approximation (Table 5), the very small acceleration caused by the predissociation is marginally more important at the lowest temperatures. What is surprising about the results in Table 7 however, is that the rate constants for decomposition of para-H_2 always exceed those for ortho-H_2 by a small margin. The reason why this happens is as follows. Counting only bound levels, ortho-H_2 has 146 and para-H_2 has 154, and as we have already shown (27) the more levels a system has, the faster will it dissociate even though a small amount more energy may be required for dissociation. We have done enough numerical experiments (17, 27) to convince ourselves that there is a variational principle here: that for a constant value of the dissociation energy, an increase in the number of (connected) levels cannot lead to a reduction in the dissociation rate; the variational principle could be stronger than stated here, but numerical experiment is not the way to establish theorems of this kind. This behavior stems from two causes, (*i*) that the transition probabilities increase as the gap size decreases, and (*ii*) that after the initial transients, most molecules find their path to dissocia-

TABLE 7. Rate constants for the dissociation of H_2 determined from the smallest eigenvalue of the full relaxation matrix, in units of cm^3 $molecule^{-1}$ s^{-1}

	para-H_2		ortho-H_2	
T (°K)	Without tunnelling	With tunnelling	Without tunnelling	With tunnelling
1500	$3.5_7\times10^{-24}$	$3.7_2\times10^{-24}$	$3.5_4\times10^{-24}$	$3.6_4\times10^{-24}$
2000	1.60×10^{-20}	1.64×10^{-20}	1.58×10^{-20}	1.61×10^{-20}
3000	5.70×10^{-17}	5.78×10^{-17}	5.67×10^{-17}	5.72×10^{-17}
4000	2.70×10^{-15}	2.72×10^{-15}	2.68×10^{-15}	2.70×10^{-15}
5000	2.34×10^{-14}	2.36×10^{-14}	2.33×10^{-14}	2.34×10^{-14}

TABLE 8. Comparison of the factored and unfactored "Δv or ΔJ only" calculations for the rate constants of dissociation (with tunnelling) of ortho-H_2 and para-H_2, in units of cm^3 $molecule^{-1}$ s^{-1}

	para-H_2		ortho-H_2	
T (°K)	Factored	Unfactored	Factored	Unfactored
1500	3.01×10^{-24}	$3.5_7\times10^{-24}$	3.94×10^{-24}	$3.4_9\times10^{-24}$
2000	1.29×10^{-20}	1.52×10^{-20}	1.61×10^{-20}	1.49×10^{-20}
3000	4.13×10^{-17}	4.79×10^{-17}	4.83×10^{-17}	4.69×10^{-17}
4000	1.84×10^{-15}	2.09×10^{-15}	2.07×10^{-15}	2.06×10^{-15}
5000	1.64×10^{-14}	1.82×10^{-14}	1.81×10^{-14}	1.82×10^{-14}

tion to be single-step processes; it appears that under these conditions it is easier to climb the activation ladder in more small steps than in fewer big ones. The fact that our factored model does not show this effect is disappointing; it probably arises because in the factored model the dissociation rate is found by solving a 20-step relaxation process for para-H_2 and a 19-step process for ortho-H_2, and this is not a sufficiently significant difference in the number of steps to offset the additional 120 cm^{-1} required to dissociate. We have remarked before (29) that the measurement of the dissociation rates for ortho- and for para-H_2 represents an intriguing experimental challenge, and it would be most interesting to know whether there is any temperature at which the rate of dissociation (or recombination) of para-H_2 is the greater as our calculations might suggest; in recombination Roberts (30) has suggested that the ortho-rate is dominant at very low temperatures, but that above 200 °K, para-recombination is somewhat favored.

It is of course possible to set up a full-matrix calculation in which all elements of the matrix are zero if both Δv and ΔJ are non-zero; thus this also is a "Δv or ΔJ only" calculation, except that each population $n(v,J)$ is free to vary independently of all others, whereas in the factored model the $n(v,J)$ were products of a vibrational with a rotational distribution. The results of this calculation are shown in Table 8 where they are compared with the corresponding results of the factored calculation taken from Table 5. Here also we find that the solution of the full (yet restricted) matrix gives rise to para-dissociation rates that are marginally faster than ortho-dissociation rates, in contrast to the factored calculations. Comparison of the second and fourth columns of rate constants between Tables 7 and 8 shows that as the temperature decreases, the more closely does the "Δv or ΔJ only" full calculation approach the correct solution without any restriction, which is to be expected since the lower the temperature, the more likely it would be that the molecules would "crawl" up the rotation–vibration ladder using the smallest steps available to them. Comparing like calculations in Table 8, it seems that as the temperature goes down, the factored calculation tends to underestimate the para-dissociation rate but overestimate the ortho-dissociation rate, to the extent that the mean of the two factored calculations is fairly close to the correct unfactored solution.

Table 9 shows the results obtained using [16*a*]

Can. J. Chem. Downloaded from www.nrcresearchpress.com by 210.87.254.42 on 09/05/12
For personal use only.

TABLE 9. The effect of simultaneous rotational and vibrational transitions on the rate of dissociation (with tunnelling) of para-H_2, in units of cm^3 $molecule^{-1}$ s^{-1}

T (°K)	Δv or ΔJ only		Unrestricted	
	Equation 16	Equation 16*a*	Equation 16	Equation 16*a*
1500	$3.5_7\times10^{-24}$	$3.5_1\times10^{-24}$	$3.7_2\times10^{-24}$	$4.4_2\times10^{-24}$
2000	1.52×10^{-20}	1.52×10^{-20}	1.64×10^{-20}	1.91×10^{-20}
3000	4.79×10^{-17}	4.82×10^{-17}	5.78×10^{-17}	6.84×10^{-17}
4000	2.09×10^{-15}	2.14×10^{-15}	2.72×10^{-15}	3.53×10^{-15}
5000	1.82×10^{-14}	1.95×10^{-14}	2.36×10^{-14}	3.56×10^{-14}

in which the $|\Delta J|$ penalty is removed. The effect of this is to change very markedly the probabilities of certain near-resonant transitions. For example the $v = 0, J = 27$ level is 6561 cm^{-1} below the dissociation limit whereas $v = 9, J = 3$ is at 6598 cm^{-1} below the limit. Because the energy difference Δ_{ij} is very small, [16*a*] will give a transition probability for the *exothermic* process of the order of e^{-5}, whereas [16] will give a probability of the order of e^{-60} since $|\Delta J| = 24$. Since it is believed that simultaneous changes in v and J are important (31) but we do not yet know whether a near-resonant change is allowed or disallowed if ΔJ is large, it is important to investigate both possibilities. We have already seen in Table 6 that in the factored calculation such a change has very little effect, which is because in the "Δv or ΔJ only" mechanism most of the dissociation flux takes single steps even without the $|\Delta J|$ penalty. This is confirmed in Table 9 where it is shown that in the full solution of the "Δv or ΔJ only" mechanism, the penalty makes essentially no difference. However, in the unrestricted mechanism, where simultaneous changes in v and J are allowed, there is a significant effect, of about 20% at 1500 °K and 50% at 5000 °K, which arises from the kinds of processes just described, since they are excluded from the "Δv or ΔJ only" description. It would seem that if this trend is maintained, simultaneous changes in v and J would be of only minor importance at lower temperatures, and could be more-or-less ignored in the description of low-temperature recombination reactions.

From the results tabulated in Tables 8 and 9, it is clear that the uncoupling of rotational and vibrational excitation, either via the factored model or via the $|\Delta J|$ penalty, has little effect on the rate of dissociation, especially so at the lower temperatures. As we have noted above, the difference between [16] and [16*a*] involves some very strong rotational–vibrational coupling; a corollary would be that under these conditions when the rotational and vibrational excitation can be treated as separable, the product-type population distribution implicit in the use of the factored model should be a reasonable approximation to the correct solution for the population distribution. One must not be misled, however, into thinking that rotational excitation and vibrational excitation *are* separable, because the second eigenvalue d_{n-2} is actually quite sensitive to changes in such coupling: the quantity $-d_{n-2}{}^{-1}$ is the relaxation time of the last transient which precedes the dissociation (13), commonly regarded as the vibrational relaxation time. Our calculations show that tunnelling has little effect on d_{n-2}, the difference being undetectable at low temperatures and amounting to about 0.1% at 5000 °K, consistent with the fact that in this range the dissociation is not strongly coupled to the internal relaxations (12). The results in Table 10 show that there is a significant change in the "vibrational" relaxation time on changing from the "Δv or ΔJ only" calculation (in which simultaneous changes in v and J are specifically forbidden) to the unrestricted calculation using probabilities given by [16] (in which such changes are weakly allowed); only one example of the "Δv or ΔJ only" relaxation times is quoted, the results are similar for ortho- or para-H_2, and for [16] or [16*a*]. Furthermore, changing the transition probabilities from those described by [16] to those described by [16*a*], the effect of which is simply to increase the rotational transition probabilities for $|\Delta J| \geqslant 4$, there is a further significant change in the "vibrational" relaxation time, of about a factor of three at 1500 °K and about a factor of ten at 5000 °K. Thus, it seems clear that the relaxation time which has hitherto been labelled a "vibrational" relaxation time in shock-

Can. J. Chem. Downloaded from www.nrcresearchpress.com by 210.87.254.42 on 09/05/12
For personal use only.

TABLE 10. The effect of changing the contribution of rotation–vibration coupling on the "vibrational" relaxation time, $-d_{n-2}^{-1}$, in s

T (°K)	para-H_2			ortho-H_2	
	Δv or ΔJ only, equation 16	Equation 16	Equation 16*a*	Equation 16	Equation 16*a*
1500	7.70×10^{-7}	1.38×10^{-7}	4.59×10^{-8}	1.37×10^{-7}	4.31×10^{-8}
2000	5.04×10^{-7}	1.09×10^{-7}	2.94×10^{-8}	1.09×10^{-7}	2.83×10^{-8}
3000	2.60×10^{-7}	8.27×10^{-8}	1.33×10^{-8}	8.29×10^{-8}	1.31×10^{-8}
4000	1.41×10^{-7}	6.33×10^{-8}	7.40×10^{-9}	6.34×10^{-8}	7.34×10^{-9}
5000	7.65×10^{-8}	4.35×10^{-8}	4.55×10^{-9}	4.37×10^{-8}	4.54×10^{-9}

TABLE 11. Arrhenius temperature coefficients for the dissociation of H_2 (with tunnelling) in kcal mol^{-1}

Temperature range (°K)	Factored model, equation 16		Full Δv or ΔJ only, equation 16		Full calculation			
					Equation 16		Equation 16*a*	
	even J	odd J	even J	odd J	even J	odd J	even J	odd J
1500–2000	99.6	99.0	100	100	100	100	100	100
2000–3000	96.2	95.4	96.1	96.1	97.4	97.5	97.6	97.1
3000–4000	90.8	89.9	90.0	90.2	91.9	91.9	94.0	94.1
4000–5000	87.5	86.6	86.2	86.5	85.8	85.9	91.2	92.0
2000–5000	93.2	92.3	92.7	92.8	93.9	94.0	95.6	95.8

tube work has really to be considered as a T–VR relaxation time, particularly so as the temperature becomes high.

The Arrhenius Temperature Coefficient of the Dissociation

We noted earlier that one of the factored calculations gave an Arrhenius temperature coefficient for dissociation which was very close indeed to the experimental value of about 92.6 kcal mol^{-1} (28); since the agreement between the factored and the unfactored methods in respect of rate constants is generally good, it follows that just about any of our approximations will have a temperature coefficient in good agreement with experiment, as shown in Table 11. It is apparent that all of the Arrhenius plots have a marked curvature, and to this extent they seem to be consistent with experimental observation of large negative recombination temperature coefficients at high temperatures, but rather small ones at low temperatures (28, 32, 33). Whilst these agreements may be fortuitous for several reasons, it is interesting to recall that our previous calculations using the energy-transfer mechanism (13) and in which only vibrational disequilibrium was considered gave a temperature coefficient of about 102 kcal mol^{-1}, and that Dove and Jones (34), using quite a different set of T–V transition probabilities found also about 102 kcal mol^{-1}; thus it appears that vibrational disequilibrium cannot easily account for the observation of low "activation energies" in diatomic dissociation reactions, but that the temperature variations in rotational disequilibrium very well could. One can also observe that in Table 11, the removal of the $|\Delta J|$ penalty raises the Arrhenius temperature coefficient in the full calculation from about 86 to 92 kcal mol^{-1} over the 4000–5000 °K temperature range. This is another indication that rotational depopulation could be a key factor in determining the temperature coefficient, and that if intramolecular rotational and vibrational transfers are unimportant there will be a tendency for the Arrhenius temperature coefficient to be lower.

We now summarize briefly other possible causes for the occurrence of these low Arrhenius temperature coefficients. We have previously shown that when strong V–V coupling is present (and the experimental measurements cannot in any sense be considered to be at infinite dilution) non-integral orders in the reactants would occur (35): those calculations referred to a temperature of 2000 °K only, slightly below the experimental

Can. J. Chem. Downloaded from www.nrcresearchpress.com by 210.87.254.42 on 09/05/12
For personal use only.

Can. J. Chem. Downloaded from www.nrcresearchpress.com by 210.87.254.42 on 09/05/12
For personal use only.

range, and were not extended to other temperatures because of a lack of any real knowledge of the relative importance of T–V *vs.* V–V coupling in H_2, and how the relative importance might change with temperature. However, it is clear from that work that it is entirely possible for the reactant orders to change slowly with temperature, and hence, if the rate constants are derived from experimental rates assuming integral reactant orders, both the rate constants and their temperature coefficients would be meaningless (35). As far as we know, no dissociation measurements have yet been directed towards the problem of how closely the rate laws are of integral order in the reactants, and until the answer is known, we will not know how important V–V coupling may be in causing anomalous Arrhenius parameters for these reactions. Then, unfortunately, there still remains the nagging suspicion that there may be a third cause, unsuspected impurity effects which are receiving much more attention from experimenters in recent years (13, 28, 29, 36). These remarks apply to only the energy-transfer component of the dissociation process: in heavier systems, one will need also to consider the radical–molecule complex or chaperon component of the process (37, 38), and in heteronuclear diatomic dissociations one can expect to find atomic chain processes which will accelerate the disappearance of the diatomic molecule; both these effects will lower the temperature coefficient of the reaction. Thus, in our view, no overall accommodation between the theoretical description and the experimental results would seem imminent until a series of experiments on the dissociation of H_2 in the presence of He (to reduce the chaperon contribution) is performed at very high dilutions (to eliminate V–V processes), paying special attention to the problem of impurities: heteronuclear molecules are far too complicated theoretically at the present time (even the HD molecule (29)), as are also heavier homonuclear molecules because of various complexities, including the existence of radical–molecule complexes and of low-lying excited electronic states from which radiation occurs.

Future Calculations

There is very considerable interest at the moment in the recombination of hydrogen atoms at low temperatures, both theoretically (18, 30, 39–41) and experimentally (32). However, in our view, both of the current theoretical approaches used to describe the recombination in hydrogen must be regarded as suspect.

The orbiting-resonance theory of Roberts, Bernstein, and Curtiss (18) was designed to deal specifically with the recombination of hydrogen and deuterium at low temperatures. The restriction to low temperatures was clearly appreciated by the original authors, but it would be useful to present some more of the reasons for this limitation which were not discussed previously. For example, for two of the six quasi-bound states of H_2 which were identified as interesting ($v = 12$, $J = 12$, and $v = 11$, $J = 13$), the loss of energy associated with the change $\Delta v = -1$ is only a little more than the loss for $\Delta J = -2$, and hence both processes are likely to occur in parallel. At low temperatures this will be fairly unimportant, but as J goes up, the vibrational gaps ($\Delta v = -1$) become markedly less than the rotational gaps ($\Delta J = -2$), so that the importance of parallel rotational and vibrational deactivations would tend to increase. Also, as was noted by Shui and Appleton (41), simultaneous rotation–vibration changes of $\Delta v = -1$, $\Delta J = +2$ are occasionally favorable, *e.g.* for $v = 14$, $J = 4$, but as J goes up $\Delta v = -2$, $\Delta J = +2$ transfers often provide deactivation paths in quite small energy steps. Our calculations (Tables 9–11) show very clearly the increasing importance of simultaneous changes in v and J as the temperature rises, but at the same time they confirm that no serious error arises from ignoring these simultaneous changes at low temperatures.

There is, however, a more fundamental difficulty with the orbiting resonance theory: that one deactivation does not make a molecule. Whenever there is a bottleneck in the deactivation ladder, the accessibility of an orbiting resonance state, or the chance that it may lose a quantum or two of rotational and/or vibrational energy is not the determining factor in deciding the rate of formation of molecules in the ground state. In such cases there is a very delicate balance, as we saw in our discussion above of the vibrational deactivation of the $J = 21$ state, between the relevant collision rates and the tunnelling rates, which will not be adequately represented in the present form of the orbiting–resonance theory. We have found repeatedly in this paper that whether one considers the existence of the wide shape resonances in a proper fashion or whether one ignores them altogether makes little difference to the calculated dissociation or recombination rates in the energy-

Can. J. Chem. Downloaded from www.nrcresearchpress.com by 210.87.254.42 on 09/05/12
For personal use only.

transfer dominated regime, both with our approximate model and with the full calculation. The interpretation of the data in Table 7 could be strained somewhat to suggest that tunnelling may be more important at the lower temperatures; the data in Table 5, from the somewhat less reliable factored method, also show a marginal but significant trend towards the increasing importance of tunnelling at the lower temperatures. One feels intuitively that it would be surprising if these small trends were to blow up into a marked divergence between the with- and without-tunnelling calculations, at least above room temperature since the extrapolation in terms of $1/T$ from our temperature range is not excessive. Of course, there is as yet no *concrete* evidence of a bottleneck in these systems; there is however much circumstantial evidence from theoretical calculations. From the reasonably close agreement we have found between the factored and the unfactored calculations (Table 8) it is probably fair to infer that the population distribution in the full calculation is moderately well represented as a product of rotational and vibrational distributions. Thus it would appear that, for example in recombination, *every* newly formed molecule must pass through some bottleneck to reach the ground state; if it is formed in a low J state, there is a vibrational bottleneck, or if it is formed in a low v state, there is a rotational bottleneck. The question arises as to whether these bottlenecks are necessary, or could sets of T–V or T–R probabilities be constructed which would not show a bottleneck? We have experimented extensively with different sets of T–V transition probabilities (12, 13, 17, 27) and always seem to find a bottleneck in vibration–dissociation coupling calculations; unfortunately, theorems connecting the eigenvalues, particularly the smallest eigenvalue, of a stochastic matrix to arbitrary changes in the matrix elements are not sufficiently well developed to define the conditions under which a bottleneck would or would not occur. We have not experimented widely with T–R transition probabilities, nor with T–VR probabilities: however, our assumed set of T–R transition probabilities is not dissimilar from those successfully used by Polanyi and Woodall (25) to explain their rotational relaxation measurements, and it would seem on this basis that the very pronounced rotational bottleneck that we find (Table 4) is fairly realistic.

On the other hand, the phase-space theory of dissociation and recombination (41, 42) does make an attempt to allow for those molecules which may be deactivated but which eventually redissociate. The major fallacy in extending this treatment to the recombination of hydrogen at low temperatures is the implicit assumption that the upper rotation–vibration levels of H_2 are sufficiently closely spaced that they may be considered classical. This assumption was mildly criticised by Pack, Snow, and Smith (40), but examination of Fig. 2 shows the assumption to be grossly optimistic. This diagram shows the distribution of gaps in the rotation–vibration spectra of ortho-H_2 and para-H_2: the left-hand ordinate is the magnitude of the gap $\omega = \Delta_{i-1,i}$ in cm^{-1} and the right-hand ordinate is $hc\omega/k$ *i.e.* the characteristic temperature for each gap; for good classical behavior, one would like to have $T > 5hc\omega/k$. *If, and only if,* the transition probabilities are governed by an equation like [16*a*], where there is no discrimination against transitions having large values of $|\Delta J|$, then Fig. 2 can be used to determine the temperature needed for effectively classical behavior amongst the upper levels. It can be seen that, excluding the quasi-bound levels which are in general more widely spaced than the bound levels, there are several transitions for both molecules in the first 5000 cm^{-1} below the dissociation limit which could not be considered classical much below 1000 °K. On the other hand, if there were a $|\Delta J|$ penalty such as is embodied in [16] for the transition probabilities, then the gaps between levels connected by only small $|\Delta J|$ changes become perhaps, on average, four or five times larger than shown in this diagram. Thus, whilst the classical phase-space theory of Shui and Appleton (41) may be applicable to most molecules at most temperatures, it certainly cannot be applied to H_2 below 500 °K, and in fact, until we know whether large changes in J are allowed or disallowed, it is not even clear that the theory can be applied to H_2 below 5000 °K.

Nor are our own calculations free from criticism. At the moment we can only simulate the energy-transfer component of the mechanism, whereas the chaperon component is thought to be significant for H_2 at low temperatures (40) and for all other molecules at all temperatures (37); however, the latter mechanism is not beyond the scope of future extensions to the present treatment, as we have shown recently (29). Neither can we solve the non-dilute problem in which V–V,

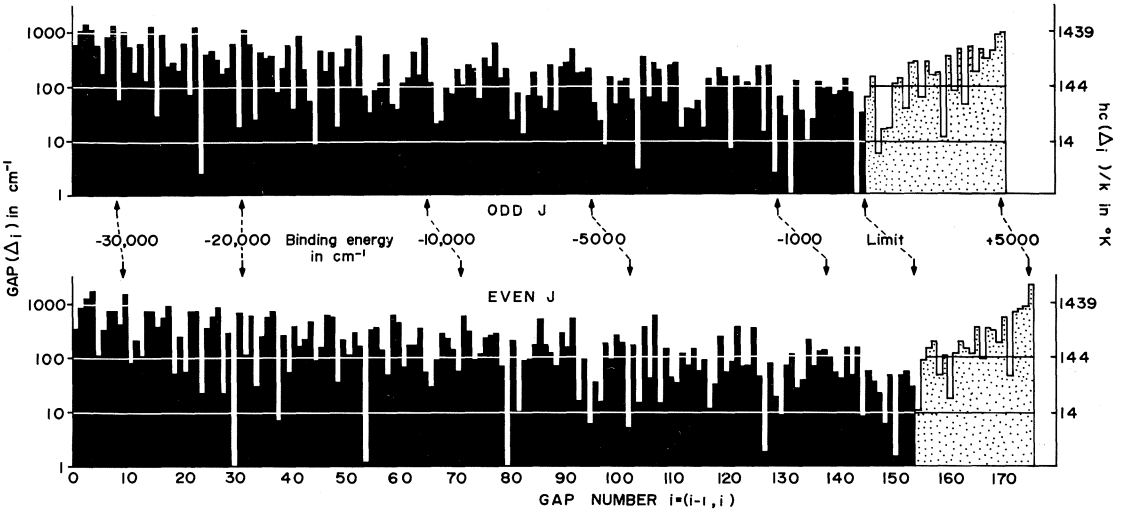

FIG. 2. Distribution of energy gaps in the rotation–vibration spectrum of ortho-H_2 (odd J) and para-H_2 (even J).

or more generally VR–VR interchanges take place, although as we have noted earlier, present theoretical indications are that when such processes are important, non-integral rate laws will occur (35), and we may hope for guidance from future experiments on this point. And, of course, there is a very long way to go before we can calculate all of the 30631 T–VR transition probabilities (15753 for even J, 14878 for odd J) required for a full solution of the energy-transfer calculation at infinite dilution! The ones we have used are based to some extent on theoretical calculation (3), guided by experimental results where available. In addition, we have performed a wide range of perturbations upon these assumed probabilities throughout this series of papers, and have consistently found gross insensitivity of the rate constants to the chosen probabilities; hence, in fact, it will only be really necessary to know a key selection of transition probabilities with reasonable precision, and as far as the remainder are concerned, a knowledge of the order of magnitude will be more than sufficient. It seems likely that in the foreseeable future, one may expect to see good calculations on T–V or T–R transition probabilities for at least a representative selection of the v or J levels of H_2 in collision with He. On the other hand, accurate treatment of simultaneous changes in rotational and vibrational energy may prove to be more difficult, and we may hope to be guided by experiments in which such changes are observed, although at the present time only for excited electronic states (43–45); our calculations suggest however that a fair calculation of the rate of dissociation or recombination can be made without knowing much about simultaneous T–VR exchanges, at least for temperatures up to and including the low end of the shock-tube temperature range.

A serious problem with our method, which stems essentially from the nature of the Boltzmann distribution, is the numerical difficulty associated with finding always the *smallest* eigenvalue of a large matrix, which becomes more and more overwhelming as the temperature is reduced. The dominant eigenvalues of these matrices are always of the order of 10^{11} s^{-1} without tunnelling, 10^{13} s^{-1} with tunnelling, and at 1500 °K, d_{n-1} is approximately 10^{-4} s^{-1}; thus, using 16-decimal-place arithmetic (IBM360/50), one really has to work hard to obtain the two-and-a-half figure accuracy on the rate constants which we quote for this temperature in Tables 7 and 9. After the completion of the work so far described, an IBM370/155 machine was installed at York University, on which it is possible to use 30-decimal-place arithmetic, enabling us, as described in the next few paragraphs, to extend these calculations down to about 700 °K. To go further would require further increases in word length, but to cover the whole experimental range (32) down to 100 °K will give rise to severe overflow and underflow problems, associated principally with the magnitudes of the Boltzmann factors for very high states of the molecules at these very low temperatures: it will be necessary

Can. J. Chem. Downloaded from www.nrcresearchpress.com by 210.87.254.42 on 09/05/12
For personal use only.

Can. J. Chem. Downloaded from www.nrcresearchpress.com by 210.87.254.42 on 09/05/12
For personal use only.

to accommodate numbers of magnitudes 10^{-300} which cannot readily be done on many commercially available computing machines. If such brute-force extension to lower temperatures fails (and in the absence of a reformulation of the problem which leaves all eigenvalues unchanged except d_{n-1} which comes out multiplied by K^{-1}), one will probably have to fall back in the last resort on the factored method. This, as we have seen, gives rise to much smaller matrices, and in at least one case (13) we have solved the $J = 0$ vibrational relaxation problem, admittedly with some difficulty, down to 300 °K. Thus, whilst the factored model cannot accommodate important rotation–vibration coupling processes, we have found that the rate constants it gives improve as the temperature falls, and it would seem that (provided the odd-J and even-J calculations do not diverge from each other too drastically, *cf.* Table 8) acceptable recombination rates could be calculated down to as low a temperature as the exponent length of the available computing machine will allow.

A Practical Test

Throughout this series of papers (11–13, 17, 27, 29, 36), we have worked with a set of transition probabilities (3, 13) which, at best, can be little better than an educated guess, and we have taken much comfort from the fact that our calculated rate constants (but not relaxation times) have been quite insensitive to perturbations in these probabilities (12, 13, 17, 27, 46). At the same time, we have been trailing far behind the modern experiments, and have been trying rather to understand or rationalize some of the puzzling features common to much of the existing mass of experimental data. Now, however, we are in a position to make some predictions, which, if they are confirmed by future experiments, will lend some confidence to our assumption that, within reason, almost any set of transition probabilities will suffice, as far as dissociation and recombination rates are concerned.

We have shown previously (27) that if only vibration–dissociation coupling is considered, the calculated rate constant for the recombination of D_2 by an inert third body is always faster than that for H_2, not only at high temperatures, but also at room temperature.[2] As we noted at the time, there is some evidence from the work of Sutton (47) that in the range 2800–4500 °K, the recombination of D_2 by argon is faster than the recombination of H_2 by argon, by a factor of about 1.25, although this conclusion is not corroborated by the work of Rink (48) at 3500 °K. However, there appears to be unambiguous evidence (32, 49, 50) that near room temperature, the rate constant for the recombination of D_2 by D_2 is significantly *less* than the rate constant for the recombination of H_2 by H_2. If, as is commonly believed (18, 39), rotational relaxation is important at lower temperatures, one would expect to obtain a different result in a rotation–vibration–dissociation calculation from that obtained in the previous vibration–dissociation calculation. We therefore performed a parallel set of calculations for D_2 to those described above for H_2, on the assumption that the T–VR transition probabilities per collision are the same function of temperature and energy gap for D_2 and for H_2, that the rotation–vibration energy levels and predissociation rates of quasi-bound states for D_2 are those calculated by LeRoy (9), and that the collision rate between D_2 and He is less than for H_2 with He by an appropriate factor (0.8165). It soon became apparent (see below) from the results obtained that it would be interesting to perform calculations for lower temperatures than 1500 °K, and the installation of IBM 370 machines at York University and at the University of Toronto, both having 30 decimal-place arithmetic, enabled us to extend these calculations down to 700 °K. However, since D_2 has 348 odd and 355 even bound and quasi-bound levels, as opposed to 172 and 177 levels respectively for H_2, the D_2 calculations were much larger and more time-consuming, and only a few were attempted. The storage requirements for H_2 in quadruple-length and for D_2 in double-length arithmetic could be accommodated on the York University IBM 370/155 installation, but for D_2 in quadruple-length arithmetic, the half-matrix describing the relaxation required almost 1.2 M bytes of storage, and those calculations were performed on the University of Toronto IBM 370/165 installation.

As for H_2, two series of calculations were performed, one using [16] in which T–VR transition probabilities are restricted to transitions having only small changes in rotational angular momentum, and the other using [16*a*] in which the probabilities are governed only by the energy difference to be transferred to or from translation. The same feature emerged for D_2 as for H_2, that

[2]Those calculations ignored the change in collision rate that would accompany the substitution of D_2 for H_2, but even if such an allowance were made, the conclusion is unchanged.

TABLE 12. (*a*) Equilibrium constants, in units of molecule cm^{-3}, calculated by standard nethods from the assumed energy-level scheme

T (°K)	Equilibrium constant	
	H_2	D_2
5000	6.00×10^{19}	5.86×10^{19}
3000	6.04×10^{16}	5.60×10^{16}
2000	9.61×10^{12}	8.13×10^{12}
1500	1.50×10^{9}	1.13×10^{9}
1000	3.74×10^{1}	2.16×10^{1}
700	6.62×10^{-9}	2.63×10^{-9}

(*b*) Comparison of calculated rate constants for dissociation and recombination of hydrogen and of deuterium by helium, determined from the smallest eigenvalue d_{n-1} of the relaxation matrix and using equilibrium constants from (*a*)

T (°K)	k_d (cm^3 molecule^{-1} s^{-1})		$\frac{k_d^{D_2}}{k_d^{H_2}}$	k_r (cm^6 molecule^{-2} s^{-1})		$\frac{k_r^{D_2}}{k_r^{H_2}}$
	H_2	D_2		H_2	D_2	
Equation 16						
5000	2.34×10^{-14}	2.57×10^{-14}	1.10	3.90×10^{-34}	4.39×10^{-34}	1.13
3000	5.72×10^{-17}	6.51×10^{-17}	1.14	9.47×10^{-34}	1.16×10^{-33}	1.22
2000	1.61×10^{-20}	1.69×10^{-20}	1.05	1.68×10^{-33}	2.08×10^{-33}	1.24
1500	3.62×10^{-24}	3.14×10^{-24}	0.87	2.41×10^{-33}	2.78×10^{-33}	1.15
1000	1.44×10^{-31}	9.30×10^{-32}	0.65	3.85×10^{-33}	4.31×10^{-33}	1.12
700	3.77×10^{-41}	1.60×10^{-41}	0.42	5.69×10^{-33}	6.08×10^{-33}	1.07
Equation 16*a*						
5000	3.53×10^{-14}	4.48×10^{-14}	1.27	5.88×10^{-34}	7.64×10^{-34}	1.30
2000	1.87×10^{-20}	2.06×10^{-20}	1.10	1.95×10^{-33}	2.53×10^{-33}	1.30
1500	4.21×10^{-24}	4.00×10^{-24}	0.95	2.81×10^{-33}	3.53×10^{-33}	1.26
1000	1.69×10^{-31}	1.14×10^{-31}	0.67	4.52×10^{-33}	5.29×10^{-33}	1.17
700	4.28×10^{-41}	1.88×10^{-41}	0.44	6.64×10^{-33}	7.15×10^{-33}	1.11

the inclusion or exclusion of the rotational predissociation contributions made very little difference to the rate constant. However, in slight contrast, the ortho- and para-dissociation rates were almost identical for D_2, presumably because in D_2 the levels are so dense that the network resistance effect, invoked above for the H_2 case, is more nearly the same for the two spin states. Hence, the results listed in Table 12 do not include all the individual rates calculated, which are available elsewhere (20), but are mean values which lie within about 1% of the rates for odd- or even-states with or without rotational predissociation at 5000 °K, and within 2 or 3% at 700 °K. The results may be summarized as follows:

(*i*) *Dissociation Rates.* At high temperatures, the rate constant for the dissociation of D_2 by He seems to be greater than that for the dissociation of H_2 by He, despite the fact that in the former case, all the eigenvalues in the system are scaled by the factor 0.8165, the ratio of the two collision rates for D_2/He and H_2/He. This is yet another example of the possible theorem to which we have alluded above, that closer level spacing leads to an increase in dissociation rate. The effect is so strong between H_2 with about 175 connected levels and D_2 with about 350 connected levels that it more than offsets *both* the unfavorable collision rate *and* the extra 631 cm^{-1} (1.8 kcal/mol) required to dissociate the D_2 molecule. However, as the temperature is reduced, this extra dissociation energy becomes an important factor and below 2000 °K, the existence of a greater number of pathways from the ground state to the continuum cannot offset the unfavorable Boltzmann factor. This amounts to about 0.55 at 1500 °K and about 0.27 at 700 °K causing a strong reversal in the calculated dissociation rate ratio. The new data in Table 12 are consistent with the trends shown in Table 11,

Can. J. Chem. Downloaded from www.nrcresearchpress.com by 210.87.254.42 on 09/05/12
For personal use only.

Can. J. Chem. Downloaded from www.nrcresearchpress.com by 210.87.254.42 on 09/05/12
For personal use only.

giving Arrhenius temperature coefficients for H_2 of about 101.5 kcal/mol between 1000 and 1500 °K, and about 102.5 kcal/mol between 700 and 1000 °K, with either set of transition probabilities; the Arrhenius temperature coefficients for D_2 are similar, roughly 2 kcal/mol higher.

(*ii*) *Recombination Rates.* The rate constant for recombination of D_2 by He seems to be greater than that for the recombination of H_2 by He throughout the temperature range accessible to us at the present time. No reversal in the isotope effect occurs because the equilibrium constants connecting k_d and k_r for the two molecules have differing temperature coefficients, mainly because of their differing dissociation energies. However, the recombination data do appear to be converging as the temperature falls, and it seems likely that a reversal could occur at lower temperatures.

(*iii*) *Experimental and Theoretical Implications.* On the basis of full rotational equilibration, as was assumed in our earlier work (27), deuterium[2] would be recombined by helium 1.36 times as fast as hydrogen at 1500 °K and 1.15 times as fast at 300 °K. The present calculations, which allow sumultaneously for T–V, T–R, and T–VR transitions, but which cannot yet be performed for temperatures below 700 °K, appear to be more realistic in that they do not seem to be inconsistent with a slower recombination rate for D_2 than for H_2 at low temperatures. This improvement can be taken as supportive of the designation of the low-temperature recombination process as being essentially rotational (18, 39). Unfortunately, we cannot yet demonstrate conclusively a trend towards a predominantly rotational mechanism without being able to calculate population distributions, and therefore fluxes between individual states during the relaxation. In principle, this can be done readily given the eigenvectors of the relaxation matrix (13), and although we have been able to generate most of the eigenvectors for a 172nd order H_2 matrix (20, 46), we have so far been unable to find all of them because of the ill-conditioned nature of the problem.

A major factor in determining the position of any possible reversal in the rate constant ratio is the ratio of the collision rates for D_2 and H_2. If, instead of choosing helium as the collision partner, we had chosen a heavier inert atom like argon, the ratio of the collision rates would have been close to 0.7. The effect of this on the rate ratios in Table 12 would then be: (*a*) the dissociation rates for H_2 and D_2 would be virtually indistinguishable at high temperatures, with D_2 always slower than H_2 (except perhaps for [16*a*] at 5000 °K); (*b*) the recombination rates would cross between 1000 and 1500 °K with the restricted set of probabilities ([16]) or between 700 and 1000 °K with the unrestricted set ([16*a*]). The same would be true of the recombination of H_2 by H_2 compared with the recombination of D_2 by D_2 (where the collision rate ratio is again 0.7) *provided* that VR–VR coupling were unimportant.

We would like to thank the University of Toronto Institute for Aerospace Studies and Computer Centre for access to their latest computing facilities.

1. L. S. KASSEL. Kinetics of homogeneous gas reactions. The Chemical Catalog Co., New York. 1932. p. 40.
2. S. GLASSTONE, K. J. LAIDLER, and H. EYRING. The theory of rate processes. McGraw-Hill, New York. 1941. p. 127.
3. H. O. PRITCHARD. J. Phys. Chem. **65**, 504 (1961).
4. H. O. PRITCHARD. *In* Transfer and storage of energy by molecules. Vol. 2. Vibrational energy. John Wiley, New York. 1969. p. 376.
5. D. G. RUSH and H. O. PRITCHARD. Eleventh Symposium (International) on Combustion. The Combustion Institute, Pittsburgh, Pa. 1967. p. 13; and discussion by S. H. BAUER and by H. O. PRITCHARD. pp. 35–36.
6. N. B. SLATER. Theory of unimolecular reactions. Methuen, London. 1959. p. 43.
7. O. K. RICE. Statistical mechanics thermodynamics and kinetics. W. H. Freeman, San Francisco. 1967. p. 495.
8. T. G. WAECH and R. B. BERNSTEIN. J. Chem. Phys. **46**, 4905 (1967).
9. R. J. LEROY. J. Chem. Phys. **54**, 5433 (1971); Report No. WIS-TCI-387, University of Wisconsin Theoretical Chemistry Institute, 1971.
10. R. E. ROBERTS. Ph.D. Thesis. University of Wisconsin, Madison, Wisconsin. 1968.
11. V. A. LODATO, D. L. S. MCELWAIN, and H. O. PRITCHARD. J. Am. Chem. Soc. **91**, 7688 (1969).
12. D. L. S. MCELWAIN and H. O. PRITCHARD. J. Am. Chem. Soc. **91**, 7693 (1969).
13. D. L. S. MCELWAIN and H. O. PRITCHARD. Thirteenth Symposium (International) on Combustion. The Combustion Institute, Pittsburgh, Pa. 1971. p. 37.
14. J.-L. LIN. J. Chem. Phys. **53**, 4567 (1970).
15. M. DOLE. Introduction to statistical mechanics. Prentice Hall, New York. 1954. p. 179.
16. JANAF Thermochemical Tables. Dow Chemical Co., Midland, Michigan. 1965.
17. E. KAMARATOS and H. O. PRITCHARD. Can. J. Chem. **49**, 2617 (1971).
18. R. E. ROBERTS, R. B. BERNSTEIN, and C. F. CURTISS. J. Chem. Phys. **50**, 5163 (1969).

19. J. TROE and H. G. WAGNER. Zeit. Phys. Chem. **55**, 326 (1967).
20. T. ASHTON. Ph.D. Thesis. York University, Downsview, Ontario. 1972.
21. R. D. LEVINE. Acc. Chem. Res. **3**, 273 (1970).
22. T. L. COTTRELL and J. C. MCCOUBREY. Molecular energy transfer in gases. Butterworths, London. 1961. p. 78.
23. L. M. VALLEY and R. C. AMME. J. Chem. Phys. **50**, 3190 (1969).
24. C. A. BOITNOTT and R. C. WARDER. Phys. Fluids, **14**, 2312 (1971).
25. J. C. POLANYI and K. B. WOODALL. J. Chem. Phys. **56**, 1563 (1972).
26. H. O. PRITCHARD and A. WALLIS. J. Chem. Phys. **42**, 3548 (1965).
27. D. L. S. MCELWAIN and H. O. PRITCHARD. Can. J. Chem. **49**, 3915 (1971).
28. A. L. MYERSON and W. S. WATT. J. Chem. Phys. **49**, 425 (1968).
29. D. L. S. MCELWAIN and H. O. PRITCHARD. Can. J. Chem. **50**, 897 (1972).
30. R. E. ROBERTS. J. Chem. Phys. **54**, 1422 (1971).
31. J. D. KELLEY. J. Chem. Phys. **53**, 3864 (1970).
32. D. O. HAM, D. W. TRAINOR, and F. KAUFMAN. J. Chem. Phys. **53**, 4395 (1970).
33. H. O. PRITCHARD. Q. Rev. (London). **14**, 46 (1960).
34. J. E. DOVE and D. G. JONES. J. Chem. Phys. **55**, 1531 (1971).
35. D. L. S. MCELWAIN and H. O. PRITCHARD. J. Am. Chem. Soc. **92**, 5027 (1970).
36. N. I. LABIB, D. L. S. MCELWAIN, and H. O. PRITCHARD. Can. J. Chem. **50**, 3832 (1972).
37. A. G. CLARKE and G. BURNS. J. Chem. Phys. **55**, 4717 (1971).
38. G. PORTER. Discuss. Faraday Soc. **33**, 198 (1962).
39. R. E. ROBERTS and R. B. BERNSTEIN. Chem. Phys. Lett. **6**, 282 (1970).
40. R. T. PACK, R. L. SNOW, and W. D. SMITH. J. Chem. Phys. **56**, 926 (1972).
41. V. H. SHUI and J. P. APPLETON. J. Chem. Phys. **55**, 3126 (1971).
42. V. H. SHUI, J. P. APPLETON, and J. C. KECK. J. Chem. Phys. **53**, 2547 (1970).
43. K. H. WELGE, S. V. FILSETH, and J. DAVENPORT. J. Chem. Phys. **53**, 502 (1970).
44. CH. OTTINGER, R. VELASCO, and R. N. ZARE. J. Chem. Phys. **52**, 1636 (1970).
45. D. L. AKINS, E. H. FINK, and C. B. MOORE. J. Chem. Phys. **52**, 1604 (1970).
46. E. KAMARATOS and H. O. PRITCHARD. To be published.
47. E. A. SUTTON. J. Chem. Phys. **36**, 2923 (1962).
48. J. P. RINK. J. Chem. Phys. **36**, 262, 1398 (1962).
49. F. S. LARKIN. Can. J. Chem. **46**, 1005 (1968).
50. J. E. BENNETT and D. R. BLACKMORE. J. Chem. Phys. **53**, 4400 (1970).

Can. J. Chem. Downloaded from www.nrcresearchpress.com by 210.87.254.42 on 09/05/12
For personal use only.

Lower Bounds to Expectation Values: Two-Electron Atoms

D. P. CHONG[1] AND F. WEINHOLD[2]

Department of Chemistry, Stanford University, Stanford, California 94305

Received July 31, 1972

Weinhold's lower bound formulas are used on rather accurate wavefunctions for the 1^1S ground states of H^-, He, and Li^+, and the 2^1S and 2^3S excited states of He. The results are found to be of very high quality, as judged by comparison with the best available variational calculations, and can be used to rule out many of the values calculated by Scherr and Knight from high-order perturbation theory.

Les formules de Weinhold concernant les niveaux de liaison de basse énergie ont été utilisées dans les fonctions d'onde plutôt précises pour les états fondamentaux 1^1S de H^-, He, Li^+ et pour les états excités 2^1S et 2^3S de He. Les résultats sont de très haute qualité par comparaison avec les meilleurs calculs variationnels disponibles et peuvent être utilisés pour éliminer plusieurs valeurs calculées par Scherr et Knight à partir de la théorie de pertubation d'ordre élevé.

[Traduit par le journal]

Can. J. Chem., **51**, 260 (1973)

Can. J. Chem. Downloaded from www.nrcresearchpress.com by 210.87.254.40 on 09/05/12
For personal use only.

Introduction

The concept of attaching rigorous error limits to theoretical estimates of quantum-mechanical properties is attractive to many chemists and physicists. Such upper and lower bounds not only provide internal and *a priori* measures of reliability, but also enable one to make more meaningful comparisons with experimental results. One of the recent developments in this direction is the application of Gramian determinantal inequalities.[3] For the lower bounds to expectation values of positive operators, Weinhold (2–5) derived a wide variety of relatively simple formulas and illustrated their use with the familiar $1s^2$ and $1s1s'$ trial functions for the 1^1S ground state of the helium atom, with promising results. The purpose of this work is to test some of these procedures on better wavefunctions. On the basis of certain preliminary results, we were encouraged to employ some rather accurate wavefunctions which could be expected to yield bounds of a definitive quality for the simple 2-electron atomic systems.

Calculations

A. Lower-Bound Formulas

In the present work, we seek lower bounds F_{LB} to the true expectation value $\langle\psi|F|\psi\rangle$ of a general positive operator $F \geqslant 0$. With one exception (when $F = r_1^{-1}$), we make use of the formulas (2, 4):

$$[1]\quad \langle\psi|F|\psi\rangle \geqslant F_{LB} = [S\langle F\rangle - \varepsilon\Delta F]^2/\langle F\rangle$$

$$[2]\quad \langle\psi|F|\psi\rangle \geqslant F_{LB} = S^2/\langle F^{-1}\rangle + [S(\langle F\rangle\langle F^{-1}\rangle - 1) - \langle F^{-1}\rangle\varepsilon\Delta F]^2 \times \{\langle F^{-1}\rangle(\langle F\rangle\langle F^{-1}\rangle - 1)\}^{-1}$$

where, in our notation, both the trial function φ and the exact wavefunction ψ are normalized,

$$[3]\quad \langle\varphi|\psi\rangle = S > 0$$

$$[4]\quad \varepsilon = (1 - S^2)^{1/2}$$

$$[5]\quad \langle F\rangle = \langle\varphi|F|\varphi\rangle$$

$$[6]\quad (\Delta F)^2 = \langle F^2\rangle - \langle F\rangle^2$$

These lower bound formulas are valid only if the expressions in square brackets are non-negative. In other words, we assume that

$$[7]\quad S/\varepsilon \geqslant (\Delta F)/\langle F\rangle$$

$$[8]\quad S/\varepsilon \geqslant (\Delta F)\langle F^{-1}\rangle/(\langle F\rangle\langle F^{-1}\rangle - 1)$$

The inequalities in eqs. 1 and 2 are sustained when the overlap S is replaced by a lower bound S_{LB} to its true value. Hence, once S_{LB} has been calculated,[4] it is straightforward to compute F_{LB} from eq. 1 or 2. It can be shown that eq. 2 gives a stronger lower bound than eq. 1. Consequently, we use eq. 1 only when $\langle F^{-1}\rangle$ is not available.

[1]On leave from the Department of Chemistry, University of British Columbia, Vancouver 8, British Columbia.

[2]Alfred P. Sloan Fellow.

[3]See ref. 1 for a review of recent progress in this area.

[4]For this purpose, we use Weinberger's formula (6). See also Weinhold (7, 8) for additional details.

TABLE 1. Quality of the wavefunctions

Parameter	Value				
	H^- 1^1S	He 1^1S	Li^+ 1^1S	He 2^1S	He 2^3S
$-E$	0.52775102*	2.90372438*	7.27991341*	2.14597404†	2.17522938†
$-\langle H\rangle$	0.52775096	2.90372437	7.27991340	2.14597368	2.17522937
$-\langle H\rangle/\langle T\rangle$	1.00000015	0.99999957	0.99999982	1.00000089	1.00000003
$(1-S_{LB}^2)^{1/2}$	0.00140508	0.00011444	0.00008100	0.00181037	0.00017006
r_1 cusp	−0.99939557	−1.99994298	−2.99977303	−1.99949450	−1.99991627
r_{12} cusp	0.49373753	0.49743221	0.49713024	0.48000644	—
$\langle\delta(\boldsymbol{r}_1)\rangle$	0.164528	1.81042	6.85194	1.30932	1.32033
	(−0.014%)	(−0.000%)	(−0.001%)	(−0.010%)	(−0.002%)
$\langle r_1^{-2}\rangle$	1.11665	6.01741	14.9276	4.14686	4.17044
		(+0.000%)			(−0.000%)
$\langle\delta(\boldsymbol{r}_{12})\rangle$	0.0027424	0.106370	0.533814	0.008676	0
	(+0.14%)	(+0.024%)	(+0.014%)	(+0.3%)	(0%)
$\langle r_{12}^{-2}\rangle$	0.155108	1.46478	4.08225	0.143742	0.0889060
		(+0.001%)			(+0.000%)

*Reference 16.
†Reference 14.

Finally, for the particular operator $F = r_1^{-1}$, the virial theorem written as[5]

[9] $$\langle\psi|r_1^{-1}|\psi\rangle = (N-1)\langle\psi|r_{12}^{-1}|\psi\rangle/(2Z) - 2E/(NZ)$$

together with the lower bound to $\langle\psi|r_{12}^{-1}|\psi\rangle$, provides a lower bound which is always found to be stronger than that calculated from eq. 2 directly.

B. Properties

For the calculation of $\langle F\rangle$, we have considered operators corresponding to delta functions and various powers of the radial and interelectronic coordinates[6]

[10] $F = \delta(\boldsymbol{r}_1)$ and r_1^n for $-2 \leqslant n \leqslant 5$

[11] $F = \delta(\boldsymbol{r}_{12})$ and r_{12}^n for $-2 \leqslant n \leqslant 2$

However, because of the assumptions in eqs. 7 and 8, the lower bound formulas 1 and 2 cannot be employed when the width ΔF is formally divergent. This rules out operators such as r_1^{-2} and r_{12}^{-2} for atoms in S states, and the delta function operators, $\delta(\boldsymbol{r}_1)$ and $\delta(\boldsymbol{r}_{12})$, for any system in any state. Additional formulas are available (5, 9) which partly avoid the difficulty, but these were not explored in the present work.

C. Wavefunctions

In order to see some aspects of the dependence on nuclear charge Z and on the degree of excitation, we have selected for study the 1^1S ground states of H^-, He, and Li^+, and the 2^1S and 2^3S excited states of neutral He. To describe the atomic states we have employed rather accurate wavefunctions which were recently obtained (10) in connection with related studies on the oscillator strengths of two-electron ions. These are of the Hylleraas type, built up from some 135–140 terms of the form

$$(1 \pm P_{12})r_1^l r_2^m r_{12}^n \exp(-\xi r_1 - \eta r_2)$$

with very rough optimization of the open-shell exponential parameters ξ, η. The general quality of these functions is indicated more specifically in Table 1, where we list such criteria of accuracy as the energy error, the overlap, and the degree of satisfaction of the virial theorem and cusp conditions. The expectation values of the operators $\delta(\boldsymbol{r}_1)$, r_1^{-2}, $\delta(\boldsymbol{r}_{12})$, and r_{12}^{-2} are also listed in Table 1, together with the percentage errors wherever accurate values are available (11–15). Energetically, these functions are of course still somewhat inferior to the well-known

[5] N, Z, and E are the number of electrons, nuclear charge, and exact energy, respectively. See ref. 3.

[6] For one-electron properties, it can be shown that ΔF in eqs. 1 and 2 may be replaced by $\Delta\bar{F}$, where $\bar{F} = \frac{1}{2}(r_1^n + r_2^n)$, in order to take advantage of the non-linearity of the lower bounds (2).

[7] In the case of r_1^{-2} and r_{12}^{-2}, these formulas (5) strengthen and generalize eqs. 1 and 2 at the cost of additional integrals over the trial function φ.

Can. J. Chem. Downloaded from www.nrcresearchpress.com by 210.87.254.40 on 09/05/12
For personal use only.

Table 2. Results for the 1^1S state of H^-, percentage errors in parentheses

F	F_{LB}	$\langle F \rangle$	Pekeris*	Scherr and Knight†
r_1^{-1}	0.682923(−0.050)	0.683262		0.688181(+0.720)
r_1	2.70658(−0.133)	2.71015(−0.001)	2.71018	2.54360(−6.146)
r_1^2	11.8719(−0.351)	11.9129(−0.007)	11.9137	9.50684(−20.20)
r_1^3	75.4519(−0.720)	75.9994		45.9546(−39.53)
r_1^4	635.469(−1.389)	644.422		264.522(−58.95)
r_1^5	6650.32(−2.571)	6825.80		1726.92(−74.70)
r_{12}^{-1}	0.3103439(−0.218)	0.311022		0.320745(+3.126)
r_{12}	4.405919(−0.154)	4.41265(−0.001)	4.41269	4.09761(−7.140)
r_{12}^2	25.11370(−0.350)	25.2004(−0.006)	25.2020	20.4348(−18.92)

*Reference 14.
†Reference 20.

TABLE 3. Results for the 1^1S state of He, percentage errors in parentheses

F	F_{LB}	$\langle F \rangle$	Pekeris*	Scherr and Knight†
r_1^{-1}	1.68827(−0.003)	1.68832(+0.000)	1.68832	1.68834(+0.001)
r_1	0.929385(−0.009)	0.929472(−0.000)	0.929472	0.929290(−0.020)
r_1^2	1.19324(−0.021)	1.19348(−0.000)	1.19348	1.19234(−0.096)
r_1^3	1.96720(−0.038)	1.96794		1.96206(−0.299)
r_1^4	3.97088(−0.067)	3.97353		3.94435(−0.734)
r_1^5	9.49271(−0.116)	9.50374		9.35833(−1.530)
r_{12}^{-1}	0.945646(−0.018)	0.945819(+0.000)	0.945818	0.945868(+0.005)
r_{12}	1.42191(−0.011)	1.42207(−0.000)	1.42207	1.42173(−0.024)
r_{12}^2	2.51585(−0.024)	2.51644(−0.000)	2.51644	2.51419(−0.089)

*Reference 12.
†Reference 20.

TABLE 4. Results for the 1^1S state of Li^+, percentage errors in parentheses

F	F_{LB}	$\langle F \rangle$	Pekeris*	Scherr and Knight†
r_1^{-1}	2.68789(−0.001)	2.68792		2.68793(+0.000)
r_1	0.572736(−0.007)	0.572774(−0.000)	0.572774	0.572768(−0.001)
r_1^2	0.446215(−0.014)	0.446279(−0.000)	0.446279	0.446255(−0.005)
r_1^3	0.441164(−0.026)	0.441278		0.441197(−0.018)
r_1^4	0.529367(−0.044)	0.529602		0.529338(−0.050)
r_1^5	0.747409(−0.076)	0.747980		0.747119(−0.115)
r_{12}^{-1}	1.56751(−0.013)	1.56772		1.56772(+0.000)
r_{12}	0.862246(−0.008)	0.862315(−0.000)	0.862315	0.862305(−0.001)
r_{12}^2	0.926910(−0.017)	0.927065(−0.000)	0.927065	0.927018(−0.005)

*Reference 13.
†Reference 20.

functions of Pekeris and co-workers (11–16), but their portability and compactness give them certain distinct advantages for our present purposes. In fact, our calculated cusp values shown in Table 1 seem to be considerably closer to the true values of $-Z$ and $+\frac{1}{2}$ for the r_1 and r_{12} cusps, respectively (17, 18), than are those reported[8] for the Pekeris functions. This in turn suggests (19) that such properties as $\langle \delta(\boldsymbol{r}_1) \rangle$ and $\langle \delta(\boldsymbol{r}_{12}) \rangle$ might also be represented to a superior accuracy by our functions.

Results and Discussion

Tables 2–6 summarize our results for the five selected states. The calculated expectation values $\langle F \rangle$ and rigorous lower bounds F_{LB} are, wherever possible, compared with the extensive variational results of Pekeris and co-workers and/or with the 6th-order perturbation theory results of Scherr and Knight (20). In the cases where the

[8]Thus, for He 1^1S, the well-known 1078-term function of Pekeris (12) gave the cusp values −1.98444 and 0.47391 for r_1 and r_{12}, respectively, compared with our values −1.99994 and 0.49743.

Can. J. Chem. Downloaded from www.nrcresearchpress.com by 210.87.254.40 on 09/05/12
For personal use only.

TABLE 5. Results for the 2^1S state of He, percentage errors in parentheses

F	F_{LB}	$\langle F \rangle$	Pekeris*
r_1^{-1}	1.13515(−0.023)	1.13541	
r_1	2.96914(−0.132)	2.97305(−0.000)	2.97306
r_1^2	16.0423(−0.291)	16.0890(−0.001)	16.0891
r_1^3	107.525(−0.489)	108.053	
r_1^4	819.250(−0.766)	825.578	
r_1^5	6939.45(−1.179)	7022.26	
r_{12}^{-1}	0.248653(−0.412)	0.249683	
r_{12}	5.26197(−0.147)	5.26968(−0.000)	5.26969
r_{12}^2	32.2064(−0.296)	32.3018(−0.001)	32.302

*Reference 15.

TABLE 6. Results for the 2^3S state of He, percentage errors in parentheses

F	F_{LB}	$\langle F \rangle$	Pekeris
r_1^{-1}	1.15465(−0.001)	1.15466(−0.000)	1.15466*
r_1	2.55015(−0.012)	2.55046(+0.000)	2.55046†
r_1^2	11.4611(−0.028)	11.4643(+0.000)	11.4643†
r_1^3	65.1833(−0.049)	65.2151	
r_1^4	428.069(−0.078)	428.403	
r_1^5	3159.58(−0.123)	3163.45	
r_{12}^{-1}	0.268154(−0.017)	0.268198(−0.000)	0.268198*
r_{12}	4.44692(−0.014)	4.44754(+0.000)	4.44754†
r_{12}^2	23.0395(−0.029)	23.0462(−0.000)	23.0462†

*Reference 12.
†Reference 15.

accurate results of Pekeris and co-workers are not available, the percentage errors listed in Tables 2–6 are based on the expectation values $\langle F \rangle$ obtained in this work.

A glance at Tables 2–6 shows that the rigorous bounds are of very high quality indeed, as judged by comparison with either the direct expectation values $\langle F \rangle$ or the corresponding Pekeris values. Only for the very high moments $\langle r_1^n \rangle$ of the most diffuse charge distributions (*e.g.*, H^- 1^1S or He 2^1S, where the moments extend into thousands of atomic units) do the discrepancies reach as much as 1%, and in many cases the true values can be guaranteed to lie no more than a few hundredths or thousandths of 1% below the calculated $\langle F \rangle$. For example, Table 6 shows that the true $\langle \psi | r_1^{-1} | \psi \rangle$ for He 2^3S could lie no further than about 1×10^{-5} a.u. below the calculated value $\langle r_1^{-1} \rangle = 1.15466$ a.u.

It is also interesting that the lower bounds can rigorously rule out most of the Scherr–Knight values for both H^- and He. In fact, the only perturbative values to survive are those which appear to lie too *high*, and thus could not be threatened by a lower-bound procedure. However, for Li^+ ($Z = 3$) the convergence of the Z^{-1} perturbation expansions has improved sufficiently that only the calculated values of r_1^4 and r_1^5 can be definitely ruled out. Thus, although the Scherr–Knight perturbation calculations yielded energy eigenvalues which closely rivalled the best variational energies, it appears that discrepancies with respect to other calculated properties should largely be resolved in favor of the variational calculations, at least for lower Z.

We are grateful to the National Science Foundation and the donors of the Petroleum Research Fund, administered by the American Chemical Society, for financial support of this research, and to Mr. Michael T. Anderson for his skillful calculation of the wavefunctions. A portion of this work was completed while one of us (F.W.) was enjoying the warm hospitality of Professor P. O. Löwdin and the Quantum Chemistry Group, University of Uppsala, Sweden, to whom sincere thanks are due.

1. F. WEINHOLD. Advan. Quantum Chem. **6**, 299 (1972).
2. F. WEINHOLD. J. Phys. A, **1**, 305 (1968).
3. F. WEINHOLD. J. Phys. A, **1**, 535 (1968).
4. F. WEINHOLD. Phys. Rev. **183**, 142 (1969).
5. F. WEINHOLD. Phys. Rev. A, **1**, 122 (1970).

Can. J. Chem. Downloaded from www.nrcresearchpress.com by 210.87.254.40 on 09/05/12
For personal use only.

6. H. F. WEINBERGER. J. Res. Natl. Bur. Std. (U.S.), **64B**, 217 (1960).
7. F. WEINHOLD. J. Math. Phys. **11**, 2127 (1970).
8. F. WEINHOLD. Proc. Roy. Soc. London, **A327**, 209 (1972).
9. L. B. REDEI. Phys. Rev. **130**, 420 (1963).
10. M. ANDERSON. M.S. Thesis. Stanford University, Stanford, California, 1972.
11. C. L. PEKERIS. Phys. Rev. **112**, 1649 (1958).
12. C. L. PEKERIS. Phys. Rev. **115**, 1216 (1959).
13. C. L. PEKERIS. Phys. Rev. **126**, 143 (1962).
14. C. L. PEKERIS. Phys. Rev. **126**, 1470 (1962).
15. Y. ACCAD, C. L. PEKERIS, and B. SCHIFF. Phys. Rev. **A4**, 516 (1971).
16. K. FRANKOWSKI and C. L. PEKERIS. Phys. Rev. **146**, 46 (1966).
17. T. KATO. Commun. Pure Appl. Math. **10**, 151 (1957).
18. C. C. J. ROOTHAAN and A. W. WEISS. Rev. Mod. Phys. **32**, 205 (1960).
19. D. P. CHONG and D. M. SCHRADER. Mol. Phys. **16**, 137 (1969).
20. C. W. SCHERR and R. E. KNIGHT. J. Chem. Phys. **40**, 3034 (1964).

Can. J. Chem. Downloaded from www.nrcresearchpress.com by 210.87.254.40 on 09/05/12
For personal use only.

Crystal Structure of $LiVO_3$

ROBERT D. SHANNON[1] AND CRISPIN CALVO

Institute for Materials Science, McMaster University, Hamilton, Ontario

Received July 21, 1972

Lithium metavanadate is monoclinic with $a = 10.158(2)$, $b = 8.4175(9)$, $c = 5.8853(9)$ Å, $\beta = 110.48(2)°$ and probable space group $C2/c$. The structure, refined by least-squares to a $\omega R = 0.033$ using 851 reflections, is isotypic with $LiAlSi_2O_6$ (spodumene) and $LiFeSi_2O_6$. Bands of Li—O edge-shared octahedra run parallel to c and are linked by chains of VO_4 tetrahedra which also run parallel to c. The mean Li(1)—O and Li(2)—O distances are significantly different, 2.153(3) and 2.284(3) Å, and are related to the degree of distortion of individual distances from the mean. The V—O distances of 1.821, 1.795, 1.662, and 1.628 Å with a mean value of 1.725 Å are consistent with bond strength sums around the oxygen atoms and empirical bond length – bond strength curves.

Le métavanadate de lithium est monoclinique avec $a = 10.158(2)$, $b = 8.4175(9)$, $c = 5.8853(9)$ Å, $\beta = 110.48(2)°$ et de groupe spatial probable $C2/c$. La structure, raffinée par les moindres carrés jusqu'à un $\omega R = 0.033$ après 851 réflexions, est isotypique avec celle de $LiAlSi_2O_6$ (spodumène) et de $LiFeSi_2O_6$. Les bandes des arêtes communes de l'octaèdre Li—O sont parallèles à c et sont reliées par des chaines tétraédrales de VO_4, également parallèles à c. Les distances moyennes Li(1)—O et Li(2)—O sont sensiblement différentes, 2.153(3) et 2.284(3) Å; elles sont dues aux distorsions des distances individuelles par rapport à la moyenne. Les longueurs de V—O de 1.821, 1.795, 1.662, et 1.628 Å avec une valeur moyenne de 1.725 Å, sont compatibles avec les sommes des forces de liaison autour des atomes d'oxygène et les courbes empiriques reliant les longueurs et les forces de liaison.

[Traduit par le journal]

Can. J. Chem., **51**, 265 (1973)

Can. J. Chem. Downloaded from www.nrcresearchpress.com by 210.87.254.6 on 09/05/12
For personal use only.

Introduction

As part of a study of vanadates containing cations of widely differing electronegativity (χ), two compounds, $LiVO_3$ and Li_3VO_4 (1), containing the electropositive ion Li($\chi \sim 1.0$), were chosen for careful structure refinement. Because $NaVO_3$ was believed by Sorum (2) to have the pyroxene-type structure, it was natural to suspect that $LiVO_3$ also belonged to the pyroxene family. Indeed, Burkert and Fritz (3) assumed $LiVO_3$ to contain corner shared chains of tetrahedral VO_4^{3-} ions, and Muller and Roy (4) assumed a pyroxene-like structure for $LiVO_3$, but the structure type was not identified from either powder or single crystal X-ray diffraction patterns. Feigelson, Martin, and Johnson (5) grew crystals of $LiVO_3$ but reported a cell different than in the present case. In this paper we report the single crystal structure refinement of the pyroxene $LiVO_3$ and compare the structural details of $LiVO_3$ and the more common silicate pyroxenes.

Experimental

Lithium metavanadate, $LiVO_3$, was prepared earlier by Canneri (6), Kohlmüller and Martin (7), Reisman and Mineo (8), and Wickham (9). Reagent grade Li_2CO_3 (B and A) and spectrographic grade V_2O_5 (Johnson–Matthey) were mixed in stoichiometric quantities, heated in a Pt crucible to 700 °C and cooled slowly. To produce larger crystals, the product was placed in a Pt boat and slowly moved through a sharp temperature change of 400 °C over a few centimeters with the highest temperature at 700 °C. The millimeter size crystals produced in this way were light green in color. Differential thermal analysis of this material showed no thermal anomalies up to the melting point of 615 °C. No change was noted in the powder pattern between 23 and 600 °C (5).

X-Ray powder diffraction patterns were obtained at 25 °C using a Hägg–Guinier camera according to a procedure described earlier (10). The pattern was indexed on a monoclinic cell consistent with space group $C2/c$. The crystal data are as follows.

$LiVO_3$ f.w. = 105.88
$a = 10.158(2)$, $b = 8.4175(9)$, $c = 5.8853(9)$ Å,
$\beta = 110.48(2)°$, $V = 471.4$ Å^3, $Z = 8$,
$\rho_c = 2.985$ g/cm^3, $\rho_o = 3.005$ g/cm^3(5).

The errors in the unit cell parameters are those derived from a least-squares fit using KCl ($a = 6.2931$ Å) as an internal standard and CuKα radiation ($\lambda_{\alpha 1} = 1.54051$ Å).

A single crystal was ground into a sphere of radius 0.021 cm ($\mu r = 0.96$). Single crystal precession patterns indicated space groups Cc or $C2/c$; we assumed space group $C2/c$ by analogy with $NaAlSi_2O_6$ (11). After collecting the diffractometer data, reflections violating c-glide symmetry were sought because such reflections had appeared in the other Li-containing pyroxenes $LiAlSi_2O_6$ (spodumene) and $LiFeSi_2O_6$ (12). Only one

[1]On leave of absence from Central Research Department, E. I. du Pont de Nemours, Wilmington, Delaware.

Can. J. Chem. Downloaded from www.nrcresearchpress.com by 210.87.254.6 on 09/05/12
For personal use only.

TABLE 1. Final atom parameters for $LiVO_3$*

Atom	x	y	z	U_{11}†	U_{22}	U_{33}	U_{12}	U_{13}	U_{23}
Li(1)	0	0.9223(6)	1/4	0.0181(22)	0.0134(21)	0.0497(35)	—	0.0180(24)	—
Li(2)	0	0.2847(7)	1/4	0.0190(22)	0.0165(23)	0.0523(36)	—	0.0146(23)	—
V	0.28829(3)	0.09485(4)	0.26694(5)	0.0082(2)	0.0120(2)	0.0098(2)	−0.0016(1)	0.0034(1)	−0.0004(1)
O(1)	0.1143(2)	0.1115(2)	0.1675(3)	0.0095(5)	0.0134(6)	0.0178(6)	0.0006(5)	0.0040(5)	0.0002(5)
O(2)	0.3555(2)	0.2719(2)	0.2824(3)	0.0236(7)	0.0183(7)	0.0283(8)	−0.0113(6)	0.0132(6)	−0.0047(6)
O(3)	0.3547(2)	−0.0280(2)	0.0760(3)	0.0117(6)	0.0237(6)	0.0117(6)	0.0008(5)	0.0038(5)	−0.0030(5)

*Standard deviations are given in parentheses.
†Calculated from $\beta_{ij} = 2\pi^2 b_i b_j U_{ij}$ where $T = \exp - (\beta_{11}h^2 + 2\beta_{12}hk + \ldots)$ is the temperature factor appearing in the structure factor equation and b_i's are the reciprocal lattice vectors.

TABLE 3. Bond distances and angles in $LiVO_3$*†

Bond	Distance (Å)	Bonds	Angle (deg)	Bonds	Angle (deg)
Li(1)—O(1), (1*c*)	2.125(4)	O(1)—Li(1)—O(1*b*)	87.8(1)	O(1*b*)—Li(1)—O(2*d*)	85.0(2)
—O(1*a*), (1*b*)	2.339(1)	—O(1*c*)	82.9(2)	—O(2*g*)	86.2(2)
—O(2*d*), (2*g*)	1.998(4)	—O(2*d*)	167.3(2)	—O(1*a*)	166.0(3)
		—O(2*g*)	88.54(1)		
⟨Li(1)—O⟩	2.153	—O(1*a*)	102.8(2)	O(2*d*)—Li(1)—O(2*g*)	101.3(3)
Li(2)—O(1), (1*c*)	2.026(4)	O(1)—Li(2)—O(1*c*)	87.9(3)	O(2*e*)—Li(2)—O(3*d*)	66.6(1)
—O(2*e*), (2*f*)	2.670(2)	—O(2*e*)	77.2(1)	—O(3*g*)	131.12(2)
—O(3*d*), (3*g*)	2.158(4)	—O(3*d*)	140.0(1)	—O(2*f*)	159.4(3)
		—O(3*g*)	106.6(1)	O(3*d*) —O(3*g*)	86.1(3)
⟨Li(2)—O⟩	2.284	—O(2*f*)	87.9(2)		
V—O(1)	1.662(1)	O(1)—V—O(2)	108.42(7)	O(2)—V—O(3)	108.39(9)
—O(2)	1.628(2)	—O(3)	114.11(6)	—O(3*a*)	103.23(7)
—O(3)	1.821(2)	—O(3*a*)	111.08(7)	O(3)—V—O(3*a*)	110.98(6)
—O(3*a*)	1.795(1)				
⟨V—O⟩	1.725				

*E.s.d.'s are given in parentheses.
†Symmetry transformations: $a = x, -y, z + 1/2$; $b = -x, -y, -z$; $c = -x, y, 1/2 - z$; $d = x + 1/2, y + 1/2, z$; $e = x + 1/2, 1/2 - y, z + 1/2$; $f = 1/2 - x, 1/2 - y, -z$; $g = 1/2 - x, 1/2 + y, 1/2 - z$.

such reflection (203 with $F_{obs} = 96$, $F_{000} = 4104$) was found.[2]

Intensities were collected on a Syntex automatic diffractometer using MoKα radiation, a graphite monochromator ($2\theta = 12°$), and a scintillation detector. Reflections were scanned in the 2θ–θ mode at variable rates from 2.0–24.0°/min, depending on the peak count, through an angle of 3° plus the α_1–α_2 separation. Background counts were made at the extreme of each scan for times equal to the peak count. A total of 851 reflections were measured over a range of 2θ from 6° to 65° of which 718 were considered to be observed. Intensities with less than 3 times the standard deviation of the background were considered to be unobserved. A number of reflections saturated the counter and were not included in the refinement (002, 02$\bar{1}$, 021, 20$\bar{2}$, 200, 22$\bar{1}$, 310, and 53$\bar{1}$). The intensities were corrected for absorption Lorentz and polarization factors using the X-ray 67 Program System for X-ray Crystallography written by Stewart, University of Maryland, and adapted to the CDC 6400 computer by Grundy. Secondary extinction coefficients were calculated for each reflection according to Zachariasen (19).

As a starting point for refinement the parameters for $LiAlSi_2O_6$ (12) were used. Several cycles of refinement using the full-matrix least squares refinement program CUDLS (20) reduced $\omega R = (\Sigma\omega||F_o| - |F_c||^2/\Sigma\omega|F_o|^2)^{1/2}$ to 0.052, using unit weights. Further refinement using anisotropic temperature factors and Cruickshank weights, $\omega = (1.005 + 0.0616|F_o| + 0.00166|F_o|^2)^{-1}$, reduced ωR to 0.033 and $R = (\Sigma||F_o| - |F_c||/\Sigma|F_o|)$ to 0.025. The weighting scheme was chosen so as to make $\omega||F_o - |F_c||^2$ independent of the variation in F_o. In the final cycle the average shift/error was 0.05. The standard deviation of an observation of unit weight, $(\Sigma\omega|F_o - F_c|^2/m - n)^{1/2}$, with m equal to the number of reflections used and n the number of variables was 1.01. The secondary extinction parameter refined according to the method of Larson (21) was $c = 2.30 \times 10^{-6}$. Scattering factors for Li^+, V^+ and O^- were taken from ref. 22. Corrections for anomalous dispersion of V were taken from Cromer (23). The final positional and thermal parameters are listed in Table 1 and the observed and calculated structure factors are listed in Table 2.[3] Table 3 lists some pertinent bond distances and angles. The final difference electron density showed no residual peaks of significant magnitude.

Results and Discussion

The pyroxene structure is characteristic of many compositions of the type $MM'X_2O_6$[4] where M = Li, Na, Mg, Fe^{2+}, and Ca; M′ = Li, Na, Mg, Fe^{2+}, Mn^{2+}, Al, Cr^{3+}, Fe^{3+}, Ti^{3+}, Sc^{3+}, and In^{3+}. Electrostatic charge balance generally requires that the combination be $M^+M^{3+}X_2O_6$ or $M_2^{2+}X_2O_6$ for X = Si^{4+} or

[2]The question of the space group of $LiVO_3$ and by analogy spodumene is an intriguing one. In both cases satisfactory structures have been obtained assuming the higher symmetry space group. Although in both cases reflections in violation of the *c*-glide plane have been noted. Both systems have been investigated by nuclear quadrupole (13, 14) resonance and in addition Mn^{2+} and Fe^{3+} in spodumene has been studied by electron paramagnetic resonance (15, 16). The former experiments in spodumene paid particular attention to the space group predictions and the results were consistent with *C*2/*c*. Those studies in $LiVO_3$ (17, 18) were consistent with space group *C*2/*c* except that a weak splitting was noted when the magnetic field was removed from the plane perpendicular to the *c* axis.

[3]Photocopy of Table 2 is available, at a nominal charge, from the Depository of Unpublished Data, National Science Library, National Research Council of Canada, Ottawa, Canada K1A 0S2.

[4]For comparison with other pyroxenes, M cations occupy the M2 site and M′ cations occupy the M1 site.

Can. J. Chem. Downloaded from www.nrcresearchpress.com by 210.87.254.6 on 09/05/12
For personal use only.

Can. J. Chem. Downloaded from www.nrcresearchpress.com by 210.87.254.6 on 09/05/12
For personal use only.

Ge^{4+} and $M_2{}^{+}X_2O_6$ for $X = V^{5+}$. There are as yet no examples of P-containing pyroxenes but there does not seem to be any reason why $LiPO_3$ or $NaPO_3$ under certain conditions would not have the pyroxene structure. Reviews of the crystal chemistry of silicate pyroxenes have been published by Prewitt and Peacor (24) and by Zussman (25) and a detailed discussion of the interatomic distances in 8 silicate pyroxenes was recently published by Clark, Appleman, and Papike (12). Zussman summarized the possible space groups: $C2/c$, $P2$, $C2$, $P2_1/c$, $Pbca$, and $Pbcn$. Clark *et al.* (12) concluded that the space group of a particular composition is determined chiefly by size and charge of the M cations: (*1*) large single or doubly charged cations lead to space group $C2/c$, *e.g.* $CaMgSi_2O_6$, $NaAlSi_2O_6$; (*2*) small singly charged cations lead to space group $C2$, *e.g.*, $LiAlSi_2O_6$ and $LiFeSi_2O_6$. (*3*) Small doubly charged cations lead to $P2/c$ or $Pbca$ *e.g.* $MgSiO_3$. Apparently the vanadate pyroxenes do not deviate from these generalities: $LiVO_3$ probably has the $LiAlSi_2O_6$ ($C2$ or $C2/c$) structure whereas $NaVO_3$ has the $NaAlSi_2O_6$ ($C2/c$) structure (2).

The pyroxene structure is generally described in terms of close-packed oxygen layers which are approximately perpendicular to a^* (10). The X ions occupy tetrahedral sites between layers whereas the larger M or M′ ions occupy six-or-eight-coordinated sites in alternate layers. The XO_4 ions are linked by corners to form continuous chains running along the c-axis. As pointed out by Prewitt and Peacor (24), the octahedra share edges to form a band running parallel to the chain. In $NaAlSi_2O_6$ the bonds are linked by the NaO_8 polyhedra whereas in $MgSiO_3$, $LiAlSi_2O_6$, and $LiVO_3$ there is a rift between the bands. Figure 1 shows the bands of Li(1) and Li(2) octahedra and the rift between these bands.

Because this is the first structure refinement of a vanadate pyroxene it is interesting to compare the molecular geometry with those of the corresponding silicates, $LiAlSi_2O_6$ and $LiFeSi_2O_6$ (12). The M2 site is occupied by Li in both cases and, as in all other pyroxenes with octahedral M2 sites, is extremely distorted. In $LiVO_3$ it is even more distorted than in $LiAlSi_2O_6$ with distances of 2.026 (2.105), 2.670 (2.278), and 2.158 Å (2.251 Å) and a mean distance of 2.284 Å (2.211 Å). The values in parentheses refer to $LiAlSi_2O_6$. If the longer bonds were to be ignored the remaining Li(2) environment would

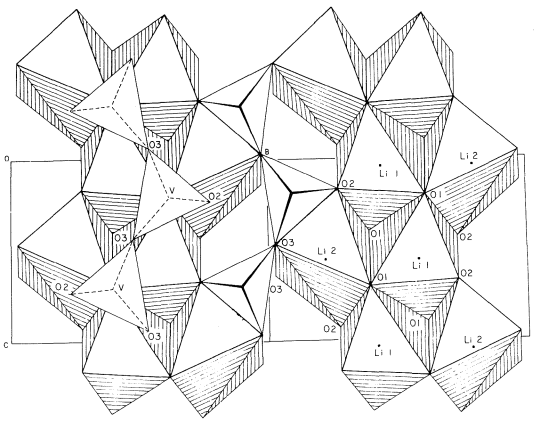

FIG. 1. Polyhedra in $LiVO_3$. The projection is down a^*.

be a distorted tetrahedron with bond angles ranging from 86 to 140°. The M1 site is also more distorted in $LiVO_3$ than $LiAlSi_2O_6$: 2.125 (1.997), 2.339 (1.943), and 1.998 Å (1.818 Å),[5] mean = 2.158 Å. In $LiFeSi_2O_6$ the M1—O(2) distance is shorter than M1—O(1) and in $LiVO_3$ the reverse is true. This is a consequence of replacing Fe^{3+} by Li^+; the Li(1)—O(1) and Li(2)—O(1) distances shorten relative to Li(2)—O(2) and Li(2)—O(2) to compensate for the loss in bond strength. The same interpretation can be made in terms of Pauling's bond strengths (26). According to this scheme O(1) is "underbonded" ($p = 1.70$) and O(2) is "overbonded" ($p = 2.17$); electrostatic balance is achieved by shortening M—O(1) bonds relative to M—O(2) bonds.

One of the most interesting and unusual features of the pyroxene structure is the large differences in mean distances for M1 and M2 sites. Table 4 shows this effect for Li, Mg, and Fe^{2+}. Although Clark *et al.* (12) claim that the mean octahedral distance in $LiAlSi_2O_6$ is in good

TABLE 4. Mean M1—O and M2—O distances in pyroxenes

Ion	M1—O	M2—O	Reference
$LiVO_3$	2.153	2.284	This work
$MgSiO_3$ clino	2.07	2.15	27
$MgSiO_3$ ortho	2.070	2.158	28
$FeSiO_3$ clino	2.137	2.224	29
$FeSiO_3$ ortho	2.145	2.240	29

[5]Distances in parentheses are Al—O distances.

TABLE 5

(*a*) Comparison of mean octahedral Li—O distances with distortion

Compound	$\bar{R}$* (Å)	*r*(Li)†	Distortion $\Delta = \langle(\Delta R/\bar{R})^2\rangle$	Reference
$LiGaO_2$	2.140(0.010)	0.740	0.0000	65 JCPSA 26 1277
$LiFePO_4$	2.154(0.002)	0.774	0.0003	68 CIWYA 68 290
$LiMnPO_4$	2.166(0.008)	0.786	0.0004	60 ACCRA 13 325
$LiAlSi_2O_6$	2.211(0.005)	0.848	0.0012	Ref. 12
$LiNbO_3$	2.153(0.011)	0.773	0.0016	66 JPCSA 27 997
$LiNb_3O_8$	2.188(0.030)	0.828	0.0019	71 ACSAA 25 3337
$LiTaO_3$	2.184(0.024)	0.804	0.0025	67 JPCSA 28 1685
$LiVO_3$	2.154(0.004)	0.790	0.0043	This work
$LiFeSi_2O_6$	2.249(0.005)	0.886	0.0044	Ref. 12
$LiC_6H_7O_7$	2.177(0.010)	0.827	0.0055	65 ACCRA 19 561
$LiVO_3$	2.285(0.004)	0.911	0.0148	This work

*$\bar{R}$ = mean octahedral Li—O distance with average e.s.d. quoted by authors in parentheses.
†*r* = effective ionic radius of Li^+. $\bar{R} = 2.158 + 8.42\Delta$, correlation coefficient = 0.81, goodness of fit = 0.030. $r = 0.784 + 9.01\Delta$, correlation coefficient = 0.79, goodness of fit = 0.036.
‡Codens for periodical titles, vol. II, ASTM Data Series DS 23A, Phila., 1966.

(*b*) Comparison of mean octahedral Mg—O distances with distortion

Compound	$\bar{R}$*(Å)	*r*(Mg)†	Distortion, $\Delta = \langle(\Delta R/\bar{R})^2\rangle$	Reference‡
MgO	2.105(0.005)	0.705	0.0000	57 AMMIA 42 39
Mg_6MnO_8	2.100(0.008)	0.710	0.0000	54 ACCRA 7 246
$CaMg(CO_3)_2$	2.095(0.008)	0.735	0.0000	59 AMMIA 44 679
$MgSO_4 \cdot 4H_2O$	2.075(0.008)	0.700	0.0000	64 ACCRA 17 863
$MgSO_4 \cdot 6H_2O$	2.065(0.008)	0.713	0.0000	64 ACCRA 17 235
$Mg(NH_4)_2(SO_4)_2 \cdot 6H_2O$	2.069(0.008)	0.713	0.0000	62 ZEGKA 117 344
$MgB_6O_7(OH)_6 \cdot 2H_2O$	2.090(0.003)	0.732	0.0001	71 AMMIA 56 1553
$MgSO_4 \cdot 6H_2O$	2.057(0.009)	0.705	0.0001	64 ACCRA 17 235
$MgNH_4PO_4 \cdot 6H_2O$	2.072(0.009)	0.712	0.0001	70 ACBCA 26 1429
$Mg_{1.8}Fe_{0.2}SiO_4$	2.103(0.003)	0.723	0.0002	68 AMMIA 53 807
$\alpha Mg_2P_2O_7$	2.105(0.009)	0.748	0.0002	67 ACCRA 23 289
$MgWO_4$	2.094(0.010)	0.734	0.0003	69 SPHCA 13 933
$MgHPO_4 \cdot 3H_2O$	2.084(0.005)	0.724	0.0003	67 ACCRA 23 418
$MgSO_4 \cdot 7H_2O$	2.065(0.008)	0.713	0.0003	64 ACCRA 17 1361
$CaMgSiO_4$	2.131(0.009)	0.751	0.0004	65 TMPMA 10 1
$Mg_3V_2O_8$	2.098(0.002)	0.738	0.0005	70 CJCHA 48 890
$Mg_3V_2O_8$	2.092(0.002)	0.732	0.0005	70 CJCHA 48 890
$MgSiO_3$	2.069(0.009)	0.703	0.0007	69 ZEKGA 129 65
$Mg_2V_2O_7$	2.124(0.002)	0.764	0.0007	Ref. 33
$MgAlBO_4$	2.094(0.008)	0.714	0.0008	65 MIASA 196
$Mg_3P_2O_8$	2.120(0.007)	0.760	0.0009	68 ACSAA 22 1466
$MgSO_4 \cdot H_2O$	2.081(0.008)	0.727	0.0011	70 BSCFA 12 4243
$Mg_{1.8}Fe_{0.2}SiO_4$	2.135(0.003)	0.755	0.0011	68 AMMIA 53 807
$Mg_2V_2O_7$	2.093(0.002)	0.733	0.0013	Ref. 33
Mg_3TeO_6	2.126(0.008)	0.746	0.0015	71 ACBCA 27 815
$Mg_2As_2O_7$	2.126(0.008)	0.766	0.0018	70 CJCHA 48 890
$MgSiO_3$	2.157(0.009)	0.791	0.0057	69 ZEKGA 129 65
MgB_4O_7	2.210(0.009)	0.853	0.0156	66 NJMMA 142

*$\bar{R}$ = mean octahedral Mg—O distance.
†*r* = effective ionic radius of Mg^{2+}. $\bar{R} = 2.093 + 8.43\Delta$, correlation coefficient = 0.70, goodness of fit = 0.019. $r = 0.723 + 8.93\Delta$, correlation coefficient = 0.67, goodness of fit = 0.019.
‡Codens for periodical titles, vol. II, ASTM Data Series DS 23A, Phila., 1966.

agreement with other values in the literature, these distances in $LiAlSi_2O_6$ and $LiFeSi_2O_6$ are actually considerably greater. Table 5*a* lists mean Li—O distances in a number of accurately refined crystal structures. The increase in mean distance is apparently caused by the very distorted M2—O polyhedron containing two very long bonds: $LiVO_3$, Li(2)—O(2) = 2.670 Å × 2,

Can. J. Chem. Downloaded from www.nrcresearchpress.com by 210.87.254.6 on 09/05/12
For personal use only.

Can. J. Chem. Downloaded from www.nrcresearchpress.com by 210.87.254.6 on 09/05/12
For personal use only.

$LiAlSi_2O_6$, Li—O(2) = 2.278 Å × 2 and in $LiFeSi_2O_6$, Li—O(3) = 2.459 Å × 2. (The fact that the long bond in $LiAlSi_2O_6$ is to O(2) and in $LiFeSi_2O_6$ is to O(3) is not understood.) In most structures containing either very short or very long distances, other bonds lengthen or shorten to compensate. Although this compensation generally results in average bond distances for coordination polyhedra which do not differ greatly from one structure to another, when the distortion becomes severe enough, a distinct dependence of mean bond length on degree of distortion can be observed. This dependence has been noted for Cu^{2+}—O and V^{5+}—O octahedra by Brown and Shannon (30) and is a consequence of the shape of the bond strength – bond length curve. For Li^+—O and Mg^{2+}—O bonds:

$$S_{Li—O} = 0.25\left(\frac{1.954}{R}\right)^{3.9}$$

$$S_{Mg—O} = 0.333\left(\frac{2.098}{R}\right)^{4.0}$$

These curves are shown in Fig. 2. As the deviation of the bond lengths from an undistorted polyhedra increase, keeping the average bond strength constant, the mean bond length must necessarily increase. In Tables 5*a* and 5*b* we have listed the mean bond lengths for a number of Li—O and Mg—O octahedra and their distortions from their mean bond length $\bar{R}$. In Figs. 3*a* and 3*b* the effective ionic radii (r) of Li^+ and Mg^{2+} have been plotted *vs.* the distortion.[6] Linear regression analyses of $\bar{R}$ and r on distortion result in correlation coefficients of about 0.70 with mean deviations of experimental from the calculated values of 0.035 Å for Li and 0.019 Å for Mg. The corresponding analyses for Cu^{2+} and V^{5+} resulted in correlation coefficients of 0.89 and 0.98, respectively, and mean deviations of the order of 0.01 Å (29). The dependence of mean bond length on distortion is easier to observe as the distortions increase; thus, there is a better fit for Cu^{2+} and V^{5+} (distortions up to 0.040 Å have been observed). Although all of the variations in Li—O and Mg—O mean bond lengths are not explained by distortion, distortion is apparently a significant factor.

In the VO_4 tetrahedra there are two bridging oxygens at 1.795 and 1.821 Å and two nonbridging oxygens at 1.628 and 1.662 Å from the vanadium ion. These distances are consistent with Baur's scheme for calculating distances from electrostatic bond strength sums around oxygen atoms (32). Table 6 shows comparison of observed and predicted distances based on an

[6]The effective ionic radius (r) is calculated by subtracting the appropriate oxygen radius from the mean bond length, $\bar{R}$ as described previously (31).

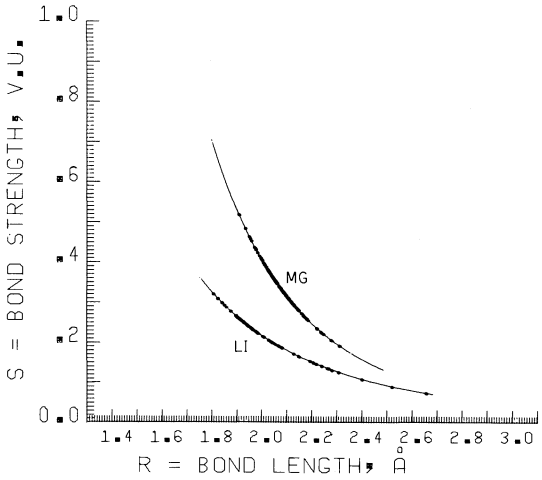

FIG. 2. Bond length – bond strength curves for Li—O and Mg—O. The individual points represent calculated bond strengths from which the curve was derived.

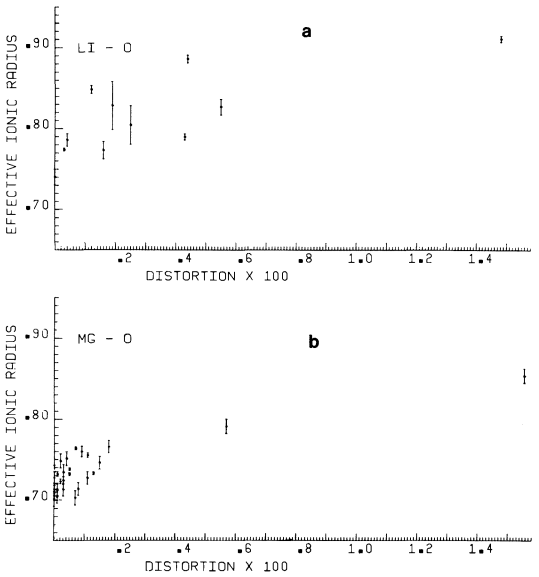

FIG. 3. (*a*) Effective ionic radius of octahedral Li^+ *vs.* distortion. Distortion is defined as $\langle(\Delta R/R)^2\rangle$ and vertical bars represent average e.s.d.'s quoted by authors; (*b*) effective ionic radius of octahedral Mg^{2+} *vs.* distortion.

TABLE 6. Comparison of observed and predicted V—O bond lengths in $LiVO_3$

	p_0	Δp_0	d_{obs} (Å)	d_{pred}* (Å)
V—O(1)	1.70	−1.45	1.662	1.65
V—O(2)	1.58	−0.57	1.628	1.63
V—O(3)	2.67	+0.52	1.821	1.80
V—O(3*a*)	2.67	+0.52	1.795	1.80
	Mean = 2.15		1.725	

*$d_{pred} = 1.721 + 0.1602(\Delta p_0)$ from ref. 34.

TABLE 7. Bond strengths in $LiVO_3$ and $LiAlSi_2O_6$

	$LiVO_3$				$LiFeSi_2O_6$			
	Li(1)	Li(2)	V	Σs_{anion}	Fe	Li	Si	Σs_{anion}
O(1)	0.18, 0.12*	0.22	1.46	1.98	0.36, 0.47	0.18	0.99	2.00
	(0.166×4)†	(0.166×2)	(1.25)	(1.70)	(0.50×4)	(0.166×2)	(1.0)	(2.17)
O(2)	0.23	0.07	1.62	1.93	0.64	0.17	1.08	1.89
	(0.166×2)	(0.166×2)	(1.25)	(1.58)	(0.50×2)	(0.166×2)	(1.0)	(1.67)
O(3)		0.17	0.92, 0.99	2.07		0.10	1.00, 0.99	2.09
		(0.166)	(1.25×2)	(2.67)		(0.166)	(1.0)	(2.17)
Σs_{cat}	1.07	0.92	4.99		2.95	0.90	4.06	
	(1.0)	(1.0)	(5.0)		(3.0)	(1.0)	(4.0)	

*Bond strengths calculated from eqs. 1 and 2 in Table 8.
†Bond strengths calculated according to Pauling's electrostatic valence principle: s = valence/CN.

equation similar to Baur's (33). The agreement is excellent with an average deviation of only 0.01 Å. Since Pauling's bond strengths are determined only by cation coordination numbers and are thus average bond strengths, rather large deviations of the anion sums from 2.0 are usually found. Using eqs. 1 and 2 in Table 8 derived from a large number of Li- and V-containing compounds to calculate bond strengths (29), Pauling's electrostatic valence principle is verified with an average deviation of about 5% from the ideal values of 1.0 for Li^+, 5.0 for V^{5+}, and 2.0 for O^{2-} (Table 7). The calculations made on $LiFeSi_2O_6$ show an average deviation of 5%. It should be noted, however, that these empirical curves as well as Pauling's classical scheme show O(2) to be "underbonded" and O(3) to be "overbonded".

In $LiM^{3+}Si_2O_6$ and $NaM^{3+}Si_2O_6$ structures, the silicate chains are relatively straight; the O(3)—O(3*a*)—O(3) angles range from 170° to 180°. In $LiVO_3$ the VO_4 chains are more kinked; the O(3)—O(3*a*)—O(3) angle is 161.8°. This deviation from linearity can be explained by reference to the relative strengths of the bonds to O(3) and O(2) (see Table 7). Referring to the lowest tetrahedron in the chain with apices pointing up in Fig. 1, a decrease in bond strengths of M(1)—O(2) and M(2)—O(2) will tend to rotate the tetrahedron clockwise and decrease the O(3)—O(3*a*)—O(3) angle from 180°; a decrease in the strength of M(2)—O(3) would have the opposite effect. Thus replacing Fe^{3+} or Al^{3+} by Li^+ will decrease the strength of M(1)—O(2) and decrease the O(3)—O(3*a*)—O(3) angle. In Table 8 it is apparent that the major change in bond strengths occur when going from $LiAlSi_2O_6$ or $LiFeSi_2O_6$ to $LiVO_3$ but in addition all the other bond strengths follow the trend indicated above.

Table 9 shows the root mean squared (r.m.s.) amplitude of vibrations for Li(1) and Li(2) in $LiVO_3$ together with the angles of the principal axes of the thermal disorder tensor. In $LiAlSi_2O_6$ the ratio of the largest to the smallest r.m.s. amplitude for the Li^+ site is 1.2 (11) compared with a factor of about 1.9 for both Li^+ sites in $LiVO_3$. Further the directions of the maximum amplitude for both Li^+ sites nearly coincide with that of the longest Li—O bond in the octahedron in each case thus suggesting positional disorder for these cations. In both cases these directions nearly parallel the c^* axis. One can easily move the Li(1) and Li(2) ions off the

Can. J. Chem. Downloaded from www.nrcresearchpress.com by 210.87.254.6 on 09/05/12
For personal use only.

TABLE 8. Comparison of O(3)—O(3*a*)—O(3) angles and the strengths (*s*) of bonds to O(2) and O(3)*

Compound	Angle O(3)—O(3*a*)—O(3)	*s*(O(2)—M1)	*s*(O(2)—M2)	*s*(O(3)—M2)
$LiVO_3$	161.8°	0.23	0.07	0.17
$LiAlSi_2O_6$	170.0°	0.61	0.14	0.14
$LiFeSi_2O_6$	180.0°	0.64	0.17	0.10

*Bond strengths calculated according to: eq. 1, $S_{Li-O} = 0.25(1.954/R)^{3.9}$; eq. 2, $S_{V^{5+}-O} = 1.25(1.714/R)^{5.1}$; eq. 3, $S_{Al-O} = 0.50(1.902/R)^{4.5}$; eq. 4, $S_{Fe^{3+}-O} = 0.50(2.012/R)^{5.3}$; eq. 5, $S_{Si-O} = 1.0(1.625/R)^{4.5}$.

TABLE 9. Magnitude and orientation of thermal ellipsoids for Li ions in $LiVO_3$

Li(1)					Li(2)				
	r.m.s. amplitude (Å)	Angle (deg) of r_i with				r.m.s. amplitude (Å)	Angle (deg) of r_i with		
i	r_i	*a*	*b*	*c*	*i*	r_i	*a*	*b*	*c*
1	0.223	88.98	90.00	21.50	1	0.230	83.64	90.00	165.88
2	0.116	90.00	0.00	90.09	2	0.130	173.64	90.00	75.88
3	0.115	1.02	90.00	111.50	3	0.128	90.00	0.00	90.00

two-fold axes, destroying this element of symmetry, yielding Li ions with five moderately strong bonds and one additional long bond. Such a displacement for Li(2), directly towards O(2*e*), shortening the Li(2)—O(2*e*) distance by 5% yields a bond strength for this ion of precisely 1.00. A comparable displacement in Li(1), shortening the Li(1)—O(1*a*) separation, increases an already high value for the bond strength of this cation. In $NaAlSi_2O_6$, $NaCrSi_2O_6$, $NaFeSi_2O_6$, and $CaMgSi_2O_6$ (11) the M2 ion also shows enhanced disorder although because the cation is now coordinated to eight oxygen atoms the direction of the maximum displacement no longer nearly coincides with *c**. It appears that a low temperature structural study might be needed to resolve these questions regarding the nature of the disorder.

The *a**, *b*, and *c* parameters reported by Feigelson *et al.* (5) agree with those reported here although β and the *a* axis length do not. Furthermore, their powder pattern of $LiVO_3$ except for the lines at $d = 3.15$ and 2.370 Å agrees with ours. Thus it is likely that the two compounds are the same and if so, their proposed study of the non-linear optic properties of these crystals might indicate whether the crystals indeed have the centro-symmetric space group proposed here.

We would like to thank Mrs. C. F. Foris and Dr. J. F Whitney of the Central Research Laboratory, E. I. du Pont de Nemours, Wilmington, Delaware for assistance with the Guinier photographs, A. Ferretti and J. Moore, also of du Pont, for preparation of the crystals, and R. Faggiani of McMaster University for assistance in collecting the intensity data. We are also grateful to C. T. Prewitt for preparing the projection of $LiVO_3$ shown in Fig. 1. This research was supported by the National Research Council of Canada.

1. R. D. SHANNON and C. CALVO. J. Solid State Chem. To be published.
2. H. SORUM. K. Norske, Vidensk. Selsk. Forh. **16**, 39 (1947); Struct. Rep. **9**, 180 (1943).
3. P. K. BURKERT and H. P. FRITZ. Z. Naturforsch. **25B**, 1053 (1970).
4. O. MULLER and R. ROY. Crystal chemistry of the ABX_3 family with particular emphasis on perovskites. Presented at the 73rd Annual Meeting of the American Ceramic Society, Chicago. April 24–29 (1971).
5. R. S. FEIGELSON, G. W. MARTIN, and B. C. JOHNSON. J. Cryst. Growth. **13/14**, 686 (1972).
6. G. CANNERI. Gazz. Chim. Ital. **58**, 6 (1928).
7. R. KOHLMÜLLER and J. MARTIN. Bull. Chim. Soc. Fr. **4**, 748 (1961).
8. A. REISMAN and J. MINEO. J. Phys. Chem. **66**, 1181 (1962).
9. D. G. WICKHAM. J. Inorg. Nucl. Chem. **27**, 1939 (1965).
10. D. B. ROGERS, R. D. SHANNON, A. W. SLEIGHT, and J. L. GILLSON. Inorg. Chem. **8**, 841 (1969).
11. C. T. PREWITT and C. W. BURNHAM. Am. Min. **51**, 956 (1966).

Can. J. Chem. Downloaded from www.nrcresearchpress.com by 210.87.254.6 on 09/05/12
For personal use only.

12. J. R. CLARK, D. E. APPLEMAN, and J. J. PAPIKE. Mineral. Soc. Am. Spec. Paper, **2**, 31 (1969).
13. G. M. VOLKOFF, H., E. PETCH, and D. W. L. SMELLIE. Can. J. Phys. **30**, 270 (1952).
14. H. E. PETCH, N. G. CRANNA, and G. M. VOLKOFF. Can. J. Phys. **31**, 837 (1953).
15. A. MANOOGIAN, F. HOLUJ, and J. W. CARSWELL. Can. J. Phys. **43**, 2262 (1965).
16. F. HOLUJ. Can. J. Phys. **46**, 287 (1968).
17. P. K. BURKERT and H. P. FRITZ. Z. Naturforsch. **25b**, 1053 (1970).
18. L. V. DMITRIEVA, Z. N. ZONN, V. A. IOFFE, and R. G. YAFAEVA. J. Struct. Chem. **11**, 862 (1970).
19. W. H. ZACHARIASEN. Acta Cryst. **16**, 1139 (1963).
20. J. S. STEPHENS. Unpublished results.
21. A. C. LARSON. Acta Cryst. **23**, 664 (1967).
22. International tables for X-ray crystallography. Vol. III. Kynoch Press, Birmingham. 1962. p. 202.
23. D. T. CROMER. Acta Cryst. **18**, 17 (1965).
24. C. T. PREWITT and D. R. PEACOR. Am. Min. **48**, 1527 (1964).
25. J. ZUSSMAN. Earth-Sci. Rev. **4**, 39 (1968).
26. L. PAULING. J. Am. Chem. Soc. **51**, 1010 (1929).
27. N. MORIMOTO, D. E. APPLEMAN, and H. T. EVANS, JR. Z. Krist. **114**, 120 (1960).
28. N. MORIMOTO and K. KOTO. Z. Krist. **129**, 65 (1969).
29. C. W. BURNHAM. Carnegie Inst. Wash. Yearbook, **65**, 285 (1967).
30. I. D. BROWN and R. D. SHANNON. To be published.
31. R. D. SHANNON and C. T. PREWITT. Acta Cryst. **B25**, 925 (1969).
32. W. H. BAUR. Trans. Am. Cryst. Assoc. **6**, 129 (1970), Am. Min. **56**, 1573 (1971).
33. R. GOPAL and C. CALVO. To be published.
34. R. D. SHANNON and C. CALVO. To be published.

Can. J. Chem. Downloaded from www.nrcresearchpress.com by 210.87.254.6 on 09/05/12
For personal use only.

Further N.M.R. Studies of the Dynamic Stereochemistry of π-Allylic Palladium(II) – Tertiary Phosphine Systems[1]

M. Oslinger and J. Powell

Lash Miller Chemical Laboratory, University of Toronto, Toronto 181, Ontario

Received June 20, 1972

A series of cations of the type 1,2-bis(diphenylphosphino)ethane(π-all)palladium(II) (all = allyl, 2-methylallyl, 2-tert-butylallyl, 1-methylallyl, 1,1-dimethylallyl, *syn*-1-tert-butyl-2-methylallyl) have been isolated as PF_6^- and/or BF_4^- salts. Variable temperature n.m.r. data fully substantiate the proposal that pyridine promoted exchange of *syn* and *anti* proton sites in such complexes occurs via a $\pi \rightarrow \sigma \rightarrow \pi$ mechanism that involves consecutive S_N2 ligand substitutions. Comparison of this variable temperature n.m.r. data with that obtained for the complexes 1,2-bis(diphenylphosphino)ethane(π-all)palladium(II) chloride (prepared *in situ*) has shown that the chloride ion, functioning as a nucleophile, is also effective in promoting $\pi \rightarrow \sigma \rightarrow \pi$ reactions. Studies of bis(dimethylphenylphosphine) (π-1,1-dimethylallyl)palladium(II) chloride in $CDCl_3$ below $-30°$ have shown that rapid consecutive S_N2 substitution reactions, in which chloride acts as a nucleophile, are also occurring in systems containing monodentate tertiary phosphine ligands. As such the PR_3 promoted *syn–syn* and *anti–anti* proton site interchange observed in complexes of the type [(π-2-methylallyl)PdCl(PR_3)] has been reinterpreted in terms of consecutive ligand substitution reactions involving PR_3 and Cl ligands instead of the original proposal which involved an in plane rotation of the π-allylic ligand.

Une série de cations du type bis(biphényl phosphino)-1,2 éthane (π-all)palladium(II) (π-all = groupement allylique, méthyl-2 allyle, tert-butyl-2 allyle, méthyl-1 allyle, diméthyl-1, 1 allyle tert-butyl-1 méthyl-2 *syn* allyle) a été isolée comme des sels de PF_6^- et/ou BF_4^-. Des données provenant de la r.m.n. à température variable renforcent pleinement l'hypothèse selon laquelle l'échange des protons des sites *syn* et *anti*, favorisé par la pyridine dans de tels complexes, s'effectue selon un mécanisme $\pi \rightarrow \sigma \rightarrow \pi$ impliquant consécutivement des substitutions S_N2 des coordinats. La comparaison des données de la r.m.n. à température variable avec celles obtenues pour les complexes du chlorure de bis-(biphényl phosphino)-1,2 éthane(π-all)palladium(II) (préparés *in situ*) a indiqué que l'ion chlorure agissant comme un nucléophile est aussi capable d'induire des réactions $\pi \rightarrow \sigma \rightarrow \pi$. Des études du chlorure de bis(diméthyl phényl phosphine)(π-diméthyl-1,1 allyl)palladium(II) dans le $CDCl_3$ en dessous de $-30°$ ont montré que les réactions rapides et consécutives de substitution S_N2, dans lesquelles la chlorure agit comme un nucléophile, se produisent aussi dand des systèmes contenant des monocoordinats de phosphine tertiaire. Comme telle l'action du PR_3 favorisant l'échange mutuel des protons des sites *syn–syn* et *anti–anti* observé dans les complexes du type [(π-méthyl-2-allyl)PdCl(PR_3)] a été repensée en termes d'une succession de réactions de substitution des coordinats impliquant les coordinats PR_3 et Cl au lieu de l'hypothèse initiale qui impliquait une rotation dans le plan des coordinats allyliques. [Traduit par le journal]

Can. J. Chem., **51**, 274 (1973)

Introduction

Since 1965, the dynamic stereochemistry of π-allylic palladium(II) halide/tertiary phosphine systems has received considerable attention (1–7). Two basic allylic proton site exchange processes are observable by p.m.r. studies of such systems. The first, involving *syn–anti* proton site exchange, has been clearly shown to occur via a short lived σ-allylic intermediate (1–8). The second process is *syn–syn* and simultaneous *anti–anti* proton site exchange. An exchange process of this type is observed on addition of PR_3 to $CDCl_3$ solutions of [(π–2–methylally)PdCl(PR_3)] (**1**); PR_3 = PPh_3, PMe_2Ph, $PMePh_2$, PEt_3 at PR_3/Pd ratios between 1.0 and 1.5 (1–5). The mechanistic pathway of this process is not clearly defined. Vrieze *et al.* (2–4) have proposed that the observed rapid exchange of *syn* protons 1 and 4 and *anti* protons 2 and 3 in **1** occurs via addition of PR_3* to give a square pyramidal intermediate (**2**) in which PR_3* occupies an axial position. A postulated 120° "in plane rotation" of the π-2-methylallyl ligand, followed by loss of the *originally co-ordinated* PR_3 (now in an axial position) results in 1–4 and

[1]Taken from the thesis of M. Oslinger, submitted to the Faculty of Graduate Studies, University of Toronto, in partial fulfillment of the requirements for the M.Sc. degree.

Can. J. Chem. Downloaded from www.nrcresearchpress.com by 210.87.254.40 on 09/05/12
For personal use only.

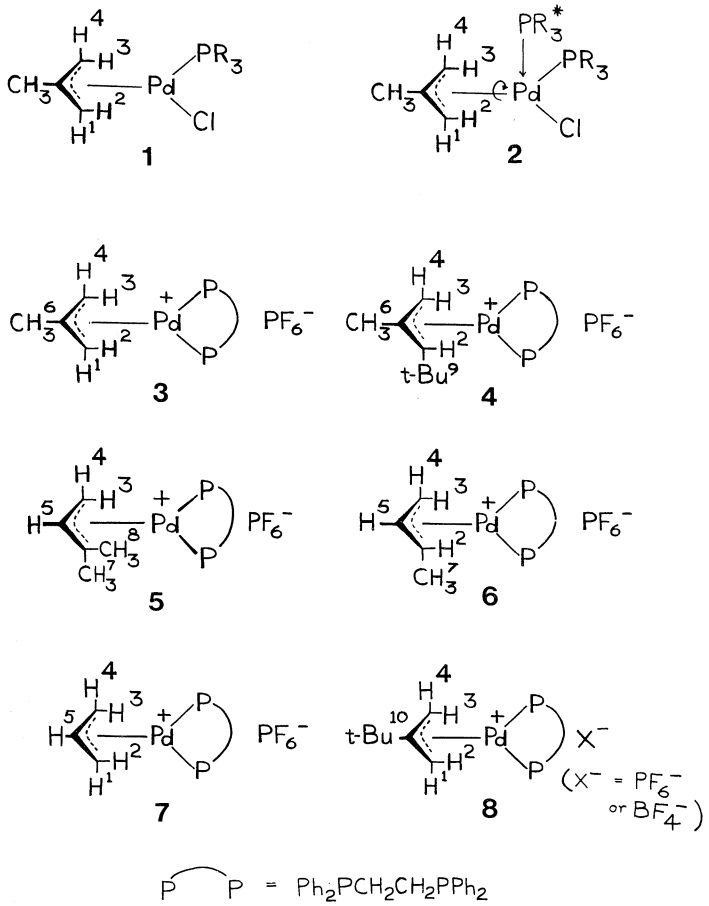

2–3 exchange. This proposal, ascribing fluxional characteristics to the π-allyl-palladium bond, is worthy of further investigation if we hope to understand the mechanism of catalytic processes involving allylic intermediates. It should be noted that the fluxional model proposed by Vrieze *et al.* (2–4) to explain *syn–syn* and *anti–anti* proton exchange in tertiary phosphine complexes of palladium(II) is not supported by direct chemical evidence. Although kinetic studies show that *syn–syn* and *anti–anti* proton exchange is first order in both monomer **1** and added PR_3, no definitive description of the intermediate can be made. The only justification proposed for a pseudorotation of the allylic ligand within a five coordinate intermediate is based on a molecular orbital treatment. Criticism of this approach centers on the assumption made that π-allyl palladium chloride complexes can be treated in an analogous fashion to sandwich compounds such as $(C_6H_6)Mo(CO)_3$ in which rapid in plane rotation of the π-benzene ligand is known to occur and for which molecular orbital calculations have been performed (9).

The inherent difficulty with the systems studied by Vrieze is that the observed *syn–syn* and *anti–anti* proton exchange cannot be related to the absolute motion of any one ligand, *i.e.*, movement of the allylic ligand (rotation) with respect to the other ligands (PR_3, Cl) cannot be distinguished from ligand exchange of PR_3 and Cl with respect to a stationary allylic ligand; either situation would result in the observed *syn–syn* and *anti–anti* proton exchange. In fact, all that one can conclude is that the allylic ligand moves *relative* to PR_3 and Cl such that each end of the allylic ligand sees a different *trans* ligand. Therefore, a real rotation of the allylic group, if it exists, cannot be demonstrated directly in the p.m.r. spectrum.

Tibbetts and Brown (7) focused their attention on the movements of the allylic ligand by em-

Can. J. Chem. Downloaded from www.nrcresearchpress.com by 210.87.254.40 on 09/05/12
For personal use only.

Can. J. Chem. Downloaded from www.nrcresearchpress.com by 210.87.254.40 on 09/05/12
For personal use only.

TABLE 1. Proton magnetic resonance data for the allylic ligand in cationic complexes of the type [(π-all)Pd(diphos)]$^+$ measured in deuteriochloroform at 34°*†

Complex	Allylic ligand	τ_1	τ_2	τ_3	τ_4	τ_5	τ_6	τ_7	τ_8	τ_9	τ_{10}
4	1-tert-Butyl-2-methylallyl	—	5.70q $J_{P_{tr}} = 10$ $J_{P_{cis}} = 1.5$	7.25d,b $J_{P_{tr}} = 10$	5.90d,b $J_{P_{tr}} = 8$	—	8.05s	—	—	9.16s	—
5	1,1-Dimethyl-allyl	—	—	6.78m,vb $J_{P_{tr}} \sim 10$	5.69m,b $J_{P_{tr}} \sim 8$	4.46q $J_3 = 14$ $J_4 = 8$	—	8.16q J_P's = 9.5 8.5	8.95t J_P's = 6.5 6.5	—	—
6	1-Methylallyl	—	*ca.*5.53 m,vb $J_{P_{tr}} \sim 10$	6.95m,vb	*ca.*5.85 m,vb	4.32m,b $J_2 \sim 13$ $J_3 \sim 13$ $J_4 \sim 8.0$	—	8.35m $J_2 = 6$ J_P's = 9.0 9.0	—	—	—
7	Allyl	5.16m,b	6.68m,b	6.68m,b	5.16m,b	4.18m $J_2,J_3 \sim 14$ $J_1,J_4 \sim 8$	—	—	—	—	—
3	2-Methylallyl	5.42b	6.75m,b	6.75m,b	5.42b	—	8.12s	—	—	—	—
8	2-tert-Butylallyl	5.46b	6.66m,b	6.66m,b	5.46b	—	—	—	—	—	9.93s

*$CHCl_3$ was used as an internal standard; s = singlet; d = 1:1 doublet; t = 1:2:1 triplet; q = 1:1:1:1 quartet; b = broad (width at half height 3–8 c/s); vb = very broad (width at half height > 8 c/s); J = coupling constant (c/s) with proton numbered x; $J_{P_{tr}}$ = coupling with *trans* ^{31}P nucleus; $J_{P_{cis}}$ = coupling with *cis* ^{31}P nucleus.
†Complex patterns due to methylene protons of diphos ligand, are observed in each spectrum *ca.* τ 7–8.

Can. J. Chem. Downloaded from www.nrcresearchpress.com by 210.87.254.40 on 09/05/12
For personal use only.

ploying the firmly bound chelating diphos ligand in (**3**). The scalar couplings of ^{31}P with the protons of the 2-methylallyl ligand provided a means by which the two ends of the 2-methylallyl group could be distinguished. Addition of pyridine to **3** in $CDCl_3$ promoted rapid *syn–anti* proton site exchange via the series of consecutive ligand substitution processes outlined in Scheme 1. The

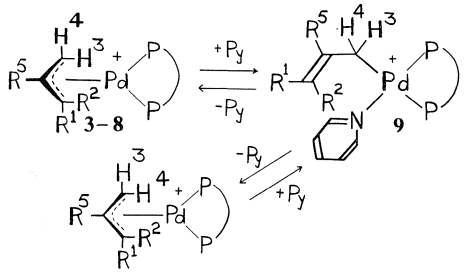

SCHEME 1. Mechanism of pyridine promoted exchange of protons 3 and 4 in the cationic complex $[(\pi\text{-all})Pd(diphos)]^+PF_6^-$.

absence of *syn–syn* and *anti–anti* proton exchange in the **3**/pyridine system prompted Tibbetts and Brown (7) to question the concept of rotation of the π-2-methylallyl ligand previously suggested by Vrieze (2–4). However, an important feature of Vrieze's mechanism is that 1–4 proton exchange and 2–3 proton exchange, *and* PR_3 ligand exchange in **1** are synonymous. In fact, in complexes such as **3** where ligand exchange between diphos and pyridine would not occur on the p.m.r. time scale owing to the stability of the chelating diphos ligand, the mechanism proposed by Vrieze predicts that a rapid in plane rotation of the π-2-methylallyl ligand would *not* occur. Thus the results of Tibbetts and Brown cannot be extrapolated to the monotertiary phosphine systems **1** where rapid PR_3 exchange is occurring.

The advantages of a complex such as **3** in studying π-allylic proton exchange (*i.e.*, the inertness of the diphos ligand to exchange and the *cis* and *trans* phosphorus 31 couplings to the protons of the allylic ligand) are attractive. As such we have prepared a series of π-allylic complexes analogous to **3** and tested the generality of the results obtained by Tibbetts and Brown. By progressively extending our p.m.r. studies from $[(\pi\text{-all})Pd(diphos)]PF_6$/pyridine systems to $\{[(\pi\text{-all})PdCl]_2 + 2diphos\}$ systems and to $\{[(\pi\text{-all})PdCl]_2 + 4PR_3\}$ systems (all = allyl, 2-methylallyl, 2-tert-butylallyl, *syn*-1-methylallyl, *syn*-1-tert-butyl-2-methylallyl, 1,1-dimethylallyl; PR_3 = Me_2PhP, Ph_3P) we have obtained sufficient evidence to show that the observed *syn–syn* and *anti–anti* proton site exchange in $[(\pi\text{-all})PdCl(PR_3)]/PR_3$ systems is in fact due to rapid consecutive S_N2 ligand substitution processes rather than a low energy in plane rotation of the π-allylic ligand.

Results and Discussion

Intramolecular Motions Occurring in a Series of $[(\pi\text{-all})Pd(diphos)]PF_6$/Pyridine Systems

The π-allylic palladium(II) diphos salts **3–8** were prepared in a manner analogous to Tibbetts and Brown (7) (reaction 1).

$$[1]\quad \tfrac{1}{2}[(\pi\text{-all})PdCl]_2 + \text{diphos} + NH_4PF_6 \xrightarrow{CHCl_3} [(\pi\text{-all})Pd(diphos)]PF_6 + NH_4Cl$$

All the salts were isolated as air stable, white crystalline solids. Complexes **3–7** were sufficiently soluble in $CHCl_3$ for p.m.r. purposes. However, the hexafluorophosphate of **8** [$X^- = PF_6^-$] was very insoluble in chloroform. As such, the tetrafluoroborate salt ($X^- = BF_4^-$) was prepared; the enhanced solubility of this latter salt enabled a p.m.r. spectrum to be recorded.

The p.m.r. data for the allylic protons in complexes **3–8** are tabulated in Table 1. The assignment of the proton resonances is based on the coupling of the *syn* protons (1 and 4) and *anti* protons (2 and 3) with the central allylic proton 5 and the *cis* and *trans* phosphorus atoms of the diphos ligand; these coupling constants agree well with previously reported values (5, 7). The *syn*-1-tert-butyl-2-methylallyl and 1,1-dimethylallyl complexes, **4** and **5**, are particularly useful in that the p.m.r. spectrum of each may be interpreted by a simple first order treatment.

The major ^{31}P coupling constants (c s^{-1}) for the *syn*-1-tert-butyl-2-methylallyl protons in **4** (Fig. 1(*a*)) are: H_2, $J_{P_{trans}} = 10$, $J_{P_{cis}} = 1.5$; H_3, $J_{P_{trans}} = 10$, $J_{P_{cis}} < 1$; H_4, $J_{P_{trans}} = 8$, $J_{P_{cis}} < 1$. For the 1,1-dimethylallyl protons of **5** (Fig. 2(*a*)), the major ^{31}P coupling constants (c s^{-1}) are: H_3, $J_{P_{trans}} \sim 10$, $J_{P_{cis}} < 1$; H_4, $J_{P_{trans}} \sim 8$, $J_{P_{cis}} < 1$; Me_7, J_P,s = 9.5 and 8.5; Me_8, J_P,s = 6.5 and 6.5. *trans*-^{31}P coupling to protons H_3 and H_4 are approximate owing to the broadness of the resonances. Furthermore, one cannot assign definitively the *cis* and *trans* ^{31}P coupling constants to the *syn* methyl protons; *cis* and *trans* ^{31}P couplings to the *anti* methyl protons are equal,

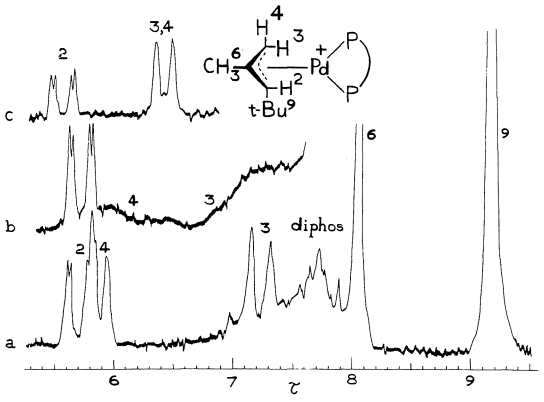

FIG. 1. The ^{1}H n.m.r. spectra of a 0.55 *M* solution of [(*t*-BuCH=C(Me)=CH$_2$)Pd(diphos)]$^+$PF$_6^-$ (**4**): (*a*) in $CDCl_3$ at 34°; (*b*) in $CDCl_3$ at 34° in the presence of 1 mol of pyridine per Pd atom; (*c*) in neat pyridine at 80°.

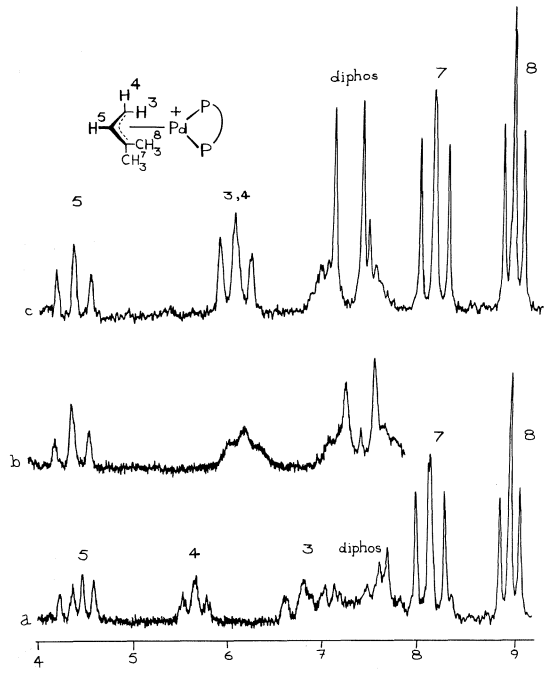

FIG. 2. The ^{1}H n.m.r. spectra of a 0.55 *M* solution of [(Me$_2$C=CH=CH$_2$)Pd(diphos)]$^+$PF$_6^-$ (**5**): (*a*) in $CDCl_3$ at 34°; (*b*) in $CDCl_3$ at 34° in the presence of one mol of pyridine per Pd atom; (*c*) in neat pyridine at 34°.

within experimental error, and the absorption is a 1:2:1 triplet.

The p.m.r. pattern of the 1-methylallyl protons in **6** is more difficult to assign owing to the very broad, ill-defined resonances observed; only the coupling pattern for the *syn*-methyl protons can be assigned with certainty (Table 1).

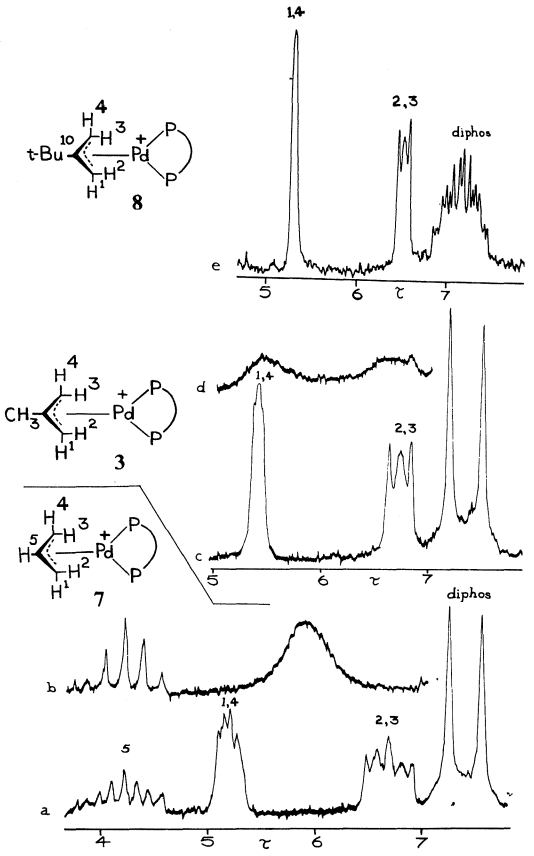

FIG. 3. The 60 MHz ^{1}H n.m.r. spectra of 0.55 *M* $CDCl_3$ solution of the complexes [(π-all)Pd(diphos)]$^+$PF$_6^-$ recorded at 34°; (*a*) π-all = π-allyl (complex **7**); (*b*) **7** plus one mol of pyridine per Pd atom; (*c*) π-all = π-2-methylallyl (complex **3**); (*d*) **3** plus 4 mol pyridine per Pd atom; (*e*) π-all = π-2-tert-butyllallyl (complex **8**) (a 0.25 *M* $CDCl_3$ solution recorded on a 100 MHz spectrometer). The line shape of the *syn* protons (1 and 4) and the *anti* protons (2 and 3) are only slightly affected by the addition of ten pyridines per Pd atom.

The p.m.r. spectrum of **7** is broad and of second order complexity (Fig. 3(*a*)). Only $J(H_{1,4}–H_5)$ and $J(H_{2,3}–H_5)$ were estimated (Table 1). No attempt was made to determine the *cis* and *trans* ^{31}P coupling constants to the terminal allylic protons in complexes **7** and **8**. As discussed by Tibbetts and Brown (7) for complex **3**, such spectra require computer analysis of the resonance shape to determine the coupling constants. However, a comparison of the spectra of **7** and **8** with that of **3** suggests ^{31}P coupling constants of a similar magnitude (see Fig. 3).

Addition of pyridine (one molecule per Pd atom) to a 0.55 *M* solution of **4** in $CDCl_3$ at 34° resulted in the broadening of the resonances of

Can. J. Chem. Downloaded from www.nrcresearchpress.com by 210.87.254.40 on 09/05/12
For personal use only.

Can. J. Chem. Downloaded from www.nrcresearchpress.com by 210.87.254.40 on 09/05/12
For personal use only.

protons 3 and 4. Proton 2 remained sharp and strongly coupled to the *cis* and *trans* ^{31}P nuclei (Fig. 1(*b*)). In neat pyridine at 80°, protons 3 and 4 gave rise to a sharp doublet ($J_{P\,trans}$ = 9 c s^{-1}) while proton 2 remained coupled to stereochemically distinct *cis* and *trans* ^{31}P (Fig. 1(*c*), Table 2).

Similarly, addition of pyridine (one molecule per Pd atom) to a 0.55 *M* chloroform-*d* solution of **5** at 34° resulted in a very broad "triplet" resonance for protons 3 and 4 while *cis* and *trans* ^{31}P coupling to the *syn* and *anti* methyl protons is preserved; proton 5 became a 1:2:1 triplet owing to coupling with protons 3 and 4 which were equivalent on the p.m.r. time scale (Fig. 2(*b*)).

In neat pyridine at 34°, the resonance for protons 3 and 4 is resolved as a broad triplet ($J(H_5–H_{3,4} \sim 11$ c s^{-1}, $J(P_{trans}–H_{3,4}) \sim 9$ c s^{-1}) while distinct *cis* and *trans* ^{31}P coupling to the *syn* and *anti* methyl protons is retained (Fig. 2(*c*), Table 2).

The addition of pyridine (one molecule per Pd atom) to 0.55 *M* chloroform-*d* solutions of **6** and **7** at 34° resulted in the collapse of resonances 3 and 4 of both spectra into a very broad single resonance (*e.g.* Fig. 3), the coupling pattern ($J(H_5–H_{3,4})$; $J(P_{trans}–H_{3,4})$) is not resolved at this stage. A higher concentration of pyridine (pyr/Pd = 4) was necessary to effect rapid *syn–anti* proton exchange in a 0.55 *M* chloroform-*d* solution of **3** (Fig. 3) while a still higher concentration of pyridine is required to effect rapid *syn–anti* proton exchange in **8**. (*e.g.* see Fig. 3). Pyridine promotion of rapid *syn–anti* proton exchange without interchange of the positions of the terminal allylic carbon atoms relative to the diphos ligand (N.B. distinct *cis* and *trans* ^{31}P coupling to allylic protons is retained in the region of fast 3–4 exchange) in the complexes **3–8** fully corroborate the findings of Tibbetts and Brown (7) in their work with complex **3** and pyridine. All the results are consistent with the concerted displacement of one end of the allylic ligand (the most substituted terminal allylic carbon in the case of complexes **4**, **5**, and **6**) by pyridine to give a short-lived σ-allylic intermediate **9**. Intermediate **9** may reform a π-allylic complex in one of the two ways thereby affecting site interchange of protons 3 and 4 as outlined in Scheme 1. During this process R_1 and R_2 retain the same configuration relative to the diphos ligand, hence distinct *cis* and *trans* ^{31}P coupling is observed for the proton resonances of R_1 and R_2 in the region of rapid *syn–anti* proton exchange. The strong *trans* ^{31}P coupling to protons 3 and 4 in neat pyridine for **4** and **5** is intermediate between $J(P_{trans}–H_3)$ and $J(P_{trans}–H_4)$ observed in the absence of exchange.

Under identical conditions of complex concentration (0.55 *M*), temperature (34°), and pyridine concentration (pyr/Pd = 1), the 1,1-dimethylallyl ligand in **5** undergoes *syn–anti* (3–4) proton exchange faster than either the 1-methylallyl or allyl ligands in **6** and **7** respectively. This is evidenced by the fact that the resonance pattern of protons 3 and 4 in **5** is approaching the fast exchange limit and coupling with the *trans* ^{31}P nucleus and protons is clearly resolved (see Fig. 2(*b*)), whereas under identical conditions of concentration and temperature the resonance patterns of protons 3 and 4 in **6** and **7** consist of a very broad single resonance typical of an intermediate exchange close to the region of coalescence. Under these same conditions, protons 3 and 4 in **4** have broadened but not coalesced while in **3** and **8**, no exchange is observed until higher concentrations of pyridine are added (*e.g.*, see Fig .3).

On the basis of such studies, a qualitative order can be cited for the relative ease of formation of the σ-allylic intermediate **9** with respect to the allylic ligand present in the complex. The ease of formation of **9** decreases in the order 1,1-dimethylallyl > 1-methylallyl ~ allyl > 1-tert-butyl-2-methylallyl > 2-methylallyl > 2-tert-butylallyl.

This order agrees well with previous studies on allylic ligand substituent effects on the rate of *syn–anti* proton exchange in the complexes [(π-all)Pd(OAc)(PMe_2Ph)] (8, 10).

Intramolecular Motions Occurring in π-Allylic Palladium Chloride – Diphos Systems at Diphos:Pd Ratios of 1:1

Because of its stability and non-lability, it was expected that the diphos ligand would occupy two coordination sites in the square plane when added to a solution of (π-all)palladium chloride (one molecule of diphos per Pd atom). If the allylic ligand occupied the remaining two coordination sites (π-allylic) in the square plane, then a species structurally analogous to the cation of complexes **3–8** would be formed. For this situation, the position of the chloride ligand relative to the square plane became of considerable interest in that it seemed reasonable that the chloride ligand might parallel the behavior of pyridine with the salts **3–8**. To explore this possi-

Can. J. Chem. Downloaded from www.nrcresearchpress.com by 210.87.254.40 on 09/05/12
For personal use only.

TABLE 2. Proton magnetic resonance data for complexes **4** and **5** in neat pyridine*

Complex	Allylic ligand	τ_2	τ_3	τ_4	τ_5	τ_6	τ_7	τ_8	τ_9
4†	1-tert-Butyl-2-methylallyl	5.58q§ $J_{P_{tr}} = 10$ $J_{P_{cis}} = 1.5$	6.42d $J_{P_{tr}} = 9.0$	6.42d $J_{P_{tr}} = 9.0$	—	8.05s	—	—	9.10s
5‡	1,1-Dimethylallyl	—	6.14t $J_5 = 11$ $J_{P_{tr}} \sim 9.0$	6.14t $J_5 = 11$ $J_{P_{tr}} = 9.0$	4.43t $J_{3,4} = 11$	—	8.22q $J_P \sim 9.5$ 8.5	9.05t $J_P = 6.5$ 6.5	—

*$CHCl_3$ was used as internal standard; J_x = coupling constant (c s^{-1}); methylene protons of diphos τ 7–8 in both systems.
†Temperature = 80°.
‡Temperature = 34°.
§d = 1:1 doublet; t = 1:2:1 triplet; q = 1:1:1:1 quartet; m = multiplet; s = singlet.

TABLE 3. Proton magnetic resonance data of allylic protons of *syn*-1-tert-butyl-2-methylallyl palladium chloride and 1,1-dimethylallyl palladium chloride in the presence of one molecule of diphos per Pd in $CDCl_3$ at 34°*

Complex	Allylic ligand	τ_2	τ_3	τ_4	τ_5	τ_6	τ_7	τ_8	τ_9
10 R^1 = *t*-Bu; R^2 = H R^5 = Me	1-tert-Butyl-2-methylallyl†	5.86q $J_{P_{tr}} = 10$ $J_{P_{cis}} = 1.5$	6.72d $J_{P_{tr}} = 9.0$	6.72d $J_{P_{tr}} = 9.0$	—	8.18s	—	—	9.93s
10 R^1 = R^2 = Me R^5 = H	1,1-Dimethyl-allyl‡	—	6.40m $J_5 = 11$ $J_{P_{tr}} \sim 9.0$	6.40m $J_5 = 11$ $J_{P_{tr}} = 9.0$	4.64t $J_{3,4} = 11$	—	8.29t J_P's ~ 9.5 9.5	9.10t J_P's = 6.5 6.5	—

*$CHCl_3$ was used as internal standard; J_x = coupling constant (c s^{-1}).
†Numbering of protons as in (**4**).
‡Numbering of protons as in (**5**).
§d = 1:1 doublet; t = 1:2:1 triplet; q = 1:1:1:1 quartet; m = multiplet; s = singlet.

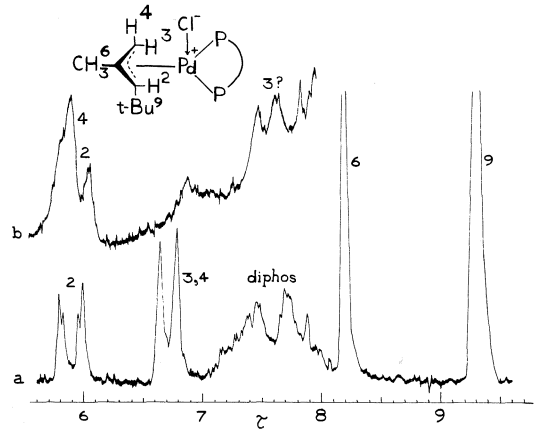

FIG. 4. The ^{1}H n.m.r. spectra of a 0.44 *M* $CDCl_3$ solution of [(*t*-BuCH=C(Me)=CH_2)Pd(diphos)Cl] (*a*) at 34° (compare with Fig. 1*c*); (*b*) at −60°.

bility, the p.m.r. spectra of a series of (π-all)palladium chloride – diphos adducts (π-all = 1-tert-butyl-2-methylallyl, 1,1-dimethylallyl, 1-methylallyl, allyl, and 2-methylallyl) were investigated.

At 34°, the p.m.r. spectrum of a 0.44 *M* chloroform-*d* solution of *syn*-1-tert-butyl-2-methylallyl palladium chloride in the presence of one molecule of diphos per Pd atom (Fig. 4(*a*), Table 3) shows a coupling pattern that is identical to that observed for **4** in neat pyridine (Fig. 1(*c*), Table 2). The major coupling constants (c s^{-1}) for the *syn*-1-tert-butyl-2-methylallyl protons are: proton 2, $J(P_{trans}–H_2) = 10$; $J(P_{cis}–H_2) = 1.5$; protons 3 and 4 (equivalent on the p.m.r. time scale), $J(P_{trans}–H_{3,4}) = 9$. These values indicate that a rapid 3–4 proton exchange is occurring *without* the loss of *cis* and *trans* ^{31}P coupling to the terminal *syn*-1-tert-butyl-2-methylallyl protons. At −60°, protons 3 and 4 are seen as separate resonances (Fig. 4(*b*)).

The *syn*-1-tert-butyl-2-methylallyl proton resonances have broadened extensively at this low temperature; this broadening, which is characteristic of all the low temperature [(π-all)Pd(diphos)Cl] spectra recorded, may be attributed to salt formation and/or viscosity effects (see later in Discussion section).

The major coupling constants (c s^{-1}) for the p.m.r. spectrum of 1,1-dimethylallyl palladium chloride and diphos (one molecule of diphos per Pd atom) in a 0.44 *M* chloroform-*d* solution recorded at 34° are: protons 3 and 4 (equivalent on the p.m.r. time scale), $J(H_5–H_{3,4}) = 11$, $J(P_{trans}–H_{3,4}) \sim 10$; *syn* methyl protons, $J(P_{cis,\ trans}–CH_{3(7)}) = 9.5, 9.5$; *anti* methyl protons, $J(P_{cis,\ trans}–CH_{3(8)}) = 6.5, 6.5$ (Fig. 5(*a*), Table 3). This spectrum exhibits an almost *identical* coupling pattern to that observed for **5** in neat pyridine at 34° (Fig. 2(*c*), Table 2).[2] At −60°, protons 3 and 4 are seen as separate, broad resonances (Fig. 5(*b*)).

Although the p.m.r. spectral patterns are more complex, similar behavior is observed when other (π-all) palladium chlorides (π-all = allyl, 1-methylallyl, and 2-methylallyl) are added to diphos (one molecule per Pd atom) in chloroform-*d* at 34°, (*i.e.*, rapid 3–4 proton exchange occurs with retention of distinct *cis* and *trans* phosphorus couplings to the terminal allylic protons. At low temperatures, protons 3 and 4 separate into two distinct absorptions while the overall spectrum is characterized by broadened proton resonances).

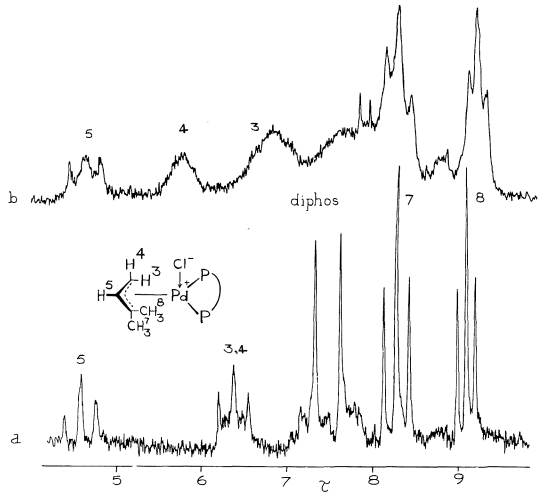

FIG. 5. The ^{1}H n.m.r. spectra of a 0.44 *M* $CDCl_3$ solution of [(Me_2C=CH=CH_2)Pd(diphos)Cl] (*a*) at 34° (compare with Fig. 2*c*); (*b*) at −60°.

[2]The similar magnitude of *cis* and *trans* ^{31}P coupling to the *syn*-methyl protons and also to the *anti*-methyl protons is confusing in that it could be taken to imply that the 1,1-dimethylallyl ligand is undergoing a site exchange relative to the ^{31}P nuclei of the diphos ligand. However, if this were the case the resonance pattern of protons 3 and 4 in the region of fast 3–4 exchange should consist of a doublet of triplets owing to coupling to H^5 and two equivalent ^{31}P nuclei. In fact the resonance pattern consists of a broad 1:2:1 triplet owing to coupling to H^5 and the *trans* ^{31}P nucleus.

Can. J. Chem. Downloaded from www.nrcresearchpress.com by 210.87.254.40 on 09/05/12
For personal use only.

Can. J. Chem. Downloaded from www.nrcresearchpress.com by 210.87.254.40 on 09/05/12
For personal use only.

The above p.m.r. data shows that phosphorus coupling to the terminal allylic protons is retained during the rapid *syn–anti* proton exchange process for each diphos–chloride system studied. This is consistent with bidentate coordination of diphos to palladium throughout the exchange process and the absence of site exchange for the terminal allylic carbons with respect to diphos. Retention of ^{31}P coupling to the allylic protons indicates that the allylic group is π-bonded to palladium a majority of the time. The close correlation of p.m.r. data (J(P–H), J(H–H)) in Tables 2 and 3 also suggests a structural similarity between the cationic species in complexes **4** and **5** and the major solution species in the analogous diphos–chloride systems. As such we propose that the major solution species in the diphos–chloride systems is **10** in which the chloride ligand occupies a fifth coordination site along the z-axis of the coordination plane, (*i.e.*, the chloride ion is closely associated with palladium, rather than being solvated by chloroform; species **10** may be considered as a contact ion pair, or a square pyramidal, five coordinate complex with a weak Pd—Cl bond in the axial position). The structure of **10** is analogous to the solid state structure of [(π-2-methylallyl)NiBr(diphos)] as determined by X-ray crystallography (11). This complex is square pyramidal with Br occupying an axial position. The Ni—Br bond length of 2.671 ± 0.002 Å is unusually long and may be equated with ionic character. That the Pd—Cl bond in **10** is weak is corroborated by conductivity studies of these systems in polar solvents such as acetone in which the ionic species **11** are formed:

$$[(\pi\text{-all})\text{Pd(diphos)Cl}] \underset{\longleftarrow}{\xrightarrow{\text{polar solvent S}}} [(\pi\text{-all})\text{Pd(diphos)}]^{+}(S)_x + Cl^{-}(S)_y$$

10 **11**

Previously Vrieze and co-workers (3) have shown that salt formation in π-2-methylallyl palladium chloride – triphenylphosphine systems in chloroform was only significant at very low temperatures. Therefore, owing to the poor solvation properties of chloroform at higher temperatures (34°), it is likely that the chloride ligand is not completely solvated but closely associated with palladium as formulated in **10**. The broadening of the allylic proton resonances, as observed in the p.m.r. of these systems at −60°, could possibly be attributed to salt formation such as **11**.

The far infrared spectrum of an equimolar mixture of (π-2-methylallyl) palladium chloride and diphos in chloroform does not show any strong absorptions in the region 325–250 cm^{-1} (see Table 4). This further substantiates the p.m.r. evidence that a normal "in plane" Pd—Cl bond is no longer present (ν(Pd—Cl) = 281 cm^{-1} in [(2-methylallyl)PdClPPh$_3$] (5)) and is consistent with the formulation of **10** as the major solution species.

With **10** as the major solution species, Scheme 2 depicts the proposed mechanism of *syn–anti* proton exchange in the diphos–chloride systems. The formation of a short-lived σ-allylic intermediate **12** is effected by the nucleophilic attack of the axial chloride on the substituted terminal allylic carbon. The π-allylic complex may be reformed in one of two ways thereby effecting site exchange of protons 3 and 4. By this mechanism, *cis* and *trans* ^{31}P coupling to the terminal protons is preserved. This mechanism is analogous to that proposed for the pyridine promoted exchange of protons 3 and 4 in the hexafluorophosphate salts (Scheme 1).

The initiation of *syn–anti* proton exchange by the solvent chloroform can be excluded on the basis that no proton exchange processes occurred for the analogous complexes **3–8** in chloroform in the absence of pyridine.

When an approximate equimolar amount of [(π-all)Pd(diphos)Cl] is added to $CDCl_3$ solutions of its [(π-all)Pd(diphos)]$^{+}PF_6^{-}$ analog equivalence of all the *syn*-protons and equivalence of all the *anti*-protons is observed together with *syn–anti* proton site exchange. This indicates that intermolecular exchange of chloride ion is fast on the n.m.r. time scale.

Further Investigations of Tertiary Phosphine Promoted Proton Exchange Mechanisms in Complexes of the Type [(π-all)PdCl(PR$_3$)]

The correlation between pyridine and chloride in terms of their nucleophilicity toward the π-allylic–palladium bond strongly suggests that analogous substitution processes should be important in dynamic (π-all) palladium chloride – mono tertiary phosphine systems.

The p.m.r. spectrum for the adduct of (π-1,1-dimethylallyl) palladium chloride with 2PMe$_2$Ph per Pd (prepared *in situ*) was recorded at several temperatures. At −50°, protons 3 and 4 appear as distinct though very broad resonances while proton 5 is a 1:2:1 triplet (J(H_5–$H_{3,4}$) = 10 cs^{-1})

TABLE 4. Far infrared data (400–250 cm^{-1}) for complexes of the type [(π-all)PdCl(L)] and the effect of excess L on the intensity of ν(Pd–Cl). Spectra recorded in 0.1*M* $CHCl_3$ solution at 31°

Complex	Far i.r. absorptions (400–250 cm^{-1})*	Added ligand (one mol per Pd)	Decrease in intensity of ν(Pd—Cl)(±5%)	Comments
[(π-2-Methylallyl)PdCl-(PMe_2Ph)]	360–340bm, *281s*	PMe_2Ph	95%	
[(π-2-Methylallyl)Pd-Cl(PPh_3)]	388w, *282s*	PPh_3	50%	Addition of *ca.* 4PPh_3/Pd eliminates ν(Pd—Cl) (No new absorptions in region 350–250 cm^{-1})
[(π-2-Methylallyl)Pd-Cl($AsPh_3$)]	382m, 338s, 326s, *283s*	$AsPh_3$	0%	Addition of *ca.* 3$AsPh_3$/Pd has no effect on intensity of ν(Pd—Cl)
[(π-1,1-Dimethylallyl)-PdCl(PMe_2Ph)]	379w, 354w, *274s*	PMe_2Ph	70%	Addition of 3PMe_2-PhP/Pd eliminates ν-(Pd—Cl) (No new absorptions in region 350–250 cm^{-1})
[(π-1,1-Dimethylallyl)-PdCl(PPh_3)]	376w, 366vw, *276s*	PPh_3	0%	
[(π-2-Methylallyl)Pd-(diphos)]PF_6	387m, 361w, 357w, 330vw			
[(π-2-Methylallyl)Pd-(diphos)Cl]	386m, 360w, 357w, 332vw			

*ν(Pd—Cl) in italics.

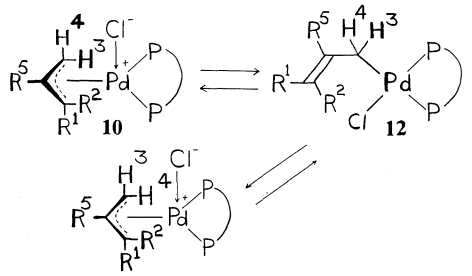

SCHEME 2. Mechanism of chloride promoted exchange of protons 3 and 4 in [(π-all)Pd(diphos)Cl].

i.e. 3–4 exchange prior to coalescence (Fig. 6(*a*)). Although partially overlapped by the methyl phosphine resonances, the *syn* and *anti* methyl protons are strongly coupled to both *cis* and *trans* ^{31}P nuclei (shaded area in Fig. 6), *anti* methyl protons: τ 8.65, *cis* and *trans* $J(P) = 6.5$ and 6.5 c s^{-1}; *syn* methyl protons: τ 8.25, *cis* and *trans* $J(P) = 10.5$ and 7 c s^{-1}. Two sharp doublets (each of relative intensity six), assigned to the methyl protons of the PMe_2Ph ligands, are observed at τ 8.50 and 8.08. Because 3–4 proton exchange is occurring at this temperature, the two methyl groups on the *same* PMe_2Ph ligand should be equivalent on the p.m.r. time scale and as such, should exhibit only one resonance instead of two. (Two Me_2PhP methyl resonances are observed for [(π-2-methylallyl)-PdCl)Me_2PhP)] in the region of no *syn–anti*

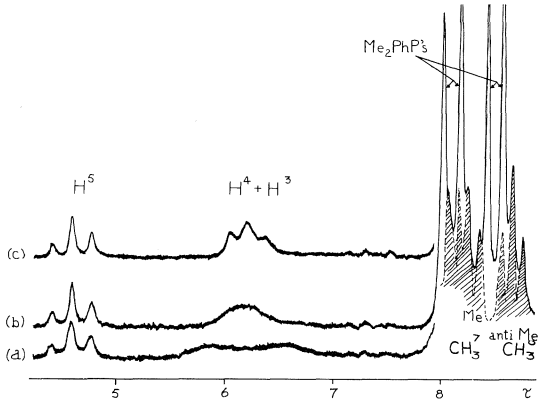

FIG. 6. The ^1H n.m.r. spectra of a 0.44 *M* $CDCl_3$ solution of [Me_2C⋯CH⋯CH_2)Pd($Me_2PhP)_2Cl$] **13** (see Scheme 3) (*a*) at −50°; (*b*) at −40°; (*c*) at −35° (compare with Fig. 5*a* and Fig. 2*c*).

Can. J. Chem. Downloaded from www.nrcresearchpress.com by 210.87.254.40 on 09/05/12
For personal use only.

Can. J. Chem. Downloaded from www.nrcresearchpress.com by 210.87.254.40 on 09/05/12
For personal use only.

proton exchange (6).) Thus the existence of two Me_2PhP doublet absorptions must indicate that each PMe_2Ph ligand is in a unique chemical environment with respect to each other.

At $-40°$, resonances 3 and 4 coalesce into a very broad singlet whereas *cis* and *trans* ^{31}P coupling to the terminal methyl protons is retained; both PMe_2Ph doublets remain sharp (Fig. 6(*b*)). At $-35°$, the resonance of protons 3 and 4 sharpens to a broad triplet ($J_5 = 10\,c\,s^{-1}$; J_P *trans* $\sim 9\,c\,s^{-1}$), whilst the terminal methyl protons, though slightly broadened, remain coupled to the *cis* and *trans* ^{31}P nuclei of the PMe_2Ph ligands. Again, the two methyl doublets of the PMe_2Ph ligands remain sharp (Fig. 6(*c*)).

At higher temperatures (above $-20°$), PMe_2Ph ligand exchange occurs as evidenced by the collapse of the Me_2PhP methyl doublets to a single broad peak (^{31}P coupling to the allylic protons is lost, the terminal methyl proton resonances become sharp singlets and protons 3 and 4 give rise to a sharp doublet ($J_5 = 10\,c\,s^{-1}$)).

Below $-35°$, the coupling pattern of the terminal methyl protons (*cis* and *trans* ^{31}P coupling) is very similar to that observed in complex **5** (Table 1, Fig. 2) in which the bidentate diphos ligand is coordinated in the square plane. By direct analogy, then, two PMe_2Ph ligands (corresponding to two sharp doublets in the p.m.r.) must occupy two *cis* coordination sites in the square plane. The presence of *trans* ^{31}P coupling to the p.m.r. equivalent protons, 3 and 4, at $-35°$ (Fig. 6(*c*)) together with the retention of *cis* and *trans* ^{31}P coupling to the terminal methyl protons indicates that the 1,1-dimethylallyl ligand is π-bonded to palladium a majority of the time, that *syn–anti* proton exchange occurs with retention of the terminal allylic carbon sites relative to the Me_2PhP ligands, and that the PMe_2Ph ligands remain coordinated to Pd throughout the rapid *syn–anti* proton exchange process (below $-20°$).[3]

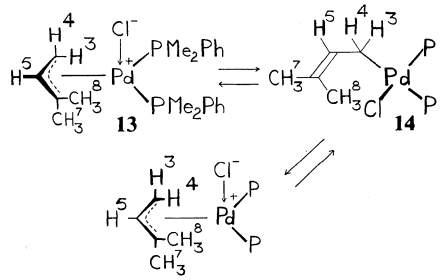

SCHEME 3. Mechanism of chloride promoted exchange of protons 3 and 4 in $[(Me_2C{=}CH{=}CH_2)Pd(Me_2PhP)_2Cl]$ (**13**).

The marked similarity in the p.m.r. data for the 1,1-dimethylallyl systems, **5** + pyridine, (**10**; $R^1 = R^2 = Me$; $R^5 = H$), and the "(π-1,1-dimethylallyl)PdCl – $2Me_2PhP$" adduct, clearly substantiates **13** as the major solution species for the latter system. (**13** is structurally analogous to **5** and **10**.) Thus when Me_2PhP is added to [(π-1,1-dimethylallyl)PdCl(Me_2PhP)] the chloride ligand is substituted by the added phosphine to give **13**. The observed *syn–anti* proton exchange can be explained by Scheme 3 which is analogous to Schemes 2 and 1, *i.e.*, nucleophilic substitution of the π-1,1-dimethylallyl ligand by the *chloride ligand* gives a short-lived σ-1,1-dimethylallyl ligand **14**. This process reforms a π-allylic complex in one of two ways thereby effecting *syn–anti* proton exchange whilst retaining distinct *cis* and *trans* ^{31}P coupling to the 1,1-dimethylallyl ligand, and stereochemically distinct Me_2PhP ligands.

At higher temperatures Me_2PhP ligand exchange in **13** is observed and this could involve Cl^- substitution of a coordinated Me_2PhP ligand to give either **15** or **16**:

[2] $[\pi\text{-(1,1-dimethylallyl)Pd(Me}_2\text{PhP)}_2\text{Cl}]$ (**13**) $\overset{\text{fast}}{\rightleftharpoons}$ (**15**) + PMe_2Ph

13 $\overset{\text{fast}}{\rightleftharpoons}$ (**16**)

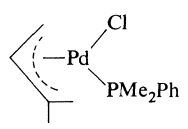

16

[3]What at first seemed a pertinent example to this study was a previous report (5) that, at 34°, the addition of PPh_3 (up to 16%) to [(π-1,1-dimethylallyl)PdCl(PPh_3)], in $CHCl_3$, effected rapid *syn–anti* proton exchange whilst retaining ^{31}P coupling to the terminal methyl protons. However, repeated attempts by us to reproduce these results proved unsuccessful.

Can. J. Chem. Downloaded from www.nrcresearchpress.com by 210.87.254.40 on 09/05/12
For personal use only.

This process is analogous to the Me_2PhP catalyzed exchange of Me_2PhP ligands in *cis*–$[MCl_2(Me_2PhP)_2]$ (M = Pd, Pt) which also occurs via consecutive $Me_2PhP \rightarrow Cl$ and $Cl^- \rightarrow$ coordinate Me_2PhP S_N2 ligand substitutions (12, 13). However, this mechanism may not be responsible for the observed Me_2PhP exchange as it involves formation of the thermodynamically less stable mono-phosphine complex **16**. Dissociation of **13** to give a small amount of **15** and free Me_2PhP followed by direct substitution of coordinated Me_2PhP by free Me_2PhP would be an equally plausible alternative. Unlike **13**, the p.m.r. spectrum of the (*syn*-1-tert-butyl-2-methylallyl)-palladium chloride – $2Me_2PhP$ adduct (prepared *in situ* in $CDCl_3$) at $-50°$ contains very broad Me_2PhP methyl proton resonances which is indicative of rapid Me_2PhP ligand exchange. Additional peaks in the spectrum suggest the formation of an appreciable amount of the *anti* isomer (*t*-Bu group in the *anti* position). Unlike the 1,1-dimethylallyl analogue, rapid *syn–anti* proton exchange along with retention of *cis* and *trans* ^{31}P coupling could not be discerned owing to the rapid phosphine ligand exchange occurring at temperatures as low as $-50°$. It is probable that steric interactions between the tert-butyl group and the *cis*-Me_2PhP ligand facilitates Me_2PhP exchange.

From the above p.m.r. studies several unifying features are apparent: (*i*) Rapid *syn–anti* proton site exchange is consistently explained by a $\pi \rightarrow \sigma \rightarrow \pi$ exchange mechanism involving a series of ligand substitution processes; (*ii*) for each system studied, the major solution species is postulated to have two phosphorus atoms (either diphos or $2PMe_2Ph$) in the square plane which remain inert to substitution during 3–4 proton exchange (this proposal is corroborated by the observance of *cis* and *trans* ^{31}P coupling throughout the occurrence of 3–4 proton exchange); (*iii*) the initiation step of 3–4 proton exchange is believed to be a nucleophilic substitution by a donor ligand (pyridine or chloride) at a Pd—C bond followed by a reverse substitution of the donor ligand by the allyl group. Furthermore addition of Me_2PhP to [(π-1,1-dimethylallyl)Pd-Cl(Me_2PhP)] results in the substitution of a Pd—Cl bond by Me_2PhP to give **13**. The extent to which such substitution occurs may be assessed by monitoring the change in intensity of ν(Pd—Cl) on addition of one PR_3/Pd to [(π-all)PdCl(PR_3)] in $CHCl_3$ at 31° (see Table **4**).

The addition of one Me_2PhP per Pd to a solution of [(π-2-methylallyl)PdCl(Me_2PhP)] (**1**; PR_3 = Me_2PhP) in $CHCl_3$ results in the complete disappearance of the ν(Pd—Cl) absorption at 282 cm^{-1}. The absence of an absorption band assignable to a ν(Pd—Cl) mode in the region 340 to 250 cm^{-1} indicates the absence of an "in plane" Pd—Cl bond. Thus the major solution species is the complex [(π-2-methylallyl)Pd(Me_2PhP)$_2$Cl] (**17**; PR_3 = Me_2PhP) (see Scheme 4) which is structurally analogous to **13** and **10** (**10**; R^1 = R^2 = H; R^5 = Me). The presence of a weak absorption at 274 cm^{-1} assignable to an in plane Pd—Cl bond in the infrared spectrum of [(π-1,1-dimethylallyl)Pd(Me_2PhP)$_2$Cl] in $CHCl_3$ at 34° is probably due to partial dissociation of an Me_2PhP ligand from **13** to give a small amount of **15** {ν(Pd—Cl) = 274 cm^{-1}} and free Me_2PhP (reaction 2; N.B. Me_2PhP ligand exchange is observed in the p.m.r. of **13** at 34°).

The addition of one PPh_3 per Pd to [(π-2-methylallyl)PdCl(PPh_3)] (**17**; PR_3 = PPh_3) decreased the intensity of the ν(Pd—Cl) absorption by *ca.* 50%. Therefore at 34° **17** and **1** (**1**; PR_3 = PPh_3) are present in *ca.* equal amounts. An addition of *ca.* 4 molecules PPh_3 per Pd atom to **1** completely eliminates the ν(Pd—Cl) absorption of **1** from the infrared spectrum as the equilibrium conditions now favor **17**. Addition of excess $AsPh_3$ to $CHCl_3$ solutions of [(π-2-methylallyl)-PdCl($AsPh_3$)] has no effect on the observed intensity of the ν(Pd—Cl) of this complex. Thus the tendency for the added ligand to give square pyramidal species of the type **17** decreases in the order $PMe_2Ph > PPh_3 > AsPh_3$. Species **17** is an intermediate in the formation of solvated ionic species. The ability of these ligands to promote salt formation also decreases in the order $PMe_2Ph > PPh_3 > AsPh_3$ (14).

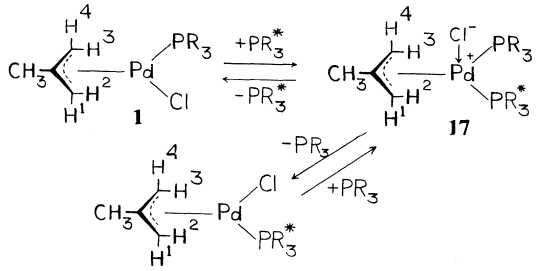

SCHEME 4. Consecutive displacement mechanism for the PR_3 promoted exchange of *syn* protons 1 and 4 with simultaneous exchange of *anti* protons 2 and 3 in the complexes [(π-2-methylallyl)PdCl(PR_3)].

The Mechanism of PR_3 Promoted Syn–Syn and Anti–Anti Proton Exchange in [(π-2-methylallyl)PdCl(PR_3)]

Our studies have shown that an added PR_3* ligand may substitute a Pd—Cl bond in [(π-2-methylallyl)PdCl(PR_3)] (**1**) to give the square pyramidal species **17** with an axial Cl ligand. Furthermore studies of *syn–anti* proton exchange in **10** and **13** have shown that consecutive S_N2 ligand substitutions involving Cl^- as a nucleophile occur very rapidly in such systems. As such the mechanism of PR_3* promoted *syn–syn* {1–4} with simultaneous *anti–anti* {2–3} proton site exchange in the complexes [(π-2-methylallyl)PdCl(PR_3)] **1** may be reconsidered in terms of the consecutive ligand substitution processes outlined in Scheme 4. Substitution of the Pd—Cl bond in **1** by PR_3* results in formation of **17**. The axial Cl^- ligand in **17** may displace either PR_3 or PR_3* with equal probability to give either **1** or **1′** thereby effecting 1–4 and 2–3 proton site exchange. Scheme 4 is very similar to the mechanism of PR_3 catalysed *cis–trans* isomerization of [$MCl_2(PR_3)_2$] (M = Pd, Pt) which also occurs via consecutive $PR_3 \rightarrow$ Cl and $Cl^- \rightarrow PR_3$ substitutions (12, 13, 15).[4]

Summary

The mechanisms of PR_3 promoted *syn–anti* proton exchange and PR_3 promoted *syn–syn* and *anti–anti* proton exchange in an extensive series of π-allylic palladium(II) – tertiary phosphine systems may be consistently and adequately explained in terms of consecutive S_N2 ligand substitutions, the lability of which are no doubt governed by the normal *trans*-influences observed in square planar d^8 complexes. Since the ease of formation of a σ-allylic intermediate depends in part on the nature and position of the alkyl substituents the observed behavior for a series of structurally similar π-allylic systems will also be a function of the alkyl substituents on the allylic ligand. Thus for example, addition of PR_3 to **1** promotes *syn–syn* and *anti–anti* proton exchange prior to *syn–anti* proton exchange and this may in part be ascribed to the relative unreactivity of the π-2-methylallyl ligand towards substitution by a nucleophile (*e.g.* Cl^-). However, *syn–anti* proton exchange is observed prior to any exchange of allylic terminal carbon sites when the π-allylic ligand has terminal alkyl substituents owing to the relative ease of formation of the σ-allylic intermediates.

Conclusions

The bulk of experimental data now available support the postulate that the ligand promoted *syn–syn* and *anti–anti* proton site exchange in π-allylic palladium(II) complexes occurs via consecutive S_N2 ligand substitutions (7, 8, 17). No firm experimental data exist which support a rotational mechanism. Thus if rotation of a π-allylic ligand about the π-allyl–Pd bond occurs at all it must be regarded as a high energy process and as such may be excluded from considerations of possible reaction pathways for palladium(II) catalyzed oligomerization reactions of unsaturated hydrocarbons.

Experimental

Proton magnetic resonance spectra were recorded on Varian Associates Model A 56/60 or HA 100 spectrometers; temperature calibrations were made using a reference methanol sample (Varian 943346-06). Infrared spectra were recorded on a Perkin–Elmer 180 spectrophotometer. Melting points were determined on a Kofler hot-stage apparatus.

π-Allylic palladium chloride complexes (π-all = allyl, 2-methyl, 1,1-dimethylallyl, and 1-methyl) were prepared by the method of Dent, Long, and Wilkinson (18). (*syn*-1-tert-Butyl-2-methylallyl)palladium chloride and (2-tert-butylallyl)palladium chloride were prepared by the method of Volger (19).

1,2-Bisdiphenylphosphinoethane(π-syn-1-tert-butyl-2-methylallyl)palladium(II) Hexafluorophosphate

(π-*syn*-1-tert-Butyl-2-methylallyl)palladium chloride (0.40 g) and (0.63 g) diphos were dissolved in 15 ml chloroform. Ammonium hexafluorophosphate (1.4 g) was added and the resultant mixture shaken for 24 h. The reaction mixture was filtered and evaporated to dryness, yielding a pale yellow oily residue. Addition of methanol gave a white solid which recrystallized from methanol as white prisms (0.90 g; 75%), m.p. 214–220°.

Anal. Calcd. for $C_{34}H_{39}F_6P_3Pd$: C, 53.66; H, 5.16. Found: C, 53.57; H, 5.21.

The following compounds were prepared in a similar fashion.

1,2-Bisdiphenylphosphinoethane(π-1,1-dimethylallyl)-palladium(II) Hexafluorophosphate

Recrystallized from chloroform–hexane solution as white prisms (0.80 g; 76%), m.p. 111–114°.

Anal. Calcd. for $C_{31}H_{33}F_6P_3Pd.CHCl_3$: C, 45.84; H, 4.08. Found: C, 46.06; H, 4.24.

The presence of one $CHCl_3$ solvent molecule per Pd atom was confirmed by p.m.r. studies in $CDCl_3$.

[4]The recent proposal (16) that the PR_3 catalyzed *cis–trans* isomerization of [$PtCl_2(PR_3)_2$] occurs via a pseudo rotation of a five coordinate intermediate has been shown to be incorrect (12).

Can. J. Chem. Downloaded from www.nrcresearchpress.com by 210.67.234.46 on 09/09/12
For personal use only.

1,2-Bisdiphenylphosphinoethane(π-1-methylallyl)palladium (II) Hexafluorophosphate

Recrystallized from methanol as white prisms (0.62 g; 83%), m.p. 175–177°.

Anal. Calcd. for $C_{30}H_{31}F_6P_3Pd$: C, 51.12; H, 4.43. Found: C, 51.21; H, 4.61.

1,2-Bisdiphenylphosphinoethane(π-allyl)palladium(II) Hexafluorophosphate

Recrystallized from methanol as white needles (0.43 g; 70%), m.p. 170–172°.

Anal. Calcd. for $C_{29}H_{29}F_6P_3Pd$: C, 50.41; H, 4.23. Found: C, 50.48; H, 4.29.

1,2-Bisdiphenylphosphinoethane(π-2-tertbutylallyl)-palladium(II) Tetrafluoroborate

Sodium tetrafluoroborate was used in place of ammonium hexafluorophosphate. The product crystallized from chloroform–hexane as white needles (0.65 g; 90%), m.p. 216–220°.

Anal. Calcd. for $C_{33}H_{37}BF_4P_2Pd.CHCl_3$: C, 45.84; H, 4.08. Found: C, 46.06; H, 4.24.

This work received financial support from the National Research Council of Canada.

1. J. Powell, S. D. Robinson, and B. L. Shaw. Chem. Commun. 78 (1965).
2. K. Vrieze, C. MacLean, P. Cossee, and C. W. Hilbers. Rec. Trav. Chim. Pay-Bas, **85**, 1077 (1966).
3. K. Vrieze, P. Cossee, A. P. Praat, and C. W. Hilbers. J. Organomet. Chem. **11**, 353 (1968).
4. K. Vrieze, A. P. Praat, and P. Cossee. J. Organomet. Chem. **12**, 533 (1968).
5. J. Powell and B. L. Shaw. J. Chem. Soc. (A), 1839 (1967).
6. P. W. N. M. van Leeuwen and A. P. Praat. Chem. Commun. 365 (1970).
7. D. L. Tibbetts and T. L. Brown. J. Am. Chem. Soc. **92**, 3031 (1970).
8. J. Powell and A. W-L. Chan. J. Organomet. Chem. **35**, 203 (1972).
9. E. M. Shustorovitch and M. E. Dyatkina. Dokl. Akad. Nauk. SSSR, **128**, 1234 (1959).
10. J. Powell. J. Chem. Soc. (A), 2233 (1971).
11. M. R. Churchill and T. A. O'Brien. Chem. Commun. 246 (1968); J. Chem. Soc. (A), 207 (1970).
12. D. G. Cooper and J. Powell. J. Am. Chem. Soc. To be published.
13. D. G. Cooper and J. Powell. To be published.
14. J. Powell and B. L. Shaw. J. Chem. Soc. (A), 774 (1968).
15. F. Basolo and R. G. Pearson. Mechanisms of inorganic Reactions. 2nd ed. Wiley, New York, New York. 1967. p. 423.
16. P. Haake and R. M. Pfeiffer. J. Am. Chem. Soc. **92**, 4996 and 5234 (1970); Chem. Commun. 1330 (1969).
17. E. Ban, A. Chan, and J. Powell. J. Organomet. Chem. **34**, 405 (1972).
18. W. T. Dent, R. Long, and A. J. Wilkinson. J. Chem. Soc. 1585 (1964).
19. H. C. Volger. Rec. Trav. Chim. Pay-Bas, **87**, 225 (1968).

Can. J. Chem. Downloaded from www.nrcresearchpress.com by 210.87.254.40 on 09/05/12
For personal use only.

Etude de quelques polymères obtenus lors de la déshydratation en système statique d'alcools allyliques disubstitués

CLAUDE ROUX ET HUBERT DAOUST

Département de chimie, Université de Montréal, Montréal, Québec

Reçu le 2 mars 1972

Les dioléfines produites lors de la déshydratation thermique en système statique d'alcools allyliques disubstitués se polymérisent simultanément à la déshydratation en donnant des polymères de bas poids moléculaires et dont la microstructure se compare à celle des polymères thermiques de diènes-1,3. Les masses moléculaires moyennes en nombre et en poids, le volume spécifique partiel et la distribution des masses ont été étudiés pour le polymère obtenu lors de la déshydratation du méthyl-3 butène-2 ol ou alcool diméthyl-3,3 allylique.

Diolefins, produced by thermal dehydration of disubstituted allyl alcohols in a static system, polymerize as they are formed giving low molecular weight polymers. The microstructure of the product is similar to that of thermal polymers of 1,3-dienes. Number- and weight-average molecular weights, partial specific volumes, and molecular weight distributions have been studied for the polymers obtained from 3-methyl-2-butene-1-ol and 3,3-dimethyl-allyl alcohol.

Can. J. Chem., **51**, 288 (1973)

Introduction

Le méthyl-3 butène-2 ol joue un rôle très important dans l'élaboration du caoutchouc naturel par l'Hevea Brasiliensis, et Lynnen et Henning (1) ont montré qu'en fait, il intervient comme premier maillon de la chaîne polyisoprénique sous la forme d'ester pyrophosphorique. La réaction de polymérisation serait amorcée par le pyrophosphate de méthyl-3 butène-2 yle, le monomère étant le pyrophosphate de méthyl-3 butène-3 yle.

Malgré toute la séduction que présente la possibilité de reproduction *in vitro* d'une telle réaction, un examen approfondi des conditions d'obtention de ces pyrophosphates d'une part et le mécanisme de polymérisation d'autre part, conduit à une impasse certaine (1).

Néanmoins, le radical alcényle du pyrophosphate responsable de l'amorçage de la réaction de polymérisation *in vivo* et plus généralement, la structure allylique disubstituée en position 3 est digne d'intérêt.

Le présent travail se rapporte donc à l'étude des polymères obtenus lors de la déshydratation thermique en système statique d'alcools allyliques disubstitués en position 3, tant du point de vue de la microstructure que de celui des masses moléculaires et de leur distribution. Ces alcools sont: le méthyl-3 butène-2 ol, les *cis* et *trans* méthyl-3 pentène-2 ols, le triméthyl-3,4,4 pentène-2 ol, et l'éthyl-3 pentène-2 ol.

Partie expérimentale

La déshydratation des alcools et la polymérisation des diènes produits ont lieu simultanément, en tubes de verres scellés sous vide, chauffés en étuve régulée à ± 1 °C à des températures variant de 150–210 °C; une étude cinétique de ce type de réaction est décrite ailleurs (2).

Les alcools, selon des quantités disponibles (3–25 g environ) sont placés dans des tubes de verre pyrex préalablement lavés et séchés soigneusement. Les tubes sont ensuite plongés dans l'azote liquide puis scellés sous un vide de l'ordre de 10^{-4} mm Hg; ils sont par la suite chauffés pendant des temps variant de 3–4 jours à 207 °C. La récupération des polymères a lieu de la façon suivante: les produits de la réaction sont dilués dans environ deux fois leur volume de chlorure de méthylène; la phase aqueuse est décantée et la phase organique traitée par le méthanol. Les polymères précipitent et le liquide surnageant est décanté. Ces opérations sont faites au total trois fois. Les polymères sont ensuite séchés sous vide. A la température ambiante, ils se présentent, une fois secs, sous forme de masses liquides très visqueuses translucides qu'il est nécessaire de conserver sous vide ou sous azote pour en éviter l'oxydation. Parmi les produits de décomposition du méthyl-3 butène-2 ol, il a été également trouvé de l'isoprène; p.é. 34–35°/760 mm Hg; n_D^{22} 1.4205. L'analyse par c.p.g. a révélé la présence, dans le liquide après précipitation, de 23 espèces différentes d'hydrocarbures éthyléniques ou poly-éthyléniques bouillant vers 180 °C sous 25 mm Hg.

Les spectres d'absorption i.r. ont été effectués soit sur appareil Beckman IR-8 soit sur appareil Perkin–Elmer 700 à partir de films obtenus de solutions.

Les spectres de r.m.n. ont été effectués sur appareil JNM-4H-100 ou C 60H de Japan Electron Optics Lab. Co. Ltd. ou sur appareil Varian T-60, le solvant utilisé est soit le benzène soit le tétrachlorure de carbone; la référence interne est le tétraméthylsilane (TMS).

Can. J. Chem. Downloaded from www.nrcresearchpress.com by 210.87.254.5 on 09/05/12
For personal use only.

Can. J. Chem. Downloaded from www.nrcresearchpress.com by 210.87.254.5 on 09/05/12
For personal use only.

La masse moléculaire moyenne en nombre a été déterminée d'une part par tonométrie sur appareil Mechrolab 301-A, le solvant étant le chloroforme, la température de l'enceinte étant de 37 °C, et d'autre part par calcul à partir de la distribution des masses par ultracentrifugation à l'équilibre, en utilisant une ultracentrifugeuse analytique Spinco modèle E-HT.

La masse moléculaire moyenne en poids a été déterminée par ultracentrifugation sur le même appareil.

Synthèse des alcools

Méthyl-3 butène-2 ol

La synthèse de cet alcool a été effectuée selon la méthode décrite par Hellin et coll. (3). Le spectre r.m.n. est celui du produit attendu; p.é. 141–142°/759 mm Hg; n_D^{21} 1.4340.

cis et trans Méthyl-3 pentène-2 ols

La réduction par l'hydrure de lithium aluminium des esters éthyliques des acides correspondants (8) fournit le mélange de ces deux alcools avec un rendement de 84%, en un produit bouillant à 80 °C sous 40 mm Hg; ces deux composés n'ont pas été séparés. Le spectre r.m.n. est celui des produits attendus.

Triméthyl-3,4,4 pentène-2 ol

La méthode utilisée pour la synthèse des méthyl-3 pentène-2 ols a été étendue à la synthèse de cet alcool. Le rendement est voisin de 23%. Le spectre r.m.n. est celui du produit attendu; p.é. 90°/20 mm Hg; n_D^{23} 1.4451.

Ethyl-3 pentène-2 ol

Cet alcool a été obtenu avec un rendement de 88% en réduisant l'ester éthylique de l'acide correspondant par l'hydrure de lithium aluminium. Le spectre r.m.n. est celui du produit attendu; p.é. 176°/760 mm Hg; n_D^{24} 1.4492. L'ester fut préparé par réaction de Wittig de la diéthylcétone sur le carboéthoxyméthylènetriphénylphosphorane en tube scellé, sans solvant, avec un rapport molaire cétone–phosphorane égal à 5, à 170 °C, pendant 96 h; le rendement est supérieur à 85%.

Les réactifs utilisés au cours de ces synthèses sont de qualité analytique; la pureté des produits obtenus a été vérifiée par c.p.g. et par spectrographie de r.m.n.

Résultats

Il a été constaté que les alcools cités ci-dessus se déshydrataient et que dans les produits de déshydratation se trouvaient des polymères insolubles dans l'acétone, le méthanol et l'éthanol, solubles dans le benzène, le cyclohexane, le chloroforme, etc.

Microstructure des polymères

Polymère obtenu lors de la déshydratation du méthyl-3 butène-2 ol

Cet alcool se déshydrate en donnant de l'isoprène dont la polymérisation conduit aux types d'addition suivants: 1,4 *cis* ou *trans*, 1,2 et 3,4. Le spectre de r.m.n. à 100 MHz dans le benzène (fig. 1) permet de calculer approximativement le pourcentage de chacune de ces additions; il y

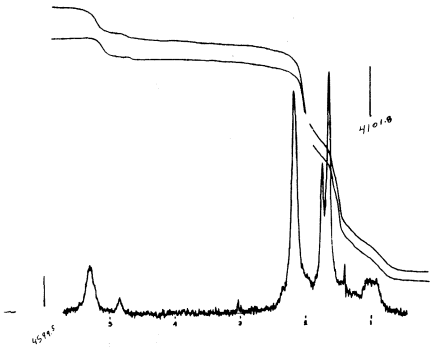

FIG. 1. Spectre à 100 MHz dans le benzène du polymère obtenu lors de la déshydratation du méthyl-3 butène-2 ol.

aurait approximativement (4–7): 53–54% de structure 1,4 *trans*; 23–24% de structure 1,4 *cis*; 2–3% de structure 1,2; 18–19% de structure 3,4.

Le spectre r.m.n. à 100 MHz dans le tétrachlorure de carbone confirme ce résultat. Le spectre i.r. (850, 885, 900, 1080, 1350, 1400, 1670, 2900 cm^{-1}) semble confirmer la présence de ces types d'addition (5, 7) et révèle ici encore l'analogie avec un polyisoprène thermique (8).

Polymère obtenu lors de la déshydratation du mélange cis–trans méthyl-3 pentène-2 ols

Ces deux alcools se déshydratent en donnant deux sortes de dioléfines: le méthyl-3 pentadiène-1,3 et l'éthyl-2 butadiène-1,3.

Chacune de ces dioléfines peut donner plusieurs types d'addition, l'analyse quantitative de chacune n'a pu être faite. La fig. 2 représente le spectre de r.m.n. du polymère obtenu. Il est à noter qu'en spectrographie de r.m.n. le signal vers 4.60 p.p.m. caractéristique de l'addition 1,2 de l'éthyl-2 butadiène-1,3 ou de l'addition 3,4 du méthyl-3 pentadiène-1,3 est pratiquement inexis-

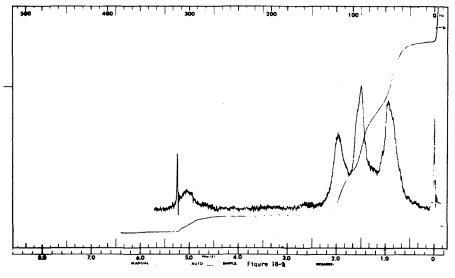

FIG. 2. Spectre de r.m.n. à 60 MHz dans le tétrachlorure de carbone du polymère obtenu lors de la deshydratation des *cis* et *trans* méthyl-3 pentène-2 ols.

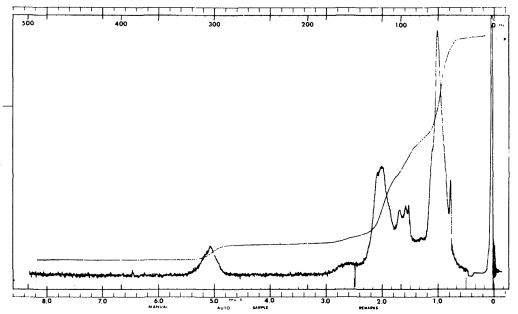

FIG. 3. Spectre de r.m.n. à 60 MHz dans le tétrachlorure de carbone du polymère obtenu lors de la déshydratation de l'éthyl-3 pentène-2 ol.

tant. Spectre i.r.: 800, 840, 870, 900, 1040, 1100, 1200, 1240, 1390, 1470, 1660, 1680, 2900 cm^{-1}.

Polymère obtenu lors de la déshydratation de l'éthyl-3 pentène-2 ol

Cet alcool se déshydrate en donnant l'éthyl-3 pentadiène-1,3 dont la polymérisation conduit à des additions 1,4 *cis* et *trans*, 1,2 et 3,4.

La fig. 3 représente le spectre de r.m.n. du polymère obtenu. Il est à noter ici également, que le signal vers 4.60 p.p.m., caractéristique de l'addition 3,4 de l'éthyl-3 pentadiène-1,3 est inexistant et que donc ce type d'addition semble exclu. Spectre i.r.: 800, 830, 900, 960, 1070, 1100, 1380, 1460, 1670, 1710, 2950 cm^{-1}.

Polymère obtenu lors de la déshydratation du triméthyl-3,4,4 pentène-2 ol

Cet alcool se déshydrate en donnant le tertiobutyl-2 butadiène-1,3 dont la polymérisation conduirait également à des additions 1,4 *cis* et *trans* 1,2 et 3,4. La fig. 4 représente le spectre de r.m.n. du polymère obtenu. L'interprétation du spectre de r.m.n. semble difficile à réaliser, néanmoins, hormis le signal inexpliqué à 7.05 p.p.m. (peut-être dû à une cyclisation) il semblerait que les trois structures 1,4, 3,4, et 1,2 soient présentes. Spectre i.r.: 800, 860, 900, 980, 1030, 1080, 1120, 1200, 1260, 1360, 1390, 1470, 1630, 1730, 2950 cm^{-1}.

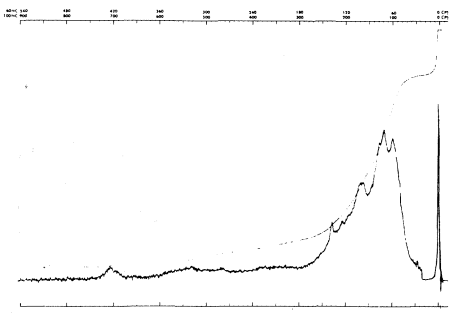

FIG. 4. Spectre de r.m.n. à 60 MHz dans le tétrachlorure de carbone du polymère obtenu lors de la déshydratation du triméthyl-3,4,4 pentène-2 ol.

Etude physico-chimique du polymère obtenu lors de la déshydratation du méthyl-3 butène-2 ol

Ce polymère a été obtenu lors de la déshydratation en système statique à 207 °C du méthyl-3 butène-2 ol. Sa masse moléculaire moyenne en nombre $\bar{M}_n$, déterminée par tonométrie, a été trouvée égale à 4750 $\pm$ 100 g mol^{-1}.

Volume spécifique partiel dans le cyclohexane de ce polymère

Cette détermination a été effectuée par la méthode dite du pycnomètre (9) à 25 $\pm$ 0.003 °C. Le graphique de la fig. 5 représente les variations de volume de la solution contenant 1000 g de solvant en fonction de la concentration massique (g/1000 g de solvant).

La pente de la courbe représentative de cette fonction, qui est ici une droite (domaine des faibles concentrations) conduit à la valeur du volume spécifique partiel $\bar{v}_2$ du polymère. Ce volume a été trouvé égal à: 0.99 $\pm$ 0.01 $cm^3\ g^{-1}$ et c'est cette valeur qui est utilisée dans les calculs relatifs à la sédimentation.

Masse moléculaire moyenne en poids

Cette détermination a été effectuée par ultracentrifugation du polymère en solution dans le cyclohexane, à 25 °C en utilisant la méthode de l'approche à l'équilibre et de la frontière synthétique (10, 11).

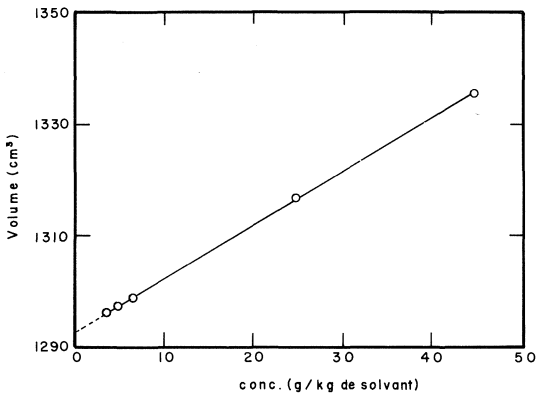

FIG. 5. Variation du volume de la solution contenant 1000 g de solvant en fonction de la concentration massique du polymère.

Can. J. Chem. Downloaded from www.nrcresearchpress.com by 210.87.254.5 on 09/05/12
For personal use only.

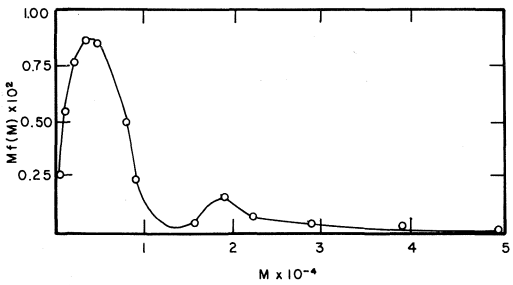

FIG. 6. Fonction de distribution en poids des masses moléculaires en fonction de la masse moléculaire (polymère obtenu lors de la déshydratation du méthyl-3 butène-2 ol).

La vitesse du rotor est de 25 980 t.p.m. La masse moléculaire moyenne en poids $\overline{M}_p$ a été calculée et trouvée égale à: 8650 ± 450 g mol^{-1}.

Distribution en poids des masses moléculaires (12–16)

La solution de polymère subit l'ultracentrifugation à 25 °C, pendant 48 h, à la vitesse de 42 040 t.p.m.

Le graphique de la fig. 6 représente la fonction de distribution en poids des masses moléculaires en fonction de la masse moléculaire.

Le calcul direct des masses moléculaires moyennes en nombre et en poids à partir de cette distribution donne comme résultats: $\overline{M}_n$ = 3 080; $\overline{M}_p$ = 7 700.

Le calcul de la masse moléculaire moyenne en poids à partir des données de l'équilibre de sédimentation (17) indique: $\overline{M}_p$ = 8 100.

Conclusion

Les polymères obtenus lors de la déshydratation en système statique d'alcools allyliques disubstitués en position 3 semblent présenter une microstructure anarchique analogue à celle des polymères thermique des diènes-1,3 avec vraisemblablement une prédominance de la structure 1,4 en configuration *trans*.

Les masses moléculaires moyennes en nombre et en poids sont faibles, la polydispersité évaluée par le rapport de $\overline{M}_p$ à $\overline{M}_n$ est relativement élevée et voisine de 2.5. La distribution en poids des masses moléculaires évaluée par ultracentrifugation est large, et il est possible de supposer qu'il existe un certain degré de branchement.

Les auteurs remercient le Conseil National de Recherches du Canada pour son aide financière au cours de cette étude. Ils remercient également le Dr. N. Ho-Duc pour sa collaboration concernant l'ultracentrifugation.

1. F. LYNNEN et L. HENNING. Angew. Chem. **72** (22), 820 (1960).
2. C. ROUX et H. DAOUST. Bull. Soc. Chim. Fr. 3332 (1972).
3. M. HELLIN, M. DAVIDSON, D. LUMBROSO, et F. COUSSMANT. Bull. Soc. Chim. Fr. 800, (1964).
4. F. ASSIOMA et J. MARCHAL. C.R. Acad. Sc. Paris. t226 série C, 195 (1968).
5. J. P. KISTLER, G. FRIEDMANN, et B. KAEMPF. Bull. Soc. Chim. Fr. 4759 (1967).
6. F. A. BOVEY. High resolution NMR of macromolecules. Academic Press, New York. N.Y. 1972.
7. Y. TANAKA, Y. TAKEUCHI, M. KOBAYASHI, et H. TADOKORO. J. Polym. Sci. Pt A2, **9**, 43 (1971).
8. Y. MORI, S. KONDO, et H. KUMAGAE. Nippon Kagaku Zasshi, **78**, 1174 (1957); C.A. **54**, 5484*f* (1960).
9. F. DANIELS, J. H. MATHEWS, J. W. WILLIAMS, P. BENDER, et R. A. ALBERTY. Experimental physical chemistry. 5th ed. McGraw-Hill, New York, N.Y. 1956. p. 86.
10. W. J. ARCHIBALD. J. Phys. Chem. **51**, 1204 (1947).
11. S. M. KLAINER et G. KEGELES. J. Phys. Chem. **59**, 952 (1955).
12. J. E. BLAIR. J. Polym. Sci. Pt C, **8**, 287 (1965).
13. T. G. SCHOLTE. J. Polym. Sci. Pt A2, **6**, 111 (1968).
14. T. G. SCHOLTE. Eur. Polym. J. **6**, 51 (1970).
15. A. YAMAMOTO, I. NODA et M. NAGASAWA. Polym. J. **1**, 304 (1970).
16. H. FUJITA. Mathematical theory of sedimentation analysis. Academic Press, New York, Londres. 1962.
17. T. G. SCHOLTE. J. Polym. Sci. Pt A2, **6**, 91 (1968).

Can. J. Chem. Downloaded from www.nrcresearchpress.com by 210.87.254.5 on 09/05/12
For personal use only.

Etude des dérivés sulfohydroxylés des halogénures de bore et des cycles dérivés du borsulfol I. Synthèses et mécanismes réactionnels

JEAN BOUIX ET ROGER HILLEL

Laboratoire de Physico-chimie minérale I, Associé au C.N.R.S. (Service du Professeur Cueilleron), Université Claude Bernard, 43, boulevard du 11 novembre 1918, 69 Villeurbanne, France

Reçu le 17 avril 1972

Par action du sulfure d'hydrogène sur un halogénure de bore autre que le fluorure, on obtient simultanément l'halogénure d'hydrogène correspondant et des dérivés de substitution nouveaux de formules BCl_2SH, BBr_2SH, $BBr(SH)_2$, BI_2SH, $BI(SH)_2$ et $B(SH)_3$.

Ces sulfohydroxohalogénoboranes sont instables et tendent à se cycliser soit en acide thioborique $(BSSH)_3$ soit en trihalogénoborsulfol $(BSX)_3$.

Dans le cas du bromure de bore, en contrôlant la composition du mélange de départ et la température de la réaction, il est possible de favoriser la formation de l'un des trois dérivés de substitution possibles et, en provoquant ensuite sa cyclisation, de préparer de façon rapide et sélective soit l'acide thioborique soit le tribromoborsulfol, ce dernier pouvant être obtenu très pur en opérant en absence de solvant.

La synthèse du trichloroborsulfol a été effectuée par dissolution de l'acide thioborique dans le chlorure de bore liquide et celle du triiodoborsulfol par action du sulfure d'hydrogène sur l'iodure de bore solide.

By the action of H_2S on boron halides (other than fluoride) one obtains the new substitution products BX_2SH, $BX(SH)_2$, and $B(SH)_3$ along with the corresponding hydrogen halide. These halogenosulfhydroboranes are unstable and cyclize to cyclic boron sulfides, either $(BSSH)_3$ or $(BSX)_3$.

In the case of boron bromide it is possible, by controlling the ratio of the reactants and the temperature of the reaction, to promote the formation of one of the three possible substitution products. Then by encouraging cyclization one may obtain, rapidly and selectively, either $(BSSH)_3$ or $(BSBr)_3$.

Synthesis of $(BSCl)_3$ was accomplished by dissolution of $(BSSH)_3$ in liquid BCl_3 and that of $(BSI)_3$ by the action of H_2S on solid BI_3. [Journal translation]

Can. J. Chem., **51**, 292 (1973)

L'action du sulfure d'hydrogène sur les halogénures de bore en absence de solvant ne donne lieu selon la littérature qu'à la formation de complexes d'addition tels que BCl_3, H_2S (1), et BCl_3, 12 H_2S (2), l'existence de ce dernier étant d'ailleurs problématique.

En remplaçant le sulfure d'hydrogène par le méthyl-mercaptan, Goubeau et Wittmeier (3) ont par contre obtenu des dérivés solides de substitution: BCl_2SCH_3, BBr_2SCH_3, $BBr(SCH_3)_2$, et $B(SCH_3)_3$. Ils préparent de plus ce dernier composé à l'état pur par action du bromure de bore sur des dérivés métalliques du mercaptan en solution dans du benzène et publient son spectre Raman, ainsi que celui du dérivé dibromé, probablement à l'état dimère. Le dérivé monobromé est par contre très instable, et son existence n'est pas certaine.

En faisant agir le sulfure d'hydrogène sur un halogénure de bore en solution dans le sulfure de carbone, Stock d'une part (4, 5) et Wiberg d'autre part (6, 7, 8) obtiennent l'acide thioborique $(BSSH)_n$ en présence d'un excès de sulfure d'hydrogène et le trihalogénoborsulfol $(BSX)_3$ en présence d'un excès d'halogénure de bore.

Notons que, dans certaines de ces réactions, Wiberg et ses collaborateurs supposent l'existence de dérivés de substitution tels que BCl_2SH (7) et BBr_2SH (9) mais n'apportent aucune preuve à l'appui de cette hypothèse.

En ce qui concerne la synthèse de l'acide thioborique, deux méthodes principales sont décrites dans la littérature: réaction à 800 °C du sulfure d'hydrogène dilué dans un courant d'hydrogène sur du bore (10, 11); action du sulfure d'hydrogène sur le bromure de bore en solution dans le sulfure de carbone suivant les réactions (6, 7, 8, 12, 13):

$$[1] \quad 3\ BBr_3 + 3\ H_2S \xrightarrow{CS_2} (BSBr)_3 + 6\ HBr$$

puis

$$[2] \quad (BSBr)_3 + 3\ H_2S \xrightarrow{CS_2} (BSSH)_3 + 3\ HBr$$

Cette synthèse dure trois semaines environ.

Comme il est impossible en pratique d'arrêter la réaction au premier stade, on prépare le trihalogénoborsulfol en traitant à reflux la solution sulfocarbonique d'acide thioborique par l'halogénure de bore correspondant, deux mécanismes étant proposés (12, 7):

Can. J. Chem. Downloaded from www.nrcresearchpress.com by 210.87.254.40 on 09/05/12
For personal use only.

Can. J. Chem. Downloaded from www.nrcresearchpress.com by 210.87.254.40 on 09/05/12
For personal use only.

[3] $(BSSH)_3 + 2\ BX_3 \rightarrow (BSX)_3 + 3\ HX + B_2S_3$

et

[4] $2(BSSH)_3 + 2\ BX_3 \rightarrow 2(BSX)_3 + 3\ H_2S + B_2S_3$

Dans le cas du dérivé iodé, Wiberg a de plus utilisé l'action en solution dans le sulfure de carbone d'un très grand excès d'iodure d'hydrogène sur l'acide thioborique (8, 18):

[5] $(BSSH)_3 + 3\ HI \rightarrow (BSI)_3 + 3\ H_2S$

Ces trihalogénoborsulfols sont des composés peu stables; en particulier le dérivé chloré se décompose dès la température ambiante en trichlorure et sulfure de bore (6, 7).

L'acide thioborique est instable au-dessus de 100 °C, et sa décomposition en sulfure d'hydrogène et en sulfure de bore est utilisée pour préparer ce dernier composé à l'état pur (13). A haute température, cette décomposition fournit également le trisulfohydroxoborane $B(SH)_3$, dérivé nouveau détecté par spectrométrie de masse et dont l'auteur a calculé le spectre i.r. (14). Le spectre i.r. de l'acide thioborique $(BSSH)_n$ avec $n = 1$ et 3 est connu (4, 14), ainsi que la structure cristalline du tribromoborsulfol (15).

Obtention des sulfohydroxohalogénoboranes en phase vapeur

Le spectre de masse des halogénures de bore gazeux, déterminé avec un faisceau d'électrons de 35 eV, comporte les pics des ions BX_3^+ et BX_2^+. En outre, il montre toujours la présence de l'halogénure d'hydrogène correspondant qui se manifeste par les pics des ions HX^+, H^+, et X^+. Dans les mêmes conditions, le sulfure d'hydrogène seul donne un spectre comportant les pics des ions H_2S^+, SH^+, et S^+ (*m/e* compris entre 32 et 36) ainsi que celui du proton.

Le spectre d'un mélange équimoléculaire de sulfure d'hydrogène et de fluorure de bore ne montre aucun pic nouveau par rapport à celui des réactifs de départ.

Par contre, si le fluorure de bore est remplacé par le chlorure, on remarque d'une part que l'intensité des pics de HCl augmente considérablement et d'autre part qu'il apparait deux massifs de pics nouveaux et peu intenses pour des rapports *m/e* compris entre 112 et 114 pour le premier et entre 77 et 79 pour le second, donc légèrement inférieurs à ceux des ions BCl_3^+ (entre 115 et 122) et BCl_2^+ (entre 80 et 85) provenant de BCl_3. Tous ces pics nouveaux atteignent simultanément leur intensité maximale pour un mélange de départ équimoléculaire. Enfin, si le rapport molaire initial H_2S/BCl_3 est supérieur à 10, d'autres pics peu intenses apparaissent entre 109 et 111 et entre 75 et 77.

Avec le bromure de bore, et pour un rapport H_2S/BBr_3 inférieur à l'unité, on note la formation simultanée de bromure d'hydrogène et d'un composé donnant deux massifs de pics situés pour le premier entre 201 et 206 et pour le second entre 121 et 125. Si le rapport précédent augmente, il apparait en outre deux autres massifs entre 154 et 160 et entre 74 et 77. Enfin, si ce rapport est supérieur à 10, tout le bromure de bore initial a disparu et il existe un pic peu intense pour un rapport *m/e* égal à 110.

Le tableau 1 montre que les intensités relatives des pics compris entre 201 et 206 correspondent sensiblement à la répartition isotopique calculée pour le dérivé BBr_2SH, les anomalies constatées s'expliquant par la formation d'ions BBr_2S^+ de masses égales à 201, 203, et 205 à partir des variétés isotopiques les plus abondantes des ions BBr_2SH^+, de masses égales à 202, 204, et 206. De la même façon, les pics situés entre 121 et 125 correspondent à des ions $BBrSH^+$ et $BBrS^+$ provenant comme les précédents de molécules BBr_2SH.

Le tableau 2 montre que les pics situés entre 154 et 160 qui apparaissent lorsque le rapport molaire initial H_2S/BBr_3 est supérieur à 1 correspondent à des ions $BBr(SH)_2^+$ dont certains ont perdu 1 ou 2 atomes d'hydrogène. Ceux compris entre 74 et 77 sont attribuables à des ions $B(SH)_2^+$, BS_2H^+, et BS_2^+ qui proviennent comme les précédents de molécules $BBr(SH)_2$.

Enfin, le pic peu intense qui se manifeste pour *m/e* 110 dans les mélanges très riches en H_2S correspond à la présence de traces du dérivé $B(SH)_3$.

On peut donc traduire la formation simultanée

TABLEAU 1. Spectre de masse du dibromosulfohydroxoborane

m/e	Intensité calculée	Intensité observée
201	4.9	6
202	19.0	17.5
203	9.9	11
204	38.9	37
205	5.5	6
206	20.6	22.5
207	0.4	—
208	0.8	—

TABLEAU 2. Spectre de masse du disulfohydroxobromoborane

m/e	Intensité calculée	Intensité observée
154	0	1.5
155	9.0	12
156	36.1	35
157	10.0	12.5
158	39.9	34
159	1.0	1.5
160	3.9	3.5
161	0.0	—
162	0.1	—

de bromure d'hydrogène et de ces trois dérivés de substitution par les équilibres:

[6] $$BBr_3 + H_2S \rightleftarrows BBr_2SH + HBr$$

[7] $$BBr_2SH + H_2S \rightleftarrows BBr(SH)_2 + HBr$$

et

[8] $$BBr(SH)_2 + H_2S \rightleftarrows B(SH)_3 + HBr$$

Conformément aux règles internationales, nous proposons pour ces composés les noms respectifs de dibromosulfohydroxoborane, bromodisulfohydroxoborane, et trisulfohydroxoborane.

Dans le cas du chlorure de bore, une réaction analogue se produit, mais la variation de masse consécutive à la substitution d'un atome de chlore par un groupement SH est trop faible pour que les pics du composé formé se distinguent nettement de ceux du chlorure de bore restant. C'est pourquoi les pics nouveaux sont peu intenses, car ils ne correspondent qu'aux ions provenant des variétés les plus légères, les autres étant masqués par les pics de BCl_3. On peut ainsi attribuer les pics situés entre 112 et 114 à des ions BCl_2SH^+ et BCl_2S^+ et ceux entre 77 et 79 à des ions $BClSH^+$ et $BClS^+$, tous ces ions provenant de la molécule BCl_2SH. De la même façon, les pics qui apparaissent dans les mélanges très riches en H_2S correspondent au dérivé disubstitué $BCl(SH_2)$. Entre le chlorure de bore et le sulfure d'hydrogène s'établissent donc les équilibres suivants:

[9] $$BCl_3 + H_2S \rightleftarrows BCl_2SH + HCl$$

et

[10] $$BCl_2SH + H_2S \rightleftarrows BCl(SH)_2 + HCl$$

L'existence des chloro- et des bromosulfohydroxoboranes a été confirmée par l'étude des spectres i.r. des mélanges précédents, seuls les composés BCl_2SH, BBr_2SH, et $BBr(SH)_2$ se formant en quantités suffisantes pour être détectés par cette méthode. L'interprétation de ces spectres, ainsi que la détermination des structures et des champs de force de ces dérivés ont été effectuées et sont en cours de publication.

Ces spectres montrent en particulier que, avec le chlorure de bore, l'équilibre est atteint de façon presque instantanée. Pour un mélange équimoléculaire, 25% du chlorure de bore initial a alors réagi. Avec le bromure, la réaction est plus lente et l'équilibre ne s'établit qu'au bout de 2 h environ. Elle est par contre plus complète, tout le bromure de bore étant consommé si sa teneur initiale est inférieure à 10%. De plus, les mélanges obtenus sont stables dans le cas du chlorure, alors que, avec le bromure, ils commencent à se décomposer spontanément dès la température ambiante s'ils contiennent plus de 90% sulfure d'hydrogène. Ils libèrent alors un solide blanc qui se dépose sur les parois du ballon.

Essais de séparation des mélanges gazeux, décomposition des sulfohydroxohalogénoboranes

Nous avons tenté d'isoler le composé BCl_2SH en soumettant un mélange en équilibre, initialement équimoléculaire de H_2S et de BCl_3, à une chromatographie préparative en phase vapeur en condensant séparément chaque fraction obtenue et en étudiant sa composition par spectrométrie i.r. Le chlorure et le sulfure d'hydrogène ne sont pas séparés et donnent un seul pic. Le second pic correspond au chlorure de bore et il possède une trainée constituée par le dichlorosulfohydroxoborane. Il n'est pas possible de séparer totalement ces deux composés, même en prélevant la queue de cette seconde fraction et en l'introduisant à nouveau dans la colonne. De plus, la moitié environ du BCl_2SH disparaît au cours de chaque passage.

En opérant par distillation sous vide du mélange liquéfié à basse température, on élimine tout d'abord le chlorure et le sulfure d'hydrogène, puis du chlorure de bore contenant des quantités croissantes de dérivé de substitution. Une partie de ce dernier se concentre dans le résidu de distillation et il s'y décompose en libérant un solide blanc. L'étude par diffraction X et absorption i.r. de ce solide montre qu'il est principalement constitué par du trichloroborsulfol $(BSCl)_3$ contenant de faibles quantités de sulfure de bore B_2S_3. La décomposition du dichlorosulfohy-

Can. J. Chem. Downloaded from www.nrcresearchpress.com by 210.87.254.40 on 09/05/12
For personal use only.

droxoborane peut donc s'écrire:

[11] $3\ BCl_2SH \rightarrow (BSCl)_3 + 3\ HCl$

puis

[12] $(BClS)_3 \rightarrow B_2S_3 + BCl_3$

Les quantités de solide obtenues sont très faibles car l'équilibre de formation de BCl_2SH est limité, et, de plus, la majeure partie de ce dérivé distille avec BCl_3 sans se décomposer. De ce fait, nous n'avons pas pu effectuer l'analyse chimique de ce solide, ni appliquer cette réaction à la synthèse du trichloroborsulfol.

Il en va autrement dans le cas des mélanges de sulfure d'hydrogène et de bromure de bore, car les dérivés de substitution se forment alors en quantité beaucoup plus importante et se décomposent plus facilement. Si on soumet à la même décomposition que ci-dessus un mélange équimoléculaire de H_2S et de BBr_3, on obtient un solide riche en $(BSBr)_3$, et, comme nous le verrons ultérieurement, les quantités obtenues sont suffisamment importantes pour que cette réaction constitue une méthode de synthèse intéressante du tribromoborsulfol.

Obtention des sulfohydroxohalogénoboranes en solution. Etude par résonance magnétique nucléaire du bore-11

Des spectres i.r. analogues à ceux déterminés en phase vapeur sont obtenus en faisant barboter du sulfure d'hydrogène dans une solution de chlorure ou de bromure de bore dans du sulfure de carbone à température ambiante.

Avec l'iodure de bore, la réaction n'avait pu être effectuée en phase vapeur en raison de la faible volatilité des dérivés iodés. En solution, on constate par spectrométrie i.r. la formation successive des composés BI_2SH, $BI(SH)_2$, et $B(SH)_3$ dont nous avons également déterminé les structures et les champs de force (publication en cours).

Il est à noter que les solutions obtenues sont très instables, et qu'elles se décomposent spontanément à température ambiante et sous pression atmosphérique en libérant, selon leur teneur en H_2S, soit le triiodoborsulfol $(BSI)_3$, soit l'acide thioborique $(BSSH)_3$ conformément aux réactions:

[13] $3\ BI_2SH \rightarrow (BSI)_3 + 3\ HI$

[14] $3\ BI(SH)_2 \rightarrow (BSI)_3 + 3\ H_2S$

et

[15] $3\ B(SH)_3 \rightarrow (BSSH)_3 + 3\ H_2S$

Nous avons également déterminé les spectres de r.m.n. du bore-11 de ces solutions en opérant en tube scellé et en utilisant le composé BF_3–Et_2O comme étalon externe. Les trois halogénures de bore seul donnent des pics situés à -47.3 p.p.m. pour BCl_3, -40 p.p.m. pour BBr_3, et $+6$ p.p.m. pour BI_3. Ces valeurs sont en bon accord avec celles données dans la littérature (16, 17).

Dans une solution contenant BCl_3 et H_2S, et quel que soit la rapport molaire H_2S/BCl_3, un seul pic nouveau, attribuable à BCl_2SH, apparaît à -55 p.p.m.

Avec le bromure de bore, un seul pic nouveau se manifeste à -49.8 p.p.m. si le rapport H_2S/BBr_3 est inférieur à 3. Il correspond au dérivé BBr_2SH. Si ce rapport augmente, le pic de $BBr(SH)_2$ apparaît à -56.2 p.p.m. et celui de BBr_3 disparaît.

Avec l'iodure de bore, un seul pic apparaît à -23.2 p.p.m. lorsque le rapport H_2S/BI_3 est inférieur à 1. Il est dû à BI_2SH. Lorsque ce rapport est compris entre 1 et 3, l'iodure de bore disparaît totalement, et le pic du dérivé disubstitué $BI(SH)_2$ se manifeste à -50 p.p.m. Enfin, si le rapport précédent est supérieur à 3, tout le dérivé monosubstitué disparaît à son tour et le dérivé trisubstitué se forme et donne un pic à -63.6 p.p.m. Ce dernier devient prépondérant si le rapport H_2S/BI_3 est supérieur à 10.

Il est à noter que l'équilibre n'est atteint qu'au bout de 12 h environ. De plus, la décomposition constatée par spectrométrie i.r. dans le cas des solutions des dérivés bromés et surtout iodés ne se produit pas dans ces conditions, car le fait d'opérer en tube scellé crée une pression en halogénure et en sulfure d'hydrogène suffisante pour stabiliser les dérivés de substitution formés: aucune trace de composés cycliques ne peut alors se former.

Synthèses de l'acide thioborique et du tribromoborsulfol

Comme nous venons de le voir, les sulfohydroxohalogénoboranes $BX_{3-n}(SH)_n$ se forment de façon intermédiaire dans la réaction entre le sulfure d'hydrogène et un halogénure de bore, réaction utilisée par Stock et par Wiberg pour préparer l'acide thioborique et les trihalogénoborsulfols. Connaissant ainsi le mécanisme de cette

Can. J. Chem. Downloaded from www.nrcresearchpress.com by 210.87.254.40 on 09/05/12
For personal use only.

Can. J. Chem. Downloaded from www.nrcresearchpress.com by 210.87.254.40 on 09/05/12
For personal use only.

synthèse, nous avons pu améliorer la méthode classique qui consiste à préparer l'acide thioborique à partir du bromure de bore et du sulfure d'hydrogène en passant par le tribromoborsulfol, puis les trihalogénoborsulfols par action de BCl_3, BBr_3, ou HI sur l'acide thioborique comme nous l'avons vu dans la bibliographie. Ces synthèses sont en effet fort longues, et, en ce qui concerne les trihalogénoborsulfols, elles ne donnent que des produits impurs avec un faible rendement, ce qui explique sans doute la rareté des données spectroscopiques relatives à ces composés.

Pour obtenir directement l'acide thioborique, il faut passer de l'halogénure de bore de départ à son dérivé trisubstitué $B(SH)_3$, puis provoquer la décomposition de ce dernier. Dans la méthode classique, cette décomposition se produit au stade des dérivés mono et disubstitués et elle fournit alors du tribromoborsulfol en partant de bromure de bore. Il faut ensuite substituer les atomes de brome du cycle par des groupements SH, ce qui explique la durée de l'opération.

Comme nous l'avons vu, c'est avec l'iodure de bore que la substitution est la plus complète. C'est donc avec cet halogénure que la synthèse de $(BSSH)_3$ sera la plus facile. Compte-tenu de la rareté de ce composé, nous avons cependant mis au point une autre méthode à partir du bromure de bore. Elle consiste à traiter ce dernier en solution dans le sulfure de carbone à -10 °C par un fort courant de H_2S. Dans ces conditions, les dérivés mono et disubstitués ne se cyclisent pas et la réaction se poursuit jusqu'au stade du dérivé trisubstitué. Il suffit alors de laisser la solution revenir à la température ambiante en maintenant le courant de H_2S, ce qui provoque la cyclisation de ce dérivé trisubstitué en acide thioborique. La synthèse dure ainsi 5 jours environ au lieu de 3 semaines.

Pour obtenir directement le tribromoborsulfol, on traite la même solution que ci-dessus par un faible courant de H_2S à la température de reflux. La décomposition se produit alors dès le stade du dérivé monosubstitué qui se cyclise à l'état de tribromoborsulfol.

Cette méthode conserve cependant l'un des inconvénients de celles décrites dans la littérature: la majeure partie du composé préparé en solution sulfocarbonique se décompose au cours de l'évaporation du solvant avec formation de sulfure de bore, ce qui explique que ce composé figure dans les équations proposées par les différents auteurs (7, 12). C'est pourquoi nous l'avons modifiée en utilisant comme solvant le bromure de bore lui-même. Dans ce but, on prépare un mélange équimoléculaire de sulfure d'hydrogène et de bromure de bore et on le laisse atteindre l'équilibre. Après refroidissement, on le distille sous vide pour éliminer HBr et H_2S, puis on le laisse revenir à température ambiante et se remettre en équilibre en fonction de sa nouvelle composition. On recommence ainsi plusieurs fois de suite cette opération, et, peu à peu, le mélange s'enrichit en BBr_3 et en BBr_2SH, ce dernier se décomposant à l'état de tribromoborsulfol qui se dissout dans le bromure de bore liquide. Il suffit alors de distiller ce solvant pour obtenir un produit très pur et bien cristallisé.

Synthèses du trichloro et du triiodoborsulfol

Comme nous l'avons vu, il est préférable d'opérer en l'absence d'un solvant tel que le sulfure de carbone pour préparer les trihalogénoborsulfols. Pour obtenir le cycle bromé, nous avons pu opérer par action directe du sulfure d'hydrogène sur le bromure de bore sans solvant, mais nous avons vu que cette réaction, dans le cas du chlorure, ne donnait que des quantités très faibles de trichloroborsulfol. C'est pourquoi, nous avons préparé ce composé en traitant de l'acide thioborique solide par un excès de chlorure de bore liquide à 0 °C. On a alors substitution sur le cycle selon la réaction:

$$[16] \quad (BSSH)_3 + 3\ BCl_3 \leftrightarrows (BSCl)_3 + 3\ BCl_2SH$$

et les dérivés formés se dissolvent dans l'excès de chlorure de bore liquide. Pour déplacer l'équilibre, on distille les composés BCl_3 et BCl_2SH et on traite le résidu par du chlorure de bore liquide. Au bout d'un certain nombre d'opérations, on constate par spectrométrie i.r. que le distillat ne contient plus que du chlorure de bore pur, ce qui prouve que la réaction est terminée. Il suffit alors de distiller l'excès de chlorure de bore pour faire cristalliser le trichloroborsulfol pur.

Pour préparer le triiodoborsulfol, et après avoir essayé diverses autres méthodes, nous avons opéré par action directe du sulfure d'hydrogène gazeux sur l'iodure de bore solide à température ambiante. Contrairement à ce qui se passait en solution, on a alors formation directe du cycle triiodé. Il suffit ensuite de sublimer sous vide l'excès d'iodure de bore pour récupérer le triiodoborsulfol pur.

Can. J. Chem. Downloaded from www.nrcresearchpress.com by 210.87.254.40 on 09/05/12
For personal use only.

Etude de quelques propriétés de l'acide thioborique et des trihalogénoborsulfols

Les trihalogénoborsulfols préparés selon les méthodes précédentes sont mieux cristallisés et beaucoup plus stables que ceux obtenus lorsque les réactions sont effectuées en solution dans le sulfure de carbone. C'est ainsi qu'on peut les purifier par sublimation sous vide secondaire vers 60 °C pour le dérivé chloré, 100 °C pour le bromé et 120 °C pour l'iodé et ceci sans décomposition. Nous avons obtenu de cette façon des produits très purs, ce qui nous a permis d'en effectuer l'étude par analyse thermique, diffraction de rayons X, et spectroscopie de vibration. Les résultats obtenus feront l'objet d'une prochaine publication.

Notons que si on les dissout dans du sulfure de carbone, ces composés donnent des pics de r.m.n. du bore-11 situés à −62 p.p.m. pour le trichloroborsulfol, à −54 pour le tribromo, à −50.2 pour le triiodo et à −57 pour l'acide thioborique.

Nous avons effectué sur ces dérivés cycliques un certain nombre de réactions en solution dans le sulfure de carbone, dans le but de préciser les mécanismes des synthèses décrites dans la littérature. Les résultats sont résumés sur les figs. 1, 2 et 3 pour les dérivés chlorés, bromés et iodés respectivement. Sur ces figures, les réactions que nous avons effectivement utilisées dans un but préparatif sont indiquées par un trait épais.

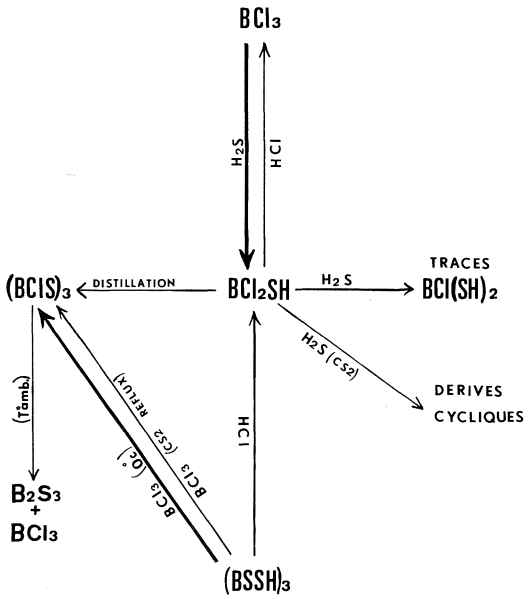

FIG. 1. Proprietés chimiques des sulfohydroxochloroboranes et du trichloroborsulfol.

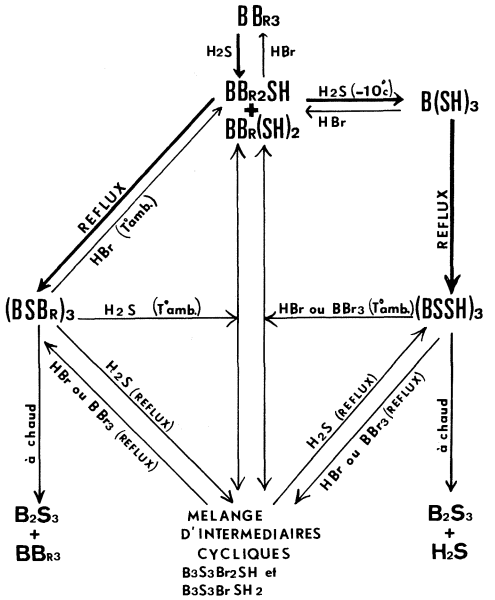

FIG. 2. Proprietés chimiques des sulfohydroxobromoboranes et du tribromoborsulfol.

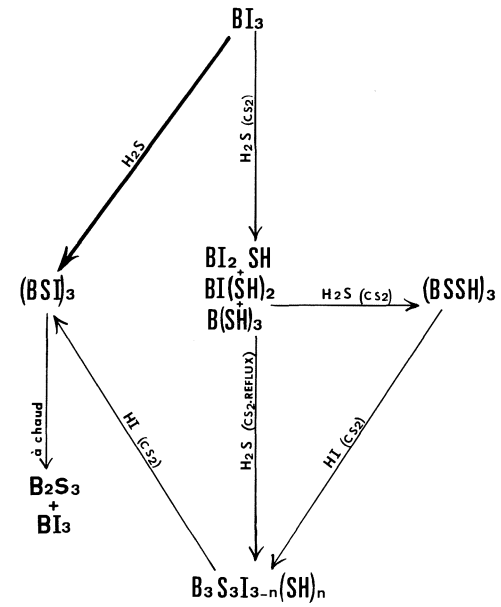

FIG. 3. Proprietés chimiques des sulfohydroxoiodoboranes et du triiodoborsulfol.

Action des halogénures d'hydrogène sur l'acide thioborique

Avec le chlorure d'hydrogène et à température ambiante aussi bien qu'à reflux, on a rupture du cycle avec formation de dichlorosulfohydroxo-

borane. Ce dernier est converti en chlorure de bore en présence d'un excès de HCl:

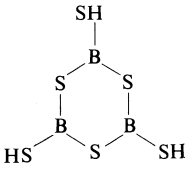

$$+ 6\,HCl \longrightarrow 3\,BCl_2SH + 3\,H_2S$$

puis $$BCl_2SH + HCl \rightleftarrows BCl_3 + H_2S$$

Avec le bromure d'hydrogène, et à température ambiante on a simultanément rupture du cycle comme ci-dessus avec le chlorure et substitution sur le cycle avec formation de composés intermédiaires entre l'acide thioborique et le tribromoborsulfol. Avec un excès de HBr, on aboutit donc à la fois à BBr_3 et à $(BSBr)_3$. Si on opère à reflux, on a uniquement substitution sur le cycle.

Enfin, avec l'iodure d'hydrogène, et quelle que soit la température, on a substitution sur le cycle et formation de triiodoborsulfol en passant par les intermédiaires $B_3S_3(SH)_2I$ et $B_3S_3(SH)I_2$. Rappelons que cette réaction a été utilisée par Wiberg pour préparer $(BSI)_3$ (8, 18).

Action des halogénures de bore sur l'acide thioborique

Dans tous les cas, on a échange entre des groupements SH du cycle et des atomes d'halogène de l'halogénure de bore:

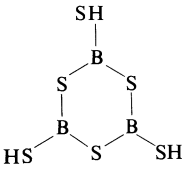

$$+ BX_3 \longrightarrow$$

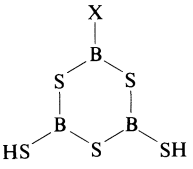

$$+ BX_2SH \text{ etc...}$$

Avec BCl_3, cette réaction est analogue à celle réalisée en l'absence de solvant pour préparer $(BSCl)_3$ à condition d'utiliser un excès d'halogénure pour substituer tous les groupements SH du cycle.

Avec le bromure et l'iodure de bore, la réaction est identique si on opère à température ambiante, mais, à la température de reflux, on a cyclisation des dérivés BX_2SH, tout le bore initial étant ainsi transformé en trihalogénoborsulfol.

Action du sulfure d'hydrogène sur les trihalogénoborsulfols

Avec le tribromoborsulfol et à température ambiante, on a simultanément substitution sur le cycle et rupture de ce cycle. A reflux, on a uniquement substitution et, en présence d'un excès suffisant d'H_2S, on obtient l'acide thioborique. Avec l'iodure de bore, et quelle que soit la température, c'est la substitution sur le cycle qui se produit.

Action du bromure d'hydrogène sur le tribromoborsulfol

Dans tous les cas, il y a rupture du cycle et, en fin de compte, formation de bromure de bore:

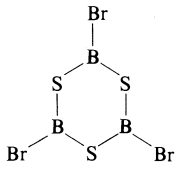

$$+ 3\,HBr \longrightarrow 3\,BBr_2SH$$

puis $$BBr_2SH + HBr \rightleftarrows BBr_3 + H_2S$$

Conclusions

Au cours de ce travail, nous avons donc mis en évidence l'existence des halogénosulfohydroxoboranes, dérivés nouveaux de formule générale $BX_{3-n}(SH)_n$, et que l'on peut obtenir soit en solution soit par simple mélange des réactifs gazeux. Ces dérivés ne sont stables qu'au sein du mélange en équilibre et, selon la valeur de n, ils se décomposent en donnant naissance soit au trihalogénoborsulfol correspondant $(BSX)_3$ soit à l'acide thioborique $(BSSH)_3$. La substitution est d'autant plus importante que l'on passe du chlore au brome et à l'iode, ce qui est conforme au fait que l'enthalpie de formation de la liaison B—X diminue lorsque le numéro atomique de l'halogène augmente.

La fig. 4 résume les résultats obtenus en r.m.n. du bore-11. Elle montre la cohérence entre les divers déplacements chimiques observés lorsqu'on passe d'un halogénure de bore à ses dérivés de substitution.

Notons que la position du pic situé à -63.6 p.p.m. et attribué au dérivé trisulfohydroxylé $B(SH)_3$ est en bon accord avec celle du pic correspondant au composé $B(SBu)_3$, situé selon la littérature à -66 p.p.m. (19).

Ces dérivés de substitution interviennent dans les réactions utilisées de façon classique pour préparer soit l'acide thioborique soit les tri-

Can. J. Chem. Downloaded from www.nrcresearchpress.com by 210.87.254.40 on 09/05/12
For personal use only.

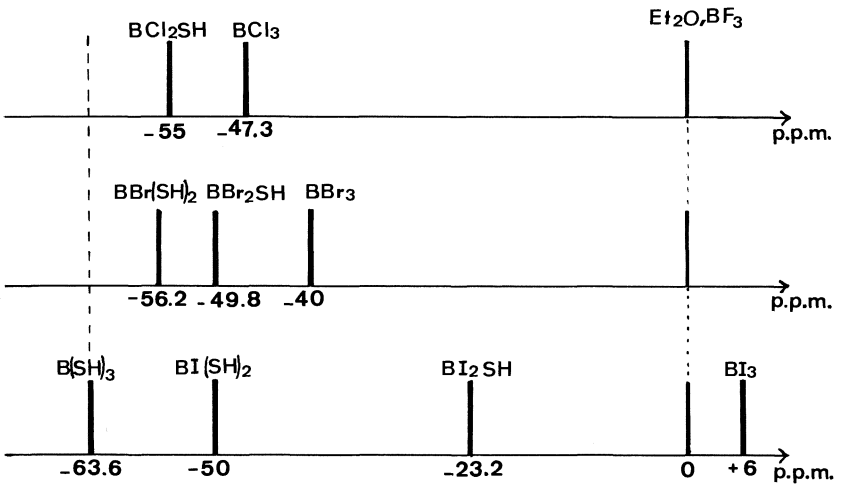

FIG. 4. Spectres de r.m.n. de ^{11}B des hologénures de bore et des sulfohydroxohalogénoboranes.

halogénoborsulfols, et, en contrôlant le déroulement de ces réactions, nous avons pu mettre au point diverses méthodes de synthèses de ces dérivés cycliques, méthodes plus rapides, plus sélectives et donnant des produits de meilleure pureté que celles décrites dans la littérature et évitant dans certains cas l'utilisation d'un solvant. Nous avons de ce fait eu la possibilité d'effectuer l'étude spectrale de ces divers composés, cette étude devant faire l'objet de prochains mémoires.

Partie expérimentale

Préparation des mélanges gazeux $BCl_3 + H_2S$ et $BBr_3 + H_2S$

Le sulfure d'hydrogène (provenance : Société Nationale des Pétroles d'Aquitaine, France) est séché par passage sur P_2O_5. Il est ensuite condensé à la température de l'azote liquide et maintenu sous vide.

Le chlorure et le bromure de bore (provenance : Koch Light, pureté indiquée : 99.8%) sont utilisés sans purification particulière. Pour BBr_3, il est cependant prudent de vérifier l'absence de BBr_2Cl décelable par son absorption i.r. à 920 et 955 cm^{-1}. ($\nu_{a^{11}B-Cl}$ et $\nu_{a^{10}B-Cl}$)

A l'aide d'une rampe à gaz de volume connu, munie d'un manomètre à mercure gradué, on prélève des quantités connues de réactifs et on les condense dans un ballon de 2.5 l. L'ensemble de l'appareillage doit être au préalable soigneusement séché sous vide. Le mélange contient au total 10^{-1} mol de réactifs, c'est-à-dire 0.5×10^{-1} de chacun dans le cas d'un mélange équimoléculaire. Dans le cas du chlorure de bore, ce mélange est entièrement gazeux à température ambiante, et sa pression est légèrement inférieure à la pression atmosphérique. Avec le bromure de bore, il subsiste en plus de la phase vapeur une partie liquide si la teneur en H_2S est inférieure à 90%.

Dosages chimiques

L'analyse élémentaire des trihalogénoborsulfols a été effectuée selon des méthodes déjà décrites (20).

Après dissolution de l'échantillon en milieu alcalin et en tube scellé, l'halogène est dosé par potentiométrie à l'aide de nitrate d'argent, le bore sous forme d'acide borique en présence de mannitol et le soufre par gravimétrie à l'état de sulfate de baryum.

La principale source d'erreur réside dans l'hygroscopicité de ces composés qui augmente lorsqu'on passe du dérivé iodé au dérivé chloré et se traduit, en particulier pour ce dernier, par un défaut de chlore dû à un départ de chlorure d'hydrogène.

Spectrométrie de masse

Les spectres sont déterminés sur un appareil Varian Mat CH5 à simple focalisation, avec des faisceaux d'électrons d'énergie égale à 35 et 70 eV. L'introduction est effectuée par l'intermédiaire d'un réservoir sous vide chauffé à 120 °C d'ou le mélange s'échappe par une fuite moléculaire.

Spectroscopie infrarouge

L'appareil utilisé est un Perkin–Elmer 337. Pour les spectres de gaz, on dispose d'une cellule étanche de 10 cm d'épaisseur en pyrex munie de faces en KBr et, pour les solutions, d'une cellule à épaisseur variable en acier inoxydable munie également de faces en KBr.

Chromatographie en phase vapeur des mélanges $BCl_3 + H_2S$

On utilise un chromatographe Carlo–Erba "Fractovap" avec détecteur à thermistances. Les colonnes en cuivre ont un diamètre de 8 mm et une longueur de 6 m. Elles sont garnies d'un mélange de chromosorb W 60/80 mesh et d'huile Kel F à 50% en poids. La température est de 0 °C, le gaz vecteur l'hélium. On introduit un mélange équimoléculaire contenant 5.10^{-3} mol de chacun des réactifs à l'aide d'un serpentin monté en dérivation.

Distillation sous vide

On prépare un mélange équimoléculaire de sulfure d'hydrogène et d'halogénure de bore (10^{-1} mol au total) dans un ballon de 2.5 l qui sert ensuite de bouilleur. La température de la distillation passe avec une vitesse de

Can. J. Chem. Downloaded from www.nrcresearchpress.com by 210.87.254.40 on 09/05/12
For personal use only.

Can. J. Chem. Downloaded from www.nrcresearchpress.com by 210.87.254.40 on 09/05/12
For personal use only.

10 °C par heure environ de celle de l'air liquide jusqu'à l'ambiante. L'ensemble est maintenu sous vide primaire, et le distillat est condensé à la température de l'azote liquide et analysé régulièrement par spectroscopie i.r.

Spectres de résonance magnétique nucléaire de ^{11}B

Le tube d'analyse est relié à la rampe à gaz. On le met sous vide, puis on y condense à la température de l'air liquide des volumes connus de sulfure d'hydrogène, de chlorure ou de bromure de bore et de sulfure de carbone (préalablement séché sur tamis moléculaire) sous des pressions mesurées grâce au manomètre à mercure. Pour l'iodure de bore solide, la mesure de volume est remplacée par une pesée en boite à gants. Une solution type contiendra par exemple 80×10^{-3} mol de CS_2, 4×10^{-3} mol de sulfure d'hydrogène et 4×10^{-3} mol d'halogénure de bore. La quantité de sulfure d'hydrogène mise en jeu est limitée par la pression supportée par le tube. Le spectre est enregistré à 33 °C sur un appareil Perkin–Elmer R 10 travaillant à 19.25 MHz, le composé $(C_2H_5)_2O$, BF_3 étant utilisé comme étalon externe. Lorsque les solutions obtenues sont peu concentrées en sulfohydroxohalogénoboranes, les spectres sont accumulés 128 fois.

Synthèses de l'acide thioborique $(BSSH)_3$

Dans un ballon de 1 l, on dissout 100 g de bromure de bore (0.4 mol environ) dans 250 cm^3 de sulfure de carbone. La solution est refroidie à −10 °C, et on y fait barboter un courant de sulfure d'hydrogène (environ 0.5 l par min). On prélève régulièrement à l'aide d'une seringue hypodermique un échantillon de la solution dont on détermine le spectre i.r. On obtient le dérivé trisubstitué $B(SH)_3$ qui se cyclise partiellement à −10 °C. Au bout de 4–5 jours, on laisse la solution revenir à température ambiante pour compléter cette cyclisation puis on filtre sur verre fritté. Le montage utilisé est dérive de celui décrit à propos d'un autre travail dans une publication précédente (21). L'acide thioborique est identifié par spectroscopie i.r. et diffraction X (13, 14) et purifié par recristallisation vers −80 °C dans le sulfure de carbone. Quantité obtenue: environ 20 g (rendement : 67% par rapport au bromure de bore).

Synthèse du tribromoborsulfol en l'absence de solvant

On prépare dans un ballon de 2.5 l un mélange de 10^{-1} mol de H_2S et 10^{-1} mol de BBr_3. La pression est voisine de l'atmosphère, et il subsiste une partie liquide. Après 24 h à température ambiante, on refroidit à la température de l'azote liquide et on laisse revenir sous vide jusqu'à −80 °C environ avec une vitesse de réchauffement de 10 °C par h. On coupe la communication avec la rampe à vide, et on laisse le mélange se remettre en équilibre pendant 4 h à température ambiante. On recommence plusieurs fois de suite la même opération en élevant à chaque fois de 10–20 °C la température maximale de la distillation jusqu'à ce qu'elle atteigne −20 °C environ. On distille ensuite le bromure de bore en excès à température ambiante pour faire recristalliser le tribromoborsulfol.

Quantité obtenue : 2.5 g environ (rendement: 20% par rapport au bromure de bore engagé dont la majeure partie sert en fait de solvant).

Anal. calc.: B, 8.79; S, 26.12; Br, 65.09. Trouvé: B, 9.0; S, 25.0; Br, 66.0.

Spectre de Debye–Scherrer: raies intenses à 3.55 et 2.87 Å; spectre d'absorption i.r. : bandes intenses vers 780, 795, et 990 cm^{-1}; p.f. 99 ± 3 °C.

Synthèse du trichloroborsulfol

On traite 10 g d'acide thioborique par 15 g de chlorure de bore liquide à 0 °C. Au bout de 4 h, on distille sous vide et on reprend le résidu solide par 15 g de chlorure de bore. On recommence l'opération jusqu'à ce que le spectre i.r. du distillat montre qu'il ne contient plus que du chlorure de bore. On reprend alors une dernière fois par BCl_3 liquide, on filtre la solution obtenue pour éliminer le sulfure de bore éventuellement formé et on fait recristalliser le $(BSCl)_3$ par distillation sous vide. Quantité obtenue : 3.5 g environ (rendement : 33% par rapport au $(BSSH)_3$ initial).

Anal. calc.: B, 13.82; S, 40.92; Cl, 45.26. Trouvé: B, 14.5; S, 43.2; Cl, 42.3.

Spectre de Debye–Scherrer: raies intenses à 3.52, 3.41, 2.78 et 2.72 Å ; spectre d'absorption i.r.: bandes intenses vers 860, 878, et 995 cm^{-1} ; p.f. 235 ± 3 °C.

Synthèse du triiodoborsulfol

On pulvérise en boite à gants 10 g d'iodure de bore préparé et purifié au laboratoire (22) qu'on place dans une nacelle. On introduit cette dernière dans un tube de pyrex monté sur un vibreur destiné à améliorer le contact gaz–solide. On traite à température ambiante par un courant de H_2S (10 l par h environ pendant 5 h). L'iodure de bore n'ayant pas réagi est ensuite sublimé sous vide vers 60 °C. Quantité obtenue : 2 g environ (rendement: 45% environ par rapport à BI_3 mis en jeu).

Anal. calc.: B, 6.37; S, 18.89; I, 74.74. Trouvé : B, 7; S, 17.4; I, 75.6.

Spectre de Debye–Scherrer : raies intenses à 4.30, 4.07, 3.25, et 2.87 Å; spectre d'absorption i.r. : bandes intenses vers 725, 740, et 980 cm^{-1}; p.f. 140 ± 3 °C.

Nous tenons à remercier Monsieur J. P. Laurent (Laboratoire de chimie inorganique, Professeur Gallais, Faculté des Sciences de Toulouse) qui a bien voulu déterminer et étudier les spectres de résonance magnétique nucléaire de nos produits en nous faisant ainsi bénéficier de ses conseils et de son expérience.

1. D. R. Martin. J. Am. Chem. Soc. **67**, 1088 (1945).
2. A. W. Ralston et J. A. Wilkinson. J. Am. Chem. Soc. **50**, 258 (1928).
3. J. Goubeau et H. W. Wittmeier. Z. anorg. Chem. **270**, 16 (1952).
4. A. Stock et M. Blix. Ber. **34**, 3099 (1901).
5. A. Stock et O. Poppenberg. Ber. **34**, 399 (1901).
6. E. Wiberg et W. Sturm. Z. Naturforsch, **8**b, 530 (1953).
7. E. Wiberg et W. Sturm. Angew. Chem. **66**, 60 (1954).
8. E. Wiberg et W. Sturm. Angew. Chem. **67**, 483 (1955).
9. E. Wiberg et W. Suterlin. Z. anorg. Chem. 202, 37 (1931).
10. P. Hagenmuller et F. Chopin. C.R. Acad. Sci. **255**, 2259 (1962).
11. F. T. Greene. Thèse. University of Wisconsin, Wisconsin. 1961.
12. H. G. Fernandez. Les hétérocycles en chimie minérale. Ed. Hermann. Paris. 1964.

13. D. THOMAS. Thèse. Université de Lille, France. 1966.
14. J. L. MACK. Thèse. Howard University, Washington D.C., 1965.
15. Z. V. ZVONKOVA. Kristallografiga. **3**, 564 (1958).
16. H. NOTT et H. WAHRENKAMP. Chem. Bencht. **99**, 1049 (1966).
17. P. ONAK, H. LANDESMAN, R. I. WILLIAMS et J. SHAPIRO. J. Phys. Chem. **63**, 1533 (1959).
18. E. WIBERG et W. STURM. Z. Naturforsch. **10**b, 114 (1955).
19. M. F. HAWTHORNE. J. Am. Chem. Soc. **83**, 1345 (1961).
20. G. CHARLOT. Analyse quantitative minérale. 2nd ed. Masson et Cie., Paris. 1961. p. 683, 640, 908.
21. P. CLAUDY et J. BOUIX. Bull. Soc. Chim. **4**, 1302 (1970).
22. J. CUEILLERON et H. MONGEOT. Bull. Soc. Chim. **1**, 76 (1966).

Can. J. Chem. Downloaded from www.nrcresearchpress.com by 210.87.254.40 on 09/05/12
For personal use only.

Preparation and Characterization of Pseudohalogeno(methyl)germanes and Related Compounds[1]

J. E. DRAKE[2] AND R. T. HEMMINGS

Department of Chemistry, University of Windsor, Windsor, Ontario

Received June 30, 1972

Synthetic routes to the series of pseudohalogeno(methyl)germanes, $MeGeH_2Ps$ and $MeGePs_3$ (Ps = N_3, CN, NCO, NCS), and the related compounds $MeGeH_2OAc$ and $Ge(N_3)_4$ are discussed. The compounds are characterized by their molecular weights, mass spectra, ^1H n.m.r. spectra and cleavage reactions. Their i.r. and Raman spectra are assigned as further confirmation of their structures.

Des approches de synthèse pour les pseudohalogéno(methyl)germanes, $MeGeH_2Ps$ et $MeGePs_3$ (Ps = N_3, CN, NCO, NCS), et les composés similaires comme $MeGeH_2OAc$ et $Ge(N_3)_4$ sont discutées. Les composés sont caractérisés par leurs poids moléculaire, spectre de masse, spectre r.m.n. du proton et leurs réactions de clivage. Leurs spectres i.r. et Raman ont aussi été utilisés comme preuves supplémentaires de leurs structures. [Traduit par le journal]

Can. J. Chem., **51**, 302 (1973)

Can. J. Chem. Downloaded from www.nrcresearchpress.com by 210.87.254.5 on 09/05/12
For personal use only.

Introduction

We recently described the preparation and characterization of the halogeno(methyl)germanes, $MeGeH_nX_{3-n}$, X = F, Cl, Br, I, n = 0, 1, or 2 (1). The work reported here is part of a continuing program on the investigation of the syntheses and vibrational analysis of species containing the $MeGeH_n$ group. We have synthesized stable mono- and tripseudohalogeno-(methyl)germanes in high yields by conventional methods and identified the products by ^1H n.m.r., i.r., Raman, and mass spectroscopy.

Unstable di-pseudohalogeno species have been identified in the ^1H n.m.r. and mass spectra although attempts to obtain them pure have been unsuccessful.

Experimental

Apparatus

A conventional Pyrex–glass vacuum system was used for all experiments. The i.r. spectra were recorded at room temperature in the range 4000–400 cm^{-1} on a Beckman IR 12 spectrometer using a gas cell (50 mm pathlength) fitted with KBr windows, or an air-tight solution cell. Raman spectra were recorded in the range 4000–50 cm^{-1} with the sample in sealed Pyrex–glass tubes (*ca.* 2 mm o.d.) on a Beckman 700 laser–Raman spectrometer using a helium–neon source. Strong bands are estimated to ± 1 cm^{-1} in the i.r. and ± 4 cm^{-1} in the Raman effect. The ^1H n.m.r. spectra were recorded at 60 MHz on a Jeol C-60 HL high resolution spectrometer in sealed tubes (*ca.* 2 or 5 mm o.d.) and the mass spectra on an AEI MS10c2 instrument, fitted with a Hitachi–Perkin–Elmer recorder, operating at an ionizing potential of 70 eV. Molecular weights were obtained from vapor density measurements of the monopseudohalides and from freezing point depression in benzene of the tripseudohalides.

Starting Materials

Methylgermane was prepared by the reaction of methyl iodide on germylpotassium (2). Commercial germane and hydrogen bromide were purified by pumping off any non-condensable gases at −196°. Commercial boron trichloride and boron tribromide (Matheson) were distilled prior to use. The i.r. spectra and vapor pressure of the middle fractions corresponded to those of the pure compounds (3, 4). The halogeno(methyl)germanes $MeGeH_2Cl$, $MeGeH_2Br$, $MeGeHBr_2$, and $MeGeH_2F$ were prepared by halogenation of methylgermane with BX_3 (X = Cl, Br) and by passing $MeGeH_2Br$ over dry lead(II) fluoride as described previously (1). The hydrides were purified by trap-to-trap distillation, fractions being taken of which the ^1H n.m.r. (1) and i.r. (5) spectra indicated a high degree of purity. Commercial trichloro-(methyl)germane and chloro(trimethyl)silane (Alfa Inorganics) were distilled to remove hydrogen chloride before use and had i.r. (6) and ^1H n.m.r. (7) spectra corresponding to the pure materials. Tribromo(methyl)germane was prepared by the reaction of trichloro(methyl)germane with excess hydrogen bromide until the ^1H n.m.r. spectrum (7) showed complete halogen exchange had occurred and the i.r. spectrum (8) corresponded to the pure compound. Reagent grade samples of the silver salts, AgCN, AgNCO, AgNCS, and AgOAc, and NaN_3 were dried in a high vacuum for several days prior to use. Azido(trimethyl)silane, Me_3SiN_3, was obtained from Me_3SiCl and NaN_3 in ether (9). Anhydrous ether (Mallinckrodt), tetrahydrofuran (B.D.H.), and benzene were distilled from fresh lithium aluminum hydride and stored in vacuum vessels. Spectral grade tetramethylsilane, germanium tetrachloride, chloroform, and carbon tetrachloride were used without further purification.

[1]Presented in part at the 55th Canadian Chemical Conference of the Chemical Institute of Canada, Quebec City, Quebec, 1972.

[2]To whom correspondence should be addressed.

Can. J. Chem. Downloaded from www.nrcresearchpress.com by 210.87.254.5 on 09/05/12
For personal use only.

Section A

Preparation of the Azido(methyl)germanes

(a) Reaction of Azido(trimethyl)silane with Monofluoro(methyl)germane

In a typical experiment Me_3SiN_3 (1.60 mmol) and $MeGeH_2F$ (1.70) mmol) were condensed into a 10 ml reaction vessel at −196°. The mixture was warmed to room temperature and allowed to react (5 min). Repeated fractionation through a trap at −78° gave Me_3SiF (*ca.* 1.55 mmol; identified by its ^1H n.m.r. (7) and i.r. (10) spectra) and a small amount of unreacted $MeGeH_2F$ (*ca.* 0.1 mmol) in a trap at −196°. Distillation of the products in the −78° trap gave pure azido(methyl)-germane, $MeGeH_2N_3$ (*ca.* 1.54 mmol; found: M, 132; calcd. for $MeGeH_2N_3$, 131.68; v.p. *ca.* 13 mm Hg at 20°) in a trap at −45° and a trace of unreacted Me_3SiN_3 in a trap at −196°. The liquid was stable, showing no signs of decomposition after 1 week at room temperature.

(b) Reaction of Azido(trimethyl)silane with Monochloro(methyl)germane

Typically Me_3SiN_3 (1.90 mmol) and $MeGeH_2Cl$ (2.00 mmol) were allowed to react at room temperature (*ca.* 30 min). Fractionation of the products gave unreacted $MeGeH_2Cl$ (1.82 mmol; v.p. 62 mm Hg at 0 °C; identified by its i.r. (5) and ^1H n.m.r. (1) spectra) in a trap at −196°; Me_3SiN_3 (*ca.* 1.70 mmol) and traces of Me_3SiCl (*ca.* 0.17 mmol) identified in the ^1H n.m.r. spectrum (7, 11) of the products in a −63° trap, and a small amount of oily material (*ca.* 0.18 mmol), which was subsequently shown to be $MeGeH_2N_3$, in a trap at −45° (found: M, 135; calcd. for $MeGeH_2N_3$, 131, 68; v.p. *ca.* 12 mm Hg at 20°).

(c) Reaction of Trichloro(methyl)germane with Sodium Azide

Typically $MeGeCl_3$ (10.5 mmol) and diethyl ether (*ca.* 20 ml) were distilled under vacuum into a 100 ml round bottomed flask fitted with a reflux condenser containing an excess of dry NaN_3 (*ca.* 4.5 g). The stirred mixture was maintained under reflux (*ca.* 100 h). Unwanted solid residue, containing NaN_3 and NaCl, was removed by vacuum filtration to give a clear ether solution which was carefully evaporated to dryness under high vacuum. Fractionation of the last portions of ether to be evaporated gave small amounts of a white subliming solid in a trap at −23° which was subsequently shown to contain mixed azido-chloro species (section *e*). $MeGe(N_3)_3$ (1.9 g; 85% yield) was isolated as a white powdery solid (found: M, 218; calcd. for $MeGe(N_3)_3$, 213.72; m.p. 44–45°). Sensitivity to percussion was not observed.

(d) Reaction of Tetrachlorogermane with Sodium Azide

In a typical reaction, $GeCl_4$ (2.1 g; *ca.* 10.0 mmol) and dry T.H.F. (*ca.* 20 ml) were distilled into a 100 ml round bottomed flask fitted with a reflux condenser containing excess dry NaN_3 (*ca.* 5.0 g). The mixture was refluxed (*ca.* 100 h) and separated by vacuum filtration to give a clear solution and a white residue containing unreacted NaN_3 and NaCl. The T.H.F. solution was carefully evaporated to dryness under high vacuum, diethyl ether being added in the latter stages to facilitate removal of the last traces of solvent. A white material, tetraazido-germane (found: M, 255; calcd. for $Ge(N_3)_4$, 240) remained in the filtration vessel. The $Ge(N_3)_4$ was apparently not sensitive to percussion but it exploded in the laser beam so only limited spectroscopic data were obtained. Small amounts of white material were sublimed with the last fractions of solvent. The i.r. spectrum in CCl_4 solution of this material showed a peak at *ca.* 450 cm^{-1} characteristic of the Ge—Cl stretching mode (5) in addition to those attributable to an azide. Thus it was assumed to be partially chlorinated $Ge(N_3)_nCl_{4-n}$.

(e) Reaction of Trichloro(methyl)germane with Azido(trimethyl)silane

Typically, $MeGeCl_3$ (*ca.* 0.5 mmol) and Me_3SiN_3 (*ca.* 1.5 mmol) were sealed together at −196° in a semi-micro n.m.r. tube and allowed to warm to room temperature. After *ca.* 10 min the ^1H n.m.r. spectrum showed resonances at 0.23 and 1.61 δ in the expected ratio 9:1 assignable to Me_3SiN_3 (11) and $MeGeCl_3$ (7), respectively. After *ca.* 5 days resonances attributable to Me_3SiCl (0.38 δ) and $MeGe(N_3)_3$ (1.39 δ) had appeared along with resonances at 1.07 and 1.20 δ. The latter resonances also appeared in the n.m.r. spectrum given by the volatile material from the reaction of $MeGeCl_3$ and NaN_3 (see section *c*) and in the n.m.r. spectrum given by a separate reaction of $MeGeCl_3$ and $MeGe(N_3)_3$ and were consistent with the formation of the azido-chloro species $MeGe(N_3)_2Cl$ and $MeGeN_3Cl_2$. Similarly, azido-bromo species $MeGe(N_3)_2Br$ (1.26 δ) and $MeGeN_3Br_2$ (1.60 δ) were observed in the n.m.r. spectrum in the reaction of $MeGeBr_3$ with $MeGe(N_3)_3$.

Characterization of the Azido(methyl)germanes

The ^1H n.m.r. parameters of mono- and triazido-(methyl)germane are listed (Table 1). The spectra, recorded in CCl_4 solution (*ca.* 5%) with internal tetramethylsilane reference, showed broadening of the resonances which was observed in the spectrum of GeH_3N_3 (12). The i.r. and Raman spectra of $MeGeH_2N_3$, $MeGe(N_3)_3$, and $Ge(N_3)_4$ are displayed (Table 2) with the assignments.

The mass spectrum of $MeGeH_2N_3$ gave fragments in the regions, *m/e* 28 (I = 1.6) (N_2^+); *m/e* 70–77 (I = 45.9) (H_nGe^+); *m/e* 83–93 (I = 100.0). (H_nCGe^+); *m/e* 101–105 (I = 8.1) ($H_nGeN_2^+$); *m/e* 114–118 (I = 30.9) ($H_nGeN_3^+$); *m/e* 129–135 (I = 17.8) ($H_nCGeN_3^+$).

Section B

Preparation of the Cyano(methyl)germanes

(a) Reaction of Chloro- and Bromo(methyl)germane with Silver(I) Cyanide

In a typical reaction, chloro- or bromo(methyl)-germane (*ca.* 1.5 mmol) was passed through a column loosely packed with a mixture of glass wool and dry silver(I) cyanide (*ca.* 25 g) at room temperature. After two double passes the silver(I) cyanide had turned from white to brown and i.r. spectroscopic examination of the volatile products indicated that almost all the starting material had been used up. Fractionation of the volatile products gave cyano(methyl)germane (1.35 mmol; found: M, 117; calcd. for $MeGeH_2CN$, 115.67; v.p. 24 mm Hg at 20°) passing through a trap at −45° but retained in one at −63°. The pure liquid showed no signs of decomposition after 5 weeks at room temperature in a sealed tube but left white deposits when distilled in the presence of Hg vapor. In the chloro system traces of unreacted $MeGeH_2Cl$ were found in a −196° following trap.

TABLE 1. The ^1H n.m.r. parameters (J in Hz ± 0.05 Hz; δ in p.p.m. ± 0.02 p.p.m.) of the pseudohalogeno(methyl)germanes*

Compound	$\lvert J(HH')\rvert$	δ(Me)	δ(Me')†	δ(GeH')
$MeGeH'_3$‡	4.22	0.29	—	3.45
$MeGeH_2'N_3$	3.08	0.69		5.23
$MeGe(N_3)_3$	—	1.07	—	—
$MeGeH_2'CN$	3.80	0.67	—	4.35
$MeGeH'(CN)_2$	n.o.§	0.98	—	5.30
$MeGe(CN)_3$	—	1.09	—	—
$MeGeH_2'NCO$	3.22	0.75		5.20
$MeGeH'(NCO)_2$	1.35	0.94	—	6.17
$MeGe(NCO)_3$	—	1.14	—	—
$MeGeH_2'NCS$	3.08	0.75	—	5.45
$MeGeH'(NCS)_2$	1.50	1.12	—	5.80
$MeGe(NCS)_3$	—	1.33	—	—
$MeGeH_2'OAc$	2.95	0.72	2.04	5.52
$MeGeH'(OAc)_2$	0.80	1.02	2.04	6.88

*The spectra were recorded at room temperature in carbon tetrachloride solutions (*ca.* 5%). Chemical shifts are in p.p.m. to low field of tetramethylsilane as internal standard.
†δ for acetoxy methyl group.
‡Reference 30.
§Not observed.

TABLE 2. Infrared and Raman spectra*† of the azides

$MeGeH_2N_3$		$MeGe(N_3)_3$		$Ge(N_3)_4$		
I.r. (gas)	Raman (liq)	I.r. (CCl_4)	Raman (CCl_4)	I.r. (CCl_4)	Raman (solid)	Assignment
3008m	3004w	2965m	2960w			$\nu_{as}CH_3$
2932m	2929mP	2930sh	2936wP			ν_sCH_3
2135s‡	2115sh‡	2146, 2121 s	2120w	2133s	2160w	$\nu_{as}N_3$¶
2080sh	2094sP					νGeH_2
1405m	1409w	1405m	1420w			$\delta_{as}CH_3$
1286s	1295mP	1275s	1285wP	1268s	1259m	ν_sN_3¶
1255sh	1255mP		1250w§			δ_sCH_3
881, 868 m	876mP					δGeH_2(sc)
867sh		865sh				ρCH_3
838s	841sh	830s	836m§			ρCH_3
733m	737mP					δGeH_2 wag, twist
670m	665wP	688s	690wP	680m	700m	$\delta N_3(\parallel)$
621m	617sP	640m	635mP			νGeC
		578m	580w	598w	592w	$\delta N_3(\perp)$
		494s br.	482§	502m		$\nu_{as}GeN$
484s‖	460sP‖		472s§		445s	ν_sGeN
	283w		320w§		300sh	Skeletal modes
			260m§		269sh	
	215mP				212sh	
	190sh		190s§			$\delta CGeN$

*In all tables: ν = stretching mode, δ = deformation, ρ = rocking, s = strong, m = medium, w = weak, sh = shoulder, P = polarized, br = broad, sc = scissors.
†Bands assignable to fundamentals are listed. Those only assignable as overtones are not included.
‡$\nu_{as}GeH_2$ displays a weak feature in this region in most $MeGeH_2X$ compounds (5).
§Observed in the solid only.
‖ρGeH_2 displays a weak feature in this region in most $MeGeH_2X$ compounds.
¶The stretching modes are strictly *pseudo*-symmetric and *pseudo*-antisymmetric but simpler terms symmetric (s) and asymmetric (as) are used throughout.

Can. J. Chem. Downloaded from www.nrcresearchpress.com by 210.87.254.5 on 09/05/12
For personal use only.

TABLE 3. Vibrational spectra* of the cyanides and of acetoxy(methyl)germane

$MeGeH_2CN$		$MeGe(CN)_3$,	$MeGeH_2OAc$†		
I.r. (gas)	Raman (liq)	I.r. (CCl_4)	I.r. (gas)	Raman (liq)	Assignments
3018m	3008w	3028m	3008m	3000w	$\nu_{as}CH_3$
2938m	2930mP	2962m	2950m	2941mP	ν_sCH_3
2202m	2190mP	2060m br			νCN
2122s 2118s	2120sP		2120s	2120sP	νGeH_2(as, s)
1430m	1429w	1409m	1423s	1424w	$\delta_{as}CH_3$
1260m	1255mP	1264m	*ca.* 1260w	1255wP	δ_sCH_3
888 879 s	878sP		880m	874m	δGeH_2 (sc)
870m		863m	870m		ρCH_3
849s	830sh	815m	840s	830w	ρCH_3
740m	735mP		730s	730w	δGeH_2 (wag and twist)
620m	618vsP	625m	622m	620vsP	$\nu GeC(Me)$
				557sP	νGeO
500m	495shP	510m			$\nu GeC(CN)$
470m	475m		480m	487m	ρGeH_2
430m	428sP	400m			$\nu Ge—NC$?
	330w			342s	Skeletal modes
	257m			289s	
	135s			226w	
				204m	

*See Table 2 footnotes.
†In the spectra of $MeGeH_2OAc$ peaks readily attributable to the OAc group are seen at 1725s (1696wP), 1372s (1374wP), 1015m (1012w), 928m (942w), 890sh (895sP). Raman values in parentheses.

(b) Reaction of Dibromo(methyl)germane with Silver(I) Cyanide

A reaction analagous to that used for the monochloro- and bromo(methyl)germanes was used with dibromo-(methyl)germane (*ca.* 2.1 mmol). An exothermic reaction occurred in which the silver(I) cyanide turned dark brown. After four double passes volatile material (1.2 mmol) was recovered after bleeding off uncondensable gas (*ca.* 0.9 mmol). Distillation of the products gave a mixture of $MeGeH_3$ and HCN (*ca.* 0.2 mmol) (identified spectroscopically) in a trap at −196°, traces of $MeGeH_2CN$ (*ca.* 0.3 mmol) in a trap at −45°, and a white involatile residue. The contents of the −45° trap sealed at −196° for n.m.r. analysis, rapidly turned white. The n.m.r. spectrum indicated the presence of $MeGeH_2CN$ (peaks at 0.67 and 4.35 δ) and traces of $MeGeH(CN)_2$ (peaks at 0.98 and 5.30 δ). Broad features at 3.95, 3.8 δ (H_nGeCN region) grew with time. Similar results were obtained when the $MeGeHBr_2$ was streamed over AgCN with N_2.

(c) Reaction of Tribromo(methyl)germane with Silver(I) Cyanide

By an analogous procedure to that described for the reaction of $MeGeCl_3$ and NaN_3, $MeGeBr_3$ (*ca.* 5 mmol), excess AgCN (*ca.* 5 g) and T.H.F. (*ca.* 15 ml) were refluxed (*ca.* 60 h). The reaction mixture turned from white to black. Filtration and removal of solvent in a high vacuum led to the isolation of tricyano(methyl)-germane, $MeGe(CN)_3$ (found: M, 170; calcd. for $MeGe(CN)_3$, 165.66). The white powdery solid liquified in moist air slowly evolving HCN, dissolved in benzene and T.H.F. but was only sparingly soluble in ether and CCl_4.

Characterization of the Cyano(methyl)germanes

The ^1H n.m.r. parameters of the cyano(methyl)-germanes are listed (Table 1). The vibrational spectra of $MeGeH_2CN$ and $MeGe(CN)_3$ are displayed (Table 3). The mass spectrum of $MeGeH_2CN$ gave the expected parent peaks, *m/e* 111–119 (H_nCGeCN^+). Confirmation of the *a priori* assignment of the unstable di-species, $MeGeH(CN)_2$, in the n.m.r. spectrum (section *b*) came from fragments at *m/e* 122–129 ($H_nGe(CN)_2^+$); *m/e* 137–144 ($H_nCGe(CN)_2^+$) given by the contents of the −45° trap. Further characterization came from hydrogen bromide cleavage reactions. The cyano(methyl)germanes $MeGeH_2CN$ (1.2 mmol) or $MeGe(CN)_3$ (0.7 mmol), were treated with excess HBr at room temperature. After *ca.* 2 h non-condensable gas was bled off at −196° and the products fractionated to isolate the product bromo(methyl) germanes, $MeGeH_2Br$ (1.1 mmol) or $MeGeBr_3$ (0.55 mmol), which were identified from vapor pressure measurements and from ^1H n.m.r. (1, 7) and i.r. (5, 8) spectra.

Section C

Preparation of the Isocyanato(methyl)germanes

(a) Reaction of Chloro- or Bromo(methyl)germane with Silver(I) Cyanate

In a typical reaction $MeGeH_2Br$ (*ca.* 2.0 mmol) was streamed through a column loosely packed with a mixture of glass wool and silver(I) cyanate (*ca.* 25 g). An exothermic reaction ensued in which the contents of the reaction tube turned black. After four double passes

Can. J. Chem. Downloaded from www.nrcresearchpress.com by 210.87.254.5 on 09/05/12
For personal use only.

TABLE 4. Vibrational spectra* of the isocyanates and isothiocyanates

$MeGeH_2NCO$		$MeGe(NCO)_3$,	$MeGeH_2NCS$		$MeGe(NCS)_3$,	
I.r. (gas)	Raman (liq)	I.r. (CCl_4)	I.r. (gas)	Raman (liq)	i.r. (CCl_4)	Assignment
3007m	3004w	3024s	3002w	3000w	2975m	$\nu_{as}CH_3$
2934m	2932mP	2970m	2930w	2926mP	2940m	ν_sCH_3
2286s	2270sh	2240s				$\nu_{as}NCO$
2098s	2109sP		2090s	2120sP		νGeH_2(as, s)
			2041s	2061m	1980s	$\nu_{as}NCS$
			1420w	1421w	1410m	$\delta_{as}CH_3$
1410m†	1409sP†	1412s†				ν_sNCO
1265m	1260mP	1265s	1260w	1256mP	1269m	δ_sCH_3
				968mP	948m	ν_sNCS
888, 874 m	879mP		882, 868 s	866mP		δGeH_2(sc)
872sh			860sh			ρCH_3
845s	832w	809s	838s	832m	831s	ρCH_3
745m	746m		714m	737m		δGeH_2 (wag, twist)
680m	682m	678s				δNCO
626s	625sP	634m	620m	618sP	625m	νGeC
		496m			413s	$\nu_{as}GeN$
481s‡	460sP‡			352mP		ν_sGeN
				472m		δNCS
			458w	450w		ρGeH_2
	286wP			290w		Skeletal
	218m			205mP		modes
	184mP			182sP		$\delta CGeN$

*See Table 2 footnotes.
†$\delta_{as}CH_3$ displays a weak feature in this region.
‡ρGeH_2 displays a weak feature in this region.

all the starting material had been consumed and isocyanato(methyl)germane, $MeGeH_2NCO$ (1.95 mmol; found: M, 131; calcd. for $MeGeH_2NCO$, 131.66; v.p. *ca.* 17 mm Hg at 20°), was obtained after fractionation in a trap at −45°. In an analogous reaction using $MeGeH_2Cl$ less than 20% conversion to the required isocyanate was obtained after ten double passes. The reaction was accompanied by formation of uncondensable gas, methylgermane, and involatile white material in the reaction tube.

Samples of $MeGeH_2NCO$ showed no signs of decomposition after 6 weeks in sealed tubes. On exposure to Hg vapor or silver(I) cyanate redistribution of the Me group was evident from the appearance of additional peaks in the ^1H n.m.r. spectrum of a fraction held at −78° at 0.94 and 6.17 δ ($MeGeH(NCO)_2$) and 0.87 δ ($Me_2Ge(NCO)_2$).

(b) Reaction of Dibromo(methyl)germane with Silver(I) Cyanate

Typically $MeGeHBr_2$ (1.5 mmol) was streamed through a column of silver(I) cyanate (*ca.* 20 g). An exothermic reaction ensued in which the contents of the reaction tube blackened. Uncondensable gas (*ca.* 0.5 mmol) was bled away through traps at −196°. The volatile material rapidly turned white at room temperature; distillation gave HNCO (*ca.* 0.1 mmol; identified spectroscopically) in a trap at −196°, $MeGeH_2NCO$ (*ca.* 0.2 mmol) and an intractable white residue in a trap at −45° and an oily material in a trap at −23°. The contents of the −23° trap, sealed for ^1H n.m.r. analysis, rapidly turned white and showed bands assignable to $MeGeH_2NCO$, 0.75, 5.20 δ; $MeGeH(NCO)_2$, 0.94, 6.17 δ; $Me_2Ge(NCO)_2$, 0.87 δ; $MeGeH_3$, 0.29, 3.45 δ with additional unidentified resonances at 3.3 and 4.15 δ.

(c) Reaction of Tribromo(methyl)germane with Silver(II) Cyanate

In a reaction analogous to that described for the preparation of tricyano(methyl)germane, $MeGeBr_3$ (*ca.* 7.5 mmol), excess silver(I) cyanate (*ca.* 8 g), and benzene (*ca.* 15 ml) were stirred under reflux (*ca.* 72 h). The reaction mixture turned brown to black and vacuum filtration followed by evaporation of solvent led to the isolation of $MeGe(NCO)_3$ (*ca.* 1.36 g, 5.2 mmol; found: M, 212; calcd. for $MeGe(NCO)_3$, 213.66; m.p. 48–51°). $MeGe(NCO)_3$ was soluble in benzene, T.H.F., and chloroform, and sparingly soluble in ether and CCl_4. No bromo-isocyanato species were detected in any reactions.

Characterization of the Isocyanato(methyl)germanes

The ^1H n.m.r. parameters of the isocyanato(methyl)germanes are listed (Table 1). I.r. and Raman spectral data are presented for $MeGeH_2NCO$ and $MeGe(NCO)_3$ (Table 4). The mass spectrum of $MeGeH_2NCO$ gave the parent peaks at *m/e* 128–132 ($H_nCGeNCO^+$). Weak fragments appeared at *m/e* 154–159 ($H_n(NCO)_2^+$) and *m/e* 166–171 ($H_nCGe(NCO)_2^+$) in the spectrum given by the contents of the −23° trap (section *b*) containing the dipseudohalide.

Can. J. Chem. Downloaded from www.nrcresearchpress.com by 210.87.254.5 on 09/05/12
For personal use only.

Can. J. Chem. Downloaded from www.nrcresearchpress.com by 210.87.254.5 on 09/05/12
For personal use only.

Hydrogen bromide cleavage reactions gave $MeGeH_2Br$ (0.8 mmol) from $MeGeH_2NCO$ (0.85 mmol) and $MeGeBr_3$ (0.85 mmol) from $MeGe(NCO)_3$ (*ca.* 1.0 mmol).

Section D

Preparation of the Isothiocyanato(methyl)germanes

(a) Reaction of Chloro- and Bromo(methyl)germane with Silver(I) Thiocyanate

A reaction analagous to that described for the syntheses of cyano- and isocyanato(methyl)germane was used. Typically, $MeGeH_2Br$ (*ca.* 2.1 mmol) was streamed through a column of silver(I) thiocyanate (*ca.* 25 g). An exothermic reaction occurred in which the silver salt turned dark brown. Isothiocyanato(methyl)germane, $MeGeH_2NCS$, (2.05 mmol; found: M, 146, calcd. for $MeGeH_2NCS$, 147.73) was recovered almost quantitatively after fractionation and condensation in a trap at $-45°$. Sealed samples showed no signs of decomposition after ten weeks at room temperature; prolonged exposure to Hg vapor or silver(I) thiocyanate resulted in the deposition of yellow residue and features assignable to disproportionation products appeared in the n.m.r. spectrum, $(Me_2Ge(NCS)_2$, 1.04 δ; $MeGeH(NCS)_2$, 1.12 and 5.80 δ; $MeGeH_3$, 0.29 and 3.45 δ; $MeGe(NCS)_3$, 1.33 δ). In a similar reaction substituting $MeGeH_2Cl$ (1.4 mmol) for $MeGeH_2Br$ no conversion to the expected thiocyanato compound was observed and $MeGeH_2Cl$ (1.35 mmol, identified by its ^1H n.m.r. (1) and i.r. (5) spectra) was recovered almost quantitatively.

(b) Reaction of Dibromo(methyl)germane with Silver(I) Thiocyanate

In a typical experiment, $MeGeHBr_2$ (1.8 mmol) was passed through a column of silver(I) thiocyanate (*ca.* 20 g). An exothermic reaction occurred in which the AgNCS turned black. Uncondensable gas (*ca.* 0.7 mmol) was bled away with the collecting bulb held at $-196°$. The volatile material contained some unreacted $MeGeHBr_2$, $MeGeH_3$, and $MeGeH_2NCS$ (*ca.* 0.3 mmol, identified in the n.m.r. spectrum) in a trap at $-45°$, and an oily liquid mixed with a yellow sublimable solid in a trap at $-23°$. The n.m.r. spectrum showed features assignable to $MeGeH(NCS)_2$, 1.12 and 5.80 δ; $Me_2Ge(NCS)_2$, 1.33 δ; $MeGe(NCS)_3$, 1.33 δ; with additional strong resonances at 3.3, 3.5, 4.4 δ. The yellow material was insoluble in CS_2 indicating that it contained no free sulfur. A CS_2 smear spectrum indicated that this material was probably polymeric thiocyanic acid.

(c) Reaction of Tribromo(methyl)germane with Silver(I) Thiocyanate

$MeGeBr_3$ (*ca.* 10.5 mmol), excess silver(I) thiocyanate (*ca.* 7.5 g), and ether (*ca.* 15 ml) were stirred under reflux (*ca.* 70 h). The reaction mixture turned dark brown and vacuum filtration followed by evaporation of solvent led to the isolation of $MeGe(NCS)_3$ (2.2g, 8.5 mmol; found: M, 265, calcd. for $MeGe(NCS)_3$, 261.87; m.p. 50–53°). $MeGe(NCS)_3$ was soluble in ether, benzene, and $CHCl_3$ and sparingly soluble in CCl_4.

Characterization of the Isothiocyanato(methyl)germanes

The ^1H n.m.r. parameters of the isothiocyanato(methyl)germanes are listed (Table 1). I.r. and Raman data are presented for $MeGeH_2NCS$ and $MeGe(NCS)_3$ (Table 4). The mass spectrum of $MeGeH_2NCS$ showed expected parent peaks at *m/e* 143–148 ($H_nCGeNCS^+$). Fragments at *m/e* 188–192 ($H_nGe(NCS)_2^+$) and *m/e* 203–207 ($H_nCGe(NCS)_2^+$) were observed in the mass spectrum given by the contents of the $-23°$ trap in section (*c*) containing the diisothiocyanate. Hydrogen bromide cleavage reactions gave $MeGeH_2Br$ (1.15 mmol) from $MeGeH_2NCS$ (1.20 mmol) and $MeGeBr_3$ (0.65 mmol) from $Me_3Ge(NCS)_3$ (*ca.* 0.8 mmol).

Section E

Preparation of Acetoxy(methyl)germane

Reaction of Bromo(methyl)germane with Silver(I) Acetate

$MeGeH_2Br$ (1.4 mmol) when streamed through dry silver(I) acetate (*ca.* 25 g) gave an exothermic reaction in which the contents of the reaction tube turned from white to black. Acetoxy(methyl)germane, $MeGeH_2OAc$ (1.3 mmol; found: M, 145; calcd. for $MeGeH_2OAc$ 148.68) was isolated after fractionation and condensation in a trap at $-45°$. In an analogous reaction substituting $MeGeH_2Cl$ (2.0 mmol) for $MeGeH_2Br$ no apparent conversion to the expected acetoxy compound was observed. The ^1H n.m.r. spectrum of the total products indicated the presence of $MeGeH_2Cl$ (*ca.* 1.7 mmol) together with small amounts of $MeGeH_3$, $MeGeHCl_2$, and Me_2GeCl_2. Samples were stable at room temperature but showed signs of disproportionation when distilled onto silver acetate. Additional peaks in the ^1H n.m.r. spectrum appearing at 0.29 and 3.45 δ ($MeGeH_3$); 1.02 and 6.88 δ ($MeGeH(OAc)_2$); 0.98 δ ($Me_2Ge(OAc)_2$) and 2.04 and 11.3 δ (HOAc).

Characterization of Acetoxy(methyl)germane

The ^1H n.m.r., i.r., and Raman spectral data for $MeGeH_2OAc$ are given (Tables 1 and 3). The mass spectrum gave the expected parent peaks at *m/e* 144–150 ($H_nCGeOAc^+$). Confirmation of the *a priori* assignment of diacetoxy-species in the ^1H n.m.r. spectrum after disproportionation, came from additional fragments at *m/e* 190–194 ($H_nGe(OAc)_2$) and *m/e* 205–211 ($H_nCGe(OAc)_2$). The HBr cleavage reaction gave $MeGeH_2Br$ (0.9 mmol) from $MeGeH_2OAc$ (0.95 mmol).

Discussion

Heavy metal salt exchange reactions have provided the most convenient routes to the cyanides, isocyanates, isothiocyanates, and acetates in silane (13, 14) and germane (15) chemistry. The long-established (13, 14) silyl-conversion series for silver salts suggested that pseudohalides might be formed from all halogeno(methyl)germanes other than the fluoride. We find that bromo(methyl)germane is quantitatively converted to the pseudohalides (reaction 1). With chloro(methyl)germane, as with chloro-

$$[1]\quad MeGeH_2Br \xrightarrow[(Ps = CN, NCS, NCO, OAc)]{AgPs} MeGeH_2Ps$$

germane (15), there is extensive conversion to the cyanide but there is only limited conversion to

Can. J. Chem. Downloaded from www.nrcresearchpress.com by 210.87.254.5 on 09/05/12
For personal use only.

the isocyanate. Chloro(methyl)germane is recovered essentially unchanged on passage over AgNCS and AgOAc.

Repeated attempts to synthesize pure samples of the dipseudohalogeno species by passage of dibromo(methyl)germane over silver salts were unsuccessful despite meticulous drying of the silver salts and dilution with nitrogen. The formation of $MeGeH(Ps)_2$, Ps = CN, NCO, NCS is accompanied by evolution of hydrogen and the formation of intractable material and the corresponding acid. Cyanic acid was found to catalyze the polymerization of SiH_3NCO (13) so presumably the presence of hydroacids catalyzes further decomposition. Although the formation of the hydroacids is suggestive of intermolecular elimination, no evidence for any Ge—Ge bonds was obtained in the vibrational or mass spectra. The ^1H n.m.r. spectra of $MeGeH(Ps)_2$ show many additional peaks arising from the continuing decomposition of the dipseudohalides.

The tripseudohalogeno(methyl)germanes are successfully prepared in high yield by the reaction of tribromo(methyl)germane with the corresponding silver salt (reaction 2), utilizing similar conditions described for the pseudohalogeno(trimethyl)germanes (16–18 and references therein). Despite the relative ease of these

$$[2]\quad MeGeBr_3 \xrightarrow[(Ps = CN, NCO, NCS)]{AgPs} MeGe(Ps)_3$$

silver salt reactions, an alternative route was sought for the azido(methyl)germane derivatives because of the instability of silver azide. Monofluorogermane reacted with azido(trimethyl)silane to form GeH_3N_3 in high yield (12, 19). The corresponding exchange between fluoro(methyl)germane and azido(trimethyl)silane gives virtually quantitative yields of azido(methyl)germane (reaction 3). By comparison the equil-

$$[3]\quad MeGeH_2F + Me_3SiN_3 \rightleftarrows MeGeH_2N_3 + Me_3SiF$$

ibrium in the reaction with chloro(methyl)germane lies far to the left at room temperature making this an unsuitable starting material.

Similarly, the reaction between trichloro(methyl)germane and azido(trimethyl)silane gives an equilibrium mixture, containing mixed species as was found for reaction of the azidosilane with dichloro(dimethyl)silane (20). These results are consistent with the generally accepted concept (21) that exchange in a silyl–germyl system favors the formation of the hard (less polarizable) moiety bound to silicon. The reaction of $MeGeF_3$ with Me_3SiN_3 was not attempted because it was not possible to prepare the required quantities of pure $MeGeF_3$ (22).

Direct reaction of an organometallic chloride with sodium azide has been successful in the syntheses of many organo-group IV azides (23) and similarly tri-azido(methyl)germane (reaction 4), and tetraazidogermane (reaction 5), may be synthesized. Unlike the related silicon com-

$$[4]\quad MeGeCl_3 + 3NaN_3 \xrightarrow{\text{ether}} MeGe(N_3)_3 + 3NaCl$$

$$[5]\quad GeCl_4 + 4NaN_3 \xrightarrow{\text{T.H.F.}} Ge(N_3)_4 + 4NaCl$$

pounds, azido(methyl)germanes do not appear to be sensitive to percussion and are stable for long periods of time above their melting points. However, a sample of $Ge(N_3)_4$ did explode in a green laser beam (*ca.* 600 mW). In the synthesis of the corresponding tin compound (24), a complex salt, $Sn(N_3)_4.2NaN_3$ was obtained. We find no evidence for similar complex formation of tetraazidogermane, which may reflect the familiar difficulty encountered in forcing germanium to increase its co-ordination number to six.

As has been indicated earlier, exchange at silicon or germanium is characteristic of the halogeno-derivatives (21). Exchange with hydrogen halide provided a convenient synthetic route to iodo- and bromo(methyl)germanes (1) because the formation of the heavier halogen bound to germanium was favored. The use of a similar route to pseudohalides would require reaction of fluoro(methyl)germanes with HPs which is not a sensible synthetic prospect. However, this type of reaction provides a convenient characterization of the pseudohalide since the parent bromo(methyl)germane is reclaimed by reaction with hydrogen bromide, consistent with reaction 6.

$$[6]\quad HBr + MeGeH_2Ps \rightarrow MeGeH_2Br + HPs$$
$$3HBr + MeGePs_3 \rightarrow MeGeBr_3 + 3HPs$$

The reactions are not suitable for the azides due to the hazardous nature of the by-product, hydrazoic acid.

Further characterization comes from molecular weight determinations and mass spectroscopy. The molecular weight of $MeGe(CN)_3$ suggests

Can. J. Chem. Downloaded from www.nrcresearchpress.com by 210.87.254.5 on 09/05/12
For personal use only.

that, unlike $Ge(CN)_4$ which is polymeric (25), it is essentially monomeric, at least in benzene solution, as are all the other mono- and tri-pseudohalides. The lack of stability of the dipseudohalides precludes the determination of their molecular weights. However, parent peaks corresponding to $MeGeHPs_2^+$ (Ps = CN, NCO, NCS, OAc) are observed in their mass spectra. The parent peaks $MeGeH_2Ps^+$ (Ps = N_3, CN, NCO, NCS, OAc) are evident in the mass spectra of the monopseudohalides. From the fragmentation patterns it becomes evident that many of the pseudohalides undergo some decomposition and analysis of the H_nCGe^+ (*m/e* 70–79) and GeH_n^+ (83–93) fragments indicates the presence of significant amounts of methylgermane (26). This is undoubtedly a result of an inevitable exposure to mercury in the sampling system of the mass spectrometer. Thus relative intensities of the peaks are not meaningful nor the fragment distribution of the region *m/e* 70–93. For $MeGeH_2N_3$, the isotopic fragmentation patterns of the H_nGe^+ and H_nCGe^+ regions are clearly not perturbed by the presence of $MeGeH_3$ so intensities are reported. The relative intensities of the fragments H_nGe^+; H_nCGe^+; H_nGeX^+; H_nCGeX^+ (X = N_3) are 46:100:31:18 which is comparable with the corresponding values for $MeGeH_2Cl$ which are 46:100:42:30 (22, 26).

The ^1H n.m.r. spectra of the pseudohalogeno-(methyl)germanes are all first order (Table 1). The $MeGeH_2'Ps$ series all give the methyl resonance as a 1:2:1 triplet, intensity 3, to high field of an associated 1:3:3:1 quartet, intensity 2, attributable to GeH_2'. The unstable dipseudohalogeno series, identified in dilute solution, give a 1:1 doublet, intensity 3, for the methyl resonance and a 1:3:3:1 quartet, intensity 1, attributable to GeH′. The tripseudohalogeno series all give the methyl resonance as a singlet at high field. Significant dilution shifts (up to 5%) were observed particularly in the mono series; in accordance with other workers we report the ^1H n.m.r. parameters for the sample in CCl_4 solution (*ca.* 5%) using an internal reference of tetramethylsilane. The spectrum of acetoxy-(methyl)germane contained an additional singlet, intensity 3, attributable to the acetoxy-methyl protons. The chemical shifts of the GeH_2' resonance in $MeGeH_2'NCS$ and $MeGeH_2'NCO$ occur very close to that of $MeGeH_2'N_3$, confirming that all three are Ge—N bonded. A comparison with the values of germyl species (GeH_3N_3, 5.1 δ (12); GeH_3NCS, 5.18 δ (27); GeH_3NCO, 5.05 δ (27); $(GeH_3)_3N$, 4.9 δ (28); $(GeH_3)_2O$, 5.3 δ; $(GeH_3)_2S$; 4.7 δ (29)) further supports this conclusion, particularly as there has been strong n.m.r. evidence that GeH_3—NCO and —NCS are truly Ge—N bonded (27). A species containing a Ge—O bond should have the larger downfield shift and this is found for $MeGeH_2'OAc$. With $MeGeH_2'CN$, the chemical shift is upfield relative to the other $MeGeH_2'Ps$ as might be expected from the value in GeH_3CN (4.33 δ) (22). In the liquid state, it has been suggested that silyl- and germylcyanides may contain significant amounts of the isocyanide form in rapid equilibrium with the *normal* structure (16, 30). The chemical shift of $MeGeH_2'CN$ (4.35 δ) although to highfield of the GeH_2' resonances of the three Ge—N bonded species is still to lowfield of the resonance in *e.g.* Me_2GeH_2' (3.73 δ) (31). This is at least consistent with the presence of the rapid equilibrium suggested above.

The shifts in the GeH_2' resonances for $MeGeH_2'X$ species, X = F, Cl, Br, I (5), are apparently controlled by an inductive effect and hence related to the electronegativity of X. Thus with increasing electronegativity of X, an increased de-shielding of the proton attached to germanium is expected, and hence a shift downfield from TMS. In this context, the order of increasing electronegativity based on the observed n.m.r. shifts is I < CN < Br < NCO ≃ N_3 < Cl < NCS < OAc, which is as expected for the relative electronegativities of C, N, and O. On the other hand, where the polarizability (or hardness) of the pseudohalides seems to be important, as in exchange reactions, the order of reactivity, I → Br → NCO, N_3 NCS, Cl, OAc → CN → F, is such that the CN group behaves more like "F" than "Br".

For the $MeGeH_nPs_{3-n}$ species (Ps = N_3, NCO, NCS, OAc; *n* = 0, 1, 2) all of the n.m.r. parameters are close to, and show similar trends to those of $MeGeH_nCl_{3-n}$ (1).

Attempts have been made to interpret the vibrational spectra of compounds such as GeH_3NCO (27) and GeH_3N_3 (12) in terms of the expected and observed fundamentals assuming C_{3v} (Ge—N—C—O, Ge—N—N—N linear) or C_s (Ge—N—C—O, Ge—N—N—N bent) symmetry. The conclusions on this basis have not been definitive so we hesitate to make extravagant claims for our proposed assignments. In

Can. J. Chem. Downloaded from www.nrcresearchpress.com by 210.87.254.5 on 09/05/12
For personal use only.

any case, for the monopseudohalides, the symmetry argument would not hold. The assignments to fundamentals (Tables 2, 3, and 4) are made by comparison with related species (5, 12, 17, 27, 32, 33). Extensive discussion must await a full normal coordinate analysis which in turn will be more meaningful if based on direct structural evidence yet to be obtained. However, a few points of interest and speculation can be raised.

The n.m.r. evidence strongly favors Ge—N bonding in the —NCO and —NCS derivatives and this is clearly supported by the vibrational spectra. The Ge—N stretching modes can be assigned to strong polarized bands at 460, 482, 480, and 352 cm^{-1} in the Raman spectra of $MeGeH_2N_3$, $MeGe(N_3)_3$ (Table 2), $MeGeH_2$-NCO, and $MeGeH_2NCS$ (Table 4) which compare with 466, 459, and 358 cm^{-1} in GeH_3N_3, GeH_3NCO and GeH_3NCS, respectively (12, 27, 33). The assignments of the NCO and NCS pseudo-symmetric stretching vibrations at *ca.* 1400 and 950 cm^{-1} are diagnostic of *N*-functional groups (34).

For the cyanides the n.m.r. evidence suggested a carbon-bonded CN group with just a possibility of some isocyanide also being present. The vibrational spectrum (Table 3) of $MeGeH_2CN$ shows bands at 2202 cm^{-1} (2190 mP in the Raman) characteristic of a carbon function $\nu_{C\equiv N}$ (32*a*). On the other hand, in $MeGe(CN)_3$ only a weak broad feature, at lower wavenumber, is observed in this region in chloroform solution. This could indicate the presence of significant amounts of the Ge—NC moiety (16) possibly resulting from association (35) despite the molecular weight evidence in benzene. Involvement of the Ge—CN moiety in association would destroy the linearity of Ge—C—N and hence the C_{3v} symmetry of $MeGe(CN)_3$. Thus association or an equilibrium mixture of *normal* and *iso* forms could account for the apparent existence of two methyl rocks in the i.r. spectrum of $MeGe(CN)_3$. In $MeGeH_2CN$ a polarized band at 495 cm^{-1} can be assigned to νGe—C(CN). The strong polarized band at 428 cm^{-1} in $MeGeH_2CN$ and a band at 400 cm^{-1} in the i.r. spectrum of $MeGe(CN)_3$ are the only ones not easily explained on a comparative basis. They compare with one in GeH_3CN at *ca.* 443 cm^{-1} which, despite its intensity, was assigned as an overtone of the Ge—CN deformation (32*a*). In $MeGeH_2CN$ an assignment to an overtone or combination band is certainly not plausible in view of the observed Raman spectrum. This band at 428 cm^{-1} could be a fundamental skeletal mode at a surprisingly high wavenumber. Alternatively, it would be reasonable to assign it to Ge–N(NC) stretch. In a spectroscopic study of the trimethylsilyl cyanide and isocyanide system it was estimated that the mole fraction of isocyanide was only 0.0015 at 25° (30). The intensity of the 428 cm^{-1} band relative to that assigned to the Ge—$C(CH_3)$ symmetric stretch is very much less than for the corresponding band at 460 cm^{-1} in $MeGeH_2N_3$.

The assignment of $MeGeH_2OAc$ is reasonably straightforward based on comparison with GeH_3OAc, Me_3GeOAc (32*c*), and acetic acid. We choose to place the Ge—O stretching mode at 557 cm^{-1} in the Raman spectrum, by comparison with the polarized band assigned to this mode in GeH_3OMe at 602 cm^{-1} (36), rather than at *ca.* 880 cm^{-1} as suggested by the earlier work on germyl acetates (32).

We wish to thank the National Research Council of Canada for financial support.

1. J. E. Drake, R. T. Hemmings, and C. Riddle. J. Chem. Soc. A, 3359 (1970).
2. D. S. Rustad, T. Birchall, and W. L. Jolly. Inorg. Synth. **11**, 128 (1968).
3. T. Wentick and V. H. Tiensu. J. Chem. Phys. **28**, 826 (1958).
4. A. Stock and E. Kuss. Ber. Deut. Chem. Ges. **47**, 3113 (1914).
5. (*a*) G. K. Barker, J. E. Drake, R. T. Hemmings, and B. Rapp. Spectrochim. Acta, **28A**, 1113 (1972). (*b*) G. K. Barker, J. E. Drake, R. T. Hemmings, and B. Rapp. J. Chem. Soc. A, 3291 (1971).
6. (*a*) D. F. Van De Vondel and G. P. Van Der Kelen. Bull. Soc. Chim. Belg. **74**, 453 (1965). (*b*) E. A. V. Ebsworth, M. Onyszchuk, and N. Sheppard. Trans. Faraday Soc. 1453 (1958).
7. (*a*) A. N. Egorochkin, A. J. Burov, V. E. Mironov, T. K. Gur, and N. S. Vyazankin. Dokl. Akad. Nauk. S.S.S.R. **180**, 861 (1968). (*b*) K. Moedritzer and J. R. Van Wazer. Rev. Chim. Minérale. **6**, 293 (1969). (*c*) E. A. V. Ebsworth and S. G. Frankiss. Trans. Faraday Soc. 1574 (1967).
8. (*a*) J. R. Aronson and J. R. Durig. Spectrochim. Acta, **20**, 219 (1964). (*b*) D. F. Van De Vondel, G. P. Van Der Kelen, and G. Van Hooydonk. J. Organomet. Chem. **23**, 431 (1970).
9. J. S. Thayer and R. West. Inorg. Chem. **3**, 899 (1964).
10. H. Kriegsmann. Z. Anorg. Allg. Chem. **294**, 113 (1958).
11. N. Wiberg and K. H. Schmid. Chem. Ber. **100**, 748 (1967).

12. S. CRADOCK and E. A. V. EBSWORTH. J. Chem. Soc. A, 1420 (1968).
13. (*a*) A. G. MACDIARMID. J. Inorg. Nucl. Chem. **2**, 88 (1956). (*b*) A. G. MACDIARMID. Q. Rev. (London), **10**, 208 (1956).
14. E. A. V. EBSWORTH and M. J. MAYS. J. Chem. Soc. 4844 (1962); 3450 (1964).
15. (*a*) S. SUJISHI and J. N. KEITH. Abst. 134th Meeting of the Am. Chem. Soc. Div. Inorg. Chem. (1958) p. 44N. (*b*) T. N. SRIVASTAVA, J. E. GRIFFITHS, and M. ONYSZCHUK. Can. J. Chem. **40**, 739 (1962).
16. D. SEYFERTH and N. KAHLEN. J. Org. Chem. **25**, 809 (1960).
17. J. S. THAYER and D. P. STROMMEN. J. Organomet. Chem. **5**, 383 (1966).
18. J. S. THAYER and R. WEST. Adv. Organomet. Chem. **5**, 169 (1966); M. F. LAPPERT and H. PYSZORA. Adv. Inorg. and Radiochem. **9**, 133 (1966).
19. S. CRADOCK and E. A. V. EBSWORTH. J. Chem. Soc. A, 1226 (1967).
20. W. SUNDERMEYER. Chem. Ber. **96**, 1293 (1963).
21. (*a*) E. A. V. EBSWORTH, A. G. LEE, and G. M. SHELDRICK. J. Chem. Soc. A, 2294 (1968). (*b*) J. E. DRAKE, R. T. HEMMINGS, and C. RIDDLE. J. Chem. Soc. A, 600 (1971). (*c*) G. K. BARKER and J. E. DRAKE. Inorg. Nucl. Chem. Lett. **7**, 39 (1971).
22. J. E. DRAKE and R. T. HEMMINGS. Unpublished results.
23. I. RUIDISCH and M. SCHMIDT. J. Organomet. Chem. **1**, 493 (1964).
24. V. E. WIBERG and H. MICHAUD. Z. Naturforsch. **9b**, 500 (1954).
25. T. A. BITHER, W. H. KNOTH, R. V. LINDSEY, JR., and W. H. SHARKEY. J. Am. Chem. Soc. **80**, 4151 (1958).
26. C. J. MCCORMICK. Ph.D. Thesis. University of Maryland, 1970.
27. K. M. MACKAY and S. R. STOBART. Spectrochim. Acta, **26A**, 373 (1970).
28. D. W. H. RANKIN. Chem. Commun. 194 (1969).
29. S. CRADOCK, E. A. V. EBSWORTH, and D. W. H. RANKIN. J. Chem. Soc. A, 1628 (1969).
30. M. R. BOOTH and S. G. FRANKISS. Spectrochim. Acta, **26A**, 859 (1970).
31. H. SCHMIDBAUR. Chem. Ber. **97**, 1639 (1964).
32. (*a*) T. D. GOLDFARB. J. Chem. Phys. **37**, 642 (1962); **41**, 3653 (1964). (*b*) J. E. GRIFFITHS. J. Chem. Phys. **48**, 278 (1968). (*c*) T. N. SRIVASTAVA and M. ONYSZCHUK. Can. J. Chem. **41**, 1244 (1963). (*d*) F. A. MILLER and G. L. CARLSON. Spectrochim. Acta, **17**, 977 (1961). (*e*) J. W. ANDERSON, G. K. BARKER, J. E. DRAKE, and R. T. HEMMINGS. Can. J. Chem. **49**, 2931 (1971).
33. G. DAVIDSON, L. A. WOODWARD, K. M. MACKAY, and P. ROBINSON. Spectrochim. Acta, **23**, 2383 (1967).
34. R. P. HIRSCHMANN, R. N. KNISELEY, and V. A. FASSEL. Spectrochim. Acta, **21**, 2125 (1965); **23A**, 109 (1967).
35. R. GUY and M. CHAIGNEAU. Bull. Soc. Chim. Fr. 257 (1956).
36. S. CRADOCK. J. Chem. Soc. A, 1426 (1968).

Can. J. Chem. Downloaded from www.nrcresearchpress.com by 210.87.254.5 on 09/05/12
For personal use only.

Calculated Geometry for Ten-Coordination[1]

YEONG C. LIN AND DONALD E. WILLIAMS

Department of Chemistry, University of Louisville, Louisville, Kentucky 40208

Received January 24, 1972

The predicted geometry for coordination of ten ligands of equal size about a central atom was found by minimizing the interligand repulsion energy. The favored arrangement of hard-sphere ligands is of the 2:4:2:2 type, of symmetry C_{2v}. The favored arrangement of soft-sphere ligands is of the 1:3:3:3 type, symmetry C_{3v}, or of the 1:4:4:1 type, symmetry D_{4d}, depending on the degree of softness. The differences in repulsion energy among the three favored arrangements were small, making it likely that any differences in ligand sizes would be an important factor in determining the structure.

La géométrie prévue pour la coordination de dix coordinats ayant des dimensions égales autour d'un atome central a été trouvée par minimisation de l'énergie répulsive entre les coordinats. L'arrangement favorisé de coordinats sphériques et durs est du type 2:4:2:2 de symétrie C_{2v}. L'arrangement favorisé de coordinats sphériques et souples est du type 1:3:3:3 de symétrie C_{3v} ou du type 1:4:4:1 de symétrie D_{4d} dépendant du degré de souplesse. Les différences dans l'énergie de répulsion entre les trois arrangements favorisés sont petites, entrainant vraisemblablement que n'importe quelle différence dans la grosseur des coordinats sera un facteur dominant dans l'attribution de la structure.

[Traduit par le journal]

Can. J. Chem., **51**, 312 (1973)

Introduction

The valence-shell-electron-pair-repulsion (VSEPR) model has proven valuable as a tool for predicting and understanding molecular geometry (1). The simplest case is the situation where a central atom is surrounded by n atoms or ligands of equal size. If some of the atoms or ligands are of different sizes, or if some of them are replaced by lone pair electrons, the situation becomes more complex. Much can be understood, however, by estimating the spatial requirements of the ligands or lone pairs in terms of a distortion from the simplest case of n equal ligands.

Chemists often assume that the potential energy of repulsion between atoms is proportional to d^{-r}, where d is an interligand distance. The repulsion exponent, r, is often taken as 12, or it may be adjusted according to some theoretical or experimental criterion. This model is referred to as the soft-sphere model.

The problem of finding the maximum angular size and orientation of n circles on a unit sphere has interested mathematicians (2). This problem may also be stated as that of finding the arrangement of points on a unit sphere which maximizes the least interpoint distance. The mathematician's statement of the problem corresponds to the chemist's statement in the limit as $r \to \infty$. This model is referred to as the hard-sphere model.

For $n \leq 12$, the solutions for the hard-sphere model are all definitely known, except for $n = 10$. Apparently the most rigorous treatment for $n = 10$ is that of Schütte and van der Waerden (2*a*), who conclude that a 2:4:2:2 arrangement of C_{2v} symmetry is probable. They give upper and lower limits for the least interligand distance as 1.14088 . . . and 1.09143 . . . , respectively.

For the soft-sphere model, the favored arrangement is known to be independent of r except for $n = 7$ and $n = 10$. The dependence on r of the $n = 7$ arrangement has been investigated by Britton (3) and by Claxton and Benson (4). For $r < 2.5$ a 1:5:1 arrangement of D_{5h} symmetry is preferred. In the range $2.5 < r < 5.6$ a 1:2:2:2 arrangement of C_2 symmetry is preferred.[2] For $r > 5.6$ a 1:3:3 arrangement of C_{3v} symmetry is obtained, similar to the hard-sphere model. The energy differences between these arrangements are small, so that any differences in ligand sizes would probably be the predominant influence in a structure with different ligands.

[1]This work supported by research grant GM 16260 from the U.S. Public Health Service.

[2]Claxton and Benson indicate that the C_2 arrangement is favored at $r = 2$; however, their energy table indicates that $E(C_2) = E(D_{5h})$ at $r = 2.5$ and that the D_{5h} structure is preferred at $r = 2$.

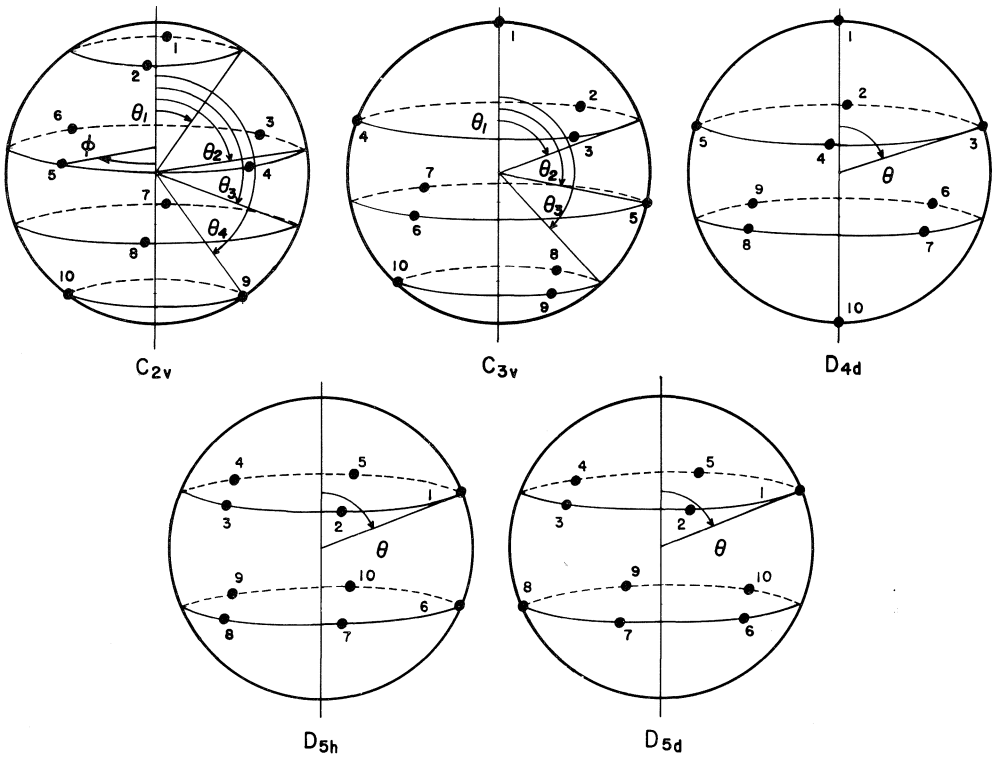

FIG. 1. Specifying parameters and ligand numbering system for ten-coordinate structures of C_{2v}, C_{3v}, D_{4d}, D_{5h}, and D_{5d} symmetry.

Method of Calculation

The model considered was an arrangement of ten points on a sphere of unit radius. The total repulsive energy (on a relative scale) was assumed to be given by

$$E = \sum_{j=1}^{9} \sum_{k=j+1}^{10} B d_{jk}^{-r}$$

where d_{jk} is the distance between points j and k, and r is the repulsion exponent. B is a constant, here taken as unity, which is included to make the equation dimensionally correct. In terms of the spherical coordinates (θ,ϕ) the square of the distance is given by

$$d_{jk}^2 = 2(1 - \sin\theta_j \sin\theta_k \cos\phi_j \cos\phi_k - \sin\theta_j \sin\theta_k \sin\phi_j \sin\phi_k - \cos\theta_j \cos\theta_k)$$

Three degrees of freedom are removed from the problem by setting the rotational origin. This may be accomplished by fixing one point at the north pole, for example, and fixing arbitrarily one additional ϕ coordinate, taking care to avoid taking the second point at the south pole. This leaves 17 degrees of freedom for the energy minimization.

A computer program was written which minimizes the replusive energy by steepest descents. A thorough analysis involving minimization of E for all 17 variables, and for various repulsion exponents, was found to be costly of computer time. We did determine the final energy minima for three values of r: 1, 12, and 30. Three different structures were obtained, of D_{4d}, C_{3v}, and C_{2v} symmetries, respectively. These arrangements may be characterized as being of 1:4:4:1, 1:3:3:3, and 2:4:2:2 coordination types, respectively (Fig. 1). In the case of $r = 30$, a false minimum structure of C_{2v} symmetry was also found. This structure has considerably shorter minimum distances and corresponds to rotating points 1 and 2 of Fig. 1 by 90° about the z axis.

For detailed examination of the energy dependence on r, we introduced symmetry constraints into the computer program. The C_{2v} structure is characterized by five parameters: θ_1,

$\theta_2, \theta_3, \theta_4$, and ϕ. The C_{3v} structure is characterized by three parameters: θ_1, θ_2, and θ_3. The D_{4d} structure is characterized by a single parameter: θ. For comparison, we also calculated the minimum energy configurations of D_{5h} (5:5, eclipsed) and D_{5d} (5:5, staggered) structures. Each of these is characterized by a single parameter, θ.

With the assumed symmetry it is possible to factor the energy expression, since several distances may be equal because of the symmetry. The factored expression for C_{2v} symmetry is

$$E(C_{2v}) = 4(d_{13}^{-r} + d_{14}^{-r} + d_{29}^{-r} + d_{47}^{-r} + d_{48}^{-r} + d_{49}^{-r} + d_{4,10}^{-r} + d_{89}^{-r}) + 2(d_{27}^{-r} + d_{28}^{-r} + d_{34}^{-r} + d_{45}^{-r} + d_{46}^{-r}) + (d_{12}^{-r} + d_{78}^{-r} + d_{9,10}^{-r})$$

Thus there are 16 unique distances, of which 5 have twofold multiplicity and 8 have fourfold multiplicity.

The energy of the C_{3v} structure may be factored as

$$E(C_{3v}) = 6(d_{35}^{-r} + d_{38}^{-r} + d_{58}^{-r}) + 3(d_{12}^{-r} + d_{15}^{-r} + d_{18}^{-r} + d_{23}^{-r} + d_{37}^{-r} + d_{39}^{-r} + d_{56}^{-r} + d_{5,10}^{-r} + d_{89}^{-r})$$

There are 12 unique distances, of which 3 have sixfold multiplicity, and 9 have threefold multiplicity.

The energy of the D_{4d} structure may be factored as

$$E(D_{4d}) = 8(d_{12}^{-r} + d_{16}^{-r} + d_{23}^{-r} + d_{46}^{-r} + d_{47}^{-r}) + 4(d_{24}^{-r}) + d_{1,10}^{-r}$$

There are 7 unique distances, of which 5 have eightfold multiplicity, and 1 has fourfold multiplicity.

The energies of the D_{5h} and D_{5d} structures may be factored as

$$E(D_{5h}) = 10(d_{12}^{-r} + d_{13}^{-r} + d_{17}^{-r} + d_{18}^{-r}) + 5(d_{16}^{-r})$$

$$E(D_{5d}) = 10(d_{12}^{-r} + d_{13}^{-r} + d_{16}^{-r} + d_{17}^{-r}) + 5(d_{18}^{-r})$$

In both cases there are 5 unique distances, of which 4 have tenfold multiplicity, and 1 has fivefold multiplicity.

The factored energy expressions were utilized to find the structure of minimum energy as a function of the characteristic parameters, for various values of the repulsion exponent. A steepest descent minimization procedure was used. No difficulties were encountered with false minima when explicit symmetry constraints were used.

Results and Discussion

Table 1 gives the minimum energies obtained for the five symmetries, for various values of the repulsion exponent. For $r \geq 25$, the C_{2v} structure is favored, confirming the symmetry prediction of Schutte and van der Waerden (2*a*) for the hard-sphere model. In the range $9 \leq r \leq 24$, the C_{3v} structure is obtained. For $r \leq 8$, the D_{4d} structure is favored. Neither of the 5:5 coordinated structures are favored for any value of r, although the energy differences become smaller for the soft-sphere model.

The differences in energy may also be expressed on a relative basis. Thus, for the frequently assigned value of $r = 12$, the C_{3v} structure is most stable. The C_{2v} structure has 0.13% more repulsion energy, the D_{4d} structure has 1.01% more repulsion energy. Clearly, only a small size difference or anisotropic effect could change the situation to favor the C_{2v} or D_{4d} structures. Larger size effects or anisotropic effects would be required to favor either of the 5:5 structures.

Gillespie (1*b*) favored the D_{4d} (bicapped square antiprism) model. This model would be appropriate for soft ligands ($r \leq 8$). To our knowledge, no one has previously predicted the C_{3v} structure, which is favored when $r = 12$. Table 2 shows the configurations of the best arrangements, for various values of the repulsion exponent. The C_{2v} structure was calculated for very large values of the repulsion exponent so as to approach the hard-sphere limit.

It appears from Table 2 that the minimum value of 1.09143 . . . given by Schütte and van der Waerden may be the exact value for hard-sphere ten-coordination. None of our runs achieved a larger value for the minimum contact distance. Our calculation with $r = 1200$ yielded a closest contact distance of 1.0913, very close to the above value.

Table 3 gives a listing of the closest interligand contacts for the three favored structures. The ranking of closest contacts remains the same, for the lowest energy structures. Thus, the closest contacts are always d_{34}, d_{25}, and d_{12} for the C_{2v}, C_{3v}, and D_{4d} structures, respectively. If $r \leq 2$, the

TABLE 1. Minimum energies for ten-coordination

	Minimum energy				
r	C_{2v}	C_{3v}	D_{4d}	D_{5h}	D_{5d}
1	32.7210	32.7214	32.7170	32.9834	32.9480
2	25.0523	25.0532	25.0414	25.7440	25.6328
4	16.6510	16.6530	16.6261	18.5118	18.1039
6	12.3620	12.3634	12.3368	15.5222	14.6367
8	9.7262	9.7250	9.7211	14.1089	12.6304
9	8.7300	8.7269	8.7416	13.6650	11.8705
10	7.8738	7.8687	7.9052	13.3154	11.2026
12	6.4646	6.4563	6.5405	12.7802	10.0467
16	4.4401	4.4298	4.5995	11.9954	8.1678
20	3.0820	3.0753	3.2937	11.3433	6.6664
24	2.1493	2.1481	2.3790	10.7451	5.4464
25	1.9650	1.9651	2.1949	10.6015	5.1784
50	0.21625	0.22049	0.30103	7.5842	1.4720
100	0.002718	0.002889	0.005745	3.8850	0.11952

TABLE 2. Characteristic parameters and closest contacts for ten-coordination

	C_{2v} symmetry						C_{3v} symmetry				D_{4d} symmetry	
r	θ_1	θ_2	θ_3	θ_4	ϕ	d(min)	θ_1	θ_2	θ_3	d(min)	θ	d(min)
1	31.95	79.16	113.91	145.47	57.48	1.0558	138.45	91.71	63.81	1.0570	65.00	1.0746
2	32.11	79.37	113.92	145.41	57.52	1.0555	138.38	91.84	64.04	1.0604	64.90	1.0731
4	32.42	79.86	114.16	145.37	57.53	1.0570	138.38	92.34	64.52	1.0644	64.79	1.0715
6	32.68	80.33	114.57	145.36	57.49	1.0597	138.47	92.89	64.96	1.0668	64.76	1.0711
8	32.87	80.74	115.04	145.36	57.43	1.0627	138.58	93.40	65.32	1.0689	64.78	1.0714
9	32.94	80.92	115.27	145.36	57.40	1.0640	138.64	93.64	65.47	1.0699	64.80	1.0717
10	33.00	81.07	115.51	145.36	57.37	1.0655	138.70	93.85	65.60	1.0709	64.82	1.0720
12	33.08	81.33	115.95	145.35	57.31	1.0678	138.80	94.21	65.80	1.0725	64.87	1.0727
16	33.16	81.71	116.72	145.31	57.21	1.0718	139.01	94.76	66.07	1.0753	64.96	1.0740
20	33.19	81.96	117.29	145.26	57.13	1.0748	139.18	95.13	66.22	1.0774	65.05	1.0753
24	33.19	82.12	117.72	145.20	57.07	1.0768	139.34	95.39	66.29	1.0789	65.11	1.0762
25	33.19	82.16	117.81	145.19	57.06	1.0773	139.38	95.44	66.30	1.0793	65.13	1.0765
50	33.17	82.50	119.04	144.59	56.88	1.0833	140.03	96.13	66.26	1.0843	65.32	1.0793
100	33.11	82.59	119.86	143.52	56.75	1.0874	140.74	96.67	66.13	1.0890	65.43	1.0809
1200	33.08	82.68	120.56	142.64	56.64	1.0913						

TABLE 3. Closest contact types

Symmetry	Range of r	Nearest	Second	Third	Fourth
C_{2v}	1,7	d_{34}	d_{13}	d_{12}	d_{37}
	8,15	d_{34}	d_{13}	d_{37}	d_{12}
	≥ 16	d_{34}	d_{37}	d_{13}	d_{12}
C_{3v}	1,2	d_{12}	d_{25}	d_{58}	
	≥ 3	d_{25}	d_{12}	d_{58}	
D_{4d}	All	d_{12}			

closest contact for C_{3v} symmetry changes to d_{12}. Table 3 indicates some other changes occurring in the second, third, and fourth closest contacts.

There are very few molecules or ions known at the present time to be ten-coordinated. Jakob and Jakob (5) report compounds of the type $Me_2[Mo(CN)_8R_2]\cdot 4H_2O$ and $Me_2[W(CN)_8R_2]\cdot 4H_2O$, where Me = Cd^{II} or Mn^{II} and R = H_2O, NH_3, or N_2H_4. They predict the D_{4d} structure with the R groups polar. The same structural prediction is given by Hoard and Silverton (6) for those compounds.

Sharp (7) has prepared the compound $PtF_8(CO)_2$. The material is light-sensitive and hydrolyzes in moist air. No prediction was made about the geometry of the structure.

Lind, Lee, and Hoard (8) have solved the crystal structure of $La(OH_2)_4AH\cdot 3H_2O$, where H_4A is ethylenediaminetetraacetic acid (EDTA). The coordination about the lanthanum is ten, but the geometry is complex because of the constraints imposed by the EDTA ligand.

NOTE ADDED IN PROOF: King (9) made a calculation for the coulombic case ($r = 1$) of ten-coordination and found a D_{4d} configuration, in agreement with this work. King gives the following additional examples of ten-coordination: the ten boron atoms in $B_{10}H_{10}^{2-}$ (10); polymeric uranium(IV) acetate (11); and yterbium diantimonide (12). The observed structures have D_{4d}, D_{4d}, and C_{2v} symmetry, respectively.

1. (*a*) R. J. GILLESPIE. Angew. Chem. Int. Ed. **6**, 819 (1967). (*b*) R. J. GILLESPIE. J. Chem. Ed. **47**, 18 (1970).
2. (*a*) K. SCHÜTTE and B. L. VAN DER WAERDEN. Math. Ann. **123**, 96 (1951). (*b*) H. S. M. COXETER. Trans. New York Acad. Sci. **24**, 320 (1962).
3. D. BRITTON. Can. J. Chem. **41**, 1632 (1963).
4. T. A. CLAXTON and G. C. BENSON. Can. J. Chem. **44**, 157 (1966).
5. W. F. JAKOB and Z. L. JAKOB. Roczniki Chem. **26**, 492 (1952); **36**, 601 (1962).
6. J. L. HOARD and J. V. SILVERTON. Inorg. Chem. **2**, 235 (1962).
7. D. W. A. SHARP. Proc. Chem. Soc. London, 317 (1960).
8. M. D. LIND, B. LEE, and J. L. HOARD. J. Am. Chem. Soc. **87**, 1611 (1965).
9. R. B. KING. J. Am. Chem. Soc. **92**, 6460 (1970).
10. W. N. LIPSCOMB. Boron hydrides. W. A. Benjamin, New York. 1963. p. 16.
11. I. JELENIC, D. GRDENIC, and A. BEZJAK. Acta Cryst. **17**, 758 (1964).
12. R. WANG, R. BODNAR, and H. STEINFINK. Inorg. Chem. **5**, 1468 (1966).

Studies of Rhenium β-Diketone Complexes. III. The Crystal and Molecular Structure of Bis(μ-*O*-1,3-diphenylpropane-1,3-dionatotricarbonylrhenium(I))

J. C. BARRICK, M. FREDETTE, AND C. J. L. LOCK[1]

Institute for Materials Research, McMaster University, Hamilton, Ontario

Received July 25, 1972

One of a series of compounds obtained by the reaction of chloropentacarbonylrhenium(I) with β-diketones has been shown by single crystal X-ray diffraction to be bis(μ-*O*-1,3-diphenylpropane-1,3-dionatotricarbonylrhenium(I)). The crystals are monoclinic with lattice parameters a = 11.988(A) Å, b = 14.441(9) Å, c = 10.298(7) Å, β = 115.25(7)°. The space group is $P2_1/c$ and there are two dimers per unit cell. A total of 1563 independent reflections were measured on a single crystal X-ray diffractometer and the structure was refined by least squares analysis to a weighted R_2 value of 0.0427. The dimer units are held together by two bridging oxygen atoms, one from each of the β-ketoenolate groups; the distance of the bridging oxygen from the rhenium atom to which it is chelated (2.162(9) Å) is shorter than the distance to the other rhenium atom (2.204(7) Å). The main part of the β-ketoenolate ring is 37° from the OReO plane.

L'un des composés obtenu par la réaction du chloropentacarbonylrhénium(I) sur les β-dicétones a été identifié par diffraction aux rayons X sur un monocristal au bis (μ-*O*-diphényl-1,3-propanedionato-1,3 tricarbonylrhénium(I)). Les cristaux sont monocliniques, les paramètres du réseau sont: a = 11.988 Å, b = 14.441(9) Å, c = 10.298(7) Å, β = 115.25(7)°. Le groupe spatial est $P2_1/c$ et il y a deux dimères par maille. Un total de 1563 reflexions indépendantes a été mesuré au diffractomètre aux rayons X sur un monocristal, la structure a été raffinée par la méthode des moindres carrés jusqu'à obtention d'une valeur pondérée sur R_2 de 0.0427. Les dimères dans la maille sont reliés entre eux par deux atomes d'oxygène formant un pont, chacun d'eux provenant des groupes β-cétoènolates; la distance de l'oxygène pont à l'atome de rhénium auquel il est chelaté (2.162(9) Å) est plus courte que celle qui le sépare de l'autre atome de rhénium (2.204(7) Å). La partie principale du cycle β-cétoènolate est située à 37° du plan OReO. [Traduit par le journal]

Can. J. Chem., **51**, 317 (1973)

Introduction

We have investigated the reaction of $Re(CO)_5Cl$ with various β-diketones and have prepared two series of compounds with apparent stoichiometries $Re_2(CO)_6(dik)_2$[2] and $Re(CO)_3Cl(dik)$. Attempts to elucidate the structure of $Re_2(CO)_6(dik)_2$ using n.m.r., infrared, Raman, and mass spectroscopy did not provide an unambiguous solution to the structure so we have examined selected compounds by single crystal X-ray diffraction. Our first study was of $Re_2(CO)_6(acac)_2$ but the crystal was apparently disordered (see below). However, a study of the structure of $Re_2(CO)_6(dbm)_2$ was successful.

[1]To whom correspondence should be addressed.

[2]dik is any β-ketoenolate anion, acac is the anion derived from acetylacetone, $C_5H_7O_2^-$, dbm is the anion derived from dibenzoylmethane, $C_{15}H_{11}O_2^-$, and thd is the anion derived from 2,2,6,6-tetramethyl-3,5-heptanedione, $C_{11}H_{19}O_2^-$.

Experiments

Analyses were performed on samples of crystals of each compound. Carbon, hydrogen, and chlorine analyses were performed by A. B. Gygli, Toronto, Canada and rhenium and chlorine were determined by neutron activation analysis (1). Molecular weights were determined by mass spectroscopy using a Consolidated Electrodynamics Corp., Model 21-110B mass spectrometer.

Bis (μ-O-pentane-2,4-dionatotricarbonylrhenium(I))

Chloropentacarbonylrhenium(I) (1 mmol) and acetylacetone (3 mmol) were refluxed in benzene (~75 ml) for 2 weeks. The pale yellow solution gradually turned dark brown during this time. Evaporation of the solvent (~20°, ~15 mm), followed by addition of ether (~100 ml) and filtration, served to remove any unreacted chloropentacarbonylrhenium(I). The filtrate was evaporated and the residues were dissolved in the minimum amount of chloroform or ether. Addition of enough petroleum ether to cause cloudiness produced a brown powder which was collected on a filter and recrystallized from methylene chloride or ether, giving small white needles.

Anal. Calcd. for $C_{16}H_{14}O_{10}Re_2$: C, 26.0; H, 1.9; Re, 50.4; mol. wt. 736, 738, 740. Found: C, 25.8; H, 2.1; Re, 51.1; mol. wt., 736, 738, 740.

Can. J. Chem. Downloaded from www.nrcresearchpress.com by 210.87.254.40 on 09/05/12
For personal use only.

Can. J. Chem. Downloaded from www.nrcresearchpress.com by 210.87.254.40 on 09/05/12
For personal use only.

Bis(μ-O-1,3-diphenylpropane-1,3-dionatotricarbonylrhenium(I))

Chloropentacarbonylrhenium(I) (1 mmol) and dibenzoylmethane (3 mmol) were refluxed for 3–4 weeks in benzene (~75 ml). Bright orange crystals of the product were removed on a filter and washed with hot benzene. More product was sometimes obtained by heating the dried residues *in vacuo* with a heat lamp for 2–3 h and then washing the melt with hot benzene.

Anal. Calcd. for $C_{36}H_{22}O_{10}Re_2$: C, 43.8; H, 2.2; Re, 37.8; mol. wt., 987. Found: C, 44.0; H, 2.2; Re, 39.7; mol. wt., >818 (highest peak in mass spectrum corresponded to $Re_2(dbm)_2^+$).

Crystallography

$Re_2(CO)_6(acac)_2$

A crystal of $Re_2(CO)_6(acac)_2$ was mounted along the needle axis. Integrated Weissenberg photographs were taken of the (*hnl*) layers (n = 0–6) with CuKα radiation and an integrated precession photograph was taken with MoKα radiation of the (0*kl*) zone and a further precession photograph of the (*h*0*l*) layer was recorded for another crystal. Systematic absences were observed for *hkl* ($h + l = 2n + 1$) and a mirror plane or two fold axis was apparent on all photographs. Assuming the crystal was orthorhombic, possible space groups were *C*222-(No.21), *Cmm*2(No.35), *Amm*2(No.38); *Cmmm*(No. 65). Patterson maps using all of these space groups did not show any self-consistent position for the rhenium atom. Trial positions were used for the rhenium atom but the lowest value of R_1[3] obtained was 0.47. Photographs taken in the (*hk*0) direction showed peculiar radial streaks as though two crystals were present and out of alignment by 1° 40′. Approximately 20 crystals from different recrystallizations were examined by X-ray diffraction and all showed this effect. The apparent unit cell dimensions were a = 15.26(1), b = 16.01(1), c = 17.68(1) Å (calibrated with a crystal of rutile (TiO_2), a = 4.5929(5) Å, c = 2.9591(3) Å (2)). Detailed examination of the photographs suggested that the crystals were either twinned, or that disorder was present giving a higher pseudo-symmetry. No further X-ray studies were made of this compound.

$Re_2(CO)_6(dbm)_2$

A single crystal 0.2 × 0.08 × 0.12 mm³, which showed complete extinction every 90° when viewed through a polarizing microscope was used for initial X-ray studies. A series of Weissenberg and precession photographs showed that the crystal was monoclinic, and the systematic absences *h*0*l*, $l = 2n + 1$, 0*k*0, $k = 2n + 1$ showed that the space group was $P2_1/c$. Precession photographs of the (100) and (010) zones, taken with MoKα radiation and calibrated with the diffraction pattern of a single crystal of TiO_2 (rutile), were used to determine the unit cell parameters. The density of a few crystals was measured by flotation in a bromoform–chloroform mixture.

$C_{36}H_{22}O_{10}Re_2$ f.w. = 986.98

Monoclinic, a = 11.988(8), b = 14.441(9), c = 10.298(7) Å, β = 115.25(7)°, V = 1612 Å³, ρ_o = 2.02, Z = 2, ρ_c = 2.03 (20 °C, MoKα, λ = 0.71069 Å), $P2_{1/c}$ (C_{2h}^5, No. 14)

Six layers perpendicular to ($\bar{1}02$) were recorded on an integrating Weissenberg camera; 4 layers perpendicular to (010) and eight layers perpendicular to (100) were recorded on an integrating precession camera. All photographs except the first three layer photographs on the Weissenberg camera were taken with MoKα radiation. The latter were taken with CuKα radiation. The intensities of all reflections were measured on a Joyce–Loebl microdensitometer. All data were corrected for Lorentz and polarization effects, but no corrections were made for absorption. These data were used to solve the crystal structure although the CuKα Weissenberg data (absorption errors) and (0*kl*) and (*h*0*l*) data (poor picture quality) were removed in later stages of the refinement (see below). Thus the original data set of ~2800 reflections was reduced to 1436 of which 966 were observed. After the structure had been solved the data were retaken using a Syntex $P\bar{1}$ automatic diffractometer. A single crystal of $Re_2(CO)_6(dbm)_2$ ground into a sphere of 0.15 mm radius was used. Data were recorded using zirconium-filtered MoKα radiation which was made monochromatic by using the 002 reflection from highly oriented graphite. The intensities were measured by the θ/2θ scan technique up to a value of 2θ = 45°. 2° scans were made over θ, and the background was counted on both sides. Peaks less than 3σ above the background were called unobserved, and peaks less than background were rejected. The intensity of a standard reflection was measured every 50 reflections. It showed a deviation of ±3.8%. The linear absorption coefficient for the compound for MoKα radiation was 81 cm^{-1}. The data were corrected for Lorentz and polarization effects but not absorption; the absorption coefficients ranged from 5.35 to 4.95. However, the error from neglect of absorption correction will be less than this since the data were collected in three batches (*1*, θ = 0–12; *2*, θ = 11–17; *3*, θ = 17–23) and each batch was given its own scale constant. Thus the maximum error which can arise from neglect of the absorption correction is 3%.

Solution and Refinement of the Structure

Using Patterson maps for the ($\bar{1}02$), (100), and (010) zones it was possible to locate the rhenium atom. Using all the film data, refinement of the rhenium atom parameters for two cycles gave R_1 = 0.16. The shortest Re—Re distance was 3.5 Å suggesting a dimeric unit. Subsequent electron density and electron difference syntheses, with calculations based on known geometries for β-diketone and phenyl groups revealed all the remaining atoms, except the hydrogen atoms. Further refinement, after elimination of CuKα and doubtful data, and using a Cruickshank weighting scheme (3) with the weights set equal to $(61 - F_o + 0.013\ F_o^2)^{-1}$ for observed reflections and zero weight for unobserved reflections, was terminated at R_2 = 0.1016. At this point the main features of the structure were apparent but M—C≡O

[3] $R_1 = (\Sigma||F_o| - |F_c||/\Sigma|F_o|)$, $R_2 = (\Sigma w|F_o^2 - F_c^2|/\Sigma w(F_o)^2)^{\frac{1}{2}}$.

TABLE 1. Atomic parameters* for $C_{36}H_{22}O_{10}Re_2 \times 10^3$

Atom	Coordinates			U_u†
	X	*Y*	*Z*	
Re	112.00(5)	85.30(3)	79.41(5)	‡
O(1)	204.1(8)	−31.2(5)	210(1)	40(2)
O(2)	−42.7(7)	17.7(5)	95(1)	29(2)
O(3)	−34(1)	248(1)	−106(1)	60(2)
O(4)	188(1)	211(1)	336(1)	71(3)
O(5)	347(1)	152(1)	59(1)	61(3)
C(1)	181(1)	−66(1)	311(1)	37(3)
C(2)	−37(1)	−14(1)	220(1)	30(3)
C(3)	67(1)	−47(1)	324(1)	37(3)
C(4)	279(1)	−125(1)	415(1)	35(3)
C(5)	396(1)	−116(1)	428(2)	51(3)
C(6)	495(2)	−173(1)	528(2)	67(5)
C(7)	464(2)	−236(1)	609(2)	69(4)
C(8)	347(2)	−245(1)	593(2)	64(4)
C(9)	250(1)	−190(1)	495(2)	53(4)
C(10)	−157(1)	−11(1)	232(1)	35(3)
C(11)	−245(1)	53(1)	148(2)	47(4)
C(12)	−351(2)	57(1)	153(2)	56(4)
C(13)	−381(2)	−4(1)	248(2)	51(4)
C(14)	−293(2)	−66(1)	330(2)	59(4)
C(15)	−179(1)	−70(1)	326(1)	36(3)
C(16)	22(1)	184(1)	963(1)	35(3)
C(17)	157(1)	163(1)	235(1)	41(3)
C(18)	254(1)	127(1)	64(1)	33(3)

*Estimated standard deviations in parentheses.
†Thermal parameters are in $Å^2 \times 10^3$.
‡For atom Re, $U_{11} = 31.5(3)$, $U_{22} = 30.0(3)$, $U_{33} = 29.0(3)$, $U_{12} = 0.0(3)$, $U_{13} = 17.9(3)$, $U_{23} = 1.3(3)$.

groups were bent (170°(2)) and the phenyl groups were badly distorted (C—C ranged from 1.28 to 1.52 Å and C—C—C angles ranged from 107 to 126°). However difference maps showed no residual peaks at more than ±1.5 e/Å^3 and no parameter shifted by more than 1/3 of its estimated standard deviation in the last few cycles of refinement. At this point the data were retaken on the diffractometer and only diffractometer data were used in subsequent refinements. The new set consisted of 1563 independent reflections, of which 1295 were observed. One cycle of refinement of the diffractometer data using the parameters determined above and varying only the scale constants dropped R_2 to 0.07. Using a Cruickshank weighting scheme with weights equal to $(29 - 0.6F_o + 0.004F_o^2)^{-1}$ for observed reflections and zero for unobserved reflections, and allowing all the parameters listed in Table 1 to vary dropped R_2 to 0.0427 when refinement was terminated. In all the refinement cycles of diffractometer data, which were done using the full matrix least squares program CUDLS written for the CDC-6400 computer by Stephens, the rhenium scattering curve of Cromer (4), including anomalous dispersion corrections (5) was used. The oxygen scattering curve was also that of Cromer, and that for carbon was taken from the International Tables (6). No anomalous dispersion corrections were applied to carbon or oxygen.

In the final cycle of refinement no parameter shifted by more than 1/10 of its estimated standard deviation and a series of electron density difference maps through the unit cell showed no residual peaks outside ±1 e/A^3. The final set of atom parameters is given in Table 1 and a comparison of $|F_o|$ and $|F_c|$ is given in Table 2.[4]

Results and Discussion

The principal interatomic distances and angles are listed in Table 3 and the molecule is illustrated in Fig. 1. The molecule is dimeric (based on the rhenium atoms) and the two halves are centro-symmetrically related. Each rhenium atom is six-coordinate, being attached to atoms at the apices of a very rough octahedron. Three positions are filled by three mutually *cis* carbonyl groups and two further positions are filled by the oxygen atoms of a chelated β-ketoenolate group. The final position is filled by one of the oxygen atoms from the β-ketoenolate group chelated to the other rhenium atom which thus

[4]Table 2 is available, at a nominal charge, from the Depository of Unpublished Data, National Science Library, National Research Council of Canada, Ottawa, Canada, KIA 0S2.

Can. J. Chem. Downloaded from www.nrcresearchpress.com by 210.87.254.40 on 09/05/12
For personal use only.

TABLE 3

(*a*) Bond distances in $C_{36}H_{22}O_{10}Re_2$*

Bond	Length (Å)	Bond	Length (Å)
Re—C(16)	1.88(1)	C(2)—C(3)	1.34(2)
Re—C(17)	1.84(1)	C(4)—C(5)	1.37(2)
Re—C(18)	1.88(2)	C(5)—C(6)	1.45(2)
Re—O(1)	2.143(8)	C(6)—C(7)	1.39(3)
Re—O(2)	2.162(9)	C(7)—C(8)	1.35(3)
Re—$O(2)_i$	2.204(7)	C(8)—C(9)	1.41(2)
C(16)—O(3)	1.17(2)	C(9)—C(4)	1.38(2)
C(17)—O(4)	1.18(2)	C(10)—C(11)	1.39(2)
C(18)—O(5)	1.19(2)	C(11)—C(12)	1.40(3)
O(1)—C(1)	1.29(2)	C(12)—C(13)	1.41(3)
O(2)—C(2)	1.34(2)	C(13)—C(14)	1.37(2)
C(1)—C(4)	1.49(2)	C(14)—C(15)	1.39(3)
C(2)—C(10)	1.49(2)	C(15)—C(10)	1.40(2)
C(1)—C(3)	1.45(2)		

*Subscript i refers to the atom related by a center of symmetry to the corresponding atom listed in Table 1. Estimated standard deviations in parentheses.

(*b*) Bond angles in $C_{36}H_{22}O_{10}Re_2$

Bond	Angle (deg)	Bond	Angle (deg)
O(1)—Re—O(2)	80.0(3)	Re—C(17)—O(4)	178(1)
O(1)—Re—$O(2)_i$	84.1(3)	Re—C(18)—O(5)	171(4)
O(1)—Re—C(16)	176.3(5)	C(9)—C(4)—C(5)	121(1)
O(1)—Re—C(17)	93.0(5)	C(4)—C(5)—C(6)	121(2)
O(1)—Re—C(18)	93.7(5)	C(5)—C(6)—C(7)	117(2)
O(2)—Re—$O(2)_i$	73.7(3)	C(6)—C(7)—C(8)	122(2)
O(2)—Re—C(16)	96.4(5)	C(7)—C(8)—C(9)	122(2)
O(2)—Re—C(17)	98.8(6)	C(8)—C(9)—C(4)	118(2)
O(2)—Re—C(18)	172.0(4)	C(15)—C(10)—C(11)	121(2)
$O(2)_i$—Re—C(16)	94.4(4)	C(10)—C(11)—C(12)	121(2)
$O(2)_i$—Re—C(17)	172.3(6)	C(11)—C(12)—C(13)	118(1)
$O(2)_i$—Re—C(18)	100.9(5)	C(12)—C(13)—C(14)	121(2)
C(16)—Re—C(17)	88.0(6)	C(13)—C(14)—C(15)	122(2)
C(16)—Re—C(18)	89.9(6)	C(14)—C(15)—C(10)	118(1)
C(17)—Re—C(18)	86.5(7)	O(1)—C(1)—C(3)	123(1)
Re—O(2)—Re_i	106.3(4)	O(1)—C(1)—C(4)	116(1)
Re—O(2)—C(2)	122.1(6)	C(3)—C(1)—C(4)	122(1)
Re_i—O(2)—C(2)	113.7(6)	C(1)—C(4)—C(5)	119(1)
O(2)—C(2)—C(3)	122(1)	C(1)—C(4)—C(9)	120(1)
O(2)—C(2)—C(10)	114(1)	C(2)—C(10)—C(11)	118(1)
C(3)—C(2)—C(10)	123(1)	C(2)—C(10)—C(15)	120(1)
C(2)—C(3)—C(1)	126(1)	C(1)—O(1)—Re	126(1)
Re—C(16)—O(3)	178(1)		

forms a bridge between the two rhenium atoms. The rhenium–rhenium distance of 3.494(1) Å is too long to allow any significant metal–metal interaction. Bridging by a β-ketoenolate group through an oxygen atom attached to two metal atoms has been observed previously in $[Ni(acac)_2]_3$ (7) and $[Co(acac)_2]_4$ (8), but it is only recently that dimeric compounds have been shown to have this form of bridging (9). It is of interest to compare features of the bridging section of $[Pr(thd)_3]_2$ (9) and our compound. The bridges in both compounds are asymmetric. The distance of the oxygen atom to the rhenium atom to which it is chelated (2.162(9) Å) is significantly shorter than the distance to the other rhenium atom (2.204(7) Å). For the praseodymium compound the situation is reversed, the corresponding distances, which are much larger, being 2.59(2) Å and 2.47(2) Å. The two Re—O (chelated) distances do not differ significantly

Can. J. Chem. Downloaded from www.nrcresearchpress.com by 210.87.254.40 on 09/05/12
For personal use only.

TABLE 4

(*a*) Selected planes* of atoms in $Re_2(CO)_6(dbm)_2$

Type	Planes	Equation
Re, O(1), O(2)	*A*	$-0.20668x+0.53029y+0.82224z=1.05592$
O(1), O(2), C(1), C(2), C(3)	*B*	$0.10774x+0.90206y+0.41794z=0.52470$
C(4), C(5), C(6), C(7), C(8), C(9)	*C*	$-0.13992x+0.68533y+0.71466z=1.30518$
C(10), C(11), C(12), C(13), C(14), C(15)	*D*	$0.05848x+0.68012y+0.73077z=1.31273$

*All planes, except *A* which is defined uniquely, are least squares planes determined by the program PALS written by Ashmore for the CDC 6400. The program transforms the cell into an orthogonal cell corresponding to the crystallographic *a*, *b*, *c** axes.

(*b*) Dihedral angles between planes

Pair of planes	Dihedral angle (deg)
AB	37
BC	25
BD	22
CD	11

(*c*) Distances in Å from the plane of *B* of selected atoms (the atoms defining ring *B* are not more than 0.08 Å out of plane)

Atom	Distance (Å)	Atom	Distance (Å)
C(4)	−0.37	C(10)	−0.08
C(5)	−0.06	C(11)	0.36
C(7)	−0.91	C(13)	−0.22
C(9)	−0.98	C(15)	−0.55
		Re	1.00

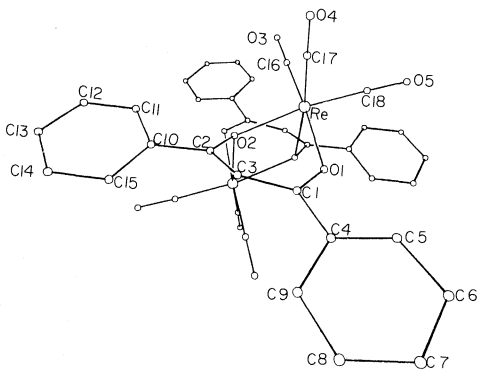

FIG. 1. The molecular structure of $Re_2(CO)_6(dbm)_2$ (the labelling of atoms corresponds to that used in Table 1).

but all Re—O distances appear to be significantly longer than the Re—O (β-ketoenolate) distances in $Re(acac)_2Cl_2$, $Re(acac)Cl_2[P(C_6H_5)_3]_2$, and $ReOCl_2(acac)P(C_6H_5)_3$ (10) where the average distance is 2.02(1) Å.

Long Pr—O distances were also observed by Erasmus *et al.* (9) for $[Pr(thd)_3]_2$ who argued that the cause was the combination of the 70° angles needed in a seven-coordinate structure and the need to keep the O—O distances above 2.8 Å. Similar steric requirements may be the cause of the longer Re—O distance in our compound, since the O(2)—Re—$O(2)_i$ angle is 74°, and the O(2)—$O(2)_i$ distance is significantly shorter (2.62(2) Å) than that observed in $[Pr(thd)_3]_2$.

Other possible reasons for the longer Re—O distance in our compound may be the destruction of any pπ–dπ interaction between the β-ketoenolate ring and the metal since as the data in Table 4 shows the dihedral angle between the plane of the β-ketoenolate ring and the MO_2(chelated) plane is 37°, the largest value ever observed for a β-ketoenolate complex. The comparable angle for $[Pr(thd)_3]_2$ is 29°.

The steric requirements of the bridging oxygen atoms and consequently the remaining chelated oxygen atoms cause a reduction in the OReO angles from the ideal octahedral angle of 90° by from 6–16° (80.0(3), 84.1(3), 73.7(3)°). However, the carbonyl groups remain nearly perpendicular to each other (C—Re—C angles 88.0(6), 89.9(6),

Can. J. Chem. Downloaded from www.nrcresearchpress.com by 210.87.254.40 on 09/05/12
For personal use only.

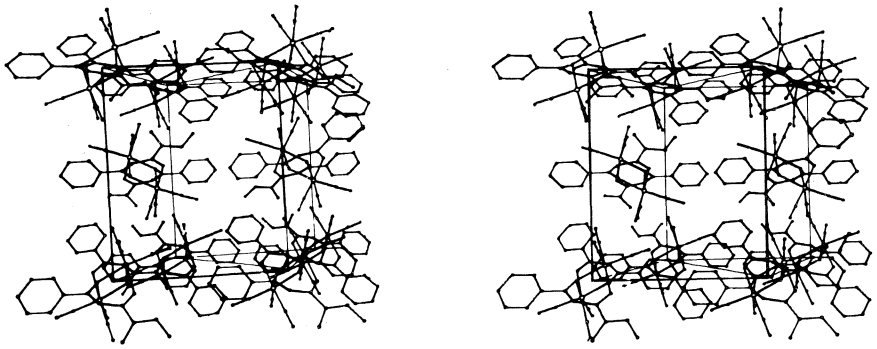

FIG. 2. Stereogram (stereoscopic pair of perspective projections) of $Re_2(CO)_6(dbm)_2$. The contents of one unit cell are shown with some projection outside the cell to show the packing; *b* and *a* are parallel to the side and top of the page respectively, and the view is down *c**.

86.5(7)) so that the angles at rhenium between the carbonyl groups and the oxygen atoms are opened up from 90° (93.0(5) to 100.9(5)). The maximum distortions in all cases are in the O(2), $O(2)_i$, Re C(17), C(18) plane:

The Re—C≡O systems are essentially linear (171(4), 178(1), 178(1)°) and the Re—C bond lengths (1.87(1) Å average) and C≡O bond lengths (1.18(2) Å average) are in good agreement with those found previously in $(B_9C_2H_{11})$-$Re(CO)_3Cs$ (11), $HRe_2Mn(CO)_{12}$ (12), and $(C_8H_7)Re(CO)_3$ (13). The corresponding angles and bond lengths within the β-ketoenolate ring are not significantly different from the average values found for a number of β-ketoenolate structures (14), but the C_1C_3 distance does appear to be significantly longer than the C_2C_3 distance (see below). The bond lengths and angles found within the phenyl rings are normal.

The planarity of certain groups of atoms within the molecule has been tested and the results are presented in Table 4, together with the dihedral angles between the planes. Both phenyl rings are essentially planar, as expected, and are quite markedly twisted from the plane of the β-ketoenolate ring, plane 3 by 25° and plane 4 by 22°. This twist may arise from a simple rotation about the C(2)—C(10) and C(1)—C(4) bonds (φ) or a tilt of the C(4)C(7) and C(13)C(10) axes out of the plane of the β-ketoenolate ring at either C(4) and C(10) or C(1) and C(2) (θ). The results in the second part of Table 4 provide information which allows separation of the two twist components.

Plane 2 is bent at C(1) (θ = 12°) and plane 3 is bent at C(2) (θ = 3°). Both plane 3 and plane 4 are rotated about the C(1)C(4) and C(2)C(10) axes (φ ~ 26°). An examination of the packing diagram suggests that the twists are probably necessary to allow the most efficient packing. The distortion at C(1) (θ) may be the reason for the apparent non-equivalence of the C(1)C(3) and C(2)C(3) distances. The bend will tend to affect the π overlap at C(1), weakening the C(1)C(3) bond, and causing a strengthening of the C(2)C(3) bond, as is observed. The errors in the CO(diketone) distances are such that it is not possible to say whether any similar effect is reflected in these bonds.

As illustrated in Fig. 2, the molecules are packed almost in layers parallel to the *ac* plane, the centers of the layers lying approximately in the unit cell *ac* face and half-way along *b*. Within the layers packing in the *c* direction is determined by the β-ketoenolate system (including the phenyl rings). The molecules are arranged such that the β-ketoenolate on one side of the molecule lies directly above the opposite β-ketoenolate group on the next molecule. Thus, considering only the β-ketoenolate parts of the molecule, the molecules are stacked like tiles on a roof, and are tilted with respect to the *c* direction. Considering alternate layers in the *b* direction the molecules are tilted in opposite directions with respect to the *c* direction. Contact in the *a* direction is provided primarily by the phenyl rings although one carbonyl group in each asymmetric half of the molecule is sandwiched between two phenyl rings, one from its own molecule and one from another.

Contact in the *b* direction is between both carbonyl and phenyl groups, with carbonyl groups on a molecule interleaving with carbonyl groups on molecules both above and below,

Can. J. Chem. Downloaded from www.nrcresearchpress.com by 210.87.254.40 on 09/05/12
For personal use only.

and phenyl groups contacting only phenyl groups in the other molecules.

We thank the National Research Council of Canada for financial support of this work.

1. W. D. COURRIER, A. GUEST, C. J. L. LOCK, and R. H. TOMLINSON. Can. J. Chem. **46**, 2965 (1968).
2. D. T. CROMER and K. HERRINGTON. J. Am. Chem. Soc. **77**, 4708 (1955).
3. D. W. J. CRUICKSHANK. Computing methods in the phase problem. Pergamon Press, Oxford. 1961.
4. D. T. CROMER. Acta Cryst. **18**, 17 (1965).
5. D. T. CROMER and J. T. WABER. Acta Cryst. **18**, 104 (1965).
6. International tables for crystallography. Vol. III. Kynoch Press, Birmingham. 1962. Table 3.3.1A.
7. G. J. BULLEN, R. MASON, and P. PAULING. Inorg. Chem. **4**, 456 (1965).
8. F. A. COTTON and R. C. ELDER. Inorg. Chem. **4**, 1145 (1965).
9. C. S. ERASMUS and J. C. A. BOEYEUS. Acta Cryst. **B26**, 1843 (1970).
10. (*a*) C. J. L. LOCK and C. WAN. Chem. Commun. 1109 (1967). (*b*) C. WAN. Ph.D. Thesis. McMaster University, Hamilton, Ontario. 1969.
11. A. ZALKIN, T. E. HOPKINS, and D. H. TEMPLETON. Inorg. Chem. **5**, 1189 (1966).
12. M. R. CHURCHILL and R. BAU. Inorg. Chem. **6**, 2086 (1967).
13. K. K. JOSHI, R. H. B. MAIS, F. NYMAN, P. G. OWSTON, and A. M. WOOD. J. Chem. Soc. (A), 318 (1968).
14. E. C. LINGAFELTER and R. L. BRAUN. J. Am. Chem. Soc. **88**, 2951 (1966).

Can. J. Chem. Downloaded from www.nrcresearchpress.com by 210.87.254.40 on 09/05/12
For personal use only.

Can. J. Chem. Downloaded from www.nrcresearchpress.com by 210.87.254.5 on 09/05/12
For personal use only.

Semimicro Determination of Sugar Configuration by Measurement of Circular Dichroism of Alditol Acetates[1]

G. M. BEBAULT, J. M. BERRY, Y. M. CHOY, G. G. S. DUTTON, N. FUNNELL, L. D. HAYWARD, AND A. M. STEPHEN[2]

Department of Chemistry, The University of British Columbia, Vancouver 8, British Columbia

Received July 13, 1972

The configuration (D or L) of a sugar may be determined conveniently by circular dichroism measurements at 213 nm on alditol acetates, or their methylated derivatives, where the acetoxy group acts as a chromophore. Only milligram quantities of material are required and the method is well suited to analyzing fractions obtained by gas–liquid chromatography. Structural information which may be derived from the c.d. spectra is briefly discussed.

La configuration (D or L) d'un sucre peut être établie par le dichroisme circulaire à 213 nm soit des alditol acétates soit de leur dérivés méthylés, où le groupement acétate joue le rôle de chromophore. On ne necessite que de très petites quantités de substance et la méthode s'adapte très bien à l'analyse des fractions obtenues par chromatographie en phase gaseuse. On discute brièvement des renseignments structuraux que fournissent les spectres d.c.

Can. J. Chem., **51**, 324 (1973)

Determination of the structure of a polysaccharide requires that the nature and proportion of the constituent sugars be known as well as the positions through which the monosaccharide units are linked in the polymer. Such investigations are facilitated by the use of gas–liquid chromatography (g.l.c.) and sugar ratios are customarily determined as trimethylsilyl ethers or as alditol acetates (1). Similarly, partially methylated sugars are conveniently separated by g.l.c. of their derived alditol acetates and the pattern of methylation is determined by mass spectrometry (2). The technique of mass spectrometry does not readily differentiate between diastereoisomers but this problem may be resolved by collection of the methylated alditol acetate from the effluent gas stream (3) followed by demethylation and characterization of the parent alditol as the peracetate (4).

None of these chromatographic methods is capable of determining the configuration (D or L) of the constituent sugars of a polysaccharide, an aspect of structural studies which is sometimes ignored. One great merit of procedures involving gas–liquid chromatography and mass spectrometry is the small quantity of material required and this is of particular value when only limited amounts of sample are available as, for example, with bacterial polysaccharides. The advantage of these techniques is lost if the determination of the configurational series must be made on macroscopic amounts of specimen. In the particular cases of D-glucose and D-galactose specific oxidases are available (*e.g.* Glucostat and Galactostat reagents, Worthington Biochemical Corporation) but no such method is available for other commonly occurring sugars; even so these are destructive methods.

We have now demonstrated that the sugar configuration (D or L) may be determined unambiguously on milligram quantities of monosaccharide derivatives from the circular dichroism (c.d.) band at *ca.* 213 nm of the corresponding alditol acetates. Just as a sugar of D-configuration may have either a positive or negative specific rotation so also D-alditol acetates may have c.d. bands of either sign. Thus, this sign must be determined empirically and a selection of such data is presented in Table 1. While the method is obviously inapplicable to *meso*-alditols, such as galactitol, it is readily extended

[1]Presented at the VIth International Symposium on Carbohydrate Chemistry, Madison, Wisconsin, August 1972.

[2]On leave from the University of Cape Town, Rondebosch, South Africa.

TABLE 1. Circular dichroism of alditol acetates

Alditol	Configuration	$\Delta\varepsilon_{213}^{MeCN}$
Threitol	L	−0.60
Arabinitol	D	+0.99
Arabinitol	L	−0.96*
Glucitol	D	+0.33
Iditol	L	−0.95
Mannitol	D	+1.7
Talitol	D	+0.73
Fucitol	D	†
Fucitol	L	+0.02
Rhamnitol	L	−1.52
2-*O*-Methylxylitol	D	+0.37
2-*O*-Methylglucitol	D	+0.71
3-*O*-Methylgalactitol	D	−0.31
3-*O*-Methylgalactitol	L	+0.43
3-*O*-Methylmannitol	D	+0.74
2,3-Di-*O*-methylgalactitol	D	+0.26
4,6-Di-*O*-methylgalactitol	D	+0.51
2,4,6-Tri-*O*-methylgalactitol	D	+1.40
2,3,4,6-Tetra-*O*-methylgalactitol	D	+0.54

*A weak band, Δε −0.11, appeared at 265 nm.
†No reliable value obtainable.

to their chiral methylated acetates obtained in structural studies. Conversely, in order to avoid the necessity of measuring c.d. bands for all possible methylated alditols these compounds may conveniently be demethylated (4) where the parent alditol is chiral.

Circular dichroism measurements were made using a Jasco J-20 automatic recording spectropolarimeter, accurately weighed milligram quantities of the alditol acetate being dissolved in acetonitrile (0.15 ml, spectroscopic grade) and placed in a quartz spectrophotometer cell with path length of 0.1 cm. The spectrometer was calibrated using the value of $\varepsilon_L - \varepsilon_R = +2.3$ for (+)-10-camphorsulfonic acid in water (5). The c.d. curves obtained at a scan-rate of 5 nm/min were bell shaped and symmetrical as far as could be ascertained (measurements below 205 nm were not reproducible). While there is no doubt about the sign of the c.d. curve in each case examined, the numerical values of Δε are sometimes hard to reproduce particularly for those compounds which have small values of Δε. This is an instrumental problem since the acetate band lies near the extreme range of the instrument used.

The initial experiments described here were carried out during an investigation, to be described later (6), into the structure of the capsular polysaccharide of *Klebsiella* K-type 7 and have subsequently been employed in other, related structural studies. Measurements have been made on the alditol acetates used for quantitative analysis of polysaccharide hydrolyzates (7), as for *Klebsiella* K-type 21, on methylated alditol acetates and on alditol acetates obtained by demethylation and acetylation. The first method is particularly convenient for mannose where no simple micromethod exists.

The capsular polysaccharide of *Klebsiella* K7 contains glucose, galactose, mannose, and glucuronic acid. From the methylated polysaccharide 2-*O*-methyl- and 2,4,6-tri-*O*-methylglucose are obtained as well as 2,4-di-*O*-methylglucose which results from reduction of the glucuronic acid residue. These compounds were separated by g.l.c. of their alditol acetates. Demethylation and acetylation of the individual fractions yielded (g.l.c.) glucitol hexaacetate, each sample of which gave a positive c.d. band with Δε values ranging from +0.28 to +0.33 depending on the amount of contaminating liquid phase caused by bleeding of the column. Thus each glucose residue in *Klebsiella* K7 is shown to be of D-configuration as is the glucuronic acid. Mannitol hexaacetate samples were obtained similarly from the methylated mannose derivatives, namely the 4,6-di- and 3,4,6-tri-*O*-methyl ethers, and each sample showed a strong positive c.d. band (Δε +1.4 to +1.7) thus demonstrating that all mannose units in the polysaccharide are of D-configuration.

The galactose in *Klebsiella* K7 gives only 2,3,4,6-tetra-*O*-methylgalactose which, on reduction and conversion to the syrupy diacetate, gave a positive c.d. band (Δε +0.54) similar to that obtained from an authentic sample of the methylated sugar of D-configuration and to that obtained by methylation of a wood galactoglucomannan (8). One sample of galactitol hexaacetate prepared by demethylation and acetylation was shown to be achiral.

In addition, a sample of 2-*O*-methyl-D-glucitol pentaacetate obtained from K7 polysaccharide was recrystallized from ethyl acetate – petroleum ether (b.p. 30–60°) and had m.p. 56–57°. The c.d. measurement showed a positive band with Δε +0.71, a value significantly greater than for D-glucitol hexaacetate. Measurements of c.d. spectra may also provide alternative means for determining the position of methoxyl substitution, distinguishing between isomers and estimating the composition of mixtures. Thus,

Can. J. Chem. Downloaded from www.nrcresearchpress.com by 210.87.254.5 on 09/05/12
For personal use only.

Can. J. Chem. Downloaded from www.nrcresearchpress.com by 210.87.254.5 on 09/05/12
For personal use only.

because of symmetry, achiral methylated alditol acetates can be expected in polysaccharide structural studies only from 3-, 2,4-, or 2,3,4-*O*-methyl derivatives of ribose and xylose and 2,4- or 2,5-*O*-methyl derivatives of galactose or allose. The significance and utility of this is demonstrated by the following experiments.

In structural studies on xylans both 2- and 3-*O*-methyl-D-xyloses are commonly encountered and this pair of compounds is not separable as alditol acetates by g.l.c. Collection of the monomethyl pentitol acetate fraction from the g.l.c., in a study on western red cedar (8), and measurement of $\Delta\varepsilon$ showed that the 2-*O*-methyl derivative was present to the extent of 35%, a value in close agreement with that (33%) obtained by integration of the well resolved methoxyl signals in the p.m.r. spectrum of the mixture of alditol acetates. A control experiment verified that 3-*O*-methyl xylitol is achiral.

The symmetry of *meso*-alditols may be destroyed on substitution thus leading to enantiomeric compounds. For example, whereas the sugars 3- and 4-*O*-methyl-D-galactose are diastereoisomers and reduction yields 3- and 4-*O*-methyl-D-galactitol, the latter compound is correctly named 3-*O*-methyl-L-galactitol indicating that the derived alditols are enantiomers. Measurement of the c.d. spectra of these two alditols as the pentaacetates shows clearly that they are of opposite sign although the numerical agreement in the $\Delta\varepsilon$ values is not good (Table 1) for the reasons given previously. The signs of the c.d. bands, however, suffice in these cases to identify the pattern of substitution in such monosaccharides.

The 3- and 4-*O*-methyl-D-galactoses were synthesized by methylation of 1,2:5,6-di-*O*-isopropylidene-D-galactofuranose (9) and of methyl 2,3,6-tri-*O*-benzoyl-α-D-galactopyranoside (10), respectively. Each sugar was crystalline and did not depress the m.p. of authentic samples (10, 11).

Measurement of c.d. spectra of chiral alditol acetates and their methylated derivatives is thus proposed as a convenient, non-destructive method for determining the configurational series of a sugar. The technique requires very small samples and is admirably suited to examining individual fractions obtained by gas–liquid chromatography. By combining these techniques with mass spectrometry most partially methylated monosaccharides may be identified completely, including the configurational assignment.

The symmetry rule relating molecular conformation and the sign of the c.d. band for alditol acetates is now under investigation as is the possibility that differences in rotational strength may be useful in distinguishing isomeric methylated alditol acetates. The c.d. spectra of sugars (12, 13) and of monoacetates of methyl glycosides (14) have been discussed recently.

We are grateful to the National Research Council of Canada for financial support, to Professor J. K. N. Jones, F.R.S. for an authentic sample of 3-*O*-methyl-D-galactose and to Mrs. E. Dumitrescu for skilled assistance in taking spectra. One of us (A.M.S.) is indebted to the University of Cape Town for study leave and to C.S.I.R. for the award of a bursary.

1. G. G. S. DUTTON. Adv. Carbohydr. Chem. In press.
2. H. BJÖRNDAL, C. G. HELLERQVIST, B. LINDBERG, and S. SVENSSON. Angew. Chem. Int. Ed. **9**, 610 (1970).
3. G. G. S DUTTON and K. B. GIBNEY. J. Chromatogr. **72**, 179 (1972).
4. G. G. S DUTTON and Y. M. CHOY. Carbohydr. Res. **21**, 169 (1972).
5. J. Y. CASSIM and J. T. YANG. Biochem. **8**, 1947 (1969).
6. G. G. S. DUTTON and A. M. STEPHEN. To be published.
7. Y. M. CHOY and G. G. S. DUTTON. Can. J. Chem. **51**, 198 (1973).
8. G. G. S. DUTTON and N. FUNNELL. To be published.
9. H. PAULSEN and H. BEHRE. Carbohydr. Res. **2**, 80 (1966).
10. E. G. GROS and I. O. MASTRONARDI. Carbohydr. Res. **10**, 318 (1969).
11. D. J. BELL. Adv. Carbohydr. Chem. **6**, 11 (1951).
12. R. G. NELSON and W. C. JOHNSON, JR. J. Am. Chem. Soc. **94**, 3343 (1972).
13. R. N. TOTTY, J. HUDEC, and L. D. HAYWARD. Carbohydr. Res. **23**, 152 (1972).
14. H. B. BOREN, P. J. GAREGG, L. KENNE, L. MARON, and S. SVENSSON. Acta Chem. Scand. **26**, 644 (1972).

Can. J. Chem. Downloaded from www.nrcresearchpress.com by 210.87.254.42 on 09/05/12
For personal use only.

Canadian Journal of Chemistry

Published by
THE NATIONAL RESEARCH COUNCIL OF CANADA

Journal canadien de chimie

Publié par
LE CONSEIL NATIONAL DE RECHERCHES DU CANADA

Volume 51 Number 3 February 1, 1973

Volume 51 numéro 3 1 février 1973

Preparation of 6′-Substituted Maltoses

LAURENCE DAVID MELTON[1] AND KEITH NORMAN SLESSOR

Department of Chemistry, Simon Fraser University, Burnaby 2, British Columbia

Received June 23, 1972

A relatively simple procedure for the preparation of 6′-substituted maltoses has been developed through the action of *Aspergillus oryzae* amylase on mono-substituted cyclohexaamyloses. 6′-Azido-, -chloro-, -bromo-, -iodo-, and -tosyl-maltose have been prepared in this way. 6′-Deoxy- and 6′-amino-6′-deoxy-maltose were easily prepared from the 6′-iodo- and 6′-azido-maltoses respectively.

Une méthode relativement simple de préparation des maltoses substitués en position 6′ a été developpée; elle fait appel à l'action de l'amylase *Aspergillus oryzae* sur des cyclohexaamyloses monosubstituées. Les azido-6′, chloro-6′, bromo-6′, iodo-6′, et tosyl-6′ maltoses ont été préparés de cette manière. Les déoxy-6′ et amino-6′ deoxy-6′ maltoses ont été préparés facilement en partant respectivement des iodo-6′ et azido-6′ maltoses. [Traduit par le journal]

Can. J. Chem., **51**, 327 (1973)

Introduction

Two general approaches to the chemical synthesis of modified disaccharides are possible. The condensation of two monomeric units, one of which has been structurally modified has been of importance primarily for the synthesis of β-linked D-glucosyl species (1). Maltose derivatives, being α-linked, are considerably more difficult to synthesize via such condensations and thus the second route, modification of a pre-existing disaccharide residue, has been more successful (2, 3). Both approaches have the disadvantages of long and arduous synthetic routes and generally give low yields. A more accessible route to modified oligosaccharides would be useful since such compounds would be of value in α-D-glucopyranosidase studies (4) and mechanistic studies (5).

The action pattern of *Aspergillus oryzae* amylase (Taka-amylase) has been established by studies on synthetic maltoside substrates (4) and partially methylated amylose (6). The effect of a substituent at the C-6 position of a glucopyranosyl residue is to prevent hydrolysis of the glucosidic bond of the substituted residue and allow hydrolysis if the substituent is in the aglycone.

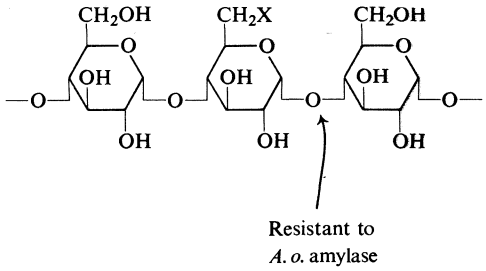

Thus, in theory, *A. oryzae* amylase action on sparsely 6-substituted amylose polymers should result in 6′-substituted maltose units as the oligomeric species. The identification of 6′-*O*-methyl-maltose in the amylase degradation of partially methylated amylose (6) is in accord with this hypothesis. Since *A. oryzae* can cleave the glucosidic bonds of cyclohexaamylose (7), mono-substituted cyclohexaamyloses (8) would appear

[1]Present address: Institut für Physiologische Chemie, Phillips Universität, Marburg (Lahn), West Germany.

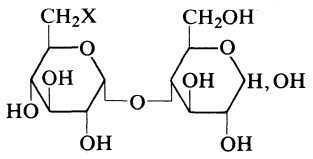

1 X = —Cl
2 X = —Br
3 X = —I
4 X = —O—SO_2—C_7H_7
5 X = —N_3
6 X = —NH_3^+
7 X = —H

Fig. 1. 6′-Substituted maltoses.

to be ideal compounds upon which to establish this concept. Assuming they can act as substrates for *A. oryzae* amylase, this should provide a convenient preparation of a homologous series of 6′-substituted maltose derivatives (see Fig. 1).

Results and Discussion

Hydrolysis of 6-substituted cyclohexaamylose derivatives by *A. oryzae* amylase was followed by the disappearance of the substrate as monitored by t.l.c. The time necessary for the disappearance of the cyclohexaamylose derivative was taken as a measure of the initial rate of hydrolysis and is reported in Table 1. It was obvious that the crude enzyme preparation, as supplied by the manufacturers, contained a maltase since little or no unsubstituted maltose was detected.

The presence of large amounts of glucose produced in the hydrolysis as well as release of monosaccharide units from the glycoproteinaceous amylase complicated the chromatography, but extended enzymatic hydrolysis of the tosyl,[2] azido, and halo cyclohexaamyloses indicated a material of intermediate R_f between glucose and the appropriate 6-substituted glucose. No 6-substituted glucoses were found to be formed. Fractionation of the enzymatic digests by charcoal column chromatography yielded the pure substituted oligosaccharides. The monotrityl[3] cyclohexaamylose enzymatic hydrolysis was extremely slow and complicated by the slow release of triphenylcarbinol and cyclohexaamylose, the latter being further degraded to glucose. Monodeoxy cyclohexaamylose was degraded completely to 6-deoxy-glucose and glucose, quite in keeping with the specificity studies on the amylase which have shown the non-recognition of the replacement of a 6-OH with H (4). Monoamino cyclohexaamylose was hydrolyzed slowly and apparently incompletely. The presence of material showing the characteristics of 6″-amino-6″-deoxy-maltotriose was detected (9). The ease with which the deoxy and amino deoxy disaccharide could be prepared from the iodo and azido disaccharide led us to abandon attempts to isolate these particular disaccharides from enzyme digests.

TABLE 1. Relative rates of the initial hydrolysis of monosubstituted cyclohexaamyloses by *A. oryzae* amylase

6-Substituent	Approximate relative rate
—OH (parent compound)	1.0
—H (monodeoxy)	1.0
—O—SO_2—C_7H_7 (monotosyl)	0.8
—Cl (monochloro)	0.8
—I (monoiodo)	0.8
—N_3 (monoazido)	0.4
—NH_3^+ (monoamino)	0.2–0.4
—O—$C_{19}H_{15}$ (monotrityl)	<0.1

Elution of the substituted oligosaccharides from charcoal columns was accomplished with various alcohols at different concentrations depending on the affinity of the sugar for the column. The tosyl and iodo derivative appeared to be most tightly held requiring 25% 1-propanol and 4% 1-butanol for elution.

Structural elucidation of the nature of the oligosaccharide was carried out in several ways. Mass spectral analysis of the pertrimethylsilyl derivatives of all the oligosaccharides showed conclusively that all were substituted disaccharides, since the molecular ion for each species was identified and higher *m/e* peaks were not present.

The monochloro disaccharide was reduced with sodium borohydride and hydrolyzed with acid to give only two products, which were identical with 6-chloro-6-deoxy-glucose and -glucitol. Assuming no change in the anomeric linkage of the disaccharide, the chloro disaccharide must then be, 6′-chloro-6′-deoxy-maltose (**1**). Further chemical evidence was derived from the iodo deoxydisaccharide by reduction to the deoxy analog with Pd/H_2 and "base peeling" of the deoxy disaccharide (10). The only reducing sugar remaining after 2 h was 6-deoxy-glucose indicating

[2]Tosyl = *p*-toluenesulfonyl.

[3]Trityl = triphenylmethyl.

Can. J. Chem. Downloaded from www.nrcresearchpress.com by 210.87.254.42 on 09/05/12
For personal use only.

Can. J. Chem. Downloaded from www.nrcresearchpress.com by 210.87.254.42 on 09/05/12
For personal use only.

that the deoxy glucose had been linked glycosidically to the glucose. The time for decomposition was typical of 1–4 linkages, 1–3 being fast (15 min), 1–6 slower (~4 h), and 1–2 stable.[4] Thus the deoxy disaccharide must be 6′-deoxy-maltose and the iodo disaccharide, 6′-deoxy-6′-iodo-maltose. Base peeling was not successful in determining the structures of derivatives **1** to **5** since the 6 substituent could complicate the transformation to saccharinic acids, leaving no reducing sugars to be identified.

Mass spectral analysis was useful not only in establishing the size of the substituted oligosaccharides, but also in determining the substitution pattern. A fragmentation pattern characteristic of the 1–4 linkage (11, 12) was observed for all the derivatives (**1**–**7**). The formation of fragment I (Table 4), which in turn decomposes to IV, is based on the fragmentation pattern observed for permethylated disaccharides (11) containing a 1–4 linkage. Pertrimethylsilyl derivatives of a 1–4 linked disaccharide have been found to form fragment II which subsequently loses a methyl radical to give fragment III (12). The decomposition of the molecular-ion to fragment V, characteristic of the reducing residue, has been demonstrated (13). In the present investigation, fragments I-IV, derived from the non-reducing moiety all had the correct *m/e* to have incorporated the substituent. These peaks were not seen in the mass spectrum of the pertrimethylsilyl derivative of maltose. On the other hand, there was no evidence that the 6-position of the reducing moiety was ever substituted with anything other than a trimethylsilyl ether. Fragments containing chlorine and bromine were relatively easily identified due to their characteristic isotopic cluster.

6′-Deoxy-maltose (**7**) and 6′-amino-6′-deoxy-maltose (**6**) are most easily prepared from the iodo (**3**) and azido (**5**) derivatives rather than directly from the deoxy- and amino-cyclohexaamylose. Both of the reactions are accomplished by reduction with hydrogen in the presence of palladium-on-carbon; conditions which do not effect the reduction of glucose to glucitol. As previously mentioned, the deoxy function was shown to be in the 6′-moiety through base peeling leaving 6-deoxy-glucose as the only reducing sugar. The position of the amino function was assigned on the basis of the specificity of the enzyme and mass spectral analysis of the azide (**5**) and amine (**6**). All of these indicated 6′-amino-6′-deoxy-maltose. Mass spectral analysis of the persilylated amine was complicated due to the presence of about 30% of the mono-*N*-trimethylsilyl derivative.

Thus, the chemical and spectroscopic evidence not only indicates the oligosaccharides to be 6′-substituted maltoses, but essentially rules out all other possibilities. This result is in complete accord with the expected specificity of *A. oryzae* amylase. The method then, allows a relatively simple preparation of a variety of 6′-substituted maltoses.

Experimental

General

Evaporations were carried out on a Buchi rotary evaporator at bath temperatures not exceeding 45°. Optical rotations were measured on a Perkin–Elmer Model P22 spectropolarimeter. Freeze-drying was done at −40°, 0.3 mm Hg generally overnight. Tes-tape, glucose analysis paper, was purchased from Eli Lilly and Co., Toronto. Activated charcoal, Darco, G-60, 20–40 mesh, was purchased from Matheson, Coleman and Bell. *A. oryzae* amylase, Type IV-A was purchased from Sigma Chemical Co. The mass spectra of pertrimethylsilyl derivatives were measured within 3 h of preparation and recorded on a Hitachi Perkin–Elmer RMU-7 spectrometer. The ionizing potential was 80 eV and the source temperature was 200°. Spectra were calibrated by direct counting of spectra recorded at high gain.

6′-Substituted Maltoses

Monosubstituted cyclohexaamylose (100–400 mg) was dissolved in 0.2 *N* acetate buffer, p*H* 5.5, containing 0.01 *M* $CaCl_2$, so that the concentration of the sugar was 10 mg/ml. *A. oryzae* amylase (10 mg/ml) was added and the solution was kept at 40° for the required time (Table 2). The amylolysis was stopped by addition of 3 *N* ammonia (0.4 ml/ml of digest). The precipitated protein was removed by centrifugation, and the supernatant liquid was evaporated. The material was dissolved in water (60 ml) and applied to an activated charcoal column (20 × 1.7 cm). The column was eluted with water (1200 ml) and 5% aqueous ethanol (1200 ml). These eluents contained salts, glucose, and traces of other reducing sugars. The column was then eluted as indicated in Table 2. The appropriate fractions were checked by t.l.c. and evaporated to dryness. The solid was extracted with 100% ethanol (3 × 0.2 ml/mg of material) and the extracts combined, filtered, and evaporated to give the pure 6′-substituted maltose. Only the iodo derivative (**3**) was crystalline, but the physical properties of all the derivatives are recorded in Table 3.

Pertrimethylsilyl Derivatives of 6′-Substituted Maltoses

The maltose derivative (3–5 mg) was dissolved in pyridine (1 ml) and hexamethyldisilazane (0.2 ml) and trimethylchlorosilane (0.1 ml) were added. The mixture

[4]T. J. Painter. Personal communication.

TABLE 2. Amylolysis of cyclohexaamyloses by *A. oryzae* amylase

Substrate cyclohexaamylose	Product maltose	Digest time (days)	Eluent	Eluent volume (l)	Yield (%)
6-Chloro-6-deoxy-	**1**	7	15% ethanol	1	60
6-Bromo-6-deoxy-	**2**	7	20% ethanol	1.5	45
6-Deoxy-6-iodo-	**3**	7	4% butanol	1	36
6-*O*-Tosyl-	**4**	5	25% ethanol	1*	
			25% 1-propanol	1	37
6-Azido-6-deoxy-	**5**	8	10% ethanol	2.5	75

*Seems to contain 6′-*O*-acetyl-maltose derived from solvolysis of the tosyl compounds in the acetate buffer.

TABLE 3. Physical properties of 6′-substituted maltoses

Compound	M.p. (°)	$[\alpha]_D^{22}$ (°)	*c* (in water)	Formula	Analysis (%) Calcd.	Found	T.l.c.* R_G	Solvent
1	—	+116	1.1	$C_{12}H_{21}ClO_{10}\cdot H_2O$	C 38.05 H 6.12	38.2 5.8	1.2	A
2	—	+105	1.0	$C_{12}H_{21}BrO_{10}$	C 35.57 H 5.22	35.3 5.2	1.3	C
3	110–112	+89	1.1	$C_{12}H_{21}IO_{10}$	C 31.87 H 4.68	31.7 4.7	1.3	C
4	—	+87	1.1	$C_{19}H_{28}O_{13}S\cdot H_2O$	C 44.36 H 5.88	44.3 5.7	1.4	B
5	—	+103	1.1	$C_{12}H_{21}N_3O_{10}\cdot H_2O$	C 37.41 H 6.02 N 10.91	37.6 5.7 10.6	1.2	B
6	—	+111 lit. (2) +88	0.64 0.3	$C_{12}H_{23}NO_{10}\cdot H_2O$	C 40.11 H 7.01 N 3.90	39.9 6.7 3.6	0.4	D
7	—	+134 lit. (2) +113	1.04 2.8	$C_{12}H_{22}O_{10}\cdot H_2O$	C 41.86 H 6.93	41.74 6.00	1.1	A

*R_G, relative to glucose. Solvent composition — butanone : methanol : water : 1 *N* acetic acid — A, 14:3:3:0; B, 145:28:27:0; C, 6:1:1:0; D, 3:1:0:1.

was shaken vigorously and kept at 40° for 1 h. The solution was evaporated to dryness and the solid extracted with hexane (4 ml). The hexane extract was filtered and the filtrate evaporated to give a colorless syrup. The characteristic peaks observed in the mass spectra are tabulated in Table 4.

*Reduction and Hydrolysis of 6′-Chloro-6′-deoxy-maltose (**1**)*

Monochloromaltose (1.5 mg) was dissolved in water (1 ml) and sodium borohydride (1.5 mg) was added. After 1 h at room temperature, the reduction was stopped by addition of 1 *N* acetic acid until the solution was p*H* 4.5. The solution was then passed through Dowex 50 (H^+) (1 ml) and evaporated three times with methanol. The residue was dissolved in 1 *N* HCl (0.3 ml), heated on a steam bath for 2 h, and neutralized with Dowex 3 (OH^-). Glucose oxidase Tes-tape gave a negative test on the neutral solution (0.2 ml) and t.l.c. (solvent A) clearly indicated only 6-chloro-6-deoxy-glucose and -glucitol to be present. These compounds were completely separable from glucose and 6-chloro-6-deoxy-glucitol in this solvent system. Clearly, the monochloromaltose is the 6′-substituted species (**1**).

*6′-Amino-6′-deoxy-maltose (**6**)*

6′-Azido-6′-deoxy-maltose (**5**) (15 mg) was dissolved in water (4 ml) and reduced with hydrogen over palladium black (5 mg) at atmospheric pressure for 3 h. The catalyst was removed by filtration and the solution evaporated to dryness, yielding 6′-amino-6′-deoxy-maltose (**6**) (13 mg) as a colorless glass. Glucose was not reduced under identical conditions. The pertrimethylsilyl derivative was prepared by dissolving **6** (3 mg) in pyridine (2 ml) at 80°, cooling to 40°, and adding hexamethyldisilazane (0.4 ml) and trimethylchlorosilane (0.2 ml). The previously described procedure was used for the isolation of this derivative. Approximately one-third of the sample was *N*-trimethylsilylated under these conditions.

*6′-Deoxy-maltose (**7**)*

Crystalline 6′-deoxy-6′-iodo-maltose (**3**) (33 mg) was dissolved in water–pyridine (9:1) (6 ml) and 5% palladium-on-charcoal (30 mg) was added. A steady but slow

Can. J. Chem. Downloaded from www.nrcresearchpress.com by 210.87.254.42 on 09/05/12
For personal use only.

Can. J. Chem. Downloaded from www.nrcresearchpress.com by 210.87.254.42 on 09/05/12
For personal use only.

TABLE 4. Mass spectra of 6′-substituted maltoses*

Species	X = Cl	(1)	Br	(2)	I	(3)	Ts	(4)	N_3	(4)	NH_2	(6)‡	H	(7)
M^+	864	(0.01)	908	(0.02)	956	(0.004)	1000	(0.009)	871	(0.003)	845	(0.0)	830	(0.02)
$(M - CH_3)^+$	849	(0.02)	893	(0.03)	941	(0.006)	985	(0.01)	856	(0.007)	830	(0.007)	815	(0.04)
(I) 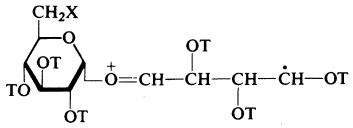	732	(0.005)	776	(0.006)	824	(0.005)	868	(0.0)	739	†	713	†	698	†
(II) 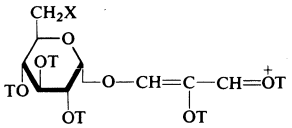	629	(0.009)	673	(0.0)	721	(0.009)	765	(0.002)	636	(0.007)	610	†	595	(0.07)
(III) 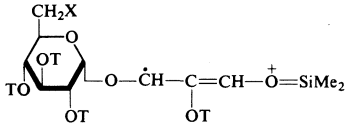	614	(0.07)	658	(0.01)	706	(0.07)	750	(0.5)	621	(0.007)	595	(0.2)	580	†
(IV) 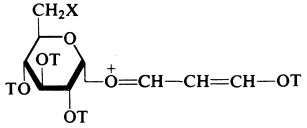	541	(0.3)	585	(0.1)	633	(0.4)	677	(0.4)	548	(0.08)	522	†	507	(0.2)
(V) 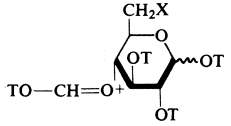	515	(0.0)	559	(0.0)	607	(0.0)	651	(0.02)	522	(0.0)	496	(0.0)	481	†
(V) 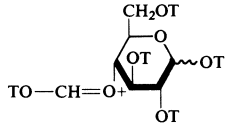	569	(0.15)	569	(0.07)	569	(0.21)	569	(0.03)	569	(0.02)	569	(0.01)	569	†

*Sample inlet temperatures: 150° **2**; 160°, **7**; 170°, **1**, **3**, **5**, **6**; 190°, **4**. Results given as *m/e* (abundance in %, relative to that of base peak). Base peak *m/e* 73 for **1**, **4**; 147 for **6**; 204 for **2**, **3**, **5**, **7**.
†Peak is part of the isotopic cluster of a more intense peak.
‡Contained ~30% mono-*N*-trimethylsilyl derivative.

stream of hydrogen was introduced through a capillary for 7 h, after which time t.l.c. indicated the reduction to be complete. Glucose was shown to be unaffected under these conditions. The catalyst was removed by filtration and the solution evaporated. The residue was dissolved in water (5 ml), passed through Dowex 3 (OH^-) (3 ml), and eluate and washings freeze-dried to provide a colorless glass (25 mg). This material was purified by elution from a charcoal column as previously described, with 4% ethanol in water, to give pure 6′-deoxy-maltose (**7**) (21 mg). The disaccharide (1 mg) was dissolved in water (0.15 ml) and 5% triethylamine in 50% aqueous methanol (0.15 ml) was added. The solution was heated at 70° for 2 h during which time the reaction was monitored by t.l.c. (solvent C, Table 3). The reaction was complete in 2 h and only 6-deoxy-glucose and some very slow running material (α-isosaccharinic acid) were observed. No glucose or reaction intermediates were seen.

We express our thanks to the National Research Council of Canada for a Fellowship (LDM) and an Operating Grant (KNS). Thanks are due also to M. K. Yang for analytical results, and G. Owen for the mass spectra, both of this department.

1. J. Stanek, M. Cerny, and J. Pacak. The Oligosaccharides. Academic Press, New York. 1965.
2. G. G. S. Dutton and K. N. Slessor. Can. J. Chem. **44**, 1069 (1966).
3. H. Arita, M. Isemura, T. Ikenaka, and Y. Matsushima. Bull. Chem. Soc. Jap. **43**, 818 (1970).
4. H. Arita, M. Isemura, T. Ikenaka, and Y. Matsushima. J. Biochem. (Tokyo), **68**, 91 (1970).
5 B. Capon. Chem. Rev. **69**, 407 (1969).
6. M. Fujinaga-Isemura, T. Ikenaka, and Y. Matsushima. J. Biochem. (Tokyo), **64**, 73 (1968).
7. V. M. Hanrahan and M. L. Caldwell. J. Am. Chem. Soc. **75**, 2191 (1953).
8. L. D. Melton and K. N. Slessor. Carbohydr. Res. **18**, 29 (1971).
9. L. D. Melton. Synthesis of monosubstituted cyclohexaamyloses and monosubstituted maltoses. Ph.D. Thesis. Simon Fraser University, Burnaby, B.C. 1972.
10. V. P. Rege, T. J. Painter, W. M. Watkins, and W. T. J. Morgan. Nature, **200**, 532 (1963).
11. N. K. Kochetkov and O. S. Chizhov. Adv. Carbohydr. Chem. **21**, 39 (1966).
12. O. S. Chizhov, N. V. Molodtsov, and N. K. Kochetkov. Carbohydr. Res. **4**, 273 (1967).
13. N. K. Kochetkov, O. S. Chizhov, and N. V. Molodtsov. Tetrahedron, **24**, 5587 (1968).

Can. J. Chem. Downloaded from www.nrcresearchpress.com by 210.87.254.42 on 09/05/12
For personal use only.

Formation and Reactions of (1-Chloroalkyl)carbamoyl Chlorides. Synthesis of 1,2,4-Triazolidine-5-ones

KINKO KOYANO AND COLIN R. MCARTHUR[1]

Department of Chemistry, York University, Downsview, Ontario

Received July 20, 1972

N-(α-Chlorobenzyl)carbaniloyl chloride and (α-chlorobenzyl)methylcarbamoyl chloride are formed by reaction of phosgene with *N*-benzylideneaniline and *N*-benzylidenemethylamine, respectively. Reaction of these carbamoyl chlorides with a number of nucleophiles is described, some of which cause cleavage of the benzyl to nitrogen bond while others give rise to substitution products without such cleavage. Of the latter type, substituted hydrazines react to effect ring closure to 1,2,4-triazolidine-5-ones. The method serves as a convenient synthesis of these new heterocyclic systems.

Le chlorure de *N*-(α-chlorobenzyl) carbaniloyle et le chlorure de (α-chlorobenzyl) méthylcarbamoyle sont formés dans la réaction entre le phosgène et la *N*-benzylidène aniline et la *N*-benzylidène méthylamine, respectivement. La réaction de ces chlorures de carbamoyle avec un certain nombre de nucléophiles est décrite, certains d'entre eux provoquent le clivage du benzyle lié à l'azote tandis que d'autres donnent lieu à des produits de substitution sans clivage. Les hydrazines substituées réagissent selon ce dernier schéma en formant un cycle de type triazolidine-1,2,4, ones-5. La méthode constitue une synthèse commode de ces nouveaux systèmes hétérocycliques. [Traduit par le journal]

Can. J. Chem., **51**, 333 (1973)

Introduction

Phosgene has been reported to react with azomethines, **1**, to produce *N*-(chloroformyl)-azomethines, **2**, and 1-chloroalkyl isocyanates, **3** (1).

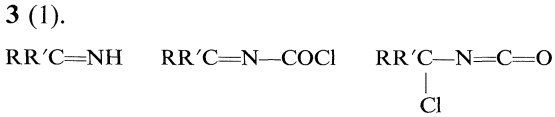

1 **2** **3**

Enolizable imines of the type **4** were reported by Chupp (2) to react with phosgene to afford (1-alkenyl)carbamoyl chlorides, **5**. In an unusual example, *N*-isobutylidinemethylamine (**4**, R = R′ = R‴ = CH_3; R″ = H) was converted to (1-chloro-2-methylpropyl)methylcarbamoyl chloride (**6**) which is surprisingly stable to dehydrochlorination (3). Kiefer (4) recently reported the reaction of phosgene with some non-enolizable *N*-substituted imines to give the corresponding (1-chloroalkyl)carbamoyl chlorides.

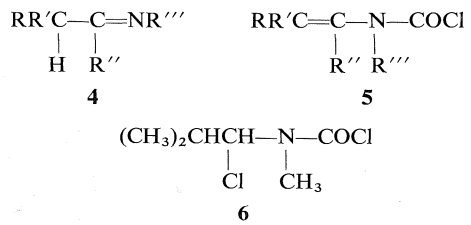

4 **5**

6

[1]Author to whom correspondence should be addressed.

The present work was undertaken to examine the reaction of non-enolizable *N*-substituted imines with phosgene as a general route to (1-chloroalkyl)carbamoyl chlorides with a view to the use of such compounds in the synthesis of heterocyclic systems. A similar study was made of *N*-(α-chlorobenzylidene)carbamoyl chloride formed from the addition of phosgene to benzonitrile (5). In this paper, we report the formation of the (α-chlorobenzyl)carbamoyl chlorides, **8**, and some of their reactions including conversion to the 1,2,4-triazolidine-5-ones, **22**.

Results and Discussion

N-Benzylideneaniline (**7***a*) and *N*-benzylidenemethylamine (**7***b*) underwent reaction with phosgene in benzene solution to afford *N*-(α-chlorobenzyl)carbaniloyl chloride (**8***a*) and (α-chlorobenzyl)methylcarbamoyl chloride (**8***b*), respectively (see Scheme 1). The (1-chloroalkyl)carbamoyl chlorides **8** were stable and could be isolated under anhydrous conditions. The struc-

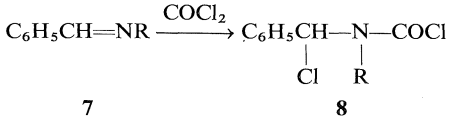

7 **8**

a, R = C_6H_5; *b*, R = CH_3

SCHEME 1

Can. J. Chem. Downloaded from www.nrcresearchpress.com by 210.87.254.105 on 09/05/12
For personal use only.

tural assignments **8** are consistent with spectral data and elemental analyses (see Experimental).

Ethanolysis of **8***a* caused cleavage to benzaldehyde diethyl acetal (**9**) and ethyl carbanilate (**10**). On the other hand, the methyl derivative, **8***b* did not undergo cleavage, but was converted to a product characterized as ethyl (α-ethoxybenzyl)-methylcarbamate (**11**) which was stable in refluxing ethanol (Scheme 2).

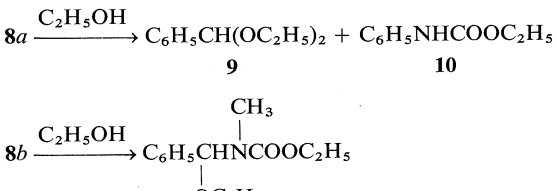

a, R = C_6H_5; *b*, R = CH_3

SCHEME 2

Reactions of the carbamoyl chlorides, **8**, with anhydrous ammonia and primary amines resulted in products which can be explained as having formed through the intermediacy of the corresponding (α-aminobenzyl)ureas, **12**, followed by base-catalyzed cleavage (see Scheme 3). From reaction with methylamine, *N*-benzylidenemethylamine (**13**, $R' = CH_3$) was obtained from both **8***a* and *b* together with 1-methyl-3-phenylurea (**14***a*, $R' = CH_3$) from **8***a*, and 1,3-dimethylurea (**14***b*, $R' = CH_3$) from **8***b*. Aniline reacted in an analogous fashion to produce *N*-benzylideneaniline (**13**, $R' = C_6H_5$) from both **8***a* and *b* along with 1,3-diphenylurea (**14***a*, $R' = C_6H_5$) from **8***a*, and 1-methyl-3-phenylurea (**14***b*, $R' = C_6H_5$) from **8***b*. Anhydrous ammonia converted **8***a* to 1,1′-benzylidenebis(3-phenylurea) (**15***a*) which, at least formally, can be viewed as having been formed through the cleavage of **12***a* (R′ = H) to benzylidene-ammonia (**13**, R′ = H) and phenylurea (**14***a*, R′ = H) which reacted further to give the bisurea. In an analogous fashion, 1,1′-benzylidene-bis-(3-methylurea) (**15***b*) was obtained from **8***b*. The bisureas **15***a* (6) and *b* (7) have been reported previously as products of the condensation of benzaldehyde with phenylurea, and methylurea, respectively.

Secondary amines also would be expected to give rise to (α-aminobenzyl)ureas analogous to the intermediates **12** but which would be stable to base-catalyzed cleavage. Dimethylamine converted **8***a* and *b* to the 1,1-dimethyl-3-(α-dimethylaminobenzyl)ureas, **16***a* and *b*, respectively. These compounds react readily with moisture in the atmosphere. On hydrolysis, each forms benzaldehyde and the corresponding urea, **17***a* or *b*. The 3-phenyl-derivative, **16***a*, undergoes what appears to be slow thermal decomposition in a dry nitrogen atmosphere at ambient temperatures as well.

Reaction of the carbamoyl chlorides, **8**, with hydrazine resulted in the formation of the semicarbazones, **19**, as the main products, together with the biureas, **20**, in smaller yields. The 1,2,4-triazolidine-5-ones, **18**, could be postulated as intermediates which underwent base-catalyzed ring opening to the semicarbazones **19** (see Scheme 4).

Under oxidizing conditions, the semicarbazone (**19***a*) is known to undergo cyclization to 3,4-diphenyl-Δ^2-1,2,4-triazolin-5-one (**21**) (8) (see Scheme 5). This result also suggests the intermediacy of the triazolidinone **18**.

The formation of the biureas, **20**, could be explained by an analogous base-catalyzed cleavage of the corresponding 1,2-bis[(α-hydrazinobenzyl)carbamoyl]hydrazine derivative which would be expected to form, in addition to **18**, by reaction of **8***a* or *b* with hydrazine.

1,2-Disubstituted 1,2,4-triazolidine-5-ones would be expected to be stable to base-catalyzed ring opening of the type **18** → **19**. Reaction of the (α-chlorobenzyl)carbamoyl chlorides, **8**, with 1,2-dimethyl- and with 1,2-diphenylhydrazine afforded convenient routes to the new heterocycles, **22**, which appear to be the first reported 1,2,4-triazolidine-5-ones (see Scheme 6). The structures are consistent with elemental analyses and spectral data (see Experimental).

Experimental

All melting points are uncorrected. The n.m.r. spectra were recorded on a Varian HA100 (100 MHz) spectrometer using tetramethylsilane as internal standard. The i.r. spectra were recorded on a Unicam SP1000 spectrometer. Mass spectra were measured on a Hitachi–Perkin–Elmer RMU-6 mass spectrometer. Microanalyses were performed by A. B. Gygli, Toronto, Ontario.

In every case in which a previously described compound was isolated as a product, the spectral data (n.m.r. and i.r.) were identical with those of an authentic sample. For each such crystalline product, the m.p. of a mixture with an authentic sample was not depressed. Each authentic sample was prepared either by the procedure cited, or if none is cited, by an unequivocal method.

Can. J. Chem. Downloaded from www.nrcresearchpress.com by 210.87.254.105 on 09/05/12
For personal use only.

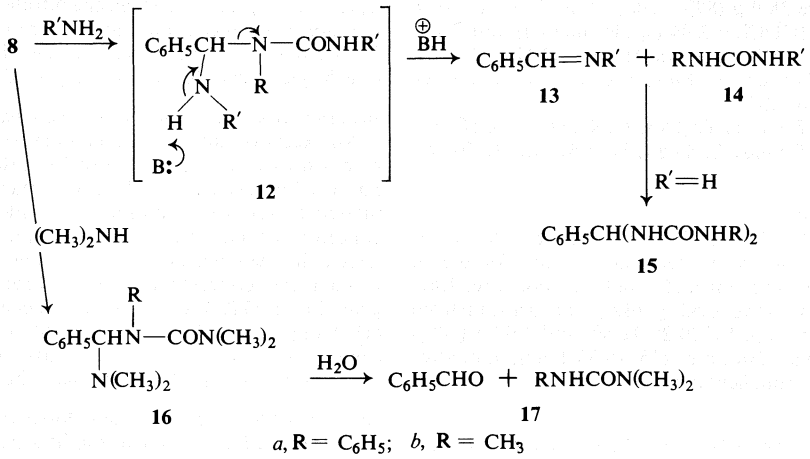

SCHEME 3

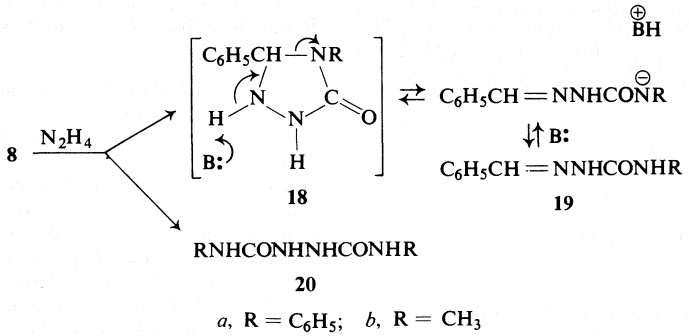

SCHEME 4

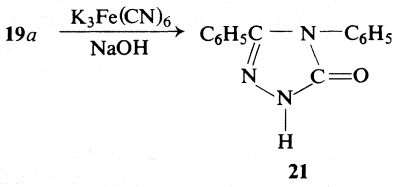

SCHEME 5

Synthesis of N-(α-Chlorobenzyl)carbaniloyl Chloride (8a)

To a stirred solution of 36.2 g (0.20 mol) of *N*-benzylideneaniline (9) in 100 ml of benzene maintained in an ice bath was added, over 1 h, 175 g of a 12.5% solution (0.22 mol) of phosgene in benzene (Matheson). The reaction mixture was stirred for an additional hour and then filtered, if necessary, to remove *N*-benzylideneaniline hydrochloride. Evaporation of solvent under reduced pressure gave 52.6 g (95% yield) of crude **8a**, m.p. 99–100.5° as white needles, m.p. after recrystallization from hexane, 102.5–103.5°; n.m.r. δ ($CDCl_3$): 7.19 (m, 10H, aromatic-H) and 7.57 p.p.m. (s, 1H, C_6H_5CH); i.r. spectrum (Nujol): $\nu_{C=O}$ 1750 cm^{-1}.

Anal. Calcd. for $C_{14}H_{11}Cl_2NO$: C, 60.03; H, 3.95; Cl, 25.32; N, 5.00. Found: C, 60.17; H, 3.85; Cl, 25.47; N, 5.00.

Synthesis of (α-Chlorobenzyl)methylcarbamoyl Chloride (8b)

By a procedure similar to that described above for the synthesis of **8a**, 22.8 g (0.20 mol) of freshly distilled *N*-benzylidenemethylamine (Aldrich) was treated with

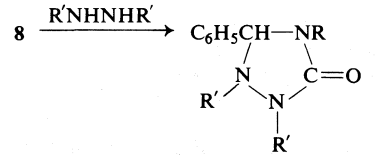

a R=C_6H_5; R′=CH_3
b R=R′=CH_3
c R=R′=C_6H_5
d R=CH_3; R′=C_6H_5

SCHEME 6

Can. J. Chem. Downloaded from www.nrcresearchpress.com by 210.87.254.105 on 09/05/12
For personal use only.

Can. J. Chem. Downloaded from www.nrcresearchpress.com by 210.87.254.105 on 09/05/12
For personal use only.

phosgene to give 38.9 g (89% yield) of **8***b*, b.p. 116° (0.1 Torr); n.m.r. δ ($CDCl_3$): 2.94 (s, 3H, methyl) and 7.40–7.55 p.p.m. (m, 6H, aromatic-H and C_6H_5CH); i.r. (neat): $\nu_{C=O}$ 1744 cm^{-1}. Mass spectrum parent peak (*m/e*): 217; calcd., 217.

Anal. Calcd. for $C_9H_9Cl_2NO$: C, 49.57; H, 4.16; Cl, 32.51; N, 6.42. Found: C, 49.83; H, 4.41; Cl, 32.76; N, 6.47.

Ethanolysis of ***8a***

A solution of 2.7 g (0.0096 mol) of **8***a* in 50 ml of anhydrous ethanol was heated under reflux for 0.5 h. After removal of ethanol under reduced pressure, fractional distillation gave 0.85 g (49%) of benzaldehyde diethyl acetal (**9**), b.p. 58° (0.25 Torr), and 1.07 g (68%) of ethyl carbanilate (**10**), b.p. 115° (0.35 Torr), m.p. after recrystallization from heptane, 49.5–50.0°.

Ethanolysis of ***8b***

A solution of 5.0 g (0.023 mol) of **8***b* in 50 ml of ethanol was heated under reflux for 0.5 h. After removal of ethanol under reduced pressure, distillation gave 3.7 g (68%) of ethyl (α-ethoxybenzyl)methylcarbamate (**11**), b.p. 118° (0.060 Torr). An analytical sample was obtained by g.l.c.; n.m.r. δ ($CDCl_3$): 1.31, 1.32 (double t, J = 7 Hz, 6H, OCH_2CH_3), 2.57 (s, 3H, NCH_3), 3.66 (q, J = 7 Hz, 2H, $C_6H_5CH(OCH_2CH_3)$), 4.27 (q, J = 7 Hz, 2H, $COOCH_2CH_3$), 6.51 (s, 1H, C_6H_5CH), and 7.2–7.7 p.p.m. (m, 5H, aromatic-H); i.r. (neat): $\nu_{C=O}$ 1710 and ν_{C-O-C} 1160, 1100, 1030 cm^{-1}.

Anal. Calcd. for $C_{13}H_{19}NO_3$: C, 65.80; H, 8.07; N, 5.90. Found C, 65.91; H, 7.99; N, 5.78.

Reactions of the Carbamoyl Chlorides ***8*** *with Methylamine and with Aniline*

(i) Methylamine

An excess of methylamine was passed through a cooled (0°) stirred solution of either **8***a* or *b* (0.02 mol) in 150 ml of dry ether over a period of 1 h. The solids produced were separated by filtration. From the reaction with **8***a*, 1-methyl-3-phenylurea (**14***a*, R′ = CH_3) was obtained in 89% yield by slurrying the solids in water to dissolve methylamine hydrochloride, collecting the remaining solids by filtration, and recrystallizing them from water, m.p. 151.0–151.5°. From **8***b*, 1,3-dimethylurea (**14***b*, R′ = CH_3) was obtained by slurrying the solids in ethanol, filtering to remove insoluble ammonium chloride, concentrating the ethanol solution, and crystallizing the residue from ether. Additional **14***b* was obtained by concentration of the ether filtrate from the reaction mixture to give a total yield of 70%, m.p. 104–106°. *N*-Benzylidenemethylamine was obtained in 59% yield from the reaction with **8***a*, and in 86% yield from **8***b* by distillation (b.p. 84°, 42 Torr) of the residue from the respective concentrated ether filtrates.

(ii) Aniline

To a stirred solution of either **8***a* or *b* (0.02 mol) in 100 ml of benzene, heated under reflux was added a solution of aniline (0.11 mol) in 150 ml of benzene. The reaction mixture was heated under reflux for an additional 1.5 h, cooled, and filtered. The solid material was slurried in water to remove aniline hydrochloride and the remaining insoluble material recrystallized from ethanol to give, from **8***a*, 1,3-diphenylurea (**14***a*, R′ = C_6H_5) in 81% yield, and from **8***b*, 1-methyl-3-phenylurea (**14***b*, R′ = C_6H_5) in 77% yield. The benzene filtrate from the reaction mixture was concentrated and the residue recrystallized from ethanol to give *N*-benzylideneaniline, m.p. 48–50° in 86% yield from **8***a*, and in 81% yield from **8***b*.

Reaction of ***8a*** *with Anhydrous Ammonia*

An excess of anhydrous ammonia was passed through a cooled (0°) stirred solution of 5.6 g (0.02 mol) of **8***a* in 50 ml of benzene over 0.5 h. The reaction mixture was filtered to remove ammonium chloride, and the filtrate concentrated under reduced pressure. The residue was heated in heptane, and after cooling, the crystals that formed were collected and recrystallized from ethanol to give 2.6 g (72%) of 1,1′-benzylidenebis(3-phenylurea) (**15***a*), m.p. 206–207° (lit. (6), m.p. 198–199°). An authentic sample was prepared as previously described (6). A satisfactory elemental analysis was obtained.

Reaction of ***8b*** *with Anhydrous Ammonia*

By a procedure similar to that described above for the reaction of **8***a*, a solution of **8***b* was treated with an excess of anhydrous ammonia. 1,1′-Benzylidenebis(3-methylurea) (**15***b*) was obtained in 55% yield, m.p. after recrystallization from methanol, 188–189.5° (lit. (7), m.p. 187–188°). An authentic sample was prepared as previously described (7). A satisfactory elemental analysis was obtained.

*Synthesis of 1,1-Dimethyl-3-(α-dimethylaminobenzyl)-3-phenylurea (****16a****)*

To a stirred, cooled (0°) solution of 5.8 g (0.021 mol) of **8***a* in 100 ml of ether was added 10 g (0.22 mol) of dimethylamine over a period of 30 min. The reaction mixture was filtered to remove dimethylamine hydrochloride, and the filtrate concentrated to give 6.2 g (100%) of crude **16***a*, m.p. after recrystallization from ether, 68–70°; n.m.r. δ ($CDCl_3$): 2.37 (s, 6H, $C_6H_5CHN(CH_3)_2$); 2.61 (s, 6H, $CON(CH_3)_2$), 5.65 (s, 1H, C_6H_5CH), and 6.9–7.4 p.p.m. (m, 10H, aromatic-H); i.r. (Nujol): $\nu_{C=O}$ 1645 cm^{-1}.

Anal. Calcd. for $C_{18}H_{23}N_3O$: C, 72.77; H, 7.77; N, 14.09. Found: C, 72.61; H, 7.76; N, 14.28.

A solution of **16***a* in ether was shaken with water. Benzaldehyde and 1,1-dimethyl-3-phenylurea (**17***a*) were isolated from the reaction mixture in essentially quantitative yields.

*Synthesis of 1,1,3-Trimethyl-3-(α-dimethylaminobenzyl)urea (****16b****)*

By a procedure similar to that described for the synthesis of **16***a*, 5 g (0.023 mol) of **8***b* was treated with 10 g (0.22 mol) of dimethylamine to give 5.1 g (94.6%) of crude **16***b*, m.p. after recrystallization from ether, 45.5–47°; n.m.r. δ ($CDCl_3$): 2.27 (s, 6H, $C_6H_5CHN(CH_3)_2$), 2.70 (s, 3H, $N(CH_3)CON(CH_3)_2$), 2.76 (s, 6H, $CON(CH_3)_2$), 5.30 (s, 1H, C_6H_5CH), and 7.25–7.65 p.p.m. (m, 5H, aromatic-H); i.r. (Nujol): $\nu_{C=O}$ 1658 cm^{-1}.

Anal. Calcd. for $C_{13}H_{21}N_3O$: C, 66.35; H, 9.00; N, 17.86. Found: C, 66.12; H, 8.88; N, 17.79.

A solution of **16***b* in ether was shaken with water. Benzaldehyde and trimethylurea (**17***b*) were isolated from the reaction mixture in essentially quantitative yields.

Reaction of ***8a*** *with Hydrazine*

To a stirred solution of 8.4 g (0.03 mol) of **8***a* in 50 ml of benzene cooled in an ice bath was added, over 15 min, a

Can. J. Chem. Downloaded from www.nrcresearchpress.com by 210.87.254.105 on 09/05/12
For personal use only.

solution of 3.2 g (0.10 mol) of anhydrous hydrazine in 10 ml of dimethylformamide. The cooled reaction mixture was stirred for an additional hour and then poured into 100 ml of ice-water. The solid product was collected, slurried in ethanol, and the remaining solid recrystallized from dimethylformamide to give 1.45 g (35%) of 1,6-diphenylbiurea (**20***a*), m.p. 255–256° (lit. (10), m.p. 270°). An authentic sample was prepared from the reaction of phenyl isocyanate with hydrazine. A satisfactory elemental analysis was obtained.

The benzene filtrate from the reaction mixture, and the ethanol filtrate were concentrated and the residues recrystallized from ethanol to give a total of 4.2 g (60%) of benzaldehyde phenylsemicarbazone (**19***a*), m.p. 182–183° (lit. (8), m.p. 180°). An authentic sample was prepared as previously described (8).

*Reaction of **8***b* with Hydrazine*

By a procedure similar to that described for **8***a*, 6.54 g (0.03 mol) of **8***b* was treated with 3.2 g (0.1 mol) of anhydrous hydrazine. From the solids that formed, 0.076 g (3.5%) of 1,6-dimethylbiurea (**20***b*), m.p. after recrystallization from dimethylformamide, 258–259° (lit. (11), m.p. 260°) was obtained. An authentic sample was prepared by the reaction of methyl isocyanate with hydrazine.

The filtrate of the reaction mixture was concentrated and the residue crystallized from ethanol to give 2.2 g (41.5%) of benzaldehyde methylsemicarbazone (**19***b*), m.p. 167–169° (lit. (12), m.p. 166°). An authentic sample was prepared as previously described (12).

*Synthesis of 1,2-Dimethyl-3,4-diphenyl-1,2,4-triazolidine-5-one (**22***a*)*

To a solution of 4 g (0.03 mol) of 1,2-dimethylhydrazine dihydrochloride (13) in 15 ml of water was added a solution of 6.1 g (0.11 mol) of potassium hydroxide in 15 ml of water. Then, 120 ml of acetone was added, and the reaction mixture was filtered to remove potassium chloride.

To 30 ml of acetone cooled in an ice bath (10–12°) were added concurrently over 1 h the 1,2-dimethylhydrazine solution and a solution of 5.6 g (0.02 mol) of **8***a* in 150 ml of acetone. The reaction mixture was stirred for another 1.5 h, filtered, and concentrated. The residue was dissolved in benzene and the benzene solution washed with water, dried over magnesium sulfate and concentrated. The solid residue was recrystallized from heptane to give 3.0 g (57%) of **22***a*, m.p. 142.5–144°); n.m.r. δ ($CDCl_3$): 2.67 (s, 3H, NCH_3), 3.01 (s, 3H, NCH_3), 5.29 (s, 1H, C_6H_5CH), and 7.0–7.5 p.p.m. (m, 10H, aromatic-H), no exchange with D_2O; i.r. (Nujol): $\nu_{C=O}$ 1698 cm^{-1}; no absorptions assignable to NH. Mass spectrum parent peak (*m/e*) 267; calcd., 267.

Anal. Calcd. for $C_{16}H_{17}N_3O$: C, 71.89; H, 6.41; N, 15.72. Found: C, 71.82; H, 6.24; N, 15.88.

*Synthesis of 1,2,4-Trimethyl-3-phenyl-1,2,4-triazolidine-5-one (**22***b*)*

By a procedure similar to that described above for the synthesis of **22***a*, **8***b* was treated with 1,2-dimethylhydrazine to give **22***b* in 42% yield, b.p. 109° (0.02 Torr); n.m.r. δ ($CDCl_3$): 2.49 (s, 3H, NCH_3), 2.57 (s, 3H, NCH_3), 2.94 (s, 3H, NCH_3), 4.43 (s, 1H, C_6H_5CH), and 7.42 p.p.m. (s, 5H, aromatic-H); i.r. (neat): $\nu_{C=O}$ 1729 cm^{-1}; no absorptions assignable to NH. Mass spectrum parent peak (*m/e*): 205; calcd., 205.

Anal. Calcd. for $C_{11}H_{15}N_3O$: C, 64.36; H, 7.37; N, 20.47. Found: C, 64.54; H, 7.46; N, 20.28.

*Synthesis of 1,2,3,4-Tetraphenyl-1,2,4-triazolidine-5-one (**22***c*)*

A solution of 4.2 g (0.015 mol) of **8***a* in 100 ml of benzene, and another solution of 5.52 g (0.03 mol) of 1,2-diphenylhydrazine (Aldrich, freshly recrystallized from ethanol) in 100 ml of benzene were added concurrently over 1 h with stirring to 30 ml of benzene. The reaction mixture was then heated under reflux for 2 h, cooled, and filtered. Evaporation of the solution and crystallization of the residue from heptane gave 2.8 g (49.5%) of **22***c*, m.p. after recrystallization from heptane, 148–148.5°; n.m.r. δ ($CDCl_3$): 6.16 (s, 1H, C_6H_5CH), and 7.0–7.75 p.p.m. (m, 20H, aromatic-H); i.r. (Nujol): $\nu_{C=O}$ 1705 cm^{-1}; no absorption assignable to NH. Mass spectrum parent peak (*m/e*): 391; calcd., 391.

Anal. Calcd. for $C_{24}H_{21}N_3O$: C, 79.77, H, 5.41; N, 10.73. Found: C, 79.71; H, 5.54; N, 10.76.

*Synthesis of 1,2,3-Triphenyl-4-methyl-1,2,4-triazolidine-5-one (**22***d*)*

By a procedure similar to that described above for the synthesis of **22***c*, **8***b* was treated with 1,2-diphenylhydrazine to give **22***d* (33.4% yield), m.p. after recrystallization from heptane, 115.5–116.5°; n.m.r. δ ($CDCl_3$): 2.69 (s, 1H, $N—CH_3$), 5.55 (s, 1H, C_6H_5CH), and 7.0–7.75 p.p.m. (m, 15H, aromatic-H); i.r. (Nujol): $\nu_{C=O}$ 1718 cm^{-1}; no absorption assignable to NH. Mass spectrum parent peak (*m/e*): 329; calcd., 329.

Anal. Calcd. for $C_{21}H_{19}N_3O$: C, 76.57; H, 5.81; N, 12.76. Found: C, 76.64; H, 5.98; N, 12.67.

We thank the National Research Council of Canada or a grant in aid of this research.

1. (*a*) L. I. Samarai, O. V. Vishnevskii, and G. I. Derkach. Chem. Ber. **102**, 2972 (1969). (*b*) L. I. Samarai, O. V. Vishnevskii, and G. I. Derkach. Angew. Chem. (Int. Ed.) **7**, 621 (1968). (*c*) L. I. Samarai, V. P. Belaya, O. V. Vishnevskii, and G. I. Derkach. Zh. Org. Khim. **4**, 720 (1968).
2. J. P. Chupp. J. Heterocycl. Chem. **8**, 557 (1971).
3. J. P. Chupp. J. Heterocycl. Chem. **8**, 677 (1971).
4. H. Kiefer. Synth. 39 (1972).
5. S. Yanagida, M. Yokoe, M. Ohoka, and S. Komori. Bull. Chem. Soc. Jap. **44**, 2182 (1971).
6. W. J. Hale and N. A. Lange. J. Am. Chem. Soc. **41**, 379 (1919).
7. H. Schiff. Ann. **291**, 370 (1896).
8. V. R. Srinivasan, G. Ramachander, and S. Naqui. Arch. Pharm. **295**, 405 (1962).
9. L. A. Bigelow and H. Eatough. *In* Organic syntheses. Coll. Vol. 1. 2nd Ed. A. H. Blatt, Editor. Wiley, New York, N.Y. 1941. p. 80.
10. O. Tsuge, I. Shinkai, and M. Tashiro. Bull. Chem. Soc. Jap. **42**, 185 (1969).
11. C Vogelesang. Rec. trav. chim. **62**, 5 (1943).
12. H. J. Backer. Rec. trav. chim. **34**, 187 (1915).
13. H. H. Hatt. *In* Organic syntheses. Coll. Vol. 2, A. H. Blatt, Editor. Wiley, New York, N.Y. 1943. p. 208.

New Synthetic Routes to Δ^2-Pyrazolin-5-ones[1]

M. J. NYE AND W. P. TANG[2]
Department of Chemistry, University of Guelph, Guelph, Ontario
Received August 10, 1972

Three new synthetic routes to Δ^2-pyrazolin-5-ones involving base-catalyzed molecular rearrangements are reported.

Trois nouvelles méthodes de synthèse des Δ^2-pyrazolidones-5 sont rapportées; elles impliquent toutes des réarrangements catalysés par les bases. [Traduit par le journal]

Can. J. Chem., **51**, 338 (1973)

Can. J. Chem. Downloaded from www.nrcresearchpress.com by 210.87.254.105 on 09/05/12
For personal use only.

Introduction

Two related base-catalyzed rearrangement reactions are the acyloin and halohydrin rearrangements (eqs. 1 and 3). Both involve push–pull mechanisms, where an oxide ion is the electron source and an electronegative atom (X) is the electron sink. In the acyloin case, X is doubly bonded, whereas in the halohydrin case it is singly bonded. Although these reactions embody an easy way of placing a migrating group on the α carbon atom of a carbonyl functional group, they have been applied only sparingly to organic synthesis. This paper shows how appropriate substitution of the archetypes leads to two new convenient syntheses of Δ^2-pyrazolin-5-ones, exemplified by eqs. 2 and 4.

Acyloin rearrangement:

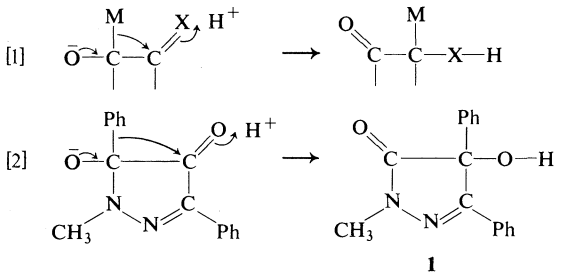

Halohydrin rearrangement:

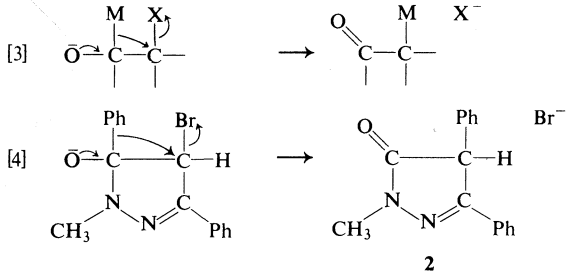

Results and Discussion

Acyloin Rearrangement:

Treatment of 5-hydroxy-3,5-diphenyl-Δ^2-pyrazolin-4-one (**3***a*) or its methyl derivative **3***b* with methanolic potassium hydroxide gave respectively 4-hydroxy-3,4-diphenyl-Δ^2-pyrazolin-5-one (**4***a*) or **4***b* in 76–80% yields. The simplest possible mechanism of this reaction involves first the removal of the OH proton from **3** followed by an acyloin rearrangement of the anion (eq. 2). It is of interest that the Δ^2-pyrazolin-5-one appears to be thermodynamically more stable than the Δ^2-pyrazolin-4-one, which can be crudely rationalized as arising from the high inherent stability of amide-like structures (3).

Chemical evidence for the structures **4***a* and *b* was provided by the alternative synthesis of **4***b* by the oxidation of 1-methyl-3,4-diphenyl-Δ^2-pyrazolin-5-one (**2**) using hydrogen peroxide. This route has been shown by Veibel (4) to be a general method for hydroxylation of the 4-position of Δ^2-pyrazolin-5-ones.[3]

The structural assignments are also supported by the similarity of the i.r. and u.v. spectra between **4***a*, **4***b*, and the model compound **5** (5) (Table 1).

4-Hydroxy-3,4-diphenyl-Δ^2-pyrazolin-5-one (**4***a*) could alternatively be obtained by boiling 4-hydroxy-3,5-diphenylpyrazole (**6**) in methanolic

[1]See also refs. 1 and 2 for preliminary communications.
[2]Present address: Department of Chemistry, University of Alberta, Edmonton, Alberta.

[3]Δ^2-Pyrazolin-5-ones might exist as at least two other tautomeric structures; however in this paper this name and structure have been arbitrarily chosen to represent the equilibrium mixture.

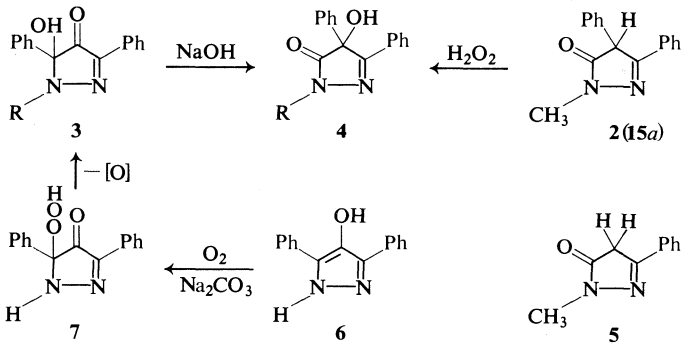

SCHEME 1

TABLE 1. Spectral data

Compound	I.r. (Nujol mull) (cm^{-1})	U.v. (95% ethanol) λ_{max} (nm)	ε
4*a*	1704	297	13 800
4*b*	1691	310	13 000
5 (5)	1698	301	12 190

sodium carbonate in the presence of air. The rationalization of this reaction (Scheme 1: **6** → **7** → **3***a* → **4***a*) is based on the established occurrence of hydroperoxide intermediates such as **8** (6) and **9** (7) in the aerial oxidation of related

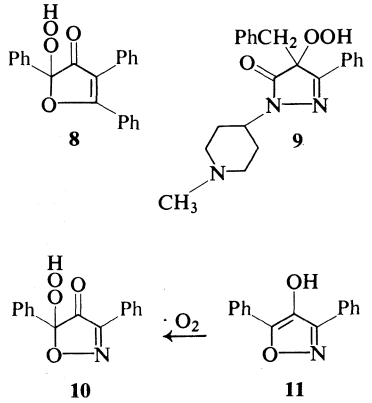

heterocycles, and on their known conversion to parent alcohols (8). The most closely related hydroperoxide in the literature is **10** which was recently proposed as an intermediate arising from aerial oxidation of **11** (9).

Halohydrin Rearrangement

Treatment of 2-bromo-1,3-diphenyl-1,3-propanedione (**12***a*) with methylhydrazine in ethanol at room temperature gave 1-methyl-3,4-diphenyl-Δ²-pyrazolin-5-one (**15***a*) in a 56% yield.

The probable reaction sequence is shown in Scheme 2 (**12***a* → **13***a* → **14***a* → **15***a*). The first two steps which are standard ketone reactions are followed by a base-catalyzed halohydrin rearrangement in step *3*. Of the several reasonable alternative mechanisms, most of which differ only in the order of occurrence of the dozen or so minor steps, the given mechanism was favored for the following reasons. (*a*) Stable analogs of the intermediate **14** have been isolated by other workers (10). (*b*) The intermediate **14** can be diverted to an alternative product, 4-hydroxy-1-methyl-3,5-diphenylpyrazole (**17**), if Z^- is a poorer leaving group than Br^-. Treatment of **12***b* with methylhydrazine gives **17** in 92% yield (3). It is seen that when the two competing reactions proceed by loss of groups of similar leaving capability (OH^- and OAc^-), then the product-controlling factor is the fact that the next step gives rise to the more stable aromatic (6π-electron system) in the observed reaction but not in the competing one (step *4 vs.* step *3*). (*c*) Steps *2* and *3* are actually a manifestation of the well-authenticated Favorskii reaction proceeding via the semibenzilic mechanism.

In the treatment of **12***b* with methylhydrazine, the stage at which the acetoxyl group is hydro-

Can. J. Chem. Downloaded from www.nrcresearchpress.com by 210.87.254.105 on 09/05/12
For personal use only.

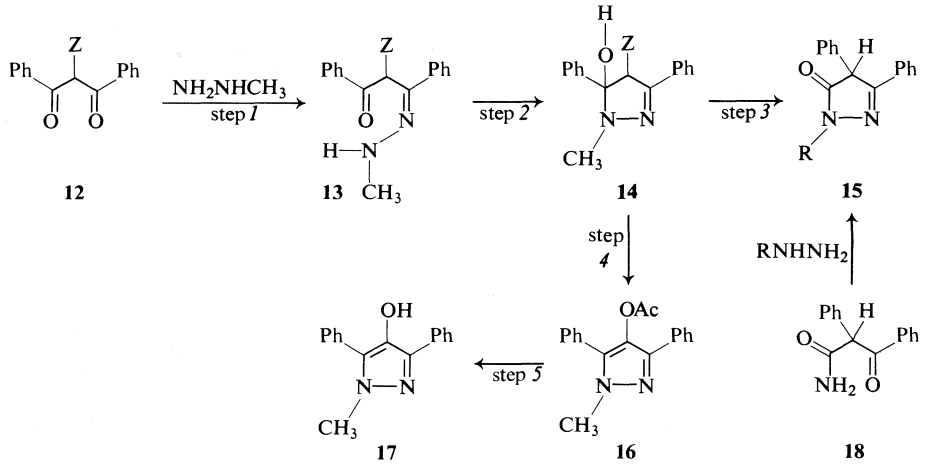

12 13 14 15 16 17 18

a, Z = Br, R = CH_3; *b*, Z = OAc, R = H; *c*, R = Ph

SCHEME 2

lyzed has not been established, but we represent this step as being the final one, since **16**, a phenolic-type ester should be hydrolyzed the fastest of all the compounds involved. If acetic acid is the solvent used in the above reaction the acetylated product **16** can be isolated.

The structure of **15***a* was established chemically by a variation of the well-known route to Δ^2-pyrazolin-5-ones from β-oxocarboxylic acid derivatives. α-Phenyl-α-benzoylacetamide (**18**) was heated with methylhydrazine dihydrochloride in refluxing ethanol for 4 h to give a 50% yield of **15***a*. When **18** was treated with hydrazine and phenylhydrazine, the expected products **15***b* and *c* were obtained and their melting points agreed with literature values (11, 12). The α-phenyl-α-benzoylacetamide was prepared by acid hydrolysis of α-phenyl-α-benzoylacetonitrile which had been made by condensing ethyl benzoate with benzyl cyanide in the presence of sodium ethoxide. Since this method of synthesis of **15** does not completely rule out the possibility of one of the tautomeric pair **19** and **20** being the actual structures, extra evidence concerning the position of the methyl group on the ring was necessary. This was afforded by the conversion of **15***a* to the alcohol **4** using hydrogen peroxide (reported earlier in paper). No alcoholic product is conceivable for a similar oxidation of **19** or **20**.

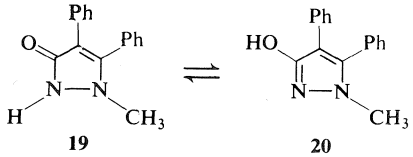

19 20

Before this final piece of evidence was obtained, there was skepticism over the structure of **15***a*, since Grünanger and Vita-Finzi had reported (11) that this compound has m.p. 272–274 °C compared with m.p. (double) 216–219, 235–237 °C obtained by us. This difference could arise through polymorphism, but we suggest that the compound obtained by those workers had, in fact, structure **19** or **20**, since their synthesis involving methylation of 5-ethoxy-3,4-diphenylpyrazole followed by hydrolytic removal of the ethyl group was ambiguous and no additional evidence was offered.

With the skeletal structure of **15***a* established, it remains to determine the position of the labile hydrogen. The three most probable tautomeric structures are **21***a*, **22***a*, and **23***a*. Katritzky and Maine (5) have studied the i.r. spectra of a number

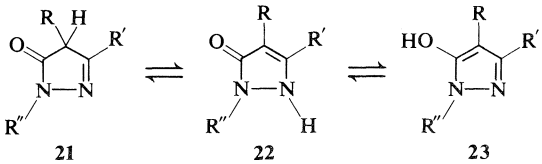

21 22 23

a, R = R′ = Ph; R″ = CH_3

of pyrazolin-5-ones and alkylated examples of the three types of tautomers and report that in chloroform solution the Δ^2-pyrazolin-5-ones (**21**) show a strong band around 1700 cm^{-1}, the Δ^3-pyrazolin-5-ones (**22**) show a strong band around 1630–1660

Can. J. Chem. Downloaded from www.nrcresearchpress.com by 210.87.254.105 on 09/05/12
For personal use only.

Can. J. Chem. Downloaded from www.nrcresearchpress.com by 210.87.254.105 on 09/05/12
For personal use only.

cm^{-1}, and the 5-hydroxypyrazoles (**23**) show no strong band between 1600 and 2000 cm^{-1}. However in the solid state (Nujol mull), whereas **21** still shows a distinctive band, **22** and **23** cannot be distinguished with certainty because both absorb in the low 1600's. In this work we obtained only solid state i.r. spectra, and no band appeared between 1620 and 2000 cm^{-1} indicating the absence of **21***a*, but not distinguishing between **22***a* and **23***a*. The tautomer **21***a* was also ruled out by the u.v. spectrum which was somewhat different from the spectra of model compounds **4***a* and *b*, and by the n.m.r. spectrum which did not show the ring CH proton but instead possessed a labile proton which only became visible by proton exchange in DMSO containing a trace of D_2O. U.v. and n.m.r. data were of no help in distinguishing between **22***a* and **23***a*.

1-Methyl-3,4-diphenyl-Δ²-pyrazolin-5-one (**15***a*) may also be prepared by treatment of 2,2-dibromo-1,3-diphenyl-1,3-propanedione with a fourfold excess of methylhydrazine in ethanol. Although this reaction must involve an extra reduction step compared with the conversion of **12***a* to **15***a*, both reactions give yields of about 55%.

Conclusion

Three new synthetic routes to Δ²-pyrazolin-5-ones have been reported in this paper. One of the advantages of each of the routes is that phenyl groups can easily be incorporated into the system. The difficulty of introducing phenyl groups using traditional syntheses is supported by the fact that neither of the two key products (**2** and **4**) reported in this paper had been prepared previously, in spite of the abundance of Δ²-pyrazolin-5-ones in the literature. It is suggested that the acyloin and halohydrin rearrangements deserve much more attention than they receive at present, especially in the synthesis of compounds bearing aryl substituents and when dealing with compounds sensitive to acid.

It is of interest that an analog of the aerial oxidation of 4-hydroxy-1-methyl-3,5-diphenylpyrazole (**6**) followed by acyloin rearrangement to 4-hydroxy-1-methyl-3,4-diphenyl-Δ²-pyrazolin-5-one (**4***a*) exists in nature in the conversion of ibogaine to iboluteine (13).

Experimental

M.p.'s were determined on a Meltemp apparatus and are uncorrected. I.r. spectra were obtained on a Beckman IR 5A spectrophotometer in Nujol mulls unless otherwise indicated, and strong bands between 1000 and 4000 cm^{-1} are quoted. U.v. spectra were measured on a Unicam SP 800 spectrophotometer in 95% EtOH at 25°. N.m.r. spectra were recorded on a Varian A60A spectrometer using an internal TMS standard. Microanalyses were performed by C. Daesslé, Organic Microanalyses, Montreal, Quebec.

*4-Hydroxy-3,4-diphenyl-Δ²-pyrazolin-5-one (**4***a*)

*(a) From 5-Hydroxy-3,5-diphenyl-Δ²-pyrazolin-4-one (**3***a*)*

A solution of **3***a* (14) (111 mg) in 1 ml 5% methanolic potassium hydroxide was refluxed for ½ h, 5 ml of water was added, and the solution refrigerated at 5° for 15 h. The solid product (85 mg, 76%) was filtered and crystallized twice from aqueous ethanol to give pure **4***a*, m.p. 210–212.5°; ν_{max} 3190, 2550 br, 1704, 1590, 1276, and 1142 cm^{-1}; λ_{max} 216 (ε 14 800) and 297 nm (13 800); δ (acetone-d_6) 6.10 (1H, s, OH), 7.25–7.60 (8H, m, aromatic), 7.78–7.94 (2H, m, aromatic), and 10.53 p.p.m. (1H, s, NH); *m/e* (70 eV): 252 (74%, M^+), 105 (100%), 77 (85%).

Anal. Calcd. for $C_{15}H_{12}N_2O_2$: C, 71.44; H, 4.80; N, 11.11. Found: C, 71.93; H, 4.87; N, 11.22.

*(b) From 4-Hydroxy-3,5-diphenylpyrazole (**6**)*

A mixture of **6** (14) (0.236 g, 0.001 mol), sodium carbonate (0.117 g, 0.0011 mol), and 90% methanol (20 ml) was refluxed for 2 h. The solids were filtered and washed with a small amount of methanol. Evaporation of the filtrate left solids which melted at 370–415°. Fractional recrystallization from ethanol gave a 32% yield of the starting material and a 31% yield of **4***a*, identified by mixture m.p. and i.r. spectrum.

*5-Hydroxy-1-methyl-3,5-diphenyl-Δ²-pyrazolin-4-one (**3***b*)

Compound **3***b* was prepared according to the method for 5-hydroxy-3,5-diphenyl-Δ²-pyrazolin-4-one (**3***a*) (14) with slight modification. A cooled (ice-bath), stirred solution of diphenylpropanetrione hydrate (15) (1.28 g, 0.005 mol) in methanol (10 ml) was treated with a solution of methylhydrazine (0.43 ml, *ca.* 0.008 mol) in methanol (1 ml). After 1 h, water (40 ml) was added to cause precipitation. Compound **3***b* was isolated in bright orange prisms, m.p. 140–141° (dec.) (from cold dilute methanol or warm benzene–petroleum) (65–75% yield); ν_{max} 3236, 1696, 1674 strong, 1204, and 1177 cm^{-1}; λ_{max} 215 (infl) (ε 13 400), 271 (15 800), and 420 nm (4660); δ ($CHCl_3$-*d*) 3.25 (3H, s, Me), 7.25–7.47 (9H, m, 8H aromatic, 1H hydroxyl exchangeable with D_2O), and 7.93–8.09 p.p.m. (2H, m, aromatic).

Anal. Calcd. for $C_{16}H_{14}N_2O_2$: C, 72.16; H, 5.30; N, 10.52. Found: C, 72.10; H, 5.18; N, 10.65.

*4-Hydroxy-1-methyl-3,5-diphenyl-Δ²-pyrazolin-5-one (**4***b*)

*(a) From 5-Hydroxy-1-methyl-3,5-diphenyl-Δ²-pyrazolin-4-one (**3***b*)*

A mixture of **3***b* (95 mg) and 1 ml 5% methanolic potassium hydroxide was refluxed for 1/2 h, 5 ml of water was added, and the solution kept at 5° for 15 h. The solid product (76 mg, 80%) was filtered and recrystallized twice from aqueous ethanol to give pure **4***b*, m.p. 179–181°; ν_{max} 3155, 2721, 2667, 1691, 1603, 1198, 1183, and 1173 cm^{-1}; λ_{max} 217 (ε 14 700) and 310 nm (13 000); δ (acetone-d_6) 3.35 (3H, s, Me), 6.08 (1H, s, OH), 7.27–7.60

(8H, m, aromatic), and 7.78–7.95 p.p.m. (2H, m, aromatic).

Anal. Calcd. for $C_{16}H_{14}N_2O_2$: C, 72.16; H, 5.30; N, 10.52. Found: C, 72.19; H, 5.21; N, 10.32.

*(b) From 1-Methyl-3,4-diphenyl-Δ²-pyrazolin-5-one (**2** or **15a**)*

The method was according to Jucker and Lindenmann (7). Hydrogen peroxide (40%) (0.87 ml) was added to a cooled (0–5°) solution of **2** (0.5 g, 0.002 mol) in 1.5% sodium hydroxide (8.5 ml). The mixture was stoppered, stirred for 1 h, and allowed to stand in a refrigerator for 24 h. The mixture was then neutralized with 5% hydrochloric acid, and the volume was reduced to one-fifth of the initial volume. A small amount of ethanol was added to dissolve the solids. On cooling crystals formed and recrystallization yielded 0.22 g (44%) of **4***b*, m.p. 178–180° identified by i.r. spectrum and mixture m.p.

Structure **2** may be converted to **4***b* by aerial oxidation, simply by heating it at its m.p. (~237°) in a m.p. tube for ½ h. The product was isolated and identified by its i.r. spectrum and mixture m.p.

*1-Methyl-3,4-diphenyl-Δ²-pyrazolin-5-one (**2** or **15a**)*

*(a) From 2-Bromo-1,3-diphenyl-1,3-propanedione (**12a**)*

Methylhydrazine (1.4 g, 0.03 mol) was added dropwise in 3 min to a warm suspension of **12***a* (16) (3.03 g, 0.01 mol) in ethanol (100 ml) under stirring. After addition, the mixture was stirred at room temperature for 1.5 h. The bulk of solvent was removed at reduced pressure and then 70% aqueous acetone (10 ml) was added. On cooling in an ice-bath, crystals formed and were collected. Recrystallization from 70% aqueous acetone gave 1.41 g (56%) of **15***a*, double m.p. 216–219° (then 235–237°); ν_{max} (KBr) 2550 br, 1601 s, 1427, 1392, 1292, 1069, and 1026 cm^{-1}; λ_{max} 240 (infl) (ε 14 700), 265 (infl) (11 200), and 300 (infl) nm (6310); δ ($CDCl_3$) 6.35 (3H, s, NMe), 7.20–7.40 (10H, m, aromatic) and deuterium exchange revealed 1 exchangeable H; *m/e* (70 eV): 250 (100%, M^+), 179 (35%), 178 (30%).

Anal. Calcd. for $C_{16}H_{14}N_2O$: C, 76.78; H, 5.64; N, 11.19; O, 6.39. Found: C, 77.22; H, 5.51; N, 11.06; O, 6.07.

(b) From 2,2-Dibromo-1,3-diphenyl-1,3-propanedione

The reaction was performed in a similar manner as in section *a*. The molar ratio of the dibromopropanedione to methylhydrazine was 1:4. Compound **15***a* was obtained in 57% yield.

*(c) From α-Phenyl-α-benzoylacetamide (**18**)*

1 ml of an aqueous solution containing methylhydrazine dihydrochloride (0.0024 mol) was added to a solution of **18** (see below) (0.48 g, 0.002 mol) in absolute ethanol (20 ml). The mixture was refluxed for 4 h. The mixture was neutralized (about p*H* 7) with 10% sodium hydroxide. The solution was reduced to half its volume, followed by cooling in an ice-bath. The crystals that formed were collected and purified giving a yield of 0.25 g (50%).

Compound **15***a* obtained from the three methods had identical spectral and physical properties.

Δ²-Pyrazolin-5-ones

α-Phenyl-α-benzoylacetamide (**18**) was prepared according to the method for the corresponding ethyl ester (17) with slight modification: α-phenyl-α-benzoylacetonitrile, obtained by condensing ethyl benzoate with benzyl cyanide in the presence of sodium ethoxide (17), was hydrolyzed in ethanol (with *ca.* 70% saturation of hydrogen chloride gas); m.p. 178.5–180° (lit. m.p. 178° (18)). The amide **18** was condensed with hydrazines to yield the Δ²-pyrazolin-5-ones.[4]

*3,4-Diphenyl-Δ²-pyrazolin-5-one (**15b**)*

This compound was obtained under conditions similar to those used for **15***a*. The refluxing time was 5 h. The yield was 68%; m.p. 234–236° (lit. m.p. 234–235° (11)); ν_{max} 3285, 3190, 1700, 1601, 1226, and 1016 cm^{-1}; λ_{max} 241 (infl) (ε 12 400) and 265 (infl) nm (10 700); δ (DMSO-d_6) 7.13 and 7.23 (10H, s, aromatic) and 10.77 p.p.m. (>1H, broad, NH; deuterium exchange revealed 2 exchangeable H).

*1,3,4-Triphenyl-Δ²-pyrazolin-5-one (**15c**)*

This compound was obtained by refluxing a mixture of the amide (**18**) (0.24 g, 0.001 mol), phenylhydrazine hydrochloride (0.18 g, 0.0012 mol), and ethanol (5 ml) for 1 h. The crystals that separated on cooling were recrystallized from ethanol, m.p. 191.5–193.5° (lit. m.p. 193–194° (12)) (64% yield); ν_{max} 1597, 1300, 1125, and 968 cm^{-1}; δ ($CHCl_3$-*d*) 7.30–8.10 (16H, m, 15H aromatic, 1H hydroxyl exchangeable with D_2O).

*4-Hydroxy-1-methyl-3,5-diphenylpyrazole (**17**) and 4-Acetoxy-1-methyl-3,5-diphenylpyrazole (**16**)*

Compound **17** was prepared (3) by refluxing a mixture of 2-acetoxy-1,3-diphenyl-1,3-propanedione (**12***b*) (16) and methylhydrazine in ethanol. The 4-acetoxypyrazole (**16**) was obtained when acetic acid was used as a solvent.

A solution of methylhydrazine (0.23 g, 0.005 mol) in acetic acid (1 ml) was added to a solution of **12***b* (1.13 g, 0.004 mol) in acetic acid (6 ml). The mixture was stirred at room temperature for 1 h. After most of the solvent was removed at reduced pressure, water (10 ml) was added. The oily product crystallized on prolonged cooling and agitation, m.p. 109–111° (from benzene–petroleum) (0.99 g, 85%). This product is identical with the one prepared by acetylation of the 4-hydroxypyrazole **17** (3).

Financial support of the National Research Council of Canada is gratefully acknowledged.

1. M. J. Nye and W. P. Tang. Chem. Commun. 1394 (1971).
2. M. J. Nye and W. P. Tang. Chem. Commun. 1395 (1971).
3. M. J. Nye and W. P. Tang. Tetrahedron, **28**, 455 (1972).
4. S. Veibel. Bull. Soc. Chim. Fr. 307 (1955), and papers cited therein.
5. A. R. Katritzky and F. W. Maine. Tetrahedron, **20**, 299 (1964).
6. E. P. Kohler, F. H. Westheimer, and M. Tishler. J. Am. Chem. Soc. **58**, 264 (1933).
7. E. Jucker and A. Lindenmann. Helv. Chim. Acta, **44**, 1249 (1961).
8. C. E. Frank. Chem. Rev. **46**, 155 (1955).

[4]Condensation of ethyl α-phenyl-α-benzoylacetate with hydrazine and phenylhydrazine gave the Δ²-pyrazolin-5-ones, **15***b* (11) and *c* (12), respectively.

Can. J. Chem. Downloaded from www.nrcresearchpress.com by 210.87.254.105 on 09/05/12
For personal use only.

9. G. BIANCHI, M. J. COOK, and A. R. KATRITZKY. Tetrahedron, **27**, 6133 (1971).
10. C. HEDBOM and E. HELGSTRAND. Acta Chem. Scand. **24**, 1744 (1970).
11. P. GRÜNANGER and P. VITA-FINZI. Atti Accad. naz. Lincei, Rend. Classe Sci. fis. mat. nat. **31**, 128 (1961).
12. W. WISLICENUS, H. EICHERT, and M. MARQUARDT. Ann. Chem. **436**, 88 (1924).
13. E. W. WARNHOFF. Molecular rearrangements. Pt. 2. *Edited by* P. de Mayo. Interscience, New York. 1964. p. 952.
14. M. J. NYE and W. P. TANG. Can. J. Chem. **48**, 3563 (1970).
15. L. A. BIGELOW and R. S. HANSLICK. Org. Syn. **2**, 244 (1943).
16. R. DE NEUFVILLE and H. v. PECHMANN. Chem. Ber. **23**, 3375 (1890).
17. B. W. HOWK and S. M. MCELVAIN. J. Am. Chem. Soc. **54**, 282 (1932).
18. E. F. J. ATKINSON, H. INGHAM, and J. F. THORPE. J. Chem. Soc. **91**, 578 (1907).

Downloaded from www.nrcresearchpress.com by 210.87.254.105 on 09/05/12
For personal use only.

The Photolysis of Propane at 123.6 nm

JAMES H. VORACHEK AND ROBERT D. KOOB

Department of Chemistry, North Dakota State University, Fargo, North Dakota 58102

Received August 2, 1972

Propane has been photolyzed at 123.6 nm, in the presence and absence of O_2, at pressures from 2–380 Torr. All products except ethane exhibit a pressure dependence which is attributed to secondary dissociation of the primary fragments, H_2, CH_4, C_2H_4, and C_3H_6. It is assumed that the range of energies carried by these fragments is broad enough that some will not dissociate even at low pressures while others of the same species cannot be stabilized even at high pressures. An internally consistent analysis rationalizes the entire observed product spectrum, with some uncertainty arising from an ambiguity in the source of acetylene. The following primary quantum yields, prior to secondary dissociation, are estimated:

$$C_3H_8 + h\nu = H_2 + C_3H_6 \quad \phi = 0.42 \text{ mol/einstein}$$
$$= C_2H_4 + CH_4 \quad \phi = 0.47 \text{ mol/einstein}$$
$$= CH_2 + C_2H_6 \quad \phi = 0.09 \text{ mol/einstein}$$

Le propane a été soumis à une photolyse à 123.6 nm, en présence et en absence de O_2, à des pressions de 2–380 Torr. Tous les produits, excepté l'éthane, manifestent une dépendance, par rapport à la pression, laquelle est attribuée à la dissociation secondaire des fragments primaires, H_2, CH_4, C_2H_4, et C_3H_6. On admet que l'étendue des énergies entraînées par ces fragments est suffisament large de sorte que certains ne se dissocieront pas même à de faibles pressions alors que d'autres de la même espèce ne peuvent être stabilisés même à de hautes pressions. Une analyse intérieurement cohérente coordonne le spectre obtenu des produits entièrement, avec certaines incertitudes provenant d'une ambiguité dans la source d'acétylène. Les premiers rendements quantiques qui suivent, précédant la seconde dissociation, ont été estimés:

$$C_3H_8 + h\nu = H_2 + C_3H_6 \quad \phi = 0.42 \text{ mol/einstein}$$
$$= C_2H_4 + CH_4 \quad \phi = 0.47 \text{ mol/einstein}$$
$$= CH_2 + C_2H_6 \quad \phi = 0.09 \text{ mol/einstein}$$

[Traduit par le journal]

Can. J. Chem., **51**, 344 (1973)

Introduction

The photochemistry of propane has been studied a good deal in the last decade (1–14) and the primary photolytic steps have been largely determined. Isotopic studies have identified precisely the origins of fragments within the molecule. Notably lacking, however, has been a measurement of quantum yields for each primary process. Two reasons for this are the uncertain actinometry in the vacuum u.v. and the extensive secondary reactions which make measurement of the yields of primary processes difficult.

While we have not improved our absolute actinometry, we have developed a two-windowed lamp which allows direct comparison of yields to those of an external standard. Thus, while absolute quantum yields may not be determined directly, yields relative to the standard may be, and the direction and magnitude of the changes in product yields may now be followed as a function of experimental conditions.

Secondary reactions are identified from the pressure dependence of all products. We sum the yields of these reactions in an attempt to estimate the overall quantum yield of the various primary processes. Yields of free radicals are obtained directly from radical combination product yields.

Experimental

Materials

Phillips research grade propane was used. After purification by gas chromatography using a silica gel column, impurity levels were below 5 p.p.m. The purified propane was dried over Drierite and vacuum distilled to a storage bulb. Linde C.P. oxygen was used without further purification.

Lamps and Cells

A krypton resonance lamp, similar to those described by Gorden *et al.* (15), was used for the photolysis. The lamp was filled on a mercury free vacuum line capable of achieving pressures less than 1×10^{-6} Torr (Veeco discharge gauge) and was gettered with a titanium gettering assembly. The chromatic purity was greater than 98%

Can. J. Chem. Downloaded from www.nrcresearchpress.com by 210.87.254.105 on 09/05/12
For personal use only.

Can. J. Chem. Downloaded from www.nrcresearchpress.com by 210.87.254.105 on 09/05/12
For personal use only.

in the region between 105 and 165 nm (McPherson 0.3 m vacuum monochromator). MgF_2 windows were attached to the lamp with Ag–AgCl seals. MgF_2 was chosen because it has a very weak dependence of its transmission properties on temperature (16). Moreover, MgF_2 is apparently less affected by irradiation history than LiF (17). Both properties were very important, as constant window properties were required for the successful use of the two-windowed lamp described in the next paragraph. The light intensity, calculated from the yield of acetylene from the photolysis of ethylene (18), was $1.7 \pm 0.1 \times 10^{14}$ quanta/s.

A "T"-shaped lamp with windows at each end of the crossbar was used to study the photolysis. The lamp was powered by a microwave generator through a tuned Evenson cavity placed on the base of the "T" nearest the crossbar. Each window looked into individual sample cells. Each cell had a 2.5 cm i.d. with a path length of 2.5 cm. The ratio of light intensities entering the two cells was determined by measuring the relative amounts of products formed in the photolysis of equal pressures of oxygen-scavenged propane. This ratio was constant throughout this work. Thus, one cell with constant sample conditions was used as an external standard to which runs made in the other cell could be compared.

The yield of methane from the photolysis of oxygen-scavenged propane at a pressure of 20 Torr was used as the external standard. The rate of formation of methane in the standard was found to be constant over the range 0.05–4% decomposition of parent to product (2).

All scavenged photolyses were conducted with 5% oxygen added to intercept free radicals and triplet methylene. No products which could be ascribed to these species were found. Except for conversion dependence runs, photolysis was carried to 0.1% conversion of parent to product. All analyses were done by gas chromatography (FID) on a 25 ft × 1/4 in. o.d., 35% (w/w) squalene column for the products containing four carbon atoms or less and a 25 ft × 1/4 in. o.d., 3% (w/w) squalene column for the product containing five or six carbons. Both columns were maintained at room temperature.

Results

Photolysis products observed in the presence of 5% oxygen at 123.6 nm include hydrogen, methane, ethane, ethylene, acetylene, propylene, and iso- and normal butane. Very small amounts of doubly unsaturated three-carbon molecules and butenes may also be observed under proper conditions. A summary of major product yields in the presence of oxygen at pressures from 2–380 Torr is given in Table 1.

As ethane was the only product found to be pressure invariant over the range investigated, all yields in Table 1 are normalized to the yield of ethane. Ethane yield serves as an internal standard and was compared directly to our external standard. The quantum yield of 0.086 reported for ethane in Table 1 was determined relative to the yield of acetylene from the photolysis of ethylene at the same wavelength, 123.6 nm, assumed equal to 0.90, as suggested by Meisels (18).[1] We make no claims for the validity of this assumption and use this number primarily for convenience. The sum of the quantum yields for the proposed primary processes in propane is near unity when the above assumption is made.

TABLE 1. Quantum yield* of nonscavengeable products in the photolysis of propane at 123.6 nm as a function of pressure

	Pressure (Torr)					
Product	2	10	20	50	100	380
CH_4	0.167	0.165	0.163	0.160	0.159	0.152
C_2H_2	0.151	0.140	0.135	0.122	0.100	0.092
C_2H_4	0.423	0.427	0.431	0.438	0.448	0.448
C_2H_6	0.086	0.086	0.086	0.086	0.086	0.086
C_3H_6	0.237	0.250	0.248	0.263	0.259	0.283

*Determined relative to the quantum yield of acetylene from ethylene equal to 0.90 at 123.6 nm.

Acetylene exhibits a striking pressure dependence. The acetylene quantum yield drops from 0.151 at 2 Torr to 0.092 at 380 Torr. The quantum yield of methane also decreases with pressure. Ethylene and propylene quantum yields increase with increasing pressure.

It is relevant to point out, in light of the recent work of Tanaka and co-workers (1), that the sum of the acetylene and ethylene yields is not independent of pressure. The difference between the ethylene yield at 380 and 2 Torr is only 50% of the difference between acetylene yields at the same pressures.

Table 2 compares the yields of products in the presence and absence of oxygen at 380 Torr. The multitude of products ascribable to radical combination in the latter case attests dramatically to the radical intercepting ability of oxygen at the levels used. Acetylene yields were not affected by the presence of oxygen. Thus, a convenient internal standard is available for comparing yields in the presence and absence of oxygen.

One may compute quantum yields of each radical relative to isopropyl by correcting the appropriate combination product for disproportionation. These products are isobutane (methyl-isopropyl) isopentane (ethyl-isopropyl),

[1]In this paper, the quantum yield of C_2H_2 from C_2H_4 is measured as 0.90.

TABLE 2. Quantum yield of all products observed in the photolysis of propane at 380 Torr

Product	No O_2	O_2, 5%	Product	No O_2
CH_4	0.181	0.152	1-Pentene	0.003
C_2H_2	0.092	0.092	Isopentane	0.029
C_2H_4	0.445	0.448	*n*-Pentane	0.006
C_2H_6	0.167	0.086	4-Methyl-1-pentene	0.026
C_3H_6	0.328	0.283	2,4-Dimethylbutane	0.080
1-Butene	0.020	—	2-Methylpentane	0.029
Isobutane	0.151	0.015	1,5-Hexatriene	trace
n-Butane	0.063	0.036	1-Hexene	0.005
3-Methyl-1-butene	0.003	—	*n*-Hexane	0.004

TABLE 3. Quantum yield of free radicals in the photolysis of propane at 380 Torr

Radical	Base product	$1 + k_d/k_c$*	Yield relative to isopropyl radical	Quantum yield of radical
Methyl	Isobutane†	1.22	0.616	0.339
Vinyl	Isopentene	1.2	0.010	0.006
Ethyl	Isopentane	1.27	0.126	0.069
Allyl	4-Methyl-1-pentene	1.3	0.124	0.068
i-Propyl	2,4-Dimethylbutane	1.68 (×2)	1.0	0.551
n-Propyl	2-Methylpentane	1.40	0.167	0.093

*Values selected from ref. 19.
†Corrected for isobutane formed by CH_2 insertion.

isopentene (vinyl-isopropyl), 4-methyl-1-pentene (allyl-isopropyl), 2-methylpentane (*n*-propyl-isopropyl), and 2,4-dimethylbutane (isopropyl-isopropyl). The sum of all products involving isopropyl radical corrected for disproportionation provides its quantum yield, 0.551. The quantum yields for all other radicals are then computed by multiplying the radical yields relative to isopropyl times the quantum yield of isopropyl radical (see Table 3).

Vinyl and allyl radicals show striking pressure dependence, both decrease with increasing pressure. The pressure dependence of allyl radical has been discussed in an earlier communication (3). It clearly results from a secondary reaction. Vinyl radical behaves similarly.

Figure 1 demonstrates the conversion dependence of the radical products *i*-pentane and 2,3-dimethylbutane over the range of 0.06% to 0.87% conversion (% conversion = (products)/(propane)$_0$ × 100). 2,3-Dimethylbutane, the product of isopropyl radical combination, increases by approximately 30% of its lowest observed yield in this range. *i*-Pentane increases by 100% over this same range. The more striking conversion dependence of *i*-pentane must arise from the conversion dependence of ethyl radical production. This result is not unanticipated in a system where both hydrogen atoms and ethylene are produced. The ratio of concentration of ethylene to propane ranges from 6×10^{-4} to 8.7×10^{-3} at these conversions. Since the ratio of the rate constants for H addition to ethylene relative to H abstraction from propane (19) is approximately 5×10^2, ethylene may compete effectively with propane for hydrogen atoms. As suggested in the discussion, the addition of H atoms to ethylene appears to provide the only "important" source of ethyl radicals as far as computing overall yields of products is concerned.

Discussion

Of many possible primary processes in the photolysis of propane, only the following have been directly demonstrated to exist (1, 9, 12, 13)

[1] $C_3H_8 + h\nu = C_3H_6 + H_2$

[2] $C_3H_8 + h\nu = C_2H_4 + CH_4$

[3] $C_3H_8 + h\nu = CH_2 + C_2H_6$

The inequity of yields between hydrogen and propylene, and methane and ethylene, as well as

Can. J. Chem. Downloaded from www.nrcresearchpress.com by 210.87.254.105 on 09/05/12
For personal use only.

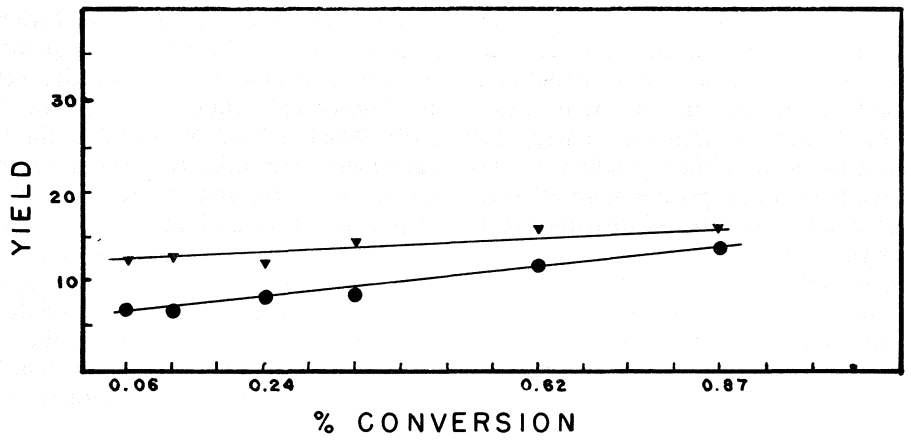

FIG. 1. The yield of isopentane, ●, in arbitrary units, as a function of percent conversion of propane to photolysis products. The actual quantum yields of isopentane at the highest and lowest conversions are 0.018 and 0.007 mol/einstein, respectively. The data were obtained in an oxygen free system of 20 Torr total pressure. For contrast the conversion dependence of 2,3-dimethylbutane is also plotted, ▼.

the appearance of acetylene, allene, and a number of products of a higher molecular weight than propane, require that other processes occur than those written as eqs. 1–3. Whether these other processes are subsequent to reactions 1–3, where any one of the fragments produced may further dissociate; or whether these other processes correspond to distinctly different processes such as reactions 4 and 5 has not been conclusively demonstrated.

[4] $C_3H_8 + h\nu = C_3H_7 + H$

[5] $C_3H_8 + h\nu = C_2H_5 + CH_3$

Photolysis of propane at 123.6 nm supplies enough energy that subsequent dissociation of any of the polyatomic fragments listed is energetically possible. Furthermore, secondary products from the dissociation of the fragments of reaction 1 are indistinguishable from the secondary products from the dissociation of fragments of reaction 4 if both occur at such a rate that they may not be quenched simply by increasing sample pressure. For example, $C_3H_6 + H + H$ may result from propyl radical dissociation in reaction 4 or from H_2 dissociation in reaction 1. The same total energy is available to each sequence as both would be initiated by a photon from the same source. It has also been demonstrated that energy is not necessarily statistically partitioned in a primary process in the photolysis of propane (20). Therefore, one cannot invoke the usual arguments regarding the number of oscillators "available" to the energy deposited by the incoming photon.

Since very rapid secondary reactions cannot be distinguished from primary processes, we will *arbitrarily* view the mechanism for the photolysis of propane as follows. The primary processes in the photolysis of propane can be generally classified as reactions 1–3. Each fragment in the primary process is generated with a broad distribution of energy. This implies that each primary fragment will have species falling into three different reactivity categories: low energy species where no further dissociation can occur; middle energy species where there will be a competition between dissociation and collisional deactivation over the pressure range studied; and high energy species which will always dissociate. "Secondary" unimolecular dissociations which must be considered are then:

[6] $H_2^* = 2H$

[7] $CH_4^* = CH_3 + H$

[8] $C_2H_4^* = C_2H_2 + H_2$

[9] $C_2H_4^* = C_2H_3 + H$

[10] $C_3H_6^* = C_2H_2 + CH_4$

[11] $C_3H_6^* = C_3H_4 + H_2$

[12] $C_3H_6^* = C_3H_5 + H$

The asterisk indicates energy in excess of the activation energy of that reaction.

Secondary dissociations of the fragments of eq. 3 are not included since ethane did not show

Can. J. Chem. Downloaded from www.nrcresearchpress.com by 210.87.254.105 on 09/05/12
For personal use only.

Can. J. Chem. Downloaded from www.nrcresearchpress.com by 210.87.254.105 on 09/05/12
For personal use only.

a pressure dependence. This lack of pressure dependence of the yield of ethane is reasonable in the framework of our assumptions. Reaction 3 is considerably more endothermic than either reaction 1 or 2, and the activation energy for further dissociation of either product of reaction 3 is relatively high (greater than 80 kcal/mol). The assumption of a broad distribution of energies suggests that some ethane molecules indeed have enough energy to further dissociate, but the fraction of ethanes having this energy would be too small for us to detect in the pressure range we have studied (20). (The maximum internal energy in the distribution of energies for any of the fragments is, of course, the energy of the photon, 10 eV, less the endothermicity of the reaction and less energy distributed to external degrees of freedom.) On the other hand, because of the large energies available and the relatively small endothermicities of [1] and [2], it may occur that high pressure limits to yields of primary products lose their meaning. Other processes, such as cage effects, may become important before pressures become sufficiently high to quench all secondary dissociation of propylene or ethylene.

The following equations show the most probable reactions of the intermediates generated in reactions 3–12.

[13] $H + C_3H_8 = C_3H_7 + H_2$

[14] $H + C_3H_6 = C_3H_7$

[15] $H + C_2H_4 = C_2H_5$

[16] $R\cdot + R'\cdot$ = combination and disproportionation products

[17] $^1CH_2 + C_3H_8 = C_4H_{10}$

[18] $^1CH_2 + M = {}^3CH_2$

Reactions 17 and 18 have been discussed for this system in a recent series of papers (21) and we will not discuss them in detail here. Reaction 17 does make a significant contribution to the overall butane yield, however, and this contribution must be considered when assigning radical yields based on observed butane. Reaction 16 is assumed to be the only important reaction of all free radicals except H and the CH_2 discussed above.

Relative rate constants for reactions 13–15 are available in the literature (19). At 380 Torr and 0.1% final conversion of propane to produce the relative yields of reactions [15]/[14] + [13] (ethyl to total propyl) is calculated from reported rate constants to be 1:9.9. The quantum yields of radicals computed in the results section show an "observed" ratio of ethyl to propyl of 0.069:0.644 or 1:9.3. We consider this to be good agreement and take this result to imply that reactions 13, 14, and 15 are the only important source of ethyl and propyl radicals. Thus, if reactions 4 and 5 are actually primary processes, the polyatomic radical fragments are not substantially stabilized at 380 Torr and do not make an important contribution to the ethyl and propyl radical yields. Similar conclusions have been reached by previous investigators (1, 5, 11[2]).

[2]Ausloos and Lias (11) would agree that stable propyl radicals are formed only in very low yields in a primary process. However, they report a yield of C_2D_5H relative to methane of 0.27 for the photolysis of 29.4 Torr of C_3D_8 in the presence of 12.9% H_2S. They interpret this product as arising from the scavenging of C_2D_5 by H_2S. Obtaining a quantum yield of C_2D_5H by comparing the relative yield to the measured quantum yield of methane in our system at a similar pressure, this implies a quantum yield of primary ethyl radicals (ostensibly from reaction 5) of 0.04 or greater than 50% of our total measured ethyl radical yield. If it were indeed the case that the C_2D_5H did arise from ethyl radicals produced in a primary process, our conclusion that such radicals make a negligible contribution to the overall ethyl radical yield would obviously be false. The simple consideration of the appropriate energetics presented below, however, shows how unlikely it is that the measured C_2D_5H could actually arise from ethyl radicals produced in a process such as reaction 5. One may compute an upper limit to the total possible quantum yield of ethyl radicals produced in reaction 5 by summing the quantum yields of acetylene, ethylene and all pentanes (measured at 30 Torr in the absence of O_2) and subtracting the yield of "molecular" methane (the quantum yield of methane in the presence of oxygen) to be 0.33. At a similar pressure the measured quantum yield of C_2D_5H has already been computed to be 0.04. Of the total possible ethyl radicals, then, 12% are stabilized at 30 Torr and 88% decompose. This is obviously a limiting case since the total ethyl radical yield computed is an upper limit on the actual possible yield. In the notation of Rabinovitch and Setser (22), $D/S = 0.73$. To obtain such a ratio for the number of ethyl radicals decomposing to the number collisionally stabilized requires that greater than 80% of the ethyl radicals produced in reaction 5 carry as vibrational energy 50 kcal or less. The reader convinces himself of the veracity of this last statement using the energy dependence of the microscopic rate constant curve presented by Rabinovitch and Setser, a critical energy of decomposition of ethyl radicals of 39.8 kcal/mol, and a specific deactivation rate of $2 \times 10^8\ s^{-1}$ (at 30 Torr). The total energy deposited in the photolyzed propane is 231 kcal. The endothermicity of reaction 5 is 84 kcal. The energy remaining to be partitioned among the various degrees of

Can. J. Chem. Downloaded from www.nrcresearchpress.com by 210.87.254.105 on 09/05/12
For personal use only.

As a means of organizing the available data we consider all photolysis products to arise from primary processes 1, 2, and 3 and secondary reactions 6–18. The contribution of each primary process will be assessed by independently considering each of the two fragments for each process 1–3. Agreement between these individual assessments will be interpreted as evidence for the completeness of our analysis.

To the yield of molecular hydrogen in the presence of a radical scavenger must be added the hydrogen which formally does not appear as H_2 because of reaction 6. This hydrogen does not appear because it reacts as H atoms. The total quantum yield of H atoms may be determined by summing the yields of propyl and ethyl radicals because only reactions 13–15 will be important H atom reactions in this system. From the total yield of H atoms must be subtracted those which arise from reactions 7, 9, and 12 as these do not represent a contribution from primary process 1. The total H atom quantum yield attributable to process 1 is then halved and added to the observed H_2 yield. Finally, H_2 arising from reactions 8 and 11 must be subtracted from the total. This last step places uncertainties on the quantum yield of reaction 1 as calculated from the hydrogen yield. Experimental difficulties prevented us from routinely determining the quantum yield of C_3H_4, reaction 11. However, this yield is small. The major uncertainty arises in determining what fraction of the observed acetylene arises from reaction 8 and what fraction arises from reaction 10. This could possibly be determined from an isotopic analysis of acetylenes produced from selectively labeled propanes; however, such an analysis has not been done at present. Thus, our estimate of the overall quantum yield for reaction 1 based on hydrogen originating products must remain in uncertainty by the observed acetylene yield. This estimate, then, has the range of 0.403–0.495 mol/einstein.

The quantum yield of reaction 1 may also be estimated by examining the propylene related fragments. To the quantum yield of propylene observed in a scavenged system one must add the yields of reactions 10, 11, and 12, all of which remove propylene in secondary unimolecular reactions. Reaction 14 need not be considered since it will not occur in a scavenged system. The same uncertainty in assigning the yield of reaction 10 occurs as was discussed in the previous paragraph. We are thus left with the estimate of the quantum yield of reaction 1 of 0.351–0.443 mol/einstein based on propylene related product yields.

Similar analyses may be accomplished for the methane and ethylene fragments expected in primary process 2. To the observed methane yield must be added the yield of methyl radicals formed in reaction 7. The methane produced in reaction 10 must be subtracted from this total. As explained above the yield of methane from reaction 10 cannot be directly determined from presently available data. Thus we are left with the range of 0.399–0.491 mol/einstein as the quantum yield of primary process 2 based on methane related reactions. To the quantum yield of ethylene observed in a scavenged system must be added the yield of acetylene resulting from reaction 8. The same uncertainty regarding the relative importance of reactions 8 and 10 still plagues us here. A range of quantum yields of 0.448–0.540 mol/einstein is thus obtained for process 2 from ethylene related reactions.

Primary process 3 is determined in a straightforward fashion. It is simply the observed ethane yield in a scavenged sample. Since ethane does not exhibit a pressure dependence, no secondary reactions of ethane need be considered. The quantum yield of reaction 3 is thus 0.086 mol/einstein. The sum of the butane yields in an oxygen scavenged system must be less than this value since all methylenes produced in reaction 3 do not survive as singlets to undergo reaction 17. The observed butane yield is 0.051 mol/einstein. The calculations of the last three paragraphs are summarized in Tables 4 and 5, where the appropriate numbers are given.

The proposed reaction scheme, [1]–[3], [6]–[18], is seen in the previous paragraphs to lead to internally consistent results. The calculated quantum yield of each of the primary processes

---

freedom of the product methyl and ethyl radicals is 147 kcal. It would be an intriguing process indeed that partitioned only 1/3 of this energy to the internal degrees of freedom of the more complex ethyl radical while the remaining 100 or so kcal went into the methyl radical and external degrees of freedom. If such considerations have any validity, it is difficult to believe that the observed C_2D_5H has primary ethyl radicals as its source, even though no obvious alternative exists. The strong conversion dependence of products arising from ethyl radical as a precursor, pentanes, reinforces our conclusion that reaction 15 is the most important source of stable ethyl radical in this system.

TABLE 4. Assessment of the yields of important secondary reactions at 380 Torr and 0.1% conversion

Reaction	Product measured	ϕ 380 Torr
[7]	CH_3	0.339
[8] + [10]	C_2H_2	0.092
[9]	C_2H_3	0.006
[11]	C_3H_4	Not determined
[12]	C_3H_5	0.068
[13] + [14]	$C_3H_7\cdot$	0.644
[15]	C_2H_5	0.069
[17]	C_4H_{10}	0.051
[6] ϕ_H	$(C_3H_7\cdot + C_2H_5—C_3H_5—C_2H_3—CH_3)$	0.299

TABLE 5. Summary of computation of quantum yield of primary processes for the photolysis of propane

Primary reaction	Fragment considered	Important yields and secondary reactions	Quantum yield
[1]	H_2	H_2*,† + [6] − [8] − [11]	0.403–0.495
	C_3H_6	C_3H_6* + [10] + [11] + [12]	0.351–0.443
[2]	CH_4	CH_4* + [7] − [10]	0.399–0.491
	C_2H_4	C_2H_4* + [8]	0.448–0.540
[3]	C_2H_6	C_2H_6*	0.086

*Quantum yield of this product in a scavenged system at 380 Torr.
†Yield estimated from data in refs. 9 and 13.

1–3 is found to be similar when calculated by considering each of its fragments individually. The major uncertainty which pervades may be traced to the acetylene forming reactions. Although we do not have direct evidence for the relative importance of reactions 8 and 10, we may speculate as to the relative importance of these two reactions. The increase in ethylene over the pressure range studied, Table 1, accounts for only 50% of the observed decrease in acetylene yield. If we assume that both reactions 8 and 10 are quenched at similar rates, then we may estimate that the observed acetylene receives approximately equal contributions from reactions 8 and 10.

If we estimate that reaction 8 contributes 50% of the observed acetylene yield at 380 Torr and reaction 10 contributes about 50%, then the following quantum yields are determined for the three postulated primary processes.

[1] $C_3H_8 = C_3H_6^* + H_2^*$ $\phi = 0.449$, based on hydrogen related reactions $= 0.397$, based on propylene related reactions

[2] $C_3H_8 = C_2H_4^* + CH_4^*$ $\phi = 0.445$, based on methane related reactions $= 0.494$, based on ethylene related reactions

[3] $C_3H_8 = C_2H_6 + CH_2$ $\phi = 0.086$, based on ethane yield

In each case the quantum yields based on individual determinations of the two fragments associated with each process overlap with a $\leqslant 5\%$ uncertainty. Considering the rather complex analysis necessary, this is most gratifying. Summing the average value for each primary process gives a total quantum yield for disappearance of propane of 0.979 mol/einstein.

Summary

Using an experimental system in which it is possible to determine quantum yields relative to an external standard for all products in the photolysis of propane, we found that all molecules observed in a scavenged system varied with pressure except ethane. This pressure dependence of product yields strongly suggests that second-

Can. J. Chem. Downloaded from www.nrcresearchpress.com by 210.87.254.105 on 09/05/12
For personal use only.

Can. J. Chem. Downloaded from www.nrcresearchpress.com by 210.87.254.105 on 09/05/12
For personal use only.

ary reactions involving primary fragments are important in determining the observed product distribution. We have postulated a scheme in which three primary processes, reactions 1–3, are the source of all unimolecularly reactive species. Secondary dissociations of H_2, C_3H_6, CH_4, and C_2H_4 provide all other reactive intermediates. The major difficulty in determining the quantum yields of each of the three primary processes lies in assessing the relative contributions to the observed acetylene yield from reactions 8 and 10, the secondary dissociation of ethylene and propylene, respectively. If indirect evidence is used to determine the relative contributions of each of these reactions, one estimates the following quantum yields for the primary processes: $\phi_1 = 0.42$; $\phi_2 = 0.47$; $\phi_3 = 0.09$. This corresponds to 43% of total primary reaction giving propylene plus hydrogen, 48% giving ethylene plus methane, and 9% giving ethane plus methylene.

Reactions 4 and 5 may be primary processes, but it has been concluded here and by previous investigators that the propyl and ethyl radicals produced in these reactions continue to dissociate by elimination of an H atom. Such sequences are not experimentally distinguishable from reaction 1 followed by 6 and reaction 2 followed by 7 and thus have not been explicitly considered. Their omission has not led to any glaring inconsistencies in our analysis.

The authors gratefully acknowledge the financial support of the National Science Foundation and Petroleum Research Fund administered by the American Chemical Society during the work reported here.

1. K. Obi, A. Akimoto, Y. Ogata, and I. Tanaka. J. Chem. Phys. **55**, 3822 (1971).
2. J. H. Vorachek. Ph.D. Thesis, North Dakota State University. *Available* University Microfilms, Ann Arbor, Michigan. 1971.
3. J. H. Vorachek and R. D. Koob. J. Phys. Chem. **74**, 4455 (1970).
4. P. Ausloos and S. G. Lias. Ber. Bunsenges. Phys. Chem. **72**, 187 (1968).
5. H. Akimoto and I. Tanaka. Ber. Bunsenges. Phys. Chem. **72**, 134 (1968).
6. A. L. Lane. Report to U.S. Atomic Energy Commission. CALT-532-34. 1968.
7. R. E. Rebbert and P. Ausloos. J. Chem. Phys. **46**, 4333 (1967).
8. D. W. L. Griffiths and R. A. Back. J. Chem. Phys. **46**, 3913 (1968).
9. J. R. McNesby. Act. Chim. Biol. Radiat. **9**, 59 (1966).
10. A. H. Laufer and J. R. McNesby. J. Phys. Chem. **70**, 4094 (1966).
11. P. Ausloos and S. G. Lias. J. Chem. Phys. **44**, 521 (1966).
12. J. R. McNesby and H. Okabe. Adv. Photochem. **3**, 157 (1964).
13. P. Ausloos, S. G. Lias, and I. B. Sandoval. Disc. Faraday Soc. **36**, 66 (1963).
14. H. Okabe and J. R. McNesby. J. Chem. Phys. **37**, 1340 (1962).
15. R. Gorden, Jr., R. E. Rebbert, and P. Ausloos. NBS Technical Note 496, U.S. Department of Commerce, Washington, D.C. 1970.
16. A. H. Laufer, J. A. Pirog, and J. R. McNesby. J. Opt. Soc. Am. **55**, 64 (1965).
17. D. F. Heath and P. A. Sacher. Appl. Opt. **15**, 937 (1966).
18. G. Meisels. Submitted.
19. A. F. Trotman-Dickenson and G. S. Milne. NSRDS-NBS 9, U.S. Department of Commerce, Washington, D.C. 1967. E. Ratajczk and A. F. Trotman-Dickenson. Supplementary Table to above. 1970.
20. (*a*) A. K. Dhingra, J. H. Vorachek, and R. D. Koob. Chem. Phys. Lett. **9**, 17 (1971). (*b*) J. H. Vorachek and R. D. Koob. J. Phys. Chem. **76**, 9 (1972).
21. (*a*) A. K. Dhingra and R. D. Koob. J. Phys. Chem. **74**, 4490 (1970). (*b*) R. D. Koob. J. Phys. Chem. **73**, 3168 (1969).
22. B. S. Rabinovitch and D. W. Setser. Adv. Photochem. **3**, 1 (1964).

Photolysis of Acylsilanes in Cyclohexane and Other Solvents

A. G. Brook and J. M. Duff

Lash Miller Chemical Laboratories, Department of Chemistry, University of Toronto, Toronto 181, Ontario

Received June 26, 1972

Whereas photolysis of acylsilanes in carbon tetrachloride has been shown to generate silyl radicals which yield chlorosilanes exclusively, and photolyses in alcohols yield siloxycarbenes which yield "mixed acetal" insertion products, it is shown that photolysis of acylsilanes in non-polar, non-halogenated solvents such as cyclohexane give complex mixtures of products which result primarily from the attack of silyl radicals on the carbonyl oxygen of an acylsilane, followed by conventional disproportionation or recombination reactions. Under some circumstances silyl radicals add to carbon–carbon double bonds. The structures of the products formed and the mechanism of their formation are described.

Alors que la photolyse des acylsilanes dans le tétrachlorure de carbone produit, comme il a été démontré, des radicaux "silyses" ce qui conduit exclusivement à des chlorosilanes, et que la photolyse dans des alcools conduit à des siloxycarbènes qui donnent des produits d'insertion d'acétales mixtes, il est démontré que la photolyse d'acylsilanes dans des solvants non-polaires et non halogénés comme le cyclohexane, donne des mélanges complexes de produits qui proviennent surtout de l'attaque des radicaux "silyles" sur l'oxygène du groupe carbonyle d'un acylsilane, suivi de réactions classiques de dismutation ou de recombinaison. Dans certains cas les radicaux "silyles" s'additionnent aux doubles liaisons carbone–carbone. Les structures des produits formés ainsi que le mécanisme de leur formation sont décrits. [Traduit par le journal]

Can. J. Chem., **51**, 352 (1973)

Can. J. Chem. Downloaded from www.nrcresearchpress.com by 210.87.254.105 on 09/05/12
For personal use only.

It has recently been shown that the photolysis of acylsilanes in carbon tetrachloride or similar halogenated solvents leads by a Norrish Type 1 cleavage to silyl and acyl radicals which subsequently react to give silyl chloride and the usual products from acyl radicals (1) (eq. 1). It has also

[1] $$R_3SiCOR' \xrightarrow[CCl_4]{h\nu} R_3Si\cdot + R'CO\cdot \rightarrow$$

$$R_3SiCl + R'COCl + R'COCCl_3 + Cl_3CCCl_3$$

been shown that photolysis in polar solvents such as alcohols gives rise to mixed acetals by way of a siloxycarbene intermediate (2, 3) (eq. 2). In view

[2] $$R_3SiCOR' \xrightarrow[MeOH]{h\nu} R_3SiO\ddot{C}R' \rightarrow R_3SiOCR'(H)(OMe)$$

of these extremes in behavior as the solvent was changed, it appeared of interest to photolyze acylsilanes in non-polar, non-halogenated solvents where, if silyl radicals were formed they would lack electronegative halogen atoms with which to react by abstraction, or where, if siloxycarbenes were formed, they would lack highly polar bonds such as OH into which they might insert.

Acetyltriphenylsilane clearly undergoes radical cleavage when photolyzed in carbon tetrachloride (3) and siloxycarbene formation when photolyzed in methanol containing a trace of pyridine (2). When photolyzed in cyclohexane using a 100 W low pressure mercury flood lamp, a complex mixture of products was formed from which three major products were separated by a combination of chromatography and crystallization.

The structures assigned to these products, their yield, and details of their structure proof are shown in eq. 3. The least soluble compound had an analysis and spectroscopic data consistent with the siloxyalkene **1**. The stereochemistry was not established but the isomer having *trans*-triphenylsilyl groups appears much more probable on steric grounds. Degradation of **1** gave almost 3 equiv of triphenylsilanol. Cleavage did not occur under milder conditions, and no reduction of the siloxy group to a silyl hydride occurred when the compound was refluxed with lithium aluminum hydride in ether. However, when treated with phenyllithium or *n*-butyllithium, both a tetra-substituted silane and a new compound **4**, which contained both an acylsilane and a β-ketosilane functionality were obtained (eq. 4). Thus **4** had n–π* u.v. absorption at 377 nm typical of an acylsilane (*e.g.* acetyltriphenylsilane λ_{max} 377 nm) and carbonyl i.r. absorption at

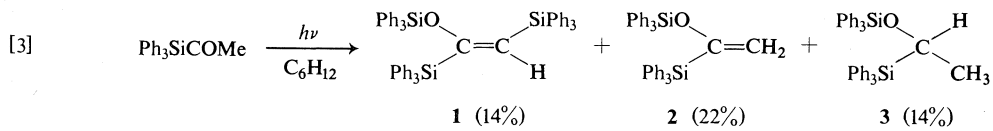

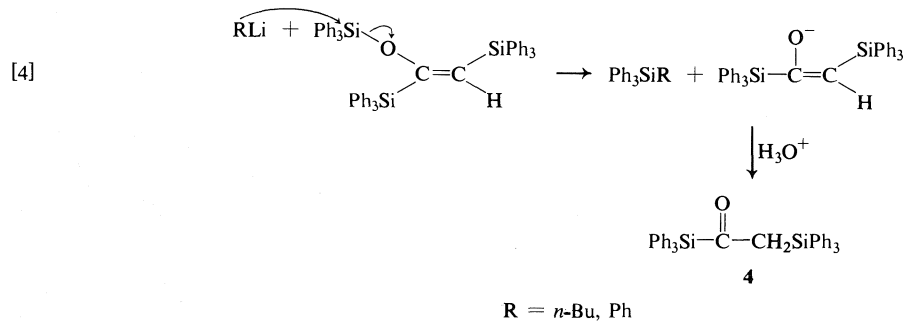

6.16 μ corresponding to the position expected for an acylsilane (acetyltriphenylsilane 6.08 μ) perturbed to longer wavelength by the expected amount by the β-silicon atom (*e.g.* Me_3CCH_2-COMe 5.82 μ, $Me_3SiCH_2COCH_3$ 5.89 μ). The structure of **4** was further confirmed when, on heating, it underwent the known thermal rearrangement of β-ketosilanes (4) to give the isomer **2** which was also synthesized by an alternate route (eq. 5).

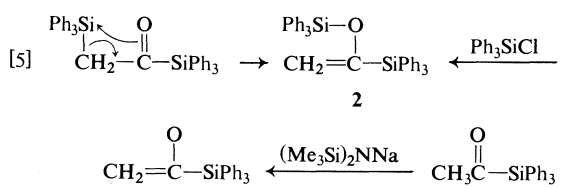

It was difficult to separate the mixture of **2** and the saturated compound **3** obtained from the original photolysis of acetyltriphenylsilane. However, when treated with dilute base, **2** was rapidly hydrolyzed to give 2 equiv of triphenylsilanol whereas **3** was relatively inert and could be isolated pure. The structure of **3** was independently confirmed by silylating the corresponding alcohol (eq. 6).

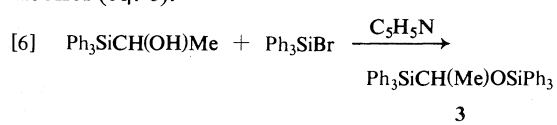

The above three products, which accounted for about 50% of the starting material, were the only ones from the photolysis reaction which were isolated and characterized. Other compounds were present, and at least some of these were unstable since on standing or on chromatography, up to 30% of triphenylsilanol and small amounts (<5%) of acetyltriphenylsilane could be isolated.

Before discussing mechanisms for the formation of the above products it is pertinent to describe the results of photolysis of another acylsilane, phenylacetyltriphenylsilane, under comparable conditions. Photolysis in cyclohexane gave three readily separable products which accounted for about 90% of the starting material. The structures and details of the structure proofs are shown in eq. 7.

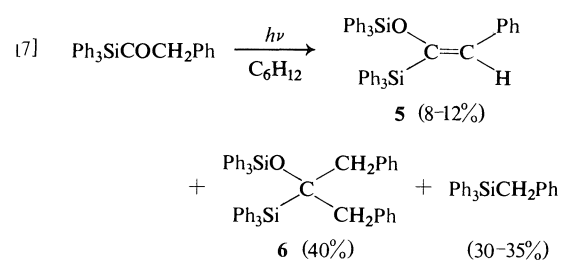

The structure of **5**, obtained in about 8–12% yield from various runs, was supported by analytical and spectroscopic data. The geometry has been assigned purely on steric arguments. Attempts to synthesize **5** by coupling the enolate ion of phenylacetyltriphenylsilane with triphenylchlorosilane, or to degrade it, by treatment with phenyl- or *n*-butyllithium, gave complex mixtures of unidentified products. Treatment with aqueous alkali gave 2 equiv of triphenylsilanol but the expected phenylacetaldehyde was not isolated, presumably due to its further reaction under the

Can. J. Chem. Downloaded from www.nrcresearchpress.com by 210.87.254.105 on 09/05/12
For personal use only.

alkaline conditions. However, reduction of **5** with lithium aluminum hydride in refluxing di-*n*-butyl ether gave a 45% yield of triphenylsilane and a 30% yield of phenylacetyltriphenylsilane together with some recovered starting material and unidentified products (eq. 8).

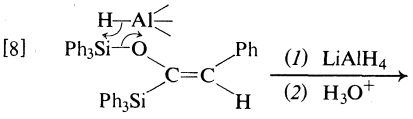

[8] $Ph_3SiH + Ph_3SiC(=O)CH_2Ph$

The structure of **6**, isolated in about 40% yield, was assigned on the basis of analytic and spectroscopic data. The compound showed no parent ion (*m/e* 728) in the mass spectrum, the highest molecular weight ions being 637 (M − CH_2Ph) and 636 (M − $PhCH_3$). Attempts to degrade **6** with the usual reagents such as lithium aluminum hydride in refluxing *n*-butyl ether, *n*-butyllithium, hydrochloric acid in aqueous acetone, or potassium hydroxide in refluxing aqueous ethanol led to almost quantitative recovery of starting material, probably because the molecule is severely sterically crowded. However, when refluxed in aqueous alkaline diglyme, conditions so harsh that phenyl groups were cleaved from silicon, 1,3-diphenyl-2-propanol (**7**), the expected carbon skeleton, was isolated in good yield (eq. 9). Rational mechanisms for this degradation involving alkoxysilane cleavage, a silylcarbinol to alkoxysilane rearrangement (5), and subsequent further cleavage can be proposed for this transformation.

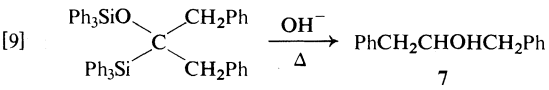

[9] $Ph_3SiO(Ph_3Si)C(CH_2Ph)_2 \xrightarrow[\Delta]{OH^-} PhCH_2CHOHCH_2Ph$ (**7**)

Further evidence for the structure of **6** was obtained by finding that it rapidly and quantitatively thermally isomerized to the disiloxane **8** at 200° (eq. 10). This appears to be a new variant of a previously recognized type of 1,2-rearrangement reaction involving silicon–oxygen bond formation and silicon–carbon bond breaking (5, 6). The structure of **8**, based on analytical and spectroscopic data, was confirmed by its hydrolysis using refluxing aqueous alkaline diglyme solution to the known 1,2,3-triphenylpropane (**9**).

The third product from the photolysis of phenylacetyltriphenylsilane was the well-known benzyltriphenylsilane.

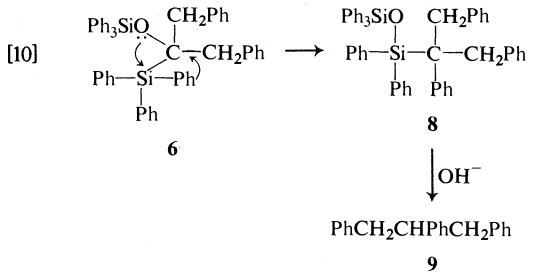

[10] $Ph_3SiO(Ph_2Si)C(CH_2Ph)_2 \rightarrow Ph_3SiO(Ph_2Si)C(CH_2Ph)_2$ (**6** → **8**)

8 $\xrightarrow{OH^-}$ $PhCH_2CHPhCH_2Ph$ (**9**)

Mechanism of the Photolyses in Cyclohexane

The products from the photolysis of acetyl- and phenylacetyltriphenylsilane are readily explained on the basis of the formation of triphenylsilyl radicals which subsequently attack the most electronegative atom in the system, namely the oxygen of an unreacted acylsilane molecule, to form a new radical species which subsequently undergoes normal (dark) radical reactions.

For acetyltriphenylsilane, a reasonable reaction path is shown in Scheme 1.

The conversion of **2** to **1** by addition of triphenylsilyl radical to the alkene **2** is not unexpected since it is known that triphenylsilyl radicals will add to alkenes (7, 8). When 2 equiv of **2** were photolyzed with any acylsilane which yielded triphenylsilyl radicals on photolysis (*e.g.* $Ph_3SiCOCH_2Ph$, *vide infra*) it was found that significant yields (20%) of **1** could be isolated, a finding consistent with the alkene **2** reacting with the silyl radicals.

The products from the photolysis of phenylacetyltriphenylsilane can be explained by the following reaction pathways (Scheme 2) where again silyl radical adds to carbonyl oxygen, followed either by loss of a hydrogen atom or addition of a benzyl radical.

Two details of this mechanism require clarification. One question concerns the initial mode of cleavage of the acylsilane, which could have occurred to give silyl and phenylacetyl radicals (path *a*), the latter of which subsequently (and totally) decarbonylated, or which could have occurred to give silylacyl and benzyl radicals (path *b*), the former of which decarbonylated. No products containing a carbonyl group are found among the products of photolysis of phenylacetyltriphenylsilane in cyclohexane, or in carbon tetrachloride, where in the latter case the products are found to be triphenylchlorosilane and benzyltriphenylsilane, together with bibenzyl, trichloroethylbenzene, and hexachloroethane, each a product reasonably derived from silyl and benzyl

Can. J. Chem. Downloaded from www.nrcresearchpress.com by 210.87.254.105 on 09/05/12
For personal use only.

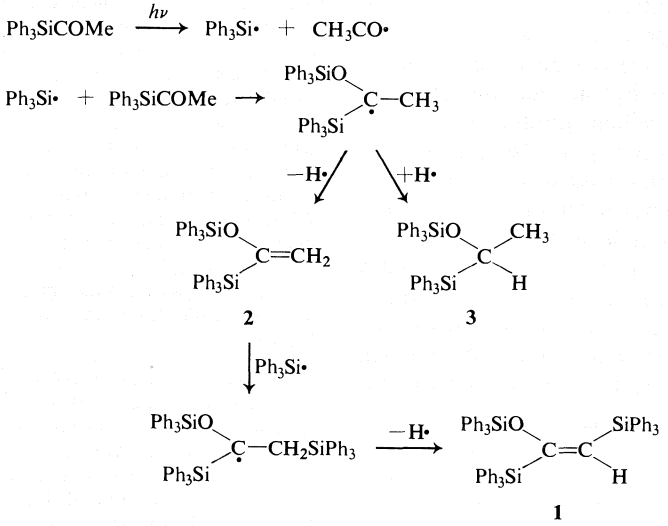

SCHEME 1. Photolysis of acetyltriphenylsilane.

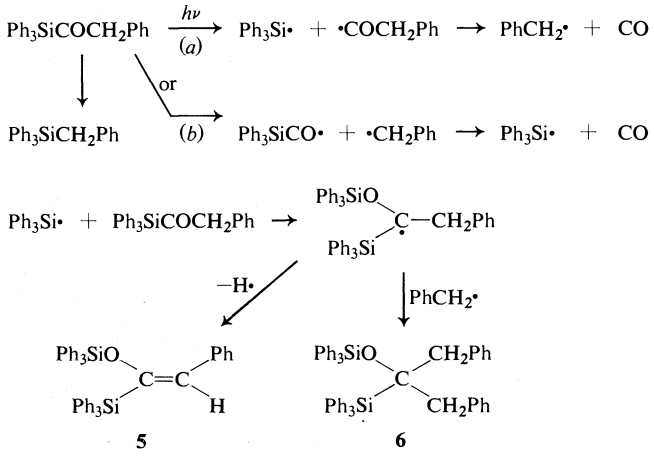

SCHEME 2. Photolysis of phenylacetyltriphenylsilane.

radicals. The known stability of benzyl radical suggests that decarbonylation of phenylacetyl radical might occur easily; nothing is known about triphenylsilylacyl radicals to date.

The second question is how the observed benzyltriphenylsilane is formed. Formally, it could arise by combination of triphenylsilyl and benzyl radicals. However, it is to be noted that almost the same yields of benzyltriphenylsilane are obtained by photolysis of the acylsilane in any of cyclohexane, carbon tetrachloride, or methanol. Since silyl radicals have been shown previously to be very reactive toward carbon tetrachloride it is not clear why they should survive in this solvent to be able to combine with benzyl radicals, nor why, if formed in methanol, their behavior should not be strongly influenced by the rather different nature of this solvent so that at least a different amount of benzylsilane would be formed. To date all acylsilanes except phenylacetyltriphenylsilane, when photolyzed in methanol, have yielded almost no products of radical reactions, but instead yielded products derived from siloxycarbenes. These various observations are rationalized by the proposal that the major source of benzyltriphenylsilane is from a separate concerted intramolecular extrusion of CO from phenylacetyltriphenylsilane (*i.e.* reaction within and relatively independent of the solvent cage), rather than from the coupling of

Can. J. Chem. Downloaded from www.nrcresearchpress.com by 210.87.254.105 on 09/05/12
For personal use only.

free silyl and benzyl radicals, which species are the sources of the other products observed as noted.

The photolyses of acetyltriphenylsilane using the di- and trichloroethylenes as solvents were briefly investigated. When photolyzed in *cis*-dichloroethylene, acetyltriphenylsilane gave a large amount of oligomerized solvent and a 34% yield of *trans*-2-triphenylsilylchloroethylene (**10**). Using *trans*-dichloroethylene, the same product was obtained in 45% yield. The *trans* geometry was assigned based on strong i.r. absorption at 10.52 μ, characteristic of a *trans*-disubstituted ethylene, and by the magnitude of the AB coupling constant of 15 Hz consistent with this geometry.

When photolyzed in trichloroethylene, acetyl chloride, triphenylchlorosilane, and 2,2-dichlorovinyltriphenylsilane (**11**) were isolated.

Both the above reactions are consistent with the cleavage of the acylsilane to radicals where the silyl radical either added to the double bond of the solvent, the new radical then losing a halogen atom, or where the silyl and acetyl radicals abstracted halogen from the solvent (Scheme 3).

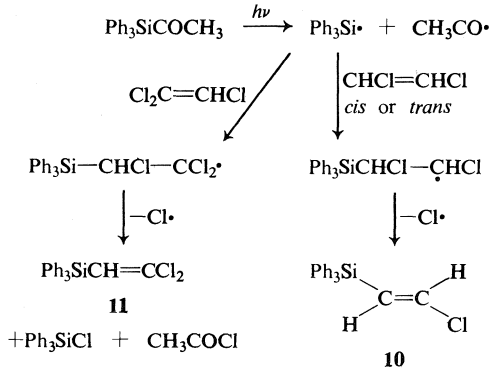

SCHEME 3. Photolysis of acetyltriphenylsilane in chloroethylenes.

The preceding data clearly demonstrate the pronounced tendency of photolytically generated silyl radicals either to abstract a highly electronegative atom (halogen) from the solvent, or to add to unsaturation (C=O or C=C) when halogen is not available for abstraction. The driving force for either process is obviously the stability achieved through the strong Si—X or Si—O bonds that are formed in this process.

Experimental

All photolyses were carried out using a 100 W PAR 38 clear mercury flood lamp, ASA code H34-4GS, which has energy maxima at 366, 405, and 436 nm, closely matching the n–π* absorption maxima of acetylsilanes which occur at about 360–380 nm. Irradiations were carried out in Pyrex flasks positioned 8–12 in. from the lamp. Solutions were flushed with nitrogen prior to irradiation to remove oxygen, and photolyses were carried out with a slight positive pressure of thoroughly dried pure nitrogen gas.

I.r. spectra were obtained on a Perkin–Elmer 237B grating spectrometer; n.m.r. spectra on Varian A60 or T60 spectrometers; u.v. spectra on a Bausch & Lomb Spectronic 505 spectrometer; mass spectra on an AEI 902 spectrometer; g.l.c. on a Varian Aerograph Series 200 dual column gas chromatograph with thermal conductivity detection. Analyses were by A. B. Gygli, Toronto, Ontario.

The Photolyses of Acetyltriphenylsilane in Cyclohexane

A solution of 3.00 g (0.0099 mol) of acetyltriphenylsilane in 75 ml of cyclohexane (dried by distillation from lithium aluminum hydride) was stirred and irradiated until all acylsilane was gone ($8\frac{3}{4}$ h).

A similar irradiation of 15.00 g of the acylsilane in 250 ml of cyclohexane required 25 h irradiation for consumption of the acylsilane; 4 g in 60 ml of solvent required $12\frac{1}{2}$ h.

A thick, faintly yellow oil, obviously a mixture, was obtained upon removal of solvent under reduced pressure. Three products giving rise to (*a*) a singlet at δ 6 p.p.m., (*b*) two doublets (J = 1.8 Hz) at 5.15 and 4.68 p.p.m., and (*c*) a quartet (J = 7.5 Hz) at 4.53 p.p.m. were identified by methods described below. Other unidentified absorption in the region 2.2–1.0 p.p.m. was observed.

The product from the photolysis of 3 g of acetyltriphenylsilane in cyclohexane was chromatographed on silica gel. Elution with 1:3 benzene – carbon tetrachloride gave 1.39 g of oil.

Further elution of the column with benzene gave about 0.15 g (4%) of starting material and 0.89 g of slightly yellow solid which was recrystallized from carbon tetrachloride – petroleum ether (60–70°) to give 0.77 g (28%) of pure triphenylsilanol, m.p. 155–156°, mixed m.p. 155–156°.

The 1.39 g of oil obtained by chromatography above was dissolved in 20 ml of benzene, methanol was added, and on standing overnight 0.43 g of white crystals, m.p. 177–183°, were obtained. Recrystallization from the same solvent mixture, and then from carbon tetrachloride – heptane gave 0.26 g (9.6%) of pure 1-triphenylsiloxy-1,2-bis(triphenylsilyl)ethylene (**1**), m.p. 180–181°: *m/e* (relative abundance, proposed origin) 818 (1, M), 741 (3, M − Ph), 559 (5, M − Ph_3Si), 457 (33, $Ph_3SiOSiPh_2$), 259 (100, Ph_3Si); i.r. (CCl_4), 7.0, 9.0 (SiPh), 9.2 μ (Si—O—C); n.m.r. (internal TMS, $CDCl_3$) δ 6.00 (1H, s, C=CH), 6.6–7.5 p.p.m. (45H, m, aryl).

Anal. Calcd. for $C_{56}H_{46}OSi_3$: C, 82.10; H, 5.66; Si, 10.28. Found: C, 82.16; H, 5.60; Si, 10.35.

Hydrolysis of 1 in Aqueous Alkaline Dioxane

A solution of 0.25 g of **1** in 6 ml of dioxane was treated with 1.5 ml of 12% aqueous potassium hydroxide at room temperature for 1 h. Work-up with dilute hydrochloric acid gave a solid which was recrystallized from petroleum ether (90–100°) to give 0.22 g (88%) of triphenylsilanol, m.p. 140–155°. Recrystallization from carbon tetrachloride – pentane gave 0.20 g (79%) of material, m.p.

Can. J. Chem. Downloaded from www.nrcresearchpress.com by 210.87.254.105 on 09/05/12
For personal use only.

Can. J. Chem. Downloaded from www.nrcresearchpress.com by 210.87.254.105 on 09/05/12
For personal use only.

155–156°, identified by mixed m.p. with the authentic material.

Lithium aluminum hydride in refluxing di-*n*-butyl ether or hydrochloric acid in refluxing aqueous acetone had little or no effect on **1**.

*Treatment of **1** with Phenyllithium; Triphenylsilylacetyltriphenylsilane (**4**)*

A solution of 1.00 g (0.00122 mol) of **1** in dry benzene was treated with 3.75 ml (0.0030 mol) of freshly-prepared phenyllithium in ether–benzene solution. Upon being refluxed for $2\frac{1}{2}$ h the solution turned deep red and gave a white precipitate. Work-up with saturated aqueous ammonium chloride (β-ketosilanes are acid-sensitive) gave a solid which upon crystallization from carbon tetrachloride gave 0.31 g (76%) of tetraphenylsilane. This was recrystallized from carbon tetrachloride to give 0.26 g (65%) of the pure compound, m.p. 240–241°.

The residual product, an oil, was dissolved in hexane and gave, in three crops, 0.78 g of solid consisting largely of triphenylsilylacetyltriphenylsilane (**4**) which melted over a wide range. Recrystallization from methylene chloride – methanol gave 0.43 g (64%) of material, m.p. 140–153°, and recrystallization from methylene chloride – pentane gave m.p. 154–158°. Subsequent recrystallization failed to sharpen the m.p.; the large range is attributed to the ready thermal decomposition of **4**.

Similar treatment of **1** with *n*-butyllithium gave *n*-butyltriphenylsilane (60%) and **4** (40%); i.r. (CCl_4) 6.16 (C=O), 7.0, 9.0 μ (Si—Ph); n.m.r. ($CDCl_3$) δ 3.42 (2H, s, CH_2), 7.2–7.4 p.p.m. (32H (30 required), m, aryl); u.v. (λ_{max}, (ε), C_6H_{12}), 338 nm (sh, 83), 350 (sh, 160), 362 (275), 376.5 (380), 391.5 (295).

Anal. Calcd. for $C_{33}H_{32}OSi_2$: C, 81.38; H, 5.75. Found: C, 80.32; H, 6.05.

The unsatisfactory elemental analysis obtained for **4** was probably a result of trapped solvent in the crystals. However, in this case heating the compound up to its melting point to remove solvent resulted in partial rearrangement to a new compound.

*Thermal Rearrangement of **4** to 1-Triphenylsiloxy-1-triphenylsilylethylene (**2**)*

A sample of 0.100 g of **4** was heated under nitrogen at 160° for 30 min. The n.m.r. and i.r. spectra of the resulting glass were identical to those of an authentic sample of 1-triphenylsiloxy-1-triphenylsilylethylene (**2**), the preparation of which is described below. Crystallization from methylene chloride – methanol gave 0.071 g (71%) of crystalline **2**, m.p. 115–118°.

*Synthesis of 1-Triphenylsiloxy-1-triphenylsilylethylene (**2**)*

To a well-stirred suspension of 3.9 g (0.10 mol) of sodium amide in 100 ml of dry benzene under nitrogen, was added 16.1 g (0.100 mol) of bis(trimethylsilyl)amine to give a suspension of sodium bis(trimethylsilyl) amide.

To the suspension containing 0.012 mol of the above material was added, all at once, 3.02 g (0.010 mol) of acetyltriphenylsilane. After stirring for 10 min at room temperature solid triphenylchlorosilane (3.25 g, 0.011 mol) was added to the deep yellow solution. The yellow color disappeared, some warming was noticed, and on stirring for 1 h at room temperature a thick white suspension was obtained. Work-up with dilute hydrochloric acid and ether gave 5.6 g of yellow oil which was dissolved in 25 ml of benzene. Addition of 200 ml of methanol and cooling the solution to −20° gave 3.82 g (68%) of 1-triphenylsiloxy-1-triphenylsilylethylene, m.p. 110–113°. Recrystallization from hexane and other hydrocarbon solvents gave very unsharp melting material containing a considerable amount of trapped solvent. The analytical sample, m.p. 120–121°, was obtained by several recrystallizations from benzene–methanol: *m/e* 560 (1, M), 546 (1, M − CH_2), 482 (5, M − PhH), 457 (23, $Ph_3SiOSiPh_2$), 379 (36, 457 − PhH), 259 (100, Ph_3Si); i.r. (CCl_4) 6.05 (weak, C=C), 7.0, 9.0 (SiPh), 8.3 (s), 9.9 μ (s); n.m.r. ($CDCl_3$); 4.67 (1H, d, J = 1.8 Hz) and 5.13 (1H, d, J = 1.8 Hz, =CH_2), 7.1–7.7 p.p.m. (30H, m, aryl).

Anal. Calcd for $C_{38}H_{32}OSi_2$: C, 81.38; H, 5.75. Found: C, 80.92; H, 5.73.

*Isolation of 1-Triphenylsiloxy-1-triphenylsilylethane (**3**) from the Photolysate*

Following the photolysis of 4.00 g of acetyltriphenylsilane in cyclohexane the product was worked-up by chromatography to give an oil upon elution with benzene – carbon tetrachloride. Crystallization of this oil from pentane gave largely **1** in the first two crops. (This was further recrystallized to give 0.30 g of pure **1**.)

Removal of solvent from the mother liquor gave 1.08 g of thin oil which on crystallization from pentane gave 0.48 g of a solid, m.p. 135–144°, judged from its n.m.r. spectrum to consist of a mixture of **2**, 5.20 and 4.72 p.p.m. (doublets, J = 1.8 Hz), and a second compound, 1-triphenylsiloxy-1-triphenylsilylethane (**3**), δ 4.56 (1H, quartet, J = 7.5 Hz) and 1.48 p.p.m. (3H, doublet, J = 7.5 Hz).

The presence of **2** was confirmed by the i.r. spectrum in which all of the bands present in the spectrum of pure **2** were seen. One-half of this solid mixture (0.24 g) after seven recrystallizations from heptane gave 0.05 g of white solid, m.p. 156–159°, which consisted of **3**, contaminated with a trace of **2**. The mixed m.p. of this solid with pure **3**, (m.p. 163–164°, prepared as described below) was 159–163°.

The second half of the solid mixture of **2** and **3** (0.26 g) was treated with 10 ml of dioxane and 3 ml of 3 *M* aqueous sodium hydroxide over 40 min at room temperature. Work-up with dilute hydrochloric acid and ether gave a solid mixture of triphenylsilanol (identified by i.r.) and **3**.

Chromatography on silica gel gave upon elution with 1:1 benzene – carbon tetrachloride a thick oily fraction which was crystallized, then recrystallized from heptane to give 0.087 g of pure **3**, m.p. 163–164°, mixed m.p. with authentic material, 163–164°.

*Synthesis of 1-Triphenylsiloxy-1-triphenylsilylethane (**3**)*

A solution of 0.70 g (0.0023 mol) of 1-triphenylsilylethanol in 40 ml of dry toluene containing 0.4 ml (0.005 mol) of pyridine and 0.0023 mol of triphenylbromosilane (prepared by the treatment of 0.60 g of triphenylsilane with bromine in carbon tetrachloride) was heated at reflux for 17 h, and then was cooled and worked-up by adding two volumes of ether and washing the solution twice with water to remove pyridinium hydrobromide. Removal of the solvent with the rotary evaporator gave an oil which, upon crystallization from petroleum ether

(60–70°) gave 0.73 g (56%) of 1-triphenylsiloxy-1-triphenylsilylethane (**3**), m.p. 159–164°. Recrystallization from heptane gave m.p. 163–164°. The mixed m.p. of this with a sample of the same compound obtained from the rearrangement of the isomeric bis(triphenylsilyl)ethanol (9) was not depressed.

*Determination of the Relative Yields of **1**, **2**, and **3***

Photolysis of 1.00 g of acetyltriphenylsilane in 60 ml of cyclohexane (over $2\frac{1}{4}$ h) and chromatography on silica gel using elution with 10% benzene in carbon tetrachloride gave 0.48 g of thick oil, whose 100 MHz expanded scale n.m.r. spectrum was utilized in the regions of (*a*) 6.0, (*b*) 5.1, and (*c*) the multiplet 4.7–4.2 p.p.m., to establish the relative yields of compounds **1**, **2**, and **3** as 28:44:28. Knowing that the mixture of the three accounts for at most 50% of the photolysate, upper limits of 14, 22, and 14%, respectively, may be assigned to the yields of **1**, **2**, and **3**.

*Isolation of **3** from the Photolysis of Acetyltriphenylsilane in Methanol Containing Pyridine*

A suspension of 0.15 g of acetyltriphenylsilane in 10 ml of methanol containing 50 μl of pyridine was irradiated for 35 min when an i.r. spectrum showed that no starting acylsilane remained. A fine precipitate was present in the solution. Cooling to −20° and filtration then gave 0.005 g of white solid, m.p. 149–155°, the n.m.r. and i.r. spectra of which indicated it to be **3**. Two recrystallizations from carbon tetrachloride – methanol gave about 2 mg of **3**, m.p. 163–165°, mixed m.p. 163–164°.

The Photolysis of Phenylacetyltriphenylsilane in Cyclohexane

A solution of 9.80 g of phenylacetyltriphenylsilane in 300 ml of dry cyclohexane was irradiated for 6 h until no starting acylsilane remained. Removal of the solvent gave a thick oil which was dissolved in 350 ml of hexane. On standing at −20° overnight 0.93 g (12%) of crude solid β-triphenylsiloxy-β-triphenylsilylstyrene (**5**) was obtained. Recrystallization from carbon tetrachloride gave 0.60 g (7.7%) of pure material, m.p. 233–235°. (In other runs, using a similar procedure pure **5** was obtained in yields of 6.6, 7.3, and 9.0%.)

The mother liquor was then evaporated to dryness and the resulting oil was dissolved in 50 ml of methylene chloride. Addition of 200 ml of methanol gave, on standing, 3.69 g of solid which was recrystallized from methylene chloride – methanol to give 3.51 g (41%) of a second product, 2-triphenylsiloxy-2-triphenylsilyl-1,3-diphenylpropane (**6**), m.p. 195–199°. (Yields of 39, 37, and 41% of this product were obtained in other runs.)

The solvent was evaporated from the mother liquor (which originally gave the 3.69 g of crude **6**) until less than 100 ml remained and on standing 3.13 g (34%) of benzyltriphenylsilane was obtained as large crystals, m.p. 97–99°. This was identified by mixed m.p. with the authentic material. (In other runs, yields of 29, 33, and 34% were obtained.)

*Characterization of β-Triphenylsiloxy-β-Triphenylsilylstyrene (**5**)*

Compound **5** on recrystallization from methylene chloride – methanol had m.p. 234–235°. The solid was heated to 234° for a few minutes to remove trapped solvent (decrepitation was observed during heating): *m/e* 636 (13, M), 559 (0.5, M − Ph), 457 (25, $Ph_3SiOSiPh_2$), 379 (23, 457 − PhH), 259 (100, Ph_3Si); n.m.r. (C_6D_6) δ 6.32 (1H, s), 6.8–7.8 p.p.m. (39H (35 required), m, aryl).

Anal. Calcd. for $C_{44}H_{36}OSi_2$: C, 82.97; H, 5.70. Found: C, 82.96; H, 5.76.

*Degradation of **5***

(a) Aqueous Alkaline Dioxane

A few milligrams of **5** in dioxane was treated with 1 ml of 10% sodium hydroxide. The solution was heated for 5 min, and then was cooled and worked-up with dilute acid and ether to give a white solid. The i.r. spectrum of this material showed it to consist of triphenylsilanol (2.70 μ) and a small amount of phenylacetic acid (3–4, (broad), 5.85 μ) which was also notable by its odor. No other products were detected.

(b) Lithium Aluminum Hydride

To a suspension of 0.33 g (0.00052 mol) of **5** in 20 ml of dry di-*n*-butyl ether was added 0.08 g (0.002 mol) of lithium aluminum hydride. The suspension was heated for 2 h. Work-up with dilute HCl gave an oil which was chromatographed on silica gel. Elution with carbon tetrachloride gave 0.11 g (83%) of triphenylsilane as an oil in the first three fractions. This was crystallized from pentane to give 0.06 g of the pure solid, m.p. 41–44°, identified by mixed m.p. with authentic material.

Further elution with carbon tetrachloride gave 0.06 g (~18%) of unidentified material.

Elution with benzene gave, in the first two fractions, 0.12 g (61%) of crude phenylacetyltriphenylsilane as an oil. Crystallization from ethanol at −20° gave 0.06 g (30%) of pure acylsilane, m.p. 93–95°, mixed m.p. 93–95°.

Further elution of the column with benzene gave 0.06 g (27%) of crude triphenylsilanol.

*Characterization of 2-Triphenylsiloxy-2-triphenylsilyl-1,3-diphenylpropane (**6**)*

Several recrystallizations from methylene chloride – methanol gave the pure material, m.p. 199–200°, which was finely ground up and was pumped on at 115°/0.1 mm prior to analysis: *m/e* 637 (3, M − $PhCH_2$), 636 (4, M − $PhCH_3$), 468 (34, M − Ph_3Si), 457 (14, $Ph_3SiOSiPh_2$), 259 (100, Ph_3Si); i.r. (CCl_4) 6.88 (C—Ph) 7.0, 9.0 μ (Si—Ph); n.m.r. (CCl_4) δ 3.58 (4H, broadened AB system, J = 14 Hz, CH_2Ph), 6.5–7.7 p.p.m. (41H, m, aryl).

Anal. Calcd. for $C_{51}H_{44}OSi_2$: C, 84.02; H, 6.08. Found: C, 84.03; H, 5.97.

*Degradation of **6** in Aqueous Alkaline Diglyme*

To a solution of 0.80 g of **6** in 50 ml of diglyme was added 5 ml of water and 1.20 g of potassium hydroxide. The solution was heated to reflux for $4\frac{1}{2}$ h, and then was acidified and extracted thrice with ether. Drying and removal of solid gave an oil which showed almost no silicon–phenyl absorption at 7 and 9 μ in the i.r. Chromatography on silica gel eluting first with benzene and then with methylene chloride gave 0.18 g (77%) of 1,3-diphenylpropan-2-ol, **7**, n_D^{23} 1.5699 (lit. n_D^{20} 1.5723 (10)).

The carbinol was treated with 0.20 g of *p*-nitrobenzoyl chloride in 1 ml of pyridine for 30 min at room temperature. Work-up with ether and saturated aqueous sodium bicarbonate gave an oil which was crystallized from hexane to give 0.25 g (63%, based on **6**) of 1,3-diphenyl-2-

Can. J. Chem. Downloaded from www.nrcresearchpress.com by 210.87.254.105 on 09/05/12
For personal use only.

propyl *p*-nitrobenzoate, m.p. 72–78°. Recrystallization from hexane gave 0.18 g of pure material, m.p. 78–79° (lit. m.p. 80–81° (11)).

Thermal Rearrangement of ***6*** *to Pentaphenyl-2-(1,2,3-triphenylpropyl)-disiloxane (****8****)*

A sample of 1.60 g of **6** was heated at 210° for 90 min. An n.m.r. spectrum of the resulting glass indicated that a quantitative isomerization to a disiloxane, **8**, had occurred. Crystallization from methylene chloride – methanol gave 1.57 g of solid which was recrystallized to give 1.36 g (85%) of pure **8**, m.p. 150–151.5°. The sample was finely ground up and was pumped on at 80°/0.1 mm prior to analysis: *m/e* 728 (0.4, M), 726 (0.2, M − H_2), 636 (0.4, M − $PhCH_3$), 457 (100, $Ph_3SiOSiPh_2$), 379 (58, 457 − PhH); i.r. (CCl_4), 6.88 (C—Ph), 7.0, 9.0 (Si—Ph), 9.3 μ (broad, SiOSi); n.m.r. δ 3.52 (4H, AB system, J = 16 Hz, CH_2Ph), 6.5–7.7 p.p.m. (40H, m, aryl).

Anal. Calcd. for $C_{51}H_{44}OSi_2$: C, 84.02; H, 6.08. Found: C, 83.99; H, 5.87.

Degradation of ***8*** *in Aqueous Alkaline Diglyme*

To a solution of 0.37 g (0.0005 mol) of **8** in diglyme was added 1 ml of 50% potassium hydroxide. Heating for 3 h followed by work-up with water gave a thin oil which showed no silicon–phenyl absorption at 7 and 9 μ in the i.r. spectrum.

Chromatography on silica gel gave, on elution with carbon tetrachloride, 0.11 g (80%) of 1,2,3-triphenylpropane, n_D^{23} 1.5858, the i.r. and n.m.r. spectra of which were identical to those of the authentic material, prepared as follows:

To a solution of 3.0 g of 1,2,3-triphenylpropan-2-ol (prepared by the addition of 2 equiv of benzylmagnesium chloride to methyl benzoate) in 95% ethanol was added 15 g of freshly prepared Raney Nickel (activity grade W1). The suspension was refluxed for 16 h. Filtration and removal of solvent gave an oil which was chromatographed on silica gel. Elution with carbon tetrachloride gave 1.30 g (46%) of 1,2,3-triphenylpropane which after distillation had n_D^{24} 1.5883 (lit. n_D^{30} 1.5864 (12)).

The Photolysis of Phenylacetyltriphenylsilane in Methanol

A suspension of 0.20 g of phenylacetyltriphenylsilane in 10 ml of methanol was irradiated for 90 min. Removal of the solvent gave a yellowish oil whose n.m.r. spectrum was almost identical to that of the crude photolysate from cyclohexane, and had the following bands: δ 2.81 (s, benzyltriphenylsilane), 3.55 (m, 2-triphenylsiloxy-2-triphenylsilyl-1,3-diphenylpropane (**6**) and superimposed singlet due to triphenylmethoxysilane), and 6.3 p.p.m. (s, β-triphenylsiloxy-β-triphenylsilylstyrene (**5**)).

The photolysis of phenylacetyltriphenylsilane in methanol containing pyridine gave virtually identical results.

Photolysis of Phenylacetyltriphenylsilane in Carbon Tetrachloride

The photolysis of 0.50 g (0.0013 mol) of phenylacetyltriphenylsilane in 15 ml of carbon tetrachloride was complete in 2 h. Removal of the solvent gave a yellow oil, whose i.r. spectrum showed only negligibly weak carbonyl absorptions. The n.m.r. spectrum of the crude product showed peaks attributable to three identifiable products: bibenzyl (2.81 p.p.m.), benzyltriphenylsilane (2.85 p.p.m.), and 1,1,1-trichloro-2-phenylethane (3.75 p.p.m.). An array of minor peaks indicated that an appreciable number of minor products were also formed.

The entire product was briefly treated with dilute potassium hydroxide in aqueous tetrahydrofuran to convert triphenylchlorosilane to triphenylsilanol. Chromatography on silica gel, eluting with carbon tetrachloride, and then with 1:1 carbon tetrachloride – benzene, gave 0.18 g of non-polar oil which was crystallized from methanol to give 0.12 g (26%) of benzyltriphenylsilane as large clear crystals, m.p. 96–97°, mixed m.p. 96–97°.

Elution of the column with ether gave a white solid which was recrystallized from heptane to give 0.19 g (52%) of triphenylsilanol, m.p. 153–154°, identified by mixed m.p.

The presence of bibenzyl and 1,1,1-trichloro-2-phenylethane, identified in the n.m.r., and of hexachloroethane, were confirmed by g.l.p.c. analysis using the following conditions: column, 20 ft × 1/4 in. 20% Carbowax 20M on Chromosorb G; column temperature, 240°; detector, 300°; injector port, 285°; flow rate 90 ml/min. Following a small scale photolysis (0.20 g of phenylacetyltriphenylsilane in 5 ml of carbon tetrachloride) the photosolution was concentrated. The g.l.p.c. trace showed peaks with retention times of 1.1, 2.1, 3.3, and 5.4 min which were identified, by injection of the authentic material, as being due to carbon tetrachloride, hexachloroethane, 1,1,1-trichloro-2-phenylethane, and bibenzyl, respectively. The origin of a fifth minor peak, at 2.7 min, is unknown.

Preparative g.l.p.c. gave a small amount of pure 1,1,1-trichloro-2-phenylethane, the n.m.r. and i.r. spectra of which were identical to those of the authentic material prepared by the coupling of trichloromethylmagnesium chloride with benzyl chloride (13).

No attempt was made to measure the yields of the latter three products but it was apparent both from the n.m.r. spectrum of the crude photolysate and from g.l.p.c. analysis that 1,1,1-trichloro-2-phenylethane was a major product, being present in greater yield than the benzyltriphenylsilane (26%). The hexachloroethane and bibenzyl are formed in somewhat lower yields.

The Photolysis of Acetyltriphenylsilane in cis-1,2-Dichloroethylene

A solution of 0.50 g (0.0017 mol) of acetyltriphenylsilane in 10 ml of freshly distilled *cis*-1,2-dichloroethylene was irradiated for 6 h. The solvent was removed to give about 2 ml of liquid. Chromatography on a 1½ in. × 3 in. silica gel column, eluting with carbon tetrachloride, gave about 1½ ml of sweet-smelling liquid (oligomerized solvent). Elution with 1:3 benzene – carbon tetrachloride gave 0.31 g of solid material which was recrystallized from methylene chloride – methanol to give 0.18 g (34%) of *trans*-1-chloro-2-triphenylsilylethylene, m.p. 127–129°. Two more recrystallizations from hexane and a final one from methylene chloride – methanol gave the analysis sample, m.p. 131–132°: *m/e* 320 (4, M), 284 (7, M − HCl), 259 (12, Ph_3Si), 242 (23, M − 78), 218 (18, Ph_2SiCl), 180 (100, unknown); i.r. (CCl_4) 7.0, 9.0 (Si—Ph), 10.52 μ (*trans*-CH=CH—); n.m.r. (CCl_4), δ 6.30, 6.63 (2H, AB system with J_{AB} = 15 Hz, *trans*-CH=CH—), 7.2–7.6 p.p.m. (15H, m, aryl).

Anal. Calcd. for $C_{20}H_{17}ClSi$: C, 74.86; H, 5.43. Found: C, 75.00; H, 5.21.

A similar procedure was used in working-up the

Can. J. Chem. Downloaded from www.nrcresearchpress.com by 210.87.254.105 on 09/05/12
For personal use only.

photolysis of acetyltriphenylsilane in *trans*-1,2-dichloroethylene. In this case, the yield of pure isolated 1-chloro-2-triphenylsilylethylene was 45%.

The Photolysis of Acetyltriphenylsilane in Trichloroethylene

A solution of 1.00 g of acetyltriphenylsilane in 100 ml of trichloroethylene was irradiated for 5 h. The solvent was distilled until only 30 ml remained. An i.r. spectrum of the distillate showed that acetyl chloride was present. Treatment of the distillate with excess aniline afforded, after work-up and recrystallization 0.08 g (18%) of acetanilide, m.p. 112–114°, identified by mixed m.p.

The solvent was removed from the residual photosolution at the rotary evaporator to give 3.85 g of sweet-smelling oil. Distillation in the Kugelrohr (110°, 0.7 mm) gave 1.55 g of volatile liquid which appeared to be largely oligomerized solvent. The nonvolatile residue, 2.13 g of brown oil, was dissolved in ether and the solution was stirred with water to convert any chlorosilane to triphenylsilanol. Work-up gave a brown oil which showed a strong silanol peak at 2.70 μ in the i.r.

Chromatography on silica gel gave, on elution with carbon tetrachloride, a small amount of oil in the first few fractions and then small amounts of white solid over many fractions. The combined solid (0.42 g) was recrystallized from methylene chloride – methanol to give 0.33 g (28%) of dichlorovinyltriphenylsilane, m.p. 125–132°. Three further recrystallizations from methylene chloride – pentane raised the m.p. to 132–133°; *m/e* 356, 354 (2, M), 319 (3, M − Cl), 318 (3, M − HCl), 278, 276 (4, 5, M − 78), 218 (100, Ph_2SiCl); n.m.r. (CCl_4), δ 6.50 (1H, S, C=CH), 7.2–7.7 p.p.m. (15H, m, aryl).

Anal. Calcd. for $C_{20}H_{16}Cl_2Si$: C, 67.70; H, 4.54. Found: C, 67.67; H, 4.56.

This research was supported by the National Research Council of Canada.

1. A. G. Brook, P. J. Dillon, and R. Pearce. Can. J. Chem. **49**, 133 (1971).
2. A. G. Brook and J. M. Duff. J. Am. Chem. Soc. **89**, 454 (1967).
3. J. M. Duff. Ph.D. Thesis. University of Toronto, Toronto, Ontario. 1970.
4. A. G. Brook, D. M. MacRae, and W. W. Limburg. J. Am. Chem. Soc. **89**, 5493 (1967).
5. A. G. Brook, G. E. LeGrow, and D. M. MacRae. Can. J. Chem. **45**, 239 (1967).
6. A. G. Brook and N. V. Schwartz. J. Org. Chem. **27**, 2311 (1962).
7. H. Merten and H. Gilman. J. Am. Chem. Soc. **76**, 5798 (1954).
8. C. Eaborn and H. Niederprüm. J. Chem. Soc. **1963**, 797.
9. A. G. Brook, C. M. Warner, and M. E. McGriskin. J. Am. Chem. Soc. **81**, 981 (1959).
10. K. Ivanov and G. Vasilev. C.R. acad. bulgare sci. **9**, 61 (1956). Chem. Abstr. **52**, 2817 (1958).
11. D. Papa, E. Schwenk, and B. Whitman. J. Org. Chem. **7**, 587 (1942).
12. K. Ishimura. Bull. Chem. Soc. Jap. **16**, 397 (1941).
13. J. Villiéras. Bull. Soc. Chim. Fr. 1520 (1967).

Can. J. Chem. Downloaded from www.nrcresearchpress.com by 210.87.254.105 on 09/05/12
For personal use only.

Retardation of AlH_2Cl Hydrogenolysis of the Ethylene Ketals of 5-Norbornen-2-one and 2-Norbornen-7-one Due to the Presence of the Double Bond[1]

H. A. Davis and R. K. Brown

Department of Chemistry, University of Alberta, Edmonton, Alberta

Received June 30, 1972

The double bond in either 5-norbornen-2-one ethylene ketal or 2-norbornen-7-one ethylene ketal provides no anchimeric assistance in the hydrogenolysis of these ketals by AlH_2Cl in ether. Instead, a marked retardation of reaction occurs, a result considered to be due to competitive association of the Lewis acid, AlH_2Cl, with the π bond.

Attack of the AlH_2Cl on the former ketal occurs from the *exo* direction to give only the *endo*-5-β-hydroxyethoxy product, whereas the latter ketal reacts with AlH_2Cl to give a 2:1 mixture of the *syn* and *anti* 7-β-hydroxyethoxy products. A rationale is provided to account for the results.

La double liaison dans soit la cétal éthylènique du norbornène-5 one-2 ou soit la cétal éthylènique du norbornène-2 one-7, ne procure pas d'assistance anchimérique lors de l'hydrogénolyse de ces cétals par AlH_2Cl dans l'éther. Plutôt, un ralentissement marqué de la réaction se produit; ce résultat semble imputable à l'association compétitive de l'acide de Lewis, AlH_2Cl, avec le lien π.

L'attaque du AlH_2Cl sur la première cétal se produit dans la direction *exo* pour donner seulement le produit *endo*-hydroxyethoxy-5-β alors que la dernière cétal réagit avec du AlH_2Cl pour donner un mélange 2:1 des produits *syn* et *anti* hydroxyéthoxy-7-β. Une explication rationnelle est proposée afin d'expliquer ces résultats. [Traduit par le journal]

Can. J. Chem., **51**, 361 (1973)

Introduction

It has been reported recently (1) that the vinyl group attached to C-2 of a 1,3-dioxolane accelerates the reductive cleavage of the dioxolane ring by AlH_2Cl in diethyl ether. This was attributed to increased stabilization of the transition state leading to the intermediate oxocarbonium ion, a species which is very rapidly and irreversibly attacked by hydride ion to produce allyl β-hydroxyethyl ether. A similar rate enhancement of hydrogenolysis by AlH_2Cl has been observed when a phenyl group is attached to C-2 of the 1,3-dioxolane ring (1, 2). Alkyl substituents on the 2-vinyl group of 2-vinyl-1,3-dioxolane further enhance the ease of the reductive cleavage of the ring (1).

It is known that the π electrons of the olefinic double bond provide anchimeric assistance in the reaction of *anti*-7-norbornenyl derivatives (3, 4). For example, the *anti*-7-tosylate is solvolyzed over 10^9 times faster than is the saturated compound 7-tosyloxynorbornane. On the other hand *exo*-2-chloro-5-norbornene undergoes solvolysis in 80% ethanol about 150 times faster than does the *endo* isomer, a difference in reactivity not much greater than that observed for the corresponding saturated compounds, *exo*- and *endo*-2-chloronorbornane (5, 6).

In view of the above information, we wished to determine whether an olefinic double bond would provide similar rate enhancement in the hydrogenolysis of 5-norbornen-2-one ethyleneketal (**1**) and 2-norbornen-7-one ethyleneketal (**2**) by AlH_2Cl in ether. This paper reports our observations concerning this question.

Results

The products obtained from the hydrogenolysis of compounds **1** and **2** are shown in Table 1, while the relative ease of the hydrogenolysis of **1** and **2** compared with other 1,3-dioxolanes, determined by competitive reactions, are shown in Table 2.

Orientation of the β-Hydroxyethoxy Substituent in the β-Hydroxyethyl Norbornenyl Ethers Obtainable From 1 and 2

The two possible products of the AlH_2Cl reduction of 5-norbornen-2-one ethyleneketal (**1**), 2-(2-*endo*-5-norbornenyloxy)ethanol, and 2-(2-*exo*-5-norbornenyloxy)ethanol, were readily

[1]Taken in part from the thesis of H. A. Davis submitted to the Faculty of Graduate Studies and Research, University of Alberta, as part of the requirements for the Ph.D. degree, 1970.

Can. J. Chem. Downloaded from www.nrcresearchpress.com by 210.87.254.40 on 09/05/12
For personal use only.

TABLE 1. Hydrogenolysis by AlH_2Cl of some norbornenone ethylene ketals in ether*

Compound	Products	
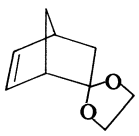 **1**	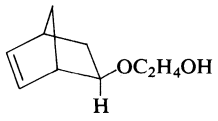 0%	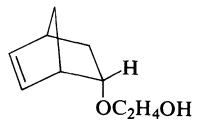 100%
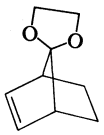 **2**	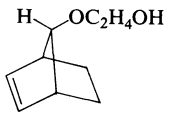 36%	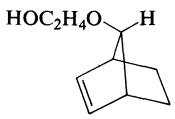 64%

*In each case the reaction was carried out at room temperature for 72 h with an excess of AlH_2Cl. The extent of reduction for **1** and **2** was 100% and 65% respectively while recovery of material in both cases was 95%.

TABLE 2. Competitive hydrogenolysis by AlH_2Cl in ether of equimolar mixtures of a norcamphor ethylene ketal with a 2-substituted-1,3-dioxolane*

Experiment number	Binary mixture†	Extent of reduction (%)
1	**1** + **3**	Trace 77
2	**2** + **3**	Trace 80
3	**1** + **4**	Trace 40
4	**2** + **4**	Trace 35

*In each case the reaction was carried out at room temperature for 30 min with sufficient AlH_2Cl to reduce completely only *one* of the two substrates.

† 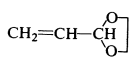

3

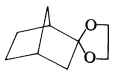

4

identified and differentiated by characteristic features of their p.m.r. spectra obtained with authentic samples. These samples were prepared from a mixture of the *exo* and *endo* isomers of 5-norbornen-2-ol, and the resulting *exo*- and *endo*-2-(5-norbornenyloxy)ethanols separated by preparative g.l.c. The two bridgehead protons of the *endo* isomer show *two* unresolved multiplets (1H for each) centered at τ 6.94 and 7.26, each with a half-width of 7 Hz, while the two bridgehead protons of the *exo* isomer show only *one* unresolved multiplet (2H) centered at τ 7.15, having $w_{1/2} \sim 10$ Hz. A similar phenomenon had been observed for the signals of the bridgehead protons in the p.m.r. spectra of *endo*- and *exo*-2-(2-norbornyloxy)ethanol (7). The observation that the p.m.r. spectrum of *endo*-5-nitro-2-norbornene shows two separate signals at τ 6.47 and 7.01 for the bridgehead protons (8) provides additional support for the above assignment. Unfortunately, the spectrum of the *exo*-5-nitro-2-norbornene was unavailable for comparison. Convincing evidence for our assignment is obtained from the portions of the signals of the C-2 protons in the p.m.r. spectrum of the *exo*- and *endo*-2-(5-norbornenyloxy)ethanols. In agreement with the well-known fact that the 2-*exo* proton is deshielded relative to the 2-*endo* proton in norbornene due to the anisotropy of the double bond (8, 9), the signal of the C-5 proton of *endo*-2-(5-norbornenyloxy)ethanol occurs as a quintet centered at τ 5.90 while the signal of the C-5 proton of the *exo* isomer lies between τ 6.3 and 6.7 in the region where the four methylene protons of the substituent absorb.

The two possible products of the AlH_2Cl hydrogenolysis of 2-norbornen-7-one ethyleneketal (**2**), 2-(7-*syn*-norbornenyloxy)ethanol, and

Can. J. Chem. Downloaded from www.nrcresearchpress.com by 210.87.254.40 on 09/05/12
For personal use only.

Can. J. Chem. Downloaded from www.nrcresearchpress.com by 210.87.254.40 on 09/05/12
For personal use only.

2-(7-*anti*-norbornenyloxy)ethanol, could also be identified and differentiated by the p.m.r. signals of the two bridgehead protons as well as by the signal of the C-7 proton. The p.m.r. spectra of authentic samples of these two hydrogenolysis products showed that for the *syn* isomer, the two bridgehead protons give rise to a narrow multiplet ($w_{1/2} \sim 5$ Hz) at τ 7.11, while those for the *anti* isomer produced a narrow multiplet at τ 7.35 ($w_{1/2} \sim 7$ Hz). Furthermore, the signal of the C-7 proton of the *syn* isomer is obscured by the signals of the four methylene protons of the hydroxyethoxy substituent τ (6.19–6.67) whereas that of the C-7 proton of the *anti* isomer experiences a diamagnetic shielding due to the double bond, a phenomenon reported by Snyder and Franzus (10), and hence appears as a broad singlet ($w_{1/2} \sim 4.5$ Hz) at τ 6.78.

Hydrogenolysis Results

There are three interesting observations from our experiments, two of which are immediately apparent from Tables 1 and 2. (*i*) The AlH_2Cl hydrogenolysis of **1** produces exclusively the 2-(2-*endo*-5-norbornenyloxy)ethanol, while similar hydrogenolysis of **2** provides an ~2:1 mixture of 2-(7-*syn*-2-norbornenyloxy)ethanol and 2-(7-*anti*-2-norbornenyloxy)ethanol (Table 1). (*ii*) The hydrogenolysis of both **1** and **2** is considerably slower than that of 2-vinyl-1,3-dioxolane (**3**) or of norcamphor ethyleneketal (**4**), the saturated analog of **1** (Table 2). Furthermore, *all* of **1** is hydrogenolyzed within a 72-h reaction period at room temperature while **2** is reduced to the extent of only 65% in 72 h under the same conditions. (*iii*) Although previous work (1) as well as the present work has shown that **3** is completely hydrogenolyzed by AlH_2Cl well within 15 min, our experiments now reveal that the presence of an equimolar quantity of **1** or **2** in an ether solution of **3** appears to retard the hydrogenolysis of **3** (Table 2, experiments 1 and 2). A similar retardation of hydrogenolysis of norcamphor ethyleneketal (**4**) occurs when ketal **4** in ether is mixed with an equimolar amount of **1** or **2** prior to the addition of AlH_2Cl. By comparison, room temperature hydrogenolysis of **4** alone in ether, by AlH_2Cl, has been shown to be complete well within 30 min (11).

Retardation of the hydrogenolysis of **3** and **4** when they are in the presence of **1** or **2** could be due to the association of the reducing agent, AlH_2Cl, with the π-electrons of the double bond of **1** or **2**, thus reducing the effective concentration of AlH_2Cl available to act as both the hydride donor and the Lewis acid which must first associate with the oxygen atom of the acetal to initiate the hydrogenolysis sequence. In support of this view, we have shown that whereas the room temperature hydrogenolysis of 2-methyl-1,3-dioxolane by AlH_2Cl in ether is complete *well* within 30 min (1), the same dioxolane in ether, mixed with an equimolar amount of cyclohexene, is hydrogenolyzed to the extent of only 90% in 30 min. A similar association of the Lewis acid, AlH_2Cl, with the double bond of **1** or **2** could account for the markedly lower rate of hydrogenolysis by AlH_2Cl of an ether solution of either **1** or **2** alone (Table 1) compared to the greater rate of such hydrogenolysis of the saturated bicyclic species, norcamphor ethylene ketal (7, 11). If such association of the AlH_2Cl with the π-bond is indeed the factor which is responsible for the decrease in rate of hydrogenolysis of **1** and **2**, it then follows that a similar retarding effect must apply in the reductive cleavage of **3**, and accordingly **3** would have cleaved even more rapidly than observed (1) if such a factor were not involved. A modifying influence in the case of **3** would be the proximity of the π-AlH_2Cl complex to C-2 of the 1,3-dioxolane ring and this might facilitate transfer of the AlH_2Cl to the oxygen of the 1,3-dioxolane ring as well as transfer of a hydride ion to C-2 to promote ring cleavage. Such a conveniently close arrangement does not occur in compounds **1** and **2**.

The exclusive formation of 2-(2-*endo*-5-norbornenyloxy)ethanol from the AlH_2Cl hydrogenolysis of **1** could be due to two factors. *Exo* approach of reagents to norbornanes is considered to be easier than is *endo* approach (7, and references therein). Hence attack by AlH_2Cl on the *exo* oxygen atom of **1** should be preferred, although the absence of two *endo* hydrogen atoms in compound **1** would decrease this steric selectivity compared with that found for the saturated analogs. Added to this is the fact that approach to the *endo* oxygen atom of **1** is complicated by the proximity of the double bond, which from the reasoning expressed in the preceding paragraphs, should provide a region of high attraction for the Lewis acid AlH_2Cl. This could interfere sufficiently with the approach of AlH_2Cl to the *endo* oxygen atom and thus

Can. J. Chem. Downloaded from www.nrcresearchpress.com by 210.87.254.40 on 09/05/12
For personal use only.

enable alternate approach of the hydrogenolyzing reagent to the *exo* oxygen atom to become sufficiently competitive so that only *exo* C—O bond cleavage is observed. This view of course must assume that the molecule of AlH_2Cl which attacks the oxygen atom and initiates C—O bond cleavage is the same one which donates the hydride ion to the developing oxocarbonium ion to complete the reductive cleavage. This is not an unreasonable assumption for compound **1** (7).

In the case of compound **2**, approach of the AlH_2Cl to the oxygen atom *syn* to the double bond could suffer the same type of interference due to the π-bond, and thus allow approach to the alternate oxygen atom to become competitive. However such alternate approach would experience sufficient steric interference from the two *exo* hydrogen atoms to prevent hydrogenolysis from occurring only with the C—O bond remote from the double bond, thus resulting in the approximately 2:1 formation of the *syn* and *anti* norbornenyloxyethanols from **2** as shown in Table 1. The generally slower reaction of **2**, compared with that of **1** could easily be due to the steric effect of the *exo* hydrogen atoms of **2**.

Experimental

Boiling and melting points are uncorrected. The g.l.c. analyses were made with an F and M Model 700 instrument equipped with 12 ft × 1/8 in. columns packed with either butanediol succinate, 20% on Gas Chrom P (60–80 mesh) or silicone rubber SE 30, 20% on Gas Chrom P (60–80 mesh). Helium was the carrier gas at a flow rate of 40 ml/min. For preparative g.l.c., an Aerograph Autoprep, Model A-700 (Wilkins Instrument and Research Co.) was employed with a 12 ft × 1/4 in. column packed with butanediol succinate on Gas Chrom P (60–80 mesh). Helium was the carrier gas. Quantitative analyses were made by measuring the areas of the peaks corresponding to the compounds obtained. These areas were compared with those obtained from known and weighed artificial mixtures. It was found that equimolar mixtures gave peaks whose areas differed by less than 5%.

The i.r. spectra were recorded with a Perkin–Elmer Model 21 instrument.

The p.m.r. spectra were recorded on either a Varian Associates A-60 or A-55/60A instrument by Mr. R. Swindlehurst and assistants in this Department. All spectra were referred to tetramethylsilane and employ the τ scale.

The p.m.r. and i.r. spectra were obtained for all compounds and were consistent with the structures assigned.

Elemental analyses were made by Mrs. Darlene Mahlow of this Department.

The drying agent for solutions was anhydrous magnesium sulfate unless otherwise indicated. Solvents were removed by rotary evaporator under reduced pressure unless otherwise stated.

Preparation of the Ketals and Acetals

*Norcamphor Ethylene Ketal (**4**)*

This compound was synthesized according to published directions (7). B.p. 78° at 14 mm; η_D^{25} 1.4756 (lit. b.p. 78–80° at 14 mm; η_D^{25} 1.4319 (7) (*note*, this value of the refractive index reported in (7) is erroneous; our measurement of the same sample used by the authors of ref. 7 gave η_D^{25} 1.4752)).

*Acrolein Ethylene Acetal (2-Vinyl-1,3-dioxolane) (**3**)*

This was prepared according to published directions (1).

*5-Norbornen-2-one Ethylene Ketal (**1**)*

This compound was prepared from 5-norbornen-2-one (12) by the same procedure used to make 2-(1-propenyl)-1,3-dioxolane (1). Yield of colorless liquid, 75%. B.p. 76° at 9 mm; η_D^{24} 1.4872.

Anal. Calcd. for $C_9H_{12}O_2$: C, 71.05; H, 7.89. Found: C, 70.92; H, 7.72.

The 60 MHz p.m.r. spectrum in CCl_4 showed a multiplet centered at τ 3.98 (2H); a singlet at 6.18 (4H); a broad singlet at 7.22 (1H), $w_{1/2}$ = 7.5 Hz; a broad singlet at 7.47 (1H), $w_{1/2}$ = 6 Hz; a multiplet between 8.06 and 9.30 (4H).

*2-Norbornen-7-one Ethylene Ketal (**2**)*

syn-7-Norbornenol (13) was converted to 2-norbornen-7-one according to the published procedure (12) and the ketone was in turn converted to the ketal **2** by the same procedure used to prepare 2-(1-propenyl)-1,3-dioxolane (1). Yield of colorless liquid, 80% B.p. 73–75° at 6 mm; η_D^{24} 1.4904.

Anal. Calcd. for $C_9H_{12}O_2$: C, 71.05; H, 7.89. Found: C, 70.91; H, 7.98.

The 60 MHz p.m.r. spectrum in CCl_4 showed a triplet centered at τ 3.98 (2H), $J \simeq 2.5$ Hz; a triplet centered at 6.26 (4H), $J \simeq 3$ Hz; a multiplet centered at 7.62 (2H); a multiplet between 7.94 and 8.32 (2H); a multiplet between 8.97 and 9.27 (2H).

Preparation of Authentic Hydrogenolysis Products

exo and endo-2-(5-Norbornen-2-yloxy)ethanol

A mixture of the *exo* and *endo* isomers of 5-norbornen-2-ol (Aldrich Chemical Co.) was converted to *ethyl exo-endo-(5-norbornen-2-yloxy)acetate* by the procedure used to prepare ethyl (2-dimethylaminoethoxy)acetate (1). Yield of colorless liquid, 43%. B.p. 73° at 0.6 mm; η_D^{24} 1.4701.

Anal. Calcd. for $C_{11}H_{16}O_3$: C, 67.54; H, 8.16. Found: C, 67.43; H, 8.33.

The 60 MHz p.m.r. spectrum in CCl_4 showed a multiplet centered at τ 3.92 (2H); a triplet at 5.92 (2H), $J \simeq 7.5$ Hz; a singlet at 6.11 (2H); a multiplet between 6.83 and 7.38 (2H); a multiplet between 7.78 and 9.28 (8H).

The i.r. spectrum in CCl_4 showed absorption bands at 3060 (vinylic C—H); 1755 and 1730 (C=O for *exo* and *endo* isomers); a broad band between 1290 and 1100 cm^{-1} (C—O).

The above acetate was converted to *exo-endo-2-(5-norbornen-2-yloxy)ethanol* by reduction with $LiAlH_4$ as described for the preparation of 2-(2-dimethylamino-

Can. J. Chem. Downloaded from www.nrcresearchpress.com by 210.87.254.40 on 09/05/12
For personal use only.

ethoxy)ethanol (1). The colorless liquid (87%) boiled at 63–65° at 1 mm; η_D^{24} 1.4895.

Anal. Calcd. for $C_9H_{14}O_2$: C, 70.10; H, 9.15. Found: C, 69.84; H, 8.73.

The i.r. spectrum in CCl_4 showed absorption between 3610 and 3280 (OH); 3080 (vinylic C—H); a broad band between 1130 and 1040 cm^{-1} (C—O).

The two isomers were separated by preparative g.l.c. and were identified by their p.m.r. spectra as described in the discussion section.

The 60 MHz p.m.r. spectrum in CCl_4 of the *endo* isomer showed a complicated doublet centered at τ 3.94 (2H); a multiplet at 5.90 (1H); a multiplet between 6.2 and 6.8 (4H); a narrow multiplet at 6.94 (1H), $w_{1/2} \simeq 7$ Hz; a narrow multiplet at 7.26 overlapping the OH signal (2H), $w_{1/2} \simeq 7$ Hz; multiplets between 7.85 and 9.40 (4H).

The 60 MHz p.m.r. spectrum in CCl_4 of the *exo* isomer showed a complicated doublet at τ 4.0 (2H); a multiplet between 6.2 and 6.8 (5H); a narrow multiplet at 7.15 (2H), $w_{1/2} \simeq 10$ Hz; a singlet at τ 8.05 (1H); a multiplet between 8.2 and 9.3 (4H).

2-(7-syn-Norbornenyloxy)ethanol

syn-7-Norbornenol (13) was converted to *ethyl (7-syn-norbornenyloxy)acetate* by the procedure used to prepare ethyl (2-dimethylaminoethoxy)acetate (1). Yield of colorless liquid, 30%. B.p. 60° at 0.1 mm; η_D^{26} 1.4768.

Anal. Calcd. for $C_{11}H_{16}O_3$: C, 67.34; H, 8.22. Found: C, 66.78; H, 8.16.

The 60 MHz p.m.r. spectrum in $CDCl_3$ showed a broad singlet at τ 3.98 (2H), $w_{1/2} \simeq 5$ Hz; a quartet at 5.79 (2H), $J \simeq 7$ Hz; a singlet at 6.01 (2H); a broad singlet at 6.37 (1H), $w_{1/2} \simeq 4.5$ Hz; a broad singlet at 7.11 (2H), $w_{1/2} \simeq 7$ Hz; a multiplet between 8.10 and 9.23 (7H).

The i.r. spectrum (neat) showed a band at 3080 cm^{-1} (vinylic C—H); a band at 1780 (C=O); a broad band between 1290 and 1110 cm^{-1} (C—O).

Reduction of the above acetate with $LiAlH_4$, as described for the preparation of 2-(2-dimethylaminoethoxy)-ethanol (1) gave the colorless liquid *2-(7-syn-norbornenyloxy)ethanol* in 80% yield. B.p. 56° at 0.2 mm; η_D^{26} 1.4915.

Anal. Calcd. for $C_9H_{14}O_2$: C, 70.10; H, 9.15. Found: C, 70.28; H, 9.32.

The 60 MHz spectrum in $CDCl_3$ showed a narrow multiplet at τ 3.96 (2H); a broad multiplet between 6.19 and 6.7 (5H); a narrow multiplet at 7.11 (2H), $w_{1/2} \simeq 5$ Hz; singlet at 7.68 (1H); a broad multiplet between 8.1 and 9.2 (4H).

The i.r. spectrum (neat) had a broad band between 3630–3200 (OH); a band at 3080 (vinylic CH) and broad absorption between 1180 and 1020 cm^{-1} (C—O).

2-(7-anti-Norbornenyloxy)ethanol

anti-7-Norbornenol (14) was converted to *ethyl (7-anti-norbornenyloxy)acetate* by the same method used to prepare ethyl (2-dimethylaminoethoxy)acetate (1). Yield of colorless liquid, 45%. B.p. 59° at 0.3 mm; η_D^{25} 1.4728.

Anal. Calcd. for $C_{11}H_{16}O_3$: C, 67.32; H, 8.22. Found: C, 67.60; H, 8.41.

The 60 MHz p.m.r. spectrum in CCl_4 showed a triplet at τ 4.08 (2H), $J \simeq 2$ Hz; a quartet at 5.83 (2H), $J \simeq 7$ Hz; a singlet at 6.09 (2H); a broad singlet at 6.75 (1H), $w_{1/2} \simeq 4.5$ Hz; a multiplet centered at 7.34 (2H); a multiplet between 8.0 and 8.37 (2H); a triplet at 8.75 (3H), $J \simeq 7$ Hz and a multiplet between 8.94 and 9.23 (2H).

The i.r. spectrum (neat) showed absorption at 3060 (vinylic C—H); a band at 1760 (C=O); a band between 1290 and 1110 cm^{-1} (C—O).

Reduction of the above acetate with $LiAlH_4$ by the procedure used to prepare 2-(2-dimethylaminoethoxy)-ethanol (1) gave colorless *2-(7-anti-norbornenyloxy)-ethanol* in 85% yield. B.p. 45° at 0.3 mm; η_D^{26} 1.4859.

Anal. Calcd. for $C_9H_{14}O_2$: C, 70.10; H, 9.15. Found: C, 70.07; H, 8.95.

The 60 MHz p.m.r. spectrum in $CDCl_3$ showed a triplet at τ 4.03 (2H); a broad multiplet between 6.2 and 6.7 (4H); a broad singlet at 6.78 (1H), $w_{1/2} \simeq 4.5$ Hz; a narrow multiplet at 7.35 (2H), $w_{1/2} \simeq 7$ Hz; a singlet at 7.49 (1H); a multiplet between 8.8 and 9.2 (2H).

Hydrogenolysis of the Ketals and Acetals

The hydrogenolysis by AlH_2Cl was carried out according to the general procedure described previously (1).

We thank the National Research Council of Canada for financial assistance for a part of this work. One of us (HAD) thanks the National Research Council of Canada for the award of a Bursary for the academic year 1969–1970.

1. H. A. Davis and R. K. Brown. Can. J. Chem. **49**, 2563 (1971).
2. B. E. Leggetter and R. K. Brown. Can. J. Chem. **42**, 990 (1964).
3. S. Winstein and M. Shatavsky. J. Am. Chem. Soc. **78**, 592 (1956).
4. W. G. Woods, R. A. Carboni, and J. D. Roberts. J. Am. Chem. Soc. **78**, 5653 (1956).
5. J. D. Roberts, W. Bennett, and R. Armstrong. J. Am. Chem. Soc. **72**, 3329 (1950).
6. J. D. Roberts, W. Bennett, and R. Armstrong. J. Am. Chem. Soc. **76**, 4623 (1954).
7. W. W. Zajec, Jr., B. Rhee, and R. K. Brown. Can. J. Chem. **44**, 1547 (1966).
8. R. R. Fraser. Can. J. Chem. **40**, 78 (1961).
9. J. I. Musher. Mol. Phys. **6**, 94 (1963).
10. E. I. Snyder and B. Franzus. J. Am. Chem. Soc. **86**, 1166 (1964).
11. Unpublished work in this laboratory.
12. R. K. Bly and R. S. Bly. J. Org. Chem. **28**, 3165 (1963).
13. W. C. Baird, Jr. J. Org. Chem. **31**, 2411 (1966).
14. P. G. Gassman and P. G. Pape. J. Org. Chem. **29**, 160 (1964).

The Elimination Reactions of Some Alkyl Cyanides in the Gas Phase

P. N. DASTOOR AND E. U. EMOVON
Department of Chemistry, University of Ibadan, Western Nigeria

Received April 28, 1972

The kinetics of the thermal decomposition of ethyl, isopropyl, and *t*-butyl cyanides into HCN and the corresponding olefines have been studied in a seasoned silica vessel in a *flow system* in the absence and presence of toluene as inhibitor. The reactions are homogeneous and the unimolecular rate constants are expressible by the following Arrhenius equations:

Ethyl cyanide (530–670 °C): $k\ (s^{-1}) = 1.30 \times 10^{13} e^{-69480/RT}$

i-propyl cyanide (547–655 °C): $k\ (s^{-1}) = 1.59 \times 10^{12} e^{-64140/RT}$

t-butyl cyanide (565–654 °C): $k\ (s^{-1}) = 1.59 \times 10^{12} e^{-63690/RT}$

Les cinétiques de la décomposition thermique des cyanures d'éthyle, isopropyle et *t*-butyle en HCN et oléfine correspondante, ont été étudiées en continu dans un récipient en silice convenablement traité, en l'absence puis en présence de toluène comme inhibiteur. Les réactions sont homogènes et les constantes de vitesse d'ordre un peuvent être exprimées par les équations d'Arrhénius suivantes:

Cyanure d'éthyle (530–670 °C): $k\ (s^{-1}) = 1.30 \times 10^{13} e^{-69480/RT}$

Cyanure d'isopropyle (547–655 °C): $k\ (s^{-1}) = 1.59 \times 10^{12} e^{-64140/RT}$

Cyanure de *t*-butyle (565–654 °C): $k\ (s^{-1}) = 1.59 \times 10^{12} e^{-63690/RT}$

[Traduit par le journal]

Can. J. Chem., **51**, 366 (1973)

Can. J. Chem. Downloaded from www.nrcresearchpress.com by 210.87.254.5 on 09/05/12
For personal use only.

Although the general reactions of the cyanides are similar to those of the halides and the cyanides have sometimes been called halogenoids, very few kinetic studies of the thermal elimination reactions of their organic derivatives have been carried out. Maccoll and coworkers (1) supported the homogenous and molecular nature of the elimination reaction of alkyl halides with β-hydrogen atoms in the gas phase. These reactions occur by concerted mechanism involving polar transition state and bear formal relationship to reactions in solution. Rabinovitch and Winkler (2) observed that methyl and ethyl cyanides pyrolyzed in the gas phase by radical mechanism but the decomposition of the ethyl compound was the more complex.

Asmus and Houser (3) studied the kinetics and products of decomposition of acetonitrile in a stirred flow reactor. The reaction was complex, involving mixed first and second order kinetics. There was no autocatalysis by HCN and the mechanism was non-chain, as the presence of a chain sensitizer, cyanogen bromide had no effect on the rate of reaction. Hunt *et al.* (4) investigated the effect of the CN group on the strengths of the adjacent C—C and C—H bonds by pyrolyzing ethyl (between 686 and 765 °C) and *t*-butyl cyanides (between 602 and 652 °C). They found that ethyl cyanide decomposed both by free radical and molecular mechanisms, with HCN and olefine as the main products of the molecular mechanism. *t*-Butyl cyanide decomposed by a free radical mechanism to form methane, hydrogen, ethane, and ethylene as gaseous products. Both these decompositions were homogeneous with first order kinetics. This observation was confirmed by this and other experimental work; the rates are not affected by the slight changes in initial concentrations of reactants at the same temperature and reasonable Arrhenius graphs are obtained by plotting the first order rates obtained at different temperatures.

This paper investigates the nature of the thermal decompositions of ethyl, isopropyl, and *t*-butyl cyanides in the gas phase and indicates their analogy to the decompositions of the alkyl halides.

Experimental

Materials

B.D.H. ethyl, isopropyl, and *t*-butyl cyanides were purified by fractional distillation and the fractions used for this work had the following physical constants: Ethyl cyanide: b.p. = 97.0 °C (746.5 mm Hg), $d^{20\,°C}$ = 0.78 g/cc; n^{30} = 1.3613 (5): b.p. = 97.5 °C (760 mm Hg), $d^{20\,°C}$ = 0.78 g/cc; n^{30} = 1.3660. Isopropyl cya-

Can. J. Chem. Downloaded from www.nrcresearchpress.com by 210.87.254.5 on 09/05/12
For personal use only.

nide: b.p. = 103 °C (745.0 mm Hg), $d^{30\,°C} = 0.77$ g/cc; $n^{30} = 1.3690$ (5): b.p. = 107.8 °C (760.0 mm Hg), $d^{20\,°C} = 0.794$ g/cc; $n^{30} = 1.3490$. *t*-Butyl cyanide: b.p. = 102.0 °C (748.0 mm Hg), $d^{25\,°C} = 0.75$ g/cc; $n^{30} = 1.3490$ (5): b.p. = 104.0 °C (760.0 mm Hg), $d^{25\,°C} = 0.758$ g/cc.

The purity of these materials was found to be not less than 98.5% by vapor phase chromatography using the flame ionization (glass) detector and a 6 ft × 3/16 in. coiled copper column packed with diethylene glycol adipate on 80–100 mesh Celite. The column oven was maintained at 60° and the flow of hydrogen and oxygen regulated to 30 ml/min.

The pyrolysis was carried out in an electrically heated silica reactor of capacity $v = 30$ cm^3, the temperature was controlled by a Sunvic RT2 controller to within ±0.5 °C. The reaction system was a conventional flow system coupled with a Toepler pump, a gas burette, and an injection system to the vapor phase chromatograph. The reactant vapor was fed from a constant volume gas burette into a stream of toluene whose flow through the reaction vessel was controlled by a capillary tube. The flow rate, F (cm^3/s), was measured by a calibrated differential manometer; the contact time, t, was calculated using the relation $t = V/F$ where V is volume of the reaction vessel.

The reaction vessel was seasoned with the products of decomposition of alkyl bromide and cyanides. The products arising from the cyanides were condensed in a trap at liquid air temperature and then analyzed in the H_2 flame v.p.c. using squalane 10% on Diatomite C, 100–120 mesh, 6 ft × 1/4 in. glass column, at room temperature. The chromatogram showed the presence of HCN and the corresponding olefines. The HCN product was further confirmed by n.m.r. spectroscopy and the v.p.c. using HCN prepared from strong NaCN solution and concentrated H_2SO_4 as standard.

The reaction was followed titrimetrically using silver nitrate and diphenyl carbazide indicator (6). The products of decomposition were passed into water and the dissolved HCN was titrated with standard silver nitrate solution. A blank titration of the alkyl cyanide in water showed no HCN produced by hydrolysis. Based on analogy to the decomposition of organic halides and cyanide results of other workers, the reaction was assumed to be the first order and the rate constant was obtained, using the relation

$$k\,(s^{-1}) = \frac{2.303}{t} \log C_0/C_f$$

where t is contact time, C_f is the final and C_0 the initial amount of the reactant. Assuming the stoichiometry R—CN → olefine + HCN, x = amount of HCN (obtained titrimetrically) = $C_0 - C_f$.

Results and Discussion[1]

The approximate equal amount of HCN from titration and the amount of olefine determined by v.p.c. confirmed this above stoichiometry. The average value of the HCN/olefine ratio in the products remained unity up to 700 °C. However, above this temperature the ratio became erratic and was observed to be 60% higher in case of ethyl cyanide, 50 to 60% lower in case of *i*-propyl cyanide and in case of *t*-butyl cyanide, it increased 3- to 4-fold. This can be attributed to decomposition of toluene and also the removal of carbonaceous coating inside the reactor.

Hunt *et al.* (4) also observed the pyrolysis of ethyl and *t*-butyl cyanides to be homogeneous. The alkyl cyanides investigated were pyrolyzed in both unpacked and packed seasoned vessel. The rate constant for the reaction was found to be independent of such surface changes and confirmed the homogeneity of the reactions.

The work of Hunt and co-workers (4) indicated that the initial process in the decomposition of ethyl cyanide is given by

$$CH_3CH_2CN \rightarrow CH_3^0 + {}^0CH_2CN$$

and for methyl cyanides:

$$CH_3CN \rightarrow H^0 + {}^0CH_2CN$$

The high bond strength for C—CN which precludes the participation of CN radical in the reaction scheme suggests that HCN is formed by a molecular mechanism only. The presence of excess toluene did not depress the rate of formation of HCN, thus confirming the absence of free radicals. The chromatograms showed essentially HCN and the corresponding olefine at the lower temperatures. Hunt *et al.* (4) obtained methane, ethane, and hydrogen in addition to the olefines and HCN in the decomposition of ethyl cyanide. The presence of large amounts of H_2 in their products is also explained by molecular mechanism. The authors could not identify these non-condensable gases and ethane by use of a gas burette fitted with Teopler pumps. At temperatures above 650 °C, particularly in inhibited runs, some other but negligible peaks appeared in the chromatogram. These could have arisen from incursion of free radicals and possibly due to decomposition of toluene. These side reactions were not investigated further. It is possible that products other than olefine and HCN observed by Hunt *et al.* could result from their higher working temperatures and the decomposition of aniline (used as a carrier). The presence of trace quantities of other products above 766°, as seen by chromatography, is attributed to decomposition of

[1]Complete set of tabular data is available, at a nominal charge, from the Depository of Unpublished Data, National Science Library, National Research Council of Canada, Ottawa, Canada, K1A 0S2.

TABLE 1. Arrhenius parameters

Parameters	Value*			
	CH_3CN	EtCN†	*i*-PrCN†	*t*-BuCN†
Temperature range (°C)		530.0–668.0	547.0–653.0	565.0–654.0
E(kcal/mol)		69.48±0.40	64.14±1.04	63.69±0.49
	72.00(3)	72.70(4)		70.20(4)
log A (s^{-1})		13.11±0.01	12.20±0.05	12.20±0.01
	11.80(3)	14.10(4)		15.20(4)
$-\Delta S$(e.u.) at 640 °C		2.26	6.44	6.42
Relative rate at 640 °C		1	2.34	3.02

*This work.
†Reference numbers in parentheses.

TABLE 2. R—X bond strength and energy of activation for elimination of HX*

C—X	C_2H_5X		*i*-C_3H_7X		*t*-C_4H_9X	
	D(C—X) (kcal mol^{-1})	E_a(kcal mol^{-1})	D(C—X) (kcal mol^{-1})	E_a(kcal mol^{-1})	D(C—X) (kcal mol^{-1})	E_a(kcal mol^{-1})
C—I	53.5(9)	49.3(11)	53.50(9)	45.0(7)	49.5(9)	38.0(7)
C—Br	69.0(1)	53.9(1)	68.00(9)	47.8(7)	63.0(1)	42.0(1)
C—Cl	81.5(1)	56.50(7)	81.00(1)	50.5(11)	78.5(1)	45.0(10)
C—F	106.0(8)	62.00(8)	105.00(8)			
		58.89(12)				
		59.0(13)				
		58.2(14)				
C—CN	122.8†	69.48‡	119.3†	64.14‡	113.40†	63.67‡
		72.70(4)				70.20(4)
C—H	98.0	77.3(5)	94.5		90.9	

*Reference numbers in parentheses.
†Calculated from standard thermodynamic quantities (15) using the relation $D(R—X) = \Delta H_f^0(R) + \Delta H_f^0(X) - \Delta H_f^0(RX)$.
‡This work.

toluene and hence the pyrolysis of cyanides beyond this temperature was terminated.

The Arrhenius parameters (Table 1) were determined from the rate constants by least square calculations using the IBM 1620 and 360/25 computer system and also from Arrhenius graphs (Figs. 1).

The R—CN bond strengths were estimated from the values for heats of formation of CN and the corresponding R radicals. These are compared with the values for the halides and corresponding energies of activation for elimination (Table 2).

The rate constant for the elimination of HCN from ethyl cyanide was expressed by Hunt *et al.* (4) by the Arrhenius equation:

$$\log k\ (s^{-1}) = 15.0 - 77\,300/2.3RT$$

These parameters are higher than the values obtained in this work. The energies of activation for the elimination of HCN are generally lower than the dissociation energy of the adjacent C—C bond, contrary to the result of Hunt *et al.* for ethyl cyanide. Their value for the activation energy predicts a predominantly free radical mechanism, leading to the formation of products other than the olefine and HCN. The values obtained in this work suggest a predominantly molecular elimination mechanism, but because of the small though significant difference, it is possible to have an incursion of free radical mechanism which may be responsible for trace peaks in the chromatogram at higher temperatures.

The thermal decompositions of ethyl, isopropyl, and *t*-butyl cyanides in the gas phase are

Can. J. Chem. Downloaded from www.nrcresearchpress.com by 210.87.254.5 on 09/05/12
For personal use only.

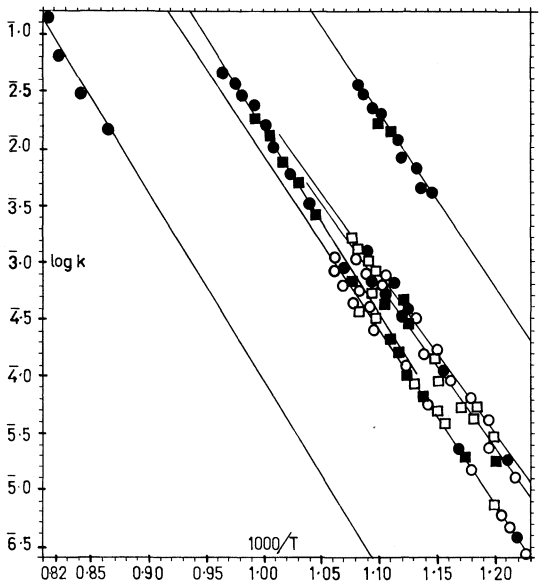

FIG. 1. Arrhenius graphs: from left to right: MeCN (ref. 3), EtCN (this work), EtCN (ref. 4), *i*-PrCN and *t*-BuCN (this work), *t*-BuCN (ref. 4). Symbols: ○ Unpacked vessel, uninhibited reaction; ● unpacked vessel, inhibited reaction; □ packed vessel, uninhibited reaction; ■ packed vessel, inhibited reaction.

homogeneous reactions occurring by molecular elimination. As for the halides, HCN is probably eliminated through a four centered cyclic transition state, in which charge development is relatively primitive.

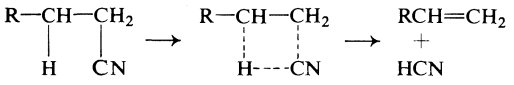

The relative rates follow the sequence EtCN < *i*-PrCN < *t*-BuCN but with very much reduced ratio by comparison with the halides. This reduced relative rate may be attributed to a small charge separation in the transition state.

1. A. MACCOLL. Adv. Phys. Org. Chem. **3**, 91 (1965).
2. B. S. RABINOVITCH and C. A. WINKLER. Can. J. Chem. **20B**, 69 (1942).
3. T. W. ASMUS and T. J. HOUSER. J. Phys. Chem. **73**, 2555 (1969).
4. A. HUNT, J. A. KERR, and A. F. TROTMAN-DICKENSON. J. Chem. Soc. 5074 (1965).
5. Handbook of chemistry and physics. 37th ed. *Edited by* C. D. Hodgman. Chemical Rubber Publishing Co. 1955–1956.
6. A. I. VOGEL. Quantitative inorganic analysis. Longmans, Green, and Co. 1951. p. 263.
7. J. WING TSANG. J. Chem. Phys. **68**, 2487 (1964).
8. A. F. TROTMAN-DICKENSON. J. Chem. Soc. (A), 3058 (1968); S. Benson and G. Haugen. J. Phys. Chem. **69**, 3898 (1965).
9. J. L. HOLMES and A. MACCOLL. Proc. Chem. Soc. 175 (1957).
10. G. B. KISTIAKOWSKY, C. H. STAUFFER, and D. BREARLEY. J. Am. Chem. Soc. **58**, 43 (1936).
11. D. H. R. BARTON and A. J. HEAD. Trans. Faraday Soc. **46**, 114 (1950).
12. G. O. PRITCHARD and R. L. THOMMARSON. J. Phys. Chem. **71**, 1674 (1967).
13. P. N. DASTOOR. J. Chem. Soc. To be published.
14. M. DAY and A. F. TROTMAN-DICKENSON. J. Chem. Soc. (A), 233 (1969).
15. S. W. BENSON. Thermochemical kinetics. John Wiley and Sons, Inc. New York. 1968. pp. 178–215. S. W. BENSON and H. E. O'NEAL. J. Phys. Chem. **71**, 2903 (1967).

Can. J. Chem. Downloaded from www.nrcresearchpress.com by 210.87.254.5 on 09/05/12
For personal use only.

Determination of the Rates of Hydrogen Atom Reaction with NO by a Modulation Technique[1]

R. ATKINSON[2] AND R. J. CVETANOVIĆ

Division of Chemistry, National Research Council of Canada, Ottawa, Canada K1A 0R6

Received August 3, 1972

A modulation technique has been used to determine from phase shift measurements the absolute values of the rate constants and the Arrhenius parameters of the reaction of hydrogen atoms with nitric oxide.

Une technique de modulation a été utilisée dans la détermination à partir des mesures de changement de phase, des valeurs absolues des constantes de vitesse et des paramètres d'Arrhénius dans la réaction des atomes d'hydrogène sur l'oxyde nitrique. [Traduit par le journal]

Can. J. Chem., **51**, 370 (1973)

Can. J. Chem. Downloaded from www.nrcresearchpress.com by 210.87.254.6 on 09/05/12
For personal use only.

Introduction

We have recently used a modulation technique to determine from phase shift measurements the absolute values of the rate constants (1) and of the Arrhenius parameters (2) for the reactions of $O(^3P)$ atoms with several olefins and with NO. Variation in the oxygen atom concentration was monitored by observing the light emission from the excited NO_2 molecules formed by the addition of $O(^3P)$ atoms to NO. Hydrogen atom concentration can be monitored in a similar manner by observing light emission from the excited HNO molecules formed by the addition of H atoms to NO. Thus, in principle, the phase shift technique can be used also to determine the rates of hydrogen atom reactions. However, the application of the technique to hydrogen atom reactions is considerably less favorable because of the low intensity of the red HNO emission and its less convenient spectral region. Nevertheless, it has proved possible to apply the technique to the reaction of H atoms with NO and to determine its rate constants at several temperatures. The results are reported in the present article.

Experimental

Hydrogen atoms were generated by the mercury photosensitization of hydrogen in a flow system. 2537 Å mercury resonance radiation was emitted by a modulated radio-frequency powered low pressure mercury arc. Hydrogen atom concentrations were monitored by the observation of the red HNO emission formed by the addition of known flows of nitric oxide to the reactant stream. The HNO emission was observed by an EMI 9558 A photomultiplier tube fitted with a Corning 2-61 cut-off filter (transmitting light of wavelengths $\geqslant 6000$ Å). A time constant of 30 s was used on the PAR-HR8 lock-in-amplifier. Otherwise the apparatus and experimental technique was as described in detail previously (1, 2) for the study of the reactions of oxygen $O(^3P)$ atoms.

For temperatures below room temperature, a refrigeration coil was fitted to the furnace enclosure. In all cases the temperatures could be held constant to ± 0.5 °C over the duration of the runs.

The gases used were Matheson C.P. grade nitric oxide and Matheson prepurified grade hydrogen. The NO was passed through a column of activated Linde Molecular Sieve 13X to remove any NO_2 present while the hydrogen flow was passed through a Deoxo unit to remove oxygen (<20 p.p.m.) and then dried by passage through a column of Drierite. Gas flows were monitored by calibrated flowmeters and regulated by needle valves. The gas stream was saturated with mercury vapor at room temperature before entering the furnace and reaction cell. A typical light input of 2×10^{17} quanta per s was obtained in the reaction cell.

Conversions of NO were always less than 2%.

Results

The reaction of H atoms with NO (with H_2 as third body) was studied at temperatures between 12 and 117 °C. For sinusoidally modulated 2537 Å radiation and the following reactions:

$$Hg(6^1S_0) + h\nu\,(2537\text{ Å}) \rightarrow Hg(6^3P_1)$$

[1] $$Hg(6^3P_1) + H_2 \rightarrow HgH + H$$
$$\rightarrow Hg(6^1S_0) + 2H$$

[2a] $$H + NO + M \rightarrow HNO + M$$

[2b] $$\rightarrow HNO^* + M$$

[3] $$HNO^* \rightarrow HNO + h\nu$$

[1]NRCC No. 12889.

[2]National Research Council of Canada Postdoctorate Fellow 1969–1971.

[4] $HNO^* + M \rightarrow HNO + M$

[5] $HgH + NO \rightarrow Hg + HNO$

The phase shift ϕ between the HNO emission and the incident 2537 Å radiation, under the conditions used, is given by (1):

$$[6] \qquad \tan \phi = \frac{\omega}{k_2[NO][M]}$$

where $k_2 = k_{2a} + k_{2b}$, $\omega = 2\pi\nu$ and ν is the modulation frequency.

The low intensity of the HNO emission and its decrease with increasing temperature necessitated working below 120 °C.

The NO pressure was varied over the range 2.4–6.7 Torr while the total pressure varied between 100 and 145 Torr at modulation frequencies of 2–4 kHz.

The values of k_2 obtained are given in Table 1. The Arrhenius plot of $k_2 = A_2 e^{-E_2/RT}$ is shown in Fig. 1. A least squares treatment gives a mean preexponential factor $A_2 = 8.9 \times 10^9$ l^2 mol^{-2} s^{-1} and an activation energy $E_2 = -0.54 \pm 0.15$ kcal mol^{-1}, where the error is twice the standard deviation.

TABLE 1. Least squares values of the rate constants k_2 for the reaction H + NO + M (M = H_2)

Temperature (°C)	$k_2 \times 10^{-10}$ (l^2 mol^{-1} s^{-1})
12.8±0.3	2.32±0.07
25.9±0.3	2.15±0.13
67.9±0.7	1.92±0.17
72.9±1.0	2.00±0.17
93.3±0.3	1.91±0.11
116.5±0.5	1.74±0.21

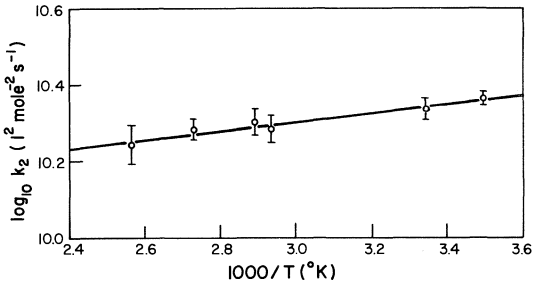

FIG. 1. Arrhenius plot for the reaction H + NO + M, with M = H_2.

Discussion

The present values are compared with the literature values in Table 2. It is seen that the activation energy obtained in this work is in excellent agreement with that of Clyne and Thrush (3) and that the value of k_2 at room temperature agrees very well with that of Hartley and Thrush (4) but is about 50% higher than the value determined recently by Hikida, Eyre, and Dorfmann (5).

A brief comment is necessary about the roles of the HgH radicals formed in the primary quenching act and of the HNO molecules formed subsequently. As shown by Callear and Wood (7) the HgH radicals are rapidly consumed by NO in reaction 5 to form HNO. On thermochemical grounds the HNO molecules thus formed will have to be in the ground electronic state and will therefore not affect directly the rate measurements. The HNO molecules, both from reaction 5 and reactions 2–4, may however interfere by consuming some H atoms,

[7] $H + HNO \rightarrow H_2 + NO$

in competition with

[8] $HNO + HNO \rightarrow H_2O + N_2O$

TABLE 2. Comparison of the values of the Arrhenius activation energy E_2 and the rate constant k_2 at room temperature obtained in the present work with those from the literature (all with M = H_2)

k_2(25 °C) $\times 10^{-10}$ (l^2 mol^{-2} s^{-1})		E_2(kcal mol^{-1})	
Present work	Literature	Present work	Literature
2.15±0.13	2.07±0.18*	−0.54±0.15	−0.6±0.2†
	1.48±0.15†		
	1.37±0.16‡		
	1.10 §		

*Reference 4.
†Reference 3.
‡Reference 5.
§Reference 6.

Can. J. Chem. Downloaded from www.nrcresearchpress.com by 210.87.254.6 on 09/05/12
For personal use only.

The ratio of the rates of reactions 7 and 2, r_7/r_2, depends (7, 8) on the [H]/[HNO] ratio under the experimental conditions employed. For the above reaction scheme the steady state approximation gives

$$[9] \qquad r_7/r_2 = (k_7/k_8^{1/2})I_a^{1/2}/k_2[M][NO]$$

I_a is the rate of absorption of light quanta, $k_7/k_8^{1/2}$ at 300 °K is (8) 1.7×10^5 $l^{1/2}$ $mol^{-1/2}$ $s^{-1/2}$ and for k_2 the present value of 2×10^{10} l^2 mol^{-2} s^{-1} can be used. For the average conditions in this work r_7/r_2 calculated from eq. 9 is about 2%. At higher temperatures $k_7/k_8^{1/2}$ (and thus also r_7/r_2) is likely, if anything, to become even smaller since k_7 is (9) about 4×10^5 l mol^{-1} s^{-1} and thus (in view of the above value (8) of $k_7/k_8^{1/2}$) k_7 is 10^8 l mol^{-1} s^{-1}. Reaction 8 is therefore likely to have larger activation energy and thus $k_7/k_8^{1/2}$ should decrease when temperature is increased. Reaction 7 can therefore be neglected in the present work.

1. R. ATKINSON and R. J. CVETANOVIĆ. J. Chem. Phys. **55**, 659 (1971); **56**, 3733 (1972).
2. R. ATKINSON and R. J. CVETANOVIĆ. J. Chem. Phys. **56**, 432 (1972).
3. M. A. A. CLYNE and B. A. THRUSH. Discuss. Faraday Soc. **33**, 139 (1962).
4. D. B. HARTLEY and B. A. THRUSH. Proc. Roy. Soc. **A297**, 520 (1967).
5. T. HIKIDA, J. A. EYRE, and L. M. DORFMANN. J. Chem. Phys. **54**, 3422 (1971).
6. R. SIMIONATIS. J. Chem. Phys. **67**, 2227 (1963).
7. A. B. CALLEAR and P. M. WOOD. Trans. Faraday Soc. **67**, 3399 (1971).
8. M. A. A. CLYNE. Tenth Symposium (International) on Combustion. The Combustion Institute. 1965. p. 311.
9. J. HEICKLEN and N. COHEN. Adv. Photochem. **5**, 157 (1968).

Can. J. Chem. Downloaded from www.nrcresearchpress.com by 210.87.254.6 on 09/05/12
For personal use only.

Reaction of Oxygen Atoms, O(^3P), with Ethylene in Liquid Nitrogen Solution[1]

SHUN-ICHI HIROKAMI[2] AND R. J. CVETANOVIĆ

Division of Chemistry, National Research Council of Canada, Ottawa, Canada K1A 0R6

Received August 3, 1972

The reaction of ground-state oxygen atoms, O(^3P), with ethylene and ethylene-d_4 in liquid nitrogen solution at 77 °K has been studied. The major and perhaps the exclusive products are ethylene oxide and acetaldehyde. The ratio of acetaldehyde to ethylene oxide is 1.2 ± 0.1 for ethylene and 0.91 ± 0.09 for ethylene-d_4. Much smaller amounts of formaldehyde and trace quantities of cyclopropane are also observed.

The effect of the concentration of ethylene on the quantum yields of addition products was measured. A limiting quantum yield of oxygen atoms scavenged by ethylene to form the addition products was 0.12±0.01. The low quantum yield suggests an appreciable cage recombination of the ground-state oxygen atoms with the trace amounts of molecular oxygen present. The effect of the concentration of added oxygen on the product yields and the relative rate constant for the addition of O(^3P) to molecular oxygen and to ethylene were determined. The ratio $k_{O+O_2}/k_{O+C_2H_4}$ is 6.0 ± 1.0 and the relative rate constant for the addition of O(^3P) to ethylene and to ethylene-d_4, $k_{O+C_2D_4}/k_{O+C_2H_4}$, is 2.0 ± 0.1.

The type of products formed and the isotope effects observed are discussed in terms of the mechanism of addition of O(^3P) atoms to ethylene.

La réaction des atomes d'oxygène à l'état fondamental, O(^3P) avec l'éthylène et l'éthylène-d_4 en solution d'azote liquide à 77 °K à été étudiée. Les produits majeurs et peut-être les seuls formés sont l'oxyde d'éthylène et l'acétaldéhyde. Le rapport d'acétaldehyde versus l'oxyde d'éthylène est 1.2 ± 0.1 pour l'éthylène et 0.91 ± 0.09 pour l'éthylène-d_4. Des quantités beaucoup plus faibles de formaldehyde ainsi que des traces de cyclopropane sont aussi obtenues.

L'effet de la concentration d'éthylène sur le rendement quantique des produits d'addition a été mesuré. Un rendement quantique limite d'atomes d'oxygène trappés par l'éthylène pour former les produits d'addition a été de 0.12 ± 0.01. Le petit rendement quantique suggère une recombinaison appréciable en cage des atomes d'oxygène dans l'état fondamental avec des quantités minimes (traces) d'oxygène moléculaire présent. L'effet de la concentration d'oxygène ajouté sur le rendement en produits et la constante de vitesse relative à l'addition de O(^3P) à l'oxygène moléculaire et à l'éthylène ont été déterminés. Le rapport $k_{O+O_2}/k_{O+C_2H_4}$ est 6.0 ± 1.0 et la constante de vitesse relative pour l'addition de O(^3P) à l'éthylène et à l'éthylène-d_4, $k_{O+C_2D_4}/k_{O+C_2H_4}$ est 2.0 ± 0.1.

Les types de produits formés et les effets isotopiques observés sont discutés en fonction du mécanisme d'addition des atomes de O(^3P) à l'éthylène. [Traduit par le journal]

Can. J. Chem., **51**, 373 (1973)

Introduction

The reaction of oxygen atoms with ethylene in the gas phase was first studied by one of the authors using the technique of mercury-photosensitized decomposition of N_2O (1). It was concluded that the primary step of the reaction involves direct addition of an oxygen atom to the double bond to form an energy-rich intermediate which then undergoes further reactions. The products formed were carbon monoxide, hydrogen, several paraffins, aldehydes, and small amounts of ethylene oxide.

The reactions of oxygen atoms with other simple olefins in the gas phase were studied in considerable detail in previous papers from this laboratory (1–6) and a general reaction mechanism has been established.

Studies of O(^3P) atom reactions with olefins in the liquid and the solid phase at low temperatures are of interest as a corollary to the gas phase studies at normal temperatures. At low temperatures any competing and secondary reactions of high activation energy tend to be suppressed and, moreover, energy-rich intermediates are rapidly stabilized by transfer of excess energy to the solvent molecules (7, 8). Thus the information obtained may complement the observations made in conventional gas phase investigations. With this prospect in mind, a study of the reaction of O(^3P) atoms with

[1]NRCC No. 12890.

[2]National Research Council of Canada Postdoctorate Fellow 1970–1972.

Can. J. Chem. Downloaded from www.nrcresearchpress.com by 210.87.254.42 on 09/05/12
For personal use only.

ethylene dissolved in liquid nitrogen at 77 °K has been carried out.

In addition to the studies of reactions of $O(^3P)$ atoms with condensed olefins at cryogenic temperatures (7–9), studies of $O(^1D)$ atom reactions in liquid argon solutions (10) and of $O(^3P)$ atoms in aqueous solutions (11) have also been recently carried out.

Experimental

Oxygen atoms are generated by photolyzing ozone, using 2537 Å line from a low pressure mercury lamp. The initially formed excited oxygen atoms, $O(^1D_2)$, are rapidly deactivated by collisions with the excess nitrogen molecules present (12).

The vacuum reaction system used was mercury-free. The 2537 Å radiation was obtained from a home-made spiral low-pressure mercury lamp and was passed through a 7–54 Corning glass filter. The reaction vessel and the Dewar flask are shown in Fig. 1.

Matheson prepurified nitrogen was used after it was passed through two spiral traps cooled with liquid oxygen. Matheson research grade oxygen was used without further purification. Matheson research grade ethylene and Merck, Sharp and Dohme ethylene-d_4 were used after thorough degassing and distillation from a trap at −160 °C. Mass spectrometric analysis showed an isotopic impurity in ethylene-d_4 of 3.0% C_2HD_3.

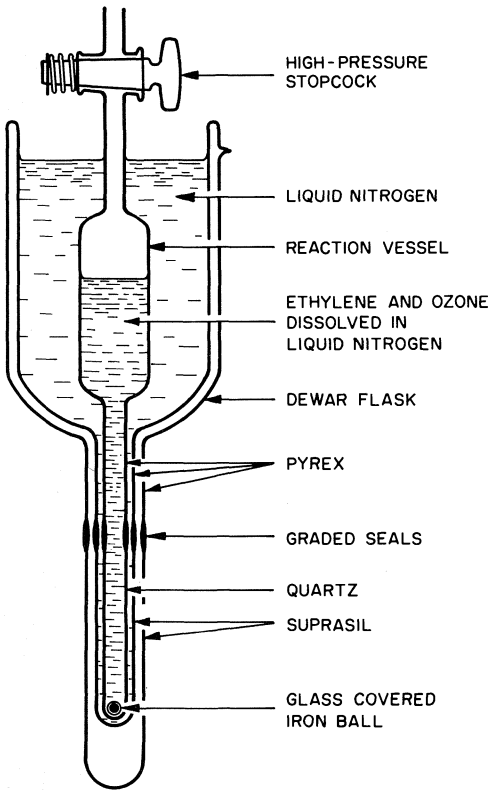

FIG. 1. Reaction vessel and Dewar flask.

To prepare a reaction sample, the nitrogen gas was first introduced into the reaction vessel under a pressure of about 1.2 to 1.5 atm, and then the gas was easily liquefied at the bottom of the reaction vessel cooled with liquid nitrogen. After a part (2–3 ml) of liquid nitrogen had been transferred, a volumetrically measured amount of ozone was introduced simultaneously with additional nitrogen. After about 5–7 ml of nitrogen and ozone were condensed in the reaction vessel, a volumetrically measured amount of ethylene was introduced and the nitrogen condensation was continued in order to dissolve completely the ethylene which tended to condense on the upper parts of the wall of the reaction vessel. (To accomplish this, the level of the liquid nitrogen in the Dewar flask was raised at this time so that further liquid nitrogen was formed higher in the reaction vessel and washed down the condensed ring of ethylene.). The total amount of liquid nitrogen solution used in each run was 50 ml.

The maximum concentration of ethylene in liquid nitrogen was calculated using the literature data for the solubility of ethylene in liquid nitrogen at 77 °K (13).

The reaction mixture was irradiated with the low pressure mercury lamp. After the irradiation, the condensable products and excess ethylene were collected in a trap at −196 °C. A cold trap at −164 °C was then used to separate the oxygenated products and lighter hydrocarbons from ethylene. The products, ethylene oxide and acetaldehyde, were analyzed at room temperature on a 2 m long polyethylene glycol-packed column and a 5 m long β,β′-thiodipropionitrile-packed column, provided with flame ionization detectors. Formaldehyde, ethylene oxide, acetaldehyde, and ethylene ozonide were analyzed on a 3.6 m long cyanosilicone-packed column at room temperature with a thermistor detector. Ethylene oxide and acetaldehyde were not completely separated on this column. The lighter hydrocarbons were analyzed on a 6 m long 2% squalane-modified activated alumina column at room temperature with a flame ionization detector. The identification of the oxygenated products was confirmed by direct mass spectrometric analysis of peaks eluted from the cyanosilicon column.

O_3 was prepared by a Tesla-coil discharge in O_2 gas which was cooled with liquid nitrogen. The number of light quanta absorbed by O_3 in liquid N_2 was estimated from the amount of N_2O produced in the reaction of $O(^1D)$ with nitrogen (12). The relative light intensity of the low pressure mercury lamp was always checked by a phototube placed behind the reaction vessel. To avoid the reaction of products with ozone after irradiation, more ethylene was added after the completion of irradiation in the experimental runs with lower concentrations of ethylene.

The following flame ionization detector molar responses relative to benzene taken as unity were used: ethylene oxide, 0.159; acetaldehyde 0.161. The molar response for ethylene ozonide was approximately obtained by extrapolating a linear plot of the peak area responses against the molecular weights (14).

Results

The observed products are ethylene oxide, acetaldehyde, formaldehyde, ethylene ozonide,

Can. J. Chem. Downloaded from www.nrcresearchpress.com by 210.87.254.42 on 09/05/12
For personal use only.

and a trace of cyclopropane. The effect of irradiation time on product yields, except for cyclopropane, is shown in Figs. 2 and 3, using 4.94×10^{-4} mol/l of ozone and 1.21×10^{-2} mol/l ethylene solution. The relative ratio of cyclopropane to the oxygenated compounds after 30 min irradiation was about 10^{-4}. The yields of

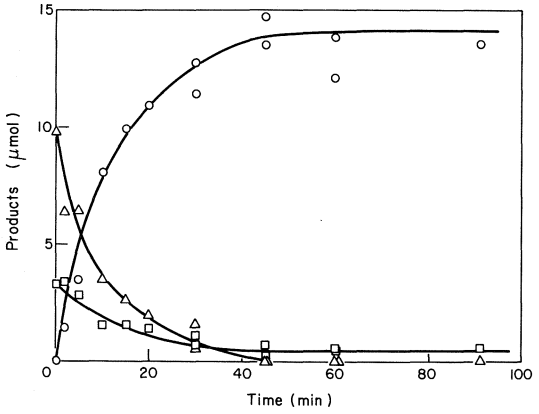

FIG. 2. Effect of irradiation on product yields (ozone concentration is 4.94×10^{-4} mol/l and ethylene concentration is 1.21×10^{-2} mol/l; ○, addition products, *i.e.* ethylene oxide plus acetaldehyde; △, ethylene ozonide; □, formaldehyde).

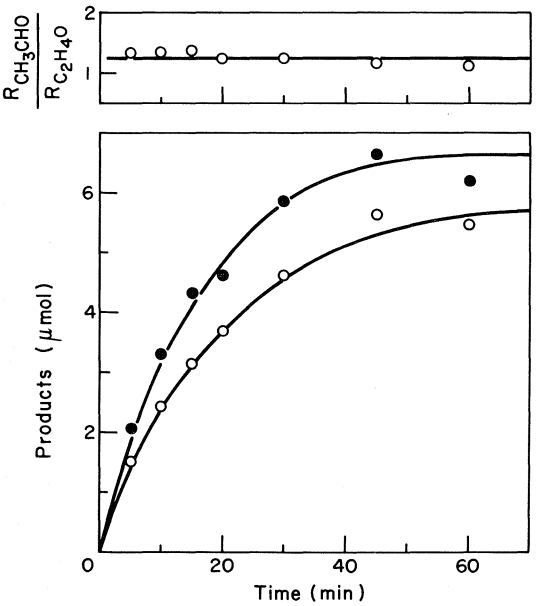

FIG. 3. Effect of irradiation on product yields and the ratio of acetaldehyde to ethylene oxide (ozone concentration is 4.94×10^{-4} mol/l and ethylene concentration is 1.21×10^{-2} mol/l; ○, ethylene oxide; ●, acetaldehyde).

ethylene oxide and acetaldehyde increased with increasing irradiation time up to constant values. The ratio of acetaldehyde to ethylene oxide remained constant within the experimental error. The yields of ethylene ozonide and formaldehyde decreased with increasing irradiation time and while the yield of ethylene ozonide approached zero after 45 min irradiation, the yield of formaldehyde approached a small constant value.

These results show that acetaldehyde and ethylene oxide are formed by direct addition of oxygen atoms to ethylene. Ethylene ozonide and the greater part of formaldehyde, on the other hand, are not photochemical products, but are formed by thermal reaction of O_3 with the residual ethylene in the solid phase (7) after the nitrogen solvent is distilled off. This explanation was confirmed by the experimental observation that the color of the unreacted ozone persisted during the distillation of the nitrogen from the reaction mixture after the irradiation, but disappeared when the temperature in the reaction vessel was raised slowly.

The effect of ethylene concentration, at a constant concentration of ozone (3.06×10^{-4} mol/l), on the product yields is shown in Tables 1 and 2 and is presented graphically in Fig. 4. The quantum yield of the total photochemical products increases with increasing ethylene concentration up to a constant value. The ratio of acetaldehyde to ethylene oxide remains constant but the yields of ethylene ozonide and formaldehyde tend to decrease with increasing ethylene concentration. An isotope effect is found in the ratio of acetaldehyde to ethylene oxide formed in the reaction. At the highest ethylene concentration used, the quantum yield of the total addition products of 0.12 to 0.13 may reflect the influence of a cage recombination of oxygen atoms with the traces of O_2 present. The effect of ethylene concentration on the quantum yield of addition products can be explained by a competition for $O(^3P)$ atoms between ethylene and O_2 (to form O_3), because the ethylene used contained no impurities except for a trace of hydrocarbons and the nitrogen used contained no impurities except for O_2.

The effect of oxygen concentration, at constant concentrations of ozone (3.06×10^{-4} mol/l) and of ethylene (2.12×10^{-2} mol/l), on product yields is shown in Table 3 and is presented graphically in Fig. 5. The quantum yield of total

Can. J. Chem. Downloaded from www.nrcresearchpress.com by 210.87.254.42 on 09/05/12
For personal use only.

TABLE 1. Effect of ethylene concentration on product yields ($[O_3] = 3.06 \times 10^{-4}$ mol/l)

Ethylene (mol/l × 10^4)	ϕ_{EO}* ($\times 10^3$)	ϕ_{AA}* ($\times 10^3$)	$\frac{\phi_{AA}}{\phi_{EO}}$*
C_2H_4			
3.54	1.50	2.06	1.38
3.86	1.63	2.06	1.26
5.26	2.43	2.68	1.10
9.24	3.84	4.55	1.18
40.4	12.4	13.0	1.05
97.2	22.6	26.4	1.17
110	26.8	32.4	1.21
212	37.9	42.2	1.11
244	40.4	41.0	1.01
336	43.9	54.0	1.23
476	47.3	55.3	1.17
480	51.9	63.3	1.22
518	54.4	59.9	1.12
534	50.2	54.0	1.08
		Ave.	1.17 ± 0.07
C_2D_4			
3.16	3.08	2.64	0.86
3.40	3.29	3.18	0.97
5.26	6.18	4.85	0.80
11.4	9.87	8.31	0.84
60.4	40.5	41.9	1.04
60.4	43.0	45.2	1.04
128	64.1	52.7	0.83
		Ave.	0.91 ± 0.09

*The subscripts EO and AA stand for ethylene oxide and acetaldehyde, respectively.

addition products decreases monotonically with increasing oxygen concentration. However, the ratio of acetaldehyde to ethylene oxide remains constant.

Discussion

Reaction Scheme and the Values of Rate Constants

The discussion and interpretation of results may be based on the following reaction scheme

[1*a*] $O_3 + h\nu \rightarrow [O^* + O_2]$

[1*b*] $[O^* + O_2] + N_2 \rightarrow N_2O + O_2$

[1*c*] $\rightarrow [O + O_2] + N_2$

[2] $[O + O_2] \rightarrow O_3$

[3] $[O + O_2] \rightarrow O + O_2$

[4] $O + C_2H_4 \rightarrow$ Products

[5] $O + O_2 \rightarrow O_3$

O* and O represent an excited ($^1D_2$) and a ground state (^3P) oxygen atom, respectively. Parentheses represent solvent cages. Reaction 1*a* represents the rate of absorption of light quanta by ozone. Reaction of $O(^3P)$ with O_3, *i.e.* $O(^3P) + O_3 \rightarrow 2O_2$, may be ruled out because it has an activation energy of about 6 kcal/mol greater than that of reaction 5 (15). Reaction of $O(^1D_2)$ with O_2, O_3, and ethylene can be ruled out because these reactions cannot compete to a significant extent for $O(^1D_2)$ with the large excess of N_2.

From a steady-state treatment of reactions 1 to 5, the following expressions are obtained for the quantum yields of N_2O and the products

[6] $$\phi_{N_2O} = \frac{k_{1b}}{k_{1b} + k_{1c}}$$

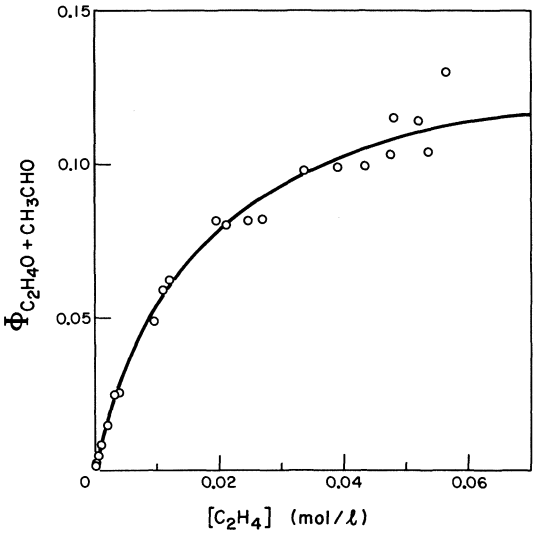

FIG. 4. Dependence of $\phi_{C_2H_4O+CH_3CHO}$ on $[C_2H_4]$ (ozone concentration is 3.06×10^{-4} mol/l).

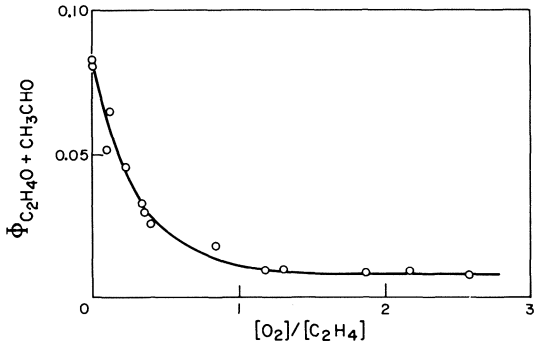

FIG. 5. Dependence of $\phi_{C_2H_4O+CH_3CHO}$ on the $[O_2]/[C_2H_4]$ ratio (ozone concentration is 3.06×10^{-4} mol/l and ethylene concentration is 2.12×10^{-2} mol/l).

Can. J. Chem. Downloaded from www.nrcresearchpress.com by 210.87.254.42 on 09/05/12
For personal use only.

TABLE 2. Effect of ethylene concentration on product yields ($[O_3] = 3.06 \times 10^{-4}$ mol/l)

Ethylene (mol/l × 10^4)	ϕ_{EO+AA}* (× 10^3)	EO + AA* (μmol)	HCHO (μmol)	Ethylene ozonide (μmol)
3.54	3.5	0.09	2.37	5.88
20.2	15.3	0.36	2.02	4.57
32.6	25.2	0.60	2.30	4.87
121	62.4	1.48	1.68	4.32
194	81.4	1.93	1.97	4.46
270	81.9	1.94	1.66	3.89
389	99.2	2.35	1.77	4.50
434	98.7	2.34	1.77	4.01
532	130	3.07	1.59	3.43

*EO and AA stand for ethylene oxide and acetaldehyde, respectively.

TABLE 3. Effect of oxygen concentration on product yields ($[O_3] = 3.06 \times 10^{-4}$ mol/l, $[C_2H_4] = 2.12 \times 10^{-2}$ mol/l)

[Oxygen]/[Ethylene]	ϕ_{EO}* (× 10^3)	ϕ_{AA}* (× 10^3)	ϕ_{AA}*/ϕ_{EO}
0	37.9	42.2	1.11
0.104	26.9	32.9	1.22
0.117	27.9	36.6	1.31
0.220	20.4	25.3	1.24
0.401	12.4	13.5	1.09
0.840	8.27	9.83	1.19
1.31	4.39	5.49	1.25
1.87	3.98	4.68	1.18
2.17	4.39	4.77	1.09
			Ave. 1.19 ± 0.07

[Oxygen]/[Ethylene]	ϕ_{EO+AA}* (× 10^3)	(EO + AA)* (μmol)	HCHO (μmol)	Ethylene ozonide (μmol)
0	82.7	1.96	1.47	4.71
0.341	32.7	0.775	1.42	5.02
0.347	29.7	0.703	1.96	5.09
1.18	9.41	0.223	1.96	5.14
2.58	7.68	0.182	1.75	5.19

*EO and AA stand for ethylene oxide and acetaldehyde, respectively.

$$[7] \quad \phi_{Products} = \frac{k_{1c}}{k_{1b} + k_{1c}} \frac{k_3}{k_2 + k_3} \times \frac{k_4[C_2H_4]}{k_4[C_2H_4] + k_5[O_2]}$$

The quantum yield of N_2O has been measured by DeMore and Raper (12). The quantum yield of the total products is approximately equal to that of the addition products (ethylene oxide and acetaldehyde), because the quantum yield of other products (cyclopropane and formaldehyde) is quite small.

In the experiments without additions of O_2, the molecular oxygen present was that initially contained in the nitrogen as an impurity. If this initial concentration of oxygen is represented by $[O_2]^0$, Equation 7 may be modified to show explicitly the dependence of the initial quantum yield (ϕ) on ethylene concentration, *i.e.*

Can. J. Chem. Downloaded from www.nrcresearchpress.com by 210.87.254.42 on 09/05/12
For personal use only.

[8] $$\phi_{EO+AA}{}^{-1} = \alpha\left(1 + \frac{k_5}{k_4}\frac{[O_2]^0}{[C_2H_4]}\right)$$

with

$$\alpha = \left(1 + \frac{k_{1c}}{k_{1b}}\right)\left(1 + \frac{k_2}{k_3}\right)$$

EO and AA represent ethylene oxide and acetaldehyde, respectively.

The plots of $\phi_{EO+AA}{}^{-1}$ *vs.* $[C_2H_4]^{-1}$ and $[C_2D_4]^{-1}$ are linear, as shown in Fig. 6.

Equation 7 may be expressed in the following form to show the effect of the concentration of oxygen added, $[O_2]$,

[9] $$\phi_{EO+AA} = \frac{1}{\alpha}\frac{k_4[C_2H_4]}{\{k_4[C_2H_4] + k_5[O_2]^0 + k_5[O_2]\}}$$

or

[10] $$\phi_{EO+AA}{}^{-1} = (\phi_{EO+AA}{}^0)^{-1} + \alpha\frac{k_5}{k_4}\frac{[O_2]}{[C_2H_4]}$$

where

$$\phi_{EO+AA}{}^0 = \frac{1}{\alpha}\frac{k_4[C_2H_4]}{k_4[C_2H_4] + k_5[O_2]^0}$$

$\phi_{EO+AA}{}^0$ is constant for constant initial concentrations of O_3 and ethylene. The plot of $\phi_{EO+AA}{}^{-1}$ *vs.* $[O_2]/[C_2H_4]$ is linear, as shown in Fig. 7.

The least squares values and standard deviations of the intercepts and the slopes of the plots in Figs. 6 and 7 for ethylene are

$$\alpha = \left(1 + \frac{k_{1c}}{k_{1b}}\right)\left(1 + \frac{k_2}{k_3}\right) = 8.66 \pm 0.55$$

$$\alpha\frac{k_5}{k_4}[O_2]^0 = (9.90 \pm 0.06) \times 10^{-2} \text{ mol/l}$$

$$\alpha\frac{k_5}{k_4} = 52.1 \pm 4.8$$

From these values it is found that the relative rate constant k_5/k_4 is 6.0 ± 1, the limiting quantum yield of addition products ($\phi_L = 1/\alpha$) is 0.12 ± 0.01, and the initial concentration of oxygen $[O_2]^0$ is $(1.9 \pm 0.2) \times 10^{-3}$ mol/l.

The relative rate constant $k_5/k_4 = 6.0 \pm 1.0$ could be compared with the value of 7.7 ± 0.6 found in aqueous solution (11). The derived value of the initial concentration of oxygen molecules (1.9×10^{-3} mol/l) is in good agreement with $\sim 3 \times 10^{-3}$ mol/l estimated from the gas-chromatographic analysis.

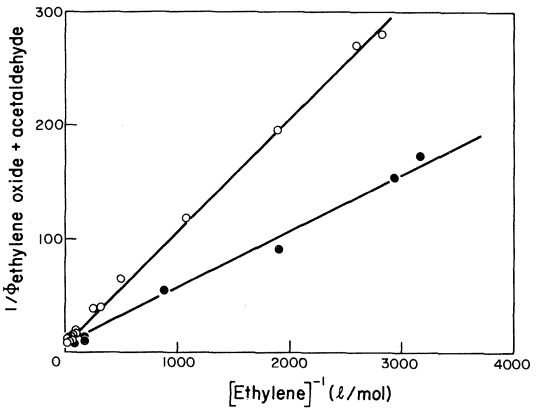

FIG. 6. The reciprocal of $\phi_{\text{ethylene oxide+acetaldehyde}}$ as a function of the reciprocal of the ethylene concentration (conditions are the same as stated in the caption to Fig. 4).

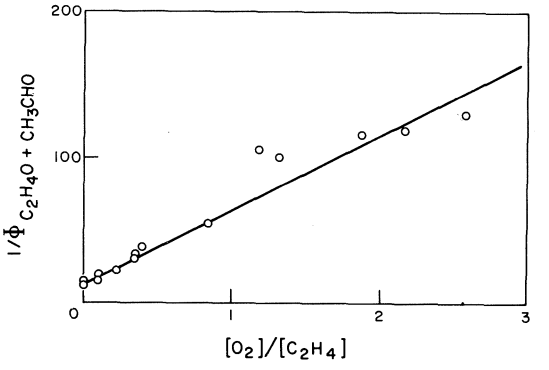

FIG. 7. The reciprocal of $\phi_{C_2H_4O+CH_3CHO}$ as a function of the $[O_2]/[C_2H_4]$ (conditions are the same as stated in the caption to Fig. 5).

For C_2D_4, the least-squares value and standard deviation of the slope of the plot in Fig. 6 are given by $\alpha(k_5/k_4)[O_2]^0 = (4.99 \pm 0.21) \times 10^{-2}$ mol/l. Taking the value for α as determined for C_2H_4, it is then seen that the relative rate constant $k_4[O + C_2D_4]/k_4[O + C_2H_4] = 2.0 \pm 0.1$.

An upper limit for k_4 may be approximately obtained by assuming that reaction 5 is diffusion controlled. An upper limit of the value of the second-order rate constant k_5 can then be calculated from the Debye equation (16),

[11] $$k_5 \leqslant \frac{8RT}{3000\eta} \text{ (l/mol s)}$$

At 77 °K the value of η is 1.58×10^{-3} (c.g.s.) (17), so that $k_5 \leqslant 1.08 \times 10^{10}$ l/mol s and therefore $k_4 \leqslant (1.8 \pm 0.3) \times 10^9$ l/mol s for ethylene.

Can. J. Chem. Downloaded from www.nrcresearchpress.com by 210.87.254.42 on 09/05/12
For personal use only.

Can. J. Chem. Downloaded from www.nrcresearchpress.com by 210.87.254.42 on 09/05/12
For personal use only.

Actually, both these values may be appreciably smaller than the indicated upper limits, in view of the measured values of k_4 and E_4 in the gas phase at higher temperatures (18) if an extrapolation of the gas phase data to liquid nitrogen solutions is permissible.

The Mechanism of $O(^3P)$ Addition to Ethylene

Addition of $O(^3P)$ atoms to simple alkene molecules is explainable (1–6) by postulating initial formation of triplet biradical intermediates which subsequently rearrange to the final products by ring closure and by migration of a hydrogen atom or an alkyl group from the C atom to which $O(^3P)$ becomes attached to the other C atom of the original double bond. This mechanism has been discussed in considerable detail in previous publications (1–6). For the case of ethylene, the mechanism predicts formation of ethylene oxide and acetaldehyde as the predominant and perhaps exclusive initial reaction products. This prediction is fully borne out by the results of the present study.

It is of interest that the acetaldehyde to ethylene oxide ratio in liquid nitrogen solution is the same as found by Ponomarev and coworkers (9) for the addition of $O(^3P)$ to solid ethylene. The reaction mechanism must therefore be the same in the two media. In the gas phase reactions the basic mechanism of $O(^3P)$ addition must again be the same, as was recognized in the very early studies (1), but the collisional stabilization of the energy rich adducts is much less efficient and extensive fragmentation occurs (1–6). Eusuf and Wagner (19) have recently observed substantial stabilization of the "hot" acetaldehyde but little or no stabilization of ethylene oxide at a helium gas pressure as high as 80 atm.

Isotope Effects

Two kinds of hydrogen–deuterium isotope effects have been found: a primary isotope effect (the greater ratio of acetaldehyde to ethylene oxide in the C_2H_4 than in the C_2D_4 reaction) and a secondary isotope effect (the greater rate of addition of $O(^3P)$ to C_2D_4 than to C_2H_4).

The observation of a primary isotope effect is consistent with the postulated mechanism of formation of acetaldehyde by hydrogen atom migration. The alternative reaction path, ring closure in the biradical intermediate to form ethylene oxide, is not likely to be susceptible to an appreciable hydrogen–deuterium isotope effect. On the other hand, internal migration of an H atom should be expected to occur more readily than migration of deuterium.

The observed secondary deuterium isotope effect is "inverse", *i.e.* C_2D_4 is found to react with $O(^3P)$ about twice as rapidly as C_2H_4. A similar inverse secondary isotope effect has been observed (20), for example, in the complexing of Ag^+ with C_2H_4 and C_2D_4, the complex being more stable in the case of C_2D_4. This similarity is probably of considerable significance since it appears likely (4) that the activated complex in the addition of $O(^3P)$ atoms to alkenes may be basically similar to a charge transfer complex. At the same time, it should be pointed out that the trends in the two processes are not always parallel. Thus, for example, Ag^+ complex with *cis*-2-butene is considerably stronger than that with *trans*-2-butene while $O(^3P)$ atoms react somewhat more rapidly with *trans*- than with *cis*-2-butene. However, the stability of the Ag^+ complexes of alkenes may reflect a delicate balance of steric and electronic interactions (20) and thus a close parallelism need not be observed.

Unambiguous interpretation of secondary deuterium isotope effects in terms of specific structural features is difficult, especially so in the case of kinetic isotope effects, since the structural parameters and vibrational characteristics of the activated complexes are generally not known. If some "plausible" values are assumed, the expected magnitude of the isotope effect may be approximately calculated from the general expressions (21, 22) based on the transition state theory. However, such calculations would be of questionable usefulness in the present case and will therefore not be attempted. Qualitatively, the effect may be discussed, for example, in terms of the differences in the "direct" and "indirect" steric effects due to the smaller nonbonded repulsions of deuterium atoms in comparison with hydrogen atoms. In a similar manner, it can be rationalized in terms of the anticipated changes on deuteration in the characteristic frequencies of CH bond vibrations or by postulating a greater effective inductive electron release from CD bonds than from the corresponding CH bonds. These possibilities have been discussed in some detail previously (20) in connection with the inverse deuterium isotope effects on the stability of Ag^+ complexes with alkenes. Somewhat similar considerations

Can. J. Chem. Downloaded from www.nrcresearchpress.com by 210.87.254.42 on 09/05/12
For personal use only.

may apply to the present case and their repetition in the present article is therefore unnecessary.

An inverse secondary deuterium isotope effect has been observed recently in the reaction of $S(^3P)$ atoms with ethylene (23). This reaction would be expected to exhibit somewhat similar behavior to the corresponding reaction of $O(^3P)$ atoms with ethylene studied in the present work.

Formation of Minor Products

As mentioned earlier, small amounts of formaldehyde and traces of cyclopropane were observed in the present study after longer irradiation times. The yield of cyclopropane is essentially negligible and the residual formaldehyde is perhaps due to a slow thermal attack of ozone on ethylene (10). However, the possibility that both these minor products may be a direct consequence of the attack of $O(^3P)$ atoms on ethylene cannot be entirely ruled out.

In the reaction of $O(^3P)$ atoms with ethylene in the gas phase, large amounts of CH_3 and HCO were found (1) to be formed in the reaction sequence

$$[12] \quad C_2H_4 + O \rightarrow C_2H_4O^* \rightarrow CH_3 + HCO$$

where $C_2H_4O^*$ represents an energy-rich molecule (1, 24). In the presence of molecular oxygen there was a large increase in the rate of formaldehyde formation. The formation of formaldehyde was attributed to the reaction of CH_3 radicals with molecular oxygen. In present experiments some molecular oxygen was always contained in the nitrogen gas as an impurity and the formation of small amounts of formaldehyde could therefore be explained by reaction of CH_3 radicals with molecular oxygen.

Another possible primary step for the formation of formaldehyde and cyclopropane is (25)

$$[13] \quad C_2H_4 + O \rightarrow CH_2 + HCHO$$

followed by reactions of CH_2 with molecular oxygen and ethylene (26)

$$[14] \quad CH_2 + O_2 \rightarrow CH_2O_2$$

$$[15] \quad CH_2 + C_2H_4 \rightarrow \text{cyclo-}C_3H_6$$

The relative ratios of the yields of cyclopropane and of formaldehyde to the sum of acetaldehyde and ethylene oxide are about 10^{-4} and 3×10^{-2}, respectively. If CH_2 is the ground state triplet, as would be likely, k_{14}/k_{15} would be (26) approximately 30 at room temperature. This value would predict, for the experimental conditions used, a ratio of cyclopropane to formaldehyde of 0.2, which is much larger than the experimental value of 3×10^{-3}. At the same time, the value of k_{14}/k_{15} at -196 °C is not known and if it is assumed to be as large as about 300, it could explain the experimentally observed low ratio of cyclopropane to formaldehyde. However, it is important to emphasize that formation of formaldehyde is at best only a very minor process in the reaction of $O(^3P)$ with ethylene at -196 °C in liquid nitrogen solution, amounting only to about 3% of the total reaction and, as mentioned, it cannot be regarded as proven that formaldehyde is indeed a primary reaction product. In the gas phase at room temperature, little or no formaldehyde is observed in the absence of molecular oxygen and no formaldehyde has been reported for the reaction of $O(^3P)$ with solid ethylene (9).

The authors are grateful to Dr. R. F. Pottie for the mass spectrometric analyses.

1. R. J. Cvetanović. J. Chem. Phys. **23**, 1375 (1955).
2. R. J. Cvetanović. J. Chem. Phys. **25**, 376 (1956).
3. R. J. Cvetanović. Can. J. Chem. **36**, 623 (1958).
4. R. J. Cvetanović. Can. J. Chem. **38**, 1678 (1960).
5. R. J. Cvetanović. Adv. Photochem. **1**, 115 (1963).
6. R. J. Cvetanović. J. Phys. Chem. **74**, 2730 (1970).
7. A. N. Hughes, M. D. Scheer, and R. Klein. J. Phys. Chem. **70**, 798 (1966).
8. M. D. Scheer and R. Klein. J. Phys. Chem. **74**, 2732 (1970).
9. A. N. Ponomarev. Kinet. Katal. **7** (1966); E. E. Kasimovskaya and A. N. Ponomarev. Kinet. Katal. **9**, 687 (1968).
10. W. B. DeMore. J. Phys. Chem. **73**, 391 (1969).
11. Ö. Amichai and A. Treinin. Chem. Phys. Lett. **3**, 611 (1969).
12. W. DeMore and O. F. Raper. J. Chem. Phys. **37**, 2048 (1962); O. F. Raper and W. B. DeMore. J. Chem. Phys. **40**, 1053 (1964).
13. N. M. Tsin. Zhur. Fiz. Khim. **14**, 418 (1940).
14. W. A. Dietz. J. Gas Chromatogr. **5**, 68 (1967).
15. S. W. Benson and A. E. Axworthy, Jr. J. Chem. Phys. **26**, 1718 (1957).
16. P. J. W. Debye. Trans. Electrochem. Soc. **82**, 265 (1942).
17. N. S. Rudenko and L. W. Schubnikow. Physik. Z. Sowjetunion, **6**, 470 (1934).
18. R. Atkinson and R. J. Cvetanović. J. Chem. Phys. **56**, 432 (1972).
19. Von M. Eusuf and H. Gg. Wagner. Berichte Bunsen-Ges. **76**, 437 (1972).
20. R. J. Cvetanović, F. J. Duncan, W. E. Falconer, and R. S. Irwin. J. Am. Chem. Soc. **87**, 1827 (1965).
21. J. Bigeleisen and M. Wolfsberg. Adv. Chem. Phys. **1**, 15 (1958).

22. M. WOLFSBERG and M. J. STERN. Pure Appl. Chem. **8**, 225 (1964).
23. O. P. STRAUSZ, I. SAFARIK, W. B. O'CALLAGHAN, and H. E. GUNNING. J. Am. Chem. Soc. **94**, 1828 (1972).
24. H. NIKI, E. E. DABY, and B. WEINSTOCK. Symp. Combust. 12th. Univ. Poitiers, Fr. 1968, 277 (1969).
25. L. I. AVRAMENKO, R. V. KOLESNIKOVA, and G. I. SAVINOVA. Izv. Akad. Nauk SSSR, Otd. Khim. Nauk, **1**, 36 (1963).
26. R. L. RUSSELL and F. S. ROWLAND. J. Am. Chem. Soc. **90**, 1671 (1968).

Can. J. Chem. Downloaded from www.nrcresearchpress.com by 210.87.254.42 on 09/05/12
For personal use only.

The Reaction Between Certain Organometallic Reagents and Benzanthrone

C. F. H. Allen

Chemistry Department, Rochester Institute of Technology, Rochester, New York

Received May 25, 1972

The action of certain organometallic reagents upon benzanthrone (7*H*-benz[*de*]anthracene-7-one) has been further investigated. Some of the components were identified, and the nature of hitherto unknown compounds was deduced. Phenylmagnesium chloride in tetrahydrofuran gave nearly double the yield of crystallizable products. The primarily-formed enol, formed by 1,4-addition and related to the principal product, 6-phenylbenzanthrone, was isolated and identified. In the presence of cuprous and cobaltous chlorides unexpected products were indicated. The formation of 3-phenylbenzanthrone is assumed to be the result of a 1,8-addition. Phenyllithium gave all the above and many others. Among them was the carbinol, formed by 1,2-addition, and a new hydrocarbon, 7-phenyl-7*H*-benzanthrene.

L'action de certains organo-métalliques sur la benzanthrone (benz[*de*]anthracène-7*H* one-7 a été étudiée de nouveau. Certains des constituants ont été identifiés et la nature de certains composés jusqu'alors inconnus en a été déduite. Le chlorure de phényl magnésium dans le tetrahydrofuranne a donné presque le double du rendement en produits cristallisables. L'énol principalement formé, obtenu par addition-1,4 et relié au produit principal, le phényl-6 benzanthrone, a été isolé et identifié. En présence des chlorures cuivreux et cobalteux des produits inespérés furent mis à jour. La formation du phényl-3 benzanthrone est semble-t-il, le résultat d'une addition-1,8. Le phenyllithium a donné tous les produits mentionnés et plusieurs autres. Parmi ceux-ci se trouvent le carbinol, formé par addition-1,2 et un nouveau hydrocarbone, le phényl-7 benzanthrène-7*H*. [Traduit par le journal]

Can. J. Chem., **51**, 382 (1973)

Can. J. Chem. Downloaded from www.nrcresearchpress.com by 210.87.254.42 on 09/05/12
For personal use only.

Earlier investigations (1–3) have shown that the product from the action of phenylmagnesium bromide on benzanthrone, under forcing conditions (ether–benzene), is the formation and isolation of 6-phenylbenzanthrone (**2**) in yields of 42–75%; this has also been formed by the use of phenylsodium (4). It was assumed that this substance resulted from an initial 1,4-addition to the double bond system, —(C=O)—CH=CH—. Because the yield was so low, it was considered worthwhile to reinvestigate the reaction making use of newly-available reagents and modern instrumental methods. The use of tetrahydrofuran as a solvent, and phenylmagnesium chloride, resulted in an initial isolation of at least an 80% yield of a solid product; this consisted not only of the aforesaid 6-phenylbenzanthrone, but a second substance which proved to be a primary adduct, the enol **3**. Furthermore, the latter relatively rapidly changed into the ketone **2** (see Scheme 1). An enol has not previously been isolated in the benzanthrone series. In practice, it was almost impossible to isolate other than the major component, the phenyl derivative **2**, except by a long, tedious, fractional crystallization. In order to avoid this, g.c. was applied to the entire reaction mixture; the ether was first treated with a silating agent to preserve the enol as its silated derivative. Interpretation of the results revealed not only a rough approximation of the amounts of the major constituent, but also the effect of changing the excess of Grignard reagent, as well as suggesting the presence of hitherto unrecognized components (Tables 1, 2).

A mixture of five known, expected components, including the hydrocarbon, $C_{28}H_{58}$, as an internal standard, for locating the various peaks, was prepared (*std.*). It will be noted that there is not much choice between the use of 3 (*372*) or 4 (*365*) equiv of the Grignard reagent. The total of silated enol plus ketone **2** is about 90 area %; this is not too far from the amount (80%) actually isolated, and indicates that our main purpose, to learn what and where the rest of the reaction products were, had been realized. The situation was similar with 5 (*379*) equiv of Grignard reagent, but there were more unidentifiable impurities. With 2 (*386*) equiv, however, there was much unused starting material. All these results as well as *385*, indicate that the enol had been formed first.

Despite the apparent separation of peaks on a

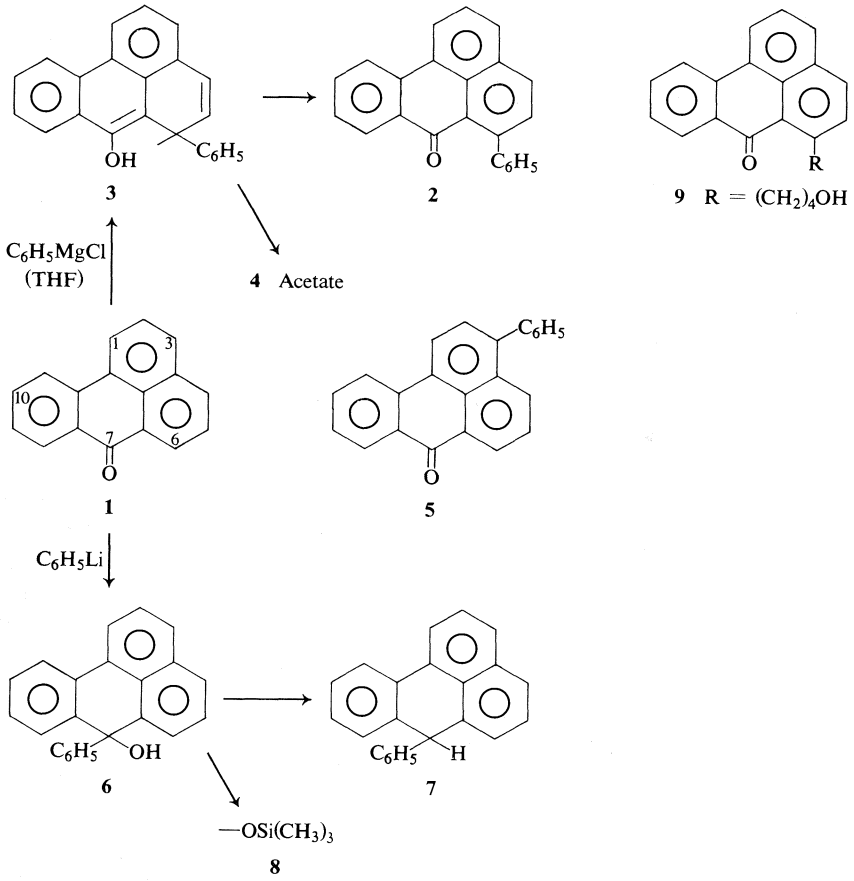

SCHEME 1

g.c. column, in practice it has proved extremely difficult to get rid of the main component, 6-phenylbenzanthrone (**2**) that accompanies attempted fractionation of crystalline products.

As it is well-known that the presence of copper in a Grignard reaction favors conjugate addition to an α,β-unsaturated ketone (5, 6), its effect was examined. Unexpectedly, an additional component, an isomeric ketone, was indicated in the g.c. It was assumed to be 3-phenylbenzanthrone (**5**) (old name, *Bz*-1-phenylbenzanthrone), because of g.c. and mass spectra (Table 3). In practice, it has not yet been possible to separate this isomer from the much more abundant **2**, because of their very similar solubilities.

In *399* the amount of cuprous chloride was doubled, and the mixture heated slightly longer. In an unsilated sample (*399*, footnote *a*, Table 1) *all* the enol had been converted to ketone **2**; the larger amounts of the ether masked the presence of isomer **5**, for it appears in the unsilated material (*399*).

Since 6-phenylbenzanthrone (**2**) is a product of 1,4-addition, the isomer **5** can be regarded as the result of conjugate, 1,8-addition. The carbon atom in the 3-position is at the end of the longest, unhindered conjugated system. 1,8-Addition is very rare; a few instances, involving the tropolone system, have been reported (8, 9).

The effect of cobalt (7) was also examined. The reaction was slowed down, as indicated by the larger amount of starting material recovered, and lesser formation of enol and ketone (*385*). Moreover, there was a new component **9**; interpretation of the mass spectral data (Table 3) indicates that the solvent, THF, had entered into its formation.

In order to ensure formation of the unknown carbinol **6**, a product of 1,2-addition, phenyllithium was employed. The situation was more complex, because of the multiplicity of products.

Can. J. Chem. Downloaded from www.nrcresearchpress.com by 210.87.254.42 on 09/05/12
For personal use only.

TABLE 1. Area % of reactions mixtures

Sample no.	Amount C_6H_5MgX and C_6H_5Li catalyst used	Ketone **5**	Ketone **2**	Enol **3**[c]	Carbinol **6**[a]	Hydrocarbon **7**	Carbinol **8**[c]	Unknowns[d] total	BA[e]
Std.	—	18.1[b]	40.4	12.5	0	0	0	0	25.5
379	5×	0	54.2	38.3	0	2.4	0	4.0	0.5
365	4×	0	55.4	37.6	0	1.3	0	2.9	2.8
378	3×	0	21.0	75.6	0	1.2	0	1.4	0.5
386[f]	2×	0	15.3	52.4	0	0	0	0.1	32.2
386[g]	2×	0	31.8	49.1	0	0	0	0.1	19.1
384	3×, Cu	5.5	35.0	50.0	0	3.5	0	0.7	5.3
399[a]	3×, Cu	0	90.0[j]	0	2.8	4.9	0	0.2	2.1
399	3×, Cu	2.5	35.8	52.4	0	6.5	0	0.1	2.8
385	3×, Co	7.3	9.2	47.1	0	3.3	1.7	16.4[h]	15
385R[i]	3×, Co	12.0	0	1.0	0	4.5	4.1	14.2	64.2
383[a]	3×, Li	[d]	45.7[j]	0	14.9	27	0	7.9	4.5
383	3×, Li	[d]	37.1	6.2	0	30.9	16	5.6	4.2
398[a,k]	3×, Li	[d]	47.3[j]	0	14.4	27.9	0	7.9	2.3
398[k]	3×, Li	[d]	43.0	3.3	0	18.7	28.6	4.4	2.0
390[l]	3×, Li, Cu	0	41.1	0	0	49.0	0	0.2	9.7

[a]Not silated.
[b]3.4 Area % of 10-phenylbenzanthrone included here in standard.
[c]Silated enol or carbinol.
[d]Areas under 1% included in unknowns.
[e]BA = unused benzanthrone.
[f]Entire run.
[g]First crop.
[h]Includes 14–14.2% product **9**, containing THF and possibly a trace of 10-phenyl-BA.
[i]RMgX added last.
[j]Includes enol.
[k]Ether only.
[l]Weak spectrum; 85% remains in column.

TABLE 2. Relative retentions of several components of the reaction mixture to benzanthrone

Elution order	t_R'/BA
Benzanthrone (BA) (**1**)	1.0
Silated carbinol (**8**)	1.36±0.01
Hydrocarbon (**7**)	1.60±0.03
Silated enol	2.39±0.01
Silated carbinol (**8**)	2.44±0.01
6-Phenyl-BA (**2**)	3.30±0.01
3-Phenyl-BA (**5**)	4.08±0.03
2-Phenyl-BA	4.71[a]
10-Phenyl-BA	5.00[a]

[a]Based on single chromatogram.

As before, unused benzanthrone, the 6-phenyl derivative **2**, and the same enol **3** were among products shown by t.l.c., and actually isolated. There was, probably, some of the 3-isomer also. Two new constituents were found; one was the expected carbinol **6**, for, after silation, the peak disappeared entirely, and a new one corresponding to its silated derivative **8**, and having a smaller retention time, appeared in a subsequent chromatogram. Mass spectrometric analysis of a trapped sample of the silyl derivative gave the calculated molecular ion at 380 *m/e*, with abundant fragment ions corresponding to the losses of silyl and phenyl groups.

The other new substance was the hydrocarbon **7**, 7-phenyl-7*H*-benzanthrene. The evidence favoring this structure is based on spectral data (u.v., i.r., mass spectrometry, and n.m.r.); the shape of the u.v. absorption curve is identical with that of 7*H*-benzanthrene (10), but the molar absorption is lower; this could be attributed to the "dilution effect" of the phenyl group. The i.r. is also similar (11); the bands at 13.4 (748 cm^{-1}) and 14.3 μ (697 cm^{-1}) suggest a monosubstituted benzene ring; the mass spectrum shows the molecular ion at 292 *m/e*, and fragment ions at 291 (24%) M − H, 289 (12%), 276 (5%), and 215 (100%) M − C_6H_5. Its n.m.r. shows 15 aromatic hydrogens to one tertiary hydrogen. The formation of 7-phenyl-7*H*-benzanthrene (**7**) presumably arises by reduction of the carbinol **6**. It appears to be present in quantity only in the organolithium runs in which the carbinol is formed.

Can. J. Chem. Downloaded from www.nrcresearchpress.com by 210.87.254.42 on 09/05/12
For personal use only.

TABLE 3. Mass spectra of benzanthrones

No.	Substituent[b]		Parent M		Fragment ions									
			M	%	M − H	%	M − OH	%	M − CO	%	M − HCO	%	M − H_2CO	%
1	None	D	230	100	229	1			202	45	201	22	200	25
	2-Phenyl	D	306	100	305	3.2	289	0.5	278	9.7	277	10	276	21
8	3-Phenyl	D		100		26		2		7		22		37
8	3-Phenyl[c]	H		100		21		1.2		6.6		19		27
8	3-Phenyl[d]	H		100		16		2		9		24		33
2	6-Phenyl	D		50		100		2[a]		8		3		8
	10-Phenyl	D		100		4		1.2		40		22		52
	X-Phenyl	H		100		15.3		1.3		22.4		30.7		35.9

[a]There is an additional peak at 287, (M − H_3O) 2%.
[b]D, DuPont 21-110B; H, Hitachi.
[c]Isolated in trap from g.l.c. of synthetic reference mixture.
[d]Separated from a Cu^+ catalyzed mixture.

Experimental

Owing to the great similarity in structures, the resemblances in physical properties of the possible isomeric benzanthrones are very close. Melting points fall in the same range. Solubilities do not differ markedly.

(I) Instrumental

Infrared Spectra

The spectra are much alike, except that of the 3-phenyl isomer **5**, which has a strong band at 7.23 μ (very difficult to detect in mixtures).

Nuclear Magnetic Resonance Spectra

These spectra are also much alike, except for the enol **3**, which has some non-aromatic bands. The n.m.r. spectra of the four available, phenyl-substituted benzanthrones are much alike, showing only aromatic hydrogen absorption, and were not decipherable in terms of individual assignments. Therefore, the position of the phenyl substitution could not be confirmed by n.m.r.

The spectrum of the enol **3** in acetone-d_6 has a complex multiplet from δ 8.0–8.8 (3H, aromatic), a complex multiplet from 7.0–7.9 (9H, aromatic). The remaining absorption is an AMX spectrum with $\delta_A = 6.67$ (1H), $\delta_M = 6.14$ (1H), $\delta_X = 5.52$ (1H), $J_{AM} = 9$, $J_{AX} = 1.5$, $J_{MX} = 5$ Hz. These do not allow distinction between the two possible allylic systems (12).

Mass Spectra

These spectra were determined by the use of two instruments, both at 7.0 eV, a DuPont-110B, and a Hitachi RMS-4. Four known phenylbenzanthrones and the parent **1** itself, as reference samples, were examined. Although the pure substances gave similar fragmentation patterns (Table 3) the relative intensities were not sufficiently different to permit their identification when they were components of a reaction mixture. All the phenylbenzanthrones are alike, except the 6-phenyl derivative **2**, which shows a fragment ion (100% at M − 1); this can be attributed to a linking with the adjacent carbonyl oxygen. A fragment at M − 28 is present in all; in this respect these ketones resemble 1-phenyl-9,10-anthraquinones (13). The fragmentation pattern of benzanthrone below 202 is entirely different from that of pure fluoranthene ($C_{16}H_{12}$).

The silated carbinol **8** gives a molecular ion at *m/e* 380 (14%) M, and fragment ions at 307 (1%) M − $(CH_3)_3Si$, 303 (100%) M − C_6H_5, 291 (15%), 289 (17%), 287 (5%), and 73 (32%) $(CH_3)_3Si$.

The enol acetate (7-acetoxy-6-phenyl-6-benz[*de*]anthracene (**4**) gives a molecular ion at *m/e* 350 (22%) M, and fragment ions at *m/e* 308 (44%) M − CH_2CO, 307 (61%) M − CH_3CO, 305 (72%) M − COOH, 291 (100%) M − $OCOCH_3$, 231 (83%), 202 (28%), and 43 (7%) CH_3CO.

The silyl derivative of the unknown substance, from the run in which phenylmagnesium chloride was "activated" with cobaltous chloride, gives a molecular ion at *m/e* 374 (80%) M, and fragment ions at 359 (40%) M − CH_3, 284 (100%) M − 90 (*i.e.*, M − $HOSi(CH_3)_3$), 256 (80%) M − 188 (loss of CO here), 215 (35%), and 73 (40%) $(CH_3)_3Si$. This is a reasonable fragmentation process for a silated derivative of a substance having the structure **9**. A partial interpretation of these observations suggests that the solvent, THF, has entered into one of the reaction products (14).

Gas Chromatography

A Barber–Colman 5000 instrument equipped with a flame ionization detector, and either an 8 ft × 1–8 in., 10% OV-1, or 4 ft, 5% Apiezon L on Chromosorb W-AWDMCS treated support, at 300 ISO, were used for all analyses. Relative retentions on either column were similar. Quantitative calculations (Tables 1, 2) were based on percentages of the volatiles, and response factors were assumed constant.

Although the reaction products were highly colored, sticky gums or hard waxes, from which, in most instances only a single crystalline component could be isolated, application of g.c. gave useful chromatograms, from which it was possible to calculate the area % of the components.

The four main fractions found in the Grignard runs were 3-phenyl- and 6-phenyl-benzanthrones, the enol of the latter, and unreacted benzanthrone. However, the lithium and cobalt runs (*383*, *385*, *398*) contained carbinols, which were estimated as their silated derivatives. Their structures were deduced by interpreting the i.r. and mass spectra. The new component **9** involving the solvent, THF, and present to the extent of about 14%, also trapped as a silated derivative, appears in the column of unknowns (*cf. 385*).

Can. J. Chem. Downloaded from www.nrcresearchpress.com by 210.87.254.42 on 09/05/12
For personal use only.

Can. J. Chem. Downloaded from www.nrcresearchpress.com by 210.87.254.42 on 09/05/12
For personal use only.

Thin-layer Chromatography

T.l.c. was of limited use. Most of the ketones were indistinguishable (had similar R_f values) on silica or alumina; the spots moved only half as fast on the latter. The solvent was benzene–chloroform, 3:1. The spot for 6-phenyl-benzanthrone (**2**), when illuminated by u.v. light (15) was brown, and masked most of the others.

(II) Preparation of Materials

Ten grams of benzanthrone (Aldrich, B 260), or Eastman's 7*H*-benz[*de*]anthracene-7-one, were recrystallized from a mixture of 70 ml of *o*-dichlorobenzene and 3.2 g of Norite, by boiling gently for 5 min and filtering through a folded filter. Alternatively, by the use of a large Soxhlet apparatus, an intimate mixture of 3 g of benzanthrone and 2 g of Norite, plus some scraps of filter paper, in the cup, was refluxed for 2 h; caking usually occurred in the bottom of the cup, and some product separated in the flask. The benzanthrone was lighter colored, and, after drying in an oven, melted at 175–176°, but the amount per run was limited to that stated. The product from dichlorobenzene was darker colored, m.p. 173–174°. Either way, the air-dried product was heated for 1 h in an oven at 93–95° before use. Other solvents (chlorobenzene, *p*-cymene, acetic or trifluoroacetic acids, dimethylformamide, and THF) were less satisfactory. 2-, 3-, and 10-Phenylbenzanthrones were prepared as given in the literature (23, 3, 24). Phenylmagnesium chloride was Fisher's (Certified reagent in THF, lot 765 225). THF was dried over sodium; air and nitrogen was bubbled through concentrated sulfuric acid. Melting points were determined on a Fisher–Johns block.

(III) The Grignard Reaction

The standardized procedure, adopted after several exploratory runs, using the usual type of apparatus, and swept with nitrogen follows: to a mixture of 25 ml of THF and 12 ml (3 equiv) of the phenylmagnesium chloride, was added 2.3 g (0.01 mol) of benzanthrone, rinsing in any adhering solid with 5 ml of THF. The solution turned a deep brown, but very little heat was evolved; the color was nearly black after 0.5 h. After the mixture had been refluxed for 1.5 h, the flask was cooled. A mixture of 6 ml of acetic acid and 16 ml of water, added cautiously at first, gave two layers. The organic solution was separated and the solvent removed. The sticky residue was taken up in chloroform and distilled with steam as long as any biphenyl (~2 g) came over.

The insoluble portion was taken up in a little chloroform. For g.c. estimation, an aliquot was dried over anhydrous calcium chloride, filtered, and the solvent evaporated; the residue was used directly or silated. To obtain the 6-phenylbenzanthrone (**2**) for further use, the insoluble residue after steam distillation was allowed to stand with a little acetone. Much of the product **2** soon crystallized; a second or even third crop might be obtained; this was followed by the enol **3**, although the separation was not sharp. Ether and methanol were helpful for removing the enol. Ether, ethyl acetate, acetone, benzene, and acetic acid were employed for recrystallization of **2**; the acid was preferred for large amounts, and acetone for small.

If the enol, which at first was isolated fortuitously, is desired, it is preferable to use a 2:1 ratio (*386*). It accumulated in the last fractions and was recrystallized from methanol; m.p., 146–147°.

Anal. Calcd. for $C_{23}H_{19}O$: C, 89.6; H, 5.8. Found: C, 89.8; H, 5.7.

The enol **3** is very readily converted to the ketone **2** (*a*) on simple standing at room temperature, and (*b*) fairly rapidly in most warmed solvents.

To show that the area percents from g.c. are reasonably similar to practical results the comparison (*379*) was made. The hard, colored residue (total weight, 3.35 g) was warmed with 6 ml of boiling acetone, the solution decanted, and the solid residue rinsed with two 4-ml portions of this solvent, followed by 6 ml of hot methanol. The residual solid (1.58 g) had a melting point of 184–185°. The acetone solution left a sticky pitch, which, after a hot ether extraction, left an additional 0.1 g of the same ketone, m.p. 183–184°, (total, 1.6 g 50%). This is in justifiable agreement with the g.c. estimation of 54.2%. It indicates that the use of results from the g.c. area percents are logical figures, and can be usefully employed.

The enol acetate **4** was prepared from 1 g of the mixture (*386*), by stirring it with 5 ml of acetyl chloride, decanting from insoluble material and allowing to cool. The crude ester was recrystallized twice, by boiling with propyl alcohol; it separated very rapidly on cooling. The pearly, yellow acetate melts at 168–169°, with very marked decomposition at 172–173°.

Anal. Calcd. for $C_{25}H_{18}O_2$: C, 85.7; H, 5.1. Found: C, 85.7; H, 5.4.

The insoluble portion, as well as residues from two recrystallizations were mixtures of the ketone **2**, and a trace of unchanged benzanthrone, identified by mixture melting points and t.l.c.

(IV) Effects of Copper and Cobalt Salts

These were employed for their possible catalytic property, *e.g.*, CuCl (5, 16) in *384* and *399*, and $CoCl_2$ (17) in *385* and *385R*. With 0.02 g of $CoCl_2$ (the hydrated reagent was allowed to stand for 10 min with 10 ml of acetyl chloride and the liquid was decanted) the residual, blue solid was rinsed into the reaction flask with 25 ml of THF, in portions. In a repeat (*385R*) of this run, with double the amount of $CoCl_2$, the phenylmagnesium chloride was inadvertently admitted last; this markedly affected the respective yields. There was no reaction with the copper and cobalt solutions by themselves, showing that the Grignard reagent was needed; this indicated that some sort of an intermediate was involved (17).

(V) Phenyllithium

This was prepared by the standard procedure (18), using 1.2 g of lithium, 90 ml of dry ether, and 12.4 g of bromobenzene (dried by distillation), to obtain 3 equiv of the reagent. To this with stirring was added, in two portions, 4.6 g of benzanthrone (0.02 mol); the second portion caused the brownish solution to boil. This was followed by 30 ml of THF, whereupon the solution became purple; all the solid dissolved without external heating, and a purple scum was formed. The ether was boiled off (10 min) on the steam bath, and the clear, dark brown solution was refluxed for 2 h without stirring. After cooling, a mixture of 5.5 ml of acetic acid and 13 ml of water was carefully added; the reaction was vigorous. The upper, ether layer was separated and distilled with steam; the residual black mass hardened. The solid from an acetone solution dispersed over silica gel (21, 22) was introduced into the top of a stainless steel column, and eluted with ligroine (b.p. 63–75°). The colored layer moved

about two-thirds of the way down the column and stopped; the colorless eluate contained 1.8 g of crude tan hydrocarbon, m.p. 142–145°. Upon recrystallization from absolute alcohol, 0.6 g (m.p. 147–148°) was recovered. It was then purified by several thin layer purifications, scraping off the bluish-green (finally, blue) areas (following by u.v. light), and extracting each time with hexane until the m.p. was 155.5–156°; the analytical sample melted at 156.5°.

Anal. Calcd. for $C_{23}H_{16}$: C, 94.5; H, 5.5. Found: C, 94.6; H, 5.8.

Both solid and solutions in hexane, benzene, and absolute alcohol showed a blue fluorescence. In t.l.c. it gives a bright blue band on SiO_2 that moves with the solvent front (visible in u.v. light only). It did not form a picrate.

With the hope of isolating additional hydrocarbon, 1.5 g of accumulated residues from previous runs (C_6H_5Li, Cu^+ (19, 20)) were chromatographed, using Al_2O_3. By employing hexane as the eluent, a faintly colored band, which was easily visualized by the u.v. light, slowly moved down the column. In this way, the hydrocarbon was free from the otherwise persistent 6-phenylbenzanthrone (**2**). The yield was 5 mg, m.p. 155–156°.

An orange band was now eluted, employing a 3:1 benzene–chloroform mixture. The fractions were concentrated, in which a few orange needles separated. After warming with ethyl formate, additional solid crystallized, m.p. 203–204°, yield 2 mg. The substance appears to be an isomeric *x*-phenylbenzanthrone, (*x* probably = 4).

The carbinol **9** was detected only in the unsilated runs (in the absence of copper), because it was very easily transformed into the hydrocarbon **7**, as already mentioned. Trapped samples, collected by g.c., were used for structure determination (i.r., mass spectrometry).

The formation of so many products from the reactants in THF solution can be expected in view of the numerous reactive species present, and is evident from the multicolored chromatogram on silica gel (22 bands).

The author takes pleasure in acknowledging the technical assistance of specialists Messrs. J. Edwards, M. Glogowski, and J. Lugert, for the g.c., (Miss) T. Davis, J. Robertson, and C. Warburton for the i.r., D. Maier for the mass spectrometry, D. Bush for the u.v., T. H. Regan for the n.m.r., and D. F. Ketchum for the microanalyses.

1. G. CHARRIER and E. GHIGI. Gazz. Chim. Ital. **62**, 928 (1932); Chem. Abstr. **27**, 1344 (1933).
2. C. F. H. ALLEN and S. C. OVERBAUGH. J. Am. Chem. Soc. **57**, 740 (1935).
3. C. F. H. ALLEN and S. C. OVERBAUGH. J. Am. Chem. Soc. **57**, 1322 (1935).
4. W. BRADLEY and F. K. SUTCLIFFE. J. Chem. Soc. 708 (1954).
5. M. S. KHARASCH and P. O. TAWNEY. J. Am. Chem. Soc. **63**, 2308 (1941).
6. H. O. HOUSE, W. L. RESPESS, and G. M. WHITESIDES. J. Org. Chem. **31**, 3128 (1966).
7. M. S. KHARASCH and O. REINMUTH. Grignard reactions of non-metallic substances. Prentice-Hall, Inc., New York. 1954. pp. 196–238.
8. R. D. HAWORTH and P. B. TINKER. J. Chem. Soc. 911 (1955).
9. O. L. CHAPMAN and D. J. PASTO. Chem. and Ind. 54 (1961).
10. E. CLAR and FR. FURNARI. Ber. **65B**, 1420 (1932).
11. H. DANNENBERG and H. J. KESSLER. Ann. **606**, 184 (1957).
12. U. E. MATTER, C. PASCUAL, E. PRETSCH, A. PROSS, W. SIMON, and S. STERNHELL. Tetrahedron, **25**, 691 (1969).
13. D. R. BUCHL and C. S. WAIGHT. Org. Mass. Spectr. **1**, 273 (1968).
14. H. GILMAN. Adv. Org. Chem. **7**, 8 (1968).
15. Spectroline, Model SL-3660. Spectronics Corp., Westbury, L.I.
16. H. O. HOUSE and R. A. LATHAM. J. Org. Chem. **31**, 2667 (1966).
17. F. W. FREY. J. Org. Chem. **26**, 5187 (1961).
18. C. F. H. ALLEN and J. C. W. EVANS. Org. Synth. Coll. Vol. II, 517.
19. G. M. WHITESIDES, W. F. FISCHER, JR., J. SANFILIPPI, JR., R. W. BASKE, and H. O. HOUSE. J. Am. Chem. Soc. **91**, 4871 (1969).
20. H. O. HOUSE and W. F. FISCHER, JR. J. Org. Chem. **33**, 949 (1968).
21. Eastman Chromagram Sheet: 6061, Silica Gel; 6063, Alumina.
22. Pre-coated preparatory T.L.C. Plates, Silica Gel, F 254. Brinkman Instruments Inc., Cantiague Road, Westbury, N. Y. 11590.
23. U.S. Patent 1 713 591 (Zentr. **100**, II, 1674 (1929)).
24. R. SCHOLL, C. SEER, and O. DISCHENDORFER. Ann. **394**, 148 (1912).

Can. J. Chem. Downloaded from www.nrcresearchpress.com by 210.87.254.42 on 09/05/12
For personal use only.

Base-catalyzed Degradations of Carbohydrates. III. Formation of a Novel Perester from 1-*O*-Acetyl-3-deoxy-2,4,6-tri-*O*-methyl-α-D-*erythro*-hex-2-enopyranose[1]

G. O. ASPINALL,[2] R. R. KING, AND ZOFIA PAWLAK[3]

Department of Chemistry, Trent University, Peterborough, Ontario

Received July 21, 1972

1-*O*-Acetyl-3-deoxy-2,4,6-tri-*O*-methyl-α-D-*erythro*-hex-2-enopyranose (**1**) reacts with *m*-chloroperbenzoic acid to give a novel perester, which has been assigned the structure 1,2-*O*-(1′-*m*-chloroperbenzoyloxyethylidene)-2-methoxy-4,6-di-*O*-methyl-α-D-glucopyranose (**2**), on the basis of spectral data and chemical degradation. The perester **2** and the derived acetate **3** undergo oxidative degradation on treatment with trifluoroacetic acid to give 3,5-di-*O*-methyl- (**4**) and 2-*O*-acetyl-3,5-di-*O*-methyl-D-arabinonolactone (**5**), respectively. Reductive decomposition of the acetylated perester **3** yields 1,3-di-*O*-acetyl-4,6-di-*O*-methyl-α-D-*arabino*-hexopyranosulose (**6**), which, on treatment with acetic anhydride in pyridine, gives successively 1,2,3-tri-*O*-acetyl-4,6-di-*O*-methyl-α-D-*erythro*-hex-2-enopyranose (**7**), 2-*O*-acetyl-1-deoxy-4,6-di-*O*-methyl-α-D-*erythro*-hex-1-enopyranose-3-ulose (**8**), and 5-acetoxy-2-(methoxymethyl)-4*H*-pyran-4-one (**9**).

Le *O*-acétyl-1 déoxy-3 tri-*O*-méthyl-2,4,6 α-D-*erythro*-hexeno-2 pyranose (**1**) réagit avec l'acide *m*-chloroperbenzoïque pour conduire à un perester nouveau auquel a été attribuée la structure *O*-(*m*-chloroperbenzoyloxy-1 éthylidène)-1,2 méthoxy-2 di-*O*-méthyl-4,6 α-D-glucopyranose (**2**), sur la base des données spectrales et dégradation chimique. Le perester **2** et le dérivé acétate **3** subissent une dégradation oxydante par traitement à l'acide trifluoroacétique qui conduit respectivement au di-*O*-méthyl-3,5 (**4**) et *O*-acétyl-2 di-*O*-méthyl-3,5 D-arabinonolactone (**5**). La décomposition du perester acétylé **3** par réduction mène au di-*O*-acétyl-1,3 di-*O*-méthyl-4,6 α-D-*arabino*-hexopyranosulose (**6**) qui, après traitement à l'anhydride acétique dans la pyridine, conduit successivement aux tri-*O*-acétyl-1,2,3 di-*O*-méthyl-4,6 α-D-*erythro*-hexeno-2 pyranose (**7**), *O*-acétyl-2 déoxy-1 di-*O*-méthyl-4,6 α-D-*erythro*-hexeno-1 pyranose ulose-3 (**8**), et acétoxy-5 (méthoxyméthyl)-2-4*H*-pyranone-4 (**9**).

[Traduit par le journal]

Can. J. Chem., **51**, 388 (1973)

3-Deoxyhex-2-enopyranoses, which are formed on alkaline degradation of 2,3-di- and higher *O*-substituted hexopyranoses, and their derivatives (1–4) are very susceptible to degradation by acid. The possible formation, by oxidation of 3-deoxyhex-2-enopyranoses, of γ-pyrones as chemically stable derivatives has been explored. 2,3,4,6-Tetra-*O*-methyl-D-glucose was chosen as an appropriate model compound for a reducing sugar so that the fate of all substituents during the transformations might be studied.

3-Deoxy-2,4,6-tri-*O*-methyl-D-*erythro*-hex-2-enopyranose (1, 2), formed on alkaline degradation of 2,3,4,6-tetra-*O*-methyl-D-glucose, was treated with acetic anhydride to give the 1-acetate **1** having the α-D-configuration. When the unsaturated sugar acetate was treated with *m*-chloroperbenzoic acid in ether a crystalline compound separated. Although this substance was relatively unstable and decomposed on prolonged standing at room temperature, a satisfactory elemental analysis was obtained for a perester of molecular formula $C_{18}H_{23}O_9Cl$ and for which structures **2**, **2***a*, and **2***b* were considered (see Scheme 1). The i.r. spectrum of the compound showed an hydroxyl band and a single carbonyl band at 3600 and 1760 cm^{-1}, and the n.m.r. spectrum showed the presence of an aromatic ring, three methoxyl groups, and a methyl group (τ 8.15) of an acetate or modified acetate. The perester furnished a syrupy monoacetate (**3**) whose n.m.r. spectrum showed an incompletely resolved doublet (τ 4.72, $J_{3,4}$ = 1.1 Hz), attributable to H-3. In the light of subsequent chemical transformations which established the D-*arabino* configuration at C-3 to -5, the n.m.r. spectrum was characteristic of a 1,2-*O*-alkylidene

[1]Presented in part at the Canadian Chemical Conference of the Chemical Institute of Canada, Halifax, Nova Scotia, May 31–June 2, 1971.

[2]Present address to which correspondence should be sent: Department of Chemistry, York University, Downsview, Ontario.

[3]On leave (1969–1970) from the Department of Organic Chemistry, University of Warsaw, Warsaw, Poland.

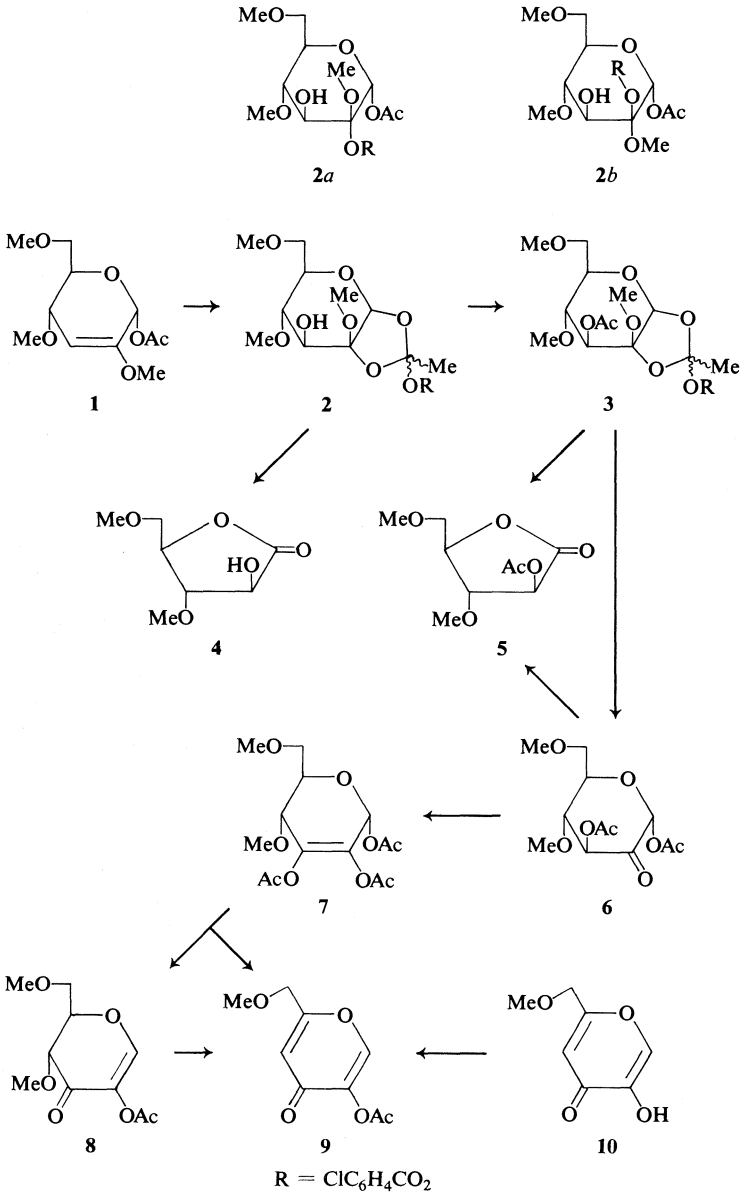

SCHEME 1

derivative having a skew–boat conformation (5–8). The mass spectra of the perester and its monoacetate **3** showed no molecular ions, but prominent fragment ions corresponded to loss of *m*-chlorobenzoylperoxy groups (*m/e* 263 and 305, respectively) and to the formation of *m*-chlorobenzoic acid (*m/e* 156 and 158) and species derived therefrom.

The presence of a peracid group in compound **2** was first suggested when treatment with trifluoroacetic acid resulted in oxidative degradation and the isolation of 3,5-di-*O*-methyl-D-arabinonolactone (**4**). The acetylated perester **3** likewise on treatment with trifluoroacetic acid underwent oxidative degradation to give 2-*O*-acetyl-3,5-di-*O*-methyl-D-arabinonolactone (**5**), whose structure was confirmed by its formation on acetylation of the lactone **4**. These parallel reactions indicate that the 3-hydroxyl group in the perester does not appear to participate in

the oxidative degradation (9, 10); furthermore, no products from C_2–C_3 cleavage were detected.

Direct evidence for the peracid function was obtained by estimation of active oxygen by treating the perester **2** with potassium iodide – acetic acid in acetone (11), the decomposition also leading to a nearly quantitative recovery of *m*-chlorobenzoic acid. Treatment of the acetylated perester **3** with zinc dust in acetic acid furnished 1,3-di-*O*-acetyl-4,6-di-*O*-methyl-α-D-*arabino*-hexpyranosulose (6), whose n.m.r. spectrum showed *inter alia* a one-proton doublet (τ 4.56, $J_{3,4}$ = 16.3 Hz) which may be assigned to H-3 in confirmation of the D-*arabino* configuration. Reaction of the glycosulose **6** with acetic anhydride in pyridine at room temperature gave a syrupy enediol acetate, 1,2,3-tri-*O*-acetyl-4,6-di-*O*-methyl-α-D-*erythro*-hex-2-enopyranose (**7**), whose structure was supported by the detection of a molecular ion peak (*m/e* 332) in the mass spectrum, the presence of an enol ester band at 1780 cm^{-1} in the i.r. spectrum, and the appearance in the n.m.r. spectrum of a new acetate signal, the disappearance of the H-3 signal, and the appearance of the H-4 signal as a doublet (τ 5.57, $J_{4,5}$ = 15 Hz). The enediol acetate **7** when heated with acetic anhydride, yielded the enediolone acetate derivative, 2-*O*-acetyl-1-deoxy-4,6-di-*O*-methyl-α-D-*erythro*-hex-1-enopyranose (**8**), and, on prolonged heating, the kojic acid derivative, 5-acetoxy-2-(methoxymethyl)-4*H*-pyran-4-one (**9**). The structure of the latter compound was confirmed by its formation on acetylation of 5-hydroxy-2-(methoxymethyl)-4*H*-pyran-4-one (monomethylkojic acid (**10**) (12)).

The observations in this and the following paper (13) indicate that oxidation of derivatives of 3-deoxy-hex-2-enopyranoses does not provide a simple route to the formation of γ-pyrones. Special comment, however, may be made on the structure of the novel perester **2**, and on the transformation of glycosuloses into γ-pyrones. Since hydroxy peresters, formed *via* epoxides, have been postulated as intermediates in the reaction of *m*-chloroperbenzoic acid with cyclic enol ethers (9, 10), structure **2***a* was first considered for the perester. However, the 3-hydroxyl group does not participate in the oxidative degradation of the perester as shown by the conversion of the hydroxy perester and its acetylated derivative, when treated with trifluoroacetic acid, into the lactones **4** and **5** respectively. Since reaction of glycosulose **6** with *m*-chloroperbenzoic acid in trifluoroacetic acid resulted in formation of the lactone **5**, it is probable that reaction of the peresters **2** and **3** with trifluoroacetic acid proceeds by hydrolysis of the ketal function, followed by intermolecular oxidation of the derived glycosulose with the liberated peracid.

We may consider here three possible structures for the perester and Scheme 2 indicates possible pathways in which reaction of the hex-2-enopyranose **1** with *m*-chloroperbenzoic acid affords a 2,3-anhydro-2-methoxy-D-*manno*-derivative as an intermediate. It is shown in the following paper (13) that the corresponding 2,3-anhydro-2-methoxy-D-*allo*-derivative does not react further with *m*-chloroperbenzoic acid. The formation of a perester of structure **2***a* by direct opening of the D-*manno*-epoxide with peracid as an external nucleophile appears unlikely. On the other hand epoxide opening by the neighboring 1-acetoxy group would give an intermediate cyclic acetoxonium ion which could react with further peracid to give a perester of structure **2** if attack took place at C-1′ or of structure **2***b* by attack at C-2. The bicyclic structure **2** for the perester is assigned since only a single carbonyl band at 1760 cm^{-1} is observed in the i.r. spectrum whereas the acetylated derivative **3** shows two bands at 1770 and 1740 cm^{-1} assignable to perester and acetate groups. More importantly the signal in the p.m.r. spectrum assigned to H-3 in the acetylated derivative is characteristic of those of H-3 in other 1,2-*O*-alkylidene-α-D-glucopyranose derivatives where ring fusion results in distortion of the pyranose ring from a chair to a skew-boat conformation (5–8). In contrast, the n.m.r. parameters for two 2,2′-di-*O*-substituted hexopyranose derivatives, which are reported in the following paper (13), indicate that both compounds exist in undistorted $^4C_1$ conformations. There is at present no experimental evidence concerning the configuration at C-1′ of the oxyethylidene group.

The overall conversion of glycosuloses into derivatives of kojic acid (14) involves eliminations of the 1-*O*- and 4-*O*-substituents, and migration of the keto function from C-2 to -3. For any particular transformation the sequence in which these steps occur will be governed in part by the nature of the leaving groups in the β-eliminations. In a recent study Lichtenthaler and Heidel (15) have isolated an intermediate enolone acetate in the formation of kojic acid in which the first step involves the elimination of the 4-*O*-substituent. Enediol derivatives have been postulated as intermediates in the migration

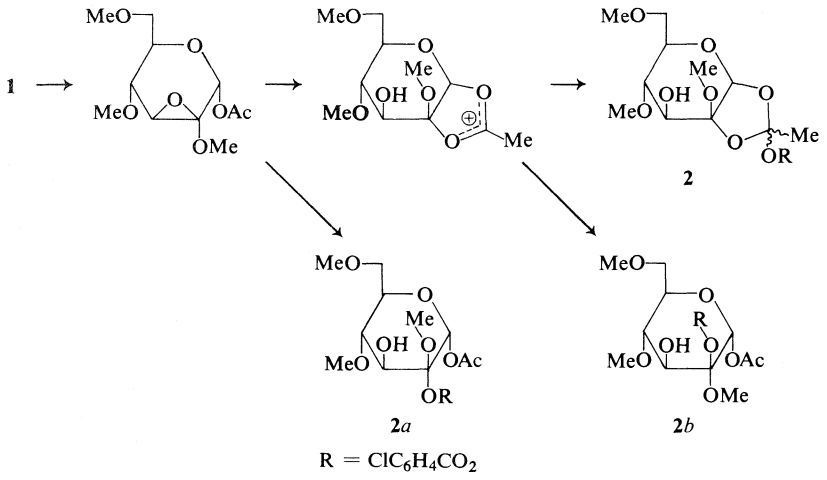

SCHEME 2

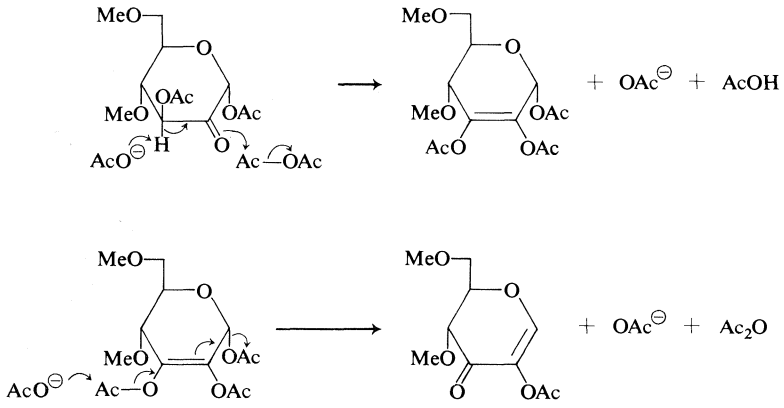

SCHEME 3

of the keto function (16), but have not previously been detected. In the present investigation an enediol acetate, **7**, has been characterized as the first product in the conversion of the glycosulose **6** into the γ-pyrone **9**. Generation of the 3-keto function and elimination of the 1-*O*-substituent take place with the formation of the enediolone **8**. The second elimination involving loss of the 4-*O*-substituent, in this case methoxy, a poor leaving group, does not take place readily. A possible mechanism for the conversion of glycosulose **6** via enediol acetate **7** into enolone acetate **8** is shown in Scheme 3.

Experimental

Melting points are uncorrected and were determined on a Kofler hot-stage microscope. Optical rotations were measured in chloroform solution with a Perkin–Elmer model 141 polarimeter at room temperature. The i.r. spectra as films or in Nujol mulls and u.v. spectra in ethanol solution were determined on Unicam SP 200 and 800A spectrophotometers. The n.m.r. spectra were recorded on a JEOL C-60HL spectrophotometer in deuterochloroform with tetramethylsilane as internal standard. Mass spectra were recorded on an A.E.I. MS 12 mass spectrometer. Plates for t.l.c. were prepared with Kieselgel GF 254 (Merck) as adsorbent, and the dried plates were sprayed with ethanolic 5% sulfuric acid. Light petroleum refers to the fraction of b.p. 40–60°. Solutions were concentrated below 50° under reduced pressure. Microanalyses were determined by A. B. Gygli, Toronto, Ontario, and by F. and E. Pascher, Bonn, West Germany.

*1-O-Acetyl-3-deoxy-2,4,6-tri-O-methyl-α-D-erythro-hex-2-enopyranose (**1**)*

3-Deoxy-2,4,6-tri-*O*-methyl-α-D-*erythro*-hex-2-enopyranose (1, 2) (0.8 g) was treated with acetic anhydride (4 ml) in pyridine (10 ml) for 18 h at 0° and 6 h at room temperature. The reaction mixture was poured into ice-water (150 ml), the solution was extracted with chloroform, and the extract was washed with sodium hydrogen

carbonate solution, dried, and concentrated. The residue was crystallized from ether–pentane to give 1-*O*-acetyl-3-deoxy-2,4,6-tri-*O*-methyl-α-D-*erythro*-hex-2-enopyranose (**1**) (0.5 g, 52%), m.p. 71–72°, $[\alpha]_D$ +45° (*c*, 1.0); ν_{max} 1735 (ester C=O), 1670 cm^{-1} (C=C); n.m.r. τ 3.91 (one-proton singlet, H-1), 5.04 (one-proton doublet, $J_{3,4}$ = 2 Hz, H-3), 6.44 (three-proton singlet, OCH_3), 6.62 (six-proton singlet, 2 × OCH_3), 7.90 (three-proton singlet, $OCOCH_3$).

Anal. Calcd. for $C_{11}H_{18}O_6$: C, 53.65; H, 7.28. Found: C, 53.76; H, 7.29.

1,2-O-(1'-m-Chloroperbenzoyloxy-ethylidene)-2-methoxy-4,6-di-O-methyl-α-D-glucopyranose (2)

The acetate **1** (0.38 g) was added to a cooled solution of *m*-chloroperbenzoic acid (0.34 g) in ether (3 ml) and the solution was kept at room temperature for 3 h and at 0° for 18 h. The crystals which separated were removed by filtration, washed with ether to remove peracid and *m*-chlorobenzoic acid, and recrystallized twice from ether to give the perester **2** (0.32 g, 48%), m.p. 123–124°; ν_{max} 3600 (OH), 1760 cm^{-1} (perester C=O); n.m.r. τ 2.12–2.73, (four aromatic protons), 4.43 (one-proton singlet, H-1), 6.60 (nine-proton singlet, 3 × OCH_3), 8.13 (three-proton singlet, C—CH_3). The supernatant liquid was washed with sodium sulfite (until the washings gave a negative reaction with starch–iodide paper), sodium hydrogen carbonate, and water, dried, and concentrated. Crystallization of the residue from ether afforded further perester **2** (0.08 g, 12%), m.p. 122–123°, $[\alpha]_D$ −14° (*c* 1.0). The same product was obtained when the oxidation was performed in dioxan or dichloromethane. T.l.c. showed that complete disappearance of starting material occurred only when 2 molar proportions of oxidant were used.

Anal. Calcd. for $C_{18}H_{23}O_9Cl$: C, 49.76; H, 5.29; Cl, 8.06. Found: C, 49.49; H, 5.16; Cl, 8.11.

The mass spectrum showed no molecular ion but prominent peaks were detected at *m/e* 263 (M − $ClC_6H_4CO_3$), and 156 and 158, and 139 and 141 (isotope pairs). Active oxygen in the perester **2** was estimated by degradation with potassium iodide – acetic acid in acetone solution followed by titration of liberated iodine with sodium thiosulfate (11). The value was 5% in excess of that calculated in the basis of the proposed structure. In addition, a virtually quantitative yield of *m*-chlorobenzoic acid (identified by m.p., mixed m.p., and i.r. spectrum) was obtained.

3-O-Acetyl-1,2-O-(1'-m-chloroperbenzoyloxy-ethylidene)-2-methoxy-4,6-di-O-methyl-α-D-glucopyranose (3)

The perester **2** (0.3 g) was kept in acetic anhydride (2 ml) and pyridine (5 ml) overnight at room temperature. The reaction product was poured into ice-water (50 ml), the solution was extracted with chloroform, and the extract was washed, dried, and concentrated to give syrupy acetylated perester **3** (0.26 g), which was homogenous on t.l.c., but was insufficiently stable for satisfactory elemental analysis; ν_{max} 1770 (perester C=O), 1740 cm^{-1} (acetate C=O); n.m.r. τ 2.14–2.73 (four aromatic protons), 4.45 (one-proton singlet, H-1), 4.62 (incompletely resolved one-proton doublet, splitting 1.1 Hz), 6.43, 6.63, 6.76 (three-proton singlets, 3 × OCH_3), 7.88 (three-proton singlet, $OCOCH_3$), 8.10 (three-proton singlet, C—CH_3). The mass spectrum showed no molecular ion but prominent peaks were detected at *m/e* 305 (M − $ClC_6H_4CO_3$), and 156 and 158, and 139 and 141 (isotope pairs).

Degradation of Perester 2 in Trifluoroacetic Acid

The perester **2** (0.44 g) was kept in trifluoroacetic acid – water (9:1, 5 ml) at room temperature for 30 min. The solution was concentrated, the residue was dissolved in ethanol, and the solution was neutralized by shaking with Amberlite resin IR-45 (OH) and concentrated. The resulting syrup crystallized from toluene to give 3,5-di-*O*-methyl-D-arabinonolactone (**4**) (0.12 g, 67%), m.p. 71°, $[\alpha]_D$ +48° (*c*, 1.0), whose i.r., n.m.r., and mass spectra were identical to those of the L-enantiomer.

Degradation of Acetylated Perester 3 in Trifluoroacetic Acid

The acetylated perester **3** (0.3 g) was kept in trifluoroacetic acid – water (9:1, 5 ml) at room temperature for 30 min. The reaction mixture was worked-up as described above and the product crystallized from ether–pentane to give 2-*O*-acetyl-3,5-di-*O*-methyl-D-arabinonolactone (**5**) (0.11 g, 58%), m.p. 53°, $[\alpha]_D$ +27° (*c*, 1.0); ν_{max} 1800 (γ-lactone), 1750 cm^{-1} (acetate C=O); n.m.r. τ 4.56 (one-proton doublet, $J_{2,3}$ = 7 Hz, H-2), 6.59 (six-proton singlet, 2 × OCH_3) 7.81 (three-proton singlet, $OCOCH_3$); M^+, 218.

Anal. Calcd. for $C_9H_{14}O_6$: C, 49.53; H, 6.42. Found: C, 49.49; H, 6.47.

The lactone **4** (0.12 g) was treated with acetic anhydride (2 ml) and pyridine (5 ml) at 0° for 1 h and then at room temperature for 24 h. The reaction product was worked-up in the usual way and crystallization from ether–pentane furnished 2-*O*-acetyl-3,5-di-*O*-methyl-D-arabinonolactone (**5**) (0.08 g), m.p. and mixed m.p. 53° $[\alpha]_D$ +27° (*c*, 1.0 in chloroform), whose i.r., n.m.r,, and mass spectra were indistinguishable from those of the previously isolated sample.

1,3-Di-O-acetyl-4,6-di-O-methyl-α-D-arabino-hexopyranosulose (6)

The acetylated perester (**3**) (1.12 g) in acetic acid (35 ml) was stirred with zinc dust at room temperature until (*ca.* 45 min) t.l.c. (ethyl acetate) indicated that decomposition was complete. Chloroform was added to the reaction mixture, and the solution was filtered, neutralized by washing with saturated aqueous sodium hydrogen carbonate, dried, and concentrated to a residue which crystallized from light petroleum to give the glycosulose **6** (0.394 g, 58%), m.p. 62–63°, $[\alpha]_D$ +47.7° (*c*, 1.3); ν_{max} 1755 cm^{-1} (C=O); n.m.r. τ 3.92 (one-proton singlet, H-1), 4.56 (one-proton doublet, $J_{3,4}$ = 16.3 Hz, H-3), 6.47, 6.57 (three-proton singlets, 2 × OCH_3), 7.76, 7.82 (three-proton singlets, 2 × $OCOCH_3$); M^+, 290.

Anal. Calcd. for $C_{12}H_{18}O_8$: C, 49.65; H, 6.25. Found: C, 49.11; H, 6.36.

Oxidative Degradation of Glycosulose 6 to Lactone 5

Glycosulose **6** (60 mg) in trifluoroacetic acid (10 ml) was treated with *m*-chloroperbenzoic acid (80 mg) for 24 h at room temperature. The reaction mixture was worked-up in the usual way and crystallization from ether–pentane furnished 2-*O*-acetyl-3,5-di-*O*-methyl-D-arabinonolactone (**5**) which was similar (m.p., and i.r. and n.m.r. spectra) to the previously prepared sample.

1,2,3-Tri-O-acetyl-4,6-di-O-methyl-α-D-erythro-hex-2-enopyranose (7)

Glycosulose **6** (310 mg) in acetic anhydride (8 ml) and pyridine (12 ml) was kept at room temperature for 4 h. The mixture was poured into ice-water, neutralized with sodium hydrogen carbonate, and extracted with chloroform. The chloroform solution was concentrated, with pyridine being removed by co-distillation with toluene to give a virtually quantitative yield of crude enediol acetate **7**. A sample of the syrupy product was purified by preparative layer chromatography (ethyl acetate – light petroleum, 1:5) and had $[\alpha]_D$ +34° (*c*, 1.0); M^+, 332; ν_{max} 1780 (enol acetate), 1760 cm^{-1} (acetate); n.m.r. τ 3.55 (one-proton singlet, H-1), 5.57 (one-proton doublet, $J_{4,5}$ = 15 Hz, H-4), 6.54, 6.58 (three-proton singlets, 2 × OCH_3), 7.79, 7.85, 7.89 (three-proton singlets, 3 × $OCOCH_3$).

Anal. Calcd. for $C_{14}H_{20}O_9$: C, 50.60; H, 6.07. Found: C, 50.45; H, 5.91.

2-O-Acetyl-1-deoxy-4,6-di-O-methyl-α-D-erythro-hex-1-enopyranose-3-ulose (8)

Enediol acetate **7** (200 mg) was heated in acetic anhydride (8 ml) and pyridine (12 ml) on a boiling-water bath for 6 h. The cooled solution was poured into ice-water, neutralized with sodium hydrogen carbonate, and extracted with chloroform, and the dried extract was concentrated to a syrup, in which t.l.c. indicated the presence of two new compounds. Preparative layer chromatography (ethyl acetate – light petroleum, 2:5) afforded the more labile major component **8** (83 mg, 52%) as a syrup which crystallized from ether – light petroleum and had m.p. 68–70°, and $[\alpha]_D$ +132° (*c*, 1.0); M^+, 230; λ_{max} 266 nm (log ε 4.16); ν_{max} 1760 (acetate), 1690 (C=O), 1630 cm^{-1} (C=C); n.m.r. τ 2.61 (one-proton singlet, H-1), 5.94 (one-proton doublet, $J_{4,5}$ = 17.5 Hz, H-4), 6.32, 6.52 (three-proton singlets, 2 × OCH_3), 7.72 (three-proton singlet, $OCOCH_3$).

Anal. Calcd. for $C_{10}H_{14}O_6$: C, 52.17; H, 6.13. Found: C, 52.69; H, 6.35.

5-Acetoxy-2-(methoxymethyl)-4H-pyran-4-one (9)

The second component from the above reaction mixture was separated chromatographically as a syrup (14 mg, 10%) which crystallized from light petroleum to give **9**, m.p. 50–51°; M^+, 198; λ_{max} 251 nm (log ε 4.00); ν_{max} 1780 (acetate), 1670 (dienone), 1642 cm^{-1} (C=C); n.m.r. τ 2.12 (one-proton singlet, H-6), 3.53 (one-proton singlet, H-3), 5.73 (two-proton singlet, CH_2), 6.53 (three-proton singlet, OCH_3) 7.17 (three-proton singlet, OCOCH).

Anal. Calcd. for $C_9H_{10}O_5$: C, 54.54; H, 5.09. Found: C, 54.77; H, 5.21.

The hex-1-enopyranos-3-ulose **8** on further treatment with hot acetic anhydride and pyridine furnished the kojic acid derivative **9**. Reaction of 5-hydroxy-2-(methoxymethyl)-4*H*-pyran-4-one (**10**) (12) with acetic anhydride and pyridine afforded the acetate **9**, which was identical (m.p. and mixed m.p., t.l.c., and i.r. and n.m.r. spectra) to the previously isolated sample.

The authors wish to acknowledge financial support from the National Research Council of Canada.

1. A. KLEMER, H. LUKOWSKI, and F. ZERHUSEN. Chem. Ber. **96**, 1515 (1963).
2. E. F. L. J. ANET. Aust. J. Chem. **18**, 837 (1965).
3. E. F. L. J. ANET. Aust. J. Chem. **19**, 1677 (1966).
4. G. O. ASPINALL, R. KHAN, and Z. PAWLAK. Can. J. Chem. **49**, 3000 (1971).
5. B. COXON and L. D. HALL. Tetrahedron, **20**, 1685 (1964).
6. R. U. LEMIEUX and A. R. MORGAN. Can. J. Chem. **43**, 2199 (1965).
7. R. G. REES, A. R. TATCHELL, and R. D. WELLS. J. Chem. Soc. C, 1768 (1967).
8. M. SCHULZ, H-F. FOEDEN, P. BERLIN, and W-R. BLEY. Ann. Chem. **715**, 172 (1968).
9. I. J. BOROWITZ, G. GONIS, R. KELSEY, R. RAPP, and G. J. WILLIAMS. J. Org. Chem. **31**, 3032 (1966).
10. H. IMMER and J. F. BAGLI. J. Org. Chem. **33**, 2457 (1968).
11. N. A. MILAS and D. M. SURGENOR. J. Am. Chem. Soc. **68**, 642 (1946).
12. A. BEÉLIK and C. B. PURVES. Can. J. Chem. **33**, 1361 (1955).
13. G. O. ASPINALL and R. R. KING. This issue.
14. A. BEÉLIK. Adv. Carbohydr. Chem. **11**, 145 (1956).
15. F. W. LICHTENTHALER and P. HEIDEL. Angew. Chem. Intl. Ed. **8**, 978 (1969).
16. H. S. ISBELL. J. Res. Nat. Bur. Stand. **32**, 45 (1944).

Base-catalyzed Degradations of Carbohydrates. IV. Formation of 2,3-Anhydro-2-methoxy-α-D-allopyranose Derivatives from 3-Deoxy-D-*erythro*-hex-2-enopyranoses

G. O. ASPINALL[1] AND R. R. KING

Department of Chemistry, Trent University, Peterborough, Ontario

Received July 21, 1972

1,4,6-Tri-*O*-acetyl-3-deoxy-2-*O*-methyl-α-D-*erythro*-hex-2-enopyranose (**4**) reacts with *m*-chloroperbenzoic acid to give the epoxide, 1,4,6-tri-*O*-acetyl-2,3-anhydro-2-methoxy-α-D-allopyranose (**6**), as the major product together with the perester, 4,6-di-*O*-acetyl-1,2-*O*-(1′-*m*-chloroperbenzoyloxy-ethylidene)-2-methoxy-α-D-glucopyranose (**5**), as a minor product. The structures of these novel compounds have been assigned on the basis of spectroscopic data and of transformations (*i*) to kojic acid diacetate and (*ii*) by oxidative degradations to substituted aldopentonolactones. Further examination of the products of the reaction of 1-*O*-acetyl-3-deoxy-2,4,6-tri-*O*-methyl-α-D-*erythro*-hex-2-enopyranose (**1**) with *m*-chloroperbenzoic acid has shown that the epoxide, 1-*O*-acetyl-2,3-anhydro-2-methoxy-4,6-di-*O*-methyl-α-D-allopyranose (**15**), is formed in addition to the previously characterized perester **2**.

Le tri-*O*-acétyl-1,4,6 déoxy-3 *O*-méthyl-2 α-D-*erythro*-hex-2-énopyranose (**4**) réagit avec l'acide *m*-chloroperbenzoïque pour donner l'époxyde, tri-*O*-acetyl-1,4,6 anhydro-2,3 méthoxy-2 α-D-allopyranose (**6**) comme produit majeur en même temps que le perester di-*O*-acétyl-4,6 (*m*-chloroperbenzoïloxy-éthylidène-1′)-1,2-*O* méthoxy-2 α-D-glucopyranose (**5**) comme un produit mineur. Les structures de ces nouveaux composés ont été assignées sur la base de données spectroscopiques et de transformations (*i*) en diacétate d'acide cojique et (*ii*) par dégradations oxidatives en aldopentono lactones substitués. Un examen plus approfondi des produits de la réaction du acétyl-1-*O* déoxy-3 tri-*O*-méthyl-2,4,6 α-D-*erythro*-hex-2-enopyranose (**1**) avec l'acide *m*-chloroperbenzoïque a montré que l'époxyde, acétyl-1 *O*-anhydro-2,3 méthoxy-2 di-*O*-méthyl-4,6 α-D-allopyranose (**15**) est formé en addition au perester **2** caractérisé précédemment. [Traduit par le journal]

Can. J. Chem., **51**, 394 (1973)

In connection with an attempt to convert 3-deoxy-hex-2-enopyranoses into chemically stable derivatives it was shown that 1-*O*-acetyl-3-deoxy-2,4,6-tri-*O*-methyl-α-D-*erythro*-hex-2-enopyranose (**1**) reacts with *m*-chloroperbenzoic acid to give the novel perester, which has been assigned the structure 1,2-*O*-(1′-*m*-chloroperbenzoyloxy-ethylidene)-2-methoxy-4,6-di-*O*-methyl-α-D-glucopyranose (**2**) (1). In order to study this unusual reaction further, the readily accessible 1,4,6-tri-*O*-acetyl-3-deoxy-2-*O*-methyl-α-D-*erythro*-hex-2-enopyranose (**4**) (2) was treated with *m*-chloroperbenzoic acid. Although a perester, 4,6-di-*O*-acetyl-1,2-*O*-(1′-*m*-chloroperbenzoyloxy-ethylidene)-2-methoxy-α-D-glucopyranose (**5**), was formed in small amount, the major product, a crystalline compound isolated in 75% yield, was 1,4,6-tri-*O*-acetyl-2,3-anhydro-2-methoxy-α-D-allopyranose (**6**), a representative of a new class of carbohydrate derivatives (see Scheme 1). We discuss the evidence for the structures of these two compounds and their transformation products and for their mode of formation.

The evidence for the structure of the perester **5** is parallel to that reported for the perester **2** which was described in the preceding paper (1) and for reasons elaborated there the 1,2-*O*-oxyethylidene structure is again preferred over alternative structures. Although the perester **5** was not sufficiently stable for a satisfactory elemental analysis to be obtained, n.m.r. and i.r. spectral data indicated the presence of two acetate groups, retention of the methoxyl group, a *m*-chlorobenzoyl (or *m*-chloroperbenzoyl) substituent, a methyl group, probably as part of an acetate or modified acetate group, and an hydroxyl group. Treatment with acetic anhydride in pyridine furnished a monoacetate (**7**). The n.m.r. signals assigned to H-3 and -4 in the perester **5** and its acetylated derivative **7** were again consistent with the existence of both compounds in the skew–boat conformation favored by 1,2-*O*-alkylidene-α-D-glucopyranose derivatives (3–6). The mass spectra of the peresters **5** and **7** did not show molecular ion peaks, but, as

[1]Present address to which correspondence should be sent: Department of Chemistry, York University, Downsview, Ontario.

Can. J. Chem. Downloaded from www.nrcresearchpress.com by 210.87.254.5 on 09/05/12
For personal use only.

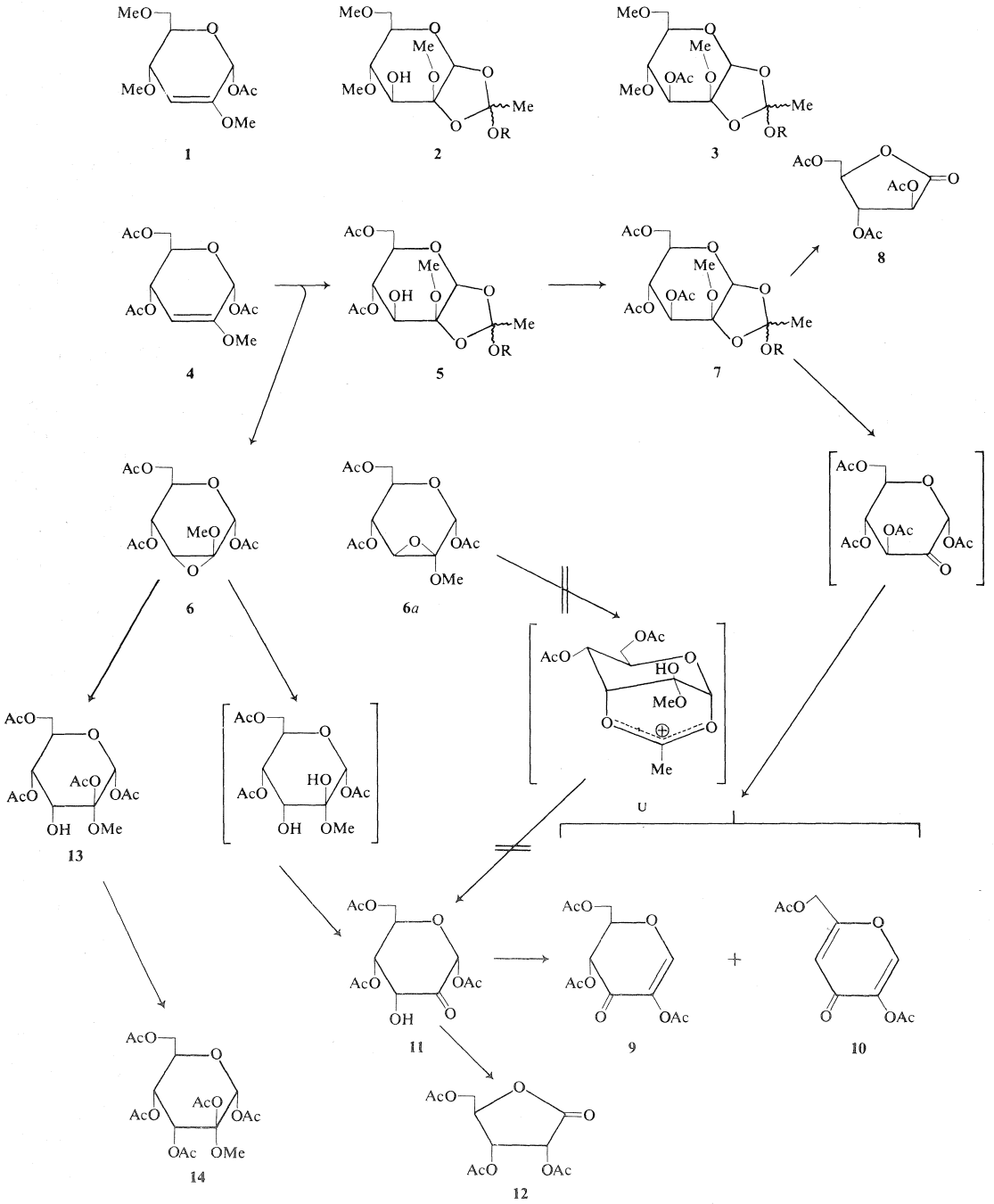

$R = ClC_6H_4CO_2$

SCHEME 1

Can. J. Chem. Downloaded from www.nrcresearchpress.com by 210.87.254.5 on 09/05/12
For personal use only.

Can. J. Chem. Downloaded from www.nrcresearchpress.com by 210.87.254.5 on 09/05/12
For personal use only.

with the previously characterized peresters (**2** and **3**), prominent fragment ions corresponding to the loss of the *m*-chloroperbenzoyloxy group and to the formation of *m*-chlorobenzoic acid and ions derived therefrom were observed. The configuration at C-3 of the acetylated perester **7** was confirmed since the compound underwent oxidative degradation on treatment with trifluoroacetic acid with the formation of 2,3,5-tri-*O*-acetyl-D-arabinonolactone (**8**).

Decomposition of the perester **7** with zinc dust in acetic acid resulted in formation of the enediolone acetate, 2,4,6-tri-*O*-acetyl-1-deoxy-α-D-*erythro*-hex-1-enopyranos-3-ulose (**9**), with some 5-acetoxy-2-(acetoxymethyl)-4*H*-pyran-4-one (kojic acid diacetate (**10**)). The enediolone **9** was converted into kojic acid diacetate (**10**) on treatment with acetic anhydride in pyridine at room temperature. 1,3,4,6-Tetra-*O*-acetyl-α-D-*arabino*-hexopyranosulose is presumably formed as an intermediate in the decomposition of the perester **7** leading to the formation of the enediolone acetate **9** but no such compound was detected. Other workers have isolated kojic acid diacetate (**10**) during attempts to oxidize 1,3,4,6-tetra-*O*-acetyl-α-D-glucopyranose with methyl sulfoxide – acetic anhydride (7, 8) and with methyl sulfoxide – sulfur trioxide (9). Although more than one pathway is possible for the conversion of 1,3,4,6-tetra-*O*-acetyl-α-D-*arabino*-hexopyranosulose into kojic acid diacetate (**10**), the isolation of the enediolone acetate **9** indicates that elimination of the 1-*O*-substituent occurs more readily than that of the 4-*O*-substituent as proposed by Lichtenthaler and Heidel (7).

The structure of the major product from the reaction of 1,4,6-tri-*O*-acetyl-3-deoxy-2-*O*-methyl-α-D-*erythro*-hex-2-enopyranose (**4**) with *m*-chloroperbenzoic acid was assigned as 1,4,6-tri-*O*-acetyl-2,3-anhydro-2-methoxy-α-D-allopyranose (**6**) on the basis of the n.m.r. spectrum in which the magnitudes of $J_{3,4} = 1.8$ and $J_{4,5} = 9.5$ Hz pointed to the 2,3-anhydro-α-D-*allo* configuration (10). Epoxide opening occurred readily with loss of methanol when the anhydro-compound **6** was heated in water. The structure of the product, which was isolated as a crystalline monohydrate, was assigned as 1,4,6-tri-*O*-acetyl-α-D-*ribo*-hexopyranosulose (**11**) on the basis of a one-proton doublet (τ 5.10, $J = 4.8$ Hz) which was attributed to H-3. Attempts to confirm this assignment by conversion of the glycosulose into its acetate failed since treatment with acetic anhydride and sodium acetate at room temperature furnished the previously characterized enediolone acetate **9** and reaction with acetic anhydride in pyridine afforded kojic acid diacetate (**10**). Evidence for the D-*ribo* configuration of the glycosulose **11** was obtained by oxidation with *m*-chloroperbenzoic acid in trifluoroacetic acid which resulted in the formation of 2,3,5-tri-*O*-acetyl-D-ribonolactone (**12**). This interesting reaction appears to involve an intramolecular 1 → 3 *O*-acetyl migration, but there is no evidence to indicate whether this migration takes place in one step or in two successive stages, 1 → 2 and 2 → 3.

The configurational assignments for the 2-methoxy epoxide **6** and the *ribo*-hexopyranosulose **11** imply that ring opening takes place by nucleophilic attack by water at C-2, the electrophilic terminus. In the light of the possible 1 → 3 *O*-acetyl migration which may occur during the above oxidative degradation of the glycosulose **11**, an alternative structure, **6***a*, for the epoxide with the 2,3-anhydro-α-D-*manno* configuration was considered. Intramolecular ring opening involving attack at C-3 and the formation of a cyclic acetoxonium ion would lead to the formation of a D-*ribo*-hexopyranosulose. The n.m.r. parameters for the glycosulose **11** rule out the possibility of acetyl migration during epoxide opening, but collapse of such an acetoxonium ion could also lead to the 1-acetate **11**. The following observations, however, argue against the second mechanism of ring opening and the alternative structure **6***a* for the epoxide. Treatment of the epoxide with acetic acid containing acetic anhydride yielded the tetra-*O*-acetate **13** which on further reaction with acetic anhydride in pyridine afforded the penta-*O*-acetate **14**. The formation of the tetra-*O*-acetate with retention of the ketalically-linked methoxyl group rather than of an unstable hemiketal indicated that ring opening occurred by nucleophilic attack at C-2. The n.m.r. spectra of the tetra-*O*-acetate **13** and the penta-*O*-acetate **14** with small coupling between H-3 and -4 ($J_{3,4}$ = 5–6 Hz) and long-range 'W' coupling between the equatorially oriented H-1 and -3 ($J_{1,3}$ = 2.3–2.8 Hz) clearly indicated the D-*ribo* configuration at C-3 to -5 of both compounds. The formation of these compounds confirms the original assignment of the 2,3-anhydro-α-D-*allo* configuration for the epoxide **6**.

Since the epoxide **6** was the major product from the action of *m*-chloroperbenzoic acid on

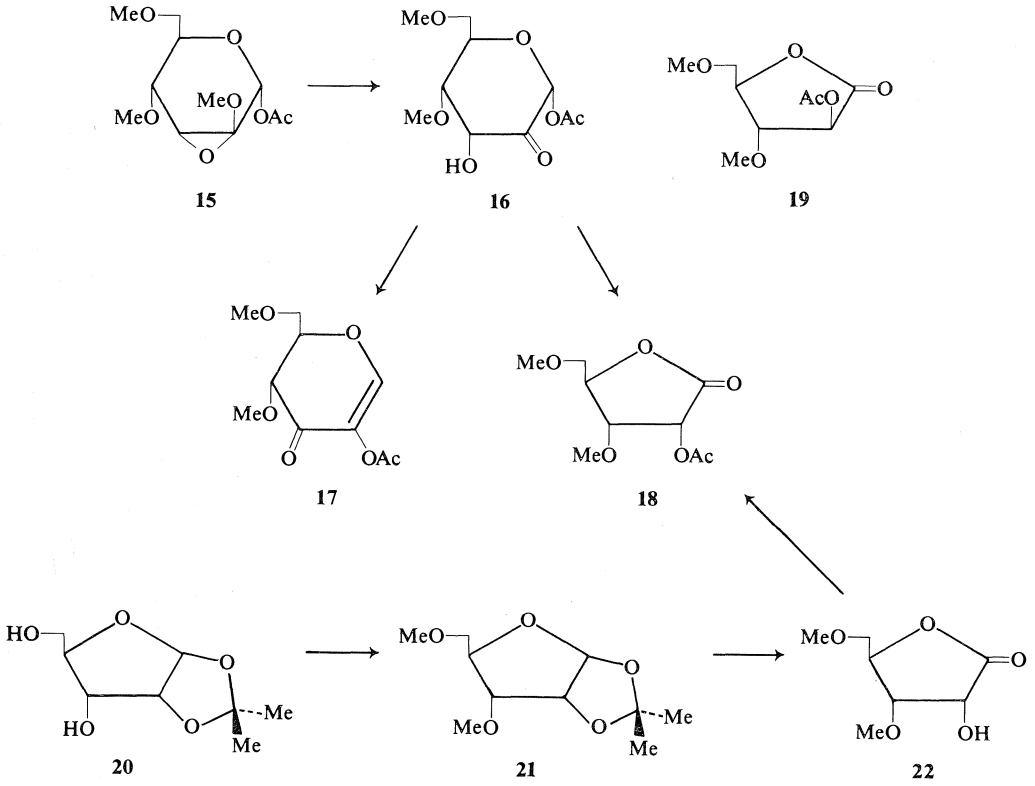

SCHEME 2

1,4,6-tri-*O*-acetyl-3-deoxy-2-*O*-methyl-α-D-*erythro*-hex-2-enopyranose (**4**), the products of the reaction of the peracid with 1-*O*-acetyl-3-deoxy-2,4,6-tri-*O*-methyl-α-D-*erythro*-hex-2-enopyranose (**1**) were re-examined. Previously no product other than perester **2** had been detected by t.l.c. of the reaction mixture. However, after crystallization of the perester, examination of the mother liquor showed the presence of another product and chromatographic separation led to the isolation of the 2-methoxyepoxide, 1-*O*-acetyl-2,3-anhydro-2-methoxy-4,6-di-*O*-methyl-α-D-allopyranose (**15**). The syrupy compound was insufficiently stable for satisfactory elemental analysis but the i.r., n.m.r., and mass spectra were consistent with the assigned structure. The structure of the epoxide **15** was established by the following transformations which were similar to those undergone by the epoxide **6**. Opening of the epoxide ring took place readily on heating in water to give the glycosulose **16**, which, on treatment with acetic anhydride in pyridine at room temperature, afforded the enediolone acetate **17**. Oxidative degradation of the glycosulose **16** with *m*-chloroperbenzoic acid in trifluoroacetic acid gave 2-*O*-acetyl-3,5-di-*O*-methyl-D-ribonolactone (**18**) in a reaction which again involved intramolecular *O*-acetyl migration. The crystalline lactone **18** was readily distinguishable from the corresponding D-arabinonolactone derivative **19**. The structure of the D-ribonolactone derivative **18** was confirmed by synthesis from 1,2-*O*-isopropylidene-α-D-ribofuranose (**20**) (11, 12) by (*a*) methylation to 1,2-*O*-isopropylidene-3,5-di-*O*-methyl-D-ribofuranose (**21**), (*b*) hydrolysis and oxidation to 3,5-di-*O*-methyl-D-ribonolactone (**22**), and (*c*) acetylation (see Scheme 2).

Two novel classes of compounds have been isolated as products of the oxidation of 3-deoxyhex-2-enopyranoses with *m*-chloroperbenzoic acid. The peresters are most closely related to the 1,2-*t*-butylperoxy orthoesters described by Schulz *et al.* (6) and prepared by the action of *O*-acyl glycosyl halides on *t*-butylhydroperoxide in collidine. Until very recently α-methoxyepoxides remained unknown carbohydrate deriv-

Can. J. Chem. Downloaded from www.nrcresearchpress.com by 210.87.254.5 on 09/05/12
For personal use only.

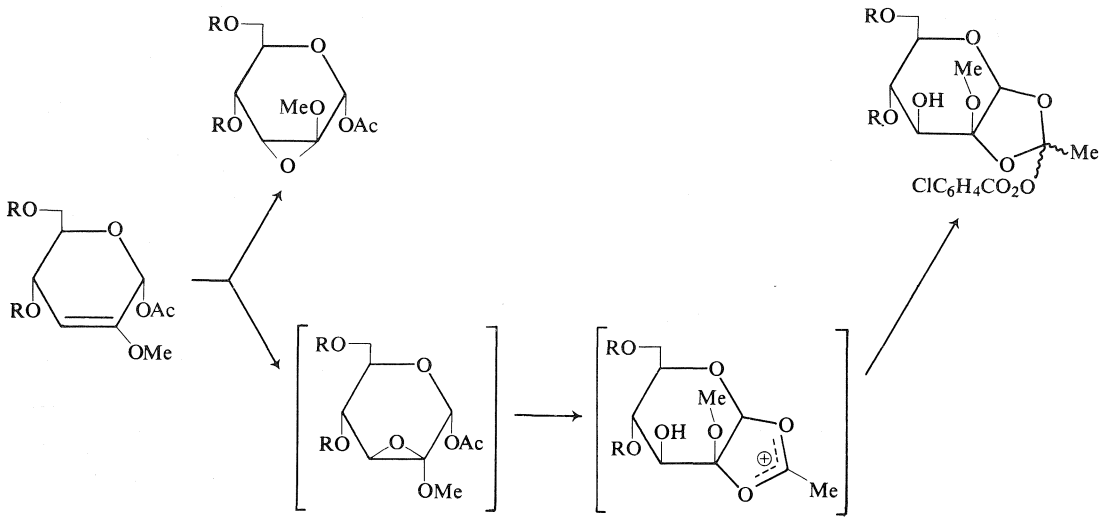

SCHEME 3

atives although an α-benzoyloxy-epoxide was reported 40 years ago by Maurer and Petsch (13). When the present work was nearly completed, Dmytraczenko *et al.* (14) reported the preparation of methyl 2,3-anhydro-4,6-*O*-benzylidene-3-methoxy-α-D-allopyranoside by the action of triethylamine in methanol on methyl 4,6-*O*-benzylidene-2-*O*-toluene-*p*-sulfonyl-α-D-*ribo*-hexopyranosid-3-ulose. The same authors (personal communication) have similarly synthesized the corresponding 2-methoxyepoxide from the 3-*O*-toluene-*p*-sulfonyl glycopyranosid-2-ulose.

In the light of the characterization of both classes of compounds we may turn to the mechanism of their formation on treatment of 3-deoxy-hex-2-enopyranoses with *m*-chloroperbenzoic acid. The 2,3-anhydro-2-methoxy-α-D-allopyranoses are relatively stable insofar as they are not susceptible to further reaction with peracid. In contrast no 2,3-anhydro-2-methoxy-α-D-mannopyranoses were detected. A possible pathway for the formation of the peresters is shown in Scheme 3 in which the α-D-*manno*-epoxide undergoes intramolecular ring opening by the neighboring *O*-acetyl group with formation of a cyclic acetoxonium ion which, in turn, reacts with further *m*-chloroperbenzoic acid. In this reaction scheme there is no clear reason why change of the 4- and 6-*O*-substituents should markedly alter the proportions of the two types of product. It may be noted, however, that whereas epoxidation of *trans*-6-acetoxymethyl-2-methoxy-5,6-dihydro-2*H*-pyran affords approximately equal proportions of methyl 2,3-anhydro-4-deoxy-6-*O*-methyl-α-DL-*lyxo*-hexopyranoside and the *ribo*-isomer (15), similar reaction of *trans*-2-methoxy-6-methoxymethyl-5,6-dihydro-2*H*-pyran gives almost exclusively the corresponding product with the *lyxo*-configuration (16). There is no evidence for the configuration at C-1′ of the oxyethylidene group in the peresters.

Experimental

Experimental procedures were as described in the preceding paper (1).

Oxidation of 1,4,6-Tri-O-acetyl-3-deoxy-2-O-methyl-α-D-erythro-hex-2-enopyranose (4) with m-Chloroperbenzoic Acid

The hex-2-enopyranose (**4**) (2.4 g) was reacted with *m*-chloroperbenzoic acid (2.8 g) in chloroform (150 ml) at room temperature for 3 h. The chloroform solution was washed with 10% sodium carbonate solution (150 ml) and water (100 ml), and concentrated to a residue which crystallized from ether – light petroleum to give 1,4,6-tri-*O*-acetyl-2,3-anhydro-2-methoxy-α-D-allopyranose (**6**) (1.71 g, 68%), m.p. 113–114°, $[\alpha]_D$ +98° (*c*, 1.0); M^+, 318; ν_{max} 1755, 1735 cm^{-1} (ester C=O); n.m.r. τ 3.68 (one-proton singlet, H-1), 5.08 (one-proton quartet, $J_{3,4}$ = 1.8, $J_{4,5}$ = 9.5 Hz, H-4), 6.17 (one-proton doublet, $J_{3,4}$ = 1.8, H-3), 6.73 (three-proton singlet, OCH_3), 7.82, 7.85, 7.94 (three-proton singlet, 3 × $OCOCH_3$).

Anal. Calcd. for $C_{13}H_{18}O_9$: C, 49.06; H, 5.70. Found: C, 48.77; H, 5.65.

The mother liquor from the crystallization was separated by preparative layer chromatography (ethyl acetate – light petroleum 1:5) to give further epoxide **6** (180 mg, 7%) and 4,6-di-*O*-acetyl-1,2-*O*-(1′-*m*-chloroperbenzoyloxy-ethylidene)-2-methoxy-α-D-glucopyranose (**5**) (386 mg, 10%) as a syrup which was too unstable for satis-

Can. J. Chem. Downloaded from www.nrcresearchpress.com by 210.87.254.5 on 09/05/12
For personal use only.

Can. J. Chem. Downloaded from www.nrcresearchpress.com by 210.87.254.5 on 09/05/12
For personal use only.

factory elemental analysis, $[\alpha]_D$ −4.2° (*c*, 1.0); λ_{max} 232 nm (log ε 4.02); ν_{max} 3700 (OH), 1765 (perester C=O), 1740 (acetate C=O), 1580 cm^{-1} (aromatic); n.m.r. τ 2.08–2.63 (four aromatic protons), 4.37 (one-proton singlet, H-1), 5.09 (one-proton quartet, $J_{3,4}$ = 2.2, $J_{4,5}$ = 6.4, H-4), 5.44 (one-proton doublet, $J_{3,4}$ = 2.2 Hz, H-3), 6.60 (three-proton singlet, OCH_3), 7.89, 7.93 (three-proton singlet, 2 × $OCOCH_3$), 8.09 (three-proton singlet, C—CH_3).

3,4,6-Tri-O-acetyl-1,2-O-(1'-m-chloroperbenzoyloxyethylidene)-2-methoxy-α-D-glucopyranose (7)

Perester **5** (300 mg) was kept in acetic anhydride (5 ml) and pyridine (10 ml) at 0° overnight and at room temperature for 2 h. The reaction mixture was poured into ice-water (100 ml), and the solution was neutralized with sodium hydrogen carbonate, and extracted with chloroform (2 × 75 ml). Concentration of the dried extract furnished the perester acetate **7** as a syrup, $[\alpha]_D$ −3.5° (*c*, 1.0); λ_{max} 233 nm (log ε 4.01); ν_{max} 1765 (perester C=O), 1745 (acetate C=O), 1578 cm^{-1} (aromatic); n.m.r. τ 2.11–2.68 (four-aromatic protons), 4.44 (one-proton singlet, H-1), 4.68 (one-proton doublet, $J_{3,4}$ = 1.8 Hz, H-3), 5.17 (one-proton quartet, $J_{3,4}$ = 1.8, $J_{4,5}$ = 6.8 Hz, H-4), 6.77 (three-proton singlet, OCH_3), 7.88, (six-proton singlet, 2 × $OCOCH_3$), 7.96 (three-proton singlet, $OCOCH_3$), 8.08 (three-proton singlet, C—CH_3). The mass spectrum showed no molecular ion but prominent peaks were detected as *m/e* 361 (M − $ClC_6H_4CO_3$), and 156 and 158, and 139 and 141 (isotope pairs). The compound was too unstable for elemental analysis.

Degradation of Acetylated Perester 7 in Trifluoroacetic Acid

The acetylated perester **7** (75 mg) was kept in trifluoroacetic acid – water (9:1, 10 ml) at room temperature for 30 min. The solution was concentrated, and the residue in chloroform (40 ml) was washed with sodium hydrogen carbonate solution and with water, dried, and concentrated. The residue was recrystallized from ether – light petroleum to give 2,3,5-tri-*O*-acetyl-D-arabinonolactone (**8**) (23 mg), m.p. and mixed m.p. 68–69°, $[\alpha]_D$ +53° (*c*, 1.0) (lit. (17) m.p. 66–69°, $[\alpha]_D$ +52.3°), whose i.r. and n.m.r. spectra were identical with those of a sample prepared from D-arabinose by bromine oxidation, followed by acetylation.

2,4,6-Tri-O-acetyl-1-deoxy-α-D-erythro-hex-1-enopyranos-3-ulose (9)

Acetylated perester **7** (200 mg) in acetic acid (10 ml) was stirred with zinc dust (100 mg) at room temperature for 1 h. Chloroform (50 ml) was added to the reaction mixture, and the filtered solution was washed with saturated sodium hydrogen carbonate solution, dried, and concentrated to a syrup which was separated by preparative layer chromatography. The major component was the syrupy hex-1-enopyranos-3-ulose **9** (83 mg, 77%), $[\alpha]_D$ +156° (*c*, 1.0); M^+ 286; λ_{max} 260 nm (log ε 4.14); ν_{max} 1745 (ester C=O), 1700 (α,β-unsaturated ketone), 1636 cm^{-1} (C=C); n.m.r. τ 2.65 (one-proton singlet, H-1), 4.42 (one-proton doublet, $J_{4,5}$ = 12.5 Hz, H-4), 7.79, 7.84, 7.90 (three-proton singlet, 3 × $OCOCH_3$).

Anal. Calcd. for $C_{12}H_{14}O_8$: C, 50.35; H, 4.93. Found: C, 50.57; H, 5.09.

The minor component was 5-acetoxy-2-(acetoxymethyl)-4*H*-pyran-4-one (kojic acid diacetate (**10**)) (~2 mg) and was identical (m.p. and mixed m.p., i.r. and mass spectra) with a sample prepared from kojic acid. Treatment of the hex-1-enopyranos-3-ulose **9** with acetic anhydride and pyridine at room temperature afforded kojic acid diacetate (**10**).

1,4,6-Tri-O-acetyl-α-D-ribo-hexopyranosulose (11)

A suspension of epoxide **6** (400 mg) in water (25 ml) was warmed on the steam bath until dissolution was complete (*ca.* 5 min). Removal of water and crystallization of the residue from ethyl acetate – light petroleum yielded the glycosulose **11** as a monohydrate (262 mg), m.p. 88–90°, $[\alpha]_D$ −38° (*c*. 1.0); ν_{max} 3660 (OH), 1745, 1718 cm^{-1} (ester C=O); n.m.r. τ 3.67 (one-proton singlet, H-1), 4.57 (one-proton quartet, $J_{3,4}$ = 4.8, $J_{4,5}$ = 2.5 Hz, H-4), 5.10 (one-proton doublet, $J_{3,4}$ = 4.8 Hz, H-3), 6.42 (broad three-proton band, exchanges with D_2O, 3 × OH), 7.84, 7.91, 7.94 (three-proton singlet, 3 × $OCOCH_3$).

Anal. Calcd. for $C_{12}H_{16}O_9.H_2O$: C, 44.72; H, 5.63. Found: C, 45.19; H, 5.85.

Attempted acetylation of the glycosulose **11** (100 mg) with acetic anhydride (5 ml) and sodium acetate (35 mg) at room temperature for 2 h, followed by work-up and preparative layer chromatography (ethyl acetate – light petroleum, 2:5), gave predominantly the hex-1-enopyranos-3-ulose **9** (64 mg) which was identical (i.r., u.v., and n.m.r. spectra) to the sample prepared previously. Alternatively, attempted acetylation of the glycosulose **11** (100 mg) at room temperature for 2 h, followed by work-up and preparative layer chromatography (ethyl acetate – light petroleum, 1:5), gave only 5-acetoxy-2-(acetoxymethyl)-4*H*-pyran-4-one (**10**) (61 mg) which was identical (m.p. and mixed m.p., i.r. and n.m.r. spectra) to a sample prepared from kojic acid.

Oxidative Degradation of Glycosulose (11)

m-Chloroperbenzoic acid (100 mg) was added to glycosulose **11** (100 mg) in trifluoroacetic acid (10 ml) and the solution was kept at room temperature for 2 h. The solution was concentrated under nitrogen and the residue in chloroform (40 ml) was washed with 10% sodium carbonate solution (30 ml) and with water (20 ml). The dried chloroform solution was concentrated and the residue was recrystallized from ether – light petroleum to give 2,3,5-tri-*O*-acetyl-D-ribonolactone (**12**) (38 mg), m.p. and mixed m.p. 55–56°, $[\alpha]_D$ +30° (*c*, 1.0) (lit. (18) m.p. 54–56°, $[\alpha]_D$ +27°), whose i.r., n.m.r., and mass spectra were identical with those of a sample prepared from D-ribose by bromine oxidation, followed by acetylation.

1,2,4,6-Tetra-O-acetyl-2-methoxy-α-D-altropyranose (13)

Epoxide **6** (400 mg) was kept in acetic acid (20 ml) containing acetic anhydride (2 ml) at room temperature until t.l.c. (ethyl acetate – light petroleum, 5:1) indicated that reaction was complete (*ca.* 3 h). The reaction mixture was poured into ice-water (100 ml) and neutralized with sodium hydrogen carbonate, and the solution was extracted with chloroform (2 × 75 ml). Concentration of the dried extract and crystallization of the residue from ether – light petroleum furnished the tetra-*O*-acetyl derivative **13** (285 mg), m.p. 40–42°, $[\alpha]_D$ +92.7° (*c*, 1.5);

ν_{max} 3600 (OH), 1740 cm^{-1} (ester C=O); n.m.r. τ 3.34 (one-proton doublet, $J_{1,3}$ = 2.8 Hz, H-1), 5.03 (one-proton quartet, $J_{3,4}$ = 5.0, $J_{4,5}$ = 16 Hz, H-4), 5.49 (one-proton quartet, $J_{1,3}$ = 2.8, $J_{3,4}$ = 5.0 Hz, H-3), 6.62 (three-proton singlet, OCH_3), 7.27 (one-proton singlet, exchanges with D_2O, OH), 7.85 (six-proton singlet, 2 × $OCOCH_3$), 7.90, 7.96 (three-proton singlet, 2 × $OCOCH_3$).

Anal. Calcd. for $C_{15}H_{22}O_{11}$: C, 47.62; H, 5.86. Found: C, 47.58: H, 5.86.

*1,2,3,4,6-Penta-O-acetyl-2-methoxy-α-D-altropyranose (**14**)*

Tetra-acetate **13** (160 mg) was kept in acetic anhydride (4 ml) and pyridine (6 ml) overnight at 0° and for 4 h at room temperature. Work-up of the reaction mixture in the usual way followed by crystallization from ether – light petroleum afforded the penta-*O*-acetate **14** (112 mg), m.p. 121–122°, $[\alpha]_D$ +91.2° (*c*, 1.0); ν_{max} 1755, 1742 cm^{-1} (ester C=O); n.m.r. τ 3.23 (one-proton doublet, $J_{1,3}$ = 2.3 Hz, H-1), 4.25 (one-proton quartet, $J_{1,3}$ = 2.3, $J_{3,4}$ = 6.0 Hz, H-3), 4.87 (one-proton quartet, $J_{3,4}$ = 6.0, $J_{4,5}$ = 17 Hz, H-4), 6.73 (three-proton singlet, OCH_3), 7.81 (three-proton singlet, $OCOCH_3$) 7.82 (six-proton singlet, 2 × $OCOCH_3$), 7.93, 7.98 (three-proton singlet, 2 × $OCOCH_3$).

Anal. Calcd. for $C_{17}H_{24}O_{12}$: C, 48.57; H, 5.76. Found: C, 48.73; H, 5.75.

*Oxidation of 1-O-Acetyl-3-deoxy-2,4,6-tri-O-methyl-α-D-erythro-hex-2-enopyranose (**1**) with m-Chloroperbenzoic Acid*

Hex-2-enopyranose **1** (2.2 g) was treated with *m*-chloroperbenzoic acid (3.1 g) in chloroform for 3 h at room temperature (t.l.c. in ethyl acetate – light petroleum (2:5) indicated that reaction was complete). The chloroform solution was washed with 10% sodium carbonate solution (150 ml) and then with water (100 ml), dried, and concentrated. Crystallization of the residue from ether–light petroleum furnished perester **2** (1.36 g) which was similar in all respects to the previously isolated sample (1). The mother liquor from the crystallization separated by preparative layer chromatography (ethyl acetate – light petroleum, 3:7) yielded further perester **2** (210 mg) together with 1-*O*-acetyl-2,3-anhydro-4,6-*O*-methyl-2-methoxy-α-D-allopyranose (**15**) (305 mg), $[\alpha]_D$ +82° (*c*, 1.0), as a syrup which was too unstable for elemental analysis; M^+, 292; ν_{max} 1744 cm^{-1} (ester C=O); n.m.r. τ 3.66 (one-proton singlet, H-1), 6.13 (one-proton doublet, $J_{3,4}$ = 1.2 Hz, H-3), 6.50, 6.63, 6.71 (three-proton singlet, 3 × OCH_3), 7.86 (three-proton singlet, $OCOCH_3$). No perester **2** was formed when the epoxide **15** was treated with further *m*-chloroperbenzoic acid.

*1-O-Acetyl-4,6-di-O-methyl-α-D-ribo-hexopyranosulose (**16**)*

A suspension of the epoxide **15** (240 mg) in water (15 ml) was warmed on the steam bath until dissolution was complete (*ca.* 5 min). Removal of water furnished the glycosulose **16** as a syrup, $[\alpha]_D$ −5.5° (*c*, 2.0); M^+, 248; ν_{max} 3580 (OH), 1745 cm^{-1} (broad, C=O); n.m.r. τ 3.67 (one-proton singlet, H-1), 5.11 (one-proton doublet, $J_{3,4}$ = 8.0 Hz, H-3), 6.52 (nine-proton singlet, 3 × OCH_3), 7.81 (three-proton singlet, $OCOCH_3$).

Anal. Calcd. for $C_{10}H_{16}O_7$: C, 48.38; H, 6.50. Found: C, 48.01; H, 6.31.

Attempted acetylation of the glycosulose **16** with acetic anhydride and pyridine at room temperature gave only 2-*O*-acetyl-1-deoxy-4,6-di-*O*-methyl-α-D-*erythro*-hex-1-enopyranos-3-ulose (**17**) which was identical (m.p., mixed m.p., and i.r. spectrum) with the previously isolated sample (1).

*Oxidative Degradation of Glycosulose (**16**)*

Glycosulose **16** (75 mg) in trifluoroacetic acid (10 ml) was treated with *m*-chloroperbenzoic acid (100 mg) at room temperature for 2 h. The solution was concentrated under nitrogen and the residue in chloroform (40 ml) was washed with 10% sodium carbonate solution (30 ml) and with water (20 ml). The dried chloroform solution was concentrated and crystallization of the residue from ether – light petroleum afforded 2-*O*-acetyl-3,5-di-*O*-methyl-D-ribonolactone (**18**) (29 mg), m.p. 54–55°, $[\alpha]_D$ −9.5° (*c*, 1.0); M^+, 218; ν_{max} 1790 (γ-lactone), 1735 cm^{-1} (acetate C=O); n.m.r. τ 4.48 (one-proton doublet, $J_{2,3}$ = 9.0 Hz), 5.85 (one-proton doublet, $J_{2,3}$ = 9.0 Hz, H-3), 6.60, 6.62 (three-proton singlet, 2 × OCH_3), 7.79 (three-proton singlet, $OCOCH_3$).

Anal. Calcd. for $C_9H_{14}O_6$: C, 49.54; H, 6.47. Found: C, 49.31; H, 6.91.

5-O-Benzoyl-1,2-O-isopropylidene-α-D-erythro-pentofuranos-3-ulose

5-*O*-Benzoyl-1,2-*O*-isopropylidene-α-D-xylofuranose (19) (2.5 g) in ethanol-free chloroform (250 ml) was added to a mixture of water (200 ml), sodium metaperiodate (20 g), sodium carbonate (1 g), and 51% ruthenium dioxide (10 g). The mixture was stirred vigorously at room temperature overnight, 2-propanol (10 ml) was added, and, after 10 min, the mixture was filtered. The organic layer was separated and the aqueous layer was extracted with chloroform. The combined organic layer and chloroform extract were dried and concentrated to give the pentofuranos-3-ulose (1.8 g), which crystallized from ether – light petroleum and had m.p. 93–95°, $[\alpha]_D$ +138° (*c*, 1.0), (lit. (11) m.p. 93–94.5°, $[\alpha]_D$ +135°).

*1,2-O-Isopropylidene-α-D-ribofuranose (**20**)*

Lithium aluminum hydride (0.75 g) was added with stirring to a cooled solution of the above pentofuranosulose (1.6 g) in tetrahydrofuran (100 ml) and the mixture was heated under reflux for 2 h. Ethyl acetate (25 ml) was added to the cooled solution, and the mixture was poured into ice-water and extracted with chloroform (2 × 150 ml). Concentration of the dried extracts and crystallization of the residue from ether afforded 1,2-*O*-isopropylidene-α-D-ribofuranose (**20**) (0.72 g), m.p. 85–86°, $[\alpha]_D$ +39.5° (*c*, 1.0), (lit. (12) m.p. 86–87°, $[\alpha]_D$ +37°).

*1,2-O-Isopropylidene-3,5-di-O-methyl-α-D-ribofuranose (**21**)*

1,2-*O*-Isopropylidene-α-D-ribofuranose (610 mg) in *N*,*N*-dimethylformamide (25 ml) was stirred with methyl iodide (0.6 ml) and silver oxide (1.5 g) for 12 h at room temperature. Insoluble salts were removed by filtration and washed, and the combined filtrate and washings were concentrated, diluted with chloroform, filtered

Can. J. Chem. Downloaded from www.nrcresearchpress.com by 210.87.254.5 on 09/05/12
For personal use only.

again, and washed several times with water. The dried chloroform solution was concentrated and crystallization of the residue from ether – light petroleum furnished **21** (492 mg), m.p. 81–83°, $[\alpha]_D$ +110° (*c*, 1.0); n.m.r. τ 4.27 (one-proton doublet, $J_{1,2}$ = 5 Hz, H-1), 6.52, 6.61 (three-proton singlet, 2 × OCH_3), 8.42, 8.63 (three-proton singlet, CMe_2).

Anal. Calcd. for $C_{10}H_{18}O_5$: C, 55.03; H, 8.31. Found: C, 55.11; H, 8.29.

3,5-Di-O-methyl-D-*ribonolactone (22)*

The isopropylidene derivative **21** (400 mg) in acetic acid (20 ml) and water (5 ml) was heated on a steam bath for 2 h and concentration of the solution gave 3,5-di-*O*-methyl-D-ribofuranose as a syrup, $[\alpha]_D$ +37° (*c*, 1.5); ν_{max} 3450 cm^{-1} (OH). Bromine (0.5 ml) was added to the sugar (150 mg) in water (15 ml) and the solution was set aside for 2 days. Excess of bromine was removed by aeration, the solution was neutralized with silver carbonate, filtered, and concentrated to yield crude **22** as a syrup. Purification of the syrup by preparative layer chromatography (ethyl acetate) followed by crystallization from ether – light petroleum gave a crystalline sample, m.p. 55–56.5°, $[\alpha]_D$ +5.6° (*c*, 1.0); M^+, 176; ν_{max} 3470 (OH), 1770 cm^{-1} (γ-lactone); n.m.r. τ 6.51, 6.67 (three-proton singlet, 2 × OCH_3), 7.14 (one-proton doublet, splitting 15 Hz, exchanges with D_2O, C—OH).

Anal. Calcd. for $C_7H_{12}O_5$: C, 47.72; H, 6.87. Found: C, 47.86; H, 6.78.

Treatment of the lactone **22** with acetic anhydride and pyridine furnished 2-*O*-acetyl-3,5-di-*O*-methyl-D-ribonolactone (**18**) which was identical (m.p. and mixed m.p., i.r., n.m.r., and mass spectra) to the previously isolated sample.

The authors wish to acknowledge financial support from the National Research Council of Canada.

1. G. O. Aspinall, R. R. King, and Z. Pawlak. This issue.
2. E. F. L. J. Anet. Aust. J. Chem. **18**, 837 (1965).
3. B. Coxon and L. D. Hall. Tetrahedron, **20**, 1685 (1964).
4. R. U. Lemieux and A. R. Morgan. Can. J. Chem. **43**, 2199 (1965).
5. R. G. Rees, A. R. Tatchell, and R. D. Wells. J. Chem. Soc. C, 1768 (1967).
6. M. Schulz, H-F. Foeden, P. Berlin, and W-R. Bley. Ann. Chem. **715**, 172 (1968).
7. F. W. Lichtenthaler and P. Heidel. Angew. Chem. Intl. Ed. **8**, 978 (1969).
8. G. J. F. Chittenden. Carbohydr. Res. **11**, 424 (1969).
9. G. M. Cree, D. W. Mackie, and A. S. Perlin. Can. J. Chem. **47**, 511 (1969).
10. R. J. Ferrier and N. Prasad. J. Chem. Soc. C, 575 (1969).
11. K. Oka and H. Wada. Yakugaku Zasshi, **83**, 890 (1963); Chem. Abstr. **60**, 1825 (1964).
12. N. A. Hughes and P. R. H. Speakman. Carbohydr. Res. **1**, 171 (1965).
13. K. Maurer and W. Petsch. Chem. Ber. **66**, 995 (1933).
14. A. Dmytraczenko, W. A. Szarek, and J. K. N. Jones. Chem. Commun. 1220 (1971).
15. A. Konowal, A. Zamojski, M. Masojidkova, and J. Kohoutova. Roczniki Chem. **44**, 1741 (1970).
16. F. Sweet and R. K. Brown. Can. J. Chem. **46**, 2283 (1968).
17. G. B. Robbins and F. W. Upson. J. Am. Chem. Soc. **62**, 1074 (1940).
18. K. Ladenburg, M. Tischler, J. W. Wellman, and R. D. Babson. J. Am. Chem. Soc. **66**, 1217 (1944).
19. P. A. Levene and A. L. Raymond. J. Biol. Chem. **102**, 317 (1933).

Can. J. Chem. Downloaded from www.nrcresearchpress.com by 210.87.254.5 on 09/05/12
For personal use only.

The Vibrational Spectra and Crystal Structure of Acenaphthylene

A. Bree, R. A. Kydd, V. V. B. Vilkos, and R. S. Williams
Department of Chemistry, University of British Columbia, Vancouver 8, British Columbia

Received June 30, 1972

A study of the polarized infrared and Raman spectra of acenaphthylene single crystals has been made. These results, together with Gordon and Yang's preliminary X-ray work, suggest that the molecules pack in some disordered arrangement in the solid at room temperature. Most of the A_1 fundamentals were identified in the Raman solution spectrum from their low depolarization ratio, and a few tentative assignments of nontotally symmetric fundamentals were made.

Une étude des spectres infrarouge et Raman en lumière polarisée a été réalisée sur des monocristaux d'acénaphtylène. Les résultats obtenus, associés à ceux des travaux préliminaires de Gordon et Yang sur les rayons X, laissent penser que les molécules suivent un arrangement désordonné à l'état solide et à la température ambiante. La plupart des fondamentales A_1 ont été identifiées sur les spectres Raman en solution à partir du faible rapport de dépolarisation, quelques attributions ont été tentées sur des fondamentales non totalement symétriques. [Traduit par le journal]

Can. J. Chem., **51**, 402 (1973)

Can. J. Chem. Downloaded from www.nrcresearchpress.com by 210.87.254.42 on 09/05/12
For personal use only.

One method of making vibrational symmetry assignments for large molecules that has proved useful (see, for example, ref. 1) is to study the polarized spectra of single crystals. This method presupposes that a knowledge of the crystal structure is available. At the turn of the century, Groth (2) found that acenaphthylene crystals were orthorhombic by examining the crystal habit, and listed the complete optical properties. More recently Gordon and Yang (3) reported in a preliminary X-ray study that the crystal has four molecules in an orthorhombic unit cell belonging to the space group *Pc2a*. These authors claim that there are two crystallographically inequivalent pairs of molecules in the acenaphthylene cell so that each molecule must occupy a special site. Their important conclusion is that the short molecular axis must lie parallel to *b*. For this structure, the activity of a molecular vibration in the crystal is shown in Table 1. Further, in the special case of a vibration allowed through a change in the polarizability tensor element α_{zz}, the scattered intensity should be exclusively in the (*bb*) Raman spectrum.

Acenaphthylene was purified by chromatography on a column of alumina using petroleum ether as both developer and eluant. On melting, acenaphthylene forms a dark red tar so that large single crystals could not be produced by the usual method of lowering the compound through a Bridgman furnace. The crystals used for the Raman experiments were grown from either benzene or ethanol solutions by slow evaporation. These crystals, having a well developed *ac* face, were at most only 2 mm thick.

The Raman spectra were recorded on a Cary 81 spectrophotometer fitted with a helium–neon laser with 33 mW power at the sample. The solution spectra were measured in benzene and benzene-d_6 because an apparent photochemical reaction producing fine white particles (acenaphthylene dimer?) occurred in such solvents as carbon tetrachloride and carbon disulfide. The results of the Raman measurements are in Table 2. The intensity distribution amongst the polarized spectra from a single crystal was not consistent with the pattern predicted for Gordon and Yang's crystal structure, and did not allow any symmetry assignments to be made. In fact, the vibrational lines appeared in all possible polarized Raman spectra of the crystal in such a way that suggested the molecular axes had nearly equal projections on the crystal frame.

Because of the crystal habit, infrared spectra of the solid were measured with the electric vector of plane polarized radiation parallel to *a* and *c* (see Fig. 1). Totally symmetric modes were unpolarized in the *ac* face and had the same intensities relative to adjacent lines in the solid as in the solution. For example, the line at 552 cm^{-1} marks an A_1 fundamental (the depolarization ratio in the Raman spectrum is 0.25) and shows this behavior. Thus, the twofold axis *z* of the molecule does not lie parallel to *b*. Further, the lowest frequency infrared active modes at

TABLE 1. Correlation table showing the selection rules for the isolated molecule and for the Gordon and Yang crystal structure with space group *Pc2a**

Molecular group C_{2v}			Site group	Factor group C_{2v}	
N	Bases	Mode	C_2	Mode	Bases
19	$xx,yy,zz;\ z$	A_1	A	a_1	$b;\ aa,bb,cc$
8	xy	A_2		a_2	ac
9	$xz;\ x$	B_1	B	b_1	$a;\ ab$
18	$yz;\ y$	B_2		b_2	$c;\ bc$

*N refers to the number of fundamentals in the free molecule and factor group symmetry species are distinguished by the use of lower case symbols.

TABLE 2. The vibrational spectra of acenaphthylene

Infrared	Raman*			Infrared	Raman*		
$\bar{\nu}_{crystal}$	$\Delta\bar{\nu}_{crystal}$	$\Delta\bar{\nu}_{solution}$	ρ	$\bar{\nu}_{crystal}$	$\Delta\bar{\nu}_{crystal}$	$\Delta\bar{\nu}_{solution}$	ρ
173 sh	163 sh			1112 w			
~185 vs				1152 ms	1151 w	1150 vw	0.37
	225 vw			1180 mw	1181 vw		
244 vs	245 vw	236 vw	dp	1204 s	1205 mw	1203 vw	dp
	370 w	374 vw	dp	1226 s	1226 w	1226 vw	p
414 s	416 mw	416 vw	0.7	1251 w	1250 m	1249 w	0.37
460 m				1259 vw			
509 m	511 s	511 mw	0.77	1280 vw			
551 s	552 s	552 m	0.25	1308 mw			
	572 vw			1333 vw			
602 mw				1361 w	1360 s	1360 m	0.16
	641 w	639 w	0.07	1372 mw	1373 vw		
660 w	661 vs	660 vs	0.04	1390 s	1389 ms	1387 vw	0.81
684 w					1413 sh	1411 sh	
727 vs				1429 vs	1429 vs	1427 s	0.12
759 sh	758 vw				1446 vw		
774 vs				1457 ms	1459 w		
789 sh				1480 s	1478 sh		
804 w	805 m	805 mw	0.07	1496 s	1493 vs	1493 s	0.07
830 vs	834 vw			1597 sh			
856 w				1607 m	1600 s	1598 ms	0.13
864 s	864 vw			1611 sh			
913 m	915 w	914 vw	dp	1623 m	1621 ms	1621 mw	0.78
938 vw				2997 w	3000 w		
971 mw	974 vw				3027 sh		
1011 mw	1014 mw	1011 vw	p	3041 s	3039 m	3042 vw	p
1032 ms	1032 ms	1032 mw	0.17	3062 s	3065 ms	3066 vw	p
	1059 vw	1053 vw	p		3077 sh		
1084 s	1083 s	1081 ms	0.11	3099 m	3099 mw		
1092 sh							

*The intensity of each Raman line in the solid refers to the strongest component amongst the six independent polarized spectra, v = very, s = strong, m = medium, w = weak, sh = shoulder, p = polarized, dp = depolarized.

185 and 244 cm^{-1} must represent B_1 fundamentals and these too appear in the *ac* spectrum, so that the molecular normal x is not parallel to b. Finally, since no out-of-plane fundamental is expected at such a high frequency, the depolarized Raman line at 1387 cm^{-1} is assigned as a B_2 fundamental; this may be the analog of the B_2 fundamental at 1351 cm^{-1} in the first excited electronic state (4). This too appears in the *ac* infrared spectrum with an intensity relative to adjacent lines undiminished from the solution spectrum so that y is not parallel to b.

Can. J. Chem. Downloaded from www.nrcresearchpress.com by 210.87.254.42 on 09/05/12
For personal use only.

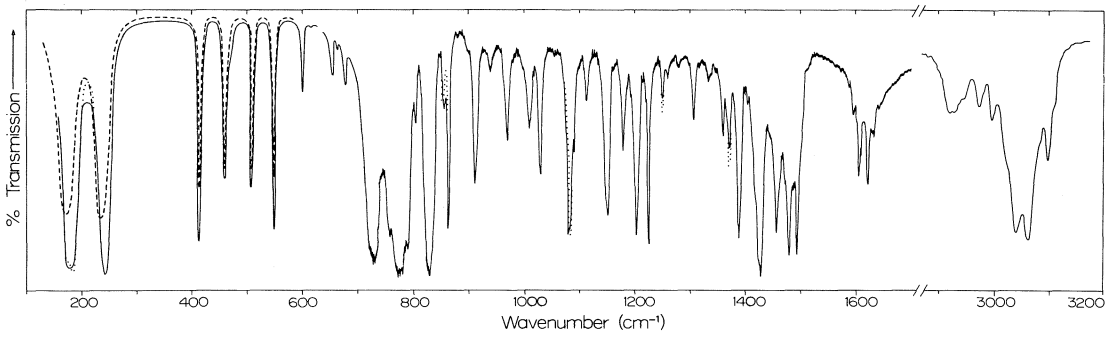

FIG. 1. The infrared spectra of acenaphthylene in solution and as an *ac* single crystal section: Full line, $||c$; dotted line, $||a$; broken line, in a benzene solution. Above 620 cm^{-1} the crystal thickness was about 50 μ and below 620 cm^{-1} it was about 100 μ.

This is confirmed by the observation that the long axis electronic transition at 21095 cm^{-1} is polarized in the *ac* plane (3).

These results appear to show that the molecules do not occupy a special site in the lattice, yet there are two layers of molecules along *b*(3). Both types of evidence, from spectroscopic and X-ray sources, can be made consistent only by assuming that the crystal structure of acenaphthylene is a considerably disordered one (5).

At this point in the argument it is important to consider the evidence which shows that the crystals were single. The thicker solution grown samples, when examined under a polarizing microscope, gave crosses as conoscopic figures and extinguished uniformly in three mutually perpendicular directions. Thin sublimation flakes, providing sections normal to the acute bisectrix, also extinguished well and reproduced the infrared results observed in thicker *ac* sections. The fact that the crystals were single is supported by the observation of factor group splittings at 854 ($||a$)/857($||c$) cm^{-1} and 1083 ($||c$)/1086($||a$) cm^{-1}.

Because of the apparent disordered nature of the crystal structure, the vibrational assignment rests largely on the depolarization ratios measured for the solution Raman spectrum, and must remain incomplete. Fundamental vibrations of A_1 symmetry are located at 552, 660, 805, 1032, 1081, 1360, 1427, 1493, 1598, 3042, 3066, and possibly 1011 and 1249 cm^{-1} from the intensities and depolarization ratios of these lines in the Raman solution spectrum. The polarized Raman lines at 1150 and 1226 cm^{-1} which are prominent in the infrared spectrum are also taken to mark A_1 fundamentals. It may be that there are two A_1 fundamentals near 1600 cm^{-1}, one at 1598 cm^{-1} seen in the Raman spectrum and a second at 1607 cm^{-1} prominent in the infrared.

The depolarized Raman lines at 1203, 1387, and 1621 cm^{-1} probably represent B_2 fundamentals since out-of-plane modes are expected at a somewhat lower energy. The very strong lines at 173 and 237 cm^{-1} in the infrared solution spectrum are taken to be B_1 fundamentals, and the weak Raman lines at about 163, 225, and possibly 370 cm^{-1} may mark A_2 fundamentals.

We would like to express our appreciation to the National Research Council of Canada for a research grant to support this work, and to Dr. R. D. Gordon and a referee for some valuable comments.

1. A. BREE, R. A. KYDD, and T. N. MISRA. Spectrochim. Acta, **25A**, 1815 (1969).
2. P. GROTH. Chem. Kryst. **5**, 421 (1919).
3. R. D. GORDON and R. F. YANG. J. Mol. Spectrosc. **34**, 266 (1970).
4. A. BREE, C. Y. FAN, and R. A. KYDD. Spectrochim. Acta, **25A**, 1375 (1969).
5. D. G. FRANKLIN, R. G. GIBB, R. D. GORDON, and R. F. YANG. Can. J. Chem. Submitted for publication.

Can. J. Chem. Downloaded from www.nrcresearchpress.com by 210.87.254.42 on 09/05/12
For personal use only.

A Mössbauer Study of the Iron Tetracarbonyl Halides

P. VASUDEV AND C. H. W. JONES

Chemistry Department, Simon Fraser University, Burnaby, British Columbia

Received June 23, 1972

The ^{57}Fe Mössbauer spectra of the *cis*-$Fe(CO)_4X_2$ compounds (X = Cl, Br, I) have been measured and the values of δ ($\sim$0.3 mm s^{-1}) and Δ ($\sim$0.3 mm s^{-1}) found to differ significantly from those previously reported for $Fe(CO)_4I_2$. The Δ values are analyzed in terms of p.q.s. values of the ligands.

The photolysis of cyclohexane solutions of $Fe(CO)_4I_2$ was studied and no evidence was found in the ^{57}Fe Mössbauer spectra of frozen samples for the previously proposed formation of *trans*-$Fe(CO)_4I_2$.

The ^{129}I Mössbauer absorption spectrum of *cis*-$Fe(CO)_4{}^{129}I_2$ is reported and the parameters found to be $\delta = +0.11 \pm 0.02$ mm s^{-1}, $e^2qQ = -980 \pm 10$ Mc s^{-1}, $\eta = 0.00 \pm 0.02$. The parameters are interpreted as evidence of *ca.* 5% 5s character on the iodine in the Fe—I bond.

Nous avons mesuré le spectre Mossbauer de ^{57}Fe des composés *cis*-$Fe(CO)_4X_2$ (où X = Cl, Br, I); les valeurs de δ ($\sim$0.3 mm s^{-1}) et Δ ($\sim$0.3 mm s^{-1}) sont significativement différentes de celles rapportées pour $Fe(CO)_4I_2$. Nous analysons les valeurs de Δ en termes de valeurs p.q.s. des ligands.

Nous avons étudié la photolyse de solution de $Fe(CO)_4I_2$ dans le cyclohexane; la formation de *trans*-$Fe(CO)I_2$, postulée antérieurement dans le cas de spectres Mössbauer de ^{57}Fe d'échantillons gelés n'a pas été confirmée.

Finalement nous rapportons le spectre Mössbauer de ^{129}I du *cis*-$Fe(CO)_4{}^{129}I_2$; les paramètres sont $\delta = +0.11 \pm 0.02$ mm s^{-1}, $e^2qQ = -980 \pm 10$ Mc s^{-1}, $\eta = 0.00 \pm 0.02$. Nous interprétons les paramètres en fonction de la manifestation de type 5s à 5% qui dénote l'oide dans la liaison Fe—I.

[Traduit par le journal]

Can. J. Chem., **51**, 405 (1973)

Can. J. Chem. Downloaded from www.nrcresearchpress.com by 210.87.254.42 on 09/05/12
For personal use only.

Introduction

The ^{57}Fe Mössbauer spectrum of *cis*-$Fe(CO)_4I_2$ has previously been reported by several workers (1–3). However, the values obtained for the isomer shift and quadrupole splitting were found to vary. We have remeasured the iron spectrum for this compound and in addition have measured the Mössbauer spectra for *cis*-$Fe(CO)_4Cl_2$ and *cis*-$Fe(CO)_4Br_2$.

A second objective of the present investigation lay in an ^{57}Fe Mössbauer study of the photolysis of *cis*-$Fe(CO)_4I_2$ in cyclohexane, where it has previously been proposed (4, 5) on the basis of i.r. data that isomerization to *trans*-$Fe(CO)_4I_2$ occurs.

Finally, the ^{129}I Mössbauer spectrum has been measured and the isomer shift and quadrupole coupling interpreted in terms of the nature of the Fe—I bond.

Results and Discussion

cis-$^{57}Fe(CO)_4X_2$

The observed isomer shifts and quadrupole splittings for *cis*-$Fe(CO)_4Cl_2$, -Br_2, and -I_2 are reported in Table 1, together with the parameters previously reported for *cis*-$Fe(CO)_4I_2$. The data for $Fe(CO)_5$ are provided to allow a further comparison of the results of these experiments with those of previous work. A sample spectrum is shown in Fig. 1. It is observed that the results for $Fe(CO)_4I_2$ are in striking disagreement with those of Herber *et al.* (1) and Fluck *et al.* (2), and while they are similar to, they are not in exact agreement with those of Collins and Pettit (3). We understand that Bancroft (6) has also studied these compounds and that the results of the present work are in reasonably good agreement with those of that investigator.

The spectra for *cis*-$Fe(CO)_4Cl_2$ and -Br_2 were found to be very similar to those of *cis*-$Fe(CO)_4I_2$.

Bancroft *et al.* (7, 8) have studied a very large number of Fe^{II} low-spin compounds and have proposed values for the partial quadrupole splittings for a number of ligands, and in particular (8): $[Cl^-] = -0.30$, $[Br^-] = -0.28$, $[I^-] = -0.29$. In the light of ^{57}Fe studies on a series of $Fe(CO)_4(SnX_3)_2$ and $Fe(CO)_4XSnX_3$ compounds we have proposed (9), in conjunction with the measurements of Bancroft *et al.* (8), that the CO ligand has a partial quadrupole splitting of $[CO] = -0.55$. The data of the present work allow a further estimate of [CO]. The point charge model predicts (7) that for the *cis*-$Fe(CO)_4$-

TABLE 1. ^{57}Fe Mössbauer parameters at 80 °K*

Compound	δ (mm s^{-1})	Δ (mm s^{-1})	2Γ (mm s^{-1})	Reference
$Fe(CO)_4Cl_2$	0.31	0.26	0.25	This work
$Fe(CO)_4Br_2$	0.32	0.31	0.24	This work
$Fe(CO)_4I_2$	0.32	0.32	0.26	This work
	0.85	0.85		1
	0.80 (147 °K)	0.74 (147 °K)		2
	0.40	0.38		3
$Fe(CO)_5$	0.17	2.51	0.28	This work
	0.17 (143 °K)	2.57 (143 °K)		1
	0.16	2.53		2

*δ with respect to sodium nitroprusside. The errors in δ, Δ, and 2Γ are 0.01 mm s^{-1}.

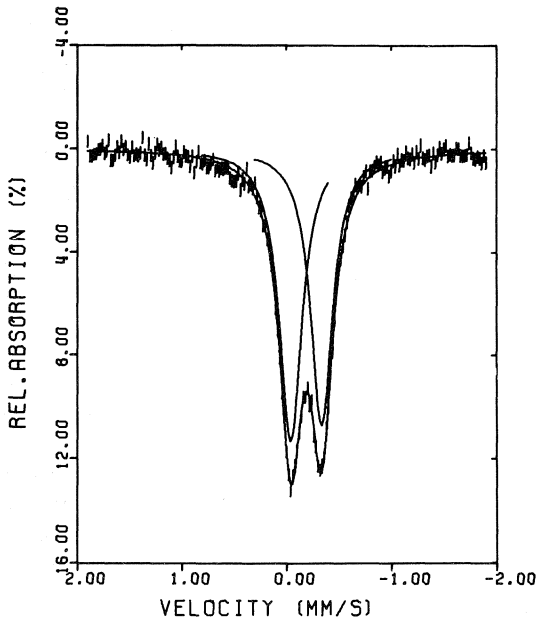

FIG. 1. The ^{57}Fe Mössbauer spectrum of $Fe(CO)_4I_2$ measured at 80 °K with the ^{57}Co/Pd source at room temperature.

X_2 compounds assuming octahedral geometry:

$$\Delta = +2[CO] - 2[X]$$

Thus using the value [X] = −0.3 and the mean Δ value for $Fe(CO)_4X_2$ we may conclude that [CO] = −0.45 or −0.15, depending on the sign of Δ in these compounds. The larger of these values is obviously nearer to the previously derived value of −0.55, although the agreement is not very good. However, the errors in this and the previously reported p.q.s. value are about 5–7% and thus the values of −0.45 and −0.55 may lie within the error limits of the measurements. Alternatively the molecules concerned may not be perfectly octahedral in which case the simple analyses presented here and in ref. 9 would not be applicable.

The Photolysis of cis-$Fe(CO)_4I_2$ in Solution

Noak (5) reported some time ago that on irradiating solutions of *cis*-$Fe(CO)_4I_2$ with visible light, a new band appeared at 2081 cm^{-1} in the i.r. spectrum, and this line was assigned to *trans*-$Fe(CO)_4I_2$. A similar observation was made by Johnson *et al.* (4), who further suggested that the *trans*-$Fe(CO)_4I_2$ might be an unstable intermediate in the photolytic decomposition of the *cis*-isomer.

In the present study we have followed the effect of irradiating cyclohexane solutions by studying both the i.r. spectrum of the liquid and the ^{57}Fe Mössbauer spectrum of frozen samples of the irradiated solution. The i.r. spectrum clearly showed the appearance of a single absorption line at 2082 cm^{-1}, as shown in Fig. 2. In contrast, the parameters of the Mössbauer spectrum showed no change within the error of the measurement, as illustrated in Fig. 2 and Table 2. The % effect in the Mössbauer spectrum decreased with irradiation time as a result of decomposition of the solution and the formation of a solid residue.

Johnson *et al.* (4) observed that the line assigned to the *trans*-isomer in the i.r. disappeared on standing irradiated solutions in the dark, and that the lines due to the *cis*-isomer did not increase in intensity. They proposed on this basis that the *trans*-isomer was unstable and decomposed on standing. It was important to establish that this process does not occur in the frozen cyclohexane glass. The i.r. spectra of samples of the irradiated solutions immediately before and following a Mössbauer experiment were found to be identical, both containing a very intense line at 2082 cm^{-1} and it is concluded that the species giving

Can. J. Chem. Downloaded from www.nrcresearchpress.com by 210.87.254.42 on 09/05/12
For personal use only.

TABLE 2. Photolysis studies*

Condition	δ† (mm s^{-1})	Δ (mm s^{-1})	2Γ‡ (mm s^{-1})	χ_i^2§
Fresh solution *cis*-$Fe(CO)_4I_2$ in cyclohexane	0.31 ± 0.01	0.33 ± 0.01	0.31	192
2 h irradiation	0.32 ± 0.02	0.37 ± 0.02	0.32	194
4 h irradiation	0.32 ± 0.02	0.35 ± 0.02	0.32	195
5½ h irradiation	0.36 ± 0.03	0.37 ± 0.03	0.32	218

*Carried out in dry cyclohexane solution under dry N_2 at room temperature. Portions of the photolyzed solutions were then frozen in liquid nitrogen.
†δ with respect to sodium nitroprusside.
‡Linewidths ±0.01 mm s^{-1}.
§χ_i^2 values for 198 degrees of freedom.

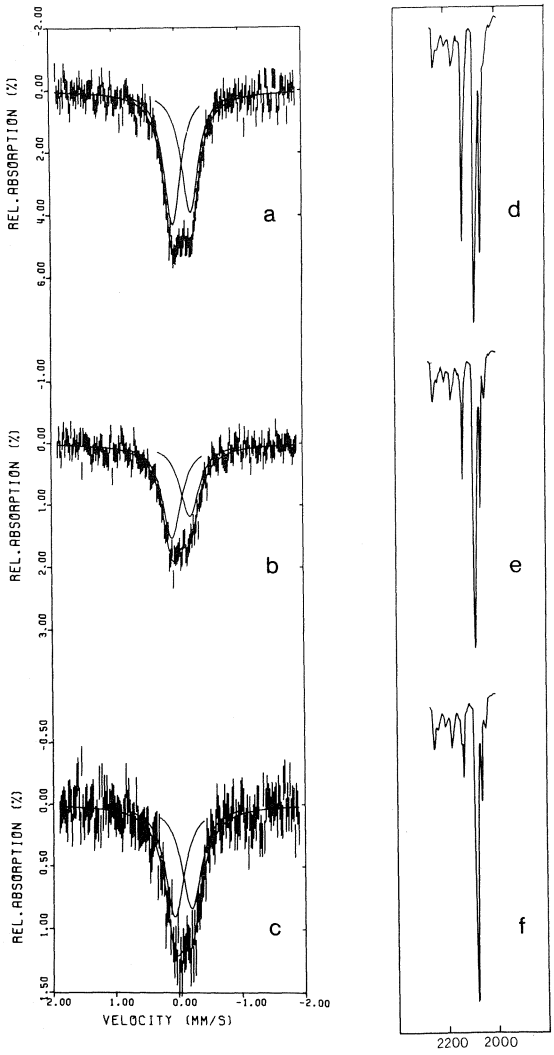

FIG. 2. The ^{57}Fe Mössbauer spectra and i.r. spectra of photolyzed cyclohexane solutions of $Fe(CO)_4I_2$, where *a*, *d* = fresh solution; *b*, *e* = 4 h irradiation; *c*, *f* = 5½ h irradiation.

rise to this absorption in the i.r. did not decompose in the frozen glass at 80 °K.

If the irradiation of the cyclohexane solution produced *trans*-$Fe(CO)_4I_2$, then it would be expected on the basis of the point charge model that the ^{57}Fe quadrupole splitting for this compound would be twice that of the *cis*-isomer. Within the error of the measurement, the Mössbauer spectrum was not found to change on irradiation. It is apparent that the Mössbauer experiment does not provide any positive evidence for the formation of *trans*-$Fe(CO)_4I_2$.

Thus, if the recoil-free fractions for *cis*- and *trans*-$Fe(CO)_4I_2$ were comparable, then lines attributable to the *trans*-isomer should be readily observable in the Mössbauer spectrum Fig. 5*c*, even though this spectrum is of poor quality. The i.r. spectra may be explained by the presence in solution of a dimer $[Fe(CO)_4I]_2$ which may fortuitously have Mössbauer parameters similar to that of *cis*-$Fe(CO)_4I_2$.

cis-$Fe(CO)_4{}^{129}I_2$

The ^{129}I Mössbauer absorption spectrum of $Fe(CO)_4{}^{129}I_2$ is shown in Fig. 3, and the computed parameters (10) for this spectrum were found to be

$$\delta = +0.11 \pm 0.02 \text{ mm s}^{-1}$$
$$e^2qQ = -980 \pm 10 \text{ Mc s}^{-1}$$
$$\eta = 0.00 \pm 0.02$$

The linewidths, constrained as equal, were found to be 1.2 mm s^{-1}.

If we assume, using the theory of Townes and Dailey (11), that the quadrupole coupling derives from the imbalance in the population of the iodine 5p orbitals, then

$$U_p = -\frac{e^2qQ_{mol}}{e^2qQ_{atom}}$$

Can. J. Chem. Downloaded from www.nrcresearchpress.com by 210.87.254.42 on 09/05/12
For personal use only.

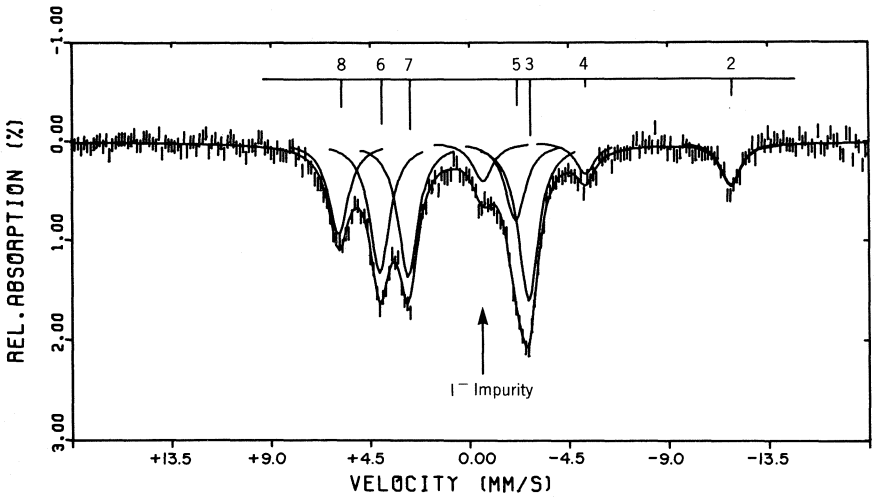

FIG. 3. The ^{129}I Mössbauer spectrum of $Fe(CO)_4{}^{129}I_2$ measured with the $Zn^{129m}Te$ source and the absorber at 80 °K. The computed independent Lorentzians are shown, and the lines had intensities in excellent agreement with the square of the Clebsch–Gordon coefficients for the respective transitions (20).

where

$$U_p = -U_z + \frac{U_x + U_y}{2}$$

and where e^2qQ_{mol} is the quadrupole coupling in the molecule of interest, e^2qQ_{atom} is that for one $5p_z$ electron ($= +1607$ Mc s^{-1} for ^{129}I) and U_x, U_y, and U_z are the population of the $5p_x$, $5p_y$, and $5p_z$ orbitals.

$$U_p = +0.61 \pm 0.01$$

The sign of e^2qQ_{mol} is consistent with the formation of a bond along the z axis and, together with the fact that $\eta = 0$, we may propose that

$$U_x = U_y = 2 \text{ when } U_z = 1.39$$

We may now turn to an examination of the isomer shift. Bukshpan *et al.* (12) have derived expressions for the dependence of the ^{129}I Mössbauer isomer shift on the number of holes in the iodine 5s (h_s) and 5p (h_p) orbitals. If it is assumed that the iodine uses only a 5p orbital in bonding to the iron, then for small values of h_p

$$\delta = 1.50h_p - 0.54$$

$$0.11 = 1.50h_p - 0.54$$

and

$$h_p = 0.43 \pm 0.03$$

It must be noted that

$$h_p = 6 - (U_x + U_y + U_z)$$

and if $U_x = U_y = 2$,

$$h_p = 2 - U_z = U_p$$

However from the above it is apparent that $h_p \neq U_p$, and it must be concluded that the bonding to the iodine does not occur exclusively through a σ-bond involving an iodine 5p orbital. One explanation for the observed h_p and U_p values may be the participation of the iodine 5s orbital in bonding. Using the expression (12)

$$\delta = -8.2\,h_s + 1.50\,h_p - 0.54$$

which approximately reflects the influence on δ of the removal of both 5s and 5p electrons, and assuming $h_p = 0.61$, $h_s = 0.03$ and thus only a 5% contribution by the iodine 5s orbital would lead to the observed isomer shift. It must be noted that the above analysis is only a tentative one, since the above expression (12) for δ in terms of h_s and h_p has never been rigorously tested. However, the participation of some 5% s-character in the bonding by the iodine would not be unexpected given the large electronegativity difference between the iron and the iodine.

An alternative explanation for the observed isomer shift and quadrupole splitting could lie in back-bonding from the filled d_{xy}, d_{yz}, and d_{xz} orbitals on the iron into the empty d orbitals on the iodine. If we assume that such an effect would not markedly influence the quadrupole coupling (11), but would decrease the isomer shift through shielding of the $5s^2$ electrons, this would be consistent with the values of h_p and U_p calculated

Can. J. Chem. Downloaded from www.nrcresearchpress.com by 210.87.254.42 on 09/05/12
For personal use only.

TABLE 3. Infrared carbonyl stretching frequencies*

Compound	ν(cm^{-1})			
$Fe(CO)_4Cl_2$-*cis*	2164w	2125s	2112m	2085m
$Fe(CO)_4Br_2$-*cis*	2155m	2112vs	2105s	2079s
$Fe(CO)_4I_2$-*cis*	2134s		2085vs	2061s

*Recorded in *n*-hexane solution on a Perkin–Elmer 457 spectrometer.

TABLE 4. Chemical analyses

	X (%)		C (%)		Fe (%)	
Compound	Found	Calcd.	Found	Calcd.	Found	Calcd.
$Fe(CO)_4Cl_2$*			18.90	20.10	23.20	23.39
$Fe(CO)_4Br_2$†	48.59	48.77	14.59	14.65	16.98	17.04
$Fe(CO)_4I_2$†	60.05	60.19	11.55	11.38	13.39	13.24

*Performed in this laboratory.
†Bernhard Mikroanal. Labs.

above. However, Perlow and Perlow (13) and Bukshpan *et al.* (12) have pointed out that shielding of iodine $5s^2$ electrons by 5d electrons should be small, consistent with the Slater shielding coefficients, and that this would particularly be the case near to a closed shell configuration on the iodine (14). On this basis it is concluded that the more probable explanation is s-participation rather back-bonding into the iodine 5d orbitals.

Experimental

The compounds used in this work were synthesized by conventional methods (15). They were characterized by their infrared spectra (Table 3) and by chemical analyses (Table 4). The more unstable chloride was analyzed in this laboratory and only C (C, H, and N Perkin–Elmer analyzer) and Fe (atomic absorption) analyses were carried out. Several samples of each compound were independently synthesized, characterized, and studied. All yielded values in good agreement with those results shown in Tables 1, 3, and 4.

The ^{129}I labelled $Fe(CO)_4{}^{129}I_2$ was prepared on a small scale by reacting *ca.* 60 mg in total of $^{129}I_2 + {}^{127}I_2$ with $Fe(CO)_5$ in dry ether under dry nitrogen. The solid residue from the reaction was extracted with dry hexane and the final product obtained on evaporation of the hexane extracts. The compound gave an ^{57}Fe Mössbauer spectrum and an i.r. spectrum identical with that of $Fe(CO)_4{}^{127}I_2$ prepared on the gram scale, the ^{57}Fe spectrum being run immediately before and after the ^{129}I spectrum. The sample contained *ca.* 20 mg of ^{129}I. The ^{129}I was obtained from Oak Ridge National Laboratories as I^- in sulfite, the iodine being obtained by oxidation and centrifugation. The ethereal solution containing added $^{127}I_2$ was dried over molecular sieve before being used in the above preparation.

The photolysis studies were carried out in dry cyclohexane under dry nitrogen, using visible light and a cold-finger device to minimize any thermal decomposition during the irradiation. About 5 ml of solution were irradiated at a time. The irradiation produced a solid residue and aliquots of the liquid removed by syringe for the i.r. and Mössbauer studies were filtered through a cotton-wool plug. The Mössbauer samples (*ca.* 0.2 ml) were transferred to Teflon thin-windowed, O-ring containers and the samples frozen by immersion in liquid nitrogen prior to placing them in the spectrometer.

The ^{57}Fe Mössbauer experiments were carried out essentially as previously described (9) using a T.M.C. constant acceleration Mössbauer drive unit and multichannel analyzer, with the absorbers at *ca.* 80 °K and the ^{57}Co/Pd source (10 mCi) at room temperature. In the ^{129}I experiment the source used was $Zn^{129m}Te$ prepared from elemental zinc and ^{129m}Te-labelled tellurium, the latter being obtained by irradiating 50 mg of ^{128}Te (enriched) for 2 weeks in the N.R.U. reactor at Chalk River Nuclear Laboratories. The ^{129}I spectra were recorded (16) on an NSEC. AM-1 spectrometer and cryoflask with the source and absorber at *ca.* 80 °K. The two spectrometers were routinely calibrated using a nitroprusside standard ($\delta = -0.442$ mm s^{-1} with respect to ^{57}Co/Pd and $\Delta = 1.712$ mm s^{-1}) and α-Fe_2O_3 for which the line spacings in ref. 17 were assumed. Computed fits to the data were obtained using a program kindly provided by Stone (ref. 18, Appendix).

The δ and e^2qQ values for ^{129}I were arrived at using least-squares fits to the line positions. Assuming that if the asymmetry parameter is small, the position of each line δ_{ij}, in the ^{129}I quadrupole split spectrum is described in terms of e^2qQ and δ by the expression (19)

$$\delta_{ij} = \frac{ce^2qQ_{gnd}}{4E_\gamma}\left[\frac{Q_{ex}}{Q_{gnd}}\frac{(C_0^* + C_2^*\eta^2)}{I^*(2I^* - 1)} - \frac{(C_0 + C_2\eta^2)}{I(2I - 1)}\right] + \delta$$

where δ_{ij} is the line position corresponding to the $m_i \rightarrow m_j$ transition, δ is the isomer shift, and C^* and C refer to the excited and ground states, respectively, where

Can. J. Chem. Downloaded from www.nrcresearchpress.com by 210.87.254.42 on 09/05/12
For personal use only.

$$C_0 = 3m^2 - I(I+1)$$

$$C_2 = \frac{1}{12}\frac{f(I,m-1)}{m-1} - \frac{f(I,m+1)}{m+1}$$

$$f(I,m) = \tfrac{1}{4}(I^2 - m^2)[(I+1)^2 - m^2]$$

and Q_{ex}/Q_{gnd} is the ratio of the quadrupole moments of the excited and ground states, taken as $+1.231 \pm 0.001$. Pasternak and Sonnino (20) have tabulated the line positions in terms of e^2qQ, δ and η^2, for small values of η. Initially lines 2, 3, 5, 6, and 7 are used in obtaining δ and e^2qQ while lines 4 and 8 are used to estimate η. Since $\eta \cong 0$, the final values of δ and e^2qQ were obtained from all seven lines.

In fitting the ^{57}Fe spectra for the solid $Fe(CO)_4X_2$ compounds no constraints were applied in the fit, while for the frozen solutions of $Fe(CO)_4I_2$ and also for the $Fe(CO)_4{}^{129}I_2$ study, the linewidths were constrained as being equal. Generally the fits obtained gave χ-squared values within the 5% confidence limit.

The authors wish to thank the National Research Council of Canada for a grant supporting this research, Dr. F. Brown, Head, Solid State Research Branch, AECL, Chalk River for his assistance in the production of the $Zn^{129m}Te$ source, and Dr. G. M. Bancroft for communicating his ^{57}Fe results to us.

1. R. H. Herber, R. B. King, and G. K. Wertheim. Inorg. Chem. **3**, 101 (1964).
2. E. Fluck, W. Kerler, and W. Neuwirth. Angew. Chem. Int. Engl. Ed. **2**, 277 (1963).
3. R. L. Collins and R. Pettit. J. Chem. Phys. **39**, 3433 (1963).
4. B. F. G. Johnson, J. Lewis, and P. W. Robinson. J. Chem. Soc. A, 1043 (1968).
5. K. Noak. Helv. Chim. Acta. **45**, 1847 (1962).
6. G. M. Bancroft. Private communication.
7. G. M. Bancroft, M. J. Mays, and B. E. Prater. J. Chem. Soc. A, 956 (1970).
8. G. M. Bancroft, R. E. B. Garrod, and A. G. Maddock. J. Chem. Soc. A, 3165 (1971).
9. N. Dominelli, C. H. W. Jones, E. Wood, and P. Vasudev. Submitted to Inorg. Nucl. Chem. Lett.
10. M. Pasternak. Symp. Faraday Soc. **1**, 119 (1967).
11. C. H. Townes and B. P. Dailey. J. Chem. Phys. **17**, 782 (1949).
12. S. Bukshpan, C. Goldstein, and S. Soriano. J. Chem. Phys. **51**, 3976 (1969).
13. G. J. Perlow and M. R. Perlow. J. Chem. Phys. **45**, 2193 (1966).
14. G. J. Perlow. Chemical applications of Mössbauer spectroscopy. *Edited by* V. I. Goldauskii and R. H. Herber. Academic Press, New York. 1968. p. 410.
15. W. Hieber and G. Bader. Ber. Deutsch. Chem. Ges. **61**, 1717 (1928).
16. J. L. Warren, C. H. W. Jones, and P. Vasudev. J. Phys. Chem. **75**, 7867 (1971).
17. M. Muir, K. J. Ando, and H. M. Coogan (*Editors*). Mössbauer Effect Data Index 1958–1965. Interscience, New York. 1966. p. 26.
18. G. M. Bancroft, W. K. Ong, A. G. Maddock, R. H. Prince and A. J. Stone. J. Chem. Soc. (A), 1966 (1967).
19. R. Bersohn. J. Chem. Phys. **20**, 1505 (1952).
20. M. Pasternak and T. Sonnino. J. Chem. Phys. **48**,1997 (1968).

Can. J. Chem. Downloaded from www.nrcresearchpress.com by 210.87.254.42 on 09/05/12
For personal use only.

Isotope Effects on Chemical Equilibria. Part I. Some Secondary Isotope Effects of the Second Kind

D. J. BARNES AND J. M. W. SCOTT

Chemistry Department and Faculty of Medicine, Memorial University of Newfoundland, St. John's, Newfoundland

Received April 5, 1972

Secondary isotope effects $K_a(H)/K_a(D)$ for the isotopic acid pairs 4-X-$C_6H_4CH_2COOH$/4-X-$C_6H_4CD_2COOH$(X = H, NO_2, OMe) have been determined at $T = 25$ °C by conductance measurements. This has involved the redetermination of the dissociation constants for the non-deuterated acids and in the case of X = NO_2, OCH_3, the new K_a values are to be preferred. The K_a of acetic acid has also been redetermined as a check on the reliability of the new data. The three isotope effects are shown to be much smaller than might have been anticipated on the basis of the e.m.f. measurements on the pair $PhCH_2COOH/PhCD_2COOH$ reported earlier (1).

Les effets isotopiques secondaires $K_a(H)/K_a(D)$ pour la paire d'acides isotopiques 4-X-$C_6H_4CH_2$-COOH/4-X-$C_6H_4CD_2COOH$ (X = H, NO_2, OCH_3) ont été évalués à $T = 25$ °C par de mesures de conductance. Ceci a impliqué une nouvelle détermination des constantes de dissociation pour les acides non-deutériés et dans le cas où X = NO_2, OCH_3 les nouvelles valeurs de K_a doivent etre préférées. Le K_a de l'acide acétique a aussi été évalué de nouveau comme standard d'exactitude des nouvelles données. Les trois effets isotopiques trouvés sont beaucoup plus petits que prévus si l'on se base sur les mesures de f.e.m. pour la paire $Ph_2CH_2COOH/PhCD_2COOH$ rapportées précédemment (1).

[Traduit par le journal]

Can. J. Chem., **51**, 411 (1973)

Introduction

The changes in dissociation constants which occur when hydrogen is replaced by deuterium in the side chains of carboxylic and ammonium acids have been studied on several occasions (1–5). The problem of predicting and understanding these subtle effects of structure on reactivity using the statistical theory of equilibria (6) has not proved particularly rewarding since a full treatment of the problem requires a complete knowledge of the reactant and product vibrational frequencies appropriate to the condensed phase in which the equilibria are examined. In practice these latter quantities are rarely available. A partial exception is exemplified by the calculation of the relative acidities of formic acid and formic acid-*d*, by Bell and Crooks (2) using the observed fundamental frequencies appropriate to the isotopic acids.

The general lack of such vibrational data has forced both theoreticians and experimentalists to devise other models to cope with secondary hydrogen–deuterium isotope effects. These latter treatments suggest that changes in reactivity resulting from the replacement of hydrogen by deuterium can be discussed in terms of hybridization, steric or non-bonded interactions, hyperconjugation or inductive effects (see references in ref. 7). Although the hyperconjugative and inductive treatments superficially appear to be electronic in origin, the Born–Oppenheimer principle is retained and the model can still be understood in terms of mass effects on vibrations. Thus, the hyperconjugative and inductive description can be recast in vibrational–statistical language, but by formally avoiding the vibrational treatment some simplification is lent to what is evidently a complex problem. The least that can be asked of this and other simplified approaches to the understanding of secondary isotope effects is that the 'as if' treatments maintain a reasonable degree of fidelity in their representation of the experimental data, *i.e.* that they be self-consistent.

Isotope effects, in which the spatial orientations of the bonds linking the isotopic atoms to the molecule are altered, are described by Streitwieser and coworkers (8) as secondary isotope effects of the first kind. Other possible processes in which spatial reorganization is absent are described as secondary isotope effects of the second kind. It has been proposed by Halevi (7), that isotope effects of the second kind behave like inductive effects. Thus, the variation of secondary isotope effects of this sort with both the structure and the position of deuteration

Can. J. Chem. Downloaded from www.nrcresearchpress.com by 210.87.254.42 on 09/05/12
For personal use only.

TABLE 1. Acid strength data related to the Taft correlation for substituted acetic acids

Acids	pK_a[a]	σ*	X_1	X_2	X_3	Σσ*
$CX_1X_2X_3COOH$						
CF_3COOH	0.23	—	F	F	F	9.30
CCl_3COOH	0.65	2.65	Cl	Cl	Cl	8.70
CBr_3COOH	0.66	—	Br	Br	Br	8.40
CHF_2COOH	1.24	2.05	F	F	H	6.69
$CHCl_2COOH$	1.29	1.74	Cl	Cl	H	6.29
$(CH_3)_3NCH_2COOH$	1.83	1.90	$(CH_3)_3N$	H	H	—
$CNCH_2COOH$	2.43	1.3	CN	H	H	4.62
CH_2FCOOH	2.59	1.10	F	H	H	4.08
$CH_2(COOH)_2$	2.83	1.05	COOH	H	H	—
$CH_2ClCOOH$	2.90	1.00	Cl	H	H	3.88
$CH_2BrCOOH$	3.07	0.92	Br	H	H	3.78
CF_3CH_2COOH	3.12	0.85	CF_3	H	H	—
$C_6H_5OCH_2COOH$	3.18	0.85	PhO	H	H	—
CH_2ICOOH	3.53	0.52	I	H	H	3.38
CH_3OCH_2COOH	3.58	0.60	CH_3O	H	H	—
HCOOH	3.77	0.49	—	—	—	—
$NO_2CH_2CH_2COOH$	3.81	0.50	NO_2CH_2	H	H	1.48
$(C_6H_5)_2CHCOOH$	3.94	0.45	C_6H_5	C_6H_5	H	2.45
$(C_6H_5)_3CCOOH$	3.96	—	C_6H_5	C_6H_5	C_6H_5	2.94
CH_2ClCH_2COOH	4.08	0.385	CH_2Cl	H	H	2.52
$C_6H_5CH_2COOH$	4.31	0.215	C_6H_5	H	H	1.58
$CF_3CH_2CH_2COOH$	4.49	0.320	CF_3CH_2	H	H	1.50
$C_6H_5CH_2CH_2COOH$	4.66	0.080	$C_6H_5CH_2$	H	H	1.195
CH_3COOH	4.76	0.00	H	H	H	1.47
$(CH_3)_2CHCOOH$	4.86	−0.19	CH_3	CH_3	H	0.49
CH_3CH_2COOH	4.88	−0.100	CH_3	H	H	0.98
$CH_3CH_2CH_2COOH$	4.82	−0.115	CH_3CH_2	H	H	0.88
$CH_3CH_2(CH_3)CHCOOH$	4.78	−0.21	CH_3CH_2	CH_3	H	0.39
$(CH_3)_3CCOOH$	5.05	−0.30	CH_3	CH_3	CH_3	0.00

[a]All pK_a values were taken from ref. 10 except those of the monohalogenoacetic acids, which were taken from ref. 11. The substituent constant parameters were taken from tabulations in ref. 9.

Can. J. Chem. Downloaded from www.nrcresearchpress.com by 210.87.254.42 on 09/05/12
For personal use only.

should be amenable to a linear free energy treatment such as that proposed by Taft (9). A test of such a hypothesis has been presented already by Streitwieser and Klein (5) and a further modification of their work will be presented here, using the Taft equation as applied to the acidities of carboxylic acids of the type XCH_2COOH.

The original correlation presented by Taft (9) for the pK_a's of a series of seven carboxylic acids (X-COOH) was of the form:

$$[1] \qquad \log K/K_0 = (1.721 \pm 0.025)\sigma^*$$

where σ* is the Taft substituent constant of the group X attached to the carboxyl group. Equation 1 can be rewritten in the form:

$$[2] \qquad pK_a = -(1.721 \pm 0.025)\sigma^* + 4.76$$

Extension of the empirical data to 26 substituted acetic acids (Table 1) gives:

$$[3] \qquad pK_a = -(1.603 \pm 0.030)\sigma^* + 4.604 \pm 0.029$$

with average r.m.s. deviation of ±0.16 pK_a units. In cases where the group X can be treated as a substituted methyl group, *i.e.* $X = CX_1X_2X_3$, it is possible to set up a modified version of eq. 3 in which the total inductive effect of the group X is measured to a first approximation, by the sum of the separate contributions of X_1, X_2, and X_3, leading to a quantity Σσ* which is defined by the equation:

$$[4] \qquad \Sigma\sigma^* = \sigma^*(X_1) + \sigma^*(X_2) + \sigma^*(X_3)$$

For the 22 substituted acetic acids listed in Table 1, for which values of Σσ* are available, a least squares treatment gives:

$$[5] \qquad pK_a = -(0.550 \pm 0.059)\Sigma\sigma^* + 5.200 \pm 0.014$$

leading to an average r.m.s. deviation of ±0.25 pK_a unit. This correlation is evidently inferior to that presented in eq. 3; nevertheless, it is possible to use the experimental $K(H)/K(D)$ ratios for the pairs CH_3COOH/CD_3COOH and $(CH_3)_3$-

Can. J. Chem. Downloaded from www.nrcresearchpress.com by 210.87.254.42 on 09/05/12
For personal use only.

$CCOOH/(CD_3)_3CCOOH$ in conjunction with eq. 5 to evaluate $\sigma^*(D)$ and $\sigma^*(CD_3)$. The $K(H)/K(D)$ ratio for the acetic acid pair is well established (5, 12), the ratio for the pivalic acid pair is that reported by Streitwieser and Klein (5). Substituting these ratios in eq. 5 gives $\sigma^*(D) = 0.482$ and $\sigma^*(CD_3) = -0.011$. These values, together with eqs. 5 and 3 make it possible to evaluate theoretical $K(H)/K(D)$ values for the remaining carboxylic acids in Table 2. Hall (13) has demonstrated that the pK_a's of primary, secondary, and tertiary amines are respectively correlated with the Taft σ^* parameter according to the equations:

$$[6] \quad pK_a(\text{primary}) = -3.14 \sum\sigma^* + 13.23$$

$$[7] \quad pK_a(\text{secondary}) = -3.23 \sum\sigma^* + 12.13$$

$$[8] \quad pK_a(\text{tertiary}) = -3.30 \sum\sigma^* + 9.61$$

where the $\sum\sigma^*$ parameter now refers to the substituents bound to nitrogen. From eqs. 6 and 7 and the value previously calculated for $\sigma^*(CD_3)$, the $K(H)/K(D)$ ratios for the ammonium acid pairs investigated by Robertson and coworkers (3, 4) can be calculated.

An examination of the predictions in Table 2 reveals that the calculated isotope ratios are qualitatively consistent with the inductive treatment. Quantitatively, however, the agreement is poor. The observed ratio for the pair $PhCH_2COOH/PhCD_2COOH$ is particularly difficult to understand since there is no obvious reason why the phenyl group should enhance the isotope effect observed in the case of acetic acid, particularly when the number of deuterium atoms per molecule is reduced.

One can conclude from the above discussion that there is clearly a need for a broader experimental basis from which to construct generalizations (14). To this end we report here a reinvestigation of phenylacetic acid. We also report $K(H)/K(D)$ ratios for the pairs 4-MeO-$C_6H_4CH_2COOH$/4-MeO-$C_6H_4CD_2COOH$ and 4-NO_2-$C_6H_4CH_2COOH$/4-NO_2-$C_6H_4CD_2$-COOH. To a first approximation, the simple inductive treatment outlined above suggests that the isotope effect on these three systems should be constant and considerably smaller than that reported by Halevi (1) for the unsubstituted isotopic pair.

TABLE 2. Predicted and observed isotope effects

Isotopic Pair	$K(H)/K(D)$ Observed (ref.)	Calculated
CH_3COOH/CD_3COOH	1.035 (12)	—
$(CH_3)_3CCOOH/(CD_3)_3CCOOH$	1.04 (5)	—
HCOOH/DCOOH	1.07 (5)	1.03
$CH_3CH_2COOH/CD_3CH_2COOH$	1.01 (1)	1.014
$CH_3CH_2COOH/CH_3CD_2COOH$	1.08 (1)	1.021
$PhCH_2COOH/PhCD_2COOH$	1.12 (1)	1.021
$CH_3{}^+NH_3/CD_3{}^+NH_3$	1.13 (3)	1.083
$(CH_3)_2{}^+NH_2/(CD_3)_2{}^+NH_2$	1.32 (3)	1.18
$(CH_3)_3{}^+NH/(CD_3)_3{}^+NH$	1.53 (4)	1.29

At the commencement of the present study isotope effects of the order of 12% were anticipated.[1] Secondary isotope effects of the second kind which reach this magnitude must be considered as large. For instance, the introduction of the methoxy substituent into the aromatic ring of phenylacetic acid produces about the same effect on acidity as replacing the methylene hydrogens in the same molecule by deuterium in the unsubstituted acid.

A careful survey of the rather extensive conductance data available for carboxylic acids suggested that it should be possible to measure individual K_a values to $\pm 0.2\%$ without undue difficulty and it was hoped that this order of accuracy would suffice to detect substituent effects on secondary isotope effects if they existed. The requirements for precise measurements of acid dissociation constants are implied in some very careful work reported by Ives and coworkers (11, 15). The high precision obtained by the Ives' group is probably a consequence of the strength of the acids studied ($K_a \simeq 10^{-3}$). It would appear that the phenylacetic acids, which are *ca.* 10 times weaker, are less suitable to the conductance technique for reasons which will be considered subsequently. Thus with respect to the individual K_a's for the protium and deuterium analogs we prefer to describe the present study as one of intermediate accuracy. However, if certain conditions are met it appears possible to determine $K(H)/K(D)$ ratios for an isotopic pair with much higher precision than the individual K_a values and in this respect the conductance method would appear to be superior to other methods which might be chosen.

Experimental

General

All melting points and boiling points are uncorrected. N.m.r. spectra were obtained using a Varian A60 spectro-

[1]Assuming the veracity of the data in ref. 1.

meter and chemical shifts are reported on the τ scale relative to tetramethylsilane (TMS) as an internal standard. Both n.m.r. and a v.p.c./combustion technique (16) were used for deuterium analysis. All organic solvents were distilled prior to use or were of known grade of purity.

Preparation of Materials

Protium Acids

The protium acids used in the present study, acetic acid, phenylacetic acid, 4-methoxyphenylacetic acid, and 4-nitrophenylacetic acid were commercial samples or samples prepared by well established routes. In some cases more than one batch of the acid was prepared and each batch was intensively purified. The constancy of the K_a as determined by conductance was taken as the main criterion of purity since the conductance technique is very sensitive to contaminants in both solvent and solute alike.

Acetic Acid

Acetic acid (A.R. Grade) was fractionally frozen twice and then fractionated using a gold spinning band column with liberal rejection of the initial and tail fractions. The fraction used for the dissociation constant measurements had a b.p. 117.5–118 °C/750 mm Hg.

Phenylacetic Acid

Runs 1–6. A commercial sample of phenylacetic acid was recrystallized twice from conductivity water and once from pentane (b.p. 40–50 °C). It was stored over phosphorus pentoxide for 2 days and then over silica gel.

Runs 9–17.[2] A sample of phenylacetic acid was crystallized twice from water and then sublimed. It was then recrystallized twice from cyclohexane and once from water. The specimen resulting from this purification procedure was dried *in vacuo* in a drying pistol at the temperature of boiling acetone.

4-Nitrophenylacetic Acid

Runs 5–8. A commercial sample of 4-nitrophenylacetic acid was recrystallized twice from conductivity water, sublimed, and then recrystallized two more times from the same solvent. The sample so purified was then dried using the same technique employed in the case of the final specimen of phenylacetic acid.

Runs 9–11. A sample of the acid was sublimed, recrystallized twice from water, and then dried in the same manner as the sample used in runs 5–8.

4-Methoxyphenylacetic Acid

4-Methoxybenzyl chloride was synthesized according to the method of Lee and co-workers (17) and was converted to the cyanide as described by Friedman and Shechter (18). The 4-methoxybenzyl cyanide was hydrolyzed with alcoholic sodium hydroxide. The resulting sodium salt was dissolved in the minimum of water and 4-methoxyphenylacetic acid precipitated by adding hydrochloric acid. The precipitated acid was collected, washed with cold water and pentane, and dried *in vacuo* over phosphorus pentoxide, m.p. 85–86 °C (lit. m.p. 86 °C (19)).

Runs 1–6. A sample of the acid was recrystallized from water, dissolved in carbonate, and treated with charcoal. The resulting solution was then treated with hydrochloric acid and the product recrystallized twice from cyclohexane. Two further recrystallizations from conductivity water were carried out and the sample was dried in the same manner as the final specimen of the unsubstituted acid.

The Deuterated Acids

The deuterated acids were all prepared by an exchange reaction in deuterium oxide using triethylamine as a catalyst. The progress of the exchange was monitored by n.m.r. using the integration of the methylene protons against the aromatic protons of the acid. It was reasonably assumed that no exchange of the aromatic protons took place under the relatively mild basic conditions used in these experiments (20).

Phenylacetic-α,α-d_2 Acid

Phenylacetic acid (10 g), dissolved in deuterium oxide (15 ml) and triethylamine (5 ml), was placed in a flask equipped with both a condenser and drying tube. The flask was heated in an oil bath at 110 °C for 52 h, and after this period n.m.r. analysis on an aliquot of the solution indicated 88.2% deuteration at the methylene position. The contents of the flask were cooled and the mixture was acidified with DCl (6 *N*) prepared from deuterium oxide and the appropriate quantity of purified thionyl chloride. The precipitated acid was washed with cold cyclohexane and dried over phosphorus pentoxide *in vacuo* for 24 h. A second exchange was carried out with the partially exchanged acid using the procedure described above at 82 °C for 96 h. Analysis of this material by n.m.r. indicated 96.7% deuteration. A further exchange (48 h) followed by recovery of the acid (see above) gave a specimen of the acid which on recrystallization from cyclohexane and water had m.p. 75–76 °C. The purified specimen contained 98% deuterium in the methylene position as judged by an n.m.r. spectrum in carbon tetrachloride (overall yield 75%). Samples of the acid prepared in this way were subjected to further purification procedures (see below) with no sensible decrease in deuterium content as judged by n.m.r. analysis. The deuterated acid purified for the conductance measurements (see below) was subjected to a combustion/v.p.c. analysis (see ref. 16) giving 1.87 D/molecule (93.6% methylene deuteration). The reason for the discrepancy between the n.m.r. and combustion/v.p.c. analysis is not understood.[3]

Phenylacetic-α,α-d_2 acid was purified for conductance measurements using the following procedures:

Runs 1–4. The deuterated acid was dissolved in carbonate solution and charcoal added. The solution was warmed and filtered hot and the filtrate treated with concentrated hydrochloric acid. The resulting acid was recrystallized twice from water and dried in a pistol for 3 days *in vacuo* at the temperature of boiling acetone.

Runs 5–10. A sample of the deuterated acid was crystallized from water, dried (see above), and then recrystallized from cyclohexane. The acid was then sublimed

[2]In some cases runs were rejected. Runs 7 and 8 in the phenylacetic acid series were not used because desiccation of a specimen of this acid over phosphorus pentoxide led to decomposition. The runs reported for all the structures examined constitute over 75% of all the data recorded.

[3]Even if the lower analytical results are correct, the influence of the low deuteration on the measured K(H)/K(D) ratios is insignificant (21).

Can. J. Chem. Downloaded from www.nrcresearchpress.com by 210.87.254.42 on 09/05/12
For personal use only.

Can. J. Chem. Downloaded from www.nrcresearchpress.com by 210.87.254.42 on 09/05/12
For personal use only.

and recrystallized twice from water and dried for 4 days in the same manner as the specimen used in runs 1–4.

Runs 11–16. A sample of the deuterated acid was sublimed, recrystallized twice from cyclohexane, and then once from water. The sample was dried for 3 days as above.

4-Nitrophenylacetic-α,α-d_2 Acid

4-Nitrophenylacetic acid (10 g) was added to deuterium oxide (15 ml) and triethylamine (5 ml) and the resulting solution heated at 50 °C for 11 h. An n.m.r. spectrum of this solution showed 89.6% deuteration of the methylene protons. Concentration of this solution followed by the addition of fresh deuterium chloride (see above) and purification of the precipitated acid by recrystallization from ether–pentane gave a product, m.p. 147–150 °C (lit. 152 °C (22)), subsequent to desiccation *in vacuo* over silica gel. A further deuteration of this product at $T =$ 50 °C, (t = 11 h) gave a sample 98.8% deuterated, m.p. 148.8–150 °C. The latter was recrystallized 3 times from cyclohexane and once from water and dried at the temperature of refluxing acetone for 24 h over silica gel. A v.p.c./combustion analysis indicated that this material contained 1.85 D/molecule (92.5% methylene deuteration). The discrepancy between the n.m.r. and combustion analysis is again apparent (see footnote 3).

4-Nitrophenylacetic-α,α,d_2 acid was purified for conductance using the following procedure:

Runs 1–5. The deuterated acid was recrystallized 3 times from cyclohexane, once from water and dried for 24 h in a pistol *in vacuo*.

4-Methoxyphenylacetic-α,α-d_2 Acid

4-Methoxyphenylacetic acid (10 g) was treated with deuterium oxide (15 ml) and triethylamine (5 ml), following the procedure for deuteration of phenylacetic acid. After a period of 23 h at 100 °C an aliquot of the solution indicated 88.2% deuteration by n.m.r. analysis. Two further exchanges of the acid in deuterium oxide increased the isotopic purity to at least 98%.

4-Methoxyphenylacetic-α,α-d_2 acid was purified for conductance measurements using the following procedures:

Conductance measurements

Runs 1–4. A sample of the deuterated acid was recrystallized from cyclohexane, sublimed, recrystallized from cyclohexane and dried in a pistol at 80 °C for 3 days.

Runs 5–6. The above material was recrystallized from water and dried for several days at 80 °C.

Potassium chloride purification

Method I. Potassium chloride (Fisher Scientific A. R. Grade) was precipitated from a saturated aqueous solution prepared from conductivity water by addition of 95% ethyl alcohol and this procedure was repeated 3 times. The salt was collected by filtration, thoroughly washed with 95% ethyl alcohol, and dried *in vacuo* for several days at 110 °C. The salt was carefully powdered with an agate mortar and pestle and returned to the drying pistol for a further 2 days.

Method II. A second sample of potassium chloride was prepared by twice precipitating a saturated solution of the salt with concentrated hydrochloric acid (A.R. Grade) and once with 95% ethyl alcohol. The subsequent treatment of this specimen was identical to that described above.

Experimental Assembly and Technique

The apparatus and techniques used follow the practice of Jones and Bradshaw (23), Shedlovsky (24), and Robertson (25).

Resistances were measured on a Jones–Joseph type conductivity bridge (23) manufactured by the Tinsley Company and on a General Radio Impedance Bridge. The Tinsley Bridge, model 4896, and accessories were assembled following the description of Robertson (25) with minor modifications made necessary because some of the components were no longer commercially available. A Hewlett Packard 1000 c.p.s. AC oscillator was connected to the bridge and the balance was detected by observing a Lissajous pattern on a Hewlett Packard model 120B oscilloscope. The detector for the General Radio impedence bridge was a G.R. 1232-A tuned amplifier and a null detector. The coarse balance on this bridge was also determined with an oscilloscope (see above). Comparison of the two bridges over the resistance range 500 – 12 000 Ω showed an agreement of better than 0.05%.

Conductivity water was prepared by passing tap water of low solid content into a deionizer (Ion Exchange Products Inc., Amberlite MB-1), followed by distillation from a Barnstead still. The distillate so produced was stored in two three-necked flasks (10 l) with teflon stoppers. The flasks were treated for 3 days with boiling nitric acid and approximately a week with steam prior to use. Final purification of the water, immediately prior to the preparation of the solutions, involved treatment with a second deionizer of Amberlite resin and the collection of the pure water under an atmosphere of purified nitrogen which had been freed from all acidic and basic contaminants. Conductivity water prepared in this manner was not used for the preparation of solutions unless the specific conductivity fell in the range 1.8×10^{-7} to 3.5×10^{-7} Ω cm^{-1}.

Conductivity cells were of the Shedlovsky type (24). The cells were constructed of Pyrex glass and the electrodes were made of shiny platinum. The resulting cell constants for the five cells used were in the range 0.08–0.20. The cells described above and all glassware required for the preparation of solutions were treated with concentrated nitric acid at a temperature of 100 °C for a period of 3 days. The glassware was then steamed for the same length of time and finally rinsed several times with conductivity water.

All solutions of potassium chloride and the carboxylic acids were prepared by weight and the concentrations reported on the molal scale.[4] Weighings were performed on a Sartorius analytical balance which could be read to 0.01 mg. Water and stock solutions were weighed on a large two pan balance to the nearest 10 mg. Weights were calibrated against a set of weights standardized by the National Physical Laboratory, England. Solutions were kept under purified nitrogen at all times.

All conductivity measurements were carried out at 25 ± 0.005 °C. A 20 gal stainless steel tank, filled with transformer oil, was maintained at 25 °C by heating and

[4]The aqueous solutions of 4-nitrophenylacetic acid were distinctly photolabile. Solutions of this acid were thus made and manipulated in the dark. This fact also accounts for the rejection of runs 1–4 for this compound (see Table 7).

TABLE 3. Cell constant determinations

10^3c (molal)	Cell 1	Cell 2	Cell 3	Cell 4	Cell 5
1.3964	0.13622	0.19832	—	0.16459	—
1.3892	0.13587	0.19847	—	0.16465	—
1.3939	0.13591	0.19832	—	0.16474	—
1.6170	0.13590	0.19852	—	0.16478	—
1.7385	0.13590	0.19823	0.086881	0.16464	0.18160
Average κ	0.13596	0.19837	0.086881	0.16468	0.18160
Deviation	±0.00017	±0.00014	—	±0.00009	—

cooling the bath simultaneously. Cooling was effected by passing cold water from a 15 gal stainless steel tank through a circulating pump into a cooling coil in the bottom of the oil bath. The rate of flow of water through the cooling coil was regulated using a by-pass arrangement incorporating two control valves. The temperature of the cooling water was maintained at 17.5 ± 0.3 °C using a Techumseh 1/4 h.p. refrigerator regulated by a Wheatstone Bridge – thermistor circuit. The temperature of the oil bath was regulated by a Sargent Thermonitor (S-82050). The basic components of this device are a background heater (125 W), controlled by a variac with an intermittent knife heater (250 W), operated by a thermistor Wheatstone Bridge circuit, coupled to a variable reactor. The voltage across the bridge was reduced from 6 to 4 V resulting in considerable improvement in the performance of this device.

A platinum resistance thermometer, calibrated by the National Physical Laboratory, was used in conjunction with a Mueller Temperature Bridge, type 4772, to measure the temperature of the regulated bath in which the conductance measurements were made. Over long periods of time the bath temperature was conveniently monitored on a Honeywell recorder connected to a Wheatstone Bridge circuit containing a Fenwal thermistor as a sensing device.

Results

Cell Constants

Cell constants were determined by measuring the resistance of aqueous solutions of two independent samples of purified potassium chloride at 25 °C over the concentration range 0.001364–0.0017385, employing both the General Radio impedance bridge and the Tinsley conductivity bridge. The weights of the salt and solvent were corrected for buoyancy. Since the equation of Fuoss (26) relating equivalent conductance of KCl solutions to the concentration

$$[9]\quad \Lambda = 149.93 - 94.65c^{1/2} + 58.74c \cdot \log c + 198.4c$$

is given using the molarity scale, conversion of the concentrations from the molal to the molarity scale was necessary. These corrections were accomplished using the expressions (27).

$$[10]\quad V = N_0V_0 + N_1Q_1$$

$$[11]\quad Q_1 = 26.52 + 2.327\,(C_2)^{1/2}$$

where V represents the volume of the solution, N_0, the number of moles of water, N_1, the number of moles of KCl, V_0 the volume of a mole of water at 25 °C, Q_1 the molal volume, and C_2 the approximate concentration of the solution. These corrections were very small.

The value of the equivalent conductance at the concentrations studied was calculated using the Fuoss expression and the cell constants were evaluated from the expression

$$[12]\quad \Lambda = \frac{10^3}{c}\kappa\left[\frac{1}{R} - \frac{1}{R_S}\right]$$

where κ represents the cell constant and R and R_S represent the resistance measurements of the solution and pure solvent respectively.

The five cell constants so determined are reported in Table 3.

Conductance Data

The conductance data calculated in the usual way for the acids acetic, phenylacetic, phenylacetic-α,α-d_2, 4-methoxyphenylacetic, and 4-methoxyphenylacetic-α,α-d_2 in water at 25 ± 0.01 °C[5] are listed in Tables 4 to 10. The thermodynamic ionization constants were calculated using a treatment of conductance data developed by Shedlovsky (28) and modified by Robinson and Stokes (29). No corrections for solvent conductivity were made to the acid solutions as there is no obvious way of making such a correction.

The details of the Robinson and Stokes method (RSM) of calculating thermodynamic equilibrium constants, along with several iteration–extrapolation methods, will be presented in

[5]The regulation of the bath was better than these limits.

Can. J. Chem. Downloaded from www.nrcresearchpress.com by 210.87.254.42 on 09/05/12
For personal use only.

TABLE 4. Conductance data for acetic acid

10^4c (molal)	Run no.	Cell number and equivalent conductance 1	2	3	4	5	10^5K_a[a] (RSM)
40.55	5	25.104	25.108	25.121	25.098	25.109	1.7575
28.424	1	29.732	29.731	29.747	29.720	29.747	1.7538
23.264	2	32.740	32.729	32.756	32.729	32.735	1.7566
11.103	6	46.447	46.431	46.470	46.419	46.432	1.7612
10.133	7	48.396	48.366	48.413	48.376	—	1.7556
14.326	3	41.160	41.159	41.187	41.153	41.159	1.7561
5.9920	4	61.624	61.602	61.654	61.586	61.604	1.7555
4.1870	8	72.461	72.422	72.482	72.419	—	1.7564

[a] $K_a = 1.7566 \pm 0.0025 \times 10^{-5}$.

TABLE 5. Conductance data for phenylacetic acid

10^4c (molal)	Run no.	Cell number and equivalent conductance 1	2	3	4	5	10^5K_a[a] (RSM)
69.879	11	31.027	31.040	31.040	31.010	31.044	4.9074
63.076	5	32.528	32.548	32.535	32.535	—	4.8955
58.984	10	33.601	33.647	33.637	—	33.657	4.9108
47.217	9	37.399	37.401	37.402	37.392	37.407	4.9236
44.067	6	38.563	38.584	38.574	38.574	—	4.9078
36.858	3	42.003	42.017	42.000	—	—	4.9251
28.300	13	47.526	47.530	47.553	47.508	47.528	4.9321
27.574	4	48.090	48.116	48.116	48.106	—	4.9328
22.612	1	—	52.603	—	52.575	—	4.9078
18.720	2	57.389	57.411	57.311	57.428	—	4.9167
17.139	12	59.864	—	59.896	59.845	59.876	4.9409
2.7688	16	130.73	130.5805	130.79	130.59	130.61	4.9368
2.5118	14	135.78	135.6734	135.90	135.67	—	4.9384
1.3591	15	170.56	170.2319	170.70	170.38	170.38	4.9252
1.0855	17	184.35	184.1449	184.56	184.19	184.15	4.9290

[a] $K_a = 4.9297 \pm 0.0150 \times 10^{-5}$.

TABLE 6. Conductance data for phenylacetic-α,α-d_2 acid

10^4c (molal)	Run no.	Cell number and equivalent conductance 1	2	3	4	5	10^5K_a[a] (RSM)
62.284	8	32.649	32.651	34.641	32.632	32.662	4.8692
49.732	7	36.343	36.344	—	36.326	36.326	4.8796
49.034	10	36.602	36.595	36.612	36.579	36.608	4.8836
34.855	6	43.006	43.002	43.015	42.985	43.001	4.8976
31.922	5	44.780	44.775	44.803	44.756	44.791	4.8936
27.031	4	48.351	48.368	48.392	48.346	48.364	4.8922
24.213	3	50.986	50.995	51.019	50.970	51.002	4.9148
23.347	2	51.859	51.838	51.886	51.839	51.865	4.9151
17.765	9	58.717	58.702	58.744	58.687	58.721	4.9067
11.034	1	72.834	72.820	72.845	72.806	72.832	4.9204
6.3995	14	92.391	92.357	92.445	92.335	92.371	4.9208
4.9907	12	102.64	102.63	102.69	102.61	102.62	4.9202
4.2937	11	109.30	109.24	109.43	109.22	109.28	4.9226
3.1564	15	123.87	123.80	124.00	123.78	123.80	4.9187
2.8839	13	128.32	128.20	128.41	128.38	128.31	4.9110
2.0516	16	146.52	146.36	146.72	146.39	146.40	4.9175

[a] $K_a = 4.9055 \pm 0.0173 \times 10^{-5}$.

Can. J. Chem. Downloaded from www.nrcresearchpress.com by 210.87.254.42 on 09/05/12
For personal use only.

TABLE 7. Conductance data for 4-nitrophenylacetic acid

10^4c (molal)	Run no.	Cell number and equivalent conductance 1	2	3	4	5	10^4K_a[a] (RSM)
16.011	11	94.833	94.909	94.934	94.868	94.932	1.3212
10.442	10	113.44	113.44	113.38	113.40	113.48	1.3231
2.8615	5	184.50	184.15	184.67	184.58	184.57	1.3277
2.6242	7	189.85	189.28	190.05	189.58	189.92	1.3260
1.5010	9	225.55	225.30	225.67	225.35	225.39	1.3281
0.94570	6	255.30	254.92	255.36	255.00	255.00	1.3375[a]
0.63893	8	278.71	—	278.99	278.72	—	1.3446[b]

[a] $K_a = 1.3241 \pm 0.0045 \times 10^{-4}$.
[b] Not included in mean K_a.

TABLE 8. Conductance data for 4-nitrophenylacetic-α,α-d_2 acid

10^4c (molal)	Run no.	Cell number and equivalent conductance 1	2	3	4	5	10^4K_a[a] (RSM)
2.4238	1	194.66	194.68	194.89	195.69	194.72	1.3250
1.1573	2	241.94	241.74	242.39	241.86	241.86	1.3264
1.3102	4	233.55	233.68	234.03	233.77	233.85	1.3203
0.57311	3	284.47	283.97	—	283.94	284.04	1.3250
0.48222	5	293.72	293.29	—	293.33	—	1.3245

[a] $K_a = 1.3240 \pm 0.0048 \times 10^{-5}$.

TABLE 9. Conductance data for 4-methoxyphenylacetic acid

10^4c (molal)	Run no.	Cell number and equivalent conductance 1	2	3	4	5	10^5K_a[a] (RSM)
10.838	1	68.711	68.976	69.016	68.959	—	4.3331
8.0969	5	78.524	78.509	78.555	—	78.527	4.3471
4.6775	2	99.521	99.489	99.556	99.460	—	4.3501
4.2055	3	104.01	104.01	104.11	103.99	—	4.3486
3.2173	6	116.25	116.20	116.30	—	116.20	4.3532
1.7463	4	147.73	147.70	147.83	—	147.67	4.3533

[a] $K_a = 4.3493 \pm 0.0053 \times 10^{-5}$.

TABLE 10. Conductance data for 4-methoxyphenylacetic-α,α-d_2 acid

10^4c (molal)	Run no.	Cell number and equivalent conductance 1	2	3	4	5	10^5K_a[a] (RSM)
10.749	6	69.028	69.049	69.081	69.031	—	4.3175
3.6980	3	109.40	109.44	109.56	109.44	109.46	4.3202
3.4958	4	111.80	111.89	111.86	111.90	—	4.3068
3.2833	1	114.86	114.91	—	114.91	114.96	4.3172
1.9913	5	140.14	140.05	140.28	140.08	140.08	4.3204
1.6582	2	150.09	149.98	150.25	150.00	150.00	4.3099

[a] $K_a = 4.3162 \pm 0.0080 \times 10^{-5}$.

Can. J. Chem. Downloaded from www.nrcresearchpress.com by 210.87.254.42 on 09/05/12
For personal use only.

TABLE 11. Comparison of equilibrium constants

Acid	$10^5 K_a$	Method[a]	Ref.
Acetic	1.757 ± 0.003 ($\Lambda_0 = 389.6$)[b]	RSM(m)	This work (33)[c]
	1.754	E.m.f.(m)	(30)
	1.76	C(c)	(22)
	1.759	I(c)	(31)
	1.758	RSM(m)	(32)
	1.753	RSM(c)	(33)
Phenylacetic	4.923 ± 0.015 ($\Lambda_0 = 379.6$)[b]	RSM(m)	This work (35)[c]
	4.88	C(c)	(22)
	4.88	E.m.f.	(34)
	4.884	C(c)	(35)
	4.95	RSM(c)	(35)
	4.928 ± 0.011	E.m.f.(m)	(36)
	4.887 ± 0.056	C(m)	(37)
	4.90	I(c)	(38, 39)
4-Nitrophenylacetic	13.25 ± 0.05 ($\Lambda_0 = 376.6$)[b]	RSM(m)	This work (22)[c]
	10.4 ($\Lambda_0 = 414$)	C(c)	(40)
	12.94 ($\Lambda_0 = 377.8$)	C(c)	(22, 40)
	14.1	C(c)	(22)
	11.91 ± 0.36	C(m)	(37)
4-Methoxyphenylacetic	4.349 ± 0.005 ($\Lambda_0 = 377.3$)[b]	RSM(m)	This work (19)[c]
	4.36	C(c)	(19)
	4.406 ± 0.031	C(m)	(37)

[a]C, conductance method; RSM, Robinson–Stokes method; I, Ives method; c, mol/l; m, mol/1000 g.
[b]Λ_0(molal) used in RSM calculations.
[c]Literature ref. for Λ_0(molar). The conversion of Λ_0(molar) to Λ_0(molal) was made in the usual way.

Part II of this series. The K_a values determined by the RSM agree very favorably with previous measurements on these acids (Table 11) apart from 4-nitrophenylacetic acid. The large discrepancy in the K_a values for the 4-nitro acid is almost certainly a consequence of the labile nature of this molecule when it is exposed to light. Since the previous workers failed to recognize this fact the value reported here is to be preferred.

A comparison of the K_a values calculated for the individual acid samples confirms the purity of each specimen used. In no case can any discrimination be made between the various samples within the precision of the results of the present study. The redetermined equilibrium constant for acetic acid is also in excellent agreement with previous values and offers further confirmation of reliability of our work.

Discussion

The thermodynamic equilibrium constants calculated using the RSM provide a method of evaluating $K(H)/K(D)$ for each of the three isotopic pairs (X = H, NO_2, OMe). A further method for calculating the isotope effect is provided by the classical plot. We deal with these methods individually below.

The RSM is a well-established treatment and has been used by several authors (41). This method requires, aside from equivalent conductance data of the acid at finite concentrations, a value of the limiting equivalent conductance. To evaluate the isotope effect we assume that $\Lambda_0(ArCH_2COO^-) = \Lambda_0(ArCD_2COO^-)$ for all the aryl groups investigated. The equilibrium constants (K_a) calculated by the RSM reveal a slight residual concentration dependence which is probably outside our experimental error. This residual concentration dependence of K_a may be a consequence of the breakdown of the theoretical expression at higher concentrations or alternatively may result from the neglect of the frequency dependence of the electrolyte resistances. In the most precise study to date (11, 15), the latter factor has been considered important. While the RSM provides a suitable method for establishing the absolute values of the individual equilibrium constants the relative values of the H and D compounds are better established using a classical plot.

The classical plot connects the quantities Λ_0,

Can. J. Chem. Downloaded from www.nrcresearchpress.com by 210.87.254.42 on 09/05/12
For personal use only.

Λ_c, c and K_c where Λ_0, Λ_c, and c have their usual significance and the quantity K_c is the classical dissociation constant, *i.e.* the K_c parameter is calculated assuming the activity coefficients for both the ions and undissociated acid are unity at all concentrations. The appropriate equation connecting these quantities for the protium acid is

$$[13] \quad \frac{1}{\Lambda_c(H)} = \frac{1}{\Lambda_0(H)} + \frac{\Lambda_c(H)c(H)}{\Lambda_0^2(H)K_c(H)}$$

Assuming $\Lambda_0(H) = \Lambda_0(D)$ (see ref. 5 and above), a least squares correlation between the variables $1/\Lambda_c$ and $\Lambda_c c$ for the H and D acids yields slopes m_H and m_D which related to the isotope effect via the equation

$$[14] \quad \frac{K_c(H)}{K_c(D)} = \frac{m_D}{m_H}^6$$

The $K(H)/K(D)$ ratios for the three isotopic pairs calculated by both RSM and classical plot are summarized in Table 12, and may be compared with Halevi's original measurement (ref. 1 and see Table 2).

Our new values are surprisingly small. Indeed, they are so small that the detection of substituent effects on isotope effects is only just inside the bounds of possibility. This is particularly unfortunate in the light of some recent comments in a review by Thornton and Thornton (42). These authors suggest that substituent effects on isotope effects are significant parameters for a detailed understanding of transition states. One of the purposes of the present study was to obtain base line data of this sort for equilibria where the detailed specification of the states involved is clearcut in contrast to rates where the nature of the transition state is always elusive.

TABLE 12. Comparison of isotope effects

	p-R-$C_6H_4CH_2COOH$/p-R-$C_6H_4CD_2COOH$ $K(H)/K(D)$	
R	Robinson–Stokes method	Classical plot
H[a]	1.004 ± 0.005	1.0072 ± 0.0004
NO_2	1.001 ± 0.005	0.997 ± 0.002
MeO	1.008 ± 0.002	1.0045 ± 0.0007

[a]Laughton and Demayo (39) have also measured $K(H)/K(D)$ for this isotopic pair and give the ratio as 1.009 ± 0.002 and 1.008 ± 0.005 depending on the method of calculation used. However the absolute value of K_a for the protium acid reported by these workers differs from that reported here and is lower than all the values given in Table 11.

A comparison of these isotope effects for the arylacetic acids with the data of Streitwieser and Klein for the isotopic pair CH_3COOH/CD_3COOH indicates that the $K(H)/K(D)$ values are less for the former structures and this observation is qualitatively in accordance with the inductive treatment, *i.e.* as the number of deuteriums decrease at a given position with respect to the carboxyl group, the isotope effect should likewise decrease. The predicted isotope effect for the pair $PhCH_2COOH/PhCD_2COOH$, based on σ^* (D) (See Table 2), is closer to the $K(H)/K(D)$ value determined in this laboratory than the ratio reported by Halevi and coworkers (1). The reasons for the difference between the result reported by Halevi and results presented here are not easily discerned.

It is now clear that Halevi's result is unduly large both in the light of the inductive treatment presented above and when examined by an alternative treatment based on the pair HCOOH/DCOOH. The inductive effect of a substituent is known to increase as the substituent is moved closer to the reaction site (10). A rough calculation shows that the isotope effect for the pair HCOOH/DCOOH based on Halevi's value of $K(H)/K(D)$ for the phenyl acetic acids would give a value of 1.15. This predicted value is much higher

[6]The complete expression for the isotope effect is $K(H)/K(D) = m(D)\Lambda_0^2(D)/m(H)\Lambda_0^2(H)$ and the validity of eq. 14 is restricted to those situations in which the ratio $\Lambda_0^2(D)/\Lambda_0^2(H)$ is closer to unity than the ratio $m(D)/m(H)$. The latter condition seems to be satisfied in previous measurements of isotope effects by conductance (3–5). In the present instance the reported isotope effects are relatively small and in consequence the proximity of $\Lambda_0^2(D)/\Lambda_0^2(H)$ to unity may represent a significant factor with respect to the validity of the isotope effect calculated on the basis of eq. 14.

The greater length of C—H bonds *vs.* C—D bonds will probably be the most important factor altering Λ_0 with isotopic substitution. Such changes in the molecular dimensions of the anions are very small but on the basis of some calculations we have made are likely to lead to differences in $\Lambda_0(H)$ and $\Lambda_0(D)$ such that the square of the ratio will differ from unity by *ca.* 1 part in 10^4.

Because our isotope effects are small our referees pointed out the desirability of measuring the limiting equivalent conductances for the isotopic anions related to the acids examined in the present study to verify the reported isotope effects. Because the estimated differences in the isotopic limiting equivalent conductances are small and because these quantities must be obtained by some sort of extrapolation procedure we doubt the feasibility of such measurements. Aspects of this problem will be considered in the second paper of the present series.

Can. J. Chem. Downloaded from www.nrcresearchpress.com by 210.87.254.42 on 09/05/12
For personal use only.

Can. J. Chem. Downloaded from www.nrcresearchpress.com by 210.87.254.42 on 09/05/12
For personal use only.

than the isotope effect (K(H)/K(D) = 1.06) measured by Bell and Miller (43).

We shall deal with the issue of these small secondary isotope effects more fully in subsequent communications together with some of our findings concerning the numerical evaluation of pK_a's from weak acid conductance data which are of interest in their own right. However, we consider that the present paper provides the best values for the pK_a's of 4-$MeOC_6H_4CH_2COOH$ and 4-$NO_2C_6H_4CH_2COOH$ and also values of the isotope effects which are worthy of theoretical attention.

The authors thank Dr. R. E. Robertson for spiritual and material encouragement, the latter involving the construction of the conductance cells. We are grateful to Professor P. Laughton and Dr. A. Demayo for the loan of a thesis relevant to the present study. We also thank Mr. Ralph Parsons and Mr. W. Gordon for sustained technical services. Finally both authors express their gratitude to the National Research Council of Canada for financial support.

1. E. A. Halevi, M. Nussim, and A. Ron. J. Chem. Soc. 866 (1963).
2. R. P. Bell and J. E. Crooks. Trans. Faraday Soc. **58**, 1409 (1962).
3. R. E. Robertson and W. Van der Linde. J. Am. Chem. Soc. **86**, 4505 (1964).
4. R. E. Robertson and D. Northcott. J. Phys. Chem. **73**, 1559 (1969).
5. A. J. Streitwieser, Jr. and H. S. Klein. J. Am. Chem. Soc. **85**, 2759 (1963).
6. J. Bigeleisen and M. Wolfsberg. Advances in chemical physics. Vol. 1. Interscience, N.Y. 1958.
7. E. A. Halevi. Progress in physical organic chemistry. Vol. 1. Interscience, N.Y. 1963.
8. A. J. Streitwieser, Jr., R. H. Jagow, R. C. Fahey, and S. Suzuki. J. Am. Chem. Soc. **80**, 2326 (1958).
9. R. W. Taft. Steric effects in organic chemistry. *Edited by* M. S. Newman. John Wiley, N.Y. 1956. Chapt. 13.
10. H. C. Brown, D. H. MacDonald, and O. Häfliger. Determination of organic structures by physical methods. *Edited by* E. A. Braude and F. C. Nachod. Academic Press Inc., N.Y. 1955. Chapt. 14.
11. D. J. G. Ives and J. H. Pryor. J. Chem. Soc. 2104 (1955).
12. R. A. Robinson, R. G. Bates, and M. Paabo. J. Phys. Chem. **70**, 540 (1966).
13. H. K. Hall. J. Am. Chem. Soc. **79**, 3411 (1957).
14. R. E. Robertson and C. Y. Wu. Chem. Ind. 195 (1965).
15. T. S. Feates and D. J. G. Ives. J. Chem. Soc. 2798 (1956).
16. R. E. Robertson. Private communication.
17. J. Lee, A. Ziering, L. Berger, and S. D. Heineman. Jubilee Vol. Emil Barell 264 (1946).
18. L. Friedman and H. Shechter. J. Org. Chem. **25**, 877 (1960).
19. F. J. Dippy and F. R. Williams. J. Chem. Soc. 1888 (1934).
20. A. I. Shatenshtein. Advances in physical organic chemistry. Vol. 1. *Edited by* V. Gold. Academic Press, N.Y. (1963).
21. D. J. Barnes, H. J. Benson and J. M. W. Scott. Unpublished work.
22. F. J. Dippy and F. R. Williams. J. Chem. Soc. 166 (1934).
23. G. Jones and B. C. Bradshaw. J. Am. Chem. Soc. **35**, 1788 (1933).
24. T. Shedlovsky. Physical methods of organic chemistry. 2nd Ed. Part II. *Edited by* A. Weissberger. Interscience, N.Y. 1949.
25. R. E. Robertson. Can. J. Chem. **33**, 1536 (1955).
26. J. E. Lind, J. J. Zwolenik, and R. M. Fuoss. J. Am. Chem. Soc. **81**, 1557.
27. S. Hamer. The structure of electrolyte solutions. John Wiley, N.Y. 1959. Chapt. 11.
28. T. Shedlovsky. J. Franklin Inst. **225**, 739 (1938).
29. R. A. Robinson and R. H. Stokes. Electrolyte solutions. Butterworths, London. 1961.
30. H. S. Harned and R. W. Ehlers. J. Am. Chem. Soc. **54**, 1350 (1932).
31. D. J. Ives. J. Chem. Soc. 731 (1933).
32. F. D. Rossini, F. T. Gucker, H. L. Johnson, L. Pauling, and G. W. Vinal. J. Am. Chem. Soc. **74**, 2699 (1952).
33. D. A. MacInnes and T. Shedlovsky. J. Am. Chem. Soc. **54**, 1429 (1932).
34. W. L. German and A. I. Vogel. J. Chem. Soc. 912 (1935).
35. G. H. Jeffery and A. I. Vogel. J. Chem. Soc. 166 (1934).
36. E. J. King and J. E. Prue. J. Chem. Soc. 275 (1961).
37. A. Fisher, B. R. Mann, and J. Vaughan. J. Chem. Soc. 1093 (1961).
38. W. C. Duer and R. A. Robinson. J. Chem. Soc. B, 2375 (1971).
39. P. Laughton and A. Demayo. Private communication.
40. G. Basterfield and J. N. Tomecko. Can. J. Res. **8**, 447 (1933).
41. R. A. Robinson and R. H. Stokes. J. Am. Chem. Soc. **76**, 1991 (1954).
42. E. K. Thornton and E. R. Thornton. Isotope effects in chemical reactions. *Edited by* C. J. Collins and N. S. Bowman. Van Nostrand Reinhold Co., N.J. 1970. Chapt. 4, p. 213.
43. R. P. Bell and W. B. T. Miller. Trams. Faraday Soc. **59**, 1147 (1963).

Synthesis and Characterization of Dipyrazolylalkanes, and Some of Their Complexes With $CoCl_2$

K. I. THÉ AND L. K. PETERSON

Department of Chemistry, Simon Fraser University, Burnaby 2, British Columbia

Received August 24, 1972

The reaction of dipyrazol-1-yl ketone with appropriate ketonic compounds is catalyzed by the presence of $CoCl_2$, to yield dipyrazolylalkanes $(C_3H_3N_2)_2CRR'$, (*a*) where R = R′ = CH_3, CD_3, C_2H_5; (*b*) where R = H, R′ = CH_3, C_6H_5; (*c*) where R = CH_3, R′ = C_2H_5; and 1,1-dipyrazolylcycloalkanes derived from cyclobutanone, pentanone, hexanone, 3-methyl and 4-methylhexanone. Cobalt(II) chloride reacts with dipyrazol-1-yl ketone, in tetrahydrofuran, to yield the complex $CoCl_2(C_3H_3N_2)_2CO$, and in acetone or acetone-d_6 to yield $CoCl_2(C_3H_3N_2)_2C(CH_3)_2$ or $CoCl_2(C_3H_3N_2)_2C(CD_3)_2$.

La réaction de la dipyrazol yl-1 cétone avec des composés cétoniques appropriés, est catalysée par la présence de $CoCl_2$ et conduit aux dipyrazolylalcanes $(C_3H_3N_2)_2CRR'$; (*a*) où R = R′ = CH_3, CD_3, C_2H_5; (*b*) où R = H, R′ = CH_3, C_6H_5; (*c*) où R = CH_3, R′ = C_2H_5; et aux dipyrazolylcycloalcanes-1,1 dérivés de la cyclobutanone, pentanone, hexanone, méthyl-3 et méthyl-4 hexanone. Le chlorure de cobalt(II) réagit avec la dipyrazol yl-1 cétone dans le tétrahydrofurane pour donner le complexe $CoCl_2(C_3H_3N_2)_2CO$ et dans l'acétone ou l'acétone-d_6 pour conduire au $CoCl_2(C_3H_3N_2)_2C(CH_3)_2$ ou au $CoCl_2(C_3H_3N_2)_2C(CD_3)_2$. [Traduit par le journal]

Can. J. Chem., **51**, 422 (1973)

Polydentate ligands may be designed with various electronic and steric characteristics, which, in conjunction with the nature of metal ion or other acceptor species, will determine the properties of complexes that may form. Because the pyrazole ring is planar (1), due to a delocalization of π-electron density, the coupling of two pyrazole rings to the sp^2 hybridized carbon atom of a carbonyl group, as in dipyrazol-1-yl ketone (**1**) (2) (structure **I**) should lead to a polydentate ligand with the four nitrogen atoms of the rings essentially coplanar with the carbonyl group. Complexation with metal ions may then lead to six-atom coplanar chelate systems, via two nitrogen atoms, or to five-atom systems, via N and O atoms (structures **II** and **III**) or ligand bridging may lead to polymeric structures.

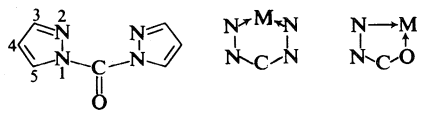

I **II** **III**

Our studies of the complexing properties of dipyrazolyl-1-ketone lead to unexpected reactions which represent the discovery of a new synthetic route to dipyrazolyl compounds (3), and to other novel organic molecules. Our synthetic work is reported in this paper.

Experimental

The manipulation of compounds was performed under anhydrous conditions, using a nitrogen-filled dry box or high vacuum system. Solvents were rigorously dried before use (4). Most of the preparative reactions were quantitative, although quoted yields of pure products are low, due to losses during work-up.

Melting points (uncorrected) were measured using Gallenkamp or Fisher–Johns m.p. apparatus. N.m.r. spectra were determined with a Varian A56/60 or Varian XL100 spectrometer, using $CDCl_3$ as solvent and with TMS as internal standard, i.r. spectra with a Perkin–Elmer 457 spectrophotometer, and mass spectra with a double focusing RMU-6E Hitachi Perkin–Elmer instrument.

Analyses, for C, N, and H, were performed by the departmental analyst.

Preparation of Dipyrazol-1-yl Ketone (1)

Sodium amide (0.26 mol) and pyrazole (0.26 mol) were placed under nitrogen into a 200 ml reaction vessel which was joined to a 2 l ballast bulb. The vessel was evacuated, dry ether (150 ml) was introduced, and after sealing, the flask was agitated for 16 h at room temperature, and for 3 h at 70 °C. Following the removal of volatile materials under vacuum, dry ether (150 ml) and phosgene (0.125 mol) were added to the residue of sodium pyrazolide, and the mixture was stirred for 3 h at room temperature, and for 14 h at 70 °C. Sodium chloride (0.252 mol) was filtered off, and the ethereal filtrate was distilled under nitrogen to yield a yellow solid, which was purified by zone fractionation under vacuum (sublimation temperatures, 85–90°) to give compound **1**, 0.112 mol, 87% yield; m.p. 61.5–62.5°.

Anal. Calcd. for $C_7N_4H_6O$: C, 51.9; N, 34.7; H, 3.7. Found: C, 52.0; N, 34.7; H, 3.7.

Mass spectrum: P_{obs} 162; P_{calcd} 162; n.m.r.: τ 2.10

Can. J. Chem. Downloaded from www.nrcresearchpress.com by 210.87.254.6 on 09/05/12
For personal use only.

Can. J. Chem. Downloaded from www.nrcresearchpress.com by 210.87.254.6 on 09/05/12
For personal use only.

(H_3) (q, $J_{3,4}$ = 2.2, $J_{3,5}$ = 0.6 Hz); 3.40 (H_4) (q, $J_{3,4}$ = 2.2, $J_{4,5}$ = 3.0 Hz); 1.27 (H_5) (q, $J_{3,5}$ = 0.6, $J_{4,5}$ = 3.0 Hz).

The $CoCl_2$-catalyzed Reaction of Dipyrazol-1-yl Ketone with Acetone

An exploratory experiment indicated that no reaction occurs in a two-component mixture of **1** and acetone. When a mixture of **1** (1.50 mmol), acetone (~5 ml), and a catalytic amount of dry $CoCl_2$ (0.005 g) was allowed to stand at room temperature, an initially purple solution, turning to dark blue, was observed. The slow evolution of a gas was noted. After 16 h, the products were separated into CO_2 (1.45 mmol), identified by its i.r. spectrum and vapor phase molecular weight (M_{obs} 44.1, M_{calcd} 44.0), and a residue of solids; extraction of the latter with ether yielded a white solid, 2,2-dipyrazolylpropane (**2**), m.p. 83.5–84.0°.

Anal. Calcd. for $C_9N_4H_{12}$: C, 61.4; N, 31.8; H, 6.8. Found: C, 61.3; N, 32.0; H, 6.9.

Mass spectrum: P_{obs} 176; P_{calcd} 176; n.m.r.: τ 7.20 (CH_3) (singlet); 2.40 (H_3) (q, $J_{3,4}$ = 1.8, $J_{3,5}$ = 0.7 Hz); 3.70 (H_4) (q, $J_{3,4}$ = 1.8, $J_{4,5}$ = 2.5 Hz); 2.57 (H_5) (q, $J_{4,5}$ = 2.5, $J_{3,5}$ = 0.7 Hz).

Other Products of the $CoCl_2$-catalyzed Reaction of Dipyrazol-1-yl Ketone with Ketonic Solvents

Reactions between **1** and various ketonic solvents, in the presence of catalytic amounts of $CoCl_2$, were carried out in essentially the same way as the reaction of **1** with acetone, as summarized below:

(*a*) Acetaldehyde yielded 1,1-dipyrazolylethane (**3**), m.p. 53.5–54.0 °C; yield 75%.

Anal. Calcd. for $C_8N_4H_{10}$: C, 59.2; N, 34.5; H, 6.2. Found: C, 59.3; N, 34.8; H, 6.1.

Mass spectrum: P_{obs} 162, P_{calcd} 162; n.m.r.: τ 7.83 (CH_3) (doublet, J = 6.8 Hz); 3.39 (CH) (q, J = 6.8 Hz); 2.46 (H_3) (q, $J_{3,4}$ = 2.0, $J_{3,5}$ = 0.6 Hz); 3.75 (H_4) (q, $J_{3,4}$ = 2.0, $J_{4,5}$ = 2.4 Hz); 2.43 (H_5) (q, $J_{3,5}$ = 0.6, $J_{4,5}$ = 2.4 Hz).

(*b*) Hexadeuteroacetone yielded 2,2-dipyrazolylhexadeuteropropane (**4**), m.p. 85.0–85.5 °C.

Anal. Calcd. for $C_9N_4H_6D_6$: C, 59.3; N, 30.8; H(D), 6.6. Found: C, 59.6; N, 31.0; H(D), 6.9.

Mass spectrum: P_{obs} 182, P_{calcd} 182; n.m.r.: τ 2.62 (H_3) (q, $J_{3,4}$ = 1.7, $J_{3,5}$ = 0.6 Hz); 3.77 (H_4) (q, $J_{3,4}$ = 1.7, $J_{4,5}$ = 2.5 Hz); 2.62 (H_5) (q, $J_{3,5}$ = 0.6, $J_{4,5}$ = 2.5 Hz).

(*c*) Methylethyl ketone yielded 2,2-dipyrazolylbutane (**5**), m.p. 54.5–55.0 °C; yield, 84%.

Anal. Calcd. for $C_{10}N_4H_{14}$: C, 63.2; N, 29.5; H, 7.4. Found: C, 63.1; N, 29.7; H, 7.3.

Mass spectrum: P_{obs} 19.0, P_{calcd} 190; n.m.r.: τ 9.12 (CH_3) (triplet, J = 7.5 Hz); 7.80 (CCH_3) (singlet); 7.27 (CH_2) (q, J = 7.5 Hz); 2.43 (H_3) (q, $J_{3,4}$ = 1.8, $J_{4,5}$ = 2.5 Hz); 2.60 (H_5) (q, $J_{3,5}$ = 0.6, $J_{4,5}$ = 2.5 Hz).

(*d*) Diethylketone yielded 3,3-dipyrazolylpentane (**6**), m.p. 55.3–56.0 °C; yield 80%.

Anal. Calcd. for $C_{11}N_4H_{16}$: C, 64.7; N, 27.4; H, 7.8. Found: C, 64.6; N, 27.8; H, 7.7.

Mass spectrum: P_{obs} 204, P_{calcd} 204; n.m.r.: τ 9.22 (CH_3) (triplet, J = 7.3 Hz); 7.25 (CH_2) (q, J = 7.3 Hz); 2.48 (H_3) (q, $J_{3,4}$ = 1.8 Hz); 3.75 (H_4) (q, $J_{3,4}$ = 1.8, $J_{4,5}$ = 2.5 Hz); 2.53 (H_5) (q, $J_{3,5}$ = 0.7, $J_{4,5}$ = 2.5 Hz).

(*e*) Benzaldehyde yielded 1,1-dipyrazolylphenylmethane (**7**), m.p. 61.6–62.0 °C; yield, 48%.

Anal. Calcd. for $C_{12}N_4H_{12}$: C, 69.6; N, 25.0; H, 5.4. Found: C, 69.8; N, 25.4; H, 5.4.

Mass spectrum: P_{obs} 224, P_{calcd} 224; n.m.r : τ 2.37 (H_3) (q, $J_{3,4}$ = 1.8, $J_{3,5}$ = 0.6 Hz); 3.60 (H_4) (q, $J_{3,4}$ = 1.8, $J_{4,5}$ = 2.4 Hz); 2.49 (H_5) (q, $J_{3,5}$ = 0.6, $J_{4,5}$ = 2.4 Hz); 2.25 (CH) (singlet). The phenyl resonances consisted of two sets of complex multiplets, centered at 2.67 τ.

(*f*) Cyclobutanone yielded 1,1-dipyrazolylcyclobutane (**8**), m.p. 79.5–80.2 °C; yield, 82%.

Anal. Calcd. for $C_{10}N_4H_{12}$: C, 63.8; N, 29.8; H, 6.4. Found: C, 63.4; N, 30.1; H, 6.3.

Mass spectrum: P_{obs} 188, P_{calcd} 188; n.m.r.: τ 2.45 (H_3) (q, $J_{3,4}$ = 1.7, $J_{3,5}$ = 0.7 H_2); 3.75 (H_4) (q, $J_{3,4}$ = 1.7, $J_{4,5}$ = 2.4 Hz); 2.62 (H_5) (q, $J_{3,5}$ = 0.7, $J_{4,5}$ = 2.4 Hz). The CH_2 protons of the cyclobutyl ring gave complex resonances centered at 6.77 and 8.93 τ.

(*g*) Cyclopentanone yielded 1,1-dipyrazolylpentane (**9**), m.p. 133.0–133.5 °C; yield, 60%.

Anal. Calcd. for $C_{11}N_4H_{14}$: C, 65.3; N, 27.7; H, 6.9. Found: C, 65.3; N; 28.0; H, 6.9.

Mass spectrum: P_{obs} 202, P_{calcd} 202; n.m.r.: τ 2.50 (H_3) (q, $J_{3,4}$ = 1.8, $J_{3,5}$ = 0.6 Hz); 3.80 (H_4) (q, $J_{3,4}$ = 1.8, $J_{4,5}$ = 2.5 Hz); 2.53 (H_5) (q, $J_{3,5}$ = 0.6, $J_{4,5}$ = 2.5 Hz). The CH_2 protons of the cyclopentyl ring gave complex resonances at 7.07 and 8.17 τ.

(*h*) Cyclohexanone yielded 1,1-dipyrazolyl cyclohexane (**10**), m.p. 76.0–76.5 °C; yield, 62%.

Anal. Calcd. for $C_{12}N_4H_{16}$: C, 66.7; N, 25.9; H, 7.4. Found: C, 66.7; N, 26.1; H, 7.5.

Mass spectrum: P_{obs} 216, P_{calcd} 216; n.m.r.: τ 2.45 (H_3) (q, $J_{3,4}$ = 1.8, $J_{3,5}$ = 0.6 Hz); 3.77 (H_4) (q, $J_{3,4}$ = 1.8, $J_{4,5}$ = 2.5 Hz); 2.58 (H_5) (q, $J_{3,5}$ = 0.6, $J_{4,5}$ = 2.5 Hz). The CH_2 protons of the cyclohexyl ring gave complex resonances at 7.17 and 8.40 τ.

(*i*) 4-Methylcyclohexanone yielded 1,1-dipyrazolyl-4-methylcyclohexane (**11**), m.p. 89.0–89.3 °C; yield, 50%.

Anal. Calcd. for $C_{13}N_4H_{18}$: C, 68.1; N, 24.5; H, 7.4. Found: C, 68.3; N, 24.4; H, 7.6.

Mass spectrum: P_{obs} 230, P_{calcd} 230; n.m.r.: τ 2.53, 2.39 (H_3 and H_3') (two quartets with identical coupling constants, $J_{3,4}$ = 1.8, $J_{3,5}$ = 0.7 Hz); 3.85, 3.67 (H_4, H_4') (two quartets, $J_{3,4}$ = 1.8, $J_{4,5}$ = 2.4 Hz); 2.29, 2.88 (H_5, H_5') (two quartets, $J_{3,5}$ = 0.7, $J_{4,5}$ = 2.4 Hz).

(*j*) 3-Methylcyclohexanone yielded 1,1-dipyrazolyl-3-methylcyclohexane (**12**), m.p. 61.2–61.5 °C; yield 30%.

Anal. Calcd. for $C_{13}N_4H_{18}$: C, 67.9; N, 24.3; H, 7.8. Found: C, 67.9; N, 24.6; H, 7.9.

Mass spectrum: P_{obs} 230, P_{calcd} 230; n.m.r.: τ 8.97 (CH_3) (doublet, J = 5.5 Hz); 6.65–8.97 (CH_2) (complex pattern); 2.52, 2.38 (H_3, H_3') (two quartets, $J_{3,4}$ = 1.8, $J_{3,5}$ = 0.6 Hz); 3.87, 3.65 (H_4, H_4') (two quartets, $J_{3,4}$ = 1.8, $J_{4,5}$ = 2.6 Hz); 2.95, 2.25 (H_5, H_5') (two quartets, $J_{3,5}$ = 0.6, $J_{4,5}$ = 2.6 Hz).

(*k*) Unsuccessful reactions: The following compounds, containing the C=O group, did not react with dipyrazol-1-yl ketone when $CoCl_2$ was used as a catalyst: 2-methylcyclohexanone, acetophenone, benzophenone, ethyl acetate, dimethylacetamide, and δ- and γ-valerolactone.

*Preparation of 2,2-Dipyrazolylpropanecobalt Dichloride (**13**)*

Cobalt(II) chloride (0.82 mmol), dried by refluxing with thionyl chloride, **1** (0.82 mmol), and dry acetone

(~5 ml) were sealed together in a reaction flask. After 16 h at room temperature, the products were CO_2 (0.80 mmol) and a non-volatile blue solid; the latter was recrystallized from acetone to yield pure 2,2-dipyrazolylpropanecobalt dichloride, $CoCl_2[(C_3H_3N_2)_2C(CH_3)_2]$ (**13**).

Anal. Calcd. for $CoCl_2[(C_3H_3N_2)_2C(CH_3)_2]$: C, 35.3; N, 18.3; H, 3.9. Found: C, 35.0; N, 18.2; H, 3.9.

A solution of **2** (0.5 mmol) in acetone (10 ml) was added with stirring to a solution of $CoCl_2$ (0.5 mmol) in acetone (25 ml), to give a dark blue solution. Upon concentrating the solution, a blue product, with the same composition and i.r. spectrum as compound **13** prepared by the above method, was obtained.

*Hydrolysis of **13***

Compound **13** (2.0 mmol) was dissolved in water (20 ml) to give a pink solution which was extracted with diethyl ether (5 × 15 ml). The work-up of the organic layer yielded a solid residue, which was purified by zone fractionation; this product (1.2 mmol, 60% yield) was identical with a sample of **2** prepared by the $CoCl_2$-catalyzed reaction of acetone with dipyrazol-1-yl ketone.

*Preparation of 2,2-Dipyrazolylhexadeuteropropanecobalt Dichloride (**14**)*

This complex was prepared in the same way as **13**, using $CoCl_2$ (4.95 mmol), and **1** (4.95 mmol) in hexadeuteroacetone as solvent. Carbon dioxide (4.70 mmol) was formed quantitatively; the blue complex (**14**) was recrystallized from hot acetone.

Anal. Calcd. for $[(C_3H_3N_2)_2C(CD_3)_2]CoCl_2$: C, 34.0; N, 18.0; H (D), 4.0. Found: C, 34.5; N, 17.9; H (D), 3.9.

*Hydrolysis of **14***

Compound **14** (3.2 mmol) was dissolved in D_2O (10 ml) and the resulting solution was extracted with diethyl ether. The work-up of the organic layer produced the free ligand (1.95 mmol 61% yield), with the same physical properties and composition as **4** prepared above.

*Preparation of Dipyrazol-1-yl Ketonecobalt Dichloride (**15**)*

A mixture of $CoCl_2$ (1.07 mmol) **1** (1.07 mmol) and dry tetrahydrofuran (10 ml) was agitated at room temperature for 16 h. The absence of CO_2 was noted, and the solution was concentrated to yield a violet solid, which was filtered off under a dry nitrogen atmosphere. The product, **15**, was extremely sensitive to moisture.

Anal. Calcd. for $[C_3H_3N_2)_2CO]CoCl_2$: C, 28.8; N, 19.2; H, 2.1. Found: C, 29.0; N, 19.3; H, 2.0.

A sample of **15** (1.05 mmol) was dissolved in dry acetone (5 ml); after 16 h, the products were CO_2 (1.00 mmol) and a blue solid, which, after recrystallization, was identified as **13** on the basis of its i.r. spectrum; this complex was hydrolyzed by the methods described above to yield the free ligand, identified by its i.r. and n.m.r. spectra as **2**.

Discussion

The new compound dipyrazol-1-yl ketone is formed quantitatively in the reaction of phosgene with sodium pyrazolide according to eq. 1:

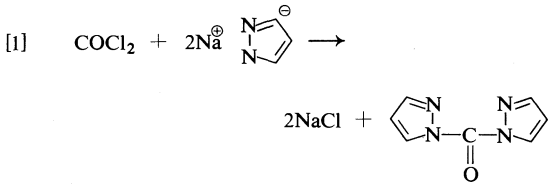

The use of lithium pyrazolide is precluded, since carbon atom lithiation occurs during the reaction of pyrazole with butyl lithium (5). The product, **1**, is very sensitive to water, yielding pyrazole and CO_2 (eq. 2). Whereas the ν(C=O)

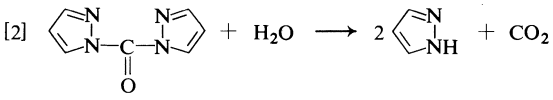

stretching vibration for amides usually occurs in the 1650 cm^{-1} region, this band appears at 1740 cm^{-1} for compound **1**, suggesting an absence of the resonance interaction postulated for amides (6):

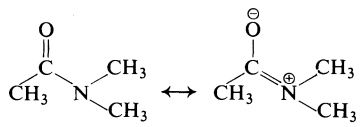

The absence of resonance may be due to aromaticity in the pyrazole ring system, requiring the lone pair of the amide nitrogen atom to be associated with the π-electron density of the ring, rather than with the carbonyl group. The monopyrazole systems, **IV**, show a trend in ν(C=O) values which may be accounted for on the basis of increasing resonance interactions with the R group, in the series R = CH_3CH_2, phenyl, and styryl, where the ν(C=O) values are 1722, 1700, and 1694 cm^{-1}, respectively (7).

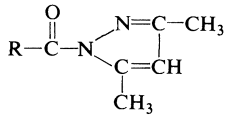

IV

The position of the ν(C=O) band for **1** indicates a similarity to the carbonyl bond in acetone (ν(C=O) = 1715 cm^{-1}), while the greater electronegativity of chloro and fluoro groups is reflected in the ν(C=O) values for $COCl_2$ (1827 cm^{-1}) and for COF_2 (1928 cm^{-1}) (8).

Compound **1** forms a violet complex with $CoCl_2$ in tetrahydrofuran solution. The car-

Can. J. Chem. Downloaded from www.nrcresearchpress.com by 210.87.254.6 on 09/05/12
For personal use only.

bonyl frequency is essentially unchanged (1735 cm^{-1}), hence coordination must involve N rather than O atoms. The complex is hydrolytically unstable, being readily converted into a cobalt–pyrazole complex, with elimination of CO_2.

Compound **1** is soluble in acetone, and in other ketonic or carbonyl solvents, without reaction; the presence of Co(II) species, even in catalytic amounts, does promote a reaction in which the carbonyl group of the solvent is exchanged for the dipyrazolylmethylene group, with evolution of carbon dioxide (2) (eq. 3).

[3] 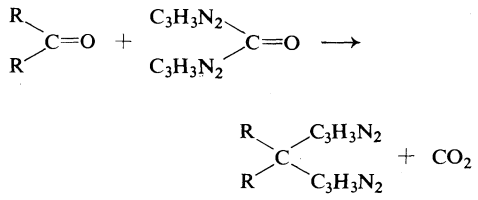

The reaction has wide applicability, to aliphatic ketones and aldehydes, to aromatic substances such as benzaldehyde, but not to benzophenone and acetophenone, and to cyclic ketones, but not to lactones. Other carbonyl systems which do not react include hexafluoro and hexachloroacetone, esters of carboxylic acids, and dimethylacetamide. It is likely that steric factors are important for benzophenone, acetophenone, and 2-methylcyclohexanone; in other cases, resonance interactions,

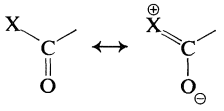

may diminish the reactivity of the carbonyl group. Further studies of the steric, electronic, and catalytic factors influencing this type of reaction are in progress. When stoichiometric proportions of compound **1** and $CoCl_2$ are dissolved in ketonic solvents, the new ligand L derived from **1** and the solvent remains complexed to the cobalt ion in a 1:1 molar ratio, giving $CoCl_2L$.

Such complexes are less susceptible to hydrolysis than those of **1**, and may be handled in the atmosphere. In aqueous solution, however, the complexes are hydrolyzed, producing free ligand which may be extracted into organic solvents. The hydrolytic stability of the dipyrazolyl alkanes is in marked contrast to the observed instability of dipyrazol-1-yl ketone, and, unlike *N*-alkylpyrazoles (9), our compounds are not hygroscopic.

Evidence for reaction between dipyrazol-1-yl ketone and acetone was first observed in the i.r. spectrum of the product, 2,2-dipyrazolylpropane, by the appearance of ν(C—H) bands at ~3000 cm^{-1}, due to CH_3 groups, and by the disappearance of ν(C=O). The ν(CH) vibrations of the "aromatic" pyrazole ring occur at 3120 and 3140 cm^{-1} (10), and hence are distinguishable from the ν(CH) stretching vibration of alkyl groups (2900–3000 cm^{-1}) for compounds **2**, **3**, **5**–**12**, and from the vibrations of the phenyl ring system (3040–3060 cm^{-1} (10)) in **7**. Comparison of the n.m.r. spectra of **1** and **2** corroborated the presence of the methyl groups in the latter molecule (at 7.2 τ); the hexadeutero analog **4** did not exhibit this resonance, showing acetone to be the source of methyl groups; the observed n.m.r. spectra of compounds **1**–**11** were in agreement with the given formulations.

The resonance positions of H_3 (2.37–2.50 τ), H_4 (3.60–3.80 τ), and H_5 (2.4–2.6 τ) were assigned on the basis of expected shielding effects associated with the carbonyl group and the nitrogen atoms; the bands were observed as quartets, due to long-range coupling with different C—H protons, ($J_{3,4}$ = 1.7–2.0, $J_{3,5}$ = 0.6–0.7, $J_{4,5}$ = 2.4–2.5 Hz) and not as doublets or triplets, as reported by Trofimenko (3). The H_x and H_x' protons of the two pyrazole rings were equivalent in all cases, except in the 1,1-dipyrazole-methylcyclohexane derivatives, where the resonances due to H_x and H_x' were observed as separate pairs of quartets, of equal intensity. The different bands presumably reflect the different positions of the pyrazole substituents, *viz.*, axial or equatorial, in the methylhexane ring. The H_3 resonance was significantly broader than that of H_5; a similar effect is reported for the two protons of substituted pyridines (11). Bands due to the R groups of compounds **2**–**12** were clearly identified, with appropriate intensities.

Mass spectra further confirmed the formulations of products; parent peaks were observed in all cases, and the larger fragments of compounds **2**–**7** were clearly identifiable as $(C_3H_3N_2)CRR'$, $C_3H_3N_2)_2CR$, and $C_3H_3N_2$. Compound **1** gave recombination products, such as *N*,*N'*-dipyrazole, as well as $(C_3H_3N_2)CO$ and $C_3H_3N_2$. The derivatives of the cycloalkanes **8**–**12**

Can. J. Chem. Downloaded from www.nrcresearchpress.com by 210.87.254.6 on 09/05/12
For personal use only.

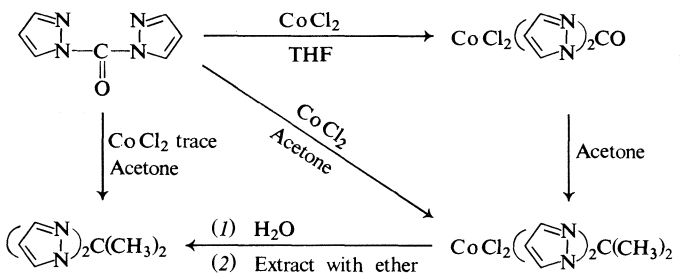

SCHEME 1

gave $(C_3H_3N_2)$C-cycloparaffin, $(C_3H_3N_2)$-$C(CH_2)_{1,3,2}$, and the free cycloparaffin fragment.

Interrelationships among various dipyrazolyl compounds are shown in Scheme 1.

Financial support from the National Research Council of Canada is gratefully acknowledged.

1. H. W. W. EHRLICH. Acta Cryst. **13**, 946 (1960).
2. L. K. PETERSON and K. I. THÉ. Chem. Commun. 841 (1972).
3. S. TROFIMENKO. J. Am. Chem. Soc. **92**, 5118 (1970).
4. A. WEISSBERGER. Technique of organic chemistry. Vol. VII. Organic Solvents. Interscience Publishers, Inc., N.Y. 1955.
5. R. HÜTTEL and M. E. SCHON. Ann. **625**, 55 (1959).
6. R. S. DRAGO. Physical methods in inorganic chemistry. Reinhold Publishing Corp. New York. 1965. p. 230.
7. W. REID and F-J. KÖNIGSTEIN. Ann. **625**, 53 (1959).
8. K. NAKAMOTO. Infrared spectra of inorganic and coordination compounds. J. Wiley and Sons, Inc., New York. 1963. p. 95.
9. G. ZERBI and C. ALBERTI. Spectrochim. Acta, **18**, 407 (1962).
10. H. A. SZYMANSKI. Theory and practice of infrared spectroscopy. Plenum Press, New York. 1964.
11. V. J. KOWALEWSKI and D. G. DE KOWALEWSKI. J. Chem. Phys. **36**, 266 (1962).

Can. J. Chem. Downloaded from www.nrcresearchpress.com by 210.87.254.6 on 09/05/12
For personal use only.

Synthesis of Some Epiminocyclohexanes by Hydride Reduction of α,β-Unsaturated Cyclohexanone Oximes and the Pyrolytic *cis*-Elimination of *N*-Acetylepiminocyclohexanes

J. R. DIMMOCK[1] AND W. A. TURNER[2]

College of Pharmacy, University of Saskatchewan, Saskatoon, Saskatchewan

AND

P. J. SMITH AND R. G. SUTHERLAND

Department of Chemistry and Chemical Engineering, University of Saskatchewan, Saskatoon, Saskatchewan

Received July 20, 1972

Reduction of several 2-benzylidenecyclohexanone oximes with lithium aluminum hydride gave the corresponding 1-benzyl-1,2-epiminocyclohexanes. Reduction of 2-benzylidenecyclohexanone oxime with lithium aluminum deuteride gave an epiminocyclohexane (**8**) which had incorporated two deuterium atoms. A reaction mechanism for the reduction is postulated. The major fragmentation pathways in the mass spectrum of **8** are outlined. Acetylation of 1-benzyl-1,2-epiminocyclohexane with acetic anhydride (15 min reflux) gave 3-acetamido-2-benzyl-1-cyclohexene by a pyrolytic *cis* elimination.

La réduction par $LiAlH_4$ de plusieurs oximes de benzylidène-2 cyclohexanones conduit aux benzyl-1 épimino-1,2 cyclohexanes correspondants. La réduction, par $LiAlD_4$ de l'oxime de la benzylidène-2 cyclohexanone donne l'épiminocyclohexane (**8**) ayant incorporé deux atomes de deutérium. Un mécanisme réactionnel est postulé pour cette réaction. Les modes majeurs de fragmentation de **8** lors de la spectrométrie de masse sont donnés généraux. L'acétylation du benzyl-1 épimino-1,2 cyclohexane avec de l'anhydride acétique (reflux de 15 min) conduit par pyrolyse impliquant une élimination *cis*, à l'acétamido-3 benzyl-2 cyclohexène-1. [Traduit par le journal]

Can. J. Chem., **51**, 427 (1973)

Introduction

Recently a series of substituted 2-benzylidenecyclohexylamines (**3**) were required as intermediates in the synthesis of some novel anticancer agents. In our earlier work,[3] we described the preparation of the ketones (**1**) shown to have the *E* configuration with relationship of the aromatic ring to the carbonyl function. These ketones were then converted to the corresponding oximes (**2**).[4] It was considered that the ketoximes could be converted to the corresponding amines (**3**) using lithium aluminum hydride (LAH), a reagent known to reduce substituted cyclohexanone oximes to amines (1, 2). The reaction sequence is shown in Scheme 1.

Results and Discussion

Reduction of **2***a* with LAH gave a colorless oil. The n.m.r. spectrum indicated the presence of 17 protons including one proton replaceable with deuterium but the olefinic proton was absent. The u.v. spectrum confirmed the absence of any styrenoid absorption. The mass spectrum indicated a parent peak at 187 with a molecular formula of $C_{13}H_{17}N$. These data show the absence of both **3***a* and the saturated primary amine, 2-benzylcyclohexylamine. The presence of one replaceable proton suggested an imine structure and aziridines have been formed by reduction of saturated cyclic oximes and α,β-unsaturated acyclic ketoximes with LAH (3, 4). The n.m.r., u.v., i.r., and mass spectral data obtained support the structure **4***a* for the compound isolated from the reduction of **2***a* with LAH. We are aware of only one other substituted cyclohexanone oxime which possessed an unsaturated linkage and gave an aziridine on reduction with LAH but in this case the double bond remained intact (5).

Reduction of **2***b* with LAH gave **4***a* which could also be obtained from **2***a* by reduction with lithium borohydride but **2***a* did not react with sodium borohydride, sodium trimethoxyborohydride, or lithium tri-(*t*-butoxy)aluminum hydride. It is interesting to note that reduction of (*Z*)-2-benzylidenecyclohexanone oxime with LAH

[1]Author to whom correspondence should be addressed.
[2]Holder of a Medical Research Council Studentship, 1968–1972.
[3]P. J. Smith, J. R. Dimmock, and W. A. Turner. Can. J. Chem. Submitted.
[4]P. J. Smith, J. R. Dimmock, and W. A. Turner. Can. J. Chem. Submitted.

Can. J. Chem. Downloaded from www.nrcresearchpress.com by 210.87.254.105 on 09/05/12
For personal use only.

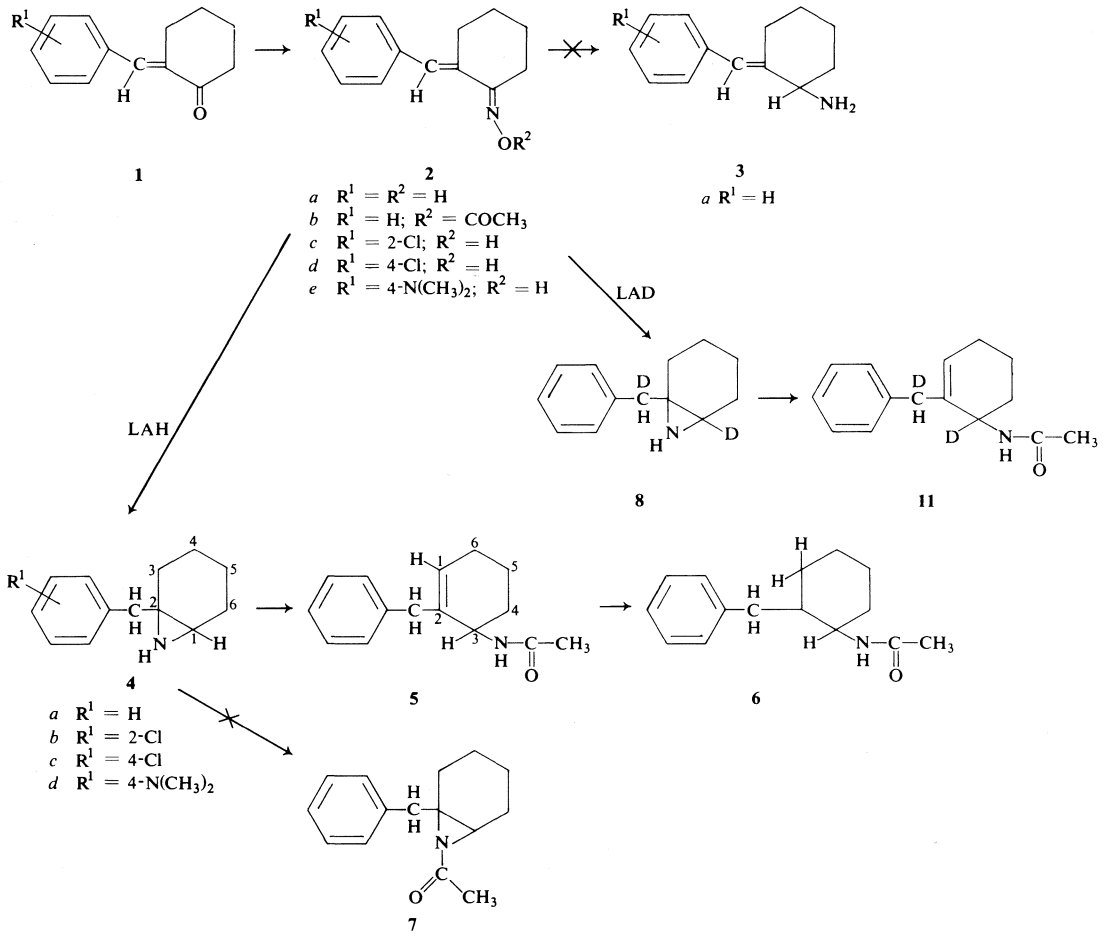

SCHEME 1

afforded **4***a* although in lower yields than reduction of **2***a*. Reduction of **2***a* with lithium aluminum deuteride (LAD) gave a compound with two deuterium atoms (**8**). The n.m.r. spectrum showed no absorption at δ 2.07–1.83 (C(2)H absent) nor the AB quartet with centers of the doublets at δ 2.92 and 2.63 ($C_6H_5CH_2$ absent). However two shaggy multiplets at δ 2.85 and 2.68 integrating for one proton were assigned to the *erythro* and *threo* forms of the product due to the CDH function in the side chain. The postulated reaction mechanism for the synthesis of the deuterated product (**8**) is shown in Scheme 2.

The mass spectrum of **8** had prominent *m/e* peaks at 189 (parent peak) and at 97 and 92 indicating the incorporation of one deuterium atom in the side chain and the other in the epiminocyclohexane portion of the molecule. The principle peaks for **4***a* and **8** are given in Table 1 and the possible fragmentation pattern for **8** is shown in Scheme 3. Work on the mass spectrometry of more complex aziridines has been published recently (6).

Reduction of **2***c* and *d* with LAH gave the corresponding aziridines (**4***b* and *c*) in good yields. In the case of reduction of **2***e*, g.l.c. of the reaction mixture indicated three components to the extent of 59, 24, and 17%. The n.m.r. spectrum of the reduction product from **2***e* was assignable to the aziridine structure **4***d*, indicating **4***d* was the major compound in the mixture. A white solid formed in the reaction mixture over a period of time (3 months) which was identified as 2-(4-dimethylaminobenzyl)cyclohexylamine by n.m.r., i.r., and mass spectral evidence. G.l.c. analysis indicated that this compound represented 24% of the reaction mixture. The third component of the reaction was not identified.

Can. J. Chem. Downloaded from www.nrcresearchpress.com by 210.87.254.105 on 09/05/12
For personal use only.

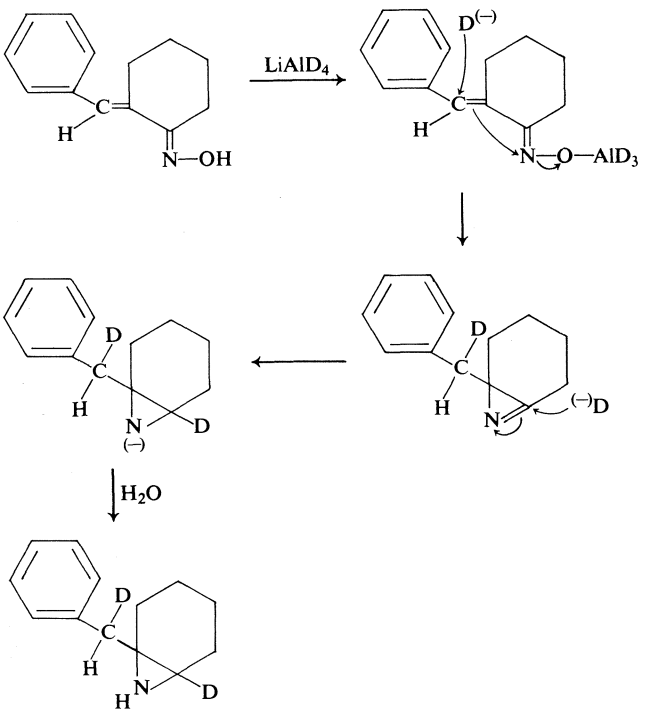

SCHEME 2

TABLE 1. Major peaks in the mass spectra of the aziridines **4*a*** and **8**

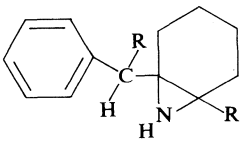

4*a* R = H
8 R = D

4*a*		**8**	
m/e	Relative abundance	*m/e*	Relative abundance
187 $[M]^+$	100	189 $[M]^+$	100
186 $[M-1]^+$	56	188 $[M-1]^+$	40
172 $[M-15]^+$	82	174 $[M-15]^+$	36
159 $[M-28]^+$	54	161 $[M-28]^+$	36
158 $[M-29]^+$	74	160 $[M-29]^+$	40
96 $[M-91]^+$	100	97 $[M-92]^+$	60
91 $[M-96]^+$	100	92 $[M-97]^+$	96

An attempt to prepare **7** by acetylation of **4*a*** with acetic anhydride (15 min reflux) gave a compound with a correct molecular weight for **7**. However, spectral evidence did not support this structure. The n.m.r. spectra indicated the presence of an olefinic group and a replaceable proton, while i.r. spectroscopy showed the presence of an NH stretching vibration as well as amide II and I bands at 1535 (NH) and 1640 cm^{-1} (CO). In view of earlier workers report of the preparation of *N*-allylcarboxamides on acylation of aziridines (7) we surmised that one of the structures **5**, **9**, or **10** may have been formed. Compound **10** may be eliminated since the u.v.

Can. J. Chem. Downloaded from www.nrcresearchpress.com by 210.87.254.105 on 09/05/12
For personal use only.

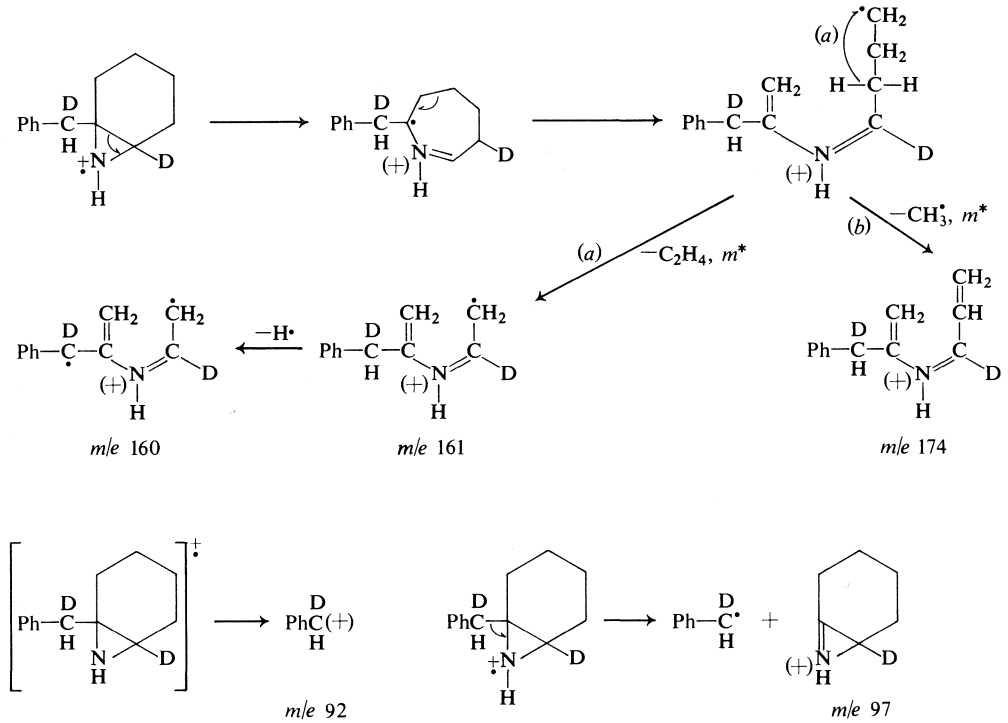

SCHEME 3

spectra indicated the absence of styrenoid absorption and the n.m.r. spectrum indicated the presence of a benzyl side chain.

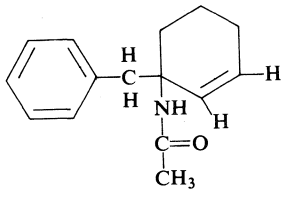

9

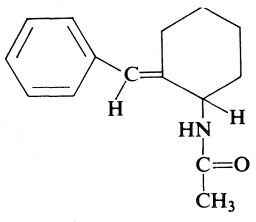

10

The n.m.r. spectrum of the amide obtained showed a broad peak at δ 5.77–5.37 integrating for two protons and a peak at δ 4.60–4.20 integrating for one proton. One of the protons at δ 5.77–5.37 could be exchanged with deuterium suggesting that an amide proton was superimposed on an olefinic proton. Catalytic hydrogenation of the amide increased the molecular weight by two mass units indicating the presence of one double bond and the n.m.r. spectra of the reduced product showed no olefinic absorptions at δ 5.77–5.37 while the amide proton was moved upfield to δ 5.71. The presence of only one olefinic proton in the unsaturated amide indicates that the structure is **5** rather than **9**. Acetylation of **8** with acetic anhydride (15 min reflux) gave **11** with no proton at δ 4.60–4.20 indicating that the absorption in **5** at δ 4.60–4.20 was due to the bridgehead proton at C-3 of the cyclohexane ring. The formation of **5** from **4***a* presumably arises by pyrolytic *cis* elimination (8, 9) of the *N*-acetylaziridine via the transition state (**12**).

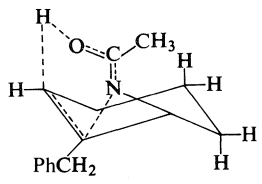

12

Can. J. Chem. Downloaded from www.nrcresearchpress.com by 210.87.254.105 on 09/05/12
For personal use only.

TABLE 2. Substituted 1-benzyl-1,2-epiminocyclohexanes

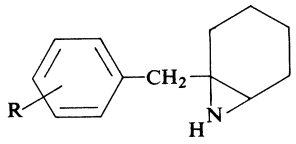

Compound **4**	R	B.p.(°/mm)	Yield*	Calcd. (%) C	Calcd. (%) H	Found (%) C	Found (%) H
a	H	78/0.2	92†,‡	83.37	9.15	83.20	9.12
b	2-Cl	100–105/0.5	91	70.42	7.27	70.50	7.41
c	4-Cl	126–128/1.3	89	70.42	7.27	70.31	7.26

*Yield is based on the weight of reaction product obtained prior to distillation. G.l.c. analysis of the material showed that one product was present to an extent greater than 99.4%.
†This compound was prepared from **2***b* in 90% yield.
‡Reaction of **2***a* with lithium borohydride using the general reduction procedure gave a product containing **4***a* (65%) and unreacted **2***a* (35%).

The anticancer activity of several of the oximes, aziridines, and related compounds described in this work will be reported elsewhere.

Experimental

General Conditions

The i.r. spectra were recorded on a Unicam SP200G spectrophotometer previously calibrated with polystyrene, using sodium chloride optics or potassium bromide discs. The n.m.r. spectra were obtained in deuterochloroform using a Varian T-60 spectrometer, with tetramethylsilane as the internal standard. Mass spectra were obtained with an AEI MS-12 spectrometer. The u.v. spectra were recorded on a Beckmann DU Spectrophotometer, in 95% ethanol, using quartz cells. All melting points were determined on a Mettler FP-1 melting point apparatus and are uncorrected. Microanalyses were carried out by Mr. O. Douglas, College of Pharmacy, University of Saskatchewan, Saskatoon, on a Coleman Model 33 Carbon–Hydrogen Analyzer. Gas chromatographic analyses were determined on a Pye 104 chromatograph equipped with 5 ft × 0.25 in. o.d. glass columns packed with 4% SE-30 adsorbed onto silanized Chromosorb W (100/120 mesh).

*General Procedure for the Preparation of Substituted 1-Benzyl-1,2-epiminocyclohexanes (**4**)*

A solution of the appropriate ketoxime or ketoxime acetate (**2**) (10) (0.037 mol) in anhydrous ether (180 ml) was added dropwise to LAH (0.057 mol) in anhydrous ether (40 ml) and heated under reflux with stirring for 8 h. The reduction complex was decomposed by the dropwise addition of water and filtered. The filtrate was dried ($MgSO_4$) and evaporation of ether gave the crude reaction product which was purified by distillation (Table 2).

*1-Benzyl-1,2-epiminocyclohexane(**4a**)*

I.r. (smear) 3250s cm^{-1} (NH); n.m.r. δ 7.40–7.00 (5H, m, C_6H_5), 2.92, and 2.63 (2H, centers of two doublets of AB quartet, J = 14 Hz, $C_6H_5CH_2$), 2.07–1.83 (1H, m, C(2)*H*), 1.90–1.50 (4H, m, C(3)H_2, C(6)H_2), 1.50–1.07 (4H, m, C(4)H_2, C(5)H_2), 0.73 (1H, broad s, exchanges with D_2O, N*H*); mass spectrum *m/e* 187 (parent peak).

The deuterium analog (**8**) was prepared in a similar manner (90% yield), using LAD. B.p. 80°/0.5 mm; i.r. (smear) 3256s cm^{-1} (NH); n.m.r. δ 7.47–7.07 (5H, m, C_6H_5), 2.85 and 2.68 (1H, centers of 2m, C_6H_5—C*H*D), 2.00–1.50 (4H, m, C(3)H_2, C(6)H_2), 1.50–1.28 (4H, m, C(4)H_2, C(5)H_2), 0.98 (1H, broad s, replaceable with D_2O, N*H*); mass spectrum *m/e* 189 (parent peak).

*1-(2-Chlorobenzyl)-1,2-epiminocyclohexane (**4b**)*

I.r. (smear) 3258s cm^{-1} (NH); n.m.r. δ 7.47–7.40 (4H, m, C_6H_4Cl), 3.13, and 2.83 (2H, centers of two doublets of AB quartet, J = 14 Hz, C_6H_4Cl—CH_2), 1.97–1.83 (1H, m, C(2)*H*), 1.97–1.60 (4H, m, C(3)H_2, C(6)H_2), 1.60–1.07 (4H, m, C(4)H_2, C(5)H_2), 0.68 (1H, broad s, exchanges with D_2O, N*H*); mass spectrum *m/e* 221 (parent peak).

*1-(4-Chlorobenzyl)-1,2-epiminocyclohexane (**4c**)*

I.r. (smear) 3257s cm^{-1} (NH); n.m.r. δ 7.43–6.97 (4H, m, C_6H_4Cl), 2.85, and 2.58 (2H, centers of two doublets of AB quartet, J = 14 Hz, C_6H_4Cl—CH_2), 2.13–1.83 (1H, m, C(2)*H*), 1.93–1.48 (4H, m, C(3)H_2, C(6)H_2) 1.48–1.07 (4H, m, C(4)H_2, C(5)H_2), 0.44 (1H, broad s, exchanges with D_2O, N*H*); mass spectrum *m/e* 221 (parent peak).

*Reduction of 2-(4-Dimethylaminobenzylidene)cyclohexanone Oxime (**2e**) with LAH*

The general reduction conditions were followed to give an oil (1.43 g), b.p. 138°/0.7 mm. G.l.c. indicated a mixture of components in concentrations of 59, 24, and 17%. The following characteristics could be assigned to 1-(4-dimethylaminobenzyl)-1,2-epiminocyclohexane as the major component of the mixture: i.r. (smear) 3286s cm^{-1} (NH); n.m.r. δ 7.23–6.80 (2H, m, aromatic C(2)*H*, C(6)*H*), 6.80–6.47 (2H, m, aromatic C(3)*H*, C(5)*H*), 2.88 (6H, s, $(CH_3)_2N$), 2.81, and 2.53 (2H, centers of two doublets of AB quartet, J = 14 Hz, $(CH_3)_2N$—C_6H_4—CH_2), 1.97–1.73 (1H, m, C(2)*H*), 2.07–1.53 (4H, m, C(3)H_2, C(6)H_2), 1.53–1.07 (4H, m, C(4)H_2, C(5)H_2), 0.68 (1H, broad s, exchanges with D_2O, N*H*).

A white solid (0.1 g), m.p. 109.5° formed in the distillate over a period of time (3 months), which was identified as 2-(4-dimethylaminobenzyl)cyclohexylamine: i.r. 3376 cm^{-1} (NH_2); n.m.r. δ 7.20–6.87 (2H, m, aromatic C(2)*H*, C(6)*H*), 6.80–6.47 (2H, m, aromatic C(3)*H*, C(5)*H*), 2.70–2.10 (2H, m, $(CH_3)_2N$—$C_6H_4CH_2$), 1.90–1.13 (10H, m, C(1)*H*, C(2)*H*, C(3)H_2, C(4)H_2, C(5)H_2,

Can. J. Chem. Downloaded from www.nrcresearchpress.com by 210.87.254.105 on 09/05/12
For personal use only.

C(6)H_2), 1.63 (2H, s, exchanges with D_2O, NH_2); mass spectrum *m/e* 232 (parent peak).

Reduction of (Z)-2-Benzylidenecyclohexanone Oxime with LAH

Reaction of (*Z*)-2-benzylidenecyclohexanone[3] with hydroxylamine by our general method[4] gave (*Z*)-2-benzylidenecyclohexanone oxime, m.p. 90–92° in a yield of 74%. Mass spectrum *m/e* 201 (parent peak).

Anal. Calcd. for $C_{13}H_{15}NO$: C, 77.58; H, 7.51. Found: C, 77.57; H, 7.49.

(*Z*)-2-Benzylidenecyclohexanone oxime (0.00994 mol) was reacted with LAH (0.0198 mol) using the general method, except that the time of heating under reflux was extended to 20 h, to give a pale yellow syrup (1.46 g). G.l.c. analysis indicated **4** (49%), unreacted oxime (33%), and two unidentified compounds (9 and 9%).

Attempted Reduction of 2a with Sodium Borohydride, Sodium Trimethoxyborohydride, and Lithium Tri-(t-butoxy)aluminum Hydride

When a mixture of **2***a* (0.05 mol), sodium borohydride (0.05 mol), ethanol (150 ml), and water (10 ml) was stirred at room temperature for 96 h or alternatively heated under reflux for 12 h, only unreacted **2***a* was isolated from the reaction.

A mixture of **2***a* (0.015 mol) and sodium trimethoxyborohydride (0.072 mol) in anhydrous tetrahydrofuran (50 ml) was heated under reflux for 96 h. The only product isolated was unreacted oxime (**2***a*).

The attempted reduction of **2***a* (0.001 mol) with lithium tri-(*t*-butoxy)aluminum hydride (0.024 mol) in anhydrous tetrahydrofuran (50 ml) heated under reflux for 8 h, gave only the unreacted oxime (**2***a*).

3-Acetamido-2-benzyl-1-cyclohexene (5)

A solution of **4***a* (2.05 g) in freshly distilled acetic anhydride (1.23 g) was heated under reflux for 15 min. The reaction mixture was poured into cold water (10 ml) and excess acetic anhydride was destroyed by the addition of 10% aqueous sodium carbonate solution (20 ml). The aqueous mixture was extracted with ether and the ether extracts were washed with water and dried ($MgSO_4$). Removal of the ether under reduced pressure gave a gummy yellow residue (2.1 g). G.l.c. analysis indicated 55% of **5**. Recrystallization of this residue from ether – Skelly F gave feathery colorless crystals of **5** (0.34 g, 14%): m.p. 103.5°; i.r. (KBr) 1535s (amide II), 1640s (amide I), 3310s cm^{-1} (NH); n.m.r. δ 7.40–7.00 (5H, m, C_6H_5), 5.77–5.37 (2H, m, C(1)H, NH, one proton replaceable by NaOD), 4.60–4.20 (1H, m, C(3)H), 3.27 (2H, s, C_6H_5—CH_2), 2.23–1.77 (2H, m, C(6)H_2), 1.78 (3H, s, CH_3CO), 1.83–1.43 (4H, m, C(4)H_2, C(5)H_2); mass spectrum *m/e* 229 (parent peak).

Anal. Calcd. for $C_{15}H_{19}NO$: C, 78.56; H, 8.35. Found: C, 78.40; H, 8.17.

The deuterium analog (**11**) was prepared by a similar acetylation procedure. G.l.c. analysis of the crude product indicated 60% of **11**. Crystallization of the crude product from ether – Skelly F gave pure **11** (3.3%): m.p. 101.5°; i.r. 1532s (amide II), 1637s (amide I), and 3310s cm^{-1} (NH); n.m.r. δ 7.37–6.90 (5H, m, C_6H_5), 5.73–5.47 (1H, m, C(1)H), 5.35 (1H, broad s, exchanges with NaOD, NH), 3.40–3.03 (1H, m, C_6H_5CHD), 2.20–1.80 (2H, m, C(6)H_2), 1.80 (3H, s, CH_3CO), 1.80–1.43 (4H, m, C(4)H_2, C(5)H_2); mass spectrum *m/e* 231 (parent peak).

1-Acetamido-2-benzylcyclohexane (6)

A solution of **5** (0.106 g) in absolute alcohol (200 ml) was hydrogenated over 10% palladium-on-charcoal (0.155 g) at 46 p.s.i. for 23 h. The catalyst was removed by filtration of the mixture through celite in a sintered glass funnel. Removal of the ethanol under reduced pressure gave colorless crystals of **6** (0.105 g, 98%): m.p. 152.5°; n.m.r. δ 7.30–6.87 (5H, m, C_6H_5), 5.71 (1H, broad s, replaceable by NaOD, NH), 4.00–3.20 (1H, m, C(1)H), 3.10–1.97 (2H, m, $C_6H_5CH_2$), 1.90 (3H, s, CH_3CO), 2.00–0.77 (8H, m, C(3)H_2, C(4)H_2, C(5)H_2, C(6)H_2); mass spectrum *m/e* 231 (parent peak).

One of the authors (W.A.T.) thanks the Medical Research Council for providing a studentship. Financial support was also provided by Smith, Kline and French Laboratories of Philadelphia, Pennsylvania for the project.

1. N. G. Gaylord. Reduction with complex metal hydrides. Interscience Publishers Inc., New York. 1956. pp. 756–757.
2. N. J. Harper, A. F. Casy, and J. R. Dimmock. J. Chem. Soc. 4280 (1964).
3. K. Kitahonoki, K. Kotera, Y. Matsukawa, S. Okada, H. Takahashi, and Y. Takano. Tetrahedron Lett. 1059 (1965).
4. K. Kotera and K. Kitahonoki. Org. Prep. Proced. **1**, 305 (1969).
5. Shionogi and Co. Ltd. Neth. Appl. 6 515 376. May 27, 1966; Chem. Abstr. **65**, 115324*e* (1966).
6. G. E. Van Lear. Tetrahedron, **26**, 2587 (1970).
7. O. C. Dermer and G. E. Ham. Ethyleneimine and other aziridines. Academic Press, New York. 1969. p. 280.
8. P. E. Fanta and A. S. Deutsch. J. Org. Chem. **23**, 72 (1958).
9. P. E. Fanta and E. N. Walsh. J. Org. Chem. **30**, 3574 (1965).

Can. J. Chem. Downloaded from www.nrcresearchpress.com by 210.87.254.105 on 09/05/12
For personal use only.

Comparison of the Complexation Constants of Some Cyclic Imides and Thioimides with Proton Acceptors

LUC LE GALL,[1] ANNE LE NARVOR,[2] JACQUES LAURANSAN,[1] AND PIERRE SAUMAGNE[2]

Université de Bretagne Occidentale, 6, Avenue Le Gorgeu, 29 N, Brest, France

Received March 8, 1972[3]

The complexation constants of some imides and thioimides in hydrogen-bonded complexes with proton acceptor molecules were determined by i.r. spectroscopy. The results permit a comparison between the proton donating abilities of these compounds. It is possible to classify them against other well-known proton donors.

Les constantes de complexation par pont d'hydrogène de quelques imides et thioimides avec des accepteurs de proton ont été déterminées par spectrométrie i.r. Les résultats permettent de comparer le pouvoir donneur de proton de ces composés et de les situer par rapport aux autres donneurs habituellement considérés.

Can. J. Chem., **51**, 433 (1973)

Can. J. Chem. Downloaded from www.nrcresearchpress.com by 210.87.254.105 on 09/05/12
For personal use only.

Introduction

Evidence for hydrogen-bonded complexes between cyclic imides or thioimides and proton acceptors has been obtained by means of i.r. spectroscopy (1–4). The complexation constants of the 1:1 complexes between pyrrolidone, thiopyrrolidone, monothiosuccinimide, dithiosuccinimide, succinimide, maleimide, phthalimide, 2,4-thiazolidinone, and rhodanine, and proton acceptors have been measured; diacetamide, a non-cyclic compound, has been used for comparison.

Complexation Constants

All compounds studied in this paper exhibit, in dilute solution in carbon tetrachloride, an absorption band near 3400 cm^{-1} due to the stretching vibration of the NH group. The absorbance of ν_{NH} decreases as the amount of proton acceptor is increased in a solution of constant concentration of the proton donor (imide, thioimide, etc.).

One molecule of the proton donor D and one molecule of the proton acceptor A form a hydrogen-bonded complex:

$$D + A \rightleftharpoons D \ldots A$$

and the complexation constant is given by the relation

$$K = \frac{C_C}{(C_D^0 - C_C)(C_A^0 - C_C)}$$

where C_C is the concentration of the complex D–A and C_D^0, C_A^0, the initial concentrations of the donor D and the acceptor A, respectively. Only a 1:1 complex is considered. In all solutions, the proton acceptor is assumed to exist in monomeric form only; this is not always the case for the proton donor. If the self association of the donor is negligible ($C_D^0 < 10^{-4}$ mol l^{-1}) the formation constant of the 1:1 complex can be determined by a method described previously (1); if the initial acceptor concentration C_A^0 is higher than the concentration of the proton donor, Becker's graphical method can be used (5). We consider two solutions with the same concentration C_D^0 of the donor, the first one containing a concentration C_A^0 of the acceptor, the second one $C_A^0 = 0$; the absorbances of ν_{NH} are respectively d and d_0. The quantity $[(1/d) - (1/d_0)]$ is plotted against C_A^0 and the complexation constant is calculated from the slope of the curve. If the self association of the donor is not negligible, one can take this into account using Pineau's method (6).

Results and Discussion

The complexation constants K_C (l mol^{-1}) of 1:1 complexes are summarized in Table 1; Becker's method has been used for most of them except for pyrrolidone, thiopyrrolidone, and diacetamide, compounds for which Pineau's method has been used.

These complexation constants permit a comparison between the proton donating ability of these compounds to form hydrogen-bonded complexes with different "bases".

[1]Laboratoire de Thermodynamique Chimique.
[2]Laboratoire de Spectrochimie Moléculaire.
[3]Revision received September 26, 1972.

Can. J. Chem. Downloaded from www.nrcresearchpress.com by 210.87.254.105 on 09/05/12
For personal use only.

TABLE 1. Complexation constants K_C* (l mol^{-1}) of some amides and imides, in carbon tetrachloride solution, with proton acceptor, near 25 °C

	Donor									
Acceptor	Pyrrolidone	Thiopyrrolidone	Diacetamide	Succinimide	Monothio-succinimide	Dithio-succinimide	Maleimide	Phthalimide	2,4-Thiazolidinone	Rhodanine
Hexamethylphosphorotriamide	21.5	107.5	183	168	225	285	255	210	1500	1300
Dimethylsulfoxide	19.3	89	135	65	63	75	60	42	190	170
Tributylphosphate	12.4	34.4	59	42	55	—	55	46	—	160
Dimethylacetamide	5.6	27	31	22	35	—	32	22	—	100
γ-Picoline	1.5	6	9.7	20	51	—	22	18	—	190
Pyridine	1.2	3.4	4	22	38	—	18	12	—	130
Eucaliptol	—	—	—	7	—	—	4.5	5.5	—	13.5
Dioxane	—	—	2.8	7	11	—	5.5	6.3	—	18
Diethylether	—	—	—	4	—	—	4	3.5	—	6.8
Isopropylether	—	—	—	3	—	—	4	3	—	6
Acetonitrile	—	—	—	2	—	—	2.5	2	—	3

*The errors in K_C were about 20%.

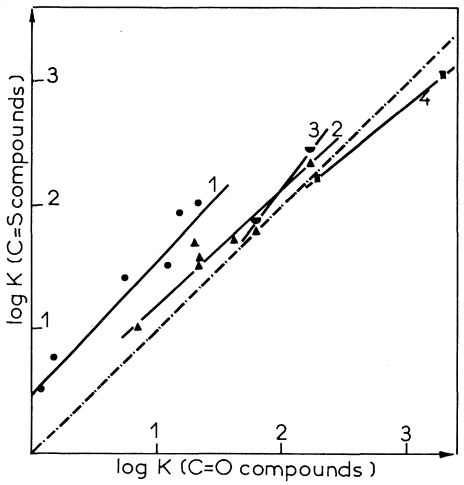

FIG. 1. Log K_C for thioamides and thioimides plotted *vs.* log K_C of the corresponding amides and imides for the same proton acceptors. Line 1, thiopyrrolidone/-pyrrolidone; line 2, monothiosuccinimide/succinimide; line 3, dithiosuccinimide/succinimide; line 4, rhodanin/-2,4-thiazolidinone (·····; 45° line).

The imides, thioimides, and related compounds are classified according to their acidic character and it is possible to observe the influence of the molecular structure, or of the presence of different atoms in the molecule, on the complexation constants.

Comparison of Thio and Oxo Compounds

In order to compare the proton-donating ability of corresponding thio and oxo compounds, log K_C of thioimides or thioamides is plotted against that of the analogous oxygen compounds (Fig. 1). For each thio/oxo pair, the plots for different acceptors are nearly linear. The 45° line suggests an equally acidic character for the two groups of compounds. The plots for thiopyrrolidone and pyrrolidone (line 1) are well above the 45° line, indicating an acidic character greater for the C═S compound than for the C═O compound. Those relating to the monothiosuccinimide, dithiosuccinimide/succinimide pairs (lines 2 and 3) are somewhat above the 45° line; an increase of acidity is again found in passing from the oxo compound to the corresponding thio compound, but this is smaller. 2,4-Thiazolidinone and rhodanine have the same behavior toward a given acceptor; the deviation of the experimental values (line 4) from the 45° line is probably not significant.

These results show that as often as not, the NH group is more acidic when it is closer to C═S groups than to C═O groups; to explain this phenomenon, it is possible for both oxo compounds (I) and thio compounds (II) to exist in the mesomeric forms (7):

(*a*) Polar form (*b*) Non-polar form

The relative electronegativity of the oxygen and sulfur atoms is insufficient to interpret the data; the atomic radius of the sulfur atom is greater than that of the oxygen atom and leads to an overlap of the atomic orbitals of the carbon atom and the X atom that is lower for X = S than for X = O. Morover, Mautner and Kumler (8) have pointed out that the ability of the 3d orbital in sulfur to accept electrons may stabilize the activated state $C^+—S^-$ (polar form (*a*)). Some authors have observed that, as a rule, the molar dipole moments (9), the chemical shift of the proton in the NH group (n.m.r.) (10, 11), and the bond order of the CN bond (11, 12) are systematically greater for compounds of group I than for those of the other group. This remark is supported by the fact that the percentage of polar form (*a*) is highest for the compounds of group II. The percentage of polar form involves an increase in the conjugation of the lone pair of the nitrogen atom with the delocalized π-electrons of the C═X bond. The hydrogen atom is now more positively charged and one finds an increase in its acidity for X = S as compared to X = O. This value agrees with Berthod and Pullman's (13) theoretical studies of 2-pyridone, uracil, guanine, and their thio-analogs: "the NH group adjacent to a double bond C═X appears more positively charged for X = S than for X = O" (13). But, for 2,4-thiazolidinone the endocyclic sulfur atom probably moderates this effect.

Comparison of Maleimide, Succinimide, and Phthalimide

The comparison of complexation constants for these compounds (Table 1) shows that they have a roughly similar acidic character. It can be seen that compared with succinimide, the introduction of an ethylenic double bond (as in maleimide), or of a benzene ring (as in phthalimide) does not alter in any significant way the complexation constant with proton acceptors:

Can. J. Chem. Downloaded from www.nrcresearchpress.com by 210.87.254.105 on 09/05/12
For personal use only.

Can. J. Chem. Downloaded from www.nrcresearchpress.com by 210.87.254.105 on 09/05/12
For personal use only.

the π-electrons of the ethylenic double bond or those of the benzene ring do not conjugate with those of the imide groups.

Comparison of Imides and Thioimides with Other Proton Donors

It is possible to compare imides and thioimides with other proton donors by means of their complexation constant with a given proton acceptor: *e.g.* dimethylsulfoxide (DMSO) in carbon tetrachloride solutions. Pyrrolidine (an aliphatic amine used for comparison) is a basic compound whose acidity is not measurable by the process used here; pyrrolidone is substantially more acidic (K_C = 19.3 l mol^{-1}) while succinimide (2 C=O groups, K_C = 65 l mol^{-1}) is more acidic still. Thus the increase in the number of adjacent carbonyl groups increases the acidity. This phenomenon is accounted for by the conjugation of the lone pair of the nitrogen atom with the π-electrons of the neighboring bonds as shown by Madec *et al.* (14) for a series of amines.

These compounds are relatively strong proton donors. In order of increasing acidity, when DMSO is chosen as the reference proton acceptor, the values are: acetylenic carbides (K_C = 0.2) (ref. 15), diphenylketimine (0.75) (ref. 3), chloroform (3.2)[4] (ref. 16), aromatic amines (2.5) (ref. 14), pyrrolidone (19.3), cyclic imides (65), cyclic thioimides (~70), thiopyrrolidone (89), diacetamide (135), phenol (188) (ref. 17), rhodanine (170), 2,4-thiazolidinone (190), and *p*-chlorophenol (476) (ref. 17). This order is slightly altered if another proton acceptor is selected for reference, hexamethylphosphorotriamide (HMPT) for example.

These results, which show that maleimide and related compounds are strong proton donors, agree with McGlynn's quantum mechanical calculations (18). According to these, the hydrogen atom of the NH group is more positively charged (q = 0.8689) and gives a stronger acidity.

Self-association of Diacetamide and Maleimide

Though the solubility of these donor compounds is very low, in a few cases, if the concentration in carbon tetrachloride is increased, self-association of the donor occurs (diacetamide, maleimide) and the absorption band ν_{NH} shows a deviation from Lambert–Beer's law. The concentration of these compounds is kept very low and we restrict our investigation to the monomer – cyclic dimer model; it is then possible to determine the self-association constant K_D for the monomer – cyclic dimer equilibrium:

$$2M \rightleftharpoons D, \qquad K_D = \frac{C_D}{C_M^2}$$

(Other models might be used for our experimental results but we have not tried them.)

Diacetamide is sufficiently soluble in this solvent for the concentration of the solutions (C_T) to be known with great accuracy. When (C_T/d) is plotted against d, a linear relationship is obtained with K_D = 223 l mol^{-1} (at 20%).

The solubility of maleimide is lower and the total concentration C_T is not known with accuracy but the self-association constant can be evaluated without a knowledge of C_T. Solutions of known dilutions, $\alpha_i \cdot C_T$, are prepared from a saturated solution (C_T unknown) and α_i/d_i is plotted against d_i (d_i is the absorbance of the ν_{NH} band for the different dilutions $\alpha_i \cdot C_T$, see Fig. 2). The straight line thus obtained gives for K_D a value of 22 ± 3 l mol^{-1}, if the molar absorptivity of maleimide is determined for very dilute solutions far-removed from saturation (it is possible to weigh very small amounts of maleimide to prepare these solutions).

Maleimide is strongly self-associated; one finds in order of increasing self-association constants (K_D) the following values: pyrrolidine (0.89) (ref. 19), diphenylketimine (0.13) (ref. 20), (0.2) (ref. 21), aniline (0.27) (ref. 22), phenol (7.4) (ref. 23), maleimide (22) (ref. 4), pyrazole (47.5) (ref. 24), pyrrolidone (197) (ref. 25), and diacetamide (223) (ref. 4). The high value for maleimide results from its high acidity.

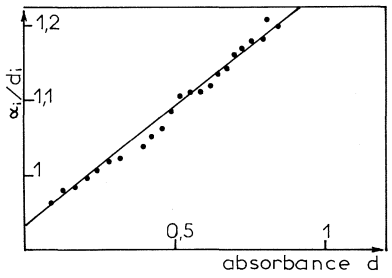

FIG. 2. α_i/d_i *vs.* d_i for maleimide in carbon tetrachloride solution at 25 °C (path length 5 mm).

[4](Mole fraction)$^{-1}$, calculated from n.m.r. studies of binary mixtures.

Experimental

All spectra were obtained with a Perkin–Elmer 225 spectrophotometer. The spectral slit width was approximately 1 cm^{-1}. Because of the low solubility of these compounds in carbon tetrachloride, cells of 5 cm path length with CaF_2 windows were used except for the study of self-association; in this case a cell of 5 mm was used. The donor compounds were commercial products from Aldrich; pyrrolidone, monothiosuccinimide, and dithiosuccinimide were kindly provided by M. Berg and M. Sandström. The proton acceptors were obtained from Prolabo and dimethylsulfoxide from Laboratoires du Bois de Boulogne. All solvents were dried by storing over Linde 4 Å molecular sieves or distilled before use. The temperature was about 25 °C.

We wish to thank Drs Berg and Sandström of the University of Lund, Sweden for the gift of the thiocompounds, Miss E. Gentric for her help and Dr J. P. Brown, Monsanto Chemicals Ltd., England, for valuable comments on the manuscript.

1. L. Le Gall, J. Lauransan, and P. Saumagne. J. Chim. Phys. **66**, 650 (1969).
2. L. Le Gall, A. Le Narvor, J. Lauransan, and P. Saumagne. C.R. Acad. Sci. Paris, **268**, 1285 (1969).
3. E. Gentric, A. Le Narvor, J. Lauransan, and P. Saumagne. J. Chim. Phys. **69**, 87 (1972).
4. L. Le Gall. Thesis of third cycle. Brest, France. 1971.
5. E. D. Becker. Spectrochim. Acta, **17**, 436 (1961).
6. P. Pineau. Thesis. Bordeaux, France. 1961.
7. N. Kulevsky and P. M. Froehlich. J. Am. Chem. Soc. **89**, 4839 (1967).
8. H. G. Mautner and W. D. Kumler. J. Am. Chem. Soc. **78**, 97 (1956).
9. L. M. Lee and W. D. Kumler. J. Org. Chem. **27**, 2052 (1962).
10. M. L. Filleux-Blanchard, F. Clesse, J. Bignebat, and G. J. Martin. Tetrahedron Lett. **12**, 979 (1969).
11. M. L. Filleux-Blanchard and A. Durand. Org. Mag. Res. **3**, 187 (1971).
12. J. Sandström. J. Phys. Chem. **71**, 2318 (1967).
13. H. Berthod and A. Pullman. C.R. Acad. Sci. Paris, **262**, 76 (1966).
14. C. Madec, J. Lauransan, and P. Saumagne. J. Phys. Chem. **75**, 8 (1971).
15. R. De Smedt and H. P. Figeys. Private communication.
16. Wet-Chuwan Lin and Shyr-Jin Tsay. J. Phys. Chem. **74**, 1037 (1970).
17. J. P. Leicknam. Thesis. Paris, France. 1966.
18. C. J. Seliskar and S. P. McGlynn. J. Chem. Phys. **56**, 1417 (1972).
19. R. H. Linnel, M. Alda, and F. Raab. J. Chem. Phys. **36**, 1401 (1962).
20. G. Geiseler and A. Jonossy. J. Mol. Struct. 393 (1972).
21. E. Gentric, A. Le Narvor, J. Lauransan, and P. Saumagne. J. Chim. Phys. **69**, 87 (1972).
22. G. Pannetier and L. Abello. Bull. Soc. Chim. France, 1645 (1965).
23. S. Singh and C. N. R. Rao. J. Phys. Chem. **71**, 1074 (1967).
24. C. M. W. Anderson, J. L. Duncan, and F. J. C. Rossotti. J. Chem. Soc. 140, 2165, 4201 (1961).
25. W. A. P. Luck. Zeit. für Natur. **23**b, 152 (1968).

Can. J. Chem. Downloaded from www.nrcresearchpress.com by 210.87.254.105 on 09/05/12
For personal use only.

Cobalt(II) Mercury Tetrathiocyanate Complexes with Lewis Bases

R. MAKHIJA, L. PAZDERNIK, AND R. RIVEST

Département de chimie, Université de Montréal, Montréal, Québec

Received August 14, 1972

A new series of octahedral cobalt(II) complexes are formed when CoX_2(X = Cl, Br, I, SCN) reacts with $Hg(SCN)_2$ in the presence of Lewis bases. These complexes of stoichiometry $CoHg(SCN)_4.2L$ (L = THF, dioxane, pyridine, aniline) are pink to violet solids which slowly decompose to the blue crystalline solid, $CoHg(SCN)_4$, the stable magnetic susceptibility standard. On further reaction of $CoHg(SCN)_4.2THF$ with mono-, bi-, and polydentate ligands in dry ethanol, complexes of the following types are obtained: $CoHg(SCN)_4.2L$ (L = $P\Phi_3$), $CoHg(SCN)_4.2LL$ (LL = trien), $CoHg(SCN)_4.3LL$ (LL = en, bipy), and $CoHg(SCN)_4.4LL$ (LL = phen). The stoichiometry of these were determined by elemental analysis. Possible structures of these are discussed with the help of mid and far infrared, visible, and ultraviolet spectroscopy, magnetic susceptibility, and X-ray powder diffraction. Some new i.r. bands like Co—P, Co—N, and Hg—S are assigned in the low region.

Une nouvelle série de complexes octaédrique du cobalt(II) a été élaborée quand du CoX_2(X = Cl, Br, I, SCN) réagit avec du $Hg(SCN)_2$ en présence de bases de Lewis. Ces complexes de stoichiométrie $CoHg(SCN)_4.2L$ (L = THF, dioxanne, pyridine, aniline) sont des solides allant du rose au violet qui se décomposent lentement en un solide cristallin bleu, $CoHg(SCN)_4$, le standard stable de mesure de susceptibilité magnétique. De plus, en poursuivant la réaction du $CoHg(SCN)_4.2THF$ avec des ligands mono, bi- et poly coordonnés dans de l'éthanol sec, on peut isoler des complexes des types qui suivent : $CoHg(SCN)_4.2L$ (L = $P\Phi_3$), $CoHg(SCN)_4.2LL$ (LL = trien), $CoHg(SCN).3LL$ (LL = en, bipy) et $CoHg(SCN)_4.4LL$ (LL = phen). La stoichiométrie de ceux-ci a été déterminée par analyse des éléments. Les structures possibles de ceux-ci sont discutées avec l'aide de l'infra-rouge moyen et lointain de la spectroscopie dans le visible et dans l'ultra-violet, de la susceptibilité magnétique et de la diffraction des rayons-X (poudre). Quelques nouvelles bandes (infra-rouge) comme Co—P, Co—N et Hg—S ont été assignées dans la région de l'infrarouge lointain. [Traduit par le journal]

Can. J. Chem., **51**, 438 (1973)

Introduction

The role of thiocyanate ion has been extensively studied in metal complexes because of its ability to coordinate either through nitrogen or sulfur or both in a bridging fashion. Infrared spectroscopy has been a valuable instrument (1–3) in studying the type of bonding *i.e.*, M—NCS, M—SCN, or M—NCS—M′. Some work has been done on complexes of the type $M^{II}Hg(SCN)_4$ where M—NCS—M′ bonding is present (4–6). Bailar and co-workers (4) have reported compounds of the type $M^{II}Hg(SCN)_4$ where M^{II}(Mn to Zn) and Hg^{II} are both tetracoordinated through thiocyanate bridging. $NiHg(SCN)_4.2H_2O$ is the only known compound where Ni atom is octahedral by co-ordinating with two molecules of water (7). Here, we report the synthesis and the characterization of compounds which can be divided into three classes, $CoHg(SCN)_4.2L$ where L is a monodentate ligand, $CoHg(SCN)_4.2P\Phi_3$, and $CoHg(SCN)_4.xLL$ where LL is a bidentate or a polydentate ligand. For each class of compounds structures will be proposed.

Experimental

Materials and Manipulations

Cobalt(II) halides (anhydrous) and mercuric thiocyanate from Alfa Inorganics Inc., triphenylphosphine, triphenylarsine, and 2,2′-bipyridine from City Chemical Corporation, New York, and 1,10-phenanthroline from Eastman Kodak Company were used after vacuum drying at room temperature. Ethylenediamine, triethylenetetramine, aniline, and triethylamine (Baker) were anhydrous and were used after distillation. Dioxane, 1,2-dimethoxyethane, tetrahydrofuran, ethanol, acetone, and methylenedichloride etc, were previously dried by standard methods and distilled onto molecular sieves (Union Carbide). All chemicals and solvents were handled in a dry box flushed with dry nitrogen or on bench top by appropriate techniques.

Physical Measurements

The infrared spectra (4000–200 cm^{-1}) of the complexes and the ligands were recorded on a Perkin–Elmer 621 spectrophotometer using CsI optics. Samples were run as Nujol mulls using CsI plates as well as CsI pellets. In the far infrared (300–33 cm^{-1}), a Perkin–Elmer 180 spectrophotometer was used and the spectra were recorded using pressed polyethylene discs, the instruments being well purged with dry air. The infrared spectra (4000–200 cm^{-1}) are given in Table 1 and those in the far infrared region in Table 2.

Ultraviolet and visible spectra were obtained on a Cary

FOR ERRATA SEE
v.51(12)1973 p.3071

Can. J. Chem. Downloaded from www.nrcresearchpress.com by 210.87.254.40 on 09/05/12
For personal use only.

Can. J. Chem. Downloaded from www.nrcresearchpress.com by 210.87.254.40 on 09/05/12
For personal use only.

TABLE 1. Infrared spectra of $CoHg(SCN)_4.x$ LL in the 4000–300 cm^{-1} region*

$CoHg(SCN)_4.2THF$	$CoHg(SCN)_4.2diox$	$CoHg(SCN)_4.2py$	$CoHg(SCN)_4.2\Phi NH_2$	$CoHg(SCN)_4.2trien$	$CoHg(SCN)_4.2trien$	$CoHg(SCN)_4.3en$	$CoHg(SCN)_4.3bipy$	$CoHg(SCN)_4.4phen$	Assignments
2144 s br	2150 s		2137 s			2097 m		2095 sh 2114 m	
2098 sh	2125 s	2095 sh	2124–45 s br	2118 s	2020–45 s br	2061 s	2100–2110 s br	2068 s	C≡N stretch
	2115 s	2064 sh		2080–90 s		2032 s	2065 sh	2076 s	
				2065 s					
			3340 m br						
			3270 m br						NH_2 stretch
1035 m	1120 vs 1070 vs			1095 s			1058 w		COC stretch
	1090 m 1045 ms						1018 s		asym
									C—H deform
920 w, 955 vw	1015 w	950 w, 930 w	925 w	931 w	886 w	1001 w	960 w	948 w	S—C≡N overtone
	935 w	898 w	890 mw	880 mw	863 w	965 w	890 w	890 w	
						870–90 w br			sym
	860 s								
752 w	755 m	750 m	795 m	799 mw		796–91 w br	805 w	797 w	Ligand
717 vw	718 w	740 w	744 ms	744 s	745 m	730 w	735 s	747 w	C—S stretch
		717 w	717 w	710–4 m		716 w		761 w	
								720 s	
672 vw	620 s	695 s	688 s	687 s				637 m	Ligand
		631 m							
			550 mw		559 w	582 m			Co–ligand*
			540 mw	521 s	513 w br	551 m			stretch
			517 mw	498 s	490 s				Ligand
			500 mw						
469 m, 448 w	470 m, 450 ms	465 m, 448 w	464 mw, 445 mw	468 mw	474 w	473 m	453 wm, 437 mw	473 mw, 448 mw	S—C≡N
		425 m		448 mw	427 w	440 m	414 m	418 m	deformation
				437 mw					Ring vibration
					360 w	372 m			Unassigned
						345 w			
				295–306 m br					Co—NCS stretch†

*vs: very broad; s: strong; m: medium; w: weak; vw: very weak; sh: shoulder; br: broad.
†Reference 33.

Can. J. Chem. Downloaded from www.nrcresearchpress.com by 210.87.254.40 on 09/05/12
For personal use only.

TABLE 2. Far infrared (300–33 cm^{-1}) spectra

	Co—NCS	Co—N(ring)	Ligand	Co—O	Hg—Cl	Hg—S	Co—P	Hg—P	Unassigned
$CoHg(SCN)_4.2P\Phi_3$	282 s br		254 sh 215 w			200 s	176 s 155 m		128 m 108 w 65 w
$CoCl_2.2P\Phi_3$							187 s* 151 w		
$Co(SCN)_2.2P\Phi_3$	293 s		256 w 220 w 210 s				175 s 138 sh		65 w
$Hg(SCN)_2.2P\Phi_3$			258 w			213 s		140—46 s 100—107 m	63 m
$HgCl_2.2P\Phi_3$					235 s 227 s			142—47 s 104—110 m	78 m
$CoHg(SCN)_4.3bipy$		265 s 232 s				204 s			188 m 98 m 168 m 76 m 140 ms
$CoHg(SCN)_4.4phen$		287 s 245 s				215 s			80 w 178 w 128 m 98 w 72 w 160 m br 94 w
$CoHg(SCN)_4.2THF$	260—2 m			236 m		215 s			196 m 78 w
$CoHg(SCN)_4.2diox$	255 w		278 sh	160 m 178 s		220 s			90 ms 78 ms 67 ms

*Given in ref. 27.

TABLE 3. Electronic spectra of Nujol mulls in kK

Complex	Color	Ultraviolet	Visible*	Near infrared
$CoHg(SCN)_4$	Blue	47.62; 41.67; 27.78	21.27; 17.48; 16.81; 16.00	8.77; 7.63
$CoHg(SCN)_4.2THF$	Pink	40.00; 36.49; 30.48; 27.93	21.14; 20.00; 16.66	12.19
$COHg(SCN)_4.2diox$	Pink	46.29; 32.79; 30.77	20.83; 19.61	8.85; 7.14
$CoHg(SCN)_4.2py$	Pink	40.00; 36.76; 32.78; 29.23	21.05; 19.05	9.34
$CoHg(SCN)_4.2\Phi NH_2$	Brownish pink	50.00; 41.15; 33.90; 29.85	20.41; 18.87	8.93
$CoHg(SCN)_4.2P\Phi_3$	Blue	40.00; 33.89; 32.26; 27.70	20.20; 17.09; 16.39; 15.87	—
$CoHg(SCN)_4.2trien$	Brown	41.66; 27.55	20.41; 16.95	12.34
$CoHg(SCN)_4.2en$	Brown	35.71; 27.03	19.31; 17.29	—
$CoHg(SCN)_4.3bipy$	Yellow	48.07; 40.82; 31.75; 27.78	20.83	11.90
$CoHg(SCN)_4.4phen$	Pink	41.66; 35.71; 31.25; 27.03	20.41	11.76

*For the blue compounds, the bands near 16.00 kK were the most intense while for the other compounds the bands near 20.00 kK were the most intense.

TABLE 4. Magnetic suspectibility measurements

Complex	Temperature (°K)	$X_M \times 10^6$ c.g.s.u.	Diamagnetic correction $\times 10^6$ c.g.s.u.	μ_{eff} (B.M.)
$CoHg(SCN)_4.2THF$	296	9559	293	4.76
	297.8	9459	293	4.82
$CoHg(SCN)_4.2diox$	298	9795	298	4.90
$CoHg(SCN)_4.2py$	296	10522	267	5.01
$CoHg(SCN)_4.2\Phi NH_2$	298	10088	313	4.98
$CoHg(SCN)_4.2P\Phi_3$	294	8368	544	4.60
$CoHg(SCN)_4.2trien$	294	1814	266	2.22(2.13)*
$CoHg(SCN)_4.3en$	294	1932	272	2.29(2.14)*
$CoHg(SCN)_4.3bipy$	294	10263	441	5.04
$CoHg(SCN)_4.4phen$	294	10081	1173	5.17

*Magnetic measurements made on Gouy's balance.

14 spectrophotometer between 50 and 5 kK. Samples were run as Nujol mulls between quartz windows. These are included in Table 3.

Magnetic susceptibility measurements were made at room temperature by Gouy's as well as Faraday's methods using $CoHg(SCN)_4$ as standard (8). The diamagnetic corrections were made by the method outlined by Figgis and Lewis (9). The results are included in Table 4.

X-Ray powder patterns were taken using 11.46 cm Debye–Scherrer Camera with nickel filtered CuKα radiation. The samples, sealed in Lindemann capillaries, were exposed for 12–15 h.

Preparation of $CoHg(SCN)_4.2THF$

Anhydrous cobalt(II) halide (10 mmol) was dissolved in the minimum amount of freshly distilled tetrahydrofuran and added to a slurry of $Hg(SCN)_2$ (20 mmol) in the same solvent. The reaction mixture was stirred magnetically for 6–8 h at room temperature. On completion of the reaction, a pink solid was obtained which was filtered, washed, dried in a dry box and finally dried in vacuum for 5 min at room temperature.

The pink solid turns blue at about 80–100 °C, does not melt till 350 °C and is insoluble in common organic solvents. It is very susceptible to moist air and mild heat under which it decomposes to $CoHg(SCN)_4$, a crystalline solid known as Gouy's standard for magnetic measurements (8).

Another route was to dissolve 10 mmol of anhydrous cobalt(II) thiocyanate in dry ethanol and add 10 mmol of mercuric thiocyanate which slowly dissolved to give a pink solution. A slight excess of 1:2 molar ratio of THF was added causing $CoHg(SCN)_4.2THF$ to crystallize as pink needles which were isolated as above. This method was used for the preparation of the dioxane complex since dioxane could not replace the THF ligand in $CoHg(SCN)_4.2THF$. With methylene dichloride or acetone as solvents, only $CoHg(SCN)_4$ is obtained from the reaction.

Preparation of $CoHg(SCN)_4.xL$

To a suspension of the dry pink solid, $CoHg(SCN)_4.2THF$ (5–6 mmol) in dry ethanol is added an excess of the appropriate ligand. The reactants are allowed to stir for 3 days, the solid is filtered, washed with dry ethanol, and dried in vacuum at room temperature. The filtrate on evaporation gives the excess of the ligand used.

Preparation of $CoHg(SCN)_4.2\Phi NH_2$

Cobalt(II) halide and mercuric thiocyanate were mixed in 1:2 molar ratio in ethanol yielding a clear red solution to which excess of anhydrous aniline is added. The resulting solution is pink and on partial removal of the solvent yields a pink powder, which is filtered and dried.

Can. J. Chem. Downloaded from www.nrcresearchpress.com by 210.87.254.40 on 09/05/12
For personal use only.

Can. J. Chem. Downloaded from www.nrcresearchpress.com by 210.87.254.40 on 09/05/12
For personal use only.

TABLE 5. Analytical results

Complex	Cobalt		Mercury		Carbon		Hydrogen		Nitrogen		Sulfur	
	Found	Calcd.	Found	Calcd.	Found	Calcd.	Found	Calcd.	Found	Calcd.	Found	Calcd.
$CoHg(SCN)_4.2THF$	8.85	9.28	31.50	31.54	22.50	22.67	2.46	2.54	8.70	8.82	20.00	20.16
$CoHg(SCN)_4.2diox$	8.16	8.82	29.26	30.02	21.76	21.57	2.67	2.42	8.49	8.39	18.50	19.20
$CoHg(SCN)_4.2py$	8.83	9.06	31.66	30.86	24.49	25.86	1.42	1.55	12.32	12.93	19.76	19.73
$CoHg(SCN)_4.2\Phi NH_2$	8.10	8.69	28.88	29.58	28.37	28.34	2.48	2.08	11.49	12.40	18.69	18.91
$CoHg(SCN)_4.2P\Phi_3$	5.61	5.80	19.83	19.73	47.77	47.26	3.56	2.98	5.25	5.51	12.43	12.62
$CoHg(SCN)_4.2trien$	—	7.51	—	25.57	23.95	24.50	4.67	4.64	21.00	21.44	16.55	16.35
$CoHg(SCN)_4.3en$	9.12	8.77	—	29.84	18.04	17.86	3.39	3.62	21.02	20.84	18.31	19.08
$CoHg(SCN)_4.3bipy$	6.05	6.14	20.38	20.88	39.30	42.52	2.46	2.49	14.50	14.58	13.31	13.55
$CoHg(SCN)_4.4phen$	5.29	4.86	—	16.54	49.84	51.47	2.38	2.64	13.40	13.86	10.72	10.56

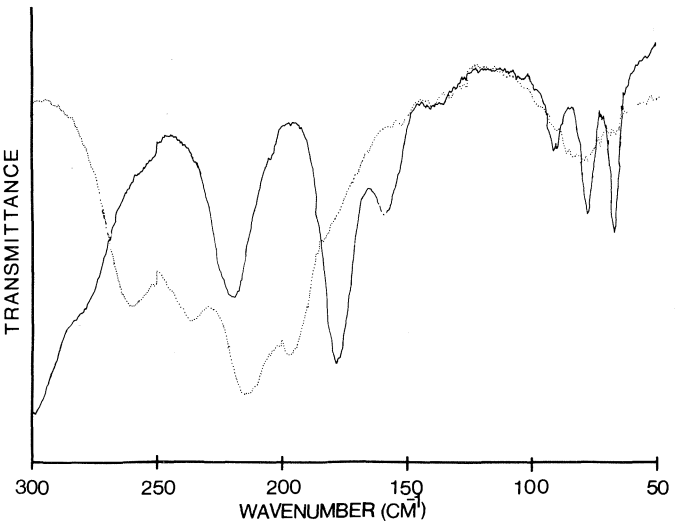

FIG. 1. $CoHg(SCN)_4.2$diox, —; $CoHg(SCN)_4.2$-THF, ···.

From the red filtrate, a second solid is obtained but this contains a small amount of mercuric halide which is formed during the reaction. The pink solid obtained slowly turns violet when dried in vacuum.

Analysis

The elemental analysis for C, H, N, S, Co, and Hg were carried out by Galbraith Laboratories Inc. and Chemalytics Inc. The results are shown in Table 5.

Results and Discussion

The results of our investigations on compounds of the type $CoHg(SCN)_4.x$Base can be easily divided into three groups *a*, *b*, and *c*, according to their stoichiometry, their infrared and visible spectra, and their magnetic moments.

Class (a) Compounds

$CoHg(SCN)_4.2L$ where L = THF, diox., py., and aniline. The infrared spectra indicate that:

(*i*) The SCN groups are bridging. The strong C≡N stretching band for these complexes lies in the frequency range 2100–2150 cm^{-1} which is the range for bridging SCN groups (6, 10, 11). These bands are in the same region as $CoHg(SCN)_4$ (4) which appears at 2142 cm^{-1}. The medium C—S stretching band in the above compounds appears in the range 740—795 cm^{-1} which is within the range for bridging SCN (1). As expected no significant change in the two S—C≡N bending vibrations as compared to $CoHg(SCN)_4$ were observed.

(*ii*) The ligands L are coordinated. The dioxane and tetrahydrofuran complexes show features typical of the coordinated molecules in the range 1250–800 cm^{-1}. In particular the absorption bands associated with the C—O—C antisymmetric stretch show the expected frequency decreased in each case (12—14), *i.e.*, the strong 1070 cm^{-1} band in tetrahydrofuran moves to 1035 (m) cm^{-1}, the strong 1120 cm^{-1} band of dioxane appears at 1045 (ms) cm^{-1}, the tetrahydrofuran band at 908 cm^{-1} moves to 877 cm^{-1} and the dioxane band at 887 to 860 cm^{-1}, respectively. The dioxane compound also shows absorption bands due to uncoordinated C—O—C.

In the aniline compound the $—NH_2$ stretching bands appear at 3340 and 3270 cm^{-1} with reduced intensity as compared to free aniline which appears at 3430 and 3360 cm^{-1}. This negative shift in frequency is indicative of aniline coordinated to a metal (15). Similarly, for the pyridine compound, the two low-lying ring vibrations (16, 17) at 405 and 604 cm^{-1} experience the positive shift and move to 425 and 631 cm^{-1}, respectively, which is due to pyridine coordinated to a metal (18, 19).

(*iii*) The Co—NCS stretching is lowered. The strong absorption band around 310–300 cm^{-1} in $CoHg(SCN)_4$ (20) which is due to Co—NCS stretching no longer appears in our complexes as it has shifted to a lower frequency 255–262 cm^{-1} as shown in Table 2 and illustrated in Fig. 1. This is expected when the geometry around the metal changes from tetrahedral to octahedral.

Can. J. Chem. Downloaded from www.nrcresearchpress.com by 210.87.254.40 on 09/05/12
For personal use only.

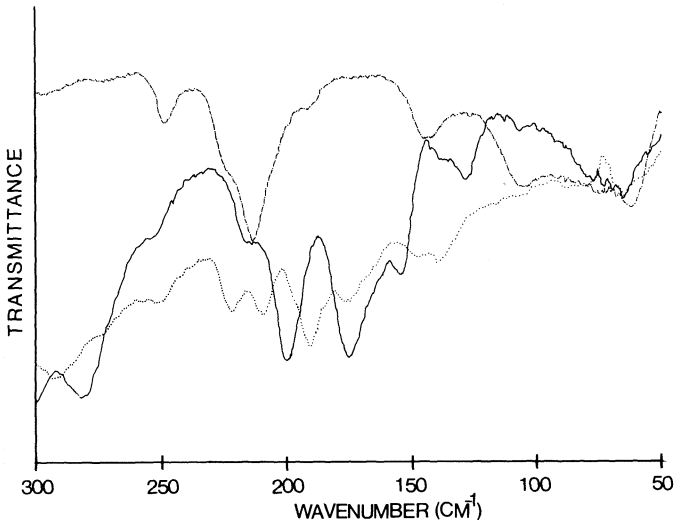

FIG. 2. $CoHg(SCN)_4.2P\Phi_3$, —; $Co(SCN)_2.2P\Phi_3$, · · ·; $Hg(SCN)_2.2P\Phi_3$, ·-·-.

The Visible Spectra

As shown in Table 3, the visible spectra are typical of an octahedral cobalt(II) in these compounds (21–23) and as expected the compounds are pink or brownish pink and have magnetic moments in the range of 4.76 to 5.01 B.M. (24).

Since these compounds are insoluble in most of the common organic solvents, no molecular weight measurements could be performed.

These different experimental results suggest that in these compounds Co(II) is attached to nitrogen of the thiocyanate group and Hg(II) to sulfur, hence both metals are attached through four SCN bridging groups while two ligand molecules are coordinated to Co(II) making it octahedral.

Class (b) Compound

In the second category we were successful in preparing only one compound, namely, $CoHg(SCN)_4.2P\Phi_3$, which is very stable in air and decomposes above 300 °C. It is slightly soluble in polar solvents like acetone or *N*,*N*′-dimethyl formamide in which it gives a blue solution. Molecular weight measurements show it to be monomeric.

The infrared spectrum of this yields four strong absorption bands at 2137, 2118, 2080, and 2065 cm^{-1} indicating both bridged and free thiocyanates (25). The *x*-sensitive *q*, *r*, and *t* absorption bands at 1095, 710–14, 437 cm^{-1} are typical of coordinated triphenyl phosphine (26). The low infrared spectrum of this compound shows bands at 176 and 155 cm^{-1} which we have assigned to be the asymmetric and symmetric Co—P stretching vibrations. This agrees with the reported bands for tetrahedral Co(II) phosphine compounds (27). This visible spectra of this compound show a strong absorption band at 15.87 and 16.34 kK which are in agreement for tetrahedral cobalt(II) (21, 28).

The far infrared spectrum was also studied. The triphenyl phosphine gives absorption bands at 251, 246, 212, 194, and 183 cm^{-1} while $CoHg(SCN)_4.2P\Phi_3$ shows absorption bands at 282, 254, 215, 200, 176, 155, and 128 cm^{-1}, respectively. Sharp and co-workers (27) have assigned Co—P stretching bands at 187 (s), 151 (w) in $(\Phi_3P)_2CoCl_2$ and at 187 (m), 142 (w) cm^{-1} for $(P\Phi_3)_2CoBr_2$ complexes. Hence our bands at 176 and 155 cm^{-1} are due to Co—P for tetrahedral species with C_{2v} symmetry. If triphenyl phosphine was attached to mercury then we should have observed bands at 137, 108 cm^{-1} as is the case for $(\Phi_3P)_2HgCl_2$ and $(\Phi_3P)_2.Hg(SCN)_2$. The absorption band at 282 cm^{-1} is due to Co—NCS and 200 cm^{-1} to Hg—S stretching. This is illustrated in Fig. 2.

A magnetic moment of 4.60 B.M. was observed.

These results suggest that in this compound both cobalt(II), and mercury(II) are tetrahedrally coordinated and that the most plausible structure is

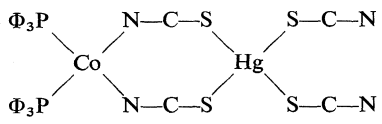

Can. J. Chem. Downloaded from www.nrcresearchpress.com by 210.87.254.40 on 09/05/12
For personal use only.

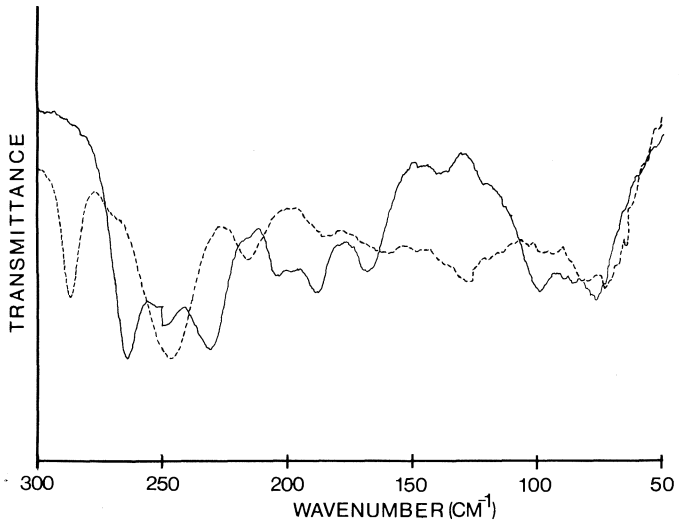

FIG. 3. $CoHg(SCN)_4.3bipy$, - - -; $CoHg(SCN)_4.4$-phen, —.

Class (c) Compounds

$CoHg(SCN)_4.xLL$ where LL = en., trien., bipy., and phen. The third type of compounds are insoluble in most of the common organic solvents, even water and DMF. They are very air stable and decompose above 300 °C. No conductance or molecular weight measurements could be performed.

The infrared spectra of all these compounds show only one type of C≡N stretch which appears below 2100 cm^{-1}, indicating only free thiocyanates (M—SCN type). The phenanthroline and bipyridine complexes are pink and yellow and have magnetic moments of 5.04 and 5.17 B.M., respectively, indicating cobalt to be high spin octahedral. This is also supported by the fact that visible spectra show absorption bands around 20–21.0 kK. On the other hand, compounds with ethylenediamine and triethylenetetraamine show magnetic moments of 2.29 and 2.22 B.M., respectively. These results were surprising as compared to the ones obtained for the other compounds and the magnetic susceptibility measurements were repeated many times confirming the above mentioned values. No interpretation of them is offered at this time.

In order to see if the complexes are ionic, we prepared the bipyridine compound starting with $K_2Hg(SCN)_4$ and $Co(bipy)_3Br_2$ in alcohol. We found the same infrared, visible spectra, and magnetic moment, which indicates that a probable structure could be $Co(bipy)_3^{2+}.Hg(SCN)_4^{2-}$. In all these complexes cobalt is believed to be hexa-coordinated and mercury tetra-coordinated with the exception of the phenanthroline complex in which both Co(II) and Hg(II) are hexa-coordinated.

Mercury thiocyanate has been used as a Lewis acid by many groups and compounds of the $Hg(SCN)_2.xL$ (x = 1 or 2 and L is ligand molecule) have been reported (29). In these compounds mercury is usually four coordinated but examples of six coordination for mercury are reported (30).

In the far infrared spectrum the free bipyridine ligand exhibits the bands at 423–404 and 168 cm^{-1}. These bands appear almost at the same frequencies in our spectrum. New bands at 375–55, 290–75, 260–35, and 240–10 cm^{-1} have been assigned to ligand vibration newly activated by complex formation. Nakamoto and co-workers (31) in their recent paper have assigned Co—N stretching at 266 and 228 cm^{-1} and we tentatively assign our bands at 265 and 232 cm^{-1} as Co—N, while the 204 cm^{-1} absorption band is due to Hg—S stretching. The Co—N stretching band is further confirmed by Strukl and Walter (32) who assigned it at 270 cm^{-1} in their bipyridine complex. Similarly in our phenanthroline complex we tentatively assign 287 and 245 cm^{-1} to Co—N stretching and 215 cm^{-1} to Hg—S stretching. The bands we observed are illustrated in Fig. 3.

These results suggest that in all these compounds Co(II) is octahedral and Hg(II) is tetrahedral with one exception, the phenanthroline

Can. J. Chem. Downloaded from www.nrcresearchpress.com by 210.87.254.40 on 09/05/12
For personal use only.

TABLE 6. X-Ray powder photograph data

$CoHg(SCN)_4.2THF$		$CoHg(SCN)_4.2P\Phi_3$		$CoHg(SCN)_4.3bipy$	
Intensity	d_{obs}	Intensity	d_{obs}	Intensity	d_{obs}
vs	7.86	vs	12.2	vs	11.1
vs	7.46	vs	11.8	mw	10.3
s	7.10	s	9.5	m	9.6
s	6.68	s	8.69	m	8.87
m	6.29	w	7.72	sm	8.08
m	5.90	s	7.23	sm	7.41
m	5.68	w	6.86	s	6.93
s	4.98	w	6.53	m	6.69
mw	4.87	m	6.22	m	6.34
mw	4.70	ms	5.97	s	6.06
s	4.56	ms	5.66	w	5.46
vs	4.16	m br	5.34	m	5.21
vs	3.999	w	5.17	w	4.89
w	3.938	w	4.94	s	4.65
mw	3.719	w br	4.58	w	4.38
w	3.554	m	4.33	w	4.25
w	3.404	mw	4.13	w	4.15
m	3.305	mw	4.04	m	4.031
w	3.156	mw	3.960	m	3.947
wm	3.020	s	3.793	mw	3.754
wm	2.9761	m	3.636	w	3.601
w	2.9029	wm	3.423	w	3.424
m	2.8488	wm	3.332	w	3.252
w	2.7364	w	3.269	m	3.142
m	2.6925	w	3.161	w	3.066
m	2.5851	w	3.055	m	2.9931
w	2.5115	w	2.9761	w	2.8892
mw	2.4813	w	2.90525	w	2.7883
w	2.4454	m	2.8312	mw	2.5960
w	2.3860	w	2.7840	wm	2.5286
m	2.3544	m	2.7283	w	2.3814
s	2.2882	w	2.6143	w	2.3223
w	2.2378	w	2.50985	w	2.2338
w	2.1974	w	2.43745	w	2.1948

complex in which it is hexa-coordinated. The experiment with $K_2Hg(SCN)_4$ and $Co(bipy)_3Br_2$ suggests that these compounds are ionic.

X-Ray powder patterns of some of the complexes were measured but due to the large number of closely packed lines, the interpretation is very difficult. We have tabulated the values of *d*-spacings (observed) and relative intensities of one compound from each class in Table 6. We have been successful in growing crystals of $CoHg(SCN)_4.2py$ and single crystal precession photographs show it to be monoclinic with systematic absences consistent for both *Cc*(noncentric) and *C*2/*c* (centric) space groups. The cell dimensions are $a = 11.46$ Å, $b = 13.29$ Å, $c = 14.50$ Å, and $\beta = 105.50°$, $Z = 4$. The complete structure is presently under investigation.

We did carry out reactions with Φ_3As, Φ_3N, Φ_2NH, Φ_3PO, and Φ_3Sb but failed to obtain any new complexes. In all these cases the starting material $CoHg(SCN)_4.2THF$ was decomposed to $CoHg(SCN)_4$. Apparently the coordinating ability of these ligands for Co(II) was insufficient to stabilize the formation of the octahedral Co(II) complex.

The authors wish to express their thanks to Dr. R. N. Jones, National Research Council of Canada, Ottawa for the use of far infrared facilities. We thank the National Research Council of Canada for financial assistance.

1. A. TURCO and C. PECILE. Nature (London), **191**, 66 (1961).
2. A. SABATINI and I. BERTINI. Inorg. Chem. **4**, 1665 (1965).
3. A. SABATINI and I. BERTINI. Inorg. Chem. **4**, 959 (1965).

Can. J. Chem. Downloaded from www.nrcresearchpress.com by 210.87.254.40 on 09/05/12
For personal use only.

4. M. M. CHAMBERLAIN and J. C. BAILAR, JR. J. Am. Chem. Soc. **81**, 6412 (1959).
5. A. TRAMER. J. Chim. Phys. **59**, 232 (1962).
6. R. A. BAILEY, S. L. KOZAK, T. W. MICHELESEN, and W. N. MILLS. Coord. Chem. Rev. **6**, 407 (1971).
7. CHOU KUO-CHAN and M. A. PORAI-KOSHITS. Kristallografiya, **5** (3), 462 (1960).
8. B. N. FIGGIS and R. S. NYHOLM. J. Chem. Soc. 4190 (1958).
9. B. N. FIGGIS and J. LEWIS. Modern coordination chemistry. *Edited by*: J. Lewis and R. G. Wilkins. Interscience Publishers Inc., New York. 1960.
10. P. C. H. MITCHELL and R. J. P. WILLIAMS. J. Chem. Soc. 1912 (1960).
11. J. L. BURMEISTER. Coord. Chem. Rev. **1**, 205 (1966).
12. G. W. A. FOWLES, P. T. GREEN, and T. F. LESTER. J. Inorg. Nucl. Chem. **29**, 2365 (1967).
13. R. J. KERN. J. Inorg. Nucl. Chem. **24**, 1105 (1962).
14. R. C. MAKHIJA and R. A. STAIRS. Can. J. Chem. **47**, 2293 (1969).
15. L. J. BELLAMY. The infrared spectra of complex molecules. Methuen and Co. Ltd., London. 1958. p. 250.
16. C. H. KLINE and J. TURKEVICH. J. Chem. Phys. **12**, 300 (1944).
17. G. ZERBI, B. CRAWFORD, and J. OVEREND. J. Chem. Phys. **38**, 127 (1963).
18. R. J. H. CLARK and C. S. WILLIAMS. Inorg. Chem. **4**, 350 (1965).
19. N. S. GILL, R. H. NUTTALL, D. E. SCAIFE, and D. W. A. SHARP. J. Inorg. Nucl. Chem. **18**, 79 (1961).
20. D. FORSTER and D. M. L. GOODGAME. Inorg. Chem. **4**, 715 (1965).
21. W. J. DAVIS and J. SMITH. J. Chem. Soc. (A), 317 (1971).
22. J. FERGUSON. J. Chem. Phys. **32**, 528 (1960).
23. D. E. BILLING and A. E. UNDERHILL. J. Chem. Soc. (A), 29 (1968).
24. RICHARD L. CARLIN. Transition metal chemistry. Vol. I. Marcel Dekker Inc., New York. 1965. pp. 1–32.
25. J. CHATT and L. A. DUNCANSON. Nature, **178**, 997 (1956).
26. G. B. DEACON and J. H. S. GREEN. Chem. and Ind. 1031 (1965).
27. J. BRADBURY, K. P. FOREST, R. G. NUTTALL, and D. W. A. SHARP. Spectrochim. Acta, **23A**, 2701 (1967).
28. F. A. COTTON, D. M. L. GOODGAME, M. GOODGAME, and A. SACCO. J. Am. Chem. Soc. **83**, 4157 (1961).
29. (*a*) S. C. JAIN and R. RIVEST. Inorg. Chim. Acta, **4**, 291 (1970). (*b*) A. R. DAVIS, C. J. MURPHY, and R. A. PLANE. Inorg. Chem. **9**, 423 (1970).
30. A. L. BEAUCHAMP, B. SAPERAS, and R. RIVEST. Can. J. Chem. **49**, 3579 (1971).
31. B. HUTCHISON, J. TAKEMOTO, and KAZUO NAKAMOTO. J. Am. Chem. Soc. **92**, 3335 (1970).
32. J. S. STRUKL and J. L. WALTER. Spectrochim. Acta, **27A**, 223 (1971).
33. D. M. ADAMS. Metal ligand and related vibrations. Arnold Publication, London. 1967. pp. 279–286.

Can. J. Chem. Downloaded from www.nrcresearchpress.com by 210.87.254.40 on 09/05/12
For personal use only.

Conductance and Conductometric Titrations of Picric Acid in Sulfolane at 30°

P. M. P. Eller and Joseph A. Caruso[1]

Department of Chemistry, University of Cincinnati, Cincinnati, Ohio 45221

Received July 13, 1972

Conductance of picric acid solutions in sulfolane resembles the behavior seen in several other aprotic solvents and is suggestive of complex solution equilibria. The effect of water on equivalent conductance of picric acid is large for concentrations greater than about 0.3 *M*. Picric acid behaves as a weak acid in conductometric titrations.

La conductance de solutions d'acide picrique dans le sulfolane se rapproche du comportement de celle rencontrée dans plusieurs autres solvants aprotiques et suggère alors des équilibres complexes en solution. L'effet de l'eau sur la conductance équivalente de l'acide picrique est considérable pour des concentrations supérieures à environ 0.3 *M*. L'acide picrique se comporte comme un acide faible lors des titrations conductimétriques. [Traduit par le journal]

Can. J. Chem., **51**, 448 (1973)

Can. J. Chem. Downloaded from www.nrcresearchpress.com by 210.87.254.5 on 09/05/12
For personal use only.

Introduction

Sulfolane (tetrahydrothiophene-1,1-dioxide) is a dipolar aprotic solvent which is finding application in titrations of acids and bases (1, 2) and in fundamental studies of acid–base equilibrium (3–5) because of its low autoprotolysis constant and moderately high dielectric constant. Conductance measurements have been limited to a few metal salts (6–8) and some moderately strong acids (9), and show limiting equivalent conductances for these solutes of about 10–12 ohm^{-1} cm^{-2} mol^{-1}. Picric acid solutions in sulfolane were found to have very stable solution resistances, and therefore the present study was undertaken in order to define further the nature of acid–base behavior in this interesting solvent.

Experimental

Apparatus

Conductance cells were made from 300 ml flasks, after the design of Daggett, Bair and Kraus (10). The electrodes were lightly platinized, at 6 C/cm^2 and the cell constants, determined with standard KCl solutions, were 0.2110 ± 0.0001 and 0.1837 ± 0.0001. A Leeds and Northrup #4666 Jones bridge, with Hewlett–Packard Audio Oscillator (Model 201-C) operating at 2000 Hz and General Radio Company Model 1232-A Tuned Amplifier/Null Detector was used to measure resistances. The cells were maintained at 30 ± 0.03 °C during experiments.

Reagents

Anhydrous sulfolane (Phillips Petroleum Company, Bartlesville, Oklahoma) was distilled (b.p. 100–105 °C, 1 mm) over concentrated sulfuric acid to prevent degradation of the solvent which occurred if it contained appreciable amounts of basic material. A second vacuum distillation was then done over sodium hydroxide pellets and resulted in a colorless distillate which contained less than 0.0007 mol/l of water (0.0013% H_2O). Specific conductance was 1–3 × 10^{-8} ohm^{-1} cm^{-1} after distillation and increased only slowly after several days of storage under dry nitrogen. Physical constants used for sulfolane at 30° were (6): density = 1.2623 g/ml, viscosity = 0.1029 P, and dielectric constant = 43.3.

The 1,3-diphenylguanidine (Eastman) was recrystallized from toluene. Tetrabutylammonium hydroxide (25% in methanol, Eastman) titrant was diluted approximately 1:10 with sulfolane. Picric acid (Eastman) was recrystallized from ethanol, then recrystallized from acetone and vacuum dried for 2 h at 80 °C.

Procedure

About 100 ml of pure solvent was weighed into a conductance cell, the resistance measured, and then a series of measurements of resistance was made after successive additions of stock solution of picric acid (*ca.* 0.04 *M*) from a weight buret.

Results and Discussion

The experimental values for equivalent conductance of picric acid solutions in sulfolane at 30° appear in Fig. 1, curve *g*. Also shown on the same figure are the data of French and Roe (11) for picric acid solutions in acetophenone at 25° (curve *h*) over the concentration range 10^{-2} to 10^{-4} *M*. The two sets of data are very similar, with slope, d log Λ/d log *C*, equal to −0.96. The magnitude of this slope was attributed by French and Roe to the formation of triple ions of the type $PiHPi^-$. However, it has been demonstrated that this mechanism cannot ade-

[1]To whom correspondence should be addressed.

Can. J. Chem. Downloaded from www.nrcresearchpress.com by 210.87.254.5 on 09/05/12
For personal use only.

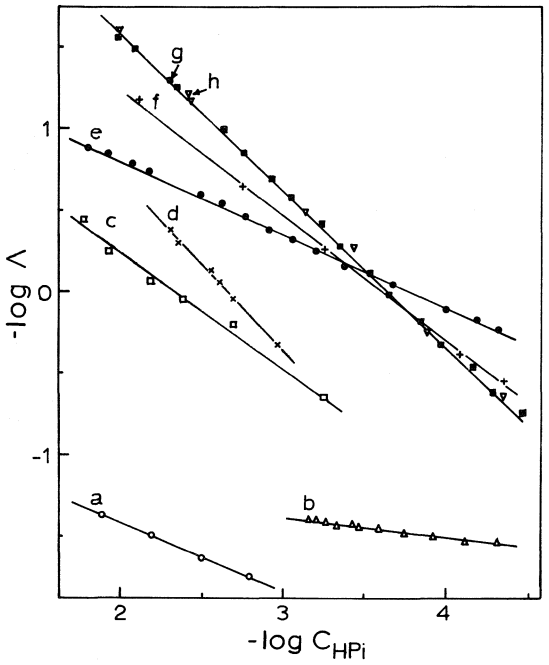

FIG. 1. Conductance of picric acid in various solvents: *a*, methanol (25°) (15); *b*, 1,1,3,3-tetramethylguanidine (25°) (14); *c*, acetone (25°) (11); *d*, acetonitrile (25°) (11); *e*, sulfolane + 1.09% by weight water (30°); *f*, α-naphthonitrile (40°) (11); *g*, sulfolane (30°); *h*, acetophenone (25°) (11).

quately explain such highly negative slopes (12). The only mechanisms which offer possible explanations for such slopes involve polymer formation. It is interesting to note that Kolthoff and co-workers have proposed $Pi(HPi)_2^-$ as the principal picric acid species at concentrations greater than 0.1 *M* (13). Implicit in their postulation, of course, is the formation of the dimer, $(HPi)_2$.

The mechanism of ionization of picric acid in sulfolane is changed by the addition of about 1% by weight water, as is seen in curve *e* of Fig. 1. In the presence of water at this level (*ca.* 0.7 *M*), the slope of the conductance line is −0.465, which is close to the −0.5 expected for the simple ionization of a weak acid according to the mechanism $HPi = H^+ + Pi^-$ (12). At concentrations of water less than 0.2 *M* the equivalent conductance of picric acid in sulfolane varies by only about 6% from that in the purified solvent, but a marked increase in Λ_{HPi} is seen (Fig. 2) for water content greater than about 0.3% by weight, with equivalent conductance

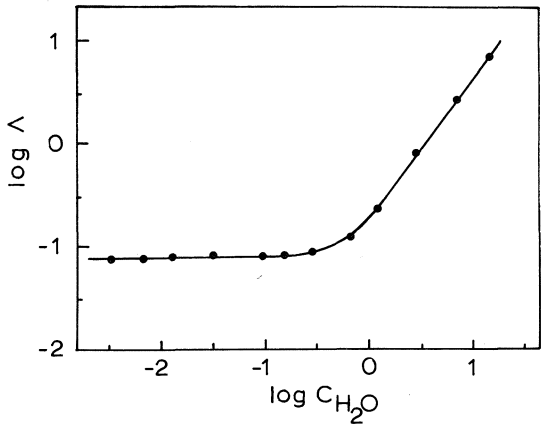

FIG. 2. Equivalent conductance of 1.98×10^{-3} *M* solution of picric acid in sulfolane at 30° as a function of added water concentration.

increasing approximately as $C^{1.3}$. The conductance of picric acid in several other solvents has been shown for comparison in Fig. 1 and the slopes listed in Table 1.

Data also have been reported for the conductance of picric acid solutions in phenol at 50°, in which the values of d log Λ/d log *C* vary from −0.53 (at 10^{-4} *M*) to −0.98 (at 10^{-2} *M*) (16).

Figure 3 shows the results of conductometric titrations of about 10^{-3} *M* picric acid in sulfolane at 30° with two bases. The titration with 1,3-diphenylguanidine (curve *b*) proceeds at low specific conductance values and gives a distinct end point characteristic of the titration of a weak acid with a weak base, with satisfactory recovery. On the other hand, the tetrabutylammonium hydroxide titrant (curve *a*) behaves as a strong electrolyte and gives an indistinct end point

TABLE 1. Conductance of picric acid in various solvents

Solvent	*T* (°C)	$\frac{d \log \Lambda}{d \log C}$	Reference
1,1,3,3-Tetramethylguanidine	25	−0.13	14
Methanol	25	−0.46	15
Sulfolane +1.09% water	30	−0.465	This work
Acetone	25	−0.72	11
α-Naphthonitrile	40	−0.78	11
Acetophenone	25	−0.95	11
Sulfolane	30	−0.96	This work
Benzonitrile	25	−0.97	11
Acetonitrile	25	−1.06	11

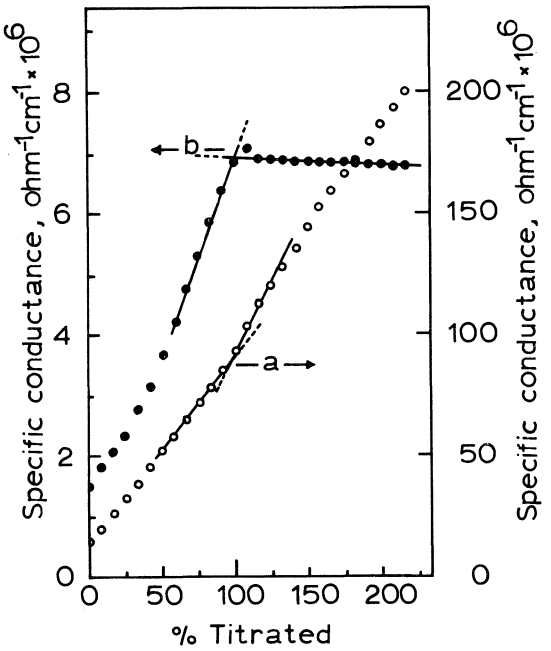

FIG. 3. Conductometric titration of picric acid in sulfolane: *a*, 7.23×10^{-4} *M* picric acid titrated with 0.1 *M* tetrabutylammonium hydroxide; *b*, 1.19×10^{-3} *M* picric acid titrated with 0.15 *M* 1,3-diphenylguanidine, at 30 °C.

(although with apparently satisfactory recovery) at much higher specific conductance values. The presence of methanol in the titrant may have contributed to slightly elevated conductances.

It may be concluded that picric acid behaves as a weak acid in sulfolane, with conductance behavior similar to that seen in several other aprotic solvents, if reasonable care is taken to exclude water.

1. D. H. MORMAN and G. A. HARLOW. Anal. Chem. **39**, 1869 (1967).
2. P. M. P. ELLER and J. A. CARUSO. Anal. Lett. **4**, 13 (1971).
3. S. K. HALL and E. A. ROBINSON. Can. J. Chem. **42**, 1113 (1964).
4. K. BOWDEN, A. BUCKLEY, and R. STEWART. J. Am. Chem. Soc. **88**, 947 (1966).
5. E. M. ARNETT and C. F. DOUTY. J. Am. Chem. Soc. **86**, 409 (1964).
6. R. FERNANDEZ-PRINI and J. E. PRUE. Trans. Faraday Soc. **62**, 1257 (1966).
7. M. DELLA MONICA, U. LAMANNA, and L. SENATORE. J. Phys. Chem. **72**, 2124 (1968).
8. M. DELLA MONICA, U. LAMANNA, and L. JANNELLI. Gazz. Chim. Ital. **97**, 367 (1967).
9. R. L. BENOIT, C. BUISSON, and G. CHOUX. Can. J. Chem. **48**, 2353 (1970).
10. H. M. DAGGETT, E. J. BAIR, and C. A. KRAUS. J. Am. Chem. Soc. **73**, 799 (1951).
11. C. M. FRENCH and I. G. ROE. Trans. Faraday Soc. **49**, 314 (1953).
12. N. G. SELLERS, P. M. P. ELLER, and J. A. CARUSO. J. Phys. Chem. **76**, 3618 (1972).
13. I. M. KOLTHOFF, S. BRUCKENSTEIN, and M. CHANTOONI. J. Am. Chem. Soc. **83**, 3927 (1961).
14. J. A. CARUSO, P. G. SEARS, and A. I. POPOV. J. Phys. Chem. **71**, 1756 (1967).
15. D. A. MACINNES. The principles of electrochemistry. Dover Publications. 1961. p. 362.
16. R. M. DOLBY and P. W. ROBERTSON. J. Chem. Soc. (London), 1711 (1930).

Can. J. Chem. Downloaded from www.nrcresearchpress.com by 210.87.254.5 on 09/05/12
For personal use only.

Production of Vibrationally Excited Carbon Monoxide by the Reaction of Oxygen Atoms with Acetylene, Methylacetylene, and Methane

S. J. ARNOLD AND G. H. KIMBELL

Defence Research Establishment Valcartier, P.O. Box 880, Courcelette, Quebec

Received July 10, 1972

Infrared chemiluminescence attributed to the first overtone of CO was observed when either C_2H_2 or CH_3C_2H was introduced into a stream of oxygen which had been passed through a microwave discharge. The addition of vibrationally cold CO to these systems was found to produce a vibrational population inversion in the chemically formed CO. CO first overtone emission was not observed when CH_4 was introduced into a similar stream of oxygen unless the CH_4 had been subjected to a microwave discharge. These observations are used to clarify the mechanisms governing the formation of CO in continuous wave air–helium–hydrocarbon electrical discharge lasers.

La chemiluminescence infrarouge attribuée à la première harmonique de CO a été étudiée quand on introduit soit du C_2H_2, ou soit du CH_3C_2H dans un courant d'oxygène lequel a préalablement subi une décharge en microondes. L'addition de CO vibrationnellement froid à ces systèmes produit une inversion des populations dans les états vibrationnels pour du CO chimiquement formé. L'émission de la première harmonique du CO n'a pas été observée quand du CH_4 est introduit dans un courant identique d'oxygène à moins que le CH_4 n'ait préalablement subi une décharge en microondes. Ces observations ont été utilisées pour clarifier les mécanismes régissant la formation du CO dans des laser à ondes continues et à décharges électriques dans un mélange air–hélium–hydrocarbones.

[Traduit par le journal]

Can. J. Chem., **51**, 451 (1973)

Introduction

Recently, workers active in studying chemical lasers have shown very great interest in chemical reactions capable of producing vibrationally excited carbon monoxide. Indeed, within the last year purely chemical laser action was observed in CO formed in a CS_2–O_2 low pressure diffusion flame (1). Several reports have also appeared describing continuous wave CO laser action occurring when a direct current discharge was sustained in mixtures such as CH_4–air–He, C_3H_8–air–He, C_2H_2–air–He, and C_2N_2–air–He (2–7). In these latter reports evidence was presented to suggest that vibrationally-excited CO formed chemically in the combustion contributed substantially to the energy of the laser.

Concurrently with this work, studies of the emission observed from the reaction of oxygen atoms with methane, acetylene, and methylacetylene were undertaken in this laboratory. The oxygen atom – acetylene system has been the subject of previous studies (8, 9); however, the need for additional experiments was felt in order to identify the role of chemically formed CO in increasing the performance characteristics of hydrocarbon–air–He continuous wave electrical discharge CO lasers.

Experimental

The apparatus used for these experiments is shown in Fig. 1. The reaction cell consisted of a 1.5 in. glass "tee" equipped with a NaCl window, which was pumped by an Edwards 660 l/min two stage pump. Oxygen atoms produced by the passage of an oxygen–helium mixture through a 2450 Mc microwave discharge entered the cell through the center tube of the concentric mixer. The hydrocarbon in a helium buffer entered through five holes in the outer tube of the concentric mixer. A second microwave discharge could be placed on the hydrocarbon–helium line. Carbon monoxide could be either premixed with the hydrocarbon–helium mixture or enter through a separate injector at right angles to the concentric mixer depending on whether one or two microwave discharges were used.

The spectra were recorded using a McPherson Model

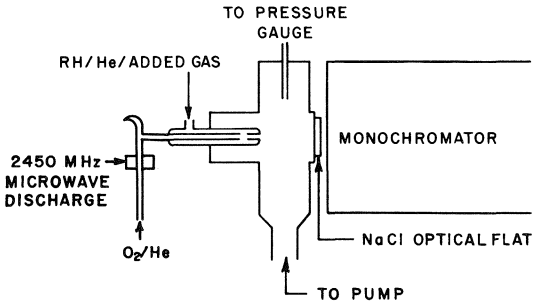

FIG. 1. Schematic diagram of the apparatus.

Can. J. Chem. Downloaded from www.nrcresearchpress.com by 210.87.254.105 on 09/05/12
For personal use only.

218 0.3 m monochromator, a Dry Ice–acetone cooled PbS detector, a phase sensitive PAR Model HR-8 amplifier and a Hewlett–Packard Model 7100B strip chart recorder. The entire optical path was flushed with dry nitrogen to minimize absorption by atmospheric water vapor. A 500 °C blackbody source was used to provide a relative measurement of the sensitivity of the detection system as a function of wavelength.

Temperatures in the reaction zone were measured with a glass-coated chromel–alumel thermocouple.

All gases were of the highest purity available from Matheson and were used without further purification. Flows were measured with Matheson rotameters.

Results and Discussion

Acetylene

When acetylene was added to a stream of oxygen which had been passed through a microwave discharge a brilliant blue violet emission filled the reaction cell. Strong infrared chemiluminescence attributed to the CO first overtone emission was observed in the region 2300 to 2800 nm. As is shown in Fig. 2, only the first 13 vibrational levels of CO were appreciably populated, although emission from up to $v = 16$ can usually be detected. Figure 3 shows a plot

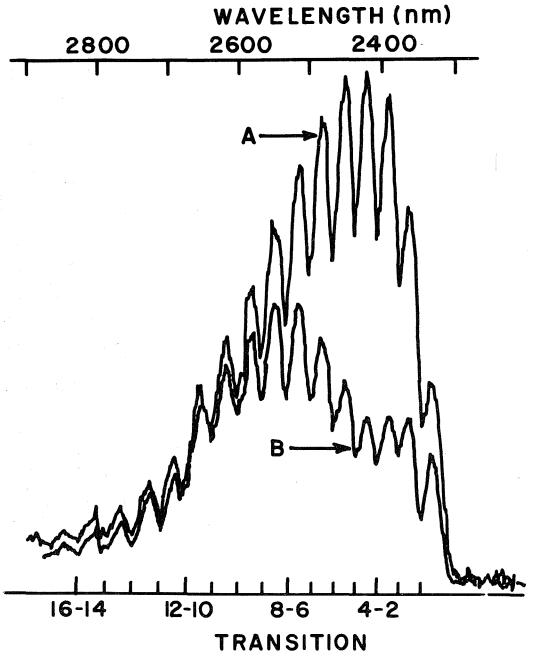

FIG. 2. The CO first overtone spectrum from the C_2H_2/O_2 atomic flame showing the effects of the addition of vibrationally cold CO. Curve *A*: flow rates, C_2H_2:O_2:He, 19:57.7:4809 μmol/s, total pressure, 8.1 Torr. Curve *B*: flow rates, C_2H_2:O_2:CO:He, 19:57.7:127:4809 μmol/s, total pressure, 8.4 Torr.

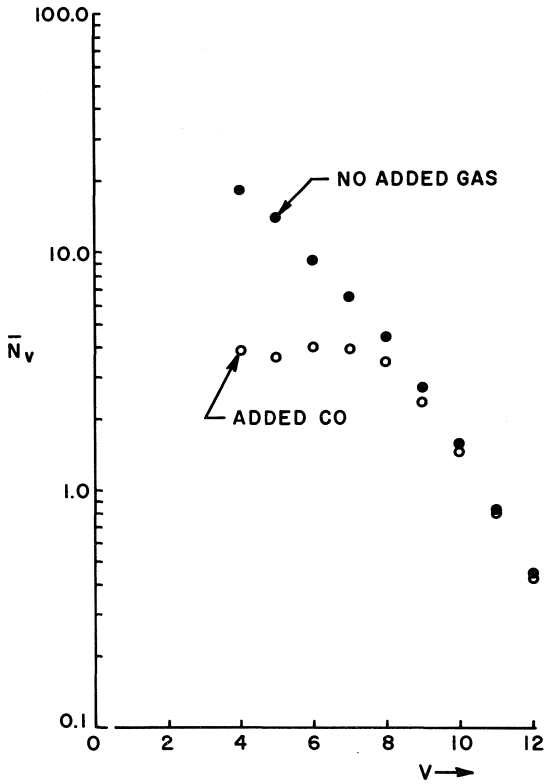

FIG. 3. Relative vibrational level population of CO† produced in the C_2H_2/O_2 atomic flame.

of the relative vibrational level population, N_v, calculated according to the method of Hancock and Smith (10), against vibrational number, v, for conditions of maximum total emission intensity (C_2H_2:O_2 ratio of 1:3). Under these conditions the system did not exhibit a population inversion.

When a second discharge cavity on the C_2H_2–He line was switched on, no marked change in the total emission intensity was observed. The spectral distribution of the emission was also unchanged. If the first discharge on the O_2–He line was shut off while that on the C_2H_2–He line remained on, no emission could be detected. These observations are entirely consistent with the mechanism for CO† formation previously proposed (8, 9)

[1] $O + C_2H_2 \rightarrow CO + CH_2 + 51$ kcal/mol

[2] $O + CH_2 \rightarrow CO + 2H + 71$ kcal/mol

with reaction 2 being sufficiently energetic to populate CO up to $v = 13$ (the highest level observed to be appreciably populated in the

Can. J. Chem. Downloaded from www.nrcresearchpress.com by 210.87.254.105 on 09/05/12
For personal use only.

Can. J. Chem. Downloaded from www.nrcresearchpress.com by 210.87.254.105 on 09/05/12
For personal use only.

present experiments). The value of the rate constant for reaction 1 is (see ref. 11):

$$k_1 = (9.2 \pm 0.4) \times 10^{10}\ \text{cm}^3\ \text{mol}^{-1}\ \text{s}^{-1}\ (298\ ^\circ\text{K})$$

Several experiments were conducted to determine the effect of changing the C_2H_2:O_2 ratio from that observed to give maximum CO emission. At lower C_2H_2 flows the total emission intensity was decreased with a slight decrease in the relative population of higher vibrational levels. At higher C_2H_2 flows a more dramatic decrease in the total emission intensity was observed. Figure 4 (curve *a*) shows the CO first overtone spectrum for a C_2H_2:O_2 ratio of 1:3, the condition of maximum total emission intensity, and Fig. 4 (curve *b*) for a C_2H_2:O_2 ratio of 2:3. When the N_v's obtained for the ratio C_2H_2:O_2 of 2:3 are divided by the comparable N_v's for the ratio C_2H_2:O_2 of 1:3 it is apparent that a rapid fall off in the relative population of higher vibrational levels is occurring. The maximum decrease was observed for $v = 8$ (see inset Fig. 4). This effect can be attributed to vibrational energy transfer from CO to the ν_2 vibration of C_2H_2 at 1973.5 cm^{-1}. Vibrational energy transfer will be more effective for higher vibrational levels of CO for which the energy discrepancy in the reaction

$$[3]\quad \text{CO}(v = n) + \text{C}_2\text{H}_2(0000^\circ0^\circ) \rightarrow \text{CO}(v = n - 1) + \text{C}_2\text{H}_2\ (01000)$$

approaches zero. Closest resonance occurs for $v = 8$. That vibrational energy transfer from CO to C_2H_2 does occur is supported by the observation of i.r. chemiluminescence from C_2H_2 in the C_2H_2–O_2 system (8).

Experiments were conducted to determine the effect of various added gases on the CO first overtone emission. Figure 2 (curve *b*) shows that when CO was premixed with the C_2H_2–He mixture, a decrease in the total emission intensity was observed. This decrease was most pronounced for lower vibrational levels with a minimum occurring for $v = 5$ which is only 29% of its value in the absence of vibrationally cold CO *vs.* $v = 10$ which is 90% of its previous value. A plot of the relative vibrational level population, N_v, against vibrational number, v, (Fig. 3) indicates that under these conditions a vibrational population inversion was marginally sustained between $v = 5$ and $v = 7$. A local vibrational temperature of ~3300 °K was calculated for levels $v = 2$ to $v = 4$ while a temperature of ~11000 °K was determined for levels $v = 6$ to $v = 10$. These observations of the effect of the addition of vibrationally cold CO are expected in view of its previously observed effect on the intensity of the CO† emission formed by the reaction of oxygen atoms with CS_2 (12).

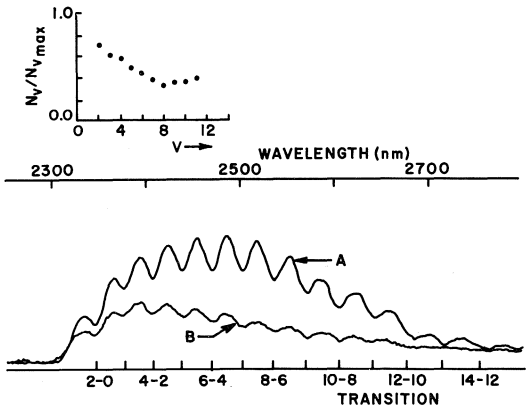

FIG. 4. The effect of changing the C_2H_2:O_2 ratio on the CO first overtone emission from the C_2H_2/O_2 atomic flame. Curve *A*: flow rates, C_2H_2:O_2:He, 19:57.7:4809 μmol/s; total pressure, 8.1 Torr. Curve *B*: flow rates, C_2H_2:O_2:He, 38:57.7:4809 μmol/s; total pressure, 8.25 Torr. Insert: Plot of the relative vibrational level population of CO† for curve *B*, (N_v), divided by the relative vibrational level population of CO† for curve *A*, ($N_{v\,max}$), against vibrational number, v.

Methylacetylene

CO first overtone emission was obtained when CH_3C_2H was added to a stream of oxygen which had been passed through a microwave discharge. As in the case of C_2H_2 only the first 13 vibrational levels of CO were appreciably populated. The relative vibrational level population was identical to that found in the C_2H_2 case with the maximum total emission intensity occurring for a CH_3C_2H:O_2 ratio of 1:3.

When CO was premixed with the CH_3C_2H–He mixture, a decrease in the total emission intensity was observed. This decrease was again most pronounced for lower vibrational levels with a minimum occurring for $v = 5$. As in the case of acetylene, a vibrational population inversion was again marginally sustained between $v = 5$ and $v = 7$.

The initial step in the reaction of oxygen atoms with methylacetylene, proposed in ref. 11:

$$[4]\quad \text{O} + \text{CH}_3\text{C}_2\text{H} \rightarrow \text{CH}_3\text{CH} + \text{CO}$$

which has a rate constant

$k_3 = (4 \pm 1) \times 10^{11}$ cm^3 mol^{-1} s^{-1} (298 °K)

yields ethylidene. Since no thermochemical data exists, the exothermicity of this reaction cannot be calculated. It can, however, be approximated as 40–50 kcal/mol exothermic by analogy with reaction 1 and is thus not sufficiently exothermic to populate CO† to $v = 13$. Chong and Kistiakowsky (13) have shown that ethylidene produced in the photolysis of methyl ketone rapidly isomerizes to an excited ethylene molecule which can either be collisionally quenched or decompose to acetylene and hydrogen. The latter course would allow formation of CO† via reactions 1 and 2, accounting for the identical spectral distributions of the CO† emission observed in the two systems.

Methane

No visible or i.r. chemiluminescence was observed when methane in a helium buffer was introduced into a stream of oxygen which had been passed through a microwave discharge. When a second microwave discharge on the CH_4–He line was switched on, a brilliant deep purple luminescent cone was visible at the end of the concentric mixer. The CO first overtone emission obtained from the methane–oxygen atom system for conditions of maximum total emission intensity, CH_4:O_2 ratio of 1:3, has a spectral distribution identical to that observed in the case of C_2H_2.

The fact that no emission was observed unless both microwave discharges were employed suggests that the CO† was not produced in the initial reaction steps. The initial step which was shown to be

[5] $\quad O + CH_4 \rightarrow CH_3 + OH + 0.4$ kcal/mol

with a rate constant (see ref. 14)

$k_5 = 3.2 \times 10^{13} \exp(-7950/(RT))$ cm^3 mol^{-1} s^{-1} (295–1000 °K)

is too slow to allow appreciable reaction to occur at the experimental temperature of ~310 °K.

When methane is passed through a microwave discharge it undergoes fragmentation. The net effect of the discharge on the CH_4, however, is to produce acetylene and hydrogen, presumably because of the very rapid reactions of the fragmentation products, CH and CH_2.[1] The O atoms then react with C_2H_2 according to reactions 1 and 2 to form CO†. The fact that a stable species is responsible for the CO† emission is supported by the following experimental evidence. The intensity of the CO† emission was unchanged when the discharge on the CH_4–He stream was moved from its normal position 6 in. from the mixing inlets to a position 40 in. from the inlets. Mass spectrometric analysis showed that C_2H_2 is a major product of discharged methane.

Air–Helium–Hydrocarbon (CO) Lasers

The mechanisms governing the formation of vibrationally excited CO in the air–helium–hydrocarbon (CO) lasers of Barry and co-workers (2–6) can be clarified in view of the previous observations on CO† formation. In these lasers emission from CO is observed upon initiation of a direct current discharge in an air–He–RH (RH = C_2H_2, CH_4, or C_3H_8) mixture. Laser emission was observed on P branch lines from $v = 3 \rightarrow v = 2$ to $v = 12 \rightarrow v = 11$ for CH_4 from $v = 5 \rightarrow v = 4$ to $v = 12 \rightarrow v = 11$ for C_3H_8 and from $v = 3 \rightarrow v = 2$ to $v = 11 \rightarrow v = 10$ for C_2H_2 and in the case of CH_4 with Q switched operation from $v = 2 \rightarrow v = 1$ to $v = 16 \rightarrow v = 15$. The authors also note that CO laser emission below 5000 nm is more readily realized by using CH_4 than with CO alone and that the power is much greater (2).

It is of interest to consider what is (*a*), the chemical mechanism responsible for CO formation in the electrical discharge and (*b*), the degree of contribution of the various methods of vibrational excitation to the laser power output, *i.e.*, electron impact, chemical excitation, collisional excitation by vibration–vibration energy transfer from N_2† or CO†.

Barry and co-worker (5) have proposed a detailed mechanism for CO formation by chemical means in their electrical discharge air–He–CH_4 laser. The initial step is proposed to be

[6] $\quad CH_4 + O_2 \rightarrow CH_3 + HO_2$

followed by CO formation via a formyl radical mechanism.

[7] $\quad HCO + O_2 \rightarrow CO + HO_2$

Reaction 6 is 57.2 kcal/mol endothermic and is, consequently, not likely to proceed rapidly at the laser operating temperature of 160 °C.

A direct current discharge through an O_2–

[1] We wish to thank the referee who made this suggestion.

Can. J. Chem. Downloaded from www.nrcresearchpress.com by 210.87.254.105 on 09/05/12
For personal use only.

CH_4–He mixture will simultaneously dissociate O_2 producing oxygen atoms and CH_4 producing fragments such as CH_2, CH, H, etc. Reactions 1 and 2 as well as the reaction

[8] $$CH + O \rightarrow CO + H + 176 \text{ kcal/mol}$$

can proceed and in all probability account for CO formation in this system. This is further supported by mass spectrometric analysis[2] wherein a strong mass peak attributable to CH_2 was observed. Since it has been shown that reaction 2, the attack of oxygen atoms on methylene radicals, can produce vibrationally excited CO with up to 13 quanta of vibrational energy, this process will undoubtedly contribute to the laser power output and is in all probability responsible for the observation of low level laser transitions in these systems. It is also reasonable to expect that electron impact and collisional excitation will contribute to the total laser power output.

In the case of the air–He–C_2H_2 laser Barry *et al.* (6) have suggested that oxidation of C_2O is responsible for CO† formation. This mechanism has been suggested by Bayes (15) to account for the formation of electronically excited CO in hydrocarbon flames not for the formation of CO† which is satisfactorily explained by the reaction sequence 1 and 2.

Summary and Conclusions

The addition of either acetylene or methylacetylene to a stream of oxygen which has been passed through a microwave discharge results in the observation of i.r. chemiluminescence from vibrationally excited carbon monoxide.

The addition of vibrationally cold CO results in a marginally sustained vibrational population inversion in the chemically formed CO.

The high vibrational temperatures observed between levels $v = 7$, $v = 6$, and $v = 5$ suggest that it should be possible to achieve gain on these transitions in a laser cavity.

In the case of methane addition to a stream of oxygen, which had been passed through a microwave discharge, no vibrationally excited CO was observed unless the methane had previously been subjected to a second microwave discharge.

In the recent work describing air–helium–hydrocarbon (CO) lasers low vibrational transitions were observed. These transitions are likely a result of the reaction

$$O + CH_2 \rightarrow CO + 2H$$

which predominates in acetylene oxidation.

[2]W. E. Boney. Private communication.

1. H. S. Pilloff, S. K. Searles, and N. Djeu. Appl. Phys. Lett. **19**, 9 (1971).
2. J. D. Barry, W. E. Boney, and J. E. Brandelik. Appl. Phys. Lett. **18**, 15 (1971).
3. J. D. Barry, W. E. Boney, and J. E. Brandelik. IEEE J. Quant. Electron. **QE-7**, 208 (1971).
4. J. D. Barry, W. E. Boney, and J. E. Brandelik. IEEE J. Quant. Electron. **QE-7**, 461 (1971).
5. W. E. Boney and J. D. Barry. Air Force Avionics Laboratory, Technical Report AFAL-TR-71-87, June 1971.
6. J. D. Barry, W. E. Boney, J. E. Brandelik, D. M. Mulder, and J. K. Woessner. Appl. Phys. Lett. **20**, 243 (1972).
7. J. E. Brandelik, J. D. Barry, and W. E. Boney. Appl. Phys. Lett. **19**, 141 (1971).
8. D. M. Creek, C. M. Melliar-Smith, and N. Jonathan. J. Chem. Soc. (A), 646 (1970).
9. P. N. Clough, S. E. Schwartz, and B. A. Thrush. Proc. Roy. Soc. Lond. **A317**, 575 (1970).
10. G. Hancock and I. W. M. Smith. Chem. Phys. Lett. **3**, 573 (1969).
11. J. M. Brown and B. A. Thrush. Trans. Faraday Soc. **63**, 630 (1967).
12. R. D. Suart, S. J. Arnold, and G. H. Kimbell. Chem. Phys. Lett. **7**, 337 (1970).
13. D. P. Chong and G. B. Kistiakowsky. J. Phys. Chem. **68**, 1793 (1964).
14. K. Schofield. Planet. Space Sci. **15**, 643 (1967).
15. K. D. Bayes. J. Chem. Phys. **52**, 1093 (1970).

Can. J. Chem. Downloaded from www.nrcresearchpress.com by 210.87.254.105 on 09/05/12
For personal use only.

Kinetics and Temperature Dependence of the Hydration of NO^+ in the Gas Phase

MARGARET A. FRENCH, L. P. HILLS, AND P. KEBARLE
Chemistry Department, University of Alberta, Edmonton, Alberta

Received June 9, 1972

The kinetics of the atmospherically important hydration sequence: $NO^+(H_2O)_{n-1} + H_2O = NO^+(H_2O)_n$ and the transfer reaction $NO^+(H_2O)_n + H_2O = HNO_2 + H^+(H_2O)_n$ were examined in nitrogen containing small quantities of NO and H_2O with a pulsed high pressure ion source mass spectrometer. The room temperature mechanism and rate constants were found to be in agreement with earlier work in other laboratories. The temperature dependence of the reaction was examined for the range 27–157 °C. The transfer reaction does not occur at higher temperatures so that the NO^+ hydration equilibria for $n = 1$ and 2 could be measured leading to $\Delta H_{1,0} = 18.5$ and $\Delta H_{2,1} = 16.1$ kcal/mol. The third order forward clustering rate constants were found to have negative temperature coefficients.

Les cinétiques de la séquence importante de l'hydratation atmosphérique: $NO^+(H_2O)_{n-1} + H_2O = NO^+(H_2O)_n$ et de la réaction de transfert $NO^+(H_2O)_n + H_2O = HNO_2 + H^+(H_2O)_n$ ont été examinées dans l'azote contenant de petites quantités de NO et H_2O, au moyen d'un spectromètre de masse ayant une source d'ionisation pulsée à haute pression. Le mécanisme à la température ambiante et les constantes de vitesses sont en accord avec un travail antérieur effectué dans d'autres laboratoires. L'influence de la température sur la réaction a été examinée entre 27 et 157 °C. La réaction de transfert ne se produit pas aux hautes températures de sorte que les équilibres d'hydratation de NO^+ pour $n = 1$ et 2 ont pu être mesurés conduisant à $\Delta H_{1,0} = 18.5$ et $\Delta H_{2,1} = 16.1$ kcal/mol. Les constantes de vitesse du troisième ordre pour l'agrégation directe ont des coefficients de température négatifs.

[Traduit par le journal]

Can. J. Chem., **51**, 456 (1973)

Can. J. Chem. Downloaded from www.nrcresearchpress.com by 210.87.254.105 on 09/05/12
For personal use only.

Introduction

The hydration of the NO^+ ion is of importance in the ionosphere (1) and in the radiation chemistry of moist air. The low ionization potential of NO makes the NO^+ ion a "charge sink" in ionized air. Studies on the kinetics of NO^+ hydration were started in this laboratory in 1969 after the completion of the O_2^+ hydration sequence (2) which is also of considerable interest. Before the present work was completed three studies of the NO^+ hydration sequence were published (3–5). The three sets of data obtained at near room temperature were in good agreement. Since the temperature dependence of the reaction mechanism had not been studied the present work was expanded to encompass studies at different temperatures. Determination of the temperature dependence of the $NO^+(H_2O)_{n-1} + H_2O = NO^+(H_2O)_n$ equilibria permitted the evaluation of some of the corresponding reaction enthalpies $\Delta H_{n-1,n}$. These enthalpies are of importance in establishing the energetics of the transfer sequence: $NO^+(H_2O)_n + H_2O = HNO_2 + H^+(H_2O)_n$. Finally the temperature dependence of the rate constants is of interest since the processes in the ionosphere occur below room temperature, while one can also conceive of radiation chemical processes in air occurring at temperatures above room temperature.

Experimental

The apparatus used was described in the earlier study of the O_2^+ hydration (2). It consisted of a high pressure ion source reaction chamber, a pulsed electron beam and a variable time delay ion gate. The ions were mass analyzed with a quadrupole mass filter. The mass dependent transmission of the quadrupole (Electron Assoc. Inc., Model 200) was determined in special calibration runs (2) and the ion intensities observed in the experimental measurements were correspondingly corrected. A mixture of N_2, NO, and H_2O passing in slow flow at some 2 Torr through the ion source was used. N_2 was the major gas, while NO and H_2O were in the 0.1 and 0.01 Torr range, respectively. The total pressure was measured with a capacitance manometer. The N_2 to NO concentration ratio was determined by measuring the N_2^+ and NO^+ peaks observed with the auxiliary low pressure ion source of the quadrupole. The measured N_2^+ and NO^+ ion intensities corrected for quadrupole and electron multiplier discrimination were assumed proportional to the partial pressure of the gases in the high pressure ion source. The gas flow through the 0.12 mm diameter ion exit leak is probably in the transition region between molecular and viscous for the pressures (1–3 Torr) used. The outflow from the vacuum chamber, in which the auxiliary ion source is located, is molecular. If the flow through the

TABLE 1. Reaction mechanism converting NO^+ hydrates to proton hydrates*

Reaction	Rate constants (present work) at 308 °K	Other determinations† at ~300 °K
[1] $N_2^+ + NO \rightarrow NO^+ + N_2$	$k_1 > 6.10^{-11}$	5×10^{-10}, 3.3×10^{-10}, ref. 6, 7
[2] $NO^+ + NO + N_2 = (NO)_2^+ + N_2$	$k_2 = 8.7 \times 10^{-30}$	5×10^{-30} (NO), ref. 4; ~30×10^{-30} (NO), ref. 8; ~33×10^{-30} (NO), ref. 9
[3] $(NO)_2^+ + H_2O = NO^+(H_2O) + NO$	$k_3 \approx 10^{-9}$	1.4×10^{-9}, $k_3 = 9 \times 10^{-14}$, ref. 4
[4] $NO^+ + H_2O + N_2 = NO^+(H_2O) + N_2$	$k_4 = 1.8 \times 10^{-28}$	1.5×10^{-28} (NO), ref. 4; 1.6×10^{-28} (N_2), ref. 3; 1.4×10^{-28} (N_2), ref. 5
[5] $NO^+(H_2O) + H_2O + N_2 = NO^+(H_2O)_2 + N_2$	$k_5 = 1 \times 10^{-27}$	1×10^{-27} (NO), ref. 4; 1×10^{-27} (N_2), refs. 3, 5
	$k_5 = 5 \times 10^{-14}$	1.4×10^{-14} (NO), ref. 4; 1.7×10^{-14} (N_2), ref. 5
[6] $NO^+(H_2O)_2 + H_2O + N_2 = NO^+(H_2O)_3 + N_2$	$k_6 = 1 \times 10^{-27}$	2×10^{-27} (NO), ref. 4; 2×10^{-27} (N_2), ref. 3 1.4×10^{-27} (N_2), ref. 5
	$k_6 = 3.4 \times 10^{-12}$	1.9×10^{-12} (NO), ref. 4; 1.3×10^{-12} (N_2), refs. 3, 5
[7] $NO^+(H_2O)_3 + H_2O = H^+(H_2O)_3 + HNO_2$	$k_7 = 3 \times 10^{-10}$	8×10^{-11}, ref. 3; 7×10^{-11}, refs. 4, 5
[8] $H^+(H_2O)_3 + H_2O + N_2 = H^+(H_2O)_4 + N_2$		

*Second order rate constants order of magnitude 10^{-9}–10^{-14}, units in cm^3 $molecule^{-1}$ s^{-1}. Third order rate constants order of magnitude 10^{-27}–10^{-30}, units in cm^6 $molecule^{-2}$ s^{-1}.
†Third body given in parentheses after rate constant value.

exit leak was purely molecular the partial pressure ratios of the component gases would be the same in the high pressure source and in the auxiliary ion source and the experimental procedure would be fully justified. This would not be the case in general for viscous flow. However, the mixture used is a special case. The masses of N_2 and NO are very close so that the fractionation induced by the molecular outflow from the vacuum chamber is minimal. The ion flow through the leak, if viscous, is governed by the major gas (N_2), which is present in large excess. Under these conditions the amount of gases entering the vacuum chamber (in mol/s) should be proportional to the partial pressure ratios. Therefore we believe that the procedure used for the N_2, NO pressure determination is justified.

The partial pressure of H_2O gas was determined by weight measurement as described in earlier publications (2).

Results and Discussion

The measured time dependence of the ion intensities after the short electron pulse is shown in Fig. 1 for a typical run. The ion intensities are normalized, *i.e.*, the intensity of each ion is divided by the total ion intensity at any given time. The normalized ion intensities will be treated as if they represented (relative) ion concentrations in a reaction vessel in which the total ion concentration remains constant with time (2).

One observes in Fig. 1 the extremely rapid disappearance of N_2^+ and a corresponding appearance of NO^+. The slow decay of NO^+ coincides with the successive appearance of NO^+H_2O and $NO^+(H_2O)_2$. The ions $NO^+(H_2O)_3$ and $H^+(H_2O)_3$ are present also but in much lower concentration. The final ion is clearly $H^+(H_2O)_4$. A detailed examination of similar results obtained in some 12 runs in which the N_2 concentration was varied from 1–3.5 Torr, NO from 0.03–0.7 Torr, and H_2O from 0–0.07 Torr permitted the establishment of the reaction mechanism shown in Table 1, which is essential-

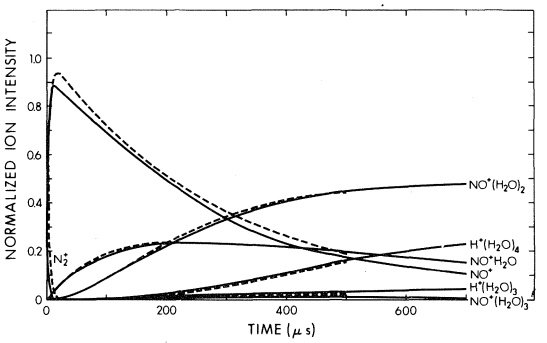

FIG. 1. Time dependence of normalized ion intensities observed at 306 °K after short (10 μs) electron pulse. Solid line experimental observations, dashed line analog computer fit calculated on basis of reaction mechanism [1]–[8]. $N_2 = 2$, $NO = 0.1$, $H_2O = 0.004$ Torr.

Can. J. Chem. Downloaded from www.nrcresearchpress.com by 210.87.254.105 on 09/05/12
For personal use only.

ly identical with the mechanisms proposed by Fehsenfeld *et al.* (3), Puckett *et al.* (4), and Howard *et al.* (5).

The rate constants determined in the present work are given in Table 1 together with the results from the above authors. The present rate constant determinations were based on a number of graphical methods (2) and analog computer fits of the normalized ion intensities. Figure 1 illustrates the type of fit that could be obtained. The analog computer was programmed to reproduce the reaction system [1]–[8]. The reaction frequencies ν_i (pseudo first order rate constants) were treated as variable parameters which were adjusted until a best fit with the normalized ion intensities was obtained. Agreement between the rate constants obtained from the reaction frequencies for runs with different concentrations established the reliability of the values.

The NO^+ is produced by charge transfer from the major gas ion N_2^+ by reaction 1. This reaction was too fast, at the high NO concentration used, to be measured accurately. The production of $NO^+(H_2O)$ via the dimer $(NO)_2^+$, *i.e.*, reactions (2) and (3) could not be avoided since it was desired to produce as little H_2O^+ as possible by direct charge transfer from N_2^+ (or N_4^+) to H_2O. This meant that the H_2O pressure had to be kept much lower than the NO pressure. The parallel reactions 2 + 3 and 4 by which NO^+ disappears and $NO^+(H_2O)$ is formed could be resolved by the plot shown in Fig. 2. The observed reaction frequency for the disappearance of NO^+ is $\nu_{obs} = k_2[NO]\,[N_2] + k_4[H_2O]\,[N_2]$. Thus a plot of $\nu_{obs}/[N_2]\,[H_2O]$ *vs.* $[NO]/[H_2O]$ should

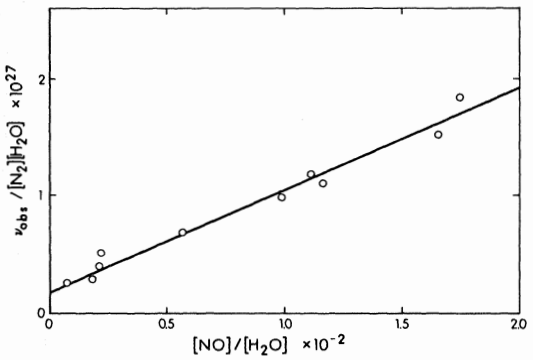

FIG. 2. Determination of rate constants k_2 and k_4 (see Table 1) from slope and intercept of plot. Observed reaction frequency $\nu_{obs} = k_2[NO]\,[N_2] + k_4[H_2O]\,[N_2]$.

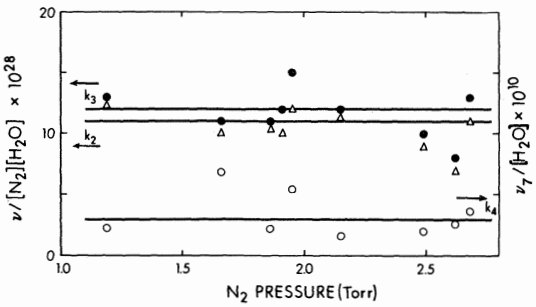

FIG. 3. Plot of $(\nu_5/[N_2][H_2O] \times 10^{28}$ (Δ) and $(\nu_6/[N_2]\,[H_2O] \times 10^{28}$ (●) *vs.* pressure of N_2 indicates that reactions 5 and 6 are third order. Similar plot of $(\nu_7/[H_2O] \times 10^{10}$ (○) indicates that reaction 7 is second order.

give a straight line with slope k_2 and intercept k_4. An independent value for k_2 in good agreement with that from Fig. 2 could be obtained in runs where the water concentration was zero. The plot of Fig. 2 is also consistent with the assigned third order for reactions 2 and 4.

The determination of the kinetic order of reactions 5, 6, and 7 is shown in Fig. 3 where $\nu_5/[H_2O]\,[N_2]$ and $\nu_6[H_2O]\,[N_2]$ are seen to be constant with N_2 pressure which indicates that k_5 and k_6 are both third order. $\nu_7/[H_2O]$ is seen to be invariant with pressure such that k_7 is second order, as expected.

On the whole there is good agreement between the present values for the rate constants and the determinations in refs. 3–5 (see Table 1). The present value for k_{-5} is higher by a factor of about 3. This difference is largely due to the higher temperature used in the present determination. (See discussion below of temperature dependence of reactions.) The same is true for the somewhat higher value for k_{-6} observed in the present work.

The present k_7 is higher by a factor of 4 than the values from refs. 3–5. Reaction 7 is a relatively fast switching reaction which is thermoneutral or only slightly endothermic. (See Table 3.) Therefore the reaction should have no, or only a very slight, temperature dependence. The difference between the present result and the earlier determinations (3–5) cannot be explained on basis of difference of temperatures. The present k_7 determination depended on computer fitting of $NO^+(H_2O)_3$ concentrations which were very low (see Fig. 1). Furthermore, the fit was not sensitive to the value of k_7 but to the combined values of k_6, k_{-6}, and k_7. Therefore the present

Can. J. Chem. Downloaded from www.nrcresearchpress.com by 210.87.254.105 on 09/05/12
For personal use only.

Can. J. Chem. Downloaded from www.nrcresearchpress.com by 210.87.254.105 on 09/05/12
For personal use only.

k_7 is of low accuracy and the value obtained by the earlier workers is probably closer to the truth.

The temperature dependence of the reaction system [1]–[8] was examined in a series of runs over the temperature range 27–156 °C. The reaction system became very simple at the highest temperatures where the only two major ions observed were NO^+ and NO^+H_2O. Their time dependence is shown in Fig. 4*a* for a temperature of 134 °C. Evidently the two ions reach equilibrium due to the operation of (−4) which at this temperature has a rate similar to the forward clustering reaction 4. The NO^+ equilibrium concentration could be conveniently observed down to 110 °C. Below this temperature the NO^+ became too small to measure reliably. The equilibrium concentrations were used for the evaluation of the equilibrium constant: $K_{0,1} = k_4/k_{-4} = [NO^+.H_2O]/[NO^+]\,[H_2O]$. A Van't Hoff plot of the values shown in Fig. 5, leads to $\Delta H_{0,1} = -18.5$ kcal/mol and $\Delta S_{0,1} = -23.0$ cal/deg (standard state 1 atm). The determinations of $K_{0,1}$ were done at a single water pressure of ~0.04 Torr. This relatively high water pressure was selected in order to speed up the achievement of equilibrium. Under these conditions, proton hydrates $H^+(H_2O)_n$ were observed as minor ions and could be accounted for as a side reaction initiated by the direct charge transfer $N_2^+ + H_2O = N_2 + H_2O^+$.

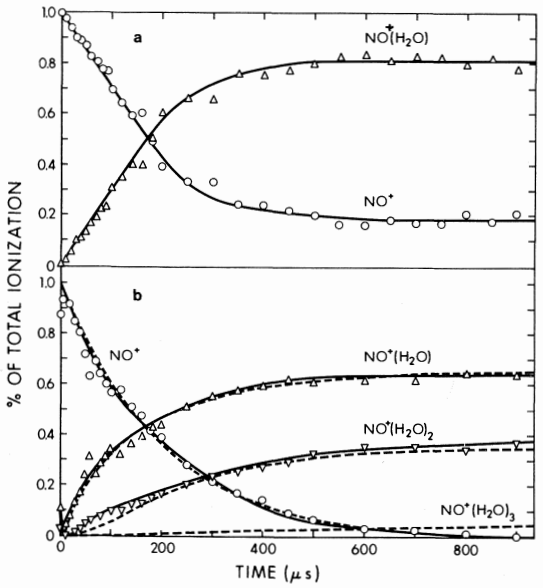

FIG. 4. (*a*) Normalized intensities in reaction system at 134 °C. Only two major ions are observed NO^+ (○), and $NO^+(H_2O)$ (Δ) which reach equilibrium at longer reaction times. The very rapidly decaying N_2^+ is not shown. $N_2 = 2.85$, $NO = 0.15$, $H_2O = 0.038$ Torr. (*b*) 67 °C, at this temperature $NO^+(H_2O)_2$ is stable such that $NO^+(H_2O)$, $NO^+(H_2O)_2$ equilibrium can be observed. $N_2 = 2.85$, $NO = 0.148$, $H_2O = 0.0067$ Torr.

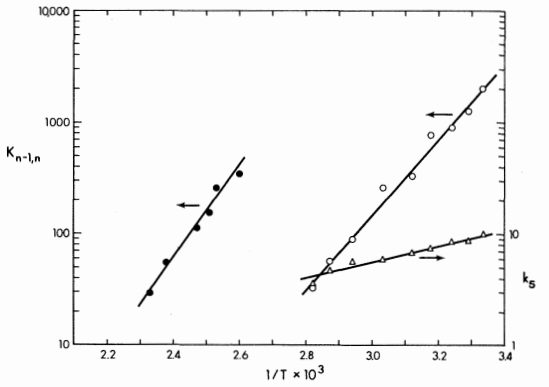

FIG. 5. Van't Hoff plot for equilibrium constants $K_{0,1}$ (●) and $K_{1,2}$ (○) (pressure in Torr) leading to ΔH and ΔS values. Arrhenius plot of rate constant $k_5 \times 10^{28}$ cm^6 $molecule^{-2}$ s^{-1} (Δ). The third order rate constant shows the expected negative temperature coefficient corresponding to "activation energy" $E_5 = -3.3$ kcal/mol.

Figure 4*b* shows that the principal ions observed at lower temperatures (67°) are NO^+, $NO^+(H_2O)$, and $NO^+(H_2O)_2$. The latter two ions reach equilibrium. Actually the production of $H^+(H_2O)_3$ via reaction 7 was still observable but was very slow because of the very low equilibrium concentration of $NO^+(H_2O)_3$. The equilibrium constant $K_{1,2} = [NO^+(H_2O)_2]/[NO^+(H_2O)]\,[H_2O]$ was determined over the temperature range shown in the Van't Hoff plot (Fig. 5). The determinations were made either by taking the concentration of the two ions at long reaction times where their ratio had become constant or by measuring k_5/k_{-5} by computer fitting the time dependence plots. The resulting values were: $\Delta H_{1,2} = -16.1$ kcal/mol and $\Delta S_{1,2} = -25.5$ e.u.

The computer fits permitted the determination of k_5 at different temperatures. It was found that the forward reaction has a negative temperature coefficient. An Arrhenius type plot of k_2 is shown in Fig. 5. The negative "activation energy" $E_2 = -3.3$ kcal/mol is of course only an experimental parameter without theoretical meaning. The temperature dependence is more meaningfully expressed in the form $k = \text{constant}\ T^{-n}$ since this expression approximates theoretically expected temperature dependence (10). The data for k_5 lead to an $n \approx 4.7$. Since the temperature

TABLE 2. Thermodynamic data for NO^+ and H^+ hydration*

Reaction	$-\Delta H^0_{n-1,n}$ (kcal/mol)	$-\Delta S^0$† (e.u.)	Reference
$NO^+ + H_2O \rightleftarrows NO^+H_2O$	18.5 ± 1.5	23.0 ± 3	This work
$NO^+H_2O + H_2O \rightleftarrows NO^+(H_2O)_2$	16.1 ± 1	25.5 ± 2.5	This work
$H^+H_2O + H_2O \rightleftarrows H^+(H_2O)_2$	31.6 ± 0.4	24.3 ± 0.5	11
$H^+(H_2O)_2 + H_2O \rightleftarrows H^+(H_2O)_3$	19.5 ± 0.3	21.9 ± 0.6	11

*The error limits given correspond to standard deviation of the least square plots. Actual error is probably larger but unknown.
†Standard state 1 atm.

TABLE 3. Energetics of the reaction $NO^+(H_2O)_n + H_2O = HNO_2 + H^+(H_2O)_n$ for $n = 0$ to 3

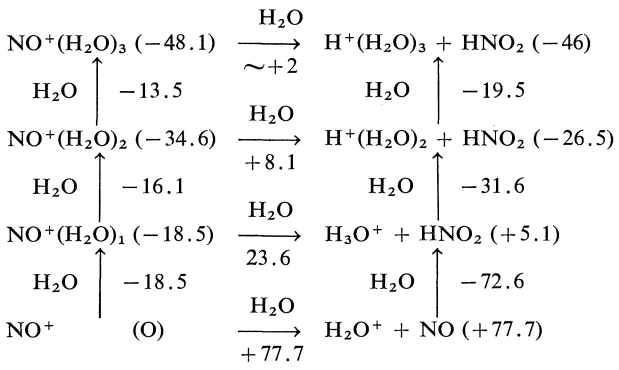

*Numerical values beside arrows represent ΔH for reaction. Numerical values in parentheses represent enthalpy difference of system relative to $NO^+ + 3H_2O$ (g). All values in kcal/mol. The value for the hydration of $NO^+(H_2O)_2 = -13.5$ kcal/mol is not based on direct measurement but estimated.

range covered is rather small and the scatter of the data considerable, a value of n as low as 4 could not be excluded.

The temperature dependence of k_4 was more difficult to determine due to the operation of the temperature dependent parallel reaction path 2 + 3 (see Table 1). An estimate indicating a dependence similar to that for reaction 5 could be obtained by considering the low temperature value for k_4 from Table 1 and the values for k_4 determined in the range 111–156 °C. At these higher temperatures high H_2O concentrations were used (see Fig. 4*a*) and the parallel reaction 2 + 3 was unimportant.

A study of the temperature dependence of k_6, k_{-6} and thus $K_{2,3} = k_6/k_{-6}$ was not successful since the concentration of $NO^+(H_2O)_3$ which was already small at 30 °C became progressively smaller as the temperature was increased. The computer fits thus became less reliable. The Van't Hoff plot of the so determined $K_{2,3}$ showed excessive scatter. The data were consistent with a value $\Delta H_{3,2} < \Delta H_{2,1} = 15.6$ kcal.

The data obtained from the temperature dependence studies are summarized in Table 2. The determination of $\Delta H_{2,1}$ and $\Delta H_{1,0}$ for the NO^+ hydration taken together with data (11) for the hydration of H_3O^+ permit one to establish the energetics of the transfer from NO^+ hydrates to H_3O^+ hydrates. These are summarized in Table 3. The additional thermochemical data needed for the table: $NO^+ + H_2O = NO + H_2O^+$, $\Delta H = +77.7$; $H_2O^+ + H_2O = H_3O^+ + OH$, $\Delta H = -24.67$; and $OH + NO = HNO_2$, $\Delta H = -48$ kcal/mol were taken from Fehsenfeld *et al.* (3).

Table 3 illustrates the gradual decrease in endothermicity for the transfer reaction

$$NO^+(H_2O)_n + H_2O = HNO_2 + H^+(H_2O)_n$$

which decreases from 14 kcals for $n = 1$ to ~2 kcal for $n = 3$. The "driving force" in this

Can. J. Chem. Downloaded from www.nrcresearchpress.com by 210.87.254.105 on 09/05/12
For personal use only.

decrease is due to the stronger hydration interaction obtained for the proton hydrates. It is interesting to note that the step at $n = 3$ appears to be still endothermic, although the thermochemical data are certainly not accurate enough to make this certain. The endothermicity, if real, could be significant in slowing down reaction 7 at temperatures around 200 °K pertaining to the D region of the ionosphere. However, this effect would be more than offset by the negative temperature coefficients of k_4, k_5, and probably k_6.

1. W. ROTH and R. S. NARCISI. Adv. Electron. Electron Phys. **28**, 79 (1970); R. S. NARCISI and A. D. BAILEY. J. Geophys. Res. **70**, 3687 (1965).
2. A. GOOD, D. A. DURDEN, and P. KEBARLE. J. Chem. Phys. **52**, 212, 222 (1970).
3. F. C. FEHSENFELD, M. MOSESMAN, and E. E. FERGUSON. J. Chem. Phys. **55**, 2120 (1971).
4. (*a*) L. J. PUCKETT and M. W. TEAGUE. J. Chem. Phys. **54**, 2564 (1971). (*b*) W. C. LINEBERGER and L. J. PUCKETT. Phys. Rev. **187**, 286 (1969).
5. C. J. HOWARD, H. W. RUNDLE, and F. KAUFMAN. J. Chem. Phys. **55**, 4772 (1971).
6. P. D. GOLDAN, A. L. SCHMELTEKOPF, F. C. FEHSENFELD, H. I. SCHIFF, and E. FERGUSON. J. Chem. Phys. **44**, 4055 (1966).
7. F. C. FEHSENFELD, D. B. DUNKIN, and E. E. FERGUSON. Planet. Space Sci. **18**, 1267 (1970).
8. S. K. SEARLES and L. W. SIECK. J. Chem. Phys. **53**, 794 (1970).
9. O. P. STRAUSZ, W. K. DUHOLKE, and H. E. GUNNING. J. Am. Chem. Soc. **52**, 4128 (1970).
10. A. GOOD. Trans. Faraday. Soc. **67**, 3495 (1971).
11. (*a*) A. J. CUNNINGHAM, J. D. PAYZANT, and P. KEBARLE. J. Am. Chem. Soc. **94**, 7627 (1972). (*b*) P. KEBARLE, S. K. SEARLES, A. ZOLLA, J. SCARBOROUGH, and M. ARSHADI. J. Am. Chem. Soc. **89**, 6393 (1967).

Can. J. Chem. Downloaded from www.nrcresearchpress.com by 210.87.254.105 on 09/05/12
For personal use only.

Kinetics and Mechanism of the Sulfonation of 2-Phenyl-1-ethanesulfonic acid[1]

A. KOEBERG-TELDER (MRS.), Z. R. H. NIENHUIS (MRS.), AND H. CERFONTAIN
Laboratory for Organic Chemistry, Nwe Achtergracht 129, University of Amsterdam, The Netherlands
Received August 8, 1972

The kinetics of the sulfonation of 2-phenyl-1-ethanesulfonic acid in 85.0–98.4% H_2SO_4 has been studied. The results are discussed in terms of sulfonation of the unionized sulfonic acid and its conjugated base, the sulfonate anion. Partial rate factors for the $—CH_2CH_2SO_3H$ substituent are reported.

La cinétique de la sulfonation de l'acide phényl-2 éthanesulfonique a été étudiée dans H_2SO_4 85.0–98.4%. Les résultats sont discutés en terme de sulfonation de l'acide non-ionisé ainsi que de sa base conjuguée, l'anion sulfonate. Des facteurs relatifs aux taux partiels de réaction sont rapportés pour le substituant $—CH_2CH_2SO_3H$. [Traduit par le journal]

Can. J. Chem., **51**, 462 (1973)

Can. J. Chem. Downloaded from www.nrcresearchpress.com by 210.87.254.42 on 09/05/12
For personal use only.

Information concerning the substituent effect of the $—SO_3H$ group is to our knowledge lacking from the literature. With the aim of obtaining information on this point, a program was set up to determine the reactivity in sulfonation of various sulfonic acids of the general structure $C_6H_5(CH_2)_nSO_3H$ (n = 0, 1, 2, 3, ...). As part of that program we now report on the homogeneous sulfonation of 2-phenyl-1-ethanesulfonic acid in sulfuric acid ranging in concentration from 85.0 to 98.4% H_2SO_4. The pseudo first order rate constants are given in Table 1. The isomer distribution of the disulfonic acid mixture resulting from the sulfonation of 2-phenyl-1-ethanesulfonic acid in 90–98% H_2SO_4 was determined by n.m.r. to be 7 ± 2%, *o*-; 3 ± 2%, *m*-; 90 ± 4%, *p*-sulfophenyl-ethanesulfonic acid, independent of the sulfuric acid concentration.

The correlation of the pseudo first order rate constant for sulfonation with the activity of $H_2S_2O_7$ is shown in Fig. 1. The slope d(log k)/d(log $a_{H_2S_2O_7}$) in the steep part of the curve, *i.e.* in the range of 93–95% H_2SO_4, is 0.86. For benzene the slope is 0.89. The similarity in slope indicates that the sulfonating entity in both cases is the same, *viz.* $H_2S_2O_7$ (2). The slope decreases at acid concentrations >95% H_2SO_4, as was observed with the halogenobenzenes (4, 5) and phenylmethanesulfonic acid (6). At these high sulfuric acid concentrations, the step in which the carbon bonded proton is removed from the 1-arenium-1-sulfonate σ-complex intermediate becomes partly rate limiting (4), and this leads to a decline in slope.

TABLE 1. Pseudo first order rate constants for the sulfonation of 2-phenyl-1-ethanesulfonic acid at 25.0°

H_2SO_4 wt. % (±0.1)	$_{ps}k_1 \times 10^4$ (s^{-1})	$-\log a_{H_2S_2O_7}$*
85.0	0.181	11.65
87.8	0.91	10.59
89.7	2.41	9.91
93.3	18.4	8.78
95.2	63.4	8.19
97.1	184	7.54
98.4	509	6.91

*$\log a_{H_2S_2O_7} = 2 \log a_{H_2SO_4} - \log a_{H_2O} + 12.25$ (2, 3).

The upwards curvature at acid concentration <90% H_2SO_4 may be explained either in terms of the occurrence of additional sulfonation by $H_3SO_4^+$ (2) or in terms of ionization of the sulfonic acid with formation of the sulfonate anion which will be more reactive towards electrophilic substitution. As for the first explanation, the reactivity of the 4-position of 2-phenyl-1-ethanesulfonic acid (see below) is about the same as that of one position in benzene, and smaller than that of the 3-position of toluene (2). The sulfuric acid concentration of equal rate contributions by the entities $H_3SO_4^+$ and $H_2S_2O_7$ for benzene and the 3-position of toluene are 79 and 80% H_2SO_4, respectively (7). The sulfuric acid concentration of equal rate contributions by the two sulfonating entities increases with increasing reactivity of the substrate position (7). This then renders the explanation in

[1]Aromatic sulfonation. Part 38 (see ref. 1).

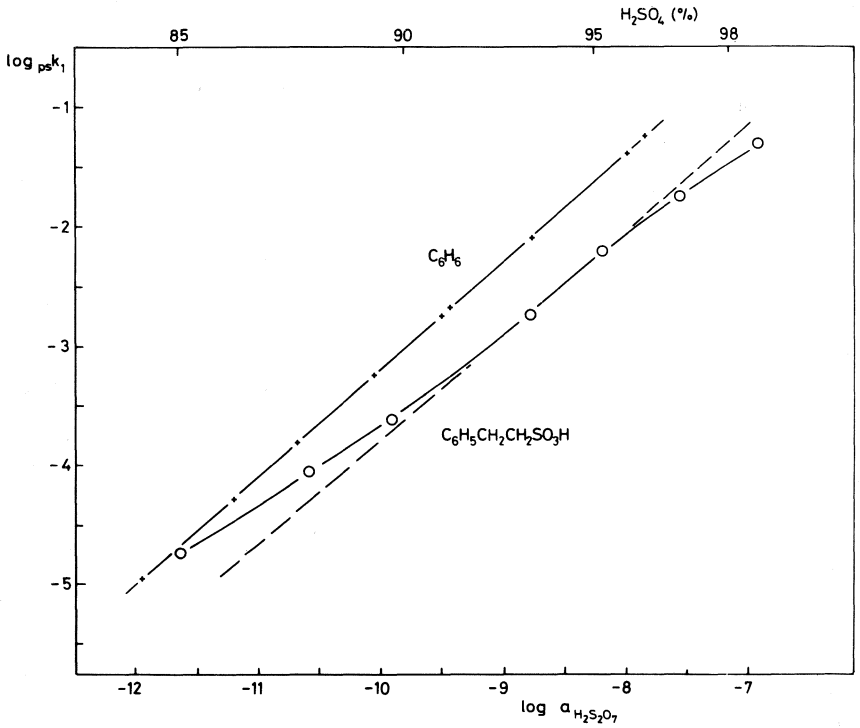

FIG. 1. Correlation of pseudo first order rate constants for sulfonation with the activity of $H_2S_2O_7$: +, benzene, slope 0.89; ○, 2-phenyl-1-ethanesulfonic acid, maximal slope 0.86.

TABLE 2. Electrophilic substitution of phenylalkanesulfonates

	$k/k_{benzene}$	
Substrate	Sulfonation, 95% H_2SO_4, 25°	Nitration, dilute aqueous* mixed acid, 30–39° (10)
$PhCH_2SO_3H$	$(1.60\pm0.12)\times10^{-4}$ (6)	0.30 ± 0.05
$PhCH_2CH_2SO_3H$	0.24 ± 0.01	3.5 ± 0.5

*68–77 mol % H_2O.

terms of additional sulfonation by $H_3SO_4^+$ improbable.

As for the second explanation, arene- and alkanesulfonic acids behave as weak acids in sulfuric acid of a lower concentration than 95% H_2SO_4, and 50% of deprotonation occurs at 82–84% H_2SO_4 (8, 9). Accordingly, with 2-phenyl-1-ethanesulfonic acid, the proportion of the more reactive sulfonate anion species increases with decreasing sulfuric acid concentration, and this will lead to an upward curvature with decreasing sulfuric acid concentration.

Further evidence that the unionized sulfonic acid is the substrate species undergoing sulfonation in 95% H_2SO_4 can be obtained from a comparison of the rates of substitution of alkali phenylmethane- and 2-phenyl-1-ethanesulfonate relative to benzene in nitration and sulfonation (Table 2). For the dilute aqueous nitric acid nitration of phenylmethanesulfonic acid it has been suggested, on the basis of a comparison between the observed and expected degree of meta-substitution for the $-CH_2SO_3H$ substituent, that the sulfonate anion is the actual species undergoing substitution (11). The very much lower relative reactivities of these substrates for

Can. J. Chem. Downloaded from www.nrcresearchpress.com by 210.87.254.42 on 09/05/12
For personal use only.

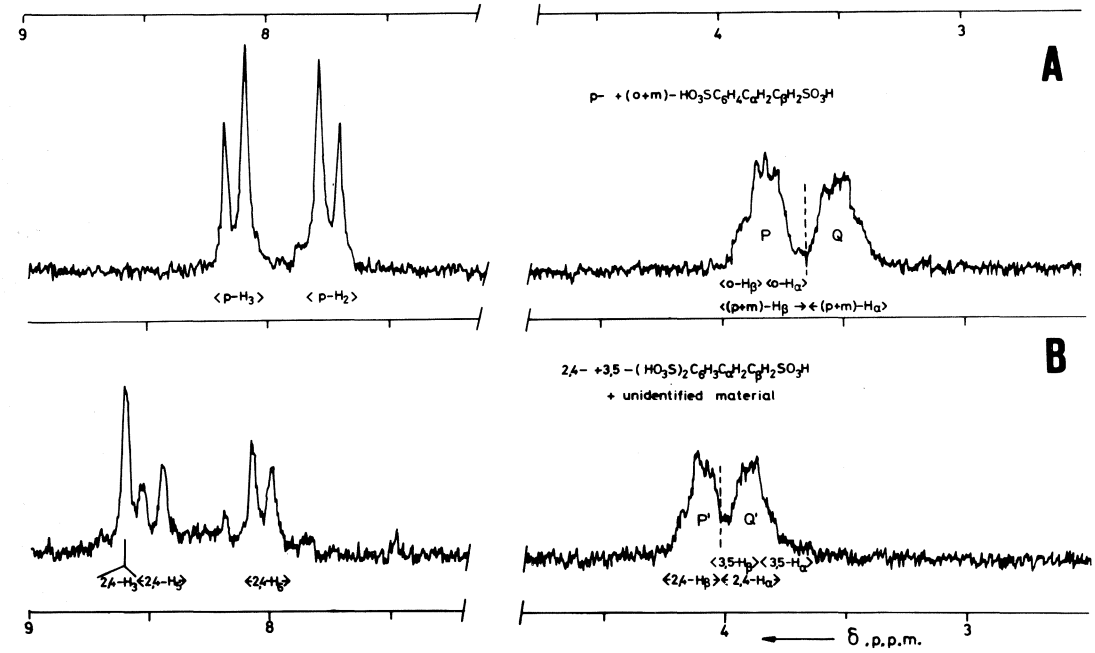

FIG. 2. N.m.r. spectra of sulfonation mixtures of 2-phenyl-1-ethanesulfonic acid after subsequent dilution to 80% H_2SO_4: A, sulfonation in an excess of 98.2% H_2SO_4; B, sulfonation, first with an excess of 98.2% H_2SO_4, then with an equal volume of 115% H_2SO_4.

TABLE 3. N.m.r. data of the sulfonic acids of 2-phenyl-1-ethanesulfonic acid (PESA) and related compounds in 80% H_2SO_4

Compounds	Aromatic H δ (p.p.m.) H_2	H_3	H_5	H_6	J_{ortho} (Hz)	CH_2, δ (p.p.m.) Benzylic (α)	Adjacent to SO_3H (β)
$C_6H_5CH_2CH_3$	singlet	7.13	(CCl_4)			2.54 (CCl_4)	
$CH_3CH_2SO_3H$							3.75 (9)
$C_6H_5CH_2CH_2SO_3H$	multiplet	7.30–7.75				3.14–3.49	3.49–3.79
$4\text{-}HO_3SC_6H_4CH_2CH_2SO_3H$	7.74	8.13			8.1	3.30–3.65	3.68–3.98
$2,4\text{-}(HO_3S)_2C_6H_3CH_2CH_2SO_3H$		8.60	8.48	8.03	8.0	3.70–4.00	4.00–4.25
$3\text{-}HO_3SC_6H_4CH_2CH_2SO_3H$						3.52*	3.82*
$2\text{-}HO_3SC_6H_4CH_2CH_2SO_3H$						3.71†	3.90†
$3,5\text{-}(HO_3S)_2C_6H_3CH_2CH_2SO_3H$						3.70†	4.00†

*The centers of the chemical shifts were taken to be equal to the centers of the chemical shifts of the 4-isomer (13).
†The centers of the chemical shifts of the α- and β-methylene hydrogen absorptions were calculated on the basis of the additivity principle of substituent shifts of the sulfonic acid substituents from:

$$\delta_{(CH_2)_i}(\text{ortho}) = \delta_{(CH_2)_i}(\text{PESA}) + \delta_{(CH_2)_i}(2,4\text{-di}) - \delta_{(CH_2)_i}(\text{para})$$
$$\delta_{(CH_2)_i}(3,5\text{-di}) = \delta_{(CH_2)_i}(\text{PESA}) + 2[\delta_{(CH_2)_i}(\text{meta}) - \delta_{(CH_2)_i}(\text{PESA})]$$

with $i = \alpha, \beta$.

sulfonation in 95% H_2SO_4 would then imply that the unionized sulfonic acid is the species undergoing sulfonation in 95% H_2SO_4.

Finally, the two complicating rate effects are minimal at 95% H_2SO_4. At that acid concentration, the rate ratio of 2-phenyl-1-ethanesulfonic acid to benzene is (0.238 ± 0.016):1. From the isomer distribution it then follows that the partial rate factors are $f_p = 1.29 \pm 0.14$, $f_m = 0.02 \pm 0.01$, and $f_o = 0.05 \pm 0.02$.

The reaction of 2-phenyl-1-ethanesulfonic acid in concentrated *aqueous* sulfuric acid

Can. J. Chem. Downloaded from www.nrcresearchpress.com by 210.87.254.42 on 09/05/12
For personal use only.

leads to clean sulfonation with formation of mainly 2-(*p*-sulfophenyl)-1-ethanesulfonic acid, the ratio of aliphatic to aromatic protons being 0.99 ± 0.02 (Fig. 2A). Further treatment of the monosulfonation mixture with *fuming* sulfuric acid (Fig. 2B leads chiefly to sulfonation with formation of mainly 2-(2,4-disulfophenyl)-1-ethanesulfonic acid, but also to some other reaction(s), possibly the formation of 2,4-styrenedisulfonic acid, since the ratio of the areas of the aliphatic to aromatic hydrogen absorption amounts only to 1.04 ± 0.03 instead of 1.33, the value required for disulfophenyl-ethanesulfonic acid.

Experimental

Sodium 2-phenyl-1-ethanesulfonate was prepared by means of the action of sodium sulfite on 1-phenyl-2-bromoethane (12).

Anal. Calcd. for $C_8H_9O_3SNa$: C, 46.15; H, 4.36; S, 15.40; Na, 11.04. Found: C, 46.04; H, 4.40; S, 15.52; Na, 11.04.

The experimental procedures and the spectrometer employed were the same as in ref. 6. The extinction measurements for the determination of the rate constants were made at λ 267 nm.

Isomer Distribution

Information concerning the products formed in the sulfonation of 2-phenyl-1-ethanesulfonic acid was obtained from an analysis of the n.m.r. spectra. The spectra were recorded after dilution of the sulfonation mixtures to the same sulfuric acid concentration (80% H_2SO_4). The results and the assignments are given in Table 3. After the spectrum of 2-phenyl-1-ethanesulfonic acid had been compared with the spectra of ethanesulfonic acid and ethylbenzene, the absorptions at δ 3.32 and 3.64 p.p.m. were assigned to the α- and β-methylene hydrogens respectively (see Table 3).

The degree of ortho-substitution was calculated from the absorption areas of the methylene hydrogens P and Q (Fig. 2A) by the equation: % ortho = $(P - Q)/(P + Q)$.

The degree of meta-substitution was estimated from the absorption areas of the methylene hydrogens P' and Q' (Fig. 2B) by the equation: % meta = $(Q' - P')/(P' + Q')$.

The authors acknowledge the assistance of Mr. H. van Oosterhout in preliminary experiments.

1. H. Cerfontain, A. Koeberg-Telder, and E. van Kuipers. J. Chem. Soc. Perkin Trans. II. In press.
2. C. W. F. Kort and H. Cerfontain. Rec. Trav. Chim. **87**, 24 (1968).
3. C. W. F. Kort and H. Cerfontain. Rec. Trav. Chim. **88**, 1298 (1969).
4. C. W. F. Kort and H. Cerfontain. Rec. Trav. Chim. **86**, 865 (1967).
5. C. W. F. Kort and H. Cerfontain. Rec. Trav. Chim. **88**, 860 (1969).
6. Z. R. H. Nienhuis, W. J. Spillane, and H. Cerfontain. Can. J. Chem. **50**, 1591 (1972).
7. H. Cerfontain and C. W. F. Kort. Int. J. Sulfur Chem. C, **6**, 123 (1971).
8. H. Cerfontain and B. W. Schnitger. Rec. Trav. Chim. **91**, 199 (1972).
9. A. Koeberg-Telder, C. van Lenten, and H. Cerfontain. Unpublished results.
10. E. S. Halberstadt, E. D. Hughes, and C. K. Ingold. J. Chem. Soc. 2441 (1950).
11. C. K. Ingold, E. H. Ingold, and F. R. Shaw. J. Chem. Soc. 813 (1927).
12. E. B. Evans, E. E. Mabbott, and E. E. Turner. J. Chem. Soc. 1161 (1927).
13. H. de Vries and H. Cerfontain. Rec. Trav. Chim. **86**, 873 (1967).

Can. J. Chem. Downloaded from www.nrcresearchpress.com by 210.87.254.42 on 09/05/12
For personal use only.

Can. J. Chem. Downloaded from www.nrcresearchpress.com by 210.87.254.105 on 09/05/12
For personal use only.

COMMUNICATIONS

The Total Synthesis of Daunomycinone[1]

CHIU MING WONG, ROBERT SCHWENK, DONALD POPIEN, AND TSE-LOK HO
Department of Chemistry, University of Manitoba, Winnipeg, Manitoba R3T 2N2

Received October 2, 1972

The aglycone of the antitumor antibiotic daunomycin, daunomycinone **1**, has been synthesized along with its C-1 isomer.

On a synthétisé la daunomycinone **1**, aglycone de l'antibiotique antitumoriale daunomycine, ainsi que son épimère en C-1. [Traduit par le journal]

Can. J. Chem., **51**, 466 (1973)

Daunomycin is currently a very important drug for clinical treatment of leukemia (1). Mild acid hydrolysis of daunomycin gives an amino sugar daunosamine and the aglycone daunomycinone **1** (2).

We wish to report a total synthesis of **1** fashioned in the CD → ABCD annelation sequence which has been successfully put to test in a model study (3). The synthesis of the antibiotic aglycone itself utilized also the bicyclic ketol **2**, obtained from 2,5-dimethoxybenzaldehyde in seven steps (**3**) or, preferably, **2** may be prepared as shown in Scheme 1.

Condensation of **2** with 3-acetoxyphthalic acid monomethyl esters (isomeric mixture) in refluxing trifluoroacetic anhydride yielded a mixture of diaryl ketones which was directly saponified (2 *N* NaOH/ethanol) and subjected to HF cyclization at room temperature. The resulting quinones **3** and **4** (overall 19%; ν 3500, 1710, 1670, 1640 cm^{-1}; *m/e* 396) were then quantitatively methylated (Me_2SO_4–K_2CO_3–acetone)(*m/e* 410; δ 2.35 (3H, s, $COCH_3$), 3.85, 3.87, 3.88, 3.92, 3.97 (9H total, singlets, OCH_3).

Since separation of isomers was not feasible at this stage, introduction of the oxygen function at C-7 was next attempted. The side-chain ketone was protected as the dioxolane group (ethanediol–TsOH–benzene; 88%; *m/e* 454; 1.40 (3H, s, CH_3), 3.88, 3.92, 3.96, 4.02 (13H total, singlets, OCH_3 and acetal CH_2), bromination (NBS) was then achieved selectively at the desired position. Methanolysis of the bromoacetals permitted isolation of two compounds by preparative t.l.c. (silica, methanol–chloroform, 1:25; R_f 0.31, 0.51) which subsequently proved to be acetals having epimeric benzylic methoxy groups (**5**, R = OCH_3 at C-1 or C-4). Only after hydrolysis (HCl – aqueous THF) of the dioxolane function could the ring A isomers be finally resolved by preparative t.l.c. (silica, methanol – ethyl acetate 1:100). From the R_f 0.51 band, the more polar daunomycinone trimethyl ether (**6**, m.p. 185–186°; *m/e* 440; ν 3460, 1715, 1680 cm^{-1}; δ 2.40 (3H, s, $COCH_3$), 3.56 (3H, s, OCH_3), 3.89 (3H, s, $ArOCH_3$), 4.00 (6H, s, $ArOCH_3$)) and the less polar isodaunomycinone trimethyl ether (**7**, m.p. 226–227°; *m/e* 440; ν 3460, 1715, 1680 cm^{-1}; δ 2.40 (3H, s, $COCH_3$), 3.56 (3H, s, OCH_3), 3.93 (3H, s, $ArOCH_3$), 4.00 (6H, s, $ArOCH_3$)) were obtained in the ratio of *ca.* 1:1. The former compound has been identified by comparison with a specimen derived from natural daunomycin.

To complete the synthesis, **6** was reacted with aluminum chloride at ambient temperature to give 4-O-demethyl-7-O-methyldaunomycinone (**8**, m.p. 246–250°; *m/e* 398; ν 3440, 1715, 1600 cm^{-1}) which was oxidized to the unstable diquinone **9** (ν 3460, 1715, 1685 cm^{-1}) by lead tetraacetate and immediately remethylated (Me_2SO_4–K_2CO_3–acetone, 25°) to provide 7-O-methyldaunomycinone (**10**; ν 3460, 1720, 1620, 1585 cm^{-1}, 10%). The benzylic methoxy was replaced by the trifluoroacetoxy group with trifluoroacetic acid (25°, 2 h), resulting in **12** (ν 3480, 1785, 1720, 1620, 1580 cm^{-1}). Treatment

[1]Part II of Synthetic Studies of Hydronaphthacenic Antibiotics.

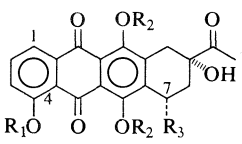

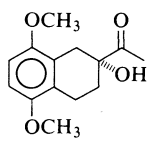

2

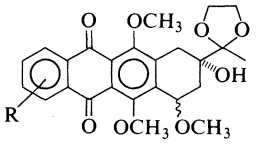

5

1 $R_1 = CH_3$, $R_2 = H$, $R_3 = OH$
3 $R_1 = R_3 = H$, $R_2 = CH_3$
6 $R_1 = R_2 = CH_3$, $R_3 = OCH_3$
8 $R_1 = R_2 = H$, $R_3 = OCH_3$
10 $R_1 = CH_3$, $R_2 = H$, $R_3 = OCH_3$
12 $R_1 = CH_3$, $R_2 = H$, $R_3 = OCOCF_3$ (epimer)

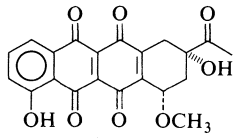

9

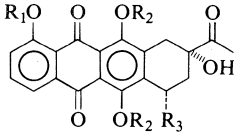

4 $R_1 = R_3 = H$, $R_2 = CH_3$
7 $R_1 = R_2 = CH_3$, $R_3 = OCH_3$
11 $R_1 = CH_3$, $R_2 = H$, $R_3 = OH$

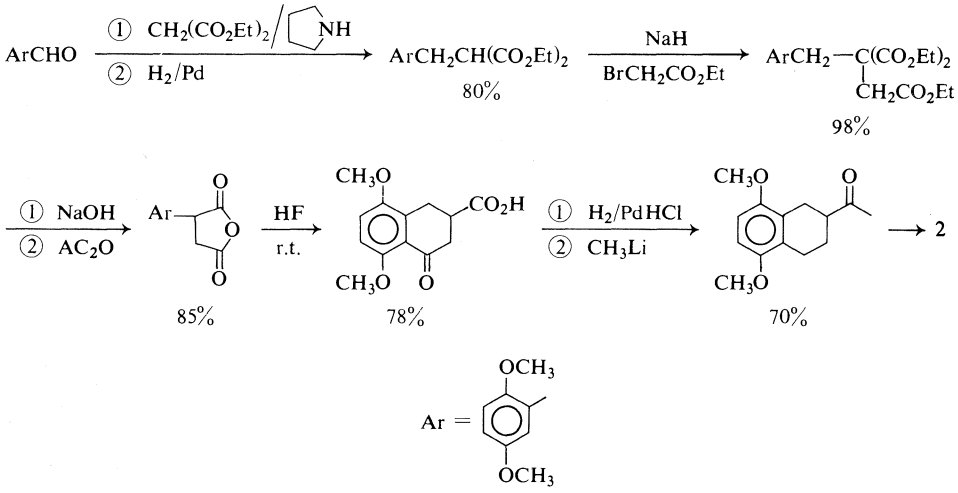

SCHEME I

of **12** with ammonium hydroxide in boiling acetone furnished daunomycinone (ν 3480, 1715, 1620, 1585 cm^{-1}). These latter two compounds are identical with samples derived from natural daunomycin.

Parallel experiments performed on isodaunomycinene trimethyl ether **7** gave isodaunomycinone (**11**, m.p. 216–218°; *m/e* 398; ν 3480, 1715, 1620, 1580 cm^{-1}). All key synthetic intermediates exhibit spectral properties consistent with assigned structures and correct elemental analyses or exact mass molecular ion.

This research was supported by the National Research Council of Canada.

1. C. TAN, H. TASAKA, K. YU, M. MURPHY, and D. KARNOFSKY. Cancer, **20**, 333 (1967).
2. F. ARCAMONE, G. FRANCESCHI, P. OREZZI, G. CASSINELLI, W. BARBIERI, and R. MONDELLI. J. Am. Chem. Soc. **86**, 5334 (1964); F. ARCAMONE, G. FRANCESCHI, P. OREZZI, S. PENCO, and R. MONDELLI. Tetrahedron Lett. 3349 (1968); F. ARCAMONE, G. CASSINELLI, G. FRANCESCHI, P. OREZZI, and R. MONDELLI. Tetrahedron Lett. 3353 (1968).
3. C. M. WONG, D. POPIEN, R. SCHWENK, and J. TERAA. Can. J. Chem. **49**, 2712 (1971).

Can. J. Chem. Downloaded from www.nrcresearchpress.com by 210.87.254.105 on 09/05/12
For personal use only.

4-Methyl-3,3-pentamethylene-1,2-dioxetane. Lack of its Formation in Ozonation of Ethylidenecyclohexane in Pinacolone[1,2]

KARL R. KOPECKY, PETER A. LOCKWOOD,[3] JOHN E. FILBY,[4] AND RONALD W. REID

Department of Chemistry, University of Alberta, Edmonton, Alberta T6G 2G2

Received October 10, 1972

The title compound has been prepared and characterized. Contrary to a previous report it is not formed on ozonation of ethylidenecyclohexane (**1**) in pinacolone. The percent yields of products formed on ozonation of **1** in Skelly B, pinacolone, and dimethyl ether are, respectively, acetaldehyde, 25, 47, 59; normal ozonide ~75, ~0, <15; and dimeric cyclohexanone peroxide 11, 17, 35.

Le composé mentionné dans le titre a été préparé et caractérisé. Contrairement à ce qui a été rapporté précédemment, il n'est pas formé par ozonolyse de l'éthylidènecyclohexane (**1**) dans la pinacolone. Les rendements de produits formés par ozonolyse de **1** dans le Skelly B, la pinacolone, et le méthioxyméthane sont respectivement 25, 47, et 59% d'acétalydéhyde; ~75, ~0, et <15% d'ozonide normal; et 11, 17, et 35% du peroxyde dimère de la cyclohexanone. [Traduit par le journal]

Can. J. Chem., **51**, 468 (1973)

Can. J. Chem. Downloaded from www.nrcresearchpress.com by 210.87.254.40 on 09/05/12
For personal use only.

Recent reports indicate that cleavage products rather than normal ozonides are formed on ozonation of alkenes in certain aldehyde or ketone solvents (1). The cleavage products were assumed to arise from decomposition of transient 1,2-dioxetanes. Several of these are claimed later to have been isolated by ozonation of some alkenes in pinacolone solution (2). In particular from ethylidenecyclohexane (**1**) was isolated a 50–75% yield of 4-methyl-3,3-pentamethylene-1,2-dioxetane (**2**) as a colorless oil which luminesced and gave cyclohexanone and acetaldehyde when heated to 170°, was reduced to 1-(1-hydroxyethyl)-cyclohexanol **3**, and was identical in all respects with **2** prepared by conventional methods (3). Also *t*-butyl acetate was found in amount presumably equivalent to the yield of **2**.

This work aroused our interest for three reasons. First, ozonation of alkenes would be a simpler and less hazardous preparation of 1,2-dioxetanes than is the present method (3). Second, a high temperature is apparently required to observe luminescence from **2**. Luminescence can be observed clearly from other 1,2-dioxetanes at temperatures as low as 50° or less (3*b*, 3*c*, 4). Finally, all of the several dioxetanes prepared so far in our laboratories are light yellow. We have now prepared **2** from the corresponding bromohydroperoxide and found that its properties are quite conventional, in contrast to the above results (2). Furthermore, we are unable to detect any **2** or *t*-butyl acetate as products of ozonation of **1** in pinacolone.

The crude bromohydroperoxide **4** of **1** was prepared (3*a*) and purified by way of the 1,4-diazabicyclo[2.2.2]octane complex (5). Pure **4** had m.p. 44.0–45.5°, 99.6% active oxygen, and satisfactory spectra. A mixture of 2.3 g **4** and 0.44 g sodium hydroxide in 10 ml of 9:1 methanol–water was stirred at 0° for 20 min. Water and carbon tetrachloride, 10 ml each, were added, solvent was removed from the dried organic layer at 20°, and then the crude product was pumped from the yellow residue under 30μ at 20° until residue became pale. A small, colorless forerun was discarded. Redistillation in this way gave bright yellow, Fig. 1, crystals (~10% yield) of **2**, m.p. ~−11°, in the −78° trap. This material had 97.8% active oxygen, molecular weight: 155 (cryoscopic, C_6H_6); n.m.r. $\tau(CCl_4)$: 4.91 (quartet, J = 6.5 Hz, 1.0 H), and 8.66 (doublet, J = 6.5 Hz) superimposed on a broad absorption from 7.8–8.8 (total 13.0H).

In benzene-d_6, **2** decomposes with a half-life

[1]This research was supported in part by a grant from the Defence Research Board of Canada, Grant Number 9530-99. We also wish to thank Professor S. Fliszár for helpful discussions.

[2]Chemical Abstracts will index the title compound as 3-methyl-1,2-dioxaspiro[3.5]nonane. We thank Dr. K. L. Loening for this information.

[3]Holder of a NRCC Scholarship, 1970–1972.

[4]Holder of a Canadian Mortgage and Housing Fellowship, 1970–1971, a NRCC Scholarship, 1971–1972, and a Province of Alberta Graduate Fellowship, 1971–1972.

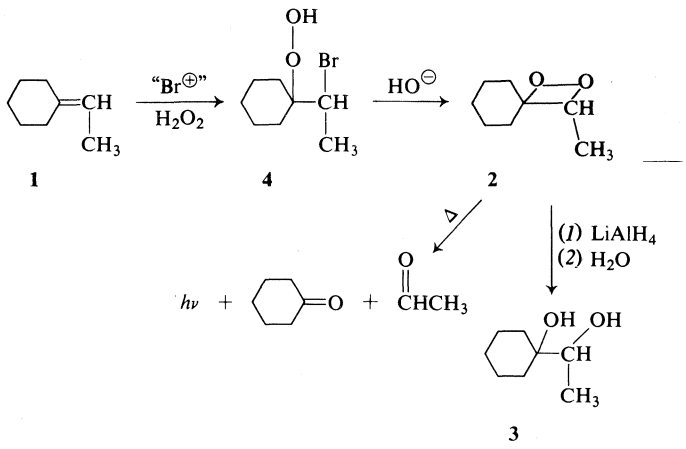

SCHEME 1

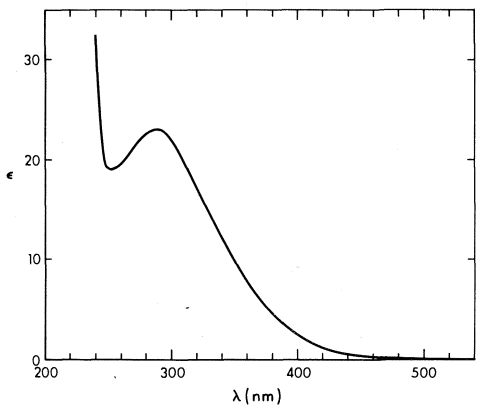

FIG. 1. Ultraviolet–visible spectrum of 0.0181 *M* 4-methyl-3,3-tetramethylene-1,2-dioxetane in heptane.

of ~15 min at 50° to give acetaldehyde, 90% (by n.m.r.), and cyclohexanone, 95% (as the 2,4-dinitrophenylhydrazone).

Reduction of **2** with lithium aluminum hydride at −40° gave **3** (87%) identical (i.r., n.m.r., t.l.c.) with an authentic sample (6). At 50°, even dilute (0.01 *M*) solutions of **2** emit a visible bluish-white luminescence. Addition of dibromoanthracene (DBA) greatly enhances its intensity (4*c*, 7). These reactions are given in Scheme 1.

We found no evidence for the formation of **2** on ozonation of **1** in pinacolone. Ozonation was carried out using ozone in nitrogen (8) and solvent was removed to give a colorless, viscous oil A as in the procedure described (2). G.l.c. analysis of A did indicate the presence of cyclohexanone and pinacolone. However, no *t*-butyl acetate could be detected either in A or in the separated pinacolone. Had 5% been formed, it would have been detected.[5,6] Also luminescence of A was not reproducible. Of eight preparations only four luminesced when heated suddenly to 170°, and none luminesced at 50° even when DBA was present. In one case, a 0.5 g sample of A (luminescent at 170°) containing DBA was heated to 50°. No luminescence could be detected. After addition of ~1 mg of **2**, a definite luminescence was seen visually. With the aid of a spectrofluorimeter it was shown that A contained less than 4×10^{-2}% of **2**.

Chemical evidence also indicates that A contains no **2**. G.l.c. analysis of the product mixture obtained on treatment of A with lithium aluminum hydride at −40° indicated that less than 5%, if any, of **3** was formed.[7] Control experiments showed that **2** survives the ozonolysis, so that it is never formed at all in this reaction.

[5]No attempt was made to detect acetaldehyde on g.l.c. analysis of A. Pinacolone as received (Aldrich Chemical Co.) contains about 1–2% of a material with a retention time (Carbowax 40 M) very near that of *t*-butyl acetate. This and other trace impurities can be removed mostly by fractional distillation and removed completely by fractional distillation followed by fractional freezing. All our experiments were done using pinacolone purified by these methods.

[6]Professor R. Criegee and P. S. Bailey have informed us that no *t*-butyl acetate could be detected among the products of ozonation of **1** in pinacalone in their laboratories, either.

[7]Professor P. S. Bailey has informed us that the same result was obtained in his laboratory (13).

Can. J. Chem. Downloaded from www.nrcresearchpress.com by 210.87.254.40 on 09/05/12
For personal use only.

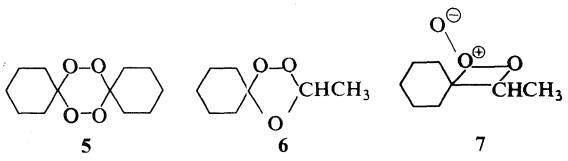

5 6 7

When A is allowed to stand even for a short time colorless crystals are deposited which were shown to be the dimeric cyclohexanone peroxide **5** by comparison (i.r., n.m.r., m.p., and mixed m.p.) with authentic material (9).

We were able to confirm that the normal ozonide **6** is not formed in pinacolone, but it is formed in 75% yield in Skelly B. Ozonolysis mixtures kept below $-30°$ until diluted with trichlorofluoromethane were analyzed at $-20°$ by n.m.r. spectroscopy at 100 MHz. In Skelly B, **6** was identified by a clean quartet, $J = 5$ Hz, at 206 Hz upfield from the chloroform internal standard signal.[8] In this region the n.m.r. spectrum of the pinacolone solution had a broad, structureless peak on which were superimposed some sharp peaks,[9] but none due to **6**. The n.m.r. spectrum of crude **6**[8] in pinacolone solvent had a clean quartet at τ 4.7.

This effect of solvent is reminiscent of that observed in ozonation of *trans*-3-hexene in dichlorodifluoromethane and in dimethyl ether-d_6 (11). Much less ozonide is formed in the latter solvent. Indeed, ozonation of **1** in dimethyl ether at $-80°$ formed only a small amount of **6** as judged from the n.m.r. spectrum taken at $-80°$. Broad, structureless absorption, due to oligomeric materials (11), was again observed near τ 5 upon which was superimposed a quartet, $J = 5$ Hz, of weak intensity.

Acetaldehyde and **5** are formed in all solvents. The percent yields of products formed on ozonation of **1** in Skelly B, pinacolone, and dimethyl ether are, respectively, acetaldehyde (by n.m.r.) 25, 47, 59; **6** (by n.m.r.) 75, ~0, <15; and **5** (by isolation) 11, 17, 35. More acetaldehyde (cleavage product) is formed in dimethyl ether than in pinacolone! Formation of large amounts of acetaldehyde is consistent with the report that the carbonyl product of the cleavage of the primary ozonide of **1** is mainly acetaldehyde (12).

It appears that pinacolone exerts a general (*e.g.*, polar), and not a specific, solvent effect on ozonation of **1**. While it is difficult to disprove the transient existence of **7**, the present results certainly do not provide support for the claim (1, 2) that **7** is an early product of reaction between ozone and **1**.

[8]Identification of **6** was made only on the basis of the n.m.r. spectrum of the concentrated oil obtained from ozonation of **1** in Skelly B. It had strong signals at $\tau(CCl_4)$ 4.81 (quartet, $J = 5$ Hz) and 8.67 (doublet, $J = 5$ Hz). The methine protons of the ozonides of *trans*-2-butene absorb at $\tau(CCl_4)$ 4.73 (10). Ozonation of **1** in acetaldehyde gives **6** (no characterization reported) in 75% yield (1*a*).

[9]The same absorption is observed in the n.m.r. spectrum of A. If, during the preparation of **2** from **4**, stirring is continued for 90 min, little **2** can be isolated and the n.m.r. spectrum of the crude product and that of A show similar absorption patterns in the region near $\tau(CCl_4)$ 4.9. This may have caused some confusion in the earlier work (2).

1. (*a*) P. R. Story, J. A. Alford, J. R. Burgess, and W. C. Ray. J. Am. Chem. Soc. **93**, 3042 (1971). (*b*) P. R. Story, J. A. Alford, W. C. Ray, and J. R. Burgess. J. Am. Chem. Soc. **93**, 3044 (1971).
2. P. R. Story, E. A. Whited, and J. A. Alford. J. Am. Chem. Soc. **94**, 2143 (1972).
3. (*a*) K. R. Kopecky, J. H. van de Sande, and C. Mumford. Can. J. Chem. **46**, 25 (1968). (*b*) W. H. Richardson and V. F. Hodge. J. Am. Chem. Soc, **93**, 3996 (1971). (*c*) W. H. Richardson, M. B. Yelvington, and H. E. O'Neal. J. Am. Chem. Soc. **94**, 1619 (1972).
4. (*a*) K. R. Kopecky and C. Mumford. Can. J. Chem. **47**, 709 (1969). (*b*) S. Mazur and C. S. Foote. J. Am. Chem. Soc. **92**, 3225 (1970). (*c*) T. Wilson and A. P. Schaap. J. Am. Chem. Soc. **93**, 4126 (1971).
5. A. A. Ostwald, F. Noel, and A. J. Stephenson. J. Org. Chem. **26**, 3969 (1961).
6. G. F. Hennion and E. J. Watson. J. Org. Chem. **23**, 656 (1958).
7. E. H. White, J. Wiecko, and D. F. Roswell. J. Am. Chem. Soc. **91**, 5194 (1969).
8. G. A. Cook, A. D. Kiffer, C. V. Klumpp, A. H. Malik, and L. A. Spence. Adv. Chem. Ser. **21**, 44 (1959).
9. R. Criegee and G. Lohaus. Ann. **583**, 6 (1953).
10. L. D. Loan, R. W. Murray, and P. R. Story. J. Am. Chem. Soc. **87**, 737 (1965).
11. F. L. Greenwood and L. J. Durham. J. Org. Chem. **34**, 3363 (1969).
12. S. Fliszár and J. Renard. Can. J. Chem. **48**, 3002 (1970).
13. P. S. Bailey, T. P. Carter, C. M. Fischer, and J. A. Thompson. Can. J. Chem. In press.

Can. J. Chem. Downloaded from www.nrcresearchpress.com by 210.87.254.40 on 09/05/12
For personal use only.

Can. J. Chem. Downloaded from www.nrcresearchpress.com by 210.87.254.5 on 09/05/12
For personal use only.

Canadian Journal of Chemistry

Published by
THE NATIONAL RESEARCH COUNCIL OF CANADA

Journal canadien de chimie

Publié par
LE CONSEIL NATIONAL DE RECHERCHES DU CANADA

Volume 51 Number 4 February 15, 1973 Volume 51 numéro 4 15 février 1973

The Photochemical Decomposition of Gaseous Formaldehyde

HENRY P. SPERLING AND SIDNEY TOBY

School of Chemistry, Rutgers University, New Brunswick, New Jersey 08903

Received June 27, 1972

The photolysis of formaldehyde was studied at 313, 334, and 366 nm in the range 80–120° and 9–40 Torr, over a 300-fold range of incident intensity. Some heterogeneous thermal decomposition was noted at these temperatures. It was found that Φ_{H_2} and Φ_{CO} were independent of intensity at low intensities which suggests that CHO → CO + H was unimportant in our system. From the zero-intensity extrapolations of Φ it was possible to obtain ϕ_I for $CH_2O + h\nu \rightarrow H + CHO$ and ϕ_{II} for $CH_2O + h\nu \rightarrow H_2 + CO$. ϕ_I and ϕ_{II} were found to vary considerably with wavelength and the values obtained are compared with literature data.

La photolyse de la formaldéhyde a été étudiée à 313, 334, et 366 nm dans les intervalles 80–120° et 9–40 Torr, en se servant d'une échelle (trois centuples) d'intensité incidente. A ces températures, quelques décompositions thermiques hétérogènes ont été observées. Il a été trouvé que Φ_{H_2} et Φ_{CO} sont indépendants de l'intensité pour de basses intensités ce qui suggère que la réaction CHO → CO + H était négligeable dans notre système. A partir de l'extrapolation, à intensité nulle, de Φ, il a été possible d'obtenir ϕ_I pour $CH_2O + h\nu \rightarrow H + CHO$ et ϕ_{II} pour $CH_2O + h\nu \rightarrow H_2 + CO$. ϕ_I et ϕ_{II} se trouvent à varier considérablement avec la longueur d'onde et les valeurs obtenues sont comparés avec celle tirées de la littérature. [Traduit par le journal]

Can. J. Chem., **51**, 471 (1973)

It is hard to overemphasize the fundamental importance of the chemistry of formaldehyde yet there is disagreement in the literature on major aspects of the thermal and photochemical decomposition. The relatively small number of investigations made with pure formaldehyde is unquestionably related to the difficulties of working with this substance: the gaseous monomer at pressures greater than a few Torr rapidly polymerizes in the temperature range −10 to 60°, building up a solid polymer on the walls of the container.

Formaldehyde has an absorption band from 220–380 nm assigned to the singlet–singlet $^1A_2 \leftarrow {}^1A_1$ transition. It is well established (1) that at the longer wavelengths, photolysis occurs via two primary processes

[I] $CH_2O + h\nu \rightarrow H + CHO$

[II] $\rightarrow H_2 + CO$

However, the values of the primary quantum yields ϕ_I and ϕ_{II}, and their variation with wavelength are uncertain. Methods used have included iodine inhibition (2), mixed isotopes (3), mercury photosensitization (4), olefin inhibition (5), and flash photolysis (6) and the discordant results will be discussed later. The method used here was the measurement of the overall quantum yields, Φ_{H_2} and Φ_{CO}, and their extrapolation to zero intensity (7). The limiting values may then be related to ϕ_I and ϕ_{II}.

Experimental Section

A conventional high vacuum system was used with greaseless valves in all sections exposed to formaldehyde or products.

All photolysis and some thermolysis runs were done in a cylindrical quartz cell of volume 0.472 l and length 20.1 cm mounted inside an oven with temperature control to within ±0.3° at 160°. The cell was connected to a Granville Phillips stainless steel valve mounted inside

Can. J. Chem. Downloaded from www.nrcresearchpress.com by 210.87.254.5 on 09/05/12
For personal use only.

the oven with a dead space of $< 1\%$. Thermolysis experiments were also performed in a spherical quartz bulb of volume 0.19 l connected to a Kontes glass valve with a Teflon/O-ring seal. Conversions were normally kept at $< 1\%$.

The optical system consisted of an Osram HBO-75W high pressure mercury arc with the beam made parallel with a quartz lens. The 313 and 334 nm regions were isolated with solution glass filters (1) and for the 366 nm region a combination of Corning 0–52 and 7–60 filters was used. Light output was checked for monochromaticity, and intensity was varied with quartz neutral density filters and monitored with an RCA 935 photodiode. Absolute incident intensities were obtained using azomethane as an actinometer assuming $\Phi_{N_2} = 1$ with the wavelengths employed. Linear Beer–Lambert plots gave the extinction coefficients of formaldehyde as $\varepsilon = 4.83$ and 1.87 l mol^{-1} cm^{-1} at 313 and 334 nm, respectively. We could not accurately measure the small value of ε at 366 nm and the value $\varepsilon = 0.07$ was taken from the spectrum given by Calvert and Pitts (1).

Formaldehyde was prepared from the polymer as described by Boyles and Toby (8). This yields a monomer of purity $> 99.9\%$, the main impurities being methanol, water, and methyl formate. The formaldehyde was stored at $-196°$.

Hydrogen and carbon monoxide were analyzed by gas chromatography using a silica gel column. No attempt was made to analyze for condensable products such as methanol and glyoxal in the presence of large amounts of unreacted formaldehyde.

Results

A thermal decomposition was studied at 80, 120, and 160°. Equal amounts of H_2 and CO were formed and a half order rate law was obeyed. The measured activation energy was 21.2 kcal/mol. This thermal decomposition was sufficient to preclude photolysis at 160°. The *maximum* correction for the dark reaction was at low intensities and was $\sim 60\%$ at 120° and $\sim 7\%$ at 80°. There is thus considerable uncertainty in the data at 120° at low intensities and most of the photolyses were performed at 80°. Thus the variables employed were wavelength, temperature, incident intensity, formaldehyde pressure, and carbon dioxide pressure. Figures 1 and 2 show the effect of incident intensity on Φ_{CO} and Φ_{H_2} at 313, 334, and 366 nm. Since we are mainly concerned with the zero-intensity values of Φ,

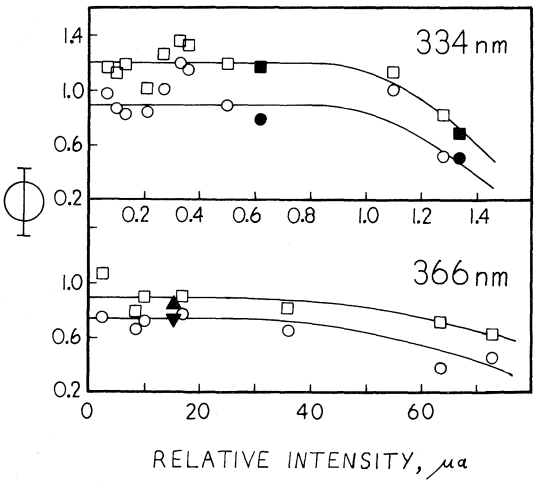

FIG. 1. Effect of incident intensity on quantum yield. Symbols: □, H_2 at 80°; ■ and ▲, H_2 at 120°; ○, CO at 80°; ● and ▼, CO at 120°. CH_2O pressure is 9 Torr except for triangular symbols = 30 Torr.

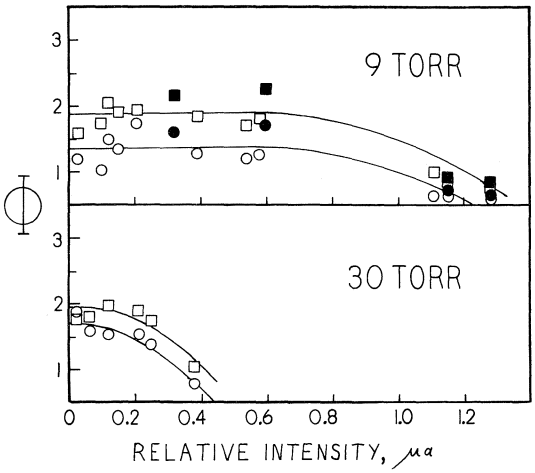

FIG. 2. Effect of incident intensity on quantum yield at 313 nm. Symbols: □, H_2 at 80°; ■, H_2 at 120°; ○, CO at 80°; ●, CO at 120°.

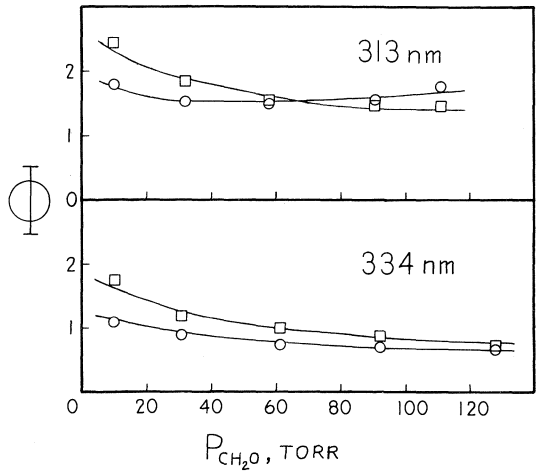

FIG. 3. Effect of CH_2O pressure on quantum yield. Symbols as in Fig. 2.

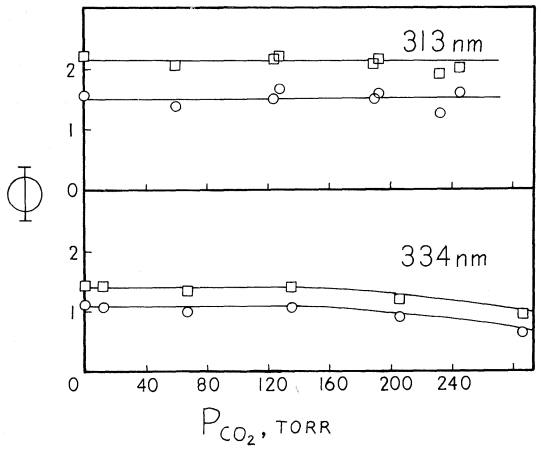

FIG. 4. Effect of added CO_2 on quantum yield. CH_2O pressure = 9 Torr. Symbols as in Fig. 2.

intensity has been plotted as the uncorrected photodiode current, for convenience. Figure 3 shows the effect of formaldehyde pressure on Φ at constant incident intensity. Figure 4 shows the effect on Φ of added carbon dioxide with up to a 30-fold excess.

Discussion

The thermolysis activation energy of 21.2 kcal/mol is incompatible with the known bond dissociation energies of CH_2O and CHO (9), and this together with the low temperatures at which decomposition occurred strongly suggests a heterogeneous process. Similar low activation energies have been found when formaldehyde was decomposed in the presence of metals (10).

To investigate whether the stainless steel valve had a catalytic effect, some experiments were carried out in a quartz bulb connected to a stopcock with a Teflon/O-ring seal. The decomposition rate fell by about a factor of 100. When pieces of stainless steel were added to the bulb, the decomposition rate increased, but silver pellets were found to have no effect. These results suggest that careful consideration must be given to the thermolysis when formaldehyde is photolyzed in the presence of metals.

The photolysis of formaldehyde in the near ultraviolet produces an excited singlet via an n,π* transition. It seems clear that dissociation and subsequent chemistry involve the excited singlet (11) and our work gives no new information on this. There is the possibility of deactivation of the excited molecule and this will be mentioned later. The dissociation $CH_2O^* \rightarrow 2H + CO$ has been shown to occur at short wavelengths by Glicker and Stief (12) but should not occur at wavelengths >271 nm.

The salient features of Figures 1–4 are that the quantum yields are (*a*) independent of incident intensity at low intensities, (*b*) independent of temperature, (*c*) somewhat dependent on pressure, and (*d*) independent of added CO_2. In addition it is clear that $\Phi_{H_2} > \Phi_{CO}$ except at the highest pressures employed.

A mechanism which gives reasonable agreement with our experimental results consists of reactions I and II followed by

[1] $H + CH_2O \rightarrow H_2 + CHO$

[2] $H + CHO \rightarrow H_2 + CO$

[3] $2CHO \rightarrow (CHO)_2$

[4] $\rightarrow 2CO + H_2$

[5] $\rightarrow CH_2O + CO$

[6] $2H (+ M) \rightarrow H_2 (+ M)$

To solve the mechanism of reactions I–II, 1–6 we make the usual steady state assumption of transient species, and also apply the cross-combination rule (13) $k_2/(k_3 + k_4 + k_5)^{1/2}k_6^{1/2} = 2$.[1] Then

$$[7]\quad \Phi_{H_2} = \phi_{II} + \frac{a\phi_I}{a + 2b} + \frac{\phi_I}{(a + 2b)^2} \times \left\{(a + b)\left[\frac{k_2\phi_I^{1/2}I_a^{1/2}}{(k_3 + k_4 + k_5)^{1/2}} + \frac{k_4(a + b)}{k_3 + k_4 + k_5}\right] + b^2\right\}$$

$$[8]\quad \Phi_{CO} = \phi_{II} + \frac{(a + b)}{(a + 2b)^2}\phi_I \times \left\{\frac{k_2\phi_I^{1/2}I_a^{1/2}}{(k_3 + k_4 + k_5)^{1/2}} + \frac{(2k_4 + k_5)(a + b)}{k_3 + k_4 + k_5}\right\}$$

where

$$a = k_1[CH_2O],\ b = (k_6\phi_I I_a)^{1/2}$$

and

$$I_a = \text{absorbed intensity}$$

Equations 7 and 8 predict that Φ will be rather insensitive to changes in intensity, with a

[1]The cross-combination rule is itself pressure dependent, (see, for example, ref. 14). Thus errors will be introduced here over a large pressure range.

Can. J. Chem. Downloaded from www.nrcresearchpress.com by 210.87.254.5 on 09/05/12
For personal use only.

TABLE 1. Values of ϕ_I/ϕ_{II}

ϕ_I/ϕ_{II} at wavelength (nm)								Temperature	
124	147	254	265	280	313	334	366	(°C)	Reference
<0.2	<0.2							25	12
		~100			~100		1.2	100	2
					5		0.5–5	140	3
		1.5						55	4
		0.18	0.23		1.1	1.4		90–130	5
				5.0	1.0	0.4	0	60–100	6
					4	2	0.4	80–120	This work

slow decrease at higher intensities. This is seen in Figs. 1 and 2. Over the limited temperature range employed Φ is independent of temperature but a pressure dependence is seen in Fig. 3 although not in Fig. 4. The pressure dependence is of small consequence at formaldehyde pressures below about 15 Torr. As intensity approaches zero we have these limiting expressions

$$[9] \quad \lim \Phi_{H_2} = \phi_{II} + \phi_I\left(\frac{k_3 + 2k_4 + k_5}{k_3 + k_4 + k_5}\right)$$

$$[10] \quad \lim \Phi_{CO} = \phi_{II} + \phi_I\left(\frac{2k_4 + k_5}{k_3 + k_4 + k_5}\right)$$

The limiting quantum yields are much less sensitive to the form of the mechanism than are eqs. 7 and 8. For example, if reaction 2 is replaced by $H + CHO \rightarrow CH_2O$, eqs. 9 and 10 are unaffected.

Our estimated values for the limiting intensity, low pressure values of Φ are as follows: 313 nm $H_2 = 1.92 \pm 0.1$, $CO = 1.30 \pm 0.1$; 334 nm $H_2 = 1.20 \pm 0.1$, $CO = 0.86 \pm 0.1$; 366 nm $H_2 = 0.88 \pm 0.15$, $CO = 0.72 \pm 0.15$.

There are too many unknowns in eqs. 9 and 10 for immediate numerical solutions of ϕ_I and ϕ_{II}. However, approximate values may be obtained indirectly. Lim Φ_{H_2} − lim $\Phi_{CO} = \phi_I k_3/(k_3 + k_4 + k_5)$ and we find this decreases as wavelength increases. Rate constants for equilibrated radicals will be independent of wavelength (λ) and thus as λ increases ϕ_I decreases. We may rewrite eqs. 9 and 10 as

$$[11] \quad \frac{\lim (\Phi_{H_2} - \phi_{II})}{\lim \Phi_{CO} - \phi_{II}} = \frac{k_3}{2k_4 + k_5} + 1$$

$$[12] \quad \frac{\lim \Phi_{H_2} - \lim \Phi_{CO}}{\phi_I} = \frac{k_3}{k_3 + k_4 + k_5}$$

and the r.h.s. must be independent of λ. Additional restraints arise because the r.h.s. of eq. 11 is clearly >1 and that of eq. 12 is <1. These restraints coupled with the assumption that ϕ_{II} varies monotonically with λ enable limits to be assigned to the values of ϕ_I and ϕ_{II} by plotting the l.h.s. of eqs. 11 and 12 against λ for different values of ϕ_I and ϕ_{II}. The results are as follows: for 313 nm, $\phi_I = 0.8 \pm 0.2$, $\phi_{II} = 0.2 \pm 0.2$; for 334 nm, $\phi_I = 0.45 \pm 0.1$, $\phi_{II} = 0.25 \pm 0.1$; for 366 nm, $\phi_I = 0.2 \pm 0.1$, $\phi_{II} = 0.45 \pm 0.1$.

Literature values for the ratio ϕ_I/ϕ_{II} (which should be more accurate than the absolute values) are given in Table 1. The lack of agreement in the data of Table 1 is discouraging. Plots of ϕ_I/ϕ_{II} (or the individual quantum yields) against wavelength show an almost random scatter. Glicker and Stief's (12) results are not strictly comparable with the others since at short wavelengths ϕ_I may be zero. The values of DeGraff and Calvert (5) show a trend at variance with all other data and probably may be discounted (6). The remaining data show rough agreement that as λ increases, ϕ_I/ϕ_{II} decreases. The dominant primary process at 366 nm is probably reaction II.

We may draw some qualitative conclusions from the trends shown in Figs. 1–4. The fact that Φ_{H_2} and Φ_{CO} do not increase at low intensities is evidence for the stability of the formyl radical up to 120°. Appreciable decomposition would lead to a chain reaction with subsequent increases in Φ_{H_2} and Φ_{CO}.

We find that $\phi_I + \phi_{II} < 1$ at 366 nm and perhaps at 334 nm. Our data are less reliable at 366 nm than at the shorter wavelengths since we were unable to measure the absorption coefficient at 366 nm. Thus we are reluctant to postulate a third, deactivating, primary process especially since a large excess of CO_2 is seen to have virtually no effect in Fig. 4. McQuigg and

Can. J. Chem. Downloaded from www.nrcresearchpress.com by 210.87.254.5 on 09/05/12
For personal use only.

Calvert (6) found $\phi_I + \phi_{II} \simeq 1.0$ for CH_2O but the sum was much less than unity for CD_2O. The possibility of a third primary process at longer wavelengths cannot be ruled out.

We thank the National Science Foundation for the support of this work.

1. J. G. CALVERT and J. N. PITTS, JR. Photochemistry. John Wiley and Sons, Inc., N.Y. 1966.
2. E. GORIN. J. Chem. Phys. **7**, 256 (1939).
3. R. KLEIN and L. J. SCHOEN. J. Chem. Phys. **24**, 1094 (1956).
4. A. G. HARRISON and F. P. LOSSING. Can. J. Chem. **38**, 544 (1960).
5. B. A. DEGRAFF and J. G. CALVERT. J. Am. Chem. Soc. **89**, 2247 (1967).
6. R. D. MCQUIGG and J. G. CALVERT. J. Am. Chem. Soc. **91**, 1590 (1969).
7. F. R. CALA, S-L. CHONG, H. P. SPERLING, and S. TOBY. Can. J. Chem. **48**, 357 (1970).
8. J. G. BOYLES and S. TOBY. J. Polymer Sci. **A-1**, **5**, 1705 (1967).
9. B. DE B. DARWENT. Bond dissociation energies in simple molecules. National Bureau of Standards NSRDS-NBS 31 (1970).
10. I. YASUMORI, T. NAKAMURA, and E. MIYAZAKI. Bull. Chem. Soc. Jap. **40**, 1372 (1967).
11. E. W. ABRAHAMSON, J. G. F. LITTLER, and K.-P. VO. J. Chem. Phys. **44**, 4082 (1966).
12. S. GLICKER and L. J. STIEF. J. Chem. Phys. **54**, 2852 (1971).
13. J. A. KERR and A. F. TROTMAN-DICKENSON. Progr. Reaction Kinet. **1**, 105 (1961).
14. F. R. CALA and S. TOBY. J. Phys. Chem. **75**, 837 (1971).

Can. J. Chem. Downloaded from www.nrcresearchpress.com by 210.87.254.5 on 09/05/12
For personal use only.

Naphthyridine Chemistry. XVII: Di-*N*-alkylated Naphthyridines

DAVID J. POKORNY AND WILLIAM W. PAUDLER[1]

Clippinger Laboratories, Department of Chemistry, Ohio University, Athens, Ohio 45701

Received September 14, 1972

It has been shown that the *N,N'*-dimethylated naphthyridines form pseudo bases by hydroxide addition in the quinolinoid rather than the isoquinolinoid ring, where possible.

The charge repulsion in the 1,8-dimethyl-1,8-naphthyridinium ion is reflected by its facile partial conversion to a mono-pseudo base at room temperature. A variable temperature study of this equilibrium reaction is described.

On a démontré que les naphthyridines diméthylées en position *N,N'* forment, si possible, des pseudo-bases par l'addition d'un groupement hydroxyle au cycle quinolinoïde plutôt qu'au cycle isoquinolinoïde.

La répulsion des charges dans l'ion diméthyl-1,8 naphthyridinium-1,8 est mise en évidence par sa conversion facile et partielle en une mono pseudo-base à la température ambiante. Une étude à diverses températures de cette réaction d'équilibre est aussi décrite.

Can. J. Chem., **51**, 476 (1973)

Can. J. Chem. Downloaded from www.nrcresearchpress.com by 210.87.254.6 on 09/05/12
For personal use only.

The recently developed facile syntheses of some naphthyridines (1–4) has made these ring systems available to extensive examinations of their reactivities. Among these studies, the electrophilic substitution reactions, Chichibabin amination (5), and behavioral patterns of the *N*-oxides (6–8) have been the subject of previous papers. A recent publication (9) delineating the reactivity of some of the mono-*N*-alkylated derivatives with base has further extended our knowledge of these ring systems.[2]

The only reported di-*N*-alkylated derivative of the naphthyridines is that of 1,5-naphthyridine (**1**) (10). This compound, when treated with zinc,

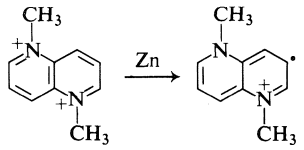

1 **2**

is said to form a free radical with the assigned structure **2**, and its other possible canonical forms.

The availability of "magic methyl" (methylfluorosulfonate) and its established ability to alkylate some difficultly alkylable functional groups prompted us to employ this compound for the syntheses of *N,N'*-dialkylated naphthyridines.

This reaction afforded the *N,N'*-dimethyl derivatives of 1,5-(**1**), 1,6-(**3**), 1,7-(**4**), 1,8-(**5**), and 2,7-naphthyridine (**6**). The structure proof of these compounds rests upon their correct elemental analyses and an analysis of their p.m.r. spectra in trifluoroacetic acid (see Table 1).

An interesting feature of these spectra involves the chemical shifts of the X-methyl protons in the 1,X-naphthyridinium derivatives. It appears that their chemical shifts are subject to an inductive effect caused by the N-1 methyl groups, whereby the 8-methyl protons in the 1,8- case absorb at τ 4.84 while the N-7 and -5 methyl protons in the 1,7- and 1,5-naphthyridinium derivatives absorb at τ 4.96 and 5.00, respectively. The 6-methyl protons in the 1,6-naphthyridinium species absorb at τ 5.08. Thus we see that, as the separation between the nitrogens increases from one carbon (1,8-naphthyridine) to two carbons (1,7- and 1,5-compounds) to three carbons (1,6-compound), the methyl protons become less and less deshielded.

A similar trend exists when one examines the effect of the X-methyl groups upon the chemical shifts of the 1-methyl protons. The p.m.r. spectra of these compounds when dissolved in deuterium oxide are rather different and these chemical shift relationships are no longer apparent.

The spectrum of the 1,8-dimethyl-1,8-naphthyridinium ion in D_2O at the p.m.r. probe temperature (33°) exhibits three broad absorption areas, two for the aromatic and one for the methyl protons. The relative peak intensities for

[1]Author to whom correspondence should be addressed.

[2]At the time of preparation of this paper we had completed a similar study and wish to comment that our results are in agreement with those reported in ref. 9, with the exception that, under our conditions no H-2 → D-2 exchange takes place in the monomethiodide of 1,8-naphthyridine.

Can. J. Chem. Downloaded from www.nrcresearchpress.com by 210.87.254.6 on 09/05/12
For personal use only.

TABLE 1. N.m.r. spectral data of the *N,N*-dimethyl-naphthyridinium difluorosulfonates

Compound	Temperature (°C)	Solvent	Chemical shifts (τ)								Coupling constants (Hz)			
			H_1	H_2	H_3	H_4	H_5	H_6	H_7	H_8	J_{23}	J_{34}	J_{56}	J_{78}
1,5-Naph*	33	D_2O	5.10	0.14	1.24	0.26	5.10	0.14	1.24	0.26				
1,6-Naph	33	D_2O	5.24	0.10	1.40	0.31	−0.38	5.15	0.69	0.94				
1,7-Naph	33	D_2O	5.21	0.14	1.34	0.54	1.01	0.80	5.12	−0.58				
1,8-Naph	95	D_2O	5.60	1.30	2.04	1.15	1.15	2.04	1.30	5.60				
1,8-Naph	33	D_2O	5.62	1.70	2.46	1.70	—	—	—	5.62				
2,7-Naph	33	D_2O	−0.45	5.20	0.89	1.16	1.16	0.89	5.20	−0.45				
1,5-Naph	33	DTFAA†	5.00	0.21	1.24	0.31	5.00	0.21	1.24	0.31	6.0	9.0	—	—
1,6-Naph	33	DTFAA	5.16	0.16	1.40	0.28	−0.32	5.08	0.73	0.98	5.0	8.0		7.0
1,7-Naph	33	DTFAA	5.09	0.20	1.32	0.56	1.02	0.86	4.96	−0.49	5.0	8.0	7.0	—
1,8-Naph	33	DTFAA	4.84	0.26	1.41	0.40	0.40	1.41	0.26	4.84				
1,8-Naph	95	DTFAA									5.0	8.0	—	—
2,7-Naph	33	DTFAA									—	8.0	—	—

*Naph, naphthyridine.
†DTFAA, deuterotrifluoroacetic acid.

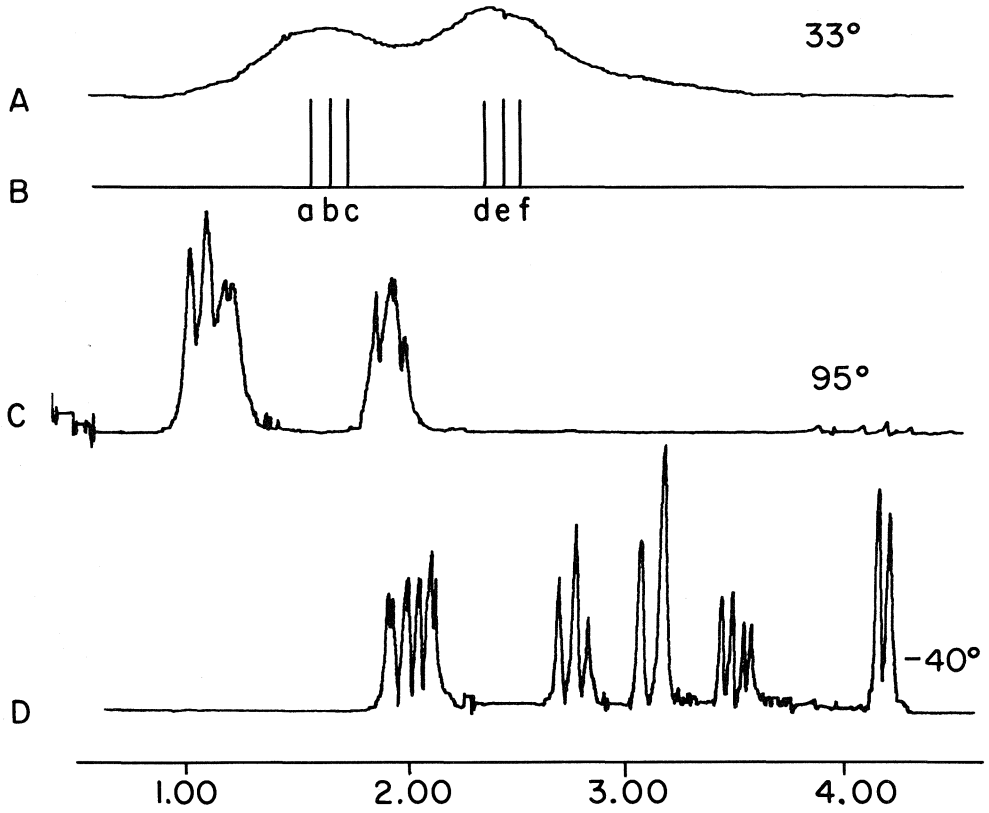

FIG. 1. Variable temperature spectra of 1,8-dimethyl-1,8-naphthyridinium di-fluorosulfonate.
(A) Room temperature spectrum of D_2O solution of 1,8-dimethyl-1,8-naphthyridinium di-fluorosulfonate. (B) Chemical shifts for a 75/25 time-averaged mixture of the 1,8-dimethyl-1,8-naphthyridinium di-fluorosulfonate and its pseudo-base derivative **7** (*cf.* text for details). (C) 1,8-Dimethyl-1,8-naphthyridinium di-fluorosulfonate in D_2O at 95°. (D) Pseudo-base derivative (**7**) observed at −40° of a CH_3OD solution of 1,8-dimethyl-1,8-naphthyridinium di-fluorosulfonate.

the two aromatic proton broad areas (see Fig. 1) are 1:1(!). This rather unexpected spectrum is highly temperature-dependent and one finds that, as the temperature is increased, the spectrum ultimately changes, at 95°, to that expected for the 1,8-dimethyl-1,8-naphthyridinium ion. On the other hand, if the temperature is lowered, one observes that the spectrum of a CD_3OD solution of this compound at −40° is that expected for a mono pseudo-base derivative (see Fig. 1). Thus, the equilibrium reaction depicted in eq. 1 is taking place.

[1] ROD + 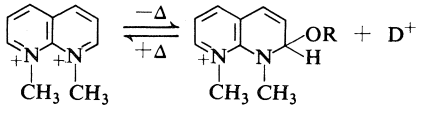 + D^+

5 **7**

That we are indeed dealing with structure **7** is evident from an analysis of its p.m.r. spectrum and a comparison of the chemical shifts and coupling constants with those of compound **8** (9).

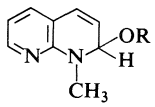

8

It now remains to analyze the curious p.m.r. spectrum at room temperature, where we are apparently observing a rapid equilibrium between compounds **5** and **7**.

Since we know the approximate chemical shifts of the protons of structures **5** and **7** which con-

Can. J. Chem. Downloaded from www.nrcresearchpress.com by 210.87.254.6 on 09/05/12
For personal use only.

Can. J. Chem. Downloaded from www.nrcresearchpress.com by 210.87.254.6 on 09/05/12
For personal use only.

tribute to the equilibrium, it becomes a simple matter to calculate the shape of the spectrum, when the two compounds are in rapid equilibrium with each other, for different concentrations of each component (11).

When this was done, the "calculated" spectrum for a 75/25 ratio of compounds **5** to **7** closely approximates the experimentally observed spectrum.

The line spectrum in Fig. 1 (graph B) represents the chemical shifts of the various time-averaged proton positions in the absence of any coupling. The lines are composed of the following proton-chemical shifts of the non-covalently hydrated species (NCH) and the mono-pseudo base compound (MPS): line *a*, H-4 of NCH and H-5 of MPS; line *b*, H-2 of NCH and H-7 of MPS; line *c*, H-4 of NCH and H-4 of MPS; line *d*, H-3 of NCH and H-6 of MPS; line *e*, H-2 of NCH and H-2 of MPS; line *f*, H-3 of NCH and H-3 of MPS. A consideration of the fact that these lines neither include the various coupling constants nor the existing lineshapes, allows one to conclude that, if they were included, a spectrum akin to the experimental one (graph A Fig. 1) would be obtained.

This facile pseudo base formation is unique to the 1,8-dimethyl-1,8-naphthyridinium ion and is not observed in the other naphthyridinium compounds examined in this study.

Thus, one is drawn to the conclusion that the expected substantial charge repulsion between the closely situated positively charged nitrogen atoms in the 1,8-naphthyridinium compound is responsible for its facile reaction with water and alcohols since these reactions relieve the charge-repulsion.[3]

The other di-*N*-alkylated naphthyridinium compounds do, however, form these pseudo bases when a stronger base (better nucleophile) than H_2O is employed. When these compounds are dissolved in D_2O containing NaOD (approximately 0.5 *N*), the p.m.r. spectra observed are those to be expected for the pseudo-base species (see Table 2). In the 1,5-, 1,6-, and 1,7-naphthyridinium compounds (**1**, **3**, and **4**) the hydroxide attacks in the quinolinoid rather than in the isoquinolinoid ring, to afford compounds of general structure:

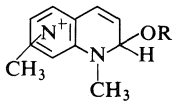

R = H, CH_3

In the absence of the highly electrophilic 2-position the attack occurs in the 1-position of the isoquinolinoid ring portion as shown by the formation of compound **9**.

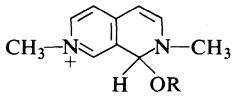

R = H, CH_3

9

Attempts at generating cation radicals of the type proposed for the 1,5-dimethyl-1,5-naphthyridinium di-methosulfate from the 1,X-dimethyl 1,6-, 1,7-, 1,8-, and 2,7-naphthyridinium di-fluorosulfonates were not successful.

Experimental

Dimethylnaphthyridinium Fluorosulfonates

To methyl fluorosulfonate (4 ml) was added the appropriate naphthyridine (200 mg, 1.5 mmol). An exothermic reaction occurred which resulted in about 90% diquaternization of the naphthyridine, as established by an n.m.r. spectrum of the crude product which indicated the presence of the mono-methylated compound. The resulting mixture was heated under reflux on the steam bath for 1 h and the supernatant liquid was removed. Additional alkylating agent was added (4 ml) and the heating was continued for an additional 0.5 h. After this time, the mixture was filtered through a sintered glass funnel to yield a white solid. This solid was repeatedly washed with dry dichloromethane, collected, and dried under vacuum (0.001 mm) for several hours. The material changed color slowly under vacuum but more rapidly in air. The 1,5-naphthyridine derivative could be recrystallized from ethanol–water mixture to yield white platelets (460 mg, 1.3 mmol, 85%; m.p. 250° (dec.)). The other derivatives could not be recrystallized since they changed color from white to red, (1,6-dimethyl-1,6-naphthyridine: 490 mg, 1.37 mmol, 90%; m.p. 207–209°), brown (1,7-dimethyl-1,7-naphthyridine: 525 mg, 1.47 mmol, 95%; m.p. 202–205°), and light brown (2,7-dimethyl-2,7-naphthyridine: 504 mg, 1.41 mmol, 92%; m.p. 217°). On standing, the compounds that could not be recrystallized presumably liberated hydrofluoric acid which etched the glass vials in which they were stored. They also developed an odor which was reminiscent of methyl sulfoxide. However, an aged sample (3 months) still gave the characteristic n.m.r. spectrum of the freshly prepared material.

Anal. Calcd. for $C_{10}H_{12}N_2O_6S_2F_2$: C, 33.51; H, 3.38;

[3]A referee suggested that another driving force for this reaction is the decreased steric repulsion between the methyl protons in the pseudo bases. We feel that this can be only a minor factor.

Can. J. Chem. Downloaded from www.nrcresearchpress.com by 210.87.254.6 on 09/05/12
For personal use only.

TABLE 2. N.m.r. spectral data of the pseudo-bases of the dimethyl-naphthyridines obtained in a basic solution*

	Chemical shifts (τ)								Coupling constants (Hz)					
Compound	H_1	H_2	H_3	H_4	H_5	H_6	H_7	H_8	J_{23}	J_{34}	J_{56}	J_{67}	J_{57}	J_{78}
1,5-Naph	6.65	4.17	3.26	2.64	5.66	1.88	2.20	2.20	5.0	10.5	—	5.0	—	—
1,6-Naph	6.66	4.20	3.77	3.16	1.88	5.94	1.88	2.96	4.0	10.0	—	—	—	7.0
1,7-Naph	6.69	4.22	3.41	2.97	2.35	1.92	5.63	1.88	5.0	10.0	6.0	—	—	—
1,8-Naph	6.43	4.37	3.67	3.35	2.23	2.95	2.11	5.92	4.0	9.0	7.0	6.0	2.0	—
2,7-Naph	3.83	6.55	2.70	4.26	2.80	1.92	5.83	1.68	—	7.0	5.0	—	—	—

*Basic solution, 0.5 *N* $NaOD/D_2O$.

N, 7.82. Found for **1**: C, 33.41; H, 3.40; N, 7.89. Found for **3**: C, 33.23; H, 3.59; N, 7.54. Found for **4**: C, 33.69; H, 3.47; N, 7.72. Found for **6**: C, 33.80; H, 3.21; N, 7.96.

*1,8-Dimethyl-1,8-naphthyridinium Di-fluorosulfonate (**5**)*

A powdered sample of 1,8-naphthyridine (0.5 g, 3.8 mmol) was added to methyl fluorosulfonate (8 ml) at 0°. The resulting mixture was heated to 100° on the steam bath at which point the white solid (mono-methylated compound) dissolved to give a clear solution. After 12 h of heating, a layer of fine white needles of product had formed. The heating was stopped and the excess methyl fluorosulfonate was removed by use of a pipette. A fresh portion of the alkylating agent was added and heating was continued for 24 h. The cooled mixture was filtered through sintered glass and washed well with dry methylene chloride. The resulting white solid was dried under vacuum for 8 h to afford pure 1,8-dimethyl-1,8-naphthyridine di-fluorosulfonate (1.23 g, 3.4 mmol, 89%; m.p. 197–199°).

Anal. Calcd. for $C_{10}H_{12}N_2O_6S_2F_2$: C, 33.51; H, 3.38; N, 7.82. Found: C, 33.53; H, 3.42; N, 7.75.

1. T. J. KRESS and W. W. PAUDLER. Chem. Commun. 3 (1967).
2. W. W. PAUDLER and S. J. CORNRICH. J. Heterocycl. Chem. **7**, 419 (1970).
3. W. W. PAUDLER and T. J. KRESS. J. Org. Chem. **32**, 832 (1967).
4. W. W. PAUDLER and T. J. KRESS. *In* Advances in heterocyclic chemistry. A. R. Katritsky and A. J. Boulton, editors. Academic Press, New York, N.Y. 1971. pp. 123ff.
5. W. W. PAUDLER and T. J. KRESS. J. Org. Chem. **33**, 1384 (1968).
6. W. W. PAUDLER and D. J. POKORNY. J. Org. Chem. **36**, 1720 (1971).
7. D. J. POKORNY and W. W. PAUDLER. J. Org. Chem. **37**, 3101 (1972).
8. D. J. POKORNY and W. W. PAUDLER. J. Heterocycl. Chem. **9**, 1151 (1972).
9. J. W. BUNTING and W. G. MEATHREL. Can. J. Chem. **50**, 917 (1972).
10. L. A. SUMMERS and L. E. PICKESON. Chem. Commun. 1183 (1967).
11. W. W. PAUDLER. Nuclear magnetic resonance. Allyn and Bacon, Inc., Boston, Mass. 1971. p. 162ff.

Can. J. Chem. Downloaded from www.nrcresearchpress.com by 210.87.254.6 on 09/05/12
For personal use only.

Lignans of Western Red Cedar (*Thuja plicata* Donn). XI. β-Apoplicatitoxin

BRUCE F. MACDONALD AND G. M. BARTON

Department of the Environment, Canadian Forestry Service, Western Forest Products Laboratory, Vancouver, British Columbia

Received August 21, 1972

The structure of the eleventh in the series of novel lignans from the heartwood of western red cedar (*Thuja plicata* Donn) has been determined as 1,4-dihydronaphthalene-6-hydroxyl-2-(hydroxymethyl)-7-methoxy-4(3′,4′-dihydroxy-5′-methoxyphenyl)-3-carboxylic acid lactone (β-apoplicatitoxin) (**1**) by spectrometric methods and by aromatization to the known compound trimethylplicatinaphthalene. This lignan provides an intermediate to the possible stereoselective synthesis of derivatives related to the picropodophyllin series.

La structure du onzième de la série des nouveaux lignanes provenant du cœur des cèdres rouges de l'ouest (*Thuja plicata* Donn) a été déterminée comme étant la lactone de l'acide dihydro-1,4 naphtalène-4 hydroxyl-6 (hydroxy méthyl) 2-méthoxy-7 (dihydroxy-3′,4′ méthoxy-5′ phényl)-4 carboxylique-3 (*β*-apoplicatitoxine) (**1**) par des méthodes spectrométriques et par aromatisation du composé connu, la triméthyl plicatinaphtalène. Ce lignane procure une intermédiaire à la synthèse stéréosélective possible de dérivés reliés à la série de la picropodophylline. [Traduit par le journal]

Can. J. Chem., **51**, 482 (1973)

Introduction

Previous work has elucidated the structural relationship of 10 lignans present in the heartwood of western red cedar (*Thuja plicata* Donn) trees, two of which were 4-aryltetrahydronaphthalenes, five were substituted dibenzyl butyrolactones, one was a 4-aryl-α-naphthol lactone, another was a naphthalene, and the latest was a butyrolactone in which a double bond was conjugated with the aromatic nucleus (1).

This new lignan is a dihydro-plicatinaphthalene, not unexpected in view of structures already elucidated in the series (1), and it is described as 1,4-dihydronaphthalene-6-hydroxyl-2-(hydroxymethyl)-7-methoxy-4(3′,4′-dihydroxy-5′-methoxyphenyl)-3-carboxylic acid lactone (**1**). It has been given the trivial name β-apoplicatitoxin because of its close association with β-apopicrosikkimotoxin (**1***a*) (2).

β-Apoplicatitoxin was isolated by ethyl acetate from the hot water extract of western red cedar heartwood. The crude material which precipitated overnight was further purified by filtering and washing several times with hot methanol. β-Apoplicatitoxin was soluble with difficulty in common organic solvents with the exception of pyridine. Initial evidence of its structure was obtained by comparison of chromatographic data (acetylated derivative) with that from earlier lignans of the series (3).

The structure of β-apoplicatitoxin was inferred from i.r. and u.v. data. A spectrographic comparison of the main features of **1***a* with related compounds of the sikkimotoxin and podophyllin series is given in Table 1. Of particularly diagnostic importance is the i.r. band 1691–1695 cm^{-1} which is indicative of a double bond not in conjugation with an aromatic ring. The close similarity in these data between **1** and β-apopicrosikkimotoxin (**1***a*) is apparent.

β-Apoplicatitoxin, which gave a positive phenolic test with the ferric–ferri-cyanide reagent (4), when chromatographed on molybdic acid-treated paper with butanol – acetic acid – water, showed a considerably reduced R_f value (0.63) compared with untreated paper R_f (0.74) and appeared as a yellow spot indicative of a pyrocatechol grouping.

Molecular weight of the acetylated derivative (**1***b*) gave a parent ion peak of *m/e* 496. Peaks were noted at *m/e* 454, 412 (base peak), and 370 corresponding to the sequential loss of three ketene molecules from the arylacetate ester groups.

The n.m.r. spectra of β-apoplicatitoxin in pyridine suggested a structure with two methoxyls, four aromatic protons, and a methylene lactone. It was noted that chemical shifts in pyridine-d_5 were strongly affected by the presence of water. Accordingly, samples were dissolved under dry nitrogen in a glove box using dry (calcium sulfate) pyridine-d_5. When the

Can. J. Chem. Downloaded from www.nrcresearchpress.com by 210.87.254.42 on 09/05/12
For personal use only.

TABLE 1. A comparison of spectral data of several related lignans

	λ_{max} (EtOH) (nm)	log ε	I.r. (lactone) (cm^{-1})	I.r. (double bond) (cm^{-1})
Trimethyl β-apoplicatitoxin (**1***a*)	281	3.61	1756	1691
α-Apopicrosikkimotoxin	285	3.91	1780	
β-Apopicrosikkimotoxin (**1***a*)	281	3.62	1756	1694
γ ± Collinusin (**3**) (7)	248 344	4.18 3.99	1750	1650
α-Apopicropodophyllin (**4**)	242 311	3.00 7.59	1775	nil
β-Apopicropodophyllin (**4**)	290	4.57	1760	1695
γ-Apopicropodophyllin (**4**)	245 295	21.00 4.45	1760	1648

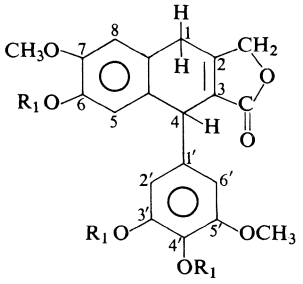

1 $R_1 = H$
1*a* $R_1 = CH_3$
1*b* $R_1 = COCH_3$

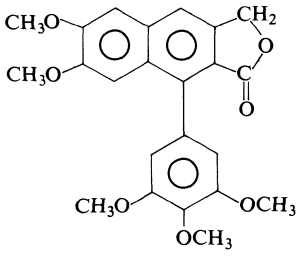

2

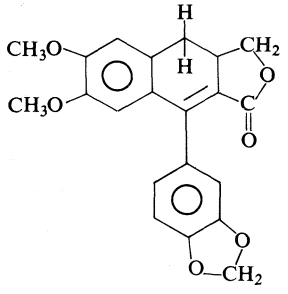

3

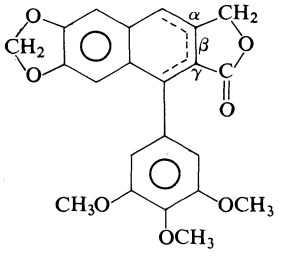

4

spectra were rerun in the presence of D_2O, the chemical shift (τ units) of some of the more important protons changed as follows: C-1, 5.06–5.21; C-2′ and -6′, 3.24–3.27; C-5, 2.81–2.87 and C-8, 3.21–3.07. It is felt that chemical shift sensitivity of the aromatic protons is due to the strong molecular association between the acidic phenolic sites and the basic nitrogen site of the pyridine. The addition of water (D_2O) is sufficient to disrupt this association, resulting in the changes noted. The magnitude of these changes, although not as large as those observable with the use of shift reagents, facilitated the identification of aromatic protons by separating them from the coincident pyridine-d_4 resonances.

The n.m.r. spectra of the methylated (**1***a*) and acetylated (**1***b*) derivatives confirmed the presence of two methoxyl and three hydroxyl groups

Can. J. Chem. Downloaded from www.nrcresearchpress.com by 210.87.254.42 on 09/05/12
For personal use only.

Can. J. Chem. Downloaded from www.nrcresearchpress.com by 210.87.254.42 on 09/05/12
For personal use only.

in the original β-apoplicatitoxin (**1**). The spectra of the methyl and acetyl derivatives also showed the usual chemical shift change of the methylene lactone proton from τ 5.19 (methylated) to 5.24 (acetylated). Protons at C-2′ and -6′ are magnetically and chemically equivalent in the methylated derivative, whereas they are not in the acetylated derivative. This indicates that the two phenolic hydroxyls in the parent β-apoplicatitoxin are in the vicinal C-3′ and -4′ positions, which is in agreement with the general structure of the previous lignans and the reduced R_f value on molybdic acid-treated paper.

An important feature of these n.m.r. spectra was the ABX system of C-1 methylene and C-4 protons; however, the AB portion was partly obscured by the methoxyl resonances. The X part C-4, which is long-range coupled with the C-1 methylene protons, appeared as a broad peak ($\Delta\frac{1}{2}h$ = 3 Hz) at τ 5.14 in the methylated and τ 5.08 in the acetylated derivative.

Definite evidence of the long-range coupling, through the double bond between C-2 and -3, in this ABX system was obtained by nuclear magnetic double resonance (n.m.d.r.) studies in deuterated dimethyl sulfoxide on the acetylated derivative (**1***b*). In this solvent, partial separation of the AB portion from the methoxyls was evident when compared with deuteriochloroform solvent. Irradiation at τ 6.07 or 6.10 (AB portion) resulted in a sharpening of the C-4 proton peak at τ 5.14 (C-4 ($\frac{1}{2}h$) = 8 → 3 Hz). Also irradiation at τ 5.14 (C-4 proton) caused the doublets at τ 6.07 and 6.10 to be significantly increased in height, with a corresponding decrease in line width. It now became apparent that methylated β-apoplicatitoxin (**1***a*) and Schrier's (2) β-apopicrosikkimotoxin had the same chemical structure. They both had similar melting points (222–224 and 224–225°, respectively) and gave almost identical spectral data (Table 1).

Ayres (5) noted that in apopicropodophyllin (**4**) the C-1 and -4 protons formed an ABX system in which the AB part was largely obscured beneath the methoxyl peaks (τ 6.25). The X part of the spectrum appeared at τ 5.20 in low-polarity solvents, resonating at lower field than normal owing to deshielding by the C_2–C_3 unsaturation.

Final proof of structure was obtained by aromatization of the methylated derivative (**1***a*) by dehydrogenation with lead tetraacetate and glacial acetic acid to give identical i.r., u.v., and n.m.r. spectra with trimethylplicatinaphthalene (**2**) (6).

Because of the non-conjugated position of the double bond between C-2 and -3, addition reactions can be controlled to give either *cis* or *trans* products. Thus, for the first time, the possibility exists of preparing *cis* compounds in the tetrahydronaphthalene cedar lignan series similar to the picropodophyllin series.

Experimental

The following equipment and materials were used: m.p, Mettler F.P. 1; i.r. spectra, Perkin–Elmer 521 grating spectrometer (KBr disks); u.v. spectra, Beckman DR-2 spectrometer (ethanol); n.m.r., Varian HA-100 (tetramethyl silane τ = 10 as internal standard); low-resolution mass spectra, MS 12, through the kind arrangements of Dr. P. J. Smith, University of Saskatoon, Saskatoon, Saskatchewan. The t.l.c. values were obtained with silica gel G (Merk) as adsorbent, toluene–ethanol (9:1) and chloroform–acetone (95:5) as developers, followed by nitric acid–sulfuric acid (1:1) spray and heat as detector. Papergrams were developed with butanol–acetic acid–water (BAW) (60:15:25) and detected with potassium ferricyanide–ferric chloride reagent (mixed 1% solutions) (4). Samples for n.m.r. analysis in dry pyridine were prepared in a dry box under a nitrogen atmosphere.

*β-Apoplicatitoxin (**1**)*

Western red cedar wood meal (3 mm Wiley mill screen, 5 kg) was boiled in water for 2 h and filtered through glass wool while still hot. The hot water extract was reduced in volume in an all-glass cyclone evaporator until a heavy precipitate formed. The evaporator was subsequently washed thoroughly with ethyl acetate (3 × 500 ml) which was then used, together with an additional quantity of ethyl acetate (1000 ml) for extracting the cooled, concentrated aqueous solution and precipitate. The ethyl acetate solution was next evaporated under reduced pressure to a small volume and, on standing overnight, a white precipitate formed. The precipitate was filtered out and washed with hot methanol. After drying, the material weighed 500 mg. The product was difficultly soluble in all common laboratory reagents except pyridine. It gave a positive phenolic test with the ferric–ferri–cyanide reagent (4). Paper chromatography (Whatman No. 1) gave a single spot R_f = 0.74 (BAW solvent). Spectra: λ_{max} (log ε) 283.5 nm (3.75); γ_{max} 3380 (broad hydroxyl), 1725 (broad lactone), 1685 and 1580 (double bond) cm^{-1}; n.m.r. τ (pyridine-d_5, dried over calcium sulfate) 2.81 (1H, singlet, aromatic C-5), 3.21 (1H, singlet, aromatic, C-8), 3.22 (1H, doublet, J = 0.75 Hz, aromatic, C-2′ or -6′), 3.24 (1H, doublet, J = 0.75 Hz, aromatic, C-6′ or -2′), 5.06 (1H, multiplet, C-4, X part of ABX), 5.28 (2H, broad singlet, lactone methylene), 6.25 (3H, singlet, methoxyl, C-5′ or -7), 6.39 (3H, singlet, methoxyl, C-7 or -5′), centered at 6.32 (2H, multiplet C-1 methylenes, AB part of ABX partially hidden by methoxyls) (three phenolic hydroxyls not observed); n.m.r. τ (pyridine-d_5, two drops of D_2O) 2.87 (1H, singlet, aromatic, C-5), 3.07 (1H, singlet, aromatic, C-8), 3.27 (2H, singlet, width at half height 1.5 Hz, aromatic C-2′ and -6′),

5.00 (2H, singlet, lactone methylene), 5.21 (1H, multiplet, C-4, X part of ABX), 6.04 (3H, singlet, methoxyl, C-5′ or -7), 6.23 (3H, singlet, methoxyl, C-7 or -5′), centered at 6.13 (2H, multiplet, C-1 methylenes, AB part of ABX hidden by methoxyls) (HOD peak at 4.45).

Trimethyl β-Apoplicatitoxin (1a)

β-Apoplicatitoxin (**1**) (50 mg) was partially dissolved in methanol (40 ml) by warming. On cooling, diazomethane in ether (5 ml) was added every 2 h for 8 h with stirring at room temperature and allowed to stand overnight. A further treatment of diazomethane in ether (5 ml) every 2 h for 6 h with stirring was necessary for complete methylation. The product (t.l.c. R_f 0.42, toluene–ethanol, 9:1) was evaporated to dryness and crystallized from hot methanol to yield 1,4-dihydronaphthalene-2-(hydroxymethyl)-6,7-dimethoxy-4(3′,4′,5′-trimethoxyphenyl)-3-carboxylic acid lactone (40 mg), m.p. 220–222°. Spectra: λ_{max} (log ε) 281.5 nm (3.61); γ_{max} 1752 (lactone), 1691 and 1585 (double bond) cm^{-1}; n.m.r. τ (deuteriochloroform) 3.31 and 3.41 (1H each, singlets, aromatic, C-5 and -8), 3.65 (2H, singlet, aromatic, C-2′ and -6′), 5.14 (1H, multiplet, C-4, X part of ABX), 5.20 (2H, singlet, lactone methylene), 6.11 (3H, singlet, methoxyl), 6.23 (6H, singlet, methoxyl), 6.25 (6H, singlet, methoxyl), centered at 6.24 (2H, multiplet, C-1 methylenes, AB part of ABX hidden by methoxyls).

Triacetyl β-Apoplicatitoxin (1b)

β-Apoplicatitoxin (**1**) (100 mg) was dissolved in a mixture of pyridine (5 ml) and acetic anhydride (5 ml). This mixture was heated under anhydrous conditions for 10 min in a boiling water bath, allowed to stand for 20 min and then evaporated to dryness under vacuum. The residue was then dissolved in hot methanol by stirring, filtered, and the filtrate cooled in a deep freeze for 4 h. The resultant crystalline product, 1,4-dihydronaphthalene-6-acetoxy-2-(hydroxymethyl)-7-methoxy-4(3′,4′-acetoxy-5′-methoxyphenyl)-3-carboxylic acid lactone (**1b**) weighed 80 mg, m.p. 243–245°. Spectra: λ_{max} (log ε) 277.5 nm (3.63); γ_{max} 1750 (broad lactone), 1685 and 1590 (double bond) cm^{-1}; n.m.r. τ (deuteriochloroform) 3.12 and 3.69 (1H each, doublet, J = 1.0 Hz, aromatic, C-2′ and -6′), 3.15 and 3.20 (1H each, singlet, aromatic, C-8 and -5), 5.08 (1H, multiplet, C-4, X part of ABX), 5.24 (2H, broad singlet, lactone methylene), 6.17 (3H, singlet, methoxyl), 6.24 (3H, singlet, methoxyl), centered at 6.23 (2H, multiplet, C-1 methylenes, AB part of ABX hidden by methoxyls), 7.76, 7.78, 7.83 (3H each, singlets, acetyls); mass spectrum (low resolution), parent ion = 496 (4%), 454 (30%), 412 (100%), 370 (70%).

Trimethyl Plicatinaphthalene (2)

Trimethyl β-apoplicatitoxin (**1a**) (100 mg), lead tetraacetate (200 mg), and glacial acetic acid (3 ml) were placed in a 100 ml conical flask fitted with an air condenser. The mixture was slowly heated from 55–70° during a 25 min period in a water bath. After cooling, water was added and the mixture was extracted several times with chloroform and the chloroform layers collected. The chloroform was then removed under vacuum and the residue dissolved in hot methanol from which yellow crystals (30 mg), m.p. 227–229° formed. This material was found to be identical with an authentic sample of trimethylplicatinaphthalene (**2**) (6) by identical u.v., i.r., and n.m.r. spectra comparisons.

The authors wish to thank Dr. J. F. Manville of the Western Forest Products Laboratory, Vancouver, British Columbia for his advice and the n.m.d.r. experiments.

1. B. F. MacDonald and G. M. Barton. Can. J. Chem. **48**, 3144 (1970).
2. E. Schreier. Helv. Chim. Acta, **46**, No. 9, 75 (1963).
3. B. F. MacDonald and E. P. Swan. J. Chromatogr. **57**, 553 (1970).
4. G. M. Barton, R. S. Evans, and J. A. F. Gardner. Nature, **170**, 249 (1952).
5. D. C. Ayres. Can. J. Chem. **47**, 2075 (1969).
6. H. MacLean and B. F. MacDonald. Can. J. Chem. **47**, 4495 (1969).
7. T. R. Gouindachari, S. S. Sathe, and V. Viswanathan. Tetrahedron Lett. **42**, 4183 (1967).

Can. J. Chem. Downloaded from www.nrcresearchpress.com by 210.87.254.42 on 09/05/12
For personal use only.

Carbon-13 Magnetic Resonance: Diterpenoid Alkaloids From the *Delphinium* Species[1]

ALAN J. JONES[2]

Department of Chemistry, University of Alberta, Edmonton, Alberta T6G 2G2

AND

M. H. BENN

The Chemistry Department, University of Calgary, Calgary, Alberta T2N 1N4

Received August 11, 1972

The carbon-13 magnetic resonance spectra of the diterpenoid alkaloids lycoctonine (**1**), deoxylycoctonine (**2**), deoxymethylenelycoctonine (**3**), browniine (**4**), isolatizidine (**5**), delphonine (**6**), lycoctonal (**7**), and their corresponding hydrochloride or perchlorate salts have been determined at 22.63 MHz in the Fourier mode. With the aid of proton decoupling techniques, additivity relationships and the effects induced by specific structural changes, self-consistent assignments of nearly all the resonances have been made. Substituent effects are often of the same order but differ in magnitude from those for simpler systems reported in the literature. The effects of protonation do not unambiguously follow the additive trends indicated in simpler systems but do exhibit a reasonably constant pattern. The data have been applied in the structural elucidation of two previously unknown bases isolated from *Delphinium bicolor* Nutt.

Les spectres de résonance magnétique du carbone-13 des alcaloïdes diterpèniques lycoctonine (**1**), deoxylycoctonine (**2**), deoxyméthylènelycoctonine (**3**), browniine (**4**), isolatizidine (**5**), delphonine (**6**), lycoctonal (**7**), et de leurs sels chlorhydrate et perchlorate, ont été déterminés à 22.63 MHz selon la technique du Fourier. Les techniques de découplage du proton, les relations d'additivité, et les effets induits par des changements structuraux spécifiques ont permis une attribution logique de presque tous les pics de résonance. Les effets de substituants sont souvent du même ordre, malgré une différence dans l'amplitude, que ceux des systèmes plus simples rapportés dans la littérature. Les effets de la protonation ne suivent pas les tendances additives indiquées pour les systèmes plus simples mais se font selon un modèle pratiquement constant. Les données ont été appliquées dans l'élucidation structurale de deux bases précédemment inconnues, isolées du "*Delphinium bicolor* Nutt".

[Traduit par le journal]

Can. J. Chem., **51**, 486 (1973)

Interest in the application of carbon-13 magnetic resonance techniques in the area of saturated nitrogen heterocyclic systems (1–4) has generated an abundance of fundamental substituent and additivity data, which exhibit two primary features. First, the substituent effects noted in the cyclohexanes (5) have been closely paralleled, although in many cases the parameters are attenuated (1), and second, the presence of a basic nitrogen center, in providing easy access to a variety of simple derivatives, can be a valuable asset in spectral assignment through a set of protonation or methiodation parameters (1–3). The second feature has also been noted for the nitrogen center in amino acids (6).

In view of the success in the application of additivity relationships in the decalins (7), perhydroanthracenes and perhydrophenanthrenes (8), and selected steroids (9), it seemed reasonable to apply the findings of the above fundamental studies to more complex analogs containing a saturated heterocyclic ring. We have chosen a series of diterpenoid alkaloids found in plants of the genera *Aconitum* and *Delphinium* (10). These alkaloids, primarily of the lycoctonine-type, have the basic C_{19}-skeleton shown in Fig. 1. Unlike the alkaloids studied by Crain *et al.* (3) they contain no aromatic rings and, therefore, *all 19–25 carbon resonances* are found in the region 10–100 p.p.m. downfield of TMS. The lycoctonine alkaloids are characterized by the high degree of oxygenated substituents, usually five or six, and although a great deal of effort was made, the skeleton completely eluded determination by chemical means, finally being solved by X-ray crystallography in 1956 (11).

[1]Presented in part at the National Research Council of Canada Symposium: "Perspectives in N.m.r. for the Seventies", Ottawa, Canada, February 21, 1972.

[2]Author to whom correspondence should be addressed.

Can. J. Chem. Downloaded from www.nrcresearchpress.com by 210.87.254.40 on 09/05/12
For personal use only.

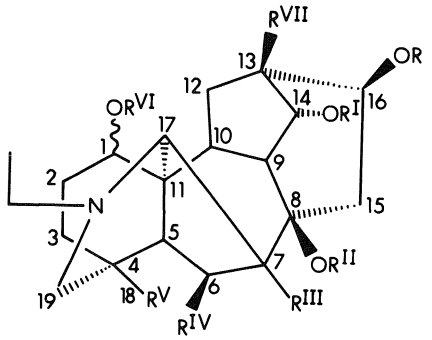

FIG. 1. Structures of the diterpenoid alkaloids studied:

1 $R^{II} = R^{VII} = H$; $R = R^{I} = R^{VI} = CH_3$; $R^{V} = CH_2OH$; $R^{III} = OH$; $R^{IV} = OCH_3$

2 $R^{II} = R^{VII} = H$; $R = R^{I} = R^{V} = R^{VI} = CH_3$; $R^{III} = OH$; $R^{IV} = OCH_3$

3 $R^{II} = R^{V} = R^{VII} = H$; $R = R^{I} = R^{VI} = CH_3$; $R^{III} = OH$; $R^{IV} = OCH_3$

4 $R^{I} = R^{II} = R^{VII} = H$; $R = R^{VI} = CH_3$; $R^{V} = CH_2OCH_3$; $R^{III} = OH$; $R^{IV} = OCH_3$

5 $R^{I} = R^{II} = R^{III} = R^{IV} = R^{VI} = R^{VII} = H$; $R = CH_3$; $R^{V} = CH_2OCH_3$

6 $R^{I} = R^{II} = R^{III} = H$; $R = R^{VI} = CH_3$; $R^{V} = CH_2OCH_3$; $R^{VII} = OH$; $R^{IV} = OCH_3$; *N*-ethyl group is replaced by *N*-methyl in this case

7 $R^{II} = R^{VII} = H$; $R = R^{I} = R^{VI} = CH_3$; $R^{V} = CHO$; $R^{III} = OH$, $R^{IV} = OCH_3$

The carbon-13 magnetic resonance spectra of these diterpenoid alkaloids reveal not only the number and type of carbon atoms in the system but also exhibit close structural and "family" resemblances and indicate the degree and sites of oxygen substitution. It may, therefore, be anticipated that these data will be of critical importance in determinations of the structure of newly isolated alkaloids of the *Aconitum*, *Delphinium*, and *Garrya* species (10, 12). We have applied the results successfully in structural determination for two previously unknown alkaloids of the *Delphinium* genus.

Experimental

Carbon-13 spectra were determined at 22.63 MHz in the Fourier mode using a Bruker HFX-90 spectrometer in conjunction with a Nicolet-1085, 20K memory, computer. The spectrometer features a deuterium lock system, a BSV-2 random noise (800 Hz band-width) proton decoupler, and a BSV-2 pulse generator-amplifier. Spectra of the bases were determined for solutions in deuterochloroform (which also provided the lock signal) with 2–5% TMS added as internal reference. For some of the hydrochloride salts dimethylsulfoxide-d_6 and heavy water were used as solvent. In these cases a mixture containing dioxane and TMS was added as reference. All samples were contained in precision ground 10 mm, o.d., tubes (Wilmad). The spectrometer was used in the cross-coil configuration. On average, a 30 μs pulse, corresponding to an approximate tilt angle of 45°, was employed. For the average spectral width of 2500 Hz the delay between pulses was 70 μs. Acquisition times averaged 4 h over 8K data points for concentrations of the order of 0.2 *M*. For off-resonance or coupled spectra this time was approximately doubled.

Some of the bases were freshly generated from their corresponding salts, while others were purified by procedures given in the literature. All hydrochlorides were prepared by bubbling dry hydrogen chloride through an ethereal solution of the base. The solid isolated was then recrystalized from the appropriate solvent.

Results

Structures and the numbering system for the alkaloids lycoctonine (**1**), deoxylycoctonine (**2**), deoxymethylenelycoctonine (**3**), browniine (**4**), isolatizidine (**5**), delphonine (**6**), and lycoctonal (**7**) are shown in Fig. 1. Substituent groups are indicated by a prime symbol on the number appropriate to the position of substitution on the C_{19}-skeleton even where oxygen atoms intervene. The carbon-13 chemical shifts for the bases **1**–**7** are given in Table 1. The general procedure for carbon-13 data acquisition and initial interpretation involved determination of (*a*) the noise decoupled carbon-13 spectrum, (*b*) the single frequency off-resonance decoupled spectrum, and (*c*) the modulated off-resonance spectrum (13). Such a sequence is shown for lycoctonal (**7**) in Fig. 2. The multiplicities generated in (*b*) enable distinction between methyl (quartet), methylene (triplet), and methine (doublet) resonances, while technique (*c*), which effectively results in irradiation of only long-range proton couplings, enables distinction of the quaternary carbon centers as shown in Fig. 2. Having established the degree of substitution for the individual carbon resonances, assignments were made on the basis of chemical shifts calculated using additivity relationships (1–5, 8) and confirmed where possible by comparing the effects of specific structural changes (14). Considerable use was made of correlation diagrams, which summarize the chemical shift data, as shown in Figs. 3 and 4.

Figures 3 and 4 show that carbon-13 shifts for the *Delphinium* alkaloids downfield of 50 p.p.m. are, in general, hetero-atom substituted, while those upfield are not. Groups such as methyl (27 p.p.m.) (5), methoxyl (56–61 p.p.m.) (15), the methyl in *N*-ethyl (*ca.* 14 p.p.m.) (16), and the carbonyl (203.6 p.p.m.) (17) in lycoctonal (**7**) are easily assigned, being distinguished by their off-

Can. J. Chem. Downloaded from www.nrcresearchpress.com by 210.87.254.40 on 09/05/12
For personal use only.

Can. J. Chem. Downloaded from www.nrcresearchpress.com by 210.87.254.40 on 09/05/12
For personal use only.

TABLE 1. Carbon-13 chemical shifts in lycoctonine and related alkaloids[a]

	Carbon position[b]																								
Compound	C-1	C-2	C-3	C-4	C-5	C-6	C-7	C-8	C-9	C-10	C-11	C-12	C-13	C-14	C-15	C-16	C-17	C-18	C-19	N-CH_2—CH_3	C-1′	C-16′	C-6′	C-14′ or C-18′
1 Lycoctonine	83.0_4	33.8_3†	31.2_4†	38.6_3	43.4_3*	90.7_5	88.3_2	~77	49.7_5*	46.1_3*	49.1_5	29.0_3†	38.0_9	84.2_8	25.7_9†	84.2_8	64.8_5	67.4_4	53.5_2	51.1_5	13.8_7	(57.7_3)	56.2_2	(55.6_8)	58.0_6
2 Deoxylycoctonine	82.8_1	33.8_0†	37.3_6	34.1_0	43.4_8*	91.5_4	88.6_0	77.6_6	(55.2_9*)	46.2_3*	49.3_0	28.9_8†	38.2_8	84.5_6	26.8_2†	84.1_3	64.3_7	26.8_2	(56.8_2)	50.9_2	14.0_7	(57.7_4)	56.2_0	(55.6_4)	58.2_2
3 Deoxymethylenelycoctonine	82.8_8	33.4_7†	29.6_2	36.9_5‡	43.8_7*	94.5_5	88.5_2	~77	49.0_8*	46.2_8*	48.7_8	29.0_6†	38.2_4‡	84.8_2	26.1_1†	84.0_7	65.0_7	—	51.0_8	50.2_7	14.0_9	(57.6_8)	56.1_7	(55.8_5)	58.3_5
4 Browniine	82.1_7	33.4_1†	32.6_0†	38.6_2	45.3_6*	90.5_9	89.2_1	76.6_4	50.2_4*	46.3_3*	48.4_9	27.8_3†	37.0_5	78.4_2	25.6_7†	85.3_0	65.3_5	75.5_7	53.2_4	51.2_4	14.1_9	(57.7_4)	56.4_7	(55.8_6)	59.2_0
5 Isolatizidine	72.4_8	29.8_7†	29.1_9†	37.4_9	44.3_4*	42.4_3	41.9_4	78.9_0	46.8_8*	45.4_2*	48.5_5	27.0_4	40.4_9	~77	25.0_7	82.5_6	63.9_1	79.2_2	56.7_1	48.8_7	13.0_5	—	56.3_4	—	59.4_6
6 Delphonine	82.4_2	36.2_2†	40.1_0†	39.7_5	42.3_4*	80.7_2	56.3_9*	76.9_4	50.7_3*	49.6_8*	50.4_6	35.0_8	72.7_9	84.7_4	26.0_5	85.9_5	63.7_0	79.7_2	51.6_2	42.5_0*	—	(57.8₂)	56.3_9	(57.3_1)	59.2_2
7 Lycoctonal	82.7_5	33.8_0†	29.8_9†	48.5_2	43.4_8*	92.0_0	88.6_6	77.6_9	49.0_9*	46.0_4*	49.7_3	29.0_3†	38.1_4	83.9_4	25.2_6†	83.5_9	64.6_1	203.6_3	50.8_1	50.0_3	13.9_6	(57.6_8)	56.1_7	(55.8_8)	59.2_2

[a]Parts per million downfield relative to TMS.
[b]Parentheses, *, †, ‡, indicate uncertainties in assignment within a given group.

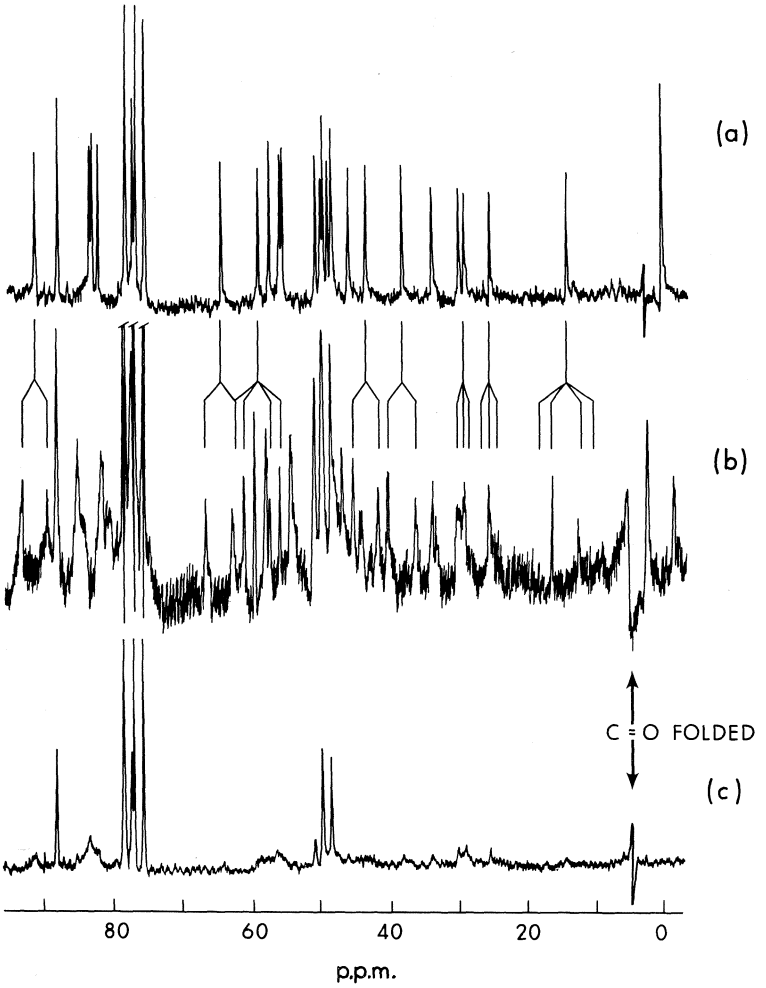

FIG. 2. The carbon-13 magnetic resonance spectrum of lycoctonal (**7**). (*a*) Noise decoupled, (*b*) off-resonance decoupled, and (*c*) modulated off-resonance decoupled.

resonance spectra and characteristic shifts. The methoxyl groups C-16′ and -18′ in isolatizidine (**5**) are the only ones common in position to those in browniine (**4**), and C-16′ is common throughout the series **1**–**7**. The narrow range (±0.2 p.p.m.) of chemical shifts exhibited by the methoxyl carbons at 56.3 p.p.m. in **1**–**7** suggests assignment to C-16′. Consequently the resonance at 59.3 ± 0.1 p.p.m. in **4** and **5** may be assigned to C-18′ (see Fig. 3). It seems probable that the resonance at 58.2 ± 0.2 p.p.m. in **1**, **2**, and **3** is due to C-14′ since this is the only carbon which differs substantially in position and shift from those in **4** and **5**. It is not possible to distinguish between the shifts for the remaining methoxyl carbons C-1′ and -6′, based on our present data.

The carbon-13 shifts for the lycoctonine skeleton are conveniently considered as follows in terms of the degree of substitution.

(a) Quaternary Carbons

These resonances are designated *q* in Figs. 3 and 4. Oxygen substitution at C-7 and -8 in lycoctonine (**1**) and C-13 in delphonine (**6**) differentiates these carbons from C-4 and -11. In isolatizidine (**5**) the C-6 and -7 oxygen functions are removed resulting in the expected upfield shifts (48.3 and 46.4 p.p.m., respectively) (15, 18), compared to **1**. The quaternary resonance at 88.3 p.p.m. in **1** is thus assigned to C-7. Figure 4 shows that the resonance at 38.6 p.p.m. may be assigned to C-4 in lycoctonine (**1**), since it is

Can. J. Chem. Downloaded from www.nrcresearchpress.com by 210.87.254.40 on 09/05/12
For personal use only.

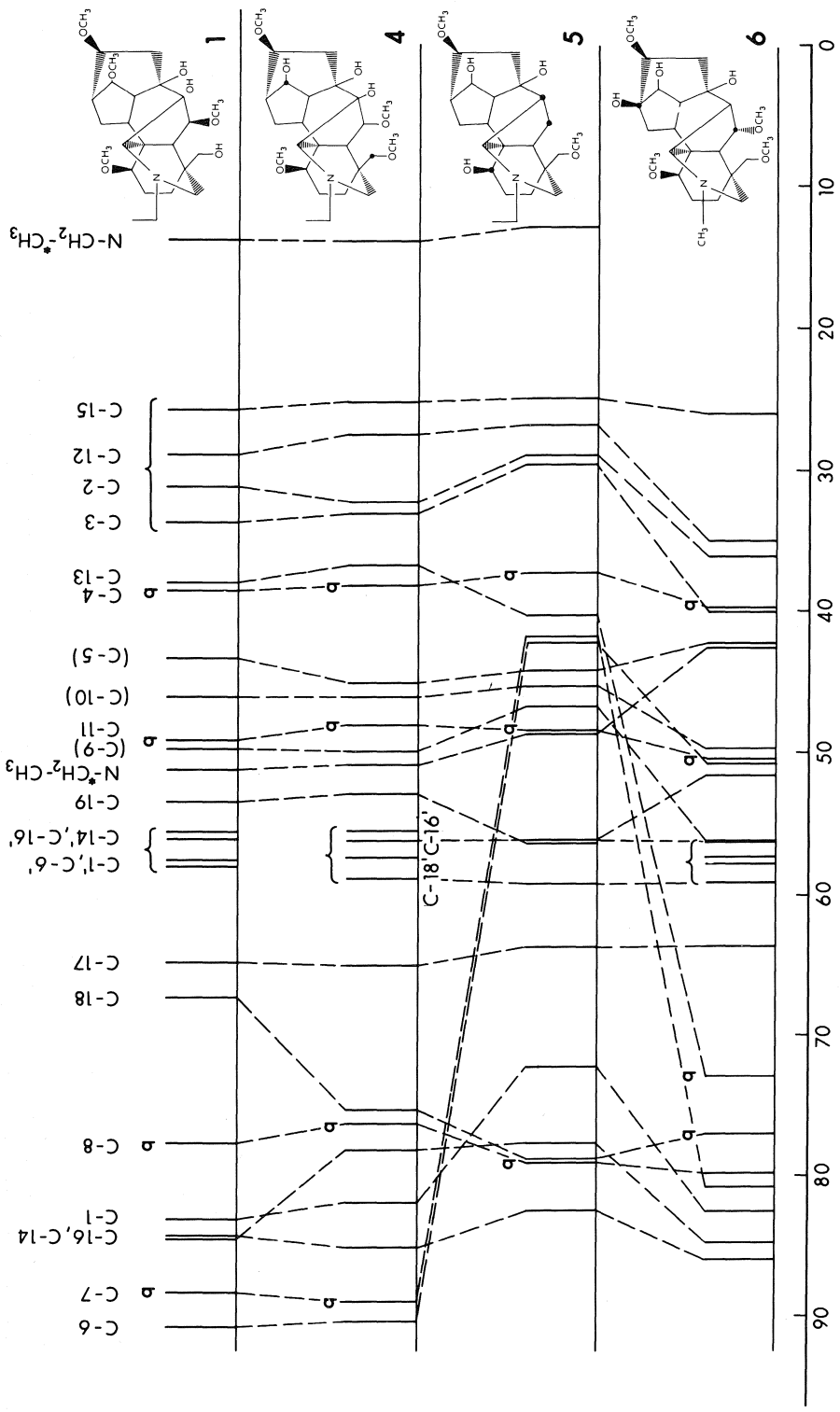

FIG. 3. Carbon-13 chemical shift correlations showing structural variations and assignments in the diterpenoid alkaloid bases lycoctonine (**1**), browniine (**4**), isolatizidine (**5**), and delphonine (**6**).

Can. J. Chem. Downloaded from www.nrcresearchpress.com by 210.87.254.40 on 09/05/12
For personal use only.

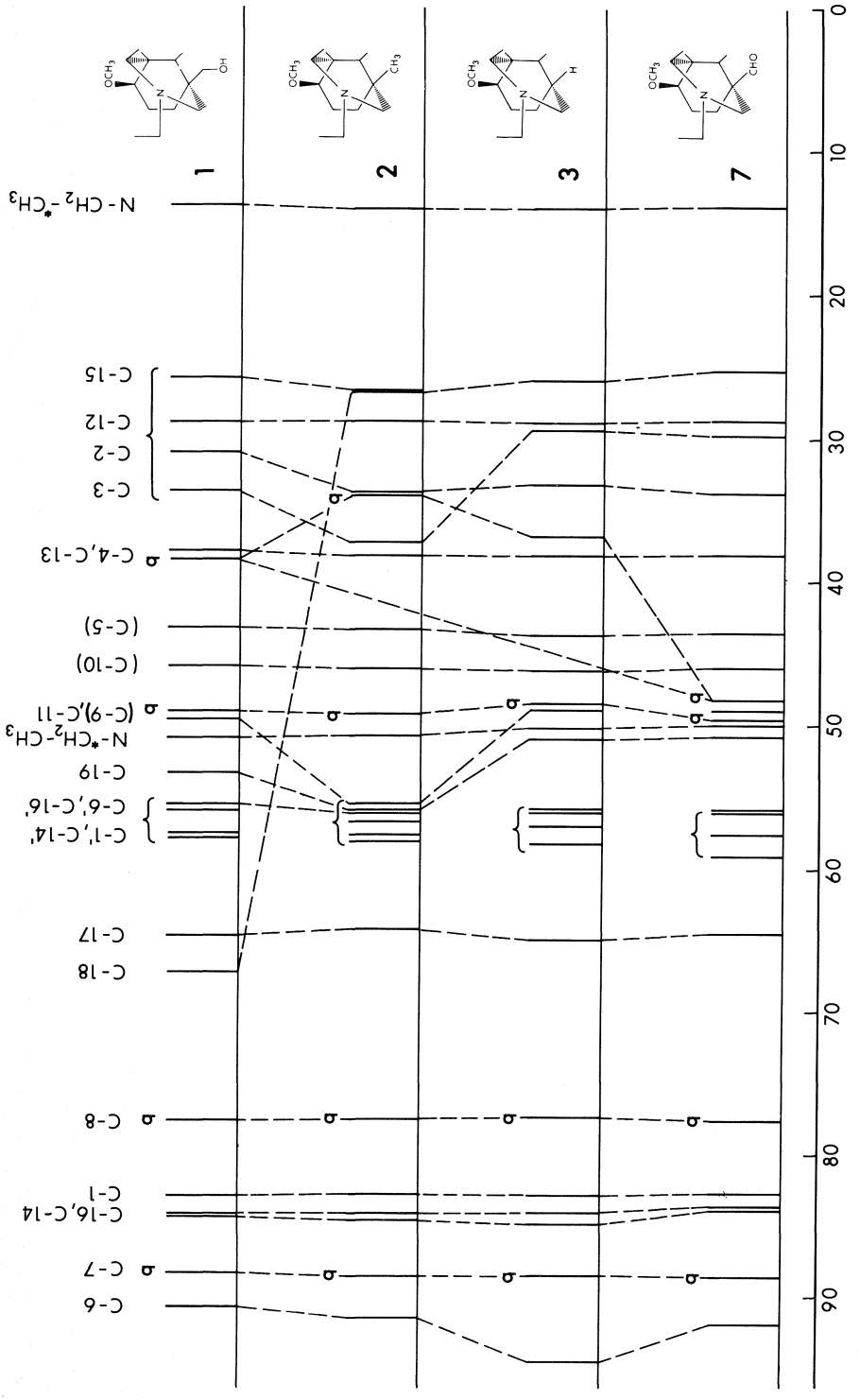

FIG. 4. Carbon-13 chemical shift correlations showing structural variations and assignments in the diterpenoid alkaloids lycoctonine (**1**), deoxylycoctonine (**2**), deoxymethylenelycoctonine (**3**), and lycoctonal (**7**).

Can. J. Chem. Downloaded from www.nrcresearchpress.com by 210.87.254.40 on 09/05/12
For personal use only.

Can. J. Chem. Downloaded from www.nrcresearchpress.com by 210.87.254.40 on 09/05/12
For personal use only.

shifted upfield (4.5 p.p.m.) as expected (15) in deoxylycoctonine (**2**) and downfield (9.9 p.p.m., see Discussion) in lycoctonal (**7**). Further, there is no resonance attributable to a quaternary carbon in the region 30–45 p.p.m. in the spectrum of deoxymethylenelycoctonine (**3**) and all other quaternary shifts remain in the same relative positions in **1**, **2**, **3** and **7**. Since the structural features at the quaternary center C-11 are similar in all the bases the resonance at 49.2 ± 0.8 p.p.m. is assigned to this carbon. However, appreciable shifts are expected at C-8, in particular, in **5** compared with **4**, but are not observed (77.8 ± 1 p.p.m.).[3] In delphonine (**6**) an obvious new quaternary resonance is observed at 72.8 p.p.m. and is, therefore, assigned to C-13 in this molecule.

(b) Methine Carbons

The upfield shift (48.3 p.p.m.) at C-6 in **5**, compared to **4**, establishes this as the lowest field *methine* resonance in the bases **1**, **2**, **3**, **4**, and **7**. An upfield shift of similar magnitude is expected at C-13 in **5**, compared to **6**. The highest field methine resonance in **5** (40.5 p.p.m.) corresponds to an α-hydroxyl substituent shift of *only* 32.3 p.p.m. However, this resonance and similar high field methine resonances in **1**, **2**, **3**, **4**, and **7** are assigned to C-13, though in **3** this resonance is not distinguished from that due to C-4. Methoxyl and hydroxyl substituent effects (15) are important in assigning the resonances due to C-1, -14, and -16 (Fig. 3). The resonance at 78.4 p.p.m. in **4** is assigned to C-14, since methoxyl replaces hydroxyl at this site in **1**. Similarly, the resonance at 72.5 p.p.m. in **5** is assigned to C-1. The most reasonable assignment for the carbons C-1 and -14 in **1** is, therefore, 83.0 and 84.3 p.p.m., respectively.[4] A β-methoxyl effect is expected at C-7 in **6**, compared to **5**, but assignment in this case is ambiguous. The remaining low-field methine resonance (84.3 p.p.m.) in **1** is assigned to C-16, since this is a methoxylated carbon. The order of the shifts for C-14 and -16 in the other bases is not established but that given is based on the shifts at C-14 in **4** and **5**. The predicted (68 p.p.m.) and observed (64.9 p.p.m.) shifts for C-17 in **1** are in reasonable agreement. This carbon is structurally similar in all the bases as verified by the small variation in shift (65.1 ± 1.4 p.p.m.) throughout this series. The remaining methine carbons C-5, -9, and -10 are not easily distinguished, and the assignments given in Table 1, and in Figs. 3 and 4 are only tentative. It is expected that a change in the substituent at C-4 in **1**, **2**, **3**, and **7** will induce a β-effect at C-5. Indeed an upfield shift (6.2 p.p.m.) is observed in the lower field resonance of this group in **3** on removal of the methyl substituent at C-4 in **2** (Fig. 4). However, the effects of other substituents in **1** and **7** are not clear. This group of resonances all move upfield on removal of the methoxyl group at C-6 in **5**, compared to **4** (Fig. 3), thus negating the opportunity to confirm the C-5 assignment on this basis. The effects observed on protonation of the nitrogen might assist in these assignments (see later). The possibility of cross-over effects for these nuclei is not excluded.

(c) Methylene Carbons

The C-18 methylene carbon resonance in lycoctonine (**1**) (67.4 p.p.m.) is assigned on the basis of the methoxyl–hydroxyl substituent effect between **1** and **4** (Fig. 3) and on the observation that it is this resonance which disappears in the spectrum of **3** and is a carbonyl carbon in **7**. The remaining methylene carbons may be considered as the *N*-alkyl type, C-19 and N—CH_2—, which are predicted to resonate at 50–55 p.p.m. (1), and the cycloalkane type, C-2, -3, -12, and -15, predicted over the range 25–35 p.p.m. (5). In the spectrum of **1** the methylene resonances at 53.5 and 51.2 p.p.m. may be tentatively assigned to the *N*-alkyl type and those at 25.8, 29.0, 31.2, and 33.8 p.p.m. to the cycloalkane type. The relief of steric interaction at C-19 on removal of the hydroxyl group at C-18′ in **2**, compared to **1**, or the methoxyl group at C-6 in **5**, compared to **4**, produces a downfield shift in the lower field resonance of the pair assigned to the *N*-alkyl type. In delphonine (**6**) an *N*-methyl group replaces the *N*-ethyl group of all other bases and the higher field line of the *N*-alkyl pair shifts upfield to 42.5 p.p.m. The carbon C-19 is thus assigned at lower field than the *N*-methylene in the bases **1**, **2**, **3**, **5**, and **7**. This order may be reversed in **4** since the methoxyl group C-18′ will

[3]In an incomplete study of the alkaloid delphinine, in which C-8 is substituted by an acetoxyl group, a downfield shift (8.2 p.p.m.) is noted (see ref. 9). This observation serves to emphasize the correctness of the C-8 assignment.

[4]Replacement of a methyl group by hydrogen is expected to give rise to an upfield shift of 4.8 p.p.m. (15). Using the assignment given, the shift at C-1 is 9.7 p.m., which is considered more reasonable than the alternative 11.8 p.p.m. if these assignments were reversed.

Can. J. Chem. Downloaded from www.nrcresearchpress.com by 210.87.254.40 on 09/05/12
For personal use only.

effectively shield the C-19 carbon in this molecule. For C-2, -3, -12, and -15 the tentatively assigned order relies on the following observations: a β-methyl effect (7.7 p.p.m.) (5) in **2**, compared to **3**. The resonances at 33.5 p.p.m. in **2** and 29.6 p.p.m. in **3** are, therefore, assigned to C-3. By analogy with **2** it is suggested that C-3 is the lowest field carbon of this group in all other bases. In isolatizidine (**5**) an upfield shift is expected and observed at C-2, since the C-1 methoxyl group in **4** is replaced by hydroxyl. However, C-3 also shifts upfield. The higher field pair of resonances in this group are assigned to C-12 and -15. Hydroxyl substitution at C-13 in **6** produces the expected β-effect (8.0 p.p.m.) (15, 16) at C-12 if the resonances at 35.0 and 27.0 p.p.m. are assigned to this carbon in **6** and **5**, respectively. The resonance due to C-15 remains relatively unperturbed (25.8 ± 1 p.p.m.) throughout these structural changes as might be anticipated.

The chemical shifts of the hydrochloride and perchlorate salts of the bases **1**–**6** are given relative to the corresponding free base in Table 2. The consistencies in these difference shifts serve to emphasize the correctness of the assignments. However, the protonation additivity parameters (1) were not applied without reservation in these cases.

In summary, the assignments for the diterpenoid alkaloids studied are given in Figs. 3 and 4.

Discussion

Attention is first drawn to the similar pattern of carbon-13 shifts exhibited by the series of lycoctonine-alkaloids studied. This pattern has made possible self-consistent and reasonably unambiguous assignment of nearly all the resonances for these compounds. A particularly important feature is the constant pattern of shifts exhibited by the quaternary carbons except in cases where major structural or substitution changes occur (*e.g.* at C-13 in **6**). This latter pattern is considered a most valuable "fingerprint" for determining the degree of, in particular, oxygen substitution in these molecules as indicated by the spectra of **5** and **6**, compared with the other bases.

The changes in the carbon-13 shifts on introduction of a substituent are indicated in Figs. 3 and 4. In most cases the effects are of the correct order but in several instances their magnitudes differ from those expected on the basis of previous reports on simpler systems. Thus, removal of the oxygenated function at C-6 and -7 in **5**, compared to **4**, is expected to produce an upfield shift of 58–60 p.p.m., since both these carbons are subject to α (48.5 p.p.m.) and β (10 p.p.m.) oxygen group substituent effects (15, 18). However, these effects are substantially attenuated (48.3 and 46.4 p.p.m.), perhaps the consequence of possible steric contributions in the compact ring structure. A similarly attenuated α-hydroxyl effect is noted at C-13 in **6** (32.3 p.p.m.). In contrast, the parameters for replacement of hydroxyl by methoxyl (or *vice versa*) are large compared with the literature values (4.8 p.p.m.) (15). Thus at C-1 in **4**, compared to **5**, at C-14 in **4**, compared to **1**, and at C-18 in **4**, compared to **1**, shifts of 9.7, 5.9, and 8.1 p.p.m. are observed, respectively. An average hydroxyl–methoxyl parameter of 8 p.p.m. is suggested in these systems.

The effect of methyl substitution at C-4 in **2**, compared to **3**, represents a typical *gem*-dimethyl effect (upfield, 2.9 p.p.m.) (5) and further justifies consideration of methylene groups as methyl substituents when dealing with additivity effects (19). On the other hand the downfield shift (9.9 p.p.m.) at C-4 in **7**, compared to **1**, resulting from substitution of an aldehyde function, is surprisingly small. This shift, however, appears to be one of very few determined for saturated carbon atoms (20), especially for one so highly substituted.[5] The limited reports (20) for this parameter for a saturated carbon center give a downfield shift of 31 p.p.m., on average, while in vinyl (21) and aromatic (22) aldehydes this parameter is nearer 10 p.p.m.

Steric contributions to the carbon-13 shifts in these alkaloids are particularly evidenced in the observed shifts at C-6. In **3**, compared to **2**, the downfield shift (3 p.p.m.) at C-6 is attributed to removal of the methyl group at C-4 which provides a steric contribution at C-6 in **2**. Resubstitution at C-4 with the bulkier aldehyde group in **7** results in C-6 shifting back upfield (2.5 p.p.m.) with a concomitant effect in the methoxyl region, presumably at C-6′.

[5]NOTE ADDED IN PROOF: In recent studies on substituted aldehydes, we observe the effect of branching rapidly attenuates the aldehyde substituent parameter. *E.g.*, in cyclohexanealdehyde a value of 12.9 p.p.m. is observed at C-α (C. P. Beeman. Private communication).

Can. J. Chem. Downloaded from www.nrcresearchpress.com by 210.87.254.40 on 09/05/12
For personal use only.

TABLE 2. Carbon-13 chemical shifts induced on protonation of the nitrogen center in lycoctonine and related alkaloids **1–6**[a]

Compound	Protonating acid	Solvent	Carbon position (relative to nitrogen)																				
			C-1(γ)	C-2(δ)	C-3(γ)	C-4(β)	C-5(γ)	C-6(γ)	C-7(β)	C-8(γ)	C-9(δ)	C-10(γ)	C-11(β)	C-12(δ)	C-13(ε)	C-14(ε)	C-15(δ)	C-16(ε)	C-17(α)	C-18(γ)	C-19(α)	*N*-CH_2—CH_3 (α)	*N*-CH_2—CH_3 (β)
1	HCl	$CDCl_3$	−0.8	−0.5	−1.3	−0.2	−0.2	−1.8	−2.6	—	−5.4	−2.5	1.2	−4.2	−0.1	−0.2	−4.4	−1.1	0.3	−1.4	3.0	1.1	−2.6
2	HCl	$CDCl_3$	−0.5	−3.8	−3.8	−0.8	−0.4	−1.7	−2.1	—	−6.6	−2.4	1.0	−0.4	−0.4	−0.7	−5.8	−1.3	−1.6	—	3.7	0.6	−3.3
3	$HClO_4$	DMSO-d_6	−1.4	0.1	−0.5	−5.8	—	−2.9	−3.5	1.1	−6.3	—	−0.2	−8.2	−0.7	−1.2	−5.7	−1.5	−0.6	—	4.6	0.6	−3.7
4	$HClO_4$	D_2O	−0.2	0.3	−2.7	−0.9	−2.0	−1.8	−3.3	2.3	−5.0	−2.0	1.7	−1.4	2.6	−3.6	−4.6	−2.5	0.7	0.9	2.8	1.3	−3.4
5	HCl	D_2O	−1.0	−0.3	−1.6	0.3	−0.6	−2.0	−1.8	−4.0	−0.2	−0.1	0.8	−1.9	−0.8	−3.0	−0.3	0.2	0.8	−2.3	0.1	0.8	−2.8
6	HCl	$CDCl_3$	−1.9	0.2	0.6	−4.0	—	−2.1	−0.2	−0.6	−8.2	−1.6	0.6	−7.6	1.1	−3.4	3.8	−3.6	4.0	−1.0	2.1	0.4	—

[a]Given in parts per million relative to the corresponding free base. Negative sign indicates an upfield shift. For comparison the following protonation parameters obtained in simple piperidines (1) are given: $CH_3NH_{C\text{-}\alpha}^+$ −2.5, $CH_3NH_{C\text{-}\beta}^+$ −4.9 $CH_3NH_{C\text{-}\gamma}^+$ −3.5 p.p.m. $CH_3NH_{C\text{-}\alpha}^+$ becomes positive where α-carbon is substituted.

Can. J. Chem. Downloaded from www.nrcresearchpress.com by 210.87.254.40 on 09/05/12
For personal use only.

With the modifications in substituent parameters and the substantial steric contributions in these molecules in mind, it seems reasonable that some of the observed shifts (*e.g.*, C-19 in **1**, **2**, and **3** or C-8 in **1**, **4**, **5**, and **6**) might be considered unusual. The general pattern of shifts exhibited by these systems does, however, enable self-consistent assignment of most of the carbon resonances in the bases.

As indicated by the difference shifts given in Table 2 there is an apparent breakdown in the additivity effects arising from protonation of the nitrogen in these alkaloids. This may be attributable to concentration or often solvent variations (23) necessary in the present study. This observation taken in conjunction with the minor ambiguities in assignment precludes detailed discussion of protonation additivity effects. However, several of the general trends observed in simple methyl-piperidines and 4-piperidones (1), in particular at sites β or γ to the nitrogen atom are reproduced. Most unusual are the large upfield shifts (*ca.* 5 p.p.m.) at the carbon atoms δ to the nitrogen, for example at C-12 and -15. These carbon atoms have the common feature that they lie in a plane, approximately 4 Å away from the nitrogen center. The carbon C-9 is similarly located with respect to the nitrogen. A comparable upfield shift (*ca.* 5 p.p.m.) is observed in the resonance at about 50 p.p.m. previously assigned to C-5, -9 or -10 in the bases. It is tempting, therefore, to assign this line to C-9. We can only speculate about the possible factors contributing to the δ-shift and presently only report the observation. In general, the shifts observed on protonation of the nitrogen exhibit reasonably close trends for each of the compounds studied and may be considered valuable in assisting with spectral assignments.

Application

We have isolated small amounts of two apparently hitherto unknown alkaloids, **A** and **B** from *Delphinium bicolor* Nutt, for which we propose the structures **8** and **9** on the basis of the following evidence.

The base A, $[\alpha]_D^{24}$ +10° ($CHCl_3$), which was not obtained crystalline, although it yielded a hydroiodide salt m.p. > 240° (methanol–ether), had composition $C_{25}H_{39}NO_6$ (M^+ calcd. 449.2777, found 449.2797 a.m.u.). The p.m.r. spectrum indicated the presence of the following groups (δ from TMS in deuterochloroform): a tertiary methyl (1.04 p.p.m.), an *N*-ethyl (CH_3 at

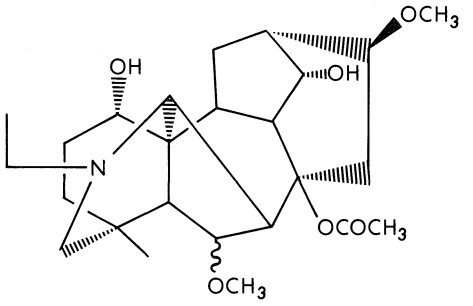

8

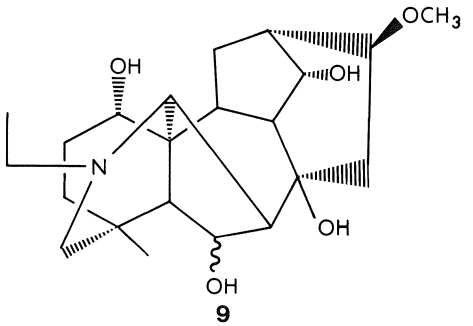

9

1.09 p.p.m., J = 7 Hz), an acetoxyl (2.10 p.p.m.), two methoxyls (3.18 and 3.46 p.p.m.), and approximately two hydroxyls (6.90 p.p.m., disappearing on addition of D_2O). I.r. absorptions at 3500, 3150, 1735, and 1238 cm^{-1} also indicated the presence of hydroxyl and acetate functions. The base **B**, m.p. 190–191°, $[\alpha]_D^{24}$ +16° ($CHCl_3$), was similarly shown to have the composition $C_{22}H_{35}NO_5$ (M^+ calcd. 393.2515, found 393.2523 a.m.u.), and to contain a tertiary methyl, an *N*-ethyl, a methoxyl, and hydroxyl groups. Given the nature of the *Delphinium* alkaloids (10), these data suggest that **A** and **B** have the lycoctonine C_{19}-skeleton shown in Fig. 1. A prominent ion in the mass spectra of **A** and **B** at *m/e* M − 17 is typical for loss of a hydroxyl group from C-1 (24). This and the observed i.r. absorptions at 3150 cm^{-1} in both bases characterize the α-hydrogen bonded configuration for this hydroxyl group (25). Pyrolysis of the base **A** in glycerol, monitored by p.m.r., indicated the generation of acetic acid, consistent with the location of the acetoxyl group at C-8 in **8** (26).

Carbon-13 chemical shifts for the bases **A** and **B** and their hydrochlorides are given in Table 3. The correlation diagram, Fig. 5, compares the carbon-13 shifts in **A** and **B** with those in deoxylycoctonine (**2**) and isolatizidine (**5**). Clearly

Can. J. Chem. Downloaded from www.nrcresearchpress.com by 210.87.254.40 on 09/05/12
For personal use only.

TABLE 3. Carbon-13 chemical shifts and assignments in the unknown alkaloids **A** and **B** and their corresponding hydrochlorides[a]

	Carbon position[b]																								
Compound	C-1	C-2	C-3	C-4	C-5	C-6	C-7	C-8	C-9	C-10	C-11	C-12	C-13	C-14	C-15	C-16	C-17	C-18	C-19	*N*-CH_2—CH_3	C-1′	C-16′	C-6′	C-14′ *or* C-18′
A[c] $C_{25}H_{39}NO_6$	**72.6**$_4$	31.6$_2$†	37.8$_2$	32.8$_9$	42.3$_2$*	72.3$_2$	44.4$_2$*	79.9$_8$	48.0$_9$*	44.4$_2$*	48.9$_5$	30 6$_5$†	40.0$_3$	75.9$_1$	29.7$_3$†	83.3$_2$	65.5$_6$	27.3$_6$	61.6$_7$	48.3$_6$	12.9$_7$	—	56.4$_7$	52.8$_6$	—
A[c]-Hydrochloride	**72.5**$_9$	30.4$_3$†	36.2$_8$	33.0$_5$	43.2$_1$*	71.7$_0$	44.2$_9$*	79.9$_5$	48.7$_1$*	43.7$_8$*	49.3$_3$	29.4$_6$†	40.0$_8$	74.6$_7$	27.5$_0$†	83.1$_3$	66.2$_6$	26.3$_6$	60.8$_7$	49.6$_8$	10.3$_0$	—	56.1$_5$	50.1$_4$	—
B $C_{22}H_{35}NO_5$	**72.9**$_7$	32.2$_7$†	42.4$_0$	32.8$_9$	44.4$_0$*	72.0$_5$	50.2$_2$*	76.0$_7$	54.8$_0$*	46.1$_2$*	48.4$_7$	29.7$_0$†	40.0$_0$	76.0$_7$	29.7$_0$†	82.4$_6$	64.9$_9$	27.4$_7$	61.8$_9$	48.4$_7$	13.0$_5$	—	56.3$_1$	—	—
B-Hydrochloride	71.7$_1$	29.7$_8$†	39.3$_5$	32.8$_0$	43.5$_0$*	70.9$_2$	50.5$_1$*	75.7$_4$	52.1$_6$*	45.0$_8$*	48.5$_0$	29.7$_8$†	39.3$_5$	74.4$_8$	27.0$_6$†	82.3$_2$	65.4$_5$	26.1$_5$	60.8$_1$	49.4$_1$	10.0$_5$	—	55.7$_4$	—	—

[a]Given in parts per million relative to TMS.
[b]* † *indicate uncertainties in assignment within a given group.*
[c]Acetyl carbons at 170.9$_9$ and 21.5$_9$ p.p.m. in free base and 170.9$_9$ and 21.5$_1$ p.p.m. in the hydrochloride.

Can. J. Chem. Downloaded from www.nrcresearchpress.com by 210.87.254.40 on 09/05/12
For personal use only.

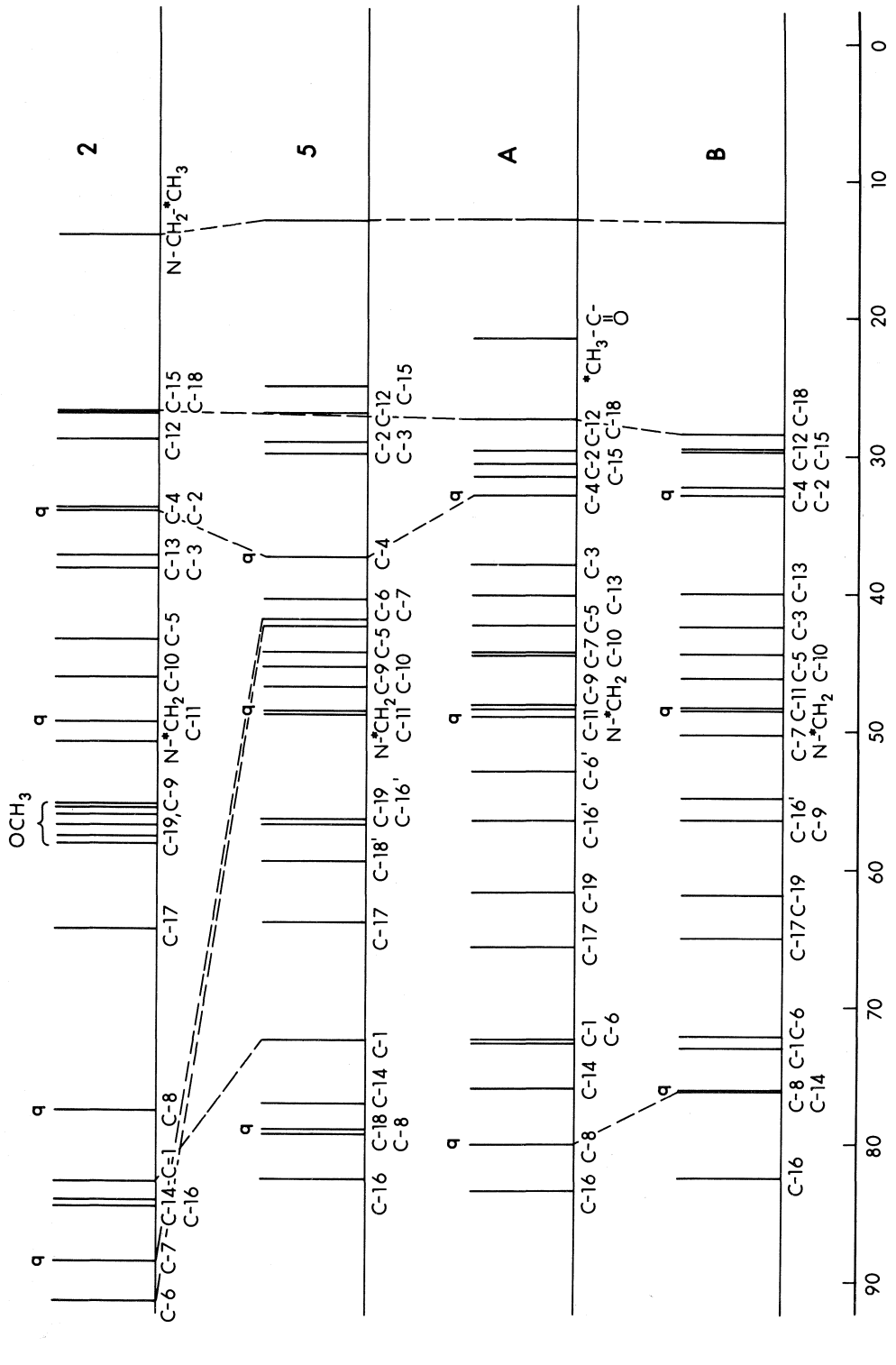

FIG. 5. Carbon-13 chemical shift correlations showing assignments in the diterpenoid alkaloids deoxylycoctonine (**2**), isolatizidine (**5**), and the unknown alkaloids **A** and **B**.

Can. J. Chem. Downloaded from www.nrcresearchpress.com by 210.87.254.40 on 09/05/12
For personal use only.

there is a close resemblance between the chemical shifts in **A** and **B** and those of the lycoctonine alkaloids. The typical chemical shifts and off-resonance results make it easy to recognize the presence of an acetoxyl group in **A** (171 and 21.6 p.p.m.), an *N*-ethyl group (methyl at 13 p.p.m.), and a C-18 methyl group (27.4 p.p.m.) in **A** and **B**, and two and one methoxyl groups in **A** and **B**, respectively. The characteristic C-16 and -16′ shifts (84.3 and 56.3 p.p.m.) enable assignment of a methoxyl group in **A** and **B** to C-16. In addition, the shift at C-4 (32.9 p.p.m.) in **A** and **B** is identical to that in **2** for the methyl substituted quaternary center. Methyl substitution at C-4 in **A** and **B** is also reflected in the shift at C-3 (37.8 and 42.4 p.p.m.) which compares favorably with that in **2** (37.4 p.p.m.).

Most noticeable is the similarity of the shifts in **A** and **B** with those in **5**, in particular, the absence of a low-field quaternary resonance. Thus C-7 must be unsubstituted in **A** and **B**. The methine signals which can be assigned to C-7 in **A** and **B** are all downfield of that in **5** indicating a substituent at C-6 (β-effect). The quaternary carbon C-8 in **A** is similar in shift to that in **5**, a feature perhaps surprising in view of the established acetoxyl group at this site in **A**. However, the upfield shift at C-8 observed in **B** is taken as indicative of replacement of the acetoxyl group in **A** by a hydroxyl group in **B**. The pattern of shifts between 70 and 85 p.p.m. in **A**, **B**, and **5** is remarkably similar. It seems reasonable to assign the methine resonances at 72.6 and 73.0 p.p.m. in **A** and **B**, respectively, to C-1 by comparison with **5** (72.5 p.p.m.), thus confirming (see mass-spectral evidence) hydroxyl substitution at this site in **A** and **B**. Similarly the shifts at 75.9 and 76.1 p.p.m. are attributed to C-14 in **A** and **B**, respectively, by comparison with **5** (*ca.* 77 p.p.m.). Thus, hydroxyl substitution at C-14 in **A** and **B** is indicated. The remaining resonances in this region 72.3 p.p.m. in **A** and 72.1 p.p.m. in **B** are attributed to C-6 since oxygen substitution is indicated at this site by the β-effects noted at C-7 and further, there are no resonances attributable to C-6 at 42 p.p.m. as in **5**. Of the remaining oxygen functions we must assign a methoxyl substituent at C-6 in **A** and hydroxyl in **B**. The possibility that the methoxyl group in **A** be assigned to C-14 is not excluded but seems unlikely in view of the methoxyl–hydroxyl effect noted at this site between **1** and **4**. However, the absence of a significant shift at C-6 between **A** and **B** is not easily reconciled.

The overriding feature which adds credence to the above assignments is the similarity in the general pattern of shifts in **A** and **B** with the model systems **1**–**7**. In effect it is this pattern which is of critical importance in ruling out substitution, particularly by oxygen, at the alternative sites available in these systems. The evidence is, therefore, compatible with the structures **8** and **9** for the bases **A** and **B**, respectively. The base **9** is the desmethyl desacetate of the base **8**. These structures are closely related to those of chasmanine and neoline systems (10), and are additions to this still poorly represented group of C_{19}-diterpenoid alkaloids with the lycoctonine skeleton *unoxygenated at C-18*.

Conclusions

We conclude that fundamental substituent and additivity data (1–8, 15, 16, 18) can be usefully applied to assignment considerations in the relatively complex diterpenoid alkaloids. Some of the parameters must be modified, in particular, in magnitude in order to meet the demands set by these more complex systems. The general pattern of carbon-13 shifts in the diterpenoid alkaloids, in particular, of the quaternary carbons can be of critical importance in structural determinations in this class of compounds.

We thank the National Research Council of Canada for support and Dr. C. P. Beeman for some experimental assistance.

1. A. J. Jones and M. M. A. Hassan. J. Org. Chem. **37**, 2332 (1972); see ref. to M. W. Duch. Ph.D. Thesis. University of Utah, Salt Lake City, Utah, February, 1970.
2. A. J. Jones, A. F. Casy, and K. M. J. McErlane. Tetrahedron Lett. 1727 (1972).
3. W. O. Crain, Jr., W. C. Wildman, and J. D. Roberts. J. Am. Chem. Soc. **93**, 990 (1971).
4. G. Ellis and R. G. Jones. J. Chem. Soc. Perkin II, 437 (1972).
5. D. K. Dalling and D. M. Grant. J. Am. Chem. Soc. **89**, 6612 (1967).
6. W. J. Horsley and H. Sternlicht. J. Am. Chem. Soc. **90**, 3738 (1968); W. Horsley, H. Sternlicht, and J. S. Cohen. J. Am. Chem. Soc. **92**, 680 (1970).
7. D. K. Dalling, D. M. Grant, and L. F. Johnson. J. Am. Chem. Soc. **93**, 3678 (1971); D. K. Dalling and D. M. Grant. J. Am. Chem. Soc. **94**, 5318 (1972).
8. D. K. Dalling and D. M. Grant. Private communication.
9. H. J. Reich, M. Jautelat, M. T. Messe, F. J. Weigert, and J. D. Roberts. J. Am. Chem. Soc. **91**, 7445 (1969).
10. S. W. Pelletier and L. H. Kieth. *In* The alkaloids, chemistry and physiology. Vol. 12. *Edited by* R. H. F. Manske. Academic Press, New York. 1970. Chapt. 1.

11. M. PRZYBYLSKA and L. MARION. Can. J. Chem. **34**, 185 (1956).
12. E. S. STERN. *In* The alkaloids. Vol. 7. *Edited by* R. H. F. Manske. Academic Press, New York. 1960. Chapt. 22.
13. E. WENKERT, A. O. CLOUSE, D. W. COCHRAN, and D. DODDRELL. J. Am. Chem. Soc. **91**, 6879 (1969).
14. For example, see: A. J. JONES, D. M. GRANT, M. W. WINKLEY, and R. K. ROBINS. J. Am. Chem. Soc. **92**, 4079 (1970); J. Phys. Chem. **74**, 2684 (1970).
15. P. C. LAUTERBUR. J. Am. Chem. Soc. **83**, 1846 (1961); K. S. DHAMI and J. B. STOTHERS. Can. J. Chem. **44**, 2855 (1966).
16. T. D. BROWN. Ph.D. Thesis. University of Utah, Salt Lake City, Utah, 1966; see also ref. 6.
17. J. B. STOTHERS and P. C. LAUTERBUR. Can. J. Chem. **42**, 1563 (1964).
18. J. D. ROBERTS, F. J. WEIGERT, J. I. KROSCHWITZ, and H. J. REICH. J. Am. Chem. Soc. **92**, 1338 (1970); L. M. JACKMAN and D. P. KELLY. J. Chem. Soc. B, 102 (1970).
19. For example, M. W. DUCH and D. M. GRANT. Macromol. **3**, 165 (1970).
20. H. SPIESECKE and W. G. SCHNEIDER. J. Chem. Phys. **35**, 722 (1961); E. LIPPMAA and T. PEHK. Eesti. NSV. Tead. Akad. Toim., Keem-Geol. **17**, 210 (1968); B. V. CHENEY, Ph.D. Thesis. University of Utah, Salt Lake City, Utah, 1966.
21. D. H. MARR and J. B. STOTHERS. Can. J. Chem. **43**, 596 (1965).
22. H. SPIESECKE and W. G. SCHNEIDER. J. Chem. Phys. **35**, 731 (1961); K. S. DHAMI and J. B. STOTHERS. Can. J. Chem. **43**, 498 (1965); **44**, 2855 (1966).
23. See for example: G. L. NELSON, G. C. LEVY, and J. D. CARGIOLI. J. Am. Chem. Soc. **94**, 3089 (1972).
24. M. S. YUNUSOV, YA V. RASHKES, V. A. TEL'NOV, and S. YUNUSOV. Khim. Prir. Soedin. 101, (1970); *c.f.* O. E. EDWARDS. *In* The alkaloids. Vol. 1. *Edited by* J. E. Saxton. Pt. 2-D. The Chemical Society: Specialist Periodical Report Series. 1970. Chapt. 16.
25. S. W. PELLETIER, L. H. KIETH, and P. C. PARTHASARATHY. J. Am. Chem. Soc. **89**, 4146 (1967).
26. L. H. KIETH and S. W. PELLETIER. J. Org. Chem. **33**, 2497 (1968).

Can. J. Chem. Downloaded from www.nrcresearchpress.com by 210.87.254.40 on 09/05/12
For personal use only.

The Interactions of Four Carbamate Pesticides with Electron-acceptor Reagents[1,2]

JAMES DANIEL MACNEIL[3] AND ROLAND WALTER FREI[4]

Trace Analysis Research Centre, Department of Chemistry, Dalhousie University, Halifax, Nova Scotia

AND

OTTO HUTZINGER

Atlantic Regional Laboratory, National Research Council of Canada, Halifax, Nova Scotia

Received May 23, 1972

The interactions between several electron-acceptor reagents and some pesticides having donor properties were investigated in solution and on cellulose thin-layers by spectrophotometric methods. In solution, formation constants and extinction coefficients were evaluated from absorbance measurements for complexes of the pesticides carbaryl, IPC, CIPC, and swep with the electron-acceptor reagent 9-dicyanomethylene-2,4,7-trinitrofluorene, using the Benesi–Hildebrand method. Values were also calculated for the carbaryl-mellitic trianhydride complex. Extinction coefficients ε_λ^{AD} for the complexes were less than 1000, while formation constants were 1–4 l mol^{-1}.

Reflectance spectroscopic measurements showed similar relationships between absorption maxima and intensities of the complexes and the donor properties of the pesticides to those observed in solution. A linear relationship between reflectance and the square root of concentration was found for all four pesticide–CNTNF complexes in the range from 5–50 μg.

Les interactions entre plusieurs réactifs accepteurs d'électrons et certains pesticides possèdant des propriétés de donneurs, ont été étudiées en solution et sur couche mince de cellulose par des méthodes spectrophotométriques. En solution, les constantes et les coefficients d'extinction ont été évalués à partir des mesures d'absorbance pour les complexes entre les pesticides carbaryle, IPC, CIPC, et "swep" le réactif électroaccepteur dicyanométhylène-9 trinitro-2,4,7 fluorène, selon la méthode de Benesi–Hildebrand. Des mesures ont été également faites pour le complexe carbaryle-trianhydride melittique. Les coefficients d'extinction ε_λ^{AD} pour ces complexes sont inférieurs à 1000, les constantes de formation sont de l'ordre de 1–4 1/mol.

Les mesures de reflexion spectroscopique donnent des relations semblables entre les maxima d'absorption, les intensités des complexes et les propriétés de donneur des pesticides, à celles observées en solution. Une relation linéaire entre la réflexion et la racine carré de la concentration a été trouvée pour tous les quatre complexes pesticides CNTNF, dans l'intervalle de 5–50 μg.

[Traduit par le journal]

Can. J. Chem., **51**, 500 (1973)

Introduction

The formation of colored π-complexes between pesticides and electron-acceptor (or donor) reagents on thin-layer chromatograms has previously been discussed (1, 2), but no attempt was made to determine formation constants of these complexes. A study of this aspect of the complex formation was undertaken in view of the part complexation is believed to play in the activity of various pesticides (3). Complexes of DDT and related compounds with tetracyanoethylene and nerve axon in solution, for example, have recently been reported (4).

There are several approaches to the determination of complexing constants, and various methods which may be applied to solution measurements have been discussed in a recent book by Foster (5). While there are objections to calculations utilizing u.v.–visible spectra (5), several considerations led us to choose this approach. Some data on the reflectance spectra of pesticide complexes *in situ* on thin-layer chromatograms had previously been obtained (2) and the comparison of spectra in solution with those in the adsorbed state was of interest. Secondly, only a measure of the relative strengths of complex formation was of interest for the purposes of this study and this appeared to be available using the Benesi–Hildebrand method (5).

[1]Issued as NRCC No. 12922.

[2]No. IV in series "Electron-donor–acceptor complexing reagents in the analysis of pesticides".

[3]Present address: Research Station, Canada Department of Agriculture, Summerland, British Columbia.

[4]To whom correspondence is to be addressed.

Can. J. Chem. Downloaded from www.nrcresearchpress.com by 210.87.254.42 on 09/05/12
For personal use only.

Can. J. Chem. Downloaded from www.nrcresearchpress.com by 210.87.254.42 on 09/05/12
For personal use only.

The quantitative determination of pesticide–acceptor π-complexes *in situ* on thin-layer chromatograms has previously been described (6, 7). It was shown that a linear relationship existed between the peak area of the complex in the reflectance scan and the concentration of the complexed pesticide over the range studied. Further studies over a larger concentration range to determine if the complexes followed the Kubelka–Munk relationships of diffuse reflectance spectroscopy or other relationships found for chromatographed species (8) were therefore indicated. It was also of interest to compare the intensity and wavelength shifts of the complex absorption bands measured in solution with those observed in the adsorbed state.

Experimental

Reagents

Analytical grade samples of the following pesticides were used in this study: carbaryl, 1-naphthyl-*N*-methylcarbamate (Union Carbide); CIPC, isopropyl *m*-chlorocarbanilate (Standard Chem); IPC, isopropyl carbanilate, (PPG Industries); swep, methyl 3,4-dichlorocarbanilate (Niagara Chem).

The following electron-acceptor reagents were used: 1,3,5-trinitrobenzene (TNB); 2,4,7-trinitro-9-fluorenone (TNF); 2,4,5,7-tetranitro-9-fluorenone (TeTNF); 9-dicyanomethylene-2,4,7-trinitrofluorene (CNTNF); 9-dicyanomethylene-2,4,5,7-tetranitrofluorene (CNTeTNF); tetracyanoethylene (TCNE); mellitic trianhydride. Sources of these compounds have been listed previously (1).

Instrumentation

Absorbance spectra were measured in solution with a Beckman DK-2A spectrophotometer using a tungsten lamp as a source and photomultipliers as detectors. Standard Beckman Pyrex cells (320–2500 nm) were used.

Reflectance spectra were recorded on a Bausch and Lomb Spectronic 505 with diffuse reflectance attachment.

Preparation of Samples

For measurements in solution, a 10^{-3} *M* solution of the complexing agent was first prepared. Samples of pesticide were weighed out and dissolved in this solution at pesticide concentrations of 0.1–0.25 *M*. Solutions (10^{-2} *M*) of the pesticides alone were also prepared, as well as solutions of carbaryl (10^{-2} *M*) in various acceptors (10^{-3} *M*).

For the reflectance measurements, solutions of the complexed pesticides carbaryl, IPC, CIPC, and swep (5 mg/ml) were prepared by dissolving weighed samples of the pesticides in a solution of the complexing agent CNTNF (5 mg/ml). The solutions were then spotted on squares (2 in. × 2 in.) cut from Eastman Chromagram sheets (cellulose, 6064, without fluorescent indicator) using Drummond microliter pipettes (Kensington Scientific Co.) of 1, 2, 3, 5, and 10 μl volumes to produce pesticide concentrations of 5, 10, 15, 25, and 50 μg/spot.

Acetone was used as solvent for all solutions.

Measurement of Spectra

In solution. absorbance spectra were measured in the double-beam mode using as reference the 10^{-3} *M* acceptor solution from 330–700 nm. The spectra of the pesticides and complexing agents were also measured individually using acetone (the solvent) as reference. Spectra were measured immediately after preparation of the samples and again after 24 h to assure that no significant variations had occurred. Both sets of data were plotted and the results were averaged.

The reflectance spectra of 50 μg samples of the four pesticide CNTNF complexes and of CNTNF (50 μg) were measured *vs.* a blank cellulose reference and the complexes were then measured against the CNTNF as reference from 400–700 nm. Dilution series of the four pesticide complexes and of the complexing agent were also measured *vs.* a blank cellulose reference from 400–700 nm. The samples were backed with white cardboard during the reflectance measurements to approximate an infinite layer thickness (8).

Results and Discussion

Measurements in Solution

The pesticide complexes in solution showed the typical broad, weak bands of π-complexes (see Fig. 1). Spectral maxima of the pesticide carbaryl with a number of acceptors are listed in Table 1. The complexes shown in Fig. 1 had a single broad absorption band and the intensities of these bands were much less than those measured in the u.v. region for the pesticides and complexing agents. Neither the pesticides nor the complexing agents showed absorption maxima in the region of the complex absorption bands.

Measurements for a series of solutions of complexing agent (at a fixed concentration) with increasing pesticide concentration produced a series of spectra such as those shown in Fig. 2 for the carbaryl–CNTNF complexes. A plot of $[A]_0/A$ *vs.* $1/[D]_0$, where $[A]_0$ and $[D]_0$ are the initial concentrations of acceptor and donor

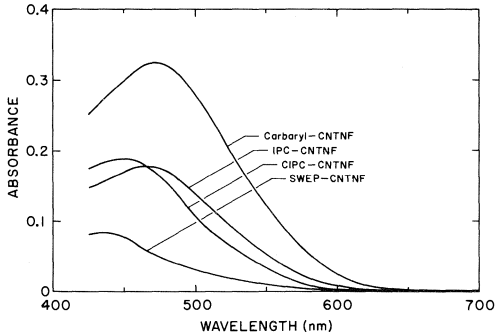

FIG. 1. Solution spectra of pesticide (0.25 *M*)–CNTNF (10^{-3} *M*) complexes *vs.* CNTNF (10^{-3} *M*).

Can. J. Chem. Downloaded from www.nrcresearchpress.com by 210.87.254.42 on 09/05/12
For personal use only.

TABLE 1. Spectral maxima of carbaryl complexes with various acceptors. [Carbaryl] = 10^{-2} M; [acceptor] = 10^{-3} M

Acceptor	λ_{max} of complex (nm)
1,3,5-Trinitrobenzene	370
2,4,5,7-Tetranitro-9-fluorenone	397
2,4,7-Trinitro-9-fluorenone	405
Mellitic Trianhydride	420
9-Dicyanomethylene-2,4,7-trinitrofluorene	475

TABLE 2. Complexing constants from Benesi–Hildebrand plots for selected pesticide–acceptor complexes in solution

Complex	λ_{max} (nm)	ε^{AD}	K_C^{AD}	$\varepsilon^{AD} \cdot K_C^{AD}$
Carbaryl–mellitic trianhydride	420	111	1.80	200
Carbaryl–CNTNF	475	613	3.89	2386
IPC–CNTNF	470	583	1.75	1020
CIPC–CNTNF	450	885	1.12	991
Swep–CNTNF	444	200	2.63	526

(pesticide), respectively, and A is the absorbance of the complex at the wavelength of measurement, was then made for each set of dilution series to calculate the complexing constants. A sample Benesi–Hildebrand plot for the carbaryl–CNTNF complex is given in Fig. 3. Extinction coefficients, ε_λ^{AD}, and formation constants, K_C^{AD}, for the complexes calculated at the wavelength of maximum absorption, λ, are presented in Table 2.

The Benesi–Hildebrand plots obtained in these experiments were linear, and previous workers have taken this as indicative of a simple 1:1 stoichiometry in the complex (9–13). Johnson and Bowen (14) have shown that this is not necessarily so, although the linearity of the plots may be taken as an indication of predominantly a stable 1:1 complex. More recently, this conclusion has been disputed by Deranleau (15), who has discussed the difficulty of determining stoichiometrics of π-complexes from spectroscopic studies. Several solid complexes prepared in a preliminary study of the use of electron-acceptors as chromatographic spray reagents were found by analysis to have 1:1 stoichiometry

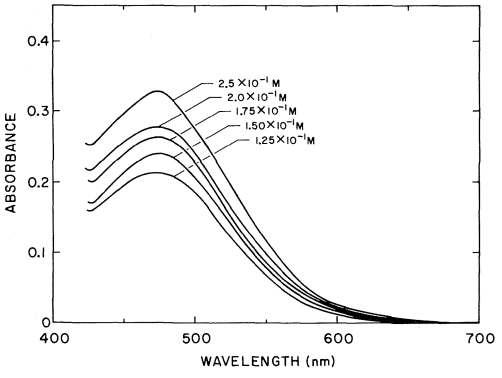

FIG. 2. Solution spectra for dilution series of carbaryl (0.125–0.25 M) – CNTNF (10^{-3} M) complexes measured *vs.* CNTNF (10^{-3} M).

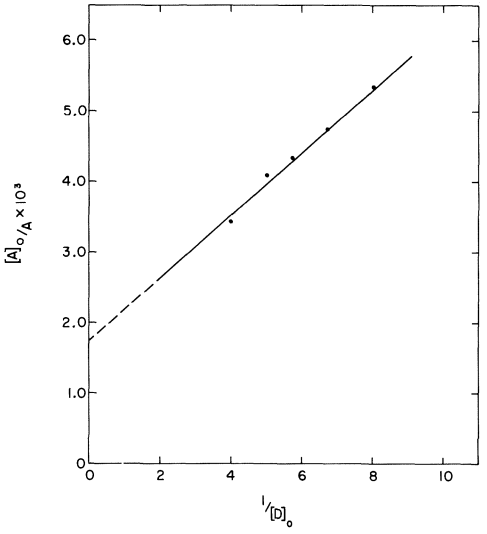

FIG. 3. Benesi–Hildebrand plot for carbaryl–CNTNF complex. $[A]_0$, initial concentration of CNTNF; $[D]_0$, initial concentration of carbaryl; A, absorbance of complex.

(16). Thus, while no analyses have been carried out in this case, there seem to be reasonable grounds to assume that the predominant species both in solution and on the chromatographic thin-layers are 1:1 complexes.

No clear pattern is evident from the extinction coefficients, ε_λ^{AD}, or the complex formation constants, K_C^{AD}. However, the product $\varepsilon_\lambda^{AD} \cdot K_C^{AD}$, which is determined directly from the slope of the Benesi–Hildebrand plot, shows a very definite trend. The four pesticides measured with CNTNF should vary in their abilities to act as donors. As the π-bonding is between the aromatic ring systems in these pesticide complexes (1), the substituent effects are quite important. Thus, while carbaryl might be expected to be the strongest π-donor in the test group due to its enlarged π-system, the relative abilities of the carbamate groups bonded to the ring either through oxygen (carbaryl) or nitrogen (IPC, CIPC, swep) to release electrons into the ring must also be considered. Furthermore, the increasing chlorine content in the series IPC, CIPC, swep should decrease their donor abilities.

The product $\varepsilon_\lambda^{AD} \cdot K_C^{AD}$ seems to follow this general trend. The small difference in the values obtained for IPC and CIPC is not surprising, as the chlorine substituent exhibits a positive resonance effect and a negative inductive effect, and thus should not appreciably alter the π-density of the aromatic system. Two chlorines, however, might be expected to exhibit a more noticeable effect. This seems to be reflected in the results. A similar trend appears in the position of the absorption maximum and the intensity of the bands, as shown in Fig. 1. Secondly, a comparison of results for the carbaryl-CNTNF and carbaryl-mellitic trianhydride complexes shows mellitic trianhydride to be the weaker of these two complexing agents.

Measurements on Cellulose

Equal weights of donor and acceptor were used in preparing these complexes to provide an approximately two-fold excess of donor over acceptor and thereby to force the complexation of the acceptor. Measured against a blank cellulose reference, the reflectance spectra of the complexes appeared as shoulders on the strong u.v.-absorption of the complexing agent CNTNF which extends slightly into the visible region of the spectrum. However, when measured against a CNTNF reference, the reflectance spectra of the complexes become more apparent, as shown in Fig. 4.

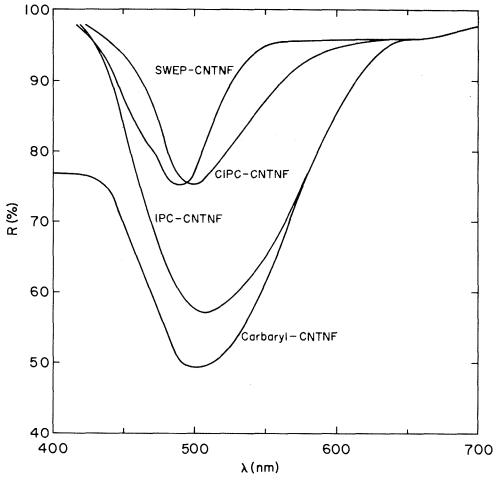

FIG. 4. Reflectance spectra of pesticide–CNTNF complexes on cellulose measured *vs.* a CNTNF reference (on cellulose).

Carbaryl and IPC–CNTNF complexes both show maximum absorption at ~505 nm, with the carbaryl complex being the more intense of the two. The CIPC and swep-CNTNF complexes have similar intensities, but show absorption maxima at ~495 and ~490 nm, respectively. The relative positions of the absorption maxima and the intensities of the bands show similar relationships to those observed in solution for these complexes. Spectral maxima are commonly observed at higher wavelengths in the adsorbed state than those measured for the same species in solution (8).

Plots of reflectance *vs.* concentration (analogous to the peak area *vs.* concentration plots (6, 7)) did not reveal a linear relationship over the larger concentration range (Fig. 5). Kubelka–Munk plots (8) show non-linearity at low concentrations. The failure of these results to satisfy the Kubelka–Munk theory may be attributed to too thin a layer to approximate an infinite layer thickness. However, a plot of reflectance versus the square root of concentration, which approximates the Kubelka–Munk functions and has been used previously in measurements on thin-layer chromatograms (8), was found to yield linear plots over the concentration range studied for all four complexed pesticides. This could thus possibly be used to extend the useful range of analysis (6, 7).

Can. J. Chem. Downloaded from www.nrcresearchpress.com by 210.87.254.42 on 09/05/12
For personal use only.

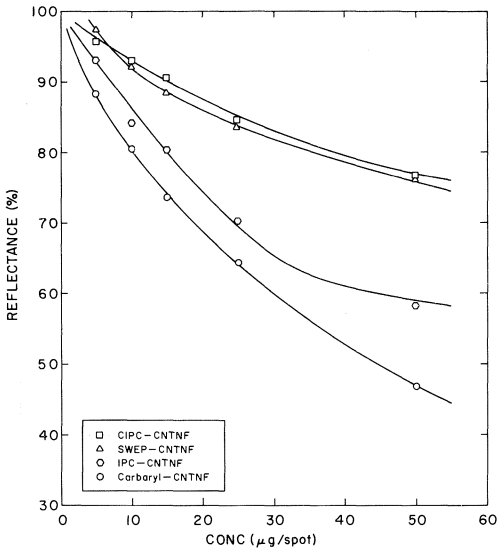

FIG. 5. Reflectance *vs.* concentration for pesticide–CNTNF dilution series, as indicated.

Conclusions

The interactions between some common pesticides and several electron-acceptor reagents resulting in π-complex formation studied in solution and on cellulose thin-layers were quite weak. Extinction coefficients measured in solution were less than 1000. Thus, detection limits for these complexes on thin-layer chromatograms are only about 1 μg, whereas metal–chelate complexes, which have much higher extinction coefficients, may be detected to 0.01 μg (8).

The Benesi–Hildebrand approach provides information as to the relative complexing abilities of various pesticides and could be of use in investigations where this type of information is desired, particularly in those cases where complexation may play a role in the pesticidal activity of the compound.

Complexation occurs more strongly in the adsorbed state on cellulose than in solution. The useful analytical range for the determination of complexed pesticides *in situ* on a thin-layer chromatogram by reflectance spectroscopy may be extended by plotting reflectance (or peak area) *vs.* the square root of concentration. The intensity, broadness, and position of the maxima of the complex absorption band in the absorbance (solution) and reflectance (adsorbed) spectra are related to the relative donor abilities of the pesticides studied.

R. W. F. wishes to thank the Canada Department of Agriculture for grants in support of this work.

J. D. M. is the recipient of a National Research Council of Canada postgraduate scholarship.

The authors thank Miss Marianne Häusler for her assistance in obtaining some of the spectral data.

1. O. HUTZINGER, W. D. JAMIESON, J. D. MACNEIL, and R. W. FREI. J. Ass. Offic. Anal. Chem. **54**, 1100 (1971).
2. J. D. MACNEIL, R. W. FREI, and O. HUTZINGER. Int. J. Environ. Anal. Chem. **1**, 205 (1972).
3. R. D. O'BRIEN. Insecticides: action and metabolism. Academic Press, New York. 1967.
4. W. E. WILSON, L. FISHBEIN, and S. T. CLEMENTS. Sci. **171**, 180 (1971).
5. R. FOSTER. Organic charge transfer complexes. Academic Press, New York. 1969.
6. R. W. FREI, J. D. MACNEIL, and O. HUTZINGER. Int. J. Environ. Anal. Chem. **2**, 1 (1972).
7. J. D. MACNEIL, R. W. FREI, S. SAFE, and O. HUTZINGER. J. Ass. Offic. Anal. Chem. In press.
8. R. W. FREI. CRC Critical Rev. Anal. Chem. **2**, 179 (1971).
9. H. A. BENESI and J. H. HILDEBRAND. J. Am. Chem. Soc. **71**, 2703 (1949).
10. R. M. KEEFER and L. J. ANDREWS. J. Am. Chem. Soc. **72**, 4677 (1950).
11. R. M. KEEFER and L. J. ANDREWS. J. Am. Chem. Soc. **73**, 462 (1951).
12. R. E. MERRIFIELD and W. D. PHILLIPS. J. Am. Chem. Soc. **80**, 2778 (1958).
13. E. M. VOIGT. J. Am. Chem. Soc. **86**, 3611 (1964).
14. G. D. JOHNSON and R. E. BOWEN. J. Am. Chem. Soc. **87**, 1655 (1965).
15. D. A. DERANLEAU. J. Am. Chem. Soc. **91**, 4050 (1969).
16. O. HUTZINGER. Anal. Chem. **41**, 1662 (1969).

Can. J. Chem. Downloaded from www.nrcresearchpress.com by 210.87.254.42 on 09/05/12
For personal use only.

The Preparation and Properties of Some Cyclic β-Diketone Diimines

KENNETH CHARLES MOSS AND FRANK PRICE ROBINSON
Department of Chemistry, University of Victoria, Victoria, British Columbia
Received August 24, 1972

The condensation reaction between a series of aliphatic diamines and a series of five- and six-membered cyclic β-diketones to form Schiff bases was investigated. Mass spectral data show that reaction occurred on the side-chain carbonyl except where steric hindrance forced condensation to occur on the ring carbonyl. N.m.r. studies show that these Schiff bases exist primarily in the ketamine form in solution, irrespective of the solvent. I.r. data confirm this. The preparation of a number of Cu(II) and Ni(II) complexes from some of the ligands is also described.

La réaction de condensation entre une série de composés diaminés aliphatiques et une serie de β-dicétones cycliques à cinq ou six membres pour former les bases de Schiff a été étudiée. Les données obtenues à partir de spectres de masse indiquent que la réaction a lieu sur le groupe carbonyle de la chaîne latérale à l'exception des cas où des contraintes stériques forcent la condensation à se faire sur le groupe carbonyle du cycle. Des études r.m.n. montrent que ces bases de Schiff sont présentes principalement en solution sous la forme cétamine, quelque soit le solvant. Ce fait est d'ailleurs confirmé par des données obtenues en i.r. La préparation d'une série de complexes du Cu(II) et du NI(II) à partir de certains coordinats est aussi décrite. [Traduit par le journal]

Can. J. Chem., **51**, 505 (1973)

Can. J. Chem. Downloaded from www.nrcresearchpress.com by 210.87.254.6 on 09/05/12
For personal use only.

There is considerable interest in the field of metal chelate catalysis, *i.e.*, reactions which are modified by metal ions through chelate ring formation, as well as reactions of metal chelates themselves (1). It has also been established that some metal chelates can act as reversible oxygen carriers (2). Of particular interest to us are the formation and reactions of Schiff bases made by the condensation of β-diketones and diamines. Metal chelates of some such bases have been shown to undergo nonenzymatic transamination similar to that thought to occur in living systems (3). As a preliminary to an investigation of the tautomerization of metal complexes of simpler analogs, thought to be an important step in transamination, we have prepared a number of Schiff bases of β-diketones with saturated five- and six-membered rings. This study was undertaken in order to ascertain which carbonyl group of

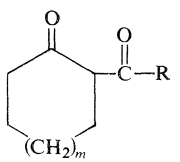

$m = 0, 1$

condenses with the diamine and whether the course of the condensation might be altered by changing the nature of R. We also wished to determine the extent of keto–enol tautomerism (Scheme 1) which esists in solutions of these Schiff bases.

Previous workers (4, 5) have shown that in bases formed with β-diketones containing a methyl group adjacent to one carbonyl function and either CH_3, C_6H_5, CF_3, p-C_6H_4Br, or p-$C_6H_4OCH_3$ adjacent to the other carbonyl, the equilibrium lies well over to the ketamine form **3** (Scheme 1). Our work describes the preparation of 17 new bases and their structure in terms of their mass, n.m.r., and i.r. spectra. Some metal chelates were also prepared.

Results and Discussion

Preparation of Schiff Bases and Metal Chelates

The β-diketones required for preparation of the Schiff bases used in this study were synthesized by acylation of the morpholino enamines of cyclopentanone and cyclohexanone (6). Condensation of the β-diketones with the appropriate diamines afforded the Schiff bases. In a few cases, metal chelates were prepared by reacting the Schiff bases with Cu(II) or Ni(II) acetate.

Mass Spectra and Structure

The bases studied showed quite characteristic behavior upon electron impact. All of the ligands exhibited parent peaks and the base peaks were dependent upon the diamine used. When the original diamine was ethylenediamine, the base

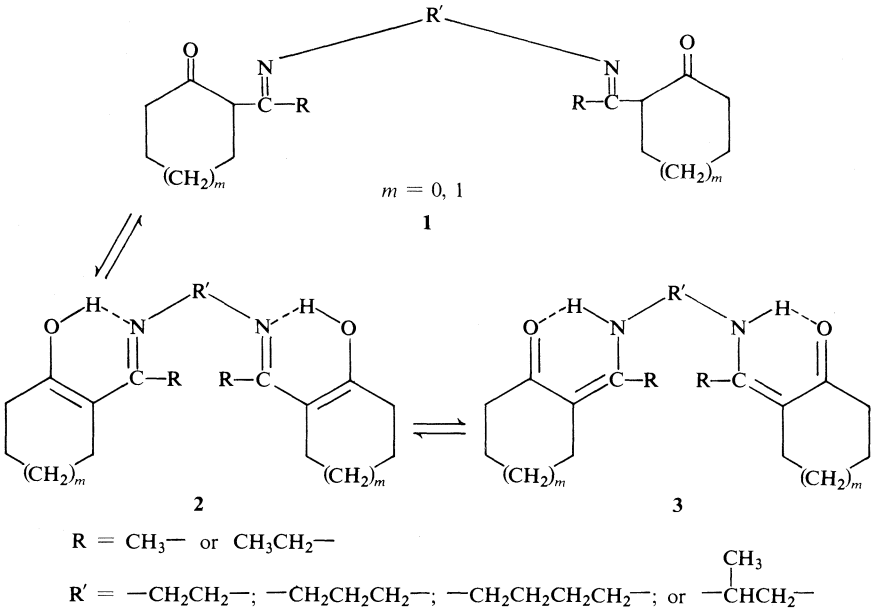

SCHEME 1

peak was one-half the *m/e* of the molecular ion. When the original diamine was 1,3-propanediamine, the base peak was due to the ion still containing two of the three methylene groups of the diamine. With 1,2-propanediamine as precursor, fragmentation occurred at the point of branching to give the more stable secondary carbonium ion as the species responsible for the base peak. With 1,4-butanediamine, symmetrical cleavage of the molecular ion is followed by loss of the alkyl side-chain of the ketone and a hydrogen atom to give the species accounting for the base peak. With the exception of the ligand derived from 2-isobutyrylcyclohexanone, all of the compounds undergo further fragmentation to the ions of cyclopentanone or cyclohexanone. Fragmentation appears to occur as outlined in Scheme 2. The different fragmentation behavior of bis-2-isobutyrylcyclohexanoneethylenediimine is taken as strong evidence that condensation between the original diamine and β-diketone occurred on the ring carbonyl rather than the side-chain carbonyl group. This suggests that if R is sufficiently large, steric hindrance becomes more important than the inductive effect which normally facilitates side-chain carbonyl condensation. The evidence that side-chain carbonyl condensation has not occurred when R = *i*-Pr, is the almost complete absence of the usually intense, characteristic peaks at *m/e* 97 and 69. These peaks are intense in all cyclohexanone-derived ligands with R = Me or Et and are assigned to the ion of cyclohexanone and the species which results from loss of CO from that ion (7). The mass spectrum of bis-2-isobutyrylcyclohexanoneethylenediimine can be adequately rationalized by the fragmentation shown in Scheme 3.

Nuclear Magnetic Resonance Spectra and Structure

The n.m.r. studies suggest that all of the Schiff bases examined exist in solution in the form of chelated hydrogen-bonded tautomers **2** and **3** (Scheme 1). We found no evidence for substantial proportions of the keto form **1** even in acetone solution, *i.e.* no signal was detected for the methine proton at the ring junction in tautomer **1**.

The n.m.r. data are summarized in Table 1 and can be conveniently discussed by considering the Schiff bases according to the diamine used. The solvent used was $CDCl_3$, unless otherwise indicated.

(1) Schiff Bases with Ethylenediamine

In each case there was a broad signal in the region 0.50 to −1.50 τ ($w_{\frac{1}{2}} \sim 20$ Hz), which must be due to a hydrogen-bonded proton. This indicates that the base is primarily in the

Can. J. Chem. Downloaded from www.nrcresearchpress.com by 210.87.254.6 on 09/05/12
For personal use only.

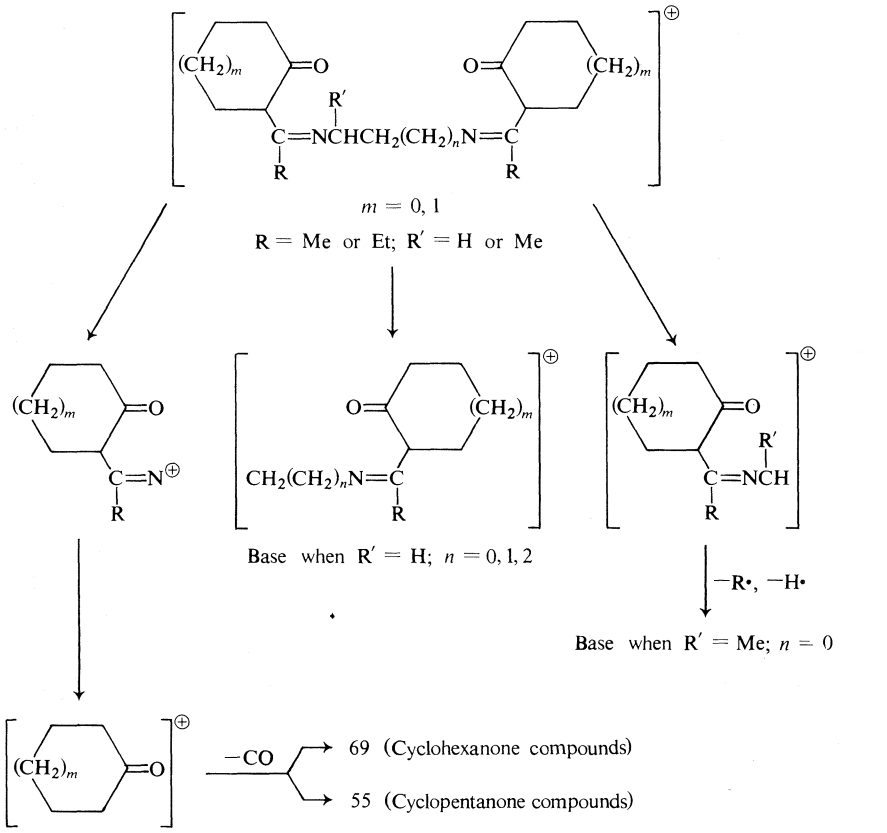

SCHEME 2

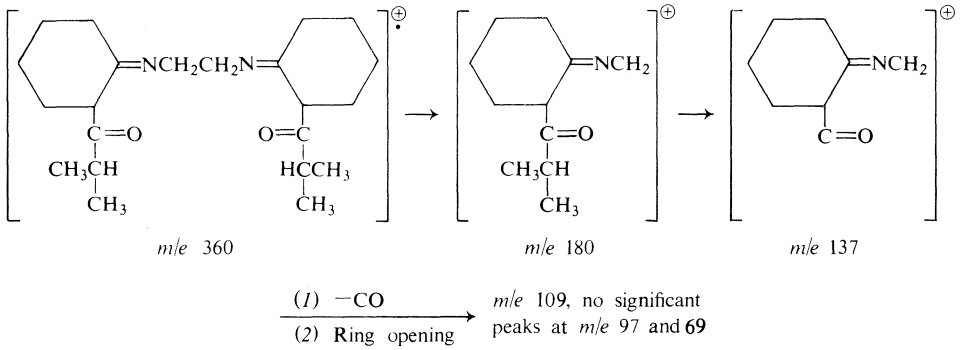

SCHEME 3

hydrogen-bonded form **2** or **3** (Scheme 1). The signal due to the methylene groups of ethylenediamine occur as a multiplet centered at about 6.6 τ. This multiplet consists of three lines of relative intensities approximately 2:1:2 and a splitting of 3.5 Hz. The unusual appearance of this multiplet must be due to coupling with the protons on the nitrogens of the diamine, an explanation used by Dudek and Holm in discussing bis-acetylacetoneethylenediimine (4). However, if the methylene groups are coupled to the proton on N, the spectrum should give a doublet. The presence of the center line probably indicates that there is more than one conformer, produced by rotation about the —C=N bond (4). The possibility that this central band is

Can. J. Chem. Downloaded from www.nrcresearchpress.com by 210.87.254.6 on 09/05/12
For personal use only.

TABLE 1. N.m.r. data of Schiff bases in $CDCl_3$

Compound	τ-Value			
	$R = CH_3$ $R' = CH_3CH_2$	N—H---O	Diamine groups adjacent to N	Cyclic system
Bis-2-acetylcyclopentanoneethylenediimine	R = 7.93	0.65	6.53[a]	8.4[b] 7.7
Bis-2-acetylcyclohexanoneethylenediimine	R = 7.92	−1.50	6.63[a]	8.4[b]
Bis-2-propionylcyclopentanoneethylenediimine	R′ = 8.95 7.72 J = 7 Hz	0.50	6.68[a]	8.2[b]
Bis-2-propionylcyclohexanoneethylenediimine	R′ = 8.98 7.76 J = 7 Hz	−1.50	6.64[a]	8.5[b] 7.7
Bis-2-isobutyrylcyclohexanoneethylenediimine	CH_3 = 8.90 CH = 7.07 J = 7 Hz	−1.82	6.62[a]	8.4[b] 7.7
Bis-2-acetylcyclopentanone-1,3-propanediimine	R = 8.05	−1.68	6.65[c] ~8.1[d]	8.4[b] 7.7
Bis-2-acetylcyclohexanone-1,3-propanediimine	R = 7.93	−0.41	6.68[c] ~8.2[d]	8.4[b] 7.7
Bis-2-propionylcyclopentanone-1,3-propanediimine	R′ = 8.98 7.72 J = 7 Hz	3.5	7.72[c] ~8.1[d]	8.4[b] 7.7
Bis-2-propionylcyclohexanone-1,3-propanediimine	R′ = 8.96 7.74 J = 7 Hz	−1.5	7.74[c] ~8.2[d]	8.4[b] 7.7
Bis-2-acetylcyclopentanonetetramethylenediimine	R = 8.08	0.75	6.77[e] 8.35[f]	7.4–8.5[b]
Bis-2-acetylcyclohexanonetetramethylenediimine	R = 7.95	−1.47	6.80[e] 8.35[f]	7.7[b] 8.4
Bis-2-propionylcyclopentanonetetramethylenediimine	R′ = 8.95 7.75 J = 7 Hz	0.50	6.80[e] 8.35[f]	7.7[b] 8.4
Bis-2-propionylcyclohexanonetetramethylenediimine	R′ = 8.96 7.76 J = 7 Hz	−1.05	6.81[e] 8.35[f]	7.7[b] 8.4
Bis-2-acetylcyclopentanone-1,2-propanediimine	R = 8.13	−0.61	6.73[g] 8.75[i] 6.45[h] J = 6 Hz	7.7[b] 8.4
Bis-2-propionylcyclopentanone-1,2-propanediimine	R′ = 8.92 7.70 J = 7 Hz	0.43	6.78[g] 8.78[i] 6.45[h] J = 6 Hz	7.7[b] 8.4
Bis-2-propionylcyclohexanone-1,2-propanediimine	R′ = 8.96 7.60 J = 7 Hz	−1.7	6.80[g] 8.78[i] 6.45[h] J = 6 Hz	7.7[b] 8.4

[a]Triplet; relative intensities 2:1:2 splitting ~3.5 Hz.
[b]Multiplets due to ring systems.
[c]Quartet; relative intensities 1:3:3:1 splitting 6 Hz.
[d]Multiplet due to central $—CH_2—$ of bridge.
[e]Quintet; relative intensities 1:3.3:2.9:3.3:1 splittings 6, 3, 3, and 6 Hz.
[f]Triplet due to $—CH_2—$ of diamine.
[g]Central methylenes of diamine.
[h]Multiplet due to —CH— of diamine.
[i]Doublet due to CH_3 of diamine.

Can. J. Chem. Downloaded from www.nrcresearchpress.com by 210.87.254.6 on 09/05/12
For personal use only.

Can. J. Chem. Downloaded from www.nrcresearchpress.com by 210.87.254.6 on 09/05/12
For personal use only.

caused by tautomer **1** (Scheme 1) may be discounted by the fact that changing the nature of the solvent has no effect on the shape of the spectrum, but merely shifts the signals. The spectra of bis-2-acetylcyclopentanoneethylenediimine and of the propionyl analog in acetone-d_6/D_2O show considerable modification of the diamine methylene groups and the disappearance of the N—H---O signal. The methylene signal still appears to be a triplet but the center peak is now more intense than the outside peaks and the multiplet is shifted upfield to about 7.5 τ, with a splitting of about 1 Hz. This confirms the assignments of the N—H---O proton and the diamine methylenes and adds weight to the suggestion that the center peak of the multiplet is due to different conformations.

The spectrum of bis-2-isobutyrylcyclohexanoneethylenediimine is basically very similar to the spectra of the other ethylenediamine bases although condensation is, in this case, on the ring and not the side-chain.

(2) Schiff Bases with 1,3-Propanediamine

The N—H---O signals are found in the region −0.5 to −1.7 τ (with the exception of bis-2-propionylcyclopentanone-1,3-propanediimine which has an unusually high field signal). The signals for the diamine occur in two regions. The methylenes adjacent to the N occur as a quartet (J = 6 Hz) and the central methylene group gives a multiplet at ~8.1 τ. Coupling with the N—H---O proton and with the central methylene protons should split the methylenes adjacent to the N into two triplets; however, if they overlap, *i.e.* $J_{CH_2-CH_2} = J_{CH_2-NH}$ = 6 Hz then a normal quartet will occur. This is consistent with the results of previous workers (4, 5) on other 1,3-propanediimine bases. The central methylene group of the diamine should give a quintet (J = 6 Hz) but is partially obscured by the signals of the cyclic systems. Spin decoupling of the deuterated bases established that the center of the multiplet is at ~8.2 τ. Deuteration (in pyridine/D_2O) caused collapse of the signal attributed to N—H---O and collapse of the quartet to a triplet (J = 6 Hz), thus confirming the assignments.

(3) Schiff Bases with 1,4-Butanediamine

The N—H---O signals occur between 0.8 and −1.5 τ. The multiplet due to the central methylene groups of the diamine bridge were shown by spin-decoupling and by comparison with the spectra of the ethylenediimine analogs to be centered at 8.35 τ in each of the four compounds. The signals due to the methylene groups adjacent to the N atoms occur as a quintet. The relative intensities of the lines are ~1:3.3:2.9:3.3:1 and the splittings are 6, 3, 3, and 6 Hz, respectively. Coupling of the terminal methylene groups with the adjacent methylene group will give a triplet. This will be further split by the N—H---O proton to give a doublet of triplets. This quintet can be explained by assuming a quartet due to $J_{CH_2-CH_2} = J_{CH_2-NH}$ = 6 Hz and the central peak due to different conformers. Deuteration of bis-2-acetylcyclohexanonetetramethylenediimine causes the N—H---O signal to disappear and the central peak of the quintet to grow. After 15 h in a pyridine/D_2O solution this peak has the form of a poorly resolved triplet (J = 6 Hz), the poor resolution being attributed to the underlying peak due to other conformers. Spin decoupling of the N—H---O signal of the same compounds in pyridine gives the same results. Low temperature spectra of deuterated and undeuterated samples showed only a broadening of the bridge proton signal and collapse of the fine structure. Consequently no real confirmation was obtained for the presence of other conformers.

(4) Schiff Bases with 1,2-Propanediamine

The absorptions due to N—H---O occur in the range ~0.5 to −2.4 τ. In these compounds there is magnetic and steric inequivalence at each end of the diamine group

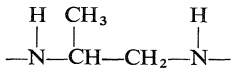

Coupling of the methine proton with the methyl group will give a doublet (~8.8 τ, J = 6 Hz). Coupling of the CH_3 group and the N—H proton with the methine proton should give a doublet of quartets; this will be further split by coupling with the bridge —CH_2— to give a 24-line multiplet. The —CH_2— signal should be a doublet of doublets due to coupling with the —CH— and —NH protons. The actual spectrum is shown in Fig. 1. The low field multiplet consists of ten lines and the high field multiplet is a distorted triplet. The integrated ratios are 1:2

and are therefore assigned to the bridge —CH— and —CH_2— groups, respectively. This is confirmed by double resonance experiments. Irradiation of the low field multiplet causes callapse

Can. J. Chem. Downloaded from www.nrcresearchpress.com by 210.87.254.6 on 09/05/12
For personal use only.

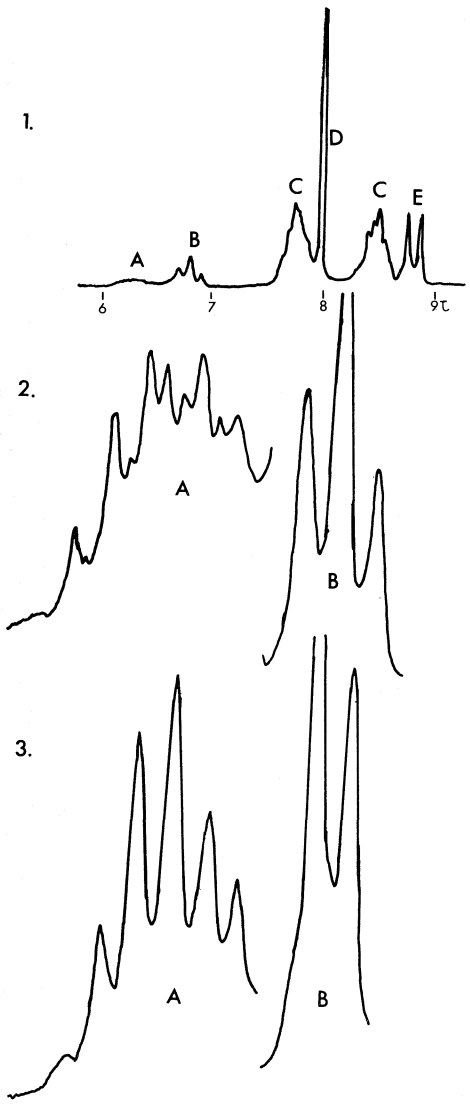

FIG. 1. (1) ^{1}H n.m.r. spectrum of bis-2-acetylcyclohexanone-1,2-propanediimine. A: —CH—; B: $—CH_2—$; C: cyclic system; D: $CH_3—C(=O)—$; E: methyl of —N(H)—CH(CH_3). (2) A and B under higher resolution. (3) A and B under higher resolution and deuterated.

of the CH_3— doublet, whereas irradiation of the high field triplet has no effect on the CH_3— signal. Deuteration of the chloroform solution with D_2O causes a rapid change in the spectrum (see Fig. 1). The low field multiplet becomes a distorted sextet (J = 6 Hz) and the high field multiplet a distorted doublet (J = 6 Hz). The distortions are partly due to the overlap of the two multiplets, but are also due to some deviation from a first order spectrum. Again irradiation of the low field multiplet causes collapse of the CH_3— doublet, whereas irradiation of the high field multiplet does not. J_{CH-CH_2} and J_{CH-CH_3} are both equal to 6 Hz and in the deuterated spectrum the —CH— multiplet would then be expected to be a regular sextet and the $—CH_2—$ multiplet a doublet. In the undeuterated spectrum and with an H—N—CH— coupling constant of 3 Hz the —CH— multiplet should consist of 12 lines of relative intensities 1:1:5:5:10:10:10:10:5:5:1:1. In the multiplet observed, only ten lines can be picked out. If the coupling constant H—N—CH_2— is 6 Hz (as in the cases with the other diamines) then the signal due to $—CH_2—$ should be a regular triplet due to the coincidence of the two doublets. To confirm the assignments of these two multiplets the spectrum of bis-trifluoroacetylacetone-1,2-propanediimine was examined. The signal of the —CH— group was again a ten line multiplet which, on deuteration, changed to a sextet; the $—CH_2—$ multiplet was again a triplet which simplified to a doublet on deuteration.

Infrared Spectra and Structure

The i.r. spectra of the ligands corroborate the conclusions drawn on the basis of the mass and n.m.r. spectra. The cyclopentanone-derived ligands all exhibit broad absorptions around 3200 cm^{-1} due to the hydrogen-bonded stretching vibration of either an O—H group (structure **2**, Scheme 1) or of a N—H group (structure **3**, Scheme 1) (8). All of these five-membered ring derivatives also show strong absorptions at 1625 cm^{-1} due to C=O stretching vibrations, shifted from the normal cyclopentanone value (9) of 1745 cm^{-1} because of both conjugation and hydrogen-bonding. The cyclohexanone-derived ligands have the corresponding absorptions at about 3450 (bonded OH or HN) and 1590 cm^{-1} (hydrogen-bonded C=O). Thus, the ligands appear to be tautomeric mixtures of structures **2** and **3** (Scheme 1). As expected, both the 3200–3450 and 1625–1590 cm^{-1} bands (1) are absent in the i.r. spectra of the metal chelates prepared.

Additional metal chelates will be prepared and both the ligands and their metal chelates

Can. J. Chem. Downloaded from www.nrcresearchpress.com by 210.87.254.6 on 09/05/12
For personal use only.

will be hydrolyzed in an attempt to observe tautomerization and determine what factors influence the course of this key reaction in the transamination process.

Experimental

Melting points were determined on a Bock-Monoscop hot stage microscope and are uncorrected. The i.r. spectra were recorded in KBr discs, thin films, or $CHCl_3$ solution on a Perkin–Elmer 337B Spectrophotometer. The n.m.r. spectra were obtained with a Varian HA-60-IL or Perkin–Elmer R-12 Spectrometer in $CDCl_3$, unless specified otherwise, using TMS as internal standard. Mass spectra were obtained on a Hitachi Perkin–Elmer RMU-6E or an AEI-MS9 Spectrometer, using an ionizing energy of 70 eV. Analyses were performed by Dr. Alfred Bernhardt, Mülheim, Germany, Dr. C. Daesslé, Montreal, Quebec, or the Microanalytical Laboratory, Chemistry Department, University of Alberta, Edmonton, Alberta.

Preparation of Ketones

1-Morpholino-1-cyclohexene

The procedure of Hünig *et al.* (6) was used. The fraction boiling at 72–75°/0.01 Torr was collected to give an 80% yield of 1-morpholino-1-cyclohexene, lit. b.p. 118–120°/10 Torr (6).

1-Morpholino-1-cyclopentene

The same procedure was used as for 1-morpholino-1-cyclohexene. The fraction boiling at 53–55°/0.1 Torr was collected to give a 95% yield of 1-morpholino-1-cyclopentene, lit. b.p. 104–106°/12 Torr (10).

2-Acetylcyclopentanone

The procedure of Stork *et al.* (10) was used to acetylate 1-morpholino-1-cyclopentene. After hydrolysis and work-up, the fraction boiling at 42–44°/0.5 Torr was collected as 2-acetylcyclopentanone, lit. b.p. 79–81°/12 Torr (11); yield 40%.

2-Propionylcyclopentanone

The same procedure (10) was used as for 2-acetylcyclopentanone. A 74% yield of 2-propionylcyclopentanone was obtained, b.p. 45–48°/0.4 Torr, lit. b.p. 96–99°/17 Torr (12).

2-Acetylcyclohexanone

The same procedure (10) as for the acylcyclopentanones was used to yield 51% of 2-acetylcyclohexanone, b.p. 53–55°/1 Torr, lit. b.p. 106–108°/14 Torr (13).

2-Propionylcyclohexanone

The preceding procedure was used to afford a 46% yield of 2-propionylcyclohexanone, b.p. 68–70°/1 Torr, lit. b.p. 110–116°/12 Torr (14).

2-Isobutyrylcyclohexanone

The procedure of Hünig *et al.* (14) was used, affording a 23% yield of 2-isobutyrylcyclohexanone, b.p. 63–64°/0.1 Torr.

Preparation of Schiff Bases

General Method

The diamine was added dropwise to a stirred solution of the β-diketone in 30–60° petroleum ether (1:2 molar ratio of diamine to β-diketone). The resulting solution was stirred for 1 h and then concentrated on a rotary evaporator. In most instances, a solid product resulted which could be purified by recrystallization. In those cases in which an oil resulted, the product was separated by chromatography on neutral Al_2O_3 (activity III) and then recrystallized.

2-Acetylcyclopentanone

(*a*) *With ethylenediamine*

White plates from heptane, m.p. 152–153°; i.r. (KBr) 3200 (bonded OH or NH), 1625 cm^{-1} (C=O); n.m.r., see Table 1; mass spectrum (70 eV) *m/e* (relative intensity) 276(50), 152(38), 138(100), 124(80), 123(13), 109(15), 96(40), 83(3), 81(24), 55(24).

Anal. Calcd. for $C_{16}H_{24}N_2O_2$: C, 69.52; H, 8.75; N, 10.13. Found: C, 69.51; H, 8.65; N, 10.18.

(*b*) *With 1,3-propanediamine*

White crystals from heptane, m.p. 80.5–81.0°; i.r. (KBr) 3200 (bonded OH or NH), 1625 cm^{-1} (C=O); n.m.r., see Table 1; mass spectrum (70 eV) *m/e* (relative intensity) 290(56), 152(100), 138(71), 137(46), 124(49), 96(24), 83(16), 55(12).

Anal. Calcd. for $C_{17}H_{26}N_2O_2$: C, 70.30; H, 9.02; N, 9.64. Found: C, 70.21; H, 8.95; N, 9.59.

(*c*) *1,4-Butanediamine*

White needles from Et_2O, m.p. 109–111°; i.r. (KBr) 3240 (bonded OH or NH), 1625 cm^{-1} (C=O); n.m.r., see Table 1; mass spectrum (70 eV) *m/e* (relative intensity) 304(71), 152(42), 138(69), 137(36), 136(100), 124(61), 109(12), 96(21), 83(8), 81(21), 55(28).

Anal. Calcd. for $C_{18}H_{28}N_2O_2$: C, 71.01; H, 9.27; N, 9.20. Found: C, 70.55; H, 9.26; N, 9.33.

(*d*) *With 1,2-propanediamine*

Pale yellow crystals from Et_2O, m.p. 127–128°; i.r. (KBr) 3250 (bonded OH or NH), 1625 cm^{-1} (C=O); n.m.r., see Table 1; mass spectrum (70 eV) *m/e* (relative intensity) 290(23), 152(100), 138(71), 124(29), 109(18), 96(20), 83(9), 81(35), 55(25).

Anal. Calcd. for $C_{17}H_{26}N_2O_2$: C, 70.30; H, 9.02; N, 9.64. Found: C, 70.17; H, 8.88; N, 9.43.

2-Propionylcyclopentanone

(*a*) *With ethylenediamine*

Tan crystals from heptane, m.p. 126–127°; i.r. (KBr) 3260 (bonded OH or NH), 1625 cm^{-1} (C=O); n.m.r., see Table 1; mass spectrum (70 eV) *m/e* (relative intensity) 304(59), 152(100), 138(31), 124(61), 123(23), 109(17), 83(7), 55(14).

Anal. Calcd. for $C_{18}H_{28}N_2O_2$: C, 71.01; H, 9.27; N, 9.20. Found: C, 70.90; H, 9.11; N, 9.36.

(*b*) *With 1,3-propanediamine*

Yellow crystals from heptane, m.p. 152–153°; i.r. (KBr) 3240 (bonded OH or NH), 1625 cm^{-1} (C=O); n.m.r., see Table 1; mass spectrum (70 eV) *m/e* (relative intensity) 318(51), 166(100), 152(38), 138(68), 83(6), 55(11).

Unstable sample, not analyzed.

(*c*) *With 1,4-butanediamine*

White plates from heptane, m.p. 135.0–135.5°; i.r. (KBr) 3250 (bonded OH or NH), 1625 cm^{-1} (C=O); n.m.r., see Table 1; mass spectrum (70 eV) *m/e* (relative intensity) 332(52), 166(21), 138(62), 137(72), 136(100), 123(13), 95(10), 83(4), 55(19).

Anal. Calcd. for $C_{20}H_{32}N_2O_2$: C, 72.24; H, 9.70; N, 8.42. Found: C, 72.38; H, 9.63; N, 8.54.

(*d*) *With 1,2-propanediamine*

Tan crystals from heptane, m.p. 85.5–86.0°; i.r. (KBr)

Can. J. Chem. Downloaded from www.nrcresearchpress.com by 210.87.254.6 on 09/05/12
For personal use only.

3240 (bonded OH or NH), 1625 (C=O); n.m.r., see Table 1; mass spectrum (70 eV) *m/e* (relative intensity) 318(33), 166(100), 138(23), 124(50), 95(8), 83(5), 55(17).

Anal. Calcd. for $C_{19}H_{30}N_2O_2$: C, 71.65; H, 9.49; N, 8.79. Found: C, 71.53; H, 9.45; N, 8.70.

2-Acetylcyclohexanone

(*a*) *With ethylenediamine*

Yellow crystals from heptane, m.p. 142.0–142.5°; i.r. (KBr) 3450 (bonded OH or NH), 1590 cm^{-1} (C=O); n.m.r., see Table 1; mass spectrum (70 eV) *m/e* (relative intensity) 304(41), 165(62), 152(100), 138(70), 123(7), 110(28), 97(6), 95(12), 69(7).

Anal. Calcd. for $C_{18}H_{28}N_2O_2$: C, 71.02; H, 9.27; N, 9.20. Found: C, 70.93; H, 9.04; N, 9.37.

(*b*) *With 1,3-propanediamine*

Yellow crystals from heptane, m.p. 115.2–115.5°; i.r. (KBr) 3450 (bonded OH or NH), 1590 cm^{-1} (C=O); n.m.r., see Table 1; mass spectrum (70 eV) *m/e* (relative intensity) 318(55), 166(100), 138(85), 124(14), 110(75), 97(5), 95(9), 69(7).

Anal. Calcd. for $C_{19}H_{30}N_2O_2$: C, 71.65; H, 9.49; N, 8.80. Found: C, 71.61; H, 9.52; N, 8.76.

(*c*) *With 1,4-butanediamine*

Yellow crystals from heptane, m.p. 141.5–144.5°; i.r. (KBr) 3450 (bonded OH or NH), 1590 cm^{-1} (C=O); n.m.r., see Table 1; mass spectrum (70 eV) *m/e* (relative intensity) 332(39), 166(18), 151(21), 150(100), 138(72), 123(12), 110(27), 97(15), 95(10), 69(14).

No analysis, compound unstable.

(*d*) *With 1,2-propanediamine*

Yellow crystals from heptane, m.p. 71.0–73.5°; i.r. (KBr) 3450 (bonded OH or NH), 1590 cm^{-1} (C=O); n.m.r., see Table 1; mass spectrum (70 eV) *m/e* (relative intensity) 318(18), 166(100), 152(24), 138(17), 123(10), 97(6), 69(7).

No analysis, compound unstable.

2-Propionylcyclohexanone

(*a*) *With ethylenediamine*

Pale yellow crystals from heptane, m.p. 97–98°; i.r. (KBr) 3450 (bonded OH or NH), 1590 cm^{-1} (C=O); n.m.r., see Table 1; mass spectrum (70 eV) *m/e* (relative intensity) 332(29), 166(100), 152(4), 150(12), 138(30), 97(1), 69(2).

Anal. Calcd. for $C_{20}H_{32}N_2O_2$: C, 72.24; H, 9.70; N, 8.42. Found: C, 72.13; H, 9.66; N, 8.44.

(*b*) *With 1,3-propanediamine*

White needles from heptane, m.p. 89.0–89.5°; i.r. (KBr) 3450 (bonded OH or NH), 1590 cm^{-1} (C=O); n.m.r., see Table 1; mass spectrum (70 eV) *m/e* (relative intensity) 346(71), 180(100), 166(35), 152(65), 137(9), 124(15), 110(61), 97(2), 69(4).

Anal. Calcd. for $C_{21}H_{34}N_2O_2$: C, 72.78; H, 9.89; N, 8.08. Found: C, 72.53; H, 10.07; N, 8.03.

(*c*) *With 1,4-butanediamine*

White needles from heptane, m.p. 85.5–86.0°; i.r. (KBr) 3450 (bonded OH or NH), 1590 cm^{-1} (C=O); n.m.r., see Table 1; mass spectrum (70 eV) *m/e* (relative intensity) 360(43), 180(20), 152(71), 151(36), 150(100), 137(15), 124(15), 110(21), 97(5), 69(4).

Anal. Calcd. for $C_{22}H_{36}N_2O_2$: C, 73.28; H, 10.06; N, 7.77. Found: C, 73.20; H, 9.92; N, 7.62.

(*d*) *With 1,2-propanediamine*

White plates from heptane, m.p. 84–85°; i.r. (KBr) 3450 (bonded OH or NH), 1590 cm^{-1} (C=O); n.m.r., see Table 1; mass spectrum (70 eV) *m/e* (relative intensity) 346(13), 180(100), 166(15), 152(16), 138(17), 124(10), 97(1), 69(2).

Anal. Calcd. for $C_{21}H_{34}N_2O_2$: C, 72.78; H, 9.89; N, 8.08. Found: C, 72.88; H, 9.54; N, 8.03.

2-Isobutyrylcyclohexanone

With ethylenediamine

White crystals from heptane, m.p. 120.5–121.5°; i.r. (KBr) 3450 (bonded OH or NH), 1590 cm^{-1} (C=O); n.m.r., see Table 1; mass spectrum (70 eV) *m/e* (relative intensity) 360(27), 193(41), 180(100), 138(45), 137(36), 122(9).

Anal. Calcd. for $C_{22}H_{36}N_2O_2$: C, 73.29; H, 10.07; N, 7.77. Found: C, 72.61; H, 10.35; N, 7.87.

Preparation of Metal Chelates

General Method

To a hot, stirred solution of the Schiff base in absolute EtOH was added an equimolar amount of anhydrous Cu(II) or Ni(II) acetate. The resulting solution was refluxed for 24 h, the volume reduced on a rotary evaporator, and cooled to precipitate the product. The product was purified in each case by recrystallization.

Bis-2-acetylcyclopentanoneethylenediimino Cu(II)

Purple crystals from EtOH, m.p. 168–173° (dec.); i.r. (KBr) 1570, 1500 cm^{-1} (C=O) (8). The 3200 and 1625 cm^{-1} bands present in the Schiff base precursor are not observed.

Bis-2-acetylcyclohexanoneethylenediimino Cu(II)

Purple crystals from EtOH, m.p. 202–204° (dec.); i.r. (KBr) 1572, 1558 cm^{-1} (C=N) (8).

Anal. Calcd. for $C_{18}H_{28}N_2O_2Cu$: Cu, 17.26. Found: Cu, 17.18.

Bis-2-acetylcyclohexanoneethylenediimino Ni(II)

Deep purple needles from acetone, m.p. 252–254° (dec.); i.r. (KBr) 1575, 1550 cm^{-1} (C=N) (8).

Anal. Calcd. for $C_{18}H_{28}N_2O_2Ni$: Ni, 16.18. Found: Ni, 15.95.

The authors thank the National Research Council of Canada and the University of Victoria Committee on Research, Leave, and Travel for generous financial support. Our thanks are also extended to J. A. Chapman, R. J. Anderson, and R. W. Britten for their help as undergraduate student assistants.

1. A. E. MARTELL. Pure and Appl. Chem. **12**, 129 (1968).
2. K. UENO and A. E. MARTELL. J. Am. Chem. Soc. **60**, 1270 (1956) and refs. cited therein.
3. D. E. METZLER and E. E. SNELL. J. Am. Chem. Soc. **74**, 979 (1952). D. E. METZLER, J. B. LONGNECKER, and E. E. SNELL. J. Am. Chem. Soc. **76**, 639 (1954). D. E. METZLER, J. OLIVARD, and E. E. SNELL. J. Am. Chem. Soc. **76**, 644 (1954).
4. G. O. DUDEK and R. H. HOLM. J. Am. Chem. Soc. **83**, 2099 (1961).
5. P. J. MCCARTHY and A. E. MARTELL. Inorg. Chem. **6**, 781 (1967).

6. S. HÜNIG, E. LÜCKE, and W. BRENNINGER. Org. Syn. **41**, 65 (1961).
7. J. H. BEYNON, R. A. SAUNDERS, and A. E. WILLIAMS. Appl. Spectrosc. **14**, 95 (1960).
8. K. UENO and A. E. MARTELL. J. Am. Chem. Soc. **59**, 998 (1955).
9. K. NAKANISHI. Infrared absorption spectroscopy—practical. Holden-Day, Inc., San Francisco. 1964. p. 42.
10. G. STORK, A. BRIZZOLARA, H. LANDESMAN, J. SZMUSZKOVICZ, and R. TERRELL. J. Am. Chem. Soc. **85**, 207 (1963).
11. B. EISTERT and R. WESSENDORF. Chem. Ber. **94**, 2590 (1961).
12. S. HÜNIG and W. LENDLE. Chem. Ber. **93**, 909 (1960).
13. G. VARON and J. M. CONIA. Compt. rend. **233**, 876 (1951).
14. S. HÜNIG, E. BENZING, and E. LÜCKE. Chem. Ber. **90**, 2833 (1957).

Can. J. Chem. Downloaded from www.nrcresearchpress.com by 210.87.254.6 on 09/05/12
For personal use only.

Isotopic Studies of the Metal–Ligand Bond. Part II. The Far Infrared Spectra of Some Binuclear and Polymeric Copper Carboxylate Derivatives; Variable Temperature and Isotopic Studies of the Copper–Ligand Vibrations

A. B. P. Lever and B. S. Ramaswamy

Department of Chemistry, York University, Downsview, Ontario, M3J 1P3

Received July 14, 1972

The far infrared spectra of 16 adducts of pyridine, quinoline, isoquinoline, urea, aniline, *o*- and *p*-toluidine with copper acetate, propionate, and butyrate, and of copper formate tetrahydrate were recorded at ambient temperature and at −196 °C. A range of derivatives were prepared containing isotopically pure ^{65}Cu. The spectra of these derivatives were used to identify, unequivocally, the copper–oxygen stretching frequencies.

Complexes believed to be polymeric (aniline and toluidine adducts) exhibit one copper–oxygen stretching vibration between 300 and 350 cm^{-1}. A second band, lying between 350 and 400 cm^{-1} is not isotopically sensitive. The dimeric complexes exhibit one or two bands in the 300–400 cm^{-1} region, all of which are isotopically sensitive. Certain of the amine adducts exhibit an isotopically sensitive band near 240 cm^{-1} assignable to a Cu—N stretching mode.

Les spectres dans l'infrarouge lointain de 16 adduits entre la pyridine, quinoléine, urée, aniline, *o*- et *p*-toluidine et l'acétate, propionate, butyrate de cuivre et formiate de cuivre tétrahydraté ont été enregistrés à la température ambiante et à −196 °C. Une série de dérivés contenant du ^{65}Cu, de pureté isotopique, ont été préparés. Les spectres de ces dérivés ont été utilisés pour identifier de façon non équivoque, les fréquences d'élongation entre le cuivre et l'oxygène. Les complexes, qu'on pense être des polymères, exibent une vibration d'élongation oxygène–cuivre, entre 300 et 350 cm^{-1} (adduits de l'aniline et de la toluidine). Une seconde bande, entre 350 et 400 cm^{-1}, n'est pas sensible à l'effet isotopique. Les complexes dimères montrent une ou deux bandes dans la région 300–400 cm^{-1}, toutes sensibles à l'effet isotopique. Pour certains adduits avec les amines, on observe une bande proche de 240 cm^{-1} et sensible à l'effet isotopique, attribuée à la vibration Cu–N.

[Traduit par le journal]

Can. J. Chem., **51**, 514 (1973)

The recent publication (1) of the X-ray structure of the *p*-toluidine adduct of copper propionate revealed that this complex has a polymeric structure (Fig. 1*a*) rather than the conventional binuclear arrangement (Fig. 1*b*) expected for most copper carboxylate derivatives (2, 3).

Magnetic studies (2, 3) had previously revealed that aniline adducts had markedly higher room temperature magnetic moments (*i.e.* lower exchange energies) than many other adducts and various proposals had been made to interpret this observation. It now seems credible that all aniline type adducts are in fact polymeric rather than dimeric. Since the electronic spectra of the aniline adducts do not differ in a significant fashion from, say, the dimeric pyridine adducts (2, 3), far infrared spectroscopy is used here to see whether a distinction might be made on the basis of the copper–oxygen stretching vibrations. Such a distinction should be possible in view of the observation (1) that the polymeric complex, copper propionate *p*-toluidine, contains at least three different types of Cu—O bond (Fig. 1*a*), whilst in the dimers the Cu—O bonds are probably all equivalent (Fig. 1*b*). Very recently, Mabbs and co-workers (4) showed that the trihydrate solvate of the *p*-toluidine adduct of copper acetate was not dimeric, but contained chains of copper atoms linked by bridging water molecules. They also suggested that the aniline type adducts may involve polymeric rather than dimeric structures and presented some magnetic and electron spin resonance data in support of this contention.

Experimental

Physical Measurements

The room temperature far infrared spectra were obtained as Nujol mulls between polythene plates utilizing a Beckman IR12 spectrophotometer. Low temperature spectra were obtained with the same instrument using a Beckman (Model VLT-2) Variable Tem-

Can. J. Chem. Downloaded from www.nrcresearchpress.com by 86.111.144.194 on 09/06/12
For personal use only.

Can. J. Chem. Downloaded from www.nrcresearchpress.com by 86.111.144.194 on 09/06/12
For personal use only.

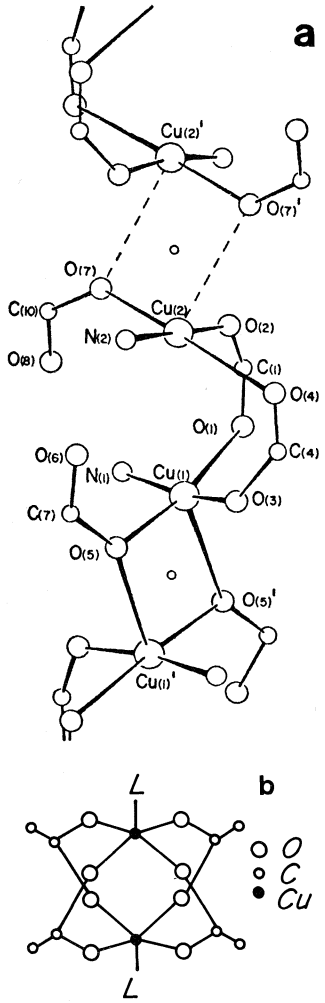

FIG. 1. (*a*) A view of a section of the one-dimensional polymeric structure of copper propionate *p*-toluidine. The copper oxygen distances are: Cu(1)—O(1) = Cu(1)—O(3) = 1.92 Å; Cu(1)—O(5) = 1.95 Å; Cu(1)—O(5)′ = 2.31 Å; Cu(2)—O(7)′ = 2.46 Å (reproduced by permission of the Authors, and of the American Chemical Society, from ref. (1)).

(*b*) Schematic structure of a dimeric copper carboxylate adduct.

perature Cell (with polythene windows), the sample having been ground intimately with regenerated polythene powder and compressed with a laboratory press into a thin opaque disc. These data were obtained with the instrument scanning at the rate of 8 cm^{-1}/min. The ^{65}Cu data and the natural copper data with which they were compared were scanned at the rate of about 1–2 cm^{-1}/min. For sharp absorption the accuracy will be ± 0.2 cm^{-1}, but for the more broad bands it was not possible to ascertain the centers of the band maxima with such accuracy. The data quoted are the average values from at least three scans.

Preparation of the Complexes

Previously described complexes were prepared by the literature route, recrystallized from an appropriate solvent and analyzed for copper. The copper analyses and bibliography are as follows: (calculated and found values for Cu (%)): copper acetate pyridine, (2, 3) 24.4, 24.4; copper acetate urea (5), 26.3, 26.1; copper acetate quinoline (6), 20.4, 20.3; copper propionate urea (5), 23.55, 23.1; copper propionate *p*-toluidine (1), 20.0, 19.8; copper propionate aniline (4), 21.0, 21.2; copper propionate pyridine (7) 22.0, 21.9; copper butyrate pyridine (3) 20.0, 19.4; copper butyrate *p*-toluidine (3), 18.4, 19.7; copper butyrate aniline (3), 18.4, 18.7; copper butyrate urea (5) 21.3, 21.1; copper formate tetrahydrate (8), 28.2, 28.1.

The isoquinoline derivatives were prepared by mixing the anhydrous copper alkanoate with isoquinoline in stoichiometric proportions in chloroform, and warming. The solid product was purified by soxhlet extraction with chloroform.

Copper Acetate Isoquinoline

Anal. Calcd. for $C_{13}H_{13}CuNO_4$: C, 50.2; H, 4.2; Cu, 20.4. Found: C, 50.35; H, 3.8; Cu, 20.5.

Copper Propionate Isoquinoline

Anal. Calcd. for $C_{15}H_{17}CuNO_4$: C, 53.2; H, 5.1; Cu, 18.75. Found: C, 52.9; H, 5.3; Cu, 18.6.

Copper Butyrate Isoquinoline

Anal. Calcd. for $C_{17}H_{21}CuNO_4$: C, 55.6; H, 5.8; Cu, 17.3. Found: C, 56.0; H, 6.0; Cu, 17.4.

Copper Propionate o-Toluidine

This compound was prepared by fusing anhydrous copper propionate with neat *o*-toluidine at 50–80° until a green product was obtained; this was then recrystallized from acetone.

Anal. Calcd. for $C_{13}H_{19}CuNO_4$: C, 49.3; H, 6.0; Cu, 20.1. Found: C, 49.2; H, 6.3; Cu, 20.4.

Results and Discussion

Despite the wealth of data which has appeared concerning copper carboxylates and their adducts, far infrared studies of the metal–ligand frequencies have, with the exception of some reports by Wasson *et al.* (9), Heyns (10), and Lorenzelli and Gesmundo (11), escaped attention. These authors assigned a series of bands between 400 and 250 cm^{-1} in copper acetate complexes to copper oxygen stretching vibrations. In order to confirm these assignments and to determine whether the far infrared region can be used to distinguish dimers from polymers, the far infrared data of a wide series of compounds were recorded and are presented in Table 1. Comparison of the spectra of the copper carboxylates with those of the corresponding alkali metal salts does indeed suggest that additional bands appearing in the copper spectra

TABLE 1. Far infrared data (200–430 cm^{-1})

Complex	Temperature*	Wavenumber†						
$Cu(HCO_2)_2.4H_2O$	r.t.	224s	271m	330s	343m	425brs		
(M)‡	l.t.	230m	277m	334s	350m	430vs		
$Cu(CH_3CO_2)_2$.Urea	r.t.	210vs	(235)	(242)	255m	273s	*355s*§	403s
(D)	l.t.	211s	237w	(247)	257m	278vs	*357vs*	398vs
$Cu(CH_3CO_2)_2$.Isoquinoline	r.t.	239s	256s	278w	*348brs*	*387m*	400w	
(D)	l.t.	220w	236s	270s	295w	*348vs*	*362vs*	389m
		400m						
$Cu(CH_3CO_2)_2$.Quinoline	r.t.	204w	235s	265s	*354vs*	*392m*	400m	
(D)	l.t.	209w	237s	273vs	*351vs*	*365vs*	*392s*	401s
$Cu(CH_3CO_2)_2$.Pyridine	r.t.	*239s*	268vs		*355vs*	419s		
(D)	l.t.	221w	*238s*	264vs	*358vs*	416m	423m	
$Cu(C_2H_5CO_2)_2$.Isoquinoline	r.t.	200s	*308s*	*372brvs*				
(D)	l.t.	206s	262brs	(306)	*315s*	(*371*)	*375vs*	*383s*
		390s						
$Cu(C_2H_5CO_2)_2$.Pyridine	r.t.	198vs	*251m*	267m	295m	*322s*	395vsbr	
(D)	l.t.	206vs	225s	*261m*	275brm	*312m*	*326s*	373vs
		384vs	400s	425s				
$Cu(C_2H_5CO_2)_2$.Aniline	r.t.	241brs	298brs	*328brs*	(340)	(360)	383brs	402m
		417m						
(P)	l.t.	220w	240s	252s	296s	*311s*	(*330*)	340s
		363m	389vs					
$Cu(C_2H_5CO_2)_2$.*p*-Toluidine	r.t.	200w	*235s*	*320brvs*	370mw	401s	430s	
(P)	l.t.	204w	*238s*	290m	*318m*	*325s*	368m	402s
$Cu(C_2H_5CO_2)_2$.*o*-Toluidine	r.t.	199vs	(245)	252m	268m	293*w*	*320vs*	396vs
(P)	l.t.	204s	264m	275m	305brm	*327s*	402s	
$Cu(C_2H_5CO_2)_2$.Urea	r.t.	205s	(225)	274m	*311m*	389brs		
(D)	l.t.	224s	270w	285s	*322brs*	351w	(378)	(395)
		401vs	(410)					
$Cu(C_3H_7CO_2)_2$.Aniline	r.t.	(230)	244brs	290brs	*346s*	370s	395brs	
(P)	l.t.	230m	243m	264s	(286)	297s	*347m*	(352)
		368s	380w					
$Cu(C_3H_7CO_2)_2$.*p*-Toluidine	r.t.	241brs	278s	295m	*313s*	368vs	427s	
(P)	l.t.	223m	242m	286m	*310s*	*324s*	348s	367s
		417s	436s					
$Cu(C_3H_7CO_2)_2$.Urea	r.t.	242brs	295s	*347s*	425brs			
(D)	l.t.	240brs	304vs	330w	*352s*	432vs		
$Cu(C_3H_7CO_2)_2$.Pyridine	r.t.	201m	245m	254m	290brs	*348vs*	415vs	(422)
(D)	l.t.	202s	242s	287s	310s	*322m*	*343s*	353s
		415vs						
$Cu(C_3H_7CO_2)_2$.Isoquinoline	r.t.	244s	291s	(*325*)	*342s*	413s		
(D)	l.t.	255s	306s	*330m*	*348s*	422vs		

*r.t. = room temperature; l.t. = low temperature.
†Shoulders are indicated in parentheses.
‡Assignments to monomeric (M), dimeric (D), and polymeric (P) species are made on the basis of previous magnetic measurements.
§See footnote to Table 2, and text, for explanation of italicized data.

below 400 cm^{-1} may reasonably be assigned to metal–oxygen modes.

The presence of a range of different axial ligands, some of which absorb in this region, does, however, complicate the issue. Comparison of the data in Table 1 reveals that the complexes may, with one or two exceptions and on the basis of their room temperature spectra, be subdivided into two groups. One group exhibits a *single* band between 300 and 400 cm^{-1} with an energy of about 350 cm^{-1} or more, and the other group exhibits *two* bands in this region, one usually below 350 and one above 350 cm^{-1}. Unfortunately this subdivision is not identical with the division into polymers and dimers suggested on the basis of the magnetic data (2, 3, 12), *i.e.* magnetic moments near 1.7 and 1.4 B.M., respectively.

The D_{4h} CuO_4 square planar chromophore should give rise to one infrared active (doubly degenerate) copper–oxygen stretching vibration, whilst the dimeric D_{4h} Cu_2O_8 unit would give rise to two ($A_{2u} + E_u$) active vibrations. Further additional active vibrations could arise through

Can. J. Chem. Downloaded from www.nrcresearchpress.com by 86.111.144.194 on 09/06/12
For personal use only.

TABLE 2. Far infrared data (200–425 cm^{-1}) for the ^{65}Cu complexes (copper–ligand vibrations in italics)

Complex	Far infrared spectra (cm^{-1})*			
$Cu(CH_3CO_2)_2$.Pyridine	*237.5(1.5)*	267(0.5)	*352.5(2.0)*	417.5(1.5)†
$Cu(C_2H_5CO_2)_2$.Isoquinoline	200(0)	*304br(4.2)*	*369.5br(2.5)*	
$Cu(C_2H_5CO_2)_2$.Urea	205br‡	273(0.5)	*308(2.5)*	*384br(5)*‡
$Cu(C_2H_5CO_2)_2$.*o*-Toluidine	252.2(0)	268(0)	293br(0)	*316.6(3.1)*
	396(0)			
$Cu(C_2H_5CO_2)_2$.*p*-Toluidine	*233.5(1.5)*	*320br*‡	370(0)	401(0) 429.5(0.5)
$Cu(C_3H_7CO_2)_2$.Pyridine	251br‡	290(0)	*347.2(1.1)*	414.5(0.5)†
$Cu(C_3H_7CO_2)_2$.*p*-Toluidine	*239(2.0)*	278(0)	295sh	*310(3.0)*
	368(0)	427(0)		

*Shift downwards (in cm^{-1}) from essentially ^{63}Cu spectrum (from Table 1) given in parenthesis immediately after band energies.
†Pyridine ring skeletal vibrations (15) evidently coupled to a metal nitrogen mode. Bands in italics near 240 cm^{-1} are Cu—N stretching vibrations; bands in italics between 300 and 400 cm^{-1} are Cu—O stretching vibrations.
‡Band too broad to ascertain shift accurately.

Can. J. Chem. Downloaded from www.nrcresearchpress.com by 86.111.144.194 on 09/06/12
For personal use only.

factor group splitting since the data are obtained in the solid state. The polymeric structure (Fig. 1*a*) has very low symmetry (C_i) with four different Cu—O distances; considering a $Cu_4O_{12}N_3$ segment of the chain, up to six Cu—O stretching modes will be infrared active, though may not all be resolvable.

The isotopic substitution method (13) was used to unequivocally confirm that these bands are indeed copper–oxygen vibrations. A range of derivatives was obtained using isotopically pure (99.7%) ^{65}Cu and the spectra compared against those obtained with natural copper (69% ^{63}Cu, 31% ^{65}Cu). Isotopic substitution of the central metal is preferred to isotopic substitution with isotopes of oxygen (or nitrogen) since the former will reveal only vibrations whose potential distribution contains metal–ligand modes, whilst use of the latter provides shifts in all vibrations involving that oxygen (C—O as well as M—O). Because of the presence of some ^{65}Cu in the natural copper samples, the isotopic shifts recorded in Table 2 probably underestimate, slightly, a true isotopic shift upon replacement of ^{63}Cu by ^{65}Cu. Calculation (14) suggests that such replacement should lead to a frequency shift of some 3–5 cm^{-1} in a vibration whose potential distribution is predominantly Cu—O in origin. *The observation that certain absorption in the 300–400 cm^{-1} region exhibits isotopic shifts of this order of magnitude confirms that these bands may be considered to be dominantly copper–oxygen stretching (presumably) vibrations* (see Fig. 2). In particular all bands exhibited by the dimeric complexes in the 300–400 cm^{-1} region were isotopically sensitive whilst for the polymeric complexes only the lower of the two bands observed in this region exhibited isotopic

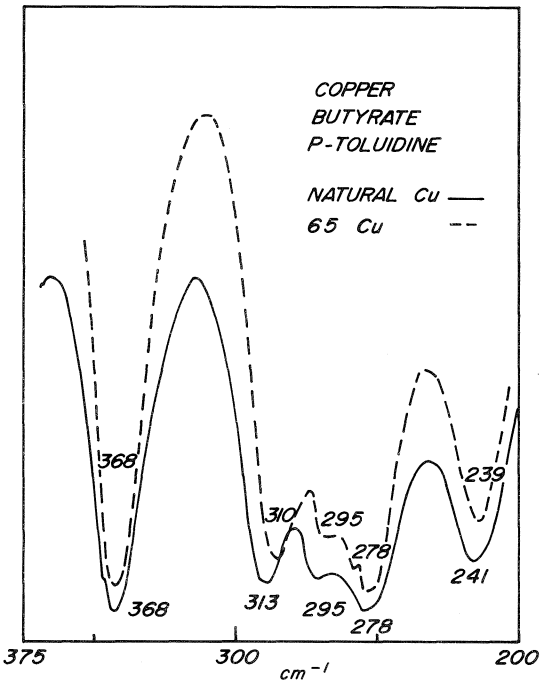

FIG. 2. The vibrational spectrum of copper butyrate *p*-toluidine containing natural copper, — and containing ^{65}Cu, ----.

sensitivity. Thus at least for those derivatives studied there is a distinction between the polymeric and dimeric species on the basis of the far infrared spectrum, albeit isotopic substitution experiments are needed to so demonstrate.

In those cases where bands shifted by less than 2.0 cm^{-1} some Cu—O contribution is indicated, but evidently the potential distribution contains some internal ligand modes. Thus those bands just above 400 cm^{-1} in the pyridine adducts and which show some slight sensitivity towards iso-

topic substitution may be assigned to a pyridine ring skeletal vibration (15, 16) coupled with a copper ligand mode (see Fig. 2).

Certain of the pyridine and toluidine adducts exhibit an isotopically sensitive band near 240 cm^{-1} assigned to the copper–nitrogen stretching vibration; such an energy is typical of a copper–nitrogen stretching mode involving such ligands (16 and references therein). However, the relatively small shifts observed suggest that this is not a very pure vibration.

In view of the broadness of the copper–oxygen modes in the room temperature spectra, the data were also taken at (or close to) −196 °C, when much more resolved spectra were obtained (see Fig. 3). Where two copper–oxygen modes were observed between 300 and 400 cm^{-1} the lower energy band was almost always resolved into two components, whilst the upper band generally shifted to higher energy. When one band was observed in this region in the room temperature spectrum, cooling led generally to a shift to high energy, and in one case to resolution into two components. One might certainly expect the polymeric complexes in particular to give a very complicated Cu—O spectrum since the crystal contains so many different kinds of Cu—O bond (1). Factor group splitting in the crystals of the dimeric molecule might also yield further bands at low temperature, so complexity in the 300–400 cm^{-1} region at low temperature, will not necessarily provide additional definitive information. Certainly splitting of the E_u modes by fields of less than four-fold symmetry might well be anticipated, such splitting being observable in the low temperature spectrum.

In comparing the room temperature data with those obtained at low temperature, problems arise because it is not always possible to draw a one to one correlation between the two spectra. Frequently a broad band will split into two components, one at lower and one at higher energy than the original band, whilst other bands will shift in energy, usually, though not always, to high energy. New features may arise in the low temperature spectrum, whilst others may disappear. Comparison is also complicated by the fact that different mulling techniques are employed to obtain the room temperature and low temperature data (see Experimental section); nevertheless there does seem to be the general trend that metal–ligand frequencies shift to higher energies on cooling as might be expected

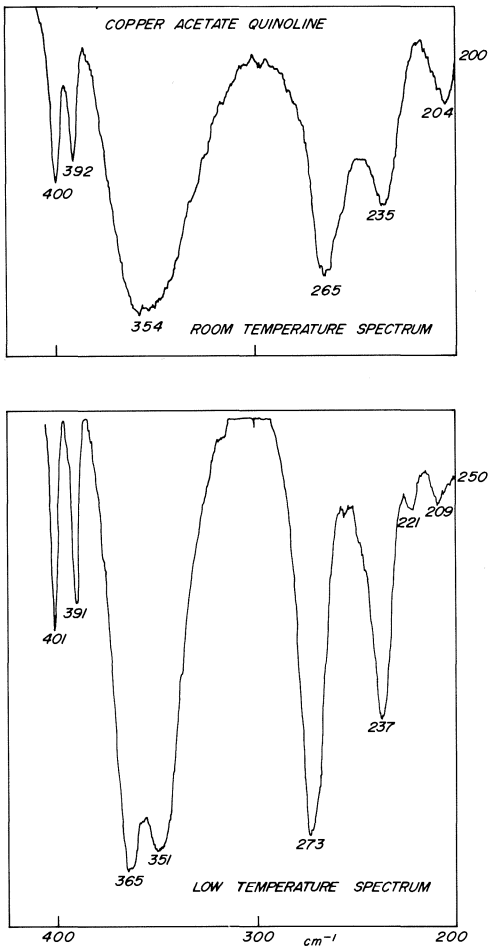

FIG. 3. The vibrational spectrum of copper acetate quinoline at room temperature (upper) and at liquid nitrogen temperature (lower).

(17, 18). Cooling frequently leads to a marked apparent increase in intensity which can aid the identification of features which are weak in the room temperature spectrum (10, 17, 18). Using the results of the low temperature studies, and the isotopic studies, as a basis, Cu—O (and in some cases Cu—N) stretching vibrations have been assigned in Table 1 for all the complexes under consideration. Although isotopic experiments were not carried out with all the complexes, it is considered that a sufficient pattern has been identified for the assignments to be secure.

NOTE ADDED IN PROOF

It is relevant that isotopic studies of the far infrared spectra of amino acid complexes of

Can. J. Chem. Downloaded from www.nrcresearchpress.com by 86.111.144.194 on 09/06/12
For personal use only.

copper(II) reveal γ(Cu—O) at *ca.* 330 cm^{-1} and γ(Cu—N) at *ca.* 380 cm^{-1} (19).

Summary

The polymeric complexes exhibit one or two bands in their room temperature infrared spectrum between 300 and 400 cm^{-1}, only the lower of which, from isotopic substitution experiments appears to be assignable to a Cu—O stretching mode. The dimeric complexes, on the other hand, have a potential distribution such that all bands between 300–400 cm^{-1} in the room temperature spectra involve copper–oxygen vibrations. Isotopic studies have also confirmed that the axial copper–nitrogen stretching vibration in certain amine adducts contributes to a band near 240 cm^{-1}.

We are indebted to the National Research Council of Canada for financial support.

1. D. B. W. Yawney and R. J. Doedens. J. Am. Chem. Soc. **92**, 6350 (1970).
2. M. Kato, H. B. Jonassen, and J. C. Fanning. Chem. Rev. **64**, 99 (1964).
3. E. Kokot and R. L. Martin. Inorg. Chem. **3**, 1306 (1964).
4. R. C. Komson, A. T. McPhail, F. E. Mabbs, and J. K. Porter. J. Chem. Soc. A, 3447 (1971).
5. M. Kishita, M. Inoue, and M. Kubo. Inorg. Chem. **3**, 237 (1964).
6. E. Borsbach. Ber. **23**, 431 (1890); Yu. V. Yablokov. Zh. Strukt. Khim. **5**, 222 (1964).
7. D. P. Graddon. J. Inorg. Nucl. Chem. **17**, 222 (1961).
8. R. L. Martin and H. Waterman. J. Chem. Soc. 2545 (1957).
9. J. R. Wasson, C. I. Shyr, and C. Trapp. Inorg. Chem. **7**, 469 (1968).
10. A. M. Heyns. J. Mol. Struct. **11**, 93 (1972).
11. V. Lorenzelli and F. Gesmundo. Atti Accad. Naz. Lincei, Cl. Sci. Fis. Mat. Natur. Rend. **36**, 485 (1964).
12. A. B. P. Lever and B. S. Ramaswamy. Can. J. Chem. To be submitted.
13. K. Nakamoto, K. Shobatake, and B. Hutchinson. Chem. Commun. 1451 (1969).
14. E. B. Wilson, J. C. Decius, and P. D. Cross. Molecular vibrations. McGraw-Hill, New York. 1955.
15. J. H. S. Green, W. Kynaston, and H. M. Paisley. Spectrochim. Acta, **19**, 549 (1963).
16. M. Keeton and A. B. P. Lever. Inorg. Chem. **10**, 47 (1971).
17. M. Keeton, A. B. P. Lever, and B. S. Ramaswamy. Spectrochim. Acta, **26A**, 2173 (1970).
18. A. B. P. Lever and B. S. Ramaswamy. Proc. XIII Int. Conf. Coord. Chem. (Poland) 123 (Abstract 66), (1970).
19. G. W. Rayner Canham and A. B. P. Lever. Spectrosc. Lett. In press.

Can. J. Chem. Downloaded from www.nrcresearchpress.com by 86.111.144.194 on 09/06/12
For personal use only.

Nitrilohexaphosphonitrilic Chloride: A Chemical and Spectroscopic Study

R. T. OAKLEY AND N. L. PADDOCK[1]

Department of Chemistry, University of British Columbia, Vancouver 8, British Columbia

Received August 16, 1972

The preparation of nitrilohexaphosphonitrilic chloride[2] $N_7P_6Cl_9$ is described; its infrared, Raman, mass and nuclear magnetic resonance spectra indicate a tricyclic condensed ring structure of C_{3v} symmetry. The molecule decomposes on attempted substitution of the chlorine atoms by fluorine and by methoxy-groups, but with dimethylamine both addition and substitution take place. One central bond is broken, and a bridged ring imide $N_6P_6(NH)(NMe_2)_8Cl_2$ is formed, in which the ring structure is sufficiently rigid for axial and equatorial groups to be distinguished. The detailed molecular structure of $N_7P_6Cl_9$ shows evidence of a compromise between the requirements for optimum σ- and π-bonding, the central N—P bonds being strained. Its substitution behavior, base strength, ultraviolet spectrum, mass spectrum, and molecular geometry are interpreted in these terms.

La préparation du chlorure de nitrilohexaphosphonitrilique[2] $N_7P_6Cl_9$ est décrite; ses spectres infrarouge, raman, résonance magnétique et son spectre de masse indiquent une structure tricyclique condensée de symétrie C_{3v}. La molécule se décompose lorsqu'une substitution des atomes de chlore par les groupes fluor ou méthoxy est tentée, avec la diméthylamine l'addition et la substitution ont lien toutes deux. Une liaison centrale se brise et un cycle imide ponté $N_6P_6(NH)(NMe_2)_8Cl_2$ se forme, dans lequel la structure cyclique est suffisamment rigide pour pouvoir distinguer les groupes axial et équatorial. La structure moléculaire détaillée de $N_7P_6Cl_9$ fournit la preuve d'un compromis entre un recouvrement optinal et nécessaire des liaisons σ et π et une tension des liaisons centrales N—P. Le comportement dans la substitution, la force basique, les spectres de masse et u.v., la géométrie moléculaire de ce composé ont été aussi interprétés en fonction de ce facteur. [Traduit par le journal]

Can. J. Chem., **51**, 520 (1973)

Introduction

In the course of his pioneer investigation of the preparation of the phosphonitrilic chlorides (2), Stokes obtained a small quantity of a compound of formula $N_7P_6Cl_9$, which he called nitrilohexaphosphonitrilic chloride. Much later, Krause (3) obtained the same compound by depolymerization of a phosphonitrilic chloride high polymer, determined some of its properties, and suggested for it a condensed ring structure (Fig. 1). Cationic fragments based on the N_7P_6 nucleus have since been detected in the mass spectra of the larger phosphonitrilic chlorides (4) and bromides (5), but there has been no detailed report of the general chemistry of this type of compound. In the present work, the condensed ring structure of $N_7P_6Cl_9$ has been established, and its reactions with typical nucleophiles investigated. The σ-bond requirements are important, causing the molecule to deviate strongly from planarity and straining the central bonds. The substitutional behavior is consequently less simple than that of monocyclic phosphonitriles, a rigid bicyclic derivative being produced on dimethylamination. The detailed structure and reactions can be understood in terms of theoretical concepts developed earlier.[3] A preliminary account of this work has been published (7).

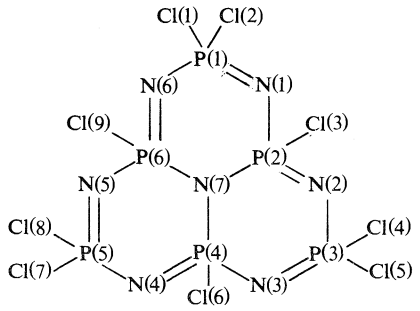

FIG. 1. Structure of $N_7P_6Cl_9$ as suggested by Krause.

Experimental

Mixtures of phosphonitrilic chlorides were prepared from phosphorus pentachloride and ammonium chloride by established methods (8). Potassium fluorosulfite was prepared by shaking finely ground dry potassium fluoride

[1]To whom correspondence should be addressed.

[2]On grounds of brevity and clarity, we use this name rather than the systematic 2,2,3*a*,5,5,6*a*,8,8,9*a*-nonachloro-2,2,5,5,8,8-hexahydro-1,3,4,6,7,9,9*b*-hepta-aza-2,3*a*,5,6*a*,8,9*a*-hexaphospha(3*a*,6*a*,9*a*-P^{v})phenalene (1).

[3]For a review and references, see ref. 6.

Can. J. Chem. Downloaded from www.nrcresearchpress.com by 210.87.254.5 on 09/05/12
For personal use only.

TABLE 1. The mass spectrum of $N_7P_6Cl_9$*

$N_7P_6Cl_9$	$N_7P_6Cl_8$	$N_7P_6Cl_7$	$N_7P_6Cl_6$		Total
3.3	12.5	0	0.9		16.7
$N_6P_5Cl_6$	$N_6P_5Cl_5$	$N_6P_5Cl_4$			
3.7	0	0.4			4.1
$N_5P_4Cl_4$					
1.3					1.3
$N_5P_5Cl_7$	$N_5P_5Cl_6$	$N_5P_5Cl_5$			
0.6	0	0.3			0.9
$N_4P_4Cl_7$	$N_4P_4Cl_6$	$N_4P_4Cl_5$	$N_4P_4Cl_4$	$N_4P_4Cl_3$	
5.2	0.2	2.2	0	0.8	8.4
$N_3P_3Cl_5$	$N_3P_3Cl_4$	$N_3P_3Cl_3$	$N_3P_3Cl_2$	N_3P_3Cl	
8.7	0.5	8.3	0	0.9	18.4
$N_3P_4Cl_6$	$N_3P_4Cl_5$	$N_3P_4Cl_4$			
1.2	0	0.5			1.7
$N_2P_3Cl_6$	$N_2P_3Cl_5$	$N_2P_3Cl_4$	$N_2P_3Cl_3$		
0.9	0.5	4.7	0.5		6.6
NP_2Cl_4	NP_2Cl_3	NP_2Cl_2	NP_2Cl	NP_2	
5.1	0	8.2	4.0	1.1	18.4
$NPCl_2$	NPCl	NP			
0.5	1.5	0.4			2.4
PCl_3	PCl_2	PCl	P		
0.2	10.1	3.6	0.6		14.5
P_2Cl	P_2	Cl			
0.8	0.4	1.8			3.0

*Singly charged fragments, percentage of whole spectrum. Abundances less than 0.1% taken as zero. Doubly charged ions: $N_7P_6Cl_7$ (0.5), $N_5P_5Cl_6$ (0.2), $N_4P_4Cl_6$ (0.5), $N_4P_4Cl_4$ (0.4), $N_3P_3Cl_4$ (0.4), $N_3P_4Cl_9$ (0.2), $N_3P_4Cl_7$ (0.3), $N_3P_4Cl_5$ (0.2), $N_2P_3Cl_5$ (0.6), NP_2Cl_5 (0.1), NP_2Cl_3 (0.2). Total 3.6.

with liquid sulfur dioxide for 3 days; its sulfur dioxide content was 98% of theoretical value. Activated potassium fluoride was obtained by heating it *in vacuo* (9). Benzene and methanol were dried by distillation from sodium; sodium methoxide was prepared from the metal and dry methanol. Silver(I) fluoride, lithium nitride, and dimethylamine were commercial products, and were used without further purification. Infrared spectra were obtained on a Perkin–Elmer 457 spectrometer, Raman spectra on a Cary 15 spectrometer with Spectra-Physics helium–neon laser excitation, and ultraviolet spectra on a Cary 14 spectrometer. A Varian HA100 spectrometer was used to obtain the ^{31}P and ^{1}H n.m.r. spectra (external 85% H_3PO_4 and internal tetramethylsilane, respectively), and an A.E.I. MS9 mass spectrograph (with conventional sampling techniques and an excitation potential of 70 V) for the mass spectra.

Preparation of Nitrilohexaphosphonitrilic Chloride

In a typical experiment, 200 g of a mixture of phosphonitrilic chlorides $(NPCl_2)_n$ (mean $n \sim 5$) was polymerized to a dark rubbery solid by heating it at 300 °C for several hours at atmospheric pressure. Extraction with benzene showed that no $N_7P_6Cl_9$ was formed at this stage. The product was depolymerized by heating it at 300 °C, <0.1 Torr, to give (mainly) a mixture (170 g) of $N_3P_3Cl_6$ and $N_4P_4Cl_8$ in the approximate weight ratio 1:2, and a residue of light flaky black ash, of unknown composition. The nitrilohexaphosphonitrilic chloride partly solidified in the condenser arm of the distillation apparatus, and partly distilled with the monocyclic chlorides, from which it was separated by taking advantage of its low solubility in petrol. The combined quantities of $N_7P_6Cl_9$ (0.5 g) were recrystallized from benzene and identified by m.p. (235°, lit. (2) 237.2°).

Anal. Calcd. for $N_7P_6Cl_9$: Cl, 52.9; N, 16.3; P, 30.8. Found: Cl, 52.8; N, 16.2; P, 30.7.

Its mass spectrum (Table 1) showed the compound to be monomeric. No improvement in yield was obtained by using the individual cyclic compounds instead of a mixture. Attempts at directed synthesis were unsuccessful; some reaction of hexaphosphonitrilic chloride $(NPCl_2)_6$ with lithium nitride took place in tetrahydrofuran, with formation of lithium chloride, but no $N_7P_6Cl_9$ was found in the product from this reaction or from those of tris-(trimethylsilyl)amine and tris(trimethylstannyl)amine with the hexameric chloride.

Reactions of Nitrilohexaphosphonitrilic Chloride

Fluorination

A slurry of $N_7P_6Cl_9$ (2.3 g, 3.85 mmol) and potassium fluorosulfite (6.5 g, 11.0 mmol) in 125 ml cyclohexane was heated under reflux in a dry atmosphere. No volatile products were trapped at −76 °C. After 16 h, the mixture was filtered and the solvent distilled off, leaving crystals of $N_7P_6Cl_9$ (1.4 g, 2.3 mmol); no $N_7P_6F_9$ or partially fluorinated derivatives were detected in the cyclohexane distillate. The insoluble residue contained chloride ion,

Can. J. Chem. Downloaded from www.nrcresearchpress.com by 210.87.254.5 on 09/05/12
For personal use only.

Can. J. Chem. Downloaded from www.nrcresearchpress.com by 210.87.254.5 on 09/05/12
For personal use only.

and, after mild hydrolysis, phosphate ion. It appeared that complete breakdown of 1.55 mmol $N_7P_6Cl_9$ had occurred, corresponding approximately to reaction of all the KSO_2F used, rather than partial fluorination of all the $N_7P_6Cl_9$. Similar results were obtained in a second experiment, in which an excess of activated potassium fluoride (3.6 g, 62 mmol) was stirred with $N_7P_6Cl_9$ (1.07 g, 1.78 mmol) at 150 °C for 48 h (a method found to give a good yield of $N_6P_6F_{12}$ from $N_6P_6Cl_{12}$). There was no visible evidence of reaction, no product was collected in the cold trap, and nothing was extracted from the reaction mixture by ethyl ether, benzene, or acetonitrile. The residue was soluble in water and gave a positive test for chloride ion, indicating that reaction of the P—Cl bonds and molecular breakdown had both occurred. In a third experiment, a finely ground mixture of $N_7P_6Cl_9$ (0.8 g, 1.34 mmol) and silver(I) fluoride (3.5 g, 27.5 mmol) was heated for 1 h at 180 °C, without obvious reaction. On further heating at 240 °C, a small quantity of an unidentified volatile product was obtained, of mean mol. wt. (vapor density) 114 (calcd. for $N_7P_6F_9$, 455). Again, breakdown of the ring evidently occurred.

Methoxylation

A solution of $N_7P_6Cl_9$ (0.3 g, 0.5 mmol) in 10 ml benzene was added slowly to a stirred suspension of sodium methoxide (0.35 g, 6.5 mmol) in 15 ml benzene. The reaction mixture was heated under reflux for 4 h, cooled, diluted with 20 ml ethyl ether and washed with water. Determination of the chloride ion showed substitution to have been quantitative. No phosphonitrilic derivative was detected either in the ethereal solution or in its aqueous extract, so that substitution was evidently accompanied by breakdown of the ring.

Amination

Dimethylamine (0.8 g, 17.9 mmol) in 12 ml benzene was added at 0 °C to a cold stirred solution of $N_7P_6Cl_9$ (0.5 g, 0.84 mmol) in 15 ml benzene. Precipitation of dimethylamine hydrochloride began at once. After 3 h, it was filtered off and the benzene evaporated from the filtrate, leaving a pale yellow oil. The oil was dissolved in petrol, filtered, and the solvent evaporated to yield 3,7,11-imino-3,11-dichlorooctadimethylamidocyclohexaphosphonitrile (0.46 g, 0.65 mmol, 77% theory) which was recrystallized from acetonitrile as colorless, flaky, triboelectric crystals, m.p. 161–163°.

Anal. Calcd. for $C_{16}H_{49}Cl_2N_{15}P_6$: C, 27.2; H, 6.9; Cl, 10.0; N, 29.8. Found: C, 27.2; H, 6.9; Cl, 10.0; N, 29.7.

Its mass spectrum showed the compound to be monomeric.

Solubility in Sulfuric Acid

A comparison of the basic behavior of the monocyclic and condensed ring compounds was made by measuring the partition coefficient P of $N_6P_6Cl_{12}$ and $N_7P_6Cl_9$ between cyclohexane and sulfuric acid of various concentrations. Solutions of the two compounds (0.001 *M*) were made in cyclohexane. The partition ratios were determined by mixing 30 ml of each solution with 30 ml of acid of known concentration, shaking the mixture for 2 min, and then finding the concentration of the chloride in the cyclohexane layer by evaporating a known volume of the solution to dryness and weighing the residue. The concentration in the acid layer was determined by difference. All measurements were made in triplicate over the range $H_0 = -8.4$ to -8.8, equal concentrations in the two layers being found for $H_0 = -8.57$ ($N_6P_6Cl_{12}$) and -8.67 ($N_7P_6Cl_9$).

Reaction with Aluminum Bromide

A solution of resublimed aluminum bromide (0.039 g, 0.145 mmol) in 9 ml carbon disulfide was added, under an atmosphere of dry nitrogen, to a stirred solution of $N_7P_6Cl_9$ (0.087 g, 0.145 mmol) in 10 ml carbon disulfide. There was no sign of a reaction after 30 min. The carbon disulfide was distilled off, and 0.083 g $N_7P_6Cl_9$ recovered from the residue by extraction with benzene.

Results

Molecular Structure of Nitrilohexaphosphonitrilic Chloride

The ^{31}P n.m.r. spectrum of $N_7P_6Cl_9$, determined in molten naphthalene, consists of two peaks of equal intensity, and is uniquely consistent with the presence of two sets of three equivalent phosphorus atoms, as implied in the structure of Fig. 1. Each peak exhibits unresolved structure. The lower chemical shift (−20.2 p.p.m.) is tentatively assigned to the PCl_2 groups by comparison with the shift (8) of $N_3P_3Cl_6$ (−20.0); the other line is at higher field (+3.5 p.p.m.), possibly because of electron release from the central nitrogen atom.

The indicated three-fold symmetry, which is independent of the detailed assignments, is confirmed by the vibrational spectra (Table 2). The symmetries D_{3h} and C_{3v} both require 33 active fundamentals, but in D_{3h} the horizontal plane of symmetry destroys the infrared activity of 14 out of 27 Raman active modes. In fact, although only 18 lines are observed, every Raman line is accompanied by an infrared counterpart. The inference of C_{3v} symmetry is supported by some detailed assignments. There have been many modifications to the vibrational assignments of the phosphonitrilic chlorides since the original work of Daasch (10), the most recent and detailed being that of Hisatsune (11, 12). In the present case, some assignments are tentative, because Raman polarization measurements were not available, owing to the compound's small solubility. The P—Cl stretching frequencies are the best established. The monocyclic phosphonitrilic chlorides, up to at least $N_6P_6Cl_{12}$, exhibit an infrared band near 600 cm^{-1} ($N_3P_3Cl_6$: 598 (11); 610 (13); 611 (14); 612 (15). $N_4P_4Cl_8$[4]: 596, 601 (15); 598, 610 (12). $N_5P_5Cl_{10}$: 601 (15); 607 (16). $N_6P_6Cl_{12}$: 603 (16); 602[5]). This is generally

[4]Two polymorphic forms.

[5]R.T. Oakley. Unpublished.

TABLE 2. Vibrational spectra of $N_7P_6Cl_9$

Raman (cm^{-1}) powder	Infrared (cm^{-1}) (Nujol)*	Assignment
149 (5)		$\rho(PCl_2)_{o.p.}$, $\tau(PCl_2)_{o.p.}$
169 (10)		
288 (0.5)	280 w	
332 (10)	330 w	$\delta(PCl_2)_{i.p.}$?
411 (1)	402 vw	
442 (6)	435 m	$\nu_s(PCl_2)_{i.p.}$
507 (1)	503 vw	Ring deformation } See Text
	525 w	$\nu_s(PCl_2)_{o.p.}$ } See Text
557 (1.5)	548 sh	$\nu(PCl)_{i.p.}$
	564 st	$\nu(PCl)_{o.p.}$
	592 vst	$\nu_{as}(PCl_2)_{i.p.}$
661 (2)	660 st	Ring deformation; see text
807 (2)	804 m	$\nu_s(NP_3)$
	870 st	Ring vibration
	903 vw	
	1188 sh	Ring vibration
	1280 vst	$\nu_{as}(PNP)$
	~1320 sh	

*CsI plates. Frequencies obtained from solutions in CS_2, CCl_4, agreed within 5 cm^{-1}, except that the line at 870 cm^{-1} was resolved into two: 858 cm^{-1} (st), 880 cm^{-1} (m). st = strong, m = medium, w = weak, v = very.

attributed to $\nu_{as}(PCl_2)_{i.p.}$[6], and the i.r. band at 592 cm^{-1} in $N_7P_6Cl_9$ is so assigned. It is broadened, and could obscure $\nu_{as}(PCl_2)_{o.p.}$. The lower limit of $\nu(PCl_2)$ is assigned as $\nu_s(PCl_2)_{i.p.}$, usually on the basis of a strong polarized Raman line, as follows (cm^{-1}). $N_3P_3Cl_6$: 363 (13); 365 (14, 15, 17, 18). $N_4P_4Cl_8$[4,6]: 385, 413 (12); 387, 413 (15); 404 (13). $N_5P_5Cl_{10}$: 439 (15). $N_6P_6Cl_{12}$: 461 (16)[7]; 451[5]. We therefore assign the strong Raman lines at 442 cm^{-1} in $N_7P_6Cl_9$ to $\nu_s(PCl_2)_{i.p.}$, its infrared activity indicating the absence of a horizontal symmetry plane. $\nu_s(PCl_2)_{o.p.}$ is then either at 503 or 525 cm^{-1}; the latter seems more likely by comparison with the spectra of the trimeric chloride–fluorides (14), but a degenerate deformation mode of the N_3P_3 ring has been assigned near this frequency (10, 11, 13, 17), and these two assignments could be reversed. The two remaining frequencies in this region (557/548, 564 cm^{-1}) are characteristic of this particular compound, and are assigned to $\nu(PCl)_{i.p.}$ (A_1) and $\nu(PCl)_{o.p.}$ (E), in agreement with assignments of $\nu(PCl)$ at 563 (19) or 575 cm^{-1} (18) in $N_3P_3Br_5Cl$, 559 cm^{-1} in $N_3P_3Cl_5Br$ (19), and 568 cm^{-1} in $N_3P_3FCl_5$, $N_3P_3F_3Cl_3$ (14).

The higher frequencies are similar to those of other phosphonitrilic derivatives, especially those with 6-membered rings. The N_7P_6 framework has one more A_1 mode than the N_6P_6 ring of the same symmetry, involving essentially the symmetric stretching of the internal PN bonds. The Raman line at 807 cm^{-1} is assigned to this mode; there is no close line in the spectra of either $N_6P_6Cl_{12}$ (16) or $N_5P_5Cl_{10}$ (15, 16), and although there is a line at 782–785 cm^{-1} in the Raman spectrum of $N_4P_4Cl_8$ (12, 13, 15, 20), it is depolarized. However, in $N_3P_3Cl_6$ the totally symmetric ring breathing frequency is established at 783–785 cm^{-1} (10, 11, 14, 15, 17, 18), and the likelihood that $N_7P_6Cl_9$ contains 6-membered rings is reinforced by the occurrence of a Raman line at 661 cm^{-1}; a totally symmetric band, attributed to a trigonal ring deformation, appears as a strong polarized band in the Raman spectrum of $N_3P_3Cl_6$ at 669–671 cm^{-1} (11, 15, 17, 18). There is a further parallelism in the occurrence of an i.r. band at 870 cm^{-1} ($N_7P_6Cl_9$) and at 872–875 cm^{-1} ($N_3P_3Cl_6$). Although the symmetry species of this last band is still uncertain (11), the assignment of the 661, 807, 870, and 1188 cm^{-1} bands as ring vibrations allied to corresponding bands in $N_3P_3Cl_6$ is generally supported by the progressive variation of similar frequencies in the series $N_3P_3Cl_{6-n}Br_n$ (19). The strongest i.r. band, that of ν_{ar} (PNP) (1280 cm^{-1}), is intermediate between the corresponding frequencies of $N_3P_3Cl_6$ (1218 cm^{-1}) and $(NPCl_2)_{4-6}$ (1315 (10), 1354 (15), 1338 (16)).

[6]In view of the complexity of the molecule, Hisatsune (12) discusses only the symmetry assignments of $N_4P_4Cl_8$.

[7]Frequency observed but unassigned.

Can. J. Chem. Downloaded from www.nrcresearchpress.com by 210.87.254.5 on 09/05/12
For personal use only.

Can. J. Chem. Downloaded from www.nrcresearchpress.com by 210.87.254.5 on 09/05/12
For personal use only.

The low frequencies are assigned with less certainty. The two lowest may correspond to the 157, 172 cm^{-1} Raman lines in $N_3P_3Cl_6$ (13) which are there of species E'', characteristic of PCl_2 rocking and torsional vibrations. The line at 332 cm^{-1} seems the natural choice for $\delta(PCl_2)_{i.p.}$, but an out-of-plane ring deformation is also expected in this region. Changes of assignments in this region are unlikely to affect the general conclusion that the molecule has the condensed ring structure of Fig. 1, but with the rings bent away from the central P_3 plane, the overall symmetry being C_{3v}.

The mass spectrum of $N_7P_6Cl_9$ (Table 1) is consistent with this conclusion, and also shows many interesting points of comparison with those of the monocyclic chlorides. Besides the parent series $N_7P_6Cl_x^{n+}$, fragments of the series $N_6P_5Cl_x^{n+}$ have been detected, the latter for the first time. Loss of $NPCl_y$, either charged or neutral, evidently occurs, without loss of the central nitrogen atom. Monocyclic and linear fragments are also formed, and, in whatever type of fragment, even-electron fragments are more abundant than odd, for both singly and doubly charged species. It is a characteristic of the monocyclic phosphonitrilic chlorides that the parent series is stable to electron impact, and when breakdown occurs, high yields of smaller rings are obtained (4). The behavior of nitrilohexaphosphonitrilic chloride is different in that the condensed ring products are the least abundant type, and breakdown occurs mainly to small linear fragments, to a much greater extent than in the monocyclic chlorides, for which the linear products typically form 10–20% of the products (4). The condensed ring structure evidently destabilizes the molecule, although condensed ring carbocyclic aromatic compounds, such as naphthalene, are less fragmented (21) than benzene (22). A similar reduced stability of the skeletal structure is found in the chemical reactions of nitrilohexaphosphonitrilic chloride, and both phenomena find an explanation in the relation between molecular and electronic structure discussed below.

Structure of $N_6P_6(NH)(NMe_2)_8NHCl_2$

In the reaction of dimethylamine with $N_7P_6Cl_9$, one of the central bonds is broken, and two of the bridgehead chlorine atoms remain unsubstituted. The evidence for the structure of $N_6P_6(NH)(NMe_2)_8Cl_2$ (Fig. 2) is based on n.m.r. spectroscopy. Its ^{31}P n.m.r. spectrum consists of three peaks at −13.7, −3.7, +1.9 p.p.m., of relative areas 1, 2, 3, assigned respectively to P_1; P_2P_6; $P_3P_4P_5$. The peak at lowest field is a triplet (J_{PP} = 40 Hz; proton coupling incompletely resolved), and the other two are broad unresolved singlets. The direct and decoupled ^1H spectra are shown in Fig. 3, together with assignments which refer to Fig. 4. The molecular symmetry is low enough for a first order treatment to be applied, and derived chemical shifts and coupling constants are given in Table 3. The analysis has three points of direct structural interest. (*a*) The largest coupling constant is 12.7 Hz. In mononuclear phosphorus(V) compounds (23) and in the dimethylamino-derivatives of trimeric phosphonitrilic chloride (24), J_{PH} decreases with increasing aminolysis, and can be used to distinguish between $\equiv PClNMe_2$ and $\equiv P(NMe_2)_2$. For the former, J_{PH} is never less than 16.3 Hz. For the latter, J_{PH} is always less than 13.9 Hz, and is only slightly dependent on ring size, decreasing from 11.2 to 10.0 Hz in the series $[NP(NMe_2)_2]_n$, (n = 3–6) (25). We conclude that the dimethylamido-groups are paired, the remaining chlorine atoms being present in the bridgehead bonds P(2)Cl(3) and P(6)Cl(9). (*b*) The molecule is rigid. If each pair of dimethylamino-groups on each phosphorus atom were equivalent, three lines with relative intensities 2:4:2 would be found in the decoupled spectrum. The observed pattern (relative intensities 1:2:3:2) shows that the pairs of substituents on three phosphorus atoms are differentiated. The high-field resonance is assigned to the (undifferentiated) L_d protons, rather than L_b (Fig. 4) on the basis of its high J_{PH} and chemical shift (24). A complete assignment

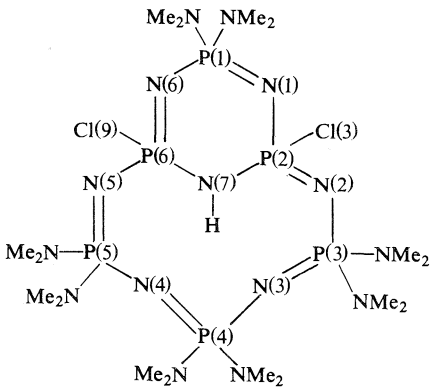

FIG. 2. Structure of $N_6P_6(NH)(NMe_2)_8Cl_2$.

TABLE 3. Proton chemical shifts and coupling constants* of $N_6P_6(NH)(NMe_2)_8Cl_2$

Type of proton†	Relative intensity	δ‡	J_{PH}(Hz)
H_a	1	2.626	10.7
H_b	2	2.606	10.7
H_c	3	2.576	10.7
H_d	2	2.551	12.7

*Dilute solution in $CDCl_3$, determined at 100 MHz. An additional proton signal, of intensity ~1/50th of the total of the high-field peaks tabulated, was found at δ = 6.15 p.p.m., and is attributed to the NH proton.
†See Fig. 4.
‡In p.p.m. downfield of internal tetramethylsilane.

of the other shifts is not possible, because the conformational structure is not unique. In terms of Fig. 4, which is based on the structure of $N_7P_6Cl_9$, the most likely interpretation is that the three equatorial dimethylamino-groups L_c have the same shift, and that one axial group L_a is differentiated from the other two, L_b, by its proximity to the central NH group. Irrespective of the exact correspondence, this is believed to be the first recorded instance of a purely conformational distinction in a phosphonitrilic derivative, the rigidity of the 10-membered ring presumably arising from the re-entrant P(6)N(7)P(2) section, and, possibly, hydrogen bonding from the NH group to the NMe_2 group L_a. (*c*) The chemical shift of the (NH) proton occurs at δ = 6.15 p.p.m., compared with δ ~ 1 for simple aliphatic secondary amines. The shift of the resonance to lower fields by electron-withdrawing groups ($C_6H_5NHCH_3$, 3.34 (26); $C_6H_5NHC_6H_5$, 5.42 (27); $C_6H_5CONHCH_3$, 8.18 (28)) is accompanied by a reduction in base strength, pK_{BH^+} for these three compounds being 4.85 (29), 0.77 (30), −0.46 (31). It is therefore likely that in the phosphonitrile the formal lone pair on the central nitrogen atom is largely delocalized into the ring system, the environment of the nitrogen atom being essentially planar, as it is in the phosphazane $N_3Me_3P_3O_3(OMe)_3$ (32). Both the infrared and mass spectra of $N_6P_6(NH)(NMe_2)_8Cl_2$ are consistent with the above structural conclusions, but are not given in detail because they are too complicated to be informative. ν_{as}(PNP) is represented by a broad complex series of bands (1150–1335 cm^{-1}) as expected for a molecule of low symmetry. The frequencies are lower than in the open ring $N_6P_6(NMe_2)_{12}$ (1340 cm^{-1}) (25). ν(NH) is present as a broad weak band centered near 3140 cm^{-1}, indicative of strong hydrogen bonding.

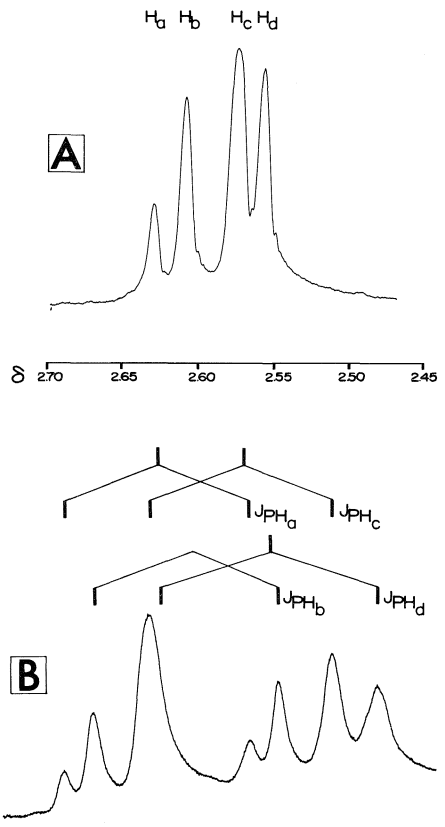

FIG. 3. The ^1H n.m.r. spectrum of $N_6P_6(NH)(NMe_2)_8Cl_2$, taken at 100 MHz. (*A*) ^{31}P–^1H decoupled, using a 2000 Hz noise band at 40.48100 MHz, (*B*) direct.

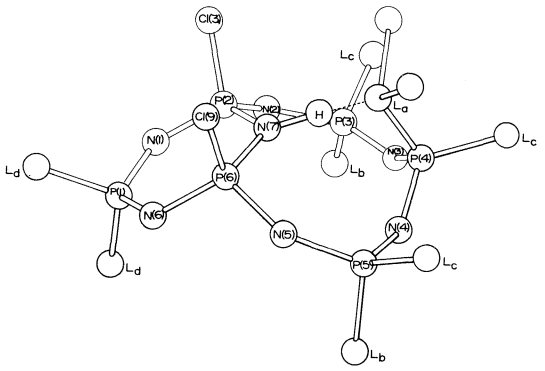

FIG. 4. Model of $N_6P_6(NH)(NMe_2)_8Cl_2$, constructed with equal bond lengths (except N–H), all ring angles at phosphorus 120°, nitrogen angles 120° in 6-membered ring, 135° elsewhere. Exocyclic groups shown as monatomic (∠ NPN = 104°) except L_a, where the angles are assumed tetrahedral. The dotted line represents the hydrogen bond referred to in the text.

Can. J. Chem. Downloaded from www.nrcresearchpress.com by 210.87.254.5 on 09/05/12
For personal use only.

Can. J. Chem. Downloaded from www.nrcresearchpress.com by 210.87.254.5 on 09/05/12
For personal use only.

Discussion

The structural features of $N_7P_6Cl_9$ deduced from its spectra have been confirmed by an X-ray determination of its crystal structure (1). The quantitative detail is important, because the nature of the bonding, the chemical reactions, and the molecular structure are inter-related. The structure is shown in Fig. 5. It consists of a central nearly planar section (the deviation of N(7) from the P(2)P(4)P(6) plane is 0.04 Å) and three 5-atom segments, typically P(6)N(6)P(1)N(1)P(2), each substantially planar, but making an angle of 25° with the central plane. It will later be more convenient to take the related angle θ_4 between the planes N(3)P(4)N(4) and P(2)P(4)P(6) as a measure of the deviation of the molecular framework from planarity. In the crystal, the small but crystallographically significant deviations from C_{3v} symmetry are believed to arise from lattice forces, and for this discussion the dimensions are averaged. The planar environment of the central nitrogen atom is consistent with complete delocalization of its unshared electrons into the ring π-system. In agreement, $N_7P_6Cl_9$ does not react with aluminum bromide, its base strength is no greater than that of the monocyclic $N_6P_6Cl_{12}$ itself, and its ultraviolet spectrum is also similar to those of the chlorides $(NPCl_2)_n$, in that there is no absorption above 210 nm, and λ_{max} is below 200 nm. In contrast, the localized n–σ* transition in dimethylamine is at 220 nm (33). Attempted interpretation of the structural information in terms of a π-system based on a planar molecule nevertheless reveals several discrepancies. The normals at N(7), P(4) to the planes P(2)P(4)P(6) and N(3)P(4)N(4) are taken as local Z_1, Z_2 axes, Y_1, Y_2, being in these planes and respectively along N(7)P(4) and the bisector of the angle N(3)P(4)N(4) (Fig. 5). If the molecule were actually planar ($\theta_4 = 0$), the two Z-axes would be parallel, and only d_{yz} would interact with p_z at N(7). For $\theta_4 > 0$, d_{z^2} and $d_{x^2-y^2}$ also participate, but since all three orbitals interact symmetrically with neighboring p_π-orbitals, to form, in monocyclic phosphonitriles, a homomorphic π-system, only a single d-orbital need be included in the simplest formal treatment. Figure 6 shows (for C_{3v} symmetry) how the scheme of levels of a P_6N_6 π-system is affected by the addition of a central p_π-orbital; the principal effect is to stabilize the two lowest A_1 orbitals.

Although this scheme makes clear how π-interactions stabilize the molecule, it is inadequate to explain the detailed properties of $N_7P_6Cl_9$, especially the length of the bonds to the central atom, which are comparatively long (1.723 Å). As a direct comparison, the mean lengths of the exocyclic PN bonds in $[NP(NMe_2)_2]_4$ (34) and $[NP(NMe_2)_2]_6$ (35) are smaller (1.68,

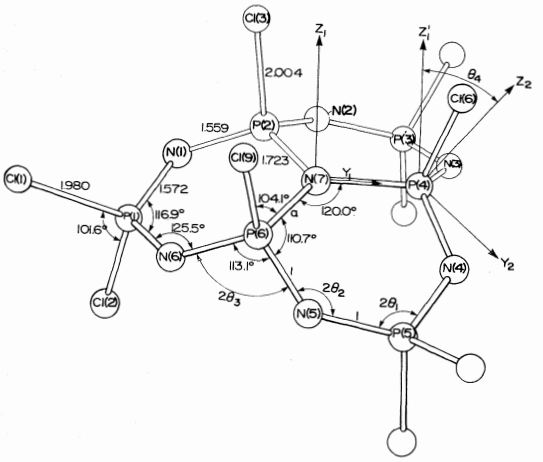

FIG. 5. Perspective view of $N_7P_6Cl_9$. Dimensions (in Å and degrees) (ref. 1) which are equivalent in C_{3v} are averaged, as are also the lengths of the equatorial and axial apical P—Cl bonds. Mean standard deviations of individual bond lengths: P—N, 0.006; P—Cl, 0.003 Å; angles: ClPCl, 0.1°; NPN, 0.3°; PNP, 0.4°; NPCl, 0.3°. The figure also shows the principal assumptions and coordinate axes used in the discussion of the structure.

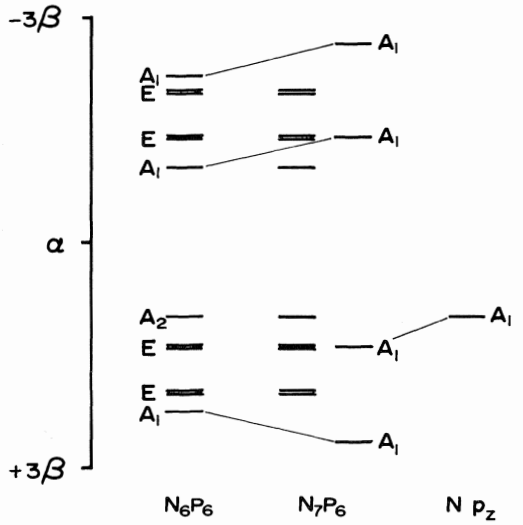

FIG. 6. π-electron levels of planar N_7P_6, related to those of N_6P_6 and a central Np_z orbital. Assumed symmetry C_{3v}. Hückel m.o.'s. $\alpha_N = \alpha_P + 2\beta$, $\alpha = (\alpha_N + \alpha_P)/2$.

1.67 Å), even though the mean sums of the angles round the nitrogen atoms are less (352°, 353°) than in $N_7P_6Cl_9$ (359.8°). The central bonds are therefore longer than expected by 0.05–0.06 Å, in spite of the apparently complete lone pair delocalization.

The paradox can be resolved if the σ-bond requirements are considered. This is not normally necessary for monocyclic derivatives because, although σ–π interaction has been recognized, the two bonding components are not mutually geometrically restrictive. In $N_7P_6Cl_9$, optimum use of both σ- and π-bonds is impossible, and the actual structure represents a compromise. The reason for the constraint can be seen if the bonds to the central atom are regarded as the equivalent of exocyclic bonds. In monocyclic derivatives, the local symmetry at phosphorus is close to C_{2v} if the two substituent groups are identical. If the σ-bonds are then formed from s–p hybrids, normalization and orthogonality require (36) that the internal and external angles 2α and 2β are related by

$$[1] \qquad C = \cot^2 \alpha + \cot^2 \beta = 1$$

Pairs of angles in phosphonitrilic derivatives often fit this relationship, values of C being for $N_3P_3Cl_6$, 1.024 (37); $N_4P_4Cl_8$ (mean), 0.955 (38); $N_5P_5Cl_{10}$ (mean), 1.011 (39). Use of d-orbitals in π-bonding need not affect the validity of this formula, so long as the electron distribution of the orbitals used is effectively spherical, but the dominant use of one d-orbital can cause the angles to vary in the same sense, rather than inversely. In $N_7P_6Cl_9$, C = 1.042 (apex), 1.112 (bridgehead), and while the angles are too small to fit the relationship accurately, they do so sufficiently closely to show the primary importance of the σ-bonds. The deviations depend on specific d-orbital interactions. Detailed consideration of the angular dependence of the overlaps of those d-orbitals which interact most strongly with the central p_π-orbital explains (1) the form and relative magnitude of the angular deviations, (2) the relative lengths of the apical and bridgehead PN ring bonds (wrongly ordered by simple "planar" m.o. theory) and (3) the relative lengths of the two types of P—Cl bond (which differ in the opposite sense to that expected on the basis of σ-hybridization).

The excessive length of the central PN bonds, crucial to the chemistry, can be interpreted with the help of a slight idealization of the real structure. The assumptions (right hand part of Fig. 5) are: symmetry C_{3v}, planarity of the central NP_3 group and the perimetric N_2P_3 segments, typically P(6)N(5)P(5)N(4)P(4), perimeter bonds of unit length, central bonds of length a. The molecular geometry is then characterized by the NPN angles $2\theta_1$ and $2\theta_3$, a PNP angle $2\theta_2$ and the dihedral angle θ_4 previously defined. The internal bond length is then

$$[2] \qquad a = (2/\sqrt{3}) \sin \theta_1 + (\sqrt{3}/3) \sin \theta_3 - \cos \theta_3 \cos \theta_4$$

It is convenient to define

$$[3] \qquad F = a - (2/\sqrt{3}) \sin \theta_1$$

a close approximation to the fractional excess bond length of central over perimeter bonds, which becomes exact for $\theta_1 = 60°$, close to the actual value. In Fig. 7, F is plotted as a function of θ_3 for typical values of θ_4. If the "pure" σ-requirement $\cot^2 \theta_3 + \cot^2 \theta_4 = 1$ is added, F is a unique function of θ_3 (dashed line), and the diagram becomes a useful basis for structural discussion. If $\theta_3 = 60°$, a normal value for the monocyclic chlorides in which the ring π-bonding is strong, a central bond length of 1.66 Å (F = 0.04) would be attained at $\theta_4 = 23°$, but only by strong violation of the σ-requirements (Fig. 7, *A*). On the other hand, if the structure is controlled entirely by the σ-bonds, the least elongation (F_{min} = 0.13) is found at $\theta_3 = 51.9°$ (*B*), an angle which corresponds to relatively weak π-bonding in the ring. The actual structure is a compromise ($\theta_4 = 49°$), but it is not accurately

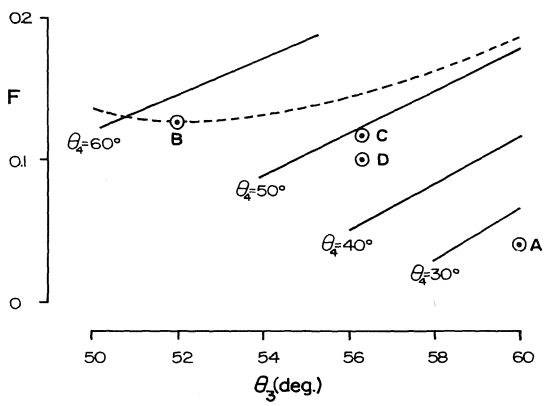

FIG. 7. Excess relative bond length F as a function of θ_3 (Fig. 5) for various θ_4. The dashed line corresponds to $\cot^2 \theta_3 + \cot^2 \theta_4 = 1$. For *A*, *B*, *C*, *D*, see text.

Can. J. Chem. Downloaded from www.nrcresearchpress.com by 210.87.254.5 on 05/05/12
For personal use only.

represented by *C*, because it does not comply with the assumptions of the model. The main inaccuracy is that the bisectors of the angles N(7)P(4)Cl(6) and N(3)P(4)N(4) are not collinear, but make a mean angle of 7.5°, in the sense that the bridgehead PN_3 groups are more nearly coplanar, and the central bonds shorter, than the σ-requirements would allow. Point *D* represents the actual values of *F* and θ_3 but not θ_4. We therefore interpret the observed fractional excess bond length of 0.1 as arising from a σ–π compromise, the bonds to the central atom being consequently strained.

It is possible to understand in this way the reduced stability of $N_7P_6Cl_9$, as compared to the monocyclic chlorides, the failure of directed syntheses from $N_6P_6Cl_{12}$, and, most important, the reactions of $N_7P_6Cl_9$ with nucleophiles. The substitution of chlorine by such electron withdrawing groups as fluorine or the methoxy-group would tend to remove electron density from the perimeter nitrogen atoms, so increasing θ_2 and θ_3 and lengthening the central bonds, and breakdown of the ring occurs with such attempted substitution. Dimethylamine would be expected to react less drastically, since the inductive effect of the nitrogen atom is offset by conjugative electron release to phosphorus. It seems most likely that the first step in the formation of $N_6P_6(NH)(NMe_2)_8Cl_2$ is the addition of Me_2NH across one central bond, sufficient strain being thereby relieved to allow normal substitution of the $P(Cl)NMe_2$ group and the remaining PCl_2 groups. If, as in phosphinate esters (40), substitution is accompanied by inversion, reaction at the bridgehead would be slow, and it is not surprising that two chlorine atoms remain.

We are grateful to the National Research Council of Canada for financial support and for an NRCC Scholarship (to R.T.O.), to Mr. P. Borda for the microanalyses, and to Dr. L. D. Hall and Mr. R. Burton for the n.m.r. spectroscopy.

1. W. Harrison and J. Trotter. J. Chem. Soc. A, 623 (1972).
2. H. N. Stokes. Am. Chem. J. **19**, 782 (1897).
3. H.-J. Krause. Z. Elektrochem. **59**, 1004 (1955).
4. C. E. Brion and N. L. Paddock. J. Chem. Soc. A, 388 (1968).
5. G. E. Coxon, T. F. Palmer, and D. B. Sowerby. J. Chem. Soc. A, 1568 (1967).
6. D. P. Craig and N. L. Paddock. *In* Nonbenzenoid aromatics. Vol. II. Academic Press, New York. 1971. p. 273.
7. W. Harrison, R. T. Oakley, N. L. Paddock, and J. Trotter. Chem. Commun. 357 (1971).
8. L. G. Lund, N. L. Paddock, J. E. Proctor, and H. T. Searle. J. Chem. Soc. 2542 (1960).
9. F. Seel, K. Rudolph, and R. Budenz. Z. Anorg. allgem. Chem. **341**, 196 (1965).
10. L. W. Daasch. J. Am. Chem. Soc. **76**, 3403 (1954).
11. I. C. Hisatsune. Spectrochim. Acta, **21**, 1899 (1965).
12. I. C. Hisatsune. Spectrochim. Acta, **25A**, 301 (1969).
13. E. Steger and R. Stahlberg. Z. Naturforsch. **17b**, 780 (1962).
14. J. Emsley. J. Chem. Soc. A, 109 (1970).
15. A. C. Chapman and N. L. Paddock. J. Chem. Soc. 635 (1962).
16. E. Steger and G. Mildner. Z. Naturforsch. **16b**, 836 (1961).
17. S. Califano. J. Inorg. Nucl. Chem. **24**, 483 (1962).
18. G. E. Coxon and D. B. Sowerby. Inorg. Chim. Acta, **1**, 381 (1967).
19. R. Stahlberg and E. Steger. Spectrochim. Acta, **23A**, 2057 (1967).
20. T. R. Manley and D. A. Williams. Spectrochim. Acta, **23A**, 149 (1967).
21. Mass Spectral Data. Res. Proj. No. 44, Spectrum No. 410. American Petroleum Institute, Pittsburgh.
22. Mass Spectral Data. Res. Proj. No. 44, Spectrum No. 175. American Petroleum Institute, Pittsburgh.
23. R. Keat and R. A. Shaw. J. Chem. Soc. 4802 (1965).
24. R. Keat, S. K. Ray, and R. A. Shaw. J. Chem. Soc. 7193 (1965).
25. G. Allen, D. J. Oldfield, N. L. Paddock, F. Rallo, J. Serreqi, and S. M. Todd. Chem. Ind. 1032 (1965).
26. Sadtler Standard Spectra. No. 3203. Sadtler Research Labs. Inc. (1968).
27. Sadtler Standard Spectra. No. 11. Sadtler Research Labs. Inc. (1968).
28. Sadtler Standard Spectra. No. 10244. Sadtler Research Labs. Inc. (1971).
29. A. L. Bacarella, E. Grunwald, H. P. Marshall, and E. L. Purles. J. Org. Chem. **20**, 747 (1955).
30. E. Högfeldt and J. Bigeleisen. J. Am. Chem. Soc. **82**, 15 (1960).
31. A. R. Goldfarb, A. Mele, and N. Gubstein. J. Am. Chem. Soc. **77**, 6194 (1955).
32. G. B. Ansell and G. J. Bullen. J. Chem. Soc. A, 3026 (1968).
33. E. Tannenbaum, E. M. Coffin, and A. J. Harrison. J. Chem. Phys. **21**, 311 (1953).
34. G. J. Bullen. J. Chem. Soc. 3193 (1962).
35. A. J. Wagner and A. Vos. Acta Cryst. **B24**, 1423 (1968).
36. K. A. R. Mitchell. J. Chem. Soc. A, 2683 (1968).
37. G. J. Bullen. J. Chem. Soc. A, 1450 (1971).
38. R. Hazekamp, T. Migchelsen, and A. Vos. Acta Cryst. **15**, 539 (1962); A. J. Wagner and A. Vos. Acta Cryst. **B24**, 707 (1968).
39. A. W. Schlueter and R. A. Jacobson. J. Chem. Soc. A, 2317 (1968).
40. M. Green and R. F. Hudson. Proc. Chem. Soc. 307 (1962).

Can. J. Chem. Downloaded from www.nrcresearchpress.com by 210.87.254.5 on 09/05/12
For personal use only.

Microwave Spectrum of Cyclohexene Sulfide

R. KEWLEY[1]

Department of Chemistry, Queen's University, Kingston, Ontario

Received August 15, 1972

The microwave spectrum of cyclohexene sulfide (7-thiabicyclo[4,1,0]heptane) has been investigated in the 26.5–40 GHz region. R-branch lines due to both *a*- and *c*-type transitions have been assigned for the ground vibrational state and for the first excited states of the ring bending and ring twisting modes. From relative intensity measurements the frequencies of these two modes are estimated as: $\nu_{bend} = 115 \pm 20$ cm^{-1} and $\nu_{twist} = 200 \pm 60$ cm^{-1}. The rotational constants for the ground vibrational state are (in MHz): $A = 3512.086 \pm 0.010$, $B = 2057.969 \pm 0.003$, and $C = 1623.023 \pm 0.003$. These values are consistent with a twisted half chair structure for the heavy atom skeleton of cyclohexene sulfide, similar to that of cyclohexene oxide.

Le spectre en microondes du sulfure de cyclohexène (thia-7 bicyclo[4,1,0]heptane) a été examiné dans la région de 26.5 à 40 GHz. Les bandes de la branche R, causées à la fois par des transitions du type *a* et du type *c*, ont été attribuées à l'état vibrationnel fondamental et au premier état excité des modes de déformation ("bending") et de torsion ("twisting") du cycle. A partir des mesures d'intensité relative, les fréquences de ces deux modes sont évaluées comme suit: $\nu_{def} = 115 \pm 20$ cm^{-1} et $\nu_{tor} = 200 \pm 60$ cm^{-1}. Les constantes rotationnelles pour l'état vibrationnel fondamental sont (en MHz) $A = 3512.086 \pm 0.010$, $B = 2057.969 \pm 0.003$, et $C = 1623.023 \pm 0.003$. Ces valeurs sont compatibles avec une structure demi-chaise croisée pour le squelette d'atomes lourds du sulfure de cyclohexène, semblable à celui de l'oxyde de cyclohexène. [Traduit par le journal]

Can. J. Chem., **51**, 529 (1973)

Introduction

In a recent microwave study of cyclohexene oxide (1) it was found that the rotational constants and electric dipole moment components of that molecule are compatible with the twisted half chair structure determined by electron diffraction (2, 3):

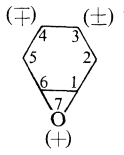

where (+) and (−) designate the heavy atoms that lie above or below the $C_1C_2C_5C_6$ plane, respectively. Although the sulfur analog cyclohexene sulfide has been studied by infrared and ultraviolet spectroscopy (4, 5) and some of its sterol-like derivatives by nuclear magnetic resonance spectroscopy (6), there appears to be no structural data whatever for this molecule in the literature. It was therefore considered that a study of the rotational spectrum of cyclohexene sulfide and a comparison of the results with those for cyclohexene oxide would be of interest.

[1]On sabbatical leave 1971–1972 at Department of Chemistry, Rice University, Houston, Texas 77001.

Experimental

The cyclohexene sulfide sample was purchased from the Aldrich Chemical Company and used without further purification. It was stored at −20 °C when not in use. The rotational spectrum was observed in the 26.5–40 GHz region using a Hewlett–Packard model 8460A MRR spectrometer. Measurements were made at room temperature and at pressures in the range 5–20 μ. The frequency measurements were made with an accuracy of about ±0.05 MHz.

Results

Ground Vibrational State

The spectrum of cyclohexene sulfide is similar to that of cyclohexene oxide (1) in that the lines most easily assigned are those due to ${}^aR_{01}$ transitions originating from nearly degenerate pairs of levels J_{0J} and J_{1J}. For cyclohexene sulfide transitions of this type with $J = 7$, 8, 9, 10, and 11 fall within the 26.5–40 GHz range of the spectrometer. The interval between the transitions $10_{0,10} \rightarrow 11_{0,11}$ and $11_{0,11} \rightarrow 12_{0,12}$ gives $2C \simeq 3245$ MHz, which provides an estimate of C to within 1 MHz of the correct value, see Table 1. Other *a*-type R-branch lines were assigned, making a total of fifty-six such lines, as well as twenty-four somewhat weaker *c*-type R-branch lines with $J = 4$, 5, 6, and 7. A least squares fit, neglecting centrifugal distortion, was performed on these eighty lines of the ground vibrational

Can. J. Chem. Downloaded from www.nrcresearchpress.com by 210.87.254.5 on 09/05/12
For personal use only.

TABLE 1. Rotational constants and moments of inertia* of cyclohexene sulfide

	Value		
		$v = 1$	
Parameter	Ground state	Bending	Twisting
A (MHz)	3512.086(0.010)	3512.416(0.030)	3512.232(0.041)
B (MHz)	2057.969(0.003)	2055.729(0.005)	2054.758(0.005)
C (MHz)	1623.023(0.003)	1622.196(0.004)	1622.139(0.004)
κ†	−0.539514	−0.541269	−0.542272
I_a (a.m.u. Å^2)	143.897	143.883	143.891
I_b (a.m.u. Å^2)	245.571	245.838	245.955
I_c (a.m.u. Å^2)	311.380	311.539	311.550

*Conversion factor 505377 MHz a.m.u. Å^2.
†Asymmetry parameter.

state giving the rotational constants in Table 1. The standard deviation of the least squares fit was 0.27 MHz. No lines of the ^{34}S isotopic form were assigned.

A careful search was undertaken for *b*-type R-branch lines even though, by analogy with cyclohexene oxide which has dipole moment $\mu_b = 0.18$ D, it was not expected that these lines would be strong enough to be observable. In fact no *b*-type lines were found. By comparing the noise level at the frequencies at which the transitions $8_{27} \rightarrow 9_{28}$, $8_{08} \rightarrow 9_{19}$, and $8_{18} \rightarrow 9_{09}$ were predicted to fall with the observed peak heights of the nearby a-type lines $8_{27} \rightarrow 9_{28}$, $8_{08} \rightarrow 9_{09}$, and $8_{18} \rightarrow 9_{19}$, respectively, it was concluded that $\mu_b \leq 0.15\,\mu_a$. Because of the fairly high J values involved and the weakness of the c-type transitions it was unfortunately not possible to measure the Stark shifts for more than two Stark lobes. A considerable amount of time and effort was spent in searching for other lobes. Attempts to find lobes for transitions falling below 26.5 GHz, using a conventional 100 kHz Stark modulation spectrometer, have not yet proved successful. The two measured lobes are:

[1] $7_{16} \rightarrow 8_{17}(M = 1)$ $\quad \Delta\nu/E^2 = (-2.10 \pm 0.05) \times 10^{-6}$ MHz cm^2 V^{-2}

[2] $7_{26} \rightarrow 8_{27}(M = 1)$ $\quad \Delta\nu/E^2 = (1.88 \pm 0.04) \times 10^{-6}$ MHz cm^2 V^{-2}

where $\Delta\nu$ = Stark shift.

The $\Delta\nu/E^2$ values for both lobes are very strongly dependent on the value of μ_c so that accurate determinations of μ_a and μ_b cannot be made from these data alone. However, an accurate value for μ_c can be obtained. Making the assumption that $\mu_b = 0.15\mu_a$ and then solving eqs. 1 and 2 for μ_a and μ_c yields $\mu_a = 1.92 \pm 0.40$ D, $\mu_c = 1.13 \pm 0.02$ D, and $\mu = 2.25 \pm 0.36$ D. If on the other hand μ_b is assumed to be zero, then the calculated dipole moment components are $\mu_a = 1.88 \pm 0.40$ D, $\mu_c = 1.13 \pm 0.02$ D, and $\mu = 2.19 \pm 0.36$ D. These values are based on $\mu_{OCS} = 0.7152$ D (7). Although the total dipole moment has large error limits, it is in quite good agreement with the solution dipole moment of cyclohexene sulfide (in CCl_4), which is 2.13 D (8). The same investigator also determined the (CCl_4 solution) dipole moment of cyclohexene oxide as 2.08 D, which is above the gas phase value of 1.91 D (1). Also the gas phase dipole moments of ethylene oxide and ethylene sulfide are, respectively, 2.00 and 1.84 D (9). This indicates that the gas phase dipole moment of cyclohexene sulfide is in the range 1.75–2.05 D and that the value of about 2.2 D in the present work is likely to be high. The μ_c component of 1.13 ± 0.02 D in cyclohexene sulfide is lower than that of cyclohexene oxide, 1.52 D, primarily because the *c*-axis makes a larger angle with the CSC angle bisector in the episulfide as compared with the angle made with the COC angle bisector in the epoxide. The increase in mass from oxygen to sulfur causes this effect.

Excited Vibrational States

In addition to the absorption lines of the ground vibrational state two sets of vibrational satellite transitions have been assigned. Intensities relative to the ground state were measured for thirteen transitions of one satellite set, yielding a vibrational frequency of 115 ± 20 cm^{-1}. Twelve

Can. J. Chem. Downloaded from www.nrcresearchpress.com by 210.87.254.5 on 09/05/12
For personal use only.

Can. J. Chem. Downloaded from www.nrcresearchpress.com by 210.87.254.5 on 09/05/12
For personal use only.

relative intensity measurements for the other weaker satellite set gave a frequency of 200 ± 65 cm^{-1}. As was the case for cyclohexene oxide the lower of the two frequencies may be attributed to the bending of the six-membered ring (about the direction C_2C_5, approximately) and the higher frequency to the twisting motion involving mainly C_3 and C_4. The corresponding frequencies for cyclohexene oxide are 156 cm^{-1} (bending) and 280 cm^{-1} (twisting) (1). The frequencies of fifty-nine rotational transitions for the first excited state of the bending mode and of fifty-five transitions of the first excited state of the twisting mode were measured. The rotational constants are given in Table 1. The standard deviations of the least squares fits were 0.35 MHz (bending mode, $v_{bend} = 1$) and 0.34 MHz (twisting mode, $v_{twist} = 1$).

Molecular Structure

As in the case of cyclohexene oxide the three measured rotational constants for the ground vibrational state of cyclohexene sulfide are insufficient to define a precise molecular structure. However, it is again possible to carry out a calculation based on reasonable assumptions for the other structural parameters in order to estimate the ring bending and twisting angles. Before doing so it may be noted that the planar moment of inertia $\sum_i m_i b_i^2 = 1/2(I_a + I_c - I_b)$ would be expected to remain about the same on going from cyclohexene oxide to cyclohexene sulfide provided that the structures are similar. The O or S atom should be very near the *a*–*c* plane. Also the C—C and C—H distances and the HCH and HCC bond angles do not change significantly between ethylene oxide and ethylene sulfide (9). Calculating from the observed moments of inertia it is found that $\sum_i m_i b_i^2 = 104.853$ a.m.u. Å^2 for cyclohexene sulfide and 104.940 a.m.u. Å^2 for cyclohexene oxide. These values give some support to the conclusion that the replacement of the oxygen atom of cyclohexene oxide by sulfur does not have a drastic effect on the rest of the structure. Therefore the procedure adopted below consists of assuming that the parameters of the epithio section are identical with those of ethylene sulfide while the other parameters are essentially the same as those assumed for cyclohexene oxide (1). The assumed $\angle C_6C_1C_2$ and the other CCC bond angles differ very slightly from the assumed cyclohexene oxide values because of the slightly different C_1C_6 distance. The angle between the H_1C_1 direction and the $C_1C_2C_5C_6$ plane in cyclohexene sulfide is assumed equal to the angle between the $H_{11}C_1$ direction and the $C_1H_{12}H_{22}C_2$ plane in ethylene sulfide (9) (Table 2).

TABLE 2. Initially assumed structure of cyclohexene sulfide*

Bond	Distance (Å)	Bonds†	Angles (deg)
C_1C_6	1.492	C_1SC_6	65.8
C_1S	1.819	$C_6C_1C_2$	121.7
C_1C_2	1.53	$C_1C_6C_5$	121.7
C_5C_6	1.53	$H_1C_1C_2$	116.8
C_2C_3	1.53	$H_6C_6C_5$	116.8
C_4C_5	1.53	All HCH	109.5
C_3C_4	1.53		
All CH	1.09		

*See Fig. 1.
†$\angle C_1C_2C_3 = \angle C_6C_5C_4$; $\angle C_2C_3C_4 = \angle C_5C_4C_3$. ∠HCH and ∠CCC have a common bisector at C_2, C_3, C_4, and C_5.

In addition there are the three ring angle parameters: the ring fusion angle θ, the twisting angle τ and the bending angle β, see Fig. 1. For cyclohexene oxide it was found that only for β close to zero could the residuals ($A_{obsd} - A_{calcd}$, etc.), in the least squares fit to the observed rotational constants, become very nearly zero. Starting from the cyclohexene sulfide structure assumed above, it is found that the residuals

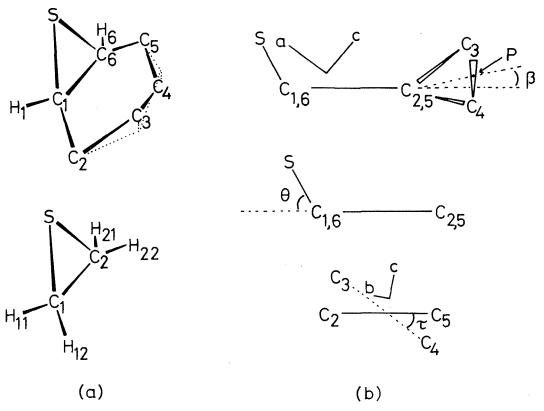

FIG. 1. (*a*) Structures of ethylene sulfide and cyclohexene sulfide. In the cyclohexene sulfide structure the hydrogen atoms attached to C_3, C_4, C_5, and C_6 have been omitted for clarity. (*b*) Definitions of the angles β (bending angle), θ (ring fusion angle), and τ (twisting angle). The point P is midway between carbon atoms C_3 and C_4. The approximate positions at the principal *a*, *b*, and *c* inertia axes are also indicated.

reach their minimum value (all less than 0.05 MHz) at $\beta = 25.7°$, $\theta = 57.2°$, and $\tau = 33.8°$. It does not seem reasonable that β should differ by as much as 25° between the two molecules. It was noticed that the value of β for minimized residuals was very sensitive to the initially assumed value of $\angle C_6C_1C_2$, which also determines the other CCC angles. A decrease of 1.1° in the value of this angle gives $\beta = 0°$, $\theta = 71.5°$ and $\tau = 27.6°$ for minimized residuals, all less than 0.05 MHz. These values appear to be quite reasonable when compared to the corresponding ones $\beta = 0°$, $\theta = 68.4°$, and $\tau = 34.4°$ obtained for cyclohexene oxide, with $\angle C_6C_1C_2 = 122°$ assumed. It should be borne in mind that these angles, for each molecule, do not represent a unique solution for the structure and that other values could be arrived at by varying $\angle C_6C_1C_2$ or the other assumed parameters.

This work was done at Rice University in the laboratory of Professor Robert F. Curl, Jr., whose interest in the problem is gratefully acknowledged. The work was supported by grant number GP 29374 from the National Science Foundation and by grant number C-071 from the Robert A. Welch Foundation. The author would also like to acknowledge a travel grant to Houston from the National Research Council of Canada.

1. T. Ikeda, R. Kewley, and R. F. Curl, Jr. J. Mol. Spectrosc. In press.
2. B. Ottar. Act. Chem. Scand. **1**, 283 (1947).
3. V. A. Naumov and V. M. Bezzubov. J. Struct. Chem. **8**, 466 (1967).
4. N. Sheppard. Trans. Faraday Soc. **46**, 429 (1950).
5. R. E. Davis. J. Org. Chem. **23**, 216 (1958).
6. K. Tori, T. Komeno, and T. Nakagawa. J. Org. Chem. **29**, 1136 (1964).
7. J. S. Muenter. J. Chem. Phys. **48**, 4544 (1968).
8. A. N. Vereshchagin. Isv. Akad. Nauk. SSSR, Ser. Khim. 1969, (3), 559 (Chem. Abstr. **71**, 21588d (1970)).
9. G. L. Cunningham, A. W. Boyd, R. J. Meyers, and W. D. Gwinn. J. Chem. Phys. **19**, 676 (1951).

Can. J. Chem. Downloaded from www.nrcresearchpress.com by 210.87.254.5 on 09/05/12
For personal use only.

Heterogeneous Interactions of Methylamines on Porous Adsorbents. Part III. The Adsorption Characteristics of Methylamines on γ-alumina and Types '3A' and '13X' 'Molecular Sieves'

WALTER GEORGE COOK AND ROBERT ANDERSON ROSS
Department of Chemistry, Lakehead University, Thunder Bay, Ontario
Received September 6, 1972

The adsorption characteristics of mono-, di-, and trimethylamine on γ-alumina have been investigated and adsorption isotherms in the regions of their boiling points determined, along with isothermal calorimetric heats of adsorption up to monolayer coverage ($\theta = 1$). From the initial heats of adsorption of 21.6 to 32.4 kcal/mol at $\theta = 0.05$, and the strong retention of the amines adsorbed at low pressures, chemisorption is considered to occur at $\theta < 0.20$. The maxima and minima displayed in the heat curves are discussed in terms of adsorbate–adsorbate interactions at sub-monolayer coverage levels. Adsorption isotherms for di- and tri-methylamine on Linde 'molecular sieves' '13X' and '3A' have been measured also, along with the trimethylamine heat curves for these materials.

Les caractéristiques d'adsorption des mono-, di-, et tri-méthylamines sur de l'alumine-γ ont été étudiées de même que les isothermes d'adsorption dans la région de leur point d'ébullition ont été déterminés en même temps que les chaleurs calorimétriques isothermales d'adsorption jusqu'à un recouvrement correspondant à une couche monomoléculaire ($\theta = 1$). A partir des chaleurs initiales d'adsorption qui correspondent à 21.6 jusqu'à 32.4 kcal/mol à $\theta = 0.05$, et de la rétention forte des amines adsorbées à basse pression, la chemisorption est prévisible pour des valeurs de $\theta < 0.20$. Les maxima et les minima observés dans les courbes de chaleur sont expliqués en terme d'interactions produit adsorbé – produit adsorbé à des niveaux de recouvrement inférieurs à la couche monomoléculaire. Les isothermes d'adsorption pour les di-, et tri-méthylamines sur de la sève moléculaire du type Linde '13X' et '3A', ont aussi été mesurés en même temps que les courbes de chaleur de la tri-méthylamine pour ces produits.

[Traduit par le journal]

Can. J. Chem., **51**, 533 (1973)

Can. J. Chem. Downloaded from www.nrcresearchpress.com by 210.87.254.42 on 09/05/12
For personal use only.

Introduction

In Parts I and II studies of the interactions of mono-, di-, and trimethylamine on silica gel and silica–alumina were reported (1, 2). The shapes of the heat curves obtained for the adsorption of these species on both materials were of particular interest as in many cases well-defined maxima and minima were observed. These phenomena were considered to arise mainly through adsorbate–adsorbate interactions. To obtain further information on the adsorption properties of the amines the work has been extended to include a study of their adsorption characteristics on γ-alumina and two types of synthetic zeolites, namely, Linde molecular sieves, '13X' and '3A'.

Experimental

The techniques of measurement, sorption balance, and calorimetry have been described (3, 4) and the physical properties of the γ-alumina adsorbent determined. Data supplied with the γ-alumina (Peter Spence and Sons Ltd.) stated it to be an aluminum trihydroxide with an X-ray structure showing 97% Gibbsite and 3% Bayerite, particle size 20 to 600 μ, and BET surface area 400 m^2/g after heat treatment at 420 °C. 'Molecular sieve' pellets were obtained from Union Carbide Corporation. A crystalline potassium aluminosilicate, type 3A, and a crystalline sodium alumino-silicate, type 13X, were used.

The purification procedures used for the amine adsorbates have been specified (1, 2).

Results

γ-*Alumina*

In all experiments alumina samples were activated at 420 °C for 3 h in air and then outgassed at 90 °C for 1 h under a vacuum of 10^{-5} Torr in the adsorption apparatus before use.

The complete adsorption–desorption isotherm for monomethylamine on γ-alumina at 266 °K is shown in Fig. 1, curve *B*. Equilibrium times were 45 min up to $p/p_0 = 0.50$ and 4 h above this pressure. The heat curve for monomethylamine adsorption on γ-alumina at 266 °K is shown in Fig. 3, curve *B*.

Figure 1 curve *A* shows the adsorption–desorption isotherm determined for dimethylamine on γ-alumina at 280 °K and Fig. 3 shows the heat curve *C* for this system. The corresponding data

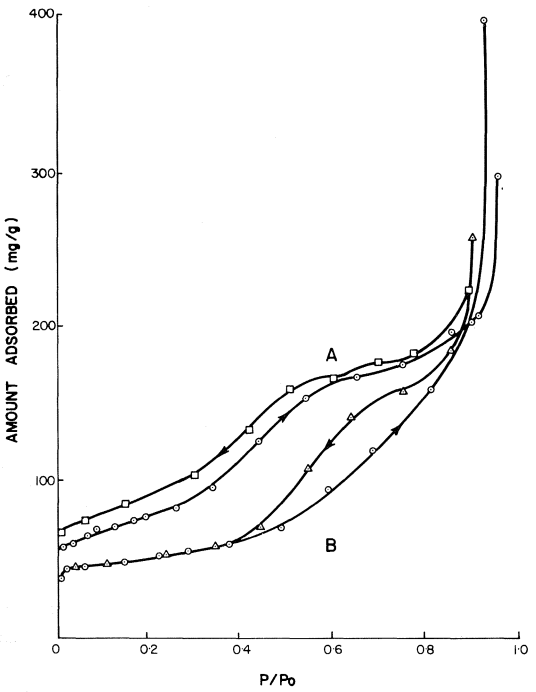

FIG. 1. Adsorption–desorption isotherms for *A*, dimethylamine at 280 °K and *B*, monomethylamine at 266 °K on γ-alumina.

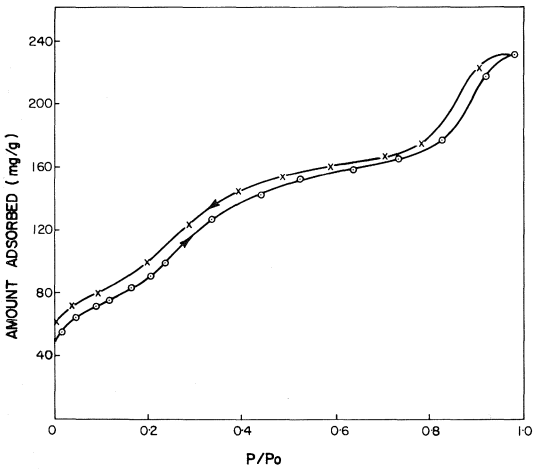

FIG. 2. Adsorption–desorption isotherm for trimethylamine at 276 °K on γ-alumina.

for trimethylamine adsorption at 276 °K are shown in Figs. 2 and 3, curves *A*.

The monolayer coverage values for mono-, di-, and tri-methylamine on γ-alumina were determined from BET plots to be 40.7, 65.0, and 72.7 mg/g, respectively, at the isotherm temperatures shown.

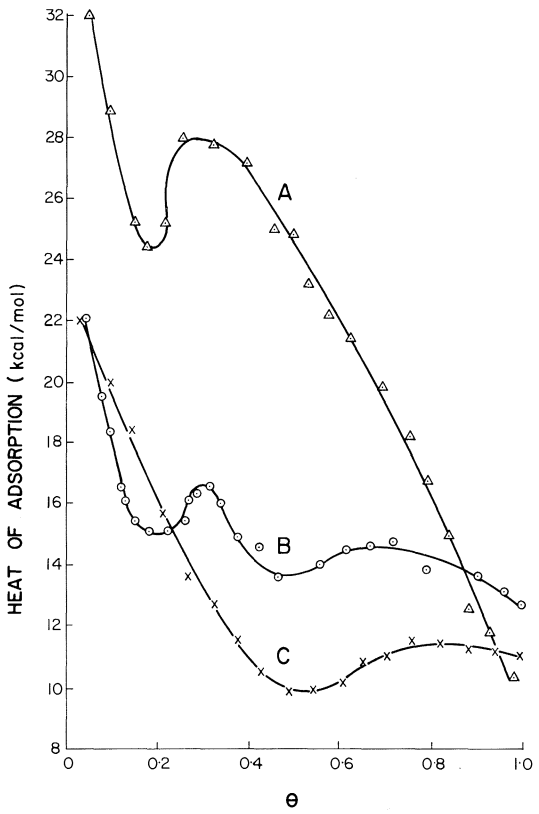

FIG. 3. Variation of isothermal calorimetric heats of adsorption with θ (fraction of surface covered) for *A*, trimethylamine at 276 °K, *B*, monomethylamine at 266 °K and *C*, dimethylamine at 280 °K on γ-alumina.

'*Molecular Sieves*'

The adsorption isotherms determined for dimethylamine adsorption on 'molecular sieves' '3A' and '13X' at 280 °K are shown in Figs. 4 and 5, curves *A*. Both materials had been activated in air at 316 °C (5) for 3 h and outgassed at 90 °C under a vacuum of 10^{-5} Torr for 1 h. In experiments with the '3A' 'molecular sieve', equilibrium was taken to be established when no measurable adsorption was detected over a 1 h period. This basis was used as an arbitrary standard since only on prolonged exposure of the 'molecular sieve' to the amine for 24 h was a further small uptake observed. The experimental error involved by adopting this procedure was estimated to be less than 0.5%. Equilibrium times for the '13X' molecular sieve' were 30 min below $p/p_0 = 0.90$ and 60 min at the highest pressures. Desorption times were consistently 60 min over the entire pressure range.

Can. J. Chem. Downloaded from www.nrcresearchpress.com by 210.87.254.42 on 09/05/12
For personal use only.

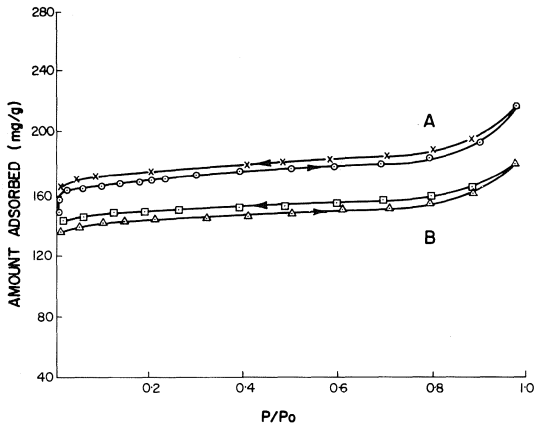

FIG. 4. Adsorption–desorption isotherms for *A*, dimethylamine at 280 °K and *B*, trimethylamine at 276 °K on 'molecular sieve' '13X'.

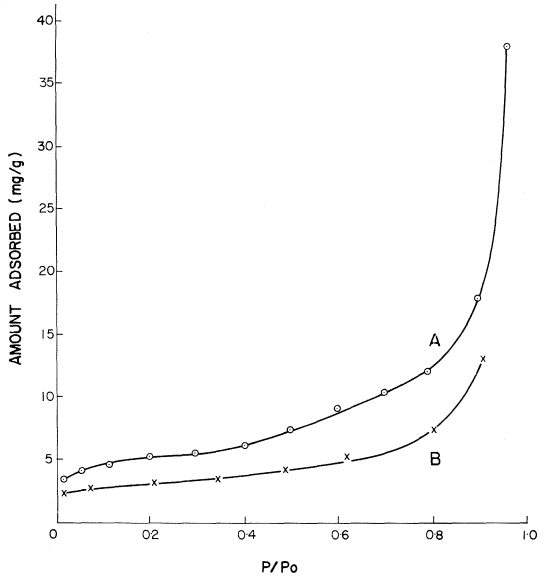

FIG. 5. Adsorption isotherms for *A*, dimethylamine at 280 °K and *B*, trimethylamine at 276 °K on 'molecular sieve' '3A'.

Trimethylamine adsorption isotherms at 276 °K on 'molecular sieves' '13X' and '3A', (Figs. 4 and 5), were of the same general form as the corresponding dimethylamine isotherms. The heat curves for trimethylamine on these materials are shown in Fig. 6.

Discussion

The adsorption of all amines on γ-alumina was initially strong, particularly in the region $p/p_0 < 0.02$. Samples of alumina equilibrated at 266

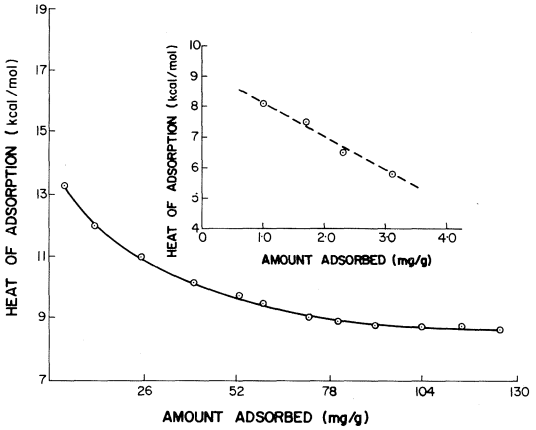

FIG. 6. Variation of isothermal calorimetric heats of adsorption with amount adsorbed for trimethylamine at 280 °K on 'molecular sieve' '13X' and 'molecular sieve' '3A' (inset).

°K in mono-methylamine vapor, $p/p_0 = 0.90$, when evacuated to 10^{-5} Torr for 1 h at this temperature retained 22.7 mg/g of the amine which corresponds to 55.7% of the monolayer coverage amount. On raising the temperature to 353 °K, the alumina still held 9.3% of the monolayer amount after being evacuated to 10^{-5} Torr for 1 h. This region of surface coverage therefore, is considered to involve strong adsorption which may involve chemisorption (6).

The adsorption isotherms of the amines on alumina show marked increases in the amounts adsorbed, after monolayer completion, beginning at $p/p_0 = 0.50$, 0.30 and 0.25 for mono-, di-, and trimethylamine, respectively. With mono- and dimethylamine, the amount adsorbed increased asymptotically above $p/p_0 = 0.90$ while trimethylamine adsorption showed a sharp increase between $p/p_0 = 0.83$ and 0.99. These effects are probably linked to the distribution of pore sizes of this adsorbent, which were determined (7) from low temperature nitrogen isotherms by the method of Cranston and Inkley (8), and which range from 20 to 300 Å in diameter with maxima occurring at 30 and 230 Å. The very steep increase in adsorption found for mono- and dimethylamine may be due to condensation of these adsorbates in the 230 Å diameter pores of the alumina. An analogous effect has been reported for the adsorption of methylamines on a "macroporous" silica gel which also showed a maximum in its pore size distribution in the range 200 to 230 Å diameter (1, 2).

Can. J. Chem. Downloaded from www.nrcresearchpress.com by 210.87.254.42 on 09/05/12
For personal use only.

Can. J. Chem. Downloaded from www.nrcresearchpress.com by 210.87.254.42 on 09/05/12
For personal use only.

The initially-high heats of adsorption of the amines on alumina, Fig. 3, are compatible with the suggestion that chemisorption is involved at low surface coverages, $\theta < 0.2$. These heats, from 21.6 to 32.4 kcal/mol, probably arise through a chemisorptive process which may involve donation of the lone pair electrons of the amine nitrogen atom to empty sp^3 hybrid orbitals of surface aluminum ions (9). In this connection it is worth noting that nuclear magnetic resonance studies of the adsorption of monomethylamine on γ-alumina indicate that the hydrogens of the amino group are more restricted than the methyl hydrogens (10). Other modes of adsorption have been suggested for ammonia on γ-alumina, including adsorption on surface oxygen species with the formation of amide ions (11), and also adsorption through coordination of the nitrogen atom to a surface aluminum ion with concurrent hydrogen bonding to surface oxide ions (11). The absence of strong Brϕnsted acidity on alumina has been deduced from both pyridine (12) and ammonia adsorption studies (11). Thus the adsorption of methylamines may not only involve interaction between amine–nitrogen electrons and surface aluminum ions but also simultaneous hydrogen bonding of amino hydrogens to surface oxide species. Thus for dimethylamine

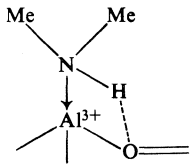

amine adsorption through interactions with surface hydroxyl groups and oxide ions may also occur.

The heats of adsorption on alumina for monomethylamine (Fig. 3, curve *B*) and trimethylamine (Fig. 3, curve *A*) fall to a minimum at $\theta = 0.20$ and 0.17, respectively, and then rise to a maximum at $\theta = 0.30$ and 0.28, respectively. The magnitude of these rises was 1.5 kcal/mol for monomethylamine and 3.6 kcal/mol for trimethylamine. This effect may result from lateral interactions between amine molecules which have been adsorbed at pressures corresponding to the minimum value of the heat curve in close proximity to amine molecules adsorbed earlier. Similar increases in the heat of adsorption to those displayed at low surface coverages with mono- and trimethylamine have been reported for ammonia adsorption on alumina (13).

The dimethylamine heats of adsorption on alumina do not show the rise which might be expected by analogy to occur at approximately $\theta = 0.29$. However, a noticeable similarity between the heat curves for mono- and dimethylamine is the occurrence of the minimum at $\theta = 0.50$ and 0.48, respectively. This fraction of monolayer coverage may correspond to the occupation of the "most active" adsorption sites by these adsorbates. Following these minima both curves show a gradual rise to a maximum at $\theta = 0.70$ and 0.81 and then a slight decrease to monolayer coverage. The increase in the heat of adsorption in this region is probably due to van der Waals interactions (14) amongst the adsorbed molecules while the subsequent decrease may occur as a result of repulsion between the partially-formed layer of polarized adsorbed molecules and molecules adsorbing subsequently in close proximity as the monolayer nears completion.

After the maximum shown at about $\theta = 0.28$ in the heat of adsorption of trimethylamine on alumina (Fig. 3), the heat evolved falls almost linearly from 28.0 to 9.9 kcal/mol at monolayer completion. The absence of a minimum at approximately $\theta = 0.5$ in this curve is difficult to explain but it may be that the large trimethylamine molecule, cross-sectional area about 30 $Å^2$ (1, 2), interacts with closely-adsorbed molecules over the entire range of surface coverage from from $\theta = 0.30$ to monolayer completion. This suggestion does not exclude any decrease in the heat of adsorption which would be expected to occur through surface heterogeneity.

The adsorption isotherms of di- and trimethylamine on 'molecular sieve' '13X', Fig. 4, are of the Langmuirian type. The effective pore diameter of this material is 10 Å (5) and these isotherms indicate that the internal cavities are almost filled by the amines at $p/p_0 = 0.01$ with little increase in adsorption below $p/p_0 = 0.70$. Between these pressures, the increase in amount adsorbed for dimethylamine was 17.0 and 13.0 mg/g for trimethylamine. Above $p/p_0 = 0.70$ both isotherms showed a considerably greater increase in the adsorbed amount, 37.0 mg/g for dimethylamine and 27.0 mg/g for trimethylamine while hysteresis occurred on desorption of both adsorbates over the entire pressure range.

In order to determine if the increased adsorption of di- and trimethylamine on 'molecular sieve' '13X' above $p/p_0 = 0.70$ could be explained by adsorption in surface discontinuities in the

pellets of the material, corresponding isotherms were determined on 'molecular sieve' '3A'. Since the effective pore diameter of this zeolite is 3 Å (5), the adsorption of di- and trimethylamine would be limited to the external surface. In both isotherms, Fig. 5, a distinct rise in the amount adsorbed took place at high pressures which seems to confirm that the final increase in adsorption on both molecular sieves did arise through intercalation and condensation of the adsorbates in the fissures and cracks in the surfaces of the pellets.

The heat of adsorption of trimethylamine on 'molecular sieve' '13X' is shown in Fig. 6. The curve falls smoothly from 13.3 kcal/mol at 5.2 mg/g adsorbed to 8.8 kcal/mol at 91.0 mg/g adsorbed and then remains constant. (It should be noted that the heats of adsorption for the 'molecular sieves' have been plotted against the amount of amine adsorbed since the basic assumptions of surface area determination do not hold for these materials (15).) A similarly-shaped heat of adsorption curve has been reported (16) for ammonia adsorption on synthetic Na faujasite. The '13X' 'molecular sieve' does not appear to contain any strong acidic adsorption sites as the initial heat evolved on trimethylamine adsorption is much lower than that observed with trimethylamine adsorption on alumina, silica–alumina or silica gel. The heats evolved on these materials were 32.4, 21.4, and 21.0 kcal/mol, respectively, at $\theta = 0.05$ (2). The fact that no irregularities are displayed in the '13X' heat curve may imply that a degree of surface heterogeniety is a factor in giving rise to increases in the heat of adsorption at low surface coverages on γ-alumina and the other siliceous adsorbents.

An attempt was made to estimate the heat evolved on trimethylamine adsorption on 'molecular sieve' '3A', Fig. 6 (inset). Extrapolation of the dotted line in this Figure gives a value of approximately 9.5 kcal/mol for initial adsorption compared with 14.0 kcal/mol for 'molecular sieve' '13X'.

1. W. G. Cook and R. A. Ross. Can. J. Chem. **50**, 1666 (1972).
2. W. G. Cook and R. A. Ross. Can. J. Chem. **50**, 2451 (1972).
3. R. A. Ross and A. H. Taylor. Proc. Brit. Ceram. Soc. **5**, 167 (1965).
4. E. Robinson and R. A. Ross. J. Chem. Soc. (A), 2521 (1969).
5. Union Carbide molecular sieves for selective adsorption. British Drug Houses. 1967. Section 5.
6. C. Clarke-Monks, B. Ellis, and K. Rowan. J. Colloid. Int. Sci. **32**, 628 (1970).
7. S. Brunauer, P. H. Emmett, and E. Teller. J. Am. Chem. Soc. **60**, 309 (1938).
8. R. W. Cranston and F. A. Inkley. Adv. Catal. **9**, 143 (1957).
9. M. L. Hair. Infrared spectroscopy in surface chemistry. Edward Arnold, London. 1967. p. 146.
10. K. Hirota, K. Fueki, and T. Sakai. Bull. Chem. Soc. Jap. **35**, 1545 (1962).
11. J. B. Peri. J. Phys. Chem. **69**, 220 (1965).
12. E. P. Parry. J. Catal. **2**, 371 (1963).
13. V. Kervorkian and R. O. Steiner. J. Phys. Chem. **67**, 545 (1962).
14. J. H. de Boer. The dynamical character of adsorption. 2nd ed. Oxford University Press, London. 1968. p. 157.
15. M. M. Dubinin. J. Colloid Int. Sci. **23**, 487 (1967).
16. L. H. Little. Infrared spectra of adsorbed species. Academic Press Inc., New York. 1966. p. 276.

Can. J. Chem. Downloaded from www.nrcresearchpress.com by 210.87.254.42 on 09/05/12
For personal use only.

Studies of Oxygen Exchange Between Trivalent Lanthanide – EDTA Complexes and Solvent Water: Evidence for a Structural Change Within the Series

R. H. Betts and R. H. Voss[1]

Department of Chemistry, University of Manitoba, Winnipeg, Manitoba R3T 2N2

Received August 30, 1972

Oxygen-18 labelled EDTA, dissolved in normal water, has been used to examine the kinetics of oxygen transfer between the solvent and a variety of metal–EDTA complexes, including most of the lanthanides, Ca and Th. The lability of the oxygens is profoundly affected by the ionic charge of the metal in the chelate. Thus oxygen exchange in the Th–EDTA–H_2O system shows a half-life of 10 min at 100 °C, while for comparable conditions, Ca–EDTA–H_2O shows a half-life in excess of 100 days. The lanthanides as a group show behavior intermediate between these extremes. Within the latter group the lability varies systematically with atomic number, Pr–EDTA (element 59) being the most reactive and Yb–EDTA (element 70) the least reactive. The maximum variation across the group is about 10-fold. Interpretation of these results is presented in terms of the polarizing effect of the metal ion on the electron density at the acetate groups. The variation in lability within the lanthanide group can be accounted for quantitatively by changes in coordination number of the central metal ion.

De l'EDTA marqué par de l'oxygène-18, dissous dans l'eau normale, a été utilisé pour examiner la cinétique du transfert d'oxygène entre le solvant et une série de complexes métal–EDTA, conprenant la plupart des lanthanides, Ca et Th. La labilité des oxygènes est profondément affectée par la charge ionique du métal dans le chélate. Par suite l'échange de l'oxygène dans le système Th–EDTA–H_2O possède une demi-vie de 10 min à 100 °C, alors que dans des conditions comparables, Ca–EDTA–H_2O possède une demi-vie supérieure à 100 jours. Les lanthanides, comme un groupe, possèdent un comportement intermédiaire entre ces 2 extrêmes. A l'intérieur de ce dernier groupe, la labilité varie systématiquement avec le numéro atomique, Pr–EDTA (élément no. 59) étant le plus réactif et Yb–EDTA (élément no. 70) le moins réactif. La variation maximum à travers le groupe se situe dans un intervalle de 10 environ. L'interprétation de ces résultats est présenté en terme d'effet polarisant de l'ion métallique sur la densité électrique des groupes acétales. La variation dans la labilité à l'intérieur du groupe des lanthanides peut être expliqué quantitativement par des changements dans le nombre de coordination de l'ion métallique central.

[Traduit par le journal]

Can. J. Chem., **51**, 538 (1973)

Introduction

In recent years increasing emphasis has been placed on the study of the types of reaction undergone by coordinated ligands as opposed to the study of the behavior of the coordinated metal ions (1–3). A familiar example of this type of study is the metal ion catalyzed hydrolysis of amino acid esters (eq. 1) discovered by Kroll in 1951 (4). The most immediate consequence of ligand coordination is an electronic polarization of the substrate which facilitates the breaking of a bond or attack by a nucleophile. In this respect, the metal ion catalyst functions as a Lewis acid withdrawing electrons from the reaction center. The proton acts similarly in the corresponding acid-catalyzed reaction. However, unlike the hydrogen ion, metal ions may operate in neutral or weakly basic solution (thus the hydrolysis of

[1] 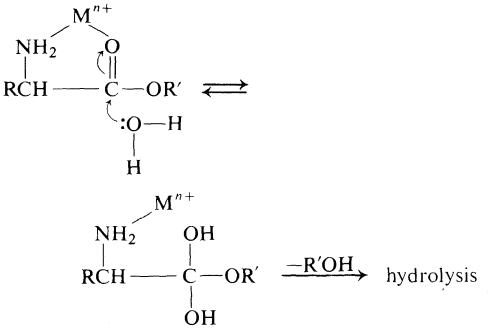

amino acid esters complexed with Co^{2+}, Cu^{2+}, Mn^{2+}, Ca^{2+}, and Mg^{2+} ions is extremely rapid even at p*H* 7–8 where the amino acid ester itself is stable (4)).

If the stability constant may be regarded as a measure of the ability of the metal ion to accept electrons, then in the cases where the acidity of the central ion is of importance in catalysis, one might expect to find a correlation between com-

[1]Holder of an N.R.C.C. Scholarship, 1971–1972.

Can. J. Chem. Downloaded from www.nrcresearchpress.com by 210.87.254.40 on 09/05/12
For personal use only.

Can. J. Chem. Downloaded from www.nrcresearchpress.com by 210.87.254.40 on 09/05/12
For personal use only.

plex stability and catalytic power. Such a relationship is indeed frequently found in nonenzymatic reactions. Kroll (4), for example, established a correspondence between the catalytic effect of the metal ions and their increasing tendency to enter into complex formation. More relevant to the present study is the observation that in the lanthanide ion catalyzed decarboxylation of oxaloacetic acid, a correlation was established between the catalytic effect of the lanthanide ion and the stability of the chelate compounds of the lanthanide oxaloacetates (5).

The present work relates to the effect of complexation of a carboxylate on the lability of its oxygen atoms with respect to exchange with water, and in particular the lanthanide (Ln)–EDTA complexes (EDTA represents ethylenediaminetetraacetic acid). The filling of the 4f subshell of the lanthanides is accompanied by a decrease of the ionic radius ("lanthanide contraction") in a regular fashion from La^{3+} (1.16 Å) to Lu^{3+} (0.93 Å) (6). Another important property of the lanthanides is that their bonding with ligands is considered to be predominantly electrostatic (7–9) largely due to the identical noble gas configurations of their outer electronic shells.

The stability constants for complexation with EDTA in aqueous solution (reaction 2) are fairly

[2] $Ln^{3+}(OH_2)_m + EDTA^{4-} \rightarrow Ln(EDTA)(OH_2)_n^- + (m - n)H_2O$

sizeable; log K values range from 15.50 for La^{3+} to 19.83 for Lu^{3+} (10) (increasing in a regular manner as the ionic size decreases).

Inasmuch as the interaction of the Ln^{3+} ions with ligands is largely electrostatic, these ions are particularly suitable for a study of the influence of the size of the central ion on its behavior in chelate formation.

Choppin has pointed out in a recent review (7) that the nature of the lanthanide complex species present in aqueous solution is still uncertain. However, ample evidence now exists (7–9) to support the view that the coordination number (C.N.) of the lanthanides is greater than six and probably 8, 9, or 10; so that even the Ln–EDTA complexes are expected to be still partially hydrated in aqueous solution.

Hoard *et al.* (11) found from crystal structure determinations of some hydrated salts that La^{3+} is coordinated to one EDTA molecule and three water molecules (giving a net coordination number (C.N.) of 9); the entire arrangement is approximately that of two hemispheres, one containing the 3 water molecules and the other, the 6 ethylenediaminetetraacetate donor sites. Such work appears to be the most convincing evidence for an expanded C.N. for the lanthanides, and if we assume that a high C.N. is preserved in aqueous solution, then a reasonable representation of the Ln–EDTA complexes is:

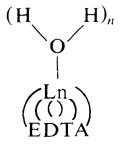

EDTA utilizes all six of its donor atoms and, in addition, there are n water molecules within the primary coordination sphere giving a net C.N. of $(6 + n)$.

Various authors have expressed the opinion that owing to the "lanthanide contraction" partially hydrated complexes (12–14) and in particular the EDTA complexes (11, 15–17) are expected to undergo a change in coordination number somewhere in the middle of the lanthanide series. Such a change is also considered to be revealed in the irregular progression of the enthalpy (ΔH) and entropy (ΔS, see Fig. 1) changes associated with the complex formation reaction (eq. 2) (11, 15–17). The explanation offered proceeds somewhat as follows. As the radius of the Ln^{3+} ion decreases from La^{3+} to Lu^{3+} (and the polarizing ability of the ion increases) EDTA can reach further around the cation. The ultimate effect of this shrinkage of the "ligand envelope" is the ejection of another water molecule from the coordination sphere occurring within the series between Sm and Tb. Because of the additional release of water, the formation of the complex containing one water molecule less $Ln(EDTA)(H_2O)_{n-1}^-$ is entropically favored, and the observed entropy increase (Fig. 1) can be explained. In the region between Sm and Tb an equilibrium is proposed (17) between two types of EDTA complexes differing in their degree of hydration which in the series

[3] $Ln(EDTA)(OH_2)_n^- \rightleftharpoons Ln(EDTA)(OH_2)_{n-1}^- + H_2O$

$$K_s = \frac{[Ln(EDTA)(OH_2)_{n-1}^-]}{[Ln(EDTA)(OH_2)_n^-]}$$

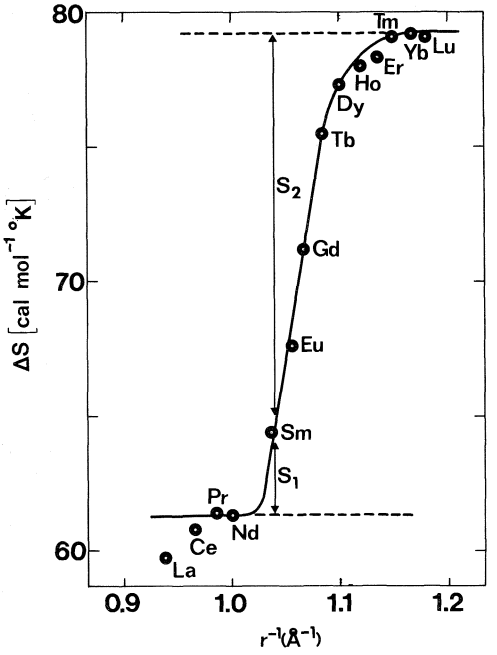

FIG. 1. Entropy change, ΔS, for Ln–EDTA complex formation reaction (eq. 2); for $\mu = 0.1$ *M*, 20 °C (33).

Sm, Eu, Gd, and Tb is gradually shifted towards the right. Geier and Karlen (17) were able to attach some quantitative significance to the above interpretation by evaluating the equilibrium constants for reaction 3. The relative amounts of the two complexes and therefore $K_s(= S_1/S_2)$ were determined from the distances S_1 and S_2 as indicated for Sm in Fig. 1. Additional evidence for the existence of an equilibrium such as [3] has been obtained at least for the europium complex from spectrophotometric (18–20) and polarographic studies (21) of aqueous solutions of the Eu–EDTA complex. The equilibrium constants, K_s, evaluated from spectrophotometric studies (18–20) were in good agreement with the values derived from thermodynamic data (17).

As regards the aquo ions, conflicting opinions have arisen. One group maintains that the C.N. of the aquo ions also changes across the series (7, 11, 22, 23) and is probably 9 for the ions from La^{3+} to Nd^{3+}, 8 for the ions from Tb^{3+} to Lu^{3+}, with the intermediate ions Sm^{3+}, Er^{3+}, and Gd^{3+} being mixtures of both types. Spedding's interpretation (22) is based on the observation that the apparent molal volumes of the Ln^{3+} ions show a non-monotonic development (becoming smaller from La to Nd, becoming larger from Nd to Tb, and then decreasing once more from Tb to Yb). On the other hand, Geier *et al.* (17–19) and Anderegg (14) are not convinced that the C.N. of the aquo ions changes. Geier considers it probable that the C.N. is 9, corresponding to a trigonal prismatic structure as found from an X-ray crystallographic study by Helmholz (24) for the $Nd(OH_2)_9^{3+}$ grouping in the solid compound $Nd(BrO_3)_3 \cdot 9H_2O$.

On the basis of (*a*) their interpretation of the thermodynamic data for EDTA complexation (as described earlier) and (*b*) the assumption that the C.N. of all the aquo lanthanide ions was constant across the series and equal to 9 (that is, $m = 9$ in eq. 2 and $n = 3$ in eq. 3), Geier and Karlen (17) investigated the thermodynamics for mixed complex formation (that is, the formation of complexes Ln(EDTA) (L) $(OH_2)_x$ where L = anions of OXS, IDA or NTA)[2] and found their data to be compatible with their original hypotheses (*a*) and (*b*). The two types of complexes in equilibrium [3] can then be represented schematically as follows

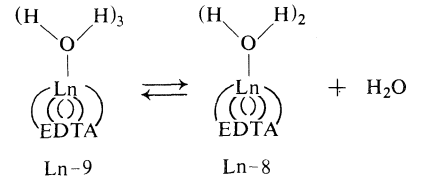

A recent study by Grenthe and Ots (25) on the lanthanide diglycolate complexes provides new evidence in support of Geier's proposed hydration equilibria [3]. A maximum in the plot of the heat capacity change (ΔC_{p_2}) for the formation of the 1:2 Ln–diglycolate complexes *vs.* atomic number was interpreted as due to the presence of hydration equilibria which (according to an expected similarity in the geometry of the Ln–EDTA complex (11) and the complex formed by the coordination of two (terdentate) diglycolate ligands to the Ln^{3+} ions) are expected to be similar to those proposed by Geier (17) for the EDTA complexes [3]. In addition, measured ΔC_p values for the corresponding EDTA complex formation (25) support Geier's claims of hydration equilibria existing among some lanthanide complexes in the middle of the series.

[2]OXS = 8-hydroxyquinoline-5-sulfonic acid, IDA = iminodiacetic acid, and NTA = nitrilotriacetic acid.

Can. J. Chem. Downloaded from www.nrcresearchpress.com by 210.87.254.40 on 09/05/12
For personal use only.

Can. J. Chem. Downloaded from www.nrcresearchpress.com by 210.87.254.40 on 09/05/12
For personal use only.

The studies of Geier and Karlen (17), Spedding *et al.* (22), Graffeo and Bear (23), and Grenthe and Ots (25) also serve to illustrate a favorite relationship employed by researchers in the field of lanthanide complexation, namely, that between some property of the individual complexes (*e.g.*, an apparent molal volume (22), enthalpy (ΔH) or entropy (ΔS) change for complex formation (17), rate constant for complex formation (23), heat capacity change (ΔC_p) for complex formation (25), or some other parameter) and the reciprocal of the cationic radius (or in some cases the atomic number). The point of view most often advanced by these (and other) researchers in the interpretation of their data is that a change in the continuity of a property as the ionic size decreases (or atomic number increases) is considered to be evidence for a change in the C.N. of the lanthanide ion. (This "discontinuity principle" has been explicitly stated by Karraker (8) and Anderegg (14)).

There is clearly a two-fold interest in examining the rate of oxygen exchange for the Ln–EDTA complexes. Such a study might provide evidence for metal ion promotion of oxygen exchange between a carboxylate group and water. In addition, an examination of the effect of the size of the Ln^{3+} ion on the rate of oxygen exchange (R) may be expected to provide further clues about variations in the structure of the group as a whole.

Experimental

Materials

Stock solutions ($\simeq$0.01 M) of the lanthanide nitrates were prepared by dissolving the respective oxides (99.99% purity; American Potash and Chemical Corp.) in a slight excess of nitric acid. The solution concentrations were determined by back titration of excess EDTA with a standard copper nitrate solution; the end point being determined potentiometrically using a mercury indicator electrode (26). Chloroacetic acid enriched in ^{18}O was prepared by dissolving 12 g of $ClCH_2COOH$ (Fisher Certified) in 36 ml of water enriched to about 1.6 atom % in ^{18}O (YEDA Research and Development Co. Ltd.) and equilibrating at 50 °C for 4–5 days. Labelled EDTA was prepared by condensation of the labelled chloroacetic acid with ethylenediamine (27). The ^{18}O-enriched EDTA (*ca.* 1.5 atom % ^{18}O as compared with *ca.* 0.2 % for natural abundance) was purified by dissolving the material in NaOH and reprecipitating it with HCl. The product was dried for several hours at 110 °C.

Sample Preparation and Isotopic Analysis

The experimental determination of the rate of oxygen exchange between Ln–EDTA complexes and solvent water involved adding weighed samples of ^{18}O-enriched EDTA to the various Ln nitrate stock solutions to give a solution $\simeq$0.01 M in the corresponding Ln–EDTA complex (generally $\simeq$5% excess of Ln^{3+} was added to ensure that the EDTA was completely complexed). For each individual run, the pH was adjusted, and six 3-ml aliquots were sealed in glass ampoules and placed in an oil bath thermostated at 104 °C. The ampoules were withdrawn at timed intervals and cooled rapidly in liquid air to "stop" the exchange reaction. To follow the progress of the exchange reaction, it was necessary to separate the EDTA from solution and analyze for its ^{18}O content. After addition of concentrated $HClO_4$ to give a medium *ca.* 1 M in acid, the separation was accomplished by passing each aliquot (generally six per run) through a cation exchange resin (Dowex AG 50 W-X8, hydrogen form). The Ln^{3+} cations were retained on the resin column and the effluent containing "free" (or uncomplexed) EDTA was brought to p$H \simeq 5$ (blue to bromocresol green indicator) by the addition of a dilute NaOH solution. (Exchange induced during this separation procedure was negligible since at room temperature and under drastic conditions ($\simeq$4 M $HClO_4$) the half-life of exchange for "free" EDTA was found to be of the order of 2 days). Approximately 1.5 ml of 0.5 M $AgNO_3$ solution was added, and the precipitate of Ag(I)–EDTA was filtered, washed with acetone, and vacuum dried. The silver salt was then pyrolyzed at 150 °C for ~5 min to give CO_2, which was collected and analyzed on a Varian-Mat GD 150 mass spectrometer for the 46/(44 + 45), ratio, $R(^{12}C^{16}O^{18}O/(^{12}C^{16}O^{16}O + {}^{13}C^{16}O^{16}O + {}^{12}C^{16}O^{17}O))$, which gave the relative abundance of ^{18}O in the CO_2 samples. The half-life of the exchange reaction ($t_{1/2}$) was derived graphically from the McKay plot (28) (for each run) of $-\log_{10}(1 - F)$ *vs.* time, where, F, the fraction exchanged at time t, was evaluated from the relationship

$$[5] \qquad F = (R_0 - R_t)/(R_0 - R_\infty)$$

where R_0, R_t, and R_∞ refer to the isotopic composition of the CO_2 samples at time zero, t, and isotopic equilibrium, respectively. The rate of oxygen exchange was then calculated using the equation

$$[6] \qquad R = \frac{ab0.693}{(a + b)t_{1/2}}$$

where a and b refer to the number of g-atoms of oxygen per l in the water and EDTA respectively.

Results and Discussion

Shown in Fig. 2 are the results for the dependence on pH of the rate of exchange for two Ln–EDTA complexes selected from opposite halves of the lanthanide series (note that the ordinate is a *negative* log plot of the rate such that the larger numbers correspond to a slower rate of exchange). Observe that beyond pH 4 the EDTA complexed by the lighter (larger) ion (Pr^{3+}) exchanges approximately ten times more rapidly than the EDTA complexed by the heavier (smaller) ion (Er^{3+}). Also shown for comparison

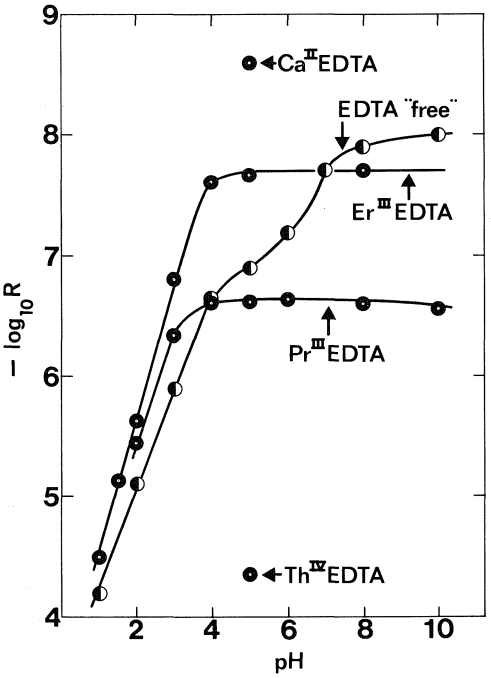

FIG. 2. pH dependence of the rate of oxygen exchange for complexed and uncomplexed ("free") EDTA at 104 °C; ≃0.01 M.

is the pH "profile" for the "free" EDTA at a comparable concentration (0.01 M) in the absence of Ln^{3+} ions. (A thorough investigation of the oxygen exchange reaction of EDTA with solvent water has been carried out by O'Connor (29) who postulated seven major mechanistic paths for this exchange. Our results (Fig. 2) are in reasonable agreement with those determined by O'Connor (29) at a comparable temperature (101 °C).)

Beyond pH 4, Pr appears to promote oxygen exchange with respect to the "free" EDTA. Er does not appear to become effective until beyond pH 7, and even then, the effect is small. In addition to the Ln complexes, preliminary investigations of a few other complexes have been made, results for two of which have been included here (Fig. 2). The tetravalent thorium ion has a very pronounced effect on the rate; EDTA complexed by this ion exchanges approximately 350 times more rapidly than the "free" EDTA (at pH 5 at least). The divalent Ca ion appears in fact to inhibit the rate of exchange.

A satisfactory explanation for the appearance of the pH "profile" for the Ln–EDTA complexes is that in the pH-independent region we have only one species, the "normal" EDTA complex (*i.e.*, EDTA 6-coordinated plus an additional "x" water molecules). At lower pH, formation of a protonated species, Ln(H EDTA) $(OH_2)_x$, must be taken into consideration (30).

We have reason to regard the eight oxygen atoms of the complexed EDTA to be equivalent although our evidence in support of this claim is not conclusive.

Figure 3 shows the effect of the size of the ionic radius on the rate of oxygen exchange for various Ln–EDTA complexes. On the basis of electrostatic arguments, one might expect the rate of exchange to increase in a regular fashion with decreasing ionic radius. The observed trend is in fact contrary to what would be expected according to our introductory remarks regarding the role of metal ions in catalysis. Perhaps a possible explanation for the observed trend in R resides in the very nature of the complex itself. The Ln–EDTA complex in aqueous solution can be classified as a mixed complex (*i.e.*, it contains two different ligands within the primary coordination sphere of the central metal ion; in this case EDTA and n water molecules). Various researchers concerned with reactions at coordinated ligands (1–3) have also stressed the im-

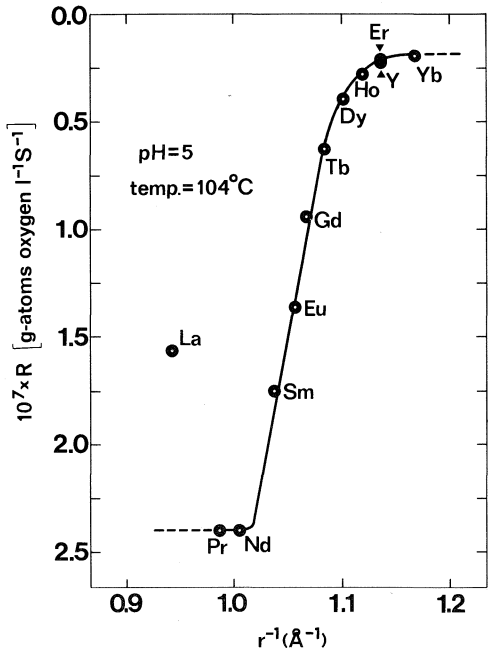

FIG. 3. Effect of the size of the central Ln^{3+} ion on the rate of oxygen exchange at pH 5 and 104 °C.

Can. J. Chem. Downloaded from www.nrcresearchpress.com by 210.87.254.40 on 09/05/12
For personal use only.

TABLE 1. Equilibrium constants for the proposed hydration equilibria [3] (all R values $\times 10^{-7}$ g-atoms oxygen l^{-8} s^{-1}) T = 104 °C

Ln	f_8*	$K_s = f_8/f_9$	R_8'	R_9'	R_{tot}†	R_{exp}
Sm	0.29	0.41(0.2)‡	0.06	1.70	1.76	1.75
Eu	0.47	0.89$^{(0.7)‡}_{(1.25)§}$	0.09	1.27	1.36	1.36
Gd	0.66	1.94(1.4)‡	0.13	0.82	0.95	0.94
Tb	0.81	4.26(10)‡	0.16	0.46	0.62	0.62
Dy	0.91	11.1	0.18	0.22	0.40	0.40
Ho	0.96	24.0	0.19	0.09	0.28	0.28
Er	0.99	99.0	0.19	0.02	0.21	0.21
Y	0.99	99.0	0.19	0.02	0.21	0.22

*f_8 = fraction of complex in 8-coordinated form.
†$R_{tot} = R_8' + R_9' = f_8R_8 + f_9R_9$ where R_9 and R_8 were obtained from the "plateau" regions of Fig. 3; $R_9 = 2.40 \times 10^{-7}$ g-atoms oxygen l^{-1} s^{-1} and $R_8 = 1.95 \times 10^{-8}$ g-atoms oxygen l^{-1} s^{-1}.
‡Reference 17; μ = 0.1, 20 °C.
§Reference 20; μ = 1.0, 70 °C.

portance of mixed complexes wherein the metal ion contributes to the ease of reaction by bringing together both components of a bimolecular reaction within its coordination sphere as well as holding the reactants in position favorable for reaction. Although a large number of investigators have admitted to the possibility that the nucleophile which initiates the reaction is also attached to the metal ion (see, for example, ref. 31 and comments therein), good evidence for such a mechanism has only recently been provided by Buckingham's study (32) of the hydrolysis of glycine esters ($NH_2CH_2CO_2R$) in $Co(en)_2(Br)(NH_2CH_2CO_2R)^{2+}$. This reaction was explained in terms of two pathways, one involving external attack by a hydroxide ion and the other occurring by internal attack on the coordinated ester by a coordinated OH^- group. In the present study, then it is possible that the Ln^{3+} ions while rendering the carbonyl carbon more susceptible to attack may also provide the water molecule as the nucleophile. In this respect we also consider as significant the close resemblance between the progression of R (Fig. 3) and ΔS (Fig. 1) *vs.* $1/r$. Rather than to regard the close similarity of these two curves as fortuitous, we propose that they are complementary evidence for a coordination number change in the Ln–EDTA complexes due to the "lanthanide contraction" (*i.e.*, the "discontinuity principle" is applicable to our study). If we adopt an explanation comparable to that of Geier and Karlen (17), then both complex series (*i.e.*, Ln-8 and Ln-9 in eq. 4) can again be recognized in the "plateau" regions, and in the region between Sm and Er hydration equilibria occur between two types of complexes differing in the number of coordinated water molecules (3 and 2). To explain the observation that EDTA complexed by Pr exchanges about ten times more rapidly than the EDTA complexed by the smaller Er ion, we suggest that structural effects are important in determining the lability of the complexed EDTA, and that the structure of the 9-coordinated mixed complex is more favorable to reaction than that of the 8-coordinated complex. Equilibrium constants were also evaluated (following the method of Geier and Karlen) for the hydration equilibria [3] and are summarized in Table 1. The good agreement between the observed rates, R_{exp}, and those calculated on the basis of a varying contribution from 8- and 9-coordinated complexes demonstrates the adequacy of this type of analysis. Also included in Table 1 are the equilibrium constants, K_s, as determined by Geier and Karlen (17) and Kostromina and Tananaeva (20); our values are in reasonable agreement considering the differences in conditions (temperature, ionic strength) and methods of evaluation.

The behavior of yttrium in Fig. 3 is worth noting. Although Y is not a true lanthanide, the rate of exchange for EDTA complexed by the Y^{3+} ion falls in the position expected from a consideration of its radius. However, we were unable to reconcile the behavior of La within this scheme.

In conclusion, the rate of oxygen exchange of the Ln–EDTA complexes appears to be sensitive to changes in the primary coordination sphere with respect to hydration; and we interpret the observed trend (Fig. 3) as evidence (admit-

Can. J. Chem. Downloaded from www.nrcresearchpress.com by 210.87.254.40 on 09/05/12
For personal use only.

tedly indirect) for a change in the coordination number of the Ln–EDTA complexes.

We thank the National Research Council of Canada for financial support of this work and a scholarship to R.H.V.

1. M. M. JONES. Ligand reactivity and catalysis. Academic Press, New York. 1968.
2. M. I. SILING and A. I. GEL'BSHTEIN. Russ. Chem. Rev. **38**, 249 (1969).
3. A. E. MARTELL. Pure Appl. Chem. **17**, 129 (1968).
4. H. KROLL. J. Am. Chem. Soc. **74**, 2036 (1952).
5. E. GELLES and J. P. CLAYTON. Trans. Faraday Soc. **52**, 353 (1956).
6. D. H. TEMPLETON and C. H. DAUBEN. J. Am. Chem. Soc. **76**, 5237 (1954).
7. G. R. CHOPPIN. Pure Appl. Chem. **27**, 23 (1971).
8. D. G. KARRAKER. J. Chem. Educ. **47**, 424 (1970).
9. T. MOELLER, D. F. MARTIN, L. C. THOMPSON, R. FERRÚS, G. R. FEISTEL, and W. G. RANDALL. Chem. Rev. **65**, 1 (1965).
10. G. SCHWARZENBACH, R. GUT, and G. ANDEREGG. Helv. Chim. Acta, **37**, 937 (1954).
11. J. L. HOARD, B. LEE, and M. D. LIND. J. Am. Chem. Soc. **87**, 1612 (1965).
12. I. GRENTHE. Acta Chem. Scand. **18**, 293 (1964).
13. L. A. K. STAVELEY, D. R. MARKHAM, and M. R. JONES. J. Inorg. Nucl. Chem. **30**, 231 (1968).
14. G. ANDEREGG. *In* Coordination chemistry. Vol. I. Am. Chem. Soc. Monograph No. 168. *Edited by* A. E. Martell. Van Nostrand Reinhold Co., New York. 1971. pp. 477–483.
15. B. LEE. Inorg. Chem. **11**, 1072 (1972).
16. G. H. NANCOLLAS. Interactions in electrolyte solutions. Elsevier, New York. 1966. pp. 159–162.
17. G. GEIER and U. KARLEN. Helv. Chim. Acta, **54**, 135 (1971).
18. G. GEIER, U. KARLEN, and A. v. ZELEWSKY. Helv. Chim. Acta, **52**, 1967 (1969).
19. G. GEIER and C. K. JØRGENSEN. Chem. Phys. Lett. **9**, 263 (1971).
20. N. A. KOSTROMINA and N. N. TANANAEVA. Russ. J. Inorg. Chem. **16**, 1256 (1971).
21. N. N. TANANAEVA and N. A. KOSTROMINA. Russ. J. Inorg. Chem. **14**, 631 (1969).
22. F. H. SPEDDING, M. J. PIKAL, and B. O. AYERS. J. Phys. Chem. **70**, 2440 (1966).
23. A. J. GRAFFEO and J. L. BEAR. J. Inorg. Nucl. Chem. **30**, 1577 (1968).
24. L. HELMHOLZ. J. Am. Chem. Soc. **61**, 1544 (1939).
25. I. GRENTHE and H. OTS. Acta Chem. Scand. **26**, 1229 (1972).
26. C. N. REILLEY, R. W. SCHMID, and D. W. LAMSON. Anal. Chem. **30**, 953 (1958).
27. A. VÀNYÓLOS. Rev. Chim. (Bucharest), **6**, 378 (1955); Chem. Abstr. **50**, 16671*f* (1956).
28. H. A. C. MCKAY. Nature, **142**, 997 (1938).
29. C. O'CONNOR. J. Inorg. Nucl. Chem. **30**, 2697 (1968).
30. R. S. KOLAT and J. E. POWELL. Inorg. Chem. **1**, 485 (1962).
31. R. J. ANGELICI and B. E. LEACH. J. Am. Chem. Soc. **89**, 4605 (1967).
32. D. A. BUCKINGHAM, D. M. FOSTER, and A. M. SARGESON. J. Am. Chem. Soc. **91**, 4102 (1969).
33. J. L. MACKEY, J. E. POWELL, and F. H. SPEDDING. J. Am. Chem. Soc. **84**, 2047 (1962).

Can. J. Chem. Downloaded from www.nrcresearchpress.com by 210.87.254.40 on 09/05/12
For personal use only.

Dielectric Constants of a Binary Solution Near the Critical Solution Temperature

I. LUBEZKY[1] AND R. MCINTOSH
Department of Chemistry, Queen's University, Kingston, Ontario
Received August 31, 1972

The dielectric constants and dielectric losses of solutions of nitrobenzene and 2,2,4-trimethyl pentane have been measured near the critical solution temperature over a concentration range of 22–75% by weight and in the frequency regions of 5–60 and 1000 – 4000 kHz. It was found that below a critical concentration of 35% maxima existed in ϵ' and ϵ'' at a temperature of 0.3 °C above the critical solution temperature. At higher concentrations the maxima disappeared and phase separation was preceded only by changes in the thermal coefficients $d\epsilon'/dT$ and $d\epsilon''/dT$. The present study combined with others indicates that two regions of loss exist for the system near the critical temperature: low frequency losses of a conductive nature and high frequency losses of the Debye type. The published experimental knowledge of such systems remains insufficient to enable a thorough test of the theoretical studies published recently by Snider.

Les constantes diélectriques et les pertes diélectriques des solutions de nitrobenzène et de triméthyl-2,2,4 pentane ont été mesurées au voisinage de la température critique de la solution, dans l'intervalle de concentration en poids de 22–75% et dans les régions de fréquences de 5–60 et 1000–4000 kHz. Au dessous d'une concentration critique de 35% des maximums existent pour ϵ' et ϵ'' à une température de 0.3 °C au dessous de la température critique de la solution. Aux plus hautes concentrations les maximums disparaissent et la séparation de phase n'est précédée que par des changements dans les coefficients thermiques $d\epsilon'/dT$ et $d\epsilon''/dT$. Cette étude, ajoutée aux précédentes, montre l'existence de deux régions de perte pour le système au voisinage de la température critique: les pertes associées aux basses fréquences de nature conductive et les pertes de hautes fréquences de nature conductive et les pertes de hautes fréquences de type Debye. Les connaissances expérimentales sur de tels systèmes publiées à ce jour, restent insuffisantes pour vérifier selon un test sûr les études théoriques recemment publiées par Snider.

[Traduit par le journal]

Can. J. Chem., **51**, 545 (1973)

Can. J. Chem. Downloaded from www.nrcresearchpress.com by 210.87.254.105 on 09/05/12
For personal use only.

Introduction

A number of publications have appeared concerning the dielectric behavior of binary solutions in the critical region and interest has increased as a result of accumulating information of the physical properties of such systems (1). Quantities such as specific heat and viscosity show a maximum at a temperature close to the transition from a one-phase to a two-phase system. The critical solution point of a binary mixture may be characterized by the vanishing of its stability coefficients such as the second derivative of the molar Gibbs free energy with respect to the mole fraction. Since the inverse of the real part of the dielectric constant ($1/\varepsilon'$) is also such a stability constant, by investigating the behavior of ε' in transitions and phase equilibria between phases, one can relate the value of $1/\varepsilon'$ to the stability or instability of a phase.

Measurements of ε' and ε'' can be made as functions of concentration, temperature, frequency of the applied field, effect of impurities and other factors. For experimental convenience, in most cases systems having upper consolute temperatures close to room temperature have been investigated. These systems consisted of solutions of nitrobenzene in some hydrocarbon for which the consolute temperature is between 20–30 °C. The experimental results for such systems obtained in several laboratories have been gathered and interpreted by Arkhangelskii and Semenchenko (2). However, the studies show disagreement concerning the behavior of the dielectric constants in the vicinity of the critical temperature. Whereas in some cases a large maximum was found in ε' and ε'' near the separation temperature, in other instances no maxima were found, and transitions to two-phase systems were accompanied only by a change in the thermal coefficients $d\varepsilon'/dT$ and $d\varepsilon''/dT$.

The present study deals with the dielectric behavior of solutions of 22–75% by weight of nitrobenzene in 2,2,4-trimethyl pentane (iso-

[1]Postdoctoral Fellow 1971–1972.

Can. J. Chem. Downloaded from www.nrcresearchpress.com by 210.87.254.105 on 09/05/12
For personal use only.

octane). This system had been investigated (3) using several concentrations and at a single frequency of 3300 MHz. It was found that the dielectric constant and loss tangent both approach a maximum at a temperature of 1.5 °C above the separation temperature. The maximum was sharpest in a concentration close to the consolute concentration, but the amplitude was higher in both ε' and tan δ with increasing concentration of nitrobenzene. Quinn and Smyth (4) tested the same system at a single solute concentration of 25% by weight and wavelengths of 575 m and 10, 3.22, and 1.26 cm (0.5, 3×10^3, 9.3×10^3, 2.4×10^4 MHz), respectively. A pronounced maximum was found in the real part of the dielectric constant at a temperature of about 2 °C above critical. It was also found that the dispersion could be characterized by a single relaxation time over much of the temperature range, meaning that a Debye absorption envelope existed for the system in the microwave range.

Experimental

Dielectric constants and losses were measured over a frequency range of 5–60 and 1000–4000 kHz. Two separate measuring circuits were employed for the two frequency ranges. A modified Schering bridge was used for the low frequency range and a resonance system served for the high frequencies. Circuit arrangements are described in an earlier work (5). The dielectric cell for the measurements consisted of a vertical coaxial capacitor which was constructed of aluminum and employed Teflon seals. The cell and lead capacitances were obtained by measuring the total capacitance with cell filled with air, benzene, ether, and chlorobenzene. The capacitance of the empty cell was found to be 20.6 pF. A careful assessment of lead capacitance and inductance was made for the frequencies employed. The overall scatter of ε' was approximately $\pm 0.05\%$ when using the bridge method, and approximately $\pm 0.2\%$ when using the resonance method. However, an uncertainty of 3% exists in the absolute value of ε'. The cell temperature was controlled in a water bath by means of a Haake thermoregulator with variable power output and cooling coils. The temperature of the thermostat was maintained to within 0.02 °C and temperature gradients along the cell were of the same order. It is believed that because of the high thermal conductivity of the cell's material the temperature gradients within it were even lower.

Nitrobenzene and 2,2,4-trimethyl pentane were obtained from Fisher Scientific Company. The certification of purity for both materials revealed less than 100 p.p.m. total impurities. Prior to measurements materials had been dried over freshly dehydrated calcium sulfate (B.D.H. analytical grade). After filling the cell with each mixture, the mother solution was placed in a sealed glass vessel beside the cell to allow observation of visual transition effects analogous to those presumably occurring in the dielectric cell under the same conditions.

Results and Discussion

In Fig. 1 the binodal curve for the system nitrobenzene–2,2,4-trimethyl pentane is shown. A review of the literature indicated that this curve had not been published previously. However, the consolute temperature deduced from the curve agrees with the value obtained by Woodburn *et al.* (6), namely, 30.4 °C. The curve was constructed from the temperatures at which the first signs of separation into two phases appeared as a sudden heavy turbidity.

In Fig. 2, ε' is described as a function of temperature for various concentrations and a frequency of 60 kHz at which the relative size of the maximum is most pronounced. It is obvious that a maximum exists in ε' and while its value increases with concentration of nitrobenzene, the amplitude of the maximum decreases until it disappears above 35% by weight of solute. Above this critical concentration the phase separation is preceded by a change in the thermal coefficient $d\varepsilon'/dT$. At a concentration of 75% of nitrobenzene it has become difficult to observe even the change of thermal coefficient. In all cases the maximum or break in the curves appeared at a temperature of 0.3 °C above separation which is indicated in the graphs by an arrow. This temperature gap does not agree with that reported in ref. 3 and the work of Quinn and Smyth (4) who found that the maximum in ε' was some 1.5–2.0 °C above separation temperature. It does agree, however, with Semenchenko's results on similar systems (7).

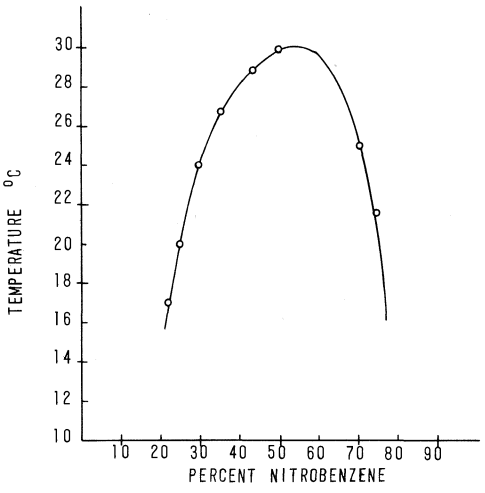

FIG. 1. Binodal curve for the system nitrobenzene-2,2,4-trimethyl pentane.

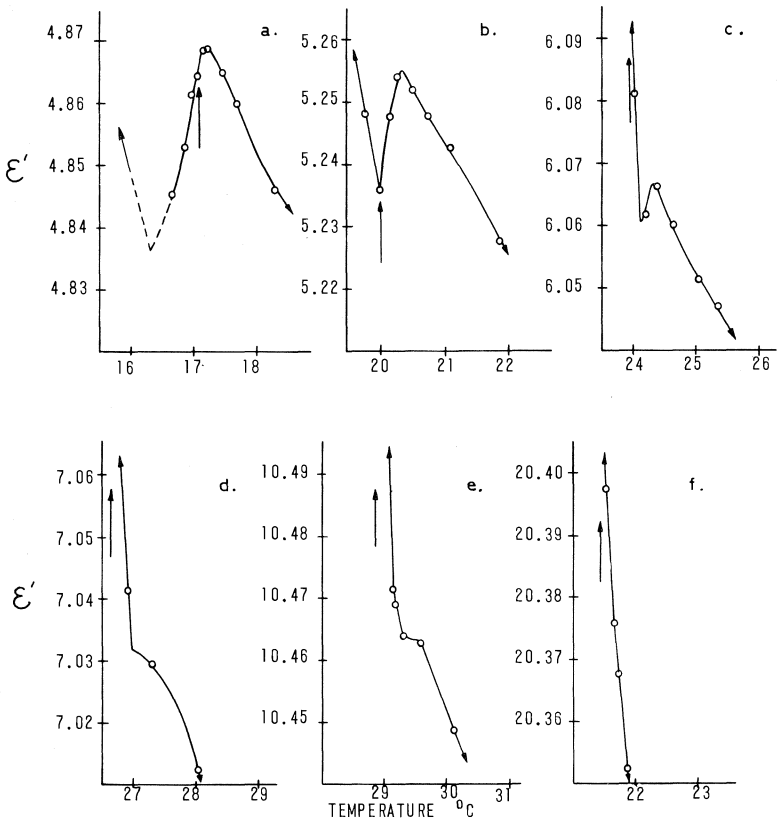

FIG. 2. ε′ as a function of temperature at a frequency of 60 kHz for the following concentrations: *a*, 22.3%; *b*, 25.0%; *c*, 30 0%; *d*, 35.3%; *e*, 50.0%; and *f*, 74.8%.

It should be noted that the frequency ranges employed by Semenchenko and in the present study were in the audio and lower radio frequencies, whereas the other two studies employed microwave frequencies. Therefore the differences could be attributed to conductance effects, which will be referred to below.

In Fig. 3, ε″ (loss factors) are plotted as a function of temperature for various concentrations and at a frequency of 5 kHz. Whereas it was found that the amplitude of the maximum in ε′ goes up, that of ε″ goes down with increasing frequency in the range of 5–60 kHz, in agreement with results of Semenchenko and co-worker (7, 8), while the frequency decreases ε′ and ε″ both increase. The effects are much more pronounced for ε″.

In Fig. 4 losses in the region of the maximum are represented for two concentrations as a function of frequency. The losses diminish with increasing frequency, and as the frequency reaches 1000 kHz, the losses are either zero or at a minimum. Beyond that frequency a new region of losses appears (note value at 4000 kHz). This region may correspond to the loss envelope in which Quinn and Smyth (4) found a single relaxation time for the system.

The audio frequency losses have the same frequency dependence even outside the critical region and indicate a contribution from conductivity effects. It seems, therefore, that in this case and others, where measurements have been made at audio frequencies, a contribution from conductivity is inherent in the losses. This effect could also account for the fact that at microwave frequencies the unusual dielectric effects were found at a temperature approximately 1° higher. In the 1000 kHz region where a smaller contribution from conductivity is expected, it is obvious from Fig. 4 that losses are either zero or at a minimum, depending upon concentration. On the other hand, ε′ retains its low frequency typical shape in the high frequency region, as seen in Fig. 5.

Can. J. Chem. Downloaded from www.nrcresearchpress.com by 210.87.254.105 on 09/05/12
For personal use only.

Can. J. Chem. Downloaded from www.nrcresearchpress.com by 210.87.254.105 on 09/05/12
For personal use only.

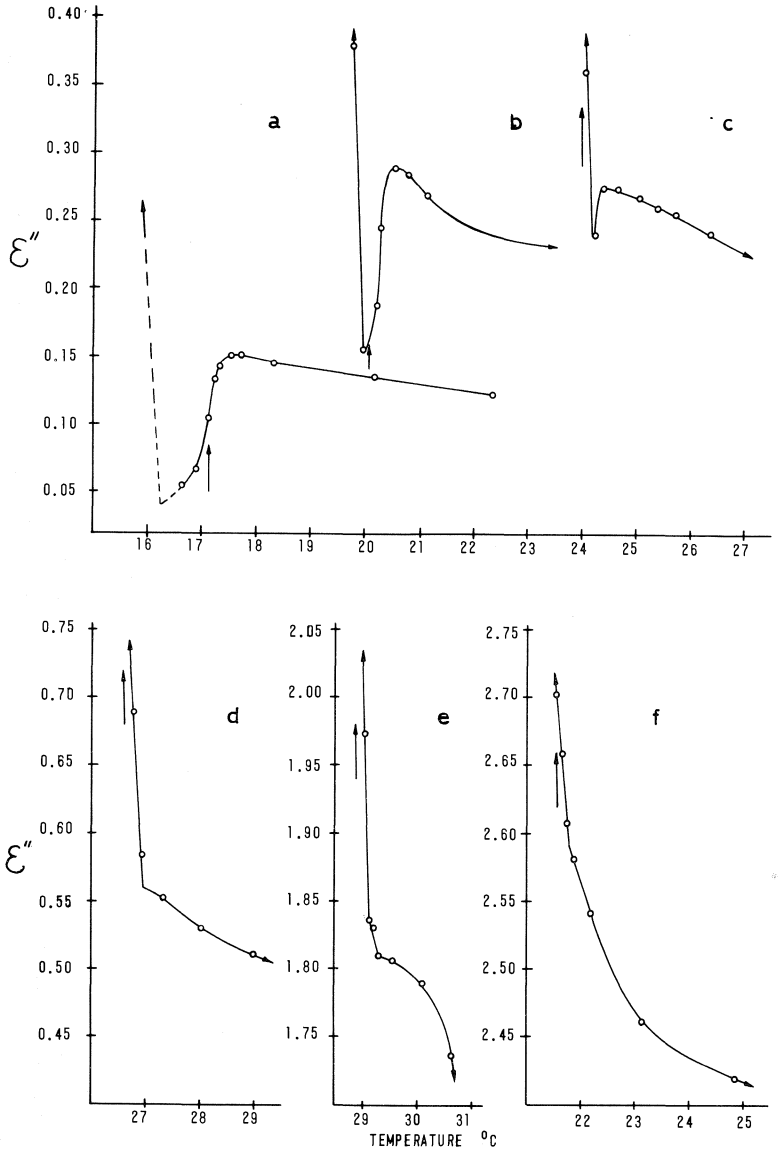

FIG. 3. ε″ as a function of temperature at a frequency of 5 kHz for the following concentrations: *a*, 22.3%; *b*, 25.0%; *c*, 30.0%; *d*, 35 3%; *e*, 50.0%; and *f*, 74.8%.

The disappearance of the maximum at a critical concentration (Figs. 2, 3, and 5) is contrary to the results given in ref. 3 as reported in the introduction. Semenchenko (2) found that for similar systems at a frequency of 1000 kHz the amplitude and sharpness of the dielectric plots reached maxima at the consolute temperature. Previous experiments of Piekara (9) and Lomova (10) showed that at the consolute temperature only a break occurred in ε′ *vs.* *T* curves and these results agree with the present findings.

Zamkov (11) tried to explain these discrepancies by showing that any value of ε′ between 0 and ∞ could be obtained at the critical temperature depending on the presence or absence of a free volume of solution outside the electric field. This explanation was adopted by Semenchenko (2).

Careful examination of Zamkov's analysis shows that it is incorrect. In the case of a cell with a free volume the expression for the free energy of the system is

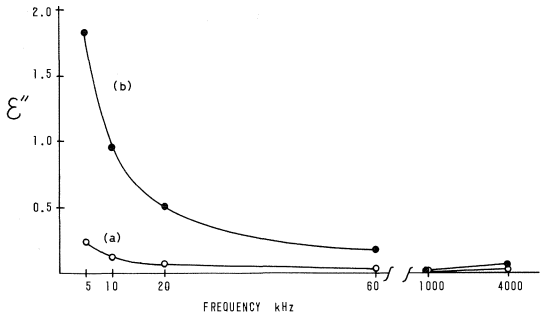

FIG. 4. ε″ at the maximum as a function of frequency: *a*, 25% solute; *b*, 50% solute.

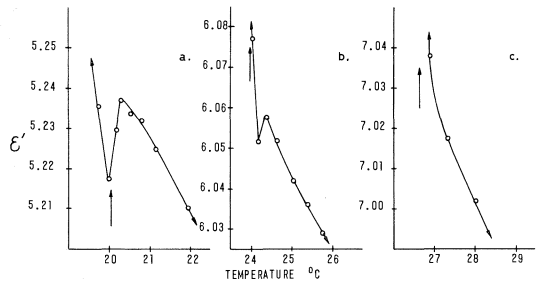

FIG. 5. ε′ as a function of temperature at a frequency of 1000 kHz for the following concentrations: *a*, 25%; *b*, 30%; *c*, 35.3%.

$$[1] \quad dG = -SdT + VdP - \frac{1}{4\pi} V_S D dE$$

where V_s is the volume confined between the electrodes, D and E are the dielectric displacement and electric field, respectively. Thus Zamkov obtains

$$[2] \quad \frac{\partial V}{\partial E} = -\frac{1}{4\pi} V_S \frac{\partial D}{\partial P}$$

and

$$[3] \quad V - V^* = -\frac{V_S}{4\pi} \int_0^E \frac{\partial D}{\partial P} dE$$

where he defines V and V^* as the volumes of material in the cell before and after applying the external field. Since there is a free volume from which to draw material, there will be no change of volume between the electrodes when the field is applied. Thus $V - V^*$ is said to be zero, which leads to the conclusion that $d\varepsilon'/dT$ is also zero.

This conclusion is incorrect as the following considerations show.

The energy of the system consists of two parts (12)

$$[4] \quad W = W_0 + W_E$$

where W_0 is the usual energy term of the system in the absence of any external perturbations and W_E is an additional term accounting for the work done by applying an external electric field.

$$[5] \quad W_E = -\frac{1}{4\pi} \int_0^V dV \int_0^E E dD$$

Therefore it is important to remember that eq. 1 applies to material both outside and inside the electric field. Consequently the integration of eq. 2 must cover the entire volume of the polarizable material. The integral of eq. 5 is evidently zero outside the cell, and this is the origin of V_s in eq. 1, but then $V - V^*$ is the change of the entire volume of the system and not necessarily equal to zero. Moreover, the electrostriction effect is well known and in polarizable materials $V - V^*$ has a definite positive value.

In the second part of Zamkov's paper in which he deals with a cell with no free volume, he again incorrectly assumes that $V - V^*$ equals zero, neglecting the electrostriction effect.

According to Zamkov's definitions the cell of the present study would be a cell with a partial free volume. Repeating the experiments and eliminating any free volume did not appreciably alter the results. With no free volume the critical concentration for the disappearance of the maxima was shifted to slightly higher values, but the differences were only of the order of the experimental error.

Conclusions

Consideration of the experiments reported here in conjunction with results already published, leads to the conclusion that apparent contradictions arise because sufficiently wide ranges of frequencies and concentrations have not been examined, even for a single system. There are now strong indications from earlier work (3, 4) and this study, that there exist at least two regions of loss for the nitrobenzene–isooctane system. The low frequency loss observed in this investigation resembles a conductive loss which is essentially eliminated as frequency is increased to 1000 kHz. However, the maximum in ε′ is still observed above the temperature of phase separation provided that solutions which contain less than 35% of nitrobenzene are examined (Fig. 5). The low frequency observations of this investigation differ from those made in the low microwave region (3, 4) in that the

Can. J. Chem. Downloaded from www.nrcresearchpress.com by 210.87.254.105 on 09/05/12
For personal use only.

low frequency effects diminish to zero with increasing concentration of nitrobenzene.

Recently Snider (13, 14) discussed the dielectric parameters of such systems theoretically on the assumption of density fluctuations in submicroscopic regions. Losses were attributed to diffusional phenomena as the critical systems change in response to the applied field. Large contributions to the dielectric constant were considered to arise from correlation effects between dipoles. Snider predicted losses at a frequency of about 500 kHz and contributions to the dielectric parameters which would be greatest at the critical composition, and which would shift to zero frequency at that composition, that is to say, at the consolute point.

Some support of these views was derived in a study of the dielectric behavior of four polar adsorbates (15). The evidence from the studies of a partially miscible liquid system has now been shown to be incomplete and no thorough test of Snider's views is as yet possible. Clearly, the intermediate frequency range from about 10 MHz to several hundred MHz must now be examined. In the meantime it is clear that results reported by Semenchenko and associates and by Smyth and associates, as well as those of Ripley and McIntosh (3), reveal anomalies in the dielectric parameters which are not due to experimental errors. Discrepancies among the experimental results are expected to disappear as further frequencies are employed. A thorough test of Snider's theoretical work will then be possible.

It is a pleasure to thank the National Research Council of Canada for financial support.

1. Symposium on critical phenomena. Ber. Bunsenges. Phys. Chem. **76**, (3/4) (1972).
2. K. V. ARKHANGELSKII and V. K. SEMENCHENKO. Zh. Fiz. Khim. **41**, 1303 (1967) (Russ. J. Phys. Chem. **41**, 692 (1967)).
3. B. D. RIPLEY and R. MCINTOSH. Can. J. Chem. **39**, 526 (1961).
4. R. G. QUINN and C. P. SMYTH. J. Chem. Phys. **39**, 3285 (1963).
5. T. MCMULLEN, E. D. CROZIER, and R. MCINTOSH. Can. J. Chem. **46**, 2945 (1968).
6. H. M. WOODBURN, K. SMITH, and H. TETEWSKY. I.E.C. **36**, 588 (1944).
7. K. V. ARKHANGELSKII and V. K. SEMENCHENKO. Zh. Fiz. Khim. **36**, 2501 (1962) (Russ. J. Phys. Chem. 1358 (1962)).
8. V. K. SEMENCHENKO and K. V. ARKHANGELSKII. Zh. Fiz. Khim. **35**, 927 (1961) (Russ. J. Phys. Chem. 454 (1961)).
9. A. PIEKARA. Bull. Acad. polon. Sci., Ser. Sci. Chim., geol. geog., Ser. A **305**, 319 (1933).
10. N. N. LOMOVA and M. I. SHAKHPARONOV. Dokl. Akad. Nauk. SSSR, **134**, 632 (1960).
11. V. A. ZAMKOV. Zh. Fiz. Khim. **36**, 1060 (1962) (Russ. J. Phys. Chem. 558 (1962)).
12. E. GUGGENHEIM. Proc. Roy. Soc. **155A**, 49 (1936).
13. N. S. SNIDER. J. Chem. Phys. **55**, 3994 (1971).
14. N. S. SNIDER. J. Chem. Phys. **56**, 233 (1972).
15. G. K. KOUVARELLIS, R. MCINTOSH, and N. S. SNIDER. J. Phys. Chem. In press.

Can. J. Chem. Downloaded from www.nrcresearchpress.com by 210.87.254.105 on 09/05/12
For personal use only.

The Dissociation Constants and Conductivities of Mono-, Di- and Triethylamine in Aqueous Solution

ALAN NEWTON CAMPBELL AND SING-YEUNG LAM

Department of Chemistry, University of Manitoba, Winnipeg, Manitoba R3T 2N2

Received September 22, 1972

The conductances of the mono-, di-, and triethylamines, and their hydrochlorides, in aqueous solution, have been determined. Corrections for the formation of amine carbonates and hydrolysis of the halides were made. By using the Kohlrausch law and the method of Shedlovsky and Kay, basic dissociation constants for the amines have been computed. The basic strength of this series has been found to conform to the usual trend for other series of aliphatic amines.

La conductivité des mono-, di-, et triethylamines et de leurs chlorhydrates a été déterminée en solution aqueuse. Des corrections pour la formation des carbonates d'amine et pour l'hydrolyse des dérivés halogénés ont été apportées. Utilisant la loi de Kohlrausch et la méthode de Shedlovsky et Kay, les constantes de dissociation basiques des amines ont été calculées. On a trouvé que la force des bases de cette série est conforme aux tendances observées pour d'autres séries d'amines aliphatiques.

[Traduit par le journal]

Can. J. Chem., **51**, 551 (1973)

Can. J. Chem. Downloaded from www.nrcresearchpress.com by 210.87.254.40 on 09/05/12
For personal use only.

Introduction

We have determined the conductivities of aqueous solutions of mono-, di-, and triethylamine, as well as those of dilute solutions of the amine hydrochlorides, so that the ionization constants of these weak bases might be known. The temperature chosen for the completely miscible systems monoethylamine–water and diethylamine–water was 25 °C. Since mixtures of monoethylamine and water containing more than about 70 mol% amine boil at 25 °C, measurements were not extended beyond this upper limit. For the system triethylamine–water the experimental temperature was 17 °C, since the system is completely miscible at this temperature.

Experimental

A. Materials

1. Conductivity water

See ref. 1.

2. Amines

See ref. 1.

3. Amine Hydrochlorides

The hydrochlorides were prepared from the amines by neutralizing chemically pure hydrochloric acid solutions with slight excess of amines. The excess quantities were expelled by gently boiling off the solutions until the condensate did not turn red litmus paper blue. The hydrochlorides were recrystallized twice from conductivity water, dried at 110 °C, then pulverized and kept in a desiccator over phosphorus pentoxide.

4. Potassium Chloride

Fisher certified A.C.S. potassium chloride was used without further purification, for the calibration of the conductance cells. It was dried at 115 °C. Standard potassium chloride solutions for calibration of the conductance cells were prepared by dissolving weighed quantities of the salt in known amounts of conductivity water.

B. Preparation and Analysis of Solutions

1. Amine Solutions

See ref. 1.

2. Amine hydrochloric solutions

Solutions for use in conductivity measurements were prepared by dissolving weighed quantities of the salts in conductivity water of known specific conductance. The weighings of the hydrochlorides were made with a microgramatic Mettler balance. Solutions of mass up to about 3 kg were weighed on a large balance having a sensitivity of 10 mg.

C. Conductance Measurements

A Leeds and Northrup conductivity bridge was used to measure the resistances of the solutions. Conductance cells of the type recommended by Jones and Bollinger (2) were used. A Shedlovsky quartz cell of the original design (3) was employed for very dilute solutions. Polarization errors were reduced by platinization.

Since the amine solutions had high vapor pressures even when chilled, rinsing the cells with amine solution might have caused a change in the original concentration of the solutions. To minimize this, dry conductance cells not rinsed by solution were used. Errors due to adsorption of amine on the platinum electrodes or to their possible attack on glass were compensated by plotting the measured resistance against time for 2 h and extrapolating the later portion, which appeared to be linear, back to zero time, when the cell was filled.

Can. J. Chem. Downloaded from www.nrcresearchpress.com by 210.87.254.40 on 09/05/12
For personal use only.

Treatment of Experimental Data and Results

The experiment equivalent conductances of the hydrochlorides of mono-, di-, and triethylamine, in which the hydrolysis effect has not been allowed for, as well as those of the free bases, as functions of their stoichiometric concentrations, are to be found in the Depository of Unpublished Data.[1] From these data, preliminary values of the basic dissociation constants were found. From these approximate values of the basic dissociation constants and the ionization constants of water at 25 °C (1.01×10^{-14}) and at 17 °C (5.33×10^{-15}), the effect of hydrolysis upon the conductivity was computed for each salt by the method of Campbell and Bock (4). The final limiting equivalent conductances computed for the substituted ammonium cations and the hydroxides are as follows:

Ion or compound	Temperature (°C)	λ^0 (cm² ohm^{-1} equiv^{-1})
Monoethylammonium ion	25	46.41
Diethylammonium ion	25	36.47
Triethylammonium ion	17	26.67
Monoethylammonium hydroxide	25	244.7
Diethylammonium hydroxide	25	234.8
Triethylammonium hydroxide	17	193.8

For ammonium ion and ammonium hydroxide, the limiting conductances at 25 °C are 73.55 and 271.9, respectively. The decrease in limiting conductance on passing from ammonia to triethylamine is no doubt due to the increase in size of the conducting species.

Our method of finding the dissociation constants of the amines is essentially that of Shedlovsky and Kay (5).

The mean activity coefficients of the free ionic species were calculated using the Davies equation (6)

$$\log y_{\pm}' = -A\left(\frac{|z_1 z_2|\sqrt{I}}{1+\sqrt{I}} - 0.3I\right)$$

with $A = 0.5115$ at 25 °C: 0.5045 at 17 °C. The ionic strength (I) was set equal to αc.

The molar activity coefficients of the free amine molecules were evaluated from the following equations

$$y_B' = \frac{kp_B}{c(1-\alpha)\cdot p_B^0}$$

and

$$k = \lim_{c\to 0} \frac{c(1-\alpha)p_B^0}{p_B}$$

where p_B and p_B^0 are the vapor pressures of B in solution and in the pure state. An example of how the limiting value of $c(1-\alpha)/a_B$ was obtained, is given for the case of monoethylamine, in Fig. 1, where $c(1-\alpha)/a_B$ is plotted against c. Since the vapor pressures of the amines in very dilute solutions were not determined we were obliged to use the data for higher concentrations, where α can only be calculated approximately ($\simeq\Lambda/\Lambda^0$). Although such an extrapolation from the plot may lead to an only approximate limiting value of k, the activity coefficient in any dilute solution is the ratio of k to the value read off from the curve at this particular concentration and it is fairly insensitive to the variation of k, provided the slope in the dilute region is not exceptionally large. In all cases, the activity coefficients of the amine molecules in dilute solutions are close to unity and this justifies the assumption often

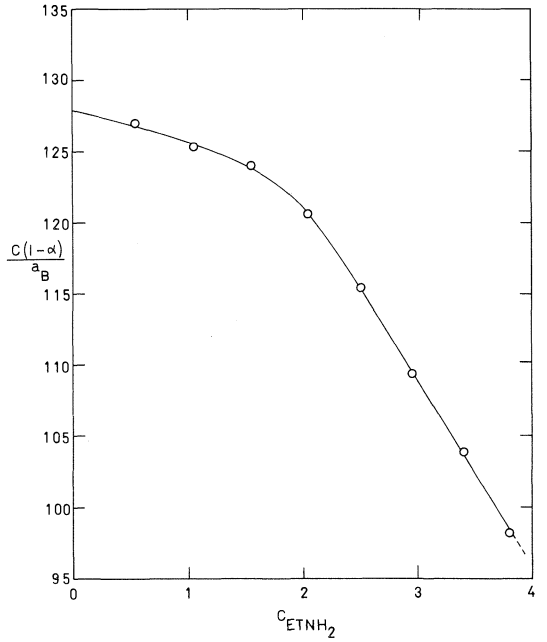

FIG. 1. Plot of $c(1-\alpha)/a_B$ *vs.* c for monoethylamine at 25 °C.

[1]Complete set of tabular data is available, at a nominal charge, from the Depository of Unpublished Data, National Science Library, National Research Council of Canada, Ottawa, Canada K1A 0S2.

made that they are unity. The activity coefficients of water in the aqueous amine solutions have been determined by us.

With these activity coefficients, water activities, and other quantities, values of

$$\frac{y_B'^{1/2} a_A^{1/2} c^{1/2}}{y_\pm' S(z)} \left[1 - \frac{\Lambda^*}{\Lambda^0} S(z)\right]^{1/2}$$

were calculated and plotted against the viscosity corrected specific conductances. The symbols, other than those well understood are: L,L_0 = specific conductance of solution and of solvent, respectively; y_B' = activity coefficient of free amine on molarity scale; a_A = activity of water; $S(z)$ = Shedlovsky function defined by

$$S(z) = 1 + z + z^2/2 + z^3/8 - z^5/12$$

$$z = \frac{(B_1\Lambda^0 + B_2)C^{1/2}\Lambda^{1/2}}{\Lambda^{0\,3/2}}$$

The intercepts of these plots give the solvent corrections, L_0, for the aqueous amine solutions. These are 4.5×10^{-6} for monoethylamine solutions, 3.5×10^{-6} for diethylamine solutions, and 4.0×10^{-6} for triethylamine solutions. These solvent corrections are several times larger than the original specific conductance of water, which contained some carbonic acid, because the amines converted the weak acid into the completely ionized salts.

The true specific conductances of the solutions were then computed. The stoichiometric concentrations of the amines were also corrected for those portions of the amines which had been converted into salt. We illustrate the method, using monoethylamine as the example. Using the limiting conductivity of monoethylammonium ion obtained above and those of the HCO_3^- and CO_3^{2-} ions at 25 °C, the concentrations of bicarbonate and of carbonate were estimated from the relation $L_0 \times 10^3/\Lambda_{salt}^0$, assuming that neutralization is complete to bicarbonate or carbonate. These concentrations are $c_{bicarbonate} = 4.9 \times 10^{-5}$; $c_{carbonate} = 2.0 \times 10^{-5}$. The concentration of monoethylammonium ion is αc. From the estimated dissociation constant of monoethylamine, $K = 4.8 \times 10^{-4}$, the ionic product of water, and the dissociation constants of carbonic acid, *viz.* $K_1 = 4.4 \times 10^{-7}$ and $K_2 = 4.7 \times 10^{-11}$, the following equilibria can be formulated

$$\frac{[\text{aminium}^+][HCO_3^-]}{[H_2CO_3][\text{aminium hydroxide}]} = \frac{\alpha}{1-\alpha} \times \frac{[HCO_3^-]}{[H_2CO_3]} = 2.1 \times 10^4$$

$$\frac{[\text{aminium}^+][CO_3^{2-}]}{[HCO_3^-][\text{aminium hydroxide}]} = \frac{\alpha}{1-\alpha} \times \frac{[CO_3^{2-}]}{[HCO_3^-]} = 2.3$$

Since the degree of dissociation is less than 0.4 for the most dilute monoethylamine solution, the ratio $[CO_3^{2-}]/[HCO_3^-]$ is larger than 3. For simplicity, we have assumed that that portion of the base was converted completely to dibasic salt. The correction for monoethylamine solutions is therefore 4.0×10^{-5} rather than 4.9×10^{-5}, and this was consequently subtracted from the concentrations of monoethylamine to obtain the corrected concentrations. In a similar manner the corrections found for diethylamine and triethylamine solutions were 3.3×10^{-5} and 4.7×10^{-5}, respectively.

From the corrected concentrations and specific conductances, new values of λ, z, $S(z)$, α and $y_\pm'$ for which the ionic strength included the contribution from the salt, were calculated. The relevant quantities are to be found in the Depository of Unpublished Data, and the final plots of corrected specific conductance against

$$\left[1 - \frac{\Lambda^*}{\Lambda^0} S(z)\left(1 - \frac{L_0}{L}\right)\right]^{1/2} \frac{y_B'^{1/2} a_A^{1/2} c^{1/2}}{S(z) y_\pm'}$$

are shown in Figs. 2, 3, and 4. Points in the low concentration regions lie on straight lines passing through the origin. The slopes were measured and, knowing the limiting conductances, the basic dissociation constants were calculated. They are 4.57×10^{-4} for monoethylamine at 25 °C, 1.02×10^{-3} for diethylamine at 25 °C, and 4.93×10^{-4} for triethylamine at 17 °C.

Separate calculations, neglecting the viscosity factor, were also made for the three systems. The results are given in the same figures, Figs. 2, 3, and 4. It is obvious that without viscosity corrections, the deviations from straight line behavior are much larger than those with viscosity correction, in the higher concentration regions. In less dilute solutions, for which values of αc are still less than 0.01, and therefore still within the working range of the Shedlovsky conductance equation, the deviations of the viscosity

Can. J. Chem. Downloaded from www.nrcresearchpress.com by 210.87.254.40 on 09/05/12
For personal use only.

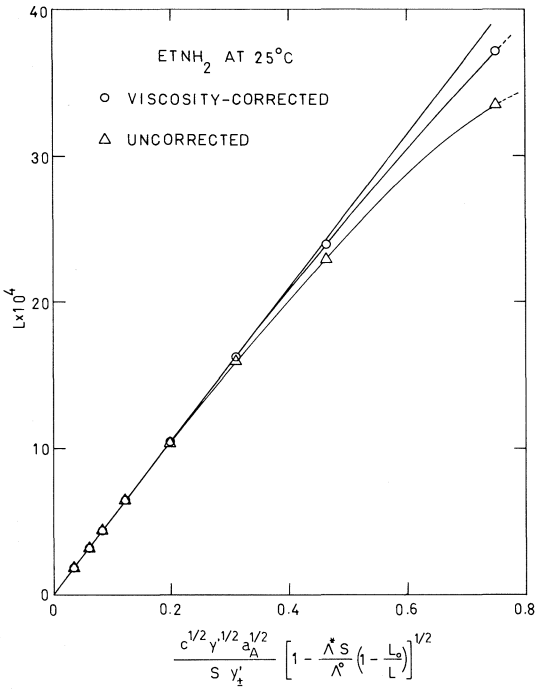

FIG. 2. Shedlovsky–Kay plot for aqueous monoethylamine solutions at 25 °C.

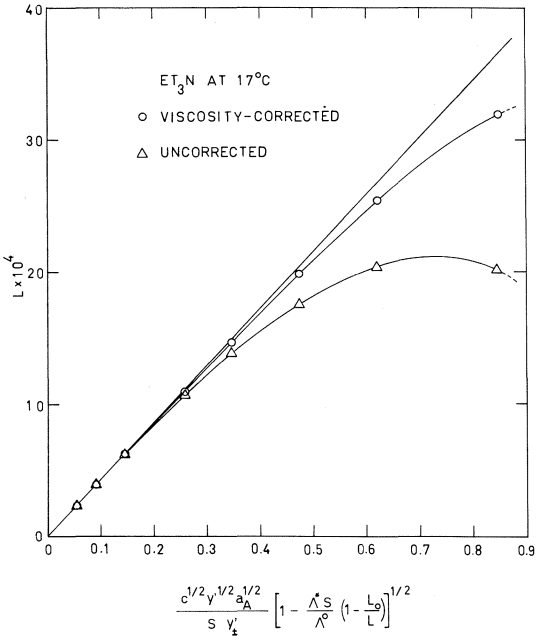

FIG. 4. Shedlovsky–Kay plot for aqueous triethylamine solutions at 17 °C.

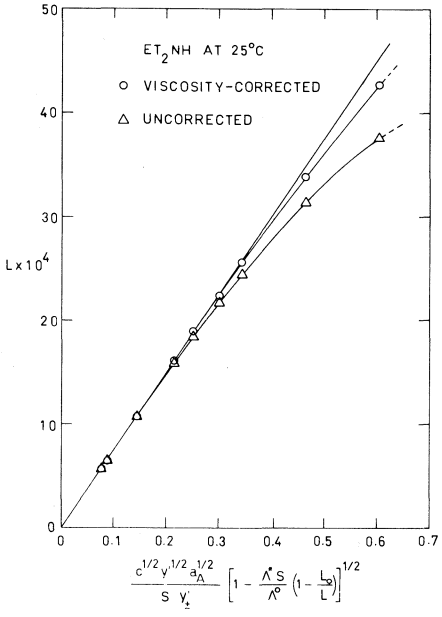

FIG. 3. Shedlovsky–Kay plot for aqueous diethylamine solutions at 25 °C.

corrected values from straight lines are presumably due mainly to the decrease of dielectric constant as the neutral amine molecules become more and more parts of the solvent media for the moving ions.

Our values of the dissociation constants agree well with the values obtained by Somerville (7), Ablard *et al.* (8), Everett and Wynne-Jones (9), Evans and Hamann (10), deLigny (11), van der Linde *et al.* (12), Moore (13), and Hansson (14). There is no doubt that for this series of substituted ammonias, diethylamine is the strongest base and ammonia the weakest ($K = 1.77 \times 10^{-5}$ mol l^{-1} at 25 °C).

1. A. N. CAMPBELL and S. Y. LAM. Can. J. Chem. In press.
2. G. JONES and G. M. BOLLINGER. J. Am. Chem. Soc. **53**, 411 (1931).
3. T. SHEDLOVSKY. J. Am. Chem. Soc. **54**, 1411 (1932).
4. A. N. CAMPBELL and E. BOCK. Can. J. Chem. **36**, 330 (1958).
5. T. SHEDLOVSKY and R. L. KAY. J. Phys. Chem. **60**, 151 (1956).
6. C. W. DAVIES. J. Chem. Soc. 2093 (1938).

Can. J. Chem. Downloaded from www.nrcresearchpress.com by 210.87.254.40 on 09/05/12
For personal use only.

7. W. C. SOMERVILLE. J. Phys. Chem. **35**. 3412 (1931).
8. J. E. ABLARD, D. S. MCKINNEY, and J. C. WARNER. J. Am. Chem. Soc. **62**, 2181 (1940).
9. D. H. EVERETT and W. F. K. WYNNE-JONES. Proc. Roy. Soc. London, **A177**, 499 (1941).
10. A. G. EVANS and S. D. HAMMER. Trans. Faraday Soc. **47**, 25 (1951).
11. C. L. DELIGNY. Rec. Trav. Chim. Pays-Bas, **79**, 731 (1960).
12. W. VAN DER LINDE, D. NORTHCOTT, W. REDMOND, and R. E. ROBERTSON. Can. J. Chem. **47**, 279 (1969).
13. T. S. MOORE. J. Chem. Soc. **91–92**, 1379 (1907).
14. J. HANSSON. Svensk. Kem. Tidskr. **67**, 256 (1955).

Can. J. Chem. Downloaded from www.nrcresearchpress.com by 210.87.254.40 on 09/05/12
For personal use only.

The Mutarotation of Glucose in Dimethylsulfoxide and Water Mixtures

N. M. Ballash and E. B. Robertson

Department of Chemistry, The University of Calgary, Calgary, Alberta T2N 1N4

Received June 7, 1972

The mutarotation of glucose is a general acid – base-catalyzed reaction which involves two proton transfers. Whether these proton transfers are carried out in a stepwise or concerted manner, the latter alternative possibly incorporating several water molecules in a cyclic transition state, is not known with certainty.

This study was undertaken in an attempt to clarify the mechanism by determining directly the number of water molecules participating in the transition state. The method chosen was to determine rates for the acid-catalyzed mutarotation of glucose as a function of solvent composition in dimethylsulfoxide and water mixtures, particularly in the water poor region. The results show that for the acid-catalyzed reaction the order with respect to water is zero. For water catalysis, the results are less reliable but suggest that about three water molecules may be involved. These facts are interpreted to mean that a stepwise mechanism is operative in the proton-catalyzed reaction, but that the solvent-catalyzed process may involve a cyclic concerted mechanism.

Rate measurements were also carried out as a function of temperature for various solvent mixtures. The calculated activation parameters remain practically constant over the solvent composition region and attest to the constancy of the mechanism over this range. Thus the results which pertain strictly to solutions of high dimethylsulfoxide content should apply to aqueous solutions as well.

La mutarotation du glucose est une réaction de catalyse acidobasique généralisée engageant deux transferts de proton. La manière dont ces protons sont transférés (c'est-à-dire selon un mécanisme par étapes ou concerté, cette dernière possibilité faisant intervenir plusieurs molécules d'eau dans un état de transition cyclique) n'est pas connue avec certitude.

Cette étude a été tentée dans le but de clarifier le mécanisme par détermination directe du nombre de molécules d'eau engagées dans l'état de transition. La méthode adoptée est la mesure des vitesses de mutarotation acido catalysée du glucose, en fonction des compositions des divers mélanges diméthylsulfoxyde-eau, particulièrement dans la région pauvre en eau. Les résultats indiquent que l'ordre de la réaction acidocatalysée est de zéro par rapport à l'eau. Les résultats pour la catalyse par l'eau sont moins sûrs mais suggèrent que trois molécules d'eau environ peuvent être engagées. L'interprétation de ces faits peut être la suivante: dans la réaction catalysée par le proton, on a un mécanisme par étapes tandis qu'un mécanisme concerté explique le processus catalysé par le solvant.

Les mesures de vitesse ont été également effectuées en fonction de la température pour divers mélanges de solvants. Les paramètres d'activation calculés restent pratiquement constants dans la zone de composition du solvant et attestent de la constance de ce mécanisme dans cette zone. Ainsi les résultats qui appartiennent strictement aux solutions riches en diméthylsulfoxyde pourraient s'appliquer également aux solutions aqueuses. [Traduit par le journal]

Can. J. Chem., **51**, 556 (1973)

Introduction

Although the mutarotation of glucose has been studied by a large number of workers over a period of many years, there is still no agreement as to the mechanism by which the reaction occurs. There are at least three mechanisms possible, plus numerous minor modifications. The most widely accepted scheme involves the formation of the free aldehyde form (γ-glucose), as in eq. 1. According to the Pedersen version of this mechanism, acids can catalyze the reaction by protonation of the ring oxygen, thereby increasing the ease with which the carbon-oxygen bond can be broken (1).

[1] 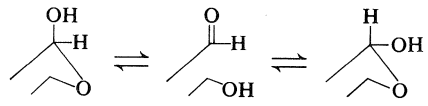

An alternative mechanism proposed by Schmid involves the removal of the proton from the C-1 hydroxyl group, as in eq. 2, and does not involve

[2] 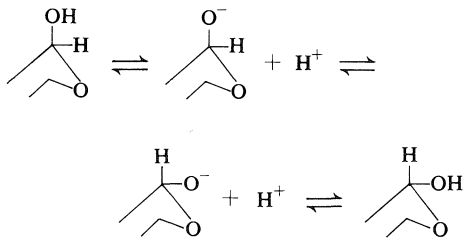

Can. J. Chem. Downloaded from www.nrcresearchpress.com by 210.87.254.42 on 09/05/12
For personal use only.

the formation of the γ-glucose (2). According to this scheme, acid catalysis would result from the polarization of the water molecules in the hydration sheath of the proton, thus increasing the ease with which a water molecule could remove the hydroxyl proton (3).

Christiansen (4) has suggested that the reaction proceeds as the result of the removal of the C-1 hydrogen as depicted in eq. 3. Again, no aldehyde

[3] 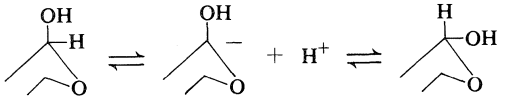

form is required. The proton may be removed from the glucose entirely, or be transferred to one of the two oxygens adjacent to the C-1 atom. Acid catalysis could presumably result from the prior protonation of the neighboring oxygen, in much the same way as in the Pedersen mechanism.

Of these three possibilities, the first seems most reasonable. It is not clear how reaction 2 can lead to mutarotation, that is, how the removal of a proton from the hydroxyl group makes easier the change in configuration of the C-1 atom involved in the transition from the second to the third species in eq. 2. The third possibility would lead to the desired reaction, but there is no reason to favor it over [1], especially since the two known equilibria of glucopyranose involve the loss of the proton from the C-1 hydroxyl (5) and the formation of the γ form. The existence of the free aldehyde form is confirmed both by the fact that D-glucose undergoes typical aldehyde reactions (6) and by its polarographic behavior (7–9).

Further, the observation that glucose -1-^{18}O undergoes oxygen exchange with water approximately 30 times more slowly than the mutarotation reaction (10) excludes other alternatives which do not proceed via ring opening.

Once reaction 1 has been accepted, the problem of the timing of the various steps remains. The Pedersen mechanism [1] considers the two proton transfers, protonation of the ring oxygen and deprotonation of the C-1 hydroxyl, to occur consecutively so that either the conjugate acid or conjugate base of glucose is an intermediate in the conversion of the sugar to the aldehyde. For the acid-catalyzed reaction, Pedersen's stepwise mechanism may be written as a fast pre-equilibrium protonation followed by a rate determining step involving simultaneous removal of the hydroxyl proton by the conjugate base of the acid and breaking of the ether linkage, eq. 4.

[4] 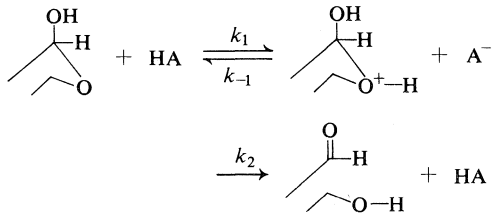

Eigen has suggested that reactions such as mutarotation which require two proton transfers may in fact proceed via a concerted mechanism involving two or more water molecules in a cyclic hydrogen-bonded transition state (11). This mechanistic view is supported by studies of other reactions, particularly the dehydration of acetaldehyde hydrate (12, 13). Both of these reactions are general acid – base-catalyzed (14), exhibit linear Brönsted plots (11), and have almost identical primary isotope effects (15). In the case of the dehydration reaction, reducing the observed rate constant into contributions from the equilibrium constant for the prior protonation and the rate constant k_2 of the deprotonation step (in the Pedersen mechanism) leads to a value of k_2 which exceeds the diffusion-controlled limit (11).

However, the comparison with the reaction of acetaldehyde does have weaknesses. For glucose, the Brönsted plot is based on data over a range of only about two powers of ten in the acid ionization constants, plus data for proton and water catalysis. It is doubtful that these latter two acids should be considered in the same plot as, for example, acetic acid. Even if only water is excluded, the plot extends over only seven pK units, instead of 18, and hence the constancy of the Brönsted α is much less significant.

Further, there is at least one major difference between the mutarotation reaction and the hydration of acetaldehyde, in that the transition state for the latter must include at least one water molecule, a restriction which is not present for the mutarotation. Thus conclusions based on the hydration reaction may or may not be applicable to the mutarotation. In addition, the isotope effect for the acid-catalyzed hydration of acetaldehyde has been questioned recently (16).

Primary solvent isotope effects on the rates of mutarotation of glucose and tetramethylglucose have been observed in deuterium oxide (17) and in $H_2O + D_2O$ mixtures (18, 19). The

Can. J. Chem. Downloaded from www.nrcresearchpress.com by 210.87.254.42 on 09/05/12
For personal use only.

Can. J. Chem. Downloaded from www.nrcresearchpress.com by 210.87.254.42 on 09/05/12
For personal use only.

k_D/k_H ratio for the mutarotation in the pure solvents is consistent with the stepwise mechanism (17). Data from experiments carried out in mixtures of light and heavy water do not lead to a clear-cut mechanistic interpretation, seemingly because for this type of reaction, changes in the rates resulting from differences in solvent participation (*e.g.*, two or three water molecules in the transition state as opposed to no solvent participation) are very small. However, there is is a slight preference for a transition state containing no water for the proton-catalyzed reaction, and for the inclusion of three water molecules in the water-catalyzed reaction (18). For the base-catalyzed reaction, there is somewhat stronger evidence for a stepwise mechanism (19).

There is considerable evidence for a cyclic concerted mechanism in some other reactions (20–26). The present work in a mixed solvent system was undertaken in the hopes of finding direct evidence concerning the role of water in the mutarotation reaction. Dimethylsulfoxide (DMSO) was chosen as the co-solvent because it is a highly polar solvent, and should not therefore contribute too large a medium effect. The essential difference between DMSO and water is that the former, being aprotic, cannot form hydrogen-bonded cyclic structures such as those proposed for water.

Experimental

Materials

Reagent grade materials were used throughout, without further treatment except as noted. β-Glucose was dried *in vacuo* before use. Tetraethylammonium perchlorate (TEAP) was prepared from tetraethylammonium bromide and sodium perchlorate, recrystallized twice from water, and dried at 60° over P_2O_5 *in vacuo*. Fisher Certified Reagent DMSO was used for most of the work at 25°; at the other temperatures and for high mole fractions of DMSO at 25°, practical grade DMSO was dried over calcium hydride for 12 h and then vacuum distilled (27).

Equilibrium Constants

The equilibrium constants were measured polarimetrically in thermostatted 20 cm tubes using the sodium D line. The initial specific rotations of α- and β-glucose were obtained by measuring the optical rotation, r, of unbuffered glucose solutions (approximately 5 wt. %). When the solvent-catalyzed reaction proceeded at a measurable rate, plots of log $(r_t - r_\infty)$ against time, using average r_∞ values obtained from rate experiments, were extrapolated to the time of mixing. For very slow reactions, a linear extrapolation of r_t as a function of time was used. In many cases, observations were made over a period of 1½ h, and the results of at least two trials were averaged in obtaining each initial value. The infinity values from the rate measurements were also used for the final, equilibrium readings required for the equilibrium constants.

Rate Constants

In order to determine the rate constant for the acid-catalyzed mutarotation of glucose, polarimetric experiments were carried out over a range of hydrochloric acid concentrations keeping the solvent composition, ionic strength, and temperature constant. At all temperatures a minimum of four runs was carried out at each mole fraction.

Mutarotation experiments were initiated by dissolving 1.25 g of α-glucose and a weighed amount of inert electrolyte (TEAP) in about 10 ml of the solvent in a 25 ml volumetric flask. An aliquot of hydrochloric acid was then added and the mixture made up to volume at the operating temperature. The temperature was checked and adjusted, if necessary, before the solution was poured into the pre-thermostatted cell.

The first optical reading could usually be taken from 3–6 min after addition of catalyst to the glucose solution. This time interval included a "settling down" time of 2 or 3 min while the solution came to thermal equilibrium.

A solution of hydrochloric acid in DMSO was obtained by slowly bubbling HCl gas into DMSO. Care was taken to cool the DMSO in an ice bath so that heat from the exothermic dissolution of HCl would not cause decomposition of the DMSO (28). Solutions of HCl in water and HCl in DMSO were standardized with a standard barium hydroxide solution which was protected from atmospheric carbon dioxide. Potentiometric titrations were carried out and equivalence points were obtained with the aid of a Gran plot (29). All DMSO and water mixtures were made up in approximately 100 ml portions by weighing on an analytical balance. The small volume changes attendant on mixing DMSO and water were taken into account when calculating the acid concentration in solvent mixtures.

Karl Fischer Reagent was used to determine the water content of solvent mixtures containing more than 0.9 mol fraction DMSO. The reagent was standardized with sodium tartrate dihydrate on the same day that it was used (30). Determination of the water content in this primary standard by drying gave the stoichiometric weight of water within 0.13%. Samples were titrated in approximately 25 ml of pre-titrated absolute methanol using the visual dead-stop end point (31). End points were reproducible to within about 0.030 ml.

Results

Equilibrium Constants

For the reversible, pseudo-first-order process

$$[5] \qquad \alpha\text{-Glucose} \underset{k^\beta}{\overset{k^\alpha}{\rightleftharpoons}} \beta\text{-Glucose}$$

the equilibrium constant, K, is given by the expression

Can. J. Chem. Downloaded from www.nrcresearchpress.com by 210.87.254.42 on 09/05/12
For personal use only.

[6] $$K = k^{\alpha}/k^{\beta} = \frac{(R_{\alpha} - R_{\infty})}{(R_{\infty} - R_{\beta})}$$

where the R's are the specific rotations of the pure α or β tautomers or of the equilibrium mixture. The results are summarized in Fig. 1. The average error is about 1.5%.

Rate Constants

The mutarotation of glucose strictly obeyed first-order kinetics under all conditions investigated (32). According to eq. 5, we are dealing with an opposing reaction scheme where k^{α} and k^{β} are pseudo-first-order rate constants. A system of this kind approaches equilibrium in a first-order fashion, with an observed rate constant $k_{obs} = k^{\alpha} + k^{\beta}$ (33).

The Guggenheim method for evaluating rate constants was employed (34) except for the fastest reactions in pure water at 35°. Here the total number of polarimetric observations was too few for the Guggenheim method to be used to advantage and rate constants were calculated using final rotation values. Slopes of Guggenheim plots were determined both graphically and by the method of averages (35). Excellent agreement was always obtained between the two methods. Except at 45° where errors are roughly doubled, estimated errors for the individual runs are less than 1%.

Under the acidic conditions used,

[7] $$k_{obs} = k_0 + k_{H^+}[H^+]$$

where H^+ represents the solvated proton. Kolthoff and Reddy have demonstrated that hydrochloric acid is completely dissociated in DMSO (28). The second-order catalytic constant, k_{H^+}, was evaluated by the method of least squares from plots of k_{obs} as a function of the molar concentration of hydrochloric acid. Extrapolation to zero acid concentration gave k_0, the solvent catalyzed rate constant. A representative plot is presented in Fig. 2.

The catalytic constants k_0, k_{H^+} and $(k_{H^+})^{\alpha}$ are listed in Table 1 along with values obtained in aqueous solutions by other workers. Acidic rate

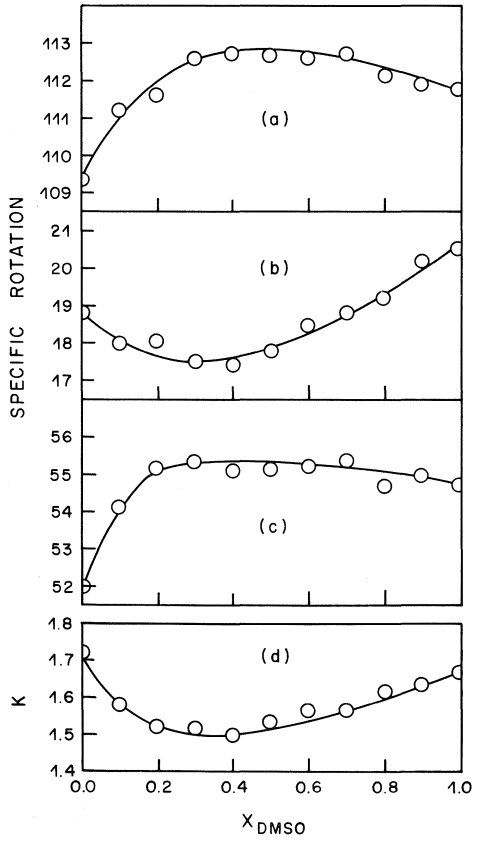

FIG. 1. Specific rotations of (*a*) α-glucose, (*b*) β-glucose, (*c*) equilibrated glucose solutions, and (*d*), K as a function of χ_{DMSO} at 24.66°.

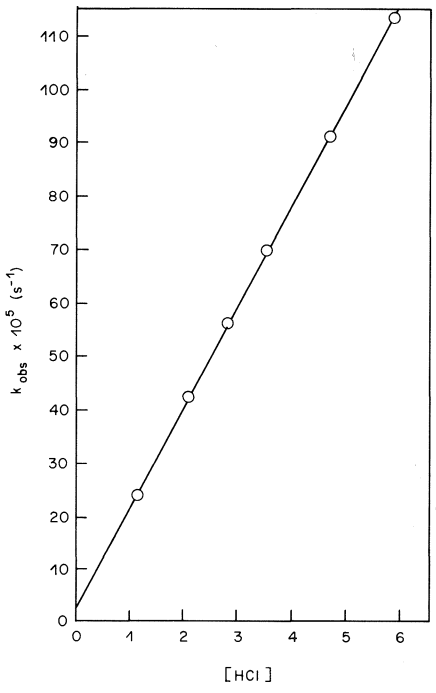

FIG. 2. k_{obs} as a function of the molar concentration of HCl for the mutarotation of glucose in 0.598 mole fraction DMSO at 24.66 °C.

TABLE 1. Catalytic rate constants k_0, k_{H^+}, and $(k_{H^+})^\alpha$ for the mutarotation of glucose in DMSO and water mixtures*

Temperature (°C)	χ_{DMSO}	$k_0 \times 10^5$ (s^{-1})	$k_{H^+} \times 10^2$ ($M^{-1}\ s^{-1}$)	$(k_{H^+})^\alpha \times 10^{-2}$ ($M^{-1}\ s^{-1}$)	Reference
15.00	0.000	15.3±1.1	0.357±0.014	0.226	This work
	0.298	1.4±1.8	0.548±0.023	0.330	This work
25.00	0.000	39.4†	1.11†	—	This work
		40.0	1.19	—	36
		40.3	1.00	—	37
		38.4	1.42	—	38
24.66	0.000	36.9±0.4	1.06±0.01	0.671	
	0.198	4.7±1.1	1.43±0.02	0.862	
	0.398	−0.4±1.9	1.70±0.05	1.02	
	0.598	2.2±0.6	1.91±0.02	1.17	
	0.798	3.3±2.0	1.98±0.06	1.22	
	0.896	5.0±1.6	1.74±0.04	1.08	
	0.942	1.6±2.0	1.62±0.06	1.01	
	0.971	0.6±0.2	1.46±0.01	0.912	
	0.992	−0.6±0.7	1.39±0.02	0.869	
35.21	0.000	99.0±0.9	3.28±0.10	2.08	
	0.298	4.4±0.3	4.60±0.03	2.77	This work
	0.598	3.7±1.4	5.51±0.14	3.36	
	0.896	0.6±2.1	5.73±0.16	3.56	
	0.942	2.2±0.3	4.94±0.02	3.08	
	0.992	2.3±1.1	4.25±0.08	2.66	
35.06	0.798	0.6±0.3	5.74±0.03	3.55	
44.44	0.298	10.9±0.2	10.64±0.04	6.40	
	0.598	2.1±1.5	13.10±0.34	8.00	
	0.798	−1.5±1.2	14.57±0.28	9.01	
	0.896	−0.1±0.0	13.98±0.01	8.68	
	0.992	1.5±0.0	10.56±0.05	6.60	

*Errors quoted are standard deviations.
†Data corrected to 25.00° by means of the activation parameters in Table 2.

coefficients for the forward reaction, $(k_{H^+})^\alpha$, have been calculated using the average equilibrium constants. Any variation of K with temperature is within experimental error at all mole fractions investigated. Plots of k_{H^+} and k_0 as a function of χ_{DMSO} are illustrated in Figs. 3 and 4 respectively. Figure 4 includes data for 25 and 35° only.

Activation Parameters

Table 2 summarizes the values of the enthalpy and entropy of activation as a function of solvent composition. At least three temperatures were used in the calculation at any given solvent composition.

Hill and Thumm obtained values of $\Delta H^\ddagger = 84.3$ kJ mol^{-1} and $\Delta S^\ddagger = -29$ J K^{-1} mol^{-1} for the acid-catalyzed reaction and $\Delta H^\ddagger = 71.5$ kJ mol^{-1} and $\Delta S^\ddagger = -113$ J K^{-1} mol^{-1} for the solvent-catalyzed reaction at 40° in pure water (39), in reasonable agreement with the present results.

Discussion

Entropy plays a very important role in determining the equilibrium properties of glucose solutions. Kendrew and Moelwyn–Hughes have measured the constant for the equilibrium between α- and β-glucose at temperatures ranging from 0–45° and have found it to be independent of temperature (40). Thus the equilibrium constant is entropy controlled.

The difference between the equilibrium constant values for glucose in water and in DMSO, 1.72 and 1.67 respectively, is just on the limits of experimental error. The plot of K against χ_{DMSO} (Fig. 1*d*) exhibits a small minimum at $\chi_{DMSO} = 0.35$. This is also the region where the viscosity and thermodynamic excess functions, including the considerable volume contraction on mixing (41), all show extremum behavior, indicative of a highly structured solvent mixture. It has been suggested that β-glucose fits into water structure more effectively than α-glucose (42, 43) possibly

Can. J. Chem. Downloaded from www.nrcresearchpress.com by 210.87.254.42 on 09/05/12
For personal use only.

Can. J. Chem. Downloaded from www.nrcresearchpress.com by 210.87.254.42 on 09/05/12
For personal use only.

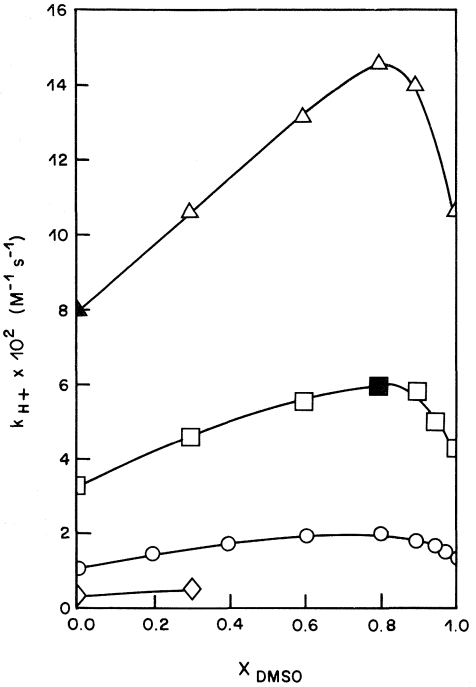

FIG. 3. k_{H+} as a function of χ_{DMSO} for the mutarotation of glucose in DMSO and water mixtures. ◇, 15°; ○, 25°; □, 35°; and △, 45°. Filled symbols represent calculated values.

TABLE 2. Activation parameters for the mutarotation of glucose in DMSO and water at 25.0°. Errors quoted are standard deviations

χ_{DMSO}	$\Delta H^{\ddagger}$ (kJ mol^{-1})	$\Delta S^{\ddagger}$ (J K^{-1} mol^{-1})
	Acid catalysis	
0.000	78±3	−24± 8
0.298	74±2	−35± 6
0.598	74±3	−36±10
0.798	77±3	−25±10
0.896	80±3	−14±12
0.992	78±3	−24±11
	Solvent catalysis	
0.000	66±2	−95± 9
0.298	71±4	−103±15

because the anomeric hydroxyl group is more easily solvated in the equatorial position. In an ordered solvent system, such as the particular solvent mixture mentioned above, β-glucose might tend to disrupt the solvent structure more than α-glucose. This would result in a shift of the equilibrium in favor of the α-anomer.

Basicity of the solvent may also affect the position of equilibrium. Los and Simpson have

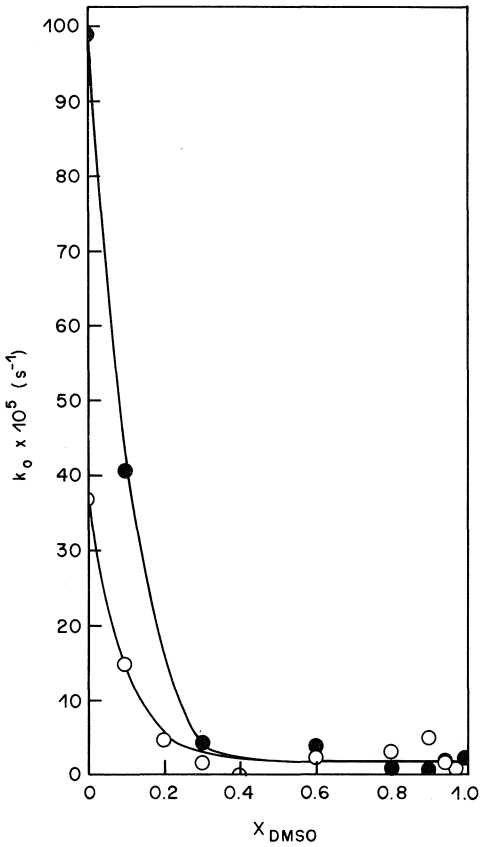

FIG. 4. k_0 as a function of χ_{DMSO} for the mutarotation of glucose in DMSO and water mixtures at 25° (○) and at 35° (●).

shown that α- and β-glucose differ in pK by about 0.3 unit (44) which is sufficient for the β-form to predominate almost exclusively in alkaline solution (45). On this basis, the equilibrium constant would be expected to remain essentially unchanged in water and in DMSO since these solvents are of comparable base strength (28). Changes in other solvent properties such as density, viscosity, and polarity may also affect the equilibrium, but the resulting solvation effects would be expected to be largely the same for both α- and β-glucose. In addition, these properties change by a relatively small amount over the entire mole fraction range.

Figure 3 shows that k_{H+} varies by less than a factor of two over the whole DMSO and water solvent composition region. Evidence that the mechanism for mutarotation remains constant over this solvent range exists in the fact that the thermodynamic activation parameters (Table 2)

Can. J. Chem. Downloaded from www.nrcresearchpress.com by 210.87.254.42 on 09/05/12
For personal use only.

are nearly constant throughout. If the energetics of the reaction do not change appreciably, there is no reason to suspect any change in the mechanism.

The function k_{H^+} increases in going from pure water to about $\chi_{DMSO} = 0.8$ where it reaches a maximum. The value of k_{H^+} in DMSO is greater than in water by a factor of 1.3. The shape of this curve must depend to a large degree on the variation of acid strength with solvent composition but the extent of this variation cannot be determined unless activities for all of the species involved are known.

In contrast to the behavior of k_{H^+}, the "spontaneous" rate constant, k_0, decreases rapidly on adding DMSO to water (Fig. 4). At $\chi_{DMSO} = 0.3$, for example, k_0 is found to be 1.7×10^{-5} s^{-1} at 25° and 4.4×10^{-5} s^{-1} at 35°. These low rates are a consequence of the fact that at this mole fraction most of the water is presumably bound to DMSO in the form of 2:1 complexes (46). The rapid decline in k_0 with increasing DMSO content is in accord with the accepted view that the mutarotation reaction requires both an acid and a base. On the addition of DMSO to water, strongly hydrogen-bonded complexes are formed. This results in a reduction of the concentration of water, the only acidic species present, which is available to act as a catalyst for the reaction. As a result, k_0 decreases as does the amount of "free" water in solution.

The mutarotation of glucose in DMSO proceeds extremely slowly, if at all, in the absence of H^+. Any observed rate is likely due to the presence of traces of catalytic impurities which are extremely difficult to remove (28).

The water dependence of glucose mutarotation can be obtained by observing the rates of the acid catalyzed reaction in various DMSO and water mixtures where the concentration of water is small. The relationship between $(k_{H^+})^\alpha$ and molar concentration of water, $[H_2O]$, can be derived by considering, for example, the stepwise mechanism depicted in eqs. 8 and 9 where α-glucose is represented by α-G and n is a number. Reactions 8 and 9 are essentially the Pedersen

$$[8] \qquad \alpha\text{-G} + H^+ \underset{k_{-1}}{\overset{k_1}{\rightleftharpoons}} \alpha\text{-GH}^+$$

$$[9] \qquad \alpha\text{-GH}^+ + nH_2O \xrightarrow{k_2} \text{Product}$$

mechanism adapted to show the water dependence of the rate determining step. The rate of reaction is

$$[10] \qquad \text{Rate} = k_2[GH^+][H_2O]^n$$

$$[11] \qquad = k_2 \frac{k_1}{k_{-1}}[G][H^+][H_2O]^n$$

assuming that $k_2 \ll k_{-1}$, *i.e.*, that the rate of removal of the hydrogen from the C-1 hydroxyl is much slower than the rate of removal of the hydrogen from the ring oxygen. The ratio k_{-1}/k_2 should be determined by the relative acidities of the two hydrogens. If the charge is localized on the ring oxygen, the ratio of acidities should be approximately the same as the ratio of the acidities of H_3O^+ as compared to H_2O.

Delocalization of the charge would involve weakening the carbon–oxygen bond, the breaking of which leads to aldehyde formation. Thus, the stability of the cyclic form as compared to the aldehyde form should indicate the extent of charge delocalization. Since the free aldehyde form is present to the extent of only 0.003% (9), very little charge delocalization occurs.[1]

The experimentally observed rate is given by

$$[12] \qquad \text{Rate} = k_{obs}{}^\alpha [G]$$

where

$$[13] \qquad k_{obs}{}^\alpha = k_0{}^\alpha + (k_{H^+})^\alpha [H^+]$$

In the solvent region under consideration ($\chi_{DMSO} = 0.8$–1.0) which is the region past the maximum in Fig. 3, $k_0{}^\alpha$ is negligible in comparison to $(k_{H^+})^\alpha$ and eq. 12 becomes

$$[14] \qquad \text{Rate} = (k_{H^+})^\alpha [G] [H^+]$$

A comparison of eqs. 11 and 14 gives

$$[15] \qquad (k_{H^+})^\alpha = k_2 \frac{k_1}{k_{-1}}[H_2O]^n$$

$$[16] \qquad \log (k_{H^+})^\alpha = n \log [H_2O] + \log k_2 \frac{k_1}{k_{-1}}$$

For the restricted solvent region mentioned above, a plot of log $(k_{H^+})^\alpha$ against log $[H_2O]$ should give a straight line with slope n. Figure 5 shows that for the mutarotation of glucose, the plot is not strictly linear, but does *not* correspond to first- or second-order kinetics and appears to approach zero order in solutions of low water

[1]We are indebted to one of the referees for suggesting this approach.

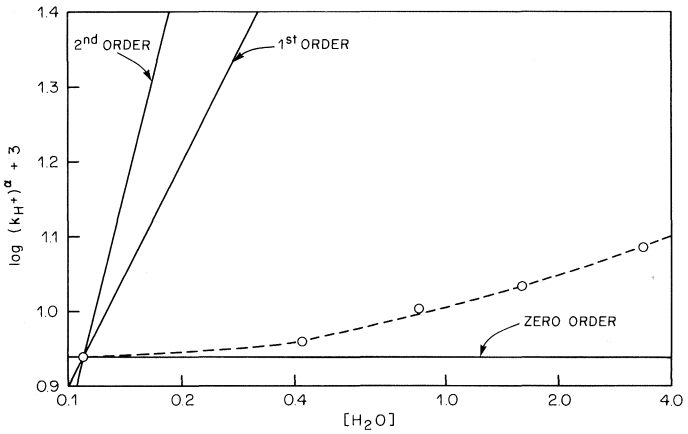

FIG. 5. Log $(k_{H+})^{\alpha}$ as a function of log [H_2O] for the mutarotation of glucose in DMSO and water mixtures at 24.66°. The solid lines represent the curves which would be obtained for various orders of reaction; the broken line connects the experimental points.

concentration. This indicates that there are *no* water molecules involved in the formation of the transition state, and excludes the possibility of a cyclic-concerted mechanism which requires a minimum of two water molecules. A stepwise mechanism on the other hand is consistent with this result and appears to be the only acceptable alternative. The fact that the plot is slightly curved is not surprising since there are many factors which may influence the slope of Fig. 5.

The solvent-catalyzed mutarotation reaction cannot be analyzed in the same way since, when $\chi_{DMSO} > 0.3$, uncatalyzed rates are exceedingly slow. For solutions containing water in concentrations of the order of 1 *M* or less, it is impossible to determine k_0 with any accuracy. However, for the region where k_0 could be measured ($\chi_{DMSO} < 0.3$), plots of log k_0^{α} against log [H_2O] were drawn up. Slopes of 3.3 ± 0.2 were obtained from data at both 25 and 35°. In aqueous solution without added catalyst, water molecules must act as an acid or base and it is possible that the mutarotation reaction does proceed *via* a cyclic-concerted mechanism involving about three water molecules. The alternative is that the solvent- and acid-catalyzed reactions proceed by way of analogous mechanisms with no solvent participation. The former possibility, based on the derived water dependence for the solvent-catalyzed reaction at high water concentrations, is certainly questionable although the amount of "free" water at $\chi_{DMSO} = 0.3$ is presumably very low (41, 47–49). This conclusion is very similar to the one drawn from a study of the solvent isotope effects (18, 19), and also agrees with the conclusions drawn by Stewart and Van Dyke from a study of the hydration of trifluoroacetophenones in aqueous sulfolane (26).

Patting and Strehlow have shown that pyruvic acid exists in aqueous solution as a "relatively stable trihydrate" (50), one water molecule being involved in the formation of the diol and the other two forming a hydrogen-bonded complex. They interpret the kinetics of the hydration and dehydration reactions as proceeding *via* a transition state similar to this trihydrate species. Inclusion of three water molecules in the kinetic expression for the hydration reaction leads to a nearly linear plot of rate as a function of HCl concentration up to levels as high as 5 *M* HCl. Their experimental conditions also involved 0.5 *M* pyruvic acid and 53 *M* water. Conclusions which are based on experimental results obtained under such extreme conditions must be treated with caution.

For the mutarotation of glucose, the enthalpies of activation were found to be practically constant over the entire range of solvent compositions. The values obtained in this study were in reasonable agreement with those reported previously (36, 40).

The entropy of activation is less negative for catalysis by proton than for catalysis by water. This order is difficult to explain since greater solvation should be observed with the charged complex resulting from an ionic catalyst unless factors other than solvation are important.

It is reasonable to propose again on the basis

Can. J. Chem. Downloaded from www.nrcresearchpress.com by 210.87.254.42 on 09/05/12
For personal use only.

of activation entropies that different mechanisms may be involved for different types of catalysis. The large negative activation entropy for water catalysis may represent the involvement of several water molecules in the transition state while the higher value for acid catalysis may simply be an expression of increased solvation of the transition state over the reacting species.

Summary

It has been demonstrated that the acid-catalyzed mutarotation of glucose proceeds by a stepwise mechanism in which there is no solvent participation in the transition state. On the other hand, conclusions regarding the mechanism for catalysis by water molecules are less definite. Both the kinetic and activation entropy results obtained in DMSO and water mixtures at high water concentrations indicate that the mechanism for solvent catalysis may be concerted involving three water molecules in a cyclic transition state.

This work was supported in part by the National Research Council of Canada.

1. K. J. PEDERSEN. J. Phys. Chem. **38**, 581 (1934).
2. H. SCHMID. Monatsh. Chem. **94**, 1206 (1963).
3. H. SCHMID. Monatsh. Chem. **95**, 454 (1964).
4. J. A. CHRISTIANSEN. J. Colloid Interface Sci. **22**, 1 (1966).
5. R. M. IZATT, J. H. RYTTING, L. D. HANSEN, and J. J. CHRISTENSEN. J. Am. Chem. Soc. **88**, 2641 (1966); J. J. CHRISTENSEN, J. H. RITTING, and R. M. IZATT. J. Chem. Soc. B, 1646 (1970).
6. R. T. MORRISON and R. N. BOYD. Organic chemistry. Allyn and Bacon, Inc., Boston, Mass. 1959. p. 768.
7. S. M. CANTOR and Q. P. PENISTON. J. Am. Chem. Soc. **62**, 2113 (1940).
8. K. WIESNER. Collection Czechoslov. Chem. Commun. **12**, 64 (1947).
9. J. M. LOS, L. B. SIMPSON, and K. WIESNER. J. Am. Chem. Soc. **78**, 1564 (1956).
10. D. RITTENBERG and C. GRAFF. J. Am. Chem. Soc. **80**, 3370 (1958).
11. M. EIGEN. Disc. Faraday Soc. **39**, 7 (1965); *In* Fast reactions and primary processes in chemical kinetics. *Edited by* S. Claesson. Interscience, New York. 1967. p. 245.
12. R. P. BELL. Advan. Phys. Org. Chem. **4**, 1 (1966).
13. J. L. KURZ. J. Am. Chem. Soc. **89**, 3528 (1967).
14. R. P. BELL and W. C. E. HIGGINSON. Proc. Roy. Soc. A**197**, 141 (1949).
15. Y. POCKER. Proc. Chem. Soc. **17**, (1960).
16. R. A. CRAIG, P. T. MCTIGUE, and J. N. RIDE. Unpublished data quoted in P. T. McTigue and P. V. Renowden. Aust. J. Chem. **23**, 297 (1970).
17. B. C. CHALLIS, F. A. LONG, and Y. POCKER. J. Chem.Soc. 4679 (1957).
18. H. H. HUANG, R. R. ROBINSON, and F. A. LONG. J. Am. Chem. Soc. **88**, 1866 (1966).
19. H. H. HUANG, A. N. H. YEO, and L. H. L. CHIA. J. Chem. Soc. B, 836 (1969).
20. R. P. BELL and B. DE B. DARWENT. Trans. Faraday Soc. **46**, 34 (1950).
21. M. L. AHRENS and H. STREHLOW. Disc. Faraday Soc. **39**, 112 (1965).
22. E. GRUNWALD and S. MEIBOOM. J. Am. Chem. Soc. **85**, 2047 (1963); Z. LUZ and S. MEIBOOM. J. Am. Chem. Soc. **85**, 3923 (1963); and E. GRUNWALD, C. F. JUMPER and S. MEIBOOM. J. Am. Chem. Soc. **85**, 522 (1963).
23. M. ANBAR, A. LOEWENSTEIN, and S. MEIBOOM. J. Am. Chem. Soc. **80**, 2630 (1958).
24. C. A. LANE, M. F. CHEUNG, and G. F. DORSEY. J. Am. Chem. Soc. **90**, 6492 (1968).
25. R. P. BELL, J. P. MILLINGTON, and J. M. PINK. Proc. Roy. Soc. A**303**, 1 (1968).
26. R. STEWART and J. D. VAN DYKE. Can. J. Chem. **50**, 1992 (1972).
27. J. N. BUTLER. J. Electroanal. Chem. **14**, 89 (1967).
28. I. M. KOLTHOFF and T. B. REDDY. Inorg. Chem. **1**, 189 (1962).
29. F. J. C. ROSSOTTI and H. ROSSOTTI. J. Chem. Educ. **42**, 375 (1965).
30. J. D. NEUSS, M. G. O'BRIEN, and H. A. FREDIANI. Anal. Chem. **23**, 1332 (1951).
31. J. MITCHELL, JR., and D. M. SMITH. Aquametry. Interscience Publishers, New York. 1948. p. 71.
32. N. M. BALLASH. M.Sc. Thesis. University of Calgary, Calgary, Alberta, 1970.
33. E. A. MOELWYN-HUGHES. Chemical statics and kinetics of solutions. Academic Press, London. 1971. p. 129.
34. E. A. GUGGENHEIM. Phil. Mag. **1**, 538 (1926).
35. F. DANIELS, J. H. MATHEWS, J. W. WILLIAMS, P. BENDER, and R. A. ALBERTY. Experimental physical chemistry. McGraw-Hill, New York. 1956. Chapt. 17.
36. G. F. SMITH and M. C. SMITH. J. Chem. Soc. 1413 (1937).
37. C. S. HUDSON and J. K. DALE. J. Am. Chem. Soc. **39**, 320 (1917).
38. J. MEYER. Z. Physik. Chem. **62**, 59 (1908).
39. D. G. HILL and B. A. THUMM. J. Am. Chem. Soc. **74**, 1380 (1952).
40. J. C. KENDREW and E. A. MOELWYN-HUGHES. Proc. Roy. Soc. A**176**, 352 (1940).
41. J. KENTTÄMAA and J. J. LINDBERG. Suomen Kemistilehti B**33**, 32, 98 (1960).
42. M. A. KALBAYAMA, D. PATTERSON, and L. PICHE. Can. J. Chem. **36**, 557 (1958).
43. M. A. KABAYAMA and D. PATTERSON. Can. J. Chem. **36**, 563 (1958).
44. J. M. LOS and L. B. SIMPSON. Rec. Trav. Chim. **73**, 941 (1954).
45. V. S. R. RAO and J. F. FOSTER. J. Phys. Chem. **69**, 636 (1965).
46. E. A. SYMONS. Can. J. Chem. **49**, 3940 (1971).
47. J. J. LINDBERG and J. KENTTÄMAA. Suomen Kemistilehti B**33**, 104 (1960).
48. E. TOMMILA and M. L. MURTO. Acta. Chem. Scand. **17**, 1947 (1963).
49. M. TAMRES and S. SEARLES, JR. J. Am. Chem. Soc. **81**, 2100 (1959).
50. H. PATTING and H. STREHLOW. Ber. Bunsenges. Physik. Chem. **73**, 534 (1969).

Can. J. Chem. Downloaded from www.nrcresearchpress.com by 210.87.254.42 on 09/05/12
For personal use only.

The Conformational Equilibrium of 1,2,3-Tribromopropane in Solution

L. ERNST[1] AND T. SCHAEFER

Department of Chemistry, University of Manitoba, Winnipeg, Manitoba R3T 2N2

Received August 3, 1972

The p.m.r. spectra of dilute solutions of 1,2,3-tribromopropane in carbon tetrachloride, acetonitrile, and dimethylsulfoxide as well as of the neat compound are examined. From the three- and four-bond spin–spin coupling constants and from a comparison between observed and calculated dipole moments it is concluded that in nonpolar solvents the title compound exists preferably in the enantiomeric conformations **a** and **i**. In polar solvents other rotamers contribute to the equilibrium but still seem to play only a minor role. Semiempirical calculations of conformational energies rule out contributions to the conformational equilibrium from rotamers having (1:3) bromine–bromine interactions, but otherwise are only in moderate agreement with experiment.

Les spectres r.m.p. de solutions diluées de tribromo-1,2,3 propane dans le tétrachlorure de carbone, l'acétonitrile, et le diméthylsulfoxide aussi bien que ceux du composé pur ont été étudiés. A partir des constantes de couplage spin–spin à trois et à quatre liaisons et à partir d'une comparaison entre les moments dipolaires calculés et observés, on a conclu au fait que dans des solvants non-polaires, le composé étudié existe préférentiellement dans les conformations énantiomériques **a** et **i**. Dans les solvants polaires, les autres rotamères contribuent à l'équilibre mais ne jouent, même là, qu'un rôle mineur. Des calculs semiempiriques des énergies conformationnelles refutent les contributions à l'équilibre conformationnel des rotamères possédant des interactions brome–brome (1:3), mais autrement ceux-ci ne sont qu'en accord partiel seulement avec l'expérience.

[Traduit par le journal]

Can. J. Chem., **51**, 565 (1973)

Can. J. Chem. Downloaded from www.nrcresearchpress.com by 210.87.254.40 on 09/05/12
For personal use only.

Introduction

There have been numerous studies in recent years on the rotational isomerism of ethane derivatives (1). 1,2-Disubstituted propanes, which can be regarded as trisubstituted ethanes, have also been investigated (2). In both types of compounds the maximum possible number of staggered conformations is three. An interesting and more complex problem is presented by the class of 1,2,3-trisubstituted propanes in which simultaneous rotation about the two C—C single bonds can occur, raising the maximum number of staggered conformations to nine. Dempster *et al.* studied the conformations of a number of polychlorinated propanes, among them 1,2,3-trichloropropane, by i.r. and n.m.r. methods (3).

We wish to report on the analyses of the p.m.r. spectra of 1,2,3-tribromopropane (**1**) in solvents of different polarity and on attempts to calculate conformational energies. The magnitudes of the three- and four-bond proton–proton coupling constants as well as the comparison between the observed (4) and calculated dipole moments allow some conclusions concerning the nature and the relative importance of the conformations involved in the rotational equilibrium.

Experimental

1,2,3-Tribromopropane, from Eastman Organic Chemicals, was used without further purification. Eight mole percent solutions in carbon tetrachloride, acetonitrile, and dimethylsulfoxide (DMSO) as well as a neat sample were prepared, all containing a small quantity of tetramethylsilane (TMS) as internal reference and locking substance. The samples were degassed by the usual freeze–pump–thaw technique. The p.m.r. spectra were recorded on a Varian HA-100 D spectrometer operating in the frequency sweep mode at a probe temperature of *ca.* 30 °C. Sweep rates were 0.02 or 0.05 Hz/s. To prevent errors arising from the nonlinearity of the spectrometer sweep, peak positions were calibrated at intervals of less than 5 Hz using a Hewlett–Packard 5323A frequency counter. The spectra which were of the AA′BB′C type were analyzed by means of the iterative computer program LAME (5).

Results and Discussion

(1) Analysis of Proton Magnetic Resonance Spectra

The spectral parameters for **1** and their standard deviations obtained in the iterative analysis are given in Table 1. In reporting the results we follow the recent recommendations of Abraham

[1]Postdoctoral Fellow 1971–1972. Present address: Badische Anilin- und Soda-Fabrik, Ludwigshafen, West Germany.

TABLE 1. Chemical shifts and coupling constants for 8 mol % solutions of 1,2,3-tribromopropane in different solvents

	Solvent			
Parameter*†‡	CCl_4	Neat	CH_3CN§	DMSO
ν_A	390.86 (1)		397.85 (1)	
ν_B	381.47 (1)		386.82 (1)	
ν_C	432.17 (1)	433.36 (1)	451.91 (0)	472.86 (1)
$^2J_{AB}$	−10.96 (1)		−11.21 (1)	
$^3J_{AC}$	4.25 (1)	4.57 (2)	4.60 (1)	4.78 (1)
$^3J_{BC}$	7.04 (1)	6.81 (2)	6.64 (1)	6.34 (1)
$^4J_{AA'}$	−0.40 (2)		−0.40 (2)	
$^4J_{BB'}$	−0.38 (1)		−0.34 (2)	
$^4J_{AB'}$	0.37 (1)		0.32 (1)	

*Chemical shifts in Hz at 100 MHz relative to internal TMS.
†Coupling constants in Hz.
‡Figures in brackets represent standard deviations as given by LAME and are to be applied to the last decimal figure.
§Chemical shifts in the CH_3CN solution were obtained relative to the solvent signal and were related to TMS by adding 196.4 Hz, the measured shift difference between CH_3CN and TMS in this solution.

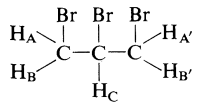

1

(6). Complete analyses could only be obtained for the solutions in CCl_4 and CH_3CN. For the neat compound and for the solution in DMSO, line widths were larger than 0.2 Hz and the fine structure of the AA'BB' parts of the AA'BB'C spectra was not well enough resolved to allow assignment of a number of transitions sufficient for the extraction of the four-bond coupling constants. Therefore only the methine proton spectrum was analyzed to yield the vicinal couplings J_{AC} and J_{BC} and the chemical shift ν_C. Root mean square (r.m.s.) errors between calculated and observed frequencies were 0.036 Hz for the neat liquid and 0.024 Hz for the DMSO solution. Fifteen of the 16 calculated transitions in the methine region were assigned in both cases. The largest deviations between calculated and observed line positions were 0.07 (neat) and 0.05 Hz (DMSO). The larger errors for the neat sample were probably caused by line broadening from viscosity effects since the melting point of **1** is 16 °C.

The complete analysis of the spectra of the CCl_4 and CH_3CN solutions offered some difficulties. While good starting values for the iterative calculation could be obtained for the three chemical shifts and for the geminal and vicinal couplings, this was not the case for the four-bond couplings. It was not possible to extract ^4J values from the methylene spectrum using first-order rules (see Fig. 1 for the CCl_4 solution). Therefore J_{AC}, J_{BC} and ν_C were initially obtained from the analysis of the methine peaks. Reasonable estimates of ν_A, ν_B, and $^2J_{AB}$ could be found from the methylene spectrum. These values were then kept constant and about 40 noniterative spectra were calculated varying $J_{AA'}$, $J_{BB'}$ and $J_{AB'}$ independently between −0.6 and +0.6 Hz. The only spectra that bore a resemblance to the experimental ones, thereby permitting assignment of the transitions, were those with $J_{AA'}$ and $J_{BB'}$ lying in the vicinity of −0.4 Hz and with $J_{AB'}$ near +0.4 Hz. For the CCl_4 (CH_3CN) solution the signs and magnitudes of the four-bond couplings were then obtained by iteration on 61 (47) out of 64 (64) calculated transitions of sufficient intensity. The r.m.s. error was 0.024 (0.019) Hz and the largest deviation between calculated and observed frequencies was 0.05 (0.05) Hz. Spin tickling experiments were not useful because only very few lines of the AA'BB' part were nondegenerate. However, the relative signs of the coupling constants were safely determined by the distinctive second-order character of the spectra. In order to illustrate the analytical quality, the experimental and the calculated spectra of the methylene protons of **1** in CCl_4 are given in Fig. 1. The calculated spectrum uses a line width of 0.15 Hz and an asymmetric line shape to simulate spectrometer conditions (7).

(2) Vicinal Couplings

To facilitate the discussion, the nine possible staggered rotamers of **1** are shown together with

Can. J. Chem. Downloaded from www.nrcresearchpress.com by 210.87.254.40 on 09/05/12
For personal use only.

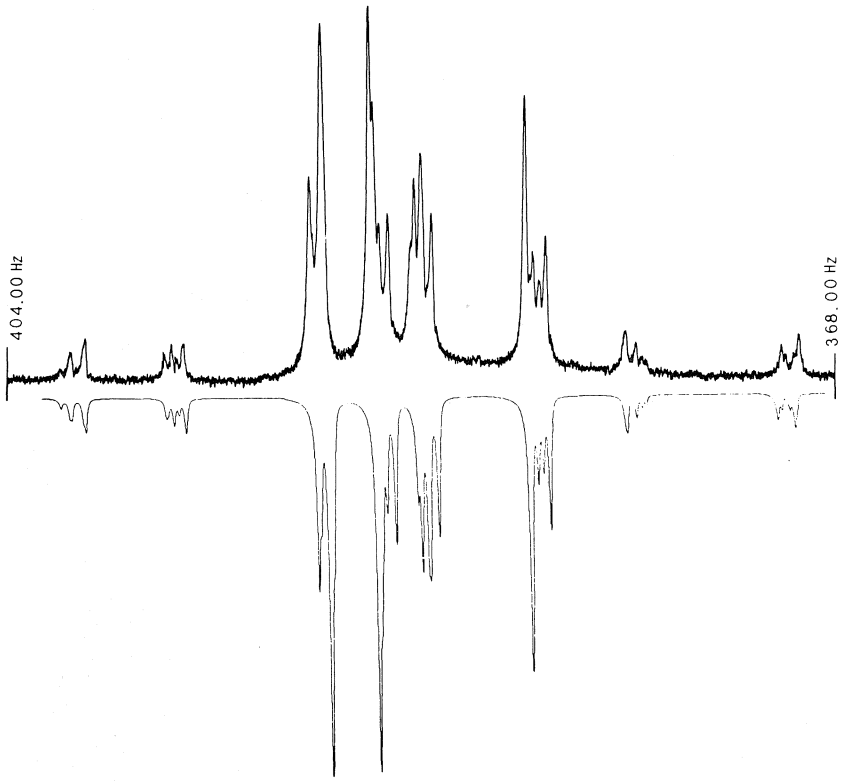

FIG. 1. Experimental (top) and calculated (bottom) p.m.r. spectra at 100 MHz of the methylene protons of an 8 mol % solution of 1,2,3-tribromopropane in CCl_4. Slight differences between the line positions of the two spectra arise from the nonlinearity of the spectrometer sweep.

the values of their dihedral angles ϕ_1 (Br^1—C^1—C^2—C^3) and ϕ_2 (C^1—C^2—C^3—Br^3). We arbitrarily define ϕ_1 as positive when Br^1 lies *in front* of the plane of the paper and ϕ_2 as positive when Br^3 lies *behind* the plane of the paper. This definition corresponds to looking along the bond from C^1 to C^2 (C^2 to C^3) with ϕ_1 (ϕ_2) being positive if an anticlockwise rotation of Br^1 (C^1) is required to cause eclipse with C^3 (Br^3). Not all nine conformations will differ in their physical properties because **a**/**i**, **b**/**f**, and **d**/**h** are pairs of enantiomers. Furthermore, conformations **c** and **g** have '(1:3) halogen–halogen interactions' and are not appreciably populated if other conformations are available to the molecule (3), a behavior well reproduced by calculations of conformational energies (see section 5). The discussion is thus limited to the four rotamers **a**, **b**, **d**, and **e** having statistical weights of 2, 2, 2, and 1, respectively. The fractional populations of **a**, **b**, **d**, and **e** are p_1, p_2, p_3, and p_4 and hence

$$[1] \qquad 2p_1 + 2p_2 + 2p_3 + p_4 = 1$$

The observed vicinal couplings J_{AC} and J_{BC} are the weighted averages of their values in the individual rotamers. It has been shown (8) that these individual couplings do not only depend on the relative orientation of the protons under consideration (*i.e.* if they are *gauche* or *trans* to each other) but also on the relative position of the substituents. Using the nomenclature of ref. 8 (subscripts to indicate the relative position of the bromine atoms and superscripts to give the relationship between the coupled protons) eqs. 2 and 3 can be written[2]

$$[2] \quad J_{AC} = p_1(J_t^g + J_g^{g'}) + p_2(J_t^g + J_g^t) + p_3(J_g^t + J_g^{g'}) + p_4 J_g^t$$

[2]See section 3 for the justification of labelling the protons A and B.

Can. J. Chem. Downloaded from www.nrcresearchpress.com by 210.87.254.40 on 09/05/12
For personal use only.

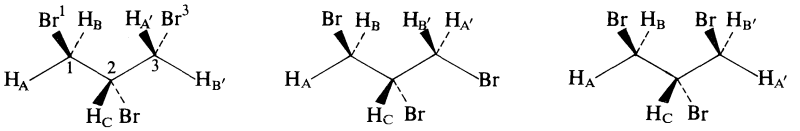

a: $\phi_1 = 60,\ \phi_2 = 60^\circ$ b: $\phi_1 = 60,\ \phi_2 = 180^\circ$ c: $\phi_1 = 60,\ \phi_2 = 300^\circ$

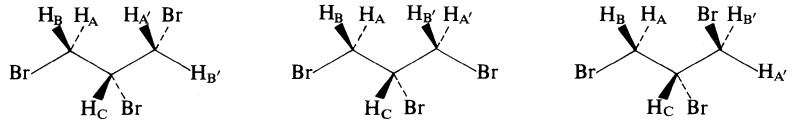

d: $\phi_1 = 180,\ \phi_2 = 60^\circ$ e: $\phi_1 = 180,\ \phi_2 = 180^\circ$ f: $\phi_1 = 180,\ \phi_2 = 300^\circ$

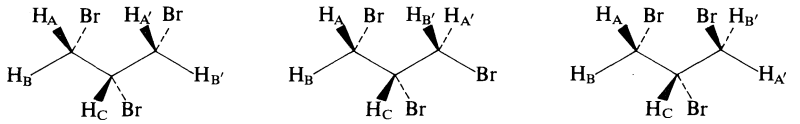

g: $\phi_1 = 300,\ \phi_2 = 60^\circ$ h: $\phi_1 = 300,\ \phi_2 = 180^\circ$ i: $\phi_1 = 300,\ \phi_2 = 300^\circ$

$$[3]\quad J_{BC} = p_1(J_t^t + J_g^g) + p_2(J_t^t + J_g^g) + p_3(J_g^g + J_g^g) + p_4 J_g^g$$

where the first entries in the brackets refer to the coupling constants across the C^1—C^2 bond, the second to the couplings across the C^2—C^3 bond. The meaning of J_g^g and $J_g^{g'}$ can be seen from formula **j**.

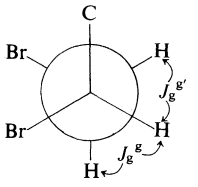

j

Abraham (8*a*) gives a set of equations describing the dependence of the coupling constants in the individual rotamers on the sum of the electronegativities of the substituents X and Y in molecules of the type X—CH_2—CH_2—Y, see eqs. 4*a–e*.

$$[4a]\quad J_t^g = 1.35 + 0.63\,(E_X + E_Y)$$

$$[4b]\quad J_t^t = 18.07 - 0.88\,(E_X + E_Y)$$

$$[4c]\quad J_g^g = 8.94 - 0.94\,(E_X + E_Y)$$

$$[4d]\quad J_g^{g'} = 10.45 - 1.43\,(E_X + E_Y)$$

$$[4e]\quad J_g^t = 16.47 - 0.60\,(E_X + E_Y)$$

For X = Y = Br, $E_X + E_Y = 5.9$ and the following values for J_t^g, J_t^t, J_g^g, $J_g^{g'}$, and J_g^t are obtained for Br—CH_2—CH_2—Br: 5.07, 12.87, 3.39, 2.01, 12.93 Hz. In the present case, Br—CH_2—$CH\langle^{C}_{Br}$, a third substituent is attached to the ethane framework and simple addition of the electronegativity of carbon to the term $E_X + E_Y$ yields values of 6.7 and −1.7 Hz for J_t^g and $J_g^{g'}$, respectively, outside the range of *gauche* couplings. As will be seen below, a compromise between these extremes proves to be most sensible.

Even if values for the individual couplings are available, there exist only three equations, 1–3, for the determination of four unknowns, p_1, p_2, p_3, and p_4. Fortunately the boundary conditions, that only solutions with positive values for the populations are possible and that p_1, p_2, and p_3 lie between 0 and 0.5 and p_4 between 0 and 1 (because of eq. 1), considerably simplify the problem. We varied p_1 in steps of 0.002 between the limits of 0 and 0.5 and calculated the remaining populations by means of eqs. 1–3. Using the individual couplings obtained directly from eqs. 4*a–e* there existed no solution for which all p's were positive. To account for the presence of the carbon substituent, the electronegativity term in eqs. 4*a–e* was augmented by 10% giving J_t^g, J_t^t, J_g^g, $J_g^{g'}$, and J_g^t as 5.44, 12.35, 2.84, 1.18 and 12.53 Hz, respectively. For this set of parameters, solutions to eqs. 1–3 could be found which satisfied the boundary conditions simultaneously for the values of J_{AC} and J_{BC} in the four different solvents.

Augmentation of $E_X + E_Y$ by 20% gave a

Can. J. Chem. Downloaded from www.nrcresearchpress.com by 210.87.254.40 on 09/05/12
For personal use only.

TABLE 2. Ranges of populations of the conformations of 1,2,3-tribromopropane in different solvents as obtained from the vicinal coupling constants

Solvent	ε*	J_{AC}	J_{BC}	p_1	p_2	p_3	p_4
CCl_4	2.45	4.25	7.04	0.40–0.44	0.05–0.00	0.06–0.01	0.00–0.09
Neat	6.40	4.57	6.81	0.36–0.42	0.06–0.00	0.08–0.02	0.00–0.12
CH_3CN	22.7	4.60	6.64	0.35–0.40	0.05–0.00	0.10–0.05	0.00–0.06
DMSO	29.2	4.78	6.34	0.32–0.37	0.05–0.00	0.13–0.09	0.00–0.09

*Calculated from eq. 5. for 8 mol % solutions.

$J_g{}^{g'}$ of 0.33 Hz, probably too small for the degree of substitution present in **1**. Nevertheless, solutions for all four solvent cases were still possible, although the vicinal couplings measured in CCl_4 allowed positive p_2, p_3, and p_4 values only in a very narrow range of p_1 (0.400–0.402). If the term $E_X + E_Y$ was made 30% larger no solutions were found with all p's positive. Consequently, if Abraham's eqs. 4*a–e* are to be applied to molecule **1**, the terms containing the sum of the electronegativities of the bromine atoms should be multiplied by a factor of 1.1 to 1.2 with 1.1 being more likely.[3]

Table 2 lists the ranges of populations which were obtained by the outlined procedure from the vicinal coupling constants in the different solvents. The dielectric constants were calculated by means of eq. 5 (ref. 9), where ε_1 ε_2, and ε_s are

$$[5]\quad \frac{\varepsilon_s - 1}{\varepsilon_s + 2} = \frac{\varepsilon_1 - 1}{\varepsilon_1 + 2}\cdot\frac{V_1}{V_1 + V_2} + \frac{\varepsilon_2 - 1}{\varepsilon_2 + 2}\cdot\frac{V_2}{V_1 + V_2}$$

the dielectric constants of solvent, solute, and solution, respectively, and V_1 and V_2 the volumes of solvent and solute. It is seen that with increasing polarity of the solution p_1 decreases from about 0.42 to 0.35, p_3 increases from 0.03 to 0.11, whereas p_2 and p_4 remain approximately constant over the solvent range at *ca.* 0.03 and 0.05, respectively. Conformations **a** and **i** are therefore the most important ones and together contribute 84% in CCl_4 and 70% in DMSO. The remaining conformations appear to be rather unimportant, except for the pair **d**/**h** which is present to the extent of about 20% in highly polar solvents.

(3) Four-bond Couplings

These couplings are less reliable as a tool in conformational analysis than are the vicinal couplings because most experimental data that are available refer either to more or less strained cyclic molecules or to molecules in which one of the protons belongs to a methyl group, thus yielding only an average over the staggered conformations. A number of INDO molecular orbital calculations (10) have been performed on propanic couplings and theoretical data are available for all possible staggered conformations. Barfield (10*a*) has shown that electronegative inductive substituents, whether bonded to the central or to the terminal carbon atoms, cause positive shifts in the coupling constants relative to propane. Comparing the theoretical coupling constants for propane and the monofluoropropanes (10*a*) and estimating the inductive effect of bromine to be about half as large as that of fluorine while assuming additivity of substituent effects, one arrives at some values for the long-range coupling constants of the individual rotamers of **1**. One can then write four equations (one for each of $J_{AA'}$, $J_{BB'}$, and $J_{AB'}$ plus eq. 1) to calculate the populations p_1 to p_4. However, this set of equations is very poorly defined and small changes in the parameters $J(\phi_1, \phi_2)$ or in the experimental coupling constants result in large variations of the calculated populations. This behavior arises because according to theory (10*a*) rather similar couplings have to be assumed for some conformations with different dihedral angles.

The long-range couplings are useful, however, in one respect. One of the experimental couplings, $J_{AB'}$, is positive and INDO (10*a*) predicts positive values only near the planar 'zig–zag' or 'W' arrangement of the coupled protons. This

[3]A referee pointed out that our treatment neglects the orientation factor for the extra carbon substituent in the fragment Br—CH_2—CH<(Br, C) as compared to Br—CH_2—CH_2—Br. Unfortunately, a decision on how to treat this factor cannot be made at the present time because of lack of evidence (experimental and theoretical) from similar compounds. We therefore emphasize that our conclusions can only be of a qualitative nature.

Can. J. Chem. Downloaded from www.nrcresearchpress.com by 210.87.254.40 on 09/05/12
For personal use only.

Can. J. Chem. Downloaded from www.nrcresearchpress.com by 210.87.254.40 on 09/05/12
For personal use only.

arrangement occurs in **a** and its mirror image **i** (**c** and **g** being ruled out because of their (1:3) Br–Br interactions). As the contributions to J_{AB}, from all conformations but **a** are negative, **a** must be very appreciably populated in order to override the negative contributions from **b**, **d**, and **e**. This conclusion justifies the labelling of protons H_A and H_B in **a** to **i** since in the major pair of rotamers **a**/**i** the coupling $J_{AC} \simeq 4.5$ Hz is smaller than $J_{BC} \simeq 6.5$ Hz, in agreement with what is inferred from the formulae, *viz.* $J_{AC} = J^g$ and $J_{BC} = (J^g + J^t)/2$, *i.e.* $J_{AC} < J_{BC}$.

(4) Dipole Moment

The dipole moment of **1** at 20° is 1.58 D in benzene solution and 1.63 D in the neat liquid (4). Assuming the geometry described in section 5 and bond moments of $\mu_{C-H} = 0$ and $\mu_{C-Br} = 1.8$ D (1), one calculates a dipole moment of 1.68 D for **a**, 1.77 D for **b**, 2.88 D for **d**, and 3.19 D for **e**. This result constitutes another strong indication of the unimportance of rotamers **d** and **e** and suggests that **1** exists almost exclusively as **a** and/or **b**. Choosing C—Br bond moments of 1.6 D does not change this conclusion. Even $\mu_{C-Br} = 1.5$ D leads to $(2p_3 + p_4) < 0.23$.

(5) Calculation of Conformational Energies and Their Solvent Dependence

The method of classical mechanics was used in an attempt to calculate the energies and populations of all possible rotamers of **1**. We follow the approach of Abraham and Parry (11) in that the energy of a given conformation in the vapor phase consists of the torsional strain plus the sum of the interactions between the atoms not bonded to a common carbon atom, as given by eq. 6. The parameter $V_0 = 2.65$ kcal/mol and

$$[6] \quad E_v = 0.5\, V_0\,(2 + \cos 3\phi_1 + \cos 3\phi_2) + \sum \{a_{ij} \exp(-b_{ij}) - c_{ij}/r_{ij}^6 + d_{ij}/r_{ij}\}$$

the values for a, b, c, and d are taken from ref. 11. The first two terms in the summation of eq. 6 represent repulsive and attractive van der Waals interactions, respectively, and the third term gives the electrostatic interaction of the polar substituents. The present approach neglects the changes in geometry occurring during the internal rotation because it uses the same bond lengths and angles for all conformations and only takes into account the variation of the dihedral angles. Therefore the calculations are rather simple when compared to the method of adjusting the geometry of every rotamer for a minimum total energy (12).

The following geometry was used: C—H bond length 1.09 Å, C—Br 1.93 Å, and C—C 1.54 Å. The bond angles BrCC and HCH at the terminal carbon atoms were set at 113 and 106°, respectively. Assuming equal magnitudes of the BrCH and CCH angles, these were calculated to be 109.4°. For the central carbon the BrCC and CCC angles were taken as 111 and 113°, giving CCH and BrCH angles of 107.2° when the latter two were assumed equal. Other geometries were tried, *e.g.* the one given in ref. 11, but gave worse agreement between calculated and experimental populations.

Solvation energies E_s for the different solvents were included in the calculations following the principles laid down in ref. 13 and using a computer program described in ref. 14. This program and the subroutine which determines the vapor phase energies were tested by the recalculation of literature values (9, 11) and produced the same results. In the calculations of E_s for **1**, dipole moments of 1.8 D for the C—Br bonds (*1a*) entailed too high a sensitivity to changes in solvent polarity. A μ_{C-Br} value of 1.5 D appeared to be more appropriate.

The total energy $E = E_v + E_s$ was calculated for simultaneous rotation about both C—C bonds by varying ϕ_1 and ϕ_2 from 0 to 360° at intervals of 6°. A step size of 2° was chosen near the energy minima. The final potential energy surface for the CCl_4 solution is shown in the contour diagram of Fig. 2. The following points represent energy minima: **a** (62, 56), **b** (66, 190), **d** (166, 54), **e** (170, 190), **f** (170, 294), **h** (300, 194), and **i** (304, 298). The numbers in brackets give ϕ_1 and ϕ_2, respectively, in degrees. In the region of dihedral angles corresponding to conformations **c** and **g** only shallow high-energy troughs are found (see Fig. 2). Their minima lie at (81, 279) and (285, 75), considerably displaced from the 'ideal' dihedral angles of 60 and 300°. The destabilizing effect of the (1:3) bromine–bromine interactions is well reproduced. While the general appearance of the calculated energy surface seems reasonable there is no agreement between the calculated order of stability of the conformations and the order deduced from the experiments. For the CCl_4 solution $p_2 > p_1 \gg p_4 \sim p_3$

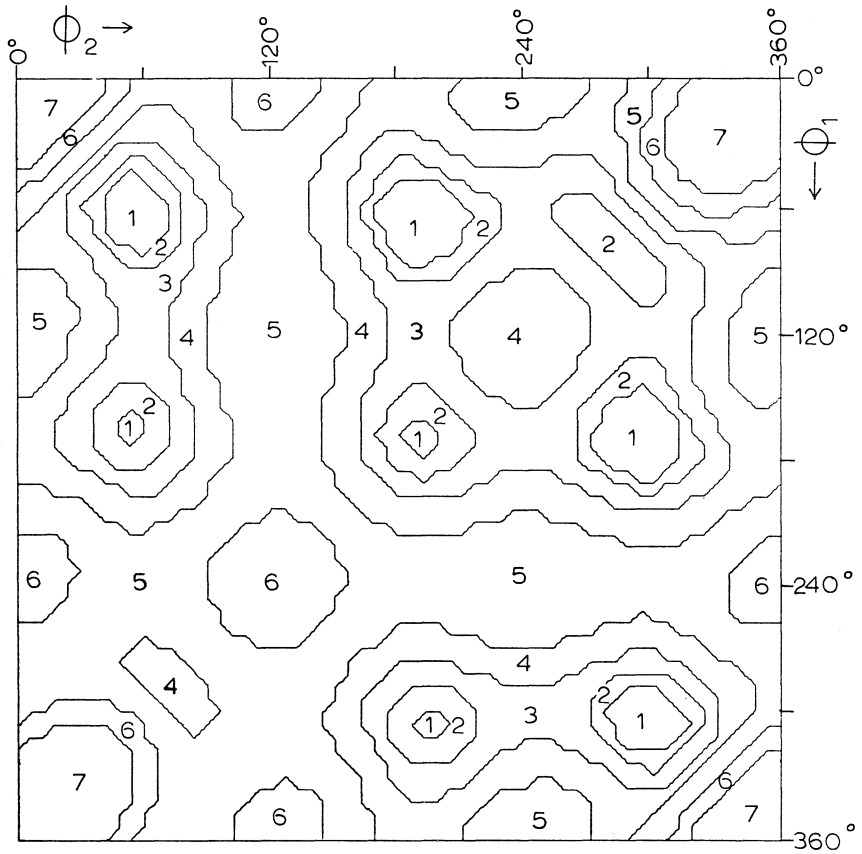

FIG. 2. Calculated energy diagram for the internal rotation of 1,2,3-tribromopropane in CCl_4. For the definition of ϕ_1 and ϕ_2 see text. The energy regions are defined as follows: 1: 0–1; 2: 1–2; 3: 2–4; 4: 4–8; 5: 8–16; 6: 16–32, and 7: >32 kcal/mol relative to the most stable conformation.

is calculated whereas the vicinal couplings lead to $p_1 \gg p_2 \sim p_3 \sim p_4$. Corresponding results for the DMSO solution are $p_2 > p_1 > p_4 > p_3$ (calculation) and $p_1 > p_3 > p_2 \sim p_4$ (experiment). These discrepancies may be due to the inadequacy of the method of calculation, *i.e.* assuming rigid bond lengths and angles over the whole range of dihedral angles. On the other hand, the functions describing the nonbonded interactions have so far only been used in calculations on ethane derivatives and on 1,2-disubstituted propanes. Perhaps they need modifications in order to describe the conformational behavior of the present, rather different, class of compounds.

We are grateful to the National Research Council of Canada for financial assistance. Dr. D. J. Wood kindly supplied the computer program for the calculation of solvation energies. Fruitful discussions with him are also appreciated.

1. (*a*) R. J. ABRAHAM and W. L. OLIVER, JR. Org. Magn. Res. **3**, 725 (1971) and earlier papers in that series; (*b*) For a review see J. P. LOWE, Progress in physical organic chemistry. Vol. 6. A. Streitwieser and R. W. Taft, editors. Interscience, New York. 1968. p. 1.
2. (*a*) H. FINEGOLD. J. Chem. Phys. **41**, 1808 (1964); (*b*) D. A. DAWSON and W. F. REYNOLDS. Can. J. Chem. **49**, 3438 (1971).
3. A. B. DEMPSTER, K. PRICE, and N. SHEPPARD. Spectrochim. Acta, **25**A, 1381 (1969); **27**A, 1563, 1579 (1971).
4. L. J. DE KREUK. Rec. trav. chim. Pays-Bas, **61**, 819 (1942).
5. C. W. HAIGH. Annual reports on NMR spectroscopy. Vol. 4. E. F. Mooney, editor. Academic Press, New York. 1971. p. 311.
6. R. J. ABRAHAM. Analysis of high resolution NMR spectra. Elsevier, Amsterdam. 1971. p. 178.
7. J. B. ROWBOTHAM and T. SCHAEFER. Can. J. Chem. **50**, 2344 (1972).

Can. J. Chem. Downloaded from www.nrcresearchpress.com by 210.87.254.40 on 09/05/12
For personal use only.

8. (*a*) R. J. ABRAHAM and G. GATTI. J. Chem. Soc. B, 961 (1969); (*b*) L. PHILLIPS and V. WRAY. J. Chem. Soc. Perkin II, 536 (1972).
9. R. J. ABRAHAM, L. CAVALLI, and K. G. R. PACHLER. Mol. Phys. **11**, 471 (1966).
10. (*a*) M. BARFIELD. J. Am. Chem. Soc. **93**, 1066 (1971); (*b*) M. S. GOPINATHAN and P. T. NARASIMHAN. J. Magn. Res. **6**, 147 (1972); (*c*) R. WASYLISHEN and T. SCHAEFER. Personal communication.
11. R. J. ABRAHAM and K. PARRY. J. Chem. Soc. B, 539 (1970).
12. J. E. WILLIAMS, P. J. STANG, and P. v. R. SCHLEYER. Ann. Rev. Phys. Chem. **19**, 531 (1968).
13. R. J. ABRAHAM and M. A. COOPER. J. Chem. Soc. B, 202 (1967).
14. D. J. WOOD. Ph.D. Thesis, University of Toronto, Toronto, Ontario. 1972.

Can. J. Chem. Downloaded from www.nrcresearchpress.com by 210.87.254.40 on 09/05/12
For personal use only.

Proton Magnetic Resonance Studies of Long-range Coupling Constants: Conformational Dependence of the ^4J Coupling Between Side Chain and Ring Protons in Formylheterocycles

BERNARD PIERRE ROQUES

Département de Chimie, Ecole Polytechnique, 17 rue Descartes, 75230 Paris Cedex 05, France

AND

SUZANNE COMBRISSON

Laboratoire de Chimie Organique, Ecole de Physique et Chimie, 10 rue Vauquelin, 75005 Paris, France

Received July 21, 1972

The ^4J coupling constant between side chain and ring protons is studied on particular models of planar heterocyclic aldehydes.

The preferential conformation of these molecules is established by use of the "zig–zag" rule for the ^5J coupling constant. This allows precise analysis of the ^4J coupling across *cc* and *ct* pathways.

The sign of some of these constants is determined and is found to be negative in either *cc* or *ct* pathways. The use of the "methyl replacement technique" shows a dominant σ electron contribution to the ^4J coupling constants. In all examples studied here, the ^4J coupling value is dependent on the pathway: $^4J^{ct}$ (−0.30 at −0.45 Hz) > $^4J^{cc}$ (−0.10 at −0.15 Hz). The existence of a stereospecificity for this coupling is in accordance with a preponderant σ electron mechanism and is useful in conformational analysis of planar aromatic aldehydes.

Le couplage ^4J entre la chaîne latérale et les protons du cycle est étudié sur différents modèles d'aldéhydes hétérocycliques de structure plane. La conformation préférentielle de ces modèles est établie par utilisation du couplage stéréospécifique ^5J. Ceci permet l'analyse détaillée des couplages ^4J au travers des enchaînements de liaisons *cc* et *ct*. Le signe de quelques-uns de ces couplages est déterminé. Il est négatif quelle que soit la disposition des liaisons. L'utilisation de la technique par remplacement d'un proton par un radical méthyle montre la prépondérance de la contribution électronique σ dans le mécanisme de ce couplage ^4J. Dans tous les exemples étudiés, le couplage ^4J est dépendant de la conformation de l'enchaînement: $^4J^{ct}$ (−0.30 à −0.45 Hz) > $^4J^{cc}$ (−0.10 à −0.15 Hz). L'existence d'une stéréospécificité de ce couplage est en accord avec la prépondérance du mécanisme de transmission σ, et peut être utilisée dans l'analyse des conformations planes d'aldéhydes aromatiques.

Can. J. Chem., **51**, 573 (1973)

Introduction

The spin–spin coupling constants over five bonds between ring and side chain protons in benzaldehydes and substituted derivatives have been studied extensively (1, 2). These couplings are stereospecific (zig-zag path) and are dominated by the σ contribution (3). In contrast, in benzaldehyde the sign of the coupling over four bonds is negative, and consequently its mechanism has been attributed to a π electron transmission. However, recently Danyluk *et al.* have shown that this coupling is dominated by a σ electron contribution (4). This conclusion is in accordance with theoretical calculations (5) which have shown negative values for ^4J coupling constants in particular conformations of saturated molecules.

In heterocyclic aldehydes (furan, thiophene, pyrrole), we have shown that the stereospecific rule for ^5J coupling is also valid (6, 7) and allows the determination of conformational preferences. In these structures, the ^4J couplings between formyl group and ring protons have not been systematically studied because of the weakness of these couplings. However, the asymetrical structures and conformational preferences of the heterocyclic aldehydes provide suitable models for a study of the ^4J coupling in two particular pathways: *cc* and *ct*. In this paper, we have

studied these couplings by the slow-passage technique in a number of α and β formylthiophenes, furans, and pyrroles. In some cases we have determined the sign of the coupling constants.

The results are discussed in terms of σ and π

Can. J. Chem. Downloaded from www.nrcresearchpress.com by 210.87.254.6 on 09/05/12
For personal use only.

Can. J. Chem. Downloaded from www.nrcresearchpress.com by 210.87.254.6 on 09/05/12
For personal use only.

electron contributions and the conformational dependence of the ^4J coupling.

Experimental

(1) Compounds

3-Formylthiophene (**6**), 2-formylpyrrole (**3**) and 1-methyl-2-formylpyrrole (**4**) were obtained from commercial sources. Other compounds were prepared by the methods quoted in references: **1** (8), **2** (9), **5** (10), **7** (11), **8** (12), **9** (13), **10** (14), and **11** (14).

(2) Nuclear Magnetic Resonance Spectra

Proton magnetic resonance spectra were recorded on a Varian HA 100 NMR spectrometer locked to HMDS at a sweep rate of 0.01 Hz/s. Double resonance experiments were accomplished using a Hewlett–Packard 200 AB oscillator. Solutions of the compounds were prepared in $CDCl_3$ that contained about 5% hexamethyldisiloxan (HMDS). All solutions were thoroughly degassed by several freeze–pump–thaw cycles. Chemical shifts are not included in this work because they are irrelevant for the present study. The coupling constants are measured directly on the spectrum and after selective irradiation. The accuracy is ± 0.05 Hz except for the compounds **1**, **2**, and **11** where the accuracy is ± 0.005 Hz. For these latter three compounds the coupling constants are computed by the "wiggle beat" technique (15).

(3) Signs

The relative signs of the coupling constants are usually obtained by the tickling technique described originally by Freeman and Anderson (16). We have determined the signs of the coupling constants in **1** and **2** by this method. However, tickling causes perturbations of any transition close ($\Delta\nu < 0.5$ Hz) to the irradiated transition and in the case of **11** the sign determination by this technique is unsuccessful. Instead, we have used the generalized Overhauser experiments described by Kaiser (17), and we have determined the sign of the coupling constants in **11** by the method of Bell *et al.* (3). In this technique, the amplitude of the second radiofrequency field is smaller than in the tickling experiments. As a consequence the connected transitions change in intensity instead of splitting into doublets.

The spin states of the nuclei coupled to other protons are given below the spectra with the convention that a positive sign under a lowfield peak of the proton denotes a positive coupling to the nucleus in question. The spin states are labelled in accordance with the signs found experimentally. The ring proton couplings are positive (18) and the signs are determined relative to them.

These experiments are illustrated by the results obtained for 4-bromo-2-formylthiophene (**2**) and 2,3-diformylthiophene (**11**).

(a) 4-Bromo-2-formylthiophene (2)

The spectrum of **2** is shown in Fig. 1. In Fig. 2, the single proton resonance spectrum of the H_3 proton is shown. The $^4J_{CHO-3}$ is clearly resolved. In Fig. 2*a* the intensity of transitions 2 and 4 of H_3 decrease by separation into unresolved doublets when transition 1 of H_5 in Fig. 1 is weakly irradiated. On the other hand no change is noted in the signal intensity of transitions 1 and 3. In Fig. 2*b* the irradiation of 4 of H_5 causes a decrease of transition 1 and 3 of H_3 while 2 and 4 remain unchanged. Hence $J_{3-5}/J_{CHO-3} < 0$. Because the couplings between ring protons and $^5J_{CHO-5}$ are positive (20), $^4J_{CHO-3}$ is negative.

(b) 2,3-Diformylthiophene (11)

We have determined by successive ticklings the signs

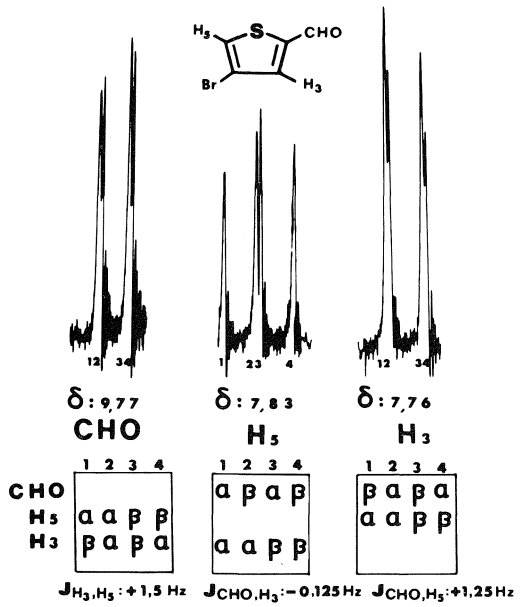

FIG. 1. Spectrum of 4-bromo-2-formylthiophene (**2**) ($\alpha = +$; $\beta = -$).

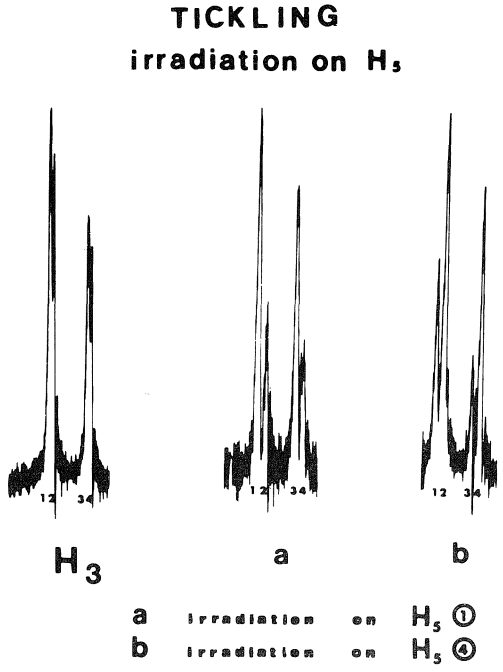

FIG. 2. Tickling on 4-bromo-2-formylthiophene (**2**).

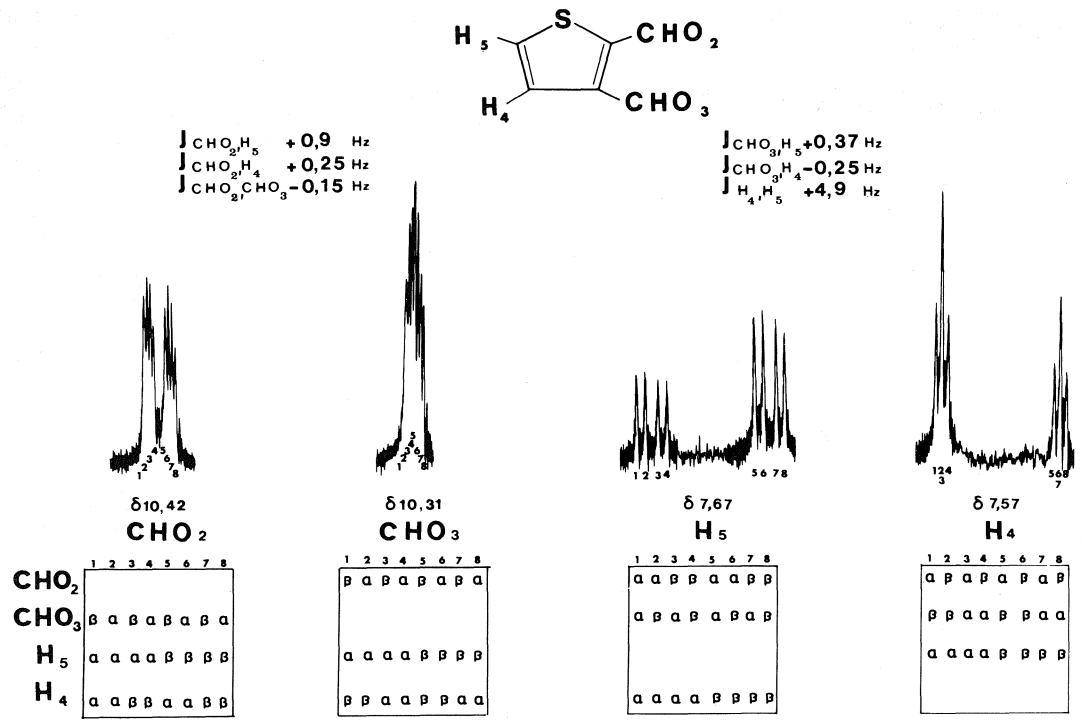

FIG. 3. Spectrum of 2,3-diformylthiophene (**11**) ($\alpha = +$; $\beta = -$).

of $^5J_{CHO_2-5}$, $^5J_{CHO_2-4}$, $^5J_{CHO_3-5}$ which are all positive and $^4J_{CHO_3-4}$ which is negative in accordance with published data (19–21).

We have also determined directly $^5J_{CHO_2-CHO_3}$ by the generalized Overhauser experiment. Fig. 3 shows the spectrum of **11**. In Fig. 4*a*, the single proton resonance spectrum of the aldehydic proton CHO_2 is shown. Fig. 4*b* shows that very weak irradiation centered on peak 1 of H_5 (Fig. 3) causes a decrease in peak 2 (regressively connected transitions) and an increase in peak 6 (progressively connected transitions). Thus $^5J_{CHO_2-4}/^5J_{CHO_2-CHO_3} < 0$, and since $^5J_{CHO_2-4} > 0$, $^5J_{CHO_2-CHO_3}$ is negative.

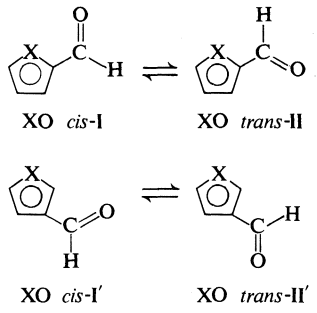

Results

^5J Coupling Constants and Conformational Preferences

All spectra are interpreted at first order and the results are reported in Table 1.

Heterocyclic aldehydes must flip between two planar conformations XO *cis* **I** or **I'** and XO *trans* **II** or **II'**.

At room temperature, we had previously determined (22, 23), by application of the ^5J stereospecific rule, the preferential conformations of all the compounds described in Table 1 except **9**.

In unsubstituted derivatives, the formyl group in the β position is almost exclusively in the XO *trans* conformation **II'**. In contrast, furfural exists in roughly equal mixtures of O–O *cis*-**I** and O–O *trans*-**II** forms. This result has been interpreted by the attendance of three interactions (24). As in benzaldehyde the stereospecific ^5J coupling must be interpreted in terms of σ transmission. We have computed the percentage of π transmission in this ^5J coupling by the "methyl replacement technique" (25). The $W_{1/2}$ width of the H_5 signal before and during irradiation of the methyl group in 2-acetyl-4-bromothiophene is determined. The difference is about 0.10 Hz. Because the $^5J_{CHO-5}$ coupling constant in 2-formyl-4-bromothiophene is 1.20

Can. J. Chem. Downloaded from www.nrcresearchpress.com by 210.87.254.6 on 09/05/12
For personal use only.

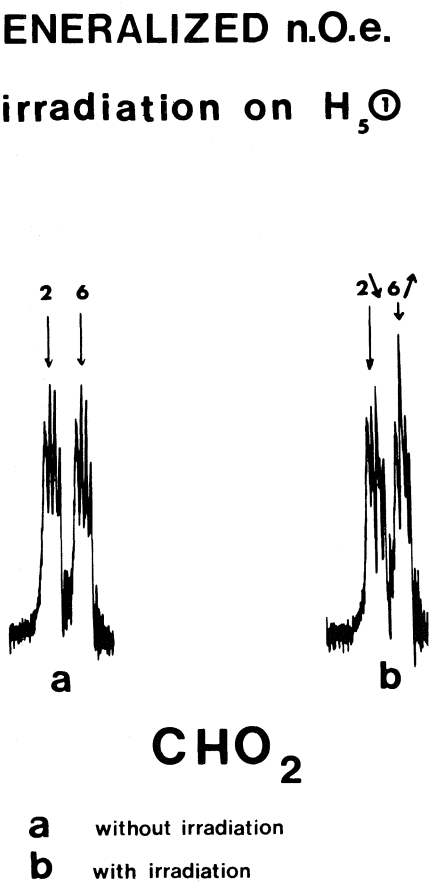

FIG. 4. Generalized Overhauser experiments on 2,3-diformylthiophene (**11**).

Hz, the percentage of π transmission is about $0.10/1.20 \times 100 \cong 8\%$.

For the present study on the ^4J coupling constants we have chosen models with conformations fixed by steric or electrostatic interactions.

Where fast inversion at room temperature occurs, the different forms are computed by application of the ^5J stereospecific rule: with the assumption that ^5J is maximum for the zig–zag pathway and ^5J is near zero for the antistereospecific pathway.

^4J Coupling Constants

There are two groups of heterocyclic compounds: α- and β-formylheterocycles. In each group two coupling pathways, *cc* and *ct*, are observed for some derivatives.

(1) α-Formylheterocycles

(a) 4-Bromo-2-formylfuran (1)

This compound shows a ^4J coupling constant $^4J_{CHO-3} = -0.085$ Hz (Fig. 5). This room temperature value is the average of the two coupling pathways: *cc* (60%) and *ct* (40%) (6). The same ^4J coupling has been measured in furfural itself by Fourier transform methods (26), $^4J_{CHO-3} = 0.06$ Hz. The introduction of a halogen in the 4 position suppresses the coupling J_{CHO-3} and allows a determination of the sign of $^4J_{CHO-3}$ as for 4-bromo-2-formylthiophene (see Experimental).

(b) 4-Bromo-2-formylthiophene (2)

This compound is entirely in the SO *cis* form **I** and the four bond coupling constant $^4J^{cc}_{CHO-3}$ is −0.125 Hz (Fig. 1).

(c) 2-Formylpyrrole (3)

As in **2**, the formyl group is completely in the *cis* conformation **I** and one observes a coupling $^4J^{ct}_{CHO-NH} = -0.32$ Hz. The sign of this coupling had been previously determined (27).

(d) 1-Methyl-2-formylpyrrole (4)

This derivative is almost exclusively in *cis* conformation **I** (28). $^4J^{cc}_{CHO-3}$ is nearly 0.12 Hz. This value is not directly measurable on the spectrum but is computed from line width measurements on the H_3 peak before and during irradiation of the CHO signal. The sign of $^4J^{cc}_{CHO-3}$ could not be determined, but on the basis of previous work, it is probably negative. Irradiation of the CH_3 signal shows no visible perturbation of the width of the CHO signal. Thus, we can assume a very weak π electron transmission for the $^4J^{ct}_{CHO-NH}$ in **3**.

(e) 1-Acetyl-2-formylpyrrole (5)

This compound is certainly planar for thermodynamic reasons, and the formyl group adopts a *trans* conformation **II** ($^5J_{CHO-4} = 0.70$, $^5J_{CHO-5} \cong 0$ Hz). The four bond coupling $^4J^{ct}_{CHO-3} = 0.37$ Hz (sign not determined but probably negative).

(2) β-Formylheterocycles

(a) 3-Formylthiophene (6), 3-Formylfuran (7), and 1-t-Butyl-3-formylpyrrole (8)

The preferential conformation of the formyl group in the β position is XO *trans*-**II**′ (22, 28). Consequently, in these derivatives the ^4J coupling constants adopt a *ct* pathway for $^4J_{CHO-4}$ and a *cc* pathway for $^4J_{CHO-2}$.

In **6**, **7**, and **8** the $^4J^{ct}_{CHO-4}$ coupling constants are in the range of −0.32 to −0.42 Hz. The signs of these couplings in β-formylthiophene and furan are known to be negative (21), and we can assume the same sign for **8**.

Can. J. Chem. Downloaded from www.nrcresearchpress.com by 210.87.254.6 on 09/05/12
For personal use only.

TABLE 1. Conformational preferences (%) and coupling constants (Hz)

Structure	*cis*	*trans*	$^5J_{CHO-5}$	$^5J_{CHO-4}$	$^4J^{cc}$	$^4J^{ct}$
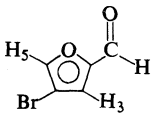 **1**	60	40	+0.6		$J_{CHO-3} = -0.085$ (av. val.)	
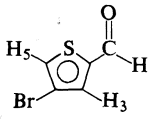 **2**	100	0	+1.25		$J_{CHO-3} = -0.125$	
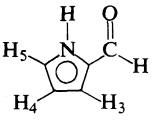 **3**	100	0	+1.13	< 0.10	J_{CHO-3}*	$J_{CHO-NH} = -0.32$
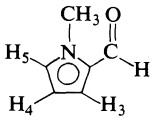 **4**	90	10	+1.05	< 0.10	$J_{CHO-3} = -0.12$†	
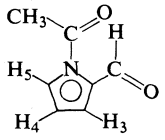 **5**	0	100	< 0.10	+0.70	$J_{CHO-3} < 0.08$	$J_{CHO-3} = -0.37$†
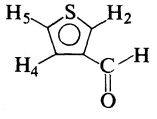 **6**	20	80	+0.8	—	$J_{CHO-2} = -0.10$†	$J_{CHO-4} = -0.35$
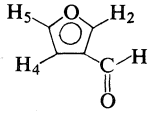 7	0	100	+0.75	—	$J_{CHO-2} < 0.08$	$J_{CHO-4} = -0.42$
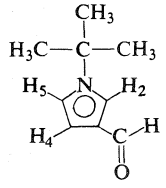 **8**	0	100	+0.70	—	$J_{CHO-2} < 0.08$	$J_{CHO-4} = -0.32$†

Can. J. Chem. Downloaded from www.nrcresearchpress.com by 210.87.254.6 on 09/05/12
For personal use only.

TABLE 1. *Concluded*

Structure	*cis*	*trans*	$^5J_{CHO-5}$	$^5J_{CHO-4}$	$^4J^{cc}$	$^4J^{ct}$
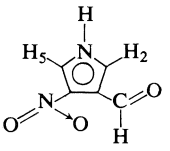 **9**	100	0	< 0.10	—		$J_{CHO-2} = -0.45$†
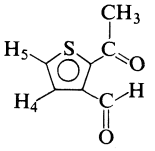 **10**	0	100	$+1.00$	—		$J_{CHO-4} = -0.42$
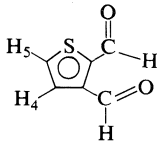 **11**	65 (CHO_3)	35 (CHO_3)	$J_{CHO_3-5} = +0.37$	—		$J_{CHO_3-4} = -0.25$ (av. val.)

*Not measurable because of J_{NH-3}.
†Signs unknown, but assumed to be negative.

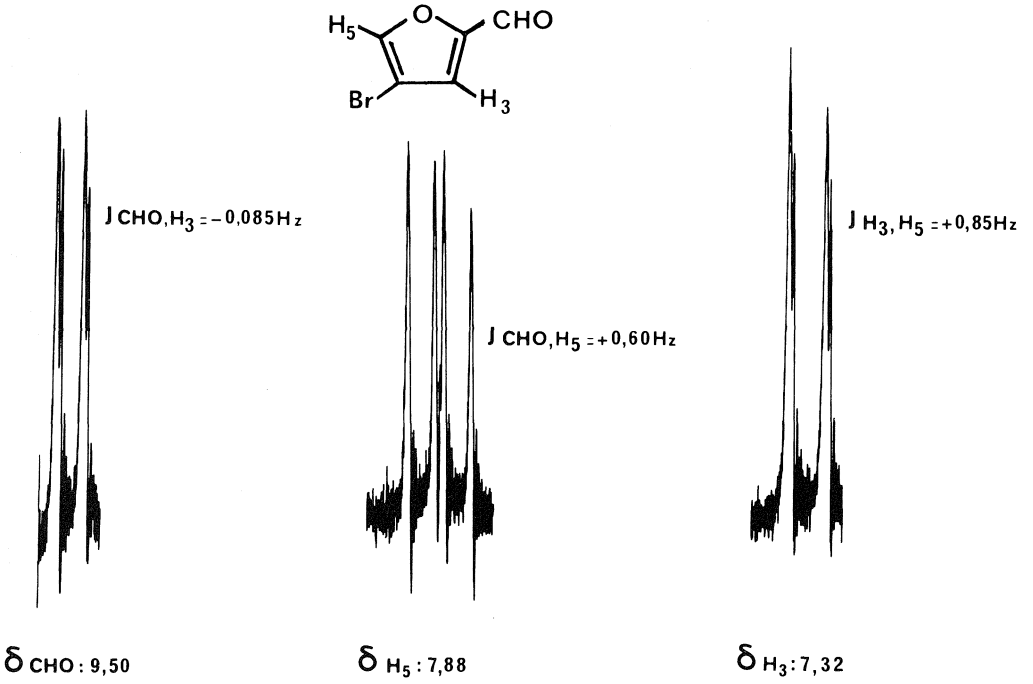

FIG. 5. Spectrum of 4-bromo-2-formylfuran (**1**).

Can. J. Chem. Downloaded from www.nrcresearchpress.com by 210.87.254.6 on 09/05/12
For personal use only.

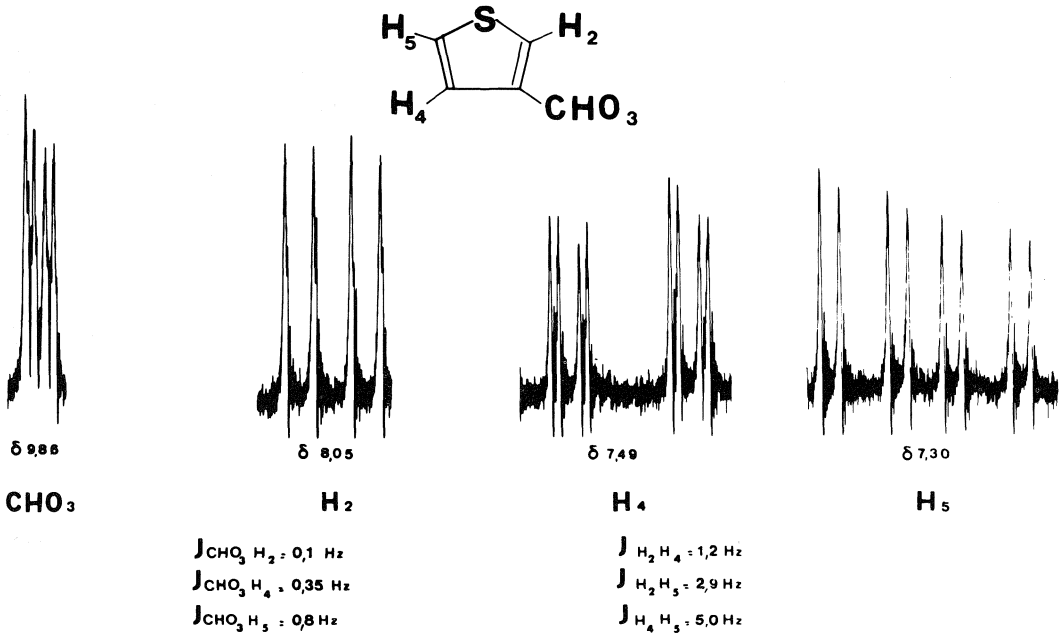

FIG. 6. Spectrum of 3-formylthiophene (**6**).

The $^4J^{cc}_{CHO-2}$ coupling has not been previously described in β-formylheterocycles. In 3-formylthiophene (**6**), $^4J^{cc}_{CHO-2} = -0.10$ Hz (Fig. 6). In the derivatives **7** and **8** this coupling is vanishingly small (<0.08 Hz) and cannot be seen in the spectrum. It is of interest to note that $^4J^{cc}_{CHO-2}$ can be observed in **6** where the formyl group is averaged at room temperature between the two forms SO *cis*-**I**′ (20%) and SO *trans*-**II**′ (80%) (22). Consequently, the value of 0.10 Hz accounts for a weak part of the $^4J^{ct}_{CHO-2}$ coupling constant.

(b) 4-Nitro-3-formylpyrrole (9)

Because of the existence of a repulsive potential between an oxygen of the nitro group and the oxygen of the formyl group, the conformation of **9** is almost exclusively HNO *cis*-**I**′. Indeed, for this compound the stereospecific $^5J_{CHO-5}$ coupling constant is undetectable. In contrast, $^4J^{ct}_{CHO-2}$ in DMSO-d_6[1] is 0.42 Hz, but the absence of $^5J_{CHO-5}$ hinders the determination of the sign of this coupling by tickling.

[1]The NH proton is exchanged by addition of a small amount of piperidine as described (13). The chemical shifts of the ring proton resonances are attributed in accordance with the additivity of the substituent effects (H_2 expt.: 7.64, calcd.: 7.77, H_5 expt.: 8 02, calcd.: 8.04 p.p.m.).

(3) 2-Acetyl-3-formylthiophene (10) and 2,3-Diformylthiophene (11)

The above compounds permit the study of the ^4J coupling constants in all pathways except for the $^4J^{cc}_{CHO-4}$ in β-formylheterocycles. Unfortunately, compounds of fixed conformation such as 2-amino- or 2-hydroxy-3-formylthiophene are unknown. (In the latter, the hydroxy group is in ketoform.) However, we can calculate the value for $^4J^{cc}_{CHO-4}$ for the two models **10** and **11**. For the former, the conformation of the CHO group is exclusively SO *cis*-**I**′ for thermodynamic and steric requirements (24). The $^5J_{CHO-5}$ is 1.00 Hz, identical to the maximum value found in 4-hydroxy-3-formylthiophene (22). Thus, we can determine in this fixed conformation the maximum value for the $^4J^{cc}_{CHO-4}$ coupling constant : −0.42 Hz. The 2,3-diformylthiophene **11** has four possible conformations, but we have concluded (23) that only two forms, **III** and **IV**, are in important concentrations.

Application of the rule of stereospecific ^5J coupling constants gives the populations : $P_{III} \cong 65\%$, $P_{IV} \cong 35\%$. The signal of the β aldehydic proton is complicated by a small coupling between the two formyl groups $^5J_{CHO_2-CHO_3} = -0.15$ Hz (see Experimental). The sign of this ^5J coupling is negative and must be due either to a

Can. J. Chem. Downloaded from www.nrcresearchpress.com by 210.87.254.6 on 09/05/12
For personal use only.

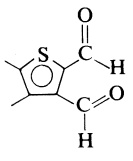

III

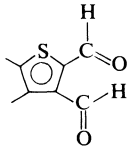

IV

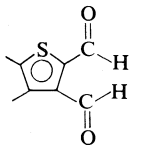

V

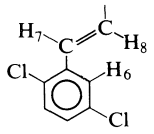

12

relatively important $\sigma-\pi$ transmission in the averaged conformations (**III** and **IV**) or, as in 2,5-dichlorostyrene (**12**), to direct interactions (29) between the proximate C—H groups on a conformation like **V**, though the contribution of **V** is certainly small.

As for the stereospecific ^5J coupling constants, the value of $^4J^{cc}_{CHO_3-4}$ is averaged over the populations of P_{III} and P_{IV}. Thus we must calculate the maximum value for this coupling : $^4J_{obs} = [^4J^{ct}_{max} \times 0.35] + [^4J^{cc}_{max} \times 0.65]$ with $^4J_{obs} = -0.25$, and $^4J^{ct}_{max} = -0.42$ Hz found in **10**. Hence $^4J^{cc}_{max} \cong -0.15$ Hz in agreement with the maximum value found for similar couplings in the *cc* pathway.

Discussion

Except for **1** where J_{CHO-3} is smaller than expected, the data of Table 1 show clearly higher values for $^4J^{ct}$ than for $^4J^{cc}$. In para-substituted benzaldehydes, the $^4J_{CHO-H_o}$ depends upon the nature of the substituents, but this effect is always weak. In our work, we have not considered this effect because even in unsubstituted derivatives, $^4J^{ct}$ remains still higher than $^4J^{cc}$.

The signs for two ^4J coupling constants corresponding to *cc* conformations are determined and are negative. The negative sign of $^4J_{CHO_3-4}$ coupling constants on β-formylthiophene and furan had been previously determined. Thus, we can assume that in all the derivatives examined in this paper, the signs of the ^4J coupling constants are negative.

On the other hand, the "methyl replacement technique" indicates a dominant σ electron mechanism for this coupling, although for the very weak coupling constant $^4J^{cc}_{CHO_2-3}$ it may be difficult to evaluate the π contribution by this technique. The negative sign for ^4J appears surprising since ^4J σ is usually positive in norm. However Barfield (5) has shown by INDO (intermediate neglect of differential overlap) computations that the sign of ^4J σ is negative for particular planar conformations *cc* and *ct* in propanic fragments.

Likewise, in propene this author has computed (INDO) values of -0.76 Hz for $^4J^{ct}$ and -1.15 Hz for $^4J^{cc}$ in planar conformations (5). Thus we should expect $^4J^{cc} > {}^4J^{ct}$ in our compounds. However, this is not the case for some conjugated aldehydes and in aromatic rings. Indeed the experimental results for acrolein indicate a higher value for $^4J^{ct}$ than for $^4J^{cc}$ (30) and in 2,5-dichlorostyrene (**12**), Barfield *et al.* (29) calculate values of -0.27 Hz for $^4J^{cc}_{6-7}$ and -0.75 Hz for $^4J^{ct}_{6-7}$. Also in para-substituted benzaldehydes (4) and fluorobenzaldehydes (31) $^4J^{ct}_{CHO-H_o} > {}^4J^{cc}_{CHO-H_o}$. In the latter compounds $^4J^{ct}_{CHO-F_o} > {}^4J^{cc}_{CHO-F_o}$ and this result is in good agreement with INDO computed values.[2]

Our results are in accordance with these latter studies and clearly prove that the ^4J coupling between side chain and ring protons is dominated by a σ-electron contribution. Consequently, this coupling is dependent on the pathway and $^4J^{ct}$ is still higher than $^4J^{cc}$. These results are useful for the conformational analysis of planar structures. It allows us to corroborate the interpretation based on the stereospecific ^5J coupling constants and to prove the preferential conformation in cases where ^5J is not accessible. It is not known whether $^4J^{ct} > {}^4J^{cc}$. This may be caused by a small positive through-space coupling in $^4J^{cc}$. We are presently studying the dependence of ^4J on electronic effects of substituent and out-of-plane arrangement of the formyl group.

1. S. Forsen and R. A. Hoffman. J. Mol. Spectrosc. **20**, 168 (1966).
2. G. P. Newseroff and S. Sternhell. Austr. J. Chem. **21**, 747 (1968).
3. C. L. Bell, S. S. Danyluk, and T. Schaefer. Can. J. Chem. **47**, 3529 (1969).
4. S. S. Danyluk, C. L. Bell, and T. Schaefer. Can. J. Chem. **47**, 4005 (1969).

[2]Calculations on furfural by INDO are not satisfactory (32). INDO results are in good agreement with experimental values but predict $^4J^{cc} > {}^4J^{ct}$. Clearly, the agreement for the ^4J couplings is poor whereas it is good for ^5J couplings.

Can. J. Chem. Downloaded from www.nrcresearchpress.com by 210.87.254.6 on 09/05/12
For personal use only.

5. M. BARFIELD. J. Am. Chem. Soc. **93**, 1066 (1971).
6. B. ROQUES, S. COMBRISSON, C. RICHE, and C. PASCARD-BILLY. Tetrahedron, **26**, 3555 (1970).
7. S. COMBRISSON, B. ROQUES, P. RIGNY, and J. J. BASSELIER. Can. J. Chem. **49**, 904 (1971).
8. Y. L. GOLDFARB, Y. B. VOL'KENSTEIN, and B. V. LOPATIN. Zh. Obshch. Khim. **34**, 969 (1964).
9. M. ROBBA and M. C. ZALUSKI. C.R. Acad. Sci. France, sér. C, **268**, 1884 (1969).
10. C. F. CANDY, R. A. JONES, and P. H. WRIGHT. J. Chem. Soc. C, 2563 (1970).
11. M. C. ZALUSKI, M. ROBBA, and M. BONHOMME. Bull. Soc. Chim. Fr. 1838 (1970).
12. C. JAUREGUIBERRY, M. C. FOURNIE-ZALUSKI, B. ROQUES, and S. COMBRISSON. Org. Mag. Res. (1972). In press.
13. P. FOURNARI, M. FARNIER, and C. FOURNIER. Bull. Soc. Chim. Fr. 283 (1972).
14. M. ROBBA, B. ROQUES, and M. BONHOMME. Bull. Soc. Chim. Fr. 2495 (1967).
15. L. M. JACKMAN and S. STERNHELL. Applications of nuclear magnetic resonance spectroscopy in organic chemistry. 2nd Ed. Pergamon Press. 1969. p. 43.
16. R. FREEMAN and W. A. ANDERSON. J. Chem. Phys. **37**, 2053 (1962).
17. R. KAISER. J. Chem. Phys. **39**, 2435 (1963).
18. A. D. COHEN and K. A. MCLAUGHLAN. Disc. Faraday Soc. **34**, 132 (1962).
19. R. A. HOFFMAN, B. GESTBLOM, S. GRONOWITZ, and S. FORSEN. J. Mol. Spectrosc. **11**, 454 (1963).
20. S. FORSEN, B. GESTBLOM, S. GRONOWITZ, and R. A. HOFFMAN. Acta Chem. Scand. **18**, 313 (1964).
21. S. FORSEN, B. GESTBLOM, R. A. HOFFMAN, and S. RODMAR. Acta Chem. Scand. **19**, 503 (1965).
22. M. C. FOURNIE-ZALUSKI and B. ROQUES. Tetrahedron Lett. **56**, 4909 (1970).
23. B. ROQUES and M. C. FOURNIE-ZALUSKI. Tetrahedron Lett. **2**, 145 (1971).
24. B. ROQUES and M. C. FOURNIE-ZALUSKI. J. Org. Mag. Res. **3**, 305 (1971).
25. R. A. HOFFMAN and S. GRONOWITZ. Ark. Kemi. **16**, 471 (1960).
26. R. FREEMAN and R. C. JONES. J. Chem. Phys. **52**, 465 (1970).
27. S. SHIMOKAWA, H. FUKUI, and J. SOHMA. Mol. Phys. **19**, 695 (1970).
28. B. ROQUES, C. JAUREGUIBERRY, M. C. FOURNIE-ZALUSKI, and S. COMBRISSON. Tetrahedron Lett. 2693 (1971).
29. M. BARFIELD, C. J. MACDONALD, I. R. PEAT, and W. F. REYNOLDS. J. Am. Chem. Soc. **93**, 4195 (1971).
30. J. E. DAVIES. J. Mol. Spectrosc. **29**, 499 (1969).
31. R. WASYLISHEN and T. SCHAEFER. Can. J. Chem. **49**, 3216 (1971).
32. R. WASYLISHEN and T. SCHAEFER. Can. J. Chem. **50**, 274 (1972).

Can. J. Chem. Downloaded from www.nrcresearchpress.com by 210.87.254.6 on 09/05/12
For personal use only.

Studies on Horseradish Peroxidase. XI. On the Nature of Compounds I and II as Determined from the Kinetics of the Oxidation of Ferrocyanide

M. L. COTTON AND H. B. DUNFORD[1]

Department of Chemistry, University of Alberta, Edmonton, Alberta

Received May 31, 1972

In order to investigate the nature of compounds I and II of horseradish peroxidase, the kinetics were studied of ferrocyanide oxidation catalyzed by these compounds which were prepared from three different oxidizing agents. The p*H* dependence of the apparent second-order rate constant for ferrocyanide oxidation by compound I, prepared from ethyl hydroperoxide and *m*-chloroperbenzoic acid, was interpreted in terms of an ionization on the enzyme with a $pK_a = 5.3$, identical to that reported previously for hydrogen peroxide. The second-order rate constant for the compound II-ferrocyanide reaction also showed the same p*H* dependence for the three oxidizing substrates. However, with more accurate results, the compound II-ferrocyanide reaction was reinterpreted in terms of a single ionization with $pK_a = 8.5$. The same dependence of ferrocyanide oxidation on p*H* suggests structurally identical active sites for compounds I and II prepared from the three different oxidizing substrates.

Pour étudier la nature des composés I et II de la peroxydase de raifort, on a examiné les cinétiques de l'oxydation du ferrocyanure catalysée par ces composés, qui ont été préparés à partir de trois agents oxydants différents. L'influence du p*H* sur la constante de vitesse apparente du deuxième ordre pour l'oxydation du ferrocyanure par le composé I préparé à partir de l'hydropéroxyde d'éthyle et de l'acide *m*-chloroperbenzoique, a été interpretée en fonction de l'ionisation de l'enzyme à un $pK_a = 5.3$, identique à celle précédemment rapportée pour l'eau oxygénée. La constante de vitesse du second ordre pour la réaction entre le ferrocyanure et le composé II, montre aussi la même relation de p*H* pour les trois substrats oxydants. Cependant, avec des résultats plus précis, la réaction entre le ferrocyanure et le composé II a été reinterprétée par rapport à l'ionisation simple à $pK_a = 8.5$. La même relation entre l'oxydation du ferrocyanure et le p*H* laisse penser à des sites actifs de structure identique pour les composés I et II, préparés à partir de trois substrats oxydants différents.

[Traduit par le journal]

Can. J. Chem., **51**, 582 (1973)

Introduction

The intermediate compounds of horseradish peroxidase (HRP), that is, compound I (HRP-I) and compound II (HRP-II), have been known for many years (1, 2). Early investigations indicated that these compounds could be formed from alkyl (3, 4) and acyl hydroperoxides (5) as well as several inorganic oxidizing agents (6). A variety of possible structures has been proposed for these compounds (7–10). Recently, it has been shown that oxygen is incorporated into compound I of chloroperoxidase upon its formation from *m*-chloroperbenzoic acid (11, 12). Clearly, in addition to the electron transfer processes occurring, a portion of the peroxide must be retained at the active site upon HRP-I formation.

Although many techniques have been applied to the study of HRP compounds (13–17), the kinetic method, in principle, provides one of the better sources of information concerning the nature of the active site. The rather complex dependence of reaction rates upon p*H* observed for different reducing substrates in HRP-catalyzed oxidations (18–20) are indicative of proton transfer processes affecting the rate-determining step. These proton transfers are a direct result of ionizable groups present on the enzyme or reducing substrate. Formation of HRP compounds with hydroperoxides may result in small structural differences if the organic fragment is retained at, or near, the active site. This bulky fragment could conceivably interfere with, or block, one or more proton transfers that have been shown to occur during the reduction of HRP compounds prepared from hydrogen peroxide. A distinctly different p*H* dependence would then emerge. Therefore, in order to investigate these possible changes in the proton transfer mechanisms, two organic hydroperoxides were chosen to study the ferrocyanide oxidation, namely, ethyl hydroperoxide and *m*-chloroperbenzoic acid. Experiments were also

[1]Author to whom correspondence should be addressed.

Can. J. Chem. Downloaded from www.nrcresearchpress.com by 210.87.254.42 on 09/05/12
For personal use only.

performed using hydrogen peroxide which supplemented a previous detailed investigation (18). The combined results of all of these experiments provide some incisive evidence concerning the nature of the enzyme's active site.

Experimental

Horseradish peroxidase was obtained from Boehringer-Mannheim as a highly purified ammonium sulfate suspension and prepared for experiments as described elsewhere (19, 20). Other experimental details are as described in the earlier study on ferrocyanide (18) except for the following.

The ethyl hydroperoxide was obtained from Polysciences Inc. as a 10% aqueous solution. A polarographic analysis of the reagent in dilute alkaline lithium sulfate solution (21) detected no hydrogen peroxide. The presence of other possible oxidizing agents known to form compounds with HRP was not observed by n.m.r. analysis. A 5×10^{-4} *M* aqueous solution of the alkyl hydroperoxide was stored at 5° and its concentration was analyzed periodically by spectrophotometry. In this method of analysis the amount of iodide oxidized was monitored quantitatively at 353 nm. A solution consisting of 0.05 *M* sodium iodide (Orion iodide standard) and 10^{-8} *M* HRP was prepared in an acetate buffer of p*H* 3.8 and $\mu = 0.01$. A 2 ml aliquot was pipetted into a cuvette, and the absorbance change observed upon the addition of 50 µl of the hydroperoxide solution. Using a molar absorptivity of $2.55 \times 10^4\ M^{-1}\ cm^{-1}$ (22), the hydroperoxide concentration was calculated. The solutions of hydrogen peroxide used to prepare the HRP compounds were also stored and analyzed in a similar manner. An independent analysis of hydrogen peroxide present in the ethyl hydroperoxide solution made use of the difference in the relative rates with which hydroperoxides and hydrogen peroxide react with iodide (23). Ammonium molybdate was used instead of HRP as a catalyst (24), and the rate of I_3^- formation was followed at 353 nm on the Cary 14 spectrophotometer. In the buffered iodide solution containing 0.005% by weight ammonium molybdate, the ethyl hydroperoxide solution was estimated to contain less than 2% hydrogen peroxide.

Technical grade *m*-chloroperbenzoic acid was obtained from the Aldrich Chemical Company. A 10% solution of the acyl hydroperoxide was made up in acetone and stored at −10°. Stock solutions of about 4×10^{-4} *M* *m*-chloroperbenzoic acid were prepared prior to each day's experimental work by adding 0.1 ml acetone solution to 100 ml of distilled water. The spectrophotometric technique described for hydroperoxide analysis was used to determine its concentration. Because of the rapid spontaneous oxidation of iodide with peracid, no HRP was required as a catalyst. Buffered iodide solutions to which HRP had been added were used to determine the total hydroperoxide and hydrogen peroxide concentration. Thus, it was estimated that slow hydrolysis (25) or contamination of the acyl hydroperoxide resulted in less than 5% of the total peroxide as hydrogen peroxide in the stock solution 8–10 h after its preparation.

All single-turnover kinetic experiments were carried out using a stopped-flow apparatus (18, 26) except at p*H* values between 9 and 10 where the Cary 14 spectrophotometer was used. The Cary 14 spectrophotometer was also used to obtain the steady-state results over the p*H* range 5–3.2 (18).

Results and Discussion

Over the p*H* range of the study HRP-I and HRP-II prepared from ethyl hydroperoxide or *m*-chloroperbenzoic acid showed identical kinetic behavior, within experimental error, to that observed for these compounds prepared from hydrogen peroxide. With excess ferrocyanide the reaction conditions become pseudo first-order and the differential rate expression for the HRP-II reaction is:

$$[1] \quad -\mathrm{d[HRP\text{-}II]}/\mathrm{d}t = k_{3,\mathrm{obs}}\,[\mathrm{HRP\text{-}II}]$$

where

$$[2] \quad k_{3,\mathrm{obs}} = k_{3,\mathrm{app}}\,[\mathrm{Fe(CN)_6}^{-4}]$$

Equation 1 was confirmed for both the alkyl and acyl hydroperoxides as oxidizing substrates by obtaining linear plots of log ΔV *vs.* time for reaction traces at many different p*H* values. Equation 2 was verified by obtaining linear relationships for k_{obs} with increasing ferrocyanide concentrations for each oxidizing substrate. Analogous results were obtained for the HRP-I reaction. Similar studies were performed at a number of other p*H* values on the stopped-flow apparatus for HRP-I, and both on the stopped-flow and spectrophotometer for HRP-II. Each stopped-flow study of k_{obs} *vs.* $[Fe(CN)_6^{-4}]$ represented 5–9 different concentrations over an order of magnitude range, and the analysis of 50–90 ΔV *vs.* time traces.

Kinetics of the HRP-II-Ferrocyanide Reaction

Values for $k_{3,app}$ were determined by the stopped-flow technique over the p*H* range 4–10.6. At high p*H* values, $k_{3,app}$ values also were determined on the Cary 14 spectrophotometer. The data appear in Table 1 and Fig. 1. Using the steady-state method, the HRP-catalyzed ferrocyanide reaction was studied in the acid p*H* region with ethyl hydroperoxide and hydrogen peroxide as oxidizing agents. The final results are presented in Table 2. Although the steady-state determinations are in good agreement with those published previously (18, 27), the second-order rate constants, $k_{3,app}$'s, determined by this method are consistently about 20% lower than those obtained by studying the HRP-

Can. J. Chem. Downloaded from www.nrcresearchpress.com by 210.87.254.42 on 09/05/12
For personal use only.

TABLE 1. The second-order rate constants determined for the HRP-II-ferrocyanide reaction at 25° and $\mu = 0.11$

pH*	$k_{3,app}$ (M^{-1} s^{-1})†	Buffer‡	Oxidizing substrate§
4.01‖	$(2.0\pm0.2) \times 10^6$	CT	M
4.20	$(1.1\pm0.1) \times 10^6$	CT	E
4.38‖	$(8.3\pm0.6) \times 10^5$	A	E
4.39	$(7.8\pm1.4) \times 10^5$	A	H
4.60‖	$(4.9\pm0.2) \times 10^5$	A	M
4.78	$(3.0\pm0.3) \times 10^5$	A	H
4.78‖	$(3.3\pm0.1) \times 10^5$	A	E
4.98	$(2.1\pm0.4) \times 10^5$	A	M
5.16	$(1.5\pm0.1) \times 10^5$	A	M
5.16	$(1.4\pm0.1) \times 10^5$	A	H
5.40	$(9.8\pm0.3) \times 10^4$	A	M
5.77	$(5.9\pm0.4) \times 10^4$	P	E
5.89	$(5.0\pm0.5) \times 10^4$	P	E
5.94	$(4.3\pm0.1) \times 10^4$	P	H
5.96‖	$(4.4\pm0.1) \times 10^4$	P	E
6.12	$(3.7\pm0.2) \times 10^4$	P	E
6.25	$(3.0\pm0.1) \times 10^4$	P	E
6.45‖	$(2.7\pm0.1) \times 10^4$	CA	E
6.61	$(2.2\pm0.1) \times 10^4$	P	M
6.92‖	$(1.8\pm0.1) \times 10^4$	P	M
7.06	$(1.8\pm0.4) \times 10^4$	P	E
7.13	$(1.7\pm0.1) \times 10^4$	P	M
7.28‖	$(1.8\pm0.1) \times 10^4$	P	M
7.50	$(1.4\pm0.1) \times 10^4$	T	M
7.73	$(1.5\pm0.2) \times 10^4$	P	E
7.95	$(1.1\pm0.1) \times 10^4$	T	M
8.57	$(7.2\pm0.9) \times 10^3$	T	E
9.00¶	$(3.4\pm0.5) \times 10^3$	T	E
9.37	$(2.2\pm0.2) \times 10^3$	C	M
9.51‖	$(2.1\pm0.1) \times 10^3$	GN	E
9.87¶	$(6.7\pm0.3) \times 10^2$	C	E
9.94¶	$(5.8\pm0.3) \times 10^2$	C	E
10.56	$(1.6\pm0.1) \times 10^2$	C	M

*Errors on pH values estimated at ± 0.02.
†Errors on rate constants represent twice the standard deviation calculated from experiments performed at a given pH.
‡Buffer abbreviations: A, acetic acid – sodium hydroxide; CA, cacodylic acid – sodium hydroxide; P, potassium dihydrogen phosphate – sodium hydroxide; T, tris-nitric acid; C, sodium bicarbonate – sodium hydroxide; CT, citric acid – sodium hydroxide; GN, glycine – sodium hydroxide.
§Oxidizing substrate abbreviations: E, ethyl hydroperoxide; M, *m*-chloroperbenzoic acid; H, hydrogen peroxide.
‖Study of the dependence of $k_{3,obs}$ on $[Fe(CN)_6^{-4}]$ from which $k_{3,app}$ was calculated from the slope of a linear least squares analysis.
¶Study of $k_{3,obs}$ *vs.* $[Fe(CN)_6^{-4}]$ performed on the Cary 14 spectrophotometer.

II-ferrocyanide reaction in isolation from other reactions involved in the steady-state cycle. Since the steady-state results are dependent on the total concentration of HRP whereas the stopped-flow results are not, the discrepancy may be caused by too small a value for the molar absorptivity of HRP at 403 nm (28). This is in agreement with recent spectral work (29, 30). However, since universal agreement has not yet been reached on the magnitude of ε_{403} for HRP, we have continued to use the previously accepted value.

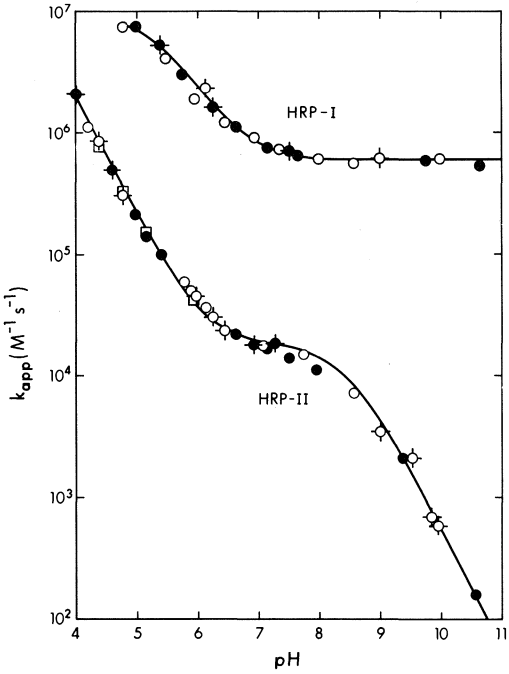

FIG. 1. Semilogarithmic plots of the apparent second-order rate constants *vs.* pH for the HRP-I-ferrocyanide and HRP-II-ferrocyanide reactions. The correlations appearing as solid curves were obtained from the nonlinear least squares analysis of the data. The error limits, to be found in Tables 1 and 4, were omitted for clarity. Different oxidizing substrates were used in the preparation of the HRP compounds. □, Hydrogen peroxide; ○, ethyl hydroperoxide; ●, *m*-chloroperbenzoic acid, -○-, -●-, study of the dependence of k_{obs} on $[Fe(CN)_6^{-4}]$ for ethyl hydroperoxide compounds and *m*-chloroperbenzoic acid compounds.

TABLE 2. The second-order rate constants for the HRP-II-ferrocyanide reaction determined from steady-state kinetics at 25° and $\mu = 0.11$

pH*	$k_{3,app}$ (M^{-1} s^{-1})†	Buffer‡	Oxidizing substrate§
3.27	$(6.9\pm1.4) \times 10^6$	CT	H
3.63	$(3.6\pm0.3) \times 10^6$	CT	E
3.85	$(2.0\pm0.2) \times 10^6$	CT	H
4.23	$(8.3\pm0.8) \times 10^5$	CT	H
4.60	$(4.9\pm0.3) \times 10^5$	A	E
5.01	$(1.9\pm0.2) \times 10^5$	A	H

*,†,‡,§The same as in Table 1.

In the stopped-flow experiments, a systematic deviation in reaction rates determined in successive experiments was observed in the acid pH region. Apparently, this was due to interference from an acid-catalyzed reaction which occurred in the stopped-flow apparatus and competed for ferrocyanide. The slow decay in ferrocyanide

Can. J. Chem. Downloaded from www.nrcresearchpress.com by 210.87.254.42 on 09/05/12
For personal use only.

Can. J. Chem. Downloaded from www.nrcresearchpress.com by 210.87.254.42 on 09/05/12
For personal use only.

concentration resulted in a gradual decline in the observed reaction rates. Interference from this competing reaction was partially overcome by preparing HRP-II in the low p*H* buffer. Therefore, for the experiments below p*H* 6, the ferrocyanide solution was unbuffered prior to the final mixing of the reactants in the stopped-flow apparatus. Under these conditions any enzyme denaturation in the acid solution was insignificant and did not affect the observed HRP-II-ferrocyanide rates. Greater precision was attained at a given p*H* by doing many experiments at different ferrocyanide concentrations. Several such studies were performed at low p*H*. Fresh ferrocyanide solutions of the correct concentration were insured by thorough flushing of the instrument with the reactant solutions prior to each experiment. Nevertheless, it was not possible to study this reaction successfully below p*H* 4 on the stopped-flow apparatus. Because these systematic errors were not detected in the previously reported work, the standard deviations for experiments performed in the earlier investigation at low p*H* were larger than originally estimated (18).

The resultant p*H* profile did not appear to justify the inclusion of an acid dissociation constant with a pK_a of 5.2 as previously reported (18). This was the case for HRP-II prepared from hydrogen peroxide, as well as the two hydroperoxides. The steady-state data confirmed this conclusion. There was no evidence for any acid dissociation constants present on the enzyme over the p*H* range 5.0–3.2. Below p*H* 3.2 the formation of HRP-I became rate-limiting so that k_3 could not be evaluated under steady-state conditions. The agreement is excellent among rate constants using all three oxidizing substrates at high p*H* for the HRP-II catalyzed oxidation of ferrocyanide (18).

For the HRP-II-ferrocyanide reaction the ionization of two acid groups, located on either the enzyme or substrate, has a major kinetic effect. Since the group having a pK_a of 8.5–8.6 cannot be associated with the ionization of any of the protonated forms of ferrocyanide, it must be assigned to the enzyme. This group also has been observed for the HRP-II-oxidation of *p*-cresol. The second group must remain largely deprotonated over the p*H* range investigated. Although substrate ionization cannot be excluded in making this group assignment, it has been shown conclusively that the enzyme has an ionizable group of p$K_a < 2$ influencing the HPR-II-iodide reaction (19). Therefore, it is not unreasonable to tentatively assign this second ionizable group to the enzyme. The simplest mechanism which adequately describes the data then becomes that depicted in eq. 3. The ground-state acid dissociation constant K_2 refers to the K_a observed at high p*H*, whereas K_1 is the ground-state acid dissociation constant of the second ionizable group. In the mechanism, $Fe(CN)_6^{-4}$ refers to all the unprotonated and protonated forms of ferrocyanide.

$$\begin{array}{ccc} & H_2P & \\ & K_1 \uparrow\downarrow & \\ HP & + \ Fe(CN)_6^{-4} \longrightarrow & \text{Products} \\ & K_2 \uparrow\downarrow & \\ & P & \end{array} \qquad [3]$$

Results from the nonlinear least-squares analysis of the data are to be found in Table 3 and a brief explanation in the Appendix. The K_2 value reported here is in good agreement with the acid dissociation constant in the alkaline p*H* region published earlier (18). The correlation shown in Fig. 2 was obtained from the steady-state data. At low p*H* values the regression line had a limiting slope of -1.0.

Kinetics of the HRP-I-Ferrocyanide Reaction

Values for $k_{2,app}$ are tabulated in Table 4 and plotted in Fig. 1 for both oxidizing substrates. Problems in the acid p*H* region were similar for HRP-I to those already discussed for HRP-II. Because of the faster rates of the HRP-I-ferrocyanide reaction, the data obtained below p*H* 5 have large experimental errors and the p*H* profile could not be precisely defined below p*H* 4.8 using the stopped-flow technique. The steady-state method is not amenable to an estimate of $k_{2,app}$. The best-fit parameters, presented in Table 5, were determined from a nonlinear least squares

TABLE 3. The parameters obtained from a nonlinear least squares analysis for the HRP-II-ferrocyanide reaction*

Parameter	Value
k_1'	$(1.8 \pm 0.1) \times 10^4$ (M^{-1} s^{-1})
K_1*	$(9.2 \pm 0.6) \times 10^{-7}$ (M)
K_1	$(3.3 \pm 0.2) \times 10^{-9}$ (M)

*The errors reported were the standard deviations obtained from the nonlinear computer analysis.

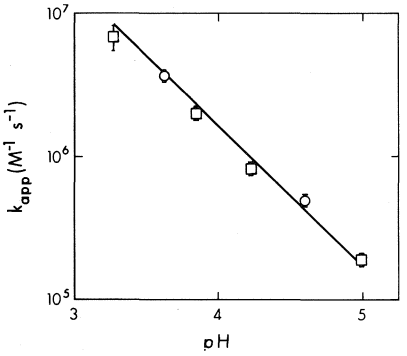

FIG. 2. Semilogarithmic plot of $k_{3,app}$ determined by steady-state kinetics *vs.* p*H* for the HRP-II-ferrocyanide reaction. Error limits were estimated as the 95% confidence limit from the linear least squares analysis at each p*H*. The correlation was obtained from a weighted nonlinear least squares analysis of the data using the $K_1{}^{\ddagger}$ and K_1 values appearing in Table 3 as fixed parameters. The variable k_1' had a calculated value of $(1.4\pm0.1) \times 10^4$ M^{-1} s^{-1}, 21% lower than that shown in Table 3. The limiting slope at the lowest p*H* was -1.0. Ethyl hydroperoxide and hydrogen peroxide were used in the preparation of HRP-II. Symbols are the same as for Fig. 1.

analysis of the data in Table 4. For comparative purposes the data reported earlier for HRP-I prepared from hydrogen peroxide (18), were reanalyzed in terms of transition-state parameters. These also appear in Table 5. The two sets of parameters are identical within the experimental errors.

Therefore, the evidence presented shows that in the reduction of each of HRP-I and HRP-II the proton transfer mechanisms are identical over a wide range of p*H* regardless of the hydroperoxide used as the substrate. This implies a structurally identical active site for each participating oxidizing agent.

Appendix

An interpretation of the p*H* dependence of the reaction based upon transition-state theory has been applied to this system and discussed in regard to experimental results obtained in deuterium oxide (27). Over the p*H* range of the combined stopped-flow and steady-state investigations of the HRP-II-ferrocyanide reaction, the data may be described in terms of one transition-state acid dissociation constant $K_1{}^{\ddagger}$, and one ground-state acid dissociation constant K_2. One may calculate $k_{3,app}$ from the relationship

$$[4] \qquad k_{3,app} = \frac{k_1'[H^+]([H^+]/K_1{}^{\ddagger} + 1)}{([H^+]/K_2 + 1)}$$

TABLE 4. The second-order rate constant determined for the HRP-I-ferrocyanide reaction at 25° and $\mu = 0.11$

p*H**	$k_{2,app}$ (M^{-1} s^{-1})†	Buffer‡	Oxidizing substrate§
4.78	$(7.3\pm2.2) \times 10^6$	A	E
4.97	$(7.5\pm1.4) \times 10^6$	A	M
5.38‖	$(5.3\pm0.3) \times 10^6$	CA	M
5.48	$(4.1\pm0.8) \times 10^6$	A	E
5.73	$(3.0\pm0.4) \times 10^6$	A	M
5.94	$(1.9\pm0.4) \times 10^6$	P	E
6.12‖	$(2.3\pm0.1) \times 10^6$	P	E
6.23‖	$(1.6\pm0.1) \times 10^6$	P	M
6.43	$(1.2\pm0.1) \times 10^6$	CA	E
6.61	$(1.1\pm0.1) \times 10^6$	P	M
6.93	$(9.1\pm0.1) \times 10^5$	P	E
7.14	$(7.5\pm0.8) \times 10^5$	P	M
7.34	$(7.5\pm1.2) \times 10^5$	P	E
7.50‖	$(6.8\pm0.3) \times 10^5$	T	M
7.62	$(6.3\pm1.2) \times 10^5$	P	M
7.98	$(6.1\pm0.6) \times 10^5$	T	E
8.57	$(5.5\pm1.4) \times 10^5$	T	E
8.99‖	$(6.1\pm0.3) \times 10^5$	T	E
9.75	$(5.9\pm0.9) \times 10^5$	C	M
9.98	$(6.0\pm0.6) \times 10^5$	T	E
10.63	$(3.3\pm0.6) \times 10^5$	C	M

*,†,‡,§The same as in Table 1.
‖Study of $k_{2,obs}$ *vs.* $[Fe(CN)_6{}^{-4}]$ from which $k_{2,app}$ was calculated from the slope of a linear least squares analysis.

TABLE 5. The parameters obtained from a nonlinear least squares analysis for the HRP-I-ferrocyanide reaction*

Parameter	Value
k_2'	$(6.0\pm0.2) \times 10^5$ (M^{-1} s^{-1})
$K_2{}^{\ddagger}$	$(2.5\pm0.2) \times 10^{-7}$ (M)
K_2	$(4.2\pm0.8) \times 10^{-6}$ (M)
k_2'†	$(6.0\pm0.2) \times 10^5$ (M^{-1} s^{-1})
$K_2{}^{\ddagger}$†	$(4.0\pm0.6) \times 10^{-7}$ (M)
K_2†	$(4.9\pm1.6) \times 10^{-6}$ (M)

*The errors reported were estimated as in Table 3.
†From previously reported data for HRP-I prepared from hydrogen peroxide (18).

In this expression k_1' represents the limiting second-order rate constant at high p*H*. The ground-state acid dissociation constant, K_1, does not appear in eq. 4 because it lies outside the p*H* range of the study; therefore, it does not affect the rates above p*H* = 3.2.

For the HRP-I-ferrocyanide reaction the data may also be described in terms of one transition-state acid dissociation constant $K_2{}^{\ddagger}$ and one ground-state acid dissociation constant K_3. One may then calculate $k_{2,app}$ from a relationship similar to eq. 4:

$$[5] \qquad k_{2,app} = \frac{k_2'([H^+]/K_2{}^{\ddagger} + 1)}{([H^+]/K_3 + 1)}$$

Can. J. Chem. Downloaded from www.nrcresearchpress.com by 210.87.254.42 on 09/05/12
For personal use only.

In this expression, k_2' is the limiting second-order rate constant at high p*H*.

The authors would like to thank J. E. Critchlow and R. S. Roman for their many helpful suggestions and the National Research Council of Canada for financial support.

1. D. Keilin and T. Mann. Proc. Roy. Soc. Ser. B, **122**, 119 (1937).
2. H. Theorell. Enzymol. **10**, 250 (1941).
3. K. G. Stern. J. Biol. Chem. **114**, 473 (1936).
4. B. Chance. Arch. Biochem. **21**, 416 (1949).
5. J. Boeseken. Proc. Acad. Sci. Amst. **33**, 134 (1930).
6. P. George. J. Biol. Chem. **201**, 413 (1953).
7. B. Chance. Science, **109**, 204 (1949).
8. P. George. Science, **117**, 220 (1953).
9. R. R. Fergusson. J. Am. Chem. Soc. **78**, 1266 (1956).
10. A. S. Brill and R. J. P. Williams. Biochem. J. **78**, 253 (1961).
11. L. P. Hager, D. L. Doubek, R. M. Silverstein, T. T. Lee, J. A. Thomas, J. H. Hargis, and J. C. Martin. *In* Oxidases and related redox systems. Proc. 2nd Int. Symp. T. E. King, H. S. Mason, and M. Morrison, Editors. University Park Press, Baltimore, Md. (In press).
12. P. F. Hollenberg and L. P. Hager. Fed. Proc. **31**, 483 Abs (1972).
13. T. H. Moss, A. Ehrenberg, and A. J. Bearden. Biochem. **8**, 4159 (1969).
14. J. Peisach, W. E. Blumberg, B. A. Wittenberg, and J. B. Wittenberg. J. Biol. Chem. **243**, 1854 (1968).
15. A. S. Brill and H. E. Sandberg. Biochem. **7**, 4254 (1968).
16. W. D. Ellis and H. B. Dunford. Can. J. Biochem. **46**, 1231 (1968).
17. G. Willick, G. R. Schonbaum, and C. M. Kay. Biochem. **8**, 3729 (1969).
18. B. B. Hasinoff and H. B. Dunford. Biochem. **9**, 4930 (1970).
19. R. Roman, H. B. Dunford, and M. Evett. Can. J. Chem. **49**, 3059 (1971).
20. R. Roman and H. B. Dunford. Biochem. **11**, 2076 (1972).
21. H. Bruschweiler and G. J. Minkoff. Anal. Chim. Acta, **12**, 186 (1955).
22. R. W. Ramette and R. W. Sandford. J. Am. Chem. Soc. **87**, 5001 (1965).
23. R. M. Johnson and I. W. Siddiqi. *In* Determination of organic peroxides. Pergamon Press, London. 1970. Chapt. 3.
24. T. C. J. Ovenston and W. T. Rees. Analyst (London), **75**, 204 (1950).
25. D. Swern. *In* Organic peroxides. Vol. I. Wiley-Interscience, New York, N.Y. 1971. Chapt. 6.
26. W. D. Ellis and H. B. Dunford. Biochem. **7**, 2054 (1968).
27. J. E. Critchlow and H. B. Dunford. J. Biol. Chem. **247**, 3714 (1972).
28. D. Keilin and E. F. Hartree. Biochem. J. **49**, 88 (1951).
29. L. M. Shannon, E. Kay, and J. Y. Lew. J. Biol. Chem. **241**, 2166 (1966).
30. K. G. Paul and T. Stigbrand. Acta Chem. Scand. **24**, 3607 (1970).

Can. J. Chem. Downloaded from www.nrcresearchpress.com by 210.87.254.42 on 09/05/12
For personal use only.

Studies on Horseradish Peroxidase. XII. A Kinetic Study of the Oxidation of Sulfite and Nitrite by Compounds I and II

R. ROMAN AND H. B. DUNFORD[1]

Department of Chemistry, University of Alberta, Edmonton, Alberta

Received May 31, 1972

The kinetics of the oxidation of sulfite and nitrite by horseradish peroxidase compounds I and II have been studied as a function of p*H* at 25° and ionic strength 0.11. The p*H* dependence of the rate of the reaction between compound I and sulfite over the p*H* range 2–7 is interpreted in terms of two ground state enzyme dissociations with pK_a values of 5.1 and 3.3, and that for the compound II reaction with sulfite in terms of a single ground state enzyme dissociation with a pK_a value of 3.9. Whereas the reaction between compound I and sulfite produces the native enzyme without the intermediate formation of compound II, the reaction of compound I with nitrite yields compound II. The second-order rate constants for the reactions of compounds I and II with nitrite increase linearly with increasing hydrogen ion concentration over the p*H* range 6–8.

Les cinétiques de l'oxydation du sulfite et nitrite par les composés I et II de la peroxydase du raifort, ont été étudiées en fonction du p*H* à 25° et à une force ionique de 0.11. L'influence du p*H* sur la vitesse de réaction entre le composé I et le sulfite, dans l'intervalle de p*H* 2–7, a été interprétée par deux dissociations enzymatiques à l'état fondamental, aux pK_a de 5.1 et 3.3; celle de la réaction entre le composé II et le sulfite a été expliquée par une dissociation enzymatique simple, à l'état fondamental, pour un pK_a de 3.9. Tandis que la réaction entre I et le sulfite conduit à l'enzyne native sans l'intermédiaire de II, la réaction de I sur le nitrite donne le composé II. Les constante de vitesse du second ordre pour les réactions de I et II sur le nitrite, croissent linéairement avec le concentration en ion hydrogène, dans l'intervalle de p*H* 6–8. [Traduit par le journal]

Can. J. Chem., **51**, 588 (1973)

Introduction

Horseradish peroxidase (EC 1.11.1.7, donor-H_2O_2 oxido-reductase) catalyzes the oxidation of a wide variety of compounds by hydrogen peroxide. The early work of Chance (1) and George (2, 3) established that the reaction normally proceeds by the following general mechanism

[1] $$HRP + H_2O_2 \rightarrow HRP\text{-}I$$

[2] $$HRP\text{-}I + AH_2 \rightarrow HRP\text{-}II + AH\cdot$$

[3] $$HRP\text{-}II + AH_2 \rightarrow HRP + AH\cdot$$

[4] $$2AH\cdot \rightarrow \text{products}$$

where HRP represents the native enzyme, HRP-I and HRP-II are the oxidized forms of the enzyme referred to as compounds I and II, and AH_2 is the reducing substrate. Work on this enzyme up to 1966 has been reviewed by Brill (4).

Previous work in this laboratory (5–7) has included kinetic studies over a range of p*H* on the oxidation of ferrocyanide, iodide, and *p*-cresol by HRP-II and iodide by HRP-I (8). The latter reaction proved to be an exception to the general mechanism illustrated in eqs. 1–4 since there is a direct two-electron transfer from iodide to HRP-I thus forming HRP without the intermediate formation of HRP-II (8). This phenomenon is of potential relevance to the mechanism of iodide oxidation by the peroxidase present in mammalian thyroid glands (9). It is of interest to determine whether other substrates of HRP could also undergo direct two-electron oxidations and sulfite and nitrite were chosen as potential two-electron donors. HRP has been shown to catalyze the oxidation of sulfite both in the presence of hydrogen peroxide (10) and its absence (11, 12). However, no kinetic data on the separate reactions of HRP-I and HRP-II with sulfite have been published. The rate of the reactions of HRP-I and HRP-II with nitrite at a single p*H* have been reported by Chance (13).

Experimental

Materials

Horseradish peroxidase was obtained from Boehringer-Mannheim as a highly purified suspension in aqueous ammonium sulfate. The technique in handling it further has been described elsewhere (6–8).

Anhydrous sodium sulfite was obtained from Fisher

[1]To whom correspondence should be addressed.

Can. J. Chem. Downloaded from www.nrcresearchpress.com by 210.87.254.105 on 09/05/12
For personal use only.

Can. J. Chem. Downloaded from www.nrcresearchpress.com by 210.87.254.105 on 09/05/12
For personal use only.

Scientific Co. (stated purity of 99.0%). Stock solutions of 0.1 M or greater were prepared fresh daily and were routinely analyzed using a molar absorptivity of $3.88 \times 10^2\ M^{-1}\ cm^{-1}$ at 276 nm for the sulfite in 0.1 F sulfuric acid (14). These sulfite solutions were found to undergo less than 1% decomposition over a period of 8 h. Sodium nitrite was obtained from the Baker Chemical Co. (stated purity 100.7%). Stock solutions of nitrite were prepared by weighing; their concentrations were checked at 355 nm using a molar absorptivity value of $23.0\ M^{-1}\ cm^{-1}$ (15). Solutions from 0.1 to $10^{-4}\ M$ were stable for several weeks when stored in the dark. Hydrogen peroxide, 30% by weight obtained from the Fisher Scientific Co., was stored in the dark as an approximately $5 \times 10^{-2}\ M$ solution, and diluted before use; its concentration was checked periodically by the HRP-catalyzed oxidation of iodide (16).

Kinetic Experiments

The majority of kinetic investigations were carried out using a stopped-flow apparatus described previously (5, 6). Kinetic experiments on the HRP-I sulfite reaction at pH values greater than 5.5 were performed on a Cary 14 spectrophotometer. Complete details of all experiments are recorded elsewhere (17). HRP-I was prepared immediately before use by adding hydrogen peroxide from a Hamilton microliter syringe to a concentration 0.8 times that of HRP. HRP-II was formed, when desired, by the addition of *p*-cresol to a concentration 0.5 times that of the enzyme, to the HRP-I solution just prior to its transfer to the stopped-flow apparatus. The reduction of HRP-I was monitored at 411 nm and that of HRP-II was usually monitored at 427 nm. In additional experiments, the HRP-II-sulfite reaction was also monitored at 411 and 403 nm.

All reactions were conducted at 25° at an ionic strength of 0.11 of which 0.01 was contributed by the buffer, and had half-lives ranging from about 10 ms to several seconds. Initial concentrations of HRP-I and HRP-II were typically about $10^{-6}\ M$. Pseudo first-order conditions were achieved by keeping the sulfite or nitrite in at least a ten-fold excess over the enzyme species.

Stoichiometric Experiments

The overall reaction stoichiometry for the HRP-catalyzed oxidation of nitrite by hydrogen peroxide was determined spectrophotometrically at pH 4.95 and 25.0°, by monitoring the decrease in nitrite concentration at 355 nm and the production of nitrate at 300 nm. Spectra of sodium nitrite and potassium nitrate were obtained from 400–270 nm on the Cary 14 spectrophotometer. The molar absorptivity of the nitrite maximum at 355 nm agreed with the published value to within 1% (15). Potassium nitrate had no observable absorbance at 355 nm. A maximum at 300 nm with a molar absorptivity of $7.3\ M^{-1}\ cm^{-1}$ was observed for the nitrate spectrum, whereas nitrite had a molar absorptivity of $8.9\ M^{-1}\ cm^{-1}$ at the same wavelength.

The stoichiometry of the reaction between HRP-I and nitrite was determined by a titration at 25.0° of HRP-I monitored at 411 nm. The initial rapid spontaneous decay of HRP-I was monitored until the rate of this reaction was slower than the reaction with nitrite (about 10% of the HRP-I was consumed), then solutions of sodium nitrite, from 2–10 μl, were added with a Hamilton microliter syringe and the changes in absorbance were measured.

Steady State Spectra

The spectra of the enzymatic species present in the steady state for the HRP-catalyzed oxidations of sulfite and nitrite were scanned on a Cary 14 spectrophotometer from 350–450 nm. Identical experiments were performed where the absorbance was monitored at a fixed wavelength (411 nm for sulfite, 431 nm for nitrite) to ensure that steady-state conditions did exist during the time taken to scan the spectrum and to estimate the number of enzymatic cycles taking place during this time.

Second Ionization Constant of Sulfurous Acid

The second ionization of sulfurous acid at an ionic strength 0.01 was measured spectrophotometrically, using a Gilford spectrophotometer with the cell-block maintained at 25.0°. Absorbance measurements were made at 212.5 nm, close to the maximum absorbance for sulfite ion, over the pH range 6.2–9.6 using phosphate or tetraborate buffers.

Results

Second Ionization Constant of Sulfurous Acid

The second ionization constant of sulfurous acid, K_s, under conditions of the present work may be defined in terms of concentrations and the operational pH scale by the relation

$$[5] \qquad pK_s = \log\frac{[HSO_3^-]}{[SO_3^{2-}]} + pH$$

The value of pK_s obtained from eq. 5 was 6.92 ± 0.02 in reasonable agreement with the published value, 6.91, obtained at unspecified ionic strength (18).

Kinetics of the HRP-I-Sulfite Reaction

With excess sulfite the observed differential rate expression is

$$[6] \qquad -d[\text{HRP-I}]/dt = k_{1,obs}[\text{HRP-I}]$$

as was verified by linear semilogarithmic plots of the change in photomultiplier output voltage *vs.* time. Values of the second-order rate constant, k_1, were obtained from the equation

$$[7] \qquad k_{1,obs} = k_1[\text{sulfite}]$$

where [sulfite] refers to the total concentrations of sodium sulfite without regard to its state of protonation. Plots of $k_{1,obs}$ *vs.* [sulfite] were linear as illustrated in Fig. 1 for the reaction at pH 3.81. Similar studies were carried out at 12 other pH values ranging from 2.7 to 7.2, in which the error in k_1 was equated to the standard deviation calculated from the linear analysis of the $k_{1,obs}$ *vs.*

Can. J. Chem. Downloaded from www.nrcresearchpress.com by 210.87.254.105 on 09/05/12
For personal use only.

TABLE 1. Second-order rate constants for the HRP-I-sulfite reaction at 25°

pH	k_1 (M^{-1} s^{-1})	Range of [sulfite] (M)	Buffer*
2.28	1.3×10^5	$(1–5) \times 10^{-4}$	C
2.42	1.2×10^5	$(1–5) \times 10^{-4}$	C
2.45	1.2×10^5	5×10^{-4}	G
2.60	1.2×10^5	$(1–5) \times 10^{-4}$	C
2.69	$(1.2 \pm 0.03) \times 10^5$	$(0.5–7.5) \times 10^{-4}$	G
2.81	1.1×10^5	5×10^{-4}	G
2.85	1.1×10^5	$(1–5) \times 10^{-4}$	C
2.96	1.0×10^5	5×10^{-4}	G
3.14	9.2×10^4	5×10^{-4}	G
3.31	$(8.8 \pm 0.06) \times 10^4$	$(0.5–5) \times 10^{-4}$	C
3.36	7.8×10^4	$(1–5) \times 10^{-4}$	C
3.53	6.7×10^4	$(1–5) \times 10^{-4}$	C
3.81	$(5.4 \pm 0.1) \times 10^4$	$(0.5–5) \times 10^{-4}$	A
3.99	$(4.7 \pm 0.04) \times 10^4$	$(1–7.5) \times 10^{-4}$	A
4.41	$(3.0 \pm 0.08) \times 10^4$	$(0.2–2) \times 10^{-3}$	A
4.65	$(2.3 \pm 0.04) \times 10^4$	$(0.4–2) \times 10^{-3}$	A
4.98	$(1.8 \pm 0.06) \times 10^4$	$(0.25–2) \times 10^{-3}$	A
5.45	$(9.5 \pm 0.5) \times 10^3$	$(0.25–2) \times 10^{-3}$	A
5.97	$(3.2 \pm 0.1) \times 10^3$	$(1–5) \times 10^{-5}$	P
6.33	$(1.3 \pm 0.03) \times 10^3$	$(1–10) \times 10^{-5}$	P
6.63	$(4.9 \pm 0.2) \times 10^2$	$(0.25–2.5) \times 10^{-4}$	P
6.89	$(2.4 \pm 0.04) \times 10^2$	$(0.5–3.5) \times 10^{-4}$	P
7.22	$(7.6 \pm 0.8) \times 10$	$(0.1–1.5) \times 10^{-3}$	P

*A, acetic acid – sodium acetate; C, citric acid – sodium citrate; G, glycine HNO_3 – glycine; P, potassium dihydrogen phosphate – disodium hydrogen phosphate.

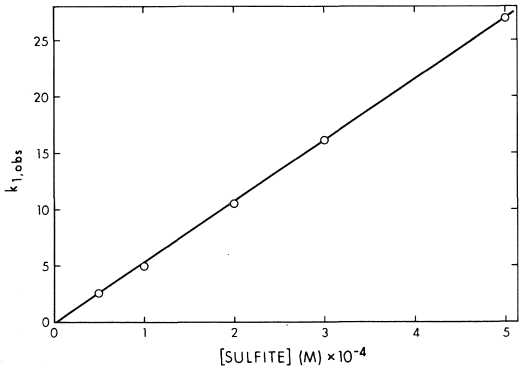

FIG. 1. Plot of $k_{1,obs}$ *vs.* [sulfite] for the reaction between HRP-I and sulfite at pH 3.81. The slope, k_1, with its standard error is $(5.4 \pm 0.1) \times 10^4$ M^{-1} s^{-1}.

[sulfite] data. The error in k_1 at the other pH values was estimated at $\pm 10\%$. Different buffers used at the same pH yielded the same kinetic results within experimental error, indicating that there were no detectable buffer effects.

Values of k_1 as a function of pH are listed in Table 1 along with the ranges of sulfite concentrations and buffers. The logarithm of k_1 is plotted *vs.* pH in Fig. 2. The pH dependence of k_1 was analyzed using the approach of Critchlow and Dunford (19) where negative and positive curvatures in the plot of log k_1 *vs.* pH are represented by ground state and transition state acid dissociation constants. The solid line in Fig. 2 illustrates the best fit to the phenomenological equation

$$[8] \quad k_1 = \frac{k_1'\left(1 + \frac{K_1^{\ddagger}}{[H^+]}\right)}{\left(1 + \frac{K_1}{[H^+]} + \frac{K_1K_2}{[H^+]^2}\right)\left(1 + \frac{K_s}{[H^+]}\right)}$$

where $K_1^{\ddagger}$ is a transition state dissociation constant associated with the positive curvature at pH 4, K_1 and K_2 are the ground state dissociation constants for acid groups of HRP-I associated with the negative curvatures at pH's 3 and 5, K_s is the sulfite dissociation constant, and k_1' is the pH independent second-order rate constant at low pH. The values of the parameters calculated from eq. 8 are listed in Table 2. The broken line in Fig. 2 is the best fit to the simpler equation

$$[9] \quad k_1 = \frac{k_1'}{\left(1 + \frac{K_2}{[H^+]}\right)\left(1 + \frac{K_s}{[H^+]}\right)}$$

Can. J. Chem. Downloaded from www.nrcresearchpress.com by 210.87.254.105 on 09/05/12
For personal use only.

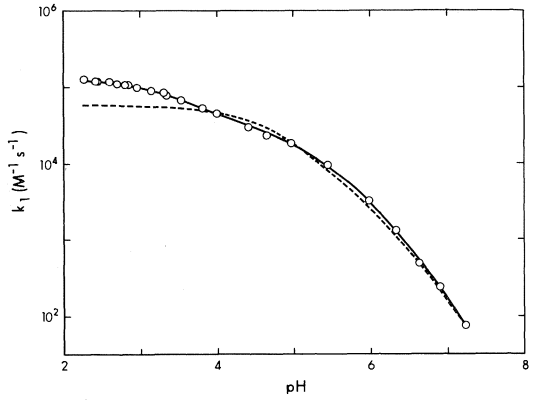

FIG. 2. Semilogarithmic plot of k_1, the second-order rate constant for the reaction of sulfite with HRP-I, *vs.* p*H*. The solid line was calculated by a weighted nonlinear least squares analysis of eq. 8 and the broken line by the comparable analysis of eq. 9.

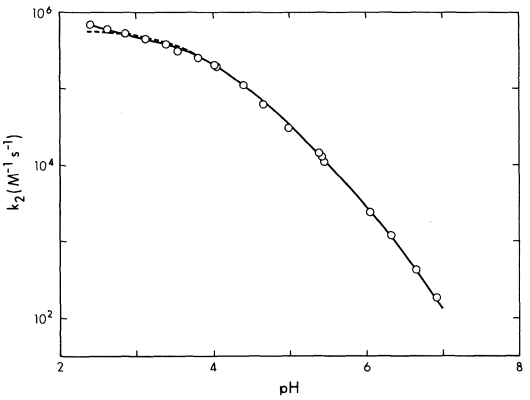

FIG. 3. Semilogarithmic plot of k_2, the second-order rate constant for the reaction of sulfite with HRP-II, *vs.* p*H*. The solid line was calculated by a weighted nonlinear least squares analysis of eq. 10 and the broken line by the comparable analysis of eq. 11.

At low p*H* there is substantial deviation between the calculated and experimental points which indicates that eq. 9 does not offer a satisfactory interpretation of the p*H* dependence of the reaction. In other words the inflections on the left side of Fig. 2 are outside the experimental error.

Kinetics of the HRP-II-Sulfite Reaction

The equations analogous to eqs. 6 and 7 were also verified for the HRP-II-sulfite reaction. The error in the second order rate constant, k_2, was equated to the standard deviation calculated from the linear analysis of the pseudo first-order rate constant *vs.* [sulfite] plots obtained at all values of p*H*. No buffer effects were observed.

Values of k_2 with their standard deviations are listed in Table 3 with the ranges of sulfite concentrations and buffers used at each p*H* and the logarithm of k_2 is plotted *vs.* p*H* in Fig. 3. The p*H* profile for the HRP-II reaction with sulfite resembles that for the analogous HRP-I reaction. At high p*H* the HRP-II rate is slightly smaller than that of HRP-I, the two rate constants are the same at p*H* 6 and at lower p*H* the HRP-II rate becomes larger than that of HRP-I. The solid line in Fig. 3 illustrates the best fit to the equation

$$[10] \quad k_2 = \frac{k_2'\left(1 + \frac{[H^+]}{K_2^{\ddagger}}\right)}{\left(1 + \frac{K_3}{[H^+]}\right)\left(1 + \frac{K_s}{[H^+]}\right)}$$

where $K_2^{\ddagger}$ is a transition state dissociation constant associated with the positive curvature at p*H* 2, K_3 is a ground state dissociation constant associated with the negative curvature at p*H* 4, K_s is the sulfite dissociation constant, and k_2' is the p*H* independent rate at p*H* 3. The broken line in Fig. 3 is the best fit to the equation

$$[11] \quad k_2 = \frac{k_2'}{\left(1 + \frac{K_3}{[H^+]}\right)\left(1 + \frac{K_s}{[H^+]}\right)}$$

which does not involve a transition state dissociation constant. Although the fit is better to eq. 10 than it is to eq. 11, this difference is small and it is not possible to distinguish between the two interpretations solely on the basis of our kinetic data. The values of the parameters calculated from eqs. 10 and 11 are listed in Table 4.

Two effects associated with the reduction of HRP-II by sulfite were observed when the reaction was monitored at 411 nm, the isosbestic point between HRP and HRP-II. If HRP-II was converted to HRP directly, as indicated in eq. 3, no change in absorbance would be expected at this wavelength, as has been observed for the reactions of iodide (6) and nitrite. For the HRP-

TABLE 2. Rate and ionization constants obtained from the p*H*-rate profile for the HRP-I-sulfite reaction (eq. 8)

Constant		pK_a values
$K_1(M)$	4.6×10^{-4}	3.3
$K_2(M)$	8.5×10^{-6}	5.1
$K_s(M)$	1.2×10^{-7}	6.9
$K_1^{\ddagger}(M)$	1.1×10^{-4}	4.0
$k_1'(M^{-1}\,s^{-1})$	1.3×10^{5}	

Can. J. Chem. Downloaded from www.nrcresearchpress.com by 210.87.254.105 on 09/05/12
For personal use only.

TABLE 3. Second-order rate constants for the HRP-II-sulfite reaction at 25°

pH	k_2 (M^{-1} s^{-1})	Range of [sulfite] (M)	Buffer*
2.43	$(6.8\pm0.4)\times10^5$	$(2–6)\times10^{-5}$	C
2.62	$(5.9\pm0.03)\times10^5$	$(2–8)\times10^{-5}$	C
2.86	$(5.3\pm0.3)\times10^5$	$(0.2–1)\times10^{-4}$	C
3.13	$(4.5\pm0.02)\times10^5$	$(0.2–1.2)\times10^{-4}$	C
3.39	$(3.7\pm0.1)\times10^5$	$(0.2–1)\times10^{-4}$	C
3.53	$(3.0\pm0.1)\times10^5$	$(0.2–1.5)\times10^{-4}$	C
3.81	$(2.5\pm0.08)\times10^5$	$(0.1–2)\times10^{-4}$	A
4.02	$(2.0\pm0.2)\times10^5$	$(0.25–2)\times10^{-4}$	A
4.03	$(1.9\pm0.06)\times10^5$	$(0.25–2.5)\times10^{-4}$	C
4.41	$(1.1\pm0.04)\times10^5$	$(0.25–3)\times10^{-4}$	A
4.66	$(6.2\pm0.2)\times10^4$	$(0.25–3)\times10^{-4}$	A
4.99	$(3.0\pm0.1)\times10^4$	$(0.375–5)\times10^{-4}$	C
5.38	$(1.5\pm0.02)\times10^4$	$(0.025–2)\times10^{-3}$	Ca
5.43	$(1.3\pm0.03)\times10^4$	$(0.1–1)\times10^{-3}$	A
5.45	$(1.1\pm0.03)\times10^4$	$(0.05–1)\times10^{-3}$	A
6.06	$(2.4\pm0.08)\times10^3$	$(0.15–2.5)\times10^{-3}$	P
6.33	$(1.2\pm0.01)\times10^3$	$(0.1–1.5)\times10^{-3}$	P
6.65	$(4.6\pm0.5)\times10^2$	$(0.5–1)\times10^{-3}$	P
6.92	$(1.8\pm0.06)\times10^2$	$(0.5–4)\times10^{-3}$	P

*A, acetic acid – sodium acetate; C, citric acid – sodium citrate; Ca, cacodylic acid – sodium cacodylate; P, potassium dihydrogen phosphate – disodium hydrogen phosphate.

TABLE 4 Rate and ionization constants obtained from the pH rate profile for the HRP-II-sulfite reaction (eqs. 10 and 11)

Constant	Eq. 10	pK_a values	Eq. 11	pK_a values
$K_3(M)$	1.3×10^{-4}	3.9	1.7×10^{-4}	3.8
$K_s(M)$	1.9×10^{-7}	6.7	1.5×10^{-7}	6.8
$K_2^{\neq}(M)$	8.1×10^{-3}	2.1		
$k_2'(M^{-1}\,s^{-1})$	4.8×10^5		5.8×10^5	

TABLE 5. First-order rate constants for the decomposition of the HRP-II-sulfite complex at 25° determined at both 403 and 411 nm

pH	[Sulfite] (M)	Rate constant (s^{-1})
6.92	4×10^{-3}	0.27
6.92	2×10^{-2}	0.31
4.99	1×10^{-4}	0.28
4.99	1×10^{-3}	0.27
4.03	2.5×10^{-5}	0.23

II-sulfite reaction however, an absorbance decrease was observed at 411 nm which corresponded to the decrease in absorbance observed for the reduction of HRP-II at 427 nm. Following this decrease in absorbance, the absorbance at 411 nm then returned exponentially to that of the native enzyme. It was found that measurements comparable to those made at 411 nm could be obtained at a variety of wavelengths from 360–420 nm. The first-order rate constants for the return of absorbance to that of the native enzyme, illustrated in Table 5, show that the reaction, measured at 411 and 403 nm, is independent of both pH and sulfite concentration. These results can be explained if the second-order process with rate constant k_2, observed at 427 nm corresponds to the formation of a spectrally distinct complex between HRP-II and sulfite and the first-order process observed at 411 nm to the decay of this complex. The spectrum of this enzymatic intermediate can be estimated from the total absorbance changes observed for the first-order reaction monitored at various wavelengths. Such experiments indicate that the molar absorptivity of the complex is about 40% of that for the native enzyme at the position of maximum absorbance by HRP (403 nm) and that the complex and native enzyme have an isosbestic point at approximately 425 nm. The similarity of the molar absorptivity values for the complex and HRP at 427 nm facilitated measurements of k_2, since no absorbance change for complex decomposition could be observed at this wavelength. At sufficiently high concentrations of sulfite, complex formation occurs more rapidly than

TABLE 6. Second-order rate constants for the HRP-I-nitrite and HRP-II-nitrite reactions at 25°

pH	k_3 (HRP-I) (M^{-1} s^{-1})	k_4 (HRP-II) (M^{-1} s^{-1})	Total [nitrite] range (M)	Buffer*
5.97	6.5×10^3		$(0.5–2.5) \times 10^{-3}$	P
5.98		$(1.8 \pm 0.04) \times 10^2$	$(0.1–4) \times 10^{-2}$	P
6.83		2.5×10	$(0.1–1) \times 10^{-1}$	P
6.93	$(6.7 \pm 0.2) \times 10^2$		$(0.025–1) \times 10^{-2}$	P
7.53		4.5	$(0.2–1) \times 10^{-1}$	P
8.21	3.7×10		$(0.2–2) \times 10^{-2}$	B
8.84	8.2		$(0.2–1) \times 10^{-1}$	B

*B, sodium tetraborate – NaOH; P, potassium dihydrogen phosphate.

complex decomposition, thus the rate of the latter reaction could be measured at 411 and 403 nm without complication. The rate constants in Table 5 were all measured with the pseudo first-order rate constant for complex formation at least ten times larger than the rate constant for complex decomposition.

Attempts to study the HRP-II-sulfite reaction at higher pH on the Cary 14 spectrophotometer were abandoned due to the presence of a slow decrease in absorbance at 427 nm which complicated the kinetic analysis. This slow absorbance decrease appeared to be independent of both pH and sulfite concentration so that it did not interfere with measurements of reaction rates which were fast enough to be observed on the stopped-flow apparatus. The similarity in rates between the reactions of HRP-I and HRP-II with sulfite coupled with the complications resulting from the slow secondary process observed at 427 nm in the latter reaction, made impractical the titration of HRP-I and HRP-II with sulfite as performed for iodide (8) and nitrite.

Kinetics of the HRP-I- and HRP-II-Nitrite Reactions

The rate equations observed for the nitrite reactions are analogous to those for sulfite. Plots of pseudo first-order rate constants *vs.* total concentration of nitrite were found to be linear for up to a 100-fold change in nitrite concentration in reactions with both HRP-I and HRP-II. Second-order rate constants, k_3 for HRP-I and k_4 for HRP-II, are listed in Table 6 along with the ranges of nitrite concentrations and buffers used at each pH. Over the limited range of pH where the reactions of nitrite were studied, the logarithms of k_3 and k_4 decreased linearly with pH. The slope of the plots of both log k_3 and log k_4 *vs.* pH is -1.0 ± 0.01.

Reaction Sequence of the HRP-I-Sulfite Reaction

Figure 4 illustrates the spectrum of the steady-state concentration of the enzymatic intermediate present in a mixture of HRP, hydrogen peroxide, and sulfite. This spectrum was scanned using the technique devised to get accurate spectra of HRP-I (8) and HRP-II (20). From Figs. 2 and 3 it can be seen that the values of k_1 and k_2 at pH 6 are the same. Thus with an excess of hydrogen peroxide the steady-state intermediate would be expected to be a 1:1 mixture of HRP-I, HRP-II,

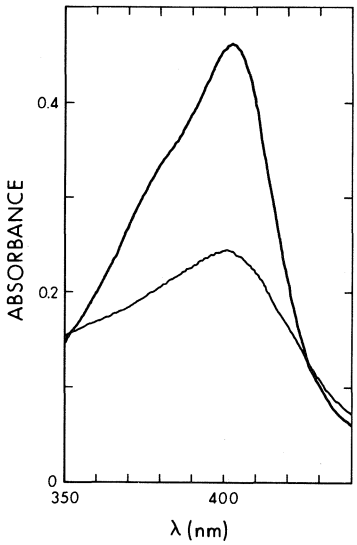

FIG. 4. Spectrum of the enzymatic species present in the steady state for the HRP reaction with sulfite (smaller maximum absorbance) compared to the spectrum of native HRP (larger maximum absorbance). The steady-state spectrum which corresponds closely to that of HRP-I, was scanned over a period of 40 s following the initiation of the reaction with hydrogen peroxide. By monitoring the same reaction at 411 nm it was estimated that the HRP had completed five reaction cycles during the time taken to scan the spectrum.

Can. J. Chem. Downloaded from www.nrcresearchpress.com by 210.87.254.105 on 09/05/12
For personal use only.

Can. J. Chem. Downloaded from www.nrcresearchpress.com by 210.87.254.105 on 09/05/12
For personal use only.

and the HRP-II-sulfite complex if HRP-I reacted to form HRP-II. The maximum in the spectrum in Fig. 4 agrees with that of the known spectrum of HRP-I within 8% and similar isosbestic points are observed (8) indicating that HRP-I is converted directly to HRP without the intermediate formation of HRP-II. The small deviation between Fig. 4 and the known spectrum of HRP-I is most probably a result of the slow spontaneous decay of HRP-I to HRP-II that was also observed for the reaction with iodide (8). The fact that HRP-II is not formed from the reaction between HRP-I and sulfite was also confirmed by studying the reaction of sulfite with a 1:1 mixture of HRP-I and HRP-II at 427 nm where the absorbance of the HRP-II-sulfite complex is negligible. If HRP-I reacted to produce HRP-II such a mixture would be expected to result in distinctly non-first-order kinetics for the HRP-II reaction, since HRP-II formation and decay would occur simultaneously. For such mixtures an exact first-order decay of HRP-II was always observed, with the same rate constant as obtained in experiments with no HRP-I present. This provides striking evidence that HRP-I is converted directly to native HRP.

Reaction Sequence of the HRP-I-Nitrite Reaction

As observed for similar experiments on the HRP-catalyzed oxidations of ferrocyanide and ascorbic acid, the spectrum of the enzymatic species present in the steady-state oxidation of nitrite closely resembles that of HRP-II (20). This steady-state spectrum reaffirms the observations of Chance (13), who reported that HRP-I reacts with nitrite in a one-electron transfer forming HRP-II.

The overall stoichiometry of the HRP-catalyzed reaction between hydrogen peroxide and nitrite is described by eq. 12 which was

$$[12] \qquad H_2O_2 + NO_2^- \xrightarrow{\text{HRP}} NO_3^- + H_2O$$

established by measuring the absorbance changes at 355 and 300 nm resulting from the steady-state oxidation of nitrite with various concentrations of hydrogen peroxide as illustrated in Fig. 5. The slope of the solid line in Fig. 5, 22.8 ± 0.4 M^{-1} cm^{-1} obtained from the linear analysis of the absorbance changes observed at 355 nm *vs.* the concentration of hydrogen peroxide is in good agreement with the value of the molar absorptivity difference between nitrite and nitrate,

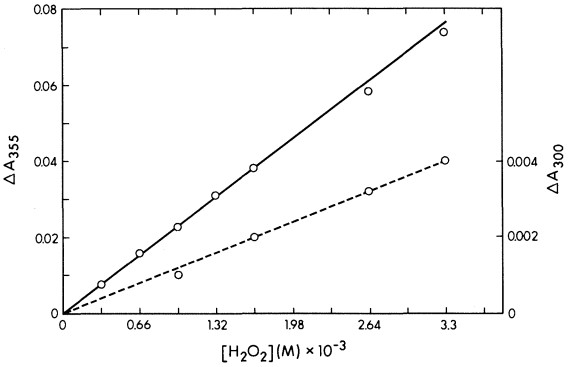

FIG. 5. Plot of the changes in absorbance at 355 and 300 nm *vs.* the concentration of hydrogen peroxide for the HRP catalyzed reaction between nitrite and hydrogen peroxide. The solid line was calculated by weighted linear least squares analysis of the observed absorbance changes at 355 and the broken line by weighted linear-least squares analysis of the observed absorbance changes at 300 nm. The slope of the solid line with its standard deviation is 22.8 ± 0.4 M^{-1} cm^{-1} and that for the broken line is 1.3 ± 0.5 M^{-1} cm^{-1}.

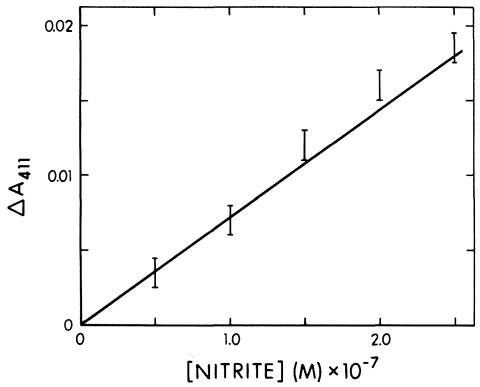

FIG. 6. Plot of the change in absorbance at 411 nm *vs.* the concentration of nitrite for the titration of HRP-I with nitrite. The solid line was calculated assuming a 2:1 ratio between HRP-I and nitrite using a difference in molar absorptivity of 3.6 × 10^4 M^{-1} cm^{-1}.

23.0 M^{-1} cm^{-1}, computed on the basis of 1 mol of nitrite being consumed for every mol of peroxide. A similar analysis at 300 nm led to a slope of 1.3 ± 0.5 M^{-1} cm^{-1} for the broken line in Fig. 5 in reasonable agreement with the difference in molar absorptivity expected if 1 mol of nitrate is formed for every mol of nitrite consumed (1.6 M^{-1} cm^{-1}).

A titration of HRP-I with nitrite was performed using the method employed for the titration of HRP-I with iodide (8). The results of the titration, as illustrated in Fig. 6, indicate that each mol of nitrite reacts with 2 mol of HRP-I.

Can. J. Chem. Downloaded from www.nrcresearchpress.com by 210.87.254.105 on 09/05/12
For personal use only.

Discussion

In general, sulfite oxidations by inorganic oxidizing agents capable of accepting two electrons always proceed via two-electron transfers producing sulfate as a product (21). The spectrum of the species present in the steady state illustrated in Fig. 4 along with the kinetic measurements made in a mixture of HRP-I and HRP-II indicate that the HRP-I-sulfite reaction involves a two-electron transfer to HRP-I without the observable formation of HRP-II. Although titrations of HRP-I and HRP-II with sulfite were not possible, it seems reasonable to assume that the stoichiometry observed for the reactions of HRP-I and HRP-II with iodide also apply to the reactions with sulfite. Thus the reaction of HRP-I with sulfite at any given pH could be described by eqs. 13 and 14 where the SO_3

$$\text{[13]}\quad \text{HRP-I} + \text{sulfite} \xrightarrow{k_1} \text{HRP} + SO_3$$

$$\text{[14]}\quad SO_3 + H_2O \xrightarrow{\text{fast}} SO_4^{2-} + 2H^+$$

does not necessarily have a discrete existence in aqueous solution.

The reaction of HRP-I with nitrite, unlike the corresponding reactions with sulfite and iodide, involves the transfer of a single electron from nitrite to HRP-I forming HRP-II. The 2:1 ratio of HRP-I to nitrite observed for the titration of HRP-I with nitrite and the 1:1 ratio between hydrogen peroxide and nitrite determined for the overall reaction indicates that the titration ratio between HRP-II and nitrite must also be 2:1. A simple mechanism for nitrite oxidation which incorporates the observed kinetics and stoichiometry for the reactions is

$$\text{[15]}\quad \text{HRP-I} + NO_2^- \xrightarrow{k_3} \text{HRP-II} + NO_2$$

$$\text{[16]}\quad \text{HRP-II} + NO_2^- \xrightarrow{k_4} \text{HRP} + NO_2$$

$$\text{[17]}\quad 2NO_2 + H_2O \xrightarrow{\text{fast}} NO_3^- + NO_2^- + 2H^+$$

where the NO_2 does not necessarily exist in aqueous solution.

It is somewhat surprising that nitrite reacts with HRP-I to produce HRP-II since it has been reported that compound I of catalase oxidizes nitrite in a direct two-electron transfer without the production of compound II (4). In addition the reaction between nitrite and hydrogen peroxide involves the transfer of two electrons and the formation of nitrate via a mechanism that is analogous to that for the reaction of sulfite with hydrogen peroxide (22). The following mechanism offers a simple rationale for the observed reactions of HRP-I with iodide, sulfite, and nitrite.

$$\text{[18]}\quad \text{HRP-I} + X \rightarrow \text{HRP-I}\overset{\delta^-\ \ \delta^+}{\ldots}X$$

$$\text{[19]}\quad \text{HRP-I}\overset{\delta^-\ \ \delta^+}{\ldots}X + H_2O \rightarrow \text{HRP-II} + \text{product}$$

$$\text{[20]}\quad \text{HRP-I}\overset{\delta^-\ \ \delta^+}{\ldots}X \rightarrow \text{HRP} + \text{product}$$

In the proposed mechanism the rate determining step is reaction 18 which is followed either by reaction 19 or 20. For the reactions of iodide and sulfite the products of single electron oxidation, atomic iodine (I·) and SO_3^-, do not react rapidly with water so that step 20 predominates. For the nitrite reaction however, the reaction between NO_2 and water is rapid (23) so that reaction 19 predominates. In the reaction of compound I of catalase, the two-electron transfer from nitrite could be due to the more transient nature of the initial enzymatic complex or perhaps to a more hydrophobic reaction site than HRP which could hinder the reaction analogous to 19.

The second-order rate constants for the reactions of HRP-I and HRP-II with the inorganic substrates iodide (6, 8), ferrocyanide (5), sulfite, and nitrite all show the same general trend of increasing values with increasing acidity. For the reactions of HRP-I and HRP-II with iodide it was possible to demonstrate that this trend resulted from the ionization of an enzyme group at low pH. For the reactions of sulfite and nitrite with HRP-I and HRP-II, the existence of substrate ionizations in the acid region (sulfite has a pK_a value of 1.8 and nitrite a pK_a of 3.4) does not allow the unambiguous establishment of the nature of the reactive protonated species, *i.e.* whether the rate influencing ionization is on the enzyme or substrate. If, however, it is assumed that the rate influencing ionizations observed for the reactions of HRP-I and HRP-II with iodide have a similar effect on the reactions with sulfite and nitrite, a good deal of consistency can be seen in the reactions of all three substrates.

For the HRP-II-sulfite reaction, the reaction of SO_3^{2-} can be shown to require a second-order rate constant of $3 \times 10^{10}\ M^{-1}\ s^{-1}$ to account for the observed rate at pH 2.4. Since the diffusion-controlled limit for a second-order rate constant

Can. J. Chem. Downloaded from www.nrcresearchpress.com by 210.87.254.105 on 09/05/12
For personal use only.

where one of the reactants is a large protein can have a maximum value of 10^{10} M^{-1} s^{-1} and is probably smaller (24), it would appear that the reactive form of the substrate is not SO_3^{2-}. If the ground state pK_a value of 3.3 and the transition state p$K_a^{\ddagger}$ value of 4.0 in Fig. 2 are considered to be paired together (a similar pairing of two inflections in close proximity was invoked for the p*H* dependence of the HRP-II-*p*-cresol reaction (20)) the reaction of HRP-I with SO_3^{2-} can also be shown to exceed the diffusion-controlled limit at low p*H*. Thus if the ionizations on HRP-I and HRP-II observed for the reactions with iodide have a similar effect on the reactions with sulfite and nitrite, then the reactive form is the singly charged anion for all three substrates.

The p*H* dependences of the second-order rate constants for the reactions of HRP-I with ferrocyanide (5), iodide (8), and sulfite all indicate enzyme ionizations with pK_a values of approximately 5. A self-consistent method for estimating the errors in these pK_a values has been developed and is reported in detail elsewhere (17). The results indicate that for the HRP-I reaction with ferrocyanide the pK_a is 5.3 ± 0.8, for reaction with iodide the pK_a is 4.6 ± 0.2 and for reaction with sulfite the pK_a is 5.1 ± 0.2. Since the difference in the pK_a values observed for the sulfite and iodide reactions is just outside the error limits on the two values, it appears reasonable to assume that the same ionizing group on HRP-I influences the reaction rate with all three substrates. The kinetics of the HRP-I-sulfite reaction indicate an enzyme pK_a of 3.3 which was not detected in the comparable reaction with iodide. Since the rapid rate of the iodide reaction prevented its study to as low a p*H* as was possible for the sulfite reaction, the influence of this enzyme ionization in the HRP-I-iodide reaction cannot be excluded. The reactions with ferrocyanide (5) and nitrite were not studied at sufficiently low p*H* to detect such a pK_a value.

The identity of the rate law and the similarity in the p*H* dependence of the second-order rate constant for the HRP-II-sulfite reaction monitored at 427 nm compared to the reactions of HRP-I and HRP-II with ferrocyanide (5), iodide (6, 8), and nitrite suggest that the former reaction is describing the same molecular process as the latter reactions. Critchlow and Dunford (20) have proposed a mechanism for the reactions of HRP-II in which this rate determining process involves (*i*) the slow displacement of a group coordinated to the iron followed by (*ii*) rapid electron transfer and (*iii*) rapid product departure. The HRP-II sulfite reaction appears to follow this three-step process but the observation of complex formation implies that one of the latter two steps is slow. The p*H* dependence of the second-order rate constant for the HRP-II sulfite reaction indicates a rate influencing ionization with pK_a of 3.9 that was not observed for the reactions of ferrocyanide (5) or iodide (6). The pK_a of this ionization suggests that the group might be a carboxylic acid residue and the electronegative character of the bisulfite ion makes plausible the postulate of a hydrogen bonding enzyme-substrate interaction.

The authors acknowledge the financial support of the National Research Council of Canada.

1. B. CHANCE. Arch. Biochem. Biophys. **41**, 416 (1952).
2. P. GEORGE. Nature (London), **169**, 612 (1952).
3. P. GEORGE. Biochem. J. **54**, 267 (1953).
4. A. S. BRILL. Comp. Biochem. **14**, 447 (1966).
5. B. B. HASINOFF and H. B. DUNFORD. Biochem. **9**, 4930 (1970).
6. R. ROMAN, H. B. DUNFORD, and M. EVETT. Can. J. Chem. **49**, 3059 (1971).
7. J. E. CRITCHLOW and H. B. DUNFORD. J. Biol. Chem. **247**, 3703 (1972).
8. R. ROMAN and H. B. DUNFORD. Biochem. **11**, 2076 (1972).
9. T. HOSOYA. Gunma Symp. Endocrinol. **5**, 219 (1968).
10. I. FRIDOVICH and P. HANDLER. J. Biol. Chem. **236**, 1836 (1961).
11. S. J. KLEBANOFF. Biochim. Biophys. Acta, **48**, 93 (1961).
12. S. F. YANG. Biochem. **9**, 5008 (1970).
13. B. CHANCE. Arch. Biochem. Biophys. **41**, 416 (1952).
14. E. T. SEO and D. T. SAWYER. J. Electroanal. Chem. **7**, 184 (1964).
15. A. P. ALTSHULLER and A. F. WARTBURG. Anal. Chem. **32**, 174 (1960).
16. M. L. COTTON and H. B. DUNFORD. Can. J. Chem. This issue.
17. R. ROMAN. Ph.D. Thesis. University of Alberta, Edmonton, Alberta. 1972.
18. Handbook of Chemistry and Physics. 48th ed. Chemical Rubber Co. Cleveland, Ohio. 1967. p. D92.
19. J. E. CRITCHLOW and H. B. DUNFORD. J. Theor. Biol. In press (1972).
20. J. E. CRITCHLOW and H. B. DUNFORD. J. Biol. Chem. **247**, 3714 (1972).
21. W. C. E. HIGGINSON and J. W. MARSHALL. J. Chem. Soc. 447 (1957).
22. J. HALPERIN and H. TAUBE. J. Am. Chem. Soc. **74**, 380 (1952).
23. F. A. COTTON and G. WILKINSON. Advanced inorganic chemistry. 2nd ed. John Wiley and Sons Inc., New York, N.Y. 1966. p. 346.
24. R. A. ALBERTY and G. G. HAMMES. J. Phys. Chem. **62**, 154 (1958).

The Hydrolysis of Disubstituted Alkyl Phosphorochloridates and *N,N,N',N'*-Tetra-substituted Phosphorodiamidic Chlorides in Water and Deuterium Oxide: Heat Capacity of Activation and Kinetic Solvent Isotope Effects

E. C. F. Ko[1] AND R. E. Robertson

Department of Chemistry, University of Calgary, Calgary, Alberta

Received August 3, 1972

The pseudo-thermodynamic parameters, $\Delta H^{\ddagger}$, $\Delta S^{\ddagger}$, and $\Delta C_p^{\ddagger}$ and the kinetic solvent isotope effects have been determined for the three alkyl-phosphorochloridates, where the alkyl group is ethylisopropyl and *n*-propyl; for tetra-methyl and tetra-ethyl phosphorodiamidic chlorides; the di-*n*-propyl and di-isopropyl analog, the di(isopropylmethylcarbinyl)phosphorochloridate and the tetra-ethylthiophosphorodiamidic chloride. These compounds have a potential relationship to compounds used as insecticides and as polymers. The mechanism of reaction is discussed on the basis of these data.

Les paramètres pseudo-thermodynamiques, $\Delta H^{\ddagger}$, $\Delta S^{\ddagger}$, et $\Delta C_p^{\ddagger}$ ainsi que les effets isotopiques et cinétiques du solvant, ont été déterminés pour les trois phosphorochloridates d'alcoyles où le groupe alcoyle est l'isopropyle d'éthyle et le *n*-propyle; pour les chlorures de tétra-méthyl et de tétra-éthyl phosphorodiamique; l'analogue di-*n*-propyl et di-isopropyl, le di-isopropyl, méthyl, carbinyl phosphorochloridate et le chlorure de tétra-éthyl thiophosphorodiamique. Ces composés ont une relation possible avec d'autres produits utilisés comme insecticides et comme polymères. Le mécanisme réactionnel est discuté sur la base de ces résultats. [Traduit par le journal]

Can. J. Chem., **51**, 597 (1973)

Introduction

The significance of pseudothermodynamic parameters derived from the temperature dependence of the rates of reaction is uncertain. Whether this is indicative of some failure of transition state theory as some suspect (1) or due to a lack of proper identification and estimation of contributing factors is an open question which calls for solution if our knowledge in this area is to advance beyond free energy correlations. Among the limited areas where recent progress has been made, we may cite the general correlation between the magnitude of the negative temperature coefficient of the enthalpy of activation ($\Delta C_p^{\ddagger}$) and mechanism for ionogenic reactions in water. Under these conditions this parameter is sensitive not only to solvent reorganization but also can provide evidence for the intrusions of competing reactions with a change of temperature whether due to "mixed kinetics" or to other causes (2) and in certain cases gives evidence of changing solvent interaction with substituents (3). Judged by this latter criteria, mixed kinetics seems far less common for solvolysis in water than occasional reference would lead one to believe. Since the coefficient $\Delta C_p^{\ddagger}$ is essentially empirical,[2] however dignified by formal title, deductions with respect to mechanism depend in large degree on the establishment of "normal values". Thus the remarkable difference in $\Delta C_p^{\ddagger}$ for the hydrolysis of dimethylsulfamoyl chloride (**1**) ($\Delta C_p^{\ddagger} = -76$ cal deg^{-1} mol^{-1}, normal for an S_N1 mechanism (5)) and that for diethylsulfamoyl chloride (**2**) ($\Delta C_p^{\ddagger} = -38$ cal deg^{-1} mol^{-1}) (6) signalled a potential difference in solvent reorganization even though both would be considered to react by an S_N1 mechanism. Thus, a mechanistic distinction not previously suspected was revealed.

In this paper our aim is to determine the values of the $\Delta C_p^{\ddagger}$ for hydrolysis in water and associated values of $\Delta H^{\ddagger}$ and $\Delta S^{\ddagger}$ for three alkyl phosphorochloridates which bear some resemblance to the alkyl chlorosulfates (7) and four *N,N,N',N'*-tetra-substituted phosphorodiamidic (see below) chlorides which have an obvious structural similarity to **1** and **2** and have been studied extensively (8–11) due to a potential

[1]Postdoctoral Fellow, 1970–1972.

[2]Granted the basic theory is a fair approximation, the value of $\Delta C_p^{\ddagger}$ as normally derived, involves the assumption that this term remains constant down to 0 °K, and is independent of temperature through the experimental range — useful but unlikely (4).

Can. J. Chem. Downloaded from www.nrcresearchpress.com by 210.87.254.42 on 09/05/12
For personal use only.

relationship to compounds used in the production of insecticides and polymers. Data for the hydrolysis of one thio-analog of the phosphorochlorides are reported as well as for di(isopropylmethylcarbinyl)phosphorochloridate.

$(R_1O)_2POCl$		$(R_1R_2N)_2POCl$	
3	R_1 = Ethyl	**7**	$R_1 = R_2$ = Methyl
4	R_1 = *i*-Pr	**8**	$R_1 = R_2$ = Ethyl
5	R_1 = *n*-Pr	**9**	R_1 = *n*-Pr; R_2 = H
6	$R_1 = R_2$ = 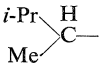	**10**	R_1 = *i*-Pr; R_2 = H

The mechanism of hydrolysis for **3** and **4** appears to be well established as an S_N2 process (8, 9). While the mechanism for the hydrolysis of **7** and **8** is less well established, the basis for possible disagreement is not very persuasive to us (10, 11). The uncertainty here, as in the case of the sulfonyl chlorides (12) and of the sulfamoyl chlorides (5, 6) arises from that uncertainty which frequently attends mechanistic deductions based on small or no rate increases above the normal value for hydrolysis following the addition of a series of nucleophiles somewhat stronger than water (9, 13). Hall argued that since **7** exhibited virtually no rate enhancement on the addition of OH^-, F^-, and EtO^-, it hydrolyzed by an S_N1 mechanism. Subsequent results obtained by Crunden and Hudson (10) and by Traylor and Westheimer (11) on **8** and **9** show that under certain conditions the hydrolysis of **7**–**9** can be expected to show specific base catalysis and nucleophilic catalysis. There is a remarkable difference toward OH^- between the results for **7** and **8** and those for **9** and **10** and presumably other amidophosphoryl chlorides having a hydrogen attached to the amido nitrogen. Traylor and Westheimer estimate that for **9**, OH^- causes a rate enhancement of at least one million times over that for **7**.

This prior information on the probable mechanism of reaction for these phosphoryl compounds provided a useful background for correlation and examination of the corresponding values of $\Delta C_p^{\ddagger}$ derived from the temperature dependence of the rates of hydrolysis in water. An attempt was made to extend the series to the thio-analog $(Et_2N)_2PSCl$, but in spite of the fact that in each separate rate determination, good first-order kinetic behavior was found, some unknown factor was introduced, which resulted in a larger experimental error than was normally found in such studies. For this reason, we have less confidence in these data than in those for the phosphoryl chlorides. For the same reason the study was terminated with the first member studied.

Results and Discussion

The rates of hydrolysis of **3**–**10** in water were determined by a conductance method described previously (14). These react in water according to first-order kinetics and on the basis of neutral equivalent determination can be assumed to follow the overall equation:

[1] 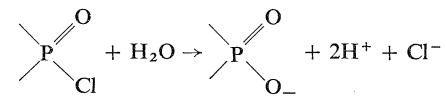

The pseudo first-order rate constants ($k < \pm 1\%$) were fitted to the three-constant equation

$$[2] \quad \log_{10} k_{obs} = A_1 + A_2/T + A_3 \log_{10} T$$

The corresponding empirical constants, A_1, A_2, A_3 are reported in Table 1 and provide a means for accurate interpolation of rates. The pseudo-thermodynamic parameters were calculated from these constants in the usual way (15) and are reported in Table 2. A sample of di(isopropylmethylcarbinyl)chlorophosphonate hydrolyzed under similar conditions to the above gave first-order rate constant of 25° and led to values of $\Delta H^{\ddagger}$ 12 735 ± 100 cal mol^{-1} and $\Delta S^{\ddagger}$ −27.44 ± 0.32 cal deg^{-1} mol^{-1} at 25°. Low solubility was considered to be the factor which prevented a more extended study.

The values of the constants corresponding to eq. 2 obtained for the hydrolysis of tetraethylthiophosphorodiamidic chloride[3] were A_1 = 54.86995, A_2 = −6264.362, and A_3 = −15.41276. The values of the derived terms were as follows: $\Delta H^{\ddagger}$ = 17 961 ± 11 cal mol^{-1}, $\Delta S^{\ddagger}$ = −17.21 ± 0.04, and $\Delta C_p^{\ddagger}$ = −32 ± 2 cal deg^{-1} mol^{-1}. The rate in D_2O at 60.20 °C was 1.216×10^{-3}. The corresponding value in H_2O is 1.561×10^{-3} giving a value of k_{H_2O}/k_{D_2O} = 1.28, a value significantly lower than found for the sulfonyl chlorides (16).

A considerable body of empirical data exists now to support the generalization that uncomplicated hydrolyses occurring by an S_N1 mechanism and leading to the creation of halide ions

[3]Rate data showing derivations >2% were discarded after a preliminary fit.

Can. J. Chem. Downloaded from www.nrcresearchpress.com by 210.87.254.42 on 09/05/12
For personal use only.

TABLE 1. Empirical constants expressing temperature dependence of the rate of hydrolysis for a series of compounds involving the P—Cl bond

Compound	R_1	R_2	A_1	$-A_2$	$-A_3$	$n_{T_1}{}^{T_2*}$
3	Et	—	60.52808	5447.116	17.77783	$30_0{}^{18}$
4	*i*-Pr	—	59.37901	5317.109	17.63455	$33_0{}^{25}$
5	*n*-Pr	—	37.7019	4377.911	9.61531	$26_0{}^{20}$
7	Me	Me	78.13629	6800.933	23.18922	$32_0{}^{30}$
8	Et	Et	69.39361	6288.947	20.46220	$34_0{}^{40}$
9	*n*-Pr	H	113.1946	8416.441	35.26286	$22_0{}^{32}$
10	*i*-Pr	H	110.4867	8227.787	34.36008	$30_0{}^{27}$

*n = number of kinetic runs within the temperature range from T_1 to T_2.

TABLE 2. Pseudo-thermodynamic activation parameters derived from the temperature dependence of rate data for hydrolysis in water

Compound	R_1	R_2	$\Delta H^{\neq}$ (kcal mol^{-1})	$\Delta S^{\neq}$ (cal mol^{-1} deg^{-1})	$\Delta C_p{}^{\neq}$ (cal mol^{-1} deg^{-1})
3	Et	—	14395.8 ± 3.8	−18.12 ± 0.01	−37 ± 2
4	*i*-Pr	—	13770.2 ± 4.6	−21.88 ± 0.02	−37 ± 1
5	*n*-Pr	—	13742 ± 51	−20.56 ± 0.18	−21 ± 3
7	Me	Me	17268.0 ± 7.8	−9.99 ± 0.03	−48 ± 1
8	Et	Et	16380.2 ± 8.8	−14.26 ± 0.03	−48 ± 2
9	*n*-Pr	H	17746.9 ± 14.8	−9.45 ± 0.05	−72 ± 3
10	*i*-Pr	H	17400.3 ± 7.8	−9.89 ± 0.03	−70 ± 1

are characterized by a more negative value of $\Delta C_p{}^{\neq}$ than those reacting by an S_N2 mechanism (14). Such a generalization is consistent with the classical observation that the ionizing mechanism involved a greater degree of charge development at the transition state (17), and hence a greater degree of solvent reorganization. Thus halides assumed to react by an S_N1 mechanism generally have values of $\Delta C_p{}^{\neq}$ about -80 ± 5 cal mol^{-1} deg^{-1} while those reacting by an S_N2 mechanism have values in the range of -40 to -55 cal mol^{-1} deg^{-1}. Exceptions are known (19), hence this distinction by itself is not a sufficient mechanistic test. While the *p*-substituted benzyl nitrates show a wider range of values for $\Delta C_p{}^{\neq}$ (18), the corresponding values for the hydrolysis of the sulfonic esters, to date, all lie in the range of -35 to -41 cal deg^{-1} mol^{-1}.

As noted above (14), for an uncomplicated reaction mechanism, whether S_N1 or S_N2, involving the displacement of halides from carbon these differences could be correlated with charge development and solvent reorganization. A simple extension of this generalization led to the expectation (14) of a corresponding correlation between mechanism and the corresponding values of the kinetic solvent isotope effect (k_{H_2O}/k_{D_2O}, k.s.i.e.) but this was not observed. The hydrolyses of alkyl halides, sulfonates, sulfates, chlorosulfates, nitrates, and phosphates, irrespective of the mechanism of displacement from a carbon center show rather low k.s.i.e. values, in the order of 1.1–1.3 whether some degree of nucleophilic interaction is required or not (19). However, substituted alkyl phosphorochloridates, phosphorodiamidic chloride, and the sulfonyl chlorides with displacement occurring from either a phosphorus or sulfur atom have significantly higher values of k.s.i.e., in the range 1.3–1.9 (Table 3). Some part of this effect may be attributed to the greater degree of nucleophilic interaction required, a conclusion supported by Rossal and Robertson by showing that a linear correlation existed between the k_{H_2O}/k_{OH^-} ratio and the k.s.i.e. for a series of para-substituted sulfonyl chlorides (20). However, these authors overlooked a second potential contributor to the k.s.i.e. In each of the second series, there is at least one oxygen α to the reaction center. The k.s.i.e. seems to increase as the number of oxygen atoms adjacent to the reaction center increases, in contrast to the lack of such an effect where the oxygen atoms lie beyond the α-position as is the case with the sulfonates, sulfates, and phosphates (Table 4). Nucleophilic attack of water by the oxygen will place the hydrogens of that molecule

Can. J. Chem. Downloaded from www.nrcresearchpress.com by 210.87.254.42 on 09/05/12
For personal use only.

TABLE 3. The first-order rate constants (10^3 s^{-1}) for the hydrolysis of P—Cl bond in compounds **3–9** in H_2O and D_2O and their k.s.i.e.

Compound	R_1	R_2	Temperature (°C)	k_{H_2O}*	k_{D_2O}†	k.s.i.e.
3	Et	—	9.991	5.000	3.343	1.50
4	*i*-Pr	—	9.991	2.294	1.370	1.67
5	*n*-Pr		9.832	4.54	—	—
7	Me	Me	20.128	5.416	3.918	1.38
8	Et	Et	20.125	2.918	2.226	1.31
9	*n*-Pr	H	20.112	3.115	2.180	1.43
10	*i*-Pr	H	20.126	4.541	3.082	1.47
11	$(Et_2N)_2$	PSCl	60.196	1.56	1.216	1.28

*Calculated from constants in Table 1.
†Observed.

TABLE 4. The k.s.i.e. and $\Delta C_p^{\ddagger}$ values compared for hydrolysis in the presence and absence of possible α-oxygens

Compound	Temperature (°C)	$-\Delta C_p^{\ddagger}$ (cal deg^{-1} mol^{-1})	k.s.i.e.	Reference
		Presence of possible α-oxygens		
5	20	48	1.31	This work
7	20	48	1.38	" "
8	20	72	1.45	" "
9	20	70	1.47	" "
3	10	37	1.50	" "
4	10	37	1.67	" "
$DiMeNSO_2Cl$	15	76	1.33	5
$MeSO_2Cl$	30	52	1.57	28
$PhSO_2Cl$	15	56	1.58	28
		Absence of possible α-oxygens		
MeCl	75	49	1.28	19
i-PrCl	75	38	1.33	19
t-BuCl	10	83	1.38	19
$MeSO_2Me$	30	38	1.06	19
i-$PrSO_2Me$	25	35	1.08	19
$MeOSO_2OMe$	30	46	1.10	19
$MeOSO_2Cl$	10	50	1.20	19
Me_3PO_4	10	50	1.07	19

in the neighborhood of unshared electrons of the sulfonyl or phosphoryl oxygens and this interaction will tend both to polarize the bond and enhance the nominal k.s.i.e. Such an effect would be analogous to the "α effect" discussed by Edwards and Pearson (21) and others (22–25) in connection with the enhanced reactivity encountered in the reaction of nucleophiles with substrates bearing unshared electrons on adjacent atoms. A similar effect has been proposed by Murto in connection with the enhanced rate of hydrolysis of picryl fluoride compared with the chloride (27) and in a sense may be regarded as a kind of intramolecular general base catalysis (23). While the possibility of such an effect seems reasonable, it cannot be large since general base catalysis normally leads to values of k.s.i.e. of 2 or larger (19) and the measured values (Table 4) combine both the isotope effect arising from such interaction and that due to normal weakening of the O—H bond as a consequence of nucleophilic interaction plus about 0.1–0.3 attributed to solvent reorganization. In the sulfonyl chloride series Rossal and Robertson reported a value of k.s.i.e. = 1.82 for the *p*-nitro and 1.40 for the *p*-MeO compound. Were the above interaction important in the sulfonyl series, the opposite order of enhancement would be expected. In that comparison, one cannot exclude the possibility that the effect is

Can. J. Chem. Downloaded from www.nrcresearchpress.com by 210.87.254.42 on 09/05/12
For personal use only.

present but is concealed by a larger opposing effect. With such an argument, any such effect could be explained and in the absence of independent supporting evidence we prefer to neglect it.

While the values of k.s.i.e. for **3** and **4** are about the same as found previously for methanesulfonyl chloride and *p*-bromobenzenesulfonyl chloride, the corresponding values of $\Delta C_p^{\ddagger}$ are significantly more positive. The latter provide two more examples of what appears to be a general phenomenon, first noted in connection with the value of $\Delta C_p^{\ddagger}$ found for the hydrolysis of *p*-methoxybenzenesulfonyl chloride (3) and supported by the corresponding value of ΔC_p derived from the ionization of benzoic acids substituted with a methoxy group (3). Further support is found in our results for the hydrolysis of β-methoxyethyl chlorosulfate (8). It was apparent from these examples that there was a temperature dependent solvent effect on the methoxy group which altered the effect of this group on $\Delta H^{\ddagger}$ and hence provided a positive component to $\Delta C_p^{\ddagger}$ which reduced the larger negative component due to solvent reorganization. Thus the less negative value of $\Delta C_p^{\ddagger}$ obtained for **3** and **4** compared to the values for **7** and **8** need not indicate a significant difference in charge development at the transition state. It follows that while it is probable that some degree of bond-making is required in the activation process for the hydrolysis of **7** and **8** as Crunden and Hudson maintain (10), the values of $\Delta C_p^{\ddagger}$ do not suggest any remarkable degree of charge development if that is implied by the term "looseness" which Traylor and Westheimer (11) introduce to account for the difference between their mechanistic conclusions and those of Hall (9) with regard to these compounds. Whether the unusually low value of $\Delta C_p^{\ddagger}$ found for the hydrolysis of **5** can be attributed to this same effect is uncertain. We see no structural reason why this should be so.

The values of $\Delta C_p^{\ddagger}$ for **9** and **10** are significantly more negative than those of **3**–**8** and hence may be taken as *prima facie* evidence of a greater degree of solvent reorganization accompanying the activation process as would be expected for an S_N1 mechanism. However, the values of k.s.i.e. are intermediate between those for **3** and **4** and those for **7** and **8**. These values are far smaller than would be expected were the amidic hydrogen (D in D_2O) strongly involved as is the case when the reaction is catalyzed by OH^- or in hydrogen participation such as occurred in the hydrolysis of **2** (6). Traylor and Westheimer report that when **9** is dissolved in D_2O, exchange of the amidic hydrogen takes place very rapidly, being essentially complete in less than 30 s. Since the rate of hydrolysis is much slower than this, the exchange process evidently does not trigger hydrolysis, after the fashion of the catalytic effect of OH^-.

An examination of Courtauld's space models for the seven phosphoryl chlorides suggests that no significant steric hindrance to nucleophilic approach exists, hence some factor other than steric hindrance (which seemed adequate in the case of the dimethylsulfamoyl chloride) (5) must determine the mechanism of hydrolysis. It seems possible that **9** and **10** can exist as a fast equilibrating mixture (eq. 3) in which a kind of hydrogen participation reduces the positive charge on

[3] 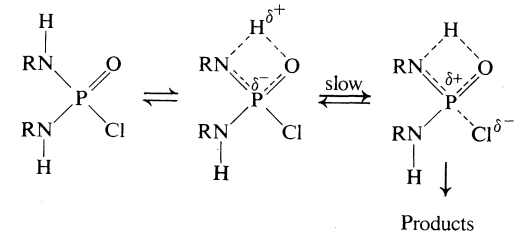

P and at the same time, on activation, facilitates the ionization of the forming chloride ion. The effect cannot be large (or the k.s.i.e. would be much greater) but may be sufficient to favor an S_N1 mechanism over some alternative. No such tautomeric forms are possible in **7** and **8**, hence these will require some degree of nucleophilic interaction in the displacement of the chloride ion. The less negative value of $\Delta C_p^{\ddagger}$ and the smaller value of k.s.i.e. are both consistent with the conclusion that the transition state is reached for this compound with a lower degree of charge separation than for the corresponding tetraalkylphosphorodiamidic chlorides.

Conclusion

No claim is made here for a reversal of mechanistic proposals based on other evidence. Where an S_N2 type mechanism is to be expected this fact is reflected in the magnitude of the k.s.i.e. and in the corresponding values of $\Delta C_p^{\ddagger}$. Quantitative differences were noted and the trends in these two parameters were shown to parallel values already obtained in other systems.

Can. J. Chem. Downloaded from www.nrcresearchpress.com by 210.87.254.42 on 09/05/12
For personal use only.

TABLE 5. Physical properties of compounds synthesized

Compound	R_1	R_2	B.p./mm Hg (°C)	N.m.r.* (H ratio)
3	Et	—	48/~2	Triplet at 8.60 and quartet at 5.74 τ (3:2)
4	*i*-Pr	—	33/~0.15	Doublet at 8.61 and multiplet at 5.28 τ (6:1)
5	*n*-Pr	—	42/~0.2	Triplet at 9.00, sextet at 8.23, and pair of triplets at 5.88 τ (3:2:2)
6	$(i\text{-PrMeCHO})_2POCl$	—	80/~1.5	Doublet at 9.00, doublet at 8.63, multiplet at 8.03, and multiplet at 5.51 τ (6:3:1:1)
7	Me	Me	54–55/~0.05	2 Equivalent singlets at 7.23 and 7.45 τ
8	Et	Et	72–73/~0.05	triplet at 8.82 and multiplet at 6.88 τ (3:2)
9	*n*-Pr	H	m.p. 94–95†	Triplet at 9.07, sextuplet at 8.47, pentaglet at 7.02, and singlet at 5.92 τ (3:2:2:1)
10	*i*-Pr	H	138–139/~0.05	Doublet at 8.75, heptuplet at 6.48, and singlet at 5.23 τ (6:1:1)

*Solvent was CCl_4 except for **9** in which $CDCl_3$ was used.
†About 10° below that reported in ref. 4.

This was not too surprising but it does provide further support for the utility of k.s.i.e. and $\Delta C_p^{\ddagger}$ values. The tetra-substituted phosphorodiamidic chlorides bearing an amido-hydrogen introduced an unusual combination of a value of k.s.i.e., which nominally would indicate bond-making with a water molecule in the activation process, contrary to the conclusions reached on the basis of other data, while the $\Delta C_p^{\ddagger}$ values indicated that the activation processes were accompanied by a more extended degree of solvent reorganization and was in the approximate range for molecules reacting by an S_N1 mechanism. These two opposed mechanistic indications were rationalized by postulating an intra-molecular interaction between an amido-hydrogen and the phosphoryl oxygen.

Experimental

The phosphorochloridates **3–6** were made in a two-step process outlined in the literature (8). Phosphorus trichloride was reacted with three-fold excess of the corresponding alcohol to give a disubstituted hydrogen phosphite which was then chlorinated with gaseous chlorine to give the phosphorochloridate. Phosphorodiamidic chlorides **6–9** were synthesized, in general, from phosphoryl chloride with four-fold excess of the corresponding amine at low temperature as previously reported (11). These compounds, except **8**, were purified by vacuum distillation two or three times, until the distillates gave homogeneous peaks on v.p.c. using a 10% neopentyl glycol sebacate on chromosorb glass column. Compound **8** was recrystallized twice from methylene dichloride and then sublimated. Their physical properties and n.m.r. spectra are summarized in Table 5.

The reaction products, acid and chloride, were analyzed by hydroxide titrations and potentiometric silver nitrate titrations, respectively. No attempts had been made to isolate the substituted phosphorus acids in the form of salts. The purification of solvents and the kinetic measurements were similarly the same as outlined in previous papers (14).

Tetraethylthiophosphorodiamidic chloride was made from diethylamine and phosphorus thiochloride by a method similar to that outlined previously (26); b.p. 50/0.25 mm Hg; n.m.r. triplet at τ 8.73 and two sets of quartets centered at 6.63 and 6.33 respectively, integration of proton ratio being 6:4.

We acknowledge with gratitude the financial support received from the National Research Council of Canada which made this work possible.

We thank Miss Eileen Huang for permission to include her kinetic results obtained in an Honors Chemistry project.

Can. J. Chem. Downloaded from www.nrcresearchpress.com by 210.87.254.42 on 09/05/12
For personal use only.

1. The transition state. Chem. Soc. (Spec. Publ.) No. 16, 1962.
2. L. J. BRUBACHER, L. TREINDL, and R. E. ROBERTSON. J. Am. Chem. Soc. **90**, 4611 (1968).
3. R. E. ROBERTSON and B. ROSSALL. Can. J. Chem. **49**, 1441 (1971).
4. G. WOLD. J. Phys. Chem. **76**, 369 (1972).
5. E. C. F. KO and R. E. ROBERTSON. J. Am. Chem. Soc. **94**, 573 (1972).
6. E. C. F. KO and R. E. ROBERTSON. Can. J. Chem. **50**, 946 (1972).
7. E. C. F. KO and R. E. ROBERTSON. Can. J. Chem. **50**, 434 (1972).
8. I. DOSTROVSKY and M. HALMANN. J. Chem. Soc. 502 (1953).
9. (*a*) H. K. HALL, JR. J. Org. Chem. **21**, 248 (1956). (*b*) H. K. HALL, JR. and C. H. LUECK. J. Org. Chem. **28**, 2818 (1963).
10. (*a*) E. W. CRUNDEN and R. F. HUDSON. Chem. & Ind. 748 (1959). (*b*) E. W. CRUNDEN and R. F. HUDSON. J. Chem. Soc. 3591 (1962).
11. P. S. TRAYLOR and F. H. WESTHEIMER. J. Am. Chem. Soc. **87**, 553 (1965).
12. R. E. ROBERTSON, B. ROSSALL, and S. E. SUGAMORI. Can. J. Chem. **47**, 4199 (1969).
13. O. ROGNÉ. J. Chem. Soc. B, 663 (1969).
14. R. E. ROBERTSON. Progr. Phys. Org. Chem. **4**, 213 (1967).
15. E. C. W. CLARKE and D. N. GLEW. Trans. Faraday Soc. **62**, 539 (1966).
16. R. E. ROBERTSON, B. ROSSALL, S. E. SUGAMORI, and L. TREINDL. Can. J. Chem. **47**, 4199 (1969).
17. C. K. INGOLD. The structure and mechanism of organic chemistry. Cornell University Press, Ithaca, N.Y. 1951. Chapt. VII.
18. K. M. KOSHY and R. E. ROBERTSON. Unpublished work.
19. P. M. LAUGHTON and R. E. ROBERTSON. Solute–solvent interactions. J. F. Coetzee and C. D. Ritchie, editors. Marcel Dekker, New York. 1969. Chapt. 7.
20. B. ROSSALL and R. E. ROBERTSON. Can. J. Chem. **49**, 1451 (1971).
21. J. O. EDWARDS and R. G. PEARSON. J. Am. Chem. Soc. **84**, 16 (1962).
22. A. L. GREEN, G. S. SAINSBURY, B. SAVILLE, and M. STANFIELD. J. Chem. Soc. 1583 (1958).
23. W. P. JENCKS. Catalysis in chemistry and enzymology. McGraw-Hill, New York. 1969. p. 107.
24. G. KLOPMAN, K. TSUDA, J. B. LOUIS, and R. E. DAVIS. Tetrahedron, **26**, 4549 (1970).
25. J. D. AUBART and R. F. HUDSON. Chem. Commun. 937 (1970).
26. B. LOEVAND and J. T. MASSENGALE. J. Org. Chem. **22**, 1186 (1957).
27. J. MURTO. Acta Chem. Scand. **20**, 310 (1966).
28. R. E. ROBERTSON, B. ROSSALL, S. E. SUGAMORI, and L. TREINDL. Can. J. Chem. **47**, 4199 (1969).

Can. J. Chem. Downloaded from www.nrcresearchpress.com by 210.87.254.42 on 09/05/12
For personal use only.

The Crystal Structure of *cis*-Dichloro(2,2′-oxydi-3-butene)platinum(II), $PtCl_2((CH_2{=}CH{-}CH(CH_3))_2O)$[1]

J. HUBERT, A. L. BEAUCHAMP, AND T. THEOPHANIDES

Département de Chimie, Université de Montréal, Montréal, Québec

Received July 24, 1972

The reaction of K_2PtCl_4 with $CH_3{-}CH{=}CH{-}CH_2{-}OH$ yields the complex *cis*-[$PtCl_2((CH_2{=}CH{-}CH(CH_3))_2O$)]. The crystals are triclinic, space group $P\bar{1}$, a = 9.420(2) Å, b = 8.359(4) Å, c = 7.837(4) Å, α = 91.10(4)°, β = 62.13(4)°, γ = 80.80(5)°, and Z = 2. The structure, solved by standard methods, has been refined anisotropically by full matrix least-squares methods to a R factor of 0.052 by use of 2441 independent observed reflections. The complex is a monomer, where both double bonds of the diolefin ether are coordinated to the platinum atom as in Zeise's salt. The usual square planar coordination of platinum(II) is completed by two chlorine atoms. The ($=CH_2$) groups of both double bonds are found on the same side of the coordination plane. Various possible conformations of the coordinated ligand in the complex are discussed.

Le complexe *cis*-[$PtCl_2((CH_2{=}CH{-}CH(CH_3))_2O$)] a été préparé par réaction de K_2PtCl_4 avec l'alcool crotylique $CH_3{-}CH{=}CH{-}CH_2{-}OH$. Les cristaux obtenus sont triclinique ($P\bar{1}$) et les paramètres cristallographiques suivants ont été obtenus: a = 9.420(2) Å, b = 8.359(4) Å, c = 7.837(4) Å, α = 91.10(4)°, β = 62.13 (4)°, γ = 80.80(5)°, et Z = 2. La structure a été résolue par la méthode de l'atome lourd et un affinement anisotrope par moindres carrés à matrice entière a conduit à un facteur R de 0.052. Le complexe est un monomère. L'éther dioléfinique est coordonné au platine par l'intermédiaire des deux doubles liaisons. La liaison entre le platine et la double liaison est du même type que celle rencontrée dans le sel de Zeise. La coordination du platine est complétée à quatre par deux atomes de chlore. Les deux groupements ($=CH_2$) sont situés d'un même côté par rapport au plan de coordination. Diverses conformations possibles du ligand dans le complexe sont discutées.

Can. J. Chem., **51**, 604 (1973)

Introduction

In their studies of the metal–olefin complexes, Hartley and Venanzi (1) have observed several interesting reactions of substituted olefins with potassium tetrachloroplatinate(II). In the case of unsaturated alcohols, the authors have noticed the occurrence of side reactions during the formation of the alcohol complex $[PtCl_3(alcohol)]^-$.

During the investigation of the reactions of K_2PtCl_4 with crotyl alcohol ($CH_3{-}CH{=}CH{-}CH_2{-}OH$), we found that one of the products is an ether complex of the formula $C_8H_{14}Cl_2OPt$.

A $PtCl_2$(allylether) has been previously prepared by Jensen (2) and described as a monomeric *cis* species. More recently, the above conclusions were confirmed by Jones (3) and the structure on Fig. 1 was proposed on the basis of n.m.r. studies. The ether ligand occupies two coordination sites and is linked to the platinum atom through the double bonds.

The ether complex prepared from crotyl alcohol gave stable single crystals and an X-ray analysis was undertaken in order to determine the nature of bonding and the configuration of the ligand.

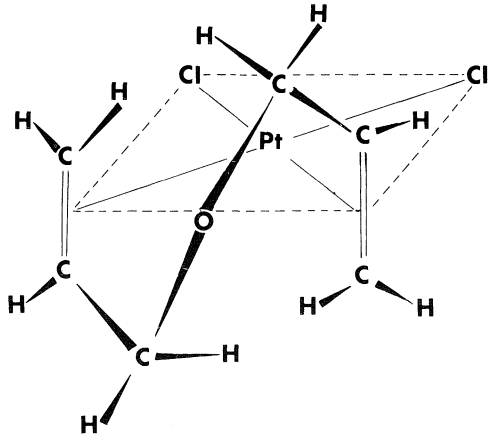

FIG. 1. Configuration proposed (3) for the *cis*-$PtCl_2$(allylether) complex.

Crystal data

$C_8H_{14}Cl_2OPt$ f.w. = 392.19

Triclinic, $P\bar{1}$, a = 9.420(2), b = 8.359(4), c = 7.837(4) Å, α = 91.10(4), β = 62.13(4), γ =

[1]Presented at the XIVth I.C.C.C. Conference, Toronto, Ontario, June 22–28, 1972.

Can. J. Chem. Downloaded from www.nrcresearchpress.com by 210.87.254.42 on 09/05/12
For personal use only.

TABLE 1. Final positional and thermal parameters* (e.s.d.'s) × 10^4

Atom	x/a	y/b	z/c	β_{11}	β_{22}	β_{33}	β_{12}	β_{13}	β_{23}
Pt	679.7(6)	2380.9(6)	40.9(7)	111.8(8)	117.2(8)	159.7(10)	−30.8(5)	−71.3(6)	23.5(5)
Cl(1)	80 (5)	1997 (5)	−2466 (5)	211 (6)	217 (7)	240 (8)	−89 (5)	−155 (6)	57 (6)
Cl(2)	−1945 (4)	3867 (5)	1912 (6)	125 (5)	187 (6)	289 (8)	4 (5)	−92 (5)	9 (6)
O	4205(11)	2312(11)	119(13)	145(15)	148(15)	224(20)	−17(12)	−104(15)	42(14)
C(1)	2662(16)	307(13)	−1296(20)	138(19)	75(15)	252(31)	−14(13)	−49(20)	12(16)
C(2)	3254(17)	1689(17)	−2139(20)	143(20)	146(20)	191(27)	−7(16)	−72(19)	43(18)
C(3)	4444(16)	2394(16)	−1827(19)	128(18)	158(20)	189(26)	−17(15)	−78(18)	37(18)
C(4)	6182(19)	1421(28)	−3161(25)	123(22)	354(44)	235(36)	1(25)	−63(24)	17(32)
C(5)	3019(17)	3699(15)	1406(19)	161(21)	127(18)	219(28)	−28(16)	−12(21)	32(18)
C(6)	3337(24)	3857(25)	3132(27)	233(33)	278(37)	293(41)	−92(28)	−17(32)	16(31)
C(7)	1274(17)	3490(18)	2157(18)	167(22)	178(22)	160(24)	−55(18)	−92(20)	12(19)
C(8)	760(15)	2063(16)	2705(17)	139(19)	156(20)	157(23)	−32(16)	−76(18)	37(17)

*Coefficients β_{ij} are defined by the expression $T = \exp[-10^{-4}(\beta_{11}h^2 + \beta_{22}k^2 + \beta_{33}l^2 + \beta_{12}hk + \beta_{13}hl + \beta_{23}kl)]$.

80.80(5)°, $V = 535.3$ Å^3, $Z = 2$, $\rho_c = 2.43$, $\rho_o = 2.33$ (flotation) at 20 °C, $\lambda MoK_{\bar{\alpha}} = 0.71068$ Å, $\lambda MoK_\beta = 0.63225$ Å, $\mu MoK_\alpha = 136.7$ cm^{-1}.

The above cell was used throughout the calculations. A conventional reduced cell of type I (angles < 90°), $a' = 7.837$ Å, $b' = 8.359$ Å, $c' = 9.007$ Å, $\alpha' = 79.40°$, $\beta' = 67.60°$, $\gamma' = 88.90°$ may be obtained by the following transformations: $a' = -c$, $b' = b$, $c' = a - c$, where the primed symbols refer to the conventional cell and the unprimed symbols to the cell used in the present work.

Experimental

The compound was synthesized by the reaction of potassium tetrachloroplatinate(II) (3 g) with an excess of crotyl alcohol (Matheson, Coleman, and Bell) (b.p. 120–122 °C) (3 ml) in 30 ml distilled water. The mixture was heated (50 °C) until the solution turned yellow. After two days a white precipitate was deposited from the clear solution. The analysis was consistent with the formula $C_8H_{14}Cl_2OPt$.

Anal. Calcd. for $C_8H_{14}Cl_2OPt$: Pt, 49.74; Cl, 18.08; C, 24.48; H, 3.57. Found: Pt, 50.00; Cl, 17.96; C, 25.01; H, 3.45.

The complex is monomeric in chloroform and non electrolyte in nitromethane.

A colorless prism with dimensions 0.160 × 0.125 × 0.095 mm was found suitable for the X-ray work. The crystals are stable in air. From precession photographs, they were found to be triclinic ($P1$ or $P\bar{1}$). The measured density corresponds to two formula units per unit cell.

The intensity data were measured on an automatic Picker FACS-1 diffractometer by using Zr-filtered MoK_α radiation. The orientation matrix and the cell constants with their estimated standard deviations were obtained by a least-squares refinement on the χ, Φ, 2θ values for 12 independent reflections. The $\theta/2\theta$ scan method was used. Each peak was scanned at a 1°(2θ)/min rate over an average range of 1.75°. Stationary background counts of 20 s were taken at each limit of the scan. Periodic check of the 061, 510, and $\bar{1}14$ reflections indicated a slow decomposition of the crystal (total intensity decrease of 8%). This effect was taken into account when the reflections were scaled on the standards in the data reduction program. The integrated intensities of 3168 independent reflections within a sphere of $2\theta < 60°$ were measured. Reflections (727) with net intensities less than 3σ (total peak count + total background count) were considered as unobserved. An absorption correction based on the equations of the crystal faces (18) was applied and each intensity was corrected for Lorentz and polarization effects.

Structure Determination

The $P\bar{1}$ group was assumed and the coordinates of the platinum atom were obtained from the Patterson map. All other atoms except hydrogens were located by structure factor and Fourier map calculations. The parameters were refined by full-matrix least-squares. The scattering factors used were those of Cromer and Waber (4). The anomalous dispersion factors $\Delta f'$ and $\Delta f''$ of platinum and chlorine (5) were included in the calculations. Only the observed reflections were used in the calculations. Isotropic refinement with unit weights converged to an R factor of 0.088. The structure was then refined anisotropically and each reflection was assigned an individual weight w based on the eq. (6): $w = a + bF_o + cF_o^2$, where $a = 15.0$, $b = -0.794$, and $c = 0.0115$. This weighting scheme yielded minimum variations of the average weighted residual as a function of F_o and $\sin\theta/\lambda$. The refinement of the scale factor, the coordinates and the anisotropic temperature factors of all the atoms except the hydrogens resulted in a residual $R = \Sigma(|F_o| - |F_c|)/\Sigma|F_o|$ of 0.052 and a weighted residual $R_w = [\Sigma w(|F_o| - |F_c|)^2/\Sigma w|F_o|^2]^{1/2}$ of 0.065. On the final difference Fourier map, the residual electron density was less than 0.8 e/Å^3 (except for three peaks of 1.5 e/Å^3 near the platinum atom), the peak height of an average carbon atom in this analysis being 6 e/Å^3. The refined parameters are given in Table 1. The programs used are described elsewhere (7).[2]

[2]The structure factor table is available, at a nominal charge, from the Depository of Unpublished Data, National Science Library, National Research Council of Canada, Ottawa, Canada, K1A 0S2.

Can. J. Chem. Downloaded from www.nrcresearchpress.com by 210.87.254.42 on 09/05/12
For personal use only.

TABLE 2. Interatomic distances and bond angles, with estimated standard deviations*

Bond	Distances (Å)	Bonds	Angle(deg)
Pt—Cl(1)	2.314(5)	Cl(1)—Pt—Cl(2)	89.3(1)
Pt—Cl(2)	2.316(8)	Cl(1)—Pt—C(1)	88.7(4)
Pt—C(1)	2.176(25)	Cl(1)—Pt—C(2)	86.7(4)
Pt—C(2)	2.183(32)	Cl(1)—Pt—C(7)	162.8(4)
Pt—C(7)	2.202(18)	Cl(1)—Pt—C(8)	159.9(4)
Pt—C(8)	2.147(15)	Cl(2)—Pt—C(1)	159.6(4)
O—C(3)	1.435(24)	Cl(2)—Pt—C(2)	162.0(4)
O—C(5)	1.446(34)	Cl(2)—Pt—C(7)	86.1(5)
C(1)—C(2)	1.406(27)	Cl(2)—Pt—C(8)	87.0(4)
C(2)—C(3)	1.458(25)	C(3)—O—C(5)	111.0(10)
C(3)—C(4)	1.542(49)	C(1)—C(2)—C(3)	123.1(14)
C(5)—C(6)	1.527(31)	C(2)—C(3)—C(4)	109.9(13)
C(5)—C(7)	1.506(35)	O—C(3)—C(2)	112.6(12)
C(7)—C(8)	1.359(25)	O—C(3)—C(4)	105.6(12)
Pt—Z(1–2)	2.069(45)	O—C(5)—C(6)	106.2(13)
Pt—Z(7–8)	2.056(40)	O—C(5)—C(7)	113.4(12)
		C(6)—C(5)—C(7)	108.2(13)
		C(5)—C(7)—C(8)	123.7(13)
		Z(1–2)—Pt—Cl(1)	87.6(4)
		Z(1–2)—Pt—Cl(2)	176.6(4)
		Z(7–8)—Pt—Cl(1)	175.4(4)
		Z(7–8)—Pt—Cl(2)	86.3(4)
		Z(1–2)—Pt—C(1)	89.2(5)
		Z(7–8)—Pt—C(8)	88.4(5)

*Z(1–2) defines the midpoint of C(1)—C(2); Z(7–8) defines the midpoint of C(7)—C(8).

Results and Discussion

The crystal structure is made up from isolated *cis*-Pt(ether)Cl_2 molecules, where the diolefin acts as a bidentate ligand (Fig. 2). The diolefin ligand is not the expected dicrotylether (CH_3—CH=CH—$CH_2)_2O$. Instead, the organic moiety is the 2,2′-oxydi-3-butene, which was obtained by isomerization and condensation (whatever the actual mechanism might be) of the original alcohol. To our knowledge, it is the first time that such an isomerization is observed during complex formation.

The chlorine atoms and the midpoints of the double bonds are arranged in a nearly square planar geometry. The angles around platinum are all close to 90° or 180° (Table 2) and the midpoints Z(1–2) (of C(1)—C(2)) and Z(7–8) (of C(7)—C(8)) are less than 0.01 Å from the Pt—Cl(1)—Cl(2) plane.

The Pt—Cl distances (2.314, 2.316 Å) are identical. They fall within the range of normal platinum–chlorine bond lengths (2.30–2.34 Å) observed in similar complexes (8–10). The π-bonding olefin does not seem to exercise any *trans*-bond-lengthening effect. The same Pt—Cl distance has been recently reported for K_2PtCl_4 (11).

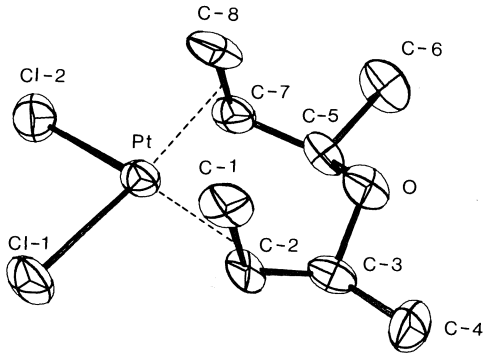

FIG. 2. Structure found for the *cis*-dichloro-(2,2′-oxydi-3-butene)platinum(II) complex.

The C(1)—C(2) (1.41(3) Å) and C(7)—C(8) (1.36(3) Å) distances are typical of those of olefins linked to platinum (8). They seem to be slightly larger than those of monosubstituted ethylene molecules (1.34–1.35 Å(12)), but these differences are not very significant. Both double bonds are nearly perpendicular to the Pt—Cl(1)—Cl(2)—Z(1–2)—Z(7–8) plane. The values obtained for ∠Pt—Z(1–2)—C(1) (89°) and ∠Pt—Z(7–8)—C(8) (88°) are very close to 90° and the dihedral angles between the Pt—Cl(1)—Cl(2) planes are 93° and 92°, respectively. The small

Can. J. Chem. Downloaded from www.nrcresearchpress.com by 210.87.254.42 on 09/05/12
For personal use only.

TABLE 3. Bond lengths and dihedral angles of platinum olefin complexes

Species	Double bond lengths (C=C)	Dihedral angles (Pt—C=C/C=C—C)	References
Propene	1.353	—	12
$[PtCl_3(C_2H_4)]^-$	1.354(15)	101	13
$PtCl_3(cis\text{-}C_4H_{10}N)$	1.40(4)	113	14
$PtCl_3(trans\text{-}C_4H_{10}N)$	1.40(4)	122 112	15
$[PtCl_3(trans\text{-}C_4H_{12}N_2)]^+$	1.416(12)	94 110	8
$[PtCl_3(cis\text{-}C_4H_8O_2)]^-$	1.40(4)	107 97	16
$PtCl_2(C_{10}H_{16})$	1.56(5) 1.53(5)	101 102 103 106	17
$PtCl_2(C_{10}H_{14}O_3)$	1.44(3) 1.39(3)	107 104 105 100	10
$PtCl_2(C_8H_{14}O)$	1.41(3) 1.36(3)	109 109	This work

distortions are probably due to packing effects and to steric constraints introduced by the rest of the ligand.

Normal values are observed for the other interatomic distances and bond angles in the coordinated ligand. The intermolecular contacts are all at least equal to the sum of the van der Waals radii.

Neutron diffraction work on Zeise's salt has shown that the hydrogen atoms are displaced away from the platinum atom and that the dihedral angles between the Pt—C—C plane and the four C—C—H planes average 101°. For an undistorted ethylene molecule in the complex, these angles would be 90°.

In the present work, dihedral angles of 109° were found between the platinum – double bond planes and the α-carbon – double bond planes (Pt—C(1)—C(2)/C(1)—C(2)—C(3) and Pt—C(7)—C(8)/C(7)—C(8)—C(5)). Although the hydrogen atoms of the double bonds could not be located, the latter dihedral angles are consistent with the structural changes taking place in the Zeise's salt. The dihedral angles and the "double bond" lengths for olefinic complexes are summarized in Table 3. It appears that these angles reflect better than the bond lengths the perturbation of the double bond on coordination.

In the *cis*-Pt(diolefin)Cl_2 molecule, the ether is the *meso* isomer and its two halves are related by an approximate mirror plane perpendicular to the coordination plane. The (=CH_2) groups of the ligand are both on the same side of the Pt—Cl(1)—Cl(2) plane. The "twisted" conformation (Fig. 1) with the two (=CH_2) groups on opposite sides of the coordination plane has been proposed by Jones (3) for the corresponding Pt(diallylether)Cl_2 complex. His conclusions were reached from solution n.m.r. spectra. Stuart molecular models of both conformations show that the present structure is favored by the following factors: (*i*) the nearly square planar geometry around the platinum atom is preserved, (*ii*) the bond angles in the ligand are not appreciably strained, and (*iii*) both "double bonds" are perpendicular to the Pt—Cl(1)—Cl(2) plane.

An interesting feature of the structure observed here is the possible existence of several isomers and conformers. Depending on the position of the oxygen with respect to the C(2)—C(3)—C(5)—C(7) plane two basic conformations are expected for the bridging ether in the complex, *i.e.*, a *boat* form (Fig. 3*a*) and a *chair* form (Fig. 3*b*). The distribution of the methyl groups on the axial (a_1,a_2) and equatorial (e_1,e_2) positions leads us to two *meso* isomers and a pair of optical

Can. J. Chem. Downloaded from www.nrcresearchpress.com by 210.87.254.42 on 09/05/12
For personal use only.

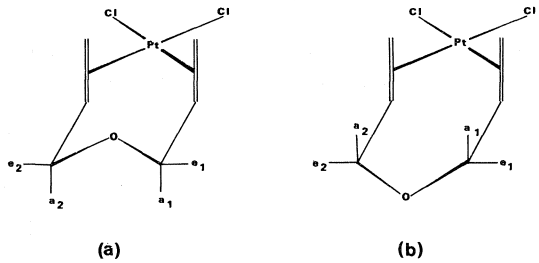

FIG. 3. Drawings of the two main conformers obtained by changing the position of the oxygen with respect to the C(2)—C(3)—C(5)—C(7) plane, in the *cis*-[$PtCl_2$(diolefinether)] complex.

TABLE 4. Possible isomers and conformers of the diolefin ether platinum(II) complex

Isomer	Conformer	a_1	a_2	e_1	e_2
meso I	Boat	H	H	CH_3	CH_3
	Chair	CH_3	CH_3	H	H
meso II	Boat	CH_3	CH_3	H	H
	Chair	H	H	CH_3	CH_3
d,l	Boat	CH_3	H	CH_3	H
		H	CH_3	H	CH_3
	Chair	CH_3	H	CH_3	H
		H	CH_3	H	CH_3

isomers, each of which might adopt both *boat* and *chair* conformations (Table 4).

For a given isomer the two conformations are not equally likely and a molecular model indicates that the interaction between the axial groups a_1,a_2 is a determining factor. On that basis, the *chair* form of meso I and the *boat* form of meso II are highly unlikely because of the close contact of the methyl groups in axial positions. An important interaction is also evident from the model between one methyl group and one hydrogen in axial positions for the boat and chair forms the *d* (or *l*) isomer. The least interaction is found in the cases of *boat* form of meso I and *chair* form of meso II. The *boat* form of meso I was found in this work, but there is no obvious reason for the non-existence of the *chair* form of meso II.

The n.m.r. spectra of the present diolefin complex are under study and our conclusions on the structures of the complex in solution and the reaction mechanisms will be published later.

The financial assistance of the National Research Council of Canada and the loan of platinum salts by the Johnson Matthey and Mallory Co. Ltd. is greatly appreciated.

1. F. R. HARTLEY and L. M. VENANZI. J. Chem. Soc. A, 330 (1967).
2. K. A. JENSEN. Acta Chem. Scand. **7**, 866 (1953).
3. R. JONES. J. Chem. Soc. A, 2477 (1969).
4. D. T. CROMER and J. T. WABER. Acta Cryst. **18**, 104 (1965).
5. D. T. CROMER. Acta Cryst. **18**, 17 (1965).
6. D. W. CRUICKSHANK. Computing methods in crystallography. Pergamon Press. 1965. p. 114.
7. A. L. BEAUCHAMP and D. GOUTIER. Can. J. Chem. **50**, 977 (1972).
8. R. SPAGNA and L. ZAMBONELLI. J. Chem. Soc. A, 2544 (1971).
9. P. G. OWSTON, J. A. JARVIS, and B. T. KILBOURN. Acta Cryst. **B27**, 366 (1971).
10. R. MASON and G. B. ROBERTSON. J. Chem. Soc. A, 492 (1969).
11. R. H. B. MAIS, P. G. OWSTON, and A. M. WOOD. Acta Cryst. **B28**, 393 (1972).
12. Tables of interatomic distances and configurations in molecules and ions. Special Publications Nos. 11 and 18. The Chemical Society of London. 1958. 1965.
13. W. C. HAMILTON. Acta Cryst. **A25**, S172 (1969).
14. R. SPAGNA, L. M. VENANZI, and L. ZAMBONELLI. Inorg. Chim. Acta, **4**, 475 (1970).
15. R. SPAGNA, L. M. VENANZI, and L. ZAMBONELLI. Inorg. Chim. Acta, **4**, 283 (1971).
16. L. ZAMBONELLI and M. COLAPIETRO. Acta Cryst. **B27**, 734 (1971).
17. N. C. BAENZIGER, R. C. MEDRUD, and J. R. DOYLE. Acta Cryst. **18**, 237 (1965).
18. W. R. BUSING and H. A. LEVY. Acta Cryst. **10**, 180 (1957).

Can. J. Chem. Downloaded from www.nrcresearchpress.com by 210.87.254.42 on 09/05/12
For personal use only.

Vibrational Spectra, Vibrational Analysis and Stereochemistries of the Pentacoordinate Molecules $SiCl_3X \cdot N(CH_3)_3$ and $SiCl_3X \cdot N(CD_3)_3$ where X = H, F, Br, or I

D. Boal and G. A. Ozin[1]

Lash Miller Chemistry Laboratory and Erindale College, University of Toronto, Toronto, Ontario

Received June 27, 1972

The thermally unstable compounds $SiCl_3X.N(CH_3)_3$ and $SiCl_3X.N(CD_3)_3$ where X=H, F, Br, or I are studied at −196 °C by infrared and Raman spectroscopy. The data are compatible with molecular five coordinate compounds having a trigonal bipyramidal stereochemistry with the ligand trimethylamine always in the axial position. Using the vibrational data and normal coordinate analyses in both the C_s and C_{3v} configurations, X is suggested to be equatorial for H and F and axial for Br and I. The factors influencing the position of X in the compounds are discussed.

Les composés thermiquement instables $SiCl_3X.N(CH_3)_3$ et $SiCl_3X.N(CD_3)_3$ où X=H, F, Br, où I ont été étudiés à −190 °C par spectroscopie infrarouge et Raman. Les résultats peuvent être attribués à des composés moléculaires de coordination cinq (5) possédant une stéréochimie bipyramidale trigonale avec le coordinat triméthylamine toujours en position axiale. En utilisant les données vibrationnelles et les analyses en coordonnées normales pour les configurations C_s et C_{3v}, on peut supposer que X est équatorial pour H et F, axial pour Br et I. Les facteurs influençant la position de X dans les composés sont discutés.
[Traduit par le journal]

Can. J. Chem., **51**, 609 (1973)

Introduction

Stereochemical information for the compounds $SiCl_3X.NMe_3$ where X = H, F, Br, or I have not previously been reported although the existence of the hydride and fluoride has been known for some time (1, 2). The compounds are found to be stable at −196 °C, yet completely dissociated into free halide and amine at room temperature. Dissociation pressure measurements have been reported for the series $SiCl_nH_{4-n}.NMe_3$ and $SiCl_nF_{4-n}.NMe_3$ where the results indicated the influence of steric and electronegativity effects on the stability order of the molecules (3, 4). With recent improvements in low temperature infrared and Raman techniques, there has been renewed interest in vibrational and structural studies of unstable co-ordination compounds.

In an attempt to study these complexes, it was assumed that the basic shape at silicon was trigonal bipyramidal, with the trimethylamine ligand lying axially. Vibrational and single crystal Raman spectra and x-ray data (5, 6) for the complexes $MX_4.NMe_3$ (M = Si, Ge, or Sn and X = F or Cl), $MX_3.2NMe_3$ (M = Al, Ga, or In and X = H, Cl, or Br) and $MX_3.NMe_3$ (M = P or As and X = Cl or Br) have been reported and the evidence is overwhelmingly in favor of the amine lying axially. Assuming this, the question is then whether the X atom will reside in the equatorial or axial position for the series $SiCl_3X.NMe_3$. An argument has been put forward (7) that for trigonal bipyramidal molecules, the most electropositive atom will lie in the equatorial plane and hence one would expect to find Cl, F, Cl, and Cl in the axial positions for the series X = H, F, Br, and I. If the trimethylamine ligand were sterically bulky enough to crowd the atoms in the equatorial plane, then one might expect to find Cl, Cl, Br, and I for the same series. A third hypothesis based on molecular orbital theory is put forward in this paper, and leads to the same predictions as the steric argument. By examining the vibrational spectra of the complexes and their perdeutero analogs, it was found that the axial atoms were Cl, Cl, Br, and I for the series X = H, F, Br, and I.

Before going into detail, it is worthwhile to discuss the spectrum of the parent molecule $SiCl_4.NMe_3$ (8, 9), which has been reported to have C_{3v} symmetry with the trimethylamine ligand in the axial position. Its spectrum is very close to that of $GeCl_4.NMe_3$ which has been shown from single crystal Raman (9) and X-ray (10) data to have the above structure. The vibrational spectrum is easily divided into ligand and acceptor modes (9), the former experiencing

[1]To whom correspondence should be addressed.

Can. J. Chem. Downloaded from www.nrcresearchpress.com by 210.87.254.6 on 09/05/12
For personal use only.

Can. J. Chem. Downloaded from www.nrcresearchpress.com by 210.87.254.6 on 09/05/12
For personal use only.

50–80 cm^{-1} shifts upon deuteration of the trimethylamine. The Si—Cl stretching modes are easily discernible because of their much smaller shifts upon deuteration. The asymmetric E mode of the equatorial chlorines is found at 582 cm^{-1} (high frequency), being strong in the infrared and weak in the Raman. The symmetrical A_1 of the equatorial chlorines comes at low frequency, 361 cm^{-1}, and is strong in the Raman. This low frequency (300–380 cm^{-1}) mode is common for light central metal atoms, for example, aluminum, silicon, and phosphorus. The other A_1 mode involves the axial silicon–chlorine stretch. This mode, because it contains motion of the silicon atom (whereas the other A_1 does not), is expected to come at higher frequencies, and indeed is observed at 385 cm^{-1}. It is significant to note that in the vibrational analysis of this complex, the axial stretching force constant was found to have one half the value of the equatorial one. In addition, the crystal structure of $AsCl_3.NMe_3$ (12) (which is based on a trigonal bipyramid with an equatorial lone pair) and $GeCl_4.NMe_3$ (10) shows the axial bond to be significantly longer than the equatorial one. The trimethylamine complex with $SiCl_3X$ can then have two possible stereochemistries

A (C_{3v})

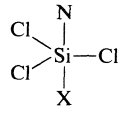

$$\Gamma_{vib}^{\nu SiCl} = A_1 + E$$

B (C_s)

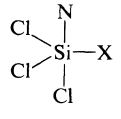

$$\Gamma_{vib}^{\nu SiCl} = 2A' + A$$

In configuration A, one would expect to find only one strong Raman peak in the Si—Cl stretching region due to the A_1 mode at about 370 cm^{-1}, as with monomeric $AlCl_3$ (11) (371 cm^{-1}). In B, however, there should be an A' mode due to the axial stretch above 380 cm^{-1}, and another A' mode having frequency greater than 400 cm^{-1} (the high frequency caused by both the motion of the silicon atom and the higher equatorial force constant compared to the axial one).

On the basis of the silicon–chlorine symmetric stretches, the stereochemistries were assigned. The perdeutero analogs were prepared to distinguish donor from acceptor modes, and normal coordinate calculations on each possible configuration were carried out.

$SiCl_3H.NMe_3$ and $SiCl_3F.NMe_3$

The spectra, observed and calculated, are tabulated in Tables 1 and 2. Both molecules show no silicon–chlorine stretching frequencies below 400 cm^{-1}, but rather two *high* frequency modes in the Raman. This strongly favors the hydrogen and fluorine atoms occupying the equatorial positions.

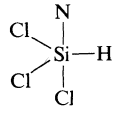

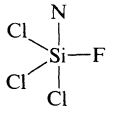

νSiCl	588 cm^{-1} A''	νSiCl	580 cm^{-1} A''
	517 cm^{-1} A'		460 cm^{-1} A'
	489 cm^{-1} A'		424 cm^{-1} A'

No serious attempt is made to assign the region under 300 cm^{-1} as the spectrum is far too complex (also indicating C_s symmetry). The low frequency calculated for the silicon–chlorine axial stretch in $SiCl_3H.NMe_3$ is due simply because of the very low force constant. If this force constant was raised to 3/4 of the equatorial, one obtains a frequency in the region observed. The calculations for a C_{3v} configuration are shown in Table 3. The Si—Cl stretching frequency calculated is significantly lower than that observed, and in order to raise this calculated value to even 470 cm^{-1}, a force constant of about double the $SiCl_4$ value must be employed. Clearly this is unacceptable since the $SiCl_4$ force constant should decrease, not increase, upon coordination. The C_{3v} model is also unable to explain the presence of two high frequency SiCl stretching modes; it predicts only one.

$SiCl_3Br.NMe_3$ and $SiCl_3I.NMe_3$

The spectra for these complexes are very different from the previous two (Tables 4 and 5). Both show only one strong band in the *low* frequency silicon–chlorine stretching region at about 370 cm^{-1}, and no acceptor modes between 400–550 cm^{-1}.

Evidence against an ionic formulation [$SiCl_3.NMe_3^+$] [X^-] for the bromide and iodide adducts stems from three observations: (*i*) the observed νSiBr and νSiI (382 and 332 cm^{-1} respectively) stretching modes are far too high and indicate normal covalently bonded halogen; (*ii*) the a_1 and e νSiCl frequencies for a "pyrami-

TABLE 1. Vibrational spectrum of $SiCl_3H.NMe_3$*

$SiCl_3H.N(CH_3)_3$† Raman (solid at −196 °C)	$SiCl_3H.N(CD_3)_3$† Raman (solid at −196 °C)	Calculated‡ $SiCl_3H.N(CH_3)_3$	Approximate description of mode
588vvw	—	593	A'' $\nu SiCl_{eq}$
517s br	*522mw*	508	A' $\nu SiCl_{eq}$
		545	A' δNMe_3
489ms	*492s*	434	A' $\nu SiCl_{ax}$
435m	434w	430	$A' + A''$ δNMe_3
		425	A' $\delta N(CD_3)_3$
423w sh			A' $\delta N(CD_3)_3$
	378w	396	A'' $\delta N(CD_3)_3$
346mw	331m		
322mw			
305w			
	296mw		
280mw			
	268mw		
252w sh	252mw		
243mw			
226ms	222ms		
	217ms		
213ms			
	192mw		
154w			
	148w		
113m			
	107m		

*Frequencies are reported in units of cm^{-1}.
†Metal–halogen skeletal stretching modes are in italics.
‡Only the Si—Cl stretching and NMe_3 deformation region is shown in the calculations.

TABLE 2. Vibrational spectrum of $SiCl_3F.NMe_3$*

$SiCl_3F.N(CH_3)_3$†		$SiCl_3F.N(CD_3)_3$†	Calculated‡	Approximate
Infrared	Raman	Raman	$SiCl_3F.N(CH_3)_3$	description of mode
857s	*868w*	*869mw*	984	A' νSiF
578vs	*580vw*	*582vw*	648	A'' $\nu SiCl_{eq}$
538m	535mw		581	A' δNMe_3
460vw	*460mw*	*464ms*	469	A' $\nu SiCl_{eq}$
			430	A''
	442w		429	A' $\delta NMe_3 + A'\delta N(CD_3)_3$
	424vs	*430vs*	434	A' $\nu SiCl_{ax}$
390s				
		392mw	396	A' $\delta N(CD_3)_3$
	378w	379w sh		
360s		362vw		
	330mw	302w br		
283w				
	268w			
254w	250mw	255m		
235w	236mw			
	225mw	223ms br		

*Frequencies are reported in units of cm^{-1}.
†Metal–halogen skeletal stretching modes are in italics.
‡Because of C_s symmetry, the region below 400 cm^{-1} is very complex and is therefore not assigned.

Can. J. Chem. Downloaded from www.nrcresearchpress.com by 210.87.254.6 on 09/05/12
For personal use only.

TABLE 3. Calculated frequencies for $SiCl_3X.NMe_3$ (X=H and F), C_{3v} symmetry*

$SiCl_3H.NMe_3$			$SiCl_3F.NMe_3$		
*H*9	Approximate description of mode	*D*9	*H*9	Approximate description of mode	*D*9
612	*E* νSiCl	612	643	*E* νSiCl	643
563	A_1 δNMe_3	532	545	A_1 δNMe_3	515
430	*E* δNMe_3	396	430	*E* δNMe_3	396
376	A_1 νSiCl	376	378	A_1 νSiCl	378
334	A_1 νSiN	328			
			269	A_1 νSiN	263
247	*E* $\rho_r NMe_3$	231	249	*E* $\rho_r NMe_3$	236
			218	*E* δFSiCl	215
161	*E* δSiCl i.p.	160			
			156	*E* δSiCl i.p.	155
135	A_1 δSiCl o.p.	130	134	A_1 δSiCl o.p.	129
84	*E* δNSiCl	82	81	*E* δNSiCl	79

*Frequencies are reported in units of cm^{-1}; i.p. = in plane, o.p. = out of plane.

TABLE 4. Vibrational spectrum of $SiCl_3Br.NMe_3$*

$SiCl_3Br.N(CH_3)_3$†		$SiCl_3Br.N(CD_3)_3$†	Calculated for C_{3v} symmetry		
Infrared	Raman	Raman	*H*9	*D*9	Assignment
580vs	*580vw*‡	*576vw*‡	636	635	*E* νSiCl
	570vw‡	*567vw*‡			
537m	539w		572	542	A_1 δNMe_3
	451w	452w	430	396	*E* δNMe_3 + $A_1\delta N(CD_3)_3$
386s	*384w*	*382w*	415	410	A_1 νSiBr§
367s	*369s*	*368s*	372	370	A_1 νSiCl§ + $E\delta N(CD_3)_3$
	342w				
		326w			
300ms	312w				
	293w	290w br			
			248	230	*E* $\rho_r NMe_3$
	228mw	221mw			
	207m	209mw			
	193w	190w			
	179ms	170ms	166	165	*E*
	161w		155	147	A_1
		136w	126	125	*E*
	103m		132	122	A_1
	96m	95m br	70	68	*E*

*Frequencies reported in cm^{-1}.
†Metal–halogen skeletal stretching modes are in italics.
‡Split degeneracy in solid.
§Very mixed modes.

dal'' C_{3v} $SiCl_3$ residue in $[SiCl_3.NMe_3^+]$ are calculated to be in the range 500–460 cm^{-1} (*c.f.* ν_1 (507 cm^{-1}) and ν_3 (494 cm^{-1}) of PCl_3) considerably higher than the observed a_1 νSiCl frequency (374–369 cm^{-1}) which is more consistent with a ''planar'' $SiCl_3$ residue in a molecular adduct $SiCl_3X.NMe_3$; (*iii*) point (*ii*) would be further emphasized by the presence of a positive charge on the cation.

On the basis of the experimental data, a molecular pentacoordinate (C_{3v}) formulation is preferred as shown below:

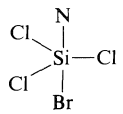

νSiCl 580 cm^{-1} *E*
369 cm^{-1} A_1

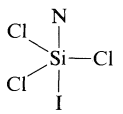

νSiCl 605 cm^{-1} *E*
374 cm^{-1} A_1

Can. J. Chem. Downloaded from www.nrcresearchpress.com by 210.87.254.6 on 09/05/12
For personal use only.

TABLE 5. Vibrational spectrum of $SiCl_3I.NMe_3$*

$SiCl_3I.N(CH_3)_3$†		$SiCl_3I.N(CD_3)_3$†	Calculated for C_{3v} symmetry		Approximate description
Infrared	Raman	Raman	*H*9	*D*9	of mode
604s br	*605vvw*	*597w br*	634	634	*E* νSiCl
	544w		569	539	A_1 δNMe_3
		→ 464w br			A_1 $\delta N(CD_3)_3$
	453w		430	396	*E* δNMe_3
		→ 393w			*E* $\delta N(CD_3)_3$
375w	*374s*	*371mw*	365	362	A_1 νSiCl
334s	*329ms*	*332s*	399	396	A_1 νSiCl + νSiI‡
281m	285vvw		247	232	*E* $\rho_r NMe_3$
240w		235vw			
213mw	215ms	217w	164	163	*E*
		197mw			
	168ms	166ms	142	134	A_1
			118	118	*E*
	109w		101	101	A_1
			66	64	*E*

*Frequencies are reported in units of cm^{-1}.
†Metal–halogen skeletal stretching modes are in italics.
‡Very mixed modes.

The calculations (Tables 4 and 5) give a very good match for C_{3v} symmetry, but a poor one for C_s. In the latter geometry, the bands were predicted to come at frequencies greater than 400 cm^{-1} as with the previous complexes, and very low force constants would have to be used to bring the frequencies down to 370 cm^{-1}.

Discussion

Having defined the configurations of the molecules $SiCl_3X.NMe_3$, it is necessary to discuss the various factors which may influence the change in stereochemistry from C_s for X = H or F to C_{3v} for X = Br and I. It has been found that for trigonal bipyramidal trimethylamine complexes (5, 6, 10, 12), the bulky NMe_3 grouping adopts an axial staggered configuration with respect to the rest of the molecule. A staggered

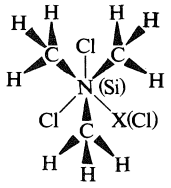

configuration of the ligand would of course present the least amount of steric strain to the molecule.

An estimate of the degree of "ligand hydrogen – equatorial halogen" steric interaction (illustrated below) can be determined from a molecular model of $SiCl_3X.NMe_3$, based on a trigonal bipyramidal stereochemistry, having an axial staggered NMe_3 with respect to a coplanar arrangement of equatorial atoms. Placing the atom X = H, F, Cl, Br, or I in either the axial or equatorial sites, assuming tetrahedral angles at N and C and using single bond covalent radii, the maximum distances of H····X closest approach were calculated.

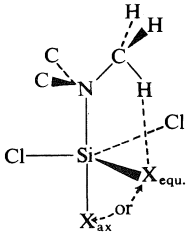

The computed H····X distances were all larger than a H—X single bond distance although the bromide H····Br (2.46 Å) and iodide H····I (2.56 Å) distances were considerably shorter than the corresponding Van der Waal's distances, 3.15 and 3.35 Å respectively.

From simple steric arguments one would tend to favor equatorial H and F atoms but axial Br and I atoms which is in agreement with our experimental observations. It is perhaps interesting to note that intramolecular ligand hydrogen – equatorial fluorine (H····F) hydrogen bonding would also probably favor an equatorial F atom in $SiCl_3F.NMe_3$.

Can. J. Chem. Downloaded from www.nrcresearchpress.com by 210.87.254.6 on 09/05/12
For personal use only.

Can. J. Chem. Downloaded from www.nrcresearchpress.com by 210.87.254.6 on 09/05/12
For personal use only.

A semi-quantitative molecular orbital approach which can be considered when discussing the configurations of these trigonal bipyramidal molecules involves the energy gain on combining the orbitals of atom X and those of the central silicon atom. The sp^3d hybridized orbitals on the central atom of the trigonal bipyramidal molecule have been considered to be approximately divided into two orbital sets (7); axial linear pd hybrids and equatorial planar sp^2 hybrids. If the greatest energy to be gained by combining two orbitals occurs when the orbitals are evenly matched in energy, it is appropriate to consider as a first approximation the valence state ionization potentials (13) of the combining atom X = H, F, Br, and I and compare them with the values for the pd axial and sp^2 equatorial orbitals on silicon shown in Scheme 1. This

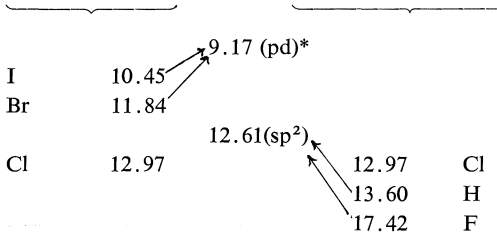

*In this approximation $E(pd) \simeq E(p_z)$.

SCHEME 1

simple scheme predicts that equatorial H and F atoms and an axial I atom are energetically favored in $SiCl_3X.NMe_3$, which agrees with our experimental observation and favors the geometries predicted from simple steric arguments. Although the fate of bromine is not clear cut on this scheme, perhaps the steric effect of Br predominates to favor the axial position.

Normal Coordinate Analysis For $SiCl_3X.NMe_3$ in C_s and C_{3v} Symmetry

The bond lengths used are listed in Table 6; the equatorial bond length is taken as the SiX_4 length while the axial one is taken as being 5% longer, in anticipation of the weakness of the axial bond, and in accordance with the $AsCl_3.NMe_3$ and $GeCl_4.NMe_3$ X-ray data (10, 12). The silicon–nitrogen length is set at 2.01 Å. The methyl groups were treated as point masses. The internal and symmetry coordinates are shown in the appendix.

The force field for the calculations on $SiCl_3X.NMe_3$ was assumed to be roughly the same as the previously published $SiCl_4.NMe_3$. The equatorial stretching force constants were set equal to the parent SiX_4 stretching constants while the axial stretching constants were given half this value. The f_β in the C_{3v} configuration was the average of the $SiCl_4$ and SiX_4 angle bending force constants and varied for each X. The f_α was given the same value as the parent SiX_4 molecule, in this case, $SiCl_4$. The f_γ was set at 3/4 of the f_α. The stretching

TABLE 6. Bond distances used in vibrational analysis

Bond	Distance (Å)
Si—N	2.01
N—Me	1.47
Si—H_{eq}	1.47
Si—H_{ax}	1.54
Si—F_{eq}	1.54
Si—F_{ax}	1.62
Si—Cl_{eq}	2.01
Si—Cl_{ax}	2.11
Si—Br_{eq}	2.28
Si—Br_{ax}	2.40
Si—I_{eq}	2.46
Si—I_{ax}	2.58

TABLE 7. Force constants for $SiCl_3X.NMe_3$ (C_{3v})

	Value for X =			
Force constant*	H	F	Br	I
f_R	2.70	2.70	2.70	2.70
f_D	1.35	3.05	0.98	0.70
f_d	1.20	1.20	1.20	1.20
f_{RR}	0.15	0.15	0.15	0.15
f_{RD}	0.15	0.15	0.15	0.15
f_α	0.489	0.489	0.489	0.489
f_β	0.648	0.665	0.669	0.642
f_γ	0.367	0.367	0.367	0.367
f_l	4.86	4.86	4.86	4.86
f_δ	1.010	1.010	1.010	1.010
$f_{\gamma'}$	0.638	0.638	0.638	0.638
$f_{l\delta}$	0.065	0.065	0.065	0.065

*In units of mdyn/Å, and mdyn/rad or mdyn Å/rad².

TABLE 8. Force constant* changes for $SiCl_3X.NMe_3$ (C_s)

X	f_R	f_r	f_D
H	2.70	1.35	2.70
F	2.70	1.35	6.11
Br	2.70	1.35	1.96
I	2.70	1.35	1.40

*In units of mdyn/Å, mdyn/rad, or mdyn Å/rad².

force constant for the Si–N bond was arbitrarily set at 1.20 mdyn/Å. The actual numbers used in the C_{3v} calculations are shown in Table 7. Only the stretching force constants changed in going to C_s symmetry, and the changes are shown in Table 8. Interaction constants not listed, as well as torsional force constants, were set equal to zero.

Experimental

Trichlorosilane (from Matheson Co.) was purified by trap-to-trap distillation and outgassed at −78 °C prior to use. Trichlorofluorosilane, trichlorobromosilane, and trichloroiodosilane were prepared by standard literature procedures (14–16) and purified by trap to trap distillation prior to use. The infrared and Raman spectra of the starting materials were found to be identical to those in the literature (17–18). Trimethylamine was dried and purified as described previously (19).

Dissociation pressure measurements have been reported for the systems $SiCl_3H/NMe_3$ and $SiCl_3F/NMe_3$ and clearly establish that only 1:1 complexes are capable of formation at low temperatures (1, 2). The $SiCl_3I.NMe_3$ adduct prepared for the first time in this study proved to be the most stable of the series and could be analyzed directly from a vacuum ampoule by hydrolysis followed by conventional argentrometric and pH titration techniques.

Anal. Calcd. for $SiCl_3I.NMe_3$: Cl, 33.2; I, 39.6; Me_3N: Si = 1. Found: Cl, 33; I, 38.7; Me_3N: Si = 1.10.

Vibrational spectra were recorded for thin films of the compounds formed by the slow deposition of a gaseous mixture of the appropriate halide with a slight excess of trimethylamine (approximately 1:1) onto the cold tip (−196 °C) of a low temperature infrared or Raman cell.

The infrared spectra were recorded on a Beckman IR 11 and Perkin–Elmer 180 and 221 spectrometers. Raman spectra were recorded on a Spex 1401 spectrometer using krypton and argon ion laser excitation.

We wish to thank the National Research Council of Canada for financial support and for an NRCC scholarship (D.B.).

Appendix

C_{3v} Internal Coordinates

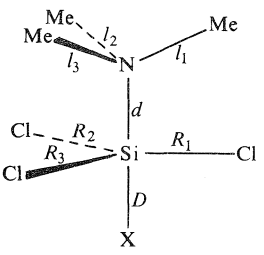

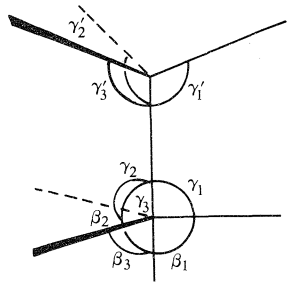

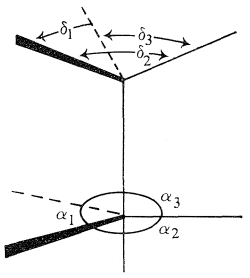

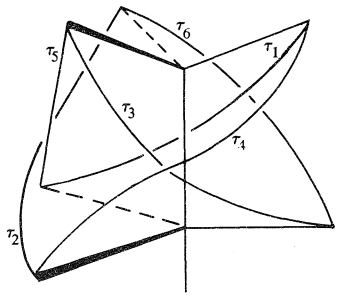

C_{3v} Symmetry Coordinates

Type A_1

$$S_1 = (1/\sqrt{3})(\Delta R_1 + \Delta R_2 + \Delta R_3)$$
$$S_2 = \Delta D$$
$$S_3 = \Delta d$$
$$S_4 = (1/\sqrt{3})(\Delta l_1 + \Delta l_2 + \Delta l_3)$$
$$S_5 = (1/\sqrt{3})(\Delta\alpha_1 + \Delta\alpha_2 + \Delta\alpha_3)$$
$$S_6 = (1/\sqrt{3})(\Delta\beta_1 + \Delta\beta_2 + \Delta\beta_3)$$
$$S_7 = (1/\sqrt{3})(\Delta\gamma_1 + \Delta\gamma_2 + \Delta\gamma_3)$$
$$S_8 = (1/\sqrt{3})(\Delta\gamma_1' + \Delta\gamma_2' + \Delta\gamma_3')$$
$$S_9 = (1/\sqrt{3})(\Delta\delta_1 + \Delta\delta_2 + \Delta\delta_3)$$
$$S_{10} = (1/\sqrt{6})(\Delta\tau_1 + \Delta\tau_2 + \Delta\tau_3 - \Delta\tau_4 - \Delta\tau_5 - \Delta\tau_6)$$

Type A_2

$$S_{11} = (1/\sqrt{6})(\Delta\tau_1 + \Delta\tau_2 + \Delta\tau_3 + \Delta\tau_4 + \Delta\tau_5 + \Delta\tau_6)$$

Can. J. Chem. Downloaded from www.nrcresearchpress.com by 210.87.254.6 on 09/05/12
For personal use only.

Can. J. Chem. Downloaded from www.nrcresearchpress.com by 210.87.254.6 on 09/05/12
For personal use only.

Type E_a

$$S_{12} = (1/\sqrt{6})(2\Delta R_1 - \Delta R_2 - \Delta R_3)$$
$$S_{13} = (1/\sqrt{6})(2\Delta l_1 - \Delta l_2 - \Delta l_3)$$
$$S_{14} = (1/\sqrt{6})(2\Delta\alpha_1 - \Delta\alpha_2 - \Delta\alpha_3)$$
$$S_{15} = (1/\sqrt{6})(2\Delta\beta_1 - \Delta\beta_2 - \Delta\beta_3)$$
$$S_{16} = (1/\sqrt{6})(2\Delta\gamma_1 - \Delta\gamma_2 - \Delta\gamma_3)$$
$$S_{17} = (1/\sqrt{6})(2\Delta\gamma_1' - \Delta\gamma_2' - \Delta\gamma_3')$$
$$S_{18} = (1/\sqrt{6})(2\Delta\delta_1 - \Delta\delta_2 - \Delta\delta_3)$$
$$S_{19} = (1/2\sqrt{3})(2\Delta\tau_1 - \Delta\tau_2 - \Delta\tau_3 - 2\Delta\tau_4 + \Delta\tau_5 + \Delta\tau_6)$$
$$S_{20} = (1/2)(\Delta\tau_2 - \Delta\tau_3 - \Delta\tau_5 + \Delta\tau_6)$$

Type E_b

$$S_{21} = (1/\sqrt{2})(\Delta R_2 - \Delta R_3)$$
$$S_{22} = (1/\sqrt{2})(\Delta l_2 - \Delta l_3)$$
$$S_{23} = (1/\sqrt{2})(\Delta\alpha_2 - \Delta\alpha_3)$$
$$S_{24} = (1/\sqrt{2})(\Delta\beta_2 - \Delta\beta_3)$$
$$S_{25} = (1/\sqrt{2})(\Delta\gamma_2 - \Delta\gamma_3)$$
$$S_{26} = (1/\sqrt{2})(\Delta\gamma_2' - \Delta\gamma_3')$$
$$S_{27} = (1/\sqrt{2})(\Delta\delta_2 - \Delta\delta_3)$$
$$S_{28} = (1/2)(\Delta\tau_2 - \Delta\tau_3 + \Delta\tau_5 - \Delta\tau_6)$$
$$S_{29} = (1/2\sqrt{3})(2\Delta\tau_1 - \Delta\tau_2 - \Delta\tau_3 + 2\Delta\tau_4 - \Delta\tau_5 - \Delta\tau_6)$$

C_s Internal Coordinates

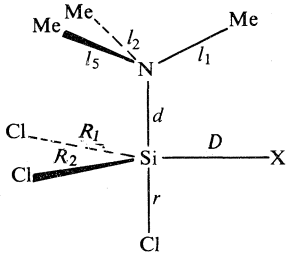

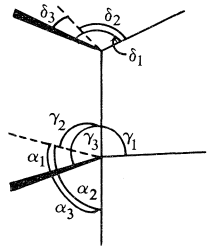

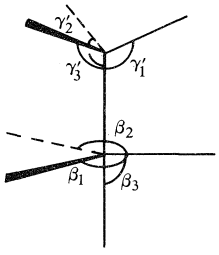

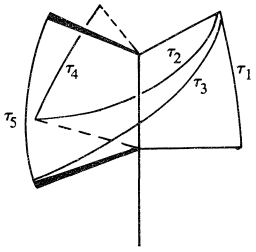

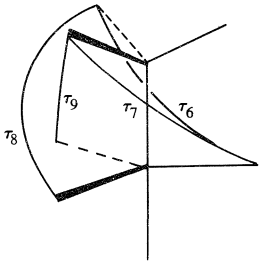

C_s Symmetry Coordinates

Type A'

$$S_1 = \Delta D$$
$$S_2 = (1/\sqrt{2})(\Delta R_1 + \Delta R_2)$$
$$S_3 = \Delta r$$
$$S_4 = \Delta d$$
$$S_5 = \Delta l_1$$
$$S_6 = (1/\sqrt{2})(\Delta l_2 + \Delta l_3)$$
$$S_7 = \Delta\alpha_1$$
$$S_8 = (1/\sqrt{2})(\Delta\alpha_2 + \Delta\alpha_3)$$
$$S_9 = (1/\sqrt{2})(\Delta\beta_1 + \Delta\beta_2)$$
$$S_{10} = \Delta\beta_3$$
$$S_{11} = \Delta\gamma_1$$
$$S_{12} = (1/\sqrt{2})(\Delta\gamma_2 + \Delta\gamma_3)$$
$$S_{13} = \Delta\gamma_1'$$
$$S_{14} = (1/\sqrt{2})(\Delta\gamma_2' + \Delta\gamma_3')$$
$$S_{15} = (1/\sqrt{2})(\Delta\delta_1 + \Delta\delta_3)$$
$$S_{16} = \Delta\delta_3$$
$$S_{17} = (1/\sqrt{2})(\Delta\tau_2 - \Delta\tau_3)$$
$$S_{18} = (1/\sqrt{2})(\Delta\tau_4 - \Delta\tau_5)$$
$$S_{19} = (1/\sqrt{2})(\Delta\tau_6 - \Delta\tau_7)$$
$$S_{20} = (1/\sqrt{2})(\Delta\tau_8 - \Delta\tau_9)$$

Type A''

$$S_{21} = (1/\sqrt{2})(\Delta R_1 - \Delta R_2)$$
$$S_{22} = (1/\sqrt{2})(\Delta l_2 - \Delta l_3)$$
$$S_{23} = (1/\sqrt{2})(\Delta\alpha_2 - \Delta\alpha_3)$$
$$S_{24} = (1/\sqrt{2})(\Delta\beta_1 - \Delta\beta_2)$$
$$S_{25} = (1/\sqrt{2})(\Delta\gamma_2 - \Delta\gamma_3)$$
$$S_{26} = (1/\sqrt{2})(\Delta\gamma_2' - \Delta\gamma_3')$$
$$S_{27} = (1/\sqrt{2})(\Delta\delta_1 - \Delta\delta_2)$$
$$S_{28} = \Delta\tau_1$$
$$S_{29} = (1/\sqrt{2})(\Delta\tau_2 + \Delta\tau_3)$$
$$S_{30} = (1/\sqrt{2})(\Delta\tau_4 + \Delta\tau_5)$$
$$S_{31} = (1/\sqrt{2})(\Delta\tau_6 + \Delta\tau_7)$$
$$S_{32} = (1/\sqrt{2})(\Delta\tau_8 + \Delta\tau_9)$$

1. A. B. Burg. J. Am. Chem. Soc. **76**, 2674 (1954).
2. J. E. Fergusson, D. K. Grant, H. H. Hickford, and C. J. Wilkins. J. Chem. Soc. 99 (1959).
3. H. J. Campbell-Ferguson and E. A. V. Ebsworth. J. Chem. Soc. (A), 1508 (1966).
4. H. J. Campbell-Ferguson and E. A. V. Ebsworth. J. Chem. Soc. (A), 705 (1967).
5. I. B. Beattie and G. A. Ozin. J. Chem. Soc. (A), 542 (1969).
6. I. R. Beattie and G. A. Ozin. J. Chem. Soc. (A), 2535 (1969).
7. E. L. Muetterties, W. Mahler, and R. Schmutzler. Inorg. Chem. **2**, 613 (1963).
8. I. R. Beattie and G. A. Ozin. J. Chem. Soc. (A), 370 (1970).
9. I. R. Beattie and T. R. Gilson. J. Chem. Soc. 6595 (1965).
10. M. S. Bitton and M. Webster. J. Chem. Soc. (A), 722 (1972).
11. I. R. Beattie and J. Horder. J. Chem. Soc. (A), 2655 (1969).
12. M. Webster and S. Keats. J. Chem. Soc. (A), 836 (1971).
13. J. Hinze and H. H. Jaffé. J. Am. Chem. Soc. **84**, 540 (1962).
14. H. H. Anderson. J. Am. Chem. Soc. **72**, 2091 (1950).
15. W. C. Schumb and H. H. Anderson. J. Am. Chem. Soc. **59**, 651 (1937).
16. R. West and E. G. Rochow. *In* Inorganic syntheses. Vol. 4. *Edited by* J. Bailar. McGraw–Hill, New York. 1953. p. 41.
17. M-L. Delwaulle. J. Phys. Chem. **56**, 355 (1952).
18. K. Hamada, G. A. Ozin, and E. A. Robinson. Can. J. Chem. **49**, 477 (1971).
19. I. R. Beattie and G. A. Ozin. J. Chem. Soc. (A), 2373 (1968).

Can. J. Chem. Downloaded from www.nrcresearchpress.com by 210.87.254.6 on 09/05/12
For personal use only.

Five Co-ordinate Complexes of Platinum(II) and Palladium(II)

K. R. Dixon and A. D. Rattray

Department of Chemistry, University of Victoria, Victoria, British Columbia

Received August 10, 1972

Reactions of 1,10-phenanthroline with halogen bridged dinuclear species, $[M_2X_2(PPh_2O)_2(PPh_2OH)_2]$ and $[M_2X_2(PR_3)_4][BF_4]_2$, give the new five co-ordinate complexes, $[MX(PPh_2O)(PPh_2OH)(Phen)]$ and $[MX(PR_3)_2(Phen)][BF_4]$, where M = Pd or Pt, X = Cl or Br, Ph = phenyl, and R = ethyl (or phenyl when M = Pd). Decomposition of the $[MX(PR_3)_2(Phen)][BF_4]$ complexes in hot solvents gives the four co-ordinate species, $[MX(PR_3)(Phen)][BF_4]$. The complexes are characterized by elemental analyses, molecular weight, and conductance measurements and infrared and nuclear magnetic resonance spectroscopy. The spectroscopic data show that $[PtCl(PEt_3)_2(Phen)][BF_4]$ has a trigonal bipyramidal structure with the phenanthroline and one triethylphosphine in the equatorial plane and a chlorine and a triethylphosphine in the axial positions.

Les réactions de la phénantroline-1,10 avec des espèces halogénées pontées et binucléaires, $[M_2X_2(PPh_2O)_2(PPh_2OH)_2]$ et $[M_2X_2(PR_3)_4][BF_4]_2$ produisent de nouveaux complexes pentacoordinés, $[MX(PPh_2O)(PPh_2OH)(Phen)]$ et $[MX(PR_3)_2(Phen)][BF_4]$ où M = Pd ou Pt, X = Cl ou Br, Ph = phényle et R = éthyle (ou phényle si M = Pd). La décomposition des complexes du type $[MX(PR_3)_2(Phen)][BF_4]$ dans des solvants chauds produit des espèces tétracoordinées $[MX(PR_3)(Phen)][BF_4]$. Les complexes ont été identifiés et caractérisés à l'aide d'analyses élémentaires, de mesures de poids moléculaire, et de conductance, de la spectroscopie infrarouge ainsi que de la résonnance magnétique nucléaire. Les données spectroscopiques montrent que le complexe $[PtCl(PEt_3)_2(Phen)][BF_4]$ possède une structure du type bupyramidale trigonale avec la phénanthroline et un groupe triéthylphosphine dans le plan équatorial et un chlore ainsi qu'un triéthylphosphine en positions axiales.

[Traduit par le journal]

Can. J. Chem., **51**, 618 (1973)

Introduction

The existence of five co-ordinate complexes of platinum(II) and palladium(II) is well established (1 and references therein). However, although some complexes of a flexible polydentate ligand (2) and some with two bidentate ligands (3–5) are known, most of the reported examples involve rather rigid polydentate ligands which may impose special constraints on the geometry of the complex. Five co-ordinate complexes of these metals involving mainly monodentate ligands are relatively rare, the principal examples being $[Pt(SnCl_3)_5]^{3-}$ (6) and $[PdBr_2(2\text{-phenyl-2-phosphaindane})_3]$ and its platinum analog (7). The present paper describes the synthesis and characterization of five co-ordinate complexes having three monodentate ligands and one bidentate ligand. One of these is of particular interest in that the nuclear magnetic resonance spectra of the ligands permit an assignment of the complex geometry.

Results and Discussion

All of the five co-ordinate complexes listed in Table 1 are prepared by cleavage reactions of halogen bridged complexes

$$[M_2X_2(PPh_2O)_2(PPh_2OH)_2] + 2\ Phen \rightarrow 2[MX(PPh_2O)(PPh_2OH)(Phen)]$$

or

$$[M_2X_2(PR_3)_4][BF_4]_2 + 2\ Phen \rightarrow 2[MX(PR_3)_2(Phen)][BF_4]$$

where M = Pd or Pt, X = Cl or Br, Phen = 1,10-phenanthroline, Ph = phenyl, and R = ethyl or phenyl. The reactions proceed rapidly in acetone solution at 25° and the products are generally stable to normal laboratory operations. However, it was noticed that in solution, particularly at elevated temperatures, the five co-ordinate $[MX(PR_3)_2(Phen)][BF_4]$ complexes tend to decompose to four co-ordinate $[MX(PR_3)(Phen)][BF_4]$ complexes. Presumably the reaction proceeds by dissociation followed by atmospheric oxidation of the tertiary phosphine and, in refluxing methanol, reaction is rapid enough to serve as a convenient preparation of the four co-ordinate species. The solid $[MX(PR_3)_2(Phen)][BF_4]$ complexes are air stable except that during melting point determinations, $[PdCl(PPh_3)_2(Phen)][BF_4]$ apparently decomposes at about 145° to form $[PdCl(PPh_3)(Phen)][BF_4]$ which finally melts close to the melting point of pure samples of the latter complex.

Can. J. Chem. Downloaded from www.nrcresearchpress.com by 210.87.254.40 on 09/05/12
For personal use only.

TABLE 1. Characterization data

Complex	Melting point (°C)	%C Calcd.	%C Found	%H Calcd.	%H Found	Molar[a] conductance (ohm^{-1} cm^2)	Infrared[b] ν(M—Cl) (cm^{-1})
$[PtCl(PEt_3)_2(Phen)][BF_4]$[c]	126–129	39.3	39.1	5.22	5.20	85	290 m
$[PtBr(PEt_3)_2(Phen)][BF_4]$	130–134	37.0	37.1	4.92	4.94	84	
$[PtCl(PEt_3)(Phen)][BF_4]$[d]	179–182	35.1	35.3	3.76	3.69	89	360 m
$[PtBr(PEt_3)(Phen)][BF_4]$	194–198	32.7	33.2	3.51	3.57	91	
$[PdCl(PEt_3)_2(Phen)][BF_4]$[e]	131–134	44.7	44.7	5.94	5.91	90	280 w
$[PdCl(PEt_3)(Phen)][BF_4]$[f]	180–184	41.0	41.0	4.40	4.47	88	365 m
$[PdCl(PPh_3)_2(Phen)][BF_4]$	145–146[g]	61.8	61.9	4.10	4.12	80	335 w
$[PdCl(PPh_3)(Phen)][BF_4]$	219–227 dec	53.7	54.1	3.45	3.65	83	365 m
$[PtCl(PPh_2O)(PPh_2OH)(Phen)]$[h]	138–142	53.1	52.4	3.59	3.79	24	300 vw
$[PtBr(PPh_2O)(PPh_2OH)(Phen)]$[i]	149–152	50.4	50.3	3.40	3.50	34	
$[PdCl(PPh_2O)(PPh_2OH)(Phen)]$[j]	125–129	59.6	59.0	4.03	3.97	11	300 vw
$[PdBr(PPh_2O)(PPh_2OH)(Phen)]$[k]	193–198 dec	56.1	55.1	3.80	3.86	14	

[a] 10^{-3} *M* solutions in nitromethane.
[b] m = medium, w = weak, vw = very weak. ν(M—Br) < 250 cm^{-1}.
[c] %N: calcd. 3.81, found 3.45.
[d] %N: calcd. 4.55, found 4.91.
[e] %N: calcd. 4.34, found 4.31.
[f] %N: calcd. 5.31, found 5.31.
[g] Partial melting occurs at 145–146° followed by resolidifying with final melting at 205–210° decomp.
[h] Molecular weight: calcd. 814, found 818.
[i] Molecular weight: calcd. 859, found 874.
[j] Molecular weight: calcd. 726, found 723.
[k] Molecular weight: calcd. 770, found 766.

The phosphinato complexes, $[MX(PPh_2O)(PPh_2OH)(Phen)]$, are characterized by elemental analyses, molecular weight, and conductance measurements and by infrared spectroscopy. The infrared spectra are similar to those reported previously (8) for the corresponding $[M_2X_2(PPh_2O)_2(PPh_2OH)_2]$ complexes and in addition show the absorptions expected for co-ordinated phenanthroline (9). Absorptions due to ν(P—O) at 995 cm^{-1} accompanied by general broadening of the spectrum in the 1200–1600 and 700–800 cm^{-1} regions show the presence of the symmetrical hydrogen bonded system, M(P=O···H···O—P) (8), and we also find that a strong band at about 330 cm^{-1} is characteristic of this system.[1] Whether this group should be regarded as a bidentate ligand or as two monodentate ligands is a moot point. These complexes are similar to the phosphinato complexes reported previously (8) in that the ν(M—Cl) frequencies give very weak absorptions and are difficult to assign. However, clear differences in the spectra of the chloro and bromo complexes show that the halogen is co-ordinated in the solid state. In solution in dibromomethane, molecular weight measurements show no dissociation and in nitromethane solution the molar conductance values (11–34 ohm^{-1} cm^2) indicate only slight dissociation when compared with values of 75–95 ohm^{-1} cm^2 expected for 1 :1 electrolytes (10).

The $[MX(PEt_3)_{1\text{ or }2}(Phen)][BF_4]$ complexes are characterized by elemental analyses, conductance measurements and by infrared and nuclear magnetic resonance spectroscopy. We have not found molecular weight determinations useful for ionic compounds because of ion pairing effects. For both the four and five co-ordinate complexes the molar conductances in nitromethane are typical of 1 :1 electrolytes (10) and demonstrate that the halides are bound to the metal even in this polar solvent.

In the solid state infrared spectra show the expected ligand and anion absorptions but several interesting differences are observed between the five and the four co-ordinate complexes: (*a*) ν(M—Cl) frequencies[2] are higher for

[1] Re-examination of our previous spectra (8) has confirmed the presence of this band in all complexes having this ligand system.

[2] These were assigned by comparison of spectra with those of corresponding bromo complexes. The $[PdBr(PR_3)_{1\text{ or }2}(Phen)][BF_4]$ complexes are not included in Table 1 since attempted preparations yielded mixtures of four and five co-ordinate species, thus preventing complete characterization. However, their infrared spectra were clearly similar to those of corresponding chloro complexes except for the absence of the bands assigned to ν(Pd—Cl).

Can. J. Chem. Downloaded from www.nrcresearchpress.com by 210.87.254.40 on 09/05/12
For personal use only.

TABLE 2. Nuclear magnetic resonance spectra

	Chemical shifts (τ)						Coupling constants (Hz)			
	Phenanthroline				PEt_3					
Compound	2/9	4/7	5/6	3/8	CH_2	CH_3	J_{2-3}/J_{9-8}	J_{2-4}/J_{9-7}	J_{3-4}/J_{8-7}	J_{Pt-2}/J_{Pt-9}
1,10-Phenanthroline hydrate[a]	0.86	1.62	2.15	2.33	—	—	4.2	1.85	8.0	—
$[PtCl(PEt_3)_2(Phen)][BF_4]$[a]	0.39	1.19	1.79	1.90	7.73 8.08	8.61 8.89	4.5	1.5	8.0	5.5
$[PtCl(PEt_3)(Phen)][BF_4]$[b,c]	0.23/ 0.76	1.10/ 1.14[d]	1.82	1.77/ 1.84[d]	7.78	8.75	4/5	1–2[e]	8/9[d]	7–15[e]/23

[a]Solvent: acetone-d_6, reference: tetramethylsilane.
[b]Solvent and reference: dichloromethane.
[c]Other coupling constants: $J_{P-2} = \sim 4$, $J_{P-CH_2} = 10$, $J_{P-CH_3} = 17.5$, $J_{CH_2-CH_3} = 7.5$ Hz.
[d]In these cases it is not possible to be certain which resonance belongs to the 3,4,5-ring and which to the 7,8,9-ring protons.
[e]Resolution was not sufficient to permit accurate determination.

tion of the three weak phenanthroline absorptions *ca.* 1600 cm^{-1} is in the range 1597–1602 cm^{-1} for the five co-ordinate complexes and 1610–1615 cm^{-1} for the four co-ordinate, (*c*) the separation of the two phenanthroline absorptions *ca.* 1500 cm^{-1} is in the range 12–20 cm^{-1} for the five co-ordinate complexes and 21–24 cm^{-1} for the four co-ordinate complexes, (*d*) the five co-ordinate triethylphosphine complexes show two absorptions (at ~440 m and 420 w) in the range 400–450 cm^{-1} whereas the four co-ordinate complexes show only one (at ~435 m).

The mean position of the *ca.* 1600 cm^{-1} absorptions and the separation of the *ca.* 1500 cm^{-1} absorptions have previously been correlated (9) with the radius of the metal ion bound to the phenanthroline[3] and we find values of 1592 and 10 cm^{-1} for the mean and separation, respectively, in 1,10-phenanthroline hydrate. A sample of $[PtCl_2(Phen)]$, prepared as previously described (11), gave corresponding values of 1611 and 20 cm^{-1}. Consequently items *a*, *b*, and *c* above are all consistent with a slightly larger radius for the five co-ordinate metals with slightly weaker metal–ligand bonding than in the four co-ordinate complexes. Although the infrared spectra of the phosphinato complexes are complicated in the 1600 cm^{-1} region by phenyl absorptions, they appear to follow the same pattern with means of 1599–1601 cm^{-1} and separations of 14–16 cm^{-1}.

Absorptions in the 400–450 cm^{-1} region of the spectra of triethylphosphine complexes were previously thought to be due to ν(M—P) vibrations. Although this has been recently shown to be incorrect (12), the available evidence (13) for planar four co-ordinate complexes still suggests that the presence of two absorption bands in this region is characteristic of two triethylphosphines in a mutually *cis* configuration whereas one band suggests a single phosphine or two phosphines in a mutually *trans* configuration. Assuming that similar considerations apply to our five co-ordinate complexes, item *d* above indicates that they have *cis* triethylphosphine ligands.

Data describing the proton nuclear magnetic resonance spectra of the triethylphosphine complexes are given in Table 2. The spectra confirm the ratios of ethyl:phenanthroline protons and for the $[MX(PEt_3)(Phen)][BF_4]$ complexes the methylene and methyl proton resonances show the expected doublet of quartets and doublet of triplets, respectively. At 60 MHz the methyl proton resonances of the $[MX(PEt_3)_2(Phen)][BF_4]$ complexes appear similar to the quintets normally observed (14) for two triethylphosphine ligands in a *trans* configuration. However, more detailed examination of the spectrum of $[PtCl(PEt_3)_2(Phen)][BF_4]$ shows this to be due to overlap of resonances from two chemically different triethylphosphines and at 220 MHz

[3]A correlation with the separation of absorptions *ca.* 850 and 725 cm^{-1} was also proposed but in our complexes the 725 cm^{-1} band is obscured by triethylphosphine absorption.

Can. J. Chem. Downloaded from www.nrcresearchpress.com by 210.87.254.40 on 09/05/12
For personal use only.

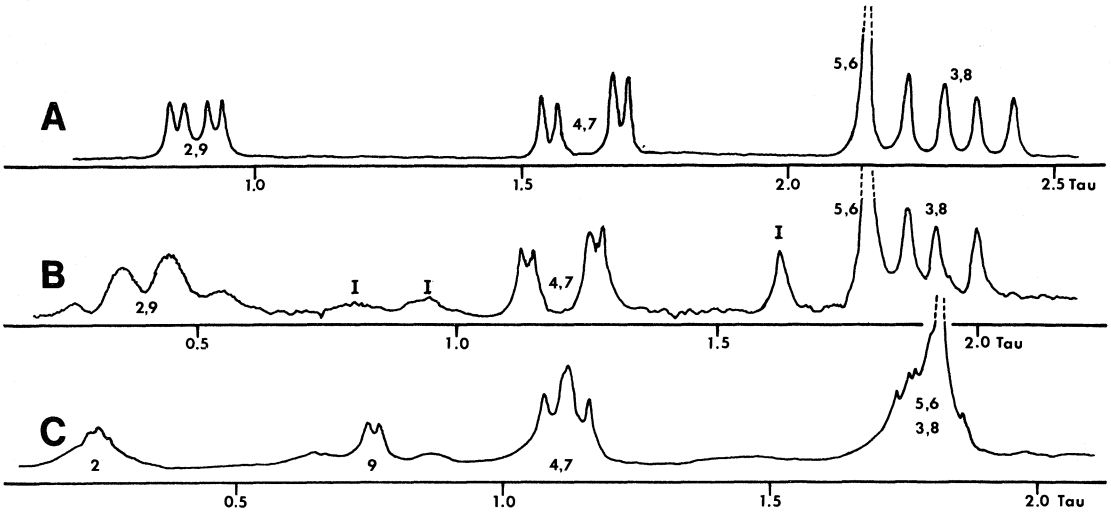

FIG. 1. Nuclear magnetic resonance spectra of phenanthroline ligands: *A*, 1,10-phenanthroline hydrate in acetone-d_6 at 60 MHz; *B*, $[PtCl(PEt_3)_2(Phen)][BF_4]$ in acetone-d_6 at 60 MHz; *C*, $[PtCl(PEt_3)(Phen)][BF_4]$ in dichloromethane at 220 MHz. Note: The 0.39 τ resonance in *B* was better resolved and more symmetrical at 220 MHz. Line width problems at 220 MHz and signal/noise problems at 60 MHz prevented the resolution of the expected 1.5 Hz couplings in *C*. *I* = Resonances due to compound *C*, present as impurity in compound *B*. Numbers adjacent to resonances refer to proton positions in the phenanthroline ring.

both methylene and methyl proton resonances show two separate multiplets. Resolution within the multiplets is poor and does not permit determination of coupling constants but the spectra are generally similar to those expected for ethyl groups coupled to one phosphorus atom, *i.e.* virtual coupling (14) between the two phosphorus atoms does not occur.

The nuclear magnetic resonance spectrum of the phenanthroline ligand in $[PtCl(PEt_3)_2(Phen)][BF_4]$ (see Table 2 and Fig. 1) is very similar to that of 1,10-phenanthroline hydrate except that (*a*) the 2/9 proton resonance in the complex has sidebands assigned to coupling with ^{195}Pt (33% abundant), (*b*) the 5/6 and 3/8 proton resonances overlap in the complex, and (*c*) the resonances shift to low field on co-ordination, in contrast to the high field shifts observed previously in octahedral complexes (15). The spectral data are generally very similar to those reported previously for phenanthroline and its complexes (15–17) and it is important to note that the simplicity of the $[PtCl(PEt_3)_2(Phen)][BF_4]$ spectrum indicates a very symmetrical environment for the co-ordinated phenanthroline. The phenanthroline spectrum in $[PtCl(PEt_3)(Phen)][BF_4]$ is more complex since the two nitrogen containing rings are *trans* to different groups:

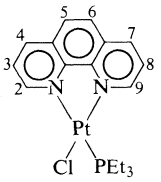

Such an asymmetry is expected to make the 2, 3, 4, and 5 positions chemically different from the 6, 7, 8, and 9 positions and in our case the 220 MHz spectrum shows chemical shift differences between 2 and 9, 3 and 8, and 4 and 7, but not between 5 and 6. The asymmetry is thus smaller than that observed previously in octahedral complexes (16, 17) but in those cases ring current effects due to proximity of another phenanthroline may be involved. Although the expected 1.5 Hz couplings are not resolved, the 9 proton resonance is easily assigned to the doublet (with ^{195}Pt sidebands) at 0.76 τ. The resonance at 0.23 τ is more complex and is therefore assigned to the proton (position 2) *trans* to phosphorus. Coupling to ^{31}P combined with broad ^{195}Pt side-bands explains the complexity of the resonance and it is interesting that the coupling constants, $J_{Pt-9} > J_{Pt-2}$, are in the order expected (18) for weakening of the metal–ligand bond *trans* to phosphorus. Moreover,

Can. J. Chem. Downloaded from www.nrcresearchpress.com by 210.87.254.40 on 09/05/12
For personal use only.

Can. J. Chem. Downloaded from www.nrcresearchpress.com by 210.87.254.40 on 09/05/12
For personal use only.

both J_{Pt-9} and J_{Pt-2} are larger than in $[PtCl(PEt_3)_2(Phen)][BF_4]$, which again indicates weaker metal–ligand bonding in the five co-ordinate complex. The assignment of the distorted triplet at ~1.1 τ as due to chemically shifted overlapping doublets (4 and 7 protons) is confirmed by the change in peak contour at 60 MHz. The 3,8 and 5,6 proton resonances are not resolved but their assignment is confirmed, together with all the other assignments, by computer simulation of the spectrum.

Nuclear magnetic resonance spectra of the other $[MX(PEt_3)_{1\text{ or }2}(Phen)][BF_4]$ complexes were recorded at 60 MHz and are generally similar to those described above except that for M = Pd resolution of the phenanthroline resonances is poor.

The nuclear magnetic resonance spectrum of $[PtCl(PEt_3)_2(Phen)][BF_4]$ was recorded in acetone-d_6. It is unlikely that the chloride would be co-ordinated in nitromethane (the solvent for our conductance measurements) and dissociated in acetone but as a check we recorded the molar conductance of the complex in acetone as 150 ohm^{-1} cm^2. Expected values for 1:1 electrolytes in acetone are not well established (10) but 150 ohm^{-1} cm^2 seems reasonable and is consistent with values obtained for other platinum complexes (19). Consequently, conductance shows the chloride to be co-ordinated, nuclear magnetic resonance shows two chemically shifted triethylphosphine resonances and a symmetrical phenanthroline and infrared shows that the chloride is co-ordinated and suggests a *cis* configuration for the triethylphosphine ligands. The only five co-ordinate structure which is consistent with these observations is a trigonal bipyramid with the phenanthroline and one triethylphosphine in the equatorial positions and a chlorine and a triethylphosphine in the axial positions. The data also exclude six co-ordinate solution species in which an acetone molecule occupies a co-ordination site. Presumably the other $[MX(PR_3)_2(Phen)][BF_4]$ complexes have similar structures and the same configuration is also possible for the $[MX(PPh_2O)(PPh_2OH)(Phen)]$ complexes. It is interesting that the bridge cleavage reaction has occurred essentially with "retention of configuration" just as observed previously (20) for cleavage by pyridine.

One aspect of these five co-ordinate complexes remains puzzling. The compounds are all pale yellow in color and their u.v./visible spectra in solution and in the solid state do not show the low energy bands previously considered characteristic of five co-ordination in platinum(II) and palladium(II) complexes (21, 22). It is possible that the high ligand field effects of phenanthroline and phosphine ligands (23) combine to move the low energy d–d bands under the charge transfer absorptions. In our complexes d–d bands at 28 000 cm^{-1} or higher energies would probably not be resolved and the previous report (21) of spectra of $[PtX\{(o\text{-}Ph_2As\cdot C_6H_4)_3\text{-}As\}][ClO_4]$ complexes gives band maxima from 21 900 cm^{-1} (X = I) to 29 200 cm^{-1} (X = CN) in dichloromethane solution. Consequently, although the required high field shifts are large, we believe this to be the most likely explanation especially since the other evidence so clearly favors five co-ordinate structures for our complexes.

Experimental

Data relating to the characterization of the complexes are given in Table 1. Microanalyses were by Schwartzkopf Microanalytical Laboratory, New York or by Chemalytics Inc., Tempe, Arizona. Molecular weights were determined in dibromomethane solution at 50° using a Hitachi–Perkin Elmer Model 115 Vapor Phase Osmometer. Conductance measurements were made on ~10^{-3} *M* solutions in nitromethane using a pipette-type cell connected to a Radiometer, Model CDM3 Conductivity Bridge. Infrared spectra were recorded from 4000–250 cm^{-1} with accuracy ±3 cm^{-1} on a Beckman IR 20 Spectrophotometer calibrated against polystyrene film and water vapor. Solid samples were examined as Nujol mulls between caesium iodide plates. Nuclear magnetic resonance spectra were recorded at 60 MHz on Perkin–Elmer R12A or Varian HA60 spectrometers and at 220 MHz by the Canadian 220 MHz NMR Centre, Sheridan Park, Ontario, using tetramethylsilane or dichloromethane as internal references. Computer simulation of spectra was achieved using the UEAITR programme (24). Ultraviolet/visible spectra were recorded on a Unicam SP700 spectrophotometer with diffuse reflectance attachment.

Analar 1,10-phenanthroline hydrate was obtained from British Drug Houses Ltd. and was used as received. The complexes, $[M_2X_2(PR_3)_4][BF_4]_2$ where X = Cl or Br and R = ethyl for M = Pt, and where X = Cl or Br and R = ethyl or phenyl for M = Pd, and $[M_2X_2(PPh_2O)_2(PPh_2OH)_2]$ where M = Pd or Pt and X = Cl or Br, were prepared as previously described (8, 20, 25). Cleavage reactions of these halogen bridged complexes by 1,10-phenanthroline were carried out in acetone solution under a nitrogen atmosphere and the preparation of $[PtCl(PEt_3)_2(Phen)][BF_4]$ is described below as an example. A representative preparation of a four co-ordinate complex, $[PtCl(PEt_3)(Phen)][BF_4]$, is also

described. Other preparations were similar and gave similar yields except for the variations noted below.

[$PtCl(PEt_3)_2(Phen)$][BF_4] and other Five Co-ordinate Complexes

[$Pt_2Cl_2(PEt_3)_4$][BF_4]$_2$ (0.492 g, 0.444 mmol) in acetone (10 ml) was added dropwise to a stirred solution of 1,10-phenanthroline hydrate (0.176 g, 0.89 mmol) in acetone (10 ml) under a nitrogen atmosphere at 25°. The order of addition of reagents was chosen to minimize the reaction of the product with [$Pt_2Cl_2(PEt_3)_4$][BF_4]$_2$ to produce [$PtCl(PEt_3)_3$][BF_4] and [$PtCl(PEt_3)$(Phen)]-[BF_4]. After stirring for 10 min, diethyl ether (100 ml) was added to yield [$PtCl(PEt_3)_2$(Phen)][BF_4] (0.552 g, 0.752 mmol) as a yellow oil which crystallized to a yellow powder. Samples for analysis were obtained by using insufficient diethyl ether to cause immediate precipitation and then cooling the reaction mixture to −15° to initiate crystallization.

The other cleavage reactions were similar except that the low solubility of the [$M_2X_2(PPh_2O)_2(PPh_2OH)_2$] complexes in acetone necessitated dropwise addition of phenanthroline solution to a stirred suspension of the appropriate starting complex. The resulting [$MX(PPh_2O)$-(PPh_2OH)(Phen)] complexes were recrystallized from dichloromethane by dropwise addition of diethyl ether.

[$PtCl(PEt_3)$(Phen)][BF_4] and other Four Co-ordinate Complexes

[$PtCl(PEt_3)_2$(Phen)][BF_4] (0.250 g, 0.341 mmol) was heated under reflux in methanol (2 ml) for 60 min in air. Ethyl acetate (5 ml) was added, followed by diethyl ether (20 ml) to yield [$PtCl(PEt_3)$(Phen)][BF_4] (0.085 g, 0.138 mmol) as a yellow precipitate which was recrystallized from methanol by dropwise addition of ethyl acetate followed by diethyl ether. The mother liquors contained mainly unreacted starting complex and higher yields could be obtained by recovering this material and re-peating the methanol reflux.

The [$PdX(PR_3)_2$(Phen)][BF_4] complexes decomposed rather more readily and brief reflux in dichloromethane was usually sufficient to yield the four co-ordinate complexes.

We thank the National Research Council of Canada and the University of Victoria for research grants and the University of Victoria for a postgraduate scholarship (to A.D.R.).

1. E. L. Muetterties and R. A. Schunn. Q. Rev. **20**, 245 (1966).
2. T. D. DuBois and D. W. Meek. Inorg. Chem. **8**, 146 (1969).
3. C. M. Harris and R. S. Nyholm. J. Chem. Soc. 4375 (1956).
4. B. Chiswell and S. E. Livingstone. J. Chem. Soc. 1071 (1960).
5. R. A. Plowman and L. F. Power. Aust. J. Chem. **24**, 303 (1971).
6. R. D. Cramer, R. V. Lindsay jun., C. T. Prewitt, and U. G. Stolberg. J. Am. Chem. Soc. **87**, 658 (1965).
7. J. W. Collier, F. G. Mann, D. G. Watson, and H. R. Watson. J. Chem. Soc. 1803 (1964).
8. K. R. Dixon and A. D. Rattray. Can. J. Chem. **49**, 3997 (1971).
9. A. A. Schilt and R. C. Taylor. J. Inorg. Nucl. Chem. **9**, 211 (1959).
10. W. J. Geary. Co-ord. Chem. Rev. **7**, 81 (1971).
11. F. A. Palocsay and J. V. Rund. Inorg. Chem. **8**, 524 (1969).
12. K. Shobatake and K. Nakamoto. J. Am. Chem. Soc. **92**, 3332 (1970).
13. P. L. Goggin and R. J. Goodfellow. J. Chem. Soc. A, 1462 (1966).
14. H. C. Clark, K. R. Dixon, and W. J. Jacobs. J. Am. Chem. Soc. **90**, 2259 (1968).
15. J. D. Miller and R. H. Prince. J. Chem. Soc. 3185, 4706 (1965).
16. J. D. Miller and R. H. Prince. J. Chem. Soc. A, 519 (1969).
17. D. J. Francis and R. B. Jordan. Inorg. Chem. **11**, 461 (1972).
18. J. F. Nixon and A. Pidcock. Ann. Rev. NMR Spectrosc. **2**, 361 (1969).
19. J. J. McFarland. Unpublished results.
20. K. R. Dixon and D. J. Hawke. Can. J. Chem. **49**, 3252 (1971).
21. G. Dyer and L. M. Venanzi. J. Chem. Soc. 2771 (1965).
22. O. St. C. Headley, R. S. Nyholm, C. A. McAuliffe, L. Sindellari, M. L. Tobe, and L. M. Venanzi. Inorg. Chim. Acta, **4**, 93 (1970).
23. P. L. Goggin, R. J. Knight, L. Sindellari, and L. M. Venanzi. Inorg. Chim. Acta, **5**, 62 (1971).
24. R. B. Johannesen, J. A. Ferretti, and R. K. Harris. J. Mag. Res. **3**, 84 (1970).
25. H. C. Clark, K. R. Dixon, and W. J. Jacobs. J. Am. Chem. Soc. **91**, 1346 (1969).

Can. J. Chem. Downloaded from www.nrcresearchpress.com by 210.87.254.40 on 09/05/12
For personal use only.

Low Energy Electron Impact Ionization and Fragmentation: Cyclobutanone

GRAHAM RICHARD BRANTON AND CLAUDIO KONG NAM PUA

Department of Chemistry, University of Victoria, Victoria, British Columbia

Received September 6, 1972

Cyclobutanone is shown to yield both $C_3H_6^+$ and $C_2H_2O^+$ ions on fragmentation under electron impact in a mass spectrometer. Using the energy distribution difference (EDD) technique the ionization energy of cyclobutanone is found to be 9.58 eV and the appearance potentials of the $C_3H_6^+$ and $C_2H_2O^+$ ions are found to be 9.85 and 10.53 eV, respectively.

Dans un spectromètre de masse, on montre que la cyclobutanone lorsque soumis à un bombardement d'électrons, libère comme fragment à la fois des ions $C_3H_6^+$ et $C_2H_2O^+$. En utilisant la technique impliquant la différence de distribution énergétique (DDE), l'énergie d'ionisation de la cyclobutanone est donnée comme étant 9.58 eV et les potentiels d'apparition des ions $C_3H_6^+$ et $C_2H_2O^+$ comme étant respectivement 9.85 et 10.53 eV. [Traduit par le journal]

Can. J. Chem., **51**, 624 (1973)

Introduction

Cyclobutanone has previously been reported (1) as showing only one major fragmentation pathway, [*a*], upon ionization by electron impact. However, the methyl substituted cyclobutanones have shown (2) fragmentation according to both of the possible fragmentation pathways [*a*] and [*b*].

[*a*] $\rightarrow CH_2CO + C_2H_4$

[*b*] $\rightarrow CO + C_3H_6$

Both of these processes have been observed for the neutral species in its thermal (3) and photolytic (4) decomposition. There has been considerable recent interest in the photolytic decomposition of cyclobutanone, and the present investigation was undertaken to test the apparent lack of similarity between the decomposition pathways of the neutral and ionic species for the unsubstituted cyclobutanone (2).

Experimental

The cyclobutanone used in the study was obtained from Aldrich Chemical Company, Inc., (C-9600-1, Lot. No. 030607, Aldrich analyzed by i.r. and g.c.) and was used without further purification, after analysis by gas chromatography and mass spectrometry showed the sample to be better than 99.9% pure.

The xenon used as a calibration gas for the electron energy scale was research grade obtained from Airco Industrial Gases, Division of Air Reduction Co. Inc.

The argon used to check the experimental set up was research grade obtained from Union Carbide.

The mass spectra were determined on an Hitachi/Perkin–Elmer model RMU-7 mass spectrometer, modified as outlined below in order to allow ionization and appearance potentials to be determined. The electron energy was controlled via a 10 turn potentiometer which could be driven by a stepping motor (manufactured by the A. W. Haydon Company) directly connected to the potentiometer. The signal from the collector was fed to a Cary 401 vibrating reed electrometer from which it was stored in a Northern Scientific NS 560 signal averaging computer prior to plotting on an X–Y recorder or to conversion to paper tape for processing on an IBM 360/50 computer.

The ionization potential and appearance potentials were determined by observing the onset for the ion production after treating the data by the energy distribution difference (EDD) technique (5), using xenon as a calibrant for the energy scale. In all runs the xenon and cyclobutanone were present in the ionization chamber at the same time.

The EDD technique is based upon the application of the formula

$$\Delta I(V) = I(V) - B \times I(V + \Delta V)$$

where $I(V)$ = ion current at electron energy V, B = a constant, ΔV = voltage increment usually about 0.1 eV, and $\Delta I(V)$ represents the ion current which would result from an electron beam with a reduced thermal energy spread.

The data were first smoothed using a 15-point 5th degree smoothing routine (6) and the best value of B was found by adjusting the slope of the curve of $\Delta I(V)$ *vs.* electron energy to be zero just prior to the onset for the production of ions. In this way it was possible to reduce the effective thermal energy spread on the electron energy and thus observe the onset of ionization much more precisely.

Results

The low resolution mass spectrum was determined at an electron energy of 70 eV and found to be consistent with that reported previously (1).

Examination of the peak at $m/e = 42$ under higher resolution showed this to be a doublet indicating that fragmentation by both pathways [*a*] and [*b*] was occurring. The accurate masses of the peaks of the doublet were found to be 42.047 and 42.010, corresponding to $C_3H_6^+$ and $C_2H_2O^+$, respectively (the calculated masses being 42.0470 and 42.0106, respectively), the peak corresponding to $C_2H_2O^+$ being about thirteen times as intense as that corresponding to $C_3H_6^+$.

The relative intensities of the two peaks were examined at various electron energies and it was observed that just above the threshold for ion production the peak due to $C_3H_6^+$ was more intense than that due to $C_2H_2O^+$, but that as the electron energy was increased the latter rapidly grew in relative intensity to become the predominant fragment ion. The ions were of approximately equal intensity at an electron energy of 2–3 eV above the threshold of ion production. At higher electron energies peaks corresponding to CO^+ and $C_2H_4^+$ were also observed, as were peaks corresponding to further fragmentation of the $C_2H_2O^+$ and $C_3H_6^+$ ions. At all electron energies the peaks at $m/e = 42$ were much larger than any other fragment ion peaks.

The ionization potential of cyclobutanone, and the appearance potentials of the two ions at $m/e = 42$, were determined by examining the onset of the ionization efficiency curves of the ions after treatment of the data by the EDD (5) technique. The applicability of this technique to the equipment used was demonstrated (7) by a study of the ionization efficiency curves of xenon and argon, when the difference in the onset of ionization was found to be 3.6 eV (literature value 3.62 eV (5)). Breaks were also observed in the ionization efficiency curves of xenon and argon and these are compared with literature values in Table 1.

For the cyclobutanone, the ion at $m/e = 70$ and the two ions at $m/e = 42$ were studied using the EDD technique. Under the operating conditions the two peaks at $m/e = 42$ overlapped but were sufficiently well resolved that the ion current due to each could be recorded with minimal contribution from the other (less than 5%). Using xenon as a calibrant for the energy scale the ionization and appearance potentials found are shown in Table 2.

The value for $C_4H_6O^+$ was the average of seven runs and the others the average of five runs. The errors on the $m/e = 42$ peaks are slightly larger than for the parent ion due to the difficulty in completely resolving the peaks.

TABLE 1. Ionization efficiency curves for argon and xenon (fine structure in eV above threshold)

(*a*) Xenon

Spectroscopic*	EDD†	Velocity selector‡	RPD§	This work
	0.33		0.35	0.28
		0.70	0.75	0.74
1.31	1.27	1.33	1.3	1.30
		2.05	1.9	1.88

(*b*) Argon

Spectroscopic*	EDD†	Velocity selector‖	This work
0.178	0.18	0.19	0.24
	0.42	0.58	0.56
		0.77	0.80
	1.01	0.97	1.04
	1.36	1.30	1.32

*Reference 14.
†Reference 5.
‡Reference 15.
§Reference 16.
‖Reference 17.

TABLE 2. Ionization and appearance potentials

Ion	*m/e*	I.P./A.P. (eV)
$C_4H_6O^+$	70	9.58±0.1
$C_3H_6^+$	42	9.85±0.15
$C_2H_2O^+$	42	10.53±0.15

Breaks were observed in the ionization efficiency curves for all of the ions in the first few volts above the onset of ionization. The reproducibility of these breaks was poor due to noise on the ionization efficiency curves, and they will not be discussed here.

Discussion

The investigation of the ionization efficiency curves of xenon and argon demonstrated that the EDD technique as applied in this study is reliable for the study of ionization efficiency curves and the measurement of the energy of the onset of ion production.

The ionization potential of cyclobutanone has been found to be 9.61 eV by the technique of photoelectron spectroscopy (8) and has been estimated to be 9.35 eV from optical spectroscopy (9). The photoelectron spectroscopy value and the value of 9.58 eV obtained in the present electron impact study correspond to the vertical

ionization potential, and the agreement between these values is remarkably good. The adiabatic ionization potential should be slightly lower than either of these values and the optical value of 9.35 eV is reasonable.

The detection of two ions at $m/e = 42$ and their identification as $C_3H_6^+$ and $C_2H_2O^+$ by accurate mass measurement clearly shows that the cyclobutanone undergoes fragmentation by the two pathways [*a*] and [*b*]. Whilst these results are in contrast to the results of Hofman (1) who observed no $C_3H_6^+$ ion, they are consistent with the mass spectral fragmentation observed for the methyl substituted cyclobutanones (2) and with the thermal and photolytic decomposition processes of neutral cyclobutanone (3, 4).

At high ionization energies the peak due to the $C_2H_2O^+$ ion was much more intense than that due to $C_3H_6^+$ and at 70 eV their relative intensities were approximately 13:1. The appearance potentials for the two ions were found to be 10.53 eV for $C_2H_2O^+$ and 9.85 eV for $C_3H_6^+$ showing that fragmentation via pathway [*b*] was occurring at lower energies than for pathway [*a*], and at ionizing energies just above the threshold of ion production the peak due to $C_3H_6^+$ ion was of greater intensity than that due to the $C_2H_2O^+$ ion. The latter peak increases much more rapidly than that due to the $C_3H_6^+$ ion and at only about 2 eV above the onset for the production of the $C_2H_2O^+$ ion it was found to be of greater intensity than the $C_3H_6^+$ ion. At higher energies further fragmentation of these ions was observed, but at the low energies these were the only fragment ions detectable.

If it is assumed that the $C_2H_2O^+$ ion is the ketene ion then the appearance potential for the production of this ion may be estimated from thermochemical data (10–12) to be 10.4 eV. The experimental data thus suggest that the $C_2H_2O^+$ ion observed is the ketene ion. Similarly the appearance potential of the $C_3H_6^+$ ion may be estimated to be either 10.4 eV, for a cyclopropane ion, or 9.7 eV for a propylene ion. The experimental data thus suggest that the observed $C_3H_6^+$ ion is the propylene ion. In each case the experimentally determined appearance potential is higher than the thermochemical estimate by about 0.15 eV; this is most likely caused by a "kinetic shift" (13).

Although such comparisons must be treated with care, it is interesting to compare the fragmentation of the ionic species with the decomposition processes observed for the neutral cyclobutanone. Thermal studies (3) have shown that although the neutral species decomposes via both processes [*a*] and [*b*], process [*a*] predominates. This correlates well with the mass spectral fragmentation at high electron energies. The photochemical processes involving neutral cyclobutanone have been recently studied in detail (4). Photochemical decomposition again occurs via both routes [*a*] and [*b*]. The relative contribution of each process depends on the energy of the exciting radiation, near to the absorption threshold, process [*b*] predominating at the lowest energies and process [*a*] predominating at energies a little higher than the absorption threshold.

The electron impact induced fragmentation of the ionic cyclobutanone is thus similar to the decomposition of the neutral species. The observation in the present study of a fragmentation process corresponding to pathway [*b*] has thus brought cyclobutanone into line with the methyl substituted cyclobutanones (2), which also show fragmentation, both of the ionic and neutral species, according to processes [*a*] and [*b*].

Grateful acknowledgment is made to the National Research Council of Canada for financial support.

1. H. J. HOFMAN. Tetrahedron Lett. 2329 (1964).
2. D. S. WEISS, R. B. GAGOSIAN, and N. J. TURRO. Org. Mass Spectrom. **3**, 145 (1970).
3. A. T. BLADES. Can. J. Chem. **47**, 615 (1969).
4. (*a*) E. K. C. LEE. *In* Excited state chemistry. *Edited by* J. N. Pitts Jr. Gordon and Breach Inc., New York. 1970 and references therein. (*b*) J. C. HEMMINGER, C. F. RUSBULT, and E. K. C. LEE. J. Am. Chem. Soc. **93**, 1867 (1971). (*c*) J. C. HEMMINGER and E. K. C. LEE. J. Chem. Phys. **56**, 5284 (1972).
5. R. E. WINTERS, J. H. COLLINS, and W. L. COURCHENE. J. Chem. Phys. **45**, 1931 (1966).
6. A. SAVITZKY and M. J. E. GOLAY. Anal. Chem. **36**, 1627 (1964).
7. C. N. K. PUA. M.Sc. Thesis, University of Victoria, Victoria, British Columbia. 1972.
8. D. CHADWICK, D. C. FROST, and L. WEILER. Tetrahedron Lett. 4543 (1971).
9. R. WHITLOCK and A. B. F. DUNCAN. J. Chem. Phys. **55**, 218 (1971).
10. S. W. BENSON and H. E. O'NEAL. Report No. NSRDS-NBS 21, U.S. Government Printing Office, Washington, D.C., 1970.
11. J. L. FRANKLIN, J. G. DILLARD, H. M. ROSENSTOCK, J. T. HERRON, K. DRAXL, and F. H. FIELD. Report No. NSRDS-NBS 26, U.S. Government Printing Office, Washington, D.C., 1969.

12. F. H. FIELD and J. L. FRANKLIN. Electron impact phenomena. Academic Press, New York. 1957.
13. F. W. MCLAFFERTY (*Editor*). Mass spectrometry of organic ions. Academic Press, New York. 1963.
14. C. E. MOORE. Atomic energy levels. National Bureau of Standards Circular 467, U.S. Government Printing Office, Washington, D.C., 1949.
15. S. N. FONER and B. H. NALL. Phys. Rev. **122**, 512 (1961).
16. C. E. MELTON and W. H. HAMILL. J. Chem. Phys. **41**, 546 (1964).
17. L. KERWIN, P. MARMET, and E. M. CLARKE. Advan. Mass Spectrom. **2**, 522 (1959).

Analysis of the Visual Spectrum of Methyl Orange in Solvents and in Hydrophobic Binding Sites

RICHARD L. REEVES AND ROBERT S. KAISER
Research Laboratories, Eastman Kodak Company, Rochester, New York 14650

AND

MARY S. MAGGIO, EDWARD A. SYLVESTRE, AND WILLIAM H. LAWTON
Management Systems Development Department, Eastman Kodak Company, Rochester, New York 14650

Received June 19, 1972

The absorption curves of methyl orange (MO) and analogous *p*-aminophenylazobenzenes in organic and aqueous organic solvents are shown to consist of two severely overlapping bands. The curves have been resolved into two skewed component bands using a regression method. The blue shift of the absorption maximum obtained when organic solvents are added to aqueous solutions of MO, or when MO is bound to bovine serum albumin or a surfactant micelle, is the result of a change in relative intensities of the component bands. The low-frequency component is assigned to a $\pi_1 \rightarrow \pi_1^*$ transition of a solvate in which there is specific hydrogen-bonding interaction between solvent and the azo nitrogens, and the high-frequency component to a $\pi_1 \rightarrow \pi_1^*$ transition of a solvate in which the interaction is absent. The low-frequency component is favored by aqueous solvent compositions and by low temperatures. The free energies of interconversion of the species in various hydrogen-bonding solvents are correlated by the solvent surface tension but not by the dielectric constant. The results show that the shift in absorption maximum accompanying binding to a protein or micelle should be interpreted as a shift in an equilibrium rather than as a shift in transition energy.

Les courbes d'absorption du méthylorange (MO) et des *p*-aminophénylazobenzènes analogues, en solvants organiques et organiques aqueux, comprennent deux bandes fortement enchevêtrées. La résolution de ces courbes en deux bandes gauches élémentaires a été faite par la méthode de régression. Le déplacement vers le bleu du maximum d'absorption, obtenu par addition de solvants organiques aux solutions aqueuses de MO ou lorsque le MO est lié à l'albumine du sérum bovin ou à une micelle surfactive, est le résultat du changement des intensités relatives des bandes composantes. La bande à basse fréquence est attribué à la transition $\pi_1 \rightarrow \pi_1^*$, d'un produit de solvatation dans lequel il y a interaction spécifique par liaison hydrogène entre le solvant et les azotes de l'azo; la bande à haute fréquence correspond à la transition $\pi_1 \rightarrow \pi_1^*$ du produit de solvatation sans interaction. La bande à basse fréquence est favorisée par la composition en eau des solvants et aux basses températures. Les énergies libres de l'interconversion des diverses espèces dans différents solvants à liaison hydrogène, ont été reliées à la tension superficielle du solvant et non à la constante diélectrique. Les résultats montrent que le déplacement du maximum d'absorption consécutif à une liaison à une protéine ou micelle devraient être interprétés plutôt comme un déplacement d'équilibre qu'un déplacement de l'énergie de transition. [Traduit par le journal]

Can. J. Chem., **51**, 628 (1973)

Methyl orange (MO, **1**) has been used as a probe for studying the interaction of organic anions with proteins (1–9), synthetic polymers (10, 11), polyelectrolytes (12), and surfactants (12–14) in aqueous solution. The interaction is usually accompanied by spectral changes that are not associated with the acid–base indicator properties of the dye. Binding to bovine serum albumin (BSA) (2, 3), to human serum albumin (HSA) at slightly acid p*H* values (3), and to surfactant micelles (13, 14) gives a shift of the absorption maximum to higher frequencies that can be duplicated by adding ethanol to aqueous solutions of MO (6, 15, 16). Binding to HSA in mildly alkaline solutions is anomalous in that the absorption curve is shifted to lower frequencies and increases in intensity (3, 7). A number of explanations have been offered for the blue shift of the absorption maximum. Forbes and Milligan (6) showed that an earlier proposal involving electrostatic interactions between protonated amino groups of the protein with the sulfonate group of MO (2) was incorrect. The importance of the *p*-dimethylamino group in giving the spectral changes was recognized (3, 6, 15) and hydrogen-bonded interactions between solvent and the amino group, azo nitrogens, and sulfonate group have

Can. J. Chem. Downloaded from www.nrcresearchpress.com by 210.87.254.5 on 09/05/12
For personal use only.

Can. J. Chem. Downloaded from www.nrcresearchpress.com by 210.87.254.5 on 09/05/12
For personal use only.

been proposed (6, 15). Forbes and Milligan predicted correctly that hydrogen-bonding to the azo nitrogens should give a red shift (17–19), and out-of-plane twisting should give a blue shift, but were incorrect in their suggestion that hydrogen-bonding to the amino group should also give a red shift (19). Brode and co-workers alone have recognized that the absorption curve of MO could consist of two overlapping bands and interpreted the low-frequency component as arising from a solvate containing a hydrogen bond between water and the azo group (15).

The demonstration that the spectral changes associated with the binding of dyes to proteins can be used quantitatively as a tool for studying the binding (2) increases the importance of understanding the factors responsible for the changes. The high correlation between spectral changes in mixed aqueous solvents and in hydrophobic binding sites suggests that the dyes experience similar changes in environment in both cases. This correlation has led some investigators to interpret the "polarity" of protein binding sites in terms of empirical solvent polarity parameters (9, 14, 20). Our recent findings that some hydrophobic dyes undergo specific solvation changes in mixed aqueous solvents that are related to changes in solvent structure (21, 22) has led us to make a detailed spectral analysis of MO and similar dyes in pure hydrogen-bonding solvents, in aqueous binaries, in a surfactant micelle, and bound in albumin. Several facts support the idea that the visual spectrum of MO consists of two unresolved bands. The shape of the absorption curve changes in mixed aqueous solvents (Fig. 1) and is not that expected for a distribution function associated with a single band. The curves are too broad and are highly skewed toward high frequencies in an aqueous environment and toward low frequencies in organic compositions. The absorption curves of the related dyes, **5** and **6**, are narrower, more symmetric, and do not give a blue shift on transfer from water to ethanol. We have resolved the absorption curves of MO and a series of *p*-aminophenylazobenzenes (**2**–**4**) into the component bands using a nonlinear least-squares method, which puts no restriction on the nature of the function used in resolution (Gaussian, Lorentzian, etc). Our results give insight into the nature of the interaction of the dyes with hydrogen-bonding solvents and with binding sites.

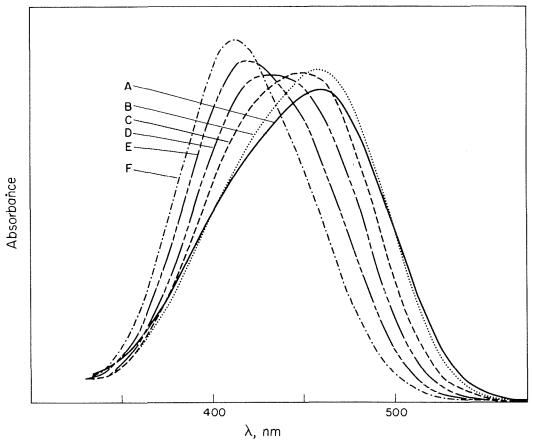

FIG. 1. Absorption curves of methyl orange in ethanol–water mixtures: *A*, water; *B*, $x_2 = 0.088$; *C*, $x_2 = 0.175$; *D*, $x_2 = 0.332$; *E*, $x_2 = 0.612$; *F*, ethanol.

Experimental

Materials

The dyes used in the study are shown in Scheme 1.

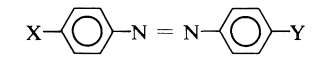

1: X = Me_2N, Y = SO_3Na
2: X = Me_2N, Y = COONa
3: X = Me_2N, Y = H
4: X = H_2N, Y = H
5: X = HO, Y = SO_3H
6: X = MeO, Y = SO_3Na

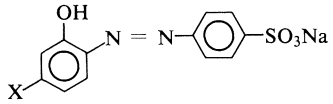

7: X = OH
8: X = Me

SCHEME 1. Dye structures

Methyl orange was certified Eastman reagent grade and was recrystallized from water. Dyes **5** and **7** were Eastman reagent grade and were recrystallized from ethanol–water and water, respectively. Dyes **2**–**4** were Eastman reagent grade and were used without further purification. Dye **6** was a sample prepared previously (19) and **8** was prepared and purified by the standard method (23). Crystalline native bovine serum albumin was purchased from Nutritional Biochemicals. The ethanol, tert-butyl alcohol, and *N*-methylformamide were the solvents used previously (21). The formamide was the center cut from freshly distilled Eastman reagent grade material. Burdick and Jackson "Distilled in Glass" DMF and DMSO were redistilled immediately before use. An unopened bottle of B and J dioxane, distilled in glass and stored under nitrogen, was used without further purification. The preparation of solutions was described previously (21).

Can. J. Chem. Downloaded from www.nrcresearchpress.com by 210.87.254.5 on 09/05/12
For personal use only.

Spectral Measurements and Analysis

Absorption curves were obtained on a Beckman DK-2A recording spectrophotometer at dye concentrations of $2.0 \times 10^{-5} - 2.5 \times 10^{-5}$ *M*. No changes in the absorption curves were seen on a 10-fold dilution. The wavelength calibration of the spectrophotometer was checked at the beginning of the study against the 546 nm mercury line and was rechecked periodically during the study with a holmium oxide glass filter. Absorbance accuracy was checked against standard NBS potassium chromate solutions (24). Solutions were thermostated at 25° and the absorption curves were obtained in a thermostated cell block.

Curve Resolutions

We assumed that each of the *n* experimental absorption curves is a linear combination of two identical-shaped component functions. Although the basic shape of the components is the same for all solvent mixtures, the amplitudes, widths, and lateral displacements of *each* component are allowed to vary independently within the mixtures. The *i*th observed curve can be modeled by

$$[1] \quad y_i(x) = f(\boldsymbol{\theta}_i; x) + \text{error} \qquad i = 1, \ldots, n$$

where

$$[2] \quad f(\boldsymbol{\theta}_i; x) = \theta_{1i} g\left(\frac{x - \theta_{2i}}{\theta_{3i}}\right) + \theta_{4i} g\left(\frac{x - \theta_{5i}}{\theta_{6i}}\right)$$

θ_{1i} and θ_{4i} are the ε_{max} for the components, since g is normalized to unit height, θ_{2i} and θ_{5i} are the respective $\bar{\nu}_{max}$, and θ_{3i} and θ_{6i} are proportional to the bandwidths at half-peak height and $g(x)$ is the shape function of the components. Instead of specifying $g(x)$ as Gaussian or Lorentzian, we used regression analysis to determine simultaneously the best $g(x)$ and the best set of parameter vectors, $\boldsymbol{\theta}_i$, *i.e.*, the g and $\boldsymbol{\theta}_i$ which minimize

$$Q = \sum_{i=1}^{n} \sum_{j=1}^{p_i} [y_i(x_{ij}) - f(\boldsymbol{\theta}_i; x_{ij})]^2$$

where x_{ij}, $j = 1, \ldots, p_i$ are the points at which the *i*th curve has been read.

In the analysis we restrict ourselves to the selection of the best function g in the set of empirical functions G which are defined by a set of points (x_k^*, y_k^*), $k = 1, \ldots, m$. The function g is defined for all x by connecting the points (x_k^*, y_k^*) by straight lines within the region $x_1^* \leqslant x \leqslant x_m$ and setting it constant (and equal to the end points) outside this region. Since any function can be approximated arbitrarily well within a finite interval by this method, we have put no restrictions on the shape of g by restricting our attention to finding the best $g \in G$. The empirical approximating function is then given by

$$g(x) \begin{cases} \displaystyle\sum_{k=1}^{m-1} \left[\frac{y_{k+1}^* - y_k^*}{x_{k+1}^* - x_k^*}(x - x_k) + y_k^*\right] \Delta_k(x) & x_1^* < x \leqslant x_m^* \\ y_1^*, \; x \leqslant x_1^* \\ y_m^*, \; x > x_m^* \end{cases}$$

where

$$\Delta_k(x) = \begin{cases} 1 & \text{for } x_k^* < x \leqslant x_{k+1}^* \\ 0 & \text{otherwise} \end{cases}$$

The analysis proceeds by selecting the points $x_1^*, \ldots, x_m^*$ at which the optimal function $g(x)$ is to be determined. Initial estimates of the n parameter vectors $\boldsymbol{\theta}_i$ are made. Each iteration of the procedure uses a linear regression to determine an improved estimate of $g(x)$, *i.e.*, of the y_k^*'s. Then n nonlinear regressions are done to produce improved estimates of the $\boldsymbol{\theta}_i$. The iterations continue until the estimate of $g(x)$ has converged to a specified number of decimal places (in our case, to three). Details of the mathematical analysis are given elsewhere (25).

Absorbance values were read from the curves at 10 nm intervals from 600 nm, where the absorbance is zero, through 360 nm, where the absorbance from the tail of a slightly overlapping u.v. band is negligible. The x_k^* were initially selected by assuming that the $g(x)$ was Gaussian. These values were subsequently modified to yield a smooth representation of $g(x)$. In the early stages we obtained starting values for the parameter vectors, $\boldsymbol{\theta}_i$, by fitting the curves visually with linear combinations of two Gaussian functions on a DuPont curve analyzer. Later, however, initial estimates were obtained by making experienced guesses.

Results and Discussion

The absorption curves of the *p*-aminophenylazobenzenes (**1**–**4**) all showed similar spectral changes in aqueous ethanol mixtures. Representative curves of MO are shown in Fig. 1. Absorption curves of MO were also measured and resolved in mixtures of water with tert-butyl alcohol, dioxane, DMF, DMSO, in 50 vol% ethylene glycol, and in neat formamide, *N*-methylformamide, and ethylene glycol. We found that linear combinations of the same function served to reconstitute the experimental absorption curves of MO in all solvents, for MO in a micelle of hexadecyltrimethylammonium bromide (HTAB), and in the adsorbed state on BSA, and of **2**–**4** in all water–ethanol mixtures.

The second derivative spectra of solutions of MO in water and in 25 mol% ethanol showed minima at about 21 000 and 24 000 cm^{-1}, corresponding to the frequencies of the maxima of the components obtained by the resolution by regression analysis. It has been shown that higher-derivative spectra of multicomponent systems with overlapping bands facilitate the detection and location of the components (26, 27).

Because the band overlap is so severe and the spectral parameters are so highly correlated, the error surface for the resolution is shallow and

Can. J. Chem. Downloaded from www.nrcresearchpress.com by 210.87.254.5 on 09/05/12
For personal use only.

rigorous criteria for convergence had to be applied to the regressions. Usually, iteration was continued until the root-mean-square differences between experimental and reconstituted absorption curves were nearly the experimental error for the spectrophotometry (about 0.016×10^4 extinction units). Using this criterion we found that replicate resolutions of four different solutions of MO in water gave standard errors for integrated intensities ($I = \int \varepsilon d\bar{\nu}$) of 1.03×10^6 cm mol^{-1} (1.65%) and 7×10^5 cm mol^{-1} (0.7%) for the low- and high-frequency components, respectively, and for ν_{max}, standard errors of 26 (0.12%) and 16 cm^{-1} (0.07%), respectively. In water the relative intensities of the low- to the high-frequency component are closest to unity (0.63), where one would expect the greatest difficulty in finding unique parameter values. The resolution should improve as one component becomes more predominant and then deteriorate as the minor component makes a relatively small contribution to the total curve. Figure 2 shows several typical resolutions.

We also attempted the resolution with two Gaussian functions on a frequency scale, but always obtained a much poorer fit than with the empirically determined skewed function. We likewise tried eq. 2 with a single component and found the fit to be inadequate. We have shown previously that an isolated band corresponding to the $\pi \rightarrow \pi^*$ transition for an azomethine dye is best described by a skewed function (22).

Absorption curves of MO in 47.8 mol% ethanol and in 50% (v/v) ethylene glycol – water were also measured at 45°, 0°, −30°, and −60°. The high-frequency component was predominant in the ethanol mixture at 25°, whereas the glycol mixture gave a curve typical of aqueous compositions. The absorption curves for the glycol – water mixture are shown in Fig. 3. In both cases, lowering the temperature increased the low-frequency component relative to the high-frequency component and gave the expected decrease in bandwidths. Both bands were shifted to slightly lower frequencies. If the experimental absorption curve were a single band, lowering the temperature should merely have decreased the width and increased the amplitude. The observed change confirms the presence of two bands, which are affected differentially by changing temperature. Further evidence for the presence of two bands comes from the fact that a clearly discernible shoulder

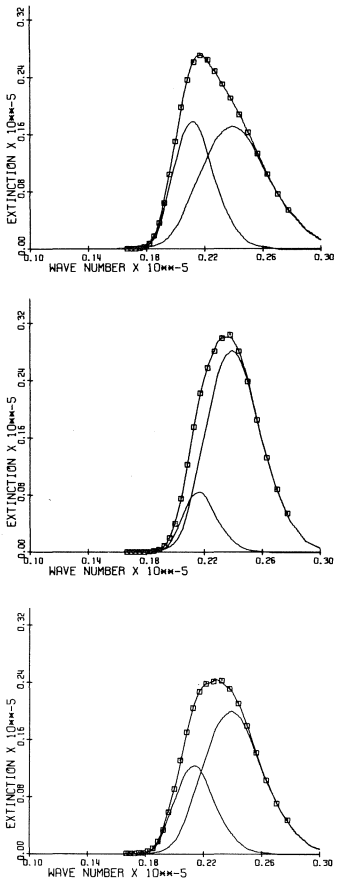

FIG. 2. Resolution of absorption curves of methyl orange. Upper curve, water; center curve, 0.677 mol fraction DMF; and lower curve, 9.0×10^{-5} *M* BSA, p*H* 7.0. The curves drawn through the data points are summations of the component curves.

is seen on the low-frequency side of the curve of **4** in 10% ethanol (15).

The principal long-wavelength absorption band of **5** and **6** and of the unsubstituted and *p*-chloro-substituted analogs are different from those of **1**–**4**, and appear to be single bands. They are nearly symmetric about the maximum on a wavelength plot and are narrower (69 nm at half-peak height for **6** in water compared to 114 nm for MO). Furthermore, transfer of **6** from water to ethanol does not give the blue shift seen with **1**–**4**, but a very small red shift (3 nm). The presence of two overlapping bands is characteristic only of the *p*-amino derivatives (15).

Hückel molecular orbital calculations on **3** show that the only electronic transition expected

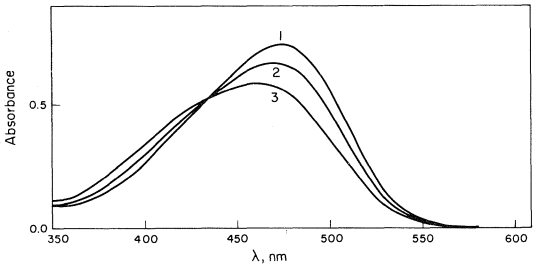

FIG. 3. The effect of temperature on the absorption curve of MO in 50% (v/v) ethylene glycol – water. Curve 1, −60°; curve 2, 0°; curve 3, 45°.

in the visual region is a single $\pi \rightarrow \pi^*$ transition (28). Using the ω-technique, Kroner and Bock calculated a transition energy that agreed with the experimental value obtained in nonpolar solvents. The low-energy band seen in aqueous solvents must be a $\pi \rightarrow \pi^*$ transition of a new absorbing species characteristic of an aqueous environment. The intensity of the low-frequency band is too great for an $n \rightarrow \pi^*$ transition. The possibility of *trans* → *cis* isomerism in the aqueous media has also been ruled out (15).

A unique solvent effect on the *p*-dimethylamino derivatives, arising from compressional forces in the structured solvents which twist this group out of coplanarity with the benzene ring, can also be ruled out. Such twisting results in a decrease in intensity of the $\pi \rightarrow \pi^*$ transition with either no frequency shift or a small blue shift (29). Furthermore, an explanation involving twisting cannot account for the fact that **4** shows the same spectral changes in the mixed solvents as **1**–**3**.

The most reasonable interpretation of the appearance of a low-frequency band in aqueous solutions of the *p*-amino derivatives is that of Brode and co-workers whereby the band is attributed to a hydrogen-bonded interaction between water and the azo nitrogens (15). The unique property of the *p*-amino group is the enhancement of the basicity of the azo nitrogens. We have calculated a pK_a of +3.6 for the azonium ion of MO, using the experimental pK_a and the azonium/ammonium tautomer ratio of the conjugate acid. The corresponding pK_a values of the next most basic derivatives, **5** and **6**, are estimated to be −1.45 and −1.49, respectively (19). The enhancement of basicity of —N=N by Me_2N— is demonstrated by the fact that an exhalted σ^+ substituent constant of −3.0 is required for Me_2N— to correlate the pK_a of MO azonium ion with the values of other ions in a homologous series. Covalent protonation of the azo nitrogens gives a pronounced red shift of the $\pi_1 \rightarrow \pi_1^*$ transition (17–19). It seems reasonable that weaker hydrogen-bonding interactions with solvent should give a smaller red shift.

Dyes **7** and **8** both have intramolecular hydrogen bonds (23). The absorption curves of both in alcohol – water mixtures showed low-frequency bands appearing either as a partially resolved shoulder or as a separate band. The relative intensities of the low-frequency components in the curves of **7** and **8** are in the same order as the relative strengths of the hydrogen bonds, as reflected in the differences in pK_a (23). Infrared (30) and electronic spectra (31) of 2- and 4-phenylazophenols show that these compounds exist as azophenols and not as quinone hydrazones in the solids and in solution.

Table 1 gives the intensities of the low-frequency (I_1) and high-frequency (I_2) components in the various neat solvents. Also listed are the solvent dielectric constants, surface tensions, and two empirical solvent "polarity" parameters, the *E* values of Reichardt and Dimroth, and δ values of Hildebrand (for a review of solvent polarity parameters for correlating spectroscopic data, see ref. 32). The *E* values are solvent-induced frequency shifts of a betaine probe and are thought to include the effect of hydrogen-bonding from solvent. The δ values are the square roots of the cohesive energy densities and are thought to be proportional to the energy required to form a solvent cavity. If we assume that the intensity ratio is equivalent to an equilibrium quotient, the logarithm of the ratio is proportional to the free energy for converting the non-hydrogen-bonded to the hydrogen-bonded solvate. Table 1 shows that the dielectric constant does not even predict the direction of change in the I_1/I_2 ratio. Figure 4 shows that there is an excellent correlation of log (I_1/I_2) with solvent surface tension (r = 0.997). A somewhat poorer correlation of log (I_1/I_2) is obtained with the *E* and δ values (r = 0.936 and 0.900, respectively). This result demonstrates the relationship between the spectral properties of the dye probe and the structural features of the hydrogen-bonding solvents. The correlation with γ suggests that the same forces that lead to high surface energies (solvent–solvent interactions) also promote sol-

Can. J. Chem. Downloaded from www.nrcresearchpress.com by 210.87.254.5 on 09/05/12
For personal use only.

TABLE 1. Intensities of the component bands of the methyl orange spectrum in hydrogen-bonding solvents at 25°

	ε (D)	γ_{25} (dyn/cm)	δ*	E^* (cm^{-1})	$I_1 \times 10^{-7}$ (cm/mol)	$I_2 \times 10^{-7}$ (cm/mol)
Water	78.5	71.97	23.4	63.1	6.26	10.00
Formamide	109.5	57.91	19.2	56.6	3.26	8.69
Ethylene glycol	37.7	46.1	14.6	56.3	2.95	12.32
N-Methylformamide	182.4	38.90	16.1	54.1	2.16	13.82
Ethanol	24.3	21.90	12.7	51.9	1.18	14.68

*From ref. 32.

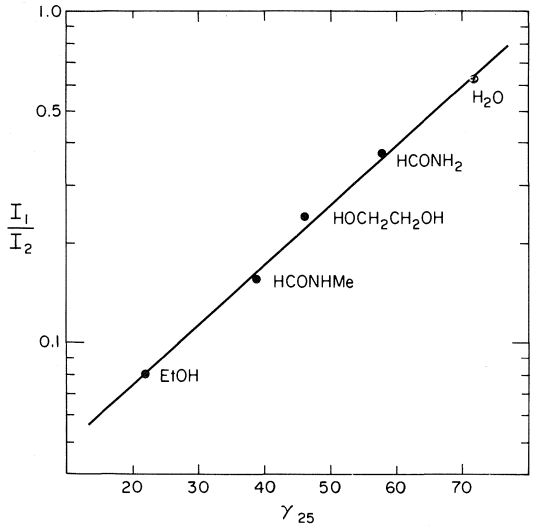

FIG. 4. Semilog plot of the intensity ratios of the component bands of MO in hydrogen-bonding solvents at 25° against the solvent surface tension.

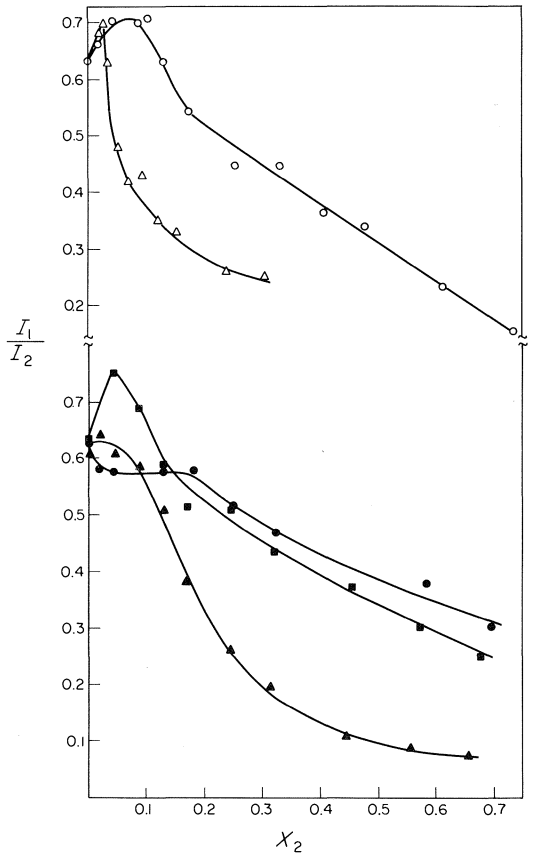

FIG. 5. Effect of solvent composition on the intensity ratios at 25° of the resolved low-frequency (subscript 1) and high-frequency (subscript 2) bands in aqueous ethanol, ○; tert-butyl alcohol, △; dioxane, ▲; DMSO, ●; and DMF, ■.

vent–solute hydrogen-bonded interaction. The correlation with γ is for an interface with air of infinite radius of curvature, and not with the more appropriate (but inaccessible) interfacial tension corrected for a radius of curvature of molecular dimensions. It has been shown that the curvature correction is appreciable (33).

The effect of solvent composition on the intensity ratios and frequency maxima of the resolved bands in the aqueous binaries is shown in Figs. 5 and 6. In the frequency plots, the data point at $x_2 = 0$ (x_2 = mole fraction of organic component) is scaled to represent 95% confidence limits estimated from four replicates. The plots show that the spectral parameters in the alcohol–water mixtures do not vary in the same way as dielectric constant and empirical polarity scales such as the Kosower Z values (34) and the Y values of Grunwald and Winstein (35) since plots of these parameters against x_2 show no extrema or inflections. Most of the irregularities in the spectral parameters of MO occur in the highly aqueous solvent compositions, suggesting that this dye is inducing some solvent sorting in the mixed solvents. We have recently

Can. J. Chem. Downloaded from www.nrcresearchpress.com by 210.87.254.5 on 09/05/12
For personal use only.

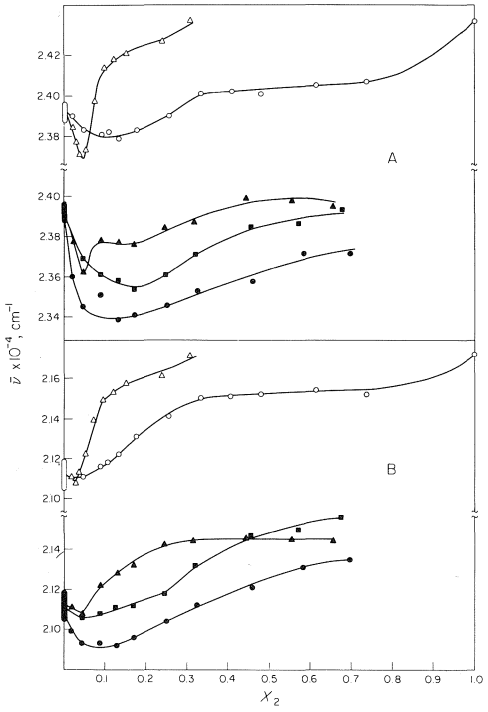

FIG. 6. Effect of solvent composition on the frequencies of maximum absorption of the resolved bands of MO in aqueous ethanol, ○; tert-butyl alcohol, △; dioxane, ▲; DMSO, ●; and DMF, ■. *A*, high-frequency component; *B*, low-frequency component.

presented evidence for induced solvent sorting from equilibrium (21), kinetic (22), and spectral studies (22) of other dyes. The effects of selective solvation on spectral properties have been treated theoretically (36).

There is a reciprocal relationship between the intensity of the low-frequency (I_1) and high-frequency (I_2) component bands that is responsible for the apparent blue shift in the experimental curves. The extrema and plateaus in the highly aqueous compositions suggest that in each case, the initial addition of the organic solvent reinforces the hydrogen-bonded interaction between solvent and dye. Similar extrema appear in the frequency plots and show that the initial addition of organic solvents shifts the resolved bands to lower frequencies. These shifts are small, but larger than experimental error. The large apparent shift of the composite curve is due primarily to the change in relative intensities.

The presence of extrema in the spectral properties of the resolved bands of MO in aqueous alcohol mixtures parallels closely the extrema that are found in many other properties of the mixtures both in the absence (37, 38) and presence of solutes (39). The generally accepted interpretation for such deviations from ideality is that the initial addition of the alcohol increases the long-range order of the solvent, and that the extrema occur at concentrations where the structure-promoting effect of the organic solvent is reversed. Our results indicate that the changes in the solvent–solvent interaction is reflected in changes in the solvent–solute interaction.

Figures 5 and 6 also show that the addition of aprotic solvents to aqueous solutions can give the same qualitative changes in the spectral parameters of MO as the two alcohols. This may not mean that similar changes in the solvent structure are induced by the protic and aprotic organic solvents. Extrema in excess thermodynamic functions of mixing (38), in viscosities (40) and in Walden product (40) occur in the water-rich dioxane–water mixtures, but these are not thought to result from enhancement of the long-range order. On the other hand, aqueous DMSO mixtures also show extrema in excess thermodynamic functions of mixing and in viscosity (41), and neutron inelastic scattering studies indicate that this solvent does increase the long-range order, with a maximum effect at $x_2 = 0.33$ (42).

The present results indicate that specific solute–solvent interactions occur in each of the binary mixtures. This fact and the failure of the spectral parameters of the resolved bands to parallel changes in solvent "polarity" scales show the difficulty in trying to conclude anything about the "polarity" of a binding site by comparing spectra of bound dye to spectra in aqueous organic solvent. By our interpretation, the spectral change accompanying the binding of MO to BSA or solubilization into a micelle is more the result of a diminution in a specific interaction with the aqueous solvent (hydrogen-bonding) than a change in polarity. The total change in the absorption curve of MO can be interpreted as a shift in the position of a ground-state equilibrium between solvation species, rather than as a change in transition energy of a single species as suggested by Williamson and Corwin (9, 14). Whereas a binding site may actually be less polar than the aqueous environment, we do not think that this is responsible for the spectral change. About all that can be

Can. J. Chem. Downloaded from www.nrcresearchpress.com by 210.87.254.5 on 09/05/12
For personal use only.

done is to compare the intensity ratios of the component bands of bound MO with the ratios in the solvent mixtures in order to find solvents showing similar spectral changes. Thus the ratio of the high-frequency to the low-frequency band in MO fully bound to BSA is 2.4, comparable to the ratio found in 30 mol% ethanol, 8 mol% tert-butyl alcohol, 15 mol% dioxane, and 40 mol% DMF and DMSO. Similarly, the intensity ratio in 0.002 *M* HTAB (cmc 9.1×10^{-4} *M* (43)) is 8.4, corresponding to the ratio found in about 84 mol% ethanol or 42 mol% dioxane. This shows that the environment of the dye in the micelle is less "waterlike" than the binding site on BSA, but we can make no numerical estimate of the "polarities" of either environment from comparison of spectral properties in the mixed solvents.

1. I. M. KLOTZ, F. M. WALKER, and R. B. PIVAN. J. Am. Chem. Soc. **68**, 1486 (1946).
2. I. M. KLOTZ. J. Am. Chem. Soc. **68**, 2299 (1968).
3. I. M. KLOTZ, R. K. BURKHARD, and J. M. URQUART. J. Am. Chem. Soc. **74**, 202 (1952).
4. F. KARUSH. J. Am. Chem. Soc. **73**, 1246 (1951).
5. G. MARCUS. Proc. Natl. Acad. Sci. U.S. **54**, 253 (1965).
6. W. F. FORBES and B. MILLIGAN. Aust. J. Chem. **15**, 841 (1962).
7. E. PROKOPOVA and P. MUNK. Collect. Czech. Chem. Commun. **28**, 957 (1963).
8. L. A. E. ASHWORTH and C. GREEN. Biochem. Biophys. Acta, **70**, 68 (1963).
9. C. E. WILLIAMSON and A. H. CORWIN. J. Colloid Interfac. Sci. **38**, 577 (1972).
10. G. OSTER. J. Polym. Sci. **16**, 235 (1955).
11. G. OSTER. J. Polym. Sci. **9**, 553 (1952).
12. F. QUADRIFOGLIO and V. CRESCENZI. J. Colloid Interfac. Sci. **35**, 447 (1971).
13. R. HAGUE and W. U. MALIK. J. Phys. Chem. **67**, 2082 (1963).
14. C. E. WILLIAMSON and A. H. CORWIN. J. Colloid Interfac. Sci. **38**, 567 (1972).
15. W. R. BRODE, I. L. SELDIN, P. E. SPOERRIC, and G. M. WYMAN. J. Am. Chem. Soc. **77**, 2762 (1955).
16. I. M. KLOTZ, R. K. BURKHARD, and J. M. URQUART. J. Phys. Chem. **56**, 77 (1952).
17. H. H. JAFFE, S. YEH, and R. W. GARDNER. J. Mol. Spectrosc. **2**, 120 (1958).
18. R. L. REEVES and W. F. SMITH. J. Am. Chem. Soc. **85**, 724 (1963).
19. R. L. REEVES. J. Am. Chem. Soc. **88**, 2240 (1966).
20. D. C. TURNER and L. BRAND. Biochem. **7**, 3381 (1968).
21. R. L. REEVES and R. S. KAISER. J. Org. Chem. **35**, 3670 (1970).
22. R. L. REEVES and R. S. KAISER. *In* Water structure at the water–polymer interface. *Edited by* H. H. G. Jellinek. Plenum Press, New York. 1972. p. 56.
23. M. C. ROSE and J. STUEHR. J. Am. Chem. Soc. **93**, 4350 (1970).
24. W. R. BRODE, J. H. GOULD, J. E. WHITNEY, and G. M. WYMAN. J. Opt. Soc. Am. **43**, 862 (1953).
25. W. H. LAWTON, E. A. SYLVESTRE, and M. S. MAGGIO. Technometrics, **14**, 513 (1972).
26. W. L. BUTLER and D. W. HOPKINS. Photochem. Photobiol. **12**, 439 (1970).
27. B. A. GULYAEV, F. F. LITVIN, and E. P. VEDENEEV. Biol. Nauk. **14**, 49 (1971).
28. J. KRONER and H. BOCK. Chem. Ber. **101**, 1922 (1968).
29. H. H. JAFFE and M. ORCHIN. Theory and applications of ultraviolet spectroscopy. John Wiley and Sons, Inc., New York. 1962. p. 389.
30. D. HADZI. J. Chem. Soc. 2143 (1956).
31. A. BURAWOY and J. T. CHAMBERLIN. J. Chem. Soc. 3734 (1952).
32. See F. W. FOWLER, A. R. KATRITZKY, and R. J. D. RUTHERFORD. J. Chem. Soc. B, 460 (1970).
33. D. S. CHOI, M. S. JHON, and H. EYRING. J. Chem. Phys. **53**, 2608 (1970).
34. E. M. KOSOWER. J. Am. Chem. Soc. **80**, 3253 (1958).
35. E. GRUNWALD and S. WINSTEIN. J. Am. Chem. Soc. **70**, 846 (1948).
36. J. MIDWINTER and P. SUPPAN. Spectrochim. Acta, **25A**, 953 (1969).
37. F. FRANKS and D. J. G. IVES. Q. Rev. **20**, 1 (1966).
38. F. FRANKS. *In* Physico-chemical processes in mixed aqueous solvents. *Edited by* F. Franks. American Elsevier Publishing Co., New York. 1967. p. 50.
39. E. M. ARNET. *In* Physico-chemical processes in mixed aqueous solvents. *Edited by* F. Franks. American Elsevier Publishing Co., New York. 1967. p. 105.
40. R. L. KAY and T. L. BROADWATER. Electrochim. Acta, **16**, 667 (1971).
41. H. H. SZMANT. *In* Dimethyl sulfoxide. *Edited by* S. W. Jacob, E. E. Rosenbaum, and D. C. Wood. Marcel Dekker, Inc., New York. 1971. p. 35.
42. G. J. SAFFORD, P. C. SCHAFFER, P. S. LEUNG, G. F. DOEBBLER, G. W. BRADY, and E. F. X. LYDEN. J. Chem. Phys. **50**, 2140 (1969).
43. P. MUKERJEE and K. J. MYSELS. Critical micelle concentrations of aqueous surfactant systems. Natl. Stand. Ref. Data Ser. Natl. Bur. Stand. (U.S.) 1971.

Can. J. Chem. Downloaded from www.nrcresearchpress.com by 210.87.254.5 on 09/05/12
For personal use only.

Erratum: Pulse Radiolysis of Aqueous Papain

J. R. CLEMENT AND D. A. ARMSTRONG
Department of Chemistry, University of Calgary, Calgary, Alberta T2N 1N4
AND
N. V. KLASSEN AND H. A. GILLIS
Division of Physics, National Research Council of Canada, Ottawa, Canada K1A 0R6

Received November 23, 1972
(Ref.: Can. J. Chem. **50**, 2833 (1972))

On page 2833, the date of receipt and the National Research Council of Canada contribution number were inadvertently omitted. The date of receipt is April 21, 1972 and the NRCC No. is 12675.

Can. J. Chem. Downloaded from www.nrcresearchpress.com by 210.87.254.6 on 09/05/12
For personal use only.

Can. J. Chem. Downloaded from www.nrcresearchpress.com by 210.87.254.5 on 09/05/12
For personal use only.

"Sideways" Bonded Dinitrogen in Matrix Isolated Cobalt Dinitrogen, CoN_2

G. A. OZIN AND A. VANDER VOET

Lash Miller Chemistry Laboratory and Erindale College, University of Toronto, Toronto, Ontario

Received October 16, 1972

Infrared spectra are reported for matrix isolated cobalt dinitrogen isotopic species, $Co^{14}N_2$, $Co^{14}N^{15}N$ and $Co^{15}N_2$, formed in the cocondensation reaction of atomic cobalt with dilute nitrogen–argon matrices at 10 °K. The data provide the first unambiguous spectroscopic evidence for a dinitrogen molecule bonded in a "sideways" fashion to a transition metal atom.

Les spectres infrarouge sont rapportés pour les espèces isotopiques cobalt diazoté, $Co^{14}N_2$, $CO^{14}N^{15}N$ et $CO^{15}N_2$, isolées par matrice et formées par condensation du cobalt atomique avec des matrices diluées d'azote–argon à 10 °K. Ces données fournissent la première preuve spectroscopique et sans ambiguité de l'existence de la molécule d'azote liée de façon latérale à l'atome métallique de transition. [Traduit par le journal]

Can. J. Chem., **51**, 637 (1973)

With the increasing number of reports of stable and matrix isolated transition metal compounds containing coordinated dioxygen or dinitrogen molecules, there has also arisen considerable interest in the mode of bonding and nature of the interaction between the metal and the ligands. Although X-ray crystallography serves to determine unambiguously the type of bonding (end-on or sideways) in stable species, in such cases where diffraction studies are not possible (*i.e.*, matrix isolation systems) vibrational spectroscopic investigations using mixed isotopically substituted ligands, ^{14}N–^{15}N or ^{16}O–^{18}O, are able to distinguish the bonding types. This is due to the *nonequivalence* of the vibrational frequencies of, for example, M—^{15}N—^{14}N and M—^{14}N—^{15}N in both the M—N and N—N stretching regions and the expected splitting of these modes. X-ray crystallography has shown that in transition metal complexes with coordinated dioxygen molecules the bonding can be sideways (1) or end-on non-linear (2). Sideways bonding has been shown in i.r. spectroscopic studies of matrix isolated binary dioxygen complexes (3) $M(O_2)_n$ (where M = Ni, Pd, or Pt and n = 1 or 2). The dinitrogen ligand, on the other hand, has always been found to be bonded in an "end-on" fashion with a linear or near linear M—N—N skeleton (4). Unequivocal i.r. spectroscopic evidence for this bonding type has been shown for the stable cation $[Ru(NH_3)_5N_2]^{2+}$ and matrix isolated NiN_2 (5, 6). In both of these systems, 1:2:1 statistical mixtures of $^{14}N_2$:$^{15}N^{14}N$:$^{15}N_2$ were used and a four-line pattern of νNN stretching modes was observed corresponding to M—$^{14}N_2$, M—$^{14}N^{15}N$, M—$^{15}N^{14}N$, M—$^{15}N_2$. The splittings of the M—$^{14}N^{15}N$/M—$^{15}N^{14}N$ central components were 4.0 and 3.8 cm^{-1} for the ruthenium and nickel complexes respectively. It is also worth noting that the matrix i.r. and Raman spectra of $Ni(^{14}N_2)_4$ in solid argon were in agreement with that expected for a *regular* tetrahedral molecule containing "end-on" bonded dinitrogen (7).

Direct evidence for the existence of a compound containing the dinitrogen molecule bonded in a "sideways fashion" has not previously been reported in the literature. It was, however, postulated (8) as a transition state in the intramolecular $^{14}N^{15}N$ exchange of the anions $[Ru(NH_3)_5$-$^{14}N^{15}N]^{2+}$/$[Ru(NH_3)_5{}^{15}N^{14}N]^{2+}$ as evidenced in the time dependent intensity changes in the Ru—N_2 stretching region. It is noteworthy that Brintzinger's dinitrogen bridged binuclear titanocene complex $(C_5H_5)_2TiN_2Ti(C_5H_5)_2$ shows no absorption in the i.r. attributable to the NN stretching mode. Of the two suggested dinitrogen-bridged centrosymmetric structures, *i.e.* end-on Ti—N≡N—Ti and edge-on

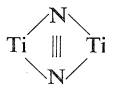

Can. J. Chem. Downloaded from www.nrcresearchpress.com by 210.87.254.5 on 09/05/12
For personal use only.

the latter was favored on the basis of chemical intuition (9).

In this communication we are reporting matrix i.r. spectroscopic evidence for the existence of cobalt dinitrogen, CoN_2, which we find to contain the dinitrogen ligand bonded in a "sideways" fashion to the cobalt atom. Our experiments consisted of cocondensing Co (McKay 99.99%) atoms with dilute nitrogen–argon matrices ($^{14}N_2$:Ar = 1:250; $^{14}N_2$:$^{15}N_2$:Ar = 1:1:2000; $^{14}N_2$:^{14}N-^{15}N:$^{15}N_2$:Ar = 1:2:1:2000 ($^{14}N_2$ Matheson 99.999%, $^{15}N_2$ Prochem 99.5%)) onto a cesium iodide plate cooled to 10 °K by an Air Products Displex closed cycle helium refrigerator. The furnace design and matrix set-up have been previously reported (10). The rate of metal atom deposition was monitored continuously throughout the experiment, using a quartz crystal microbalance as described previously (11). The probability of a Co atom having another Co atom as a nearest neighbor in the matrix was arranged to be less than 10^{-3}. Under these conditions one can be sure of producing mononuclear species. I.r. spectra were recorded on a Beckmann IR 12.

When Co atoms were cocondensed with $^{14}N_2$/Ar = 1:250 matrix gases a single sharp i.r. absorption was observed at 2101.0 cm^{-1} (Fig. 2). When the experiment was repeated with $^{14}N_2$/$^{15}N_2$/Ar = 1:1:2000, a *doublet* was observed at 2101.0 and 2029.5 cm^{-1}, which with $^{14}N_2$/$^{14}N^{15}N$/$^{15}N_2$/Ar = 1:2:1:2000 became a *triplet* at 2101.0, 2066.5, and 2029.5 cm^{-1}. These three i.r. absorptions are clearly assignable to νNN stretching modes of a binary dinitrogen complex of Co containing a *single* dinitrogen molecule, that is CoN_2 (Fig. 1).

The three-line spectrum was carefully examined under conditions of high resolution. All three absorptions were found to have *identical* band widths of 2.5 ± 0.2 cm^{-1} at half height. The slit width used for the highest resolution scan was 0.36 cm^{-1} with a scan speed of 0.4 cm^{-1}/min. At slit widths lower than 1.5 cm^{-1} intensity loss was observed, which indicates that a slit width of 0.36 cm^{-1} is below the 2.5 cm^{-1} band width at half height of the central νNN $Co^{14}N^{15}N$ component. If some splitting of the central component had remained undetected, it must be less than 0.4 cm^{-1}.

Unlike $Ni(N_2)$ (Fig. 2) the central νNN component of $Co^{14}N^{15}N$ is *not* split and has an absorption intensity approximately *twice* that

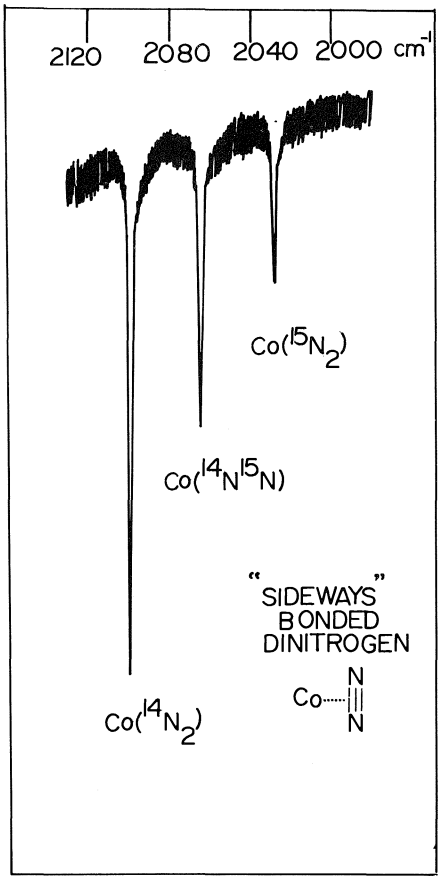

FIG. 1. The matrix i.r. spectrum of the products of the cocondensation reaction of Co atoms with $^{14}N_2$:$^{14}N^{15}N$:$^{15}N_2$:Ar = 1:2:1:2000 at 10 °K. The intensity of the NN stretching mode assigned to $Co(^{14}N_2)$ is larger than expected because of trace quantities of residual $^{14}N_2$ gas either in the vacuum line or in the Ar matrix gas.

of the νNN component belonging to $Co^{15}N_2$. These two spectral observations, when taken in conjunction with the identical band widths at half height of νNN for $Co^{14}N_2$, $Co^{14}N^{15}N$ and $Co^{15}N_2$ and the 3.8–4.0 cm^{-1} doublet splitting of the central component for "end-on" bonded dinitrogen in the nickel and ruthenium complexes (5, 6), are overwhelmingly in favor of dinitrogen bonded in a "sideways" fashion to cobalt in CoN_2.

The dinitrogen ligand in CoN_2 is clearly bonding in a manner similar to that of olefins in transition metal olefin complexes (12). This is unlike dinitrogen in, for example, Andrews' matrix isolated lithium supernitride species (13) which shows an NN stretching mode characteristic of

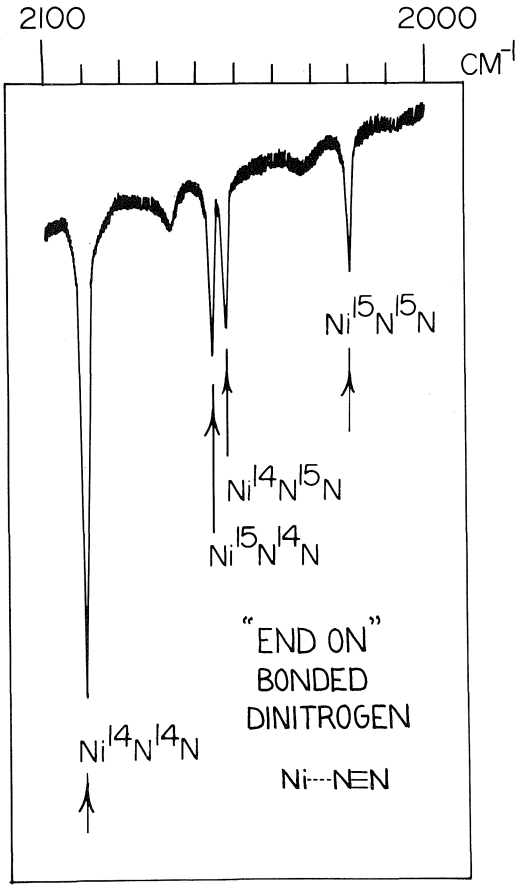

FIG. 2. The matrix i.r. spectrum of the products of the cocondensation reaction of Ni atoms with $^{14}N_2$:$^{14}N^{15}N$:$^{15}N_2$:Ar = 1:2:1:2000 at 10 °K. The intensity of the NN stretching mode assigned to Ni($^{14}N_2$) is larger than expected because of trace quantities of residual $^{14}N_2$ gas either in the vacuum line or in the Ar matrix gas.

reduced dinitrogen at 1800 cm^{-1} (*cf.* 1836–1807 cm^{-1} from the Raman spectra of the supernitride ion N_2^- in potassium halide lattices (14)) and which is best described as an electrostatically bound ion pair $Li^+N_2^-$ (similar to matrix isolated lithium superoxide (15), $Li^+O_2^-$).

Orgel (16) was first to consider the stability of $M-\overset{N}{\underset{N}{|||}}$ relative to M—N≡N by invoking a two way charge-transfer process for the bonding picture of dinitrogen in terms of neutral excited states of the metal and ligand. This simple approach does not yield a clear distinction between side-on and end-on bonded N_2, as the n–π upper state of N_2 is 7.3 eV which is comparable to the π–π excited state of N_2 at 6–8 eV. However, extended Hückel molecular orbital calculations have recently been reported by Yatsimirskii *et al.* (17) for FeN_2 in both the side-on and end-on configurations. The calculated energies indicated that the sideways bonded species would be less stable than the end-on bonded. From considerations of the n_σ and n_π orbital populations for the N—N and N—Fe bonds and their relationships to bond strengths, one would have expected the ν_{NN} stretching frequency of sideways bonded N_2 to lie at a considerably lower frequency than end-on bonded N_2. In actual fact the NN stretching frequency for CoN_2 lies about 10 cm^{-1} *above* that of NiN_2.

The existence of side-on bonded N_2 in CoN_2 may give some clues as to possible new routes to stable complexes containing side-on N_2 and their relationship to the fixation of N_2. For example, synthesis might possibly be directed towards species isoelectronic with Co(0) in CoN_2, namely, Mn(−II), Fe(−I) or Ni(I). One finds in fact, that dinitrogen complexes of these low or negative valence state metals have not yet been investigated. Apparently the anticipated fixation of N_2 via "hydridic" dinitrogen complexes, such as $(Ph_3P)_3Co(H)N_2$ was unsuccessful. A breakthrough might possibly be realized with compounds of the type $L_nM-\overset{N}{\underset{N}{|||}}$ (where M = Mn(−II), Fe(−I), Co(0) or Ni(I)) using acidic rather than hydridic conditions.

We wish to thank Dr. Martin Moskovits for helpful discussion, the National Research Council of Canada and the Research Corporation for financial support.

1. J. A. McGinnety, N. C. Payne, and J. A. Ibers. J. Am. Chem. Soc. **91**, 6301 (1969) and refs. therein.
2. G. A. Rodley and W. T. Robinson. Nature, **235**, 438 (1972).
3. H. Huber and G. A. Ozin. Can. J. Chem. **50**, 3746 (1972).
4. F. Bottomley and S. C. Nyburg. Acta Cryst. B**24**, 1289 (1968); B. R. Davis, N. C. Payne, and J. A. Ibers. Inorg. Chem. **8**, 2719 (1969).
5. Yu. J. Borodko, A. K. Shilova, and A. E. Shilov. Russ. J. Phys. Chem. **44**, 349 (1970).
6. G. A. Ozin and M. Moskovits. J. Chem. Phys. In press.
7. H. Huber, E. P. Kündig, M. Moskovits, and G. A. Ozin. J. Am. Chem. Soc. In press.
8. J. N. Armor and H. Taube. J. Am. Chem. Soc. **92**, 2560 (1970).
9. J. E. Bercaw, R. H. Marvich, L. G. Bell, and H. H. Brintzinger. J. Am. Chem. Soc. **94**, 1219 (1972).

Can. J. Chem. Downloaded from www.nrcresearchpress.com by 210.87.254.5 on 09/05/12
For personal use only.

10. E. P. KÜNDIG, M. MOSKOVITS, and G. A. OZIN. J. Mol. Struct. **14**, 137 (1972).
11. M. MOSKOVITS and G. A. OZIN. J. Appl. Spectry. **26**, 481 (1972).
12. J. CHATT. J. Chem. Soc. 2939 (1953); M. J. S. DEWAR. Bull. Soc. Chim. Fr. **18**, C71 (1951).
13. R. C. SPIKER, L. ANDREWS, and C. TRINDLE. J. Am. Chem. Soc. **94**, 2401 (1972).
14. W. HOLZER, W. F. MURPHY, and H. J. BERNSTEIN. J. Mol. Spectry. **32**, 13 (1969).
15. L. ANDREWS. J. Chem. Phys. **50**, 4288 (1969); L. ANDREWS and A. HATZENBUHLER. J. Chem. Phys. **56**, 3398 (1972); H. HUBER and G. A. OZIN. J. Mol. Spectry. **41**, 595 (1972).
16. L. E. ORGEL. An introduction to transition-metal chemistry. Methuen. 1966.
17. K. B. YATSIMIRSKII and YU. A. KRAGLYAK. Dok. Akad. Nauk SSSR, **186**, 885 (1969).

Can. J. Chem. Downloaded from www.nrcresearchpress.com by 210.87.254.5 on 09/05/12
For personal use only.

Can. J. Chem. Downloaded from www.nrcresearchpress.com by 210.87.254.40 on 09/05/12
For personal use only.

Canadian Journal of Chemistry

Published by
THE NATIONAL RESEARCH COUNCIL OF CANADA

Journal canadien de chimie

Publié par
LE CONSEIL NATIONAL DE RECHERCHES DU CANADA

Volume 51 Number 5 March 1, 1973

Volume 51 numéro 5 1 mars 1973

X-Radiolysis Ion Yields and Electron Ranges in Liquid Xenon, Krypton, and Argon: Effect of Electric Field Strength

MAURICE G. ROBINSON AND GORDON R. FREEMAN

Chemistry Department, University of Alberta, Edmonton, Alberta, T6G 2G2

Received July 21, 1972

X-Radiolysis ion yields were measured at electric fields between 1 and 60 kV/cm in argon at 87 °K, krypton at 148 °K, and xenon at 183 °K. The results were analyzed according to a theoretical model to obtain the total ion yields G_{tot}, the free ion yields at zero field strength G_{fi}^0 and the most probable penetration ranges b of the secondary electrons in the liquids. The respective values were: Ar, 7.3, 2.9, 1330 Å; Kr, 13.0, 5.8, 880 Å; Xe, 13.7, 7.0, 720 Å. The total ionization yields in these substances are greater in the liquid than in the gas phase, probably due to smaller ionization potentials in the condensed phase (polarization energy effect). Field dependent electron mobilities are also reported.

Les rendements en ions libres produits par les rayons X dans l'argon à 87 °K, le krypton à 148 °K, et le xenon à 183 °K ont été mesurés à des champs électriques allant de 1 à 60 kV/cm. Les resultats ont été analysés à l'aide d'un modèle théorique en vu d'obtenir pour chaque liquide le rendement total en ions, G_{tot}, le rendement en ions libres en l'absence de champ électrique, G_{fi}^0, et la distance de penetration la plus probable, b, pour les électrons secondaires. Les valeurs sont respectivement: Ar, 7.3, 2.9, 1330 Å; Kr, 13.0, 5.8, 880 Å; Xe, 13.7, 7.0, 720 Å. Le rendement total en ions pour ces substances est plus élevé en phase liquide qu'en phase condensée (effect de l'energie de polarisation). Les mobilités électroniques en fonction du champ électrique sont presentées.

Can. J. Chem., **51**, 641 (1973)

Introduction

Relationships between the ranges and mobilities of electrons in liquids and the properties of the liquids have aroused considerable interest recently (1–11). Ranges of radiolytically produced secondary electrons and mobilities of thermal electrons in liquid alkanes increase with increasing sphericity of the molecules (1). It has been suggested that anisotropy of molecular polarizability has a major influence on the electron behavior (1, 12).

In this respect the liquified rare gases are worthy of study, having isotropic polarizabilities. Electron behavior in liquid argon (7) is similar to that in methane (5, 7), which seems surprising in spite of the nearly isotropic polarizability of methane. Methane has a more complex structure and much lower molecular energy levels than does monatomic argon. One suspects that interactions of an electron with two or more argon atoms at once are important in the liquid (7). It is therefore of interest to do measurements in krypton and xenon.

Thermal electron mobilities in these liquids are limited by scattering interactions (13–18).

Experimental

Materials and Sample Preparation

Ultrapure grade, 99.999%, argon and Research Grade krypton (5 p.p.m. xenon, no other detectable impurities) were obtained from Matheson. The Research Grade, 99.995%, xenon from Linde contained < 1 p.p.m. oxygen.

The materials were handled in a vacuum rack that was initially evacuated to $< 10^{-6}$ Torr.

Traces of oxygen were removed from argon in the

TABLE 1. Properties of materials

Material	T (°K)	d (g/cm^3)	ε	α (Å^3)*	Z†	Electron density (10^{23} electrons/cm^3)	Vapor pressure (atm)*
Ar	87	1.40‡	1.50§‖	1.63	18	3.80	1
Kr	148	2.15*	1.57‖	2.47	36	5.56	6
Xe	183	2.93*	1.88‖	4.01	54	7.25	3
Au	293	19.3‡			79	46.6	
Pb	293	11.4‡			82	27.1	
LiF	293	2.64‡			~8 for τ	7.35	
Fricke	293	1.02			~8 for τ	3.41	

*Reference 20. Reference 20*b* is obtainable from the U.S. Department of Commerce.
†Atomic number.
‡Reference 19.
§Reference 21.
‖Calculated from the polarizability α and density d, using the Clausius–Mosotti equation.

manner described previously (1, 7). Attempts to similarly purify xenon were unsuccessful. Purification of xenon and krypton was not pursued because it was found that the desired measurements could be made with the materials as supplied.

Physical Properties of the Liquids

These are summarized in Table 1. Values were taken or estimated from data in refs. 19–21.

Conductance Cells

A variety of cells were used, particularly in the case of argon. The large (25 cm^3) cell with a guard ring has already been described (5). Other cells had a much smaller capacity (5 cm^3) and were either of the simple two plate type (Fig. 1*a*) or the guard ring variety (Fig. 1*b*).

The cell constants were measured conductiometrically using standard KCl solutions.

Cooling Baths

The refrigerants were liquid argon 87 °K, *n*-pentane slush 148° K, and methanol slush 183 °K.

Determination of the Free Ion Yield

The free ion yields were measured using the charge clearing method (2, 5). A schematic diagram of the circuit is shown in Fig. 2. Signals were usually generated by 100 ns pulses of 1.70 MeV X-rays. Alternate signals and blanks (no pulse from the van de Graaff accelerator) were fed into a low drift high sensitivity integrator and averaged with the Fabritek model 1062 Instrument Computer. The clearing field was applied continuously and each current integration sweep, which normally lasted for 2 s, was begun about 100 ns before the X-ray pulse.

On two occasions 1 μs X-ray pulses were used for argon, and the results were within experimental error of those obtained with 0.1 μs pulses.

Electron Conductance Transient (ECT)

Measurement of the ECT was effected using the circuits shown schematically in Fig. 3. When the half life ($t_{1/2}$) of the ECT was greater than 1 μs circuit *a* was used. This circuit had a decay $t_{1/2} = 0.8$ μs and a gain of 10^6. For $t_{1/2} < 1$ μs circuit *b* was used. It had a decay $t_{1/2} = 50$ ns and a gain of 10^4.

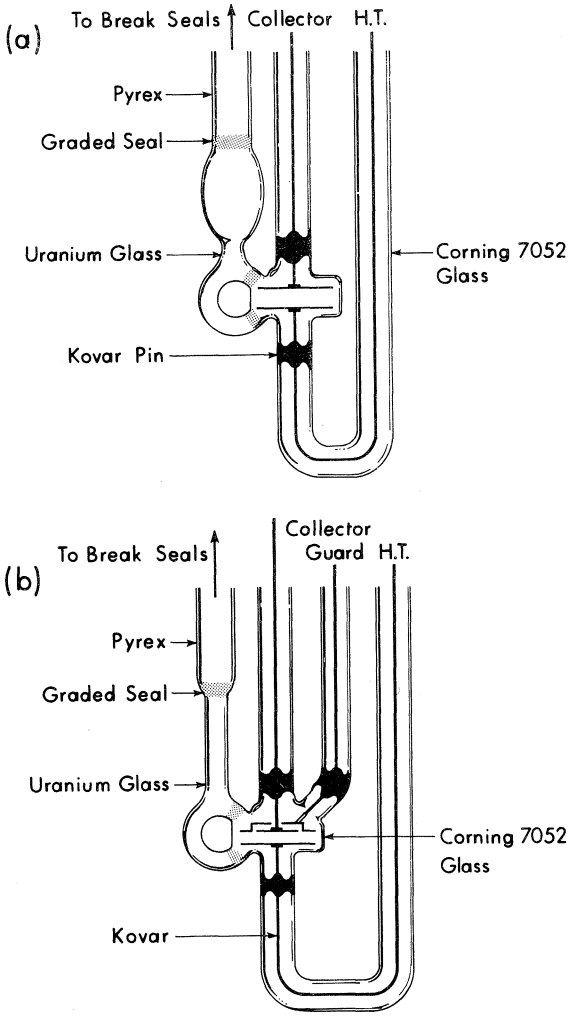

FIG. 1. Conductance cells: (*a*) electrode separation 0.50 cm, area 3.71 cm^2; (*b*) collecting electrode effective area 1.77 cm^2, separation 0.30 cm.

Can. J. Chem. Downloaded from www.nrcresearchpress.com by 210.87.254.40 on 09/05/12
For personal use only.

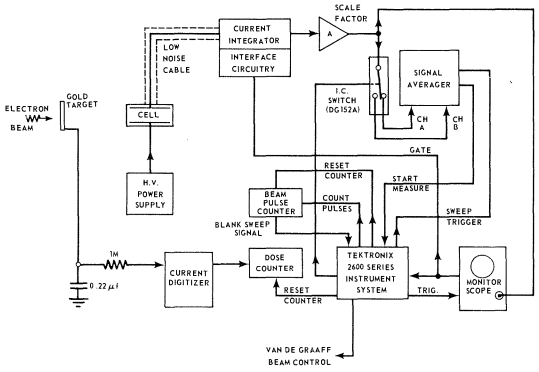

FIG. 2. Circuit for measuring free ion yields.

Dosimetry

The monitor used for every pulse was the charge collected on the gold target of the accelerator (5). The monitor was calibrated by thermoluminescence dosimetry with lithium fluoride crystals, which in turn were calibrated against the Fricke dosimeter in a low intensity (10–100 r/h) gamma source.

The amounts of photoelectric absorption in krypton and xenon had to be determined. To do this, several types of experiment were done: (*1*) apparent free ion yields were measured in each of the liquids with the normal 1.7 MeV beam, and with this beam filtered through 7 mm and 14 mm of lead; (*2*) apparent free ion yields were measured in xenon with the van de Graaff set at 0.75 MeV; (*3*) energy absorption calculations were done with X-ray spectra and absorption coefficients.

X-ray spectra were constructed from data in refs. 22

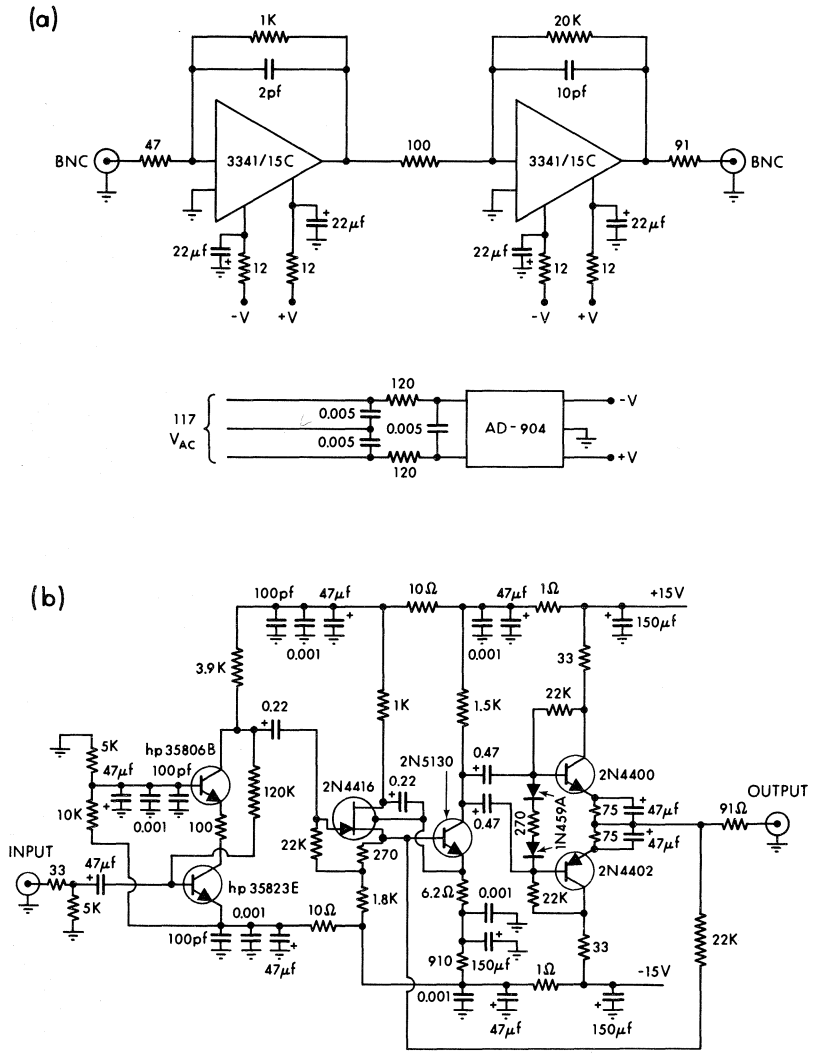

FIG. 3. Circuits for measuring the electron conductance transient. Response $t_{1/2}$ (*a*) 0.8 μs; (*b*) 50 ns.

Can. J. Chem. Downloaded from www.nrcresearchpress.com by 210.87.254.40 on 09/05/12
For personal use only.

TABLE 2. Dosimetry factors per electron of absorber M relative to that for LiF

M	Van de Graaff energy (MeV)	Pb filter (mm)	Factor* A†	Factor* B‡
LiF	1.70	0	1.00	1.00
	1.70	7	0.57 (0.54§)	1.00
	1.70	14	0.35 (0.33§)	1.00
Ar	1.70	0	1.03	1.03
	1.70	7	0.58	1.02
	1.70	14	0.36	1.02
Kr	1.70	0	1.16	1.16
	1.70	7	0.60	1.05
	1.70	14	0.37	1.04
Xe	0.75	0	2.14	2.14
	1.70	0	1.56	1.56
	1.70	7	0.70	1.24
	1.70	14	0.42	1.20

*Factor $= \int_0^{h\nu_{max}} {}_e\mu_a(M,h\nu)N(h\nu)h\nu dh\nu / \int_0^{h\nu_{max}} {}_e\mu_a(LiF,h\nu)N(h\nu)h\nu dh\nu$. The assumed fractional amount of gold K radiation in the normal beam (no Pb) was adjusted to give the correct ratio between the Xe ion yields with 0 and 7 mm Pb for the 1.7 MeV beam. The resulting fraction, 0.2% of the normal beam energy relative to 0.0% for the filtered beam, was assumed to be constant for all other absorbers. The same fraction gave good agreement for the 0.75 MeV beam results.
†Factor relative to LiF in normal (zero Pb) beam.
‡Factor relative to LiF in beam with same filter.
§Measured.

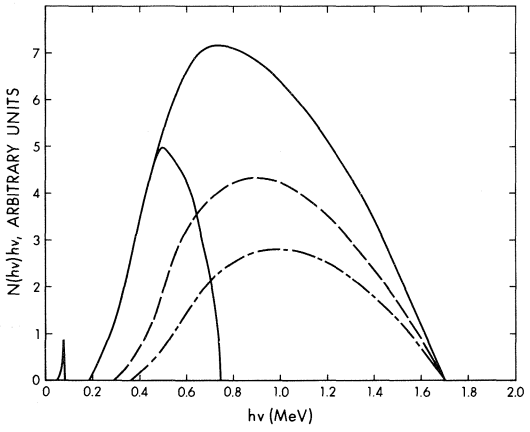

FIG. 4. X-ray spectra: $N(h\nu)$ is the number of photons of energy $h\nu$ per cm². —, normal beam; ---, filtered by 7 mm lead; -·-·-, filtered by 14 mm lead. The small peak at 0.08 MeV is gold K radiation; it contains 0.2% of the energy of the normal beam and corresponds to the difference between the amount of K radiation from Au in the normal beam and that from Pb in the filtered beam. The latter appears to be negligible.

and 23. The spectrum of an unfiltered X-ray beam with the desired $h\nu_{max}$ was simulated as in ref. 23. Attenuation by the gold target (effective thickness 2.8–2.9 mm) was estimated with the aid of absorption spectra constructed by interpolation between data in ref. 22.

The "normal" beam was the one emerging from the gold target. The shapes for 1.7 and 0.75 MeV peak energies are shown in Fig. 4 (full lines). Comparison of observed with calculated results indicates that the K radiation peak contains 0.2% of the beam energy in both cases.

Shapes of 1.7 MeV beams filtered by 7 mm and 14 mm of lead are also shown in Fig. 4 (broken lines). The calculated extent of beam attenuation agreed with that measured by LiF dosimetry when Pb absorption coefficient values lying between μ and μ_a were used (see eqs. 1 and 2 and discussion of build-up factors in ref. 24):

$$[1] \qquad \mu = \tau + \sigma_a + \sigma_s + \pi$$

$$[2] \qquad \mu_a = \tau + \sigma_a + \pi$$

where τ is the photoelectric absorption coefficient, σ_a and σ_s are the "actual" and "scatter" Compton coefficients, and π is the pair production coefficient (22).

The amount of dose D_M absorbed from the beam in material M relative to the amount absorbed in LiF is given by eq. 3.

$$[3] \qquad \frac{D_M}{D_{LiF}} = \frac{n_M \int_0^{h\nu_{max}} {}_e\mu_a(M,h\nu)N(h\nu)h\nu dh\nu}{n_{LiF} \int_0^{h\nu_{max}} {}_e\mu_a(LiF,h\nu)N(h\nu)h\nu dh\nu}$$

where n_M and n_{LiF} are the numbers of electrons/cm³ in M and LiF, respectively, ${}_e\mu_a(M,h\nu)$ is the "actual" absorption coefficient per electron of M for photons of energy $h\nu$, and $N(h\nu)$ is the relative number of photons of energy $h\nu$. The integrations were done numerically, using values of ${}_e\mu_a(M,h\nu)$ from Fig. 5 and the X-ray spectra in Fig. 4.

Values of the ratio of integrals in eq. 3 are listed in Table 2.

Normal doses were 1×10^{10} and 3×10^{10} eV/cm³ argon, for 0.1 and 1 μs pulses, respectively.

Can. J. Chem. Downloaded from www.nrcresearchpress.com by 210.87.254.40 on 09/05/12
For personal use only.

Can. J. Chem. Downloaded from www.nrcresearchpress.com by 210.87.254.40 on 09/05/12
For personal use only.

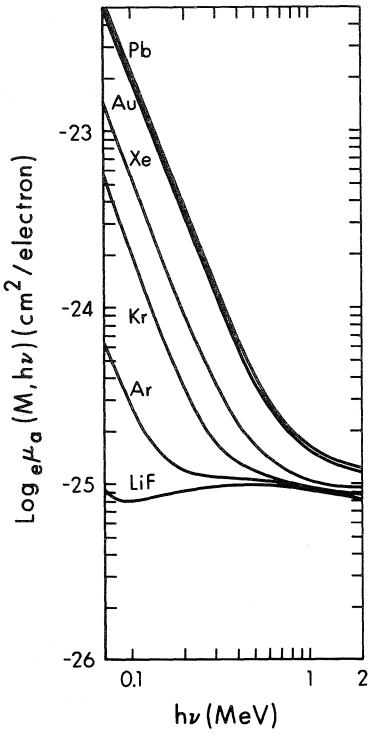

FIG. 5. Absorption coefficients per electron of material M, as functions of X-ray energy. ${}_e\mu_a = {}_e\tau + {}_e\sigma_a + {}_e\pi$. The values were interpolated and calculated from data in ref. 22.

Results

Free Ion Yields

Argon, 87 °K

Eleven series of experiments were done using different cells, different dosimeter crystals, different radiation pulse lengths (0.1 and 1 μs), and different preparations of argon. The measured values of $G_{fi}{}^{E}$, the free ion yield at applied electric field strength E, were reproducible to ±10%. The averaged results are shown in Fig. 6. The free ion yield increases rapidly from $G_{fi}{}^{E} = 4.6$ at 1.1 kV/cm to 7.0 at 12 kV/cm, then increases relatively slowly at higher fields.

Measurements were also done after placing lead filters between the X-ray target and the sample. Blocks of lead 7 mm and 14 mm thick reduced the beam strength, as measured by the LiF crystals, to 0.54 and 0.33, respectively, of the normal value. The amount of charge collected in argon per unit of dose measured with the LiF dosimeter was independent of whether the X-rays were filtered by lead. This agrees with the constancy of the dosimetry factors in Table 2.

Krypton, 148 °K

Free ion yields were higher in krypton than in argon, but the effect of field strength was similar in the two liquids (Figs. 6 and 7).

Filtering the X-rays through 7 mm of lead reduced by 12% the amount of charge collected in krypton per unit of dose measured with the LiF crystals. Increasing the filter thickness to 14 mm did not decrease this "apparent G value" further, thereby confirming the dosimetry factors in Table 2. The dosimetry factors account for the photoelectric absorption process, which is negligible in the LiF crystals but is appreciable in krypton. Filtration through lead reduces the fraction of lower energy photons in the X-ray beam and thereby decreases the importance of photoelectric absorption relative to the Compton process (22, 23).

The yields in Figs. 6–8 were calculated using the factors under B in Table 2, and are "true G

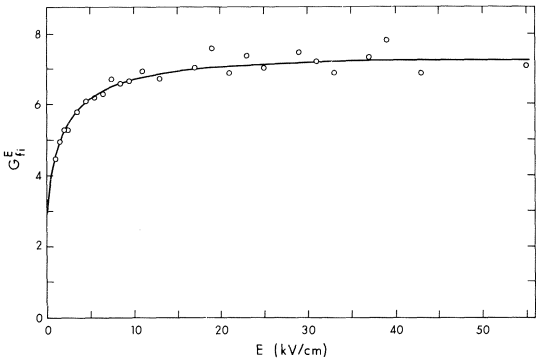

FIG. 6. Yields of ions collected at field strength E in argon at 87 °K. The points are the averages from eleven samples. The curve was calculated (see text).

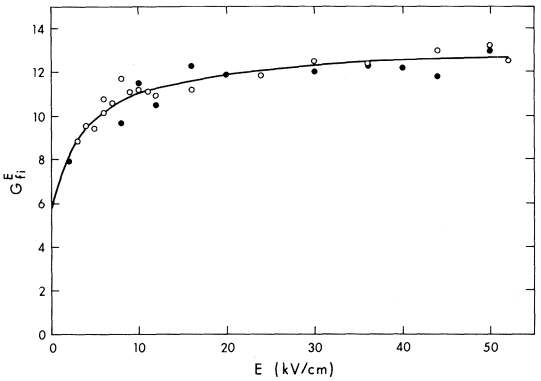

FIG. 7. Yields of ions collected at field strength E in krypton at 148 °K: ○, normal 1.7 MeV X-rays; ●, 1.7 MeV X-rays filtered by 14 mm Pb. The curve was calculated (see text).

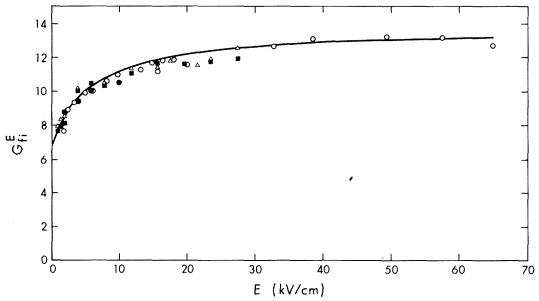

FIG. 8. Yields of ions collected at field strength E in xenon at 183 °K. 1.7 MeV rays: ○, normal beam; ■, 7 mm Pb filter; △, 14 mm Pb filter. 0.75 MeV X-rays, normal beam, ●. The curve was calculated (see text).

values", as distinguished from the "apparent G values" that were calculated directly from the LiF dosimetry.

Xenon, 183 °K

Xenon exhibits the highest ion yields measured thus far (Fig. 8). The field strength effect is similar to those in argon and krypton.

Filtering the 1.7 MeV X-rays through 7 mm of lead reduced the apparent G values by 25%; 14 mm of lead reduced the apparent G values an additional 2%. The effects of the lead filters are consistent with the dosimetry factors in Table 2.

Reducing the accelerator energy to 0.75 MeV increased the apparent G values by 35% over those at 1.7 MeV, with no lead filter. At the lower energy photoelectric absorption is more important, relative to the Compton process (22, 23), and the dosimetry factor is given in Table 2.

ECT and Electron Mobility

Argon, 87 °K

Argon that had been purified by the charcoal electrolysis technique (7) gave an ECT with a relatively long half life. The half life $t_{1/2}$ decreased with increasing field strength and pulse dose (Fig. 9). The decay of the ECT was first order at higher field strengths. The order increased at the lower field strengths but was still less than 2.0 at 4 V/cm with a pulse dose of 3×10^{10} eV/cm^3.

An idealized peak current i_0 at the end of the pulse was obtained by correcting the measured ECT for signal decay during the pulse and for circuit response characteristics (which varied from amplifier to amplifier). From i_0 one can obtain the electron mobility u through eq. 4 (7, 12, 25). The mobilities of the positive ions are negligible in these systems (26).

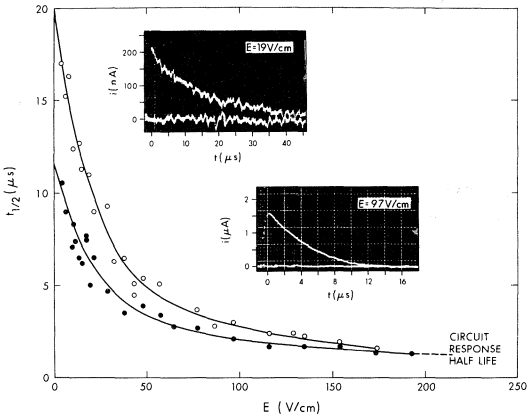

FIG. 9. Half life of ECT in argon as functions of applied field strength E and pulse dose: ○, 1.0×10^{10} eV/cm^3; ●, 3.6×10^{10} eV/cm^3. The inset pictures were obtained with 100 ns pulses of 1.3×10^{10} eV/cm^3.

$$[4] \qquad G_{fi}^{E}\, u = 6.24 \times 10^{20}\, i_0/\text{dose}\, AE$$

where i_0 is in A, the pulse dose is in eV/cm^3, A is the area of the collecting electrode in cm^2, E is the applied field strength (V/cm), G_{fi}^{E} is the free ion yield at E.

Values of u obtained from i_0 and G_{fi}^{E} (Fig. 6) are given in Fig. 10. Measurements were made at 1 and 6×10^{10} eV/cm^3 per pulse. The mobilities at $E > 80$ V/cm were independent of pulse dose and of field strength. The apparent decrease of u at low field strengths was somewhat more marked for the larger pulse dose and may be partly attributed to space charge effects.

Krypton, 148 °K

The half life of the ECT in krypton after a 100 ns pulse was 320 ns (amplifier response $t_{1/2} = 50$ ns) and was independent of field strength from 20 to 600 V/cm. A typical oscilloscope trace is shown in Fig. 11. The decay was first order and was attributed to reaction of the electrons with a trace of impurity, such as oxygen, in the liquid.

Values of i_0 and u were determined as described above, using a pulse dose of 1×10^{10} eV/cm^3. The electron mobility decreased steadily with increasing field strength, but was always much higher than that in argon (Fig. 10).

Xenon, 183 °K

The ECT had $t_{1/2} = 400$ ns, independent of field strength from 40 to 200 V/cm. The decay was first order, as in krypton.

Can. J. Chem. Downloaded from www.nrcresearchpress.com by 210.87.254.40 on 09/05/12
For personal use only.

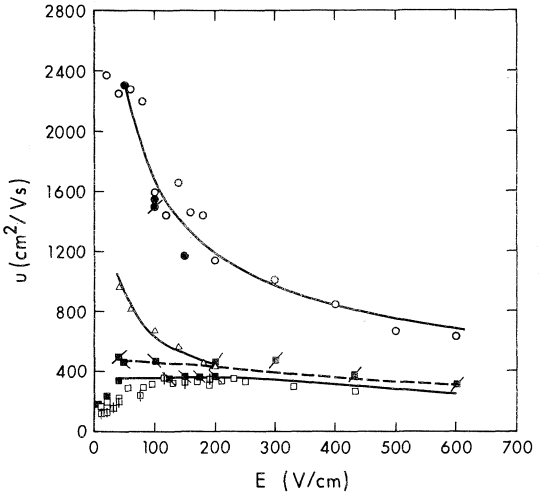

FIG. 10. Electron mobilities in liquids krypton, xenon, and argon. Krypton: ○, present results, 148 °K, v.p. = 6 atm, pulse dose 1×10^{10} eV/cm³; ◐, ref. 13, 148 °K, 6 atm; ●, ref. 13, 152 °K, v.p. = 15 atm; —, $u = 16{,}900\ E^{-1/2}$. Xenon: △, present results, 183 °K, v.p. = 3 atm, pulse dose 1×10^{10} eV/cm³; —, $u = 6{,}350\ E^{-1/2}$. Argon: present results, 87 °K, v.p. = 1 atm, □, pulse dose 1×10^{10} eV/cm³, ⊞, 6×10^{10} eV/cm³; ■, ref. 7, 87 °K, 1 atm, pulse dose 4×10^{10} eV/cm³; ◪, ref. 14, 85 °K, 0.7 atm; ▣, ref. 13, 90 °K, 6–7 atm; ---, Shockley theory, ref. 14; —, Cohen and Lekner theory, ref. 14.

The electron mobility decreased with increasing field strength (Fig. 10). The curve fell between those for krypton and argon.

Discussion

Yields and Ranges of Secondary Electrons

The results in Figs. 6–8 were analyzed to obtain values of the free ion yield at zero field $G_{fi}{}^0$, the total ionization yield G_{tot}, and the most probable penetration range b of the secondary electrons in the liquid. The computer method of analysis has been described in detail elsewhere (27, 28), so only illustrative equations are given.

The free ion yield $G_{fi}{}^E$ in the presence of an applied field E (V/cm) is given by eq. 5.

$$[5] \quad G_{fi}{}^E = G_{tot}\int_0^\infty F(y)e^{-r/y} \times [1 + \beta r + 0.375\beta^2 r^2 - 0.750\beta^2 ry + ...]dy$$

where $F(y)dy$ is the fraction of thermalized electron–ion pairs that have initial intrapair separation distances between y and $y + dy$, $r = \xi^2/\varepsilon kT$, $\xi = 4.80 \times 10^{-10}$ e.s.u., ε is the dielectric constant of the medium, k is Boltzmann's constant, T is the Absolute temperature, and $\beta = \xi E/600kT$. At zero field $\beta = 0$ and one obtains $G_{fi}{}^0$ from eq. 5.

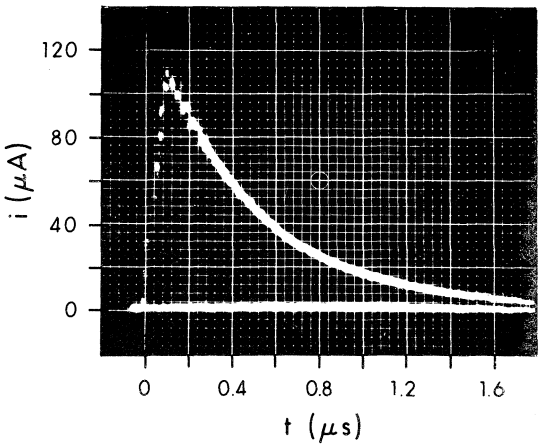

FIG. 11. Oscilloscope trace of ECT signal from krypton at 148 °K. $E = 140$ V/cm, pulse dose $= 1.3 \times 10^{10}$ eV/cm³, collecting electrode area = 3.65 cm².

For liquids in which the free ion yield is large, such as the present ones, the distribution $F(y)$ is well approximated by the Gaussian function, eq. 6 (28).

$$[6] \quad F(y) = (4y^2/\pi^{1/2}b^3)\exp(-y^2/b^2)$$

where b is the dispersion parameter. The separation distance y corresponds to the penetration range of the secondary electron into the liquid away from its parent ion, and b is the most probable value of y.

Values of b and G_{tot} were chosen to obtain the smallest mean deviation of the yields calculated by eq. 5 from the experimental yields for a given liquid. The best-fit values of b and G_{tot} are listed in Table 3 and the calculated curves are shown in Figs. 6–8. The resulting values of $G_{fi}{}^0$ are also given in Table 3.

One finds that the total ionization yield in liquid argon is nearly double the gas phase yield (29), whereas in krypton and xenon the ionization yields in the liquid are triple those in the gas phase (Table 3). Ionization in these liquids is evidently greatly facilitated by polarization energy, as it is in many solids (30, 31). For example, the ionization potential of anthracene is 7.2 eV in the gas phase (32) and $\leqslant$4.0 eV in the crystal (31). The lowering of the ionization potential is real. The generation of negative

Can. J. Chem. Downloaded from www.nrcresearchpress.com by 210.87.254.40 on 09/05/12
For personal use only.

TABLE 3. Electron yields and ranges

	T (°K)	$G_{t=t}$	G_{fi}^{0}	b (Å)	G_{ion}^{gas}*	G_{tot}/G_{ion}^{gas}	I.P. (eV)†	$E(^3P_2)$ (eV)†
Ar	87	7.3	2.9	1330	3.8	1.9	15.7	11.6
Kr	148	13.0	5.8	880	4.1	3.2	14.0	9.9
Xe	183	13.7	7.0	720	4.5	3.0	12.1	8.3

*Reference 29. $G_{ion}^{gas} = 100/W$, where W = average energy expended per ion pair.
†Gas phase I.P. = ionization potential. $E(^3P_2)$ = excitation energy of the lowest excited state. References 20 and 47.

charge carriers in the bulk crystal is linearly dependent on the light intensity (33), so it is not a two-quantum process (34).

The secondary electron ranges in krypton and xenon are smaller than those in argon (Table 3). This might be partly due to the decreasing size of the subelectronic-excitation energy region and partly due to an increase in $(-dT/dx)$ in the subelectronic region as one proceeds from argon to xenon.

The energy of the lowest excited state $^3P_2$ in the gas phase (Table 3) is probably higher than that of the lowest excited electronic state in the liquid, although the trends from argon to xenon should be the same.

Electrons in the subelectronic excitation region probably lose energy to intermolecular modes via transient M_2* states, where M is Ar, Kr, or Xe (35–43). Comparison with Brouilloin scattering of light (44) leads to the speculation that larger clusters M_n might also contribute to energy degradation of the electrons.

Thermal Electron Mobilities

The present values of the electron mobilities in krypton at 148 °K (Fig. 10) agree with those reported earlier for the same temperature (13). At the field strengths used the mobility decreases as $E^{-1/2}$, which has been attributed to an increase of electron "temperature" with E (13, 14, 45).

The electron mobility in xenon at 183 °K also decreases as $E^{-1/2}$ (Fig. 10). The mobilities are nearly a factor of two lower than those reported earlier for xenon at 163 °K (14). The temperature dependence of electron mobilities in these liquids is complex and is not understood (13–15, 18).

For argon at 87 °K the present mobility values are within experimental error of those in ref. 13 but are lower than those in ref. 14 (Fig. 10). The present results at $E > 100$ V/cm agree with the theory of Cohen and Lekner (14, 46) but not with that of Shockley (14, 45). The apparent decrease in mobility at $E < 100$ V/cm was previously attributed to space charge effects (7), but one would have expected a larger dependence upon pulse dose if space charge were the only cause. At 10 V/cm a six-fold increase in pulse dose decreased the apparent mobility by only 50% (Fig. 10). Ten different samples in four different cells gave the same results over the entire field range, within ±10%. The samples were given several radiation pulses at zero field before each field-on measurement, to remove polarization effects in the cell. The behavior at low fields is not understood, but the difference between the results from different laboratories (Fig. 10) indicates that experimental artifacts are important.

The study of electron mobilities will be continued.

We would like to thank J.-P. Dodelet for doing the calculations for Figs. 6–8 and the staff of the Radiation Research Center for aid with the electronics. This work was supported by the National Research Council of Canada. R. Schiller is thanked for a preprint of ref. 11.

1. P. H. TEWARI and G. R. FREEMAN. J. Chem. Phys. **49**, 4394 (1968); **51**, 1276 (1969).
2. W. F. SCHMIDT and A. O. ALLEN. J. Phys. Chem. **72**, 3730 (1968).
3. R. M. MINDAY, L. D. SCHMIDT, and H. T. DAVIS. J. Chem. Phys. **50**, 1473 (1969); **54**, 3112 (1971).
4. W. F. SCHMIDT and A. O. ALLEN. J. Chem. Phys. **50**, 5037 (1969); **52**, 2345, 4788 (1970).
5. M. G. ROBINSON, P. G. FUOCHI, and G. R. FREEMAN. Can. J. Chem. **49**, 3657 (1971).
6. R. A. HOLROYD and M. ALLEN. J. Chem. Phys. **54**, 5014 (1971).
7. P. G. FUOCHI and G. R. FREEMAN. J. Chem. Phys. **56**, 2333 (1972).
8. H. T. DAVIS, L. D. SCHMIDT, and R. M. MINDAY. Chem. Phys. Lett. **13**, 413 (1972).
9. K. FUEKI, D.-F. FENG, and L. KEVAN. Chem. Phys. Lett. **13**, 616 (1972).
10. R. M. MINDAY, L. D. SCHMIDT, and H. T. DAVIS. J. Phys. Chem. **76**, 442 (1972).
11. R. SCHILLER. J. Chem. Phys. Submitted.
12. J.-P. DODELET and G. R. FREEMAN. Can. J. Chem. **50**, 2667 (1972).
13. H. SCHNYDERS, S. A. RICE, and L. MEYER. Phys. Rev. **150**, 127 (1966).
14. L. S. MILLER, S. HOWE, and W. E. SPEAR. Phys. Rev. **166**, 871 (1968).

Can. J. Chem. Downloaded from www.nrcresearchpress.com by 210.87.254.40 on 09/05/12
For personal use only.

15. J. A. JANKE, L. MEYER, and S. A. RICE. Phys. Rev. A, **3**, 734 (1971).
16. J . LEKNER. Phys. Rev. **158**, 130 (1967).
17. S. A. RICE. Acc. Chem. Res. **1**, 81 (1968).
18. J. A. JAHNKE, N. A. W. HOLZWARTH, and S. A. RICE. Phys. Rev. A, **5**, 463 (1972).
19. Handbook of chemistry and physics. 50th ed. *Edited by* C. D. Hodgman *et al.* Chemical Rubber Co., Cleveland, Ohio. 1969.
20. (*a*) G. A. COOK (*Editor*). Argon, helium, and the rare gases. Interscience Publishers, New York. 1961. pp. 151, 360. (*b*) V. G. FASTOVSKII, A. E. ROVINSKII, and YU. V. PETROVSKII. Inert gases. Israel Program for Scientific Translations, Jerusalem. 1967. pp. 28, 47, 48, 50.
21. J. R. PARTINGTON. An advanced treatise on physical chemistry. Vol. 5. Longmans, Green and Co., London. 1962. p. 349.
22. H. E. JOHNS and J. S. LAUGHLIN. *In* Radiation–dosimetry. *Edited by* G. J. Hine and G. L. Brownell. Academic Press, New York. 1956. Chapt. 2.
23. W. J. MEREDITH and J. B. MASSEY. Fundamental physics of radiology. John Wright and Sons, Bristol. 1968. Chapt. 5 and 12.
24. B. T. PRICE, C. C. HORTON, and K. T. SPINNEY. Radiation shielding. Pergamon Press, London. 1957. Chapt. 2.
25. E. E. CONRAD and J. SILVERMAN. J. Chem. Phys. **51**, 450 (1969).
26. H. T. DAVIS, S. A. RICE, and L. MEYER. J. Chem. Phys. **37**, 947, 2740 (1962).
27. G. R. FREEMAN. J. Chem. Phys. **39**, 1580 (1963).
28. J.-P. DODELET, P. G. FUOCHI, and G. R. FREEMAN. Can. J. Chem. **50**, 1617 (1972).
29. W. P. JESSE and J. SADAUSKIS. Phys. Rev. **107**, 766 (1957).
30. D. R. KEARNS and M. CALVIN. J. Chem. Phys. **34**, 2026 (1961).
31. N. GEACINTOV and M. POPE. J. Chem. Phys. **47**, 1194 (1967).
32. R. W. KISER. Introduction to mass spectrometry and its applications. Prentice–Hall, Englewood Cliffs, N.J. 1965. Appendix IV.
33. N. GEACINTOV and M. POPE. J. Chem. Phys. **45**, 3884 (1966).
34. L. P. GARY, K. DE GROOT, and R. C. JARNAGIN. J. Chem. Phys. **49**, 1577 (1968).
35. N. BERNARDES and H. PRIMAKOFF. J. Chem. Phys. **30**, 691 (1959).
36. R. E. LECKENBY and E. J. ROBBINS. Proc. Roy. Soc. (London), **291A**, 389 (1966).
37. J. H. HOLLOWAY. Noble-gas chemistry. Methuen, London. 1968. pp. 41–58.
38. J. P. MCTAGUE and G. BIRNBAUM. Phys. Rev. Lett. **21**, 661 (1968).
39. J. P. MCTAGUE, P. A. FLEURY, and D. B. DUPRE. Phys. Rev. **188**, 303 (1969).
40. J. P. MCTAGUE and G. BIRNBAUM. Bull. Am. Phys. Soc. **14**, 344 (1969).
41. W. S. GORNALL, H. E. HOWARD-LOCK, and B. P. STOICHEFF. Phys. Rev. **A1**, 1288 (1970).
42. J. A. BUCARO and T. A. LITOVITZ. J. Chem. Phys. **54**, 3846 (1971).
43. M.-C. CASTEX and N. DAMANY. Chem. Phys. Lett. **13**, 158 (1972).
44. T. R. GILSON and P. J. HENDRA. Laser raman spectroscopy. Wiley–Interscience, London. 1970. pp. 14–15.
45. W. SHOCKLEY. Bell System Tech. J. **30**, 990 (1951).
46. M. H. COHEN and J. LEKNER. Phys. Rev. **158**, 305 (1967).
47. Y. YAMAMOTO, S. TAKAMUKU, and H. SAKURAI. Bull. Chem. Soc. Jap. **44**, 2104 (1971).

Can. J. Chem. Downloaded from www.nrcresearchpress.com by 210.87.254.40 on 09/05/12
For personal use only.

Kinetics of Quasifree Electron Reactions in the Liquids Methane, Krypton, and Xenon

MAURICE G. ROBINSON AND GORDON R. FREEMAN

Chemistry Department, University of Alberta, Edmonton, Alberta, T6G 2G2

Received July 21, 1972

The encounter efficiency of $e^- + N_2O \rightarrow N_2O^-$ in the liquids methane, krypton, and xenon at 183 °K is $f \approx 10^{-5}$. The parameter β, for the nonhomogeneous kinetics of reactions in γ radiolysis spurs in the liquids, has values similar to those (10^{13}–10^{14} V/cm²) obtained earlier for liquids such as cyclohexane, methanol, and water at 298 °K, in which f is approximately unity. Previous results for nitrous oxide in neopentane at 296 °K have been reinterpreted to obtain $f \approx 10^{-2}$. For solvents in which the electron mobility is very high (~10^3 cm²/Vs) the value of f is low. As the electron mobility decreases f increases to a maximum of unity.

La probabilité, f, de reaction par rencontre de $e^- + N_2O \rightarrow N_2O^-$ dans des liquides tels que le méthane, le krypton et le xenon à 183 °K est environ 10^{-5}. Le parametre β de cinetique nonhomogène (relatif aux reactions dans les grappes se produisant lors de l'irradiation γ) dans ces liquides a des valeurs comparables (10^{13}–10^{14} V/cm²) à celles déterminées précédemment à 298 °K pour des liquides tels que le cyclohexane, le méthanol, et l'eau pour lesquels f vaut pratiquement l'unité. Des resultats antérieurs concernant l'oxyde nitreux dans le néopentane à 296 °K ont été réinterprétés; ils donnent $f \approx 10^{-2}$. Pour des solvants à haute mobilité électronique (~10^3 cm²/Vs) la valeur de f est petite. Lorsque cette mobilité électronique décroît, f croît jusqu'à sa valeur maximum qui est l'unité.

Can. J. Chem., **51**, 650 (1973)

Can. J. Chem. Downloaded from www.nrcresearchpress.com by 210.87.254.6 on 09/05/12
For personal use only.

Introduction

It has been demonstrated that the kinetics of the reaction of electrons with nitrous oxide in liquid hydrocarbons is influenced by the molecular structure of the solvent (1, 2). The efficiency of the reaction in neopentane (1) appears to be anomalously low. To determine whether the low efficiency correlates with the quasifree behavior of electrons (3, 4), the study has been extended to the liquids methane, krypton, and xenon. Electrons have a larger degree of freeness[1] in these liquids (5–8) than in neopentane (4, 6, 9), as indicated by the mobilities. The present work verifies that the encounter efficiency of the reaction between electrons and nitrous oxide decreases with increasing degree of freeness of the electrons.

Experimental

Materials and Apparatus

The vacuum system was grease free and was evacuated to $< 10^{-6}$ Torr, with baking of appropriate sections, before introducing the substances for sample preparation.

Matheson Ultrapure methane contained 5 p.p.m. oxygen and < 10 p.p.m. carbon dioxide. It was transferred from the cylinder to the vacuum system through a system of valves that was kept above atmospheric pressure and was thoroughly flushed with methane before a sample was collected. Each sample (several cm³) was condensed in a trap, subjected to several trap-to-trap distillations with occasional pumping on the receiver and retaining only the middle fraction each time, then pumped on until half of the remaining liquid evaporated.

Matheson Research Grade krypton (5 p.p.m. xenon, no other detectable impurities) and Linde 99.995% xenon (< 5 p.p.m. nitrogen, < 1 p.p.m. oxygen) were used as received, taking care to prevent the introduction of impurities.

Small samples (0.1–0.2 g) of each gas containing known amounts of nitrous oxide were condensed at 77 °K in 4 mm o.d. Pyrex tubes and sealed off (0.3 cm³). After equilibration at 193 °K for 30 min the colorless and homogeneous solutions were irradiated in a methanol slush bath at 183 °K to a dose of 4×10^{19} eV/g, in a ^{60}Co Gammacell-220. The dose rate was 5×10^{15} eV/g s in methane. Samples were frozen at 77 °K in a stainless steel "bomb" incorporated into the carrier gas flow line of a Hewlett–Packard 5750 gas chromatograph. The helium flow rate was 76 cm³/min. On warming, the sample tube exploded and its contents were swept by the carrier gas onto a 48 ft molecular sieve 5A column at 296 °K. Nitrogen and oxygen were measured by a thermal conductivity detector operated at 280 mA. Calibration of the system was effected using irradiated solutions of nitrous oxide in ethane and relating the nitrogen peak areas to the known $G(N_2)$ values determined by *P.V.T.* measurements and mass spectrometry (2).

[1]It has been customary to distinguish between "quasifree" and "localized" states of electrons in liquids. However, recent work (24) indicates that a continuous variation in electron behavior between "free" and "localized" is possible and one may speak of the "degree of freeness" of the electron.

Can. J. Chem. Downloaded from www.nrcresearchpress.com by 210.87.254.6 on 09/05/12
For personal use only.

The g.c. sensitivity of oxygen was shown to be 10% greater than that of nitrogen by injecting samples of air into the gas chromatograph.

Dosimetry

The Fricke dosimeter is suitable for use when the sample does not contain a large concentration of heavy elements ($Z > 16$). It was therefore used to determine the dose rate in methane and nitrous oxide; conversion from system to system was done on the basis of their relative electron densities. Energy absorption by light elements from the photons in a Gammacell occurs nearly exclusively by the Compton process.

In the krypton ($Z = 36$) and xenon ($Z = 54$) samples both photoelectric and Compton absorption were important. The relative contribution of the photoelectric process increases as Z^4 (10).

Gammacell radiation is comprised mainly of photons with energies 1.17 and 1.33 MeV, with a smaller amount of lower energy photons scattered from the shielding into the irradiation chamber. It is difficult to measure the actual energy spectrum of the radiation inside the chamber. The relative contributions of the low and high energy photons were estimated by comparing the induced electrical conductances in cyclohexane and xenon, with and without lead shielding. Similar measurements were made using a d.c. beam of 1.7 MeV peak energy X-rays from the van de Graaff, at a dose rate similar to that in the Gammacell. Dosimetry of the X-ray beam is reported in the adjoining article (11), and is used as the basis for the present calculations.

Measurement of the induced conductances in the unshielded cells was straightforward with both sources. When shielding was used with the van de Graaff, it was a 20 cm × 20 cm annulus of lead 1.4 cm thick. The geometry of the radiation field in the Gammacell and the awkward shape of the conductance cell prevented complete shielding to be accomplished in that source. However, the same shielding was used for xenon and cyclohexane in a given source.

About 0.1% of oxygen was added to the xenon to capture the electrons and reduce space charge effects. The cyclohexane was not deaerated.

The ratio of the unshielded/shielded conductances at low electric field strengths was measured for each substance with the two radiation sources. Only Compton absorption is important in the cyclohexane; both Compton and photoelectric absorption are important in the xenon. The cyclohexane ratio was therefore used as a standard to which the xenon ratio was compared: xenon/cyclohexane = 1.25 in the Gammacell and 1.28 with the van de Graaff. These values are the same within experimental error, which fortuitously allows the van de Graaff dosimetry factors (11) for xenon and krypton to be used for the Gammacell. The relative average absorption coefficients per electron of the medium are: 1.0 for C_6H_{12}, CH_4, N_2O, Fricke solution, LiF; 1.2 for Kr; 1.6 for Xe.

Accurate dosimetry for samples containing heavy elements is difficult to obtain. The total ion yields reported in this and the adjoining article agree within < 10%, which may be taken as the uncertainty in the dosimetry for xenon and krypton. That for methane and nitrous oxide is ~1%.

TABLE 1. Liquid and molecular (gas phase) properties

Liquid	T (°K)	ε	d (g/cm³)	α (Å³)	I.P. (eV)[h]
Kr	183	1.46[a]	1.80[d]	2.47[d]	13.99
Xe	183	1.87[a]	2.93[d]	4.01[d]	12.08
	193	1.85[a]	2.86[d]		
N_2O	183	2.01[b,c]	1.23[e]	3.00[g]	12.89
	193	1.98[b]	1.20[e]		
CH_4	183	1.36[a]	0.26[f]	2.60[g]	12.98
C_3H_8	183	1.90[a]	0.637[f]	6.3[g]	11.07
	193	1.88[a]	0.625[f]		

[a]Calculated from the Clausius–Mosotti equation. For propane the effect of the small dipole moment μ = 0.084 D was included by using the Debye equation.
[b]Reference 12.
[c]Reference 13.
[d]References 15 and 16.
[e]Reference 17.
[f]Reference 14.
[g]Reference 18.
[h]Reference 19.

Liquid and Molecular (Gas Phase) Properties

The dielectric constants ε of the liquids were obtained from refs. 12 and 13 or calculated from the Clausius–Mosotti equation (12). Densities d were obtained from refs. 14–17. The values are listed in Table 1, along with those for the gas phase molecular polarizabilities α (15, 18) and ionization potentials I.P. (19).

Results

Nitrogen Yields

The yields of nitrogen from the γ radiolysis of solutions of nitrous oxide in methane, krypton, and xenon at 183 °K are shown in Fig. 1. Three xenon solutions were irradiated at 193 °K to be

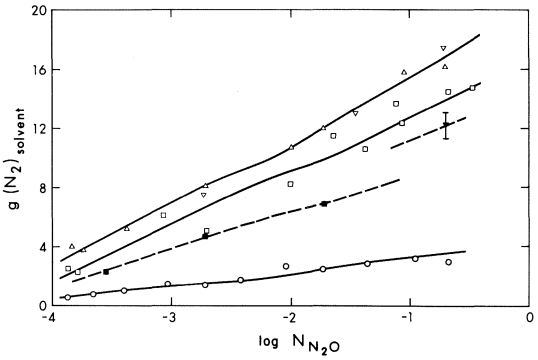

FIG. 1. Yields of nitrogen from nitrous oxide scavenging species in methane (○), krypton (□), and xenon (△) at 183 °K. N_{N_2O} is the mole fraction of N_2O. Other reaction conditions are xenon at 193 °K (▽); xenon containing 0.8–7 mol % propane at 193 °K (▼); krypton containing 2.7 mol % propane at 183 °K (■). All lines were calculated (see text); the broken lines refer to the samples containing propane and correspond simply 0.71 × the yields from samples without propane.

Can. J. Chem. Downloaded from www.nrcresearchpress.com by 210.87.254.6 on 09/05/12
For personal use only.

certain that nitrous oxide (triple point 182 °K) was all in solution; the results were the same within experimental error at the two temperatures (Fig. 1). The yields were corrected for the direct radiolysis of nitrous oxide and refer to the energy absorbed initially in the solvent. The nitrogen yield from the direct radiolysis of nitrous oxide in methane solutions was assumed to equal that from nitrous oxide containing propane, $g(N_2)_{N_2O} = 11$ (Table 2); that in krypton and xenon solutions was assumed to equal the yield in pure nitrous oxide, $g(N_2)_{N_2O} = 13$ (20, 21). The largest correction in the xenon solutions was 0.3 g units. The net yield $g(N_2)_{solvent}$ resulted from the scavenging by nitrous oxide of solvent radiolysis intermediates.

In all three liquids $g(N_2)_{solvent}$ increased steadily as the mole fraction of scavenger was increased from 10^{-4} to 0.2. The yields in xenon and krypton were much larger than those in methane.

Oxygen Yields

The oxygen yields from solutions of nitrous oxide in krypton and xenon are displayed in Fig. 2. The yields were corrected for the direct radiolysis of nitrous oxide and refer only to the scavenging of species generated by the radiolysis of the solvent. The shapes of the curves are similar to those in Fig. 1. The ratio of the oxygen to the nitrogen yield was constant over the entire concentration range, within experimental error, and equalled 0.17 ± 0.01 in both krypton and xenon; the corresponding ratio for pure nitrous oxide, averaged over the three studies reported in Table 2, is 0.21 ± 0.01.

Oxygen was not formed in the methane solutions.

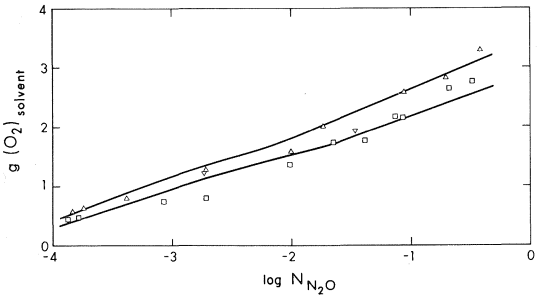

FIG. 2. Yields of oxygen from nitrous oxide scavenging species in krypton (□) and xenon (△) at 183 °K, plotted against the mol fraction N_{N_2O}. Xenon solutions were also measured at 193 °K (▽). The lines were calculated (see text).

TABLE 2. Yields of nitrogen and oxygen from the radiolysis of liquid nitrous oxide containing propane, at 193 °K

Mole fraction propane	$g(N_2)_{N_2O}$*	$g(O_2)_{N_2O}$
0.000	12.5	2.8
	12.9†	2.6†
	13.1‡	2.7‡
0.010	12.3	1.2
0.034	11.0	0.3
0.089	10.9	0.0

*Corrected for the nitrogen that results from energy absorption in propane, using $g(N_2)_{propane} = 5$ (2).
†Reference 20.
‡Reference 21.

Addition of Propane to Krypton and Xenon Solutions

The fact that the nitrogen and oxygen yields were so much greater from the xenon and krypton systems than from the methane solutions seemed to be related to the chemical reactivity of the hydrocarbon. Propane, which is more reactive than methane, was therefore added to the xenon and krypton systems to observe its effect.

To an initially 20% N_2O/80% Xe mixture was added 0.8, 2.4, and 6.7 mol% of propane. The three solutions gave the same results, within experimental error: $g(N_2)_{Xe} = 12.2 \pm 0.9$ and $g(O_2) = 0.0$. In the absence of propane the yields were $g(N_2)_{Xe} = 17$ and $g(O_2)_{Xe} = 3.0$. Thus a small amount of hydrocarbon eliminated the oxygen and reduced the nitrogen yield to a plateau value 0.7 times the original value.

Since 2% of propane was more than sufficient to reduce $g(N_2)$ and $g(O_2)$ to plateau values in a highly concentrated N_2O/Xe solution, 2.7% of propane was added to three low concentration N_2O/Kr solutions. As in xenon, the oxygen yield was eliminated and nitrogen was reduced to 0.7 of the yield at the corresponding N_2O concentration in the absence of propane.

Addition of propane to liquid nitrous oxide reduced the oxygen yield to zero but the nitrogen yield decreased only to 0.9 of the value for pure nitrous oxide (Table 2).

Discussion

Kinetic Analysis

The values of $g(N_2)_{max}$ in xenon and krypton containing propane were estimated to be 14 and 13, respectively (see later discussion), which agree with the total ionization yields estimated

Can. J. Chem. Downloaded from www.nrcresearchpress.com by 210.87.254.6 on 09/05/12
For personal use only.

by the charge clearing technique, 13.7 and 13.0, respectively (11). It therefore appears that one nitrogen molecule results from the scavenging of one electron in the hydrocarbon containing systems.

[1] $$e^- + N_2O \rightarrow N_2O^-$$

[2] $$N_2O^- + \ldots \rightarrow N_2 + \ldots$$

The nitrogen yields from the methane solutions are also consistent with the suggestion that one electron scavenged leads to the formation of one nitrogen molecule. It will be assumed that $g(N_2)_{max} = g(\text{ionization}) = 4$ in methane (5).

In the absence of hydrocarbon in xenon and krypton $g(N_2)_{solvent}/g(e^-\text{ scavenged}) = 1.4$. Speculation about the mechanism is not presented here.

Details of the kinetics model were published earlier (22, 23), but a brief outline is given here for convenience.

In pure liquid M the relevant reactions are:

[3] $$M \rightsquigarrow [M^+ + e^-]$$

[4] $$[M^+ + M] \rightarrow [N^+ + P]$$

[5] $$[N^+ + e^-] \rightarrow \text{geminate neutralization}$$

[6] $$[N^+ + e^-] \rightarrow N^+ + e^- \text{ (free ions)}$$

[7] $$N^+ + e^- \rightarrow \text{random neutralization}$$

Square brackets about reactants or products indicate that the enclosed species are in a spur. The ion N^+ is probably CH_5^+ in methane, Kr_2^+ in krypton, and Xe_2^+ in xenon.

In the presence of electron scavenger S:

[8] $$e^- + S \rightarrow S^-$$

[9] $$S^- + N^+ \rightarrow \text{products}$$

[10] $$[e^- + S] \rightarrow [S^-]$$

[11] $$[S^- + N^+] \rightarrow \text{products}$$

Reactions 7–9 involve only free ions and obey homogeneous kinetics: reactions 5, 6, and 10 are described by nonhomogeneous kinetics.

The free ion yield g_{fi} is given by

[12] $$g_{fi} = g(\text{ionization}) \times \int_0^\infty F(y) \exp(-\xi^2/\varepsilon kTy)\, dy$$

where $F(y)dy$ is the fraction of thermalized electron–ion pairs that have initial intrapair distances between y and $y + dy$, $\xi = 4.8 \times 10^{-10}$ e.s.u., ε is the dielectric constant of the medium, k is Boltzmann's constant, and T is the absolute temperature.

The distribution $F(y)$ in systems that have large free ion yields, such as the present ones, is suitably approximated by a Gaussian function (24)

[13] $$F(y) = (4y^2/\pi^{1/2}b^3) \exp(-y^2/b^2)$$

where b is the dispersion parameter. Furthermore, in such systems the product of b and the liquid density d has been found to be independent of temperature (24) and will be assumed to be so in the present solvents.

In methane at 120 °K $bd = 2.1 \times 10^{-6}$ g/cm^2 (5), so at 183 °K one obtains $b = 2.1 \times 10^{-6}/0.26 = 8.1 \times 10^{-6}$ cm. Using $g(\text{ionization}) = 4$ one obtains $g_{fi} = 1.8$ from eqs. 12 and 13. Thus the curve for methane in Fig. 1 should be governed by homogeneous kinetics between $g(N_2) = 0$ and 1.8; that at $g(N_2) > 1.8$ should be governed by nonhomogeneous kinetics.

Homogeneous Kinetics

A peculiarity is introduced into the kinetics by the fact that the mobility of electrons (6–8) is about six orders of magnitude greater than those of the positive and negative ions in these liquids (6, 25). Thus $k_7 \gg k_9$, and the steady state concentration of ions in the absence of scavenger ($\propto k_7^{-1/2}$) is about three orders of magnitude smaller than that when all the free ion electrons have been scavenged ($\propto k_9^{-1/2}$). At all practical scavenger concentrations greater than zero, one may write $[e^-] \ll [S^-] \approx [N^+]$. With this approximation steady state treatment gives:

[14] $$g(N_2)_{fi} = g_{fi}/[1 + ([N^+]/a)]$$

[15] $$[N^+]^3 + a[N^+]^2 = ab$$

[16] $$a = k_8[N_2O]/k_7$$

[17] $$b = Rg_{fi}/k_9$$

where R is the dose rate in units appropriate to those of g_{fi} and k_9. The cubic equation 15 was solved by trial and error at each nitrous oxide concentration, using a Hewlett–Packard HP-35 calculator.

In the present liquids the electron mobilities are $\sim 10^3$ cm^2/V s (6–8) and the positive and negative ion mobilities are $\sim 10^{-3}$ cm^2/V s (6, 25). Reactions 7 and 9 are both approximately diffusion controlled, so $k_7 \approx 10^{18}$ l/mol s and $k_9 \approx 10^{12}$ l/mol s (6). At the present dose rate in methane $Rg_{fi} = 4 \times 10^{-8}$ mol/l s. Fitting eq.

TABLE 3. Kinetic parameters for reactions of electrons with nitrous oxide in liquids

Liquid	T (°K)	g (ionization)	g_{fi}	b (Å)	f	β (10^{13} V/cm^2)	u_e (cm^2/V s)
CH_4	183	4	1.8	800	1×10^{-5}	20	$\sim 10^3$ [e]
Kr	183	12.6 (18[b])	6.7 (9.6)[b]	1000	1×10^{-5}	2	2200 [f]
Xe	183	14 (20[b])	7.1 (10.2)[b]	720	3×10^{-5}	3	$\sim 10^3$ [g]
$C(CH_3)_4$[a]	296	4.7	1.0	176	$\sim 10^{-2}$ [c]	~ 5[c]	~ 50[h]
c-$C_5H_9CH_3$[a]	296	4.9	0.13	61	1	4[d]	$\leqslant 1$[i]
c-C_6H_{12}[a]	296	5.0	0.13	59	1	3[d]	0.4[h]
CH_3OH[a]	298	4.6	2.0	20	1	4[d]	0.0006[j]
H_2O[a]	298	4.0	2.7	18	1	31[d]	0.0018[k]

[a]Reference 23.
[b]$g(N_2)_{max}$ and $g(N_2)_{fi}$ in the absence of hydrocarbon equal 1.4 g(ionization) and 1.4 g_{fi}, respectively.
[c]Revised value.
[d]Calculated by assuming $f = 1$.
[e]300 at 120 °K (6).
[f]Value at 100 V/cm.
[g]References 8 and 11.
[h]References 4 and 24.
[i]By comparison with the values in cyclopentane and cyclohexane (4).
[j]Reference 27.
[k]Reference 28.

14 to the lower part of the methane curve in Fig. 1 gave $k_8 = 3 \times 10^{10}$ l/mol s, and the calculated curve is that shown between 1×10^{-4} and 4×10^{-3} mole fraction nitrous oxide.

The diffusion controlled value of k_8 would have been $\sim 4\pi(3 \times 10^{-8}$ cm) $(10^3$ cm^2/V s) (0.016 V) $(6 \times 10^{20}) \approx 3 \times 10^{15}$ l/mol s. Thus the encounter efficiency of reaction 8 is $\sim 10^{-5}$.

Nonhomogeneous Kinetics

The relevant equations are (23)

$$[18] \quad g(N_2) = g(N_2)_{fi} + g_{gn} \int_0^\infty F(y) \times [1 - \exp(-\xi^2/\varepsilon kTy)][1 - (1 - fN_s)^{\beta\nu}]\, dy$$

where $g_{gn} = [g(\text{ionization}) - g_{fi}]$, f is the encounter efficiency of reaction 10 and is taken equal to that of reaction 8, N_s is the mole fraction of scavenger, β is an adjustable parameter, and ν is given by

$$[19] \qquad \nu = 1.4 \times 10^7 \varepsilon y^3 \quad \text{cm}^2/\text{V}$$

where y is in cm.

The methane curve at $N_{N_2O} > 4 \times 10^{-3}$ in Fig. 1 was calculated from eq. 18 using $f = 10^{-5}$ and the best fit value of β was 2×10^{14} V/cm^2.

The krypton and xenon systems were similarly analyzed and the results are summarized in Table 3. The calculated curves are shown in Fig. 1.

In all three solvents the encounter efficiency of the electron reaction with nitrous oxide was very low, $\sim 10^{-5}$, and the values of β were in the vicinity of those that had been obtained for compounds such as cyclohexane and methanol (23, 26, and Table 3).

Attempts were also made to fit the methane results by arbitrarily taking $f = 10^{-6}, 10^{-5}, 10^{-4}$, etc., and varying β to get a best value in each case. A good fit could not be obtained with $f = 10^{-6}$, but for $f \geqslant 10^{-5}$ the same best-fit curve was obtained with values of β such that βf = constant. The same was true of the krypton and xenon systems. Thus, analysis of only the nonhomogeneous portion of the results furnishes only the value of βf. One needs separate information about either β or f. In the present three solvents the values of f were obtained from the homogeneous kinetics portion of the results.

It appears that $\beta \approx 10^{13}$–10^{14} V/cm^2 in a wide variety of systems, from krypton to methanol (Table 3). Earlier work on neopentane involved the assumption that $f = 1$ in that liquid, and the resulting low value $\beta = (5$–$8) \times 10^{11}$ V/cm^2 (1, 23) was not understood. One may now assume that β would be normal in neopentane, with $f \approx 10^{-2}$ (Table 3).

Values of β in the vicinity of 10^{14} V/cm^2 are readily understood in terms of the diffusion model (22).

The encounter efficiency of the reaction between electrons and nitrous oxide is very low in liquids in which the electron mobility is very high. As the mobility decreases f increases to its maximum value of unity (Table 3). This behavior is understandable in terms of the dependence of reaction probability on the electron–reactant interaction time per encounter.

Part of the decrease in f from 10^{-2} in neopen-

Can. J. Chem. Downloaded from www.nrcresearchpress.com by 210.87.254.6 on 09/05/12
For personal use only.

tane at 296 °K to 10^{-5} in methane at 183 °K is probably due to a temperature dependence of $f(e^- + N_2O)$.

Oxygen Yields

Oxygen was not a product in the systems that contained an organic compound.

The curves in Fig. 2 were obtained by multiplying the upper two calculated curves in Fig. 1 by 0.17. Agreement between calculated and measured yields is satisfactory, which indicates that the mechanism following the scavenging of intermediates by nitrous oxide is constant over a wide concentration range.

We are grateful to J.-P. Dodelet for doing many of the calculations. This work was supported by the National National Research Council of Canada.

1. K. Horacek and G. R. Freeman. J. Chem. Phys. **53**, 4486 (1970).
2. M. G. Robinson and G. R. Freeman. J. Chem. Phys. **55**, 5644 (1971).
3. P. M. Tewari and G. R. Freeman. J. Chem. Phys. **49**, 4394 (1968).
4. W. F. Schmidt and A. O. Allen. J. Chem. Phys. **52**, 4788 (1970).
5. M. G. Robinson, P. G. Fuochi, and G. R. Freeman. Can. J. Chem. **49**, 984, 3657 (1971).
6. P. G. Fuochi and G. R. Freeman. J. Chem. Phys. **56**, 2333 (1972).
7. H. Schnyders, S. A. Rice, and L. Meyer. Phys. Rev. **150**, 127 (1966).
8. L. S. Miller, S. Howe, and W. E. Spear. Phys. Rev. **166**, 871 (1968).
9. R. M. Minday, L. D. Schmidt, and H. T. Davis. Phys. Rev. Lett. **26**, 360 (1971).
10. H. E. Johns and J. S. Laughlin. *In* Radiation dosimetry. *Edited by* G. J. Hine and G. L. Brownell. Academic Press, New York. 1956. Chap. 2.
11. M. G. Robinson and G. R. Freeman. Can. J. Chem. This issue.
12. J. R. Partington. An advanced treatise on physical chemistry. Vol. 5. Longmans, London. 1954. Section XI.
13. Handbook of chemistry and physics. 50th ed. Chemical Rubber Publishing Co., Cleveland, Ohio. 1969.
14. R. W. Gallant. Physical properties of hydrocarbons. Vol. 1. Gulf Publishing Co., Houston, Texas. 1968.
15. V. G. Fastovskii, A. E. Rovinskii, and Yu. V. Petrovskii. Inert gases. Israel Program for Scientific Translations, Jerusalem. 1967. Obtainable from the U.S. Dept. of Commerce.
16. G. A. Cook (*Editor*). Argon, helium, and the rare gases. Vol. 1. Interscience, New York. 1961.
17. Matheson gas data book. Matheson Co., Newark, Calif. 1961. p. 339.
18. Londolt–Börnstein. Zahlenwerte und Funktionen. I Bd. 6 Teil. Springer–Verlag, Berlin. 1951. p. 511.
19. R. W. Kiser. Introduction to mass spectrometry and its applications. Prentice–Hall, Englewood Cliffs, N.J. 1965. Appendix IV.
20. M. G. Robinson and G. R. Freeman. J. Phys. Chem. **72**, 1394 (1968).
21. T. E. Sambrook. Unpublished.
22. G. R. Freeman. J. Chem. Phys. **46**, 2822 (1967).
23. J.-P. Dodelet and G. R. Freeman. Can. J. Chem. **49**, 2643 (1971); **50**, 2729 (1972).
24. J.-P. Dodelet and G. R. Freeman. Can. J. Chem. **50**, 2667 (1972).
25. H. T. Davis, S. A. Rice, and L. Meyer. J. Chem. Phys. **37**, 947, 2470 (1962).
26. K. N. Jha and G. R. Freeman. J. Chem. Phys. **48**, 5480 (1968).
27. P. Fowles. Trans. Faraday Soc. **67**, 428 (1971).
28. K. Schmidt and W. Buck. Science, **151**, 70 (1966).

Can. J. Chem. Downloaded from www.nrcresearchpress.com by 210.87.254.6 on 09/05/12
For personal use only.

Reactions of Hot Hydrogen Atoms in Gaseous Hydrogen Chloride and Hydrogen Bromide

D. K. JARDINE,[1] N. M. BALLASH, AND D. A. ARMSTRONG
Department of Chemistry, The University of Calgary, Calgary, Alberta
Received August 18, 1972

Hydrogen atoms of initial kinetic energy $E_0 = 1.15$ or 2.1 eV were produced photolytically and their reactions with HCl were studied at 300 °K using bromine as a scavenger. The fraction, F_H, undergoing reaction 2 while hot was found to be 0.79 ± 0.02 and 0.55 ± 0.02 for $E_0 = 2.1$ and 1.15 eV, respectively.

[2] $$H + HCl \rightarrow H_2 + Cl$$

For 2.1 eV atoms a similar result was obtained at 200 °K with chlorine as scavenger. On the addition of carbon dioxide as a moderator F_H decreased in a manner consistent with the kinetic theory of hot atom reactions. Comparison of the present results with previous work on the D + DCl abstraction reaction showed that the cross section of the latter is probably 20 to 50% higher than that of H + HCl. The cross section of reaction 2 appears to increase with energy over most of the 0.1 to 1.1 eV range and possibly also above it. Its average magnitude over this energy region was estimated to be $\lesssim 0.35$ Å^2.

For atoms of $E_0 = 1.15$ eV reacting in HBr F_H is close to unity. The threshold of reaction 3′

[3′] $$H + Br_2 \rightarrow HBr + Br$$

is near zero energy and its cross section rises rapidly, becoming $\gtrsim 7$ Å^2 in the thermal region for 300 °K.

Des atomes d'hydrogène d'énergie cinétique initiale $E_0 = 1.15$ ou 2.1 eV ont été produits photolytiquement et leurs réactions avec HCl ont été étudiées à 300 °K en utilisant du brome comme fixateur. La fraction, F_H, impliquée dans la réaction 2 lorsque chaude s'est révélée être 0.79 ± 0.02 et 0.55 ± 0.02 pour $E_0 = 2.1$ et 1.15 eV, respectivement.

[2] $$H + HCl \rightarrow H_2 + Cl$$

Pour les atomes possédant $E_0 = 2.1$ eV, un résultat semblable a été obtenu à 200 °K avec du chlore comme fixateur. En additionnant du dioxyde de carbone comme modérateur, F_H a diminué en accordance avec la théorie cinétique des réactions impliquant des atomes chauds. La comparaison des résultats obtenus avec des travaux antérieurs sur la réaction d'abstraction D + DCl a montré que la coupe transversale de cette dernière est probablement plus élevé de 20 à 50 pour cent que celle de H + HCl. La coupe transversale de la réaction 2 semble s'accroître avec l'énergie tout au long de l'intervalle de 0.1 à 1.1 eV et probablement aussi au-dessus de celui-ci. Son amplitude moyenne pour cette région énergétique a été evaluée à $\lesssim 0.35$ Å^2.

Pour les atomes ayant $E_0 = 1.15$ eV et réagissant dans HBr, F_H est proche de l'unité. Le début de la réaction 3′ se situe

[3′] $$H + Br_2 \rightarrow HBr + Br$$

près de l'énergie nulle et sa coupe transversale augmente rapidement pour devenir $\gtrsim 7$ Å^2 dans la région thermique correspondant à 300 °K. [Traduit par le journal]

Can. J. Chem., **51**, 656 (1973)

Introduction

Atoms or radicals with excess translational energy are commonly referred to as "hot". They may be formed by nuclear recoil reactions, when their initial energy is in the 10^2 to 10^4 eV range (1, 2), or with lesser energy (0.5 to 5 eV) by the dissociation of molecules in repulsive excited states (3, 4). Since the cross sections for electronic transitions to repulsive states are often large in small molecules (5, 6), hot atoms and radicals are frequently encountered as primary species in photochemistry and radiation chemistry. However, in spite of this, the magnitudes and energy dependences of the cross sections for their reactions have only been studied in a relatively few systems. This publication is concerned with the reactions of hot *H* atoms with gaseous HCl and HBr. The experiments consisted of photolysing HCl, HBr, or HCl–HBr

[1]Present address: Capilano College, West Vancouver, British Columbia.

Can. J. Chem. Downloaded from www.nrcresearchpress.com by 210.87.254.105 on 09/05/12
For personal use only.

Can. J. Chem. Downloaded from www.nrcresearchpress.com by 210.87.254.105 on 09/05/12
For personal use only.

mixtures in the presence of chlorine or bromine which competed very efficiently for thermalyzed atoms and less efficiently for hot atoms. By studying the hydrogen yields as a function of scavenger concentration, it was possible to determine the fraction of atoms which reacted hot and to estimate relative cross sections and some absolute cross sections. The effects of changing the initial energy of the atoms and of moderating them with carbon dioxide were also investigated. In addition to providing information which is vital for a more complete understanding of the mechanism of radiolysis of HCl, the results add to the present body of knowledge of hot hydrogen atom reactions and can be compared with those of other recent studies, including an investigation of the behavior of D atoms in DCl under similar conditions (7).

Experimental

Reagents

Hydrogen chloride, chlorine, and carbon dioxide were all obtained from the Matheson Company. Hydrogen chloride was purified as previously described to remove HBr, water, halogens, and other impurities (8, 9). After passage over KOH pellets to remove HCl and other acidic impurities, chlorine was carefully degassed and further purified by sublimation at −125 °C. Carbon dioxide was simply degassed and sublimed before use and reagent grade bromine was treated similarly.

Apparatus and Procedure

After purification the reagents were all stored at liquid nitrogen temperature in storage tubes attached to a mercury-free vacuum line. Samples were prepared for photolysis by measuring the desired pressure of each reagent in a standard volume using a diaphragm gauge. The photolysis cells were 6 cm long and 4.6 cm in diameter with the end windows of Suprasil and the cylindrical walls of quartz. Attached to the cells were a cold trap and a magnetically driven stirring vane which ensured complete mixing of the reagents. The Hanovia SC2537 low pressure mercury lamp for HCl photolyses was constructed with a Suprasil envelope. It was situated about 13 cm from the end window of the photolysis cell. Both were in a light proof box which could be purged with nitrogen, and the cell compartment could be thermostated at different temperatures. The lamp was allowed to stabilize for some 30 min before the shutter between it and the cell was removed to start a photolysis. In preliminary experiments the lamp was monitored continuously during each run, using a platinum photocell. Since the output was found to be constant over the short periods (1 to 10 min) involved, this procedure was abandoned and the lamp was simply checked for long term variations in intensity by measuring the hydrogen yield from HCl at a standard pressure. While a deterioration in the intensity of the 1849 Å line occurred over the lifetime of the lamps, examination of their emission spectra with a McPherson Model 218 vacuum u.v. spectrometer showed that this remained the only line of measurable intensity at wavelengths below that of the strong line at 2537 Å. For the photolysis of HCl–HBr mixtures a standard SC2537 lamp with a quartz envelope was used. This did not produce any hydrogen from HCl alone and showed no detectable emission at 1849 Å.

Photolyses with no scavenger in the cell were performed before and after each series of experiments with added scavenger. Yields in the presence of scavenger at a given concentration were determined relative to the yield from pure HCl at the same pressure as in the HCl–scavenger mixture. For 1849 Å photolyses HCl pressures were always such that over 99% of the incident light intensity was absorbed ($\varepsilon \simeq 80\ M^{-1}\ cm^{-1}$ at 1849 Å (10, 11)). For the 2537 Å photolysis the fraction of light absorbed by HBr is very small and proportional to the HBr concentration since $\varepsilon = 1.0\ M^{-1}\ cm^{-1}$ (12). A correction was made for absorption by bromine.

At the end of each photolysis the hydrogen halide, carbon dioxide, and halogen were condensed at liquid nitrogen temperature in the cold trap attached to the photolysis cell. The hydrogen was then pumped into an analysis line using an oil diffusion pump followed by a cold trap and toepler pump. The amount of hydrogen was determined by techniques already described (8).

Results

Since there is evidence for complex formation between HCl and polarizable molecules (13) we investigated the spectrum of bromine and HCl–bromine mixtures with a Cary Model 15 Spectrophotometer to determine whether such complexes were formed and if they absorbed between 1800 and 2000 Å, this being the region of absorption of the Br_4 complex (14). It was shown that any absorption at 1849 Å by an HCl–Br_2 complex or by Br_2 itself at the pressures used in this study was negligible compared to the absorption by HCl. The absorption by chlorine at this wavelength was also shown to be negligible. The extinction coefficient of bromine at 2537 Å was found to be $1.8\ M^{-1}\ cm^{-1}$ at the pressures used.

The upper line in Fig. 1 shows a plot of hydrogen concentration *vs.* photolysis time for a sample of initially pure hydrogen chloride. At sufficiently long photolysis times these plots tend to bend over toward a limiting hydrogen concentration. As illustrated by the lower curve this occurs at much shorter photolysis times at high chlorine concentrations. Since the small amount of chlorine formed during photolysis does not change $[Cl_2]$ significantly, the tendency to a limiting hydrogen concentration cannot be caused by an increasing consumption of H atoms in the reaction

$$H + Cl_2 \rightarrow HCl + Cl$$

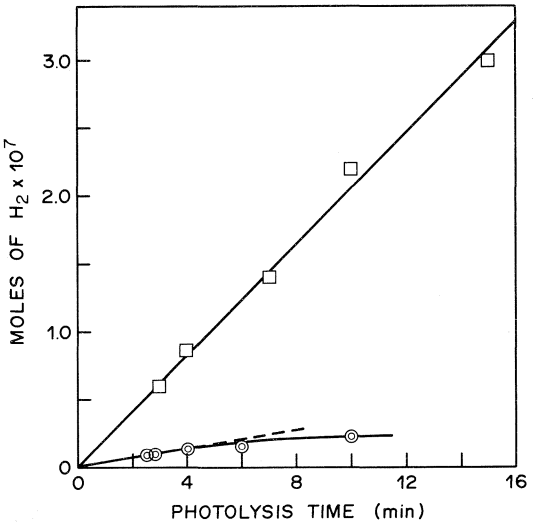

FIG. 1. Yield–time plots for the 1849 Å photolysis of HCl at 300 °K: □, initially pure HCl; ◎, HCl with added CO_2 and Cl_2 such that $[CO_2]/[HCl] = 5$, and $[Cl_2]/[HCl] = 0.05$.

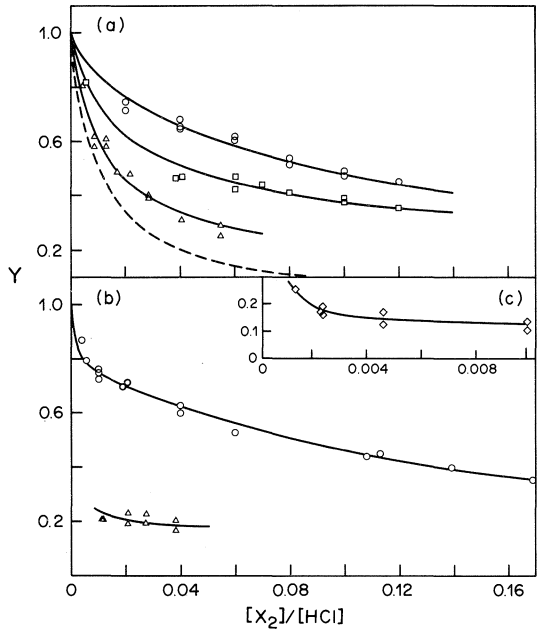

FIG. 2. Effect of scavengers on hydrogen yields from the 1849 Å photolysis of HCl in the presence and absence of carbon dioxide moderator: (*a*) chlorine as scavenger: ○, HCl only at 200 °K; □ and △, HCl + CO_2 at 300 °K with $[CO_2]/[HCl] = 1.00 \pm 0.04$ and 5.00 ± 0.05, respectively. The curves through these data are calculated (see text); the dashed line is calculated from ref. 23 and shows the yields expected for thermal atoms; (*b*) bromine as scavenger at 300 °K: ○, HCl only; △, $[HCl]/[CO_2] = 5.0 \pm 0.1$; (*c*) bromine as scavenger at 300 °K: $[HCl]/[CO_2] = 8.2 \pm 0.1$.

It must therefore be attributed to

$$Cl + H_2 \rightarrow HCl + Cl$$

which will increase in importance as $[H_2]$ builds up (9).

All hydrogen yields were obtained from the linear initial regions of plots such as those in Fig. 1. Hydrogen yields from hydrogen chloride – scavenger mixtures relative to those in standard runs with HCl alone (or HCl and CO_2, see below) are designated by the symbol Y and plotted as a function of scavenger concentration in Fig. 2(*a*) for chlorine and 2(*b*) for bromine. Results are shown for different moderator:HCl ratios. The relative yields were found to be reproducible to within $\pm 5\%$ or better. Figure 2(*c*) shows the effect of very low concentrations of bromine on hydrogen yields from an HCl–CO_2 mixture with a $[CO_2]/[HCl]$ ratio of 8.2.

Yields from the 2537 Å photolysis of HCl–HBr mixtures of fixed composition and of HBr were determined in the presence of varying concentrations of bromine. They were also expressed as relative yields, taking the yield in the absence of scavenger as a standard. They are plotted as a function of bromine concentration in Fig. 3 in accord with the mathematical analysis presented below.

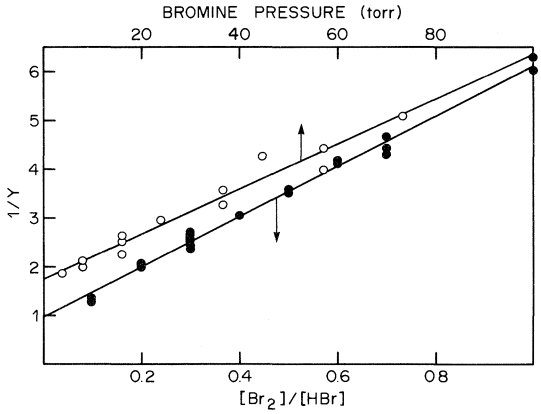

FIG. 3. Reciprocal plots of relative hydrogen yields from the 2537 Å photolysis of pure HBr (●), and a 0.98:0.02 HCl:HBr mixture (○). (Plotted in accord with expressions vi and vii, respectively; see text.)

Can. J. Chem. Downloaded from www.nrcresearchpress.com by 210.87.254.105 on 09/05/12
For personal use only.

Can. J. Chem. Downloaded from www.nrcresearchpress.com by 210.87.254.105 on 09/05/12
For personal use only.

Discussion

Mechanism

The vacuum u.v. spectrum of HCl has been studied by Romand (10) and Myer and Samson (11). Absorption begins at 2200 Å and only the 1849 Å line emitted by the SC2537 Å lamps with Suprasil windows will be absorbed. As explained elsewhere this leads to photodissociation with an excess kinetic energy of 2.1 eV going to the hydrogen atoms (7, 15)

[1] $$HCl + h\nu \rightarrow \underline{H}(^2S_{1/2}) + Cl(^2P_{3/2})$$

The photolysis of HBr with 2537 Å mercury radiation is similar, giving $\underline{H}$ atoms with an average kinetic energy of 1.15 eV (16, 17). Broadening of these energies by ~0.05 eV in both cases results from the distribution of rotational (and translational) energies of the dissociating molecules (16). The production of $X(^2P_{1/2})$ atoms is assumed to be negligible for both HCl and HBr (18).

The strong 2537 Å line from the SC2537 lamps will also be absorbed by chlorine and bromine when they are added as scavengers. This causes dissociation (5). Both of the resulting halogen atoms (X)

$$X_2 + h\nu \rightarrow X(^2P_{3/2}) + X(^2P_{1/2}) \text{ or } (^2P_{3/2})$$

are hot and the $^2P_{1/2}$ atom is also electronically excited, giving it a total excess energy of 1.26 and 1.69 eV for Cl_2 and Br_2, respectively. In both instances this is less than the threshold energy of the reaction

$$X + XH \rightarrow X_2 + H,$$

which must exceed the value of ΔE calculated from bond dissociation energies (ΔE = 1.95 eV for X = Cl and 1.80 eV for X = Br (19)). Hydrogen atom formation by this process should not therefore compete with the recombination of the halogen atoms (see below).

For the case of the HCl photolysis at 1849 Å the threshold energies for collisionally induced dissociation of HCl and Cl_2

$$\underline{H} + HCl \rightarrow 2H + Cl \qquad \Delta E = 4.43 \text{ eV}$$

$$\underline{H} + Cl_2 \rightarrow H + 2Cl \qquad \Delta E = 2.48 \text{ eV}$$

must each exceed the corresponding ΔE (19). They are both larger than the initial energy of the $\underline{H}$ atoms and these reactions may be neglected. Thus, as has been pointed out in previous publications dealing with the photolysis of deuterium chloride (7) and the radiolysis of hydrogen chloride (9, 15), the effect of chlorine may be interpreted in terms of the following reactions

[2] $$\underline{H} + HCl \rightarrow H_2 + Cl$$

[2] $$H + HCl \rightarrow H_2 + Cl$$

[3] $$\underline{H} + Cl_2 \rightarrow HCl + Cl$$

[3] $$H + Cl_2 \rightarrow HCl + Cl$$

[4] $$\underline{H} + M \rightarrow H + M$$

[5] $$Cl + H_2 \rightarrow HCl + H$$

[6] $$H + Cl + M \rightarrow HCl + M$$

[7] $$H + H + M \rightarrow H_2 + M$$

[8] $$Cl + Cl + M \rightarrow Cl_2 + M$$

Reaction 4 is composite in the sense that M can be hydrogen halide, carbon dioxide, or halogen. Unlike reactions 2 and 3 it occurs many times during the lifetime of an $\underline{H}$ atom, reducing the excess translational energy in small decrements until it falls below the minimum energy E_M for reaction 2. The atom is then designated as H. Shizgal and Karplus (20) have calculated a threshold energy of 0.113 eV for reaction 2 by fitting the experimental data of Westenberg and de Haas (21) for the thermal reaction to a line-of-centers model and this appears to be the best value available for E_M.[2]

In the presence of bromine as a scavenger reactions 3 and 3 will be replaced by the analogous reactions of Br_2. Also the ΔE (19) for reaction 9′

[9′] $$\underline{H} + Br_2 \rightarrow H + 2Br \qquad \Delta E = 1.97 \text{ eV}$$

shows that it may be possible with 2.1 eV $\underline{H}$ atoms. However, it would be manifested in terms of the efficiency of bromine as a moderator and would in fact be included in the bromine counterpart of reaction 4. Since reaction 10

[2]For reaction with a stationary HCl molecule momentum conservation actually requires that the minimum laboratory energy of $\underline{H}$ be ~2.8% higher than the reaction threshold energy (4). However, this is negligible when compared to the uncertainty in E_M arising from: (*a*) the fact that the cross section may rise more steeply than predicted by the line of centers model as has in fact been observed for the H + *n*-C_4D_{10} → HD + C_4D_9 abstraction, and (*b*) the contribution to the collision energy from the Maxwellian energy distribution of the target molecules. While (*a*) would raise the threshold energy, the effect of (*b*) would be compensatory, allowing atoms of lower energy to react. Though uncertain, E_M = 0.113 eV is therefore at present a reasonable choice.

Can. J. Chem. Downloaded from www.nrcresearchpress.com by 210.87.254.105 on 09/05/12
For personal use only.

[10] $Cl + Br_2 \rightarrow ClBr + Br$

will convert Cl atoms to Br atoms (22), reactions 5, 6, and 8 will therefore be almost entirely eliminated in favor of their bromine atom counterparts. To avoid an unnecessary proliferation of reaction numbers we shall use the same ones for analogous bromine and chlorine reactions, inserting a prime next to those which refer to bromine.

Since $[H_2]$ is always much smaller than [HCl], and $k_{5'} \ll k_{2'}$ and $k_5 \ll k_2$ (19), the concentration of H atoms will be much less than that of the halogen atoms. Hence, reactions 6 and 7 can be neglected. Under these circumstances the steady state approximation gives

[i] $$\frac{d[H_2]}{dt} = \phi I_{abs}(F_H + F_M f_t) - \text{rate of reaction 5} \times (1 - f_t)$$

The symbols F_H, F_M, and f_t are identified as follows, the rate constants being those for the case of chlorine as scavenger:

[ii] $$F_H = \left\{\begin{matrix}\text{fraction of } \underline{H} \\ \text{reacting with HCl} \\ \text{while hot}\end{matrix}\right\} = \left(1 + \frac{\sum_M \underline{k}_4[M]}{\underline{k}_2[HCl]} + \frac{\underline{k}_3[Cl_2]}{\underline{k}_2[HCl]}\right)^{-1}$$

[iii] $$F_M = \left\{\begin{matrix}\text{fraction of } \underline{H} \text{ moderated} \\ \text{to energies below the} \\ \text{threshold of reaction 2}\end{matrix}\right\} = \frac{\sum_M \underline{k}_4[M]}{\underline{k}_2[HCl]}\left(1 + \frac{\sum_M \underline{k}_4[M]}{\underline{k}_2[HCl]} + \frac{\underline{k}_3[Cl_2]}{\underline{k}_2[HCl]}\right)^{-1}$$

[iv] $$f_t = \left\{\begin{matrix}\text{fraction of} \\ \text{moderated H} \\ \text{reacting with HCl}\end{matrix}\right\} = \left(1 + \frac{k_3[Cl_2]}{k_2[HCl]}\right)^{-1}$$

For the case of the 2537 Å photolysis of HBr–HCl mixtures 1.15 eV atoms are produced in reaction 1′

[1′] $HBr + h\nu \rightarrow \underline{H} + Br(^2P_{3/2})$

and the following two reactions must be included in the mechanisms and accounted for in expressions *ii*, *iii*, and *iv*.

[2′] $\underline{H} + HBr \rightarrow H_2 + Br$

[2′] $H + HBr \rightarrow H_2 + Br$

Otherwise the mechanism and analysis of data are the same as for HCl.

Reaction 5 is the major reason for the approach to limiting hydrogen concentrations and it is clearly negligible in the linear initial region of the concentration:time plots (see Fig. 1) where our yields were measured. Thus, expression *i* becomes simply $d[H_2]/dt = \phi I_{abs}(F_H + F_M f_t)$ and the hydrogen yield in the presence of the scavenger relative to that in its absence may be written

[v] $$Y = F_H + F_M f_t$$

Expression v has a complex dependence on the halogen concentration and cannot be used without further simplification, the usual one being $F_M f_t = 0$.

Analysis

HCl and Scavengers Only

Assuming $F_M f_t = 0$ (*i.e.* k_3/k_2 equal to infinity), expression v simplifies to $Y = F_H$. Inverting and substituting proper terms for F_H from expression ii one has for the chlorine case

[vi] $$\frac{1}{Y} = 1 + \frac{k_4^{HCl}}{k_2} + \frac{(k_4^{Cl_2} + k_3)[Cl_2]}{k_2[HCl]}$$

where superscripts are used to identify the molecules to which each $\underline{k}_4$ refers. This is identical to the expression used in ref. 7 for the analysis of $\underline{D}$ atom reactions in DCl. Figure 4 shows plots of $1/Y$ *vs.* $[Br_2]/[HCl]$ and $[Cl_2]/[HCl]$. The slopes $((\underline{k}_4^{X_2} + \underline{k}_3)/\underline{k}_2$, X = Cl or Br) and intercepts $(1 + \underline{k}_4^{HCl}/\underline{k}_2)$ are presented in Table 1.

In practice k_3/k_2 (and $k_{3'}/k_2$) are not infinite. Their magnitudes will depend on the mean energy of the moderated atoms, reaching maximum values in completely thermalized systems. Figure 2(*c*) shows that for a carbon dioxide moderated

TABLE 1. Experimental data for the reactions of hot H atoms in HCl and D atoms in DCl

E_0 (eV)	Temperature (°K)	Reactant	$[CO_2]/[HCl]$	$1+\frac{k_4^{HCl*}}{k_2}$	F_H*	Scavenger	$\frac{k_4^{X_2}+k_3*}{k_2}$
2.1	303±2	DCl†	0	1.65±0.07	0.61±0.02	Cl_2	7.48±0.38
2.1	303±2	DCl†	0.90		0.37		
2.1	303±2	DCl†	1.87		0.26		
2.1	200±5	HCl	0	1.17±0.06	0.85±0.04	Cl_2	8.60±0.40
2.1	300±5	HCl	0	1.26±0.04	0.79±0.02	Br_2	9.24±0.24
2.1	300±2	HCl	1.0		0.49±0.0‡	Cl_2	7.4 ±0.6
2.1	300±2	HCl	5.0		0.19±0.06	Cl_2	
2.1	300±2	HCl	5.0		0.20±0.03	Br_2	
1.15	300±2	HCl	0	1.82±0.07§	0.55±0.02	Br_2	20±2

*Uncertainties shown are standard deviations.
†Data of ref. 7.
‡Calculated from $k_3^{CO_2}/k_2 = 0.80$ and shown to be consistent with data in Fig. 2(*a*). See text.
§Corrected from 1.76 for the effect of HBr.

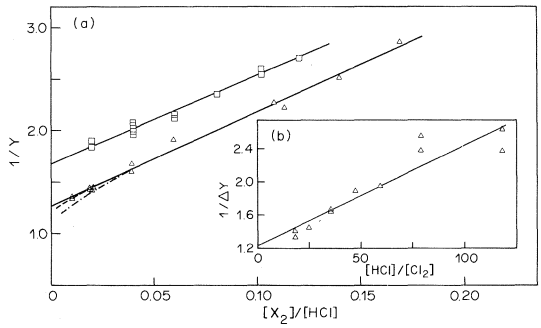

FIG. 4. Reciprocal plots of relative hydrogen yields from the 1849 Å photolysis of HCl: (*a*) □, HCl at 200 °K with Cl_2 as scavenger; △, HCl at 300 °K with Br_2 as scavenger; (*b*) $[CO_2]/[HCl] = 5.00 \pm 0.05$ mixture at 300 °K with Cl_2 as scavenger.

system with $[CO_2]/[HCl] = 8.2$, 80% of all hydrogen atoms were scavenged at $[Br_2]/[HCl] = 2.5 \times 10^{-3}$, whence it can be shown that $k_{3'}/k_2 \geq 1600$ for thermal H at 300 °K. To determine the effects of finite $k_{3'}/k_2$ ratios in the region of 1600 or less, values of $1/Y$ were calculated from expression v using the appropriate $(\underline{k}_4^{Br_2} + \underline{k}_{3'})/\underline{k}_2$ and $1 + \underline{k}_4^{HCl}/\underline{k}_2$ from bromine from Table 1. The dashed and dot-dashed curves in Fig. 4*a* demonstrate the curvature[3] obtained taking $k_{3'}/k_2 = 1600$ and 100, respectively. Over the $[Br_2]/[HCl]$ range 0.01 to 0.05 the experimental points show a better fit to the dashed curve (or the straight line) than to the dot-dashed curve, implying that $k_{3'}/k_2$ is much greater than 100 and probably close to 1600.

It is convenient to note here that for thermal H $k_2 = 1.11 \times 10^{-13}$ cm^3 molecule^{-1} s^{-1} at 300 °K (21) and therefore with $k_{3'}/k_2 > 1600$, $k_{3'}$ must be $> 1.8 \times 10^{-10}$ cm^3 molecule^{-1} s^{-1}. Taking a value of zero for the activation energy it follows from the collision theory expression $k = \sigma_{AB}(8kT/\pi\mu)^{1/2} \exp(-E/RT)$ (19) that the cross section of reaction 3′ in the thermal region must be $\gtrsim 7$ Å^2.

The chlorine data, which are displaced upward by 0.5 on the ordinate scale in Fig. 4(*a*), are less extensive, but the linearity is good showing that, as for bromine, k_3/k_2 is at least an order of magnitude larger than $(\underline{k}_4^{Cl_2} + \underline{k}_3)/\underline{k}_2$. However, presently available data show that E_3 (= 1700 to 2200 cal mol^{-1} (15)) is much larger than $E_{3'}$ and the thermal rate constant ratio for k_3/k_2 at 200 °K is known (15, 23) to be only 340 ± 40. Thus the maximum value of k_3/k_2 is substantially smaller than $k_{3'}/k_2$ and chlorine will not be as effective a scavenger of H as bromine. The fact that the chlorine results give a smaller value of $1 + \underline{k}_4^{HCl}/\underline{k}_2$ than the bromine data (1.17 as opposed to 1.26, see Table 1) may in part be due to this.[3] However, the discrepancy lies within the combined experimental uncertainty of the two measurements. The mean value of F_H for 2.1 eV $\underline{H}$ in pure HCl calculated from the two results, 0.82 ± 0.04, is relatively large, confirming an earlier conclusion that reactions of hot hydrogen atoms would be important in the HCl system (9).

HBr and HCl–HBr Mixtures

The lower line in Fig. 3 shows hydrogen yields from the 2537 Å photolysis of HBr plotted as a function of $[Br_2]/[HBr]$ in accordance with

[3]Actually in addition to causing curvature at low $[X_2]/[HCl]$ values of $\underline{k}_3/\underline{k}_2$ less than 1600 cause a downward shift in the linear portion and this has not been shown. For $\underline{k}_3/\underline{k}_2 = 100$ it amounts to a shift of approximately 0.06 on the ordinate scale.

Can. J. Chem. Downloaded from www.nrcresearchpress.com by 210.87.254.105 on 09/05/12
For personal use only.

Can. J. Chem. Downloaded from www.nrcresearchpress.com by 210.87.254.105 on 09/05/12
For personal use only.

expression vi. In agreement with Fass' data (17) the intercept ($= 0.97 \pm 0.04$) is essentially unity, showing that in HBr the analysis cannot distinguish between atoms which react hot and after moderation. From Fass' results for complete moderation with carbon dioxide $k_{3'}/k_{2'}$ is 23 at 300 °K and $E_{2'} - E_{3'} = 0.8 \pm 0.3$ kcal mol^{-1}. Since $E_{3'} \simeq 0$ (see above) then $E_{2'}$ must be $\simeq 0.8$ kcal mol^{-1}. The threshold energy of reaction 2′ will be less than $E_{2'}$ and therefore lies in the region of $(3/2)RT$, where the average fractional energy loss of $\underline{H}$ per collision is reduced due to the thermal motion of the moderator molecules (see eq. 12 of ref. 24). This feature and the much smaller difference between $k_{3'}/k_{2'}$ and $(\underline{k}_4^{Br_2} + \underline{k}_{3'})/\underline{k}_{2'}$ (see below) than for the corresponding ratios in the HCl system may be partly responsible for the inability to detect any moderated atoms. However, it must be realized that F_H in HBr *should* be greater than in HCl and much closer to unity, since the cross section for reaction 2′ is about twice that of reaction 2 and moderation of $\underline{H}$ by HBr is probably less efficient than by HCl due to the greater molecular weight (see below). Assuming all $\underline{H}$ atoms react hot in HBr the slope of the lower line in Fig. 3 gives

$$\frac{\underline{k}_4^{Br_2} + \underline{k}_{3'}}{\underline{k}_{2'}} = 5.2 \pm 0.1$$

in good agreement with Fass' value of 5.3 ± 0.4.

The data in Fig. 3 for the 2537 Å photolysis of the 2% HBr in HCl mixture can be interpreted[4] in terms of expression vii

$$[\text{vii}] \qquad \frac{1}{Y} = 1 + \frac{\sum_M \underline{k}_4[M] + \underline{k}_{3'}[Br_2]}{\underline{k}_2[HCl] + \underline{k}_{2'}[HBr]}$$

The slope and intercept are then respectively

$$(\underline{k}_4^{Br_2} + \underline{k}_{3'})(\underline{k}_2[HCl] + \underline{k}_{2'}[HBr])^{-1}$$

and

$$\left[1 + \frac{\underline{k}_2}{\underline{k}_4^{HCl}[HCl]} + \frac{\underline{k}_{2'}[HBr]}{\underline{k}_4^{HCl}[HCl]}\right]$$

The values of $\underline{k}_4^{HCl}/\underline{k}_2$ and $(\underline{k}_4^{Br_2} + \underline{k}_{3'})/\underline{k}_2$ for $\underline{H}$ atoms of 1.15 eV initial energy in Table 1 were calculated with corrections for the HBr terms assuming the same value of $(\underline{k}_4^{Br_2} + \underline{k}_{3'})/\underline{k}_{2'}$ as in pure HBr and neglecting $\underline{k}_4^{HBr}$. The contributions of the HBr terms are in any case only about 10%, and errors resulting from the foregoing assumption should be small.

HCl–CO_2 Mixtures

Carbon dioxide is not entirely non-reactive toward $\underline{H}$. In fact in the present study the absolute hydrogen yields were consistently 3–4% lower when it was added to HCl in proportions of 1:1 or larger. This reduction in hydrogen yield should correspond to F_H for the reaction of 2.1 eV $\underline{H}$ atoms with CO_2: $\underline{H} + CO_2 \rightarrow HO + CO$, and it indeed compares very favorably with 2.8×10^{-2} measured by Oldershaw and Porter (25) for 2.02 eV $\underline{H}$ atoms in a region where F_H is rising steeply. It should be noted that in the present work an allowance for the small consumption of $\underline{H}$ by carbon dioxide was made by calculating the Y values in Fig. 2(*a*) and (*b*) with respect to standard runs containing the appropriate ratio of $[CO_2]$:[HCl].

Returning to expression v and assuming that $k_{3'}/k_2 \simeq 1600$ it can be shown that f_t should be negligible for $[Br_2]/[HCl] \geqslant 2 \times 10^{-2}$. Hence, it is apparent from the lower points in Fig. 2(*b*) that F_H is reduced to 0.20 ± 0.03 in the 5:1 CO_2–HCl mixture. For the case of chlorine at room temperature f_t is not negligible as is shown by the dashed line in Fig. 2(*a*), which gives values of Y calculated from the data of ref. 23 for the case of complete moderation and thermalization of all atoms (*i.e.* $F_H = 0$ and $Y = 1 \times f_t$). Thus the foregoing simple procedure cannot be used. However, with $F_H \simeq 0.20$ the reduction in Y caused by the scavenging or moderation of $\underline{H}$ by chlorine should be small below $[Cl_2]/[HCl] = 4 \times 10^{-2}$. Therefore, taking F_H as independent of $[Cl_2]$, the chlorine results for the 1:5 HCl–CO_2 mixture can be analyzed in terms of expression viii.

$$[\text{viii}] \qquad \frac{1}{1 - Y} = \frac{1}{F_M(1 - f_t)} = \frac{1}{\Delta Y} = \frac{1}{F_M}\left\{1 + \frac{k_3[HCl]}{k_2[Cl_2]}\right\}$$

Figure 4(*b*) shows the data plotted in accord with this expression. The intercept gives $F_M = 0.81 \pm 0.06$ and hence $F_H = 0.19 \pm 0.06$ which is consistent with the result obtained above from the bromine data.

From the ratio of the slope to the intercept of Fig. 4(*b*) k_3/k_2 is found to be 100 ± 10. The good agreement with the known rate constant ratio of 93 ± 14 for thermal H atoms at 300 °K

[4]It should be noted that $k_3/(k_2 + 0.02\ k_{2'})$ is 680 fulfilling the requirement that $F_M f_t$ is negligible for $[Br_2]/HX] > 2 \times 10^{-2}$ in the 2% HBr in HCl mixture.

Can. J. Chem. Downloaded from www.nrcresearchpress.com by 210.87.254.105 on 09/05/12
For personal use only.

(23) implies that although F_M is not unity those atoms which fall below E_M approach a Maxwellian energy distribution before finally reacting with HCl or chlorine. This is expected to occur provided the distribution of thermal velocities of the target molecules is such that few of them can make a significant contribution to the relative velocity and energy of collision (26). For HCl molecules with a Maxwellian velocity distribution at 300 °K it can be shown that less than 20% of the collisions of a 0.10 eV H atom will have relative kinetic energy exceeding 0.113 eV.[5] Thus thermalization of a significant fraction of the moderated H atoms should be possible even in pure HCl. The present data suggest that it is the dominant fate of moderated atoms in the system with $[CO_2]/[HCl] = 5$. Other results not presented in detail provide evidence for a similar behavior in a system with $[CO_2]/[HCl] = 1.8$. They also give $F_M = 0.69 \pm 0.03$ (see Fig. 5 below).

Analysis of the chlorine scavenging results in Fig. 2(*a*) for $[CO_2]/[HCl] = 1.0$ at 300 °K by expression vi gave

$$(\underline{k}_4^{Cl_2} + \underline{k}_3)/\underline{k}_2 = 7.4 \pm 0.6$$

showing that this ratio is not markedly changed for the above carbon dioxide concentration. The intercept of the plot corresponded to $F_H = 0.53$ or $F_M = 0.47$, whence using expression iii $\underline{k}_4^{CO_2}/\underline{k}_2$ is 0.60. However, with $F_M \simeq 0.47$ the $F_M f_t$ term is again significant, though not as large as for the $[CO_2]:[HCl] = 5:1$ system. Thus the above values of both F_M and $\underline{k}_4^{CO_2}/\underline{k}_2$ must be regarded as lower limits. In fact it can be seen from Fig. 2(*a*) that the data for $[CO_2]/[HCl] = 1$ and 5 are all consistent with $\underline{k}_4^{CO_2}/\underline{k}_2 = 0.80$, the curves through the points having been drawn using $k_3/k_2 = 93$, $\underline{k}_4^{CO_2}/\underline{k}_2 = 0.80$, and $(\underline{k}_4^{Cl_2} + \underline{k}_3)/\underline{k}_2 = 8.6$.

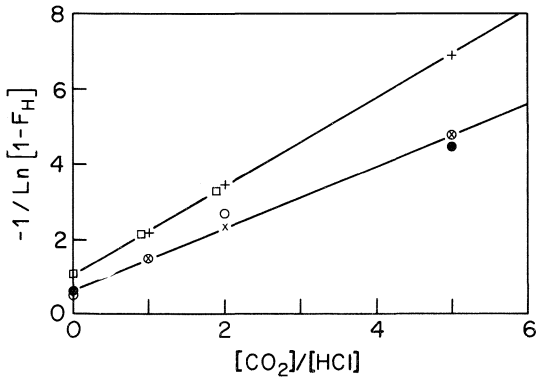

FIG. 5. Effect of CO_2 on the fraction of atoms reacting hot: □, experimental values of F_H for D + DCl from ref. 7; +, values of F_H calculated with expression *ii* taking $\underline{k}_4^{CO_2}/\underline{k}_2 = 1.15$ from ref. 7 for D + DCl; ●,○, experimental values of F_H for H + HCl from this study (open circle = chlorine, closed = bromine); ×, values of F_H calculated with expression *ii* taking $\underline{k}_4^{CO_2}/\underline{k}_2 = 0.80$ for H + HCl (see text).

[5]See expression (A4) of ref. 27.

Comparison with Other Systems

The purpose of this section is to examine the present results within the framework of the theory of hot atom reactions so that comparisons with data for related systems can be made. The basic equations for the analysis of hot atom reactions have been discussed by Wolfgang and his coworkers (see refs. 1 and 2 and citations therein). The fraction of atoms, F_M, moderated to energy E_M in pure reactant is given by

$$[ix] \qquad -\ln F_M = -\ln (1 - F_H) = \int_{E_M}^{E_0} \frac{P_r(E)}{F_r(E)} dE$$

where E_0 is the initial energy of the atoms. $P_r(E)$ is the probability of reaction per collision with reactant and $F_r(E)$ the reciprocal of the collision density for $\underline{H}$ atoms of energy E. For the case with moderator present, following Wolfgang's approach, we write

$$-\ln (1 - F_H) = \int_{E_M}^{E_0} \frac{f_r P_r(E)}{f_r F_r(E) + (1 - f_r) F_m(E)} dE,$$

where f_r is the collision fraction of the reactant. If the reciprocal collision densities $F_r(E)$ and $F_m(E)$ have the same functional dependence on E but differ by a constant factor, then:

$$[x] \qquad -\frac{1}{\ln (1 - F_H)} = \frac{\alpha_r}{I} + \frac{\alpha_m}{I} C \frac{[M]}{[R]}$$

C is the ratio of collision cross sections, $I = \int_{E_M}^{E_0} (P_r(E)/\phi(E))dE$, and the α terms are defined by $\phi(E) = F_r(E)/\alpha_r = F_m(E)/\alpha_m$. This form of expression is easily justified for systems with moderation by elastic hard sphere collisions, for which the kinetic theory model yields $\phi(E) = E$ and $\alpha = \ln \langle (E_{\text{before collision}}/E_{\text{after collision}}) \rangle$. De-

Can. J. Chem. Downloaded from www.nrcresearchpress.com by 210.87.254.105 on 09/05/12
For personal use only.

tailed theoretical calculations show that actual values of α for the inert gases are smaller than those calculated from the hard sphere model, because of the softness of the interaction potentials. For example, $\alpha_{Xe+\underline{H}} \simeq 0.005$ as opposed to the hard sphere value of 0.0153 (24). However, the *form* of expression x holds extremely well when applied to experimental data for inert gases as moderators (1, 2). In general it also holds well for polyatomic gases (1, 2, 28), and therefore provides a useful framework for the analysis of experimental data although its limitations for quantitative predictions must be recognized.

As shown in Fig. 5 the experimental determinations of F_H for 2.1 eV $\underline{H}$ atoms in Table 1 and values calculated from expression iii with $\underline{k}_3^{CO_2}/\underline{k}_2 = 0.8$ and $\underline{k}_3^{HCl}/\underline{k}_2 = 0.26$ obeyed expression x over the range $[CO_2]/[HCl] = 0$ to 5. This was also true of the corresponding data of Wood and White for the D atom – DCl – CO_2 system. Table 2 summarizes α_{HCl}/I and α_{CO_2}/I derived from the intercepts and slopes of plots of $\{-\ln(1 - F_H)\}^{-1}$ against $[CO_2]/[HCl]$. The constant C in expression x was calculated from the collision diameters $d_{DCl} = d_{HCl} = 3.3$, $d_{CO_2} = 3.9$, and $d_D = d_H = 2.5$ Å taken from viscosity data as in ref. 7. The kinetic theory model predicts $\alpha_{CO_2}/\alpha_{HCl} \simeq 0.85$ for both the H–HCl and D–DCl systems, and it is interesting to note that the experimental values are 1.04 and 0.85 respectively, showing a better agreement for the more massive D atoms. The absence of a marked discrepancy in favor of the halides implies that the displacement reaction

$$\underline{H}' + HCl \rightarrow H'Cl^v + H,$$

where $H'Cl^v$ has excess vibrational energy, does not play a major role in the moderation process for these molecules. There is no direct experimental information on this particular reaction, but the recent work of Wood (29) shows that at thermal energies the isotopic analog

$$H + DCl \rightarrow HCl + D$$

has an "A" factor ~850 times less than the abstraction process

$$H + DCl \rightarrow HD + Cl$$

although the latter has a higher activation energy. Thus the displacement reaction would not appear to be highly efficient.

The large fraction of atoms which cascade from the 1.15 to 2.1 eV energy range to the 0.113 to 1.15 eV range makes it difficult to state whether σ_2, the cross section of reaction 2, increases primarily below 1.15 eV or also above it. However, it appears from a comparison of α_{H+HCl}/I_{H+HCl} for $E_0 = 2.1$ and 1.15 eV in Table 2 that σ_2 is increasing with energy over most of the range between the threshold and 1.15 eV and possibly also above 1.15 eV. Substitution of the hard sphere value of $\alpha_{H+HCl} = 0.052$ into the α_{H+HCl}/I_{H+HCl} terms leads to average cross sections of ~0.35 and ~0.7 Å^2 over the energy ranges 0.113 to 1.15 and 0.113 to 2.1 eV, respectively. Although admittedly crude[6] these estimates show that at the energies used here σ_2 is only about 5% (or less) of the total collision cross section of 27.2 Å^2. The magnitude of the cross section for reaction 2 is thus comparable to that of reaction 11

[11] $\underline{H} + n\text{-}C_4D_{10} \rightarrow HD + C_4D_9$ (sec)

for which a maximum value of 0.35 Å^2 at 1.1 eV has recently been reported (30). If one accepts the kinetic theory prediction that the α values for $\underline{D}$ atoms colliding with DCl and CO_2 will be twice those for the corresponding collisions of $\underline{H}$ atoms, then the 2.1 eV data in Table 2 suggest that σ_2 may be significantly (20 to 50%) larger when H is replaced by D. This result is interesting since trajectory calculations (31) predict that mass effects, including isotopic substitution, are very important in determining the magnitude of cross sections for abstraction reactions. However, there are at present no detailed calculations for the H + HCl and D + DCl reactions.

The $(\underline{k}_4^{X_2} + \underline{k}_3)/\underline{k}_2$ ratios are complex functions of the reaction cross sections and collision densities in the hot atom region and cannot be eas-

TABLE 2. Kinetic theory parameters for the reactivity and moderation of hot atoms in DCl and HCl

Atom	E_0	Reactant (r)	α_r/I	$\frac{\alpha_{CO_2}}{I} C$
D	2.1	DCl	1.07	1.11
H	2.1	HCl	0.63	0.83
H	1.15	HCl	1.62	—

[6]Using $\alpha_{Xe+H} = 0.005$ as a standard the comparative data of ref. 25 show that α_{CO_2+H} should be ~0.024 as opposed to the hard sphere value of 0.044. α_{HCl+H} should be reduced by a similar proportion from the hard sphere value of 0.052 and the average cross sections reported in the text are therefore likely to be high.

Can. J. Chem. Downloaded from www.nrcresearchpress.com by 210.87.254.105 on 09/05/12
For personal use only.

ily related to physical parameters for individual processes. However, from certain comparisons a few interesting conclusions concerning the magnitudes of reaction cross sections for the HBr–Br_2 system can be drawn. As pointed out above Fass' value of $(\underline{k}_4^{Br_2} + \underline{k}_{3'})/\underline{k}_{2'} = 5.3 \pm 0.4$ for $E_0 =$ 1.15 eV is in good agreement with ours. Fass also observed the same $(\underline{k}_4^{Br_2} + \underline{k}_{3'})/\underline{k}_{2'}$ for $E_0 =$ 2.9 eV. More recently White and Su (32) have reported $(\underline{k}_4^{Br_2} + \underline{k}_{3'})/\underline{k}_{2'} = 5.48 \pm 0.22$ for $E_0 =$ 1.65 eV and 4.11 ± 0.16 at $E_0 = 2.9$ eV. Their value for $E_0 = 2.9$ eV does not agree with Fass'. However, the discrepancy is only about 20% and $(\underline{k}_4^{Br_2} + \underline{k}_{3'})/\underline{k}_{2'}$ is obviously not strongly dependent on E_0. Since few if any atoms are moderated before reaction it is reasonable as a first approximation to neglect $\underline{k}_4^{Br_2}$ and to associate the experimental values of $(\underline{k}_4^{Br_2} + \underline{k}_{3'})/\underline{k}_{2'}$ with $\underline{k}_{3'}/\underline{k}_{2'}$ or in fact with $\bar{\sigma}_{3'}/\bar{\sigma}_{2'}$, where the cross sections are averaged over the energy range of the reacting atoms.[7] Gann and Dubrin (33) have recently reported a mean cross section of 1.6 ± 0.3 Å^2 for reaction 2′ over the energy range 0.33 to 1.7 eV, based on the collision density distributed in xenon. From this and using our hot atom rate constant ratio of 5.2 as a measure of $\bar{\sigma}_{3'}/\bar{\sigma}_{2'}$, $\bar{\sigma}_{3'}$ is calculated to be $\simeq 8.5$ Å^2. Comparison with the estimate of > 7 Å^2 above (Analysis: HCl and Scavengers Only) for the thermal energy range confirms that $\sigma_{3'}$ must rise rapidly to its maximum value.[8] The constancy of $(\underline{k}_4^{Br_2} + \underline{k}_{3'})/\underline{k}_{2'}$ requires a similar rapid rise in $\sigma_{2'}$ which must be close to if not above its energy of maximum value at 1.15 eV.[8] The strong dependence of $(\underline{k}_4^{Br_2} + \underline{k}_{3'})/\underline{k}_2$ on energy (see Table 2) is in direct contrast implying, in support of earlier statements, that σ_2 is increasing more slowly with energy and may still be rising in the region above 1 eV.

The authors wish to acknowledge financial support from the National Research Council of Canada and also the University of Calgary which provided graduate scholarships for D.K.J. They are also grateful to Dr. G. Miller for valuable discussions and to Drs. W. G. Laidlaw and F. C. Adam who made many helpful contributions during the course of this work.

1. R. Wolfgang. J. Chem. Phys. **39**, 2983 (1963).
2. R. Wolfgang. Prog. in react. kinet. **3**, 97 (1965).
3. H. A. Schwarz, R. R. Williams, and W. H. Hamill. J. Am. Chem. Soc. **74**, 6007 (1953).
4. R. M. Martin and J. E. Willard. J. Chem. Phys. **40**, 2999 (1964); **40**, 3007 (1964).
5. J. G. Calvert and J. N. Pitts. Photochemistry. John Wiley and Sons, New York. 1966.
6. G. Herzberg. Molecular spectra and molecular structure. I. Spectra of diatomic molecules. D. Van Nostrand, New York. 1950.
7. G. O. Wood and J. M. White. J. Chem. Phys. **52**, 2613 (1970).
8. D. A. Armstrong. Can. J. Chem. **40**, 1385 (1962).
9. R. S. Davidow, R. A. Lee, and D. A. Armstrong. J. Chem. Phys. **45**, 3364 (1966).
10. J. Romand. Ann. Phys. (Paris), **4**, 527 (1949).
11. J. A. Myer and J. A. R. Samson. J. Chem. Phys. **52**, 266 (1970).
12. K. T. Wong. Ph.D. Thesis. University of Calgary, Calgary, Alberta. 1966.
13. D. H. Rank, P. Sitaram, W. A. Glickman, and T. A. Wiggins. J. Chem. Phys. **39**, 2673 (1963).
14. E. A. Ogryzlo and B. C. Sanctuary. J. Phys. Chem. **69**, 4422 (1965); A. A. Passchier, J. D. Christian, and N. W. Gregory. J. Phys. Chem. **71**, 937 (1967).
15. D. E. Wilson and D. A. Armstrong. Radiat. Res. Rev. **2**, 297 (1970).
16. R. G. Gann, W. M. Ollison, and J. Dubrin. J. Am. Chem. Soc. **92**, 450 (1970).
17. R. A. Fass. J. Phys. Chem. **74**, 984 (1970).
18. R. S. Mulliken. J. Chem. Phys. **8**, 382 (1940).
19. S. W. Benson. The foundations of chemical kinetics. McGraw-Hill, New York. 1960.
20. B. Shizgal and M. Karplus. J. Chem. Phys. **54**, 4345 (1971).
21. A. A. Westenberg and N. de Haas. J. Chem. Phys. **48**, 4003 (1968).
22. M. I. Christie, R. S. Roy, and B. A. Thrush. Trans. Faraday Soc. **55**, 1139 (1959).
23. F. S. Klein and M. Wolfsberg. J. Chem. Phys. **34**, 1494 (1961).
24. C. Rebick and J. Dubrin. J. Chem. Phys. **53**, 2079 (1970).

[7]If one uses the average of $\bar{\sigma}_{2'} = 1.6$ Å^2 reported by Gann and Dubrin for the energy range 0.35 to 1.7 eV and a kinetic theory

$$\alpha \simeq \frac{2\mu_{H+HBr}}{m_H + m_{HBr}},$$

it can be shown that in pure HBr 70% of H are consumed between 0.6 eV and E_0 for $E_0 = 1.15$ eV and between 1.5 eV and E_0 for $E_0 = 2.9$ eV. Therefore, unless the real value of α is much larger than the kinetic theory prediction, Fass' two $\underline{k}_6^{Br_2}/\underline{k}_{2'}$ ratios correspond to average ratios of cross sections over these limited energy ranges. For the HCl competitions with bromine the lower reaction cross section and higher α would cause the energy range to be spread much more as indeed is indicated by the significant fraction of atoms moderated for $E_0 = 1.15$ and 2.1 eV.

[8]Trajectory calculations (32) actually show both $\sigma_{2'}$ and $\sigma_{3'}$ as decreasing in the region of 1.7 to 2.9 eV (32). Note, however, that $\sigma_{2'}$ may rise to a second maximum in the energy range where collisions with a large angle of approach relative to the molecular axis become important (31).

25. G. H. OLDERSHAW and D. A. PORTER. Nature, **223**, 490 (1969).
26. D. M. CHAPIN and M. D. KOSTIN. J. Chem. Phys. **46**, 2506 (1967).
27. R. N. PORTER. J. Chem. Phys. **45**, 2284 (1966).
28. G. A. OLDERSHAW and D. A. PORTER. J. Chem. Soc., Faraday Trans. I, **68**, 709 (1972).
29. G. O. WOOD. J. Chem. Phys. **56**, 1723 (1972).
30. R. G. GANN, W. M. OLLISON, and J. DUBRIN. J. Chem. Phys. **54**, 2304 (1972).
31. P. J. KUNTZ, E. M. NEMETH, J. C. POLANYI, and W. H. WONG. J. Chem. Phys. **52**, 4654 (1970).
32. J. M. WHITE and H. Y. SU. J. Chem. Phys. In press.
33. R. G. GANN and J. DUBRIN. J. Phys. Chem. **76**, 1321 (1972).

Can. J. Chem. Downloaded from www.nrcresearchpress.com by 210.87.254.105 on 09/05/12
For personal use only.

The Preparation and Properties of Complexes of Antimony and Bismuth Trifluorides with Strong Fluoride Acceptors

T. BIRCHALL, P. A. W. DEAN,[1] B. DELLA VALLE, and R. J. GILLESPIE

Department of Chemistry, McMaster University, Hamilton, Ontario

Received August 10, 1972

The reactions of antimony and bismuth trifluorides with the pentafluorides of antimony and arsenic in liquid sulfur dioxide yield the adducts $SbF_3 \cdot SbF_5$ (type A), $SbF_3 \cdot AsF_5$, $BiF_3 \cdot 3SbF_5$, and $BiF_3 \cdot AsF_5$; no adducts of the trifluorides with BF_3 were isolated. Antimony metal reacts with excess of antimony pentafluoride and arsenic pentafluoride in liquid sulfur dioxide giving a second form of $SbF_3 \cdot SbF_5$ (type B) and the same form of $SbF_3 \cdot AsF_5$ as produced from SbF_3, respectively. $BiF_3 \cdot 3SbF_5$ can be formulated as $Bi(SbF_6)_3$, but its Raman spectrum indicates the presence of extensive cation–anion fluorine-bridging. Their Raman spectra suggest that $BiF_3 \cdot AsF_5$, $SbF_3 \cdot AsF_5$, and $SbF_3 \cdot SbF_5$ (type B) have similar structures, possibly containing polymeric fluorine-bridged cations, but that $SbF_3 \cdot SbF_5$ (type A) has a different structure probably like that of $AsF_3 \cdot SbF_5$. The ^{121}Sb Mössbauer spectra of the SbF_3 adducts support the assignment of similar structures to $SbF_3 \cdot AsF_5$ and $SbF_3 \cdot SbF_5$ (type B), and the suggestion that $SbF_3 \cdot AsF_5$ and both forms of $SbF_3 \cdot SbF_5$ contain antimony (III) fluoro-cations. ^{19}F n.m.r. shows that SbF_3 has appreciable solubility in SO_2 solutions of SbF_5 and indicates the possible formation of "fluxional" SbF_2–Sb_nF_{5n+1} molecules in SbF_3–SbF_5 solutions.

Les réactions des trifluorures d'antimoine et de bismuth avec les pentafluorures d'antimoine et d'arsenic dans le dioxyde de soufre liquide donnent les produits d'addition, $SbF_3 \cdot SbF_5$ (type A), $SbF_3 \cdot AsF_5$, $BiF_3 \cdot 3SbF_5$ et $BiF_3 \cdot AsF_5$; aucun produit résultant de l'addition des trifluorures avec BF_3 n'a été isolé. Lorsque l'antimoine métallique réagit avec un excès de trifluorure d'antimoine et d'arsenic dans le dioxyde de soufre liquide, on obtient alors une seconde forme de $SbF_3 \cdot SbF_5$ (type B) ainsi que la forme identique de $SbF_3 \cdot AsF_5$ tel qu'obtenu à partir de SbF_3. On peut formuler la forme $BiF_3 \cdot 3SbF_5$ comme étant $Bi(SbF_6)_3$, cependant son spectre Raman indique un apport considérable de ponts fluorés entre les cations et les anions. Selon leurs spectres Raman, les composés $BiF_3 \cdot AsF_5$ et $SbF_3 \cdot SbF_5$ (type B) possèdent, semble-t-il, une structure similaire comportant vraisemblablement des cations liés par des ponts fluorés polymériques alors que $SbF_3 \cdot SbF_5$ (type A) possède une structure différente se comparant probablement à celle du $AsF_3 \cdot SbF_5$. Les spectres Mossbauer ^{121}Sb des produits d'addition du SbF_3 confirment l'attribution de structures semblables pour $SbF_3 \cdot AsF_5$ et $SbF_3 \cdot SbF_5$ (type B) et l'hypothèse selon laquelle le $SbF_3 \cdot AsF_5$ ainsi que les deux formes de $SbF_3 \cdot SbF_5$ contiennent des fluorocations (III). La spectroscopie r.m.n. du ^{19}F indique que SbF_3 possède une solubilité appréciable dans des solutions de SbF_5 dans le SO_2 et montre ainsi la formation possible de molécules "fluxionales" SbF_2–Sb_nF_{5n+1} dans des solutions de SbF_3–SbF_5. [Traduit par le journal]

Can. J. Chem., **51**, 667 (1973)

Introduction

Although PF_3 (1) and AsF_3 (2) form well-defined complexes with antimony pentafluoride, the situation with regard to similar complexes of SbF_3 is more confused. Ruff and Plato (3) reported an exothermic reaction between SbF_3 and SbF_5 which, on distillation of the reaction mixture, led to the compounds $SbF_5 \cdot nSbF_3$ (n = 2,5 and possibly 3,4). They found no evidence for a 1:1 compound. Woolf (4), however, found that SbF_3 was insoluble in SbF_5 and did not increase the conductivity of the pentafluoride. More recently, Davies and Moss (5) have been unable to repeat the work of Ruff and Plato. Nevertheless there is some indication that SbF_3–SbF_5 complexes are formed when carbonium ions (6) or hydrocarbons (7) are oxidized by SbF_5 in sulfur dioxide solution.

We have now reinvestigated the interaction between SbF_3 and fluoride-acceptors, and in addition have studied similar reactions of BiF_3, about the fluoro-basic character of which there has been no previous report.

Antimony metal reacts with excess arsenic or antimony pentafluoride in liquid sulfur dioxide to form Sb(III) containing fluorocomplexes and discussion of these complexes is also included in this report. It should be noted that if the pentafluorides are not in excess, antimony(I) salts can be produced in the reaction of antimony with SbF_5 or AsF_5 (8, 9).

[1]Present address: Department of Chemistry, University of Western Ontario, London 72, Ontario.

Can. J. Chem. Downloaded from www.nrcresearchpress.com by 210.87.254.42 on 09/05/12
For personal use only.

Can. J. Chem. Downloaded from www.nrcresearchpress.com by 210.87.254.42 on 09/05/12
For personal use only.

TABLE 1. Raman spectra of adducts of BiF_3 and SbF_3 and related compounds in cm^{-1}*

$BiF_3 \cdot AsF_5$	$BiF_3 \cdot 3SbF_5$	$SbF_3 \cdot AsF_5$	$SbF_3 \cdot SbF_5$(B)	$SbF_3 \cdot SbF_5$(A)	$AsF_3 \cdot SbF_5$	$CsAsF_6$†	$CsSbF_6$‡	Tentative assignments
					738 m 728 mw			ν_1 AsF_2^+
	714 w			719 vw				?
689 vs	690 m sh 685 vs ~673 mw br 643 m	705 m sh 693 m sh 678 s 639 mw	678 w br 658 ms 651 s 625 w br	700 m 685 m 678 m 668 ms 642 s	699 mw 685 s 681 m sh 641 s	699 i.r. 685 R	674 i.r. 658 i.r. 659 R	ν_1,ν_3 MF_6^-
				605 ms				ν_1 SbF_2^+
570 m 546 m	581 mw 537 mw 528 mw 525 mw	605 m sh 589 s 557 mw	578 m br 563 m sh br	555 mw	561 mw	576 i.r.	572 R	ν_2 MF_6^-
~511 m vbr	490 mw 481 sh	~499 m vbr ~450 m vbr	~521 m vbr ~445 m vbr	495 mw br 456 m vbr				ν(M—F—M)
391 sh 371 m 319 mw br	293 mw 287 mw 272 m	271 w 251 mw	295 w sh 280 mw	298 m 276 mw	301 mw 279 mw	392 i.r. 372 R	287 R 285 i.r. 279 i.r.	ν_4,$\nu_5$$MF_6^-$
241 w 226 w	186 sh 169 mw 94 m br		~139 w br	206 w	219 mw 172 mw 121 mw 84 w 59 m			Lattice vibrations

*v = very, w = weak, m = medium, s = strong, br = broad, sh = shoulder. I.r. and R indicated observed in the infrared and Raman spectrum, respectively.
†Reference 17.
‡Reference 18.

Can. J. Chem. Downloaded from www.nrcresearchpress.com by 210.87.254.42 on 09/05/12
For personal use only.

Results and Discussion

Neither SbF_3 nor BiF_3 react with boron trifluoride under the experimental conditions reported here. However, BiF_3 reacts with excess AsF_5 or SbF_5 to give a 1:1 or 1:3 adduct, respectively, while SbF_3 gives 1:1 adducts with both pentafluorides. Inconclusive results were obtained while trying to prepare, from SbF_3,[2] SbF_3–SbF_5 complexes with other than a 1:1 stoichiometry. It is interesting that $SbF_3 \cdot AsF_5$ is an isomer of the known $AsF_3 \cdot SbF_5$ (2).

Antimony metal reacts with excess arsenic pentafluoride to give $SbF_3 \cdot AsF_5$ which is identical in all respects with the complex prepared directly from antimony trifluoride. In contrast, the reaction of antimony metal with excess antimony pentafluoride normally gives a form of $SbF_3 \cdot SbF_5$ quite different from that obtained starting with SbF_3. It was found that the two forms of $SbF_3 \cdot SbF_5$ could not be interconverted either thermally or by extended treatment with antimony pentafluoride in liquid sulfur dioxide. For the purposes of further discussion, the $SbF_3 \cdot SbF_5$ formed from SbF_3 will be called A, that formed from Sb, B.

Raman Spectra

The Raman spectra of the new metal trifluoride adducts are given in Table 1 together with the Raman spectra of $AsF_3 \cdot SbF_5$ and cesium hexafluoro-arsenate and antimonate for comparison.

The Raman spectra of $BiF_3 \cdot AsF_5$, $SbF_3 \cdot AsF_5$ and $SbF_3 \cdot SbF_5$ (B) are quite similar, but they differ from those expected for structures containing recognizable MF_2^+ cations and $M'F_6^-$ anions. Such basically ionic formulations might have been expected by analogy with the postulated structure of $PF_3 \cdot SbF_5$, *i.e.* $PF_2^+SbF_6^-$ (1) and in light of the partly ionic character of $AsF_3 \cdot SbF_5$ (11). An isolated MF_6^- anion of O_h symmetry has three Raman-active vibrations, $\nu_1(A_{1g})$, $\nu_2(E_g)$, and $\nu_5(T_{2g})$ while an isolated (bent) MF_2^+ ion with C_{2v} symmetry should also have three Raman-active modes, $\nu_1(A_1)$, $\nu_2(A_1)$, and $\nu_3(B_1)$. The majority of the bands observed in the Raman spectra of the above three compounds fall in the same regions as the bending and deformation modes of either AsF_6^- ($BiF_3 \cdot AsF_5$ and $SbF_3 \cdot AsF_5$) or SbF_6^- ($SbF_3 \cdot SbF_5$(B)), and, following accepted procedure, we have assigned these bands as being related to the normal modes of the MF_6^- with O_h symmetry. There are, however, many more bands than can be accounted for by assuming isolated octahedral MF_6^- anions to be present. We associate this complexity with the occurrence of a significant amount of cation–anion fluorine-bridging, a situation expected in these compounds which contain very acidic cations. Where fluorine-bridging is appreciable, both distortion of the anion and factor group splitting may contribute to the complexity of a spectrum (12).

Surprisingly the spectra of none of $BiF_3 \cdot AsF_5$, $SbF_3 \cdot AsF_5$, and $SbF_3 \cdot SbF_5$ (B) show bands which are obviously due to a cation, though clearly a cation must be present. This situation contrasts with that found for $PF_3 \cdot SbF_5$ (1) and $AsF_3 \cdot SbF_5$. The vibrational spectrum of the former shows two P—F stretches as expected for a bent PF_2^+ cation, and the Raman spectrum of the latter (see Table 1) has bands at 728 and 738 cm^{-1} which can reasonably be assigned to ν_1 of the AsF_2^+ cation (the doubling of ν_1 is probably a factor group splitting). The ν_1 frequency of AsF_2^+ is comparable to, but higher than, that found for gaseous GeF_2 (692 cm^{-1} (13)), as expected. Further comparison with the spectrum of GeF_2 suggests ν_3 for AsF_2^+ might be found at $\sim$700 cm^{-1}, a region obscured by the bands of the SbF_6^- anion. The situation with respect to ν_2 of AsF_2^+ is similar.

It is possible that the difference between the SbF_3 and BiF_3 adducts and the adducts of AsF_3 and PF_3 is related to the difference propensities for fluorine-bridging of the two heavy and two light elements. Both PF_3 and AsF_3 are monomolecular in the gas liquid phases (14) and presumably form molecular lattices, but SbF_3 (15) and BiF_3 (16) are extensively fluorine-bridged in the solid state. Therefore it is reasonable that any strong fluorine-bridging in $PF_2^+SbF_6^-$ and $AsF_2^+SbF_6^-$ should be between the cation and the anion. This is known to be the case for $AsF_3 \cdot SbF_5$ (11). For adducts of SbF_3 and BiF_3, on the other hand, two extreme possibilities can be envisaged: ether cation–anion fluorine-bridging is predominant (as in $AsF_2^+SbF_6^-$) or cation–cation bridging is stronger, *i.e.* a polymeric fluorine-bridged cation is formed. Provided all the fluorines in this cation are involved in strong fluorine-bridging no M(III)—F stretching vibrations will be seen. Thus it seems that the BiF_3 and SbF_3 adducts discussed above contain polymeric

[2]4 moles of antimony and 11 moles of SbF_5 react in liquid SO_2 giving Sb_3F_{11} but this is, in fact, an Sb(I) salt, $Sb(I)Sb_2F_{11}$ (10).

Can. J. Chem. Downloaded from www.nrcresearchpress.com by 210.87.254.42 on 09/05/12
For personal use only.

cations, *i.e.* they are $(SbF_2)_n^{n+}(MF_6^-)_n$ and $(BiF_2)_n^{n+}(AsF_6^-)_n$, and this suggestion receives support from the observation, in the spectra of all three adducts, of a broad band or bands in the region ~400–500 cm^{-1}, a region which appears characteristic of fluorine-bridged systems.

The Raman spectrum of $SbF_3 \cdot SbF_5$ (A) is markedly dissimilar to that of $SbF_3 \cdot SbF_5$ (B) showing that the two compounds must have different structures. The Raman spectrum of the former is more complicated than would be expected if it arose only from a distorted SbF_6^- anion; in particular, the quite strong band at 605 cm^{-1} is at too low a frequency to be due to an Sb(V)—F stretch and it seems clear that it must be assigned to a terminal Sb(III)—F stretch. This fact, together with the distinct similarity between the Sb(V)—F stretching regions of the spectra of $AsF_3 \cdot SbF_5$ and $SbF_3 \cdot SbF_5$ (A), allows the tentative conclusion that $SbF_3 \cdot SbF_5$ (A) has the $AsF_3 \cdot SbF_5$ structure or something quite similar to it, *i.e.* it is $SbF_2^+SbF_6^-$, and that the band at 605 cm^{-1} is, in fact, the ν_1 vibration of an SbF_2^+ cation. The proposed structure, involving fluorine-bridging only between Sb(V) and Sb(III), and not between Sb(III) and Sb(III) represents a second extreme type of fluorine-bridged structure as outlined above. If this is the correct structure, it is not unreasonable that a type A $SbF_3 \cdot AsF_5$ could not be prepared, since the AsF_6^- anion does not enter as readily into extensive fluorine-bridging as does SbF_6^-.

$BiF_3 \cdot 3SbF_5$ can presumably be formulated $Bi(SbF_6)_3$, and in agreement with this formulation its Raman spectrum (see Table 1) does exhibit bands in the stretching and deformation regions of the SbF_6^- anion. However, the large number of bands observed once more provides good evidence for strong cation–anion interactions, *i.e.* fluorine-bridging, a situation not unexpected in view of the anticipated very high acidity of Bi^{3+}.

^{121}Sb Mössbauer Spectra

Details of the Mössbauer data for the SbF_3 adducts are presented in Table 2 together with data for some related antimony fluorides. The chemical isomer shift, being a measure of "s" electron density at the antimony nucleus, can give valuable information about oxidation states. For example Sb^{3+} with a 5s electron pair would have a relatively high "s" electron density at the Sb nucleus, whereas Sb^{5+} with no 5s electrons would have a much lower "s" electron density. Since the nuclear term in the isomer shift expression is negative for the nucleus in question, compounds of Sb(III) will have less positive isomer shifts than compounds of Sb(V). This is clearly evident from Table 2 and ref. 19: antimony trifluoride has an isomer shift of −6.04 mm/s while SbF_5 and SbF_6^- salts have shifts of ~ +11 mm/s. One also notes the effect of the stereochemically active lone pair in SbF_3 which gives rise to a large quadrupole coupling constant. On the other hand, Sb(V) compounds have small or as yet undetected quadrupole coupling constants.

Both $SbF_3 \cdot SbF_5$ adducts gave Mössbauer spectra which contained two resonances of equal area, which immediately eliminates the possibility that these compounds are "$Sb(IV)F_4$". In both cases, the resonance absorption at the more positive velocity is typical of Sb(V) in a six coordinate environment, such as SbF_6^-. Note however that, in the adducts, the Sb(V) environment is much more distorted than that in the SbF_6^- salts. This confirms the Raman data discussed above where the deviations from O_h symmetry were postulated to arise from appreciable fluorine-bridging. The data would suggest that the Sb(V) environment in the (B) adduct is more symmetric than in the (A) adduct. Presumably the extent of bridging is less for (B) than for (A). However, attention should be drawn to the large error in the quadrupole splitting parameter.

The other resonance absorption in each of these spectra, and that in the spectrum of $SbF_3 \cdot AsF_5$, occurs at negative velocities with respect to InSb, is broad, and very asymmetric. This is typical of Sb(III) in a very distorted environment

TABLE 2. ^{121}Sb Mössbauer parameters for SbF_3 adducts and related compounds at 80 °K

Compound	Isomer shift* (± 0.2 mm/s)		Quadrupole coupling (± 2.0 mm/s)	
$SbF_3 \cdot SbF_5$(A)	−8.3	+11.3	+18.2	+8.0
$SbF_3 \cdot SbF_5$(B)	−7.5	+11.2	+18.3	+5.4
$SbF_3 \cdot AsF_5$	−7.3		+19.4	
SbF_3†	−6.04		+19.6	
SbF_5†		+10.8		
$NaSbF_6$‡		+10.4		
$KSbF_6$		+11.5		+3.1

*Isomer shifts are relative to InSb at 80 °K.
†Reference 19.
‡Reference 20.

Can. J. Chem. Downloaded from www.nrcresearchpress.com by 210.87.254.42 on 09/05/12
For personal use only.

such as that in SbF_3. The recently redetermined crystal structure of SbF_3 (15) shows a polymeric, rather than a molecular lattice, in which the antimony is at the center of a distorted octahedron of six fluorines, three at 1.93 Å and three at 2.61 Å. The gross distortion of the octahedron can be attributed to the influence of the 5s electron pair. Further, the magnitude of the isomer shift indicates that the 5s electron pair is participating to a considerable extent in the bonding scheme (21). Adduct formation with either SbF_5 or AsF_5 does not appear to result in drastic changes in the asymmetry about the Sb(III) since the quadrupole coupling is not significantly altered: the variations observed are within experimental error and a similar coordination number therefore seems probable for each compound.

The Sb(III) isomer shifts of these adducts are however appreciably different from SbF_3. The shift to more negative velocities on adduct formation can be rationalized in terms of placing at least some positive charge on the Sb(III): this would have the effect of contracting the orbitals, hence increasing the "s" electron density and causing a shift to more negative velocities. The isomer shifts for the $SbF_3{\cdot}AsF_5$ and $SbF_3{\cdot}SbF_5$ (B) adducts suggest that these are of the same structure type, again confirming the Raman data, but that $SbF_3{\cdot}SbF_5$ (A) has a different structure. A polymeric cation, as in $SbF_3{\cdot}SbF_5$ (B), having strong Sb(III)—F—Sb(III) bridge bonds and, presumably, two weak Sb(III)—F—Sb(V) bonds, would be expected to have a different isomer shift than the (A) adduct, where, by analogy to $AsF_3{\cdot}SbF_5$ (11), there are presumably two strong Sb(III)—F bonds and four weaker Sb(III)—F—Sb(V) bridge bonds. Since the more weakly bound fluorines would be less effective at removing electron density than strongly bound fluorines, a more negative isomer shift results for the $SbF_3{\cdot}SbF_5$ (A) adduct.

^{19}F *N.M.R. Spectra*

Because of its possible formation when carbonium ions (6) and hydrocarbons (7) are oxidized by SbF_5, it was of interest to measure the ^{19}F n.m.r. spectrum of $SbF_3{\cdot}SbF_5$ in SO_2. It was found however, that this complex, once isolated, was virtually insoluble in SO_2. Therefore the spectrum of the supernatant liquid over a mixture with $SbF_3/SbF_5/SO_2 = 1/4.0/17.8$ (a typical ratio for the preparation of $SbF_3{\cdot}SbF_5$) was measured and is shown in Fig. 1.

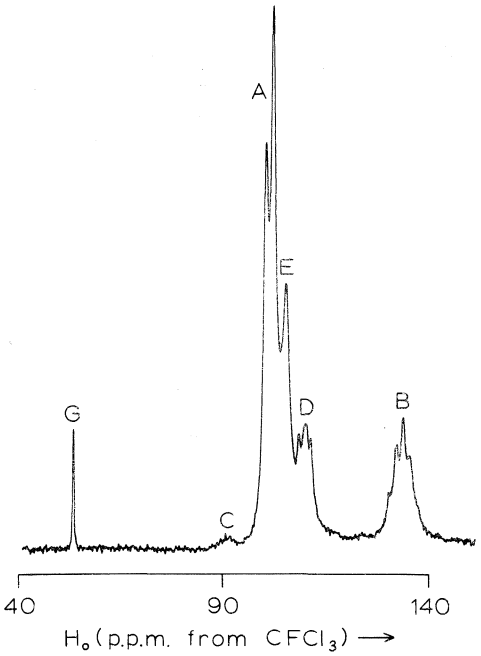

FIG. 1. The −85 °C 56.4 MHz ^{19}F n.m.r. spectrum of the supernatant liquid over a mixture of composition $SbF_5/SbF_3/SO_2 = 1/4.0/17.8$.

The resonance *G*, at ϕ 52.1, is almost certainly due to F-on-Sb(III) since the −90° ^{19}F n.m.r. spectrum of a saturated fluorosulfuric acid solution of $SbF_3{\cdot}SbF_5$ shows, in addition to signals from SbF_6^- and $SbF_5{\cdot}SO_3F^-$, a line at similarly low applied field, ϕ 65.9. The doublet *A* and quintet *B* (ϕ 100.5, 133.0; *J* 100 Hz) arise mainly from $SbF_5{\cdot}SO_2$ (6, 22), and the broad signal *C* (ϕ 90.5) and triplet-like resonance *D* (ϕ 109.8), which is, in fact, a double-doublet, from $Sb_2F_{11}^-$ (6, 23). The signal *E*, at ϕ 105.2, is in the same position as a resonance observed previously (6) in the spectrum of *t*-BuF/3.8SbF_5 in SO_2, which was thought to be due to a species involving Sb(III) and Sb(V). The position of *E* is consistent with its resulting from SbF_6^-. It appears therefore that SbF_3 has appreciable solubility in SO_2 in the presence of SbF_5 and that the SbF_6^- and $Sb_2F_{11}^-$ anions are formed together with an Sb(III) species which is presumably SbF_2^+. (Due to overlap of the somewhat broad signals in the region of F-on-Sb(V) we could not determine accurate intensities and hence the stoichiometries of the species involved.) However an earlier study (6) has shown that large amounts of SbF_6^- cannot coexist with $SbF_5{\cdot}SO_2$; the two combine to give $Sb_2F_{11}^-$. In the light of this earlier result,

Can. J. Chem. Downloaded from www.nrcresearchpress.com by 210.87.254.42 on 09/05/12
For personal use only.

the distribution of Sb(V) species in the present solution is somewhat anomalous. Recently, a similarly irregular distribution of species in NbF_5 (or TaF_5)–SbF_5–SO_2ClF has been interpreted (24) in terms of "fluxional" molecules, which, though they give n.m.r. spectra typical of ionic species are in fact covalent *i.e.* NbF_4–Sb_nF_{5n+1}. It seems possible that in SbF_3–SbF_5–SO_2 the III–V complexes formed are also "fluxional" and of the general form SbF_2-Sb_nF_{5n+1}.

To further determine the conditions under which the SbF_3–SbF_5 complexes exist in SO_2 solution, we prepared solutions similar to that above but also containing Et_4NSbF_6. When $SbF_6^-/SbF_5 > 1$, the only n.m.r. signals observed were from $Sb_2F_{11}^-$ or a mixture of $Sb_2F_{11}^-$ and SbF_6^-, no signal attributable to F-on-Sb(III) was seen. We conclude that SbF_3–SbF_5 complexes can only be formed in fluoride-containing SO_2 solution when $SbF_5/F^- > 2$.

Experimental

Reagents

Antimony pentafluoride (Ozark Mahoning Co.) and fluorosulfuric acid (Baker and Adamson Co.) were purified by standard procedures. Tetraethylammonium hexafluoroantimonate was prepared according to Bacon *et al.* (6). Boron trifluoride (Matheson of Canada Ltd.), arsenic pentafluoride (Ozark Mahoning Co.) and sulfur dioxide (Matheson of Canada Ltd., anhydrous grade), antimony trifluoride (K and K Laboratories, 99%) and bismuth trifluoride (Ozark Mahoning Co., 99%) were all used without further purification. The Raman spectra of the last two were:

SbF_3: 546 (mw.br.), 500 (s), 457 (ms), 275 (w), 249 (vw), 211 (vw), 117 (w), 90 (w) cm^{-1}.

BiF_3: 289 (m.br.), 270 (m), 245 (m), 198 (m.br.), 122 (m), 111 (ms), 80 (s), 65 (ms) cm^{-1}.

Reagents of Antimony and Bismuth Trifluorides with Boron Trifluoride, Arsenic Pentafluoride and Antimony Pentafluoride

The reactions were carried out in essentially the same manner previously reported (18) for complexes of stannous fluoride. As in the rest of this study, all manipulations, except those requiring use of a vacuum line, were carried out in a dry box. In typical preparations *ca.* 1 g of the trifluoride was treated with a large excess of Lewis acid (4 mol/mol). The reactions involving SbF_5 appeared complete after standing overnight at room temperature (without stirring), but to ensure completion, the reactions were normally allowed to stand for several days. An attempted stoichiometric preparation of $2SbF_3{\cdot}SbF_5$ gave an obviously inhomogeneous product even after a reaction time of several weeks. In the preparations of the AsF_5 adducts and the attempted preparations of the BF_3 adducts, the SO_2 suspension of the trifluoride and products was stirred for 1 week at room temperature. The solids isolated from the BF_3 reactions analyzed as the initial trifluorides.

Typical analyses are:

Anal. Calcd. for $SbF_3{\cdot}SbF_5$: F, 38.43; Sb, 61.57; Sb(III), 30.78. Found: F, 36.38; Sb, 61.5, 62.2, 62.4, 62.6; Sb(III), 33.0, 33.2, 31.6, 30.8.

Anal. Calcd. for $SbF_3{\cdot}AsF_5$: F, 43.59; Sb + As, 56.40. Found: F, 43.57; Sb + As, 55.99.

Anal. Calcd. for $BiF_3{\cdot}3SbF_5$: Bi, 22.81; F, 37.32; Sb, 39.87. Found: Bi, 22.70; F, 37.33; Sb, 38.50.

Anal. Calcd. for BiF_3AsF_5: As, 17.19; Bi, 47.95; F, 34.87. Found: As, 16.84; Bi, 47.19; F, 34.18.

Reactions of Antimony Metal with Arsenic and Antimony Pentafluorides

The apparatus and procedure were very similar to that used for the reactions of the trifluorides (above). Finely ground antimony (1 mol) was stirred, in liquid SO_2, with an excess of the pentafluoride (> 4 mol of SbF_5 or > 2.5 mol AsF_5). The reactions take place according to

$$2Sb + 8SbF_5 \rightarrow 5SbF_3{\cdot}SbF_5$$

or $$2Sb + 5AsF_5 \rightarrow 2SbF_3{\cdot}AsF_5 + 3AsF_3$$

The reaction involving SbF_5 is complete in *ca.* 24 h, that involving AsF_5 takes about 1 week at room temperature. The products were isolated after washing with liquid SO_2 and removal of volatiles. The Raman and Mössbauer spectra of the $SbF_3{\cdot}AsF_5$ prepared this way were identical with those of a sample prepared from SbF_3.

Anal. Calcd. for $SbF_3{\cdot}SbF_5$: F, 38.43; Sb, 61.57. Found: F, 38.69; Sb, 61.49.

$AsF_3{\cdot}SbF_5$

This was prepared according to ref. 2.

Analyses

Except for the determination of antimony in $SbF_3{\cdot}SbF_5$ which was achieved iodimetrically, analyses were performed by Alfred Bernhardt, West Germany.

Raman Spectra

The Raman spectra of the solids were obtained using a Spex Industries Model 1400 spectrometer with Ar^+ excitation (5145 or 4880 Å) from a Spectra Physics 140 laser. The 90° viewing technique of Gillespie and Pez (25) was used. Samples were contained in sealed Pyrex (melting point) capillary tubes.

Mössbauer Spectra

Mössbauer Spectra were recorded with an Austin Science Associates constant acceleration drive unit, used in conjunction with a Victoreen PIP 400A multichannel analyzer operating in multiscalar mode. The source was $Ba^{121m}SnO_3$ (0.5 mCi) obtained from New England Nuclear Ltd. All isomer shifts were reported relative to InSb at liquid nitrogen temperature. The detector was a Xe–CO_2 filled proportional counter with the window of the single channel analyzer set on the escape peak of the 37 keV ^{121}Sb gamma ray. The velocity scale was calibrated with a Pd(^{57}Co) source and a metallic iron foil. The $SbF_3{\cdot}SbF_5$ and $SbF_3{\cdot}AsF_5$ absorbers, which were mounted in the manner used for stannous fluoride complexes (18), were cooled to liquid nitrogen temperature; they contained 40 mg/cm² and 30 mg/cm² of antimony

respectively. The spectra were analyzed by means of the curve-fitting program previously described (26).

^{19}F N.M.R. Spectra

The n.m.r. spectra were obtained using a Varian DA-60 spectrometer modified as reported earlier (27). Samples were prepared by mixing the non-volatile components in an n.m.r. tube in the dry box and then condensing the requisite amount of SO_2 into the tube *in vacuo* prior to sealing. Chemical shifts were measured relative to $CFCl_3$ by sample interchange.

We thank the National Research Council of Canada for generous financial assistance. We are grateful to Mr. J. Ballard for preparing and obtaining the Raman spectrum of $AsF_3 \cdot SbF_5$.

1. R. D. W. KEMMITT, V. M. MCRAE, R. D. PEACOCK, and I. L. WILSON. J. Inorg. Nucl. Chem. **31**, 3674 (1969).
2. A. A. WOOLF and N. N. GREENWOOD. J. Chem. Soc. 2201 (1950).
3. O. RUFF and PLATO. Ber. **37**, 674 (1904).
4. A. A. WOOLF. J. Chem. Soc. 279 (1955).
5. T. K. DAVIES and K. C. MOSS. J. Chem. Soc. (A), 1054 (1970).
6. J. BACON, P. A. W. DEAN, and R. J. GILLESPIE. Can. J. Chem. **47**, 1655 (1969).
7. J. BACON and R. J. GILLESPIE. Unpublished work.
8. P. A. W. DEAN and R. J. GILLESPIE. Chem. Commun. 853 (1970).
9. R. J. GILLESPIE and O. C. VAIDYA. Chem. Commun. 40 (1972).
10. P. A. W. DEAN and R. J. GILLESPIE. Unpublished work.
11. A. J. EDWARDS and R. J. C. SILLS. J. Chem. Soc. (A), 942 (1971).
12. K. O. CHRISTE and C. J. SCHACK. Inorg. Chem. **9**, 2296 (1970); H. A. CARTER and F. AUBKE. Can. J. Chem. **48**, 3456 (1970).
13. J. W. HASTIE, R. HAGUE, and J. L. MARGRAVE. J. Phys. Chem. **72**, 4492 (1966).
14. R. D. W. KEMMITT and D. W. A. SHARP. Advances in fluorine chemistry. Vol. 4, *Edited by* M. STACEY, J. C. TATLOW, and A. G. SHARPE. Butterworths, London. 1965. p. 142.
15. A. J. EDWARDS. J. Chem. Soc. (A), 2751 (1970).
16. W. H. ZACHARIASEN. U.S. Atomic Energy Commission, Argonne Natl. Lab. Report AA1L-4400 (January, 1950); A. ZALKIN and D. H. TEMPLETON. J. Am. Chem. Soc. **75**, 2453 (1953).
17. G. M. BEGUN and A. C. RUTENBERG. Inorg. Chem. **6**, 2212 (1967).
18. T. BIRCHALL, P. A. W. DEAN, and R. J. GILLESPIE. J. Chem. Soc. (A), 1777 (1971).
19. J. F. STEVENS and C. H. BOWEN. Mössbauer Effect Methodol. **5**, 27 (1969).
20. V. A. BRYUKHANOV, B. Z. IOFA, V. KOTKHAKAR, S. I. SEMENOV, and V. S. SHPINEL. Sov. Phys. J.E.T.P. **26**, 912 (1968).
21. T. BIRCHALL, B. P. DELLA VALLE, E. MARTINEAU, and J. B. MILNE. J. Chem. Soc. (A), 1055 (1971).
22. J. W. MOORE, H. W. BAIRD, and H. B. MILLER. J. Am. Chem. Soc. **90**, 1358 (1965).
23. R. J. GILLESPIE and K. C. MOSS. J. Chem. Soc. (A), 1170 (1966).
24. P. A. W. DEAN and R. J. GILLESPIE. Can. J. Chem. **49**, 1736 (1971).
25. R. J. GILLESPIE and G. P. PEZ. Inorg. Chem. **8**, 1229 (1969).
26. T. BIRCHALL and B. P. DELLA VALLE. Can. J. Chem. **49**, 2808 (1971).
27. P. A. W. DEAN and R. J. GILLESPIE. J. Am. Chem. Soc. **91**, 7260 (1970).

Can. J. Chem. Downloaded from www.nrcresearchpress.com by 210.87.254.42 on 09/05/12
For personal use only.

Magnetic Susceptibilities of some Compounds of Sulfur

M. B. KENNEDY, M. W. LISTER, R. MARSON, AND R. B. POYNTZ
Department of Chemistry, University of Toronto, Toronto 181, Ontario

Received July 12, 1972

Magnetic susceptibilities are reported for a number of compounds containing sulfur–oxygen bonds; the sulfur may also be bonded to organic groups or to halogen. The results are compared with earlier measurements on the phosphorus–oxygen or halogen–oxygen systems, and with other data on the sulfur–oxygen compounds which give information on the bond order. Though some trends similar to those in phosphorus–oxygen or halogen oxygen systems are noted, it does not seem to be possible to correlate the magnetic susceptibilities with the bond orders in any simple way.

Les susceptibilités magnétiques ont été rapportées pour un certain nombre de composés contenant des liaisons soufre–oxygène, soufre-groupes organiques ou halogène. Les résultats ont été comparés aux mesures précedentes concernant les systèmes phosphore–oxygène, halogène–oxygène ainsi qu'aux autres données sur les composés soufre–oxygène; des informations sur l'ordre de liaison ont aussi été obtenues. Bien qu'on note une certaine similitude dans les tendances pour les systèmes phosphore–oxygène ou halogène oxygène, il ne semble pas possible de relier d'une façon simple les susceptibilités magnétiques aux ordres de liaison. [Traduit par le journal]

Can. J. Chem., **51**, 674 (1973)

Can. J. Chem. Downloaded from www.nrcresearchpress.com by 210.87.254.42 on 09/05/12
For personal use only.

In an earlier paper (1), two of the present authors reported measurements on the diamagnetic susceptibilities of compounds containing oxygen linked to nitrogen or phosphorus. The results were considered in terms of the degree of double bonding of the oxygen, and possible delocalization of the π-electrons; and were related to the stretching force constants and bond lengths in some of the compounds. The results supported a singly bonded oxygen in amine oxides, R_3NO, but doubly bonded in phosphine oxides. Phosphate esters showed a large enhancement in susceptibility over the corresponding phosphite esters, $OP(OR)_3$ as compared with $P(OR)_3$, in spite of the apparent double bonding of the unique oxygen in phosphate esters. This was also true, but to a lesser extent in the oxyhalides as compared with the halides, OPX_3 as compared with PX_3, where X is chlorine or bromine.

Analogous measurements on sulfur compounds were made at the time of the above work, and amplified by other more recent measurements. The object of the present paper is to report the results, and to apply similar considerations to them. Some of the compounds have been measured by other workers, as mentioned in detail below, but it seemed worthwhile to report our results, as confirmation of values of diamagnetic susceptibilities have often proved useful.

Experimental

Apparatus

The susceptibility measurements were made as in the earlier paper (1). The standard substance was benzene, carefully freed from oxygen. It was assumed to have a volume susceptibility of -0.6187×10^{-6} e.m.u/ml at 25 °C, or -0.7081×10^{-6} e.m.u/g, as reported by Eggleston, Evans, and Richards (2). This was checked by measurements on water which gave a value of $-0.719 \pm 0.002 \times 10^{-6}$ e.m.u/ml, as a mean of eight determinations.

Densities of liquids were measured in a 10 ml pyknometer. Densities of solids were measured directly in the tube used for magnetic measurements, from the weight and length of the sample in the tube. These are, of course, apparent densities of the solids.

Chemicals

Thionyl and Sulfuryl Chlorides

Samples (500 ml) were distilled under nitrogen to give constant boiling middle fractions, boiling at 79.0 and 69.5 °C, respectively.

Dimethyl Sulfoxide

This was prepared by oxidation of dimethyl sulfide by 30% hydrogen peroxide. The product, after fractional distillation, melted at 18.5 °C, in agreement with Douglas' value (3), though Addison and Sheldon (4) report a melting point of 19 to 20 °C. A large sample, from the Crown Zellerbach corporation, after drying and fractionation, melted at 19 °C. Both samples had the same magnetic susceptibility within experimental error.

Diethyl Sulfoxide

This was prepared by oxidation of diethyl sulfide in acetone by 30% hydrogen peroxide (5). After repeated drying and distillation under vacuum, a sample melting

Can. J. Chem. Downloaded from www.nrcresearchpress.com by 210.87.254.42 on 09/05/12
For personal use only.

at 20.8 °C was obtained (20 °C in ref. (4)). The infrared spectrum showed no detectable diethyl sulfone.

Anal. Calcd. for $C_4H_{10}OS$: C, 45.24; H, 9.49; S, 30.20. Found: C, 45.23; H, 9.49; S, 30.11.

Dimethyl Sulfone

Dimethyl sulfone (200 g), from the Crown Zellerbach Corporation, was twice recrystallized from benzene, then fractionally sublimed under vacuum. It melted at 108.5 °C; Douglas (3) gives 108.1 to 108.5 °C.

Di (n-propyl) Sulfone

A sample from Distillation Products Industries Ltd. was fractionally distilled under vacuum. The melting point was 29.5 °C, as compared with the literature value (6) of 29 °C.

Dimethyl Sulfite

A sample from the Columbia Chemical Company was fractionally distilled, first under nitrogen and then under vacuum, to give a product boiling at 126 °C (7, 8).

Di(n-propyl) Sulfite

A sample was fractionally distilled under vacuum to give a middle fraction boiling at 192 °C; literature value (7) is 191 °C.

Methyl Sulfonyl Chloride

A sample from the Pennsalt Chemical Company was fractionally distilled to give a middle fraction boiling at 161 °C; literature values vary from 159 to 161.5 °C (9).

Sodium and Potassium Sulfite

Fisher Certified Reagent Grades were recrystallized twice under nitrogen, ground to a fine powder, and dried over phosphorus pentoxide. The products in both cases had a purity of 99.5%, by iodometric analysis.

Sodium Bisulfite

This was recrystallized from a mixture of water and ethanol under nitrogen. The product, after drying was 99.3% pure, by iodometric analysis.

Sodium and Potassium Bisulfate

Fisher Reagent Grade samples were recrystallized, ground to a fine powder, and dried over phosphorus pentoxide.

Fluorosulfuric Acid

A sample from the Allied Chemical Company was fractionally distilled; boiling point 162 °C, in agreement with the literature value (10).

Chlorosulfuric Acid

This was a reagent grade provided by the British Drug Houses.

Potassium and Cesium Fluorosulfites

These were prepared from the alkali metal fluoride and sulfur dioxide.

Anal. Calcd. for KSO_2F: K, 32.00; F, 15.55. Found: K, 32.28; F, 15.33.

Anal. Calcd. for $CsSO_2F$: Cs, 61.5; F, 8.79. Found: Cs, 61.0; F, 8.60.

Potassium Fluorosulfate

A sample from K and K Rare Chemicals Company analyzed as follows.

Anal. Calcd. for KSO_3F: K, 28.30; F, 13.75; S, 23.21. Found: K, 28.42; F, 13.46; S, 23.06.

Sodium and Potassium Chlorosulfates

These were prepared by the reaction of the alkali metal chloride with chlorosulfuric acid, the excess acid being then removed by distillation. The salts were analyzed for chlorine, and for the equivalents of acid produced on hydrolysis.

Anal. Calcd. for $NaSO_3Cl$: Cl, 25.60; weight to produce one equivalent of acid, 69.26. Found: Cl, 25.23; weight to produce one equivalent of acid, 70.13.

Anal. Calcd. for KSO_3Cl: Cl, 22.93; weight to produce one equivalent of acid, 77.3. Found: Cl, 22.06; weight to produce one equivalent of acid, 80.1.

The main impurity was the corresponding bisulfate.

Sodium Sulfide

A sample was recrystallized to give crystals of $Na_2S.9H_2O$. These were dehydrated by prolonged drying under vacuum over sulfuric acid. The product gave on analysis 97.0% Na_2S, and it was assumed that the rest was water.

Results

Table 1 gives the results for the molar diamagnetic susceptibilities for the various compounds. The units are -10^{-6} e.m.u/mol, and these units will be used throughout the discussion. Table 1 also contains values for the densities of the liquids; for solids only effective densities were obtained, or needed, and as these depend on the packing of the particular sample, they are not worth reporting. It might be added that dimethyl sulfone gave an effective density of 1.313 g/ml; as this was melted into the tube, and showed

TABLE 1. Density and molar susceptibility of various compounds

Compound	Density (g/ml at 25 °C)	Molar susceptibility (-10^{-6}e.m.u./mol)
$(CH_3)_2SO$	1.091	44.3
$(C_2H_5)_2SO$	1.001	67.3
$(CH_3)_2SO_2$	—	50.3
$(C_3H_7)_2SO_2$	1.112	97.1
$(CH_3)_2SO_3$	1.212	53.4_5
$(C_3H_7)_2SO_3$	1.018	100.5
$SOCl_2$	1.628	45.2
SO_2Cl_2	1.656	50.7
CH_3SO_2Cl	1.450	49.9_5
Na_2SO_3	—	41.0
K_2SO_3	—	52.2
$NaHSO_3$	—	32.9_5
KSO_2F	—	41.2
$CsSO_2F$	—	61.6
$NaHSO_4$	—	43.8
$KHSO_4$	—	48.9_5
HSO_3F	1.737	37.4
KSO_3F	—	51.6_5
HSO_3Cl	1.745	46.2
$NaSO_3Cl$	—	50.7_5
KSO_3Cl	—	58.6_5
Na_2S	—	32.8

Can. J. Chem. Downloaded from www.nrcresearchpress.com by 210.87.254.42 on 09/05/12
For personal use only.

little shrinkage on solidification, it is probably close to the true density. The susceptibilities are the means of at least three measurements, which agreed to 0.3%. The results for sodium and potassium chlorosulfates require comment, in that the samples, as analyzed, contained 2–3% of the alkali metal bisulfate. The susceptibilities per gram of these compounds are: $NaSO_3Cl$ 0.367, $NaHSO_4$ 0.364, KSO_3Cl 0.380, $KHSO_4$ 0.359. Therefore 3% of the bisulfates as impurity would change the g-susceptibility (and hence the molar susceptibility) of sodium chlorosulfate by 0.025% and of potassium chlorosulfate by 0.16%. These are less than other errors in measurement.

Discussion

A number of results on these, and related compounds, are available in the literature, some of them published after our own experimental work was completed. Relevant data on molar susceptibilities are: $(CH_3)_2SO$, 44.4 (11); $(C_2H_5)_2SO$, 67.0 (12); $(C_3H_7)_2SO$, 91.0 (11); $(C_4H_9)_2SO$, 112.5 (11); $(CH_3)_2SO_2$, 51.3 (11), 49.62 (13); $(C_3H_7)_2SO_2$, 97.3 (11), 96.7 (14); $(CH_3)_2SO_3$, 53.7 (11); $(C_3H_7)_2SO_3$, 100.6 (11).

Hameka (15) has shown that the diamagnetic susceptibility of a compound can be expressed as the sum of terms, firstly for each atom, secondly for each bond, and thirdly for the interactions of any two bonds with an atom in common. In general it is not possible to obtain a value for every term in such a sum from experimental data, but the terms can be grouped into a number of parameters, for which values can be found. In a homologous series containing only *n*-alkyl groups, the increment per CH_2 should be constant from the ethyl compound onwards. The methyl compound, or the hydrogen compound, might be expected to deviate from the constant increment, though the deviation in practice seems to be fairly small (16). O'Sullivan and Hameka (16) also suggest that the CH_2 increment is not constant from one series to another, but depends on the polar nature of the compounds.

If we apply their method to a compound RX, where R is an *n*-alkyl group, and X is any functional group, we obtain

$$\chi_M = a_0 + a_1 n$$

where n is the number of carbon atoms in R, provided n is two or more. The parameter a_1 is given by

$$a_1 = \chi_C + \chi_{CC} + 2\chi_{CH} + \chi_{CCC} + 4\chi_{CCH} + \chi_{HCH}$$

Here (and later), χ with one subscript is the contribution from the atom indicated by the subscript, χ with two subscripts is the contribution from the bonds between the two atoms indicated, and χ with three subscripts is the contribution from the interaction of two bonds starting from the central atom in the subscript and ending in the outside two. It can be seen that a_1 should be independent of the nature of the group X. It is assumed that χ_H is zero, as hydrogen has no inner electrons. If X is a single atom, a_0 is given by

$$a_0 = \chi_X - \chi_{CC} + \chi_{CH} + \chi_{CX} - 2\chi_{CCC} - 3\chi_{CCH} + 2\chi_{HCH} + \chi_{CCH} + 2\chi_{HCX}$$

This term depends on X; if X is polyatomic, a_1 is unchanged, but a_0 will contain other terms from bonds or interactions within X. For the methyl compound, CH_3X

$$\chi_M = a_0 + a_1 + \delta$$

where

$$\delta = \chi_{CCC} - \chi_{CCH} - \chi_{CCX} + \chi_{HCX}$$

Similarily for a compound R_2Y

$$\chi_M = a_0' + 2a_1 n$$

where each R contains n carbon atoms, provided n is two or more. a_1 has the same meaning as before, and a_0' if Y is monatomic, is given by

$$a_0' = \chi_Y - 2\chi_{CC} + 2\chi_{CH} + 2\chi_{CY} - 4\chi_{CCC} - 6\chi_{CCH} + 4\chi_{HCH} + 2\chi_{CCY} + 4\chi_{HCY} + \chi_{CYC}$$

The coefficients in most cases are double those of the corresponding term in a_0. For the methyl compound, $(CH_3)_2Y$, $\chi_M = a_0' + 2a_1 + 2\delta$, where δ is the same as before, with Y substituted for X.

For any series, a_0 (or a_0') and a_1 can be found by least squares. If this is done, the data in Table 1, refs. 11, 14, and 17, give the results in Table 2. In Table 2, the a_1 values, which are in fact the methylene increments, differ somewhat from Hameka's value of 11.26 for the alkanes. However it is not apparent that the a_1 values are related in any simple way to the structures of the series. The same applies to the values of δ in Table 2, though they are all rather small quantities, as has been found in other series (16).

If we look at the a_0 (or a_0') values in Table 2 we see firstly a very small increase in going from

Can. J. Chem. Downloaded from www.nrcresearchpress.com by 210.87.254.42 on 09/05/12
For personal use only.

TABLE 2. a_0 or a_0', a_1, and δ values of a series of S compounds

Compound	a_0 or a_0'	a_1	δ
R_2S	22.42	11.50	−0.26
R_2SO	22.47	11.30	−0.39
R_2SO_2	24.97	11.80	+0.87
R_2SO_3	30.3	11.7	−0.13
R_2SO_4	39.2	11.7	−0.5
RSOCl	32.83	11.55	—
RSO_2Cl	40.76	11.06	1.87

the R_2S to the R_2SO series, similar to the change between R_3P and R_3PO, or between X^- and XO^-, where X is Cl or Br (18). This increase for the sulfur compounds equals

$$\chi_O + \chi_{SO} + 2\chi_{CSO}$$

and for the phosphorus compounds

$$\chi_O + \chi_{PO} + 3\chi_{CPO}$$

Hence, if the small increase in the phosphorus compounds is taken as evidence for a largely doubly bound oxygen, the same should be true of the sulfur series. The increase in a_0' from R_2SO to R_2SO_2 equals

$$\chi_O + \chi_{SO} + 2\chi_{CSO} + \chi_{OSO}$$

This is found to be appreciably larger than the increase from R_2S to R_2SO, and it is unlikely that this change can be ascribed to the extra χ_{OSO} term. Consequently the magnetic results suggest less double bonding in the sulfone, if it is assumed that doubly bound oxygen has a smaller diamagnetic contribution than singly bound, as is true of ketones and aldehydes, as compared with ethers and alcohols. However, the S—O distance is 1.47 ± 0.03 Å (19) in $(CH_3)_2SO$, and 1.43 ± 0.02 Å (20) in $(CH_3)_2SO_2$. The S—O stretching frequency is 1109 cm^{-1} in $(CH_3)_2SO$, which Gillespie and Robinson (21) interpret as a bond order of 1.56; the frequencies are $(CH_3)_2SO_2$ are $\nu_{sym} = 1143$, $\nu_{antisym} = 1310\ cm^{-1}$, which they interpret as a bond order of 1.77.

The best comparison for the sulfite is probably with the sulfoxide, where the increase in a_0' (sulfite–sulfoxide) is

$$2\chi_O - 2\chi_{CS} + 2\chi_{CO} + 2\chi_{SO} - 2\chi_{SCC} + 2\chi_{OCC} - 4\chi_{SCH} + 4\chi_{OCH} - 2\chi_{CSO} + 2\chi_{COS} - \chi_{CSC} + 3\chi_{OSO}$$

There will evidently be considerable cancellation in the bonding and interaction terms, but exactly how much is uncertain. The increase in a_0' is 7.8, or 3.9 per oxygen; somewhat smaller than for an ether oxygen, and considerably smaller than the increment of 7.5 per oxygen for the rather similar change from an alkyl phosphine oxide to an alkyl phosphate (1). If the sulfoxide contains a double bond, one can perhaps conclude that the sulfite does also. The increase in a_0' from sulfites to sulfates is

$$\chi_O + \chi_{SO} + 3\chi_{OSO}$$

which should not be very different from that from sulfoxide to sulfone. The actual increase is 8.9, which is large; but similar to that found in going from a ketone to an ester (about 8.6), or from a phosphite to a phosphate (about 9.4), this latter being a very similar structural change. The S—O distances in sulfuric acid (22) are fairly short (1.425 and 1.535 Å), with fairly high stretching frequencies (1368 and 968 cm^{-1}), which Gillespie and Robinson interpret as bond orders of 1.84 and 1.35. The relatively high magnetic susceptibility of both sulfuric acid and the sulfate esters presumably indicates considerable delocalization of the π-electrons.

In the acid halide series, it may first be noted as a basis for comparison that the average difference in magnetic susceptibility between a chlorine and a hydrogen atom is about 15.3 (data mostly from ref. 17). Consequently the difference of 15.8 between a_0 for R_2SO_2 and RSO_2Cl is in line with other covalent chlorides. However, the susceptibility of SO_2Cl_2 is only 9.9 higher than a_0 for RSO_2Cl. The S—O distances are much the same (about 1.43 Å) in all these compounds, but the S—O stretching frequencies increase along the series R_2SO_2, RSO_2Cl, SO_2Cl_2, being interpreted (21) as bond orders of 1.77, 1.82, and 1.87, respectively. This seems a somewhat small increase in double bond character to account for the considerable decrease in increment. The terms in these two increases should be

$$a_0(RSO_2Cl) - a_0'(R_2SO_2) = -\chi_H + \chi_{Cl} + \chi_{CC} - \chi_{CH} - \chi_{CS} + \chi_{SCl} + 2\chi_{CCC} + 3\chi_{CCH} - 2\chi_{HCH} - \chi_{SCC} - 2\chi_{SCH} - 2\chi_{SCO} + 2\chi_{OSO} - \chi_{CSC} + \chi_{CSCl}$$

$$\chi(SO_2Cl) - a_0(RSO_2Cl) = -\chi_H + \chi_{Cl} + \chi_{CC} - \chi_{CH} - \chi_{CS} + \chi_{SCl} + 2\chi_{CCC} + 3\chi_{CCH} - 2\chi_{HCH} - \chi_{SCC} - 2\chi_{SCH} - 2\chi_{CSO} + 2\chi_{OSO} - \chi_{CSCl} + \chi_{OSCl}$$

Can. J. Chem. Downloaded from www.nrcresearchpress.com by 210.87.254.42 on 09/05/12
For personal use only.

These are sufficiently similar expressions, so that we can attribute differences in increment to differences in bonding.

The series: R_2SO, $a_0' = 22.5$; RSOCl, $a_0 = 32.8$; $SOCl_2$, $\chi = 45.2$ is more regular. The S—O distances are a little longer for R_2SO and the stretching frequency lower, as noted above; data for $SOCl_2$ are similar: S—O = 1.45 ± 0.02 Å (23), and 1229 cm^{-1} (24) which is interpreted as a bond order of 1.75. This agrees with the small increase in susceptibility along the series.

Turning now to the inorganic compounds, we must first consider what differences to expect from the different alkali metals used, or from the free acid. Selwood (25) gives as ionic susceptibilities: Na^+, 5; K^+, 13; Cs^+, 31; and similar values are quoted by Dorfman (26), though with a somewhat higher value of 36 for Cs^+. A comparison of salts of the same anion gives an average difference of 8.0 between Na^+ and K^+, and 20.6 between K^+ and Cs^+. Individual cases differ appreciably from these averages, since the susceptibilities are not strictly additive in terms of the ions they contain. If we accept the value of 5.0 for Na^+, and hence 13.0 for K^+ and 33.6 for Cs^+, the susceptibilities from the anions are as shown in Table 3, which also includes data by Trew *et al.* on sulfates (27), and on hydrogen sulfide (17).

The magnetic susceptibilities of HSO_3^- and SO_3^{2-}, or HSO_4^- and SO_4^{2-} are not very different, though HSO_4^- is somewhat less than SO_4^{2-}. These species differ only in a proton, and though the extent of delocalization of the π electrons must be somewhat different, this evidently has only a small effect on the susceptibility. Taking the average for each series we get: S^{2-}, 22.8; SO_3^{2-}, 28.6; SO_4^{2-}, 42.45; that is a rise of only 1.93 per oxygen in going from sulfide to sulfite, but a further rise of 11.85 in going to sulfate. In the latter increase, there is some resemblance to the phosphorus system. Gillespie and Robinson deduce bond orders 1.13 in sulfite and 1.50 in sulfate, so that it does not seem possible to correlate these with the magnetic susceptibilities in any simple fashion.

TABLE 3. Ionic susceptibilities

	Susceptibility				
Anion/cation	Na^+	K^+	Cs^+	Free acid	a_0
S^{2-}	22.8	—	—	25.5	22.4
SO_3^{2-}	31.0	26.2	—	—	30.3
HSO_3^-	27.95	—	—	—	—
SO_4^{2-}	42.45	41.2	43.7	39.8	39.2
HSO_4^-	38.8	36.0	—	—	—
SO_2F^-	28.2	28.0	—	—	—
SO_3F^-	—	38.65	—	37.4	—
SO_3Cl^-	45.75	45.65	—	46.2	—

As regards the halogen containing species, a comparison of the susceptibilities of a number of organic compounds, containing Cl, F, or OH (in alcohols), makes the average differences in susceptibility: Cl − OH, 10.3; Cl − F, 9.4; though with deviations from the average of up to 2.2. These are for covalent compounds; the differences for ions (mostly from alkali halides) are 13.6 for $Cl^- - F^-$, and, less certainly, 15.0 for $Cl^- - OH^-$. Selwood (25) gives values which make $Cl^- - F^-$ 15, and $Cl^- - OH^-$ 14. The differences observed for the ions in Table 3 are $SO_2F^- - HSO_3^-$ 0.25, and $SO_3F^- - HSO_4^-$ 1.25; both close to the average difference for covalent compounds of 0.9. Hence magnetically these behave as if the F and OH are similarly bound. The difference $SO_3Cl^- - HSO_4^-$ is 8.3; which is somewhat below the covalent average. This may indicate somewhat greater π-delocalization in HSO_4^- as compared with SO_3Cl^-, as might be expected from their formulae.

1. M. W. LISTER and R. MARSON. Can. J. Chem. **42**, 1817 (1964).
2. B. C. EGGLESTON, D. F. EVANS, and R. E. RICHARDS. J. Chem. Soc. 941 (1954).
3. T. B. DOUGLAS. J. Am. Chem. Soc. **68**, 1972 (1946).
4. C. C. ADDISON and J. C. SHELDON. J. Chem. Soc. 2705 (1956).
5. D. S. TARBELL and C. WEAVER. J. Am. Chem. Soc. **63**, 2939 (1941).
6. G. W. FENTON and C. K. INGOLD. J. Chem. Soc. 2338 (1929).
7. S. I. VOGEL and D. M. COWAN. J. Chem. Soc. 22 (1943).
8. L. P. KYRIDES. J. Am. Chem. Soc. **66**, 1006 (1944).
9. O. C. BILLETER. Ber. **38**, 2015 (1905); I. BEILSTEIN. Handbuch der Organischer Chemie. 1st ed. Vol. 4. 1922. p. 5.
10. J. BARR and R. GILLESPIE. J. Inorg. Chem. **3**, 1149 (1964).
11. G. ROBINET, P. DAGNAC-AMANS, and J. F. LABARRE. J. Chim. Phys. Physiochim. Biol. **66**, 63 (1969).
12. P. PASCAL. C. R. **173**, 712 (1921).
13. H. FRANCOIS. Bull. Soc. Chim. Fr. 513 (1962).
14. V. BALIAH, C. SRINIVASAN, and M. M. ABUBUCKER. Indian J. Chem. **8**, 981 (1970).
15. H. F. HAMEKA. J. Chem. Phys. **34**, 1996 (1961).

16. P. S. O'SULLIVAN and H. F. HAMEKA. J. Am. Chem. Soc. **92**, 25 (1970).
17. G. FOËX. Tables de constantes et données numériques. 7. Diamagnetisme et paramagnetisme. Masson, Paris. 1957.
18. M. B. KENNEDY and M. W. LISTER. Can. J. Chem. In press.
19. O. BASTIANSEN and H . VIERROL. Acta Chem. Scand. **2**, 702 (1948).
20. R. E. RUNDLE. Dissertation Calif. Inst. Techn. Pasadena, Calif. 1941.
21. R. J. GILLESPIE and E. A. ROBINSON. Can. J. Chem. **41**, 2074 (1963).
22. R. PASCARD. C. R. **240**, 2162 (1955).
23. K. J. PALMER. J. Am. Chem. Soc. **60**, 2360 (1938).
24. R. J. GILLESPIE and E. A. ROBINSON. Can. J. Chem. **40**, 644 (1962).
25. P. W. SELWOOD. Magnetochemistry. Interscience Publishers. 1956. p. 78.
26. Y. G. DORFMAN. Diamagnetism and the chemical bond. Edward Arnold (London). 1965. p. 51.
27. V. C. G. TREW, S. F. A. HUSSAIN, and A. J. SIDDIQI. Trans. Faraday Soc. **61**, 1086 (1965).

Can. J. Chem. Downloaded from www.nrcresearchpress.com by 210.87.254.42 on 09/05/12
For personal use only.

The Infrared and Raman Spectra of 3,4-Dichloro-1,2,5-thiadiazole

A. W. RICHARDSON

Department of Chemistry, Bishop's University, Lennoxville, Quebec

Received June 27, 1972

The i.r. and Raman spectra of 3,4-dichloro-1,2,5-thiadiazole have been recorded and assignments made for all 15 fundamental vibrations. Preliminary data from the vapor-phase u.v. absorption spectrum have been used to confirm some assignments.

Les spectres i.r. et Raman du dichloro-3,4 thiadiazole-1,2,5 ont été déterminés et les 15 vibrations fondamentales ont été assignées. Des données préliminaires dérivées des spectres d'absorption u.v. en phase vapeur ont été utilisées pour confirmer quelques-unes des attributions.

[Traduit par le journal]

Can. J. Chem., **51**, 680 (1973)

Can. J. Chem. Downloaded from www.nrcresearchpress.com by 210.87.254.42 on 09/05/12
For personal use only.

Introduction

We are currently investigating the vibrational and electronic spectra of compounds of the type

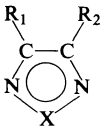

with the goal of determining the effects of the substituents R_1 and R_2 and heteroatom X on the ground and first excited states of these molecules. We have reported on the u.v. vapor-phase absorption spectra of 1,2,5-thiadiazole (**1**, $R_1 = R_2 = H$, X = S) (1) and furazan (or 1,2,5-oxadiazole) (**2**, $R_1 = R_2 = H$, X = O) (2). A report has also been given on the i.r. and Raman spectra of 3-chloro-1,2,5-thiadiazole (**3**, $R_1 = H$, $R_2 = Cl$, X = S) (3) in preparation for a study of its u.v. spectrum.

In the same way, we now present the results of a study of the i.r. and Raman spectra of 3,4-dichloro-1,2,5-thiadiazole (**4**, $R_1 = R_2 = Cl$, X = S). As in the study of **3**, the assignment of the fundamental vibrations is based primarily on the i.r. and Raman spectra, but some use of u.v. spectral data has been made to confirm the assignments of the totally symmetric vibrational modes.

Experimental

Compound **4** was prepared by the reaction of α-aminoacetonitrile bisulfate with sulfur dichloride in dimethylformamide followed by the addition of chlorine gas (4). After distillation through an 8 in. Vigreux column, the product was purified by g.l.c. using a 20 ft × 3/8 in. column of 30% SE30 on 45/60 Chrom W with a Varian Aerograph autoprep 700 gas chromatograph. Analytical g.l.c. on polar and non-polar columns showed the sample purity to be in excess of 99%.

The i.r. spectra were recorded on a Perkin–Elmer model 621 i.r. spectrophotometer. Spectra of the gas were recorded with the sample at its vapor pressure around room temperature in a 10 cm cell with KBr or CsI windows while those of the liquid were recorded for a capillary film between KBr plates or sheets of polyethylene. The Raman spectrum of the liquid sealed in a melting point tube was excited by an argon ion laser and recorded on a Spex double monochromator with a rotatable analyzer to measure depolarization ratios ρ.

Results

The measured wavenumbers of all bands observed for **4** in the i.r. and Raman spectra are listed in Table 1. Also included are other data such as estimated relative intensities, band types, depolarization ratios, etc. The accuracy of the measured wavenumbers is estimated to be about $\pm 2\ cm^{-1}$ for strong bands and somewhat worse for weaker bands. The i.r. spectrum of **4** in the gas phase is illustrated in Fig. 1.

Interpretation of Spectra

Compound **4** was assumed to be a planar molecule of C_{2v} symmetry like **1** (5). Thus, the 15 normal modes of vibration can be classified by symmetry as $6A_1 + 2A_2 + 2B_1 + 5B_2$.[1]

The A_1, B_1, and B_2 vibrations are allowed in the i.r., with types *A*, *C*, and *B* band contours, respectively, in the vapor phase. To facilitate making assignments for **4**, types *A*, *B*, and *C*

[1]The axis system used here has the *z* axis as the C_2 axis and the *x* axis perpendicular to the plane of the molecule. This recommended axis system was not used in earlier work on related molecules, thus leading to interchange of the B_1 and B_2 symmetry species as used here.

TABLE 1. The i.r. and Raman spectra of 3,4-dichloro-1,2,5-thiadiazole

Liquid		Vapor			Raman			
ν	Intensity	ν	Intensity	Band type	ν	Intensity	ρ	Assignment*
2879	1							2 × 1444
2651	1							2 × 1326
2608	1							1326 + 1275
2542	1	2535	1					2 × 1275
2069	1							1326 + 738
2017	1							1275 + 738
1823	1							1023 + 812
1762	2	1748	1					2 × 883 1275 + 476
1690	1							883 + 812 1326 + 360
1633	3	1632	1					1275 + 360
1552	1	1551	1					812 + 738
1540	1							1275 + 271
1503	2	1508 1501	1	*B*?				1023 + 476
1483	3	1490	1	*C*?	1473	1		1023 + 451
1444	46	1454 1447	31	*B*	1441	3	0.65	Ring stretch (B_2)
1386	10	1394	4 b†	*A*?	1383	4	0.03	1023 + 360
					1361	1	0.3	883 + 476
		1338						
1326	98	1334 1330	100	*A*	1325	45	0.08	Ring stretch (A_1)
1310 sh	16				1307	2	~0.2	827 + 476
					1286	3	0.2	812 + 476
		1282						
1275	94	1278 1274	88	*A*	1274	5	0.27	Ring stretch (A_1)
1213	4	1225 1216	2	*B*?	1211	1	0.4	1023 + 190 738 + 476
1180	3							812 + 360
1148	2							883 + 271
1141 sh	1							
1101	2							738 + 360
1080	2	1089	4 b†	*C*?				812 + 271
					1042	1	0.06	2 × 521
1023	100	1034 1027	92	*B*	1022	1	0.8	X-Sensitive (ring in-plane bend) (B_2)
1009 sh	16							827 + 178
929	2	933	1					738 + 190
883	2	878 870	1	*B*				X-Sensitive (ring in-plane bend) (B_2)
827	57	836 830	21	*B*				X-Sensitive (CCl antisymmetric stretch) (B_2)
		819						
812	50	814 808	36	*A*	808	55	0.07	Ring in-plane bend (A_1)
					796 sh	6	0.03	521 + 271
738	2				737	23	0.13	X-Sensitive (CCl symmetric stretch) (A_1)
712	1							2 × 360
655	1							476 + 178
645	1							451 + 190
557	1				547 br	1	0.04	2 × 271

Can. J. Chem. Downloaded from www.nrcresearchpress.com by 210.87.254.42 on 09/05/12
For personal use only.

TABLE 1 (*Concluded*)

Liquid		Vapor			Raman			
ν	Intensity	ν	Intensity	Band type	ν	Intensity	ρ	Assignment*
		531						
521	61	525	22	*C*	518	2	0.6	Ring out-of-plane bend (B_1)
		516						
476	17	471	4		475	100	0.09	X-Sensitive (ring in-plane bend) (A_1)
					451	6	0.58	X-Sensitive (ring out-of-plane bend (A_2)
360	5	358	2		362	19	0.79	X-Sensitive (CCl in-plane bend) (B_2)
271	3				271	10	0.75	X-Sensitive (CCl out-of-plane bend) (B_1)
					190	10	0.74	X-Sensitive (CCl in-plane bend) (A_1)
					178	43	0.75	X-Sensitive (CCl out-of-plane bend) (A_2)

*For the X-sensitive modes, the motion which most likely predominates in the normal mode is given in parentheses. Liquid frequencies have been used throughout for the assignment of overtone and combination bands.
†b = broad.

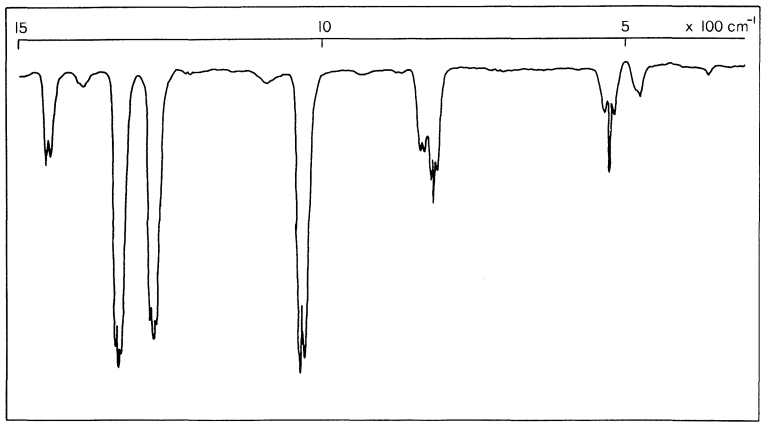

FIG. 1. The i.r. spectrum of 3,4-dichloro-1,2,5-thiadiazole in the vapor-phase.

band contours were calculated in the rigid asymmetric rotor approximation (6) using a computer program written by Pierce. Band contours calculated using the rotational constants $A = 0.06384$, $B = 0.04959$, and $C = 0.02791$ cm^{-1} for both the lower and upper states are shown in Fig. 2. These rotational constants were calculated by assuming the structure of **4** to be exactly the same as **1** (5) and r(C—Cl) = 1.70 Å (7).

All 15 fundamental vibrations are allowed in the Raman spectrum. The $6A_1$ fundamentals should be polarized ($\rho < 0.75$) while all others should be depolarized ($\rho = 0.75$). Because of experimental errors in measuring intensities, ρ values calculated from observed spectra may differ from the theoretical values. This was previously found to be particularly noticeable for low frequency bands in **3** recorded under the same conditions as used here (3).

Particular assignments for the fundamentals of **4** are based on assignments in related molecules. For the ring modes, the assignments made previously for **1** (8, 9) and **3** (3) were used as guides. Since it has been shown that **1** has aromatic character (5), it was felt that the effect of replacing two adjacent H atoms by Cl atoms might be similar to that in benzene. Thus, the X-sensitive modes of *o*-dichlorobenzene were used as guides in assigning the related modes of **3**.

Can. J. Chem. Downloaded from www.nrcresearchpress.com by 210.87.254.42 on 09/05/12
For personal use only.

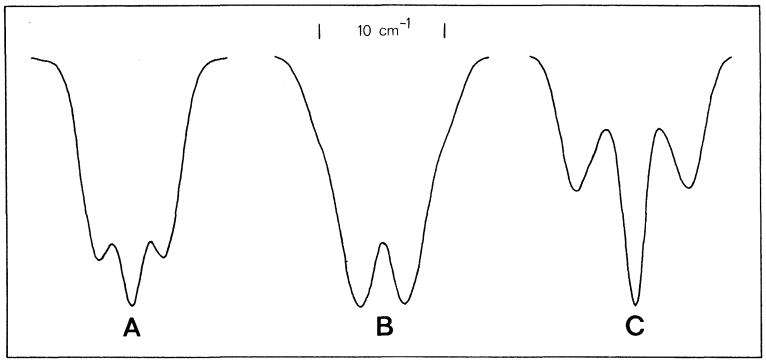

FIG. 2. Calculated type *A*, *B*, and *C* band contours for 3,4-dichloro-1,2,5-thiadiazole.

Normal coordinate calculations have shown that the vibrations involving the chlorine substituents are strongly coupled with the ring vibrations in *o*-dichlorobenzene (11). Therefore, it is to be expected that the same situation obtains in **3**. Since there are likely no "pure" vibrations, it is clear that definitive assignments of observed frequencies to particular atomic motions cannot be made and the safest procedure to follow at this point would be to label vibrations as ring modes or as X-sensitive modes as is done in *o*-dichlorobenzene (10). However it was thought useful to attempt to classify the X-sensitive vibrations further in terms of the principal components of the normal modes. Examination of the potential energy distribution calculated for *o*-dichlorobenzene (11) and the assignments made for other molecules having similar C—Cl bonds allowed reasonable conclusions as to which vibrational motion predominates in a particular normal mode to be reached and these are indicated below. These assignments are, of course, quite qualitative; more detailed assignments can be made only after a normal coordinate calculation.

A_1 Fundamental Vibrations

From consideration of the intensities of the observed bands plus the requirements that the band contours in the vapor-phase i.r. spectrum should be type *A* and the measured depolarization ratios in the Raman spectrum should be less than 0.75, it is clear that five of the A_1 fundamentals are 1334, 1278, 814, 738, and 471 cm^{-1}. For reasons detailed below, the sixth A_1 fundamental is chosen to be the band observed at 190 cm^{-1} in the Raman spectrum of the liquid.

By comparison with the assignments for **1** and **3**, it is clear that 1334 and 1278 cm^{-1} are ring stretching fundamentals and 814 cm^{-1} is a ring in-plane bending fundamental. That the bands at 738, 471, and 190 cm^{-1} are due to X-sensitive modes is clear from comparison to assignments for **1** and **3**. The band at 738 cm^{-1} may be assigned as largely due to the symmetric C—Cl stretching motion since it is the only strong A_1 band in the expected range. Similarly, the band at 471 cm^{-1} must be largely due to a ring in-plane bending motion. The remaining A_1 fundamental at 190 cm^{-1} is assigned as being largely due to C—Cl symmetric in-plane bending motion. This assignment was initially made by analogy to *o*-dichlorobenzene where an A_1 band largely due to the C—Cl symmetric in-plane bending motion is observed at 202 cm^{-1} (10, 11); this was done in spite of the fact that its measured depolarization ratio of 0.74 is greater than expected since there is confirmation of the assignment from the u.v. studies.

Preliminary analysis of the vapor-phase u.v. absorption spectrum of **4** in the 2900–2400 Å region (which undoubtedly is due to an allowed electronic transition) has shown the presence of hot bands at intervals of 1276 ± 3 (7), 814 ± 3 (9), 744 ± 2 (9), 471 ± 6 (10), and 202 ± 2 (9) cm^{-1} to long wavelengths of common bands in several places.[2] Obviously, the first four of these correspond to the A_1 fundamentals at 1278 (vapor), 814 (vapor), 738 (liquid), and 471 (vapor) cm^{-1}, previously assigned. The 202 cm^{-1} interval observed in the vapor must correspond to the 190 cm^{-1} band observed in the liquid and so provides conclusive evidence for its assignment as an A_1 fundamental.

[2]The figures given are the average value and standard deviation for the number of intervals given in parentheses observed in the vapor-phase u.v. absorption spectrum.

Can. J. Chem. Downloaded from www.nrcresearchpress.com by 210.87.254.42 on 09/05/12
For personal use only.

TABLE 2. Frequencies (cm^{-1}) of normal vibrations of 3,4-dichloro-1,2,5-thiadiazole

Symmetry		Frequency (cm^{-1})	Approximate description*
A_1	ν_1	1334	Ring stretch
	ν_2	1278	Ring stretch
	ν_3	814	Ring in-plane bend
	ν_4	738†	X-Sensitive (C—Cl stretch)
	ν_5	471	X-Sensitive (ring in-plane bend)
	ν_6	190‡	X-Sensitive (C—Cl in-plane bend)
A_2	ν_7	451‡	X-Sensitive (ring out-of-plane bend)
	ν_8	178‡	X-Sensitive (C—Cl out-of-plane bend)
B_1	ν_9	525	Ring out-of-plane bend
	ν_{10}	271†	X-Sensitive (C—Cl out-of-plane bend)
B_2	ν_{11}	1451	Ring stretch
	ν_{12}	1031	X-Sensitive (ring in-plane bend)
	ν_{13}	874	X-Sensitive (ring in-plane bend)
	ν_{14}	833	X-Sensitive (C—Cl stretch)
	ν_{15}	358	X-Sensitive (C—Cl in-plane bend)

*For the X-sensitive modes, the motion which most likely predominates in the normal mode is given in parentheses.
†Measured in i.r. of neat liquid.
‡Measured in Raman of neat liquid.

A_2 Fundamental Vibrations

Since these two vibrations are forbidden in the i.r. but allowed in the Raman, the assignments here should be straightforward. The band observed at 451 cm^{-1} in the Raman must therefore be an A_2 fundamental and is assigned as ν_7, an X-sensitive mode largely due to ring out-of-plane bending motion, by analogy to **1**. The fact that the measured depolarization ratio is less than the expected value of 0.75 must be caused by experimental errors in the intensity measurements which are probably due to the weakness of the band.

The remaining A_2 fundamental is expected to occur at low frequency, the analogous mode in *o*-dichlorobenzene occurring at 152 cm^{-1} (10). Therefore, ν_8 is assigned as the band observed at 178 cm^{-1} in the Raman; this mode is X-sensitive, but is expected to be largely due to C—Cl out-of-plane bending motion.

B_1 Fundamental Vibrations

These vibrations are allowed in the i.r., with a type *C* band contour in the vapor-phase, and in the Raman with a depolarization ratio of 0.75. From its observed type *C* band contour, the band at 525 cm^{-1} must be due to a B_1 vibration, and by analogy to **1** and **3** it is assigned as ν_9, a ring out-of-plane bending. ν_{10} is expected to be X-sensitive and to have a major contribution from C—Cl out-of-plane bending motion. Since the analogous vibration in *o*-dichlorobenzene is observed at 239 cm^{-1} (10), ν_{10} is assigned to the band at 271 cm^{-1}.

B_2 Fundamental Vibrations

These five vibrations are allowed in the i.r. with type B band contours in the vapor phase and in the Raman with depolarization ratios of 0.75. Examination of the observed spectra shows that the bands at 1451, 1051, and 833 cm^{-1} must be B_2 fundamentals. By comparison with **1** and **3**, 1451 cm^{-1} must be assigned as a ring in-plane stretching vibration. The 1031 and 833 cm^{-1} bands are clearly X-sensitive since there is no simple correlation with bands of **1** and **3**. The

Can. J. Chem. Downloaded from www.nrcresearchpress.com by 210.87.254.42 on 09/05/12
For personal use only.

TABLE 3. Comparison of the frequencies (cm^{-1}) of the fundamental vibrations of the ring in 1,2,5-thiadiazole, 3-chloro-1,2,5-thiadiazole, and 3,4-dichloro-1,2,5-thiadiazole

	Description*	$C_2H_2N_2S$ (8)	C_2HClN_2S (3)	$C_2Cl_2N_2S$
$A_1(A')$	Ring stretch	1350	1325	1334
	Ring stretch	1294	1287	1278
	Ring in-plane bend	806	825	814
	Ring in-plane bend‡	688	430	471
$A_2(A'')$	Ring out-of-plane bend‡	500†	649	451
$B_1(A'')$	Ring out-of-plane bend	520	518	525
$B_2(A')$	Ring stretch	1461	1460	1451
	Ring in-plane bend‡	895	949	1031
	Ring in-plane bend‡	780	786	874

*The C_{2v} symmetry species apply for $C_2H_2N_2S$ and $C_2Cl_2N_2S$ while the C_s symmetry species apply for C_2HClN_2S.
†Fundamental not observed.
‡X-Sensitive normal modes.

TABLE 4. Comparison of the frequencies (cm^{-1}) of some X-sensitive normal vibrations of 3,4-dichloro-1,2,5-thiadiazole and *o*-dichlorobenzene

	Description*	$C_2Cl_2N_2S$	*o*-$C_6H_4Cl_2$ (10, 11)
A_1	C—Cl symmetric stretch	738	660
	C—Cl symmetric in-plane bend	190(202)†	202
A_2	C—Cl out-of-plane bend	178	152
B_1	C—Cl out-of-plane bend	271	239
B_2	C—Cl antisymmetric stretch	833	740
	C—Cl antisymmetric in-plane bend	360	336

*The description gives the motion which most likely predominates in the particular normal mode (see text).
†Value in parentheses is for the vapor-phase as determined from the u.v. absorption spectrum.

most probable assignments would seem to be that 1031 cm^{-1} involves largely ring in-plane bending motion while 833 cm^{-1} involves mainly C—Cl antisymmetric stretching motion.

There now remain two B_2 fundamentals to be assigned; these will both likely be X-sensitive but one will consist largely of ring in-plane bending motion while the other will consist largely of C—Cl in-plane bending motion. There is only one band at low wavenumbers which is not assigned; this band at 358 cm^{-1} is easily assigned to an X-sensitive normal mode largely involving C—Cl in-plane bending motion since the corresponding vibration in *o*-dichlorobenzene occurs at 336 cm^{-1}. The assignment of the remaining fundamental presents more of a problem since there are no strong type *B* bands left. By reference to **1** and **3**, this X-sensitive vibration might be expected to fall in the 400–1000 cm^{-1} range. The only unassigned type *B* band in this range is at 874 cm^{-1} and so it must be assigned the X-sensitive mode largely involving the ring in-plane bending motion. This assignment is supported by the fact that this band cannot be assigned as a first overtone or binary combination band of B_2 symmetry.

Other Assignments

All except one of the other bands observed can be assigned as first overtones or binary combinations using the assignment of fundamentals given above; in a few cases more than one assignment is possible for a particular band. The details of these assignments are given in Table 1. In a few cases of weak bands, the assignments may be questioned (*e.g.* A_2 combination observed in the i.r. of the liquid), but in the absence of other suitable assignments these are left as indicated.

Conclusion

The assignments of the fundamental vibrations of 3,4-dichloro-1,2,5-thiadiazole are summarized in Table 2. These are consistent with the molecule being planar and having C_{2v} symmetry.

Can. J. Chem. Downloaded from www.nrcresearchpress.com by 210.87.254.42 on 09/05/12
For personal use only.

The assignments for the ring modes can be correlated with those of the parent molecule 1,2,5-thiadiazole and 3-chloro-1,2,5-thiadiazole as shown in Table 3. The correlation is particularly good for the three ring stretching vibrations, the ring in-plane bend near 815 cm^{-1}, and the ring out-of-plane bend near 520 cm^{-1} but rather poorer for the four remaining vibrations due to their X-sensitive nature. The correlation obviously supports the assignments made and gives a better understanding of the form of these normal modes in these molecules.

A comparison of the frequencies of the remaining (X-sensitive) normal vibrations in 3,4-dichloro-1,2,5-thiadiazole with analogous vibrations of *o*-dichlorobenzene is given in Table 4 and shows that although the values for the former molecule are generally larger than for the latter molecule, the correlation is sufficiently good to give confidence in the assignments made.

The author thanks the National Research Council of Canada for providing financial assistance for this work. Thanks are also due to Dr. A. Cabana of l'Université de Sherbrooke, Sherbrooke, Québec for use of the Perkin–Elmer Model 621 Spectrophotometer, to Dr. G. W. King of McMaster University, Hamilton, Ontario for having the Raman spectra recorded, to Dr. L. Pierce of the University of Notre Dame, South Bend, Indiana for use of the asymmetric rotor band contour program, and to the Département de l'Education du Québec for the use of computing facilities.

1. E. Firkins and A. W. Richardson. Chem. Commun. 1368 (1971).
2. B. J. Forrest and A. W. Richardson. Can. J. Chem. **50**, 2088 (1972).
3. A. W. Richardson. Can. J. Chem. **50**, 627 (1972).
4. L. M. Weinstock, P. Davis, B. Handelsman, and R. Tull. J. Org. Chem. **32**, 2823 (1967).
5. V. Dobyns and L. Pierce. J. Am. Chem. Soc. **85**, 3553 (1963).
6. H. C. Allen, Jr. and P. C. Cross. Mol. Vibrotors. John Wiley and Son, Inc., New York, N.Y. 1963.
7. Interatomic Distances. Special Publ. No. 11. The Chemical Society, London. 1958.
8. B. Soptrajanov and G. E. Ewing. Spectrochim. Acta, **22**, 1417 (1966).
9. E. Benedetti, G. Sbrana, and V. Bertini. Gazz. Chim. Ital. **97**, 379 (1967).
10. J. H. S. Green. Spectrochim. Acta, **26** A, 1913 (1970).
11. J. R. Scherer. Planar vibrations of chlorinated benzenes. The Dow Chemical Co., Midland, Michigan. 1963.

Can. J. Chem. Downloaded from www.nrcresearchpress.com by 210.87.254.42 on 09/05/12
For personal use only.

The Kinetics of the Ethanolysis Reaction of Some 4-Nitro-substituted Triphenylmethyl Chlorides

ELEANOR L. KULIN AND K. T. LEFFEK
Chemistry Department, Dalhousie University, Halifax, Nova Scotia

Received July 31, 1972

The kinetics of the ethanolysis of three triphenylmethyl chlorides, the 4-nitro, 4,4′-dinitro, and 4,4′,4′′-trinitrophenylmethyl compounds, have been studied. The effect of change in substrate and solvent composition on the activation parameters, $\Delta H^{\ddagger}$ and $\Delta S^{\ddagger}$, has been determined. For these compounds, $\Delta H^{\ddagger}$ appears to be controlled by substrate structure while $\Delta S^{\ddagger}$ varies predominantly with solvent composition.

The attempted reaction of pyridine with 4,4′,4′′-trinitrophenylmethyl chloride to form the quaternary ammonium salt is also reported.

The reactions are interpreted to be proceeding via a carbonium ion-pair mechanism.

La cinétique de l'éthanolyse de trois chlorures de triphénylméthyl, le nitro-4, le dinitro-4,4′ et le trinitro-4,4′,4′′ phénylméthyl, a été étudiée. L'effet causé par le changement du substrat et par la composition des solvants sur les paramètres d'activation, $\Delta H^{\ddagger}$ et $\Delta S^{\ddagger}$, a été déterminé. Pour ces composés, il semble que le soit controlé par la structure du substrat alors que le $\Delta S^{\ddagger}$ varie essentiellement avec la composition du solvant.

La tentative pour réaliser la réaction entre la pyridine et le chlorure de trinitro-4,4′,4′′ phénylméthyl en vue de former le sel d'ammonium quaternaire est aussi relatée.

Un mécanisme impliquant une paire d'ions dont un ion carbonium est envisagé pour ces réactions.
[Traduit par le journal]

Can. J. Chem., **51**, 687 (1973)

Can. J. Chem. Downloaded from www.nrcresearchpress.com by 210.87.254.6 on 09/05/12
For personal use only.

Introduction

Nucleophilic substitution reactions on the central carbon atom of triphenylmethyl chloride have attracted a number of investigators because of the relative stability of the derived carbonium ion under a variety of conditions (1). This compound reacts via a carbonium ion mechanism even under conditions adverse to the ionization process. Thus in a benzene solution, which is colorless, the second-order reactions observed are in fact bimolecular attacks of the reagent on the triphenylmethyl chloride carbonium ion-pair (2–11). In order to observe an S_N2 reaction the substrate molecule must have its ionizing capability reduced by electron-withdrawing substituents on the phenyl rings. Patai and Zabicki (12) studied the acetolysis of 4,4′,4′′-trinitrophenylmethyl chloride, but found no reaction in glacial acetic acid at 30 °C, although solvolysis took place in aqueous acetic acid via a carbonium ion mechanism. However, Miotti and Fava (13) investigated the radiochloride exchange in acetone solvent between the same substrate and tetraethylammonium radiochloride and presented evidence that the reaction was a direct S_N2 attack on the covalent molecule.

In the present paper we report the rate constants and activation parameters for the 4-nitro, the 4,4′-dinitro, and the 4,4′,4′′-trinitrotriphenylmethyl chloride undergoing ethanolysis in two solvents.

Results and Discussion

Ethanolysis Reaction

First-order rate constants were obtained for the ethanolysis of each of the substituted triphenylmethyl chlorides at a minimum of seven different temperatures over a 35–40° range. At most temperatures, three or four runs were made, although with the very slow reactions only two runs were carried out. Since the 4-nitrotriphenylmethyl chloride was found to react with ethanol at about the same rate as it dissolves, the ethanolysis of this compound was measured in a solvent consisting of 30% v/v dioxane in ethanol. The 4,4′-dinitrotriphenylmethyl chloride was measured in both this mixed solvent and pure ethanol and the 4,4′,4′′-trinitrotriphenylmethyl chloride was studied only in ethanol. The results given in Table 1 were calculated by a least squares analysis of the data obtained by either the Guggenheim method (14) or from the

TABLE 1. First-order rate constants for the ethanolysis of substituted triphenylmethyl chlorides

Temperature (°C)	No. of runs	$10^4 k_1$ (s^{-1})
(a) 4-Nitrotriphenylmethyl chloride in 30% v/v dioxane in ethanol		
−6.1	3	2.75±0.08
0.0	3	4.98±0.15
5.3	3	7.96±0.04
10.0	3	12.4±0.06
15.0	3	19.2±0.06
20.0	3	29.5±0.10
25.0	3	44.5±0.28
29.9$_5$	3	63.3±0.35
(b) 4,4'-Dinitrotriphenylmethyl chloride in 30% v/v dioxane in ethanol		
29.9	3	0.339±0.004
40.0	3	0.855±0.001
45.0	3	1.263±0.007
50.0	3	2.039±0.011
55.0	3	3.005±0.015
60.0	3	4.403±0.020
65.0	3	6.476±0.034
(c) 4,4'-Dinitrotriphenylmethyl chloride in ethanol		
20.0	2	0.845±0.005
24.9	4	1.476±0.002
30.0	3	2.47±0.02
35.0	4	3.91±0.005
40.0	4	6.33±0.035
45.0	3	9.69±0.04
50.0	3	14.79±0.07
55.0	3	22.24±0.10
(d) 4,4',4''-Trinitrotriphenylmethyl chloride in ethanol		
25.0	3	0.00432±0.00001
31.6	3	0.0103±0.0001
35.0	3	0.0148±0.00002
41.6	3	0.03135±0.00014
45.0	2	0.0444±0.0003
50.0	2	0.0746±0.00003
55.0	2	0.122±0.001
60.0	4	0.198±0.001
65.0	3	0.348±0.001

integrated first-order rate equation. The latter was used only for the runs which were too slow to follow over the three half-lives required by the Guggenheim method.

The rate constants of Table 1 were fitted to the transition state theory eq. 1 by a least squares computation. An example plot is shown

$$[1] \quad \log_{10}(k_1/T) = \log(k/h) + \Delta S^{\ddagger}/2.303R - \Delta H^{\ddagger}/2.303RT$$

in Fig. 1 from which it can be seen that, within the precision of the results there is no evidence of non-linearity in the dependence of $\log_{10}(k_1/T)$ on $1/T$. The derived activation parameters are shown in Table 2.

Since there was no discernible temperature dependence of the enthalpy of activation, the heat capacity of activation, $\Delta C_p^{\ddagger}$ seems to be indistinguishable from zero. This means it is less than about -30 cal deg^{-1}, which corresponds to a change of 0.1 kcal mol^{-1} in $\Delta H^{\ddagger}$ over a 30° temperature range.

The rate constants in Table 1 show that the order of solvolytic reactivity is trinitro < dinitro < mononitro derivative, which immediately suggests that we are dealing with a reaction, the mechanism of which involves an ionization as a rate determining step. This mechanism would be a classical S_N1 mechanism (15), which is at variance with the findings of Miotti and Fava

Can. J. Chem. Downloaded from www.nrcresearchpress.com by 210.87.254.6 on 09/05/12
For personal use only.

TABLE 2. Activation parameters for the ethanolysis of substituted triphenylmethyl chlorides

Substituents:	4-Nitro	4,4′-Dinitro		4,4′,4″-Trinitro
Solvent:	Dioxane/ethanol	Dioxane/ethanol	Ethanol	Ethanol
$\Delta H^{\ddagger}$ (kcal mol^{-1})	13.5±0.1	16.5±0.1	17.1±0.1	20.1±0.2
$\Delta S^{\ddagger}$ (cal deg^{-1} mol^{-1})	−23.9±0.2	−24.6±0.3	−18.6±0.4	−17.2±0.5

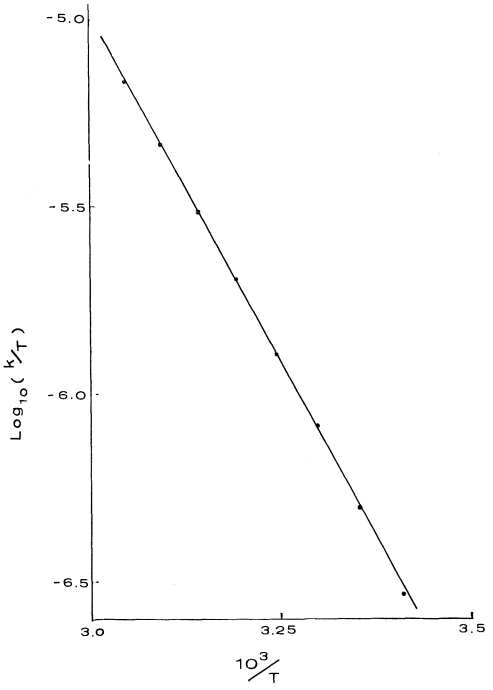

FIG. 1. Activation parameter plot for the solvolysis of 4,4′-dinitrotriphenylmethyl chloride in ethanol.

(13). However, the latter authors claimed a simple S_N2 reaction only for the radiochloride exchange of the trinitro-derivative in acetone solvent. They noted that in acetonitrile solvent the first-order component of the reaction increased and the second-order component decreased. Nevertheless, in both solvents, both the first- and second-order rate constants were greater for the dinitro than for the trinitro compounds, *i.e.* the same order as we observe. To explain this the authors suggested that "bond breaking may well be predominant in these bimolecular substitutions". It is very difficult philosophically and experimentally to distinguish between a simple S_N2 reaction with predominant bond breaking and a two-step mechanism with an ion-pair intermediate, although some erudite attempts have been made, particularly by Sneen and coworkers (16–20) and by Scott (21). Sneen *et al.* have suggested that S_N reactions go via ion-pair mechanisms and that direct attack on the covalent substrate seldom, if ever, occurs. This postulate is based on a detailed analysis of only a few S_N reactions, although Scott (21) has expanded the scope of the theory by applying it to solvolysis reactions of primary alkyl compounds. Sneen's theory is analogous to saying that there are no covalent or ionic bonds in chemistry but only bonds intermediate between the two. For S_N reactions he has cut back the range for the pure S_N1 and S_N2 mechanisms to practically nothing, and increased the range for intermediate mechanisms and at the same time described the intermediate mechanisms in more concrete terms. This is the direction in which the study of reaction mechanisms ought to be going, but this does not necessarily mean that Sneen's description of S_N reactions is, at this time, more useful than Ingold's S_N1 and S_N2. It seems clear that Miotti and Fava observed a reaction of trinitrotriphenylmethyl chloride in acetone, at least very close to a simple S_N2 displacement, whereas it seems most likely that in the more polar ethanol solvents, the solvolysis reactions probably proceed through a carbonium ion-pair, *i.e.* the present results are consistent with Sneen's theory, although the solvolysis of this substrate molecule is not a rigorous test of the theory.

A comparison of the rates in the two solvents for the dinitro compound also shows that this substrate reacts about seven times faster in the more polar ethanol than in the less polar mixed solvent, again indicating that the transition state of the rate determining step has more charge separation than the initial state.

The activation parameters in Table 2 exhibit an interesting pattern in that the enthalpy of activation, $\Delta H^{\ddagger}$, changes with substrate structure but not significantly with solvent change. On the other hand, the entropy of activation, $\Delta S^{\ddagger}$, remains constant when the alkyl group is changed but is distinctly different for the two solvents.

The enthalpies of activation increase with

Can. J. Chem. Downloaded from www.nrcresearchpress.com by 210.87.254.6 on 09/05/12
For personal use only.

Can. J. Chem. Downloaded from www.nrcresearchpress.com by 210.87.254.6 on 09/05/12
For personal use only.

increasing number of nitro substituents, qualitatively as would be expected for a rate determining ionization step, since each strongly electron-attracting nitro group would make it more difficult for the electrons of the carbon–chlorine bond to be transferred to the chlorine atom.

The fact that the entropies of activation do not change with substrate structure indicates, according to the criterion of Long and Schalager (22), that the mechanism of the reaction is the same for all three substrate molecules. However, the large negative values of $\Delta S^{\ddagger}$ would classify these reactions on Long's criterion as S_N2, although Long set up the $\Delta S^{\ddagger}$ test on the basis of hydrolysis reactions and cautioned that the complexity of the $\Delta S^{\ddagger}$ parameter precluded a too quantitative use of its size as an indicator of mechanism. Since it can be seen that about -6 cal mol^{-1} deg^{-1} can be added to this parameter by the introduction of the non-reacting co-solvent dioxane, the $\Delta S^{\ddagger}$ values cannot be considered evidence against an S_N1 mechanism but nevertheless may indicate non-typical behavior.

In a carbonium ion-pair mechanism either the first ionization step may be rate controlling (S_N1) or the second nucleophilic attack step may be rate controlling (S_N2 C^+). For solvolysis reactions, in particular, intermediate mechanisms may be envisaged in which neither step is completely rate controlling. The mechanism for the ethanolysis of 4-nitro substituted triphenylmethyl chlorides is most probably an intermediate mechanism but well over towards S_N1, *i.e.* the ionization step to yield a carbonium ion-pair is clearly the most important in controlling the rate but not necessarily exercising complete control. It is then easy to imagine that this mechanism changes to S_N2 with predominant bond breaking when the solvent is changed to acetone and the nucleophile to chloride ion, as found by Miotti and Fava (13).

Reaction of 4,4′,4′′-Trinitrophenylmethyl Chloride with Pyridine

Although the early literature contains many reports of the reaction of triphenylmethyl chloride itself with pyridine to form the quaternary ammonium salt, more recent work (4) shows that this reaction does not take place at atmospheric pressure, although Okamoto and Shimakawa (23) have prepared the salt at 4000–5000 atm pressure.

4,4′,4′′-Trinitrotriphenylmethyl chloride (10^{-3} *M*) in pyridine solution was maintained at 60–65 °C for 17 days, during which time the conductance of the solution increased by only a very small amount. If the quaternization reaction takes place it must be at least 500 times slower than the ethanolysis, or alternatively there is an equilibrium which overwhelmingly favors the reactants. Either of these alternatives is consistent with the proposition that an S_N2 reaction is not easily accomplished in the solvolysis of this type of substrate.

Experimental

4,4′,4′′-Trinitrotriphenylmethyl Chloride

This was prepared in a two-step process from triphenylmethane. The nitration was carried out according to the method of Shoesmith *et al.* (24) using a mixture of nitric and sulfuric acids at -5 to 0 °C. The nitrated methane was dried and recrystallized from chloroform – petroleum ether, m.p. 210–211 °C (lit. 212.5 °C (24)).

The chlorination of the trinitro derivative was carried out by the procedure given by Patai and Zabicky (12) using a similar apparatus. The reaction was carried out with 4 g of starting material and yielded 2.5 g of yellow crystals of 4,4′,4′′-trinitrotriphenylmethyl chloride, m.p. 199–204 °C (lit. 196–198 °C and 208 °C (12)). The n.m.r. spectrum ($CDCl_3$) gave δ 8.22, d, $J = 9$ Hz, 6H; 7.45, d, $J = 9$ Hz, 6H.

4,4′-Dinitrotriphenylmethyl Chloride

Ziegler and Mathes (25) described the preparation of this compound in 1930 using the method which Baeyer and Villiger (26) used for the preparation of 4-nitrotriphenylmethyl chloride in 1904 (see below). This method was found to work much more poorly for the dinitro derivative than for the mononitro derivation. Although on one attempt some product was obtained, it was not possible to purify it for kinetic measurements. The dinitro derivative was, therefore, prepared by the seven step procedure shown in Scheme 1.

Step 1. Diphenylmethane (75 g) was added in a fine stream to a vigorously stirred solution of nitric acid (390 g) and sulfuric acid (470 g) maintained at -10 to $-20°$. Stirring was continued for 45 min, the temperature not rising above -10 °C, then the solution was poured into an excess of ice water, the yellow precipitate filtered off, and washed with water, methanol, and hot diethyl ether. Yield of 4,4′-dinitrophenylmethane was 60 g, m.p. 186–189 °C (lit. 183 °C (27)).

Step 2. 4,4′-Dinitrophenylmethane (60 g) was dissolved in glacial acetic acid (700 ml) and the mixture refluxed. A solution of chromic anhydride (10 g) in water (110 ml) was slowly added through the top of the condenser and refluxing was continued for 2 h. The cooled solution was then added to an excess of ice-water, whereupon the crude 4,4′-dinitrobenzophenone precipitated. This was filtered, washed with water, $NaHCO_3$ solution, and water again, then dried at 90 °C. The i.r. spectrum contained a peak at 1675 cm^{-1} ($CHCl_3$). The yield was 68 g, m.p. 183–186 °C (lit. m.p. 189 °C (27)).

Step 3. 4,4′-Dinitrobenzophenone (68 g) was added to 95% ethanol (500 ml), followed by $NaBH_4$ (3 g) and the

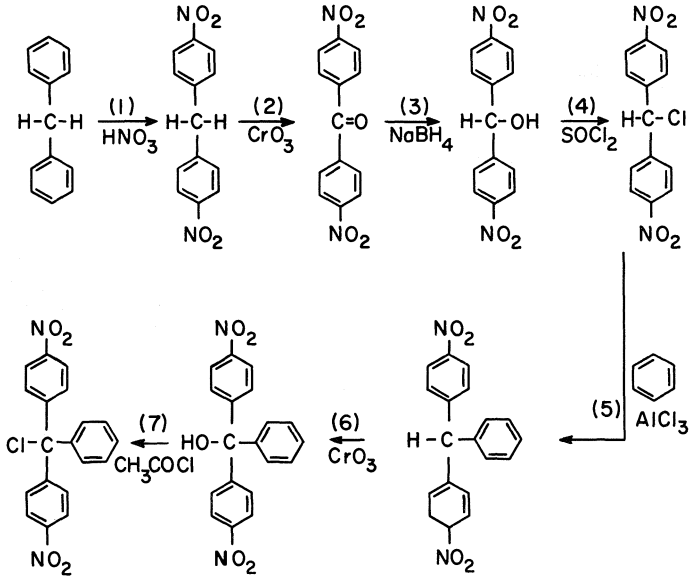

SCHEME I

solution was allowed to stand 10 h, then poured into an excess of water. The yellow precipitate of 4,4′-dinitrodiphenylmethanol was collected and dried. The yield was 45 g, m.p. 160–162 °C. The i.r. spectrum showed a peak at 3570 cm^{-1} ($CHCl_3$), but none at 1675 cm^{-1}.

Step 4. 4,4′-Dinitrodiphenylmethanol (45 g) was dissolved in dry benzene (700 ml). Freshly distilled thionyl chloride (59 g) was slowly added and the solution refluxed 8 h. The benzene and excess thionyl chloride were distilled off under reduced pressure leaving a brown oil. This oil was dissolved in a minimum quantity of hot benzene, and warm petroleum ether (90–120 °C) was added until the solution became cloudy. On allowing to stand overnight, yellow crystals formed. The yield of the 4,4′-dinitrodiphenylmethyl chloride was 30 g, m.p. 109–111 °C. The i.r. spectrum showed no peak at 3570 cm^{-1}.

Step 5. 4,4′-Dinitrodiphenylmethyl chloride (30 g) was dissolved in dry benzene (800 ml). Freshly sublimed anhydrous aluminum chloride (30 g) was added slowly, and the solution refluxed for $3\frac{1}{2}$ h with vigorous stirring. On cooling, ice and dilute HCl were added to the stirred mixture. The whole mixture was poured into a separatory funnel and the aqueous layer drawn off. The benzene layer was washed twice with dilute HCl and the acid layers were collected and washed once with fresh benzene. The combined benzene layers were dried for at least 12 h over anhydrous $CaCl_2$, filtered, and the benzene was evaporated off at a rotary evaporator. The brown oil which remained was dissolved in the minimum quantity of benzene, and warm petroleum ether (b.p. 90–120 °C) was added until the solution became cloudy. Benzene was added to just clear the cloudiness and the mixture was allowed to cool slowly. After about 2 h, yellow crystals and a red oil formed. The residue was recrystallized several more times by the same procedure before a pure product, free from oily residue, could be separated. The yield of 4,4′-dinitrotriphenylmethane was 15 g, m.p. 160–165 °C.

Step 6. The methane (5 g) was dissolved in glacial acetic acid (150 ml) and heated under reflux, then a solution of chromic anhydride (7.5 g) dissolved in water (50 ml) was slowly added through the top of the condenser, after which refluxing was continued for 1 h. The reaction mixture was added to an excess of ice water, the yellow 4,4′-dinitrophenylmethanol which precipitated was collected, washed with water, $NaHCO_3$, and water again. The product was dried overnight, yield 4 g, m.p. 143–146 °C. The i.r. spectrum ($CHCl_3$) gave a peak at 3600 cm^{-1}.

Step 7. The alcohol (4 g) was added to freshly distilled acetyl chloride (50 ml) and refluxed 12 h. Dry benzene (20 ml) was added and the excess acetyl chloride distilled off under reduced pressure. The volume of the benzene was reduced to about 10 ml on a rotary evaporator, and petroleum ether (b.p. 90–120 °C) was added until the solution became cloudy. On standing overnight yellow crystals of 4,4′-dinitrotriphenylmethyl chloride formed and were recrystallized from benzene – petroleum ether. The n.m.r. spectrum ($CDCl_3$) gave δ 7.2–7.5, m, 5H; 8.17, d, $J = 9$ Hz, 4H; 7.53, d, $J = 9$ Hz, 4H. The i.r. spectrum ($CHCl_3$) gave no peak at 3600 cm^{-1}. Potentiometric titration indicated 97% purity, by chloride analysis. The yield was 3.5 g, m.p. 139–140 °C (lit. m.p. 141 °C (25)).

4-Nitrotriphenylmethyl Chloride

This was prepared in a two-step reaction from nitrobenzophenone by the method of Baeyer and Villiger (26). The latter material was converted to 4-nitrobenzophenone dichloride using PCl_5. The product was crystallized from hot petroleum ether (90–120 °C). Yellow crystals were obtained, m.p. 54–55 °C (lit. 56–57 °C (26)). The dichloride was reacted with $AlCl_3$ in dry benzene. The crude product was recrystallized several times from hot petroleum ether (90–120°) before oil-free yellow crystals were obtained. Two final recrystallizations were made from petroleum ether in the presence of acetyl chloride. The

Can. J. Chem. Downloaded from www.nrcresearchpress.com by 210.87.254.6 on 09/05/12
For personal use only.

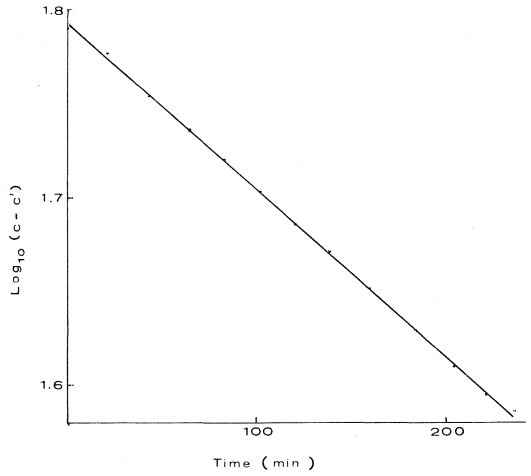

FIG. 2. Run No. 192. Guggenheim plot for the solvolysis of 4,4′-dinitrotriphenylmethyl chloride in ethanol–dioxane (70:30 v/v) at 29.9 °C.

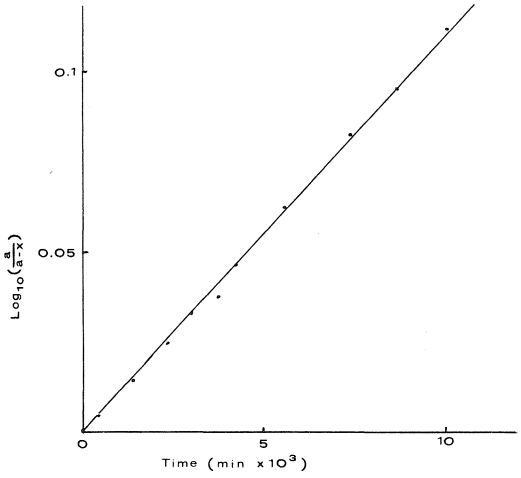

FIG. 3. Run No. 152. First-order plot for the solvolysis of 4,4′,4″-trinitrotriphenylmethyl chloride in ethanol at 25.0 °C.

yield of the second step was about 4%, m.p. 90–92 °C (lit. 92–93 °C (26)). The n.m.r. spectrum ($CDCl_3$) gave δ 7.25–7.35, m, 10H; 8.15, d, J = 9 Hz, 2H; 7.47, d, J = 9 Hz, 2H.

Solvents

Ethanol was dried with Mg turnings and fractionally distilled. Dioxane was dried with anhydrous $CaCl_2$ for 24 h, then sodium metal for another 24 h, followed by 6 h refluxing over sodium metal. The dioxane was then fractionally distilled.

Kinetic Procedure

The rates were determined by following the change in conductance with time, using cells of *ca.* 25 ml capacity, shiny platinum electrodes, and cell constants of about 0.01. The conductances were measured with a Wayne–Kerr bridge, type B221. The initial concentrations of the substrates were about 2×10^{-4} M or less and at such concentrations the relation between the produced HCl and measured conductance was found by experiment to be linear. Thus, most of the rate constants were calculated directly from the conductance readings using the Guggenheim method (14). However, the trinitro-derivative reacted too slowly below 50 °C to be followed over the minimum three half-lives, so the integrated first-order rate equation was used for these runs; the concentration of unreacted chloride being calculated from the HCl concentration read from a calibration plot. The calibration plots were set up using the precision burette described by Martin *et al.* (28). Two example runs are shown in Figs. 2 and 3.

The authors are grateful for financial support by the National Research Council of Canada, to Dr. R. E. Robertson for the loan of the precision burette, and to Dr. T. P. Forrest for helpful discussions on synthetic problems.

1. A. STREITWIESER, JR. Solvolytic displacement reactions. McGraw-Hill Book Co., New York. 1962. p. 39.
2. C. G. SWAIN. J. Am. Chem. Soc. **70**, 1119 (1948).
3. C. G. SWAIN and M. M. KREEVOY. J. Am. Chem. Soc. **77**, 1122 (1955).
4. C. G. SWAIN and E. E. PEGUES. J. Am. Chem. Soc. **80**, 812 (1958).
5. E. D. HUGHES, C. K. INGOLD, S. F. MOK, S. PATAI, and Y. POCKER. J. Chem. Soc. 1220 (1957).
6. E. D. HUGHES, C. K. INGOLD, S. PATAI, and Y. POCKER. J. Chem. Soc. 1230 (1957).
7. E. D. HUGHES, C. K. INGOLD, S. F. MOK, and Y. POCKER. J. Chem. Soc. 1238 (1957).
8. E. D. HUGHES, C. K. INGOLD, S. PATAI, and Y. POCKER. J. Chem. Soc. 1256 (1957).
9. E. D. HUGHES, C. K. INGOLD, S. F. MOK, S. PATAI, and Y. POCKER. J. Chem. Soc. 1265 (1957).
10. K. T. LEFFEK and R. G. WATERFIELD. Can. J. Chem. **45**, 1497 (1967).
11. K. T. LEFFEK. Can. J. Chem. **48**, 1 (1970).
12. S. PATAI and J. ZABICKI. J. Chem. Soc. 5479 (1961).
13. U. MIOTTI and A. FAVA. J. Am. Chem. Soc. **88**, 4274 (1966).
14. E. A. GUGGENHEIM. Phil. Mag. **2**, 538 (1926).
15. C. K. INGOLD. Structure and mechanism in organic chemistry. Cornell University Press, Ithaca, N.Y. 1969. p. 428–430.
16. H. WEINER and R. A. SNEEN. J. Am. Chem. Soc. **85**, 2181 (1963).
17. H. WEINER and R. A. SNEEN. J. Am. Chem. Soc. **87**, 287 (1965).
18. R. A. SNEEN and J. W. LARSEN. J. Am. Chem. Soc. **91**, 362 (1969).
19. R. A. SNEEN and F. R. ROLLE. J. Am. Chem. Soc. **91**, 2140 (1969).
20. R. A. SNEEN and J. W. LARSEN. J. Am. Chem. Soc. **91**, 6031 (1969).
21. J. M. W. SCOTT. Can. J. Chem. **48**, 3807 (1970).

Can. J. Chem. Downloaded from www.nrcresearchpress.com by 210.87.254.6 on 09/05/12
For personal use only.

22. F. A. LONG and L. L. SCHALAGER. Advances in physical organic chemistry. Vol. 1. *Edited by* V. Gold. Academic Press, London. 1963. p. 1.
23. Y. OKAMOTO and Y. SHIMAKAWA. J. Org. Chem. **35**, 3752 (1970).
24. J. B. SHOESMITH, C. E. SOSSON, and A. C. HETHERINGTON. J. Chem. Soc. 2221 (1927).
25. K. ZIEGLER and W. MATHES. Ann. der Chemie, **479**, 111 (1930).
26. A. BAEYER and V. VILLIGER. Ber. **37**, 597 (1904).
27. Dictionary of organic compounds. 4th. Ed. Eyre and Spottiswoode Ltd., London. 1969.
28. J. MARTIN, R. E. ROBERTSON, and G. C. BENSON. J. Sci. Instrum. **41**, 237 (1964).

Can. J. Chem. Downloaded from www.nrcresearchpress.com by 210.87.254.6 on 09/05/12
For personal use only.

Biosynthesis of Mycophenolic Acid[1]

C. T. Bedford, P. Knittel, T. Money, G. T. Phillips, and P. Salisbury
Chemistry Department, University of British Columbia, Vancouver 8, British Columbia

Received May 8, 1972

Comparative incorporation experiments with (1′-^{14}C)-orsellinic acid (**2**) and (1′-^{14}C)-4,6-dihydroxy-2,3-dimethylbenzoic acid (**3**) suggest that only the latter compound is a specific precursor of mycophenolic acid; the implication of this result in terms of the early stages of the biosynthetic sequence is noted.

Des expériences comparatives d'incorporation avec l'acide orsellinique (1′-^{14}C) (**2**) et l'acide dihydroxy-4,6 diméthyl-2,3 benzoïque (1′-^{14}C) (**3**) suggèrent que seulement, le dernier composé nommé est un précurseur spécifique de l'acide mycophénolique; l'implication de ce résultat en ce qui a trait aux premières étapes de la séquence biosynthétique est aussi relatée.

[Traduit par le journal]

Can. J. Chem., **51**, 694 (1973)

Can. J. Chem. Downloaded from www.nrcresearchpress.com by 84.22.46.98 on 09/08/12
For personal use only.

The structure (2, 3), synthesis (4), biosynthesis (1, 5–9), and biological activity (10) of mycophenolic acid (**1**), a metabolite of *P. brevicompactum*, have been the subject of considerable investigation. Current interest in the compound is centered primarily on its potential use in chemotherapy (10). At the outset of our investigations little was known of the sequence of reactions or intermediates involved in the biosynthesis of this important mold metabolite. Previous studies by Birch and co-workers (5) had shown (Scheme 1) that the basic carbocyclic skeleton of the molecule was acetate-derived and that methionine provided the *O*- and *C*-methyl groups attached to the aromatic nucleus (5, 7). In addition the terpenoid nature of the aliphatic side chain was established (5) by specific incorporation of mevalonic acid into this structural unit (Scheme 1). The combined results of previous research had therefore established the origin of every carbon atom in structure **1** but the order and nature of steps involved in the biosynthetic sequence remained unknown.[2]

Our initial studies were designed to determine the nature of the least complex polyketide intermediate in the biosynthetic route since this information would allow definite conclusions to be made regarding the nature of the β-tetraketo enzyme-bound precursor and exclude some of the possible operational sequences leading from basic units (acetate, mevalonate, etc.) to final product. For this purpose we decided to test the precursor activity of (1′-^{14}C)-orsellinic acid (**2**) and (1′-^{14}C)-4,6-dihydroxy-2,3-dimethylbenzoic acid (**3**). The synthesis of **2** and **3** followed procedures described by Thomas (11) and Pettersson (12), respectively. After purification, the acids **2** (2.5×10^{-3} mCi/mmol) and **3** (5.4×10^{-4} mCi/mmol) were separately administered to shake cultures of *P. brevicompactum* grown on Raulin–Thom medium.[3] The p*H* of the broth at the time of administration was 5.2–5.6 and when p*H* 7 had been reached (10–14 days later) mycophenolic acid was isolated from the parallel experiments and purified to constant radioactivity. Mycophenolic acid isolated from the orsellinic acid experiment was radioinactive while the sample from the experiment using acid **3** as precursor had specific activity of 6.3×10^{-5} mCi/mmol (specific incorporation 11.7%). To determine if the incorporation of radioactivity into mycophenolic acid was random or specific a variety of degradative methods were investigated. Ozonolysis of the dimethyl derivative **4** in dimethyl sulfide (13) or water (2) gave variable yields of fragmentation products **5** and **6** (see Scheme 2). Reductive cleavage of the intermediate ozonide with lithium aluminum hydride

[1]Much of this work has been described in a preliminary communication (1).

[2]Preliminary investigations by Birch and his colleagues (6) indicated that radioactive orsellinic acid (**2**) was incorporated into mycophenolic acid (**1**) with partial randomization of the label. It was also suggested that the sequence from orsellinic acid to mycophenolic acid could involve acid **3** as an intermediate.

[3]It was found that if *P. brevicompactum* was grown on Czapek–Dox medium the correct p*H* was reached in shorter time but the recovered mycophenolic acid was much less pure.

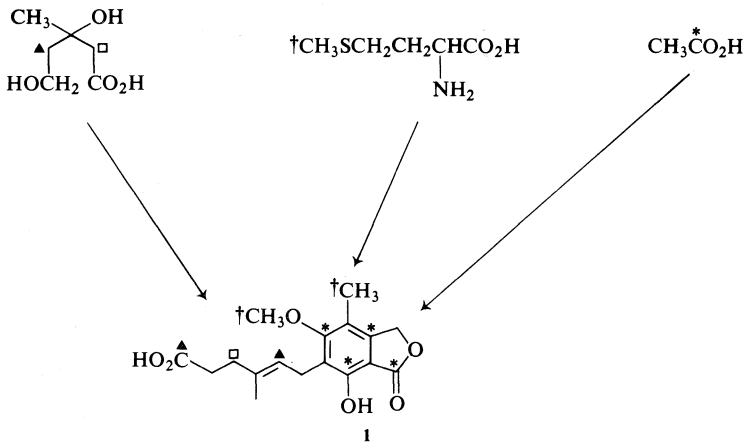

SCHEME 1

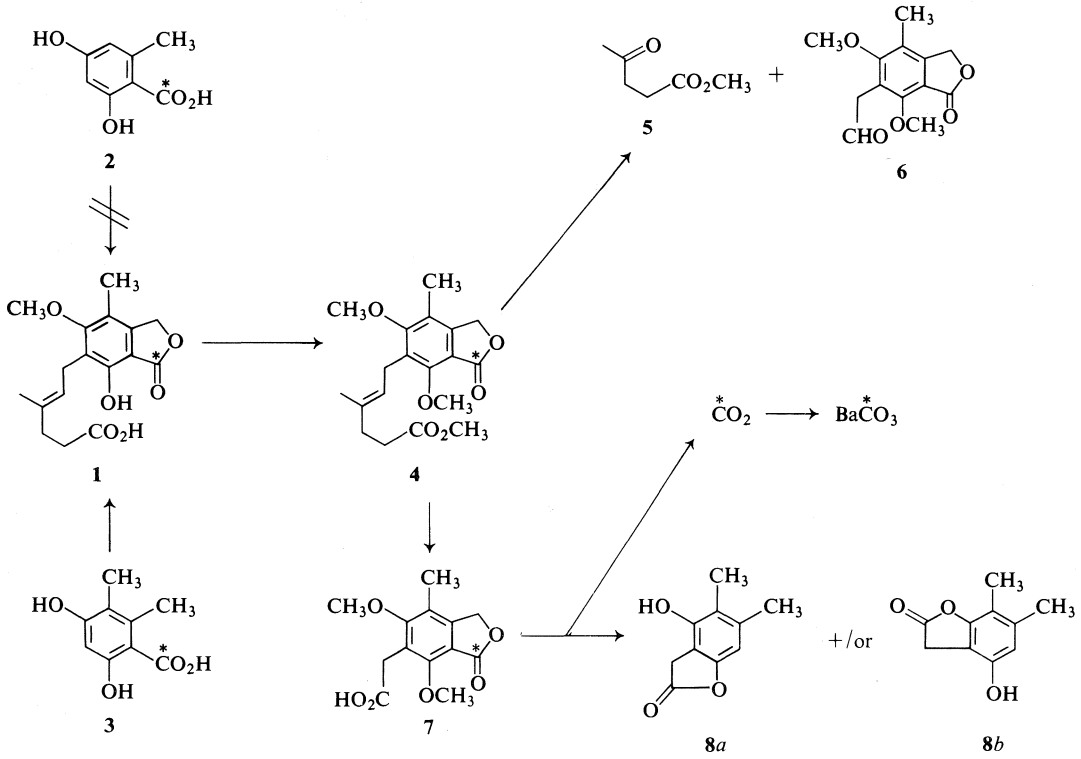

SCHEME 2

also failed to give a satisfactory result. However, when ozonolysis of the dimethyl derivative **4** (after dilution, 1.78×10^{-5} mCi/mmol) was followed by treatment with 30% hydrogen peroxide – formic acid a good yield of 6-carboxymethyl-5,7-dimethoxy-4-methylphthalide (**7**) (1.77×10^{-5} mCi/mmol) was obtained with total retention of radioactivity. The specific location of the radioactive carbon atom in this compound was determined by further degradation. Treatment of **7** with red phosphorus and hydriodic acid (2) yielded radioinactive 4-hydroxy-6,7-dimethyl-2-oxocoumaran (**8***a*) and/or isomer (**8***b*) and 1 mol equiv of carbon dioxide (counted as

Can. J. Chem. Downloaded from www.nrcresearchpress.com by 84.22.46.98 on 09/08/12
For personal use only.

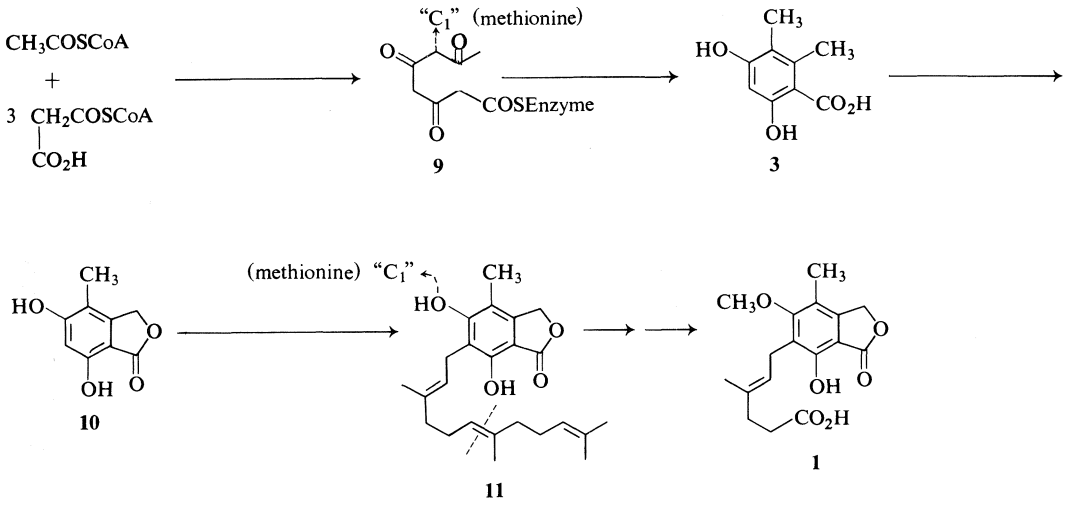

SCHEME 3

$BaCO_3$ (14); 1.71×10^{-5} mCi/mmol) which possessed 96% of the original activity. These results show that specific incorporation of radioactivity from (1′-^{14}C)-4,6-dihydroxy-2,3-dimethylbenzoic acid (**3**) into mycophenolic acid (**1**) had occurred and support the role of this acid[4] as the least complex aromatic precursor in the biosynthetic sequence[5] (1). In addition the contrasting results obtained with acids **2** and **3** lead to the exclusion of several possible biosynthetic sequences. Thus *C*-methylation is occurring before aromatization[6] of the β-tetraketo enzyme-bound thio-ester (**9**) (Scheme 3) and other secondary transformations (*O*-methylation, phthalide ring formation, and construction of the C_7 side-chain) are occurring after formation of acid **3**. The next step in the biosynthetic route seems to be the formation of the phthalide ring since Canonica and his colleagues have recently reported the specific incorporation of (7-^{14}C)-5,7-dihydroxy-4-methylphthalide (**10**) into mycophenolic acid (**1**) (8).

A solution to the problem presented by the construction of the C_7 terpenoid side-chain has been provided recently by the studies of Canonica and co-workers (9). 6-Farnesyl-5,7-dihydroxy-4-(methyl-^{14}C)-phthalide (**11**) was shown to be efficiently incorporated into mycophenolic acid and although degradation studies were not reported it seems certain that this compound is the next intermediate beyond phthalide **10** and that oxidative fission of the appropriate double bond in **11** (or its *O*-methyl ether) could produce the C_7 acidic side-chain present in mycophenolic acid. A biosynthetic scheme based on the cumulative efforts of several independent groups is depicted by Scheme 3.

Experimental

U.v spectra were recorded in methanol on a Unicam SP800 spectrophotometer. I.r. spectra were recorded on a Perkin–Elmer 137B spectrophotometer with sodium chloride cells using either Nujol mulls or chloroform solutions. N.m.r. spectra were recorded on Varian T-60, Varian A-60 or Jeolco C-60H instruments using tetramethylsilane as internal standard. Melting points (Kofler block) are uncorrected.

Radioactivity was measured with a Nuclear Chicago Mark 1 Liquid Scintillation System in counts per minute (c.p.m.). The radioactivity of the sample was subsequently calculated using the counting efficiency which was determined for each sample by the external standard technique utilizing a built in barium-133 gamma source.[7] The counting error[8] (% deviation) was 1.6% at a confi-

[4]It is interesting to note that we have detected 4,6-dihydroxy-2,3-dimethylbenzoic acid as a normal metabolite of *P. brevicompactum* (15). The acid has previously been isolated from *A. terreus* (16) and *G. roseum* (17).

[5]Low incorporation of **2** and high incorporation of **3** were simultaneously reported by Canonica and co-workers (9).

[6]*C*-Methylation before *and* after aromatization of polyketide precursors has previously been demonstrated (18, 19). Recent enzymic studies by Gatenbeck and co-workers have shown that the biosynthesis of **3** in *A. flaviceps* involves *C*-methylation at a pre-aromatic stage (20).

[7]Mark I Liquid Scintillation Systems Instruction Manual, Sect. 1, Nuclear-Chicago Corp., Des Plaines, Illinois (1966).

[8]Nuclear Chicago Publication No. 710-711580 (3rd Ed.), p. 13 (1969).

Can. J. Chem. Downloaded from www.nrcresearchpress.com by 84.22.46.98 on 09/08/12
For personal use only.

Can. J. Chem. Downloaded from www.nrcresearchpress.com by 84.22.46.98 on 09/08/12
For personal use only.

dence level of 90%. The organic scintillation solution used was made up of the following components: toluene (1 l), 2,5-diphenyloxazole (4 g), and 1,4-bis-[2-(5-phenyloxazole)]benzene (0.05 g). In practice the sample was dissolved in benzene (1 ml) or methanol (1 ml) in a counting vial and the volume made up to 15 ml with the above solution. For each sample counted, the background was determined using a vial filled with scintillator solution and solvent.

Administration of Radioactive Compounds to Penicillium brevicompactum

Cultures of *Penicillium brevicompactum* (1M1 17456) were grown on Raulin–Thom medium (100 ml) in 250 ml flasks until the p*H* of the broth was 5.2–5.6. Solutions of the radioactive compounds in ethanol or water (emulsified with Tween 20) were added directly to the broth. The time from inoculation until addition of radioactive substrates was 12–15 days and the optimum generation time (approximately 10 days) was measured by u.v. absorption at 303 nm and corresponded to a rise of approximately 1.6 p*H* units. In the case of (1′-^{14}C)-orsellinic acid 5.1 mg was administered to each of ten flasks (total radioactivity fed; 7.6×10^{-4} mCi) and for (1′-^{14}C)-4,6-dihydroxy-2,3-dimethylbenzoic acid 5.4 mg was administered to each of five flasks (total radioactivity fed; 8.0×10^{-5} mCi). The mycelium was filtered off and both the mycelium and the broth were extracted with large amounts of ether. Drying and removal of the ether yielded mycophenolic acid as a yellow gum. Purification was accomplished by crystallization from ethyl acetate to constant specific activity, m.p. 136–138 °C; mixed m.p. 137–139 °C.

*Ozonolysis of Mycophenolic Acid (**1**)*

Radioactive mycophenolic acid was diluted with radioinactive material and the mixture recrystallized from ethyl acetate. A typical degradative procedure is outlined below.

Mycophenolic acid (**1**) (75 mg, 0.23 mmol) was treated with ethereal diazomethane to give the dimethyl derivative **4**. The crude product was dissolved in methanol (10 ml), cooled to −78 °C, and ozone was passed through the solution until a permanent blue color was present. Excess ozone was removed in a stream of nitrogen and the solvent was removed under vacuum with very gentle heating. To the residual pungent yellow oil was added formic acid (0.38 ml) and 30% hydrogen peroxide (0.26 ml). The solution was heated at 100 °C for 30 min, excess formic acid was removed under vacuum, and saturated sodium bicarbonate solution was added to the residue. After extraction with ether, the aqueous layer was acidified. Extraction of the aqueous layer with ether followed by evaporation of the solvent provided a yellow solid which, on trituration with ether and crystallization from ether–petroleum ether (30–60°), gave 6-carboxymethyl-5,7-dimethoxy-4-methylphthalide (**7**) as white needles, m.p. 150–152 °C (lit. (2) m.p. 150–151 °C); ν_{max} (Nujol) 3300–2600, 1760, 1705, 1601 cm^{-1}; τ ($CDCl_3$) 1.59 (s, 1H), 4.83 (s, 2H), 5.90 (s, 3H), 6.21 (m, 5H), 7.82 (s, 3H).

*Reduction, Decarboxylation, and Demethylation of (**7**)*

A mixture of 6-carboxymethyl-5,7-dimethoxy-4-methylphthalide (**7**) (100 mg, 0.4 mmol), red phosphorus (0.3 g), and hydriodic acid (3 ml) was refluxed in an atmosphere of carbon dioxide–free nitrogen. The resulting carbon dioxide was converted to barium carbonate by bubbling through a barium hydroxide solution and after 19 h the filtered, dried barium carbonate was counted as a suspension (14). Excess phosphorus was removed by filtration, the filtrate extracted with ethyl acetate (4 × 15 ml), and the ethyl acetate extracts washed with water, and aqueous sodium thiosulfate. Drying and removal of the ethyl acetate yielded a gummy yellow solid. Sublimation at 120 °C/0.05 mm and subsequent crystallization from benzene gave 4-hydroxy-6,7-dimethyl-2-oxocoumaran (**8***a*) and/or isomer (**8***b*) as white needles, m.p. 179–183 °C (lit. (2) m.p. 184–185 °C); ν_{max} ($CHCl_3$) 3200–3500, 1801, 1745, 1650 cm^{-1}; τ ($CDCl_3$) 3.60 (s, 1H), 6.32 (s, 2H), 7.78 (s, 3H), 7.86 (s, 3H); *m/e* M^+ 178.

We are grateful to the National Research Council of Canada for generous financial support (NRCC A2267).

1. C. T. Bedford, J. C. Fairlie, P. Knittel, T. Money, and G. T. Phillips. Chem. Commun. 323 (1971).
2. J. H. Birkinshaw, H. Raistrick, and D. J. Ross. Biochem. J. **50**, 630 (1952) and refs. cited therein.
3. A recent X-ray analysis has provided confirmation for structure **1**; W. Harrison, H. Shearer, and J. Trotter. J. Chem. Soc. Perkin II, 1542 (1972).
4. A. J. Birch and J. J. Wright. Aust. J. Chem. **22**, 2635 (1969).
5. A. J. Birch, R. J. English, R. A. Massy Westropp, and H. Smith. Proc. Chem. Soc. 233 (1957); J. Chem. Soc. 369 (1958); A. J. Birch. Chem. Weekblad, **56**, 597 (1960).
6. A. J. Birch. Proc. Chem. Soc. 3 (1962); Science, **156**, 202 (1967); Ann. Rev. Plant Physiol. **19**, 321 (1968).
7. G. Jaureguiberry, G. Farrugie-Fougerouse, H. Audier, and E. Lederer. C.R. **259**, 3108 (1964).
8. L. Canonica, W. Kroszczynski, B. M. Ranzi, B. Rindone, and C. Scolastico. Chem. Commun. 1357 (1970).
9. L. Canonica, W. Kroszczynski, B. M. Ranzi, B. Rindone, and C. Scolastico. Chem. Commun. 257 (1971).
10. T. J. Franklin and J. M. Cook. Biochem. J. **113**, 515 (1969); S. B. Carter, T. J. Franklin, D. F. Jones, B. J. Leonard, S. D. Mills, R. W. Turner, and W. B. Turner. Nature, **223**, 848 (1969).
11. R. Thomas. Biochem. J. **78**, 748 (1961).
12. G. Pettersson. Acta Chem. Scand. **19**, 1724 (1965).
13. J. T. Pappas and W. P. Keaveney. Tetrahedon Lett. 4273 (1966).
14. H. J. Cluley. Analyst, **87**, 170 (1962).
15. C. T. Bedford. Unpublished observations.
16. R. F. Curtis, P. C. Harries, C. H. Hassall, and J. D. Levi. Biochem. J. **90**, 43 (1964).
17. G. Pettersson. Acta Chem. Scand. **19**, 414 (1965).
18. E. Lederer. Quart. Rev. **23**, 453 (1969) and refs. cited therein.
19. G. Pettersson. Svensk kem. Tidskr. **78**, 3 (1966) and references cited therein.
20. S. Gatenbeck, P. O. Eriksson, and Y. Hansson. Acta Chem. Scand. **23**, 699 (1969).

Vibrational Spectroscopic Studies of Aqueous Alkali Metal Bicarbonate and Carbonate Solutions[1]

BARRY G. OLIVER[2] AND ANTHONY R. DAVIS[3]

Water Quality Research Division, Department of the Environment, Ottawa, Canada

Received August 24, 1972

The laser Raman and infrared spectra of Li, Na, K, Rb, Cs bicarbonates and carbonates in H_2O and D_2O have been determined at 25 °C. The relative integrated intensities of the Raman bands have been measured for each salt from 0.01 *M* up to saturation. Changes observed in the carbonate spectrum with concentration have been interpreted in terms of solvation and ion-pairing of the carbonate ion. Based on the vibrational spectrum, there was no evidence for ionic interactions in the bicarbonate solutions. The hydrogen–deuterium exchange on the bicarbonate ion in H_2O–D_2O mixtures has been followed using Raman spectroscopy and the concentration quotients for the pertinent reactions have been calculated.

Les spectres en Raman laser et en infrarouge des bicarbonates de Li, Na, K, Rb, et Cs, ainsi que des carbonates dans l'H_2O et dans le D_2O ont été déterminés à 25 °C. Les intensités relatives intégrées des bandes du spectre Raman ont été mesurées pour chaque sel à partir de 0.01 *M* jusqu'à saturation. Les changements observés dans le spectre du carbonate par rapport à la concentration ont été interprétés en fonction de la solvatation et de la formation en paire d'ions de l'ion carbonate. En se basant sur le spectre vibrationnel, il n'y a aucune raison pour envisager des interactions ioniques dans les solutions de bicarbonate. L'échange hydrogène–deutérium sur l'ion bicarbonate dans des mélanges H_2O–D_2O a été suivi en utilisant la spectroscopie Raman et les quotiens de concentration pour les réactions correspondantes ont été calculés. [Traduit par le journal]

Can. J. Chem., **51**, 698 (1973)

Introduction

An understanding of the bicarbonate–carbonate equilibrium is important in a study of natural waters, since it is largely responsible for controlling the water's p*H* and thus directly affects many of the chemical equilibria in the water (1). The Raman and infrared spectra of saturated aqueous potassium bicarbonate and carbonate solutions have been used to determine the structure of bicarbonate and carbonate ions in these concentrated solutions (2). It is of interest to extend these studies to lower concentrations approaching natural water levels to see whether the structure of the ions is changed by dilution.

Considerable information about ion–ion and ion–solvent interactions in aqueous nitrate systems has been obtained using vibrational spectroscopy (3–7). The relative importance of the ion-pairing and solvation effects can be assessed by varying the cation and by changing the solvent. In this study the laser Raman and infrared spectra of Li, Na, K, Rb, Cs bicarbonates and carbonates in H_2O and D_2O are reported.

Experimental

Raman and complementary infrared spectra were measured for aqueous solutions of each salt from about 0.01 *M* up to the solubility limit. The solutions were prepared using reagent grade salts and filtered through Solvinert Millipore filters (0.25 μ) prior to recording the spectra. The samples in precision Pyrex cells were placed in a holder thermostated at 25 °C and the Raman spectra measured with a Jarrell-Ash Model 25-300 Raman spectrometer (8). A Spectra Physics Model 125 Helium–Neon laser (632.8 nm, 50 mW) or a Coherent Radiation Model 54A Argon laser (488.0 nm, 200 mW) was used as the excitation source. Infrared spectra were obtained as smears between AgCl plates with a Perkin–Elmer Model 457 Grating Spectrometer. Band contours were resolved with a Dupont Curve Resolver using a Lorentz–Gaussian distribution function. All Raman band intensities were measured relative to the 459 cm^{-1} band of CCl_4. An accuracy of ±2% for band intensities is attainable with this instrumentation for strong well-resolved bands (*e.g.* 1069 cm^{-1} band of carbonate). Decomposition of the bicarbonate solutions results in larger errors for these solutions. In the case of weak or overlapping bands the accuracy of the intensity measurements is about ±10%.

[1]Presented, in part, at the 55th Canadian Chemical Conference of the Chemical Institute of Canada, Quebec City, Quebec, June 6, 1972.

[2]Present address: Water and Wastewater Treatment Research Subdivision, Department of the Environment, Canada Centre for Inland Waters, P.O. Box 5050, Burlington, Ontario.

[3]To whom correspondence should be addressed.

Can. J. Chem. Downloaded from www.nrcresearchpress.com by 210.87.254.105 on 09/05/12
For personal use only.

Can. J. Chem. Downloaded from www.nrcresearchpress.com by 210.87.254.105 on 09/05/12
For personal use only.

Results and Discussion

A typical Raman spectrum observed for carbonate solutions is shown in Fig. 1. The relative intensities of the major Raman bands are graphed as a function of concentration in Fig. 2. The plots are linear over the whole concentration range. The bands in the 600 and 1400 cm^{-1} regions have much lower relative intensities than the band in the 1000 cm^{-1} region; so low in fact that feeble water bands in these regions have sufficient intensity to make curve resolving more difficult. Using D_2O as the solvent does alleviate this problem to some extent. The Raman and infrared band positions for potassium carbonate at different concentrations in H_2O and D_2O are shown in Table 1. The carbonate frequencies are virtually independent of alkali metal cation. The Raman band positions are seen to change by a few wave numbers with concentration.

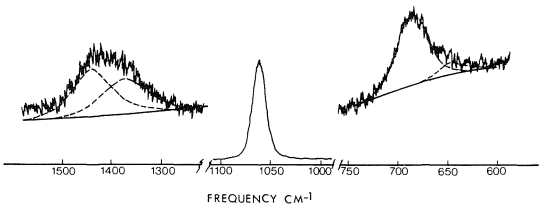

FIG. 1. Resolved Raman spectrum of 8 M Rb_2CO_3 in H_2O. Full scale equals 1×10^4 counts per s for the 100–1100 cm^{-1} region and 2×10^2 c.p.s. for the 600–750 cm^{-1} and the 1300–1500 cm^{-1} region. The weak Raman band at 880 cm^{-1} is observed only at high gain and is not shown in the figure.

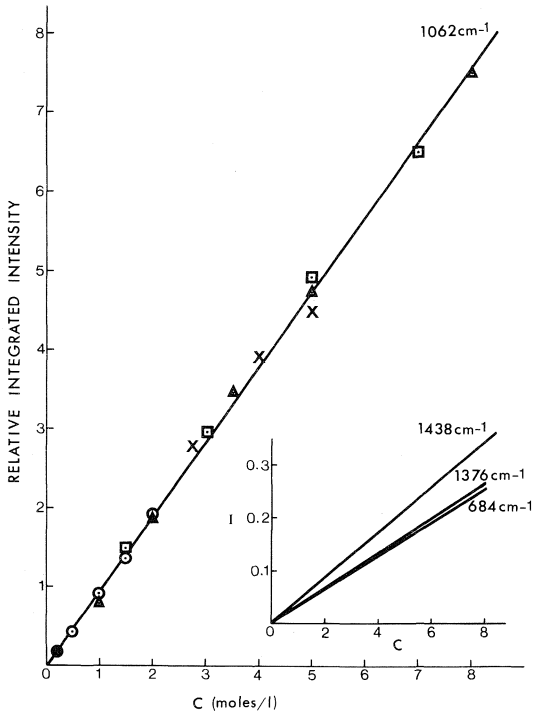

FIG. 2. A plot of relative integrated intensity *vs.* concentration for the major Raman bands of carbonate. ●, Li_2CO_3; ○, Na_2CO_3; △, K_2CO_3; □, Rb_2CO_3; ×, Cs_2CO_3. Only best fit lines shown for weaker bands for clarity.

The symmetry point group for an unperturbed carbonate ion is D_{3h} and the Raman and infrared activity of the expected vibrations are: $\nu_1(A_1')$ R ~1065 cm^{-1}, $\nu_2(A_2'')$ i.r. ~880 cm^{-1}, $\nu_3(E')$ i.r., R ~1400 cm^{-1}, and $\nu_4(E')$ i.r., R ~685 cm^{-1}. The vibrational spectrum of carbonate in aqueous solution is at variance with these selection rules. The infrared forbidden ν_1 band appears in the infrared spectrum of the concentrated solutions at 1052 cm^{-1}. Also the Raman forbidden ν_2 band appears in the Raman spectrum of the concentrated solutions at 880 cm^{-1}. In addition the $\nu_3(E')$ vibration appears to be split into two bands in both the infrared and Raman spectra at all concentrations.

These observations are in many ways similar to those made for alkali metal nitrates by Irish and Davis (3). They interpreted their data in terms of nitrate–water and nitrate–metal interactions. The persistent splitting of the $\nu_3(E')$ band in dilute carbonate solutions where interionic effects should be small, probably indicates that this splitting is due to carbonate–water interaction. This is supported by the fact that the splitting of the $\nu_3(E')$ band is different in the solvent D_2O. Also the band positions in the 1400 cm^{-1} and the 600 cm^{-1} region are different in the two solvents, another indication that the dilute solution spectrum is that of the solvated carbonate ion. The weak bands at 1052 cm^{-1} in the infrared and at 880 cm^{-1} in the Raman could also be features of the solvated carbonate ion spectrum. The weak band at 650 cm^{-1} which is present only in the ultraconcentrated solutions can be assigned to a carbonate ion–water restricted rotation or libration similar to modes found in pure water (9) and those observed for the solvated nitrate ion (3).

Lee and Wilmshurst (10) also observed that the $\nu_3(E')$ band of aqueous K_2CO_3 was split but attributed this to ion-pair formation. Previous studies of aqueous alkali metal nitrates (3, 5, 6)

TABLE 1. Concentration variation of the Raman and infrared band positions of the carbonate ion dissolved in H_2O and D_2O*

Concentration (mol/l)	Spectra (cm^{-1})						
			Raman for H_2O solutions				
8.0	(650)	684	880	1062	1376	1438	1762
6.0	—	684	880	1063	1377	1437	1762
4.0	—	684	—	1065	1379	1436	1761
2.0	—	686	—	1066	1380	1435	1762
1.0	—	687	—	1067	1380	1434	1761
0.1	—	—	—	1069	—	—	—
0.01	—	—	—	1069	—	—	—
			Raman for D_2O solutions				
8.0	—	702	880	1062	1398	1451	1759
2.0	—	703	—	1065	1395	1446	1760
0.1	—	—	—	1068	—	—	—
			Infrared for H_2O solutions				
8.0	—	—	880	1056	~1375	~1430	—
2.0	—	—	880	1060	1370	1425	—
0.1	—	—	—	—	1374	1427	—
			Infrared for D_2O solutions				
8.0	—	695	877	1052	~1390	~1445	1750
2.0	—	—	877	1056	1385	1434	—
0.1	—	—	—	—	1386	1436	—

*For detailed assignment see ref. 2.

have shown that the $\nu_4(E')$ band is split into two bands when contact ion-pairs are present. Only a single band was observed in the $\nu_4(E')$ region for the aqueous carbonate solutions. Bates, Brooker, Quist, and Boyd (11) have shown that the $\nu_4(E')$ band is not split even for molten alkali metal carbonates. Therefore, the spectral results indicate that contact ion-pairs may not be formed in this system. However, the results do not rule out the possibility of ion-pair formation. The $\nu_4(E')$ band is extremely weak in carbonates so recording and resolving the spectrum in this region is difficult. It could be that the $\nu_4(E')$ band for carbonate is split but to a much smaller extent than for nitrate. In any case, it is evident that in these solutions the carbonate ion symmetry has been altered by solvent and possibly cation interactions.

The Raman spectrum for bicarbonate in H_2O is shown in Fig. 3. The 1067 cm^{-1} Raman band is due to carbonate. About 10% of the bicarbonate decomposes to CO_2 and carbonate when it is dissolved in water at 25 °C.

[1] $$2HCO_3^- \rightarrow CO_2 + CO_3^{2-} + H_2O$$

Therefore, twice the carbonate concentration, determined from Raman relative intensity data

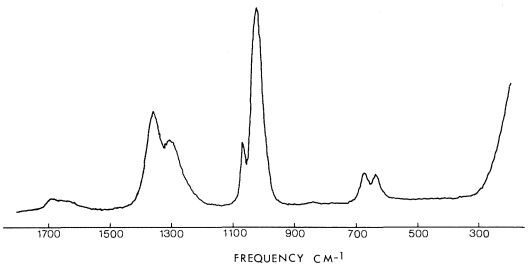

FIG. 3. Raman spectrum of 4 *M* $CsHCO_3$ in H_2O.

(Fig. 2), must be subtracted from the bicarbonate concentration, determined by weight, to obtain the correct concentration of bicarbonate in the aqueous solutions. The relative intensities of the major Raman spectral bands of potassium bicarbonate are plotted against this corrected concentration in Fig. 4. Three other fundamentals at 841, 1630, and 2650 cm^{-1} and one overtone band at 1684 cm^{-1} are also present in the Raman spectrum, but they are very weak. The plots are linear over the whole concentration range.

The Raman and infrared band positions for bicarbonate in H_2O and D_2O are compiled in Table 2. The structure of bicarbonate in a concentrated $KHCO_3$ solution and the assignment

Can. J. Chem. Downloaded from www.nrcresearchpress.com by 210.87.254.105 on 09/05/12
For personal use only.

Can. J. Chem. Downloaded from www.nrcresearchpress.com by 210.87.254.105 on 09/05/12
For personal use only.

TABLE 2. Raman and infrared band positions for a 3.5 *M* solution of $KHCO_3$ in H_2O and D_2O*

Raman (cm^{-1})		Infrared (cm^{-1})	
H_2O	D_2O	H_2O	D_2O
632	600	—	—
672	672	—	670
841	841	840	835
1017	980	1000	975
1302	1030	1300	1025
1360	1360	1355	1355
1630	1630	1620	1620
1682	1682	—	—
2650	2030	2620	2020

*For detailed assignment see ref. 2.

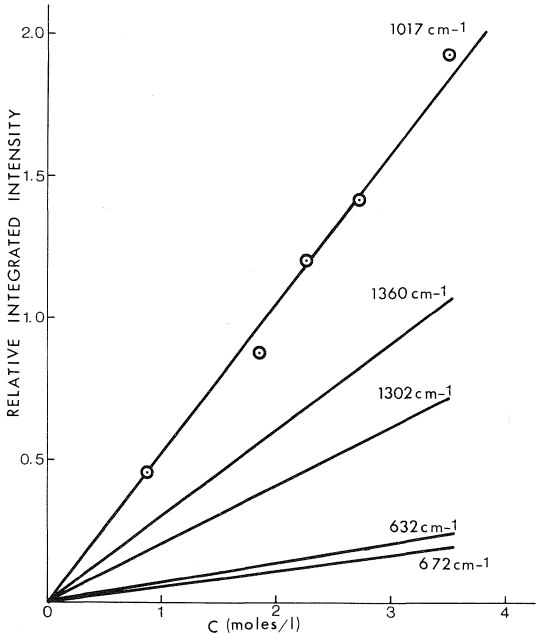

FIG. 4. A plot of relative integrated intensity *vs.* concentration for the major Raman band of potassium bicarbonate. Only best fit lines shown for weaker bands for clarity.

of frequencies to approximate modes of vibration has been deduced from the band positions, band shifts on deuteration, and Raman depolarization ratios (2). The replacement of $KHCO_3$ with Li, Na, Rb, or Cs bicarbonate proved to have little effect on the Raman or infrared band positions or the Raman relative intensities. Changing the bicarbonate molarity essentially has no effect on the spectra either. Thus it appears that the $C_s(\sigma_h)$ structure deduced for bicarbonate in concentrated $KHCO_3$ solutions holds for all concentrations and for all alkali metals. Certainly there is no evidence for ionic interactions from the vibrational spectrum.

The bicarbonate ion has an ionizable hydrogen atom which is replaceable by deuterium. This can occur when the bicarbonate ion is dissolved in D_2O and then the vibrations of the OH part of the ion will shift to lower frequencies due to the formation of OD. The 2650 cm^{-1} line shifts to 2030 cm^{-1} in D_2O, the 1302 cm^{-1} to 1030 cm^{-1}, the 1017 cm^{-1} to 980 cm^{-1}, and the 632 cm^{-1} to 600 cm^{-1}. Since the concentration of HCO_3^- in any solution can be found from the Raman intensity data (Fig. 4), it is possible to follow the hydrogen–deuterium exchange on the bicarbonate ion in H_2O–D_2O mixtures. The 900–1100 cm^{-1} region of the Raman spectrum of 2.9 *M* K_2CO_3 in H_2O–D_2O mixtures is shown in Fig. 5. The solution containing only DCO_3^- (spectrum (*d*)) was prepared by adding DCl to a D_2O solution of K_2CO_3 until no carbonate was detected in the Raman spectrum. Four bands appear in this region of the spectrum: the easily resolvable 1067 cm^{-1} carbonate band, the 1017 cm^{-1} HCO_3^- band, and the 980 and 1030 cm^{-1} DCO_3^- bands. The overlap of the latter three bands makes curve resolving difficult. But if it is kept in mind that both the 980 cm^{-1} and the 1030 cm^{-1} bands are generated by DCO_3^- and since it is possible to set the shapes of the two bands using the DCO_3^- spectrum, the total band contour for the two bands can be

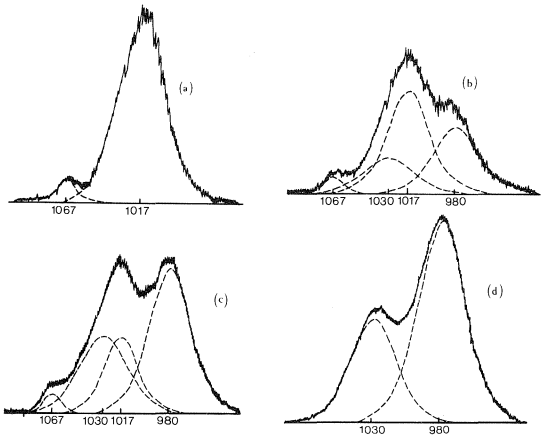

FIG. 5. Resolved Raman spectra of the 900–1100 cm^{-1} region for 2.9 *M* $KHCO_3$ in (*a*) H_2O, (*b*) 50 mol% H_2O – 50 mol% D_2O, (*c*) 25 mol% H_2O – 75 mol% D_2O, and (*d*) D_2O.

TABLE 3. Species concentrations and concentration quotients determined by Raman spectroscopy for the system $KHCO_3$–H_2O–D_2O*

Solution	$[HCO_3^-]$	$[DCO_3^-]$	$[H_2O]$	[HOD]	$[D_2O]$	Q_3	Q_4
2.9 *M* $KHCO_3$ in 50 mol% H_2O – 50 mol% D_2O	1.57	1.33	14.66	27.25	13.33	1.73	0.46
2.9 *M* $KHCO_3$ in 25 mol% H_2O – 75 mol% D_2O	0.96	1.94	4.06	21.42	29.72	1.46	0.38
2.9 *M* $KHCO_3$ in 10 mol% H_2O – 90 mol% D_2O	0.37	2.52	0.87	11.82	42.47	1.90	0.50

*Mean concentration quotients $Q_3 = 1.7 \pm 0.2$, $Q_4 = 0.45 \pm 0.05$.

treated as a single band and the missing gap filled with the 1017 cm^{-1} band. In this way it was possible to obtain excellent reproducible fits for the experimental spectrum. The concentration of HCO_3^- was then determined from the 1017 cm^{-1} band intensity and the concentration of DCO_3^- obtained by subtraction. A check on the accuracy of the determination was made using the 1302 cm^{-1} band intensity. The HCO_3^- concentrations from both regions of the spectrum were found to be in good agreement.

The important reactions for the exchange equilibrium are as follows

[2] $H_2O + D_2O \rightleftarrows 2HOD$

$$Q_2 = [HOD]^2/[H_2O][D_2O]$$

[3] $HCO_3^- + D_2O \rightleftarrows DCO_3^- + HOD$

$$Q_3 = [DCO_3^-][HOD]/[HCO_3^-][D_2O]$$

[4] $HCO_3^- + HOD \rightleftarrows DCO_3^- + H_2O$

$$Q_4 = [DCO_3^-][H_2O]/[HCO_3^-][HOD]$$

The value of the concentration quotient Q_2 for reaction 2 at 25 °C is 3.8 (12).

Since $[HCO_3^-]$ and $[DCO_3^-]$ have been obtained experimentally there are five unknowns in the equations: $[H_2O]$, $[D_2O]$, [HOD], Q_3, and Q_4. It is possible to write equations for the known total concentration of hydrogen and deuterium in the solutions.

[5] $[H]_{total} = 2[H_2O] + [HOD] + [HCO_3^-]$

[6] $[D]_{total} = 2[D_2O] + [HOD] + [DCO_3^-]$

From these five equations it is now possible to calculate the concentration quotients Q_3 and Q_4. The species concentrations obtained from Raman intensity data for three 2.9 *M* $KHCO_3$ solutions in H_2O–D_2O mixtures and the calculated concentration quotients are shown in Table 3. The experiment was repeated for 1 *M* $NaHCO_3$ solutions in two H_2O–D_2O mixtures and the quotients, $Q_3 = 1.9 \pm 0.2$, $Q_4 = 0.50 \pm 0.05$, are in close agreement with the $KHCO_3$ results. Therefore, the concentration quotients appear to be independent of cation and molarity.

The authors are grateful to Mrs. Jocelyn Larabie for technical assistance.

1. R. A. HORNE. Marine chemistry. Wiley–Interscience, New York, N.Y., 1969. p. 203.
2. A. R. DAVIS and B. G. OLIVER. J. Sol. Chem. **1**, 329 (1972).
3. D. E. IRISH and A. R. DAVIS. Can. J. Chem. **46**, 943 (1968).
4. D. E. IRISH. *In* Ionic interactions from dilute solutions to fused salts. *Edited by* S. Petrucci. Vol. 2. Academic Press, New York, N.Y. 1971. p. 187.
5. D. E. IRISH, D. L. NELSON, and M. H. BROOKER. J. Chem. Phys. **54**, 654 (1971).
6. J. D. RIDDEL, D. J. LOCKWOOD, and D. E. IRISH. Can. J. Chem. **50**, 2951 (1972).
7. B. G. OLIVER and A. R. DAVIS. J. Inorg. Nucl. Chem. **34**, 2851 (1972).
8. A. R. DAVIS and C. CHONG. J. Inorg. Chem. **11**, 1891 (1972).
9. G. E. WALRAFEN. J. Chem. Phys. **40**, 3249 (1964).
10. H. LEE and J. K. WILMSHURST. Aust. J. Chem. **17**, 943 (1964).
11. J. B. BATES, M. H. BROOKER, A. S. QUIST, and G. E. BOYD. J. Phys. Chem. **76**, 1565 (1972).
12. I. KIRSHENBAUM. Physical properties and analysis of heavy water. McGraw-Hill, New York, N.Y., 1951. p. 54.

Can. J. Chem. Downloaded from www.nrcresearchpress.com by 210.87.254.105 on 09/05/12
For personal use only.

Bimolecular Reactions of Trapped Ions. V. Ionic Chemistry of Simple Oxygen-containing Molecules[1]

ALAN S. BLAIR AND ALEX. G. HARRISON

Department of Chemistry, University of Toronto, Toronto 181, Ontario

Received July 20, 1972

The ion-molecule reactions occurring in a number of one-component and two-component systems involving oxygen-containing compounds have been studied using an ion trapping technique. The variable reaction time possible (up to 3.2 ms) has permitted a study of the sequential ion–molecule reactions occurring. In one-component systems (M = CH_3CHO, $(CH_3)_2O$, or $(CH_3)_2CO$) the MH^+ ion formed initially reacts to produce M_2H^+ in a rapid third order reaction (k in the range 10^{-24} to 10^{-25} cm^6 $molecule^{-2}$ s^{-1}). No M_2H^+ was observed in ethylene oxide. In two-component systems a rapid proton transfer reaction $M_1H^+ + M_2 \rightarrow M_2H^+ + M_1$ occurs when the proton affinity of M_2 is greater than the proton affinity of M_1; consequently, the third order solvation reactions normally will involve only reactions of M_2H^+.

The reactions of isomeric $C_2H_5O^+$ ions have been studied. The $CH_3OCH_2^+$ ion reacts slowly by H^- abstraction and/or CH_3^+ transfer. The $CH_3CH{=}OH^+$ ion rapidly (and essentially completely) transfers a proton to $(CD_3)_2O$ and to $(CH_3)_2CO$. By contrast the $C_2H_5O^+$ ion obtained by protonation of ethylene oxide does not react completely with $(CD_3)_2O$ or $(CH_3)_2CO$. In the former case a quasi-equilibrium is reached while in the latter case there is evidence that the $C_2H_5O^+$ ions have rearranged to a $CH_3OCH_2^+$ structure by an unknown mechanism.

Considerable detail has been obtained concerning the primary ion–molecule reactions occurring, particularly for systems containing ethylene oxide.

Les réactions ion–molécule qui se produisent pour un certain nombre de systèmes à une ou deux composantes engageant des composés à oxygène, ont été étudiées par la technique du piègeage ionique. La possibilité de jouer sur la variable temps de la réaction (jusqu'à 3.2 ms) a permis une étude séquentielle des réactions ion–molécule. Dans les systèmes à une composante (M = CH_3CHO, $(CH_3)_2O$, ou $(CH_3)_2CO$), l'ion MH^+ initialement formé réagit et donne M_2H^+ selon une réaction rapide d'ordre trois (k de l'ordre de 10^{-24} à 10^{-25} cm^6 $molécule^{-2}$ s^{-1}). Pour l'oxyde d'éthylène, aucun M_2H^+ n'a été observé. Pour les systèmes à deux composantes, une réaction de transfert rapide de proton $M_1H^+ + M_2 \rightarrow M_2H^+ + M_1$, se produit lorsque l'affinité pour le proton de M_2 est supérieure à celle de M_1; en conséquence, les réactions de solvatation d'ordre trois n'engageront normalement que les réactions de M_2H^+.

Les réactions des ions isomères $C_2H_5O^+$ ont été étudiées. L'ion $CH_3OCH_2^+$ réagit lentement par abstraction de H^- et (ou) transfert de CH_3^+. L'ion $CH_3CH{=}OH^+$ transfère rapidement (et de façon pratiquement totale) son proton à $(CD_3)_2O$ et à $(CH_3)_2CO$. Au contraire l'ion $C_2H_5O^+$, obtenu par protonation de l'oxyde d'éthylène, ne réagit pas complètement sur $(CD_3)_2O$ ou $(CH_3)_2CO$. Dans le premier cas on atteint une quasi-équilibre tandis que pour le second, un réarrangement des ions $C_2H_5O^+$ en $CH_3OCH_2^+$ selon un mécanisme inconnu, a été mis en évidence.

Des informations détaillées ont été aussi obtenues pour les réactions primaires ion–molécules, surtout pour les systèmes contenant l'oxyde d'éthylène. [Traduit par le journal]

Can. J. Chem., **51**, 703 (1973)

Introduction

The ion–molecule reactions of a considerable number of oxygen-containing molecules have been studied by pressure variation at constant repeller field (1–7), by ion cyclotron resonance (i.c.r.) techniques (7–10), and by the zero-field pulsing technique (3, 11). It is well-established that the major reactions occuring involve formation of the protonated molecule (monosolvated proton) and in many cases more highly solvated protons are observed at higher pressures. Although rate constants for many of the reactions forming the monosolvated proton have been measured, there is little quantitative information available concerning the subsequent reactions of this species.

We have found (12–14) that the trapped ion technique (15) is particularly suited to the study of sequential ion–molecule reactions. The present work was undertaken, in part, to study the reactions of monosolvated protons in a number of one-component and two-component systems in-

[1]The work reported here will constitute part of the Ph.D. Thesis to be submitted by A. S. Blair to the University of Toronto.

Can. J. Chem. Downloaded from www.nrcresearchpress.com by 210.87.254.42 on 09/05/12
For personal use only.

Can. J. Chem. Downloaded from www.nrcresearchpress.com by 210.87.254.42 on 09/05/12
For personal use only.

volving oxygen-containing molecules. The work necessarily involved a study of the reactions forming the monosolvated protons. This has, on the whole, confirmed the earlier work, but has provided additional details in several cases, particularly for systems containing ethylene oxide.

An additional objective of the present work was to study quantitatively the reactions of isomeric $C_2H_5O^+$ ions and the systems have been chosen with this objective in mind. Several structures (**I** to **III**) have been proposed for the

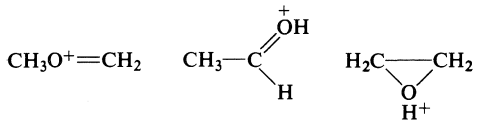

I II III

$C_2H_5O^+$ ions observed in the electron impact fragmentation of alcohols and ethers (16–19). While the present work was in progress Beauchamp and Dunbar (10) reported that $C_2H_5O^+$ ions derived from ethers (structure **I**) react by H^- abstraction and/or methyl cation transfer while $C_2H_5O^+$ ions of nominal structures **II** and **III** both react by proton transfer and therefore cannot be distinguished from each other by reaction type. However, this i.c.r. study reported no rate coefficients and the possibility remained that structures **II** and **III** might be distinguishable from the rate of reaction.

Experimental

The work was carried out using the mass spectrometer and ion-trapping techniques described previously (15). In this technique ions are produced during a short (1 μs) pulse of electrons of suitable energy and are trapped in the negative space charge of a continuous electron beam of energy insufficient to cause ionization. A positive voltage pulse applied to the repeller electrode a known and variable time after the ionizing pulse removes the ions for mass analysis. In the present work delay times between the ionizing and withdrawal pulses (and hence reaction times) of up to 3.2 ms were used. Rate coefficients were obtained from observations of the ion intensities (normalized as a fraction of the total recorded ion intensity) as a function of the reaction time.

Source concentrations were not measured directly but were related to the gas pressure in the inlet system. Tests showed that the source concentration was a linear function of sample inlet pressure and that the gas composition in the ion source was the same as that of the mixture in the inlet system. The relation between source concentration and inlet pressure was established by observation of the rate of the $CH_4^+ + CH_4$ reaction in pure methane; all rate constants are therefore relative to the value (11) of 1.20×10^{-9} cm^3 molecule^{-1} s^{-1} for this reaction. Gas mixtures were made up accurately by pressure and normally at least three different mixtures were used in establishing rate data. The error limits quoted represent the mean deviation of three or more determinations.

All unlabelled compounds were commercially available. Acetaldehyde-d_4, acetaldehyde-d_3, dimethyl-d_6 ether, methyl-d_3 ethyl ether, and ethylene oxide-d_4 were obtained from Merck, Sharp, and Dohme, Montreal. The unlabelled acetaldehyde contained a small diethyl ether impurity which was removed by gas chromatography. The remaining compounds showed no detectable impurities in their mass spectra and were used without purification.

Results and Discussion

Acetaldehyde

Figure 1 shows typical results obtained for this system at an ionizing electron energy such that CH_3CHO^+, CH_3CO^+, and CHO^+ were the only primary ions.[2] Although CH_3CO^+ shows an initial small decrease this was not observed at lower electron energies and we conclude that this ion is essentially unreactive with acetaldehyde, in agreement with the conclusions derived from earlier pressure studies (1, 2).

The reactions observed in the acetaldehyde system can be described by the scheme

[1] $CH_3CHO^+ + CH_3CHO \rightarrow CH_3CHOH^+ + C_2H_3O$

[2] $CHO^+ + CH_3CHO \rightarrow CH_3CHOH^+ + CO$

[3] $CH_3^+ + CH_3CHO \rightarrow C_2H_3O^+ + CH_4$

[4] $CH_3CHOH^+ + 2CH_3CHO \rightarrow (CH_3CHO)_2H^+ + CH_3CHO$

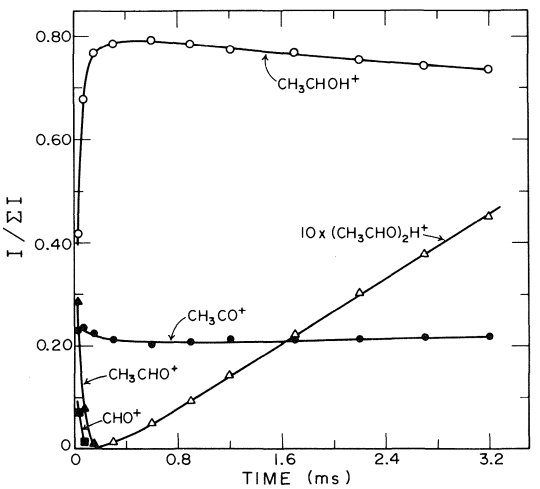

FIG. 1. Ion intensities *vs.* time, acetaldehyde [M] = 1.03×10^{13} molecules cm^{-3}.

[2]The mass spectrum of CD_3CHO indicates that the $(M - 1)^+$ ion of acetaldehyde is predominantly CH_3CO^+.

Can. J. Chem. Downloaded from www.nrcresearchpress.com by 210.87.254.42 on 09/05/12
For personal use only.

The rate coefficients measured for reactions 1 to 3 are summarized in Table 1 and compared with previous literature values (2) obtained from pressure studies. The present value for k_1 is higher than the pressure study result; the lower value was obtained in the present work when unpurified acetaldehyde was used. Using CD_3CHO it was established that reaction 1 proceeds almost exclusively by transfer of the aldehydic hydrogen (as H or H^+), in agreement with the results of Meisels and co-workers (20).

The kinetic order of reaction 4 was not rigorously established but was assumed to be third order by analogy with the similar reactions in dimethyl ether and acetone (see below). The third order rate coefficient was found to be $k_4 = 1.2 \times 10^{-25}$ cm^6 molecule^{-2} s^{-1} from the decrease in the CH_3CHOH^+ intensity with reaction time at long delay times.

Ethylene Oxide

Figure 2 shows typical results obtained at a source concentration of 1.17×10^{13} molecules cm^{-3}. The CHO^+ ion reacts rapidly by proton transfer, the rate coefficient (Table 1) being in good agreement with that obtained from the pressure studies (2). As in acetaldehyde the $C_2H_3O^+$ ion is unreactive.

The remaining reactions in ethylene oxide can be described by the scheme

[5] $C_2H_4O^+ + C_2H_4O \rightarrow C_2H_5O^+ + C_2H_3O$

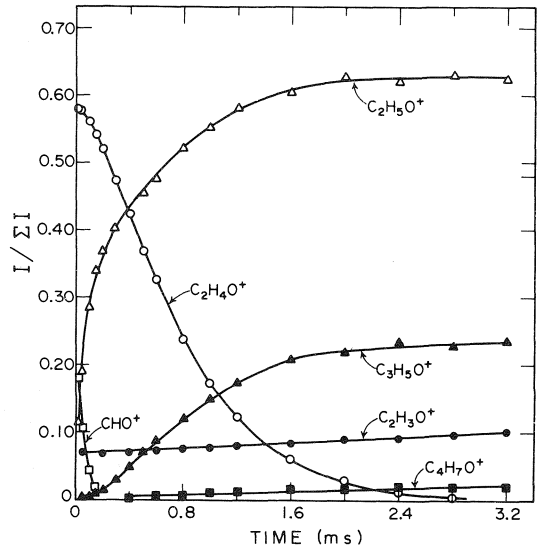

FIG. 2. Ion intensities *vs.* time, ethylene oxide [M] = 1.17×10^{13} molecules cm^{-3}.

[6] $C_2H_4O^+ + C_2H_4O \rightarrow C_2H_4O^{+*} + C_2H_4O$

[7*a*] $C_2H_4O^{+*} + C_2H_4O \rightarrow C_2H_5O^+ + C_2H_3O$

[7*b*] $\rightarrow C_3H_5O^+ + CH_2O$

[8] $C_2H_5O^+ + C_2H_4O \rightarrow C_2H_3O^+ + (H_2 + C_2H_4O)$

[9] $C_2H_5O^+ + C_2H_4O \rightarrow C_4H_7O^+ + H_2O$

The $C_2H_4O^+$ ion current does not decrease in the exponential fashion expected for a quasi-first order reaction but shows an initial sigmoidal shape. This behavior was also observed when $C_2H_4O^+$ was the only primary ion and therefore cannot be attributed to formation of $C_2H_4O^+$ by ion–molecule reactions. In addition the $C_3H_5O^+$ product species shows an initial induction period characteristic of the product of a sequence of bimolecular reactions. Both of these observations can be explained by assuming that the $C_2H_4O^+$ ions formed initially by electron impact react only slowly to form detectable products (reaction 5) but considerably more rapidly (reaction 6) to form a structurally or energetically modified ion, $C_2H_4O^{+*}$, which subsequently reacts to produce both $C_2H_5O^+$ and $C_3H_5O^+$ (reaction 7).[3] A similar type of reaction sequence has been observed in vinyl fluoride (12). It does not appear possible that the $C_2H_4O^{+*}$ can be formed by inelastic collisions between electrons and the trapped ions. Simple calculations show that the collision cross-section would have to be 10^{-10} to 10^{-12} cm^2 which does not appear possible for 5–8 eV electrons.

The proposed mechanism receives further support from the plot in Fig. 3 of $I_{C_3H_5O^+}$ and $\sum I_{C_2H_5O^+}$ *vs.* $\Delta I_{C_2H_4O^+}$, the *m/e* 44 which has reacted.[4] $\sum I_{C_2H_5O^+} = I_{C_2H_5O^+} + I_{CHO^+} + I_{C_2H_3O^+} + I_{C_4H_7O^+}$ and the increase in $\sum I_{C_2H_5O^+}$ with time thus represents the $C_2H_5O^+$ formed by reactions 5 and 7*a*. The plot of $\sum I_{C_2H_5O^+}$ *vs.* $\Delta I_{C_2H_4O^+}$ clearly shows two linear regions. The initial region, with a slope of 1.0, corresponds to formation of $C_2H_5O^+$ by reaction 5, and during this time no $C_3H_5O^+$ is formed. The second region has a slope of 0.52 ± 0.04 (average of several determinations) and corresponds to the fractional yield of $C_2H_5O^+$ by reaction 7. The $I_{C_3H_5O^+}$ plot has an onset corresponding to the

[3]In C_2D_4O the *m/e* 57 ($C_3H_5O^+$) ion moved to *m/e* 62 ($C_3D_5O^+$) confirming the ionic composition.

[4]The data of Fig. 3 were obtained at a lower ionizing electron energy than the data in Fig. 2.

TABLE 1. Rate constants for ion molecule reactions

Reaction	$k \times 10^9$ (cm^3 molecule^{-1} s^{-1}) This work	Literature (ref.)
$CH_3CHO^+ + CH_3CHO$	$2.4_9 \pm 0.1$	1.91(2)
$CHO^+ + CH_3CHO$	$2.5_3 \pm 0.1$	2.45(2)
$CH_3^+ + CH_3CHO$	$2.4_9 \pm 0.05$	
$CD_3CDO^+ + CD_3CDO$	2.4_6	
$CHO^+ + \overline{CH_2CH_2O}$	1.65 ± 0.3	1.75(2)
$C_2H_4O^{+*} + \overline{CH_2CH_2O}$	0.15 ± 0.03	
$C_2D_4O^{+*} + \overline{CD_2—CD_2O}$	0.19 ± 0.02	
$(CH_3)_2O^+ + (CH_3)_2O$	$1.5_8 \pm 0.15$	1.45(2)
$CHO^+ + (CH_3)_2O$	$1.7_4 \pm 0.15$	1.55(2)
$CH_3O^+ + (CH_3)_2O$	$1.1_6 \pm 0.15$	
$CH_3^+ + (CH_3)_2O$	2.0 ± 0.3	2.6(2)
$CH_3OCH_2^+ + (CH_3)_2O$	0.013 ± 0.009	
$(CD_3)_2O^+ + (CD_3)_2O$	1.5_8	
$CD_3OC_2H_5^+ + CD_3OC_2H_5$	$1.4_3 \pm 0.05$	
$CD_3OCH_2^+ + CD_3OC_2H_5$	$0.17_5 \pm 0.005$	
$(CH_3)_2CO^+ + (CH_3)_2CO$	0.65 ± 0.03	0.51(7), 0.54(7)
$CH_3CO^+ + (CH_3)_2CO$	0.22 ± 0.02	0.30(7), 0.43(7)
$CH_3OCH_2^+ + (CH_3)_2CO$	0.033 ± 0.010	
$(CH_3)_2OH^+ + (CH_3)_2CO$	1.0 ± 0.1	
$CH_3CHOH^+ + (CD_3)_2O$	1.88 ± 0.05	
$CH_3CHOH^+ + (CH_3)_2CO$	2.25	
This Work		
$CH_3CHOH^+ + 2CH_3CHO \rightarrow (CH_3CHO)_2H^+ + CH_3CHO$	1.2×10^{-25} cm^6 molecule^{-2} s^{-1}	
$(CH_3)_2OH^+ + 2(CH_3)_2O \rightarrow ((CH_3)_2O)_2H^+ + (CH_3)_2O$	$1.0 \pm 0.2 \times 10^{-25}$ cm^6 molecule^{-2} s^{-1}	
$(CH_3)_2COH^+ + 2(CH_3)_2CO \rightarrow ((CH_3)_2CO)_2H^+ + (CH_3)_2CO$	$6.5 \pm 0.5 \times 10^{-25}$ cm^6 molecule^{-2} s^{-1}	

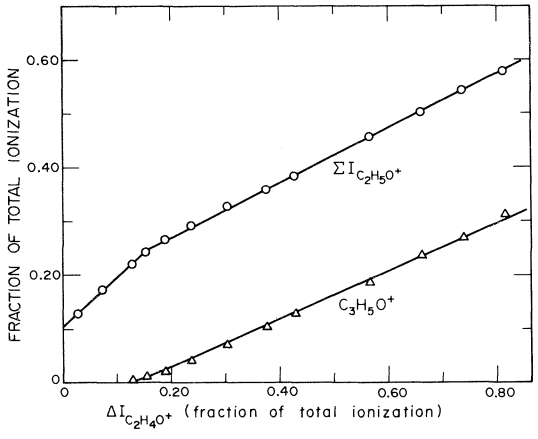

FIG. 3. Ethylene oxide, $\Sigma I_{C_3H_5O^+}$ and $I_{C_2H_4O^+}$ *vs.* $\Delta I_{C_2H_4O^+}$ (see text).

break in the $\sum I_{C_2H_5O^+}$ plot and a slope of 0.45 $\pm$ 0.04. Apparently $C_3H_5O^+$ is produced only by reactions of $C_2H_4O^+$ ions which have been modified by collision (reaction 6) and not by those formed initially by electron impact. From the position of the change in slope in Fig. 3 we estimate that k_6 is in the range 2–3 $\times$ 10^{-9} cm^3 molecule^{-1} s^{-1}. The total rate constant k_7 is given in Table 1.

The alternative explanation that $C_3H_5O^+$ is formed by reaction 10 is discarded as a major source of $C_3H_5O^+$ because

[10] $C_2H_5O^+ + C_2H_4O \rightarrow C_3H_5O^+ + CH_4O$

double resonance i.c.r. experiments (10) confirm *m/e* 44 as the precursor and because the $C_3H_5O^+$ yield does not increase significantly after the

Can. J. Chem. Downloaded from www.nrcresearchpress.com by 210.87.254.42 on 09/05/12
For personal use only.

Can. J. Chem. Downloaded from www.nrcresearchpress.com by 210.87.254.42 on 09/05/12
For personal use only.

m/e 44 has disappeared even though $C_2H_5O^+$ is present in abundance. Experiments at higher source pressures did confirm that reaction 10 occurred but much too slowly to account for a significant fraction of the $C_3H_5O^+$ produced.

The $C_3H_5O^+$ product was not reported in the earlier pressure study (2) and a re-examination of the records shows that this region of the mass spectrum was not recorded. It was reported in the i.c.r. study (10) although neither the reaction order nor the fractional yield were established. Although the disolvated proton was reported in the i.c.r. study we did not observe this product even at our highest pressures ($\sim 4 \times 10^{13}$ molecule cm^{-3}) and longest reaction times. A small yield of a product of *m/e* 71 (probably $C_4H_7O^+$) corresponding to loss of H_2O from the $C_2H_5O^+ + C_2H_4O$ collision complex was observed (reaction 9).

Dimethyl Ether

Typical results are illustrated in Fig. 4. The results are consistent with the following reaction scheme which is in agreement with previous studies (1, 2, 10).

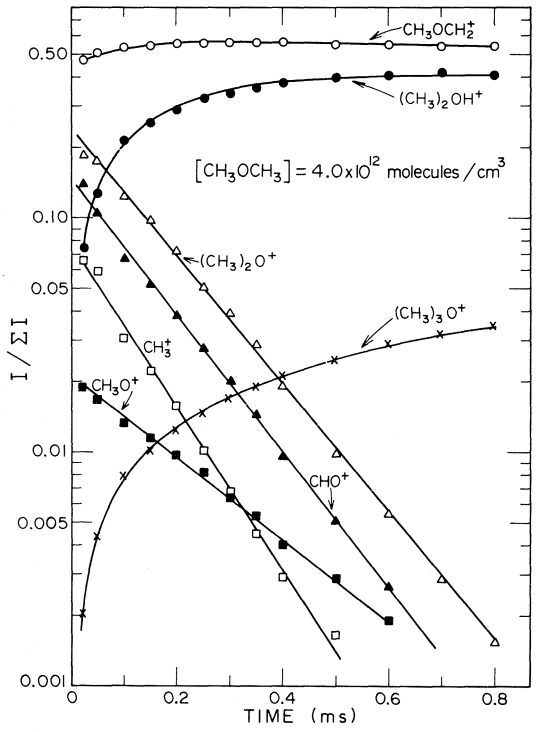

FIG. 4. Dimethyl ether, ion intensities *vs.* time [M] = 4.00×10^{12} molecules cm^{-3}.

[11] $(CH_3)_2O^+ + (CH_3)_2O \rightarrow (CH_3)_2OH^+ + CH_3OCH_2$

[12] $CHO^+ + (CH_3)_2O \rightarrow (CH_3)_2OH^+ + CO$

[13] $CH_3^+ + (CH_3)_2O \rightarrow CH_3OCH_2^+ + CH_4$

[14] $CH_3O^+ + (CH_3)_2O \rightarrow CH_3OCH_2^+ + CH_4O$

[15] $CH_3OCH_2^+ + (CH_3)_2O \rightarrow (CH_3)_3O^+ + CH_2O$

The rate coefficients measured are summarized in Table 1 and are in good general agreement with those obtained at 2.4 eV ion exit energy in the pressure studies (2). Reaction 15, methyl cation transfer, is one of the characteristic reactions of $C_2H_5O^+$ ions of structure **I** (10), however it is extremely slow ($k = 1.3 \pm 0.9 \times 10^{-11}$ cm^3 $molecule^{-1}$ s^{-1}) and consequently it was difficult to obtain an accurate rate coefficient. The other reaction characteristic of structure **I** ions, H^- abstraction, is not observable in this system since it regenerates the reactant ion.

Figure 5 shows results obtained at a higher source pressure and an electron energy such that $(CH_3)_2O^+$ was the major primary ion. The monosolvated proton clearly reacts to form both $(CH_3)_3O^+$ and the disolvated proton $((CH_3)_2O)_2H^+$, presumably by the following reactions.

[16] $(CH_3)_2OH^+ + (CH_3)_2O \rightarrow (CH_3)_3O^+ + CH_3OH$

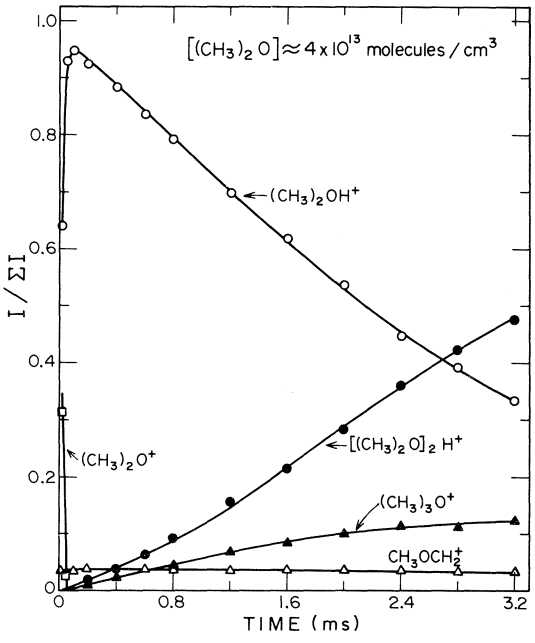

FIG. 5. Dimethyl ether system, [M] $\approx 4 \times 10^{13}$ molecules cm^{-3}.

[17] $(CH_3)_2OH^+ + 2(CH_3)_2O \rightarrow ((CH_3)_2O)_2H^+ + (CH_3)_2O$

Assuming these two reactions we may derive eq. 18 for reaction times greater than that necessary for complete reaction of $(CH_3)_2O^+$.

$$[18] \quad \log[(CH_3)_2OH^+] = \frac{-(k_{16}[(CH_3)_2O] + k_{17}[(CH_3)_2O]^2)t}{2.303} + \text{constant}$$

From eq. 18 we note that the slope of the plot of $\log[(CH_3)_2OH^+]$ *vs.* t when plotted in the form $2.303 \times \text{slope}/[(CH_3)_2O]$ *vs.* $[CH_3OCH_3]$ should yield a straight line with an intercept of k_{16} and a slope of k_{17}. A typical plot is shown in Fig. 6 covering a factor of two in $[CH_3OCH_3]$. A satisfactory least-squares straight line is observed leading from three separate determinations to the average values $k_{16} = 2.7 \pm 0.3 \times 10^{-12}$ cm^3 molecule^{-1} s^{-1} and $k_{17} = 1.0 \pm 0.2 \times 10^{-25}$ cm^6 molecule^{-2} s^{-1}.

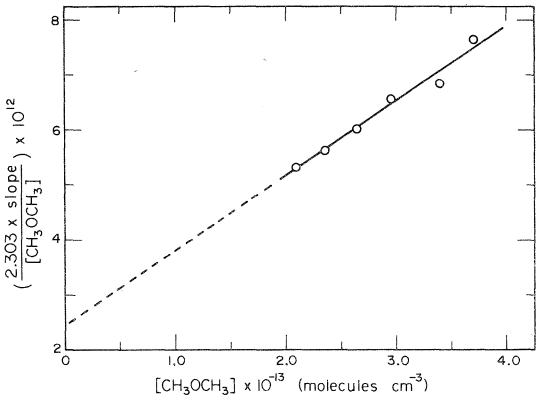

FIG. 6. Dimethyl ether, determination of k_{16} and k_{17} (see text).

Methyl-d_3 Ethyl Ether

Typical results for this system are shown in Fig. 7. The initial curvature in the $CD_3OCH_2^+$ plot is unexplained. The $CD_3OC_2H_5^+$ ion reacts to form $CD_3OC_2H_5{\cdot}H^+$ and $CD_3OC_2H_5{\cdot}D^+$ in the ratio 1.0:1.1 in excellent agreement with the ratio reported by Beauchamp and Dunbar (10) in the i.c.r. study. The $CD_3OCH_2^+$ ion reacts mainly by reactions 19 and 20 in the ratio $k_{19}:k_{20} = 0.05:0.95$.

[19] $CD_3OCH_2^+ + CD_3OC_2H_5 \rightarrow C_2H_5O(CD_3)_2^+ + CH_2O$

[20] $CD_3OCH_2^+ + CD_3OC_2H_5 \rightarrow CD_3OC_2H_4^+ + CD_3OCH_3$

This ratio is in good agreement with the thermal energy ratio of 0.04:0.96 obtained in the i.c.r. study (10). Although reaction 20, H^- abstraction, predominates over D^- abstraction from the methyl group of the neutral ether we do observe a low yield of $C_2H_5OCD_2^+$ which appears to react further, probably by H^- abstraction to yield $CD_3OC_2H_4^+$.

The total rate constants for reaction of $CD_3OC_2H_5^+$ and $CD_3OCH_2^+$ are recorded in Table 1. These rates have not been measured previously. The rate coefficient for reaction of $CD_3OCH_2^+$ with $CD_3OC_2H_5$ is approximately a factor of ten greater than that for reaction of

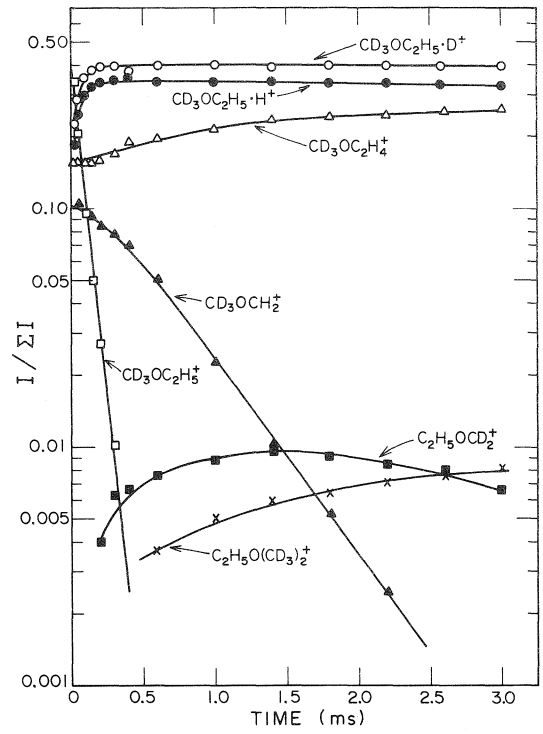

FIG. 7. Methyl-d_3 ethyl ether, intensities *vs.* time, $[M] = 1.02 \times 10^{13}$ molecules cm^{-3}.

$CH_3OCH_2^+$ with CH_3OCH_3, primarily because the H^- abstraction reaction is observable in the former system. However, the total rate constant is still much lower (at least a factor of ten) than the rate coefficient calculated from ion-induced dipole interactions (21) indicating that the majority of the collisions are non-reactive.

Can. J. Chem. Downloaded from www.nrcresearchpress.com by 210.87.254.42 on 09/05/12
For personal use only.

Can. J. Chem. Downloaded from www.nrcresearchpress.com by 210.87.254.42 on 09/05/12
For personal use only.

Acetone

Typical results for this sytem at an ionizing electron energy sufficient to produce only $(CH_3)_2CO^+$ and CH_3CO^+ as primary ions are shown in Fig. 8. The molecular ion reacts by two major channels, reactions 21 and 22, with the

[21] $(CH_3)_2CO^+ + (CH_3)_2CO \rightarrow (CH_3)_2COH^+ + CH_3COCH_2$

[22] $(CH_3)_2CO^+ + (CH_3)_2CO \rightarrow CH_3COCH_3 \cdot COCH_3^+ + CH_3$

relative rates $k_{21}:k_{22} = 0.78:0.22$ (average of seven determinations). Recently, MacNeil and Futrell (7) have reported a ratio 0.67:0.33, while Terry and Tiernan (6), from tandem experiments, have reported a ratio 0.48:0.52. Our results are in better agreement with those of MacNeil and Futrell. The slight increase and the curvature in the initial portion of the CH_3CO^+ plot indicate that this ion also is being produced to a minor extent by reaction of the molecular ion. Terry and Tiernan (6) have also reported a small yield of CH_3CO^+ when $(CH_3)_2CO^+$ is reacted with acetone in a tandem mass spectrometer.

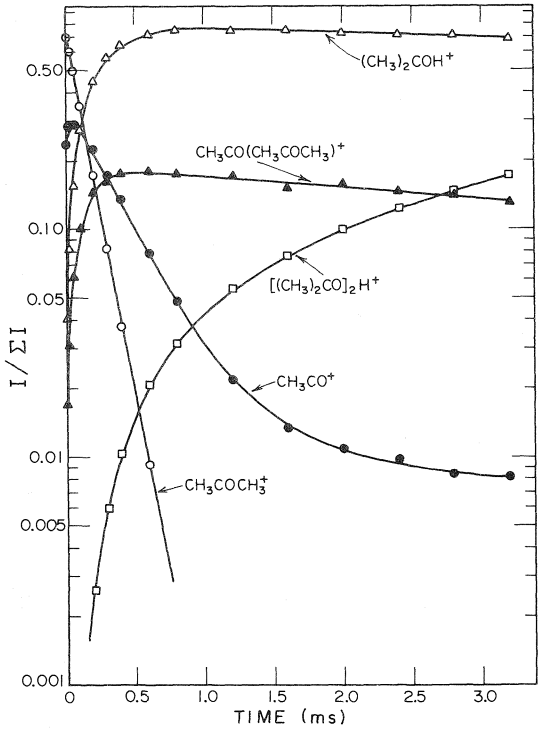

FIG. 8. Acetone, ion intensities *vs.* time, [M] = 1.14×10^{13} molecules cm^{-3}.

The total rate coefficient for reaction of $(CH_3)_2CO^+$, 6.5×10^{-10} cm^3 $molecule^{-1}$ s^{-1} (Table 1) is in satisfactory agreement with the thermal energy value of 5.4×10^{-10} cm^3 $molecule^{-1}$ s^{-1} and the pressure plot value of 5.1×10^{-10} cm^3 $molecule^{-1}$ s^{-1}, both reported by MacNeil and Futrell (7).

The major portion of the CH_3CO^+ ion is reactive, although the intensity levels off at approximately 0.4% of the total ionization indicating a possible non-reactive component. The only reaction detected was [23].

[23] $CH_3CO^+ + (CH_3)_2CO \rightarrow (CH_3)_2COH^+ + CH_2CO$

Terry and Tiernan (6) report that reaction 23 accounts for 99% of the reaction of CH_3CO^+, while MacNeil and Futrell report a 10% charge transfer to acetone at thermal energies. A small amount of charge transfer probably would not be detectable in our experiments. Values of $\Delta H_f((CH_3)_2COH^+)$ ranging from 110 kcal mol^{-1} (22) to 125 kcal mol^{-1} (23, 24) have been reported. The lower value makes reaction 23 6 kcal mol^{-1} exothermic while the higher value makes the reaction 9 kcal mol^{-1} endothermic for ground state reactants. It is possible that the reaction is indeed endothermic and that the unreactive component of the CH_3CO^+ signal represents that portion with insufficient energy to overcome the activation energy barrier for the reaction. The analogous reaction of CH_3CO^+ with acetaldehyde is 16 kcal mol^{-1} endothermic and CH_3CO^+ is completely unreactive with acetaldehyde (see above).

The $(CH_3)_2COH^+$ ion reacts further to form the disolvated proton $[(CH_3)_2CO]_2H^+$. To determine the order of this reaction the slopes of the log $[(CH_3)_2COH^+]$ *vs.* t plots at various concentrations of acetone were plotted in the manner 2.30 × slope/$[(CH_3)_2CO]$ *vs.* $[(CH_3)_2CO]$ (see eq. 18 and relevant discussion) as shown in Fig. 9. Within experimental error the intercept is zero indicating no second order contribution while the slope leads to a third order rate coefficient for the disappearance of $(CH_3)_2COH^+$ of $6.5 \pm 0.2 \times 10^{-25}$ cm^6 $molecule^{-2}$ s^{-1}. MacNeil and Futrell (7) have reported a second order rate coefficient for reaction of $(CH_3)_2COH^+$, however it is not clear that they have definitely established the reaction order.

As the results in Fig. 8 show the $CH_3COCH_3 \cdot COCH_3^+$ product reacts slowly at longer re-

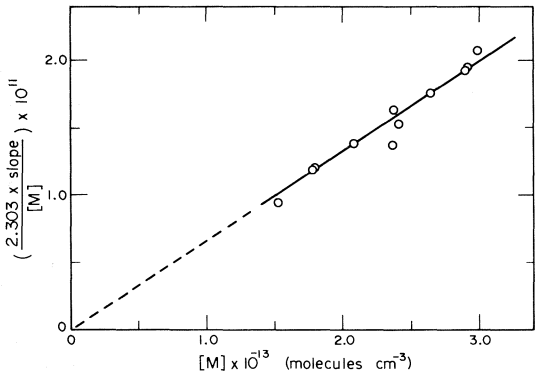

FIG. 9. Third-order plot for disappearance of $(CH_3)_2COH^+$, acetone.

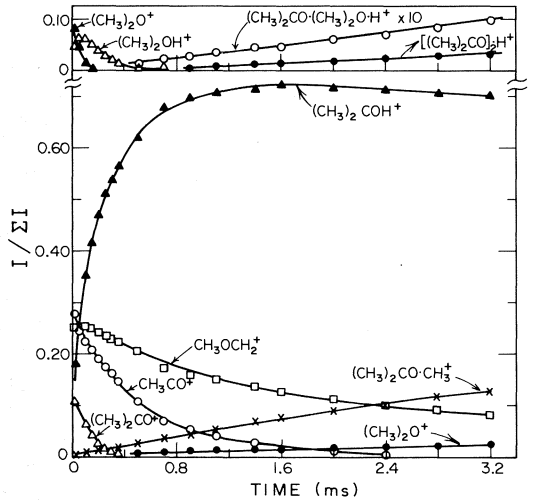

FIG. 10. Dimethyl ether – acetone system $[CH_3OCH_3] = [CH_3COCH_3] = 5.62 \times 10^{12}$ molecules cm^{-3}.

action times, probably to give the disolvated proton by reaction 24.

[24] $CH_3COCH_3{\cdot}COCH_3^+ + (CH_3)_2CO \rightarrow [(CH_3)_2CO]_2H^+ + CH_2CO$

Dimethyl Ether – Acetone

This system was studied to obtain quantitative information concerning the reaction of $CH_3OCH_2^+$ ions (structure **I**) with acetone. Typical results for a 1:1 mixture are shown in Fig. 10. Both the molecular ions react rapidly to give $(CH_3)_2OH^+$ and $(CH_3)_2COH^+$ and we estimate for the cross-sections $(CH_3)_2CO^+ + (CH_3)_2O$ and $(CH_3)_2O^+ + (CH_3)_2CO$ rate coefficients of $0.7 \pm 0.05 \times 10^{-9}$ and $2.8_5 \pm 0.05 \times 10^{-9}$ cm^3 $molecule^{-1}$ s^{-1} respectively, although we cannot determine the relative importance of H atom abstraction and H^+ transfer in either case. The CH_3CO^+ ion reacts only with acetone yielding a rate coefficient of 2.4×10^{-10} cm^3 $molecule^{-1}$ s^{-1} in good agreement with the value obtained in pure acetone. Proton transfer from CH_3CO^+ to dimethyl ether would be 13 kcal mol^{-1} endothermic while H^- abstraction from the ether would be 7 kcal mol^{-1} endothermic.

The $(CH_3)_2OH^+$ reacts at longer delay times by proton transfer to acetone with a rate constant (Table 1) of $1.0 \pm 0.1 \times 10^{-9}$ cm^3 $molecule^{-1}$ s^{-1}. This reaction is consistent with the relative proton affinities (23), $PA((CH_3)_2O) =$ 186 kcal mol^{-1} and $PA((CH_3)_2CO) =$ 190 kcal mol^{-1}.

There appears to be an unidentified reaction forming $CH_3OCH_2^+$ at short reaction times. However, at longer times $CH_3OCH_2^+$ reacts slowly with $(CH_3)_2O$ to give $(CH_3)_3O^+$ and more rapidly by CH_3^+ transfer to acetone, reaction 25.

[25] $CH_3OCH_2^+ + (CH_3)_2CO \rightarrow (CH_3)_2CO{\cdot}CH_3^+ + CH_2O$

From the rate of disappearance of $CH_3OCH_2^+$ we estimate $k_{25} = 3.3 \pm 1.0 \times 10^{-11}$ cm^3 $molecule^{-1}$ s^{-1} compared to the value of $1.3 \pm 0.9 \times 10^{-11}$ cm^3 $molecule^{-1}$ s^{-1} for reaction of $CH_3OCH_2^+$ with dimethyl ether.

Acetaldehyde – Dimethyl-d_6 Ether

In pure acetaldehyde $C_2H_5O^+$ ions presumably of structure **II** are formed in abundance and react only slowly with acetaldehyde. The acetaldehyde – dimethyl-d_6 ether system was studied to elucidate the reactions of CH_3CHOH^+ ions with the ether.

Typical results are shown in Fig. 11. The primary CH_3CO^+ and $CD_3OCD_2^+$ ions are essentially unreactive[5] while CH_3CHO^+, CHO^+, and $(CD_3)_2O^+$ react rapidly to form the protonated and deuteronated forms of both neutral molecules. For the cross-reactions $CH_3CHO^+ + (CD_3)_2O$ and $(CD_3)_2O^+ + CH_3CHO$ we obtain rate coefficients of $1.6 \pm 0.4 \times 10^{-9}$ and $1.5 \pm 0.4 \times 10^{-9}$ cm^3 $molecule^{-1}$ s^{-1} respectively. In neither case could the reaction channels

[5]At higher pressures and over longer reaction times a small yield of $CH_3CHO{\cdot}CD_3^+$ (*m/e* 62) was observed, presumably from the slow reaction of $CD_3OCD_2^+$ with CH_3CHO.

Can. J. Chem. Downloaded from www.nrcresearchpress.com by 210.87.254.42 on 09/05/12
For personal use only.

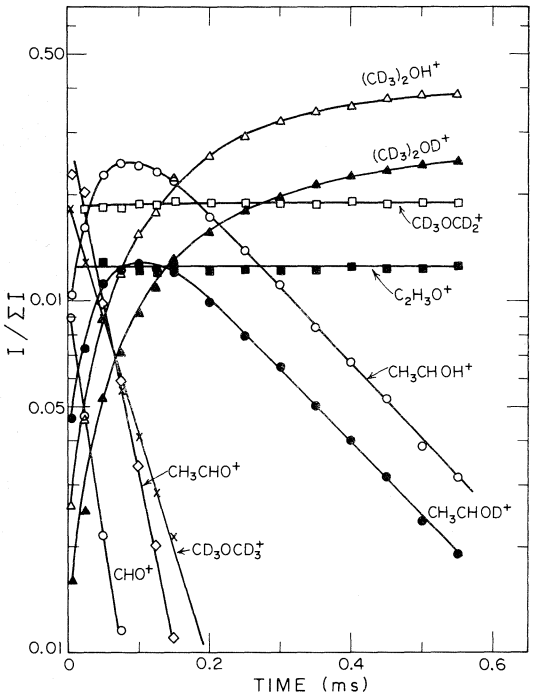

FIG. 11. Acetaldehyde – dimethyl-d_6 ether system $[CH_3CHO] = 7.22 \times 10^{12}$ molecules cm^{-3}, $[CD_3OCD_3] = 2.\overline{0} \times 10^{12}$ molecules cm^{-3}.

be clearly identified and probably both hydron transfer and atom abstraction occur.

At longer reaction times the semi-logarithmic plots for both CH_3CHOH^+ and CH_3CHOD^+ decrease linearly through occurrence of the reactions.

[26] $CH_3CHOH^+ + (CD_3)_2O \rightarrow (CD_3)_2OH^+ + CH_3CHO$

[27] $CH_3CHOD^+ + (CD_3)_2O \rightarrow (CD_3)_2OD^+ + CH_3CHO$

These reactions are anticipated since the proton affinity of dimethyl ether is greater than the proton affinity of acetaldehyde (23). The rate coefficients for the two reactions are identical within experimental error and several determinations led to the average value listed in Table 1.

Beyond 0.2 ms (*i.e.*, after the primary ions had reacted) the sums $CH_3CHOH^+ + (CD_3)_2OH^+$ and $CH_3CHOD^+ + (CD_3)_2OD^+$ remain constant indicating that reaction 27 occurs exclusively by D^+ transfer. Beauchamp and Dunbar (10) have noted that CD_3CHOH^+ ions produced by electron impact on $(CD_3)_2CHOH$ react with diisopropyl ether only by H^+ transfer below 12 eV ionizing electron energy. However, as the electron energy was increased above this value D^+ transfer was observed to increase rapidly in importance. Since $AP(CD_3CHOH^+) = 11.4$ eV they concluded that a maximum of 0.6 eV internal excitation was required to cause hydrogen randomization in the CD_3CHOH^+ ion. In our system the possible reactions forming CH_3CHOD^+ *i.e.*, $(CD_3)_2O^+ + CH_3CHO$ and $CH_3CHO^+ + (CD_3)_2O$, are 0.2 and 0.5 eV exothermic. Apparently either this excess energy is not retained by the product ion or it is insufficient to cause hydrogen randomization.[6]

One run was also carried out in a 10:1 CH_3CHO–$(CD_3)_2O$ mixture at approximately 2.5×10^{13} molecules cm^{-3} ion source concentration. The CH_3CHOH^+ signal peaked at ~0.05 ms (~47% of total ionization) and then decreased rapidly with a corresponding increase in the $(CD_3)_2OH^+$ signal. However, the CH_3CHOH^+ ion did not react completely but became constant at approximately 1.5% of the total ionization between 2 and 3 ms.

The origin of this apparent unreactive component is uncertain, however, it may indicate the attainment of a steady-state or quasi-equilibrium.[7] From the constant ionic concentrations and the relative neutral concentrations we calculate an apparent equilibrium constant for reaction 26 of ~400. This value is not inconsistent with the reported difference of 3 kcal mol^{-1} in the proton affinities of acetaldehyde and dimethyl ether (23). As discussed below a much larger non-reactive component is observed for $C_2H_5O^+$ in ethylene oxide – dimethyl-d_6 ether mixtures under similar conditions.

Ethylene Oxide – Dimethyl-d_6 Ether

These mixtures were studied in an attempt to obtain quantitative information concerning the reaction of $C_2H_5O^+$ ions of structure **III** with the ether. Because of the low reactivity of $C_2H_4O^+$ with C_2H_4O it was necessary to work

[6]In addition the reactant ions probably have an average kinetic energy of 0.4 eV (15). This does not appear to be converted to internal energy of the product ion to any significant extent since hydrogen randomization does not occur.

[7]Since the system is not at thermal equilibrium a true chemical equilibrium cannot be established. Hence we will refer to these steady-state conditions as quasi-equilibria.

Can. J. Chem. Downloaded from www.nrcresearchpress.com by 210.87.254.42 on 09/05/12
For personal use only.

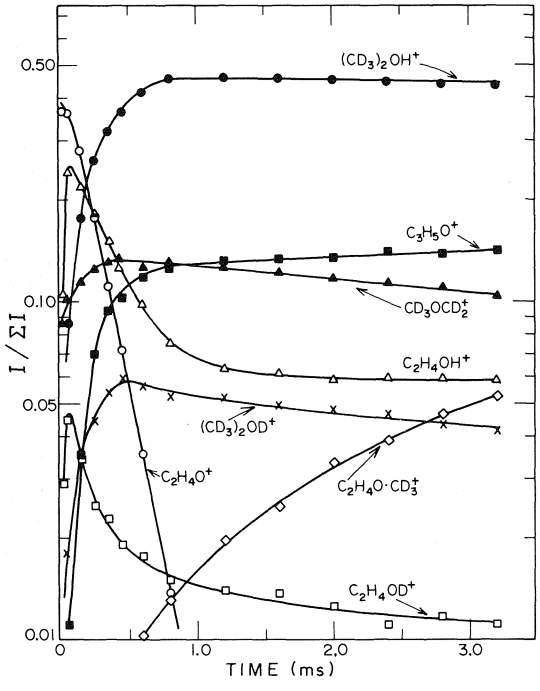

FIG. 12. Ethylene oxide – dimethyl-d_6 ether system, approximately 3.5×10^{13} molecules cm^{-3} $[C_2H_4O]$: $[CD_3OCD_3] = 10:1$.

at higher source pressures and with mixtures rich in ethylene oxide so that rapid conversion of $C_2H_4O^+$ to $C_2H_5O^+$ could be achieved.

Figure 12 shows results obtained in a 10:1 mixture at approximately 3.5×10^{13} molecules cm^{-3} total ion source concentration. At this concentration the ethylene oxide molecular ion disappears moderately rapidly not only by reactions 5 to 7 but also by reactions 28 to 30.[8]

[28] $C_2H_4O^+ + (CD_3)_2O \rightarrow (CD_3)_2OH^+ + C_2H_3O$

[29] $C_2H_4O^+ + (CD_3)_2O \rightarrow C_2H_4O{\cdot}D^+ + CD_3OCD_2$

[30] $C_2H_4O^+ + (CD_3)_2O \rightarrow CD_3OCD_2{}^+ + C_2H_4DO$

Reaction 30, D^- abstraction, is indicated by the initial significant increase in the $CD_3OCD_2{}^+$ ion current. The corresponding reaction is not observed in the acetaldehyde–ether system even though it is an exothermic reaction for both the acetaldehyde and ethylene oxide molecular ions. The reaction therefore appears to be characteristic of $C_2H_4O^+$ ion originating from ethylene oxide.

[8]It is probable that these reactions involve the $C_2H_4O^{+*}$ ion formed in reaction 6.

The rate of the proton transfer reaction 31

[31] $C_2H_4O{\cdot}H^+ + (CD_3)_2O \rightarrow (CD_3)_2OH^+ + C_2H_4O$

involving $C_2H_5O^+$ ions presumably of structure **III** could not be determined accurately. As shown in Fig. 12, the $C_2H_5O^+$ intensity, after reaching a maximum at ~0.1 ms, initially drops rapidly through the occurrence of reaction 31, but levels off at ~5.8% of the total ionization and no further reaction occurs. In a 120:1 ethylene oxide – $(CD_3)_2O$ mixture the $C_2H_5O^+$ intensity reached a maximum value of 52% of the total ionization at short delay times followed by a rapid decrease to a value of 32% which did not change between 2 and 3 ms.

The explanation of this apparent unreactive component of the $C_2H_5O^+$ signal may lie in the attainment of a quasi-equilibrium. From the experimental results we estimate apparent equilibrium constants for reaction 31 of 78 in the 10:1 mixture and 75 in the 120:1 mixture. The reported (23) proton affinities, $PA(C_2H_4O) = 183$ kcal mol^{-1} and $PA((CH_3)_2O) = 186$ kcal mol^{-1}, lead to a calculated equilibrium constant of 58 (for 373 °K, the approximate source temperature) assuming $\Delta S°$ is negligibly small.

Although this agreement supports the postulate of an equilibrium an alternative explanation is possible. The $C_2H_5O^+$ ion derived from ethylene oxide may have rearranged to structure **I** with the result that the experimental data really represent a steady-state achieved between reaction 26 and proton transfer from $(CD_3)_2OH^+$ to the oxide. These are two separate reactions which do not combine as a single reversible reaction and the steady-state conditions have no interpretation as a chemical equilibrium.

Although we are inclined to believe that the first explanation holds and that the different equilibrium constants for the ethylene oxide – ether and acetaldehyde ether systems indicate different structures for the $C_2H_5O^+$ ions, the results are not conclusive. More substantial evidence for the non-identity of the $C_2H_5O^+$ ions is obtained from the studies of the mixtures with acetone reported below.

In addition to the ions shown in Fig. 12 a small yield of the disolvated proton $((CD_3)_2O)(C_2H_4O)H^+$ was observed at high pressures and long reaction times in mixtures rich in ethylene oxide. This result is in contrast to the pure ethylene oxide system where no disolvated protons were observed even at the highest pressures used.

Can. J. Chem. Downloaded from www.nrcresearchpress.com by 210.87.254.42 on 09/05/12
For personal use only.

Can. J. Chem. Downloaded from www.nrcresearchpress.com by 210.87.254.42 on 09/05/12
For personal use only.

Acetaldehyde-d_4 – Acetone

This system was studied briefly to examine the reactions of CD_3CDOD^+ ions (structure **II**) with acetone. Results for a 3.9:1.0 mixture are shown in Fig. 13. Both CDO^+ and CD_3CDO^+ react with acetone to produce mainly $(CH_3)_2COD^+$. From the slope of the semi-logarithmic plot for CD_3CDO^+ we obtain, after correction for the $CD_3CDO^+ + CD_3CDO$ reaction, a rate coefficient of 3×10^{-10} cm^3 molecule^{-1} s^{-1} for the reaction of CD_3CDO^+ with acetone. Both CH_3CO^+ and CD_3CO^+ react with acetone only and we calculate rate coefficients of 3.0×10^{-10} and 2.6×10^{-10} cm^3 molecule^{-1} s^{-1}, respectively, in good agreement with the results obtained in pure acetone.

The CD_3CDOD^+ ion reacts rapidly and completely by D^+ transfer to acetone, the rate coefficient being 2.25×10^{-9} cm^3 molecule^{-1} s^{-1}. A complete reaction is to be expected since $PA((CH_3)_2CO)$ is at least 7 kcal mol^{-1} greater than $PA(CH_3CHO)$ (23). However, the result for this system is to be contrasted with the results obtained for the similar ethylene oxide – acetone system discussed below.

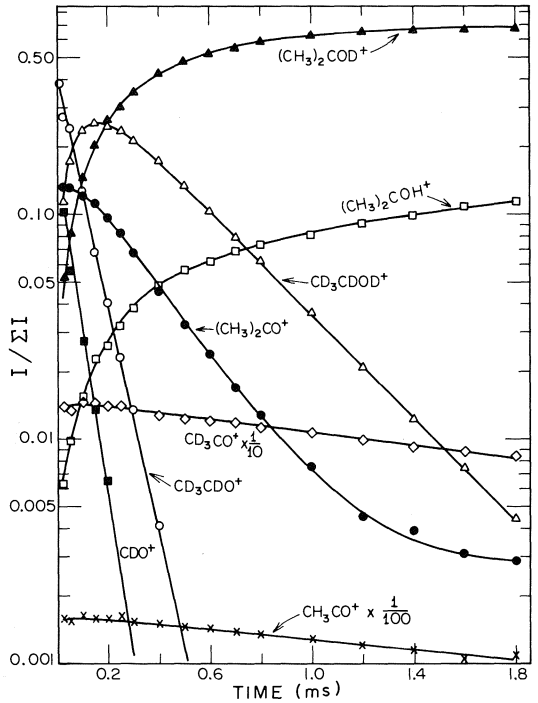

FIG. 13. Acetaldehyde-d_4 – acetone system, $[CD_3CDO] = 4.54 \times 10^{12}$ molecules cm^{-3}, $[CH_3COCH_3] = 1.16 \times 10^{12}$ molecules cm^{-3}.

Ethylene Oxide – Acetone

These mixtures were examined in an attempt to obtain quantitative information concerning the reaction of $C_2H_5O^+$ ions of structure **III** with acetone. Figures 14 and 15 present the results obtained in an 8:1 ethylene oxide – acetone mixture.

Several products are observed in this system which are not observed in acetaldehyde–acetone mixtures. A secondary ion is formed at *m/e* 72, shifting to *m/e* 74 in C_2D_4O–$(CH_3)_2CO$ mixtures, which corresponds to the addition of CH_2^+ to acetone (reaction 32).[9]

[32] $C_2H_4O^+ + (CH_3)_2CO \rightarrow C_4H_8O^+ + CH_2O$

A similar reaction between $C_2H_4O^+$ and acetaldehyde is also observed. A product ion is also observed at *m/e* 87, shifting to *m/e* 91 in C_2D_4O–$(CH_3)_2CO$ mixtures, which we attribute to the acetylation reactions 33 and 34.

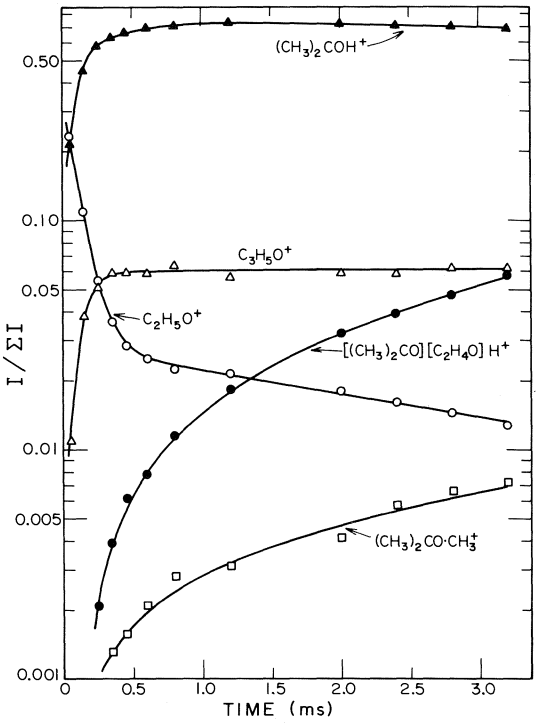

FIG. 14. Ethylene oxide – acetone system, $[C_2H_4O] = 4.96 \times 10^{13}$ molecules cm^{-3} $[CH_3COCH_3] = 0.63 \times 10^{13}$ molecules cm^{-3}.

[9] $C_4H_8O^+$ also appears to be formed by a further unidentified reaction since its intensity continues to rise slowly even after the $C_2H_4O^+$ ion has reacted completely.

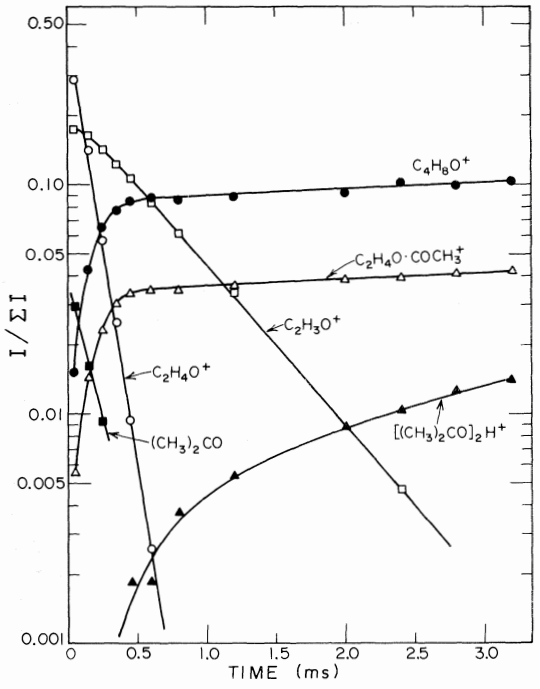

FIG. 15. Ethylene oxide – acetone system, conditions as for Fig. 14.

[33] $(CH_3)_2CO^+ + C_2H_4O \rightarrow C_2H_4O{\cdot}COCH_3^+ + CH_3$

[34] $(CH_3)_2COH^+ + C_2H_4O \rightarrow C_2H_4O{\cdot}COCH_3^+ + CH_4$

The latter reaction is included since the *m/e* 87 product intensity continues to increase after the $(CH_3)_2CO^+$ ion has reacted completely. Additional products are the disolvated proton $((CH_3)_2CO)(C_2H_4O)H^+$ (*m/e* 103) and $((CH_3)_2CO)_2H^+$ (*m/e* 117) observed in low yield at long reaction times.

As in the ethylene oxide – ether mixtures the rate of reaction of the $C_2H_5O^+$ ion could not be established accurately. As shown in Fig. 15 the $C_2H_5O^+$ intensity, which reached a maximum before 0.05 ms, initially decreases rapidly with a corresponding increase in $(CH_3)_2COH^+$. However, the reaction apparently does not go to completion and beyond 0.5 ms, the rate of decrease of the $C_2H_5O^+$ signal is much slower. Similar results were observed in 4:1 and 40:1 mixtures. The change in the rate of reaction cannot be due to the approach to a steady-state, as appears to be the case in the mixtures with $(CD_3)_2O$, since from the relative proton affinities (23) we calculate that the equilibrium in the proton transfer reaction should lie far to the side of protonated acetone ($K \approx 1 \times 10^4$).[10] Rather the change in rate of reaction appears to result from a change in structure of the $C_2H_5O^+$ ion.

There are two pieces of evidence which indicate that the slow reaction of $C_2H_5O^+$ at longer times represents reaction of structure **I** ions rather than structure **III** ions. In the region between 1.0 and 3.2 ms the linear semi-logarithmic plot for $C_2H_5O^+$ (Fig. 15) leads to a rate constant for the disappearance of $C_2H_5O^+$ of 4.2×10^{-11} cm^3 molecule^{-1} s^{-1} assuming reaction only with acetone.[11] An almost identical rate constant, 4.0×10^{-11} cm^3 molecule^{-1} s^{-1}, is obtained by a similar analysis of the results in a 4:1 mixture. Both these values are in good agreement with the value $k_{25} = 3.3 \pm 1.0 \times 10^{-11}$ cm^3 molecule^{-1} s^{-1} measured for the reaction in dimethyl ether – acetone mixtures. The occurrence of reaction 25

[25] $CH_3OCH_2^+ + (CH_3)_2CO \rightarrow (CH_3)_2CO{\cdot}CH_3^+ + CH_2O$

in the present system also is supported by the observation of a product species of *m/e* 73 ($(CH_3)_2CO{\cdot}CH_3^+$) which increases significantly over the time range from 1.0 to 3.2 ms (Fig. 14). In the 4:1 mixture where the decrease in $C_2H_5O^+$ over this time range is greater the *m/e* 73 intensity was considerably higher (maximum 2% of total ionization).

The mechanism by which $C_2H_5O^+$ ions of structure **I** are formed is not clear. It obviously must occur only in the mixtures with acetone since no reaction of $C_2H_5O^+$ by CH_3^+ addition was observed either in the pure ethylene oxide or ethylene oxide – $(CD_3)_2O$ systems.[12] A collision-induced isomerization is thermochemically permitted ($\Delta H_f(CH_3OCH_2^+)$) = 156 kcal mol^{-1} (26). $\Delta H_f(C_2H_4O{\cdot}H^+)$ = 170 kcal mol^{-1} (10), however, there is no apparent reason why it should be specific to the ethylene oxide – acetone

[10]Experimentally at long delay times we find that the ratio $[C_2H_4O]\,[(CH_3)_2COH^+]/[(CH_3)_2CO]\,[C_2H_5O^+]$ varies from 200 to 800 for the mixtures studied.

[11]The reaction of $C_2H_5O^+$ ions of either structure **I** or **III** with ethylene oxide is much slower.

[12]If the incomplete reaction of $C_2H_5O^+$ in ethylene oxide – $(CD_3)_2O$ mixtures was due to formation of $CH_3OCH_2^+$ ions the $C_2H_5O^+$ signal should not become constant but should continue to drop in Fig. 12 with the same slope as the $CD_3OCD_2^+$ signal.

Can. J. Chem. Downloaded from www.nrcresearchpress.com by 210.87.254.42 on 09/05/12
For personal use only.

Can. J. Chem. Downloaded from www.nrcresearchpress.com by 210.87.254.42 on 09/05/12
For personal use only.

mixture. Comparison with the results obtained in the acetaldehyde–acetone mixture shows once again differences for the $C_2H_5O^+$ ions formed in the two systems.

Ethylene Oxide – Acetaldehyde

The ionic reactions in the mixtures C_2H_4O–CH_3CHO, C_2D_4O–CH_3CHO, C_2H_4O–CD_3CDO, and C_2D_4O–CD_3CDO were examined. Figure 16, showing results for a 1:1 C_2D_4O:CH_3CHO mixture, is typical of the results obtained. In no case did we observe significant net proton transfer from one protonated form to the other neutral although the results from mixtures of each of the two components with $(CD_3)_2O$ do suggest that the proton affinity of ethylene oxide is slightly greater than the proton affinity of acetaldehyde.

From the rate of disappearance of CH_3CHO^+ we calculate that this ion reacts rapidly ($k = 1.9 \times 10^{-9}$ cm^3 molecule^{-1} s^{-1}) with C_2D_4O to produce both CH_3CHOD^+ and $C_2D_4OH^+$. This rapid rate of reaction rules out the possibility that the modified molecular ion $C_2H_4O^+$* produced in ethylene oxide (reaction 6) has the acetaldehyde structure since the rate of reaction 7 is much lower ($k_7 = 0.15 \times 10^{-9}$ cm^3 molecule^{-1} s^{-1}).

The plot of the $C_2D_4O^+$ ion current shows the characteristic sigmoid shape (compare Fig. 2) and it appears that $C_2D_4O^+$* is the major species reacting with acetaldehyde. From the linear region of the semi-logarithmic plot at longer reaction times we calculate $k \approx 6 \times 10^{-10}$ cm^3 molecule^{-1} s^{-1} for the reaction. The major product is $C_3H_4D_2O^+$ (*m/e* 60) whose graph of intensity *vs.* time shows an initial shape

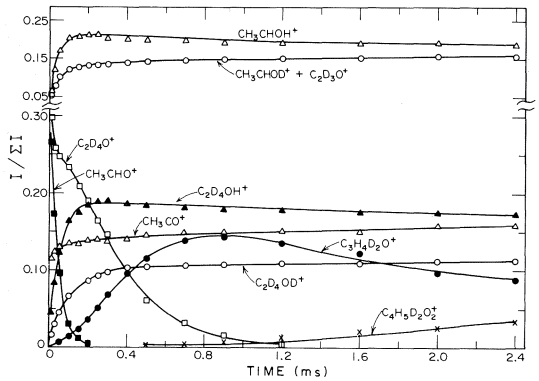

FIG. 16. Acetaldehyde – ethylene-d_4 oxide [CH_3CHO] = [C_2D_4O] = 5.49×10^{12} molecules cm^{-3}.

expected for the product of a sequential reaction series (compare $C_3H_5O^+$ in Fig. 2). The identity of the product was confirmed by the observation of the following reactions in the appropriate mixtures.

[35] $C_2H_4O^+ + CH_3CHO \rightarrow C_3H_6O^+$(*m/e* 58) $+ CH_2O$

[36] $C_2D_4O^+ + CH_3CHO \rightarrow C_3H_4D_2O^+$ (*m/e* 60) $+ CD_2O$

[37] $C_2H_4O^+ + CD_3CDO \rightarrow C_3H_2D_4O^+$ (*m/e* 62) $+ CH_2O$

[38] $C_2D_4O^+ + CD_3CDO \rightarrow C_3D_6O^+$ (*m/e* 64) $+ CD_2O$

The reaction clearly corresponds to $C(H,D)_2^+$ transfer from the reactant ion to the neutral acetaldehyde and occurs without isotopic mixing. The reaction is analogous to reaction 33 observed in ethylene oxide – acetone mixtures and thus appears to be typical of the reaction of ethylene oxide molecular ions with a carbonyl function.

The ions produced in reactions 35 to 38 react further in the isotopically specific reactions 39 to 42

[39] $C_3H_6O^+ + CH_3CHO \rightarrow C_4H_7O_2^+$ (*m/e* 87) $+ CH_3$

[40] $C_3H_4D_2O^+ + CH_3CHO \rightarrow C_4H_5D_2O_2^+$ (*m/e* 89) $+ CH_3$

[41] $C_3D_4H_2O^+ + CD_3CDO \rightarrow C_4D_5H_2O_2^+$ (*m/e* 92) $+ CD_3$

[42] $C_3D_6O^+ + CD_3CDO \rightarrow C_4D_7O_2^+$ (*m/e* 94) $+ CD_3$

which account for the major part of the $C_3(H,D)_6O^+$ ion which reacts. In each case the reaction corresponds to condensation of the ion with acetaldehyde and elimination of a methyl radical as the neutral fragment. Although the reactions are isotopically specific it cannot be determined from the present work whether the methyl radical is derived from the ionic or neutral reactant, however, it does not contain any of the hydrogens derived from the ethylene oxide precursor to the $C_3(H,D)_6O^+$ ion.

Conclusions

The present work has shown that in the one-component acetaldehyde, acetone, or dimethyl ether systems the monosolvated protons react

predominantly to form the disolvated proton. Under our conditions (up to 0.4 eV average ion kinetic energy) the reactions are third order with rate constants in the range 10^{-24} to 10^{-25} cm^6 molecule^{-2} s^{-1}. The rate coefficients for the thermal energy reactions should be even larger with the result that at moderate pressures in these systems extensive solvation of the proton should occur. The ethylene oxide system is unique in that no disolvated protons were observed, although in mixed systems solvates of the type $M(C_2H_4O)H^+$ ($M = (CD_3)_2O$ or $((CH_3)_2CO)$ were observed.

In two-component systems bimolecular reactions of the type

$$[43] \qquad M_1H^+ + M_2 \rightarrow M_2H^+ + M_1$$

occur rapidly if the proton affinity of M_2 is significantly greater than that of M_1 ($\sim$3 kcal mol^{-1}). The rate coefficients of several of these reactions have been measured and are in the range 1.0 to 2.2 $\times$ 10^{-9} cm^{-3} molecule^{-1} s^{-1}. Consequently in many of the mixed systems reaction 43 will be more rapid than the third order solvation reactions with the result that the latter reactions will involve mainly the M_2H^+ species.

In a number of systems the proton transfer reaction 43 did not go to completion but reached a steady-state or apparent equilibrium. Since there is little doubt that in our system the reactant species are not at thermal equilibrium the observation of a quasi-equilibrium situation illustrates the hazards of using such measurements to derive equilibrium constants and associated thermochemical data. Steady-state conditions appear to be relatively easy to attain, however, true equilibrium conditions may be much more difficult to attain.

The present work and i.c.r. work (10) both have shown that $C_2H_5O^+$ ions of structure **I** ($CH_3OCH_2^+$) undergo CH_3^+ transfer and, in some cases H^- abstraction reactions. However, in all cases studied a large fraction of the ion–molecule collisions are unreactive since the measured rate coefficients are in the 10^{-11} cm^3 molecule^{-1} s^{-1} range for CH_3^+ transfer and in the 10^{-10} cm^3 molecule^{-1} s^{-1} range for H^- abstraction. Neither in this work nor in the i.c.r. study (10) is there any evidence that $C_2H_5O^+$ ions of structure **I** undergo proton transfer reactions. Recently, Haney and Franklin (27) have proposed that ions of nominal structure **I** rearrange to structure **II** (CH_3CHOH^+) on formation from ethers by electron impact. The ion of structure **II** reacts rapidly by proton transfer and the failure of the $C_2H_5O^+$ ion from ethers to react similarly is strong evidence that the rearrangement has not occurred. Haney and Franklin's proposal was based on the measurement of the excess kinetic energy of the fragment ion at the appearance potential threshold. Assuming that the excess energy was randomized among all degrees of freedom they derived from the appearance potential, corrected for the excess energy involved, an ionic heat of formation for the $C_2H_5O^+$ ion of nominal structure **I** identical with the known value for ions of structure **II**. It is possible that in the work of Haney and Franklin (27) the assumption of complete randomization of the excess energy is not valid and that the fraction appearing as kinetic energy is correspondingly high.

The present work has revealed a number of unique features concerning the ionic reactions involving the molecular ion derived from ethylene oxide. The $C_2H_4O^+$ ion formed initially in the electron impact process is quite unreactive but apparently undergoes a rapid collisional modification to a more reactive species which reacts with neutral ethylene oxide to form $C_3H_5O^+$ and with carbonyl compounds by CH_2^+ addition. These reactions are not observed for $C_2H_4O^+$ (acetaldehyde) ions and the differences appear to provide a means of distinguishing between the two structures. However, one cannot rule out the possibility that these differences may arise from energy effects rather than structural effects since $\Delta H_f(\overline{CH_2—CH_2O^+}) =$ 231 kcal mol^{-1} while $\Delta H_f(CH_3CHO^+) = 196$ kcal mol^{-1} (25).

The authors are indebted to the National Research Council of Canada for financial support and for the award of studentships (1968–1971) to A.S.B.

1. M. S. B. Munson. J. Am. Chem. Soc. **87**, 5313 (1965).
2. H. Pritchard and A. G. Harrison. J. Chem. Phys. **48**, 5623 (1968).
3. J. C. J. Thynne, F. K. Amenu-Kpodo, and A. G. Harrison. Can. J. Chem. **44**, 1351 (1966).
4. H. Pritchard, J. C. J. Thynne, and A. G. Harrison. Can. J. Chem. **46**, 2141 (1968).
5. D. J. Hyatt, E. A. Dodman, and M. J. Henchman. Adv. Chem. Ser. **58**, 131 (1966).
6. J. O. Terry and T. O. Tiernan. Paper presented at 16th Annual Conference on Mass Spectrometry, Pittsburgh, 1968.

Can. J. Chem. Downloaded from www.nrcresearchpress.com by 210.87.254.42 on 09/05/12
For personal use only.

7. K. A. MacNeil and J. H. Futrell. J. Phys. Chem. **76**, 409 (1972).
8. J. M. S. Henis. J. Am. Chem. Soc. **90**, 844 (1968).
9. R. C. Dunbar. J. Chem. Phys. **52**, 2780 (1970).
10. J. L. Beauchamp and R. C. Dunbar. J. Am. Chem. Soc. **92**, 1477 (1970).
11. S. K. Gupta, E. G. Jones, A. G. Harrison, and J. J. Myher. Can. J. Chem. **45**, 3107 (1967).
12. N. A. McAskill and A. G. Harrison. Int. J. Mass Spectrom. Ion Phys. **5**, 193 (1970).
13. A. A. Herod, A. G. Harrison, and N. A. McAskill. Can. J. Chem. **49**, 2217 (1971).
14. A. S. Blair, E. J. Heslin, and A. G. Harrison. J. Am. Chem. Soc. **94**, 2935 (1972).
15. A. A. Herod and A. G. Harrison. Int. J. Mass Spectrom. Ion Phys. **4**, 415 (1970).
16. D. Van Raalte and A. G. Harrison. Can. J. Chem. **41**, 3118 (1963).
17. A. G. Harrison and B. G. Keyes. J. Am. Chem. Soc. **90**, 5046 (1968).
18. T. W. Shannon and F. W. McLafferty. J. Am. Chem. Soc. **88**, 5021 (1966).
19. F. W. McLafferty and H. D. R. Schuddemage. J. Am. Chem. Soc. **91**, 1866 (1969).
20. L. G. Leger, G. G. Meisels, and T. O. Tiernan. J. Chem. Phys. **52**, 4319 (1970).
21. G. Gioumousis and D. P. Stevenson. J. Chem. Phys. **29**, 294 (1958).
22. L. Hellner and L. W. Sieck. J. Res. Nat. Bur. Stds. **75A**, 487 (1971).
23. J. L. Beauchamp. Annu. Rev. Phys. Chem. **22**, 527 (1971).
24. A. G. Harrison, A. Ivko, and D. Van Raalte. Can. J. Chem. **44**, 1625 (1966).
25. Ionization potentials, appearance potentials, and heats of formation of gaseous positive ions. NSRDS-NBS *26*, Washington, D.C. 1969.
26. C. D. Finney and A. G. Harrison. Int. J. Mass Spectrom. Ion Phys. **9**, 221 (1972).
27. M. A. Haney and J. L. Franklin. Trans. Faraday Soc. **65**, 1794 (1969).

Can. J. Chem. Downloaded from www.nrcresearchpress.com by 210.87.254.42 on 09/05/12
For personal use only.

Computer-assisted Generation of IUPAC Names of Polycyclic Bridged Ring Systems

D. VAN BINNENDYK AND A. C. MACKAY

Canada Packers Limited, Research and Development Laboratories, 2211 St. Clair Avenue West, Toronto, Ontario

Received January 28, 1972[1]

A computer program for the generation of IUPAC names of polycyclic bridged ring systems has been devised. It enables the names of complex molecules to be arrived at easily from conventionally drawn structures.

On a mis au point un programme qui, à l'aide d'ordinateur peuvent dégénérer les noms systématiques (UICPA) de composés polycicliques. Ce programme permet de trouver facilement les noms de molécules complexes en faisant appel aux structures représentées d'une manière conventionnelle.

[Traduit par le journal]

Can. J. Chem., **51**, 718 (1973)

Can. J. Chem. Downloaded from www.nrcresearchpress.com by 210.87.254.6 on 09/05/12
For personal use only.

In 1966 it was pointed out by Meinwald and Crandall (1) that the IUPAC rules for the nomenclature of bridged polycyclic hydrocarbons (2) were not being complied with by all authors. More recently, Eckroth (3) has reported on a method intended to facilitate the generation of correct names for "von Bayer hydrocarbons". In spite of these papers, erroneous names for bridged ring compounds continue to appear in the literature (4, 5, 6) (see Table 1).

The IUPAC rules (2) may be summarized:

(*1*) Select as the *main ring* the ring that has the greatest number of atoms.

(*2*) Select as the *main bridge* the bridge spanning the main ring that has the greatest number of atoms; if there is a choice between two or more bridges of equal length select the bridge which divides the main ring most symmetrically.

(*3*) The system is now numbered along the longest arm of the main ring such that the superscripts describing the location of the other bridges are as low as possible.

Considering each of the rules in turn, while the first appears to be straightforward, it is not obvious that for a given compound there may be several ways in which the main ring may be generated. The possibilities for **4** (**5–8**) are illustrated and each of these must be considered in turn in arriving at the best name for the molecule. The second rule can result in several more possible names being generated, especially if two or more bridges fulfil the requirements of the rule. As far as the third rule is concerned, Eckroth (3) has already noted that there are three possible interpretations:

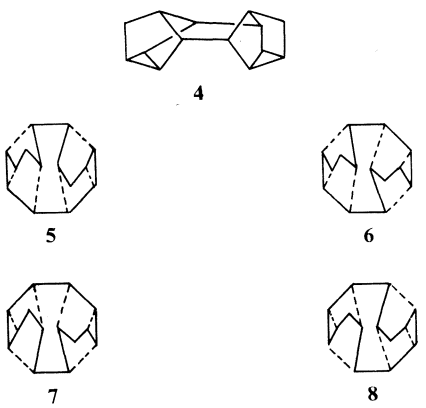

(*a*) The name selected will have, at the first difference in the first of the superscripts, the lower number. If this does not result in a discrimination between two different names, then the second superscripts are considered.

(*b*) Only the first superscripts are considered and if this does not enable a choice to be made, then selection is made on the basis of position of substituents or other features of the molecule such as a site of unsaturation.

(*c*) Chemical Abstracts uses the lower at the first possible difference of either of each pair of superscripts.

By following (*a*) above, which he suggests be adopted by IUPAC, a suggestion endorsed by the present authors, Eckroth gives **4** the name *endo,cis,endo*-heptacyclo[8.4.0.$0^{2,12}$.$0^{3,7}$.$0^{4,9}$.$0^{6,8}$.$0^{11,13}$]tetradecane. However, by selecting an

[1]Revision received August 23, 1972.

TABLE 1. Correct and erroneous names for some bridged ring compounds

Compound	Reference	Assigned name	Correct name
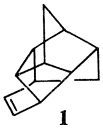 1	4	Pentacyclo[7.2.1.$0^{2,8}$.$0^{3,11}$.$0^{6,10}$]-dodec-4-ene	Pentacyclo[5.5.0.$0^{2,6}$.$0^{3,10}$.$0^{4,8}$]-dodec-11-ene
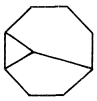 2	5	Tricyclo[6.1.0.$0^{5,9}$]nonane	Tricyclo[4.3.0.$0^{2,9}$]nonane
3	6	Tetracyclo[5.2.1.$0^{2,6}$.$0^{3,10}$]-deca-4,8-diene	Tetracyclo[4.4.0.$0^{2,8}$.$0^{3,7}$]-deca-4,9-diene

alternative main ring (**6** as opposed to **5**) a better name may be arrived at: *endo,cis,endo*-heptacyclo[8.4.0.0^{2,12}.0^{3,8}.0^{4,6}.0^{5,9}.0^{11,13}]tetradecane.

If no decision has been reached for the name by this stage, the position of hetero atoms and substituents may be taken into consideration.

With the synthesis of increasingly complex molecules, the generation of the correct name becomes correspondingly more difficult and time-consuming.

In light of the ever increasing use of automated systems for the retrieval of information, it is more than ever desirable that authors name their compounds correctly along the lines recommended by IUPAC. Without this, chemistry, and particularly the chemistry of bridged ring systems, will become hopelessly confused and information irretrievably buried; this should be self-evident since formula indices locate specific compounds, not members of a given system. Eckroth's paper only serves to emphasize the difficulties encountered in the manual generation of IUPAC names. Conversion of familiar three-dimensional representations into Schlegel diagrams (7) is not always easy and requires considerable practice. Furthermore, once the molecule is represented in this way, there is no assurance that the investigator will obtain the best possible name. However, conversion of the 3-D representation into a planar graph serves to change the point of view of the investigator and thus assists in a more objective analysis. Symmetrical molecules are particularly amenable to this method of name generation.

Conrow (8) reported in 1966 a Fortran program for the computer generation of IUPAC names for bridged bicyclic, tricyclic, and tetracyclic hydrocarbons. Its most severe limitation is that polycyclic compounds having more than four rings are excluded. Furthermore, in the case of a tetracyclic compound that is topologically twisted, absurd names are generated. The input required is in the form of a connection matrix; however, this limitation could be overcome by supplying simpler data together with a program for the generation of the connective matrix. Finally, quaternary atoms in the molecule under consideration result in no further processing of the name.

In noting the deficiencies of the above methods of name generation, it was felt that in order to consider exhaustively all possible names for a given system, a more comprehensive computer program would be necessary. A Fortran program[2] has now been written which will facilitate the generation of the correct IUPAC name for polycyclic bridged ring systems. The use of the program can be illustrated for a simple example. The molecule is drawn as usual. *e.g.*

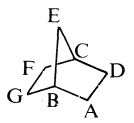

9

[2]A listing of the program may be obtained on request from the authors.

Can. J. Chem. Downloaded from www.nrcresearchpress.com by 210.87.254.6 on 09/05/12
For personal use only.

Can. J. Chem. Downloaded from www.nrcresearchpress.com by 210.87.254.6 on 09/05/12
For personal use only.

The carbon atoms forming the ring system are labelled alphabetically in any order. All of the bonds (with AB and BA regarded as separate bonds) are written down and counted. In preparing the list of atoms for the computer, the first atom in the list should be the tertiary or quarternary carbon dividing the longest chain of secondary carbon atoms incorporated in the bridged ring system. In cases of multiple choice, any one of the equivalents may be selected. (In Table 2 these atoms have been circled.) This ensures that the computer will determine the correct main ring. As described below, the computer starts its search for the best main ring from the first tertiary or quaternary carbon mentioned on the list. In the following example, listing from A, the best name will not be obtained. Starting the search from B, which fulfills the above condition, will give the correct name.

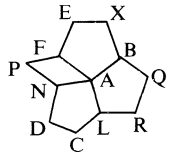

The above example is the only case encountered where the restriction on starting point has been found important. Other examples considered to date have given the correct IUPAC name in the list of names produced by random choice of starting point. On supplying these data, and the program, to the computer, the following output is obtained:

(*a*) The sequence of atoms in the main ring is printed and any atoms not part of the main ring are identified and printed.

(*b*) The bonds not used in the main ring are identified and printed.

(*c*) If two or more atoms are excluded from the main ring, the name has to be generated from the above data.

(*d*) If all, or all but one, atoms are involved in the main ring, the main bridge is selected by the computer and the name of the ring system is generated.

Some further elaboration of the above points is necessary, considering each in turn. Point (*a*) is the essential function of the computer program. The identification of the sequence of atoms in the main ring is accomplished by the complete enumeration of all possible rings. The first tertiary or quaternary atom given on the input list is selected as a starting point. There are then three or four possible starting routes, which are stored in computer memory. Proceeding to the second atom on the first route, it is determined (*i*) if secondary, the route is augmented with the third atom or (*ii*) if tertiary, a fourth route, from the original starting point, is enumerated or (*iii*) if quaternary, two additional routes must be enumerated. The program will continue in this way, enumerating all possible routes. If a route returns to the original starting point, thus becoming a ring, but other routes still continue, that ring is eliminated thus sparing computer storage. Similarly eliminated is any route which cannot proceed except by doubling back on itself. The storage of all possible routes takes up a large portion of the computer memory. For example, with the IBM 360 Model 40 computer used for this work, with a 100 k memory, it was found that a maximum of approximately 900 routes could be stored. This could be increased by using disk storage, or breaking down the analysis into parts, but the 900 routes were found to be sufficient for the analysis of some of the more complex polycyclic compounds given in the literature. The time taken on the computer also increases to a significant amount, that is, to 10 min and more, when analyzing nonacyclic compounds. When the program has run to completion, all routes are eliminated and those last to return to the original starting point are printed out as the longest. This method will generate twice the number of *different* possible rings fitting IUPAC rule no. 1 above; the factor 2 takes into account the necessity to discriminate between clockwise and anti-clockwise progression round the ring. Point (*b*) requires no further discussion. While (*c*) appears to be a definite limitation, most of the errors in naming bridged polycyclic ring systems seem to arise from the failure of the authors concerned to find the main ring in their molecules. It is a relatively simple matter to generate the name, given a complete list of the main rings (see example 1). For molecules fitting the criteria of (*d*), names are printed for each main ring generated. From the list of names printed, a selection may be made by inspection. Further refinement at this stage resulting in a single name being chosen by the computer does not seem advisable until one of the alternatives of IUPAC rule no. 3 is generally accepted.

As has been mentioned above, many of the wrong names found in the literature appear to

TABLE 2. Computer-generated names

Structure	Total number of names generated	Detail of different names generated
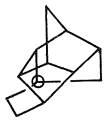	4	*Pentacyclo[5.5.0.0^{2,6}.0^{3,10}.0^{4,8}]dodecane Pentacyclo[5.5.0.0^{2,10}.0^{4,9}.0^{8,12}]dodecane Pentacyclo[5.5.0.0^{2,6}.0^{4,12}.0^{5,10}]dodecane Pentacyclo[5.5.0.0^{4,11}.0^{6,10}.0^{8,12}]dodecane
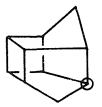	16	Pentacyclo[5.3.0.0^{3,6}.0^{4,10}.0^{5,8}]decane Pentacyclo[5.3.0.0^{2,5}.0^{3,10}.0^{4,8}]decane *Pentacyclo[5.3.0.0^{2,5}.0^{3,9}.0^{4,8}]decane Pentacyclo[5.3.0.0^{2,6}.0^{3,10}.0^{5,9}]decane Pentacyclo[5.3.0.0^{2,6}.0^{4,10}.0^{5,8}]decane Pentacyclo[5.3.0.0^{2,6}.0^{3,9}.0^{5,8}]decane Pentacyclo[5.3.0.0^{3,6}.0^{4,10}.0^{5,9}]decane Pentacyclo[5.3.0.0^{2,6}.0^{3,10}.0^{4,8}]decane
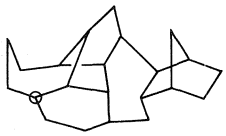	2	Heptacyclo[17.2.1.0^{2,18}.0^{4,13}.0^{7,14}.0^{11,15}.0^{12,17}]docosane *Heptacyclo[17.2.1.0^{2,18}.0^{3,8}.0^{5,9}.0^{6,13}.0^{7,16}]docosane
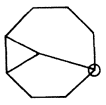	2	*Tricyclo[4.3.0.0^{2,9}]nonane Tricyclo[4.3.0.0^{5,7}]nonane
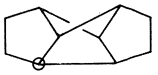	4	*Tetracyclo[4.4.0.0^{2,8}.0^{3,7}]decane Tetracyclo[4.4.0.0^{4,10}.0^{5,9}]decane
	12	Pentacyclo[4.3.0.0^{2,5}.0^{3,9}.0^{4,7}]nonane Pentacyclo[4.3.0.0^{2,5}.0^{3,9}.0^{4,8}]nonane *Pentacyclo[4.3.0.0^{2,5}.0^{3,8}.0^{4,7}]nonane
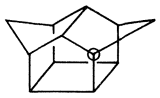	20 (18)	Hexacyclo[5.4.1.0^{2,6}.0^{3,10}.0^{4,8}.0^{9,12}]dodecane Hexacyclo[5.4.1.0^{2,6}.0^{3,10}.0^{5,9}.0^{8,11}]dodecane Hexacyclo[5.4.1.0^{2,6}.0^{4,11}.0^{5,9}.0^{10,12}]dodecane Hexacyclo[5.4.1.0^{3,10}.0^{4,12}.0^{5,9}.0^{8,11}]dodecane *Hexacyclo[5.4.1.0^{2,8}.0^{3,7}.0^{4,11}.0^{6,10}]dodecane
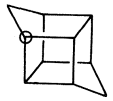	16	Pentacyclo[5.3.0.0^{2,6}.0^{4,10}.0^{5,9}]decane *Pentacyclo[5.3.0.0^{2,6}.0^{3,9}.0^{4,8}]decane
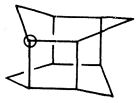	16	*Pentacyclo[6.4.0.0^{2,7}.0^{4,11}.0^{5,10}]dodecane
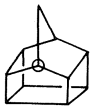	4	*Pentacyclo[5.4.0.0^{2,6}.0^{3,10}.0^{5,9}.0^{8,11}]undecane
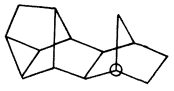	4	Hexacyclo[9.2.1.0^{2,10}.0^{3,7}.0^{4,9}.0^{6,8}]tetradecane *Hexacyclo[9.2.1.0^{2,10}.0^{3,8}.0^{4,6}.0^{5,9}]tetradecane

Can. J. Chem. Downloaded from www.nrcresearchpress.com by 210.87.254.6 on 09/05/12
For personal use only.

TABLE 2 (*Continued*)

Structure	Total number of names generated	Detail of different names generated
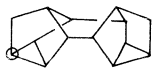	16	Heptacyclo[8.4.0.$0^{2,7}$.$0^{3,5}$.$0^{4,8}$.$0^{9,13}$.$0^{12,4}$]tetradecane *Heptacyclo[8.4.0.$0^{2,12}$.$0^{3,7}$.$0^{4,9}$.$0^{6,8}$.$0^{11,13}$]tetradecane Heptacyclo[8.4.0.$0^{2,12}$.$0^{3,8}$.$0^{4,6}$.$0^{5,9}$.$0^{11,13}$]tetradecane Heptacyclo[8.4.0.$0^{2,6}$.$0^{3,8}$.$0^{5,7}$.$0^{9,13}$.$0^{12,4}$]tetradecane
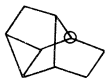	8	Tetracyclo[4.3.0.$0^{2,9}$.$0^{3,7}$]nonane Tetracyclo[4.3.0.$0^{3,5}$.$0^{4,9}$]nonane Tetracyclo[4.3.0.$0^{4,9}$.$0^{5,7}$]nonane *Tetracyclo[4.3.0.$0^{2,4}$.$0^{3,7}$]nonane
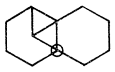	4	Tetracyclo[5.4.0.$0^{1,6}$.$0^{5,7}$]undecane Tetracyclo[5.4.0.$0^{2,7}$.$0^{2,11}$]undecane *Tetracyclo[5.4.0.$0^{1,3}$.$0^{2,7}$]undecane Tetracyclo[5.4.0.$0^{1,6}$.$0^{6,8}$]undecane
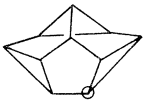	12	Hexacyclo[4.4.0.$0^{2,4}$.$0^{3,9}$.$0^{5,7}$.$0^{8,10}$]decane *Hexacyclo[4.4.0.$0^{2,10}$.$0^{3,5}$.$0^{4,8}$.$0^{7,9}$]decane
	4	Tricyclo[3.2.1.$0^{4,6}$]octane *Tricyclo[3.2.1.$0^{2,7}$]octane

*IUPAC names.

have arisen through incorrect choice of the main ring. The program may be divided, giving a sub-program which will generate with greatly reduced computer memory requirements, only the possible main rings. Thus smaller computers may be employed to overcome one of the major obstacles to correct nomenclature in bridged ring systems. For extremely complex cases, even with this reduced memory requirement, the number of possible routes being considered by the computer may exceed the space available.

A few ring systems subjected to this method of name generation are shown in Table 2.

Example 1: Manual Generation of the IUPAC Name from the Main Rings

Schleyer *et al.* (9) reported the synthesis of **I** to which they assigned the name nonacyclo-[11.7.1.1^{2,18}.$0^{3,16}$.$0^{4,13}$.$0^{5,10}$.$0^{6,14}$.$0^{7,11}$.$0^{15,20}$]-docosane. Computer print-out was in the form depicted in Chart 1. A total of 16 entries was

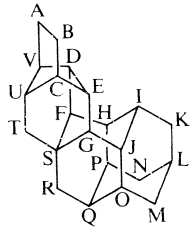

I

FOR THE MAIN RING OF 20 ATOMS, NAMELY
CUTSRQPHIKLMOJGEDVAB

THE NUMBER OF ATOMS NOT IN
THE MAIN RING 2
F N

THE FOLLOWING BONDS WERE NOT USED
20 CE DF EZ FD FH FS GS HF IJ JI LN NL
NP OZ PN QO SF SG UV VU

CHART 1

obtained; this represents eight pairs, thus after excluding one from each pair, eight rings have to be considered. The steps followed were:

(*1*) Determine if any two atoms not in the main ring were joined; in this example they were not.

(*2*) For each of the eight rings, consider in turn each of the atoms as the main bridge in order to determine the most symmetrical bridge; in this example F forms the main bridge.

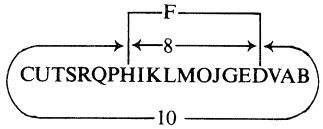

(*3*) Insert the remaining atom and the missing links then number the molecule in accordance with IUPAC rule 3 above:

Can. J. Chem. Downloaded from www.nrcresearchpress.com by 210.87.254.6 on 09/05/12
For personal use only.

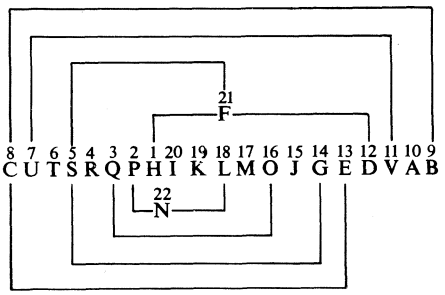

(4) The name of the compound, by inspection, is thus: nonacyclo[10.8.1.1^{2,18}.0^{3,16}.0^{5,14}.0^{5,21}-.0^{7,11}.0^{8,13}.0^{15,20}]docosane, which, according to the IUPAC rules is a more acceptable name than the one assigned by the authors.

In all the literature examples of bridged ring systems examined, in no case has the computer, controlled by this program, failed to make it possible to produce a name, as good as or better than the literature name.

In the case of the first compound in Table 2 only one main ring is found by the computer. Four names are generated since the main bridge divides the main ring equally and thus it is theoretically possible to start numbering from either bridgehead and to proceed in either direction. While programming the computer to produce a single name would be straightforward, the current confused situation with IUPAC rule 3 makes it expedient that all possible names be listed.

Dr. T. F. Massiah is cordially thanked for his interest and encouragement throughout the course of this work.

1. J. MEINWALD and J. K. CRANDALL. J. Am. Chem. Soc. **88**, 1292 (1966).
2. IUPAC nomenclature of organic chemistry, 1957. Butterworth and Co. Ltd., London. 1958.
3. D. R. ECKROTH. J. Org. Chem. **32**, 3362 (1967).
4. I. A. AKHTAR, D. M. BRATBY, and G. I. FRAY. J. Chem. Soc. C, 2716 (1968).
5. J. K. CRANDALL and R. J. WATKINS. Tetrahedron Lett. 1251 (1971).
6. R. M. SMITH, R. WEST, and V. MARK. J. Am. Chem. Soc. **93**, 3621 (1971).
7. A. F. WELLS. The third dimension in chemistry. Oxford University Press, London. 1956. p. 28.
8. K. CONROW. J. Chem. Doc. **6** (4), 206 (1966).
9. P. VON R. SCHLEYER, E. OSAWA, and M. G. B. DREW. J. Am. Chem. Soc. **90**:18, 5035 (1968).

Can. J. Chem. Downloaded from www.nrcresearchpress.com by 210.87.254.6 on 09/05/12
For personal use only.

Photolyse du pentène-1 dans l'ultraviolet à vide

PATRICK M. PERRIN ET GUY J. COLLIN

Département des Sciences Pures, Université du Québec à Chicoutimi, Chicoutimi, Québec

Reçu le 24 août 1972

La décomposition de la molécule pentène-1 excitée produite dans la photolyse aux raies de résonnance du xénon (8.4 eV) et du krypton (10.0 eV), a été étudiée. Les principaux produits de décomposition sont l'éthylène, l'allène, le butadiène-1,3, et l'acétylène ainsi que d'autres produits mineurs. Les atomes d'hydrogène s'additionnent sur la double liaison du monomère et forment ainsi un radical pentyle excité, qui se décompose en propène et radical éthyle à très basse pression ($P < 1$ Torr). Enfin l'isomérisation de la molécule excitée pentène-1 à ces énergies est de peu d'importance.

Photolysis of 1-pentene molecules at 8.4 eV (xenon photolysis) and 10.0 eV (krypton photolysis) was studied. Excited molecules decompose to produce mainly ethylene, propadiene, 1,3-butadiene, acetylene, and other minor products. Hydrogen atoms add to the double bond of the monomer and the resulting excited pentyl radical decomposes at low pressure ($P < 1$ Torr) into propene and ethyl radical. Isomerization of excited 1-pentene molecules is unimportant at these energies.

Can. J. Chem., **51**, 724 (1973)

Introduction

Nous avons récemment étudié la photolyse dans l'u.v. lointain des *cis*- et *trans*-butène-2 (1) et du butène-1 (2). L'étude du pentène-1 est un prolongement de ces travaux. Nous avons étudié l'importance des réactions de dégradation de la molécule de pentène-1 excitée, les réactions de recombinaisons radicalaires et la fragmentation des radicaux pentyles formés dans l'addition des atomes d'hydrogène sur la double liaison. L'effet de l'hydrogène sulfuré, comme intercepteur de radicaux vinyles en particulier, était au centre de nos préoccupations.

Procédés expérimentaux

Toutes les expériences de photolyse du pentène-1 ont été effectuées, en utilisant l'émission photonique dans l'u.v. lointain, produite par une lampe contenant du xénon ou du krypton sous faible pression, excitée à l'aide d'une antenne micro-onde. Ces lampes ont été décrites (3) et leurs caractéristiques ont été rappelées dans la littérature (1, 4). Au cours des irradiations du pentène-1 seul, ou en présence d'hélium ou d'oxygène, nous n'avons pas observé de baisse de rendement appréciable de la lampe. Par contre, dans les irradiations en présence d'hydrogène sulfuré, il se forme un dépôt de soufre sur la fenêtre cristalline que l'on nettoie périodiquement avec du disulfure de carbone. L'actinométrie a été faite comparativement à celle de l'isobutylène (5).

Le pentène-1 provient de Chemical Sample Co.; il a été purifié par chromatographie. Le pentène-1 perdeutéré a été fourni par Merck, Sharp and Dohme of Canada. L'hydrogène sulfuré et l'oxygène, fournis par les établissements Matheson, ont été utilisés après dégasage sur un système à haut vide. Les irradiations sont analysées par c.p.g. sur des colonnes de squalane et d'alumine. Les produits de l'irradiation des mélanges perdeutérés ont été piégés à la sortie du chromatographe à basse température et analysés séparément dans un spectromètre de masse CEC 21-104.

Résultats

L'irradiation du pentène-1 a été menée à des énergies de 8.4 eV (147 nm) et 10.0 eV (123.6 nm) dans les domaines de pression variant de 0.015–100 Torrs (tableaux 1 et 2).

Les figs. 1 et 2 montrent la variation du rendement de certains produits relativement au pentène en fonction du temps d'irradiation. La pente de ces courbes représente leur vitesse de formation et elle est constante. Il n'y a donc pas de réaction secondaire provenant de l'interaction des photons et des produits réactionnels. Cela reste valable tant que le temps d'irradiation reste inférieur à 100 min pour l'intensité utilisée. Le taux de conversion du pentène est alors de 1% environ. Au delà de ce délai, la pente des courbes diminue et le rendement quantique des produits décroît. Les autres résultats sont résumés dans les tableaux et figures qui suivent.

Discussion

Le potentiel d'ionisation du pentène normal est de 9.5 eV (6). Donc à 123.6 nm, soit 10.0 eV, une part importante des molécules excitées conduisent à l'ionisation et forment ainsi l'ion $C_5H_{10}^+$. Comme aucun effet de capteurs d'ions positifs ou d'électrons n'a été observé, il faut en conclure que les processus de réactions ioniques qui ont lieu à 123.6 nm ne participent pas à la formation des produits étudiés ici. Les seules

Can. J. Chem. Downloaded from www.nrcresearchpress.com by 210.87.254.6 on 09/05/12
For personal use only.

TABLEAU 1. Rendements quantiques dans l'irradiation du pentène-1 (λ = 147 nm)

Pentène-1[a]	0.4	0.4	0.4	1.5	1.5	1.5	1.32	1.32	1.32
O_2[a]	—	0.04	—	—	0.15	—	—	0.13	—
H_2S[a]	—	—	0.08	—	—	0.08[b]	—	—	0.07[b]
He[a]	—	—	—	—	—	—	100	100	100
CH_4	0.01_5	—	0.22	0.02_5	—	0.22_4	0.01_8	0.00_4	0.22_2
C_2H_2	0.05_1	0.03_3	0.04_3	0.05_3	0.03_3	0.03_7	0.06_8	0.05_8	0.08
C_2H_4	0.40_5	0.40	0.45_8	0.40	0.40	0.53_5	0.46	0.44_7	0.63
C_2H_6	0.05_5	0.00_8	0.51_5	0.05_5	0.01	0.37_5	0.06_7	0.01	0.31
C_3H_6	0.28_5	0.27	0.33_3	0.15_6	0.15_7	0.21_4	0.05_6	0.04_1	0.05_6
C_3H_8 / C_3H_4[c]	0.07_8	0.01_8	0.06_1	0.07	0.01_2	0.06	0.07_1 / 0.00_6	0.01_2 / 0.00_6	0.06[o]
C_3H_4[d]	0.128	0.128	0.128	0.128	0.128	0.128	0.128	0.128	0.128
C_4H_6[e] / C_4H_8[f]	0.16_3	0.13_2	0.01_3	0.16_4	0.13_8	0.02_2	0.17_5[h] / 0.03_7	0.145[h] / 0.01_2	0.03
n-C_4H_{10}	0.09_2	0.00	0.00	0.06_5	0.00	0.00	0.03_3	0.00	0.00
C_5H_8[g]	0.03_3	0.03_3	0.02	0.04_5	0.04_5	0.04_5	0.06	0.06	0.06
n-C_5H_{12}	0.03_1	0.00	0.035	0.08_4	0.00	0.91	0.13	0.00	0.70

[a]En Torr.
[b]Ces expériences ont été faites avec 5, 10, et 20% d'H_2S. Les trois résultats sont comparables.
[c]Propyne.
[d]Allène.
[e]Butadiène-1,3 + butyne-1.
[f]Butène-1 + isobutène.
[g]Pentadiènes-1,3 et -1,4.
[h]Butadiène-1,3.

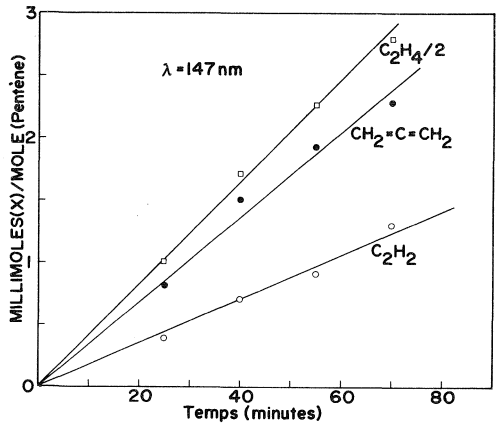

FIG. 1. Rendements relatifs en fonction du temps d'irradiation (pression, 100 Torr).

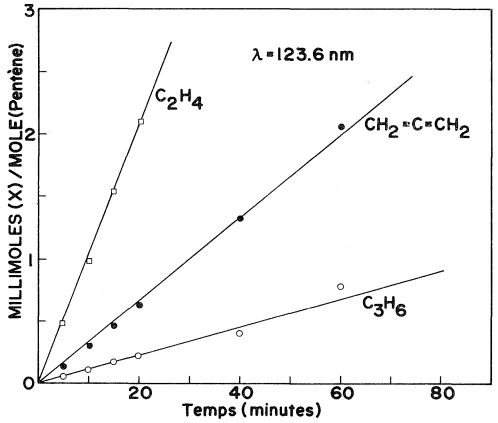

FIG. 2. Rendements relatifs en fonction du temps d'irradiation (pression, 100 Torr).

réactions retenues seront celles de la décomposition de la molécule de pentène excitée (éq. 1).

[1] $$C_5H_{10}\text{-}1 + h\nu \rightarrow (C_5H_{10})^{**}$$

L'énergie emmagasinée par la molécule est de 194 kcal mol^{-1} à 147.0 nm et 231 kcal mol^{-1} à 123.6 nm. Statistiquement, une importante partie de cette énergie peut se localiser au voisinage d'une liaison C—C ou d'une liaison C—H et en provoquer la rupture. Ces réactions sont très rapides et interviennent avant une collision moléculaire, du moins dans le domaine de pression étudié ici. Les rendements des produits ainsi obtenus sont indépendants de la pression et ne sont pas affectés par la présence de faibles proportions d'additifs (0, 10%). En général, les réactions de fragmentation sont donc de la forme de l'éq. 2. R_1 est un fragment radicalaire

[2] $$(C_5H_{10})^{**} \rightarrow R_1 + R_2^*$$

stable, et R_2 est un fragment radicalaire excité. Rompre une liaison C—H nécessite environ 100 kcal mol^{-1} et une liaison C—C, 90 kcal mol^{-1}. Il reste donc une quantité suffisante pour que l'un des deux fragments se scinde à son tour et globalement la molécule de pentène produira

Can. J. Chem. Downloaded from www.nrcresearchpress.com by 210.87.254.6 on 09/05/12
For personal use only.

Can. J. Chem. Downloaded from www.nrcresearchpress.com by 210.87.254.6 on 09/05/12
For personal use only.

TABLEAU 2. Rendement quantique dans l'irradiation du pentène-1 ($\tilde{\lambda}$ = 123.6 nm)

n-Pentène-1	Additif (Torr)	CH_4	C_2H_2	C_2H_4	C_2H_6	C_3H_6	C_3H_8 + C_3H_4[a]	C_3H_4[b]	C_4H_6[c] + C_4H_8[d]	*n*-C_4H_{10}	C_5H_8[e]	*n*-C_5H_{12}
1.32	—	0.049	0.103	0.45	0.089	0.29	0.096	0.190	0.155	0.059	0.020	0.018
1.32	O_2:0.07	0.033	0.100	0.43	0.025	0.26	0.018_5	0.190	0.103	0.0	0.015	nm[f]
1.32	O_2:0.07 He:100	0.020_6	0.093	0.46	0.026	0.078	0.017	0.190	0.163	0.0	0.018_5	0.0

[a]Propyne.
[b]Allène.
[c]Butadiène-1,3 + butyne-1.
[d]Butène-1 + isobutène.
[e]Pentadiènes-1,3 + -1,4.
[f]Non mesuré.

TABLEAU 3. Photolyse du mélange C_5H_{10}:C_5D_{10} (1:1) (λ = 123.6 nm); analyses isotopiques

Composé: R	R-d_0	R-d_1	R-d_3	R-d_4	R-d_5	R-d_6	R-d_8	R-d_{10}
Ethylène	66.2	—	—	33.8				
Allène	67	—	—	33				
Propène	44	33	—	—	9.5	12.6		
Propane	37	—	22	—	22	—	18	
Butyne-1 + butadiène-1,3	64.5	—	—	—	—	35.5		
Butène-1 + isobutène	32.7	—	26.4	—	24.6	—	16.3	
n-Butane	50±25	—	—	—	40±10	—	—	10

deux fragments radicalaires et un élément composé moléculaire stables. Les réactions 3–8 rendent compte de la dégradation de la molécule de pentène-1 excitée.

[3*a*] $(C_5H_{10})^{**} \rightarrow 2H\cdot + C_5H_8$ ΔH = 135 kcal mol^{-1}

[3*b*] $(C_5H_{10})^{**} \rightarrow H_2 + C_5H_8$ ΔH = 30 kcal mol^{-1}

[4*a*] $(C_5H_{10})^{**} \rightarrow H\cdot + CH_3\cdot + C_4H_6$ ΔH = 115 kcal mol^{-1}

[4*b*] $(C_5H_{10})^{**} \rightarrow CH_4 + C_4H_6$ ΔH = 15 kcal mol^{-1}

[5*a*] $(C_5H_{10})^{**} \rightarrow H\cdot + C_2H_5\cdot + C_3H_4$ ΔH = 126 kcal mol^{-1}

[5*b*] $(C_5H_{10})^{**} \rightarrow C_2H_6 + C_3H_4$ ΔH = 30 kcal mol^{-1}

[6*a*] $(C_5H_{10})^{**} \rightarrow H\cdot + C_3H_7\cdot + C_2H_2$ ΔH = 133 kcal mol^{-1}

[6*b*] $(C_5H_{10})^{**} \rightarrow C_3H_8 + C_2H_2$ ΔH = 34 kcal mol^{-1}

[7*a*] $(C_5H_{10})^{**} \rightarrow H\cdot + \cdot C_2H_3 + C_3H_6$ ΔH = 145 kcal mol^{-1}

[7*b*] $(C_5H_{10})^{**} \rightarrow H\cdot + \cdot C_3H_5 + C_2H_4$ ΔH = 100 kcal mol^{-1}

[7*c*] $(C_5H_{10})^{**} \rightarrow C_3H_6 + C_2H_4$ ΔH = 22.5 kcal mol^{-1}

[8] $(C_5H_{10})^{**} \rightarrow \cdot CH_3 + \cdot C_2H_3 + C_2H_4$ ΔH = 132 kcal mol^{-1}

Les tableaux 1 et 2 montrent que la plupart des produits analysés ont des rendements indépendants de la pression. Ils montrent aussi que les réactions de fragmentation, menant à la formation de deux composés moléculaires stables (réactions 3*b*–6*b* et 7*c*), sont beaucoup moins importantes que celles qui mènent à la formation de trois fragments stables: deux radicaux et une molécule neutre. Ainsi les rapports $k_{[4b]}/k_{[4a]}$ et $k_{[5b]}/k_{[5a]}$ sont inférieurs ou égaux à 0.05 à 147 nm et 0.10 à 123.6 nm. De plus ce schéma réactionnel se trouve en accord avec les analyses isotopiques de l'éthylène, de l'allène et du butadiène-1,3 (tableau 3). Ces produits sont tous perprotonés, ou perdeutérés. De plus l'irradiation du pentène-1,5d_1 (CH_2=$CHCH_2$-CH_2CH_2D) produit du butadiène-1,3 en majorité perhydrogéné.

Les pentynes n'ayant pas été mesurées, il en résulte que les rendements en pentadiènes donnent une valeur par défaut du rendement des réactions 3*a* et 3*b*. L'allène a été choisi comme composé de référence, car son rendement quantique reste constant quelle que soit la pression ou bien que l'on opère avec ou sans oxygène ou hydrogène sulfuré. Les processus donnant lieu à la formation du radical méthylène ne peuvent être importants (éq. 9). En effet ceux-ci,

[9] $(C_5H_{10})^{**} \rightarrow :CH_2 + R_1 + R_2$ (ou C_4H_8)

étant donné l'énergie utilisée, sont en majorité, des méthylènes singulets (7, 8). A basse pression, ils réagissent avec le pentène-1 (9) pour donner des composés d'insertion soit dans une liaison C—C, soit dans une liaison C—H pour donner les hexènes linéaires ou substitués, soit sur la double liaison pour donner alors le propyl-cyclopropane qui peut s'isomériser à basse pression et redonner des hexènes linéaires. Des expériences d'irradiation en présence d'oxygène, à 147.0 et 123.6 nm ont été menées à faible pression et l'analyse chromatographique n'a pas permis d'observer des composés hydrocarbonés en C_6. Sachant que l'oxygène ne gêne pas la réactivité des méthylènes singulets envers le pentène (7) et supprime tous les produits d'addition radicalaire, on en conclut que la quantité de radicaux méthylènes produite

Can. J. Chem. Downloaded from www.nrcresearchpress.com by 210.87.254.6 on 09/05/12
For personal use only.

Can. J. Chem. Downloaded from www.nrcresearchpress.com by 210.87.254.6 on 09/05/12
For personal use only.

est négligeable, ou que les produits d'insertion obtenus ne sont pas assez importants pour être observés. La quantité de C_4H_8 produite est, elle aussi, négligeable: de l'ordre de 0.01–147 nm.

Réactions radicalaires

Les réactions d'atomes d'hydrogène avec les oléfines sont bien connues (10–13) et le mécanisme réactionnel en est bien établi (éqs. 10–12).

[10] $H\cdot + C_5H_{10}\text{-}1 \rightarrow (\cdot C_5H_{11})^*$
$\Delta H = -33.5$ kcal mol^{-1}(11)

[11] $H\cdot + C_5H_{10}\text{-}1 \rightarrow \cdot C_5H_9 + H_2$

[12] $H\cdot + \cdot C_5H_{11} \rightarrow H_2 + C_5H_{10}$

La réaction 12 doit être négligée vis-à-vis de la réaction 11, étant donné la faible concentration des radicaux pentyles relativement à celle du pentène. Pour la même raison, on néglige les réactions d'addition de l'atome d'hydrogène sur les oléfines produites au cours de l'irradiation (pas de processus secondaire). Cvetanović et son équipe (10, 12) ont détermine le rapport $k_{[11]}/k_{[10]}$ pour le propène et le butène-1, soit 0.045 et 0.093. En l'absence de valeur pour le pentène normal, on peut estimer que la majorité des atomes d'hydrogène produits s'additionnent sur le pentène-1. Le radical pentyle formé est soit primaire, soit secondaire (éqs. 13 et 14).

[13*a*] $(s\text{-}C_5H_{11})^* \rightarrow \dot{C}_2H_5 + C_3H_6$
(D_s) $\Delta H = 15.5$ kcal mol^{-1}

[13*b*] $(s\text{-}C_5H_{11})^* + M \rightarrow s\text{-}\dot{C}_5H_{11} + M$ (S_s)

[14*a*] $(n\text{-}C_5H_{11})^* \rightarrow \dot{C}_3H_7 + C_2H_4$ (D_n)

[14*b*] $(n\text{-}C_5H_{11})^* + M \rightarrow n\text{-}\dot{C}_5H_{11} + M$ (S_n)

Ce mécanisme réactionnel est en accord avec la variation du rendement quantique du propène, en fonction de la pression: figs. 3 et 4. La variation du rendement en éthylène indique également une certaine quantité des radicaux pentyles primaires excités. Ce schéma est aussi en accord avec les données de la littérature (11) et la composition isotopique du propène exprimée dans le tableau 3. La variation du rapport S/D (stabilisation/décomposition), en fonction de la pression pour les deux énergies considérées, confirme également ce mécanisme:

$$\frac{S_s}{D_s} = \frac{(s\text{-}C_5H_{11})^* - (C_3H_6)_{[13a]}}{(C_3H_6)_{[13a]}} = \frac{k_{[13b]}M}{k_{[13a]}}$$

Les courbes S/D en fonction de la pression sont linéaires tant que le rapport S/D est

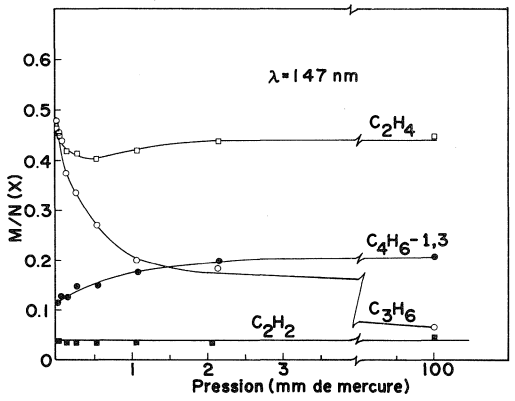

FIG. 3. Rendements quantiques en fonction de la pression.

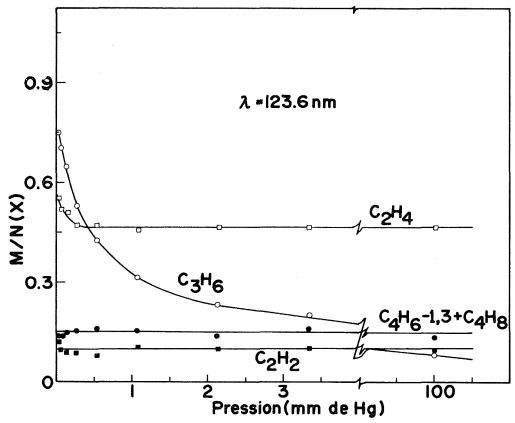

FIG. 4. Rendements quantiques en fonction de la pression.

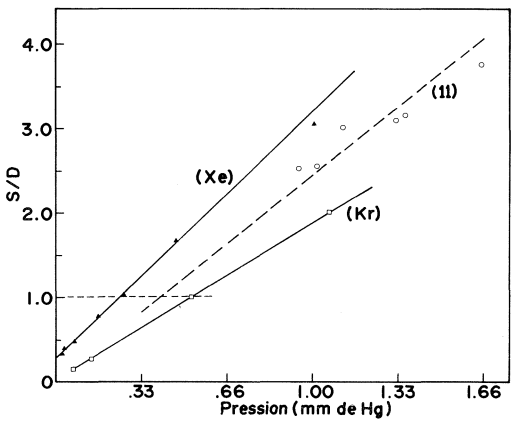

FIG. 5. Variation du rapport S/D en fonction de la pression; (Xe) : 147.0 nm; (Kr) : 123.6 nm; (11) : référence bibliographique.

TABLEAU 4. Rendements quantiques des radicaux (λ = 147 nm)

Pression de l'échantillon		$\cdot CH_3$	$\cdot C_2H_3$	$\cdot C_2H_5$	$\cdot C_3H_5$	$\cdot C_3H_7$	$\cdot C_5H_{11}$
0.4	A[a]	0.22	0.05_8	0.50_5	0.06	0.04_3	0.35
0.4	B[b]	0.30	0.18	0.38_5	0.24	0.07	0.38
1.5	A	0.22	0.13_5	0.36_4	0.05_8	0.04_5	0.51
1.5	B	0.30	0.18	0.25_5	0.24	0.06	0.52_5
100.0	A	0.21_8	0.19_3	0.30	0.01_5	0.05_1	0.70
100.0	B	0.30	0.18	0.14	0.24	0.05	0.65

[a]A: Valeurs obtenues en utilisant H_2S comme intercepteur radicalaire.
[b]B: Valeurs calculées à l'aide du mécanisme réactionnel proposé.

inférieur à 3 (fig. 5). Les pressions de demi-stabilisation à 8.4 et à 10.0 eV sont différentes, montrant ainsi qu'au moins à 10.0 eV, les atomes d'hydrogène ont une énergie cinétique supérieure à l'énergie thermique ordinaire. Bien que la pression la plus basse de travail (0.033 Torr) soit encore trop haute pour déterminer les rendements en propène et éthylène à pression "nulle" (figs. 3 et 4), les rendements en radicaux pentyles excités ont pu être estimés convenablement, en particulier à l'aide de l'effet de l'hydrogène sulfuré et des réactions radical–radical. A 147 nm, les résultats sont résumés dans le tableau 4. A 123.6 nm, la décroissance du rendement en éthylène est nette (fig. 5) et les rendements sont: $(s\text{-}\cdot C_5H_{11})^* = 0.9_5 \pm 0.1_5$ et $(n\text{-}\cdot C_5H_{11})^* = 0.18 \pm 0.04$. Alors qu'à 8.4 eV, 7% des radicaux pentyles sont primaires, ils sont de l'ordre de 17% à 10.0 eV, confirmant ainsi que les atomes d'hydrogène, au moins à 10.0 eV, ne peuvent plus être considérés comme thermiques. Ces résultats sont en accord avec ceux qu'on obtient avec les butènes (1, 2). La constante de vitesse de la réaction d'addition de l'atome d'hydrogène étant au moins de deux ordres de grandeur plus rapide sur pentène-1 que sur l'oxygène, la présence de 10% d'oxygène ne gêne donc pas la formation des radicaux pentyles (14).

L'irradiation du pentène-1 a été menée avec 5, 10 et 20% d'hydrogène sulfuré à deux pressions différentes, soit 1.5 et 100 Torrs et à différents temps d'irradiation. Les résultats concordent entre eux (tableau 1) (4*a*) (éq. 15). Même en

[15] $$R\cdot + H_2S \rightarrow RH + HS\cdot$$

opérant avec un maximum de 20% d'hydrogène sulfuré on peut en négliger la photolyse. La valeur du coefficient d'extinction de l'hydrogène sulfuré n'a pas été déterminé directement aux longueurs d'ondes utilisées. Toutefois il s'avère qu'il est très inférieur à celui du pentène-1 (15, 16). Le radical HS· produit dans la réaction 15 ne gêne pas le mécanisme réactionnel global. Il faut cependant noter la disparition presque totale du butadiène-1,3 lors des irradiations en présence d'hydrogène sulfuré en accord avec une observation déjà faite (4*b*). De plus on a noté que, sur la colonne de squalane, l'hydrogène sulfuré donne un signal correspondant au temps de passage du propène et, donc, empêche la détermination certaine du rendement quantique des radicaux allyles. En l'absence de tout intercepteur radicalaire, les réactions du type radical–radical étant athermiques, on a admis que chaque radical a autant de chance de réagir avec n'importe quel autre (12). Les valeurs des constantes de réaction de recombinaison–dismutation des principaux processus radicalaires ont été trouvés dans la littérature (14, 17, 18). Les principaux produits radicalaires sont le méthane, l'éthane, le propane, le butane, et le pentane dont les rendements quantiques varient avec la pression (figs. 4 et 6). Puisque la décomposition des radicaux pentyles est sensible à la pression, les rendements des radicaux éthyles et propyles sont aussi fonction de la pression. Donc le rendement des produits de combinaison du radical éthyle avec les radicaux propyle, méthyle ou lui-même décroît quand la pression croît. Cela se passera inversement pour le radical pentyle, dont la variation a été étudiée à travers celle du pentane. Il est alors possible de calculer en retour les rendements des radicaux libres (figs. 6 et 7). Il faut cependant noter que la majorité des produits formés par voies radicalaires sont des hydrocarbones saturés, mettant en évidence la formation intermédiaire de radicaux saturés. Il est cependant très probable que des radicaux insaturés, tels les radicaux vinyles et allyles, réagissent très vite avec le monomère et qu'ils ne participent pas aux ré-

Can. J. Chem. Downloaded from www.nrcresearchpress.com by 210.87.254.6 on 09/05/12
For personal use only.

TABLEAU 5. Décomposition de la molécule pentène-1 excitée

Réactions	Energie d'excitation 147 nm, 8.4 eV	Energie d'excitation 123.6 nm, 10.0 eV
$(C_5H_{10})^{**} \rightarrow C_5H_8 + H_2$ (2H·)	0.06±0.01[a]	0.02
$(C_5H_{10})^{**} \rightarrow C_4H_6 + \cdot CH_3 + H\cdot$ (CH_4)	0.15±0.01	0.10
$(C_5H_{10})^{**} \rightarrow C_4H_8 + :CH_2$	0.01±0.01	
$(C_5H_{10})^{**} \rightarrow C_3H_4 + \cdot C_2H_5 + H\cdot$ (C_2H_6)	0.14±0.01	0.21
$(C_5H_{10})^{**} \rightarrow C_2H_2 + \cdot C_3H_7 + H\cdot$ (C_3H_8)	0.05±0.01	0.09
$(C_5H_{10})^{**} \rightarrow C_2H_4 + \cdot C_3H_5 + H\cdot$ (C_3H_6)	0.26±0.01	0.43
$(C_5H_{10})^{**} \rightarrow C_3H_6 + H\cdot + \cdot C_2H_3$ (C_2H_4)	0.02±0.02	
$(C_5H_{10})^{**} \rightarrow C_2H_4 + \cdot CH_3 + \cdot C_2H_3$	0.16±0.02	
Total	0.85±0.10	0.85

[a]Rendements quantiques.

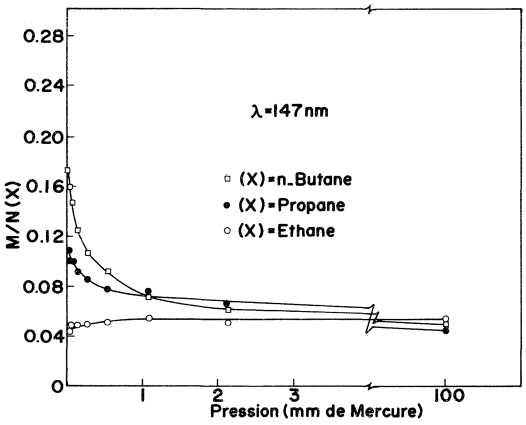

FIG. 6. Rendements quantiques en fonction de la pression des dérivés radicalaires.

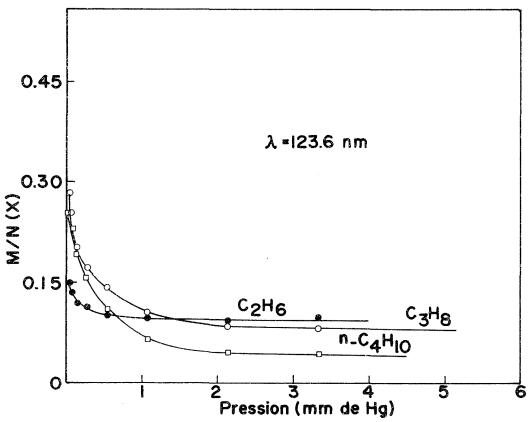

FIG. 7. Rendements quantiques en fonction de la pression des dérivés radicalaires.

actions radical–radical et ne sont pas interceptés par l'hydrogène sulfuré. Il est enfin difficile pour le moment d'expliquer l'effet de l'hydrogène sulfuré sur le rendement en éthylène, en fonction de la pression. Les rendements des radicaux libres sont ainsi rassemblés dans le tableau 4.

Conclusion

Dans le tableau 5 sont résumées les différentes réactions de décomposition de la molécule pentène-1 excitée. Conformément à un résultat déjà connu, le processus essentiel est celui de la fragmentation en deux radicaux et une molécule neutre stable (1), abstraction faite des ions $C_5H_{10}^+$ produits à 123.6 nm. Le rendement total des réactions de fragmentation est par défaut car d'autres réactions mineures peuvent s'ajouter à celles indiquées. Par exemple, l'importance de la réaction 16 est minime dans un travail

[16] $(C_5H_{10})^{**} \rightarrow H\cdot + \cdot C_5H_9$

similaire (1). Enfin il faut noter la faible importance des réactions d'isomérisation du pentène-1 excité à ces énergies en accord avec les résultats obtenus à ces longueurs d'onde avec les butènes (1, 2, 5) et contrairement à ceux obtenus avec des énergies plus faibles comme par exemple dans la photosensibilisation par le mercure (19, 20). Il est vrai que la pression des échantillons est ici trop faible pour permettre la stabilisation de la molécule surexcitée.

Nous remercions l'Université du Québec à Chicoutimi pour le traitement qu'elle a accordé à l'un de nous (P.M.P.) et le Conseil National de Recherches du Canada qui nous a assisté financièrement. Nous remercions

Can. J. Chem. Downloaded from www.nrcresearchpress.com by 210.87.254.6 on 09/05/12
For personal use only.

également le Centre de Recherches pour la Défense de Valcartier qui a mis son spectromètre de masse à notre disposition.

1. G. J. COLLIN et P. M. PERRIN. Can. J. Chem. **50**, 2823 (1972).
2. G. J. COLLIN et P. AUSLOOS. 5ième Conférence Intl. Photochim. Yorktown Heights, N.Y. 1969.
3. R. GORDEN, JR., R. E. REBBERT et P. AUSLOOS. N.B.S., Note technique 496 (1969).
4. (*a*) G. J. COLLIN, P. M. PERRIN et C. M. GAUCHER. Can. J. Chem. **50**, 2391 (1972). (*b*) G. J. COLLIN et P. M. PERRIN. Can. J. Chem. **50**, 2400 (1972).
5. J. HERMAN, K. HERMAN et P. AUSLOOS. J. Chem. Phys. **52**, 28 (1970).
6. J. L. FRANKLIN, J. G. DILLARD, H. M. ROSENSTOCK, J. T. HERRON, K. DRAXL et F. H. FIELD. NSRDS-NBS 26. 1969.
7. T. W. EDER et R. W. CARR. JR., J. Phys. Chem. **73**, 2074 (1969).
8. A. K. DHINGRA et R. D. KOOB. J. Phys. Chem. **74**, 4490 (1970).
9. F. H. DORER et B. S. RABINOVITCH. J. Phys. Chem. **69**, 1952 (1965).
10. (*a*) K. R. JENNINGS et R. J. CVETANOVIĆ. J. Chem. Phys. **34**, 1233 (1961). (*b*) G. R. WOOLLEY et R. J. CVETANOVIĆ. J. Chem. Phys. **50**, 4697 (1969).
11. M. J. PEARSON et B. S. RABINOVITCH. J. Chem. Phys. **42**, 1624 (1969).
12. R. J. CVETANOVIĆ et L. C. DOYLE. J. Chem. Phys. **50**, 4705 (1969).
13. J. A. COWFER, D. G. KEIL, J. V. MICHAEL et C. YEH. J. Phys. Chem. **75**, 1584 (1971).
14. A. F. TROTMAN-DICKENSON et G. S. MILNE. NSRDS-NBS 9. 1967.
15. P. AUSLOOS et S. G. LIAS. J. Chem. Phys. **44**, 521 (1966).
16. L. C. JONES, JR. et L. W. TAYLOR. Anal. Chem. **27**, 228 (1955).
17. M. H. J. WIJNEN. J. Am. Chem. Soc. **83**, 3752 (1961).
18. J. O. TERRY et J. H. FUTTREL. Can. J. Chem. **45**, 2327 (1967).
19. J. R. MAJER, J. F. T. PINKARD et J. C. ROBB. Trans. Faraday Soc. **60**, 1247 (1964).
20. D. W. PLACZEK et B. S. RABINOVITCH. Can. J. Chem. **43**, 820 (1965).

Can. J. Chem. Downloaded from www.nrcresearchpress.com by 210.87.254.6 on 09/05/12
For personal use only.

Fluorinated Alkoxides. Part VII. Complexes of 2-Acetamidohexafluoro-2-propanol with First-row Transition and Lanthanide Elements

CELIA MACDONALD AND C. J. WILLIS

Department of Chemistry, University of Western Ontario, London 72, Ontario

Received July 27, 1972

2-Acetamidohexafluoro-2-propanol (HAcfp), $CH_3CONHC(CF_3)_2OH$, may act as a bidentate, uninegative, ligand to give complexes of the type $M(Acfp)_2$ ($M = Co^{2+}$, Ni^{2+}, Cu^{2+}, Zn^{2+}); $M(Acfp)_3$ ($M = Fe^{3+}$); $M(Acfp)_4$ ($M = Ce^{4+}$); or $[M(Acfp)_4]^-$ (M = lanthanide(III)). Coordination is through the two oxygen atoms, except in the case of copper, where nitrogen also enters into coordination. In the complex $Cu(Acfp)_2$, the amido proton may be removed with NaH to give $Na_2[Cu(Acfp)_2]$, which undergoes addition reactions with carbonyl groups.

Formamide similarly undergoes reaction with hexafluoroacetone to give $HCONHC(CF_3)_2OH$, which chelates to copper in the same manner as HAcfp, while succinic acid diamide reacts with hexafluoroacetone to give the compound $[—CH_2CONHC(CF_3)_2OH]_2$, which acts as a tetradentate, dinegative, ligand.

Possible structures of the above complexes are discussed.

L'acétamido-2 hexafluoropropanol-2 (HAcfp) $CH_3CONHC(CF_3)_2OH$ réagit comme ligand bidentique, mononégatif pour conduire aux complexes du type $M(Acfp)_2$ ($M = Co^{2+}$, Ni^{2+}, Cu^{2+}, Zn^{2+}), $M(Acfp)_3$ ($M = Fe^{3+}$); $M(Acfp)_4$ ($M = Ce^{4+}$); ou $[M(Acfp)_4]^-$ (M = lanthanide(III)). La coordination se fait par les deux atomes d'oxygène excepté pour le cuivre où l'azote entre aussi en coordination. Dans le complexe $Cu(Acfp)_2$, le proton de l'amide peut être arraché par NaH pour conduire à $Na_2[Cu(Acfp)_2]$, qui donne des réactions d'addition sur les groupes carbonyles.

Le formamide donne des réactions semblables avec l'hexafluoroacétone et conduit à $HCONHC(CF_3)_2OH$ qui entre en chélation avec le cuivre de la même façon que HAcfp tandis que la diamide de l'acide succinique donne avec l'hexafluoroacétone, le composé $[—CH_2CONHC(CF_3)_2OH]_2$ réagissant en tant que ligand tétradentique[1] et binégatif.

Les structures possibles des complexes ci-dessus sont discutées.

[Traduit par le journal]

Can. J. Chem., **51**, 732 (1973)

Can. J. Chem. Downloaded from www.nrcresearchpress.com by 210.87.254.42 on 09/05/12
For personal use only.

In previous investigations on fluorinated alkoxides, we have demonstrated that fluorinated tertiary alcohols are sufficiently acidic to act as donor ligands in an ionized form, *i.e.*, the hexafluoro-2-propanol group, $—C(CF_3)_2OH$, coordinates as $—C(CF_3)_2O^-$. We have thus prepared complexes of perfluoropinacol, $(CF_3)_2C(OH)C(OH)(CF_3)_2$, (PFP), with main group (1) and transition metals (2) and complexes of hydroxyhexafluoroisobutyric acid, $(CF_3)_2C(OH)COOH$ (3), both of these molecules acting as bidentate, dinegative, ligands.

Various compounds of the type $R—C(CF_3)_2OH$ may readily be made by the addition of hexafluoroacetone to suitable R—H bonds, and its reaction with acetamide is known to give 2-acetamidohexafluoro-2-propanol[1] (**1**) (4). This compound is of considerable interest as a potential ligand, as it has three possible donor sites; the hydroxyl group, the amido nitrogen atom, and the carbonyl group. We have therefore prepared a series of complexes of HAcfp with various transition metals and we have investigated the reactions of the ligand in both the free and coordinated states.

[1]Throughout this paper, the name of this compound is abbreviated to HAcfp, while its ionized forms are denoted as Acfp.

Ligands

The free ligand **1**, like most carbonyl-substituted alcohols, contains considerable intramolecular hydrogen-bonding. This would be

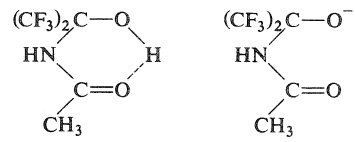

1 **2**

absent in the ionized form **2**, in contrast to perfluoropinacol, where the ion is stabilized by hydrogen-bonding (5), and, consistent with this, we find the pK_a of HAcfp to be 8.3, whereas that of perfluoropinacol is 5.95. However,

Can. J. Chem. Downloaded from www.nrcresearchpress.com by 210.87.254.42 on 09/05/12
For personal use only.

HAcfp is still sufficiently acidic to give a detectable end-point on titration in aqueous solution, and in the formation of complexes it appears to react as structure **2**, that is, a bidentate, uninegative, ligand. Although this bears some structural resemblance to the familiar ligand acetylacetone (acac), the ligand lacks the delocalization of electron density present in acac.

As would be expected, the second proton in the HAcfp could not be removed by titration in aqueous medium, but reaction of the ligand with sodium hydride in tetrahydrofuran (THF) gave the stable disodium salt of the doubly ionized species **3**. In this case, delocalization of

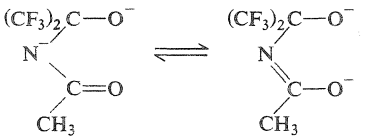

3

the second negative charge between the nitrogen and the carbonyl oxygen atoms would lead to some increased stability, but, as before, complete delocalization around the ring of a chelated ion would not be possible. Although moisture-sensitive and intensely reactive, the disodium salt when kept *in vacuo* was more stable than the parent ligand. As described below, it proved possible to isolate complexes of the ligand in the doubly ionized form, but it was convenient to prepare these by deprotonation of complexes already formed from the singly ionized form. Hexafluoroacetone did not condense with trifluoroacetamide, nor with secondary amides, presumably because of steric hindrance (6).

With formamide, hexafluoroacetone underwent condensation readily to give 2-formamidohexafluoro-2-propanol, $HCONHC(CF_3)_2OH$. This product was similar in behavior to the acetamide adduct, but more stable with respect to decomposition into constituent amide and ketone. With amide, however, the adduct slowly decomposed at room temperature. Succinic acid diamide gave a stable 1:2 adduct with hexafluoroacetone.

Transition Metal Complexes

The reaction of HAcfp with the appropriate metal ion in methanol solution at a p*H* of approximately 8 gave a series of neutral complexes $M(Acfp)_2$ ($M = Co^{2+}$, Ni^{2+}, Cu^{2+}, Zn^{2+}) or $M(Acfp)_3$ ($M = Fe^{3+}$). Various other methods of complex preparation were attempted, without success, such as reacting the ligand with metal carbonyls or other low-valency metal compounds. With tetrakis(triphenylphosphine)-platinum(0), the ligand decomposed cleanly to give the product $[(C_6H_5)_3P]_2Pt(CF_3)_2CO$, known previously (7) from the reaction of that platinum compound with hexafluoroacetone.

Using tetramethylethylenediamine (TMED), the copper complex $[(TMED)Cu(Acfp)]^+$ was prepared, but HAcfp did not yield the extensive range of mixed ligand complexes which are readily formed with perfluoropinacol (8) and hydroxyhexafluoroisobutyric acid (3).

In assigning structures to the complexes of HAcfp, the main problem is concerned with the mode of attachment of the ligand, which, as mentioned earlier, has three possible donor sites. Based largely on i.r. spectral evidence, we suggest that the principle mode of attachment is through the two oxygen atoms of structure **2**, although the presence of both O—H and N—H frequencies, often hydrogen-bonded, makes a definite assignment difficult.

The ligand HAcfp in the solid state shows strong, broad, i.r. absorption at 3260 and 3090 cm^{-1}, associated with hydrogen-bonded O—H and N—H bonds, respectively. Unfortunately, the compound is not soluble in non-polar solvents, but in diethyl ether solution the intensity of absorptions in this region was much reduced, and positions of the peaks had moved to 3540 cm^{-1} (intramolecularly hydrogen-bonded O—H) and 3410 cm^{-1} (free N—H). Other characteristic absorption peaks were the "amide I" band (carbonyl absorption) at 1640 (solid) or 1675 cm^{-1} (solution) and the "amide II" band (N—H deformation) at 1560 (solid) or 1575 cm^{-1} (solution).

Positions of the amide I and II bands in the complexes $Fe(Acfp)_3$ and $M(Acfp)_2$ (M = Co, Ni, Cu, Zn) are shown in Table 1. The spectra are generally similar, with the amide II band at 1530–1540 cm^{-1}, somewhat lower than in the free ligand, while the amide I band varies over a slightly wider range from 1615–1680 cm^{-1}. In the region above 3000 cm^{-1}, however, there is a striking difference between the copper complex and the other four (Fig. 1). While complexes of Fe, Co, Ni, and Zn show a strong, extremely sharp absorption at 3440 cm^{-1}, the complex $Cu(Acfp)_2$ shows broad absorptions of medium intensity between 3200 and 3580 cm^{-1}. The

TABLE 1. Infrared spectra (cm^{-1})

	Amide I	Amide II
HAcfp	1640	1560
HAcfp*	1675	1575
$Fe(Acfp)_3$	1620	1535
$Co(Acfp)_2$	1655	1535
$Ni(Acfp)_2$	1660	1540
$Cu(Acfp)_2$	1615	1530
$Zn(Acfp)_2$	1680	1530
$[(TMED)Cu(Acfp)]_2SO_4$	1635	1525
$Na_2[Cu(Acfp)_2]$	1665	—
$Ce(Acfp)_4$	1650	1530
$NH_4[Er(Acfp)_4]$	1670	1540

*Diethyl ether solution, otherwise as Nujol mulls.

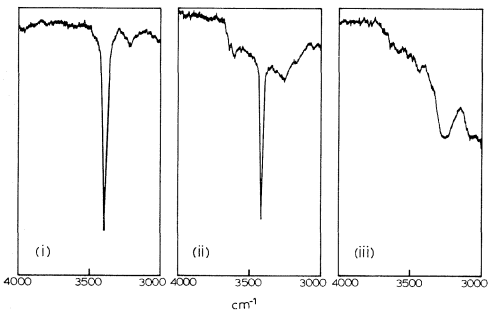

FIG. 1. I.r. spectra of Acfp complexes, Nujol mulls. (*i*) $Fe(Acfp)_3$, (*ii*) $Ni(Acfp)_2$, (*iii*) $Cu(Acfp)_2$.

sharp absorption at 3440 cm^{-1} is clearly associated with a free N—H stretching frequency, confirming that the mode of attachment of the ligand in these compounds is through the two oxygen atoms. In the case of the copper complex, the shift to lower frequency and considerable broadening of the N—H absorption could be caused either by hydrogen-bonding or by coordination of the nitrogen atom to a metal atom. The former explanation is unlikely, since the amide II band (N—H deformation) is at the same frequency as in the other complexes. Furthermore, if hydrogen-bonding were present, it would presumably involve an oxygen or nitrogen atom on an adjacent ligand, and it seems unlikely that such interaction would occur in the copper complex, but not in the complexes of similar stoichiometry of other metals.

We therefore favor the explanation of coordination by the nitrogen atom, in view of the considerable body of evidence (9) that this causes a lowering of N—H stretching frequencies, although other workers (10) have questioned this theory as an over-simplification. Coordination of the nitrogen atom to copper could occur in either of two ways; by the ligand acting in a tridentate manner, or by the ligand coordinating through the alcoholic oxygen and amide nitrogen atoms, leaving the carbonyl oxygen uncoordinated. The latter possibility may be rejected in this case, since the carbonyl absorption frequency (amide I) of a free carbonyl group would be at higher frequency, whereas the amide I band in the copper complex is actually the lowest of those measured in this work. We suggest, therefore, that the Acfp ion is tridentate in the copper complex, but bidentate in the other four complexes studied. A mode of attachment in which the three donor atoms in the ligand coordinate to the same copper atom seems most unlikely, as the formation of the two required four-membered rings introduces an unreasonable degree of strain. Instead, it would seem probable that the copper atom is surrounded by four oxygen atoms in a plane from two ligands, with additional coordination perpendicular to the plane from nitrogen atoms in adjacent molecules of complex. In this way, the copper would achieve a basically square planar environment with weaker axial interactions, an arrangement frequently found for this element (11).

The mixed ligand complex, $[(TMED)Cu(Acfp)]^+$, was isolated as two salts, the sulfate and the fluorophosphate. Here again a difference in spectra in the N—H region was observed, the sulfate showing the broad absorption similar to $Cu(Acfp)_2$, while the fluorophosphate showed the very sharp band at 3440 cm^{-1} found in the complexes of other metals. Present evidence is insufficient to distinguish between hydrogen-bonding from anion to cation, or possible nitrogen coordination, as the cause of this difference.

The visible spectra and magnetic moments of the cobalt and nickel complexes suggest that the metal ion is octahedrally coordinated in both of them. Accepting that the appearance of the sharp N—H i.r. absorption precludes the possibility of coordination from the nitrogen atom in the ligand, such coordination could be achieved by polymerization through bridging oxygen atoms, a phenomenon well characterized in the trimeric $Ni(acac)_2$ (12) and the tetrameric $Co(acac)_2$ (13). Molecular weight measurements in methanol solution were of little assistance on this point, as most of the complexes were dissociated to a molecular weight of the monomer or less, but the cobalt complex did show some association as concentration was increased.

Can. J. Chem. Downloaded from www.nrcresearchpress.com by 210.87.254.42 on 09/05/12
For personal use only.

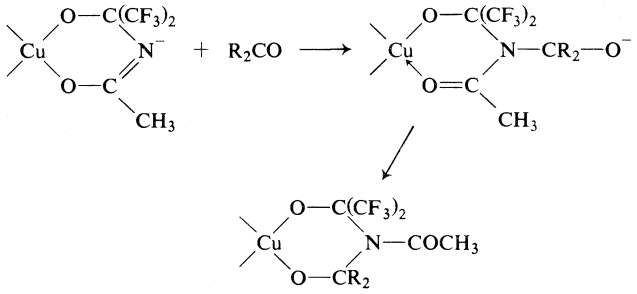

SCHEME 1

Reactions of the Coordinated Ligand

The isolation of the disodium salt of HAcfp suggested that the ligand might be capable of coordinating in a dinegative form. In practice, it was easier to form a complex of this type by deprotonation of the coordinated ligand using sodium hydride, but this reaction was only successful with the copper complex $Cu(Acfp)_2$. With complexes of other metals, reaction with sodium hydride led only to decomposition. The product, $Na_2[Cu(Acfp)_2]$ showed no O—H or N—H absorption in its i.r. spectrum, while the amide I band was at 1665 cm^{-1}. As would be expected, this complex was reactive and easily hydrolyzed, when the protonated complex $Cu(Acfp)_2$ was regenerated.

On attempted recrystallization of the salt $Na_2[Cu(Acfp)_2]$ from acetone, its properties changed markedly and it was no longer air-sensitive. Analysis showed that two molecules of acetone had been incorporated for each molecule of complex, and a similar reaction occurred with methyl ethyl ketone or ethyl acetate. The acetone was firmly held, being still present after keeping *in vacuo* at 70° for 24 h, but was lost when the adduct was dissolved in other solvents, unless they were scrupulously dry, $Cu(Acfp)_2$ being regenerated. In the formation of the acetone adduct, however, no particular precautions had to be taken to exclude moisture.

A similar adduct was formed with some difficulty from hexafluoroacetone by reacting excess of the ketone with $Na_2[Cu(Acfp)_2]$ in tetrahydrofuran (THF) in a sealed tube, then recrystallizing from solvents saturated with hexafluoroacetone.

The stability and ready formation of these adducts of carbonyl compounds makes it unlikely that they are simple 2:1 adducts in which donation is occurring from carbonyl oxygen to the copper atom. The i.r. spectrum of the acetone adduct showed no O—H or N—H bands, but the amide I band had split to give two peaks, at 1720 and 1600 cm^{-1}. Similarly, the methyl ethyl ketone adduct gave peaks at 1715 and 1600 cm^{-1}. It appears, therefore, that reaction of the ketone with the coordinated ligand has occurred, and Scheme 1 shows a possible sequence in which attack by the nucleophilic nitrogen atom on the carbonyl group is followed by a rotation of the ligand to displace the acetyl group. Such a structure for the products would account for the presence of two amide I bands in the i.r. spectrum, the higher frequency being that of the free acetyl group and the lower frequency that of the coordinated $—CR_2O$ group. With the hexafluoroacetone adduct, however, the higher frequency absorption of the free acetyl group was not seen, the strong amide I band being at 1680 cm^{-1}. The fluorinated ketone, with the basicity of the oxygen greatly reduced by the electronegative trifluoromethyl groups, would be even less likely than would acetone to coordinate as a simple donor molecule, so it must have reacted with the ligand. Although a definite decision cannot be made, we suggest that, in this case, reaction has stopped at the second stage of the above scheme, with one $—C(CF_3)_2O^-$ group coordinated to the sodium ion rather than the copper ion. The remarkable stability of fluorinated sodium alkoxides of this type has been demonstrated by the properties of the sodium derivative of perfluoro-*t*-butanol, $(CF_3)_3CONa$, which may be distilled without decomposition (14).

Lanthanide Complexes

Previous work on lanthanide complexes has shown that these elements form stable complexes with β-diketone ligands, and that bulky fluorine-substituted ligands give greatest stability, presumably through shielding the metal ion (15). In view of the resemblance of HAcfp to acac and

Can. J. Chem. Downloaded from www.nrcresearchpress.com by 210.87.254.42 on 09/05/12
For personal use only.

Can. J. Chem. Downloaded from www.nrcresearchpress.com by 210.87.254.42 on 09/05/12
For personal use only.

similar ligands, it was thought probable that stable lanthanide–Acfp complexes could be prepared.

Reaction of a lanthanide 3^+ ion (typically, Er^{3+} or Dy^{3+}) with a considerable excess of HAcfp, neutralized with ammonium hydroxide, precipitated complexes with a 4:1 ligand–metal ratio, *e.g.* $NH_4[Er(Acfp)_4]$. The i.r. spectrum showed the strong, sharp, peak at 3440 cm^{-1} assigned to free N—H, and other bands (Table 1) typical of the coordinated ligand, and there is no reason to doubt that the lanthanide ion is eight-coordinate in these complexes. The ammonium salts could be sublimed unchanged, as can the analogous derivatives of hexafluoroacetylacetone (15).

The above complexes were, however, unstable in solution in the absence of excess ligand. When dissolved in organic solvent, or when a synthesis was attempted with a lower ligand–metal ratio, a product of different formulation was produced. Although this latter type of complex was prepared for ten different lanthanides (La, Pr, Nd, Sm, Eu, Tb, Dy, Ho, Er, Yb), no definite decision on its formulation was possible. Analytical data (average of ten complexes) gave a F:C ratio of 1.10 ± 0.01, whereas HAcfp ($C_5F_6H_4NO_2$) requires a ratio of 1.20. The observed F:C ratio could be produced by a stoichiometry $C_{10}H_{11}$ (ratio 1.10) or $C_{11}F_{12}$ (ratio 1.09). The former ratio implies loss of a fluorine atom from a trifluoromethyl group, which was rejected as impossible under the mild conditions employed, so the complex appears to contain one extra carbon atom for each two molecules of ligand. Incorporation of a solvent molecule was ruled out, as the product obtained was independent of the solvent used, so the extra carbon appears to come from ligand decomposition.

The i.r. spectra of these complexes showed that the strong peak at 3440 cm^{-1} was still present, but an additional sharp absorption at 3660 cm^{-1} was also present. Partial deuteriation of the complex produced corresponding peaks at 2685 and 2520 cm^{-1} (Fig. 2), and they may be assigned to free N—H and O—H respectively. The usual amide bands were present at 1650 and 1535 cm^{-1}.

The position and sharpness of the O—H band in the i.r. spectrum suggests an hydroxide, rather than coordinated water. Taking into account the other evidence, the composition of these complexes corresponds to a formulation in which a molecule of acetamide, arising from ligand degradation, is incorporated for every two lanthanide atoms, giving the composition $M_2(Acfp)_4(OH)_2 \cdot CH_3CONH_2$. Direct evidence of the presence of acetamide is lacking, since its i.r. spectrum would be obscured by that of the Acfp ligand, so this conclusion rests mainly on analytical data and must be regarded as tentative.

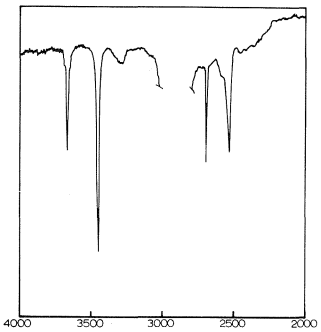

FIG. 2. I.r. spectra of partially deuteriated lanthanide complexes of Acfp.

When preparation of a complex of cerium(III) was attempted, using the same method as had been employed for the other lanthanides, the only product isolated was the neutral eight-coordinate Ce(IV) complex, $Ce(Acfp)_4$. This ready oxidation of cerium, apparently by air during the reaction, is surprising, but a similar effect has been noted in the preparation of a Ce(IV) complex of dipivaloylmethane using Ce(III) as starting material (16). The latter complex was red and relatively high-melting (276°), which the authors suggested as criteria for distinguishing Ce(IV) complexes, but our Acfp complex was pale yellow and melted at 118°.

Complexes of Other Ligands

A brief investigation was made of the complexing ability of ligands formed by the condensation of hexafluoroacetone with other amides. The benzamide adduct, as described above, was of limited stability. It was hoped that it might be stabilized by incorporation into complexes, but although complex formation occurred, the products were unstable and satisfactory analytical data could not be obtained.

The formamide adduct, $HCONHC(CF_3)_2OH$, gave a stable copper complex similar to HAcfp. Its i.r. spectrum in the region above 3000 cm^{-1} showed the same broad N—H absorption as $Cu(Acfp)_2$. However, attempts to deprotonate

Can. J. Chem. Downloaded from www.nrcresearchpress.com by 210.87.254.42 on 09/05/12
For personal use only.

it with sodium hydride led only to decomposition.

A preliminary investigation was made of the possibility of synthesizing multidentate ligands by the reaction of hexafluoroacetone with molecules containing several amide groups. Urea, the simplest diamide, was tried first, but the product was of limited stability and satisfactory characterization could not be achieved. With succinic acid diamide, however, a stable 1:2 adduct with hexafluoroacetone was prepared. The expected hydrogen-bonded structure for this product would be:

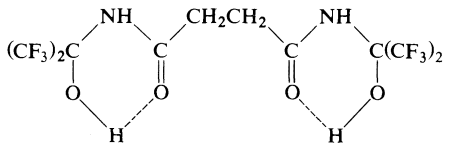

and examination of molecular models suggested that this should be capable of tetradentate coordination to a single metal ion, via the four oxygen atoms. This was confirmed by the isolation of a neutral, monomeric, complex of copper(II), very similar to the complex Cu(Acfp)$_2$. Studies on this and related multidentate ligands are continuing.

Experimental

General Techniques

Volatile materials were manipulated on a standard vacuum manifold. I.r. spectra were recorded on a Beckman model IR-10 instrument, visible spectra on a Beckman DK-1, n.m.r. spectra on a Varian HA-100 instrument at 100 or 94.1 MHz for ^{1}H and ^{19}F respectively (references: $(CH_3)_4Si$ and $CFCl_3$), and mass spectra on a Varian M-66 instrument. Magnetic moments were determined at room temperature by the Gouy method. Molecular weights were determined on a Hitachi–Coleman osmometer. Microanalyses were performed by Alfred Bernhardt Laboratories; all analytical data are in Table 2. Petroleum ether refers to 30–60° light petroleum spirit.

2-Acetamidohexafluoro-2-propanol (HAcfp)

The preparation followed the published procedure (4). Yield was virtually quantitative. The ^{19}F n.m.r. spectrum (acetone solution) showed a singlet at 82.5 p.p.m. The equivalent weight was determined by titration with standard base in 50% aqueous methanol: found, 226; calcd., 225.

Reaction of HAcfp with Sodium Hydride

Sodium hydride (1.0 g) was added to dry tetrahydrofuran (THF) (20 ml) under nitrogen, and HAcfp (4.0 g) in dry THF (30 ml) added slowly with stirring. After gas evolution had ceased (2 h), the solution was filtered and evaporated to dryness, the residue taken up in dry THF, filtered, and concentrated to precipitate the disodium salt, which was stored *in vacuo*. ^{19}F n.m.r. (THF solution) gave a singlet at 75.2 p.p.m.

Reaction of HAcfp with Cu(II), Ni(II),Co(II), and Zn(II)

Copper(II) sulfate (2.2 g) and HAcfp (4.0 g) were dissolved in methanol and methanolic potassium hydroxide added with stirring to p*H* 8. The solution was evaporated to dryness, and the residue dissolved in THF, filtered, and concentrated. Dropwise addition of petroleum ether precipitated light blue crystals of Cu(Acfp)$_2$, m.p. 180° (dec.), μ_{eff} = 1.73 B.M. The visible spectrum (acetone solution) gave a single peak at 15 600 cm^{-1} (ε 26) and two bands at 15 400 and 13 800 (sh) cm^{-1} by diffuse reflectance. The highest peak in the mass spectrum was at m/e = 444, corresponding to the parent molecule (protonated) less a trifluoromethyl group.

For nickel(II), the preparation was carried out in the same manner, using nickel nitrate. The product was noticeably less soluble in organic solvents than was the copper complex, and was recrystallized from methanol to give pale green crystals of Ni(Acfp)$_2$, m.p. 190° (dec.), μ_{eff} = 2.84 B.M. The visible spectrum (acetone solution) gave peaks at 8800 (ε 11), 14 100 (23), and 25 000 (61) cm^{-1} and peaks at 8200, 14 100, and 24 500 cm^{-1} by diffuse reflectance. The mass spectrum gave no peaks corresponding to nickel-containing fragments.

For cobalt(II), the preparation was carried out in the same manner, using cobalt(II) nitrate. The product was purified by washing with 2-propanol, followed by recrystallization from acetone – petroleum ether, m.p. 195° (dec.), μ_{eff} = 4.85 B.M. The visible spectrum (acetone solution) showed peaks at 17 000 (ε 13), 19 000 (17), and 20 400 (20) cm^{-1}, and poorly resolved peaks at 17 100, 19 000, and 23 000 cm^{-1} by diffuse reflectance. The highest peak in the mass spectrum was at m/e = 507, corresponding to the parent ion.

For zinc(II), the preparation was carried out in the same manner, using zinc sulfate. The crude product contained some oily impurity which was removed by heating *in vacuo* at 60°. The residue was then recrystallized from THF – petroleum ether. The ^{19}F n.m.r. spectrum showed a singlet at 81.6 Hz.

Molecular weight measurements on complexes in this group were attempted, but were not conclusive. The cobalt complex, Co(Acfp)$_2$, gave a value of 510 (calcd., 507) when extrapolated to zero concentration in methanol solution, but showed some association, rising to 700 at 3×10^{-2} *m*. The copper and zinc complexes both appeared to dissociate in dilute solution and gave low molecular weights. The nickel complex was not sufficiently soluble in methanol for reliable figures to be obtained, but appeared to be monomeric.

Reaction of HAcfp with Iron(III)

To a solution of ferric chloride (0.43 g) and HAcfp (2.0 g) in methanol (20 ml) was added ammonium hydroxide (6 *M* in 50% water–methanol) with stirring to p*H* 9. Diethyl ether (40 ml) was then added and the solution filtered to remove precipitated ammonium chloride. The filtrate was evaporated to dryness *in vacuo*, redissolved in diethyl ether, and filtered through anhydrous magnesium sulfate. Petroleum ether was added to the cloud point and green crystals of Fe(Acfp)$_3$ formed on

Can. J. Chem. Downloaded from www.nrcresearchpress.com by 210.87.254.42 on 09/05/12
For personal use only.

TABLE 2. Analytical data

Compound	Formula	Carbon		Hydrogen		Fluorine	
		Calcd.	Found	Calcd.	Found	Calcd.	Found
$Na_2(Acfp)$	$C_5H_3F_6NO_2Na_2$	22.3	22.3	1.1	1.4	42.4	42.0
$Fe(Acfp)_3$	$C_{15}H_{12}F_{18}N_3O_6Fe$	24.7	24.8	1.7	1.7	47.0	46.7
$Co(Acfp)_2$	$C_{10}H_8F_{12}N_2O_4Co$	23.7	23.1	1.6	1.3	45.0	44.7
$Ni(Acfp)_2$	$C_{10}H_8F_{12}N_2O_4Ni$	23.7	23.2	1.6	1.3	45.0	44.2
$Cu(Acfp)_2$	$C_{10}H_8F_{12}N_2O_4Cu$	23.5	23.3	1.6	1.4	44.6	44.1
$Zn(Acfp)_2$	$C_{10}H_8F_{12}N_2O_4Zn$	23.4	23.6	1.6	1.7	44.4	44.8
$[(TMED)Cu(Acfp)]_2SO_4$	$C_{22}H_{20}F_{12}N_6O_8SCu$	29.2	29.1	4.4	4.5	25.3	24.9
$[(TMED)Cu(Acfp)]PF_6$	$C_{11}H_{10}F_{12}N_3O_2PCu$	24.1	24.3	3.7	3.8	41.6	41.4
$Na_2[Cu(Acfp)_2]\cdot THF$	$C_{14}H_{14}F_{12}N_2O_5Na_2Cu$	28.2	28.6	2.4	2.6	38.4	39.9
$Na_2[Cu(Acfp)_2][(CH_3)_2CO]_2$	$C_{16}H_{18}F_{12}N_2O_6Na_2Cu$	28.6	28.3	2.7	2.6	33.9	34.2
$Na_2[Cu(Acfp)_2][CH_3COC_2H_5]_2$	$C_{18}H_{22}F_{12}N_2O_6Na_2Cu$	30.9	30.7	3.2	3.3	32.6	32.2
$Na_2[Cu(Acfp)_2][(CF_3)_2CO]_2$	$C_{16}H_6F_{24}N_2O_6Na_2Cu$	21.6	21.4	0.7	1.6	51.4	54.5
$HCONHC(CF_3)_2OH$	$C_4H_3F_6NO_2$	22.7	22.6	1.4	1.5	54.1	54.3
$Cu[HCONHC(CF_3)_2O]_2$	$C_8H_4F_{12}N_2O_4Cu$	19.9	19.5	0.8	0.7	47.2	46.9
$[—CH_2CONHC(CF_3)_2OH]_2$	$C_{10}H_8F_{12}N_2O_4$	26.7	26.9	1.8	1.8	50.8	51.1
$[—CH_2CONHC(CF_3)_2O]_2Cu$	$C_{10}H_6F_{12}N_2O_4Cu$	23.6	23.4	1.2	1.3	44.7	44.5
$Ce(Acfp)_4$	$C_{20}H_{16}F_{24}N_4O_8Ce$	23.2	23.4	1.6	1.7	44.1	43.9
$NH_4[Er(Acfp)_4]$	$C_{20}H_{20}F_{24}N_5O_8Er$	22.2	22.9	1.9	1.8	42.2	42.9*
$NH_4[Dy(Acfp)_4]$	$C_{20}H_{20}F_{24}N_5O_8Dy$	22.3	22.3	1.9	1.5	42.3	41.9†
$Eu_2(Acfp)_4(OH)_2\cdot CH_3CONH_2$	$C_{22}H_{23}F_{24}N_5O_{11}Eu_2$	20.4	20.6	1.8	1.7	35.3	35.5‡

*Nitrogen: Calcd., 6.5. Found, 6.7.
†Nitrogen: Calcd., 6.5. Found, 6.3.
‡Nitrogen: Calcd., 5.4. Found, 4.8. Analysis typical of 10 lanthanide complexes; see text.

Can. J. Chem. Downloaded from www.nrcresearchpress.com by 210.87.254.42 on 09/05/12
For personal use only.

standing, m.p. 130° (dec.), μ_{eff} = 5.68 B.M. The visible spectrum (methanol solution) showed one weak peak at 22 200 cm^{-1} (ε 6) before onset of a charge-transfer band. The highest peak in the mass spectrum was at m/e = 504, corresponding to the loss of one Acfp group from the parent molecule.

Reaction of HAcfp with Tetrakis(triphenylphosphine)-platinum(0)

The $[(C_6H_5)_3P]_4Pt$ (1.0 g) and HAcfp (4.0 g) were dissolved in dry THF (20 ml) under nitrogen, and the solution kept at 60° for 48 h, by which time the original yellow color had faded. After partial removal of solvent, petroleum ether was added and a white solid precipitated. This was recrystallized from benzene–pentane and identified as bis(triphenylphosphine)platinum(hexafluoroacetone), $[(C_6H_5)_3P]_2PtOC(CF_3)_2$, by analysis and by comparison of its ^{19}F n.m.r. spectrum with published data (7).

Attempted Reaction of HAcfp with Cr(III), Mn(III), and Fe(II)

The synthetic route described above for Cu(II) did not give complexes of Cr(III), Mn(III), or Fe(II). Standard methods for the preparation of acac complexes were therefore attempted, such as reaction of Cr(III) with aqueous HAcfp in the presence of urea, reaction of Fe(II) with HAcfp in acetate buffer solution, and reaction of permanganate with Mn(II) and HAcfp. No success was achieved. HAcfp also failed to give identifiable products on reaction with nickel carbonyl or chromium hexacarbonyl.

Reaction of HAcfp with Copper(II) and TMED

Copper sulfate (2.22 g) and HAcfp (2.0 g) were dissolved in methanol (60 ml) and TMED added dropwise with stirring to p*H* 8. The solution was filtered, evaporated to dryness, redissolved in methanol, filtered, and concentrated, then added dropwise to 200 ml of rapidly stirred dry acetone. The hygroscopic blue crystals precipitating were quickly filtered from the solution and dried *in vacuo* to give $[(TMED)Cu(Acfp)]_2SO_4$. The visible spectrum (methanol solution) showed a single peak at 16 000 cm^{-1} (ε 11). Reaction of a methanolic solution of the sulfate with potassium fluorophosphate precipitated potassium sulfate. Concentration of the remaining solution yielded dark purple crystals of $[(TMED)Cu(Acfp)]PF_6$, having the same visible spectrum as the sulfate.

Reaction of $Cu(Acfp)_2$ with Sodium Hydride

$Cu(Acfp)_2$ (10 g, 19.5 mmol) in dry THF (100 ml) was added slowly with stirring to a suspension of sodium hydride (1.0 g, 21.0 mmol) in THF (50 ml) under nitrogen. There was a vigorous initial evolution of gas which ceased after stirring for 2 h, by which time the blue color of the solution had faded and a dark blue precipitate formed. The solution was filtered and the solid washed with dry THF and dried immediately *in vacuo* to give the air-sensitive disodium salt, $Na_2[Cu(Acfp)_2]$. A similar reaction sequence with the nickel and zinc HAcfp complexes led only to decomposition products.

Reaction of $Na_2[Cu(Acfp)_2]$ with Carbonyl Compounds

The sodium salt was dissolved in acetone and the solution filtered and concentrated. Dropwise addition of petroleum ether caused precipitation of the acetone adduct as pale blue crystals, recrystallized from acetone, m.p. 147° (dec.). The same procedure was followed using methyl ethyl ketone or ethyl acetate in place of acetone. To prepare the hexafluoroacetone adduct, the sodium salt was suspended in dry THF in a glass reaction tube and excess hexafluoroacetone condensed in the tube. The tube was sealed and kept at 25° with shaking for 4 h, then the tube opened and the solution filtered. Addition of pentane saturated with hexafluoroacetone caused precipitation of the blue adduct, recrystallized from THF–pentane saturated with hexafluoroacetone, m.p. 114–115°.

Preparation of 2-Formamidohexafluoro-2-propanol

Formamide and hexafluoroacetone were reacted together under the same conditions as were used for the preparation of HAcfp, giving a virtually quantitative yield of 2-formamidohexafluoro-2-propanol, m.p. 120–121°, equivalent weight by titration, 215 (calcd., 211).

Reaction of 2-Formamidohexafluoro-2-propanol with Copper(II)

The procedure was the same as that followed for HAcfp, the product being recrystallized from methanol. The i.r. spectrum showed broad N—H absorptions at 3400 and 3190 cm^{-1}, while amide I and II bands were at 1640 and 1585 cm^{-1} respectively.

Reaction of Hexafluoroacetone with Succinic Acid Diamide

The diamide had only very limited solubility in suitable organic solvents, so reaction was much slower than with acetamide. In a typical preparation, succinic acid diamide (10 g) was suspended in dry THF (30 ml) in a Carius tube (100 ml) and excess hexafluoroacetone (30 g) condensed in. The tube was sealed and kept at 25° for 7 days, then opened and the solution filtered to remove unreacted diamide, then concentrated, when the adduct crystallized out. Recrystallization from THF gave *N,N'*-bis[1-hydroxyperfluoro-(1-methylethyl)] succinic acid diamide (H_2Fsda), m.p. 227° (dec.).

Reaction of H_2Fsda with Copper(II)

H_2Fsda (1.0 g) and copper(II) sulfate pentahydrate (0.56 g) were dissolved in methanol (20 ml) and methanolic potassium hydroxide added to p*H* 9. The solution was filtered and evaporated to dryness, the residue dissolved in THF, filtered, and petroleum ether added to the cloud point. The copper complex, Cu(Fsda), crystallized on standing. It had molecular weight in methanol of 516 (calcd., 524) and showed a single absorption at 15 400 cm^{-1} (ε 39) in methanol. The i.r. spectrum showed the same broad N—H absorption above 3000 cm^{-1} as was found for $Cu(Acfp)_2$, with the amide I and II bands at 1615 and 1580 cm^{-1} respectively.

Attempted Reaction of Hexafluoroacetone with Other Amides

No reaction could be detected between hexafluoroacetone and *N*-methylacetamide, trifluoroacetamide, or *N*-methyltrifluoroacetamide. Reaction of hexafluoroacetone with benzamide gave the expected adduct in 80% yield, but reversion to starting materials occurred slowly on standing and rapidly in solution when recrystallization was attempted. Satisfactory analytical data could not be obtained. Metal complexes (Cu, Co, Zn) were pre-

pared using the crude ligand, but these also decomposed on standing.

Reaction of HAcfp with Lanthanides

(*i*) As a typical example, erbium(III) chloride (1.0 g, 3.5 mmol) and HAcfp (1.8 g, 8.0 mmol) were dissolved in methanol (20 ml) and methanolic ammonium hydroxide added to p*H* 9. Diethyl ether was added to precipitate ammonium chloride, the solution filtered, evaporated to dryness, the residue taken up in ether, filtered, and benzene added to the cloud point. Subsequent slow evaporation gave pale pink needles of a complex whose analysis corresponded to the composition $Er_2(Acfp)_4(OH)_2 \cdot CH_3CONH_2$. By a similar reaction, analogous complexes were prepared for La, Pr, Nd, Sm, Eu, Tb, Dy, Ho, and Yb. Colors and magnetic moments were those usual to these lanthanides, and analytical data gave the respective F:C ratios of 1.08, 1.09, 1.09, 1.09, 1.09, 1.09, 1.12, 1.11, and 1.12 (average, 1.10). The lanthanum complex (the only one to be diamagnetic) showed two peaks in its ^{19}F n.m.r. spectrum, at 81.4 and 82.1 p.p.m.

(*ii*) The above procedure was repeated using cerium(III) nitrate. The product was the cerium(IV) complex $Ce(Acfp)_4$, pale yellow crystals, m.p. 118°. The complex was diamagnetic and the ^{19}F n.m.r. spectrum showed a singlet at 80.7 p.p.m. The proton n.m.r. spectrum showed a broad peak at 2.75 p.p.m., and the i.r. spectrum showed the sharp N—H peak at 3440 cm^{-1}.

(*iii*) A different procedure was adopted using a considerable excess of ligand. HAcfp (0.94 g, 4.2 mmol) was suspended in water (20 ml) and ammonium hydroxide added dropwise until solution was complete. The resulting solution was added slowly to aqueous erbium chloride (0.2 g, 0.7 mmol), giving a pale pink precipitate of $NH_4[Er(Acfp)_4]$, which could not be recrystallized without decomposition to give a complex of type (*i*). It had μ_{eff} = 9.80 B.M. and N—H absorptions in the i.r. spectrum at 3440 (sharp), 3380 (broad), and 3280 (broad) cm^{-1}. The similar dysprosium complex was white and had μ_{eff} = 10.6 B.M.

We thank the National Research Council of Canada for financial support of this work in the form of an operating grant and a scholarship (to C.M.).

1. M. Allan, A. F. Janzen, and C. J. Willis. Can. J. Chem. **46**, 3671 (1968).
2. M. Allan and C. J. Willis. J. Am. Chem. Soc. **90**, 5343 (1968).
3. J. T. Price, A. J. Tomlinson, and C. J. Willis. Can. J. Chem. **50**, 939 (1972).
4. P. E. Newallis and E. J. Rumanowski. J. Org. Chem. **29**, 3114 (1964).
5. W. J. Middleton and R. V. Lindsey. J. Am. Chem. Soc. **86**, 4948 (1964).
6. R. S. Drago, D. W. Meek, M. D. Joesten, and L. Laroche. Inorg. Chem. **2**, 124 (1963).W. E. Bull, S. K. Mactan, and J. E. Willis. Inorg. Chem. **2**, 303 (1963).
7. B. Clarke, M. Green, R. B. L. Osborn, and F. G. A. Stone. J. Chem. Soc. A, 167 (1968).
8. W. S. Cripps and C. J. Willis. Unpublished observations.
9. F. A. Cotton. *In* Modern coordination chemistry. *Edited by* J. Lewis and R. G. Wilkins. Interscience, New York, N.Y. 1960. p. 361. J. Fujita, K. Nakamoto, and M. Kobayashi. J. Am. Chem. Soc. **78**, 3295 (1956).
10. J. G. Gibson and E. D. McKenzie. J. Chem. Soc. A, 1667 (1971).
11. N. F. Curtis and H. K. J. Powell. J. Chem. Soc. A, 3069 (1968).
12. J. G. Bullen, R. Mason, and P. Pauling. Inorg. Chem. **4**, 456 (1965).
13. F. A. Cotton and R. C. Elder. Inorg. Chem. **4**, 1145 (1965).
14. R. E. A. Dear, W. B. Fox, R. J. Fredericks, E. E. Gilbert, and D. K. Huggins. Inorg. Chem. **9**, 2590 (1970).
15. M. F. Richardson and R. E. Sievers. Inorg. Chem. **10**, 498 (1971).
16. J. Selbin, N. Ahmad, and N. Bhacca. Inorg. Chem. **10**, 1383 (1971).

Can. J. Chem. Downloaded from www.nrcresearchpress.com by 210.87.254.42 on 09/05/12
For personal use only.

Interactions intramoleculaires. XIV.[1] Interactions *gauches* avec un groupement *t*-butyle (séries cyclohexanique et cyclohexénique)[2]

JEAN-PIERRE AYCARD ET HUBERT BODOT

Laboratoire de chimie organique structurale (Associé au CNRS n°109), Université de Provence, Centre de Saint-Jérôme, 13013 Marseille, France

Reçu le 8 décembre 1971[3]

Pour les 3-*t*-butyl cyclohexènes substitués en 4 (X = $COOC_2H_5$ ou C≡N) et disubstitués en 4,5 (X = $COOC_2H_5$), leurs homologues saturés et le 1,2-diméthyl 4-méthoxycarbonyl 5-*t*-butyl cyclohexène, les différences d'enthalpie libre entre stéréoisomères sont déterminées, et discutées en termes de différences d'interactions *gauches*.

Pour les composés cyclohexaniques disubstitués, les valeurs de ($I_{ae} - I_{ee}$) sont +0.2 (X = $COOC_2H_5$) et −1.7 kcal mol^{-1} (X = C≡N) pour les interactions avec un groupement *t*-butyle vicinal; dans le dernier cas, l'isomère à C≡N axial est nettement plus stable que celui à C≡N équatorial.

Pour les composés cyclohexéniques disubstitués, les valeurs ($I_{ae} - I_{ee}$) sont +2.1 (X = $COOC_2H_5$) et +0.6 kcal mol^{-1} (X = C≡N).

Pour les composés trisubstitués, les résultats s'expliquent par un renforcement des interactions I_{ee} pour les stéréoisomères ayant tous les substituants équatoriaux.

Les synthèses et les identifications des isomères sont rapportées.

For the 4-substituted (X = $COOC_2H_5$ or C≡N) and 4,5-disubstitued (X = $COOC_2H_5$) 3-*t*-butyl cyclohexenes, their saturated homologs and for 1,2-dimethyl 4-methoxycarbonyl 5-*t*-butyl cyclohexene, the free energy differences are determined and discussed in terms of *gauche* interaction differences.

For disubstitued cyclohexane compounds, ($I_{ae} - I_{ee}$) values are +0.2 (X = $COOC_2H_5$) and −1.7 kcal mol^{-1} (X = C≡N) for interactions with a vicinal *t*-butyl group; in the last case, the axial cyano isomer is clearly more stable than the equatorial cyano isomer.

For disubstitued cyclohexene compounds, ($I_{ae} - I_{ee}$) values are +2.1 (X = $COOC_2H_5$) and +0.6 kcal mol^{-1} (X = C≡N).

For trisubstitued compounds, the results can be explained by an increase of diequatorial interactions in all equatorial stereoisomers.

The synthesis and the isomer identifications are reported.

Can. J. Chem., **51**, 741 (1973)

Introduction

Dans le cadre d'une série d'études conformationnelles de composés cyclohexaniques et cyclohexéniques à contraintes stériques progressives (2, 3), nous avons évalué les interactions *gauches* (*I*) entre deux substituants éthoxycarbonyles (—$COOC_2H_5$) vicinaux (en position 4,5 en série cyclohexénique). Comme Sicher et Tichy (4, 5) l'avaient mis en évidence, nos résultats ont confirmé, en série cyclohexanique, l'inégalité des interactions I_{ae} (entre deux substituants *cis*) et I_{ee} (entre deux substituants *trans* diéquatoriaux): $I_{ae} > I_{ee}$. Par contre, nous avons montré, qu'en série cyclohexénique (positions 4,5), ces interactions sont peu différentes ($I_{ae} \simeq I_{ee}$); l'interprétation de ces résultats a montré qu'à côté du simple facteur stérique dû à l'inégalité des angles dièdres entre substituants vicinaux, il était nécessaire de tenir compte de la déformation des cycles, plus aisée quand les deux substituants sont en position *trans* diéquatoriale.

Nous abordons ici, dans chacune des deux séries (fig. 1), l'étude: (*a*) des interactions *gauches* entre le groupement *t*-butyle et les substituants cyano, méthoxycarbonyle, ou éthoxycarbonyle situés en positions 1,2 sur le cyclohexane, ou 3,4 et 4,5 sur le cyclohexène; (*b*) d'un groupe de quatre stéréoisomères impliquant simultanément une interaction *gauche* *t*-butyle-éthoxycarbonyle, et celle entre deux groupements éthoxycarbonyles.

Ce choix de structures fortement contraintes a pour but de mettre en évidence les limites des interprétations évoquées ci-dessus; ces limites

---

[1]Partie XIII: réf. 1.

[2]Cette publication constitue une partie de la thèse de Doctorat ès Sciences physiques que doit soutenir M.J-P. Aycard devant l'Université de Provence. Une partie des résultats ont été présentés devant le XXIII rd Congress of Pure and Applied Chemistry, Boston, juillet 1971.

[3]Révision reçue le 13 octobre 1972.

Can. J. Chem. Downloaded from www.nrcresearchpress.com by 210.87.254.105 on 09/05/12
For personal use only.

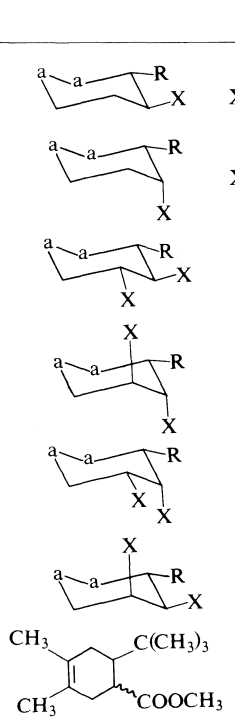

FIG. 1. Désignation des composés R = $(CH_3)_3C$; X = $COOC_2H_5$ (sauf pour **3** et **4**).

étaient prévisibles compte tenu de certains résultats récents de la littérature (6, 7).

Les synthèses, les séparations, et les identifications des différents stéréoisomères sont décrites en partie expérimentale, ainsi que leurs mises en équilibre; celles-ci conduisent aux valeurs des constantes d'équilibre et aux différences d'enthalpie libre du tableau 1.

Discussion

Pour les composés disubstitués **1**–**4**, les constantes d'équilibre varient de 10^{-2}–8. Dans chaque série, il intervient une forte diminution de la différence d'enthalpie libre en passant du groupement éthoxycarbonyle au groupement cyano (**1** → **3** et **2** → **4**); de l'ordre de 2.7 kcal mol^{-1}, ces variations sont beaucoup plus importantes que celles des enthalpies libres conformationnelles (ΔG_X^0) des groupements (environ 1 kcal mol^{-1}). D'autre part, pour les 2-*t*-butyl cyanocyclohexanes (**4**), l'isomère à cyano axial est nettement plus stable que celui à cyano équatorial ($\Delta G^0 = +1.47$ kcal mol^{-1}); ce renversement de la préférence conformationnelle est encore plus marqué qu'avec le substituant hydroxyle ($\Delta G^0 = +0.26$) (réf. 8).

Une analyse en termes d'interactions *gauches* peut être effectuée en admettant le blocage conformationnel du groupement *t*-butyle en position équatoriale ou pseudoéquatoriale (série cyclohexénique):

$$G^0_{cis} - G^0_{trans} = -\Delta G_X{}^0 + I_{ae} - I_{ee}$$

Les valeurs des enthalpies libres conformationnelles $\Delta G_X{}^0$ des groupements sont données dans le tableau 2.

Pour la série cyclohexanique, la différence des interactions *gauches* ($I_{ae} - I_{ee}$) diminue quand on passe du groupement méthyle au *t*-butyle (tableau 3), que le substituant vicinal soit un éthoxycarbonyle, un cyano, ou un hydroxyle; pour les deux derniers, qui ont un encombrement stérique faible ou modéré, l'inégalité $I_{ae} < I_{ee}$ est nettement marquée quand ils sont en interaction avec le groupement *t*-butyle. Ces résultats ne sont pas en accord avec l'interprétation élémentaire, évoquée dans l'introduction, qui ne considère que les modifications

Can. J. Chem. Downloaded from www.nrcresearchpress.com by 210.87.254.105 on 09/05/12
For personal use only.

TABLEAU 1. Constantes d'équilibre $K = n_b/n_a$ et différences d'enthalpie libre (kcal mol^{-1}) entre stéréoisomères*

Equilibres	$K \times 10^2$	$(G_b^0 - G_a^0)$ Expér.	Calc.
1 *trans* ⇄ **1** *cis*	1.0±0.3	+3.2 ±0.2	—
2 *trans* ⇄ **2** *cis*	12.9±0.4	+1.43±0.02	—
3 *trans* ⇄ **3** *cis*†	40.7±0.3	+0.63±0.02	—
4 *trans* ⇄ **4** *cis*†	807±3	−1.47±0.03	—
5 ⇄ **7**	1.4±0.6	+3.0 ±0.3	$4.3 - I_{ee}$
5 ⇄ **9**	1.7±0.5	+2.8 ±0.2	3.4
5 ⇄ **11**	77±2	+0.18±0.02	1.3
6 ⇄ **8**	19.0±0.5	+1.17±0.02	2.4
6 ⇄ **10**§	8.3±0.6	+1.74±0.05	2.4
6 ⇄ **12**§	61±1	+0.34±0.01	2.2
13 *trans* ⇄ **13** *cis*‡	11.8	+1.4	—

*Sauf pour les composés **3**, **4** et **13**; solvant éthanol, $(C_2H_5ONa) = 0.8$ mol l^{-1}; $t = 78.5$ °C.
†Solvant *t*-butanol; $((CH_3)_3CONa) = 3$ mol l^{-1}; $t = 82.0$ °C.
‡Solvant méthanol; $(CH_3ONa) = 0.8$ mol l^{-1}; $t = 65.0$ °C; pour ce couple de stéréoisomère, les fractions molaires ont été obtenues directement à partir des surfaces des pics chromatographiques sans correction (*cf.* partie expérimentale).
§Le rapport des fractions molaires des isomères **10** et **12** (non séparable en c.p.p.v.) à l'équilibre a été déterminé par r.m.n. (signaux des groupements *t*-butyles).

TABLEAU 2.

Série:	Cyclohexanique	Cyclohexénique (position 4 ou 5)
$X = COOC_2H_5$	−1.24(22)	−1.1(3, 17)
$X = C{\equiv}N$	−0.19(5)	0.0(3)

énergétiques associées à des variations d'angles dièdres. Les calculs semi-empiriques (modèle de Westheimer) réalisés sur les isomères *cis–trans* et *trans–cis* du 2,5-di-*t*-butyl cyclohexanol (9) montrent la difficulté d'une interprétation selon un modèle simple; la rotation du *t*-butyl semble jouer un rôle déterminant.

L'importance des interactions *gauches* diéquatoriales I_{ee} impliquant un groupement *t*-butyle, se manifeste également dans les deux résultats suivants: (*a*) l'isomère *trans–cis–trans* du 2-*t*-butyl 5-méthyl cyclohexane 1,4-diol est partiellement sous forme flexible (7); (*b*) la mise en équilibre des isomères *trans–cis* et *trans–trans* du 3-*t*-butyl 1,2-dibromo cyclohexane (10) est réalisée presque exclusivement au profit du dernier ($K > 99$), l'isomère *trans–cis* impliquant une interaction *gauche* $(CH_3)_3C \ldots Br$ diéquatoriale.

Pour la série cyclohexénique, lorsque les deux substituants sont en positions 4,5 (tableau 3, dernière ligne), le seul résultat dont nous disposons (composés **13**) nous conduit à une valeur de la différence $(I_{ae} - I_{ee})$ à peu près égale à celle de la série cyclohexanique, alors que pour l'interaction entre deux groupements éthoxycarbonyles vicinaux, la différence $(I_{ae} - I_{ee})$ était nettement plus importante en série cyclohexanique (2).

Pour les positions 3,4 de la série cyclohexénique (tableau 3, avant-dernière ligne), l'interaction I_{ae} est nettement plus importante que I_{ee}, même avec le groupement cyano. D'autre part, avec un groupement méthoxycarbonyle, cette interaction croit en passant du groupement méthyle au *t*-butyle.[4] Ces deux remarques s'expliquent bien sur la base de contraintes stériques importantes pour les isomères *cis*, l'angle dièdre entre les substituants étant nettement plus faible que celui de l'isomère *trans*; en effet, pour le 3,4-diméthyl cyclohexène, il a été calculé un angle dièdre de 47° (11).

Pour les composés trisubstitués **5–12**, les différences d'enthalpie libre entre stéréoisomères ont été évaluées (ΔG^0 calc. du tableau 1) en admettant l'additivité des enthalpies libres conformationnelles ΔG_X^0 et des différentes inter-

[4]Pour l'interaction avec le groupement méthyle, la différence $(I_{ae} - I_{ee})$ est estimée à environ 1 kcal mol^{-1}, d'après la différence d'enthalpie libre entre les isomères *cis* et *trans* du 3-méthyl 4-méthoxycarbonyl cyclohexène, et une analyse conformationnelle par r.m.n. des composés deutériés (travaux non publiés de R. Geuss et J. P. Aycard).

Can. J. Chem. Downloaded from www.nrcresearchpress.com by 210.87.254.105 on 09/05/12
For personal use only.

TABLEAU 3. Différences entre les interactions *gauches* ($I_{ae} - I_{ee}$) (kcal mol^{-1})

	R	X = C≡N		X = COOR′ (R′ = CH_3 ou C_2H_5)		X = OH	
		ΔG^{0*}	($I_{ae} - I_{ee}$)	ΔG^{0*}	($I_{ae} - I_{ee}$)	ΔG^{0*}	($I_{ae} - I_{ee}$)
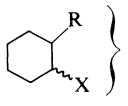	H	−0.2(5)	—	−1.2(5, 22)	—	−0.8(4)	
	CH_3	−0.2(5)	0.0	−2.2(5)	+1.0	−1.1(4)	+0.3
	$(CH_3)_3C$	+1.5	−1.7	−1.4	+0.2	+0.3(8)	−1.1
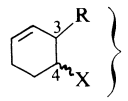	$(CH_3)_3C$	−0.6	+0.6	−3.2	+2.1	—	—
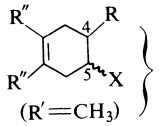	$(CH_3)_3C$	—	—	−1.4	+0.3	—	—

*Différence d'enthalpie libre associée au processus: (pour les composés du tableau 1, $\Delta G^0 = G_a^0 - G_b^0$).

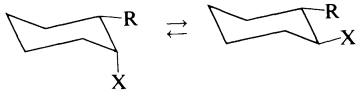

actions gauches R . . . X (tableau 3) et X . . . X,[5] ainsi que le blocage conformationnel du groupement *t*-butyle en position équatoriale ou pseudoéquatoriale. Par rapport aux valeurs expérimentales, les valeurs calculées sont toutes systématiquement surestimées d'environ 1 kcal mol^{-1} (2 kcal mol^{-1} pour le composé **12**). Ceci peut résulter d'une sous-estimation des interactions dans les stéréoisomères de référence (**5** et **6**). Ceux-ci adoptent vraisemblablement la conformation avec tous les substituants équatoriaux. Il peut être envisagé l'hypothèse d'un renforcement des interactions I_{ee} (*t*-Bu . . . $COOC_2H_5$) et I_{ee} ($COOC_2H_5$ . . . $COOC_2H_5$) résultant de l'impossibilité, pour le groupement éthoxycarbonyle central, de minimiser simultanément chacune de ces interactions par déplacement dans le plan équatorial de la molécule (effet de butoir des groupements vicinaux équatoriaux).[6]

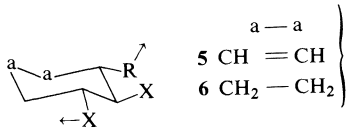

Partie expérimentale

(i) Composés disubstitués ***1–4***

Les composés cyclohexéniques **1** et **3** ont été synthétisés par condensation diénique (13, 14) entre le 5,5-diméthyl 1,3-hexadiène (15, 16) et l'acrylate d'éthyle (14 h à 170 °C) ou l'acrylonitrile (24 h à 150 °C), respectivement. Dans le premier cas, le produit obtenu (eb_{10} = 78 °C; rendement 75%) est un mélange des 3-*t*-butyl 4-éthoxycarbonyl cyclohexène **1** *cis* (49%) et **1** *trans* (38%) et des 3-*t*-butyl 5-éthoxycarbonyl cyclohexène **14** *trans* (7%) et **14** *cis* (6%). Dans le second cas, le produit obtenu (eb_{20} = 100 °C; rendement 55%) est un mélange constitué des 3-*t*-butyl 4-cyano cyclohexène **3** *cis* (42%) et **3** *trans* (53%) et des 3-*t*-butyl 5-cyano cyclohexène **15** (5%).

Les séparations des différents stéréoisomères ont été effectuées par chromatographie de partage en phase vapeur (c.p.p.v.) (pour les temps de rétention, *cf.* tableau 4). Dans le premier cas, si le composé **14** *cis* a un temps de rétention plus grand que les autres isomères, il n'est pas possible de séparer **1** *cis* (88%) et **14** *trans* (12%) (pourcentages estimés par r.m.n.).

Chacune des fractions a été hydrogénée pour donner les composés cyclohexaniques **2** et **4** correspondants, en présence d'oxyde de platine dans l'acide acétique pour **1**, et en présence de palladium-sur-charbon (5%) dans l'alcool éthylique pour **2** (500 mg de produit sont traités dans 25 cm^3 de solvant avec 10 mg de catalyseur). Il a

[5]Pour les interactions $COOC_2H_5$ . . . $COOC_2H_5$, ($I_{ae} - I_{ee}$) = +1.0 et 0.2 kcal mol^{-1} respectivement en séries cyclohexanique et cyclohexénique (positions 4,5) (2).

[6]Le déplacement du groupement central dans le plan équatorial pourrait expliquer la diminution de ΔpK observée (12) à la fois pour les isomères *trans–trans* et *cis–trans* du 2-amino 6-*t*-butyl cyclohexanol.

Can. J. Chem. Downloaded from www.nrcresearchpress.com by 210.87.254.105 on 09/05/12
For personal use only.

TABLEAU 4. Temps de rétention* en c.p.p.v. et déplacements chimiques† en r.m.n. $\delta \times 10^6$†

	t*	—CH(CO—O—)— (m)	—CH_2— (cycle) —CH(—$C(CH_3)_3$)— (m)	$(CH_3)_3C$— (s)	—CH_2—O—CO— (q)	CH_3—CH_2—O— (t)	CH=CH (m)
1 *trans*	8.0(*a*)	—	1.5 –2.5	0.88	4.00	1.20	5.60
1 *cis*	10.0(*a*)	2.6–2.9	1.6 –2.4	0.92	4.00	1.25	5.65
2 *trans*	6.3(*a*)	—	1.1 –2.1	0.82	3.90	1.20	—
2 *cis*	4.3(*a*)	2.8–3.0	1.1 –2.5	0.80	4.00	1.20	—
3 *trans*	45.9(*b*)	—	1.6 –2.8	1.0	—	—	5.75
3 *cis*	52.8(*b*)	2.85–3.3	1.56–2.6	1.06	—	—	5.70
4 *trans*	39.9(*c*)	—	1.06–2.35	1.06	—	—	—
4 *cis*	32.8(*c*)	2.8–3.1	1.0 –2.25	1.0	—	—	—
5	24.7(*d*)	—	1.8 –2.0	0.88	3.95	1.20	5.68
7	27.2(*d*)	2.8–3.0	2.0 –2.5	0.90	4.00	1.20	5.70
9	30.0(*d*)	3.0–3.2	2.0 –2.4	0.92	3.95	1.18	5.62
11	21.2(*d*)	3.0–3.1	2.0 –2.4	0.90	3.95	1.18	5.60
6	22.8(*e*)	—	1.1 –2.5	0.88	3.90	1.18	—
8	14.7(*e*)	2.5–2.7 3.2–3.3	1.2 –2.1	0.85	4.05	1.25	—
10	18.3(*e*)	2.9–3.1	1.1 –2.4	0.90	4.00	1.29	—
12	18.3(*e*)	2.7–2.9	1.1 –2.4	0.85	3.90	1.27	—
13 *trans*	17.0(*f*)	—	1.4 –2.5	0.85	3.50‡	—	1.45§
13 *cis*	13.0(*f*)	2.9	—	—	—	—	—

*t en min; phase stationnaire: 10% Reoplex 400 sur Chromosorb W 60/80; long. 1.5 m; diam. 3.5 mm; températures: (*a*) 100, (*d*) 137, (*e*) 142, (*f*) 105 °C; gaz vecteur (N_2): (*a*) 25, (*d*) 26, (*e*) 27.3, (*f*) 25 $cm^3\ mn^{-1}$. (*b*) phase stationnaire: 10% P.E.G. 1500 sur chromosorb W 60/80; long. 3 m; diam. 3.5 mm; température 115 °C; gaz vecteur (N_2): 26 $cm^3\ mn^{-1}$. (*c*) phase stationnaire: 10% P.E.G. 4000 sur chromosorb W 60/80; long. 3 m; diam. 3.5 mm; température 145 °C; gaz vecteur (N_2): 25 $cm^3\ mn^{-1}$.
†δ par rapport au TMS; solvant CCl_4 ou CS_2; (m) massif; (s) singulet; (q) quadruplet; (t) triplet.
‡CH_3—O—CO—.
§CH_3—C=C—CH_3.

été contrôlé, par c.p.p.v. et r.m.n., que l'hydrogénation est totale.

L'identification de ces différents composés a été assurée dans le cadre de l'hypothèse de conformations chaises (ou demi-chaises) et de la préférence conformationnelle du groupement *t*-butyle pour la position équatoriale (ou pseudo-équatoriale). Les arguments sont développés ci-dessous.

La mise en equilibre (par l'éthylate de sodium dans l'alcool éthylique) du composé **1** *trans* (temps de rétention: 8.0 min), conduit à un mélange de **1** *trans* (>99%) et de **1** *cis* (<1%) de temps de rétention 10.0 min; la mise en équilibre du mélange **1** *cis* (88%) + **11** *trans* (12%) conduit à un nouveau mélange: **1** *trans* (87%); **1** *cis* + **11** *trans* (4%); **11** *cis* (9%). Ces résultats montrent que le composé **1** *cis* correspond bien au second pic chromatographique (il se transforme essentiellement en son isomère **1** *trans*); d'autre part, la différence d'enthalpie libre associée à l'équilibre **1** *trans* ⇄ **1** *cis* ($\Delta G^0 = 3.2$ kcal mol^{-1}) (tableau 3) est très nettement différente de celle que l'on peut prévoir pour l'équilibre **11** *cis* ⇄ **11** *trans* ($\Delta G^0 \simeq 1.1$ kcal mol^{-1}) d'après l'enthalpie libre conformationnelle du groupement éthoxycarbonyle (3, 17, 18) situé en position 4 (ou 5) sur le cyclohexène[7]; dans ce cas, le groupement *t*-butyle, relativement éloigné, ne doit pas modifier sensiblement cette valeur. Enfin, l'épimérisation du 4-carboxyl 3-*t*-butyl cyclohexène (14) conduit à une proportion similaire des isomères *cis* et *trans* (5% et 95% respectivement).

La mise en équilibre (par le *t*-butylate de potassium dans l'alcool *t*-butylique) de **3** *cis* ou de **3** *trans* conduit à un mélange 28.9/71.1 de ces deux isomères.

En c.p.p.v., pour la série cyclohexanique, il a été remarqué (2, 19) que les composés à groupements éthoxycarbonyles équatoriaux ont des temps de rétention supérieurs à ceux de leurs isomères axiaux; cette inégalité est respectée pour les composés **2** *cis* et **2** *trans*. Par contre, en série cyclohexénique, les temps de rétention sont inversés (*cf.* tableau 4, composés **1** *cis* et **1** *trans*); cette observation est en accord avec les résultats d'Inukai et Kojima (20) concernant les 3-méthyl 4-méthoxycarbonyl cyclohexènes *cis* et *trans*, et avec nos propres résultats (*cf.* paragraphe (*ii*) concernant les isomères **5** et **7**. Les composés à groupement cyano ont des comportements analogues.

En r.m.n., les signaux d'un proton situé en α du groupement éthoxycarbonyle ou du groupement cyano se distinguent nettement, vers les champs faibles ($\delta \simeq 3.0 \times 10^{-6}$), quand ce groupement est axial; par contre, lorsqu'il est situé en position équatoriale, les signaux r.m.n. du proton axial correspondant sont situés dans le massif des autres protons du cycle (2, 19); pour chacun des isomères *cis* des composés **1**–**4**, il apparaît (tableau 4) un massif distinct entre 2.6 et 3.0×10^{-6} (et dont

[7]Le même argument a été utilisé pour identifier les composés **11** *cis* et **11** *trans*; toutefois, la précision expérimentale sur les pourcentages de ces isomères à l'équilibre n'est pas suffisante pour envisager une détermination quantitative de la différence d'enthalpie libre.

Can. J. Chem. Downloaded from www.nrcresearchpress.com by 210.87.254.105 on 09/05/12
For personal use only.

Can. J. Chem. Downloaded from www.nrcresearchpress.com by 210.87.254.105 on 09/05/12
For personal use only.

l'intégration correspond à un proton) confirmant la position axiale du substituant éthoxycarbonyle ou cyano.

Ainsi, les différentes remarques ci-dessus sont toutes en accord avec les identifications du tableau 4.

(ii) Composés trisubstitués à groupements éthoxycarbonyles trans ***5***, ***7***, ***6***, ***8***

La condensation diénique (18 h à 200 °C) entre le 5,5-diméthyl 1,3-hexadiène et le fumarate d'éthyle conduit à un mélange ($eb_{1.5}$ = 114–117 °C; rendement 70%) des 3-*t*-butyl 4,5-diéthoxycarbonylcyclohexène *trans–cis*[8] **5** (39%) et *cis–trans* **7** (61%); après séparation par c.p.p.v. préparative, chacun de ces isomères a été hydrogéné pour accéder aux composés cyclohexaniques correspondants (**6** et **8** respectivement).

L'identification des isomères a été réalisée grâce aux observations suivantes.

En r.m.n. (tableau 4), le composé **8** présente deux massifs centrés à 2.6×10^{-6} (intégration: 1 H) et à 3.3×10^{-6} (1 H) correspondant manifestement (*cf.* remarque ci-dessus) à deux protons équatoriaux en α des substituants éthoxycarbonyles diaxiaux; par contre, pour le composé **6**, les massifs correspondants ne se distinguent pas des signaux des protons du cycle.

En c.p.p.v. (tableau 4), le temps de rétention du composé **8** est inférieur à celui de son isomère **6**, en bon accord avec la remarque du paragraphe (*i*) ci-dessus.

Puisque les composés **6** et **8** résultent respectivement de l'hydrogénation des isomères **5** et **7**, l'identification de ces derniers est également assurée. Nous constatons d'autre part que: pour le composé **7**, les protons en α des groupements éthoxycarbonyles donnent lieu à une résonance à champ faible (massif entre 2.8 et 3.0×10^{-6}) confirmant la position diaxiale de ces deux groupements; et le temps de rétention de ce composé (27.2 mn) est supérieur à celui de l'isomère **5** à groupements éthoxycarbonyles diéquatoriaux (24.7 mn), soit un ordre inverse par rapport à celui de la série cyclohexanique.

(iii) Composés trisubstitués à groupements ethoxycarbonyles cis ***9***, ***11***, ***10***, ***12***

La condensation diénique (18 h à 200 °C) entre le 5,5-diméthyl 1,3-hexadiène et le maléate d'éthyle conduit à un mélange ($eb_{1.5}$ = 114–118 °C; rendement 60%) des 3-*t*-butyl 4,5-diéthoxycarbonylcyclohexène *cis–cis* **9** (46%) et *trans–trans* **11** (54%); après séparation par c.p.p.v. préparative, chacun de ces isomères a été hydrogéné pour accéder aux composés cyclohexaniques correspondants (**10** et **12** respectivement).

Pour chacun de ces quatre composés, le spectre r.m.n. fait apparaître un massif (intégration: 1H) pour des déplacements chimiques compris entre 2.7 et 3.2×10^{-6}; ce résultat confirme la présence d'un substituant éthoxycarbonyle axial pour chacun. D'autre part, en série cyclohexénique, pour le signal des protons du groupement *t*-butyle, le déplacement chimique est plus grand pour le composé dont le groupement éthoxycarbonyle vicinal est axial (*cf.* tableau 4; comparer les valeurs pour les couples **1** *cis*/**1** *trans* et **7**/**5**). Si l'on admet qu'il en est de même pour le couple des composés **9**/**11**, le composé ayant le plus faible temps de rétention (tableau 4) est identifié avec le composé **11**.

La mise en équilibre effectuée à partir de l'un de ces composés cyclohexéniques **5**, **7**, **9** ou **11** conduit à un mélange identique de ces composés dans les proportions suivantes: 55.7, 0.8, 1, et 42.6% respectivement. Le très faible pourcentage du composé **7** à l'équilibre est en accord avec la très forte interaction *gauche* (mise en évidence par l'équilibre **1** *trans* ⇄ **1** *cis*) entre le groupement *t*-butyle et un groupement éthoxycarbonyle vicinal situé en position axiale. Cet accord constitue une indication relativement nette en faveur de l'identification effectuée pour les isomères **9** et **11**; elle assure celle des composés **10** et **12**.

(iv) 1,2-Diméthyl 4-méthoxycarbonyl 5-t-butylcyclohexènes ***13***

Compte-tenu de l'impossibilité de condenser le 1,3-butadiène avec l'ester méthylique du 4,4-diméthyl 2-pentenoïque *trans*,[9] nous avons réalisé la synthèse diénique entre ce dernier et le 2,3-diméthyl 1,3-butadiène (48 h à 170 °C). Elle conduit, avec un rendement de 30% après séparation en c.p.p.v., à l'isomère **13** *trans*.

L'absence de signaux r.m.n. entre 2.5 et 3.2×10^{-6} est en accord avec la position équatoriale du groupement méthoxycarbonyle. La mise en équilibre, par le méthylate de sodium dans l'alcool méthylique, du composé **13** *trans* conduit à un mélange constitué de ce dernier et de son isomère **13** *cis* (10.6%). Celui-ci n'a pas été isolé, mais le spectre r.m.n. du mélange présente un signal de faible intensité à 2.9×10^{-6} correspondant au proton équatorial en α du groupement méthoxycarbonyle de **13** *cis*.

Il est à noter que le temps de rétention de l'isomère *cis* est inférieur à celui de l'isomère *trans* (tableau 4) comme pour les 1,2-diméthyl 4,5-diéthoxycarbonyl cyclohexènes (2), mais contrairement à ce que nous avons observé pour le couple **1** *cis*/**1** *trans* et pour les 4,5-diéthoxycarbonyl cyclohexènes (2).

(v) Mises en equilibre

Elles ont été réalisées dans les conditions décrites dans des publications antérieures (2, 5). Lorsque deux isomères ont des temps de rétention identiques (**1** *cis* et **14** *trans*; **10** et **12**), il a été considéré que le facteur correctif des aires des pics chromatographiques était le même pour ces deux isomères; leur proportion a été déterminée par r.m.n.

La mise en équilibre des isomères **13** a été effectuée dans le méthanol anhydre sous l'action du méthylate de sodium. Comme l'isomère *cis* n'a pas été isolé à l'état pur, un facteur correctif de 1.0 a été arbitrairement choisi.

---

[8]Ces deux suffixes se rapportent aux substituants éthoxycarbonyles (respectivement en positions 4 et 5) par rapport au groupement *t*-butyle.

[9]Ce diénophile a été préparé par la méthode de Brändström (21); sa structure *trans* a été confirmée par r.m.n. (δ × 10^6; s, singulet; d, doublet)

$$(CH_3)_3C\text{—}CH{=}CH\text{—}COOR$$
a b c e

R = H (solvant $CDCl_3$); a, 1.09 (s); b, 5.7 (d); c, 7.5 (d) (J = 16.5 Hz); e, 10.9 (s).

R = CH_3 (solvant (CCl_4); a, 1.09 (s); b, 5.8 (d); c, 6.8 (d) (J = 16.0 Hz); e, 3.6 (s).

Une partie de ces résultats a été exposée au cours de plusieurs conférences au Canada en juillet 1971; au cours des discussions qui ont suivi, des critiques et des suggestions ont été faites par de nombreux collègues Canadiens; nous les remercions pour leur contribution et pour leur accueil très chaleureux. Nous remercions également les deux rapporteurs pour leurs critiques constructives.

1. J. TORRI et H. BODOT. C. R. Acad. Sc. Paris. **274**, 89 (1972).
2. J-P. AYCARD, H. BODOT et R. LAURICELLA. Bull. Soc. Chim. Fr. 3516 (1969).
3. J-P. AYCARD, H. BODOT, R. GARNIER, R. LAURICELLA et G. POUZARD. Org. Mag. Res. **2**, 7 (1970).
4. J. SICHER et M. TICHY. Coll. Czech. Chem. Comm. **32**, 3687 (1967).
5. M. TICHY et J. SICHER. Coll. Czech. Chem. Comm. **33**, 68 (1968).
6. R. D. STOLOW, A. A. GALLO et J. L. MARINI. Tetrahedron Lett. 4655 (1969).
7. R. S. STOLOW et J. L. MARINI. Tetrahedron Lett. 1449 (1971).
8. D. J. PASTO et D. R. RAO. J. Am. Chem. Soc. **92**, 5151 (1970).
9. D. H. FABER et C. ALTONA. Chem. Commun. 1210 (1971).
10. P. L. BARICI, G. BELLUCI, G. BERTI, F. MARIONI, A. MARSILI et I. MORELLI. Chem. Commun. 1437 (1970).
11. R. BUCOURT et D. HAINAUT. Bull. Soc. Chim. Fr. 1366 (1965).
12. C. FREPPEL, J. C. RICHER, A. TCHAPLA et Z. WELWART. Can. J. Chem. Soumis pour publication.
13. K. ALDER, K. HEIMBACH et E. KUHLE. Chem. Ber. **96**, 1364 (1953).
14. G. P. KUGATOVA-SHEMYAKINA et V. B. BERZIN. Zhur. Org. Khim. **7**, 85 (1971).
15. G. P. STEVENS. J. Am. Chem. Soc. **57**, 1112 (1935).
16. Z. N. KOLYASKINA et A. A. PETROV: Zhur. Obshchei Khim. **32**, 1067 (1962).
17. N. S. ZEFIROV, V. N. CHEKULAEVA et A. I. BELOZEROV. Tetrahedron, **25**, 1997 (1969).
18. N. S. ZEFIROV, N. M. SERGEEV, V. N. CHEKULAEVA et L. G. GURVICH. Dokl. Akad. Nauk, SSSR, **190**, 345 (1970).
19. B. J. ARMITAGE, G. W. KENNER et M. J. T. ROBINSON. Tetrahedron, **20**, 747 (1964).
20. T. INUKAI et T. KOJIMA. J. Org. Chem. **32**, 869 (1967).
21. A. BRÄNDSTRÖM. Acta Chem. Scand. **13**, 610 (1959).
22. N. L. ALLINGER et L. A. FREIBERG. J. Org. Chem. **31**, 894 (1966).

Can. J. Chem. Downloaded from www.nrcresearchpress.com by 210.87.254.105 on 09/05/12
For personal use only.

Post-infectional Inhibitors from Plants. IV. The Structure of Capsidiol, an Antifungal Sesquiterpene from Sweet Peppers[1]

M. GORDON, A. STOESSL, AND J. B. STOTHERS

University of Western Ontario and Research Institute, Canada Agriculture, University Sub Post Office, London 72, Ontario

Received August 28, 1972

Chemical and spectroscopic studies of the title compound have led to **1** as a representation of its structure.

A la suite d'études chimiques et spectroscopiques la représentation **1** est proposée comme structure du composé mentionné dans le titre. [Traduit par le journal]

Can. J. Chem., **51**, 748 (1973)

Can. J. Chem. Downloaded from www.nrcresearchpress.com by 210.87.254.5 on 09/05/12
For personal use only.

Capsidiol, an antifungal compound produced by the fruit of sweet peppers in response to inoculation with fungi, may have importance in the natural resistance of the plant to fungal disease (1). It can be assigned structure **1** on the basis of the chemical and spectral data reported here.

Capsidiol is optically active and has the molecular constitution $C_{15}H_{24}O_2$ as established by elemental analysis and high resolution mass spectrometry. The i.r. spectrum indicates the absence of carbonyl and the presence of hydroxyl functions. The latter are identifiable as two secondary alcohols by acetylation of **1** to an oily diacetate **2** which exhibits characteristic downfield shifts, relative to their resonance position in the proton spectrum of capsidiol, of two one-proton multiplets (Table 1). An isopropenyl group in capsidiol is responsible for a three-proton signal at δ 1.74 (vinylic methyl), two one-proton multiplets at δ 4.70 and 4.73, and i.r. absorption (in $CHCl_3$) at 888 cm^{-1} (1,1-disubstituted double bond). On hydrogenation of **1** to dihydrocapsidiol **3**, these bands vanish while two doublets appear at δ 0.88 and 0.90. The proton spectrum of **1** reveals, in addition, the presence of one other secondary and one tertiary methyl group as well as of a trisubstituted double bond (one-proton multiplet at δ 5.91); since capsidiol is transparent to light above 215 nm, this bond is not conjugated with the isopropenyl group.

The sum of these data accounts for all the functional groups of capsidiol and requires it to be bicyclic. Further information is available from a closer examination of the hydroxyl functions. Splitting patterns in the proton spectrum of **1** show that one of the alcoholic methine protons is vicinal to three other protons, while the second is flanked by only two protons. Their partly superimposed resonance signals appear as an eight-line pattern at δ 4.59 and as a triplet at δ 4.35, respectively. A decoupling experiment at 220 MHz demonstrated that the two protons are not vicinal to each other but suggested instead that both are coupled to the same methylene group; that is, that they are in a 1,3-relationship. This inference was confirmed and extended by chemical means.

Oxidation of capsidiol with dilute Jones' reagent furnished a mixture of capsenone (**4**) and the unconjugated ketone **5**. Both compounds were isolated in small amounts as oils.

Capsenone (**4**) became more readily available when it was discovered that the compound, identified by i.r., u.v., n.m.r., and mass spectra, was produced in pepper fruit after inoculation with certain fungi or on supplying capsidiol to cultures of these fungi in a synthetic medium (2). It is a conjugated ketone, ν_{max} 1692 cm^{-1}, whose u.v. absorption (λ_{max} 238 nm, ε 6300) recalls that of 3β-hydroxy-4-cholesten-6-one (λ_{max} 239 nm, ε 6300) (3*a*). The proton spectrum is in accord with the formulation of **4** as a six- or higher-membered cyclic ketone conjugated with an exocyclic double bond. The absorption of the lone olefinic proton (H-5) is shifted downfield from δ 5.91 in **1** to 6.71 in **4** with its splitting

[1]Contribution No. 536 from the Research Institute and Part XXV in the series NMR Studies (for Part XXIV see ref. 7).

TABLE 1. Proton magnetic resonance data: chemical shifts

Compound	1	2	3	4	5	6	7
H-1	1.72					2.25	2.15
H-2	4.59	5.57	4.56	4.47	—	6.00	—
H-3a	1.67	1.70		2.36	2.78		
						6.82	5.75
H-3e	1.35	1.90		2.70	2.46		
H-4	4.35	5.40	4.32	—	4.65	—	6.91
H-5	5.91	6.10	5.88	6.71	6.12	6.91	6.32
H-6, H′-6	1.90	1.88, 2.13		2.25	1.97, 2.10		2.00, 2.12
H-7		1.89		2.25	2.10		2.22
H-8, H′-8						1.41, 1.94	1.43, 1.86
$=CH_2$	4.70, 4.73	4.68, 4.72	—	4.72, 4.76	4.65, 4.71	4.73, 4.77	4.72, 4.76
Me-1	0.88	0.90	0.83	1.05	1.14	1.13	1.08
Me-9	1.37	1.33	1.34	1.11	1.27	1.23	1.18
Me-vinyl	1.74	1.72	0.88, 0.90	1.75	1.76	1.76	1.76
OAc	—	2.02, 2.04	—	—	—	—	—

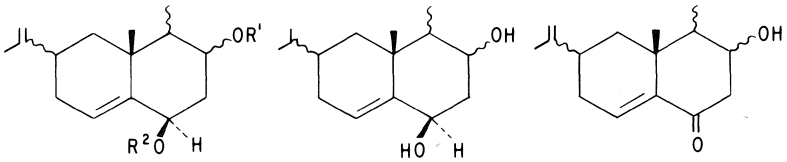

1 R' = R² = H
2 R' = R² = Ac
8 R' = SO_2Me, R² = H

3 4

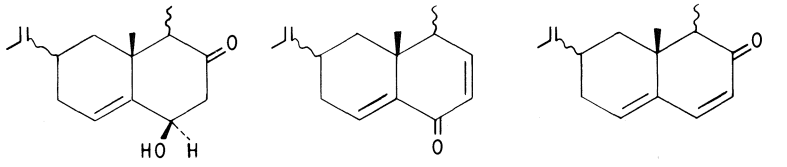

5 6 7

pattern unchanged, indicating a β-*cis*-relation to the carbonyl at C-4; the intervening carbon atom must be a ring junction. Capsenone is stable to dilute base but on treatment with alkoxide in deuteriomethanol, two deuterium atoms are substituted for the two hydrogens on C-3. This collapses the eight-line pattern arising from H-2 into a doublet and confirms the 1,3-disposition of the two oxygen functions. On treatment of **4** with acid under mild conditions, the hydroxyl attached to C-2 is eliminated, with the formation of isocapsidienone which may be formulated as the cross-conjugated ketone **6**.

Compound **5** absorbs at 1718 cm^{-1} (unstrained nonconjugated ketone). Unlike capsenone, **5** is extremely labile to very dilute base which converts it instantaneously into capsidienone **7**. This compound exhibits carbonyl absorption at 1678 cm^{-1} but no hydroxyl absorption while its maximum at 290 nm (ε 12 200) corresponds to that reported for 3,5-cholestadien-2-one (λ_{max} 290 nm, ε 12 600) (3*b*).

Capsidienone is more conveniently accessible by manganese dioxide oxidation of capsidiol, in a slow reaction proceeding via **5** as an intermediate. Capsenone (**4**), the expected product of allylic oxidation, is generated in this reaction in only barely detectable traces. This evidently reflects severe steric hindrance of the C-4 hydroxyl group. The same inference may be drawn from the reaction of capsidiol with an excess of methanesulfonyl chloride, to form the 2-monomesylate **8** as the only major product. The mesylate was characterized unambiguously by its proton spectrum, having methanesulfonyl

Can. J. Chem. Downloaded from www.nrcresearchpress.com by 210.87.254.5 on 09/05/12
For personal use only.

Can. J. Chem. Downloaded from www.nrcresearchpress.com by 210.87.254.5 on 09/05/12
For personal use only.

absorption at δ 3.01 and the eight-line pattern for H-2 at δ 5.49, well separated from the H-4 doublet of doublets at δ 4.39. The instability and pronounced tendency of **8** to yield intractable products precluded its use in further studies.

To account for the splitting pattern of H-2 in capsidiol and its derivatives, only one proton can be located at C-1. A ring junction at C-1 must be excluded because the ring cannot be smaller than six-membered and one junction has already been identified at C-10. Of the two remaining candidates for C-1 substitution, the isopropenyl group must also be excluded. Its presence at C-1 in compounds **5**, **6**, and **7** would provide extra deshielding of H-1, which would then be expected to absorb in the unobscured region of the proton spectra below δ 2.3. No such absorption can be observed. The substituent at C-1 is therefore the secondary methyl group, whose resonance does in fact undergo downfield shifts on oxidation of the hydroxyl functions. Further, irradiation of the secondary methyl in **7** simplifies part of the spectrum between δ 1.95 and 2.40 with the appearance of a singlet at 2.15. The singlet must represent the decoupled absorption of H-1 which cannot, therefore, be vicinal to protons other than those of the methyl group. This result implies that C-1 is situated between the carbonyl group and a fully substituted carbon atom.

The olefinic proton H-5 in capsidiol and its derivatives is characterized by splitting patterns which require it to be adjacent to an unsubstituted methylene group, thus excluding C-6 as a possible site for the isopropenyl group. A decoupling experiment showed that the latter is equatorially bonded to a carbon bearing at least one hydrogen atom. Irradiation at δ 2.22 (H-7) removed the 12.2 Hz coupling observed for the signal centered about δ 1.43 while the 14.4 Hz coupling, assigned to the geminal interaction, remained. These data lead to the following part structure for capsidiol.

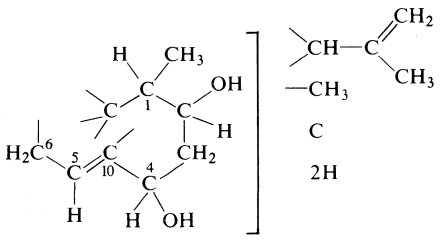

The only biogenetically-plausible, bicyclic structure in which these fragments can be combined is that presented by **1**. The observed coupling constants and shielding effects indicate its stereochemistry to be as in **9** *if the B ring is a chair*. Deshielding effects on the angular methyl group and the coupling constants of H-4 indicate that the C-4 hydroxyl and angular

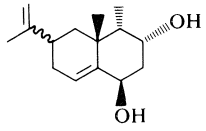

9

methyl groups are *syn*-diaxial. Since $J_{2,3a}$ is 12.0 Hz, H-2 is axial and since $J_{1,2} = 4.8$ Hz, it follows that H-1 is equatorial and consequently, the secondary methyl is axial. In the closely related eremophilanes, the corresponding methyl groups are *cis* (4). If this were the case for capsidiol, the B ring must exist in a boat conformation and from the presently available ^{1}H n.m.r. results, this possibility cannot be unequivocally excluded, although examination of models suggests that the boat conformation would not be as rigid as the 12.0 Hz coupling implies. Since preliminary ^{13}C n.m.r. data also appear to support the unexpected *trans*-diaxial disposition of the methyl groups, a detailed ^{13}C study is underway.

Experimental

Solvents were redistilled. Ethanol refers to 96% ethanol, light petroleum to the fraction boiling at 37–67°. T.l.c. was done on silica gel (Camag DF5) or alumina (Camag DSF5) in tanks saturated with solvent vapor, column chromatography on BDH silica gel (60–120 mesh). Melting points were determined on the Kofler block; i.r. spectra with a Unicam SP 1000 spectrophotometer; u.v. spectra on ethanolic solutions with a Beckman DK instrument. N.m.r. spectra were determined on deuteriochloroform solutions with tetramethylsilane as internal reference. The data given in Tables 1 and 2 were obtained with a Varian HA-100 spectrometer after the samples had been shaken with a drop of D_2O. Coupling constants (±0.05 Hz) were averaged from several scans at 100 or, more frequently, 50 Hz sweep-widths calibrated every 5 Hz. Decoupling experiments were carried out using stacked General Radio 1310 and 1310A oscillators and chemical shifts determined in this way were the measured difference frequencies when the appropriate maximum decoupling was achieved. Most of the chemical shifts, ±0.01 p.p.m., were determined from calibrated 250 or 100 Hz wide spectra. A 220 MHz spectrum and decoupling experiments on a degassed sample of **1** were

TABLE 2. Proton magnetic resonance data: coupling constants

Compound	1	2	3	4	5	6	7
1e, 2a	4.8_0	5.8_0	4.7_1	4.8_8	—	5.7_5	—
1e, Me-1	7.0_0	7.0_0	7.1_0	7.0	7.3_8	7.2_5	7.4_0
2a, 3a	12.0_0	11.5_0	11.9_5	11.1_7	—		—
						10.0_3	
2a, 3e	4.8_0	5.8_0	4.7_1	6.1_4	—		—
3a, 3e	13.0_0			16.8_1	15.3_8	—	—
3a, 4e	3.7_1	3.4_8	3.7_3	—	5.4_0	—	
							9.8_5
3e, 4e	2.5_2	2.5_3	2.5_4	—	1.8_7	—	
3e, 5				1.1_3	1.7_5		0.6_1
4, 5				—		—	0.8_3
5, 6	2.4_2	2.3_8		2.3_6	2.3_6	2.3_4	2.4_0
5, 6′	6.2_7	6.1_2		6.6_4	6.2_1	6.3_9	6.4_0
7a, $=CH_2$	0.8_0	0.8_0		0.7_9	0.9_8	0.7_5	0.7_0
7a, 8a						12.6_5	12.2_0
7a, 8e						2.9_3	2.6_0
8a, 8e						14.1_3	14.4_0
$=CH_2$	1.8_0	1.8_0		1.6_9	1.8_4	1.7_5	1.7_0

provided by the Canadian 220 MHz NMR Centre, Sheridan Park, Ontario. Other spectra were obtained with a Varian A60A instrument and their assignments were not confirmed by decoupling experiments. Molecular weights were obtained by Dr. D. B. MacLean and T. Martin by mass spectrometry. Specific rotations were determined on a Schmidt–Haensch polarimeter.

Capsidiol (1)

The isolation of capsidiol (**1**) from aqueous diffusates from fungus-inoculated fruit of *Capsicum frutescens* L. has been described (1). When other components of the crude ether extract are not required for study, it is advantageous to replace chromatography over silica gel (1) by chromatography over alumina (Woelm 200 neutral, grade III) with chloroform as eluant. Only the latter system was effective in the isolation of capsidiol from the more complex ether extracts obtained from tissue homogenates of inoculated fruit.

Pure capsidiol, m.p. 152–153°, is obtained by recrystallization from ether or ether – light petroleum. A form melting at 167–169° was obtained occasionally but reverted to the form, m.p. 152–153°, on recrystallization. Capsidiol is very soluble in methanol and ethanol, more sparingly in ether and chloroform, and almost insoluble in water. It has $[\alpha]_D^{22°}$ +21° (*c*, 2.1 in chloroform) and ν_{max} (KBr) 3430, 1651, 1472, 1455, 1382, 1217, 1060, 1022, 900, and 720 cm^{-1}.

Anal. Calcd. for $C_{15}H_{24}O_2$ (mol. wt. 236): C, 76.22; H, 10.24. Found (236): C, 76.07; H, 10.19.

Capsidiol diacetate (2)

Capsidiol (7 mg) was treated with acetic anhydride (0.3 ml) in pyridine (0.5 ml) at room temperature overnight. Evaporation gave the diacetate **2** as a syrup, homogeneous by t.l.c. and proton spectrum, and further characterized by ν_{max} (CCl_4) 1737, 1643, 1468, 1442, 1372, 1242, 1219, 1027, 1013, and 889 cm^{-1}.

Dihydrocapsidiol (3)

Capsidiol (125 mg) in isopropanol was hydrogenated by the standard procedure (5) in the Brown hydrogenator except that acetic acid was used instead of hydrochloric acid. Absorption of hydrogen ceased with 0.85 mol equiv. The product was filtered, the filter-cake washed with hot ethanol, and the combined filtrates evaporated to dryness. The residue was extracted with benzene, the extracts were re-evaporated, and the product refiltered in ether after addition of Celite. After concentration to *ca.* 1 ml and addition of light petroleum, dihydrocapsidiol (60 mg) crystallized out and was recrystallized from ether as needles, m.p. 153–155°, depressed on admixture with capsidiol, $[\alpha]_D^{23°}$ −3° (*c*, 1.00 in chloroform); ν_{max} (KBr) 3440, 1472, 1390, 1230, 1052, 1031, and 720 cm^{-1}.

Anal. Calcd. for $C_{15}H_{26}O_2$ (mol. wt. 238): C, 75.58; H, 11.00. Found (238): C, 75.55; H, 11.07.

Oxidation of Capsidiol

(*i*) Capsidiol (70.2 mg, 0.3 mmol) in acetone (18 ml) was chilled to ice-temperature, removed from the cooling bath, and treated dropwise and with vigorous shaking with 0.6 *N* chromic oxide in 0.6 *N* sulfuric acid (1.0 ml) during 15 min. After being shaken at room temperature for another 60 min, the product was diluted with water (20 ml) and extracted with ether (3 × 40 ml). The syrup obtained on evaporation of the washed and dried extracts was chromatographed over a column of silica gel (8 g; 105 fractions, 20 ml each; increasing concentrations of ether in light petroleum to ether). Suitably combined fractions were rechromatographed over silicic acid (Mallinckrodt) – Celite (4:1) with ether (15%) in light petroleum or by preparative t.l.c. (silica; 5% methanol in chloroform; also used to monitor the fractionation), and again over silica gel (25–30% ether in light petroleum).

The compounds isolated in essentially pure form were: (*a*) Unreacted capsidiol (16.5 mg). (*b*) Capsenone (**4**) (9.5 mg), viscous oil, ν_{max} ($CHCl_3$) 3780, 3460, 3030 (sh),

Can. J. Chem. Downloaded from www.nrcresearchpress.com by 210.87.254.5 on 09/05/12
For personal use only.

2980, 2960, 1692, 1685 (sh), 1633, 1468, 1380, and 896 cm^{-1}.

Mol. Wt. Calcd. for $C_{15}H_{22}O_2$: 234. Found: 234.

(*c*) The ketone **5**, (4.4 mg), viscous oil, ν_{max} ($CHCl_3$) 3790, 3470, 3040 (sh), 2990, 2960, 1718, 1650, 1468, 1382, 990, and 900 cm^{-1}.

Mol. Wt. Calcd. for $C_{15}H_{22}O_2$: 234. Found: 234.

The u.v. spectrum showed end-absorption and a band (ε 300) near 286 nm, possibly attributable to an impurity. Addition of 0.10 *N* sodium hydroxide solution (0.10 ml) to the alcoholic solution (3.0 ml) containing **5** (6×10^{-3} mg) and immediate redetermination of the spectrum (< 30 s) gave an intense maximum at 290 nm (ε 11 400) stable during at least 0.5 h and to subsequent acidification.

(*ii*) The ether-soluble product from a similar oxidation of capsidiol (93.6 mg) was dissolved in ethanol (100 ml) and 1.0 *N* sodium hydroxide solution (1.0 ml) was added. After 2 min, the solution was acidified (10.0 ml 1.0 *N* hydrochloric acid), diluted with water, and extracted with ether. After washing, drying, and evaporating, the extract was chromatographed over silica gel (20 g). Fractions 11–28 (10–15% ether in light petroleum, 2.5 ml per fraction) furnished chromatographically homogeneous capsidienone (**7**) (15.4 mg) as a colorless oil, ν_{max} (liquid) 3100, 2990, 2950, 2890, 1678, 1635, 1589, 1465, 1455, 1398, 1373, 1250, 1209, 1060, 1009, 894, 875, and 842 cm^{-1}.

Mol. Wt. Calcd. for $C_{15}H_{20}O$: 216. Found: 216.

Fractions 44–49 (30% ether) gave capsenone (7.9 mg). More capsenone (6.8 mg) and capsidiol (14.3 mg) were obtained by preparative t.l.c. of fractions eluted subsequently (50%, 100% ether).

(*iii*) Capsidiol (104 mg) in benzene (10 ml) was stirred with active manganese dioxide (1 g) (6) at room temperature. T.l.c. indicated that slow conversion of **1** into **7** occurred with **5** as an intermediate accumulating only in traces. More oxidant was added after 6 and 10 days (0.60, 0.84 g respectively). After another day, the mixture was diluted with benzene, filtered, and the filter cake washed with ether. The residue (56 mg) from the combined filtrates was chromatographed over silica gel (5 g) in ether – light petroleum (1:4) to furnish pure **7** (n.m.r., u.v., i.r., t.l.c.; 49 mg).

Dideuteriocapsenone

To capsenone (16.6 mg) dissolved in methanol-d_4 (0.4 ml) was added potassium *tert*-butoxide (11.2 mg) in methanol-d_4 (0.6 ml). After 5 min, the yellow color of the solution was discharged by the dropwise addition of acetic acid-d_4 and deuterium oxide was added. The product was extracted with carbon tetrachloride, the extracts were washed with a little deuterium oxide, dried (sodium sulfate) and evaporated. Mass spectrometry was done on a sample further purified by t.l.c. (silica; *sec*-butanol – ethyl acetate – acetic acid 5:95:0.1) with substitution of hydrogen for the hydroxylic deuterium.

Mol. Wt. Calcd. for $C_{15}D_2H_{20}O_2$: 236. Found: 236.

Isocapsidienone (6)

To capsenone (15 mg) in ethanol (3 ml) was added concentrated hydrochloric acid (0.05 ml). Reaction was complete after about 8 h at room temperature. The solution was neutralized by addition of calcium carbonate and evaporated. The residue was extracted with chloroform, the extract washed with water, and freed from minor impurities by preparative t.l.c. on silica (methanol–chloroform 5:95). The resultant oil had ν_{max} (liquid) 3095, 3045, 2980, 2945, 2890, 1678, 1632, 1468, 1388, 1262, 892, and 808 cm^{-1} and λ_{max} 238 nm (ε 7800), λ_{sh} 267 nm (ε 4300).

Mol. Wt. Calcd. for $C_{15}H_{20}O$: 216. Found: 216.

Mesylation of Capsidiol

Capsidiol (121 mg) in pyridine (2.4 ml) at −5° was treated with freshly distilled methanesulfonyl chloride (0.10 ml; *ca.* 2.5 equiv). After 18 h at room temperature, the product was poured on ice (10 ml), acidified with concentrated hydrochloric acid (3.3 ml added dropwise), and extracted with chloroform. The oil obtained by evaporation of the washed and dried extract was chromatographed over silica gel (16.5 g). Fractions 45–50 (20 ml each; ether – light petroleum 1:1) and 51–60 (ether) contained material (94 mg) consisting predominantly of capsidiol-2-monomesylate (only traces of impurities detectable in the proton spectrum). On attempted remesylation at room temperature during 48 h, the material decomposed to an intractable product.

We are grateful to Prof. D. B. MacLean and Mr. T. Martin for providing us with mass spectrometric data and to the National Research Council of Canada for financial support of this study.

1. A. Stoessl, C. H. Unwin, and E. W. B. Ward. Phytopathol. Z. **74**, 141 (1972).
2. E. W. B. Ward and A. Stoessl. Phytopathol. **62**, 1186 (1972).
3. A. I. Scott. Interpretation of the ultraviolet spectra of natural products. Pergamon Press, New York. 1964. (*a*) p. 399, (*b*) p. 407.
4. A. R. Pinder. Perfum. and Essent. Oil Record, **59**, 280 (1968).
5. C. A. Brown and H. C. Brown. J. Org. Chem. **31**, 3989 (1966).
6. L. A. Carpino. J. Org. Chem. **35**, 3971 (1970).
7. M. Gordon, A. Stoessl, and J. B. Stothers. Can. J. Chem. **50** 122 (1972).

Can. J. Chem. Downloaded from www.nrcresearchpress.com by 210.87.254.5 on 09/05/12
For personal use only.

Some Electron Spin Resonance Observations in the Photoreduction of Nitrobenzenes

S. K. WONG AND J. K. S. WAN

Department of Chemistry, Queen's University, Kingston, Ontario

Received October 10, 1972

The photoreduction of some nitrobenzenes in various organic solvents was re-investigated by e.s.r. and the rapid scan e.s.r. method. The present study resolved the contradicting e.s.r. assignments of the radical observed in the photoreduction of nitrobenzene in tetrahydrofuran and confirmed the identification of the radical PhN(Ȯ)OR. All other radicals observed in various solvents were identified and their formation can be explained by secondary processes in the photoreduction.

La photoréduction de certains nitrobenzènes a été étudiée de nouveau dans plusieurs solvants organiques par r.s.e. (résonance de spin électronique) et par r.s.e. en balayage rapide. L'étude présente permet d'élucider les attributions contradictoires en r.s.e. du radical observé lors de la photoréduction du nitrobenzène dans le tétrahydrofuranne et confirme l'identification du radical PhN(Ȯ)OR. Tous les autres radicaux observés dans différents solvants ont été identifiés et leur formation peut s'expliquer par des processus secondaires dans la photoréduction. [Traduit par le journal]

Can. J. Chem., **51**, 753 (1973)

Introduction

Electron spin resonance spectroscopy has been widely used to identify paramagnetic intermediates in photochemical reactions; conversely photochemical reactions have provided convenient methods of generating radicals for e.s.r. study of their structures (1). The application of e.s.r. technique to investigate the photoreduction of nitro-compounds is one of the more controversial examples. In 1962 Lagercrantz and Yhland (2) first observed the e.s.r. spectra of a photoparamagnetic species in a tetrahydrofuran (THF) solution of *s*-trinitrobenzene. The authors (2) proposed the assignment of an *s*-trinitrobenzene radical anion, produced by a charge-transfer mechanism. Briegleb and Lind (3) later confirmed the charge-transfer process but the assignment of the e.s.r. spectra to the trinitrobenzene radical anion was challenged by Ward (4). Using deuterium-labelled THF as solvent in the photolysis of nitrobenzene, Ward (4) has observed a further hyperfine splitting due to a hydrogen atom from the solvent. Thus, he reassigned the spectra of the photoparamagnetic intermediate to the radical PhN(Ȯ)OH and suggested that the excited nitrobenzene abstracted a hydrogen atom from the solvent as the initial step in the photoreduction of aromatic nitro-compounds. This interpretation has gained general acceptance in the past (5–8). However, Cowley and Sutcliffe (9) have recently reported some good evidence that the photointermediate in the photolysis of nitrobenzene has the structure PhN(Ȯ)OR, in which R is the solvent radical.

Most of the e.s.r. studies of the photoreduction of aromatic nitro-compounds were carried out in ether or alcohol solvents, but many other studies involving product analysis of the photoreduction have been done using amines and hydrocarbons as solvents. We wish to report here a re-investigation of the photolysis of aromatic nitro-compounds in a variety of solvents by e.s.r. spectroscopy with the hope that some, if not all, of the previous contradicting assignments on the radical intermediates can be resolved.

Experimental

Nitrobenzene was purified by distillation, and *m*-dinitrobenzene and *s*-trinitrobenzene were recrystallized from ether. All solvents used were the highest grade available commercially.

Solutions of the nitro-compounds contained in 5 mm o.d. Pyrex tubings were degassed to 10^{-4} Torr before they were photolyzed at room temperature in the cavity of a Varian V4502 e.s.r. spectrometer with 100 kHz modulation. The light source was an unfiltered 200 W super pressure mercury lamp.

E.s.r. spectra simulation was performed on an IBM 360-50 computer using a modified programme made available by Bell Telephone Laboratory. The technique and the experimental assembly of the rapid scan e.s.r. method, using a Fabri-tek 1074 instrument computer, have been described elsewhere (10).

Can. J. Chem. Downloaded from www.nrcresearchpress.com by 210.87.254.42 on 09/05/12
For personal use only.

Can. J. Chem. Downloaded from www.nrcresearchpress.com by 210.87.254.42 on 09/05/12
For personal use only.

TABLE 1. Hyperfine coupling constants for radicals observed in the photolyses of nitrobenzenes in organic solvents

Substrate	Solvent	Hyperfine coupling constants (G)						Radical assigned
		a_N	a_H^o	a_H^m	a_H^p	a_H(R)	a_H^{NH}	
Nitrobenzene	THF	15.0	2.9	1.0	3.2	0.35	—	PhN(Ȯ)OR
Nitrobenzene	THF + H_2O	15.0	2.9	1.0	3.2	0.35	—	PhN(Ȯ)OR
		9.1	2.8	0.95	3.2	—	12.1	PhN(Ȯ)H
Nitrobenzene	THF + D_2O	15.0	2.9	1.0	3.2	0.35	—	PhN(Ȯ)OR
		9.1	2.8	0.95	3.2	—	1.8 (a_D)	PhN(Ȯ)D
Nitrobenzene	Isopropanol	13.5	3.5	1.1	3.5	—	—	PhN(Ȯ)OC$(CH_3)_2$OH
Nitrobenzene	CH_3OH + NH_4OH	12.8	3.3	1.1	3.6	—	—	$PhNO_2^-$
Nitrobenzene	$(CH_3)_2NH_2$ + H_2O	13.4	3.3	1.1	3.5	—	—	$PhNO_2^-$
Nitrobenzene	Morpholine	12.0	3.5	1.1	3.7	—	—	$PhNO_2^-$
Nitrobenzene	Cyclohexane	10.5	3.0	—	3.0	3.0	—	PhN(Ȯ)R
Nitrobenzene	Dimethylformamide	15.5	3.0	1.0	3.0	—	—	PhN(Ȯ)OC(O)N$(CH_3)_2$
		9.0	3.0	1.0	3.0	—	12.1	PhN(Ȯ)H
Dinitrobenzene	Toluene	10.1	2.8	0.7	2.8	5.5	—	PhN(Ȯ)CH_2Ph
Dinitrobenzene	Cumene	10.8	2.5	0.6	2.5	—	—	PhN(Ȯ)C$(CH_3)_2$Ph
Dinitrobenzene	Diphenylmethane	10.2	2.6	0.8	2.6	3.6	—	PhN(Ȯ)$CHPh_2$
Trinitrobenzene	THF	13.0	2.9	0.2	3.2	0.4	—	PhN(Ȯ)R
Trinitrobenzene	Dioxane	13.0	2.9	0.2	3.2	0.2	—	PhN(Ȯ)R
Trinitrobenzene	Toluene	9.5	2.6	—	2.6	5.2	—	PhN(Ȯ)CH_2Ph
Trinitrobenzene	Indene	9.5	2.5	—	2.5	2.5	—	PhN(Ȯ)R
Trinitrobenzene	Cyclohexane	9.0	3.0	—	3.0	3.0	—	PhN(Ȯ)R

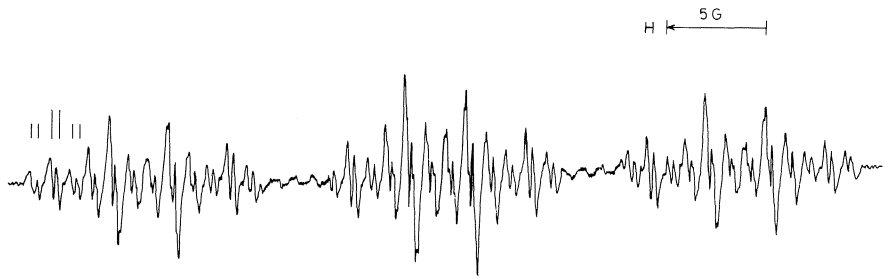

FIG. 1. E.s.r. spectrum observed during the photolysis of nitrobenzene in THF.

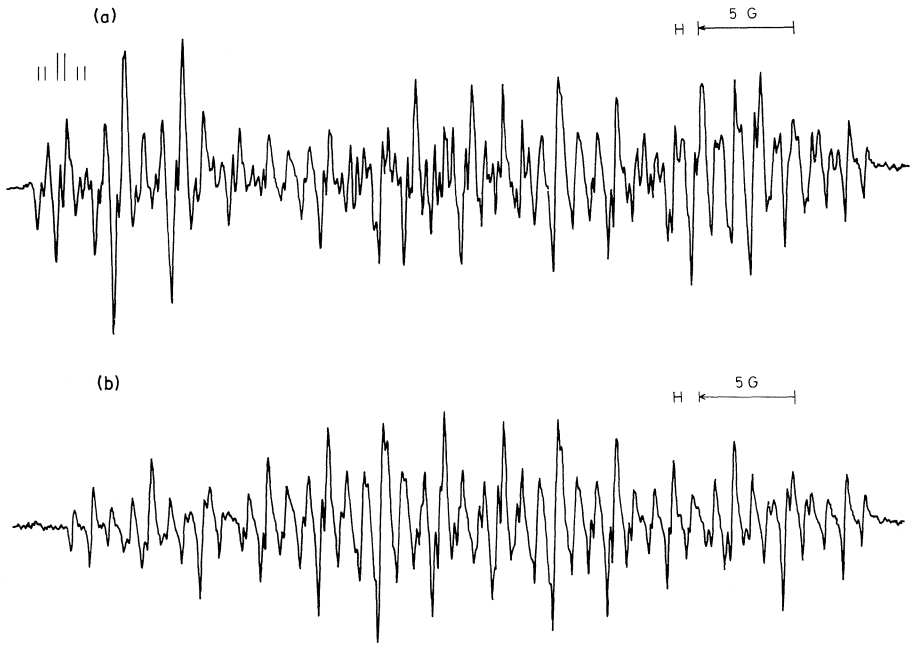

FIG. 2. E.s.r. spectra observed (*a*) during and (*b*) after the photolysis of nitrobenzene in THF + H_2O.

Results

Photolysis in Ethers

The photolysis of nitrobenzene in pure THF led to the observation of an e.s.r. spectrum given in Fig. 1. This spectrum is similar to that reported by Ward (4), except that the present spectrum was better resolved to show the small difference in the ortho and para proton splittings of the nitrobenzene ring. This spectrum is assigned to the radical PhN(Ȯ)OR (where R is the tetrahydrofuranyl radical) and its hyperfine coupling constants are given in Table 1. To support the assignment of the PhN(Ȯ)OR radical, further experiments were carried out in mixed solvents of THF and D_2O. It is reasonable to predict that radicals such as the PhN(Ȯ)OH would undergo proton exchange with water and therefore the doublet hydroxy proton splitting would collapse.

In a controlled experiment using THF and H_2O as solvent (9:1 in volume), the observed e.s.r. spectra *during* and *after* the photolysis were shown in Figs. 2*a* and *b*, respectively. Computer analysis revealed that the spectrum in Fig. 2*a* is the composite of the two spectra in Figs. 1 and 2*b*. When the experiment was carried out with 9:1 volume ratio of THF and D_2O, the observed e.s.r. spectra *during* and *after* the photolysis (Figs. 3*a* and *b*) again showed that the spectrum during photolysis (Fig. 3*a*) is the composite of Figs. 1 and 3*b*. Our interpretation is that the spectrum in Fig. 1 is correctly assigned

Can. J. Chem. Downloaded from www.nrcresearchpress.com by 210.87.254.42 on 09/05/12
For personal use only.

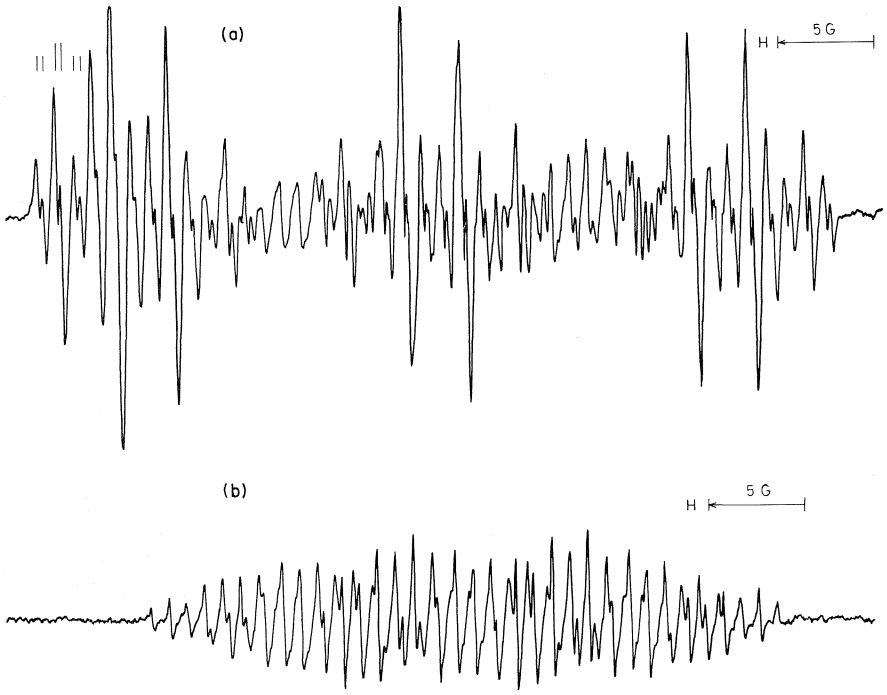

FIG. 3. E.s.r. spectra observed (*a*) during and (*b*) after the photolysis of nitrobenzene in THF + D_2O.

to the radical PhN(Ȯ)OR, which is not affected by the change of H_2O to D_2O in the mixed solvents. On the other hand, the additional species observed in the mixed solvent systems is assigned to the radical Ph(Ȯ)H, or the PhN(Ȯ)D, respectively. The latter radical probably resulted from proton–deuteron exchange between the PhN(Ȯ)H and D_2O. The hyperfine coupling constants of these radicals are reported in Table 1. We conclude that these experiments have demonstrated that the photoradical produced in the reduction of nitrobenzene in THF is indeed the radical PhN(Ȯ)OR as proposed by Cowley and Sutcliffe (9), and not the radical PhN(Ȯ)OH (4).

Photolysis of *s*-trinitrobenzene was also carried out in pure THF, in dioxane, and in perdeuteriated ethers. The spectra observed were substantially the same as those reported by Briegleb and Lind (3), and are given in Table 1.

Photolysis in Alcohols

Photolysis of nitrobenzene in methanol gave extremely weak e.s.r. signals which were difficult to detect. In isopropanol, however, a reasonable spectrum was observed which can be interpreted as due to PhN(Ȯ)$C(CH_3)_2OH$ (see Table 1). These results are quite different from those reported by Chachachaty and Forchioni (11). These authors claimed that they observed the radical PhN(Ȯ)CH_2OH in methanol and the radical PhN(Ȯ)H in isopropanol.

When the alcohols were made alkaline with ammonium hydroxide, the radicals observed were the nitrobenzene radical anion, during photolysis. Solutions of *m*-dinitrobenzene and *s*-trinitrobenzene in alkaline alcohol gave a deep red color probably due to the formation of the Meisenheimer σ-complexes (12). Photolysis of these solutions did not produce any observable e.s.r. spectra.

Photolysis in Amines

Photolyses of nitrobenzene in cyclopentamine, in morpholine, in tetrahydropyridine, in 40% aqueous dimethylamine, and in 40% aqueous diethylamine, all produced stable e.s.r. spectra which can be readily assigned to the nitrobenzene radical anion.

Solutions of *m*-dinitrobenzene and *s*-trinitro-

Can. J. Chem. Downloaded from www.nrcresearchpress.com by 210.87.254.42 on 09/05/12
For personal use only.

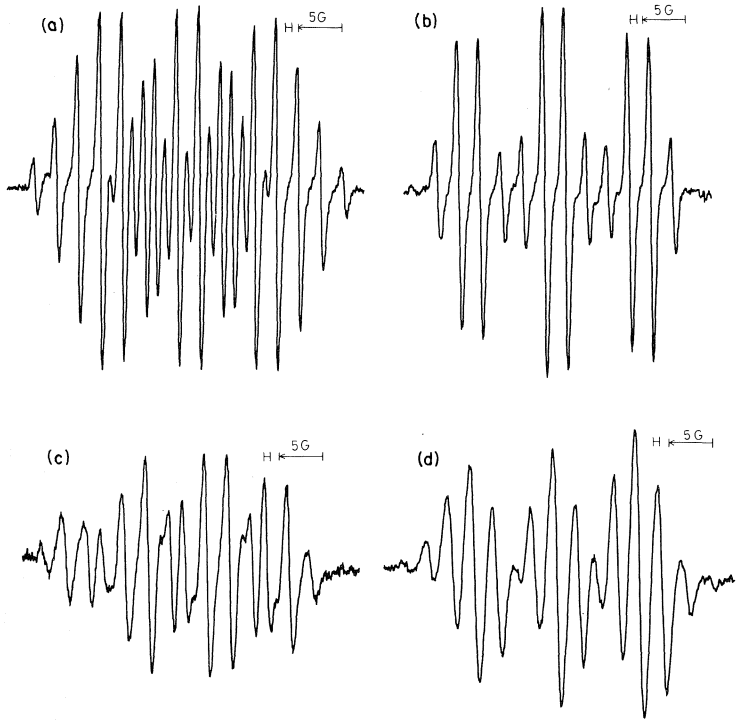

FIG. 4. E.s.r. spectra observed in the photolysis of trinitrobenzene in (*a*) toluene, (*b*) cumene, (*c*) diphenylmethane, and (*d*) indene.

benzene in various amine solvents also gave deep red or purple color and photolyses of these solutions produced no observable e.s.r. signal.

Photolysis in Hydrocarbons

In toluene, cumene, indene, diphenylmethane, and cyclohexane, the photolyses of *s*-trinitrobenzene gave fairly stable and well-resolved e.s.r. spectra (Fig. 4). These spectra are assigned to radicals of the type PhN(Ȯ)R, in which R is the hydrocarbon fragment after one of the α-hydrogens has been abstracted by the substrate. Their hyperfine parameters are reported in Table 1. These assignments were confirmed by experiments using 98% *s*-trinitrobenzene-d_3, generously supplied by E. Buncel of this Department.

When *m*-dinitrobenzene was photolyzed in these hydrocarbon solvents, the observed e.s.r. spectra were also due to the similar type of PhN(Ȯ)R radicals and were listed in Table 1.

Photolysis in Dimethylformamide

When nitrobenzene was photolyzed in dimethylformamide, the e.s.r. spectrum observed upon initial irradiation was very complex. After 10–20 min of continuous irradiation the spectrum changed gradually to a simple pattern which can be readily identified as the radical PhN(Ȯ)H. This simple spectrum can also be obtained directly by a pulse of light with observation appropriately delayed.

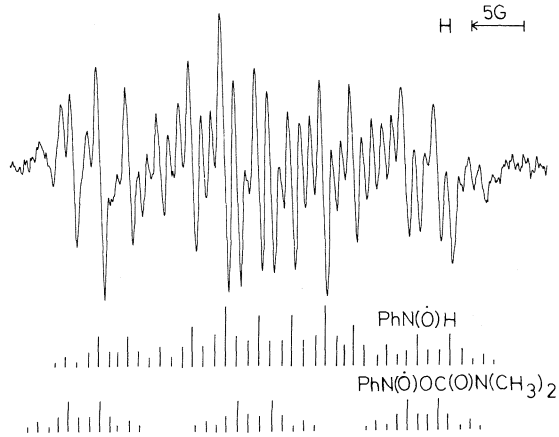

FIG. 5. Rapid scan e.s.r. spectrum observed in the photolysis of nitrobenzene in dimethylformamide.

Can. J. Chem. Downloaded from www.nrcresearchpress.com by 210.87.254.42 on 09/05/12
For personal use only.

Can. J. Chem. Downloaded from www.nrcresearchpress.com by 210.87.254.42 on 09/05/12
For personal use only.

Because of the rapid changes in the initially observed e.s.r. spectra, it was hoped that the initial radical species could be captured before decay by the rapid scan e.s.r. method (10). About 3000 scans can be made within a minute during the short light exposure. The spectrum thus obtained is shown in Fig. 5. A careful analysis of this spectrum with the aid of computer simulation revealed that the initial spectrum was a composite of spectra due to both the PhN(Ȯ)H and the $PhN(\dot{O})OC(O)N(CH_3)_2$ radicals. The assignment of the latter radical (Table 1) must be treated as tentative, but its nitrogen splitting is similar to the type PhN(Ȯ)OR and quite different from that of the radicals PhN(Ȯ)R.

Discussion

The e.s.r. results in the present study confirmed the complexity of the solvent effect in the photoreduction of simple aromatic nitro-compounds as suggested by other studies (5, 13–15) involving product analysis. It is rather unfortunate that the presumably primary radical PhN(Ȯ)OH which would be expected from hydrogen abstraction of the excited nitrobenzene molecule, was not observed and identified in this study. However, analogous radicals resulting from photolyses of 2,3,5,6-tetrachloronitrobenzene and 2,3,6-trichloronitrobenzene have been claimed (9) to exist. While it is reasonable to postulate the role of the radical PhN(Ȯ)OH in the mechanism of the photoreduction of aromatic nitro-compounds, it must be recognized that direct e.s.r. evidence is still lacking. Nevertheless, we should discuss here the roles of those radicals detected by e.s.r. in the present investigation, in the mechanism of the photoreduction.

Radicals of the type PhN(Ȯ)OR, which have been observed in ethers, isopropanol, and dimethylformamide solvents, presumably are formed by addition of the solvent radical R to nitrobenzene. The solvent radicals R can be initially produced by losing a hydrogen atom to an excited triplet nitrobenzene. Indeed, the addition reaction 1 has been demonstrated by McMillan and Norman (16). Furthermore, the

[1] $$\dot{R} + RhNO_2 \rightarrow PhN(\dot{O})OR$$

intermediate tetrahydrofuranyl radical has also been trapped using phenyl-*t*-butyl nitrone (17). The decay kinetics of the 2,3,5,6-tetrachlorophenyl alkoxy nitroxide radical was found to follow the first-order rates under various conditions and was probably due to unimolecular decomposition (9*b*), as shown in reaction 2. The

[2] $$PhN(\dot{O})OR \rightarrow PhNO + R\dot{O}$$

radical RȮ produced in reaction 2 can further abstract a hydrogen atom from the solvent leading to a chain mechanism in the photoreduction. However, Hurley and Testa (5) have measured the quantum yield of the nitrobenzene in degassed isopropanol solution and their low value of $1.14 \pm 0.08 \times 10^{-2}$ seemed to be incompatible with a chain mechanism. Perhaps the low quantum yield could be due to a combination of factors, such as low efficiency in the intersystem crossing to the triplet state of the nitrobenzene and the rapid deactivation of the triplet nitrobenzene compared to the chemical abstraction reaction.

The phenyl nitroxide PhN(Ȯ)H, which was observed in aqueous THF and in dimethylformamide solvents, has been regarded as a possible precursor to one of the reduction products, phenylhydroxylamine (5). Ayscough and coworkers (18) proposed the step shown in reaction 3 for the formationof the phenyl nitroxide rad-

[3] $$PhNO + PhN(\dot{O})OH \rightarrow PhN(\dot{O})H + PhNO_2$$

ical. This, however, cannot be confirmed due to the illusiveness of the primary radical PhN(Ȯ)OH.

In amine or aqueous alkaline solutions, it has been demonstrated that the photolysis of nitrobenzene results in the observation of its radical anion. Barltrop and Bunce (14) have suggested that the anion radical is formed by loss of a proton from the primary PhN(Ȯ)OH radical (see eq. 4). While this again cannot be confirmed

[4] $$PhN(\dot{O})OH \rightleftharpoons Ph\dot{N}O_2^- + H^+$$

at present because of the lack of e.s.r. evidence for the primary PhN(Ȯ)OH radical, the subsequent decomposition of the nitrobenzene radical anion has been studied in detail in aqueous solutions by a variety of polarographic, e.s.r., pulsed radiolysis, and u.v. spectrometric methods (19–24). The result can be summarized and presented by reactions 5 and 6. Thus in these

[5] $$Ph\dot{N}O_2^- + PhN(\dot{O})OH \rightarrow PhNO_2 + PhN(O)OH^-$$

[6] $$PhN(O)OH^- \rightarrow PhNO + OH^-$$

aqueous solvents, nitrobenzene is photoreduced

by a different mechanism involving its radical anions as the major intermediate.

Another type of radical, PhN(Ȯ)R, which has been detected in hydrocarbon solvents, is likely to be a secondary radical formed by the addition of solvent radicals Ṙ to one of the intermediate product nitrosobenzene. The preference of the hydrocarbon radicals attacking the nitrosobenzene in presence of a higher concentration of nitrobenzene could partly be attributed to the fact that nitrosobenzene is a more powerful electron acceptor (9, 16).

This research was supported by the National Research Council of Canada.

1. J. K. S. WAN. *In* Advances in Photochemistry. To be published.
2. C. LAGERCRANTZ and M. YHLAND. Acta Chem. Scand. **16**, 1043, 1799 (1962).
3. G. BRIEGLEB and G. LIND. Z. Naturforsch, A**23**, 1747, 1752 (1968).
4. R. L. WARD. J. Chem. Phys. **38**, 2588 (1963).
5. R. HURLEY and A. C. TESTA. J. Am. Chem. Soc. **88**, 4330 (1966).
6. A. CARRINGTON, A. HUDSON, and H. C. LONGUET-HIGGINS. Mol. Phys. **9**, 377 (1965).
7. W. FOX, J. M. GROSS, and M. C. R. SYMONS. J. Chem. Soc. A, 448 (1966).
8. J. K. BROWN and W. G. WILLIAMS. Chem. Commun. 495 (1966).
9. D. J. COWLEY and L. H. SUTCLIFFE. Chem. Commun. 201 (1966); J. Chem. Soc. B, 569 (1970); Trans. Faraday Soc. **65**, 2286 (1969).
10. L. FABES. Ph.D. Thesis. Queen's University, Kingston, Ontario. 1971; S. K. WONG, L. FABES, W. GREEN, and J. K. S. WAN. J. Chem. Soc. Faraday I. **68**, 2211 (1972).
11. C. CHACHATY and A. FORCHIONI. Tetrahedron Lett. 307 (1968).
12. E. BUNCEL, A. R. NORRIS, and K. E. RUSSELL. Quart. Rev. **12**, 123 (1968).
13. J. W. WELLER and G. A. HAMILTON. Chem. Commun. 1390 (1970).
14. J. A. BARLTROP and N. J. BUNCE. J. Chem. Soc. C, 1467 (1968).
15. H. A. MORRISON. *In* The Chemistry of the Nitro and Nitroso Groups. *Edited by* H. Feuer. Pt. 1. Interscience, New York. 1969. p. 165.
16. M. MCMILLAN and R. O. C. NORMAN. J. Chem. Soc. B, 590 (1968).
17. E. G. JANZEN and J. GERLOCK. J. Am. Chem. Soc. **91**, 3108 (1969).
18. P. B. AYSCOUGH, R. C. SEALY, and D. E. WOONDS. J. Phys. Chem. **75**, 3454 (1971).
19. K. D. ASMUS, A. WIGGER, and A. HENGLEIN. Ber Bunsenges Phys. Chem. **70**, 862 (1966).
20. G. FARNIA, G. MENGOLI, and E. VIANELLO. Ricerca Sci. **37**, 668 (1967).
21. L. H. PIETTE, P. LUDWIG, and R. N. ADAMS. J. Am. Chem. Soc. **83**, 3909 (1961).
22. P. KOOPMANN and H. GERISCHER. Ber. Bunsenges Phys. Chem. **70**, 127 (1966).
23. B. KASTENING and S. VAVRICHA. Ber. Bunsenges Phys. Chem. **72**, 27 (1968).
24. A. R. METCALFE and W. A. WATERS. J. Chem. Soc. B, 918 (1969).

Can. J. Chem. Downloaded from www.nrcresearchpress.com by 210.87.254.42 on 09/05/12
For personal use only.

Iridoids of *Mentzelia decapetala* (Pursh). I. Mentzeloside[1,2]

TERRY JOHN DANIELSON AND EDWARD MILES HAWES
College of Pharmacy, University of Saskatchewan, Saskatoon, Saskatchewan

AND

CARMAN ARTHUR BLISS
College of Pharmacy, University of New Mexico, Albuquerque, New Mexico

Received July 20, 1972

Mentzeloside (**1**), *rel*-(1*R*,4*aR*,5*R*,6*R*,7*S*,7*aR*)-6,7-epoxy-1-*O*-β-D-glucosyl-5-hydroxy-1,4*a*,5,6,7,7*a*-hexahydro-4-methylcyclopenta(*c*)pyran, was isolated from flowers and seed pods of *Mentzelia decapetala*. The preparation of various chemical derivatives and the examination of spectral (i.r., u.v., and ^{1}H n.m.r.) data allowed a complete structure to be proposed for the title compound.

La mentzeloside (**1**), *rel*-(1*R*,4*aR*,5*R*,6*R*,7*S*,7*aR*) époxy-6,7-*O*-β-D-glucosyl-1 hydroxy-5, hexahydro-1,4*a*,5,6,7,7*a* méthyl-4 cyclopenta(*c*)pyranne, a été isolée à partir des fleurs ainsi que des cosses de la graine du *Mentzelia decapetala*. La préparation de plusieurs dérivés chimiques et l'examen de données spectrales (i.r., u.v., et r.m.n. ^{1}H) ont permis d'élaborer une structure complète pour le composé mentionné dans le titre. [Traduit par le journal]

Can. J. Chem., **51**, 760 (1973)

Mentzelia decapetala is the only member of the family Loasaceae found on the Canadian prairies. Previous work on the nature of the secondary constituents of the genus *Mentzelia* is limited to an investigation of their seed oil content (1). The present paper reports the structure elucidation of an iridoid glycoside, mentzeloside (**1**, Scheme 1) isolated from *M. decapetala*.

Compound **1** was isolated from a methanolic extract of the flowers and seed pods of *M. decapetala*. Separation on a Florisil column yielded an optically active white crystalline material. The empirical formula $C_{15}H_{22}O_9$ was established by elemental analysis and mass spectrometry. Preliminary examination of the i.r. (1665 cm^{-1}) and u.v. spectra (λ_{max} 204 nm) indicated the presence of an enol ether function (2). **1** gave black polymers on acid treatment, a property which has been shown to be characteristic of most iridoid compounds (3, 4). The latter designation gained further support by the presence of a one-proton signal at 6.13 p.p.m. in the ^{1}H n.m.r. spectrum (Fig. 1) assignable to the olefinic proton on C-3 of an iridoid skeleton.

A few other features of the n.m.r. spectrum were discernable. The 6.13 p.p.m. absorption displayed weak (J = 0.5 Hz) coupling to a high field (1.60 p.p.m.), three-proton signal, which was attributed to an allylic methyl function at C-4. Two upfield, one-proton signals centered at 2.31 and 1.91 p.p.m. were assigned to the two bridgehead protons, C-7*a* and -4*a* respectively. The 8 Hz interaction displayed between these protons was similar to the couplings observed in other *cis*-ring fused iridoids (5). Also the downfield tertiary proton (2.31 p.p.m.) was coupled (J = 10 Hz) with an ethereal proton signal at 4.68 p.p.m. The latter was assigned to the acetal proton at C-1. The large coupling was indicative of a dihedral angle approaching 180° and a *trans*-diaxial relationship between the protons on C-7*a* and -1.

Acetylation of **1** yielded a crystalline pentaacetate (**2**) of molecular formula $C_{25}H_{32}O_{14}$. Catalytic hydrogenation of **2**, or of **1** followed by acetylation, gave the dihydro-derivative (**3**). Comparison of the n.m.r. spectra of **2** and **3** showed loss of the C_3-olefinic proton at 6.07 p.p.m. and changes in the three-proton methyl resonance. This signal at 1.60 p.p.m. in **2** had undergone an upfield shift of 0.45 p.p.m. due to loss of the deshielding influence of the double bond. New protons appeared in the spectrum of **3** in the 2.12–1.47 and 3.79–3.41 p.p.m. regions. These were assigned to C-4 and -3 respectively. Irradiation at 1.70 p.p.m. affected collapse of the C-8 methyl from a broad doublet (J = 7 Hz)

[1]Presented in part at the American Society of Pharmacognosy, Iowa City, Iowa, July 1968.

[2]Abstracted in part from the University of Saskatchewan Ph.D. Thesis of T.J.D. (1972).

Can. J. Chem. Downloaded from www.nrcresearchpress.com by 210.87.254.42 on 09/05/12
For personal use only.

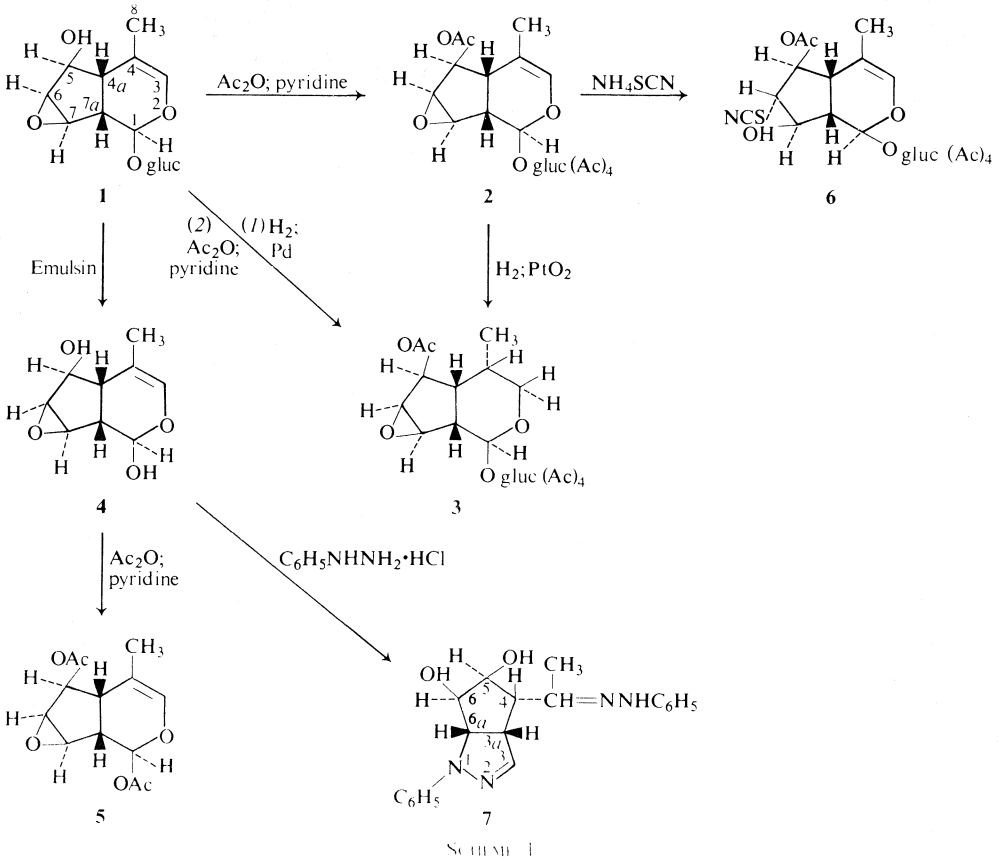

SCHEME 1

to a singlet. These changes in the spectrum of **3** served to prove the initial presence and subsequent saturation of an enol ether olefinic bond, and indicated a correct assignment for the C_4-methyl function in **1**.

The sharpness of the C-8 methyl resonance in the n.m.r. spectrum of **3** indicated that the reduction had been stereospecific. Approach to the catalyst surface from the least hindered β side of the molecule should give rise to a product in which the C-8 methyl group is α-orientated (2).

Enzymatic hydrolysis with emulsin of **1** yielded mentzelol (**4**) (a reducing aglycone) and glucose. The latter was confirmed by gas chromatography of the TMS–ether derivative. The glucose moiety must be at C-1 in **1**, due to the generation of reducing properties upon hydrolysis and by analogy with other iridoid glucosides. A β-configuration for glucose was indicated by the ease of hydrolysis with emulsin and by the signal of the glucose anomeric proton in the n.m.r. spectrum of **1** (4.54 p.p.m., $J = 7.5$ Hz) (6). There was no definite evidence for epimerization about C-1 in **4**. The n.m.r. spectrum did not show the C-1 axial proton epimer, which would be expected to occur as a narrowly split doublet at a somewhat higher field (7).

Acetylation of **4** produced a crystalline diacetate (**5**). The similarity of the n.m.r. (see Fig. 2) to that of unedol diacetate (**8**) (5) allowed tentative assignment of all structural features of **5** and by analogy **1** also. A low field signal at 6.10 p.p.m.

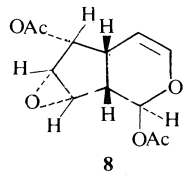

8

was assigned to the C-3 olefinic proton, while a high field three-proton doublet at 1.52 p.p.m. was attributed to the C-8 methyl function. A broad doublet at 5.51 p.p.m. which had undergone a downfield shift of 1.1 p.p.m. (relative to **4**) upon acetylation was shown by spin decoupling to be

Can. J. Chem. Downloaded from www.nrcresearchpress.com by 210.87.254.42 on 09/05/12
For personal use only.

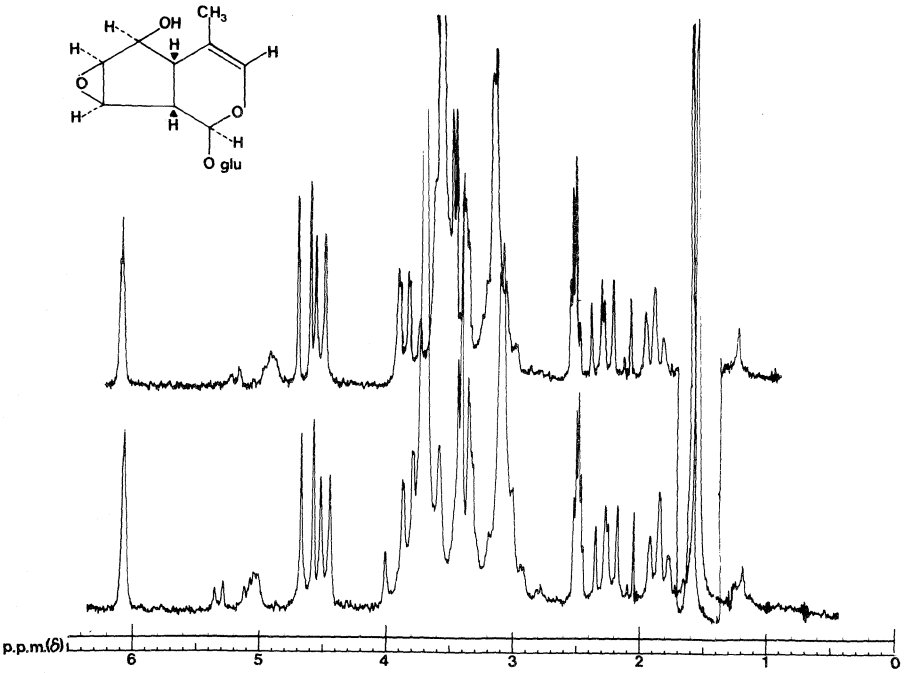

FIG. 1. The 100 MHz ^{1}H n.m.r. spectrum of mentzeloside; lower tracing, room temperature; upper tracing, 70°; solvent DMSO-d_6; DSS internal standard.

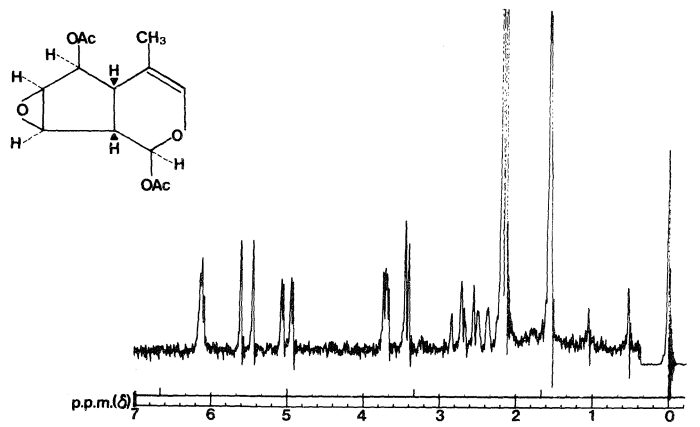

FIG. 2. The 60 MHz ^{1}H n.m.r. spectrum of mentzelol diacetate; solvent $CDCl_3$; TMS internal standard.

coupled with the C-7*a* bridgehead proton (J = 10 Hz). This signal was therefore the C-1 acetal proton and the retention of the large coupling indicated that the configuration at C-1 had not been affected by hydrolysis and acetylation. The C-7*a* bridgehead proton was coupled to a second bridgehead proton at 2.36 p.p.m. (J = 7.5 Hz), which was in turn coupled with a one-proton signal at 5.0 p.p.m. (J = 8 Hz). This latter signal had been shifted downfield 1.2 p.p.m. by acetylation and was assigned to a secondary acetate methine on C-5. Two coupled, one-proton, signals at 3.70 and 3.42 p.p.m. (J = 2.75 Hz) were the oxirane protons on C-6 and -7 of **5**. The magnitude of the coupling and the chemical shift of these signals were characteristic of the protons of an epoxide on a five-membered ring (5, 8). The downfield epoxide proton was coupled to the C-5 acetate methine (J = 1.5 Hz) and is thus positioned at C-6. The upfield epoxide proton is

Downloaded from www.nrcresearchpress.com by 210.87.254.42 on 09/05/12
For personal use only.

Can. J. Chem. Downloaded from www.nrcresearchpress.com by 210.87.254.42 on 09/05/12
For personal use only.

then attributed to C-7. Coupling between this proton and the C-7*a* bridgehead proton was absent. This lack of observable coupling is characteristic of a *trans*-interaction between vicinal protons in cyclic epoxides and thus the epoxide ring must be *trans* to the C_1—C_{7a} bond. The epoxide ring is then in a β-position, above the general plane of the iridoid nucleus. The configuration of the C-5 proton could also be deduced from the observed coupling of 1.5 Hz. This is characteristic of a *cis*-interaction and the C-5 proton must therefore be placed *cis* to the C-6 epoxide proton (8).

When mentzeloside pentaacetate (**2**) was allowed to react with the ammonium thiocyanate in *N*,*N*-dimethylformamide (DMF) under reflux a compound (**6**) incorporating CHNS was isolated ($C_{26}H_{33}O_{14}S$). The n.m.r. spectrum of **6**, as compared to that of **2**, showed loss of the epoxide protons centered at 3.68 p.p.m. and the appearance of three new signals. A low field multiplet at 4.08 p.p.m. and an upfield doublet of doublets at 3.30 p.p.m. were attributed to a secondary alcohol methine and a thiocyanate methine respectively. An intermediate signal at 3.55 p.p.m. was shown by deuterium exchange to be a hydroxyl proton. Spin decoupling experiments indicated that the thiocyanate methine was coupled to the C-5 acetate methine (5.12 p.p.m., J = 5 Hz) and to the 4.08 p.p.m. signal (J = 9.7 Hz), which allowed placement of the thiocyanate group at C-6. **6** thus resulted from S_N2 cleavage of the C_6—O bond by thiocyanate ion, accompanied by the appropriate inversion at C-6 and retention of configuration at C-7.

Epoxide cleavage with ammonium thiocyanate was also attempted in tetrahydrofuran under reflux, but resulted in the recovery of starting material. Goodman has reported that cleavage of vicinally substituted epoxides only under the vigorous DMF conditions was indicative of one *cis*- and one *trans*-vicinal substituent (9). This observation is in agreement with the steric assignment of a *cis*-relationship between the protons on C-5 and -6 in **5**.

An interesting feature in the n.m.r. spectrum of **6** was the collapse of the C-1 acetal proton signal in **2** from a broad doublet (J = 9 Hz) to a narrow doublet (J = 1 Hz), which was shifted downfield 0.79 p.p.m. This is interpreted as being due to a conformational inversion of the dihydropyran ring, resulting in an axial–equatorial inversion at C-1 and a change in dihedral angles from about 180 to about 90°. Although this ring inversion would cause the bulky tetra-*O*-acetylglucosyl group to assume an axial position, Drieding models show any 1,3- or 1,4-interactions to be minimal. This conformation should also be stabilized by the "anomeric effect" (10).

Unexpected confirmation of the presence of the epoxide function and its steric relationship to the C-5 hydroxyl group in **1** was obtained from the product (**7**) derived from the reaction of mentzelol (**4**) with phenylhydrazine hydrochloride. **7** was assigned the pyrazoline structure since the n.m.r. spectrum clearly lacked any signals assignable as epoxide protons, the u.v. spectrum did not contain a maximum near 320 nm characteristic of α,β-unsaturated phenylhydrazones (11), and exposure to bromine vapor produced an olive green color characteristic of pyrazolines (12). The product formed from the reaction of catalpol aglycone (**9**) with 2,4-dinitro-

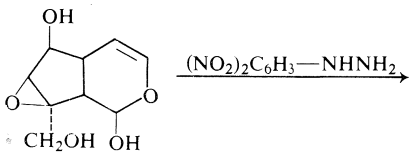

9

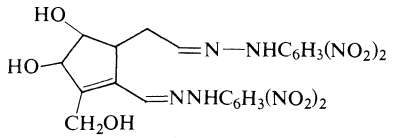

10

phenylhydrazine has been assigned as an α,β-unsaturated 2,4-dinitrophenylhydrazone (**10**) (13); however the use of phenylhydrazine would be expected to more readily yield a pyrazoline (14).

In the n.m.r. spectrum of **7** the bridgehead protons on C-3*a* and -6*a* appear as an octet at 3.92 and a doublet at 4.17 p.p.m. respectively. The latter signal displayed coupling only to the C-3*a* proton (J = 11 Hz), indicating that the dihedral angle to the proton on C-6 must approach 90°. Dreiding models show that this is only possible if these protons are *trans* and the cyclopentane ring has a "V_5 boat" conformation. This conformation is preferred in various rigidly fused bicyclic cyclopentane derivatives (8). Table 1 compares the observed couplings for the C-4, -5, and -6 protons of **7** to those recorded in the literature for the model compounds **11** and

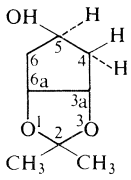

11

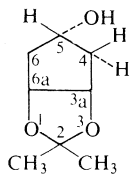

12

TABLE 1. Observed couplings (Hz) in compounds **7**, **11**, and **12**.

Compound		$J_{4,5}$	$J_{5,6}$
7		10	4
11*	*cis*	6	
	trans	9.3	
12*	*cis*	4.7	
	trans	1.2	

*Reference 8.

12 (8). These latter structures have been shown to exist in the "V_5 boat" conformation, and the similarity of the coupling constants for **11** to those observed in **7** allows one to assign the hydroxyl of C-5 the same relative stereochemistry. Therefore, the C-5 hydroxyl group is indicated as being *cis* to the oxirane ring in **4** and **1** and the proton at this center must be α, thus completing all assignments of the relative stereochemistry of **1**.

Experimental

The n.m.r. spectra were run on Varian T-60 or HA-100 instruments. TMS was used as internal standard for $CDCl_3$ or acetone-d_6 solutions, while DSS was used for DMSO-d_6 solutions. Chemical shifts are recorded in p.p.m. (δ) units downfield from the internal standard. The i.r. spectra were recorded as potassium bromide discs on a Unicam SP200 spectrometer and the u.v. spectra on a Unicam SP800 recording spectrometer. Optical rotations were determined with a Bellingham and Stanley polarimeter. Melting points were determined with a Gallenkamp melting point apparatus and are uncorrected. Florisil (Floridin Company, 30–60 mesh or Fisher Scientific 60–100 mesh) or silica gel powder (Baker 3405, 60–200 mesh) were used for column chromatography. Microanalyses were carried out by Mr. R. M. Smith of the College of Pharmacy and Dr. Strauss, Oxford, England. Mass spectra were determined with an AEI-MS 12 single focusing mass spectrometer (70 eV) with a heated inlet system operating near or at the melting points of the compounds. Samples were introduced by direct probe.

Extraction and Isolation of Mentzeloside (1)

Flowers and seed pods of *Mentzelia decapetala* (fresh weight 12.2 kg) were immersed in methanol containing calcium carbonate immediately after collection. This plant material was further treated with boiling methanol, filtered, and air dried. The partially extracted dry plant material was then ground to a fine powder and exhaustively percolated with aqueous methanol (70%). The combined methanolic extracts were evaporated to an aqueous solution and washed with chloroform. The volume of the aqueous solution was then adjusted to 7 l with water.

An aliquot portion (500 ml) of the above aqueous solution was stirred with basic lead hydroxide (2 h) and filtered. Removal of solvent *in vacuo* yielded a brown syrup (39 g) which was successively extracted with hot absolute ethanol (400 ml), ethanol (500 ml), and methanol (300 ml). Concentration *in vacuo* of the combined extracts produced a brown syrup (30 g) which was redissolved in methanol, evaporated onto aluminum oxide (110 g), and placed in a soxhlet extractor. Exhaustive extraction with absolute ethanol yielded, after removal of solvent, a brown syrup (11 g) which was placed on a column of Florisil (400 g). Elution with benzene–methanol (3:1) yielded in the fraction between 1500 and 1900 ml of total eluate, **1**, which recrystallized from methanol as white crystals (0.240 g): m.p. 266–270° dec. $[\alpha]_D^{23}$ −100.88° (*c* 1.021 in H_2O); u.v. max 205 nm (log ε 3.53); i.r. 1665 (C=C—O) and 3420 cm^{-1} (O—H); n.m.r. (DMSO-d_6) δ 6.13 (m, 1, $J_{3,4a}$ = 0.5 and $J_{3,8}$ = 0.5 Hz, C_3-*H*), 4.68 (d, 1, $J_{1,7a}$ = 10 Hz, C_1-*H*), 4.54 (d, 1, $J_{1',2'}$ = 7.5 Hz, glucose), 3.89 (dd, 1, $J_{5,4a}$ = 8 and $J_{5,6}$ = 1.5 Hz, C_5-*H*), 3.83 (m, 2, glucose), 3.50 (d, 1, $J_{7,6}$ = 2.75 Hz, C_7-*H*), 3.39 (m, 1, C_6-*H*), 3.14 (m, 4, glucose), 2.31 (dd, 1, $J_{7a,1}$ = 10 and $J_{7a,4a}$ = 7.5 Hz, C_{7a}-*H*), 1.91 (m, 1, $J_{4a,5}$ = 8, $J_{7a,4a}$ = 7.5, and $J_{4a,3}$ = 0.5 Hz, C_{4a}-*H*), and 1.60 p.p.m. (d, 3, $J_{8,3}$ = 0.5 Hz, C_8-H_3); mass spectrum *m/e* (relative intensity) 184(80), 167(41), 166(4), 138(10), 137(60), 95(82), and 73(100).

Anal. Calcd. for $C_{15}H_{22}O_9$: C, 52.02; H, 6.40. Found: C, 52.10; H, 6.45.

Mentzeloside Pentaacetate (2)

To a solution of mentzeloside (**1**, 0.310 g) in anhydrous pyridine (5 ml) was added acetic anhydride (1 ml). The solution was stirred on a steam bath (2 h). Cooling and addition of ice water yielded **2** which recrystallized from methanol as fine white needles (0.417 g, 85%): m.p. 199°; $[\alpha]_D^{26}$ −103.32° (*c* 0.974 in $CHCl_3$); i.r. 1665 (C=C—O) and 1740 cm^{-1} (ester C=O); n.m.r. ($CDCl_3$) δ 6.07 (m, 1, $J_{3,8}$ = 0.5 and $J_{3,4a}$ = 0.5 Hz, C_3-*H*), 4.77–5.33 (c, 5, C_5-*H* and glucose 4H), 4.57 (d, 1, $J_{1,7a}$ = 9 Hz, C_1-*H*), 4.13 (m, 2, glucose), 3.6–3.75 (c, 3, C_6-*H*, C_7-*H* and glucose), 2.50 (dd, 1, $J_{7a,1}$ = 10 and $J_{7a,4a}$ = 7.5 Hz, C_{7a}-*H*), 2.30 (ddd, 1, $J_{4a,5}$ = 8, $J_{4a,7a}$ = 7.5 and $J_{4a,3}$ = 0.5 Hz, C_{4a}-*H*), 2.0 (c, 15, 5 CH_3COO—), and 1.53 p.p.m. (d, 3, $J_{8,3}$ = 0.5 Hz, C_8-H_3).

Anal. Calcd. for $C_{25}H_{32}O_{14}$: C, 53.95; H, 5.80. Found: C, 53.89; H, 5.80.

Dihydromentzeloside Pentaacetate (3)

(*a*) Compound **1** (0.200 g) in water (15 ml) was added to a suspension of hydrogen saturated 10% palladium/charcoal (0.125 g) in ethyl alcohol (80%, 85 ml) and was stirred under a hydrogen atmosphere at room temperature for 16 h. Removal of the catalyst and evaporation of solvent yielded a glassy residue (0.190 g) which was pure to paper chromatography and lacked olefinic stretching in the i.r. spectrum.

To the above residue in pyridine (5 ml) was added acetic anhydride (1 ml). The solution was allowed to

Can. J. Chem. Downloaded from www.nrcresearchpress.com by 210.87.254.42 on 09/05/12
For personal use only.

Can. J. Chem. Downloaded from www.nrcresearchpress.com by 210.87.254.42 on 09/05/12
For personal use only.

stand at room temperature for 16 h and was poured into cold water (10 ml). Filtration and recrystallization from methanol yielded **3** (0.165 g, 55%): m.p. 184–185°; $[\alpha]_D^{26}$ −84.6° (*c* 0.654 in $CHCl_3$); n.m.r. ($CDCl_3$) δ 4.75–5.31 (c, 5, C_5-*H* and glucose 4H), 4.37 (d, 1, $J_{1,7a}$ = 9 Hz, C_1-*H*), 4.16 (m, 2, glucose), 3.79–3.41 (m, 5, C_3-H_2, C_6-*H*, C_7-*H*, and glucose 1H), 2.33 (dd, 1, $J_{7a,1}$ = 9 and $J_{7a,4a}$ = 8 Hz, C_{7a}-*H*), 2.12–1.47 (m, 17, C_4-*H*, C_{4a}-*H* and 5CH_3COO—), and 1.05 p.p.m. (d, 3, $J_{8,4}$ = 7 Hz, C_8-H_3).

(*b*) Compound **2** (0.250 g) in glacial acetic acid (10 ml) was added to a suspension of hydrogen-saturated platinum oxide (0.250 g) in ethyl alcohol – acetic acid (1:1, 50 ml) and was stirred at room temperature under a hydrogen atmosphere. After 3 h the catalyst was removed and the solvent evaporated yielding **3** which recrystallized from ethyl alcohol (0.180 g, 72%), and was identical to the product isolated above.

Mentzeloside Aglycone; Mentzelol (4)

To a solution of **1** (2 g) in water (350 ml) was added a suspension of emulsin (0.130 g) in water (50 ml). The resultant suspension was allowed to stand at room temperature (18 h), after which the solvent was removed *in vacuo* to yield a gummy residue. Extraction of this residue with hot chloroform–ethanol (4:1, 150 ml) yielded, after filtration and removal of solvent, crude aglycone (1.71 g). Crystallization from ethyl acetate yielded **4** as white crystals (0.654 g, 62%): m.p. 153–155°; $[\alpha]_D^{23}$ −122.35° (*c* 0.425 in CH_3OH); u.v. max 203 nm (log ε 3.56); n.m.r. (DMSO-d_6) δ 7.0 (d, 1, *J* = 7 Hz, O*H*, exchanges readily with D_2O), 6.05 (m, 1, C_3-*H*), 5.1 (d, 1, *J* = 7 Hz, O*H*, exchanges readily with D_2O), 4.4 (dd, 1, $J_{1,7a}$ = 9.5 and $J_{H,OH}$ = 7 Hz, D_2O exchange, d, $J_{1,7a}$ = 9.5 Hz, C_1-*H*), 3.8 (dd*, 1, $J_{5,4a}$ = 8 and $J_{H,OH}$ = 7 Hz, D_2O exchange, d, $J_{5,4a}$ = 8 Hz, C_5-*H*), 2.1 (dd, 1, $J_{7a,1}$ = 9.5 and $J_{7a,4a}$ = 7.5 Hz, C_{7a}-*H*), 1.8 (dd, $J_{4a,7a}$ = 7.5 and $J_{4a,5}$ = 8 Hz, C_{4a}-*H*), and 1.6 p.p.m. (d, 3, $J_{8,3}$ = 0.5 Hz, C_8-H_3); mass spectrum *m/e* (relative intensity) 184(100), 167(16), 166(3), 138(10), 137(54), and 95(75).

Anal. Calcd. for $C_9H_{12}O_4$: C, 58.69; H, 6.56. Found: C, 58.44; H, 6.38.

Mentzelol Diacetate (5)

To a solution of **4** (0.650 g) in anhydrous pyridine (7.5 ml) was added acetic anhydride (2.5 ml). This solution was heated on a steam bath (0.5 h), cooled, and poured into saturated aqueous sodium bicarbonate (150 ml). Extraction with chloroform (3 × 20 ml) yielded, after drying ($CaCl_2$) and evaporation, the diacetate (0.585 g, 62%). Vacuum sublimation (1 mm Hg, 114°) yielded **5** as white needle-like crystals: m.p. 109–111°; $[\alpha]_D^{23}$ −182.01° (*c* 0.467 in $CHCl_3$); n.m.r. ($CDCl_3$) δ 6.10 (m, 1, $J_{3,8}$ = 0.5 and $J_{3,4a}$ = 0.5 Hz, C_3-*H*), 5.51 (d, 1, $J_{1,7a}$ = 10 Hz, C_1-*H*), 5.0 (dd, 1, $J_{5,4a}$ = 8 and $J_{5,6}$ = 1.5 Hz, C_5-*H*), 3.70 (dd, 1, $J_{6,5}$ = 1.5 and $J_{6,7}$ = 2.75 Hz, C_6-*H*), 3.42 (d, 1, $J_{7,6}$ = 2.75 Hz, C_7-*H*), 2.68 (dd, 1, $J_{7a,1}$ = 10 and $J_{7a,4a}$ = 7.5 Hz, C_{7a}-*H*), 2.36 (ddd, 1, $J_{4a,5}$ = 8, $J_{4a,7a}$ = 7.5 and $J_{4a,3}$ = 0.5 Hz, C_{4a}-*H*), 2.18 (s, 3, CH_3COO—), 2.14 (s, 3, CH_3COO—), and 1.52 p.p.m. (d, 3, $J_{8,3}$ = 0.5 Hz, C_8-H_3).

Anal. Calcd. for $C_{13}H_{16}O_6$: C, 58.20; H, 6.01. Found: C, 58.43; H, 6.18.

Thiocyanate (6)

To a solution of mentzeloside pentaacetate (**2**, 0.420 g) in *N*,*N*-dimethylformamide (20 ml) was added ammonium thiocyanate (0.075 g, 1.3 equiv). The solution was heated under reflux (17 h) after which the solvent was removed *in vacuo*. The non-volatile residue was placed on a column of silica gel (30 g) and was developed with chloroform. Evaporation of the first 150 ml of solvent yielded starting material (**2**, 0.057 g). Further elution with chloroform (550 ml) and chloroform – ethyl acetate (19:1, 300 ml) yielded **6** as white crystals (0.068 g, 15%): m.p. 199.5–201.5°; i.r. 1670 (C=C—O), 2155 (—S—C≡N) and 3520 cm^{-1} (—OH); n.m.r. ($CDCl_3$) δ 6.0 (m, 1, C_3-*H*), 5.36 (d, 1, $J_{1,7a}$ = 1 Hz, C_1-*H*), 5.26–4.8 (m, 5, C_5-*H* and glucose 4H), 4.2 (m, 2, glucose), 4.08 (m, 1, C_7-*H*), 3.75 (m, 1, glucose), 3.55 (m, 1, exchanges readily with D_2O, O-*H*), 3.30 (dd, 1, $J_{6,5}$ = 5 and $J_{6,7}$ = 9.7 Hz, C_6-*H*), 2.55 (m, 2, C_{4a}-*H* and C_{7a}-*H*), 1.9–2.2 (c, 15, 5 CH_3COO—), and 1.65 p.p.m. (d, 3, $J_{8,3}$ = 0.5 Hz, C_8-H_3).

Anal. Calcd. for $C_{26}H_{33}NO_{14}S$: C, 50.72; H, 5.40; N, 2.28; S, 5.21. Found. C, 50.62; H, 5.34; N, 2.22; S, 5.50.

Mentzelol Phenylhydrazone Pyrazoline (7)

To a solution of mentzelol (**3**, 0.100 g) in water (5 ml) was added sodium acetate (0.200 g) and phenylhydrazine hydrochloride (0.230 g, 3 equiv). The reaction mixture was shaken until crystals began to appear and was then allowed to stand at room temperature overnight. Filtration yielded orange–brown crystals (0.196 g) which recrystallized from methanol–water to yield **7** (0.096 g, 50%): m.p. 209–210°; u.v. max 243 (log ε 4.11) and 276 nm (log ε 4.44); n.m.r. (acetone-d_6) δ 7.4–6.5 (c, 12, 10 aryl-*H*, C_3-*H*, and C_8-*H*), 4.17 (d, 1, $J_{6a,3a}$ = 11 Hz, C_{6a}-*H*), 3.92 (ddd, 1, $J_{3a,6a}$ = 11, $J_{3a,4}$ = 7, and $J_{3a,3}$ = 1.5 Hz, C_{3a}-*H*), 3.90 (d, 1, $J_{6,5}$ = 4 Hz, C_6-*H*), 3.68 (ddd, 1, $J_{5,6}$ = 4, $J_{5,4}$ = 10, and $J_{5,3}$ = 0.5 Hz, C_5-*H*), 2.90 (s, 3, exchange readily with D_2O, 2O*H*, N*H*), 2.55 (m, 2, C_4-*H* and C_7-*H*), and 1.30 p.p.m. (d, 3, $J_{9,7}$ = 6.5 Hz, C_9-H_3).

Anal. Calcd. for $C_{21}H_{24}N_4O_2$: C, 69.22; H, 6.62. Found: C, 69.23; H, 6.62.

The authors wish to express sincere appreciation to Dr. R. A. Abramovitch for valuable comments. The support of the project by the Medical Research Council of Canada (Grant No. Ma-3802) is gratefully acknowledged.

1. F. R. Earle, C. A. Glass, Q. C. Geisinger, I. A. Wolfe, and Q. Jones. J. Am. Oil Chem. Soc. **37**, 440 (1960).
2. M. L. Scarpati and M. Guiso. Tetrahedron, **23**, 4709 (1967).
3. For a review of iridoids, see J. M. Bobbitt and K.-P. Segebarth. Organic substances of natural origin. Vol. 2. *Edited by* W. I. Taylor and A. R. Battersby. Marcel Dekker, Inc., New York. 1969. Chapt. 1.
4. L. H. Briggs, B. F. Cain, P. W. LeQuesne, and J. N. Shoolery. Tetrahedron Lett. 69 (1963).
5. T. A. Geissman, W. F. Knaack, Jr., and J. O. Knight. Tetrahedron Lett. 1245 (1966).

6. R. U. LEMIEUX, R. K. KULLNIG, H. J. BERNSTEIN, and W. G. SCHNEIDER. J. Am. Chem. Soc. **80**, 6098 (1968).
7. C. DJERASSI, T. NAKANO, A. N. JAMES, L. H. ZALKO, E. J. EISENBRAUN, and J. N. SHOOLERY. J. Org. Chem. **26**, 1192 (1961).
8. R. STEYN and H. Z. SABLE. Tetrahedron, **27**, 4429 (1971).
9. L. GOODMAN. Chem. Commun. 219 (1968).
10. E. L. ELIEL, N. L. ALLINGER, S. J. ANGYAL, and G. A. MORRISON. Conformational analysis. Interscience Publishers, New York. 1965. Chapt. 6.
11. G. F. DUFFIN and J. D. KENDALL. J. Chem. Soc. 408 (1954).
12. L. C. RAIFORD and W. J. PETERSON. J. Org. Chem. **1**, 544 (1937).
13. W. H. LUNN, D. W. EDWARD, and J. T. EDWARD. Chem. Ind. 1488 (1961).
14. L. C. BEHR, R. FUSCO, and C. H. JARBO. Pyrazoles, pyrazolines, pyrazolidines, indazoles and condensed rings. Interscience Publishers, New York. 1967. Chapt. 7.

Can. J. Chem. Downloaded from www.nrcresearchpress.com by 210.87.254.42 on 09/05/12
For personal use only.

^{13}C Nuclear Magnetic Resonance Spectra of Bridged 10π-Electron Systems. The Extent of Electron Delocalization

A. V. KEMP-JONES, ALAN J. JONES, M. SAKAI, C. P. BEEMAN, AND S. MASAMUNE

Department of Chemistry, University of Alberta, Edmonton, Alberta T6G 2G2

Received September 29, 1972

The ^{13}C n.m.r. spectrum of the cation **4** suggests the presence of considerable 1,7-bonding, indicating that it should be described as a substituted homotropylium cation rather than a monocyclic 10π-electron system. The intra-annular carbon atoms of **3** and **4** do not show a significant upfield shift due to the ring current. Explanations are offered.

Le spectre r.m.n. du ^{13}C du cation **4** suggère la présence d'une liaison importante entre 1 et 7; ce résultat indique que l'ion devrait être représenté sous forme d'ion homotropylium substitué plutôt que sous forme d'un système monocyclique contenant 10 électrons π. Les atomes de carbone intra-annulaires de **3** et **4** ne sont pas déplacés d'une façon significative vers les hauts champs à cause des courants de cycle. Des explications sont proposées. [Traduit par le journal]

Can. J. Chem., **51**, 767 (1973)

Can. J. Chem. Downloaded from www.nrcresearchpress.com by 210.87.254.40 on 09/05/12
For personal use only.

Our recent demonstration that both *cis*- and *trans*-[10]annulenes (**1** and **2**) are non-planar olefinic hydrocarbons (1) contrasts with the behavior of 1,6-methano[10]annulene (**3**), the p.m.r. spectrum of which indicates the presence of the diamagnetic ring current associated with

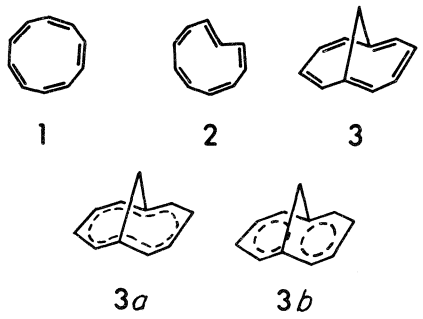

aromatic electron delocalization (2). The remarkable aromaticity of **3** might be partially caused by the possibility of some 1,6-bonding overlap; this interaction must be invoked in order to explain the u.v. spectrum of **3** (3). For this reason we investigated the ^{13}C n.m.r. spectrum of bicyclo[5.4.1]dodecapentaenylium fluoroborate (**4**) (4). ^{13}C n.m.r. shifts provide a sensitive probe for local charge and might, therefore, indicate to what extent the positive charge in **4** is delocalized over the π system. Estimation of the charge at the various carbon atoms of **4** requires a comparison of the chemical shifts with those in a neutral model compound having the same geometry, since ^{13}C shifts are also sensitive to changes in the geometry of the molecule (5); we have used bicyclo[5.4.1]dodecapenta-2,5,7,9,11-ene (**5**) (6) as the model compound. The ^{13}C n.m.r. spectra of **4** and **5** are shown in Fig. 1 and the chemical shifts relative to internal tetramethylsilane are given in Table 1. The choice of acetonitrile-d_3 as the solvent was determined by the solubility of the fluoroborate; no appreciable solvent-induced shifts were noted for a solution of **5** in dichloromethane-d_2. Analysis of the ^{13}C spectra of **4** and **5** first requires analysis of their proton spectra. The proton spectrum of **4** was previously recorded, but not analyzed (4). Four distinct multiplet patterns (H-α τ 0.7 (2H), H-β 1.15 (3H), H-γ 1.35 (2H), and H-δ 1.6 (2H)) appear in the aromatic region, in addition to two doublets of triplets (H-ε τ 10.3 (1H), H-ζ 11.8 (1H)) in the aliphatic region. Irradiation at H-α resulted in a general simplification of the H-β signal, but did not affect the signals of H-γ and -δ; the H-α, -β multiplets remained unchanged on irradiation at H-δ. Thus, the aromatic protons appeared to consist of two separate systems: H-α,β (5H) and -γ,δ (4H). Irradiation at H-ζ induced a significant change in the H-γ signal shape to give a typical, symmetrical AA'BB' pattern for H-γ and -δ, while H-α and -β remained unchanged. A reciprocal effect was noted on irradiation at H-γ and H-ζ became a doublet. Thus, it is now clear that H-γ,δ,ζ constitute an AA'BB'X system. In a similar manner, irradiation at H-ε resulted in a simplification of the H-α multiplet; irradiation at H-α caused the H-ε

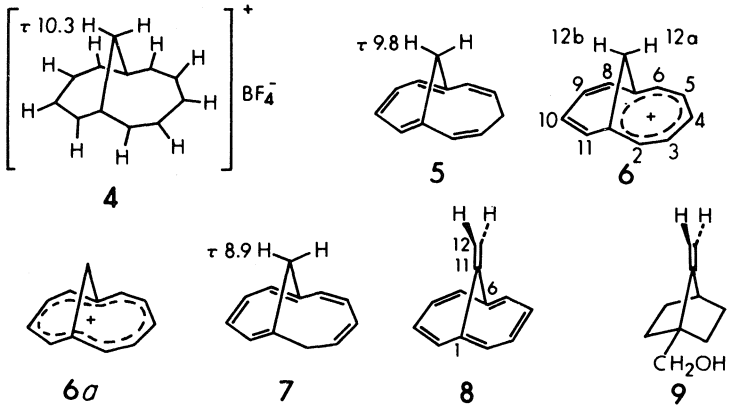

signal to collapse to a doublet. Therefore the remaining group of six protons is safely concluded to be an AA'BB'CX system. If one applies the well-documented, long-range coupling (W-pattern) effect (7) to the present system, then the observation of the typical AA'BB' pattern on irradiation of H-ζ is consistent only with the assignment that H-γ,δ,ζ are H-8,11, -9,10 and -12a and that H-α,β,ε are H-2,6, -3,4,5 and -12b. The proton spectrum of **5** had been analyzed previously (6). The analysis of the proton spectra permitted assignment of the ^{13}C absorptions by means of the selective decoupling technique (8) as illustrated for **5** in Fig. 2. Because of the similar chemical shifts of some of the proton resonances of **4** (H-3,5 and -8,11) and **5** (H-2,6 and -8,11), complete assignment of the ^{13}C spectrum is not possible. However, when the proton resonances overlap, the corresponding ^{13}C absorptions are often close together, and in fact the resulting ambiguities in the chemical shifts are quite small and do not detract from the subsequent discussion. Strikingly, the downfield shifts of the carbon atoms C-8,11 and -9,10 are

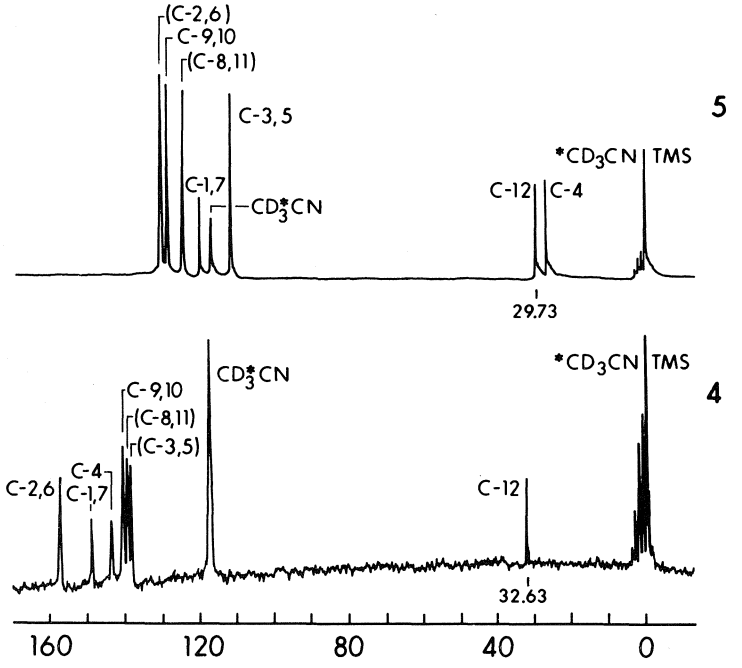

FIG. 1. The ^{13}C spectra of bicyclo[5.4.1]dodecapentaene (**5**) and bicyclo[5.4.1]dodecapentaenylium fluoroborate (**4**) for solutions in acetonitrile-d_3. Parentheses indicate uncertainties in assignment.

Can. J. Chem. Downloaded from www.nrcresearchpress.com by 210.87.254.40 on 09/05/12
For personal use only.

TABLE 1. ^{13}C chemical shifts in some bridged 10π-electron systems

	Carbon position*						
Compound	-1,7	-2,6	-3,5	-4	-8,11	-9,10	-12
5†	120.6	130.8 or 125.1	112.3	26.8	125.1 or 130.8	129.1	29.7
4‡	149.6	158.0	139.3 or 140.1	144.3	140.1 or 139.3	141.2	32.6
	-1,6		-2,5,7,10		-3,4,8,9		-11
3‡	115.1		129.2		126.6		35.2

*Positive numbers indicate p.p.m. downfield from TMS.
†In CD_3CN. Solvent-induced shifts of 0.1–0.3 p.p.m. were noted for the solution in CD_2Cl_2.
‡In CD_3CN.

both in the range 9–15 p.p.m., whereas those of C-1,7, -2,6, and -3,5 are all substantially higher at 27–33 p.p.m. The latter range is remarkably similar to the 29.6 p.p.m. downfield shift observed between the tropylium cation and cycloheptatriene (9). The narrow range of the ^{13}C shifts in the seven-membered ring and their value suggests that **4** is best represented as a substituted homotropylium cation **6** rather than **6***a* (4).[1] The downfield shifts of C-8,11 and -9,10 can be attributed to the inductive effect of the homotropylium substituent. Representation of **4** as **6** rather than **6***a* is also consistent with the small shift of the bridge proton H-12b on converting **5** to **4**. Furthermore, this small shift of H-12b suggests that little change in the geometry of the framework occurs on converting **5** to **4**, since the chemical shift of H-12b is sensitive to changes in the geometry of the system, as is shown by comparing **5** and **7** (6). If the homoaromaticity (6π) of the C-7,8,9,10,11,1 system is more extensively attained in **4** than that implied by **6** (see footnote 1), then the degree of diamagnetic anisotropy due to the three double bonds of **5** may be approximately equated to that of the ring current effect of the same part of **4**. Obviously the representation of **4** as **6** implies that 1,7-homoconjugative overlap is important in stabilizing the cation **4**. This conclusion does not necessarily require that 1,6-overlap is important in stabilizing the ground state of **3**, but it does emphasize that the problem requires further investigation.

Another feature of the c.m.r. spectra of **4** and **5** which deserves comment is the small *downfield* shift of the bridge carbon C-12 on converting **5** to **4**; it might have been expected that C-12 would be shielded by the ring current of **4**. Similarly the bridge carbon (C-11) of 1,6-methano[10]annulene (**3**) resonates downfield from C-12 of **5** (see Table 1). No unequivocal shielding effects of ring currents on ^{13}C shifts have in fact been observed for any systems thus far, but this may be attributed to the positioning of the carbon atoms of all previously examined molecules in a 'null' shielding region between the shielding and deshielding regions (10). While this argument *might* still be applicable to **4**, especially when representation **6** is considered,[2] it seems less likely to apply to **3**. Not only the hydrogen atoms attached to C-11 are shielded, but also the methylene hydrogen atoms of **8** (11), which lie in the C-1, -11, -6 plane, resonate at τ 6.8, which represents a shielding of about 1.3 p.p.m.[3] The hydrogen atoms at C-12 of **8** should be in a much less favorable position than C-11 of **3** for shielding by the ring current. Therefore, C-11 of **3** appears to be in the shielding region regardless of whether we choose 1,6-methano[10]annulene

[1]The degree of homoaromaticity of the system involving C-1, -7, -8, -9, -10, and -11 is not certain at present. Therefore a highly electron-delocalized formula similar to **3***b* could possibly be more suitable as a structure. **6***a* means no electron overlap between C-1 and -7, whereas **6** is used to emphasize the presence of such an interaction, the degree of which of course remains to be determined.

[2]The substantial shielding of H-12a does not *necessarily* require that C-12 will be in a shielding region since the orientation of H-12a and C-12 with respect to the ring current is different.

[3]For comparison, methylene cyclohexane resonates at τ 5.18 and the 7-methylene-norbornane **9** (12) (a suggested model system (**11***b*)) absorbs at τ 5.38 and 5.48.

Can. J. Chem. Downloaded from www.nrcresearchpress.com by 210.87.254.40 on 09/05/12
For personal use only.

Can. J. Chem. Downloaded from www.nrcresearchpress.com by 210.87.254.40 on 09/05/12
For personal use only.

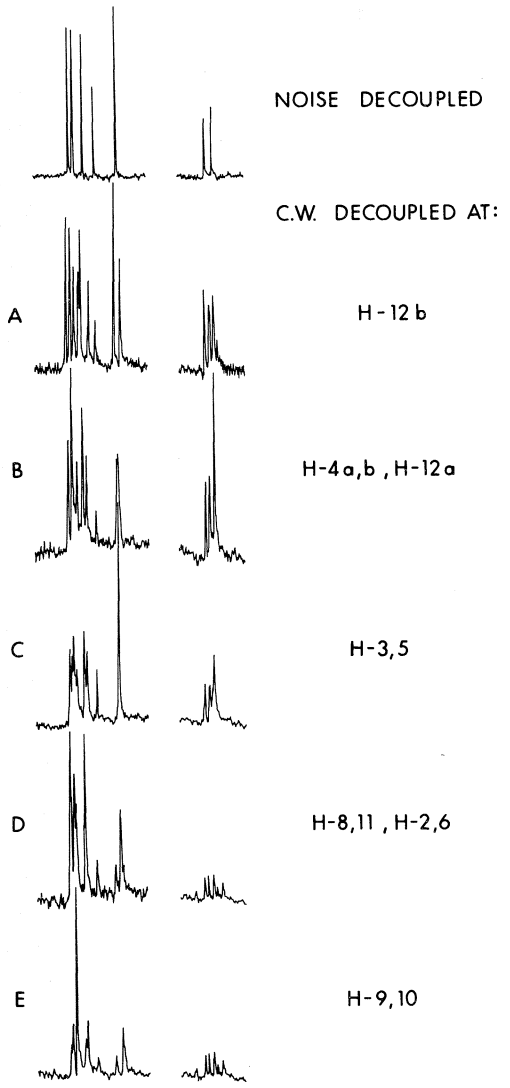

FIG. 2. Selective decoupling experiments on bicyclo-[5.4.1]dodecapentaene (**5**) in methylenechloride-d_2. A through E show the effects of stepping the decoupler through the proton resonance frequencies.

(**3***a*, monocyclic 10π) or 9,10-methanonaphthalene (**3***b*, bicyclic homoaromatic) as the model for the diamagnetic current induced in **3**. Although we still cannot rigorously exclude the possibility of a small null shielding region around C-11 as the reason for the lack of an upfield shift for C-11 in **3**, we feel that a much more likely explanation is that ^{13}C absorptions may be *relatively* insensitive to ring current effects. If the absolute value of the ring current effect (a few p.p.m. at most for ^1H) is independent of the nucleus involved then the effect in ^{13}C spectra would be outweighed by shifts due to changes in geometry and local charge.

The spectra of other molecules having intra-annular carbon atoms, such as **10** (13) and **11** (14), would be of interest in further examining this question, but the improbability of obtaining completely satisfactory model compounds (*e.g.* **12** for **10**) means that only a large shielding effect due to the ring current would be detectable (presumably 20 p.p.m. would be sufficient).

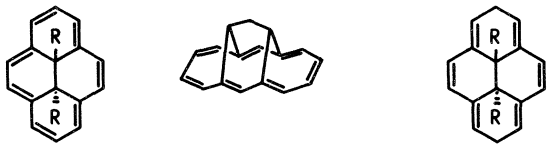

10 **11** **12**

Experimental

Compounds **3** (2), **4** (4), and **5** (6) were prepared by the literature procedures. The ^{13}C n.m.r. spectra were determined in the Fourier mode using a Bruker HFX-90 spectrometer operating at 22.63 MHz with deuterium lock.

ADDED IN PROOF: Professors E. Vogel and H. Günther, commenting on our manuscript, generously provided us (Dec. 11 and 14, 1972) with information concerning (*i*) p.m.r. spectral analysis of **4** (K. Müllen, Dissertation, Köln, 1971) and their C.m.r. studies on their bridged annulenes. We thank the National Research Council of Canada for financial support.

1. (*a*) S. MASAMUNE, K. HOJO, K. HOJO, G. BIGAM, and D. L. RABENSTEIN. J. Am. Chem. Soc. **93**, 4966 (1971); (*b*) S. MASAMUNE and N. DARBY. Acc. Chem. Res. **5**, 272 (1972).
2. E. VOGEL and H. D. ROTH. Angew. Chem. Int. Ed. Engl. **3**, 228 (1964). For a recent review see E. Vogel. Proc. Robert A. Welch Found. Conf. Chem. Res. **12**, 215 (1968).
3. H.-R. BLATTMAN, E. HEILBRONNER, and G. WAGNIERE. J. Am. Chem. Soc. **90**, 4786 (1968). Also see H. GÜNTHER. Z. Naturforsch. **20**b, 948 (1965) and E. VOGEL. 23rd Int. Cong. Pure Appl. Chem. **1**, 275 (1971).
4. W. GRIMME, H. HOFFMANN, and E. VOGEL. Angew. Chem. Int. Ed. Engl. **4**, 354 (1965).
5. (*a*) A. J. JONES, E. L. ELIEL, D. M. GRANT, M. C. KNOEBER, and W. F. BAILEY. J. Am. Chem. Soc. **93**, 4772 (1971); (*b*) D. K. DALLING and D. M. GRANT. J. Am. Chem. Soc. **89**, 6612 (1967).
6. E. VOGEL, R. FELDMANN, and H. DÜWEL. Tetrahedron Lett. 1941 (1970).
7. For application of this effect to a system similar to the present case, see P. AHLBERG, D. L. HARRIS, M. ROBERTS, P. WARNER, M. SAKAI, D. COOK, A. DIAZ, J. P. DIRLAM, H. HAMBERGER, and S. WINSTEIN. J. Am. Chem. Soc. **94**, 7063 (1972).

8. A. J. JONES, T. D. ALGER, D. M. GRANT, and W. M. LITCHMAN. J. Am. Chem. Soc. **92**, 2386 (1970).
9. H. SPIESECKE and W. G. SCHNEIDER. Tetrahedron Lett. 468 (1961); see also G. A. OLAH and G. D. MATEESCU. J. Am. Chem. Soc. **92**, 1432 (1970).
10. For discussion of the possible effect of ring currents on ^{13}C shifts, see ref. 7 and: (*a*) T. D. ALGER, D. M. GRANT, and E. G. PAUL. J. Am. Chem. Soc. **88**, 5397 (1966); (*b*) A. J. JONES and D. M. GRANT. Chem. Commun. 1670 (1968); (*c*) A. J. JONES, P. D. GARDNER, D. M. GRANT, W. M. LITCHMAN, and V. BOEKELHEIDE. J. Am. Chem. Soc. **92**, 2395 (1970); (*d*) D. DODDRELL and W. S. CAUGHEY. J. Am. Chem. Soc. **94**, 2510 (1972). Also see H. GÜNTHER, R. WENZL, and W. GRIMME. J. Am. Chem. Soc. **91**, 3808 (1969).
11. (*a*) E. VOGEL, F. WEYRES, H. LEPPER, and V. RAUTENSTRAUCH. Angew. Chem. Int. Ed. Engl. **5**, 732 (1966); (*b*) F. WEYRES. Dissertation. University of Cologne, Cologne, W. Germany. 1966.
12. E. BAGGIOLINI, H. P. HAMLOW, and K. SCHAFFNER. J. Am. Chem. Soc. **92**, 4906 (1970).
13. V. BOEKELHEIDE and T. A. HYLTON. J. Am. Chem. Soc. **92**, 3669 (1970).
14. E. VOGEL, A. VOGEL, H.-K. KUBBELER, and W. STURM. Angew. Chem. Int. Ed. Engl. **9**, 514 (1970).

Can. J. Chem. Downloaded from www.nrcresearchpress.com by 210.87.254.40 on 09/05/12
For personal use only.

Electrochemical Oxidation of Trifluoroacetic Acid in an Organic Medium. II. In Presence of Propionic Acid[1]

ROGER N. RENAUD AND DONALD E. SULLIVAN[2]

Division of Chemistry, National Research Council of Canada, Ottawa, Canada

Received September 5, 1972

Trifluoropropane could not be prepared by the "crossed" Kolbe reaction from a mixture of trifluoroacetic acid and propionic acid. Instead, a mixture consisting of 3,3,3-trifluoropropene, 1,2-bis(trifluoromethyl)ethane, 1,1,2-tris(trifluoromethyl)ethane, and 1,2,4-tris(trifluoromethyl)butane was obtained. The probable mechanism for the reaction is discussed.

Le trifluoropropane n'a pu être synthétisé par la réaction de Kolbe à partir d'un mélange d'acide trifluoroacétique et d'acide propionique. Au lieu du trifluoropropane, le trifluoro-3,3,3-propène, le bis-(trifluorométhyle)-1,2-éthane, le tris(trifluorométhyle)-1,1,2-éthane, et le tris(trifluorométhyle)-1,2,4-butane furent obtenus. Le mécanisme probable de la reaction est démontré.

Can. J. Chem., **51**, 772 (1973)

Can. J. Chem. Downloaded from www.nrcresearchpress.com by 210.87.254.42 on 09/05/12
For personal use only.

Introduction

In the first part of this series (1), the preparation of deuterio-trifluoroethane and deuteriopentafluoropropane by the "crossed" Kolbe reaction of a mixture of the corresponding fluoroacids and acetic-d_3 acid was described. The series was continued using propionic acid instead of acetic acid in order to synthesize trifluoropropane.

It is known that the electro-oxidation of propionic acid anions gives ethane, ethylene, and, under certain conditions, butane (2). It is also reported in the literature that the electrolysis of a mixture of acetic acid and propionic acid gives some propane (3). Therefore, a series of electrolyses was carried out in order to optimize the experimental conditions for the preparation of trifluoropropane from trifluoroacetic acid and propionic acid. The results are shown in Table 1.

At high concentrations of sodium propionate (3) (run 1) or at high temperature (run 2), butane and esters were obtained, while at low current densities (run 3), practically no gaseous products were formed. However, under the conditions shown for run 4, a liquid with a low vapor pressure at −130 °C was obtained, which contained practically no butane, but consisted of a mixture of 3,3,3-trifluoropropene, 1,2-bis(trifluoromethyl)ethane, 1,1,2-tris(trifluoromethyl) ethane, and 1,2,4-tris(trifluoromethyl)butane as the major products.

[1]NRCC No. 12955.

[2]NRCC Summer Student 1971–1972.

Experimental

In run 4, a solution of trifluoroacetic acid (13.5 g) in water (25 ml) was added at a rate of one drop per 10 s to a solution of propionic acid (125 ml) and sodium propionate (15.7 g) in water (250 ml) at 20 °C in a 500 ml round-bottom flask equipped with a pressure equilibrated funnel, a thermometer, a reflux condenser, a magnetic bar stirrer, a salt bridge filled with a saturated KCl solution, and two pieces of smooth platinum foil (5 × 2.8 cm), 10 mm apart. The rest of the apparatus was essentially the same as described in the previous paper (1) except that a spiral side-arm trap at −78° was placed before the Stock trap. The electrolysis was carried out at a potential of 2.8 V *vs.* s.c.e. (current density: 0.20 A/cm^2) and continued for 1 h after the addition of the trifluoroacetic acid.

The trap in liquid nitrogen was attached to a vacuum line and the high vapor pressure fraction at −130 °C was discarded. The low vapor pressure residue proved on analysis by v.p.c. and mass spectrometry to be nearly pure 3,3,3-trifluoropropene when compared with an authentic sample. The yield was 23.7% (2.7 g).

The liquid collected in the trap at −78 °C (3.5 ml) was washed with 50 ml of a 20% sodium hydroxide solution at room temperature for 12 h under stirring, in a flask equipped with a Dry-Ice cold-finger, to remove any esters present. The supernatant oil (≈2.6 ml) was collected on the vacuum line, dried over $MgSO_4$, and fractionally distilled at atmospheric pressure through a semi-micro distilling column. Each fraction was analyzed by mass spectrometry, v.p.c., and elemental analysis.

The first fraction (b.p. ≈25 °C) was 1,2-bis(trifluoromethyl)ethane (1 g; yield 10%) identified by comparison with an authentic sample (4).

The second fraction (b.p. 52–53 °C) was 1,1,2-tris(trifluoromethyl)ethane (1.3 g; yield 14%); mass spectrum: *m/e* 215 $(M - F)^+$ and 195 $(M - HF_2)^+$.

Anal. Calcd. for $C_5H_3F_9$: C, 25.64; H, 1.28. Found: C, 25.47; H, 1.41.

The third fraction (b.p. 92–100 °C) and the residue (0.9 g; yield 8.7%) were most likely 1,2,4-tris(trifluoro-

TABLE 1. Electrochemical oxidation of a mixture of $CF_3COO^{\ominus}$ and $CH_3CH_2COO^{\ominus}$

Run	Na propionate (*N*)	Current density (A/cm^2)	*E* (s.c.e.)	*T* (°C)	Products
1	5	0.36	2.8	20	Butane and esters
2	0.4	0.40	2.8	45	
3	0.45	0.05	2.8	18	No reactions
4	0.45	0.20	2.8	20	$CF_3CH{=}CH_2$ $CF_3CH_2CH_2CF_3$ $(CH_3)_2CHCH_2CF_3$ $CF_3(CH_2)_2CH(CF_3)CH_2CF_3$

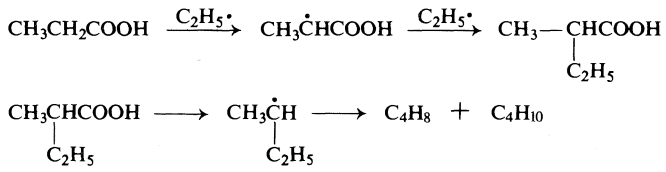

SCHEME 1

methyl)butane (mass spectrum: *m/e* 243 $(M - F)^+$ and 223 $(M - HF_2)^+$) contaminated with a small quantity of 1,2,6-tris(trifluoromethyl)butane (mass spectrum: *m/e* 271 $(M - F)^+$ and 251 $(M - HF_2)^+$).

Anal. Calcd. for $C_7H_7F_9$: C, 32.06; H, 2.68. Found: C, 33.14; H, 3.09.

Discussion

Goldschmidt *et al.* (5) identified a trace of butene-1, as its dibromoderivative, from the electrolysis of propionic acid, and postulated the mechanism depicted in Scheme 1 for its formation.

Therefore, in the presence of trifluoromethyl radicals, the formation of α-trifluoromethylpropionic acid is expected. This acid could be the precursor of trifluoropropene by oxidative decarboxylation followed by elimination or disproportionation. However, when the reaction was done with α,α-dideuteriopropionic acid, a 42/58 mixture of mono- and dideuterio-trifluoropropene was obtained, a result not explicable by the above mechanism. The result could be explained, however, by an attack of a trifluoromethyl radical on adsorbed ethylene which is always formed during the electrolysis of propionic acid. However, in no instance in the literature is it mentioned that ethylene functions as an adsorbed radical acceptor. Dienes and substituted ethylenes are generally good radical acceptors (6–11), to produce mainly the adjacent methyl acetoxy derivatives in acetic acid. The mechanism for these reactions is further complicated by the fact that the half-wave potentials of these olefinic compounds are all in the same range as the potential normally used for the Kolbe reaction. According to Fleischmann and Pletcher (12), the half-wave potential of ethylene is 3.3 V *vs.* s.c.e., a potential much higher than the potential used in this work. Therefore, ethylene can only react as a radical acceptor. To verify this statement, ethylene gas was bubbled between the two electrodes in a methanolic solution of sodium methylate to which trifluoroacetic acid was added. The products of this reaction were the same as when the reaction was done with propionic acid. No condensation products were obtained in an aqueous solution, probably due to the low solubility of ethylene in water. The electrolysis of acetic acid in the presence of ethylene gave no condensation products in a methanolic solution.

The fact that the electrolysis of propionic acid in the presence of acetic acid gives propane (3) and in the presence of trifluoroacetic acid, trifluoropropene, seems to follow the general trend of the relative reactivities of a methyl radical and a trifluoromethyl radical towards an ethyl radical and an ethylene molecule in the gas phase (13, 14) or in solution (15). However, it could be erroneous to compare free-radical reactions and adsorbed radical reactions. Moreover, the complete absence of trifluoropropane formation at

Can. J. Chem. Downloaded from www.nrcresearchpress.com by 210.87.254.42 on 09/05/12
For personal use only.

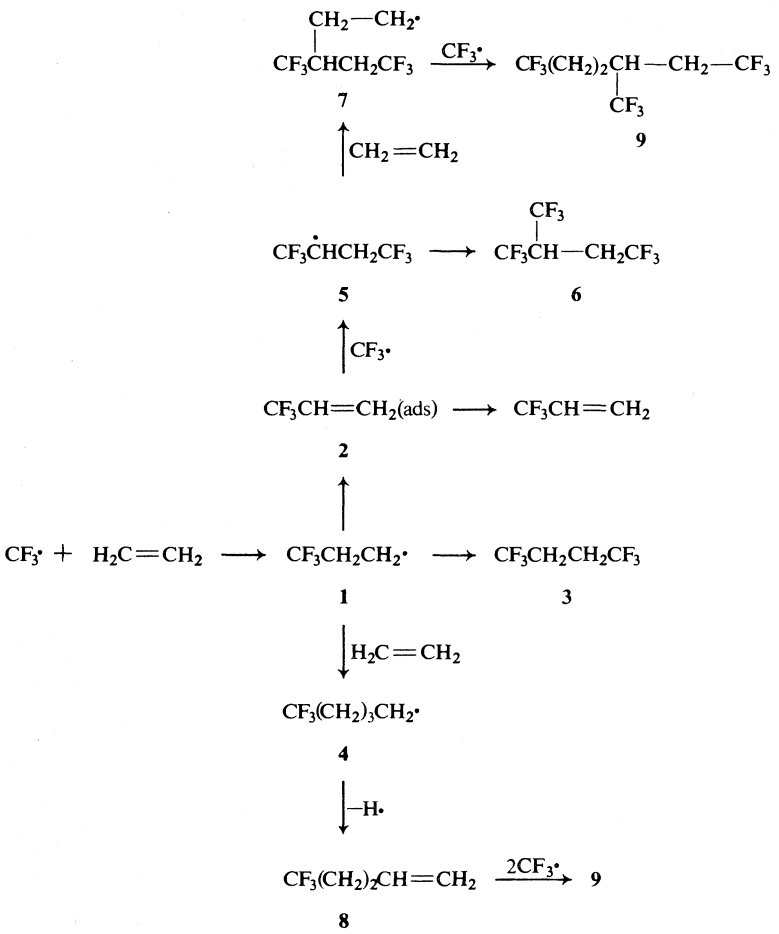

SCHEME 2

high ethyl radical concentration in the presence of trifluoromethyl radicals (Table 1, run 1) and the formation of polytrifluoromethylated compounds (run 4), a result which has no parallel in free-radical reactions, seems to indicate that an orientation effect and a strong adsorption effect of the fluorinated radicals at the anode surface might play an important role in the formation of the products observed. Orientation effects at the electrode surface were used by many authors to explain their observations in anodic (16–20) and in cathodic (21–23) processes. Even though no definite evidence has as yet been presented to support the control of product formation by the electrode surface, it often does point in this direction. More work is in progress in order to bring support to these effects on the course of the reaction.

It was found that at high propionate anion concentration (Table 1, run 1), butane was the major product, while at low anion concentration (run 4), the major product was trifluoropropene. At high anion concentration, the concentration of ethyl radicals at the surface of the anode, at any given time, is high and, consequently, the possibility of two radicals combining is also high. On the other hand, at low anion concentration, the chances of an isolated ethyl radical combining with another one are tremendously diminished and, therefore, the ethyl radical can lose a hydrogen radical to form ethylene. As the ethylene concentration in the medium increases, the formation of trifluoropropene also increases.

Assuming that the reasoning above is correct, then the mechanism for the formation of the other compounds isolated from the reaction can be illustrated as shown in Scheme 2.

Can. J. Chem. Downloaded from www.nrcresearchpress.com by 210.87.254.42 on 09/05/12
For personal use only.

The adsorbed trifluoropropyl radical, **1**, can either lose a hydrogen radical to give an adsorbed trifluoropropene molecule, **2**, or have a long lifetime and react with another trifluoromethyl radical, which is kept in low concentration, to form 1,2-bis(trifluoromethyl)ethane (**3**), or react with another ethylene molecule to form trifluoropentyl radical, **4**. Compound **2** can either desorb or react with a trifluoromethyl radical to form 1,2-bis(trifluoromethyl)ethyl radical, **5**. 1,1,2-Tris(trifluoromethyl)ethane (**6**) can result from **5**. Two routes are possible for the formation of compound **9**. The first is via radical **5** by consecutive reactions with an ethylene molecule and a trifluoromethyl radical to give radical **8** and then **9**. The second route is via radical **4** to form **8** by the loss of a hydrogen radical and then to compound **9** in presence of a trifluoromethyl radical. Even though both routes are possible, the second is doubtful since neither hexafluorohexane nor trifluoropentene were isolated from the reaction mixture.

We are grateful to Dr. K. O. Kutschke for helpful discussions.

1. R. N. RENAUD and D. E. SULLIVAN. **50**, 3084 (1972).
2. G. S. PANDE and S. N. SHUKLA. Electrochim. Acta, **4**, 215 (1961).
3. R. C. PETERSEN, M. FINKELSTEIN, and S. D. ROSS. J. Org. Chem. **32**, 564 (1967).
4. W. R. HASEK, W. C. SMITH, and V. A. ENGELHART. J. Am. Chem. Soc. **82**, 543 (1960).
5. S. GOLDSCHMIDT, W. LEICHER, and H. HAAS. Ann. Chem. **577**, 153 (1952).
6. S. GOLDSCHMIDT and E. STÖCKL. Chem. Ber. **85**, 630 (1952).
7. W. B. SMITH and H.-G. GILDE. J. Am. Chem. Soc. **81**, 5325 (1959).
8. R. V. LINDSEY, JR. and M. L. PETERSON. J. Am. Chem. Soc. **81**, 2073 (1959).
9. W. B. SMITH and H.-G. GILDE. J. Am. Chem. Soc. **83**, 1355 (1961).
10. P. COURBIS and A. GUILLEMONAT. C.R. Acad. Sc. Paris, **262**, 1435 (1966).
11. W. B. SMITH and Y. HYON YUH. Tetrahedron, **24**, 1163 (1968).
12. M. FLEISCHMANN and D. PLETCHER. Tetrahedron Lett. 6255 (1968).
13. G. O. PRITCHARD and J. R. DACEY. Can. J. Chem. **38**, 182 (1960).
14. S. J. W. PRICE and K. O. KUTSCHKE. Can. J. Chem. **38**, 2128 (1960).
15. A. P. STEFANI, L. HERK, and M. SZWARC. J. Am. Chem. Soc. **83**, 4732 (1961).
16. F. D. MANGO and W. A. BONNER. J. Org. Chem. **29**, 1367 (1964).
17. S. TSUTSUMI and K. KOYAMA. Disc. Faraday Soc. **45**, 247 (1968).
18. T. INOUE, K. KOYAMA, T. MATSUOKA, and S. TSUTSUMI. Bull. Chem. Soc. Japan, **40**, 162 (1967).
19. N. L. WEINBERG and E. A. BROWN. J. Org. Chem. **31**, 4058 (1966).
20. N. L. WEINBERG and E. A. BROWN. J. Org. Chem. **33**, 4326 (1968).
21. R. DIETZ and M. E. PLOVER. Disc. Faraday Soc. **45**, 154 (1968).
22. R. N. GOURLEY, J. GRIMSHAW, and P. G. MILLER. Chem. Commun. **3**, 1278 (1967).
23. L. HORNER and D. DEGNER. Tetrahedron Lett. 5889 (1968).

Can. J. Chem. Downloaded from www.nrcresearchpress.com by 210.87.254.42 on 09/05/12
For personal use only.

The Chemistry of the Aminochromes. Part XVI. Proton Magnetic Resonance Spectroscopy[1,2]

W. S. POWELL,[3,4] R. A. HEACOCK,[5] D. G. SMITH,[5] AND A. G. MCINNES[5]

Chemistry Department, Dalhousie University, Halifax, Nova Scotia, and Atlantic Regional Laboratory, National Research Council of Canada, Halifax, Nova Scotia

Received August 21, 1972

The p.m.r. spectra of a number of aminochromes and aminochrome monosemicarbazones have been measured and the major features of the spectra discussed. The synthesis of a new aminochrome, 2-methylnoradrenochrome is described.

Les spectres de r.m.n. d'un certain nombre d'aminochromes et de semicarbazones d'aminochromes ont été mesurés et leurs principales caractéristiques sont discutées. La synthèse d'un nouvel aminochrome, le méthyl-2 noradrénochrome est décrite. [Traduit par le journal]

Can. J. Chem., **51**, 776 (1973)

Can. J. Chem. Downloaded from www.nrcresearchpress.com by 210.87.254.40 on 09/05/12
For personal use only.

Robinson (1) in 1965 reported some p.m.r. data for adrenochrome (compound **1**, Table 1) which had previously been assigned a zwitterionic mesomeric structure by Harley-Mason (2). The spectrum was recorded in DMSO-d_6 solution and resonances at 5.47 and 6.50 δ were assigned to the hydrogens at C-4 and -7. However in a personal communication to one of us (R. A. Heacock) in 1966, Dr. Robinson stated that the assignments for these hydrogens should have been reversed. Since his original paper (1) no further p.m.r. data on adrenochrome or related aminochromes have been reported. To fill this gap in the literature we have recorded the p.m.r. spectra of some aminochromes and aminochrome monosemicarbazones (see structures listed in Table 1) in DMSO-d_6 at 60 MHz. All p.m.r. parameters in Table 2 were obtained by comparing the experimental spectra with those simulated with the Varian Spectro System 100. Because the spectra were comparatively simple it was not considered necessary to check the results at a second radiofrequency.

In all of the compounds examined, except **2**, **2***a*, and **4**, two resonances with chemical shifts characteristic of "aromatic" type hydrogens (3) were observed for H-4 and -7. Moreover H-7 could be assigned to the resonance at higher field (5.30–5.47 δ) because the low field signal for H-4 (6.42–6.80 δ) was absent from the spectra of **2** and **2***a* which are of known structure with $R_4 = CH_3$ (4). It follows, therefore, that the iodine atom in **4** must be located at C-7 since a characteristic resonance was observed for H-4 (6.56 δ) whereas no signal at higher field was observed for H-7. This work therefore confirms that the iodine atom in iodoaminochromes is at C-7 (5) rather than at C-2 as was originally suggested (6).

The "benzylic" type methylene hydrogens at C-3 in **8** were readily assigned (3) to the high field multiplet at 3.00 δ whereas the corresponding hydrogens at C-2, which also bears a nitrogen atom, occurred as expected at lower field at 3.80 δ (3). For those compounds in which there is an hydroxyl or methoxyl group at position 3, the hydrogen at C-3 exhibited a characteristic downfield shift appearing in the range 4.50–5.00 δ. On the other hand, replacement of one of the methylene hydrogens at C-2 with a methyl substituent as in **7** did not appreciably affect the chemical shift of the hydrogen at C-2 which appeared as expected at 3.76 δ. The remaining signals in all the spectra were readily identified on the basis of their chemical shifts, multiplicities, and/or intensities, or their ease of replacement with deuterium. Assignments were confirmed by decoupling experiments.

Compound **7** was synthesized from 1-(3,4-dihydroxyphenyl)-2-aminopropan-1-ol, the side chain of which has an *erythro* configuration, thus requiring that the methyl and hydroxyl substituents on C-2 and -3, and therefore H-2a

[1]For Part XV, see ref. 12.
[2]NRCC No. 12932.
[3]Taken, in part, from the Ph.D. Thesis of W. S. Powell, Dalhousie University, 1972.
[4]Holder of NRCC Scholarship, 1967–1971.
[5]Reprint requests can be addressed to any of these authors at the Atlantic Regional Laboratory.

TABLE 1. Structures of aminochromes and monosemicarbazone derivatives

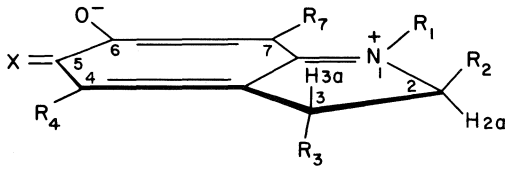

	Compound	X	R_1	R_2	R_3	R_4	R_7
1	Adrenochrome	O	CH_3	H-2b	OH	H	H
1*a*	Adrenochrome monosemicarbazone	$H_2NCONHN$	CH_3	H-2b	OH	H	H
2	4-Methyladrenochrome	O	CH_3	H-2b	OH	CH_3	H
2*a*	4-Methyladrenochrome monosemicarbazone	$H_2NCONHN$	CH_3	H-2b	OH	CH_3	H
3	Adrenochrome methyl ether	O	CH_3	H-2b	OCH_3	H	H
4	7-Iodoadrenochrome methyl ether	O	CH_3	H-2b	OCH_3	H	I
5	Noradrenochrome	O	H	H-2b	OH	H	H
5*a*	Noradrenochrome monosemicarbazone	$H_2NCONHN$	H	H-2b	OH	H	H
6	1-Isopropylnoradrenochrome	O	$CH(CH_3)_2$	H-2b	OH	H	H
7	2-Methylnoradrenochrome	O	H	CH_3	OH	H	H
8	Epinochrome	O	CH_3	H-2b	H-3b	H	H

and -3a, have a *trans* relationship to one another. This follows because the experimental conditions for cyclization preclude epimerization at the two asymmetric carbons (see Experimental). From Table 2 it can be seen that, apart from the typical geminal coupling constants (7, 8), the spin–spin couplings between hydrogens on C-2 and -3 fall either in the range 1.8–4.0 or 6.2–7.0 Hz. The data for **7**, ($J_{trans} = J_{2a,3a} = 3.6$ Hz), together with known trends in the behavior of spin–spin couplings in other similar five-member ring systems (8), enabled the lower range of values discussed above to be assigned to *trans*, and the higher range of values to *cis*, spin–spin couplings for the compounds listed. It is also worth noting that for those compounds with a methylene group at position 2, the hydrogen (H-2a) *cis* to R_3 = OH or OCH_3, occurred at highest field and was *trans* coupled to H-3a. In the case of compound **8** which bore no electronegative substituent at C-3 the *trans* ($J_{2a,3a} = J_{2b,3b} = 4.0$ Hz) and *cis* ($J_{2a,3b} = J_{2b,3a} = 7.0$ Hz) couplings were the largest observed throughout the series of compounds investigated, as would be expected (8).

For those compounds in which R_4 = H long-range coupling ($1.5 \leqslant J_{3,4} \leqslant 2.3$ Hz) was observed between this hydrogen and all hydrogens directly bonded to C-3. When $R_4 = CH_3$, long-range coupling (8) was observed between H-3a and these methyl hydrogens in **2** but surprisingly not in **2***a*. The presence of long-range coupling between one of the aromatic hydrogens (H-4) and H-3a in the iodoaminochrome **4** is of course further evidence that the iodine atom must be attached to C-7 in this compound.

Experimental

Aminochromes

Methods described in the literature were used to prepare adrenochrome (9), adrenochrome methyl ether (10), 7-iodoadrenochrome methyl ether (10), 4-methyladrenochrome (4), 1-isopropylnoradrenochrome (10), noradrenochrome (11), and epinochrome (12).

2-*Methylnoradrenochrome* was prepared in a manner analogous to that for noradrenochrome (11). The free base 1-(3,4-dihydroxyphenyl)-2-aminopropan-1-ol (3,4-dihydroxynorephedrine; 2 g), prepared according to one of the standard procedures (*cf.* ref. 4) from the corresponding hydrochloride, was treated with silver oxide (8.3 g) in methanol (200 ml) for 8 min and the reaction mixture subsequently filtered through anhydrous sodium sulfate and then Dowex-1 × 8 (Cl^-). Crystallization was initiated by adding ethyl acetate (250 ml) and reducing the volume to ≈30 ml at <25° *in vacuo* followed by the further addition of ethyl acetate (30 ml) and once again reducing the volume of the solution to ≈25 ml. 2-Methylnoradrenochrome (515 mg; 26% yield) was obtained as dark red microcrystals which completely decomposed without melting by 115°; λ_{max} (H_2O) nm (ε): 216 (26 800), 295 (9600), 488 (3690); ν_{max} (Nujol): 3235, 3210, 1667, 1617, 1582, 1543 cm^{-1}.

Anal. Calcd. for $C_9H_9NO_3$: C, 60.33; H, 5.06; N, 7.82. Found: C, 59.94; H, 4,86; N, 7.79%.

Aminochrome Monosemicarbazones

Methods in the literature were used to prepare 4-methyladrenochrome and noradrenochrome monosemi-

Can. J. Chem. Downloaded from www.nrcresearchpress.com by 210.87.254.40 on 09/05/12
For personal use only.

Can. J. Chem. Downloaded from www.nrcresearchpress.com by 210.87.254.40 on 09/05/12
For personal use only.

TABLE 2. The p.m.r. data (60 MHz spectra) for aminochromes and monosemicarbazone derivatives in DMSO-d_6 with TMS as internal reference*

Compound	Chemical shifts δ‡	System§	Hz† ν_{2a}	ν_{2b}	ν_{3a}	ν_{3b}	ν_4	Coupling constants (Hz) $J_{p,q}$ 2a,2b	2a,3a	2b,3a	3a,4
1	3.08(R_1 = CH_3, s), 5.39(H-7, s) 6.02(OH,bd)	A(H-2a)B(H-2b)M(H-3a)X(H-4)H-4, 6.42 δ	174.2	143.8	86.0		0.0	−12.0	3.2	6.8	2.0
1*a*	3.00(R_1 = CH_3, s), 5.38(H-7, s) 5.75(OH, bd) 7.00(NH_2, bs) 14.72(NH, bs)	A(H-2a)B(H-2b)M(H-3a)X(H-4)H-4, 6.75 δ	198.0	169.0	106.0		0.0	−11.9	3.0	7.0	1.5
2	3.07(R_1 = CH_3, s), 5.33(H-7, s) 5.85(OH, s)	A(H-2a)B(H-2b)M(H-3a)X_3(R_4 = CH_3)H-3a, 5.03 δ	90.6	59.8	0.0		184.8 (R_4=CH_3)	−12.5	2.4	6.2	1.1 (J_{3a,CH_3})
2*a*	2.18(R_4 = CH_3, s), 2.98(R_1 = CH_3, s) 5.30(H-7, s), 5.55(OH,bd) 6.88(NH_2, bs), 14.98(NH, bs)	A(H-2a)B(H-2b)M(H-3a)H-3a, 5.03 δ	94.8	66.0	0.0			−12.0	1.8	6.6	
3‖	3.13(R_1 = CH_3, s), 3.47(OCH_3, s) 5.33(H-7, s)	A(H-2a)B(H-2b)M(H-3a)X(H-4)H-4, 6.46 δ	164.0	140.0	98.0		0.0	−11.9	2.6	6.2	1.6
4	3.30(R_1 = CH_3, s), 3.60(OCH_3, s)	A(H-2a)B(H-2b)M(H-3a)X(H-4)H-4, 6.56 δ	166.0	145.2	112.0		0.0	−12.5	2.3	6.3	1.6
5¶	5.47(H-7, s)	A(H-2a)B(H-2b)M(H-3a)X(H-4)H-4, 6.45 δ	180.3	146.3	86.0		0.0	−12.5	3.3	6.7	2.0
5*a*	5.38(H-7, s), 5.70(OH, bd) 7.02(NH_2, bs), 8.55(R_1 = H, bs) 14.83(NH, bs)	A(H-2a)B(H-2b)M(H-3a)X(H-4)H-4, 6.80 δ	204.5	174.0	106.0		0.0	−11.9	3.1	6.8	1.5
6	1.23, 1.25, 4.07(R_1 = $HC(CH_3)_2$) 5.47(H-7, s), 6.03(OH, bs)	A(H-2a)B(H-2b)M(H-3a)X(H-4)H-4, 6.43 δ	182.0	145.3	87.0		0.0	−12.0	3.1	6.9	2.0
7	5.42(H-7, s), 6.07(OH, bs) 9.35(NH, bs)	A(H-4)M(H-3a)P(H-2a)X_3(R_{2b} = CH_3)H-4, 6.42 δ	159.4	305.0 (R_{2b} = CH_3)	115.0		0.0	6.3 (J_{H_{2a},CH_3})	3.6		2.2
8	3.11(R_1 = CH_3, s), 5.40(H-7, s)	A(H-2a)A′(H-2b)X(H-3a)X′(H-3b)H-4, 6.37 δ	154.0	154.0	201.0	201.0	0.0	$J_{2a,2b} = -12.0, J_{3a,3b} = -8.0$ $J_{2a,3a} = J_{2b,3b} = 4.0$ $J_{2a,3b} = J_{2b,3a} = 7.0$ $J_{3a,4} = J_{3b,4} = 2.3$			

*Spectra were recorded on a Varian A-60A n.m.r. spectrometer equipped with a V-6058 spin decoupler.
†For computer purposes the chemical shift of the lowest-field proton was empirically given a value of 0.0 Hz and all others were measured relative to it.
‡b = broad, d = doublet, s = singlet.
§Chemical shifts reported in this column refer to the centroid of the H-4 (**1**, **1*a***, **3**, **4**, **5**, **5*a***, **6**, **7**), H-3a (**2**, **2*a***), or AA′XX′ (**8**) multiplets.
‖Spectrum was recorded in acetone-d_6.
¶Signals for the protons H-1 and OH (R_3) were too broad to be observed; exchangeable protons established by exchange with D_2O.

carbazones (4, 11). Adrenochrome monosemicarbazone was obtained from the Koch-Light Laboratories.

The authors wish to thank Mr. J. van Ingen for recording some of the spectra.

1. B. ROBINSON. J. Pharm. Pharmacol. **17**, 89 (1965).
2. J. HARLEY-MASON. Experientia, **4**, 307 (1948).
3. L. M. JACKMAN and S. STERNHELL. Applications of nuclear magnetic resonance spectroscopy in organic chemistry. Pergamon Press, New York. 1969. Part 3.
4. R. A. HEACOCK and O. HUTZINGER. Can. J. Chem. **43**, 2535 (1965).
5. R. A. HEACOCK, O. HUTZINGER, B. D. SCOTT, J. W. DALY, and B. WITKOP. J. Am. Chem. Soc. **85**, 1825 (1963).
6. D. RICHTER and H. BLASCHKO. J. Chem. Soc. 601 (1937).
7. R. CAHILL, R. C. COOKSON, and T. A. CRABB. Tetrahedron, **25**, 4681 (1969).
8. S. STERNHELL. Quart. Rev. **23**, 236 (1969).
9. R. A. HEACOCK, C. NERENBERG, and A. N. PAYZA. Can. J. Chem. **36**, 853 (1958).
10. R. A. HEACOCK and B. D. SCOTT. Can. J. Chem. **38**, 516 (1960).
11. W. S. POWELL and R. A. HEACOCK. Can. J. Chem. **49**, 341 (1971).
12. W. S. POWELL and R. A. HEACOCK. Can. J. Chem. **50**, 3360 (1972).

Can. J. Chem. Downloaded from www.nrcresearchpress.com by 210.87.254.40 on 09/05/12
For personal use only.

Reactions of Thiyl Radicals. X. Photolysis of Ethyl Sulfide Vapor[1]

CONRAD S. SMITH AND ARTHUR R. KNIGHT

Department of Chemistry and Chemical Engineering, University of Saskatchewan, Saskatoon, Saskatchewan S7N 0W0

Received September 22, 1972

The photolysis of ethyl sulfide vapor at 2537 Å has been investigated as a function of substrate and CF_4 pressure, time, and temperature. Reaction products with quantum yields in parentheses are ethyl disulfide (0.178), ethane (0.138), butane (0.086), ethanethiol (0.096), 4-methyl-3-thiahexane (0.034) and 4-methyl-3,5-dithiaheptane.

Ethyl and ethylthiyl radicals are formed in the primary process and the product yields indicate a net primary decomposition quantum yield of 0.48. A reaction mechanism involving subsequent reactions of the primary fragments is proposed and explains the observed products and the observed variation in rates. Excited radicals and hot radical combination products play a minor role in this system, in contrast to the behavior of lower molecular weight sulfides. Secondary photolysis of the disulfide produced and consumption of ethanethiol are important factors in determining the time dependence of reaction rates in this system.

La photolyse de la vapeur de sulfure d'éthyle à 2537 Å a été étudiée en fonction de la nature du substrat et de la pression de CF_4 ainsi que du temps et de la température. Les produits de la réaction, dont les rendements quantiques sont donnés entre parenthèses, sont les suivants, disulfure d'éthyle (0.178) éthane (0.138), butane (0.086) éthanethiol (0.096), méthyl-4 thia-3 hexane (0.034), et méthyl-4 dithia-3,5 heptane.

Les radicaux éthyle et éthylthiyle sont formés dans la première phase et les rendements de produits indiquent fort nettement un rendement quantique de la décomposition primaire égal à 0.48. Un mécanisme réactionnel impliquant des réactions subséquentes des fragments primaires est proposé: celui-ci permet d'ailleurs d'expliquer la formation des produits observés ainsi que les fluctuations observées dans les vitesses de formation. Les radicaux excités et les produits de combinaison de radicaux chauds jouent, en réalité, un rôle négligeable dans ce système, ce qui va à l'encontre du comportement des sulfures ayant des poids moléculaires plus bas. La photolyse secondaire du composé disulfuré obtenue ainsi que la consommation d'éthanethiol sont des facteurs importants pour déterminer dans ce système la dépendance existant entre le temps et les vitesses de la réaction. [Traduit par le journal]

Can. J. Chem., **51**, 780 (1973)

Introduction

As part of a continuing series of investigations of the photochemical kinetics of sulfur compounds that are thiyl radical sources we have studied and report on here the vapor phase photolysis of $C_2H_5SC_2H_5$ at 254 nm. In comparison with the lower molecular weight sulfides, this substrate provides a relatively labile source of abstractable hydrogen atoms. In addition, the thiyl radical combination product $C_2H_5SSC_2H_5$ would be expected to be relatively stable to the unimolecular decomposition that would regenerate ethylthiyl radicals.

The photolysis of ethyl sulfide vapor has not been investigated previously. Methyl sulfide vapor has been studied in direct photolysis (1, 2) and in mercury photosensitization (3, 4). The direct photolysis of methyl ethyl sulfide has also been investigated (5). In each case the products of the reaction can be rationalized on the basis of a C—S bond cleavage in the primary process, followed by reactions of the alkyl and thiyl radicals formed thereby. It has been shown (4) that the thiyl radical disproportionation:combination ratio determined from thiol and disulfide yields is pressure sensitive and that only at high total pressures are the observed yields of these products indicative of the actual relative contribution of the two processes.

Experimental

The photolyses were conducted in a mercury-free system constructed of stainless steel and Pyrex glass. The vacuum line could be heated to 75 °C to facilitate the transfer of relatively non-volatile materials. The lamp was a Hanovia 30620 medium pressure mercury arc fitted with a Vycor 7910 filter. The filter, along with the absorption characteristics of the substrate (6) limited the effective wavelengths to between 2300 and 2600 Å; principally, the reversed Hg-line at 2537 Å. The reaction cell was a quartz

[1]From the Ph.D. Thesis of C. S. Smith, to be submitted to the University of Saskatchewan, Saskatoon, Saskatchewan.

Can. J. Chem. Downloaded from www.nrcresearchpress.com by 210.87.254.105 on 09/05/12
For personal use only.

Can. J. Chem. Downloaded from www.nrcresearchpress.com by 210.87.254.105 on 09/05/12
For personal use only.

cylinder, 4.4 cm o.d. by 20 cm long fitted with a demountable furnace.

Ethyl sulfide (Eastman) and diethyl ketone (B.D.H.) were freed from impurities by preparative scale gas chromatography. In some experiments, A.P.I. standard sample ethyl sulfide, free from detectable impurities, was used without further purification. Carbon tetrafluoride (Matheson) was degassed and fractionated at low temperature in the line before use.

Reaction products were identified by comparison of g.c. retention times, confirmed by mass spectrometric analysis of the g.c. effluent.

For experiments involving the photolysis of the substrate alone, the reaction products and undecomposed substrate were fractionated by low temperature distillation at −160.5 °C. Products non-condensable at this temperature, C_2H_4 and C_2H_6, were analyzed on a 10 ft Poropac-Q column at 25 °C, while the substrate and other products were eluted with temperature programming on a 6 ft tricresyl phosphate column. In the experiments with CF_4 present, the addend was removed at −160.5 °C along with the C_2 fraction before analysis.

The absorbed intensity for the actinometry experiments was determined utilizing the photolysis of 12 Torr diethyl ketone at 170 °C, assuming a quantum yield of unity for CO production (7), with a Hanovia model 688A45 low pressure mercury lamp. The percent absorption at 2537 Å by both the actinometer, 19.1%, and the substrate, 18.4% at P = 30 Torr, were determined in the reaction cell using a Zeiss Model PMQ-II spectrophotometer. The emission spectrum of the lamp was determined and corrections made for the relative weak emission lines between 2655 and 3132 Å that are absorbed by the ketone but not by the sulfide. The carbon monoxide formed in the ketone photolysis was removed through a liquid nitrogen trap to an auxiliary system and determined in a gas burette. The absorbed light intensity was 0.134 μ einsteins min^{-1}. A comparison of the yields of products from the photolysis of 30 Torr sulfide in the actinometry experiments and in the experiments using the medium pressure Hg lamp indicated that the effective intensity of the latter light source is within 10% of the low pressure lamp. Thus the quantum yield determinations here were at effectively the same intensity as the other experiments.

Results

The photolysis of ethyl sulfide vapor at 30 °C and 20 Torr pressure gives the following reaction products listed in decreasing order of importance: C_2H_6, $C_2H_5SSC_2H_5$, C_4H_{10}, C_2H_4, C_2H_5SH, and 4-methyl-3-thiahexane (MTH), $C_2H_5CH(CH_3)$-SC_2H_5. In addition, a product too non-volatile to permit routine quantitative analysis was tentatively identified as 4-methyl-3,5-dithiaheptane (MDTH), $C_2H_5SC_2H_4SC_2H_5$. Thioacetaldehyde, if formed, would not have been detected.

A mass balance in carbon and sulfur may be estimated on the following basis. A rate for carbon-containing products can be determined from the observed product rates of products analyzed quantitatively via eq. 1. The analogous

$$[1]\quad R_c = 2R_{C_2H_4} + 2R_{C_2H_6} + 4R_{C_4H_{10}} + 2R_{C_2H_5SH} + 4R_{C_2H_5SSC_2H_5} + 6R_{MTH}$$

rate expression for sulfur-containing products is given by eq. 2. From the stoichiometry of the

$$[2]\quad R_s = R_{C_2H_5SH} + R_{MTH} + 2R_{C_2H_5SSC_2H_5}$$

$C_2H_5SC_2H_5$ decomposition R_c should be identical to $4R_s$. Although this kind of calculation is a valuable tool with respect to product accountability, it is insensitive to products with a c/s ratio of 4. The most likely such product would be the dimer of the "substrate radical", $CH_3\dot{C}HSC_2H_5$. A non-volatile product of that type and its isomers would not have been detected by the analytical techniques used here. If eqs. 1 and 2 are modified to include R_{MDTH}, the net effect would be the addition of a $2R_{MDTH}$ term to the right hand side of $R_c = 4R_s$. It is to be expected therefore that there would be a deficiency in sulfur products when the calculation excludes the MDTH whose rates were not determined.

Equations 1 and 2 do not include the possible yield of thioacetaldehyde that would result from the disproportionation between C_2H_5S radicals or between C_2H_5 and C_2H_5S radicals. The effect of incorporating this C_2H_4S yield would be to increase the $4R_s$ term more than R_c. Thus an apparent sulfur product deficiency indicated by eqs. 1 and 2 as written may be the result of not taking these disproportionation processes into account. However, the appearance of MTH and MDTH as products is evidence that abstraction reactions do occur in this system, since both products originate with the $C_2H_5S\dot{C}HCH_3$ radical. Thus at least some of the observed C_2H_6 and C_2H_5SH must be formed via H-atom abstraction from the substrate.

Figures 1 and 2 show the variation in rate of product formation as a function of ethyl sulfide pressure for an exposure time of 60 min. All rates show a continuous increase, indicating that absorption of the incident radiation is incomplete up to 50 Torr, the maximum pressure that can be examined at room temperature. This is consistent with the absorption measurements made in connection with the actinometry experiments.

Stoichiometric calculations utilizing eqs. 1 and 2 give $R_c = 0.133 \pm 0.004$ and $4R_s = 0.126 \pm 0.004$ μmol min^{-1} at 20 Torr sulfide pressure while at $P_{C_2H_5SC_2H_5} = 40$ Torr, $R_c = 0.220 \pm 0.007$ and $4R_s = 0.192 \pm 0.006$ μmol min^{-1}. The fact that the two rates are the same within experi-

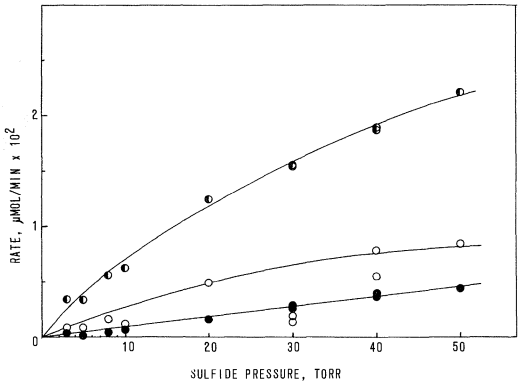

FIG. 1. Variation in rate of formation of ethyl disulfide, ◐; ethanethiol, ○; and MTH, ●, as a function of substrate pressure for the photolysis of ethyl sulfide at an exposure time of 60 min.

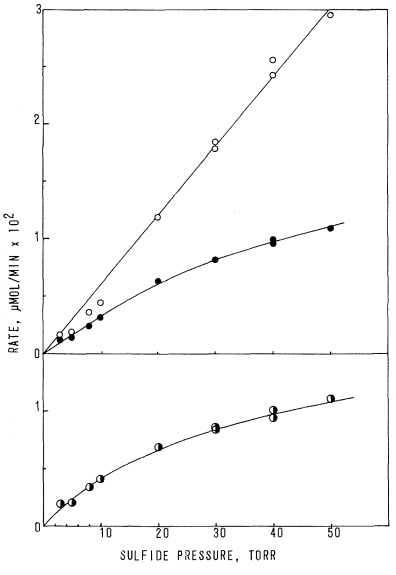

FIG. 2. Variation in rate of formation of ethane, ○; ethylene, ●; and butane, ◑; as a function of substrate pressure for the photolysis of ethyl sulfide at an exposure time of 60 min.

mental error is likely fortuitous since some sulfur deficiency should result from the exclusion of the MDTH yields, but is evidence against a very large contribution from C_2H_5S disproportionation. The sulfur product deficiency pointed to by the calculations from the rates at 40 Torr will be due in part to the MDTH yield. Because of its origin in abstraction from the substrate by primary radicals, the relative importance of this product would be expected to increase with substrate pressure.

The rate of consumption of the substrate is given by $R_c/4$, where R_c is defined by eq. 1. At an ethyl sulfide pressure of 50 Torr, the data in Figs. 1 and 2 indicate that for 60 min exposure there is 0.6% decomposition.

The variation in rates with exposure time for the photolysis of 20 Torr ethyl sulfide is shown in Fig. 3. The rates for C_2H_4 and MTH are time independent within experimental error. Ethyl disulfide and ethanethiol show rates that pass through a shallow maximum and decline at the longer exposure times. The C_2H_6 rate exhibits a pronounced increase while there is a concomitant decline in $R_{C_4H_{10}}$. The total rate of C_2H_5 radical consumption, however, calculated from eq. 3,

$$[3] \quad R_{-C_2H_5} = R_{C_2H_6} + R_{C_2H_4} + 2R_{C_4H_{10}} + R_{MTH}$$

remains essentially constant at $3.2 \pm 0.2 \times 10^{-2}$ μmol min^{-1} between 10 and 240 min.

The values, in μmol min^{-1} calculated from eq. 1 at 45 and 240 min for R_c are, respectively 0.124 ± 0.004 and 0.116 ± 0.004, while the corresponding $4R_s$ values computed using eq. 2 are 0.114 ± 0.004 and 0.099 ± 0.003. Although part of the increased S-product deficiency at longer times would be expected because of their greater susceptibility to secondary decomposition, the influence of MDTH formation is also significant. The effect of exposure time on the relative MTH and MDTH yields was estimated[2] to illustrate this point. For 60 min exposure of 20 Torr sulfide R_{MDTH}/R_{MTH} was 1.3 ± 0.2 while in an experiment corresponding to 480 min exposure, this ratio was 1.7 ± 0.1. If a $2R_{MDTH}$ term (see above) is included in eq. 2, the values of $4R_s$ at 45 and 240 min (assuming $R_{MDTH}/R_{MTH} = 1.5$) become 0.119 ± 0.004 and 0.104 ± 0.004 μmol min^{-1}, respectively. Thus there is a mass balance within experimental error at the short times while a sulfur deficiency, albeit somewhat reduced, remains in the observed rates at 240 min.

Table 1 lists the results of an investigation of

[2]The relative yields were approximated by comparing the g.c. peak areas for the two products assuming the same molar response. The longer experiment was carried out at a somewhat higher intensity and corresponded, on a percent decomposition basis, to 480 min exposure in the series described in Fig. 3. The retention time of the MDTH peak, even with temperature programming, was such that peak areas could not be determined accurately in the routine analysis of yields from experiments with exposure times up to 240 min where MDTH yields are on the order of 0.03 μmol or less.

Can. J. Chem. Downloaded from www.nrcresearchpress.com by 210.87.254.105 on 09/05/12
For personal use only.

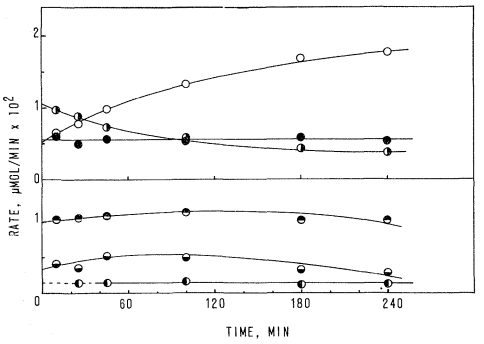

FIG. 3. Variation in rate of formation of ethane, ○; ethylene, ●; butane, ◑; ethyl disulfide, ◓; ethanethiol, ◒; and MTH, ◐; as a function of exposure time for the photolysis of 20 Torr ethyl sulfide.

TABLE 1. Effect of added CF_4 on the photolysis of 20 Torr ethyl sulfide*

	Rate (μmol min^{-1} × 10^3)			
$P(CF_4)$ (Torr)	$C_2H_5SSC_2H_5$	MTH	C_2H_5SH	C_4H_{10}
0	7.6	1.3	4.0	4.9
50	8.5	1.6	3.6	5.1
100	8.3	1.5	3.5	5.7
165	8.4	1.8	4.6	5.2
250	8.4	1.7	4.6	5.3
500	7.8	1.6	5.3	5.2

*Exposure time = 60 min; T = 25 °C.

the effect of added CF_4 on the photolysis of 20 Torr $C_2H_5SC_2H_5$ for 60 min. As in previous investigations of addend effect with methyl sulfide (2) and methyl ethyl sulfide (5), there is some scatter in the observed rates but apart from a possible small increase in thiol yields, the rates appear to be essentially unaffected by inert addend.

A series of experiments was carried out to determine the effect of temperature on the reaction. Twenty Torr $C_2H_5SC_2H_5$ measured at 30 °C was photolyzed for 25 min at temperatures from 30–92.5 °C. The results are shown in Figs. 4 and 5. Application of eqs. 1 and 2 to the data at 80 °C gives R_c = 0.151 and $4R_s$ = 0.135 μmol min^{-1}. Comparison of these values with R_c and $4R_s$ for 20 Torr substrate at 30 °C indicates an apparent small increase in overall decomposition of 11% for carbon-containing products and 7% for S-compounds. Thus the principal effect of temperature is a redistribution of the products. Three products have rates that increase significantly with temperature, C_2H_6, C_2H_5SH, and

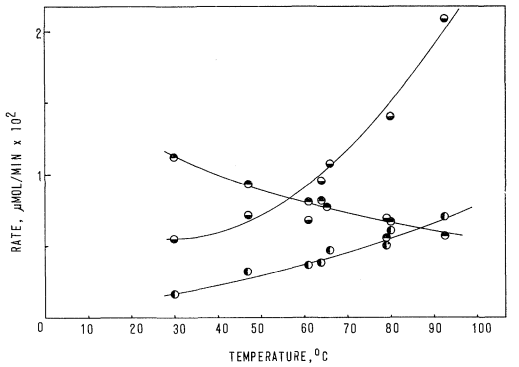

FIG. 4. Variation in rate of formation of ethanethiol, ◒; MTH, ◐; and ethyl disulfide, ◓; as a function of temperature for the photolysis of 20 Torr (measured at 30 °C) ethyl sulfide for 25 min.

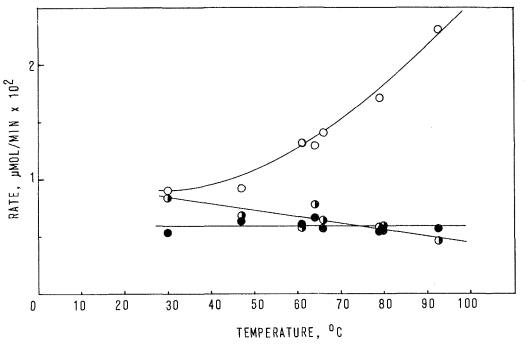

FIG. 5. Variation in the rate of formation of ethane, ○; ethylene, ●; and butane, ◑; as a function of temperature for the photolysis of 20 Torr (measured at 30 °C) ethyl sulfide for 25 min.

MTH. Arrhenius plots of $R_{C_2H_6}/R^{\frac{1}{2}}_{C_4H_{10}}$ and $R_{C_2H_5SH}/R^{\frac{1}{2}}_{C_2H_5SSC_2H_5}$ are linear between 30 and 80 °C (values at 92.5 being slightly higher than indicated by an extrapolation of the graph) and give apparent activation energies of 3.4 and 5.2 kcal mol^{-1} for C_2H_6 and C_2H_5SH, respectively. MTH is a secondary product and the variation with temperature of the concentration of radicals involved in its formation cannot be eliminated in a simple ratio. However, an Arrhenius plot of the MTH rates indicates an overall apparent activation energy of 5 kcal mol^{-1}.

Finally, utilizing the low pressure mercury lamp, the quantum yields of products were determined by photolysing 30 Torr ethyl sulfide for 30 min. The values are listed in Table 2. Comparison of the product ratios in this series with the data for 30 Torr at an exposure time of 60 min (Figs. 1 and 2) or 20 Torr at t = 30 min (Fig. 3)

Can. J. Chem. Downloaded from www.nrcresearchpress.com by 210.87.254.105 on 09/05/12
For personal use only.

TABLE 2. Quantum yields in the photolysis of ethyl sulfide at 2537 Å

Product	Φ (mol einstein^{-1})
C_2H_4	0.086
C_2H_6	0.138
C_4H_{10}	0.110
C_2H_5SH	0.096
MTH	0.034
$C_2H_5SSC_2H_5$	0.178

shows that there is no significant difference in product distribution between the two lamps. The primary decomposition quantum yield, Φ_p, can be computed from the yields of products that result from ethyl radicals using eq. 4, which gives

$$[4] \quad \Phi_p = \Phi_{C_2H_6} + \Phi_{C_2H_4} + 2\Phi_{C_4H_{10}} + \Phi_{MTH}$$

a value of 0.48, or from C_2H_5S radical products, via eq. 5. The thiol and disulfide yields alone

$$[5] \quad \Phi_p = \Phi_{C_2H_5SH} + \Phi_{C_2H_5SSC_2H_5} + \Phi_{MDTH}$$

give $\Phi_p = 0.43$ indicating a value of Φ_{MDTH} of *ca.* 0.05, consistent with the estimated value of 1.3 for R_{MDTH}/R_{MTH} and Φ_{MTH} (observed) of 0.034.

Discussion

The kind of reaction products observed in this system and their similarity to those that have been found previously to characterize the photodecomposition of other sulfides points to C—S bond cleavage in the primary process, reaction 6.

$$[6] \quad C_2H_5SC_2H_5 + h\nu \rightarrow C_2H_5S + C_2H_5$$

The fact that product yields are essentially unaffected by inert addend pressure rules out the possibility of the formation of a long-lived excited sulfide molecule in the primary process.

In attempting to explain product formation on the basis of subsequent reactions of the primary radicals, particularly with respect to the relative contributions of the several possibilities, a number of factors must be considered. As will become apparent, the lack of data on the kinetics of C_2H_5S radical reactions gives rise to some uncertainties in the interpretation of the results. The kinetic data that can be extracted from this study, however, provide useful information on the kinetics of this species, particularly indicating that its behavior is significantly different from that of CH_3S.

As with the lower molecular weight sulfides, there will be energy carry-over in the primary process. The S—C bond strength in $C_2H_5SC_2H_5$ is 71 kcal mol^{-1} (8). Therefore at 2537 Å, there is a 42 kcal mol^{-1} energy excess in reaction 6. If the carry-over is inversely proportional to mass, then $E_{C_2H_5} = 28$ and $E_{C_2H_5S} = 13$ kcal mol^{-1}. However, because of the larger number of degrees of freedom in the primary fragments, their excess energy, whether or not apportioned in that way, would be expected to be less important than in CH_3SCH_3.

The presence of relatively large amounts of thiol as a product in this system gives rise to the possibility, not a factor in CH_3SCH_3 or $C_2H_5SCH_3$ photolyses, that because of the lability of the sulfhydryl hydrogen the abstraction of hydrogen atoms from this molecule may be an important reaction. Radical attack on the S—H bond would be expected to have an appreciably lower activation energy than attack on the C—H bonds in the substrate.

Secondary photolysis of the ethyl disulfide produced would also be important. The absorption measurements carried out for the actinometry calculations give $\varepsilon_{C_2H_5SC_2H_5} = 5.3$ l/mol cm at 2537 Å while for $C_2H_5SSC_2H_5$, the molar extinction coefficient is 315 (6). Thus, for example, in the photolysis of 20 Torr ethyl sulfide, after 240 min exposure 25% of the absorbance is due to the 2.5 μmol of disulfide present.

On the basis of these considerations, the sequence of reactions depicted by eqs. 7–19 is suggested for the ethyl sulfide photolysis. The primary process, reaction 6, will be followed by [7], etc.

$$[7] \quad 2C_2H_5 \rightarrow C_2H_4 + C_2H_6$$

$$[8] \quad 2C_2H_5 \rightarrow C_4H_{10}$$

$$[9] \quad 2C_2H_5S \rightarrow C_2H_5SH + C_2H_4S$$

$$[10] \quad 2C_2H_5S \rightarrow C_2H_5SSC_2H_5$$

$$[11] \quad C_2H_5 + C_2H_5S \rightarrow C_2H_5SC_2H_5$$

$$[12] \quad C_2H_5 + C_2H_5S \rightarrow C_2H_4 + C_2H_5SH$$

$$[13] \quad C_2H_5 + C_2H_5S \rightarrow C_2H_6 + C_2H_4S$$

$$[14] \quad C_2H_5 + C_2H_5SC_2H_5 \rightarrow C_2H_6 + C_2H_5S\dot{C}HCH_3$$

$$[15] \quad C_2H_5S + C_2H_5SC_2H_5 \rightarrow C_2H_5SH + C_2H_5S\dot{C}HCH_3$$

$$[16] \quad C_2H_5 + C_2H_5S\dot{C}HCH_3 \rightarrow MTH$$

$$[17] \quad C_2H_5S + C_2H_5S\dot{C}HCH_3 \rightarrow MDTH$$

$$[18] \quad C_2H_5 + C_2H_5SH \rightarrow C_2H_6 + C_2H_5S$$

$$[19] \quad C_2H_5SC_2H_5 + h\nu \rightarrow 2C_2H_5S$$

Can. J. Chem. Downloaded from www.nrcresearchpress.com by 210.87.254.105 on 09/05/12
For personal use only.

Can. J. Chem. Downloaded from www.nrcresearchpress.com by 210.87.254.105 on 09/05/12
For personal use only.

The initial rates obtainable from Fig. 3 by extrapolation to zero exposure time are not influenced by reactions 18 and 19. Although the results at short exposure times are subjected to relatively large experimental errors because of the small amounts of products involved, some limiting values can be established that indicate the observed rates are consistent with the reactions proposed and with the kinetic information about these processes available from other systems.

The rate constant ratio $k_9/k_{10} = 0.07$, determined in the photolysis of methyl ethyl sulfide vapor (5) gives the initial rate of ethanethiol formation in reaction 9 from the observed value of $R^0_{C_2H_5SSC_2H_5} = 1.0 \times 10^{-2}$ μmol min^{-1} as 0.07 via eq. 20, where here, and in subsequent equa-

$$[20] \qquad R_9^0 = 0.07 R_{10}^0$$

tions and discussion, rates are quoted in μmol min$^{-1} \times 10^2$. The observed $R^0_{C_2H_5SH}$ value is 0.35 and thus from equation 21, the combined

$$[21] \qquad R^0_{C_2H_5SH} = R_9^0 + R_{12}^0 + R_{15}^0$$

rate of thiol production in reactions 12 and 15 is 0.28. This represents a *maximum* value for R_{12}^0, were reaction 15 to make a negligible contribution to C_2H_5SH formation. Proceeding on that assumption, since the initial ethylene rate can be expressed as in eq. 22, and $R^0_{C_2H_4} = 0.55$, the

$$[22] \qquad R^0_{C_2H_4} = R_7^0 + R_{12}^0$$

minimum value of R_7^0 is therefore 0.27. This value together with the observed $R^0_{C_4H_{10}}$ value of 1.05 gives $k_7/k_8 \geq 0.26$. Values of 0.1 (7), 0.2 (9), and 0.14 (10, 11) have been reported for this disproportionation:combination ratio of ethyl radicals. The fact that the minimum value estimated here from the stoichiometry is larger may be evidence that either the C_2H_5 radicals are "hot" or that C_2H_4 is formed in an additional primary process. Other aspects of the data, however, as indicated below, can be interpreted in terms of thermalized ethyl radicals and ethylene production solely via radical–radical reactions.

For ethane, the total initial yield is given by eq. 23. Figure 3 shows the initial rate to be 0.50,

$$[23] \qquad R^0_{C_2H_6} = R_7^0 + R_{13}^0 + R_{14}^0$$

and thus, using the R_7^0 minimum value of 0.27, $(R_{13}^0 + R_{14}^0) \leq 0.23$. On the basis of the known small contribution of the disproportionation mode to the total rate of thiyl radical reactions of the radical–radical type that has been rationalized principally on the basis of the tendency of organosulfur compounds not to undergo reactions in which C—S bonds are converted to C=S bonds (4, 12), it would be expected that R_{13}/R_{14} is quite minute and therefore that the 0.23 likely represents essentially the maximum value of R_{14}.

To complete the stoichiometric analysis, the rate of $C_2H_5S\dot{C}HCH_3$ radical formation is required. The very small yield of MTH and, more particularly of MDTH, precludes measurement of their rates at short exposure times. The rate for the dimer of the substrate radical, which product is likely formed to some extent, would also be required. Thus, although the data available do not permit definitive calculations, they nevertheless provide evidence for the main features of the proposed mechanism.

The observed variation in reaction rates that occurs within the framework of a constant calculated amount of decomposition as the exposure time is lengthened is evidence that the redistribution of reaction products arises from secondary reactions, of which processes 18 and 19 would be the most important. The reaction analogous to [18] involving C_2H_5S radicals amounts to an exchange process that would have no net effect on observed rates.

As the concentration of thiol increases in the system with time, reaction 18 will become progressively a more important source of ethane. Increased importance of this process has two effects. The rates of reactions 7 and 8 will decrease; the observed decline in $R_{C_4H_{10}}$ reflecting the reduction in the rate of the latter process. The second effect will be to regenerate ethylthiyl radicals whose most important reaction here is recombination forming ethyl disulfide. The secondary photolysis of this product, however, evidently limits the amount of disulfide that can accumulate with the result that $R_{C_2H_5SSC_2H_5}$ rises slightly with time but after longer periods shows a slight decline. The regeneration of thiyl radicals and the resultant increase in their steady state concentration is manifested in several ways. Ethanthiol declines only slightly with time; its consumption in reaction 18 evidently being compensated for by its secondary formation following C_2H_5S reformation from the disulfide photolysis. The relative amount of MDTH compared to MTH is found to increase. Finally, there is evidently an increase in the rate of reaction 12, giving additional ethylene that compensates for the decline in $R_{C_2H_4}$ from process 7, so that no net

Can. J. Chem. Downloaded from www.nrcresearchpress.com by 210.87.254.105 on 09/05/12
For personal use only.

change in the rate of C_2H_4 production is observed. Both reactions 7 and 12 are influenced by ethyl radical concentration but $R_7 \propto [C_2H_5]^2$ while $R_{12} \propto [C_2H_5]$. The increased sulfur product deficiency observed at the longer exposure times may reflect an increase in the rate of reaction 13, giving unanalyzable thioacetaldehyde, that parallels the rise in R_{12}.

The change in reaction rates with temperature is influenced by the same considerations, except that secondary disulfide photolysis will be essentially a constant factor. Because of the increases in the rate of abstraction processes with temperature, the recombination reaction involving ethylthiyl radicals cannot compete as effectively as at room temperature and the rate of disulfide formation is reduced. As more and more thiol is formed in primary radical–radical reactions, and in process 15 as reflected in the increase in rate for products coming from the $C_2H_5S\dot{C}HCH_3$ radical, its concentration will increase and again, through reaction 18, result in a higher C_2H_5S radical concentration. As with increasing exposure time, the latter alteration leads to an increase in the rate of reaction 12 counteracting the decline in R_7 that results from abstraction by C_2H_5 radicals becoming more important. This combination of effects then gives rise to the observed temperature independence of $R_{C_2H_4}$. Thus the observed rate can be explained on the basis of the interdependence of the proposed radical–radical reactions, but the arguments do not preclude the formation of ethylene and ethanethiol in an additional primary process.

These arguments also imply that some portion of the ethane yield comes from reaction 18 and thus the observed apparent activation energy of C_2H_6 formation represents the net effect of both reactions 14 and 18. Therefore the value of 3.4 kcal mol^{-1} for C_2H_6 does not necessarily indicate an important contribution from abstraction by hot ethyl radicals since the activation energy of reaction 18, even with thermalized radicals, would not be large. For example, Kerr and Trotman-Dickenson (13) report $E_a = 5.2$ kcal mol^{-1} for the abstractive attack of CH_3 radicals from the photolysis of acetone on C_2H_5SH. The observed yields of ethanethiol are less than those originating in the first instance from the radical reactions and process 15 (the former presumably being temperature independent) because of the secondary consumption of C_2H_5SH. If the latter reaction were not occurring, $R_{C_2H_5SH}$ would increase more rapidly with temperature. That would indicate an actual activation energy larger than the 5.2 kcal mol^{-1} observed, a prediction consistent with the suggestion that excess energy of the radicals in this system, although exerting some influence, is not as important as in the case of lower molecular weight sulfides.

The fact that the quantum yields in this system are less than unity may be an indication that some recombination of primary fragments is taking place, as indicated in reaction 11. In addition, the inefficiency of photodecomposition in this system may have the same origin as the more pronounced similar effect observed in methyl sulfide and methyl ethyl sulfide.

Further investigations to determine the rate of ethyl and ethylthiyl radical attack on the substrate will be required to elucidate further the relative importance of some of the processes that contribute to the decomposition. The examination of the triplet mercury sensitized decomposition will also be useful, as it has been shown to be in the case of methyl sulfide (4), in evaluating the role of the various reactions in the mechanism and the efficiency of the primary decomposition. An investigation of the latter system is currently underway in this laboratory.

The authors gratefully acknowledge the financial support of the National Research Council of Canada for this work.

1. T. Inaba and H. Ogoro. Kogyo Kogaku Zasshi, **72**, 114 (1969).
2. P. M. Rao and A. R. Knight. Can. J. Chem. **50**, 844 (1972).
3. A. Jones, S. Yamashita, and F. P. Lossing. Can. J. Chem. **46**, 833 (1968).
4. D. R. Tycholiz and A. R. Knight. J. Am. Chem. Soc. In press.
5. D. R. Tycholiz and A. R. Knight. Can. J. Chem. **50**, 1734 (1972).
6. J. G. Calvert and J. N. Pitts, Jr. Photochemistry. Wiley, New York, N.Y. 1966. p. 489.
7. K. O. Kutschke, M. H. J. Wijnen, and E. W. R. Steacie. J. Am. Chem. Soc. **74**, 714 (1952).
8. H. Mackle. Tetrahedron **19**, 1159 (1963).
9. K. J. Ivin and E. W. R. Steacie. Proc. Roy. Soc. A**208**, 25 (1951).
10. D. G. L. James and G. E. Troughton. Trans. Faraday Soc. **65**, 763 (1969).
11. A. C. R. Brown and D. G. L. James. Can. J. Chem. **43**, 660 (1965).
12. O. P. Strausz, J. Font, E. L. Dedio, P. Kebarle, and H. E. Gunning. J. Am. Chem. Soc. **89**, 4805 (1967).
13. J. A. Kerr and A. F. Trotman-Dickenson. J. Chem. Soc. 3322 (1957).

Nuclear Magnetic Resonance Studies of Solute–Solvent Interactions. Improved Methods of Proton Chemical Shift Determinations for Completely Associated and Unassociated Solutes

R. E. KLINCK[1]

Department of Chemistry, University of Connecticut, Storrs, Connecticut 06268

Received August 28, 1972

Previous data for the temperature dependence of the proton chemical shifts of two para-substituted benzaldehydes in toluene solution are re-investigated using improved methods for obtaining the proton chemical shifts in the associated and unassociated solutes. The calculations provide ΔH and ΔS values of -1.13 ± 0.07 kcal/mol and -4.0 ± 0.3 e.u., respectively. Attempts to determine the solute–solvent ratio gave inconclusive results.

Des données antérieures concernant l'influence de la température sur les déplacements chimiques des protons de deux benzaldéhydes substitués ont été réexaminées en solution dans le toluène en utilisant des méthodes améliorées pour obtenir les déplacements chimiques des molécules de soluté associées et non-associées. Les calculs ont permis d'évaluer que le ΔH et le ΔS sont respectivement de 1.13 ± 0.07 kcal/mol et -4.0 ± 0.3 u.e. Des essais en vue de déterminer le rapport soluté–solvant ont donné des résultats non concluants. [Traduit par le journal]

Can. J. Chem., **51**, 787 (1973)

Introduction

In a previous paper (1*a*), the thermodynamic parameters governing the postulated association (2) between *p*-substituted benzaldehydes (**1**) and toluene-d_8 were reported. To simplify analysis, it was assumed that the solute and solvent interact in a 1:1 ratio. The main disadvantages

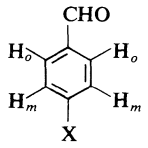

1

in the method of analysis were the determinations of the chemical shifts of the unassociated aldehyde (ν_A) and the complex (ν_C). The present work was undertaken to try out improved methods for the determination of the above parameters as well as to obtain an estimate for the solute–solvent ratio which best fits the data.

Experimental

All experimental data used in this work are those obtained from the previous study (1). Chemical shift values are given in Hz relative to tetramethylsilane (TMS) as internal standard.

[1]Present address: Department of Chemistry, Urbana College, Urbana, Ohio 43078.

Treatment of Experimental Data and Results

For an unknown solute–solvent ratio, the association can be described by the dynamic equilibrium,

[1] aldehyde (A) + x solvent (S) $\rightleftharpoons$ complex (C)

where C is AS_x and x is the number of solvent molecules involved in the complex.[2] Letting p be the fraction of solute complexed at equilibrium, eq. 2 is obtained for the equilibrium con-

$$[2] \quad K = \exp(-\Delta H/RT)\exp(\Delta S/R) = \frac{p}{1-p} \times \left[\frac{1 - xpX_A^0}{X_S^0 - xpX_A^0}\right]^x$$

stant, where ΔH and ΔS are the enthalpy and entropy of formation of the complex, and X_A^0 and X_S^0 are the initial mole fractions of aldehyde and solvent. The fraction p is obtained as previously (1) from the observed proton shift (ν),

[2]To be completely general one should also include the possibility that more than one aldehyde molecule is involved in the complex. This was considered in a more general analysis of the data which provided a best value of one aldehyde molecule per complex molecule. It simplifies the treatment to use this result in the development above. The equations derived are satisfactory for describing all concentrations of solute provided that no self-association of the solute occurs.

Can. J. Chem. Downloaded from www.nrcresearchpress.com by 210.87.254.42 on 09/05/12
For personal use only.

Can. J. Chem. Downloaded from www.nrcresearchpress.com by 210.87.254.42 on 09/05/12
For personal use only.

such that

$$[3] \qquad p = (\nu - \nu_A)/(\nu_C - \nu_A)$$

A plot of ln K *vs.* $1/T$ should yield a straight line of slope $-\Delta H/R$ and intercept $\Delta S/R$. Note that for a given temperature the value of K must be the same for all concentrations. (An indication that the previous analysis is in need of improvement can be seen from Fig. 1*a*. Only one straight line should be obtained for all concentrations. Comparison with Fig. 1*b* shows the improvement from the present method of analysis.) The unknowns to be determined in eq. 2 are ν_A, ν_C, and x. The determination of these parameters will be discussed in detail for the *N*-methyl protons of *p*-*N*,*N*-dimethylaminobenzaldehyde.

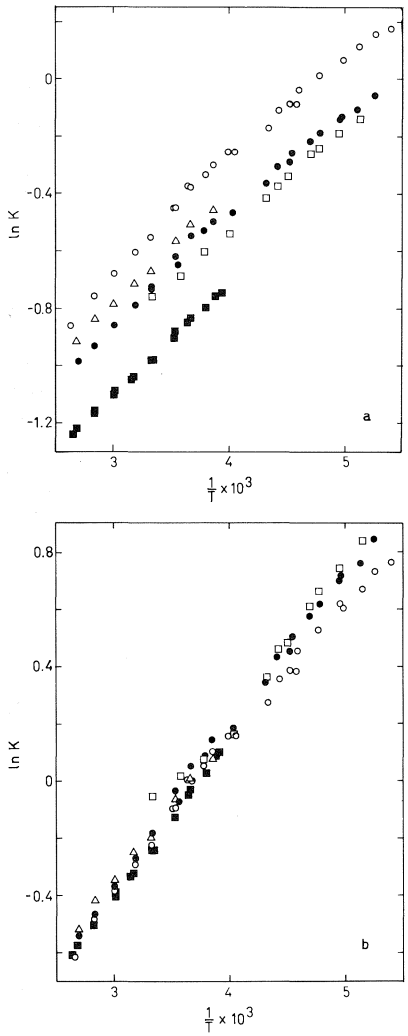

FIG. 1. Plots of ln K *vs.* $1/T$ for the methyl protons of *p*-*N*,*N*-dimethylaminobenzaldehyde in toluene-d_8: (*a*) from previous study (1); (*b*) from present treatment (solution concentrations in mol %: □, 0.5; ●, 1.0; ○, 2.5; ■, 5.0; △, 10.0).

Determination of ν_A

In the original treatment of the data (1), the value of the chemical shift of the unassociated solute was taken to be the value obtained in CCl_4 solution. However, in the complex, the solvent aromatic ring will have a different effect on each of the solute protons depending on its relative position (2). It has also been shown by Kotowycz and Schaefer that there can be a specific association between aromatic solutes and CCl_4 (3). Thus the values in CCl_4 are not a good approximation for ν_A. The present treatment provides more reliable values for the chemical shift of the unassociated solute.

As the temperature is increased, the equilibrium represented by eq. 1 will be shifted towards the unassociated solute. At infinite temperature, the aldehyde will be present only in the unassociated form. A plot of the observed chemical shift *vs.* reciprocal temperature gives a linear relationship at high temperatures. Therefore, extrapolation of the plot to $1/T = 0$ will give a value for ν_A. This is illustrated in Fig. 2 for four of the five concentrations (the 0.5 mol % solution was not studied above room tem-

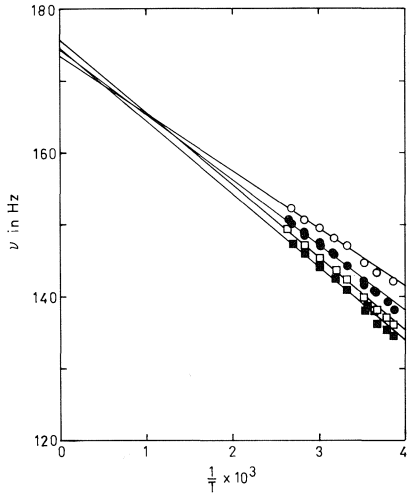

FIG. 2. Extrapolation of the ν *vs.* $1/T$ plot for the methyl protons of *p*-*N*,*N*-dimethylaminobenzaldehyde in toluene-d_8 to obtain ν_A (solution concentrations in mol %: ■, 1.0; □, 2.5; ●, 5.0; ○, 10.0).

Can. J. Chem. Downloaded from www.nrcresearchpress.com by 210.87.254.42 on 09/05/12
For personal use only.

perature) of *p-N,N*-dimethylaminobenzaldehyde using the chemical shift of the methyl protons. The straight lines represent the best least squares fit of the data above room temperature. A value for ν_A of 175 ± 2 Hz is obtained upon averaging the results for the four concentrations. Similar plots are obtained for the other protons of this solute and for the various protons of *p*-nitrobenzaldehyde. A check on the above values for ν_A can be made by conducting the same extrapolation on the chemical shift values obtained from deuterochloroform solution. Excellent agreement is found between the proton shifts in the two solvents as indicated in Table 1.

Determination of ν_C

In the previous calculations (1), the value of the chemical shift of the complex protons (ν_C) was obtained by extrapolating the ν *vs.* T plot to $T = 0$. Since the lowest temperature at which spectra were observed was 170 °K, there is considerable error involved with such an extrapolation. The present method uses a curve fitting procedure to obtain the best value of ν_C consistent with the experimental data. Taking the logarithm of eq. 2 yields eq. 4. For the proper

$$[4]\quad \ln\frac{p}{1-p} + x\ln\left[\frac{1 - xpX_A^0}{X_S^0 - xpX_A^0}\right] = \frac{-\Delta H}{RT} + \frac{\Delta S}{R}$$

values of x, ν_A, and ν_C a plot of the left hand side of eq. 4 *vs.* $1/T$ should give a linear relationship, with $-\Delta H/R$ as the slope and $\Delta S/R$ as the intercept. A computer program was written which allows a variation of the value of ν_C for a given value of x and performs a least squares fit of the data for each value of ν_C chosen. The value of ν_C which gives the maximum value of r (correlation coefficient) is taken as the best value (4). This analysis was carried out for each proton of the solute and each concentration studied. Initially the value of x was taken as unity to determine the general range of ν_C values and to determine if ν_C is concentration dependent. The randomness found for ν_C indicates there is no specific trend with concentration. The values of r ranged from 0.994–0.999 indicating very good fitting of the data points.

Estimation of x

As mentioned earlier for a given temperature, K must have the same value for all concentrations. Therefore, eq. 4 should yield only one straight line for all concentrations. The computer program also enables one to obtain the best fit of the data for all concentrations. The value of ν_C is varied as before and in addition the value of x is varied. Again, a maximum value for r is the criterion for a best fit. The best integer value for x in all cases is found to be 3, although the deviation is about ±0.4. Typical values of r found for integer values of x are shown in Table 2. The best values for ν_C, ΔH, and ΔS are 98 Hz, −1.07 kcal/mol, and −4.0 e.u., respectively. Using the values of ν_C and x obtained from this determination one can calculate the ΔH and ΔS values for each proton for all concentrations. These results are summarized in Tables 3 and 4.

Discussion

The present method of analysis provides a number of advantages. A much improved method of determining the chemical shift of the unassociated solute protons is employed. The validity of this method is shown by the good agreement obtained for all concentrations studied and for the two solvents used. Further studies of the applicability of the method to other systems are currently under way. The

TABLE 1. Proton chemical shifts for the unassociated *p*-substituted benzaldehydes in toluene-d_8 and chloroform-*d*

	Substituents			
	p-NO_2		*p*-$N(CH_3)_2$	
Protons	C_7D_8 ν_A (Hz)	$CDCl_3$ ν_A (Hz)	C_7D_8 ν_A (Hz)	$CDCl_3$ ν_A (Hz)
ortho	464	468	454	455
meta	486	486	402	401
Formyl	598	603	586	586
N-Methyl	—	—	175	175

TABLE 2. Correlation coefficients for various values of x obtained for the *N*-methyl protons of *p-N,N*-dimethylaminobenzaldehyde

x	r	$-\Delta H$ (kcal/mol)	$-\Delta S$ (e.u.)
1	0.983	1.12	4.3
2	0.992	1.11	4.2
3	0.995	1.07	4.0
4	0.991	1.02	3.7

TABLE 3. Thermodynamic parameters for complex formation of *p*-*N*,*N*-dimethylaminobenzaldehyde in toluene-d_8

	Non-equivalent sites			
	N-Methyl protons*		meta-Protons†	
Solute concentration (mol %)	$-\Delta H$ (kcal/mol)	$-\Delta S$ (e.u.)	$-\Delta H$ (kcal/mol)	$-\Delta S$ (e.u.)
0.5	1.13	4.2	1.24	4.4
1.2	1.08	4.0	1.10	3.9
2.5	0.98	3.7	1.03	3.6
5.0	1.10	4.1	1.08	3.8
10.0	1.01	3.7	1.05	3.5
Averaged values‡	1.06 ± 0.06	3.9 ± 0.2	1.10 ± 0.07	3.8 ± 0.3
All concentrations§	1.07	4.0	1.06	3.7

*ν_C = 98 Hz.
†ν_C = 344 Hz.
‡These are statistical averages with the standard deviation shown.
§Obtained from the best fit of the data for all concentrations simultaneously.

TABLE 4. Thermodynamic parameters for complex formation of *p*-nitrobenzaldehyde in toluene-d_8

	Non-equivalent sites					
	Formyl protons*		ortho-Protons†		meta-Protons‡	
Solute concentration (mol %)	$-\Delta H$ (kcal/mol)	$-\Delta S$ (e.u.)	$-\Delta H$ (kcal/mol)	$-\Delta S$ (e.u.)	$-\Delta H$ (kcal/mol)	$-\Delta S$ (e.u.)
1.0	1.15	3.7	1.15	4.0	1.03	3.7
2.5	1.23	4.0	1.23	4.3	1.09	4.0
5.0	1.33	4.4	1.27	4.5	1.13	4.2
Averaged values§	1.23 ± 0.07	4.0 ± 0.3	1.22 ± 0.05	4.3 ± 0.2	1.08 ± 0.04	4.0 ± 0.2
All concentrations‖	1.21	4.0	1.21	4.2	1.10	4.0

*ν_C = 520 Hz.
†ν_C = 383 Hz.
‡ν_C = 422 Hz.
§These are statistical averages with the standard deviation shown.
‖Obtained from the best fit of the data for all concentrations simultaneously.

chemical shift values obtained for the protons of the associated solute are also much more reliable than those obtained earlier. For these reasons the thermodynamic parameters obtained are more reliable and self-consistent. The agreement between the values obtained from different protons of the same solute is much better than that obtained earlier (1).

The best values of the thermodynamic parameters obtained from this treatment appear to be $\Delta H = -1.08 \pm 0.06$ kcal/mol, $\Delta S = -3.9 \pm 0.3$ e.u. for *p*-*N*,*N*-dimethylaminobenzaldehyde and $\Delta H = -1.18 \pm 0.07$ kcal/mol, $\Delta S = -4.1 \pm 0.3$ e.u. for *p*-nitrobenzaldehyde. These values for the enthalpy and entropy changes represent the statistical averages of the results obtained for all protons and all concentrations. The Chauvenet principle (4) was employed to eliminate widely divergent values. The error limits indicated represent the standard deviations (σ). The fact that the ΔH values are larger than those obtained with the previous treatment is due to the more reliable ν_A and ν_C values resulting from this analysis. The difference between the ΔH values from the meta protons and those from the ortho and formyl protons in the latter solute could be due to association taking place in the proximity of the nitro group as well as the formyl group as suggested by Ronayne and Williams (5).

Although the possibility of more than one solvent molecule being involved in the association has been accounted for in the present treatment, the conclusions regarding the nature of the

Can. J. Chem. Downloaded from www.nrcresearchpress.com by 210.87.254.42 on 09/05/12
For personal use only.

solute–solvent associations remain the same as reported earlier (1). The interactions are very weak. The present analysis substantiates this further when one considers the solute–solvent ratio found. From Table 2 it is apparent that the ratios of 1:2 or 1:4 would fit the data within the error limits for ΔH and ΔS. In addition there is no drastic change in the correlation coefficient r in going to these ratios. The specificity of the interaction is considerably obscured since it is difficult to envisage a reasonable physical model for a complex with a 1:3 solute–solvent ratio. These observations support the conclusions of recent reviewers of solvent effects (5, 6) in which the oversimplification of the 1:1 complex model and the inappropriateness of pictorial descriptions of such complexes are indicated.

We thank the National Science Foundation for support of this work through Grant GJ-9 to the Computer Center of the University of Connecticut.

1. (*a*) R. E. KLINCK and J. B. STOTHERS. Can. J. Chem. **44**, 37 (1966). (*b*) R. E. KLINCK. Ph.D. Thesis. The University of Western Ontario, London, Ontario, 1965. pp. 96–130.
2. R. E. KLINCK and J. B. STOTHERS. Can. J. Chem. **40**, 2329 (1962).
3. G. KOTOWYCZ and T. SCHAEFER. Can. J. Chem. **46**, 3110 (1968).
4. J. F. KENNEY and E. S. KEEPING. Mathematics of statistics. Pt. 2. 2nd Ed. D. Van Nostrand Co. Inc., New York. 1953.
5. J. RONAYNE and DUDLEY H. WILLIAMS. *In* Annual review of NMR spectroscopy. Vol. 2. E. F. Mooney, Editor. Academic Press, New York. 1969. pp. 83–124.
6. P. LASZLO. *In* Progress in N.M.R. spectroscopy. Vol. 3. J. W. Emsley, J. Feeney, and L. H. Sutcliffe, Editors. Pergamon Press, New York. 1967. Chapt. 6.

Can. J. Chem. Downloaded from www.nrcresearchpress.com by 210.87.254.42 on 09/05/12
For personal use only.

The Wittig Reaction of Indole-2-methyltriphenylphosphonium Iodide with 4-Piperidone Derivatives and Aromatic Aldehydes[1]

JOHAN A. EENKHOORN, S. OSMUND DE SILVA, AND VICTOR SNIECKUS
Department of Chemistry, University of Waterloo, Waterloo, Ontario

Received July 17, 1972

2-(4-Piperidylidene)methylindole (**8***a–e*, **21**) and 2-(2-aryl)vinyl indole (**25***a–e*, **27**, **32**) derivatives have been obtained from the Wittig reaction of indole-2-methyltriphenylphosphonium iodides (**6**, **20**, **26**) with 4-piperidones (**7***a–e*) and aromatic aldehydes (**24***a–e*), respectively. Yields have been optimized by studying a variety of base-solvent combinations. The reaction failed in the case of **6** with 3-ethyl-4-piperidones (**10**); instead of compound **11**, 2-methylindole (**12**) was produced. The utility of phosphonium salts **9***a–c* and phosphonate ester **33***a* has been tested: compounds **9***a* and **33***a* showed some advantage in the preparation of Wittig adducts **8***e* and **25***c* respectively but the steric problems associated with hindered ketones (**10**) were not overcome even with the reactive phosphonium salts **9***b* and *c*. A mechanism is advanced for the formation of 2-methylindole analogous to that proposed for the base-promoted decomposition of benzylphosphonium salts (Scheme 2). Aromatic aldehydes yield mainly *trans*-Wittig adducts (**25**) with the exception of pyridine-2-aldehyde which produces exclusively *cis*-**25***c* in nonpolar solvent due to preferred formation of the hydrogen-bonded betaine **29**. Interconversion of *cis*-**25***c* ⇄ *trans*-**25***c* and their photochemical reaction to pyridocarbazole **28** are reported (Scheme 5). The chemistry of some 2-(4-piperidylidene)methylindoles has been briefly studied (Scheme 3).

Les dérivés du (piperidylidène-4 méthyl)-2 indole (**8***a–e*, **21**) et de l'(aryl-2 vinyl)-2 indole (**25***a–e*, **27**, **32**) ont été obtenus par la réaction de Wittig entre les iodures de méthylphosphonium-2 indoles (**6**, **20**, **26**) et les pipéridones-4 (**7***a–e*) et aldéhydes aromatiques (**24***a–e*) respectivement. Les rendements ont été optimalisés par l'étude de diverses combinaisons base-solvant. La réaction échoue dans le cas de **6** avec les éthyl-3 pipéridones-4 (**10**), on obtient le méthyl-2 indole (**12**) au lieu de **11**. L'utilité des sels de phosphoniums **9***a–c* et de l'ester phosphonique **33***a* a été testée: les composés **9***a* et **33***a* présentent un avantage certain dans la préparation respective des adduits **8***e* et **25***c* selon la réaction de Wittig mais les problèmes stériques des cétones encombrées (**10**) n'ont pas été résolus même avec les sels de phosphoniums réactifs **9***b* et *c*. Le mécanisme avancé pour la formation du méthyl-2 indole est analogue à celui proposé pour la décomposition basique des sels de benzylphosphoniums (schéma 2). Les aldéhydes aromatiques donnent surtout des adduits de Wittig *trans* **25** à l'exception de la pyridinealdéhyde-2 qui conduit exclusivement au *cis* **25***c*, en solvant non polaire, par la formation préférentielle de la bétaine 29 liée par pont hydrogène. L'interconversion du *cis*-**25***c* ⇄ *trans* **25***c* et leur réaction photochimique en pyrido-2 carbazole **28** sont rapportées (schéma 5). La chimie de quelques (piperidylidène-4 méthyl)-2 indoles a été brièvement étudiée (schéma 3). [Traduit par le journal]

Can. J. Chem., **51**, 792 (1973)

The most general reaction of indole compounds is manifest in their propensity to undergo facile electrophilic substitution at the 3-position (2). As a result, 3-functionalized indoles are readily available which may be modified to a variety of carbon chain-extended derivatives (3). On the contrary, direct electrophilic attack at the 2-position of the indole nucleus can be achieved only in special situations: (*a*) by inter- or intramolecular reaction of a 3-substituted derivative (**1**) (4); (*b*) via a 2-lithio derivative (**2**) (5); (*c*) in a 4-oxo-4,5,6,7-tetrahydroindole system (**3**) (6); (*d*) using activation at the 3-position, *i.e.* **4**, Y = CO_2Et, X = OH (*7a*); Y = H, X = OMe (*7b*) but not Y = H, X = NR_2 (8) for alkylation and Claisen rearrangement, *i.e.*, **4**, Y = CO_2Et, X = $OCH_2CH = CR_2$ (7); and (*e*) by reaction of π-allyl nickel dibromide with 2-bromoindole derivatives (9).[2] All of these possess certain synthetic limitations: in (*a*) further transformation at the 3-position is not possible while in (*b*) protection of the nitrogen by alkylation is required, a step which is not reversible. Cases (*c*) and (*d*) necessitate further steps to attain the indole oxidation state and both these as well as (*e*) may be limited to the preparation of 2-allyl derivatives. Alternate, although in some cases lengthy, routes to use-

[1]A portion of this work has appeared in preliminary form, see ref. 1.

[2]The mechanism of this reaction is not known although it most probably is not an electrophilic substitution.

Can. J. Chem. Downloaded from www.nrcresearchpress.com by 210.87.254.40 on 09/05/12
For personal use only.

Can. J. Chem. Downloaded from www.nrcresearchpress.com by 210.87.254.40 on 09/05/12
For personal use only.

fully functionalized 2-substituted indoles are available using benzenoid precursors. The most significant of these are: (*a*) the classical Reissert reaction (10); (*b*) the well-known Madelung reaction in which renewed interest has been expressed (11); (*c*) recently developed routes via *o*-azido- and *o*-nitrostyrenes (12); and finally (*d*) the Fischer synthesis which is only moderately useful for this purpose (13).

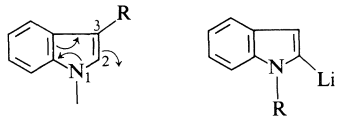

1

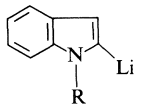

2

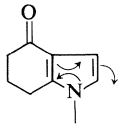

3

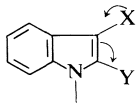

4

In spite of the above documentation, we observed that relatively few reports are available which deal with carbon chain extension or modification of 2-substituted indoles (14, 15, 16)[3,4] and that, in general, synthetic methodology in this area has been underdeveloped. In order to rectify this situation, we have explored the Wittig reaction of indole 2-methyltriphenylphosphonium iodide (**6**) and related compounds with 4-piperidone derivatives (**7**) and aromatic heterocyclic aldehydes (**24**) with the intent to develop a new '2-substituted indole' approach to complex indole alkaloids[5] and to establish new synthetic routes to certain heteroaromatic systems (15, 18). Specifically, we focused our attention initially on the uleine alkaloids[6] for which the key intermediate **11** was envisaged. While we have not succeeded in preparing the desired compound (**11**), we have developed a general Wittig synthesis of 2-alkylidene indoles[7] and we have delineated its scope and certain limitations insofar as both phosphorus and carbonyl components are concerned.

Indole 2-methyltriphenylphosphonium iodide (**6**) was prepared in high yield from the known 2-dimethylaminomethylindole methiodide (**5***a*) (21) or 2-diethylaminomethylindole methiodide (**5***b*) by treatment with triphenylphosphine in refluxing dimethyl formamide (DMF). The Wittig reaction (22) of **6** with 1-methyl-4-piperidones **7***a–d* in ethanol in the presence of metal (lithium, potassium, and sodium) ethoxides gave, with one exception, good yields of the adducts **8***a–d* (Scheme 1). Compound **8***e* was best obtained from the *p*-dimethylaminophosphonium salt (**9***a*) and **7***e* while **8***f* could not be prepared by this reaction due to its instability during isolation (*vide infra*).

The structures of the adducts are supported by spectral evidence, in particular the diagnostic u.v. absorption of a 2-vinyl indole chromophore (19). The n.m.r. spectra also agreed with the proposed structures in that they exhibited characteristic vinyl proton singlets and deshielded indole C_3-hydrogens (see Table 1). The low yield of **8***b* may be attributed in large part to attack of ethoxide ion on the carbophenoxy function resulting in the formation of phenol and **8***f*. Phenol was in fact obtained from the reaction mixture but **8***f* was not isolated. This was no doubt due to its inherent instability as evidenced from the observation that the reaction of **6** with 1-carbethoxy-4-piperidone (**7***f*) took place readily (u.v. evidence) but the expected product could not be isolated by the normal methods. In the case of compound **8***e* we experienced extreme difficulties in effecting clean separation of product from triphenylphosphine oxide. This problem was overcome by using the ylide derived from **9***a* which produces a phosphine oxide with a basic handle (22*b*, 23).[8] Separation was now readily achieved by extraction with dilute hydrochloric acid. Attempts to use **9***a* for the preparation of the *N*-carbethoxy Wittig product (**8***f*) only led to extensive decomposition.

Application of the most efficient set of condi-

[3]A heuristic principle not explicitly stated in texts dealing with indole chemistry is that attempts to modify a 2-substituent by electrophilic or oxidative reagents is inherently dangerous due to the presence of the exposed and highly reactive 3-position whereas the reverse is usually not true.

[4]For some indole 2-methyl functionalizations now widely used in indole alkaloid synthesis and transformations, see ref. 17.

[5]Such approaches are relatively rare, *cf.* refs. 5*b* and 16.

[6]For recent total syntheses, see ref. 19.

[7]A survey of the literature reveals very few examples of Wittig reactions involving simple indole derivatives, *cf.* refs. 5*b* and 20.

[8]We thank Dr. J. Muchowski for discussion regarding this method.

Can. J. Chem. Downloaded from www.nrcresearchpress.com by 210.87.254.40 on 09/05/12
For personal use only.

TABLE 1. I.r., u.v., and n.m.r. spectra of 2-(4-piperidylidene)indole derivatives (**8***a–e*, **21**, **22**)

Compound	ν_{max} cm^{-1}	λ_{max} (ε) mμ	τ-Values					
			Indole N—H[a]	Aromatic	Indole 3-H[a]	Vinyl H[a]	Piperidine CH_2	Other
8*a*	3430 2780 1650	240 (19 800) 307 (22 600) 313 (sh, 20 700)	1.9	2.35–3.1 (m, 4H)	3.58	3.87	7.1–7.8 (br m, 8H)	7.7 (s, 3, NCH_3)
8*b*	3400 1700 1600	240 (25 000) 307 (23 400) 314 (21 000)	1.95	2.3–3.1 (m, 9H)	3.59	3.78	6.17–6.67[b], 7.34[c], 7.69[c]	
8*c*	3390 1660	243 (15 900) 307 (22 300) 313 (sh, 21 100)	2.1	2.33–3.06 (m, 9H)	3.6	3.87	7.1–7.8 (br m, 8H)	6.5 (s, 2, $CH_2C_6H_5$)
8*d*	3410 1710	245 (15 800) 307 (22 200) 313 (21 100)	2.02	2.2–3.0 (m, 4H)	3.57	3.75	6.15–6.67[b], 7.25[c], 7.53[c]	5.18 (s, 2H, $CO_2CH_2CCl_3$)
8*e*	3300[d] 1630	241 (26 400) 308 (22 000) 314 (20 500)	−1.87[e]	2.0–3.0 (m, 9H)	3.33	3.47	6.0–6.67[b], 7.38[c], 7.67[c]	
21	2780 1650	243 (20 400) 301 (16 500)		2.2–3.0 (m, 4H)	3.73	3.92	7.2–7.75 (br m, 8H)	6.57 (s, 3H, indole 1-CH_3), 7.8 (s, 3H, NCH_3)
22	3430[f] 1660	240 (19 100) 307 (21 900) 313 (20 100)	1.98	2.3–3.1 (m, 4H)	3.55	3.85	6.8–7.2[b], 7.25[c], 7.64[c]	5.8 (br s, 1H, NH)

[a]Broad singlet, 1H.
[b]Broad multiplet, 4H.
[c]Triplet, 2H, J = 6 Hz.
[d]Measured as a Nujol mull.
[e]N.m.r. spectrum measured in pyridine-d_5.
[f]Measured in CH_2Cl_2 solution.

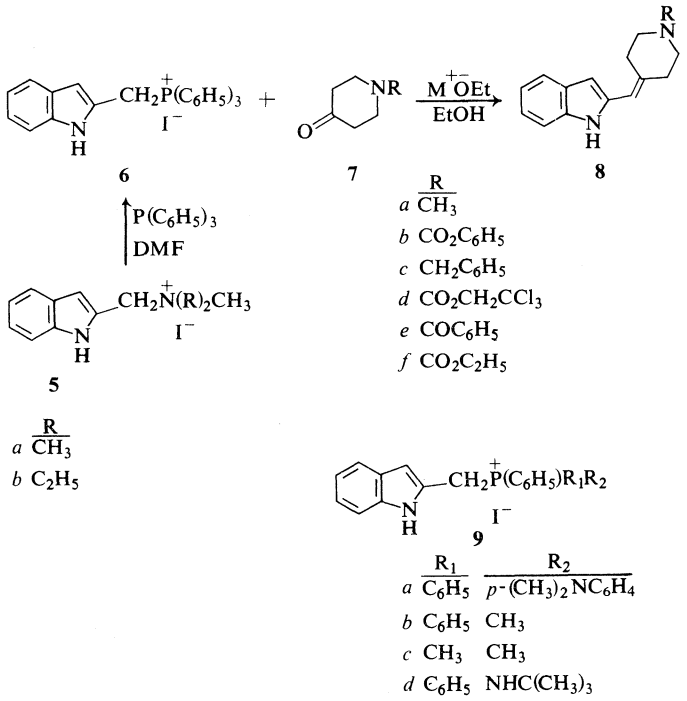

SCHEME 1

tions (lithium ethoxide in ethanol) for the formation of Wittig adducts **8***a–e* to the reaction of **6** with 3-ethyl-4-piperidone derivatives **10***a* and *b* gave disappointing results in that the expected products **11***a* and *b* were not detected even after prolonged reaction times and only substantial amounts of 2-methylindole were isolated.

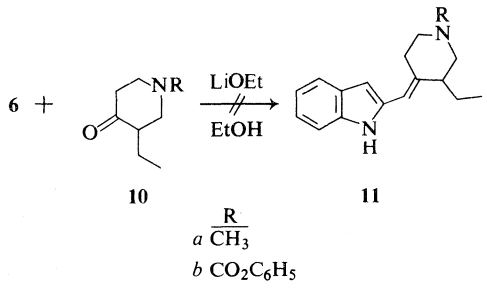

In order to optimize yields of the Wittig adducts **8***a–e* and to overcome the problems associated with compounds **10***a* and *b*, we also studied the reaction of **6** with the representative ketones **7***a* and *b* under a variety of other conditions. Instead of the desired reaction, formation of 2-methylindole (**12**) was invariably observed irrespective of the nucleophilicity of the base (potassium *t*-butoxide, dimsyl sodium) or polarity of the solvent (DMF, DMSO, THF, benzene). Under some conditions, *e.g.*, dimsylsodium, DMSO, 70–80°, 70–80% yields of **12** were isolated. Although this type of side reaction in a Wittig synthesis has not been documented (22*b*), it may be likened to the well-known base-promoted decomposition of benzylophosphonium salts to toluene derivatives (24) and its mechanism may be analogously represented (Scheme 2). In support of this formulation, we found that prolonged treatment of **6** with sodium ethoxide in ethanol in the absence of carbonyl reagents gave compound **12** and triphenylphosphine oxide. If ylide **14** is a benzylic ylide and therefore classified as moderately stable (25), current mechanistic thought (22*a*) stipulates that **14** + $R_2CO \rightleftarrows$ **17** is fast and reversible and that **17** → **19** is the rate-determining step. This is in accord with its rather sluggish behavior in reactions with ketones **8***a–e* (22*b*) and its ready reactivity with aromatic aldehydes (*vide infra*). In cases (**10***a* and *b*) where the equilibrium to betaine **17** is not far advanced due to serious steric hindrance problems presented by the 3-ethyl group, the formation of 2-methylindole may be understood in terms of an escape route which proceeds via a small equilibrium con-

Can. J. Chem. Downloaded from www.nrcresearchpress.com by 210.87.254.40 on 09/05/12
For personal use only.

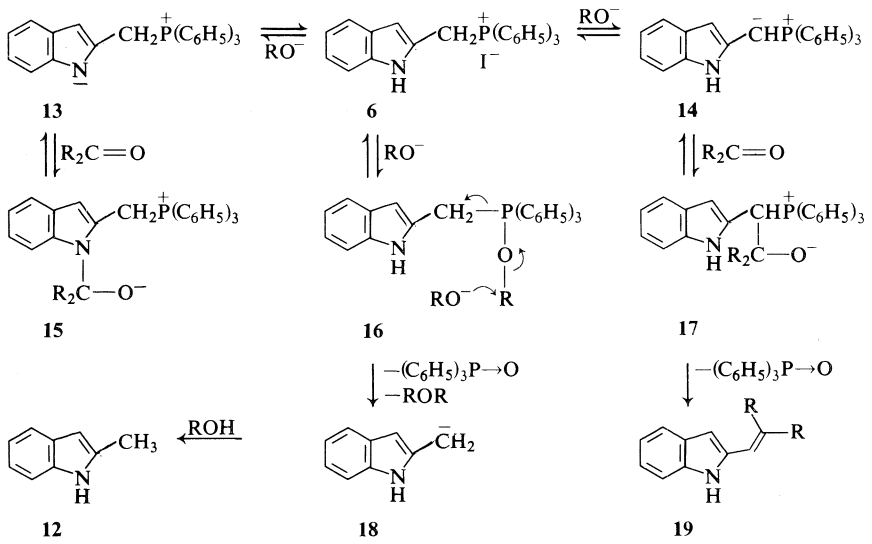

SCHEME 2

centration of the phosphonium salt **6** and thence through **16** → **18** → **12** and which becomes important under conditions of thermodynamic control.

We were also interested in determining if the potential formation of anion **13** and therefore of carbinol amine **15** had any influence on the yields in the Wittig reaction. That the anion **13** is in fact formed was shown by complete deuterium exchange of both the methylene and C_3-protons of **6** under comparable conditions using sodium ethoxide in ethanol-O-*d* (see Experimental).[9] However, since the Wittig reaction of the *N*-methyl analog, **20** with *N*-methyl-4-piperidone (**7***a*) gave olefin **21** in similar yield to that observed in the case of olefin **8***a* (Scheme 1), it would appear that the reversible formation of

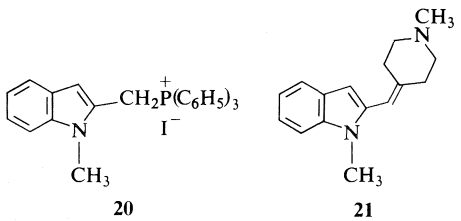

15 has little if any effect on the overall outcome of the reaction.[10] Treatment of **20** with sodium ethoxide in ethanol for extended periods of time or with dimsylsodium in DMSO gave 1,2-dimethylindole, a result which indicates that the indole NH is not obligatory for the formation of 2-methylindole.[10,11]

In order to determine to what extent the steric interference can be relieved and ylide reactivity can be increased in the Wittig reaction, we undertook to study two other phosphonium salts **9***b* and *c*. Since previously it had been observed that replacement of phenyl groups by alkyl groups on phosphorus facilitates reaction in case of stabilized ylides but impedes it for unstabilized ylides (28), we prepared **9***b* and *c* by standard methods (see Experimental section) and subjected each of them first to reaction with **7***a* under the most favorable conditions (sodium ethoxide in absolute ethanol at reflux). In both cases, the product **8***a* was formed in high yield within minutes as evidenced by t.l.c. and u.v. spectroscopy (compared to hours needed in the

[9]Under these conditions, indole incorporated deuterium at the 3-position at a slower rate (50% by n.m.r.) (H. Waterman, these laboratories). This may be due to the comparatively greater NH acidity of **6** as a result of an inductive effect of the positively charged phosphorus.

[10]Other deuterium exchange studies of **20** are given in the Experimental section.

[11]An alternate mechanism involving reductive cleavage to produce 2-methylindole and triphenylphosphine has ample analogy in indole chemistry (26) and has been observed for benzyltriphenylphosphonium salts (27). The failure to detect triphenylphosphine in all experiments rules out this pathway.

Can. J. Chem. Downloaded from www.nrcresearchpress.com by 210.87.254.40 on 09/05/12
For personal use only.

Can. J. Chem. Downloaded from www.nrcresearchpress.com by 210.87.254.40 on 09/05/12
For personal use only.

case of **6**). In a preparative reaction of **9***c* with **7***a*, a yield of compound **8***a* comparable to that obtained by using phosphonium salt **6** was isolated. Nevertheless, when the identical conditions were applied to the reaction of either **9***b* or *c* with the 3-ethyl-4-piperidone **10***a*, slight development of the 2-vinylindole chromophore in the u.v. spectrum was noted over long reaction times and only 2-methylindole was isolated. Thus it would appear that the ylides derived from phosphonium salts **9***b* and *c* may be destablilized and more reactive than that formed from **6**. Nevertheless, since ketone **10***a* does not undergo reaction with either **9***b* or *c*, a combination of an unfavorable steric requirement for the formation of the betaine (**17**, Scheme 2) and/or olefin and possibly an enhanced facility for attack at the less encumbered phosphorus by alkoxide (29) must be responsible for the predominance of 2-methylindole formation in these two cases. Parenthetically, the ylide derived from the phosphonium salt **9***a* was also totally unreactive towards **10***a* even though an enhanced reactivity may have been expected on the basis of a $+I$ contribution from the *p*-dimethylamino group (22*a*).

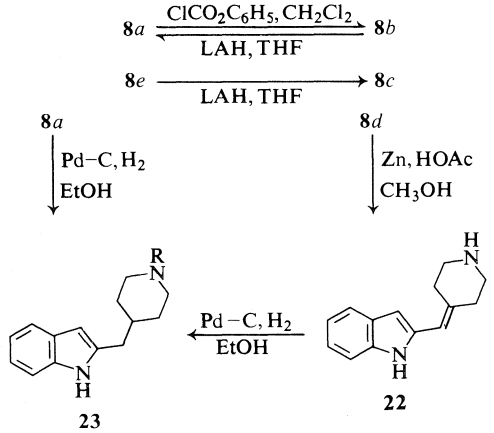

a R = H
b CH_3
c $CO_2C_6H_5$

SCHEME 3

Several chemical interrelationships among the Wittig products and other potentially useful reactions were carried out (Scheme 3). The *N*-methyl derivative **8***a* was transformed into **8***b* by treatment with phenyl chloroformate according to the very useful procedure devised by Hobson and McCluskey (30). The reversal of this transformation could be achieved by lithium aluminum hydride reduction. The *N*-benzyl adduct **8***c* was obtained in overall 36% yield by direct lithium aluminum hydride reduction of the crude product **8***e* from the Wittig reaction of **6** with 1-benzoyl-4-piperidone (**7***e*). Deblocking of the trichlorocarboethoxy function in **8***d* was readily effected according to a known method (31) to yield compound **22**. Catalytic hydrogenation of both the *N*-methyl and N–H Wittig products **8***a* and **22** gave the dihydro compounds **23***a* and *b* respectively. Finally, as in the case of the *N*-methyl adduct **8***a*, compound **23***b* could be converted into the corresponding *N*-carbophenoxy derivative **23***c*.

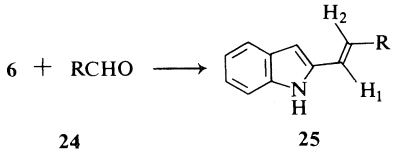

a R = C_6H_5
b R = *p*-$NO_2C_6H_4$
c R = 2-pyridyl
d R = 3-pyridyl
e R = 4-pyridyl

SCHEME 4

For reasons discussed earlier, it was desirable to extend the Wittig reaction to benzaldehyde and pyridine aldehydes. As expected, the reaction of **6** with aldehydes **24***a–e* proceeded much more readily and gave high yields of adducts **25***a–e* (Scheme 4). Some indication of the scope of this reaction was given by the reaction of the readily available tryptophol 2-methylphosphonium salt **26** (see Experimental section) with pyridine 3-aldehyde to give a moderate yield of the adduct **27**, a potential precursor to Aspidosperma alkaloids (16).[12] In this series, isolation

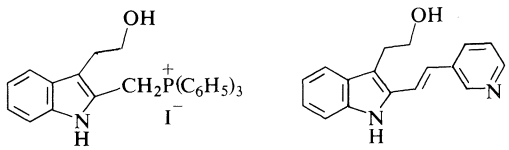

26 **27**

[12]We have also recently prepared the analogous 4-pyridyl adduct in high yield.

Can. J. Chem. Downloaded from www.nrcresearchpress.com by 210.87.254.40 on 09/05/12
For personal use only.

TABLE 2. I.r., u.v., n.m.r. and mass spectra of 2-(2-aryl)vinylindole derivatives (**25***a–e*, **27**, and **32**)

Compound	KBr ν_{max} cm^{-1}	λ_{max} (ε) mμ	τ Values[a] NH[b]	Pyridine α-H	Indole 3-H[c]	Other	*m/e* (relative abundance)[d]
trans-**25***a*	3325(w), 1630(w), 1580(w), 954(s), 790(s), 755(s), 738(s)	264 (31 400) 285 (26 600) 335 (37 000) 345 (38 800) 363 (27 200)	−0.5		3.31	2.28–3.04 (m, 11H, aromatic, H_1, H_2)	219(M^+, 100), 218(98), 217(29), 204(23), 189(13), 188(7), 187(8)
trans-**25***b*	3325(w), 1625(w), 1585(w), 1505(s), 1330(s), 978(s), 955(s), 865(m), 833(m), 793(m), 763(m), 748(m)	306 (11 700) 410 (32 000)	−1.9		3.4	1.73 (d, 2H, J = 9 Hz) and 2.18 (d, 2H, J = 9 Hz) (p-$NO_2C_6H_4$), 2.42–3.14 (m, 6H, aromatic, H_1, H_2)	*e*
cis-**25***c*	3400(w), 1615(m), 1585(s), 820(s), 740(s), 725(s)	268.5 (10 500) 285 (7000) 298 (8400) 373 (23 600)	−4.2	1.05 (m, 1H)	3.23	1.97–3.15 (m, 7H, aromatic, pyridine β- and γ-H), 3.18 (d, 1H, J = 14 Hz, H_1 or H_2), 3.53 (d, 1H, J = 14 Hz, H_1 or H_2)	220(M^+, 74), 219(100), 192(18), 191(29)
			−4.0[f]	1.37 (m 1H)	3.32	2.2–3.03 (m, 7H, aromatic, pyridine β- and γ-H), 3.25 (d, 1H, J = 14 Hz, H_1 or H_2), 3.76 (d, 1H, J = 14 Hz, H_1 or H_2)	
trans-**25***c*	3200(w), 1625(m), 1585(s), 955(s), 790(s), 770(w), 750(s), 738(s)	263 (10 400) 359 (36 000)	−1.37	1.38 (br d, 1H)	3.32	2.08–3.07 (m, 9H, aromatic pyridine β- and γ-H, H_1, H_2)	220(M^+, 41), 219(100), 218(16), 191(5)
trans-**25***d*	3400(w), 1630(s), 955(s), 795(s), 750(m), 735(w)	264 (11 700) 355 (34 500)	−0.6[g]	1.3 (m, 1H) 1.56 (m, 1H)	3.33	2.04 (m, 1H, pyridine γ-H), 2.35–3.19 (m, 5H, aromatic, pyridine β-H), 2.50 (br d, 1H, J = 14 Hz, H_1 or H_2), 2.85 (br d, 1H, J = 14 Hz, H_1 or H_2)	220(M^+, 79), 219(100), 218(23), 192(7), 191(10)
trans-**25***e*	3320(w), 1625(m), 1580(s), 970(m), 955(m), 810(m), 750(m), 735(m)	258.5 (9500) 364 (32 300)	−1.5	1.4 (br d, 2H)	3.23	2.2–3.03 (m, 8H, aromatic, pyridine β-H, H_1, H_2)	220(M^+, 100), 219(87), 218(21), 193(18), 192(14), 191(18), 149(13)

Can. J. Chem. Downloaded from www.nrcresearchpress.com by 210.87.254.40 on 09/05/12
For personal use only.

TABLE 2. (*Concluded*)

Compound	KBr ν_{max} cm^{-1}	λ_{max} (ε) mμ	τ Values[a] NH[b]	Pyridine α-H	Indole 3-H[c]	Other	*m/e* (relative abundance)[d]
cis-**25***e*	3400(w)[h], 795(m), 735(m)	265 (11 300) 357 (16 600)	1.73	1.4 (br d, 2H)	3.43	2.36–3.0 (m, 6H, aromatic, pyridine β-H), 3.2(d, J = 14 Hz, H_1 or H_2), 3.5 (d, J = 14 Hz, H_1 or H_2)	220(M^+, 100), 219(86), 218(20), 192(10), 191(9), 190(12)
trans-**27**	3200(br), 1630(m), 795(m), 740(s), 705(s)	261 (4700) 360 (14 600)	−2.25	1.22 (br s, 1H) 1.5 (br s, 1H)		1.88 (br d, 1H, pyridine γ-H, J = 8 Hz), 2.2–3.1 (m, 7H, pyridine β-H, aromatic, vinyl-H), 5.35 (OH)[b], 6.44 (br t, 2H, J = 7 Hz, —CH_2O), 6.6 (br t, 2H, J = 7 Hz, CH_2)	265(M^+ + 1, 7.5), 264(M^+, 37.5), 234(20), 233(100), 232(16), 231(20), 218(15.5)
cis-**32**	1640(m)[i], 1600(s), 1570(m), 1475(s), 1335(s), 970(m), 920(m), 825(m)			1.37 (d, J = 5 Hz, 1H)	3.43	2.31–3.1 (m, 7H, pyridine β- and γ-H, aromatic), 3.2 (s, 2H, vinyl-H), 6.50 (s, 3H, CH_3)	
trans-**32**	1640(m)[i], 1590(s), 1540(m), 1475(s), 1350(m), 1330(m), 965(m)	280 (8000)[j] 423 (22 200)		1.43 (d, J = 5 Hz, 1H)	3.14	2.08–3.08 (m, 10H, pyridine β- and γ-H, aromatic, vinyl-H), 6.32 (s, 3H, CH_3)	

[a]Recorded in polysol-*d*.
[b]Broad singlet, 1H, exchanged with D_2O.
[c]Broad singlet, 1H.
[d]Only peaks with > 5% relative abundance are tabulated.
[e]Could not be obtained due to low volatility.
[f]Recorded in $CDCl_3$.
[g]Recorded in acetone.
[h]Recorded in CS_2.
[i]Recorded in $CHCl_3$.
[j]Spectrum of methiodide derivative, see footnote [i], Table 5.

problems were again encountered. In some cases, an alternate method using 1,5-diazabicyclo(4,3,0)non-5-ene (DBN) (32) in DMSO or THF was adapted which gave better yields of products. Other variations from the general procedure are recorded in the Experimental section (Table 5).

The structures of adducts **25***a–e* and **27** are assigned on the basis of analytical and spectral evidence (Table 2). In our preliminary work (1), we assigned *trans* stereochemistry to the Wittig products **25***c* (m.p. 118°, prepared by method A) and **25***d* (prepared by methods A and B) by virtue of the observed large coupling constants (J = 14 Hz) for the vinyl protons. Although the complexity of the spectra for all other Wittig products precluded stereochemical assignment, it was nevertheless assumed to be *trans* by analogy and on the basis of previous experience with similar reaction conditions (22*a*). Further investigation of **25***c* presented inconsistencies between chemical and spectral data which have now led us to assign *cis* stereochemistry to the 118° m.p. product (**25***c*) on the basis of the following evidence. Its n.m.r. spectrum showed a broad absorption at τ −4.2 (1H, exchanged over several hours with D_2O), previously undetected (1), which is typical of strongly hydrogen bonded protons (33). Its i.r. spectrum in chloroform solution showed absorption at 3000 cm^{-1} whose position was unaffected by high dilution (34). Furthermore, it was converted to an isomeric compound, m.p. 210–211° by treatment with 1 *N* sulfuric acid. The latter was also obtained from the Wittig reaction carried out under a different set of conditions (Table 5, method B). Photolysis of the m.p. 210–211° compound in methylene chloride solution gave the m.p. 118° isomer and both were converted to the pyridocarbazole derivative **28** under the photolytic conditions described previously (18) (Scheme 5). These observations are consistent with the assignment of structure *cis*-**25***c* to the m.p. 118° isomer and *trans*-**25***c* to the m.p. 210–211° isomer.[13] The hydrogen-bonded structure, clearly seen by examination of models, must also be responsible for the lower energy transition observed in the u.v. spectrum of *cis*-**25***c* when compared to the *trans*-**25***c* structure (Table 2). The intensities of the high wavelength

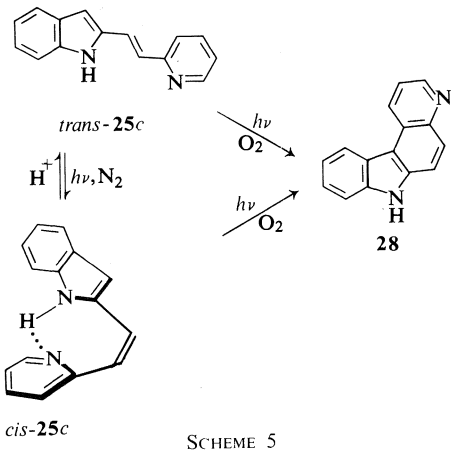

SCHEME 5

absorptions of the two isomers are as expected for stilbene-like compounds (36).

In view of the above results, it was essential to obtain chemical evidence for the stereochemistry of all other Wittig products. Treatment of **25***a*, *b*, *d*, and *e* with 1 *N* sulfuric acid gave recovered starting material in greater than 80% yields. Compound **25***a* was stable to the photochemical conditions[14] which led to the isomerization of *trans*-**25***c* while *b* and *d* underwent extensive decomposition. Photolysis of *trans*-**25***e* gave a small amount of *cis*-**25***e* which rapidly reverted to the *trans* isomer in warm methanolic solution (see Experimental section). The *trans* stereochemistry of **27** is assured from the similarity of its u.v. spectrum to that of **25***d*. Clearly, with the exception of **25***c* which was isolated as the *cis* or a mixture of *cis* and *trans* isomers depending on reaction conditions, all Wittig products were obtained exclusively as the *trans* isomers. The exception was briefly investigated and the results obtained (Table 5) may be understood by a slight modification of the presently accepted formulation for the Wittig reaction of 'moderated' (moderately stable) ylides with reasonably reactive aldehydes (25, 37).

In an aprotic solvent (THF) with DBN as base, the slow irreversible formation of the *erythro* betaine **29** from **6** and the highly reactive pyridine 2-aldehyde (38) is expected to be strongly enhanced by the intramolecular hydrogen bonding between the indole NH and the pyridine

[13]The vinyl hydrogens in *trans*-**25***c* are deshielded in comparison with those of *cis*-**25***c* as expected (35).

[14]In one experiment, a small amount of a compound suspected to be *cis*-**25***a* was obtained. However, its rapid isomerization to the *trans* isomer during purification precluded characterization.

Can. J. Chem. Downloaded from www.nrcresearchpress.com by 210.87.254.40 on 09/05/12
For personal use only.

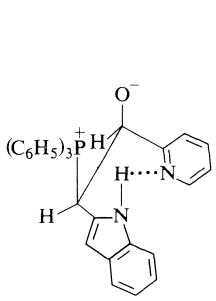

29

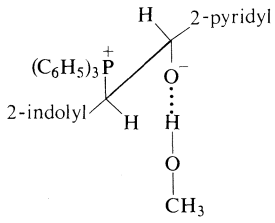

30

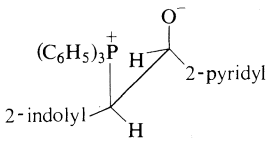

31

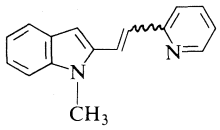

32

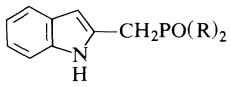

33

a $\frac{R}{OC_2H_5}$

b C_6H_5

nitrogen and thus lead exclusively to the production of *cis*-**25***c* as observed. The change to a protic solvent (methanol) and sodium methoxide as base should favor the formation of the intermolecularly hydrogen-bonded *erythro* betaine **30**. However, the stability of betaines should now be greater and their decomposition to olefins and triphenylphosphine oxide should be slower. Therefore, the 'reversibility factor' (39) would be larger and there would be opportunity for leakage to the thermodynamically more stable *threo* betaine **31** which should lead to some *trans*-**25***c* product. In agreement with this rationale a 1:1 *cis–trans* ratio of **25***c* was obtained using sodium methoxide in refluxing methanol. A control experiment showed that no isomerization *cis*-**25***c* → *trans*-**25***c* was occurring under these conditions. No change in yields or *cis–trans*-**25***c* isomer composition was observed when the reaction was carried out in the presence of lithium methoxide and soluble lithium chloride in refluxing methanol solution. These results show that the enhanced stabilization of the *erythro* betaine **30** by coordination of the lithium ion with the oxygen function is not an important consideration and that the *cis–trans* isomer ratio is largely determined by the thermodynamic stability of the *erythro* (**30**) and *threo* (**31**) betaines (40). This contention is further supported by the observation that the *cis–trans* ratio remained the same when the reaction was carried out in the presence of lithium methoxide in methanol solution at *room temperature* (39). Finally, it is of interest to note that the Wittig reaction of the *N*-methyl phosphonium salt **20** with pyridine 2-aldehyde also produced a 1:1 mixture of *cis* and *trans* adducts (**32**) in refluxing methanol using sodium methoxide as the base, supporting the view that in a polar protic solvent *erythro* betaine **29** plays an insignificant role in determining the geometrical isomer ratio of the Wittig product.

In view of the results with pyridine 2-aldehyde (**24***c*), experiments were undertaken to vary the conditions of the reaction of **6** with the aldehydes **24***a*, *d*, and *e* in order to force the formation of the corresponding *cis* Wittig products. In all these cases, Wittig reaction in THF solution was very slow even at 80° (ylide **6** color persisted for 4 days), *cis* adducts were not detected, and decomposition of the ylide was eventually observed. The highly reactive *p*-nitrobenzaldehyde (**24***b*) gave exclusively *trans* product (**25***b*) (Table 5). If *cis* compound was formed in this case, then isomerization to *trans* product must be occurring rapidly even at room temperature. Therefore, from a stereochemical point of view it appears that two factors impart a special

Can. J. Chem. Downloaded from www.nrcresearchpress.com by 210.87.254.40 on 09/05/12
For personal use only.

Can. J. Chem. Downloaded from www.nrcresearchpress.com by 210.87.254.40 on 09/05/12
For personal use only.

position to pyridine 2-aldehyde in the reaction with ylide **6**: (1) its highly electrophilic carbonyl function (41) and, more importantly, (2) its ability to form a strong intramolecular hydrogen bonded *erythro* betaine **29**.

A recent demonstration of the successful Wadsworth–Emmons reaction (42) between triethylphosphonoacetate and hindered 3-ethyl-4-piperidone derivatives (43) led us to explore the reactivity of diethyl indole-2-methylphosphonate (**33***a*). Although this compound was readily prepared[15] from the methiodide **5***a*, it was found to be totally unreactive towards ketone **10***a* and, surprisingly, even **7***a* and **24***c* under several sets of previously mentioned conditions. We reasoned that perhaps the acidity of the indolic NH is much greater than that of the methylene protons in **33***a* and thus that the required carbanion for the Wittig reaction was not generated under these conditions. When **33***a* was treated with 2 equiv of each of sodium hydride and *N*-methyl-4-piperidone **7***a* in DMF solution, the adduct **8***a* was obtained, albeit in very low yield. However, application of these conditions to the reaction of **33***a* with pyridine-2-aldehyde (**24***c*) gave a *cis–trans* mixture of **25***c* in 44% overall yield offering some support for the above proposal. Although the yield is somewhat lower than that obtained using phosphonium salt **6** (Table 5), this method may be more convenient for the preparation of compounds **25***d* and *e* in that problems of separation of triphenylphosphine oxide encountered in the latter cases are circumvented.

Finally, an attempt was made to prepare indole-2-methyldiphenylphosphine oxide (**33***b*) since evidence in the literature indicated that this type of system was highly effective in reactions with hindered carbonyl compounds (46). Although the immediate precursor (**9***d*) for compound **33***b* was readily prepared, its hydrolysis with base by the prescribed method (47) gave 2-methylindole (**12**) instead of the expected product. This result may be explained by a mechanism analogous to that proposed for the production of **12** in the abortive Wittig reaction attempts (Scheme 2). Credibility for this proposal and thus for the behavior of 2-methylindole carbanion **18** as a good leaving group is further strengthened when it is realized that normally N—P bonds are broken more readily than C—P bonds in these systems (48).

[15]Our unambiguous synthesis of **33***a* corroborates the structural assignment for this compound which has caused some concern (44, 45).

Experimental

General Methods

Melting points were measured on a Fisher-Johns apparatus and are uncorrected. Microanalyses were performed by A. B. Gygil, Toronto; W. Boos, Uniroyal Laboratories, Guelph; Microtech Laboratories, Skokie, Illinois; Scandinavian Microtechnical Laboratory, Herlev, Denmark; and Microanalytical Laboratory, Bonn, Germany. I.r. spectra were determined with a Beckman IR-5A instrument in chloroform solution unless otherwise indicated. U.v. spectra were recorded on a Coleman-Hitachi EPS-3T spectrophotometer in methanol solution. N.m.r. spectra were obtained on Varian T-60, A-60A, and HA-100 spectrometers in deuteriochloroform solution unless otherwise stated. Mass spectra were determined with a Hitachi–Perkin–Elmer RMU-6E spectrometer at 70 eV. T.l.c. was carried out with Merck silica gel GF 254 and column chromatography with Merck silica gel (0.05–0.2 mm) obtained from Brinkmann (Canada) Ltd. unless otherwise stated. Benzene and THF were dried by refluxing over sodium and benzophenone until a deep blue color persisted in solution. DMF and DMSO were dried by allowing them to stand for several days over Linde molecular sieves (Type 4A) unless otherwise indicated.

The following compounds were purchased from Aldrich Chemical Co.: 1-methyl-4-piperidone (**7***a*), 2,2,2-trichloroethyl chloroformate, chlorodiphenylphosphine, dichlorophenylphosphine, diphenylphosphinic acid, and 1,5-diazabicyclo(4.3.0)nonene-5 (DBN). With the exception of **7***a* which was distilled, all of these were used without further purification.

Preparation of 4-Piperidone Derivatives

The following compounds were prepared by literature methods with minor modifications: 4-piperidone hydrochloride (49) (m.p. 145–150°; lit. (50) m.p. 147–149°); 1-benzyl-4-piperidone (**7***c*) (51) (b.p. 108–110°, 0.1 mm; lit. (50) b.p. 114–116°, 0.3 mm); 1-benzoyl-4-piperidone (**7***e*) (51) (b.p. 158–160°, 0.2 mm; lit. (50) b.p. 158–160°, 0.2 mm); 1-methyl-3-ethyl-4-piperidone (**10***a*) (51, 52) (b.p. 74–76°, 13 mm; lit. (52) b.p. 102°, 33 mm).

1-Carbophenoxy-4-piperidone (7b)

In an adaptation of a literature procedure (30), a solution of 15.7 g (0.10 mol) of phenyl chloroformate in 50 ml of methylene chloride was added dropwise to a stirred solution of 11.3 g (0.10 mol) of 1-methyl-4-piperidone (**7***a*) in 50 ml of methylene chloride. The mixture was refluxed for 18 h, cooled, and diluted with 50 ml of water. The methylene chloride layer was separated, washed with saturated salt solution, and dried (Na_2SO_4). After filtration, the solvent was removed *in vacuo* and the resulting oil was distilled to give 10.8 g (49%) of **7***b*, b.p. 150–160° (0.1 mm) which solidified upon standing. Two recrystallizations from carbon tetrachloride – petroleum ether (30–60°) gave an analytical sample, m.p. 76–78°; i.r. ν_{max} 1700 (C=O) cm^{-1}; n.m.r. (CCl_4) τ 2.3–3.0 (m, 5H, aromatic), 6.2 (t, 4H, J = 6 Hz, CH_2N), 7.64 (t, 4H, J = 6 Hz, CH_2CO).

Can. J. Chem. Downloaded from www.nrcresearchpress.com by 210.87.254.40 on 09/05/12
For personal use only.

Anal. Calcd. for $C_{12}H_{13}NO_3$: C, 65.74; H, 5.98; N, 6.39. Found: C, 65.49; H, 5.91; N, 6.36.

1-(2,2,2-Trichlorocarboethoxy)-4-piperidone (7d)

To a stirred solution of 7.0 g (50 mmol) of 4-piperidone hydrochloride in 50 ml of water was added a solution of 10.5 g (50 mmol) of 2,2,2-trichloroethyl chloroformate in 100 ml of ether followed by a solution of 85 g (100 mmol) of sodium bicarbonate in 100 ml of water. An additional 100 ml of ether was added and the reaction mixture was stirred at room temperature for 17 h. The ether layer was separated and the aqueous layer was extracted with ether. The combined ether extract was washed consecutively with 2 *N* hydrochloric acid solution, water, and a saturated sodium chloride solution. The ether layer was dried (Na_2SO_4) and evaporated to dryness. The residue was distilled to give 13.3 g (97%) of a colorless liquid, b.p. 138–140°, 0.4 mm which solidified. Recrystallization from carbon tetrachloride – petroleum ether (30–60°) gave an analytical sample of **7d**, m.p. 47–48°, i.r. ν_{max} 1720 (C=O) cm^{-1}; n.m.r. (CCl_4) τ 5.20 (s, 2H, $CO_2CH_2CCl_3$), 6.20 (t, 4H, J = 6 Hz, CH_2N), 7.56 (t, 4H, J = 6 Hz, CH_2CO).

Anal. Calcd. for $C_8H_{10}Cl_3NO_3$: C, 35.00; H, 3.67; N, 5.10. Found: C, 35.34; H, 3.56; N, 5.12.

1-Carboethoxy-4-piperidone (7f)

This compound was prepared in 56% yield from **7a** and ethyl chloroformate by the procedure described for **7b**. It showed b.p. 99–100°, 0.3 mm (lit. (53) b.p. 93°, 1 mm) and required storage at 0° under nitrogen.

1-Carbophenoxy-3-ethyl-4-piperidone (10b)

The procedure was that used for the preparation of **7b**. From 7.0 g (0.05 mol) of **7a** and 7.8 g (0.05 mol) of phenyl chloroformate there was obtained 7.0 g (57%) of **10b** as a thick colorless oil, b.p. 152–154°, 0.03 mm; i.r. (neat) ν_{max} 1710 (C=O) cm^{-1}; n.m.r. (CCl_4) τ 2.5–3.1 (m, 5H, aromatic), 5.7–7.2 (m, 4H, CH_2N), 7.67 (t, 2H, J = 6 Hz, CH_2CO), 7.4–8.2 (m, 1H, CHCO), 8.2–9.0 (m, 2H, CH_2CH_3), 9.23 (t, 3H, J = 7 Hz, CH_3).

Anal. Calcd. for $C_{14}H_{17}NO_3$: C, 68.00; H, 6.93; N, 5.66. Found: C, 67.77; H, 7.06; N, 5.46.

*Preparation of Phosphonium Salts **6**, **9a–d**, **26** and Phosphonate Ester **33a** (Table 3)*

2-Diethylaminomethylindole Methiodide (5b)

This compound was prepared in 96% yield by lithium aluminum hydride reduction of indole-2(*N*,*N*-diethyl) carboxamide (m.p. 168–170°; lit. (54) m.p. 163–164°) followed by treatment with methyl iodide according to the method of Schindler (21). After recrystallization from methanol, it showed m.p. 167°.

Anal. Calcd. for $C_{14}H_{21}IN_2$: C, 48.83; H, 6.10; N, 8.14; I, 36.93. Found: C, 49.02; H, 6.14; N, 7.99; I, 37.01.

Indole-2-methyltriphenylphosphonium Iodide (6)

This compound was prepared by modification of a literature method (55). A stirred solution of 35 g (0.11 mol) of 2-dimethylaminomethylindole methiodide (**5a**) (21) and 45 g (0.17 mol) of triphenylphosphine in 350 ml of dry DMF was refluxed for 24 h. The solvent was removed *in vacuo* and the residue was triturated with 500 ml of benzene. The solid was collected and washed with benzene to yield 41 g (71%) of product. Recrystallization from ethanol provided an analytical sample of **6**, m.p. 254–255°.

Compound **6** was also prepared by treatment of 2-diethylaminomethylindole methiodide (**5b**) with 1.2 equiv of triphenylphosphine in DMF. In this case, however, the mixture was not refluxed; instead, diethylmethylamine was collected by distillation through a Vigreux column over a 1 h period. Isolation as described above afforded **6** in 90% yield.

Anal. Calcd. for $C_{27}H_{23}INP$: C, 62.44; H, 4.46; N, 2.70. Found: C, 62.42; H, 4.42; N, 2.66.

Indole-2-methyl(p-dimethylaminophenyl)diphenylphosphonium Iodide (9a)

This compound was prepared by the method outlined for **6**. From 12.6 g (0.04 mol) of **5a** and 18.3 g (0.06 mol) of *p*-dimethylaminophenyldiphenylphosphine (56) there was obtained 21.0 g (93%) of **9a** as a colorless solid, m.p. 275–277°.

Anal. Calcd. for $C_{29}H_{28}IN_2P$: C, 61.91; H, 5.02; N, 4.98. Found: C, 62.25; H, 5.09; N, 5.18.

Indole-2-methyldiphenylmethylphosphonium Iodide (9b)

A solution of 3.2 g (0.01 mol) of **5a** and 2.5 g (0.0125 mol) of diphenylmethylphosphine (57) in 50 ml of dry DMF was stirred and refluxed for 18 h in a carbon dioxide atmosphere. The solvent was removed *in vacuo* and the residue was triturated with a mixture of benzene and carbon tetrachloride to give a semisolid which was recrystallized twice from ethanol to yield 3.2 g (70%) of **9b** as a slightly pink, crystalline material, m.p. 231–233° (sinter 218°).

Anal. Calcd. for $C_{22}H_{21}INP$: C, 57.78; H, 4.63; N, 3.06. Found: C, 57.78; H, 4.68; N, 3.12.

Indole-2-methyldimethylphenylphosphonium Iodide (9c)

A stirred solution of 3.4 g (0.01 mol) of **5b** and 1.8 g (0.01 mol) of dimethylphenylphosphine (57) in 100 ml of dry DMF under a carbon dioxide blanket was brought to gentle reflux and diethylmethylamine was collected by distillation through an attached Vigreux column over a period of 1 h. The solvent was removed *in vacuo* and the resulting residue was dissolved in methylene chloride. This solution was successively washed with water and saturated salt solution, and dried (Na_2SO_4). The solvent was evaporated *in vacuo* to give a yellow resin which was recrystallized from acetone to yield 1.3 g (32%) of **9c**, m.p. 99–100° (sinter 95°).

Anal. Calcd. for $C_{17}H_{19}INP$: C, 51.66; H, 4.85; N, 3.54. Found: C, 51.69; H, 5.41; N, 3.41.

Indole-2-methyldiphenyl-N-t-butylaminophosphonium Iodide (9d)

In an adaptation of a literature method (47), a solution of 3.2 g (10 mmol) of **5a** and 5.2 g (20 mmol) of diphenyl-*t*-butylaminophosphine (47) in 50 ml of dry DMF was stirred and refluxed for 18 h. The solvent was removed *in vacuo* and the residue was triturated with carbon tetrachloride to give 5.5 g of yellow solid which, after two recrystallizations from ethanol at 0°, afforded 2.1 g (41%) of **9d**, m.p. 155–156°.

Anal. Calcd. for $C_{25}H_{28}IN_2P$: C, 58.38; H, 5.49; N, 5.45. Found: C, 58.39; H, 5.54; N, 5.43.

When compound **9d** was treated with aqueous potassium hydroxide according to Sisler and Smith (47), 2-methylindole (**12**) was obtained in 89% crude yield.

Can. J. Chem. Downloaded from www.nrcresearchpress.com by 210.87.254.40 on 09/05/12
For personal use only.

TABLE 3. Spectral data for indole-2-methylphosphonium salts (**6**, **9***a–d*, **20**, **26**) and phosphonate ester (**33***a*)

Compound	λ_{max} (ε) mμ	τ Values[a]			
		Indole N—H[b]	Indole 3-H[b]	—CH_2P[c]	Other
6	271 (11 200), 278 (11 000) 287 (9800), 293 (9100)	−0.80	4.20	4.82	2.1–3.3 (m, 19H, aromatic)
9*a*	297 (30 000), 304 (29 400)				
9*b*	271 (11 700), 277 (11 800) 285 (10 900), 293 (9300)	−0.77	4.08	5.14	2.0–3.4 (m, 14H, aromatic), 7.52 (d, 3H, J = 15 Hz, PCH_3)
9*c*	271 (9900), 276 (10 100) 285 (9700), 293 (7900)	−0.58	3.67[d]	5.37	1.7–3.2 (m, 9H, aromatic), 7.77 (d, 6H, J = 14 Hz, PCH_3)
9*d*	272 (11 000), 278 (11 000) 284 (10 100), 293 (8000)	−0.48	4.37[e]	5.27	2.0–3.1 (m, 14H, aromatic), 4.20 (br d, 1H, J = 8 Hz, NH), 8.87 (s, 9H, CH_3)
20	274 (12 600), 281 (12 300) 283 (sh, 10 700), 284 (sh, 10 400)		3.80[d]	4.40	1.8–3.0 (m, 19H, aromatic), 6.83 (br s, NCH_3)
26	262 (sh, 3600), 268 (sh, 4200) 276 (4300), 285 (sh, 3800) 294 (sh, 3400)	−0.45		4.70	1.8–3.05 (m, 19H, aromatic), 6.40 (br s, 1H, OH), 6.70 (br t, 2H, J = 6 Hz, —CH_2O), 7.70 (br t, 2H, J = 6 Hz, CH_2)
33*a*[f]	275 (8600), 282 (8400) 291 (6600)	1.57	3.67	6.67	2.3–3.1 (m, 4H, aromatic), 5.9 (q, 2H, J = 7 Hz, CH_2CH_3), 6.03 (q, 2H, J = 7 Hz, CH_2CH_3), 8.77 (t, 6H, J = 7 Hz, CH_2CH_3)

[a]Measured in DMSO-d_6 in all cases except **9***b* and **33***a* which were determined in polysol-*d* and $CDCl_3$ respectively. Insolubility precluded determination of the n.m.r. spectrum of **9***a*.
[b]Broad singlet, 1H.
[c]Doublet, 2H, J = 15 Hz.
[d]Doublet, 1H, J = 3 Hz.
[e]Broad doublet, 1H, J = 4 Hz.
[f]I.r. ν_{max} 3360, 1220, 1050, 1030 cm^{-1}, *cf.* ref. 60.

Can. J. Chem. Downloaded from www.nrcresearchpress.com by 210.87.254.40 on 09/05/12
For personal use only.

*Indole-1-methyl-2-methyltriphenylphosphonium Iodide (**20**)*

Sodium hydride (50% dispersion in mineral oil) (3.12 g, 65 mmol) placed in a flask under a slow stream of nitrogen was washed twice with dry petroleum ether (35–60°). The flask was immersed into a Dry Ice – carbon tetrachloride bath (−15°) and 150 ml of DMF (freshly distilled from calcium hydride) was added. To the stirred mixture was added dropwise a solution of 9.4 g (50 mmol) of indole-2(*N*,*N*-dimethyl)carboxamide (21) in 100 ml of dry DMF and stirring was continued for 45 min. Dried and freshly distilled methyl iodide (14.2 g, 100 mmol) in 50 ml of dry DMF was similarly added and the temperature of the mixture was allowed to rise to −10° over a 1 h period. After further periods of stirring at 0° (1 h) and room temperature (10 h), most of the solvent was removed *in vacuo* and the resulting residue was extracted with three 100 ml portions of ether. The combined extracts were evaporated to yield an oil which formed a solid upon addition of ice-water and vigorous agitation. Recrystallization from benzene – petroleum ether (60–80°) gave 9.1 g (91%) of *indole-1-methyl-2(N,N-dimethyl)carboxamide*, m.p. 95°, i.r. ν_{max} 1627 (C=O) cm^{-1}; u.v. λ_{max} 287 (11 700) mμ; n.m.r. τ 2.2–3.0 (m, 4H, aromatic), 3.37 (s, 1H, indole 3-H), 6.20 (s, 3H, indole 1-CH_3), 6.88 (s, 6H, $N(CH_3)_2$).

Anal. Calcd. for $C_{12}H_{14}N_2O$: C, 71.26; H, 6.98; N, 13.85. Found: C, 71.22; H, 7.26; N, 13.88.

Lithium aluminum hydride reduction of indole-1-methyl-2(*N*,*N*-dimethyl)carboxamide according to the method of Schindler (21) gave a quantitative yield of *1-methyl-2-dimethylaminomethylindole*, b.p. 130°, 0.05 mm, n.m.r. τ 2.3–3.07 (m, 4H, aromatic), 3.85 (s, 1H, indole 3-H), 6.34 (s, 3H, indole 1-CH_3), 6.57 (s, 2H, CH_2N), 7.84 (s, 6H, $N(CH_3)_2$), which was converted into its methiodide also in quantitative yield. Recrystallization from benzene–methanol gave an analytical sample of *1-methyl-2-dimethylaminomethylindole methiodide*, m.p. 217–219° (dec.), λ_{max} 278 (10 000), 288 (sh, 7400), 300 (sh, 3900) mμ; n.m.r. (DMSO-d_6) τ 2.2–3.0 (m, 4H, aromatic), 3.1 (s, 1H, indole 3-H), 5.6 (br s, 2H, CH_2N^+), 6.12 (s, 3H, indole 1-CH_3), 6.82 (br s, 9H, $^+N(CH_3)_3$).

Anal. Calcd. for $C_{13}H_{19}N_2I$: C, 47.28; H, 5.77; N, 8.49; I, 38.49. Found: C, 47.58; H, 5.43; N, 8.54; I, 38.55.

The above compound was converted to *indole-1-methyl-2-methyltriphenylphosphonium iodide* (**20**) according to the method used for **6** except that the reflux time was abbreviated (3.5 h). Recrystallization from methanol gave a 60% yield of **20**, m.p. 240–241° (dec.). The compound was found to be very air sensitive.

Anal. Calcd. for $C_{28}H_{25}INP$: C, 63.05; H, 4.70; N, 2.63; I, 23.83; P, 5.82. Found: C, 62.70; H, 4.74; N, 2.65; I, 24.08; P, 5.44.

*Indole-2-[3-hydroxyethyl]-2-methyltriphenylphosphonium Iodide (**26**)*

Using the method for the preparation of **6**, 3.64 g (0.01 mol) of indole-3-[2-hydroxyethyl]-2-dimethylaminomethyl methiodide (58) was treated with 7.92 g (0.03 mol) of triphenylphosphine in 30 ml of dry DMF to give 5.60 g (99%) of compound **26**. Recrystallization from methanol gave a sample, m.p. 258–260° (dec.).

Anal. Calcd. for $C_{29}H_{27}INOP$: C, 61.82; H, 4.84; N, 2.49; I, 22.56; P, 5.51. Found: C, 61.49; H, 4.77; N, 2.52; I, 22.82; P, 5.49.

*Diethyl Indole-2-methylphosphonate (**33a**)*

The procedure of Harvey *et al.* (59) was adapted. To a stirred suspension of 0.46 g (9.6 mmol) of sodium hydride (50% suspension in mineral oil) in 25 ml of dry THF was added a solution of 1.6 g (11.6 mmol) of diethyl phosphite (59) in 25 ml of THF. The reaction mixture was refluxed until the solid had disappeared, cooled, and treated with a solution of 2.0 g (6.3 mmol) of **5***a* in 50 ml of DMF. The mixture was refluxed for 18 h and evaporated to dryness *in vacuo*. The residue was treated with water and the resulting solution was extracted with ether. The ether extract was washed with saturated sodium chloride solution and dried (Na_2SO_4). There was obtained 1.5 g of solid which was chromatographed (chloroform eluent) to yield 1.1 g (66%) of crystalline product. Recrystallization from methanol at −20° and repeatedly from ether gave a pure sample of **33***a* as colorless crystals, m.p. 105–107° (lit. (60) m.p. 119–120°), i.r. identical bands to those reported (60).

*Preparation of 2-(4-Piperidylidene)methylindole Derivatives (**8***a–e and **21**) (Table 4)*

*General Method 2-(1-Methyl-4-piperidylidene)-methylindole (**8***a)*

To a stirred solution of lithium ethoxide in ethanol under nitrogen (prepared from 125 mg (18 mmol) of lithium and 25 ml of absolute ethanol) were added consecutively 9.3 g (18 mmol) of indole-2-methyltriphenylphosphonium iodide (**6**), 50 ml of absolute ethanol, and a solution of 2.1 g (18 mmol) of 1-methyl-4-piperidone (**7***a*) in 40 ml of ethanol. An additional 50 ml of ethanol was added and the reaction mixture was stirred and refluxed for 21 h. The solvent was removed *in vacuo* and the residue was dissolved in ether. After removal of triphenylphosphine oxide by filtration, the solution was treated with an equimolar amount of citric acid monohydrate in benzene. The resulting precipitate was collected and washed with ether. It was then suspended in a mixture of water and methylene chloride and the mixture was basified with solid sodium bicarbonate. The organic layer was separated and the aqueous mixture was extracted further with methylene chloride. The combined extract was washed with saturated sodium chloride solution and dried (Na_2SO_4). There was obtained 3.4 g (84%) of product which was recrystallized from methanol to give 2.5 g of pure **8***a*.

*2-(1-Benzoyl-4-piperidylidine)methylindole (**8***e)*

To a stirred solution of lithium ethoxide in absolute ethanol under nitrogen (prepared from 24 mg (3.5 mmol) of lithium in 50 ml of ethanol) at reflux there was added 2.02 g (3.6 mmol) of **9***a* and 50 ml of ethanol, followed immediately by a solution of 0.72 g (3.6 mmol) of 1-benzoyl-4-piperidone (**7***e*) in 50 ml of ethanol. The reaction mixture was refluxed for 18 h and evaporated to dryness *in vacuo*. The residue was treated with 200 ml of benzene and the resulting precipitated phosphine oxide was removed by filtration. The filtrate was washed consecutively with water, four 50 ml portions of a 5% hydrochloric acid solution, and saturated salt solution. The benzene solution was dried (Na_2SO_4) and evaporated to dryness *in vacuo* to give 1.2 g of crude material which was recrystallized three times from ethanol to yield a pure sample of **8***e*.

TABLE 4. Preparation[a] and physical data of 2-(4-piperidylidene)indole derivatives (**8***a–e*, **21**, **22**)

Compound	M.p. (°C) (solvent)	Yield[b] (%)	Formula	Analysis %C Calcd.	%C Found	%H Calcd.	%H Found	%N Calcd.	%N Found
8*a*	143–145 (MeOH)	57	$C_{15}H_{18}N_2$	79.61	79.32	8.02	7.90	12.38	12.31
8*b*	164–165 (MeOH)	14	$C_{21}H_{20}N_2O_2$	75.88	75.91	6.06	6.12	8.43	8.44
8*c*	132–133 (MeOH)	50	$C_{21}H_{22}N_2$	83.40	83.34	7.33	7.40	9.26	9.25
8*d*	153–154 (EtOH)	44	$C_{17}H_{17}N_2O_2Cl_3$	52.67	52.83	4.42	4.40	7.22	7.02
8*e*[c]	191–193 (EtOH)	52	$C_{21}H_{20}N_2O$	79.72	79.53	6.37	6.48	8.85	8.66
21	87 (ligroin, 60–80°)	59	$C_{16}H_{20}N_2$	79.96	79.69	8.39	8.40	11.66	11.91
22[d]	193–194 (EtOH)	52	$C_{14}H_{16}N_2$	79.21	79.34	7.60	7.59	13.20	12.93

[a]Compounds **8***a* and *c* were prepared by the Wittig reaction according to the general method described for **8***a*, Compounds **8***b*, **8***d*, and **21** were prepared by the same method except that the isolation procedure involved chromatography (**8***b*, neutral alumina; **8***d*, silica gel; **21**, basic alumina, grade III) with benzene as eluent. The preparation of **8***e* is described separately. The reactions were carried out on 1–9 mmol scale and the recrystallizations were effected at −20° to 0°.
[b]Reported yields are of crystallized material.
[c]The *p-N,N*-dimethylaminophenylphosphonium salt **9***a* was used in this preparation.
[d]This compound was obtained from **8***d*.

Interconversions and Transformations of Wittig Products (Scheme 3)

*Reaction of **8**a with Phenyl Chloroformate: Alternate Preparation of **8**b*

To a suspension of 450 mg (2 mmol) of **8***a* in 15 ml of dry benzene was added dropwise a solution of 320 mg (2 mmol) of phenyl chloroformate in 20 ml of benzene–chloroform (1:1). The thick mixture was stirred and refluxed for 4 h, cooled, and washed consecutively with water, dilute hydrochloric acid, water, sodium bicarbonate, and saturated salt solution. The benzene solution was taken to dryness to give a pale brown solid which was recrystallized from methanol to yield 255 mg (39%) of **8***b*, which was shown to be identical by m.p. and mixture m.p. comparison to an authentic sample prepared by the Wittig reaction.

*Lithium Aluminum Hydride Reduction of **8**b*

A solution of 68 mg (0.2 mmol) of **8***b* and 0.14 g (3.7 mmol) of lithium aluminum hydride in 5 ml of dry tetrahydrofuran was refluxed for 2.5 h. Normal isolation procedure yielded 23 mg (50%) of **8***a*, identical by i.r. and n.m.r. spectral comparison with an authentic sample prepared by the Wittig reaction.

*Lithium Aluminum Hydride Reduction of **8**e*

A sample of **8***e* prepared by the Wittig reaction of **6** with **7***e* was not purified but directly subjected to lithium aluminum hydride reduction (10-fold excess of LAH, reflux for 20 h in THF) as above to give **8***c* in 36% yield after purification via the citrate salt method as described for the preparation of **8***a*. The material was shown to be identical by m.p. and mixture m.p. comparison to an authentic sample of **8***c* prepared by the Wittig reaction.

*2-(4-Piperidylidene)methylindole (**22**)*

To a solution of 1.8 g (2.8 mmol) of **8***d* in 30 ml of methanol there was added 5 ml of glacial acetic acid and 1.1 g of zinc dust and the mixture was refluxed for 3 days (31). The inorganic material was removed by filtration and the filtrate was concentrated *in vacuo*. The residue was dissolved in water and the resulting solution was extracted with methylene chloride. The aqueous solution was basified with solid sodium bicarbonate and extracted with methylene chloride. The organic extract was washed with saturated salt solution and dried (Na_2SO_4). There was obtained 0.5 g of yellow solid which upon recrystallization from acetone at −20° gave 0.31 g (52%) of compound **22**.

*2-(4-Piperidyl)methylindole (**23**a)*

A solution of 0.7 g (3.3 mmol) of compound **22** in 140 ml of ethanol was hydrogenated over 0.4 g of 5% palladium-on-charcoal (50% water) at 3.5 atm and room temperature for 23 h. Normal isolation procedure and recrystallization from acetone at 0°, gave 0.5 g (73%) of **23***a*. An additional recrystallization from acetone afforded an analytical sample, m.p. 177–179° (sinter 168°); i.r. ν_{max} 3400 cm^{-1}; u.v. λ_{max} 275 (7700), 281 (7700), 291 (5900) mμ; n.m.r. τ 1.9 (br s, 1H, indole NH), 2.3–3.1 (m, 4H, aromatic), 3.8 (br s, 1H, indole 3-H), 6.7 (m, 4H, CH_2N), 7.35 (d, 2H, J = 6 Hz, indolyl-2-CH_2), 7.8–9.0 (m, 6H, $CHCH_2CH_2N$, NH).

Anal. Calcd. for $C_{14}H_{18}N_2$: C, 78.46; H, 8.47; N, 13.07. Found: C, 78.13; H, 8.43; N, 12.89.

*2-(1-Methyl-4-piperidyl)methylindole (**23**b)*

Compound **8***a* (1.49 g, 6.6 mmol) was reduced according to the procedure described for the preparation of **23***a*. There was obtained 0.81 g (54%) of **23***b* which was recrystallized from ethanol to give an analytical sample, m.p. 141–142°; i.r. ν_{max} 3400 (NH), 2780 (NCH_3) cm^{-1}; u.v. λ_{max} 275 (7500), 281 (7500), 291 (5800) mμ; n.m.r. τ 2.0 (br s, 1H, indole NH), 2.3–3.1 (m, 4H, aromatic), 3.7 (br s, 1H, indole 3-H), 7.3 (d, 2H, J = 6 Hz, indolyl-2-CH_2), 7.67 (s, 3H, NCH_3); 6.9–9.0 (m, 9H, piperidine).

Anal. Calcd. for $C_{15}H_{20}N_2$: C, 78.90; H, 8.83; N, 12.27. Found: C, 78.78; H, 8.80; N, 12.19.

*2-(1-Carbophenoxy-4-piperidyl)methylindole (**23**c)*

Compound **23***b* was treated with phenyl chloroformate according to the method used for the conversion **8***a* → **8***b*. Recrystallization from ethanol gave a 20% yield of **23***c*, m.p. 151–153° (sinter 148°); i.r. ν_{max} 3410 cm^{-1}; u.v. λ_{max} 275 (8100), 282 (8000), 291 (6400) mμ; n.m.r. τ 1.9 (br s, 1H, indole NH), 2.2–3.2 (m, 9H, aromatic), 3.7 (br s, 1H, indole 3-H), 5.75 (br d, 2H, J = 12 Hz,

Can. J. Chem. Downloaded from www.nrcresearchpress.com by 210.87.254.40 on 09/05/12
For personal use only.

piperidine α-CH_2), 7.08 (br d, 2H, J = 12 Hz, piperidine α-CH_2 shielded by —$CO_2C_6H_5$ function due to NCO_2-C_6H_5 hindered rotation), 7.31 (d, 2H, indolyl-2-CH_2), 7.8–9.1 (m, 5H, $CHCH_2CH_2N$).

Anal. Calcd. for $C_{21}H_{22}N_2O_2$: C, 75.42; H, 6.63; N, 8.38. Found: C, 75.56; H, 6.67; N, 8.27.

*Preparation of 2-(2-Aryl)vinylindole Derivatives (**25***a–e*, **27**, and **32**)*

Reactions were carried out with 1.93–3.85 mmol of **6** and equivalent amounts of base and aromatic aldehydes in 1:100 w/v of **6**:THF or DMSO (method A) or in 1:20 w/v of **6**:absolute methanol (method B). The preparation method, isolation procedure, and physical properties for compounds **25***a–e* and **32** are recorded in Table 5.

*2-(2-(p-Nitrophenyl)vinyl)indole (**25***b*)*

Method A. With DBN in THF or DMSO solution

To a stirred solution of 1.04 g (2 mmol) of **6** in 60 ml of dry THF at 40° (oil bath) under nitrogen there was added simultaneously and dropwise from two separatory funnels solutions of 0.30 g (2 mmol) of *p*-nitrobenzaldehyde in 10 ml of THF and 0.25 g (2 mmol) of DBN in 10 ml of THF. The reaction mixture was stirred at 40° for 1 h and then heated at 80° for 2 h. Heating was discontinued and the mixture was stirred for an additional 24 h. The solvent was removed *in vacuo* and the residue was chromatographed (methylene chloride) to give 0.52 g of **25***b*.

Method B. With sodium methoxide in methanol solution

To a stirred solution of 1.00 g (1.93 mmol) of **6** in 175 ml of absolute methanol at 40° (oil bath) under nitrogen there was added dropwise and simultaneously from two separatory funnels solutions of 0.29 g (1.93 mmol) of *p*-nitrobenzaldehyde in 25 ml of methanol and 0.08 g (1.93 mmol) of sodium methoxide in 25 ml of methanol. The reaction mixture was stirred at 40° for 2 h and then refluxed for 15 h. The solvent was removed *in vacuo* and the residue was stirred and refluxed with 200 ml of benzene for 10 h. The benzene extract was evaporated to dryness and the residue was chromatographed (methylene chloride) to give 0.42 g (81%) of **25***b* which was shown to be identical to the sample obtained by method A by m.p. and mixture m.p. determination.

*2-(2-(2-Pyridyl)vinyl)indole (cis-, trans-**25***c*) Using Diethyl Indole-2-methylphosphonate (**33***a*)*

A mixture of sodium hydride (0.288 g, 6 mmol) in dry DMF (75 ml) was prepared at −10° as in the experiment dealing with the synthesis of **20**. A solution of **33***a* (0.791 g, 3 mmol) in dry DMF (25 ml) was added dropwise to the stirred mixture over 30 min and stirring was continued for 1 h during which time the dark green reaction mixture was allowed to warm to room temperature. A solution of pyridine-2-aldehyde (0.642 g, 6 mmol) was added dropwise and the resulting yellow solution was stirred at room temperature for 16 h. The reaction mixture was concentrated and the brown gum was suspended in water. This suspension was extracted with ether (2 × 250 ml) and methylene chloride (250 ml) and the combined extracts were dried (Na_2SO_4) and evaporated to dryness. The residue was chromatographed over basic alumina (grade III, methylene chloride) to give 0.115 g (18%) of *cis*-**25***c* and 0.172 g (26%) of *trans*-**25***c* which were identified by m.p., mixture m.p., and spectral comparison with samples prepared by the Wittig reaction of **6** with **24***c*.

*Reaction of Indole-2-methyltriphenylphosphonium Iodide (**6**) with Sodium Methoxide. Formation of 2-Methylindole (**12**)*

To a stirred solution of 0.519 g (1.0 mmol) of **6** in 100 ml of anhydrous methanol under nitrogen was added dropwise a solution of 0.023 g (1.0 mmol) of sodium in 25 ml of anhydrous methanol. The mixture was refluxed for 48 h. The solvent was removed *in vacuo* and the residue was extracted with 100 ml of warm petroleum ether (60–80°). Concentration of the extract gave 0.081 g (62%) of 2-methylindole (**12**) shown to be identical to an authentic sample (50) by t.l.c. and u.v. and n.m.r. spectroscopy. The residue remaining from the petroleum ether extraction was extracted with 300 ml of hot ether. Concentration of this extract yielded 0.161 g (60%) of triphenylphosphine oxide. The remaining residue was recrystallized from methanol to give 0.175 g (33%) of starting material (**6**).

Deuterium Exchange Experiments

*(a) Phosphonium Salt **6***

A solution of 0.0046 g (0.2 mmol) of sodium metal in 3 ml of anhydrous ethanol-*O-d* (Stohler Isotope Chemicals, Montreal) was prepared under nitrogen. The mixture was allowed to cool to room temperature and 0.103 g (0.2 mmol) of **6** was added. The solution was stirred for 30 min and quenched with 5 ml of D_2O and excess Dry Ice. The solvent was removed *in vacuo*. The resulting residue showed m.p. 245–247° (dec.) and a u.v. spectrum identical to that of **6**. T.l.c. showed the absence of 2-methylindole. Its n.m.r. spectrum in DMSO-d_6 lacked absorption at τ −0.80, 4.20, and 4.82 indicating essentially complete deuterium exchange of NH, indole 3-H, and methylene protons in **6** (see Table 3).

*(b) Phosphonium Salt **20***

The procedure described above was performed using 0.0092 g (0.4 mmol) of sodium, 8 ml of ethanol-*O-d*, and 0.214 g (0.4 mmol) of **20**. After the normal work-up, t.l.c. examination of the solid showed the presence of triphenylphosphine oxide and a compound with an R_f value identical to that of 1,2-dimethylindole. Extraction of the solid with warm petroleum ether (60–80°) gave 0.037 g of 1-methyl-2-trideuteriomethylindole, m.p. 53–54°, which showed u.v. spectral and t.l.c. behavior in several solvent systems identical with those of an authentic sample of 1,2-dimethylindole (50). Its n.m.r. spectrum was superimposable on that of 1,2-dimethylindole except that it lacked a signal at τ 7.60 (2-CH_3). The residue remaining after the petroleum ether extract was treated with hot ether to give 0.071 g of triphenylphosphine oxide. The remaining residue was recrystallized from ethanol-*O-d* to give 0.635 g of deuterated starting material, m.p. 230–232° (dec.), which showed a u.v. spectrum identical to that of **20** and differed in the n.m.r. spectrum from the latter compound only in the absence of an absorption at τ 4.4 indicating that only the methylene protons had undergone deuterium exchange (see Table 3).

*cis–trans Isomerization of Compound **25***c*

*(a) Acid-catalyzed (cis-**25***c* → *trans-**25***c*)*

A solution of 0.100 g of *cis*-**25***c* in 25 ml of 1 *N* sulfuric

Can. J. Chem. Downloaded from www.nrcresearchpress.com by 210.87.254.40 on 09/05/12
For personal use only.

Can. J. Chem. Downloaded from www.nrcresearchpress.com by 210.87.254.40 on 09/05/12
For personal use only.

TABLE 5. Preparation and physical data of 2-(2-aryl)vinylindole derivatives (**25***a–e*, **27**, and **32**)

Compound	Preparation method	M.p. (°C) (solvent)	Yield[a] (%)	Analysis: Formula	%C Calcd.	%C Found	%H Calcd.	%H Found	%N Calcd.	%N Found
25*a*	A (DMSO, room temperature, 12 h; 80°, 1 h)[b,c]	210 (EtOH)	39	$C_{16}H_{13}N$	87.64	87.40	5.98	5.87	6.39	6.38
	B		49							
25*b*[d]	A (THF)	260–262 (C_6H_6)	99	$C_{16}H_{12}N_2O_2$	72.72	72.81	4.58	4.61	10.60	10.47
	B		81							
25*c*	A (THF)[e]	118 (petroleum ether, 60–80°)	58(*cis*)	$C_{15}H_{12}N_2$	81.79	81.78	5.49	5.46	12.72	12.61
	B[f]	210–211 (EtOH)	34(*trans*) 34(*cis*)	$C_{15}H_{12}N_2$	81.79	81.67	5.49	5.70	12.72	12.75
	B (LiOMe)[f]		29(*cis*) 45(*trans*)							
	B (LiOMe, room temperature)[f]		47(*cis*) 47(*trans*)							
	B (LiOMe, 2 equiv LiCl)[f]		30(*cis*) 33(*trans*)							
25*d*	A (DMSO)[c,g]	194 (MeOH)	47	$C_{15}H_{12}N_2$	81.79	81.48	5.49	5.51	12.72	12.73
	B[g]		56							
25*e*	A (THF)[g]	215–217 (MeOH)	59(*trans*)	$C_{15}H_{12}N_2$	81.79	81.71	5.49	5.63	12.72	12.61
	B[g]		43(*trans*)							
	B (LiOMe)[g]		61(*trans*)							
		137–138 (MeOH)	5(*cis*)	$C_{15}H_{12}N_2$	81.79	81.54	5.49	5.59	12.72	12.65
27	B[h]	183–184 (H_2O–MeOH)	28	$C_{17}H_{16}N_2O$	77.25	77.20	6.10	6.16	10.64	10.34
32[i]	B[h]	oil	32(*cis*)							
		oil	37(*trans*)	$(C_{16}H_{14}N_2 \cdot CH_3I)$[j]	54.25	54.05	4.52	4.55	7.45	7.33

[a]Reported yields are of crystallized material except in the case of **32**.
[b]Isolation procedure: the reaction mixture was poured into ice-water and the resulting cloudy solution was exhaustively extracted with ether. The ether extract was dried (Na_2SO_4), concentrated and the residue was chromatographed (benzene).
[c]Poor results were obtained when THF was used as a solvent.
[d]The m.p. of **25***b* was incorrectly reported as 165–166° (dec.) and the yield of its formation has been improved from 74% to 99% (*cf.* ref. 1).
[e]Chromatography using chloroform as eluent.
[f]The reaction mixture was concentrated and extracted with cold petroleum ether (60–80°) to give *cis*-**25***c*. The residue was suspended in ether and repeatedly extracted with 5% hydrochloric acid solution. The combined acid extracts were basified with solid sodium carbonate and the solution was extracted with ether. The ether extract was dried (Na_2SO_4) and concentrated to yield *trans*-**25***c*.
[g]The reaction mixture was processed as in footnote [b] but the ether extract was treated with a saturated solution of citric acid in ether–ethanol (100:1). The resulting precipitate was washed with ether and then stirred with 10% sodium carbonate solution (200 ml) for 3 h. The aqueous solution was extracted with ether to yield reasonably pure product.
[h]Work-up as in footnote [f] followed by preparative t.l.c. on silica gel (Merck GF254, 9:1 MeOH:CH_2:Cl_2).
[i]Treatment of oily *cis*- or *trans*-**32** with methyl iodide in $CHCl_3$ at room temperature gave the same *trans*-**32** methiodide, m.p. 271 °C (MeOH) (identical i.r., u.v., mixture m.p. undepressed).
[j]Hygroscopic and unstable.

acid was stirred at room temperature for 36 h. The solution was basified with sodium carbonate and extracted with ether. Chromatography over basic alumina (grade III, methylene chloride) yielded 0.041 g of *trans*-**25***c* and 0.058 g of *cis*-**25***c*.

(b) Photochemical (trans-25c → cis-25c)

A solution of 0.100 g of *trans*-**25***c* in 200 ml of methylene chloride was irradiated under nitrogen at 3500 Å in a Rayonet Photochemical Reactor for 4 h. The solution was evaporated to dryness to give 0.0995 g of crystalline *cis*-**25***c*.

Photocyclization of trans-25c to 7H-Pyrido(2,3-c)-carbozole (28)

The photocyclization of *cis*-**25***c* (m.p. 118°) originally assumed to be the *trans* isomer (1) to **28** has been described (18). Under these conditions, *trans*-**25***c* (m.p. 210–211°) gave a 48% yield of **28** which was shown to be identical to an authentic sample (18).

We thank the National Research Council of Canada for financial support. Partial support from the University of Waterloo and the Ontario Mental Health Foundation is also gratefully acknowledged. We warmly thank Dr. D. B. MacLean, Mr. B. Sayer, Dr. L. W. Reeves, and Mr. R. Shaddick for some of the n.m.r. spectra, and Drs. R. H. F. Manske and J. Muchowski for suggestions and discussion. N. Burnett and E. R. Vrscay ably aided in large scale preparations. Dr. F. Grail of the Chemical Abstracts Service kindly solved some nomenclature problems.

1. J. A. EENKHOORN, O. S. DE SILVA, and V. SNIECKUS. Chem. Commun. 1095 (1970).
2. R. J. SUNDBERG. The chemistry of indoles. Academic Press, New York. 1970. Chapt. 1.
3. Reference 2, Chapts. 4 and 9.
4. (*a*) Acylation: intermolecular, ref. 2, p. 412; intramolecular, M. NARISADA, F. WATANABE, and W. NAGATA. Tetrahedron Lett. 3681 (1971); F. E. ZIEGLER, J. A. KLOEK, and P. A. ZORETIC. J. Am. Chem. Soc. **91**, 2342 (1969); (*b*) Alkylation: M. WAKSELMAN, G. DECODTS, and M. VILKAS. C. R. Acad. Sci., Paris, Ser. C. **266**, 1089 (1969), and G. CASNATI, M. FRANCIONI, A. GUERESCHI, and A. POCHINI. Tetrahedron Lett. 2485 (1969); (*c*) Mannich reaction: J. WOLINSKY and J. E. SUNDEEN. Tetrahedron, **26**, 5427 (1970) and refs. therein; N-to-C_2 rearrangement: G. CASNATI and A. POCHINI. Chem. Commun. 1328 (1970).
5. (*a*) J. KEBRLE, A. ROSSI, and K. HOFFMANN. Helv. Chim. Acta, **42**, 907 (1959); J. KEBRLE and K. HOFFMANN. Gazz. Chim. Ital. **93**, 238 (1963); (*b*) F. E. ZIEGLER and E. B. SPITZNER. J. Am. Chem. Soc. **92**, 3492 (1970); (*c*) C. R. GANELLIN and H. F. RIDLEY. J. Chem. Soc. C, 1537 (1969) and refs. therein.
6. W. A. REMERS and M. J. WEISS. J. Org. Chem. **36**, 1241 (1971).
7. (*a*) H. PLIENINGER, H. SIROWEJ, and D. RAU. Ber. **104**, 1863 (1971); H. PLIENINGER and H. SIROWEJ. Ber. **104**, 1869 (1971); (*b*) M. HAMANA and I. KUMADAKI. Chem. Pharm. Bull. (Tokyo) **19**, 1669 (1971).
8. M.-S. LIN and V. SNIECKUS. J. Org. Chem. **36**, 645 (1971).
9. H. PLIENINGER and H. SIROWEJ. Ber. **104**, 2027 (1971).
10. (*a*) Reference 2, p. 176 ff.; P. ROSENMUND, J. BAUER, and D. SAUER. Ber. **104**, 1379 (1971).
11. F. YONEDA, T. MIYAMAE, and Y. NITTA. Chem. Pharm. Bull. (Tokyo) **15**, 8 (1967); G. GRETHE, H. L. LEE, and M. R. USKOKOVIC. Syn. Commun. **2**, 55 (1972); R. L. AUGUSTINE and S. F. WANAT. Syn. Commun. **2**, 63 (1972).
12. H. HEMETSBERGER, D. KNITTEL, and H. WEIDMANN. Monatsh. Chem. **101**, 161 (1970); R. J. SUNDBERG, H. F. RUSSELL, W. V. LIGON, JR., and L.-S. LIN. J. Org. Chem. **37**, 719 (1972).
13. Reference 2, pp. 159, 417.
14. Reference 2, pp. 97–99.
15. H.-P. HUSSON, C. THAL, P. POTIER, and E. WENKERT. J. Org. Chem. **35**, 442 (1970).
16. (*a*) E. WENKERT, K. G. DAVE, I. DAINIS, and G. D. REYNOLDS. Austr. J. Chem. **23**, 73 (1970); (*b*) H.-P. HUSSON, C. THAL, P. POTIER, and E. WENKERT. Chem. Commun. 480 (1970).
17. I. K. KIM and K. L. ERICKSON. Tetrahedron, **27**, 3979 (1971) and refs. therein; L. J. DOLBY and S. SAKAI. Tetrahedron, **23**, 1 (1967); J. HARLEY-MASON and ATTA-UR-RAHMAN. Chem. Commun. 208 (1967); R. T. BROWN, G. F. SMITH, K. S. J. STAPLEFORD, and D. A. TAYLOR. Chem. Commun. 190 (1970).
18. O. DE SILVA and V. SNIECKUS. Synthesis, 254 (1971).
19. A. JACKSON, N. D. V. WILSON, A. J. GASKELL, and J. A. JOULE. J. Chem. Soc. C, 2738 (1970); L. J. DOLBY and H. BIERE. J. Org. Chem. **35**, 3843 (1970); T. KAMETANI and T. SUZUKI. J. Org. Chem. **36**, 191 (1971); T. KAMETANI and T. SUZUKI. J. Chem. Soc. C, 1053 (1971); G. BUCHI, S. J. GOULD, and F. NAF. J. Am. Chem. Soc. **93**, 2492 (1971); T. KAMETANI and T. SUZUKI. J. Org. Chem. **37**, 1291 (1972).
20. N. N. SUVOROV, I. A. ORLOVA, and K. F. TURCHIN. Khim. Geterosikl. Soedin. 250 (1969); Chem. Abstr. **71**, 21964*y* (1969); E. E. SCHWEIZER and K. K. LIGHT. J. Org. Chem. **31**, 870 (1966); M. VON STRANDTMANN, M. P. COHEN, C. PUCHALSKI, and J. SHAVEL, JR. J. Org. Chem. **33**, 4306 (1968); S. HÜNIG and H.-C. STEINMETZER. Tetrahedron Lett. 643 (1972); F. E. ZIEGLER, E. B. SPITZNER, and C. K. WILKINS. J. Org. Chem. **36**, 1759 (1971); H. PLIENINGER, C. WAGNER, and H. IMMEL. Ann. **743**, 95 (1971); For a failure, see F. A. CAREY and J. R. NEERGAARD. J. Org. Chem. **36**, 2731 (1971).
21. W. SCHINDLER. Helv. Chim. Acta, **40**, 2156 (1967).
22. For reviews see, (*a*) A. W. JOHNSON. Ylide chemistry. Academic Press, New York. 1966. p. 132 ff.; (*b*) A. MAERCKER. Org. React. **14**, 270 (1965).
23. S. TRIPPETT and D. M. WALKER. J. Chem. Soc. 2130 (1961).
24. M. GRAYSON and P. T. KEOUGH. J. Am. Chem. Soc. **82**, 3919 (1960); see also ref. 22*a*, pp. 88–92.
25. M. SCHLOSSER. Topics Stereochem. **5**, 1 (1970).
26. L. J. DOLBY and D. L. BOOTH. J. Org. Chem. **30**, 1550 (1965); K. M. BISWAS and A. H. JACKSON. Tetrahedron, **24**, 1145 (1968).
27. A. W. HERRIOTT. Tetrahedron Lett. 2547 (1971).
28. A. W. JOHNSON and R. B. LACOUNT. Tetrahedron, **9**, 130 (1960).

Can. J. Chem. Downloaded from www.nrcresearchpress.com by 210.87.254.40 on 09/05/12
For personal use only.

29. J. R. CORFIELD, N. J. DE'ATH, and S. TRIPPETT. J. Chem. Soc. C, 1930 (1971) and refs. therein.
30. J. D. HOBSON and J. G. MCCLUSKEY, J. Chem. Soc. C, 2015 (1967).
31. T. B. WINDHOLZ and D. B. R. JOHNSTON. Tetrahedron Lett. 2555 (1967).
32. H. OEDINGER, H.-J. KNABE, F. MOLLER, and K. EITER. Ber. **99**, 2012 (1966).
33. L. M. JACKMAN and S. STERNHELL. Nuclear magnetic resonance spectroscopy in organic chemistry. 2nd ed. Pergamon Press, Oxford. 1969. p. 382.
34. K. NAKANISHI. Infrared absorption spectroscopy. Holden-Day, Inc., San Francisco. 1962. p. 32.
35. Reference 33, p. 224.
36. H. H. JAFFE and M. ORCHIN. Theory and applications of ultraviolet spectroscopy. John Wiley and Sons, Inc., New York. 1962. p. 430.
37. R. F. HUDSON. Chem. Brit. **7**, 287 (1971).
38. J. L. R. WILLIAMS, R. E. ADEL, J. M. CARLSON, G. A. REYNOLDS, D. G. BORDEN, and J. A. FORD, JR. J. Org. Chem. **28**, 387 (1963).
39. M. E. JONES and S. TRIPPETT. J. Chem. Soc. C, 1090 (1966).
40. S. TRIPPETT. Pure Appl. Chem. **9**, 255 (1964).
41. K. SCHOFIELD. Hetero-aromatic nitrogen compounds. Butterworths, London. 1967. p. 311.
42. H. O. HOUSE. Modern synthetic reactions. 2nd ed. W. A. Benjamin, Inc., Menlo Park, California. 1972. p. 690.
43. R. J. SUNDBERG and F. O. HOLCOMBE, JR. J. Org. Chem. **34**, 3273 (1969).
44. Reference 2, p. 163.
45. D. REDMORE. Chem. Rev. **71**, 315 (1971).
46. L. HORNER, H. HOFFMANN, H. G. WIPPEL, and G. KLAHRE. Ber. **92**, 2499 (1959).
47. H. H. SISLER and N. L. SMITH. J. Org. Chem. **26**, 611 (1961).
48. A. J. KIRBY and S. G. WARREN. The organic chemistry of phosphorus. Reaction mechanisms in organic chemistry. Vol. 5. Elsevier Publ. Co., Amsterdam. 1967. p. 260.
49. F. E. ZIEGLER and P. A. ZORETIC. Tetrahedron Lett. 2639 (1968).
50. I. HEILBRON. Dictionary of organic compounds. Oxford University Press, New York. 1965.
51. S. M. MCELVAIN and R. E. MCMAHON. J. Am. Chem. Soc. **71**, 901 (1949).
52. A. ZIERING, A. MOTCHANE, and J. LEE. J. Org. Chem. **22**, 1521 (1957).
53. S. MOROSAWA. Bull. Chem. Soc. Jap. **33**, 1108, 1113 (1960).
54. K. LENARD and J. BORSY. Acta Chim. Acad. Sci. Hung. **34**, 439 (1962); Chem. Abstr. **59**, 542*b* (1963).
55. H. HELLMAN and O. SCHUMACHER. Ann. **640**, 79 (1961).
56. W. C. DAVIS and F. G. MANN. J. Chem. Soc. 276 (1964).
57. J. MEISENHEIMER, J. CASPER, M. HORING, W. LAUTER, L. LICHTENSTADT, and W. SAMUEL. Ann. **449**, 213 (1926).
58. E. WENKERT, K. G. DAVE, C. T. GNEWUCH, and P. W. SPRAGUE. J. Am. Chem. Soc. **90**, 5251 (1968).
59. R. G. HARVEY, T. C. MYERS, H. I. JACOBSON, and E. V. JENSEN. J. Am. Chem. Soc. **79**, 2612 (1957).
60. A. I. RAZUMOV and P. A. GUREVICH. Zhur. Obshch. Khim. **37**, 1615 (1967).

Can. J. Chem. Downloaded from www.nrcresearchpress.com by 210.87.254.40 on 09/05/12
For personal use only.

Halogen Ring Monosubstituted Benzoic Acid Hydrazides as Ligands. II.[1] Ultraviolet Spectra and pK Determination

GEORGE MANOUSSAKIS, DEMETRIUS HARISTOS, AND CATHERINE YOURI
Laboratory of Inorganic Chemistry, University of Thessaloniki, Thessaloniki, Greece

Received September 14, 1972

The u.v. spectra of 12 halogen-substituted benzoic acid hydrazides are reported. A very intense band in the region 225–260 mμ and a second one of low intensity at 270–290 mμ are assigned to $\pi \rightarrow \pi^*$ and $n \rightarrow \pi^*$ transitions, respectively.

The pK_1 and pK_2 of the mentioned hydrazides, corresponding to the Brönsted acids $XC_6H_4C(O)\overset{+}{N}H\overset{+}{N}H_3$ and $XC_6H_4C(OH)=NNH_2$ respectively, were obtained spectrophotometrically (X = F, Cl, Br, or I in *o*-, *m*-, and *p*-position). The influence of the nature and the position of the halogen atom on the pK values is discussed.

Les spectres u.v. de 12 hydrazides d'acides benzoïques substitués par des halogènes sont rapportés. Une bande très intense dans la région de 225–260 mμ et une autre de faible intensité à 270–290 mμ ont été assignées respectivement aux transitions $\pi \rightarrow \pi^*$ et $n \rightarrow \pi^*$.

Les pK_1 et pK_2 des hydrazides mentionnés, correspondant respectivement aux acides de Brönsted $XC_6H_4C(O)\overset{+}{N}H\overset{+}{N}H_3$ et $XC_6H_4C(OH)=NNH_2$ ont été obtenus spectrophotométriquement (X = F, Cl, Br, ou I en position *o*-, *m*-, ou *p*-). L'influence de la nature et de la position des atomes d'halogène sur les valeurs de pK est discutée. [Traduit par le journal]

Can. J. Chem., 51, 811 (1973)

Introduction

The present paper deals with the effect of substitution on the proton dissociation constants of halogen-substituted benzoic acid hydrazides (HBAH) and with their chelate-forming tendency. This investigation was undertaken because of our interest in the equilibria between these hydrazides and several metal ions in solution.

As far as we know, very limited attempts have been made to study spectrophotometrically and to elucidate the stabilities of halogen-substituted benzoic acid hydrazides. A notable work on this subject was that of Titov *et al.* (2, 3) who determined the pK of several ring-substituted hydrazides, including the *m*- and *p*-chloro-derivatives.

Results and Discussion

At lower pH values, the u.v. spectra of the studied hydrazides show two characteristic bands: a low intensity band at 270–290 mμ which is possibly due to an $n \rightarrow \pi^*$ transition, and a second one in the region 225–260 mμ that is possibly due to a $\pi \rightarrow \pi^*$ transition. The intensities of both these bands depend on pH values, as is shown in the representative spectra (Fig. 1). The intensity of the second band ($\pi \rightarrow \pi^*$) decreases markedly with an increase in pH while at the same time, the intensity of the first band ($n \rightarrow \pi^*$) increases, resulting in the appearance of two isosbestic points.

The presence of two isosbestic points is an indication that the equilibrium in question involves three absorbing species. This is more obvious from the diagram of Fig. 2, which shows the correlation between optical density (D) and pH values at 250 mμ, for the *o*-Cl derivative. In the analogous curves for the other 11 hydrazides, the inflection points are at almost the same place. The first section (A) of the curve in Fig. 2 corresponds to the equilibrium between the Brönsted acid $XC_6H_4C(O)\overset{+}{N}H\overset{+}{N}H_3$, designated LH^+, and the neutral form, $XC_6H_4C(O)NHNH_2$ (LH); the horizontal section (B) corresponds only to the neutral form; and the third section, at p$H > 10$, corresponds to equilibrium between the enolic $XC_6H_4C(\bar{O})=NNH_2$ (L^-) and neutral forms.

The wavelengths and molecular absorption coefficients of $\pi \rightarrow \pi^*$ bands of species LH and LH_2^+ of *p*-derivatives are tabulated in Table 1. *p*-Derivatives are specially selected, because their λ_{max} of $\pi \rightarrow \pi^*$ bands are in the accessible part of the spectrum (4). The $\pi \rightarrow \pi^*$ bands show considerable shifting to higher wavelengths and increase in ε_{max} from fluoro- to iodo-derivatives.

[1]For part I, see ref. 1.

Can. J. Chem. Downloaded from www.nrcresearchpress.com by 210.87.254.40 on 09/05/12
For personal use only.

Can. J. Chem. Downloaded from www.nrcresearchpress.com by 210.87.254.40 on 09/05/12
For personal use only.

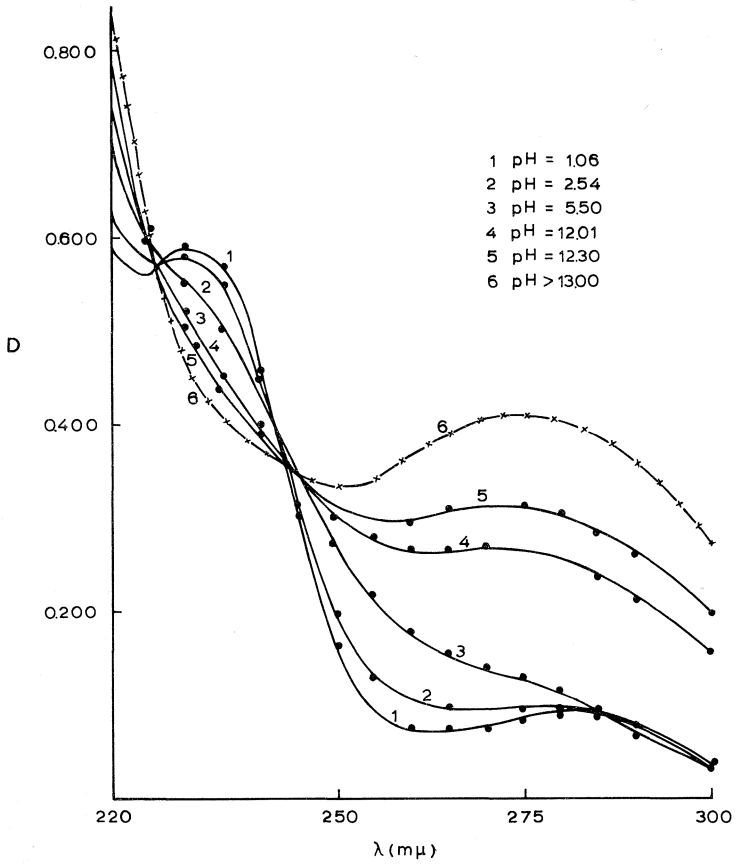

FIG. 1. Absorption spectra of *m*-Cl benzoic acid hydrazide in different p*H* values. Curve 6 is calculated.

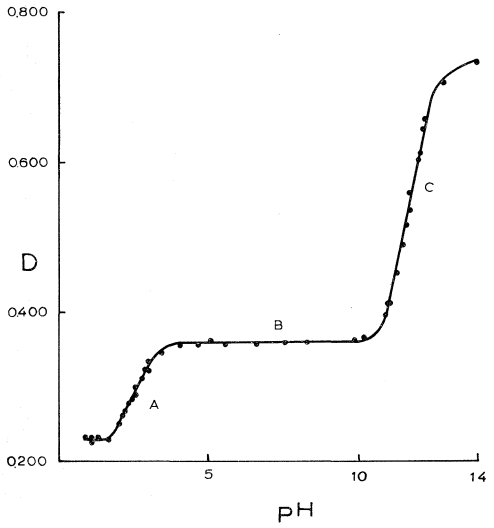

FIG. 2. Correlation between optical density and p*H* values at 250 mμ of *o*-Cl derivative.

TABLE 1. The λ_{max} and ε_{max} values of free benzoic acid hydrazide and HBAH in *p*-position

	LH		LH^{2+}	
Hydrazides	λ_{max} (mμ)	ε_{max}	λ_{max} (mμ)	ε_{max}
Free	226	8714	230	9620
p-F	229	8950	233	10150
p-Cl	237	13150	241	14700
p-Br	242	14050	247	15375
p-I	252	15025	257	14560

These variations are attributed mainly to the inductive effect ($-I$) and resonance effect ($+R$), which are introduced by the halogen substituent. These effects influence the polarity of the C—O bond; the first of them ($-I$) decreases the polarity and the second one ($+R$) increases it.

The increasing of ε_{max} values from fluoro- to iodo-derivatives (Table 1), could be explained by

TABLE 2. The optical densities of species LH_2^+, LH and L^- and pK values of HBAH at 25 °C

Hydrazides	$D_{LH_2^+}$ pH < 1.8	D_{LH} p$H \simeq$ 5–10	D_{L^-}* pH > 13	λ_{anal}	Calculated pK at 25 °C† pK_1	pK_2
$C_6H_5CONHNH_2$	0.215	0.528	—	260	3.05 ± 0.02 3.05 ± 0.03 (3) 3.03 ± 0.01 (6)	
	—	0.261	1.171	275		12.56 ± 0.04 12.52 ± 0.03 (2) 12.45 ± 0.03 (6)
o-$FC_6H_4CONHNH_2$	0.212	0.531	0.875	255	2.85 ± 0.02	12.04 ± 0.05
m-$FC_6H_4CONHNH_2$	0.604	0.500	0.381	230	2.92 ± 0.03	12.16 ± 0.05
p-$FC_6H_4CONHNH_2$	0.401	0 337	0.240	235	3.03 ± 0.03	12.35 ± 0.04
o-$ClC_6H_4CONHNH_2$	0.230	0.358	0.736	250	2.56 ± 0.03	11.79 ± 0.03
m-$ClC_6H_4CONHNH_2$	0.569	0.504	0.404	235	2.76 ± 0.04 2.89 ± 0.03 (3)	11.98 ± 0.04 11.95 ± 0.03 (2)
p-$ClC_6H_4CONHNH_2$	0.570	0.458	0.211	245	2.98 ± 0.03 3.02 ± 0.03 (3)	12.15 ± 0.04 12.09 ± 0.03 (2)
o-$BrC_6H_4CONHNH_2$	0.222	0.304	0.568	248	2.71 ± 0.04	11.90 ± 0.02
m-$BrC_6H_4CONHNH_2$	0.524	0.484	0.339	236	2.85 ± 0.04	12.03 ± 0.04
p-$BrC_6H_4CONHNH_2$	0.538	0.432	0.244	252	3.00 ± 0.03	12.15 ± 0.05
o-$IC_6H_4CONHNH_2$	0.252	0.292	0.562	260	2.81 ± 0.03	11.96 ± 0.03
m-$IC_6H_4CONHNH_2$	0.224 —	0.423 0.206	— 0.761	258 275	2.90 ± 0.04	12.05 ± 0.04
p-$IC_6H_4CONHNH_2$	0.356 —	0.478 0.570	— 0.341	242 255	3.00 ± 0.03	12.16 ± 0.03

*The optical density of species L^- is calculated.
†Numbers in parentheses are references.

assuming that the chromophore action of HBAH is due to the following resonance form:

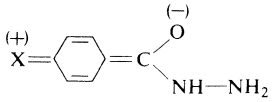

The value of ε_{max} will depend on the contribution of this form, which is favored by the polarization of the halogen atom and the strength of +R effect. The resonance effect varies according to series F < Br < Cl < I.

The values of λ_{max} and the corresponding ε values change slightly in going from neutral (LH) to ionic form (LH_2^+) of hydrazides (Table 1). This change is also attributed to the increased polarity of the C—O bond, which is affected as well by the form of the hydrazino group. The ionic form, $-NHNH_3^+$, makes the C—O bond more polar. The unique exception is the iodo-derivatives. This exception is possibly due to the greater tendency of the iodo-derivatives to form stronger intramolecular hydrogen bonding of the type,

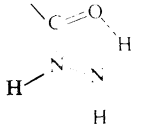

because of the more pronounced resonance effect (+R). The increased tendency of the *p*-I derivatives to form strong intramolecular coupling of this type is obvious from the similarity of their i.r. spectra in the region of the amide I band, to those of the *o*-derivatives which also have a tendency to undergo intramolecular coupling (1).

The stability constants for the proton–ligand complexes have been determined spectrophotometrically (5). The method consists in determining the relative proportion of ions to molecules when a hydrazide is dissolved in a series of solutions of accurately known pH values. This has been done at the analytical wavelength, λ_{anal}, at which the greatest difference in optical densities between ion and molecule has been observed. For this purpose, the optical density of hydrazide solutions has been measured over the whole spectrum in a large range of pH values. Table 2 contains (*a*) the optical densities of the species LH_2^+, LH, and L^- at the corresponding region of the pH values, (*b*) the calculated pK values, and (*c*) the analytical wavelength used in each case. Since D_{L^-} values are not directly obtainable, they are calculated indirectly using a graphical method. The pK_1 and pK_2 values, in Table 2, which correspond to Brönsted acids $XC_6H_4C(O)NHNH_3^+$

Can. J. Chem. Downloaded from www.nrcresearchpress.com by 210.87.254.40 on 09/05/12
For personal use only.

and $XC_6H_4C(OH)=NNH_2$ respectively, were calculated from eqs. 1 and 2, where D_L is the observed optical density of species L^-, D_M that of a mixture of L^- and LH, and D_{LH} of LH respectively at the analytical wavelength in the proper region of pH.

$$[1] \qquad pK_1 = pH + \log \frac{D_{LH} - D_M}{D_M - D_{LH_2^+}}$$

$$[2] \qquad pK_2 = pH + \log \frac{D_{L^-} - D_M}{D_M - D_{LH}}$$

The obtained values agree well with those in the literature (2, 3, 6) for the non-substituted benzoic acid hydrazide thus confirming the reliability of the method used. Also in the cases of *m*- and *p*-chloro-derivatives, some data were available in the literature, but since these values were required as the basis of the present investigation, they were freshly collected under the conditions of this study. For these compounds our values, when converted into approximate thermodynamic constants, agree well with the values reported by Titov *et al.* (2, 3).

As it is shown from the calculated pK values (Table 2), *o*-derivatives are stronger acids than meta, and meta are stronger than *p*-derivatives. Such a change will be expected if we take into consideration that the strength of $-I$ inductive effect varies according to the series *o*-, *m*-, *p*-; this means a stronger withdrawal of electron charge by the substituent, according to the above-mentioned series.

The pK values of fluoro derivatives are higher than those of the corresponding chloro, bromo, and iodo compounds. This unusual phenomenon may be due to the possibility that fluoro-derivatives form stronger intra- or intermolecular hydrogen bonds.

Experimental

Preparation of Hydrazides

The hydrazides were prepared by the same method as described in an earlier communication (1).

Physical Measurements

A Zeiss PMQ II u.v. spectrophotometer was used. The pH values were measured by a Beckman pH meter (glass–calomel electrode). The ionic strength was 0.01 M with KCl.

1. G. E. Manoussakis, D. A. Haristos, and C. E. Youri. Chim. Chronika. **1** (3), 182 (1972).
2. E. V. Titov, N. G. Korzhenevskaya, and V. I. Rybachenko. Ukr. Khim. Zh. 34(12), 1253 (1968).
3. E. V. Titov, L. M. Kapkan, V. I. Rybachenko, and N. G. Korzhenevskaya. Reakts. Sposobnost. Org. Soedin, **5**, 673 (1968).
4. P. Grammaticakis. Bull. Soc. Chim. Fr. 933 (1970).
5. A. Albert and E. P. Serjeant. The determination of ionization constants. Chapman and Hall Ltd., London. 1971. pp. 45, 52.
6. A. Albert. Nature, **177**, 525 (1956).

Can. J. Chem. Downloaded from www.nrcresearchpress.com by 210.87.254.40 on 09/05/12
For personal use only.

Canadian Journal of Chemistry

Published by
THE NATIONAL RESEARCH COUNCIL OF CANADA

Journal canadien de chimie

Publié par
LE CONSEIL NATIONAL DE RECHERCHES DU CANADA

Volume 51 Number 6 March 15, 1973

Volume 51 numéro 6 15 mars 1973

Can. J. Chem. Downloaded from www.nrcresearchpress.com by 210.87.254.6 on 09/05/12
For personal use only.

Electrochemical Studies of Organotitanium Nitrogen Fixation Systems

T. CHIVERS AND E. D. IBRAHIM

Department of Chemistry, The University of Calgary, Calgary 44, Alberta

Received August 28, 1972

The electrochemical reduction of compounds of the type $(\pi\text{-Cp})_2\text{Ti(R)Cl}$ (R = Cl, CH_3, C_6H_5, C_5F_5, $OTiCl(\pi\text{-Cp})_2$) in ether solvents has been studied using the techniques of polarography, controlled potential electrolysis, and cyclic voltammetry. The one-electron reduction products, presumably $(\pi\text{-Cp})_2\text{TiR}$ (R = CH_3, C_6F_5), are initially green in tetrahydrofuran but, in a dinitrogen or argon atmosphere, they form intensely blue solutions which result from the reaction of $(\pi\text{-Cp})_2\text{TiR}$ with tetrahydrofuran solvent.

La réduction électrochimique des composés du type $(\pi\text{-Cp})_2\text{Ti(R)Cl}$ (R = Cl, CH_3, C_6H_5, C_6F_5, $OTiCl(\pi\text{-Cp})_2$) dans des solvants éthérés a été étudiée en utilisant les techniques de la polarographie, de l'électrolyse à potentiel contrôlé et de la voltamétrie cyclique. Les produits des réductions n'impliquant qu'un seul électron, probablement $(\pi\text{-Cp})_2\text{TiR}$ (R = CH_3, C_6F_5) sont initialement verts dans le tétrahydrofuranne mais, sous un atmosphère d'azote (N_2) ou d'argon, ceux-ci forment des solutions bleues très intenses qui sont les résultat de la réaction entre le produit $(\pi\text{-Cp})_2\text{TiR}$ et le solvant tétrahydrofuranne.
[Traduit par le journal]

Can J. Chem., **51**, 815 (1973)

Introduction

A number of systems which involve bis(π-cyclopentadienyl)titanium dichloride, $(\pi\text{-Cp})_2\text{TiCl}_2$, in the presence of an excess of a reducing agent are active in nitrogen fixation (1–11). The identity of the reduced titanium species responsible for nitrogen fixation has not been definitely established, however, although numerous suggestions have been made (Table 1). Brintzinger and co-workers (12, 13) have provided supporting evidence for the role of titanocene monomer in the coordination step, originally suggested by van Tamelen and co-workers (5–8), by isolation of the intensely blue complex $[(\pi\text{-Cp})_2\text{Ti}]_2\text{N}_2$ stable at room temperature. It is not certain, however, that the identity or even the oxidation state of the active titanium intermediate is the same for all the reducing systems described in Table 1. Indeed an intensely blue complex formed between dinitrogen and $(\pi\text{-Cp})_2\text{Ti}^{III}\text{Ph}$ of composition $[(\pi\text{-Cp})_2\text{TiPhN}]_n$ has been isolated, but is unstable above 0° (14).

The use of electrochemical techniques, whereby the extent of reduction of Ti(IV) can be controlled precisely, to study the reduction of $(\pi\text{-Cp})_2\text{TiCl}_2$ in the presence and absence of dinitrogen has been recognized (13, 15). Dessy and co-workers observed the formation of a deep blue species in the controlled potential reduction of $(\pi\text{-Cp})_2\text{TiCl}_2$ in dimethoxyethane after uptake of 2 electrons and attributed it to monomeric $(\pi\text{-Cp})_2\text{Ti}$ (16). More recently, Doisneau and Marchon (15) reported that the blue color appears under an atmosphere of dinitrogen, but not under helium, suggesting that the blue dinitrogen complex $[(\pi\text{-Cp})_2\text{Ti}]_2\text{N}_2$ might be generated in these electrolytic reductions. However, Brintzinger and co-workers have challenged this conclusion since they find that blue solutions are obtained under argon as well

TABLE 1. Nitrogen fixation systems based on $(\pi\text{-Cp})_2TiCl_2$

Reducing agent	Active species	Oxidation state of titanium	Reference
EtMgBr	$(C_5H_6)_2Ti$	0	2
Li, Na, K, Rb, Cs	Complex of Ti^0	0	3
Mg, Ca, La, Ce Pr^iMgCl	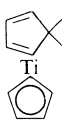	+1	4
Li^+Np^-	$(\pi\text{-Cp})_2Ti$	+2	5
Mg	$(\pi\text{-Cp})_2Ti$	+2	6
Na sand	$[(\pi\text{-Cp})_2Ti]_{1-2}$ "Active titanocene"	+2	8
Li^+Np^- or Na^+Np^-	$[(\pi\text{-Cp})_2TiH_2Ti(\pi\text{-Cp})_2]^-$	+2,+3	9
EtMgCl, EtLi, Pr^iMgCl or Pr^iLi	$[(\pi\text{-Cp})_2TiH_2]^-$	+3	10
PhLi	$(\pi\text{-Cp})_2TiPh$	+3	11

as in a dinitrogen atmosphere. They suggest the formation of the blue species is due to reaction of monomeric $(\pi\text{-Cp})_2Ti$ with either solvent or supporting electrolyte.

We have studied the electrochemical reduction of compounds of the type $(\pi\text{-Cp})_2Ti(R)Cl$ (R = Cl, CH_3, C_6H_5, C_6F_5, $OTiCl(\pi\text{-Cp})_2$) in ether solvents in order to determine the role of their one-electron reduction products $(\pi\text{-Cp})_2TiR$ in the coordination of dinitrogen. When this work was begun compounds of the type $(\pi\text{-Cp})_2TiR$ were unknown although $(\pi\text{-Cp})_2TiPh$ had been proposed as an intermediate in the $(\pi\text{-Cp})_2TiCl_2$/PhLi nitrogen fixation system (11) and in the thermal decompsition of $(\pi\text{-Cp})_2TiPh_2$ in hydrocarbon solvents (17) or in the presence of diphenylacetylene (18). $(\pi\text{-Cp})_2TiMe$ was presumed to be stable at room temperature from the persistence of its e.s.r. spectrum (10). During the course of this work brief reference has been made to the preparation of some $(\pi\text{-Cp})_2TiR$ derivatives (R = $\sigma\text{-}C_5H_5$, C_6F_5, $\sigma\text{-}CH_2C_6H_5$, $o\text{-}C_6H_4CH_2NMe_2$) (19). Previous electrochemical studies of organotitanium compounds in aprotic solvents have included the dihalides $(\pi\text{-Cp})_2TiX_2$ (X = F, Cl, Br, I) (24) and some $(\pi\text{-Cp})_2TiR_2$ derivatives (R = CH_3, C_6H_5, and $-CH_2-CH-CH)$ (25).

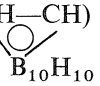

Experimental

Apparatus

Polarography

Polarographic measurements were carried out using a Metrohm Polarecord E261R in conjunction with an *iR* compensator E446. The dropping mercury electrode (d.m.e.) had the following characteristics: $m = 4.58$ mg/s and $t = 1.96$ s with open circuit and $h = 63.5$ cm. A saturated aqueous calomel electrode (s.c.e.) was used as a reference electrode. An agar salt bridge connected to a tube containing $(n\text{-Bu})_4NClO_4$ (10^{-1} *M*) in dimethoxyethane and a fine porosity frit was used to separate the s.c.e. from the solution under investigation. A two compartment cell in which the electrodes were separated by a 25 mm medium porosity frit was used and the auxiliary electrode was a platinum wire. Polarograms were recorded for solutions in both tetrahydrofuran and dimethoxyethane. Solutions were *ca.* 10^{-3} *M* in electroactive substance for polarography and 10^{-1} *M* in supporting electrolyte $(n\text{-Bu})_4NClO_4$ for all electrochemical work. These solutions were degassed for 15 min (N_2) or 40 min (Ar) and polarographic measurements were made at 25°.

Controlled Potential Electrolysis

Microcoulometric measurements were carried out in the same cell using a Heath Malmstadt-Enke EUW-401 polarography system in conjunction with a EUW-19A operational amplifier. The recorder of the Metrohm Polarecord was used for current–time curves, and *n* values were determined by measuring the area under these curves. The working electrode was a mercury pool, and electrical contact was made via a platinum wire pinch-sealed into glass. Stirring was achieved by bubbling inert gas into the solutions during electrolysis. Solutions were *ca.* 10^{-6} *M* in electroactive substance for microcoulometric measurements and the initial current was *ca.* 0.7–0.8 mA. Solutions were *ca.* 2×10^{-3} *M* for the formation of the blue species.

Cyclic Voltammetry

Cyclic potential sweeps were generated by a Hewlett–Packard 3300A function generator with trigger/phase lock plugin 3302A. The working electrode was a hanging mercury drop which could be adjusted by means of a micrometer screw. Read out devices were a Hewlett-Packard 7034A X–Y recorder (slow sweeps) and a Tektronix storage oscilloscope equipped with a Polaroid camera C12 (fast sweeps). Solutions were *ca.* 10^{-4} *M* in electroactive substance.

Can. J. Chem. Downloaded from www.nrcresearchpress.com by 210.87.254.6 on 09/05/12
For personal use only.

Can. J. Chem. Downloaded from www.nrcresearchpress.com by 210.87.254.6 on 09/05/12
For personal use only.

Materials

Argon and dinitrogen (prepurified 99.997% min.) were passed through a 30 cm column of freshly activated Ridox reagent (Fisher Scientific Co.) and a 30 cm column of phosphorus pentoxide and were then presaturated with ether solvent before passing into the solutions under electrochemical investigation. Ether solvents were predried (Na) and then freshly distilled from $LiAlH_4$ under argon before use. It was particularly important to ensure that dimethoxyethane was free of peroxide. Tetra-*n*-butylammonium perchlorate, prepared from tetra-*n*-butylammonium hydroxide and perchloric acid, was recrystallized from ethanol/water and dried overnight at 110°/0.01 mm in an Aberhalden pistol.

$(\pi\text{-Cp})_2TiCl_2$ was supplied by Strem Chemicals Inc. and was recrystallized from toluene before use. $(\pi\text{-Cp})_2Ti(C_6F_5)Cl$ was prepared from pentafluorophenyl-lithium and $(\pi\text{-Cp})_2TiCl_2$ (20) and after recrystallization from benzene/hexane had m.p. 201–203° (lit. m.p. 201–203° (20); 187–188° (21)).

Anal. Calcd. for $C_{16}H_{10}ClF_5Ti$: C, 50.5; H, 2.7. Found C, 49.9; H, 3.3.

$(\pi\text{-Cp})_2Ti(Cl)O(Cl)Ti(\pi\text{-Cp})_2$ was prepared by air oxidation of the green solution formed by reducing $(\pi\text{-Cp})_2TiCl_2$ with zinc dust in acetone and had m.p. 226–230° after recrystallization from acetone (lit. m.p. 230° dec. (22)).

Anal. Calcd. for $C_{20}H_{20}Ti_2Cl_2O$: C, 54.2; H, 4.6. Found: C, 54.2; H, 4.9.

$(\pi\text{-Cp})_2Ti(Me)Cl$ was prepared from $(\pi\text{-Cp})_2TiCl_2$ and methylmagnesium chloride in dry methylene chloride at −30° and recrystallized from hexane/toluene to give orange-yellow crystals of $(\pi\text{-Cp})_2Ti(CH_3)Cl$ which had an infrared spectrum identical to that reported in the literature (23). The ^1H n.m.r. spectrum in $CDCl_3$ showed two peaks at 3.72τ (π-C_5H_5) and 9.19τ (CH_3) with relative intensities 29:9.5 (lit. 3.66τ (π-C_5H_5); 9.28τ (CH_3) (23)). $(\pi\text{-Cp})_2Ti(C_6H_5)Cl$ was prepared according to the literature (23) but was not sufficiently stable as a dilute solution in dimethoxyethane for detailed electrochemical studies.

Spectroscopic Measurements

Solutions for spectroscopic investigations were removed from the electrochemical cell under vacuum and then transferred to a Vacuum Atmospheres dry-box. The following instruments were used: ^1H n.m.r. spectra (Varian A60), infrared spectra (Perkin–Elmer 337, and 621), ultraviolet/visible spectra Beckman DB-G. Analyses were carried out in this department by Mrs. S. Swaddle and by Alfred Bernhardt, W. Germany.

Results and Discussion

The data for the polarographic and controlled potential reduction of $(\pi\text{-Cp})_2Ti(R)Cl$ (R = CH_3, C_6H_5, C_6F_5, Cl, $OTiCl(\pi\text{-Cp})_2$) derivatives are summarized in Table 2.

$(\pi$-Cp$)_2$Ti(CH$_3$)Cl (1)

The polarogram of **1** shows one anodic and three cathodic waves. The anodic wave and first cathodic wave have very small diffusion currents which increase in intensity if the solution is stirred with mercury before imposition of potential indicating that these waves result from a reaction of **1** with mercury, as previously observed by Gubin and Smirnova (24) in their electrochemical studies of bis(π-cyclopentadienyl)titanium dihalides. The limiting currents of these two waves are independent of concentration and $\sqrt{h}$, suggesting kinetic behavior. The second cathodic wave shows absorption behavior up to a mercury height of 45 cm followed by a linear dependence on $\sqrt{h}$. A graph of potential against log $i/(i_d - i)$ for this wave had a slope of −0.096 V indicative of an irreversible electrode process, as expected for cleavage of a Ti—Cl bond. Controlled potential electrolysis on the plateau of the first wave (−1.80 V) gave an n value of 1.1, suggesting that this wave involves a one-electron reduction. The third cathodic wave at −2.32 V is very irreversible and c.p.e. on the plateau of this wave gave an n value of 2.2.[1] Since the limiting currents for the second and third cathodic waves are 4.0 and 0.5 μA, respectively, the following mechanism is postulated to explain the coulometric results,

TABLE 2. Polarographic and microcoulometric data for the reduction of $(\pi\text{-Cp})_2Ti(IV)$ derivatives in dimethoxyethane, 0.1 *M* Bu_4NClO_4

Compound	$-E_{1/2}$ (V)*	i_d (μA)	n†
(1) $(\pi\text{-Cp})_2Ti(CH_3)Cl$	−0.12	0.5	
	0.72	0.45	
	1.26	4.0	1.1
	2.32	0.5	2.2
(2) $(\pi\text{-Cp})_2Ti(C_6F_5)Cl$	0.84	4.8	1.1
	2.55	~14.4	
(3) $(\pi\text{-Cp})_2Ti(C_6H_5)Cl$	0.33	0.4	
	0.97	3.3	‡
	2.64	1.2	
(4) $(\pi\text{-Cp})_2TiCl_2$	0.19	0.1	
	0.80	3.2	0.8§
	2.04	1.9	1.85§
(5) $[(\pi\text{-Cp})_2TiCl]_2O$	0.06	0.30	
	0.17	0.56	
	1.19	5.20	2.0
	2.38	1.35	

**Versus* saturated calomel electrode. $E_{1/2}$ values were independent of the degassing agent (N_2 or Ar).
†Values determined by microcoulometry.
‡Insufficiently stable at these concentrations for microcoulometric studies.
§Reference 16.

[1]Gubin and Smirnova (24) reported only two waves for the polarographic reduction of **1** in dimethylformamide; an anodic wave at 0.14 V and a poorly defined cathodic wave at −1.17 V (*vs.* s.c.e.).

Can. J. Chem. Downloaded from www.nrcresearchpress.com by 210.87.254.6 on 09/05/12
For personal use only.

$$(\pi\text{-Cp})_2\text{Ti(CH}_3\text{)Cl} + e^- \rightarrow (\pi\text{-Cp})_2\text{TiCH}_3 + \text{Cl}^- \quad \text{(wave 2)}$$

$$(\pi\text{-Cp})_2\text{TiCH}_3 + \text{solvent} \xrightarrow{k_c} \text{Y}$$

$$\text{Y} + e^- \rightarrow \text{Z} \quad \text{(wave 3)}$$

where k_c has a value such that the chemical reaction occurs completely on the timescale for coulometry but not on that for polarography. The cyclic voltammogram of a 10^{-3} *M* solution of **1** with cathodic hold is shown in Fig. 1 and confirms the irreversible nature of the polarographic reduction at -1.26 V (peak A). The anodic sweep, however, reveals an oxidative wave (B) which, on reverse cathodic sweep, has associated with it a cathodic wave (C) with $E_{1/2}$ corresponding to the first cathodic polarographic wave. We are thus dealing with the process

$$(\pi\text{-Cp})_2\text{TiCH}_3 \underset{+e^-,\,(C)}{\overset{-e^-,\,(B)}{\rightleftharpoons}} (\pi\text{-Cp})_2\text{TiCH}_3^+$$

During electrochemical reduction (1 h) at -1.8 V, the orange solution of **1** in tetrahydrofuran turns green, consistent with the formation of $(\pi\text{-Cp})_2\text{TiCH}_3$ (26). After completion of the reduction the green solution becomes deep blue ($\frac{1}{2}$ h) either under a dinitrogen *or* an argon atmosphere. The appearance of the blue solution in the electrochemical reduction is not, therefore, due to the formation of a dinitrogen complex of the type $[(\pi\text{-Cp})_2\text{Ti(CH}_3\text{)N}]_n$ (14).

$(\pi$-Cp$)_2$Ti(C_6F_5)Cl (2)

The polarogram of **2** shows two cathodic waves at -0.84 V and -2.55 V. A very small pre-wave at -0.28 V results from the interaction of **1** with mercury before imposition of potential since its limiting current increases if the solution is stirred with mercury as indicated by polarograms recorded at regular time intervals. The first cathodic wave is well-defined and its limiting current is proportional to concentration and $\sqrt{h}$ indicating a diffusion-controlled process. The slope of the curve log $(i/i_d - i)/E$ is -0.120 V suggesting an irreversible reduction, as expected for cleavage of a Ti—Cl bond, and this is confirmed by the cyclic voltammogram which shows similar features to the cyclic voltammogram of **1** (Fig. 2). Controlled potential electrolysis at the first wave (-1.1 V) gives an *n* value of 1.1 suggesting a one-electron reduction. The orange solution of **2** in tetrahydrofuran turns green and then blue during electrochemical reduction (1 h) at the first wave under a dinitrogen *or* an argon atmosphere. As with **1** the appearance of the blue solution is not, therefore, due to the formation of a dinitrogen complex.

$(\pi$-Cp$)_2TiCl_2$ (4)

The polarographic reduction of **4** in dimethoxyethane proceeds via two one-electron steps (16) (Table 2). During the electrolysis of a 2×10^{-3} *M* solution of **4** in tetrahydrofuran (2 h) with *n*-Bu_4NClO_4 as supporting electrolyte at -2.4 V *vs.* s.c.e. (*i.e.* on the plateau of the *second* polarographic wave) we observed the following color changes: orange → yellow → green → blue *either* under a dinitrogen or under an argon atmosphere. These observations are consistent with the results of Brintzinger and co-workers (13) who used dimethoxyethane as solvent. Although monomeric $(\pi\text{-Cp})_2\text{Ti}$ is un-

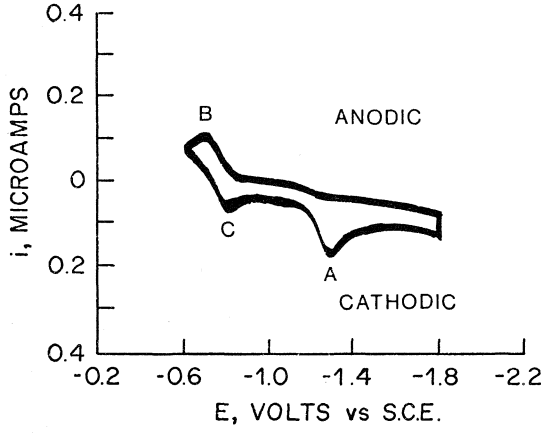

FIG. 1. Cyclic voltammogram of $(\pi\text{-Cp})_2\text{Ti(CH}_3\text{)Cl}$ in dimethoxyethane containing 0.1 *M* *n*-Bu_4NClO_4.

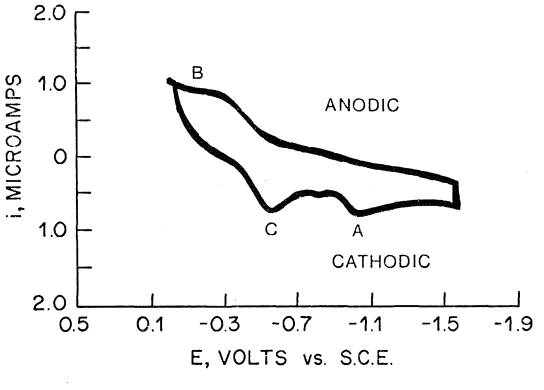

FIG. 2. Cyclic voltammogram of $(\pi\text{-Cp})_2\text{Ti}(C_6F_5)\text{Cl}$ in dimethoxyethane containing 0.1 *M* *n*-Bu_4NClO_4.

Can. J. Chem. Downloaded from www.nrcresearchpress.com by 210.87.254.6 on 09/05/12
For personal use only.

doubtedly the primary product of electrolysis under these conditions, it is clear that the blue solutions do not result from dinitrogen uptake to give the known complex $[(\pi\text{-Cp})_2\text{Ti}]_2\text{N}_2$ (12, 13).

$[(\pi\text{-Cp})_2TiCl]_2O$ (5)

The polarogram of **5** shows one anodic wave and three cathodic waves.[2] The first two waves are kinetic in nature, their limiting currents being independent of $\sqrt{h}$. The cathodic wave at -0.77 V is diffusion controlled, as indicated by the linear dependence of the limiting current on concentration and $\sqrt{h}$. The slope of the curve $\log (i/i_d - i)/E$ is 0.154 V indicative of an irreversible electrochemical process. The irreversibility was confirmed by cyclic voltammetry. Controlled potential electrolysis (2 h) on the plateau of this wave (-1.45 V) gave an n value of 2, suggesting the following electrochemical reduction

$$(\pi\text{-Cp})_2\text{Ti(Cl)O(Cl)Ti}(\pi\text{-Cp})_2 + 2e^- \rightarrow (\pi\text{-Cp})_2\text{TiOTi}(\pi\text{-Cp})_2 + 2\text{Cl}^- \quad (6)$$

The color of the reduced solution, under dinitrogen, was green and remained green after completion of electrolysis, unlike the solutions containing the one-electron reduction products of **1** and **2**. The third cathodic wave of **5** at -2.38 V was poorly defined and clearly irreversible. Controlled potential electrolysis on the plateau of this wave gave an intensely blue solution consistent with the electrochemical cleavage of a Ti—O bond in **6** to give monomeric $(\pi\text{-Cp})_2\text{Ti}$ and an oxyanion *e.g.* $(\pi\text{-Cp})_2\text{TiO}^-$.

Conclusions

Nature of the Blue Solutions

The green, one-electron reduction products of $(\pi\text{-Cp})_2\text{Ti(R)Cl}$ (R = CH_3, C_6F_5), presumably $(\pi\text{-Cp})_2\text{TiR}$, in tetrahydrofuran turn blue under either a dinitrogen *or* an argon atmosphere. The blue species cannot, therefore, be a dinitrogen complex of the type $[(\pi\text{-Cp})_2\text{Ti(R)N}]_n$ but it may be a secondary product resulting from the interaction of electrochemically generated $(\pi\text{-Cp})_2\text{TiR}$ with either the solvent or the electrolyte. Although the blue solutions formed in the electrolytic reductions are thermally more stable than the blue dinitrogen complex $[(\pi\text{-Cp})_2\text{Ti}(C_6H_5)\text{N}]_n$ (14), they are extremely air-sensitive and it is not a practical proposition to separate the small amount of blue species from the large excess of electrolyte. Consequently we have prepared $(\pi\text{-Cp})_2\text{TiR}$ derivatives (R = CH_3, C_6F_5) by chemical reduction of $(\pi\text{-Cp})_2\text{Ti(R)Cl}$ (26) and we find that *ca.* 10^{-3} *M* solutions of the green $(\pi\text{-Cp})_2\text{TiR}$ compounds in tetrahydrofuran slowly become blue (λ_{max} 580 nm, R = CH_3; λ_{max} 582 nm, R = C_6F_5) either under a dinitrogen atmosphere or *in vacuo*. Furthermore green solutions of $[(\pi\text{-Cp})_2\text{TiCl}]_2$ (*ca.* 10^{-3} *M*) in tetrahydrofuran, but not in benzene, become an intense violet blue color (λ_{max} 575 nm) during the course of one week at room temperature either under dinitrogen or *in vacuo*.[3] Thus the blue solutions must be formed by interaction of $(\pi\text{-Cp})_2\text{Ti}^{III}$ derivatives with solvent tetrahydrofuran or by isomerization induced by the solvent. Removal of solvent from the blue solutions gives thermally stable, air-sensitive blue-black crystalline solids.

The characterization of these solids and the preparation of $(\pi\text{-Cp})_2\text{Ti}^{III}\text{R}$ derivatives by chemical reduction will be the subjects of future publications.

We are grateful to Dr. I. Drummond for help with the cyclic voltammetry experiments and to the National Research Council of Canada for financial support.

1. M. E. Vol'pin and V. B. Shur. Nature (London), **209**, 1236 (1966); Dokl. Akad. Nauk SSSR, **156**, 1102 (1964).
2. R. Maskill and J. M. Pratt. Chem. Commun. 950 (1967).
3. E. Bayer and V. Schurig. Chem. Ber. **102**, 3378 (1969).
4. A. E. Shilov, A. K. Shilova, E. F. Kvashina, and T. A. Vorontsova. Chem. Commun. 1590 (1971).
5. E. E. van Tamelen, D. Seeley, S. Schneller, H. Rudler, and W. Cretney. J. Am. Chem. Soc. **92**, 5251 (1970).
6. E. E. van Tamelen and H. Rudler. J. Am. Chem. Soc. **92**, 5253 (1970).
7. E. E. van Tamelen. Acc. Chem. Res. **3**, 361 (1970).
8. E. E. van Tamelen, W. Cretney, N. Kluentschi, and J. S. Miller. Chem. Commun. 481 (1972).
9. G. Henrici-Olivé and S. Olivé. Angew. Chem. Int. Ed. Engl. **8**, 650 (1969).
10. H. Brintzinger. J. Am. Chem. Soc. **89**, 6871 (1967).

[2]It has previously been reported that the polarographic reduction of **5** (solvent not specified) showed a wave at ~ -0.9 V *vs.* s.c.e. compared to -0.44 V for $(\pi\text{-Cp})_2\text{TiCl}_2$ (22).

[3]$[(\pi\text{-Cp})_2\text{TiCl}]_2$ was prepared by reduction of $(\pi\text{-Cp})_2\text{TiCl}_2$ with aluminum metal. We are grateful to Dr. P. C. Wailes for the unpublished experimental details of this preparation.

11. M. E. VOL'PIN, V. B. SHUR, R. V. KUDRYAVTSEV, and L. A. PRODAYKO. Chem. Commun. 1038 (1968).
12. J. E. BERCAW and H. H. BRINTZINGER. J. Am. Chem. Soc. **93**, 2045 (1971); R. H. MARVICH and H. H. BRINTZINGER. J. Am. Chem. Soc. **93**, 2046 (1971).
13. J. E. BERCAW, R. H. MARVICH, L. G. BELL, and H. H. BRINTZINGER. J. Am. Chem. Soc. **94**, 1219 (1972).
14. J. H. TEUBEN and H. J. DE LIEFDE MAJER. Rec. Trav. Chim. Pays Bas, **90**, 360 (1970).
15. R. G. DOISNEAU and J. C. MARCHON. J. Electroanal. Chem. Interfacial Electrochem. **30**, 487 (1971).
16. R. E. DESSY, R. B. KING, and M. WALDROP. J. Am. Chem. Soc. **88**, 5112 (1966).
17. G. A. RAZUVAEV, V. N. LATYAEVA, L. I. VYSHINSKAYA, and G. A. KILYAKOVA. Zhur. obschchei Khim. **36**, 1491 (1966).
18. H. MASAI, K. SONOGASHIRA, and N. HAGIHARA. Bull. Chem. Soc. Jap. **41**, 750 (1968).
19. H. J. DE LIEFDE MEIJER and F. JELLINEK. Inorg. Chim. Acta, **4**, 651 (1970).
20. M. A. CHAUDHARI, P. M. TREICHEL, and F. G. A. STONE. J. Organometal. Chem. **2**, 206 (1964).
21. M. D. RAUSCH. Inorg. Chem. **3**, 300 (1964).
22. S. A. GIDDINGS. Inorg. Chem. **3**, 684 (1964).
23. J. A. WATERS and G. A. MORTIMER. J. Organometal. Chem. **22**, 417 (1970).
24. S. P. GUBIN and S. A. SMIRNOVA. J. Organometal. Chem. **20**, 229 (1969).
25. S. P. GUBIN and S. A. SMIRNOVA. J. Organometal. Chem. **20**, 241 (1969).
26. T. CHIVERS and E. D. IBRAHIM. Unpublished observations.

Can. J. Chem. Downloaded from www.nrcresearchpress.com by 210.87.254.6 on 09/05/12
For personal use only.

Pressure Effects upon the Rates of Aquation of Halopentaamminechromium(III) Ions: Evidence for an Associative Mechanism

G. GUASTALLA AND T. W. SWADDLE[1]

Department of Chemistry, The University of Calgary, Calgary, Alberta T2N 1N4

Received September 13, 1972

For the replacement of X^- by H_2O in $Cr(NH_3)_5X^{2+}$, ΔV_0^* (the value of the volume of activation ΔV^* at zero pressure) at 25.0° in 0.1 *m* NH_4ClO_4 is −10.8, −10.2, and −9.4 $cm^3\ mol^{-1}$ respectively for $X^- = Cl^-$, Br^-, and I^-, while ΔV, the molar volume of reaction, is −8.4, −7.2 and −6.0 $cm^3\ mol^{-1}$. The pressure-dependence of ΔV^* can be expressed in terms of the number x of water-molecules which are electrostricted as the systems go from ground-state to transition-state; for $X^- = Cl^-$, Br^-, and I^-, $x = 1.9$, 2.0, and 1.7. These data, combined with $\Delta V^* = -5.8\ cm^3\ mol^{-1}$ for the aquo-exchange of $Cr(NH_3)_5OH_2^{3+}$, indicate an associative mechanism for these reactions, as does the contrast with ΔV_0^* data for the formally analogous, but dissociatively-activated, reactions of $Co(NH_3)_5X^{(3-n)+}$.

Dans le remplacement de X^- par H_2O dans $Cr(NH_3)_5X^{2+}$, ΔV_0^* (valeur du volume d'activation ΔV^* à la pression zéro) à 25.0° dans NH_4ClO_4 0.1 *m* est de −10.8, −10.2, et −9.4 $cm^3\ mol^{-1}$ respectivement pour $X^- = Cl^-$, Br^-, et I^-, tandis que ΔV, volume molaire de la réaction, vaut −8.4, −7.2, et −6.0 $cm^3\ mol^{-1}$. L'influence de la pression sur ΔV^* peut être exprimée en fonction du nombre x de molécules d'eau, conditionné électrostatiquement lorsque le système passe de l'état fondamental à l'état de transition; pour $X^- = Cl^-$, Br^-, et I^-, $x = 1.9$, 2.0, et 1.7. Ces données, combinées à $\Delta V^* = -5.8\ cm^3\ mol^{-1}$ pour l'échange à l'eau de $Cr(NH_3)_5OH_2^{3+}$, indiquent un mécanisme associatif pour ces réactions, de même que les données contraires sur ΔV_0^* concernant les analogues formels, mais activés par dissociation, des réactions de $Co(NH_3)_5X^{(3-n)+}$. [Traduit par le journal]

Can. J. Chem., **51**, 821 (1973)

Introduction

We have recently shown (1–5) that the effect of pressure P upon the rates of substitution reactions of transition-metal complexes in aqueous solution can lead to useful mechanistic information if *either* the reaction is suitably simple *or* there is an independent criterion with which the derived parameters (the volume of activation, ΔV^*, and its pressure dependence, if significant) can be compared. Thus, for the ideally simple aquo-exchange reaction of $Co(NH_3)_5OH_2^{3+}$, ΔV^* is $+1.2\ cm^3\ mol^{-1}$ and is pressure-independent within the experimental uncertainty (6), which suggests a dissociative mechanism. This conclusion is reinforced by the observation that for $X^{n-} = SO_4^{2-}$, Cl^-, Br^-, NO_3^-, *and* H_2O in the reaction

[1] $$Co(NH_3)_5X^{(3-n)+} + H_2O \rightarrow Co(NH_3)_5OH_2^{3+} + X^{n-}$$

there is an excellent linear correlation of slope 1.0 between ΔV_0^* ($=\Delta V^*$ at zero pressure) and the molar volume of reaction ΔV, which indicates that the Co—X is completely broken, and the solvation of X^{n-} fully provided for, in the transition state (1–3).

On the other hand, the ΔV^* values for the aquo-exchange reactions of $Cr(H_2O)_6^{3+}$ and $Cr(NH_3)_5OH_2^{3+}$ are respectively −9.3 and $-5.8\ cm^3\ mol^{-1}$ and are apparently pressure-independent (2, 4, 5). It would be very difficult to rationalize these latter data except in terms of an associative interchange (I_a) mechanism (7) in which a water molecule from the second coordination sphere (solvation sheath) of the complex displaces an existing aquo-ligand from the first coordination sphere in a synchronous process on a time scale which is short compared with the time scale of the exchange of water molecules in the second coordination sphere with bulk solvent. In this mechanism, as in the dissociative mechanism proposed for the Co(III) system, only the water-molecules of the relatively incompressible first and second coordination spheres are involved, independently of bulk solvent, so that ΔV^* is not a function of pressure in either case (4, 5). Since it has become common practice to assume *dissociative* activation to be operative in octahedral substitutions in general, we have sought further evidence for an associ-

[1]To whom correspondence should be addressed.

Can. J. Chem. Downloaded from www.nrcresearchpress.com by 210.87.254.42 on 09/05/12
For personal use only.

Can. J. Chem. Downloaded from www.nrcresearchpress.com by 210.87.254.42 on 09/05/12
For personal use only.

ative mechanism at cationic chromium(III) centers through high-pressure kinetic studies analogous to those which were successful with cobalt(III) complexes (1–3).

We have previously presented other evidence (8) favoring an I_a mechanism for substitutions in complexes of the type $Cr(H_2O)_5X^{(3-n)+}$, although Ferraris and King (9) have published data which appear to favor a D mechanism (7), *i.e.*, one in which a $Cr(H_2O)_5^{3+}$ intermediate with a lifetime greater than the relaxation time of the second coordination sphere is formed, for cases in which X^{n-} is a "good leaving group." The apparently contradictory evidence can be reconciled in favor of an associative mechanism for spontaneous $Cr(H_2O)_5X^{(3-n)+}$ substitutions (see below), but in any case these reactions involve uncertainties arising from the apparent activation of the aquo-ligand *trans* to X in the iodo-complex at least (10), as well as difficulties stemming from the incursion of inversely hydrogen-ion-dependent competitive reaction pathways, even in strongly acidic solutions. We have therefore turned our attention to the analogous reactions

$$[2]\quad Cr(NH_3)_5X^{(3-n)+} + H_2O \rightarrow Cr(NH_3)_5OH_2^{3+} + X^{n-}$$

which have the added advantage of being directly comparable with the $Co(NH_3)_5X^{(3-n)+}$ series previously examined (1–3).

Experimental

Materials

$[Cr(NH_3)_5OH_2](NO_3)_3.NH_4NO_3$ was prepared by the standard method (11) and converted to $[Cr(NH_3)_5OH_2](ClO_4)_3$ by precipitation with perchloric acid; the product was recrystallized from water containing $HClO_4$.

Anal. Calcd. for $[Cr(NH_3)_5OH_2](ClO_4)_3$: N, 15.5; H, 3.8. Found: N, 15.5; H, 4.0.

$[Cr(NH_3)_5Cl](ClO_4)_2.2H_2O$ was prepared from the chloride (12, 13).

Anal. Calcd. for $[Cr(NH_3)_5Cl](ClO_4)_2.2H_2O$: N, 17.1; H, 4.4. Found: N, 17.2; H, 4.6.

$[Cr(NH_3)_5Br](ClO_4)_2$ was made from the bromide (11) by precipitation from warm aqueous solution with perchloric acid; it was washed once with ice-cold water, then dried with alcohol and ether.

Anal. Calcd. for $[Cr(NH_3)_5Br](ClO_4)_2$: N, 16.8; H, 3.6. Found: N, 16.5; H, 3.9.

$[Cr(NH_3)_5I]I_2$ was prepared by heating solid $[Cr(NH_3)_5OH_2]I_3$ (made by precipitation with NaI from a solution of the double nitrate) at 120° for 1 h; the product was washed several times with water and dried with alcohol and ether. It could not be converted to the perchlorate salt because of its low solubility and rapid aquation.

The positions and molar absorbancy indices of the maxima in the visible spectra of all the above compounds were in excellent agreement with published values (14). All these compounds were stored in the dark over P_2O_5.

Fisher Certified NH_4ClO_4 was used without further purification.

Kinetic Measurements

These were made *in situ* in a Cary Model 15 spectrophotometer, using the high-pressure optical cell assembly previously described (15). The temperature of the high-pressure cell was maintained at 25.0 ± 0.1° by circulating water from a thermostat bath through the walls of the spectrophotometer sample compartment, thermal contact being made through an aluminum mounting-block, and the temperature was measured with a calibrated Atkins thermistor inserted in a narrow well drilled close to the solution cavity.

The solutions were about 3.0×10^{-3} *m* in chromium(III) complex and 0.1 *m* in NH_4ClO_4. For the chloro- and bromo-complexes, the decrease in optical absorbance was measured continuously as a function of time at 240 and 265 nm respectively over periods of at least 2–3 half-lives of the first-order aquation reaction. The "infinite time" absorbances had to be estimated from measurements on fresh solutions of $[Cr(NH_3)_5OH_2](ClO_4)_3$ and the appropriate halide ion, since some loss of the ammonia ligands was anticipated after several half-lives of the halo-aquation processes. In the case of the iodo-complex, however, the halide replacement was sufficiently rapid to be followed for fully ten half-lives at 360 nm.

Duplicate kinetic experiments conducted using various spectrophotometer slit-widths gave the same rate coefficients (within the experimental uncertainty) as did runs made in ordinary 2 cm quartz cells and runs carried out in the pressure assembly at atmospheric pressure. Thus, neither photo-effects nor interactions with the pressure vessel influenced the reaction rates under our experimental conditions.

Dilatometry

Volume changes accompanying the aquation of the various $Cr(NH_3)_5X^{2+}$ ions were measured at atmospheric pressure and 25.00 ± 0.01°, using a 50.0 ml vessel fitted with an upright capillary outlet tube of 0.0991 mm internal diameter. The procedure resembled that described by Spiro *et al.* (16). Typically, a weighed quantity ($\sim 2 \times 10^{-4}$ mol) of the powdered complex was dissolved rapidly at a selected "zero-time" in 60.0 ml of a 0.10 *m* NH_4ClO_4 solution which was already at 25.00°, and the dilatometer (also at 25.00°) was filled at once to overflowing with the solution, so that a drop remained standing on the level top of the capillary tube. When temperature perturbations caused by the filling process had subsided (10–15 min), the drop of excess solution was removed carefully, and the fall of the resulting meniscus in the tube was followed with a cathetometer as a function of time *t* elapsed since "zero-time."

For the bromo- and iodo-complexes the level (h_t) of the meniscus was recorded until it became stationary (h_∞) and the hypothetical level (h_0) corresponding to the start

Can. J. Chem. Downloaded from www.nrcresearchpress.com by 210.87.254.42 on 09/05/12
For personal use only.

of the aquation at "zero-time" was obtained by extrapolation of the function[2] log $(h_t - h_\infty)$, which was accurately linear with respect to t, back to "zero-time." First-order rate coefficients k, obtained from these data, were in good agreement with those measured spectrophotometrically. The molar volume of reaction ΔV was calculated from $(h_0 - h_\infty)$, the cross-sectional area of the capillary, and the number of moles of the halo-complex which would have been present at "zero-time" in the dilatometer.

For the chloro-complex, and for some runs involving the bromo-, the reaction was not followed beyond ~70% completion in the dilatometer; rather, the values of k obtained from the spectrophotometric measurements were used to calculate the amounts of unreacted halo-complex which would be present at times t_1, t_2, etc., whence ΔV could be calculated from measurements of the corresponding heights h_1, h_2, etc. These two procedures gave identical results, within the experimental uncertainty, for the bromo-complex.

Results

The spectrophotometric rate data were accurately first-order in halo-complex concentration up to at least 90% completion of reaction for $X^{n-} = I^-$ or Br^-, or 70% for Cl^-. Some slight deviations from strict first-order behavior after long reaction times in the latter case seemed to originate in minor degrees of ammonia loss from the aquo- or chloro-complexes. First-order rate coefficients k were reproducible to within 1% at worst, and were the same (within this limit) in both 0.1 m NH_4ClO_4 and 0.1 m $HClO_4$; the values of k measured at 1 bar pressure agreed satisfactorily with those reported by Levine, Jones, Harris, and Wallace (17). These data are summarized in Table 1.

The dependence of ln k upon P is non-linear for $X^{n-} = Cl^-$, Br^- and I^-, but the data can be represented to within the experimental uncertainty by the purely empirical equation

$$[3] \qquad \ln k_P = \ln k_0 + BP + CP^2$$

which assumes $(\partial \Delta V^*/\partial P)_T$ to be constant $(= -2RTC)$ and yields $\Delta V_0^* = -RTB$. Alternatively, if we assume instead that the pressure-dependence of ΔV^* is due exclusively to electrostriction of solvent (which is justified (3, 5), since ΔV^* is independent of P for the case $X^{n-} = H_2O$, in which there is no electrostrictional contribution) and acknowledge that electrostricted water is virtually incompressible as compared with bulk water, we can adapt the Tait equation for the compressibility of water to obtain the relationship

$$[4] \quad \ln k_P = \ln k_0 - P\Delta V_0^*/RT - (0.251x/RT) \times [(P + 3060) \ln (1 + P/3060) - P]$$

where P is in bars and x is the mean number (or at least a *lower limit* to the mean number) of water molecules added to the solvation sheath of the complex as it goes from the initial state to the transition state (3). These two equations represent the data equally well in this instance, and the respective parameters are listed in Table 2. In the following discussion, the parameters from eq. 4 are used, since the number x has a more obvious physical meaning than does $(\partial \Delta V^*/\partial P)_T$.

The volumes of reaction ΔV obtained from the dilatometric measurements were reliable to ± 0.3 cm^3 mol^{-1}, and are summarized in Table 3.

TABLE 1. Mean first-order rate coefficients k for the aquation of $Cr(NH_3)_5X^{2+}$ at 25.0° in 0.1 m NH_4ClO_4

	k ($\times 10^5$, s^{-1})		
P (kbar)	X = Cl	X = Br	X = I
0.001	1.034	9.64	103.4
0.500	—	11.67	123.6
1.00	1.548	14.20	—
1.05	—	—	149.1
1.50	1.874	16.63	171.3
2.00	2.25	19.30	—
2.45	2.57	—	—
2.50	—	23.1	234
2.90	—	—	258
3.00	—	26.7	—
3.10	3.18	—	—
3.50	—	30.6	296
4.00	—	33.5	—

Discussion

If the ΔV_0^* values for reaction 2 are scaled against those for reaction 1 (1–3, 5), as in Fig. 1 (to which Gay and Nalepa's (18) ΔV^* value for the aquation of $Cr(NH_3)_5NCS^{2+}$ has been added), it is seen at once that ΔV_0^* varies only about *half* as rapidly with changing X^{n-} in the Cr series as in the Co series. If one accepts that the Co—X bond is essentially completely broken and the solvation of X^{n-} fully provided for in the transition state of reaction 1, then it must be

[2]It is easily shown that, for a first-order reaction in a dilatometer of the type described, ln $[h_0 - h_\infty)/(h_t - h_\infty)] = kt$, where k is the first-order rate coefficient.

TABLE 2. Activation parameters for reaction 2, derived from eqs. 3 and 4

X^{n-} in $Cr(NH_3)_5X^{(3-n)+}$	ΔV_0*(eq. 3) ($cm^3\ mol^{-1}$)	$10^3(\partial\Delta V^*/\partial P)_T$ ($cm^3\ bar^{-1}\ mol^{-1}$)	ΔV_0*(eq. 4) ($cm^3\ mol^{-1}$)	x
Cl^-	-10.6 ± 0.3	1.04 ± 0.19	-10.8 ± 0.3	1.9 ± 0.3
Br^-	-9.9 ± 0.3	1.04 ± 0.14	-10.2 ± 0.3	2.0 ± 0.3
I^-	-9.2 ± 0.2	0.96 ± 0.13	-9.4 ± 0.3	1.7 ± 0.3
H_2O*	-5.8 ± 0.2	$0.0\ \pm0.3$	-5.8	0

*References 2 and 5.

TABLE 3. Molar volume changes ΔV accompanying reaction 2 at 25.0° in 0.1 *m* NH_4ClO_4

X	Quantity of $Cr(NH_3)_5X^{2+}$ aquated (mmol)	Volume change (μl)	Mean ΔV. ($cm^3\ mol^{-1}$)
Cl	0.126	−1.05	−8.4
	0.180	−1.53	
Br	0.200	−1.49	−7.2
	0.151	−1.04	
	0.083	−0.61	
I	0.195	−1.19	−6.0
	0.179	−1.04	

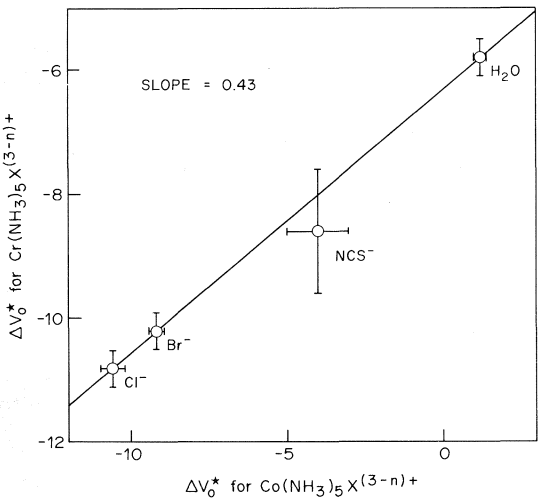

FIG. 1. ΔV_0* values for aquations of $Cr(NH_3)_5X^{(3-n)+}$ compared to those for $Co(NH_3)_5X^{(3-n)+}$.

acknowledged that these processes are only about *half* as far advanced in the transition state of reaction 2. This interpretation is supported by the observation that the mean numbers x of electrostricted water molecules in the transition state of reaction 1 for $X^{n-} = Cl^-$ and Br^- are 4.1 and 3.9 (5), as against *half* as many (Table 2) for the aquations of the analogous Cr(III) complexes.

An alternative approach (2, 3) is to divide ΔV_0* into a bond-making and -breaking part, ΔV_b*, which remains almost constant as X^{n-} is changed[3] and can be identified with ΔV* for the case $X^{n-} = H_2O$, and an electrostrictive part, ΔV_{el}*, which varies significantly with X^{n-} because of the markedly different solvational requirements of the various X^{n-}. We see that, for $X^{n-} = Cl^-$, Br^-, and NCS^-, ΔV_{el}* is −11.8, −10.4, and −5.0 $cm^3\ mol^{-1}$ for reaction 1, but only −5.0, −4.4, and −2.8 $cm^3\ mol^{-1}$ respectively for reaction 2; once again, electrostrictive effects are only about *half* as fully developed in the Cr(III) system as in the analogous Co(III) series.

However, the most convincing evidence to the effect that the separation of X^{n-} and provision for its solvation are only about half complete in the transition state of reaction 2 is the slope of 0.5_9 found for the linear relationship between ΔV_0* and ΔV (Fig. 2). This result stands in sharp contrast to that obtained for reaction 1, for which the slope of the ΔV_0* *vs.* ΔV plot is 1.0 (1–3) and which characterizes an I_d mechanism. Attempts to extend the correlation of Fig. 2 to include $X^{n-} = SO_4^{2-}$ and NO_3^- were thwarted by our failure to prepare and characterize $Cr(NH_3)_5SO_4^+$, and by the anomalous behavior of the nitrato complex, which aquates to yield *cis*-$Cr(NH_3)_4(OH_2)_2^{3+}$: these facts appear to be related mechanistically, and will be reported upon in detail in a forthcoming article. The *N*-thiocyanato complex could not be included because the loss of some coordinated ammonia, combined with the difficulty of adequate temperature control at the high tempera-

[3]The strongly negative value of ΔV* for the $Cr(NH_3)_5OH_2^{3+}$ aquo-exchange is considered (2, 4, 5) to originate in the "hole" left in the solvation sheath when the attacking water molecule moves to the first coordination sphere; this quantity will be virtually constant for a given type of solvation sheath, *i.e.*, for a given series of complexes such as $Cr(NH_3)_5X^{(3-n)+}$.

Can. J. Chem. Downloaded from www.nrcresearchpress.com by 210.87.254.42 on 09/05/12
For personal use only.

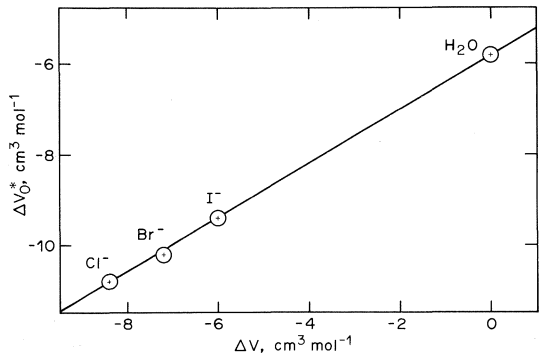

FIG. 2. Volume of activation ΔV_0^* (at zero pressure) *vs.* molar volume of reaction ΔV for the replacement of X^{n-} by H_2O in $Cr(NH_3)_5X^{(3-n)+}$ at 25.0° in 0.1 *m* NH_4ClO_4. Slope = 0.59.

tures necessary to study this hydrolysis, prevented our obtaining a meaningful ΔV value by dilatometry.

Clearly, the mechanism of substitution in the $Cr(NH_3)_5X^{(3-n)+}$ series is *not* the same as the I_d process which is considered to be operative in the analogous Co(III) systems. If we accept that the bond-breaking process is only about half as far advanced in the transition-state of reaction 2 as in the I_d mechanism of reaction 1, then consideration of the principle of microscopic reversibility requires that *either* bond-*making* (by incoming H_2O) must be as important as and synchronous with bond-breaking (an I_a mechanism), *or*, less plausibly, a long-lived[4] five-coordinated intermediate $[\{Cr(NH_3)_5\}(H_2O)_y]^{3+}$ is formed. In the latter case, bond-making and bond-breaking processes could be of comparable importance but would be *separate* in time; the bond-breaking transition state would lead to $Cr(NH_3)_5^{3+}$, and a bond-making transition state would lead onward from this intermediate toward the products.

However, the D mechanism can be discounted for at least three reasons. Firstly, it is in effect an extreme development of an I_d mechanism, and we have seen that the kinetic characteristics of reaction 2 do not correspond to those of reaction 1, which is considered to typify I_d behavior. Secondly, it is very hard to believe that a solvated, five-coordinate cationic species $[\{Cr(NH_3)_5\}(H_2O)_y]^{3+}$ would not collapse to the very stable $Cr(NH_3)_5OH_2^{3+}$ (aq) species in a time which would be somewhat less than the time-constant for the exchange of the yH_2O of the second coordination sphere with bulk solvent. Thirdly (and most importantly) the correlation of Fig. 2 very obviously includes the aquo-exchange reaction of $Cr(NH_3)_5OH_2^{3+}$, *which has a strongly negative volume of activation*; it would be exceedingly difficult to reconcile this observation with any kind of dissociative mechanism, and so we conclude that an associative mechanism is indeed operative in reaction 2 for the cases $X^{n-} = H_2O$, *N*CS^-, I^-, Br^-, and Cl^- at least. The mechanism is likely to be I_a rather than A (7), since steric compression (see below) would work against the survival of a long-lived seven-coordinate intermediate, and indeed no such Cr(III) species have been characterized to date.

Duffy and Earley (19) measured the anation rates and spectrophotometric ion-pair formation constants *K* for the reactions of $Cr(NH_3)_5OH_2^{3+}$ with Cl^- and NCS^-. Their data show that, if one assumes the reaction sequence

$$[5]\quad Cr(NH_3)_5OH_2^{3+} + X^- \overset{K}{\rightleftharpoons} \{Cr(NH_3)_5OH_2^{3+}, X^-\} \xrightarrow{k_i} \{Cr(NH_3)_5X^{2+}, OH_2\} \xrightarrow{\text{fast}} Cr(NH_3)_5X^{2+} + H_2O$$

then k_i is apparently significantly slower than the rate of aquo-exchange. This can be independently checked for the case $X^- = NCS^-$ (but not Cl^-) by plotting the reciprocals of Duffy and Earley's observed pseudo-first-order rate coefficients k_{obs} against $[NCS^-]^{-1}$; the intercept on the k_{obs}^{-1} axis gives $k_i = 3.7 \times 10^{-5}$ s^{-1} at 45°, while the slope ($= 1/k_iK$) gives $K \sim 12$ (which is close to the spectrophotometric value of 10). Our aquo-exchange rate data (5) show that NCS^- entry into the first coordination sphere from within the ion pair is thus about 18 times slower than aquo-replacement at 45°.

The latter observation is obviously consistent with an I_d mechanism, for which anation could only be consequent upon, and so not faster than, aquo-ligand separation. However, it is also

[4]"Long-lived" signifies that five-coordination persists longer than the average residence-time of molecules or ions in the second coordination sphere. An incoming ligand from bulk solution would have to enter the second coordination sphere of the intermediate complex before it could form a bond to the central metal ion; thus, the distinguishing feature of the intermediate of reduced coordination number in a D mechanism is that reduced coordination must persist longer than the time needed for exchange between the second coordination sphere and the solution at large.

Can. J. Chem. Downloaded from www.nrcresearchpress.com by 210.87.254.42 on 09/05/12
For personal use only.

Can. J. Chem. Downloaded from www.nrcresearchpress.com by 210.87.254.42 on 09/05/12
For personal use only.

entirely consistent with an I_a process in which NCS^- competes rather inefficiently with water as a nucleophile. Such is likely to be the case in a stereoretentive flanking replacement of the departing aquo-ligand, as seems to be usual for Cr(III) centers (14); the water molecules solvating the complex ion will tend to be concentrated around the acidic aquo-ligand, because of efficient hydrogen-bonding (5), while X^{n-} in an ion-pair will tend to be situated on the least heavily solvated side of the complex, remote from the replaceable aquo-group, where closest approach to the charged central metal-ion is possible. In any event, there is considerable disparity between the k_i values for Cl^- and NCS^- in Scheme 5 (19), whereas Langford and Muir (20) found the k_i values for the I_d anations of $Co(NH_3)_5OH_2^{3+}$ by Cl^-, NCS^-, and even SO_4^{2-} to be essentially equal; the obvious explanation of this difference in behavior between Cr and Co is that Cl^- and NCS^- are displaying their different nucleophilic powers against $Cr(NH_3)_5OH_2^{3+}$ in an I_a mechanism.

The assignment of an I_a mechanism to reaction 2 is supported by the observation (21) that the rate coefficients for the aquations of the pentaamine complexes $Cr(NH_2R)_5Cl^{2+}$ *decrease* 33-fold on going from R = H to R = CH_3, largely because of an increase of 4.0 kcal mol^{-1} in the activation enthalpy, ΔH^*. This is very likely due to increased steric hindrance to the entry of a seventh ligand in an I_a mechanism, since Foxman (22) has shown that there is severe steric congestion in the ground state of the analogous ion $Co(NH_2CH_3)_5Cl^{2+}$. It is particularly significant that the aquation rate of this last ion is 22 times *faster* than that of $Co(NH_3)_5Cl^{2+}$, in accordance with steric decompression on going to the transition state via an I_d mechanism (23). Solvational differences will also contribute to the rate differences, as pointed out by Parris and Wallace (21), and it is therefore not surprising that the aquation rates increase in *both* the $Cr(NH_2R)_5Cl^{2+}$ and $Co(NH_2R)_5Cl^{2+}$ series as the alkyl chain R is extended beyond methyl; alkyl chain lengthening will make the complexes increasingly "hydrophobic," without significantly increasing steric congestion, as the latter will originate almost entirely in the α carbon atoms.

The assignment of an I_a mechanism to acid-independent chromium(III) aquations and an I_d scheme to their cobalt(III) analogs provides an answer to the long-standing question (24) of why the ratio of base hydrolysis rates to aquation rates should be so much greater in cobalt(III) complexes than in their chromium(III) and rhodium(III) analogs. The hypothetical I_d process for Cr(III) aquations, which would be truly comparable with that operating at Co(III) centers, is evidently "undercut" by the more energetically accessible I_a path; thus, if both series of base hydrolyses proceed via a similar conjugate-base dissociative mechanism (as seems likely), the difference in rates between base hydrolysis and aquation for Cr(III) will seem anomalously small, and the relative importance of base hydrolysis in Cr(III) systems will be reduced as compared with Co(III). The same argument explains the apparent inertness (*vis-à-vis* aquation) of Rh(III) ammines toward base hydrolysis, since an I_a mechanism seems to be operative in the reactions of $Rh(NH_3)_5OH_2^{3+}$ at least (5, 25, 26). The point is then not that the base hydrolyses of Cr(III) and Rh(III) complexes are unusually *slow*, but rather that the corresponding aquations are unusually *fast*.

In the light of the above discussion and our previous arguments (2, 4, 8) in favor of an associative mechanism in substitution reactions of complexes of the type $Cr(H_2O)_5X^{(3-n)+}$, we consider it appropriate to make the general statement that *an I_a mechanism is operative in acid-independent substitution reactions of cationic chromium(III) complexes in aqueous solution.* This may appear to be inconsistent with Ferraris and King's observation (9) that the induced solvolysis of azido- and halo-pentaaquochromium(III) ions, and the spontaneous solvolysis of iodopentaaquochromium(III) ion extrapolated to zero extent of reaction, in aqueous methanol give essentially the same relative amounts of $Cr(H_2O)_6^{3+}$ and $Cr(H_2O)_5(CH_3OH)^{3+}$, for a given solvent composition. This observation *suggests* (but, as Ferraris and King emphasize (9), does not *prove*) that a common intermediate is produced, *i.e.*, that a D mechanism is operative in these solvolyses of various $Cr(H_2O)_5X^{(3-n)+}$ species.

However, it should be borne in mind that the two entering reagents $H_3C—OH$ and H—OH will both present essentially the same attacking group (—OH) to the Cr(III) center in an associative process, and consequently there will be very little *electronic* discrimination between the two nucleophiles by the Cr—X group. Accordingly, the CH_3OH/HOH ratio in the products is

Can. J. Chem. Downloaded from www.nrcresearchpress.com by 210.87.254.42 on 09/05/12
For personal use only.

not likely to vary significantly from one X to another, especially since all the X^{n-} studied in this connection are "good leaving groups," so that the degree of bond-making in an I_a mechanism need not be great in order to provide the energetic assistance needed to facilitate the bond-breaking process. The greater "nucleophilic power" of water over methanol toward metal ion centers can be ascribed partly to steric factors (by analogy with Foxman's findings (22)).

On the other hand, when two competing nucleophiles *do* differ appreciably in their electronic structures, as for example H_2O *vs.* Cl^- (aq), the product ratios in a substitution reaction can be expected to vary with the nature of the departing ligand X^{n-} if the mode of activation is associative, but not if a D mechanism is operative. We have observed a significant variation in the yield of $Cr(H_2O)_5Cl^{2+}$ relative to $Cr(H_2O)_6^{3+}$ when various $Cr(H_2O)_5X^{2+}$ are aquated in 1.0 *M* HCl (8), and this, coupled with the strongly negative ΔV^* value for the $Cr(H_2O)_6^{3+}$ aquo-exchange (4) and a striking dependence of the anation rate of $Cr(H_2O)_6^{3+}$ upon the nature of the entering ligand X^{n-} (*e.g*, anation by NCS^- is $\sim 2 \times 10^3$ times faster than by I^-) (8), constitutes strong support for our view that an I_a mechanism is indeed operative in hydrogen-ion-independent substitutions in complexes of the $CrL_5X^{(3-n)+}$ type in aqueous solution. These considerations do not preclude the possibility that the *induced* solvolyses of $Cr(H_2O)_5X^{2+}$ species proceed by a D mechanism, as proposed by Ferraris and King (9); indeed, Birk and Ingerman (27) have recently presented evidence which suggests that the mechanisms of the spontaneous and induced aquation mechanisms differ in precisely this way.

We thank the National Research Council of Canada for financial assistance, Ms. S. J. Swaddle for microanalyses, and Drs. E. L. King and C. H. Langford for stimulating discussions.

1. W. E. Jones and T. W. Swaddle. Chem. Commun. 998 (1969).
2. T. W. Swaddle. Proc. XIV Int. Conf. Coord. Chem. 17–19 (1972).
3. W. E. Jones, L. R. Carey, and T. W. Swaddle. Can. J. Chem. **50**, 2739 (1972).
4. D. R. Stranks and T. W. Swaddle. J. Am. Chem. Soc. **93**, 2783 (1971).
5. T. W. Swaddle and D. R. Stranks. J. Am. Chem. Soc. **94**, 8357 (1972).
6. H. R. Hunt and H. Taube. J. Am. Chem. Soc. **80**, 2642 (1958).
7. C. H. Langford and H. B. Gray. Ligand substitution processes. W. A. Benjamin, New York, N.Y. 1965.
8. L. R. Carey, W. E. Jones, and T. W. Swaddle. Inorg. Chem. **10**, 1566 (1971).
9. S. P. Ferraris and E. L. King. J. Am. Chem. Soc. **92**, 1215 (1970).
10. P. Moore, F. Basolo, and R. G. Pearson. Inorg. Chem. **5**, 223 (1966).
11. M. Mori. Inorg. Synth. **5**, 134 (1957).
12. G. Schlessinger. Inorg. Synth. **6**, 138 (1960).
13. E. Zinato, R. Lindholm, and A. W. Adamson. J. Inorg. Nucl. Chem. **31**, 449 (1969).
14. C. S. Garner and D. A. House. Transition Met. Chem. **6**, 59 (1970).
15. T. W. Swaddle and P.-C. Kong. Can. J. Chem. **48**, 3223 (1970).
16. T. G. Spiro, A. Revesz, and J. Lee. J. Am. Chem. Soc. **90**, 4000 (1968).
17. M. A. Levine, T. P. Jones, W. E. Harris, and W. J. Wallace. J. Am. Chem. Soc. **83**, 2453 (1961).
18. D. L. Gay and R. Nalepa. Can. J. Chem. **48**, 910 (1970).
19. N. V. Duffy and J. E. Earley. J. Am. Chem. Soc. **89**, 272 (1967).
20. C. H. Langford and W. R. Muir. J. Am. Chem. Soc. **89**, 3141 (1967).
21. M. Parris and W. J. Wallace. Can. J. Chem. **47**, 2257 (1969).
22. B. M. Foxman. Chem. Commun. 515 (1972).
23. D. A. Buckingham, B. M. Foxman, and A. M. Sargeson. Inorg. Chem. **9**, 1790 (1970).
24. F. Basolo and R. G. Pearson. Mechanisms of inorganic reactions. 2nd ed. J. Wiley and Sons, Inc., New York. 1967. p. 182.
25. H. L. Bott, A. J. Poë, and K. Shaw. Chem. Commun. 793 (1968).
26. F. Monacelli. Inorg. Chem. Acta, **2**, 263 (1968).
27. J. P. Birk and C. M. Ingerman. Inorg. Chem. **11**, 2019 (1972).

Oxodichlororhenium(IV), $ReOCl_2$

P. W. Frais, H. E. Howard-Lock, and C. J. L. Lock[1]

Institute for Materials Research, McMaster University, Hamilton, Ontario

Received August 22, 1972

The preparation and some physical and chemical properties of $ReOCl_2$ are described.

On décrit la préparation ainsi que quelques propriétés physiques et chimiques de $ReOCl_2$.

[Traduit par le journal]

Can. J. Chem., **51**, 828 (1973)

Can. J. Chem. Downloaded from www.nrcresearchpress.com by 210.87.254.5 on 09/05/12
For personal use only.

Introduction

Until recently only two oxochlorides of rhenium have been clearly established, namely $ReOCl_4$ and ReO_3Cl (1). Very recently there have been reports of $ReOCl_3$ (2) and the mixed complexes $ReO_3Cl \cdot ReOCl_4$ (3) and $Re_2O_3Cl_6$-$(ReO_3Cl)_2$ (4). We now report the existence of yet another simple oxochloride, namely oxodichlororhenium(IV), $ReOCl_2$.

Experiments

Rhenium and chlorine analyses were performed by the neutron activation method described previously (5). Infrared spectra were recorded for solid samples ground into a mull with Nujol. The Nujol had been dried by refluxing with phosphorus pentoxide followed by vacuum distillation. The mull samples were mounted between potassium bromide plates and spectra were recorded on Perkin–Elmer 337, 521, and 301 spectrometers. Raman emission was excited by 10 mW of radiation from a He–Ne laser (λ6328 Å), and spectra were recorded with a Coderg PHO double monochromator with photoelectric detection. X-Ray diffraction photographs of powdered samples were recorded on a Debye–Scherrer camera. Samples were sealed inside fused quartz tubes and nickel-filtered CuKα radiation was used for recording the photographs. Line intensities were measured from the photographs with a Joyce–Loebl microdensitometer. $ReOCl_2$ was prepared by a number of different chemical reactions. Typical reaction conditions are described below unless changes in the conditions made significant differences in the distribution of products, in which case different runs are described.

Analysis and Identification of Products

For qualitative identification of products only infrared spectroscopy (volatile materials) or X-ray diffraction (involatile materials) was used. Combination of these techniques with quantitative analysis (see below) applied to pure and known "impure" samples (*i.e.* mixtures of known composition) has shown that infrared spectroscopy could identify as little as 5% of an impurity (and in many cases $< 1\%$) while X-ray diffraction could detect as little as 5% of impurity in a single substance and 10% in a mixture of two compounds. For X-ray diffraction it is possible that large quantities of an amorphous product were present but we have no other evidence for this in any of our experiments. For each type of reaction reported below many runs were made (typically 5–10) and in most runs attempts were made not only to separate volatile and involatile products, but to separate the products into individual components. This was hard to do for volatile products, but for involatile products was achieved by hand-picking crystals. Parts of both volatile and involatile samples were examined by X-ray and infrared techniques to confirm that only the expected products were present.

For quantitative analysis of a reaction, the nature of the products was established by a series of qualitative runs first. In the quantitative run the amounts of starting materials and volatile and involatile products were weighed on a microbalance. The remainder of the sample (which was weighed) was then analyzed by the neutron activation analysis technique described previously (5) to give (*1*) Re:Cl atom ratio, (*2*) percentage Re and Cl, (*3*) average oxidation state of rhenium. From the above data it was possible to calculate the amount of each individual product present, within the error limits we have given.

Reaction a: ReO_3 + $ReCl_5$

(*i*) ReO_3(1.0 g) and $ReCl_5$(1.55 g) were sealed in an evacuated Pyrex tube (25 mm diameter, approximate volume 40 ml) fitted with a break-seal, and heated at 350 °C for 17 h in a tube furnace. On cooling, the tube was sealed to a vacuum line, the seal was broken, and materials, volatile at room temperature, were distilled into a U-trap cooled by a Dry Ice/acetone bath. The volatile products were $ReOCl_4$ and ReO_3Cl (i.r. spectroscopy) and the residue was shown by X-ray powder diffraction to be a mixture of Re_3Cl_9, $ReOCl_2$, and ReO_3.

(*ii*) Experiment (*i*) was repeated except that the tube was heated to 400 °C for 5 days, care being taken to minimize the thermal gradient in the tube. In this case the involatile products were only $ReOCl_2$ and Re_3Cl_9. The $ReOCl_2$ was present as a cluster of metallic-purple acicular crystals and the Re_3Cl_9 was present as small compact crystals. The two types of crystals were readily identified under a microscope. Separation of the two components was accomplished by washing the mixture several times with dry acetonitrile, and in this way dissolving all the Re_3Cl_9. Thus far, this has been the only source of larger crystals of $ReOCl_2$, and these were used for all experiments performed with $ReOCl_2$.

[1]To whom correspondence should be addressed.

TABLE 1. Analysis of $ReOCl_2$

Parameter	Value		
		Found	
	Calculated	Neutron activation	H_2 reduction
Cl/Re atom ratio	2.00	2.0(1)	—
%Re	68.1	65(3)	68(1)
%Cl	26.0	25(2)	—

Reaction b: ReO_3 + $ReOCl_4$

(*i*) ReO_3 (0.38 g) and $ReOCl_4$ (~0.4 g) were sealed in a tube (20 mm diameter, 20 cm long) fitted with a breakseal. The materials were placed in opposite ends of the tube and the tube was arranged in a furnace such that the ReO_3 was at ~235 °C and $ReOCl_4$ was at ~100 °C. No reaction occurred in 48 h and the temperatures were raised to ~280 °C and ~120 °C. After a further 72 h a coating of metallic-purple material had formed in the ~200 °C zone. The weight was not recorded, but X-ray powder photography showed the material was mostly $ReOCl_2$ with some Re_3Cl_9 impurity. An infrared spectrum of the residual volatile material showed it was a mixture of ReO_3Cl and $ReOCl_4$.

(*ii*) The experiment was repeated with 0.61 g ReO_3 and ~0.45 g $ReOCl_4$ placed in a tube with a constriction between the 285 and 200 °C zones. The reaction was allowed to proceed for ~7 days, and the products were separated. The products occurred as three groups in the tube, the two groups of involatiles occurring on either side of the constriction, and the volatile material condensed in the cool end. Examination of the three groups of products by suitable combination of weighing, infrared spectroscopy and X-ray powder photography showed the products were: product from 280 °C zone: > 90% ReO_3, trace of $ReOCl_2$, trace of Re_3Cl_9 (0.52 g); product from 200 °C zone: $ReOCl_2$ ~100%, trace of ReO_3 (probably from walls when filling tube), no Re_3Cl_9 (0.01 g); volatile products: mostly $ReOCl_4$ with some ReO_3Cl (0.54 g by difference).

Reaction c: Decomposition of $ReOCl_4(OH_2)$ (6)

When $ReOCl_4(OH_2)$ was distilled quickly under vacuum, at least partial decomposition occurred, giving a volatile mixture of $ReOCl_4$ and ReO_3Cl and a black residue remaining where the $ReOCl_4(OH_2)$ had been. Powder photography has shown this black residue was a mixture of $ReOCl_2$ and Re_3Cl_9.

Similarily, when $ReOCl_4(OH_2)$ crystals are allowed to sit exposed to a nitrogen atmosphere in a good dry box (Vacuum Atmospheres Corp., Calif. model HE493 DRI-TRAIN) a black surface layer formed, even in the short time required to mount a crystal in a capillary tube. This black material was also shown by powder photography to be a mixture of $ReOCl_2$ and Re_3Cl_9.

Reaction d: $ReOCl_4$ + $SnCl_2$

$ReOCl_4$ (~0.30 g) and $SnCl_2$ (0.15 g) were sealed in an evacuated Pyrex tube fitted with a breakseal at opposite ends of the tube. The tube was placed in a tube furnace such that the $SnCl_2$ was at ~210 °C and $ReOCl_4$ at ~70 °C. After 48 h the volatile colorless liquid (assumed to be $SnCl_4$) was removed through the breakseal, and the involatile products analyzed by powder photography. These were found to be a mixture of ReO_3 and Re_3Cl_9 with minor amounts of $ReOCl_2$ being present.

Reaction e: ReO_3 + $ReCl_3$

ReO_3 (0.10 g) and $ReCl_3$ (0.25 g) were reacted at 500 °C for ~72 h. The volatile component of the products were distilled through a breakseal and analyzed by infrared and neutron activation analysis. It was shown to be > 90% $ReOCl_4$ with ReO_3Cl as a minor impurity. The involatiles consisted of a mixture of Re metal and ReO_2 (identified by powder photography).

Analysis and Characterization of $ReOCl_2$

Neutron activation analysis was performed 12 times on six samples of crystalline $ReOCl_2$ prepared by preparation *a*. In addition a sample of $ReOCl_2$ weighing 14.2(1) mg was reduced in a gentle stream of hydrogen at ~250 °C for ~90 h. The $ReOCl_2$ was in a porcelain boat, and the apparatus was fitted with a U-trap cooled in a Dry Ice/acetone bath to trap any volatile rhenium products. The final weight of the reduced product was 9.6(1) mg, and neutron activation analysis showed only ~0.02 mg of Re in the U-trap. The results are summarized in Table 1.

Oxodichlororhenium(IV) was insoluble in dry acetonitrile, acetone or diethylether, but reacted with moisture present in the atmosphere or in these solvents to form a metallic-gold colored surface coating. With cold distilled water, immediate reaction occurred giving a fibrous black precipitate. The physical appearance of $ReOCl_2$ crystals was very similar to the published photographs of $MoOCl_2$ (7) and $WOCl_2$ (8), both of which were also described as possessing a metallic lustre.

Infrared spectra were recorded over the range 4000 cm^{-1} to 120 cm^{-1}, and Raman spectra were recorded in the range 20–1100 cm^{-1} from the exciting line. Infrared bands were observed at 906(w) and 128 cm^{-1}(m) and Raman bands were observed at 497, 460, and 370 cm^{-1} from the exciting line. Infrared bands were estimated to have a maximum error of ± 2 cm^{-1} in the 4000–400 cm^{-1} range and ± 5 cm^{-1} in the 400–100 cm^{-1} range. Errors in the Raman bands were estimated to be ± 2 cm^{-1} over the whole range.

Crystallography

Crystallographic examination was made on crystals of $ReOCl_2$. Without exception, needles of $ReOCl_2$ obtained from reaction *a*, examined with both precession and Weissenberg methods, yielded diffraction patterns indicating serious disorder in at least one direction. Attempts to obtain a full Weissenberg photograph rotating about the needle axis gave only streaks. It was possible to get

Can. J. Chem. Downloaded from www.nrcresearchpress.com by 210.87.254.5 on 09/05/12
For personal use only.

Can. J. Chem. Downloaded from www.nrcresearchpress.com by 210.87.254.5 on 09/05/12
For personal use only.

unit cell parameters from rotation and precession photographs. Data obtained were

Cl_2ORe f.w. = 273.1

Orthorhombic or monoclinic $a = 3.69(1)$, $b = 14.7(1)$, $c = 6.63(1)$ Å, $\beta = 90.0(1)°$, $V = 360$ Å^3, $\rho_c = 5.04$ g cm^{-3}, $Z = 4$, ρ_o, not determined, (22 °C, λMoKα = 0.71069 Å).

Powder photographs of $ReOCl_2$ were of mediocre quality, but were consistent in line position and intensity with precession photographs. Data are given in Table 2.

Reactions of $ReOCl_2$

(a) Thermal Decomposition

Accurately weighed amounts of $ReOCl_2$ (<60 mg) were sealed in evacuated 4 mm Pyrex tubes fitted with break-seals. The $ReOCl_2$ was heated in one end of the tube while the other end was at room temperature. At ~380 °C, $ReOCl_2$ began to decompose visibly. At 500 °C, decomposition occurred according to the equation

$$4ReOCl_2 \xrightarrow{500\ °C} Re + \tfrac{1}{3}Re_3Cl_9 + ReOCl_4 + ReO_3Cl$$

This was confirmed by a combination of X-ray powder photography, infrared spectroscopy and neutron activation analysis (3). The data obtained for two independent decompositions are shown in Table 3.

At lower temperatures, the decomposition of $ReOCl_2$ was incomplete and only $ReCl_3$, $ReOCl_4$, and ReO_3Cl were observed as products.

(b) Reaction of $ReOCl_2$ and $ReCl_5$

Equimolar amounts of $ReOCl_2$ and $ReCl_5$ were sealed in an evacuated reaction tube and reacted at 200 °C in such a way that separation of $ReCl_5$ was not possible. As expected, the much more thermodynamically stable products $ReOCl_4$ and Re_3Cl_9 are formed. The results are summarized in Table 4.

Results and Discussion

Analyses showed clearly that we had prepared a compound of the type $ReCl_2X$, where X was probably an amount of oxygen or OH group. Possible compounds were $ReOCl_2$, ReO_2Cl_2, $ReOCl_2 \cdot OH_2$, $ReOCl_2OH$. The analytical results suggested the first formulation but were not conclusive. However, we feel that by the determination of the weights of the reactants and products in various preparation and decomposition reactions we have shown unambiguously that we have prepared $ReOCl_2$.

The crystal structure studies of $ReOCl_2$ did not reveal the structure because of the presence of multiple crystals and possibly twinning or disordering. The unit cell is either orthorhombic or monoclinic with $\beta = 90°$. One distance is particularly short and suggests possible structures for the compound. They are shown in Figs. 1*a* and 1*b*. The short distance (3.69 Å = *a*) is very close to 3.73 Å observed for the linear Re—O—Re distance in ReO_3 (9). Two possible arrangements exist for the chlorine atoms and the layer arrangement shown in Fig. 1*a* seems more probable, considering the fibrous nature of the material. The *b* distance of 14.7 Å, which corresponds almost exactly to four $ReCl_2Re$ distances (as shown in Fig. 1) based on parameters for Re_2Cl_{10} (10), does not allow a choice between the two structures.

TABLE 2. X-Ray diffraction data for powdered $ReOCl_2$

d_{obs}(Å)	d_{calcd}*(Å)	*hkl*	I_{obs}
7.35	7.350	020	100
3.68	3.675	040	<5
3.60	3.579	110	58
3.32	3.315	002	15
3.15	3.149	111	6
2.46	2.450	060	10
1.85	1.845	200	8
1.83	1.825	170	6
1.80	1.789	220	6

*Indexed in terms of an orthorhombic cell $a = 3.69$ (1), $b = 14.7(1)$, $c = 6.63(1)$ Å.

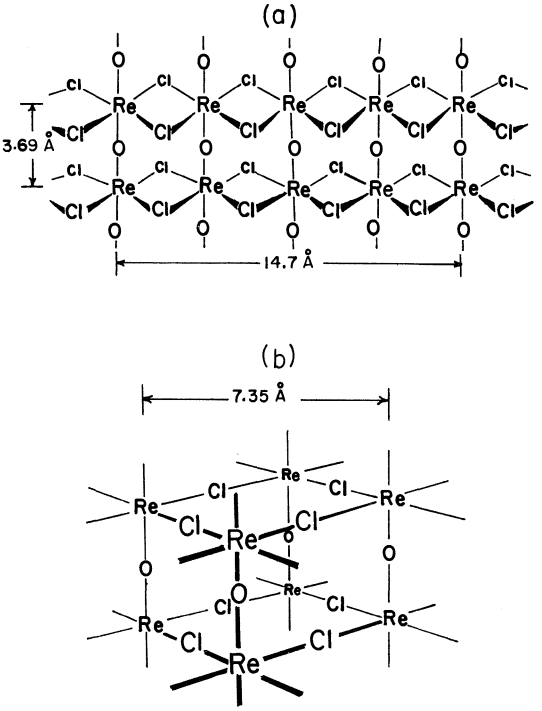

FIG. 1. Possible structures of $ReOCl_2$: (*a*), layer structure; (*b*), three dimensional net structure.
Note: The diagrams do not show distortions which would allow Re—Re interactions.

TABLE 3. Thermal decomposition of $ReOCl_2$

Compound	Decomposition 1 (weight in mg) Found	Decomposition 1 (weight in mg) Calculated*	Decomposition 2 (weight in mg) Found	Decomposition 2 (weight in mg) Calculated*
$ReOCl_2$†	28(2)		52(2)	
Re‡	4.6(2)	4.8(2)	8.8(2)	9.0(4)
Re_3Cl_9	7.1(2)	7.5(6)	13.6(2)	13.9(7)
$ReOCl_4$§	9.0(9)	8.8(7)	16.0(8)	16.4(8)
ReO_3Cl§	7.0(7)	6.9(6)	15.1(8)	12.7(6)

*Calculated from the equation $4\ ReOCl_2 \rightarrow Re + \frac{1}{3}Re_3Cl_9 + ReOCl_4 + ReO_3Cl$.
†Starting product. All calculated weights based on this figure. The uncertainty results from difficulties in transferring all the $ReOCl_2$ needles to the bottom of the decomposition tube. Uncertainties in the calculated values also arise from this source.
‡Obtained by weighing.
§Obtained by neutron activation analysis.

TABLE 4. Reaction of $ReOCl_2$ and $ReCl_5$

	Reaction 1 (weight in mg) Found	Reaction 1 (weight in mg) Calculated*	Reaction 2 (weight in mg) Found	Reaction 2 (weight in mg) Calculated
Starting materials				
$ReCl_5$	27.3(5)	—	57.8(5)	—
$ReOCl_2$	20.5(5)	—	42.3(5)	—
Unreacted materials				
$ReCl_5$	7.5(7)	9(1)	—	—
$ReOCl_2$	6.8(7)	6.8(7)	—	—
Reaction products				
Re_3Cl_9	17(1)	15(2)	46.1(5)	45.3(5)
$ReOCl_4$	17(1)	17(2)	52(1)	53.3(5)

*Calculations are based on 6.8 mg of unreacted $ReOCl_2$. The values are calculated from the equation $ReOCl_2 + ReCl_5 \rightarrow ReOCl_4 + \frac{1}{3}Re_3Cl_9$.

The vibrational spectra of $ReOCl_2$ are characterized by the absence of many significant features. Even for the most concentrated mulls or pellets, only two weak bands were observed in the infrared spectrum (906, 128 cm^{-1}) and for the solid (crystal or powder) only three bands were observed in the Raman spectrum (497, 460, 370 cm^{-1}).

Only two vibrations can be assigned with any confidence. The band at 906 cm^{-1} corresponds to a linear Re—O—Re asymmetric stretch (11) and is observed at the same frequency for ReO_3. Similarly a band at ~370 cm^{-1} has been assigned to an Re—Cl stretch for $ReOCl_4$ (12). The bands in the 460–497 cm^{-1} region are too high for transitions except those associated with the —O—Re—O—Re— system. For *bent* Re—O—Re systems the symmetric Re—O—Re stretch occurs in this region (11) but not, supposedly, for linear systems. Frequencies for the symmetric —O—Re—O— stretch and bend have not been reported. We have no explanation as to why we observed no infrared absorptions in the Re—Cl stretch region.

$ReOCl_2$ is one of the fourteen products which have now been identified as arising from the reaction of ReO_3 and $ReCl_5$ in the presence of small amounts of moisture (see refs. 2, 4, 6). $ReOCl_2$ is important in that our decomposition studies show clearly that it is the intermediate in the very unusual formation of rhenium metal from the reaction of two rhenium compounds in a high oxidation state.

Compared to the other oxochlorides of rhenium, $ReOCl_2$ is relatively stable with respect to reaction with air and moisture and one wonders why it has not been observed before. It is markedly thermally unstable, but it is found as a product in so many of the reactions tried. Perhaps one explanation is that it is relatively involatile and thus occurs with Re_3Cl_9 in most reactions. Unless one was looking for $ReOCl_2$

Can. J. Chem. Downloaded from www.nrcresearchpress.com by 210.87.254.5 on 09/05/12
For personal use only.

it is possible not to recognize it in a sample of Re_3Cl_9, particularly if the $ReOCl_2$ is in the powder form. The presence of some $ReOCl_2$ in Re_3Cl_9 may explain some of the conflicting reports on the properties of different samples of Re_3Cl_9, such as solubility and magnetic properties (13 and references therein). Re_3Cl_9 is diamagnetic, but $ReOCl_2$ should be paramagnetic. Unfortunately we have been unable to prepare sufficient pure $ReOCl_2$ to perform magnetic measurements.

We thank the National Research Council of Canada for financial support of this work and the grant of a Scholarship to P.W.F.

1. A. Bruckl and K. Ziegler. Chem. Ber. **65**, 916 (1932).
2. P. W. Frais, C. J. L. Lock, and A. Guest. Chem. Commun. 75 (1971).
3. K. I. Petrov, V. V. Kravchenko, D. V. Drobot, and V. A. Aleksandrova. Russ. J. Inorg. Chem. **16**, 928 (1971).
4. C. Calvo, P. W. Frais, and C. J. L. Lock. Can. J. Chem. **50**, 3607 (1972).
5. W. D. Courrier, A. Guest, C. J. L. Lock, and R. H. Tomlinson. Can. J. Chem. **46**, 2965 (1968).
6. P. W. Frais and C. J. L. Lock. Can. J. Chem. **50**, 1797 (1972).
7. H. Schäfer and J. Tillack. J. Less Common Met. **20**, 171 (1970).
8. S. S. Eliseev, I. A. Glukhov, and N. V. Gaidaenko. Russ. J. Inorg. Chem. **14**, 328 (1969).
9. K. Meisel. Z. Anorg. Allgem. Chem. **207**, 121 (1932).
10. K. Mucker, G. S. Smith, and Q. Johnson. Acta Cryst. **B24**, 874 (1968).
11. R. M. Wing and K. P. Callahan. Inorg. Chem. **8,** 871 (1969).
12. A. Guest and C. J. L. Lock. Can. J. Chem. **49**, 603 (1971).
13. R. Colton. The chemistry of rhenium and technetium. Interscience–Wiley, London. 1965.

Can. J. Chem. Downloaded from www.nrcresearchpress.com by 210.87.254.5 on 09/05/12
For personal use only.

A Comparison of the Conformations of Uridine, β-Pseudouridine, and Dihydrouridine in Dimethyl Sulfoxide and Water. A ^{1}H Nuclear Magnetic Resonance Study[1]

ROXANNE DESLAURIERS AND IAN C. P. SMITH

Division of Biological Sciences, National Research Council of Canada, Ottawa, Canada K1A 0R6

Received July 6, 1972

The ^{1}H n.m.r. spectra of the nucleosides uridine (U), dihydrouridine (D), and β-pseudouridine (β-ψ) in deuterated dimethyl sulfoxide (DMSO-d_6) have been analyzed and the results compared with those obtained from analyses of spectra taken in deuterated water (D_2O). The conformations of the ribose rings in DMSO-d_6 and D_2O solutions are similar. The conformation about the exocyclic $C_{4'}$—$C_{5'}$ bond shows a greater preference for the *gauche–gauche* rotamer in DMSO-d_6 than in D_2O. No changes in the sugar–base torsion angle were detectable in the spectra taken with the two solvents. The resonances of the sugar ring hydroxyl protons were assigned and the spin–spin couplings measured. In the three nucleosides studied the hydroxyl groups are rotating rapidly with only slight preferences for the particular rotamers. When preferences are manifest, they are for the *gauche* rotamers at 2′ and 3′, and the symmetrical *gauche–gauche* rotamer at 5′.

On a analysé les spectres de r.m.n. ^{1}H des nucléosides uridine (U), dihydrouridine (D), et β-pseudouridine (β-ψ) dans le diméthylsulfoxide-d_6 (DMSO-d_6) et l'oxyde de deutérium (D_2O). On compare les conformations dans les deux solvants. Les cycles riboses sont semblables, mais les groupements exocycliques CH_2—OH manifestent une plus grande préférence pour l'isomère *gauche–gauche* dans le DMSO-d_6 que dans le D_2O. On ne trouve aucune différence conformationelle autour de la liaison glycosidique dans le DMSO-d_6 et dans le D_2O. Les groupements hydroxyles dans les trois composés sont en rotation rapide et montrent une faible préférence pour certains conformères, pour les rotamères *gauches* à 2′ et 3′, et pour le rotamère *gauche–gauche* à 5′.

Can. J. Chem., **51**, 833 (1973)

Introduction

In all transfer RNA sequenced to date, the modified nucleosides β-pseudouridine (β-ψ) and dihydrouridine (D) occupy special locations. However, no special structural role for them has yet been demonstrated. The conformations of uridine (U), β-ψ, and D have been compared in aqueous solution by ^{1}H n.m.r. and suggestions have been made for their structural roles in transfer RNA (1–3). One aspect of the conformations that could not be compared in aqueous solution is the preference for rotational isomers of the hydroxyl groups. We report here a study of this aspect in dry dimethyl sulfoxide. A study in this solvent is also of interest because so many biological compounds are studied in it for reasons of solubility, and a comparison of the overall conformations in each solvent is an indication of the usefulness of such data.

Experimental

Uridine (Sigma Chemicals), β-pseudouridine (Calbiochem, A grade), and dihydrouridine (Calbiochem, B grade) were used without further purification and revealed no impurities in the n.m.r. spectra. Deuterated dimethyl sulfoxide (Merck, Sharp and Dohme of Canada) was stored over molecular sieve (Linde 3A) to remove traces of water. Solutions (0.1 *M*) of nucleosides were prepared in the following manner. One sample of each was dissolved in D_2O, lyophilyzed, and then redissolved in DMSO-d_6 in order to exchange the protons of the hydroxyl groups, and gain a clearer spectrum of the ribose ring protons. Another was dissolved in DMSO, lyophilyzed, and redissolved in DMSO-d_6 to remove adsorbed water molecules. All manipulations were carried out in a dry box under dry nitrogen. Spectra were recorded using Varian XL-100 and HR-220 spectrometers (Canadian 220 MHz Centre, Sheridan Park, Ontario). Assignment of the hydroxyl protons was done by successively decoupling the 2′, 3′, and 5′ ribose ring protons. Spectral analysis was carried out using the computer program Hydra (4). Solutions were considered satisfactory only when the simulated spectra resembled the experimental spectra in every respect. The results of the analyses of the n.m.r. spectra of the three compounds are presented in Table 1. A typical spectrum of the hydroxyl protons is shown in Fig. 1.

Discussion

(a) Hydroxyl Group Conformation

H—C—O—H′ coupling constants are known to depend on the dihedral angle between the

[1]NRCC No. 12958.

Can. J. Chem. Downloaded from www.nrcresearchpress.com by 210.87.254.105 on 09/05/12
For personal use only.

TABLE 1. Proton chemical shifts and coupling constants of U, β-ψ, and D in D_2O and DMSO-d_6*

Chemical shifts (p.p.m.)	Uridine		β-Pseudouridine		Dihydrouridine	
	D_2O (ref. 1)	DMSO	D_2O (ref. 2)	DMSO	D_2O (ref. 3)	DMSO
$\nu_{1'}$	5.901	5.790	4.674	4.471	5.864	5.682
$\nu_{2'}$	4.341	4.028	4.279	3.925	4.303	3.949
$\nu_{3'}$	4.222	3.969	4.141	3.877	4.164	3.857
$\nu_{4'}$	4.128	3.850	4.009	3.706	4.030	3.678
$\nu_{5_B'}$	3.907	3.625	3.840	3.601	3.804	3.501
$\nu_{5_C'}$	3.803	3.556	3.726	3.450	3.727	3.442
ν_{5_A}	5.887	5.640			2.75	2.5
ν_{5_B}					2.75	
ν_{6_A}	7.862	7.880	7.660	7.546	3.59	3.3
ν_{6_B}					3.53	
$\nu_{OH\text{-}2'}$		5.312		4.855		5.016
$\nu_{OH\text{-}3'}$		5.012		4.655		4.880
$\nu_{OH\text{-}5'}$		5.038		4.743		4.760
Coupling constants (Hz)						
$J_{1'2'}$	4.4	5.1	5.0	4.5	6.3	6.0
$J_{2'3'}$	5.3	4.8	5.0	4.5	6.0	5.3
$J_{3'4'}$	5.5	4.3	5.2	5.3	3.6	3.7
$J_{4'5_B'}$	3.0	2.8	3.2	3.0	3.6	3.8
$J_{4'5_C'}$	4.4	3.0	4.6	3.5	4.8	4.0
$J_{5'_B5'_C}$	−12.7	−12.3	−12.7	−11.9	−12.6	−12.1
$J_{OH_2'-H_2'}$		5.0		4.8		5.4
$J_{OH_3'-H_3'}$		4.0		5.3		4.4
$J_{OH_5'-H_5'}$		4.0		4.8, 6.2		5.4

*Chemical shifts of U and β-ψ in D_2O were reported with respect to internal 2-trimethyl-silyl-propanesulfonic acid, sodium salt (DSS), those of D in D_2O with respect to internal sodium-3-trimethyl-silyl-propionate-2,2,3,3-d_4 (TSP). Chemical shifts of the nucleosides in DMSO-d_6 are reported from internal TMS. The correction factors at 30 °C are: internal DSS – external TMS in D_2O = 0.41; internal DSS – internal TSP in D_2O = 0.02; internal TMS – external TMS in DMSO = 0.37 p.p.m. The corrections between the internal references used are less than 5 Hz at 30 °C.

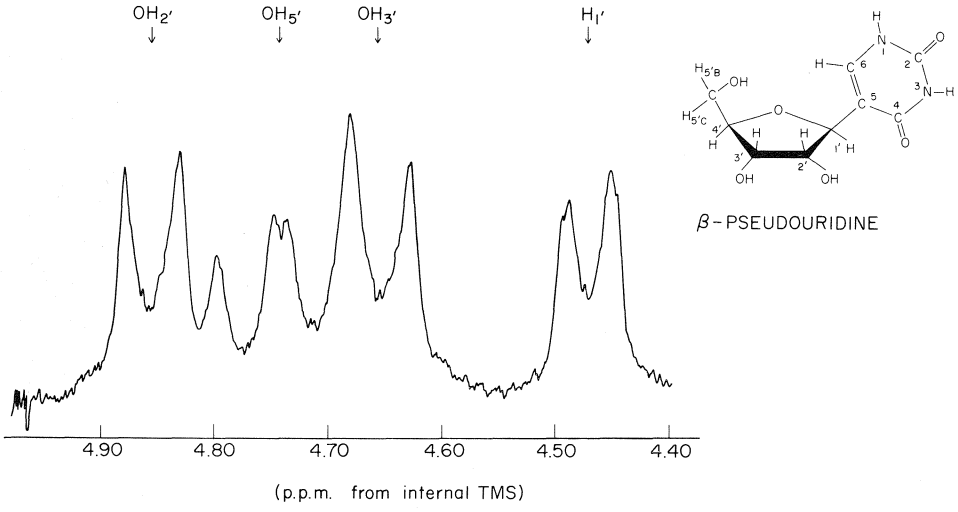

FIG. 1. The 100 MHz spectrum of the hydroxyl region of β-ψ in DMSO-d_6. Chemical shifts are reported in p.p.m. downfield from internal TMS.

Can. J. Chem. Downloaded from www.nrcresearchpress.com by 210.87.254.105 on 09/05/12
For personal use only.

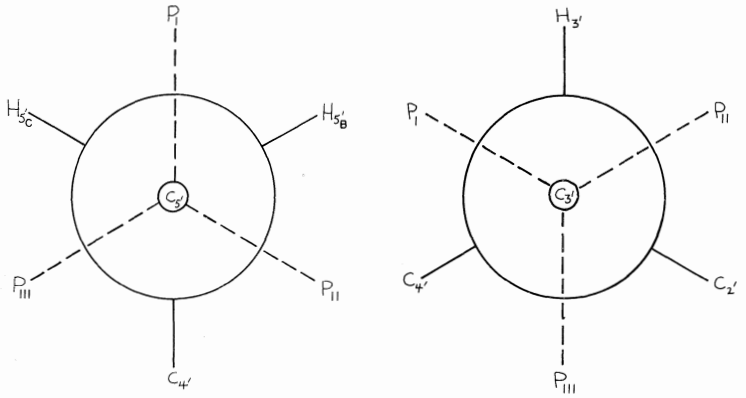

FIG. 2. Possible rotamers for the hydroxyl and phosphate groups at the 5′ and 3′ positions in nucleosides and nucleotides, respectively.

vicinal protons. A relationship similar to that proposed by Karplus (5) has been derived to account for this dependence (6),

$$[1]\quad J_{HCOH'} = 10.4\cos^2\phi - 1.5\cos\phi + 0.2$$

where ϕ is the dihedral angle formed between the H—C—O and C—O—H′ planes. This relationship has already been applied to the study of common nucleosides in mixtures of dimethyl sulfoxide and benzene (7). Our data for uridine, the only nucleoside common to both studies, demonstrate a significant difference in hydroxyl conformations in DMSO and in 40% benzene – 60% DMSO.

For a rapidly rotating hydroxyl group with equal lifetimes (populations) of the three possible rotamers an average coupling constant ($\bar{J}$) of 5.4 Hz would be observed. This arises from a weighted average of two *gauche* and one *trans* coupling.

$$[2]\quad \bar{J}_{observed} = P_I J_g + P_{II} J_g + P_{III} J_t$$

$$[3]\quad 1 = P_I + P_{II} + P_{III}$$

where J_g, using eq. 1, is 2.1 Hz and J_t is 12.1 Hz. P_i is the population of each rotamer; $P_I = P_{II} = P_{III} = 0.33$ for a freely rotating system. None of the measured couplings corresponds to that for either a *gauche* or a *trans* conformation. This indicates that the hydroxyl groups are interconverting rapidly between rotamers. It is possible that they may have a longer lifetime (larger population) in one rotamer state than the other.

Rotamer populations corresponding to the $H_{2'}$–$OH_{2'}$ and $H_{3'}$–$OH_{3'}$ couplings (Fig. 2) were calculated using eqs. 4 and 5.

$$[4]\quad \bar{J}_{observed} = 2.1\,P_g + 12.1\,P_t$$

$$[5]\quad 1 = P_g + P_t$$

There are two *gauche* conformers and the preceding set of equations measures only the total population.

For the 5′ hydroxyl group it is necessary to define the relationship between the OH-5′ proton and each of the H-5_B′ and -5_C′ protons (Fig. 2). In this case we call the rotamers *gauche–gauche* (I), *gauche–trans* (II), and *trans–gauche* (III). The relative populations of each rotamer can be estimated using eqs. 6–8

$$[6]\quad \bar{J}_{OH_{5'}-H_{5_B'}} = P_I J_g + P_{II} J_g + P_{III} J_t$$

$$[7]\quad \bar{J}_{OH_{5'}-H_{5C'}} = P_I J_g + P_{II} J_t + P_{III} J_g$$

$$[8]\quad 1 = P_I + P_{II} + P_{III}$$

where P_i is the mole fraction of each rotamer. J_g and J_t are the *gauche* and *trans* couplings determined from [1]. $\bar{J}_{OH_{5'}-H_{5_B'}}$ and $\bar{J}_{OH_{5'}-H_{5C'}}$ are the values obtained from the spectra. These are average values due to rapid rotation, on the n.m.r. time scale, about the exocyclic $C_{5'}$—$O_{5'}$ bond. We should emphasize here that the

Can. J. Chem. Downloaded from www.nrcresearchpress.com by 210.87.254.105 on 09/05/12
For personal use only.

TABLE 2. Calculated rotamer populations* about C—O bonds and the observed couplings (Hz) of the hydroxyl protons in U, β-ψ, and D

	β-ψ			D			U		
Spin–spin coupling	Observed J	P_t	P_g	Observed J	P_t	P_g	Observed J	P_t	P_g
$J_{OH_{2'}-H_{2'}}$	4.8	0.27	0.74	5.4	0.33	0.67	5.0	0.29	0.71
$J_{OH_{3'}-H_{3'}}$	5.3	0.32	0.68	4.4	0.23	0.76	4.0	0.19	0.80
		P_{t-g} P_{g-t}	P_{g-g}		P_{t-g} P_{g-t}	P_{g-g}		P_{t-g} P_{g-t}	P_{g-g}
$J_{OH_{5'}-H_{5'}}$	4.8 6.2	0.41	0.32	5.4	0.33	0.33	4.0	0.19	0.62
		0.27			0.33			0.19	

*P_g, population of *gauche* rotamer (total population of two *gauche* rotamers at 2′ and 3′). P_t, population of *trans* rotamer. P_{t-g}, P_{g-t}, population of *trans–gauche* and *gauche–trans* rotamers at 5′. P_{g-g}, population of *gauche–gauche* rotamer at 5′.

method cannot distinguish the *gauche–trans* rotamer (II) from the *trans–gauche* rotamer (III) since absolute assignments of H-5_B′ and -5_C′ cannot be made.

The results of the rotamer calculations are shown in Table 2. At the 2′ position, D manifests no preference for any rotamer whereas both β-ψ and U have slight preferences for the *gauche* rotamers. At the 3′ position, β-ψ manifests no preference for any rotamer but D and U have slight preferences for the *gauche* rotamers. At the 5′ position, β-ψ slightly favors one of the unsymmetrical rotamers (II or III of Fig. 2), D has equal populations of all three, and U has a strong preference for the *gauche–gauche* rotamer.

Because the corresponding experiment cannot be done in water, comparison of the hydroxyl group conformations in DMSO-d_6 and D_2O cannot be made. However, recently it has been found that rotamer populations about C—O bonds can be estimated by means of the couplings between ^{13}C and ^{31}P in the group ^{13}C—C—O—^{31}P of nucleotides (8–11). The data for the 2′-, 3′-, and 5′-phosphates of U indicate that the 2′-phosphate group prefers the $C_{1'}$-*trans*, $C_{3'}$-*gauche* rotamer, the 3′-phosphate the $C_{2'}$-*gauche*, $C_{4'}$-*trans* rotamer, and the 5′-phosphate, the $C_{4'}$-*trans* rotamer (I of Fig. 2). No data are available for the phosphates of D and β-ψ. The bulkier phosphate groups have greater preferences for particular rotamers than do the hydroxyl groups of the compounds studied here. In the case of 2′-UMP, 3′-UMP, and 5′-UMP the preferences manifest by the phosphate group are similar to, although more pronounced than, those found for the corresponding hydroxyl groups of U.

(b) Ribose Ring Conformation

The expected angles and coupling constants for different ribofuranose ring conformations and the arguments used in the conformational analysis have been described in detail earlier (1, 2, 12), and justified by recent experimental (10) and theoretical (13) studies. The chemical shifts and coupling constants of the ribose ring protons are given in Table 1. The data indicate that within the reliability of the method there are no significant changes in the ribose ring conformation when changing the solvent from D_2O to DMSO-d_6.

(c) Conformation About the Exocyclic $C_{4'}$—$C_{5'}$ Bond

In DMSO-d_6, the vicinal (4′–5_B′ and 4′–5_C′) couplings for all three nucleosides are smaller and more alike than in D_2O. This indicates an even greater preference for the *gauche–gauche* rotamer in DMSO. The relative populations of each rotamer can be estimated using eqs. 3, 6, and 7 where J_g and J_t are determined using the Karplus relationship (5). The method, which assumes rapid interconversion between rotamers, has been described in detail elsewhere (1–3). Results of the calculations are presented in Table 3. Because an unambiguous assignment of H-5_B′ and -5_C′ cannot easily be made, the method cannot distinguish between the *gauche–trans* and *trans–gauche* rotamers. In the present case this is an insignificant limitation since the

Can. J. Chem. Downloaded from www.nrcresearchpress.com by 210.87.254.105 on 09/05/12
For personal use only.

TABLE 3. Limits for the relative populations of 60° staggered rotamers around the exocyclic $C_{4'}$—$C_{5'}$ bond of U, β-ψ, and D in DMSO-d_6 solutions

	Uridine		β-Pseudouridine		Dihydrouridine	
J_0 (0–90°)	9.4	9.4	9.4	9.4	9.4	9.4
J_0 (90–180°)	10.4	12.0	10.4	12.0	10.4	12.0
$J_{4'5_B'}$	2.8	2.8	3.0	3.0	3.8	3.8
$J_{4'5_C'}$	3.0	3.0	3.5	3.5	4.0	4.0
P_I	0.79	0.82	0.70	0.75	0.53	0.61
P_{II}	0.12	0.10	0.18	0.15	0.25	0.21
P_{III}	0.09	0.08	0.12	0.10	0.22	0.18

gauche–gauche rotamers are preferred. If we use the argument proposed recently by Remin and Shugar (14) the assignments represented by Fig. 3 of ref. 3 are correct, and states I, II, and III of Table 3 are the *gauche–gauche*, *gauche–trans*, and *trans–gauche* states, respectively.

(d) Chemical Shift Changes

In DMSO-d_6, most of the proton resonances shift upfield. The H-2′, -3′, -4′, -5_B′, and -5_C′ resonances do so by 24–35 Hz. This does not appear to be caused by any change in the sugar–base torsion angle. Such changes are usually measured by preferential shifts in the resonances of the ribose ring protons (15–17). The 2′ and 3′ protons should be deshielded and the 4′, 5_B′, and 5_C′ protons should be shielded if there is a change of base conformation from *anti* to *syn*. Such changes have not been observed, all proton resonances have shifted upfield by similar amounts.

The chemical shift changes induced in the base proton resonances by DMSO-d_6 are less uniform than the shifts induced in the ribose ring protons. In U, the H-5 resonance is shifted upfield 25 Hz but the H-6 resonance is shifted downfield 2 Hz. In β-ψ, the H-6 resonance is shifted upfield 11 Hz. In D, where the H-5_A, -5_B, -6_A, and -6_B resonances give rise to 'deceptively simple' spectra, the resonances appear shifted upfield 25–30 Hz. The anomalous behavior of U in this case may be due to specific solvent–base interactions, which have been invoked to explain abnormal temperature dependences of the base proton resonances of U and related oligonucleotides (18), and the solvent effects on the ^{13}C n.m.r. spectra of uridine (19).

Conclusion

Analyses of the n.m.r. spectra of U, D, and β-ψ in DMSO-d_6 do not show any large conformational differences in the ribose ring when compared with data taken in D_2O; the greatest difference is an increased preference by the exocyclic CH_2—OH group for the *gauche–gauche* rotamer. In the three nucleosides the hydroxyl groups are rotating rapidly and manifest only slight preferences for particular rotamers. When a preference is manifest, it is for the *gauche* rotamers at positions 2′ and 3′, and the *gauche–gauche* rotamer at position 5′. No changes were detected in the sugar–base torsion angle. The principal conformational difference observed in DMSO between uridine and the modified nucleosides dihydrouridine and β-pseudouridine is the strong preference of the 5′-hydroxyl group of uridine for the *gauche–gauche* rotamer.

1. B. J. BLACKBURN, A. A. GREY, I. C. P. SMITH, and F. E. HRUSKA. Can. J. Chem. **48**, 2866 (1970).
2. F. E. HRUSKA, A. A. GREY, and I. C. P. SMITH. J. Am. Chem. Soc. **92**, 4088 (1970).
3. R. DESLAURIERS, R. D. LAPPER, and I. C. P. SMITH. Can. J. Biochem. **49**, 1279 (1971).
4. R. D. LAPPER. Private communication.
5. M. KARPLUS. J. Chem. Phys. **30**, 11 (1959).
6. R. R. FRASER, M. KAUFMAN, P. MORAND, and G. GOVIL. Can. J. Chem. **47**, 403 (1969).
7. D. B. DAVIES and S. S. DANYLUK. Can. J. Chem. **48**, 3112 (1970).
8. H. H. MANTSCH and I. C. P. SMITH. Biochem. Biophys. Res. Commun. **46**, 808 (1972).
9. I. C. P. SMITH, H. H. MANTSCH, R. D. LAPPER, R. DESLAURIERS, and T. SCHLEICH. *In* Conformations of biological molecules and polymers. Proc. Vth Jerusalem Symposium on Quantum Chemistry and Biochemistry. *Edited by* E. D. Bergmann and B. Pullman. Academic Press, New York. In press.
10. R. D. LAPPER, H. H. MANTSCH, and I. C. P. SMITH. J. Am. Chem. Soc. **94**, 6243 (1972).
11. R. D. LAPPER, H. H. MANTSCH, and I. C. P. SMITH. J. Am. Chem. Soc. In press.
12. T. SCHLEICH, B. J. BLACKBURN, R. D. LAPPER, and I. C. P. SMITH. Biochem. **11**, 137 (1972).

Can. J. Chem. Downloaded from www.nrcresearchpress.com by 210.87.254.105 on 09/05/12
For personal use only.

13. C. GIESSNER-PRETTRE and B. PULLMAN. J. Theor. Biol. In press.
14. M. REMIN and D. SHUGAR. Biochem. Biophys. Res. Commun. **48**, 636 (1972).
15. H. DUGAS, B. J. BLACKBURN, R. K. ROBINS, R. DESLAURIERS, and I. C. P. SMITH. J. Am. Chem. Soc. **93**, 3468 (1971).
16. M. P. SCHWEIZER, J. T. WITKOWSKI, and R. K. ROBINS. J. Am. Chem. Soc. **93**, 277 (1971).
17. F. E. HRUSKA. J. Am. Chem. Soc. **93**, 1795 (1971).
18. I. C. P. SMITH, B. J. BLACKBURN, and T. YAMANE. Can. J. Chem. **47**, 513 (1969).
19. H. H. MANTSCH and I. C. P. SMITH. Can. J. Chem. In press.

Can. J. Chem. Downloaded from www.nrcresearchpress.com by 210.87.254.105 on 09/05/12
For personal use only.

6,8,8-Trimethyl-6-(*o*-methylthiobenzoyl)-4-thia-benzocyclooctenone. A Novel Product from the Attempted Base-catalyzed Methylation of 3-Methylthiochroman-4-one

IAN W. J. STILL, MOHINDER S. CHAUHAN, AND M. THOMAS THOMAS

Lash Miller Chemical Laboratories, Department of Chemistry, University of Toronto, Toronto, 181, Ontario

Received October 6, 1972

The structure of the unusual eight-membered cyclic ketone **3** obtained on treatment of 3-methylthiochroman-4-one with methyl iodide in the presence of potassium *t*-butoxide has been assigned on the basis of n.m.r. (^{13}C and ^{1}H), i.r., and mass spectrometric evidence. A mechanism has been proposed to account for the formation of both abnormal and expected methylation products from 3-methylthiochroman-4-one under varying conditions.

La structure de la cétone inusitée **3**, cyclique à huit membres, obtenue en traitant le méthyl-3 thiochromanone-4 avec de l'iodure de méthyle en présence de *t*-butoxide de potassium, a été élucidée en se basant sur la r.m.n. (^{13}C et ^{1}H) l'i.r., et la spectrométrie de masse. Un mécanisme est proposé tenant compte de la formation des deux produits de méthylation, l'un anormal l'autre prévu, à partir du méthyl-3 thiochromanone-4, et ce sous différentes conditions.

[Traduit par le journal]

Can. J. Chem., **51**, 839 (1973)

As part of a continuing investigation of the chemical and photochemical reactions of thiochromanone derivatives (1, 2) we wished to prepare 3,3-dimethylthiochroman-4-one (**2**) (3) from 3-methylthiochromanone (**1**) (4). In spite of some indication (5) that similar alkylation at the 3-position in the chromanones was likely to prove difficult, we have now succeeded in achieving the required conditions for the conversion of **1** into **2**. The details of an interesting rearrangement discovered during our search for the appropriate conditions have now been elucidated and will form the subject of the following discussion.

The treatment of 3-methylthiochroman-4-one with potassium *t*-butoxide and methyl iodide in refluxing *t*-butyl alcohol produced a solid product which was clearly not identical with the expected simple methylation product **2**. This ketone had i.r. bands at 1685 and 1655 cm^{-1} (C=O) and the presence of two carbonyl groups was further confirmed by the ^{13}C n.m.r. spectrum which showed signals at δ 210.6 and 198.5 p.p.m. The mass spectrum showed a molecular ion at *m/e* 384 with major fragments appearing at *m/e* 233 and 151. Chemical confirmation of the existence of two carbonyl groups was provided by sodium borohydride reduction which led to the formation of a diol.[1]

[1]Attempted desulfurization of the rearrangement product with Raney nickel led only to a complex mixture of products.

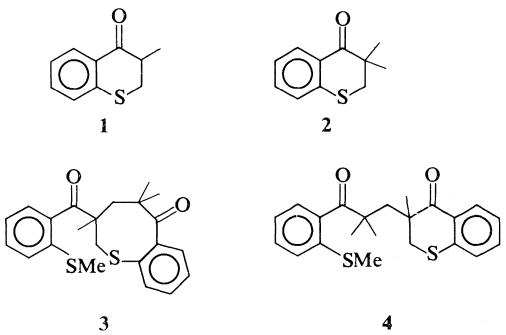

Two structures which might be expected to be compatible with the above evidence and the molecular formula of $C_{22}H_{24}O_2S_2$, and which can also be accounted for by reasonable mechanistic pathways are those of **3** and **4**. Our preference for structure **3** has been based on a thorough examination of the spectroscopic evidence not only from the rearrangement product but from model compounds such as **1**, **2**, and thiochroman-4-one itself. Our rejection of the thiochromanone structure **4** rests mainly on the following observations:

(*1*) The i.r. carbonyl stretching bands of **1**, **2**, and the parent thiochromanone are in the range 1665–1675, whereas the rearrangement product has carbonyl bands at 1685 and 1655 cm^{-1}.

(*2*) The ^{13}C chemical shifts of the carbonyl carbons of **1**, **2**, and thiochroman-4-one lie in the range δ 193.7–198.2, whereas the chemical shifts of the carbonyl carbons in the rearrange-

Can. J. Chem. Downloaded from www.nrcresearchpress.com by 210.87.254.40 on 09/05/12
For personal use only.

Can. J. Chem. Downloaded from www.nrcresearchpress.com by 210.87.254.40 on 09/05/12
For personal use only.

ment product are δ 210.6 (eight-membered ring) and 198.5 p.p.m. (acyclic carbonyl) (6). (Other assignments in the ^{13}C n.m.r. spectrum of **3** were made by examination of partially decoupled spectra and appear in the Experimental section.)

(*3*) The base peak in the mass spectra of four simple thiochromanones already examined, including **1** and the parent member of the series, corresponds to a retro-Diels–Alder fragmentation process (7). Occurrence of such a fragmentation in **4** would lead to a fragment of *m/e* 136. The spectrum of the rearrangement product indeed reveals a peak at *m/e* 136, but with an intensity less than 5% of that of the base peak (*m/e* 151). Structure **3** can better accommodate the fragmentations leading to peaks at *m/e* 233 ($C_{14}H_{17}OS$) and 151 (C_8H_7OS), whose constitution has been confirmed by accurate mass measurement, and also to a major peak at *m/e* 328, corresponding to loss of isobutylene from the molecular ion.

(*4*) Mechanistic arguments also favor formation of **3** rather than **4** and will be discussed in a later section.

It is of interest to point out one feature of interest in the ^1H n.m.r. spectrum of **3**, namely a well-marked distinction in the appearance of the two methylene group signals of the eight-membered ring. In the case of the —SCH_2— group, the expected doublet of doublets was evident, at δ 2.93 and 3.48 p.p.m., with a geminal coupling constant of 13.5 Hz. However, the non-equivalence of the protons of the —CCH_2— group was too small to be observable (8) on a 60 MHz spectrometer and was only just discernible on a 100 MHz spectrometer (slightly resolved peak centered at δ 2.50 p.p.m.). The addition of relatively small increments of the lanthanide shift reagent Eu(fod)$_3$ rapidly increased the non-equivalence of the —CCH_2— protons while affecting each diastereotopic proton of the —SCH_2— group almost equally, thus enabling us to obtain two well-resolved AB quartets and assign a geminal coupling constant of 14 Hz to the —CCH_2— hydrogens.

A series of methylation experiments on **1** using a variety of basic reagents (potassium *t*-butoxide, sodium amide, sodium hydride) in a variety of solvents (benzene, *t*-butyl alcohol, 1,2-dimethoxyethane) under nitrogen, for varying lengths of time and at different temperatures, has revealed that the product of the reaction is, in most cases, the expected 3,3-dimethylthiochroman-4-one (**2**). Only when potassium *t*-butoxide was employed as the base was any of the rearrangement product **3** obtained. Interestingly, **3** was the major product using potassium *t*-butoxide in refluxing solutions of benzene or *t*-butyl alcohol, although in each case minor amounts of **2** were also observed. In the former experiment we were able to isolate a small amount (*ca.* 5%) of 2-methyl-2′-methylthioacrylophenone (**5**), the structure of which has been established by n.m.r., i.r., and mass spectrometry, and also by catalytic reduction to the isobutyrophenone analog, and which we believe is involved in the formation of **3** as an intermediate (Scheme 1). However, even in the presence of potassium *t*-butoxide, **1** could be efficiently converted to **2** by carrying out the reaction in *t*-butyl alcohol at 25°.

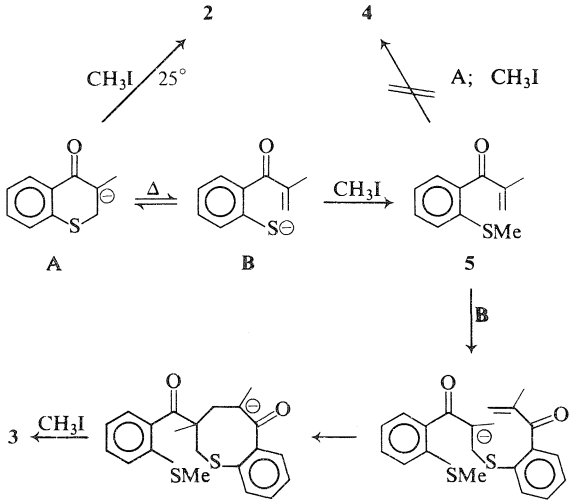

SCHEME 1

Our view of the mechanistic route to **3** from **1**, summarized in Scheme 1, is based in part on the observation that higher temperatures appear to promote the formation of the 'abnormal' product in the base-catalyzed methylation reaction and in part on the isolation of compound **5** as a minor product from the potassium *t*-butoxide catalyzed reaction of **1** with methyl iodide in benzene. The equilibrium mixture of the anion **A** and the ring-opened thiolate ion **B** thus leads predominantly, if not exclusively, to **2** in the presence of methyl iodide at 25°, but predominantly to **5** at temperatures around 80°. The observed preferential attack on **5** by **B** rather than **A** is expected on steric grounds, while sub-

Can. J. Chem. Downloaded from www.nrcresearchpress.com by 210.87.254.40 on 09/05/12
For personal use only.

sequent cyclization (intramolecular Michael-type addition) and methylation account for the observed product **3**.

Our study has shown that while base-catalyzed alkylation at the 3-position in thiochroman-4-one derivatives is possible, it is markedly sensitive to the reaction conditions employed.

Experimental

General

The i.r. spectra (cm^{-1}) were recorded as specified on a Perkin–Elmer Model 337 grating spectrophotometer and the p.m.r. spectra (δ) on Varian A-60 and HA-100 spectrometers with tetramethylsilane as the internal standard.

The ^{13}C n.m.r. spectra were obtained on a Varian Associates XL-100-15 machine with tetramethylsilane as the internal standard. Mass spectra were recorded on a Bell and Howell 21-490 spectrometer and accurate mass measurements on the A.E.1. MS-902 instrument. The elemental analyses were performed by the Scandinavian Microanalytical Laboratory, Box 25, Herlev, Denmark. V.p.c. was conducted on a Varian Aerograph Autoprep Model A-700 instrument using a Ucon column (12 ft × $\frac{3}{8}$ in.) containing 60–80 mesh Chromosorb W. Column chromatography was performed using silica gel (Davison Chemical, Grade 923, 100–200 mesh) or neutral alumina (Fisher Grade I, 80–200 mesh) and Fisher A.C.S. grade solvents. All melting points and boiling points are uncorrected.

3-Methylthiochroman-4-one

This compound was prepared by the method of Arndt (4).

Methylation of 3-Methylthiochroman-4-one

Method A

A solution of potassium *t*-butoxide prepared by refluxing potassium (1.17 g) in *t*-butyl alcohol (40 ml) under nitrogen was cooled to 40° and 3-methylthiochroman-4-one (1.78 g in 5 ml dry benzene) added with stirring. The mixture was immediately cooled in ice and methyl iodide (4 ml) was added. After stirring for 10–15 min, the reaction mixture was refluxed for a further 90 min. Water (40 ml) was added to the cooled reaction mixture and the *t*-butyl alcohol evaporated. The residual solution was extracted with ether and the combined ethereal extracts washed and dried ($MgSO_4$). The ether was evaporated and the residue chromatographed over alumina. Elution with benzene – petroleum ether mixture (40–50% benzene) gave 3,3-dimethylthiochroman-4-one (**2**) (70 mg). Further elution with benzene – petroleum ether mixtures (70% benzene), benzene, and finally benzene–ether mixtures (2–6% ether) gave the dimer **3** (1.2 g, 63%) which was crystallized from acetic acid and finally recrystallized from a mixture of benzene – petroleum ether, m.p. 112–113°. I.r. (KBr) 1685 and 1655 (C=O); n.m.r. ($CHCl_3$-d_1) 1.16 (3H, s), 1.26 (3H, s), 1.33 (3H, s), 2.31 (3H, s), 2.50 (2H, unresolved AB quartet), 2.93 (1H, d, J = 13.5 Hz), 3.48 (1H, d, J = 13.5 Hz), 6.90–7.40 (7H, m), 8.01 (1H, dd, J_1 = 8.5, J_2 = 2.0 Hz); ^{13}C n.m.r. 210.6 (s, cyclic C=O), 198.5 (s, acyclic C=O), 141.2, 140.2, 136.5, and 130.6 (each s, aromatic quaternary carbon), 133.7–123.5 (m, 8 aromatic carbon), 48.3, 44.9 (each s, quaternary carbon), 44.5 (t, C—CH_2), 38.6 (t, S—CH_2), 28.5, 26.3, and 24.2 (each q, C—CH_3), 17.5 (q, S—CH_3). The mass spectrum showed the expected molecular ion at *m/e* 384 (6), 328 (10), 233 (25), 194 (5), 177 (11), 151 (100), 136 (5), 108 (5). Mass measurements (*m/e* 233 and 151). Calculated for $C_{14}H_{17}OS$ and C_8H_7OS; 233.0999 and 151.0217. Found: 233.1013 and 151.0222.

Anal. Calcd. for $C_{22}H_{24}O_2S_2$: C, 68.75; H, 6.25; S, 16.66. Found: C, 68.61; H, 6.33; S, 16.43.

Method B

To a solution of potassium *t*-butoxide (1.17 g) in benzene (125 ml) was added 3-methylthiochroman-4-one (1.78 g in 10 ml benzene). Methyl iodide (4 ml) was then added to the brown solution at 25° and the temperature maintained at 25° for 15 min. The mixture was then refluxed for 1½ h and cooled. Water (40 ml) was added to the reaction mixture and the solution extracted thoroughly with ether, the combined extracts being washed and dried ($MgSO_4$). The ether was evaporated and the residue chromatographed over silica gel (100–200 mesh, 200 g). Elution with benzene – petroleum ether mixture (1:1) gave 3,3-dimethylthiochroman-4-one (**2**) (5 mg) and 2-methyl-2′-methylthioacrylophenone (**5**) (70 mg, 4%) which was purified by v.p.c. at 180°. I.r. (**5**) (neat liquid): 1650, 1580, 1430, 1350; n.m.r. ($CHCl_3$-d_1) 2.05 (3H, m, J < 1 Hz), 2.40 (3H, s), 5.50 (1H, m), 5.92 (1H, m), 7.10–7.60 (4H, m). The mass spectrum showed the expected molecular ion at *m/e* 192. Calculated for $C_{11}H_{12}OS$: 192.060874. Found: 192.061535.

Further elution with benzene and benzene methylene – chloride mixture (2% methylene chloride) gave the dimer **3** (1.3 g, 68%).

Method C

To a solution of 3-methylthiochroman-4-one (0.85 g) in dry benzene (10 ml) was added methyl iodide (1 ml in 5 ml of benzene). The mixture was cooled and sodium hydride (0.4 g) added with stirring during 30 min and the mixture refluxed for 5 h. Water (40 ml) was added, and the solution extracted with benzene. The combined benzene extracts were washed and dried ($MgSO_4$). The benzene was evaporated and the residue chromatographed over alumina. Elution with benzene – petroleum ether mixture (2:3) yielded 3,3-dimethylthiochroman-4-one (**2**) (0.3 g, 40%) and starting material (0.15 g).

Methylation of Thiochroman-4-one

To a solution of thiochroman-4-one (20.3 g) in freshly distilled 1,2-dimethoxyethane (50 ml) was added methyl iodide (20 ml) and the mixture cooled to −10°. A slurry of sodium hydride (12.5 g) in pentane was added in small amounts with vigorous stirring, keeping the temperature below 10°, and then the reaction mixture was maintained at room temperature for 4 h. During this period the red color gradually faded and finally the mixture was heated to 80° for 5 min by which time the red color had disappeared completely. The reaction mixture was cooled, water added, and the solution extracted with ether. Washing and drying ($MgSO_4$) of the combined extracts and evaporation of the solvent gave 3,3-dimethylthiochroman-4-one (**2**) (11.2 g, 46%) which was purified by distillation under reduced pressure, b.p. 120–122° (1.5 mm). I.r. (neat liquid) 1668, 1587, 1307, 1075, 985, and 892; n.m.r. ($CHCl_3$-d_1) 1.30 (6H, s), 3.00 (2H, s), 7.00–7.30 (3H, m), 8.05 (1H, dd, J_1 = 8.5, J_2 = 2.0 Hz).

Reduction of Dimeric Rearrangement Product **3** *with* $NaBH_4$

Compound **3** (200 mg) in dioxane (20 ml) was added to sodium borohydride (400 mg) in dioxane–water mixture (1:1) (16 ml) and the solution allowed to stand at room temperature for 1 h. The dioxane was removed under vacuum while keeping the bath temperature at 40–50°. The solution was acidified with dilute hydrochloric acid and the product (180 mg, 90%) collected as a white solid which was crystallized from a mixture of ethanol – petroleum ether, m.p. 172–174°. I.r. (Nujol) 3350, 3265, 1600, 1590. The mass spectrum showed the expected molecular ion at *m/e* 388 (4), 370 (7), 236 (19), 235 (24), 217 (17), 162 (100), 153 (57), 147 (45), 135 (24), 109 (16), 83 (16), 77 (17).

Hydrogenation of 2-Methyl-2′-methylthioacrylophenone (**5**)

2-Methyl-2′-methylthioacrylophenone (30 mg) was dissolved in ethyl acetate (15 ml) and hydrogenated over Pd (5% on C) (20 mg) at 25° and 760 Torr. After the uptake of 1 mol of hydrogen was complete the solution was filtered and the solvent evaporated. The residue was molecularly distilled to give *o*-methylthio-isobutyrophenone (25 mg). I.r. (neat liquid) 1655, 1580, 1550, 1450, 1425, 1260, 1220, 972, 730; n.m.r. ($CHCl_3$-d_1) 1.20 (6H, d, J = 7.0 Hz), 2.34 (3H, s), 3.41 (1H, m, J = 7.0 Hz) 7.00–7.80 (4H, m). The mass spectrum showed the expected molecular ion at *m/e* 194. Calculated for $C_{11}H_{14}OS$: 194.0765. Found: 194.0775.

We thank Mr. N. Plavac for recording the ^{13}C n.m.r. spectra and Mr. Ian Peat for helpful discussion regarding the use of the lanthanide shift reagent. Financial support of this work by the National Research Council of Canada is gratefully acknowledged.

1. I. W. J. Still and M. T. Thomas. J. Org. Chem. **33**, 2730 (1968).
2. I. W. J. Still and M. T. Thomas. Tetrahedron Lett. 4225 (1970).
3. K.-H. Wünsch, K.-H. Stahnke, and A. Ehlers. Chem. Ber. **103**, 2302 (1970).
4. F. Arndt. Chem. Ber. **58**, 612 (1925).
5. Heterocyclic Compounds. Vol. 2. *Edited by* R. C. Elderfield. John Wiley and Sons Inc., New York. 1951. p. 379.
6. G. C. Levy and G. L. Nelson. Carbon-13 nuclear magnetic resonance for organic chemists. John Wiley and Sons, Inc., New York, N.Y. 1972. pp. 110–116.
7. A. G. Harrison, I. W. J. Still, and M. T. Thomas. Org. Mass Spectrom. **3**, 899 (1970).
8. A. K. Bose, B. Dayal, H. P. S. Chawla, and M. S. Manhas. Tetrahedron Lett. 3599 (1972) and refs. cited therein.

Can. J. Chem. Downloaded from www.nrcresearchpress.com by 210.87.254.40 on 09/05/12
For personal use only.

The Alkylation of Cyclic Diketone Thallium(I) Salts

JOHN M. MCINTOSH[1] AND P. M. BEAUMIER
Department of Chemistry, University of Windsor, Windsor, Ontario

Received September 25, 1972

The *C*/*O* alkylation ratios of a series of alkyl halides and α-haloesters with the thallium(I) salts of 1,3-cyclohexanedione and 1,3-cyclopentanedione have been investigated. Unlike the alkylation of acyclic diketone salts, the predominant process in most cases is *O*-alkylation.

On a déterminé les pourcentages relatifs de *C* et de *O*-alkylation obtenus lors de la réaction des sels de thallium(I) de la cyclohexanedione-1,3 et de la cyclopentanedione-1,3 avec une série d'halogénures d'alkyle et d'esters halogénes en α. Contrairement aux résultats obtenus en séries acycliques, le processus prédominant dans la plupart des cas est la *O*-alkylation.

[Traduit par le journal]

Can. J. Chem., **51**, 843 (1973)

Can. J. Chem. Downloaded from www.nrcresearchpress.com by 210.87.254.42 on 09/05/12
For personal use only.

Much of the recent activity in organic synthesis has been focussed on the development of regiospecific reactions. The advances made in this area have allowed the synthesis of many compounds which would have been otherwise difficult if not impossible. Notable among these developments has been the regiospecific *C*-alkylation and -acylation of 1,3-diketones through the mediation of their thallium(I) salts in heterogeneous media (1). The problems involved in the alkylation of these compounds using more usual conditions are well known (for an excellent summary of these problems, see ref. 2).

Our interest in this procedure stemmed from the need to prepare 2-alkyl-1,3-cyclopentanediones and 2-alkyl-1,3-cyclohexanediones for other work. The alkylations of 1,3-cyclopentanedione and 1,3-cyclohexanedione are known to be unusually difficult (3, 4). When our investigation was initiated, no reports of the alkylation of *cyclic* 1,3-diketones via their thallium salts had appeared.[2] We, therefore, undertook a survey of these reactions with thallium salts **1** and **5** and a series of alkyl halides and α-haloesters in order to determine the *C*/*O* alkylation ratios.

Results and Discussion

Our initial attempts involved the reactions of **1** and **5** with methyl iodide (**2***a*) and ethyl bromide (**2***b*) (Scheme 1). The results in terms of *C*-alkylation, especially with **2***b*, were disappointing. However, it was felt that the use of a bifunctional alkylating agent, as well as affording more useful products, might well allow an increase in the amount of *C*-alkylation. Since most of the charge on the ambident ion will reside on the oxygen atom, an initial coordination of one of the two positively polarized atoms in **2** at this position might occur. The remaining electrophilic site in **2** might then orient itself towards the β-carbon atom of **1** or **5**, thus improving the chance for *C*-alkylation.

The results are summarized in Scheme 1 and Tables 1, 2, and 3. All reactions were run employing the salt as a suspension in the alkylating agent which also served as the solvent, conditions reported to maximize the yield of *C*-alkylated product (1*b*).

The regiospecificity of the alkylation of acyclic 1,3-diketone thallium salts has been attributed to the crystal structure of the salt. The metal and two oxygen atoms are inside the crystal, exposing only the carbon skeleton to the action of the alkylating agent (1*b*). The evidence for this has been summarized (1*a*). However, the data presented in Table 1 clearly indicate that this predilection of *acyclic* 1,3-diketone thallium salts for *C*-alkylation is not shared by their cyclic relatives. Although we have no evidence as to the crystal structure of **1** or **5**, we attribute our results to the steric prohibition of such a cyclic chelation and the shielding of the carbon atom of the ambident nucleophile by the ring methylene groups. Another proposal (ref. 2, p. 523) has suggested that the regiospecificity in the acyclic cases is due to the fact that the reactions are both heterogeneous and involve a cation which is tightly bound to oxygen, factors which are

[1]To whom correspondence should be addressed.
[2]However, for recent examples see refs. 5 and 14.

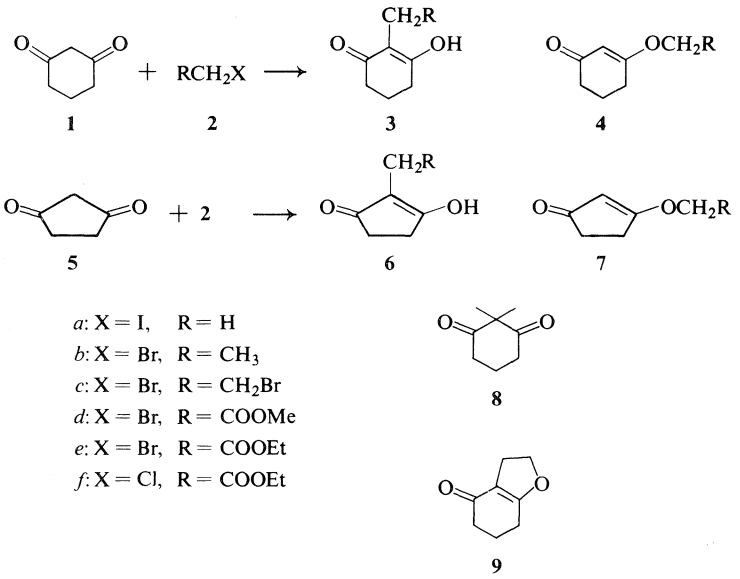

SCHEME 1

TABLE 1. Products and yields from alkylations of salts **1** and **5**

Run No.	Reactants	Catalyst	Temperature (°C)	Reaction % Conversion	*O*-alkylation	*C*-alkylation	Other
1	**1** + **2***a*	—	41	92	22 (**4***a*)	51 (**3***a*) 27 (**8**)	—
2	**1** + **2***b*	—	70*	15	100 (**4***b*)	—	—
3	**1** + **2***c*	—	70	15	82 (**4***c*)	13 (**9**)†	5
4		Et_3N	70	68	90 (**4***c*)	8 (**9**)†	2
5	**1** + **2***d*	—	70	68	69 (**4***d*)	—	31‡
6	**1** + **2***f*	—	70	22	62 (**4***f*)	—	38‡
7		Et_3N	70	98	94 (**4***f*)	—	6
8	**5** + **2***a*	—	41	98	95 (**7***a*)	5 (**6***a*)	—
9	**5** + **2***b*	—	70*	18	100 (**7***b*)	—	—
10	**5** + **2***c*	—	70	15	100 (**7***c*)	—	—
11		Et_3N	70	85	100 (**7***c*)	—	—
12		—	100	42	100 (**7***c*)	—	—
13	**5** + **2***d*	—	70	96	81 (**7***d*) 19 (**7***a*)	—	—
14	**5** + **2***e*	—	70	87	100 (**7***e*)	—	—
15	**5** + **2***f*	—	70	31	100 (**7***f*)	—	—

*Sealed tube reaction.
†Unstable.
‡Comprised of at least 4 compounds whose stability precluded further identification.

known to favor *C*-alkylation. Clearly our results do not support this postulate.

The isolation of a 13% yield of 4-oxo-2,3,4,5,6,7-hexahydrobenzofuran (**9**) from the reaction of **1** and ethylene dibromide (**2***c*) indicated the occurrence of some *C*-alkylation and gave some support to our hopes for improved yields of **3** from bifunctional alkylating agents. However, when **1** was treated with **2***d* or **2***f*, complex mixtures resulted, from which could be isolated the ethers **4***d* and **4***f*. The remainder of the products all showed strong carbonyl absorptions but their n.m.r. spectra were unintelligible in terms of simple alkylation procedures, and they decomposed rapidly on exposure to air and light.

The esters **3***d* and **3***f* have been prepared by

Can. J. Chem. Downloaded from www.nrcresearchpress.com by 210.87.254.42 on 09/05/12
For personal use only.

Can. J. Chem. Downloaded from www.nrcresearchpress.com by 210.87.254.42 on 09/05/12
For personal use only.

TABLE 2. N.m.r. spectra of the alkylation products*†

Compound No.	Nuclear magnetic resonance spectra
3*a*‡	2.50 (t, 4, J = 6, ring), 2.15 (s, 3, CH_3), 1.88 (q, 2, J = 6, ring).
4*a*	5.40 (s, 1, —C=C*H*—), 3.76 (s, 3, —OCH_3), 2.57–1.75 (m, 6, ring).
8	2.75 (t, 4, J = 6, ring), 2.05 (q, 2, J = 6, ring), 1.36 (s, 6, CH_3—C—CH_3).
4*b*	5.20 (s, 1, C=C*H*), 3.55 (q, 2, J = 7, O$CH_2$$CH_3$), 2.60–1.72 (m, 6, ring), 1.36 (t, 3, J = 7, CH_2CH_3).
9	4.52 (t, 2, J = 10, CH_2—CH_2—O), 3.00–1.82 (m, 8).
4*c*	5.37 (s, 1, C=C*H*—), 4.20 (t, 2, J = 6, —O$CH_2$$CH_2$—), 3.61 (t, 2, J = 6, O—CH_2CH_2Br), 2.65–1.8 (m, 6, ring).
4*d*	5.11 (s, 1, —C=C*H*—), 4.47 (s, 2, —O—CH_2—COOR), 3.78 (s, 3, —COOCH_3), 2.7–1.7 (m, 6, ring).
4*f*	5.17 (s, 1, —C=C*H*—), 4.45 (s, 2, —O—CH_2COOR), 4.20 (q, 2 —$CO_2CH_2CH_3$), 2.7–1.7 (m, 6, ring), 1.30 (t, 3, J = 7, $CO_2CH_2CH_3$).
6*a*‡	9.56 (s, 1, O*H*), 2.60 (m, 4, ring), 2.00 (s, 3, CH_3).
7*a*	5.45 (s, 1, —C=C*H*), 3.97 (s, 3, —OCH_3), 2.82–2.40 (m, 4, ring).
7*b*	5.23 (s, 1, C=C*H*—), 4.02 (q, 2, J = 6.5, OCH_2—CH_3), 2.73 (m, 4, ring), 1.38 (t, 3, J = 6.5 CH_2—CH_3).
7*c*	5.23 (s, 1, C=C*H*), 4.33 (t, 2, J = 5.3, —O—CH_2—CH_2), 3.59 (t, 2, J = 5.3, CH_2CH_2—Br), 2.75–2.3 (m, 4, ring).
7*d*	5.20 (s, 1, C=C*H*), 4.57 (s, 2, O—CH_2—COOR), 3.80 (s, 3, COOCH_3), 2.8–2.3 (m, 4, ring).
7*e*§	5.15 (s, 1, C=C*H*), 4.60 (s, 2, —O—CH_2—COOR), 4.26 (q, 2, J = 7.5, CO_2—CH_2—CH_3), 2.80–2.25 (m, 4, ring), 1.25 (t, 3, J = 7.5, $CO_2CH_2CH_3$).

*Tabulation follows the order chemical shift (δ value), multiplicity (s = singlet, d = doublet, t = triplet, q = quartet, m = multiplet), number of protons, coupling constant, and assignment of protons.
†In deuteriochloroform unless otherwise noted.
‡In pyridine-d_6.
§In carbon tetrachloride.

TABLE 3. Infrared spectra of the alkylation products (cm^{-1})*

Compound No.	Infrared spectra (cm^{-1})
3*a*†	3100, 1580
4*a*	1670, 1645, 1610
8	1730, 1700, 1464
4*b*‡	1680, 1660(sh), 1610
9	1630(vs)
4*c*‡	1650, 1600
4*d*	1768, 1750(sh), 1670, 1620
4*f*	1761, 1740(sh), 1660, 1615
7*b*	1705, 1680, 1600
7*c*	1710, 1687, 1592
7*d*	1765, 1705, 1685, 1605
7*e*‡	1765, 1740, 1710, 1608

*In chloroform solution unless otherwise specified.
†As potassium bromide dispersion.
‡In carbon tetrachloride solution.

the action of α-haloesters on the potassium salts of 1,3-cyclohexanedione (6), but in our hands, none of these materials could be isolated. Since our interest was simply in the *C*/*O* alkylation ratios, we have not investigated these reactions further.

The data also indicate that *C*-alkylation is a more favorable process for **1** than for **5**. As proposed previously (3) this result may be ascribed to the fact that *O*-alkylation of **1** forces the product to assume the half chair conformation whereas *C*-alkylation allows the product to exist in the more stable chair conformation. In the case of **5**, both the *O*- and *C*-alkylation products are relatively rigid and therefore the stability gained by the formation of the conjugated ketone takes precedence. Similar reasoning has been used to rationalize the difference in the acidities of 1,3-cyclohexanedione and 1,3-cyclopentanedione (7).

One further point is of interest. When the enol ether **7***d* was allowed to stand at room temperature and exposed to the atmosphere, a clean conversion to **7***a* occurred over a period of some weeks. Although the enol ethers **7***a*, **4***a*, and **4***c* did decompose under analogous conditions, many products were produced. We have no further information on this rather novel decomposition.

NOTE ADDED IN PROOF: A recent paper (15) has presented results which also bring into doubt the ability of thallium enolate salts to promote exclusive *C*-alkylation in acyclic cases.

Experimental

Unless otherwise noted infrared spectra were recorded on a Beckmann IR12 spectrometer in chloroform solution and n.m.r. spectra were obtained on a JEOLCO C6OHL spectrometer in deuteriochloroform and are reported in δ units relative to TMS. The g.l.c. analyses were carried out on F and M Models 720 and 5750 gas chromatographs utilizing an 8 ft × 0.25 in. 20% SE-30 on Chromosorb W column. Preparative g.l.c. was performed using an 8 ft × 0.375 in. column packed as above. Composition of mixtures was determined using a disc integrator. Microanalyses were performed by A. B. Gygli, Microanalysis Laboratory, Toronto, Ontario.

*Preparation of Salts **1** and **5***

1,3-Cyclohexanedione or 1,3-cyclopentanedione (8) was dissolved in a mixture of benzene and ethanol (2:1) and thallium ethoxide (9) was added dropwise with stirring. The salt precipitated from solution, was collected by filtration, and recrystallized from ethanol. The yields were quantitative.

1,3-Cyclohexanedione thallium salt **1**; m.p. 191–192°; i.r.(KBr): 3410, 2940, 1655, 1540, 1415, 1375, 1320 cm^{-1}.

1,3-Cyclopentanedione thallium salt **5**; m.p. 205–206°; i.r.(KBr): 3380, 2920, 1635, 1560, 1360, 1280 cm^{-1}.

General Alkylation Procedure

The thallium(I) salt (**1** or **5**) was suspended in 15 ml of the alkylating agent and heated at constant temperature. The cooled reaction mixture was filtered and the residue was washed with 30 ml of benzene. The combined filtrates (fraction A) were evaporated to afford crude material which was immediately subjected to g.l.c. analysis. Preparative g.l.c. afforded samples of each of the components for spectral and elemental analysis. The residue from the filtration was then washed with absolute methanol to remove the thallium halide; the filtrate (fraction B) was evaporated and the crude material was analyzed. In each case, most of the unreacted **1** or **5** was recovered from this fraction. Only other products are mentioned below. The relative amounts of products are shown in Table 1 and the spectral data are summarized in Tables 2 and 3. Catalysis was accomplished by adding three drops of triethylamine to the reaction mixture.

*Methyl Iodide and **1***

Fraction A (0.5 g) containing 41% of **8** (10) and 59% of **4***a* (6) which were identical in all respects with authentic samples was obtained from 3.1 g of **1** (9.8 mmol). Fraction B afforded 0.7 g of **3***a* m.p. 198–200° (lit. (4) 204°).

*Methyl Iodide and **5***

Fraction A (0.7 g), identical in all respects with **7***a* (11), was obtained from 2.0 g (6.78 mmol) of **5**. Fraction B gave 0.3 g of **6***a*, m.p. 207–208° (lit. (12) 208–209°).

*Ethyl Bromide and **1***

Fraction A (0.1 g) was obtained from 1.5 g (4.92 mmol) of **1** and consisted entirely of **4***b*, identical with an authentic sample (6).

*Ethyl Bromide and **5***

Fraction A (0.1 g) identified as **7***b* was obtained from 1.3 g (4.45 mmol) of **5** in the usual manner.

Anal. Calcd. for $C_7H_{10}O_2$: C, 66.65; H, 7.99. Found: C, 66.61; H, 8.22.

Fraction B afforded **5** as the only isolable material.

Can. J. Chem. Downloaded from www.nrcresearchpress.com by 210.87.254.42 on 09/05/12
For personal use only.

1,2-Dibromoethane and ***1***

Fraction A (0.4 g) was obtained from 3 g (9.85 mmol) of **1**. From this material **4***c* could be isolated by g.l.c.

Anal. Calcd. for $C_8H_{11}BrO_2$: C, 43.57; H, 5.04; Br, 36.47. Found: C, 43.86; H, 5.06; Br, 35.84.

Two other compounds were present, one of which presented spectral data consistent with **9**. Mass spectral analysis gave a molecular weight of 138 (P + 1 = 9%, P + 2 = 1%). $C_8H_{10}O_2$ requires P + 1 = 8.9%, P + 2 = 0.7% (13). Other prominent peaks in the mass spectrum occurred at *m/e* 111, 110 (base), 80, 68. The instability of the compound prevented our obtaining a satisfactory elemental analysis.

Again, fraction B afforded **1** as the only product.

1,2-Dibromoethane and ***5***

Fraction A (0.2 g) identified as **7***c* was obtained from 2.0 g (6.78 mmol) of **5**.

Anal. Calcd. for $C_7H_9BrO_2$: C, 40.98; H, 4.39. Found: C, 41.02; H, 4.34.

Fraction B afforded **5** as the only isolable material. Increasing the temperature to 100° raised the yield of **7***c* to 42% while adding three drops of triethylamine to the reaction afforded **7***c* in 85% yield.

Methyl Bromoacetate and ***1***

Fraction A (0.96 g) was obtained from 2.4 g (7.72 mmol) of **1**. From this material could be isolated 69% of **4***d*.

Anal. Calcd. for $C_9H_{12}O_4$: C, 58.69; H, 6.57. Found: C, 58.49; H, 6.75.

The remainder of this fraction was comprised of four compounds in approximately equal amounts whose spectral characteristics indicated that they were not products of simple alkylation of **1** and which rapidly decomposed on standing.

Methyl Bromoacetate and ***5***

Fraction A (1.7 g) which consisted of 18% **7***a* and 77% of **7***d* was obtained from 2.0 g (6.78 mmol) of **5**.

Anal. Calcd. for $C_8H_{10}O_4$: C, 56.47; H, 5.92. Found: C, 56.44; H, 5.89.

That **7***a* was a product of decomposition of **7***d* was shown by analysis of a sample of **7***d* which had been allowed to stand at room temperature for a period of several days. It had been cleanly converted to **7***a*. No rearrangement took place when air was excluded.

Fraction B consisted entirely of unreacted **5**.

Ethyl Bromoacetate and ***5***

Fraction A (1.6 g) was obtained from 2.8 g (9.36 mmol) of **5**. The major (93%) component was identified as **7***e*. The remainder of the fraction was composed of several small impurities which were not investigated.

Anal. Calcd. for $C_9H_{12}O_4$: C, 58.69; H, 6.57. Found: C, 58.77; H, 6.69.

Again, fraction B was entirely unreacted **5**.

Ethyl Chloroacetate and ***1***

Fraction A (0.47 g) was obtained from 3 g (9.85 mmol) of **1**. From this material **4***f* was isolated.

Anal. Calcd. for $C_9H_{14}O_4$; C, 60.50; H, 7.14. Found: C, 60.59; H, 7.12.

The remainder of the product was comprised of at least four compounds whose i.r. and n.m.r. spectra were not consistent with products of simple alkylation and which rapidly decomposed.

Fraction B afforded only unreacted **1**.

Ethyl Chloroacetate and ***5***

Fraction A (0.25 g) was obtained from 1.3 g (4.35 mmol) of **5** in the usual manner. This material consisted entirely of the *O*-alkylated product **7***e* (=**7***f*). Unreacted **5** was the only compound in fraction B.

The financial assistance of the National Research Council of Canada and the technical assistance of Mr. D. Hill are greatly appreciated. The assistance of Professor R. D. Bach (Wayne State University) in obtaining the mass spectrum is also gratefully acknowledged.

1. (*a*) E. C. TAYLOR and A. McKILLOP. Acc. Chem. Res. **3**, 330 (1970); (*b*) E. C. TAYLOR, G. H. HAWKS, and A. McKILLOP. J. Am. Chem. Soc. **90**, 2421 (1968).
2. H. O. HOUSE. Modern synthetic reactions. 2nd ed. Benjamin, New York, N.Y. 1972. p. 511 ff.
3. D. ROSENTHAL and K. H. DAVIS. J. Chem. Soc. (C), 1973 (1966).
4. H. STETTER. *In* Newer methods of preparative organic chemistry. Vol. 2. p. 51.
5. J. W. HUFFMAN and T. M. HSU. Tetrahedron Lett. 141 (1972).
6. H. STETTER and W. DIERICHS. Chem. Ber. **85**, 61 (1952).
7. C. B. C. BOYCE and J. S. WHITEHURST. J. Chem. Soc. 2022 (1959).
8. J. M. McINTOSH and P. M. BEAUMIER. J. Org. Chem. **37**, 2905 (1972).
9. G. BRAUER. *Editor*. Handbook of preparative inorganic chemistry. Vol. 1. 2nd ed. Academic Press, New York, N.Y. 1963. p. 877.
10. S. SWAMINATHAN, S. RAMACHANDRAN, and S. K. SANKARAPPA. Tetrahedron, **20**, 1119 (1964).
11. H. O. HOUSE and G. H. RASMUSSON. J. Org. Chem. **28**, 27 (1963).
12. J. PANOUSE and C. SANNIE. Bull. Soc. Chim. Fr. 1036 (1955).
13. R. SILVERSTEIN and G. C. BASSLER. Spectrometric identification of organic compounds. John Wiley, New York, N.Y. 1964. p. 26.
14. W. M. B. KONST, J. BRYNSVOORT, W. N. SPECKAMP, and H. O. HUISMAN. Rec. trav. Chim. **91**, 869 (1972).
15. J. HOOZ and J. SMITH. J. Org. Chem. **37**, 4200 (1972).

Can. J. Chem. Downloaded from www.nrcresearchpress.com by 210.87.254.42 on 09/05/12
For personal use only.

The New Synthesis of 5,6-Dimethyl-5-hepten-2-one from 2,3-Dimethyl-1,3-butadiene

SHOJI WATANABE, KYOICHI SUGA, AND TSUTOMU FUJITA

Department of Applied Chemistry, Faculty of Engineering, Chiba University, Yayoicho, Chiba, Japan 280

Received August 3, 1972

The reaction of 2,3-dimethyl-1,3-butadiene (**1**) with methyl acetoacetate in the presence of a catalyst composed of palladous chloride and *p*-phenyl-1-phospha-3-methyl-3-cyclopentene gave 3-carbomethoxy-5,6-dimethyl-5-hepten-2-one (**2**) (1:1 adduct). Alkali decomposition of **2** gave 5,6-dimethyl-5-hepten-2-one (**3**), which was a key intermediate for the preparation of α-irone. Similarly, isoprene gave a mixture of 5- and 6-methyl-5-hepten-2-one.

La réaction du diméthyl-2,3 butadiène-1,3 (**1**) avec l'acétoacétate de méthyle en présence d'un catalyseur composé de chlorure de palladium et de *p*-phénylphospha-1 méthyl-3 cyclopentène-3, conduit au carbométhoxy-3 diméthyl-5,6 heptène-5 one-2 (**2**) (adduit de type 1:1). La décomposition alcaline de **2** conduit à la diméthyl-5,6 heptène-5 one-2 (**3**) qui est l'intermédiaire clé dans la préparation de l'α-irone. De la même façon, l'isoprène donne un mélange de méthyl-5 et -6 heptène-5 one-2.

[Traduit par le journal]

Can. J. Chem., **51**, 848 (1973)

The ketone irone, found in oil of orris root, is used extensively in perfumery, because of its odor of violets. 5,6-Dimethyl-5-hepten-2-one (**3**) is an important key compound for the synthesis of α-irone. Ruzicka prepared 5,6-dimethyl-5-hepten-2-one (**3**) from 2,3-dimethyl-2-buten-1-bromide and ethyl acetoacetate (1). We have found the new preparative method for compound **3** from 2,3-dimethyl-1,3-butadiene and methyl acetoacetate using a new catalyst.

The reaction of active methylene compounds with 1,3-dienes has been reported (2). An active and easily available catalyst is prepared by mixing dichlorobis(triphenylphosphine)palladium and basic sodium compounds such as sodium phenoxide. The reaction of ethyl acetoacetate with 1,3-butadiene in the presence of $PdCl_2$-$(PPh_3)_2$–PhONa catalyst gives mixtures of 1:2 and 1:4 adducts (2). However, the reaction of 2,3-dimethyl-1,3-butadiene (**1**) with ethyl acetoacetate results in the exclusive formation of ethyl 2-acetyl-2,3,6,7-tetramethyl-2,7-decadienoate (1:2 adduct) in very low yields (7%). We have investigated the reaction of 2,3-dimethyl-1,3-butadiene (**1**) with methyl acetoacetate, and found that a new catalyst consisting of palladous chloride and *p*-phenyl-1-phospha-3-methyl-3-cyclopentene is very effective for the selective preparation of a 1:1 adduct. When a mixture of 2,3-dimethyl-1,3-butadiene (**1**) and methyl acetoacetate was heated for 10 h at 100 °C in the presence of a catalyst composed of palladous chloride, *p*-phenyl-1-phospha-3-methyl-3-cyclopentene, and sodium phenoxide, 3-carbomethoxy-5,6-dimethyl-5-hepten-2-one (**2**) (1:1 adduct) was selectively obtained in a yield of about 50% (see Scheme 1). This catalyst is a new special catalyst for the preparation of a 1:1 adduct (**2**). 5,6-Dimethyl-5-hepten-2-one (**3**) was prepared by the alkaline decomposition of **2**. Similarly, the reaction of isoprene (**4**) with methyl acetoacetate using this catalyst gave a mixture of methylheptenone (**7**), an important intermediate for the synthesis of terpene compounds, and 5-methyl-5-hepten-2-one (**8**), as shown in the Experimental. The method mentioned above is superior to the well-known method, the acetoacetate-rearrangement route (Carroll reaction) (4).

Experimental

Reaction of 2,3-Dimethyl-1,3-butadiene (1) with Methyl Acetoacetate

In a glass-sealed autoclave under nitrogen a mixture of 0.21 g (1 mmol) of palladous chloride, 0.29 g (2.5 mmol) of sodium phenoxide, 5 g (61 mmol) of 2,3-dimethyl-1,3-butadiene (**1**), and 0.35 g (2 mmol) of *p*-phenyl-1-phospha-3-methyl-3-cyclopentene was stirred at 25 °C for 5 min in an atmosphere of nitrogen. To this mixture, 10 g (122 mmol) of **1** was added. After 15 min, 22 g (190 mmol) of methyl acetoacetate was added. The mixture was heated at 100 °C for 10 h. The solution was directly distilled to give the following fractions: (A) b.p. ~85 °C/30 mm, yield 8 g; (B) b.p. 85–125 °C/30 mm, yield 2 g; and (C) b.p. 125–130 °C/30 mm, yield 16 g. Fraction A was a mixture of unchanged **1** and methyl acetoacetate. Fraction B was a mixture of 3-carbo-

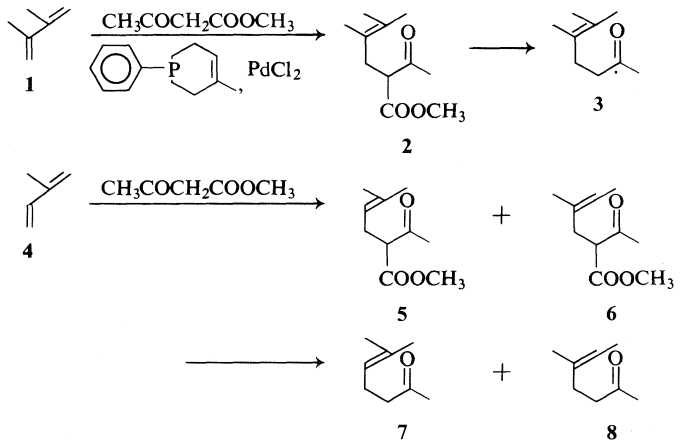

SCHEME 1

methoxy-5,6-dimethyl-5-hepten-2-one (**2**) (yield 8%), **1**, and methyl acetoacetate. Fraction C was compound **2** (yield 44%); i.r.: 1745, 1720 cm^{-1}.

Anal. Calcd. for $C_{11}H_{18}O_3$: C, 66.67; H, 9.09. Found: C, 66.52; H, 9.06.

5,6-Dimethyl-5-hepten-2-one (3)

A mixture of 9.9 g (0.05 mol) of compound **2** and 5% sodium hydroxide solution was agitated for 4 h at room temperature. To this solution, 7.84 g of 50% sulfuric acid was added. The solution was directly distilled at atmospheric pressure. The distillate was extracted with isopropylether. The ether extract was washed with water, dried over anhydrous sodium sulfate, and distilled to give the following fractions: (A) b.p. ~92 °C/31 mm, yield 0.5 g; (B) b.p. 92–93.5 °C/31 mm, yield 4.5 g (yield 70%). Fraction B was 5,6-dimethyl-5-hepten-2-one (**3**); i.r.: 1717 cm^{-1}; n.m.r. (δ, p.p.m.): 1.6 (s, CH_3—C, 9H), 2.0 (s, CH_3—C(=O)—, 3H), 2.3 (t, —CH_2—, 4H); mass spectrum (*m/e*): M^+ 140.

Anal. Calcd. for $C_9H_{16}O$: C, 77.64; H, 11.59. Found: C, 77.62; H, 11.56.

Synthesis of Methylheptenone (7) from Isoprene and Methyl Acetoacetate

In a glass-sealed autoclave, a mixture of 0.21 g (1 mmol) of palladous chloride, 0.29 g (2.5 mmol) of sodium phenoxide, 5 g (74 mmol) of isoprene, and 0.35 g (2 mmol) of *p*-phenyl-1-phospha-3-methyl-3-cyclopentene was stirred at 25 °C for 5 min in an atmosphere of nitrogen. To this mixture, 15 g (221 mmol) of isoprene was added. After 15 min, 22 g (190 mmol) of methyl acetoacetate was added. The mixture was heated at 50 °C for 13 h. The solution was directly distilled to give the following fractions: (A) b.p. ~85 °C/30 mm, yield 4 g; (B) b.p. 85–110 °C/30 mm, yield 2 g; (C) b.p. 110–115 °C/30 mm, yield 22 g; and (D) b.p. 103–104 °C/0.05 mm, yield 4 g. Fraction A was a mixture of unchanged isoprene and methyl acetoacetate. Fraction B was a mixture of 1:1 adduct (**5** and **6**, yield 4%), isoprene, and methyl acetoacetate. Fraction C was a mixture of 3-carbomethoxy-6-methyl-5-hepten-2-one (**5**) and 3-carbomethoxy-5-methyl-5-hepten-2-one (**6**) in yield of 37%. The mixture consisted of 85% of **5** and 15% of **6** by gas-chromatographic analysis; i.r.: 1680, 1745, 1720, 880 cm^{-1}.

Anal. Calcd. for $C_{10}H_{16}O_3$: C, 65.22; H, 8.70. Found: C, 65.20; H, 8.64.

Fraction D was an adduct of 2 mol isoprene with 1 mol methyl acetoacetate. Its structure was not determined.

Fraction C (9.2 g, 0.05 mol) was treated with sodium hydroxide solution in a manner similar to the preparation of **3** to give a mixture (7 g) of 6-methyl-5-hepten-2-one (**7**) and 5-methyl-5-hepten-2-one (**8**) in yield of 44%. The mixture consisted of **7** (85%) and **8** (15%) by gas-chromatographic analysis. Compounds **7** and **8** were separated by gas-chromatographic trapping using a column of Silicone DC 200 (20%) on Celite 545 (2 m). The structures of these compounds were confirmed by comparison of their authentic samples using g.l.c. and i.r. spectra.

Synthesis of p-Phenyl-1-phospha-3-methyl-3-cyclopentene

Dichlorophenylphosphine was prepared as reported previously (3), b.p. 90–92 °C/10 mm. In a dry glass equipment, a mixture of dichlorophenylphosphine (179 g), isoprene (89 g), and copper stearate (3.5 g) was left for 48 h to give a white solid, *p*-phenyldichloro-1-phospha-3-methyl-3-cyclopentene. This crude solid was washed with *n*-hexane several times. A mixture of the solid (124 g), tetrahydrofuran (300 ml), and Mg dust (18 g) activated by a small amount of ethyl bromide was refluxed for 1 h. The tetrahydrofuran solution was treated with water, made alkaline with diluted sodium hydroxide solution, and extracted with benzene. Distillation under nitrogen gave 69.7 g of *p*-phenyl-1-phospha-3-methyl-3-cyclopentene, b.p. 120–125 °C/5 mm.

Anal. Calcd. for $C_{11}H_{13}P$: C, 74.98; H, 7.43; P, 17.58%. Found: C, 74.93; H, 7.39; P, 17.42.

1. L. RUZICKA. Helv. Chim. Acta, **23**, 959 (1940).
2. G. HATA, K. TAKAHASHI, and A. MIYAKE. J. Org. Chem. **36**, 2116 (1971).
3. B. BUCHNER, L. B. LOCKHART. Org. Syn. Coll. Vol. **4**, 784 (1963); J. Am. Chem. Soc. **73**, 755 (1951).
4. M. F. CARROLL. J. Chem. Soc. 507 (1941).

Marine Organic Chemistry. I. Isolation of 3β,6α-Dihydroxy-5α-pregn-9(11)-en-20-one from the Saponins of the Starfish *Asterias forbesi*. A Rapid Method for Extracting Starfish Saponins[1]

JOHN W. APSIMON, JOHN A. BUCCINI,[2] AND SATYANAND BADRIPERSAUD
Department of Chemistry, Carleton University, Ottawa, Canada K1S 5B6

Received November 3, 1972

The major aglycone from the saponins of *Asterias forbesi* has been identified as 3β,6α-dihydroxy-5α-pregn-9(11)-en-20-one (**1**). A simplified procedure for extracting saponins from starfish is reported which reduces the required working time from 7–14 to 1–3 days.

L'aglycone majeur obtenu des saponosides de l'*Astérias forbesi* a été identifié comme étant le dihydroxy-3β,6α pregn-5α ène-9(11) one-20 (**1**). Une méthode simplifiée pour l'extraction des saponosides de l'étoile de mer est rapportée; celle-ci réduit le temps nécessaire requis par l'extraction de 7–14 jours à 1–3 jours. [Traduit par le journal]

Can. J. Chem., **51**, 850 (1973)

Introduction

The phylum Echinodermata is comprised of some 6500 species of marine invertebrate animals, of which there are five classes (1): (*1*) Holothuridea (sea cucumbers), (*2*) Asteroidea (starfish), (*3*) Echinoidea (sea urchins and sand dollars), (*4*) Ophiuroidea (brittle stars and basket stars), and (*5*) Crinoidea (sea lilies and feather stars).

For many years, organic chemists have investigated the naphthaquinone and anthraquinone pigments (2), the carotenoids (2), and the sterols (3) produced by these animals. Chemically, the echinoderms are unique in that the holothuroids and asteroids produce saponins (4–6) while no other animals — including the echinoids, ophiuroids, and crinoids — have been shown to do so (7). Since the first reports of saponin in sea cucumbers (4, 5), several papers have appeared dealing with the physiological properties and chemical composition of the holothuroid saponins and aglycones (2, 8). Several workers have shown that starfish saponins are the active principles of starfish which induce the "avoidance" or "escape" responses in many species of mollusc, thereby reducing predation by starfish of susceptible species of mollusc (9, 10). The saponin mixture has recently been identified as the spawning inhibitor in the Japanese starfish *Asterias amurensis* (11). Despite extensive investigations of their biological properties, little attention has been paid to the chemical composition of the starfish saponins which are complex mixtures, incorporating steroidal and nortriterpenoid aglycones, several different sugars, and a sodium sulfate half-ester. Only within the last year have the results of chemical investigations of the starfish aglycones appeared in print (12–15). As part of a continuing investigation of biologically active marine organic compounds, we have examined the saponin mixture of a common North Atlantic starfish, *Asterias forbesi*, and wish to report here the results of our recent investigations.

(A) The Saponins of Asterias forbesi

Specimens of *A. forbesi* were collected at South Bristol, Maine in August, 1971 and immediately frozen with Dry Ice for shipment. Upon receipt the animals were thawed and extracted by the published procedure (6) to obtain the saponin mixture (Fig. 1). This material was hydrolyzed (2 *N* HCl, steam bath) and the precipitated aglycones obtained by chloroform extraction. Repeated t.l.c. on silica gel resolved the aglycone mixture into two bands, one being a mixture of compounds of molecular weight 414 and the other, crystallized from benzene to give pure **1**, m.p. 151–153 °C, $[\alpha]_D^{20}$ +60° (ethanol). The

[1]Presented at the 55th Canadian Chemical Conference of the Chemical Institute of Canada, Quebec City, Quebec, June 5–7, 1972.

[2]Present address: Food Advisory Bureau, Department of National Health and Welfare, Ottawa, Canada K1A 0L2.

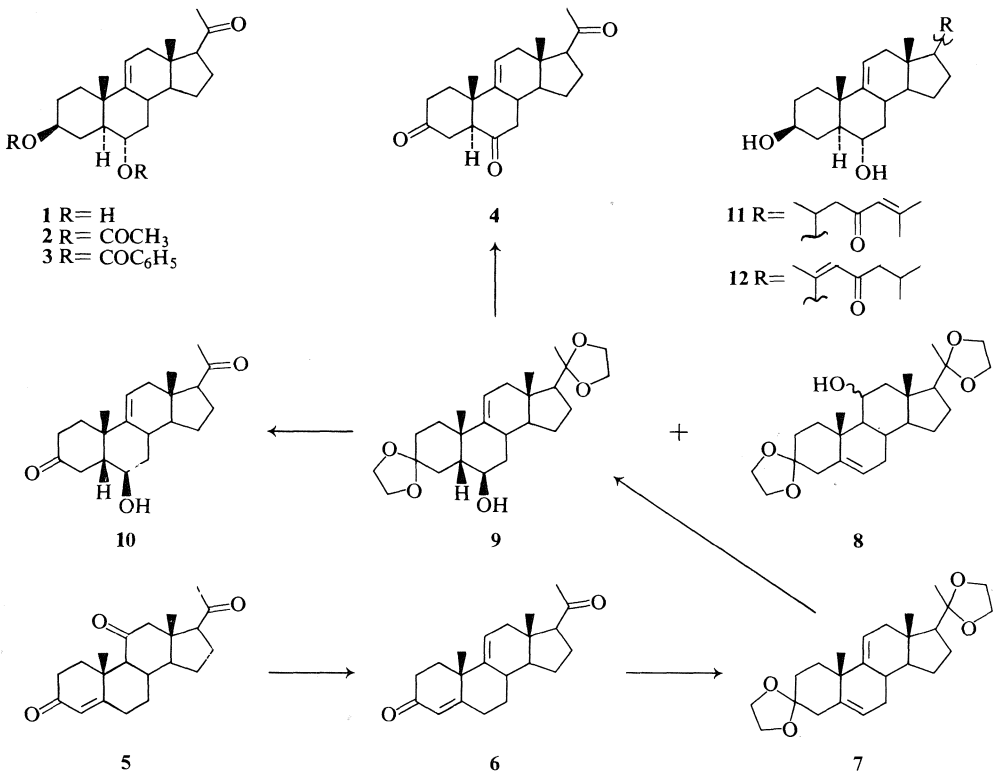

SCHEME 1

molecular formula was established as $C_{21}H_{32}O_3$ by high resolution mass spectrometry and the i.r. spectrum showed absorptions for hydroxy and carbonyl groups (3280, 1700 cm^{-1}, respectively). Aglycone (**1**) was shown to be a diol by conversion to the oily diacetate **2** [M^+ 416, ν_{max} (neat) 1735, 1700 cm^{-1}]. The n.m.r. spectrum of **1** indicated the presence of an acetyl group and from the general appearance of the spectrum, **1** was assumed to be a dihydroxy derivative of pregn-20-one. The n.m.r. spectrum of **1** exhibited an absorption at 5.36 δ corresponding to one olefinic proton indicating the presence of a trisubstituted olefinic bond.

Jones oxidation of **1** gave a crystalline triketone **4** whose molecular formula was established as $C_{21}H_{28}O_3$ by high resolution mass spectrometry. The u.v. spectrum of **4** in ethanol and NaOH/ethanol showed only end absorption, indicating that **4** did not possess an α,β-unsaturated ketone, a 1,2- or 1,3-diketone group. With these restrictions, there remained 72 possible structures for **4** *i.e.* for a pregn-20-one with one trisubstituted olefinic bond and two ketones in addition to the 17-acetyl group. Of this number, only two compounds had calculated (16, 17) angular methyl group chemical shifts which agreed with the experimental values for **4** (Table 1): these were pregn-5-en-2,11,20-trione and 5α-pregn-9(11)-en-3,6,20-trione. The former possibility was eliminated by a similar comparison of the calculated methyl group shifts of all possible 2,11-diols and -diacetates with the experimental methyl shifts of **1** and **2**. Thus, **4** was assumed to be 5α-pregn-9(11)-en-3,6,20-trione; this has been confirmed by the

TABLE 1. Angular methyl group chemical shifts in $CDCl_3$ (δ, p.p.m. downfield from internal TMS)

	C-19 H_3		C-18 H_3	
Compound	Exper.	Calcd.*	Exper.	Calcd.*
1	0.95	0.95	0.55	0.56
2	1.03	1.02	0.55	0.56
4	1.12	1.12	0.63	0.60
9	1.28	1.28	0.72	0.72
10	1.36	1.37	0.62	0.63

*From tables in refs. 16 and 17.

synthesis of **4** from commercially available pregn-4-en-3,11,20-trione (**5**, Scheme 1).

Conversion of **5** to pregn-4,9(11)-dien-3,20-dione (**6**) was carried out following the published procedures (18, 19). Slow distillation of a mixture of **6**, benzene, ethylene glycol, and *p*-toluenesulfonic acid resulted in the formation of diketal **7**. Reaction of **7** with 1.3 equiv of BH_3/tetrahydrofuran was followed by oxidation with sodium hydroxide/hydrogen peroxide to give a mixture of two monohydroxy diketals (**8** and **9**) which were separated by t.l.c. on silica gel. Deketalization of the isomer of larger R_f (**8**) gave an enone, demonstrating that the olefinic bond in **8** was in the 5,6-position. The slower moving isomer was then assumed to be **9** and the stereochemistry at C-5 and -6 follows from a comparison of the experimental and calculated angular methyl group chemical shifts of **9** and of the diketone **10** obtained by deketalization of **9** (Table 1). Furthermore, in the n.m.r. spectra of **9** and **10**, the C-6 methine hydrogen signal appeared as a broad absorption with a half-intensity bandwidth of 8 Hz, clearly consistent with a C-6 equatorial proton (17). From precedents (20, 21) we had expected an α-attack in the hydroboration/oxidation of the 5,6-olefinic bond: the observed β-attack must reflect a severe steric effect on the α-face of the steroid system. Such steric hindrance would account for the results of our earlier attempts to reduce **7** in which we used up to 10 equiv of disiamylborane and still recovered **7** intact.

Collins oxidation of **9** followed by deketalization gave crystalline triketone **4**, shown to be identical to the sample obtained from **1** by comparison of i.r., n.m.r., and mass spectra and t.l.c. behavior on silica gel (chloroform, and ethyl acetate/benzene).

From the structure of **4**, it followed that the aglycone **1** must be one of the four possible isomers of 3,6-dihydroxy-5α-pregn-9(11)-en-20-one. Consideration of the methyl group chemical shifts led to the conclusion that **1** was either the 3α,6α- or 3β,6α-diol. The stereochemistry of the hydroxy groups was determined by obtaining the circular dichroism (c.d.) spectrum of the dibenzoate ester **3** and application of the dibenzoate chirality rule (22). The observed c.d. Cotton effects in methanol were +12.5 at 236 nm and −7.8 at 222 nm which are consistent only with a 3β,6α-stereochemistry: thus the complete structure of **1** is 3β,6α-dihydroxy-5α-pregn-9(11)-en-20-one.

Since completion of this work, three independent reports have appeared in which **1** has been proposed for the structure of the major aglycone from the saponins of *Asterias amurensis* (14), *A. forbesi* (15), and *Acanthaster planci* (13, 15). In these reports, the structure of **1** was postulated after hydrogenation of the olefinic bond (*presumed* to be in the 9(11)-position) and correlation with known saturated pregn-20-ones. Our synthesis of **4** firmly establishes the position of the olefinic bond and we report a novel demonstration of the hydroxy group stereochemistry of **1**.

In addition to **1**, two aglycones from starfish saponins have been identified: they are Marthasterone **11** from *Marthasterias glacialis* (12) and **12**, a minor aglycone from *Acanthaster planci* (13). It is striking that the three aglycones differ only in the composition of the C-17 side chain and would perhaps suggest a common biosynthetic route to these compounds. In view of the fact that starfish are characterized by Δ^7-sterols (3), it would be of interest to determine if the $\Delta^{9(11)}$-aglycones are biosynthetic or dietary in origin.

(B) A Simplified Extraction Procedure for Starfish Saponins

It is apparent from the recent literature that there is an increasing interest in the starfish saponins and we wish to report a simplified extraction procedure which we believe to be a significant improvement on the published procedure (6) shown schematically in Fig. 1. Working with 1–10 kg batches of starfish, we encountered several problems: (*a*) large volumes of alcohol/water were required to effectively extract the animals, (*b*) the rotary evaporation of large volumes of saponin extract was a tedious and time-consuming task, (*c*) defatting with benzene or ether gave emulsions which required 12–48 h to break, (*d*) using alcohol in the extracting solvent resulted in the extraction of large amounts of fats which were difficult to remove and contaminated the final sample of saponin. We have found that saponin may be successfully extracted merely by soaking live starfish in distilled water for 2-4 h at room temperature (Fig. 2). Removal of the animal bodies leaves an aqueous solution of saponin which contains but a minimal amount of fats and does not require defatting with ether or benzene. The aqueous solution can be immediately worked-up and the saponin extracted with *n*-butanol, etc.. It has

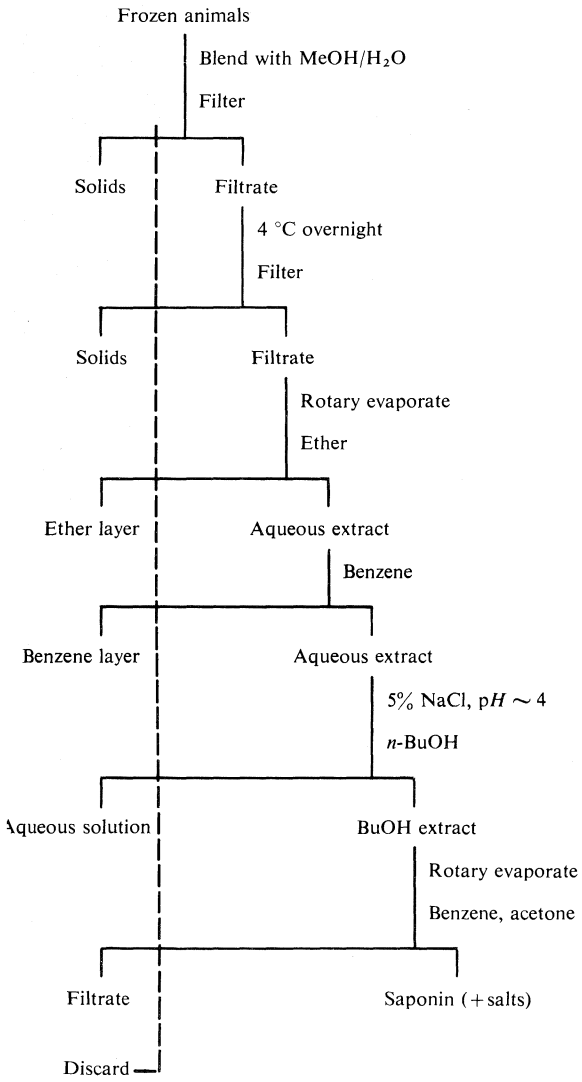

FIG. 1. Extraction procedure based on method in ref. 6.

been our experience that batches of 5–10 kg of starfish may be worked-up in 2–3 days to yield the saponin as compared with 10–14 days via the procedure in Fig. 1. The savings in time, solvents, and equipment are obvious.

Applying this technique to four species of starfish, we have succeeded in extracting from 33–94% of the saponin available in the animals, depending upon the species (Table 2). While the method would be of limited value in the 7- to 14-rayed *Solaster* species, it works very well with the 5-rayed *Asterias* and *Henricia* species. Further studies are currently underway to determine the generality of the extraction technique.

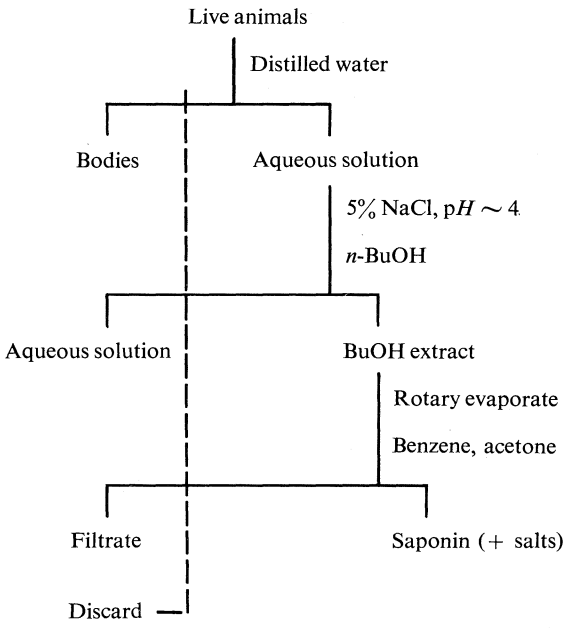

FIG. 2. Schematic representation of simplified extraction procedure.

TABLE 2. Extraction of starfish saponins via the simplified procedure (Fig. 2)

Species	Conditions	Saponin extracted (%)
Henricia sanguinolenta	1 × 2 h	60
	3 × 2 h	94
Asterias vulgaris	1 × 15 min	33
Crossaster papposus	3 × 2 h	33
Solaster endeca	3 × 1 h	37

Work on the constituents of a variety of echinoderms is also in progress in our laboratory.

Experimental

Melting points were determined on a Kofler hot stage and are corrected. The n.m.r. spectra were obtained on a Varian T-60 or Varian XL-100 spectrometer with tetramethylsilane as internal standard. Chemical shifts are expressed in the δ scale and the following abbreviations apply: s, singlet; d, doublet; t, triplet; m, multiplet. The i.r. spectra were determined on a Perkin–Elmer 237B grating spectrophotometer. Low resolution mass spectra were obtained on an AEI MS 12 instrument. The t.l.c. was performed using pre-coated plates obtained from E.M. Reagents (silica gel F-254, 0.25 or 2.0 mm).

Specimens of *Asterias forbesi* were collected in August, 1971 at South Bristol, Maine by representatives of the New England Aquarium, Boston, Mass. and immediately frozen with Dry Ice. The specimens of *Henricia sanguinolenta* (Feb./72), *Asterias vulgaris* (Aug./71), *Solaster endeca* (Oct./71), and *Crossaster papposus* (Dec./71) were collected at Deer Island in the Bay of Fundy by Marine

Research Associates, New Brunswick and were received live within 48 h of shipment.

Classical Extraction Procedure (Fig. 1)

Upon receipt, the frozen block of *A. forbesi* (5–10 kg) was divided into small pieces and thawed for 4–5 h under methanol/water (3/1) solution (15 l). The thawed mixture was homogenized using a Waring Commercial Blender and allowed to stand for 3 h. The animal pulp was separated by suction filtration and extracted twice more with methanol/water (10 l). The filtrates were stored in a cold room overnite at 4° and filtered once more. The filtrate was concentrated (to 4 l) by rotary evaporation, using bath temperatures of 45° or less to minimize thermal decomposition. The resulting mixture of oils and aqueous solution was diluted to 6 l with water and extracted with ether (3 l) and then benzene (3 l). In both extractions, emulsions were obtained: the ether emulsions separated in 2–4 h but those of benzene required 12–48 h for acceptable separation. The defatted aqueous solution was made up to 5% sodium chloride and the p*H* adjusted to 4 with dilute hydrochloric acid. The resulting mixture was extracted with water-saturated 1-butanol (3 × 2 l) and the water layer discarded. The butanol extract was suction-filtered through Whatman 1 filter paper and then gravity-filtered through a cotton plug to remove a sticky suspension. The butanol filtrate was concentrated (to 100–200 ml) by rotary evaporation and the saponin precipitated by the addition of benzene (1.5 l). The supernatant solution was decanted and the precipitate washed with acetone and collected by suction filtration. This precipitate contained large amounts of NaCl (silver nitrate test) and was freed of inorganic salts and small organic molecules (*e.g.* sugars) by dialysis in a cellophane bag against running tap water for 6–10 h. The clear solution in the cellophane bag was free of chloride (silver nitrate test) and lyophilization gave the saponin mixture (10 g).

Rapid Isolation Procedure (Fig. 2)

Live animals were completely immersed in distilled water at room temperature and allowed to soak for varying periods of time (Table 2). The animals were removed and the resulting solution gravity-filtered through a cotton plug, made up to 5% sodium chloride, and the p*H* adjusted to 4 with dilute hydrochloric acid. The saponin was then extracted with 1-butanol, etc. as in the classical procedure.

*3β,6α-Dihydroxy-5α-pregn-9(11)-en-20-one (**1**) from the Saponins of A. forbesi*

A solution of the saponin mixture from *A. forbesi* (4.3 g) in aqueous 2 *N* HCl (400 ml) was placed under a nitrogen atmosphere and warmed on a steam bath. Within 30 min, the clear solution became cloudy and after 2 h a clear supernatant and an oily deposit were observed. The mixture was cooled, extracted with chloroform (4 × 200 ml) and the aqueous solution discarded. Flash evaporation of the dried (Na_2SO_4) chloroform extract gave a gum (1.8 g) which was chromatographed on 2 mm silica gel plates, with the plates being developed twice (ethyl acetate, ethyl acetate/methanol = 20/1). Viewing the plates under u.v. light (360 nm), two dark bands were observed in the R_f range 0.5–0.8. The band of greater R_f was eluted and the spectral data indicated that it was probably a derivative of one of the sugars released during hydrolysis of the saponin. The second band visible under u.v. light was found to have a molecular weight of 414 and it is believed to be a mixture of several isomers (480 mg). This mixture is currently being investigated.

Elution of the area from R_f 0.1 to 0.5 gave a gum (180 mg) which was re-chromatographed to give pure aglycone **1** (120 mg). Crystallization from benzene gave **1** as a white solid, m.p. 151–153° (lit. m.p. 157–160 (14), 162–163 (13), 193–196° (15)); $[\alpha]_D^{20°}$ +60° (*c* 0.328, ethanol); $C_{21}H_{32}O_3$, M^+ 332.2350 (required 332.2351); ν_{max} (Nujol) 3280, 1700, 1040 cm^{-1}; n.m.r. ($CDCl_3$) δ 0.55 (s, 3H, C-18 H_3), 0.95 (s, 3H, C-19 H_3), 2.13 (s, 3H, $COCH_3$), 3.3–3.8 (broad m, 2H, C-3 and -6 methine H), and 5.36 (broad m, 1H, C-11 H); *m/e* at 332, 317, 314, 299, 296, 281, 230.

*3β,6α-Diacetoxy-5α-pregn-9(11)-en-20-one (**2**)*

The aglycone **1** (8 mg) was acetylated (pyridine (0.1 ml) and acetic anhydride (3 ml) for 36 h) and the crude product purified by t.l.c. on silica gel (benzene/ethyl acetate = 20/1, then = 10/1). The diacetate **2** was obtained as a clear oil (6 mg) ν_{max} (film) 1735, 1700, 1250, 1035 cm^{-1}; n.m.r. ($CDCl_3$) δ 0.55 (s, 3H, C-18 H_3), 1.03 (s, 3H, C-19 H_3), 2.03 (s, 6H, $OCOCH_3$), 2.12 (s, 3H, $COCH_3$), 4.4–5.1 (broad m, 2H, C-3 and -6 methine H), and 5.36 (broad m, 1H, C-11 H); *m/e* at 416, 356, 341, 296, 281, 226, 211.

*3β,6α-Dibenzoyloxy-5α-pregn-9(11)-en-20-one (**3**)*

The aglycone **1** (8 mg) was benzoylated (anhydrous pyridine (1 ml) and benzoyl chloride (0.5 ml), steam bath for 4 h) and routine work-up followed by t.l.c. on silica gel (benzene, then benzene/ethyl acetate = 20/1) gave the dibenzoate ester **3** as a clear gum (5 mg); ν_{max} (film) 1720–1700, 1600, 1580, 1490 cm^{-1}; n.m.r. ($CDCl_3$) δ 0.60 (s, 3H, C-18 H_3), 1.15 (s, 3H, C-19 H_3), 2.16 (s, 3H, $COCH_3$), 4.84–5.33 (m, 2H, C-3 and -6 methine H), 5.40–5.60 (m, 1H, C-11 H), and 6.5–8.2 (m, 10H, ArH). The c.d. spectrum was run in methanol solution (*c* 5 mg/100 ml): maximum at 236 nm (+12.5), minimum at 222 nm (−7.8).

*5α-Pregn-9(11)-en-3,6,20-trione (**4**)*

An excess of Jones reagent (23) was added to a stirred, cooled (0°) solution of aglycone **1** (9 mg) in acetone (5 ml). After 15 min, the reaction mixture was diluted with water and extracted with chloroform (3 × 15 ml). Rotary evaporation of the dried (Na_2SO_4) chloroform extract gave an oil which was purified by t.l.c. on silica gel (benzene/ethyl acetate = 3/1, then = 1/1) to give the trione **4** (6 mg) which crystallized on standing, m.p. 180–182°; $C_{21}H_{28}O_3$, M^+ 328.2073 (required 328.2037); ν_{max} (Nujol) 1715–1700 cm^{-1}; n.m.r. ($CDCl_3$) δ 0.63 (s, 3H, C-18 H_3), 1.12 (s, 3H, C-19 H_3), 2.15 (s, 3H, $COCH_3$), and 5.64 (broad m, 1H, C-11 H).

*Conversion of Pregn-4-en-3,11,20-trione (**5**) to the Trione **4***

The synthesis of pregn-4,9(11)-dien-3,20-dione (**6**) from **5** was carried out following the published procedures (18, 19). A mixture of **6** (200 mg), benzene (100 ml), ethylene glycol (2 ml), and *p*-toluenesulfonic acid (5 mg) was slowly distilled over a 2 h period to leave a small volume (5–10 ml) of liquid remaining in the reaction

flask. The reaction mixture was cooled, washed with saturated aqueous sodium bicarbonate solution (15 ml), water (15 ml), and then dried (Na_2SO_4) and flash evaporated to give an oil. This material was chromatographed on silica gel plates (chloroform/methanol = 50/1) and the major band eluted to give the diketal **7** (130 mg); ν_{max} (film) 1675–1650 cm^{-1} (C=C); n.m.r. ($CDCl_3$) δ 0.77, 1.22, and 1.32 (3s, 3H each, C-18, -19, and -21 methyls), 3.99 (m, 8H, OCH_2CH_2O), and 5.37–5.60 (broad m, 2H, C-6 and -11 H).

A solution of diketal **7** (100 mg, 0.25 mmol) in anhydrous tetrahydrofuran (15 ml) was placed under a nitrogen atmosphere, cooled to 0° and reacted with 0.33 *M* BH_3/tetrahydrofuran (1 ml). After standing for 2 h at room temperature, the mixture was reacted with 3 *N* NaOH (3 ml) and 30% hydrogen peroxide (0.5 ml) and stirred for 1 h. Tetrahydrofuran was removed by vacuum evaporation and the resulting mixture extracted with ether. Flash evaporation of the dried (Na_2SO_4) organic extract gave an oily mixture which was chromatographed on silica gel plates to give two main bands. Elution of the band at R_f 0.5 gave crystalline material, m.p. 150–154°, assigned structure **9** on the basis of the following spectral data (see Table 1 and Discussion); ν_{max} (Nujol) 3475 cm^{-1} (OH); n.m.r. ($CDCl_3$) δ 0.72 (s, 3H, C-18 H_3), 1.28 (s, 3H, C-19 H_3), 1.32 (s, 3H, C-21 H_3), 3.7–3.9 (m, 1H, C-6 methine), 3.97 (m, 4H, OCH_2CH_2O), and 5.3–5.6 (m, 1H, C-11 H); *m/e* at 418, 403, 400, 358.

A mixture of acetone (20 ml), 2 N sulfuric acid (5 ml), and **9** (10 mg) was stirred at room temperature for 12 h, diluted with water, and extracted with chloroform to give the hydroxy-diketone **10** (6 mg); ν_{max} (film) 3450 (OH), 1700 (C=O) cm^{-1}; n.m.r. ($CDCl_3$) δ 0.62 (s, 3H, C-18 H_3), 1.36 (s, 3H, C-19 H_3), 2.16 (s, 3H, $COCH_3$), 3.7–3.9 (broad m, 1H, C-6 methine), and 5.5–5.8 (broad m, 1H, C-11 H).

Chromium trioxide (50 mg, 0.50 mmol) was dried in a vacuum dessicator over phosphorus pentoxide and then added to a stirred solution of anhydrous pyridine (83 mg, 1.05 mmol) in anhydrous methylene chloride (5 ml). After stirring this mixture for 30 min, a solution of hydroxy-diketal **9** (30 mg, 0.072 mmol) in methylene chloride (2 ml) was added dropwise and stirring continued for 1 h. The supernatant solution was decanted, leaving a black residue which was washed with ether (3 × 10 ml) and the combined ether and methylene chloride solutions were flash evaporated. The residue was taken up in ether and chromium salts removed by filtration. The ether filtrate was washed with 1 *N* sodium hydroxide (2 × 15 ml) and saturated sodium chloride solution. The ether was removed by flash evaporation and the residue refluxed for 1 h with acetone (5 ml) and 5% sulfuric acid (1 ml). Dilution with water and chloroform extraction gave crude trione **4**, purified by t.l.c. on silica gel to give crystalline material (11 mg), m.p. 175–177°. This sample of **4** was shown to be identical to that obtained by oxidation of **1** by comparison of i.r., n.m.r., and mass spectra and t.l.c. behavior on silica gel (chloroform, or ethyl acetate/benzene).

We wish to thank Mr. P. Montreuil (Montreal Aquarium, Montreal, Quebec) for valuable discussions, Mr. A. MacKay (Marine Research Associates, Lord's Cove, Deer Island, New Brunswick), and Mr. E. H. Taylor (Curator, New England Aquarium, Boston, Mass.) for providing the animals used in this work. Professor K. Nakanishi (Columbia University, New York, N.Y.) kindly determined the c.d. spectra and Professors D. B. MacLean (McMaster University, Hamilton, Ontario) and J. Holmes (University of Ottawa, Ottawa, Ontario) the high resolution mass spectra. The generous financial assistance of the National Research Council of Canada is gratefully acknowledged.

1. L. H. HYMAN. The invertebrates. Vol. 4, McGraw–Hill, New York. 1955.
2. J. S. GROSSERT. Chem. Soc. Rev. **1**, 1 (1972) and refs. therein.
3. L. J. GOAD, I. RUBINSTEIN, and A. G. SMITH. Proc. R. Soc. Lond. B, **180**, 223 (1972).
4. R. F. NIGRELLI. Zoologica (New York), **37**, 89 (1952).
5. T. YAMANOUCHI. Publ. Seto Mar. Biol. Lab. **IV** (2–3), 183 (1955).
6. Y. HASHIMOTO and T. YASUMOTO. Bull. Jap. Soc. Sci. Fish. **26**, 1132 (1960).
7. T. YASUMOTO, M. TANAKA, and Y. HASHIMOTO. Bull. Jap. Soc. Sci. Fish. **32**, 673 (1966).
8. G. HABERMEHL and G. VOLKWEIN. Toxicon, **9**, 319 (1971).
9. H. M. FEDER and A. M. CHRISTENSEN. *In* Physiology of echinodermata. R. A. Boolootian, editor. J. Wiley and Sons Inc., New York, N.Y. 1966. p. 87.
10. H. M. FEDER. Sci. Am. **227**, 93 (1972).
11. S. IKEGAMI, Y. KAMIYA, and S. TAMURA. Agr. Biol. Chem. (Tokyo), **36**, 1087 (1972).
12. A. B. TURNER, D. S. H. SMITH, and A. M. MACKIE. Nature, **233**, 209 (1971).
13. Y. M. SHEIKH, B. M. TURSCH, and C. DJERASSI. J. Am. Chem. Soc. **94**, 3278 (1972); Tetrahedron Lett. 3721 (1972).
14. S. IKEGAMI, Y. KAMIYA, and S. TAMURA. Tetrahedron Lett. 1601 (1972); 3725 (1972).
15. Y. SHIMIZU. J. Am. Chem. Soc. **94**, 4051 (1972).
16. N. S. BHACCA and D. H. WILLIAMS. Applications of NMR spectroscopy in organic chemistry: illustrations from the steroid field. Holden-Day Inc., London. 1964. Chapt. 2.
17. J. E. BRIDGEMAN, P. C. CHERRY, A. S. CLEGG, J. M. EVANS, E. R. H. JONES, A. KASAL, V. KUMAR, G. D. MEAKINS, Y. MORISAWA, E. E. RICHARDS, and P. D. WOODGATE. J. Chem. Soc. C, 250 (1970).
18. B. J. MAGERLEIN and R. H. LEVIN. J. Am. Chem. Soc. **75**, 3654 (1953).
19. C. W. SHOPPEE and T. REICHSTEIN. Helv. Chim. Acta, **24**, 351 (1941).
20. S. WOLFE, M. NUSSIM, Y. MAZUR, and F. SONDHEIMER. J. Org. Chem. **24**, 1034 (1959).
21. G. ZWEIFEL and H. C. BROWN. Org. React. **13**, 1 (1963).
22. N. HARADA, S. SUZUKI, H. UDA, and K. NAKANISHI. J. Am. Chem. Soc. **93**, 5577 (1971) and refs. therein.
23. L. F. FIESER and M. FIESER. Reagents for organic synthesis. John Wiley and Sons, Inc., New York, N.Y. 1967. p. 142.

Studies Relating to Aziridine Antitumor Antibiotics. Part I. Asymmetric Syntheses. Part II.[1] Chiral Aziridines and their Conversion to α-Aminoacids

J. W. LOWN, T. ITOH,[2] AND N. ONO[3]

Department of Chemistry, University of Alberta, Edmonton, Alberta

Received September 18, 1972

Separable diastereomeric *cis-l*-menthyl 2-phenyl-3-aziridinecarboxylates (**4** and **5**) were prepared by the Gabriel reaction. *N*-Acylation with *p*-nitrobenzoyl chloride or *p*-anisoyl chloride of **4** and **5** gives **7** and **8**, and **23** and **24**, respectively. Sodium iodide-catalyzed rearrangement of the *N*-acylated aziridines is regiospecific with exclusive attack at C-2 and from **8** is obtained the chiral 2-oxazolines *cis*-**9** and *trans*-**10** in a ratio of 30:70 together with the unsaturated amide **11**. The structure of the latter was proven by independent synthesis. The intermediate *l*-menthyl *N-p*-nitrobenzoyl-3-iodophenyl-alaninate (**18**) was isolated at lower temperatures and shown to form the equilibrium mixture of **9** and **10** with triethylamine owing to partial racemization by a Finkelstein identity reaction. Use of an *N-p*-anisoyl substituent in the aziridine improves the yield of chiral 2-oxazolines by preventing the formation of **11**, and allows the separation of pure *cis*- and *trans*-oxazolines for characterization. The aziridines bearing *N-p*-anisoyl substituents display a greater sensitivity to attack by weaker nucleophiles than the *p-N*-nitrobenzoyl analogs.

Acid hydrolysis of **9** and **10** gives D-*allo*-β-phenylserine in an optical yield of about 17% from which **5** and **8** are tentatively assigned the 2R,3R configuration. Similar acid hydrolysis of the 2-*p*-anisyl-2-oxazoline (**26***b*) allowed the isolation of the intermediate *l*-menthyl *O*-anisoyl-*allo*-β-phenylserinate (**30***a*), hydrolysis of which gave D-*allo*-β-phenylserine in about 18% optical yield. The isolation of *allo*-β-phenylserine only from *cis*- and *trans*-2-oxazolines is attributed to acid-catalyzed inversion at the benzylic center to the conformationally more stable *allo* form.

Les diastéréoisomères séparables, *cis l*-menthyl, phényl-2 aziridine carboxylates-3 (**4** et **5**) ont été préparés à partir de la réaction de Gabriel. La réaction de *N*-acylation avec le chlorure de *p*-nitrobenzoyle ou avec le chlorure de *p*-anisoyle sur les produits **4** et **5** conduit aux produits **7** et **8**, et **23** et **24** respectivement. Le réarrangement catalysé par l'iodure de sodium des aziridines acylées est régiospécifique avec une attaque exclusivement sur le C-2; à partir de **8**, on obtient alors les formes optiquement actives oxazolines-2 *cis*-**9** et *trans*-**10** dans le rapport 30:70 ainsi que l'amide insaturée **11**. La structure de ce dernier produit fut d'ailleurs prouvée par synthèse indépendante. L'intermédiaire *l*-menthyl *N-p*-nitrobenzoyle iodo-3 phénylalaninate (**18**) a été isolée à des températures plus basses de même qu'il a été montré que celui-ci conduisait à un mélange en équilibre de **9** et **10** en présence de triethylamine à cause d'une racémisation partielle par une réaction du type Finkelstein. L'utilisation d'un substituant *N-p*-anisoyle sur l'aziridine conduit à une amélioration du rendement en oxazolines-2 optiquement actives en empêchant la formation de **11**, de même qu'il permet la séparation des oxazolines *cis* et *trans* pour des fins de caractérisation. De la même manière, les azirdines portant des substituants *p-N*-anisoyle deviennent plus susceptibles d'être attaquées par des nucléophiles plus faibles que les analogues de *p-N*-benzoyle.

L'hydrolyse acide de **9** et **10** conduit au D-*allo*-β-phénylserine avec un rendement optique d'environ 17% à partir duquel on a tenté d'assigner aux produits **5** et **8** les configurations 2R,3R. L'hydrolyse acide similaire de la *p*-anisyl-2 oxazoline-2 (**26***b*) a permis d'isoler l'intermédiaire *l*-menthyl *O*-anisoyl *allo*-β-phenylserinate (**30***a*) lequel hydrolysé, conduit au D-*allo*-β-phenyl serine avec un rendement optique d'environ 18%. L'isolation de l'*allo*-β-phenylserine à partir des oxazolines *cis* et *trans* seulement, est attribuée à une inversion catalysée par l'acide du centre benzylique de la forme *threo* pour donner la forme *erythro* représentant la conformation la plus stable.

[Traduit par le journal]

Can. J. Chem., **51**, 856 (1973)

The Mitosane class of potent antitumor antibiotics **1** isolated in 1956 (1) from *Streptomyces caespitos* is in clinical use in Japan in the control of tumors (2). These compounds have yet to be synthesized and the mode of action is not fully understood, preventing rational structural modification to enhance antitumor properties (3, 4).

It has been established that the antitumor activity of the Mitosanes depends on their bifunctional alkylating ability through the carbamate side chain at C-10 and the chiral aziridine function at C-1 (5, 6). These initiate the introduction

[1]For part I see ref. 28.

[2]NRCC Postdoctoral Fellow, 1971–1973, on leave of absence from Kitasato University, Tokyo, Japan.

[3]NRCC Postdoctoral Fellow, 1971–1972.

Can. J. Chem. Downloaded from www.nrcresearchpress.com by 210.87.254.6 on 09/05/12
For personal use only.

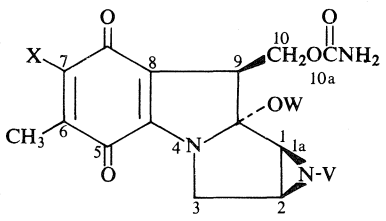

1

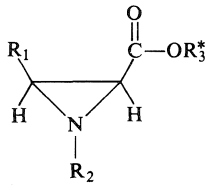

2

of covalent linkages and result in cross-linking of complementary strands in DNA (3). Irreversible loss of cross-linking activity upon opening of the aziridine ring attests to its role (6*b*). The principal intracellular consequences and lethal action of the administration of Mitomycin C lie in the inhibition of DNA synthesis resulting from this irreversible cross-linking (7–9). Despite the fact that Mitomycin C contains only one aziridine ring, it shows activity and specificity higher than all polyfunctional agents (8*a*). This suggests a highly specific mode of binding to the DNA and that the chirality of the aziridine may well be the determining factor.

Whereas studies on chiral aziridines hitherto have concentrated on chirality induced by restricted inversion of the 1-substituent in *N*-halo (10) and *N*-amino (11) aziridines, little or no attention has been paid to aziridines which owe their chirality to a 2-substituent such as exists in the aziridine moiety in the Mitosanes or in, *e.g.* **2**, where R_3* = *l*-menthyl, *l*-bornyl, 2-octanyl.

As part of a program designed to elucidate the mode of antitumor action of the Mitosanes and to develop more active analogs, we undertook to examine the chemistry of some chiral aziridines of type **2** especially with regard to configurational stability, preferred site of alkylation, and the stereochemistry of certain transformations.

In addition, chiral 2-carboalkoxyaziridines of type **2** contain the essential structural features for a possible asymmetric synthesis of α-aminoacids.

We report synthetic approaches that have been made via the Gabriel reaction. The reactions in the subsequent development to the α-aminoacids proved to be sensitive to steric hindrance effects with respect to stereospecificity and sensitive to substituent effects with regard to elimination and stereospecificity, but to exhibit the desired regiochemistry of ring opening (contrary to some literature precedents) and retention of configuration on nitrogen substitution and acid-catalyzed *trans*-esterification.

Just as the novel asymmetric synthesis of α-aminoacids from alkyl nitriles employing diisopinocampheylborane as a chiral agent described in Part 1 (27) is formally related to enzymatic transaminations (12), the synthesis described here, involving the formal addition of the elements of ammonia to a chiral olefin, resembles the aminations catalyzed by aspartase (13). A distinction is made, however, for while the former method qualifies as an asymmetric synthesis, in the latter a different approach is adopted in that the diastereomers are separated.

Bromination of *l*-menthyl cinnamate proceeded normally and treatment of the *l*-menthyl 2,3-dibromo-2,3-dihydrocinnamate (**3**) with methanolic ammonia proceeded stereoselectively to give a readily separable mixture of the diastereomeric and thermodynamically more stable *cis-l*-menthyl 2-phenyl-3-aziridinecarboxylates (**4** and **5**) as crystalline solids (see Scheme 1). This result is consistent with, but does not necessarily require (14) stereospecific *trans* addition of ammonia to the more stable intermediate *l*-menthyl 2-bromocinnamate (**6**) followed by *trans* internal S_N2 displacement of the *threo* intermediate. Treatment of **3** with triethylamine gives a single *l*-menthyl 2-bromocinnamate (**6**) which upon treatment with methanolic ammonia gives **4** and **5** (see Scheme 2). Both **4** and **5** were acylated with retention of configuration with *p*-nitrobenzoyl chloride in the presence of triethylamine to give the diastereomeric *cis-N-p*-nitrobenzoyl derivatives **7** and **8**.

When compound **8** was treated with a solution of sodium iodide (15) or potassium thiocyanate in refluxing acetone three products were obtained; the *cis*- and *trans*-2-oxazolines (**9** and **10**) and the unsaturated amide, **11** (see Scheme 3). Compounds **9** and **10** were produced in a ratio of 30:70. The assignments are based on comparison of the n.m.r. line positions and coupling constants of the methine protons with those of literature values (16). In this series, with both 2-*p*-nitrophenyl and 2-*p*-anisyloxazolines, the *cis* isomers had consistently larger coupling

Can. J. Chem. Downloaded from www.nrcresearchpress.com by 210.87.254.6 on 09/05/12
For personal use only.

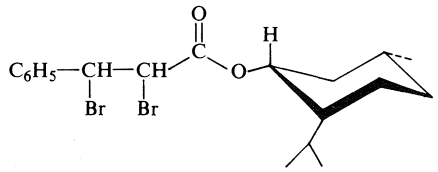

3

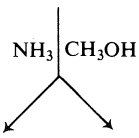

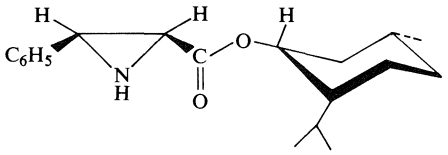

4

m.p. 156–158°
$[\alpha]_D^{23}$ −18.78°

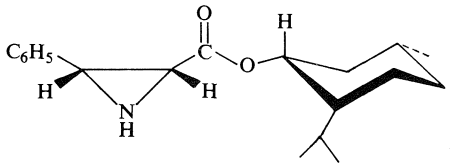

5

m.p. 124°
$[\alpha]_D^{23}$ − 51.75°

SCHEME 1

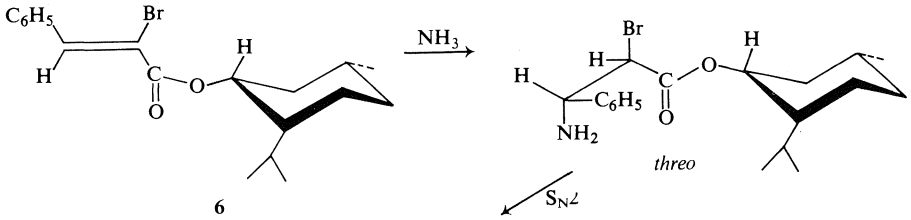

6

4 and 5

SCHEME 2

constants and larger chemical shift difference than the *trans* isomers. The bulky *l*-menthyloxy group reduced the difference in the magnitude of the coupling constants compared with the methyl esters (16). However, the correlation which is possible between the analogous *cis*- and *trans*-5-methyl analogs and the corresponding α-aminoacids of known absolute configuration

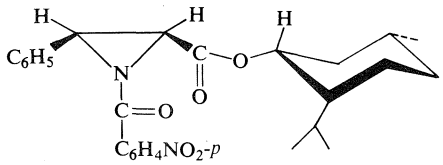

7

m.p. 157–158°
$[\alpha]_D^{23}$ − 33.4°

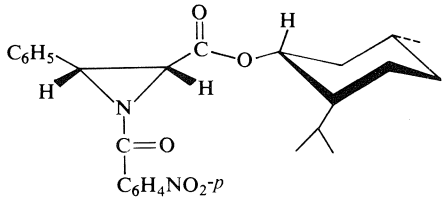

8

m.p. 176–177°
$[\alpha]_D^{23}$ − 27.12°

places these assignments on a firm foundation (see ref. 28).

Rearrangement of compound **7** under similar conditions gave pure *trans*-**10** and compound **11**. The structure of **11** was proven by its independent synthesis from glycine by the route depicted in Scheme 4, a modification of a synthesis due

Can. J. Chem. Downloaded from www.nrcresearchpress.com by 210.87.254.6 on 09/05/12
For personal use only.

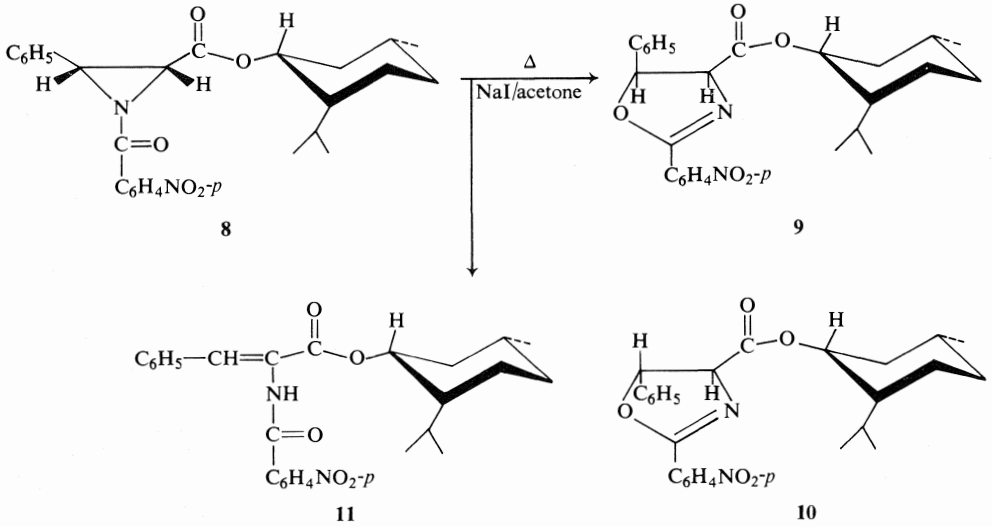

SCHEME 3

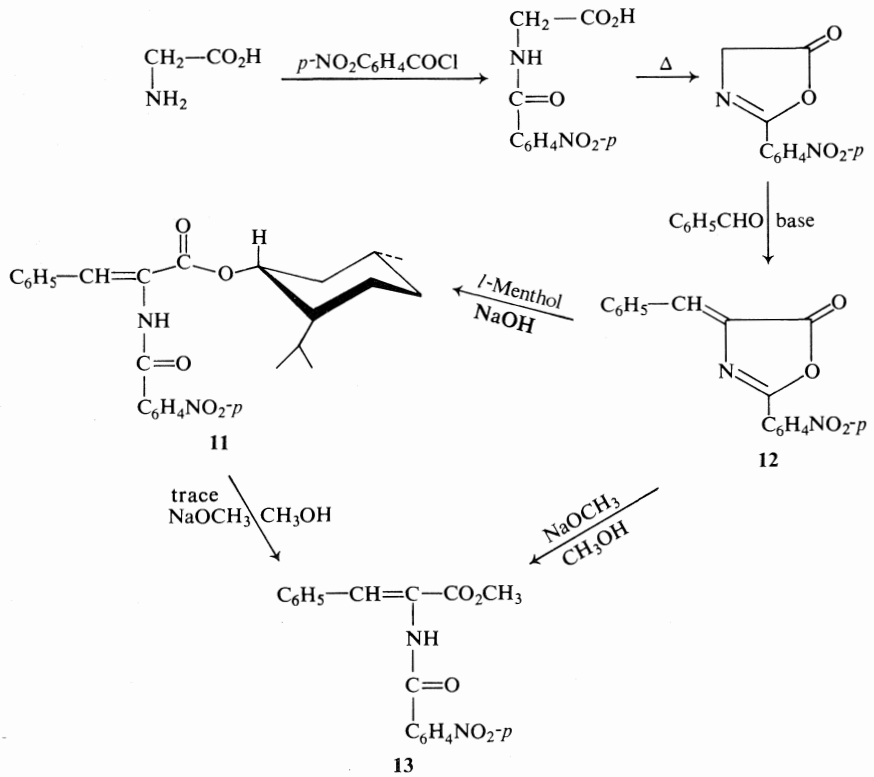

SCHEME 4

to Yamada and coworkers (17). Treatment of the benzaloxazoline **12** with methanol and sodium methoxide also afforded **13** which was identical with the product obtained by *trans*-esterification of **11** with sodium methoxide in methanol.

The iodide-catalyzed rearrangement of **7** and **8** is regiospecific in that nucleophilic attack occurs exclusively at the C-2 aziridine position to give **9** and **10**. The ultimate proof of the orientation of the groups in the oxazolines is the isolation

Can. J. Chem. Downloaded from www.nrcresearchpress.com by 210.87.254.6 on 09/05/12
For personal use only.

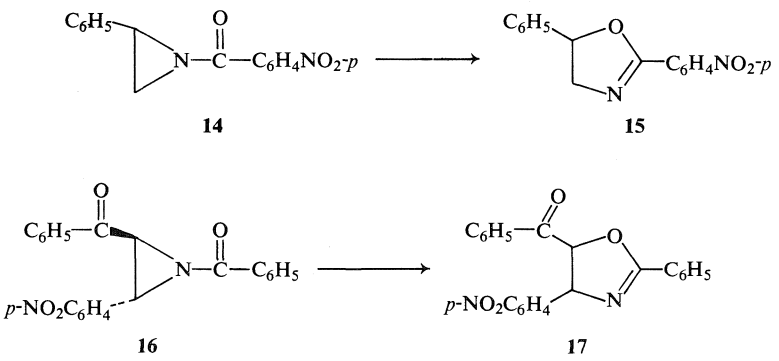

SCHEME 5

of *allo*-β-phenylserine by acid hydrolysis (see below). The regiochemistry observed, while desired from the viewpoint of α-aminoacid synthesis, was contrary to expectation based on some literature reports. Thus Heine and Kaplan (18) report the nucleophile-catalyzed rearrangement of 1-*p*-nitrobenzoyl-2-phenyl- and *trans*-1,2-dibenzoyl-3-*p*-nitrophenylaziridines (**14** and **16**) (see Scheme 5). In both cases the products **15** and **17** suggested that steric hindrance factors are not dominant in the opening, *i.e.* the nucleophile attacks the more positive and more hindered carbon in the case of **14** and **16**.

It seems plausible that in the case of **7** and **8**, however, the increased bulk offered by the carbomenthoxy group is sufficient to ensure exclusive attack at C-2. The *l*-menthyl group thus serves the several purposes in the synthesis of allowing the easy separation of diastereomers, controlling the regiochemistry of the rearrangement, and inducing asymmetry in the resulting α-aminoacid.

This dependence of the regiochemistry of nucleophilic ring opening in chiral aziridines on the steric bulk of the 2-substituent leads to the important conclusion, with regard to the mechanism of Mitomycin induced DNA cross-linking, that the site of alkylation in the antibiotic could be changed from C-1 to -2 provided W or the C-10 side chain in Mitomycin analogs were made sufficiently bulky. The "normal" Mitomycin bifunctional alkylation at C-1 and -10, *i.e.* across a four-carbon span, limits the alkylation sites on DNA effectively to guanine units on adjacent complementary strands (3). Shifting the alkylation site to C-2, *i.e.* across a five-carbon span, would increase the scope of cross-linking property.

Compounds **9**, **10**, and **11** arise from a common intermediate, the *l*-menthyl *N*-*p*-nitrobenzoyl-3-iodo-phenylalaninate (**18**) which could be isolated by a controlled room temperature iodide-catalyzed ring opening.

Compound **18** was identified by its spectral characteristics and in giving positive sodium fusion and Beilstein tests for iodine. Treatment of a solution of **18** with triethylamine at ambient temperature gave a mixture of **9** and **10** in a ratio of 25:75 in quantitative yield. Since this ratio is close to that obtained directly from *cis*-**8** it represents the equilibrium value for the Finkelstein reaction (see Scheme 6). Elimination of hydrogen iodide from **18** to give **11** is favored over ring closure by heating.

The isolation of the intermediate β-haloamide in the rearrangement of aziridines is comparatively rare and has been reported in only a few isolated instances (19). Presumably ring closure of **18** to **9** and **10** with triethylamine is favored over elimination to **11** because the NH proton in **18** is rendered more acidic by the *p*-nitrobenzoyl group.

Acid-catalyzed hydrolysis of the mixture of **9** and **10** obtained from *cis*-**8** gave D-*allo*-β-phenylserine containing a trace of phenylserine. The α-aminoacids were conveniently identified by the paper chromatographic procedure developed by Shaw and Fox (20) and by their characteristic i.r. spectra (21). The aminoacids have specific rotation of $[\alpha]_D^{25}$ −14.4 (*c*, 2, 6 *N* HCl) representing an approximate optical yield of 17.5%. This result in which the major product has the D-*erythro* configuration is closely comparable with that obtained from *l*-menthyl 2R,3R-2-methyl-1-*p*-nitrobenzoyl-3-aziridinecarboxylate (see ref. 28). On this basis we tentatively

Can. J. Chem. Downloaded from www.nrcresearchpress.com by 210.87.254.6 on 09/05/12
For personal use only.

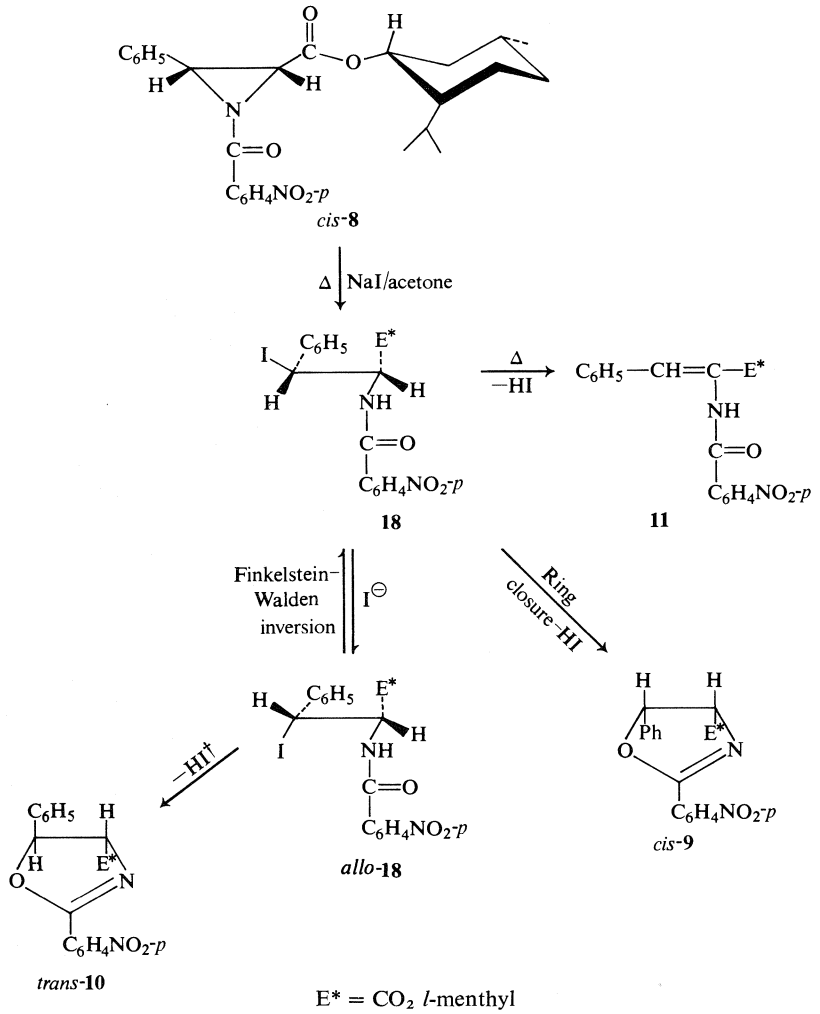

†When **18** was isolated in a room temperature reaction, treatment with Et_3N also gave *cis*-**9** *trans*-**10** quantitatively in a ratio of 25:75.

SCHEME 6

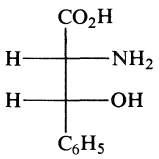

19

D-*allo*-β-Phenylserine

assign the configuration of the aziridine diastereomers **5** and **8** as 2R,3R as implied by their formulae given earlier in Schemes 1 and 3.

The fact that rearrangement of a diastereomerically pure *cis*-aziridine (**8**) leads to a mixture of *cis*- and *trans*-oxazolines which are subsequently hydrolyzed to D-*allo*-β-phenylserine with an optical yield of 17% implies that partial racemization occurs at both C-2 and -3 of **8** during the rearrangement and hydrolysis steps.

Similar behavior has been observed in the sodium iodide-catalyzed rearrangement of *cis*-1-*p*-nitrobenzoyl-2,3-diphenylaziridine (**20**) which in that case resulted in total inversion to give *trans*-2-*p*-nitrophenyl-4,5-diphenyl-2-oxazoline (**21**) (22) (Scheme 7). This was attributed to a Finkelstein identity reaction resulting in a Walden inversion of the intermediate promoted by the steric restrictions imposed upon formation of a *cis*-4,5-diphenyl-2-oxazoline. In the

Can. J. Chem. Downloaded from www.nrcresearchpress.com by 210.87.254.6 on 09/05/12
For personal use only.

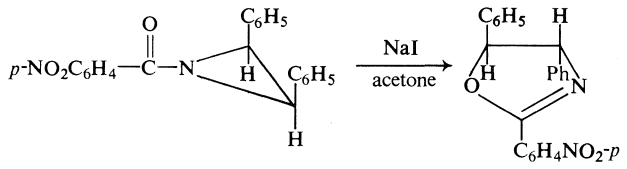

cis-**20** *trans*-**21**

SCHEME 7

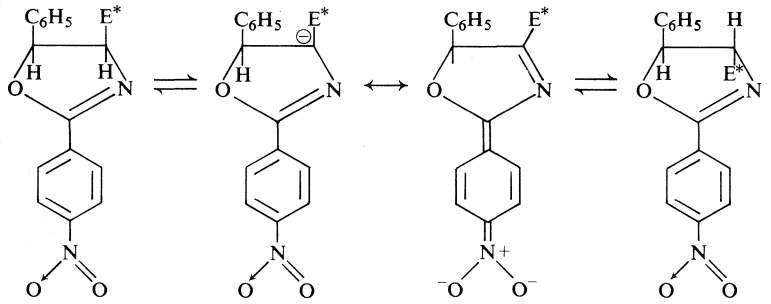

22

$E^* = CO_2$-*l*-menthyl

SCHEME 8

present case the most plausible explanation for partial racemization at C-2 of the aziridine, in view of the isolation of **18**, is a Finkelstein reaction on the latter (accompanied by some irreversible loss of hydrogen iodide to form **11**) leading to an equilibrium ratio of **18**:*allo*-**18** of 25:75 (see Scheme 6). In addition, the vigorous acid conditions necessary to hydrolyze **9** and **10** to *allo*-β-phenylserine may also result in further racemization at C-3 of **19** in view of the benzylic nature of the latter position.

Thus the problems encountered in a projected asymmetric synthesis of α-aminoacids from chiral aziridines in using *N*-aroyl substituents in general and *N*-*p*-nitrobenzoyl group in particular are (*i*) facile elimination to give **11** which limits the yield of aminoacids; (*ii*) the non-separability of the *cis*- and *trans*-oxazolines (**9** and **10**); and (*iii*) Finkelstein inversion of the intermediate β-iodoamide promoted by the bulky aryl group at C-2 of the aziridine. In addition, the use of a nitro substituent increases the danger of racemization at C-4 of the oxazoline by nucleophiles or bases by the mechanism depicted in Scheme 8 (23).

These problems were obviated in part by employing a *N*-substituent (*p*-anisoyl) which bears an electron-releasing group. This resulted in prevention of elimination to **11**, allowed the separation of *cis*- and *trans*-oxazolines for characterization, and also resulted in a substantial change in the reactivity of the chiral aziridines towards regiospecific nucleophilic attack. While partial racemization due to the Finkelstein reaction was still encountered here, its total elimination by the use of a smaller C-2 substituent with the attendant dramatic increase in optical yield of α-aminoacids is described in ref. 28.

The pure diastereomeric aziridines **4** and **5** were acylated with *p*-anisoyl chloride in the presence of triethylamine to give **23** and **24**, respectively. Treatment of **24** with sodium

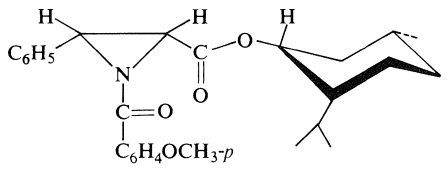

23
m.p. 152–154°
$[\alpha]_D^{23}$ −33.8°

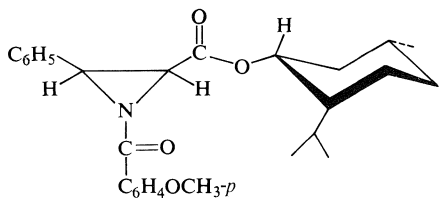

24
m.p. 145–146°
$[\alpha]_D^{23}$ −42.8°

Can. J. Chem. Downloaded from www.nrcresearchpress.com by 210.87.254.6 on 09/05/12
For personal use only.

Can. J. Chem. Downloaded from www.nrcresearchpress.com by 210.87.254.6 on 09/05/12
For personal use only.

iodide in hot acetone gave geometrically pure *trans*-2-oxazoline (**25**) (*i.e.* retention) or geometrically pure *cis*-2-oxazoline (**26***a*) (*i.e.* overall inversion). In contrast to the rearrangement of the *p*-nitrobenzoyl analog, no concomitant elimination to form the analog of **11** occurred.

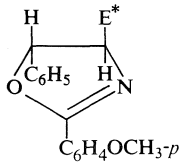

25

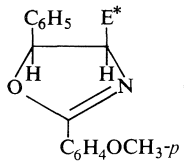

26

a $[\alpha]_D$ −20°
b $[\alpha]_D$ −80.5°

E* = CO_2-*l*-menthyl

The *cis* and *trans* configurations were assignable on the basis of their characteristic methine n.m.r. absorptions as explained earlier. Again the rearrangements were regiospecific in the required direction and involve the exclusive attack by the nucleophile at C-2 of the aziridine. This was proven subsequently by acid-catalyzed hydrolysis to *allo*-β-phenylserine.

The *N*-*p*-anisoyl aziridines (**23** and **24**) displayed a greater sensitivity towards nucleophiles than the *p*-nitrobenzoyl analogs in that they are opened quantitatively under mild treatment with methanol to give **27***a* and *b*, respectively. Similar sodium iodide-catalyzed rearrangement of aziridine **23** gave only the *cis*-2-oxazoline (**26***b*) under all reaction conditions. The latter had a specific rotation quite different from that of **26***a*.

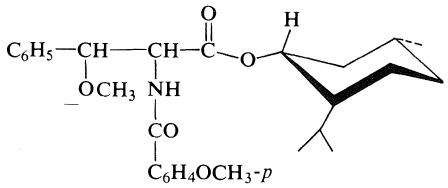

27

a $[\alpha]_D^{23}$ −11.0°
b $[\alpha]_D^{23}$ −10.5°

The fact that the observed rotations in **26***b* and **25** are not due merely to the presence of the *l*-menthyl residues and that they differ in diastereomeric composition is shown by the acid-catalyzed *trans*-esterification with methanol and anhydrous hydrogen chloride with retention of configuration at C-4 to form respectively the *cis*- and *trans*-methyl-2-oxazoline 4-carboxylates (**28** and **29**), both of which showed non-zero rotations. Thus the oxazolines **25**, **26***a*, and **26***b* retain chirality in the heterocyclic ring after the nucleophile-catalyzed rearrangement.

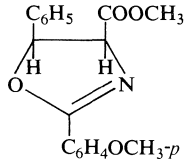

28

$[\alpha]_D^{23}$ −28°

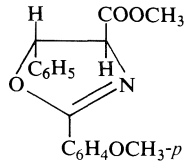

29

$[\alpha]_D^{23}$ +2.9°

Controlled hydrolysis of the *cis*-oxazoline (**26***b*) with 10% aqueous hydrochloric acid gave the *l*-menthyl *O*-anisoyl-*allo*-β-phenylserinate (**30***a*). Further acid hydrolysis of compound **30***a* afforded D-*allo*-β-phenylserine which exhibited a rotation of $[\alpha]_D^{23}$ (6 *N* HCl) −14.8°, representing 18% optical yield. The aminoacid was identified by paper chromatography (20) and also characterized by the preparation of the methyl ester **31** (24).

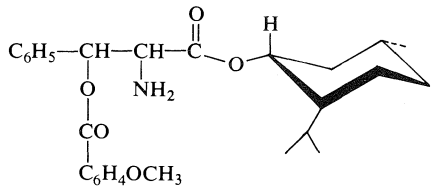

30

a m.p. 134–135°; $[\alpha]_D$ −27.3°
b m.p. 142–143°; $[\alpha]_D$ −33°

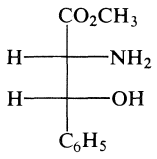

31

While the oxazoline yields have been improved by using a *p*-methoxy substituent in the synthesis, and regiospecificity is maintained in the rearrangement of **23** and **24**, stereoselectivity is obtained for **23** to **26***b* (retention) and **24** to **25** (inversion), and chirality is induced in both isomeric oxazolines (*cf.* **28** and **29**), nevertheless the optical yield obtained 18% is still low. Moreover only the *allo* isomer of the aminoacid is obtained. It seems likely that the relatively harsh acid conditions necessary to hydrolyse **25** and **26** results in partial racemization and equilibration to give the more stable *allo*-β-phenylserine (see Scheme 9).

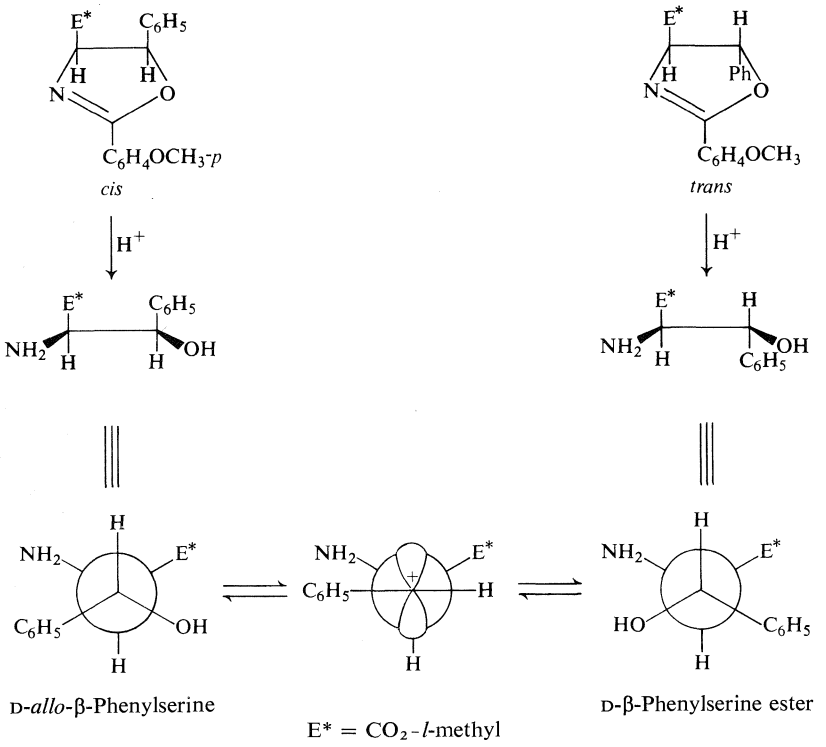

SCHEME 9

In summary, chiral ester functions may be used in the Gabriel synthesis of aziridines to permit the separation of diastereomeric chiral aziridines and their derivatives and to induce asymmetry in the synthesis of α-aminoacids. The nucleophile-catalyzed rearrangements exhibit the required regiochemistry. The overall stereospecificity and hence the optical yield is limited by (*i*) racemization resulting from a Finkelstein identity reaction on the isolable β-iodoamide, although this is only partial in contrast to literature reports of the rearrangement of aryl substituted aziridines, (*ii*) racemization accompanying acid hydrolysis of benzylic derivatives, and (*iii*) elimination to an unsaturated amide in the case of the *p*-nitrobenzoyl derivatives. The observation on the regiospecificity of the nucleophilic attack on chiral aziridines is pertinent to the design of Mitomycin analogs.

Experimental

Melting points were determined on a Fisher–Johns apparatus and are uncorrected. The i.r. spectra were recorded on a Perkin–Elmer model 421 spectrophotometer, and only the principal, sharply defined peaks are reported. The n.m.r. spectra were recorded on Varian A-60 and A-100 analytical spectrometers. The spectra were measured on approximately 10–15% (w/v) solutions in $CDCl_3$, with tetramethylsilane as a standard. Line positions are reported in p.p.m. from the reference. Mass spectra were determined on an Associated Electrical Industries MS-9 double focusing high resolution mass spectrometer. The ionization energy, in general, was 70 eV. Peak measurements were made by comparison with perfluorotributylamine at a resolving power of 15 000. Kieselgel DF-5 (Camag, Switzerland) and Eastman Kodak precoated sheets were used t.l.c. Microanalyses were carried out by Dr. C. Daesslé, Organic Microanalysis Ltd., Montreal, Quebec and by Mrs. D. Mahlow of this department.

l-Menthyl Cinnamate

A solution of 99.96 g (0.6 mol) of cinnamoyl chloride in 50 ml of dry benzene was added dropwise to a stirred solution of 93.76 g (0.6 mol) of *l*-menthol in 150 ml of dry benzene. The mixture was stirred for 48 h at room temperature. Evaporation of the solvent afforded a yellow oil, fractionation of which gave 166 g (97% yield) of *l*-menthyl cinnamate, b.p. 175°/0.5 mm, as a colorless oil; $[\alpha]_D^{23}$ −76.14 (*c*, 1.06 EtOH).

Anal. Calcd. for $C_{19}H_{26}O_2$ (mol. wt. 286.1933): C, 79.68; H, 9.15. Found (286.1927 (mass spectrum)): C, 79.72; H, 9.03.

The n.m.r. spectrum δ_{TMS} ($CDCl_3$): 0.7–2.5 (m, 18H, menthyl protons), 4.65–5.07 (m, 1H, menthyl methine); AB quartet centered at 6.43 and 7.68, J = 16 Hz (2H,

Can. J. Chem. Downloaded from www.nrcresearchpress.com by 210.87.254.6 on 09/05/12
For personal use only.

Can. J. Chem. Downloaded from www.nrcresearchpress.com by 210.87.254.6 on 09/05/12
For personal use only.

trans-vinyl), and aryl absorption. The i.r. spectrum ν_{max}(film): 1700 cm^{-1} (conjugated ester C=O).

l-Menthyl 2,3-Dibromo-3-phenylpropionate (3)

The dibromo derivative **3** was prepared by bromination of the *l*-menthyl cinnamate in chloroform according to the usual procedure in 92% yield, m.p. 74–76° (CH_3OH); $[\alpha]_D^{23}$ −19.90 (*c*, 1.09 EtOH).

Anal. Calcd. for $C_{19}H_{26}Br_2O_2$: C, 51.45; H, 5.86; Br, 35.74. Found: C, 51.45; H, 5.72; Br, 35.56.

The n.m.r. spectrum $\delta_{TMS}(CDCl_3)$: AB quartet centered at 4.8 and 5.37, J = 12 Hz (CHBr—CHBr), and aryl and *l*-menthyl absorption. The i.r. spectrum $\nu_{max}(CHCl_3)$: 1730 cm^{-1} (saturated ester C=O).

l-Menthyl 2-Bromocinnamate (6)

To a solution of 26.7 g (0.6 mol) of *l*-menthyl 2,3-dibromo-3-phenylpropionate in 50 ml of dry benzene was added dropwise with stirring a sample of 6.50 g (0.65 mol) of triethylamine. The solution was stirred for 16 h at room temperature then washed with water and dried ($MgSO_4$). Removal of the solvent *in vacuo* gave a pale yellow oil which solidified on cooling. Crystallization from methanol gave *l*-menthyl 2-bromocinnamate (**6**) 21.59 g (98% yield), m.p. 93–95°.

Anal. Calcd. for $C_{19}H_{25}BrO_2$ (mol. wt. 364.1038): C, 62.05; H, 6.88; Br, 21.82. Found (364.1045 (mass spectrum)): C, 62.27; H, 6.70; Br, 21.53.

The n.m.r. spectrum $\delta_{TMS}(CDCl_3)$: 8.23 (1H, s, vinyl proton) and menthyl and aryl absorption.

Preparation of Diastereomeric cis-l-Menthyl 2-Phenyl-3-aziridinecarboxylates (4 and 5)

Dry ammonia gas was introduced into a solution of 11.25 g (25 mmol) of *l*-menthyl 2,3-dibromocinnamate in 200 ml of methanol in a pressure bottle until the solution was saturated, the bottle stoppered, and the solution stirred for 3 days at room temperature. After removal of the solvent, the resulting residual oil was treated with 40 ml of dichloromethane and the solution was washed with water (2 × 20 ml) and dried ($MgSO_4$). Removal of the solvent and treatment of the residual oil with 40 ml of methanol precipitated 1.8 g (26% yield) of one of the diastereomeric *cis-l*-menthyl 2-phenyl-3-aziridinecarboxylates (**4**), m.p. 156–158°, as white crystals; $[\alpha]_D^{23}$ −18.78 (*c*, 0.74 benzene).

Anal. Calcd. for $C_{19}H_{27}O_2N$ (mol. wt. 301.2042): C, 75.71; H, 9.03; N, 4.05. Found (301.2038 (mass spectrum)): C, 75.75; H, 9.04; N, 4.12.

The n.m.r. spectrum $\delta_{TMS}(CDCl_3)$: 0.3–2.2 (m, 18H, menthyl protons), AB quartet centered at 3.04 and 3.54, J = 6 Hz (*cis*-aziridine ring protons), 4.36–4.80 (m, 1H, menthyl methine), 7.4 (s, 5H, aryl). The i.r. spectrum $\nu_{max}(CHCl_3)$: 1710 (C=O), 3325 and 3270 cm^{-1} (NH).

The filtrate was kept at 0° for 2 days when 1.5 g (22% yield) of the second diastereomeric *cis-l*-menthyl 2-phenyl-3-aziridinecarboxylate (**5**), m.p. 124° (MeOH), was obtained; $[\alpha]_D^{23}$ −51.75 (*c*, 0.80 benzene).

Anal. Calcd. for $C_{19}H_{27}NO_2$ (mol. wt. 301.2042): C, 75.71; H, 9.03; N, 4.05. Found (301.2041 (mass spectrum)): C, 75.75; H, 9.04; N, 4.12.

The n.m.r. spectrum $\delta_{TMS}(CDCl_3)$: 0.3–2.2 (m, 18H, menthyl protons), AB quartet centered at 2.97 and 3.46, J = 6 Hz (*cis*-aziridine ring protons), 4.2–4.8 (m, 1H, menthyl methine), 7.30 (m, 5H aryl absorption).

Preparation of Diastereomeric cis-l-Menthyl 1-p-Nitrobenzoyl-2-phenyl-3-aziridinecarboxylates (7 and 8)

(*a*) To a solution of 1.5 g (5 mmol) of aziridine **4** and 0.5 g (5 mmol) of triethylamine in 20 ml of dry benzene was added with stirring a solution of 0.92 g (5 mmol) of *p*-nitrobenzoyl chloride in 10 ml of dry benzene and the mixture stirred for 18 h. The triethylamine hydrochloride which had precipitated, was collected and the filtrate washed with water (2 × 15 ml) and dried ($MgSO_4$). Removal of the solvent and recrystallization of the residual gum from a mixture of methanol, ethanol, and dichloromethane gave *cis-l*-menthyl 1-*p*-nitrobenzoyl-2-phenyl-3-aziridinecarboxylate (**7**) 1.3 g (58% yield), m.p. 157–158°; $[\alpha]_D^{23}$ −33.4° (*c*, 0.93 benzene).

Anal. Calcd. for $C_{26}H_{30}N_2O_5$ (mol. wt. 450.2155): C, 69.31; H, 6.71; N, 6.22. Found (450.2142 (mass spectrum)): C, 69.29; H, 6.53; N, 6.13.

The n.m.r. spectrum $\delta_{TMS}(CDCl_3)$: 0.3–2.3 (m, 18H, menthyl protons), AB quartet centered at 3.66 and 4.05, J = 7 Hz (*cis*-aziridine ring protons), 4.3–4.8 (m, 1H, menthyl methine), 7.3–7.7 (m, 5H, phenyl), 8.30 (s, 4H, *p*-nitrophenyl).

The i.r. spectrum $\nu_{max}(CHCl_3)$: 1780 (ester C=O), 1680 cm^{-1} (amide).

(*b*) Reaction of the diastereomeric aziridine **5**, 1.50 g (5 mmol), and 0.92 g (5 mmol) of *p*-nitrobenzoyl chloride by a similar procedure gave 2.23 g (99% yield) of *cis-l*-menthyl 1-*p*-nitrobenzoyl-2-phenyl-3-aziridinecarboxylate (**8**) which was purified by recrystallization from ethanol and dichloromethane, m.p. 176–177°; $[\alpha]_D^{23}$ −27.12 (*c*, 0.73 benzene).

Anal. Calcd. for $C_{26}H_{30}N_2O_5$ (mol. wt. 450.2155): C, 69.31; H, 6.71; N, 6.22. Found (450.2172, mass spectrum): C, 69.38; H, 6.69; N, 6.37.

The n.m.r. spectrum $\delta_{TMS}(CDCl_3)$: 0.2–1.90 (m, 18H, menthyl protons), AB quartet centered at 3.66 and 4.06, J = 7 Hz (*cis*-aziridine ring protons), 4.3–4.90 (m, 1H, menthyl methine), 7.27–7.70 (m, 5H, phenyl), 8.30 (s, 4H, nitrophenyl).

Reaction of Diastereomeric cis-l-Menthyl 1-p-Nitrobenzoyl-2-phenyl-3-aziridinecarboxylates with Sodium Iodide in Acetone

While ordinarily treatment of **7** or **8** with a refluxing solution of sodium iodide in acetone gives both **10** and **11**, it was found that a molar ratio of aziridine:NaI of 1:4.6 favored formation of **9** and **10** and a ratio of 1:5 favored elimination to **11** as described below.

(i) Molar Ratio of Aziridine:NaI = 1:4.6

(a) Rearrangement of aziridine 8

A solution of 2.25 g (5 mmol) of aziridine **8** and 3.45 g (23 mmol) of sodium iodide in 30 ml of dry acetone was heated under reflux for 30 h. After removal of the solvent the residual oil was dissolved in 20 ml of dichloromethane and the solution washed with water (2 × 15 ml) and dried ($MgSO_4$). Removal of the solvent *in vacuo* gave a yellow solid and crystallization from methanol gave a 30:70 mixture of *cis*- and *trans-l*-menthyl 2-*p*-nitrophenyl-5-phenyl-2-oxazoline-4-carboxylate, 1.2 g (53% yield), m.p. 95–96°; $[\alpha]_D^{23}$ −32.6° (*c*, 1.03 benzene).

Anal. Calcd. for $C_{26}H_{30}N_2O_5$ (mol. wt. 450.2154): C, 69.31; H, 6.71; N, 6.22. Found (450.2154 (mass spectrum)): C, 69.18; H, 6.79; N, 6.27.

Can. J. Chem. Downloaded from www.nrcresearchpress.com by 210.87.254.6 on 09/05/12
For personal use only.

The n.m.r. spectrum $\delta_{TMS}(CDCl_3)$: 0.6–2.35 (m, 18H, menthyl protons), 4.62–5.2 (m, 1H, menthyl methine), AB quartet centered at 4.97 and 5.50, $J = 6$ Hz (*trans*-oxazoline 4,5 methines); AB quartet centered at 4.90 and 5.92, $J = 8$ Hz (*cis*-oxazoline 4,5 methines) (ratio of *cis*:*trans* AB quartets by integration is 30:70) 7.40 (s, 5H, phenyl), 8.33 (s, 4H, nitrophenyl). The i.r. spectrum $\nu_{max}(CHCl_3)$: 1732 (ester C=O), 1650 cm^{-1} (oxazoline C=N).

(b) Rearrangement of aziridine **7**

A solution of 2.25 g (5 mmol) of aziridine **7** and 3.45 g (23 mmol) of sodium iodide in a similar manner gave 1.8 g (80% yield) of *trans-l*-menthyl 2-*p*-nitrophenyl-5-phenyl-2-oxazoline-4-carboxylate, m.p. 96°; $[\alpha]_D^{23}$ −33.1° (*c*, 1.03 benzene).

The n.m.r. spectrum $\delta_{TMS}(CDCl_3)$: 0.6–2.3 (m, 18H, menthyl protons), 4.62–5.2 (m, 1H, menthyl methine), AB quartet centered at 4.97 and 5.52, $J = 6$ Hz (*trans*-oxazoline 4,5 methines), 7.46 (s, 5H, phenyl), 8.37 (s, 4H, nitrophenyl). The material was otherwise very similar to that obtained in section (*i·a*) above.

(ii) Molar Ratio of Aziridine:NaI = 1:5

A solution of 0.9 g (2 mmol) of aziridine **8** and 1.49 g (10 mmol) of sodium iodide in 15 ml of dry acetone was heated under reflux for 30 h. After removal of the solvent, the residual oil was taken up in 20 ml of dichloromethane and the solution washed with water (2 × 15 ml) and dried ($MgSO_4$). Removal of the solvent *in vacuo* gave *l*-menthyl 2-*p*-nitrobenzamidocinnamate (**11**), 0.80 g (88% yield) purified by recrystallization from methanol, m.p. 165°; $[\alpha]_D^{23}$ −23.56 (*c*, 1.18 benzene).

Anal. Calcd. for $C_{26}H_{30}N_2O_5$ (mol. wt. 450.2155): C, 69.31; H, 6.71; N, 6.22. Found (450.2166 (mass spectrum)): C, 69.30; H, 6.52; N, 6.16.

The n.m.r. spectrum $\delta_{TMS}(CDCl_3)$ 0.6–2.3 (m, 18H, menthyl protons), 4.66–4.94 (1H, sextet, menthyl methine), 7.20–7.40 (6H, aryl and vinyl protons), AB quartet at 8.20 and 7.95, $J = 9$ Hz (4H, aryl and NH protons). The i.r. spectrum $\nu_{max}(CHCl_3)$: 1690 (NHCO—), 1695 (ester), 3470 cm^{-1} (NH).

Similar treatment of 270 g (6 mmol) of aziridine **7** with 0.5 g (33 mmol) of sodium iodide in 10 ml of dry acetone afforded compound **11** identical with that obtained above.

*Isolation and Cyclization of l-Menthyl N-p-Nitrobenzoyl-3-iodophenylalaninate (**18**)*

A solution of 2.25 g (5 mmol) of aziridine **8** and 1.50 g (10 mmol) of sodium iodide in 70 ml of dry acetone was stirred at room temperature for 48 h. After removal of the solvent *in vacuo*, the residual oil was dissolved in 30 ml of chloroform and the solution washed with water (2 × 15 ml) and dried ($MgSO_4$). Removal of the solvent gave **18** as a pale yellow oil which gave strong positive Lassaigue and Beilstein tests for iodine.

The n.m.r. spectrum $\delta_{TMS}(CDCl_3)$: 0.6–2.4 (m, 18H, menthyl protons) 3.50–4.0 (s, broad 1H, NH), 4.6–5.1 (m, 1H, menthyl methine), AB quartet centered at 4.94 and 5.46, $J = 7$ Hz (2H, methines), and aryl absorption. The i.r. spectrum ν_{max}(film): 1650 (amide C=O), 3360 cm^{-1} (broad NH).

A solution of 1.04 g (18 mmol) of **18** and 2.16 g (12 mmol) of triethylamine in 35 ml of dry acetone was stirred for 16 h at room temperature. After removal of the acetone *in vacuo* the residue was dissolved in 35 ml of chloroform and the solution washed with water (2 × 20 ml) and dried ($MgSO_4$). Removal of the solvent *in vacuo* afforded a mixture of *cis* and *trans* **9** and **10** in a ratio of 25:75 as shown by the integrals of the AB quartets in the n.m.r.

Independent Synthesis and Structure Proof of l-Menthyl 2-p-Nitrobenzamidocinnamate and Methyl 2-p-Nitrobenzamidocinnamate

*(a) 4-Benzal-2-p-nitrophenyl-5-oxazolone (**12**)*

This material was prepared from *p*-nitrohippuric acid and benzaldehyde in 60% yield by a literature procedure, m.p. 229° (lit. m.p. 225–228° (26)).

*(b) l-Menthyl 2-p-Nitrobenzamidocinnamate (**11**)*

This material was prepared from **12** and sodium *l*-menthylate according to a similar procedure described by Yamada and coworkers (17) in 75% yield, m.p. 165°. The spectral and physical data of this compound were identical with that obtained from aziridine **8** as described above.

*(c) Methyl 2-p-Nitrobenzamidocinnamate (**13**)*

A solution of 294 mg (1 mmol) of **12** in 50 ml of benzene was added to a solution of 63 mg (1.1 mmol) of sodium methoxide in 50 ml of methanol. The reaction mixture was stirred for 3 h at ambient temperature. Removal of the solvents *in vacuo* gave compound **13** as a white solid 264 mg (81% yield) which was purified by recrystallization, m.p. 189–190° (aqueous MeOH).

Anal. Calcd. for $C_{17}H_{14}N_2O_5$ (mol. wt. 326.0902): C, 62.57; H, 4.32; N, 8.59. Found (326.0902 (mass spectrum)); C, 62.34; H, 4.41; N, 8.93.

The n.m.r. spectrum $\delta_{TMS}(CDCl_3)$: 3.85 (s, 3H, CO_2CH_3), 7.34 (m, 6H, phenyl and vinyl protons), 8.10 (s, 4H, nitrophenyl). The i.r. spectrum $\nu_{max}(CHCl_3)$: 1688 (amide C=O), 1710 (ester C=O), 3420 cm^{-1} (NH). This material was identical with that obtained from **11** by *trans*-esterification with sodium methoxide in methanol.

Acid-catalyzed Hydrolysis of l-Menthyl 2-p-Nitrophenyl-5-phenyl-2-oxazoline-4-carboxylate

A solution of 0.9 g (2 mmol) of oxazolines **9** and **10** in 50 ml of concentrated hydrochloric acid and 30 ml of dioxane was heated under reflux for 3 days. The filtered solution was evaporated to dryness under reduced pressure and the residual solid subjected to chromatography on an ion exchange resin (J. T. Baker Chemical Co).

The main fraction afforded D-*allo*-β-phenylserine containing a little phenylserine as a white solid, 0.250 g (69% yield), m.p. 230°; $[\alpha]_D^{23}$ −14.4 (*c*, 2.0 6 *N* HCl) (lit. $[\alpha]_D^{25}$ 82.0 (*c*, 2.0 6 *N* HCl) (25)). The R_f values of D-*allo*-β-phenylserine and phenylserine on paper chromatography were 0.30 and 0.40 respectively by ninhydrin visualization.

Esterification of 0.226 g (1.25 mmol) of the amino acid with methanol according to the procedure described below gave methyl *allo*-β-phenylserinate, m.p. 78–80° (from ether) (lit. m.p. 110° (24)), $[\alpha]_D^{23}$ −3.0 (*c*, 2.0, EtOH). Mass spectrum calcd. for $C_8H_{10}NO$ fragment ion 136.0762; observed 136.0760.

*Preparation of Diastereomeric cis l-Menthyl 1-p-Anisoyl-2-phenyl-3-aziridinecarboxylates (**23** and **24**)*

(*a*) Aziridine **4** (1.50 g, 5 mmol) was acylated with 0.85 g (5 mmol) of *p*-anisoyl chloride in the presence of 0.5 g (5 mmol) of triethylamine according to the usual

Can. J. Chem. Downloaded from www.nrcresearchpress.com by 210.87.254.6 on 09/05/12
For personal use only.

procedure affording the *N*-anisoylaziridine (**23**), 2.1 g (96% yield) as a white solid, m.p. 152–154°; $[\alpha]_D^{23}$ −33.8 (*c*, 1.05 benzene).

Anal. Calcd. for $C_{27}H_{33}NO_4$ (mol. wt. 435.2409): C, 74.45; H, 7.64; N, 3.22. Found (435.2400 (mass spectrum)): C, 74.36; H, 7.65; N, 3.32.

The n.m.r. spectrum $\delta_{TMS}(CDCl_3)$: 0.2–2.0 (m, 18H, menthyl protons), AB quartet centered at 3.55 and 3.92, J = 7.0 Hz (*cis*-aziridine ring protons), 3.81 (s, 3H, OCH_3), 4.3–4.90 (m, 1H, menthyl methine), AB quartet centered at 6.84 and 8.03, J = 8.5 Hz (4H, anisoyl ring protons), 7.2–7.7 (m, 5H, phenyl protons). The i.r. spectrum $\nu_{max}(CHCl_3)$: 1680 (amide C=O), 1730 cm^{-1} (ester C=O).

(*b*) The diastereomeric aziridine (**5**) (1.50 g, 5 mmol) was acylated with 0.85 g (5 mmol) of *p*-anisoyl chloride in the presence of 0.5 g (5 mmol) of triethylamine according to the same procedure to give the *N*-anisoylaziridine (**24**), 2.13 g (98% yield), as a white solid purified by recrystallization from MeOH, m.p. 145–146°; $[\alpha]_D^{23}$ −42.8 (*c*, 0.75 benzene).

Anal. Calcd. for $C_{27}H_{33}NO_4$ (mol. wt. 435.2409): C, 74.45; H, 7.64; N, 3.22. Found (435.2405 (mass spectrum)): C, 74.34; H, 7.66; N, 3.44.

The n.m.r. spectrum $\delta_{TMS}(CDCl_3)$: 0.3–2.2 (m, 18H, menthyl protons), AB quartet centered at 3.58 and 3.97, J = 7.0 Hz (*cis*-aziridine ring protons), 3.85 (s, 3H, OCH_3), 4.3–4.8 (m, 1H, menthyl methine), AB quartet centered at 6.90 and 8.10, J = 9.0 Hz (4H, anisoyl ring protons), 7.1–7.7 (m, 5H) phenyl protons). The i.r. spectrum $\nu_{max}(CHCl_3)$: 1665 (amide C=O), 1730 cm^{-1} (ester C=O).

Reaction of Diastereomeric cis-l-Menthyl 1-p-Anisoyl-2-phenyl-3-aziridinecarboxylates with Methanol to Form 27a and b

(*a*) A solution of 217 mg (0.5 mmol) of aziridine **24** in 10 ml of methanol was heated under reflux for 30 min. The solvent was removed *in vacuo* and the residual solid purified by recrystallization from light petroleum giving **27***b* as a white solid, 210 mg (90% yield), m.p. 125–127°; $[\alpha]_D^{23}$ −10.5 (*c*, 1.34 benzene).

Anal. Calcd. for $C_{28}H_{37}NO_5$ (mol. wt. 467.2672): C, 71.92; H, 7.98; N, 3.00. Found (467.2681 (mass spectrum)): C, 71.84; H, 7.76; N, 3.02.

The n.m.r. spectrum $\delta_{TMS}(CDCl_3)$: 0.7–2.3 (m, 18H, menthyl protons), 3.38 (s, 3H, OCH_3), 3.89 (s, 3H, aryl OCH_3), 4.8–5.2 (m, 4H, 3 methines and NH absorption), AB quartet centered at 6.94 and 7.72 (4H, anisoyl protons), 7.37 (s, 5H, phenyl protons). The i.r. spectrum $\nu_{max}(CHCl_3)$: 1715 (ester C=O), 3440 cm^{-1} (amide NH).

(*b*) Similarly a reaction of 435 mg (1 mmol) of the diastereomeric aziridine **23** with refluxing methanol gave 430 mg (99% yield) of **27***a* as a white solid, m.p. 94–95° (from light petroleum); $[\alpha]_D^{23}$ −11.0 (*c*, 0.96 benzene).

Anal. Calcd. for $C_{28}H_{37}NO_5$ (mol. wt. 467.2672): C, 71.92; H, 7.98; N, 3.00. Found (467.2672); C, 71.87; H, 8.01; N, 2.95.

The n.m.r. spectrum $\delta_{TMS}(CDCl_3)$: 0.7–2.3 (m, 18H, menthyl protons), 3.38 (s, 3H, OCH_3), 3.89 (s, 3H, aryl OCH_3), 4.8–5.2 (m, 4H, 3 methine peaks and NH), AB quartet centered at 6.94 and 7.72 (2H, anisoyl protons), 7.37 (s, 5H, phenyl protons). The i.r. spectrum ν_{max} ($CHCl_3$): 1740 (amide C=O), 1720 (ester C=O); 3440 cm^{-1} (amide NH).

Reaction of Diastereomeric cis-l-Menthyl 1-p-anisoyl-2-phenyl-3-aziridinecarboxylates with Sodium Iodide in Acetone

(*a*) A solution of 870 mg (2 mmol) of aziridine **23** and 1.20 g (8 mmol) of sodium iodide in 30 ml of dry acetone was heated under reflux for 15 h. After removal of the solvent the residual oil was taken up in 20 ml of chloroform and the solution washed with water (2 × 15 ml) and dried ($MgSO_4$). The solvent was removed *in vacuo* and crystallization of the resulting solid from light petroleum and methanol gave *cis-l*-menthyl 2-*p*-anisyl-5-phenyl-2-oxazoline-4-carboxylate (**26***b*), 0.635 g (73% yield), m.p. 89–90°. $[\alpha]_D^{23}$ −80.6 (*c*, 1.26 benzene).

Anal. Calcd. for $C_{27}H_{33}NO_4$ (mol. wt. 435.2409): C, 74.45; H, 7.64; N, 3.22. Found (435.2403 (mass spectrum)): C, 74.64; H, 7.70; N, 3.34.

The n.m.r. spectrum: $\delta_{TMS}(CDCl_3)$: 0.65–2.2 (m, 18H, menthyl protons); 3.80 (s, 3H, OCH_3); AB quartet centered at 4.74 and 5.77, J = 7.5 Hz (2H *cis*-oxazoline protons); 4.6–5.1 (m, 1H, menthyl methine); AB quartet centered at 6.90 and 7.99, J = 9.0 Hz (4H anisyl ring protons), 7.32 (s, 5H, phenyl protons). The i.r. spectrum $\nu_{max}(CHCl_3)$: 1630 (oxazoline N=C), 1715 cm^{-1} (ester C=O).

(*b*) A reaction of 0.870 g (2 mmol) of the diastereomeric aziridine (**24**) with 1.20 g (8 mmol) of sodium iodide in acetone according to similar conditions gave *trans-l*-menthyl 2-*p*-anisyl-5-phenyl-oxazoline-4-carboxylate (**25**), 0.827 g (94% yield), as an oil. $[\alpha]_D^{23}$ −45.7 (*c*, 1.46 benzene).

Anal. Calcd. for $C_{27}H_{33}NO_4$ (mol. wt. 435.2409): C, 74.45; H, 7.64; N, 3.22. Found (435.2400 (mass spectrum)): C, 74.23; H, 7.51; N, 3.17.

The n.m.r. spectrum $\delta_{TMS}(CDCl_3)$: 0.7–2.3 (m, 18H, menthyl protons), 3.85 (s, 3H, OCH_3), AB quartet centered at 4.83 and 5.38, J = 6.0 Hz (2H, *trans*-oxazoline protons), 4.6–5.1 (m, 1H, menthyl methine), AB quartet centered at 6.95 and 8.03 (4H, anisyl ring protons), 7.33 (s, 5H, phenyl protons). The i.r. spectrum $\nu_{max}(CHCl_3)$: 1640 (C=N) 1725 cm^{-1} (ester C=O).

(*c*) A comparable reaction of 0.870 g (2 mmol) of the aziridine **24** with 1.20 g (8 mmol) of sodium iodide in acetone in a similar procedure gave 0.732 mg (84% yield) of *cis-l*-menthyl 2-*p*-anisyl-5-phenyl-oxazoline-4-carboxylate (**26***a*), m.p. 90°; $[\alpha]_D^{23}$ −20.0 (*c*, 1.65 benzene).

The spectral and physical data of this material were identical with that of the material obtained in the rearrangement of **23** described in section *a* above.

trans-Esterification of cis- and trans-l-Menthyl 2-p-Anisyl-5-phenyl-2-oxazoline-4-carboxylates

(*a*) A solution of 0.435 g (1 mmol) of **26***b* in 20 ml of methanol was saturated with dry hydrogen chloride at room temperature and the solution stirred at room temperature for 4 days. The solvent was removed *in vacuo* and the residue taken up in 10 ml of chloroform and the solution washed with (*i*) 5% sodium hydroxide (2 × 7 ml), and (*ii*) water (2 × 7 ml), then dried ($MgSO_4$). The solvent and displaced *l*-menthol were removed *in vacuo* at 50–60° in 20 h and the residual yellow oil decolorized by treatment with charcoal in benzene affording **28** as a colorless oil; $[\alpha]_D^{23}$ −28 (*c*, 1.83 benzene).

Anal. Calcd. for $C_{18}H_{17}NO_4$ (mol. wt. 311.1158): C, 69.44; H, 5.50; N, 4.50. Found (311.1154 (mass spectrum)): C, 69.32; H, 5.75; N, 4.78.

Can. J. Chem. Downloaded from www.nrcresearchpress.com by 210.87.254.6 on 09/05/12
For personal use only.

The n.m.r. spectrum $\delta_{TMS}(CDCl_3)$: 3.86 (s, 6H, CO_2CH_3 and $—OCH_3$), AB quartet centered at 6.80 and 5.88, $J = 7.5$ Hz (2H, *cis* oxazoline 4,5 coupling), AB quartet centered at 6.94 and 8.0, $J = 9.0$ Hz (2H, anisyl ring protons), 7.38 (s, 5H, phenyl protons). The i.r. spectrum $\nu_{max}(CHCl_3)$: 1635 (C=N), 1725 cm^{-1} (ester C=O).

(*b*) A similar *trans*-esterification was carried out with 0.435 g (1 mmol) of the diastereomeric *trans*-oxazoline **25** and 20 ml of methanol which was saturated with dry hydrogen chloride and worked-up as described above to give **29** as an oil 0.265 g (85% yield); $[\alpha]_D^{23}$ +2.9 (*c*, 1.0 benzene).

Anal. Calcd. for $C_{18}H_{17}NO_4$ (mol. wt. 311.1158): C, 69.44; H, 5.50, N, 4.50. Found (311.1154 (mass spectrum)): C, 69.26; H, 5.32; N, 4.41.

The n.m.r. spectrum $\delta_{TMS}(CDCl_3)$: 3.85 (s, 6H, CO_2CH_3 and OCH_3), AB quartet centered at 4.90 and 5.42, $J = 6.5$ Hz (*trans*-oxazoline 4,5 protons, AB quartet centered at 6.97 and 8.06, $J = 9.0$ Hz (anisyl ring protons), 7.35 (s, 5H, phenyl protons). The i.r. spectrum $\nu_{max}(CHCl_3)$: 1640 (C=N), 1730 cm^{-1} (ester C=O).

Acid Catalyzed Hydrolysis of cis- and trans-l-Menthyl 2-p-Anisyl-5-phenyl-2-oxazoline-4-carboxylates

(A) Hydrolysis to Intermediates O-Anisoyl-allo-β-phenylserinates

(*a*) A solution of 0.435 g (1 mmol) of oxazoline **26***b* in 20 ml of 10% aqueous hydrochloric acid was heated under reflux for 18 h. Upon cooling, a crystalline precipitate of *l*-menthyl-*O*-anisoyl-*allo*-β-phenylserinate hydrochloride had separated and was collected. A vigorous stream of dry ammonia was passed through a suspension of the crystalline solid in 70 ml of ether. The granular ammonium chloride was collected and washed with ether. Removal of the solvent from the filtrate and washings gave *l*-menthyl-*O*-anisoyl-*allo*-β-phenylserinate (**30***a*) 0.345 g (77% yield), m.p. 134–135° (CCl_4); $[\alpha]_D^{23}$ −27.3 (*c*, 1.9 hydrochloride salt in CH_3OH).

Anal. Calcd. for $C_{27}H_{35}NO_5$ (mol. wt. 453.2515): C, 71.49; H, 7.78; N, 3.09. Found (453.2508 (mass spectrum)): C, 71.21, H, 7.81; N, 3.06.

The n.m.r. spectrum $\delta_{TMS}(CDCl_3)$: 0.6–2.1 (m, 18H, menthyl protons), 8.3–11 (bs, 2H, NH_2), 3.83 (s, 3H, OCH_3), 4.9–5.4 (m, 3H, 3 methines), AB quartet centered at 6.85 and 7.65, $J = 9.0$ Hz (4H, anisoyl protons), 7.33 (s, 5H, phenyl protons). The i.r. spectrum $\nu_{max}(CHCl_3)$: 1660 (anisoyl C=O); 1720 (ester C=O); 3460 cm^{-1} (NH_2).

(*b*) Acid-catalyzed hydrolysis of 0.43 g (1 mmol) of the isomeric *trans*-oxazoline **25** with 20 ml of 20% aqueous hydrochloric acid by a similar procedure gave 0.38 g (87% yield) of *l*-menthyl-*O*-anisoyl-*allo*-β-phenylserinate (**30***b*) which was purified by recrystallization from benzene, m.p. 142–143°; $[\alpha]_D^{23}$ −33 (c, 1.65, benzene).

Anal. Calcd. for $C_{27}H_{35}NO_5$ (mol. wt. 453.2515): C, 71.49; H, 7.78; N, 3.09. Found (453.2509); C, 71.25; H, 7.63; N, 3.02.

The n.m.r. spectrum was very similar to that obtained in the hydrolysis of **26***b*. Mixed m.p. of this material with **30***a* was depressed to 125–30°.

(B) Hydrolysis to α-Aminoacids. Preparation of allo-β-Phenylserine and Methyl allo-β-Phenylserinate

(*a*) A solution of 2.718 g (6 mmol) of compound **30** in 50 ml of concentrated hydrochloric acid and 30 ml of dioxane was heated under reflux for 5 days. The filtered solution was concentrated under reduced pressure and the residual solid was subjected to chromatography on ion exchange resin AGC-244 (J. T. Baker Chem. Co.). Removal of the solvents afforded allophenylserine **19**, 0.450 g, (45% yield), $[\alpha]_D^{25}$ (6 *N* HCl) −14.8 (*c*, 2.0), (lit. $[\alpha]_D^{25}$ (6 *N* HCl) −82.0 (*c*, 2.0) (25)). A stream of dry hydrogen chloride was passed through a suspension of 181 mg (1 mmol) of **31** in 20 ml of dry methanol for 45 min under reflux. The clear solution was concentrated almost to dryness and a stream of ammonia passed through a suspension of the residual oil in 60 ml of dry ether for 10 min. The precipitated ammonium chloride was collected and washed with ether (2 × 7 ml). Removal of the solvent *in vacuo* gave methyl *allo*-β-phenylserinate, 0.136 g (70% yield), m.p. 98–100° (from ether) (lit. m.p. 110° (20)); $[\alpha]_D^{23}$ −2.2 (*c*, 0.9 $CHCl_3$).

Anal. Calcd. for $C_{10}H_{13}NO_3$: C, 61.52; H, 6.71; N, 7.18, Found: C, 61.63; H, 6.67; N, 7.13.

Mass spectrum Calcd. for fragment ion $C_8H_{10}NO$ ($C_6H_5CHOHCH{=}\overset{+}{N}H_2$): 136.0762). Found: 136.0760.

The α-aminoacid was identified by ascending paper chromatography according to the procedure by Shaw and Fox during 16 h. The respective R_f values of the spots visualized by the ninhydrin method were 0.30 (*allo*-β-phenylserine main product) and 0.44 (phenylserine present in trace amounts). The n.m.r. spectrum $\delta_{TMS}(CDCl_3)$: 2.34 (2H, bs, D_2O exchangeable, NH_2 and OH), 3.74 (s, 3H, CO_2CH_3), 4.26 (s, 2H, 2 methines), 7.33 (s, sh, phenyl protons). The i.r. spectrum $\nu_{max}(CHCl_3)$: 1725 (ester C=O), 3390, 3520 cm^{-1} (NH_2,OH).

(*b*) Hydrolysis of 2.718 g (6 mmol) of **30***b* with concentrated hydrochloric acid under similar conditions gave allophenylserine, 0.75 g (76% yield), m.p. 225–257°; $[\alpha]_D^{23}$ −3.5 (*c* 1.0 CH_3OH as hydrochloride salt.)

Paper chromatography showed one spot with an R_f value of 0.30 (ninhydrin) identifying *allo*-β-phenylserine. Esterification of the *allo*-β-phenylserine with methanol and hydrogen chloride gave methyl *allo*-β-phenylserinate, m.p. 88–90° (from ether), in 87% yield. No m.p. depression with the product from section (*a*).

Anal. Calcd. for $C_{10}H_{13}NO_3$: C, 61.52; H, 6.71; N, 7.18. Found: C, 61.63; H, 6.83; N, 6.99.

Mass spectrum Calcd. for fragment ion $C_8H_{10}NO$ ($C_6H_5CHOHCH{=}\overset{+}{N}H_2$): 136.0762. Found: 136.0760.

This research was supported by a National Research Council of Canada grant to J.W.L. and by the Chemistry Department, University of Alberta, Edmonton, Alberta. We thank Mr. R. Swindlehurst and Dr. A. Hogg for the n.m.r. and mass spectra.

1. (*a*) T. Hata, Y. Sano, R. Sugawara, A. Matsumae, K. Kanamori, T. Shima, and T. Hoshi. J. Antibiot. (Tokyo), Ser. A, **9**, 141 (1956). (*b*) S. Wakaki, H. Marumo, T. Tomioka, G. Shimizu, E. Kato, H. Kamada, S. Kudo, and Y. Fujimoto. Antibiot. Chemother. **8**, 228 (1958). (*c*) S. Wakaki. Cancer Chemother. Rept. **13**, 79 (1961). (*d*) J. S. Webb, D. B. Cosulich, J. H. Mowat, J. B. Patrick, R. W. Broschard, W. E. Meyer, R. P. Williams, C. F. Wolf, W. Fulmor, C. Pidacks, J. E. Lancaster. J. Am. Chem. Soc. **84**, 3185 (1962).

2. (*a*) W. FRANK and A. E. OSTERBURG. Cancer Chemother. Rept. **9**, 114 (1960). (*b*) K. SUGIURA. Cancer Chemother. Rept. **13**, 51 (1961). (*c*) A. E. EVANS. Cancer Chemother. Rept. **14**, 1 (1961). (*d*) J. S. EVANS, E. A. MUSSER, and J. E. GRAY. Antibiot. Chemother. **11**, 445 (1961).
3. W. SZYBALSKI and V. N. IYER. *In* Antibiotics I: mechanism of action. *Edited by* D. Gottleib and P. D. Shaw. Springer-Verlag, New York. 1967. p. 211.
4. E. J. KIRSCH. *In* Antibiotics II. *Edited by* D. Gottleib and P. D. Shaw. Springer-Verlag, New York. 1967. p. 66.
5. J. A. MONTGOMERY, T. P. JOHNSTON, and Y. F. SHEALY. *In* Medicinal chemistry. Part I. 3rd Ed. *Edited by* A. Burger. Wiley-Interscience, New York. 1970. p. 698.
6. (*a*) Reference 3, p. 227; (*b*) Reference 3, p. 230.
7. M. N. LIPSETT and A. WEISSBACH. Biochem. **4**, 206 (1965).
8. (*a*) H. S. SCHWARTZ, J. E. SODERGREN, and F. S. PHILIPS. Science, **142**, 1181 (1963). (*b*) H. MURAKAMI. J. Theoret. Biol. **10**, 236 (1966). (*c*) J. F. COLLINS. Brit. Med. Bull. **21**, 223 (1965).
9. V. N. IYER and W. SZYBALSKI. Proc. Natl. Acad. Sci. U.S. **50**, 355 (1963).
10. (*a*) S. J. BROIS. J. Am. Chem. Soc. **90**, 508 (1968). (*b*) D. FELIX and A. ESCHENMOSER. Angew. Chem. Intl. Ed. Engl. **7**, 224 (1968). (*c*) J. M. LEHN and J. WAGNER. Chem. Commun. 148 (1968). (*d*) R. G. KOSTYANOVSKY, Z. E. SAMOJLOVA, and I. I. TCHERVIN. Tetrahedron Lett. 719 (1969).
11. D. J. ANDERSON, D. C. HORWELL, and R. S. ATKINSON. J. Chem. Soc. (C) 624 (1971).
12. J. D. MORRISON and H. S. MOSHER. Asymmetric organic reactions. Prentice-Hall Inc., Englewood Cliffs, N.J. 1971. p. 325.
13. (*a*) O. GAWRON and T. P. FONDY. J. Am. Chem. Soc. **81**, 6333 (1959). (*b*) H. J. BRIGHT, R. E. LUNDIN, and L. L. INGRAHAM. Biochem. **3**, 1224 (1964).
14. (*a*) K. D. BERLIN, L. G. WILLIAMS, and O. C. DERMER. Tetrahedron Lett. 873 (1968). (*b*) N. M. CROMWELL. J. Am. Chem. Soc. **81**, 4702 (1959).
15. H. W. HEINE. Angew. Chem. Intl. Ed. Engl. **1**, 528 (1962).
16. S. H. PINES, M. A. KOZLOWSKI, and S. KARADY. J. Org. Chem. **34**, 1621 (1969).
17. S. YAMADA, T. FUJII, and T. SHIOIRI. Chem. Pharm. Bull. (Tokyo), **10**, 680 (1962).
18. H. W. HEINE and M. S. KAPLAN. J. Org. Chem. **32**, 3069 (1967).
19. (*a*) P. E. FANTA and E. N. WALSH. J. Org. Chem. **30**, 3574 (1965). (*b*) P. E. FANTA, R. J. SMAT, and J. R. KRIKAU. J. Heterocycl. Chem. **5**, 419 (1968). (*c*) W. L. NELSON and D. D. MILLER. J. Org. Chem. **35**, 1185 (1970).
20. K. N. F. SHAW and S. W. FOX. J. Am. Chem. Soc. **75**, 3421 (1953).
21. R. J. KOEGEL, J. P. GREENSTEIN, M. WINITZ, S. N. BIRNBAUM, and R. A. MCCALLUM. J. Am. Chem. Soc. **77**, 5708 (1955).
22. H. W. HEINE, D. C. KING, and L. A. PORTLAND. J. Org. Chem. **31**, 2662 (1966).
23. E. E. HAMEL and E. P. PAINTER. J. Am. Chem. Soc. **76**, 919 (1954).
24. J. H. LOOKER and D. N. THATCHER. J. Org. Chem. **22**, 1233 (1957).
25. W. S. FONES. J. Biol. Chem. **204**, 323 (1953).
26. V. G. ZUBENKO. Dopov. Akad. Nauk. Ukr. RSR. Ser. B (1968) **30**. (6), 547; Chem. Abstr. **69**, 106596p.
27. U. E. DINER, M. WORSLEY, J. W. LOWN, and J. FORSYTHE. Tetrahedron Lett. 3145 (1972).
28. J. W. LOWN, N. ONO, and T. ITOH. Can. J. Chem. Submitted.

Can. J. Chem. Downloaded from www.nrcresearchpress.com by 210.87.254.6 on 09/05/12
For personal use only.

The Bimolecular Self-reactions of Secondary Peroxy Radicals. Product Studies[1]

D. LINDSAY, J. A. HOWARD, E. C. HORSWILL, L. ITON,[2] K. U. INGOLD, T. COBBLEY, AND A. LL

Division of Chemistry, National Research Council of Canada, Ottawa, Canada K1A 0R9

Received September 29, 1972

The principal products formed from 1-ethoxyethyl hydroperoxide and 1,2-diphenylethyl hydroperoxide on oxidation with reagents that are presumed to generate the corresponding *sec*-alkylperoxy radicals (Ce(IV), *tert*-butoxy, and Ag_2O) have been identified. The products formed when the corresponding alkoxy radicals are generated in pairs have also been identified. It is concluded that the Russell (1) concerted cyclic mechanism in which tetroxide decomposed to molecular products is not the exclusive route for the bimolecular self-reaction of *sec*-alkylperoxy radicals. It is suggested that there is also a second tetroxide decomposition process which yields radical products. The second process may yield "free" alkoxy radicals or it may, perhaps, yield the products of β-scission of the alkoxy radicals in a step concerted with O—O homolysis of the tetroxide. The relative importance of tetroxide decomposition to molecular and to radical products will depend on the structure of the alkyl groups, the temperature and, perhaps, the solvent.

Les principaux produits formés dans l'oxydation de l'éthoxy-1 éthylhydroperoxyde et diphémyl-1,2 éthyl hydroperoxyde par des réactifs susceptibles d'engendrer les radicaux *sec*-alkylperoxy correspondants (Ce(IV), *ter*-butoxy, et Ag_2O) ont été identifiés. Les produits issus des radicaux alkoxy correspondants, lorsque ceux ci étaient formés par pairs, ont été également identifiés. Le mécanisme cyclique concerté de Russell (1) selon lequel le tétroxyde se décompose en produits moléculaires, n'est donc pas la voie exclusive dans l'autoréaction bimoléculaire des radicaux *sec*-alkylperoxy. Une seconde voie pour la décomposition du tétroxyde en produits radicalaires a été proposée. Ce second processus peut conduire aux radicaux alkoxy libres, ou aux produits de scission β des radicaux alkoxy selon une étape concertée avec homolyse O—O du tétroxyde. L'importance relative de la décomposition du tétroxyde en produits moléculaires ou radicalaires dépendra de la structure des groupes alkyles, de la température et peut être du solvant.

[Traduit par le journal]

Can. J. Chem., **51**, 870 (1973)

In 1957 Russell (1) suggested that the bimolecular self-reaction of secondary alkylperoxy radicals involved the concerted decomposition (reaction *2*) of an initially formed tetroxide (see Scheme 1).

The most frequently postulated alternative mechanism involves decomposition of the tetroxide to give two alkoxy radicals and oxygen (reaction *3*). According to the Russell mechanism the ketone, RR′CO, and the alcohol, RR′CHOH, will be formed in equimolar quantities. The same will be true of the non-concerted mechanism provided that all the alkoxy radicals that escape the cage (reaction *5*) undergo β-scission,

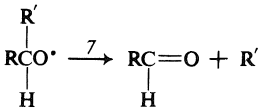

If, however, the free alkoxy radicals abstract a hydrogen atom there will be a preponderance of alcohol.

The Russell, or concerted, mechanism is supported by a considerable body of experimental evidence (2–5), most of which has been obtained at ambient temperatures (20–60°). The non-concerted decomposition will be favored at higher temperatures because it will have a higher activation energy than the concerted process. For example, it has been estimated (6) that with *s*-butylperoxy radicals k_3/k_2 is ~0.04 at 30° and ~0.3 at 100°.

Two experimental observations have prevented the unreserved acceptance of the Russell mechanism as the dominant process at ambient temperatures and below. Firstly, thermochemical calculations suggest that if the overall reaction proceeded by the concerted route it should have a negative activation energy of several kilocalories per mole (7). However, experimental measurements in the temperature range −16 to −90° indicate a positive activation energy of ~3 kcal/mol for a number of *sec*-alkylperoxy radicals (8, 9). Secondly, Diaper (10) has reported that 1-methoxy (**1***a*) and 1-*tert*-butoxynonane-1-hydroperoxide (**1***b*) were smoothly oxidized to di-(1-alkoxyalkyl)peroxides by 1 equiv of

[1]NRCC No. 12962.
[2]NRCC Summer Student, 1969.

Can. J. Chem. Downloaded from www.nrcresearchpress.com by 210.87.254.105 on 09/05/12
For personal use only.

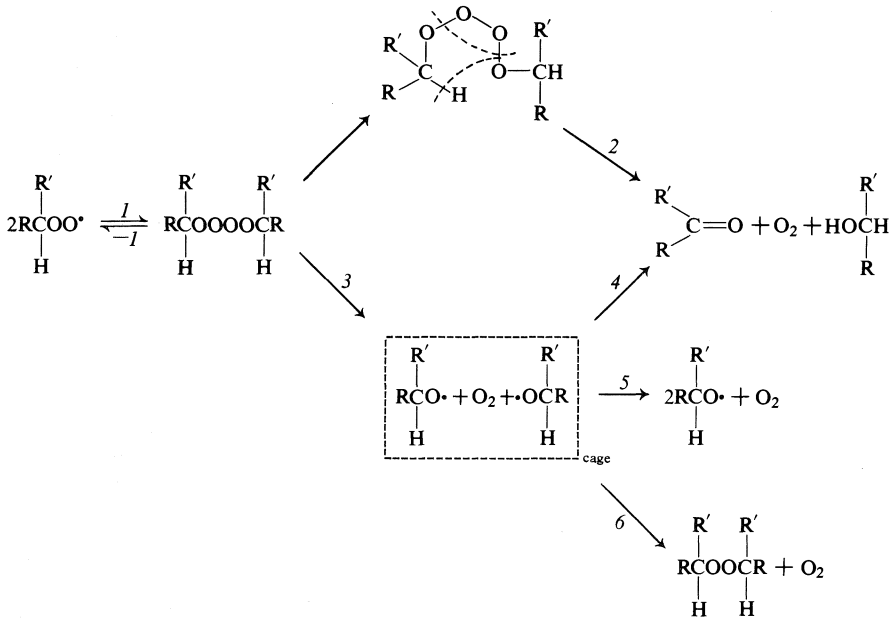

SCHEME 1

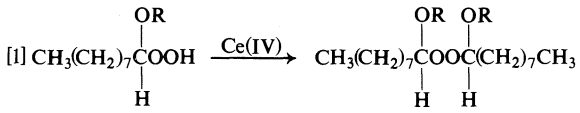

1

a R = CH_3

b R = $(CH_3)_3C$

Ce(IV) in methanol at 0° (eq. 1). Since Ce(IV) oxidizes alkyl hydroperoxides to the corresponding peroxy radicals in high yield (11, 12) it seems not unreasonable to suppose that 1-alkoxyalkylperoxy radicals react by the radical pathway and that the caged alkoxy radicals combine (reaction *6*, Scheme 1) rather than disproportionate.

Diaper's products contrast sharply with the products normally found in processes which are presumed to involve the bimolecular self-reaction of secondary alkylperoxy radicals. Numerous studies (1, 4, 6, 9, 13–16) attest to the fact that such products are the appropriate alcohol and ketone and that these are formed in high yield and in *approximately* equimolar amounts. Diaper's results prompted us, therefore, to investigate the products formed from an analogous peroxy radical, 1-ethoxyethylperoxy. Although little or no di-(1-ethoxyethyl)peroxide was formed, the other products suggested that alkoxy radicals played a significant role in the reaction. Our product studies were, therefore, extended to the 1,2-diphenylethylperoxy radical which was chosen because any free alkoxy radical should undergo a relatively rapid β-scission to yield benzaldehyde which could be easily detected in the reaction mixture (eq. 2). Attempts

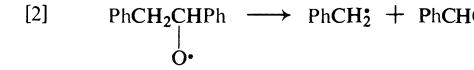

were also made to study the behavior of caged pairs of 1-ethoxyethoxy and 1,2-diphenylethoxy radicals in order to avoid some of the assumptions otherwise necessary in interpreting the results of the peroxy radical studies (*cf.* refs. 3 and 4).

Results and Discussion

1-Ethoxyethylperoxy Radicals

These peroxy radicals were most conveniently prepared by oxidation of 1-ethoxyethyl hydroperoxide either by ceric ammonium nitrate, *tert*-butoxy radicals, or silver oxide. The principal reaction products expected from their self-reaction are shown in Scheme 2 while the yields of the products actually found are listed in Tables 1 and 2.

Ethanol was presumably formed by decomposition of the hemiacetal (eq. 3). The acetalde-

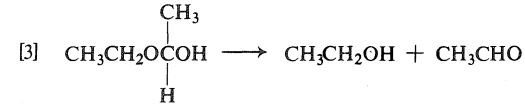

Can. J. Chem. Downloaded from www.nrcresearchpress.com by 210.87.254.105 on 09/05/12
For personal use only.

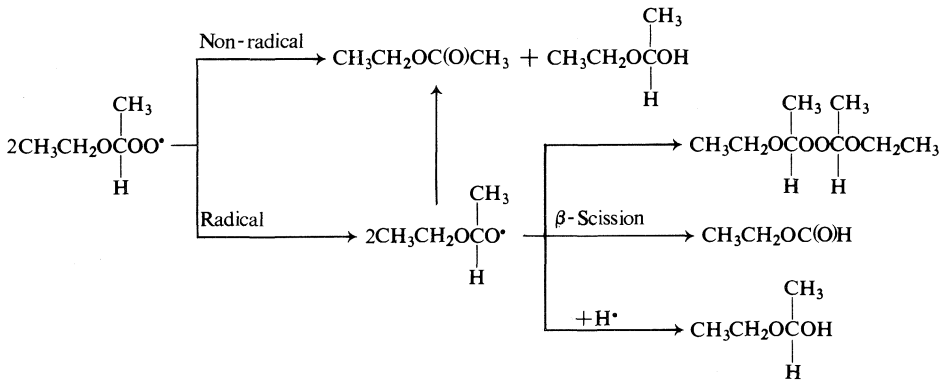

SCHEME 2

TABLE 1. Products from the Ce(IV) oxidation of 1-ethoxyethyl hydroperoxide in methanol at 0° (yields are mol/mol of hydroperoxide)

Initial hydroperoxide concentration (*M*)	Methyl formate	Ethyl formate	Ethyl acetate	Ethanol	1,1-Dimethoxyethane	Oxygen
0.18	0.09	0.17	0.47	0.58	0.4	0.4
0.25[a]	[b]	0.03	0.3	[c]	0.2[d]	[e]
0.33	0.05	0.06	0.06	0.25	0.08	[e]
0.45	0.09	0.10	0.3	0.53	0.22	0.4
0.83	0.08	0.16	0.4	0.5	0.22	0.4

[a]In ethanol.
[b]Not present.
[c]Solvent.
[d]1,1-Diethoxyethane.
[e]Not measured.

hyde formed in this process appeared as the appropriate dialkoxyethane in alcoholic solvents (eq. 4). The presence of methyl formate in

[4] $CH_3CHO + 2ROH \rightarrow CH_3CH(OR)_2 + H_2O$

methanol but not in ethanol, CCl_4 or benzene was probably the result of a *trans*-esterification of ethyl formate (eq. 5).

[5] $CH_3OH + CH_3CH_2OCHO \rightarrow CH_3CH_2OH + CH_3OCHO$

Diaper (10) obtained di-(1-*tert*-butoxynonyl)-peroxide in 45% yield by the oxidation of **1***b* with Ce(IV). In contrast, we could detect no di-(1-ethoxyethyl)peroxide among the products from the Ce(IV) oxidation of 1-ethoxyethyl hydroperoxide under similar experimental conditions. Although the product balances were not too good the sum of [formate] + [acetate] + ½([ethanol] + [dimethoxyethane]) for the Ce(IV) experiments with initial hydroperoxide concentrations of 0.18, 0.45, and 0.83 *M* were such that less than 10% of the hydroperoxide could have been converted to peroxide. This difference in products is surprising but is not necessarily inconsistent with the radical reaction playing an important role in the bimolecular self-reactions of these peroxy radicals. That is, high molecular weight alkoxy radicals will diffuse from the cage more slowly than low molecular weight radicals and so they will yield more peroxide if reaction *6* of Scheme 1 is the principal cage process. The cage lifetime may also be increased by hydrophobic bonding between the 1-*tert*-butoxynonoxy radical pair. That is, methanol is a hydrophilic solvent and as such will rather poorly solvate such large alkoxy radicals and so they will tend to remain in the cage for longer than the small, readily solvated, 1-ethoxyethoxy radicals. While the different peroxide yields can be rationalized in this way, it is by no means certain that the metal ion does not play a role in peroxide formation, the extent of this role depending on the hydroperoxide. An example of

Can. J. Chem. Downloaded from www.nrcresearchpress.com by 210.87.254.105 on 09/05/12
For personal use only.

Can. J. Chem. Downloaded from www.nrcresearchpress.com by 210.87.254.105 on 09/05/12
For personal use only.

TABLE 2. Products from the *tert*-butyl hyponitrite induced decomposition of 1-ethoxyethyl hydroperoxide at 40° (yields are mol/mol of hydroperoxide)

Initial hydroperoxide concentration (*M*)	Solvent	Methyl formate	Ethyl formate	Ethyl acetate	Ethanol	Acetaldehyde	1,1-Dimethoxyethane
0.1	Methanol	[a]	[a]	[b]	1.0	[c]	0.3
0.25	Methanol	[a]	[a]	[b]	0.92	[c]	0.24
0.33	Methanol	0.14	0.18	0.18	0.76	[c]	0.25
0.4	Methanol	0.03	[a]	0.38	0.6	[c]	~1.0
0.25	Ethanol	[c]	0.12	1.0	[d]	[c]	0.76[e]
0.1	CCl_4	[c]	0.06	0.5	0.21	0.2	[c]
0.2	CCl_4	[c]	0.05	0.38	0.14	0.3	[c]
0.4	CCl_4	[c]	0.05	0.41	0.18	0.13	[c]
0.4	Benzene	[c]	0.04	0.54	0.05	0.08	[c]
Oxidation with silver oxide at 23°[f]							
0.05	Benzene	[c]	0.12	0.12	0.52	0.36	[c]

[a]Not detected.
[b]Obscured by other v.p.c. peaks.
[c]Not present.
[d]Solvent.
[e]1,1-Diethoxyethane.
[f]Hydroperoxide destroyed in 2 days. In the absence of Ag_2O the hydroperoxide is stable for this length of time.

Can. J. Chem. Downloaded from www.nrcresearchpress.com by 210.87.254.105 on 09/05/12
For personal use only.

the difficulties involved in interpreting products is provided by the observation that 3% di-*sec*-butyl peroxide is formed in the Co(II)-catalyzed decomposition of *sec*-butyl hydroperoxide (17) but none is produced in the *tert*-butoxy radical induced decomposition (4).

The yields of the products formed by the oxidation of 1-ethoxyethyl hydroperoxide in methanol by Ce(IV) and by *tert*-butoxy were quite similar. The average yields for the Ce(IV) oxidation of 0.18, 0.45, and 0.83 *M* hydroperoxide and the yield for the *tert*-butoxy oxidation of 0.33 *M* hydroperoxide (which gave a good product balance) are, respectively, methyl formate, 0.09 and 0.14; ethyl formate, 0.14 and 0.18; ethyl acetate, 0.39 and 0.18; ethanol, 0.54 and 0.76; dimethoxy ethane, 0.28 and 0.25. This similarity implies that both reactions involve similar intermediates, *i.e.* peroxy radicals (eqs. 6 and 7). Irrespective of the mechanism of the

[6] $ROOH + Ce(IV) \rightarrow ROO\cdot + Ce(III) + H^+$

[7] $ROOH + t\text{-}BuO\cdot \rightarrow ROO\cdot + t\text{-}BuOH$

subsequent reactions of the peroxy radicals the fact that the yield of ethanol was two or three times that of dimethoxyethane can only be accounted for if the latter compound was unstable under the reaction conditions. In separate experiments it was shown that dimethoxyethane was stable to Ce(IV) but was oxidized by *tert*-butoxy to form methyl acetate (among other products). Methyl acetate was one of the minor products identified in the *tert*-butoxy oxidations of the hydroperoxide (eq. 8). In the Ce(IV) reactions

[8] $(CH_3O)_2CHCH_3 \xrightarrow{(-H\cdot)} (CH_3O)_2\dot{C}CH_3 \longrightarrow CH_3OC(O)CH_3 + CH_3\cdot$

the dimethoxyethane may be oxidized by the radicals formed in this reaction.

The yields of ethanol and acetaldehyde were more nearly equal in CCl_4 and in benzene (both *t*-butoxy and Ag_2O oxidations). However, there is no obvious reason why [acetate] was so much less than $\frac{1}{2}$([ethanol] + [acetaldehyde(dimethoxy ethane)]) for the Ag_2O oxidation and for *t*-butoxy oxidation in methanol, whereas the reverse was the case for *t*-butoxy oxidation in CCl_4 and in benzene. For the Ce(IV) oxidation these quantities were equivalent as we would expect if they arose from tetroxide by way of reactions *2* or *3* + *4* of Scheme 1. Excess ethyl

[9] 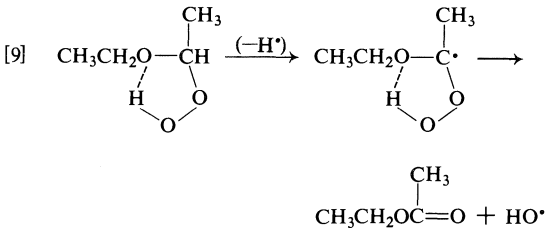

acetate might arise from abstraction of the tertiary hydrogen of the hydroperoxide (eq. 9), but a deficiency is difficult to account for.

With regard to the mechanism of the peroxy radical self-reaction, the most significant product is formate. In methanol it is conceivable that this could be formed by way of an oxidation of the solvent to formic acid. However, formate was also formed in CCl_4 and in benzene. It seems most likely that it was produced principally by β-scission of 1-ethoxyethoxy radicals (eq. 10). If

[10] 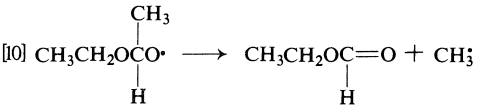

this is correct, it implies that alkoxy radicals were present in these systems and hence that at least some tetroxide probably decomposed by reaction *3* of Scheme 1, with some of the alkoxy radicals escaping from the cage (reaction *5*). The relative importance of reactions *2* and *3* cannot be estimated without some knowledge of the behavior of caged ethoxyethoxy radical pairs (reactions *4*, *5*, and *6*).

Decomposition of Di-(1-ethoxyethyl)-peroxide

The principal products formed by thermal decomposition of di-(1-ethoxyethyl)peroxide in cumene at 130° are listed in Table 3. The production of hydrogen can probably be best explained by a non-radical concerted decomposition of the peroxide (eq. 11) (3, 18). This

[11] 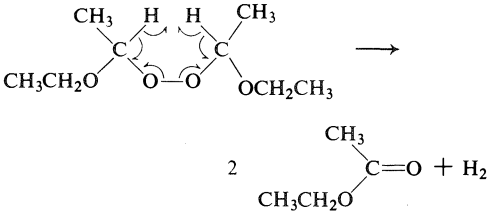

process accounts for about one quarter of the peroxide, *i.e.* ~0.25 mol H_2 and ~0.5 mol ethyl acetate. The remaining ethyl acetate and the

TABLE 3. Products from the thermal decomposition of di-(1-ethoxyethyl)peroxide in cumene at 130° (yields are mol/mol of peroxide)

Initial peroxide concentration (M)	Ethyl formate	Ethyl acetate	Ethanol	Acetaldehyde	Hydrogen	Methane	Dicumyl
0.46	0.45	1.1	0.5	0.45	[a]	[a]	0.14
0.20	0.50	1.05	[b]	[b]	0.24	0.47	[a]
0.10	0.45	1.05	[b]	[b]	0.25	0.37	0.18
0.05	0.37	0.95	[b]	[b]	0.27	0.40	0.16

[a]Not measured.
[b]Not detected.

other products are presumed to arise by processes involving free radicals.

The data can be interpreted in two extreme ways depending on the importance assigned to alkoxy radical disproportionation in the cage (reaction *4*, Scheme 1). If it is assumed that there is no cage disproportionation[3] then the approximately equal concentrations of ethanol and acetaldehyde (at the highest initial concentration of peroxide[4]) can be explained by hydrogen abstraction by free alkoxy radicals (eq. 12),

$$[12]\quad CH_3CH_2OCH(CH_3)O^{\bullet} + SH \longrightarrow S^{\bullet} + [CH_3CH_2OCH(CH_3)OH] \longrightarrow CH_3CH_2OH + CH_3CHO$$

where SH is either cumene (hence the bicumyl) or peroxide (hence the remaining ethyl acetate[5]).

$$[13]\quad CH_3CH_2O\underset{\underset{H}{|}}{\overset{\overset{CH_3}{|}}{C}}OO\overset{\overset{CH_3}{|}}{\underset{\bullet}{C}}OCH_2CH_3 \longrightarrow CH_3CH_2O\underset{\underset{H}{|}}{\overset{\overset{CH_3}{|}}{C}}O^{\bullet} + O{=}\overset{\overset{CH_3}{|}}{C}OCH_2CH_3$$

On the alternative assumption that cage disproportionation is very important, the ethanol, acetaldehyde, and remaining ethyl acetate are assumed to be formed in the cage (eq. 14).

$$[14]\quad \boxed{2CH_3CH_2OCH(CH_3)O^{\bullet}}_{cage} \longrightarrow CH_3CH_2OH + CH_3CHO + CH_3CH_2OC(O)CH_3$$

Attempts to distinguish between these alternative mechanisms were unsuccessful.[6,7]

Ethyl formate and methane were formed in approximately equal amounts and constitute about one third of the products formed from alkoxy radical precursors. This presumes that these products arose by β-scission of free alkoxy radicals, the expelled methyl being converted to methane by solvent or peroxide (eq. 15). In

$$[15]\quad CH_3^{\bullet} + SH \rightarrow CH_4 + S^{\bullet}$$

the hydroperoxide oxidations at 0–40°, formate constituted a rather similar fraction of the products (say 20 ± 10% for those experiments in which the product balance was reasonable). On the basis of the first assumption (*i.e.* all alkoxy radical pairs escape the cage with one third undergoing β-scission and two thirds abstracting H at 130°) it is difficult to predict what fraction of the product from a caged pair of alkoxy radicals would be formate at temperatures 100° lower. For *sec*-alkoxy radicals β-scission would

[3]Under similar conditions it has been reported both that "there is very little, if any, disproportionation of two *sec*-butoxy radicals in the solvent cage" (3), and that there is a significant amount of cage disproportionation of the *sec*-butoxy radicals (19).

[4]It is uncertain whether our failure to detect either of these compounds at lower peroxide concentrations was due to their further reaction under the experimental conditions or to poor resolution on the v.p.c.

[5]In this connection, it is worth noting that di-*sec*-butyl peroxide is not subject to induced decomposition under similar conditions (3). However, di-(1-ethoxyethyl)-peroxide should be a much better H donor than di-*sec*-butyl peroxide.

[6]Although the yield of acetate decreased with decreasing peroxide concentration (which argues in favor of an induced decomposition) the yield of formate also decreased rather than increasing as it should if the peroxide was the principal H donor to the alkoxy radicals.

[7]The product yield with 0.10 M peroxide initially was unaffected by the addition of 0.2 M 2,6-di-*tert*-butyl-4-methylphenol. This does not rule out induced decomposition of the peroxide since a sufficiently rapid attack of the alkoxy radicals on the solvent would prevent their interception by the phenol. If this is true, it must be cumyl radicals that induce decomposition of the peroxide.

Can. J. Chem. Downloaded from www.nrcresearchpress.com by 210.87.254.105 on 09/05/12
For personal use only.

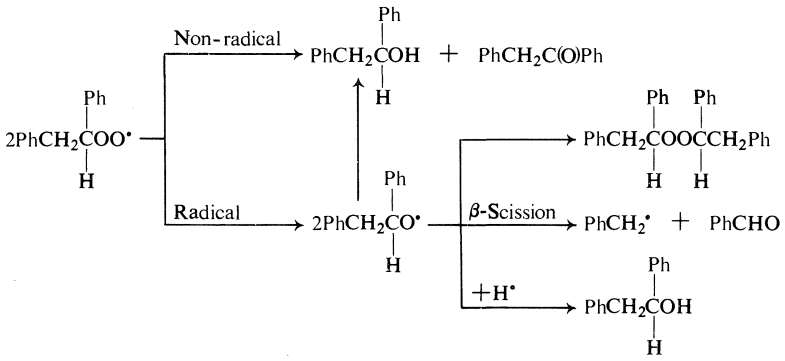

SCHEME 3

decrease in importance relative to hydrogen abstraction as the temperature was lowered. *If* this is also the case for *sec*-α-alkoxyalkoxy radicals then the high yields of formate in the hydroperoxide oxidations imply that most (say ≥80%) of the bimolecular self-reactions of the peroxy radicals yield alkoxy radicals and that the concerted process is relatively unimportant. On the other hand, if β-scission predominates over hydrogen abstraction as the temperature is decreased, then approximately 20% of the peroxy radicals react to give alkoxy radicals. On the basis of the second assumption (*i.e.* that one third of the alkoxy radical pairs escape the cage while two thirds disproportionate in the cage) one would predict that most peroxy radical pairs yield alkoxy radicals. This is because the ratio of alkoxy diffusion from the cage to disproportionation in the cage is not expected to be very dependent on the temperature.

The production of formate in the hydroperoxide oxidations argues in favor of some of the peroxy–peroxy reactions yielding free alkoxy radicals. Although far from definitive, the peroxide decomposition experiments suggest that the majority of such reactions yield alkoxy radicals and that the non-radical process is relatively unimportant (probably ≤20% of the total reaction).

1,2-Diphenylethylperoxy Radicals

The possible self-reactions of these peroxy radicals are shown in Scheme 3. 1,2-Diphenylethylperoxy radicals were conveniently produced for product studies either by oxidation of 1,2-diphenylethyl hydroperoxide or by autoxidation of bibenzyl.

Oxidation of 1,2-Diphenylethyl Hydroperoxide

The products formed by the oxidation of this hydroperoxide with *tert*-butoxy radicals, with Ce(IV), and with silver oxide, are listed in Table 4. In the Ce(IV) oxidations the yield of 1,2-diphenylethanol was reduced and the yield of benzaldehyde enhanced by the facile and quantitative oxidation of this alcohol to the aldehyde (20). If some allowance is made for this side-reaction, then the yields of the four oxygen-containing compounds were reasonably similar in the different experiments. These products are, therefore, presumed to arise from 1,2-diphenylethylperoxy radicals.

Autoxidation of Bibenzyl

The major product formed during the autoxidation of bibenzyl was of course, 1,2-diphenylethyl hydroperoxide (eq. 16). Benzaldehyde and

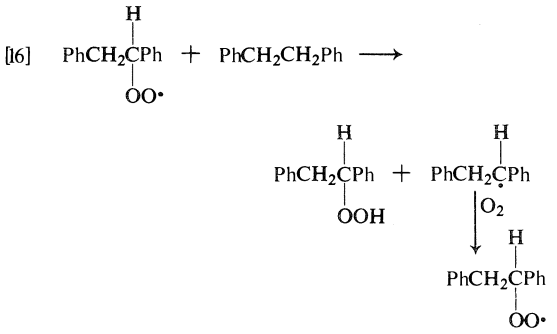

benzoin were minor products (see Table 4) and were probably formed in the chain terminating step. It is uncertain whether or not 1,2-diphenylethanol was formed in termination since our analytical procedure (v.p.c.) required the rather large amount of hydroperoxide to be reduced to the alcohol (with Ph_3P) before the actual analysis. The error in the estimation of "termination" alcohol from the total yield of alcohol and the iodiometrically measured yield of hydroperoxide would be of similar magnitude to the

Can. J. Chem. Downloaded from www.nrcresearchpress.com by 210.87.254.105 on 09/05/12
For personal use only.

TABLE 4. Products from the oxidation of 1,2-diphenylethyl hydroperoxide and from the autoxidation of bibenzyl

Products	Hydroperoxide oxidation[a]				
	t-BuO· in benzene at 56°[b]	Ce(IV) in methanol at 0°[c]	Ce(IV) in methanol at 0°[d]	Ag_2O in benzene at 60°[e]	Bibenzyl autoxidation at 56°[f]
PhCHO	0.27	0.41	0.75	0.27	0.24
$PhCH_2OH$	0.09	0.1	0.21	trace	[g]
$PhCH_2CH(OH)Ph$	0.30	0.15	(~1.0)[h]	0.41	(~2.1)[i]
$PhCH_2C(O)Ph$	0.30	0.34	0.37	0.30	0.65
$PhCH_2CH_2Ph$	trace	trace	trace	trace	[j]

[a]Yields are mol/mol of hydroperoxide.
[b][*t*-$BuON_2OBu$-*t*]/[hydroperoxide] = 0.1 *M*/0.18 *M*
[c][Hydroperoxide]/[Ce(IV)] = 0.1 *M*/0.1 *M*
[d][Hydroperoxide]/[Ce(IV)] = 0.2 *M*/0.1 *M*
[e][Ag_2O]/[hydroperoxide] = 0.25 *M*/0.25 *M*
[f]Yields are mol/mol of initiating (or terminating) radicals.
[g]Not detected.
[h]Excess hydroperoxide (~1.0) was reduced quantitatively to diphenylethanol with triphenylphosphine. The yield of diphenylethanol formed in the Ce(IV) oxidation was therefore ~0. It was presumed that the alcohol was formed and was oxidized to benzaldehyde (see text).
[i]Hydroperoxide (~2.0) formed in the autoxidation chain was reduced with Ph_3P. Because of the large amount of diphenylethanol produced in this way, it was not possible to estimate how much was formed in chain termination (see text).
[j]Substrate.

TABLE 5. Products formed from thermal decomposition of bis-(1,2-diphenylethyl)hyponitrite (yields are mol/mol of hyponitrite[a])[b]

Solvent	Temperature (°C)	PhCHO	$PhCH_2$ | PhCHOH	$PhCH_2$ | PhC=O	$PhCH_2$ | $PhCH_2$
CCl_4	78[c]	1.5	0	0.1	0.3
Cyclohexane	81	1.2	0.4	0.1	0.4
V.p.c.	260	1.7	0.04	0.2	0.5

[a]Based on the assumption that B (as defined in the Experimental) was bis-(1,2-diphenylethyl)-hyponitrite.
[b]Mean yields based on a number of experiments with different batches of hyponitrite and at initial hyponitrite concentrations in the range 0.03–0.12 *M*.
[c]Almost identical product yields were obtained in a decomposition at 30°.

amount of alcohol expected to be formed in termination.

It seems likely that the bimolecular self-reactions of 1,2-diphenylethylperoxy radicals yield benzaldehyde, benzyl alcohol, 1,2-diphenylethanol, and benzoin. The last two compounds may be formed either by the non-radical or radical reactions.

The benzaldehyde and the benzyl alcohol and bibenzyl detected in the hydroperoxide oxidations were presumably formed via free 1,2-diphenylethoxy radicals (Scheme 4).

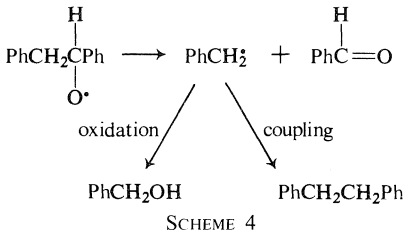

SCHEME 4

Bis-(1,2-diphenylethyl)hyponitrite

An attempt was made to study the chemistry of caged pairs of 1,2-diphenylethoxy radicals by the preparation and decomposition of bis-(1,2-diphenylethyl)hyponitrite. Unfortunately this hyponitrite could not be prepared with a purity better than 30% (see experimental). However, we feel confident that the four products listed in Table 5 resulted from the thermal decomposition of this hyponitrite according to Scheme 5.

The sum of the yields of benzaldehyde, diphenylethanol, and benzoin was 1.94 in the decomposition at 260° which is in good agreement with the expected value of 2.0. Product balances were less satisfactory for the decompositions in CCl_4 or cyclohexane.

The principal fate of 1,2-diphenylethoxy radical pairs is diffusion from the cage, followed in

Can. J. Chem. Downloaded from www.nrcresearchpress.com by 210.87.254.105 on 09/05/12
For personal use only.

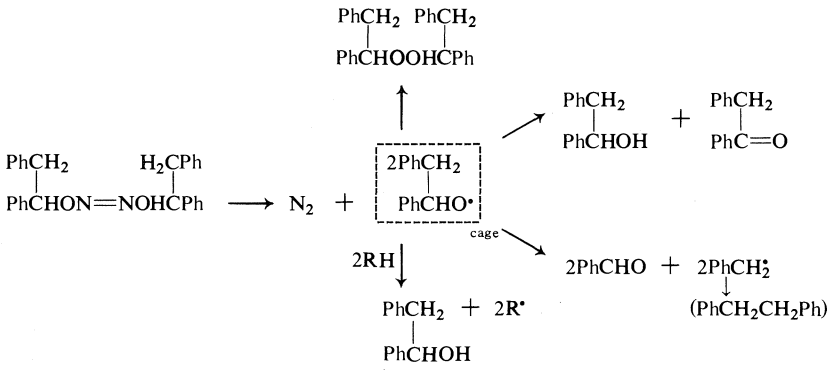

SCHEME 5

CCl_4 by β-scission, while in cyclohexane, at 80°, β-scission predominates but hydrogen abstraction from the solvent plays a significant role. Since there was relatively little benzoin or (in CCl_4) diphenylethanol, disproportionation in the cage cannot be important. However, carbonyl yields determined by i.r. spectroscopy were generally about 10–20% less than the yields of benzaldehyde and benzoin[8] measured by v.p.c. and recorded in Table 5. This suggests that some of the benzaldehyde found by v.p.c. arose from decomposition (in the injection port) of bis-(1,2-diphenylethyl)peroxide. In summary, the majority of the alkoxy radicals escape the cage and undergo β-scission or, in a suitable donor, abstract a hydrogen. About 10–20% of the caged pairs probably combine to yield peroxide but less than 10% of the pairs disproportionate in the cage. Hiatt's results (3, 4) suggest that caged *sec*-butoxy radical pairs behave rather similarly.

With regard to the bimolecular self-reactions of peroxy radicals, the data in Table 4 indicate that 1,2-diphenylethylperoxy radicals react together to give *approximately* equal quantities of benzaldehyde, diphenylethanol, and benzoin. The benzaldehyde is presumably formed from diphenylethoxy radicals. According to the data in Table 5 the other two compounds must be formed by a process *not* involving diphenylethoxy radicals. This latter process is, presumably, the concerted decomposition of the tetroxide. That is, approximately one third of the 1,2-diphenylethylperoxy radical pairs react via reactions *3* and *5* of Scheme 1 and two thirds via reaction *2*.

[8]I.r. spectroscopy only gives the sum of benzaldehyde and benzoin since the C=O fundamental stretching bands for these two compounds occur at almost the same frequency.

Conclusion

The present results provide evidence that not all secondary alkylperoxy radicals undergo their bimolecular self-reactions entirely by the concerted cyclic mechanism at ambient temperatures. A significant fraction of the overall reaction can apparently yield free alkoxy radicals. However, it is far from clear why, at similar temperatures, 1-ethoxyethylperoxy pairs yield alkoxy radicals in (probably) ≥80% yield, while 1,2-diphenylethylperoxy pairs yield alkoxy radicals in ~33% yield, and *sec*-butylperoxy pairs yield *sec*-butoxy radicals in only ~4% yield (4, 6). Possibly dialkyl tetroxides that can yield alkoxy radicals, that are very subject to β-scission, decompose by multiple bond scission, *i.e.* by a concerted but non-cyclic mechanism. Thus, although di-*tert*-butyl tetroxide probably undergoes one-bond scission (eq. 17) (21, 22), most

$$[17]\quad Me_3COOOOCMe_3 \xrightarrow{slow} Me_3CO^{\bullet} + (^{\bullet}OOOCMe_3) \xrightarrow{fast} O_2 + {}^{\bullet}OCMe_3$$

other di-*tert*-alkyl tetroxides are less stable than the *tert*-butyl compound (21–23) and their stability decreases as the derived alkoxy radicals become more unstable with respect to β-scission. This suggests that β-scission may be synchronized with (and therefore assist) O—O scission of the tetroxide. Suitably substituted tetroxides (both di-*tert*-alkyl and di-*sec*-alkyl) may therefore, perhaps, decompose by two-bond (or more) scission, *e.g.* as in eq. 18.

If this explanation of our analytical data is

Can. J. Chem. Downloaded from www.nrcresearchpress.com by 210.87.254.105 on 09/05/12
For personal use only.

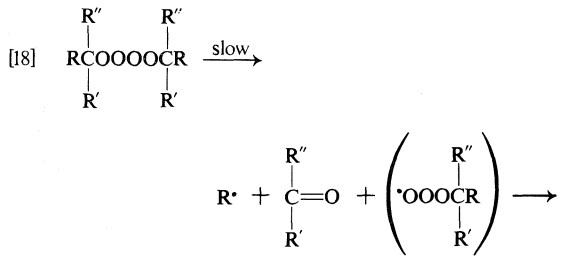

correct, it suggests that structural factors may have a profound effect not only on the rates of the bimolecular self-reactions of *sec*-alkylperoxy radicals, but also on their mechanism of reaction. Thus, for example, diphenylmethylperoxy radicals (24) should decompose principally by the concerted cyclic mechanism since neither phenyl nor hydrogen are readily cleaved from alkoxy radicals and since the hydrogen that must be transferred in the cyclic process will be quite labile. Evidence favoring the Russell mechanism for this peroxy radical has been presented previously (24). In contrast, peroxy radicals such as $(PhCH_2)_2CHOO^{\bullet}$ or $(Ph_3C)_2CHOO^{\bullet}$ are expected to react principally by the concerted non-cyclic route since they would yield unstable alkoxy radicals and since the central hydrogen is not particularly labile. It is expected that these two peroxy radicals would react more rapidly than, for example, $(CH_3CH_2)_2CHOO^{\bullet}$. For this radical the concerted non-cyclic process would be less favored so that reaction would be more likely to occur by the concerted cyclic process. Evidence favoring the cyclic process for $CH_3CH_2(CH_3)CHOO^{\bullet}$ has been obtained (25).

In conclusion, *sec*-alkylperoxy radicals can react both by the concerted cyclic (Russell) mechanism and by a process which yields either "free" alkoxy radicals or the products of β-scission of the alkoxy radicals in a step concerted with O—O homolysis of the tetroxide. The relative importance of these two processes will depend on the nature of the alkyl groups, the temperature and, perhaps, the solvent.

Experimental

Materials

1-Ethoxyethyl hydroperoxide was prepared from H_2O_2 and ethyl vinyl ether by the method of Milas *et al.* (26). Iodiometric titration indicated that the product was >90% pure. Reduction with a slight excess of triphenyl phosphine gave only acetaldehyde and ethanol. Ethyl formate was not formed in this reduction, nor was it present in the hydroperoxide.

Di-(1-ethoxyethyl)peroxide was prepared from H_2O_2 and ethyl vinyl ether in the presence of a small amount of thionyl chloride by the method of Lederer and Weissermel (27). Titration for peroxide indicated that the product was >90% pure.

1,2-Diphenylethyl hydroperoxide was prepared from H_2O_2 and 1,2-diphenylethanol (Aldrich, recrystallized from benzene:hexane, 1:20) by the method of Davies *et al.* (28). This hydroperoxide is a white crystalline material, m.p. 55°, purity >90% by iodiometric titration. Reduction of the hydroperoxide with Ph_3P gave only 1,2-diphenylethanol. Benzaldehyde was not formed in this reduction, nor was it present in the hydroperoxide. The hydroperoxide is stable at 56° yielding no benzaldehyde even after 8 days at this temperature.

Anal. Calcd. for $C_{14}H_{14}O_2$: C, 78.48; H, 6.59. Found: C, 78.33; H, 6.64.

Bis-(1,2-diphenylethyl)hyponitrite was probably prepared in about 30% yield by reaction of 1,2-diphenylethyl bromide with silver hyponitrite according to the procedure of Partington and Shah (29). The bromide was prepared in 86% yield by reaction of 1,2-diphenylethanol with anhydrous HBr in benzene at its freezing point (30). The bromide was purified by dry column chromatography on silica using trichloroethylene as the solvent. The purified bromide, n_D^{20} 1.6019 (lit. (30) n_D^{20} 1.6019), showed no OH or C=O absorption bands in the i.r. V.p.c. confirmed that it contained no benzaldehyde, 1,2-diphenylethanol, benzoin, or bibenzyl.

The bromide (2.1 g) was dissolved in 20 ml of purified ether and cooled to −10°. Silver hyponitrite (2.2 g, 100% excess) was added in small portions with continuous stirring, the ether being kept under a blanket of dry argon. At the end of the addition all organic bromide was gone (copper wire test). The silver bromide and excess silver hyponitrite were removed by filtration. Removal of the ether in an air stream at 0° (or under vacuum) resulted in a vigorous evolution of nitrogen and the separation of oily white crystals. At this stage, the i.r. spectrum (mull) showed a large, hydrogen-bonded, OH band but little or no C=O band. On warming the crystalline mass, nitrogen evolution began again and became rapid at ~50°. The crystals remaining were *trans*-stilbene. The oily contaminant and/or some of the crystalline material is believed to be bis-(1,2-diphenylethyl)hyponitrite. Nitrogen evolution experiments indicated that the compound decomposing rapidly at 0° (compound A) was formed in ~10% yield based on starting bromide while that decomposing rapidly at 50° (the hyponitrite, compound B) was formed in ~30% yield. The balance of the material (~60%) was stilbene. All attempts to separate B from stilbene by fractional crystallization or by trituration from the stilbene crystals were frustrated by its low yield (relative to stilbene) and by its instability. However, we believe that B is the desired dialkyl hyponitrite and that compound A may be the mono-alkyl hyponitrite or, perhaps, hyponitrous acid. The raw product gave an intense i.r. absorption at 980 cm^{-1} which appears to be a characteristic of hyponitrites (31, 32). This band disappeared as B decomposed and the decomposition products and their yields were consistent with B being bis-(1,2-diphenylethyl)hyponitrite. Various modifications of the preparation described above such as changing the solvent, did not increase the yield of B.

Can. J. Chem. Downloaded from www.nrcresearchpress.com by 210.87.254.105 on 09/05/12
For personal use only.

Can. J. Chem. Downloaded from www.nrcresearchpress.com by 210.87.254.105 on 09/05/12
For personal use only.

The half-life for decomposition of B was ~6 h at 30°. This may be compared with half-lives of ~40 h at this temperature for di-*tert*-butyl hyponitrite (31) and ~4 h for dibenzyl hyponitrite (33) and for dicumyl hyponitrite (34).

tert-Butylhyponitrite was prepared by the method of Kiefer and Traylor (31). All other compounds were commercial materials that were purified by standard procedures before use.

Hydroperoxide Decompositions

Ceric ammonium nitrate (1.0 *M*) in methanol was added slowly with stirring to a 0.2 *M* solution of the hydroperoxide in methanol at 0°. Addition was continued until the color of the added ceric solution was not completely destroyed. The solution was stirred for a further 15 min at 0° and the reaction products were then analyzed by v.p.c. The products formed in the hydroperoxide oxidation were treated similarly. Only 1,2-diphenylethanol reacted, and that only slightly, under these conditions.

tert-Butyl hyponitrite (0.1 *M*) in benzene was heated with the hydroperoxide (0.18 *M*) in benzene, under vacuum, for ten half-lives of the hyponitrite before the samples were analyzed.

Silver oxide (freshly prepared) was reacted with the hydroperoxide (0.18 *M*) in benzene under vacuum until the hydroperoxide had been destroyed.

Peroxide Decomposition

Di-(1-ethoxyethyl)peroxide was decomposed for 8 h in undiluted cumene under vacuum at 130°.

Autoxidation of Bibenzyl

Bibenzyl (5.3 *M*) containing α,α′-azo-bis-isobutyronitrile (0.19 *M*) was shaken under 1 atm of oxygen at 56°. The oxygen absorption rate was $\sim 3 \times 10^{-6}\ M\ s^{-1}$, corresponding to a chain length of ~2. After 67 h the bibenzyl had absorbed 0.7 *M* of oxygen. The accumulated hydroperoxide was reduced with a slight excess of Ph_3P before v.p.c. analysis of the products.

Hyponitrite Decomposition

These experiments were carried out on the raw product obtained by reacting 1,2-diphenylethyl bromide with silver hyponitrite. After the preparation of each batch of hyponitrite the solvent was evaporated under reduced pressure and the raw product was divided into portions which were dissolved in CCl_4 or cyclohexane. I.r. spectra were recorded after the samples had stood at room temperature for 15–30 min (in order to destroy compound A). Only very small amounts of carbonyl- and hydroxyl-containing compounds were present at this time. One sample of B was decomposed at 50° in a system that allowed the nitrogen yield, and hence the purity of the hyponitrite, to be measured. A second sample was injected directly into the v.p.c. to determine the products of rapid thermal cracking (at 260°). The remaining samples were decomposed in refluxing CCl_4 or cyclohexane or at 30°, under a blanket of argon, and were analyzed by i.r. spectroscopy (for C=O) and by v.p.c.

The authors are grateful to Dr. T. Pearce. We also wish to thank Dr. K. F. Preston for analyzing the methane and hydrogen formed in the di-(1-ethoxyethyl)peroxide decompositions.

1. G. A. Russell. J. Am. Chem. Soc. **79**, 3871 (1957).
2. K. U. Ingold. Acc. Chem. Res. **2**, 1 (1969).
3. R. Hiatt and S. Szilagyi. Can. J. Chem. **48**, 615 (1970).
4. R. Hiatt and L. Zigmund. Can. J. Chem. **48**, 3967 (1970).
5. J. A. Howard. Adv. Free Rad. Chem. **4**, 49 (1971).
6. T. Mill, F. R. Mayo, H. Richardson, K. Irwin, and D. L. Allara. J. Am. Chem. Soc. **94**, 6802 (1972).
7. D. F. Bowman, T. Gillan, and K. U. Ingold. J. Am. Chem. Soc. **93**, 6555 (1971).
8. J. E. Bennett, D. M. Brown, and B. Mile. Trans. Faraday Soc. **66**, 386 (1970).
9. J. A. Howard and J. E. Bennett. Can. J. Chem. **50**, 2374 (1972).
10. D. G. M. Diaper. Can. J. Chem. **46**, 3095 (1968).
11. J. R. Thomas. J. Am. Chem. Soc. **87**, 3935 (1965).
12. J. R. Thomas and K. U. Ingold. Adv. Chem. Ser. **75**, 258 (1968).
13. G. Dobson and G. Hughes. J. Phys. Chem. **69**, 1814 (1965).
14. A. Maclachlan. J. Am. Chem. Soc. **87**, 960 (1965).
15. R. Blackburn and A. Charlesby. Trans. Faraday Soc. **62**, 1159 (1966).
16. W. A. Cramer. J. Phys. Chem. **71**, 1112, 1171 (1967).
17. R. Hiatt, K. C. Irwin, and C. W. Gould. J. Org. Chem. **33**, 1430 (1968).
18. L. J. Durham, C. F. Wurster, and H. S. Mosher. J. Am. Chem. Soc. **80**, 332 (1958); L. J. Durham and H. S. Mosher. J. Am. Chem. Soc. **82**, 4537 (1960); **84**, 2811 (1962).
19. W. A. Pryor, E. V. Morkved, and H. T. Bickley. J. Org. Chem. **37**, 1999 (1972).
20. P. M. Nave and W. S. Trahanovsky. J. Am. Chem. Soc. **90**, 4755 (1968); **93**, 4536 (1971).
21. K. Adamic, J. A. Howard, and K. U. Ingold. Can. J. Chem. **47**, 3803 (1969).
22. J. E. Bennett, D. M. Brown, and B. Mile. Trans. Faraday Soc. **66**, 397 (1970).
23. J. A. Howard, K. Adamic, and K. U. Ingold. Can. J. Chem. **47**, 3793 (1969).
24. J. A. Howard and K. U. Ingold. J. Am. Chem. Soc. **90**, 1058 (1968).
25. J. A. Howard and K. U. Ingold. J. Am. Chem. Soc. **90**, 1056 (1968).
26. N. A. Milas, R. L. Peeler, Jr., and O. L. Mageli. J. Am. Chem. Soc. **76**, 2322 (1954).
27. M. Lederer and K. Weissermel. Ger. Pat. 1 081 893 (1960); Chem. Abstr. **55**, 15347*f*.
28. A. G. Davies, R. V. Foster, and A. M. White. J. Chem. Soc. 1541 (1953).
29. J. R. Partington and C. C. Shah. J. Chem. Soc. 2589 (1932).
30. D. Y. Curtin and D. B. Kellorn. J. Am. Chem. Soc. **75**, 6011 (1953).
31. H. Kiefer and T. G. Traylor. Tetrahedron Lett. 6163 (1966).
32. L. Kuhn and E. R. Lippincott. J. Am. Chem. Soc. **78**, 1820 (1956).
33. J. B. DeSousa and S. K. Ho. Nature, **186**, 776 (1960); **199**, 64 (1963).
34. H. Kiefer and T. G. Traylor. Abstract of paper presented to the International Symposium on the Chemistry of Organic Peroxides. September 1967. Berlin-Adlershof.

Condensation Reactions of 2-Amino-*N*-acylphenethylamines and 2-Amino-β-acylaminostyrenes

F. M. F. Chen and T. P. Forrest

Chemistry Department, Dalhousie University, Halifax, Nova Scotia

Received August 8, 1972

Molecular sieves have been used to catalyze the condensation reaction of *cis*-β-(*o*-acetotoluidino)-2-aminostyrene (**4**) to yield 2-methyl-3-(*o*-tolyl)-3*H*-1,3-benzodiazepine (**11**). A second major product from the reaction was 2-(*o*-toluidino)-*N*-acetylindole (**13**), an example of the type of compound presumed to be an intermediate in the Fischer indole synthesis. The formation of *N*-acetylindole from **13** occurred on treatment of **13** with silica or alumina.

The *trans* isomer, **5**, and the reduced analog, **6**, were unreactive with molecular sieves but **6** could be converted to 4,5-dihydro-2-methyl-3-(*o*-tolyl)-3*H*-1,3-benzodiazepine by reaction with phosphorous oxychloride.

De la sève moléculaire a été utilisée pour catalyser la réaction de condensation du *cis*-β-(*o*-acetotoluidino) amino-2 styrène (**4**) pour produire la méthyl-2 (*o*-tolyl)-3-3*H* benzo-1,3 diazépine (**11**). Un second produit majeur de la réaction à été l'(*o*-toluidino)-2 *N*-acétylindole (**13**), un exemple du type de composé supposé être un intermédiaire dans la synthèse selon Fischer de l'indole. La formation du *N*-acétylindole à partir de **13** se produit lorsque l'on traite **13** avec de la silice ou de l'alumine.

L'isomère *trans*, **5**, et l'analogue réduit, **6**, ne réagissaient pas avec la sève moléculaire mais **6** pouvait être transformé en dihydro-4,5 méthyl-2 (*o*-tolyl)-3-3*H* benzo-1,3 diazepine par réaction avec l'oxychlorure de phosphore. [Traduit par le journal]

Can. J. Chem., **51**, 881 (1973)

Introduction

A potentially very useful method for the synthesis of 1,3-benzodiazepines by the internal condensation of 2-amino-*N*-acylphenethylamines is illustrated in Scheme 1. Although this type of

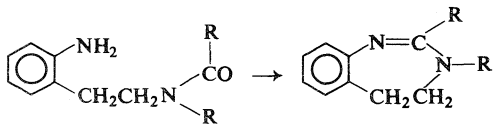

Scheme 1

condensation has been used in the synthesis of the six-membered quinazolines (1) and the five-membered benzimidazoles (2), attempts to employ it in the formation of the seven-membered 1,3-benzodiazepines have proven to be unsuccessful (3, 4). Treatment of 2-amino-*N*-benzoyl-4,5-dimethoxyphenethylamine (**1**) with the usual reagents employed in similar cyclizations led only to starting material or intractable tars (3). The acid-catalyzed rearrangement of ethyl-2-amino-α-benzamidocinnamate (**2**) yielded no 1,3-benzodiazepine derivatives (5). Thermal or acid-catalyzed condensations of 2-acetamido-3-(*o*-aminophenyl)-2-butene (**3**) led to excellent yields of 2,3-dimethylindole and no 1,3-benzodiazepines (6). We have investigated the reactivity of some 2-amino-*N*-acetylphenethylamine derivatives under various conditions and wish to report our findings.

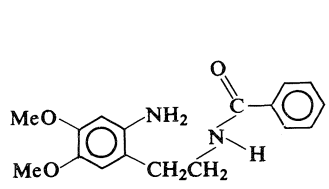

1

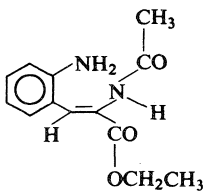

2

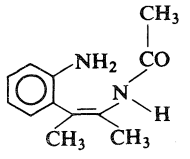

3

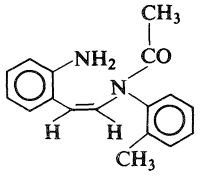

4

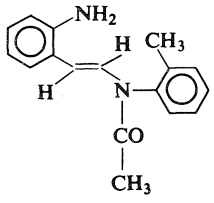

5

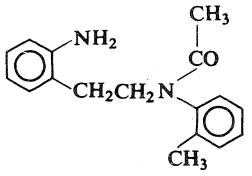

6

Can. J. Chem. Downloaded from www.nrcresearchpress.com by 210.87.254.42 on 09/05/12
For personal use only.

Can. J. Chem. Downloaded from www.nrcresearchpress.com by 210.87.254.42 on 09/05/12
For personal use only.

Results and Discussion

The compounds on which we chose to carry out our investigations were the *cis* and *trans* isomers of β-(*o*-acetotoluidino)-2-aminostyrene, **4** and **5**, and the dihydro analog, **6**. These were prepared by the addition of *o*-acetotoluidide (**7**) to *o*-nitrophenyl-acetylene (**8**) to form the β-(*o*-acetotoluidino)-2-nitrostyrenes, (**9** and **10**) (Scheme 2), which were then reduced. The addition reaction was catalyzed by sodium hydride and yielded a mixture of the *cis* and *trans* addition products. The spectral parameters which permitted the structural verification of these new compounds are presented in the Experimental.

The selective reduction of the nitro group of **9** and **10** was carried out by ferrous ammonium sulfate in a water–methanol mixture. Hydrogenation of **10** over palladium–charcoal reduced both the carbon–carbon double bond and the nitro group producing **6** in good yield.

No 1,3-benzodiazepines were obtained by treating the compounds with aqueous acid as was employed by Plieninger and Nogradi (7) in the cyclization of α-imino-β-(2-acetaminophenyl)-γ-butyrolactone; **4** and **5** yielded indole and *o*-acetotoluidine whereas **6** was recovered unchanged. The reaction of **6** with PCl_3 or $POCl_3$ was successful in producing the 4,5-dihydro-2-methyl-3-(*o*-tolyl)-3*H*-1,3-benzodiazepine, in contrast to the behavior of the similar compound **1**, which was reported (3) to give no 1,3-benzodiazepine under similar conditions. The reaction of **4** or **5** with $POCl_3$ or PCl_3 yielded only intractable tars.

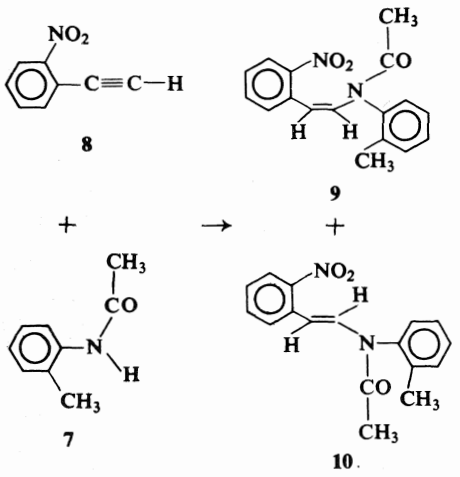

SCHEME 2

Heating **4** with molecular sieves provided a successful method for carrying out the condensation of the *cis* isomer to yield the corresponding 1,3-benzodiazepine. The best yield of 2-methyl-3-(*o*-tolyl)-3*H*-1,3-benzodiazepine (**11**) from **4** was obtained using molecular sieve 4A in benzene at reflux temperature. The *trans* isomer **5** and the saturated analog **6** yielded only starting materials when treated with molecular sieves.

The mass spectrum of **11** showed a molecular ion at *m/e* 248 and the n.m.r. spectrum exhibited peaks due to two singlet methyl groups at δ 1.63 and 2.40, eight aromatic protons between δ 6.60 and 7.40, and an AB system for the olefinic protons (δ 5.15, 5.67, J_{AB} = 8 Hz). Hydrolysis of **11** occurred on contact with water yielding **4**, thereby verifying the structure of **11**.

A second major product from the reaction of **4** with molecular sieves was 2-(*o*-toluidino)-*N*-acetylindoline (**13**). The mass spectrum of **13** exhibited a molecular ion at *m/e* 266 (6) and major fragment ions at 159 (5), 158 (10), 118 (60), 117 (55), 107 (100). The n.m.r. spectrum showed singlet methyl peaks at δ 2.06 and 2.14, a multiplet at 6.65–7.30 for seven aromatic protons, a broad doublet at 8.20 for the aromatic H-7 proton, a broad singlet at 4.0 for the NH and an ABX system for the heterocyclic ring protons (δ 3.07, d, H-3, A of ABX; 3.52, dd, H-3, B of ABX; 5.89, H-2, X of ABX; J_{AB} = 17, $J_{AX} < 1$, J_{BX} = 7 Hz). The structure was verified by the conversion of **13** to *N*-acetylindole and *o*-toluidine by chromatography on alumina or silica.

A plausible mechanism for the product formation is shown in Scheme 3. The latter part of this scheme has the same sequence of steps as the mechanism commonly accepted (8) for the Fischer indole synthesis. The formation of *N*-acetyl compounds **13** and **14** supports the conclusion of Yamamoto (9, 10, 13) that acyl derivatives of the Fischer indole intermediates do not require deacylation prior to closing the heterocyclic ring. It had been previously suggested (11) that the amide nitrogen had to be converted to the more basic amine nitrogen in order to add to the imine function of the indoline precursor (**12**). This isolation of 2-(*o*-toluidino)-*N*-acetylindoline (**13**) represents the first isolation of a 2-aminoindoline derivative which could eliminate the amino group to produce an indole as proposed for the last step of the Fischer indole synthesis. The feasibility of this step has been

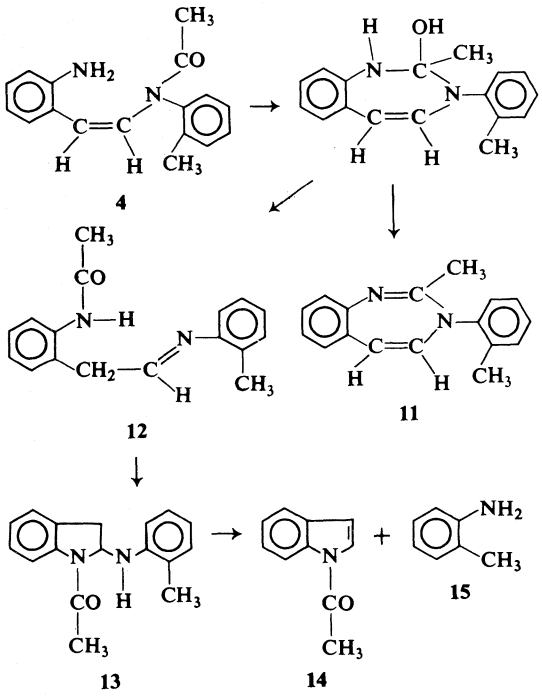

SCHEME 3

demonstrated by the conversion of **13** to *N*-acetyl indole (**14**) and *o*-toluidine (**15**) by chromatography on alumina or silica. These products, **14** and **15**, were also isolated directly from the reaction of **4** on some molecular sieves.

Although molecular sieves have been commonly used as dehydrating agents, their use as catalysts in condensation reactions is not well established. A recent report (12) describes the marked catalytic effect of molecular sieves on the formation of ketimines and enamines. The molecular sieves are particularly useful catalysts in that relatively mild reaction conditions may be employed and simple isolation procedures permit their use where the products are sensitive to aqueous acid or base.

Experimental

N.m.r. spectra were recorded on a Varian T60 spectrometer using $CDCl_3$ as solvent and tetramethylsilane as internal standard. Mass spectra were recorded on a C.E.C. model 21-104 spectrometer. I.r. spectra were recorded in chloroform solution on Perkin–Elmer model 237 B spectrometer. Silica gel (silicar CC7 100 mesh) and alumina (neutral, activity 1, 80–200 mesh) were used as chromatographic stationary phases. Melting points are uncorrected.

*β-(o-Acetotoluidino)-2-nitrostyrenes (**9** and **10**)*

To a solution of *o*-acetotoluidide (1.65 g, 0.011 mol) in dry dimethylsulfoxide, under nitrogen, was added a 50% sodium hydride oil dispersion (0.1 g, 0.002 m). The mixture was stirred for 30 min followed by dropwise addition of a solution of *o*-nitrophenylacetylene (1.47 g, 0.01 m) in dimethylsulfoxide (10 ml). The mixture was stirred at room temperature for about 20 h and then made acidic with acetic acid. The solvent was removed under reduced pressure (35°/0.1 mm) and the residue transferred to a silica gel column (50 g) and eluted with 10% ether in hexane (0.85 g, 27% of *trans* product and 1.5 g, 52% of *cis* product). *trans*-β-(*o*-Acetotoluidino)-2-nitrostyrene (**10**), m.p. 80 °C; n.m.r. ($CDCl_3$): δ 1.88 (s, CH_3), 2.23 (s, CH_3), 5.70 (d, J = 14 Hz, 1H), 7.0–8.0. (m, 9H); i.r.: 1690 (C=O) 1635 cm^{-1} (C=C); mass spectrum: 296 (8), 251 (6), 236 (8), 149 (28), 132 (32), 120 (48), 118 (91), 107 (50), 91 (89), 43 (100). *cis*-β-(*o*-Acetotoluidino)-2-nitrostyrene (**9**), m.p. 100 °C; n.m.r.: δ 1.77 (s, CH_3), 2.08 (s, CH_3), 6.16 (d, J = 9, 1H), 6.7–7.7. (m, 9H); i.r.: 1680 (C=O), 1640 cm^{-1} (C=C); mass spectrum: 296 (4), 251 (8), 236 (10), 149 (27), 132 (30), 120 (49), 118 (90), 107 (49), 91 (88), 43 (100).

*β-(o-Acetotoluidino)-2-aminostyrenes (**4** and **5**)*

A solution of *cis*-β-(*o*-acetotoluidino)-2-nitrostyrene (**9**) (0.6 g, 0.002 mol) and $FeSO_4 \cdot 7H_2O$ (5 g, 0.018 mol) in 40 ml of a methanol–water mixture (1:1) was heated to reflux. Concentrated ammonium hydroxide (4 ml) was added and the mixture refluxed for 30 min. The mixture was cooled, filtered, and the filtrate concentrated under reduced pressure to one-half the original volume, then extracted with chloroform. The chloroform layer was then extracted with a 2 *N* HCl solution. The aqueous layer was basified with NH_4OH and extracted with chloroform. The chloroform layer, after drying and removal of solvent, yielded *cis*-β-(*o*-acetotoluidino)-2-aminostyrene (**4**) (0.3 g, 50% yield), m.p. 77 °C; n.m.r.: ($CDCl_3$): δ 1.77 (s, CH_3), 2.12 (s, CH_3), 3.50 (s, NH_2), 5.71; (d, J = 9 Hz, 1H), 6.2–7.0 (m, 8H), 7.21 (d, J = 9 Hz, 1H); i.r.: 3380, 3480. (NH_2), 1660 cm^{-1} (C=O); mass spectrum: 266 (16), 248 (8), 223 (10), 208 (19), 149 (30), 119 (36), 118 (100), 107 (45).

Anal. Calcd. for $C_{17}H_{18}N_2O$: C, 76.66; H, 6.81; N, 10.52. Found: C, 76.60; H, 6.86; N, 10.21.

trans-β-(*o*-Acetotoluidino)-2-nitrostyrene (**10**) (0.3 g, 0.001 mol) when reduced under the same conditions yielded *trans*-β-(*o*-acetotoluidino)-2-aminostyrene (**5**) (0.18 g, 61%), m.p. 155 °C; n.m.r. ($CDCl_3$): δ 1.83 (s, CH_3), 2.20. (s, CH_3), 3.37 (s, NH_2), 5.20 (d, J = 14 Hz, 1H), 6.44–7.37 (m, 8H), 8.00 (d, J = 14 Hz, 1H); i.r.: 3380, 3450 (NH_2), 1650 cm^{-1} (C=O); mass spectrum: 266 (7), 223 (5), 208 (5), 149 (17), 118 (34), 117 (100), 107 (50).

*N-2-(o-Aminophenyl)-ethyl-N-(o-tolyl)acetamide (**6**)*

trans-β-(*o*-Acetotoluidino)-2-nitrostyrene (**10**) (0.6 g, 0.002 mol) and 5% palladium-on-carbon (0.1 g) in ethanol (10 ml) was stirred under hydrogen at atmospheric pressure for 4 h. The solution was filtered and the solvent removed *in vacuo* to yield compound **6** (0.6 g, 95% yield), m.p. 113–115 °C; n.m.r. ($CDCl_3$): δ 1.8 (s, 3H), 2.3 (s, 3H), 2.7–4.2 (m, 4H) 4.5 (bs, 2H, D_2O exchangeable), 6.5–7.4 (m, 8H); i.r.: 1650, 3370, 3490 cm^{-1}; mass

Can. J. Chem. Downloaded from www.nrcresearchpress.com by 210.87.254.42 on 09/05/12
For personal use only.

spectrum: 268 (6), 149 (6), 120 (65), 119 (75), 106 (16), 84 (35), 56 (75), 43 (100).

4,5-Dihydro-2-methyl-3-(o-tolyl)-3H-1,3-benzodiazepine

Compound **6** (0.6 g, 0.002 mol) and phosphorous oxychloride (0.17 g, 0.0011 mol) in methylene chloride (20 ml) was heated under reflux for 16 h. After cooling, pyridine (0.4 g, 0.005 m) was added and the mixture stirred at room temperature for 30 min. The mixture was concentrated *in vacuo* to a small volume and the residue distributed between ether and an aqueous sodium carbonate solution (10%). The ether layer, after removal of the solvent and distillation (160 °C/0.1 mm), yielded 4,5-dihydro-2-methyl-3-(*o*-tolyl)-3*H*-1,3-benzodiazepine (0.4 g, 70%); n.m.r. ($CDCl_3$): δ 1.85 (s, CH_3), 2.24 (s, CH_3), 3.07–3.27 (m, 2H), 3.57–3.77 (m, 2H), 6.8–7.2 (m, 8H); i.r. 1620 cm^{-1} (C=N); mass spectrum: 250 (57), 235 (7), 132 (50), 131 (100), 130 (70), 119 (50), 91 (68), 90 (54), 77 (35), 65 (43), 43 (35).

*Reaction of **4** with Molecular Sieves*

cis-β-(*o*-Acetotoluidino)-2-aminostyrene (**4**) (1.1 g, 0.0045 mol) and freshly activated (by heating at 170° for 24 h) molecular sieve (Davison Chemical, 4A, 14–30 mesh granules) in dry benzene (50 ml) was heated under reflux for 16 h. The mixture was then filtered and the molecular sieve washed with fresh benzene. The solvent was removed *in vacuo* and an ether–hexane mixture (9:1, 10 ml) was added. The solid which formed was recrystallized from ether–hexane to yield compound **13** (0.36 g. 32%), m.p. 138–140 °C; i.r. 3400. (NH), 1660 cm^{-1} (C=O).

The mother liquors on distillation yielded 2-methyl-3-(*o*-tolyl)-3*H*-1,3-benzodiazepine (**11**), (b.p. 140 °C/0.05 mm) (0.15 g, 25%); i.r.: 1680 cm^{-1} (C=N); mass spectrum: 248 (20), 131 (100), 117 (35), 116 (30), 105 (40). A better yield of **13** (60%), could be obtained by using molecular sieve 3A in refluxing benzene for 72 h.

This research was supported by grants from the National Research Council of Canada and the Faculty of Graduate Studies of Dalhousie University.

1. K. HOFMANN. *In* Chemistry of heterocyclic compounds: imidazole and derivatives. Vol. 6. Part. 1. Interscience Publishers Inc., New York, N.Y. 1953. p. 266.
2. W. L. F. ARMAREGO. Adv. Heterocycl. Chem. **1**, 281 (1963).
3. H. R. RODRIGUEZ, B. ZITO, and G. DE STEVENS. J. Org. Chem. **33**, 670 (1968).
4. G. DE STEVENS. *In* Topics in heterocyclic chemistry. Wiley-Interscience, New York, N.Y. 1969. p. 154.
5. A. P. MARTINEZ, W. A. SKINNER, W. W. LEE, L. GOODMAN, and B. R. BAKER. J. Org. Chem. **26**, 860 (1961).
6. N. N. SUVOROV, N. P. SOROKINA, and YU. P. SKEINKER. Zhur. Obshchei Khim. **28**, 1090 (1958). Chem. Abstr. **52**, 18373*e* (1958).
7. H. PLIENINGER and I. NOGRADI. Chem. Ber. **88**, 1965 (1955).
8. B. ROBINSON. Chem. Rev. **69**, 227 (1969).
9. H. YAMAMOTO. Bull. Chem. Soc. Jap. **40**, 425 (1967).
10. H. YAMAMOTO. J. Org. Chem. **32**, 3693 (1967).
11. N. N. SUVOROV and N. P. SOROKINA. Dokl. Akad. Nauk. SSSR, **136**, 840 (1961). Chem. Abstr. **55**, 17621*f* (1961).
12. K. TAGUCHI and F. H. WESTHEIMER. J. Org. Chem. **36**, 1570 (1971).
13. T. P. FORREST and F. M. F. CHEN. J. Chem. Soc. Chem. Commun. 1067 (1972).

Can. J. Chem. Downloaded from www.nrcresearchpress.com by 210.87.254.42 on 09/05/12
For personal use only.

The Formation and Decay of the Paramagnetic Species Formed on the Surface of Al_2O_3–MoO_3 with Anthracene/Benzene Solution

HISASHI UEDA AND NAOYUKI TODO

National Chemical Laboratory for Industry, Meguro-ku, Tokyo, Japan

Received May 30, 1972

MoO_3 supported on alumina in a flow-through type sample tube was fixed in an e.s.r. cavity and anthracene solutions in benzene were passed through it at 20 °C. Three paramagnetic species were observed. One was Mo^{5+}, one was the anthracene cation R^+, and the remaining one was R^+O^{*2-} previously reported. Formation of R^+ and R^+O^{*2-} was complete within a few minutes after the contact of the solution after which the decay of R^+ became apparent. R^+ disappeared in a pseudo-first order reaction which actually was a second order reaction with the water dissolved in the solution. The rate constant for the reaction, $R^+ + H_2O \rightarrow$ diamagnetic products, was 0.34 l mol^{-1} s^{-1}. R^+O^{*2-} was completely stable during the measurement and even after draining the solvent or after drying the oxide particles with N_2 gas. It was concluded that Mo^{5+} was formed from two R^+ and H_2O molecules. The time dependence of the concentration of R^+ was found to be $[R^+] = [R^+]_0 \exp(-kt)$ and that of Mo^{5+}, $[Mo^{5+}] = [Mo^{5+}]_\infty (1 - \exp(-kt))$ where the subscripts zero and infinity indicate the time $t = 0$ and $t = \infty$ respectively. The present results seem to indicate that the more important paramagnetic species which influences the catalytic processes is not the cation R^+ but the complex ion R^+O^{2-}.

Le MoO_3 fixé sur alumine dans un tube à échantillon à flux continu, est placé dans la cavité d'un appareil RPE puis traversé par des solutions benzéniques d'anthracène à 20 °C. Trois espèces paramagnétiques ont été observées: Mo^{5+}, R^+ cation anthracène et R^+O^{*2-} précédemment rapporté. La formation de R^+ et R^+O^{*2-} est totale en quelques minutes, après contact de la solution, dès que la disparition de R^+ devient apparente. Cette disparition de R^+ se fait selon une réaction de pseudo-premier ordre qui est, en réalité, une réaction d'ordre deux avec l'eau dissoute dans la solution. La constante de vitesse de la réaction $R^+ + H_2O \rightarrow$ produits diamagnétiques, vaut 0.34 l mol^{-1} s^{-1}. R^+O^{*2-} est d'une stabilité complète durant la mesure et même après élimination de solvant ou sèchage des particules d'oxyde par N_2 gazeux. On a conclu à la formation de Mo^{5+} à partir de deux molécules de R^+ et H_2O. L'influence du temps sur la concentration de R^+ s'exprime en $[R^+] = [R^+]_0 \exp(-kt)$ et celle de Mo^{5+} en $[Mo^{5+}] = [Mo^{5+}]_\infty (1 - \exp(-kt))$ où les indices indiquent les temps $t = 0$ et $t = \infty$. Ces résultats semblent indiquer que les espèces paramagnétiques les plus importantes qui influent sur les processus catalytiques, ne sont pas le cation R^+ mais l'ion complexe R^+O^{*2-}. [Traduit par le journal]

Can. J. Chem., **51**, 885 (1973)

Introduction

The formation of charge transfer complexes and carbonium ions on the surface of silica–alumina particles was first established by visible absorption spectroscopy using 1,1-diphenylethylene and triphenylethylene (ref. 1, papers 62 and 65). Subsequently several attempts were made to detect these ionic molecular species by electron spin resonance (e.s.r.) method. The e.s.r. spectra of cations of hydrocarbons such as naphthalene, anthracene, and perylene (2–5) and the cations of 1,1-diphenylethylene, aniline, and diphenylamine (6, 7) were successfully observed by adsorbing the hydrocarbons on silica–alumina from a solution. These cations were considered to arise from the Lewis acid points on silica–alumina after charge transfer from these points to the added hydrocarbons, or as charge transfer complexes. As hydrocarbon cations are quickly decomposed by water, the removal of the last traces of water from these systems by a vacuum technique was essential in those experiments (2–7).

A different method to observe paramagnetic species on the surface of zinc oxide (8), alumina (9), and other oxides (10) was employed by Ueda and co-worker. The oxide powder was dipped in the benzene solution of an aromatic hydrocarbon or its derivative, the solution was then evaporated at room temperature. The paramagnetic species thus formed were stable and their e.s.r. spectra did not show any hyperfine structures. It was concluded that these species were complex ions R^+O^{*2-}, formed by an active O^{2-} surface ion(s), O^{*2-}, and the aromatic hydrocarbon, R.

Until now the relation between these two paramagnetic species, *viz.* the one formed on the

Can. J. Chem. Downloaded from www.nrcresearchpress.com by 210.87.254.42 on 09/05/12
For personal use only.

surface of silica–alumina in vacuum and the one formed on the surface of various oxides in air (with some humidity) was unknown. The rate constants for reactions by which the hydrocarbon cations are formed from hydrocarbon and Lewis acid points on the oxide surface have not been known. Nor have those for the disappearance of the hydrocarbon cations when reacted with water and other poisoning substances. In the present work the relation between these two paramagnetic species and the rate constants of their reactions with water have been studied and are reported.

Experimental

An anthracene solution was passed through a layer of the oxide particles supported on a fused silica filter in a silica sample tube placed inside the resonant cavity. Only a small portion of the solute in the solution was consumed and therefore the overall rate of formation of the paramagnetic species was only slightly affected by the flow rate. A JES-3BX type x-band e.s.r. spectrometer was used. The incident microwave power to the sample cavity was attenuated to 15 mW. A silica tube (5 mm o.d.) containing the filter section was inserted into the sample cavity. The benzene solution of anthracene was stored in a 500 ml reservoir and was delivered by a syringe pump into the top end of the silica sample tube through a flow meter. The solution which passed through the oxide layer was discarded from the lower end of the sample tube. The flow rate of the solution was 6.0 ml/min, therefore the measurement could be continued for 90 min. The anthracene used was purified by passing its solution through an activated alumina powder and then by recrystallization. The oxide particles used contained 8.5% MoO_3 supported on γ-alumina. Molybdenum was first supported as ammonium molybdate on γ-alumina from an aqueous solution and then was calcined at 550 °C for 1 h. Particle size was 10–20 mesh. The solvent benzene used contains 0.050% water, which is equivalent to 2.4×10^{-2} mol/l. This small amount of dissolved water was slowly adsorbed by the oxide and so that the "Q" of the resonant cavity was slowly reduced, which reduced the sensitivity of detection. To correct the variation in the sensitivity of the apparatus, one of the absorption lines of Mn^{2+} also present inside the cavity was repeatedly measured between the sample measurements. The time dependent intensity of the Mn^{2+} signal thus obtained was used for the sensitivity calibration. The spin concentration, c, was calculated as $c = c_0 I/I_0$ where c_0 is the concentration of the standard DPPH sample, I is the e.s.r. intensity of the unknown sample and I_0 is the e.s.r. intensity of the standard DPPH sample. $I = sh$ was used to determine the e.s.r. intensity, where s is the area enclosed by an integral e.s.r. absorption curve of a standard height and h is the height of the integral absorption curve of each spectrum.

Results

In Fig. 1 the e.s.r. absorption intensities of the Mn^{2+} line appearing at $g \simeq 2.14$ (or belonging

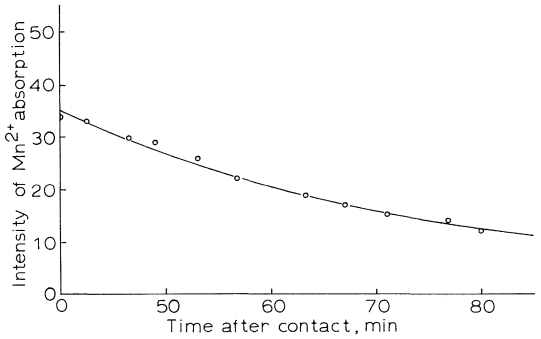

FIG. 1. Intensities of the experimental Mn^{2+} lines. The data in this figure were obtained from a 1 mmol/l solution of anthracene. The line measured belongs to $M_I = +5/2$ of the manganese nucleus.

to the nuclear spin quantum number of $+5/2$) are shown as a time dependent curve; the sensitivity calibration was made from this curve. Figure 1 was obtained when the anthracene concentration was 1 mmol/l, but similar results were observed at other anthracene concentrations. The approximately linear decrease with respect to time of the Mn^{2+} line at t, $m(t)$, will be proportional to the intensity of the sample absorption $I(t)$ with a proportionality factor $i(t)$

$$I(t) = i(t)m(t)$$

$m(0)$ is now used as a standard reference, where $t = 0$ means the moment at which the benzene solution was introduced. If $I'(t)$ is defined as

$$I'(t) = I(t)m(0)/m(t)$$

it represents the e.s.r. intensity compensated for the sensitivities of the e.s.r. detection system. As $I(t)$ is equal to $i(t)m(t)$, $I'(t)$ is equal to $i(t)m(0)$ and gives the relative e.s.r. intensity. Figure 2 shows the time dependence of $I'(t)$ obtained by the anthracene solution of 2 mmol/l. Two absorptions were observed, one at $g = 1.933$ and another at $g = 2.003$. The line at $g = 1.933$ is due to Mo^{5+} (11). The intensity of this line, y, as a function of time is given by

$$y = y_\infty(1 - \exp(-kt))$$

where k is the rate constant concerned. The initial dotted part of the curve means that no detection of the signal was made in this period because here the solution begins to flow into the cavity section of the sample tube and therefore adjustment of the microwave frequency must be done manually. Before the solution flowed in, the concentrations of both paramagnetic species were

Can. J. Chem. Downloaded from www.nrcresearchpress.com by 210.87.254.42 on 09/05/12
For personal use only.

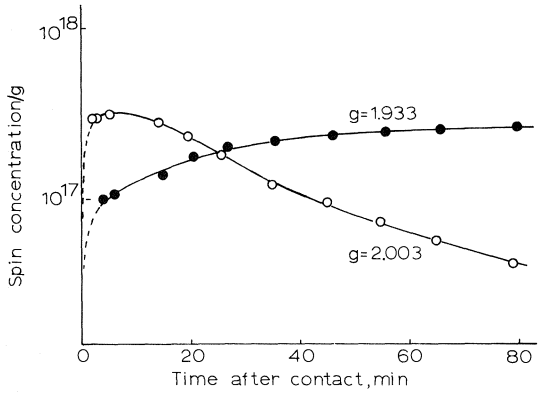

FIG. 2. Spin concentrations observed in Al_2O_3–MoO_3. The dotted initial parts of the curves were drawn as an extrapolation. The concentration of anthracene was 2 mmol/l.

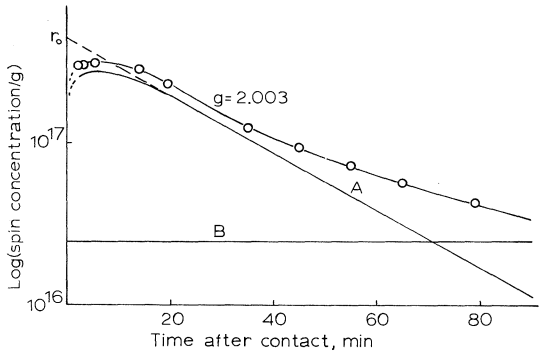

FIG. 3. The analysis of the intensity curve for $g = 2.003$ in Fig. 2, r_0 was obtained as an extrapolation of the component A to $t = 0$.

less than 1×10^{15} spins/ml ($g = 2.003$) and 5×10^{15} spins/ml ($g = 1.933$). The intensity curve of $g = 2.003$ in Fig. 2 can be separated into two components A and B as shown in Fig. 3. The component A can be written as

$$r = r_0 \exp(-kt)$$

except in the initial formation period, where r is the e.s.r. intensity, r_0 is the extrapolated value at $t = 0$, Fig. 3, and k is the rate constant already mentioned. The rate constant calculated from these data as

$$k = \log(r_1/r_2)/0.43294(t_2 - t_1)$$

is shown in Table 1, and is observed to be independent of anthracene concentration. The numerical values for the k calculated from y and those calculated from r are experimentally identical.

TABLE 1. The decay rate constant k and the concentrations of the paramagnetic species*

Anthracene (mmol/l)	k ($\times 10^{-4}$ s^{-1})†	b ($\times 10^{17}$ spins/g)	r_0 ($\times 10^{17}$ spins/g)
0.54	7.76	0.042	1.29
1.03	7.84	0.154	2.61
2.02	7.45	0.247	4.64
3.02	7.70	0.281	1.97
4.04	7.07	0.281	2.81
6.01	7.09	0.422	5.30
8.21	7.23	0.464	3.84

*The values obtained at 15 mW of incident microwave power.
†The average value is 7.45×10^{-4} s^{-1}.

The component B is a stable species and its concentration, b, is constant in the time scale of 90 min. However, the slope in Fig. 4 (2 h–20 h region) yield a decay rate constant of 5×10^{-6} s^{-1} for component B, *cf.* 7×10^{-4} s^{-1} for component A. The values b and r_0 are also shown in Table 1.

All the paramagnetic species have been thus far assumed to exist on the surface of Al_2O_3–MoO_3 particles, and not in the solution. In fact, as shown in Fig. 4, the change of e.s.r. intensities observed in the solution-flow-and-drainage, and N_2-purge treatments indicate that the assumption has been correct. Most of the unpaired electrons did not escape from the sample section by the drainage. As there is oxygen in the anthracene–benzene solution, one might suspect that the chemical species which destroys the paramagnetic species of the component A in Fig. 3 might be oxygen atoms or molecules.

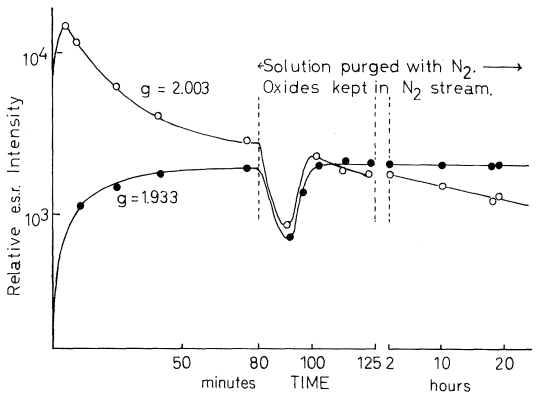

FIG. 4. The relative e.s.r. intensities observed during a solution-flow-N_2-purge period. The time axis after 125 min is in hours. The drop of both curves, after the N_2-purge was started, is due to cooling of the sample section in the cavity caused by the evaporation of benzene.

Can. J. Chem. Downloaded from www.nrcresearchpress.com by 210.87.254.42 on 09/05/12
For personal use only.

Can. J. Chem. Downloaded from www.nrcresearchpress.com by 210.87.254.42 on 09/05/12
For personal use only.

This is disproved by shaking the benzene solution with concentrated sulfuric acid and then distilling in a vacuum line three times. Well degassed Al_2O_3–MoO_3 particles and anthracene were added in vacuum, the anthracene cation thus formed was measured by e.s.r., again in vacuum. Oxygen was then introduced into the sample tube but it had no effect on the e.s.r. spectrum. Oxygen is thus not responsible for the decay of component A in Fig. 3.

Figure 5 indicates the e.s.r. spectra observed during 2–3 min period after contact of anthracene solution with the oxide layer. It is a composite of the e.s.r. spectra of component A and component B. The hyperfine component in the figure is ascribed to the component A because of its first order decay rate, $7.5 \times 10^{-4}\ s^{-1}$. As the spectral shape depends on the power of the incident microwave, the ratio of component A to component B in Fig. 5 is to be understood as that for 15 mW. At a lower incident microwave power such as 2 mW, a larger ratio of component A to component B was observed. Under the observed spectrum, an ideal e.s.r. spectrum, based upon the one obtained by the anthracene cation observed in concentrated H_2SO_4 but with zero line width, is shown with proton splittings of -6.53 G (9- and 10-positions), -3.06, and 1.38 G (1, 4, 5, 8- and 2, 3, 6, 7-positions, respectively) (12). The two spectra were compared by a simulation method. If one assumes the functional shape of each absorption line (*i.e.* $\exp(-aH^2)$) and a reasonable line width constant ($a = 50\ G^{-2}$ in the preceding formula) a simulated absorption curve in which the peak positions and the peak intensity is quite similar to the observed hyperfine structure is obtained. Only the positions of the major anion e.s.r. lines are shown at the bottom of Fig. 5. The corresponding cation e.s.r. lines (with the same relative intensities) are connected with the broken lines. Anion proton hyperfine splittings are -5.34, -2.74, and -1.51 G respectively (12). It was not found possible, with any simulation parameters tried, to fit the ideal anion spectrum to the experimentally observed hyperfine spectrum, although the cation ideal spectrum can be fitted to the experimental spectrum very easily. Therefore, the e.s.r. spectrum shown in Fig. 5 is from the anthracene cation and not from the anion.

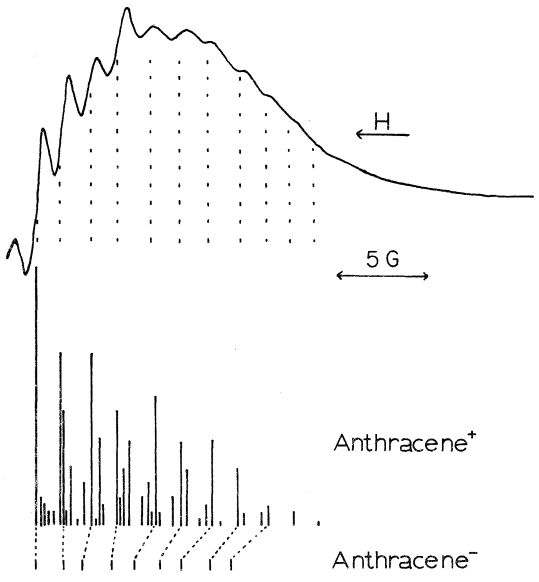

FIG. 5. The hyperfine structure of the species giving rise to the component A in Fig. 3. An ideal (width = 0) e.s.r. spectrum for anthracene cation is shown in the middle. The positions of the corresponding stronger lines of the anion spectrum are shown at the bottom of the figure.

The component B does not exhibit a hyperfine structure, and the shape of the spectrum is identical to that already reported for R^+O^{*2-} complex ion on alumina surface (10). In Fig. 6, the concentration of Mo^{5+}, y, is plotted against that of anthracene cation R^+, r; the equation

$$r + 2y = \text{constant}$$

fits these data approximately.

Figure 7 shows the effect of C_6H_6 and H_2O on the paramagnetic species formed on the sur-

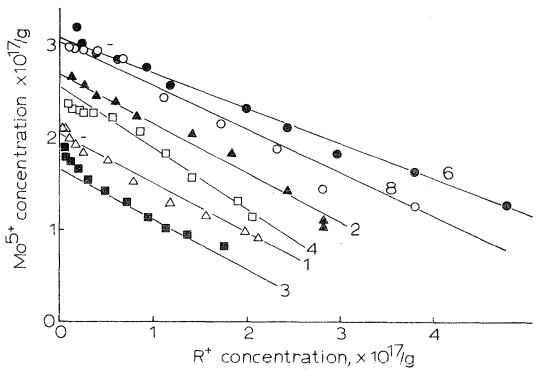

FIG. 6. The relation between the concentration of R^+ and Mo^{5+}. The figures shown at the end of each line indicate the concentration of anthracene in mmol/l.

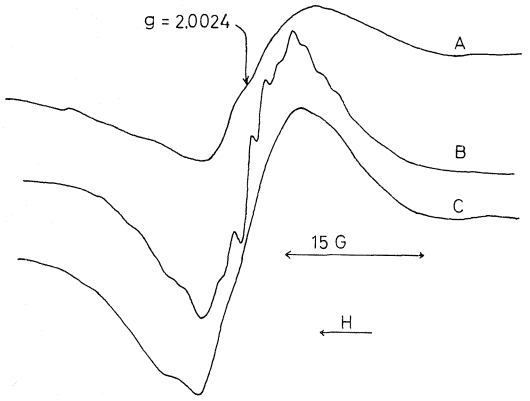

FIG. 7. The effects of benzene and water on the e.s.r. of anthracene–Al_2O_3–MoO_3 system. A: 0.07 g anthracene + 0.7 g Al_2O_3–MoO_3 evacuated. B: after 70 mm Hg of benzene introduced. C: after further addition of 20 mm Hg of water vapor. The overlapped hyperfine structure in B is due to anthracene cation.

face of Al_2O_3–MoO_3. A was obtained by 0.07 g of anthracene powder mixed with 0.7 g of Al_2O_3–MoO_3 after evacuation to 10^{-4} mm Hg for 10 min; B was obtained by introducing 70 mm Hg of benzene vapor into the sample which gave A; C was obtained by introducing 20 mm Hg of H_2O vapor into the sample which gave B.

Discussion

Two Paramagnetic Species

Figures 3 and 7 indicate the existence of two paramagnetic species. The reactive one has been shown to be anthracene cation in Fig. 5. The results in Fig. 4 indicate that the paramagnetic species giving rise to component B in Fig. 3 is identical to the stable paramagnetic species R^+O^{*2-} proposed by Ueda (9, 10). The concentration of B, *b*, does depend on the concentration of the solute, as shown in Table 1, but by Ueda's method of preparing R^+O^{*2-} the concentration of the solution immediately before the complete evaporation of the solvent reaches the solubility limit of the solute except in the case of a very dilute solution in which all the solute has been adsorbed by the oxide surface before complete evaporation of the solvent. Therefore, the concentration (per gram) of R^+O^{*2-} on the oxide surface depends only on the magnitude of the surface area and the surface properties of the oxide particle.

Some information on the relation between R^+ and R^+O^{*2-} are found in Figs. 3 and 7. As both species have cationic properties (if one considers O^{2-} in the lattice as an electronically neutral species in the sense that the ionization potential of O^{2-} in the lattice is not low), it may be anticipated that the two species are related in the following manner

$$R^+ \rightarrow X \rightarrow R^+O^{*2} \rightarrow Y \rightarrow \text{decay}$$

and so on. However, as shown in Fig. 7, the formation of anthracene cation requires the presence of benzene vapor while the formation of R^+O^{*2-} does not. Therefore, it should be concluded that the immediate origins of these two species are different and in that sense they exist independently. No perylene cation is formed when perylene solution is mixed with unsupported silica although perylene cation is formed on MoO_3-supported silica and mixed with perylene solution in the same way.[1] It is therefore concluded that R^+ is formed by a charge transfer reaction between anthracene and Mo^{6+}. R^+O^{*2-}, however, has been shown to be formed by anthracene and an active surface anion, O^{*2-} (9, 10).

Reaction of Anthracene Cation

The following shows that the apparent first order decay rate of R^+ is caused by the pseudo-first order reaction with water. The solution fed through the catalyst layer in the sample tube in the resonance cavity contains only benzene, anthracene, O_2, N_2, and H_2O. N_2 is known to be inactive with aromatic cations. In the present work, benzene and O_2 have been found to have no effect on the cation e.s.r. spectrum. On the other hand, H_2O destroyed the anthracene cation very effectively, as shown in Fig. 7. As the concentration of H_2O was always constant (2×10^{-2} mol/l), there is no way to interpret the apparent first order decay rate of R^+ other than by considering it to be a pseudo-first order reaction with H_2O. The average value of the pseudo-first order reaction rate constant in Table 1 is 7.45×10^{-4} s^{-1}. The reaction actually taking place is, therefore, a second order reaction,

$$[1] \qquad R^+ + H_2O \xrightarrow{k'} P + Q$$

where P and Q denote the reaction products. If the concentration of water is contained in *k*,

[1]H. Ueda, unpublished results. Similar results have recently been reported (ref. 14).

Can. J. Chem. Downloaded from www.nrcresearchpress.com by 210.87.254.42 on 09/05/12
For personal use only.

Can. J. Chem. Downloaded from www.nrcresearchpress.com by 210.87.254.42 on 09/05/12
For personal use only.

k' can then be calculated and is 3.10×10^{-2} l mol^{-1} s^{-1}. It can be assumed that the reaction 1 is essentially the reaction between R^+ and OH^- existing in H_2O. If so,

$$[2] \qquad R^+ + OH^- \xrightarrow{k''} P' + Q'$$

As $[OH^-]$ is 10^{-7} mol/l, $k'' = 3.10 \times 10^5$ l mol^{-1} s^{-1} is obtained. This value is not far from the neutralization reaction rate constant between NH_4^+ and e_{aq}^- observed by pulse radiolysis, $\simeq 10^6$ l mol^{-1} s^{-1}, (13) so that the reaction scheme 2 is not unreasonable.

The formation of Mo^{5+}

It is shown in Fig. 6 that

$$r + 2y = \text{constant}$$

If y is differentiated with respect to r

$$dy/dr = -1/2.$$

This indicates that one Mo^{5+} is formed when two R^+ are lost. Therefore

$$[2'] \qquad 2R^+ + 2OH^- + Mo^{6+} \rightarrow Mo^{5+} + X$$

will be taking place. An electronically negative species, Mo^{5+} $(= Mo^{6+} + e^-)$ formed from R^+ is rather puzzling, but

$$[2''] \quad 2R^+ + 2OH^- \rightarrow 2RO + 2H$$

$$[3] \qquad 2H + Mo^{6+} \rightarrow Mo^{5+} + H^+ + 0.5H_2$$

will explain [2']. Only 50% of hydrogen atoms formed are assumed to reduce Mo^{6+} in [3]. As

$$y = \text{constant} - 0.5r$$

and

$$r = r_0 \exp(-kt)$$

$$y = \text{constant} - 0.5r_0 \exp(-kt)$$

is obtained. As

$$y = y_\infty (1 - \exp(-kt))$$

is observed experimentally, then

$$y = 0.5r_0 (1 - \exp(-kt))$$

should hold with

$$y_\infty = 0.5r_0$$

Some deviation from this last relation is found in Fig. 6, but, it is satisfied approximately.

Initial Reaction Rate

In Fig. 2, no measurements were made between $t = 0$ and $t = 2$, though the value at $t = 0$ was observed. Under the present experimental conditions, the linear flow rate of the solution was 1.41 cm/s and so the time required to wet all the oxide particles (filled length was 45 mm) was 3 s. This value is negligible when compared with 2 min. However, the space among oxide particles is filled with air which must be replaced with the solution. Not all the air among the particles is removed at the first contact of the solution and some bubbles are observed during the first minute. As the wave length of light in air and in benzene is considerably different, the automatic frequency control does not work during this period. Thus, the present experimental procedures cannot eliminate the 2 min period without measurement. One possible solution to this problem will be to fill the space among oxide particles with pure benzene and then switch to anthracene solution. But the initial anthracene concentration will then change greatly and this makes the analysis of the results complicated. A variation of this method is to inject anthracene solution into the flow path of pure benzene as a pulse. The analysis of this pulse method will also be complicated, and for this reason these experiments were not included in this work.

However, if a few assumptions are made, the initial rate of formation of anthracene cation can be estimated. The anthracene cation is formed by the reaction

$$R + L^+ \rightarrow R^+ + L$$

where R signifies anthracene molecule and L^+ signifies the Lewis acid point. If the concentration of L^+ is written as l, and its initial value as l_0, and the concentration of R^+ is written as r,

$$(dr/dt)_{\text{formation}} = k_i[R][L^+] = -dl/dt$$

By writing

$$k_i[R] = k_j$$

$$l = l_0 \exp(-k_j t)$$

is obtained. R^+ decays by reaction with H_2O with an apparent first order decay rate constant k_d. Therefore,

$$dr/dt = k_i[R][L^+] - k_d r = k_j l_0 \exp(-k_j t) - k_d r$$

is solved, and r thus obtained is

$$r = r_0 \exp(-k_d t) - k_j l_0 \exp(-k_j t)/(k_j - k_d)$$

The experimental results show that $k_j > k_d$.

When $t \to 0$, $r \to 0$, so that

$$r_0 - k_j l_0/(k_j - k_d) = 0$$

By approximating

$$k_j l_0/(k_j - k_d) \simeq l_0$$

$$r_0 = l_0$$

is obtained. The maximum point of the r–t curve is then given by

$$dr/dt = 0 = l_0(k_j \exp(-k_j t) - k_d \exp(-k_d t))$$

The time, t, obtained by solving this equation is

$$t = (\log_e (k_j/k_d))/(k_j - k_d)$$

The time for the maximum point observed in Fig. 3 is about 305 s. The k_d value observed is 7.45×10^{-4} s^{-1}, whence the value of k_j is estimated as 8.9×10^{-3} s^{-1}. As the value of [R] is 2×10^{-3} mol/l, $k_i = 4.5$ l mol^{-1} s^{-1} is obtained.

Implications for Catalyst Activity

Acid points on the surface of oxide catalysts are said to be the active point for isomerization reactions. The Lewis acid point, which makes the anthracene cation, has been deduced to be such a point. However, on the oxide surface another point exists at which paramagnetic species are formed, namely O^{*2-} sites. As shown in Fig. 3, the cation-forming points were destroyed in the earliest period of the flow of the anthracene solution containing water and were never regenerated again, at least at 20 °C. In other words, they are too sensitive to poisoning. Compared with it, R^+O^{*2-} was stable and resistant to poisoning. Therefore, repeated catalytic reactions seem to be possible with the O^{*2-} surface ions although not with the Lewis acid points at which the anthracene cation is formed. However, the results in Fig. 3 have been observed at 20 °C. At higher temperatures, poisoned acid points might be regenerated. These points will be investigated in future studies.

The authors wish to thank Mr. K. Ogawa for his assistance in the preparation of the mixed oxide.

1. A. N. Webb. 2nd International Congress on Catalysis. Editions Technip, Paris. 1960.
2. J. J. Rooney and R. C. Pink. Proc. Chem. Soc. 70 (1961).
3. D. M. Brouwer. Chem. Ind. London, 177 (1961).
4. D. M. Brouwer. J. Catal. **1**, 372 (1962).
5. J. K. Fogo. J. Phys. Chem. **61**, 1919 (1961).
6. H. P. Leftin, M. C. Hobson, and J. S. Leigh. J. Phys. Chem. **62**, 1214 (1962).
7. W. K. Hall. J. Catal. **1**, 53 (1962).
8. H. Ueda. Can. J. Chem. **46**, 891 (1968).
9. H. Ueda and N. Todo. Bull. Chem. Soc. Jap. **43**, 3698 (1970).
10. H. Ueda. Bull. Chem. Soc. Jap. **43**, 319 (1970).
11. J. Masson and J. Nachtschein. Bull. soc. chim. Fr. 3933 (1968). K. S. Seshadri, F. E. Masoth, and L. J. Petrakis. J. Catal. **19**, 95 (1970). K. S. Seshadri and L. J. Petrakis. J. Phys. Chem. **74**, 4102 (1970).
12. J. R. Bolton and G. K. Fraenkel. J. Chem. Phys. **40**, 3307 (1964). A. Carrington, F. Dravnieks, and M. C. R. Symons. J. Chem. Soc. 947 (1959). The nuclear spin splitting values in this paper were adopted from the former literature.
13. F. S. Dainton. *In* Fast reactions and primary processes in chemical kinetics. Stig Claesson, ed. Almquist and Wiskell, Stockholm. 1967. p. 185.
14. C. Naccache, J. Bandiera, and M. Dufaux. J. Catal. **25**, 334 (1972).

Can. J. Chem. Downloaded from www.nrcresearchpress.com by 210.87.254.42 on 09/05/12
For personal use only.

The Barrier to Rotation in 2,2′-iminobis (acetamidoxime) and its Nickel(II) and Zinc(II) Complexes

ROGER E. CRAMER[1] AND ROBERT DERYKE

Department of Chemistry, University of Hawaii, 2545 The Mall, Honolulu, Hawaii 96822

Received July 19, 1972

The free energy of activation at the coalescence temperature was measured for the rotational barrier about the amide bond in 2,2′-iminobis(acetamidoxime) (IBO) and its Ni(II) and Zn(II) complexes. The barrier is 10.5 ± 0.3 kcal/mol and increases by about 1 kcal/mol upon coordination of Ni(II) and Zn(II). By means of INDO molecular orbital calculations it is shown that the amide proton *trans* to the donor nitrogen experiences the largest isotropic shift in $Ni(IBO)_2(NO_3)_2$ and that the major portion of spin delocalization takes place through the oxime nitrogen σ donor orbital, which is not the highest filled orbital of the ligand.

L'énergie libre d'activation à la température de coalescence a été mesurée pour la barrière de rotation autour de la liaison amide pour le 2,2′-iminobis(acétamidoxime) (IBO) et pour ses complexes avec le Ni(II) et Zn(II). Cette barrière vaut 10.5 ± 0.3 kcal/mol et augmente d'environ 1 kcal/mol par coordination avec le Ni(II) et Zn(II). Les calculs des orbitales moléculaires selon la méthodes INDO montrent que le proton amide *trans* par rapport à l'azote donneur subit le déplacement isotrope le plus grand dans $Ni(IBO)_2(NO_3)_2$ et que la majeure partie de la délocalisation de spin se produit à travers l'orbitale donneur de l'azote de l'oxime, qui n'est pas l'orbitale occupée du ligand la plus élevée.

[Traduit par le journal]

Can. J. Chem., **51**, 892 (1973)

Introduction

While the barrier to rotation about C—N bonds in amides has been an active area of research for some time (1), there have been no reports of such a barrier in an amidoxime. In addition while limited information is available about the change in the magnitude of the rotational barrier of amides upon coordination to the amido oxygen of such Lewis acids as H^+ (2) and BF_3 (3), apparently no similar information is available for transition metal Lewis acids. The recent synthesis of 2,2′-iminobis(acetamidoxime) (4), $HN[—CH_2—C(NH_2)NOH]_2$, has provided access to amidoximes, and the crystal structures (5) of the Ni(II) and Cu(II) complexes of this ligand have shown that the C—NH_2 bond length is comparable to that found in many amides. Accordingly we have estimated the barrier to rotation about this bond for 2,2′-iminobis(acetamidoxime) (abbreviation, IBO) and its complexes with Ni(II) and Zn(II) by approximate n.m.r. methods.

Experimental

IBO

IBO was synthesized by the method of Eddy *et al.* (4).

$Ni(IBO)_2(NO_3)_2$

This complex was prepared by the method of Eddy (4) substituting $Ni(H_2O)_6(NO_3)_2$ for $Ni(H_2O)_6Cl_2$. Since the nitrate complex is much more soluble in H_2O than is the Cl complex, it was necessary to isolate the complex by evaporation of the H_2O. The crystals were washed with MeOH and dried.

Anal. Calcd. for $Ni(IBO)_2(NO_3)_2$: C, 19.03; H, 4.39; N, 33.28. Found: C, 19.44; H, 4.32; N, 32.73.

$Zn(IBO)_2(NO_3)_2$

This complex was prepared in the same manner as was $Ni(IBO_2)(NO_3)_2$.

Anal. Calcd. for $Zn(IBO)_2(NO_3)_2$: C, 18.78; H, 4.33; N, 32.85. Found: C, 19.14; H, 4.38; N, 33.00.

N.M.R. Spectra

Spectra were obtained using a Varian Associates HA-100 spectrometer operating in the HA mode and chemical shifts are reported with respect to internal TMS. Temperature was controlled by means of Varian Variable Temperature Controller Model V-6040. The estimated error in the temperature measurements is ±2 °C.

Barrier Calculations

The free energy of activation at coalescence ($\Delta G^{\neq}_c$) for the rotation was calculated from the Eyring equation (1*a*)

$$[1] \qquad \Delta G^{\neq}_c = 4.57T(10.32 + \log T_c/K_r)$$

where T_c is the coalescence temperature, K_r is the rate constant for the exchange of the two amide protons at this temperature, and is given by

$$[2] \qquad K_r = \pi\Delta\nu/\sqrt{2}$$

where $\Delta\nu$ is the separation between the amide peaks in the absence of exchange. For IBO and for $Zn(IBO)_2(NO_3)_2$, $\Delta\nu$ was obtained from spectra recorded at temperatures in the slow exchange region. In the case

[1]To whom correspondence should be addressed.

TABLE 1. Chemical shifts for amidoximes

Compound	Solvent	Chemical shift*			
		N*H*	C*H*$_2$	O*H*	N*H*$_2$
IBO	DMSO	−3.25	−3.10	−8.98	−5.43
Zn(IBO)$_2$(NO$_3$)$_2$	DMSO	−4.10	−3.44	−8.84	−6.51
Ni(IBO)$_2$(NO$_3$)$_2$	DMSO	†	−96	−2.70	−25

*In p.p.m. from TMS. Negative sign indicates downfield.
†Unobserved.

TABLE 2. The free energies of activation for amidoxime rotational barriers

Compound	Solvent	Δν (Hz)	T_c (C°)	$\Delta G^{\neq}$ (kcal/mol)
IBO	DMF	25±1	−60±2	10.5±0.3
Zn(IBO)$_2$(NO$_3$)$_2$	MeOH	15±1	−47±2	11.5±0.3
Ni(IBO)$_2$(NO$_3$)$_2$	DMSO	3000±300	+17±2	11.8±0.4

of IBO the DMF solution froze at −80 °C and Δν became constant below −70 °C while for Zn(IBO)$_2$-(NO$_3$)$_2$ the freezing point of the solution was far below the coalescence temperature. In the case of Ni(IBO)$_2$-(NO$_3$)$_2$, the separation of the nonexchanging amide peaks is temperature dependent due to the paramagnetism of the molecule (for a recent review of the n.m.r. of paramagnetic molecules, see ref. 6). In order to estimate Δν at the coalescence temperature the position of the two amide peaks for temperatures below T_c was plotted *vs.* 1/*T*. Straight lines were realized between +7 °C and the freezing point of the solution at −5 °C which indicates slow exchange in this temperature region. These straight lines were extrapolated to T_c where Δν was taken as the difference between the extrapolated chemical shifts, as suggested by Ho and Reilley (7). Although this method produces a rather large error in Δν (see Table 2) the resultant uncertainty in $\Delta G^{\neq}_c$ is acceptable due to the logarithmic nature of eq. 1.

Results

The chemical shifts for the compounds studied here at room temperature are reported in Table 1. The data necessary for the calculation of the barriers to rotation from eqs. 1 and 2, as well as values for $\Delta G^{\neq}_c$ are reported in Table 2. We place no significance on the small (0.3 kcal/mol) difference reported for the Ni^{2+} and Zn^{2+} complexes due to the difficulty in measuring the paramagnetically broadened peaks in the Ni^{2+} case, and due to possible errors in the extrapolation procedure (*vide supra*). Considering the wide differences in the parameters which characterize these two systems, we feel that the small difference in the reported barriers supports their validity.

The p.m.r. spectrum of acetamide exhibits a broad featureless peak with a width at half-height of 70–80 Hz (8) due to relaxation caused by the quadrupolar ^{14}N (9). Roberts (10) has pointed out that the ^{14}N broadening is temperature sensitive, since slower molecular motion leads to more rapid relaxation of ^{14}N and thus sharper amide proton signals. It is found that larger amides have less broad proton peaks (10, 11) and that the peak width of any given proton decreases with decreasing temperature (8). The large size of the compounds reported here would lead us to expect narrow proton peaks at room temperature and the observed peak widths of 5–6 Hz for IBO and Zn(IBO)$_2$(NO$_3$)$_2$ are among the smallest reported for amido protons (10–12). The amide peaks also show a decrease in line width with decreasing temperature and at −10 °C both IBO and Zn(IBO)$_2$(NO$_3$)$_2$ exhibit line widths of 4 Hz. Attempts to decouple the ^{14}N from the protons at room temperature caused the line widths to decrease from 5–6 Hz to about 4 Hz, thus confirming that the ^{14}N is experiencing rapid relaxation and that its contribution to the proton line width is negligible at room temperature. Since the ^{14}N relaxation time decreases with decreasing temperature we conclude that quadrupolar broadening of the amido proton peaks will be negligible at the coalescence temperature, thus allowing the application of eqs. 1 and 2.

Discussion

Rotational Barrier of Amidoximes

The barrier to rotation about the C—NH$_2$ bond for IBO reported in Table 2 is among the lowest ever reported for an amide. It can be

compared to the value of 17.7 kcal/mol reported by Drakenberg and Forsin (13) for formamide. The lower barrier in the amidoximes compared to formamide is consistent with the trend in X groups pointed out by Kessler (1*a*) in that it closely resembles those found for other amides where X contains an imino nitrogen. Accordingly the barrier in IBO is quite similar to the values of 12 to 13 kcal/mol reported for some *N*-arylamidines (X = *N*—Aryl, R = $(CH_3)_2N$, H_a = H_b = Me) (14). The slightly higher barrier in this latter case may be due to the fact that the amido nitrogen substituents are methyl groups which are known to lead to barriers slightly higher than the corresponding protonic compounds (13). The low barrier reported here is also consistent with the failure of Neuman and Young (15) to observe two peaks for dimethylacetamidine (X = NH, R = H_a = H_b = Me) down to −40 °C. Thus we conclude that in amides containing the imino nitrogen, including the oxime group X = NOH, structure **1** is more favored than **2** for compounds containing nitrogen than oxygen, *i.e.*, there is more double bond character in the bond to an imino nitrogen than to a carbonyl oxygen.

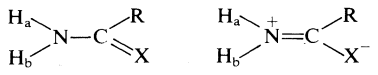

1 **2**

Coordination of either Zn^{2+} or Ni^{2+} is seen to increase the barrier by about 1 kcal/mol or nearly 10%. This increase in the barrier of IBO upon coordination of Zn^{2+} and Ni^{2+} is comparable to that observed by other workers with similar systems. For example, Kessler (14) found that protonation of the imino nitrogen in *N*-arylamidines raised $\Delta G^{\neq}_c$ from 12.1 to 12.6 kcal/mol. Gore *et al.* (3) studied the effect of coordination of BF_3 upon the barrier in *N*,*N*-dimethylformamide, and treatment of their data by eqs. 1 and 2 shows that the barrier has increased to 21.9 kcal/mol (1*b*) from 20.9 kcal/mol for DMF. Although they had difficulty in measuring the coalescence temperature for the BCl_3 adduct, the approximate value given yields a $\Delta G^{\neq}_c$ of 22.1 kcal/mol. Due to the wide variations in these systems, detailed comparisons are not justified. Yet it does seem apparent that coordination of a Lewis acid at the X site does favor structure **2**, as expected, although the increase in barrier is only about 1 kcal/mol without regard to the details of the system.

Chemical Shifts

The chemical shifts of the protons of IBO and $Zn(IBO)_2(NO_3)_2$ are normal. The differences observed between IBO and $Zn(IBO)_2(NO_3)_2$ can be explained by the drain of electron density from the ligand upon coordination to the electrophilic Zn^{2+}. The NH_2 resonances of these compounds exhibit an interesting temperature dependence. In the case of IBO dissolved in MeOH this peak shifts from −5.43 p.p.m. at room temperature to −6.16 p.p.m. (average for two NH peaks observed at this temperature) at −75 °C, while in the case of the Zn^{2+} complex dissolved in DMF the shift is from −6.64 p.p.m. at 30 °C to −6.94 p.p.m. at −75 °C. Similar shifts as a function of temperature have been observed by Sunners *et al.* (16) for formamide in acetone and were attributed to a decrease in hydrogen bonding to the solvent at higher temperature. This explanation would also be expected to hold here, with the difference between the two systems being due to the greater acidity of the NH_2 protons in $Zn(IBO)_2^{2+}$ and the stronger Lewis base strength of DMF.

Isotropic Shifts

The chemical shifts of $Ni(IBO)_2(NO_3)_2$ are dominated by the isotropic shift resulting from the paramagnetism of the complex. The methylene shift is in close agreement with the values found for the methylene protons of $Ni(en)_3(Cl)_2$ (7). The only other report of a contact shifted hydroxyl proton of an oxime is by Baucom and Drago (17) who report a shift of −75 p.p.m. for this type of proton in *bis*(2,6-diacetylpyridine dioxime)nickel(II). Since the chemical shifts which we report here are the first to be reported for an amidoxime there is no other data with which to compare the NH_2 contact shift. The moderate downfield shift (18–19 p.p.m.) can however be contrasted with the large (≈100 p.p.m.) upfield shift found for the amino protons of $Ni(CH_3NH_2)_6^{2+}$ (18). Our inability to find the N—*H* proton is in accord with the very large line widths usually found for protons on amines coordinated to nickel(II) (7). The chemical shifts assignments reported here are supported by relative intensity and line width data as well as H–D exchange experiments.

Below the coalescence temperature, the chemical shifts of the two diasterotopic amido protons

of $Ni(IBO)_2(NO_3)_2$ are -10.0 p.p.m. and -40.0 p.p.m. respectively, at 0 °C. Subtracting the chemical shift of the amido protons of $Zn(IBO)_2(NO_3)_2$ to obtain isotropic shifts we have $\Delta\nu = -3.5$ p.p.m. and $\Delta\nu = -33.5$ p.p.m. From the spectra alone we have no way of assigning which of these two peaks is due to H_a and which is due to H_b of structure **1**. In a study of *N*-methyl lactams (19) coordinated to Ni(II), a larger isotropic shift was observed for the *N*-methylene group than for the *N*-methyl group. Thus the larger shift was found for the group *trans* to the carbonyl group. Since both the *N*-methyl lactams and IBO are amides with σ donor orbitals, and since all unpaired electrons of Ni(II) are in σ orbitals, we would expect a similar σ delocalization mechanism for the two ligands. Thus we might expect that H_a would experience the greatest isotropic shift.

In order to confirm these ideas we carried out INDO (20) molecular orbital calculations on the model compound acetamidoxime (R = CH_3, X = NOH). The highest filled molecular orbital in this compound is of π symmetry while the oxime nitrogen σ donor orbital, through which coordination to the Ni^{2+} ion takes place, is about 2.1 eV more stable than this π orbital. The usual method of estimating isotropic shifts from INDO calculations involves removing an electron from the highest filled molecular orbital (21), or replacing a nitrogen donor atom with a carbon atom (22). In the case of acetamidoxime both methods place unpaired spin in the highest filled orbital, which is of π symmetry. From our foregoing arguments we would not expect such a π mechanism to reproduce our experimental results for $Ni(IBO)_2^{2+}$, and this expectation is fulfilled. The radical cation predicts *upfield* shifts for both amido hydrogens, $R = A(H_a)/A(H_b) = -10.7G/-10.1G = 1.05$, while for the replacement by carbon we have $R = -7.8G/-8.7G = 0.89$. Experimentally, we find *downfield* shifts with an experimental ratio $R = -33.5$ (p.p.m.)/-3.5 (p.p.m.) = 9.6.

In order to test the σ mechanism we are faced with the problem of introducing spin into the oxime σ donor orbital. We could accomplish this by removing 3 electrons, *i.e.*, a 3+ cation, or by replacing the oxime nitrogen with a Be atom. It seems likely that both of these procedures would be so drastic as to render the results unreliable. We have therefore chosen to model the system in another way. We have placed a hydrogen atom in the position which would be occupied by the Ni(II) ion, *i.e.*, about 2.0 Å from the oxime nitrogen. Since the hydrogen atom has an unpaired electron, and is only capable of σ bonding with the ligand, it should be a reasonable qualitative, but not quantitative, probe for spin delocalization springing from a Ni(II) ion. The results of this calculation confirm our expectation that H_a has the larger coupling constant, and hence the larger contact shift. Thus this system is analogous to the *N*-methyl lactam system in that the greater shift is experienced by the amido nitrogen substituent *trans* to the donor atom. Comparison of the calculated ratios, $R = 0.508G/0.075G = 6.76$, with the experimental ratio 9.6 (*vide supra*) indicates reasonable agreement in view of the approximations necessary. The agreement is certainly much better than that discussed above for delocalization in a π orbital, and would indicate the primary spin delocalization is through the σ orbital. This is the first reported case where the delocalization is primarily found to be into the second highest filled orbital, rather than the highest filled.

We would like to thank Tom Bopp and John Gilje for useful discussions on this topic and to acknowledge the donors of the Petroleum Research Fund, administered by the American Chemical Society, for partial support of this research.

1. (*a*) H. KESSLER. Angew. Chem. Int. ed. **9**, 219 (1970); (*b*) W. E. STEWART and T. H. SIDDALL III. Chem. Rev. **70**, 517 (1970).
2. G. FRAENKEL and C. FRANCONI. J. Am. Chem. Soc. **82**, 4478 (1960).
3. E. S. GORE, D. J. BLEARS, and S. S. DANYLUK. Can. J. Chem. **43**, 2135 (1965).
4. L. P. EDDY, W. W. LEVENHAGEN, and S. K. MCEWEN. Inorg. Synth. **11**, 89 (1968).
5. D. L. CULLEN and E. C. LINGAFELTER. Inorg. Chem. **9**, 1865 (1970).
6. R. H. HOLM. Acc. Chem. Res. **2**, 307 (1969).
7. F. F.-L. Ho and C. N. REILLEY. Anal. Chem. **42**, 600 (1970).
8. R. J. GILLESPIE and T. BIRCHALL. Can. J. Chem. **41**, 148 (1963).
9. L. H. PIETTE, J. D. RAY, and R. A. OGG. J. Mol. Spectrosc. **2**, 66 (1968).
10. J. D. ROBERTS. J. Am. Chem. Soc. **78**, 4495 (1956).
11. G. V. D. TIERS and F. A. BOVEY. J. Phys. Chem. **63**, 302 (1959).
12. G. S. HAMMOND and R. C. NEUMAN, Jr. J. Phys. Chem. **67**, 1655 (1963).
13. T. DRAKENBERG and S. FORSIN. J. Phys. Chem. **74**, 1 (1970).

14. H. KESSLER. Angew. Chem. Int. Ed. **7**, 898 (1968).
15. R. C. NEUMAN, Jr., and L. B. YOUNG. J. Phys. Chem. **69**, 2570 (1965).
16. B. SUNNERS, L. H. PIETTE, and W. G. SCHNEIDER. Can. J. Chem. **38**, 681 (1960).
17. E. I. BAUCOM and R. S. DRAGO. J. Am. Chem. Soc. **93**, 6469 (1971).
18. R. J. FITZGERALD and R. S. DRAGO. J. Am. Chem. Soc. **90**, 2523 (1968).
19. B. B. WAYLAND, R. S. DRAGO, and H. F. HENNEIKE. J. Am. Chem. Soc. **88**, 2455 (1966).
20. D. A. DOBOSH. CNINDO, Program 141, Quantum Chemistry Program Exchange, Indiana University, 1969.
21. M. J. SCARLETT, A. T. CASEY, and R. A. CRAIG. Aust. J. Chem. **23**, 1333 (1970).
22. W. DEW. HORROCKS, Jr., and D. L. JOHNSTON. Inorg. Chem. **10**, 1835 (1971).

Investigations of Substituent Effects by Nuclear Magnetic Resonance Spectroscopy and All-valence Electron Molecular Orbital Calculations. I. 4-Substituted Styrenes

GORDON K. HAMER,[1] IAN R. PEAT,[2] AND WILLIAM F. REYNOLDS

Department of Chemistry, University of Toronto, Toronto 181, Ontario

Received June 14, 1972

^1H and ^{13}C chemical shifts have been determined for over 20 4-substituted styrenes under conditions corresponding to infinite dilution in a non-polar medium. Correlations of the internal chemical shift difference for the β vinyl protons, $\Delta\delta(B - C)$ with electric field components estimated by a classical electrostatic calculation, with the field parameter *F*, and with hydrogen charge densities estimated by CNDO/2 MO calculations provide conclusive evidence for the existence of a through-space field effect. CNDO/2 calculations for 4-substituted 1-vinylbicyclo[2.2.2]octanes and ethylene–methylX pairs indicate that this through-space field effect has a geometric dependence similar to that predicted by the Buckingham equation.

Correlations of vinyl ^1H and ^{13}C chemical shifts and charge densities with field, *F*, and resonance, *R*, parameters provide a self-consistent picture of electronic effects in these compounds. ^1H chemical shifts for some derivatives are affected by magnetic effects but this does not obscure the overall pattern of electronic effects. This pattern of electronic effects can be completely accounted for by a model which assumes that substituent effects can be transmitted through space (field effects), via conjugative interactions (resonance effects) or by polarization of the styrene π electron system by the polar C—X bond (π polarization effects). The latter effect appears to be more important than previously realized.

^1H correlations with *F* and *R* are used to estimate self-consistent and apparently reasonable $\Delta\chi$ values for C≡N and C≡C—H groups and *F* and *R* values for carbonyl substituents and $(CH_3)_3M$ substituents (M = Si, Ge, Sn, and Pb). The halogens give anomalous results. A comparison of various correlations suggests that these anomalies are magnetic in origin.

Les déplacements chimiques de ^1H et ^{13}C ont été déterminés sur plus de vingt styrènes substitués en -4 dans des conditions de dilution infinie, en milieu non polaire. Les corrélations entre la différence de déplacement chimique interne pour les protons β vinyliques, $\Delta\delta(B - C)$ et les composantes du champ électrique évaluées par calcul classique d'électrostatique, le paramètre de champ *F*, et les densités de charge sur l'hydrogène obtenues par calcul CNDO/2 MO fournissent une preuve concluante de l'existence d'un effet de champ à travers l'espace. Les calculs CNDO/2 sur les vinyl-1 bicyclo[2.2.2]octanes substitués en 4 et sur les couples éthylène–méthyleX, montrent que cet effet spatial de champ dépend de la géométrie selon l'équation de Buckingham.

Les corrélations entre les déplacements chimiques du ^1H vinyle et ^{13}C, des densités de charge avec le champ *F* et les paramètres de résonance *R* fournissent une image cohérente des effets électroniques dans ces composés. Dans certains dérivés les déplacements chimiques du ^1H sont affectés par les effets magnétiques mais cela ne change pas l'allure générale des effets électroniques qui peut être totalement expliquée par un modèle qui suppose que les effets de substituants peuvent être transmis à travers l'espace (effets de champ), via des interactions de conjugaison (effets de résonance) ou par polarisation du système électronique π du styrène par la liaison C—X (effets de polarisation π). Ce dernier effet est plus important qu'on ne le pensait précédemmant.

Les corrélations entre ^1H avec *F* et *R* ont été utilisées pour apprécier les valeurs $\Delta\chi$ cohérentes et apparemment raisonnables pour les groupes C≡N et C≡C—H et les valeurs *F* et *R* pour les substituants du carbonyle et de $(CH_3)_3M$ (M = Si, Ge, Sn, et Pb). Les halogènes conduisent à des résultats anormaux. Une comparaison entre les diverses corrélations suggère que ces anomalies sont d'origine magnétique. [Traduit par le journal]

Can. J. Chem., **51**, 897 (1973)

Introduction

Zürcher (1) and Allinger and coworkers (2), have shown that the substituent dependence of proton chemical shifts for many aliphatic compounds can be accounted for in terms of the dipolar electric field effect and the anisotropic magnetic susceptibility of the substituent. The substituent dependence of proton chemical shifts (S.C.S.) for aromatic compounds is less certain. Miller and co-workers have summarized the results of approximately 100 correlations of S.C.S. for aromatic derivatives with Hammett

[1]NRCC Scholarship holder, 1967–1970.

[2]NRCC Scholarship holder, 1968–1971. Gulf Oil Fellowship holder, 1971–1972.

Can. J. Chem. Downloaded from www.nrcresearchpress.com by 210.87.254.105 on 09/05/12
For personal use only.

Can. J. Chem. Downloaded from www.nrcresearchpress.com by 210.87.254.105 on 09/05/12
For personal use only.

substituent constants (3):

$$[1] \qquad \delta^3 = \rho\sigma + \delta_0$$

However, many of the correlations were unsatisfactory (correlation coefficient, $r < 0.90$) and they concluded that the observed ρ values were not reliable measures of the efficiency of transmission of substituent effects (3). More recently, Wiley and Miller (4) have correlated S.C.S. with the divided field, F, and resonance, R, substituent constants of Swain and Lupton (5).

$$[2] \qquad \delta = fF + rR + \delta_0$$

While much better correlations were obtained, it was concluded that the correlations were physically meaningless since unrealistic values of the weighting factors, f and r, were found (4).

However, almost all of these investigations were carried out in interacting solvents (CCl_4 cannot be regarded as an inert solvent for p.m.r. measurements (6)) and often at finite solute concentrations. Consequently, the chemical shifts may reflect both solvent–solute and solute–solute interactions. In addition many investigations have involved a limited range of substituents, often including halogens or other substituents with uncertain magnetic anisotropy effects.

By contrast with ^1H chemical shifts, ^{13}C chemical shifts are relatively insensitive to magnetic anisotropy effects (due to the much greater chemical shift range (7)) and to solvent and concentration effects (8). Consequently ^{13}C chemical shift measurements have provided a considerable amount of information about electronic substituent effects in aromatic derivatives (9). ^{13}C chemical shifts primarily reflect substituent effects transmitted through the bonding network of the molecule.

An alternative approach for interpreting S.C.S. is to compare chemical shifts with electron densities determined by molecular orbital calculations. All-valence electron calculations of the CNDO/2 type (10) have proved to be particularly useful for investigations of ^1H (11, 12), ^{13}C (8, 13), and ^{19}F (14) chemical shifts of aromatic derivatives since they provide information about electronic effects transmitted through both π and σ electron systems. In addition, we have shown that they also reflect through space field effects (15).

In view of the uncertainties surrounding S.C.S. in aromatic derivatives, we decided to carry out a detailed investigation of a large family of closely related compounds, determining ^1H and ^{13}C chemical shifts under as inert conditions as possible and estimating electron densities by CNDO/2 (all-valence electron) molecular orbital calculations. The purpose of the investigation was threefold: to determine as completely as possible the electronic distributions in these compounds, to determine to what extent ^1H chemical shifts reflect this electronic distribution, and to interpret the three parameters listed above in terms of mechanisms of transmission of substituent effects. In order to fulfil this last aim it was decided to correlate chemical shifts with divided substituent constants. F and R were chosen since these are claimed to have the most complete division of field and resonance effects (5). However, since the use of F and R correlations has been severely criticized, we decided to use three criteria to test the validity of our correlations. First, ^1H and ^{13}C chemical shifts and charge densities should reveal similar patterns of substituent effects. Second, it should be possible to rationalize the f and r values for the correlations in terms of a reasonable model for mechanisms of transmission of substituent effects. Finally, the same model should account for variations in f and r between closely related series of compounds.

For our initial investigation, we chose 4-substituted styrenes as model compounds. The advantages of these compounds for investigations of S.C.S. has been previously discussed (16). While there have been several investigations of S.C.S. for these compounds (16–20), all of them suffered from one or more of the weaknesses outlined above. We report below the results of an investigation in which ^1H and ^{13}C chemical shifts of more than 20 4-substituted styrenes were measured in an inert medium and compared with charge densities determined by CNDO/2 molecular orbital calculations.

Experimental

(a) Preparation and Purification of Compounds

4-Methylstyrene and 4-vinylbiphenyl were obtained commercially from Aldrich Chemical Company, Inc. 4-Ethoxystyrene and 1,4-divinylbenzene were purchased from Pfaltz and Bauer, Inc. 4-*t*-Butylstyrene was ob-

[3]Chemical shifts in p.p.m. are defined according to the δ scale, *i.e.* with high frequency (low field) shifts positive.

Can. J. Chem. Downloaded from www.nrcresearchpress.com by 210.87.254.105 on 09/05/12
For personal use only.

tained from Professor K. Yates, University of Toronto. All of the remaining 4-substituted styrenes were known compounds and were synthesized using previously reported procedures. Physical constants were in good agreement with values from the literature. Full details of syntheses are reported elsewhere (21).

4-Vinylbiphenyl was sublimed at 80 °C and 0.1 mm immediately before use. Other styrenes were purified by vacuum distillation or recrystallization just before use. Purities were checked by n.m.r. spectroscopy and, in some cases, by v.p.c.

(b) Recording of Nuclear Magnetic Resonance Spectra

^{1}H spectra were recorded on a Varian HA-100 spectrometer operating in frequency sweep mode at a probe temperature of 30 ± 2 °C. Solvent cyclohexane was used as the lock and reference peak. Spectra were recorded and calibrated using previously reported procedures (16). The cyclohexane (Fisher A.C.S. grade) was fractionally distilled from sodium and stored over Linde 4A molecular sieve. Dissolved oxygen was purged by aeration with dry nitrogen immediately before sample preparation. Three styrene solutions were measured with concentrations in the range 1–5 mol %.

^{13}C spectra were obtained at 25.160 MHz using a Varian XL-100-15 spectrometer operating in pulsed Fourier transform mode with proton decoupling (probe temperature 32 ± 3 °C). Fourier transformations were performed using a Varian 620i computer (16K memory) and standard software. Spectra were recorded for 0.4 *M* solutions in CCl_4 with 8% C_6D_{12} as a lock signal and 1% tetramethylsilane as internal reference. ^{13}C spectra were not recorded for NH_2, CO_2CH_3, and $CO_2C_2H_5$ derivatives since these compounds were produced in very low yield.

Results

The vinyl proton spectra of 4-substituted styrenes were initially analyzed as ABC spectra by the exact method (22), using the computer program EXAN. The parameters from the exact method were further refined using the iterative computer programs LAOCN3 (23) or LACX (24). Computed r.m.s. errors between calculated and observed transition frequencies were <0.022 Hz.

No dilution shifts were observed for a number of compounds (OCH_2CH_3, SCH_3, CH_3, $C(CH_3)_3$, $Si(CH_3)_3$, $Ge(CH_3)_3$, $Sn(CH_3)_3$, and $Pb(CH_3)_3$) over the concentration range studied. The infinite dilution shifts were taken as the observed shifts at 2 mol % concentration. For other compounds, infinite dilution chemical shifts were estimated from least-squares plots of the dilution shifts. Dilution shifts were linear within experimental error. Standard deviations of the zero-concentration intercept were <0.0008 p.p.m. It is estimated that individual infinite dilution chemical shifts are accurate to 0.002 p.p.m. and that the internal chemical shift difference for the β protons, Δδ(B − C), is accurate to 0.001 p.p.m. Infinite dilution chemical shift data are reported in Table 1. Protons are labeled as shown in **1**. Although chemical

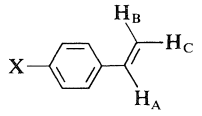

1

shifts were measured relative to cyclohexane they have been expressed relative to tetramethylsilane by adding 1.4457 p.p.m., the experimentally-determined chemical shift of cyclohexane, relative to tetramethylsilane at infinite dilution.[4] Coupling constant data are also given in Table 1.

^{13}C chemical shift data (relative to $^{13}CH_3Si(CH_3)_3$) are given in Table 2. Repeated runs for styrene with different frequency offsets, different spectral widths and concentrations from 0.1 to 0.4 *M* gave chemical shifts which were reproducible to 0.02 p.p.m. Consequently we believe that chemical shifts are accurate to at least 0.04 p.p.m. (1 Hz). Phenyl ^{13}C chemical shifts were assigned by assuming that S.C.S. for the styrene derivatives are very similar to those for phenyl derivatives (8, 25).

CNDO/2 calculations were performed using a standard program (26). Calculations were performed for two values of the styrene valence angle α (see Discussion) while standard parameters were used for other bond angles and bond lengths. For 4-aminostyrene, calculations were performed assuming both a planar NH_2 group and the previously reported pyramidal geometry (27). Full details of assumed geometrics for other substituents are tabulated elsewhere (21). Vinyl hydrogen and carbon charge densities and C-1 charge densities for α = 120° are given in Table 3 (other phenyl carbon charge densities and charge densities for α = 130° are on deposit in the Depository of Unpublished Data, National Science Library, National Research Council of Canada, Ottawa, Canada K1A 0S2).

Results of CNDO/2 calculations for 4-substituted 1-vinylbicyclo[2.2.2]octanes and methyl-X-ethylene pairs are summarized in Table 4.

Correlations of chemical shifts with *F* and *R*

[4]The previously reported value of 1.4438 (16) is in error. The data from ref. 16 have been corrected by adding 0.0019 p.p.m.

TABLE 1. Vinyl proton chemical shifts (in p.p.m. relative to $(CH_3)_4Si$) and coupling constants (Hz) for 4-substituted styrenes at infinite dilution in C_6H_{12}.

Substituent	δ(A)	δ(B)	δ(C)	Δδ(B − C)	J_{AB}	J_{AC}	J_{BC}
H	6.6289	5.6302	5.1135	0.5167	17.56	10.90	1.09
F	6.5914	5.5522	5.1012	0.4510	17.56	10.93	0.93
Cl	6.5821	5.6120	5.1469	0.4651	17.56	10.89	0.87
Br	6.5676	5.6300	5.1575	0.4725	17.55	10.89	0.87
I	6.5498	5.6417	5.1490	0.4927	17.56	10.89	0.89
Me	6.5742	5.5576	5.0353	0.5223	17.58	10.90	1.11
t-Bu	6.5943	5.5772	5.0513	0.5259	17.56	10.89	1.20
CF_3	6.6610	5.7309	5.2612	0.4697	17.55	10.91	0.73
NH_2	6.4942	5.4037	4.8909	0.5128	17.55	10.90	1.20
NMe_2	6.5032	5.3937	4.8637	0.5300	17.51	10.87	1.26
OMe	6.5612	5.4819	4.9867	0.4952	17.55	10.89	1.12
OEt	6.5404	5.4617	4.9647	0.4970	17.56	10.89	1.11
SMe	6.5624	5.5757	5.0684	0.5074	17.53	10.89	1.03
NO_2	6.7014	5.8069	5.3629	0.4440	17.57	10.93	0.58
C≡N	6.6302	5.7442	5.2999	0.4443	17.56	10.94	0.62
CH=CH_2	6.6002	5.6178	5.0981	0.5197	17.56	10.90	1.07
Ph	6.6553	5.6621	5.1287	0.5334	17.57	10.89	1.05
C≡CH	6.5968	5.6428	5.1601	0.4827	17.57	10.92	0.93
COMe	6.6636	5.7394	5.2427	0.4967	17.56	10.92	0.89
COOMe	6.6547	5.7288	5.2301	0.4987	17.54	10.91	0.89
COOEt	6.6587	5.7267	5.2264	0.5003	17.57	10.91	0.93
$SiMe_3$	6.6127	5.6445	5.1083	0.5362	17.58	10.87	1.15
$GeMe_3$	6.6285	5.6525	5.1151	0.5374	17.57	10.89	1.17
$SnMe_3$	6.5971	5.6293	5.0875	0.5418	17.54	10.90	1.14
$PbMe_3$	6.6131	5.6327	5.0864	0.5463	17.55	10.89	1.16

TABLE 2. ^{13}C chemical shifts for 4-substituted styrenes (in p.p.m. to low field of $^{13}CH_3Si(CH_3)_3$ at 25.160 MHz)

	Chemical shifts					
Group	C-4	C-3,5	C-2,6	C-1	C-α	C-β
H	127.46	128.15	126.00	137.40	136.96	113.20
F	162.77	115.59	127.87	133.95	136.11	113.43
Cl	133.53	128.49	127.13	135.69*	135.69*	113.97
Br	121.61	131.43	127.46	136.20	135.76	114.10
I	93.00	137.36	127.69	136.67	135.84	114.19
CH_3	136.73*	128.86	125.97	134.78	136.73*	112.20
$C(CH_3)_3$	150.06	124.96	125.78	134.67	136.69	112.39
CF_3	129.99	125.32	126.14	140.68	135.64	116.02
$N(CH_3)_2$	149.83	112.18	126.93	126.49	136.67	108.93
OCH_3	159.22	113.59	127.07	130.23	136.29	110.98
OC_2H_5	158.63	114.13	127.08	130.13	136.37	110.84
SCH_3	137.95	126.30†	126.47†	134.31	136.21	112.64
NO_2	147.41	123.65	126.43	143.08	135.03	117.90
C≡N	112.05	131.94	126.44	141.21	135.39	117.05
CH=CH_2	136.88	126.13	126.13	136.88	136.49	113.20
C_6H_5	—‡	—	—	—	136.47	113.23
C≡CH	121.64	132.04	125.80	137.60	136.22	114.44
$COCH_3$	136.53	128.35	125.95	141.35	136.07	115.91
$Si(CH_3)_3$	139.27	133.15	125.37	137.78	136.98	113.45
$Ge(CH_3)_3$	141.41	132.73	125.56	137.29	136.98	113.22
$Sn(CH_3)_3$	141.05	135.58	125.67	137.32	137.07	113.22
$Pb(CH_3)_3$	148.04	136.29	126.13	136.72	137.06	113.00

*Overlapping peaks.
†Assignment uncertain.
‡Phenyl carbons not assigned.

Can. J. Chem. Downloaded from www.nrcresearchpress.com by 210.87.254.105 on 09/05/12
For personal use only.

Can. J. Chem. Downloaded from www.nrcresearchpress.com by 210.87.254.105 on 09/05/12
For personal use only.

were performed using LMCL2, a linear least-squares multiple correlation program written by Unger and Swain (28) or the IBM SSP subroutine MULTR (29). A step-wise multiple regression subroutine, STPRG (29) was used for correlations with three independent variables (*i.e.* F, R, and $|R|$) in order to determine the relative significance of the variables entering the regression. All correlations and CNDO/2 calculations were performed on an IBM 360/65 computer.

Discussion

(a) Geometry of Styrene

The expected magnitudes of field and resonance effects in 4-substituted styrenes are very sensitive to the assumed geometry of styrene. While this is not precisely known, all available experimental data indicates that styrene is planar or nearly planar (30–32).

Calculated electric field effects upon the internal chemical shift of the β protons, $\Delta\delta(B - C)$, are particularly sensitive to the angle α between C-1, -α, and -β. Recently, it has been shown that α for *trans*-stilbene is accurately reproduced by CNDO/2 energy minimization calculations (33). Consequently, we attempted similar calculations for styrene.

Only the C_1—C_α bond length r, the C-α valence angle α, and the vinyl–phenyl dihedral angle ρ were treated as variables. A rigorous energy optimization was not attempted; instead r, α, and ρ were varied independently. Minima were found for r = 1.45–1.46 Å, α = 129–130°, and ρ = 90°. The values of r and α are consistent with experimental results for *trans*-stilbene (1.46 Å, 128°) (34) but the calculated value of ρ is completely inconsistent with available experimental evidence (30–32). The failure of CNDO/2 calculations to predict the most stable dihedral angle in conjugated aromatic molecules appears to be general since calculations for stilbene (31), benzaldehyde (35), and biphenyl (36) all give a minimum energy for ρ = 90°. Significantly, more sophisticated *ab initio* calculations for styrene give values of r and α similar to those for the CNDO/2 calculations (r = 1.46 Å, α = 128°) but predict minimum energy when ρ = 0° (37). In view of the above results, two geometries of the styrene molecule were employed in calculations: (*i*) standard (STD) geometry with α = 120°, r = 1.46 Å, and ρ = 0°, (*ii*) calculated (CNDO) geometry with α = 130°, r = 1.45 Å, and ρ = 0°. It is suspected that the correct value of α falls between these two extremes.

(b) Consideration of Possible Solute–Solute and Solvent–Solute Interactions

All of the styrene derivatives showed small dilution shifts which were linear, within experimental error, at low concentrations. Consequently, we are confident that the extrapolated infinite dilution ^1H chemical shifts are not affected by solute–solute interactions. Raynes and Raza have recently discussed the nature of cyclohexane solvent effects (38). They concluded that cyclohexane behaves as a magnetically isotropic molecule, does not show specific solvent effects, and that van der Waals' interactions should affect the different solute protons equally. However, their results suggest the presence of a reaction field effect. The reaction field should have a direction parallel to the solute electric dipole moment, μ (39):

$$[3] \qquad R = \tfrac{2}{3}\left(\frac{\varepsilon - 1}{2\varepsilon + n^2}\right)(n^2 - 1)\frac{\mu}{\alpha}$$

where n and α are respectively the refractive index and the polarizability of the solute and ε is the solution dielectric constant. According to this formula, the reaction field should, in many cases, cause shifts which are similar in sign and magnitude to those due to intramolecular field effects. However, Weiner and Malinowski concluded that eq. 3 should be modified by replacing ε by the effective dielectric constant, ε′ (40). For cyclohexane, ε′ = 1.0, *i.e.* it should not exert any reaction field effect. Our results support this viewpoint. If intramolecular field effects are dominant then $\Delta\delta(B - C)$ should depend upon the dipole moment of the C—X σ bond (16) while if reaction field effects are dominant, $\Delta\delta(B - C)$ will be determined by the molecular dipole moment. As shown below, $\Delta\delta(B - C)$ correlates very well with calculations based on C—X σ bond moments even for substituents such as OCH_3 where the C—X bond moment and the molecular dipole moment are grossly different (41). In addition, it has been shown that solvent shifts for 4-substituted styrenes are completely inconsistent with the reaction field model (16). Consequently, we believe that reaction field effects are much less important than intramolecular field effects for 4-substituted styrenes in cyclohexane and that cyclohexane

Can. J. Chem. Downloaded from www.nrcresearchpress.com by 210.87.254.105 on 09/05/12
For personal use only.

TABLE 3. Excess charge densities ($\times 10^4$, relative to unsubstituted styrene for 4-substituted styrenes (STD geometry))

	$N(CH_3)_2$	NH_2*	NH_2†	OH‡	OCH_3‡	CH_3	$C(CH_3)_3$	$CH{=}CH_2$‡	$C{\equiv}CH$	$COCH_3$‡	F	CF_3	CN	NO_2	Cl¶	SCH_3‡¶	$Si(CH_3)_3$¶	$Si(CH_3)_3$**
C-1_σ	+211	+231	+167	+147	+141	+58	+74	+19	+7	−80	+70	−96	−43	−158	+9	+49	+13	−145
C-1_π	− 560	−611	−452	−417	−400	−153	−213	−65	−36	+196	−240	+259	+90	+387	−86	−143	−22	+378
C-α_σ	−14	−16	−11	+1	−1	−6	−9	−1	+6	+18	+23	+40	+22	+66	+26	+8	−7	+3
C-α_π	+86	+94	+66	+49	+50	+26	+32	+8	−8	−49	0	−85	−45	−130	−21	+9	+8	−55
H_A	−37	−40	−27	−16	−18	−10	−14	−3	+6	+23	+9	+48	+27	+73	+18	0	−4	+23
C-β_σ	+86	+95	+69	+55	+55	+24	+33	+8	−2	−43	+15	−68	−32	−105	−7	+15	+6	−57
C-β_π	−211	−230	−164	−132	−131	−59	−78	−19	+8	+104	−33	+167	+82	+255	+19	−35	−15	+142
H_B	−30	−33	−24	−20	−19	−8	−11	−3	+1	+14	−7	+21	+10	+32	+1	−6	−1	+21
H_C	−31	−33	−22	−10	−11	−9	−12	−2	+7	+23	+17	+51	+29	+79	+23	+3	−4	+17
Δ§	+1	0	−2	−10	−8	+1	+1	−1	−6	−9	−24	−30	−19	−47	−22	−9	+3	+4
ΣC_π‖	−1012	−976	−688	−673	−693	−129	−237	+39	+46	+376	−473	+139	+179	+224	−289	−287	+37	+424

*Planar NH_2 group.
†Pyramidal NH_2 group.
‡Average of two planar conformations.
§$\Delta = \Delta q\ (H_B - H_C)$.
‖ ΣC_π = total change in π charge density.
¶3s and 3p orbitals only.
**3s, 3p, and 3d orbitals.

TABLE 4. Excess charge densities ($\times 10^4$, relative to the H substituent); methane–ethylene isolated molecules model (IM), 4-substituted 1-vinylbicyclo[2.2.2]octanes (VBCO), and 4-substituted styrenes (STY) (see text for details)

	NH_2*			OH†			F			NO_2		
	IM	VBCO	STY	IM	VBCO	STY	IM	VBCO	STY	IM	VBCO	STY
H_A	+2	+2	−40	+8	+11	−15	+13	+21	+9	+24	+44	+73
H_B	−1	−2	−33	−1	+1	−21	+5	+7	−7	+8	+16	+32
H_C	0	+1	−33	+8	+12	−10	+19	+27	+17	+37	+56	+79
Δ‡	−1	−3	0	−9	−11	−11	−14	−20	−24	−29	−40	−47

*Planar conformation of NH_2 group.
†Planar (syn) conformation of OH group.
‡$\Delta = \Delta q\,(H_B - H_C)$.

can be regarded as an inert solvent for investigations of ^1H S.C.S.

In order to confirm that CCl_4 was an inert solvent for ^{13}C chemical shift measurements, ^{13}C chemical shifts were determined for styrene and its 4-nitro and 4-*N*,*N*-dimethylamino derivatives in C_6D_{12}. S.C.S. for the latter two compounds were identical within 0.10 p.p.m. (0.05 p.p.m. for vinyl carbons) with those in CCl_4. Consequently, we believe that the ^{13}C chemical shifts in Table 2 are not affected by solvent effects.

(c) Predicted Nature of Substituent Effects in Styrene Derivatives

Three types of through-bond substituent effects will be considered: σ inductive effects, resonance effects, and π inductive effects. The latter two are respectively defined as involving (*i*) charge transfer between the substituent and the styrene π electron system and (*ii*) redistribution of π electron density without charge transfer. The σ inductive effect should contribute positively to *f*. Assuming that it depends on the number of intervening bonds, this effect should be greater for C-α than C-β. Similarly it should be greater for H_A and smaller and equal for H_B and H_C. By contrast, resonance effects should primarily affect π electron density at C-β (17*a*). Consequently, δ_{H_B} and δ_{H_C} correlations should have nearly identical *r* values with a smaller *r* value for δ_{H_A}. Similarly $\delta_{C\text{-}\beta}$ should show a greater *R* dependence than $\delta_{C\text{-}\alpha}$. π inductive effects should also affect δ_{H_B} and δ_{H_C} equally by altering electron density at C-β. However, the exact nature of these effects is controversial (42) and further comment will be reserved until section (*e*).

Through-space field effect contributions to individual protons can be estimated using the Buckingham equation which assumes that the field effect depends upon the electric field component acting along a C—H bond (43). Using STD geometry and assuming a dipole moment of 1.0 D located 0.9 Å along the C_4—X bond, calculated field components are: $E_z(A) = 7.5 \times 10^3$, $E_z(B) = -0.9 \times 10^3$, $E_z(C) = 7.0 \times 10^3$, and $\Delta E_z(B - C) = -7.9 \times 10^3$ e.s.u./cm^2. Through-space field contributions to *f* values for the individual proton correlations should be in approximately the same ratio. On the basis of the above discussion, δ_{H_B} and δ_{H_C} should be equally affected by through-bond effects and the only electronic substituent effect contributing to Δδ(B − C) should be the field effect.

S.C.S. for individual compounds may also be affected by the anisotropic magnetic susceptibility of the substituent. The contribution due to this term is given by:

$$[4] \qquad \delta_M = (1/3r^3) \sum_{i=1}^{3} \chi_i (3\cos^2\theta_i - 1)$$

where *r* is the distance between the centre of the induced magnetic dipole and the proton and θ_i is the angle between the *r* vector and the axis of one of three principal magnetic susceptibilities, χ_i (44). Finally, the substituent could alter the ring current effect of the phenyl group by resonance (45). The change in ring current depends upon the importance of quininoid structures:

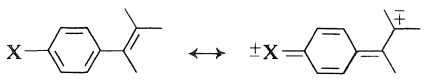

Following Yamada *et al.* (46), this effect should depend upon |*R*|.

(d) Field Dependence of Δδ(B − C)

The internal chemical shift difference for the β protons, Δδ(B − C), should depend upon the difference in substituent-induced electric fields acting along the C_β—H_B and C_β—H_C bonds, $\Delta E_z(B - C)$ (16). Following Cumper's sugges-

Can. J. Chem. Downloaded from www.nrcresearchpress.com by 210.87.254.105 on 09/05/12
For personal use only.

Can. J. Chem. Downloaded from www.nrcresearchpress.com by 210.87.254.105 on 09/05/12
For personal use only.

tion of assigning $\mu = 0$ for the C—H bond moment (47), the field dependence of $\Delta\delta(B - C)$ should be given by:

$$[5] \quad \Delta\delta(B - C) = A\Delta E_z(B - C) + \Delta\delta_0(B - C)$$

where $\Delta\delta_0(B - C)$ is the chemical shift difference for styrene and A is the constant in the Buckingham equation (43). We have expanded our previous correlation of this type to include three additional groups, CH_3, $C(CH_3)_3$, and CF_3 which have dipole moments acting along the phenyl-substituent bond. Groups whose dipole moment axes are poorly defined were avoided as far as possible. Aliphatic group moments (47) were chosen to eliminate resonance effects from the calculations. Calculations were performed for STD geometry with E_z evaluated both at the proton and halfway along the C—H bond[5] and for CNDO geometry with fields evaluated at the same position (parameters used in the calculations are given elsewhere (21)). In each case, A was estimated from the slope of the best straight line for eq. 5. Excellent correlations were obtained when halogens were omitted (correlation coefficients, $r > 0.998$) with respective A values for the four correlations listed above of 4.6×10^{-12}, 3.1×10^{-12}, 6.5×10^{-12}, and 4.0×10^{-12}. The second correlation is illustrated in Fig. 1. While A is extremely sensitive to the chosen geometry, the observed values are reasonably consistent with previous values which have ranged from 2 to 4.2×10^{-12} (1, 43) (A is positive for the δ scale). Evidence is presented in the following paper (49) which suggests that the larger A values may be significant. When the halogens were included, the correlations were worse but the A values were almost unchanged (*e.g.*, $r = 0.968$, $A = 3.2 \times 10^{-12}$ for the correlation in Fig. 1). Thus inclusion of the halogens does not alter the conclusion that $\Delta\delta(B - C)$ primarily reflects the field effect of the substituent. It is well established that halogens show deviations in plots of S.C.S. which cannot be attributed to magnetic anisotropy effects (16, 50, 51). Possible origins for the deviations are discussed below.

Electrostatic calculations were also performed for 4-ethynyl and 4-cyanostyrene. After correction for the magnetic anisotropy effect of the triple bonds (see section (*f*)) these points lie close to the straight line in Fig. 2.

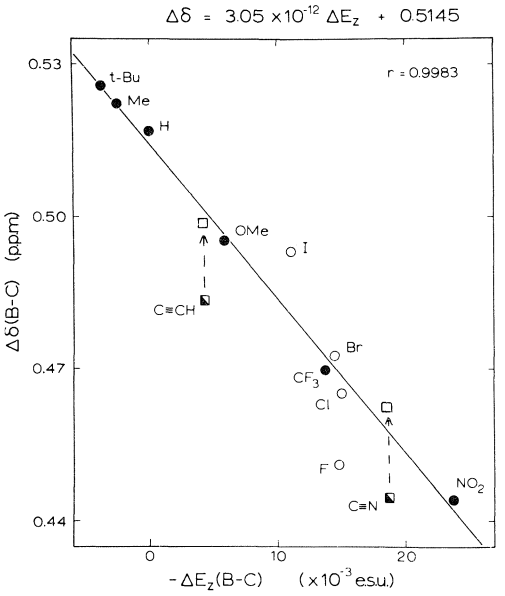

FIG. 1. Correlation of β proton chemical shift difference, $\Delta\delta(B - C)$ *vs.* difference in electric field along C_β—H_B and C_β—H_C bond, $\Delta E_z(B - C)$. Solid points are used for correlation. Uncorrected chemical shifts for the cyano and ethynyl groups (◪) and values corrected for magnetic anisotropy effects (□) (see section (*f*)) are also plotted.

An alternative approach for demonstrating the through-space field dependence of $\Delta\delta(B - C)$ is to correlate $\Delta\delta(B - C)$ with the field substituent parameter F. However, in view of the criticism of Wiley and Miller of the use of F and R for investigations of S.C.S. (4), F was first correlated with $\Delta E_z(B - C)$ to confirm that F was a measure of the electric field effect as calculated by the Buckingham equation. A very good correlation was obtained ($r = 0.989$) confirming that F is a valid measure of the through-space field effect. No deviations were noted for the halogens. Since F and $\Delta E_z(B - C)$ both measure only electronic effects, this suggests that the deviations for the halogens in the chemical shift plots are magnetic in origin.

The initial correlation of F *vs.* $\Delta\delta(B - C)$ was performed for 19 styrenes. F and R values were available for all substituents except the dimethylamino and ethynyl groups. F and R values can be calculated from σ_m and σ_p values (5). A variety of σ_p values have been reported for the dimethylamino group (52). $\sigma_p = -0.622$ (52) was chosen because it was determined for

[5]Buckingham suggested that E_z should be evaluated at the proton (43) while Musher argued that it should be evaluated halfway along the C—H bond (48).

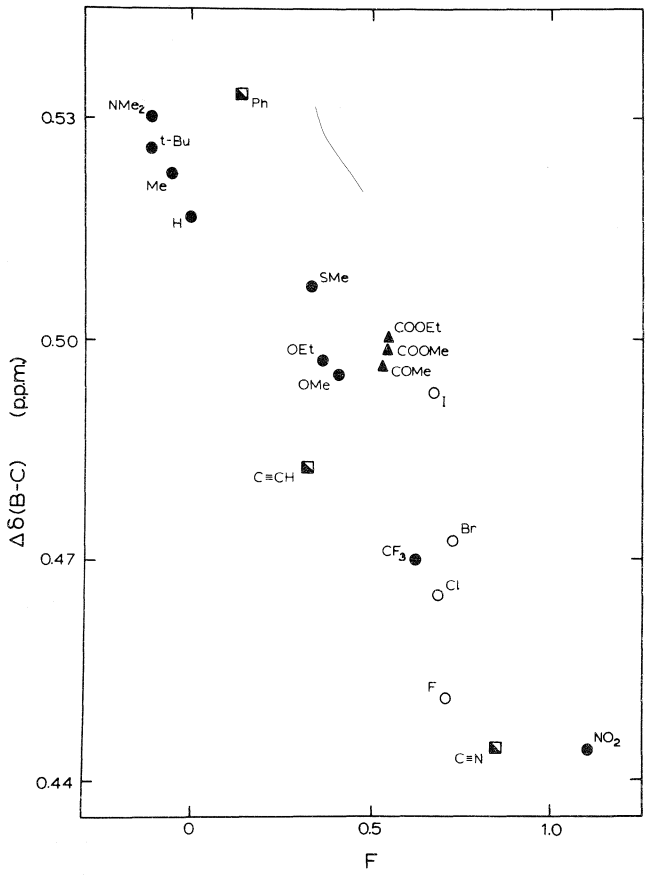

FIG. 2. Plot of β proton chemical shift difference *vs.* *F*. ◪ represents points for which anisotropic corrections are estimated while ▲ represents points for which revised *F* values are estimated (see section (*f*)).

reactants (*e.g.* $XC_6H_4CH{=}CHC_6H_5$ and $XC_6H_4CH{=}NOH$) which are electronically similar to styrene. *F* and *R* were then estimated as respectively −0.097 and −0.568. For the ethynyl group, σ_m and σ_p values from Landgrebe and Rynbrandt (53) were used to estimate $F = +0.317$, $R = +0.055$. Other *F* and *R* values were taken from the original tabulation (5).

A correlation of $\Delta\delta(B - C)$ *vs.* *F* for 19 4-substituted styrenes is shown in Fig. 2. A general relationship is apparent although the correlation coefficient is not very good ($r = 0.891$). A correlation with *F* and *R* gave a statistically insignificant *r* value, indicating that the scatter is not due to resonance contributions. However, closer inspection indicated that most of the larger deviations could be due to the expected magnetic anisotropy effect of the substituent. The cyano and ethynyl groups should shield all protons of the vinyl group while phenyl and carbonyl groups should deshield them (54, 55). Since H_B is closer to the substituent than H_C, this will decrease $\Delta\delta(B - C)$ for the first two groups and increase it for the other substituents, as noted in Fig. 2. The anomalous behavior of the halogens has been previously discussed.

Removal of the ten above-mentioned substituents left nine ($N(CH_3)_2$, $C(CH_3)_3$, CH_3, H, OCH_3, OC_2H_5, SCH_3, CF_3, and NO_2). All except NO_2 contain only single bonds and all except SCH_3 involve only first row elements. Consequently they would be expected to have small anisotropic effect. Available evidence (56, 57) indicates that the magnetic anisotropy effect of the NO_2 group should be small compared to S.C.S. (*e.g.* $\Delta\delta_M(B - C) = -0.005$ p.p.m. for $\Delta\chi$ values from ref. 56). Consequently no magnetic anisotropy corrections were applied for the NO_2 derivative. In the case of the 4-

Can. J. Chem. Downloaded from www.nrcresearchpress.com by 210.87.254.105 on 09/05/12
For personal use only.

TABLE 5. Test for possible corrections to experimental chemical shifts due to anisotropic magnetic susceptibility effects and to F values for carbonyl substituents

	C_6H_5			C≡N ($\Delta\chi = -28.8 \times 10^{-30}$ cm^3/molecule)		
	$\delta_{exp.} - \delta_{calcd.}$*	δ_M†	Corrected‡ $\delta_{exp.}$	$\delta_{exp.} - \delta_{calcd.}$	δ_M§	Corrected $\delta_{exp.}$
δ_{H_A}	+0.0487	+0.0593	6.5960	−0.0636	−0.0572	6.6874
δ_{H_B}	+0.0545	+0.0612	5.6009	−0.0448	−0.9535	5.7977
δ_{H_C}	+0.0305	+0.0380	5.0907	−0.0286	−0.0348	5.3347
$\Delta\delta$(B − C)	+0.0227	+0.0231	0.5103	−0.0187	−0.0187	0.4630

	C≡C—H ($\Delta\chi = -25.0 \times 10^{-30}$ cm^3/molecule)			F	Cl	Br	I
	$\delta_{exp.} - \delta_{calcd.}$	δ_M§	Corrected $\delta_{exp.}$	$\delta_{exp.} - \delta_{calcd.}$	$\delta_{exp.} - \delta_{calcd.}$	$\delta_{exp.} - \delta_{calcd.}$	$\delta_{exp.} - \delta_{calcd.}$
δ_{H_A}	−0.0456	−0.0491	6.6459	+0.0011	−0.0397	−0.0553	−0.0643
δ_{H_B}	−0.0409	−0.0460	5.6888	−0.0104	−0.0204	+0.0001	+0.0258
δ_{H_C}	−0.0271	−0.0299	5.1900	+0.0131	−0.0114	−0.0007	+0.0087
$\Delta\delta$(B − C)	−0.0160	−0.0160	0.4897	−0.0214	−0.0085	+0.0014	+0.0178

	$COCH_3$(corrected $F = +0.347$)				CO_2CH_3, $CO_2C_2H_5$ (corrected $F = +0.306$)	
	$\delta_{exp.} - \delta_{calcd.}$	$\delta_{M(1)}$‖	$\delta_{M(68)}$¶	$f\Delta F$**	$\delta_{exp.} - \delta_{calcd.}$††	$f\Delta F$**
δ_{H_A}	−0.0173	+0.0133	+0.0173	−0.0097	−0.0137	−0.0128
δ_{H_B}	−0.0241	+0.0146	+0.0129	−0.0185	−0.0140	−0.0244
δ_{H_C}	−0.0418	+0.0079	+0.0064	−0.0308	−0.0333	−0.0404
$\Delta\delta$(B − C)	+0.0126	+0.0069	+0.0064	+0.0126	+0.0166	+0.0166

*Experimental chemical shift − calculated chemical shift (from eight point correlation equations) in p.p.m.
†Estimated magnetic anisotropy contribution, determined by ring current calculation (58).
‡$\delta_{exp.} - \delta_M$.
§Estimated magnetic anisotropy contribution, using $\Delta\chi$ value estimated from $\Delta\delta(B - C)_{exp.} - \Delta\delta(B - C)_{calcd.}$ and eq. 4.
‖Calculated using $\Delta\chi$ values from ref. 1.
¶Calculated using $\Delta\chi$ values from ref. 68.
**Correction factor for calculated chemical shifts, obtained by estimating a new F value from the eight point correlation equation for $\Delta\delta$(B − C).
††Using average chemical shifts for the two esters.

phenyl derivative, it was found that the deviations between calculated and observed ^{1}H chemical shift both for $\Delta\delta$(B − C) and for the individual protons closely corresponded to the calculated ring current effect of the phenyl group as determined by the approach of Johnson and Bovey (58) (assuming a dihedral angle between the phenyl groups of 21° since ρ = 19–23° for biphenyl in cyclohexane (30)). Consequently ^{1}H chemical shifts for the phenyl derivative were corrected for ring current effects (see Table 5) and included in the correlation. Results of the ten point correlation are given in Table 6. $\Delta\delta$(B − C) still depends only upon F but with a much improved correlation coefficient. However, the most important observation is that the f value for the correlation in which groups with uncertain magnetic effects are eliminated is the same within experimental error as the f value for the original 19 point correlation. Consequently, we conclude that deviations of individual points due to magnetic contributions do not obscure overall trends in electronic effects upon ^{1}H S.C.S. *provided that enough points are included in the correlation.* Both the full correlation and the restricted correlation indicate that $\Delta\delta$(B − C) is dominated by field effects.

The dipolar electric field due to a substituent should polarize a C—H bond (48), altering the electron density in the hydrogen 1s orbital. Consequently, the difference in charge density between H_B and H_C of a 4-substituted styrene should reflect the field effect of the substituent.[6] We designate this difference, measured relative to styrene, as $\Delta(\Delta = (q_{H_B} - q_{H_C})_X - (q_{H_B} - q_{H_C})_H)$. A plot of Δ *vs.* $\Delta\delta$(B − C) (with anisotropic corrections for the cyano and ethynyl

[6]A preliminary account of part of this work has appeared elsewhere (15).

Can. J. Chem. Downloaded from www.nrcresearchpress.com by 210.87.254.105 on 09/05/12
For personal use only.

TABLE 6. Correlation of vinyl proton chemical shifts (δ scale) *vs.* field, *F*, and resonance, *R*, substituent parameters (*f* and *r* values used to estimate Δχ or *F* and *R* values are given to four significant figures)

Points	Chemical shift	*f**	*r**	δ_0	*r*	S.d.† (p.p.m.)
19	δ(A)	0.013±0.021	0.181±0.029	6.616	0.852	0.027
	δ(B)	0.086±0.017	0.376±0.025	5.625	0.977	0.023
	δ(C)	0.162±0.014	0.371±0.019	5.100	0.989	0.018
	Δδ(B − C)‡	−0.074±0.009	—	0.521	0.891	0.013
10§	δ(A)	0.047±0.018	0.176±0.026	6.612	0.951	0.018
	δ(B)	0.094±0.017	0.409±0.025	5.629	0.990	0.017
	δ(C)	0.160±0.016	0.418±0.024	5.110	0.993	0.017
	Δδ(B − C)	−0.069±0.004	—	0.521	0.984	0.005
8‖	δ(A)	0.0520±0.014	0.1851±0.022	6.616	0.973	0.014
	δ(B)	0.0991±0.015	0.4088±0.024	5.630	0.993	0.015
	δ(C)	0.1646±0.014	0.4182±0.023	5.112	0.995	0.015
	Δδ(B − C)	−0.0674±0.002	—	0.520	0.996	0.003
19¶	δ(A)	0.025±0.015	0.201±0.022	6.616	0.927	0.021
	δ(B)	0.096±0.012	0.408±0.016	5.630	0.990	0.016
	δ(C)	0.166±0.010	0.410±0.014	5.109	0.994	0.014
	Δδ(B − C)	−0.070±0.005	—	0.521	0.951	0.008
15**	δ(A)	0.046±0.013	0.184±0.017	6.613	0.972	0.014
	δ(B)	0.095±0.014	0.408±0.018	5.630	0.993	0.016
	δ(C)	0.161±0.013	0.417±0.017	5.111	0.995	0.015
	Δδ(B − C)	−0.069±0.003	—	0.521	0.987	0.004
13‖	δ(A)	0.0507±0.009	0.1816±0.012	6.614	0.987	0.010
	δ(B)	0.1004±0.011	0.4142±0.014	5.632	0.996	0.012
	δ(C)	0.1661±0.010	0.4196±0.014	5.113	0.997	0.012
	Δδ(B − C)	−0.0674±0.002	—	0.520	0.997	0.002

*Coefficients for equation $\delta = fF + rR + \delta_0$ plus standard errors in coefficients.
†Standard deviation between calculated and experimental chemical shifts.
‡Correlation with *F* only.
§F, Cl, Br, I, C≡N, C≡C—H, $COCH_3$, CO_2CH_3, $CO_2C_2H_5$ omitted, C_6H_5 δ values corrected for magnetic anisotropy effects.
‖SCH_3, CF_3 omitted.
¶C_6H_5, C≡N, C≡CH δ values corrected for magnetic anisotropy effects, revised *F* values for $COCH_3$, CO_2CH_3, $CO_2C_2H_5$.
**F, Cl, Br, I omitted.

groups) is shown in Fig. 3. For STD geometry (Fig. 3) the slope of the plot of Δδ(B − C) *vs.* Δ is 18.0 p.p.m./hydrogen 1s electron while for CNDO geometry (not shown) the slope is 23.2 p.p.m./hydrogen 1s electron. Both values are in excellent agreement with previously determined scaling factors which have ranged from 17.8 (59) to 26.6 (60) p.p.m./hydrogen 1s electron. However, deviations are again noted for some substituents. Field effects for CF_3 and NO_2 groups appear to be overestimated while the effect of the cyano group is underestimated. Similar deviations have been noted for dipole moments of $C_6H_5NO_2$ and $C_6H_5C{\equiv}N$ (14), indicating that CNDO/2 calculations do not precisely reproduce the charge distributions induced by these substituents.[7] However, this quantitative failure of the calculations for individual substituents does not obscure the overall trend shown in Fig. 3. This provides further evidence for the existence of a through-space electric field effect which affects ^1H chemical shifts by polarizing C—H bonds.

We have now shown that three independent measures of the electric field effect (classical electrostatic calculations, field substituent constants and charge densities estimated by MO calculations) indicate that Δδ(B − C) is dominated by field effects. In the first and third approaches, scaling factors relating field components and charge densities with chemical shifts are in good agreement with previously reported scaling factors (there is no *a priori* method for predicting a value of *f* for the second correlation). We believe that the results in this section represent the most convincing evidence yet presented for the existence of an intramolecular field effect upon proton chemical shifts.

[7]The correlation coefficient is significantly improved ($r = 0.967$) if charge densities for nitro and cyano derivatives are scaled to correctly reproduce the dipole moments.

Can. J. Chem. Downloaded from www.nrcresearchpress.com by 210.87.254.105 on 09/05/12
For personal use only.

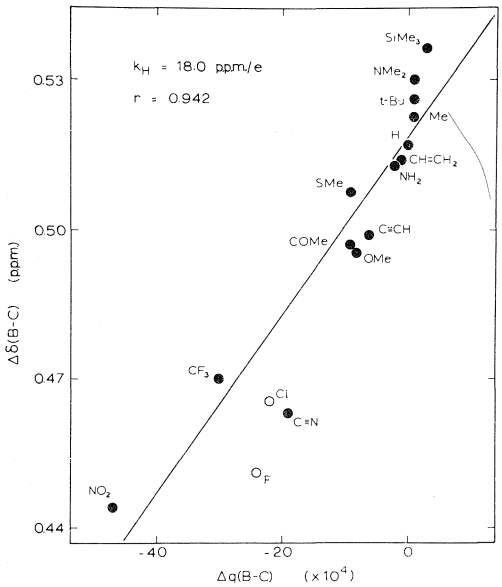

FIG. 3. Correlation of $\Delta\delta(B - C)$ with difference in calculated charge density for β protons of 4-substituted styrenes (halogens excluded).

(e) Substituent Effects upon Individual Vinyl Protons and Carbons

Correlations of vinyl proton chemical shifts with F and R were performed for the original 19 point set, for the restricted set of ten outlined in section (*d*) and for a further set in which two of the ten styrenes (CF_3 and SCH_3) were eliminated since they showed significantly larger deviations than the other eight. Results for the three sets of correlations are summarized in Table 6. The restricted set correlations were carried out in order to get the best possible lines to be used in evaluating magnetic anisotropy effects and unknown or uncertain F and R parameters (see section (*f*)). While the correlation coefficients are significantly improved for the ten and eight point correlations, it is most important to note that the pattern of f and r values is nearly identical for the three sets of correlations. This provides further evidence that magnetic effects upon individual protons do not obscure the overall pattern of electronic effects. Correlations were also performed against F, R and $|R|$. In each case the t test (61) indicated a less than 60% probability of a non-zero coefficient for $|R|$ with particularly small values in the case of δ_{H_A} ($\ll 50\%$) which should be most sensitive to variation in ring current. By contrast both f and r always exceeded 95% confidence limits and usually exceeded 99% confidence limits. Consequently, we conclude that there is a statistically insignificant contribution to S.C.S. for 4-substituted styrenes from the variation of ring current with substituent.

In addition to having similar values for the different sets of data points, the f and r values are consistent with the model of substituent effects outlined in section (*c*). For each set, r values for δ_{H_B} and δ_{H_C} are identical within the uncertainty in r and are much larger than the r values for δ_{H_A}. In all cases the correlation of $\Delta\delta(B - C)$ *vs.* F is insignificantly improved by a correlation with R, confirming that $\Delta\delta(B - C)$ is dominated by field effects. f is larger for δ_{H_C} than for δ_{H_B}, as predicted. However, f values for the individual proton correlations indicate that some additional effect is operative. Based on $f = -0.067_4$ for the correlation of $\Delta\delta(B - C)$ with F, predicted f values for δ_{H_A}, δ_{H_B}, and δ_{H_C} (using the values of E_z quoted in section (*c*)) are respectively $+0.064$, -0.007 and $+0.060$. The difference between predicted and observed values is $-(0.01 - 0.05)$ for δ_{H_A} and $+(0.09 - 0.11)$ for δ_{H_B} and δ_{H_C}. These residual f values are completely inconsistent with expected contributions due to σ inductive effects, indicating that these effects are insignificant in this system. However, ^{13}C chemical shifts and π charge densities for the vinyl group indicate that the residual field dependence can be attributed to a form of π inductive effect.

All available styrene derivatives were included in correlations of ^{13}C chemical shifts with F and R since magnetic effects should be negligible compared to the large ^{13}C S.C.S. (results presented in section (*f*) indicate $\delta_M < 0.10$ p.p.m. for vinyl carbons and protons). Interestingly, halogens fitted about as well as other points, providing further evidence that the deviations for these points in ^1H S.C.S. investigations are magnetic in origin. Results of the correlations are given by eqs. 6 and 7. One

$$[6]\quad \delta_{C\text{-}\alpha} = -(1.30 \pm 0.07)F - (0.35 \pm 0.13)R \quad (r = 0.974)$$

$$[7]\quad \delta_{C\text{-}\beta} = +(2.82 \pm 0.15)F + (7.14 \pm 0.27)R \quad (r = 0.991)$$

important observation is that the f values for C-α and C-β are very similar in pattern to the residual f values for the corresponding protons,

Can. J. Chem. Downloaded from www.nrcresearchpress.com by 210.87.254.105 on 09/05/12
For personal use only.

Can. J. Chem. Downloaded from www.nrcresearchpress.com by 210.87.254.105 on 09/05/12
For personal use only.

i.e. positive for C-β and smaller and negative for C-α.

The MO calculations indicate that substituent induced changes in vinyl charge density are dominated by changes in π electron density. This is particularly apparent for C-β where changes in σ charge density simply mirror changes in π charge density, as previously suggested (14):

$$[8] \qquad \text{C-}\beta_\sigma \approx -0.4\text{C-}\beta_\pi$$

Consequently, π charge densities were correlated with F and R:

$$[9] \quad \text{C-}\alpha_\pi = -(0.0075 \pm 0.0010)F - (0.0132 \pm 0.0014)R$$

$$[10] \quad \text{C-}\beta_\pi = +(0.0140 \pm 0.0022)F + (0.0314 \pm 0.0029)R$$

Again the f values are similar in pattern to those observed for the ^{1}H and ^{13}C chemical shift correlations. In addition, the ratios of f for chemical shift and charge densities are respectively 173 and 201 p.p.m./π electron for C-α and C-β, in excellent agreement with previously reported scaling factors for ^{13}C chemical shifts of 160–200 p.p.m./π electron (62, 63).[8] The charge densities indicate that the field dependence of the vinyl carbons and the residual field dependence of the vinyl protons (after subtraction of through-space field effects) arise from some mechanism which alters the π electron density but is proportional to F. We suggest that the mechanism is a polarization of the styrene π electron system by the polar C—X bond, leading to a polarization of the vinyl group. The exact nature of this π polarization effect is discussed in greater detail in the following paper (49). Further evidence for π polarization effects in phenyl derivatives has been obtained from ^{13}C spectra of phenylalkanes with α and β substituents (64). In addition, ^{13}C spectra of *trans*-1-substituted 1,3-butadienes also provide evidence of π polarization effects in these compounds (65). Consequently, we believe that π polarization effects are more important than previously realized (42).

The ^{13}C chemical shifts and charge densities also provide information about resonance effects. The C-β correlations indicate a substantial resonance effect at this carbon, as predicted in section (*c*) (with a reasonable ratio of r values of 228 p.p.m./π electron). However, the correlations suggest a negligible or slight negative resonance contribution for C-α (the calculations apparently overestimate this contribution since the ratio of r values is only 27 p.p.m./π electron). This is apparently anomalous since the proton correlations indicate a significant positive R dependence for δ_{H_A}. However, the vinyl proton charge densities indicate that this is not really an anomaly at all. For example, for 4-methoxystyrene, q_{H_A} is negative even though C-α_π is positive and through-space field effects should also make q_{H_A} positive. The negative charge for q_{H_A} apparently reflects the effect of the large negative π charge density at C-1 (see Table 3). C-1_π is primarily determined by resonance effects:

$$[11] \quad \text{C-}1_\pi = +(0.017 \pm 0.006)F + (0.086 \pm 0.007)R$$

This is confirmed by the ^{13}C chemical shift correlations:

$$[12] \quad \delta_{\text{C-1}} = +(2.98 \pm 0.37)F + (15.78 \pm 0.69)R \quad (r = 0.985)$$

(the ratio of f values is 175 p.p.m./π electron while the ratio of r values is 1.83 p.p.m./π electron, in good agreement with accepted values (62, 63)). We believe that the resonance dependence of δ_{H_A} arises from a through-space transmission of the effect of the large π charge density at C-1 (and to a lesser extent at C-β).

The above results indicate that a substantial fraction of the substituent effects in 4-substituted styrenes are transmitted through the π electron system. In an attempt to separate through-space field effects from effects transmitted through the π electron system and to confirm the validity of the Buckingham equation for field effects (43), calculations were performed for model compounds with no intervening π electron system. The compounds were 4-substituted 1-vinylbicyclo[2.2.2]octanes (VBCO) and pairs of molecules; ethylene and CH_3X molecules arranged so that the C—X bond and the ethylene molecule were in the same orientation as the C—X bond and the vinyl group in VBCO. Substituent-induced changes in vinyl charge densities (see Table 4) are in both cases consistent

[8]The validity of relating ^{13}C S.C.S. due to remote substituents with carbon charge densities is discussed elsewhere (64).

with the predictions of the Buckingham equation, *i.e.* $q_{H_A} \approx q_{H_C} \gg q_{H_B}$, confirming that the latter equation correctly predicts the geometric dependence of the electric field effect. However, the sensitivity of the vinyl protons to field effects (as measured by Δ) apparently depends upon the nature of the intervening molecular framework. This point is further discussed in the following paper (49).

In summary, correlations of ^1H chemical shifts (after correction for through-space field effects), ^{13}C chemical shifts, and carbon charge densities with F and R provide a consistent picture of electronic effects transmitted through the carbon framework of styrene. It is concluded that the two mechanisms of transmission of these through-bond effects are resonance and π polarization interactions. These two mechanisms plus a field effect similar to that predicted by the Buckingham equation can completely account for the f and r values for the ^1H and ^{13}C chemical shift correlations as well as the pattern of calculated charge densities.

(f) Estimation of Δχ Values or F and R Values for Individual Substituents

As pointed out in section (*d*), individual points showed deviations which might be due to magnetic anisotropy effects. We decided to use the individual ^1H correlations in conjunction with eq. 4 in an attempt to determine Δχ values. For substituents with axially symmetric magnetic susceptibilities, Δχ was estimated from the difference between the observed Δδ(B − C) value and the value calculated from the eight point correlation equation for Δδ(B − C) *vs.* F (see Fig. 4), using eq. 4. This Δχ value was then tested to see whether it could account for the deviations from the individual proton correlations. This is a rigorous test since the three individual proton correlations with F and R should be completely independent.

Results for C≡N, C≡C—H, F, Cl, Br, and I substituents are summarized in Table 5. The calculated correction factors for the first two groups are in good agreement with the differences between calculated and experimental chemical shifts. Assuming STD geometry, the correction factor for C≡N corresponds to $\Delta\chi = -29 \times 10^{-30}$ cm^3/molecule while for CNDO geometry it is $\Delta\chi = -39 \times 10^{-30}$ cm^3/molecule. Corresponding values for C≡C—H are respectively -25×10^{-30} and -34×10^{-30}

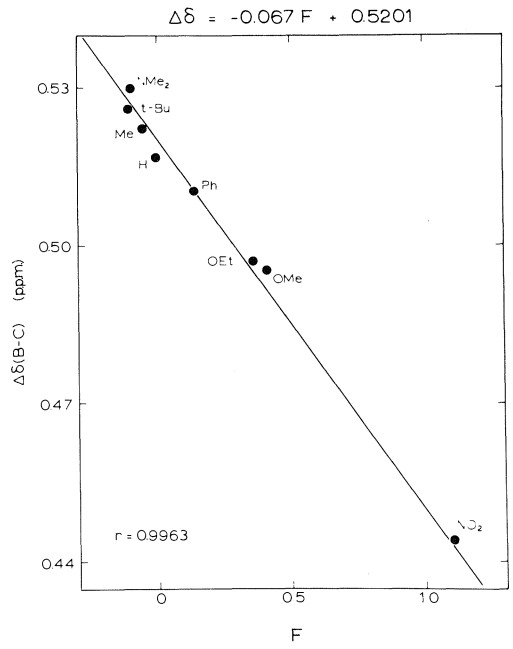

FIG. 4. Eight point correlation of Δδ(B − C) *vs.* F (phenyl corrected for ring current effects) used in section f to estimate Δχ and revised F values.

cm^3/molecule. All values are in good agreement with previously reported values which have ranged from -27×10^{-30} (66) to -34×10^{-30} cm^3/molecule (67) for both substituents. By contrast, deviations for the halogens are totally erratic and cannot be accounted for in terms of magnetic anisotropy effects. However, the correlation of F *vs.* ΔE_z(B − C) and the ^{13}C chemical shift correlations both indicate that the deviations are due to some type of magnetic effect, although the exact nature of the effect is unclear.

Since substituents containing the carbonyl group are characterized by two Δχ values (and two non-equivalent conformations of the vinyl group), correction factors cannot be estimated from the Δδ(B − C) correlation by itself. Instead, previously reported Δχ values for the C=O group (1, 68) were used to calculate correction factors. The calculated correction factors for the individual protons all have the wrong sign (Table 5). However, it was noted that the deviations parallel the signs and magnitudes of the f values for the four correlations, suggesting incorrect F values for carbonyl substituents. Consequently, we used the Δδ(B − C) correlation to estimate new F values (using an average deviation for the two esters). In

Can. J. Chem. Downloaded from www.nrcresearchpress.com by 210.87.254.105 on 09/05/12
For personal use only.

TABLE 7. Estimated F and R values for various substituents estimated from the 13 point correlations for δ(B) and δ(C)

Substituent	F	R	$\delta(A)_{exp.}$	$\delta(A)_{calcd.}$	Δ
$Si(CH_3)_3$	-0.26_6	$+0.09_5$	6.613	6.619	−0.006
$Ge(CH_3)_3$	-0.28_6	$+0.11_9$	6.629	6.622	+0.007
$Sn(CH_3)_3$	-0.35_2	$+0.07_9$	6.597	6.611	−0.014
$Pb(CH_3)_3$	-0.42_1	$+0.10_4$	6.613	6.612	+0.001
NH_2	$+0.14_5$	-0.58_6	6.494	6.516	−0.022
$CH{=}CH_2$	-0.00_4	-0.03_3	6.600	6.609	−0.009

each case, the agreement for all three protons is improved using the new, smaller F values. It is interesting to note that the corresponding σ_I values for carbonyl substituents determined from chemical shift measurements in aprotic solvents are approximately 50% smaller than those determined from reactivity measurements (69). This was the only type of substituent for which an effect of this type was noticed. Therefore, we believe it is reasonable that F for carbonyl substituents determined from chemical shifts in inert solvents appear to be significantly smaller than F values determined from reactivity measurements, even though this is contrary to the original assumption of Swain and Lupton that F and R are independent of the system (5). While this implies an insignificant magnetic anisotropy effect for the carbonyl group, anticipated δ_M values are small and might be difficult to detect by our approach. Deviations for CF_3 and SCH_3 groups could not be accounted for by any single correction involving F, R, or $\Delta\chi$. However, the deviations may be due to some combination of these effects.

Corrected δ values for C≡N and C≡C—H derivatives and corrected F values for carbonyl substituents were included in new 19 point, 15 point (halogen omitted), and 13 point (CF_3, SCH_3 omitted) correlations. Results are summarized in Table 6. With the corrected values, correlation coefficients are further improved but the f and r values are not significantly altered.

In view of the excellent correlations for the corrected 13 point set, it was decided to use these correlations to estimate F and R parameters for other substituents. Consequently, the 4-$(CH_3)_3$M-styrenes (M = Si, Ge, Sn, Pb) were synthesized. F and R were evaluated by simultaneously solving the 13 point correlations for δ_{H_B} and δ_{H_C}. The results are summarized in Table 7. The derived F and R values were checked by using them to evaluate δ_{H_A}. δ_{H_A} should be a sensitive probe for anisotropic effects since these effects should be relatively larger for δ_{H_A} than for δ_{H_B} and δ_{H_C} while field and resonance effects should be smaller. In fact, differences between calculated and observed δ_{H_A} values are small and show no evidence of persistent deviations due to anisotropic effects. Swain and Lupton (5) calculated $F = -0.047$ and $R = -0.044$ for the $(CH_3)_3Si$ group from measurements of benzoic acid dissociation constants. There have been several other determinations of σ constants for the $(CH_3)_3Si$ group (70). All of these give F negative and R positive with an average of $F = -0.23$ and $R = +0.15$, in good agreement with our results. The other $(CH_3)_3M$ substituents show increasingly negative F values on going from Si to Pb, consistent with previous conclusions concerning the inductive effects of these substituents (70). By contrast, the R values are essentially constant throughout the series. The $+R$ values could be taken as an indication of d(π)—p(π) bonding although we would not have anticipated that this effect should be constant throughout the series. The CNDO/2 calculations throw further light on the possibility of d(π)—p(π) bonding. The total change in π electron density, $\sum C_\pi$ is a measure of the resonance effect of the substituent (14). In the case of the $(CH_3)_3Si$ group (see Table 3), $\sum C_\pi$ is positive even when 3d orbitals are excluded from the calculation, indicating that it is not necessary to invoke d(π)—p(π) bonding to account for the $+R$ effect of the $(CH_3)_3Si$ group.

4-Aminostyrene was not included in the original correlations since it was not obtained in sufficient yield and purity until the correlations were completed. Consequently, it was decided to evaluate F and R from δ_{H_B} and δ_{H_C} and compare them with reported values. Results are given in Table 7. Calculated values of F and R are both more positive than those given by Swain and

Can. J. Chem. Downloaded from www.nrcresearchpress.com by 210.87.254.105 on 09/05/12
For personal use only.

Can. J. Chem. Downloaded from www.nrcresearchpress.com by 210.87.254.105 on 09/05/12
For personal use only.

Lupton (respectively +0.037 and −0.681) (5) although deviations are not much greater than the estimated probable error of ±0.05. It is interesting to compare the derived F and R values for NH_2 with those calculated for $N(CH_3)_2$ from σ constants estimated for electronically similar systems (see above). The R values are very similar but the F values are of opposite sign. By contrast, σ_I for NH_2 and $N(CH_3)_2$ are reported to have an identical value of +0.10 (69). However, both the values of Δδ (B − C) (Table 1) and the Δ values (Table 3) for the NH_2 and $N(CH_3)_2$ derivatives indicate that F has opposite signs for the two substituents. The CNDO/2 calculations also indicate the resonance effects of these groups are extremely sensitive to geometry. This may account for the sensitivity of σ_p values for amino groups to the nature of the reaction (52). F and R values for the vinyl group correlations are also given in Table 7. While it is possible that these values may not be very accurate due to magnetic anisotropy effects, they do suggest that the substituent effect of the vinyl group is small. This is confirmed by the charge densities for divinylbenzene (Table 3). This suggests that the vinyl group is a particularly useful probe for electronic effects since it is nearly electronically neutral. In summary, the correlations of δ *vs.* F and R have been used to obtain self-consistent Δχ values for several substituents which are in good agreement with previously reported values. They have also been used to estimate self-consistent and reasonable F and R values for other substituents. However, results for the halogens are anomalous and these substituents should be avoided in investigations of S.C.S., or at very least not included in limited data sets.

(g) Vinyl Proton Coupling Constants

The geminal coupling constants for 4-substituted styrenes are equally sensitive to field and resonance effects:

$$[13]\quad J_{BC} = (-0.38F - 0.37R + 1.07)\text{Hz} \qquad (r = 0.988)$$

By contrast, vicinal coupling constants are constant within experimental error. This is very surprising since both vicinal and geminal coupling constants vary with substituent in most vinyl compounds (71). At present we have no explanations for these observations.

Conclusions

Correlations of the chemical shift difference for the β protons, Δδ(B − C), with electrostatic calculations based on the Buckingham equation, with the field substituent parameter F, and with hydrogen charge densities estimated by CNDO/2 MO calculations demonstrate conclusively that Δδ(B − C) reflects a through-space electric field effect. In the absence of an intervening π electron system, calculated hydrogen charge densities for individual vinyl protons show a pattern similar to that predicted by the Buckingham equation.

Correlations of ^1H chemical shifts (corrected for through-space field effects), ^{13}C chemical shifts, and carbon charge densities with F and R provide a consistent picture of electronic effects transmitted through the carbon framework of styrene. While ^1H SCS for individual derivatives sometimes appear to reflect magnetic as well as electronic effects, the overall pattern of electronic effects deduced from f and r values is identical whether one includes all derivatives or if one removes derivatives with suspected magnetic effects. The through-bond electronic effects can be explained in terms of resonance and π polarization effects. These two effects plus through-space field effects can completely account for the f and r values for the ^1H and ^{13}C chemical shift correlations as well as the pattern of calculated charge densities. Since the three approaches give a self-consistent picture of electronic effects which can be rationalized in terms of field, resonance, and π polarization effects, we believe that we have fulfilled the primary aims of the project. We also have fulfilled two of the three criteria which we suggested for determining the validity of F and R correlations. The third criterion (comparison of f and r values for closely related compounds) is considered in the following paper. The combination of ^1H and ^{13}C chemical shifts measured under inert conditions with calculated charge densities appears to be a useful technique for investigating electronic distributions in molecules (provided that a sufficiently large set of substituents is investigated) since the check of self-consistency provides a basis for evaluating the reliability of the conclusions.

The ^1H chemical shift correlations have also been used to estimate self-consistent Δχ values for C≡N and C≡C—H groups which are in good agreement with previously reported values,

revised F values for carbonyl substituents which are consistent with σ_I values determined from chemical shift measurements, and apparently reasonable F and R values for several other substituents.

Financial support from the National Research Council of Canada is gratefully acknowledged. We thank Professor S. I. Miller for providing a preprint of a paper before publication and I.R.P. thanks Gulf Oil Canada, Ltd. for a Fellowship.

1. R. F. ZÜRCHER. *In* Progress in NMR spectroscopy. Vol. 2. J. W. Emsley, J. Feeney, and L. H. Sutcliffe, editors. Pergamon Press, Oxford. 1967. Chapt. 5.
2. M. T. TRIBBLE, M. A. MILLER, and N. L. ALLINGER. J. Am. Chem. Soc. **93**, 3894 (1971).
3. T. YOKOYAMA, G. R. WILEY, and S. I. MILLER. J. Org. Chem. **34**, 1859 (1969).
4. G. R. WILEY and S. I. MILLER. J. Org. Chem. **37**, 767 (1972).
5. C. G. SWAIN and E. C. LUPTON. J. Am. Chem. Soc. **90**, 4328 (1968).
6. P. LASZLO. *In* Progress in NMR spectroscopy. Vol. 3. J. W. Emsley, J. Feeney, and L. H. Sutcliffe, editors. Pergamon Press, Oxford. 1967, Chapt. 6.
7. J. B. STOTHERS. Quart. Rev. **19**, 144 (1965).
8. (*a*) G. C. LEVY, G. L. NELSON, and J. D. CARGIOLI. Chem. Commun. 506 (1971). (*b*) G. L. NELSON, G. C. LEVY, and J. D. CARGIOLI. J. Am. Chem. Soc. **94**, 3089 (1972).
9. G. C. LEVY and G. L. NELSON. Carbon-13 nuclear magnetic resonance for organic chemists. J. Wiley & Sons, New York. 1972. Chapt. 4.
10. J. A. POPLE and G. A. SEGAL. J. Chem. Phys. **43**, 3289 (1966).
11. J. W. EMSLEY. J. Chem. Soc. A, 1387 (1968).
12. J. F. SEBASTIAN and J. R. GRUNWELL. Can. J. Chem. **49**, 1779 (1971).
13. J. E. BLOOR and D. L. BREEN. J. Phys. Chem. **72**, 716 (1968).
14. R. T. C. BROWNLEE and R. W. TAFT. J. Am. Chem. Soc. **92**, 7007 (1970).
15. G. K. HAMER and W. F. REYNOLDS. Chem. Commun. 1218 (1971).
16. G. K. HAMER and W. F. REYNOLDS. Can. J. Chem. **46**, 3813 (1968).
17. (*a*) K. S. DHAMI and J. B. STOTHERS. Can. J. Chem. **43**, 510 (1965). (*b*) GURUDATA, J. B. STOTHERS, and J. D. TALMAN. Can. J. Chem. **45**, 731 (1967).
18. (*a*) J. E. DUBOIS, J. A. MILLER, and J. E. DOUCET. J. Chim. Phys. **63**, 1283 (1966). (*b*) J. E. DUBOIS and J. P. DOUCET. J. Chim. Phys. **64**, 1145 (1967). (*c*) J. P. DOUCET, B. ANCIAN, and J. E. DUBOIS. J. Chim. Phys. **69**, 188 (1972).
19. T. A. WITTSTRUCK and E. N. TRACHTENBERG. J. Am. Chem. Soc. **89**, 3803 (1967).
20. F. W. WEHRLI, E. PRETSCH, and W. SIMON. Helv. Chim. Acta, **50**, 2189 (1967).
21. G. K. HAMER. Ph.D. Thesis. University of Toronto, Toronto, Ontario, 1973.
22. (*a*) S. CASTELLANO and J. S. WAUGH. J. Chem. Phys. **35**, 1960 (1961). (*b*) J. R. CAVANAUGH. J. Chem. Phys. **36**, 2644 (1962).
23. S. CASTELLANO and A. A. BOTHNER-BY. LAOCN3. Mellon Institute Publication, Pittsburgh, Pa. 1967.
24. C. W. HAIGH. Private communication.
25. W. F. REYNOLDS. Unpublished results.
26. Quantum Chemistry Program Exchange program 141.
27. D. G. LISTER and J. K. TYLER. Chem. Commun. 152 (1966).
28. S. UNGER and C. G. SWAIN. Linear multiple correlation by least squares. Version 2. Document 9970, AD1 Auxiliary Publications Project, Library of Congress, Washington, D.C.
29. IBM System 360 Scientific Subroutine package III.
30. P. L. BRITTON, C. L. CHENG, R. J. W. LEFEVRE, L. RADOM, and G. L. RITCHIE. J. Chem. Soc. B, 2100 (1971).
31. H. SUZUKI. Electronic absorption spectra and geometry of organic molecules. Academic Press, New York. 1967, Chapt. 13.
32. M. BARFIELD, C. J. MACDONALD, I. R. PEAT, and W. F. REYNOLDS. J. Am. Chem. Soc. **93**, 4195 (1971).
33. S. LJUNGGREN and G. WETTERMARK. Theor. Chim. Acta. **19**, 326 (1970).
34. J. M. ROBERTSON and I. WOODWARD. Proc. Roy. Soc. (London), A**162**, 568 (1937).
35. O. GROPEN and H. M. SEIP. Chem. Phys. Lett. **11**, 445 (1971).
36. B. TINLAND. Theor. Chim. Acta, **11**, 452 (1968).
37. W. J. HEHRE, L. RADOM, and J. A. POPLE. J. Am. Chem. Soc. **94**, 1496 (1972).
38. W. T. RAYNES and M. A. RAZA. Mol. Phys. **20**, 339 (1971).
39. A. D. BUCKINGHAM, T. SCHAEFER, and W. G. SCHNEIDER. J. Chem. Phys. **32**, 1227 (1960).
40. P. H. WEINER and E. R. MALINOWSKI. J. Phys. Chem. **75**, 3971 (1971).
41. L. E. SUTTON. *In* Determination of organic structures by physical methods. Vol. 1. E. A. Braude and F. C. Nachod, editors. Academic Press, New York. 1955.
42. A. R. KATRITZKY and R. D. TOPSOM. J. Chem. Ed. **48**, 427 (1971).
43. A. D. BUCKINGHAM. Can. J. Chem. **38**, 300 (1960).
44. H. M. MCCONNELL. J. Chem. Phys. **27**, 226 (1957).
45. H. P. FIGEYS and R. FLAMMANG. Mol. Phys. **12**, 481 (1967).
46. H. YAMADA, Y. TSUNO, and Y. YUKAWA. Bull. Chem. Soc. Jap. **43**, 1459 (1970).
47. C. W. N. CUMPER. Tetrahedron **25**, 3131 (1969).
48. J. I. MUSHER. J. Chem. Phys. **37**, 34 (1962).
49. G. K. HAMER, I. R. PEAT, and W. F. REYNOLDS. Can. J. Chem. This issue.
50. (*a*) J. S. MARTIN. Ph.D. Thesis. Columbia University, New York, N.Y., 1962. (*b*) J. S. MARTIN and B. P. DAILEY. J. Chem. Phys. **39**, 1722 (1963).
51. Y. NOMURA and Y. TAKEUCHI. Tetrahedron Lett. 639 (1969).
52. H. H. JAFFÉ. Chem. Rev. **35**, 191 (1953).
53. J. A. LANDGREBE and R. H. RYNBRANDT. J. Org. Chem. **31**, 2585 (1966).
54. A. A. BOTHNER-BY and J. A. POPLE. Ann. Rev. Phys. Chem. **16**, 43 (1965).
55. L. M. JACKMAN and S. STERNHELL. Applications of NMR spectroscopy in organic chemistry. 2nd Ed. Pergamon Press, Oxford. 1969. Chapt. 2.
56. I. YAMAGUCHI. Mol. Phys. **6**, 105 (1963).

Can. J. Chem. Downloaded from www.nrcresearchpress.com by 210.87.254.105 on 09/05/12
For personal use only.

57. P. R. WELLS. Aust. J. Chem. **17**, 967 (1964).
58. C. E. JOHNSON and F. A. BOVEY. J. Chem. Phys. **29**, 1012 (1958).
59. J. A. POPLE, W. G. SCHNEIDER, and H. J. BERNSTEIN. High resolution N.M.R. McGraw-Hill, New York. 1959. Chapt. 7.
60. J. I. MUSHER. *In* Advances in magnetic resonance. Vol. 2. J. S. Waugh, editor. Academic Press, New York. 1966. p. 177.
61. W. J. YOUDEN. Statistical methods for chemists. John Wiley and Sons, New York. 1951.
62. P. C. LAUTERBUR. J. Am. Chem. Soc. **83**, 1838 (1961).
63. H. SPIESECKE and W. G. SCHNEIDER. Tetrahedron Lett. 468 (1961).
64. W. F. REYNOLDS, I. R. PEAT, M. H. FREEDMAN, and J. R. LYERLA, Jr. Can. J. Chem. Submitted.
65. O. KAJIMOTO and T. FUENO. Tetrahedron Lett. 3329 (1972).
66. W. ZEIL and H. BUCHERT. Z. Phys. Chem. **38**, 47 (1963).
67. G. S. REDDY and J. H. GOLDSTEIN. J. Chem. Phys. **39**, 3509 (1963).
68. J. W. APSIMON and H. BEIERBECK. Can. J. Chem. **49**, 1328 (1971).
69. P. R. WELLS, S. EHRENSON, and R. W. TAFT. Prog. Phys. Org. Chem. **6**, 147 (1966) and refs. therein.
70. E. A. V. EBSWORTH. *In* Organometallic chemistry of the group IV elements. Vol. 1. A. G. Macdiarmid, editor. Marcel Dekker, New York. 1968.
71. T. SCHAEFER. Can. J. Chem. **40**, 1 (1962).

Can. J. Chem. Downloaded from www.nrcresearchpress.com by 210.87.254.105 on 09/05/12
For personal use only.

Investigations of Substituent Effects by Nuclear Magnetic Resonance Spectroscopy and All-valence Electron Molecular Orbital Calculations. II. 4-Substituted α-Methylstyrenes and α-*t*-Butylstyrenes

GORDON K. HAMER,[1] IAN R. PEAT[2] AND W. F. REYNOLDS

Department of Chemistry, University of Toronto, Toronto 181, Ontario

Received June 14, 1972

Substituent-induced ^1H chemical shifts (S.C.S.) for 19 4-substituted α-methyl- and α-*t*-butylstyrenes have been determined at infinite dilution in C_6H_{12} and ^{13}C S.C.S. have been determined for 0.4 *M* solutions in CCl_4. S.C.S. are correlated with field and resonance substituent parameters and compared with charge densities determined by CNDO/2 MO calculations. The variation of S.C.S. with the dihedral angle, ρ, between phenyl and vinyl groups and the overall pattern of S.C.S. can be largely accounted for by a model of substituent effects based on field, resonance, and π polarization effects, with conjugative interactions varying as $\cos^2\rho$. Both ^{13}C chemical shifts and charge densities indicate that the π polarization effect consists of two components: (*1*) a through-space polarization of the vinyl system by the polar C—X bond and (*2*) polarization of the entire conjugated styrene π electron system. However, significant deviations are noted for some of the ^1H S.C.S. correlations. The CNDO/2 calculations indicate that these deviations are primarily due to electronic effects not predicted by the model outlined above. CNDO/2 calculations for related compounds provide a partial explanation by indicating that the magnitude of the field effect depends upon the nature of the molecular framework.

Les déplacements chimiques en ^1H induits par des substituants (S.C.S.) pour 19 α-méthyl et α-*t*-butylstyrènes substitués en position 4 ont été déterminés à dilution infinie dans le C_6H_{12}; ceux-ci en ^{13}C ont été déterminés en solution 0.4 *M* dans le CCl_4. Les déplacements chimiques induits par des substituants sont reliés aux paramètres de champ et de résonance caractéristiques des substituants et comparés avec les densités de charge obtenues par des calculs CNDO/2 MO. La variation dans les déplacements chimiques avec l'angle dièdre, ρ, entre les groupes phényle et vinyl ainsi que le schéma général de ces déplacements chimiques peuvent très bien s'interpréter à partir d'un modèle des effets de substituants basé sur le champ, la résonance et des effets de polarisation π avec des interactions de conjugaison variant selon le $\cos^2\rho$. Les déplacements chimiques en ^{13}C et les densités de charge indiquent tous les deux, que l'effet de polarisation π possède deux composantes: (*1*) une polarisation à travers l'espace du système vinylique par la liaison polaire C—X et (*2*) une polarisation du système d'électrons π du styrène conjugué en entier. Cependant, des écarts notables ont été observés pour quelques-unes des correlations dans les déplacements chimiques en ^1H. Les calculs CNDO/2 montrent que ces écarts sont imputables principalement à des effets électroniques imprévisibles selon le modèle illustré précédemment. Les calculs CNDO/2 pour des composés voisins permettent une explication partielle en montrant que l'amplitude des effets de champ dépend de la nature du squelette moléculaire.

[Traduit par le journal]

Can. J. Chem., **51**, 915 (1973)

Introduction

In the preceding paper (1), ^1H and ^{13}C chemical shifts for 4-substituted styrenes were correlated with field (*F*) and resonance (*R*) substituent parameters (2):

$$[1] \qquad \delta = fF + rR + \delta_0$$

These correlations of substituent-induced chemical shifts (S.C.S.) were used in conjunction with charge densities estimated by CNDO/2 molecular orbital calculations (3) to deduce mechanisms of transmission of substituent effects in these compounds. However, since the use of *F* and *R* correlations for this purpose has been severely criticized (4), several criteria were proposed to test the validity of the correlations (1). One of these criteria was that *f* and *r* values should vary in a regular and predictable fashion for related series of compounds. To test this criterion, a series of 4-substituted derivatives of 2-phenylpropene (**1**) and 2-phenyl-3,3-dimethylbutene (**2**) were synthesized. These compounds will hence-

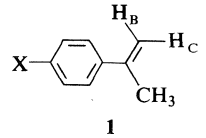

1

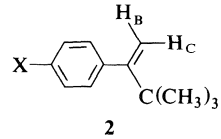

2

[1]NRCC Scholarship holder, 1967–1970.

[2]NRCC Scholarship holder, 1968–1971. Gulf Oil Fellowship holder 1971–1972.

forth be referred to as derivatives of α-methylstyrene (AMS) and α-*t*-butylstyrene (ATBS). These compounds were chosen on the assumption that through-bond electronic effects should vary as a function of the dihedral angle, ρ, between phenyl and vinyl groups.

Results of investigations of S.C.S. for AMS and ATBS derivatives are presented below.

Experimental

(a) Preparation and Purification of Compounds

α-Methylstyrene and its 4-fluoro and 4-chloro derivatives were obtained from Aldrich Chemicals, Inc. Other AMS derivatives were known compounds and were synthesized by previously reported methods. Full details are reported elsewhere (5).

Of the ATBS derivatives only the parent α-*t*-butylstyrene (6, 7) and its 4-methoxy derivative (7) have been previously described in the literature. The remaining compounds were synthesized by modifying known methods; in most cases, the olefin was obtained by catalytic dehydration of the appropriate 3,3-dimethyl-2-phenyl-2-butanol over activated alumina. Synthetic procedures and analytical data are outlined below.

3,3-Dimethyl-2-phenyl-1-butene

3,3-Dimethyl-2-phenyl-2-butanol, b.p. 108–109.5°/10 mm (lit. 128°/20 mm (6), 95.5°/4.5 mm (7)), was obtained from the reaction of 3,3-dimethyl-2-butanone and phenyllithium in refluxing ether (6). The alcohol was dehydrated over activated alumina and purified by v.p.c. An analytical sample had b.p. 56.5–57°/3.4 mm (lit. 75°/10 mm (6)).

Anal. Calcd. for $C_{12}H_{16}$: C, 89.93; H, 10.07. Found: C, 90.02; H, 10.13.

3,3-Dimethyl-2-(4′-methylphenyl)-1-butene

The required butanol, b.p. 93–97°/2 mm (lit. 98°/2.5 mm (7)), was prepared from 4-methylphenyllithium and 3,3-dimethyl-2-butanone and dehydrated over alumina. Purification by v.p.c. gave the styrene, b.p. 74.8–75°/2.6 mm.

Anal. Calcd. for $C_{13}H_{18}$: C, 89.59; H, 10.41. Found: C, 89.50; H, 10.39.

3,3-Dimethyl-2-(4′-t-butylphenyl)-1-butene

4-Bromo-*t*-butylbenzene, b.p. 82–84°/5 mm (lit. 113–114°/20 mm (8)), was obtained by addition of chlorosulphonic acid to an ice-cold solution of bromobenzene and *t*-butanol (9). The lithium reagent prepared from this product was treated with 3,3-dimethyl-2-butanone to give the required butanol, b.p. 99–102°/2 mm. Dehydration of the alcohol with alumina, followed by preparative v.p.c., gave a white crystalline solid, m.p. 46.5–47.5°, b.p. 86–86.3°/0.8 mm.

Anal. Calcd. for $C_{16}H_{24}$: C, 88.82; H, 11.18. Found: C, 88.64; H, 11.29.

3,3-Dimethyl-2-(4′-N,N-dimethylaminophenyl)-1-butene

The required butanol was prepared from 4-*N*,*N*-dimethylaminophenyllithium (10) and 3,3-dimethyl-2-butanone. The butanol did not readily dehydrate during distillation. Consequently the crude alcohol was refluxed with potassium hydrogen sulfate for 5 min at 140°, and vacuum distilled. An analytical sample of the olefin, recrystallized from methanol, had m.p. 26–27°.

Anal. Calcd. for $C_{14}H_{21}N$: C, 82.70; H, 10.41; N, 6.89. Found: C, 82.88; H, 10.31; N, 6.95.

3,3-Dimethyl-2-(4′-fluorophenyl)-1-butene

The reaction of 3,3-dimethyl-2-butanone with 4-fluorophenylmagnesium bromide gave the required alcohol, b.p. 90–97°/5 mm. The alcohol was dehydrated over alumina. The olefin, purified by v.p.c., had b.p. 58°/1.9 mm.

Anal. Calcd. for $C_{12}H_{15}F$: C, 80.86; H, 8.48; F, 10.66. Found: C, 80.72; H, 8.51; F, 10.48.

3,3-Dimethyl-2-(4′-chlorophenyl)-1-butene

4-Chlorophenylmagnesium chloride (11) was converted to 3,3-dimethyl-2-(4′-chlorophenyl)-2-butanol, b.p. 98–103°/2 mm, by treatment with 3,3-dimethyl-2-butanone. The alcohol was dehydrated over alumina; purification of the distillate by v.p.c. gave the styrene, b.p. 81–81.2°/1.9 mm.

Anal. Calcd. for $C_{12}H_{15}Cl$: C, 74.02; H, 7.77; Cl, 18.21. Found: C, 73.95; H, 8.04; Cl, 17.96.

3,3-Dimethyl-2-(4′-bromophenyl)-1-butene

The bromophenylbutanol, b.p. 110–115°/2 mm, was obtained from the reaction of 3,3-dimethyl-2-butanone with 4-bromophenylmagnesium bromide. Purification of the alumina catalyzed dehydration product by v.p.c. gave the desired olefin, b.p. 98–99°/2 mm.

Anal. Calcd. for $C_{12}H_{15}Br$: C, 60.26; H, 6.32; Br, 33.42. Found: C, 60.46; H, 6.27; Br, 33.24.

3,3-Dimethyl-2-(4′-methoxyphenyl)-1-butene

4-Methoxypivalophenone, b.p. 130–132°/5 mm (lit. 138–140°/8 mm (12)), was prepared by Friedel–Crafts acylation of anisole with pivaloyl chloride and aluminum chloride (12). The ketone was converted directly to the required styrene by the Wittig synthesis (13) and the crude reaction product purified by v.p.c. (column A; 160°, 200 ml/min helium). An analytical sample had b.p. 84°/1 mm (lit. 63°/0.6 mm (7)).

Anal. Calcd. for $C_{13}H_{18}O$: C, 82.06; H, 9.53. Found: C, 82.18; H, 9.33.

3,3-Dimethyl-2-(4′-nitrophenyl)-1-butene

3,3-Dimethyl-2-butanol was added to an ice-cold suspension of aluminum chloride in benzene while dry hydrogen chloride was bubbled into the mixture (14). The isolated product, 3,3-dimethyl-2-phenylbutane, b.p. 205–207°/756 mm (lit. 205–207°/760 mm (14)), was nitrated by the method of Stirling and Bogert (15). Distillation of the crude 3,3-dimethyl-2-(4′-nitrophenyl)-butane gave a fraction, b.p. 119–124°/2 mm (lit. 117–124°/2 mm (14)), which solidified on standing; m.p. 37.5–38.5°, recrystallized from methanol. Treatment of this material with *N*-bromosuccinimide and benzoyl peroxide (16) gave the benzyl bromide, m.p. 122–123°, recrystallized from methanol. The bromide was dehydrohalogenated with ethanolic potassium hydroxide (4 h at 60°) (16) to give 3,3-dimethyl-2-(4′-nitrophenyl)-1-butene, m.p. 42–43°, recrystallized from pentane.

Anal. Calcd. for $C_{12}H_{15}NO_2$: C, 70.22; H, 7.37; N, 6.83. Found: C, 70.16; H, 7.32; N, 6.94.

Catalytic dehydrations were carried out using activated alumina (Matheson Coleman and Bell; 8–14 mesh) which was washed with ammonium hydroxide and dried for 24 h at 100° before packing into the reaction tube. 3,3-Dimethyl-2-phenyl-2-butanols were passed through the heated (250°) reaction tube at a flow rate of 0.5 ml/min, using N_2 as a carrier gas and with the apparatus main-

TABLE 1. Vinyl proton chemical shifts (in p.p.m. relative to $(CH_3)_4Si$) and coupling constants (in Hz) for 4-substituted α-methylstyrenes at infinite dilution in C_6H_{12}

Substituent	δ_{H_B}	δ_{H_C}	$\Delta\delta$(B − C)	$^4J_{AB}$	$^4J_{AC}$	J_{BC}
H	5.2751	4.9965	0.2786	−0.82	−1.51	1.62
CH_3	5.2285	4.9306	0.2979	−0.81	−1.50	1.68
$C(CH_3)_3$	5.2511	4.9503	0.3008	−0.81	−1.47	1.70
F	5.2219	4.9843	0.2376	−0.81	−1.49	1.53
Cl	5.2639	5.0173	0.2466	−0.81	−1.49	1.36
OCH_3	5.1848	4.8957	0.2891	−0.81	−1.49	1.60
$N(CH_3)_2$	5.1533	4.8125	0.3408	−0.79	−1.47	1.74
NO_2	5.4266	5.2041	0.2225	−0.82	−1.50	1.07
$Si(CH_3)_3$	5.2811	4.9963	0.2848	−0.82	−1.50	1.63
$Sn(CH_3)_3$	5.2581	4.9710	0.2873	−0.81	−1.48	1.65

tained at 130–150 mm pressure. Products were trapped in a receiver flask immersed in a Dry Ice – acetone slurry.

ATBS derivatives were dried over Linde 4A molecular sieve. They were then purified by preparative v.p.c., using a Varian Aerograph Autoprep 700 and a 20 ft × 3/8 in. column packed with 30% SE-30 on 45/60 mesh Chromosorb W. Melting points were determined on a Fisher–Johns hot-stage apparatus and are uncorrected. Elemental analyses were carried out by A. B. Gygli, Microanalyses Laboratories Limited, Toronto, Ontario.

(b) Sample Preparations and Recording of Spectra

All styrene derivatives were either used immediately after synthesis and purification or else were redistilled or recrystallized immediately before use. AMS derivatives were dissolved in cyclohexane which was used as a lock and reference signal. The cyclohexane (Fisher A.C.S. grade) was fractionally distilled from sodium and stored over Linde 4A molecular sieve. ATBS derivatives were dissolved in cyclohexane-d_{12} (Merck Sharp and Dhome Canada Ltd.) with 4% tetramethylsilane as lock and reference signal, to avoid interference between *t*-butyl and cyclohexane peaks. Measurements were made at three concentrations in the range of 1–5 mol %.

Proton spectra were obtained on a Varian HA-100 operating in frequency sweep mode at a probe temperature of 30°. Experimental conditions were identical to those previously described (17). Nuclear Overhauser effects for α-*t*-butylstyrene were determined according to the procedure of Bell and Saunders (18), using the electronic integrator of the HA-100 and a Hewlett–Packard 4204A digital oscillator. The sample (5 mol % in $CDCl_3$ containing 5 mol % tetramethylsilane as lock and reference) was filtered, degassed by five freeze–pump–thaw cycles on a high vacuum line and sealed at 0.01 mm.

^{13}C n.m.r. spectra were obtained in CCl_4 for 0.4 *M* solutions, using previously reported procedures (1).

Results

A complete A_3BC spectral analysis was carried out for the α-methyl and vinyl proton spectrum of α-methylstyrene, using the iterative computer program LAME (19) (protons are not labelled conventionally in order of increasing field but rather by analogy to styrene (1) to facilitate comparisons between different series).

TABLE 2. Vinyl proton chemical shifts (in p.p.m. relative to $(CH_3)_4Si$) and coupling constants (in Hz) for 4-substituted α-*t*-butylstyrenes at infinite dilution in cyclohexane-d_{12}

Substituent	δ_{H_B}	δ_{H_C}	$\Delta\delta$(B − C)	J_{BC}
H	4.7200	5.1367	−0.4167	1.79
CH_3	4.7256	5.1513	−0.4257	1.68
$C(CH_3)_3$	4.7247	5.1538	−0.4291	1.60
F	4.7247	5.1518	−0.4271	1.58
Cl	4.6958	5.1092	−0.4134	1.87
Br	4.7110	5.1156	−0.4046	1.87
OCH_3	4.6896	5.0776	−0.3880	2.07
$N(CH_3)_2$	4.7035	5.1088	−0.4053	1.91
NO_2	4.7780	5.2399	−0.4619	1.19

However, it was found that all chemical shifts and coupling constants and also the chemical shift difference $\Delta\delta$(B − C) agreed within 0.05 Hz of those obtained from a first order A_3MX analysis. Consequently, all AMS spectra were analyzed by first order analysis. ATBS derivatives were analyzed as AB spectra (there was no resolvable coupling to the *t*-butyl group).

Infinite dilution proton chemical shifts were determined by least squares fitting of the linear dilution curves. Standard errors of intercepts never exceeded 0.0008 p.p.m. Proton chemical shifts and coupling constants for AMS derivatives are summarized in Table 1 with results for ATBS derivatives in Table 2. ^{13}C chemical shift data for both compounds are given in Table 3.

CNDO/2 calculations were carried out on an IBM 360-65 computer using a standard program (19). Most bond lengths and bond angles for styrene were identical to those previously reported (1) with the C_1—C_α—C_β valence angle α fixed at 120°. The C_1—C_α bond length was varied as a function of ρ

[2] $$r_{C_1—C_\alpha} = (1.52 - 0.06 \cos \rho)\text{Å}$$

TABLE 3. ^{13}C chemical shifts (in p.p.m. relative to $^{13}CH_3Si(CH_3)_3$) for 0.4 *M* solutions of 4-substituted α-methyl- and α-*t*-butylstyrene derivatives in CCl_4

Substituent	C-4	C-3,5	C-2,6	C-1	C-α	C-β
(a) α-Methylstyrenes						
H	127.05	127.87	125.25	141.07	142.97	112.13
CH_3	136.23	128.53	125.18	138.26	142.74	111.28
$C(CH_3)_3$	149.55	124.66	125.02	138.21	142.74	111.39
F	162.21	114.78	126.84	137.15	141.99	112.09
Cl	133.20	128.14	126.50	139.42	141.89	112.73
OCH_3	158.98	113.28	126.30	133.61	142.30	110.37
$N(CH_3)_2$	149.59	112.03	125.97	129.62	142.28	108.65
NO_2	147.23	123.27	125.85	146.96	141.50	115.82
$Si(CH_3)_3$	138.62	132.93	124.65	141.49	143.04	112.23
$Sn(CH_3)_3$	140.36	135.35	124.96	141.05	143.08	112.03
(b) α-t-Butylstyrenes						
H	126.05	127.05	128.70	143.08	159.43	111.39
CH_3	134.99	127.73	128.64	140.21	159.34	111.27
$C(CH_3)_3$	148.31	123.84	128.51	140.23	159.33	111.29
F	161.55	113.99	130.15	138.86	158.49	112.06
Cl	132.05	127.38	130.01	141.40	158.39	112.04
Br	120.53	130.35	130.35	141.85	158.39	112.03
OCH_3	158.09	112.52	129.61	135.39	159.04	111.49
$N(CH_3)_2$	148.79	111.68	129.30	131.90	159.37	111.03
NO_2	146.96	122.40	129.37	149.59	157.94	112.86

TABLE 4. Excess charge densities ($\times 10^4$, relative to the parent styrene) for C-1 and vinyl protons and carbons of 4-substituted styrenes with $\rho = 90°$ (phenyl and vinyl groups at right angles)

	$N(CH_3)_2$	NH_2	OCH_3	CH_3	$C(CH_3)_3$	C≡CH	F	Cl*	CF_3	C≡N	NO_2	$Si(CH_3)_3$*
$C\text{-}1_\sigma$	+214	+176	+145	+54	+76	+8	+70	−17	−109	−51	−178	+10
$C\text{-}1_\pi$	−574	−460	−409	−159	−215	−30	−245	−86	+263	+94	+396	−24
$C\text{-}\alpha_\sigma$	−2	+2	+11	−4	−4	+11	+37	+36	+44	+26	+72	−7
$C\text{-}\alpha_\pi$	+41	+31	+15	+11	+17	−12	−27	−36	−78	−45	−118	+4
$C\text{-}\beta_\sigma$	+9	+3	−4	+5	+5	−6	−23	−23	−34	−19	−53	+5
$C\text{-}\beta_\pi$	−41	−30	−12	−11	−17	+14	+35	+43	+88	+52	+133	−5
H_B	−18	−11	−7	−5	−8	+3	+7	+11	+25	+14	+38	−3
H_C	−25	−18	−8	−7	−10	+7	+17	+22	+46	+27	+71	−3
Δ†	+7	+7	+1	+2	+2	−4	−10	−11	−21	−13	−33	0

*3s and 3p orbitals only.
†$\Delta = \Delta q(H_B - H_C)$.

to allow for decreased conjugation in the non-planar forms. Assumed geometries for other substituents are tabulated elsewhere (5). For reasons of computational economy, most calculations were carried out for 4-substituted styrenes with $\rho = 90°$ rather than for α-alkylstyrenes using the experimental ρ. Vinyl carbon and hydrogen charge densities are given in Table 4 (complete charge densities are on deposit in the Depository of Unpublished Data, National Science Library, National Research Council of Canada, Ottawa, Canada K1A 0S2). However, calculations were also performed for a limited number of styrene derivatives with $\rho = 30$ and 60° and AMS derivatives with the experimental ρ of 30°. These calculations showed that charge densities varied smoothly with ρ. In addition, nearly identical results were obtained for the substituent dependence of charge densities of styrene and AMS derivatives with $\rho = 30°$, demonstrating that no complications were introduced by the presence of the alkyl substituent.

Discussion

(a) Determination of Conformation of α-Alkylstyrenes

^1H and ^{13}C S.C.S. in 4-substituted α-alkylstyrenes are very sensitive to the dihedral angle, ρ, between the phenyl and vinyl groups. Consequently we attempted to determine this angle as accurately as possible. ρ was estimated from the

TABLE 5. Calculated ring current and charge density contributions to $\Delta\delta_0$(B − C), the β proton chemical shift difference in unsubstituted styrene, AMS and ATBS
(*a*) Calculated charge densities for H_B and H_C in styrene, AMS and ATBS

	Charge density ($\times 10^4$)				
Proton	Styrene(0°)	Styrene(30°)	AMS(30°)	Styrene(64°)	ATBS(64°)
H_B	+169	+144	+58	+126	+30
H_C	+63	+66	+46	+70	+78

(*b*) Calculated ring current (r.c.) and charge density (c.d.) contributions to δ_0(B), δ_0(C) and $\Delta\delta_0$(B − C)

		δ (p.p.m.)		
Proton	Contribution	Styrene	AMS(30°)	ATBS(64°)
H_B	r.c.*	0.561	0.438	0.123
	c.d.†	0.355	0.122	0.063
	Total	0.916	0.560	0.186
	δ_0(calcd.)‡	5.630	5.274	4.900
	δ_0(exp.)	5.630	5.275	4.720
H_C	r.c.	0.258	0.246	0.218
	c.d.	0.132	0.097	0.164
	Total	0.390	0.343	0.382
	δ_0(calcd.)	5.104	5.057	5.096
	δ_0(exp.)	5.113	4.997	5.137
$H_B - H_C$	$\Delta\delta_0$(calcd.)§	0.526	0.217	−0.196
	$\Delta\delta_0$(exp.)	0.517	0.279	−0.417

*Calculated using Bovey–Johnson (42) calculations.
†Calculated assuming a scaling factor of 21 p.p.m./hydrogen 1s electron and expressed relative to zero charge density.
‡Calculated δ_0 obtained by assuming that the calculated value for δ(B) for styrene is equal to the experimental value and expressing other values relative to this value.
§Difference in total ring current and charge density contributions for H_B and H_C. It is not necessary to assume any chemical shift in this case.

electronic absorption spectrum using two different techniques.

Experimentally determined λ_{max} values for the conjugation bands of styrene AMS and ATBS were respectively 248, 243 and 223 mμ while the corresponding extinction coefficients were 14 310, 10 900, and 2630. ρ can be estimated from the extinction coefficients using the approach of Braude and Sondheimer (20):

$$[3] \qquad \varepsilon/\varepsilon_{0^\circ} = \cos^2\rho$$

where ε_{0° is the extinction coefficient for styrene (assumed planar (1)). This approach gives ρ = 29° for AMS and ρ = 65° for ATBS. Alternatively one can determine ρ from conjugation band transition frequencies, using the method of Suzuki (21). This method yields ρ = 30° for AMS and ρ = 63° for ATBS (full details of the calculation are given elsewhere (5)). The two methods are in excellent agreement and average values of ρ = 30° for AMS and ρ = 64° for ATBS will be used in the following discussion.

(b) Assignment of H_B and H_C for AMS and ATBS and Discussion of Factors Determining $\Delta\delta_0$(B − C)

H_B and H_C for AMS have been previously assigned on the basis of specific deuteration experiments (22). It was found that $\delta_{H_B} > \delta_{H_C}$, as in styrene. However, $\Delta\delta_0$(B − C) is much smaller for AMS (+0.279 p.p.m.) than for styrene (+0.517 p.p.m.). H_B and H_C for ATBS have not been previously assigned. These were assigned by utilizing the nuclear Overhauser effect (n.O.e.) (23,24). Irradiation of the *t*-butyl group gave a positive n.O.e. of 11 ± 2% for the low field vinylidene proton and negative n.O.e. of 3 ± 2% for the high field proton. This allows unambiguous assignment of the low field peak as H_C and the high field peak as H_B. This means that $\Delta\delta_0$(B − C) has changed sign and now has a large negative value (−0.417 p.p.m.) for ATBS.

It is interesting to consider why this occurs. As shown in Table 5, δ_{H_C} is nearly constant while

δ_{H_B} moves continuously to low frequency (high field) on going from styrene to ATBS. It is known that the vinyl proton chemical shifts in styrene are not solely due to ring current effects (25). The CNDO/2 calculations indicate that differences in charge density for H_B and H_C contribute substantially to $\Delta\delta_0(B - C)$. Assuming an average scaling factor of 21 p.p.m./hydrogen 1s electron (1), then $\Delta\delta_0(B - C)$ for styrene and AMS are almost quantitatively predicted by a combination of ring current and charge density effects (Table 5). A somewhat larger error is found for ATBS although chemical shift trends are well reproduced, particularly for H_C. The large positive charge density for H_B in styrene (**3**) apparently is due to the steric interaction between H_B and H_2 since q_{H_B} decreases as ρ increases: Similarly, H_2 has a less

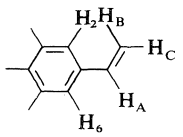

3

negative charge (-18×10^{-4}) than H_6 (-54×10^{-4}) with q_{H_2} becoming more negative as ρ increases. By contrast, q_{H_C} is much less sensitive to ρ. Thus, there are apparently two electronic contributions to the high field shift of H_B on going from styrene to ATBS: (*1*) relief of steric hindrance and (*2*) the electron-releasing effect of the alkyl substituent (as evidenced by the additional negative contribution to q_{H_B} for the alkylstyrenes as compared to styrene for the same ρ). This combines with the decreased ring current effect to give a large high field shift for H_B. By contrast, the near constancy of δ_{H_C} reflects a lesser sensitivity to both ring current and charge density effects. It is also possible that there is a van der Waals' or dispersion interaction (26) contributing to the low field shift of H_B in styrene. However, the results can be explained without invoking an effect of this kind.

One final conclusion can be drawn from the above discussion and the data in Table 5: for a given styrene derivative, δ_{H_B} should be much more sensitive than δ_{H_C} to small changes in ρ.

(c) Interpretation of Substituent-induced Chemical Shifts

π-Conjugative effects should vary as $\cos^2\rho$ (27). Consequently, the expected weighting factors, *r*, for correlations of S.C.S. with *F* and *R* can be estimated from the observed values for styrene (1):

$$[4] \qquad r_{H_B} = 0.414 \cos^2\rho$$

$$[5] \qquad r_{H_C} = 0.420 \cos^2\rho$$

$$[6] \qquad r_{C\text{-}\alpha} = -0.35 \cos^2\rho \approx 0$$

$$[7] \qquad r_{C\text{-}\beta} = 7.15 \cos^2\rho$$

It is more difficult to make predictions from the observed *f* values since they should reflect both through-space field effects and π polarization effects (1). As a first approximation it seemed reasonable to assume that the through-space field effect upon proton chemical shifts should be independent of ρ. To predict how π polarization effects vary with ρ it is necessary to determine the exact nature of these effects.

The $N(CH_3)_3^+$ group should have a large field effect and small resonance effect (zero according to Swain and Lupton (2)). Since σ inductive effects are unimportant (1), vinyl ^{13}C chemical shifts for $N(CH_3)_3^+$ derivatives should primarily reflect π inductive effects. Chemical shift data for $N(CH_3)_3^+$ derivatives of styrene and ATBS as well as charge densities for the styrene derivative at $\rho = 0$ and $\rho = 90°$ are given in Table 6. Comparison of π charge densities for $\rho = 90$ and $\rho = 0°$ suggests that there are two mechanisms of transmission of π inductive effects. For $\rho = 90°$, the phenyl and vinyl π electron systems appear to be independently polarized towards the positive group, leading to equal but opposite changes in π electron density for C-α and -β. This effect, which is probably transmitted through space, should be the only mechanism affecting the vinyl group for large values of ρ. For small values of ρ, the vinyl and phenyl groups are conjugated and the entire π electron system can be polarized. This additional polarization mechanism leads to electron transfer from the vinyl to the phenyl group with loss of electron density from C-β but little change in electron density for C-α. These two mechanisms can account for the *f* values obtained from the correlations of vinyl ^{13}C chemical shifts for 4-substituted styrenes with *F* and *R* (1). These correlations showed a small negative *f* value for C-α and a larger positive *f* value for C-β. The C-α and -β chemical shifts for $N(CH_3)_3^+$ derivatives of styrene and ATBS are also consistent with this interpretation of π

TABLE 6. (*a*) Calculated charge densities for 4-*N*,*N*,*N*-trimethylammoniostyrene at $\rho = 0°$ and $\rho = 90°$ ($\times 10^4$, relative to styrene)

ρ	C-4	C-3,5	C-2,6	C-1	C-α	C-β
0°	+707*	−173	+163	+274	−145	+339
	(−902)	(−187)	(+185)	(+464)	(−343)	(+580)
90°	+737	−185	+201	+238	−116	+231
	(−840)	(−212)	(+257)	(+447)	(−360)	(+413)

(*b*) Comparison of substituent-induced ^{13}C chemical shifts for *N*,*N*,*N*-trimethylammonio and *t*-butyl derivatives of styrene and α-*t*-butylstyrene in CD_3OD (in p.p.m. relative to parent styrenes)

Compound	Substituent	C-4	C-3,5	C-2,6	C-1	C-α	C-β
Styrene	$N(CH_3)_3^+$	+18.95	−7.90	+1.98	+2.42	−2.13	+3.90
	$C(CH_3)_3$	+22.69	−3.20	−0.18	−2.75	−0.26	−0.83
	Δ†	−3.74	−4.70	+2.16	+5.17	−1.87	+4.73
α-*t*-Butylstyrene	$N(CH_3)_3^+$	+18.60	−7.19	+2.08	+2.48	−1.82	+1.58
	$C(CH_3)_3$	+22.35	−3.22	−0.20	−2.84	−0.09	−0.13
	Δ	−3.75	−3.97	+2.28	+5.32	−1.73	+1.71

*Total charge density and (in brackets) π charge density.
†S.C.S. for $N(CH_3)_3^+$ derivative − S.C.S. for $C(CH_3)_3$ derivative.

polarization effects. Assuming a $\cos^2\rho$ dependence for the conjugative π polarization mechanism, this indicates that the residual through-space π polarization effect upon $\delta_{C-\beta}$ at $\rho = 90°$ should be approximately 30% of the total π polarization effect at C-β for the planar styrene. By contrast, C-α is much less sensitive to ρ, as suggested by the calculations. Of the phenyl carbon chemical shifts, C-1 and -2,6 are consistent with the presence of a π polarization effect but C-3,5 and -4 apparently are not. However, the latter chemical shifts are likely to reflect structural effects similar to the α and β effects for linear hydrocarbons (28).[3] Since the $N(CH_3)_3^+$ group is isoelectronic with the $C(CH_3)_3$ group and similar in size, a comparison of chemical shifts for these pairs of styrene derivatives should minimize if not completely eliminate structural effects. The chemical shift differences should then reflect the effect of the positive charge on the $N(CH_3)_3^+$ group. As seen in Table 6, these chemical shift differences indicate a strong π polarization effect (the relatively small shift for C-4 may be due to the counteracting σ inductive effect of the $N(CH_3)_3^+$ group). This is a particularly interesting observation since π polarization effects are usually regarded as unimportant (32). However, we have obtained corroboratory evidence for π polarization effects from the ^{13}C chemical shifts of a large number of phenylalkane derivatives (31). In addition, ^{13}C chemical shift data and π charge densities for *trans*-1-substituted 1,3-butadienes indicate that π polarization effects are important in these derivatives (33).

The evidence presented above concerning the nature of π polarization effects can be used to predict *f* values for δ_{H_B}, δ_{H_C}, and $\delta_{C-\beta}$ as a function of ρ. Total *f* values for H_B and H_C of styrene are respectively 0.100 and 0.166 with estimated through-space field components of −0.007 and 0.060 and π polarization components of 0.107 and 0.106 (1). Assuming that 30% of the π polarization effect remains at $\rho = 90°$ (see above) and that the field effect is independent of ρ:

[3]The exact nature of these effects is still unclear (29) although it has been suggested that the α effect may be due to contributions to the diamagnetic and paramagnetic terms in the chemical shift equation arising from the electron distribution on the α substituent (29, 30). In any case, it appears improbable that the α and β effects will be totally reflected by changes in the ground state charge density at the carbon in question. γ-Effects were also noted for hydrocarbons (28). However, these effects apparently reflect *gauche* steric interactions (29) and should be insignificant in the case of C-2,6 S.C.S. since these carbons are *trans* to the substituent. The validity of correlating ^{13}C S.C.S. due to more remote substituents with ground state charge densities is discussed in detail elsewhere (31).

TABLE 7. Correlations of ^1H and ^{13}C S.C.S. (in p.p.m.) for styrene, α-methylstyrene (AMS) and α-*t*-butylstyrene (ATBS) derivatives with F and R

Compound	δ	f*	r*	S.D.†	r‡
(*a*) ^1H S.C.S.					
Styrene	H_B	+0.100±0.011	+0.414±0.014	0.012	0.996
	H_C	+0.166±0.010	+0.420±0.014	0.012	0.997
	$H_B - H_C$	−0.067±0.002	—	0.002	0.997
AMS	H_B	+0.094±0.011 (+0.08)§	+0.234±0.020 (+0.31)	0.014	0.987
	H_C	+0.140±0.008 (+0.15)	+0.313±0.013 (+0.32)	0.010	0.997
	$H_B - H_C$	−0.046±0.007 (−0.07)	−0.079±0.011 (0)	0.008	0.977
ATBS	H_B	+0.044±0.010 (+0.04)	+0.055±0.016 (+0.08)	0.009	0.974
	H_C	+0.077±0.008 (+0.11)	+0.104±0.014 (+0.08)	0.008	0.995
	$H_B - H_C$	−0.032±0.003 (−0.07)	−0.049±0.006 (0)	0.004	0.994
(*b*) ^{13}C S.C.S.					
Styrene	C-2,6	+0.89±0.17	−1.90±0.32	0.34	0.898
	C-1	+2.98±0.37	+15.78±0.69	0.73	0.985
	C-α	−1.30±0.07	−0.35±0.13	0.15	0.974
	C-β	+2.82±0.15	+7.15±0.27	0.29	0.991
AMS	C-1	+3.11±0.29	+18.03±0.58	0.43	0.996
	C-α	−1.02±0.13 (≈−1.3)	+0.44±0.25 (≈0)	0.20	0.947
	C-β	+2.32±0.09 (+2.3)	+5.88±0.19 (+5.4)	0.15	0.997
ATBS	C-1	+3.03±0.31	+18.79±0.62	0.41	0.997
	C-α	−1.18±0.10 (≈−1.3)	−0.14±0.20 (≈0)	0.13	0.980
	C-β	+1.04±0.05 (+1.2)	+0.57±0.10 (+1.4)	0.07	0.994

*Weighting coefficients for equation $\delta = fF + rR + \delta_0$.
†Standard deviation between calculated and observed chemical shifts (in p.p.m.).
‡Correlation coefficient.
§Values for f and r estimated from **eqs.** 4–10 (in brackets).

$$[8]\quad f_{H_B} = -0.007 + 0.107\,(0.30 + 0.70 \times \cos^2\rho) = +0.025 + 0.075\cos^2\rho$$

$$[9]\quad f_{H_C} = +0.060 + 0.106\,(0.30 + 0.70 \times \cos^2\rho) = +0.092 + 0.074\cos^2\rho$$

$\delta_{C\text{-}\beta}$ should only reflect π polarization effects and resonance effects. Since $f_{C\text{-}\beta}$ for styrene $= +2.82$;

$$[10]\quad f_{C\text{-}\beta} = +2.82\,(0.30 + 0.70\cos^2\rho) = +0.85 + 1.97\cos^2\rho$$

By contrast, both calculations and chemical shift data for $N(CH_3)_3^+$ derivatives suggest that $f_{C\text{-}\alpha}$ should be nearly independent of ρ. While eqs. 4–10 appear complex, they are based on a very simple model for mechanisms of transmission of substituent effects, *i.e.*, that any conjugative interaction should vary as $\cos^2\rho$.

Results of correlations of ^1H and ^{13}C chemical shifts with F and R are summarized in Table 7. Halogens were excluded from the ^1H correlations but included in the ^{13}C correlations for reasons discussed in the previous paper (1). Previously determined F and R values were used for the $N(CH_3)_2$, $Sn(CH_3)_3$, and $Si(CH_3)_3$ groups (1) with other values taken from the original tabulation (2).

The f and r values predicted from eqs. 4–8 are also given in Table 7. In the case of ^{13}C correlations, there is a generally good agreement between predicted and observed f and r values. In particular the f values are entirely consistent

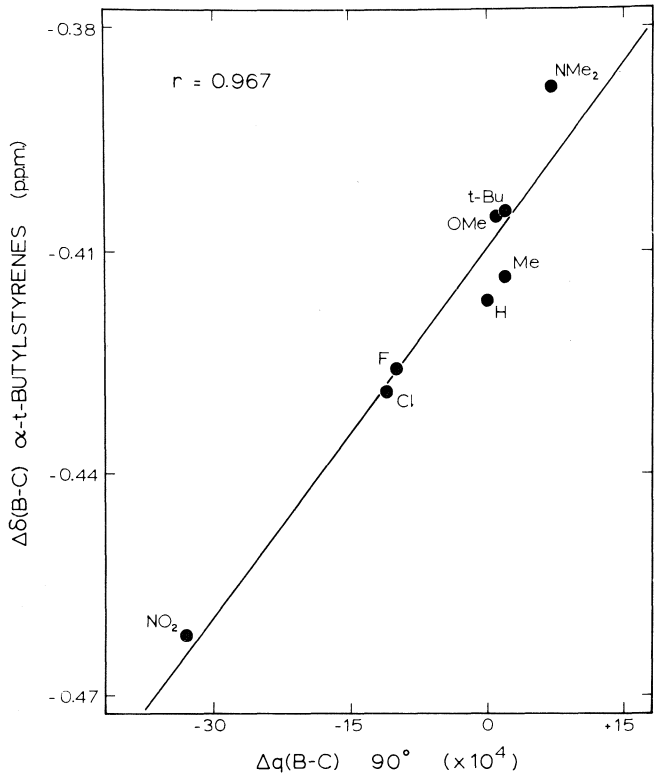

FIG. 1. Correlation of the β proton chemical shift difference, Δδ(B − C) of ATBS derivatives with the difference in charge density for the β protons of styrene derivatives (relative to styrene with ρ = 90°).

with the postulated nature of π polarization effects. The signs and magnitudes of the *f* values for C-2,6 and -1 are also consistent with phenyl group π polarization while the *r* values are consistent with normal pictures of resonance interactions (the increase in *r* with ρ for C-1 is logical since the resonance effect should be isolated in the phenyl group as conjugation between phenyl and vinyl groups decreases). No correlations were performed for C-3,5 and -4 because these chemical shifts are likely to be affected by structural effects. The ^{1}H chemical shift correlations also show good agreement between predicted *f* and *r* values. However, it appears that *f* for δ_{H_C} and *r* for δ_{H_B} both decrease more rapidly than predicted by eqs. 9 and 4. Consequently, Δδ(B − C) for AMS and ATBS derivatives depends upon both *F* and *R* with a smaller field dependence for Δδ(B − C) than in the case of styrene (1).

While the ^{1}H S.C.S. for H_B and H_C do not precisely follow the predictions based upon the model of electronic substituent effects outlined above, charge densities determined by the CNDO/2 calculations indicate a probable electronic origin for the deviations. For planar 4-substituted styrenes, $\Delta(\equiv q_{H_B} - q_{H_C}$, relative to styrene) is linearly related to *F*:

$$[11] \qquad \Delta(0°) = -(33 \pm 4) \times 10^{-4}F$$

with a statistically insignificant dependence on *R*. On the other hand, when ρ = 90°, Δ depends upon both *F* and *R*:

$$[12] \quad \Delta(90°) = -(20 \pm 3) \times 10^{-4}F - (17 \pm 4) \times 10^{-4}R$$

Thus it is seen that both the decreased field dependence and the negative resonance dependence of Δδ(B − C) on going from styrene to non-planar α-alkylstyrenes are reproduced by the CNDO/2 calculations. This has been further confirmed by plotting Δδ(B − C) for ATBS *vs.* Δ(90°) (Fig. 1). There is a good correlation (better than for styrene (1)) and the slope of 17 p.p.m./hydrogen 1s electron is consistent with previously suggested scaling factors for proton chemical shifts (34, 35). While the good

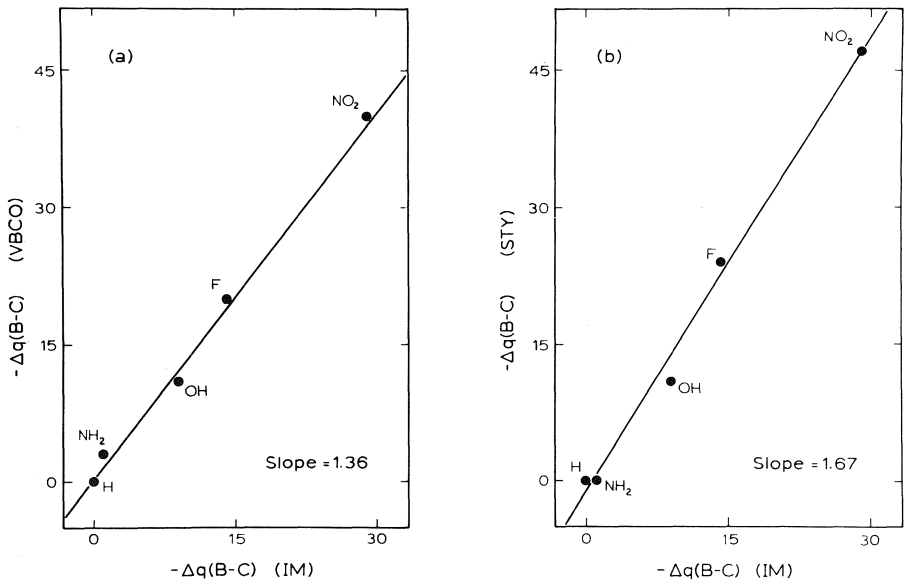

FIG. 2. Plots of differences in charge densities for H_B and H_C of (*a*) 4-substituted 1-vinylbicyclo[2.2.2]octanes (VBCO) and (*b*) 4-substituted styrenes (STY), both plotted against the corresponding difference in ethylene proton charge density for CH_3X—C_2H_4 pairs of molecules (IM).

correlation may be partly fortuitous since the calculations were carried out for styrene at 90° rather than ATBS at 64°, it is highly improbable that the agreement could be completely accidental. In addition, plots of $q_{H(90°)}$ *vs.* $q_{H(0°)}$ for each proton (not shown) revealed a linear plot for H_C while the plot for H_B was irregular, particularly for groups with large R values. This supports the conclusion from the F and R correlations that there is an unexpected resonance contribution to δ_{H_B}.

Thus the CNDO/2 calculations for 4-substituted styrenes with $\rho = 90°$ provide evidence for electronic effects which can apparently account for all deviations between predicted and observed f and r values for AMS and ATBS derivatives. In addition, CNDO/2 calculations for 4-substituted 1-vinylbicyclo[2.2.2]octanes (VBCO) and ethylene–CH_3X pairs (oriented so that the C—X bond and the ethylene group are in an identical orientation to the C—X bond and the vinyl group in VBCO) (1) provide a possible explanation for the reduced field dependence of δ_{H_B} and $\Delta\delta(B - C)$ on going from styrene to AMS to ATBS. These calculations indicate that the field effect of the substituent (as measured by Δ) strongly depends upon the nature of the intervening molecular framework (see Fig. 2). The field effect of the substituent should vary inversely as the effective dielectric constant within the cavity (36) where ε_{eff} is a function of both the molecule and the surrounding medium. Hermann (37) has calculated that ε_{eff} for 4-substituted bicyclo[2.2.2]octane carboxylic acids in vacuum is less than unity (0.73). This corresponds to an enhancement of the field effect by 1.37, in exact agreement with the calculated enhanced field effect for VBCO derivatives relative to CH_3X–ethylene pairs. The field effect is apparently even larger for styrene where the field acts in the nodal plane of the phenyl π system, *i.e.* in a cavity inside a polarizable system. It is entirely conceivable that ε_{eff} is increased by rotating the vinyl group so that the field no longer acts through the cavity formed by the phenyl π electron system. An increased ε_{eff} would lead to a decreased field effect. This would primarily effect the f coefficient for δ_{H_C}, as observed.

Previous experimental investigations (1, 38, 39) of field effects upon proton chemical shifts provide support for the suggestion that the A constant in the Buckingham equation (40) depends upon the system (see Table 8). Calculated A values are based upon Musher's calculated value of 3.1×10^{-12} for the effect of an isolated dipole upon a C—H bond (39) and the proportionality factors shown in Fig. 2. An experimental investigation of 1-vinylbicyclo[2.2.2]octane derivatives has been undertaken in an attempt to confirm this point.

TABLE 8. Comparison of observed and calculated values of A constant in the Buckingham equation for various systems

System	$A(\times 10^{12})$ Observed	Calculated
CH bond in gas phase	2.9*	3.1§
CH bond in alicyclic compounds	4.2†	4.2‖
CH bond in aromatic compounds	4.6–6.5‡	5.5‖

*Estimated from CHF_3 in gas phase (43).
†Estimated from S.C.S. for steroids (38) (field evaluated at the proton).
‡Estimated from S.C.S. for 4-substituted styrenes (1) (field evaluated at the proton).
§Calculated value for isolated C—H bond in gas phase (39).
‖Calculated values for 4-substituted 1-vinylbicyclo[2.2.2]octanes and styrenes, using $A = 3.1 \times 10^{-12}$ for a C—H bond in the gas phase and the slopes of the plots of Δ for these compounds *vs.* Δ for C_2H_4–CH_3X pairs (Fig. 2).

The CNDO/2 calculations strongly suggest that the smaller than predicted R dependence of δ_{H_B} for AMS and ATBS derivatives is, at least in part, due to electronic interactions. Since there is no apparent reason why conjugative interactions should affect δ_{H_B} and δ_{H_C} differently, the small r values apparently reflect some additional negative resonance contribution to δ_{H_B}, *i.e.* a contribution by which electron-withdrawing ($+R$) groups cause high field shifts while $-R$ groups cause low field shifts. This is unexpected and the nature of the electronic effect is unclear to us. However, it is possible that it may be associated with an interaction of the C_α—C_β—H_B σ bond system with the phenyl π electron system. C_β—H_C would be much less likely to interact with the π electron system.

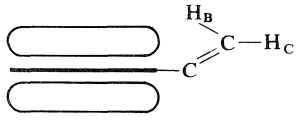

4

While the CNDO/2 calculations indicate that S.C.S. for the vinyl protons of AMS and ATBS derivatives are primarily due to electronic effects, one substituent effect which is primarily magnetic in origin may also be present. This is associated with substituent-induced changes in the dihedral angle ρ. The vinyl group can either accept or donate electrons by resonance. Therefore any substituent with a significant resonance effect should increase the conjugation between phenyl and vinyl groups. This is supported by CNDO/2 calculations since the calculated C_1—C_α bond order is greater for both 4-*N*,*N*-dimethylaminostyrene (0.2949) and 4-nitrostyrene (0.2952) than for styrene (0.2919).

As shown in Table 5, δ_{H_B} is much more sensitive than δ_{H_C} to changes in ρ, primarily due to changes in ring current effect. Since δ_{H_B} increases with decreasing ρ, substituent-induced changes in ρ should be reflected by a positive dependence of δ_{H_B} and $\Delta\delta(B - C)$ on $|R|$ (since both $+R$ and $-R$ substituents should decrease ρ).[4] Since all substituents had either $-R$ effects or very small $+R$ effects, this is difficult to distinguish from the observed negative R dependence (*i.e.* $-R \approx +|R|$). Based on the data from Table 5, the predicted angular dependence of δ_{H_B} at $\rho = 30°$ is approximately -0.01 p.p.m./degree. Thus the additional resonance contribution to δ_{H_B} could arise from very small changes in ρ, probably not exceeding 5°. This does not appear unreasonable.

There is conflicting evidence for the existence of a magnetic effect due to changes in ρ. In support of an effect of this type is the observation that the negative R dependence for $\Delta\delta(B - C)$ is apparently greater for AMS than for ATBS, whereas a purely electronic effect might be expected to have a maximum for $\rho = 90°$. However, the CNDO/2 results provide strong evidence for the presence of an electronic effect. It is probable that both effects are present, but their relative importance is uncertain.

In conclusion, correlations of vinyl ^1H and ^{13}C S.C.S. for AMS and ATBS derivatives with F and R give f and r values which are in good agreement with values predicted from experimental results for styrenes and a model for transmission of substituent effects which assumes a $\cos^2\rho$ dependence for transmission of any conjugative interaction. In cases where discrepancies are observed between calculated and observed f and r values, CNDO/2 calculations indicate that the deviations are primarily due to unanticipated electronic interactions, although one possible magnetic effect is postulated. Since the ^1H and ^{13}C chemical shifts and CNDO/2 charge densities all reflect similar trends in substituent effects and since the variation of f and r with ρ is in overall good agreement with a simple model of substituent effects, we conclude that the F and R

[4]This effect is completely different from a substituent-induced decrease in the total ring current effect of the phenyl group (38). The latter effect, which should have a *negative* $|R|$ dependence, is not important in 4-substituted styrenes (1) and therefore is unlikely to be important here.

correlations reflect electronic effects for these compounds and can be used to deduce mechanisms of transmission of substituent effects. As in the case of 4-substituted styrenes (1), the three main mechanisms of transmission of substituent effects are through-space field effects, resonance or mesomeric effects and π polarization effects. The magnitude of the field effect appears to depend upon the nature of the intervening molecular framework. Both CNDO/2 calculations and vinyl and phenyl ^{13}C chemical shifts suggest that the π polarization effect can be divided into two effects. When there is no conjugation between phenyl and vinyl groups ($\rho = 90°$) the two groups are independently polarized by the substituent (presumably acting through space) but for $\rho < 90°$ an additional polarization of the entire conjugated styrene π electron system can occur. The observation of π polarization effects is particularly important since these effects have often been considered to be unimportant.

Our conclusion that the correlations of S.C.S. for styrene derivatives with F and R reflect intramolecular electronic effects in these compounds is contradictory to the conclusion of Miller and Wiley based on S.C.S. for other systems (4). We have reinvestigated some of the systems on which the latter conclusions were based. This is the subject of the following paper.

W.F.R. thanks the National Research Council of Canada for financial support. I.R.P. thanks Gulf Oil Canada Ltd. for a Fellowship.

1. G. K. HAMER, I. R. PEAT, and W. F. REYNOLDS. Can. J. Chem. This issue.
2. C. G. SWAIN and E. C. LUPTON. J. Am. Chem. Soc., **90**, 4328 (1968).
3. J. A. POPLE and G. A. SEGAL. J. Chem. Phys. **44**, 3289 (1966).
4. S. I. MILLER and G. R. WILEY. J. Org. Chem. **37**, 767 (1972).
5. G. K. HAMER. Ph.D. Thesis. University of Toronto, Toronto, Ontario, 1973.
6. B. B. CORSON, H. E. TIEFENTHAL, G. R. ATWOOD, W. J. HEINTZELMAN, and W. L. REILLY. J. Org. Chem. **21**, 584 (1956).
7. G. A. OLAH, M. B. COMISAROW, and C. J. KIN. J. Am. Chem. Soc. **91**, 1458 (1969).
8. C. H. YODER, R. H. TUCK, and R. E. HESS. J. Am. Chem. Soc. **91**, 539 (1969).
9. W. H. C. RUEGGEBERG, M. L. CUSHING, and W. A. COOK. J. Am. Chem. Soc. **68**, 191 (1946).
10. H. GILMAN, E. A. ZOELLNER, and W. M. SELBY. J. Am. Chem. Soc. **55**, 1252 (1933).
11. H. E. RAMSDEN, A. E. BALINT, W. R. WHITFORD, J. J. WALBURN, and R. CSERR. J. Org. Chem. **22**, 1202 (1957).
12. E. ROTHSTEIN and R. W. SAVILLE. J. Chem. Soc. 1950 (1949).
13. N. C. DENO, F. A. KISH, and H. J. PETERSON. J. Am. Chem. Soc. **87**, 2157 (1965).
14. R. C. HUSTON and I. A. KAYE. J. Am. Chem. Soc. **64**, 1576 (1942).
15. E. C. STIRLING and M. T. BOGERT. J. Org. Chem. **4**, 25 (1939).
16. G. BRUBACHER and E. SUTER. Helv. Chim. Acta, **33**, 256 (1950).
17. G. K. HAMER and W. F. REYNOLDS. Can. J. Chem. **46**, 3813 (1968).
18. R. A. BELL and J. K. SAUNDERS. Can. J. Chem. **48**, 1114 (1970).
19. Quantum Chemistry Program Exchange program 141.
20. E. A. BRAUDE and F. SONDHEIMER. J. Chem. Soc. 3754 (1955).
21. H. SUZUKI. Electronic absorption spectra and geometry of organic molecules. Academic Press, New York. 1967. Chapts. 9 and 13.
22. D. R. DAVIS and J. D. ROBERTS. J. Am. Chem. Soc. **84**, 2252 (1962).
23. R. KAISER. J. Chem. Phys. **42**, 1838 (1965).
24. F. A. L. ANET and A. J. R. BOURN. J. Am. Chem. Soc. **87**, 5250 (1965).
25. J. A. POPLE, W. G. SCHNEIDER, and H. J. BERNSTEIN. High resolution NMR. McGraw-Hill, New York. 1959. p. 241.
26. (*a*) T. SCHAEFER, W. F. REYNOLDS, and T. YONEMOTO. Can. J. Chem. **41**, 2969 (1963). (*b*) T. YONEMOTO. Can. J. Chem. **44**, 223 (1966).
27. (*a*) E. G. MCRAE and L. GOODMAN. J. Mol. Spectrosc. **2**, 464 (1958). (*b*) E. G. MCRAE and L. GOODMAN. J. Chem. Phys. **29**, 334 (1958).
28. D. M. GRANT and E. G. PAUL. J. Am. Chem. Soc. **86**, 2984 (1964).
29. D. K. DALLING and D. M. GRANT. J. Am. Chem. Soc. **94**, 5318 (1972).
30. J. MASON. J. Chem. Soc. A, 1038 (1971).
31. W. F. REYNOLDS, I. R. PEAT, M. H. FREEDMAN, and J. R. LYERLA, JR. Can. J. Chem. Submitted.
32. A. R. KATRITZKY and R. O. TOPSOM. J. Chem. Ed. **48**, 427 (1971).
33. O. KAJIMOTO and T. FUENO. Tetrahedron Lett. 3329 (1972).
34. Reference 25. Chapt. 7.
35. J. I. MUSHER. *In* Advances in magnetic resonance. Vol. 2. J. S. Waugh, editor. Academic Press, New York. 1966.
36. J. G. KIRKWOOD and F. W. WESTHEIMER. J. Chem. Phys. **6**, 506 (1938).
37. R. B. HERMANN. J. Am. Chem. Soc. **91**, 3152 (1969). K. S. DHAMI and J. B. STOTHERS. Can. J. Chem. **43**, 510 (1965).
38. R. F. ZURCHER. *In* Progress in NMR spectroscopy. Vol. 2. J. W. Emsley, J. Feeney, and L. H. Sutcliffe, editors. Pergamon Press, Oxford. 1967. Chapt. 5.
39. J. I. MUSHER. J. Chem. Phys. **37**, 34 (1962).
40. A. D. BUCKINGHAM. Can. J. Chem. **38**, 300 (1960).
41. H. P. FIGEYS and R. FLAMMANG. Mol. Phys. **12**, 581 (1967).
42. C. E. JOHNSON and F. A. BOVEY. J. Chem. Phys. **29**, 1012 (1958).
43. L. PETRAKIS and H. J. BERNSTEIN. J. Chem. Phys. **37**, 2731 (1962).

Stereochemical and Steric Effects in Nucleophilic Substitution of α-Halo Ketones

J. William Thorpe and John Warkentin

Department of Chemistry, McMaster University, Hamilton, Ontario

Received August 11, 1972

Bimolecular substitution reactions of α-halo ketones with acetate and azide ions are remarkably insensitive to steric hindrance. 1-Bromo-4,4-dimethyl-2-pentanone (bromomethyl neopentyl ketone) is only slightly less reactive than bromo acetone in spite of the fact that the carbonyl group in the former is neopentylic. The results are interpreted in terms of a normal S_N2 transition state, not involving either special alignment of entering and leaving group with the π-orbital of the carbonyl function (conjugation) or covalent interaction between nucleophile and carbonyl carbon (bridging) for reaction of conformationally-mobile systems. Conformationally-fixed systems, on the other hand, may be affected by such factors. *trans*-2-Chloro-4-*t*-butylcyclohexanone is 61-fold more reactive than the *cis*-isomer, in the S_N2 reaction with acetate. Activation parameters support the conclusion that only those α-halo ketones which are stereochemically set up for conjugation and bridging undergo substitution by a mechanism significantly different from that operating in corresponding reactions of alkyl halides.

Possible significance of the results to the mechanism of bimolecular elimination is discussed.

Les réactions de substitution bimoléculaire des α-halocétones avec les ions acétate et azoture sont remarquablement insensibles à l'empêchement stérique. La bromo-1 diméthyl-4,4 pentanone-2 (bromométhyl néopentyl cétone) n'est que légèrement moins réactive que la bromoacétone malgré un groupe carbonyle néopentylique. Les résultats sont interprétés par un état de transition normal S_N2 qui n'implique ni un alignement spécial du groupe entrant ou partant ave l'orbitale π du carbonyle (conjugaison) ni une interaction covalente entre le nucléophile et le carbone du carbonyle (pontage) pour la réaction des systèmes conformationnellement mobiles. Les systèmes de conformation rigide peuvent être affectés par de tels facteurs. La *trans* chloro-2 *t*-butyl-4 cyclohexanone est 61 fois plus réactive que le *cis* dans la réaction S_N2 avec l'acétate. Les paramètres d'activation permettent de conclure que seules ces α-halocétones, où la stéréochimie se prête à une conjugaison et à un pontage, subissent une substitution selon un mécanisme nettement différent de celui des halogénures d'alkyle.

L'apport possible de ces résultats au mécanisme de l'élimination bimoléculaire a été discuté.

[Traduit par le journal]

Can. J. Chem., **51**, 927 (1973)

Introduction

The enhanced reactivity of α-halo ketones, relative to alkyl halides, in bimolecular nucleophilic substitution has been known for many years. For example, phenacyl chloride and chloroacetone were reported to react 97 000 and 33 000 times as fast, respectively, as *n*-propyl chloride with iodide ion in acetone at 50° (1). Somewhat smaller rate factors, lying between 10^2 and 10^3, were reported for the same compounds reacting at 30° in methanol with acetate, azide, cyanate, and thiocyanate ions (2).

Many mechanisms have been proposed to account for the enhancement of reactivity conferred by the carbonyl group. Hughes (3) suggested that the inductive effect of the carbonyl group enhances the normal polarity of the carbon–halogen bond by increasing electron deficiency at the α-carbon. The more polar the C—X bond the faster would be the attack of nucleophiles in bimolecular displacement. Baker (4*a*) suggested that the first and rate-determining step is addition to the carbonyl carbon from which the addend is then transferred to the α-position, with displacement of halogen, in a fast step. A variant of that mechanism, which includes epoxide formation (eq. 1), has been considered by Pearson and coworkers (4*b*).

Other modes of interaction of the nucleophile

[1] $$RCOCH_2X + B \rightleftharpoons R-\underset{\displaystyle B^+}{\overset{\displaystyle O^-}{\underset{|}{\overset{|}{C}}}}-CH_2X \rightarrow$$

$$R-\overset{O}{\underset{\displaystyle B^+}{\overset{/\backslash}{C}}}-CH_2 + X^-$$

$$\downarrow B' \text{ fast}$$

$$RCOCH_2B' + B$$

Can. J. Chem. Downloaded from www.nrcresearchpress.com by 210.87.254.5 on 09/05/12
For personal use only.

Can. J. Chem. Downloaded from www.nrcresearchpress.com by 210.87.254.5 on 09/05/12
For personal use only.

with the carbonyl function have been suggested. Dewar (5) postulated that the C—X bond being broken and the new bond being formed at the transition state are aligned with the π-plane of the carbonyl group. Excess negative charge can then be accommodated in a molecular orbital encompassing the carbonyl group (conjugation) with consequent lowering of the activation free energy. A modification of that transition state picture, with partial covalent bonding of the nucleophile to both the carbonyl carbon and the α-carbon (bridging) has been suggested also (6). These last mechanisms have in common a strict geometric requirement but they differ with respect to the carbonyl-to-nucleophile[1] bond distance.

Another rationale for the enhanced S_N2 reactivity of α-halo carbonyl compounds does not invoke such a geometric restriction. Pearson and coworkers (4*b*) reached the conclusion that interaction between carbonyl group and nucleophile is largely electrostatic and that α-halo carbonyl compounds owe their high S_N2 reactivity to polarization interaction which is particularly important in those compounds because of the smaller steric requirement of RCO compared to RCH_2.

Finally, the possibility that α-halo ketones might give substitution products via the enolization–solvolysis mechanism, eq. 2, was considered in 1938 by Richard (7). Many cases have

[2]
$$RCH_2COCH_2X \rightleftharpoons RCH{=}C(OH){-}CH_2X \rightarrow RCH{=}C(OH)^{+}{=}CH_2X^{-} \xrightarrow{B^-} RCH_2COCH_2B + RCH(B)COCH_3$$

now been reported in which that mechanism is probably operative (8, 9). Possibly a given fast rate of substitution could result from fast enolization–solvolysis in which case comparison with S_N2 rates in corresponding alkyl halides would be meaningless.

For substitutions on α-halo ketones by weakly basic nucleophiles, many of the potential rationales (above) for fast rates are untenable or weak. The explanation of Hughes would require that electron-withdrawing α-substituents other than carbonyl should also enhance the rate of S_N2 reaction of a halide. However, what is found is that α-halogen, α-alkoxy, and α-sulfonyl substituents retard the rate of bimolecular substitution of alkyl halides. Baker's mechanism fails to fit the general observation that the rate of substitution of α-halo ketones is strongly dependent on the identity of the halogen (4*b*, 10); bromo ketones reacting faster than chloro ketones.

Epoxides have been isolated or shown to be intermediates in reactions of some α-halo ketones, particularly those containing the α-halo benzyl group, with bases (11–16). Alkoxide bases are the most common ones leading to epoxides and other products, such as ketals, derived from them. Whether or not epoxide intermediates lead to normal S_N2 products seems to depend on the system under investigation. Good kinetic evidence against epoxide intermediates in substitutions of α-halo ketones with nitrogen and sulfur bases was provided by Pearson and coworkers (4*b*). Lutz (17) used a stereochemical probe for the epoxide mechanism. He showed that optically active desyl chloride undergoes exchange and racemization, with radioactive Cl^-, at the same rate. For the epoxide mechanism exchange without racemization is predicted. On the other hand, Turro, Rappe, and coworkers (18) claim that the epoxide mechanism is a major route to α-methoxy ketones in reactions of several α-bromo ketones with methoxide in methanol.

The enolization–solvolysis mechanism should be easily recognized by examination of the products and of unreacted halo ketone. Unless high selectivity for capture of the allylic cation intermediate at the original halogen-bearing site is built in, the absence of rearranged substrate and rearranged product can be taken as evidence against ion-pair intermediates.

It is more difficult to rule out the remaining explanations; namely conjugation (5), bridging (6) and electrostatic/steric factors (4*b*). Evidence pointing to a definite geometric requirement as

[1]In the bridging mechanism, the leaving group as well as the nucleophile could bridge the two carbon atoms. Such bridging would have to be the same for both entering and leaving groups in cases of displacement on $RCOCH_2X$ by X^-.

TABLE 1. Rates of S_N2 reactions in aqueous 1,2-DME at 54.8°

Compound	$10^3 k^{AcO^-}$ (M^{-1} s^{-1}) X = Cl[a]	$10^3 k^{AcO^-}$ (M^{-1} s^{-1}) X = Br[a]	$10^2 k^{N_3^-}$ (M^{-1} s^{-1}) X = Br[a]
CH_3COCH_2X	1.14 (3.40)	1.46 (2.47)[b]	9.48 (1.63)
$CH_3CH_2COCH_2X$	1.05 (3.14)	1.46[c] (2.47)	—
$(CH_3)_2CHCOCH_2X$	0.710 (2.12)	1.05[d] (1.77)	9.24 (1.59)
$(CH_3)_3C\,COCH_2X$	0.335 (1.00)	0.592 (1.00)[b]	5.81 (1.00)
$CH_3CH_2COCH_2X$	1.05 (18.3)	1.46[c] (2.43)	9.24 (1.55)
$CH_3CH_2CH_2COCH_2X$	0.620 (10.8)	1.18 (1.97)	8.68 (1.46)
$(CH_3)_2CHCH_2COCH_2X$	0.129 (2.24)	0.922 (1.53)	5.94 (1.00)
$(CH_3)_3C\,CH_2COCH_2X$	0.0575 (1.00)	0.601 (1.00)	—

[a]In each group the bracketed numbers next to the rate constants are relative rates referred to the last entry for that group.
[b]At 0.2°, the ratio of rate constants (bromoacetone/bromopinacolone) is 5.98.
[c]For *n*-butyl bromide under the same conditions, $k^{AcO^-} = 2.06 \times 10^{-5}$ M^{-1} s^{-1}.
[d]This is a composite rate constant for the S_N2 reaction and the enolization/solvolysis mechanism, as indicated by the product composition: $(CH_3)_2CHCOCH_2OAc$, 72.5%; $(CH_3)_2CHCOCH_2OH$, 17.2%; $(CH_3)_2C(OAc)COCH_3$, 5.5%; $(CH_3)_2C(OH)COCH_3$, 4.8%. In reaction of the bromo ketone with azide, and in reaction of the chloro ketone with either nucleophile, solvolytic products were not detected.

demanded by the conjugation and bridging pictures was provided by Bartlett and Trachtenberg (19), who studied bimolecular substitution of pseudo halides **1** and **2**. In each case the leaving group is a dinitro phenoxide ion,

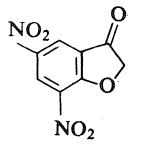

1

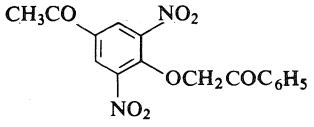

2

attached α to ketonic carbonyl. In **1**, however, the leaving group departs in a plane perpendicular to the carbonyl π-orbital, making bridging or conjugation impossible. Compound **2**, in which there is no such restriction, reacted 9000 times as fast with iodide in acetone at 0°; the net result of lower values of both $\Delta H^{\ddagger}$ (10 *vs.* 31 kcal mol^{-1} for **1**) and $\Delta S^{\ddagger}$ (−30 *vs.* +25 e.u. for **1**). Although these results were considered to be consistent with either the conjugation mechanism or the bridging mechanism (19), the authors cautioned that Pearson's electrostatic model might also suffice to explain the sluggishness of **1**, to which the nucleophile must approach along a line parallel to the C=O dipole but from the negative end. Sisti and Lowell (2) concluded, however, that the electrostatic model is insufficient. They found that highly-polarizable nucleophiles like cyanate and azide react faster with α-halo carbonyl compounds than with alkyl halides by factors no larger than those in corresponding reactions with less polarizable nucleophiles. If electrostatic interaction with the polar C=O group were a dominant source of stabilization, the extent of this interaction should depend critically on the polarizability of the nucleophile. Temnikova and coworkers (20) also favor a Dewar–Winstein transition state, with its geometric constraint, over one dominated by electrostatic factors.

The objectives of the work described in this paper were to find stronger evidence for or against the Dewar–Winstein transition states in substitution reactions of α-halo ketones and, if possible, to distinguish between them. The features on which probes were based are the strict geometric requirement common to both and the steric hindrance by R of $RCOCH_2X$ that should be appreciable if significant bonding to carbonyl carbon (bridging) were involved in displacements of the halogen.

Methods, Results, and Discussion

Rates of displacement of chloride or bromide ions from α-halo ketones by acetate or azide ions in homogeneous, dilute solutions of aqueous 1,2-dimethoxyethane (DME) were followed with appropriate ion-specific electrodes. Second order kinetics was established and products were isolated and identified. With two exceptions (see footnotes to Table 1) all the substrates gave unrearranged substitution products, without a trace of solvolytic products. Moreover, in those cases where stereochemistry could be demonstrated, substitution proceeded with inversion. Traces of α,β-unsaturated ketones, the expected products of E2 reactions, were looked for with u.v. spectroscopy in a few cases but none were

Can. J. Chem. Downloaded from www.nrcresearchpress.com by 210.87.254.5 on 09/05/12
For personal use only.

TABLE 2. Rates of S_N2 reactions in aqueous 1,2-DME at 54.8°

Compound	$10^5 k^{AcO^-}$ (M^{-1} s^{-1}) X = Cl[a]		$10^5 k^{AcO^-}$ (M^{-1} s^{-1}) X = Br[a]		$10^3 k^{N_3^-}$ (M^{-1} s^{-1}) X = Br[a]	
CH_3COCH_2X	114	(306)	146	(64.0)	94.8	(9.60)
$CH_3COCHXCH_3$	40.4	(109)	61.2	(26.8)	57.6	(5.83)
$CH_3CO\ CX(CH_3)_2$	0.372	(1.00)	2.28[b]	(1.00)	9.88	(1.00)
$CH_3COCHXCH_3$	40.4	(7201)	61.2	(744)	57.6	(172)
$CH_3COCHXCH_2CH_2$	2.78	(495)	20.0	(243)	—	
$CH_3COCHXCH(CH_3)_2$	0.0852	(15.2)	1.26	(15.3)	3.70	(11.0)
$CH_3COCHX\ C(CH_3)_3$	0.00561	(1.00)	0.0823	(1.00)	0.335	(1.00)

[a]In each group the bracketed numbers following the rate constants are relative rates referred to the east entry in that group.
[b]This rate constant, like that for reaction of the isomeric bromo ketone (Table 1, footnote *d*) is a composite value from competing S_N2 and enolization/solvolysis reactions. The value 2.28×10^{-5} M^{-1} s^{-1} is only an upper limit for the S_N2 rate constant and relative rates (26.8 and 64.0) in that column are nothing more than lower limits.

detected. It is therefore safe to conclude that the reactions followed, save for the exceptional cases, were purely bimolecular substitution processes.

Table 1 holds rate data for reaction of α-halo ketones in which the site of substitution is primary but in which the steric bulk of the other carbonyl substituent is varied, first by successive increases in the number of α-methyl groups (entries 1–4) and then by analogous changes in the extent of β-branching (entries 5–8). It is striking that in the first series the rate factors caused by substituting *t*-butyl for methyl at carbonyl carbon are only 3.4, 2.5, and 1.6 for displacement of Cl^- by AcO^-, Br^- by AcO^-, and Br^- by N_3^-, respectively, at 54.8°. For the second reaction run at 0.2°, the rate factor is increased to 6.0 (Table 1, footnote *b*). Steric hindrance to attack at neopentyl positions has been well documented. For example, saponification of ethyl acetate in 85% ethanol at 50° is 161 times as fast as the same reaction of ethyl trimethylacetate (21). In acid-catalyzed hydrolysis the same esters show a rate ratio of 35 at 25° (22). Other models for the steric effect in addition to neopentylic, sp^2-carbon include hydroboration of alkenes and carbene additions to alkenes. In hydroboration by disiamyl borane in THF at 0°, *cis*-2-butene is about 30 times as reactive as *cis*-4,4-dimethyl-2-pentene (23). Dichlorocarbene reacts 35 times faster with 1-butene than with 3,3-dimethyl-1-butene at −10° (24). These reactions are not equally good models for the steric effect to be expected for reaction of α-halo ketones via a three-membered transition state and differences in medium and in temperature compound the problem of choosing the best model. However, that choice is unnecessary because the steric effects found in this work (Table 1, entries 1–4) are considerably smaller than those in any of the above-mentioned model reactions and are therefore not compatible with appreciable bonding of the nucleophile to carbonyl carbon. This conclusion is supported by the activation parameter data, which are discussed below.

The larger rate factors resulting from β-branching of chloro ketones, but not of bromo ketones (Table 1), can be accounted for qualitatively. The neopentyl substituent at carbonyl carbon can hinder not only addition to that atom but also reaction at the remote α-site. Examination of molecular models reveals that the latter hindrance can be larger in the β- than in the α-branched series. Presumably chloro ketones are more sensitive than bromo ketones to steric hindrance at the halogen-bearing carbon because the nucleophile must bond more tightly to that site at the transition state for displacement of the poorer leaving group.

Table 2 shows the effects of steric hindrance resulting from branching in the halogen-bearing carbonyl substituent. As expected for a bimolecular substitution process, the rate factors are substantial. For substitution by acetate, changing CH_2X to $CHXC(CH_3)_3$ brings about a 20 000-fold rate reduction for X = Cl and a 1800-fold reduction for X = Br. Again the greater sensitivity of the chloro ketones to steric hindrance is in keeping with a tighter transition state for displacement of a poor leaving group.

The observed effects on rates, of changing the nucleophile from acetate to azide (Tables 1, 2), are similar to those reported by Sisti and Lowell (2) who found azide 126-fold and 46-fold faster than acetate in displacement of chloride from

Can. J. Chem. Downloaded from www.nrcresearchpress.com by 210.87.254.5 on 09/05/12
For personal use only.

TABLE 3. Rates and activation parameters

Compound	$10^5 k_{54.8°}^{AcO^-}$ (M^{-1} s^{-1})	$\Delta H^{\ddagger}$ (kcal mol^{-1})	$\Delta S^{\ddagger}$ (e.u.)
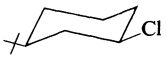	0.118	16.0±0.8[a]	−37±3[a]
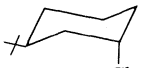	0.254	15.0±1.0[a]	−39±3[a]
	0.832	18.1±0.3[b]	−27±1[b]
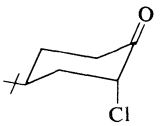	50.6	10.2±0.3[b]	−43±1[b]
$CH_3CH_2CH_2CH_2Br$	2.06	20.7±0.6[c]	−17±2[c]
$CH_3CH_2COCH_2Br$	146	21.8±0.3[d]	−5±1[d]

[a]From rates at 54.8 and 75.0°.
[b]From rates at 35.0, 54.8, and 75.0°.
[c]From rates at 40.0, 54.8, and 70.0°.
[d]From rates at 0.20, 30.0, and 54.8°.

$C_6H_5COCH_2Cl$ and CH_3COCH_2Cl, respectively, in methanol at 30°. Lower sensitivity of azide to steric factors is usually accounted for in terms of a more reactant-like transition state; the complementary rationale for the one accounting for leaving group effects (above).

Table 3 contains rate data and activation parameters for S_N2 reactions of some alkyl halides and halo ketones, including conformationally-locked systems. The *t*-butylcyclohexyl chlorides are nearly identical in both rate at 54.8° and parameters of activation. Two striking features emerge when these compounds are compared with the corresponding chloro cyclohexanones. First, both chloro ketones are more reactive than either cyclohexyl chloride. Even if the geometry precludes conjugative and bridging interactions between nucleophile and carbonyl group, the latter causes an appreciable rate enhancement. The second striking feature is that the origin of that enhancement is entirely entropic in the case of the *cis*-chloro ketone; the enthalpic effect of introducing the CO function is actually rate retarding. This feature is not peculiar to cyclohexyl systems nor to chloro compounds as the last two entries indicate. It is also not unique to the aqueous solvent system used here, or to acetate as nucleophile. Bordwell and Brannen (25) found that the faster rate of reaction of $C_6H_5COCH_2Cl$ (relative to that of *n*-BuCl) with I^- in acetone is largely the result of a more favorable entropy of activation. The third notable feature is that the reactivity of the *trans*-chloro ketone is quite different in origin. Here $\Delta H^{\ddagger}$ and $\Delta S^{\ddagger}$ are both lowered relative to those parameters for the *trans*-cyclohexyl chloride.

Any interpretation of these results in terms of mechanism must recognize the similarity between the sets of data for *cis*-cyclohexyl chloride and *cis*-chlorocyclohexanone on the one hand and for 1-bromobutane and 1-bromo-2-butanone on the other. In both *cis*-cyclic, secondary chloro compounds and acyclic, primary bromo compounds, the result of changing $CH_2\underset{|}{C}HX$ to $\underset{|}{C}OCHX$ is to increase rate, $\Delta H^{\ddagger}$, and $\Delta S^{\ddagger}$. Since the geometry precludes conjugation and bridging in the conformationally-fixed systems, one must conclude that such factors are not important either in the S_N2 reactions of acyclic α-bromo ketones; a conclusion that is supported by the data in Table 1.

The data for *trans*-2-chloro-4-*t*-butylcyclo-

Can. J. Chem. Downloaded from www.nrcresearchpress.com by 210.87.254.5 on 09/05/12
For personal use only.

Can. J. Chem. Downloaded from www.nrcresearchpress.com by 210.87.254.5 on 09/05/12
For personal use only.

hexanone (Table 3) are consistent with either the Dewar or the Winstein picture. In the Dewar mechanism, activation enthalpy would be lowered by virtue of better charge redistribution (delocalized bonding) which is also achieved in the Winstein mechanism by more localized bonding. In either mechanism the enthalpic gain would be partly offset by entropic loss which follows from the reduction in degrees of freedom imposed by a strict geometric requirement.

In summary, we suggest that the Dewar–Winstein mechanisms of S_N2 reactions of α-halo ketones apply only in exceptional cases, where molecular geometry is already appropriately constrained in the substrate. Our present data are not extensive enough to permit selection of one of the two closely related mechanisms as the more likely in such cases.

For the S_N2 reactions of those acyclic α-halo ketones which were studied, electrostatic attraction between nucleophile and carbonyl carbon, coupled with a low steric requirement for RCO (4*b*, 25) appears to be adequate to explain both rates and activation parameters. To fit the results of Bartlett and Trachtenberg (19, see above) to this picture, one can invoke a substantial unfavorable electrostatic effect in reaction of **1**, rather than a large favorable conjugative or bridging effect in reaction of **2**. As was pointed out in the introduction, those authors considered such an alternative explanation.

Our results concerning substitutions may be relevant also to the mechanism of bimolecular elimination which, it has been suggested (26–28), proceeds through a bridged transition state having features of both elimination and substitution. This mechanism has been called

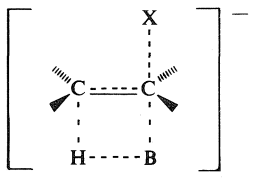

3

"E2C" and is pictured as having a transition state somewhat like **3**. Evidence against appreciable involvement of B^- at carbon, based on a probe of steric requirements similar to the one described in this paper, has been published (29). Our results also point to the low probability of E2C mechanisms, for it is unlikely that bridging to sp^3-carbon can be important if bridging to carbonyl carbon is not.

Experimental

Acyclic α-Halo Ketones

All halo ketones, except the 4-*t*-butyl chlorocyclohexanones, were purified by gas–liquid partition chromatography (g.l.p.c.) until samples were obtained which eluted as single peaks from analytical g.l.p.c. columns and which showed no evidence of extraneous signals in n.m.r. spectra run at high spectrum amplitudes. The bromo ketones listed in the tables were prepared either by bromination of the appropriate ketones (30) or by reacting a diazo ketone with hydrogen bromide. Chloro ketones were obtained by analogous reactions of ketones with chlorine (30). The following procedures are typical. Data for the purified products, all of which were known compounds, are listed in Table 4.

3-Bromo-4,4-dimethyl-2-pentanone and 1-Bromo-4,4-dimethyl-2-pentanone

Gradual addition of bromine (1.87 g, 0.0117 mol) to a well-stirred solution of 4,4-dimethyl-2-pentanone (2.40 g, 0.0211 mol) in water (100 ml) containing potassium chlorate (0.350 g, 2.87×10^{-3} mol) at 50–60° gave a mixture of bromo ketones as a dense layer on the bottom of the flask. Separation was followed by washing with water, shaking with magnesium oxide, further washing with water, and drying with calcium chloride. Preparative g.l.p.c. on a QF-1 column (10 ft × 3/8 in., 10% liquid phase) at 145° and 60 ml min^{-1} flow rate of helium gave, in order of their elution: 3-bromo-4,4-dimethyl-2-pentanone; 1-bromo-4,4-dimethyl-2-pentanone; 1,1-dibromo-4,4-dimethyl-2-pentanone; and 1,3-dibromo-4,4-dimethyl-2-pentanone.

1-Bromo-3-methyl-2-butanone

Isobutyryl chloride, b.p. 40° at 150 mm (24.5 g, 0.230 mol) was treated with diazomethane (19.3 g, 0.460 mol) in ether (31). The resulting diazo ketone was reacted with hydrogen bromide (31) to afford 1-bromo-3-methyl-2-butanone which was separated from minor impurities by preparative g.l.p.c. on the same column (above) at 150° and 24 ml min^{-1} flow rate of helium.

3-t-Butylcyclohexyl Chlorides

Following the procedure of Eliel and Martin (32), the chloroformate from *cis*-3-*t*-butylcyclohexanol (4.53 g, 2.90×10^{-2} mol) and phosgene (3.72, 3.71×10^{-2} mol) was converted to the *trans*-chloride by treatment with dry pyridine. After concentration with a rotary evaporator the solution was chromatographed on QF-1 (10 ft × 3/8 in. column, 10% liquid phase) at 135° and 50 ml/min. The first component to emerge was a cyclohexene; the second was *trans*-3-*t*-butylcyclohexyl chloride, as judged from the chemical shift of the equatorial CHCl proton (270 Hz) which is reported (32) to be 269.8 Hz from TMS. The *cis*-isomer (5% *trans*) was donated by Professor E. L. Eliel; its properties were the same as those reported in the literature (32). Gas chromatography removed the *trans*-isomer.

2-Chloro-4-t-butylcyclohexanones

These compounds were prepared and purified according to methods described by Teo (33).

TABLE 4. Refractive indices of reactants and products

Structure	n_D^{25} X = Cl	X = Br	X = OAc	X = OH
CH_3COCH_2X	1.4431	1.4680	1.4153	
$CH_3CH_2COCH_2X$	1.4422	1.4658[a]	1.4177	
$(CH_3)_2CHCOCH_2X$	1.4241	1.4412[b]	1.4191	1.4249
$(CH_3)_3CCOCH_2X$	1.4337	1.4630	1.4182	
$CH_3CH_2CH_2COCH_2X$	1.4326	1.4623[a]	1.4196	
$(CH_3)_2CHCH_2COCH_2X$	1.4277	1.4581[a]	1.4195	
$(CH_3)_3CCH_2COCH_2X$	1.4371	1.4617[a]	1.4187	
$CH_3CHXCOCH_3$	1.4205	1.4560[a]	1.4118[a]	
$(CH_3)_2CXCOCH_3$	1.4366	1.4532[a]	1.4146	1.4103
$CH_3CH_2CHXCOCH_3$	1.4280	1.4555	1.4158	
$(CH_3)_2CHCHXCOCH_3$	1.4313	1.4605	1.4153	
$(CH_3)_3CCHXCOCH_3$	1.4341	1.4620[a]	1.4153	

[a]22°.
[b]20°.

Dry chlorine was passed into formic acid (340 ml) with stirring until the solution was 0.21 *M* in chlorine. The concentration was determined by adding 10 ml of 20% aqueous KI to 1 ml of the solution and titration of the resulting iodine with thiosulfate to the starch end point. This solution of chlorine in formic acid (7.14×10^{-2} mol of Cl_2) was added to 4-*t*-butylcyclohexanone (10.0 g, 6.50×10^{-2} mol) in 10 ml of formic acid. The solution was stirred for 1 h at 0–10° before water was added and the crude product was extracted into CH_2Cl_2. The latter solution was washed with saturated bicarbonate, water, and brine before it was dried with magnesium sulfate. Evaporation of the solvent left 11.0 g of a pale yellow oil; a mixture containing the isomeric chloro ketones.

Separation of the isomers was accomplished by column chromatography on silica gel, using 250 g of adsorbent in a 5 cm tube. The following solvents were used for elution, in the quantity and in the order given: (*1*) petroleum ether, b.p. 60–80°, 250 ml; (*2*) 99% petroleum ether/1% benzene, 250 ml; (*3*) 98% petroleum ether/2% benzene, 250 ml; (*4*) 95% petroleum ether/5% benzene, 250 ml; (*5*) 90% petroleum ether/10% benzene, 1000 ml; (*6*) 85% petroleum ether/15% benzene, 500 ml; (*7*) 80% petroleum ether/20% benzene, 4 l; (*8*) 70% petroleum ether/30% benzene, 750 ml; (*9*) 50% petroleum ether/50% benzene, 2 l; (*10*) benzene, 1750 ml; (*11*) 50% benzene/50% ether, 500 ml; and (*12*) ether, 500 ml.

Fraction *7* contained nearly pure *trans*-2-chloro-4-*t*-butylcyclohexanone (2.68 g) while fraction *8* was a mixture of that compound and a 2,6-dichloro ketone. Fraction *9* contained pure dichloroketone and fraction *10* held the desired *cis*-2-chloro-4-*t*-butylcyclohexanone (4.30 g). Fractions *11* and *12* were, respectively, a mixture of *cis*-2-chloro ketone with unreacted ketone and pure starting material. The *trans*-compound was purified by bulb-to-bulb distillation at low pressure and the *cis*-isomer was recrystallized from pentane to m.p. 58–59°. Spectra of both matched those supplied by Teo and Warnhoff (33).

Substitution Products

The isomeric 3-*t*-butylcyclohexyl chlorides were refluxed separately for several days in the acetate buffer used for kinetics (below). Extraction and chromatography on 10% QF-1 (10 ft × 1/8 in.) showed only starting material and one new component in each case. Preparative g.l.p.c. (10% QF-1, 10 ft × 3/8 in.) gave pure samples of the substitution products, which were shown by n.m.r. (32) and i.r. to be the isomeric 3-*t*-butylcyclohexyl acetates, formed by substitution with inversion of configuration.

Similarly, *cis*- and *trans*-2-chloro-4-*t*-butylcyclohexanone reacted with acetate ion to give, respectively, only *trans*- and *cis*-2-acetoxy-4-*t*-butylcyclohexanone. Of the latter, the *trans*-compound absorbed at 250 Hz ($AcOCH_{eq}$), compared to 255 Hz ($ClCH_{eq}$) in the *trans*-chloro ketone (33) and the *cis*-compound absorbed at 274 Hz ($AcOCH_{ax}$), compared to 270 Hz ($ClCH_{ax}$) in the *cis*-chloro ketone (33).

Substitution products from reaction of all acyclic halo ketones (Tables 1, 2) with acetate ion in aqueous DME were isolated by preparative g.l.p.c. and were identified by n.m.r. and i.r. spectroscopy. Because of the simplicity of these products and the ease with which they can be isolated and identified, details are not given. Some physical properties are gathered in Table 4.

α-Azido ketones were isolated from only a few reactions of azide ion with the halo ketones. 3-Bromo-4-methyl-2-pentanone, for example, gave only one product which was isolated by g.l.p.c. and identified from its spectra as the known (34) 3-azido-4-methyl-2-pentanone. Halo ketones which reacted solvolytically when acetate was the nucleophile (Tables 1, 2, footnotes) gave only one product (g.l.p.c.) from reaction with azide.

Ion-specific Electrodes

Bromide ion activity electrode, Model 94-35, and chloride ion activity electrode, Model 94-17, both by Orion, were used to measure halide ion concentrations. These electrodes develop potentials which are proportional to the logarithm of the activity of the ion in question (35). Potential *vs.* concentration curves were prepared for each electrode with standard solutions of the appropriate ion in the solvent used for kinetics (below). The bromide ion electrode was used in conjunction with a saturated calomel electrode (Fisher, Model 13-639-52) while the chloride electrode was used with a double junction reference electrode (Orion, Model 90-02). Potential

Can. J. Chem. Downloaded from www.nrcresearchpress.com by 210.87.254.5 on 09/05/12
For personal use only.

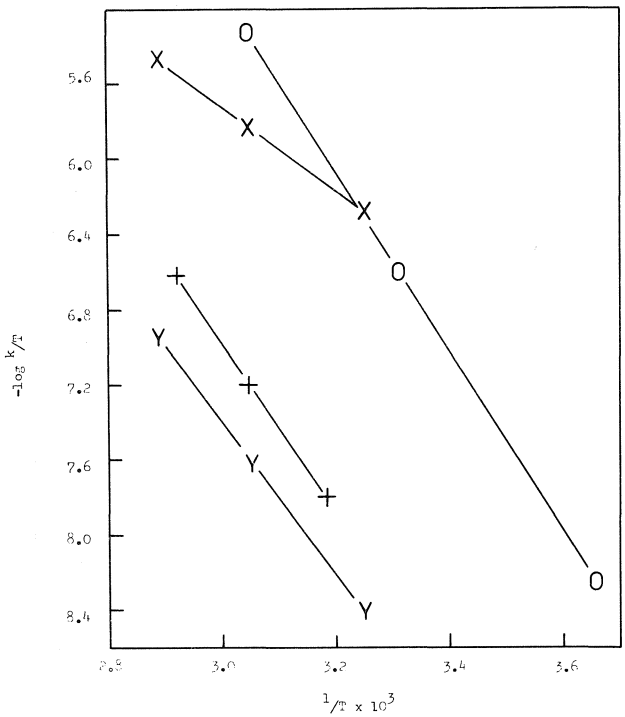

FIG. 1. Activation parameter plots for substitution by acetate: Y = *cis*-2-chloro-4-*t*-butylcyclohexanone; X = *trans*-2-chloro-4-*t*-butylcyclohexanone; + = *n*-butyl bromide; O = 1-bromo-2-butanone.

was measured with an expanded-scale p*H* meter (Fisher Accumet, Model 310), used in the expanded millivolt mode. A 1 mV recorder was used for following reactions with short (< 20 min) half-lives.

The bromide electrode was calibrated between 5.6×10^{-6} and 3.3×10^{-3} *M* in Br^-, readings being taken approximately every 10 mV. Log $[Br^-]$ *vs.* potential was linear in that range; the potential change being 120 mV. Its calibration was unchanged during 6 months of use. The chloride electrode was similarly calibrated. At the low end of its effective concentration range (5.0×10^{-5} *M*) that electrode's output was not proportional to log $[Cl^-]$. Gradual changes in the output of the chloride electrode required recalibration about once a month.

Kinetics

The reaction vessel, which was used for kinetics as well as for calibration, was a 125 ml three-necked flask of which the central neck was B-24/40 and the outer necks were B-19/40 ground joints. Electrodes were fitted snugly to these by means of machined Teflon rings, the halide electrode to the central neck and the reference electrode to an outer neck. This flask was supported in a water bath kept at 54.80 ± 0.04°, which contained an immersed magnetic stirrer (Tri-R Instruments) to drive the 1/2 in. Teflon-covered bar magnet in the flask.

For displacements by acetate the flask, mounted in the bath, was charged with 100 ml of a solution prepared from acetic acid (6.00 g, 0.100 mol), sodium acetate (8.20 g, 0.100 mol), 1,2-dimethoxyethane (24.0 ml) and water to make 100 ml. For substitution by azide, sodium azide (3.25 g, 0.050 mol) was added instead of acetate and the quantity of acetic acid was reduced to 3.00 g (0.050 mol). The necks were closed with glass stoppers during the time required for thermal equilibration. Electrodes were then inserted and, after about 20 min when the potential became steady, the halo ketone was injected from a syringe which was weighed before and after injection. Reaction was followed to two half-lives or more except for a few very slow reactions which were followed to 50% reaction only. In all cases where infinity values were taken, the agreement between the observed final halide concentration and that calculated from the quantity of halo ketone weighed in was within 3%. All halo ketones were run at least twice; the stoichiometric concentration of halo ketone being changed by factors between two and four. Agreement among the rate constants from these runs was to within 5% or better.

Pseudo first-order rate constants were obtained by plotting log $([X^-]_\infty - [X^-]_t)$ *vs.* time, where $[X^-]$ is the halide concentration. Values of $[X^-]_\infty$ were either measured or, in the case of slow reactions, obtained from the calculated initial concentration of organic halide. The slope of such a plot was set equal to $-k/2.303$. Division of such rate constants by the concentration of nucleophile gave the second order constants of Tables 1–3.

Activation parameters were obtained by fitting log k/T and $1/T$ data to a straight line (Fig. 1) with a linear least-squares computer program. The relationships (2.303 *R*) (slope) = $-\Delta H^{\ddagger}$ and (2.303 *R*) (intercept $-\log k/h$) = $\Delta S^{\ddagger}$ were applied to the computer values of the best slope and intercept. Errors were estimated from the maximum

Can. J. Chem. Downloaded from www.nrcresearchpress.com by 210.87.254.5 on 09/05/12
For personal use only.

and minimum slopes of lines fitting the extremes of the kinetic data.

The authors are indebted to Dr. K. E. Teo, Professor E. W. Warnhoff, and Professor E. L. Eliel for procedures, copies of spectra, and/or chemicals, as described in the manuscript. Financial support from the National Research Council of Canada, and an Ontario Graduate Fellowship to J. W. T., are also gratefully acknowledged.

1. J. B. CONANT, W. R. KIRNER, and R. E. HUSSEY. J. Am. Chem. Soc. **47**, 488 (1925).
2. A. J. SISTI and S. LOWELL. Can. J. Chem. **42**, 1896 (1964).
3. (*a*) E. D. HUGHES. Trans. Faraday Soc. **37**, 603 (1941). (*b*) E. D. HUGHES. Quart. Rev. (London), **5**, 245 (1951).
4. (*a*) J. W. BAKER. J. Chem. Soc. **848**, (1938). (*b*) R. G. PEARSON, S. H. LANGER, F. V. WILLIAMS, and W. J. MCGUIRE. J. Am. Chem. Soc. **74**, 5130 (1952).
5. M. J. S. DEWAR. The electronic theory of organic chemistry. Clarendon Press, Oxford. 1949. p. 73.
6. S. WINSTEIN, E. GREENWALD, and H. W. JONES. J. Am. Chem. Soc. **73**, 2700 (1951), footnote 16.
7. G. RICHARD. Bull. Soc. Chim. Fr. **5**, 286 (1938).
8. (*a*) V. ROSNATI, D. MISITI, and F. DE MARCHI. Gazz. Chim. Ital. **96**, 497 (1966). (*b*) V. ROSNATI, G. PAGANI, and F. SANNICOLO. Tetrahedron Lett. 124 (1967). (*c*) V. ROSNATI, F. SANNICOLO, and G. PAGANI. Gazz. Chim. Ital. **98**, 1085 (1968). (*d*) V. ROSNATI, G. PAGANI, and F. SANNICOLO. Tetrahedron Lett. 4545 (1967). (*e*) V. ROSNATI, F. SANNICOLO, and G. PAGANI. Tetrahedron Lett. 4649 (1968). (*f*) V. ROSNATI, F. SANNICOLO and G. PAGANI. Gazz. Chim. Ital. **99**, 152 (1969). (*g*) V. ROSNATI, F. SANNICOLO, and G. ZECCHI. Gazz. Chim. Ital. **99**, 651 (1969). (*h*) V. ROSNATI, F. SANNICOLO, and G. ZECCHI. Tetrahedron Lett. 599 (1970).
9. (*a*) F. G. BORDWELL and R. G. SCAMEHORN. J. Am. Chem. Soc. **90**, 6751 (1968). (*b*) F. G. BORDWELL, R. G. SCAMEHORN, and W. R. SPRINGER. J. Am. Chem. Soc. **91**, 2087 (1969). (*c*) F. G. BORDWELL, M. W. CARLSON, and A. C. KNIPE. J. Am. Chem. Soc. **91**, 3949 (1969). (*d*) F. G. BORDWELL and M. W. CARLSON. J. Am. Chem. Soc. **91**, 3951 (1969).
10. H. T. CLARK. J. Chem. Soc. **97**, 416 (1910).
11. A. M. WARD. J. Chem. Soc. 1541 (1929).
12. E. P. KOHLER and F. W. BROWN. J. Am. Chem. Soc. **55**, 4299 (1933).
13. C. PREVOST and A. SOMMIÈRE. Bull. Soc. Chim. Fr. **2**, 1151 (1935).
14. T. I. TEMNIKOVA and V. A. KROPACHEVA. J. Gen. Chem. U.S.S.R. **19**, 1917 (1949).
15. C. L. STEVENS, W. MALIK, and R. PRATT. J. Am. Chem. Soc. **72**, 4758 (1950).
16. (*a*) T. I. TEMNIKOVA, G. A. UGOLNIKOVA, O. A. NETSETSKAYA, and T. B. REMIZOVA. J. Gen. Chem. U.S.S.R. **27**, 2550 (1957). (*b*) T. I. TEMNIKOVA and N. A. OSHUEVA. J. Gen. Chem. U.S.S.R. **28**, 3252 (1958). (*c*) T. I. TEMNIKOVA and N. S. KIRIKOVA. J. Gen. Chem. U.S.S.R. **34**, 386 (1964). (*d*) T. I. TEMNIKOVA and O. A. KAUROV. J. Gen. Chem. U.S.S.R. **34**, 389 (1964). (*e*) T. I. TEMNIKOVA and N. A. KAUROV. J. Gen. Chem. U.S.S.R. **34**, 712 (1964). (*f*) T. I. TEMNIKOVA and A. S. DNEPROVSKII. J. Gen. Chem. U.S.S.R. **34**, 2878 (1964). (*g*) T. I. TEMNIKOVA and V. S. KARAVAN. J. Gen. Chem. U.S.S.R. **34**, 3204 (1964). (*h*) T. I. TEMNIKOVA and O. A. KAUROV. J. Gen. Chem. U.S.S.R. **34**, 3211 (1964).
17. R. P. LUTZ. J. Am. Chem. Soc. **90**, 3788 (1968).
18. N. J. TURRO, R. B. GAGOSIAN, C. RAPPE, and L. KNUTSSON. Chem. Commun. 270 (1969).
19. P. D. BARTLETT and E. N. TRACHTENBERG. J. Am. Chem. Soc. **80**, 5808 (1958).
20. V. S. KARAVAN, T. E. ZHESKO, and T. I. TEMNIKOVA. Zh. Org. Khim. **4**, 1000 (1968).
21. D. P. EVANS, J. J. GORDON, and H. B. WATSON. J. Chem. Soc. 1439 (1938).
22. R. W. TAFT, JR. Steric effects in organic chemistry. M. S. Newman, Editor. John Wiley and Sons, Inc. New York. 1956. p. 598.
23. H. C. BROWN and A. W. MOERIKOFER. J. Am. Chem. Soc. **83**, 3417 (1961).
24. R. A. MOSS and A. MAMANTOV. Tetrahedron Lett. 3425 (1968).
25. F. G. BORDWELL and W. T. BRANNEN, JR. J. Am. Chem. Soc. **86**, 4645 (1964).
26. S. WINSTEIN, D. DARWISH, and N. J. HOLNESS. J. Am. Chem. Soc. **78**, 2915 (1956).
27. D. N. KEVILL, G. A. COPPENS and N. H. CROMWELL. J. Org. Chem. **28**, 567 (1963).
28. A. J. PARKER, M. RUANE, G. BIALE, and S. WINSTEIN. Tetrahedron Lett. 2113 (1968).
29. D. ECK and J. F. BUNNETT. J. Am. Chem. Soc. **91**, 3099 (1969).
30. J. R. CATCH, D. F. ELLIOTT, D. H. HEY, and E. R. H. JONES. J. Chem. Soc. 272 (1948).
31. J. R. CATCH, D. F. ELLIOTT, D. H. HEY, and E. R. H. JONES. J. Chem. Soc. 278 (1948).
32. E. L. ELIEL and R. J. L. MARTIN. J. Am. Chem. Soc. **90**, 689 (1968).
33. K. E. TEO. The University of Western Ontario. Personal communication from K. E. Teo and E. W. Warnhoff, 1970.
34. J. H. BOYER and D. STRAW. J. Am. Chem. Soc. **74**, 4506 (1952).
35. G. A. RECHNITZ. Chem. Eng. News. **45** (25), 146 (1967).

Can. J. Chem. Downloaded from www.nrcresearchpress.com by 210.87.254.5 on 09/05/12
For personal use only.

Iron Carbonyl Complexes of the Diastereomers of *cis*-$(C_6H_5)(CH_3)AsC(CF_3)=C(CF_3)As(CH_3)(C_6H_5)$

W. R. CULLEN AND L. MIHICHUK

Chemistry Department, University of British Columbia, Vancouver 8, British Columbia

Received October 16, 1972

The reaction of $CF_3{\equiv}CCF_3$ with $(C_6H_5)(CH_3)As{-}As(CH_3)(C_6H_5)$ gave both *cis*- and *trans*-$(C_6H_5)(CH_3)AsC(CF_3){=}C(CF_3)As(CH_3)(C_6H_5)$, (L—L), in nearly equal amounts. When hexafluoroacetone is used as solvent the *cis*-isomer predominates (88%). The two diastereomers of the *cis*-adduct were isolated and reacted with $Fe(CO)_5$ to afford (L—L)$Fe(CO)_3$ and (L—L)$Fe_2(CO)_6$. Two of the three possible geometric isomers of the latter were obtained and their properties allowed assignment of the configuration of the starting ligands. Minor amounts of the symmetric and asymmetric forms of $[Fe(CO)_3As(CH_3)(C_6H_5)]_2$ were also obtained through loss of fluorocarbon.

La réaction du $CF_3{\equiv}CCF_3$ avec du $(C_6H_5)(CH_3)As{-}As(CH_3)(C_6H_5)$ donne à la fois les produits *cis* et *trans* $(C_6H_5)(CH_3)AsC(CF_3){=}C(CF_3)As(CH_3)(C_6H_5)$, (L—L) dans des proportions pratiquement égales. Quand l'hexafluoroacétone est utilisé comme solvant, l'isomère *cis* prédomine (88%). Les deux diastéréoisomères du produit d'addition *cis* ont été isolés et ont réagi avec le $Fe(CO)_5$ pour donner alors le (L—L)$Fe(CO)_3$ et le (L—L)$Fe_2(CO)_6$. Deux des trois isomères géométrique possibles de ce dernier produit ont été obtenus et leurs propriétés ont permis l'attribution de la configuration des coordinats de départ. Des quantités moindres des formes symétriques et asymétriques du $[Fe(CO)_3As(CH_3)(C_6H_5)]_2$ ont aussi été obtenus par la perte de carbones fluorés.

[Traduit par le journal]

Can. J. Chem., **51**, 936 (1973)

Introduction

Ligands of the type $RC{=}CR'(CF_2)_nCF_2$ (R = $As(CH_3)_2$, $P(C_6H_5)_2$; R′ = $As(CH_3)_2$, $P(C_6H_5)_2$; n = 1–4, but not all combinations) have been found to react with iron carbonyls giving a variety of products (1–4). The related acyclic ditertiary arsine *cis*-$(CH_3)_2AsC(CF_3){=}C(CF_3)As(CH_3)_2$, (L—L)′, seems to form only complexes of the type (L—L)′$Fe(CO)_3$ and (L—L)′$Fe_2(CO)_6$(2, 5). The former has a five-coordinate structure which is probably undergoing positional exchange in solution (4, 6). In the latter the double bond takes part in the bonding and the structure is as shown in **A** (R = CH_3). This triligate behavior is rare for acyclic ditertiary arsines (4) although the cyclic ligands $RC{=}CR'(CF_2)_nCF_2$ have a propensity to act in this way forming $Fe_2(CO)_6$ complexes

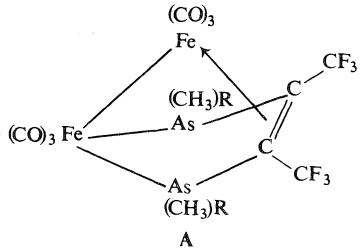

A

related to **A**. In order to investigate this phenomenon further it was decided to study another acyclic ditertiary arsine *cis*-2,3-bis(methylphenylarsino)hexafluorobutene-2 (**B**).

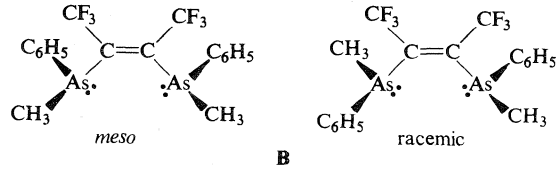

B

In this paper we report on the separation of **B** into its two diastereomers and describe the complexes formed by them.

Recently Bosnich and Wild (7) have prepared dichloropalladium complexes containg the *meso* and racemic isomers of $(C_6H_5)(CH_3)AsCH_2{-}CH_2As(CH_3)(C_6H_5)$ and have separated them using chromatography. Other platinum complexes of these same diastereomers have been studied by Cheney and Shaw (8).

Experimental

A standard vacuum system was used for the manipulation of volatile reactants. All reactions were carried out using degassed solvents in sealed evacuated Carius tubes. I.r. spectra were recorded on a Perkin–Elmer 457 spectrophotometer and calibrated using polystyrene and cyclohexane. N.m.r. spectra were run on a Varian T-60 spectrom-

Can. J. Chem. Downloaded from www.nrcresearchpress.com by 210.87.254.105 on 09/05/12
For personal use only.

Can. J. Chem. Downloaded from www.nrcresearchpress.com by 210.87.254.105 on 09/05/12
For personal use only.

eter. Chemical shifts are given in p.p.m. downfield from internal TMS for ^1H and upfield from internal $CFCl_3$ for ^{19}F spectra. Melting points were determined using a Gallenkamp melting point apparatus and are uncorrected.

U.v. irradiations were performed using a 200 W Hanovia lamp situated ~20 cm away from the reaction tube. The tube was continuously shaken, and cooled by an air stream. Microanalyses were made by Mr. Peter Borda of this department.

Hexafluorobutyne-2 and hexafluoroacetone were purchased from Peninsular Chemresearch Inc., iron pentacarbonyl from Alfa Inorganics Inc., and benzenearsonic acid from Eastman Organic Chemicals. All were used without further purification.

The experimental details reported have been selected from a number of related experiments and describe the conditions that have been found to result in the highest yields of the desired compounds.

*Preparation of cis-2,3-Bis(methylphenylarsino)-hexafluorobutene-2 (**B**)*

Methylphenylarsonic acid was prepared from benzene arsonic acid by the method of Cragoe *et al.* (9) and was reduced to 1,2-dimethyl-1,2-diphenyldiarsine as described by Reesor and Wright (10).

The diarsine (8 g, 24 mmol), dissolved in 25 ml of petroleum ether (b.p. 30–60°), and excess hexafluoroacetone (14 g, 84 mmol) were sealed together in a Pyrex tube and allowed to stand (with occasional shaking) for 4 h at 20°. The tube was then opened and hexafluorobutyne-2 was added (6 g, 36 mmol). The tube contents were allowed to react at 20° for 5 days. Excess volatile starting materials and solvent were taken into the vacuum system leaving a viscous yellow liquid to which hexane (50 ml) was added until the solution turned cloudy. Upon cooling in Dry Ice, white crystals of the racemic isomer of *cis*-2,3-bis(methylphenylarsino)hexafluorobutene-2 were isolated (m.p. 79–81°).

Anal. Calcd. for $C_{18}H_{16}F_6As_2$: C, 43.6; H, 3.2. Found: C, 43.6; H, 3.1.

The n.m.r. spectra (CCl_4 solution) consisted of a singlet at 1.20 (As—CH_3), a multiplet centered at 7.40 (As—C_6H_5), and a singlet at 53.2 p.p.m. (CF_3).

The solvent was removed under reduced pressure leaving a yellow liquid which was warmed to 34° at 10^{-3} mm to remove a small amount of impurity. The substantially pure *meso* isomer of *cis*-2,3-bis(methylphenylarsino)hexafluorobutene-2 remained. It was not possible to distill the product without decomposition.

Anal. Calcd. for $C_{18}H_{16}F_6As_2$: C, 43.6; H, 3.2. Found: C, 43.5; H, 3.1.

The n.m.r. spectra (CCl_4 solution) consisted of a singlet at 1.50 (As—CH_3), a multiplet centered at 7.20 (As—C_6H_5), and a singlet at 53.0 p.p.m. (CF_3). Traces of the *trans*-isomer were also present in this fraction, as evidenced by the presence of absorption at 50.0 and 50.8 p.p.m. (see Results and Discussion).

Reactions with Iron Pentacarbonyl

A number of reactions between iron pentacarbonyl and the ligands **B** are given in Table 1. Also included are some reactions of 1,2-dimethyl-1,2-diphenyldiarsine. In all cases the crude reaction mixture was evaporated to dryness and the residue was chromatographed on Florisil using nitrogen saturated solvents as indicated in Table 1. Analytical and spectroscopic data for the products of all these reactions are listed in Tables 2 and 3.

Results and Discussion

When tetramethyldiarsine reacts with hexafluorobutyne-2 at 20°, facile quantitative addition across the triple bond occurs with the formation of an approximate 1:1 mixture of the *cis*- and *trans*-isomers of 2,3-bis(dimethylarsino)-hexafluorobutene-2 (eq. 1, R = CH_3) (11). How-

[1] 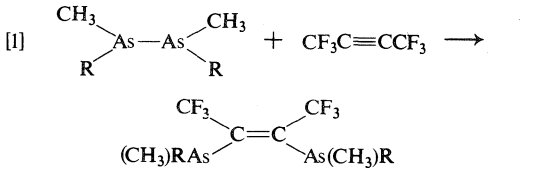

C

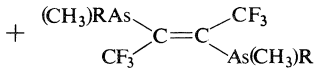

D

ever, when hexafluoroacetone is used as solvent and if the diarsine is first allowed to mix with the solvent before the acetylene is added then the product is predominantly the *cis*-adduct (~90%) (12). The stereospecificity is probably due to the initial formation of a complex between the diarsine and hexafluoroacetone such as **E** (R = CH_3) which allows attack of the acetylene on only one side of the arsenic–arsenic bond (12). Other workers have evidence for the existence of similar adducts (13).

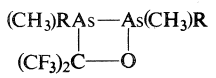

E

We have now found that 1,2-dimethyl-1,2-diphenyldiarsine reacts similarly with hexafluorobutyne-2. Figure 1*a* shows the ^{19}F n.m.r. spectrum of the reaction product obtained in the absence of hexafluoroacetone. Figure 1*b* shows the spectrum of the product obtained when hexafluoroacetone is present.

The two lowfield peaks in the spectra can be assigned to the *meso* and racemic forms of the *trans*-adduct **D** (R = C_6H_5) and the two high field peaks to the *meso* and racemic forms of the *cis*-adduct **C** (R = C_6H_5). The latter are drawn explicitly as **B**. It can be seen that the

Can. J. Chem. Downloaded from www.nrcresearchpress.com by 210.87.254.105 on 09/05/12
For personal use only.

TABLE 1. Reactions with iron pentacarbonyl*

No.	$Fe(CO)_5$	Ligand	Conditions	Products	Yield (%)	Purification†
1	5 g (25 mmol)	racemic 1 g (2 mmol)	U.v. irradiation benzene solution (25 ml), 3 days	rac-(L—L)$Fe(CO)_3$ rac-(L—L)$Fe_2(CO)_6$	40 10	C (1) C (3)
2	5 g (25 mmol)	racemic 1 g (2 mmol)	Pyrolysis in benzene (20 ml) at 150°, 2 days	rac-(L—L)$Fe(CO)_3$ rac-(L—L)$Fe_2(CO)_6$	15 35	C (1) C (3)
3	5 g (25 mmol)	racemic 1 g (2 mmol)	Pyrolysis in benzene (20 ml) at 150°, 3 days	$Fe_2(CO)_6[As(CH_3)(C_6H_5)]_2$‡ rac-(L—L)$Fe_2(CO)_6$	10 15	C (1) C (2)
4	5 g (25 mmol)	*meso* 1 g (2 mmol)	U.v. irradiation benzene solution (25 ml), 3 days	$Fe_2(CO)_6[As(CH_3)(C_6H_5)]_2$‡ *meso*-(L—L)$Fe(CO)_3$	trace 25	C (1) C (2)
5	5 g (25 mmol)	*meso* 1 g (2 mmol)	Pyrolysis in benzene (20 ml) at 150°, 2 days	$Fe_2(CO)_6[As(CH_3)(C_6H_5)]_2$‡ *meso*-(L—L)$Fe_2(CO)_6$	10 15	C (1) C (2)
6	5 g (25 mmol)	*meso* 1 g (2 mmol)	Pyrolysis in benzene (20 ml) at 150°, 3 days	$Fe_2(CO)_6[As(CH_3)(C_6H_5)]_2$‡ *meso*-(L—L)$Fe_2(CO)_6$	35 15	C (1) C (2)
7	4 g (20 mmol)	$[As(CH_3)(C_6H_5)]_2$ 2 g (6 mmol)	Pyrolysis in benzene (25 ml) at 150°C, 3 days	$Fe_2(CO)_6[As(CH_3)(C_6H_5)]_2$ (symmetric) $Fe_2(CO)_6[As(CH_3)(C_6H_5)]_2$ (asymmetric)	33 6	Reaction mixture was washed with petroleum ether leaving the symmetric isomer which is less soluble. The solution was chromatographed. C (1) gives the asymmetric and C(1)–C(3) the symmetric isomer
8	5 g (25 mmol)	$[As(CH_3)(C_6H_5)]_2$ 2 g (6 mmol)	U.v. irradiation in 20 ml of benzene, 3 days	$Fe_2(CO)_6[As(CH_3)(C_6H_5)]_2$‡	3	As in experiment 7

*(L—L) = $(CH_3)(C_6H_5)AsC(CF_3)=C(CF_3)As(CH_3)(C_6H_5)$ (**B**) and is the ligand unless otherwise stated.
†C indicates chromatography on Florisil. The arabic numeral indicates the solvent required to elute the product: (1) is 100% petroleum ether (b.p. 30–60°), (2) is 98% petroleum ether, 2% diethylether, (3) is 95% petroleum ether, 5% diethylether.
‡This is mainly the symmetric isomer with trace amounts of the asymmetric one.

TABLE 2. Analytical data for new complexes*

Compound	Color	M.p.(°C)	% C		% H	
			Calcd.	Found	Calcd.	Found
$Fe_2(CO)_6[As(CH_3)(C_6H_5)]_2$ (symmetric)	Orange	162–164	39.2	39.0	2.6	2.8
$Fe_2(CO)_6[As(CH_3)(C_6H_5)]_2$ (asymmetric)	Orange	93–95	39.2	39.5	2.6	2.8
rac-(L—L)$Fe(CO)_3$	Brown	142–143†	39.6	39.4	2.5	2.5
meso-(L—L)$Fe(CO)_3$	Brown	117–120†	39.6	39.3	2.5	2.5
rac-(L—L)$Fe_2(CO)_6$	Red–brown	173–175	37.1	37.4	2.1	2.3
meso-(L—L)$Fe_2(CO)_6$	Red–brown	144–146	37.1	37.4	2.1	2.2

*(L—L) = $(CH_3)(C_6H_5)AsC(CF_3)=C(CF_3)As(CH_3)(C_6H_5)$.
†With decomposition.

TABLE 3. I.r. and n.m.r. data for new complexes*

Compound	^1H	^{19}F	ν(CO) (cm^{-1})
$Fe_2(CO)_6[As(CH_3)(C_6H_5)]_2$ (symmetric)	Singlet at 1.93 (CH_3); multiplet centered at 6.93 (C_6H_5)	—	2052s, 2009vs, 1979vs, 1965vs, 1955m
$Fe_2(CO)_6[As(CH_3)(C_6H_5)]_2$ (asymmetric)	Singlets at 0.93, 2.0 (CH_3); multiplets centered at 6.93 and 7.4 (C_6H_5)	—	2052s, 2007vs, 1977vs, 1965vs, 1955m
rac-(L—L)$Fe(CO)_3$	Singlet at 2.2 (CH_3); multiplet centered at 7.4 (C_6H_5)	Singlet at 51.0 (CF_3)	2003vs, 1937s, 1919vs
meso-(L—L)$Fe(CO)_3$	Singlet at 2.23 (CH_3); multiplet centered at 7.53 (C_6H_5)	Singlet at 51.8 (CF_3)	2003vs, 1939s, 1921vs
rac-(L—L)$Fe_2(CO)_6$	Singlets at 1.23 (CH_3) and 2.57 (CH_3); multiplets centered at 7.0 and 7.5 (C_6H_5)	Quartets centered at 41.0 and 46.8 (CF_3) $J_{F,F}$ = 11.3 Hz	2064m, 2023s, 1999m, 1985m, 1971w, 1959w
meso-(L—L)$Fe_2(CO)_6$	Singlet at 2.57 (CH_3); multiplet centered at 7.0 (C_6H_5)	Singlet at 44.5 (CF_3)	2064m, 2023s, 1995m, 1983m, 1967w, 1955w

*N.m.r. spectra from $CDCl_3$ solutions; i.r. spectra from cyclohexane solutions.

effect of the hexafluoroacetone is to change the ratio from 55% *trans*:45% *cis* in its absence to 12% *trans*:88% *cis* in its presence.

Confirmation of this assignment comes from the result that the *meso* and racemic isomers **B** can be separated by virtue of their different solubility in hexane. One isomer which is obtained as a pure solid and which will be shown below to be the racemic one is responsible for the absorption at 53.2 p.p.m. The other isomer which will be shown to be the *meso* form of **B** is obtained as an oil, free of the racemic form, but contaminated with traces of the two forms of the *trans*-adduct **D** (R = C_6H_5).

The *cis*-diastereomers **B**, once separated, are stable. The *cis*-configuration allows them to act as monometallic bidentate (chelating) ligands or as bimetallic tridentate ligands as in **A**. The results given in Table 1 show that both the racemic and *meso* isomers give complexes (L—L)$Fe(CO)_3$ and (L—L)$Fe_2(CO)_6$ ((L—L) = $(CH_3)(C_6H_5)AsC(CF_3)=C(CF_3)As(CH_3)(C_6H_5)$) when reacted with iron pentacarbonyl. This confirms their *cis*-geometry.

The (L—L)$Fe(CO)_3$ complexes which as usual (2) are best prepared by u.v. irradiation show the expected three bands in the ν(CO) region of the i.r. spectrum. The slight differences in frequencies for the two isomers are probably not significant. The n.m.r. spectra show singlets for the CF_3 and CH_3 resonances indicating a symmetrical structure in solution. Thus, in solution, the ligand is either bound to two equatorial positions of a distorted trigonal bipyramidal structure, or, more likely, the molecule is undergoing positional exchange (6), possibly the turnstile mechanism (14). The spectroscopic results for these (L—L)-$Fe(CO)_3$ complexes do not allow a decision to be

Can. J. Chem. Downloaded from www.nrcresearchpress.com by 210.87.254.105 on 09/05/12
For personal use only.

Can. J. Chem. Downloaded from www.nrcresearchpress.com by 210.87.254.105 on 09/05/12
For personal use only.

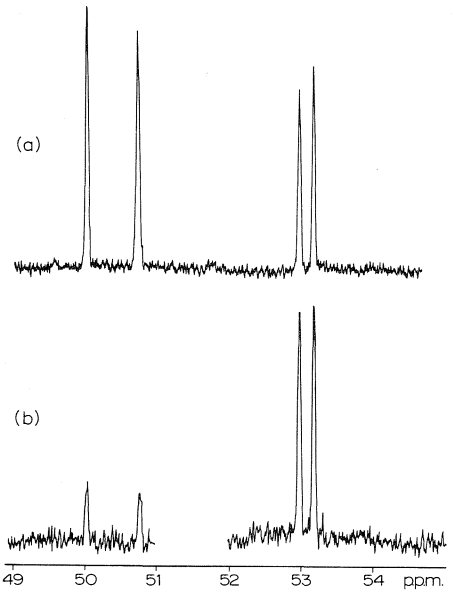

FIG. 1. The ^{19}F n.m.r. spectrum of the product of eq. 1 (R = C_6H_5) (*a*) in the absence of hexafluoroacetone and (*b*) in the presence of hexafluoroacetone.

made regarding the structure of the initial ligand, *i.e.*, whether it is racemic or *meso*, since the complexes are too symmetrical; one having CH_3 groups *cis* with respect to the chelate ring (the *meso* complex) and the other *trans*.

The (L—L)$Fe_2(CO)_6$ complexes **A** (R = C_6H_5) are best prepared by heating the reagents (the (L—L)$Fe(CO)_3$ complexes are probably intermediates (Table 1) (2)). The i.r. spectra of these compounds in the ν(CO) region show the typical pattern (1), but in this case the differences in frequencies could be significant since three geometric isomers are possible. If it is assumed that no interconversion of the ligands **B** occurs during the reaction, the racemic isomer should give one complex **F** and the *meso* would give two isomers **G** and **H**.

The crystalline ligand affords a $Fe_2(CO)_6$ complex whose n.m.r. spectrum shows two As—CH_3 and two CF_3 absorptions. The two CF_3 groups belong to the same molecule since there is spin–spin coupling between them ($J_{F,F}$ = 11.3 Hz). Such a spectrum would be expected only for **F** and thus the solid starting ligand is the racemic form of **B**. The n.m.r. spectrum of the $Fe_2(CO)_6$ complex obtained from the oily ligand showed only one type of As—CH_3 group to be present and only one CF_3 group. Such a spectrum would be possible for either **G** or **H**, but not from a mixture of both. Thus the oily product is the *meso* form of **B** and gives the same product, probably **G**, on heating and u.v. irradiation. The reason for preferring **G** is that phenyl–phenyl repulsions appear to be less than methyl–methyl in this sort of system (q.v.).

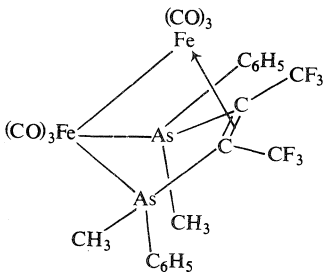

F

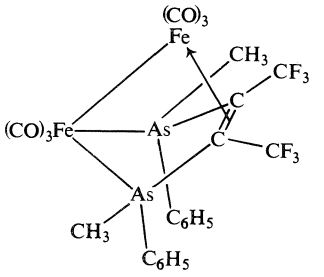

G

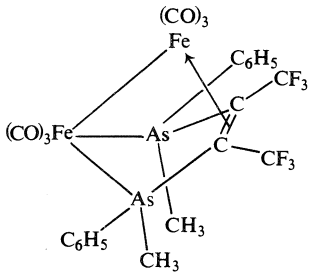

H

Also isolated from the thermal reactions of **B** with iron pentacarbonyl was a compound having the empirical formula $Fe(CO)_3As(CH_3)(C_6H_5)$. This proved to be identical with the product obtained by heating the iron carbonyl with 1,2-dimethyl-1,2-diphenyldiarsine: lower yields are obtained on irradiation.

The major unfluorinated product has the structure **I** (E = As). The n.m.r. spectrum shows only one type of As—CH_3 group hence the structure is symmetrical. The ν(CO) bands are very similar to the phosphorus analog (15) which has the two phenyl groups axial as in **I** (E = P)

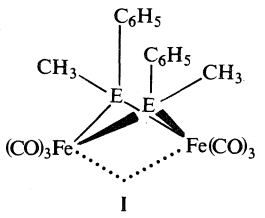

I

(16) and it is reasonable to believe the arsenic analog would be iso-structural.

The minor reaction product of the reactions of the diarsine with iron pentacarbonyl is an isomer of **I** which has the asymmetric structure **J**, since the ^1H n.m.r. spectrum shows two distinct singlets in the As—CH_3 region.

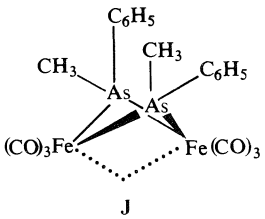

J

One of these resonances is at relatively high field (0.93 p.p.m.) and this can be assigned to the methyl group which is adjacent to the phenyl group on the other arsenic atom. The i.r. spectra of **I** and **J** in the ν(CO) region are identical (E = As) as is the case for the two phosphorus analogs (15).

More detailed study has shown that at 150° in benzene the symmetric and asymmetric forms **I** and **J** are in equilibrium with the ratio of **I** to **J** being 6:1. Thus n.m.r. spectrum of an initially pure sample of the asymmetric isomer when heated to 150° soon showed signals due to the symmetric form. A limiting spectrum was obtained after 15 h. Similarly a sample of the symmetric compound showed a comparable spectrum after heating at 150° for 90 h. The greater stability of the symmetric form **I** suggests that phenyl–phenyl repulsion is less than phenyl–methyl or methyl–methyl interactions. The symmetric isomer is 'rigid' in solution while the asymmetric one undergoes positional exchange (it 'flaps') (17). Considerations such as these form the basis for the choice made above that **G** would be more stable than **H**.

As mentioned above, the bridging arsenido compounds **I** and **J** are produced when the ligands **B** react with iron pentacarbonyl. Their yield is low after prolonged irradiation but heating to 150° for 3 days affords significant amounts. The *meso* isomer is a better source of the fluorocarbon-eliminated product. In fact the yield is almost that which is obtained by treating iron pentacarbonyl with the diarsine under identical conditions. The (L—L)$Fe_2(CO)_6$ complexes are stable by themselves in benzene solution at 150° for at least 5 days so they are not the unique source of the arsenido-bridged complexes.

The reaction mixture is very complex and it is difficult enough to establish when the fluorocarbon is lost, let alone rationalize the differences in behavior between the two ligands **B**. We have spectroscopic evidence for the existence of tetrakis(trifluoromethyl)cyclopentadienoneiron tricarbonyl in solution. This would be formed by reaction of the free acetylene with iron pentacarbonyl (18).

The authors are grateful to the National Research Council of Canada for financial support. We would also like to thank Dr. R. K. Pomeroy for assistance and Dr. P. M. Treichel for preprints of his relevant papers.

1. W. R. Cullen, D. A. Harbourne, B. V. Liengme, and J. R. Sams. Inorg. Chem. **8**, 95, 1464 (1969); **9**, 702 (1970).
2. L. S. Chia, W. R. Cullen, and D. A. Harbourne. Can. J. Chem. **50**, 2182 (1972).
3. L. S. Chia and W. R. Cullen. Unpublished results.
4. W. R. Cullen. Adv. Inorg. Chem. Radiochem. **15**, 323 (1972).
5. J. P. Crow, W. R. Cullen, J. R. Sams, and J. E. H. Ward. J. Organomet. Chem. **22**, C29 (1970).
6. W. R. Cullen and D. A. Harbourne. Inorg. Chem. **9**, 1839 (1970).
7. B. Bosnich and S. B. Wild. J. Am. Chem. Soc. **92**, 459 (1970).
8. A. J. Cheney and B. L. Shaw. J. Chem. Soc. A, 3549 (1971).
9. E. J. Cragoe, R. J. Andres, R. F. Coles, B. Elpern, J. F. Morgan, and C. S. Hamilton. J. Am. Chem. Soc. **69**, 925 (1947).
10. J. W. B. Reesor and G. F. Wright. J. Org. Chem. **22**, 382 (1957).
11. W. R. Cullen and N. K. Hota. Can. J. Chem. **42**, 1123 (1964).
12. W. R. Cullen and G. E. Styan. J. Organomet. Chem. **4**, 151 (1965).
13. E. W. Abel. Personal communication.
14. I. Ugi, D. Marquarding, H. Klusacek, P. Gillespie, and F. Ramirez. Acc. Chem. Res. **4**, 288 (1971).
15. P. M. Treichel, W. M. Douglas, and W. K. Dean. Inorg. Chem. **11**, 1615 (1972).
16. L. F. Dahl and J. J. Huntsman. Submitted for publication and quoted in ref. 15.
17. W. R. Cullen and L. Mihichuk. Unpublished results.
18. J. L. Boston, D. W. A. Sharp, and G. Wilkinson. J. Chem. Soc. 3488 (1962).

Can. J. Chem. Downloaded from www.nrcresearchpress.com by 210.87.254.105 on 09/05/12
For personal use only.

The Beckmann Rearrangement on Ketoximes Initiated by Hexamethylphosphoric Triamide

RICHARD S. MONSON AND BRUCE M. BROLINE
Department of Chemistry, California State University, Hayward, California 94542

Received August 24, 1972

Ketoximes are found to undergo the Beckmann rearrangement in hexamethylphosphoric triamide at 225–240°, affording the corresponding amides in good yield.

On a observé que les cétoximes subissent le réarrangement de Beckmann dans le HMPT à 225–240° en conduisant avec de bons rendements aux amides correspondantes. [Traduit par le journal]

Can. J. Chem., **51**, 942 (1973)

Can. J. Chem. Downloaded from www.nrcresearchpress.com by 210.87.254.40 on 09/05/12
For personal use only.

Hexamethylphosphoric triamide (HMPT), in addition to its well known uses as a reaction medium (1), shows promise of becoming a useful reagent in several dehydration and substitution reactions (2, 3). Continuing our studies on the uses of this versatile reagent, we now report that the Beckmann rearrangement of ketoximes can be successfully carried out in HMPT.

When aromatic ketoximes are heated in approximately a three-fold molar excess of HMPT (pot temperatures of 225–240°), a copious evolution of dimethylamine is observed. After a brief reflux, the solution is cooled and subjected to a water work-up. Good yields of the corresponding crude anilides are obtained as shown in Table 1.

TABLE 1. Amides by HMPT initiated Beckmann rearrangement on ketoximes

Oxime	Crude yield of corresponding amide (%)
Benzophenone oxime	54
Acetophenone oxime	52
p-Methoxyacetophenone oxime	71
p-Methylacetophenone oxime	85
p-Chloroacetophenone oxime	75
p-Bromoacetophenone oxime	89

Our prior work on reactions in refluxing HMPT (2) has suggested that dehydration reactions occur after initial formation of phosphorodiamidate derivatives. In the present case, these considerations lead to the reaction pathway shown in eqs. 1 and 2.

As in other reactions conducted in HMPT, the reaction products include a gummy precipitate which has previously been shown (4) to consist primarily of bis(dimethylammonium)dihydrogen pyrophosphate, $(Me_2NH_2)_2H_2P_2O_7$.

The yields of crude amides obtained by the reaction of ketoximes in HMPT compare favorably with those obtained by conventional reagents (5). Moreover, conventional reagents (for example H_2SO_4, H_3PO_4, or PCl_5) are frequently acidic and are usually extremely reactive towards many functional groups. On the other hand, HMPT is mildly basic and neither it nor its reaction products are highly reactive. This fact may offer a possible advantage in the preparation of sensitive amides.

Experimental

Oximes were prepared in the usual way from commercially available ketones, hydroxylamine hydrochloride, and aqueous sodium acetate. They were recrystallized from aqueous ethanol before use. HMPT was distilled before use, b.p. 120–122°/21 mm. Products were identified by their i.r. spectra and by comparison of their melting points with literature values.

Beckmann Rearrangement. General Procedure

The oxime (0.1 mol) is dissolved in 65 ml of HMPT and brought to reflux. The solution turns cloudy at 210–230°, and refluxing commences at 225–235°. When the pot temperature reaches approximately 240°, the reaction

[1] $$\mathrm{Ar{-}C(=NOH){-}CH_3} + (Me_2N)_3PO \rightarrow \mathrm{Ar{-}C(=N{-}O{-}P(O)(NMe_2)_2){-}CH_3} + Me_2NH$$

[2] $$\mathrm{Ar{-}C(=N{-}O{-}P(O)(NMe_2)_2){-}CH_3} \rightarrow \left[\mathrm{Ar{-}C(=N^{\oplus}){-}CH_3}\right] \rightarrow [\mathrm{Ar{-}N{=}\overset{\oplus}{C}{-}CH_3}] \rightarrow \mathrm{Ar{-}NH{-}C(=O){-}CH_3}$$

becomes noticeably exothermic. The total reflux time is 10 min, and the resulting solution is dark red.

The cooled reaction mixture is poured into 550 ml of ice water with rapid stirring. The solution is saturated with sodium chloride whereupon the crude amide separates. An additional portion of amide may be obtained by extracting the aqueous solution with ether – ethyl acetate (1:1), drying the organic solution (anhydrous Na_2SO_4), and evaporating the solvent. The crude amide may be purified by recrystallization from benzene or benzene–cyclohexane.

The authors wish to express their appreciation to the Research Foundation, California State University, Hayward, California, for financial support.

1. (*a*) H. NORMANT. Angew. Chem. Int. Ed. **6**, 1046 (1967); (*b*) H. NORMANT. Colloq. Int. Centre Nat. Rech. Sci. No. 182, 207 (1970).
2. R. S. MONSON, D. N. PRIEST, and J. C. ULLREY. Tetrahedron Lett. 929 (1972), and references cited therein.
3. J. S. LOMAS, D. S. SAGATYS, and J. E. DUBOIS. Tetrahedron Lett. 165 (1972).
4. R. S. MONSON and D. N. PRIEST. J. Org. Chem. **36**, 3826 (1971).
5. L. G. DONARUME and W. Z. HELDT. Org. React. **11**, 1 (1960).

Can. J. Chem. Downloaded from www.nrcresearchpress.com by 210.87.254.40 on 09/05/12
For personal use only.

The Temperature Dependence of the Diffusion Coefficients of Ar, CO_2, CH_4, CH_3Cl, CH_3Br, and $CHCl_2F$ in Water

DOW M. MAHARAJH AND JOHN WALKLEY

Chemistry Department, Simon Fraser University, Burnaby 2, British Columbia

Received March 2, 1972[1]

Diffusion coefficient values are reported over a 0 to 35 °C temperature range for Ar, CO_2, CH_4, CH_3Br, CH_3Cl, and $CHCl_2F$ in water. Various empirical theories relating these diffusion coefficient values to the viscosity of water (η) and the size of the diffusing solute molecule are examined. None are found valid though a linear relationship is found to hold between log D and log η for all systems. McLaughlin's hard sphere theory is examined and found in surprisingly good agreement with experiment. It is seen, however, that this theory cannot adequately predict the temperature dependence of the diffusion coefficient of the solute.

Les valeurs des coefficients de diffusion pour Ar, CO_2, CH_4, CH_3Br, CH_3Cl, et $CHCl_2F$ dans l'eau, ont été rapportées dans l'intervalle de température de 0 à 35 °C. Diverses théories empiriques reliant les valeurs des coefficients de diffusion à la viscosité de l'eau (η) et à la taille de la molécule de soluté qui diffuse, ont été examinées. Aucune n'a été trouvée correcte bien qu'une relation linéaire existe entre le log D et le log η pour tous les systèmes. La théorie de la sphère dure de McLaughlin, en accord surprenant avec l'expérience, a été examinée. Cependant cette théorie ne peut prévoir de façon convenable la relation entre la température et le coefficient de diffusion du soluté.

[Traduit par le journal]

Can. J. Chem., **51**, 944 (1973)

Introduction

It is well established that a wide range of gases form solid water–gas clathrates in which the interaction between solute and water is of the van der Waals type (1). The range of stability of these clathrates varies considerably, the hydrate decomposition pressure of argon, at 0 °C, is 105 atm and for xenon is 1.5 atm. The hydrate decomposition temperature at 1 atm is −42.8 °C for argon and −3.4 °C for xenon. In general, these gases are only slightly soluble in water at 0 °C but have a "solubility" in the solid state often some powers of ten greater.

The development of an adequate theory for the equilibrium thermodynamic solubility properties of gases in water suffers because there is no adequate theory for pure water itself (2). The entropy and enthalpy of solution of gases in water are appreciably lower than those found in other solvents, their partial molal volumes far smaller (3). Early theories developed the concept that in water the gas molecule builds up an "iceberg" around it (4). More recent theories use the "two-structure" model of pure water and it is suggested that the dissolved gas solute stabilizes the large compact "clusters" already present (5). The early theory of Eley has been extended using recent developments in hard sphere theory (6). This theory predicts the observed thermodynamic properties with remarkable success and essentially treats both solute and water as hard sphere molecules (3, 6).

Hildebrand has recently suggested that the comparison of diffusion coefficient data for gases in water and in non-polar solvents may help to distinguish the role of the "water cage structure" (7). He argues that the diffusion coefficient for a solute is largely dependent upon the size of the solute. Thus the considerably greater size of a solute surrounded by a "water structure" cage should be revealed by a smaller diffusion coefficient. In a comparison of data for gases in water and in carbon tetrachloride solvent, no gross differences in the diffusion coefficient values are found.

In this paper we present diffusion coefficient data for argon, carbon dioxide, methane, methyl chloride, methylbromide, and dichlorofluoromethane in water over a temperature range of 0 to 35 °C. We describe the inverted tube method used for the measurement of the rates of dissolution of these gases into water. This method was devised in order to overcome the density gradient convection term often found operating in other methods.

In terms of the solid water clathrate, the gases

[1]Revision received October 20, 1972.

Can. J. Chem. Downloaded from www.nrcresearchpress.com by 210.87.254.42 on 09/05/12
For personal use only.

Can. J. Chem. Downloaded from www.nrcresearchpress.com by 210.87.254.42 on 09/05/12
For personal use only.

studied cover a hydrate decomposition pressure (at 0 °C) from 311 atm (CH_3Cl) to 12.3 atm (CO_2) and a decomposition temperature (at 1 atm pressure) from +11.1 °C (CH_3Br) to −42.8 °C (Ar). The gases span a molar volume (at boiling point V_b) range from 28 cc mol^{-1} (Ar) to 55 cc mol^{-1} (CH_3Br). The measured diffusion coefficient values (10^5 D cm^2 s^{-1}) range from 1.85 (CO_2) to 1.35 (CH_3Br). All gases give linear log D *vs.* $1/T$ plots, the slopes lying between 6.71×10^2 (CH_4) and 14.85×10^2 ($CHCl_2F$).

We discuss our data in terms of the accepted empirical relationships often proposed to correlate diffusion data and also in terms of the hard sphere diffusion model of McLaughlin (8). In terms of the former relationships, a generally uniform type of behavior is found for the range of gases examined. McLaughlin showed his extension of Thorne's hard sphere theory to the diffusion of hard sphere mixtures gave good comparison for a wide range of gases in water at 25 °C and for the diffusion of CO_2 in water over a wide temperature range. We find this theory disappointing in its prediction of the temperature dependence of the diffusion coefficient of the gases we ourselves have measured.

Experimental

Inverted Tube Method

The diffusion cell is made from precision bore tubing (1 mm diameter) and is some 15 cm long. A small bulb of about 1 ml capacity is blown 2 cm from one end and the other end is sealed. To load the cell, it is first placed in a desiccator vessel and evacuated thoroughly. The whole apparatus is then flushed with the gas under investigation and re-evacuated several times. It is finally filled with gas at 1 atm pressure and a few drops of the degassed solvent are transferred into the bulb of the diffusion cell through a serum cap, using a hypodermic syringe. The diffusion cell is then placed in a thermostat and after 30 min, more degassed solvent at the same temperature as the thermostat is quickly introduced into the capillary, displacing the gas, until a gas slug of some 5 mm in length is left at the end of the capillary. The change in position of the solvent meniscus accompanying the dissolution of the gas is followed with a microscope fitted with a calibrated filar eye piece (Gaertner Scientific Corp.). The magnification of the microscope is ×100 and the position of the meniscus can be measured as a function of time to within 0.005 mm. The whole apparatus is mounted on a concrete block to avoid mechanical vibration. A typical run lasts about 5000 s and during this time the meniscus moves some 1.5 mm. In preliminary runs, capillaries of 1, 2, and 3 mm in diameter were used for the cells. The rate of absorption of CO_2 into water is found to be independent of the diameter of the cell to within the accuracy of the experiment. The solvent, water, is purified by distillation in a Pyrex vessel and all gases were supplied by Matheson.

The whole system is kept at a constant pressure and the rate of absorption of the gas into the solvent is followed by measuring the position of the gas/solvent interface as a function of time. The moving boundary method for non-steady state diffusion has been treated extensively by Booth (9) and by Danckwerts (10). Experimental conditions with respect to the method of placing the gas below the solvent are suitable only for the measurements made at large t values and under these conditions the relationship between the volume of gas dissolved, V, and the time, t, is

$$V = \frac{2ARTX_2}{V_1}\sqrt{\frac{Dt}{\pi}}$$

where A is the area of the diffusion cell; X_2 is the saturation solubility mole fraction of the gas; R is the gas constant; T is absolute temperature; and V_1 is the molar volume of the solvent.

Results

Measurements have been made for the rate of absorption into water of Ar, CO_2, CH_4 over the temperature range 0 to 35 °C and of CH_3Cl, CH_3Br, and $CHCl_2F$ over the range 10 to 35 °C. Tables 1–6 give slope values of the V *vs.* $\sqrt{t}$ plots, estimated to be accurate to 2%. Diffusion coefficient values, (D_2 cm^2 s^{-1}) are also given in Tables 1–6. For all gases a linear ln D_2 *vs.* $1/T$ relationship was found, the coefficients of the equation $\ln D_2 = B/T + C$ are given in Table 7.

Diffusion coefficient values were calculated for argon using the solubility data of Ben-Naim *et al.* (11) for the range 0 to 30 °C and the value of Smith and co-workers (12) at 35 °C. We may compare our 25 °C value of $D_2 = 1.44 \times 10^{-5}$ cm^2 s^{-1} with that value obtained by Smith and co-workers using the "Ringboem" technique (13)

TABLE 1. Slope values of V *vs.* $\sqrt{t}$ plots and D_2 values for Ar–H_2O system

T (±0.01 °K)	Slope of V *vs.* $\sqrt{t} \times 10^2$ (cc $s^{-1/2}$)	$10^5 D_2$ (cm^2 s^{-1}) Experimental	$10^5 D_2$ (cm^2 s^{-1}) Exact solution from eq. 2*
273	1.63±0.01	0.72	0.65
278	1.59±0.02	0.85	0.76
283	1.54±0.02	0.97	0.90
288	1.48±0.01	1.09	1.03
293	1.45±0.01	1.23	1.19
298	1.44±0.02	1.44	1.36
303	1.60±0.03	1.65	1.54
308	1.50±0.02	1.82	1.77

*Using $(\sigma_{22}/\sigma_{11})^c$ values, Table 7.

TABLE 2. Slope values of V vs. $\sqrt{t}$ plots and D_2 values for CO_2–H_2O system

T (±0.01 °K)	Slope of V *vs.* $\sqrt{t} \times 10^2$ (cc $s^{-1/2}$)	10^5 D_2 (cm^2 s^{-1})		
		Experimental	Solution from eq. 2	
			Approximate*	Exact†
273	6.11±0.03	1.00	0.84	0.51
278	5.39±0.04	1.16	0.99	0.61
283	5.04±0.03	1.32	1.17	0.72
288	4.67±0.03	1.52	1.34	0.82
293	4.43±0.01	1.74	1.55	0.95
298	4.07±0.01	1.85	1.78	1.08
303	3.66±0.02	2.19	2.01	1.23
308	3.62±0.01	2.41	2.30	1.41

*Using $(\sigma_{22}/\sigma_{11})^c$ values, Table 7.
†Using $(\sigma_{22}/\sigma_{11})^a$ values, Table 7.

TABLE 3. Slope values of V *vs.* $\sqrt{t}$ plots and D_2 values for CH_4–H_2O system

T (± 0.01 °K)	Slope of V *vs.* $\sqrt{t} \times 10^2$ (cc $s^{-1/2}$)	10^5 D_2 (cm^2 s^{-1})	
		Experimental	Exact solution from eq. 2*
273	2.00± 0.03	1.05	0.68
278	1.86± 0.04	1.10	0.80
283	1.71± 0.01	1.22	0.95
288	1.61±0.05	1.33	1.09
293	1.53±0.01	1.47	1.26
298	1.51±0.02	1.64	1.44
303	1.44±0.03	1.74	1.64
308	1.43±0.02	1.96	1.87

*Using $(\sigma_{22}/\sigma_{11})^c$ values, Table 7.

of 1.46×10^{-5} cm^2 s^{-1}. The experimental techniques are quite different, the agreement between the two values is excellent. The recent measurement of Boerboem and Kleyn (14) give values of 0.633×10^{-5} cm^2 s^{-1} at 0 °C and of 0.78×10^{-5} cm^2 s^{-1} at 25 °C. Wise and Houghton (15) using the collapsing bubble method, found D values higher than our own but this is expected from their method. For the CO_2/H_2O system the measured D_2 values agree well with those reported by Unver and Himmelblau (16) obtained using the laminar method. In obtaining D_2 values for methane we can use either the saturation solubility data of Lange or that of Claussen and Polgase (20). The data of Lange gave a linear $\ln D_2$ *vs.* $1/T$ plot, the data of Claussen and Polgase did not. Our data for methane using the Lange solubility values (17) agrees well with those values obtained by Witherspoon and Saraf (18) measured using the capillary cell method of Wang (19). Wise and Houghton using the collapsing bubble method report values again considerably higher than those of our own. For the remaining gases, we can make comparison only to the values obtained by Chiang and Toor (21) who, using the diaphragm method, obtained a value of $D_2 = 1.39 \times 10^{-5}$ cm^2 s^{-1} for CH_3Cl in water, agreeing well with our value of 1.40×10^{-5} cm^2 s^{-1} (at 25.0 °C).

Discussion

In a previous paper (22) we discussed the "open tube" method for measuring the diffusion of a gas into a solvent. In that method the gas is placed *above* the solvent and the rate of dissolution measured by finding the change in gas volume (at constant pressure) as a function of time. For benzene and carbon tetrachloride solvents, data were obtained in good agreement with values published by other workers. For the dissolution of gases into water this technique cannot be used. For these systems, the dissolution of the gas produces a layer of solvent of density greater than the bulk density. The simple diffusion controlled dissolution is enhanced by a density convection mechanism. This is a complex mechanical instability problem and has been discussed by several authors (23, 24). It is worth commenting that with this density induced convection term plus the natural diffusion term, the dissolution of the gas can be observed to follow a pseudo non-steady state mechanism (as in the case of argon into water) where volume uptake of gas is proportional to time$^{1/2}$ or to follow a

Can. J. Chem. Downloaded from www.nrcresearchpress.com by 210.87.254.42 on 09/05/12
For personal use only.

TABLE 4. Slope values of V *vs.* $\sqrt{t}$ plots and D_2 values for CO_2–H_2O system

T (±0.01 °K)	Slope of V *vs.* $\sqrt{t} \times 10^2$ (cc $s^{-1/2}$)	$10^5 D_2$ (cm^2 s^{-1})		
		Experimental	Solution from eq. 2	
			Approximate*	Exact†
283	1.35±0.04	0.83	1.25	0.89
288	1.24±0.03	0.98	1.44	1.01
293	1.16±0.03	1.18	1.63	1.17
298	1.09±0.04	1.40	1.90	1.35
303	1.03±0.02	1.65	2.16	1.52
308	0.985±0.03	2.07	2.47	1.75

*Using $(\sigma_{22}/\sigma_{11})^c$ values, Table 7.
†Using $(\sigma_{22}/\sigma_{11})^a$ values, Table 7.

TABLE 5. Slope values of V *vs.* $\sqrt{t}$ plots and D_2 values for CH_3Br–H_2O system

T (±0.01 °K)	Slope of V *vs.* $\sqrt{t} \times 10^2$ (cc $s^{-1/2}$)	$10^5 D_2$ (cm^2 s^{-1})		
		Experimental	Solution from eq. 2	
			Approximate*	Exact†
283	2.25±0.08	0.85	1.04	0.57
288	2.01±0.02	1.03	1.18	0.65
293	1.78±0.03	1.16	1.37	0.75
298	1.60±0.03	1.35	1.57	0.86
303	1.48±0.02	1.64	1.77	0.97
308	1.35±0.01	2.00	2.03	1.12

*Using $(\sigma_{22}/\sigma_{11})^c$ values, Table 7.
†Using $(\sigma_{22}/\sigma_{11})^a$ values, Table 7.

TABLE 6. Slope values of V *vs.* $\sqrt{t}$ plots and D_2 values for $CHCl_2F$–H_2O system

T (±0.01 °K)	Slope of V *vs.* $\sqrt{t} \times 10^2$ (cc $s^{-1/2}$)	$10^5 D_2$ (cm^2 s^{-1})		
		Experimental	Solution from eq. 2	
			Approximate*	Exact†
283	1.36 ±0.10	0.98	1.07	0.56
288	1.19 ±0.11	1.20	1.22	0.64
293	1.03 ±0.08	1.50	1.42	0.74
298	0.912±0.06	1.80	1.62	0.96
303	0.758±0.04	2.20	1.83	1.03
308	0.677±0.04	2.60	2.10	1.11

*Using $(\sigma_{22}/\sigma_{11}) = 1$.
†Using $(\sigma_{22}/\sigma_{11})^a$ values, Table 7.

mechanism linear with time (as for CO_2 into water). The former mechanism gives rise to reproducible data and allows an "apparent" D_2 value to be obtained. Such D_2 values are far greater than the real D_2 (diffusion coefficient) value. For argon into water an apparent D_2 value of 10.3×10^{-5} cm^2 s^{-1} is found, a factor of 7 larger than the real value. Results for gases in water from our earlier "constant size bubble" method (25) were again found to give relatively higher D_2 values, presumably again due to the presence of the density convection term.

For the gases studied, the "inverted tube method" gives results in good agreement with those values obtained by other workers. It would seem that with the gas diffusing *upwards* into the solution, the dissolution process has no density convection term.

Can. J. Chem. Downloaded from www.nrcresearchpress.com by 210.87.254.42 on 09/05/12
For personal use only.

Can. J. Chem. Downloaded from www.nrcresearchpress.com by 210.87.254.42 on 09/05/12
For personal use only.

TABLE 7. Diffusion coefficient values for gases in water at 25.00 ± 0.01 °C

Gas	$10^5 D_2$ (cm^2 s^{-1})	Coefficients of $\ln D_2 = B/T + C$		ΔE (kcal mol^{-1})	$10^5 D_2 V_b^{2/3}$	Average $\frac{D_2\eta_1}{T} \times 10^3$	$(\sigma_{22}/\sigma_{11})^a$	$(\sigma_{22}/\sigma_{11})^b$	$(\sigma_{22}/\sigma_{11})^c$	σ_{22} (Å)
		$-B \times 10^3$	$-C$							
Ar	1.44	2.236	3.6443	4.43	13.28	4.31	1.24	0.86	1.32	3.42*
CO_2	1.89	2.264	3.2164	4.48	20.91	5.97	1.454	1.05	1.10	4.00*
CH_4	1.64	1.545	5.8556	3.06	18.47	5.15	1.34	1.38	1.81	3.70*
CH_3Cl	1.40	3.109	0.7415	6.15	19.00	4.28	1.22	1.26	0.96	3.37*
CH_3Br	1.35	2.337	3.4027	4.63	19.53	4.10	1.61	1.65	1.05	4.43*
$CHCl_2F$	1.80	3.419	−0.5389	6.77	29.72	5.19	1.62	—	0.60	2.66†

*Reference 30.
†Reference 32.
‡$(\sigma_{22}/\sigma_{11})^a$: using σ_{22} as listed and $\sigma_{11} = 2.75$ (ref. 6). $(\sigma_{22}/\sigma_{11})^b$: from gas viscosity data. $(\sigma_{22}/\sigma_{11})^c$: from slope of D *vs.* $D_1{}^0$ plot.

Can. J. Chem. Downloaded from www.nrcresearchpress.com by 210.87.254.42 on 09/05/12
For personal use only.

Over the temperature range studied, all gases exhibited good, linear, ln D_2 *vs.* $1/T$ plots (Fig. 1), suggesting there is no change in the immediate environment of the gas over this temperature range. If activation energies (ΔE) are meaningful, the values obtained from the ln D_2 *vs.* $1/T$ plots, given in Table 7, show reasonable constancy. The value for methane (3.06 kcal) is in good agreement with the 2.900 kcal value for the diffusion of a wide range of hydrocarbons in water as reported by Witherspoon and Saraf (18).

Various empirical relationships have been suggested for the diffusion coefficients of gases in liquids. The diffusion of a gas through a dense solvent is controlled mainly by the size of the diffusing solute molecule and by the viscosity of the solvent. Hildebrand has suggested that the product $D_2V_b^{2/3}$, where V_b is the solute molar volume at the boiling point, should be approximately constant (7). As seen in Table 7, a rough constancy is observed though the value of this product for argon is considerably less, and the value $D_2V_b^{2/3} = 53.9$ for $CHCl_2F$ is far higher, than the other gases. A linearity exists between $10^5D_2V_b^{2/3}$ and the activation energy ΔE for CH_4, CH_3Cl, and CH_3Br as might be expected from Hildebrand's arguments for the use of the $V_b^{2/3}$ term. The data of Witherspoon (18) give for CH_4, C_2H_6, and C_3H_8 a $D_2V_b^{2/3}$ value of 21.5 ($\pm$0.4).

Othmar and Thakar (26) have suggested that as both diffusion and viscosity are rate processes, both varying as an exponential function of temperature, a plot of log D *vs.* log η (the solvent viscosity) should give a straight line. We give such a plot in Fig. 2 and observe that all six gases give a good linear relationship over the temperature range measured. Wilke and Chang (27) have proposed an equation relating the diffusion coefficient of a solute to the physical properties of both solute and solvent, *viz.*

$$[1] \qquad D_2 = \frac{7.4 \times 10^{-13} \times (2.6\,M)^{1/2}T}{\eta V_b^{0.6}}$$

It is found that this equation is totally unable to represent our observed data; typical systems are plotted in Fig. 3. Neither do the various improvements of the Wilke–Chang equation show any better agreement with experiment. If we

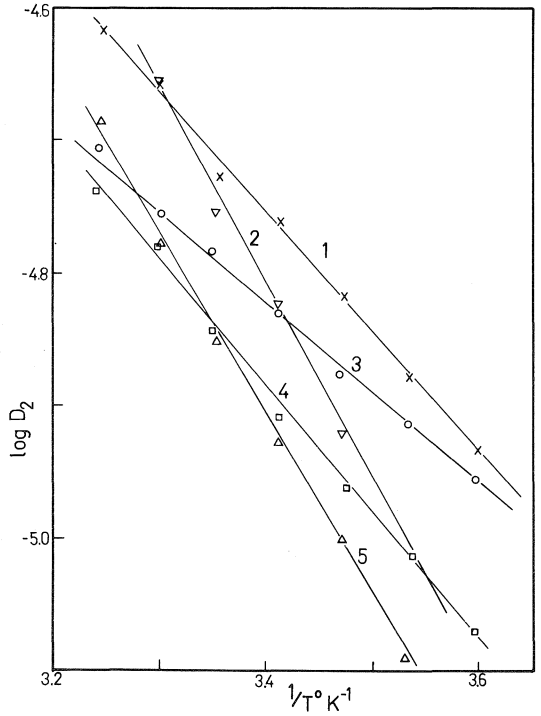

FIG. 1. Dependence of log D_2 on the reciprocal absolute temperature ($1/T$ °K^{-1}). Legend: CO_2, 1 (×); $CHCl_2F$, 2 (▽); CH_4, 3 (○); Ar, 4 (□); CH_3Cl, 5 (△). Lines through data points are drawn using coefficients given in Table 7.

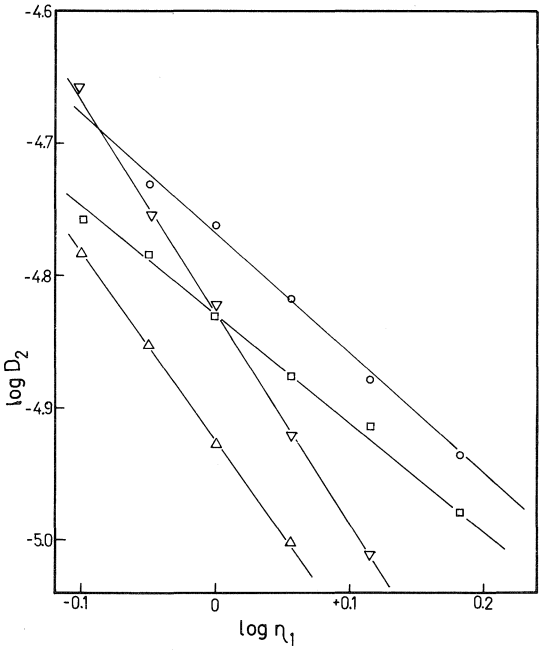

FIG. 2. Dependence of gas diffusion coefficient (log D_2) on the viscosity of water (log η_1). Legend: CO_2, ○; CH_4, □; $CHCl_2F$, ▽; $CHCl_3$, △.

examine the simple Stokes–Einstein relation

$$D_2\eta_1 = kT/3\pi\sigma_{22}$$

we find a reasonable consistency for the $D_2\eta_1/T$ term for all systems over the temperature range studied. If we plot the average value of $D_2\eta_1/T$ against $(1/\sigma_{22})$ we find that though a linear relationship exists for the CO_2, CH_4, Ar, and CH_3Cl, the slope of the line is of the wrong sign.

The McLaughlin (8) formulation of the diffusion equation, based upon the theory of Enskog (28), offers an alternative to the Stokes–Einstein equation and the many empirical relationships based upon it, some of which are discussed above. The resulting equation of the McLaughlin treatment for that case where X_1 (mole fraction of solvent) $\rightarrow 1$ and $X_2 \rightarrow 0$ is

$$[2]\quad \frac{D_2}{D_1^0} = \frac{(M_1 + M_2)^{1/2}}{2M_2}\left(\frac{\sigma_{11}}{\sigma_{22}}\right)^2 \times \left[\frac{(2 + b_{11}^0)}{(1 - b_{11}^0)^2 + 3b_{11}^0\sigma_{22}/\sigma_{12}}\right]$$

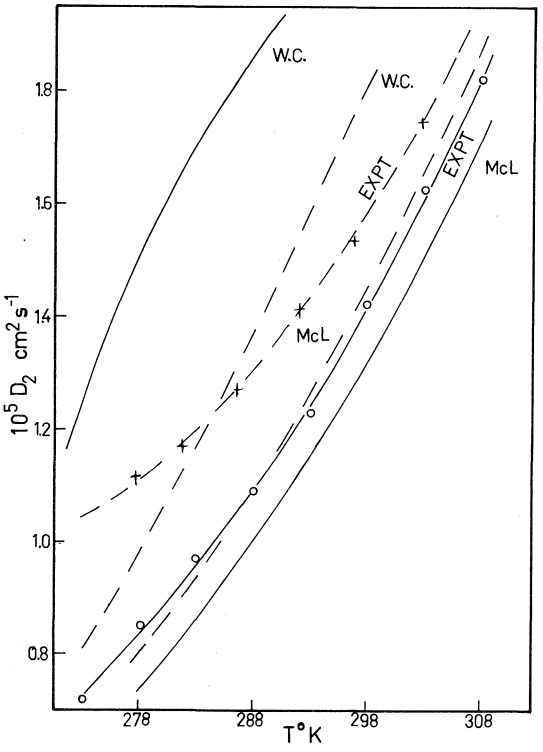

FIG. 3. Temperature dependence of diffusion coefficient of argon and of methane, with Wilke–Chang and McLaughlin approximations. Legend: argon data, full line; methane data, dashed line.

where D_2 is the coefficient of diffusion of the gas (solute) in the solvent, D_1^0 the self-diffusion coefficient of the solvent, M_i and σ_{ii} the molecular mass and hard-sphere diameter of solvent (*1*) and solute (*2*), and $b_{11}^0 = (\pi\eta_1\sigma_{11}^3/6)$. To obtain D values from this equation we need values of the self-diffusion coefficient D_1^0 of water over the temperature range of the experiment. We obtained these values from the data of Wang, Robinson, and Edelman (29). We also need hard-sphere diameter values (σ_{ii}) of the solvent and of the various solutes. For water we use a value $\sigma = 2.75$ Å (6). For the solutes we use the generally accepted 12–6 Lennard–Jones potential σ values (30).

As may be seen in Tables 1–6, a reasonable agreement of eq. 2 with experiment is observed. We have used D_1^0 data obtained with D_2O as the tracer molecule (29*b*) using $H_2{}^{18}O$ tracer data (29*a*) gives no overall better agreement. We compare data predicted by eqs. 1 and 2 with experimental data for argon and methane in Fig. 3. In general, the temperature dependence of D_2 is not well predicted by eq. 2. We note that we have not considered the hard-sphere diameter values to vary with temperature. We test the validity of this by plotting in Fig. 4 the diffusion coefficient of the solute (D_2) against the self-diffusion coefficient of water (D_1^0) at the same temperature. For all systems examined a good linear relationship exists. This suggests that the r.h.s. of eq. 1 can indeed be considered independent of temperature.

It is seen from Table 2 that for the CO_2–H_2O system the agreement between the theoretical eq. 2 values and experimental values is not only worse than the Wilke–Chang values but far worse than those values predicted from his theory, for this system, by McLaughlin (8). McLaughlin made two approximations when using eq. 2. He obtained the σ_{22}/σ_{11} ratio from data on the low density gas viscosities of water and of CO_2 over the temperature range of the D values. The ratio is obtained from the relationship (8)

$$(\eta_i)_{gas} = 1.015\,(5/16\sigma_{ii}^2)(M_i kT/\pi)^{1/2}$$

In this range, 0–55 °C, he found the σ_{22}/σ_{11} ratio to vary from 0.98 to 1.01. Having found this ratio close to unity he could then set the last term in eq. 2 equal to unity. The very small variations in σ_{22}/σ_{11} (from gas viscosity data)

Can. J. Chem. Downloaded from www.nrcresearchpress.com by 210.87.254.42 on 09/05/12
For personal use only.

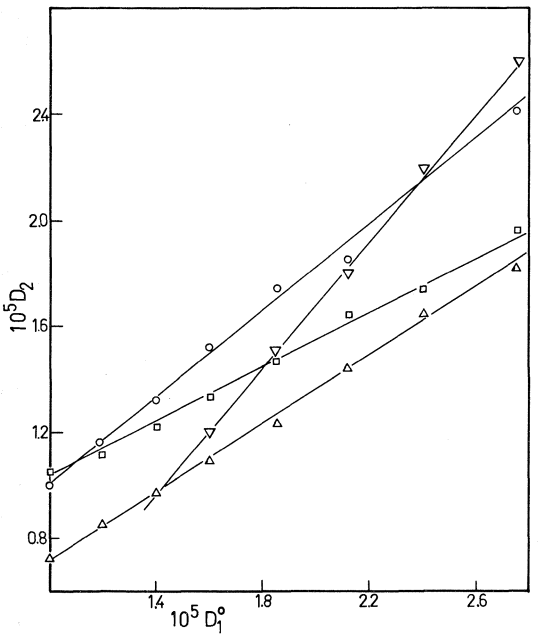

FIG. 4. Diffusion coefficient of gas (D_2) plotted against the self-diffusion coefficient of water (D_1°) at the same temperature. Legend: CO_2, ○; Ar, △; CH_4, □; $CHCl_2F$, ▽.

over the temperature range studied support our interpretation of the linearity of the D *vs.* D_1^0 plot. If we make the assumption that the final term in eq. 2 *is* unity, we can then obtain the σ_{22}/σ_{11} ratio from the slope of the D *vs.* D_1^0 plot. These are given in Table 7 and it is seen that for the CO_2–H_2O system the value of $\sigma_{22}/\sigma_{11} = 1.10$ is, in fact, self-consistent with the assumption that the final term in eq. 2 is approximately unity. It agrees with the σ_{22}/σ_{11} ratio obtained from the gas viscosity data for CO_2–H_2O but does not agree with the ratio obtained from accepted σ values. Using the σ_{22}/σ_{11} ratio obtained from the D_2 *vs.* D_1^0 plot, the D_2 values obtained from eq. 2 are in better agreement with the experimental values (see Table 2). For the CH_3Cl–H_2O and the CH_3Br–H_2O systems the D_2 *vs.* D_1^0 plot gives σ_{22}/σ_{11} ratios close to unity. As can be seen from Tables 4 and 5 using these σ ratios and making the assumption that the final term in eq. 2 is unity does *not* improve the agreement with experiment. We note, however, that for the latter two systems the σ_{22}/σ_{11} ratios from the D_2 *vs.* D_1^0 plot do not agree with the ratios obtained from gas viscosity data. For the $CHCl_2F$–H_2O system using a σ_{22} value of 4.45 Å (for source see Table 7), the diffusion values obtained are in rather poor agreement with the experimental values. From the D_2 *vs.* D_1^0 plot the σ ratio is found to be 0.60 but this ratio is not self-consistent with the assumption that the final term in eq. 2 is unity. We do not have dilute gas viscosity data for $CHCl_2F$ but it would appear that eq. 2 cannot predict the D_2 value for $CHCl_2F$ in water with any real success. In his examination of the CO_2–H_2O system McLaughlin (8), noting the difference in the reported D_1^0 values for water (obtained using different tracer molecules) (29*a*, *b*), showed that using $H_2{}^{18}O$ data better agreement could be obtained. Whilst this is so, an examination of the six systems here presented shows no overall improvement. For some systems a better agreement with experiment is observed, for others a worse agreement. We note, however, that D_1^0 data obtained using the $H_2{}^{18}O$ tracer give linear D_2 *vs.* D_1^0 plots just as were obtained using the D_2O tracer data.

As a final test of the McLaughlin equation we see that from eq. 2 we may obtain an expression for the ratio of the diffusion coefficients of two gas solutes in the same solvent, *viz.*

$$\frac{D_{2A}}{D_{2B}} = \frac{\left(\frac{M_1 + M_A}{M_A}\right)^{1/2}}{\left(\frac{M_1 + M_B}{M_B}\right)^{1/2}} \frac{(\sigma_{1B})^2}{(\sigma_{1A})^2} \times \frac{[(1 - b_{11}{}^0)^2 + 3b_{11}{}^0\sigma_{AA}/\sigma_{1A}]}{[(1 - b_{11}{}^0)^2 + 3b_{11}{}^0\sigma_{BB}/\sigma_{1B}]}$$

To a good approximation we may set the final term to unity, thus obtaining the expression

$$[3] \quad \frac{D_{2A}}{D_{2B}} = \left[\frac{M_B(M_1 + M_A)}{M_A(M_1 + M_B)}\right]^{1/2} \times \left[\frac{1 + \sigma_{BB}/\sigma_{11}}{1 + \sigma_{AA}/\sigma_{11}}\right]^{1/2}$$

Using argon as one of the two solutes (2A) we may compare the slope of the D_{2A} *vs.* D_{2B} plots (over the temperature range of the data) with the calculated slope as given by eq. 3. For all pairs of systems examined good linear plots are obtained but comparison of experimental and calculated slope values is very bad. We give a typical comparison in Table 8 in which the theoretical slope values are calculated using both the $(\sigma_{22}/\sigma_{11})^a$ and $(\sigma_{22}/\sigma_{11})^b$ values of Table 7.

Can. J. Chem. Downloaded from www.nrcresearchpress.com by 210.87.254.42 on 09/05/12
For personal use only.

TABLE 8. D_{2A}/D_{2B} slope values (eq. 3) using the value for Ar–H_2O system for D_{2A}

System for D_{2B}	D_{2A}/D_{2B} Experimental	Theoretical *i**	Theoretical *ii*†
CH_4–H_2O	1.217	0.903	1.348
CO_2–H_2O	0.781	1.161	1.172
CH_3Cl–H_2O	0.838	1.016	1.523
CH_3Br–H_2O	0.838	1.484	2.222
$CHCl_2F$–H_2O	0.576	0.846	

*Using $(\sigma_{22}/\sigma_{11})^a$ values, Table 7.
†Using $(\sigma_{22}/\sigma_{11})^b$ values, Table 7.

Conclusion

The six gases studied cover a wide range of gas–hydrate stability. No outstanding differences in actual diffusion coefficient values nor in the temperature dependence of the D values is observed. Agreement of measured values and of various empirical theories is, in general, poor, but this is obviously a matter of the poverty of the empirical relationships. Huq and Wood (31) have examined a wide range of empirical and semi-empirical equations relating D values to the properties of solute and solvent and found a similar disparity between the experimental data and the expected correlation.

The McLaughlin diffusion equation, considering its simplicity (*i.e.* that it comes from hard sphere theory), its sensitivity to the σ_{ii} values used and even more so to the self-diffusion value of water (see ref. 8) gives reasonable agreement with experiment. We see, however, that even in the comparison of the D_2 value of one gas in water to the D_2 value of another gas in water the hard sphere theory lacks acceptable predictive success.

This research was carried out under a grant from the Defense Research Board and under a grant from the Water Resources Board, Department of the Environment.

1. G. A. JEFFREY and R. K. MCMULLAN. Adv. Chem. Phys. **9**, 43 (1966).
2. R. A. HORNE. Prog. Chem. **16**, 1 (1970).
3. A. PURKAYASTHA and J. WALKLEY. To be published.
4. H. S. FRANK and M. W. EVANS. J. Chem. Phys. **13**, 507 (1945).
5. A. BEN-NAIM. J. Phys. Chem. **69**, 3240 (1965).
6. R. A. PIEROTTI. J. Phys. Chem. **69**, 281 (1965).
7. J. H. HILDEBRAND. Proc. Nat. Acad. Sci. **64**, 1329 (1969).
8. E. MCLAUGHLIN. J. Chem. Phys. **30**, 1254 (1969); Mol. Phys. **16**, 501 (1969).
9. P. BOOTH. Trans. Faraday Soc. **44**, 1796 (1948).
10. P. V. DANKWERTS. Trans. Faraday Soc. **46**, 701 (1950).
11. A. BEN-NAIM and S. BAER. Trans. Faraday Soc. **59**, 2735 (1963).
12. J. T. ASHTON, R. A. DAWE, K. W. MILLER, E. B. SMITH, and B. J. STICKINS. J. Chem. Soc. (*c*), 1793 (1969).
13. R. G. SMITH, G. T. KRIESS, and M. F. MORALER. J. Phys. Chem. **59**, 382 (1955).
14. A. J. H. BOERBOOM and G. KLEYN. J. Chem. Phys. **50**, 1086 (1969).
15. D. L. WISE and G. HOUGHTON. Chem. Exp. Sci. **21**, 999 (1966).
16. A. A. UNVER and D. M. HIMMELBLAU. J. Chem. Eng. Data, **9**, 428 (1964).
17. N. A. LANGE. Handbook of chemistry. 10th ed. McGraw-Hill Co. Inc., New York. 1961.
18. P. A. WITHERSPOON and D. N. SARAF. J. Phys. Chem. **69**, 3752 (1965).
19. J. H. WANG. J. Am. Chem. Soc. **73**, 510 (1951).
20. W. F. CLAUSSEN and M. F. POLGASE. J. Chem. Phys. **74**, 4817 (1952).
21. S. H. CHIANG and H. L. TOOR. A.I. Chem E. I. **6**, 539 (1960).
22. L. J. BENNETT, W. Y. NG, and J. WALKLEY. J. Phys. Chem. **72**, 4699 (1968).
23. L. M. BLAIR and J. A. QUINN. Fluid Mech. **36**, 385 (1969).
24. W. N. GILL and R. SANKARASUBRAMANIAN. Proc. Roy. Soc. A, **316**, 341 (1970).
25. W. Y. NG and J. WALKLEY. Can. J. Chem. **47**, 1075 (1969).
26. D. F. OTHMAR and M. S. THAKAR. Ind. Eng. Chem. **45**, 589 (1953).
27. C. R. WILKE and P. CHANG. J.A.I. Chem. E. **1**, 264 (1955).
28. S. CHAPMAN and T. G. COWLING. The mathematical theory of non-uniform gases. Cambridge University Press, England. 1939.
29. (*a*) J. H. WANG, C. U. ROBINSON, and I. S. EDELMAN. J. Am. Chem. Soc. **75**, 466 (1953); (*b*) J. H. WANG. J. Am. Chem. Soc. **73**, 511 (1951).
30. J. O. HIRSCHFELDER, C. F. CURTISS, and R. B. BIRD. Molecular theory of gases and liquids. John Wiley and Sons, Inc., New York. 1945.
31. A. HUQ and T. WOOD. J. Chem. Eng. Data, **13**, 256 (1968).
32. J. O. HIRSCHFELDER, F. T. MCCLURE, and I. F. WEEKS. J. Chem. Phys. **10**, 201 (1942).

Can. J. Chem. Downloaded from www.nrcresearchpress.com by 210.87.254.42 on 09/05/12
For personal use only.

Experimental and Theoretical Estimates of Sigma and Pi Electron Contributions to Long-range Spin–Spin Coupling Constants in Coumarin and its Methyl Derivatives

J. B. ROWBOTHAM[1] AND T. SCHAEFER

Department of Chemistry, University of Manitoba, Winnipeg, Manitoba R3T 2N2

Received July 17, 1972

A full analysis of the p.m.r. spectra of coumarin and five of its methyl derivatives allows the assignment of σ and π electron components to the inter-ring proton–proton spin–spin coupling constants. Magnitudes of up to 0.3 Hz are observed over a coupling path of eight bonds. The σ and π components can be combined on the basis of the appropriate valence bond structures to predict closely the observed parameters in naphthalene, suggesting only weak participation of the ether oxygen atom in the π electron system of coumarin. Calculations of the inter-ring coupling constants at the INDO and CNDO/2 levels of molecular orbital theory are helpful in the interpretation of the observed data, the agreement with experiment being quantitative in many instances. Comparison of the observed coupling constants in coumarin and styrene with the INDO results for an assumed planar form of the latter suggests that styrene exists in a nonplanar conformation.

Une étude complète des spectres r.m.n. du coumarin et de cinq de ses dérivés méthylés permet l'attribution des composantes σ et π aux constantes de couplages déduites spin–spin des interactions proton–proton. Des amplitudes allant jusqu'à 0.3 Hz sont observées pour une zone de couplage incluant huit liaisons. Les composantes σ et π peuvent être combinées en se basant sur les structures appropriées (obtenues par la théorie du lien de valence) pour prédire avec précision les paramètres observés pour le naphtalène suggérant une faible participation seulement de l'atome d'oxygène du groupe éther dans le système d'électrons π du coumarin. Les calculs des constantes de couplage déduites aux niveaux INDO et CNDO/2 de la théorie des orbitales moléculaires sont utiles dans l'interprétation des données obtenues, l'accord avec les données expérimentales étant très souvent quantitatif. La comparaison des constantes de couplage observées pour le coumarin et le styrène avec les résultats INDO pour une structure supposée planaire pour ce dernier suggère que le styrène existe dans une conformation non-planaire.

[Traduit par le journal]

Can. J. Chem., **51**, 953 (1973)

Introduction

The dependence on conformation and on bonding situation of the spin–spin coupling constants between protons on a side-chain and ring protons in benzene and pyridine derivatives has been extensively studied by experimental and theoretical methods (1–20). Less extensive investigations of inter-ring long-range proton coupling constants in fused aromatic systems (21, 22) have been reported for naphthalene (23), acridine (24), isoquinoline (25), and for several coumarin derivatives (26). The use of the 'methyl group replacement technique' (27–29) and of approximate molecular orbital theory at the INDO and CNDO/2 levels (30) is enlightening in the elucidation of the coupling mechanisms operating in the single ring compounds (7, 8, 14). In this paper we apply these methods to the inter-ring coupling constants in coumarin (**1**). Comparisons are made with experimental data for naphthalene, a fused aromatic molecule, and with theoretical data for styrene, a single ring compound.

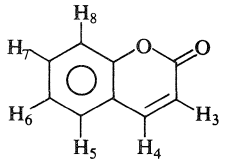

1

Experimental

Coumarin and its 3- and 6-methyl derivatives were obtained from Aldrich Chemical Co. The 4-, 7-, and 8-methylcoumarins were prepared by standard procedures (31–33). Analytical samples contained tetramethylsilane (TMS) as internal reference and locking material and were degassed by the freeze–pump–thaw technique. The solvents and concentrations of solute (given in Table 1) were dictated by considerations of spectral complexity of the multispin systems. P.m.r. spectra were recorded in the frequency sweep mode on an HA-100D spectrometer

[1]Postdoctoral Fellow, 1970–1972.

Can. J. Chem. Downloaded from www.nrcresearchpress.com by 210.87.254.40 on 09/05/12
For personal use only.

TABLE 1. Proton chemical shifts* and coupling constants† in coumarin and some methylcoumarins

	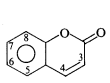	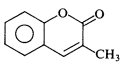	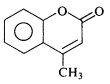	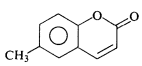	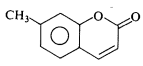	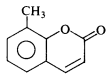
Solvent:	$CDCl_3$	Acetone-d_6	$CDCl_3$	$CDCl_3$	$CDCl_3$	$CDCl_3$
concentration (mol%):	20	12	10	14	12	16
ν_3	636.24	—	618.13	631.40	629.18	634.06
ν_4	769.67	763.25	—	759.07	763.79	765.52
ν_5	745.94	748.89	756.60	720.40	732.57	727.30
ν_6	722.63	724.18	725.82	—	704.46	711.88
ν_7	746.79	746.73	747.96	725.64	—	730.66
ν_8	722.33	722.99	725.42	711.20	704.12	—
ν_{CH3}	—	211.28	239.97	235.12	240.52	237.81
$^3J_{34}(^4J_{34})$	+9.58	(−1.37)	((−)1.28)	9.56	+9.50	+9.51
$^5J_{35}(^6J_{35})$	+0.32	(−0.27)	0.36	0.32	0.31	+0.30
$^6J_{36}(^7J_{36})$	+0.13‡	(+0.10‡)	0.12‡	(0.10‡)	+0.13	+0.10
$^7J_{37}(^8J_{37})$	+0.34	(−0.26)	0.27	0.34	(−0.29)	+0.32
$^6J_{38}(^7J_{38})$	−0.13	(+0.10‡)	0.01	(−)0.03	−0.12	(+0.10‡)
$^4J_{45}(^5J_{45})$	−0.31	−0.36	(0.06‡)	(−)0.32	−0.31	−0.33
$^5J_{46}(^6J_{46})$	0.01	0.01	(0.00‡)	(0.00)	0.08	0.00‡
$^6J_{47}(^7J_{47})$	−0.10‡	(−)0.09	(0.04‡)	(−)0.03	(0.12)	(−)0.10‡
$^5J_{48}(^6J_{48})$	+0.65	+0.64	(0.06‡)	0.65	0.70	(0.00‡)
$^3J_{56}(^4J_{56})$	+7.70	+7.75	7.98	((−)0.81)	+7.89	7.71
$^4J_{57}(^5J_{57})$	+1.64	+1.62	1.56	2.10	(+0.32)	+1.58
$^5J_{58}(^6J_{58})$	0.49	+0.50	0.48	0.44	+0.45§	−0.60
$^3J_{67}(^4J_{67})$	+7.39	+7.41	7.35	((−)0.60)	((−)0.62)	+7.50
$^4J_{68}(^5J_{68})$	1.13	1.11	1.20	(0.31)	1.66	(0.35)
$^3J_{78}(^4J_{78})$	+8.38	+8.35	8.32	8.44	((−)0.76)	−0.81

*In Hz at 100 MHz to low field of internal TMS.
†In Hz. When sign is omitted or given in brackets, it was not determined. When the *value* is in brackets, it concerns a methyl group.
‡Adjusted manually for best line shape.
§Or possibly +0.17 Hz. See text.

at a sweep width of 1 Hz/cm and a sweep rate of 0.02 Hz/s. They were repeatedly calibrated by reading sweep and manual oscillator frequencies at intervals of 5 Hz or less. Double irradiation experiments (34) employed an HP-4204A audio oscillator.

Results and Discussion

(1) Spectral Analysis

(a) Proton Assignments

In general the olefinic proton H_3 resonated at a higher field than the aromatic protons while H_4 resonated at lower field. However, the peaks from H_4 overlapped those from the aromatic protons in 3-methylcoumarin when dissolved in chloroform or benzene. But in acetone-d_6 solution these peaks were well separated. Variation of solute concentrations minimized the overlap of peaks belonging to different aromatic protons, those from H_5 and H_7 usually being centered 20–25 Hz to low field of those from H_6 and H_8.

(b) Computer Simulations

The program LAME (35), coupled to a plotting routine (36), was initially used in the non-iterative mode until the computed spectra closely resembled the experimental recordings. As many lines as practical were then assigned, followed by iterative computer runs. Typically about 300 of 800 transitions were assigned.[2] The r.m.s. error and the standard deviations in the derived parameters were better than 0.03 and 0.01 Hz, respectively. Two of the correlation coefficients involving the long-range coupling–coupling constants were sizeable. These were 0.45 for J_{35}–J_{37} in 6-methylcoumarin and 0.61 for ν_3–J_{36} in 8-methylcoumarin. Hence the sums of the indicated parameters in these two cases are rather more precise than the individual values. Often the smaller couplings were not reproduced as well as desired and consequently these were then adjusted by trial and error to yield the best simulations of the experimental spectra. Changes of a few hundredths of a Hz produced noticeable

[2]The presence of three magnetically equivalent methyl protons causes a large number of transitions so that the ratio of 3:8 is less severe than first appears.

Can. J. Chem. Downloaded from www.nrcresearchpress.com by 210.87.254.40 on 09/05/12
For personal use only.

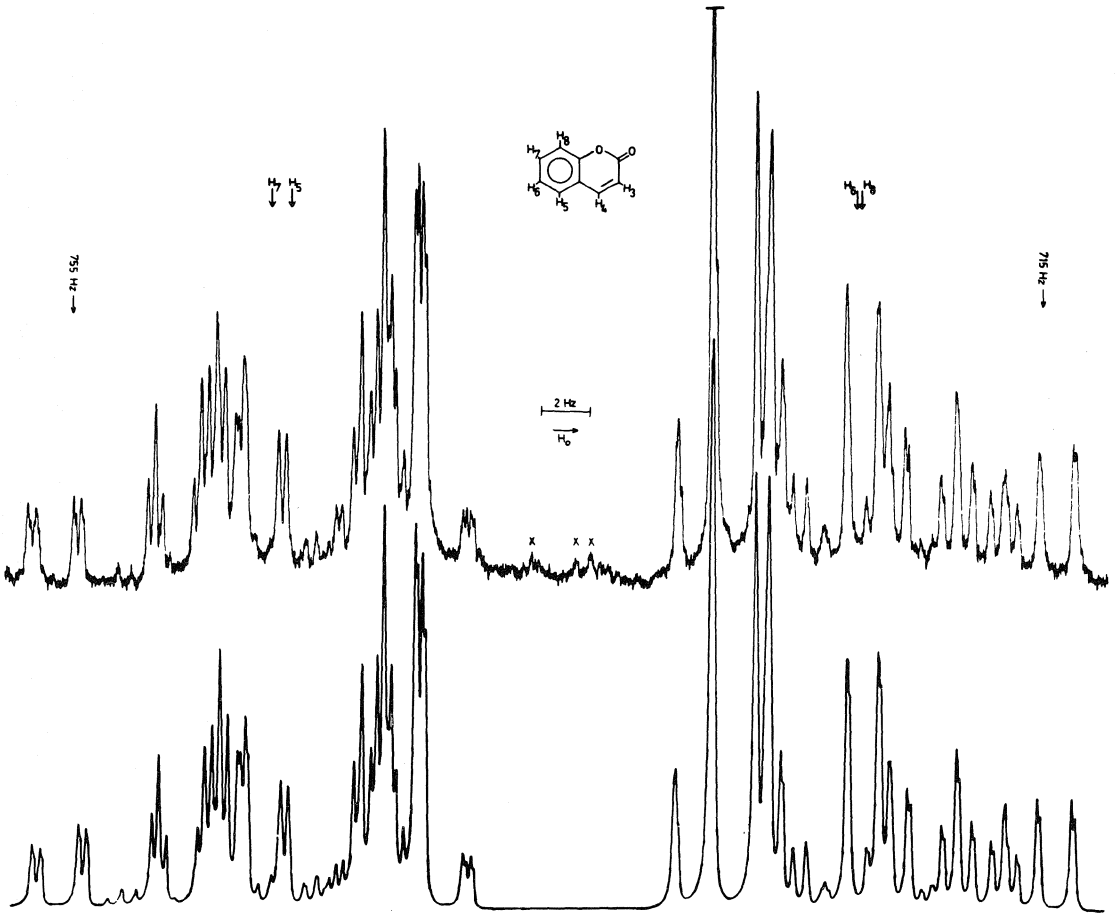

FIG. 1. The p.m.r. spectrum at 100 MHz of the ring protons in coumarin as a 20 mol % solution in chloroform-*d*. The shifts of the protons are indicated by vertical arrows. The calculated spectrum employs the parameters in Table 1 with $\Delta\nu_{1/2} = 0.15$ Hz and an asymmetry factor of 0.70 (see text). The peaks marked by crosses arise from impurities.

change in the spectra. Figure 1 displays the observed ring proton spectrum for coumarin together with the computed spectrum based on the parameters in Table 1 (assumed line width at half height of 0.15 Hz and an asymmetry parameter (36) of 0.70).

(c) 7-Methylcoumarin

The spectrum of this compound proved difficult to analyze accurately, as the chemical shifts of H_6 and H_8 are separated by only 0.3 Hz, and the coupling parameters are therefore less certain ($\pm$0.05 Hz) than for the other compounds in Table 1. Moreover, the peak positions of H_8 for this compound were not affected significantly by small variations of $^5J_{58}$, while the splittings in the H_5 region were not linearly dependent on the variations. As a result, equally good simulations were obtained when $^5J_{58}$ was set at 0.17 or 0.45 Hz. The former value was rejected as improbable.

(d) Determination of Signs of Couplings

In Table 1 the signs of the coupling constants[3] were determined by weak irradiation experiments (34) whenever possible and are given relative to the signs of the vicinal couplings, known to be positive. When the signs are not given or are enclosed in brackets they are not based on tickling experiments, these proving impossible or ambiguous because of difficulties in choosing

[3]In the nomenclature used here a left superscript on the coupling, *J*, indicates the number of bonds separating the coupled nuclei, their positions in **1** being given by right subscripts.

Can. J. Chem. Downloaded from www.nrcresearchpress.com by 210.87.254.40 on 09/05/12
For personal use only.

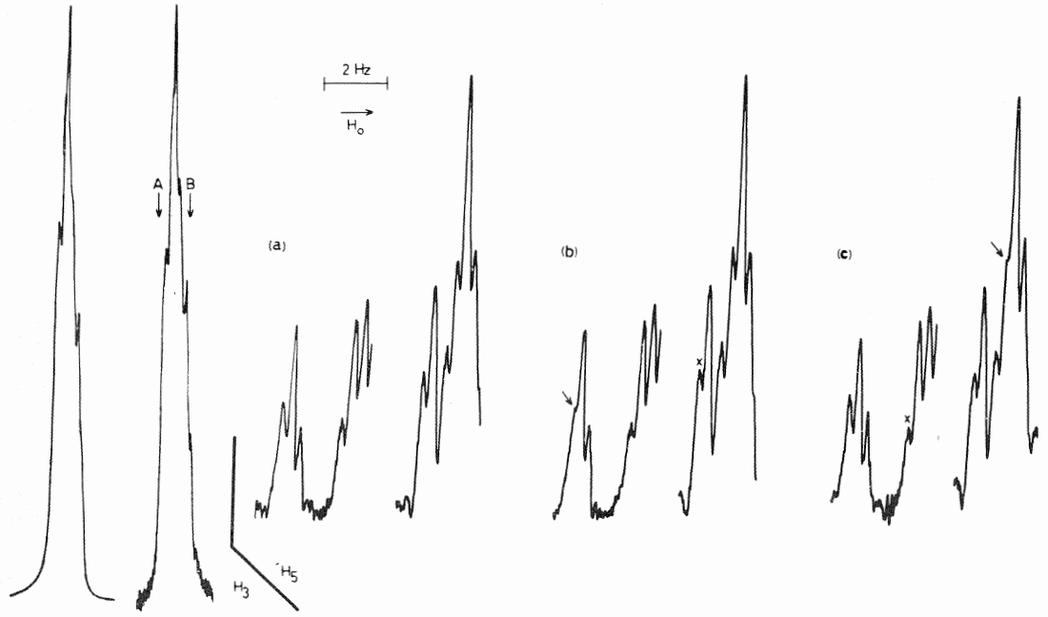

FIG. 2. On the left the high-field half of the p.m.r. spectrum of the olefinic proton H_3 in coumarin is shown together with the calculated spectrum; experimental and computational conditions as in Fig. 1. In the spectra of ring proton H_5 (easily matched to the left-hand part of Fig. 1) the conditions are (*a*) single resonance, (*b*) weak irradiation at the point marked A in resonance of H_3, (*c*) weak irradiation at point B in resonance of H_3. Arrows mark the peaks affected by the irradiation and crosses indicate those peaks which *would* have been affected had $^6J_{36}$ been negative; *i.e.*, of opposite sign to $^3J_{56}$.

the necessary triplets of couplings whose presence is reflected in well-resolved spectral splittings.

In only one case was a sign found opposite to expectation, that of $^6J_{36}$. When the high-field peaks from H_3 in coumarin are weakly irradiated at points marked A and B in Fig. 2, the peaks from H_5 are perturbed as shown. In brief, irradiation of a "low-field" H_3 peak perturbs a "low-field" H_5 peak and hence $^6J_{36}/^3J_{56} > 0$. It also follows from these experiments that $^3J_{34}/^4J_{45} < 0$ and $^7J_{37}/^4J_{57} > 0$.

(2) Intra-ring Coupling Constants

(a) Between Ring Protons

Most of these couplings are unexceptional (Table 1). Thus, the couplings in the aromatic ring of coumarin agree to within 0.2 Hz with the values calculated by assuming additivity (37–39) of the substituent effects from methoxyl and vinyl groups, as deduced from data on anisole (39), 3-bromostyrene (7), and bromobenzene (39), data for styrene itself being unavailable. The presence of a methyl group on the benzene ring alters the couplings in the manner expected from their values in benzene (37) and toluene (1). However, in 4-methylcoumarin $^3J_{56}$ is 0.3 Hz larger than in coumarin, possibly because of steric interference by the methyl group with the electron distribution in the C—H_5 bond. A similar situation is found in 9-methylacridine (24).

Again, the olefinic coupling $^3J_{34}$ in coumarin is smaller than in styrene derivatives (7) but by the amount expected from the difference observed in this coupling between methyl propenoate (40) and ethylene (41).

(b) Between Ring and Methyl Protons

The couplings between methyl and ring protons over five and six bonds, $^5J_m^{H,CH_3}$ and $^6J_p^{H,CH_3}$, lie within experimental error of those in toluene (1). The benzylic couplings over four bonds, $^4J_o^{H,CH_3}$, either lie near -0.80 Hz or near -0.60 Hz. A rationalization of these values depends on a contribution from structures **2** or **3**

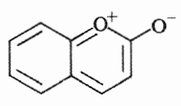

2

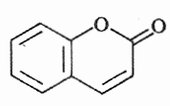

3

TABLE 2. Inter-ring coupling constants in coumarins compared with those in naphthalene and those calculated by INDO and CNDO/2 for coumarin and planar styrene

	Coumarins, obs.*			Coumarin, calcd.†		Styrene, calcd.‡	Naphthalene§
	H,H		H,CH_3	INDO	CNDO/2	INDO	obs.
$^3J_{34}$	9.50 to 9.58	$^4J_{34}$	−1.28 to −1.37	9.07	7.76	—	—
$^7J_{37}$	0.27 to 0.34	$^8J_{37}$	−0.26 to −0.29	0.35	0.02	0.29	0.25
$^6J_{36}$	0.10 to 0.13	$^7J_{36}$	0.10	0.21	0.24	0.12	0.10
$^6J_{38}$	−0.01 to −0.13	$^7J_{38}$	0.10	−0.24	0.00	−0.18	−0.10
$^6J_{47}$	−0.03 to −0.10	$^7J_{47}$	0.04 to 0.12	−0.26	−0.01	−0.24	−0.10
$^5J_{35}$	0.30 to 0.32	$^6J_{35}$	−0.27	0.50	0.21	0.50	0.23
$^5J_{46}$	0.00 to 0.08	$^6J_{46}$	0.00	0.21	0.09	0.22	0.23
$^5J_{48}$	0.64 to 0.70	$^6J_{48}$	0.00 to −0.06	1.31	0.81	1.28	0.85
$^4J_{45}$	−0.31 to −0.36	$^5J_{45}$	0.06	−0.26	0.22	−0.27	−0.45

*In Hz from Table 1.
†Calculated for the H,H couplings in coumarin, see text for geometry.
‡For a planar molecule, ref. 7.
§Reference 23.

because the magnitude of $^4J_o^{H,CH_3}$ is known (19, 42–45) to depend on the bond order of the intervening C···C bond. Indeed those couplings in Table 1 which involve bonds C_5—C_6 or C_7—C_8 in the coupling path have a magnitude near 0.8 Hz and those involving the C_6—C_7 bond are near 0.6 Hz in magnitude. Precisely similar arguments apply to, and magnitudes occur in, a series of benzene (19) and pyridine (6, 36) derivatives.

The allylic couplings, $^4J_{cis}^{H,CH_3}$, in 3- and 4-methylcoumarin are about 0.4 Hz smaller in magnitude than in propene (46), as is qualitatively expected if structure **2** (giving C_3—C_4 single bond character) is of importance. But substituent effects (—C═O linkage) may well occur in coumarin, although their prediction (47) is not easy.

(3) Long-range Inter-ring Coupling Constants

(a) The Methyl Group Replacement Results

As originally suggested by Hoffman (27, 28) the π electron contribution to a proton coupling constant $J^{H,H}$ can be estimated by substitution of one of the coupled protons by a methyl group. The negative of the ensuing coupling J^{H,CH_3} is a measure of the π contribution to $J^{H,H}$. When used with the realization that $^4J^{H,CH_3}$ (14, 47) and even $^5J^{H,CH_3}$ (14, 15) may contain residual σ electron contributions, the technique is of wide applicability (4, 6, 15, 19, 29).

In Table 2 the ranges of inter-ring proton–proton and proton – methyl proton coupling constants for the coumarins are abstracted from Table 1. Beginning with $^7J_{37} = 0.30 \pm 0.03$ Hz, one finds $^8J_{37}^{H,CH_3} = -0.28 \pm 0.02$ Hz. There exist no known proton coupling constants over seven bonds in saturated systems, so that this result is an excellent example of the methyl replacement technique.

Turning to ^6J, the technique implies that $^6J_{38}$ and $^6J_{47}$ are accounted for by a π electron contribution of −0.1 Hz. On the other hand, a value of +0.10 Hz for both $^6J_{36}$ and $^7J_{36}^{H,CH_3}$ indicates a σ electron contribution of +0.2 Hz to $^6J_{36}$. The three ^6J values are accounted for if there exists a π electron contribution of near −0.1 Hz to each but a σ contribution of +0.2 Hz to one of them only, $^6J_{36}$. It is interesting[4] that the bonds between H_3 and H_6 form a zig-zag or all-*trans* path (49), known to give rise to substantial magnitudes of ^5J.

The largest ^5J is $^5J_{48} = 0.67 \pm 0.03$ Hz. This ubiquitous coupling found, for example, in isoquinoline (21, 22, 25), acridine (24), indene (50), and benzofuran (50), occurs whenever a zig-zag configuration exists. Replacement of H_4 or H_8 in coumarin by a methyl group reduces $^6J_{48}^{H,CH_3}$ to almost zero; a σ mechanism therefore dominates. The other two five-bond couplings, $^5J_{46}$ and $^5J_{35}$ do not involve an all-*trans* pathway. $^5J_{35}$ is clearly π electron dominated ($^5J_{35} \simeq -^6J_{35}^{H,CH_3}$), while $^5J_{46}$ is very small, if not zero, and so is $^6J_{46}^{H,CH_3}$.

The methyl replacement method suggests that the *peri* coupling, $^4J_{45}$, arises from a σ electron mechanism. However, the methyl protons in 4-methylcoumarin can approach H_5 rather close-

[4]A coupling of ±1 Hz over six bonds in a saturated system occurs in the cyclopentadiene Diels–Alder adduct of bicyclo[2.1.0]pent-2-ene (48). The coupled protons are related via an all-*trans* or zig-zag bonding path.

Can. J. Chem. Downloaded from www.nrcresearchpress.com by 210.87.254.40 on 09/05/12
For personal use only.

Can. J. Chem. Downloaded from www.nrcresearchpress.com by 210.87.254.40 on 09/05/12
For personal use only.

ly and a through-space (51, 52) and/or a direct (52) coupling interaction is possible and may well vitiate this suggestion.[5] Therefore, the question of mechanism cannot be settled by this method.

(b) INDO and CNDO/2 Molecular Orbital Calculations

The use of the finite perturbation technique with molecular orbitals at the INDO level of SCF MO theory (30, 53, 54) presents a useful guide to the interpretation of long-range coupling constants (7, 8, 14, 47, 55). Furthermore, the difference between coupling calculated at the INDO and CNDO/2 levels can be an *approximate* measure of the role of the π-electrons in the coupling mechanism (30).

In Table 2 the results of such computations on coumarin assume a planar form, **4**, the geometry of the molecule being unknown. Standard bond

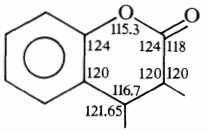

4

lengths (30, 56) and trigonal angles very nearly closed the pyran ring but distorted the C—O—C angle by 11°. The chosen angles in **4** reduce the distortion of this angle to 5.9° (from tetrahedral). Up to 100 SCF cycles were performed (14, 57) on an IBM 360/65 computer, H_3 and H_4 being perturbed, and convergence to better than 0.01 Hz was obtained for the quoted numbers in Table 2.

(c) Comparison of INDO and CNDO/2 Results With Experiment

In Table 2 the INDO results for coumarin reproduce the observed signs of all the long-range inter-ring coupling constants but, in general, overestimate their magnitude. A similar situation was found in benzaldehyde and its derivatives (8).

The magnitude of $^7J_{37}$, a π-electron coupling, is correctly calculated by INDO while CNDO/2 calculates only 0.02 Hz: a good illustration of how INDO incorporates π electron effects.[6]

A comparison of INDO and CNDO/2 computations of ^6J is also instructive. INDO overestimates $^6J_{38}$ and $^6J_{47}$ by about −0.1 Hz and the vanishing values estimated by CNDO/2 confirm the π electron mechanism[7] for these couplings, as inferred from the methyl replacement technique. For $^6J_{36}$ this latter technique implied a π electron contribution of −0.1 Hz and a σ electron contribution of +0.2 Hz while CNDO/2 properly computes 0.24 Hz. This agreement is emphasized by the very small CNDO/2 estimates for $^7J_{37}$, $^6J_{38}$, and $^6J_{47}$: an all-*trans* configuration, as for H_3 and H_6 must exist for a σ electron involvement in ^6J. INDO overestimates $^6J_{36}$ by 0.1 Hz.

The all-*trans* or zig-zag configuration is also important for large σ electron contributions to ^5J (8, 49), as illustrated by $^5J_{48}$ in Table 2. CNDO/2 is in rather close agreement with observation for this constant but INDO overestimates its magnitude substantially, in much the same way as it does for $^5J^{H,CHO}$ in benzaldehyde and its derivatives (8). INDO also overestimates $^5J_{35}$ and $^5J_{46}$ by as much as 0.2 Hz. CNDO/2 gets $^5J_{46}$ right but disagrees with the methyl group replacement technique for $^5J_{35}$. However, the difference between the two theoretical estimates for $^5J_{35}$ is 0.29 Hz, in good agreement with the observed number. In this sense the theory could be said to be in agreement with experiment.

INDO computes $^4J_{45}$ correctly in sign and is close to experiment in magnitude. CNDO/2 disagrees in sign with experiment, the implication therefore being that $^4J_{45}$ is dominated by a π electron mechanism. The fact that $^5J_{45}{}^{H,CH_3}$ is only 0.06 Hz, instead of the 0.3 Hz expected for a π mechanism, may have its origin in the through-space (interaction of the hydrogen 1s orbitals on H_5 and CH_3) or direct (only the two C—H bond orbitals interacting) mechanism. These two mechanisms very likely produce negative coupling interactions (see footnote 5) and could reduce the π coupling of 0.3 Hz to the 0.06 Hz actually observed for $^5J_{45}{}^{H,CH_3}$.

(d) Comparison With INDO Calculations for Planar Styrene

In Table 2 the relevant long-range couplings between ring and olefinic protons, computed (7) by INDO methods for a planar styrene molecule,

[5]Some INDO MO calculations (14) in which a hydrogen molecule and a methane molecule, or two methane molecules, are brought to within van der Waals distances of each other predict *negative* couplings between protons in different molecules.

[6]For the vicinal coupling, $^3J_{34}$ in Table 2, the difference between INDO and CNDO/2 is 1.31 Hz, almost exactly equal to the magnitude of $^4J_{34}{}^{H,CH_3}$. The excellent agreement may be coincidental but is nevertheless encouraging.

[7]A referee emphasizes that the modification from CNDO/2 to INDO may introduce mechanisms which are neither σ nor π; *caveat emptor*.

Can. J. Chem. Downloaded from www.nrcresearchpress.com by 210.87.254.40 on 09/05/12
For personal use only.

are very similar to those tabulated for the INDO calculations on coumarin. In fact, for many of the couplings the styrene calculations are in slightly better agreement with the observed data on coumarin than are the calculations for the latter, which also assume a planar molecule. Furthermore, the agreement is much better than that between the styrene calculations and the observations on a number of styrene derivatives (7). Therefore the O—C=O group in the pyran ring does not alter the computed couplings to a marked extent and probably the styrene molecule is not planar, in contrast to the benzaldehyde molecule (58).

(e) Comparison With Long-range Couplings in Naphthalene

The inter-ring coupling constants in coumarin and naphthalene (Table 2) follow the same trends, the couplings lying within 0.2 Hz of each other in the two compounds while the algebraic sums of the eight couplings lie within 0.05 Hz. The ether linkage in coumarin redistributes the long-range interactions to some extent but does not radically alter them from their values in naphthalene.

Another point from which to view this comparison invokes a valence bond picture. With reference to Table 2[8] it is likely that the π electron components of the long-range couplings fall into three groups. First, when a resonance structure connecting the coupled protons can be drawn, such as **5**, the π contribution is $+0.3$ Hz. Second, when it is possible to link only one

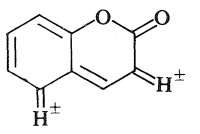

5

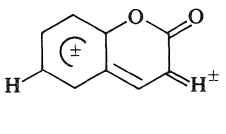

6

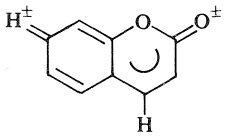

7

of the protons with the other ring, as in **6** or **7**, then the π component is -0.1 Hz. Third, if it is impossible to write a resonance structure linking a coupled hydrogen and involving both rings *without* including the p orbitals of the ether oxygen atom, then the π component of the coupling is zero (not detectable by our experiments). Again, the σ electron contribution is zero, except for an all-*trans* coupling path where it is 0.65 and 0.20 Hz respectively for five and six intervening bonds.

When these σ and π components are used to predict the coupling constants in naphthalene, using the appropriate resonance structures, the agreement with experiment is gratifying except for $^5J_{15}^{H,H}$, where the disagreement is as large as 0.1 Hz. Very probably, therefore, structure **3** and not **2** is an important one, the ether oxygen atom playing predominantly a "saturated" role in the pyran ring. The allylic coupling, $^4J_{34}^{H,CH_3}$, may after all be smaller than in propene because of the substituent effects discussed in detail by Barfield (47); hence **2** need not be important.

Conclusions

The inter-ring proton–proton coupling constants in coumarin may be separated into σ and π electron components by means of the methyl group replacement technique. By applying these components to the appropriate resonance structures of naphthalene, rather good agreement is found with the observed inter-ring coupling constants. Theoretical estimates at the INDO and CNDO/2 levels of molecular orbital theory are helpful in the interpretation of these couplings, although INDO somewhat overestimates the magnitudes of some of them. Comparison with the observed and calculated coupling constants in styrene suggests a nonplanar conformation for that molecule.

We are grateful to the National Research Council of Canada for financial support.

1. M. P. Williamson, R. J. Kostelnik, and S. M. Castellano. J. Chem. Phys. **49**, 2218 (1968).
2. S. Sternhell. Quart. Rev. **23**, 236 (1969).
3. G. Kotowycz and T. Schaefer. Can. J. Chem. **44**, 2743 (1966).
4. R. Wasylishen and T. Schaefer. Can. J. Chem. **49**, 94 (1971).
5. M. Barfield and B. Chakrabarti. Chem. Rev. **69**, 757 (1969).
6. J. B. Rowbotham, R. Wasylishen, and T. Schaefer. Can. J. Chem. **49**, 1799 (1971).
7. M. Barfield, C. J. Macdonald, I. R. Peat, and W. F. Reynolds. J. Am. Chem. Soc. **93**, 4195 (1971).
8. R. Wasylishen and T. Schaefer. Can. J. Chem. **49**, 3216 (1971).

[8]The valence bond picture is not to be confused with the tabulated molecular orbital results.

9. S. FORSÉN and R. A. HOFFMAN. J. Mol. Spectrosc. **20**, 168 (1966).
10. D. G. DEKOWALEWSKI and S. CASTELLANO. Mol. Phys. **16**, 567 (1969).
11. R. FREEMAN. Mol. Phys. **6**, 535 (1963).
12. H. M. HUTTON, J. B. ROWBOTHAM, B. H. BARBER, and T. SCHAEFER. Can. J. Chem. **49**, 2033 (1971).
13. M. BARFIELD and B. CHAKRABARTI. J. Am. Chem. Soc. **91**, 4346 (1969).
14. R. WASYLISHEN and T. SCHAEFER. Can. J. Chem. **50**, 1852 (1972).
15. C. J. MACDONALD and W. F. REYNOLDS. Can. J. Chem. **48**, 1002 (1970).
16. G. P. NEWSOROFF and S. STERNHELL. Austral. J. Chem. **21**, 747 (1968).
17. A. D. COHEN and K. A. MCLAUCHLAN. Mol. Phys. **9**, 49 (1965).
18. K. D. BARTLE, D. W. JONES, and R. S. MATTHEWS. Tetrahedron, **25**, 2701 (1969).
19. D. J. BLEARS, S. S. DANYLUK, and T. SCHAEFER. J. Chem. Phys. **47**, 5037 (1967); Can. J. Chem. **46**, 654 (1968).
20. R. WASYLISHEN, J. B. ROWBOTHAM, L. ERNST, and T. SCHAEFER. Can. J. Chem. **50**, 2575 (1972).
21. T. SCHAEFER. Can. J. Chem. **39**, 1864 (1961).
22. F. A. L. ANET. J. Chem. Phys. **32**, 1274 (1960).
23. R. W. CRECELY and J. H. GOLDSTEIN. Org. Magn. Reson. **2**, 613 (1970).
24. O. SCIACOVELLI and W. VON PHILIPSBORN. Org. Magn. Reson. **3**, 339 (1971).
25. F. BALKAU and M. L. HEFFERNAN. Austral. J. Chem. **24**, 2311 (1971).
26. M. W. JARVIS and A. G. MORITZ. Austral. J. Chem. **21**, 2445 (1968).
27. R. A. HOFFMAN. Mol. Phys. **1**, 326 (1958).
28. R. A. HOFFMAN. Arkiv Kemi, **17**, 1 (1961).
29. R. A. HOFFMAN and S. GRONOWITZ. Acta Chem. Scand. **13**, 1477 (1959).
30. J. A. POPLE and D. L. BEVERIDGE. Approximate molecular orbital theory. McGraw-Hill Book Co., New York. 1970.
31. Organic Syntheses, **24**, 68 (1944).
32. K. FRIES and W. KLOSTERMAN. Ber. **39**, 871 (1906).
33. E. N. MARVELL, B. RICHARDSON, R. ANDERSON, J. L. STEPHENSON, and T. CRANDALL. J. Org. Chem. **30**, 1032 (1965).
34. R. FREEMAN and W. A. ANDERSON. J. Chem. Phys. **37**, 2053 (1962).
35. C. W. HAIGH and J. M. WILLIAMS. J. Mol. Spectrosc. **32**, 398 (1969).
36. J. B. ROWBOTHAM and T. SCHAEFER. Can. J. Chem. **50**, 2344 (1972).
37. S. CASTELLANO and R. KOSTELNIK. Tetrahedron Lett. 5211 (1967).
38. T. SCHAEFER, G. KOTOWYCZ, H. M. HUTTON, and J. W. S. LEE. Can. J. Chem. **46**, 2531 (1968).
39. J. M. READ, JR., R. W. CRECELY, R. S. BUTLER, J. E. LOEMKER, and J. H. GOLDSTEIN. Tetrahedron Lett. 1215 (1968).
40. W. BRÜGEL, T. ANKEL, and F. KRÜCKEBERG. Z. Elektrochem. **64**, 1121 (1960).
41. N. SHEPPARD and R. M. LYNDEN-BELL. Proc. Roy. Soc. (London), **269**A, 385 (1962).
42. H. M. MCCONNELL. J. Chem. Phys. **30**, 126 (1959).
43. M. J. S. DEWAR and R. C. FAHEY. J. Am. Chem. Soc. **85**, 2704 (1963).
44. H. ROTTENDORF and S. STERNHELL. Tetrahedron, **20**, 1289 (1963).
45. K. D. BARTLE and J. A. S. SMITH. Spectrochim. Acta, **23**A, 1689 (1967).
46. A. A. BOTHNER-BY and C. NAAR-COLIN. J. Am. Chem. Soc. **83**, 231 (1961).
47. M. BARFIELD. J. Am. Chem. Soc. **93**, 1066 (1971).
48. J. E. BALDWIN and R. K. PINSCHMIDT, JR. J. Am. Chem. Soc. **92**, 5247 (1970).
49. C. N. BANWELL and N. SHEPPARD. Disc. Faraday Soc. **34**, 115 (1962).
50. J. A. ELVIDGE and R. G. FOSTER. J. Chem. Soc. 590 (1963).
51. M. BARFIELD and M. KARPLUS. J. Am. Chem. Soc. **91**, 1 (1969).
52. P. C. MYHRE, J. W. EDMONDS, and J. D. KRUGER. J. Am. Chem. Soc. **88**, 2459 (1966).
53. J. A. POPLE, J. W. MCIVER, JR., and N. S. OSTLUND. J. Chem. Phys. **49**, 2960, 2965 (1968).
54. J. A. POPLE, D. L. BEVERIDGE, and P. A. DOBOSH. J. Chem. Phys. **47**, 2026 (1967).
55. M. BARFIELD and S. STERNHELL. J. Am. Chem. Soc. **94**, 1905 (1972).
56. J. A. POPLE and M. S. GORDON. J. Am. Chem. Soc. **89**, 4253 (1967).
57. P. A. DOBOSH. Program 141, Quantum Chemistry Program Exchange, Bloomington, Indiana.
58. S. FORSÉN and P. N. SKANCKE. *In* Selected topics in structure chemistry. *Edited by* P. Anderson, O. Bastiansen, and S. Furberg. Universitetsforlaget, Oslo, Norway. 1967.

Can. J. Chem. Downloaded from www.nrcresearchpress.com by 210.87.254.40 on 09/05/12
For personal use only.

INDO Molecular Orbital Calculations of Nuclear Spin–Spin Coupling Constants Over Three Bonds Between ^{13}C and ^{1}H in Some Simple Molecules

R. WASYLISHEN[1] AND T. SCHAEFER

Department of Chemistry, University of Manitoba, Winnipeg, Manitoba R3T 2N2

Received August 16, 1972

Molecular orbital calculations, at the INDO level, of the spin–spin coupling constants over three bonds between carbon-13 and protons are reported for a number of simple molecules. In propane the coupling depends on dihedral angle in the Karplus manner. Fluorine substituents cause changes in the computed coupling which are best described as alternating with the number of bonds intervening between the substituent and the coupled nuclei. Finer details of this phenomenon are discussed and calculations on propyllithium are performed. Replacement of a central carbon atom in propane by a heteroatom does not radically alter the computed couplings. The presence of a carbonyl group in the coupling path results in an overestimate of the magnitude of the coupling. In propene the coupling between ^{13}C in position 1 and a methyl proton displays a maximum when the C—H bond of the methyl group lies parallel to the π orbitals. In toluene the coupling to a methyl proton is insensitive to the dihedral angle over half its range, a result of importance to structural studies. Among other molecules under consideration are methylacetylene, propionaldehyde, and the strained bicyclobutane. It is suggested that in certain instances the mean of the predictions from the INDO and CNDO/2 procedures may agree better with experiment than will the prediction from either procedure alone. Calculations on fluorobenzene and 1,2-difluorobenzene suggest that the main experimental trends of the couplings between carbon and protons within the benzene ring are reproduced. Such is perhaps not true for the five-membered heterocycles.

Les calculs INDO appliqués aux orbitales moléculaires, des constantes de couplage spin–spin à travers trois liaisons entre le carbone-13 et les protons, sont rapportés pour un certain nombre de molécules simples. Dans le propane, le couplage dépend de l'angle dièdre selon la loi de Karplus. Les substituants fluorés provoquent des changements dans le couplage calculé qui alternent avec le nombre de liaisons séparant le substituant et le noyau couplé. Une analyse plus détaillé de ce phénomène et des calculs sur le propyl lithium sont donnés. La présence d'un groupe carbonyle sur le trajet du couplage a pour résultat une surestimation de l'amplitude du couplage. Dans le propène, le couplage entre le carbone-13 de la position 1 et un proton du méthyle passe par un maximum lorsque la liaison C—H du groupe méthyle est parallèle aux orbitales. Dans le toluène, le même couplage avec un proton du méthyle reste insensible à l'angle dièdre sur plus de la moitié de l'intervalle, résultat important dans les études de structure. Les autres molécules considérées sont le méthylacétylène, le propionaldéhyde et le bicyclobutane tendu. Pour certains exemples on pense que les prévisions selon les méthodes INDO et CNDO/2 donnent un meilleur accord avec l'expérience que ne le ferait chacune des méthodes seule. Les calculs sur les fluorobenzène et difluoro-1,2 benzène reproduisent les tendances expérimentales majeures pour les couplages entre carbone et protons du cycle benzènique. Cela n'est peut être plus valable pour les hétérocycles à cinq membres. [Traduit par le journal]

Can. J. Chem., **51**, 961 (1973)

Introduction

Approximate molecular orbital theory at the INDO level (1, 2) is relatively successful in reproducing the observed trends of nuclear spin–spin coupling constants for a variety of organic molecules (1–9). In particular, the calculated coupling constants over three bonds between protons (1, 4, 5) and between protons and other first-row elements (10, 11) display the Karplus relationship (12) with dihedral angles; and their dependence on substituent effects agrees fairly well with experiment (4, 5).

Recent advances in instrumentation facilitate the measurement of ^{13}C magnetic resonance spectra, and their use in structural and conformational studies is developing rapidly (13). The extraction of coupling constants over three bonds between ^{13}C and protons, $^{3}J(^{13}C,H)$, will therefore become common and their use in structural work (14) will likely be aided by theoretical predictions of their magnitudes for some model compounds.

In this paper we report the results of the

[1]Holder of an NRCC scholarship, 1971–72.

Can. J. Chem. Downloaded from www.nrcresearchpress.com by 84.22.46.98 on 09/08/12
For personal use only.

Can. J. Chem. Downloaded from www.nrcresearchpress.com by 84.22.46.98 on 09/08/12
For personal use only.

calculations of $^3J(^{13}C,H)$ in a number of common bonding situations. The computations are carried out by the finite perturbation technique (15*a*) at the INDO level of molecular orbital theory and yield the Fermi contact contribution to $^3J(^{13}C,H)$.

Computational Procedure

In the finite perturbation formalism, the Fermi contact contribution to nuclear spin–spin coupling between two nuclei A and B is given by eq. 1 (6–8), where h_B is the perturbation due

$$[1] \quad J_{AB} = \frac{\hbar}{2\pi}[(8\pi/3)\beta]^2\gamma_A\gamma_B S_A^2(0)S_B^2(0) \times [(\delta/\delta h_B)\rho^{spin}_{S_AS_A}(h_B)]_{(h_B=0)}$$

to the nuclear moment μ_B and has the form

$$h_B = \frac{8}{3}\pi\beta\mu_B S_B^2(0)$$

$\rho^{spin}_{S_AS_A}(h_B)$ is the diagonal element of the spin density matrix (in the presence of the contact perturbation h_B) corresponding to the valence s orbital of atom A, γ_A and γ_B are the magnetogyric ratios of nuclei A and B, β is the Bohr magneton, and $S_A^2(0)$ and $S_B^2(0)$ are the valence s-orbital electron densities of atom A and atom B at their respective nuclei. Using the method of finite differences Pople *et al.* (2, 15*a*) have shown that the derivative in eq. 1 can be approximated by $\rho^{spin}_{S_AS_A}(h_B)/h_B$. Thus the coupling constant (in Hz) is approximated by eq. 2. The error in the

$$[2] \quad J_{AB} = \frac{\hbar}{2\pi}[(8\pi/3)\beta]^2\gamma_A\gamma_B S_A^2(0)S_B^2(0) \times [\rho^{spin}_{S_AS_A}(h_B)/h_B]$$

approximation has a minimum when h_B is approximately 10^{-3} hartrees and $\rho^{spin}_{S_AS_A}(h_B)$ is calculated using open-shell semi-empirical molecular orbitals at the INDO level of approximation (1).

All coupling constants were calculated (15*b*) using eq. 2 with the same parameterization as used previously by Pople *et al.* (1, 15*a*). Because all other terms in eq. 2 are taken as constant, it is the sensitivity of the spin density in the orbital S_A to the presence of the perturbation h_B which determines the the spin-spin coupling constants. Because h_B is small, the spin densities are extremely small and therefore the spin density matrix must be known very accurately in the calculation of coupling constants. For carbon–proton coupling constants $J(^{13}C,H) = 285958.6283\ \rho^{spin}_{H_sH_s}$ Hz when $h_C = 10^{-3}$ hartrees. In order to obtain reasonably accurate coupling constants the usual energy criterion for convergence of the SCF iteration was changed to the requirement that

$$[3] \quad 10^{-4} \leq \frac{\rho_{ii}^{old} - \rho_{ii}^{new}}{\rho_{ii}^{old}}$$

for all *i*. By this criterion one can estimate the accuracy of the calculated coupling constants since J_{AB} is directly proportional to ρ^{spin}_{AA}/h or ρ^{spin}_{BB}/h depending on whether A or B is perturbed. For example, consider the accuracy of a calculated $J(^{13}C,H)$ with a magnitude of 28.60 Hz. If the convergence criterion given by eq. 3 is satisfied then the change in $J(^{13}C,H)$ in one SCF cycle is less than 0.00286 Hz. When coupling constants did not converge in 90 SCF cycles using the criterion given by eq. 3, 100 SCF cycles were carried out. If, after 100 SCF cycles the energy and the coupling constants did not converge, *e.g.* for $CH_3N{=}C{=}O$, the results of the calculations were discarded.

The input data for a calculation required the Cartesian coordinates of all atoms, the total charge, and the multiplicity of the molecule. Since the calculated coupling constants were sometimes sensitive to the molecular geometry, an attempt was made to use the best available structural parameters. The atomic coordinates were usually calculated from these structural parameters with the aid of the "Model-Builder" programme MBLD (15*c*). The sources of the structural parameters or atomic coordinates are given at appropriate places in the text.

All calculations were carried out on an IBM 360/65 computer.

Results and Discussion

(1) $^3J(^{13}C{-}C{-}C{-}H)$ in Propane, 1-Fluoropropane, 2-Fluoropropane, and 2,2-Difluoropropane

Standard geometries (1, 16) are assumed, yielding the results in Table 1. The dihedral angle and the conformations are depicted in **1**, **2**, **2***a*, **3**, and **4**. Note that staggered conformations about the C—C bonds are initially assumed and that one of the methyl groups (containing H_1) is then rotated so as to define a series of dihedral angles θ.

TABLE 1. Dependence of $^3J(^{13}C, H)$ in Hz on dihedral angle in propane, 1-fluoropropane, 2-fluoropropane, and propyllithium

Angle* (degrees)	Propane	1-Fluoropropane†		2-Fluoropropane†	Propyllithium‡
		2‡	***2a***‡	**3**	
0(360)	6.820	8.173	6.926(6.926)	5.628(5.628)	5.374
15(345)	6.364	—	6.556(6.373)	— —	5.018
30(330)	5.148	6.106	5.392(5.067)	4.752(3.688)	4.086
35(325)	4.634	—	— (4.527)	— —	3.688
45(315)	3.543	—	3.793(3.393)	— —	2.848
60(300)	2.000	2.213	2.208(1.824)	2.054(1.125)	1.624
75(285)	0.944	—	1.062(0.808)	— —	0.684
85(275)	0.677	—	0.716 —	— —	0.309
90(270)	0.698	0.761	0.695(0.668)	0.404(0.774)	0.210
105(255)	1.405	—	1.281(1.500)	— —	0.274
120(240)	2.950	3.931	2.752(3.140)	1.876(3.485)	0.824
135(225)	4.961	—	4.764(5.181)	— —	1.682
150(210)	6.914	9.225	6.790(7.112)	5.511(6.988)	2.588
165(195)	8.309	—	8.287(8.454)	— —	3.265
180(180)	8.812	11.737	8.884(8.884)	7.942(7.942)	3.514

*The angles in brackets correspond to the J values in brackets.
†See the text for the conformations of these molecules. The fluorine atom is attached to ^{13}C in **2** and ***2a***.
‡In **2** and in propyllithium the fluorine atom and lithium atom lie *trans* to the methyl group containing the coupled proton. In ***2a*** the fluorine atom lies *gauche* to this methyl group.

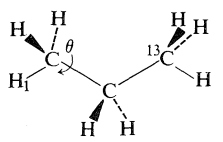

$\theta = 180°$ for H_1

1

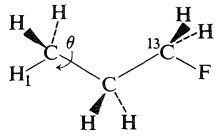

2

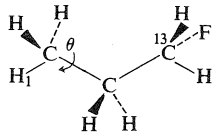

2a

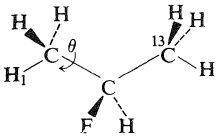

$\theta = 180°$ for H_1

3

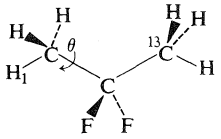

4

(i) Propane (1)

$^3J(^{13}C,H)$ was calculated at intervals of 15° or less between 0 and 180° and has been tabulated (17). The curve of $^3J(^{13}C,H)$ *vs.* θ is given for purposes of comparison in Fig. 1. It is represented by eq. 4 to within an average deviation of 0.013 Hz and a maximum deviation of 0.03 Hz. In eq. 4 the first coefficient, 4.26 Hz,

$$[4]\quad {}^3J(^{13}C,H) = 4.26 - 1.00\cos\theta + 3.56\cos 2\theta$$

corresponds to the average coupling constant for free rotation or, alternatively, to the average of $^3J(^{13}C,H)$ at angles of 60, 180, and 300° (the latter situation is realistic because the barrier to internal rotation of the methyl group is 3.575 kcal/mol (18)). The second coefficient, −1.00 Hz, is half the difference between the coupling constants at $\theta = 0°$ and $\theta = 180°$. The minimum in $^3J(^{13}C,H)$ occurs, not at $\theta = 90°$, but at $85° < \theta < 90°$. The shape of the curve is not surprising[2] in view of the work of Karplus (12) on ^3J(H—C—C—H) and in view of what is known for coupling over three bonds between other nuclei (17 and refs. therein).

(ii) 1-Fluoropropane (2 and 5)

The fluorine atom is attached to ^{13}C in **2** and lies *trans* to the methyl group containing the coupled proton. The computed coupling constants in Table 1 are plotted against θ in Fig. 1 and are reproduced by eq. 5 with an accuracy similar to that described for eq. 4. The computed

[2]Exact agreement with previous calculations (3, 4) of ^3J(H,H) and $^1J(^{13}C,^{13}C)$ in propane was found.

Can. J. Chem. Downloaded from www.nrcresearchpress.com by 84.22.46.98 on 09/08/12
For personal use only.

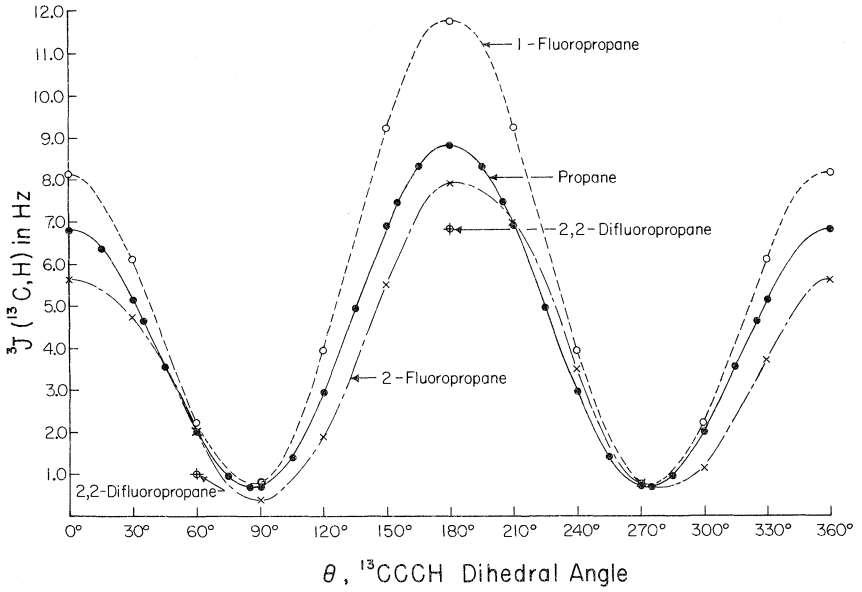

FIG. 1. The coupling constant (in Hz) over three bonds between ^{13}C and protons is plotted as a function of dihedral angle in propane, 1-fluoropropane, and 2-fluoropropane. The detailed conformations are depicted in the text. Note that J values are plotted for conformation **2** of 1-fluoropropane, in which fluorine lies *trans* to the methyl group containing the coupled proton.

[5] $^3J(^{13}C,H) = 5.34 - 1.78 \cos\theta + 4.62 \cos 2\theta$

couplings are always larger than those for propane. On the other hand, when the fluorine atom is not attached to the ^{13}C site, as in **5**, one calculates $^3J(^{13}C,H) = 1.10$ Hz, *i.e.*, at $\theta = 60°$. The corresponding value for propane is 2.00 Hz and is 2.21 Hz for **2**.

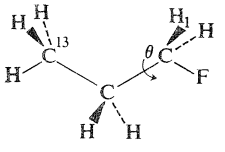

$\theta = 60°$ for H_1

5

Subtraction of eq. 5 from eq. 4 yields the substituent effect, ΔJ, as represented by eq. 6. Clearly, the magnitude of ΔJ is minimal at

[6] $-\Delta J = 1.08 - 0.78 \cos\theta + 1.06 \cos 2\theta$

$\theta = 90°$, *i.e.*, when the C—H_1 bond lies perpendicular to the plane containing the carbon and fluorine atoms. The magnitude of ΔJ has a maximum at $\theta = 180°$. On the other hand, the relative substituent effect, $\Delta J/J$, where J is the value in propane, has a somewhat different dihedral angle dependence. For example, between $\theta = 120$ and 180° its value does not deviate appreciably from 1/3.

(iii) 1-Fluoropropane (2a)

In **2***a* the fluorine atom lies *gauche* to the methyl group containing the coupled proton. A plot *vs.* θ of the computed $^3J(^{13}C,H)$ values in Table 1 (not shown here) does not substantially deviate from that for propane. The two values in different quadrants generally bracket that for a given angle in propane, their mean falling within about 0.1 Hz of the coupling in propane (see Table 1). The average $^3J(^{13}C,H)$ for the staggered form (**2***a*) is 4.43 Hz (θ = 60, 180, and 300°), very near the corresponding value of 4.27 Hz for propane. In contrast, for **2** the average is 5.39 Hz.

Comparison of the results for **1**, **2**, and **2***a* in Table 1 suggests that when the C—H_1 bond lies perpendicular to the C—C—^{13}C plane, the values of ΔJ and $\Delta J/J$ will be small. If, in addition, the C—F bond also approaches perpendicularity to the C—C—^{13}C plane, the value of $\Delta J/J$ never becomes very large, no matter what the orientation of the C—H_1 bond. Although the experimental values may well turn out to differ somewhat from the computed values, the trends embodied by these rules should be of use in structural work.

The contrasting behavior of $^3J(^{13}C,H)$ in the

Can. J. Chem. Downloaded from www.nrcresearchpress.com by 84.22.46.98 on 09/08/12
For personal use only.

Can. J. Chem. Downloaded from www.nrcresearchpress.com by 84.22.46.98 on 09/08/12
For personal use only.

staggered conformations **2** and **2***a* can complicate the prediction of its magnitude in 1-fluoropropane and in analogous propane derivatives. If the two *gauche* forms, **2***a*, and the *trans* form, **2**, were equally populated, the predicted magnitude of $^3J(^{13}C,H)$ would be $(2 \times 4.43 + 5.39)/3 = 4.74$ Hz as compared to 5.39 Hz if only the *trans* form, **2**, were appreciably populated. We compute **2***a* as 1.8 kcal/mol less stable than **2**, in which the greater substituent dependence of $^3J(^{13}C,H)$ is predicted. Substituents larger than fluorine will no doubt increase the relative stability of the *trans* form.

(iv) 2-Fluoropropane (3 and 6)

In Table 1 the computed couplings are presented at 30° intervals between 0 and 360° of the dihedral angle θ and are plotted in Fig. 1. This curve in Fig. 1 is not symmetrical about θ = 180° and is represented to within an average deviation of 0.02 Hz by eq. 7. As implied by **6**, there exists an additional dependence of $^3J(^{13}C,H)$

$$[7]\quad {}^3J(^{13}C,H) = 3.69 - 1.16\cos\theta + 3.10\cos 2\theta - 0.19\sin\theta + 0.70\sin 2\theta$$

on the dihedral angle φ in the fragment H—C—C—F containing the coupled proton. In parti-

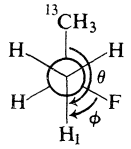

θ = 180° and φ = 60° for H_1

6

cular, when φ = 90°, corresponding to 210° for θ, the curves for propane and 2-fluoropropane coincide in Fig. 1. These curves also coincide at φ = 300° (or −60°), corresponding to θ = 60°. At φ = 270° (or −90°), corresponding to θ = 30°, the value for propane is decreased by less than 8%. To a good approximation, therefore, the substituent effect is small when the C—F bond is perpendicular to the C—H_1 bond. On the other hand, when φ = 180° (θ = 300°) the value for propane has been decreased by 44% and when φ = 0° (θ = 120°) the decrease is 37%. Again, to a good approximation, the substituent effect is relatively large when the C—F and C—H_1 bonds are near coplanarity.

Note, however, that between θ = 210° and about 270° the substituent causes an increase in $^3J(^{13}C,H)$ relative to propane, reaching a maximum of about 18% at θ = 240°. In practice, of course, the all-staggered conformation is the stable one and the angles 210 ≤ θ ≤ 270° do not occur. In fact the predicted value of $^3J(^{13}C,H)$ is 1/3(2.054 + 7.942 + 1.125) = 3.71 Hz, (as can also be deduced from the first term of eq. 7), about 0.55 Hz smaller than in propane.

(v) 2,2-Difluoropropane (7)

Only the staggered conformation, **7**, was considered. For θ = 180° (H_1 in **7**) one com-

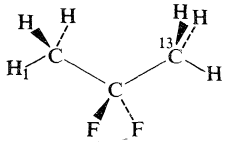

7

putes $^3J(^{13}C,H)$ = 6.81 Hz and for θ = 60° the value is 1.00 Hz. These numbers are also entered in Fig. 1. The expense of the computations is such that calculations at other angles θ are hardly justified, the effect of a second fluorine substituent being as expected.

(vi) Propyllithium

The geometry of **2** was assumed, with lithium replacing fluorine and with a C—Li bond length of 2.10 Å. The computed values of $^3J(^{13}C,H)$ at intervals of 15° or less in the dihedral angle θ are to be found in Table 1. These values can be approximated by eq. 8 to within a maximum

$$[8]\quad {}^3J(^{13}C, H) = 2.25 + 0.93\cos\theta + 2.04\cos 2\theta$$

deviation of 0.15 Hz (at θ = 0 and 180°) and a mean deviation of 0.078 Hz. At a given angle the magnitude of $^3J(^{13}C, H)$ is smaller than in propane.

In addition, the maximum in $^3J(^{13}C,H)$ is smaller at 180° than at 0°, in contrast to propane or 1-fluoropropane, although the greatest substituent effect occurs at θ = 180°, as in form **2** of 1-fluoropropane. The positive coefficient of cos θ in eq. 8 describes the fact that $J(180°) < J(0°)$, the implication being that this happens whenever the substituent in a structure of type **2** is less electronegative than hydrogen.

The computed average $^3J(^{13}C,H)$ values for the staggered forms **1** (4.27 Hz), **2** (5.39 Hz), and propyllithium (2.25 Hz) imply a nonlinear dependence on the electronegativity of the substituent, different from the observed behavior of ^3J(H—C—C—H) in H—C—C—H. However,

the former situation is qualitatively different in that the substituent is bonded directly to one of the coupled nuclei, ^{13}C.

(vii) Calculated Substituent Effects

A decreasing, alternating substituent effect on ^3J(H—C—C—H) occurs (19, 20) and is qualitatively reproduced by INDO molecular orbital calculations (4, 5). In **8** a substituent X, more electronegative than the hydrogen which it replaces, causes a decrease in $^3J(H_1,H_2)$, an

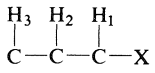

8

increase in $^3J(H_2,H_3)$, and so forth. The magnitude of the effect decreases with the number of intervening bonds between the substituent and the coupled nuclei.

A natural extension of this scheme suggests that bonding of X to one of the coupled nuclei, as in **9**, will lead to an increase of $^3J(^{13}C,H)$ over that observed when X = H. The results in Table 1 and Fig. 1 confirm the suggestion for 1-fluoropropane. Then, when X is attached to C-2 in **9** a decrease in $^3J(^{13}C,H)$ is expected and is so calculated for 2-fluoropropane (with the qualifications noted in section 1.iv). Again, bonding of X to C-3 in **9** must also diminish $^3J(^{13}C,H)$, as calculated: at $\theta = 60°$ one has $^3J(^{13}C,H)$ as 1.10 Hz in **5** and as 2.00 Hz in propane (**1**).

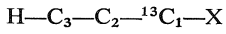

9

These substituent effects must be considered when using $^3J(^{13}C,H)$ values in structural work. Note, however, that even the highly electronegative fluorine substituent is predicted to cause substantial changes in $^3J(^{13}C,H)$ only at certain angles θ (Fig. 1).

(viii) Comparison with an Experimental Datum

In 2,2-dimethyl-1-chloropropane (**10**), the observed value of $^3J(^{13}C,H)$ is 5.63 Hz (21), representing an average of the couplings to the

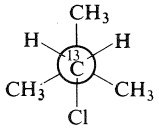

10

protons of the three methyl groups. The chlorine substituent lies *gauche* to two of the methyl groups, analogous to structure **2***a*, and *trans* to the third methyl group, analogous to structure **2**. If **2** and **2***a* can be used for purposes of comparison, one has a predicted value of $^3J(^{13}C,H)$ of $(2 \times 4.43 + 5.39)/3 = 4.75$ Hz (see section 1.iii). The agreement between observed and calculated values is not impressive, particularly as fluorine is more electronegative than chlorine.

(2) Cyclohexane

Standard geometries are assumed for the chair conformation and the calculated vicinal proton coupling constants agree exactly with literature values (4). The computations find that $^3J(^{13}C,H) = 1.70$ ($\theta = 60°$, axial proton) and $^3J(^{13}C,H) = 7.66$ Hz ($\theta = 180°$, equatorial proton). The corresponding values for propane are 2.00 and 8.81 Hz. At room temperature the rapid interchange of axial and equatorial proton positions entails an average $^3J(^{13}C,H)$ of 4.68 Hz (the different averaging procedure, over three angles, in propane yields 4.26 Hz).

Experimental data for cyclohexane itself are unavailable but for rigid β-1,2,3,4,5,6-hexachlorocyclohexane, where the chlorine atoms take up equatorial positions (22), one has $^3J(^{13}C, H) = 1.08 \pm 0.04$ Hz ($\theta = 60°$). Each of the carbon atoms in the ^{13}C—C—C—H fragment carries a chlorine atom, the one on ^{13}C causing an increase in $^3J(^{13}C, H)$ and the other two causing a decrease (see Fig. 1 and Table 1); so that the observed value is in qualitative agreement with expectations based on the 1.70 Hz calculated for cyclohexane.

*(3) Dimethylamine (**11**) and Dimethylether*

(i) Dimethylamine

In this molecule a heteroatom replaces the central carbon atom in propane. Atomic coordinates were provided by a microwave study (23). The barrier to rotation of the methyl group is 3.2 kcal/mol (24) and calculations were done for the stable conformation, **11**, in which two C—H bonds lie in the C—N—C plane (23, 24*a*). The results were that $^3J(^{13}C,H_1) = 8.47$ ($\theta = 180°$), $^3J(^{13}C,H_2) = 0.955$ ($\theta = 300°$), $^3J(^{13}C, H_3) = 2.30$ Hz ($\theta = 60°$). Clearly, the coupling depends on the orientation of the lone-pair electrons but the conformational average is 1/3(2.30 + 8.47 + 0.96) or 3.91 Hz, not very different from the analogous average of 4.26 Hz

Can. J. Chem. Downloaded from www.nrcresearchpress.com by 84.22.46.98 on 09/08/12
For personal use only.

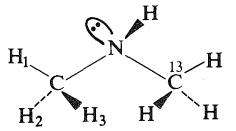

11

for propane, where the individual values are 8.81 (180°), 2.00 (300°), and 2.00 Hz (60°).

For the standard geometry of **11** the computations yield 8.39 ($\theta = 180°$), 1.34 ($\theta = 300°$), and 1.74 Hz ($\theta = 60°$) for $^3J(^{13}C,H)$. The individual values differ from those entailed by the microwave geometry above but the average of 3.82 Hz is close to the average for the latter geometry. Calculations at 15° intervals in θ for the standard geometry give an average of 3.90 Hz over 25 points on the period of 360° in θ.

(ii) Dimethylether

Calculations at 15° intervals between $\theta = 0°$ and 180° for dimethylether, assuming a standard geometry with a structure analogous to **11** (C—H bonds and lone-pairs staggered), resulted in an average value over 13 points of 3.24 Hz for $^3J(^{13}C,H)$. For the equilibrium conformation the mean of the values[3] at 180° (7.24 Hz) and at 60° (1.03 Hz twice) is 3.10 Hz.

A plot of $^3J(^{13}C,H)$ *vs.* θ for dimethylether can be represented by eq. 9 (the plot for dimethylamine is similar to that for 2-fluoropropane in Fig. 1) with an average deviation of 0.056 Hz. A comparison of eq. 9 with eq. 4 for propane

$$[9] \quad ^3J(^{13}C,H) = 3.10 - 1.14 \cos\theta + 3.05 \cos 2\theta$$

indicates the negative shift of the curve for the ether (a similar but smaller shift occurs for the amine).

Thus the computations predict that a heteroatom in the chain does not alter the calculated magnitudes by large amounts but that nitrogen and oxygen atoms act to decrease $^3J(^{13}C,H)$ relative to its value in a hydrocarbon fragment.

The observed value of $^3J(^{13}C,H)$ in dimethylether in solution is 5.7 ± 0.1 Hz (24*b*), much larger than the calculated 3.1 to 3.2 Hz. Observations are lacking on propane, so that the predicted negative shifts may be qualitatively correct. If so, the measured value in dimethylether suggests that $^3J(^{13}C,H)$ lies near 7 Hz in propane itself and should be easily observable in 2,2-dideuteropropane.

(4) Propene (12) and 1,1-Difluoropropene (13)

The geometry of propene was taken from the paper by Scarzafava and Allen (25*a*). In Table 2 the computed $^3J(^{13}C,H)$ magnitudes are given as a function of θ for propene. In contrast to its behavior in propane, $^3J(^{13}C,H)$ in propene displays a minimum at $\theta = 0°$ and a maximum

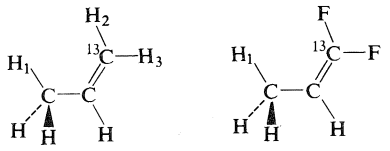

$\theta = 0°$ for H_1

12 13

near $\theta = 90°$ (see Fig. 2); indicating the importance of the π electrons in the transmission of spin information between the two nuclei. The predicted conformational average of $^3J(^{13}C,H)$ is 1/3(5.237 (0°) + 10.882 (120°) + 10.882 (120°)) = 9.00 Hz, more than twice as large as in propane.

The use of a standard geometry has the consequence that $^3J(^{13}C,H)$ is calculated as 5.277 Hz at $\theta = 0°$ and 10.199 Hz at $\theta = 120°$, giving a conformational average of 8.56 Hz.

The employment of a standard geometry for **13** yields 6.353 Hz for $^3J(^{13}C,H)$ at $\theta = 0°$ and 12.015 Hz at 120°. The average at the equilibrium conformation is 10.13 Hz, larger than in propene

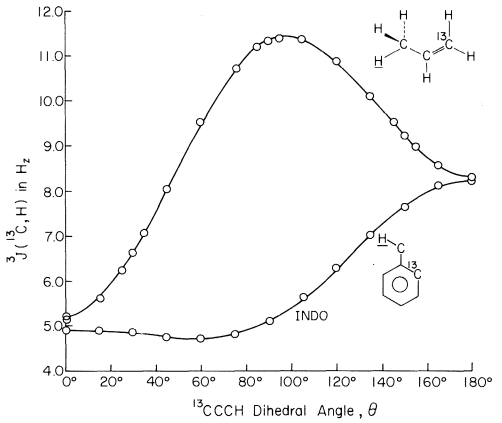

FIG. 2. The coupling constant (in Hz) over three bonds between ^{13}C and protons in propene and toluene is plotted against dihedral angle for the conformations shown in the text and sketched in the figure.

[3]The individual values at 15° intervals for dimethylether and dimethylamine are available from the authors.

Can. J. Chem. Downloaded from www.nrcresearchpress.com by 84.22.46.98 on 09/08/12
For personal use only.

TABLE 2. Dependence of $^3J(^{13}C, H)$ in Hz on dihedral angle in propane, toluene, and the monofluorotoluenes*

Angle (Degrees)		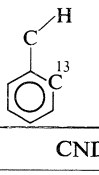 INDO	CNDO/2	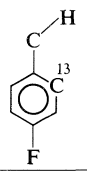	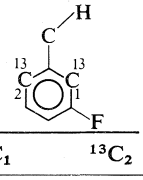 $^{13}C_1$	$^{13}C_2$	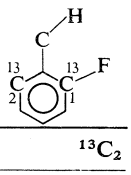 $^{13}C_1$	$^{13}C_2$
0	5.237 Hz	4.855	3.744	4.881	5.010	4.866	4.785	5.051
15	5.605	4.829	—	4.857	4.978	4.843	4.762	5.026
25	6.226	—	—	—	—	—	—	—
30	6.626	4.761	2.762	4.795	4.892	4.782	4.717	4.958
35	7.072	—	—	—	—	—	—	—
45	8.049	4.682	—	4.725	4.794	4.712	4.693	4.872
60	9.522	4.654	0.798	4.705	4.752	4.685	4.726	4.823
75	10.695	4.749	—	4.813	4.848	4.793	4.885	4.888
85	11.187	—	—	—	—	—	—	—
90	11.331	5.030	0.004	5.110	5.148	5.073	5.159	5.133
95	11.407	—	—	—	—	—	—	—
105	11.362	5.517	—	5.616	5.674	5.553	5.560	5.582
120	10.882	6.167	1.619	6.287	6.373	6.192	6.063	6.179
135	10.086	6.877	—	7.014	7.145	6.886	6.606	6.847
145	9.497	—	—	—	—	—	—	—
150	9.216	7.508	4.378	7.661	7.831	7.503	7.101	7.428
155	8.956	—	—	—	—	—	—	—
165	8.546	7.940	—	8.103	8.299	7.925	7.448	7.822
180	8.295	8.094	5.704	8.259	8.471	8.071	7.569	7.959

*Note that for meta and ortho fluorotoluene the two values are given for the appropriate angles θ. For example, when θ = 0° for C_1 it is 180° for C_2.

(a positive shift in J on substitution at ^{13}C by fluorine was also calculated above for propane). In 1,1-dichloropropene the observed value of $^3J(^{13}C,H)$ is ± 9.5 Hz (25*b*), in good agreement with theory if it is considered that chlorine is less electronegative than fluorine.

When ^{13}C in **12** is placed in the methyl group the calculations yield $^3J(^{13}C—C=C—H_2)$ = 5.96 (*cis* or θ = 0°) and $^3J(^{13}C—C=C—H_3)$ = 12.43 Hz (*trans* or θ = 180°).

(5) Toluene (14) and the Monofluorotoluenes

For toluene, **14**, and *p*-fluorotoluene standard geometries were assumed and the ensuing

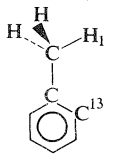

θ = 0° for H_1

14

computations resulted in the angular dependence of $^3J(^{13}C\cdots C—C—H)$ in Table 2. In Fig. 2 the plotted dependence on angle of $^3J(^{13}C,H)$ contrasts strongly with that in propene, being largely independent of θ between 0 and 90°.

A comparison of the curves for propane, propene, and toluene (Figs. 1 and 2) allows the inference that in toluene, where the intervening $^{13}C—C$ bond possesses only a partially double bond character, the angular behavior of $^3J(^{13}C\cdots C—C—H)$ is a composition of that for propene and of one very similar to that for propane. The inference is strengthened by the near coincidence of the curves for propene and toluene at θ = 0 and 180°. At these angles the π electrons need not be significantly involved in the coupling mechanism, but between 0 and about 90° their increasing participation in toluene is roughly cancelled by the mechanism analogous to that represented for propane in Fig. 1. Then, between 90 and 180° the latter mechanism predominates.

This interpretation was examined by the calculation of $^3J(^{13}C,H)$ for **14** using the CNDO/2 molecular orbitals because these tend to reflect the contributions of the σ electrons to the transmission of spin information (1). In Table 2 the resultant values do indeed display a minimum of 0 Hz near θ = 90°, showing a Karplus-type

Can. J. Chem. Downloaded from www.nrcresearchpress.com by 84.22.46.98 on 09/08/12
For personal use only.

Can. J. Chem. Downloaded from www.nrcresearchpress.com by 84.22.46.98 on 09/08/12
For personal use only.

behavior as for propane. The interpretation above is evidently a reasonable one.

The curve for toluene should be remembered when the ^{13}C nucleus is bonded into a structure with delocalized electrons and a Karplus curve is being assumed. Note that between 90 and 180° such an assumption is qualitatively valid but is invalid between 0 and 90°.

This somewhat unexpected behavior is confirmed by the computations given in Table 2 for the fluorotoluenes. The $^3J(^{13}C,H)$ values differ only slightly from those in toluene when fluorine is situated meta or para to the methyl group. When fluorine is bonded to ^{13}C the values are up to 0.5 Hz *smaller* than in toluene, in contrast to the behavior calculated for propane and 1-fluoropropane.

The average $^3J(^{13}C,H)$ values in toluene and *p*-fluorotoluene are found by taking the means of the numbers at 15° intervals between 0 and 180°. The averages are 5.82 Hz for toluene and 5.91 Hz for *p*-fluorotoluene, rather closer to that for propane (4.26 Hz) than that for propene (9.00 Hz). The averaging procedure for toluene is correct because the barrier to internal rotation of the methyl group is only 0.014 kcal/mol (26) whereas in propene, **12** is more stable than other conformations by 2 kcal/mol (27).

When ^{13}C occurs in the methyl group of toluene and a standard geometry is assumed with one C—H bond of the methyl group eclipsing a C—H bond on the ring, the computations yield $^3J(^{13}C,H)$ as 5.02 Hz for the proton in the eclipsing C—H bond and as 4.69 Hz for the other ortho proton in the ring. In principle this dependence on conformation could be applicable to the study of various alkyl derivatives of benzene.

(6) N-Methylmethylenimine (15)

In **15** a nitrogen atom replaces C-2 in propene. The calculation is performed for the molecule in which ^{13}C occurs in the methyl group because a measurement is available on **16**. The microwave geometry (28) of **15** is utilized to compute $^3J(^{13}C—N=C—H_1) = 9.09$ (*cis*) and $^3J(^{13}C—N=C—H_2) = 18.34$ Hz (*trans*) whereas a standard geometry yields 11.54 and 15.71 Hz, respectively. In *N*-benzylidenemethylamine (**16**), the observed value of *cis* $^3J(^{13}C—N=C—H)$ is 11.9 ± 0.6 Hz (29). The agreement between calculated and observed values is reasonable, particularly if the anticipated increase in $^3J(^{13}C,H)$ caused by the electronegative phenyl group in **16** is considered. Note also that replacement of C-2 in propene by a nitrogen atom leads to an increase in the calculated magnitude of the coupling, in contrast to the analogous situation for propane and dimethylamine (section 3).

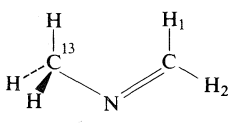

15

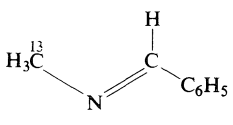

16

(7) Acetone (17)

In acetone (**17**), a trigonally hybridized carbon atom lies in the coupling path but the double

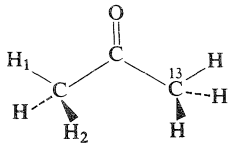

17

bond, in contrast to propene, is peripheral to the path. The atomic coordinates of the stable conformation **17** are known from a microwave investigation (30) and their use yields $^3J(^{13}C—C—C—H_1) = 7.29$ ($\theta = 180°$) and $^3J(^{13}C—C—C—H_2) = 3.08$ Hz ($\theta = 60°$). Corresponding numbers for propane are 8.81 and 2.00 Hz, respectively. When $\theta = 180°$ the oxygen substituent decreases $^3J(^{13}C,H)$ in a manner similar to fluorine in 2-fluoropropane (section 1). However, when the C—H bond containing the coupled proton does not lie in the nodal plane of the π electron cloud, the calculations predict an increase in $^3J(^{13}C,H)$ from its value in propane; indicating a positive contribution from the π electrons.

The barrier to internal rotation is only 0.778 ± 0.010 kcal/mol in the gas phase (31) so that conformations other than **17** are appreciably populated at room temperature. Nevertheless, a reasonable surmize from the above discussion is of a shallower curve for acetone than for propane (Fig. 1) and therefore the average $^3J(^{13}C,H)$ will hardly be smaller than 4 Hz. The experimental value is 1.46 Hz (32) and the conclusion that a substantial theoretical overestimate exists for this bonding situation is inescapable. The disagreement cannot be attributed to the use of a wrong or a standard geometry (the calculated

dipole moment of 2.90 D agrees exactly with the gas phase measurement (31)).

A more likely cause of the discrepancy resides in an overestimate of the π electron contribution to $^3J(^{13}C,H)$ in acetone.[4] For example, the INDO approximation finds $J(^{13}C—C—C—H)$ = 9.40 Hz in benzene while at the CNDO/2 level of calculation, which does not allow for nonzero π spin density inductions, yields 5.51 Hz (1). The experimental value is 7.4 Hz (33). It may well be, then, that for ketones the CNDO/2 prodecure will also be needed in order to arrive at better predictions for $^3J(^{13}C, H)$.

(8) Propionaldehyde-3-^{13}C and its Oxime

These compounds were chosen because experimental estimates of $^3J(^{13}C,H)$ are available and because they contain an aldehydic functional group. Standard geometries were assumed. In the gas phase the *cis* form, **18**, of the aldehyde is more stable than the *gauche* form, **19**, by 0.900 ± 0.100 kcal/mol (34) and the four heavy atoms are coplanar. In **18** the aldehyde proton,

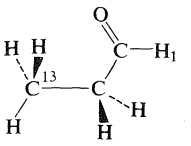

18

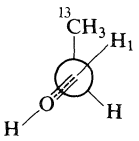

19

H_1, and ^{13}C are *trans* to each other (θ = 180°) and the calculations predict $^3J(^{13}C—C—C—H_1)$ as 4.98 Hz whereas in the *gauche* form, **19**, they predict 1.40 Hz (θ = 60°). From the temperature dependence of $(^3J_g + {}^3J_t)/2$ in solution rough estimates of 3.5 Hz for J_t and 0.2 Hz for J_g were made (35*a*).

For the oximes of **18** and **19** standard geometries (C=N—O—H atoms in a plane and a CNO angle of 109.47°) give rise to predicted values

NOH
||

of $^3J(^{13}C—C—C—H_1)$ as 6.38 (θ = 180°) and 3.58 Hz when θ = 60°. When applied to the oxime O-methyl ether, $^{13}CH_3CH_2—CH=N—O—CH_3$, the experimental method above suggested 7.8 and 0.7 Hz for these two couplings (35*a*). It appears, therefore, that the theoretical overestimates may not be confined to the carbonyl compounds.

*(9) Acrolein (**20** and **20a**)*

In **20** and **20***a* one has a carbonyl group conjugated with the double bond in propene.

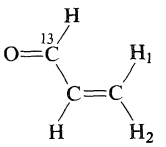

20

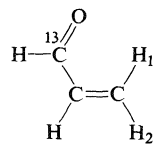

20*a*

For the *s-trans* form, **20**, the standard geometry entails $^3J(^{13}C,H_1)$ = 11.14 and $^3J(^{13}C,H_2)$ = 20.24 Hz. The corresponding values for the *s-cis* form are 9.47 and 16.95 Hz. The observed values (35*b*) are 10.1 and 15.9 Hz, respectively. The *s-trans* form is the more stable and hence the theory is not in satisfactory agreement with experiment, substantially overestimating the magnitudes and their ratio for the two couplings.

(10) Methylacetylene

The microwave geometry (36) yields $^3J(^{13}C{\equiv}C—C—H)$ = 7.89 and $^3J(^{13}C—C{\equiv}C—H)$ = 4.87 Hz, both considerably larger than the observed (37) values of 4.8 and 3.6 Hz, respectively. Standard geometry entailed 7.43 and 4.80 Hz as the calculated values. From the CNDO/2 (6.55 Hz) and INDO (10.99 Hz) values of $^3J(H—C{\equiv}C—H)$ in acetylene (1), compared to the experimental measurement of 9.5 Hz (38), one may infer that the mean result from the two methods will also produce better agreement with experiment for $^3J(^{13}C{\equiv}C—C—H)$ and $^3J(^{13}C—C{\equiv}C—H)$.

*(11) Bicyclo [1.1.0] butane (**21**)*

As an example of a strained molecule, **21** was subject to the calculations based on the microwave structure (39). INDO predicts $^3J(^{13}C,H_1)$

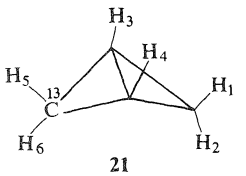

21

= 11.33 and $^3J(^{13}C,H_2)$ = 2.72 Hz while the experiment (40) finds 16.0 ± 0.5 and 5.3 ± 0.2 Hz, respectively. The calculated quantities are too

[4]A referee suggests that for the carbonyl compounds the contact density at the carbon nucleus may differ from the optimum parameter determined by Pople and coworkers.

Can. J. Chem. Downloaded from www.nrcresearchpress.com by 84.22.46.98 on 09/08/12
For personal use only.

Can. J. Chem. Downloaded from www.nrcresearchpress.com by 84.22.46.98 on 09/08/12
For personal use only.

small,[5] a point to note when considering other strained molecules.

(12) Fluorobenzene (23) and 1,2-Difluorobenzene (24)

In this section the influence of electronegative substituents on $^3J(^{13}C,H)$ in the benzene ring is investigated. Standard geometries are assumed for both molecules. For ease of comparison, the diagrams display the calculated couplings in a serial fashion.

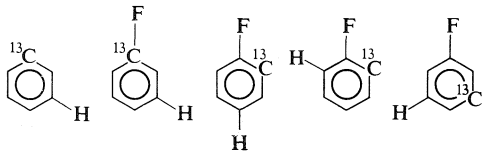

9.40 Hz	12.43	9.96	7.36	10.21
22	**23***a*	**23***b*	**23***c*	**23***d*

Relative to benzene the marked increase of $^3J(^{13}C,H)$ in **23***a* and the decrease in **23***c* is similar to that calculated respectively for 1-fluoropropane (**2**) and 2-fluoropropane relative to propane. No experimental data are available for compounds related to **23**.

Such data are available for 1,2-dichlorobenzene (41) and in the diagrams they are compared to the INDO calculations on 1,2-difluorobenzene. Noting that the observed value in benzene is 7.4 Hz (33), that the calculated value is 9.40 Hz (1) and that chlorine is less electronegative than fluorine, the calculations may be considered

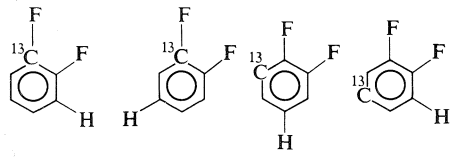

Calcd. 10.52 Hz	12.95	10.74	10.31
Obs. 7.92	11.57	8.41	8.63
(1,2-di Cl)			
24*a*	**24***b*	**24***c*	**24***d*

to reproduce the observed trends at least partially. It may well be helpful in disentangling the complex ^{13}C spectra of benzene derivatives (see ref. 41 and the last sentence of ref. 42).

[5]The vicinal proton coupling constants were calculated as $^3J_{3,4} = 5.67$ (10.4 ± 0.2), $^3J_{1,4} = 1.57$ (2.9 ± 0.2), $^3J_{2,3} = 2.08$ (1.2 ± 0.2) Hz, the experimental quantities being given in brackets.

(13) Pyridine (25) and Pyridinium Ion (26)

The atomic coordinates of pyridine were those of Bak *et al.* (43). The same coordinates were used for the ion but with an N—H bond length of 1.03 Å. It was calculated that $^3J(^{13}C_2,H_4) = 9.27$ (10.08) $^3J(^{13}C_2,H_6) = 13.53$ (5.40), $^3J(^{13}C_3,H_5) = 8.60$ (8.06), and $^3J(^{13}C_4,H_2) = 8.93$

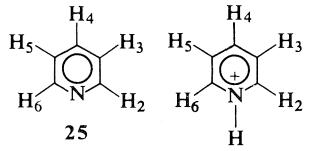

25 **26**

(7.48) Hz, where the values for the ion occur in the brackets. In **25** only $^3J(C_2,H_6)$ is calculated to be larger than in benzene (compare propane and dimethylether where the opposite shift is predicted) while in the ion, **26**, $^3J(C_2,H_4)$ is predicted as larger than in benzene.

(14) Methylbenzoate (27)

Couplings from the carbon nucleus in the carboxylate group to protons have recently been measured (44). A standard geometry was assumed in the calculation. The conformation of the methyl group, shown in **27**, was indicated by the known structure of methyl formate (45).

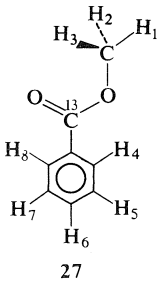

27

One computes $^3J(^{13}C,H_1) = 5.38$ and $^3J(^{13}C,H_2) = 0.75$ Hz, yielding an average of 2.29 Hz. The observed number is 3.73 Hz. Again, the computed values of $^3J(^{13}C,H_4)$ and $^3J(^{13}C,H_8)$ are 6.71 and 5.98 Hz, respectively, as compared to the observed mean value of 4.08 Hz. The relative magnitudes of the two calculated couplings are correctly reproduced, but one is too small and the other too large (compare dimethylether and acetone or acrolein above).[6] In planar benzaldehyde we compute

[6]One computes $^4J(^{13}C,H_5)$ as 0.47 and $^4J(^{13}C,H_7)$ as 0.83 Hz. The observed mean of $^4J(^{13}C,H)$ is 1.11 Hz. On the other hand, the calculated value of $^5J(^{13}C,H_6)$ is 1.53 Hz while the observed number is 0.48 Hz.

the analogous couplings as $^3J(^{13}C,H_4)$ equal to 7.53 Hz and $^3J(^{13}C,H_8)$ equal to 6.52 Hz. The stereospecificity displayed by the computed couplings of a carbonyl carbon to ring protons can probably be used as a probe in conformational work when it is combined with observation.

(15) Furan (28) and Pyrrole (29)

The atomic coordinates for **28** were taken from ref. 46, for **29** from ref. 47. The computations yield for **28**, $^3J(^{13}C_2,H_4) = 9.02$,

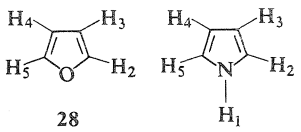

28

29

$^3J(^{13}C_2,H_5) = 6.64$, and $^3J(^{13}C_3,H_5) = 9.30$ Hz. The observed values are 10.8, 7.0, and 5.8 Hz, respectively (48). It is tempting to ascribe the disagreement between theory and experiment to a wrong assignment of the experimental spectrum (42, 48).

For **29** one calculates $^3J(^{13}C_2,H_4) = 9.69$, $^3J(^{13}C_2,H_5) = 6.04$, $^3J(^{13}C_3,H_5) = 9.55$, and $^3J(^{13}C_3,H_1) = 6.84$ Hz. Experiment suggests that both of the latter two couplings equal 7.8 Hz (48), while in 2,5-dimethylpyrrole $^3J(^{13}C_2,H_4)$ is 7.3 Hz (48). The theory is in difficulty in this respect with five-membered heterocycles.

Conclusions

In general the INDO MO computations of spin–spin coupling over three bonds between ^{13}C and protons may well be useful in conformational work when combined with experimental data. In particular, certain pitfalls connected with arguments based on analogies to H,H and H,^{19}F couplings over three bonds may be avoided by reference to the theory. However, the exploratory calculations reported here emphasize that the quantitative aspects of the theory must be treated with circumspection.

We are grateful to the National Research Council of Canada for financial support and to the staff of the Computing Center of the University of Manitoba for their cooperation. We thank the referees for some very helpful comments.

1. J. A. Pople and D. L. Beveridge. Approximate molecular orbital theory. McGraw–Hill Book Co., New York. 1970.
2. J. A. Pople, J. W. McIver, Jr., and N. S. Ostlund. Chem. Phys. Lett. **1**, 465 (1967).
3. G. E. Maciel, J. W. McIver, Jr., N. S. Ostlund, and J. A. Pople. J. Am. Chem. Soc. **92**, 1, 11, 4151 (1970).
4. G. E. Maciel, J. W. McIver, Jr., N. S. Ostlund, and J. A. Pople. J. Am. Chem. Soc. **92**, 4497, 4506 (1970).
5. P. D. Ellis and G. E. Maciel. Mol. Phys. **20**, 433 (1971).
6. M. Barfield. J. Am. Chem. Soc. **93**, 1066 (1971).
7. M. Barfield, C. J. Macdonald, I. R. Peat, and W. F. Reynolds. J. Am. Chem. Soc. **93**, 4195 (1971).
8. M. Barfield and S. Sternhell. J. Am. Chem. Soc. **94**, 1905 (1972).
9. R. Wasylishen and T. Schaefer. Can. J. Chem. **49**, 3216 (1971); **50**, 1852 (1972).
10. M. S. Gopinathan and P. T. Narasimhan. Mol. Phys. **21**, 1141 (1971).
11. R. Wasylishen and T. Schaefer. Can. J. Chem. **50**, 2989 (1972).
12. M. Karplus. J. Chem. Phys. **30**, 11 (1959); J. Am. Chem. Soc. **85**, 2870 (1965).
13. E. Breitmaier, G. Jung, and W. Voelter. Angew. Chem. Int. Ed. **10**, 673 (1971).
14. R. U. Lemieux, T. L. Nagabhushan, and B. Paul. Can. J. Chem. **50**, 773 (1972).
15. (*a*) J. A. Pople, J. W. McIver, Jr., and N. S. Ostlund. J. Chem. Phys. **49**, 2960, 2965 (1968). (*b*) P. A. Dobosh. Program 141, Q.C.P.E., Indiana University, Bloomington, Indiana. (*c*) Program 135, Q.C.P.E., Indiana University, Bloomington, Indiana.
16. J. A. Pople and M. S. Gordon. J. Am. Chem. Soc. **89**, 4253 (1967).
17. R. Wasylishen and T. Schaefer. Can. J. Chem. **50**, 1710 (1972).
18. J. H. Holland. J. Chem. Phys. **49**, 1908 (1968).
19. A. D. Cohen and T. Schaefer. Mol. Phys. **10**, 209 (1965).
20. S. Castellano and R. Kostelnik. J. Am. Chem. Soc. **90**, 141 (1968).
21. G. J. Karabatsos and C. E. Orzech. Jr. J. Am. Chem. Soc. **87**, 560 (1965).
22. O. Yamamoto and K. Hayamizu. J. Mag. Res. **5**, 429 (1971).
23. J. E. Wollrab and V. W. Laurie. J. Chem. Phys. **48**, 5058 (1968).
24. (*a*) V. W. Laurie and J. Wollrab. Bull. Am. Phys. Soc. Ser II, **8**, 327 (1963). (*b*) H. Dreeskamp, K. Hildenbrand, and G. Pfisterer. Mol. Phys. **17**, 429 (1969).
25. (*a*) E. Scarzafava and L. C. Allen. J. Am. Chem. Soc. **93**, 311 (1971). (*b*) E. Sackmann and H. Dreeskamp. Spectrochim. Acta, **21**, 2005 (1965).
26. H. Rudolph, H. Dreizler, A. Joeschke, and P. Wendling. Z. Naturforsch., **22a**, 940 (1967).
27. E. Hirota. J. Chem. Phys. **45**, 1984 (1966).
28. K. V. L. N. Sastry and R. F. Curl, Jr. J. Chem. Phys. **41**, 77 (1964).
29. V. M. S. Gil and A. C. P. Alves. Mol. Phys. **16**, 527 (1969).

Can. J. Chem. Downloaded from www.nrcresearchpress.com by 84.22.46.98 on 09/08/12
For personal use only.

30. R. NELSON and L. PIERCE. J. Mol. Spectrosc. **18**, 344 (1965).
31. J. D. SWALEN and C. C. COSTAIN. J. Chem. Phys. **31**, 1562 (1959).
32. A. R. TARPLEY, JR. and J. H. GOLDSTEIN. Mol. Phys. **21**, 549 (1971).
33. F. J. WEIGERT and J. D. ROBERTS. J. Am. Chem. Soc. **89**, 2967 (1967).
34. S. S. BUTCHER and E. B. WILSON, Jr. J. Chem. Phys. **40**, 1671 (1964).
35. (*a*) G. J. KARABATSOS, C. E. ORZECH, Jr., and N. HSI. J. Am. Chem. Soc. **88**, 1817 (1966). (*b*) K. M. CRECELY, R. W. CRECELY, and J. H. GOLDSTEIN. J. Mol. Spectrosc. **37**, 252 (1971).
36. C. C. COSTAIN. J. Chem. Phys. **29**, 864 (1958).
37. J. N. SHOOLERY, L. F. JOHNSON, and W. A. ANDERSON. J. Mol Spectrosc. **5**, 110 (1960).
38. R. M. LYNDEN-BELL and N. SHEPPERD. Proc. Roy. Soc. (London), A**269**, 385 (1962).
39. K. W. COX, M. D. HARMONY, G. NELSON, and K. B. WIBERG. J. Chem. Phys. **50**, 1976 (1969).
40. K. WÜTRICH, S. MEIBOOM, and L. S. SNYDER. J. Chem. Phys. **52**, 230 (1970).
41. A. R. TARPLEY, Jr. and J. H. GOLDSTEIN. J. Mol. Spectrosc. **37**, 432 (1971).
42. K. TAKAHASHI, T. SONE, and K. FUJIEDA. J. Phys. Chem. **74**, 2765 (1970).
43. B. BAK, L. HANSEN-NYGAARD, and J. RASTRUP-ANDERSON. J. Mol. Spectrosc. **2**, 361 (1958).
44. A. M. IHRIG and J. L. MARSHALL. J. Am. Chem. Soc. **94**, 3268 (1972).
45. R. F. CURL, Jr. J. Chem. Phys. **30**, 1529 (1959).
46. B. BAK, D. CHRISTENSEN, W. B. DIXSON, L. HANSEN-NYGAARD, J. RASTRUP-ANDERSON, and M. SCHOTTLÄNDER. J. Mol. Spectrosc. **9**, 124 (1962).
47. L. NYGAARD, J. T. NIELSEN, J. KIRCHHEIMER, G. MALTESEN, J. RASTRUP-ANDERSEN, and G. O. SØRENSEN. J. Mol. Struct. **3**, 491 (1971).
48. F. J. WEIGERT and J. D. ROBERTS. J. Am. Chem. Soc. **90**, 3543 (1968).

Can. J. Chem. Downloaded from www.nrcresearchpress.com by 84.22.46.98 on 09/08/12
For personal use only.

A Synthesis of 2-Amino-2,6-dideoxy-D-(and L-)galactose (Fucosamine) and 2-Amino-2,6-dideoxy-D-(and L-)talose (Pneumosamine)[1]

MALCOLM B. PERRY AND VIRGINIA DAOUST

Division of Biological Sciences, National Research Council of Canada, Ottawa, Canada K1A 0R6

Received October 10, 1972

5-Deoxy-D-lyxose underwent base-catalyzed addition with nitromethane to give a mixture of 1,6-dideoxy-1-nitro-D-galactitol and 1,6-dideoxy-1-nitro-D-talitol (*ca.* 2:1). Acetylation of the crystalline 1,6-dideoxy-1-nitro-D-galactitol gave 2,3,4,5-tetra-*O*-acetyl-1,6-dideoxy-1-nitro-D-galactitol which on treatment with methanolic ammonia afforded 2-acetamido-1,2,6-trideoxy-1-nitro-D-talitol and 2-acetamido-1,2,6-trideoxy-1-nitro-D-galactitol (*ca.* 3:1) which under the modified Nef reaction conditions gave 2-acetamido-2,6-dideoxy-D-talose and 2-acetamido-2,6-dideoxy-D-galactose respectively. The glycoses were converted to 2-amino-2,6-dideoxy-D-talose hydrochloride and 2-amino-2,6-dideoxy-D-galactose hydrochloride on hydrolysis with hydrochloric acid.

A similar reaction sequence applied to 5-deoxy-L-lyxose afforded the L-enantiomorphic intermediates, and gave 2-amino-2,6-dideoxy-L-talose hydrochloride and 2-amino-2,6-dideoxy-L-galactose hydrochloride as final products.

Le déoxy-5-D-lyxose s'additionne sur du nitrométhane en milieu basique pour conduire au mélange de didéoxy-1,6-nitro-1-D-galactitol et de didéoxy-1,6 nitro-1-D-talitol (*ca.* 2:1). L'acétylation du didéoxy-1,6 nitro-1-D-galactitol cristallin fournit le tétra-*O*-acétyl-2,3,4,5 didéoxy-1,6 nitro-1-D-galactitol qui, en présence d'ammoniac méthanolique, conduit à l'acétamido-2 tridéoxy-1,2,6 nitro-1-D-talitol et à l'acétamido-2 tridéoxy-1,2,6 nitro-1-D-galactitol (*ca.* 3:1); dans les conditions de la réaction modifiée de Nef, ce mélange donne respectivement l'acétamido-2 didéoxy-2,6-D-talose et l'acétamido-2 didéoxy-2,6-D-galactose. Les glycoses sont convertis en chlorhydrates d'amino-2 didéoxy-2,6-D-talose et d'amino-2 didéoxy-2,6-D-galactose dans l'hydrolyse par l'acide chlorhydrique.

La même séquence réactionnelle sur le déoxy-5-L-lyxose conduit aux intermédiaires L-énantiomorphes puis aux chlorhydrates d'amino-2 didéoxy-2,6-L-talose et d'amino-2 didéoxy-2,6-L-galactose comme produits finals. [Traduit par le journal]

Can. J. Chem., **51**, 974 (1973)

Can. J. Chem. Downloaded from www.nrcresearchpress.com by 210.87.254.5 on 09/05/12
For personal use only.

The following 2-amino-2,6-dideoxyhexoses have been identified as components of bacterial polysaccharides: 2-amino-2,6-dideoxy-D-glucose (quinovosamine) (1–5), 2-amino-2,6-dideoxy-L-mannose (rhamnosamine) (6, 7), 2-amino-2,6-dideoxy-D-galactose (fucosamine) (8–13), 2-amino-2,6-dideoxy-L-galactose (14–16), and 2-amino-2,6-dideoxy-L-talose (pneumosamine) (15, 17, 18). A survey of the carbohydrate components of *Pseudomonas* species made in this laboratory revealed many unusual aminoglycoses, including 2-amino-2,6-dideoxyhexoses. The synthesis of the series of these latter compounds was undertaken to provide glycoses for the development of analytical procedures and for the preparation of methyl ethers required in structural studies.

Although methods have been described for the synthesis of 2-amino-2,6-dideoxy-D-talose (18), 2-amino-2,6-dideoxy-L-talose (19, 20), 2-amino-2,6-dideoxy-L-galactose (20, 21), and 2-amino-2,6-dideoxy-D-galactose (13), it was considered that the series might be conveniently synthesized from available 5-deoxypentoses by the nitromethane method which has found general application in the synthesis of 2-amino-2-deoxyaldoses (22). This paper records the successful synthesis of 2-amino-2,6-dideoxy-D-talose and 2-amino-2,6-dideoxy-D-galactose from 5-deoxy-D-lyxose, and the corresponding L-enantiomorphs from 5-deoxy-L-lyxose, using the nitromethane method.

5-Deoxy-D-lyxose, prepared by the degradation of D-fucose diethyl dithioacetal (21, 23) underwent addition with nitromethane in the presence of sodium methoxide and the resulting precipitated sodium salts of 1,6-dideoxy-1-nitro-D-galactitol (66%) and 1,6-dideoxy-1-nitro-D-talitol (34%) were deionized with hydrogen form ion-exchange resin and the product afforded crystalline 1,6-dideoxy-1-nitro-D-galactitol which on acetylation gave 2,3,4,5-tetra-*O*-acetyl-1,6-

[1]NRCC No. 12975.

Can. J. Chem. Downloaded from www.nrcresearchpress.com by 210.87.254.5 on 09/05/12
For personal use only.

dideoxy-1-nitro-D-galactitol. Treatment of the 2,3,4,5-tetra-*O*-acetyl-1,6-dideoxy-1-nitro-D-galactitol with saturated methanolic ammonia (24) afforded a mixture of 2-acetamido-1,2,6-trideoxy-1-nitro-D-galactitol (27%) and 2-acetamido-1,2,6-trideoxy-1-nitro-D-talitol (73%), the latter compound being obtained pure by crystallization from ethanol solution. The 2-acetamido-1,2,6-trideoxy-1-nitro-D-talitol on treatment under the mild modified Nef conditions (24) gave chromatographically pure 2-acetamido-2,6-dideoxy-D-talose. The crude 2-acetamido-1,2,6-trideoxy-1-nitro-D-galactitol remaining after the removal of crystalline 2-acetamido-1,2,6-trideoxy-1-nitro-D-talitol, underwent the modified Nef reaction to give a mixture of 2-acetamido-2,6-dideoxy-D-talose and 2-acetamido-2,6-dideoxy-D-galactose, the latter compound being separated by crystallization from the ethanol solution of the mixture.

The 2-acetamido-2,6-dideoxy-D-talose and 2-acetamido-2,6-dideoxy-D-galactose were each hydrolyzed with hot dilute hydrochloric acid to yield crystalline 2-amino-2,6-dideoxy-D-talose hydrochloride and 2-amino-2,6-dideoxy-D-galactose hydrochloride respectively which had physical properties in agreement with those recorded in the literature for these compounds.

The synthesis of the two 2-acetamido-2,6-dideoxy-hexoses performed without the isolation of the intermediates gave improved yields. The final products of 2-acetamido-2,6-dideoxy-D-talose and 2-acetamido-2,6-D-galactose were obtained in 44 and 17% yields respectively, based on 5-deoxy-D-lyxose used. The final mixture can be separated by preferential crystallization of the 2-acetamido-2,6-dideoxy-D-galactose leaving essentially pure 2-acetamido-2,6-dideoxy-D-talose which is readily purified by conversion to 2-amino-2,6-dideoxy-D-talose hydrochloride which is obtained pure in good yield. Alternatively, the two 2-acetamido-2,6-dideoxy-hexoses are easily separated by cellulose column chromatography using aqueous 1-butanol as the mobile phase.

5-Deoxy-L-lyxose, prepared either by the degradation of L-fucose diethyl dithioacetal (21) or from D-galactono-1,4-lactone (25), underwent the same synthetic reaction sequence as that described for 5-deoxy-D-lyxose to yield the corresponding L-enantiomorphic intermediates and to give, as final products, 2-amino-2,6-dideoxy-L-talose hydrochloride and 2-amino-2,6-dideoxy-L-galactose hydrochloride.

Experimental

Paper chromatography was performed by the descending method (26) on Whatman No. 1 filter paper using either (A) pyridine – ethyl acetate – water (2:5:5 v/v; top layer) or (B) 1-butanol–ethanol–water (4:1:5 v/v; top layer) as the mobile phase. Glycoses were detected with either (*i*) 2% silver nitrate in acetone followed by 3% sodium hydroxide in ethanol (27), (*ii*) 2% *p*-anisidine hydrochloride in ethanol (28), or (*iii*) 2% ninhydrin in acetone. The rates of movement of the glycoses are quoted relative to D-galactose (R_{Gal}) or to 2-amino-2-deoxy-D-glucose hydrochloride (R_{GN}).

Gas–liquid partition chromatography (g.l.p.c.) was carried out using a Hewlett-Packard model 402 gas chromatograph with a hydrogen flame detector and fitted with glass U-tubes (4 ft × 6 mm × 3 mm internal diameter) packed with 10% neopentyl-glycol sebacate polyester on 80–100 mesh acid washed Chromosorb W. Retention times of the compounds are quoted relative to penta-*O*-acetyl-L-arabinitol (T_A) or to 2-acetamido-2-deoxy-1,3,4,5,6-penta-*O*-(trimethylsilyl)-D-glucitol (T_{GN}).

Melting points were determined on a Fisher-Johns apparatus and are corrected. Solutions were concentrated under reduced pressure and below 40 °C. Optical rotations were determined at 20 °C using a Perkin–Elmer 141 polarimeter.

(A) Synthesis of 2-Amino-2,6-dideoxy-D-talose Hydrochloride and 2-Amino-2,6-dideoxy-D-galactose Hydrochloride

(1) 1,6-Dideoxy-1-nitro-D-talitol and 1,6-Dideoxy-1-nitro-D-galactitol

To a solution of 5-deoxy-D-lyxose (21) (4.4 g) in a mixture of methanol (50 ml) and nitromethane (15 ml) was added 1.7 *N* sodium methoxide in methanol (23 ml) and the mixture was kept at 20 °C for 18 h. Following the addition of ether (140 ml), the precipitated product was collected by filtration, washed with cold methanol, ether, and light petroleum (b.p. 30–60 °C) and dried under vacuum. The product dissolved in cold water (70 ml) was passed down a column of Rexyn 101(H^+) ion-exchange resin (120 ml) and the eluate and water washings were concentrated to a syrup (5.5 g).

A portion of the product (20 mg) was dissolved in 2 *N* sodium hydroxide (0.2 ml) and the solution was added dropwise to 6 *N* sulfuric acid (0.3 ml) at 0 °C. After 2 h at room temperature the mixture was diluted with water (5 ml) and following neutralization ($BaCO_3$), filtration, and passage of the filtrate through a column of mixed Rexyn 101(H^+) and Rexyn RG6(OH^-) ion-exchange resins (2 ml), the solution was concentrated to a syrup (*ca.* 12 mg). Paper chromatographic examination of the syrup (solvent A) revealed two spots having R_{Gal} 2.37 and 4.26 corresponding in mobilities and color reaction, with authentic 6-deoxy-D-galactose and 6-deoxy-D-talose respectively (visual ratio 2:1). G.l.p.c. (180 °C) of a reduced ($NaBH_4$) and acetylated (29, 30) portion of the latter syrup gave two peaks corresponding with penta-*O*-acetyl-6-deoxy-D-talitol (T_A 0.72, 34%) and penta-*O*-acetyl-D-6-deoxy-D-galactitol(T_A 0.77, 66%).

On keeping, a methanolic solution of the mixed 1,6-dideoxy-1-nitro-hexitols (5.4 g) gave crystals (2.8 g), m.p. 170–176 °C (mixture of *talo*- and *galacto*-epimers, *ca.* 1:5 by Nef reaction) which after three recrystallizations from

Can. J. Chem. Downloaded from www.nrcresearchpress.com by 210.87.254.5 on 09/05/12
For personal use only.

ethanol afforded pure 1,6-dideoxy-1-nitro-D-galactitol (2 g) having m.p. 180 °C and $[\alpha]_D$ +6° (*c*, 0.3 in water).

Anal. Calcd. for $C_6H_{13}O_6N$: C, 36.92; H, 6.71; N, 7.18. Found: C, 37.10; H, 6.53; N, 6.99.

A small sample of the pure product on treatment under the Nef conditions (as above) gave only 6-deoxy-D-galactose.

(2) 2,3,4,5-Tetra-O-acetyl-1,6-dideoxy-1-nitro-D-galactitol

1,6-Dideoxy-1-nitro-D-galactitol (2 g) in acetic anhydride (20 ml) was treated with 1 drop of concentrated sulfuric acid and the mixture was heated on a boiling water bath for 30 min. The cooled reaction mixture was poured onto crushed ice (150 ml) and the precipitated derivative (3.9 g) was collected and washed with cold water. The product after two recrystallizations from ethanol gave crystalline 2,3,4,5-tetra-*O*-acetyl-1,6-dideoxy-1-nitro-D-galactitol having m.p. 138–139 °C and $[\alpha]_D$ −18.5° (*c*, 0.7 in chloroform).

Anal. Calcd. for $C_{14}H_{21}O_{10}N$: C, 46.28; H, 5.83; N, 3.86. Found: C, 46.41; H, 5.86; N, 3.76.

Acetylation of the mixed 1,6-dideoxy-1-nitro-D-galactitol and -D-talitol (3.4 g) remaining after removal of the -D-galactitol component afforded further crystalline 2,3,4,5-tetra-*O*-acetyl-1,6-dideoxy-1-nitro-D-galactitol (1.6 g) and a syrup mixture of 2,3,4,5-tetra-*O*-acetyl-1,6-dideoxy-1-nitro-D-galactitol and 2,3,4,5-tetra-*O*-acetyl-1,6-dideoxy-1-nitro-D-talitol (4.3 g).

(3) 2-Acetamido-1,2,6-trideoxy-1-nitro-D-galactitol and 2-Acetamido-1,2,3-trideoxy-1-nitro-D-talitol

2,3,4,5-Tetra-*O*-acetyl-1,6-dideoxy-1-nitro-D-galactitol (4.1 g) in dry methanol (45 ml) was cooled to 0 °C and ammonia gas was passed into the solution for 30 min and the saturated mixture was then kept for 18 h at 20 °C. The mixture was concentrated to a syrup which was triturated with warm chloroform (3 × 30 ml) to remove acetamide and the light brown syrup remaining was dissolved in hot ethanol, treated with charcoal (2 g), filtered, and, following concentration of the ethanol solution, crystalline 2-acetamido-1,2,6-trideoxy-1-nitro-D-talitol (1.2 g) was obtained, which had, after recrystallization from ethanol, m.p. 166–167 °C and $[\alpha]_D$ +20° (*c*, 0.4 in water).

Anal. Calcd. for $C_8H_{16}O_6N_2$: C, 40.67; H, 6.83; N, 11.86. Found: C, 40.83; H, 6.76; N, 11.69.

A portion of the product (10 mg) resulting from the action of ammonia on the 2,3,4,5-tetra-*O*-acetyl-1,6-dideoxy-1-nitro-D-galactitol on treatment under the Nef conditions gave two 2-acetamido-2,6-dideoxy-hexoses which on paper chromatography gave two spots having R_{Gal} 3.02 and 4.10 corresponding in mobility and color reactions with 2-acetamido-2,6-dideoxy-D-galactose and 2-acetamido-2,6-dideoxy-D-talose respectively (visual ratio 1:2) while quantitative g.l.p.c. analysis (190 °C) of the trimethylsilylated product (31) indicated the mixture to be composed of 27% 2-acetamido-2,6-dideoxy-D-galactose and 73% 2-acetamido-2,6-dideoxy-D-talose.

(4) 2-Amino-2,6-dideoxy-D-talose Hydrochloride

2-Acetamido-1,2,6-trideoxy-1-nitro-D-talitol (0.96 g) was dissolved in a solution of $Ba(OH)_2 \cdot 8H_2O$ (1.18 g) in water (18 ml) and the mixture was added dropwise with stirring to a solution of concentrated sulfuric acid (1.2 ml) in water (11 ml) cooled in ice. The mixture was kept at 20 °C for 18 h and following neutralization ($BaCO_3$) and filtration, the filtrate was treated with Dowex-1 (CO_3^{2-}) ion-exchange resin (8 ml) and 4 drops of acetic anhydride and, after 20 min, the solution was passed down a column of mixed Rexyn 101(H^+) and Rexyn RG6(OH^-) ion-exchange resins and the eluate and washings were concentrated to dryness (0.62 g).

Paper chromatographic analysis of the product (solvent A) gave a single spot having R_{Gal} 4.10 corresponding with authentic 2-acetamido-2,6-dideoxy-D-talose and g.l.c. (190 °C) of the trimethylsilylated (31) equilibrated product showed four peaks having T_{GN} 0.53 (17%), 0.62 (46%), 0.98 (25%), and 1.07 (12%). The 2-acetamido-2,6-dideoxy-D-talose (0.6 g) which failed to crystallize was hydrolyzed with 3 *N* hydrochloric acid for 2 h at 100 °C and following concentration to dryness the product afforded pure 2-amino-2,6-dideoxy-D-talose hydrochloride (0.48 g) which gave a single ninhydrin positive spot on paper chromatography (solvent B) with R_{GN} 1.70 and had m.p. 164–165 °C and $[\alpha]_D$ +7 → −10° (*c*, 0.5 in water) (lit. (18) m.p. 161.5–163.5 °C and $[\alpha]_D$ +8 → −10° (water); L-enantiomorph (20) m.p. 162–163 °C and $[\alpha]_D$ −4 → +10° (water) and (19) m.p. 163–164 °C and $[\alpha]_D$ +9° (water)).

Anal. Calcd. for $C_6H_{14}O_4NCl$: C, 36.09; H, 7.07; N, 7.01; Cl, 17.75. Found: C, 36.12; H, 7.02; N, 7.15; Cl, 17.55.

(5) 2-Acetamido-2,6-dideoxy-D-galactose

The syrupy mixture of 2-acetamido-1,2,6-trideoxy-1-nitro-D-talitol and 2-acetamido-1,2,6-trideoxy-1-nitro-D-galactitol (1.42 g) remaining from the ammonia treatment of 2,3,4,5-tetra-*O*-acetyl-1,6-dideoxy-1-nitro-D-galactitol and removal of the crystalline 2-acetamido-1,2,6-trideoxy-1-nitro-D-talitol (section 3 above) was treated under the modified Nef conditions (as in section 4 above) to give a mixture of 2-acetamido-2,6-dideoxy-D-talose and 2-acetamido-2,6-dideoxy-D-galactose (1.1 g) which from concentrated ethanol solution gave crystalline 2-acetamido-2,6-dideoxy-D-galactose (0.48 g) which was removed leaving essentially pure 2-acetamido-2,6-dideoxy-D-talose as a syrup.

The 2-acetamido-2,6-dideoxy-D-galactose on paper chromatography (solvent A) gave a single spot R_{Gal} 3.02 and after recrystallization from ethanol the crystals (0.37 g) had m.p. 201–202 °C and $[\alpha]_D$ +109 → +87° (*c*, 0.4 in water) (lit. (13) m.p. 196–197 °C and $[\alpha]_D$ +129 → +92° (water); L-enantiomorph (21) m.p. 197–198 °C and $[\alpha]_D$ −119 → −82° (water)).

Anal. Calcd. for $C_8H_{15}O_5N$: C, 46.82; H, 7.37; N, 6.83. Found: C, 46.69; H, 7.44; N, 7.01.

G.l.c. (190 °C) of the trimethylsilylated (31) crystalline 2-acetamido-2,6-dideoxy-D-galactose gave a single peak T_{GN} 1.03 while the water equilibrated glycose gave two peaks having T_{GN} 1.03 (56%) and 1.75 (44%).

(6) 2-Amino-2,6-dideoxy-D-galactose Hydrochloride

2-Acetamido-2,6-dideoxy-D-galactose (0.2 g) after hydrolysis with 3 *N* hydrochloric acid for 2 h at 100 °C afforded crystalline 2-amino-2,6-dideoxy-D-galactose hydrochloride from methanol–acetone solution which gave a single ninhydrin positive spot on paper chromatography (solvent B) with R_{GN} 1.52 and had m.p. 192–193 °C and $[\alpha]_D$ +120 → +93° (*c*, 0.4 in water) (lit. (13) m.p. 192 °C and $[\alpha]_D$ +117 → +92° (water); L-enantiomorph (21) m.p. 192–193 °C and $[\alpha]_D$ −119 → −92° (water)).

Anal. Calcd. for $C_6H_{14}O_4NCl$: C, 36.09; H, 7.07; N, 7.01: Cl, 17.75. Found: C, 36.01; H, 6.98; N, 7.10; Cl, 17.60.

(B) 2-Amino-2,6-dideoxy-D-talose Hydrochloride and 2-Amino-2,6-dideoxy-D-galactose Hydrochloride

(1) 2-Acetamido-2,6-dideoxy-D-talose and 2-Acetamido-2,6-dideoxy-D-galactose

5-Deoxy-L-lyxose (21, 25) (5 g) was condensed with nitromethane (as in Section A.1) to yield the sodium salts of the 1,6-dideoxy-1-nitro-hexitols which were deionized (Rexyn 101(H^+)) and concentrated to a syrup (6.4 g). Acetylation of the syrup (as in Section A.2) gave the tetra-*O*-acetates of 1,6-dideoxy-1-nitro-L-talitol and 1,6-dideoxy-1-nitro-L-galactitol (11.3 g) which were treated with methanolic ammonia (as in Section A.3) and, following the removal of acetamide, the mixture of 2-acetamido-1,2,6-trideoxy-1-nitro-L-talitol and 2-acetamido-1,2,6-trideoxy-1-nitro-L-galactitol (7 g) was obtained as a syrup. The mixed 2-acetamido-1,2,6-trideoxy-1-nitro-hexitols were treated under the modified Nef reaction conditions (as in Section A.4) to yield 2-acetamido-2,6-dideoxy-L-talose and 2-acetamido-2,6-dideoxy-L-galactose (4.9 g). On keeping at room temperature, the concentrated ethanol solution of the product gave crystals of 2-acetamido-2,6-dideoxy-L-galactose (0.98 g) leaving essentially pure (*ca.* 90%) 2-acetamido-2,6-dideoxy-L-talose as a syrup (3.7 g).

The 2-acetamido-2,6-dideoxy-L-galactose after recrystallization from ethanol gave a single spot on paper chromatography (solvent A) R_{Gal} 3.02 and g.l.p.c. of the trimethylsilylated product gave a chromatogram identical with the D-enantiomorph. The crystals had m.p. 195–198 °C and $[\alpha]_D$ $-116 \rightarrow -83°$ (*c*, 0.2 in water).

Anal. Calcd. for $C_8H_{15}O_5N$: C, 46.82; H, 7.37; N, 6.83. Found: C, 46.59; H, 7.30; N, 7.02.

(2) 2-Amino-2,6-dideoxy-L-galactose Hydrochloride

2-Acetamido-2,6-dideoxy-L-galactose (0.3 g) was hydrolyzed with 3 *N* hydrochloric acid for 3 h at 100 °C and the concentrated product gave crystalline 2-amino-2,6-dideoxy-L-galactose (0.23 g) which gave a single ninhydrin positive spot on paper chromatography R_{GN} 1.52 (solvent B) and had m.p. 191–193 °C and $[\alpha]_D$ $-115 \rightarrow -95°$ (*c*, 0.5 in water).

Anal. Calcd. for $C_6H_{14}O_4NCl$: C, 36.09; H, 7.07; N, 7.01. Found: C, 36.00; H, 7.11; N, 7.07.

(3) 2-Amino-2,6-dideoxy-L-talose Hydrochloride

The impure 2-acetamido-2,6-dideoxy-L-talose (3.7 g) was hydrolyzed with 3 *N* hydrochloric acid (50 ml) for 3 h at 100 °C and following concentration, the methanol–acetone solution of the residue gave crystalline 2-amino-2,6-dideoxy-L-talose hydrochloride (2.3 g) which gave a single ninhydrin positive spot on paper chromatography R_{GN} 1.71 (solvent B) and had m.p. 163–164.5 °C and $[\alpha]_D$ $-5 \rightarrow +10°$ (*c*, 0.4 in water).

Anal. Calcd. for $C_6H_{14}O_4NCl$: C, 36.09; H, 7.07; N, 7.01. Found: C, 36.02; H, 7.11; N, 7.00.

1. E. J. SMITH. Biochem. Biophys. Res. Commun. **15**, 593 (1964).
2. O. LÜDERITZ, J. GMEINER, B. KICKHÖFEN, H. MEYER, and R. WHEAT. J. Bacteriol. **95**, 490 (1968).
3. R. R. COLWELL, E. J. SMITH, and G. B. CHAPMAN. Can. J. Microbiol. **14**, 165 (1968).
4. N. SUZUKI, A. SUZUKI, and A. FUKASAWA. J. Jap. Biochem. Soc. **42**, 130 (1970).
5. S. G. WILKINSON and K. A. CARBY. J. Gen. Microbiol. **66**, 221 (1971).
6. B. JANN and K. JANN. Eur. J. Biochem. **5**, 173 (1968).
7. F. ØRSKOV, I. ØRSKOV, B. JANN, E. MÜLLER-SEITZ, and O. WESTPHAL. Acta path. microbiol. scandinav. **71**, 339 (1967).
8. M. J. CRUMPTON and D. A. L. DAVIES. Biochem. J. **70**, 729 (1958).
9. R. WHEAT, E. L. ROLLINS, and J. LEATHERWOOD. Nature, **202**, 492 (1958).
10. R. W. WHEAT, E. L. ROLLINS, and J. M. LEATHERWOOD. J. Biol. Chem. **238**, 26 (1963).
11. J. D. HIGGINBOTHAM and M. HEIDELBERGER. Carbohydr. Res. **23**, 165 (1972).
12. N. SHARON, I. SHIF, and U. ZEHAVI. Biochem. J. **93**, 210 (1964).
13. U. ZEHAVI and N. SHARON. J. Org. Chem. **29**, 3654 (1964).
14. G. T. BARRY and E. ROARK. Nature, **202**, 493 (1964).
15. S. A. BARKER, J. S. BRIMACOMBE, M. J. HOW, and M. STACEY. Nature, **189**, 303 (1961).
16. J. A. CIFONELLI, P. A. REBERS, M. B. PERRY, and J. K. N. JONES. Biochem. **5**, 3066 (1966).
17. S. A. BARKER, M. STACEY, and J. M. WILLIAMS. Bull. Soc. Chim. Biol. **12**, 1611 (1960).
18. J. S. BRIMACOMBE and M. J. HOW. J. Chem. Soc. 5037 (1962).
19. P. M. COLLINS and W. G. OVEREND. Chem. Ind. (London), 375 (1963).
20. J. S. BRIMACOMBE, J. G. H. BRYAN, and M. STACEY. Carbohydr. Res. **1**, 258 (1965).
21. R. KUHN, W. BISTER, and W. DAFELDECKER. Ann. **628**, 186 (1959).
22. H. H. BAER. Advan. Carbohydr. Chem. Biochem. **24**, 67 (1969).
23. L. HOUGH and T. J. TAYLOR. J. Chem. Soc. 3544 (1955).
24. C. SATOH and A. KIYOMOTO. Chem. Pharm. Bull. Tokyo, **12**, 615 (1964).
25. R. K. HULYALKAR and M. B. PERRY. Can. J. Chem. **43**, 3241 (1965).
26. S. M. PARTRIDGE. Biochem. J. **42**, 238 (1948).
27. W. E. TREVELYAN, D. D. PROCTER, and J. S. HARRISON. Nature, **166**, 444 (1950).
28. L. HOUGH, J. K. N. JONES, and W. H. WADMAN. J. Chem. Soc. 1702 (1950).
29. S. W. GUNNER, J. K. N. JONES, and M. B. PERRY. Chem. Ind. (London), 255 (1961).
30. S. W. GUNNER, J. K. N. JONES, and M. B. PERRY. Can. J. Chem. **39**, 1892 (1961).
31. M. B. PERRY. Can. J. Biochem. **42**, 451 (1964).

Can. J. Chem. Downloaded from www.nrcresearchpress.com by 210.87.254.5 on 09/05/12
For personal use only.

Radical Intermediates in Chloramine and *N*-Chloroimide Reactions[1]

OLIVER EDWARD EDWARDS, DONALD H. PASKOVICH, AND ALLAN H. REDDOCH

Divisions of Chemistry and of Biological Sciences, National Research Council of Canada, Ottawa, Canada K1A 0R6

Received October 10, 1972

Nitrogen-centered radicals produced by the action of Ag(0) or Ag(I)-amine systems on *N*-chloroazacyclononane, *N*-chloropiperidine, and *N*-chlorosuccinimide have been trapped using 2-methyl-2-nitrosopropane. The resulting nitroxides exhibited e.p.r. spectra consistent with structures **1**, **2**, and **3**. Hydrogen gas evolved during reaction of the chloramines with Ag(0) was shown to arise completely from the amine derivatives.

Excess Ag(0) reduced the succinamidyl radical to give the silver salt of succinimide.

Les radicaux centrés sur l'azote et obtenus par action des systèmes Ag(0) ou Ag(I)-amine sur le *N*-chloroazacyclononane, *N*-chloropipéridine, et *N*-chlorosuccinimide ont été piégés en utilisant du méthyl-2 nitroso-2 propane. Les nitroxydes qui en résultent, montrent des spectres r.p.e. compatibles avec les structures **1**, **2**, et **3**. Le dégagement gazeux obtenu dans la réaction des chloramines sur Ag(0) provient uniquement des dérivés aminés.

L'excès d'Ag(0) réduit le radical succinamidyle et conduit au sel d'argent du succinimide.

[Traduit par le journal]

Can. J. Chem., **51**, 978 (1973)

Can. J. Chem. Downloaded from www.nrcresearchpress.com by 210.87.254.105 on 09/05/12
For personal use only.

In connection with our studies of chloramine decomposition by silver ions or metallic silver (1) it seemed desirable to have independent evidence for the postulated nitrogen-centered radicals. The products from reaction of hypochlorites (2), hypobromites, and aliphatic chloramines (1) with finely divided silver were consistent with reduction to give the oxygen and nitrogen-centered radicals respectively. However the reaction of aliphatic chloramines with silver salts was more controversial. While considerable evidence has been provided by Gassman for heterolytic fission of the N—Cl bonds in a number of cases (3), our studies showed that this did not take place at room temperature with *N*-chloropiperidine or medium ring chloramines. The need for amine to initiate reaction, the formation of parent secondary amine, and the sensitivity of the reactions to oxygen led us to conclude that traces of metallic silver were initiating these reactions also. This conclusion is now supported by radical trapping evidence.

No radicals were detected when a degassed solution of *N*-chloroazacyclononane, indolizidine, and silver perchlorate in 90% aqueous acetonitrile was examined in the e.p.r. spectrometer. However if 2-methyl-2-nitrosopropane (4) was present during the reaction, a nitroxide with hyperfine splitting consistent with structure **1** was observed. The same nitroxide was formed when the chloramine was treated *in vacuo* with

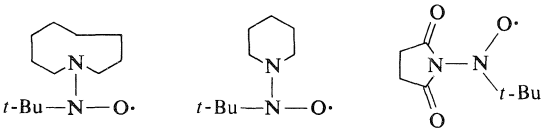

1 **2** **3**

metallic silver in the presence of the nitroso compound. In a similar manner the radical **2** was identified in reaction of *N*-chloropiperidine with silver.

We conclude that silver induces homolytic fission of the chloramines as in eq. 1. A comparable reaction of *N*-chlorosuccinimide and *N*-bromosuccinimide takes place and the succinimidyl radical was trapped in the *N*-chloro case as nitroxide **3**. However preparative runs

[1] $$R_2NCl + Ag(0) \rightarrow R_2N\cdot + AgCl$$

with *N*-bromosuccinimide showed that the succinamidyl radical was rapidly reduced further to the anion (eq. 2). This provides a convenient

[2] 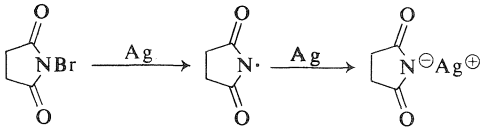

high yield route to the silver salt of succinimide. The stability of the anion must contribute markedly to the ease of reduction of the imidyl radical. A comparable reduction of the medium ring amidyl radicals such as **4** probably accounts for the puzzlingly high yield of parent lactam

[1]NRCC No. 12976.

TABLE 1. Summary of e.p.r. spectra

System	Solvent	Coupling constants (G) a_N	$a_{N'}$	a_H*	$a_{N''}$†
N-Chloroazacyclononane	Dioxane–H_2O	16.1	1.24	0.78(4)	16.4
N-Chloroazacyclononane	2-MTHF–D_2O	15.4	1.26	0.56(4)	
N-Chloropiperidine	Dioxane–H_2O(80:20)	18.8	0.88	0.88(2)	16.2
N-Chloropiperidine	2-MTHF–H_2O	18.6			15.0
N-Chlorosuccinimide	2-MTHF–D_2O	16.4	1.80		7.7

*Numbers in brackets indicate the number of equivalent protons.
†The coupling constant $a_{N''}$ refers to a second nitrogen-containing radical coexisting with the first.

produced when the corresponding *N*-chlorolactam was treated with silver (5).

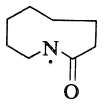

4

Aldimines were shown to be important products arising from cyclic nitrogen-centered radicals (1). These could arise by disproportionation (eq. 3) (6), radical attack

[3] $2RN\dot{-}CH_2R' \rightarrow RN(H)-CH_2R' + RN{=}CHR'$

on chloramine (eq. 4), or hydrogen atom loss from the nitrogen-centered radical (eq. 5).

[4] $X\cdot + RN(Cl)-CH_2R' \rightarrow$

$RN(Cl)-\dot{C}HR' \xrightarrow{Ag(0)} RN{=}CHR' + AgCl$

$RN(Cl)-\dot{C}HR' \rightarrow RN{=}CHR' + Cl\cdot$

[5] $RN\dot{-}CH_2R' \rightarrow RN{=}CHR' + H\cdot$

When *N*-chloroazacyclononane or *N*-chloropiperidine were treated with silver *in vacuo*, vigorous gas evolution was observed. We hence examined the nature of the gas produced when aqueous dioxane, aqueous dioxane-d_8, and dioxane-D_2O were the solvents. Pure hydrogen was produced in all cases. This observation seems to demand that hydrogen atoms are only formed on the silver surface (eq. 5) and that they either combine to give hydrogen gas before leaving the surface or selectively abstract hydrogen from other radicals on the surface (eq. 6).

[6] $RN\dot{-}CH_2R' + H\cdot \rightarrow RN{=}CHR' + H_2$

This may only be a minor reaction of the amine radicals, and it is not known what proportion of the aldimines arise by the routes shown in eqs. 3, 4, and 5.

Electron Paramagnetic Resonance Results

The coupling constants of the various e.p.r. spectra are summarized in Table 1. The spectra from *N*-chloroazacyclononane are consistent with a radical of structure **1**. The smaller coupling constants may be slightly uncertain because these splittings are not fully resolved. The two nitrogen couplings of 16.1 and 1.24 G are reasonable for a structure $\diagdown N\dot{-}NO-\diagup$ as shown by the radicals derived from *N*-chlorosuccinimide by Lagercrantz and Forschult (4*b*) (16.4 and 1.81 G) and from carbazole by Terabe and Konaka (8) (16.77 and 1.37 G). The four equivalent protons also support structure **1** if the radical is rapidly interconverting among various conformations.

Similarly the spectra support radical **2** as the product from *N*-chloropiperidine on the basis of magnitude and number of the coupling constants. The coupling with only two protons shows that the conformational inversion is slow relative to the e.p.r. time scale. The rather large a_N of 18.8 G may arise from such steric effects, as well as from solvent polarity (7).

The second radical found in both the above systems with a coupling constant of 16 G is probably di-*t*-butyl-nitroxide (7).

The *g* values of the radicals derived from *N*-chloroazacyclononane and *N*-chloropiperidine in aqueous dioxane are less by 0.00009 and 0.00032 respectively than that of the di-*t*-butyl-nitroxide in the corresponding solution. These values are within the range usually found for nitroxides.

N-Chlorosuccinimide yields the same spectrum as that obtained by Lagercrantz and Forschult (4*b*) on u.v. irradiation of that compound in chloroform in the presence of 2-methyl-

Can. J. Chem. Downloaded from www.nrcresearchpress.com by 210.87.254.105 on 09/05/12
For personal use only.

2-nitrosopropane (a_N 16.4 and 1.81 G). This points to the presence of radical **3**. The second radical species with $a_N = 7.7$ G and a g value of 0.00098 greater than that of the first was also seen by these authors.

Experimental

The analysis for H_2, HD, and D_2 by g.l.c. was done using a 2 m column packed with alumina containing $MnCl_3$ at −196 °C (9).

The *in vacuo* experiments were done in two-compartment all-glass cells. The solution was separated from the silver by a fritted glass filter and a break seal. The liquid was degassed by three freeze–thaw cycles in high vacuum, and the silver was pumped free of volatile solvents and gases. Both arms were then sealed and the solution added to the silver via the break seal. For the e.p.r. study a 4 mm tube was provided on the solution arm and for the gas analysis a branch, with a standard taper joint and a break seal, was provided on the solution side. The gas samples were prepared by freezing all condensable components in liquid nitrogen. These were then sealed off from the gas-containing compartment.

Electron Spin Resonance Experiments

The dioxane used had been distilled over sodium and stored over sodium wire under nitrogen. It may still have contained traces of peroxides (5). The 2-methyltetrahydrofuran had been purified by drying over lithium aluminum hydride followed by distillation *in vacuo* into a high vacuum storage flask containing pyrene and sodium. It was distilled under high vacuum before use.

N-Chloropiperidine and N-Chloroazacyclononane

The typical experiment involved 1 ml of solvent, 2–3 mg of the dimer of 2-methyl-2-nitrosopropane, and Tollens' silver (1) from 0.75 g of silver nitrate. When D_2O was used as a co-solvent the silver was washed with the organic solvent to remove water prior to evacuation. The quantity of chloramine used was approximately 30 mg of *N*-chloropiperidine or *N*-chloroazacyclononane.

The experiments using *N*-chloroazacyclononane, indolizidine and silver perchlorate were performed in acetonitrile as follows:

To a solution of 5 ml of acetonitrile containing 90 mg of *N*-chloroazacyclononane, 7 mg of the dimer of 2-methyl-2-nitrosopropane and 121 mg of silver perchlorate was added 0.5 ml of acetonitrile containing 12 mg of indolizidine. A 1 ml aliquot was degassed twice and sealed *in vacuo*. The solution gave e.p.r. signals with the same parameters as those obtained from the silver-initiated reactions. Comparable runs without the nitroso compound gave no detectable e.p.r. signal.

N-Bromosuccinimide

A solution of 109 mg of *N*-bromosuccinimide and 3.3 mg of 2-methyl-2-nitrosopropane in 1 ml of acetonitrile was degassed. The deep yellow solution gave no e.p.r. signal. When mixed with Tollens' silver from 0.5 g of silver nitrate *in vacuo*, vigorous gas evolution resulted and the yellow color disappeared. Again no e.p.r. signal was detected.

N-Chlorosuccinimide

A solution of 51 mg of *N*-chlorosuccinimide (m.p 149°) and 3 mg of the dimer of 2-methyl-2-nitrosopropane was degassed and added *in vacuo* to approximately 300 mg of fresh Tollens' silver. The e.p.r. spectrum of a filtered solution is reported in Table 1.

Nature and Source of the Gas in Ag^0 Reactions

(*a*) A mixture of 189 mg of *N*-chloroazacyclononane in 1 ml of dioxane and 0.2 ml of deuterium oxide was degassed three times *in vacuo*, then added *in vacuo* to Tollens' silver from 0.7 g of silver nitrate. The gas evolved during 96 h was analyzed by g.l.c. and shown to be pure hydrogen free from HD or D_2.

(*b*) A repetition of (*a*) using 1 ml of dioxane-d_8 and 0.2 ml of water as solvent also gave pure hydrogen.

(*c*) Fresh Tollens' silver from 1 g of silver nitrate was added *in vacuo* to a degassed solution of 139 mg of *N*-chloropiperidine in 1 ml of dioxane and 0.1 ml of deuterium oxide. Vigorous gas evolution ensued. G.l.c. analysis showed this to be pure hydrogen.

(*d*) An identical experiment to (*c*) using dioxane-d_8 and deuterium oxide as solvents and dioxane-washed silver again gave pure hydrogen.

N-Bromosuccinimide With Tollens' Silver

A solution of 1.25 g of *N*-bromosuccinimide in 20 ml of acetonitrile was purged with nitrogen. After addition of freshly prepared Tollens' silver from 2.49 g of silver nitrate the mixture was stirred under nitrogen at 24 °C. The extent of reaction was 48% in 0.5 h, 63% in 1 h and 73.5% in 2 h. Silver from 1 g of silver nitrate was added to speed the reaction to completion. The mixture was filtered from solids (A) then the filtrate taken to small volume under reduced pressure. The residue was suspended in methylene chloride, then filtered. The soluble portion was fairly pure succinimide (60 mg). The insoluble white granular solid remaining (513 mg) proved to be the silver salt of succinimide. When suspended in dilute hydrochloric acid it gave silver chloride and succinimide.

The original solids (A) consisted of more silver salt of succinimide, unreacted silver, and silver bromide. This was treated with nitric acid to dissolve the silver and silver salt. The well-washed residue of silver bromide weighed 1.15 g. The calculated amount for 1 mol equiv from 18.5 ml of the original solution is 1.19 g.

1. O. E. Edwards, D. Vocelle, and J. W. ApSimon. Can. J. Chem. **50**, 1167 (1972).
2. V. Boido and O. E. Edwards. Can. J. Chem. **49**, 2664 (1971).
3. P. G. Gassman. Acc. Chem. Res. **3**, 26 (1970).
4. (*a*) M. J. Perkins, P. Ward, and A. Horsfield. J. Chem. Soc. B, 395 (1970); (*b*) C. Lagercrantz and S. Forschult. Acta Chem. Scand. **23**, 708 (1969); (*c*) A. Mackor, Th. J. W. Wajer, and Th. J. de Boer. Tetrahedron, **24**, 1623 (1968).
5. O. E. Edwards, J. M. Paton, M. H. Benn, R. E. Mitchell, C. Watanatada, and K. N. Vohra. Can. J. Chem. **49**, 1648 (1971).
6. D. Mackay and W. A. Waters. J. Chem. Soc. C, 813 (1966); B. G. Gowenlock and D. R. Snelling. Adv. Chem. Ser. **36**, 150 (1962); M. A. Ratcliffe and J. K. Kochi. J. Org. Chem. **37**, 3268 (1972).
7. S. Forschult, C. Lagercrantz, and K. Torssell. Acta Chem. Scand. **23**, 522 (1969).
8. S. Terabe and R. Konaka. J. Am. Chem. Soc. **91**, 5655 (1969).
9. I. Yasumori and S. Ohno. Bull. Chem. Soc. Jap. **39**, 1302 (1966).

Can. J. Chem. Downloaded from www.nrcresearchpress.com by 210.87.254.105 on 09/05/12
For personal use only.

Can. J. Chem. Downloaded from www.nrcresearchpress.com by 210.87.254.42 on 09/05/12
For personal use only.

The Synthesis of Trisubstituted Enol Ethers and of Methyl Ketones from Ketones

GILLES CARON AND JEAN LESSARD

Département de chimie, Université de Sherbrooke, Sherbrooke, Québec

Received November 22, 1972

A reliable method for the synthesis of trisubstituted enol ethers (and of the corresponding methyl ketones) is described involving the condensation of the α-lithiated 2-methoxypropionic acid salt with a ketone to give a β-hydroxy acid, the cyclization to a β-lactone which is then decarboxylated (and mild acid hydrolysis of the enol ether).

On décrit une méthode efficace pour la synthèse d'éthers énoliques trisubstitués (et des méthyl cétones correspondantes). Les étapes de cette synthèse sont: la condensation du dérivé α-lithien du sel de l'acide méthoxy-2 propionique avec une cétone pour donner un β-hydroxy acide, sa cyclisation en β-lactone qui est ensuite décarboxylée (et l'hydrolyse acide de l'éther énolique dans des conditions douces).

Can. J. Chem., **51**, 981 (1973)

The Wittig reaction of α-methoxyethyl triphenyl phosphorane with ketones has been reported (1). However the trisubstituted enol ethers were not isolated as such but the crude reaction mixture was hydrolyzed to give the corresponding methyl ketones in low to moderate yields in the presence of the starting ketone. Furthermore, this Wittig reaction was not successful with cyclopentanone.

We wish to report a reliable and convenient method for the synthesis of trisubstituted enol ethers (and of the corresponding methyl ketones) from ketones. The reaction sequence of this synthesis is illustrated in Scheme 1. Although each step is well documented (2), the use of an α-lithio-α-alkoxycarboxylate is quite novel, and the usefulness and convenience of the method do make it of real interest to the synthetic chemist.[1] The yields of the different products[2] from four representative ketones are recorded in Table 1.

The 2-methoxypropionic acid (**1**) was prepared as described by Petrov *et al.* (3). The same experimental conditions as those described by Adam *et al.* (2) were used for the generation of the α-lithiocarboxylate salt **2**, its condensation with ketones as well as for the cyclization of the β-hydroxy acids **3** into the β-lactones **4**. The decarboxylation of the β-lactones **4** was carried out in the presence of solid anhydrous potassium carbonate (5–10% relative to the β-lactone) to prevent the isomerization of the trisubstituted enol ethers **5** into their monosubstituted isomers **7**.[3] The methyl ketones **6** were obtained by stirring, at room temperature, an ethereal solution of the enol ethers **5** with 0.2 *N* aqueous HCl (10–60 h) or more conveniently by saturating the ethereal solution with 70% aqueous $HClO_4$ (10 min) (4).

The synthesis of 2-methoxy-3-*n*-propyl-2-hexene (**5**, $R_1 = R_2 = n\text{-}C_3H_7$) is representative of the standard experimental procedure. Lithium α-lithio-2-methoxypropionate (**2**) was

[1]To our knowledge, this is the first reliable method for the synthesis of pure trisubstituted enol ethers from ketones.

[2]All compounds had spectral (i.r., n.m.r.) data compatible with their structures. All new compounds gave satisfactory compositional analyses and/or mass spectroscopic data. Known crystalline derivatives (semicarbazones or oximes) of the methyl ketones were prepared and their melting points compared with those of the literature.

[3]This isomerization occured quite extensively (40–70%) without the presence of base even with very pure samples of β-lactones. The less substituted isomers are more stable and the results of the equilibration studies will be reported later.

5 7

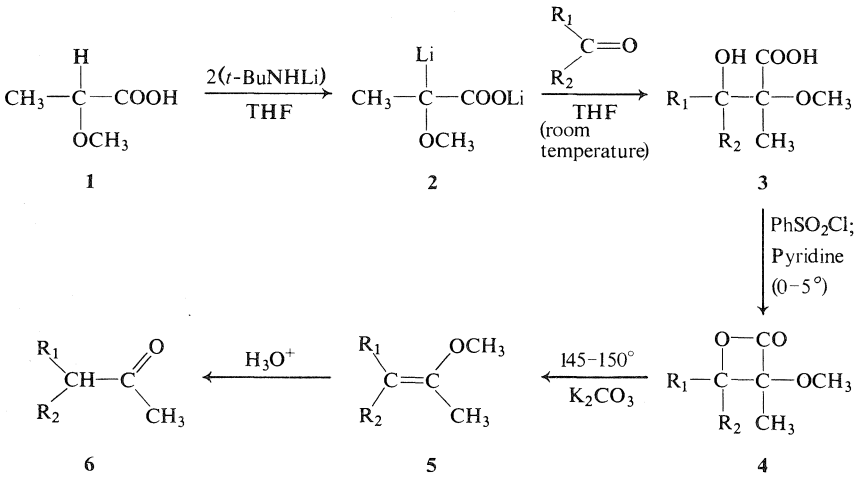

1 2 3 4 5 6

SCHEME 1

TABLE 1. The preparation of trisubstituted enol ethers **5** and methyl ketones **6** via the formation of β-hydroxy acids **4** and β-lactones **5** from ketones

	3		4		5	6
Ketone	Yield* (%)	M.p. (°C)	Yield* (%)	M.p. (°C)	Yield* (%)	Yield (%)
Cyclohexanone	64† 61‡	89.5–90.5	82	93.5–94	quant.	96§
Cyclopentanone	59† 42‡	123–123.5	83		quant.	95§
4-Heptanone	67‡		77		quant.	88§
2-Octanone	85† 69‡		91‖		quant.‖	96*

*Of isolated pure product.
†Based on the ketone (mole ratio of acid to ketone of 5).
‡Based on the acid (mole ratio of acid to ketone of 0.20).
§By vapor phase chromatography (compound **6** was the sole compound of the ethereal solution).
‖Approximately 1 :1 *cis*/*trans* mixture by n.m.r.

prepared by adding, under a nitrogen stream, 5.20 g (50 mmol) of 2-methoxypropionic acid (**1**) to a magnetically stirred ice-cold (freshly prepared (2)) solution of *t*-butylamide (100 mmol) in 100 ml tetrahydrofuran, then stirring at *ca.* 25° for 1 h. To this solution was added dropwise at *ca.* 25° 28.55 g (250 mmol) of 4-heptanone in 60 ml tetrahydrofuran and stirring was continued for 20 h. The usual working-up (2) gave 7.23 g (67%) of 3-hydroxy-2-methoxy-2-methyl-3-*n*-propylhexanoic acid (**3**, $R_1 = R_2 = n\text{-}C_3H_7$), 100–110° (0.8–1.0 mm).[4]

[4]The analytical sample was obtained by microdistillation.

Anal. Calcd. for $C_{11}H_{22}O_4$: C, 60.52; H, 10.16. Found: C, 60.46; H, 10.38.

To an ice-cold solution of 5.30 g (24 mmol) of the β-hydroxy acid in 120 ml anhydrous pyridine, 8.83 g (50 mmol) of benzenesulfonyl chloride was added. The mixture was shaken and placed in the refrigerator for 12 h. The usual working-up (2) gave 3.70 g (77%) of 3-methoxy-3-methyl-4,4-di-*n*-propyloxetan-2-one (**4**, $R_1 = R_2 = n\text{-}C_3H_7$), 70–72° (0.4 mm).[4]

Anal. Calcd. for $C_{11}H_{20}O_3$: C, 65.97; H, 10.07. Found: C, 65.70; H, 10.33.

A mixture of 754 mg (3.76 mmol) of the β-lactone and 49 mg of K_2CO_3 was heated at 145° at atmospheric pressure for 55 min to yield

Can. J. Chem. Downloaded from www.nrcresearchpress.com by 210.87.254.42 on 09/05/12
For personal use only.

589 mg (100%) of 2-methoxy-3-*n*-propyl-2-hexene, 58–60° (20–25 mm).[4]

Anal. Calcd. for $C_{10}H_{20}O$: C, 76.86; H, 12.90. Found: C, 77.17; H, 13.03.

The condensation of the α-lithiocarboxylate salt **2** with a 17-ketosteroid, androst-5-en-3β-ol-17-one tetrahydropyranyl ether, gave none of the expected β-hydroxy acid and 93% of the starting ketone was recovered. Thus it appears that steric hindrance of the ketone is an important factor in this reaction, a fact that can be an advantage or a limitation.

Further studies are in progress to explore the possibility of a general synthesis of alkyl ketones from ketones and to extend this reaction to aldehydes.

We thank the National Research Council of Canada and "le Ministère de l'Education du Québec" for financial support.

1. D. R. COULSON. Tetrahedron Lett. 3323 (1964).
2. W. ADAM, J. BAEZA. and J. C. LIU. J. Am. Chem. Soc. **94**, 2000 (1972).
3. A. A. PETROV, B. V. GANTSEVA, and O. A. KISELEVA. Zhur. Obscheĭ Khim. **23**, 737 (1954).
4. S. G. LEVINE. J. Am. Chem. Soc. **80**, 6150 (1958).

Can. J. Chem. Downloaded from www.nrcresearchpress.com by 210.87.254.42 on 09/05/12
For personal use only.

Can. J. Chem. Downloaded from www.nrcresearchpress.com by 210.87.254.5 on 09/05/12
For personal use only.

Canadian Journal of Chemistry

Published by
THE NATIONAL RESEARCH COUNCIL OF CANADA

Journal canadien de chimie

Publié par
LE CONSEIL NATIONAL DE RECHERCHES DU CANADA

Volume 51 Number 7 April 1, 1973

Volume 51 numéro 7 1 avril 1973

A Low Temperature Infrared Study on the Association of Thiols with Pyridine and Triethylamine

R. BICCA DE ALENCASTRO[1] AND C. SANDORFY

Département de Chimie, Université de Montréal, Montréal, Québec

Received September 20, 1972

The infrared spectra of solutions containing propane-1-thiol or benzenethiol as proton donors, and pyridine or triethylamine as proton acceptors were measured down to about −100 °C. The dependence of hydrogen bond formation on concentration and temperature was studied at the fundamental and overtone region of the S—H stretching vibration. The predominant species is found to be a 1:1 S—H---N type complex. In addition, evidence was found for the existence of more highly associated species at low temperatures. Thiol–thiol S—H---π type hydrogen bonds are also present in the case of benzenethiol–pyridine mixtures.

Les spectres infrarouges de solutions contenant du propanethiol-1 ou du benzènethiol comme donneurs de proton et de la pyridine ou de la triethylamine comme accepteurs de proton ont été mesurés à des températures allant de 20 °C à −100 °C. Les effets de la concentration en base d'une part et de la température d'autre part sur la formation de la liaison hydrogène, ont été étudiés aux niveaux de la fondamentale et de la première harmonique de la vibration de valence du groupement S—H. L'espèce prédominante est un complexe 1:1 de type S—H---N. D'autre part, l'existence d'espèces plus associées a été mise en évidence aux températures les plus basses. Des liaisons hydrogène de type S—H---π auto-associées ont été trouvées dans les mélanges benzènethiol–pyridine.

Can. J. Chem., 51, 985 (1973)

Introduction

In a previous publication (1) we studied the self-association of both aliphatic and aromatic thiols in solution at low temperatures. Although the S—H---S hydrogen bonds formed are relatively weak, the existence of two or three differently associated species could be ascertained in most cases. As a second step in the study of the hydrogen bonds formed by S—H groups, we have examined some systems in which stronger bonds are expected. In the present paper we deal with S—H---N type bonds.

Solutions of mercaptans in organic nitrogen bases are known to undergo both self-association and association with the proton accepting solvent molecules. As early as in 1940, Gordy and Stanford (2) studied the variation of the infrared spectrum, in the region of the S—H stretching vibration, when mercaptans are dissolved in solvents such as pyridine, aniline, or benzylamine, and attributed these changes to association of the S—H---N type. Bulanin, Denisov, and Pushkina (3) observed association between propane-1-thiol and triethylamine. N.m.r. and u.v. studies (4, 5) confirmed this, and suggested that these complexes were of the 1:1 type.

We have studied the association of propane-1-thiol and benzenethiol with pyridine and triethylamine as proton acceptors over a wide temperature range, and have measured the fundamentals as well as the overtones of the S—H stretching vibration. The solvent used was

[1]Brazil–Canada exchange fellow. On leave of absence from Instituto de Química, Universidade Federal de Rio de Janeiro, Rio de Janeiro, Brazil.

Can. J. Chem. Downloaded from www.nrcresearchpress.com by 210.87.254.5 on 09/05/12
For personal use only.

CCl_3F (Freon 11) which enabled us to work at temperatures down to -100 °C. We hoped to be able to follow the changing pattern of association with temperature, and to identify the bands due to the complexes formed between the thiols and the bases.

Experimental

The fundamentals were measured on a Perkin–Elmer Model 621 spectrometer and the overtones on a Cary 17 instrument. In the fundamental region, we used a 0.9 mm cell with silver bromide windows for low temperatures, and commercial 1.0 and 0.1 mm sodium chloride cells for room temperature spectra. A 1 cm quartz cell was used for the overtone region. More details of the experimental techniques are given elsewhere (6). Temperatures were measured with a copper–constantan thermocouple.

CCl_3F (Freon 11) obtained from the E.I. Dupont de Nemours of Canada Co., was distilled and kept over phosphorus pentoxide. Spectrograde quality carbon tetrachloride from Anachemia Chems. Ltd., Montreal, was dried on molecular sieves of the type 4A.

The mercaptans were the same as those used in our previous work (1). Pyridine, a spectroquality reagent from the Matheson, Coleman, and Bell Co., was treated with KOH pellets for at least 24 h before distillation. Triethylamine, from the same company, was dried over $CaSO_4$, and distilled. None of the i.r. spectra of these bases showed water absorption.

All solutions were prepared gravimetrically in a dry-box filled with nitrogen to avoid oxidation or moisture absorption. The concentrations were *not* corrected for solvent contraction since intensities measured at different temperatures were not compared. The correction should not exceed 15% at -100 °C in any case. All curves were corrected for solvent absorption. Figures 1 and 4 show the spectrum of the thiol in an inert solvent, the spectrum of the base in the same solvent, the spectrum of the thiol–base mixture, and the spectrum of the mixture, obtained by subtracting the absorption of the base. In the other figures only the first and the last are shown.

The solutions were used immediately after preparation. After 24 h, ternary solutions of mercaptans and triethylamine in CCl_3F, and solutions of mercaptans in triethylamine give a white crystalline precipitate. This solid shows (in Nujol) a band between 2650 and 2700 cm^{-1}, characteristic of the NH^+ absorption (for a discussion on quaternary ammonium salts see ref. 7). After being in contact with the silver bromide windows of the low temperature cells for several hours, the pyridine solutions gave a white solid deposit, soluble in acetone, which is probably a silver–pyridine complex. This deposit, however, showed no appreciable absorption in our spectral region.

Results and Discussion

Figures 1 and 2 show the effect of temperature and pyridine concentration on the spectrum of the complex between propane-1-thiol and pyridine. The maximum of the S—H---N band is near 2520 cm^{-1}, at room temperature, and at 2485 cm^{-1}, at -101 °C. The increased half-width seems to indicate that this band is actually due to more than one species. The band center must receive most of its intensity from the 1:1 complex, that is, from S—H---N type bonds. On the high frequency side, both free and S—H ---S bonds can contribute to the intensity. On

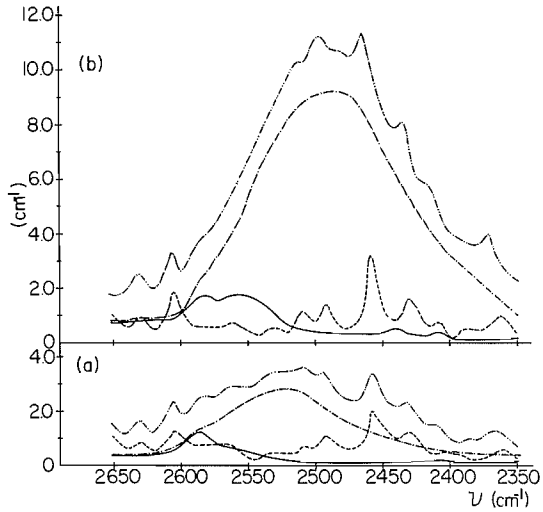

FIG. 1. The infrared spectrum (2350–2650 cm^{-1}) of (—), a 0.98 *M* solution of propane-1-thiol in CCl_3F; (---), a 2.86 *M* solution of pyridine in CCl_3F; (-·-·-), a mixture of 0.98 *M* propane-1-thiol and 2.86 *M* pyridine in CCl_3F; (-··-), a mixture of 0.98 *M* propane-1-thiol and 2.86 *M* pyridine in CCl_3F with the absorption due to pyridine subtracted. (*a*) 20 °C; (*b*) -101 °C. Vertical axis: $1/l \log I_0/I$ in cm^{-1} units.

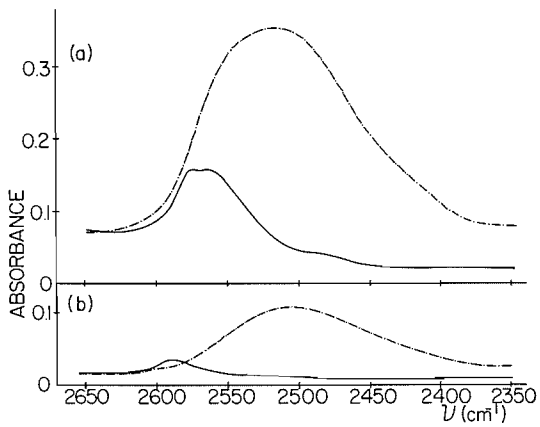

FIG. 2. The infrared spectrum (2350–2650 cm^{-1}) of (*a*) 5.92 *M*; (*b*) 1.43 *M* solutions of propane-1-thiol (—) in CCl_4 and (-··-) in pyridine, at 20 °C with the absorption due to pyridine subtracted.

Can. J. Chem. Downloaded from www.nrcresearchpress.com by 210.87.254.5 on 09/05/12
For personal use only.

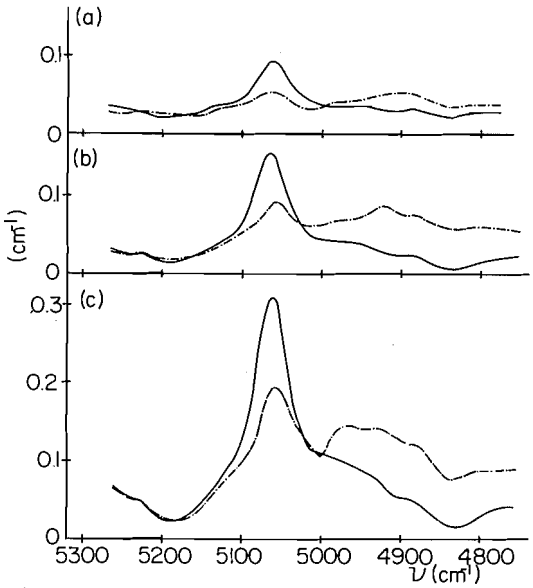

FIG. 3. The infrared spectrum (4750–5250 cm^{-1}) of (*a*) 1.43 *M*; (*b*) 2.75 *M*; (*c*) 5.92 *M* solutions of propane-1-thiol (—) in CCl_4 and (- - -) in pyridine, at 20 °C with the absorption due to pyridine subtracted. Vertical axis: $1/l \log I_0/I$ in cm^{-1} units.

the low frequency side, S—H---N type bonds of more highly associated species of the type S—H---S—H---N come in. Of course, the S—H---S group of the latter may contribute to the intensity on the high frequency side. The breadth and the intensity increase of this band on its low frequency side as the temperature decreases, can be taken as an indication of the presence of such more highly associated complexes.

Figures 3 and 4 show that, at the first overtone, the free band is present up to a thiol–pyridine ratio of 1:7, (Fig. 3*a*) but is absent at higher pyridine concentrations. In all cases, however, the presence of pyridine decreases the intensity of the free band showing that S—H---N type association occurs. At lower temperatures and higher concentrations a broad band appears near 4900 cm^{-1}. This must be the S—H---N band of the 1:1 complex. As we are limited by the crystallization temperature of pyridine and by the stronger bands near 4800 cm^{-1} of pyridine (still strong enough in pyridine-d_5 to prevent concentration or temperature studies) we cannot observe the band of the more associated species at the overtone level. Studies in solution of inert solvents at lower temperatures are not possible because we are dealing with very weak bands.

Figures 5 and 6 show the results we obtained for the benzenethiol–pyridine complex. This is known to be a 1:1 complex at room temperature (4). The spectrum shows, at 20 °C, a broad and rather symmetrical band centered near 2430 cm^{-1}. This spectrum yields two interesting results. First, the band is very broad. Secondly, even with a 3:1 excess of pyridine to thiol the band near 2572 cm^{-1} still persists. The latter band is assigned to thiol–thiol S—H---π type hydrogen bonds. The free band is weaker and cannot be seen in the spectrum. However, it can be observed for similar concentrations at the overtone (see below). At low temperature (−101 °C) the broad band is asymmetrical on the lower frequency side. This is again probably

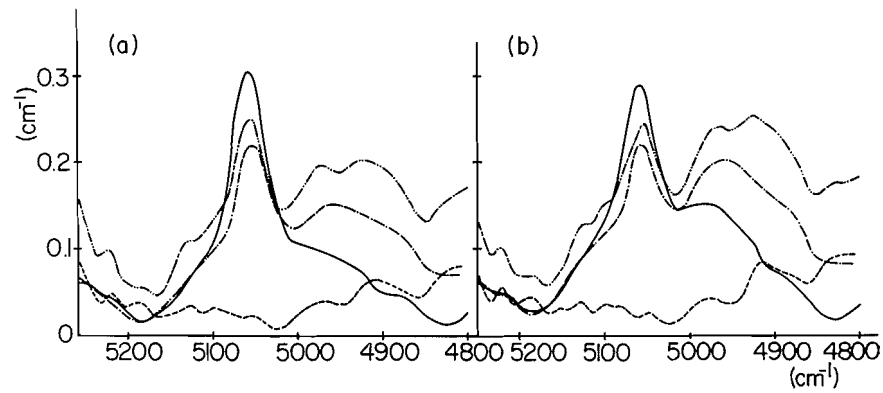

FIG. 4. The infrared spectrum (4800–5250 cm^{-1}) of (—), a 5.74 *M* solution of propane-1-thiol in CCl_3F; (---), a 5.54 *M* solution of pyridine in CCl_3F; (-·-·-), a mixture of 5.74 *M* propane-1-thiol and 5.54 *M* pyridine; (-·-), a mixture of 5.74 *M* propane-1-thiol and 5.54 *M* pyridine with the absorption due to pyridine subtracted. (*a*) 20 °C; (*b*) −20 °C. Vertical axis: $1/l \log I_0/I$ in cm^{-1} units.

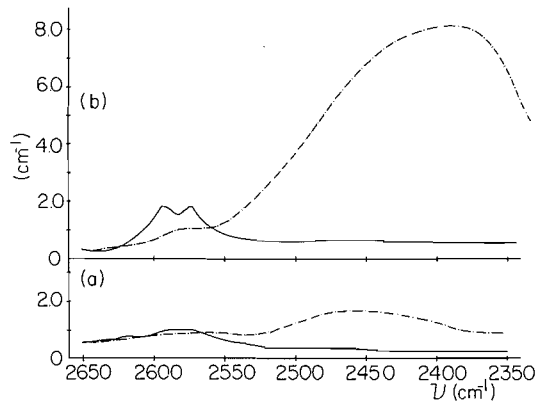

FIG. 5. The infrared spectrum (2350–2650 cm^{-1}) of (—), a 0.27 *M* solution of benzenethiol in CCl_3F; (···), a mixture of 0.27 *M* benzenethiol and 0.92 *M* pyridine in CCl_3F. (*a*) 20 °C; (*b*) −101 °C. The absorption due to pyridine is subtracted. Vertical axis: $1/I \log I_0/I$ in cm^{-1} units.

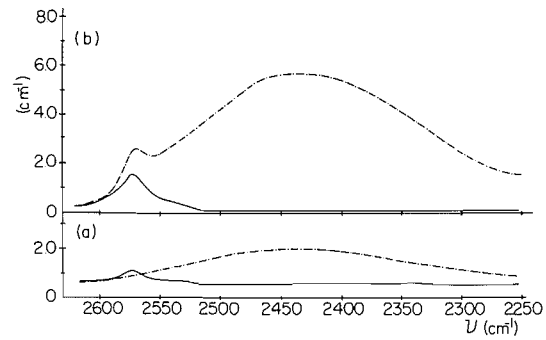

FIG. 6. The infrared spectrum (2250–2630 cm^{-1}) of (*a*) 0.68 *M* and (*b*) 2.54 *M* solutions of benzenethiol (—) in CCl_3F and (---) in pyridine, at 20 °C with the absorption due to pyridine subtracted. Vertical axis: $1/I \log I_0/I$ in cm^{-1} units divided by ten.

due to a more associated species. Another interesting observation is the breaking of some of the self-associated S—H---π bands at low temperatures. At the first overtone level (Fig. 7) the spectra are less conclusive due to the severe overlap with the much stronger bands of pyridine near 4800 cm^{-1}. Nevertheless some interesting remarks can be made. The "free" band loses intensity when the concentration of pyridine is raised and is shifted toward lower frequencies. A band, partially overlapped by pyridine absorption, can be seen at lower frequencies and should be ascribed to the S—H---N vibration of the 1:1 complex. As we showed in our previous work (1) the "free" band of benzenethiol is due, at the overtone level, to the actual free band and to the self-associated S—H---π type band. This is further confirmed in the present work by concentration studies at the overtone level (compare (*a*), (*b*), and (*c*) of Fig. 7). In the presence of pyridine we expect that the S—H---N complexes are formed by preferentially using the free S—H groups still present, rather than breaking existing weaker complexes. In a dilute solution of an inert solvent, the benzenethiol free band is expected to predominate over the S—H---π type band, but the reverse is true if the solvent is pyridine. Increasing the concentration of benzenethiol should favor the S—H---π bonds in both solvents. This is translated by two effects in the spectra of Fig. 7. First, the apparent maximum of the overlapping free S—H and S—H---π bands is at higher frequencies when pyridine is absent. Secondly, the difference between these two frequencies is greater for dilute solutions of benzenethiol. In addition, the S—H---π type band is seen to persist for similar concentrations (compare Figs. 6(*b*) and 7(*b*)) at the fundamentals. We therefore think that the band which remains at higher pyridine concentrations, near 5050 cm^{-1}, is not a free S—H band but the remaining S—H---π band of the self-associated benzenethiol.

The spectra obtained with the stronger base triethylamine are quite similar (Figs. 8 and 9). At the fundamentals the bands are again very broad and their maxima are, as expected, at lower frequencies than in the case of the pyridine complexes. As triethylamine has relatively strong bands in this part of the spectrum we had to use dilute solutions of propane-1-thiol and triethylamine in CCl_3F. The S—H---N band at room temperature is not well defined at these concentrations (it is located at 2420 cm^{-1} in a 5.72 *M* solution of propane-1-thiol in triethylamine, at 20 °C). However, it can be readily seen at lower temperatures. Its maximum is at 2360 cm^{-1}, at −101 °C, and it is clearly asymmetrical, indicating that at lower temperatures, as in the case of pyridine complexes, some more associated complex is also present. On the high frequency side of the 2360 cm^{-1} band, which corresponds to the S—H---S region, some increase of intensity is observed also. Since this spectrum is obtained by subtraction, this is somewhat doubtful (a strong band of triethylamine exists in this region). However, if this

Can. J. Chem. Downloaded from www.nrcresearchpress.com by 210.87.254.5 on 09/05/12
For personal use only.

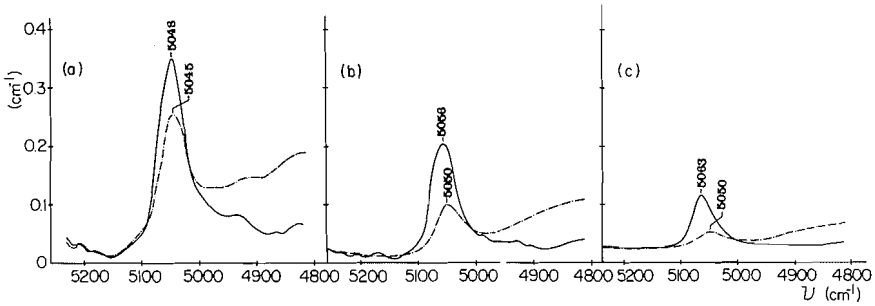

FIG. 7. The infrared spectrum (4800–5250 cm^{-1}) of (*a*) 5.55 *M*; (*b*) 2.77 *M*; and (*c*) 0.99 *M* solutions of benzenethiol (—) in CCl_4 and (---) in pyridine, at 20 °C with the absorption due to pyridine subtracted. Vertical axis: $1/l \log I_0/I$ in cm^{-1} units.

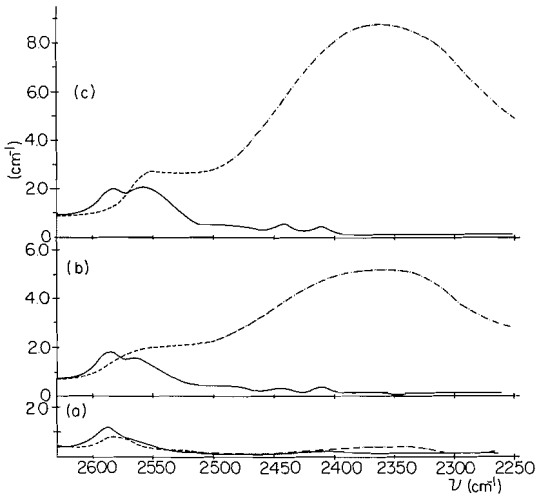

FIG. 8. The infrared spectrum (2250–2630 cm^{-1}) of (—), a 0.94 *M* solution of propane-1-thiol in CCl_3F, and (---), a mixture of 0.94 *M* propane-1-thiol and 0.91 *M* triethylamine, in CCl_3F. (*a*) 20 °C; (*b*) −73 °C; (*c*) −101 °C. (---) region of comparatively strong bands of triethylamine. The absorption due to triethylamine is subtracted. Vertical axis: $1/l \log I_0/I$ in cm^{-1} units.

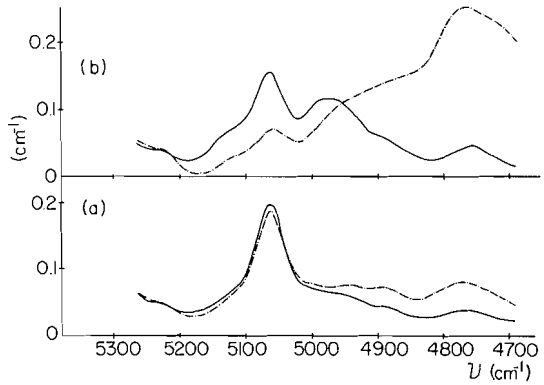

FIG. 9. The infrared spectrum (4700–5250 cm^{-1}) of a 3.23 *M* solution of propane-1-thiol (—) in CCl_3F and (---) in triethylamine. (*a*) 20 °C; (*b*) −98 °C. The absorption due to triethylamine is subtracted. Vertical axis: $1/l \log I_0/I$ in cm^{-1} units.

band really exists it would confirm the presence of a higher complex of the S—H---S—H---N type at lower temperatures. At the overtone (Fig. 9) the maximum is near 2480 cm^{-1} at −98 °C. This is probably due to the S—H---N type association of the 1:1 complex. Some S—H---S absorption remains and again we cannot say whether it is due to the remaining self-associated S—H---S bond, to some more associated S—H---N species, or to both.

Conclusions

The main associated species in solutions containing propane-1-thiol or benzenethiol as proton donors, and pyridine or triethylamine as proton acceptors, is a 1:1 complex with a hydrogen bond of the S—H---N type. The related band in the spectrum appears at distinctly lower frequencies than the S—H---S bands. At low temperatures we find evidence for the formation of a more highly associated species of the S—H---S—N type. The overtone of the 1:1 S—H---N complex has been identified.

Free S—H bands persist in these solutions at donor–acceptor ratios lower than 1:3. S—H---π type hydrogen bonds of the self-associated thiol are found for benzenethiol–pyridine mixtures even in the presence of a large excess of pyridine.

We would like to express our thanks to the National Research Council of Canada for financial help. One of us (RBA) would like also to express his gratitude to the National Research Council of Canada and the Conselho Nacional de Pesquisas, Rio de Janeiro, Brazil, for financial assistance under the Brazil–Canada Program for Scientific

Can. J. Chem. Downloaded from www.nrcresearchpress.com by 210.87.254.5 on 09/05/12
For personal use only.

Exchange, and to the Instituto de Química da Universidade Federal do Rio de Janeiro, Rio de Janeiro, Brazil, for a special leave of absence.

1. R. BICCA DE ALENCASTRO and C. SANDORFY. Can. J. Chem. **50**, 3594 (1972).
2. W. GORDY and S. C. STANFORD. J. Am. Chem. Soc. **62**, 497 (1940).
3. M. O. BULANIN, G. S. DENISOV, and R. A. PUSHKINA. Opt. and Spectrosc. **6** (6), 491 (1959).
4. R. MATHUR, E. D. BECKER, R. B. BRADLEY, and N. C. LI. J. Phys. Chem. **67**, 2190 (1963).
5. S. SINGH, A. S. N. MURTHY, and C. N. R. RAO. Trans. Faraday Soc. **62**, 1056 (1966).
6. M. ASSELIN and C. SANDORFY. J. Mol. Struct. **8**, 145 (1971).
7. L. J. BELLAMY. The infrared spectra of complex molecules. 2nd ed. Methuen and Co., Ltd. London. 1958. p. 259.

Can. J. Chem. Downloaded from www.nrcresearchpress.com by 210.87.254.5 on 09/05/12
For personal use only.

Charge Distributions and Chemical Effects. III.[1] A Comparison with PCILO and CNDO/2 Calculations

S. FLISZÁR AND J. SYGUSCH

Département de Chimie, Université de Montréal, Montréal, Québec

Received July 14, 1972

The PCILO charge distributions of a number of alkanes are in excellent agreement with charge distributions derived on the assumption that the inductive effects can be described in a Taft-like manner. This agreement with "quantitative chemical intuition" stresses the strong chemical character of the PCILO method. The CNDO/2 results are only in qualitative agreement with "chemical expectancy" and suffer apparently from the same difficulties as PCILO used with zero C—C and C—H polarities.

Pour une série d'alcanes, les distributions de charges calculées par la méthode PCILO sont en excellent accord avec celles dérivées de l'hypothèse que les effets inductifs puissent être décrits à la manière de Taft. Cet accord avec l'"intuition chimique quantitative" met en relief le fort caractère chimique de PCILO. Les résultats CNDO/2 ne sont qu'en accord qualitatif avec l'"intuition chimique" et connaissent les mêmes difficultés que PCILO, lorsque cette dernière méthode est utilisée avec des polarités C—C et C—H nulles.

Can. J. Chem., **51**, 991 (1973)

Can. J. Chem. Downloaded from www.nrcresearchpress.com by 210.87.254.40 on 09/05/12
For personal use only.

The success of a quantum mechanical description of a molecule is usually evaluated by its ability of reproducing correctly some observable quantity, such as spectroscopic information, rotational barriers, conformations, etc. However, different quantum mechanical approaches though each one may be "successful" in its own right, are known to generate quite different information on charge distributions; quantities which are not, at present, subject to direct control. This is disturbing if one tends to consider molecular wave functions, or at least their densities, as part of the description of the molecular reality.

In this situation, one is thus restricted to express satisfaction with the fact that the different methods of calculation usually reproduce the same *trends* in charge distributions.[2] Although such an attitude is not free from difficulties, it may be justified, at least in part, on the grounds that the trends predicted by a variety of theoretical methods seem intuitively correct, *i.e.*, that they often agree with what one would expect from chemical evidence. In other words, theoretical trends are accepted when they make sense with the vague intuition derived from experimental facts.

The difficulty, arising from the fact that charge distributions are not measured, is that the "chemical intuition" had not been formulated in a sufficiently quantitative manner. Recently, however, charge distributions in simple hydrocarbons have been calculated on purely chemical grounds (2, 3). The object of the present study is a comparison of these charge distributions, based only on "chemical expectation", with those calculated by the PCILO ("Perturbative Configuration Interaction using Localized Orbitals" (4)) method and to discuss some aspects regarding the internal consistency of both these methods as far as electron populations are concerned. The interest in this bond orbital perturbation theory resides in its computational suitability for the conformational study of large molecules (5–7).

The "Chemical" Population Analysis

This calculation rests on the assumption[3] that the electron-withdrawing or -releasing ability of

[1]For parts I and II, see refs. 2 and 3.

[2]An interesting example is given in ref. 1

[3]The nature of the chemical information used in setting up this approach can best be described by the following examples. If it is assumed that the ethyl group is a better electron-donor than the methyl group, any H atom in ethane is expected to be electron-richer than a methane H atom. For similar reasons, the tertiary H atom in isobutane is expected to carry more electrons than an ethane H atom, because the tert-butyl group is a better electron-donor than the ethyl group. In a similar way, neopentane can be considered as a tert-butyl group attached to a methyl group. Since the tert-butyl group is, in common experience, a better electron-donor than methyl, a net positive charge should be carried by the

groups (inductive effects) can be evaluated and described by numbers in a Taft like manner (eqs. 1 and 2) and on eq. 3 which, crudely, expresses the idea of charge alternation: "a positive site is best favored when embedded in a negative surrounding, and conversely" (2, 3, 8). Equation 4 expresses the fact that the sum of the net atomic charges Q over the whole molecule is 0.

$$[1] \qquad Q_H = a\sigma^* + b$$

$$[2] \qquad Q(CH_3) = -a'\sigma^*$$

$$[3] \qquad Q_i = \sum(\alpha_j Q_j + \beta_j) \; (j \text{ adjacent to } i)$$

$$[4] \qquad \sum Q = 0$$

The request for the *simultaneous* validity of eqs. 1–4, which are individually verified by a variety of MO calculations (2), generates in a first approximation the charge distributions indicated in ref. 3. This approximation utilized the assumption that the parameters in eq. 3 are the same for primary to quaternary atoms. Although these calculated charge distributions were in satisfactory agreement with a variety of quantum-mechanical results, we now wish to remove this restriction, and calculate the charge distributions using only eqs. 1 and 2, inserting the appropriate Taft polar constants (9). For example, (average)Q_{Hprim}(propane) $= -0.115a + b$, with a and b as in Table 1, and $Q_{Cprim} = Q(CH_3) - 3Q_{Hprim}$.

It should be noted that the present calculation affects only the distributions within the CH_3 groups in propane, isobutane, and neopentane, the other results being those of ref. 3. For large n values[4] ($\gtrsim 10$), the difference between the two modes of evaluating the charges on the primary H atoms is small ($\lesssim 2\%$) and could therefore be neglected (3). For small n values, however, the differences between the two alternative solutions is considerable and, thus, useful in the discussion of the results.

TABLE 1. Parameters and net atomic charges, in relative units $Q_C(C_2H_6) = -1.000$

Compound	Charge*
	$a = -a' = 10/3n$
	$b = (n + 1)/3n$
Methane	$Q_C = -4(n + 1)/3n$
Ethane	$Q_C = -1.000$
Propane	$Q_{Cprim} = -(3n + 0.55)/3n$
	$Q_{Csec} = 2(2 - n)/3n$
	$Q_{Hprim} = (n - 0.15)/3n$
	$Q_{Hsec} = (n - 1)/3n$
Isobutane	$Q_{Cprim} = -(3n + 1.25)/3n$
	$Q_{Ctert} = (8 - n)/3n$
	$Q_{Hprim} = (n - 0.25)/3n$
	$Q_{Htert} = (n - 2)/3n$
Neopentane	$Q_{Cprim} = -(n + 0.35)/n$
	$Q_{Cquat} = 4/n$
	$Q_H = (n - 0.65)/3n$

*The usual Taft polar σ^* constants (9) were used *i.e.*, $\sigma^*(n\text{-}C_3H_7) = -0.115$, $\sigma^*(i\text{-}C_4H_9) = -0.125$, and $\sigma^*(neo\text{-}C_5H_{11}) = -0.165$.

Methods of Calculation

The PCILO semi-empirical all valence electrons method (4) considers, from a conceptual point of view, that the chemical formula is a good zeroth order approximation and looks at the molecule as an assembly of chemical bonds in interaction, the interaction being treated by perturbation theory. This method lies beyond the SCF approximation and uses the CNDO/2 hypotheses (10) for the integrals. Because of the inclusion of the CNDO/2 hypotheses on the atomic integrals in the PCILO calculations, the results obtained by a CNDO/2 calculation of charge distributions are also presented, for comparison. In PCILO, the hybrid atomic orbitals are constructed following Del Re's method (11), *i.e.*, hybrids with maximum overlap on the chemical bonds, adding to the strong chemical character of PCILO.

The PCILO program uses a polarity parameter δ for each bond, such that the coefficients c_{i1} and c_{i2} of the bonding orbitals are $c_{i1} = [(1 + \delta)/2]^{1/2}$ and $c_{i2} = [(1 - \delta)/2]^{1/2}$. These polarities may be determined empirically from bond dipole moments $\mu_i = 2\delta_i \times l_i$, where l_i = length of bond i. In the calculations reported below,

tert-butyl group and an equal net negative charge by the CH_3 group. Hence, a net positive charge is carried by the quaternary C atom, since the four methyl groups are equivalent. In isobutane, the net negative charge on the CH_3 groups is expected to be lower than in the case of neopentane, because isobutane is isopropy-methyl and the isopropyl group is less electron-donating than tert-butyl.

[4]This is the only parameter required for describing the charge distributions in simple alkanes (3) (Table 1). The meaning of n can be deduced from $a = 10/3n$, where a, in a way, measures the sensitivity of charge transfers to substituent effects (eqs. 1 and 2). Small n values indicate strong substituent effects; if, on the contrary, inductive effects were non-existent, the charge distributions would be those corresponding to $n = \infty$, *i.e.*, $a = 0$.

Can. J. Chem. Downloaded from www.nrcresearchpress.com by 210.87.254.40 on 09/05/12
For personal use only.

TABLE 2. A comparison between PCILO, CNDO/2 and "inductive" charge distributions (me)

Compound	Atom	PCILO $\delta = 0.035$	"Inductive" $n = 1.3$	PCILO $\delta = 0$	"Inductive" $n = 0.223$	CNDO/2	"Inductive" $n = 0.35$
Methane	C	−55.0	−52.6	−31.5	−31.4	−50.3	−39.1
Ethane	C	−22.3	−22.3	+3.2	−4.3	−7.6	−7 6
Propane	C_{prim}	−29.4	−25.4	+0.2	−7.9	−8.8	−11.6
	C_{sec}	+8.8	+8.0	+31.2	+22.9	+23.6	+23.9
	H_{prim}	+6.9	+6.6	+3.2	+0.5	+0.7	+1.4
	H_{sec}	+1.3	+1.7	−9.2	−5.0	−5.0	−4.7
Isobutane	C_{prim}	−34.7	−29.4	−2.1	−12.4	−9.1	−16.6
	C_{tert}	+39.4	+38.3	+56.5	+50.1	+46.1	+55.4
	H_{prim}	+6.7	+6.0	−4.7	−0.2	−0.9	+0.7
	H_{tert}	−3.3	−4.0	−15.7	−11.4	−11.0	−11.9
Neopentane	C_{prim}	−38.5	−28.3	−3.4	−11.1	−8.7	−15.2
	C_{quat}	+67.8	+68.6	+77.3	+77.3	+61.5	+86.8
	H	+6.4	+3.7	−6.1	−2.8	−2.2	−2.2

several choices for δ(CC) and δ(CH) have been considered, for comparison.

Results and Discussion

The PCILO results calculated assuming zero carbon–carbon polarity and two different carbon–hydrogen polarities are compared in Table 2 with the results obtained from Table 1, using in each case the best n value. The CNDO/2 results are also given, for comparison. In our "inductive" calculations, the net atomic charges are obtained in charge units by multiplying the expressions of Table 1 by a unity factor β, such that $-\beta = Q_C(C_2H_6)$.

The use of the carbon–hydrogen polarity $\delta = 0.035$ ($\delta(CC) = 0$) seems reasonable if a C—H bond dipole moment of ≈0.4 D is assumed. The agreement between the PCILO results and those calculated for $n = 1.3$ is reasonable, but the primary C atoms of propane, isobutane, and neopentane are somewhat more negative for the PCILO approach than in the "inductive" calculation.[5]

With $\delta(CH) = \delta(CC) = 0$, on the contrary, the net PCILO charges on the primary C atoms of propane, isobutane, and neopentane are *less* negative than those calculated with $n = 0.223$, using the "inductive" formulas. Of course, the previous approximation (3) would give rise to an even more pronounced disagreement with the PCILO results, because the relevant charges would be more negative than those given by the "inductive" calculation (*e.g.* −71 me for the primary C atom in neopentane, with $n = 0.223$). It is clear from these results that the chemical picture obtained with $\delta(CH) = 0$ is not satisfactory, even more so when the C atoms in ethane are found to carry a net positive charge. Indeed, the energies (Table 3) indicate that $\delta(CH) = 0.035$ should be preferred over $\delta(CH) = 0$.

The CNDO/2 charge distributions (2) (Table 2) for methane and neopentane are similar to those calculated by the PCILO method, using $\delta(CH) = 0.035$. For the other molecules between these extreme cases only erratic or at best qualitative agreement is obtained in comparison to the results using the best n value of 0.35. As in PCILO with zero polarities, the propane, isobutane, and neopentane primary C atoms are less negative in CNDO/2 than in the corresponding "inductive" calculation. However, although these CNDO/2 results apparently suffer from the zero C—H polarities, they still appear to be more acceptable in the chemical sense than those calculated by PCILO with $\delta(CH) = 0$. It must be noted that no attempt has been made here to improve the CNDO/2 results, although this could probably be done by an adequate choice of parameters.

The results presented in Table 2 clearly indicate that the PCILO charge distributions and their consistancy with the "chemical intuition" largely depends on the assumed C—H

[5]With this low n value, the difference between the present "inductive" results and those derived from the approximation described earlier (3) would be considerable. The latter approximation gives (with $n = 1.3$) the following results for the primary C atoms (in me): −35.5 (propane), −48.7 (isobutane), and −61.8 (neopentane), *i.e. more negative* values than the corresponding PCILO figures.

Can. J. Chem. Downloaded from www.nrcresearchpress.com by 210.87.254.40 on 09/05/12
For personal use only.

Can. J. Chem. Downloaded from www.nrcresearchpress.com by 210.87.254.40 on 09/05/12
For personal use only.

TABLE 3. Zeroth order (E_0) and final energies (kcal/mol)

	Energy (kcal/mol)				
	Methane	Ethane	Propane	Isobutane	Neopentane
$\delta(CH) = 0.035$					
$E_0 =$	−0.63462196E+04	−0.11770087E+05	−0.17193810E+05	−0.22617401E+05	−0.28040882E+05
$E =$	−0.63705661E+04	−0.11846228E+05	−0.17318829E+05	−0.22788541E+05	−0.28255542E+05
$\delta(CH) = 0.00$					
$E_0 =$	−0.63461713E+04	−0.11770125E+05	−0.17193888E+05	−0.22617476E+05	−0.28040915E+05
$E =$	−0.63703303E+04	−0.11845911E+05	−0.17318317E+05	−0.22787725E+05	−0.28254310E+05
δ minimum					
$E_0 =$	−0.63465937E+04	−0.11770769E+05	−0.17194751E+05	−0.22618557E+05	−0.28042204E+05
$E =$	−0.63705732E+04	−0.11846329E+05	−0.17318954E+05	−0.22788607E+05	−0.28255442E+05

TABLE 4. A comparison of "optimized" PCILO with "inductive" net atomic charges

Compound	Atom	Atomic charge (me) PCILO	$n = 0.525$ $\beta = 11.0$
Methane	C	−43.3	−42.6
Ethane	C	−10.4	−11.0
Propane	C_{prim}	−14.6	−14.8
	C_{sec}	+20.2	+20.6
	H_{prim}	+2.0	+2.6
	H_{sec}	−3.9	−3.3
Isobutane	C_{prim}	−19.6	−19.7
	C_{tert}	+51.3	+52.2
	H_{prim}	+1.1	+1.9
	H_{tert}	−10.5	−10.3
Neopentane	C_{prim}	−19.9	−18.4
	C_{quat}	+82.0	+83.8
	H	+0.2	−0.9

polarity. The following results (Table 4) were obtained by an energy minimization with respect to both C—C and C—H polarity.[6,7]

The agreement between these "optimized" PCILO results and those obtained with $n = 0.525$ ($\beta = 11.0$ me) by means of the "inductive" formulas is far superior to what has been observed for the cases discussed above. Although these optimizations are probably not perfect, they are certainly close to the best values. Any further refinement would, however, lead only to small improvements. These would not become apparent in a comparison with the corresponding "inductive" results because the PCILO charges are not exactly normalized. In fact, at the level of the results of Table 4, the discrepancies between the two modes of calculation are not significant.

Conclusions

The PCILO method, properly optimized, reproduces the net atomic charges predicted on the assumption that the inductive effects of the alkyl groups can be described by numbers in a Taft-like manner. The best agreement is achieved by the charge distributions corresponding to the molecular energy minima. The CNDO/2 results, while of the order of magnitude of the PCILO net charges, are only in qualitative agreement with the "inductive" results and seem to suffer from the same difficulties as PCILO used with zero C—C and C—H polarities.

The close agreement between the "inductive" and selected LCAO results has been discussed earlier (3); the EHT, Del Re's method and the Pariser–Parr approach are characterized by their small inductive effects ($n \geqslant 9.5$) and large charge separations. In PCILO, on the contrary, the small n value, corresponding to important inductive effects, enables their discussion on a refined basis (inductive formulas). The fact that the PCILO and the "inductive" charge distributions agree so closely suggests that the usual interpretation of the inductive effects, in terms of net electron release, is appropriate and that the ordering of the electron releasing abilities, as described by Taft's polar σ^* constants, is adequate.

The use of the "inductive" formulas does not alter the spirit of "charge alternation" represented by eq. 3. This is indicated by the fact (Table 1) that in the methane-C, ethane-C, C_{sec}, C_{tert}, and C_{quat} atoms the net charge becomes more positive by the amount $\beta(4 + n)/3n$ for every substitution of H by a CH_3 group. Despite the restrictions on eq. 3, the concept of charge alternation can be used as a rule-of-thumb for the evaluation the effect of α-substitution of hydrogen atoms by methyl groups, as illustrated in the case of carbonium ions (3).

Finally, it may be considered that the close agreement between the PCILO charge distributions and their counterpart based on quantitative chemical intuition supports the claim, by the authors of PCILO, that "there is a lot of chemistry in PCILO".

[6]The polarities corresponding to this optimization are as follows: δ(CH) = 0.019 (CH_4), and 0.018 for all the other C—H_{prim} bonds. For secondary H atoms, δ(CH) = 0.017; for tertiary H atoms, δ(CH) = 0.015. The δ(CC) polarities are 0 (ethane), 0.002 (propane), 0.0025 (isobutane), and 0.003 (neopentane).

[7]The calculated rotational barriers were 2.1 kcal/mol (ethane), and 2.8 kcal/mol (propane), average obtained by taking one-half of the difference in energy between the completely staggered and eclipsed conformations. These results compare favorably with the observed barriers, *i.e.*, 2.8 kcal/mol (ethane) (12) and 3.4 kcal/mol (propane) (13).

The financial aid by the National Research Council of Canada is gratefully acknowledged.

1. B. PULLMAN and A. PULLMAN. Progr. Nucleic Acid Res. and Mol. Biol. **9**, 327 (1969).
2. S. FLISZÁR. J. Am. Chem. Soc. **95**, 1068 (1972).
3. S. FLISZÁR. J. Am. Chem. Soc. **95**, 7386 (1972).
4. S. DINER, J. P. MALRIEU, and P. CLAVERIE. Theor. Chim. Acta (Berl.), **13**, 1 (1969). J. P. Malrieu, P.

Can. J. Chem. Downloaded from www.nrcresearchpress.com by 210.87.254.40 on 09/05/12
For personal use only.

Claverie, and S. Diner. Theor. Chim. Acta (Berl.), **13**, 18 (1969). S. Diner, J. P. Malrieu, F. Jordan, and M. Gilbert. Theor. Chim. Acta (Berl.), **13**, 101 (1969).
5. J. LANGLET, B. PULLMAN, and M. BERTHOD. J. Mol. Struct. **6**, 139 (1970).
6. B. MAIGRET, B. PULLMAN, and J. CAILLET. Biochim. Biophys. **40**, 808 (1970).
7. J. LANGLET, B. PULLMAN, and H. BERTHOD. J. Chim. Phys. **67**, 480 (1970).
8. S. FLISZÁR, J. RENARD, and D. Z. SIMON. J. Am. Chem. Soc. **93**, 6953 (1971).
9. R. W. TAFT. J. Am. Chem. Soc. **75**, 4231 (1953).
10. J. A. POPLE and G. A. SEGAL. J. Chem. Phys. **44**, 3289 (1966).
11. G. DEL RE. Theor. Chim. Acta, **1**, 188 (1963).
12. K. S. PITZER. Discuss. Faraday Soc. **10**, 66 (1951).
13. K. S. PITZER. Chem. Rev. **27**, 39 (1940).

Can. J. Chem. Downloaded from www.nrcresearchpress.com by 210.87.254.40 on 09/05/12
For personal use only.

A Field Ion Investigation of Oxygen on Tungsten

R. A. SHIGEISHI[1]

Inorganic Chemistry Laboratory, University of Oxford, Oxford, England

Received June 28, 1972

The adsorption of oxygen on tungsten was investigated with a field ion microscope. Two experimental procedures were followed. In the first, a tungsten tip previously annealed to 973 or 1173 °K was held at 78 °K while exposed to oxygen. Coverages ranged from less than a monolayer to saturation. After the ambient oxygen was removed, the tip was heated to the annealing temperature. In the second, oxygen adsorption occurred on a hot tip held at 973 °K. Estimated coverages were significantly less than a monolayer.

Results reveal a dramatic difference in the extent of surface diffusion, rearrangement, disruption, and oxygen penetration for the two procedures, the latter producing more extensive effects. Possible explanations for these differences are considered.

L'adsorption de l'oxygène sur le tungstène a été étudiée avec un miscroscope à champ ionique. Deux méthodes expérimentales furent suivies. Dans la première, un filament de tungstène recuit à 973 ou 1173 °K a été soumis à l'action de l'oxygène à 78 °K. On enregistre des recouvrements inférieurs à la couche monomoléculaire jusqu'à la saturation. Après avoir enlevé l'oxygène du milieu, le filament a été chauffé à la température de recuit. Dans la seconde, l'adsorption d'oxygène se passe sur un filament chaud maintenu à 973 °K. Les recouvrements estimés étaient de beaucoup inférieurs à la couche monomoléculaire.

Les résultats montrent alors des différences importantes en ce qui a trait à l'étendue de la diffusion en surface au réarrangement, à la rupture et à la pénétration de l'oxygène, pour les deux procédés; le dernier produisant des effets encore plus marqués. Des explications possibles pour ces différences sont présentées. [Traduit par le journal]

Can. J. Chem., **51**, 997 (1973)

Introduction

The oxygen–tungsten system has been extensively studied for many years and recently, much new information has been obtained on surface structures, work function changes, surface diffusion, adsorption states, and kinetics of oxide formation by a variety of techniques including Leed, electron desorption spectrometry, flash desorption, and field emission microscopy. Recent reviews by McCarroll (1) and Musket (2) summarize these findings and hence need not be repeated here.

There are, however, comparatively few reports of the systematic investigation of the tungsten–oxygen system at elevated temperatures by means of field ion microscopy (3). It is now generally recognized that oxygen atoms on tungsten cannot be imaged since they are either field desorbed from the surface before imaging voltages are reached or else are buried within the surface (4). Nevertheless, it is also known that when oxygen is chemisorbed, tungsten–tungsten bonds are weakened with the result that in field desorption, both oxygen and an adjacent tungsten atom are stripped off together in the form of tungsten oxide molecular ions. Müller and co-workers' initial atom probe studies (5) have shown that these ions are WO^{3+}, WO_2^{3+}, and WO_3^{3+}. Thus the combination of chemisorption and field desorption results in an "etched" surface and from a comparison of the images of clean and etched surfaces the position of the oxygen can be inferred. Field ion microscopy should therefore be valuable in studying among other things, surface diffusion, preferential adsorption, and penetration of adsorbate into the substrate.

This paper is a report of the field ion investigation of the oxygen–tungsten system for coverages ranging from less than a monolayer to saturation, for the temperatures 973 °K and 1173 °K. This narrow temperature range is of particular interest since irreversibility as defined by Gomer and Hulm (6) occurs in this range. A preliminary report of this work has been presented by Anderson (7).

Two types of experiments were conducted. In the first, oxygen was adsorbed at 78 °K and following evacuation the tungsten tip was heated. In the second, oxygen was admitted to the tip

[1]Present address: Department of Chemistry, Carleton University, Ottawa, Canada K1S 5B6.

Can. J. Chem. Downloaded from www.nrcresearchpress.com by 210.87.254.40 on 09/05/12
For personal use only.

held at 973 °K. As will be shown, these procedures result in surfaces that are disrupted to substantially different degrees.

Experimental

The all glass field ion microscope was of conventional design (8) with an outer Dewar and a re-entrant cold finger to cool the tungsten tip and electrical leads.

The tip temperature could be altered by resistive heating via an electronic feedback circuit of a type designed by Klein (9). The temperature itself was calculated by measuring, potentiometrically, the resistance of a small central portion of the loop to which the tungsten tip was spot welded and using a temperature *vs.* resistance calibration curve (10). Approximately 5 s were required for the temperature to stabilize to within 5 °K for any chosen temperature between 900 and 1200 °K. While this method only measures the temperature at the central portion of the loop, van Oostrum (11) and Pichaud *et al.* (12) have shown that the temperature at the sharp tip is not significantly different.

Pure oxygen and helium could be admitted to the microscope by thermal diffusion through silver and Pyrex thimbles respectively.

Prior to beginning experiments, the tip was heated to temperatures greater than 2200 °K in 10^{-6} Torr oxygen for 24 h to rid the tungsten of internal carbon impurities. This was followed by outgassing the tip at greater than 2200 °K till a base pressure of 5×10^{-10} Torr was achieved. The re-entrant tube was then demounted, the tip re-etched and the unit sealed into the microscope. After a vacuum of 5×10^{-10} Torr was obtained, the tip was momentarily flashed to rid the shank of contaminants and then field evaporated to a perfect endform. Finally, the tip was heated to 973 or 1273 °K.

For the first set of experiments the tip was cooled to 78 °K and the oxygen leaked in to the desired pressure. After adsorption had occurred, the ambient oxygen was pumped out and the tip heated. The surface was then examined by controlled field desorption. In the second set, the tip was heated to 973 °K, the oxygen leaked in and after a set time pumped out. The surface was then examined as before. In both cases, in order to reduce the production of CO the leak thimbles had been previously calibrated so that the ion gauge was not in operation while oxygen or helium was being admitted.

Results

Low Temperature Adsorption

Figure 1 shows the sequence of micrographs for a tip at 78 °K exposed to 7×10^{-9} Torr oxygen for 40 min and heated to 973 °K for 2 min after the oxygen was pumped out. The first micrograph, that of a clean tip annealed to 973 °K reveals the usual structure described previously by Bassett (13). As compared to a field evaporated endform, the surface is disordered and the low index {211}, {110}, and {100} planes have grown in area and appear to be atomically flat. As well, multiple height steps are formed between the {211} and central (110) plane. The field emission micrograph subsequent to the oxygen and heat treatment shows prominent emission mainly from the low work function regions around and including the {111} and the viscinals of the {100}. While these might appear to be built up regions, the initial field ion micrographs indicate that the most prominent surface atoms are located at the edges of the {111} and in the {411} regions. Surprisingly, however, no atoms are to be seen in the triangular region centered on the (111) pole, which appears to be atomically flat. On the clean tip (Fig. 1*a*) atoms are visible in this area even though no crystallographic order is present. Furthermore, since little or no field desorption occurs from this area oxygen is not present here.

As the voltage is raised field desorption occurs predominantly from the viscinals of the {100}, especially {411}, and to a lesser extent from the edges of {211} planes. These areas are thus identified as being particularly rich in oxygen. However, after the initially bright atoms have been removed and most of the surface is imaged (Fig. 1*d*), it is apparent from a comparison of Figs. 1*d* and 1*a* that the surface is structurally similar to that of the clean annealed tip. The two exceptions are the {111} regions which have been remarked upon previously and the {211} planes. A color comparison of these same photographs leads to the observation that the {211} planes of the oxygenated surface have grown slightly in area.

As field evaporation voltage is approached and the rings of the central (110) become more visible, field desorption begins to occur in this region, but the comparatively low frequency of such events indicates only a light disruption of this plane.

Figures 1*e* and 1*f* are images of the surface just prior to and after the field evaporation of the top atom layer of the (110). The surface is almost atomically perfect except for the slight disorder around the {100} which is usually present in tips of large radius of curvature.

Comparison of voltages required to field evaporate the top atomic layer of the central (110) for the clean and treated tip (23.0 and 23.1 kV) indicates little or no thermal blunting of the tip.

Similar experiments at higher and lower oxygen exposures and at 1173 °K result in an almost identical surface disruption pattern as described

Can. J. Chem. Downloaded from www.nrcresearchpress.com by 210.87.254.40 on 09/05/12
For personal use only.

Can. J. Chem. Downloaded from www.nrcresearchpress.com by 210.87.254.40 on 09/05/12
For personal use only.

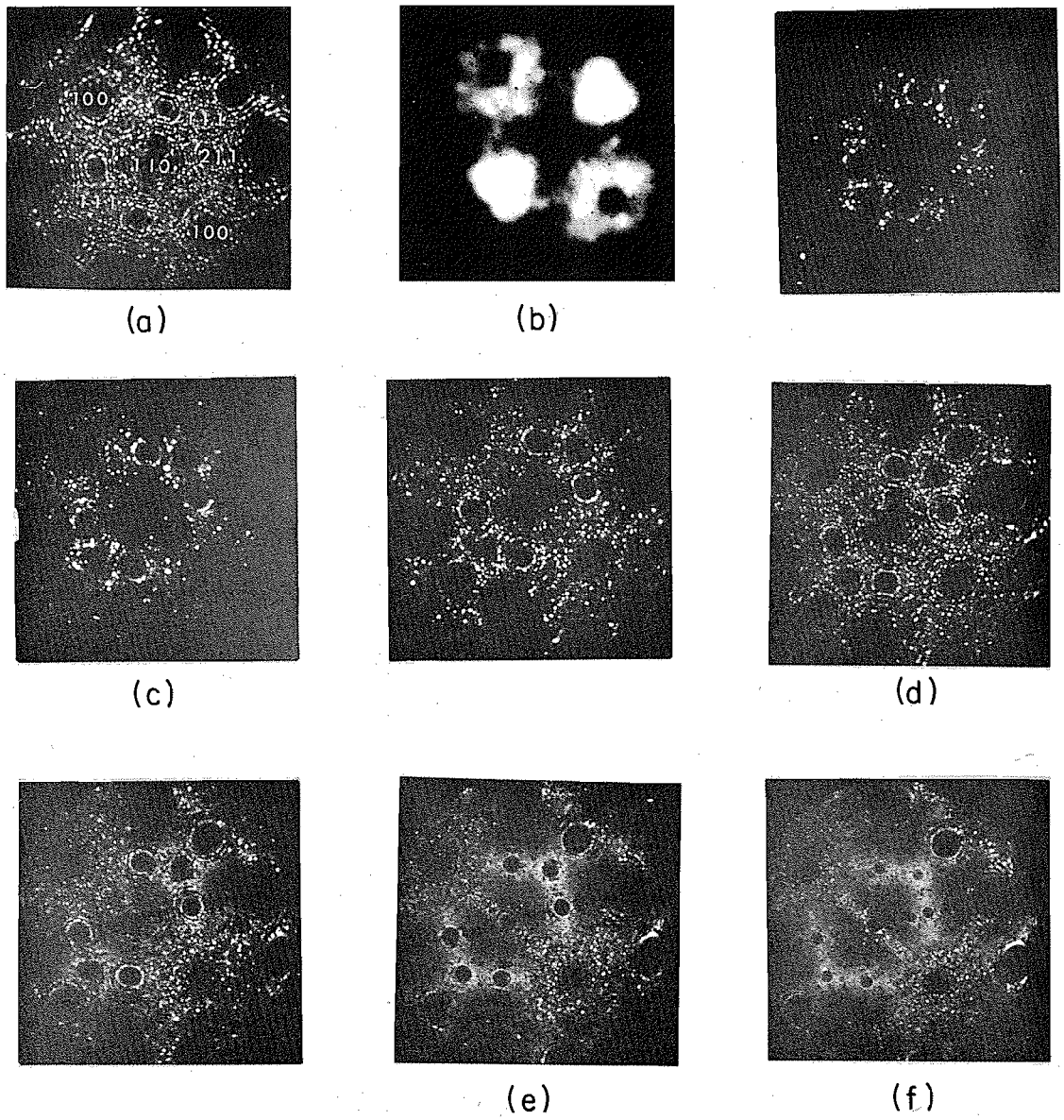

FIG. 1. (*a*) Clean tip annealed to 973 °K; 23.0 kV (20.0); (*b*) field emission; (*c*) 15.8 kV; (*d*) 18.5 kV; (*e*) 22.7 kV (19.4); (*f*) 23.1 kV (20.0). Figures in parentheses indicate best image voltage.

above, except that for very low coverages very little change in the surface is observed. Also the length of time the oxygenated surface was heated, whether 2 min or 1 h made little difference to the state of the surface. At 1173 °K the only change was a slight blunting of the tip. In all other respects, the flat {111} planes, the bright atoms at the periphery of the {111} and at the {411}, the slight growth of {211}, the high oxygen concentration at {411} and viscinals of {100} and the slight oxygen penetration, the results were the same.

Adsorption at 973 °K

Figure 2 shows the surface at progressively higher voltages of a tip that had been held at 973 °K for 3.5 min while the oxygen pressure built up to 5×10^{-9} Torr. For unit sticking

Can. J. Chem. Downloaded from www.nrcresearchpress.com by 210.87.254.40 on 09/05/12
For personal use only.

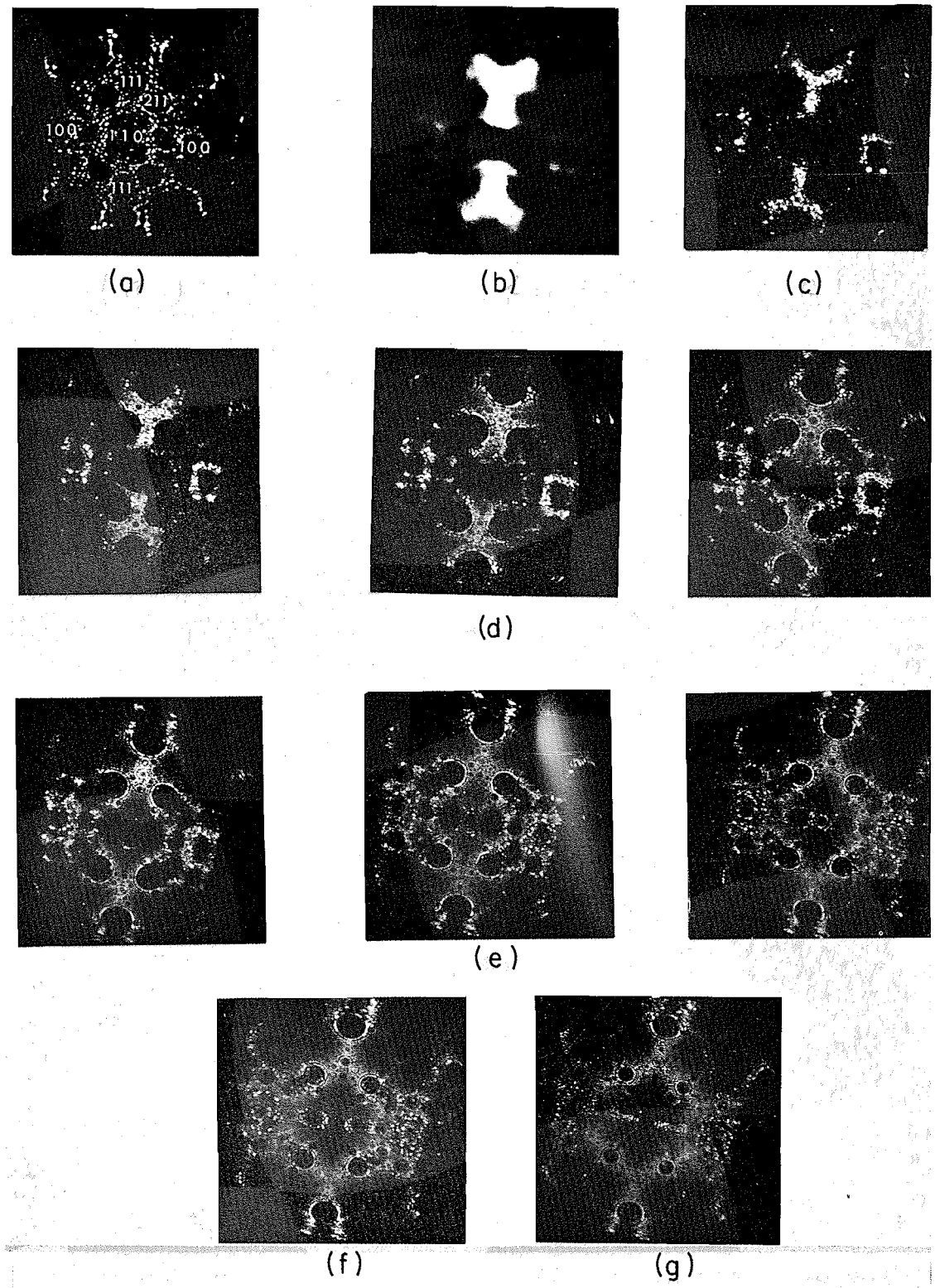

FIG. 2. (*a*) Clean tip annealed to 973 °K; 24.4 kV; (*b*) Field emission; (*c*) 16.8 kV (15.3); (*d*) 20.8 kV (17.2); (*e*) 23.8 kV (19.0); (*f*) 24.8 kV (20.0); (*g*) 25.2 kV (20.3).

Can. J. Chem. Downloaded from www.nrcresearchpress.com by 210.87.254.40 on 09/05/12
For personal use only.

coefficient this corresponds to approximately 1/5 monolayer coverage. The characteristic square and trigon pattern in the field emission micrograph (Fig. 2*b*) implies prominent structures around the {100} and {111}. This is confirmed by the initial field ion micrographs which, unlike the previous case, reveal a narrow three pronged ridged structure centered on the (111) pole with each ridge pointing towards a (110) plane. After field desorption of the bright irregular clumps of atoms around the {111}, this region is atomically perfect and further field evaporation occurs very regularly. This implies that although the bright clumps may contain oxygen, once these are removed, oxygen is absent from the {111}. It would appear, then, in view of the subsequent perfection of the built-up ridge that the major diffusing species in this region is tungsten.

The other built-up structure which is located around the cube edges of the {100} is composed of clumps of bright atoms which show some order and which are comparatively stable with respect to field desorption, *i.e.*, as many as five to six (111) layers may be field evaporated before some of these bright atoms are removed. Unlike the ridge structure, however, the irregular manner of field evaporation from this built-up region implies the presence of oxygen in this structure. Diffusion to this region, therefore, must involve oxygen, whether as atoms or in the form of tungsten–oxygen complexes. It should be noted that the pattern of field desorption indicates only whether oxygen is present or not but gives no clue as to the structural or chemical relationship between the oxygen and tungsten. At the temperatures and pressures used here, an ordered bulk oxide phase seems unlikely. Rather, a solution of oxygen and tungsten (whether in the form of tungsten–oxygen complexes, reconstructed layers (19), or oxide nuclei (20)) reflecting the initial stages of oxidation seems probable.

Visual observation of the frequency of desorbing image points reveals, as in the previous case, that the regions of high oxygen concentration are viscinals of the {100}, and especially the {411} and the side of the {211} bordering {411} which is not imaged. The overall pattern of surface damage is seen in Fig. 2*e*. Comparison of this with Fig. 1*d* clearly reveals the dramatic difference in the effects of the two adsorption and heating procedures.

Figures 2*f* and 2*g* show the state of the surface after the removal of one and four layers of the central (110). Penetration of the oxygen is much more extensive in this case and even after the removal of four layers a small region near the {100} and {411} still shows some disorder.

Finally, while no overall blunting of the tip occurred, these micrographs indicate that the area of the {211} increased significantly due to facetting of the {111} and its viscinals.

Discussion

There is much documented evidence that adsorbed gases cause an enhanced surface diffusion of substrate metal atoms, the driving force being the resulting decrease in surface free energy (14, 16). That such a process occurs in these experiments is evident from the growth of {211} planes after the oxygen and heat treatment. Ehrlich and Hudda (15) have shown that surface diffusion of tungsten atoms on the {211} planes occurs most readily along the close packed rows in the [111] direction toward the {111} and {411}. As Anderson has pointed out (7), such an anisotropic diffusion of tungsten atoms from the top layer(s) of the {211} would explain the deposition of atoms at the {411} and the viscinals of the {111} and hence the bright atoms initially seen in these areas. However, in the case of low temperature adsorption, the micrographs indicate that some of these bright atoms diffused from the (111) plane itself. On the clean annealed surface the {111} is flat and structureless but it does contain atoms that are sufficiently prominent to be imaged. For the low temperature case these atoms have disappeared and the {111} planes are totally devoid of image spots. Either the {111} have become atomically flat as a result of diffusion or else the prominent atoms have been field desorbed in the form of tungsten–oxygen complexes. No desorptions are seen to occur from this area, however. While it is still possible that field desorption of these complexes may have occurred prior to the initial image formation this also seems unlikely, since in other regions of the surface field desorption of prominent atoms or complexes can be seen. It is only from regions like the center of a (211) plane which has become atomically flat by diffusion that no desorption is seen.

While surface diffusion of substrate metal atoms is assisted by the presence of oxygen (14), its extent in the instance of a chemisorbed layer rearranged at 973–1173 °K must be limited since no significant restructuring of the surface is

Can. J. Chem. Downloaded from www.nrcresearchpress.com by 210.87.254.40 on 09/05/12
For personal use only.

evident in the micrographs. In particular, no prominent ridges are formed around the {111} and {100}. This is confirmed by Gomer and Hulm (6) and by Bell *et al.* (17). The latter workers measured work function changes and Fowler–Nordheim pre-exponential factors and concluded that no significant facetting or ridge formation occurs on the {100} and {111} regions when an oxygen layer adsorbed at 78 °K was heated to 1200 °K. However, it is significant that heating to 1600 °K did result in ridge formation and surface reconstruction in these areas. It seems, therefore, that the same surface endform may be achieved by heating a low temperature layer to 1600 °K as by adsorbing oxygen at 1000–1200 °K.

For high temperature adsorption, surface diffusion is much more extensive. Here, the three {211} planes around the (111) grow to such an extent at the expense of the (111) viscinals (facetting) that they tend to intersect each other and form a prominent three pronged ridge on top of which, a few bright atom clumps (probably these contain oxygen) are randomly distributed. Once these are removed gradual field evaporation reveals an atomically perfect (111) and viscinals with no trace of incorporated oxygen.

The pattern of field desorption indicates that the dramatic difference in the extent of diffusion facetting and surface restructuring for the low and high adsorption temperature procedures is due to the degree of oxygen–tungsten interaction in the formation of complexes or oxide nuclei. In this regard it is of interest to review the results of Ptushinskii and Chuikov (20) and Tracey and Blakely (25).

From a mass spectrometric analysis of flash desorption products of the O_2/W system, the former authors showed that oxide formation is much more extensive when oxygen is adsorbed on a hot (1050 °K) tungsten ribbon than when oxygen was adsorbed at 300 °K and subsequently heated to 1050 °K. Furthermore, they determined the rate law for oxide desorption and concluded that oxides are formed immediately when oxygen is adsorbed on a hot ribbon, but that they are only formed in the flashing process when the adsorption temperature is 300 °K. This implies for the latter case that oxide formation is a two step process, the first of which is probably governed by diffusion of oxygen atoms.

Tracey and Blakely observed the facetting of W(211) to W(110) under conditions similar to those used here. They found that the activation energy for facetting was 0.15 and 1.5 eV for high and low temperature adsorption. Since the activation energy for oxygen diffusion on tungsten is of the order of 1.5 eV it would appear that facetting following the latter procedure is hindered by diffusional barriers while in the former it is governed by the supply of gas phase oxygen to dissociation sites.

Thus the preceding evidence supports the results obtained here of the enhanced surface processes when the adsorption temperature is high. The more extensive formation of tungsten–oxygen complexes would naturally result in more damage to the surface since tungsten–tungsten bonds are being broken. Furthermore, these species should be relatively loosely bound to the surface compared to chemisorbed oxygen (*e.g.*, desorption energies of oxide and chemisorbed oxygen are 4.5 and 6.5 eV (20)) so that they should diffuse more easily. This results not only in a regeneration of adsorption sites for more complex formation but also in greater mass transport of tungsten to the appropriate areas (viscinals of {411} and {111}), hence resulting in greater facetting than in the case when chemisorbed oxygen must diffuse to the proper sites for complex formation. Although in the latter case complex formation is very limited at 1000 °K, heating to higher temperatures should enhance the reaction so that at some temperature ridge formation and facetting should occur. As mentioned previously, the results of Bell *et al.* show that this temperature is about 1600 °K.

A second major difference in the effects of the two procedures is the depth of oxygen penetration into the substrate. This is confined to the surface layer in the first case while in the second, it extends more than four layers. The micrographs indicate that the regions where greatest penetration occur coincide with those of greatest oxygen concentration, namely, the viscinals of the {100} planes and especially the {411}. While, previously, penetration of oxygen into tungsten had not been observed at low exposures of oxygen, more recent investigation by Singleton (21), Lee and Pethica (22), and Zingerman and Ishchuk (24) indicates a solution process confined to a few surface layers when oxygen is adsorbed on tungsten heated to 850–1050 °K. However, they were unable to indicate the crystal planes where the penetration was occurring. The difference in penetration depth can again be rationalized by the difference in complex formation and consequent surface diffusion, facetting,

Can. J. Chem. Downloaded from www.nrcresearchpress.com by 210.87.254.40 on 09/05/12
For personal use only.

and reconstruction involving incorporation of oxygen into the substrate lattice.

An alternative explanation for the differences in the results of the two procedures, involving the liberated heat of adsorption, is suggested by the work of both May (18) and Zingerman and Ishchuk (23, 24). May has suggested that for highly exothermic adsorption such as oxygen on tungsten, not all of the heat of adsorption is immediately dissipated by the substrate lattice at the moment of dissociative chemisorption but rather that part of this energy is available for the creation of a "hot" oxide molecule (or some tungsten–oxygen complex) which temporarily has a high kinetic energy parallel to the surface. The availability of part of the heat of adsorption combined with a high substrate temperature when adsorption occurs would help to rationalize the enhanced surface diffusion and restructuring which follows the second procedure. In the first procedure, the heat of adsorption is dissipated prior to heating the surface and hence is not available for overcoming surface diffusion.

With respect to penetration of oxygen into the lattice, the latter authors have suggested that this occurs only during the actual time of interaction between oxygen and tungsten with the liberated heat of adsorption providing the means of overcoming the activation barrier for the penetration process. If this suggestion regarding the availability of the heat of adsorption is correct it would account for the greater penetration when the adsorption temperature is high.

Summary and Conclusion

Heating a tungsten tip saturated with oxygen at 78 to 973 or 1173 °K produces relatively little change in the surface compared to a clean tip annealed to the same temperatures. Surface diffusion results in a slight growth of {211} planes and deposition of tungsten atoms at the periphery of {111} and {411}. The greatest concentration of oxygen is located in the atomically rough viscinals of the {100}. Penetration of oxygen beyond the first surface layer is not observed. For smaller oxygen coverages even less surface disruption occurs.

Adsorption on a tungsten surface at 973 °K of significantly less than a monolayer of oxygen causes much more extensive surface restructuring and build up around {111} and {100}. Growth of {211} planes occurs to such an extent that they intersect to form a ridge structure centered on the (111). Penetration of oxygen into the metal occurs to a depth of more than four atomic layers.

The extensive surface disruption for high temperature adsorption is tentatively explained in terms of the enhanced formation of oxygen–tungsten species although a second explanation in terms of the liberated heat of adsorption is also considered.

The author wishes to thank Professor J. S. Anderson who supervised this work and Dr. G. K. L. Cranstoun who gave freely of advice and assistance. The author also thanks the National Research Council of Canada for the award of a postdoctoral fellowship.

1. B. McCarroll. J. Chem. Phys. **46**, 863 (1967).
2. R. G. Musket. J. Less-Common Metals, **22**, 175 (1970).
3. S. S. Brenner. High temperature, high resolution metallography. *Edited by* H. I. Aaronson and G. S. Ansell. Gordon and Breach, New York. 1967. p. 281.
4. D. W. Bassett. Brit. J. Appl. Phys. **18**, 1753 (1967).
5. E. W. Müller, J. A. Panitz, and S. B. McLane. Rev. Sci. Instrum. **39**, 83 (1968).
6. R. Gomer and J. K. Hulm. J. Chem. Phys. **27**, 1363 (1957).
7. J. S. Anderson. Surface phenomena of metals. Society of Chemical Industry Monograph No. 28. 1968. p. 109.
8. J. S. Anderson. Aust. Acad. Sci. **1**, 109 (1967).
9. R. Klein. Rev. Sci. Instrum. **29**, 770 (1958).
10. C. J. Smithells. Metals reference book. 4th ed. Butterworths, London. 1967.
11. A. van Oostrum. Phillips Res. Repts. Suppl. **1**, 40 (1966).
12. M. Pichaud, A. Muller, and M. Drechsler. Surf. Sci. **26**, 14 (1971).
13. D. Bassett. Proc. Roy. Soc. A, **286**, 191 (1965).
14. A. J. W. Moore. Metal surfaces: structure, energetics, and kinetics. American Society for Metals, Metals Park, Ohio. 1963.
15. G. Ehrlich and F. G. Hudda. J. Chem. Phys. **44**, 1039 (1966).
16. W. W. Mullins. Metal surfaces: structure, energetics, and kinetics. American Society for Metals, Metals Park, Ohio. 1963.
17. A. E. Bell, L. W. Swanson, and L. C. Crouser. Surf. Sci. **10**, 254 (1968).
18. J. W. May. Surf. Sci. **18**, 431 (1969).
19. J. Anderson and W. Danforth. J. Franklin Inst. **279**, 160 (1965).
20. Yu. G. Ptushinskii and B. A. Chuikov. Surf. Sci. **6**, 42 (1967).
21. J. H. Singleton. J. Chem. Phys. **47**, 73 (1967).
22. A. E. Lee and B. A. Pethica. Proc. Roy. Soc. A, **309**, 141 (1969).
23. Ya. P. Zingerman and V. A. Ishchuk. Sov. Phys.-Solid State, **6**, 904 (1964).
24. Ya. P. Zingerman and V. A. Ishchuk. Sov. Phys.-Solid State, **7**, 173 (1965).
25. J. C. Tracey and J. M. Blakely. Surf. Sci. **13**, 313 (1968).

Crystal Structure of α-$Zn_2V_2O_7$

RAMANATHAN GOPAL[1] AND CRISPIN CALVO
Department of Chemistry, McMaster University, Hamilton, Ontario

Received July 19, 1972

α-$Zn_2V_2O_7$ is monoclinic with lattice parameters $a = 7.429(5)$, $b = 8.340(3)$, $c = 10.098(3)$ Å, $\beta = 111.37(5)°$, $Z = 4$ and space group $C2/c$. The structure was refined using a full matrix least-squares with 1034 reflections measured with a quarter-circle General Electric automatic X-ray diffractometer to a final R value of 0.066. The anion consists of a pair of VO_4 tetrahedra sharing an oxygen atom which lies on a two-fold axis. The bridging V—O bond length is 1.775(4) Å while the three independent terminal ones are 1.728(4), 1.704(7), and 1.658(8) Å long. These bond lengths are consistent with the charge character around the individual oxygen atoms. The Zn ions are coordinated to five oxygen atoms with Zn—O bonds ranging from 1.973 to 2.088 Å. The structure is similar to that of α-$Cu_2P_2O_7$ and transforms to the thortvietite structure at about 615 °C.

L'α-$Zn_2V_2O_7$ est monoclinique avec les paramètres de maille $a = 7.429(5)$, $b = 8.340(3)$, $c = 10.098(3)$ Å, $\beta = 111.37(5)°$, $Z = 4$ et le groupe est $C2/c$. La structure a été raffinée en utilisant une matrice des moindres carrés avec 1034 réflections mesurées avec un diffractomètre à rayons-X au quart de cercle automatique General Electric jusqu'à une valeur finale de R égale à 0.066. L'anion consiste en une paire de tétrahèdres VO_4 partageant un atome d'oxygène qui se trouve sur un axe binaire. La longueur de la liaison V—O faisant le pontage est de 1.775(4) Å alors que celle des trois autres liaisons terminales indépendantes, est de 1.728(4), 1.704(7) et 1.658(8) Å. Ces longueurs de liaisons sont compatibles avec le caractère de la charge autour des atomes individuels d'oxygène. Les ions Zn sont coordinés à cinq atomes d'oxygène avec les liens Zn—O s'échelonnant de 1.973 à 2.088 Å. La structure est semblable à celle de l'α-$Cu_2P_2O_7$ et adopte la structure de la thortvietite vers 615 °C.

[Traduit par le journal]

Can. J. Chem., **51**, 1004 (1973)

Introduction

Recently determined structures containing pentavalent vanadium ions in tetrahedral coordination have shown that the V—O bond length is very sensitive to the environment of the oxygen atoms. For example, in the isotypic $Mg_3(VO_4)_2$ (1), $Co_3(VO_4)_2$ (2), and $Ni_3(VO_4)_2$ (3) the V—O bond lengths are 1.809, 1.813, and 1.815 Å respectively for that particular oxygen atom bonded to three divalent cations, while the remaining V—O bond lengths involving oxygen atoms bonded to only two divalent cations lie between 1.695 and 1.716 Å. α-$Zn_3(VO_4)_2$, which is also isotypic with these compounds, shows a similar but somewhat smaller effect (4).

$M_2X_2O_7$ compounds, when the radius of M is less than about 0.9 Å and X is tetrahedrally bonded to oxygen atoms, commonly crystallize in either the thortveitite structure or some modification of it. This seems universally true for X = P and As and for the two divanadate structures, that of $Mn_2V_2O_7$ (5) and $Cd_2V_2O_7$ (6), with cations in this range previously reported. In the thortvietite-like phase the coordination of M is six-fold, while in each of the various low-temperature α phases some fraction of the cations reduce their coordination to five oxygen atoms (7–10). Thus these phases are suitable for the study of environmental effects on bond lengths since in the α phases the terminal oxygen atoms will not all be bonded to the same number of cations.

Pollard (11), Brown and Hummel (12), Angenault (13) and Makarov, Foliev, and Serebryakova (14) have studied the phase diagram of the ZnO–V_2O_5 system. The general conclusion is that $Zn_2V_2O_7$ is polymorphic with a fast reversible phase transformation at 615 °C. Angenault concluded that α-$Zn_2V_2O_7$ is orthorhombic with lattice parameters of $a = 7.441$, $b = 8.337$, and $c = 18.84$ Å from powder diffractometry, contrary to the results reported here. A further point of interest is the thermochromic nature of $Zn_2V_2O_7$ which is light yellow in the α phase and changes to red in the β phase (12).

Experiments

Crystals of α-$Zn_2V_2O_7$ were prepared in a platinum crucible by the reaction of stoichiometric amounts of ZnO and V_2O_5 at 925 °C. The melt was slowly cooled

[1]Present address: Queen's University, Kingston, Ontario.

Can. J. Chem. Downloaded from www.nrcresearchpress.com by 210.87.254.105 on 09/05/12
For personal use only.

Can. J. Chem. Downloaded from www.nrcresearchpress.com by 210.87.254.105 on 09/05/12
For personal use only.

through the melting point (877 °C (12)) and quenched when the temperature was about 750 °C.

Accurate unit cell parameters were obtained from a least-squares refinement of sixteen 2θ values measured with a General Electric semi-automatic quarter-circle diffractometer utilizing filtered MoKα radiation (λ = 0.71069 Å) with standard errors 3X those obtained from the refinement. The crystal data are:

α-$Zn_2V_2O_7$ f.w. = 363.28

a = 7.429(3), b = 8.340(3), c = 10.098(3) Å, β = 111.37 (5)°, volume = 580.1 Å^3 space group: $C2/c$, Z = 4, ρ_o = 4.1 ± 0.1 g/cm^3, ρ_c = 3.93 g/cm^3.

The space group possibilities are Cc and $C2/c$ since preliminary photographic work showed that reflections were extinct in general when $h + k$ was odd and for $h0l$ when l was odd. The centric space group was chosen since electron paramagnetic resonance measurements on Mn^{2+} doped crystals showed only one unique cation site (15).

The structure was refined with data taken with a crystal whose size was 0.13 × 0.12 × 0.08 mm. Filtered MoKα radiation was used in conjunction with a General Electric quarter-circle semi-automatic diffractometer using a 2θ–θ scan. All the reflections in a hemisphere up to 2θ = 55° were scanned at a rate of 2° per min and an angular range dependent upon the value of 2θ. The background was determined under stationary conditions by a 20 s count at either side of the peak. Those reflections whose intensity measure, after correction for background, was less than zero were not considered in the refinement. The unobserved limit was set at 3σ with σ determined by the counting statistics. All the intensities were corrected for Lorentz and polarization effects and for absorption ($\langle \mu R \rangle$ = 0.7). The final data set contained 1034 unique reflections of which 653 were observed.

The structure was refined starting with the parameters reported for α-$Cu_2P_2O_7$ (7). A full-matrix least-squares program written by J. S. Stephens for the CDC 6400 was used. Atomic scattering factors, corrected for dispersion, were obtained from the International Tables for X-ray Crystallography (16). Weights were assigned according to the relationship $\omega = (7.00 + 0.097|F_o| + 0.0073|F_o|^2)^{-1}$ where the coefficients were determined so that $\omega|F_o - F_c|^2$ would be independent of the local average observed structure factor. Unobserved reflections whose calculated structure factors, F_{calc}, was less than the value derived from the 3σ limit were given zero weight in the refinement. The refinement was terminated when all the calculated shifts were less than 1/3 of the standard errors derived from the least-squares. The final R value was 0.066 while $\omega R = (\Sigma\omega||F_o| - |F_c||/\Sigma\omega|F_o|^2)^{1/2}$ was 0.086. The final parameters are in Table 1 and the calculated and observed structure factors are compared in Table 2.[2]

The phase transformation in $Zn_2V_2O_7$ was investigated by examining the diffraction pattern of a single crystal at elevated temperatures using a precession camera. The crystal was heated with a stream of hot air. All l odd reflections disappeared beyond the transition and no evidence of a stacking disorder, as had been found in $Cu_2P_2O_7$ (7), was detected. It is thus presumed that the high temperature phase has space group $C2/m$ and is isotypic with thortvietite (17).

Description of the Structure

The structure of α-$Zn_2V_2O_7$ is based upon a perturbed hexagonally packing of oxygen atoms with c as the stacking direction. The cations occupy sites with five oxygen atom neighbors under 3.0 Å. The sixth oxygen atom, O(4f), lies 3.35 Å away and the Zn—O(4f) bond corresponds to the one that is ruptured in transforming from a thortveitite-like high temperature phase to that of α-$Zn_2V_2O_7$ structure (Fig. 1). Because of the bent V—O—V moiety, showing an angle of 149.3°, the anion pulls away from the cation at each of its ends.

As Fig. 2 shows, the structure contains the layers of oxygen atoms stacked perpendicular to (001). Zn ions and V—O—V groups lie in octahedrally coordinated sites in alternate layers of oxygen atoms. These latter groups lie in sites, containing a crystallographic two-fold axis through the oxygen atom, elongated roughly along a with each vanadium ion sharing two oxygen atoms with one layer and one with the next.

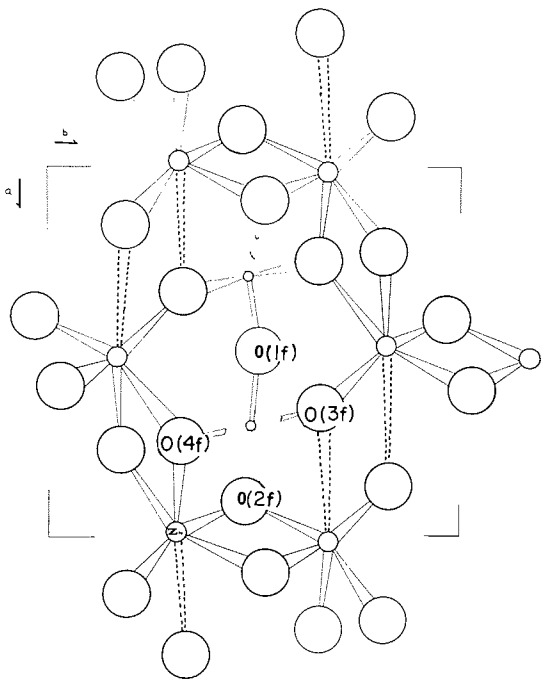

FIG. 1. The structure of α-$Zn_2V_2O_7$ projected onto the ac plane.

[2]Table 2 is available, at a nominal charge, from the Depository of Unpublished Data, National Research Council of Canada, Ottawa, Canada K1A 0S2.

Can. J. Chem. Downloaded from www.nrcresearchpress.com by 210.87.254.105 on 09/05/12
For personal use only.

TABLE 1. Atomic parameters for α-$Zn_2V_2O_7$ with estimated standard deviations in parentheses

	Positional			Thermal					
Atom	x	y	z	U_{11}*	U_{22}	U_{33}	U_{12}	U_{13}	U_{23}
Zn	−0.04958(9)	0.3239(1)	0.51955(8)	0.0073(3)	0.0104(6)	0.0097(3)	−0.0000(3)	−0.0001(3)	0.0010(3)
V	0.2016(1)	0.0049(2)	0.2058(1)	0.0030(4)	0.0103(7)	0.0052(3)	−0.0009(3)	−0.0007(2)	0.0010(4)
O(1)	0	0.0612(16)	1/4	0.011(3)	0.039(7)	0.023(3)	—	0.010(2)	—
O(2)	0.3984(7)	−0.0189(8)	0.3620(5)	0.009(2)	0.016(3)	0.009(1)	−0.002(1)	−0.002(1)	0.001(2)
O(3)	0.2440(7)	0.1541(8)	0.1056(6)	0.006(1)	0.016(3)	0.014(2)	0.003(1)	0.004(1)	0.007(2)
O(4)	0.1531(8)	−0.1647(8)	0.1138(7)	0.013(2)	0.017(4)	0.018(2)	−0.003(2)	−0.004(1)	−0.002(2)

*Calculated from $\beta_{ij} = 2\pi^2 b_i b_j U_{ij}$ where $T = \exp[-(\beta_{11}h^2 + 2\beta_{12}hk\ldots)]$ is the thermal factor appearing in the structure factor expression and b_{ij}'s are the reciprocal lattice vectors.

TABLE 3. Bond length and angles in α-$Zn_2V_2O_7$ with estimated standard deviations in parentheses*

Bond	Length (Å)	Bonds	Angle (deg)	Bonds	Angle (deg)
ZnO_5 group					
Zn—O(2*f*)	1.988(6)	O(2*f*)—Zn—O(3*a*)	94.2(2)	O(3*a*)—Zn—O(3*g*)	81.7(2)
—O(3*a*)	2.088(6)	—O(3*g*)	109.1(2)	—O(4*c*)	94.2(2)
—O(3*g*)	2.027(6)	—O(4*c*)	136.2(3)	—O(2*h*)	169.9(2)
—O(4*c*)	1.973(7)	—O(2*h*)	81.5(2)	O(3*g*)—Zn—O(4*c*)	114.7(2)
—O(2*h*)	2.087(6)	O(4*c*)—Zn—O(2*h*)	95.3(2)	—O(2*h*)	91.0(2)
V_2O_7 group					
V—O(1*a*),—O(1*b*)	1.775(4)	O(1*a*)—V—O(2*a*)	108.2(2)	O(2*a*)—V—O(3*a*)	110.4(3)
—O(2*a*),—O(2*b*)	1.728(4)	—O(3*a*)	108.2(4)	—O(4*a*)	110.6(3)
—O(3*a*),—O(3*a*)	1.704(7)	—O(4*a*)	109.6(4)	O(3*a*)—V—O(4*a*)	109.9(3)
—O(4*a*),—O(4*a*)	1.658(8)	V(1)—O(1*a*)—V(2)	149.3(8)		

*Transformations: $a = -x, y, 1/2 - z$; $b = x, y, z$; $c = x, -y, 1/2 + z$; $d = -x, -y, -z$; $e = 1/2 - x, 1/2 + y, 1/2 - z$; $f = 1/2 + x, 1/2 + y, z$; $g = 1/2 + x, 1/2 - y, 1/2 + z$; $h = 1/2 - x, 1/2 - y, -z$.

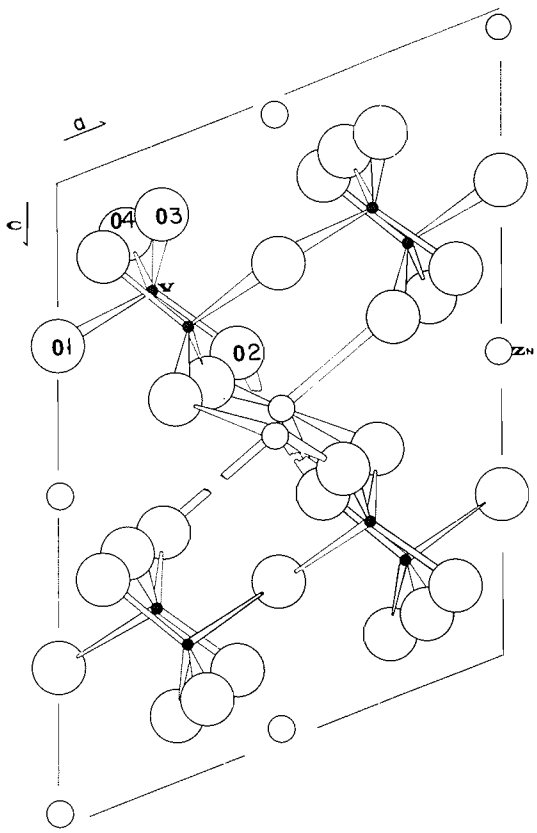

FIG. 2. The structure of α-$Zn_2V_2O_7$ showing the arrangement of the cations and their coordination environment.

The individual bond distances and angles are found in Table 3. The Zn—O bonds range from 1.973 Å (Zn—O(4*c*)) to 2.088 Å (Zn—O(3*a*)). O(4) is that oxygen atom bonded to only one Zn ion and V^{5+} ion while the remaining terminal oxygen atoms are bonded to two cations. The ZnO_5 polyhedra is a distorted trigonal bipyramid with the longer ZnO bonds in the axial direction.

The bridging V—O bond length at 1.775(4) Å is significantly longer than any involving terminal oxygen atoms. The V—O(4) bond length is the shortest, as one expects for that oxygen atom which is underbonded. The angular deviations from ideal tetrahedral values are small in comparison to comparable pyrophosphate systems (7–10). Two of the three O(1)—V—O bond angles are significantly smaller than ideal, while the remaining one does not differ significantly from the ideal value. The three O—V—O bond angles among terminal oxygen atoms are larger than ideal, but again one of them, O(3)—V—O(4), is not significantly larger.

Discussion

A comparison of the structure of α-$Zn_2V_2O_7$ with that of α-$Cu_2P_2O_7$ highlights many points of interest. α-$Cu_2P_2O_7$ has the largest P—O—P angle among those pyrophosphates with non-linear P—O—P bonds. By the same token α-$Zn_2V_2O_7$ also shows the largest V—O—V angle (149.3°) for the analogous divanadates. At the moment this group encompasses $Mg_2V_2O_7$ (17) (140.4°), $Co_2V_2O_7$ (2) (117.5°), β-$Sr_2V_2O_7$ (18) (123°), and $Pb_2V_2O_7$ (19) (122°).

The bridging oxygen atom in α-$Cu_2P_2O_7$ (7), as in $Zn_2V_2O_7$, shows enhanced disorder in the plane perpendicular to the vector connecting the centers of the tetrahedra forming the anion, as seen in Tables 4 and 5. It is not unexpected that the former compound would show a larger amplitude for this oxygen atom relative to the remaining ones as room temperature lies sub-

Can. J. Chem. Downloaded from www.nrcresearchpress.com by 210.87.254.105 on 09/05/12
For personal use only.

TABLE 4. Root mean squared amplitudes and angles of the principal axes of the thermal ellipsoids to the unit cell axes in $Zn_2V_2O_7$

Atom	r_i	Root-mean-squared amplitude (Å)	Angle between r_i and the crystal axis		
			a	*b*	*c*
Zn	r_1	0.118	46.8	105.2	152.0
	r_2	0.101	105.0	163.7	78.7
	r_3	0.077	132.9	84.2	115.3
V	r_1	0.106	70.9	153.4	113.8
	r_2	0.084	126.3	116.4	32.7
	r_3	0.047	42.6	87.7	68.9
O(1)	r_1	0.197	90.0	0.0	90.0
	r_2	0.152	96.4	90.0	152.2
	r_3	0.087	6.4	90.0	117.8
O(2)	r_1	0.139	48.5	128.2	129.3
	r_2	0.118	118.7	141.6	57.2
	r_3	0.071	55.0	86.0	56.5
O(3)	r_1	0.149	88.6	138.9	128.4
	r_2	0.092	113.6	127.6	38.4
	r_3	0.072	28.9	104.2	92.2
O(4)	r_1	0.176	40.8	92.2	152.1
	r_2	0.134	99.7	17.7	100.0
	r_3	0.084	50.8	72.5	64.2

TABLE 5. Root-mean-squared amplitudes and angles of the principal axes of the thermal ellipsoids to the unit cell axes in α-$Cu_2P_2O_7$

Atom	r_i	Root-mean-squared amplitude	Angle between r_i and the crystal axis		
			a	*b*	*c*
Cu	r_1	0.140	144.3	95.2	35.4
	r_2	0.117	86.9	174.4	95.4
	r_3	0.083	125.5	88.0	124.9
P	r_1	0.130	73.7	158.7	108.2
	r_2	0.091	112.1	109.2	19.6
	r_3	0.079	32.6	81.1	83.0
O(1)	r_1	0.254	90.0	0.0	90.0
	r_2	0.175	94.7	90.0	14.9
	r_3	0.099	13.8	90.0	104.9
O(2)	r_1	0.181	91.2	177.2	87.2
	r_2	0.147	52.4	92.7	161.7
	r_3	0.083	38.4	89.4	71.9
O(3)	r_1	0.132	28.8	112.9	124.2
	r_2	0.110	67.8	79.1	43.3
	r_3	0.089	107.4	154.4	66.8
O(4)	r_1	0.176	26.1	91.0	135.6
	r_2	0.120	106.1	40.9	117.9
	r_3	0.114	70.0	49.1	58.6

stantially closer to the transition temperature in the case of $Cu_2P_2O_7$. Further, the transformation is continuous leading to disorder streaks parallel to a^* in $Cu_2P_2O_7$; but no streaking was noted in $Zn_2V_2O_7$. Some indication of the effect of the disorder on the apparent geometry of the anion can be obtained by examining the difference in the maximum correction to the X—O bond lengths between the X—O bond involving the bridging oxygen atom and the average value in-

Can. J. Chem. Downloaded from www.nrcresearchpress.com by 210.87.254.105 on 09/05/12
For personal use only.

Can. J. Chem. Downloaded from www.nrcresearchpress.com by 210.87.254.105 on 09/05/12
For personal use only.

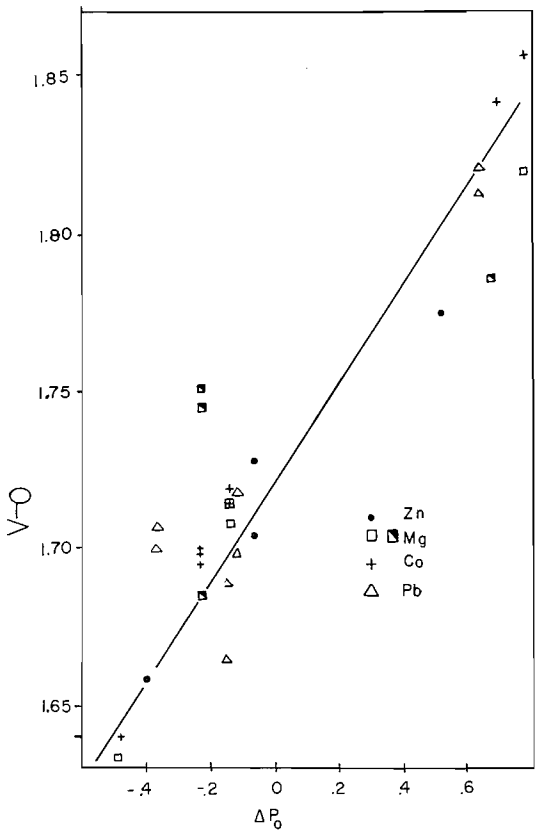

FIG. 3. V—O bond lengths in $M_2V_2O_7$ compounds *vs.* Δp_O. $Mg_2V_2O_7$ values indicated by ◥ represent the side of the anion with an additional weak V—O interaction.

volving the terminal oxygen atom. In $Zn_2V_2O_7$ this excess is 0.010 Å while in α-$Cu_2P_2O_7$ it is 0.024 Å, leading to maximum possible X—O—X angle decreases of 2 and 6°, respectively.

In $Zn_2V_2O_7$, as in α-$Cu_2P_2O_7$, the X—O bond involving the oxygen atom bonded strongly to only one cation, in addition to the pentavalent ion, is contracted. Baur has shown that for P—O bonds, the P—O bond length, d_{P-O}, is given by $d_{P-O} = 1.534 + 0.11\Delta p_O$ (20) and the analogous relationship for the vanadates is $d_{V-O} = 1.721 + 0.16\Delta p_O$ (19). The value of p_O is obtained by summing the ratios of the valency to the coordination number for each of the neighbors of the oxygen atom and Δp_O is the difference between p_O and its mean value in the specific compound. Figure 3 shows a plot of bond length versus Δp_O for the divanadates investigated in this laboratory. In $Mg_2V_2O_7$ one side of the V_2O_7 shows a fifth V—O interaction of about 2.4 Å and leads to large deviations as shown by the points in the plot. Generally the agreement with the linear correlation as shown in Fig. 3 is good. The predicted V—O(—V) bond length in $Zn_2V_2O_7$ lies substantially higher than the experimental ones, suggesting that the disorder indicated by the thermal parameters have significantly contracted this bond length.

Finally the question of the nature of the $Zn_2V_2O_7$ phase report by Angenault should be considered. His orthorhombic cell with space group *F*222, *Fmm*2, or *Fmmm* is somewhat reminiscent of the single crystal data that we have obtained on $Cu_2V_2O_7$ whose unit cell is orthorhombic with $a = 8.404$, $b = 20.670$, and $c = 6.442$ Å with space group *Fdd*2. The intensity distribution reported by Angenault is similar to that measured by us for $Cu_2V_2O_7$. It would appear that perhaps Angenault's $Zn_2V_2O_7$ is a high temperature modification from the manner in which it was prepared.

This research was supported by grant number A-940 from the National Research Council of Canada.

1. N. KRISHNAMACHARI and C. CALVO. Can. J. Chem. **49**, 1629 (1971).
2. E. E. SAUERBREI. M.Sc. Thesis, McMaster University, Hamilton, Ontario. 1972.
3. R. FAGGIANI and C. CALVO. Unpublished results.
4. R. GOPAL and C. CALVO. Can. J. Chem. **49**, 3056 (1971).
5. E. DORM and B. MARINDER. Acta Chem. Scand. **21**, 590 (1967).
6. P. K. L. AU and C. CALVO. Can. J. Chem. **45**, 2297 (1967).
7. B. E. ROBERTSON and C. CALVO. Acta Cryst. **22**, 665 (1967).
8. B. E. ROBERTSON and C. CALVO. J. Solid State Chem. **1**, 120 (1970).
9. C. CALVO. Acta Cryst. **23**, 289 (1967).
10. N. KRISHNAMACHARI and C. CALVO. Acta Cryst. **B28**, 2883 (1972).
11. A. J. POLLARD. U.S. Dept. Commer. Off. Tech. Serv. AD 412635 (1963).
12. J. J. BROWN and F. A. HUMMEL. Trans. Brit. Ceram. Soc. **64**, 419 (1965).
13. J. ARGENAULT. Rev. Chem. Miner. **7**, 651 (1970).
14. V. A. MAKAROV, A. A. FOTIEV, and N. SEREBRYAKOVA. Russ. J. Inorg. Chem. **16**, 1515 (1971).
15. HOK NAM NG. Unpublished results.
16. International tables for X-ray crystallography. Vol. III. Kynoch Press, Birmingham. 1962.
17. R. GOPAL. Ph.D. Thesis. McMaster University, Hamilton, Ontario. 1972.
18. J. A. BAGLIO and J. N. DANN. J. Solid State Chem. **4**, 87 (1972).
19. R. D. SHANNON and C. CALVO. Can. J. Chem. **51**, 70 (1973).
20. W. H. BAUR. Trans. Am. Cryst. Assoc. **6**, 129 (1970).

Radiolysis Free Ion Yields and Electron Ranges in Polar and Nonpolar Liquids: Fluoromethanes[1]

MAURICE G. ROBINSON AND GORDON R. FREEMAN

Chemistry Department, University of Alberta, Edmonton, Alberta, T6G 2G2

Received October 23, 1972

The free ion yields at zero applied electric field strength in the liquid fluoromethanes are $G_{fi}^0 = 1.6$ in CH_3F, 1.9 in CH_2F_2 and 1.1 in CHF_3, all at 183 °K, and 0.07 in CF_4 at 143 °K. Median ranges y_{med} of the secondary electrons were estimated by fitting the electric field dependence of G_{fi} to a model equation: $y_{med} = 41$ Å in CH_3F, 39 Å in CH_2F_2 and CHF_3, and 132 Å in CF_4, at the above-mentioned temperatures. The average number of collisions, n, required to thermalize a secondary electron is about 64 000 in liquid Ar, 7 700 in CH_4, 660 in $C(CH_3)_4$, 360 in CF_4, 110 in C_3H_8, 44 in CH_3F, 39 in CH_2F_2, 35 in CHF_3, 17 in H_2O, and 12 in CH_3OH. The value of n with nonpolar molecules (up to neopentane in size) tends to decrease with increasing molecular complexity and with decreasing sphericity. Presence of a large dipole moment in the molecule decreases n further, and hydrogen bonds reduce n still more. Energy transfer between the electrons and rotational modes of the molecules appears to be important.

Le rendement en ions libres en l'absence de champ électrique, G_{fi}^0, est à 183 °K: 1.6 pour le CH_3F, 1.9 pour le CH_2F_2 et 1.1 pour le CHF_3; 0.07 pour le CF_4 à 143 °K. La distance médiane de pénétration, y_{med}, des électrons secondaires dans chaque liquide a été déduite de la meilleure distribution utilisée pour le calcul de l'effet du champ électrique sur le rendement en ions libres. Ces distances médianes sont aux températures mentionnées: $y_{med} = 41$ Å pour le CH_3F, 39 Å pour le CH_2F_2, 39 Å pour le CHF_3, et 132 Å pour le CF_4. Le nombre moyen de collisions, n, subies par un électron secondaire jusqu'à thermalisation est environ: 64 000 pour l'argon liquide, 7 700 pour le méthane, 660 pour le néopentane, 360 pour le CF_4, 110 pour le propane, 44 pour le CH_3F, 39 pour le CH_2F_2, 35 pour le CHF_3, 17 pour l'eau et 12 pour le méthanol. La valeur de n dans des liquides non polaires dont les molécules ont une taille ne dépassant pas celle du néopentane tend à diminuer avec l'accroissement de la complexité moléculaire et avec l'écart progressif de la forme sphérique. La présence dans la molécule d'un moment dipolaire élevé réduit n, et s'il y a liaisons hydrogènes n est réduit d'avantage. Le transfert d'énergie entre les électrons et les modes de rotation des molécules semble être important.

Can. J. Chem., **51**, 1010 (1973)

Introduction

Electron behavior in liquid hydrocarbons is affected by the structure of the molecules (1–5). The rate of energy loss by epithermal electrons in a liquid alkane correlates inversely with the sphericity of the molecules (3, 5). The electron–molecule energy transfer interaction apparently involves rotational modes of the molecules and may operate through the anisotropic polarizability of nonpolar molecules (5). Presence of a permanent electric dipole in a molecule should enhance the electron–molecule interaction (6). To obtain information about the effect of a permanent dipole moment, radiolysis free ion yields were measured and electron ranges estimated in CH_3F, CH_2F_2, CHF_3, and CF_4; the first three compounds have dipole moments $\mu > 1.6$ D, whereas that of CF_4 is zero (7). The results are reported below.

[1]This work received financial assistance from the National Research Council of Canada.

Experimental

Materials

The methyl fluoride and difluoromethane were obtained from Columbia Organic Chemicals and the fluoroform and tetrafluoromethane from Matheson.

Each gas was introduced into the high vacuum system via two purification columns at 298 °K. One contained sodium hydroxide pellets and the other silica gel; the latter was activated under vacuum for 4 h at 520 °K. After condensation at 77 °K the compounds were distilled repeatedly from trap to trap, the receiver being continually open to vacuum. Prior to use the compounds were electrolyzed as liquids at 143 °K and 1–2 kV/cm for 1 h. The samples were then distilled into the conductance cell at 77 °K and the cell unit sealed off with a flame.

The densities, dielectric constants, dipole moments, and mean polarizabilities of the four fluoromethanes are listed in Table 1.

Conductance Cell

The collecting electrode was guarded in a manner similar to that reported earlier (8), but the total cell volume was reduced to about 5 cm^3. The effective electrode area was 1.77 cm^2 and the separation 0.30 cm.

Determination of the Free Ion Yields

The free ion yields were measured as a function of

Can. J. Chem. Downloaded from www.nrcresearchpress.com by 210.87.254.105 on 09/05/12
For personal use only.

TABLE 1. Physical properties of the fluoromethanes

Liquid	T (K)	d (g/cm^3)	ε	μ (D)	α (Å^3)
CF_4	143	1.62[a,b]	1.64[c]	0.0[d]	2.9[e]
CHF_3	183	1.48[a,b]	21.4[c]	1.65[d]	2.8[e]
CH_2F_2	183	1.30[b]	38.9[c]	1.97[d]	2.7[f]
CH_3F	183	0.903[a] 0.905[b]	27.9[c]	1.85[d]	2.6[e]

[a]Reference 25.
[b]K. Shinsaka. To be published.
[c]P. Tremaine and M. G. Robinson. To be published.
[d]Reference 7.
[e]Reference 26 and citations therein.
[f]By interpolation between the other values in this series.

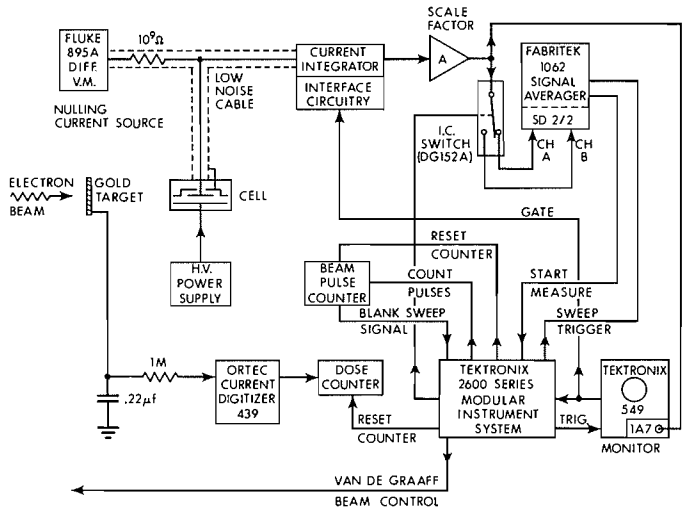

FIG. 1. Schematic diagram of circuit for measurement of free ion yields. Odd numbered sweeps of the integration system were blanks, in which no radiation pulse occurred. The nulling current source was used to cancel the background conductance of the sample. Details of the current integrator are in Fig. 3*b* of ref. 8.

applied voltage by the charge clearing method (2, 8–10). The circuit used was similar to that recently described (8) with the important exception that the clearing field was on continuously during an experiment. This eliminated the problems associated with a high voltage switch. A schematic diagram of the circuit used is shown in Fig. 1.

Signals were generated by 1 μs pulses of 1.7 MeV X-rays. At each field strength eight alternate signals and blanks (no radiation pulse) were fed into a low drift high sensitivity integrator and averaged with a Fabritek model 1062 Instrument Computer. The averaged signals and blanks were displayed on an oscilloscope and photographed (see Fig. 2). A Tektronix 549 B oscilloscope with a type 1A7 plug-in monitored the integrator output from each signal and blank. The integration time for each signal and blank was 2 s.

Despite the great care taken to purify these compounds the liquids CH_3F, CH_2F_2, and CHF_3 contained sufficient ionic impurities (ionic dissociation?) to give an appreciable background conductance. Additional treatment with sodium hydroxide or electrolysis had no effect. In order to take measurements of the radiation induced conductance the background conductance was nulled by an opposing voltage across a 10^9 ohm resistor. The nulling currents at the maximum field strengths used were 1.6 nA in CH_3F, 0.7 nA in CH_2F_2, and 0.1 nA in CHF_3.

Dosimetry

The absorbed dose per X-ray pulse was $\sim 3 \times 10^{10}$ eV/cm^3, measured by thermoluminescent dosimetry (8). The dose absorbed in the desired liquid was calculated from that absorbed in the thermoluminescent lithium chloride crystals, using the relative electron densities. Each pulse was monitored by the charge collected on the gold target.

Results and Discussion

Free Ion Yields and Their Field Dependence

The free ion yields increased in the order $CF_4 \ll CHF_3 < CH_3F < CH_2F_2$ (Fig. 3). The dielectric constants of the liquids increase in the same order (Table 1).

The free ion yield $G_{fi}{}^E$ increased with applied field strength E in all liquids, but the relative

Can. J. Chem. Downloaded from www.nrcresearchpress.com by 210.87.254.105 on 09/05/12
For personal use only.

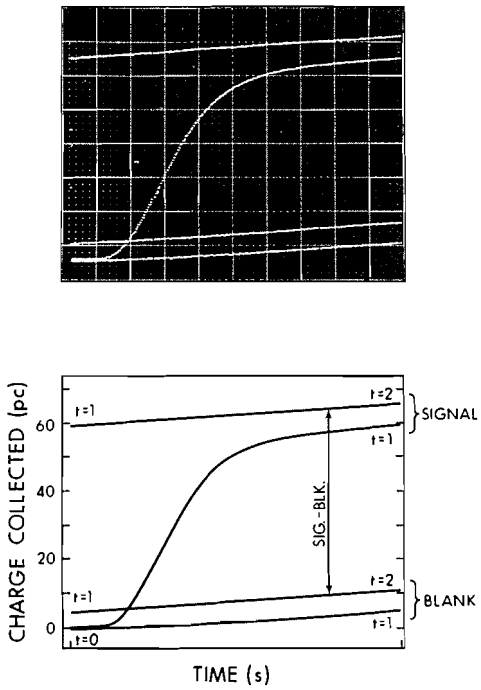

FIG. 2. Typical averages of four signals and four blanks from charge integrator output. Liquid methyl fluoride, 2.3 kV/cm, average pulse dose 3.8×10^{10} eV/cm^3, oscilloscope sweep time 1 s, total integration time 2 s.

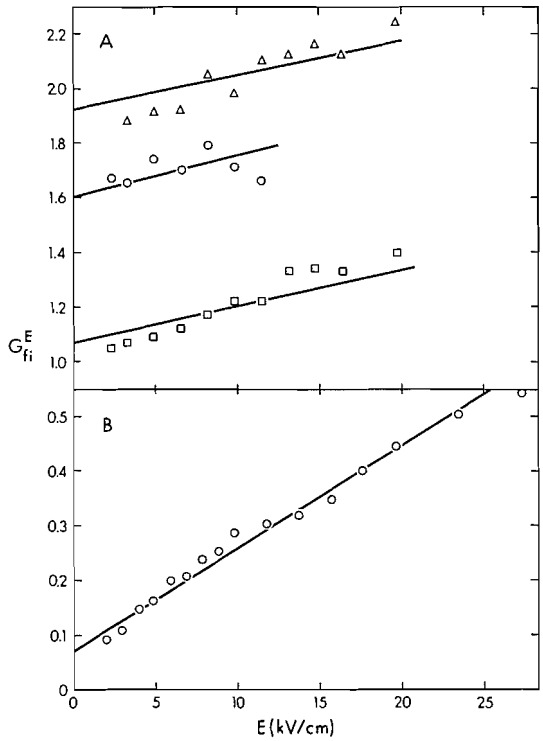

FIG. 3. Free ion yields $G_{fi}{}^E$ at applied electric field strength E. *A*, all liquids at 183 °K: ○, CH_3F; △, CH_2F_2; □, CHF_3. *B*, CF_4 at 143 °K. The curves were calculated from eq. 1, using the $F(y)$ distributions mentioned in the text.

increase was much greater in the nonpolar CF_4 than in the polar liquids CHF_3, CH_2F_2, and CH_3F (Fig. 3).

The influence of applied field strength on the free ion yield in a liquid irradiated by low LET radiation is approximately described by eq. 1 (11, 12).

$$[1] \quad G_{fi}{}^E = G_{tot} \int_0^\infty F(y)\, e^{-r/y} (1 + \beta r + 0.375\beta^2 r^2 - 0.750\beta^2 r y + \ldots)\, dy$$

where G_{tot} is the total number of ion–electron pairs generated per 100 eV absorbed by the liquid, $F(y)dy$ is the fraction of thermalized electron–ion pairs with initial intrapair separation distances between y and $y + dy$, $r = \xi^2/\varepsilon kT$, ξ is the electronic charge, ε is the dielectric constant of the liquid, k is Boltzmann's constant, T is the absolute temperature, and $\beta = \xi E/600kT$. At zero field strength $\beta = 0$ and

$$[2] \quad G_{fi}{}^0 = G_{tot} \int_0^\infty F(y)\, e^{-r/y}\, dy$$

By inserting the values of the appropriate constants one finds that $\beta r = 9.69E/\varepsilon T^2$. Furthermore

$$[3] \quad G_{fi}{}^E = G_{fi}{}^0 \left\{ 1 + \frac{9.69E}{\varepsilon T^2} + \frac{35.2E^2}{\varepsilon^2 T^4} - \frac{4.21 \times 10^4 E^2}{\varepsilon T^3} \frac{\int_0^\infty F(y) y\, e^{-r/y}\, dy}{\int_0^\infty F(y)\, e^{-r/y}\, dy} + \ldots \right\}$$

Under the conditions used in the present work the free ion yields increased approximately linearly with field strength. The fractional increase in yield with increasing field is given approximately by the second term in the brackets of the right hand side of eq. 3, $9.69E/\varepsilon T^2$. The relatively large field effect observed in CF_4 is due mainly to the low value of ε of that liquid compared to those of the other liquids (Table 1).

Can. J. Chem. Downloaded from www.nrcresearchpress.com by 210.87.254.105 on 09/05/12
For personal use only.

TABLE 2. Ion yields and electron ranges

Liquid	T (K)	G_{tot}[a]	G_{fi}^0	b (Å)	y_{med} (Å)
CF_4	143	2.9[b]	0.07[d]		132[e]
CHF_3	183	3.3[c]	1.1[d]	36	39[e]
CH_2F_2	183	3.7[c]	1.9[d]	36	39[e]
CH_3F	183	3.7[c]	1.6[d]	38	41[e]

[a]Assumed equal to the gas phase values.
[b]Reference 27.
[c]Estimated by comparison with those of CF_4 and CH_4 ($G_{tot} = 3.7$ in CH_4 (see ref. 28)). The ionization potentials (eV) are: CF_4, < 15.0; CHF_3, 13.8; CH_2F_2, 12.6; CH_3F, 12.8; CH_4, 13.0.
[d]Free ion yield extrapolated to zero field strength.
[e]Median range of the electrons.

Ranges of the Secondary Electrons

The observed values of G_{fi}^E were fitted to eq. 1, using the Gaussian range distribution [4] for CH_3F, CH_2F_2, and CHF_3.

$$[4] \qquad F(y) = (4y^2/\pi^{1/2}b^3) \exp(-y^2/b^2)$$

where b is the dispersion parameter, and is also the most probable value of y. The Gaussian function has been found to be suitable for liquids in which $G_{fi}^0 > 0.2$ (12). The value of b in each of the three liquids is listed in Table 2. The calculated values of G_{fi}^E are represented by the full curves for these compounds in Fig. 3.

The Gaussian form of $F(y)$ distribution did not allow satisfactory agreement to be obtained between calculated and observed values of G_{fi}^E in CF_4; the calculated field dependence was larger than that observed. It had been found earlier (12) that a power function [5] gave satisfactory results when G_{fi}^0 was <0.2.

$$[5] \quad \begin{cases} F(>y) = (y_{min}/y)^x & y \geq y_{min} \\ F(>y) = 1 & y \leq y_{min} \end{cases}$$

where

$$F(>y) = \int_y^\infty F(y)\,dy$$

This function worked well in eq. 1 for CF_4, and the best values of the parameters were found to be $y_{min} = 100$ Å and $x = 2.5$. The calculated yields are shown in Fig. 3.

The median range y_{med} can be used to compare typical range values in systems where different $F(y)$ distributions apply. The arithmetic-mean range is not appropriate for this purpose because it gives too much weight to the long-range tail in some distributions.

In the Gaussian function [4], $y_{med} = 1.09b$; in the power function [5] with $x = 2.5$, $y_{med} = 1.32\ y_{min}$. The values of y_{med} obtained for the fluorocarbons are listed in Table 2. Electron ranges are approximately equal in CH_3F, CH_2F_2, and CHF_3, while those in CF_4 are three times larger.

Comparison with Other Systems: Secondary Electron Energy Loss Rates

Medium ranges of secondary electrons in a number of liquids are listed in Table 3 (8, 12–14). The liquid density has been used successfully to normalize ranges in hydrocarbons (2, 5, 9, 12), but density is less suitable for the normalization of ranges in different kinds of compounds. A more meaningful comparison might be obtained by estimating the average number n of collisions required to thermalize the secondary electrons in the liquids.

The detailed shape of the electron path is determined by both elastic and inelastic scattering, but the length of the path is limited by inelastic scattering. The latter process is mainly responsible for the de-energization of the electron. The elastic (momentum transfer) scattering cross sections of all of the substances in Table 3 for 1 eV electrons are probably of the order of 10 Å^2(15*a*, 16, 17); the inelastic cross sections are in general smaller than elastic cross sections for electrons with energies less than 10 eV (16, 17).

The relation between the average number of collisions n undergone during thermalization and the median penetration range y_{med} is, assuming random scattering (15*b*):

$$[6] \qquad y_{med} = 1.09b = 1.09\sqrt{2n}\,\lambda$$

where λ is the mean free path. Therefore

$$[7] \qquad n = y^2{}_{med}/2.4\lambda^2$$

The secondary electrons in liquid hydrocarbons appear to interact with molecules or parts of molecules up to the size of neopentane (5), which is the largest molecule being considered

Can. J. Chem. Downloaded from www.nrcresearchpress.com by 210.87.254.105 on 09/05/12
For personal use only.

TABLE 3. Comparison of electron median ranges in several liquids

Liquid	T (°K)	y_{med} (Å)	n^f (collisions)	α^a (Å^3)	μ^k (D)	$N^{-1/3}$ (Å)	N (10^{21}molecules/cm^3)
Ar[a]	87	1 420	64 000	0.0[g]	0.00	3.6	21.1
CH_4[b]	120	545	7 700	0.0[g]	0.00	4.0	15.6
$C(CH_3)_4$[c]	294	234	660	0.0[g]	0.00	5.9	4.93
CF_4	143	132	360	0.0[g]	0.00	4.5	11.1
CH_3CH_3	183	~114[e]	~270	0.7[g]	0.00	4.5	11.0
$CH_2(CH_3)_2$[b,c]	183	79	110	0.9[g]	0.08	4.9	8.71
$CH(CH_3)_3$[a,c]	183	102	160	0.7[g]	0.13	5.2	7.1
CH_3F	183	41	44	0.8[h]	1.85	4.0	16.0
CH_2F_2	183	39	39	—	1.97	4.1	15.1
CHF_3	183	39	35	0.3[i]	1.65	4.2	13.2
CH_3OH[d]	298	22	12	0.7[j]	1.70	4.1	14.8
H_2O[d]	296	20	17	~0.5[j]	1.85	3.1	33.3

[a]Reference 13.
[b]Reference 8.
[c]Reference 12.
[d]Reference 14.
[e]Estimated by comparison of the b values for C_2H_6 and C_3H_8 in ref. 8 with the more appropriate y_{med} value for C_3H_8 in ref. 12.
[f]Calculated from eq. 9.
[g]Polarizability anisotropies α^a calculated from information in ref. 29. See also footnote *a* in Table IV of ref. 5, concerning inaccuracies in the values listed in ref. 30.
[h]Reference 31.
[i]Reference 32.
[j]Reference 33.
[k]Reference 7, gas phase.

here. One might therefore take λ approximately equal to the molecular diameter for these small molecules, whence

$$\lambda \approx N^{-1/3} \quad [8]$$

and

$$n \approx y^2_{med} N^{2/3}/2.4 \quad [9]$$

where N is the number of molecules/cm^3.

Values of n are given in Table 3. The average number of collisions required to thermalize a secondary electron in liquid argon is an order of magnitude greater than that required in methane, which in turn is an order of magnitude greater than that in neopentane. The decrease in n corresponds to an increase in energy transfer per collision, $-dT/dn$, and correlates with the increasing molecular complexity in the series Ar, CH_4, $C(CH_3)_4$.

On going from $C(CH_3)_4$ to CF_4 n decreases by a factor of two. Thus CF_4 is somewhat more efficient than is $C(CH_3)_4$ at accepting energy from an epithermal electron. The difference might be due to a more accessible transient negative ion state in CF_4 than in $C(CH_3)_4$. Transient negative ion states are often invoked as intermediates in the vibrational excitation of molecules by electrons (18–22).

In the series CH_4, CH_3CH_3, $CH_2(CH_3)_2$, $CH(CH_3)_3$, $C(CH_3)_4$ n decreases 30-fold from methane to ethane, a further 2.5-fold to propane, then increases again 1.5-fold to isobutane and a further 4-fold to neopentane (Table 3). Two influences combine to give a minimum n value at propane: n tends to decrease with increasing molecular complexity and decreasing molecular sphericity. Molecular complexity increases throughout the series from methane to neopentane, but sphericity is at a minimum at propane. The less sphere-like alkanes have the greater anisotropies of polarizability α^a (Table 3). The magnitude of the rotational excitation cross section of a nonpolar molecule for slow electrons depends on the anisotropy (16). The selection rules for excitation by slow electrons (16) are similar to those for Raman excitation (23).

The value of n in CH_3F is 6-fold smaller than that in CH_3CH_3. This difference is presumably due to the large dipole moment in CH_3F (Table 3) and is consistent with the suggestion (5) that electrons lose their energy mainly to rotational modes of the molecules.

The small decrease in n from CH_3F to CHF_3 might be related to easier vibrational excitation of the latter, which presumably possesses a lower lying negative ion state and a lower vibrational excitation threshold (F—C—F bending) than does the former.

The 4-fold decrease in n on going from CH_3F

Can. J. Chem. Downloaded from www.nrcresearchpress.com by 210.87.254.105 on 09/05/12
For personal use only.

to CH_3OH is not due to differences in the molecular dipole moments or anisotropies of polarizability (Table 3). These properties are similar for the two substances. It appears that hydrogen bonds are efficient energy sinks for low energy electrons. Hydrogen bonds have extremely high polarizabilities (24), and presumably large anisotropies. Furthermore, the strong solvating power of —OH groups for electrons might cause the electron to become localized before it has been completely "thermalized". The electron range would thereby be shortened.

Methanol appears to be a more efficient energy sink than is water for low energy electrons, n being smaller in the former than in the latter (Table 3). This difference is not understood, although it correlates with the relative optical absorption energies of solvated electrons in the two liquids: $E_{\lambda_{max}} = 1.9$ and 1.7 eV in methanol and water, respectively.

We would like to thank the staff of the Radiation Research Center for aid with the electronics and J.-P. Dodelet for calculating the curves in Fig. 2.

1. R. GIBAUD. J. Chim. phys. **64**, 521 (1967).
2. W. F. SCHMIDT and A. O. ALLEN. (*a*) Science, **160**, 301 (1968); (*b*) J. Phys. Chem. **72**, 3730 (1968).
3. P. H. TEWARI and G. R. FREEMAN. (*a*) J. Chem. Phys. **49**, 954 (1968); (*b*) **49**, 4394 (1968).
4. R. M. MINDAY, L. D. SCHMIDT, and H. T. DAVIS. (*a*) Phys. Rev. Lett. **26**, 360 (1971); (*b*) J. Chem. Phys. **54**, 3112 (1971).
5. J.-P. DODELET and G. R. FREEMAN. Can. J. Chem. **50**, 2667 (1972).
6. H. S. W. MASSEY, E. H. S. BURHOP, and H. B. GILBODY. Electronic and ionic impact phenomena. 2nd ed. Vol. 2. Clarendon Press, Oxford. 1969.
7. R. D. NELSON, JR., D. R. LIDE, JR., and A. A. MARYOTT. Selected values of electric dipole moments for molecules in the gas phase. NSRDS-NBS 10. 1967.
8. M. G. ROBINSON, P. G. FUOCHI, and G. R. FREEMAN. Can. J. Chem. **49**, 3657 (1971).
9. W. F. SCHMIDT and A. O. ALLEN. J. Chem. Phys. **52**, 2345 (1970).
10. P. H. TEWARI and G. R. FREEMAN. J. Chem. Phys. **51**, 1276 (1969).
11. G. R. FREEMAN. J. Chem. Phys. **39**, 1580 (1963).
12. J.-P. DODELET, P. G. FUOCHI, and G. R. FREEMAN. Can. J. Chem. **50**, 1617 (1972).
13. P. G. FUOCHI and G. R. FREEMAN. J. Chem. Phys. **56**, 2333 (1972).
14. J.-P. DODELET and G. R. FREEMAN. Can. J. Chem. **50**, 2729 (1972).
15. E. W. MCDANIEL. Collision phenomena in ionized gases. John Wiley and Sons, New York. 1964; (*a*) Chapt. 4; (*b*) pp. 38–50, 492.
16. D. E. GOLDEN, N. F. LANE, A. TEMKIN, and E. GERJUOY. Rev. Mod. Phys. **43**, 642 (1971).
17. Y. ITIKAWA. ANL-7939 (Argonne National Lab.). April 1972.
18. R. HAAS. Z. Phys. **148**, 177 (1957).
19. J. C. Y. CHEN and J. L. MAGEE. J. Chem. Phys. **36**, 1407 (1962).
20. T. L. COTTRELL and I. C. WALKER. Q. Rev. **20**, 153 (1966).
21. A. V. PHELPS. Rev. Mod. Phys. **40**, 399 (1968).
22. L. G. CHRISTOPHOROU. Atomic and molecular radiation physics. Wiley–Interscience, New York. 1971. Chapt. 5.
23. G. HERZBERG. Infrared and Raman spectra of polyatomic molecules. Van Nostrand, New York. 1945. Chapt. 1.
24. R. JANOSCHEK, E. G. WEIDEMANN, H. PFEIFFER, and G. ZUNDEL. J. Am. Chem. Soc. **94**, 2387 (1972).
25. F. Richter (*Editor*). Beilsteins handbuch der organischen chemie. 4 Auflage. 3 Ergänzungswerk. I Band. 1 Teil. Springer–Verlag, Berlin. 1958. pp. 33–36.
26. J. APPLEQUIST, J. R. CARL, and K.-K. FUNG. J. Am. Chem. Soc. **94**, 2952 (1972).
27. R. COOPER and R. M. MOORING. Aust. J. Chem. **21**, 2417 (1968).
28. G. G. MEISELS. J. Chem. Phys. **41**, 51 (1964); P. ALDER and H. K. BOTHE. Z. Naturforsch. **20a**, 1700 (1965).
29. R. J. W. LEFÈVRE. Rev. Pure and Appl. Chem. **20**, 67 (1970); Adv. Phys. Org. Chem. **3**, 1 (1965).
30. LANDOLT–BÖRNSTEIN. Zahlenwerte und Funktionen. I Bd. 3 Teil. 1951. p. 290.
31. C. G. LEFÈVRE and R. J. W. LEFÈVRE. Rev. Pure Appl. Chem. **5**, 261 (1955).
32. N. J. BRIDGE and A. D. BUCKINGHAM. Proc. Roy. Soc. **A295**, 334 (1966).
33. C. G. LEFÈVRE, R. J. W. LEFÈVRE, B. P. RAO, and A. J. WILLIAMS. J. Chem. Soc. (London), 123 (1960).

Can. J. Chem. Downloaded from www.nrcresearchpress.com by 210.87.254.105 on 09/05/12
For personal use only.

Reactivity of Substituted Benzenethiols Towards Chlorotris(triphenylphosphine)iridium(I) and Chlorotris(triphenylarsine)iridium(I)[1]

JOSEPH L. HERDÉ AND CAESAR V. SENOFF[2]

Department of Chemistry, University of Guelph, Guelph, Ontario

Received July 6, 1972

A series of substituted benzenethiols, HSC_6H_4Y (Y = 4-Br, 4-F, 4-H, 4-CH_3, or 4-CH_3O) have been shown to react with $IrCl(Ph_3M')_3$ (M′ = P or As) in benzene to form dimeric iridium(III) complexes of the type, $[IrHCl(SC_6H_4Y)(Ph_3M')_2]_2$, **1**. The thiol, 4-nitrobenzenethiol, reacts with $IrCl(Ph_3M')_3$ (M′ = P or As) to form complexes of the type $[IrCl_2(SC_6H_4NO_2)(Ph_3M')_2]_2$, **2**. Complexes **1** undergo reductive elimination with carbon monoxide to form *trans*-$[Ir(CO)_2(Ph_3M')_2]Cl$ whereas complexes **2** do not react with carbon monoxide. Spectroscopic properties (i.r. and n.m.r.) of these complexes are discussed in relation to their structure in the solid state and in solution.

Une série de benzènethiols substitués, HSC_6H_4Y (Y = Br-4, F-4, H-4, CH_3-4, ou CH_3O-4) réagit, comme il est montré, avec $IrCl(Ph_3M')_3$ (M′ = P ou As) dans le benzène pour former des complexes dimériques de l'iridium(III) du type $[IrHCl(SC_6H_4Y)(Ph_3M')_2]_2$, **1**. Le thiol, nitro-4 benzènethiol réagit avec $Ir(PH_3M')_3$ (M′ = P ou As) pour former des complexes du type $[IrCl_2(SC_6H_4NO_2)(Ph_3M')_2]_2$, **2**. Les complexes **1** subissent une élimination réductive avec du monoxide de carbone pour former le *trans*-$[Ir(CO)_2(Ph_3M')_2]Cl$ alors que les complexes **2** ne réagissent pas avec le monoxyde de carbone. Les caractéristiques spectroscopiques (i.r. et r.m.n.) de ces complexes sont discutées en fonction de leurs structures dans l'état solide de même qu'en solution. [Traduit par le journal]

Can. J. Chem., 51, 1016 (1973)

Chlorotris(triphenylphosphine)iridium(I) and related iridium(I) complexes have been investigated by several workers (1–7). The ability of these complexes to participate in oxidative addition reactions and their ability to function as homogeneous catalysts have also been of particular interest (2, 3). As part of a general investigation into the reactivity of substituted benzenethiols towards low valent transition metal complexes (8–10) we have undertaken a study of the reactivity of a series of 4-substituted benzenethiols, HSC_6H_4Y (Y = 4-NO_2, 4-Br, 4-F, 4-H, 4-CH_3, or 4-CH_3O) towards $IrCl(Ph_3M')_3$ (M′ = P or As). The results of this investigation are reported at this time.

Results and Discussion

At the outset of this study it was anticipated that the complexes, $IrCl(Ph_3M')_3$ (M′ = P or As) would oxidatively add HSC_6H_4Y (Y = an electron releasing or electron withdrawing substituent) to form $IrHCl(SC_6H_4Y)(Ph_3P)_3$ according to reaction 1. This expectation was not realized. The substituted benzenethiols do not simply oxidatively add to $IrCl(Ph_3M')_3$ but form dimeric complexes, the nature of which is markedly dependent upon the nature of the substituent, Y. Accordingly, it was found that HSC_6H_4Y (Y = 4-Br, 4-F, 4-H, 4-CH_3, or 4-CH_3O) reacted with $IrCl(Ph_3M')_3$ (M′ = P or As) to form cream-colored precipitates over a prolonged period of time according to reaction 2.

[1] $IrCl(Ph_3M')_3 + HSC_6H_4Y \rightarrow IrHCl(SC_6H_4Y)(Ph_3M')_3$

[2] $2IrCl(Ph_3M')_3 + 2HSC_6H_4Y \rightarrow [IrHCl(SC_6H_4Y)(Ph_3M')_2]_2 + 2Ph_3M'$

The time of reaction and yield of product are

TABLE 1. Reaction times and yields for the complexes $[IrHCl(SC_6H_4Y)(Ph_3M')_2]_2$

Complex	Reaction time (h)	% yield
$[IrHCl(SC_6H_4Br)(Ph_3P)_2]_2$	24	86
$[IrHCl(SC_6H_4F)(Ph_3P)_2]_2$	20	87
$[IrHCl(SC_6H_5)(Ph_3P)_2]_2$	40	69
$[IrHCl(SC_6H_4CH_3)(Ph_3P)_2]_2$	48	80
$[IrHCl(SC_6H_4OCH_3)(Ph_3P)_2]_2$	30	74
$[IrHCl(SC_6H_4Br)(Ph_3As)_2]_2$	72–96	38
$[IrHCl(SC_6H_4F)(Ph_3As)_2]_2$	72–80	26
$[IrHCl(SC_6H_5)(Ph_3As)_2]_2$	90–100	45
$[IrHCl(SC_6H_4CH_3)(Ph_3As)_2]_2.C_6H_6$	48–72	60
$[IrHCl(SC_6H_4OCH_3)(Ph_3As)_2]_2$	48–72	50

[1]Taken from the M.Sc. Thesis of J.L.H., August, 1971.
[2]To whom all correspondence to be addressed.

Can. J. Chem. Downloaded from www.nrcresearchpress.com by 210.87.254.40 on 09/05/12
For personal use only.

Can. J. Chem. Downloaded from www.nrcresearchpress.com by 210.87.254.40 on 09/05/12
For personal use only.

dependent on the nature of Y. These data are given in Table 1. The formation of these dimeric complexes may be *conceptually* rationalized by the following scheme where L = Ph_3P or Ph_3As, and Ar = YC_6H_4, *i.e.*,

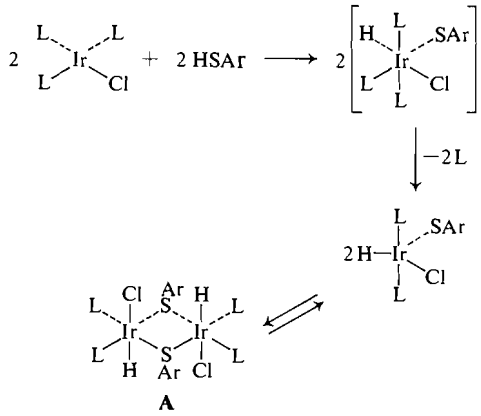

A

The first step involves a simple *cis*-oxidative addition of the substituted benzenethiol to the iridium(I) substrate to form an octahedral iridium(III) "intermediate" followed by elimination of L to form a 5-coordinate iridium(III) derivative which then dimerizes to form the observed product, **A**. The triphenylphosphine complexes, $[IrHCl(SC_6H_4Y)(Ph_3P)_2]_2$, **1**, are air stable in the solid state and are sparingly soluble in common organic solvents (*e.g.*, acetone, benzene, chloroform, etc.) whereas the corresponding triphenylarsine complexes, $[IrHCl(SC_6H_4Y)(Ph_3As)_2]_2$, **2**, are also air stable in the solid state but are more soluble in organic solvents.

The complexes, **1**, are characterized by a strong, sharp band in the region 2231–2110 cm^{-1}, which may be assigned to the ν_{Ir-H} vibration. The corresponding iridium–hydrogen stretching vibration for the complexes, **2**, was observed between 2203–2184 cm^{-1}. Metal–chlorine stretching vibrations are expected to occur below 400 cm^{-1} (11). Complexes **1** and **2** exhibited a band of medium intensity in the regions 248–242 and 260–249 cm^{-1}, respectively, which has been assigned to the ν_{Ir-Cl} vibration. These infrared data are presented in Table 2.

Complexes **1** were too insoluble to observe the high field resonance expected for a hydrido ligand bonded to iridium. However, the complexes **2** were sufficiently soluble to observe this resonance as a single peak at ~21 p.p.m. in $CDCl_3$. The n.m.r. data are given in Table 3.

Molecular weight measurements confirm that the complexes are indeed dimeric. Typical molecular weight data (osmometry in $CHCl_3$ or C_6H_6) are given in Table 4. These data indicate that the complexes dissociate in solution into two five coordinate species according to reaction 3. Unfortunately, the complexes **1** were too insoluble

[3] $[IrHCl(SC_6H_4Y)(Ph_3M')_2]_2 \rightleftharpoons 2[IrHCl(SC_6H_4Y)(Ph_3M')_2]$

to permit a measurement of their molecular weights. Presumably, these complexes are also dimeric in view of their similar properties (*vide supra et vide infra*) to the complexes **2**.

It is possible to visualize several different structures for the complexes **1** and **2**. The four most likely structures are shown below

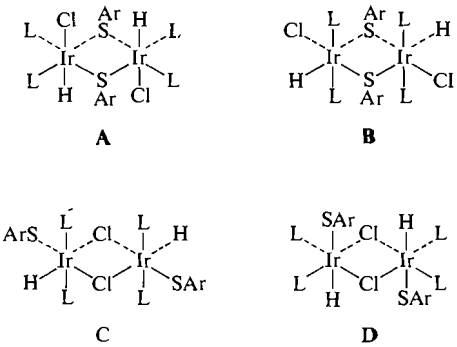

A B C D

If one considers the propensity that an arenethiolato ligand has for functioning as a bridging group, then structures **C** and **D** may be eliminated from any further consideration. The fact that a single resonance due to the hydrido ligand bonded to iridium was observed in the ^1H n.m.r. spectra of complexes **2**, the fact that only one ν_{Ir-Cl} vibration and one ν_{Ir-H} vibration was observed in the infrared spectra of complexes **1** and **2** and the fact that molecular weight measurements for complexes **2** indicate that these complexes are dimeric are all consistent with structures A and **B** (C_{2h} local symmetry) having arenethiolato bridging groups. A δ value of ~21 p.p.m. in the ^1H n.m.r. spectra of complexes **2** (see Table 3) is consistent with the hydrido ligand being *trans* to a ligand of low *trans*-influence such as Cl^- or $YC_6H_4S^-$ (12 and references therein). Hence, the position of the highfield resonance of the hydrido ligand in complexes **2** does not unambiguously distinguish between structure **A** and structure **B**.

A plot of ν_{Ir-H} *vs.* the Hammett substituent parameter, σ_p, for the complexes **2** is shown in

TABLE 2. Infrared data*

Complex	ν_{Ir-H} (cm^{-1})	ν_{Ir-Cl} (cm^{-1})	Other bands (cm^{-1})
$[IrHCl(SC_6H_4Br)(Ph_3P)_2]_2$	2231(s)	243(m)	415(m) 438(m) 455(m) 497(s) 515(m) 530(s)
$[IrHCl(SC_6H_4F)(Ph_3P)_2]_2$	2234(s) 2210(sh)	243(m)	422(m) 443(m) 460(m) 498(s) 519(s) 536(s)
$[IrHCl(SC_6H_5)(Ph_3P)_2]_2$	2237(s)	248(m)	431(m) 457(m) 473(m) 516(s) 530(s) 547(s)
$[IrHCl(SC_6H_4CH_3)(Ph_3P)_2]_2$	2230(s)	243(m)	420(m) 452(m) 471(m) 500(s) 516(s) 534(s)
$[IrHCl(SC_6H_4OCH_3)(Ph_3P)_2]_2$	2222(s)	242(m)	420(m) 445(m) 461(m) 502(s) 516(s) 543(s)
$[IrHCl(SC_6H_4Br)(Ph_3As)_2]_2$	2196(s) (2225)†(m)	249(m)	231(vw) 287(w) 334(sh) 344(sh) 349(s) 471(s) 483(s) 500(m)
$[IrHCl(SC_6H_4F)(Ph_3As)_2]_2$	2203(s) 2192(sh) (2195)†(m)	260(m)	231(vw) 290(w) 344(s) 400(w) 428(vw) 476(s) 485(s) 519(m)
$[IrHCl(SC_6H_5)(Ph_3As)_2]_2$	2202(sh) 2184(s) (2209)†(m)	255(m)	230(vw) 289(w) 333(sh) 346(s) 465(s) 487(s)
$[IrHCl(SC_6H_4CH_3)(Ph_3As)_2]_2.C_6H_6$	2194(s) (2192)†(m)	251(m)	231(vw) 290(w) 321(sh) 345(s) 403(vw) 470(s) 482(s) 502(m)
$[IrHCl(SC_6H_4OCH_3)(Ph_3As)_2]_2$	2201(sh 2190 (s) (2205)†(m)	258(m)	232(vw) 291(w) 308(sh) 320(sh) 331(sh) 380(vw) 466(s) 488(s) 517(w)
$[IrCl_2(SC_6H_4NO_2)(Ph_3P)_2]_2$	—	310(m) 269(w) 262(w) 238(w)	443(m) 468(m) 520(s) 529(s)
$[IrCl_2(SC_6H_4NO_2)(Ph_3As)_2]_2$	—	338(s) 330(s) 297(w) 221(vw)	484(sh) 477(s) 446(m)

*s = strong, sh = shoulder, m = medium, w = weak, vw = very weak.
†Measured in chloroform.

TABLE 3. ^1H n.m.r. data for $[IrHCl(SC_6H_4Y)(Ph_3As)_2]_2$*

Complex	^1H chemical shift For Ir—H (p.p.m.)
$[IrHCl(SC_6H_4Br)(Ph_3As)_2]_2$	†
$[IrHCl(SC_6H_4F)(Ph_3As)_2]_2$	21.36
$[IrHCl(SC_6H_5)(Ph_3As)_2]_2$	21.36
$[IrHCl(SC_6H_4CH_3)(Ph_3As)_2]_2.C_6H_6$	21.37
$[IrHCl(SC_6H_4OCH_3)(Ph_3As)_2]_2$	21.33

*Measured in $CDCl_3$ with TMS as internal reference.
†Not measured because of low solubility of complex.

Fig. 1. The non-linearity of this plot is interpreted as indicating that the *full* electronic effect of the para-substituent does not manifest itself in the position of the ν_{Ir-H} vibration as has been observed when a para-substituted benzenethiolato ligand is *trans* to a hydrido ligand (9). In this later situation a linear correlation was observed between ν_{Ir-H} and σ_p. The observed variation in ν_{Ir-H} for complexes **2** together with the fact that the high-field chemical shift of the hydrido ligand bonded to iridium(III) is invariant to the nature of the substituent, Y (see

Can. J. Chem. Downloaded from www.nrcresearchpress.com by 210.87.254.40 on 09/05/12
For personal use only.

TABLE 4. Molecular weight measurements*

Complex	Concentration (mg ml^{-1})	Molecular weight Observed	Molecular weight Calculated
$[IrHCl(SC_6H_5)(Ph_3As)]_2$	9.243	1071	
	5.346	971	1899
	4.220	935	
$[IrHCl(SC_6H_4CH_3)(Ph_3As)_2]_2$	8.380	1041	
	6.435	995	1926
	4.518	960	
$[IrHCl(SC_6H_4F)(Ph_3As)_2]_2$	14.650	1465	
	9.880	1449	1933
	5.030	1424	
$[IrHCl(SC_6H_4OCH_3)(Ph_3As)_2]_2$	15.490	1645	
	10.880	1584	1959
	5.450	1545	
$[IrHCl(SC_6H_4Br)(Ph_3As)_2]_2$	18.039	1520	2057
$[IrCl_2(SC_6H_4NO_2)(Ph_3P)_2]_2$†	2.80	1436	
	2.63	1384	
	2.13	1374	1883
	1.60	1333	
	1.40	1273	
$[IrCl_2(SC_6H_4NO_2)(Ph_3As)_2]$†	2.50	1250	
	2.04	1244	2058
	1.39	1108	

*Measured in chloroform unless indicated otherwise.
†Measured in benzene.

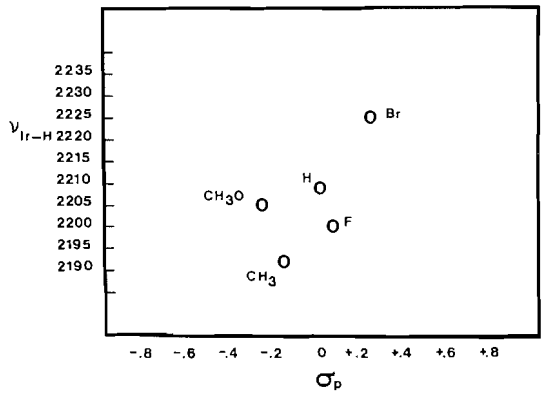

FIG. 1. Hammett plot for $[IrHCl(SC_6H_4Y)(Ph_3As)_2]_2$.

Table 3), are consistent with the arenethiolato moiety being *cis* to the hydrido ligand (8). These observations favor structure **A**.

Finally, for a large number of octahedral iridium(III) complexes it has been noted that ν_{Ir-Cl} appears at $\sim$250 cm^{-1} when Cl is *trans* to H (13). This particular vibration for complexes **1** and **2** has been observed between $\sim$240–260 cm^{-1} (see Table 2) and also lends support for structure **A**.

The product formed when 4-nitrobenzenethiol reacts with $IrCl(Ph_3M')_3$ is not of the type **1** or **2** but rather an iridium(III) complex which does not contain an iridium–hydrogen bond. These particular complexes have been formulated as $[IrCl_2(SC_6H_4NO_2)(Ph_3P)_2]_2$, **3**, and $[IrCl_2(SC_6H_4NO_2)(Ph_3As)_2]_2$, **4**, in the solid state. Molecular weight measurements (see Table 4) confirm that these complexes are indeed dimeric and also indicate that they are dissociated in solution according to reaction 4. The precise

[4] $[IrCl_2(SC_6H_4Y)(Ph_3M')_2]_2 \rightleftharpoons 2[IrCl_2(SC_6H_4Y)(Ph_3M')_2]$

reason for $HSC_6H_4NO_2$ behaving differently towards $IrCl(Ph_3M')_3$ is not clearly understood at present. The two most likely structures for **3** and **4** involve either Cl^- or $O_2NC_6H_4S^-$ bridging groups and are shown below where L = Ph_3P or Ph_3As and Ar = $C_6H_4NO_2$. Structure

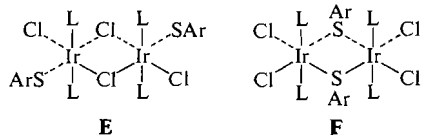

E **F**

Can. J. Chem. Downloaded from www.nrcresearchpress.com by 210.87.254.40 on 09/05/12
For personal use only.

Can. J. Chem. Downloaded from www.nrcresearchpress.com by 210.87.254.40 on 09/05/12
For personal use only.

E (C_{2h} local symmetry) would be expected to exhibit at least two ν_{Ir-Cl} vibrations ($2B_u$, bridging and terminal) whereas structure **F** (D_{2h} local symmetry) would be expected to show at least four ν_{Ir-Cl} vibrations ($2B_{2u}$ and $2B_{3u}$). Structure **F** appears to be more likely in view of the proposed structures for complexes **1** and **2** although structure **E** cannot be completely rejected on the basis of the available spectroscopic data (Table 2). Attempts to replace Cl by Br in the complexes **3** and **4** were not successful. Hence, the bands observed in the region 340–220 cm^{-1} could not be positively assigned to ν_{Ir-Cl} vibrations. Accordingly, the assignments for ν_{Ir-Cl} for **3** and **4** given in Table 2 must be regarded as tentative.

The reactivity of carbon monoxide with the complexes **1**–**4** has been investigated. Complexes of the type, **1** and **2** were found to readily undergo "reductive elimination" by reaction with CO at 1 atm and at room temperature to form *trans*-$[Ir(CO)_2(Ph_3M')_2]Cl$ where M′ = P or As, *i.e.*,

[5] $[IrHCl(SC_6H_4Y)(Ph_3M')_2]_2 + 4CO \rightarrow 2\ trans\text{-}[Ir(CO)_2(Ph_3M')_2]Cl + 2HSC_6H_4Y$

On the other hand, complexes **3** and **4** do not react with carbon monoxide and may be recovered unchanged after prolonged exposure to 1 atm carbon monoxide at room temperature, *i.e.*,

[6] $[IrCl_2(SC_6H_4NO_2)(Ph_3M')_2]_2 + 4\ CO \nrightarrow 2\ trans\text{-}[Ir(CO)_2(Ph_3M')_2]Cl + 2ClSC_6H_4NO_2$

Apparently, the hydrido ligand is necessary for reductive elimination of occur. The complexes *trans*-$[Ir(CO)_2(Ph_3P)_2]Cl$ and *trans*-$[Ir(CO)_2(Ph_2As)_2]Cl$ behave as 1:1 electrolytes in acetone and nitromethane (see Experimental section). The low molar conductivities associated with these complexes are similar to those reported recently by Collman and co-workers (14) for $[Ir(CO)_2(TDPME)]Cl$ where TDPME = 1,1,1-tris(diphenylphosphinomethyl)ethane. These low molar conductivities could be due to the loss of Ph_3M' in solution according to reaction 7.[3]

[7] $[Ir(CO)_2(Ph_3M')_2]Cl \rightleftharpoons [Ir(CO)_2(Ph_3M')Cl] + Ph_3M'$

These particular four coordinate iridium(I) complexes are similar to *trans*-$[Ir(CO)_2(Ph_3M')_2][ALCl_4]$ which have been reported by Hieber and Frey (15). The *trans*-arrangement of the CO ligands is supported by the fact that only one ν_{CO} vibration (D_{2h} local symmetry) was observed in the infrared at ~2000 cm^{-1}. The ν_{CO} vibration for *trans*-$[Ir(CO)_2(Ph_3P)_2]Cl$ was observed at 2025 cm^{-1} (Nujol), 2029 cm^{-1} ($CHCl_3$), and at 2020 cm^{-1} (Nujol), 2024 cm^{-1} ($CHCl_3$) for *trans*-$[Ir(CO)_2(Ph_3As)_2]Cl$. In order to eliminate the possibility that these dicarbonyl complexes were in fact not tricarbonyl derivatives of the type $[Ir(CO)_3(Ph_3M')_2]Cl$ (16, 17), the tetraphenylborate derivative, $[Ir(CO)_2(Ph_3P)_2](BPh_4)$ was prepared (see Experimental section) which also exhibited only one ν_{CO} band at 2024 cm^{-1} (Nujol).

Since the complexes **1** and **2** appear to be dissociated in solution (reaction 3), the observed reductive elimination (reaction 5) may be compared to the reaction of the five coordinate iridium(III) complexes, $[IrHCl_2(Ph_3P)_2]$ and $[IrHCl(O_2CCF_3)(Ph_3P)_2]$, with CO which undergo simple nucleophilic addition to form $[IrHCl_2(CO)(Ph_3P)_2]$ and $[IrHCl(O_2CCF_3)(CO)(Ph_3P)_2]$, respectively (18).

Experimental

Materials

Triphenylphosphine was purchased from Eastman Organic Chemicals, Inc. and was recrystallized from ethanol. A generous supply of cyclooctene was provided by the Columbian Carbon Co., Inc., Princeton, New Jersey. Other chemicals used were commercially available samples. All reactions were normally carried out under an atmosphere of nitrogen.

Di-μ-chlorotekrakis(cyclooctene)diiridium(I), $[IrCl(C_8H_{14})_2]_2$

This was prepared according to the method of Herdé and Senoff (19).

Chlorotris(triphenylphosphine)iridium(I), $IrCl(Ph_3P)_3$

This was prepared according to the method of Bennett and Milner (2) from the reaction of triphenylphosphine with $[IrCl(C_8H_{14})_2]_2$.

Chlorotris(triphenylarsine)iridium(I), $IrCl(Ph_3As)_3$

This complex was generated *in situ* from the reaction of triphenylarsine with $[IrCl(C_8H_{14})_2]_2$ according to the method of Bennett and Milner (2). The complex was not isolated because of its extreme reactivity with oxygen.

Di-μ-arenethiolatodihydridodichlorotetrakis(triphenylphosphine)diiridium(III), $[IrHCl(SC_6H_4Y)(Ph_3P)_2]_2$

The following general procedure was used to prepare these complexes. To a degassed benzene solution (20 ml) of chlorotris(triphenylphosphine)iridium(I) (0.50 g) was added an excess of the appropriate substituted benzenethiol (0.25 g or 0.5 ml). The solution immediately changed

[3]We thank a referee for bringing this point to our attention.

TABLE 5. Analytical data

Complex	Analysis (%) Calculated C	Calculated H	Found C	Found H	M.p. (dec.) (°C)
$[IrHCl(SC_6H_4Br)(Ph_3P)_2]_2$	53.56	3.72	52.90	3.87	199–206
$[IrHCl(SC_6H_4F)(Ph_3P)_2]_2$	57.27	3.98	57.62	4.18	>223
$[IrHCl(SC_6H_5)(Ph_3P)_2]_2$	58.47	4.18	57.73	4.11	172–176
$[IrHCl(SC_6H_4CH_3)(Ph_3P)_2]_2$	58.90	4.34	58.10	4.43	187–195
$[IrHCl(SC_6H_4OCH_3)(Ph_3P)_2]_2$	57.85	4.26	58.43	4.39	192–210
$[IrHCl(SC_6H_4Br)(Ph_3As)_2]_2$	48.98	3.40	49.20	2.45	197–202
$[IrHCl(SC_6H_4F)(Ph_3As)_2]_2$	52.07	3.62	52.80	4.26	175–184
$[IrHCl(SC_6H_5)(Ph_3As)_2]_2$	53.05	3.79	53.57	3.72	176–180
$[IrHCl(SC_6H_4CH_3)(Ph_3As)_2]_2.C_6H_6$	55.28	3.93	54.98	3.91	172–175
$[IrHCl(SC_6H_4OCH_3)(Ph_3As)_2]_2$	52.65	3.88	53.58	4.13	185–192

color from orange to green and was stirred for a prolonged period of time (see Table 1). The cream-yellow precipitate was then filtered, washed with benzene and dried *in vacuo* over boiling benzene overnight. Analytical data are presented in Table 5.

Di-μ-arenethiolatodihydridodichlorotetrakis(triphenylarsine)diiridium(III), $[IrHCl(SC_6H_4Y)(Ph_3As)_2]_2$

The following general procedure was used to prepare these complexes. To a degassed benzene solution (20 ml) of di-μ-chlorotetrakis(cyclooctene)diiridium(I) (0.50 g) was added an excess of triphenylarsine (1.25 g). This solution was stirred for 4–6 h whence an excess of appropriate substituted benzenethiol (1.0 g or 1.0 ml) was added. The reaction was allowed to proceed over a prolonged period of time (see Table 1). The cream-yellow product was then collected by filtration, washed with benzene, and dried *in vacuo* over boiling benzene overnight. Analytical data are given in Table 5.

Di-μ-arenethiolatotetrachlorotetrakis(triphenylphosphine)diiridium(III), $[IrCl_2(SC_6H_4NO_2)(Ph_3P)_2]_2$

To a degassed benzene solution (20 ml) containing chlorotris(triphenylphosphine)iridium(I) (0.50 g) was added 4-nitrobenzenethiol (0.25 g). The solution immediately changed color from orange to brick-red and was stirred for 12–24 h whence brick-red crystals precipitated upon the addition of ligroin (b.p. 63–75°; 50 ml). The crystals were then filtered, washed with ligroin and dried *in vacuo* at 25°. Yield = 0.33 g (71%). M.p. > 190° (dec.).

Anal. Calcd. for $C_{84}H_{68}Cl_4N_2O_8P_4S_2Ir_2$: C, 53.53; H, 3.62. Found: C, 52.91; H, 3.77.

Di-μ-arenethiolatotetrachlorotetrakis(triphenylarsine)diiridium(III), $[IrCl_2(SC_6H_4NO_2)(Ph_3As)_2]_2$

To a degassed benzene solution (20 ml) containing di-μ-chlorotetrakis(cyclooctene)diiridium(I) (0.50 g) was added an excess of triphenylarsine (1.25 g). This solution was then stirred for 4–6 h whence an excess of 4-nitrobenzenethiol (0.80 g) was added. The reaction was then allowed to proceed for 12–24 h after which time brick-red crystals precipitated upon the addition of ligroin (63–75°; 50 ml). The crystals were filtered, washed with ligroin, and dried *in vacuo* at 25°. Yield = 0.64 g (56%). M.p. > 145° (dec).

Anal. Calcd. for $C_{84}H_{68}Cl_4As_4N_2O_8S_2Ir_2$: C, 48.95, H, 3.30. Found: C, 49.82, H, 3.85.

trans-Dicarbonylbis(triphenylphosphine)iridium(I) Chloride, $[Ir(CO)_2(Ph_3P)_2]Cl$

This complex may be prepared starting with any complex **1**. A typical preparation is presented below.

Di-μ-(4-methoxybenzenethiolato)dihydridodichlorotetrakis(triphenylphosphine)diiridium(III) (0.50 g) was added to 100 ml of chloroform which was previously saturated with carbon monoxide. Carbon monoxide was then bubbled through the solution for 2–3 h. The volume of solution was then reduced to about 10–15 ml under reduced pressure at room temperature. Ligroin (b.p. 63–75°; 50 ml) was then added to precipitate the product as bright yellow crystals which were collected by filtration. The product was recrystallized from acetone–ligroin. Yield = 0.38 g (84%). M.p. 167–71° (dec.). Molar conductance of a 4.70×10^{-4} *M* solution in acetone at 25° was 54.7 ohm^{-1} cm^2 mol^{-1} and of a 3.47×10^{-4} *M* solution in nitromethane at 25° was 21.41 ohm^{-1} cm^2 mol^{-1}.

Anal. Calcd. for $C_{38}H_{30}ClP_2O_2Ir$: C, 56.45; H, 3.71; Cl, 4.38; Ir, 23.76. Found: C, 56.44; H, 4.60; Cl, 4.11; Ir, 24.65.

trans-Dicarbonylbis(triphenylarsine)iridium(I) Chloride, $[Ir(CO)_2(Ph_3As)_2]Cl$

This complex may be prepared using any complex **2** as starting material. The procedure followed to prepare this complex was essentially the same as that noted above for *trans*-$[Ir(CO)_2(Ph_3P)_2]Cl$. Yields were in the range 50–70%. M.p. 169–73° (dec.). Molar conductance of a 4.80×10^{-4} *M* solution in acetone at 25° was 46.9 ohm^{-1} cm^2 mol^{-1} and of a 4.69×10^{-4} *M* solution in nitromethane at 25° was 18.5 ohm^{-1} cm^2 mol^{-1}.

Anal. Calcd. for $C_{38}H_{30}As_2O_2Ir$: C, 50.89; H, 3.34; Cl, 4.02; Ir, 21.43. Found: C, 51.04; H, 3.72; Cl, 4.22; Ir, 22.50.

trans-Dicarbonylbis(triphenylphosphine)iridium(I)-tetraphenylborate, $[Ir(CO)_2(Ph_3P)_2](BPh_4).CH_2Cl_2$

A sample of *trans*-$[Ir(CO)_2(Ph_3P)_2]Cl$ (0.2 g) was dissolved in 10 ml of methylene chloride and 5 ml of methanol containing 0.1 g of sodium tetraphenylborate was added. The resulting solution was stirred at room tem-

Can. J. Chem. Downloaded from www.nrcresearchpress.com by 210.87.254.40 on 09/05/12
For personal use only.

perature for 45 min whereupon it was filtered. The volume of filtrate was reduced under vacuum and an excess of methanol was added to precipitate the desired product as a yellow solid which was dried *in vacuo* at 25°.

Anal. Calcd. for $C_{63}H_{52}BCl_2O_2P_2Ir$: C, 64.27, H, 4.42. Found: C, 63.93, H, 4.64.

Physical Measurements

Infrared Spectra

These were recorded on a Beckman IR-12 spectrophotometer as Nujol mulls between NaCl or CsI plates in the region 4000–650 cm^{-1}. In the region 650–200 cm^{-1}, Nujol mulls between CsI or polyethylene plates were used. Solution spectra ($CHCl_3$) were recorded with 0.2 or 0.4 mm NaCl liquid cells. Sharp bands were scanned at 16 cm^{-1} min^{-1} and at about 25 cm^{-1} min^{-1} for all other bands.

^1H N.M.R. Spectra

These were recorded on a Varian HA100 spectrometer in $CDCl_3$ with tetramethylsilane as internal reference.

Conductivity Measurements

Electrical conductivities were measured at 25° with a Beckman Model RC-18H conductivity bridge using a glass cell with platinized electrodes (cell constant = 0.20 cm^{-1}).

Melting points were determined with a Fisher–Johns melting point apparatus and are uncorrected. Molecular weight measurements were performed on a Hitachi–Perkin Elmer 115 molecular weight apparatus, by the Schwarzkopf Microanalytical Laboratory, Woodside, N.Y., or by the Alfred Bernhardt Microanalytical Laboratory, West Germany.

The authors wish to thank the National Research Council of Canada for financial support (C.V.S.). One of us (J.L.H.) wishes to thank the government of the province of Ontario for a fellowship. The authors also thank Mr. J. C. Lambert for experimental assistance, Mr. B. G. Sayer for obtaining the n.m.r. spectra, and the Department of Chemistry, McMaster University, Hamilton for the use of the HA100 spectrometer.

1. J. P. COLLMAN, M. KUBOTA, F. D. VASTINE, J. Y. SUN, and J. W. KANG. J. Am. Chem. Soc. **90**, 5430 (1968).
2. M. A. BENNETT and D. L. MILNER. J. Am. Chem. Soc. **91**, 6983 (1969).
3. H. VAN GAAL, H. G. A. M. CUPPERS, and A. VAN DER ENT. Chem. Commun. 1694 (1970).
4. M. KUBOTA and D. M. BLAKE. J. Am. Chem. Soc. **93**, 1368 (1971).
5. E. W. AINSCOUGH and S. D. ROBINSON. J. Chem. Soc. **A**, 3413 (1971).
6. M. A. BENNETT and R. CHARLES. Aust. J. Chem. **24**, 427 (1971).
7. M. A. BENNETT and R. CHARLES. J. Am. Chem. Soc. **94**, 666 (1972).
8. C. V. SENOFF. Can. J. Chem. **48**, 2444 (1970).
9. A. E. KESKINEN and C. V. SENOFF. J. Organomet. Chem. **37**, 201 (1972).
10. J. R. GAYLOR and C. V. SENOFF. Can. J. Chem. **50**, 1868 (1972).
11. D. M. ADAMS. Metal–ligand and related vibrations. E. Arnold Publishers, London. 1967.
12. H. D. KAESZ and R. B. SAILLANT. Chem. Rev. **72**, 231 (1972).
13. J. M. JENKINS and B. L. SHAW. J. Chem. Soc. 6789 (1965).
14. W. O. SIEGL, S. J. LAPPORTE, and J. P. COLLMAN. Inorg. Chem. **10**, 2158 (1971).
15. W. HIEBER and V. FREY. Chem. Ber. **99**, 2614 (1966).
16. M. J. CHURCH, M. J. MAYS, R. N. F. SIMPSON, and F. P. STEFANINI. J. Chem. Soc. **A**, 2909 (1970).
17. A. J. DEEMING and B. L. SHAW. J. Chem. Soc. **A**, 2705 (1970).
18. D. M. BLAKE and M. KUBOTA. J. Am. Chem. Soc. **92**, 2578 (1970).
19. J. L. HERDÉ and C. V. SENOFF. Inorg. Nucl. Chem. Lett. **7**, 1029 (1971).

Can. J. Chem. Downloaded from www.nrcresearchpress.com by 210.87.254.40 on 09/05/12
For personal use only.

Raman Spectra of Hexagonal Ethylsulfates of Yttrium and of some Rare Earths[1]

G. SCHAACK[2] AND J. A. KONINGSTEIN

Department of Chemistry, Carleton University, Ottawa, Canada K1S 5B6

Received May 4, 1970[3]

The phonon Raman spectra of single crystals of $Y(C_2H_5SO_4)_3 \cdot 9H_2O$, $Ce(C_2H_5SO_4)_3 \cdot 9H_2O$, $Nd(C_2H_5SO_4)_3 \cdot 9H_2O$, $Sm(C_2H_5SO_4)_3 \cdot 9H_2O$ have been studied at low temperatures with laser excitation. Some information has also been obtained of the compounds of Ho^{3+} and Er^{3+}. The types of symmetry of the observed modes have been determined and compared with the results of a group theoretical calculation. The internal modes of the C_2H_5 and SO_4 groups and of the H_2O molecules can be completely attributed to observed transitions. There is some evidence to attribute the librational modes of the H_2O molecules to transitions which show a very pronounced temperature dependence of the line-widths. Reasons for this temperature dependence are discussed. No lines have been found that can be attributed uniquely to electronic transitions.

La spectrophonie Raman de monocristaux de $Y(C_2H_5SO_4)_3 \cdot 9H_2O$, $Ce(C_2H_5SO_4)_3 \cdot 9H_2O$, $Nd(C_2H_5SO_4)_3 \cdot 9H_2O$ et $Sm(C_2H_5SO_4)_3 \cdot 9H_2O$ a été étudiée à basse température par excitation laser. Des informations ont également été obtenues sur les composés de Ho^{3+} et Er^{3+}. Les types de symétrie des modes de vibration observés ont été déterminés et comparés avec les résultats du calcul théorique sur les groupes. Les modes de vibration internes des groupes C_2H_5, SO_4 et des molécules d'eau peuvent être complètement attribués aux transitions observées. L'attribution des modes de vibration des molécules d'eau a été prouvée d'une certaine façon par l'influence très prononcée de la température sur les largeurs des raies dont les causes ont été discutées. Il n'existe pas de raies qui ne soient uniquement attribuées aux transitions électroniques. [Traduit par le journal]

Can. J. Chem., 51, 1023 (1973)

Introduction

The rare-earth ethylsulfates $(M) \cdot (C_2H_5SO_4)_3 \cdot 9H_2O$, where M is one of the 14 rare-earth ions (R.E.) in the trivalent state or the yttrium ion, are an isomorphous series of crystals, which have attracted considerable interest for the studies of ions with an unfilled 4f shell in the crystalline matrix. In a series of investigations planned to study the electronic Raman scattering of low lying levels of the R.E. ions we have observed the Raman spectra due to the optical phonons of these crystals. The knowledge of these phonon levels is prerequisite for a study of electronic effects in these crystals, because both processes have scattering cross-sections of comparable magnitude and spectral lines between phonon or electronic levels have thus similar appearance (1). Information about the phonon levels is also needed for investigations on the 4f-electron–phonon interaction, especially for the interpretation of vibronic spectra (2).

In this paper we report on the Raman spectra of single crystals of yttrium ethylsulfate (Y-E.S.), Ce-E.S., Nd-E.S., Sm-E.S., Ho-E.S. and Er-E.S. Clear crystals (about $1.5 \times 1.0 \times 0.4$ cm^3) were grown from aqueous solutions at constant temperature. The well developed faces of the crystals were used to orient the cut and polished probes.

The Raman spectra of Nd-E.S., Sm-E.S., Ho-E.S., and Er-E.S. were excited with the 6328 Å radiation of a commercial He–Ne laser with a power of 80 mW, the spectra of Y-E.S. and of Ce-E.S. were studied with the 4880 or 5145 Å radiation of an Ar^+ laser (500 mW). The crystals were mounted on a cold-finger of a He research Dewar (3) or in the case of Ce-E.S. and Nd-E.S. immersed in superfluid helium at 2 K. A description of this second type of cryostat will be given elsewhere. Some samples were also studied at 77 and 300 K.

To discriminate between the three different types of Raman active transitions (see Structure), the plane of polarization of the incoming laser beam was rotated by means of half-wave plates and the scattered light analyzed in directions parallel and perpendicular to the Poynting vector of the laser beam under 90°-scattering geometry.

[1]Research supported in part by grants of the National Research Council of Canada and the Defence Research Board.

[2]Permanent address: Institute für Technische Physik der Technischen Hochschule, Darmstadt, Germany.

[3]Revision received November 23, 1972.

Can. J. Chem. Downloaded from www.nrcresearchpress.com by 210.87.254.5 on 09/05/12
For personal use only.

TABLE 1. Group theoretical enumeration of the normal modes of the R.E.-E.S. in different spectral ranges

(*a*) Normal mode containing internal modes

Group	Site symmetry	No. of molecules per cell	Type and spectral range of vibration	Modes of 1 molecule	Modes of the unit cell
H_2O	C_s	6	O—H valence 3000 cm^{-1}	$1A'$ $1A''$	A_g,E_{2g},B_u,E_{1u} B_g,E_{1g},A_u,E_{2u}
			O—H deformation 1600 cm^{-1}	$1A'$	A_g,E_{2g},B_u,E_{1u}
	C_1	12	O—H valence 3000 cm^{-1}	$2A$	$2(A_g,B_g,A_u,B_u,$ $E_{1g},E_{2g},E_{1u},E_{2u})$
			O—H deformation 1600 cm^{-1}	A	A_g,B_g,A_u,B_u $E_{1g},E_{2g},E_{1u},E_{2u}$
C_2H_5	C_s	6	C—H valence 2900–3000 cm^{-1}	$3A'$ $2A''$	$3(A_g,E_{2g},B_u,E_{1u})$ $2(B_g,E_{1g},A_u,E_{2u})$
			C—H deformation 1300–1500 cm^{-1}	$3A'$ $2A''$	Same as above Same as above
			C—C 800–1100 cm^{-1}	$3A'$ $2A''$	Same as above Same as above
SO_4	C_s	6	ν_3 (F_2) 1150 cm^{-1}	$2A'$ A''	$2(A_g,E_{2g},B_u,E_{1u})$ (B_g,E_{1g},A_u,E_{2u})
			ν_4 (F_2) 600 cm^{-1}	$2A'$ A''	Same as above Same as above
			ν_1 (A_1) 1050 cm^{-1}	A'	A_g,E_{2g},B_u,E_{1u}
			ν_2 (E) 450 cm^{-1}	A' A''	A_g,E_{2g},B_u,E_{1u} B_g,E_{1g},A_u,E_{2u}

(*b*) Normal modes containing external modes*

Group	Site symmetry	No. of molecules per cell	Type and spectral range of vibration	Modes of 1 molecule	Modes of the unit cell
$9H_2O$	C_{3h}	2	Internal modes of the $(9H_2O)$-group (T),(L) 200–800 cm^{-1}	$8A'$ $8A''$ $8E'$ $8E''$	$8(A_g,B_u)$ 5T,3L $8(B_g,A_u)$ 3T,5L $8(E_{2g},E_{1u})$ 4T,4L $8(E_{1g},E_{2u})$ 4T,4L
			External modes of the $(9H_2O)$-group (T),(L) 100 cm^{-1}	A' A'' E' E''	A_g,B_u L A_u,B_g T E_{2g},E_{1u} T E_{1g},E_{2u} L
R.E. or Y^{3+}	C_{3h}	2	(T) 400 cm^{-1}	E' A''	E_{2g},E_{1u} T A_u,B_g T
C_2H_5	C_s	6	(T),(L) 400 cm^{-1}	$3A'$ 2T,1L $3A''$ 1T,2L	$3(A_g,E_{2g},B_u,E_{1u})$ $3(B_g,E_{1g},A_u,E_{2u})$
SO_4	C_s	6	Same as above	Same as above	Same as above

*T: translation; L: libration.

Structure

The crystal structure of the R.E.-E.S. has been determined by X-ray methods (4, 5). The compounds crystallize in the space group C_{6h}^2 ($P6_3/m$) with 2 formula units per hexagonal unit cell. The R.E. ions have the site symmetry C_{3h} and 9 water molecules are the nearest neighbors. Six of them are situated above and below the mirror plane forming a trigonal prism and have a point symmetry C_1. The other three water molecules (C_s) are lying in this plane together with the three ethylsulfate groups (C_s), which fill the space between the metal-hydrate complexes.

In Table 1, results of the group theoretical calculations of the number and symmetry of

Can. J. Chem. Downloaded from www.nrcresearchpress.com by 210.87.254.5 on 09/05/12
For personal use only.

Can. J. Chem. Downloaded from www.nrcresearchpress.com by 210.87.254.5 on 09/05/12
For personal use only.

the optical phonons at zero wavevector are given. Here each molecule or molecular group is treated as a separate unit and the number and the symmetry of the internal and external (translational and librational) vibrations are tabulated together with the wavenumber region where the fundamental transitions are to be expected.

In the point group C_{6h} normal vibrations transforming according to the following irreducible representations are Raman-active: A_g ($\alpha_{xx} = \alpha_{yy},\alpha_{zz}$); $E_{1g}(\alpha_{xz},\alpha_{yz})$; $E_{2g}(\alpha_{xx} = \alpha_{yy},\alpha_{xy})$. The infrared active modes belong to $A_u(P_z)$ and $E_{1u}(P_x,P_y)$. The modes B_g, B_u, E_{2u} are optically inactive. In total, we should expect 35 A_g modes (20 + 15), 28 E_{1g} (13 + 15), 36 E_{1u} (20 + 16), 36 E_{2g} (20 + 16), and 28 E_{2u} (13 + 15) types of transitions including the two modes ($1A_u$, $1E_{1u}$) with zero frequency. The numbers in brackets give the internal and external modes, respectively. It must be emphasized, however, that the separation of the modes into internal and external motions of different molecules as in Table 1, is an enumeration of symmetry coordinates, the actual normal modes are a superposition of symmetry coordinates of equal species. The classification of the modes given in Table 1 is based on the following assumptions:

(*a*) The 6 water molecules with C_s symmetry are arranged in the unit cell with the plane of the molecules perpendicular to the mirror plane in the crystal. This arrangement gives plausible distances for H bonds to neighboring oxygen atoms (5) and is in agreement with intensity measurements of the Raman bands in the 3000 cm^{-1} region (6).

(*b*) The SO_4 and the C_2H_5 groups of the ethylsulfate complex can be treated as separate units, as far as their vibrational properties are concerned (6).

(*c*) The shell of 9 water molecules around a R.E. ion from a complex of coupled molecules. Accordingly, the translations and librations of the single H_2O molecules are coupled to form "internal" vibrations within this complex. The existence of such coupled modes in a tetrahedral arrangement of $4H_2O$ molecules has been demonstrated (7). In the present case, we can assume that the force constants acting on both the C_s and C_1 molecules are about the same. Values of the interatomic distances of the oxygen atoms in these complexes (5) indicate that the influence of ion–ion repulsion and alignment of the permanent dipole moment of the H_2O molecules in the central field of the R.E. ion and the strength of the H-bonds are very nearly the same for both types of molecules.

Spectra

Raman spectra of Y-E.S., Ce-E.S., and Nd-E.S. were studied in detail and the tensor components $z(xx)y$, $z(yx)y$, $z(xz)y$, and $x(zz)y$, $x(zx)y$, $x(yx)y$ were investigated (8). The A_g transitions can be observed in the (xx) and (zz) spectra, the E_{1g} modes in the (xz) spectra, the E_{2g} modes in the (xx) and (xy) spectra. In good samples, unique polarization properties were found, and a straightforward determination of the symmetry species was possible. Only the strong A_g transitions in the 700–1100 cm^{-1} region were present also in the (xy) and (xz) spectra (9), making the assignment of factor group split E_{2g} modes near the A_g modes somewhat uncertain. The region of the O—H and C—H stretching vibrations has been studied only for Y-E.S.

Similar experiments have been performed for Sm-E.S. However, due to electronic and vibronic transitions in this crystal, the scattered light was reabsorbed in broad wavenumber regions, leaving some unexplored gaps in the Raman spectrum. The same difficulties, on an extended scale, have been encountered for Ho-E.S. and Er-E.S. Symmetry species were not determined for phonons of these last two crystals. The symmetry of these observed phonons was found from a comparison of Raman lines of Y-E.S., Ce-E.S., and Nd-E.S. crystals of equal frequencies and similar shapes.

As an example of Raman spectra of R.E.-E.S. crystals, the spectrum of Ce-E.S. at 2 K is shown in Fig. 1. At room temperature (Fig. 2), the observed wavenumbers are shifted to lower values (2–5 cm^{-1}). A survey of the spectrum of Y-E.S. at 80 K between 2900 and 3500 cm^{-1}, the C—H— and O—H— valence region is depicted in Fig. 3. In Table 2, the wavenumbers observed at low temperatures and assignments are given. For completeness, the wavenumbers of the infrared active phonons of types A_u and E_{1u} are also included. The wavenumbers above 450 cm^{-1} were taken from ref. 6 (values of La-E.S.), the wavenumbers below 380 cm^{-1} are the values of Hill and Wheeler (10) for La-E.S., Sm-E.S., and Er-E.S., taken at helium temper-

TABLE 2. Observed wavenumbers in Raman spectrum of Y–E.S. (77K), Ce-E.S. (2K), Nd-E.S. (2K), Sm-E.S. (4.2K) and Er-E.S. (4.2K)

Observed wavenumbers (cm^{-1}) in						
Y-E.S.	Ce-E.S.	Nd-E.S.	Sm-E.S.	Er-E.S.	Assignment	Remarks
40	25	25	26	33	E_{1g}	
	42	(43)	45		A_g, E_{2g}	
		47	54		A_g, E_{2g}	
		(45)	(44)	(44)	(i.r.)	
		(54)	(52)	(55)	(i.r.)	
		(64)	(62)	(63)	(i.r.)	
68	66	66	69	67	E_{1g}	
72	65	68	69		A_g, E_{2g}	
		(69)	(71)	(70)	(i.r.)	
80	74	77	80		$E_{2g}, (A_g)$	
		(80)	(78)	(80)	(i.r.)	
94	89	90	92	96	E_{1g}	
100	96	97	100		A_g	
	99	98			E_{2g}	
115	112	112	114	116	E_{1g}	
		(118)		(110)	(i.r.)	
135	128	127	130	131	E_{2g}	
142(?)	130	133	139		E_{1g}	
		(150)		(148)	(i.r.)	
	158	169			E_{1g}	
		(166)		(159)	(i.r.)	
179	166	167			A_g	$(zz) \gg (xx), (yy)$
	168	174	178	185(?)	E_{2g}	
	192	191	193		A_g	
195	196	193	197	198	E_{1g}	
		(195)		(192)	(i.r.)	
		(209)		(205)	(i.r.)	
218	222	223			E_{2g}	
230	242	243	223		E_{1g}	
		229	231(?)	235(?)	A_g	
		(240)		(237)	(i.r.)	
257	252	251	256		E_{1g}	
270	261	258			A_g	$(zz) \gg (xx), (yy)$
		(259)		(258)	(i.r.)	
270	264	266	268	274	E_{2g}	
		(282)		(284)	(i.r.)	
	280				E_{2g}	
328	316	321	323		E_{1g}	
340	342	340	342	341	A_g, E_{2g}	s
349	351	350	352	351	E_{2g}	
		(360)		(360)	(i.r.)	
372	365	364	371		A_g	$(zz) \gg (xx), (yy)$
380					(E_{1g})	
419	425	422	423		A_g	$(zz) \gg (xx), (yy)$
422	420	416	419		E_{1g}	SO_4, ν_2; S
425	424	422	423		E_{2g}	
432	432	429	432		E_{1g}	
494	490	489	490		$A_g, (E_{1g}), E_{2g}$	
		(490)			(E_{1u})	
		(530)			(A_u)	
528	521	525			A_g, E_{2g}	
	542	542			E_{1g}	
559	577				E_{2g}	
		(566)			(E_{1u})	
576	573	576	576		E_{1g}	

Can. J. Chem. Downloaded from www.nrcresearchpress.com by 210.87.254.5 on 09/05/12
For personal use only.

TABLE 2 (*Concluded*)

Observed wavenumbers (cm^{-1}) in						
Y-E.S.	Ce-E.S.	Nd-E.S.	Sm-E.S.	Er-E.S.	Assignment	Remarks
576	578	576	576		A_g	
		(592)			(A_u)	
	616				E_{1g}	(SO_4), ν_4
618	616	618	618		E_{2g}	
		(620)			(E_{1u})	
627	623	624			A_g	(SO_4), ν_4
		(637)			(A_u)	
644	632	637			E_{2g}	
	643				(E_{1g})	
		(678)			(E_{1u})	
710	686	685			E_{2g}, E_{1g}	
	694	685			A_g	
		(735)			(E_{1u})	
737	755				A_g	
		(802)	(802)		(E_{1u})	A', A''
	804	802		805	E_{2g}, (H_2O?)	s
811	810	808	809	810	A_g, E_{2g}; E_{1g}	
		(925)			(E_{1u})	
927	929	927	929		E_{2g}	A'
	934	927	936		A_g	
		(1007)			E_{1u}	A'; s
1013	1011	1010	1013	1012	A_g, E_{2g}	
1058					E_{1g}	A''
		(1066)			E_{1u}	ν_1, (SO_4); s
1073	1073	1073	1075	1074	A_g, E_{2g}	
1115	1110	1111	1114		A_g	A', comb (?)
	1114	1111			E_{2g}	
1201	1199	1197	1200(?)		E_{1g}	
		(1204)			(A_u)	ν_3, (SO_4)
			1210(?)		A_g	
		(1227)			(E_{1u})	
1295	1291	1290	1294		E_{1g}	A''
1396	1395	1395			E_{2g}, (A_g)	A' C—H, deformation
1449	1447	1444			E_{1g}, E_{2g}, A_g	$A' + A''$; s
1465	1466	1467			A_g	A'
1476	1473	1471			E_{2g}	
2922					A_g, E_{2g}	A'
2938					E_{1g}	A''
2946					A_g (E_{1g}), E_{2g}	A'; s C—H, valence
2978					A_g (E_{2g})	A'
2990					E_{1g}	A''; s
3380					E_{1g} (E_{2g})	sh
3397					E_{1g}, E_{2g}	s
3422					E_{2g}	O—H, valence
3450					A_g, E_{2g}, E_{1g}	s
3465					A_g	sh

*The wavenumbers in parentheses are infrared data on La-E.S. (in this table cited in the column of Nd-E.S.) and on Sm-E.S. and Er-E.S. (6, 10). For Ho-E.S. the following Raman shifts have been observed: 41, 66, 93, 115 cm^{-1}. s = strong, sh = shoulder, comb = combination. The horizontal lines in this table separate the wavenumber-regions according to the different origin of the modes: external modes, internal modes of the C_2H_5 and SO_4 groups and of the H_2O molecules.

ature. Assignments were not offered by these authors for the phonon spectrum.

It is seen from Tables 1 and 2 that good agreement exists between the numbers of expected and observed modes. There are $3A'$ and $2A''$ modes of the C_2H_5-group in the site-symmetry C_s in both the regions of C—H valence and deformation vibrations, although the factor group splitting is in some cases not fully resolved. In the region of the C—C vibrations, $3A'$ and $2A''$ modes are observed. Another mode $A_g + E_{2g}$ at 1114 cm^{-1} may be interpreted

Can. J. Chem. Downloaded from www.nrcresearchpress.com by 210.87.254.5 on 09/05/12
For personal use only.

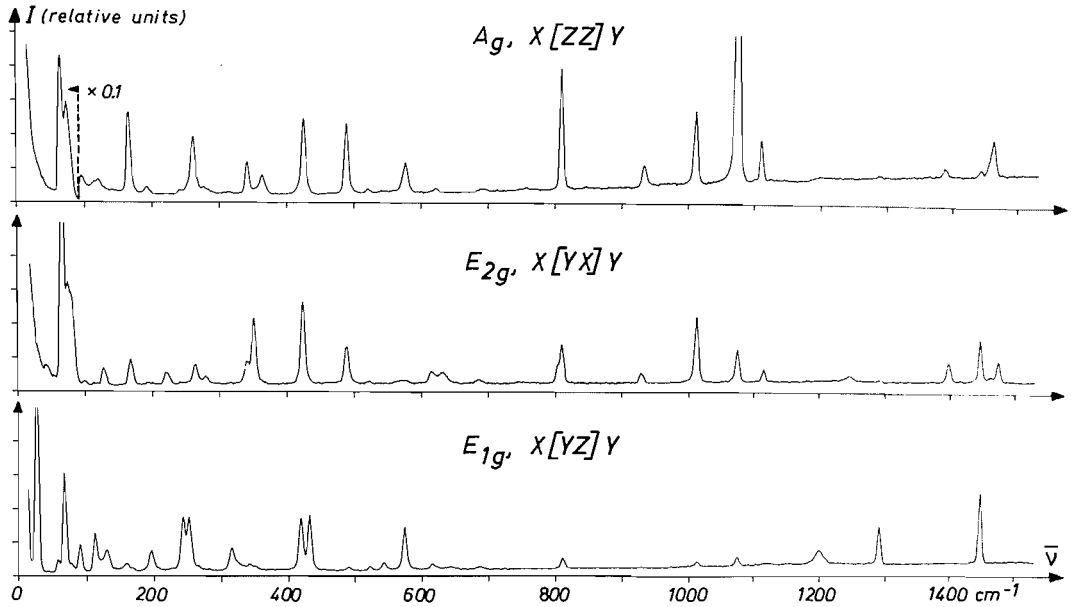

FIG. 1. Raman spectrum of Cerium-ethylsulfate at $T = 2$ K below 1500 cm^{-1}. Excitation wavelength $\lambda =$ 5145 Å, speed: 50 cm^{-1} min^{-1}, slits: 3.5 cm^{-1}. The spectrum has not been corrected for the wavelength dependent sensitivity of the photo-cathode (S 20) or the grating efficiency.

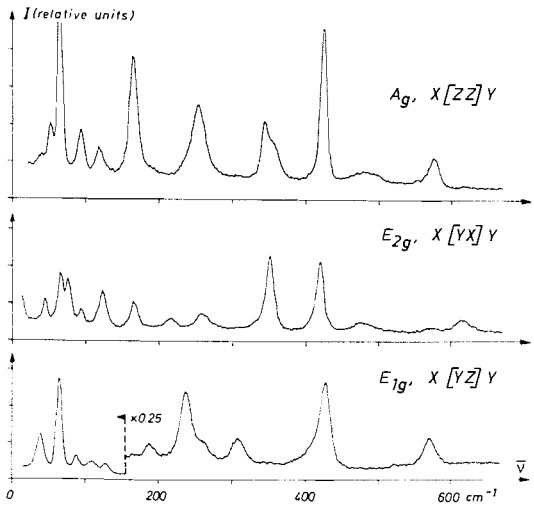

FIG. 2. Raman spectrum of Ce-E.S. below 600 cm^{-1} at $T = 300$ K. Other conditions same as in Fig. 1.

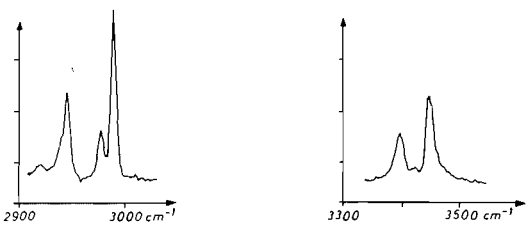

FIG. 3. Raman spectrum of Y.-E.S. at $T = 77$ K, region of O—H and C—H valence vibrations. The spectrum is a superposition of $z(yx)y$ and $z(yz)y$ ($E_{1g} + E_{2g}$).

as a combination of the very strong Raman active mode at 1073 cm^{-1} (ν_1 of SO_4) with the strong external (A_g,E_{2g}) mode at 43 cm^{-1}. In the region of the very broad O—H-transitions at 3000 cm^{-1}, reliable assignments of the observed bands to molecules with C_1 and C_s site symmetry cannot be given here. Transitions were not found in the region where O—H deformation vibrations are normally observed.

Below 800 cm^{-1} the external lattice modes are to be expected, together with the internal ν_2 and ν_3 modes of the SO_4 group. Not taking the latter into account, $15A_g$, $15E_{1g}$, and $16E_{2g}$ modes have been observed. From Table 1 we expect exactly these numbers. For this comparison, some weak and questionable bands which have been put into brackets in Table 2 have not been counted. Some may be due to electronic effects (see below), others may be due to second-order transitions or due to fluorescence from other rare-earth impurities. For the infrared active modes, the agreement between the calculated and observed number of modes is less satisfying. Twenty modes have been observed, while 32 were expected ($16A_u + 16E_{1u}$). However, the

Can. J. Chem. Downloaded from www.nrcresearchpress.com by 210.87.254.5 on 09/05/12
For personal use only.

Can. J. Chem. Downloaded from www.nrcresearchpress.com by 210.87.254.5 on 09/05/12
For personal use only.

infrared spectrum between 360 and 490 cm^{-1} is still unknown, and the wavenumber region above 500 cm^{-1} has been studied only in reflection where weak transitions were not detected.

There does not seem to be a direct correspondence between the phonon wavenumbers given here and the wavenumbers derived by Wong and Erath (2) from vibronic transitions of different R.E.-E.S. spectra. The frequencies of the latter were determined by the maxima of the density of phonon states at certain wavevectors ($\boldsymbol{k} > 0$) in the Brillouin zone. Due to the $\boldsymbol{k}$-dispersion of the external phonons, only in a few cases (determined by selection rules) will the wavenumbers of these maxima coincide with the values observed here for $\boldsymbol{k} = 0$. There is, however, some correspondence in both cases concerning the number of phonon frequencies within a certain interval. Both methods give a slowly decreasing "density of observed phonon levels" with increasing wavenumbers from 20 to 250 cm^{-1}.

Discussion

The internal vibrations of the C_2H_5-group, the SO_4-group and the water molecules have been discussed in ref. 6. Our present investigation fully supports the earlier assignments and conclusions. Here we treat the low frequency modes. Unfortunately, due to the complicated structure, only a few qualitative remarks can be made.

As a general experience in hydrated crystals, vibrations consisting predominantly of translations of the water molecules are found between 1000 and 350 cm^{-1}. In the ($Be \cdot 4H_2O$) complex (7) molecular motions of this type have been identified between 1014 and 488 cm^{-1}. If the same relative frequency spread is assumed for the ($R.E. \cdot 9H_2O$) system, corresponding modes should be expected between 750 and 350 cm^{-1}.[4] In this region $5A_g$, $4E_{1g}$, $4E_{2g}$ modes are observed, while $5A_g$, $4E_{1g}$, and $5E_{2g}$ modes are calculated (Table 1).[5] As a consequence, there is some reason to interpret the lines observed in this region as mainly due to translatory motions of the water molecules.

Enumerating these observed modes, the levels at 620 and 420 cm^{-1} (ν_2 and ν_4 of SO_4) have not been counted as well as the group of 3 levels at 490 cm^{-1}. This latter group we assign to librations of the H_2O molecules around the axis of the smallest moment of inertia (Fig. 4). There are several reasons for this assignment:

(*a*) Usually, because of the weak interaction of librating molecules within a metal hydrate complex, the correlation splitting is small (7). This is observed for the group at 490 cm^{-1} (LI), where the splitting between the 3 modes with different symmetry is within the precision of the measurements.

(*b*) There are two other groups of levels in the spectrum at 340 cm^{-1} (LII) and at 270 cm^{-1} (LIII) demonstrating the same features. These are assigned to the librations around axes II and III (Fig. 4).

The three frequencies ω_I, ω_{II}, and ω_{III} roughly obey the relation: $\omega_I^2 : \omega_{II}^2 : \omega_{III}^2 = \theta_I^{-1} : \theta_{II}^{-1} : \theta_{III}^{-1}$, where θ_I, θ_{II}, θ_{III} are the moments of inertia (e.g. ref. 11). Consequently, the potential well is about the same for the three librational motions.

(*c*) The H_2O molecule has a permanent intrinsic electric dipole moment parallel to the symmetry axis of the molecule. This dipole moment gives rise to strong infrared active transitions coupled with the librations around the axes I and III, while librations around axis

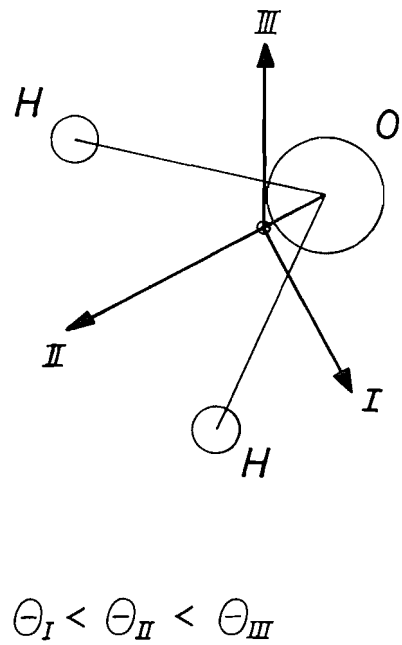

FIG. 4. Water molecule and the orientation of the axis of inertia. θ: moment of inertia.

[4]The region of the internal vibrations of the C_2H_5 group starts at 750 cm^{-1}.

[5]The missing E_{2g} mode might be the one at 804 cm^{-1} in Ce-E.S. This mode does not belong to the internal modes of the C_2H_5 group.

TABLE 3. Observed linewidths $\Delta\bar{\nu}$(full width at half intensity) of some characteristic lines in the Raman spectrum of neodymium-ethylsulfate at different temperatures

A_g					E_{2g}			
		$\Delta\bar{\nu}(cm^{-1})$					$\Delta\bar{\nu}(cm^{-1})$	
$\bar{\nu}$ (cm^{-1})	Assignment	300K	77K	4.2K	$\bar{\nu}$ (cm^{-1})	Assignment	300K	77K
68	?	9.1	*6.0*	*5.4*	68	?	7.8	*5.4*
127	?	18.5	*5.9*	*5.4*	167	?	18	6.4
173	?	12.7	*5.4*	*5.4*	258	(H_2O)	22.4	10
266	(H_2O)	>25	10.2	7.1	340	(H_2O)	11.5	*5.8*
340	(H_2O)	9.8	7.0	*5.7*	422	(SO_4)	10.5	6.2
422	(SO_4)	16.5	6.8	*5.7*	488	(H_2O)	32	9.6
488	(H_2O)	>40	11	7.5	576	Translation (H_2O)	19	8.1
					809	(C—C)	8.3	*5.2*
ΔS		4.6	4.6	4.0			5.4	4.9

*The values have not been corrected for finite slit-widths ΔS. Accordingly, values of $\Delta\bar{\nu} < 6\ cm^{-1}$ (in italics) are fully due to instrumental broadening effects.

II remain infrared inactive in accordance with the observations.

(*d*) A strong temperature dependence of the line-width is generally encountered in low frequency levels of hydrated crystals. The two groups at 270 cm^{-1} (LIII) and at 490 cm^{-1} (LI) show an extraordinarily strong temperature dependence of the Raman line-width (Table 3) and Fig. 2. In the room temperature spectra, these groups are extremely broad and some components are barely visible. The group at 340 cm^{-1} (LII) has a smaller temperature dependence than the groups LI and LIII. The reason for this behavior of LII may be related to the fact that neither the O atom nor the electric dipole moment participate in this motion.

As is demonstrated in Table 3 and in Fig. 2, the temperature dependence of the line-widths is small in the region of the internal modes ($\nu > 800\ cm^{-1}$) and in the region of the modes at very low wavenumbers ($\nu < 100\ cm^{-1}$, translations of entire groups (SO_4, C_2H_5, R.E.)) (Table 3). In the region within these limits there is a considerable broadening with increasing temperature with a maximum effect occurring in the groups assigned to LI and LIII. In the case of the ($Be{\cdot}4H_2O$) complex (7), it was observed that translational motions of this complex are strongly coupled (mixed) with librations, while there exist pure librational modes with essentially no admixture of translations. There are good reasons to assume that this behavior is not a special property of the ($Be{\cdot}4H_2O$) tetrahedron, but is more generally encountered. Therefore, we can attribute the strong temperature effect for wavenumbers 100 $cm^{-1} < \nu < 800\ cm^{-1}$ to an admixture of librational motions of the water molecules with all the other modes of the crystal of appropriate symmetry in this region. The behavior of the librational modes can be understood by considering two possibilities:

(*1*) a potential of the librations that is more anharmonic than the potential of translational motions; or

(*2*) the potential energy of a librating H_2O molecule is strongly dependent on the metal–oxygen distance. Consequently, the thermal excitation of translatory motions at elevated temperatures will change, and in general reduce, this potential energy and lower the frequency of the librations of H_2O molecules in a thermally excited translatory state. Accordingly, the librational bands will spread with increasing temperature.

It is evident that more work has to be done to clarify this situation.

One of the motives of this investigation was to observe phonons that involve the translational motions of the R.E. ions. An assignment of these motions, which is of interest for crystal-field considerations, could be achieved in the case of the R.E. garnets (1) with the help of a mass dependent frequency shift. Such a shift can be expected in the Raman active irreducible representation containing these translations

Can. J. Chem. Downloaded from www.nrcresearchpress.com by 210.87.254.5 on 09/05/12
For personal use only.

Can. J. Chem. Downloaded from www.nrcresearchpress.com by 210.87.254.5 on 09/05/12
For personal use only.

(Table 1*b*). Unfortunately, this shift is completely masked by a frequency shift of all modes due to changes in the dimensions of the unit cell (5).

Electronic Effects

A search for electronic Raman transitions in the R.E.-E.S. crystals yielded no unique results even at temperatures of 2 K. There are weak bands observed in the expected wavenumber regions; however, the interpretation of these bands, mentioned above, is ambiguous. They are usually one or two orders of magnitude weaker in intensity than the neighboring phonon transitions. The application of a strong external magnetic field would be very helpful to identify these weak transitions. A careful search in the region of the excited multiplet components $2F_{7/2}$ of Ce^{3+} near 2200 cm^{-1} and $4I_{11/2}$ of Nd^{3+} near 2000 cm^{-1} also had only negative results. This finding is unexpected because in $CeCl_3$ (12, 13) most electronic transitions are easily detected. The density per unit volume of scattering R.E.-ions is higher by a factor of 5.8 in the hexagonal R.E.-chlorides than in the R.E.-E.S., but even this factor does not explain the extraordinary weak signals due to electronic effects. One has to consider however, the fact that the states of the 4f"-configuration have, on the average, larger widths in the R.E.-E.S. than in the chlorides due to the presence of phonons with much higher energy in the former crystal. The existence of such a direct coupling between the 4f electrons and the phonons has been demonstrated by the anomalous specific heat of Ce-E.S. near 3 K (14) which is found to be larger than the Schottky-type anomaly expected, due to the first excited Kramers-doublet at 4.7 cm^{-1} above the ground level of the Ce^{3+} ion. This anomaly was successfully calculated (15) by assuming an interaction between this excited electronic level and the acoustic phonons.

It will be the object of a further study to see if the surprising differences in frequencies and relative intensities of the low-lying optical phonons ($\nu < 100$ cm^{-1}) in Ce-E.S. between room temperature and 2 K (see Figs. 1 and 2) are due to a similar electron–phonon coupling mechanism. In Nd-E.S., where the first excited Kramers doublet is at 149.4 cm^{-1} (16), and in Y-E.S., the differences between room temperature and low temperature spectra are much less pronounced than in Ce-E.S.

Conclusions

The optically active phonon frequencies for this important crystalline matrix are now well known except for a small gap in the infrared spectrum. For a study of electronic Raman spectra, this matrix may offer some advantages: there are wavenumber regions free of phonon lines (1500 $cm^{-1} < \nu < 2900$ cm^{-1}; $\nu > 3500$ cm^{-1}) which are well suited for studies of $\Delta J = 1$ transitions of the Ce^{3+}, Pr^{3+}, Nd^{3+}, and Tb^{3+} ions. On the other hand, the large number of phonon levels may facilitate a study of an interaction between 4f electrons and resonant phonons.

1. G. MACE, G. SCHAACK, TOANING NG, and J. A. KONINGSTEIN. Z. Phys. **230**, 391 (1970); J. A. KONINGSTEIN and G. SCHAACK. Phys. Rev. **B2**, 1242 (1970).
2. E. Y. WONG and E. H. ERATH. J. Chem. Phys. **39**, 1629 (1963).
3. J. A. KONINGSTEIN and O. S. MORTENSEN. J. Mol. Spectrosc. **27**, 343 (1968).
4. J. A. A. KETELAAR. Physica, **4**, 619 (1937).
5. D. R. FITZWATER and R. E. RUNDLE. Z. Kristallogr. **112**, 362 (1959).
6. H. P. GESERICH, K. H. HELLWEGE, and G. SCHAACK. Z. Naturforsch. **20a**, 289 (1965).
7. P. DIEM, K. H. HELLWEGE, J. JÄGER, G. SCHAACK, and F. J. SCHEDEWIE. Phys. kondens. Materie, **7**, 52 (1968).
8. J. F. SCOTT and S. P. S. PORTO. Phys. Rev. **142**, 570 (1966).
9. S. P. S. PORTO, J. A. GIORDMAINE, and T. C. DAMEN. Phys. Rev. **147**, 608 (1966).
10. J. C. HILL and R. G. WHEELER. Phys. Rev. **152**, 482 (1966).
11. G. HERZBERG. Infrared and Raman spectra of polyatomic molecules. D. van Nostrand Co., New York. 1945. p. 488.
12. A. KIEL, T. C. DAMEN, S. P. S. PORTO, S. SINGH, and F. VARSANYI. Phys. Rev. **178**, 1518 (1969).
13. G. SCHAACK and J. A. KONINGSTEIN. J. Phys. Chem. Solids, **31**, 2417 (1970).
14. H. MEYER and P. L. SMITH. J. Phys. Chem. Solids, **9**, 285 (1959); C. E. JOHNSON and H. MEYER. Proc. Roy. Soc. (London), Ser. A, **253**, 199 (1959).
15. E. BECKER and R. B. CLOVER. Phys. Rev. Lett. **21**, 1327 (1968).
16. G. H. DIEKE and L. HEROUX. Phys. Rev. **103**, 1227 (1956).

Solid–Liquid Phase Equilibria for the Ternary Systems V_2O_5–Na_2O–Fe_2O_3, V_2O_5–Na_2O–Cr_2O_3, and V_2O_5–Na_2O–MgO

R. C. KERBY

Extraction Metallurgy Research Section, Mines Branch, Department of Energy, Mines and Resources, Ottawa, Canada

AND

J. R. WILSON

Department of Metallurgical Engineering, Queen's University, Kingston, Ontario

Received June 1, 1972

The phase equilibrium relationships of several vanadate systems have been studied by a combination of differential thermal analysis (DTA) and X-ray powder diffraction methods. All systems studied were eutectic in nature. The liquidus temperatures of the sodium vanadates were found to depend on the oxygen partial pressure for sodium oxide concentrations between 1.0 and 36 mol%. This effect was not observed for the ferric vanadate, chromic vanadate or magnesium vanadate systems. The solid–liquid phase equilibria for the ternary vanadate systems V_2O_5–Na_2O–Fe_2O_3, V_2O_5–Na_2O–Cr_2O_3, and V_2O_5–Na_2O–MgO were measured by determining the temperature–composition data for various quasi-binary systems within each ternary system. Liquidus temperatures between 500 and 700 °C were found for those compositional ranges containing greater than 40 mol% V_2O_5 and between 10 and 60 mol% Na_2O. The liquidus temperatures decreased with increasing oxygen partial pressure over much of the same compositional range.

Les relations d'équilibre de phases de plusieurs systèmes impliquant des vanadates ont été étudiées par combinaison de deux méthodes à savoir l'analyse thermale différentielle et la diffraction de rayons-X (poudre). Tous les systèmes qui furent étudiés, étaient du type eutectique. Les températures liquidus des vanadates de sodium se sont révélées dépendantes de la pression partielle de l'oxygène pour des concentrations d'oxyde de sodium dans l'intervalle compris entre 1.0 et 36 mol%. Cet effet ne fut pas observé pour les systèmes de vanadate ferrique, de vanadate chromique et de vanadate de magnésium. Les équilibres de phase solide–liquide pour les systèmes ternaires de vanadates, V_2O_5–Na_2O–Fe_2O_3, V_2O_5–Na_2O–Cn_2O_3 et V_2O_5–Na_2O–MgO, ont été mesurés en déterminant des données sur la température et la composition pour des systèmes presque binaires à l'intérieur de chacun des systèmes ternaires. Les températures liquidus entre 500 et 700 °C ont été trouvées pour les domaines de composition comprenant plus que 40 mol% en V_2O_5 et entre 10 et 60 mol% en Na_2O. Les températures liquidus diminuent si la pression partielle de l'oxygène augmente et ce, pour la plupart des domaines similaires de composition. [Traduit par le journal]

Can. J. Chem., **51**, 1032 (1973)

Introduction

The use of residual fuel oils of high vanadium and sodium contents (100 p.p.m.) as a low-cost fuel for power generation can often lead to severe corrosion problems (1). Particularly severe corrosion occurs on metal and refractory components which have been in direct contact with hot (>500 °C) fly ash deposits (2). This form of corrosion is often called "catastrophic" vanadate corrosion and is considered to be due to the presence of liquid vanadates in the fly ash deposits. The liquid vanadates are thought to increase the corrosion rate by fluxing or altering the normally protective oxide layers present on the surface of the alloys and by providing a source of oxide ion for the corrosion reaction (1).

Several vanadates are commonly found in the fly ash deposits which exhibit severe corrosion characteristics (3). The liquid sodium vanadates centering about the composition $Na_2O{\cdot}6V_2O_5$ are considered to be the most corrosive (4, 5). Ferric vanadates and chromic vanadates are often present in the fly ash deposits as corrosion products. The presence of magnesium vanadates is caused by magnesium-based additives in the fuel oil for controlling corrosion (6).

A number of phase studies have been made on the system V_2O_5–Na_2O. The solid–liquid phase equilibria have been examined by Canneri (7), Illarionov *et al.* (8), and Slobodin *et al.* (9). The meta-, pyro-, and ortho-vanadates were shown to be present, but there were some discrepencies in the reported melting points. Oxygen was evolved on freezing at compositions between 1 and 32 mol% sodium oxide, with the formation of vanadyl vanadates or sodium vanadium

Can. J. Chem. Downloaded from www.nrcresearchpress.com by 210.87.254.105 on 09/05/12
For personal use only.

Can. J. Chem. Downloaded from www.nrcresearchpress.com by 210.87.254.105 on 09/05/12
For personal use only.

"bronzes" (7, 10). These compounds have been the subject of a number of investigations because of their semiconducting properties (11, 12). Phases which have been identified include Na_x-V_2O_5, where $0.1 < x < 0.67$, and $Na_{1+y}V_3O_8$, where $0.0 < y < 0.8$ (13–15).

The systems V_2O_5–Fe_2O_3 and V_2O_5–Cr_2O_3 have been reported by Burdese (16) to exhibit eutectic melting together with the formation of the incongruently melting compounds $FeVO_4$ and $CrVO_4$. A miscibility gap has been reported for the system V_2O_5–Fe_2O_3 (17). The eutectic system V_2O_5–MgO was reported to contain the incongruently melting compounds: MgV_2O_6, $Mg_2V_2O_7$, $Mg_3(VO_4)_2$, and $Mg_3V_4O_{13}$ (18–20). The crystal structures of $FeVO_4$ (21), $CrVO_4$ (22), and $Mg_3(VO_4)_2$ (23) have been determined.

Because catastrophic vanadate corrosion is dependent on the presence of liquid vanadates in the fly ash deposits, it is important to have accurate data on the temperature–oxygen partial pressure–compositional ranges in which the liquid vanadates can occur. The solid–liquid phase equilibria of several vanadate systems have been determined.

Experimental

The liquidus and solidus lines of the vanadate systems were determined using differential thermal analysis (DTA). The samples were contained in 6 mm i.d. Vycor tubes open at one end. The sample tubes were contained in an Inconel 600 block, and chromel–alumel reference and sample thermocouples were placed next to the Vycor tubes. The melts were too corrosive to allow the thermocouples to be placed in the melts. A limited amount of attack of the Vycor tubes was observed when the melts contained more than 50 mol% sodium oxide (1). The samples and sample holder were enclosed in a gas-tight Vycor tube, allowing the oxygen partial pressures over the melt to be accurately controlled. High purity oxygen and argon were used to give controlled atmospheres above the melt. Reagent grade vanadium pentoxide, sodium carbonate, ferric oxide, chromic oxide, and magnesium oxide were used to prepare the vanadate mixtures. Johnson and Matthey "specpure" vanadium pentoxide was used to provide a temperature calibration standard.

A programmed rate of 10 deg per min was used for the DTA experiments. The sample was heated and cooled several times. The peak temperatures obtained from the heating DTA curves were used to plot the phase diagrams. Several temperature calibration experiments using high-purity lead and silver indicated that the temperature measurements were accurate to within ± 2 °C. "Specpure" vanadium pentoxide (m.p. 670 $\pm$ 2 °C) was used to provide a temperature calibration standard for every sample run. Powder diffraction spectra were made on selected air-quenched samples using a Norelco X-ray diffractiometer and zirconium-filtered molybdenum radiation.

Results

The System V_2O_5–Na_2O

The measured phase diagram of the system V_2O_5–Na_2O is shown in Fig. 1. The oxygen partial pressure was found to have a significant effect on the melting points for compositions between 1 and 36 mol% Na_2O; *i.e.*, for the sodium–vanadium bronzes. The sodium–vanadium bronzes lose oxygen on freezing (10):

$$[1]\quad Na_2O{\cdot}6V_2O_5(l) \rightleftharpoons Na_2O{\cdot}xV_2O_4{\cdot}(6-x)V_2O_5 + (x/2)O_2(g)$$

so that a change in oxygen partial pressure would be expected to change the composition of the solid. This was verified experimentally (Fig. 2) by measuring the weight change of the sodium vanadates as they were cooled under various oxygen partial pressures. As would be expected the V^{4+} ion concentration, as determined from the weight change, increased as the oxygen partial pressure was decreased. The melting points of these sodium vanadates increased initially as the oxygen partial pressure was decreased, but the melting point remained constant for oxygen partial pressures less than 0.2 atm (Fig. 3). The phase relationships shown in the quasi-binary phase diagram of Fig. 1 can also be represented as a portion of the ternary phase system V_2O_5–Na_2O–V_2O_4.

Five compounds, $Na_2O{\cdot}xV_2O_4{\cdot}(6-x)V_2O_5$, $5Na_2O{\cdot}xV_2O_4{\cdot}(12-x)V_2O_5$, $Na_2O{\cdot}V_2O_5$ or $NaVO_3$, $2Na_2O{\cdot}V_2O_5$, and $3Na_2O{\cdot}V_2O_5$ or Na_3VO_4, were identified by X-ray powder diffraction methods, using previously reported spectral data (24–26). No significant differences

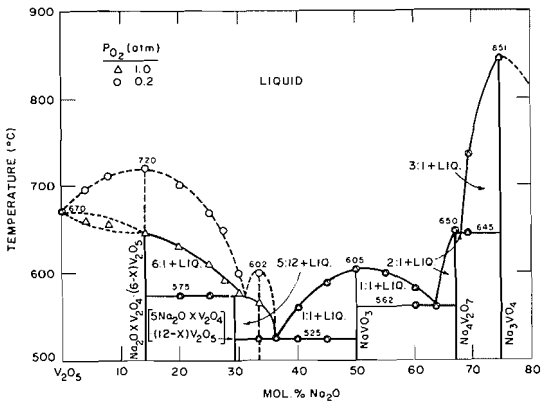

FIG. 1. The V_2O_5–Na_2O phase diagram at two oxygen partial pressures.

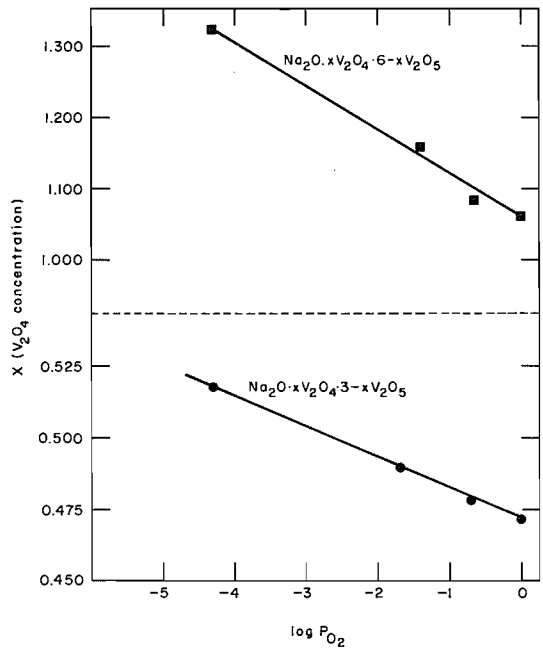

FIG. 2. Change in composition with oxygen partial pressure on freezing of the sodium vanadates $Na_2O \cdot xV_2O_4 \cdot (6 - x)V_2O_5$ and $Na_2O \cdot xV_2O_4 \cdot (3 - x)V_2O_5$.

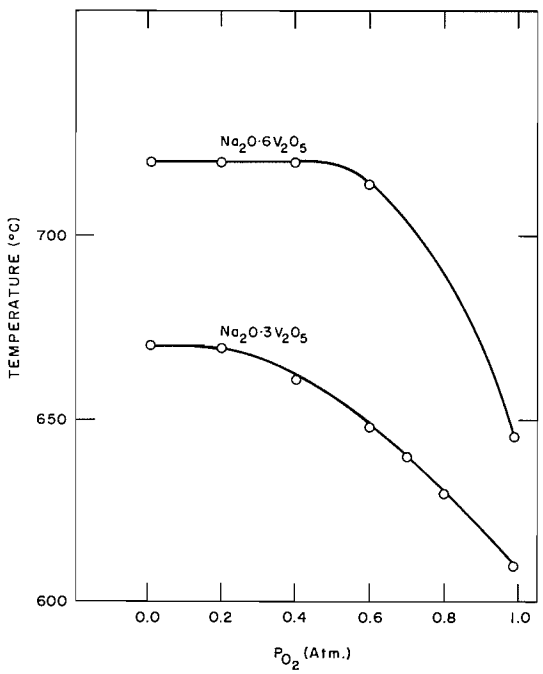

FIG. 3. The dependence of the melting point of the sodium vanadates $Na_2O \cdot xV_2O_4 \cdot (6 - x)V_2O_5$ and $Na_2O \cdot xV_2O_4 \cdot (3 - x)V_2O_5$ on the oxygen partial pressure.

in the X-ray diffraction spectra of the same vanadates frozen under various oxygen partial pressures were observed. The compositions and temperatures of the three eutectics and one peritectic are reported in Table 1. The differences in the previously reported phase diagrams (7–9) are at least partially due to the effect that oxygen partial pressure has on the liquidus points in the composition range of the sodium–vanadium bronzes. The lack of a clearly defined eutectic between the compounds V_2O_5 and $Na_2O \cdot xV_2O_4 \cdot (6 - x)V_2O_5$ probably indicates considerable solid solubility.

The System V_2O_5–Na_2O–Fe_2O_3

No effect of oxygen partial pressure on the melting temperatures was found for the system V_2O_5–Fe_2O_3 (Fig. 4). The orthovanadate, $Fe_2O_3 \cdot V_2O_5$ or $FeVO_4$, was identified by X-ray powder diffraction methods, using previously reported spectral data (27). No evidence was found for the existence of the metavanadate, $Fe_2O_3 \cdot 3V_2O_5$ or $Fe(VO_3)_3$, the pyrovanadate, $2Fe_2O_3 \cdot 3V_2O_5$ or $Fe_4(V_2O_7)_3$, or the previously reported compound $Fe_2O_3 \cdot 2V_2O_5$ (28). The compositions and temperatures of the two eutectics and the peritectic are reported in Table 1. Both the eutectic temperature (645 °C) and the peritectic temperature (870 °C) were higher than the eutectic temperature (635 °C) and peritectic temperature (840 °C) reported by Burdese (16). A liquid–liquid miscibility gap was found in the compositional region about $FeVO_4$, which is in agreement with data reported by Schlapfer *et al.* (17).

The liquidus phase diagram of the ternary system V_2O_5–Na_2O–Fe_2O_3 (Fig. 5) at an oxygen partial pressure of 1 atm was measured by deter-

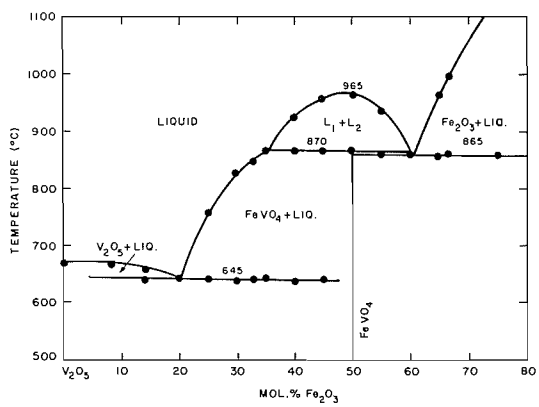

FIG. 4. The V_2O_5–Fe_2O_3 phase diagram.

Can. J. Chem. Downloaded from www.nrcresearchpress.com by 210.87.254.105 on 09/05/12
For personal use only.

TABLE 1. Invariant points

Composition (mol%)			Temperature (°C)	Type of invariant	Equilibrium solid phases
V_2O_5	Na_2O				
69	31		575	Peritectic	$Na_2O{\cdot}xV_2O_4{\cdot}(6-x)V_2O_5$, $5Na_2O{\cdot}xV_2O_4{\cdot}(12-x)V_2O_5$
64	36		525	Eutectic	$5Na_2O{\cdot}xV_2O_4{\cdot}(12-x)V_2O_5$, $NaVO_3$
37	63		562	Eutectic	$NaVO_3$, $Na_4V_2O_7$
32	68		645	Eutectic	$Na_4V_2O_7$, Na_3VO_4
V_2O_5	Fe_2O_3				
80	20		645	Eutectic	V_2O_5, $FeVO_4$
64	36		870	Peritectic	$FeVO_4$
40	60		870	Peritectic	$FeVO_4$
38	62		865	Eutectic	$FeVO_4$, Fe_2O_3
V_2O_5	Na_2O	Fe_2O_3			
81	2	17	610	Eutectic	V_2O_5, $FeVO_4$, $Na_2O{\cdot}xV_2O_4{\cdot}(6-x)V_2O_5$
58	18	24	530	Peritectic	$Na_2O{\cdot}xV_2O_4{\cdot}(6-x)V_2O_5$, $FeVO_4$, $5Na_2O{\cdot}xV_2O_4{\cdot}(12-x)V_2O_5$
42	24	34	515	Peritectic	$NaVO_3$, $FeVO_4$, $5Na_2O{\cdot}xV_2O_4{\cdot}(12-x)V_2O_5$
38	18	44	510	Eutectic	$FeVO_4$, $NaVO_3$, Fe_2O_3
22	50	28	535	Eutectic	$NaVO_3$, $Na_4V_2O_7$, Fe_2O_3
V_2O_5	Cr_2O_3				
76	24		655	Eutectic	V_2O_5, $CrVO_4$
52	48		902	Peritectic	$CrVO_4$, Cr_2O_3
V_2O_5	Na_2O	Cr_2O_3			
76	3	21	630	Eutectic	V_2O_5, $Na_2O{\cdot}xV_2O_4{\cdot}(6-x)V_2O_5$, $CrVO_4$
56	26	18	545	Peritectic	$Na_2O{\cdot}xV_2O_4{\cdot}(6-x)V_2O_5$, $CrVO_4$, $5Na_2O{\cdot}xV_2O_4{\cdot}(12-x)V_2O_5$
52	28	20	505	Eutectic	$5Na_2O{\cdot}xV_2O_4{\cdot}(12-x)V_2O_5$, $NaVO_3$, $CrVO_4$
43	17	40	555	Eutectic	$CrVO_4$, $NaVO_3$, Cr_2O_3
35	39	26	520	Eutectic	$NaVO_3$, $Na_4V_2O_7$, Cr_2O_3
V_2O_5	MgO				
77	23		604	Eutectic	V_2O_5, $Mg_2V_6O_{17}$
72	28		640	Peritectic	$Mg_2V_6O_{17}$, MgV_2O_6
56	44		742	Peritectic	MgV_2O_6, $Mg_2V_2O_7$
37	63		980	Peritectic	$Mg_2V_2O_7$, $Mg_3(VO_4)_2$
V_2O_5	Na_2O	MgO			
77	1	22	602	Eutectic	V_2O_5, $Mg_2V_6O_{17}$, $Na_2O{\cdot}xV_2O_4{\cdot}(6-x)V_2O_5$
61	23	16	535	Peritectic	$Na_2O{\cdot}xV_2O_4{\cdot}(6-x)V_2O_5$, $5Na_2O{\cdot}xV_2O_4{\cdot}(12-x)V_2O_5$, $Mg_2V_6O_{17}$
49	30	21	510	Peritectic	$Mg_2V_6O_{17}$, $NaVO_3$, $5Na_2O{\cdot}xV_2O_4{\cdot}(12-x)V_2O_5$
46	21	33	540	Peritectic	$Mg_2V_6O_{17}$, $Mg_2V_2O_7$, MgV_2O_6
47	26	27	505	Eutectic	$NaVO_3$, $Mg_2V_6O_{17}$, $Mg_2V_2O_7$
24	37	39	495	Peritectic	$NaVO_3$, $Mg_3(VO_4)_2$, $Mg_2V_2O_7$
15	44	41	470	Peritectic	$Mg_3(VO_4)_2$, $Na_4V_2O_7$, —
22	48	30	480	Peritectic	$Mg_3(VO_4)_2$, $Na_4V_2O_7$, $NaVO_3$

mining the temperature–composition data for the following quasi-binary systems; V_2O_5–($Na_2O{\cdot}Fe_2O_3$), V_2O_5–($2Fe_2O_3{\cdot}Na_2O$), and Na_2O–($FeVO_4$). The data for these systems have been submitted to the Depository of Unpublished Data.[1] The temperatures and approximate compositions of three eutectic points and peritectic points found in the ternary system were determined separately and are reported in Table 1. A previous study of a portion of this ternary system has shown that the iron vanadate, $FeVO_4$, and sodium vanadium bronzes exist over a wide concentration range (29). The partial solution of V_2O_5 in Fe_2O_3 was also found.

The vanadium pentoxide-rich portion of the ternary system had melting points less than

[1]Complete set of tabular data is available, at a nominal charge, from the Depository of Unpublished Data, National Science Library, National Research Council of Canada, Ottawa, Canada K1A 0S2.

Can. J. Chem. Downloaded from www.nrcresearchpress.com by 210.87.254.105 on 09/05/12
For personal use only.

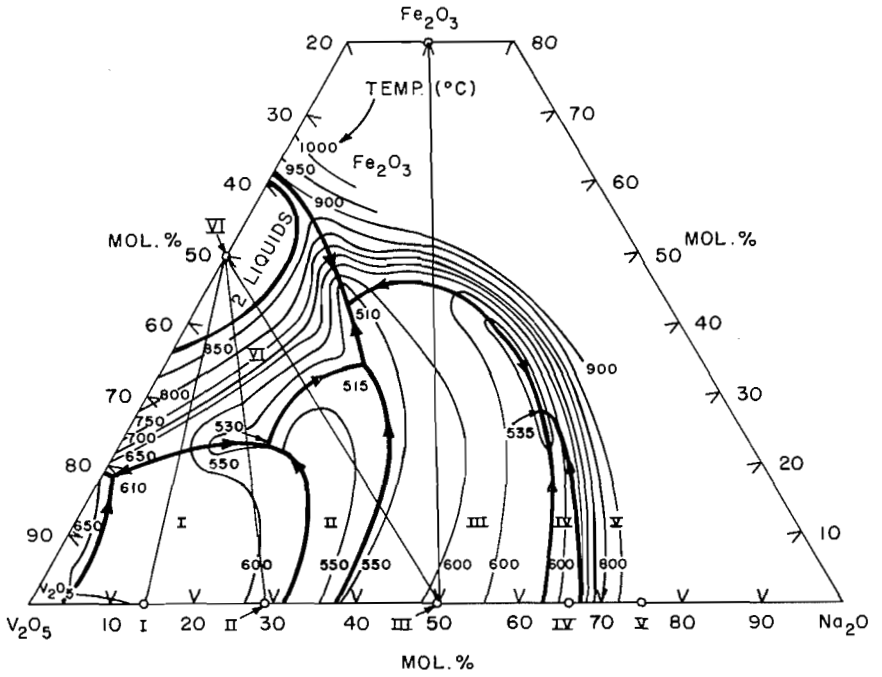

FIG. 5. Proposed ternary phase diagram V_2O_5–Na_2O–Fe_2O_3. Binary phase compositions: I = $Na_2O{\cdot}xV_2O_4{\cdot}(6 - x)V_2O_5$, II = $5Na_2O{\cdot}xV_2O_4{\cdot}(12 - x)V_2O_5$, III = $NaVO_3$, IV = $Na_4V_2O_7$, V = Na_3VO_4, VI = $FeVO_4$.

700 °C. Much of this same region also showed an increase in the temperature of the liquidus with a decrease in oxygen partial pressure, although the maximum liquidus points observed were still less than 720 °C (Fig. 6).

The System V_2O_5–Na_2O–Cr_2O_3

The phase diagram for the system V_2O_5–Cr_2O_3 is given in Fig. 7. The melting points were found to be independent of oxygen partial pressure. The compound $CrVO_4$ was identified from published X-ray diffraction data (30). No evidence was found for the existence of the metavanadate or the pyrovanadate (31, 32). The compositions and temperatures of the eutectic and peritectic are reported in Table 1. The peritectic temperature of 902 °C which was observed in the present work agrees more closely with the temperature 907 °C reported by Lucas *et al.* (33) than with the temperatures 810 °C and 886 °C reported by Burdese (16) and Amiel *et al.* (34), respectively. An eutectic temperature of 655 °C was found in this work. Amiel *et al.* (34) reported an eutectic temperature of 650 °C and Burdese (16) found the eutectic temperature to be 665 °C.

The liquidus phase diagram of the ternary system V_2O_5–Na_2O–Cr_2O_3 (Fig. 8) at an oxygen partial pressure of 1 atm was measured by determining the temperature–composition data for

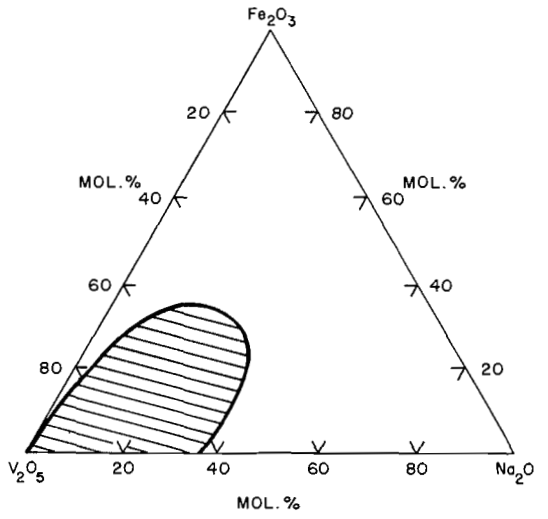

FIG. 6. Region of V_2O_5–Na_2O–Fe_2O_3 phase system which shows a change in melting point with oxygen partial pressure (shaded portion).

Can. J. Chem. Downloaded from www.nrcresearchpress.com by 210.87.254.105 on 09/05/12
For personal use only.

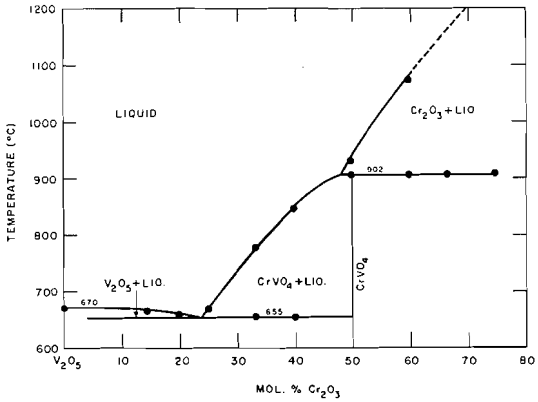

FIG. 7. The V_2O_5–Cr_2O_3 phase diagram.

the following quasi-binary systems: V_2O_5–($Cr_2O_3 \cdot 2Na_2O$), V_2O_5–($Cr_2O_3 \cdot Na_2O$), and V_2O_5–($2Cr_2O_3 \cdot Na_2O$). The data for these systems have been submitted to the Depository of Unpublished Data. The temperatures and approximate compositions of the four eutectic points and one peritectic point found in the ternary system were determined separately and are reported in Table 1.

Chromic oxide (Cr_2O_3) was found over a wider concentration range in this system than the other ternary systems. The portion of the vanadium pentoxide-rich section of the phase diagram in which the liquidus temperatures were less than 700 °C was less extensive than that found for the other ternary systems. However, the portion of the diagram in which the temperature of the liquidus was affected by the oxygen partial pressure was found to be much the same (Fig. 6).

The System V_2O_5–Na_2O–MgO

The phase diagram for the system V_2O_5–MgO is shown in Fig. 9. The oxygen partial pressures were found to have no effect on the liquidus temperatures. The metavanadate, $MgO \cdot V_2O$ or $MgVO_3$, the pyrovanadate, $2MgO \cdot V_2O_5$, and the orthovanadate, $3MgO \cdot V_2O_5$, were identified by X-ray powder diffraction methods, using previously reported spectral data (35–37).

A fourth compound, $2MgO \cdot 3V_2O_5$, was identified and the spectral data are reported in Table 2. This compound appears to be the stoichiometric equivalent of the oxygen-deficient compound α-MgV_3O_8 or $2MgO \cdot V_2O_4 \cdot 2V_2O_5$, which was prepared by Galy and Pouchard (35) under reducing conditions. The compound $3MgO \cdot 2V_2O_5$ has been reported (20, 38) but it was not identi-

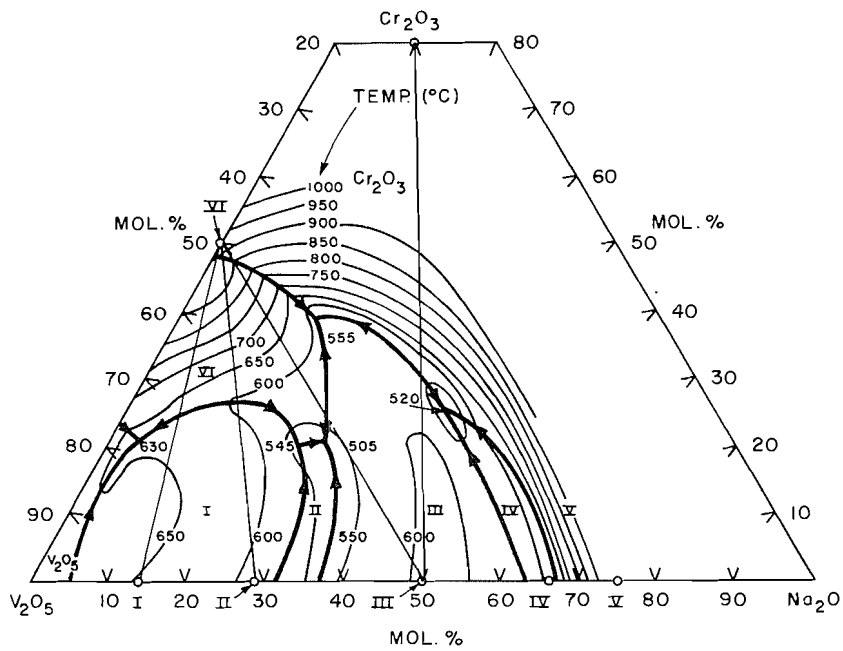

FIG. 8. Proposed ternary phase diagram V_2O_5–Na_2O–Cr_2O_3. Binary phase compositions: I = $Na_2O \cdot xV_2O_4 \cdot (6 - x)V_2O_5$, II = $5Na_2O \cdot xV_2O_4 \cdot (12 - x)V_2O_5$, III = $NaVO_3$, IV = $Na_4V_2O_7$, V = Na_3VO_4, VI = $CrVO_4$.

Can. J. Chem. Downloaded from www.nrcresearchpress.com by 210.87.254.105 on 09/05/12
For personal use only.

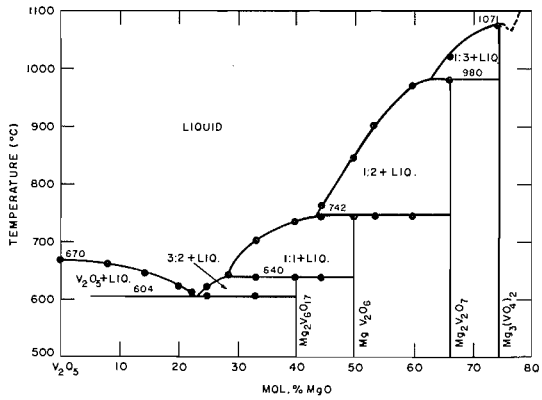

FIG. 9. The V_2O_5–MgO phase diagram.

TABLE 2. Powder diffraction data for $2MgO{\cdot}3V_2O_5$

Intensity*	*d*-spacing (Å)
5	4.33
1	4.03
8	3.86
1	3.39
1	3.21
2	3.10
10	3.04
1	2.94
3	2.848
2	2.685
2	2.173
1	2.070
2	1.974
1	1.731

*Intensities were estimated visually with the strongest line as 10.

fied in these studies. The eutectic nature of the magnesium vanadate system as shown in Fig. 6 agrees in general with that reported by Pollard (18), Kohlmuller and Perraud (19), and Speranskaya (20), although there are some discrepencies in the eutectic and peritectic temperatures. All of the magnesium vanadates except the orthovanadate, $Mg_3(VO_4)_2$, were found to melt incongruently.

The liquidus phase diagram of the ternary system V_2O_5–Na_2O–MgO (Fig. 10) at an oxygen partial pressure of 1 atm was measured by determining the temperature–composition data for the following quasi-binary systems: V_2O_5–$(2MgO{\cdot}Na_2O)$, V_2O_5–$(MgO{\cdot}Na_2O)$, and V_2O_5–$(2Na_2O{\cdot}MgO)$. The data for these systems have been submitted to the Depository of Unpublished Data. The temperatures and approximate compositions of the two eutectic points and six peritectic points found in the ternary system were determined separately and are reported in Table 1.

The vanadium pentoxide-rich portion of the phase diagram in which the liquidus temperature was less than 700 °C was more extensive than for either system previously shown. The portion of the phase diagram in which the temperature of the liquidus was affected by the oxygen partial pressure was much the same as that indicated for the two previous systems (Fig. 6).

Discussion

An interesting aspect of the vanadate systems examined in this report is the effect that oxygen partial pressure has on the liquidus temperatures when concentrations of 1 to 36 mol% sodium oxide are present. A number of vanadates containing 1 to 32 mol% of the univalent cation lose oxygen on freezing to form nonstoichiometric oxides (7), and can be represented as:

$$[2]\quad M_2O{\cdot}xV_2O_5(l) \rightleftharpoons M_2O{\cdot}yV_2O_4{\cdot}(x-y)V_2O_5 + (y/2)O_2$$

where $M_2O{\cdot}yV_2O_4{\cdot}(x-y)V_2O_5$ is often called a vanadate "bronze". These vanadate "bronzes" are frequently semiconducting and include the sodium, lithium, potassium (39), silver, and cuprous vanadates (40). The loss of oxygen is usually credited to the stabilizing influence of the lattice structure of solid V_2O_5, so that the compounds can often be formulated as $M_xV_2O_5$ (13–15). For example, the sodium ions in the sodium vanadates are considered to be situated in "tunnels" in the V_2O_5 lattice. Vanadate bronzes can also be formed with multivalent cations if highly reducing conditions are used (35, 41, 42).

As the oxygen partial pressure over the freezing sodium vanadates was reduced, there was an increase in the V^{4+} ion concentration, in the oxygen vacancy concentration of the solid sodium vanadates, and in the liquidus temperature. However, at still lower oxygen partial pressures (less than 0.2 atm), the V^{4+} ion concentration continued to increase, but the liquidus temperature remained constant. The eutectic points were not affected by the oxygen partial pressure. The increase in V^{4+} ion concentration apparently stabilized the compound $Na_2O{\cdot}xV_2O_4{\cdot}(6-x)$-$V_2O_5$, resulting in an increase in its melting point from 645 to 720 °C. The sodium vanadate

Can. J. Chem. Downloaded from www.nrcresearchpress.com by 210.87.254.105 on 09/05/12
For personal use only.

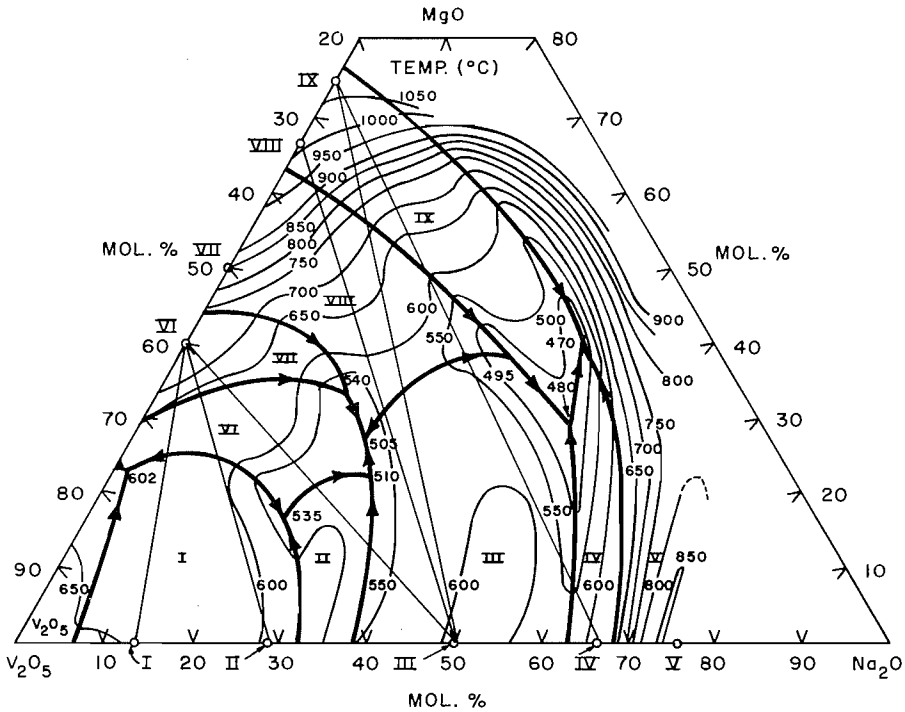

FIG. 10. Proposed ternary phase diagram V_2O_5–Na_2O–MgO. Binary phase compositions: I = $Na_2O{\cdot}xV_2O_4{\cdot}(6 - x)V_2O_5$, II = $5Na_2O{\cdot}xV_2O_4{\cdot}(12 - x)V_2O_5$, III = $NaVO_3$, IV = $Na_4V_2O_7$, V = Na_3VO_4, VI = $Mg_2V_6O_{17}$, VII = MgV_2O_6, VIII = $Mg_2V_2O_7$, IX = $Mg_3(VO_4)_2$.

phase diagram (Fig. 1) also appeared to indicate that the compound $Na_2O{\cdot}xV_2O_4{\cdot}(2 - x)V_2O_5$ may be stable at lower oxygen partial pressures, although X-ray powder diffraction analysis was unable to confirm this. Both of these oxygen-deficient compounds can be represented as ternary compounds in the system V_2O_5–Na_2O–V_2O_4.

The ferric vanadates, chromic vanadates, and magnesium vanadates did not show an increase in liquidus temperatures with decreasing oxygen partial pressures. The compounds evolved little, if any, oxygen on freezing. However, on the addition of sodium oxide to these vanadates, there was oxygen evolution on freezing in certain compositional ranges (Fig. 6), with a consequent increase in liquidus temperatures with decreasing oxygen partial pressures. The presence of a univalent cation appears necessary for the formation of oxygen-deficient vanadates under the conditions used in this study, *i.e.*, in an oxidizing atmosphere.

The large compositional ranges in the ternary vanadate systems in which the liquidus lies between 500 and 700 °C is of importance in relation to catastrophic vanadate corrosion because the corrosion mechanism is dependent on the presence of molten vanadates (1). For example, the operating temperatures of residual oil-fired boilers is at present limited to a maximum temperature of 500 °C, because of severe corrosion at higher temperatures (2). An examination of the ternary phase diagrams indicates that the sodium vanadates present in the fly ash deposits must dissolve at least their own weight in corrosion products or other oxides before the liquidus temperatures will rise above 700 °C. Therefore, it is difficult to control catastrophic vanadate corrosion by methods which raise the liquidus temperatures of the vanadates present in the fly ash, without accumulating large volumes of modified fly ash deposits.

Conclusions

The vanadate systems which were examined were predominately eutectic systems, although there may be some solid solubility of the metal oxides in vanadium pentoxide. The ternary sys-

Can. J. Chem. Downloaded from www.nrcresearchpress.com by 210.87.254.105 on 09/05/12
For personal use only.

tems V_2O_5–Na_2O–Fe_2O_3, V_2O_5–Na_2O–Cr_2O_3, and V_2O_5–Na_2O–MgO exhibited large compositional ranges between 40 and 100 mol% V_2O_5 and between 10 and 60 mol % Na_2O for which the liquidus temperatures were between 500 and 700 °C.

The liquidus temperatures of the sodium vanadates decreased with increasing oxygen partial pressure for compositions containing between 1 and 36 mol% sodium oxide. The same effect occurred in the case of the ternary systems examined in this study when more than 35 mol% of these same sodium vanadates were present. The effect appears to be related to the stabilization of the oxygen-deficient vanadyl vanadates at low oxygen partial pressures.

This work was supported by grants from the Defence Research Board of Canada.

1. J. R. Wilson and R. C. Kerby. J. Eng. Power, Trans. ASME. **95** (1), 36 (1973).
2. K. Sachs. Metallurgia, **57**, 123, 167, 224 (1958).
3. H. R. Johnson and D. J. Littler (*Editors*). Mechanism of corrosion by fuel impurities. Butterworths, London. 1963.
4. G. W. Cunningham and A. de S. Brasunas. Corrosion, **12**, 389 (1956).
5. W. R. Foster, M. H. Leipold, and T. S. Shevlin. Corrosion, **12**, 539 (1956).
6. D. W. McDowell, Jr. and J. R. Milhalisin. ASME Paper No. 60-WA-260 (1960).
7. G. Canneri. Gaz. Chem. Ital. **58**, 6 (1928).
8. V. V. Illarionov, R. P. Ozerov, and E. V. Kil'desheva. Zh. Neorg. Khim. **2**, 884 (1957).
9. B. V. Slobodin and A. A. Fotiev. Zh. Priklad. Khim. **38**, 801 (1965).
10. L. B. Johnson. Ind. Eng. Chem. **52**, 55A (1960).
11. J. H. Perlstein and M. J. Sienko. J. Chem. Phys. **44**, 174 (1968).
12. B. G. Golovkin, A. A. Fotiev, and A. A. Neuimin. Zh. Fiz. Khim. **45**, 2247 (1971).
13. A. D. Wadsley. Acta Cryst. **8**, 695 (1955); **10**, 261 (1957).
14. R. P. Ozerov, G. A. Gol'der, and G. S. Zhdanov. Sov. Phys. Crystallogr. **2**, 211 (1957).
15. J. Galy, J. Darriet, A. Casalot, and J. B. Goodenough. J. Solid State Chem. **1**, 339 (1970).
16. A. Burdese. Ann. Chim. (Rome), **47**, 801, 804 (1957).
17. P. Schlapfer, P. Amgverd, and H. Preiss. Schweiz Arch. Wiss. Techn. **15**, 291 (1949).
18. A. J. Pollard. NASA Accession No. N 65/17008, Contract No. NRL-6038. 1964. 11 pp.
19. R. Kohlmuller and J. Perraud. Bull. Soc. Chim. Fr. **3**, 642 (1964).
20. E. I. Speranskaya. Izv. Akad. Nauk. SSSR, Neorg. Mater. **7**, 1804 (1971).
21. B. Robertson and E. Kostiner. J. Solid-State Chem. **4**, 29 (1972).
22. K. Brandt. Arkiv. Kemi. Mineral Geol. **17A**, No. 6, 1 (1943).
23. E. F. Bertant, A. Durif, and R. Pauthenet. Acta Cryst. **13**, 1015 (1960).
24. P. T. Davies, B. D. Caddock, C. Orman, and G. C. S. Waghorn. Shell Res. Ltd., Thornton Report M 193 (1959).
25. D. G. Baldwin. Shell Research Ltd., Thornton Report M 186 (1958).
26. G. LeFlem, R. Olazcuaga, J. P. Parant, J. E. Reau, and C. Fouassier. C.R. Acad. Sci. Ser. C, **275** (20), 1358 (1971).
27. F. C. Monkman and N. J. Grant. Corrosion, **9**, 460 (1953).
28. Y. Otsubu and K. Utsumi. Nippon Kagaku Zasshi, **92**(8), 737 (1971).
29. N. G. Moleva, N. A. Vatolin, N. N. Belyaeva, and F. K. Korovychenko. Tr. Inst. Met., Akad. Nauk. SSSR Ural. Filial, (17), 102 (1969).
30. J. Amiel, D. Olivier, and M. Dessolin. C.R. Acad. Sci. Ser. C, **246**, 1045 (1967).
31. D. Olivier. C.R. Acad. Sci. Ser. C, **272**(13), 1225 (1971).
32. D. Olivier and P. Rabette. C.R. Acad. Sci. Ser. C, **265**, 1451 (1967).
33. G. Lucas, M. Weddle, and A. Preece. J. Iron Steel Inst. **174**, 342 (1955).
34. J. Amiel, D. Colaitis, and D. Olivier. C.R. **C263**, 224 (1966).
35. J. Galy and M. Pouchard. Bull. Soc. Chim. Fr. (**1**), 261 (1967).
36. A. J. Elshout. Mitt. der V.G.B. **49**, 182 (1969).
37. ASTM Powder Diffraction File, No. 12–405.
38. B. W. King and L. L. Suber. J. Am. Cer. Soc. **38**, 306 (1955).
39. I. Lukacs, C. Strusievici, and C. Liteanu. Rev. Roum. Chem. **13**, 953 (1968).
40. M. V. Volzhenskii, M. V. Pashkovskii, and L. C. Svekolkina. Russ. J. Inorg. Chem. **8**, 129 (1963).
41. J. Galy, A. Casalot, J. Darriet, and P. Hagenmuller. Bull. Soc. Chim. Fr. (**1**), 227 (1967).
42. A. A. Fotiev, V. L. Volkov, and B. G. Golovkin. Zh. Neorg. Khim. **15**(10), 2637 (1970).

Can. J. Chem. Downloaded from www.nrcresearchpress.com by 210.87.254.105 on 09/05/12
For personal use only.

Pyrochlores. IX. Partially Oxidized $Sn_2Nb_2O_7$ and $Sn_2Ta_2O_7$: A Mössbauer Study of Sn(II,IV) Compounds[1]

DAVID J. STEWART[2] AND OSVALD KNOP
Department of Chemistry, Dalhousie University, Halifax, Nova Scotia

AND

ROY E. MEADS AND WILLIAM G. PARKER
Department of Physics, University of Exeter, Exeter, England

Received September 13, 1972

Partially oxidized tin(II) niobate and tantalate pyrochlores are homogeneous cubic phases. They have been shown by Mössbauer ^{119}Sn spectroscopy to contain both Sn(II) and Sn(IV). Each valency state is segregated on its own, crystallographically distinct sublattice as a consequence of the size disparity of Sn^{2+} and Sn^{4+} atoms. The strong temperature dependence of the Mössbauer Sn^{2+}:Sn^{4+} area ratios between room temperature and 4.2 °K indicates that the recoil-free fractions of the Sn^{2+} and Sn^{4+} atoms in these structures are noticeably different. The values of the recoil-free fractions at 0 °K, which were estimated from simple Einstein and Debye models, were used to obtain Sn^{2+}:Sn^{4+} population ratios from the Mössbauer area ratios extrapolated to 0 °K. The area ratios were shown to differ from the population ratios by 15–20% at 0 °K and by as much as 70% at room temperature. The formulae of the two nonstoichiometric pyrochlores based on the population ratios are $Sn_{2-2u}^{2+}(Sn_u^{4+}B_{2-u}^{5+})O_{7-(5/2)u}$ (B = Nb, Ta; u = 0.18–0.20). These formulae are consistent with chemical and other evidence. Mössbauer parameters and the limitations of using a Mössbauer area ratio to determine the Sn^{2+}:Sn^{4+} population ratio in Sn(II,IV) compounds are discussed.

Le niobate et le tantalate d'étain(II) partiellement oxydés sont des phases cubiques homogènes du type pyrochlore. Elles contiennent à la fois Sn(II) et Sn(IV) comme le prouvent les spectres Mössbauer de ^{119}Sn. Ces deux types d'atomes occupent chacun son sous-réseau cristallin à cause de la disparité dans la taille des atomes Sn^{2+} et Sn^{4+}. Les deux sous-réseaux sont cristallographiquement distincts. Les rapports des surfaces des pics d'absorption Mössbauer Sn^{2+}:Sn^{4+} varient fortement entre 4.2 et 290 °K, ce qui indique que, dans ces structures, les fractions d'effet Mössbauer sans recul des atoms Sn^{2+} diffèrent sensiblement de celles des atomes Sn^{4+}. On s'est servi de modèles simples d'Einstein et de Debye pour calculer les valeurs correspondantes à ces fractions à 0 °K. Ces valeurs ont été utilisées pour obtenir les rapports des populations atomiques Sn^{2+}:Sn^{4+} à partir des rapports des surfaces des pics Mössbauer extrapolés à 0 °K. On a démontré que l'écart de 15 à 20% qui existe, à 0 °K, entre les rapports de population et les rapports des surfaces, peut atteindre jusqu'à 70% à la température ambiante. Les deux pyrochlores non-stoechiométriques ont été formulés sur la base des rapports de population: $Sn_{2-2u}^{2+}(Sn_u^{4+}B_{2-u}^{5+})O_{7-(5/2)u}$ (B = Nb, Ta; u = 0.18–0.20); ces formules sont compatibles avec les preuves chimiques et autres. On discute des paramètres spectraux Mössbauer et des limites que pose la méthode pour déterminer le rapport de population Sn^{2+}:Sn^{4+} dans les composés Sn(II,IV) à partir du rapport des surfaces des pics d'absorption Mössbauer.

Can. J. Chem., **51**, 1041 (1973)

Previously we reported the preparation of cubic pyrochlores of the intended compositions $Sn_2^{2+}Nb_2^{5+}O_7$ and $Sn_2^{2+}Ta_2^{5+}O_7$ (1). The first attempt (samples *i*) resulted in products which were slightly inhomogeneous, but on repeating the preparations pyrochlores free from detectable foreign phases were obtained (samples *ii*, Table 1 of ref. 1). However, in refining the crystal structures of these two pyrochlores from powder diffractometer intensities, the discrepancy indices R could not be reduced below about 7%; the values of some of the parameters of refinement, as well as the measured densities, suggested that the niobate and tantalate might be nonstoichiometric. Since Bodiot (2), who also has described the preparation of such pyrochlores, considered his products as stoichiometric, we were curious to see whether the suspected lack of stoichiometry of our material could be traced to oxidation of some of the Sn(II) and therefore detected by Mössbauer ^{119}Sn spectroscopy. Preliminary spectra indeed indicated that both Sn(II) and Sn(IV) were present. This settled the problem of nonstoichiometry of our preparations quali-

[1]For Part VIII see ref. 1.

[2]Present address: Invermay Research Centre, Private Bag, Mosgiel, New Zealand.

Can. J. Chem. Downloaded from www.nrcresearchpress.com by 210.87.254.5 on 09/05/12
For personal use only.

Can. J. Chem. Downloaded from www.nrcresearchpress.com by 210.87.254.5 on 09/05/12
For personal use only.

tatively. However, the simultaneous presence of the two valencies of tin seemed to merit a detailed investigation by itself, as these pyrochlores are, to our knowledge, the first authenticated examples of oxidic mixed-valency tin compounds that have been reported. They afford an opportunity to study the recoil-free fractions of Sn atoms in different valency states and different coordinations but contained in the same crystal structure, and thus to assess the validity of the method of determining Sn(II):Sn(IV) ratios of such compounds from the area ratios of the two Mössbauer absorptions. We have carried out such a study and the results are described in the following.

Experimental

Details of preparation and the lattice parameters of the tin niobate and tantalate samples are given in ref. 1. Densities of the powders were determined as described in ref. 3.

Mössbauer spectra were recorded under conditions of constant geometry and for a fixed analyzer live time. Details of the apparatus are given in refs. 4 and 5. The source used was 5 mCi $BaSnO_3$ at room temperature. Absorbers were prepared by dispersing the sample powders in acrylic resin. Since the spectra were to be analyzed to give $Sn^{2+}:Sn^{4+}$ ratios, it was of particular importance to ensure that the areas and line widths of resonances were not distorted by the effects of nonlinear absorption in thick absorbers. The absorber thickness was therefore restricted to *ca.* 3 mg/cm^2 of natural Sn in each case. A check experiment using a thinner absorber showed no significant change in the relative intensities and line widths of the spectral features, and so it was concluded that the requirement of thin absorbers had been satisfied.

As discussed later, determination of $Sn^{2+}:Sn^{4+}$ population rations requires knowledge of the area of a spectral component as a function of temperature. Spectra were therefore obtained with the sample at 4.2, 77, 194.5 °K, and at room temperature. They were fitted to Lorentzian lines using the computer program developed by Clark (6), which provides for a variety of constraints. No correction for a curved baseline count was included, as at the source-to-detector distance used the curvature is known to be negligible and the spectra fitted to straight baselines all had acceptable χ^2 values. Isomer shifts are reported relative to $BaSnO_3$ at room temperature. To convert to β-Sn subtract 2.570 mm/s and to α-Sn, subtract 1.92 mm/s (7).

Results

Identification of the Mössbauer Absorption Peaks

Apart from varying relative intensities the same features were present in the Mössbauer spectra at all temperatures. These were a well-resolved doublet with isomer shift characteristic of Sn^{2+} and a singlet with isomer shift characteristic of Sn^{4+} (Fig. 1). Statistically acceptable fits were obtained by the use of Lorentzian line shapes assuming that the spectrum contained a total of three resonances and imposing no constraints on area or line width. The line widths were approximately 1 mm/s and were typical of thin-absorber ^{119m}Sn spectra obtained with the $BaSnO_3$ source. They are larger than the minimum (0.62 mm/s) calculated from the known lifetime of the ^{119m}Sn excited state. This increased line width may arise from resonant self-absorption in the source which may not be ideally thin, and from a fluctuating electric field gradient due to the presence of defects and distortions in source and absorber materials. The spectra of the

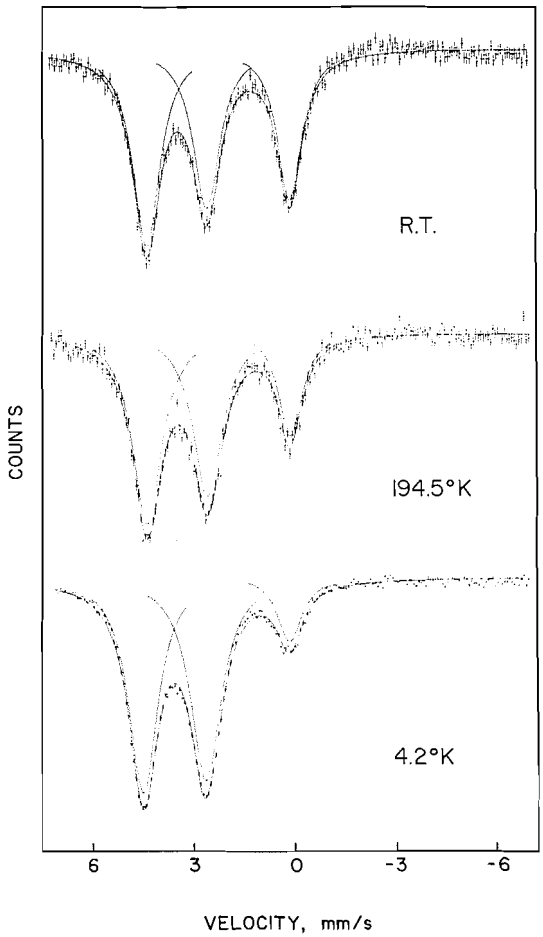

FIG. 1. Mössbauer spectra of tin tantalate (sample *ii*) at different temperatures. The zero of the velocity scale refers to the center of the $BaSnO_3$ calibration spectrum. The counts per channel (in thousands) for the spectra shown ranged from 5785 to 5875 (room temperature), 1660 to 1710 (194.5 °K), and 1535 to 1640 (4.2 °K).

TABLE 1. Mössbauer ^{119}Sn parameters (in mm/s) of tin niobate and tantalate*

	Sn^{2+} absorption				Sn^{4+} absorption		Area ratio
T, °K	IS	QS	Γ_1	Γ_2	IS	Γ_3	$A^{2+}:A^{4+}$
			Niobate				
290	3.58(2)	1.87(2)	1.04(2)	0.99(2)	0.21(1)	0.95(2)	2.68(2)
194.5	3.46(2)	1.87(2)	1.00(2)	0.92(2)	0.09(1)	0.95(3)	3.86(4)
77	3.48(2)	1.90(2)	1.04(1)	0.96(1)	0.16(4)	0.93(3)	6.07(4)
4.2	3.54(2)	1.89(2)	1.08(1)	1.01(1)	0.23(2)	0.97(3)	7.64(6)
			Tantalate				
290	3.49(1)	1.83(2)	1.05(2)	0.96(2)	0.08(1)	1.03(2)	2.42(2)
194.5	3.50(1)	1.83(2)	1.11(2)	1.03(2)	0.10(1)	0.97(3)	3.80(3)
77	3.56(1)	1.88(2)	1.12(2)	1.03(2)	0.08(1)	1.07(3)	5.55(5)
4.2	3.59(1)	1.89(2)	1.13(1)	1.04(1)	0.08(1)	0.97(3)	7.30(5)

*IS, isomer shift relative to $BaSnO_3$ at room temperature; QS, quadrupole splitting; Γ, line width (full width at half height). The standard deviations are quoted in units of the second decimal place.

niobate and the tantalate were very similar. They were reproducible on repeated cooling and warming up of the Mössbauer specimens between liquid–helium and room temperatures.

The Sn^{2+} absorption cannot correspond to free SnO as the isomer shift for the Sn^{2+} doublet is larger than would be expected for this oxide (*cf.* Table 1). Furthermore, no SnO lines were present in the X-ray powder patterns of the samples, and it is most unlikely that free SnO would have remained stable at the final firing temperatures of 750 °C or higher. The Sn^{2+} doublet must thus be due to Sn^{2+} within the *P* structure. The asymmetry of the doublet, which increases with temperature, arises from the Gol'danskii-Karyagin effect.

The well-defined Sn^{4+} resonance cannot be attributed to free SnO_2. If unreacted SnO_2 (formed by disproportionation of SnO) were present in an amount suggested by the relative intensity of the Sn^{4+} resonance, SnO_2 lines would have been observed in the powder patterns, which was not the case. Even if free SnO_2 were initially X-ray amorphous, it is unlikely to have remained in this state after heating to 750 °C.

Comparison of the Mössbauer spectra and parameters of samples *i* with those of samples *ii* shows little or no difference. There was no detectable resonance due to free tin in sample *i* of the niobate, and the interpretation of the Mössbauer results is therefore not affected by its presence. The results of measurements on samples *ii* are given in Table 1.

It seems clear that the spectra must arise from the presence of both Sn^{2+} and Sn^{4+} in a single homogeneous cubic *P* phase of mixed-valency character in both the niobate and the tantalate. Their Sn:*B* ratios must be 1:1 as intended, but allowance must be made for possible change in the oxygen content during firing or for the occurrence of an internal redox process (*vide infra*). In the first case the overall formula of the products can be written as $Sn_2B_2O_{7+z}$; in the second, $z = 0$ and formulae like $(Sn^{2+},Sn^{4+})_2(Nb^{5+},Nb^{4+})_2O_7$, for example, become a possibility.

The $Sn^{2+}:Sn^{4+}$ Ratio from the Mössbauer Spectrum

The relative areas of the Sn^{2+} and Sn^{4+} features of the Mössbauer spectra vary substantially with temperature (Fig. 1 and Table 1). This indicates that the recoil-free fractions of the two ionic species are unequal, implying a significantly different lattice vibrational spectrum for each. Moreover, the fractions will not be equal at 0 °K, owing to the effect of differences of zero-point motion. Hence considerable care must be exercised in interpreting the spectra in terms of relative ionic populations.

The following procedure was adopted for obtaining the $Sn^{2+}:Sn^{4+}$ ratio of each material. Assuming that the lattice vibrational spectrum of the solid is of the Einstein, single-frequency type, the recoil-free fraction f would be expected (21) to depend on temperature as

$$\ln f^E = -(\hbar^2/2\lambda^2 Mk\theta_E) \times \{1 + 2[\exp(\theta_E/T) - 1]^{-1}\}$$

where λ = γ-ray wavelength, M = mass of emitting nucleus, k = Boltzmann constant, and θ_E = the Einstein characteristic temperature. At

Can. J. Chem. Downloaded from www.nrcresearchpress.com by 210.87.254.5 on 09/05/12
For personal use only.

Can. J. Chem. Downloaded from www.nrcresearchpress.com by 210.87.254.5 on 09/05/12
For personal use only.

TABLE 2. Characteristic temperatures, recoil-free fractions and ionic populations for Sn^{2+} and Sn^{4+} (E, Einstein model; D, Debye model)

Parameter	Value	
	Niobate	Tantalate
$\theta_E(Sn^{2+})$	111 °K	100 °K
$\theta_D(Sn^{2+})$	192 °K	173 °K
$f_0^E(Sn^{2+})$	0.763	0.742
$f_0^D(Sn^{2+})$	0.792	0.772
$\theta_E(Sn^{4+})$	242 °K	170 °K
$\theta_D(Sn^{4+})$	424 °K	295 °K
$f_0^E(Sn^{4+})$	0.884	0.838
$f_0^D(Sn^{4+})$	0.900	0.859
$f_0^E(Sn^{2+}):f_0^E(Sn^{4+})$	0.863	0.884
$f_0^D(Sn^{2+}):f_0^D(Sn^{4+})$	0.880	0.899
Ionic population, %		
Sn^{2+}	90(2)	89(2)
Sn^{4+}	10(2)	11(2)

$T = 0$, $\ln f_0^E = -(\hbar^2/2\lambda^2 Mk\theta_E)$. If a Debye model is assumed, the corresponding results are

$$\ln f^D = -(3\hbar^2/4\lambda^2 Mk\theta_D) \times \left\{1 + 4(T/\theta_D)^2 \int_0^{\theta_D/T} x(e^x - 1)^{-1}\,dx\right\}$$

$$\ln f_0^D = -(3\hbar^2/4\lambda^2 Mk\theta_D)$$

The areas A^{2+} and A^{4+} (in arbitrary units) of the Sn^{2+} and Sn^{4+} components of the Mössbauer spectrum were obtained as a function of temperature from the constant-geometry, constant live time measurements. These were plotted as log A *vs.* T and fitted first to an Einstein and then to a Debye function. This procedure leads to values of θ_E and θ_D, and to values of f_0^E and f_0^D (Table 2). It was found that good fits were obtained to the data using either assumption.

The measured area ratio at 4.2 °K will not change significantly below this temperature. It may be corrected for the ratio of recoil-free fractions at $T = 0$ using the Einstein or the Debye value and leads then to a corrected population ratio $Sn^{2+}:Sn^{4+}$. The result is not particularly model sensitive. Taking a mean leads to the values for ionic populations given in Table 2, where due (and generous) allowance has been made in assessing the error for the dependence on model.

The $Sn^{2+}:Sn^{4+}$ Ratio from Total Oxidation

Assuming that the final oxidation states of Sn, Nb, and Ta in air are Sn^{4+}, Nb^{5+}, and Ta^{5+} respectively, firing the mixed-valency pyrochlores to constant weight at a sufficiently high temperature in air and noting the weight gain will give the total reducing power, *i.e.* the amount of oxygen required for complete oxidation of all the Sn^{2+} to Sn^{4+} and any B^{4+} to B^{5+}.

Typically, heating a 0.6 g sample each of the niobate and tantalate (preparations *ii*) for 24 h at 900 °C resulted in weight increases of 5.28 and 3.74% respectively. The color of both products was white. On the assumption that the weight gain was due solely to the oxidation of Sn^{2+}, the formula and the $Sn^{2+}:Sn^{4+}$ ratio are $Sn_2Nb_2O_{7.22(3)}$ and 8.1(12) for the niobate and $Sn_2Ta_2O_{7.32(4)}$ and 5.3(8) for the tantalate.[3] In the presence of Nb^{4+} or Ta^{4+} smaller $Sn^{2+}:Sn^{4+}$ ratios would be obtained, so the above values may be regarded as the upper limits of the ratios from the total oxidation experiments.

Lattice Parameter and Density

The values obtained for samples *ii* compare reasonably well with Bodiot's:

Compound	Parameter	Value	
		This work	Reference 2
Niobate	a_0 (Å)	10.588(1)	10.581(2)
	d (g/cm^3)	5.33(1)	5.64
Tantalate	a_0 (Å)	10.565(1)	10.550(2)
	d (g/cm^3)	6.58(5)	8.33

The exception is the density of the tantalate, which will be commented upon later.

The $a_0(P)$ values of the two $Sn_{1+x}B_2O_{6+x}$ phases increase with x (Fig. 2). Not all of the stated intended compositions represent the true stoichiometries; this uncertainty is undoubtedly responsible, at least in part, for the observed spread of the points for the tantalate.

Discussion

In the idealized P structure the cations are located in sites of two types, 16(*c*) and 16(*d*), both of symmetry $\bar{3}m$ (*cf.* ref. 8). A 16(*c*) site is coordinated by 6+2 oxygen atoms and accommodates the larger cation. A 16(*d*) site is coordinated by six oxygens and accommodates the smaller cation. The effective size of an Sn^{2+} atom for a particular coordination number is

[3]An arbitrary error of ±0.5 mg was assumed to be associated with the difference weighing and handling of the samples.

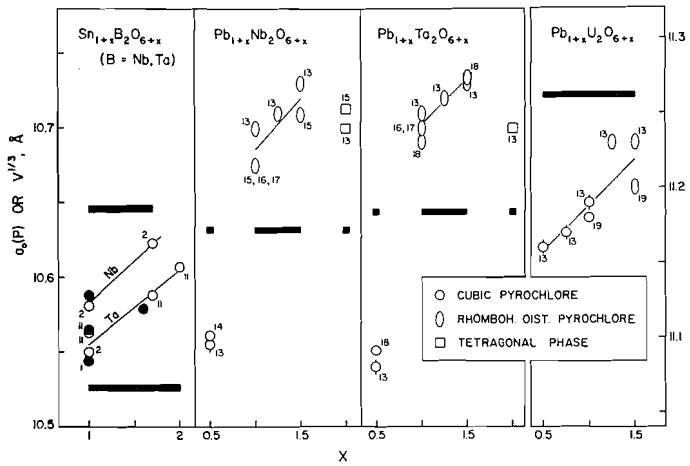

FIG. 2. Variation of the lattice parameter with composition for cubic $Sn_{1+x}B_2O_{6+x}$ (B = Nb, Ta) pyrochlore phases. Similar plots for $Pb_{1+x}B_2O_{6+x}$ (B = Nb, Ta, U) are shown for comparison (see text). Homogeneity ranges are indicated by black horizontal bars, references by numbers. Full circles, this work.

appreciably greater than that of an Sn^{4+} atom. Since A^{2+} ions in stoichiometric *2–5* pyrochlores, $A_2{}^{2+}B_2{}^{5+}O_7$, are located in 16(*c*) sites and B^{4+} ions in stoichiometric *3–4* pyrochlores, $A_2{}^{3+}B_2{}^{4+}O_7$, in 16(*d*) sites, it is plausible to assume that in the partially oxidized tin niobate and tantalate Sn^{2+} ions will be located in 16(*c*) and Sn^{4+} ions in 16(*d*). The separation of the valency states would then coincide with segregation into two crystallographically nonequivalent sets of sites, each having its own distinct coordination. The Mössbauer results are consistent with this view.

In general, the occurrence of markedly different recoil-free fractions for identical nuclei in ions of equal mass within the same crystal structure, is to be ascribed to (*i*) the dominance (in determining f) of modes of vibration characteristic for the ions of their bonding to immediate neighbors, and (*ii*) marked differences in the local bonding forces for the two ionic species. This latter would certainly be the case if the ions were located in different sites of unequal coordination.

Stoichiometry

The Sn^{2+}:Sn^{4+} ratios estimated from the corrected Mössbauer area ratios, 9.0(20) for the niobate and 8.1(18) for the tantalate, are indistinguishable within the stated errors, suggesting that the extent of oxidation to Sn^{4+} was much the same in all our preparations. The Mössbauer area ratio for the niobate leads to the formula $Sn_{1.64(4)}{}^{2+}Sn_{0.18(4)}{}^{4+}Nb_{1.82}{}^{5+}O_{6.55(9)}$. The maximum possible occupancy of the unit cell which is permitted for this composition by the experimental density is 97(2)%. The contents 16(*c*)|16(*d*)|48(*f*) + 8(*a*) of the unit cell can then be formulated as $12.8(3)\,Sn^{2+}|1.4(3)\,Sn^{4+} + 14.2\,Nb^{5+}|51.1(7)\,O^{2-}$. This agrees surprisingly well with the result obtained from the total oxidation experiment, $12.5(3)\,Sn^{2+}|1.5(3)\,Sn^{4+} + 14.0(1)\,Nb^{5+}|50.6(8)\,O^{2-}$, considering the so far unsupported assumption that all the niobium is present as Nb^{5+}.

The formula and unit-cell occupancy resulting from the Mössbauer area ratio and experimental density for the tantalate are

$$Sn_{1.60(4)}{}^{2+}Sn_{0.20(4)}{}^{4+}Ta_{1.80}{}^{5+}O_{6.50(9)}$$

and

$$11.7(4)Sn^{2+}|1.5(4)Sn^{4+} + 13.1Ta^{5+}|47.4(8)O^{2-}$$

the number of formula units calculated from d(exp) is only 7.27(14). The formula and unit-cell occupancy based on the total oxidation experiment

$$Sn_{1.45(4)}{}^{2+}Sn_{0.28(4)}{}^{4+}Ta_{1.72}{}^{5+}O_{6.30(4)}$$

and

$$11.0(4)Sn^{2+}|2.1(3)Sn^{4+} + 13.0(1)Ta^{5+}|47.8(4)O^{2-}$$

agree less well with those derived from the

Can. J. Chem. Downloaded from www.nrcresearchpress.com by 210.87.254.5 on 09/05/12
For personal use only.

Can. J. Chem. Downloaded from www.nrcresearchpress.com by 210.87.254.5 on 09/05/12
For personal use only.

Mössbauer area ratio than in the case of the niobate. It should be realized, however, that an error $d\Delta w$ of 0.5 mg in a weight Δw of 0.025 g gained by a 0.5 g ($= w$) sample in a total oxidation experiment will produce a change of 0.8 in the Sn^{+2}:Sn^{4+} ratio Q of the niobate and 2.3 in that of the tantalate.[4]

The Q(Mössbauer) and Q(oxidation) values for the niobate are in reasonable agreement even though Q(oxidation) has been calculated on the assumption that Nb^{5+} is the only valency of niobium present. Since no attempt was made in this investigation to secure *direct* evidence of Nb^{4+} in the structure, the agreement of the Q values precludes the presence *or* the absence of Nb^{4+} being argued with any conviction. The bright orange-yellow color of the niobate *would* suggest the possibility that Nb^{4+} atoms are present: they would be expected to reside on the 16(d) sublattice in a statistical mixture with Nb^{5+} and Sn^{4+} atoms and thus be in a situation favorable for the existence of electronic exchange processes which are characteristic of many mixed-valency compounds and manifest by striking colors.[5] Unfortunately not enough is known about mixed Nb(IV,V) oxide compounds for the color to be used as evidence in support of Nb^{4+} in the niobate. Certain apparently stoichiometric oxygen compounds of Nb^{5+} which are colorless at room temperature turn characteristically bright orange when hot. If this reversible phenomenon has its analogy in the well-known color change in ZnO on heating in air, very small amounts of Nb^{4+}, of no consequence to bulk stoichiometry, would be responsible for the room-temperature color of the niobate. Those of Sleight's (9) $Hg_2B_2O_7$ (B = Nb, Ta) pyrochlores that were most nearly stoichiometric were yellow, while samples somewhat more deficient in mercury and oxygen were red to black and their unit-cell size was decreased. Similarly, the color of $Cd_2NbB^{IV}O_6F$ (B = Ti, Zr, Hf, Ge, Sn) pyrochlores (10) ranged from pale yellow to brick red; often there was a color variation from one preparation to another.

Inasmuch as the Sn^{4+} content of the tantalate, as estimated from the weight gain, is already somewhat greater than indicated by the Mössbauer area ratio, any Ta^{4+} assumed to be present would imply an even lower Sn^{2+} content and make the discrepancy worse. However, without an internal redox process involving lower valency states of Ta or Nb the question of the source of oxygen necessary to convert Sn^{2+} to Sn^{4+} in all our preparations becomes embarrassing. The Mössbauer spectrum of the black SnO used as a starting material did not show visible Sn^{4+} absorption; the pentoxides had been calcined before use; the quartz ampoules were kept under vacuum (better than 10^{-5} Torr) for several hours before sealing. Oxidation of the samples on storage in air would have increased the Mössbauer area ratio in the right direction; the initial Sn^{4+} content might therefore be even smaller than that estimated. A possible explanation might be oxygen adsorbed on the surface of the reactant powders. As for the correction factor applied to the Mössbauer area ratio, even *before* correcting for unequal recoil-free fractions the area ratio gives an Sn^{2+}:Sn^{4+} value higher than the "total oxidation" value. At present we cannot offer a satisfactory reason why the Sn^{2+} should have oxidized.

The question of whether strictly stoichiometric $Sn_2Nb_2O_7$ and $Sn_2Ta_2O_7$ can be prepared remains to be answered. Bodiot assumed that his preparations were stoichiometric, for his results gave him no reason to believe otherwise. However, the difference between the formula weights of $Sn_2B_2O_7$ and $Sn_2B_2O_{7.3}$ (a typical composition of our preparations) is only about 1% for Nb and about 0.7% for Ta, so that small departures from stoichiometry might escape attention in thermogravimetric experiments unless specifically looked for. Nonstoichiometry would not be much noticed in $a_0(P)$, as a decrease in $a_0(P)$ arising from deficient occupancy of

---

[4]For a composition $Sn_{2-y}^{2+}Sn_y^{4+}B_2^{5+}O_{7+y}$ the variation of Q is given by $dQ = -2y^{-2}dy = (K+1)wd\Delta w/(w - K\Delta w)^2$, where $K \sim 17$ for the niobate and ~ 22 for the tantalate. In the vicinity of the singularity at $w = K\Delta w$, dQ varies very steeply.

[5]In a P structure with fully occupied 16(d) and 48(f) sublattices the three-dimensional B—O_2 network forms $B_4(O_2)_6$ clusters of symmetry $\bar{4}3m$ about the empty 8(a) sites. These clusters are similar in shape to the P_4O_6 and As_4O_6 molecules in the vapor or to the As_4O_6 or Sb_4O_6 units in cubic As_2O_3 and Sb_2O_3 and may be described as tetrahedra with broken edges. The vertices of the tetrahedron are occupied by B and the points where the edges are broken are occupied by O_2. The unique BO_2B angle of the isosceles B—O_2—B triangle is about 135°, the B—O_2 distance is typically 1.96–2 Å, and the B—B distance is equal to $a_0\sqrt{2}/4$, *i.e.* typically about 3.6 Å. It is conceivable that such a compact local configuration of high symmetry is favorable for the occurrence of fast B^{4+},B^{5+} exchange interactions.

Can. J. Chem. Downloaded from www.nrcresearchpress.com by 210.87.254.5 on 09/05/12
For personal use only.

16(*c*) and 48(*f*) + 8(*a*) is partially compensated by the greater effective ionic radius of Sn^{4+} relative to Nb^{5+} and Ta^{5+}.[6] For a composition difference as large as $Sn_2Ta_2O_7$ and $Sn_3Ta_2O_8$ the difference in $a_0(P)$ is, according to ref. 11, 0.044(5) Å, *i.e.* only about 0.4%. This suggests that effects produced by differences in the oxygen stoichiometry of $Sn_2B_2O_{7+z}$ preparations would probably be small enough to pass for spread between different sets of measurements, especially since the spread in the values reported for $a_0(P)$ of "$Sn_2Ta_2O_7$" alone amounts to 0.021(2) Å (Fig. 2).

Bodiot's *d*(exp) value for the tantalate, 8.33 g/cm^3, yields $Z = 8.36$ for the formula $Sn_2Ta_2O_7$. However, a value of Z greater than 8 cannot be reconciled with the standard occupancy of a pyrochlore unit cell. If the discrepancy were to be attributed to experimental error, the error would have to be substantial, since density determinations on powders invariably tend to give values lower than *d*(X-ray).

For our preparations *ii* the fraction of 16(*c*) sites occupied by Sn^{2+} is only about 78% in the niobate and about 71% in the tantalate. The theoretical lower limit of the $Sn^{2+}:Sn^{4+}$ ratio consistent with $Sn:B^{5+} = 1$ and with full occupancy of the 16(*d*) and 48(*f*) sites is 3, corresponding to the unit-cell occupancy $Sn_{9.6}{}^{2+}|Sn_{3.2}{}^{4+}B_{12.8}{}^{5+}|O_{48}{}^{2-}|\square_8$.[7] In this case only 60% of the 16(*c*) sites are occupied, *i.e.* for every three Sn^{2+} atoms there are two vacancies, and the 8(*a*) sites are empty.

The site occupancy and unit-cell contents of the cubic phases deriving from $Sn_2B_2O_7$ with $Sn:B$ ratios greater than unity are not known at present. The composition ranges of these $Sn_{1+x}B_2O_{6+x}$ ($x \geqslant 1$) pyrochlores are substantial: Trunov *et al.* (11) have reported $x = 2$ as the upper limit for the tantalate (Fig. 2). For $x < 1$ the existence of only one phase has been ascertained in the SnO–Nb_2O_5 system (2). This is the congruently melting $SnNb_2O_6$; it has a complex powder pattern and a narrow, if any, homogeneity range. In the SnO–Ta_2O_5 system, in addition to $SnTa_2O_6$ (possibly related to the rhombohedral $PbTa_2O_6$) a tetragonal phase $SnTa_4O_{11}$ stable to at least 1400 °C has been found (2, 11).

These phase and structure relationships differ from those described for the systems PbO–Nb_2O_5, PbO–Ta_2O_5, and PbO–"U_2O_5" by Kemmler-Sack and Rüdorff (13) and by earlier authors (see Fig. 2). In the $Pb_{1+x}B_2O_{6+x}$ (B = Nb, Ta) compositions cubic P phases do exist but are restricted to $x = 0.5$, *i.e.* to unit-cell occupancies $Pb_{12}{}^{2+}|B_{16}{}^{5+}|O_{52}$; in this respect they are very similar to our Sn niobate and tantalate. The rhombohedrally distorted P phase which occurs from $x = 1$ to 1.5 is followed by a tetragonal phase of unknown structure at $x = 2$. The existence of the homogeneity range of the rhombohedral P phase is accounted for (13) from experimental evidence by a progressively smaller proportion of B^{5+} in 16(*d*) while 16(*c*) + 16(*d*) remain fully occupied, *i.e.* presumably (though this has not been demonstrated) $Pb_{16}{}^{2+}|Pb_{\delta}{}^{2+}B_{16-\delta}{}^{5+}|O_{56-(3/2)\delta}$. The size disparity of the Pb^{2+} and B^{5+} atoms occupying 16(*d*) and the simultaneous presence of oxygen vacancies are held responsible for the rhombohedral distortion and the eventual emergence of the tetragonal phase at $x = 2$. The alternative possibility of 16(*d*) being incompletely occupied and the excess Pb atoms being located elsewhere in the structure (presumably in 8(*a*) or 8(*b*)) has also been suggested (13).

In the $Pb_{1+x}U_2O_{6+x}$ pyrochlores the situation is reported to be different again (13). The cubic structure which exists at $x = 0.5$ is retained up to $x = 1$, after which a progressive rhombohedral distortion is observed to $x = 1.5$; a discrete $Pb_3U_2O_8$ phase could not be prepared. Experimental densities are consistent with unit-cell occupancies $Pb_{32(1+x)/(3+x)}{}^{2+}U_{64/(3+x)}{}^{5+}O_{32(6+x)/(3+x)}$ for $0 \leqslant x \leqslant 1$,[8] while interstitial

[6]The relative insensitivity of a_0 to variations of composition is responsible for the a_0 values of our and Bodiot's $Sn_2Nb_2O_7$ and $Sn_2Ta_2O_7$ samples being accommodated at $r^{VIII}(Sn^{2+}) = 1.22$ Å (12) on the straight line of Fig. 3, ref. 1, correlating $a_0(P)$ of $A_2{}^{2+}B_2{}^{5+}O_7$ (B = Nb, Ta) with $r^{VIII}(A^{2+})$. In this limited sense Shannon and Prewitt's value for the radius of Sn^{2+} in 8-coordination may be regarded as acceptable.

[7]This is apparently the limit of the oxygen content which the P structure can tolerate. It is, however, possible that in defect pyrochlores the oxygen atoms are distributed statistically over 48(*f*) + 8(*a*), leaving a small fraction of vacancies on the 48(*f*) sublattice.

[8]This occupancy requires some of the oxygen atoms to occur in interstitial positions and some of the U^{5+} atoms in the 8-coordinated 16(*c*) sites. Magnetic susceptibility measurements (20) seem to be consistent with this proposal. If the Pb and U atoms were distributed at random over 16(*c*) + 16(*d*) rather than 16(*d*) being occupied exclusively by U, the structure would approximate the defect fluorite structure.

Can. J. Chem. Downloaded from www.nrcresearchpress.com by 210.87.254.5 on 09/05/12
For personal use only.

accommodation of lead and oxygen atoms is postulated for $x > 1$: $Pb_{8(1+x)}{}^{2+}U_{16}{}^{5+}O_{8(6+x)}$.

This variety of behavior shows the importance of the relative sizes of A^{2+}, B^{5+} and O^{2-} in determining the type of defect structure and rules out predictions for $Sn_{1+x}B_2O_{6+x}$ based on analogy with other $A_{1+x}B_2O_{6+x}$ compounds.

Mössbauer Parameters

The room-temperature isomer shifts of Sn^{2+} in the niobate and tantalate fall between the values reported by Lees and Flinn (7) for SnF_2 and SnC_2O_4, 3.46(4) and 3.59(4) mm/s respectively. The temperature dependence of the isomer shift is small. The quadrupole splitting is large and comparable with that of $Sn_3(PO_4)_2$, 1.90(3) mm/s (7). When our values are plotted in Fig. 4 of ref. 7, the points for the two pyrochlores are almost indistinguishable and lie considerably above the upper straight line. It is uncertain whether Lees and Flinn's interpretation of the Sn^{2+} isomer shift is applicable here. As pointed out above, the site symmetry at a 16(*c*) site is $\bar{3}m$, *i.e.* containing a center of symmetry. Sn^{2+} in these two pyrochlores is probably the first known case of a divalent tin atom in a centrosymmetric situation; or, more correctly, it would be if the two pyrochlores were stoichiometric.

The occupation of not more than about 78% of the 16(*c*) sites has several important consequences. Assuming that in an "essentially ionic" crystal only the immediate environment of a Mössbauer-active atom affects the spectrum, we shall consider the six 16(*c*), the six 16(*d*), and the two 8(*a*) sites adjacent to an Sn^{2+} atom. The sites of the first two types are arranged at the vertices of a cuboctahedron of edge length $a_0\sqrt{2}/4$ Å in such a way that the six corners of two opposing triangular faces are at the 16(*c*) sites and the remaining six, coplanar, vertices coincide with the 16(*d*) sites. All twelve sites are at a distance of $a_0\sqrt{2}/4$ Å from the Sn^{2+} atom. The two 8(*a*) sites are on a threefold rotation axis passing through the centers of the two opposing 16(*c*) triangles, at $a_0\sqrt{3}/8 = 2.28$ Å from the Sn^{2+} atom.

In a strictly stoichiometric $Sn_2{}^{2+}B_2{}^{5+}O_7$ pyrochlore all the Sn^{2+} atoms would be equivalent, at centers of coordination cuboctahedra of symmetry $\bar{3}m$, and only one, simple Sn^{2+} spectrum would be expected. This would very likely consist of a quadrupole doublet broadened only by crystal imperfections and by instrumental factors. However, the reduced occupancy of 16(*c*) in our preparations results, on the average, in a replacement of about 10% of the B^{5+} atoms in 16(*d*) by Sn^{4+} and about 5% by cation vacancies, and in the removal of about 83% of the O_1 atoms in 8(*a*) if 48(*f*) is assumed to be completely filled. As a consequence (assuming Bernoulli distribution, *i.e.* in the absence of preferential interactions) only about 5% of all the Sn^{2+} atoms have immediate environments of the type

$$Sn_6{}^{2+} \textit{ or } \square_6|B_6{}^{5+} \textit{ or } Sn_6{}^{4+} \textit{ or } \square_6|(O_1)_0 \textit{ or } (O_1)_2$$

i.e. of symmetry $\bar{3}m$. All the other Sn^{2+} atoms have environments of lower symmetries. Considering the very short Sn^{2+}—O_1 distance, one would expect the absence of one of the two nearest O_1 neighbors to have a substantial effect on the electric field gradient at Sn^{2+} and on the type of bond such as an Sn^{2+} atom engages in, and hence on the Mössbauer parameters. Moreover, there will be a variety of environments owing to the different configurations of the Sn^{2+}, Sn^{4+}, B^{5+} and $\square$ nearest neighbors at the vertices of the coordination cuboctahedra, corresponding to a range of point-group symmetries; the oxygen atoms may be distributed statistically over 48(*f*) + 8(*a*), leaving anion vacancies in 48(*f*) and consequently in the immediate O_2-environment of the Sn^{2+} (and Sn^{4+}) atoms; and there may be significant contributions from more distant neighbors in the defect pyrochlore structure. The observed Mössbauer Sn^{2+} spectrum is thus the resultant of a large number of spectra, each arising from an individual local situation and having its own isomer shift and quadrupole splitting. This is consistent with the observed line broadening. It is thus not strictly true that the values of the isomer shift and quadrupole splitting, as obtained by fitting the experimental spectrum to a Lorentzian quadrupole doublet, are those of Sn^{2+} in a centrosymmetric environment of the majority, $Sn_6{}^{2+}B_6{}^{5+}$ type, the contribution of such Sn^{2+} atoms to the overall spectrum being less than 5%. Otherwise it would be tempting to interpret the isomer shift in terms of Lees and Flinn's diagram (Fig. 4 of ref. 7) as corresponding to 0.5p electrons, which would be suggestive of linear $s^1(sp)^{\frac{1}{2}}$ or trigonal $s^{1\frac{1}{2}}(sp^2)^{\frac{1}{2}}$ orbital hybrids; the symmetries of both are compatible with the $\bar{3}m$ symmetry at 16(*c*).

Can. J. Chem. Downloaded from www.nrcresearchpress.com by 210.87.254.5 on 09/05/12
For personal use only.

The vacancies in 8(*a*) may also be held responsible for the markedly different recoil-free fractions of the Sn^{2+} and Sn^{4+} atoms. The amplitude of thermal vibration of the Sn^{2+} atom must be, on the average, strongly anisotropic by virtue of the absence of one or both of the nearest-neighbor O_I atoms. Support for this is found in the occurrence of the Gol'danskii-Karyagin effect manifested by the asymmetry of the Sn^{2+} spectra.

Conclusions

(*1*) The partially oxidized cubic pyrochlores $Sn_2Nb_2O_7$ and $Sn_2Ta_2O_7$ were found to contain Sn^{2+} and Sn^{4+}, each valency being segregated in its own crystallographic equipoint and corresponding to a distinct characteristic (Einstein or Debye) temperature. The two oxides appear to be the first well-authenticated cases of oxidic Sn(II,IV) compounds.

(*2*) When Sn(II) and Sn(IV) are simultaneously present in a crystal structure, it is almost certain that the Sn(II) and Sn(IV) atoms will occupy crystallographically nonequivalent sites and hence have different environments. This difference will manifest itself in unequal recoil-free fractions. The Sn(II):Sn(IV) population ratio cannot then be obtained from the corresponding ^{119}Sn Mössbauer area ratio without first determining the temperature dependence of the latter and correcting for the dissimilarity of the recoil-free fractions at 0 °K. In the present case use of simple Einstein and Debye models has shown that without such corrections, the mean value of the Sn(II):Sn(IV) Mössbauer area ratio may differ from the Sn(II):Sn(IV) population ratio by as much as 20% even at 4.2 °K. The ultimate accuracy of the population ratio derived in this manner will depend significantly, even with spectra collected to high statistics, on the closeness with which the function assumed for the shape of the baseline represents the actual baseline.

(*3*) Using corrected Mössbauer area ratios, experimental densities and lattice parameters leads to the formula $Sn_{2-2u}{}^{2+}(Sn_u{}^{4+}B_{2-u}{}^{5+})O_{7-(5/2)u}$ (B = Nb, Ta; u = 0.18–0.20) for the two pyrochlore phases. This formula is consistent with the results of total oxidation experiments.

We wish to express our gratitude to Miss Rosemary Watkins for assistance in the calculation of population ratios from the Mössbauer data. Financial support of this investigation by the National Research Council of Canada is hereby acknowledged.

1. F. Brisse, D. J. Stewart, V. Seidl, and O. Knop. Can. J. Chem. **50**, 3648 (1972).
2. D. Bodiot. Rev. Chim. Minér. **5**, 569 (1968).
3. O. Knop, C.-H. Huang, and F. W. D. Woodhams. Am. Miner. **55**, 1115 (1970).
4. O. Knop, F. Brisse, R. E. Meads, and J. Bainbridge. Can. J. Chem. **46**, 3829 (1968).
5. P. E. Clark, A. W. Nichol, and J. S. Carlow. J. Sci. Instr. **44**, 1001 (1967).
6. P. E. Clark. Unpublished program. University of Exeter, Exeter, England.
7. J. K. Lees and P. A. Flinn. J. Chem. Phys. **48**, 882 (1968).
8. O. Knop, F. Brisse, L. Castelliz, and Sutarno. Can. J. Chem. **43**, 2812 (1965).
9. A. W. Sleight. Inorg. Chem. **7**, 1704 (1968).
10. D. Laguitton and J. Lucas. C.R. C, **269**, 105 (1969).
11. V. K. Trunov, Yu. P. Simanov, and L. M. Kovba. Zh. Strukt. Khim. **4**, 277 (1963).
12. R. D. Shannon and C. T. Prewitt. Acta Cryst. B**25**, 925 (1969); B**26**, 1046 (1970).
13. S. Kemmler-Sack and W. Rüdorff. Z. Anorg. Allgem. Chem. **344**, 23 (1966).
14. W. R. Cook, Jr., and H. Jaffe. Phys. Rev. **89**, 1297 (1953).
15. R. S. Roth. J. Res. Natl. Bur. Std. **62**, 27 (1959).
16. F. Jona, G. Shirane, and R. Pepinsky. Phys. Rev. **98**, 903 (1955).
17. I. G. Ismailzade. Izv. Akad. Nauk SSSR, ser. fiz., **22**, 1485 (1958).
18. E. C. Subbarao. J. Am. Ceram. Soc. **44**, 92 (1961).
19. W. Rüdorff, S. Kemmler, and H. Leutner. Angew. Chem. Int. Ed. **1**, 329 (1962).
20. S. Kemmler-Sack, E. Stumpp, W. Rüdorff, and H. Erfurth. Z. Anorg. Allgem. Chem. **354**, 287 (1967).
21. R. H. Nussbaum. *In* Mössbauer effect methodology. Vol. 2. *Edited by* I. J. Gruverman. Plenum Press, New York. 1966. p. 8.

Matairesinol-4,4′-di-*O*-β-D-glucopyranoside from *Trachelospermum asiaticum* var. *intermedium*[1]

SANSEI NISHIBE, SUEO HISADA, AND ISAO INAGAKI

Faculty of Pharmaceutical Sciences, Nagoya City University, Mizuho-ku, Nagoya 467, Japan

Received August 15, 1972

A new lignan diglucoside was isolated from the stems of *Trachelospermum asiaticum* Nakai var. *intermedium* Nakai (Apocynaceae) and the structure has been determined as matairesinol-4,4′-di-*O*-β-D-glucopyranoside (**1**).

Un nouveau diglucoside de la lignine a été isolé des tiges des *trachelospermum asiaticum* Nakai var. *intermedium* Nakai (Apocynaceae) et la structure a été identifié au matairesinol di-*O*-β-D-glycopyranoside-4,4′ (**1**). [Traduit par le journal]

Can. J. Chem., **51**, 1050 (1973)

In our previous papers (1–4), the structures of four lignan glucosides from the stems of *Trachelospermum asiaticum* Nakai var. *intermedium* Nakai were elucidated.

In this paper a new lignan diglucoside, matairesinol-4,4′-di-*O*-β-D-glucopyranoside (**1**) was isolated. The only other lignan diglucoside previously reported is liriodendrin (5). The co-occurrence of matairesinol-4,4′-di-*O*-β-D-glucopyranoside (**1**) and matairesinoside (matairesinol-4′-*O*-β-D-glucopyranoside) are subjects of interest from the biogenetic point of view and suggests the possibility of occurrence of another matairesinol monoglucoside possessing a glucose moiety linked with phenolic hydroxy group at C-4. Actually the isolation of matairesinol monoglucoside (matairesinol-4-*O*-β-D-glucopyranoside) from safflower meal has been reported (6–7).

The chloroform–methanol (2:1, v/v) extract described in the Experimental was subjected to a column chromatography on activated charcoal followed by chromatography on a silica gel column, chloroform–ethanol (3:2, v/v) being used as eluant.

Compound **1**, m.p. 104–106°, was obtained from the fraction showing R_f 0.16 spot on t.l.c. using chloroform–ethanol (3:1) as developer. The i.r. spectrum of **1** showed a γ-lactone band at 1765 cm^{-1}. The peaks at 225 and 279 nm in the u.v. spectrum were unchanged when adding sodium ethoxide, thus indicating the absence of free phenolic hydroxy group.

The acid hydrolysis of **1** yielded aglycone (**3**) and D-glucose. The i.r. spectrum of **3** showed a γ-lactone band at 1775 cm^{-1} and the u.v. spectrum showed the peaks at 231.5 and 283 nm, giving bathochromic shift to 250.5 and 298.5 nm with sodium ethoxide. The properties of **3** were identical with those of matairesinol. Compound **3** was identified with an authentic sample by a mixed melting point and i.r. spectra. The presence of D-glucose was proven by paper chromatography.

Compound **1** was treated with acetic anhydride and pyridine at room temperature to give the acetylated derivative (**2**). The n.m.r. spectral data of **2** are as described in the Experimental. The similar assignments of the protons of sugar and aglycone parts in the n.m.r. spectrum are reported in those of matairesinoside pentaacetate (8) and arctiin tetraacetate (9).

Compound **1** was suggested, therefore, to be a matairesinol derivative having two glucose moieties linked with phenolic hydroxy group at C-4 and -4′. The analytical data of **1** was satisfactory for $C_{32}H_{42}O_{16}\cdot H_2O$. The molecular weight determination of **2** by vapor pressure osmometry also agreed with the formula $C_{48}H_{58}O_{24}$. The proof of two glucosidic linkages rather than a glucosyl–glucosidic linkage was achieved as follows. The permethyl ether prepared by the methylation of **1** with sodium hydride, dimethyl sulfoxide, and methyl iodide (Hakomori's method (10)) afforded only methyl 2,3,4,6-tetra-*O*-methyl-D-glucopyranoside on methanolysis with 3% methanolic hydrogen chloride. The glucosyl–glucoside was omitted since it was not the only type of dissacharide moiety possible.

The stereochemistry of the glucosidic linkages could not be determined from the n.m.r. spectrum of **2** (11). The comparison of the experi-

[1]Part IV in the series "Lignans of *Trachelospermum asiaticum* var. *intermedium*".

Can. J. Chem. Downloaded from www.nrcresearchpress.com by 210.87.254.40 on 09/05/12
For personal use only.

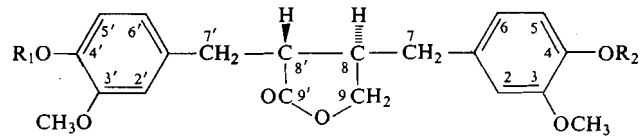

1 R_1 = glucosyl; R_2 = glucosyl
2 R_1 = $(Ac)_4$ glucosyl; R_2 = $(Ac)_4$glucosyl
3 R_1 = H; R_2 = H

TABLE 1. Values of the specific molecular rotation

Calcd. $[M]_D^\circ$ in ethanol*		Found $[M]_D^\circ$ in ethanol
Lignans		Lignans
4′-β,4-β linkages	−250.7	**1** −168.2
4′-β,4-α or 4′-α,4-β linkages	+119.3	**3** −124.7
4′-α,4-α linkages	+489.3	

*The following $[M]_D$-values were used for the calculation: methyl-α-D-glucopyranoside, +307°, and methyl-β-D-glucopyranoside, −63°.

mental value of the specific molecular rotation ($[M]_D$) of **1** with those calculated with α- and β-glucose moieties are as shown in Table 1.

The $[M]_D$-value and the enzymatic hydrolysis of **1** with emulsin proved the β-linkage of glucose moieties with the aglycone. Thus the structure of **1** has been established as matairesinol-4,4′-di-*O*-β-D-glucopyranoside (4,4′-dihydroxy-3,3′-dimethoxy-lignan-olid(9,9′)-4,4′-di-β-D-glucopyranoside by the nomenclature of Freudenberg and Weinges (12)).

Experimental

All melting points were not corrected. The following equipment was used: i.r. spectra, infrared spectrophotometers IR-S, IR-E, and IRA-2 (Jasco); u.v. spectra, Hitachi recording spectrophotometer Model EPS-3T (ethanol); n.m.r. spectra, JNM-MH-60 (Jeol) with tetramethylsilane (δ = 0) as internal standard in deuteriochloroform; optical rotation, Yanagimoto OR-10; molecular weight, Hitachi Perkin–Elmer 115 molecular weight apparatus with benzil as reference compound; g.l.c., JGC-1100 (Jeol) with flame ionization detector.

The t.l.c. values were obtained with silica gel G (Merck) as adsorbent; the spots were detected by spraying with 10% sulfuric acid and heating. For paper chromatography Toyo filter paper No. 51 (2 cm × 40 cm) was used.

Extraction

The dried stems of *Trachelospermum asiaticum* Nakai var. *intermedium* Nakai (25 kg) were extracted with hot methanol (4 × 36 l) and the methanol solution was evaporated to a small volume, diluted with water, and filtered. The filtrate was extracted successively with light petroleum (4 × 1.5 l), ether (4 × 1.5 l), and chloroform (5 × 1.5 l). The aqueous layer was concentrated to a syrup and extracted with hot ethyl acetate (4 × 1.8 l). The residue was extracted with chloroform–methanol (2:1, v/v) (5 × 1.5 l). The chloroform–methanol extract (82 g) was chromatographed on a column of activated charcoal (Wako, 400 g, 9 cm × 32 cm). Fractions (1 l each) were eluted by methanol–water (1:99, v/v) (nos. 1–2), methanol–water (1:1, v/v) (nos. 3–7), and methanol alone (nos. 8–13), respectively.

Matairesinol-4,4′-di-O-β-D-glucopyranoside (1)

The eluate of fraction no. 10 (1.7 g) was chromatographed on a silica gel column (Mallinckrodt, 100 g, 4.5 cm × 26 cm) with chloroform–ethanol (3:2, v/v) as eluting solvent. Fractions (50 ml each) were monitored by t.l.c. using chloroform–ethanol (3:1, v/v) as developer. The R_f 0.16 fraction was evaporated and final purification was achieved by re-chromatography on a silica gel column to give colorless powder **1**, 51.4 mg, m.p. 104–106°, $[\alpha]_D^{14}$ −24.0 (*c*, 0.5 in ethanol).

Anal. Calcd. for $C_{32}H_{42}O_{16}\cdot H_2O$: C, 54.85; H, 6.33. Found: C, 54.52; H, 6.24.

Spectra: λ_{max} in nm (log ε) 225 (4.09), 279 (3.65); ν_{max} (KBr) 3560–3240 (hydroxyl), 1765 (γ-lactone), 1595, 1510 cm^{-1} (aromatic).

Acid Hydrolysis of Matairesinol-4,4′-di-O-β-D-glucopyranoside (1)

The solution of matairesinol-4,4′-di-*O*-β-D-glucopyranoside (45 mg) in 10% sulfuric acid (25 ml) was heated on a boiling water bath for 2 h. The oily product separated was extracted with ether and the ether solution was washed with water, dried over sodium sulfate, and evaporated to dryness. The residue was chromatographed on a silica gel column (Mallinckrodt, 30 g, 2.5 cm × 12 cm) with chloroform–ethyl acetate (4:1, v/v) as eluting solvent. Fractions were monitored by t.l.c. using chloroform–ethyl acetate (1:1, v/v) as developer. The R_f 0.62 fraction was evaporated to dryness. The residue was recrystallized from 30% aqueous acetic acid to give colorless needles, 6 mg, m.p. 118.5–119.5°, $[\alpha]_D^{23}$ −34.8 (*c*, 0.3 in ethanol) an authentic sample $[\alpha]_D^{8}$ −40.0 (in ethanol) (9); lit. $[\alpha]_D^{25}$ −37.9, −35.7, −40.5 (in acetone) (6).

Spectra: λ_{max} in nm (log ε) 231.5 (4.10), 283 (3.79), shifting to 250.5 (4.33), 298.5 (4.03) in sodium ethoxide; ν_{max} ($CHCl_3$) 3560 (hydroxyl), 1775 (γ-lactone), 1610, 1510 cm^{-1} (aromatic).

The product was identified with an authentic sample of matairesinol by a mixed melting point and i.r. spectral comparison.

The water layer was neutralized with barium carbonate and evaporated to dryness. Paper chromatography of this

Can. J. Chem. Downloaded from www.nrcresearchpress.com by 210.87.254.40 on 09/05/12
For personal use only.

residue (solvent: butanol – acetic acid – water (4:1:1, v/v), color reagent: aniline hydrogen phthalate) showed only one spot of D-glucose.

Matairesinol-4,4′-di-O-β-D-glucopyranoside Octaacetate (2)

Matairesinol-4,4′-di-*O*-β-D-glucopyranoside (40 mg) was dissolved in pyridine (1 ml) and acetic anhydride (1 ml). The mixture was left standing overnight at room temperature. The reaction product was added to the ice water with stirring and then extracted with ether. The ether solution was washed with water, dried over sodium sulfate, and evaporated to dryness. The residue was recrystallized from methanol to give colorless powder, 31.1 mg, m.p. 88–89°.

Anal. Calcd. for $C_{48}H_{58}O_{24}$ (mol. wt. 1018.98): C, 56.58; H, 5.74. Found ((vapor pressure osmometry in chloroform) 976.4): C, 56.77; H, 5.94.

Spectra: λ_{max} in nm (log ε) 227 sh (4.11), 279 (3.66); ν_{max} (KBr) 1760 (γ-lactone and acetyl), 1595, 1515 cm^{-1} (aromatic); n.m.r. 7.10–6.35 (6H, aromatic H, multiplet), 5.50–4.75 (8H, multiplet), 4.30–4.00 (6H, broad singlet), 4.00–3.80 (2H, C-9, multiplet), 3.75 (6H, methoxyl, singlet), 3.00–2.75 (2H, C-8, -8′, broad), 2.75–2.40 (4H, C-7, -7′, broad), 2.02 and 2.05 (24H, acetyl, two singlets).

Gas–Liquid Chromatography on Methanolysate of Permethyl Ether of Matairesinol-4,4′-di-O-β-D-glucopyranoside (1)

The carbanion prepared from sodium hydride (40 mg) and dimethyl sulfoxide (1 ml) was added to solution of matairesinol-4,4′-di-*O*-β-D-glucopyranoside (8 mg) in dimethyl sulfoxide (1 ml) under nitrogen gas and the mixture was stirred at room temperature. After 1 h, methyl iodide (0.2 ml) was added and the mixture was left standing overnight. The water was added to the reaction mixture, which was extracted with chloroform. The chloroform solution was washed with water, dried over sodium sulfate, and evaporated to dryness. The residue (6.6 mg) was heated with 3% methanolic hydrogen chloride in a sealed tube placed in boiling water bath for 10 h. The reaction mixture was diluted with water and extracted with chloroform. The chloroform solution was washed with water, dried, and concentrated. The presence of methyl 2,3,4,6-tetra-*O*-methyl-D-glucopyranoside only in the concentrated solution was demonstrated by g.l.c. (condition: column, 15% poly-butanediol glycol succinate on Celite 545 (2 m × 3 mm); column temperature, 175°; carrier gas, N_2 (30 ml/min); t_R (min), 5.5 and 7.5).

Enzymatic Hydrolysis of Matairesinol-4,4′-di-O-β-D-glucopyranoside (1)

The emulsion (1 mg) (Tokyo Chemical Industry Co.), was added to matairesinol-4,4′-di-*O*-β-D-glucopyranoside (5 mg) in purified water (5 ml) and the mixture was left standing at room temperature for 2 weeks. The mixture was extracted with ether. The ether layer was dried and evaporated. The presence of matairesinol in the residue was proved by co-t.l.c. with an authentic sample. The water layer was evaporated to dryness. In the residue, only the presence of D-glucose was shown by the paper chromatography.

The authors are indebted to the Analytical Center of Nagoya City University for n.m.r. spectral measurements and elemental analyses.

1. I. INAGAKI, S. HISADA, and S. NISHIBE. Chem. Pharm. Bull. (Tokyo), **16**, 2307 (1968).
2. I. INAGAKI, S. HISADA, and S. NISHIBE. Phytochem. **10**, 211 (1971).
3. S. NISHIBE, S. HISADA, and I. INAGAKI. Chem. Pharm. Bull. (Tokyo), **19**, 866 (1971).
4. S. NISHIBE, S. HISADA, and I. INAGAKI. Chem. Pharm. Bull. (Tokyo), **20**, 2075 (1972).
5. E. DICKEY. J. Org. Chem. **23**, 179 (1958).
6. R. PALTER and R. E. LUNDIN. Phytochem. **9**, 2407 (1971).
7. R. PALTER, W. F. HADDON, and R. E. LUNDIN. Phytochem. **10**, 1587 (1971).
8. K. MATSUO, T. TOKOROYAMA, and T. KUBOTA. Phytochem. **11**, 1522 (1972).
9. I. INAGAKI, S. HISADA, and S. NISHIBE. Chem. Pharm. Bull. (Tokyo). **20**, 2710 (1972).
10. S. HAKOMORI. J. Biochem. **55**, 205 (1964).
11. A. VON WARTBURG, M. KUHN, and H. LICHTI. Helv. Chim. Acta, **47**, 1203 (1964).
12. K. FREUDENBERG and K. WEINGES. Tetrahedron, **15**, 115 (1961).

Can. J. Chem. Downloaded from www.nrcresearchpress.com by 210.87.254.40 on 09/05/12
For personal use only.

Conformational Preferences of ortho-Substituted Benzophenones. Correlations Between Carbon-13 Nuclear Magnetic Resonance Shieldings and Calculated Torsional Angles

GERALD WALLACE BUCHANAN[1]
Department of Chemistry, Carleton University, Ottawa, Canada K1S 5B6

AND

GIORGIO MONTAUDO AND PAULO FINOCCHIARO
Institute of Industrial Chemistry of the University, Viale Doria 8, Catania, Italy

Received October 6, 1972

The results of an investigation of the conformational properties of some benzophenones are reported. Carbon-13 n.m.r. spectra provide a generally applicable method to study the conformational preference of these compounds through the C=O shifts. Semi-empirical conformational energy calculations have been used to build contour maps of relative conformational energy as a function of the two internal rotation angles of these molecules. Conformations of minimum energy, as detected from the contour maps, have been assumed as the most stable. The phenyl torsional angles corresponding to these conformations, plotted against the C=O shifts, furnish linear relationships.

Les résultats d'une étude des propriétés conformationnelles de quelques benzophénones sont présentés. Les spectres r.m.n. du carbone-13 procure une méthode généralement applicable pour étudier la préférence conformationnelle de ces composés en se servant des déplacements du carbonyl C=O. Des calculs semi-empiriques de l'énergie conformationnelle ont été utilisés pour élaborer des diagrammes d'énergie conformationnelle relative en fonction des deux angles de rotation interne de ces molécules. Les conformations d'énergie minimum, obtenues à partir des diagrammes, ont été acceptées comme étant les plus stables. Les angles de torsion du phényl correspondant à ces conformations sont reliés linéairement avec les déplacements du C=O. [Traduit par le journal]

Can. J. Chem., **51**, 1053 (1973)

Introduction

The application of proton n.m.r. spectroscopy to the study of conformational preferences in ortho-substituted acetophenones and benzophenones has been recently reported (1). For acetophenones it has been shown that the carbon-13 carbonyl group shieldings can be employed effectively for the determination of the angle of twist between the C=O group and the benzene ring in these conjugated molecules (2). Potentially the carbon-13 n.m.r. (c.m.r.) method should have valuable application for the study of benzophenone conformation as well, however no c.m.r. data for benzophenones have been available in the literature to date.

We herein report results of a c.m.r. examination of nine benzophenones and detailed calculations of their preferred conformations.

In our approach, semi-empirical conformational energy calculations have been used to build contour maps of relative conformational energy as a function of the two internal rotation angles of these molecules.

Conformations of minimum energy, as detected from the contour maps, have been assumed the most stable.

The phenyl torsional angles corresponding to these conformations, plotted against the C=O shifts, furnish good linear relationships, thus providing a valuable method of conformational analysis.

Results

Table 1 contains the carbon-13 chemical shifts (downfield from internal TMS) for the benzophenones presently examined. To facilitate discussion the C=O shifts for related acetophenones are included in parentheses.

Assignments of the carbonyl resonances are straightforward, these carbons appearing at the lowest field position in the spectrum. Other carbons bearing no directly bonded hydrogens are easily recognized by their retention of singlet structure in the off resonance decoupling experi-

[1]To whom correspondence should be addressed.

Can. J. Chem. Downloaded from www.nrcresearchpress.com by 210.87.254.40 on 09/05/12
For personal use only.

TABLE 1. ^{13}C n.m.r. chemical shifts for benzophenones (p.p.m. from TMS ± 0.1)*

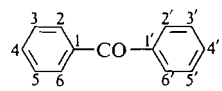

Compound:		1	2	3	4	5	6	7	8	9
Substitution position	CH_3	—	2	2,4,6	2,4,6,2′	—	—	2	2,4,6	2,4,6,
	OCH_3	—	—	—	—	4′	2′,4′	2′,4′	2′,4′	4′
	C=O	195.5	197.2	199.3	200.7	193.3	193.9	195.5	197.0	197.7
	(C=O)†	196.3	200.1	206.9		194.9	194.8			
	C-1	137.0	137.9	137.6	138.6	136.9	135.9	139.8	139.3	136.5
	C-2	129.2	135.8	133.3	133.1	128.1	126.5	135.3	132.9	132.3
	C-3	127.6	130.2	127.8	127.3	126.7	125.2	128.6	127.5	126.7
	C-4	131.6	130.3	136.2	137.0	130.3	129.0	129.4	136.8	135.8
	C-5	127.6	124.5	127.8	127.3	126.7	125.2	123.9	127.5	126.7
	C-6	129.2	129.5	133.3	133.1	128.1	126.5	127.4	132.9	132.3
	C-1′		137.1	136.6	137.4	128.7	118.7	120.9	120.6	129.1
	C-2′		129.2	128.4	135.9	130.9	158.4	159.6	161.1	130.1
	C-3′		127.7	127.5	130.8	112.3	96.1	98.5	98.5	112.6
	C-4′		132.8	132.5	130.9	161.5	162.2	163.0	164.3	163.0
	C-5′		127.7	127.5	124.7	112.3	102.3	104.5	104.7	112.6
	C-6′		129.2	128.4	130.5	130.9	129.3	132.2	133.9	130.1
	2-CH_3		19.1	18.5	18.5			20.0	19.1	18.6
	4-CH_3			20.4	20.7				20.9	20.4
	2′-CH_3				20.1					
	2′-OCH_3						55.3	55.3	55.4	
	4′-OCH_3					55.1	55.3	55.3	55.4	55.3

*0.5 *M* in $CDCl_3$.
†Shifts for corresponding acetophenones.

ment. In several compounds the ortho-aromatic carbons were assigned from specific ^1H decoupling since it is known (1) that aromatic protons ortho to the carbonyl group of acetophenones and benzophenones resonate at lower fields than those in meta- and para-positions. Remaining benzophenone ring carbon assignments were made by analogy with acetophenones (2) or by using well-established substituent effects on aromatic carbon shieldings (3).

Assignments of ring methyl and methoxy carbon resonances are unambiguous, the methyls appearing in the range $\delta = 18$–21 and methoxys near $\delta = 55$. It is clear that ortho-methyl groups resonate at *ca.* 2 p.p.m. higher field than their para counterparts, but the shieldings do not vary significantly with conformation.

Comparison of the ring-carbon shifts for benzophenones with the related acetophenones (2) reveals a striking similarity in the shieldings. Evidently there is no appreciable interaction between the two benzene rings in the diphenyl-ketones which affects these carbon shifts. In the proton spectra of these molecules, long range anisotropy effects are measurable (1); however, contributions to the carbon-13 shifts from anisotropic factors are of relatively minor importance (4). Accordingly, a detailed discussion of all ring-carbon shieldings seems unwarranted since the trends in acetophenones are well documented (2).

Carbonyl-carbon shieldings in these compounds, however, follow clear patterns. Interpretations are based on the well-established findings that conjugated carbonyl-carbon nuclei are shielded relative to their unconjugated counterparts (5). This effect is attributed to an increase in the electron density at the C=O in the conjugated systems. In the present series the C=O shifts for benzophenones are at higher field than for the corresponding acetophenones, an observation consistent with the presence of the second aromatic ring in the diphenyl-ketones. Also, within a series, as the degree of steric interference increases at the ortho-position, the carbonyl-carbon becomes deshielded, indicating the presence of steric inhibition of resonance. For acetophenones, Dhami and Stothers have correlated the torsional angle between the ring and the C=O group with the carbonyl shift and ob-

Can. J. Chem. Downloaded from www.nrcresearchpress.com by 210.87.254.40 on 09/05/12
For personal use only.

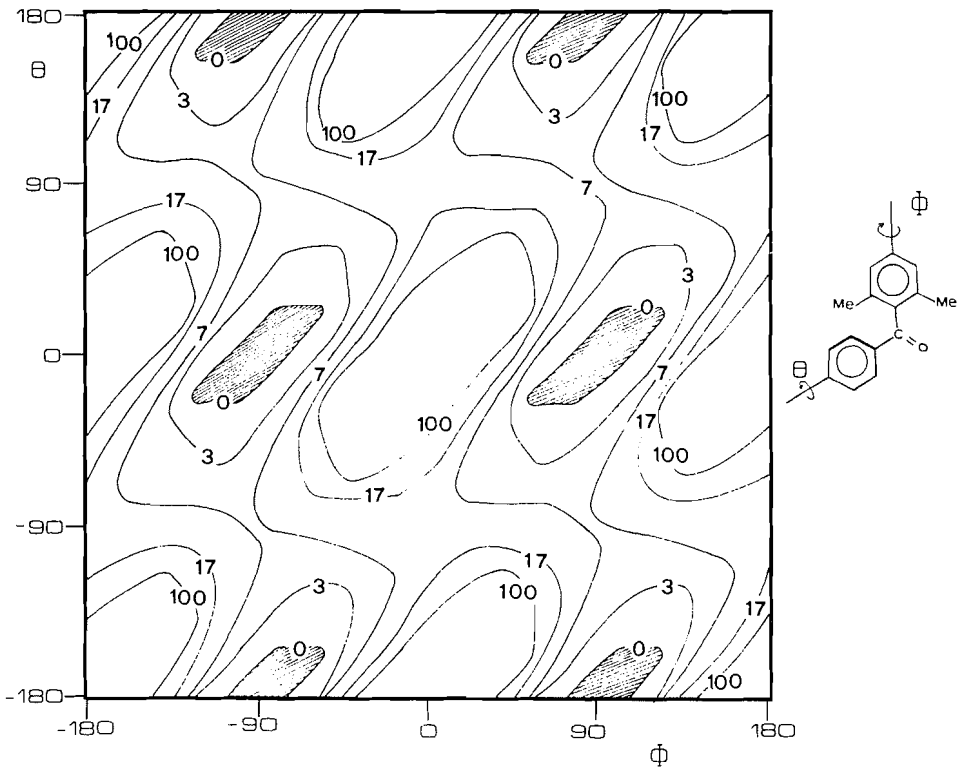

FIG. 1. Energy contour map of 2,6-dimethylbenzophenone. The planar starting conformation ($\phi = \theta = 0°$) is represented in the upper right side. The shaded area corresponds to the energetically "allowed" region. Numbers contained in the figure are energies in kcal/mol.

tained reasonable geometries (2). The situation in benzophenones is more complex since two torsional angles must be estimated.

Accordingly, we have calculated (see Experimental for details) the energy contour maps of some ortho-methyl substituted benzophenones as a function of the two internal rotation angles ϕ and θ. Relevant data are summarized in Table 2 and an example is given in Fig. 1.

The energy minimum for the unsubstituted benzophenone (Table 2) is found at $\phi = 30$, $\theta = -30°$.

This value compares favorably with that found (6) by Extended Huckel (EH) calculations for the same molecule ($\phi = 38$; $\theta = -38°$) and with a number of experimental figures from various techniques (7*b*, 7*c*, 8).

Also the position of the barrier to internal rotation (Table 2) is coincident with that found (6) by EH calculations, but its value (2.5 kcal/mol) is about twice as high.

As evidenced by the data in Table 2 the positions of the minima vary sensibly according to the substitution pattern. Molecular conformations identified by these energy minima have been assumed as the most stable and the corresponding phenyl torsional angles have been used in the correlations with spectral data.

Methyl Benzophenones

For the methyl benzophenones a plot of the observed ^{13}C carbonyl shift *vs.* $\cos^2 \phi + \cos^2 \theta$ is shown in Fig. 2. A correction factor for the presence of an ortho-methyl group has been suggested based on the finding that in ortho-xylenes, methyl carbons appear at slightly higher field (1 p.p.m.) than for cases where the methyls are further separated (9). Support for including this 1 p.p.m. per ortho-methyl correction in carbonyl compounds is gained from results for ortho-tolualdehyde, mesityaldehyde, and acetophenones (2). A plot which includes these corrections for ortho-methyl benzophenones is shown by the dotted line in Fig. 2.

Clearly, as the degree of steric hindrance at the ortho-position increases, the C=O group is

Can. J. Chem. Downloaded from www.nrcresearchpress.com by 210.87.254.40 on 09/05/12
For personal use only.

Can. J. Chem. Downloaded from www.nrcresearchpress.com by 210.87.254.40 on 09/05/12
For personal use only.

TABLE 2. Relative conformational energy data (kcal/mol) for ortho-methyl substituted benzophenones

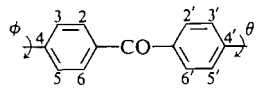

Positions of methyl groups	Energy minima		φ = 90° θ = 90°	φ = 90° θ = −90°	φ = 0° θ = 90°	φ = 180° θ = 90°	φ = 90° θ = 180°	φ = 90° θ = 0°	Saddle point		
	φ	θ							φ	θ	*E*
—	30°	−30°	8.0	8.0	2.5	2.5	2.5	2.5	0°	−90°	2.5
6	55°	−5°	6.5	6.5	3.5	5.5	0.5	0.5	0°	−90°	3.5
2,6	90°	0°	6.0	6.0	9.0	9.0	0.0	0.0	90°	−90°	6.0*
									0°	−90°	9.0†
2,6,6′	90°	30°	13.0	13.0	3.5	3.5	2.3	0.0	−100°	−100°	11.0

*Value for the unsubstituted ring.
†Value for the substituted ring.

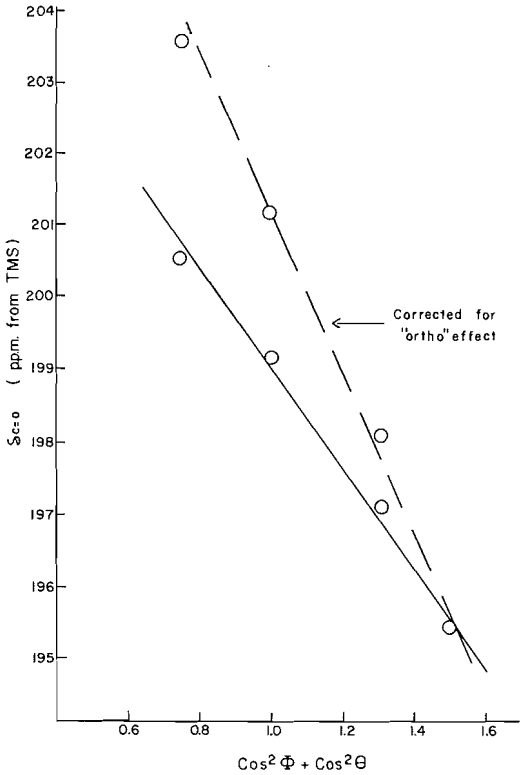

FIG. 2. Plot of carbonyl-carbon shielding *vs.* calculated phenyl torsional angles for benzophenone and ortho-methylbenzophenones.

less shielded, reflecting a decrease in the electron density at this carbon due to the attenuated conjugation with the benzene ring.

A check on the origin of the downfield C=O shifts with bulky ortho-substitution is provided by examination of the variation of the shielding of the aromatic carbon para to the C=O group. For both acetophenones and benzophenones the para-carbon is deshielded relative to benzene (δ = 128.7), due to the conjugative electron-withdrawing effect of the C=O group. In acetophenone where the torsional angle is 0°, the para-carbon resonates at 132.0 p.p.m. For benzophenone the calculated torsional angles are 30° and accordingly an upfield shift for the para-carbon is expected since the degree of resonance between *a single* aromatic ring and the C=O group should be decreased relative to the acetophenone. Indeed a small upfield shift to 131.6 p.p.m. is seen for the para-carbon of benzophenone. For ortho-methyl benzophenone the para-carbon is shifted upfield to 130.3 p.p.m. reflecting the decrease in resonance interaction on substitution of a bulky ortho-group. In the mesitylbenzophenones **3** and **4**, the trend is evident at the C-4′ position. Addition of the ortho-methyl group in **4** increases the calculated angle of twist to 30° and shifts the C-4′ resonance up to 130.9 p.p.m., whereas without this group a shielding of 132.5 p.p.m. is found. An apparent inconsistency in the C-4 shifts is present for compounds **6** and **7**. From the above argument the C-4 resonance in **7** is expected to be at higher field than in **6**, but a small effect (129.0 $\pm$ 0.1) *vs.* (129.4 $\pm$ 0.1) in the opposite direction is found. No ready explanation for this is available. In the following discussion, additional reasons for viewing the data for ortho-methoxy compounds with caution are presented.

Methoxy Benzophenones

Conformational calculations are not available for these compounds and thus only a qualitative discussion of trends is permitted. Addition of a para-methoxy group to benzophenone shields the C=O by 2.2 p.p.m., an effect which may be due to conjugative electron release by the para-oxygen atom. In the acetophenones (2) a similar albeit smaller effect is present. An ortho-methoxy function as in **6** deshields the carbonyl by 0.6 p.p.m. relative to **5** which may be indicative of some steric inhibition of resonance by this ortho-group. Direct comparison with benzophenone is not possible since a sample of ortho-methoxy benzophenone was not available. A comparison of acetophenones (2) however, shows a deshielding effect of 1.8 p.p.m. in the ortho-methoxy derivative.

In compounds **6**, **7**, and **8** it is clear that addition of ortho-methyl groups to the second aromatic ring increases the steric inhibition of resonance, causing the C=O shieldings to move to lower field. For compound **9** the low field C=O shift of 197.7 p.p.m. is puzzling. If indeed there is steric interference to resonance due to the ortho-methoxy group, the C=O shift in **7** should be at lower field than in **9**, which is not observed. A similar discrepancy occurs with the corresponding acetophenones (3).

It is apparent that successive addition of ortho-methyl groups gives rise to predictable changes in c.m.r. C=O shifts which are useful for estimating torsional angles in benzophenones. Results for molecules bearing ortho-methoxy groups, however, must be viewed with some caution.

Can. J. Chem. Downloaded from www.nrcresearchpress.com by 210.87.254.40 on 09/05/12
For personal use only.

Can. J. Chem. Downloaded from www.nrcresearchpress.com by 210.87.254.40 on 09/05/12
For personal use only.

It is of interest to compare the ^{13}C n.m.r. method with u.v. spectroscopy, which has been used extensively for studying steric inhibition of resonance. For methyl benzophenones with identically substituted rings, Rekker and Nauta (10) found that ortho-substitution causes a measurable decrease in the intensity of absorption of the K band (also termed the conjugative or C band). A value of 15° for the benzophenone torsional angle was obtained which is somewhat smaller than the present result of 30°.

The difficulties in obtaining accurate band intensity measurements from u.v. spectra are well known (11). In the benzophenone u.v. spectra (10) the B and K bands overlap partially further limiting the precision of the technique. At best one is employing an energy difference between an electronically excited state and ground state to evaluate a property of the ground electronic state.

^{13}C shifts, however, arise from the ground electronic state only, and the possibility of overlapping bands is remote, since the C=O resonances are at characteristically low field. Furthermore, contributions from non-steric effects can often be corrected as illustrated for the methyl group in Fig. 2.

We conclude that ^{13}C n.m.r. is a valuable technique for the examination of conformational preferences in Ar—X—Ar systems. Results for compounds having X = O, S, SO_2, and CH_2 will be reported in the near future.

Experimental

Spectra

The carbon n.m.r. spectra were obtained at 25.2 MHz using a Varian XL-100-12 n.m.r. spectrometer, most commonly under conditions of complete proton noise decoupling. Spectral accumulations were accomplished with a Varian C-1024 time-averaging computer. Samples were contained in 8 mm tubes and were examined as 0.5 *M* solutions in $CDCl_3$, containing 2% TMS as an internal standard. Off resonance decoupling experiments were carried out with the proton frequency offset approximately 500 Hz from the center of the proton spectral region. During the specific proton decoupling experiments the noise modulation was turned off.

Calculations

These were performed with help of a microcomputer Hewlett-Packard 9100 B. The starting conformation ($\phi = \theta = 0°$) for the compounds studied was taken with both rings planar, and the origin of the axes was placed at the bridge carbon atom. Interatomic distances and natural bond angles were taken from pertinent literature data (7).

Distances among interacting atoms were computed for each pair of ϕ and θ values calculating first (trigonometrically) the atomic coordinates for each interacting atom for a fixed conformation and then applying the usual rotation matrix methods (12). Non-bonded interactions were obtained from the calculated distances according to the Lennard-Jones potential (13). Torsional energies were not taken into account because they were found to be negligible (14).

Individual energy values for each one of the interacting pairs considered were added together obtaining the total strain energy (unminimized) for each pair of ϕ and θ values from 0–360°, with a 10° increment.

The strain energies found were minimized according to a procedure described in a previous paper (6).

The molecular-mechanical approach of computing the molecular energy does not normally include resonance interaction. In order to take into account this term we have subtracted, from the total strain energy of the methyl benzophenones studied, the theoretical conjugative energy (15) (E_0) of 6.0 kcal/mol which was assumed to vary (15, 17) as a function of the two internal rotation angles: $E = E_0 (\cos^2 \phi + \cos^2 \theta)$.

Compounds

Syntheses and physical properties of the benzophenones were reported previously (1).

We thank the National Research Council of Canada, Carleton University President's Research Fund, and the North Atlantic Treaty Organization for generous financial support of this work.

1. G. MONTAUDO, P. FINOCCHIARO, and P. MARAVIGNA. J. Am. Chem. Soc. **93**, 4214 (1971).
2. K. S. DHAMI and J. B. STOTHERS. Tetrahedron Lett. 631 (1964); Can. J. Chem. **43**, 479 (1965).
3. P. C. LAUTERBUR. J. Am. Chem. Soc. **83**, 1846 (1961).
4. M. KARPLUS and J. A. POPLE. J. Chem. Phys. **38**, 2803 (1963).
5. J. B. STOTHERS and P. C. LAUTERBUR. Can. J. Chem. **42**, 1563 (1964).
6. G. MONTAUDO and P. FINOCCHIARO. J. Am. Chem. Soc. **94**, 6745 (1972).
7. (*a*) L. E. SUTTON. *In* Tables of interatomic distances and configuration in molecules and ions. Suppl. 1956–1959, Burlington House, London 1965; (*b*) G. M. LOBANOVA. Kristallogr. **13** (6), 984 (1969); (*c*) E. G. FLEISCHER, NAKO SUNG, and S. HAWKINSON. J. Phys. Chem. **72**, 4311 (1968).
8. (*a*) R. BRADLEY and R. J. W. LE FEVRE. J. Chem. Soc. 56 (1962); (*b*) P. H. GORE, J. A. HOSKINS, R. J. W. LE FEVRE, L. RADSON, and G. L. RITCHIE. J. Chem. Soc. B, 741 (1967); (*c*) R. N. JONES. J. Am. Chem. Soc. **67**, 2127 (1945).
9. P. LAUTERBUR. J. Chem. Phys. **38**, 1406, 1415, 1432 (1963).
10. R. E. REKKER and W. TH. NAUTA. Rec. Trav. Chim. Pays-Bas, **73**, 969 (1954).
11. H. H. JAFFE and M. ORCHIN. Theory and applications of ultra violet spectroscopy. J. Wiley and Sons, New York. 1962.
12. H. A. ELLIOTT, K. D. FRYER, J. D. GARDNER, and N. J. HILL. Vectors and matrices. Holt, Toronto, Ontario. 1966. p. 254.

13. R. A. SCOTT and H. A. SCHERAGA. J. Chem. Phys. **45**, 209 (1966); **46**, 4410 (1967); H. A. SCHERAGA. *In* Advances in physical organic chemistry. Vol. 6. V. Gold, Editor. Academic Press, N.Y. 1968. p. 103.
14. J. F. YAN, G. VANDERKOOI, and H. A. SCHERAGA. J. Chem. Phys. **49**, 2713 (1968); N. C. COHEN. Tetrahedron, **27**, 789 (1971).
15. R. HOFFMANN and J. R. SWENSON. J. Phys. Chem. **74**, 415 (1970) and refs. therein. The theoretical value for the conjugative energy is in reasonable agreement with the experimental (16).
16. R. E. KLINK, D. H. MARR, and J. B. STOTHERS. Chem. Commun. 409 (1967); F. A. L. ANET and M. AHMAD. J. Am. Chem. Soc. **86**, 119 (1964).
17. E. A. BRAUDE and F. SONDHEIMER. J. Chem. Soc. 3754 (1955); C. L. CHENG, R. J. W. LE FEVRE, G. L. RITCHIE, P. A. GORE, and M. YNSUF. J. Chem. Soc. B, 1579 (1971).

Can. J. Chem. Downloaded from www.nrcresearchpress.com by 210.87.254.40 on 09/05/12
For personal use only.

The Photo-addition of Naphthalene and Acrylonitrile. An X-ray and Nuclear Magnetic Resonance Study of the Cycloadducts

R. M. BOWMAN, C. CALVO, J. J. MCCULLOUGH, R. C. MILLER, AND I. SINGH

Department of Chemistry, McMaster University, Hamilton, Ontario

Received August 2, 1972

The photoaddition of naphthalene and acrylonitrile has been reinvestigated. It was found that the cyclobutane adduct described previously is *endo*-7-cyano-2,3-benzobicyclo[4.2.0]-octa-2,4-diene (**7**), and not the *exo*-8-cyano compound. The structure was determined from an X-ray diffraction study on the *p*-bromophenylurethane of the carbinol derived from the cyano-compound. The structural details are described. The crystallographic data are $a = 13.85(1)$, $b = 7.976(2)$, $c = 12.752(4)$ Å, $\alpha = 90.80(3)$, $\beta = 87.02(6)$, $\gamma = 90.99(5)°$ space group $P\bar{1}$, $Z = 2$ units of $C_{20}H_{18}O_2NBr$. The least-squares residual R was 0.085 for 651 X-ray reflections measured on a Syntex P1 diffractometer using graphite-monochromatized Mo radiation. The methine proton resonances in the 220 MHz n.m.r. spectrum of **7** were resolved using pyridine solvent, and the coupling constants are consistent with the structure and geometry, as derived from the X-ray work. A small fraction (7%) of 8-cyano-2,3-benzobicyclo[4.2.0.]octa-2,4-diene was also formed. This is tentatively assigned as the *endo* isomer, and on base treatment it isomerizes to a new compound, identified as the *exo* isomer. In contrast, the major cycloadduct **7** is recovered unchanged from base treatment. The folded geometry of the four-membered ring in these adducts apparently determines the stabilities of the epimers, and the proton–proton vicinal coupling constants.

La photoaddition du naphtalène et de l'acrylonitrile a été réétudiée. On a trouvé que l'adduit cyclobutane précédemment décrit est l'*endo*-cyano-7 benzo-2,3 bicyclo[4.2.0] octadiène-2,4 (**7**) et non l'*exo*-cyano-8. La structure a été déterminée par la diffraction de rayons X sur le *p*-bromophényluréthane du carbinol dérivé du composé cyano. Des détails sur la structure sont fournis. Les données cristallographiques sont: $a = 13.85(1)$ $b = 7.976(2)$, $c = 12.752(4)$ Å, $\alpha = 90.80(3)$, $\beta = 87.02(6)$, $\gamma = 90.99(5)°$, le groupe spatial est $P\bar{1}$ et $Z = 2$ unités de $C_{20}H_{18}O_2NBr$. La méthode des moindres carrés donne un R résiduel de 0.085 pour 651 réflexions de rayons X prises sur diffractomètre syntex P1, avec une radiation Mo rendue monochromatique par le graphite. Les résonances du proton méthine en r.m.n. à 220 MHz, ont été résolues avec la pyridine comme solvant; les constantes de couplage sont compatibles avec la structure et la géométrie fournies par les rayons X. Une petite fraction (7%) de cyano-8 benzo-2,3 bicyclo[4.2.0] octadiène-2,4 a été également formée. On a tenté de l'identifier à l'isomère *endo*, ce dernier s'isomérise par traitement basique en un nouveau composé identifié à l'isomère *exo*. Le cycloadduit **7** a été retrouvé inchangé après traitement basique. La géométrie plissée du cycle à quatre membres dans ces adduits détermine apparemment les stabilités des épimères et les constantes de couplage vicinal entre protons. [Traduit par le journal]

Can. J. Chem., **51**, 1060 (1973)

During the past few years, we have reported studies of products (1, 2) and mechanism (3, 4) of the photoaddition of naphthalene and acrylonitrile in hydroxylic solvents. The products were assigned the structures **1**, **2**, and **3**.

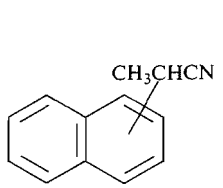

1, 2

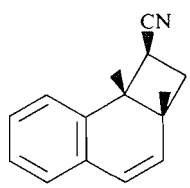

3

The cycloadduct was assigned the structure *exo*-8-cyano-2,3-benzobicyclo[4.2.0]-octa-2,4-diene (**3**) on the basis of n.m.r. evidence, equilibration behavior, and unit cell dimensions in the crystal (1, 2). However, in the course of the quantitative work on this reaction (3, 4) a second cycloadduct was found (7% yield) whose n.m.r. spectrum suggested that it was 8-cyano-2,3-benzobicyclo[4.2.0]-octa-2,4-diene. Since this minor adduct was not an epimer of the major one (see below), considerable doubt was cast on structure **3** for the latter. It was therefore decided to reinvestigate the structure of the major cycloadduct, and of the methods available, X-ray was chosen since this would reveal the position and stereochemistry of the cyano-group.

Results

Preparation of Derivative for X-ray Study

The major cycloadduct m.p. 98°, from photolysis of naphthalene and acrylonitrile (1, 2) was

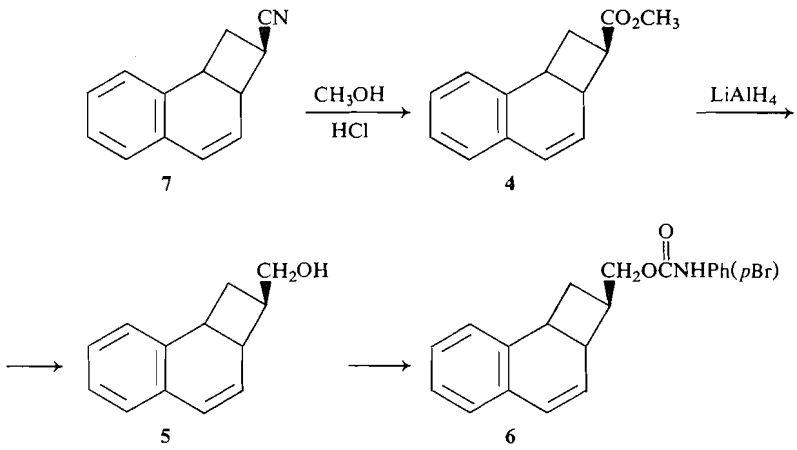

SCHEME 1

converted to the methyl ester **4** by treatment with methanol and hydrogen chloride in ether (5). Reduction of the ester with $LiAlH_4$ gave the carbinol **5** as an oil. The latter reacted with *p*-bromophenylisocyanate in cyclohexane at reflux to give the *p*-bromophenylurethane **6**, m.p. 155–157°. This derivative gave single crystals from 95% ethanol, which were used in the X-ray work. The route from the photoadduct to the derivative **6** is shown in Scheme 1.

Structure of Photoadduct

The X-ray work on the *p*-bromophenylurethane **6** is described in detail in the Experimental. The structure of **6** is shown in Fig. 1, and the bond distances and angles in Table 1. It can be seen that the carbinol CH_2 group in **6** is bonded at C-7, and has the *endo*-configuration. The major photoadduct must therefore be *endo*-7-cyano-2,3-benzobicyclo[4.2.0]octa-2,4-diene **7**, and not **3** as previously assigned.

Some interesting structural features of the benzobicyclo[4.2.0]octa-2,4-diene ring system follow from the X-ray structure. It is found, Table 2, that C-1, -2, -3, -4, -5 are coplanar, with C-6 0.16 Å out of this plane. The four-membered ring is *cis*-fused at C-1 and -6, and is non-planar, being folded about the C6–C8 diagonal by 21°. The dihedral angle in this compound is considerably smaller than in cyclobutane (33°), and somewhat smaller than in a number of substituted cyclobutanes (6, 7). The dihedral angle of 21° does allow the C-7 *endo*-substituent to adopt the more stable, equatorial conformation (7*d*, 8). The conformation of **7** is shown in Fig. 2.

It was reported previously (1, 2) and confirmed in more recent experiments that **7** did not epimerize on treatment with base, even though one proton was exchanged for deuterium under mild, basic conditions. We must conclude, therefore, that **7** is appreciably more stable than the (unknown) epimer. This is understandable

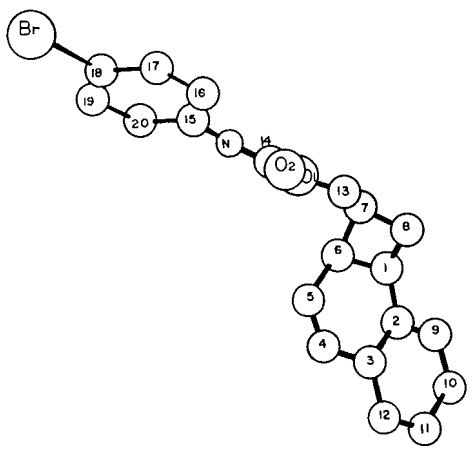

FIG. 1. Molecular structure of *p*-bromophenylurethane **6**; numbering agrees with that used in the Tables and in the text.

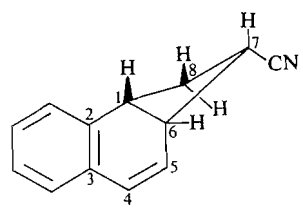

FIG. 2. Conformation of four-membered ring in photoadduct **7**.

TABLE 1. Bond distances and angles in *p*-bromophenylurethane derivative of *endo*-2,3-benzobicyclo[4.2.0]octa-2,4-diene-8-carbinol

Atoms	Bond lengths (Å)	Bond angle	(Degrees)
C1—C2	1.51(3)	C2—C1—C6	118(2)
		C2—C1—C8	115(2)
		C6—C1—C8	89(2)
C2—C3	1.47(3)	C1—C2—C3	120(2)
		C1—C2—C9	120(2)
		C3—C2—C9	120(2)
C3—C4	1.46(3)	C2—C3—C4	117(2)
		C2—C3—C12	118(2)
C1—C6	1.58(3)	C4—C3—C12	125(2)
C4—C5	1.34(3)	C3—C4—C5	127(2)
C5—C6	1.55(3)	C4—C5—C6	121(2)
C6—C7	1.60(3)	C1—C6—C5	114(2)
		C1—C6—C7	89(2)
		C5—C6—C7	113(2)
C7—C8	1.56(3)	C6—C7—C8	89(2)
		C6—C7—C13	122(2)
C8—C1	1.58(3)	C1—C8—C7	90(2)
C9—C2	1.36(3)	C2—C9—C10	120(2)
C9—C10	1.47(3)		
C10—C11	1.39(3)	C9—C10—C11	118(2)
C11—C12	1.37(3)	C10—C11—C12	122(2)
C12—C3	1.43(3)	C3—C12—C11	121(2)
C13—O1	1.45(2)	O1—C13—C7	106(2)
C13—C7	1.50(3)		
C14—O1	1.30(3)	O1—C14—O2	122(2)
C14—O2	1.25(3)	O1—C14—N	115(2)
C14—N	1.36(3)	O2—C14—N	123(2)
C15—N	1.37(3)	N—C15—C16	123(2)
C15—C16	1.44(3)	N—C15—C20	119(2)
		C16—C15—C20	118(2)
C16—C17	1.39(3)	C15—C16—C17	118(2)
C17—C18	1.40(3)	C16—C17—C18	123(2)
C18—C19	1.41(3)	C17—C18—C19	119(2)
C18—Br	1.86(2)		
C19—C20	1.38(3)	C18—C19—C20	119(2)
C20—C15	1.43(3)	C15—C20—C19	123(2)
		C12—O1—C14	119(2)
		C14—N—C15	128(2)

in terms of the geometry of **7**, since the epimer would have the cyano-group axial, if the cyclobutane ring is folded as shown.

Structure of the Minor Cycloadduct

The minor cycloadduct was present in about 7% of the total photoadduct yield, as estimated by v.p.c. analysis, and was isolated by column chromatography. The adduct **8** had m.p. 56–58° and isomerized on treatment with base to a compound **9**, m.p. 47–48°. Both **8** and **9** (and **7**) had mass spectra typical of cyclobutanes (9), in that the parent ion peaks at *m/e* 181 (3) were weak, and the base peaks at *m/e* 128 (100) corresponded to naphthalene cation. It is obvious that **8** and **9** must be the epimeric 8-cyano-2,3-benzobicyclo[4.2.0]octa-2,4-dienes, but the question of which is which cannot be answered with certainty. However, if it is assumed that the four-membered ring is folded in the same way as in **7**, the structures of **8** and **9** can be assigned, as shown in Scheme 2.

The equilibrium composition is 88% of **9** and 12% of **8**. The cyano-group will be equatorial in the *exo*-compound, which should therefore correspond to the more stable isomer, **9**. The *endo*-isomer should therefore be the photoadduct, **8**.

This tentative assignment is supported by the n.m.r. spectra, which are described in Table 2. In the spectrum of **9**, H-8 (α to cyano-group) appears as a quartet, $J = 10.0$ Hz. That is, all

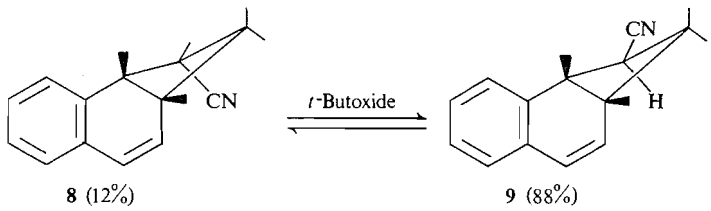

8 (12%) **9** (88%)

SCHEME 2

TABLE 2. Least-squares planes and out-of-plane distances*

Atom	Out-of-plane deviations (Å)
(a) Plane defined by C-1, -2, -3, -4, -5, -9, -10, -11, -12 is 9.18X − 3.65Y + 3.08Z = 11.04 with a standard of 0.05 Å	
C-6	0.16
C-7	−1.18
C-8	−1.58
C-13	−2.20
(b) Plane defined by C-6, -7, and -8 is −8.6X + 4.04Y + 7.31Z = 5.64	
C-1	−0.41
C-13	1.12
(c) Plane defined by C-1, -6, and -8 is 4.58X + 4.14Y + 5.62Z = 8.83	
C-2	1.17
C-3	2.44
C-4	2.43
C-5	1.39
C-7	−0.41
C-9	1.10
C-10	2.28
C-11	3.46
C-12	3.56
C-13	0.27

*The acute angle between planes (*a*) and (*c*) is 21.33° and that between (*b*) and (*c*) is 72.59°. The out-of-plane (*a*) distance of C-7 and -8 support the stereochemistry proposed as does the fact C-1 and -13 are on opposite sides of plane (*b*). Further support is provided by the fact that C-7 is on the opposite side of all the remaining atoms reported out-of-plane (*c*) and in particular C-13.

the vicinal coupling constants for H-8 are large. In **8** however, the H-8 resonance appears as a doublet of triplets, $J = 6.0$ and 8.5 Hz (a further splitting of $J = 2.0$ Hz is present, due to coupling with H-8). The coupling constant of 6.0 Hz may be due to a vicinal equatorial–equatorial coupling, since this is variable in magnitude (10). All the couplings in **9** however, should be axial–axial or axial–equatorial, and should therefore be large (10).

To check the above assignments, a spin decoupling experiment was performed on **8**. The multiplet at 3.20 δ (assigned to H-6) was irradiated, and the following changes were noted. The H-5 doublet of doublets became a doublet; the triplet at 3.92 δ (H-1) collapsed to a broad peak, and a small change was observed in the multiplet at 3.45 δ (H-8).

Interpretation of the Nuclear Magnetic Resonance Spectrum of the Major Cycloadduct

The n.m.r. spectrum of **7** ($CDCl_3$) at 100 MHz was described previously (1, 2). It was reported that the three methine protons gave rise to a complex multiplet at 3.54 δ, and the protons of the methylene group gave a multiplet at 2.65 δ, and this can be seen in Fig. 3A. No coupling constants could be measured from these multiplets. Since the geometry of the four-membered ring is known from our X-ray study, it seemed worthwhile to obtain values for the vicinal proton–proton coupling constants in this ring. Interpretation of cyclobutane p.m.r. spectra is difficult, in spite of the considerable amount of data which is available (11), and it was of interest to see if the spectrum of **7** could be interpreted by taking the shape of the cyclobutane ring into account (10).

During deuterium exchange experiments on **7**, using pyridine as solvent, it was noted that the methine multiplet was partially resolved at 100 MHz. By utilizing this solvent, which is known to shift protons near a polar functional group (12), and by use of a 220 MHz instrument, the three resonances in the methine multiplet were resolved. The coupling constants and chemical shifts are given in Table 3, and the spectra in pyridine (220 MHz) and in $CDCl_3$ (100 MHz) are shown in Fig. 3.

The vicinal coupling constants for H-1 and -7 (the latter assigned by deuterium exchange) are large (8.5–10.0 Hz), which is reasonable for structure **7**. There is no equatorial–equatorial splitting to these protons, and this apparently is the only vicinal coupling in cyclobutanes which can be small (10).

A repeat of the spin decoupling experiment

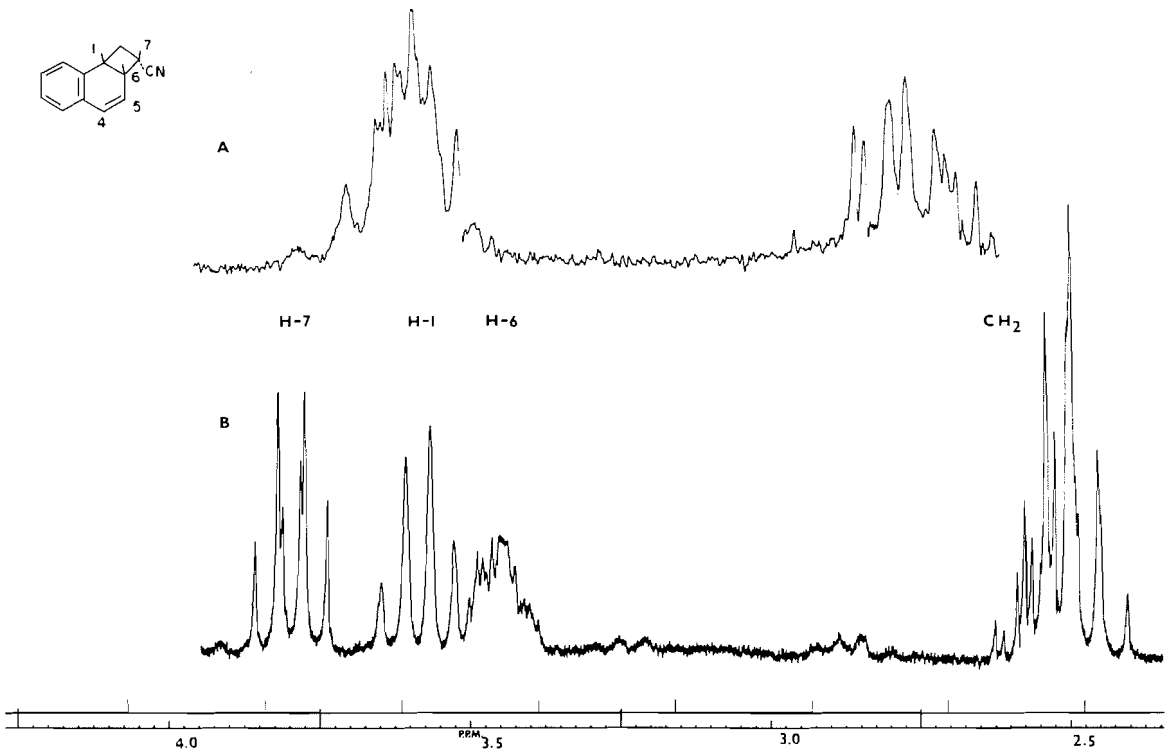

FIG. 3. N.m.r. spectra of cycloadduct **7**. (A) Spectrum at 100 MHz, $CDCl_3$ solvent; (B) spectrum at 220 MHz, pyridine solvent. The chemical shift scales for A and B are in approximate agreement, and chemical shifts should be taken from Table 2.

reported previously (2) revealed that the vinylic proton H-5 is coupled to the methine proton H-6, and not to the protons of the methylene group.

A discussion of the orientation in this photoaddition is included in the paper on substituent effects on the reaction (13).

Experimental

Materials

Reagents and solvents not listed here were obtained and purified as described previously (2). Acrylonitrile was Eastman Practical Grade, purified by the method of Bevington and Eaves (14).

Instrumentation

N.m.r. spectra were obtained with a Varian HA-100 instrument and chemical shifts are given in p.p.m. (δ) downfield from tetramethylsilane. I.r. spectra were run on a Beckman IR-5 or on a Perkin–Elmer 337 instrument. Mass spectra were normally measured on a Hitachi-Perkin–Elmer MRU 6 instrument. V.p.c. was carried out on a Varian 204B dual column instrument, using helium at 35 ml/min. Melting points were taken on a Kofler hot stage and are reported corrected. Microanalyses were by the Spang Microanalytical Laboratory, Ann Arbor, Michigan.

Photolysis of Naphthalene and Acrylonitrile

Naphthalene (1.025 g; 0.008 mol) and acrylonitrile (21.2 g, 0.4 mol) in 400 ml of 1:1 *tert*-butyl alcohol–*iso*-propyl alcohol were irradiated under argon, using the Hanovia 450 W lamp and a Pyrex filter, for 4 h. The solution was evaporated under vacuum, and the mixtures from seven identical runs were combined. The total crude yield was extracted with 250 ml of 5:1 hexane–ether mixture and filtered, and the filtrate was evaporated. The polymer-free mixture thus obtained was chromatographed on a 70 × 4.0 cm column of silica gel, slurry-packed in benzene, and eluted with this solvent. 200 ml fractions were collected. Fractions 1 and 2 contained naphthalene (2.15 g) and fractions 12–15 contained the substituted naphthalenes **1** and **2** (160 mg). The major cyclobutane **7** was found in fractions 16–29 (4.13 g, m.p. 97–98° from light petroleum). Fractions 30–40 contained the new cyclobutane, **8** mixed with **7** (total weight 750 mg). The latter fractions were combined and chromatographed on a 55 × 2.0 cm column of silica gel, again elution was with benzene, and 200 ml fractions were collected. Fractions 8–17 contained 500 mg of *8*, m.p. 55–60°, from light petroleum. The material was homogeneous by v.p.c. and t.l.c. Sublimation at 55–60°/0.1 mm, and further crystallization from light petroleum afforded *endo*-8-cyano-2,3-benzobicyclo[4.2.0]octa-2,4-diene (**8**), m.p. 56–58°.

Anal. Calcd. for $C_{13}H_{11}N$: C, 86.15; H, 6.12; N, 7.73. Found: C, 86.20; H, 6.12; N, 7.69.

TABLE 3. N.m.r. spectral data for cyclobutane adducts of naphthalene and acrylonitrile

Cyclobutane isomer	Chemical shifts,* multiplet structure,† coupling constant (*J*)‡						
	H-1	H-4	H-5	H-6	H-7(7′)	H-8(8′)	Other
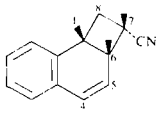 7	3.61,q* *J*=9.0	6.63,d *J*=10.0	5.93,dd *J*=10.0, 3.0	3.47,m*	3.82,dt* *J*=8.5, 10.0	2.55,m	7.0,m
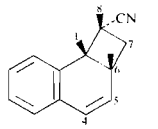 8	4.02,t *J*=9.0	6.37,dd *J*=10.0, ~1.0	5.75,dd *J*=10.0, 4.0	3.25 sym. m	2.25, 2.75 both m	3.55,ddt *J*=8.5, 6.0, 2.0	7.05, 7.20 both m
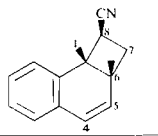 9	3.91,t *J*=9.0	6.40,dd *J*=10.0, 1.5	5.75,dd *J*=10.0, 3.5	3.25,m	2.25, 2.75 both m	3.35,dq *J*=9.0, 1.0	7.0–7.2 m

*Measured at 100 MHz using $CDCl_3$ as solvent, except for 7 where H-1, -6, and -7 resonances were resolved at 220 MHz in pyridine solution; shifts given in p.p.m. downfield from tetramethylsilane.
†m = multiplet; d = doublet; dd = doublet of doublets; dt = doublet of triplets; ddt = doublet of doublets of triplets; q = quartet.
‡Coupling constants (*J*) given in Hz.

In the i.r. the CN stretch showed at 2265 cm^{-1} (CCl_4). The n.m.r. spectrum is described in Table 2 and in the text. Analysis of the photolysis mixture by v.p.c. (5 ft × 1/8 in. of 5% QF-1 on Chromosorb W, at 170°) showed the following ratios and retention times: **7**, 89%, 3.4 min; **8**, 7.0% 3.9 min; **1** and **2**, 4.0%, 2.6 min. The peaks of **7** and **8** overlapped and the ratio was measured using a Dupont Analog Curve Resolver.

Epimerization of endo-8-Cyano-2,3-benzobicyclo[4.2.0-]octa-2,4-diene (8)

Compound **8** (130 mg, 0.717 mmol) was dissolved in 15 ml of 0.1 *M* potassium *tert*-butoxide in *tert*-butyl alcohol. The mixture was stirred at ambient temperature in a nitrogen atmosphere, and the aliquots were withdrawn periodically and analyzed by v.p.c. on the above QF-1 column. A new peak of retention time 2.9 min appeared, and after 4 h of reaction, the area of this peak showed no further increase with time. This peak is identified as **9**, and the equilibrium mixture of **8** and **9** contained 88% of the latter. After 6 h, the mixture was poured into ether, and the solution was washed with 0.5 *N* HCl, then with saturated NaCl solution, and dried ($MgSO_4$). The oil obtained on evaporation of the solvent was chromatographed on a 2 × 65 cm column of silica gel. Elution was with benzene and 200 ml fractions were collected. Fractions 5–8 contained **9** (101 mg, m.p. 46–48°) and **8** (15 mg) was recovered in fractions 10–16. *exo*-8-Cyano-2,3-benzobicyclo[4.2.0]octa-2,4-diene had the CN band at 2265 cm^{-1}, and the n.m.r. spectrum is described above. Sublimation at 60°/0.1 mm, and crystallization from light petroleum gave colorless prisms, m.p. 47–48°.

Anal. Calcd. for $C_{13}H_{11}N$: C, 86.15; H, 6.12; N, 7.73 Found: C, 86.26; H, 6.13; N, 7.67.

Since the retention times of **1**, **2** and **9** are very similar, it is difficult to know if **9** is formed in the photolysis. Since its presence was not noted during chromatography of the photolysis mixture, it can only be present in very minor amount.

Deuterium Exchange of endo-7-Cyano-2,3-benzobicyclo-[4.2.0]octa-2,4-diene (7)

To the cyano-compound **7** (20 mg) in dry pyridine (0.3 ml) was added 0.05 ml of 0.05 *M* NaOD, and the mixture was heated at 50° for 12 h. in an n.m.r. tube. Integration of the methine and methylene proton multiplets showed that one methine proton had been exchanged for deuterium. In this solution at 100 MHz the three methine proton resonances were partially resolved, and it was possible to identify the lowest field doublet of triplets with the proton removed by exchange.

Conversion of endo-7-Cyano-2,3-benzobicyclo[4.2.0]octa-2,4-diene (7) to endo-7-Carbomethoxy-2,3-benzobicyclo[4.2.0]octa-2,4-diene (4)

A mixture of methyl alcohol and anhydrous ether (7:20) (54 ml) at 0° was saturated with HCl from a tank by bubbling the gas through for 1 h. The cyano-compound **7** (1.0298 g, 0.00568 mol) was then added, and the solution was stirred (magnetic stirrer) for 8 h. Water (20 ml) was added dropwise at 0°, the mixture was warmed at 25°, and stirred 3 h. On pouring into water (500 ml) and extracting with ether, 144 mg of ester **4** was obtained. On allowing the aqueous layer from the extraction to stand 12 h, crystals of **4** (891 mg) m.p. 84–89° were deposited. The combined products were crystallized from ethanol–water to afford *endo*-7-carbomethoxy-2,3-benzobicyclo[4.2.0]octa-2,4-diene, 1.0200 g, 84%, m.p. 91–93°.

Anal. Calcd. for $C_{14}H_{14}O_2$: C, 78.48; H, 6.59. Found: C, 78.44; H, 6.63.

$LiAlH_4$ Reduction of endo-7-Carbomethoxy-2,3-benzobicyclo[4.2.0]octa-2,4-diene

The ester **4** (700 mg, 3.267 mmol) in ether (20 ml) was added dropwise to a stirred slurry of lithium aluminum

TABLE 4. Atomic parameters of the *p*-bromophenylurethane derivative

Atom	*x*	*y*	*z*	*B*(Å²)
Br	0.3752(2)	0.0754(7)	1.4106(3)	*
O-1	0.7541(10)	0.047(3)	0.891(1)	4.7(3)
O-2	0.674(1)	0.382(3)	0.973(1)	6.1(4)
N	0.661(1)	−0.047(3)	1.036(1)	3.8(4)
C-1	1.011(1)	0.101(4)	0.672(2)	4.4(5)
C-2	1.099(1)	0.287(4)	0.673(2)	4.2(6)
C-3	1.122(2)	0.436(4)	0.769(2)	4.2(5)
C-4	1.064(2)	0.369(5)	0.865(2)	5.2(6)
C-5	0.994(2)	0.181(4)	0.876(2)	4.9(6)
C-6	0.965(2)	0.004(4)	0.781(2)	4.8(5)
C-7	0.861(1)	0.075(4)	0.741(2)	4.8(5)
C-8	0.913(1)	0.240(4)	0.650(2)	4.8(5)
C-9	1.152(2)	0.334(5)	0.581(2)	5.9(6)
C-10	1.231(2)	0.536(5)	0.578(2)	6.6(6)
C-11	1.249(2)	0.677(5)	0.670(2)	5.7(6)
C-12	1.198(2)	0.630(5)	0.763(2)	5.4(6)
C-13	0.788(1)	0.229(4)	0.808(2)	4.1(5)
C-14	0.696(2)	0.139(5)	0.966(2)	4.5(5)
C-15	0.594(1)	−0.010(4)	1.118(2)	3.9(5)
C-16	0.521(1)	0.192(4)	1.120(2)	4.5(5)
C-17	0.457(1)	0.210(4)	1.208(2)	4.6(5)
C-18	0.460(2)	0.035(5)	1.293(2)	5.5(6)
C-19	0.533(2)	−0.159(5)	1.293(2)	6.1(6)
C-20	0.597(2)	−0.183(5)	1.206(2)	5.3(6)

*Anisotropic thermal components (Å²) for Br are:

B_{11}†	B_{22}	B_{33}	B_{12}	B_{13}	B_{23}
7.06	10.03	8.18	−0.64	0.94	−1.28

†The expression for the thermal ellipsoid used in the structure amplitude calculations includes the terms

$$\exp[-\tfrac{1}{4}(h^2a^{*2}B_{11} + 2hka^*b^*B_{12} + \ldots.)].$$

hydride (2.0 g) in ether (100 ml). The mixture was stirred and heated under reflux for 12 h. Excess hydride was decomposed by the dropwise addition of water, and the ether was filtered and dried ($MgSO_4$). Evaporation gave an oil (524 mg, 85%) which declined to crystallize, but showed a broad i.r. absorption in the 3000–3500 cm^{-1} region (OH). This was assumed to be 2,3-benzobicyclo-[4.2.0]octa-2,4-dienyl-*endo*-7-carbinol (**5**) and was converted to the required derivative without further purification.

Preparation of the p-Bromophenylurethane of Carbinol (7)

The carbinol **5** (245 mg, 1.287 mmol) dried by azeotropic distillation of benzene, and *p*-bromophenylisocyanate (274 mg, 1.383 mmol) in cyclohexane (20 ml) were heated under reflux for 1 h. Crystals were deposited while the solution was still hot. The mixture was cooled and filtered to afford 272 mg (55%) of the *p*-bromophenylurethane of **5**, which gave needles, m.p. 155–157°, from 95% ethanol.

Anal. Calcd. for $C_{20}H_{18}O_2NBr$: C, 62.50; H, 4.72; N, 3.65; Br, 20.80. Found: C, 62.43; H, 4.64; N, 3.54; Br, 20.92.

These crystals were used in the X-ray study described below.

Description of X-ray Work on p-Bromophenylurethane (6)

Crystal Data

$C_{20}H_{18}O_2NBr$ f.w. = 384.26

Triclinic, space group $P\bar{1}$ with $a = 13.85(1)$, $b = 4.976(2)$, $c = 12.752(4)$ Å, $\alpha = 90.80(3)$, $\beta = 87.02(6)$, $\gamma = 90.99(5)°$, $V = 877.44$ Å³ $D_o = 1.39 \pm 0.08$ g/cm³, $Z = 2$, $D_c = 1.45$ g/cm³ (20 °C, λ(MoKα) = 0.71069 Å).

The derivative was crystallized from methanol–chloroform to obtain suitable plate-shaped crystals. The dimensions of the unit cell were obtained from a least-squares refinement of 15 values of 2θ measured with MoKα radiation using a Syntex automatic diffractometer. The calculated density assuming two molecules per unit cell agrees with the density measured using a solution of potassium iodide in water, and this leads to the space group $P\bar{1}$.

A crystal with dimensions 0.02 × 0.03 × 0.08 mm was used to collect data on the Syntex diffractometer. The MoKα used for intensity data collection was monochromatized using graphite. All the data are a hemisphere with a maximum radius defined by $2\theta \leq 35°$ were recorded using a θ–2θ scan with a scan rate determined by the intensity at the peak and scan range dependent upon the value of θ. Backgrounds were recorded on either side of the peak and used to determine the integrated

intensity together with an estimated standard deviation based upon counting statistics. The final reflections whose intensity were less than 36 were regarded as unobserved. Of the total 1113 reflections, 651 had observable intensities. The data were corrected for Lorentz and polarization but not absorption.

The bromine atom position was determined from the Patterson function. The signs determined from the subsequent structure factor calculation were used to calculate an electron density map from which the remaining atoms were found. The structure was further refined utilizing full matrix least squares programs. This and other calculations were done using 'X-ray 67' program system for X-ray crystallography published by the University of Maryland and adopted for use with the CDC 6400 by H. D. Grundy. The atomic scattering curves were taken from the International Tables for X-ray Crystallography (15). Weights, ω, were chosen so that $\omega|F_o - F_c|^2$ would locally be independent of the, F_o, observed structure factor and the function obtained was $\omega = [15 - 0.05|F_o|]^{-1/2}$. The unobserved reflections were weighted as the observed were and also included in the refinement. The final R value is 0.105 while the least-squares residual is 0.115.[1] The refinement was terminated when the calculated shifts were less than 1/3 of the estimated standard deviations. A final difference synthesis showed no missing structural features although peaks as 1/5 of a carbon atom were noted.

The final atomic parameters are recorded in Table 4, and the observed and calculated structure factors are compared in Table 5.[2] Table 1 contains a list of the pertinent bond lengths and angles with standard deviations calculated from the standard errors derived from the least-squares matrix. The structure is shown in Fig. 1.

We thank Mr. B. Sawyer for obtaining the 100 MHz n.m.r. spectra, and Dr. A. Grey and Mrs. V. Robinson of the Canadian 220 MHz n.m.r. center for the 220 MHz spectrum of 7. We are grateful to Dr. Grey for drawing our attention to ref. 10, and to Dr. R. F. Childs for suggesting the conditions for deuterium exchange of 7. We thank the National Research Council of Canada for financial support.

[1]The weighted $R = \left\{\frac{\Sigma\omega|F_o - F_c|^2}{\Sigma\omega|F_o^2}\right\}^{1/2}$

[2]These tabular data (Table 5) are available from the Depository of Unpublished Data, National Science Library, National Research Council of Canada, Ottawa, Canada K1A 0S2.

1. J. J. McCULLOUGH, C. CALVO, and C. W. HUANG. Chem. Commun. 1176 (1968).
2. J. J. McCULLOUGH and C. W. HUANG. Can. J. Chem. **47**, 757 (1969).
3. R. M. BOWMAN, T. R. CHAMBERLAIN, C. W. HUANG, and J. J. McCULLOUGH. J. Am. Chem. Soc. **92**, 4106 (1970).
4. R. M. BOWMAN and J. J. McCULLOUGH. Chem. Commun. 948 (1970).
5. R. M. BOWMAN, J. J. McCULLOUGH, and J. S. SWENTON. Can. J. Chem. **47**, 4503 (1969).
6. T. UEDA and T. SHIMANOUCHI. J. Chem. Phys. **49**, 470 (1968).
7. (*a*) H. P. LEMAIRE and R. L. LIVINGSTON. J. Am. Chem. Soc. **74**, 5732 (1952); (*b*) T. B. OWEN and J. L. HOARD. Acta Cryst. **4**, 172 (1951); (*c*) W. G. ROTHSCHILD and B. P. DAILEY. J. Chem. Phys. **36**, 2931 (1962); (*d*) J. B. LAMBERT and J. D. ROBERTS. J. Am. Chem. Soc. **85**, 3710 (1963).
8. E. L. ELIEL, N. L. ALLINGER, S. J. ANGYAL, and G. A. MORRISON. *In* Conformational analysis. Interscience Publishers, New York. 1965. pp. 199–200; J. M. CONIA, J. L. RIPOL, L. A. TUSHAUS, C. L. NEUMANN, and N. L. ALLINGER. J. Am. Chem. Soc. **84**, 4982 (1962).
9. G. SUGOWDZ, P. J. COLLIN, and W. H. F. SASSE. Tetrahedron Lett. 3843 (1969); M. L. GROSS and C. L. WILKINS. Tetrahedron Lett. 3875 (1969); N. SUGIYAMA, Y. SATO, and C. KASHIMA. Bull. Chem. Soc. Jap. **43**, 3205 (1970); P. SINGH. J. Org. Chem. **36**, 3334 (1971).
10. E. B. WHIPPLE and G. R. EVANEGA. Org. Mag. Res. **2**, 1 (1970).
11. (*a*) I. FLEMING and D. H. WILLIAMS. Tetrahedron, **23**, 2747 (1967). (*b*) L. PAOLILLO, H. ZIFFER, and O. BUCHARDT. J. Org. Chem. **35**, 38 (1970).
12. P. V. DEMARCO, E. FARKAS, D. DODDRELL, B. L. MYLARI, and E. WENKERT. J. Am. Chem. Soc. **90**, 5480 (1968), and refs. cited therein.
13. T. R. CHAMBERLAIN, J. J. McCULLOUGH, and J. K. SAUNDERS. Can. J. Chem. Submitted.
14. J. C. BEVINGTON and D. E. EAVES. Trans. Faraday Soc. **55**, 1777 (1957). *Cited in* L. F. FIESER and M. FIESER, Reagents for organic synthesis. John Wiley and Sons, Inc., New York, N.Y. 1967. p. 14.
15. International Tables for X-ray Crystallography. Volume III. Kynoch Press, Birmingham, England. 1962.

Oligoribonucleotide Synthesis. V.[1] Preparation of 2′-O-Tetrahydropyranyl Derivatives of Guanosine and Their Insertion into a General Stepwise Synthesis

THOMAS NEILSON, EDWARD V. WASTRODOWSKI, AND EVA S. WERSTIUK

Department of Biochemistry, McMaster University, Hamilton, Ontario

Received September 7, 1972

The syntheses of N^2-benzoyl-2′-*O*-tetrahydropyranylguanosine (**5**) and its corresponding 5′-*O*-triphenylmethoxyacetyl derivative (**6**) are described. Compounds **5** and **6** are the protected derivatives of guanosine required for insertion into a phosphotriester synthesis for oligoribonucleotides. Syntheses of GpC and GpG were carried out to illustrate incorporation of **5** and **6** into a sequence.

Les synthèses de la *N*-benzoyl-2 *O*-tetrahydropyranyl-2′ guanosine (**5**) et de son dérivé *O*-triphénylmethoxyacétyl-5′ correspondant (**6**) ont été décrites. Les composés **5** et **6** sont des dérivés protégés de la guanosine requis pour l'insertion dans la synthèse d'un phosphotriester d'oligoribonucléotides. Les synthèses du GpC et GpG ont été realisées pour illustrer l'incorporation de **5** et **6** dans une séquence.
[Traduit par le journal]

Can. J. Chem., 51, 1068 (1973)

Oligoribonucleotides isolated from enzymic digestions of native RNAs vary in length and sequence. In order to synthesize any of these fragments or their modifications, for example, single base changes, a general synthesis for oligoribonucleotides of any length and sequence, is essential.

In one of our previous communications (2), a convenient stepwise synthesis for protected triribonucleotides of predetermined sequence containing adenine, cytosine, and uracil base residues, was described. Corresponding 2′-*O*-tetrahydropyranyl-nucleoside derivatives were coupled together using β,β,β-trichloroethyl 3′-5′-phosphotriester linkages to give protected triribonucleotide derivatives which on deblocking gave free trinucleoside diphosphates.

In this communication we report the syntheses of 2′-*O*-tetrahydropyranylguanosine derivatives and their incorporation into some sample diribonucleotides. This extension of our previous studies allows the assembly of sequences containing the guanine base residue at any position within the sequence and not just at the 3′-terminal position.

Since the *N*-benzamide grouping was used to protect adenine and cytosine bases in these current studies, it seemed the logical choice for protection of the 2′-amino group of guanosine. As well as giving better solubility to intermediates, the benzoyl group should provide more stable protection than would the acetyl group which has been used in earlier synthesis (3).

N^2-Benzoylguanosine (**1**) (4) was treated with excess trimethyl orthoacetate in the presence of *p*-toluenesulfonic acid to give the cyclic orthoacetate derivative **2** as the major product (see Scheme 1). Immediate benzoylation using benzoyl chloride in anhydrous pyridine converted **2** to its corresponding 5′-*O*-benzoate ester (**3**). Aqueous acetic acid cleaved the orthoacetate ring to give a mixture of the 2′- and 3′-acetates of N^2-5′-*O*-dibenzoyl guanosine in 67% overall yield. P.m.r. analysis of the acetate methyl signals revealed a 1:1 mixture. Fractional crystallization from ethanol gave pure 3′-*O*-acetyl-N^2-benzoylguanosine (**4**) in 40% yield. Routine reaction of **4** with dihydropyran followed by careful de-*O*-benzoylation gave a diastereoisomeric mixture of N^2-benzoyl-2′-*O*-tetrahydropyranylguanosine (**5**). Silica gel chromatographic resolution of this mixture gave low R_F isomer **5***a* (50% yield) and high R_F isomer **5***b* (20% yield).

In accordance with normal practice, the less soluble low R_F isomer **5***a* was used exclusively for the 5′-terminal position of a short sequence to be assembled by stepwise synthesis, while the more soluble isomer **5***b* was "ear-marked" for guanosine insertion in positions other than the 5′-terminal slot. Before **5***a* could be incorporated into a sequence, conversion to its 5′-*O*-triphenylmethoxyacetate (**6**) was necessary to ensure phosphorylation only at the 3′-hydroxyl. This

[1]For part IV, see ref. 1.

Can. J. Chem. Downloaded from www.nrcresearchpress.com by 210.87.254.105 on 09/05/12
For personal use only.

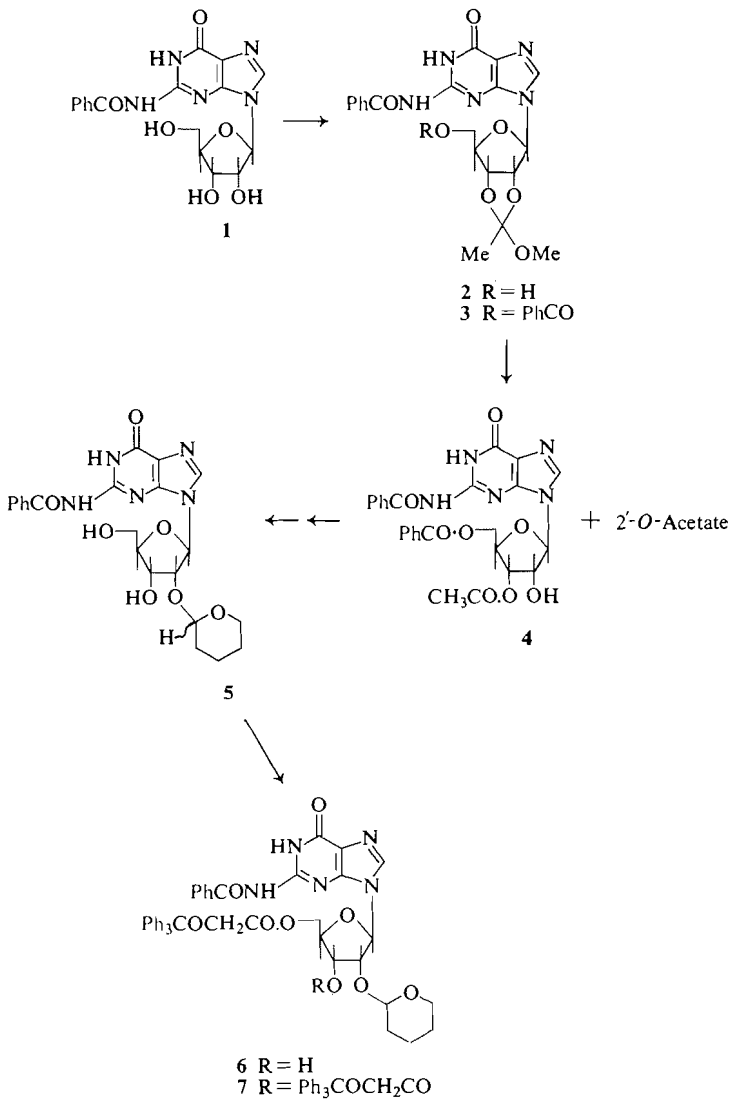

SCHEME 1

protecting group can be cleaved specifically using very dilute alkaline treatment (1). Once a protected di- or triribonucleotide has been prepared starting with **6** and coupling successive 2′-*O*-tetrapyranylnucleoside derivatives by means of 3′–5′-phosphotriester linkages, regeneration of its 5′-terminal hydroxyl would allow the partially deblocked di- or trinucleotides to participate in block synthesis, thus giving much longer oligoribonucleotides.

Treatment of **5***a* with sodium triphenylmethoxyacetate (1) and tri-isopropylbenzenesulfonyl chloride (TPS) in pyridine gave the desired product (**6**) in 52% yield accompanied by some disubstituted material (**7**) (16%) (see Scheme 2). Dilute aqueous ammonia treatment on **6** regenerated **5***a* completely within 2 h. Further treatment (>2.5 h) resulted in detectable hydrolysis of the benzamide grouping. This difference in hydrolysis rates will guarantee selective cleavage of the trityloxyacetyl group at the oligoribonucleotide level.

The bis-cyclohexylammonium salt of β,β,β-trichloroethyl phosphate (5) was converted to its corresponding pyridinium salt and activated in pyridine using 2 equiv of TPS. Phosphoryla-

Can. J. Chem. Downloaded from www.nrcresearchpress.com by 210.87.254.105 on 09/05/12
For personal use only.

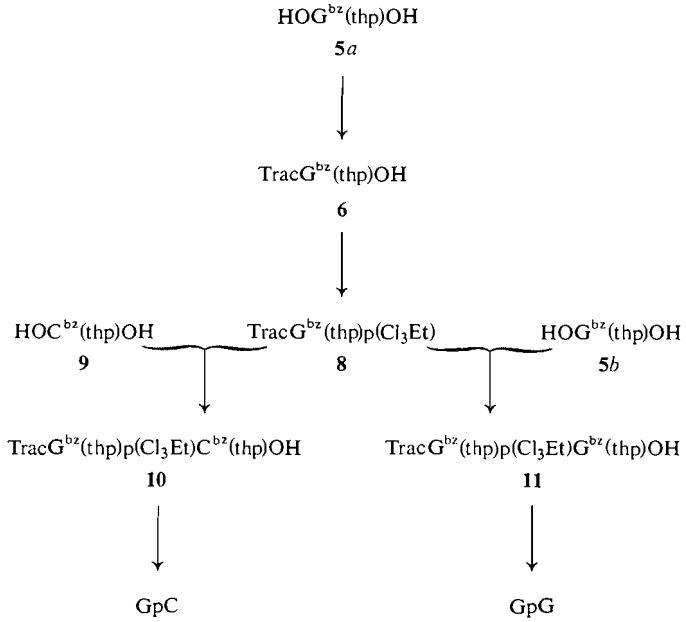

SCHEME 2

tion of **6** was carried out in pyridine to give protected Gp **8** as its pyridinium salt. Immediate activation with 1 equiv of TPS and coupling with the 5′-hydroxyl of the higher R_F diastereoisomer of N^4-benzoyl-2′-*O*-tetrahydropyranylcytidine (**9**) (6) gave protected GpC **10**[2] in 30% yield over two steps. In another experiment protected Gp **8** was coupled to the 5′-hydroxyl of the higher R_F diastereoisomer of N^2-benzoyl-2′-*O*-tetrahydropyranylguanosine (**5***b*) to give protected GpG **11** in 28% yield over the two steps. These yields were lower than the previous protected dinucleotide preparations; however, in both couplings substantial percentages of protected Gp **8**, 35 and 38% respectively, were left unreacted and recovered. Apparently, reaction of TPS with the incoming nucleoside derivative competes with phosphotriester formation involving protected Gp **8**. Protected dinucleotide derivatives **10**[2] and **11** appeared as elongated spots on t.l.c. because each in reality is a diastereoisomeric pair resulting from the asymmetry of 3′–5′-phosphotriesters. No attempt was made to resolve these pairs as the chirality disappears on deblocking (1).

Complete deblocking of **10** and **11** using the three-step procedure described previously (2) gave the free dinucleoside phosphates, GpC and GpG, respectively, in *ca.* 80%.

Snake venom diesterase treatment on GpC gave G and pC in the correct ratio, similarly GpG gave G and pG. Complete digestions in each case confirmed the fidelity of the 3′–5′-diphosphate linkages (< 1% 2′–5′ linkage) thus confirming that specific 2′-*O*-tetrahydropyranyl protection exists in the guanosine derivatives, **5** and **6**.

Experimental

The p.m.r. spectra were recorded on a Varian T60 or Varian HA-100 spectrometer in 10–15% (w/v) DMSO-d_6 – D_2O solutions, and line positions are reported in p.p.m. from the reference (TMS).

Silica gel (Baker Analyzed Reagent) was used for column chromatography; and Analtech prescored silica gel plates were employed for t.l.c. The plates were usually developed in 5 or 10% methanol in methylene chloride mixtures. The t.l.c. detection was carried out using a ceric sulfate spray (1 g $H_4Ce(SO_4)_4$ in 10% aqueous sulfuric acid solution) and followed by heating the plates at 300–400 °C. Compounds containing a trityl group develop as yellow spots, while others appear as brown colorations.

[2]To condense the large structural formulae necessary to describe protected dinucleotides shown in Scheme 2, a shorthand method suggested by the IUPAC–IUB commission on Biochemical Nomenclature is adopted (8).

For example, N^2-benzoyl-2′-*O*-tetrahydropyranyl-5′-*O*-triphenylmethoxyacetylguanylyl (3′-β,β,β-trichloroethyl-5′)N^4-benzoyl-2′-*O*-tetrahydropyranylcytidine can be written as TracG^{bz}(thp)p(Cl$_3$Et)C^{bz}(thp)OH where Trac is trityloxyacetyl.

Can. J. Chem. Downloaded from www.nrcresearchpress.com by 210.87.254.105 on 09/05/12
For personal use only.

TABLE 1. The R_{Up}'s of free dinucleotides and markers

Compound	Paper chromatography (Whatman No. 1) solvent A	Thin layer chromatography		
		Solvent A	Solvent B	Solvent C
GpC	0.95 (0.94)*	0.90	0.33	1.06
GpG	0.78 (0.80)*	0.67	0.23	
Up	1.0	1.0	1.0	1.0
G	1.81	4.9	1.52	3.5
pC	0.70	0.23	0.74	0.62
pG	0.50	0.21	0.48	

*Literature values ref. 7.

Paper chromatography was performed using the descending technique on Whatman No. 1 or 3 MM paper. Analtech pre-coated cellulose plates (Avicel F) were used for t.l.c. of deblocked nucleotides. The solvent systems employed for paper chromatography and t.l.c. on cellulose were (A) ethanol – 1 *M* ammonium acetate, p*H* 7.5 (7:3, v/v); (B) 1-BuOH – glacial HOAc – H_2O (5:3:2, v/v); (C) 2-PrOH – concentrated NH_4OH – H_2O (7:1:2, v/v). A short wave u.v. lamp was used for detection.

It was essential that moisture be excluded from all coupling reactions. After evaporation *in vacuo* of the pyridine solution, normal pressure was restored with dry nitrogen and *not* atmospheric air. All such evaporations were carried out in the temperature range of 30–40 °C.

Emulsion, frequently obtained during methylene chloride extractions of aqueous pyridine solutions, was broken by the addition of a few milliliters of saturated sodium chloride solution.

N^2-Benzoyl-2′,3′-O-methoxyethylideneguanosine (2)

Trimethyl orthoacetate (10.0 ml) was added to a stirred suspension of N^2-benzoylguanosine (4) (3.75 g, 9.70 mmol) and *p*-toluenesulfonic acid monohydrate (0.2 g, 1.05 mmol) in anhydrous dimethylformamide (7.5 ml). After 30 min, t.l.c. indicated *ca.* 50% conversion into a major product (R_F 0.06 → 0.5 in 10% CH_3OH–CH_2Cl_2). Further addition of *p*-toluenesulfonic acid monohydrate (0.2 g, 1.05 mmol) completed the reaction. The mixture was then cooled and neutralized with concentrated ammonia solution, then evaporated *in vacuo* to half volume. Pyridine (10 ml) was added and this solution was used for the next reaction without any further purification.

N^2-5′-O-Dibenzoyl-2′,3′-O-methoxyethylideneguanosine (3)

Benzoyl chloride (2.5 ml, 21 mmol) was added dropwise, with stirring to a cooled (ice) solution containing N^2-benzoyl-2′,3′-*O*-methoxyethylideneguanosine (**2**) prepared above. After 30 min, t.l.c. indicated complete conversion into a major product of R_F 0.85 in 10% CH_3OH–CH_2Cl_2. Ice (*ca.* 5 g) was then added, and after 30 min the reaction mixture was poured into ice-water (50 ml) and repeatedly extracted with methylene chloride (3 × 25 ml). The combined organic extracts were washed with saturated sodium bicarbonate solution (50 ml), followed by water (2 × 25 ml) and evaporated *in vacuo* to a yellow oil (R_F 0.85 in 10% CH_3OH–CH_2Cl_2) which was used in the next reaction without further purification.

3′-O-Acetyl-N^2-5′-O-dibenzoylguanosine (4)

A mixture of crude N^2-5′-*O*-dibenzoyl-2′,3′-*O*-methoxyethylideneguanosine (**3**) prepared above, and 10% acetic acid (25 ml) was stirred at room temperature. After 16 h t.l.c. indicated complete reaction (R_F 0.85 → 0.63 in 10% CH_3OH–CH_2Cl_2). The reaction mixture was then repeatedly extracted with methylene chloride (3 × 25 ml), the combined organic extracts were washed with saturated sodium bicarbonate solution (50 ml) and evaporated to dryness *in vacuo*. The yellow glass (4 g) was purified by chromatography on silica gel (100 g) in methylene chloride. Elution with 3.0 (1 l) and 3.5% (1 l) methanol – methylene chloride mixtures gave a mixture of 2′ and 3′-*O*-acetates (3.5 g, 67%; R_F 0.64 in 10% CH_3OH–CH_2Cl_2). The p.m.r. spectrum of the mixture showed signals (δ TMS) at 6.2 (1H, doublet; $J \simeq 4.5$ Hz; 1′-anomeric proton of 2′-*O*-acetate); 6.0 (1H doublet; $J \simeq 6.0$ Hz; 1′-anomeric proton of 3′-*O*-acetate); 2.20 (3H, sharp singlet; 3′-$COCH_3$ protons); and 2.15 (3H, sharp singlet; 2′-$COCH_3$ protons). The p.m.r. spectrum indicated a *ca.* 1:1 mixture of the two isomeric acetates. Pure 3′-*O*-acetyl-N^2-5′-*O*-dibenzoylguanosine (**4**), (2.10 g, 40%; m.p. 214–216°) was obtained by crystallization from absolute ethanol. The p.m.r. spectrum showed signals (δ TMS) at 8.25 (1H, singlet, 8 proton of G); 8.2–7.4 (10H, multiplet; two C_6H_5CO protons); 6.00 (1H, doublet; $J \simeq 6.0$ Hz; 2′-sugar proton) and at 2.20 p.p.m. (3H, sharp singlet; CH_3CO protons).

Anal. Calcd. for $C_{26}H_{23}N_5O_8$ (mol. wt. 533.30): C, 58.54; H, 4.35; N, 13.13. Found: C, 58.80; H, 4.27; N, 13.14.

Concentration of the mother liquor to a small volume yielded only varying mixtures of N^2-5′-*O*-dibenzoyl-2′,(3′)-*O*-acetates.

N^2-Benzoyl-2′-O-tetrahydropyranylguanosine (5)

A solution of *p*-toluenesulfonic acid monohydrate (0.20 g; 1.1 mmol) in dry dioxan (20 ml) containing molecular sieves (0.4 g) was cooled in ice until solidified. Dihydropyran (7.37 g, 8 ml; 88 mmol) was then added dropwise with stirring, followed by a suspension of 3′-*O*-acetyl-N^2-5′-*O*-dibenzoylguanosine (**4**) (2.13 g; 4.0 mmol; m.p. 215°, R_F 0.63 in 10% CH_3OH–CH_2Cl_2) in dry dioxan (20 ml). After 2 h the reaction was allowed to return to room temperature and t.l.c. indicated formation

Can. J. Chem. Downloaded from www.nrcresearchpress.com by 210.87.254.105 on 09/05/12
For personal use only.

Can. J. Chem. Downloaded from www.nrcresearchpress.com by 210.87.254.105 on 09/05/12
For personal use only.

of a major product (R_F 0.75 in 10% CH_3OH–CH_2Cl_2). This colorless solution was cooled in ice, and neutralized with concentrated ammonia. The precipitated ammonium tosylate was filtered off, washed well with methylene chloride, and the combined filtrate and washings evaporated *in vacuo* to give a yellow oil which was dissolved in a mixture of ethanol (20 ml) and pyridine (10 ml). Ethanolic sodium hydroxide (containing 10 ml 2 *N* NaOH and 10 ml absolute ethanol) was added with stirring. After 5 min t.l.c. indicated two products of R_F 0.35 and 0.30 in 10% CH_3OH–CH_2Cl_2 in the approximate proportion of 2:3. The p*H* of the solution was then adjusted to *ca.* 7.0 with Dowex 50W-X8 resin (pyridinium form). The resin was filtered off, washed well with ethanol, and the combined filtrate and washings evaporated *in vacuo*. The resulting mixture of diastereoisomers (**5**) was separated on silica gel (60 g) in methylene chloride. Elution with 2.5% methanol – methylene chloride mixture (500 ml) yielded the low m.p. diastereoisomer **5***b* (0.375*g*, 20%; R_F 0.35 in 10% CH_3OH–CH_2Cl_2). Continued elution with 3.0–3.5% methanol – methylene chloride mixtures (500 ml + 500 ml) gave a mixture of diastereoisomers (0.30 g, R_F 0.35 and 0.30 in 10% CH_3OH–CH_2Cl_2). Finally, the high m.p. diastereoisomer **5***a* (0.94 g, 50%; R_F 0.30 in 10% CH_3OH–CH_2Cl_2) was obtained on elution with 3.5–4.0% methanol – methylene chloride mixtures (500 ml + 500 ml). Total yield of **5***a* and *b* was 86%. An analytically pure sample of the high R_F diastereoisomer **5***b* of m.p. 152–154°, R_F 0.35 was obtained by crystallization from ethyl acetate containing a trace of methanol. Its p.m.r. spectrum showed signals (δ TMS) at 8.40 1H, singlet, 8 proton of G); 8.2–7.4 (5H, multiplet, C_6H_5CO protons); 6.18 (1H, doublet, $J \simeq 7.0$ Hz; 1′-anomeric proton); 5.00 (1H, multiplet, 2′-sugar proton); and a broad peak at 1.50 p.p.m. (6H, multiplet, thp protons).

Anal. Calcd. for $C_{22}H_{25}N_5O_7.H_2O$ (mol. wt. 489.49): C, 53.98; H, 5.56; N, 14.31. Found: C, 53.95; H, 5.58; N, 14.12.

Crystallization from ethyl acetate – methanol (2:1) provided an analytical sample of m.p. 192–194° of the other isomer (**5***a*) of R_F 0.30. Its p.m.r. spectrum showed signals (δ TMS) at 8.38 (1H, singlet, 8 proton of G); 8.2–7.4 (5H, multiplet, C_6H_5CO protons); 6.15 (1H, doublet, $J \simeq 8$Hz; 1′-anomeric proton); 5.20 (1H, multiplet, 2′-sugar proton); and a broad peak at 1.50 p.p.m. (6H, multiplet, thp protons).

Anal. Calcd. for $C_{22}H_{25}N_5O_7.H_2O$ (mol. wt. 489.49): C, 53.95; H, 5.56; N, 14.31. Found: C, 54.12; H, 5.54; N, 14.27.

N^2-Benzoyl-2′-O-tetrahydropyranyl-5′-O-triphenylmethoxyacetylguanosine (6)

Sodium triphenylmethoxyacetate (1) (550 mg, 1.72 mmol) was evaporated *in vacuo* from anhydrous pyridine (3 × 15 ml), and finally its volume reduced to *ca.* 5 ml. The solution was sealed under nitrogen, TPS (236 mg, 0.78 mmol) added, and the reaction mixture allowed to stand at room temperature for 2 h. The low R_F diastereoisomer of N^2-benzoyl-2′-*O*-tetrahydropyranylguanosine (**5***a*) (0.336 g, 0.72 mmol; R_F 0.30 in 10% CH_3OH–CH_2Cl_2) was evaporated from anhydrous pyridine (3 × 15 ml) and finally its volume reduced to *ca.* 5 ml. This solution was then added to the triphenylmethoxyacetic acid – TPS complex (prepared above), and the reaction set aside at room temperature for 1–2 days in the dark. Further portions of TPS (2 × 50 mg) were added to ensure complete esterification. After 5 days t.l.c. indicated complete conversion into a product (R_F 0.30 → 0.65 in 10% CH_3OH–CH_2Cl_2). Ice (*ca.* 2 g) was then added, and the mixture stirred for a further hour. The reaction mixture was then poured into ice-water (40 ml) and repeatedly extracted with methylene chloride (3 × 10 ml). The combined organic extracts were washed, and evaporated to dryness *in vacuo*. The yellow glass obtained was purified by chromatography on silica gel (20 g) in methylene chloride. Elution with 1.0% methanol – methylene chloride mixture (500 ml) yielded N^2-benzoyl-3′,5′-*O*-di-triphenylmethoxyacetyl-2′-*O*-tetrahydropyranylguanosine (**7**) (120 mg, 16%; R_F 0.85 in 10% CH_3OH–CH_2Cl_2). The p.m.r. spectrum of **7** showed signals (δ TMS) at 8.20 (1H, singlet; 8 proton of G); 9.2–7.4 (35H, multiplet; C_6H_5CO and trityl aromatic protons); 6.00 (1H, doublet; $J \simeq 7$ Hz, 1′-anomeric proton); 5.5 (1H, multiplet; 2′-sugar proton); 5.1 (1H, multiplet; 3′-sugar proton); 3.8 (4H, singlet; —OCH_2CO protons); and a broad peak at 1.5 p.p.m. (6H, multiplet; thp protons). Pure N^2-benzoyl-2′-*O*-tetrahydropyranyl-5′-*O*-triphenylmethoxyacetylguanosine (**6**) (0.282 g, 52% R_F 0.66 in 10% CH_3OH–CH_2Cl_2) was obtained on elution with 2.0–2.5% methanol – methylene chloride mixtures. An analytically pure sample of **6** of m.p. 110° (dec.) was prepared by crystallization from methylene chloride – hexane. The p.m.r. spectrum showed signals (δ TMS) at 8.25 (1H, singlet; 8 proton of G); 8.2–7.1 (20H, multiplet; C_6H_5CO and trityl aromatic protons); 6.14 (1H, doublet; $J \simeq 6$Hz, 1′-anomeric proton); 5.45 (1H, multiplet; 2′-sugar proton); 4.75 (1H, multiplet; 3′-sugar proton); 3.8 (2H, singlet; —OCH_2CO protons); and 1.5 p.p.m. (6H, multiplet; thp protons).

Anal. Calcd. for $C_{43}H_{41}N_5O_9$ (mol. wt. 771.83): C, 66.92; H, 5.35; N, 9.07. Found: C, 67.03; H, 5.46; N, 8.98.

N^2-Benzoyl-2′-*O*-tetrahydropyranyl-5′-*O*-triphenylmethoxyacetylguanosine (**6**) (3 mg, R_F 0.65 in 10% CH_3OH–CH_2Cl_2) was dissolved in dilute methanolic ammonia (0.3 ml, prepared by 100-fold dilution of concentrated ammonia with methanol) and stirred at room temperature. After 2 h, t.l.c. indicated complete regeneration of starting material (**5***a*) (R_F 0.31 in 10% CH_3OH–CH_2Cl_2). After 2.5 h, t.l.c. indicated the appearance of a further product (R_F 0.24 in 10% CH_3OH–CH_2Cl_2) obtained by hydrolysis of the benzamide group.

N^2-Benzoyl-2′-O-tetrahydropyranyl-5′-O-triphenylmethoxyacetylguanosine-3′-β,β,β-trichloroethyl phosphate (8)

Bis-cyclohexylamine salt (360 mg, 0.81 mmol; 3 equiv) of mono-β,β,β-trichloroethyl phosphate (5) was dissolved in anhydrous pyridine (20 ml) with warming, and converted to its pyridinium salt by repetitive evaporation *in vacuo* and solution in pyridine (5 × 20 ml). TPS (496 mg, 1.62 mmol; 6 equiv) was then added to the pyridinium salt in pyridine (10 ml). After 1 h, a pyridine solution of N^2-benzoyl-2′-*O*-tetrahydropyranyl-5′-*O*-triphenylmethoxyacetylguanosine (**6**) (200 mg, 0.27 mmol; 1 equiv; R_F 0.65 in 10% CH_3OH–CH_2Cl_2) was added to the yellow solution and the reaction mixture sealed under nitrogen and set aside at room temperature in the dark. After 1.5 days, t.l.c. indicated complete conversion into a product

Can. J. Chem. Downloaded from www.nrcresearchpress.com by 210.87.254.105 on 09/05/12
For personal use only.

of R_F *ca.* 0.20 in 10% CH_3OH–CH_2Cl_2. Ice (*ca.* 2 g) was added and the quenched reaction left for 30 min, poured into ice-water (50 ml), and repeatedly extracted with methylene chloride (4 × 20 ml). The combined organic extracts were washed with distilled water (2 × 20 ml). Methylene chloride was removed by evaporation *in vacuo* and replaced by anhydrous pyridine (10 ml). This pyridine solution, containing the pyridinium salt **8** was used immediately to form blocked dinucleotide phosphate derivatives.

*N^2-Benzoyl-2′-O-tetrahydropyranyl-5′-O-triphenylmethoxyacetylguanylyl (3′-β,β,β-trichloroethyl-5′)N^4-benzoyl-2′-O-tetrahydropyranylcytidine (**10**)*

TPS (91 mg, 0.3 mmol; 1.1 equiv) was added to the pyridine solution of the blocked guanylate derivative (**8**), and activation allowed to proceed for 30 min at room temperature in the dark. The high R_F diastereoisomer of N^4-benzoyl-2′-*O*-tetrahydropyranylcytidine (**9**) (6) (173 mg, 0.4 mmol; 1.5 equiv; R_F 0.6 in 10% CH_3OH–CH_2Cl_2) dissolved in anhydrous pyridine (5 ml) was added and the reaction mixture sealed under nitrogen and set aside at room temperature for 7 days in the dark. Further portions of TPS (3 × 40 mg) were added till all the cytidine derivative (**9**) disappeared. T.l.c. indicated *ca.* 60% conversion into a product of R_F 0.60 in 10% CH_3OH–CH_2Cl_2. Ice (5 g) was then added, and after 30 min the aqueous pyridine solution was poured into ice-water (30 ml) and repeatedly extracted with methylene chloride (4 × 20 ml). The combined organic extracts were washed with water (2 × 20 ml) and evaporated *in vacuo*. The last traces of pyridine were removed by co-distillation with toluene (2 × 10 ml). Methylene chloride (100 ml) was then added and the solution mixture resolved by chromatography on silica gel (20 g) in methylene chloride. Elution with 1% methanol – methylene chloride mixture gave a fast moving material, tentatively identified as the TPS-derivative of **9**. Elution with 3.0% methanol – methylene chloride mixture yielded a mixture of the diastereoisomers of **10** (1) (60 mg, R_F 0.65–0.60 in 10% CH_3OH–CH_2Cl_2). An enriched sample of the lower R_F isomer **10** (50 mg) was obtained by eluting the column with 3.5% methanol – methylene chloride mixtures. Total yield of **10**, 30%. Further elution with 6.0–7.0% methanol – methylene chloride mixtures gave the uncoupled guanylate derivative **8** (97 mg; 35%). The p.m.r. spectrum of compound **10** showed signals (δ TMS) at 8.25 (1H, singlet; 8 proton of G); 8.2–7.15 (25H, multiplet; C_6H_5CO and trityl aromatic protons); 6.1 and 5.7 (2H, two doublets superimposed; 1′-anomeric protons); 3.75 (2H, singlet; —OCH_2CO protons); and a broad peak centered at 1.55 p.p.m. (12H, multiplet; thp protons).

Guanylyl(3′–5′)cytidine (GpC)

A solution of N^2-benzoyl-2′-*O*-tetrahydropyranyl-5′-*O*-triphenylmethoxyacetylguanylyl (3′-β,β,β-trichloroethyl-5′)N^4-benzoyl-2′-*O*-tetrahydropyranylcytidine (**10**) (10 mg, R_F 0.60 in 10% CH_3OH–CH_2Cl_2) in *N*,*N*-dimethylformamide (1.0 ml) was stirred at 50° with Cu–Zn couple (*ca.* 20 mg). After 1 day, t.l.c. indicated complete conversion of starting material into a product of R_F origin in 10% CH_3OH–CH_2Cl_2. Half saturated methanolic ammonia (1 ml) was then added, and the reaction mixture stirred at room temperature for 2 days. *N* Ammonia solution (1 ml) was added, and the Cu–Zn couple filtered off, and washed well with dilute ammonia. The combined filtrate and washings were carefully concentrated *in vacuo* and the solution p*H* brought to 8–10. Dowex 50 W (NH_4^+ form, *ca.* 1 g) was added, and the mixture stirred at room temperature for 15 min. The resin was filtered off, and washed well with water. The combined filtrate and washings were concentrated *in vacuo* to *ca.* 20 ml. The p*H* of the solution was then adjusted to 2.0 with 0.1 *N* hydrochloric acid solution, and the reaction mixture stirred at room temperature. After 2 days, t.l.c. on cellulose indicated that the hydrolysis was complete (R_{Up} 6.0 → 0.90). GpC (80 o.d.$_{260}$, 85%; R_{Up} 0.90 in solvent A) was isolated and purified by preparative paper chromatography in solvent A. Enzymic analysis of the ammonium salt of GpC (20 o.d.$_{260}$) in tris buffer (0.2 ml, 0.1 *M*; p*H* 8.0) with snake venom diesterase (100 λ) (Worthington, 1 mg/ml) at 35° for 16 h showed complete digestion. Paper chromatographic and t.l.c. analyses in various solvents showed the expected products (G + pC) in the correct ratio.

*N^2-Benzoyl-2′-O-tetrahydropyranyl-5′-O-triphenylmethoxyacetylguanylyl (3′-β,β,β-trichloroethyl-5′)N^2-benzoyl-2′-O-tetrahydropyranylguanosine (**11**)*

TPS (91 mg, 0.3 mmol; 1.1 equiv) was added to the pyridinium solution of the blocked guanylate derivative **8**, and activation allowed to proceed for 30 min at room temperature in the dark. The high R_F diastereoisomer of N^2-benzoyl-2′-*O*-tetrahydropyranylguanosine (**5***b*) (170 mg, 0.35 mmol; 1.3 equiv; R_F 0.35 in 10% CH_3OH–CH_2Cl_2) dissolved in anhydrous pyridine (5 ml) was added and the reaction mixture sealed under nitrogen and set aside at room temperature for 7 days in the dark. Further portions of TPS (3 × 40 mg) were added till all of **5***b* had disappeared. T.l.c. indicated *ca.* 50% conversion into a product of R_F 0.60 in 10% CH_3OH–CH_2Cl_2. Ice (5g) was then added, and after 30 min the aqueous pyridine solution was poured into ice-water (30 ml) and repeatedly extracted with methylene chloride (4 × 20 ml). The combined organic extracts were washed with saturated sodium bicarbonate solution (2 × 20 ml) and then with water (2 × 20 ml) and evaporated *in vacuo*. The last traces of pyridine were removed by co-distillation with toluene (2 × 10 ml). Methylene chloride (100 ml) was then added, and the reaction mixture purified by chromatography on silica gel (20 g) in methylene chloride. Elution with 3.5% methanol – methylene chloride mixture gave a mixture of the diastereoisomers of **11** (107 mg; 28%). Further elution with 7% methanol – methylene chloride mixture gave uncoupled guanylate derivative **8** (105 mg; 38%). The p.m.r. spectrum of **11** showed signals (δ TMS) at 8.2 and 8.15 (2H, singlet; 8 protons of Gs); 8.15–7.10 (25H, multiplet; C_6H_5CO and trityl aromatic protons); 6.2 and 6.05 (2H, two doublets superimposed; 1′-anomeric protons of Gs); 3.75 (2H, singlet; —OCH_2CO protons); and a broad peak centered at 1.55 p.p.m. (12H, multiplet; thp protons of Gs).

Guanylyl(3′–5′)guanosine (GpG)

A solution of N^2-benzoyl-2′-*O*-tetrahydropyranyl-5′-*O*-triphenylmethoxyacetylguanylyl (3′-β,β,β-trichloroethyl-5′)N^2-benzoyl-2′-*O*-tetrahydropyranylguanosine (**11**) (5 mg, R_F 0.4 in 10% CH_3OH–CH_2Cl_2) in *N*,*N*-di-

methylformamide (1.0 ml) was stirred at 50° with Cu–Zn couple (*ca.* 20 mg). After 1 day t.l.c. indicated complete conversion of starting material into a product of R_F origin in 10% CH_3OH–CH_2Cl_2. Half saturated methanolic ammonia (1 ml) was then added, and the reaction mixture stirred at room temperature for 2 days. *N* ammonia solution (1 ml) was added, and the Cu–Zn couple filtered off, and washed well with dilute ammonia. The combined filtrate and washings were carefully concentrated *in vacuo* and the solution p*H* brought to 8–10. Dowex 50W (NH_4^+ form; *ca.* 1 g) was added, and the mixture stirred at room temperature for 15 min. The resin was filtered off, and washed well with water. The combined filtrate and washings were concentrated *in vacuo* to *ca.* 20 ml. The p*H* of the solution was then adjusted to 2.0 with 0.1 *N* hydrochloric acid solution, and the reaction mixture stirred at room temperature. After 2 days t.l.c. on cellulose indicated that the hydrolysis was complete. (R_{Up} 4.5 → 0.81). GpG (40 o.d.$_{260}$, 76%; R_{Up} 0.81 in solvent A) was isolated and purified by preparative paper chromatography in solvent A. Enzymic analysis of the ammonium salt of GpG (20 o.d.$_{260}$) in tris buffer (0.2 ml, 0.1 *M*; p*H* 8.0) with snake venom diesterase (100 λ) (Worthington, 1 mg/ml) at 37° for 16 h showed complete digestion. Paper chromatographic and t.l.c. analyses in various solvents showed the expected products (G + pG) in the correct ratio.

1. E. S. Werstiuk and T. Neilson. Can. J. Chem. **50**, 1283 (1972).
2. T. Neilson and E. S. Werstiuk. Can. J. Chem. **49**, 3004 (1971).
3. R. Lohrmann, D. Söll, H. Hayatsu, E. Ohtsuka, and H. G. Khorana. J. Am. Chem. Soc. **88**, 819 (1966).
4. C. Chládek and J. Smrt. Coll. Czech. Chem. Commun. **29**, 214 (1964).
5. F. Eckstein. Chem. Ber. **100**, 2228 (1967).
6. T. Neilson and E. S. Werstiuk. Can. J. Chem. **49**, 493 (1971).
7. R. Lohrmann and H. G. Khorana. J. Am. Chem. Soc. **86**, 4188 (1964).
8. IUPAC-IUB Commission on Biochemical Nomenclature. Biochem. **9**, 4022 (1970).

Can. J. Chem. Downloaded from www.nrcresearchpress.com by 210.87.254.105 on 09/05/12
For personal use only.

Low Temperature Infrared Study of Hydrogen Bonding in Dissolved Pyrrole and Indole

MARIE-CLAUDE BERNARD-HOUPLAIN AND C. SANDORFY

Département de Chimie, Université de Montréal, Montréal, Québec

Received September 21, 1972

Self-association by hydrogen bonding in the case of pyrrole was studied by i.r. spectroscopic methods. The fundamental first and second overtones of the NH stretching vibration were measured at different concentrations and at temperatures ranging from 22 to −190 °C. The existence of at least two associated species in solution has been ascertained. 2,5-Dimethylpyrrole and indole were also studied and gave similar results.

L'autoassociation du pyrrole par liaisons hydrogène a été étudiée par spectroscopie i.r. Les transitions fondamentales ainsi que les premières et deuxièmes transitions harmoniques de la vibration de valence NH ont été mesurées à différentes concentrations et à différentes températures allant de 22 à −190 °C. On a établi l'existence d'au moins deux espèces associées en solution.

Le 2,5 diméthylpyrrole et l'indole ont été étudiés dans les mêmes conditions et ont donné des résultats similaires.

Can. J. Chem., **51**, 1075 (1973)

Can. J. Chem. Downloaded from www.nrcresearchpress.com by 210.87.254.42 on 09/05/12
For personal use only.

Introduction

In an attempt to elucidate the nature of self-association by hydrogen bonding in the case of the NH group, we examined the i.r. spectra of three molecules taken as representatives of the different types of secondary amines, dimethylamine, *N*-methylaniline, and pyrrole. The technique used in this work consisted in measuring the fundamental, the first and, when possible, the second overtone of the N—H stretching vibration in mixed solvents which can be used down to liquid nitrogen temperature where these solvents become rigid glasses. Our work on dimethylamine and *N*-methylaniline was reported in two previous publications (1, 2).

In this paper we report our results on pyrrole (P). We have also studied indole (I) and 2,5-dimethylpyrrole (DMP).

The work done on the association of pyrrole with different bases has been reviewed by Bellamy (3). Self-association of pyrrole at room temperature has been studied by i.r. spectroscopy, as well as cryoscopic, calorimetric, dielectric, and n.m.r. methods (4–14).

Recently Lautié and Novak (15) measured the i.r. and Raman spectra of pyrrole in the solid state at −190 °C. They found that in the crystal, pyrrole forms long chains in which the individual molecules are associated by hydrogen bonds.

Neither low temperature nor overtone studies seem to have been reported on the self-association of pyrrole in solution up to the present time. We measured the i.r. spectra in both the fundamental, first and, when possible second overtone region of the N—H stretching vibration down to −190 °C in order to follow the pattern of molecular associations over a wide range of temperature.

Experimental

Pyrrole and 2,5-dimethylpyrrole were supplied by Aldrich Chem. Co. Inc. These products were distilled twice under vacuum; fresh samples were used for the preparation of the solutions. Indole was purchased from Fisher Scientific Co. Ltd. and was used without further purification; it was a "certified" Fisher product and its melting range was 51.0–51.7 °C.

Pyrrole-d_4 (minimum isotopic purity of about 99%) was supplied by Merck, Sharp and Dohme of Canada Ltd. and was used without further purification. Pyrrole-*N-d* was made by exchange between pyrrole and heavy water (16); we obtained a sample about 95% rich in pyrrole-*N-d*. The solvents were 1:1 mixtures of CCl_3F and CF_2Br–CF_2Br (FR) and of CCl_3F and methylcyclohexane (FM). These mixtures form rigid glasses near liquid nitrogen temperature (17–18). The freons were supplied by Dupont de Nemours Co. of Canada and the methylcyclohexane by Phillips Petroleum Company. Carbon tetrachloride was also used as a solvent and was purchased from Anachemia Chem. Ltd. All the solvents were distilled and kept over phosphorus pentoxide.

The preparation of solutions and filling of sample cells were done entirely in a dry box, under an inert atmosphere.

The NH fundamentals were measured on a Perkin–Elmer model 621 spectrometer and the overtones on a Cary 17 instrument.

Other experimental details were given in previous publications from this laboratory (17–18).

Can. J. Chem. Downloaded from www.nrcresearchpress.com by 210.87.254.42 on 09/05/12
For personal use only.

Results

Pyrrole

Figure 1 shows the results of a concentration study at 20 °C. In a dilute solution the free N—H band has its peak at 3498 cm^{-1}. A weak band appears at 3475 cm^{-1} on the side of the *free* band. This band was first assigned by Linnell (19) to a hot band involving the NH stretching vibration (ν_s) and the 565 cm^{-1} out-of-plane NH bending vibration (ν_i). The transition goes from ($\nu_{s,\,v=0} + \nu_{i,\,v=1}$) to ($\nu_{s,\,v=1} + \nu_{i,\,v=1}$) and the separation between ν_s and the hot band is equal to the anharmonic coupling constant between the two modes. As we shall see below our low temperature and overtone spectra confirm this assignment.

At higher concentrations a broad associated band appears whose center shifts to lower frequencies with increasing concentration. For the pure liquid the peak is at 3401 cm^{-1} with a shoulder near 3430 cm^{-1}. The half width of the free band is 14 cm^{-1} for the most dilute solution while it is 81 cm^{-1} for the associated band in the pure liquid. The hydrogen bond shift is of the order of 100 cm^{-1}.

At the same time in the first overtone region we find a free band at 6854 cm^{-1} for the most dilute solution (Fig. 2). The hot band is again observed and, as expected, its distance from the main peak is twice that in the fundamental region (42 and 23 cm^{-1}, respectively). The relative intensity of the associated band with respect to the free band is much less than in the fundamental region. It is not until about a 4 *M* concentration is reached that it is clearly distinguished as a shoulder. It becomes a band for the liquid with its maximum at 6757 cm^{-1}. This weakness of the overtone of the associated band is a general

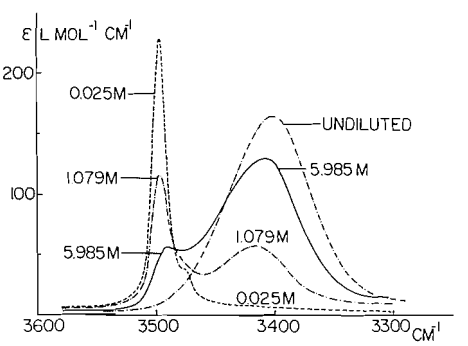

FIG. 1. The NH stretching fundamental of pyrrole at different concentrations, at 22 °C, in CCl_4.

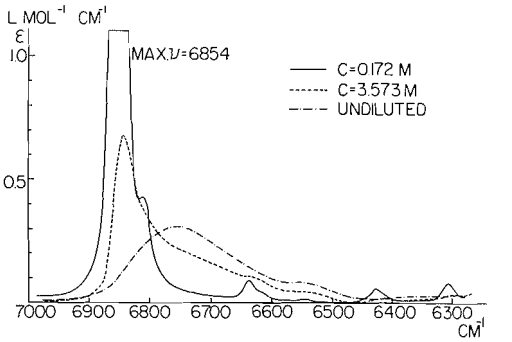

FIG. 2. The first overtone of the NH stretching vibration of pyrrole at different concentrations in CCl_4. Temperature: 22 °C.

phenomenon first observed by Luck and Ditter (20). An explanation for it was put forward recently by Di Paolo *et al.* (21).

In order to ascertain that CH + NH type combination tones make no significant contribution to the observed bands we measured the spectrum of C_4D_4NH (pyrrole-d_4). Only some weaker bands disappear below about 6640 cm^{-1}. The main band at 6757 cm^{-1} (or 6761 in C_4D_4NH) persists as well as a pronounced shoulder on its low frequency side (at about 6660 cm^{-1}).

Now, the question arises if the main maximum of the fundamental at 3401 cm^{-1} is due to the same associated species as the main peak at 6757 cm^{-1} of the overtone? The answer is that it is almost certainly not. Assigning the two apparent peaks to the same species would yield an anharmonicity constant ($\omega ex_e = \nu_{01} - \nu_{02}/2$) equal to only 23 cm^{-1} while the corresponding free bands give 71 cm^{-1}. A similar situation exists in the aliphatic amines and we were able to show previously that the apparent decrease in the value of the anharmonicity constant was due to an erroneous assignment. Since the less associated species are highly favored from the point of view of the intensity of their overtone bands it is reasonable to assume that the 6757 cm^{-1} peak corresponds to the shoulder at about 3430 cm^{-1} and the shoulder at about 6660 cm^{-1} to the peak at 3401 cm^{-1}.

The half width of the free overtone is 26 cm^{-1} and that of the broad associated band (in the liquid) is of the order of 190 cm^{-1}.

We also measured the second overtone for pyrrole. The free band is at 10 075 cm^{-1} (0.1 *M*), the hot band at 10 010 cm^{-1} and the associated band at 9883 cm^{-1} (pure liquid). The half widths

Can. J. Chem. Downloaded from www.nrcresearchpress.com by 210.87.254.42 on 09/05/12
For personal use only.

are 42 cm^{-1} for the free band and about 340 cm^{-1} for the associated band. The anharmonicity constant computed from $\nu_{02}/2 - \nu_{03}/3$ is 69 cm^{-1} for the free band and about 80 cm^{-1} for the associated band.

Since the free:associated intensity ratios are similar in the first and second overtone region the correspondence between these bands is unambiguous and confirms our assignments of the first overtones.

These concentration studies were performed in a CCl_4 solution in which pyrrole has a very good solubility. Solute–solvent interaction between pyrrole and CCl_4 has only a weak influence on the spectra (9).

Figure 3 shows the spectra at a variety of temperatures in FM solution. The free band is slowly shifted to lower frequencies when temperature decreases. (The shift amounts to about 12 cm^{-1} from 20 to -140 °C for a 0.1 *M* solution). In a 0.1 *M* solution the free band is still present at -140 °C and at 0.014 *M* it is present even at -190 °C. Linnell's hot band appears as a shoulder at about 3475 cm^{-1} and fades away as temperature is lowered. The associated band shifts faster and very probably contains two bands, one at about 3425 which disappears rapidly when temperature is lowered and one, the main peak, at 3392 cm^{-1} (at -40 °C and 0.124 *M* in FM). The observed shift must be the result of a certain amount of real shift and of changing overlap conditions due to the varying intensities of the two bands. They can be assigned to two different associated species; we shall tentatively call them dimer and oligomer, respectively. At -190° practically only the oligomer is present. The free band has some asymmetry at its low frequency side but we do not see sufficient evidence for a different species there. It is probably due to Linnell's band and, perhaps, to the free end-NH group of associated species.

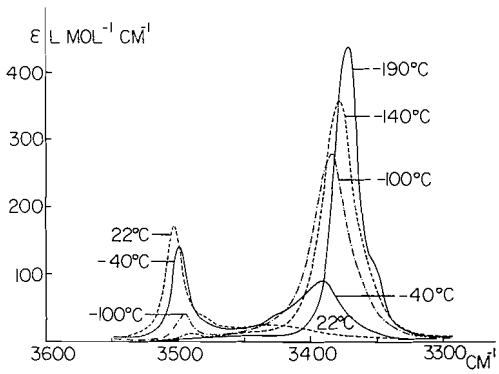

FIG. 3. The NH stretching fundamental of pyrrole at different temperatures in a 1:1 mixture of CCl_3F and methylcyclohexane. Concentration at 22 °C: 0.124 *M*.

The 3401 cm^{-1} peak found in the pure liquid at room temperature probably corresponds to the 3392 cm^{-1} peak (-40 °C) which shifts to 3375 cm^{-1} at -190 °C. However, the band of the liquid is broad and complex and does not reflect the same proportions of species as the low temperature spectrum of the dilute solution.

There is a shoulder becoming an almost separate narrow band at the low frequency side of the main peak, near 3355 cm^{-1} at -190 °C. It could correspond to a more highly associated species but its sharpness is surprising. Otherwise it could only be a ternary combination. Its persistance at low temperatures seems to rule out an assignment to a hot band. For the time being we shall consider it as a combination band.

These temperature variation studies lead to the same observations for initial concentrations varying from 0.01 to 0.4 *M*, which were the limits of our measurements.

The general appearance of these spectra places pyrrole somewhere between aliphatic secondary amines and alcohols. The relatively large shift from the free to the associated bands is reminiscent of alcohols. It amounts to about 80 cm^{-1} for our "dimer". The more moderate shift between "dimer" and "oligomer" is consistent with the assumption that in the case of alcohols where this latter shift is much larger, the change in anharmonicity upon hydrogen bond formation is responsible for a part of the shift (22). The half width of the 3375 cm^{-1} peak at -190 °C is only about 25 cm^{-1} so the band is quite sharp. This again may be due to relatively moderate anharmonicity (hardly higher than for the free band; see below) which does not favor strong environmental interactions (23) and to the existence of relatively well defined associated species.

In the bromine containing FR solvent the free band's relative strength is greater than in FM. This is another manifestation of the hydrogen bond weakening property of bromine containing solvents which we described previously (24). It slows down hydrogen bond formation which would otherwise occur more rapidly as temperature is decreased.

All the spectra given in Fig. 3 remain practically the same if we take C_4D_4NH instead of

Can. J. Chem. Downloaded from www.nrcresearchpress.com by 210.87.254.42 on 09/05/12
For personal use only.

TABLE 1. Wave numbers of the fundamental (ν_{01}), first overtone (ν_{02}), and second overtone (ν_{03}) of the NH stretching frequency; anharmonicity constants* and frequency shifts ($\Delta\nu$) for dimethylamine, *N*-methylaniline, and pyrrole

	Monomer					Associated species in solution							
	ν_{01}	ν_{02}	ν_{03}	X_{12}	X_{23}	ν_{01}	$\Delta\nu = \nu_{01}^{Free} - \nu_{01}^{Ass.}$	ν_{02}	$\Delta\nu = \nu_{02}^{Free} - \nu_{02}^{Ass.}$	ν_{03}	$\Delta\nu = \nu_{03}^{Free} - \nu_{03}^{Ass.}$	X_{12}	X_{23}
Dimethylamine (ref. 1)	3355	6547	9589	81	78	3288	67	6432	115	9463	126	72	62
						3235	120	—	—	—	—	—	—
N-Methylaniline (ref. 2)	3446	6739	9876	76.5	77.5	3413	33	6676	63	9790	86	75	74.7
						3377	69	6601	138	9673	203	76.5	76.2
						3290	156	—	—	—	—	—	—
Pyrrole	3504	6870	10101	69	68	3425	79	—	—	—	—	—	—
						3375	129	6575	295	9615	486	88	83

*$X_{12} = \nu_{01} - \nu_{02}/2$; $X_{23} = \nu_{02}/2 - \nu_{03}/3$.

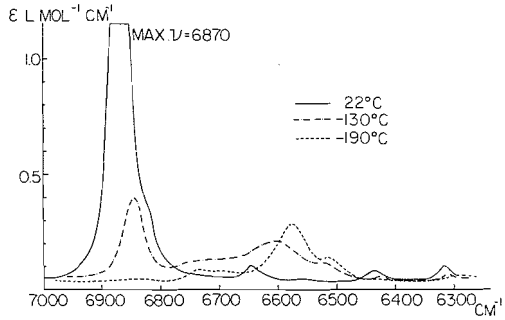

FIG. 4. The first overtone of the NH stretching vibration of pyrrole at different temperatures in a 1:1 mixture of CCl_3F and CF_2Br–CF_2Br. Concentration at 22 °C: 0.127 *M*.

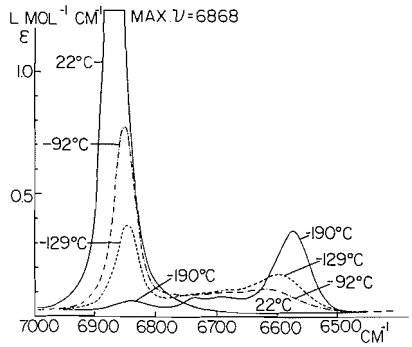

FIG. 5. The first overtone of the NH stretching vibration of pyrrole-d_4 at different temperatures in a 1:1 mixture of CCl_3F and CF_2Br–CF_2Br. Concentration at 22 °C: 0.123 *M*.

C_4H_4NH. On the other hand all the above described bands "disappear" in C_4H_4ND.

In the region of the first overtone (Fig. 4) we observe the expected strong free band (6870 cm^{-1} at 20 °C in FR). At the lowest temperature, however, the free band is very weak (6840 in FR); it is followed by two weak associated bands at 6735 and 6690 cm^{-1} and a strong band at 6575 cm^{-1}. The weaker band at 6514 cm^{-1} is a CH + NH combination band as can be ascertained by comparing the spectrum of C_4H_4-NH to that of C_4D_4NH (Fig. 5). All other bands remain the same (CH + NH type combinations are much less disturbing than the analogous CH + OH bands of alcohols).

With the 3375 cm^{-1} main peak in the fundamental region the 6575 cm^{-1} band yields an anharmonicity constant of 88 cm^{-1}. We think that the moderate increase with respect to the corresponding value of the free NH vibration (69 cm^{-1}) is significant and illustrates the relative strength of this hydrogen bond. On the other hand, its "normal" value confirms the assignment of the 6575 cm^{-1} band to the overtone of the 3375 cm^{-1} fundamental.

Thus the observations made on the overtones underscore the important difference in the nature of the association between the pure liquid (room temperature) and the dilute solutions taken at low temperatures. As we have seen, in the pure liquid, the 6757 cm^{-1} band is predominant meaning that the most abundant species is a less associated species for the liquid than for the solutions at low temperatures. The weak and somewhat broad band at 3425 cm^{-1} (Fig. 3) is likely to contain the fundamentals of the weak bands at 6735 and 6690 cm^{-1}.

In the FR solvent we again see the delaying effect of the bromine containing solvent molecule and the greater relative strength of the free band.

In the region of the second overtone we see the free band at 10 101 cm^{-1} (0.133 *M* in FR) at 20 °C and Linnell's hot band at 10 020 cm^{-1}. At −190 °C the free band is reduced to a broad feature almost lost in the background. The associated species give a shoulder at 9740 and a band at 9615 cm^{-1}. The correspondence with the respective fundamentals and overtones seems to be straightforward (Table 1).

2,5 Dimethylpyrrole (DMP)

Self association of DMP was studied at 22 °C, in the region of the fundamental by Abraham *et al.* (25). They identified the bands of the free and one associated species; from the Δν(NH) value they concluded that the steric hindrance by the α-methyl group has no effect on the strength of the hydrogen bond.

We carried out similar studies on DMP as on pyrrole; the spectra can be interpreted on the same basis as previously and need not be discussed in detail.

Figures 6 and 7 show the spectra, at different temperatures, of a solution of DMP in FR. At 22 °C, the free band is observed at 3486 cm^{-1} and a hot band is found at about 3465 cm^{-1}. At the lowest temperature, at the fundamental level, we observe a strong associated band at 3337 cm^{-1} (half width 30 cm^{-1}) with a shoulder at approximatively 3370 cm^{-1} which is more pronounced than in the case of pyrrole. This indicates again the presence of at least two species at the lowest temperatures. At the overtone level,

Can. J. Chem. Downloaded from www.nrcresearchpress.com by 210.87.254.42 on 09/05/12
For personal use only.

Can. J. Chem. Downloaded from www.nrcresearchpress.com by 210.87.254.42 on 09/05/12
For personal use only.

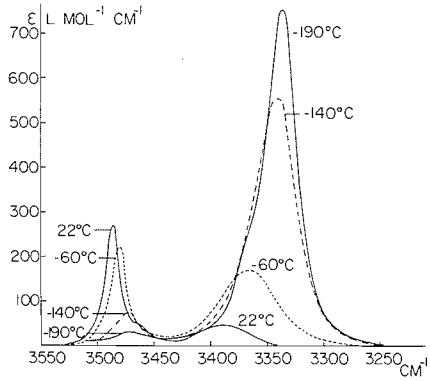

FIG. 6. The NH stretching fundamental of DMP at different temperatures in a 1:1 mixture of CCl_3F and CF_2Br–CF_2Br. Concentration at 22 °C: 0.086 *M*.

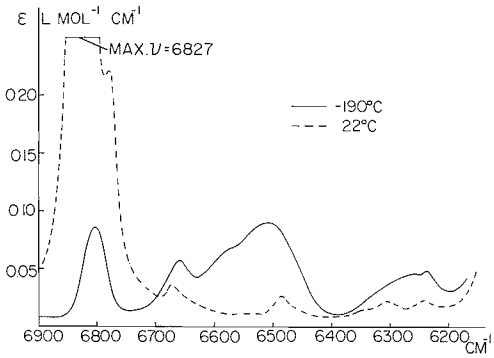

FIG. 7. The first overtone of the NH stretching vibration of DMP at different temperatures in a 1:1 mixture of CCl_3F and CF_2Br–CF_2Br. Concentration at 22 °C: 0.091 *M*.

at −190 °C, the free band at 6803 cm^{-1} is still fairly strong; this can be taken as an indication of the lesser degree of association in DMP than in pyrrole, due to the steric hindrance by the α-methyl groups. (However, the HB are approximately of the same strength in the two amines as indicated by the values of the Δν(NH)).

The 6510 cm^{-1} band and a shoulder on its high frequency side are assigned to the overtones of the associated bands at 3337 and 3370 cm^{-1}, respectively. The band near 6660 cm^{-1} is present in dilute solution and does not change very much in frequency or in intensity when the temperature is gradually lowered and we assign it to a combination tone, not containing NH stretching motion; the same applies to the weak bands between 6300 and 6200 cm^{-1}.

The main point is that the existence of two associated species at low temperatures is confirmed by the observations made on DMP.

Indole

The effect of solvent and concentration on the n.m.r. spectra of several indoles has been investigated recently by Reinecke *et al.* (26) and by Saitô and Nukada (27). When the temperature of a 0.041 *M* solution of indole is gradually lowered, the intensity of the free band diminishes while its frequency is shifted from 3503 at 22 to 3490 cm^{-1} at −190 °C. The associated band located at 3435 cm^{-1} at room temperature is shifted to 3400 cm^{-1} with a strong shoulder appearing at its low frequency side. A comparison of the spectra of pyrrole and indole leads to the conclusion that the less associated species is favored in the case of indole; the more highly associated species comes in strongly at lower temperatures only. The coexistence of the two species in comparable proportions explains the greater width of the band measured at low temperatures (Fig. 8). Turning our attention to the first overtone

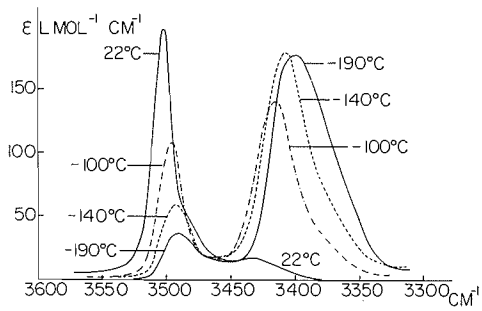

FIG. 8. The NH stretching fundamental of indole at different temperatures in a 1:1 mixture of CCl_3F and CF_2Br–CF_2Br. Concentration at 22 °C: 0.041 *M*.

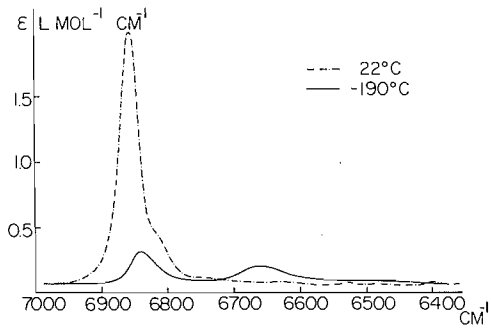

FIG. 9. The first overtone of the NH stretching vibration of indole at different temperatures in a 1:1 mixture of CCl_3F and CF_2Br–CF_2Br. Concentration at 22 °C: 0.041 *M*.

Can. J. Chem. Downloaded from www.nrcresearchpress.com by 210.87.254.42 on 09/05/12
For personal use only.

region, at -190 °C, we still find a fairly strong free band at 6840 cm^{-1} (Fig. 9). Only one associated band can be distinguished at 6659 cm^{-1}, without any shoulder on its low frequency side. The main reason for this is probably that the overtone of the less associated band contributes most of the intensity of the observed band. We often encountered the fact that the relative intensities of two associated bands are different for the overtones from those for the fundamentals, so that the less associated species is favored at the overtone level.

Discussion and Conclusions

Dimethylamine, *N*-methylaniline, and pyrrole represent three different types of secondary amines and a comparison between their behavior from the point of view of molecular associations is instructive (Table 1 summarizes some of the main observations).

DMA consists essentially of monomers and dimers in solutions as well as in the pure liquid. Only at low temperatures, in solutions, did we find evidence for a more highly associated species. The shift that occurs upon hydrogen bond formation is of the order of $\Delta\nu = 67$ cm^{-1} for the dimer and about $\Delta\nu = 120$ cm^{-1} for the more highly associated species (at the fundamental level).

In the case of NMA we see the formation of three associated species as the temperature is lowered, with $\Delta\nu$ equal to 33, 69, and 156 cm^{-1}. The spectrum of the liquid gives a relatively well-defined band at about the same frequency as that of the dimer in solution with a low frequency tail containing the bands due to higher associated species. The case of NMA is closer to the case of weakly associating (sterically hindered) alcohols (28).

Pyrrole is even more associative. As in alcohols, in solutions of pyrrole the dimer located near 3425 cm^{-1} is difficult to find, it probably only exists in a narrow range of concentrations and temperatures.

The center of the broad associated band which we observe for pure pyrrole at room temperature is at a $\Delta\nu = 103$ cm^{-1} from the free band, indicating that the most abundant species in this case is no more a dimer but an oligomer even at room temperature. The breadth of this band must then be due to contributions from other associated species and a variety of solvent configurations. This situation is more like what we encounter for alcohols than that for DMA and NMA.

The sharp band which we find in the low temperature solution spectra of pyrrole at the fundamental level has a lower frequency than the center of the broad band of the liquid but remains relatively close to it. The sharpness of the band suggests that it belongs to well defined oligomer species with relatively little variation in their environments.

The anharmonicities for the oligomers are slightly higher than for the related free species, a fact that again emphasizes the resemblance of the hydrogen bonds formed by pyrrole to those of alcohols. The observed frequencies and shifts show, however, that the degree of association must be lower than in most alcohols.

It appears that in dilute solutions, at low temperatures we have a small number of relatively highly associated species while in the pure liquid, at room temperature, a greater variety of species exists which, on the average is less highly associated.

We express our thanks to the National Research Council of Canada for financial assistance.

1. M. C. Bernard-Houplain and C. Sandorfy. J. Chem. Phys. **56**, 3412 (1972).
2. M. C. Bernard-Houplain, G. Bélanger, and C. Sandorfy. J. Chem. Phys. **57**, 530 (1972).
3. L. J. Bellamy. Advances in infrared group frequencies. Methuen & Co. Ltd. 1968. p. 282.
4. N. Fuson, M. L. Josien, R. L. Powell, and E. Utterback. J. Chem. Phys. **20**, 145 (1952).
5. M. L. Josien, P. Pineau, M. Paty, and N. Fuson. J. Chem. Phys. **24**, 1261 (1956).
6. S. N. Vinogradov and R. H. Linnell. J. Chem. Phys. **23**, 93 (1955).
7. J. A. Happe. J. Phys. Chem. **65**, 72 (1961).
8. G. M. Badger, R. L. N. Harris, P. A. Jones, and J. M. Sasse. J. Chem. Soc. 4329 (1962).
9. M. Gomel and H. Lumbroso. Bull. Soc. Chim. Fr. 2200 (1962).
10. H. Lumbroso. J. Chim. Phys. **61**, 132 (1964).
11. A. Weisbecker. J. Chim. Phys. **63**, 838 (1966).
12. T. Schaefer and W. G. Schneider. J. Chem. Phys. **32**, 1224 (1960).
13. M. T. Chenon and N. Lumbroso-Bader. C. R. Acad. Sc. Paris, **266**, 293 (1968).
14. J. Dos Santos, F. Cruege, and P. Pineau. J. Chim. Phys. **67**, 826 (1970).
15. A. Lautié and A. Novak. J. Chem. Phys. 2479, **56**, (1972).
16. B. Bak, D. Christensen, L. Hansen, and J. Rastrup-Andersen. J. Chem. Phys. **24**, 720 (1956).
17. G. Durocher and C. Sandorfy. J. Mol. Spectrom. **20**, 410 (1966).

18. M. ASSELIN and C. SANDORFY. J. Chem. Phys. **52**, 6130 (1970).
19. R. H. LINNELL. J. Chem. Phys. **41**, 3274 (1964).
20. W. A. P. LUCK and W. DITTER. Ber. Bunsenges. Phys. Chem. **72**, 365 (1968).
21. T. DI PAOLO, C. BOURDERON, and C. SANDORFY. Can. J. Chem. **50**, 3161 (1972).
22. M. ASSELIN and C. SANDORFY. J. Mol. Struct. **8**, 145 (1971).
23. M. ASSELIN and C. SANDORFY. Chem. Phys. Lett. **8**, 601 (1971).
24. M. C. BERNARD-HOUPLAIN, C. BOURDÉRON, J. J. PÉRON, and C. SANDORFY. Chem. Phys. Lett. **11**, 149 (1971).
25. R. J. ABRAHAM, E. BULLOCK, and S. S. MITRA. Can. J. Chem. **37**, 1859 (1959).
26. M. G. REINECKE, H. W. JOHNSON, and J. F. SEBASTIAN. J. Am. Chem. Soc. **91**, 3817 (1969).
27. H. SAITÔ and K. NUKADA. J. Am. Chem. Soc. **93**, 1072 (1971).
28. C. BOURDÉRON, J. J. PÉRON, and C. SANDORFY. J. Phys. Chem. **76**, 864 (1972).

Can. J. Chem. Downloaded from www.nrcresearchpress.com by 210.87.254.42 on 09/05/12
For personal use only.

The Influence of Coordinating Solvents on the Thermal Decomposition of Methyl Titanium Trichloride

JAMES D. MCCOWAN
Department of Chemistry, Queen's University, Kingston, Ontario
Received November 2, 1972

The mechanism of decomposition of CH_3TiCl_3 in coordinating solvents is shown not to involve free radicals in some cases. An analysis of published work on the decomposition of titanium alkyls suggests mechanisms of decomposition similar to those postulated for alkyls of other transition metals.

On démontre que dans certain cas le mécanisme de décomposition du CH_3TiCl_3 dans des solvants coordinants n'implique pas de radicaux libres. Une analyse des résultats publiés sur la décomposition des alkyl titanium suggère que leurs mécanismes de décomposition sont similaires à ceux des dérivés alkylés des autres métaux de transition. [Traduit par le journal]

Can. J. Chem., 51, 1083 (1973)

Can. J. Chem. Downloaded from www.nrcresearchpress.com by 210.87.254.42 on 09/05/12
For personal use only.

A free radical mechanism of thermal decomposition is widely accepted for many alkyl–transition metal compounds (1, 2), particularly those involving methyl groups. In the particular case of CH_3TiCl_3, there is conclusive evidence (3) that free radicals do not form in non-coordinating solvents but it has become accepted (4) that a free radical mechanism is predominant in coordinating solvents. Such a mechanism was originally proposed (5) on the basis of mass balance considerations and of the relatively fast decompositions in coordinating solvents, and it was given substantial support by the observation (6) that the decomposition kinetics are first order, and that CH_3D is among the products, when the decomposition is carried out in a mixed solvent tetrahydrofuran and perdeuterotoluene. The observation of unambiguous first order kinetics is consistent with the postulate that the homolytic breaking of the carbon–metal bond is the rate determining step. Moreover, the existence of CH_3D among the products tended to confirm that a radical had formed, capable of attacking toluene-d_8 molecules which were, presumably, well beyond the coordination sphere.

The assumption of a free radical path as the general case in such systems, while plausible on the evidence, proves to be unjustified.

Experimental Methods

Materials

$(CH_3)_2Zn$ was Alfa Inorganics "Electronic Grade" and was used as received. $TiCl_4$ was reagent grade, once distilled under vacuum. $(C_2D_5)_2O$ (98% deuterated), $CD_3C_6D_5$ (99.5% deuterated), and C_8D_{18} (98% deuterated) were obtained from Merck, Sharp, and Dohme, from Stohler Inc., and from Wilmad Co. Inc., respectively, and were used as received. Non-deuterated solvents were purchased in reagent grade and were distilled under vacuum, the middle cut being used. Both ethers were first refluxed over sodium.

Preparation of CH_3TiCl_3

All steps of the preparation were carried out within a box of dry nitrogen.

$(CH_3)_2Zn$ (3.1×10^{-3} mol) was added slowly to a solution of 6.2×10^{-3} mol of $TiCl_4$ in 5 ml of CCl_3F at about 0 °C. After a few minutes shaking as the solution warmed to room temperature, the precipitated zinc chloride was filtered off. Three 1 ml amounts of CCl_3F were used to wash remaining CH_3TiCl_3 solution from the preparation vessel and the filter.

Using ungreased ground glass joints to prevent reaction, a vacuum trap-to-trap distillation at −35° separated the CH_3TiCl_3 from the more volatile CCl_3F. The purple crystals were then dissolved in the working solvent or transferred directly to the reaction vessel. Precipitation techniques of the sort usually employed (3, 4, 7) invariably result in the occlusion of some solvent (even heptane) in the CH_3TiCl_3 crystals and were therefore unsatisfactory for the work in this paper. Two or three distillations are required where complete solvent removal is obligatory.

Decomposition Studies and Results

A series of decompositions was carried out at room temperature in a variety of solvents, as shown in Table 1. Concentrations of CH_3TiCl_3 in the original solution were determined, for deuterated octane and toluene solutions, by comparison of ten or more integrals of the proton n.m.r. spectrum with those of a reference material, cyclohexane or trichloroethylene, added in known amount. Spectra were obtained on a Bruker HX-60 spectrometer.

In the case of solutions in heptane, or in diethyl ether, the amount was estimated from the known yield found in deuterated solvents.

In all samples except K, the non-coordinating solvent was measured into the distillation receiver, and the resulting CH_3TiCl_3 solution was then transferred to the decomposition vessels and, in some cases, to an n.m.r. tube. Coordinating solvents were then added as required

Can. J. Chem. Downloaded from www.nrcresearchpress.com by 210.87.254.42 on 09/05/12
For personal use only.

TABLE 1. Systems examined

Sample	Reagents used (mmol)							Remarks
	CH_3TiCl_3	$(C_2H_5)_2O$	$(C_2D_5)_2O$	C_4H_8O	C_7H_{16}	C_8D_{18}	C_7D_8	
A	2.9	—	1.92	—	4.5	—	—	Solution turns dark red-purple and opaque on addition of ether. Precipitate probable. Observations in A′ same.
A′	1	—	1.44	—	2.1	—	—	
B	2.7	1.92	—	—	—	7.3	—	Similar to A.
C	1	1.44	—	—	—	1.8	—	Kept in dark throughout.
D	1	1.44	—	—	—	1.8	—	Irradiated throughout by fluorescent lamp at 10 cm. Observations as in A.
E	1.0	—	1.92	—	—	1.5	—	Handled as samples A and B. Observations as in A.
F	2.7	—	—	4.3	—	—	9.2	Red precipitate and much heat produced on adding THF. Kept in dark during decomposition.
G	2.7	—	—	4.3	—	—	9.2	Observations as in F. Handled as in D.
H	1.1	—	—	—	—	1.6	—	Transparent yellow solution irradiated as in D. Brown precipitate appears within 5 min. Observations in H′ similar.
H′	1.2	—	—	—	—	3.7	—	
I	1.2	0.96	—	—	—	—	1.2	Kept in dark throughout. Dark red precipitate with little colorless liquid after decomposition.
J	1.3	—	—	—	—	—	1.4	
K	1.2	—	1.06	—	—	—	—	Decomposition very rapid.

TABLE 2. Volatile products

Sample	Ratio CH_3D/CH_4	Other species				
		C_2H_6	H_2	HD	D_2	CH_3Cl
A	0.062	Trace	Trace	Trace	No	?
A′	0.149	Yes	?	?	?	?
B	0.000	Yes	Trace	Trace	Trace	No
C	0.000	Trace	?	?	?	?
D	0.000	Trace	?	?	?	?
E	0.079	Yes	Trace	Trace	Trace	?
F	0.522	Trace	No	No	No	?
G	0.513	Trace	No	No	No	?
H	0.002	Yes	Yes	Yes	Yes	No
H′	0.026	Yes	Yes	Yes	Yes	No
I	0.026	No	Trace	No	No	?
J	0.130	No	No	No	No	?
K	0.724	Yes	Yes	Yes	Yes	Trace

and the vessels sealed. In sample K, CH_3TiCl_3 was distilled into the decomposition vessel. The ether was added, and the vessel sealed.

Sample vessels have a total volume of approximately 3 ml. Each was stored, in darkness or in u.v. according to the experiment, until decomposition was near complete. Those products volatile at liquid nitrogen temperature were then released into the inlet system of the AEI MS10 mass spectrometer. In some cases, a second subsequent release at −80 °C was made in a search for the less volatile methyl chloride. Results are shown in Table 2.

Estimation of Errors

Quantities of liquid reagents were measured volumetrically using microliter syringes. Amounts are accurate to at least 3% in all cases.

In those samples where CH_3TiCl_3 concentration was determined by n.m.r., the concentration is known to within 10%. In all other cases, the estimate is very rough but the reproducibility of the preparation is such that estimates are probably within 30% of being correct and quite possibly better. In any event, exact knowledge of concentrations is not essential.

The relative amounts of CH_3D and CH_4 were established on the basis of measurements of mass 16 (corrected for contributions from CH_3D) and of mass 17 (corrected for contributions from CH_4 and from background water). Reproducibility in successive spectra was better than 10%. In most cases, an average of two spectra was used in calculating the relative amounts.

The presence or absence of H_2, HD, D_2, C_2H_6, and CH_3Cl was determined in some cases, but no quantitative estimates were attempted. Not only are there solubility differences at −195 °C but there is certain to be variable occlusion of gases in the crystals of frozen solvent. The relative amounts of CH_4 and CH_3D, however, are unaffected by these factors.

Discussion

Limited Occurrence of Free Radical Mechanism

D'yachkovskii's conclusion (6) that the mechanism of decomposition of $CH_3TiCl_3 \cdot 2THF$ in toluene-d_8 is a free radical one is borne out by the data from samples F and G. Moreover, these experiments show that the mechanism producing CH_3D does not require irradiation, removing any suspicion that the production of CH_3D arose from continuous irradiation in the u.v. spectrometer.

However, samples A to E show unequivocally that it is incorrect to apply this mechanism generally to other coordinating solvents, including the diethyl ether case of Beermann and Bestian (5). In the formation of methane by decomposition of CH_3TiCl_3 in noncoordinating solvents, the solvent is not the source of the fourth hydrogen (3, 7). In diethyl ether/alkane mixtures, the fourth hydrogen is to some extent obtained from the ether but never from the alkane. A free radical mechanism is therefore ruled out.

On the other hand, a free radical mechanism is supported by the evidence for the system $CH_3TiCl_3 \cdot 2THF$ in toluene-d_8, although an alternative explanation is available. Garnett has reviewed the mechanisms of transition metal catalysis of hydrogen exchange (8). His dissociative π-complex mechanism provides a route whereby a D atom from toluene-d_8 could find its way to subsequent elimination as CH_3D. Such exchanges are well established for alkyl benzenes and even for alkanes, and while one is reluctant to compare Garnett's acidic Pt(II) systems with those of the present work, it should be noted that there is evidence of catalysis of hydrogen exchange by reduced titanium. Coordination of aromatics to CH_3TiCl_3 has already

Can. J. Chem. Downloaded from www.nrcresearchpress.com by 210.87.254.42 on 09/05/12
For personal use only.

Can. J. Chem. Downloaded from www.nrcresearchpress.com by 210.87.254.42 on 09/05/12
For personal use only.

been suggested on the basis of both decomposition (7) and n.m.r. (9) data. The possibility of catalyzed hydrogen exchange has also been suggested (7) as the explanation of the scrambling of hydrogens in the products of deuterolysis (7, 10, 11). The presence of traces of CH_3D among the products of decomposition of CH_3TiCl_3 in toluene-d_8 (sample J) and its complete absence in heptane and cyclohexane (3) support the suggestion that toluene coordinates to titanium and can transfer a hydrogen to the metal, thus providing an alternative explanation to the free radical one, at least for sample I.

While the balance of evidence supports a free radical mechanism in tetrahydrofuran, other alternatives should continue to be examined in all cases, and must be examined for solvents like diethyl ether where the free radical mechanism is invalid.

An Alternative Mechanism for Diethyl Ether

Alkane elimination involving abstraction of a hydrogen from an atom β to the metal by an alkyl attached to the same metal is well established as the mechanism of decomposition of many transition metal alkyls (1) including those of titanium (3). Moreover, such abstraction has been observed in molecules having atoms other than carbon in the α position (12, 13) although it is uncertain from the data in the cases cited if decomposition occurs in the liquid or solid. Related examples can be found elsewhere in transition metal chemistry, such as the formation of iridium hydrides from alcohols (14).

Abstraction from coordinated diethyl ether offers this pathway in samples A to E. Such a mechanism explains why deuterium is obtained from the ether but never from the alkane. Cyclic ethers have "β-hydrogens" further removed from the metal, and their complexes decompose markedly more slowly (4, 5). Ethers lacking a hydrogen on the atom β to the metal might be expected not to produce rapid decomposition. Preliminary experiments with diphenyl ether confirm this. Such a solvent has important possibilities both for fundamental studies and for the development of novel Ziegler catalysts.

Initiation of Autocatalysis

These experiments reveal a second point. In those systems involving deuterated ether (samples A, A′, E, and K), CH_4 and not CH_3D is the major product. Since this is true even in samples where other solvents are either deuterated (sample E) or absent (sample K), CH_3TiCl_3 itself must be the source of the fourth hydrogen. Thus while the presence of diethyl ether increases the rate of decomposition by several orders of magnitude, only a small part of the methane is formed through direct abstraction of a hydrogen from the ether.

Methane is formed in non-coordinating solvents without any contribution of hydrogen from the solvent (3) but at relatively slow rates (7). However the process is autocatalytic (5, 7), the solid decomposition products acting as the catalyst. If the solid produced in the ether systems catalyzed this reaction, as well as initiating the autocatalysis, a large amount of CH_4 would result.

Such an explanation gains additional support from samples H and H′. Here decomposition occurs in a non-polar but irradiated solvent. The rate of decomposition is at least two orders of magnitude greater than in the absence of irradiation, but we find relatively little CH_3D, the expected product of photodecomposition. Catalysis of decomposition by small nuclei of solid products, produced photolytically throughout the solution, is suggested, in analogy with the ether case where the "β-mechanism" serves to provide the initial catalyst.

Ethane is produced at accelerated rates when such decompositions occur in some coordinating solvents but it is much less abundant relative to methane than is the case for comparable concentrations and temperatures in non-coordinating solvents (7). While the production of ethane without solvent contribution must involve at least two CH_3TiCl_3 molecules, the complete absence of ethane among the products of $(CH_3)_2TiCl_2$ (7) strongly suggests that this latter species is not an intermediate. The mechanism is therefore likely to involve binuclear elimination. Strong coordination of tetrahydrofuran or toluene would interfere with this mechanism, as is observed in samples F, G, I, and J, providing further evidence of the active role of aromatic solvents.

Relationship to Thermal Decomposition of Other Transition Metal Alkyls

Recent work suggests that where the "β-mechanism" involves an alkyl group, there is a hydride/olefin intermediate (18–20). In the case

Can. J. Chem. Downloaded from www.nrcresearchpress.com by 210.87.254.42 on 09/05/12
For personal use only.

of dialkyls, the reductive elimination of an alkane from such an intermediate would account for the observed product distribution.

In the decomposition of $(C_2H_5)_2Ti(C_5H_5)_2$, it has been shown that ethane is evolved more rapidly than ethylene, with both eventually appearing in equal quantities (15). Since titanium systems are efficient polymerization catalysts, the olefin predicted on the basis of this mechanism would be expected as polymer. Polyolefins have been reported by several investigators (5, 7). The proposed mechanism is also supported by the formation of CH_4 and C_2H_4 but never of C_2H_6 in mixed methyl and ethyl titanium systems (5); by the olefinic terminations of polyolefins produced on titanium based Ziegler catalysts (16, 17); and by the evidence of equilibria producing olefin/hydride species in related systems (18–20). Postulation of a slower, analogous α-elimination for methyl compounds, involving a carbene intermediate, is much more speculative, but such a route has been proposed (21, 22) for methyl chromium(III) compounds.

The hydride intermediate mechanism requires at least one vacant coordination site. Thus factors which lead to five or six coordinate configurations, providing that they do not block all sites, would enhance the rate of both eliminations. Absorptions of $(CH_3)_2TiCl_2$ on a β-$TiCl_3$ substrate would achieve this, as would coordination with suitable solvents. Strongly coordinating solvents, however, will retard the decomposition by blocking the vacancy necessary for the formation of the intermediate. This last point has already been put forward in a general way (23) and has been convincingly demonstrated for di-*n*-butylbis(triphenyl phosphine) platinum(II) (20). It explains why rates of CH_3TiCl_3 are slower in strongly coordinating tetrahydrofuran than in weakly coordinating diethyl ether, and are slower still with bidentate ligands (24), although, contrary to the last reference, solutions of uncoordinated CH_3TiCl_3 decompose more slowly still (7, 25).

Multiple Effects of Coordinating Species

Coordination may be expected to have at least two other influences on the rate and path of decomposition of CH_3TiCl_3 as well as other transition metal compounds.

Where the product solid catalyzes decomposition, the product species may itself be coordinated. This may alter its catalytic properties completely, even rendering it soluble.

Moreover, in certain cases where equilibria are involved, such as the proposed route (7) whereby CH_3TiCl_3 yields CH_4 through a disproportionation into $(CH_3)_2TiCl_2$ and $TiCl_4$, preferential coordination to one species could shift the equilibrium and increase or decrease the equilibrium concentration of the intermediate species. This particular effect has no analogy in many related cases, such as in the decomposition of $(CH_3)_4Ti$. Indeed, in this case, there is neither a catalyzing solid product nor an equilibrium, and the only effect of coordinating solvents is to block coordination sites needed for the decomposition path. Thus coordinating solvents invariably slow the decomposition, with the greatest effect from strongly coordinating bidentate ligands (26), and with those having a hydrogen on a β atom showing some decomposition by this route (27, 28).

The Similarities of Titanium Alkyls to the Alkyls of Other Transition Metals

The similarity of the mechanisms proposed to those proposed by other authors for other metal alkyls is worth emphasis. There has been a suggestion, sometimes explicit (2), that titanium alkyls are markedly different, and in particular that "promotional pathways . . . play a major role at the beginning of the transition metal series" whereas these pathways "do not operate at the end of the transition series" where "concerted pathways" are believed to dominate. The present work, and the accompanying analysis, suggest for titanium alkyls the same three mechanisms described by Braterman and Cross for the end of the series; β-elimination, reductive elimination, and binuclear elimination. These are all "concerted pathways" in the sense used by Braterman and Cross. It is "the availability of such pathways that controls the lability of the metal carbon bond" for titanium as for other metals.

Thanks are due to Queen's University for financial support of this research; to Dr. J. A. Stone for provision of the MS10 and for much kind advice on its use; and to Drs. M. C. Baird and B. K. Hunter for provocative discussions.

1. M. L. H. Green. Organometallic compounds. Vol. 2. 3rd ed. Methuen, London. 1968. p. 221.
2. P. S. Braterman and R. J. Cross. J.C.S. Dalton, 657 (1972).

3. H. DE VRIES. Rec. Trav. Chim. **80**, 866 (1961).
4. R. J. H. CLARK and A. J. MCALEES. J. Chem. Soc. A, 2026 (1970).
5. C. BEERMANN and H. BESTIAN. Angew. Chem. **71**, 618 (1959).
6. F. S. D'YACHKOVSKII, N. E. KHRUSHCH, and A. E. SHILOV. Kin. i Katal, **9**, 1006 (1968).
7. J. D. MCCOWAN and J. F. HANLAN. Can. J. Chem. **50**, 755 (1972).
8. J. L. GARNETT. Catal. Rev. **5**, 229 (1971).
9. J. F. HANLAN and J. D. MCCOWAN. Can. J. Chem. **50**, 747 (1972).
10. L. A. M. RODRIGUEZ, J. GABANT, and B. HARGITAY. Tetrahedron Lett. **17**, 7 (1959).
11. L. A. M. RODRIGUEZ and J. GABANT. J. Polym. Sci. **57**, 881 (1962).
12. H. BURGER and H. J. NEESE. J. Organomet. Chem. **20**, 129 (1969).
13. H. BURGER and H. J. NEESE. J. Organomet. Chem. **21**, 381 (1970).
14. L. VASKA and J. W. DILUZIO. J. Am. Chem. Soc. **84**, 4989 (1962).
15. H. SINN and F. PATAT. Angew. Chem. Int. **3**, 93 (1964).
16. G. NATTA. J. Polym. Sci. **34**, 21 (1959).
17. A. SCHINDLER. Makromol. Chem. **70**, 94 (1964).
18. R. J. O'BRIEN, J. DVORAK, and W. SANTO. Chem. Commun. 411 (1970).
19. M. TSUTSUI, M. HANCOCK, J. ARIYOSHI, and M. N. LEVY. Angew. Chem. Int. **8**, 410 (1969).
20. G. M. WHITESIDES, J. F. GAASCH, and E. R. STREDONSKY. J. Am. Chem. Soc. **94**, 5258 (1972).
21. M. MICHMAN and H. H. ZEISS. J. Organomet. Chem. **13**, P23 (1968).
22. J. R. C. LIGHT and H. H. ZEISS. J. Organomet. Chem. **21**, 391 (1970).
23. G. YAGUPSKY, W. MOWAT, A. SHORTLAND, and G. WILKINSON. Chem. Commun. 1369 (1970).
24. G. W. A. FOWLES, D. A. RICE, and J. D. WILKINS. J. Chem. Soc. A, 1920 (1971).
25. K. H. THIELE, P. ZDUNNECK, and D. BAUMGART. Z. anorg. allg. Chem. **378**, 62 (1970).
26. J. MÜLLER and K. H. THIELE. Z. anorg. allg. Chem. **362**, 120 (1968).
27. G. A. RAZUVAEV, V. N. LATYAEVA, and A. V. MALYSHEVA. Dokl. **173**, 1353 (1967).
28. V. N. LATYAEVA, A. P. BATALOV, A. V. MALYSHEVA, and V. I. KULEMIR. J. Gen. Chem. U.S.S.R. **38**, 282 (1968).

Can. J. Chem. Downloaded from www.nrcresearchpress.com by 210.87.254.42 on 09/05/12
For personal use only.

Pyrrole Chemistry. XV. The Chemistry of Some 3,4-Disubstituted Pyrroles[1]

JOHN KINGTON GROVES, NIVEN EDDY CUNDASAWMY, AND HUGH JOHN ANDERSON
Department of Chemistry, Memorial University, of Newfoundland, St. John's, Newfoundland

Received October 13, 1972

The syntheses of a variety of 3,4-disubstituted pyrroles including the antimitotic agent Verrucarin E are described. 3,4-Pyrroledicarboxylic esters were prepared through a Diels–Alder reaction. Partial hydrolysis of the diesters gave the 4-ester-3-acids which were modified to achieve the synthesis of a variety of unsymmetrically 3,4-disubstituted pyrroles. Raney nickel reduction of a thiolester gave hydroxymethyl under conditions which left acyl or carbalkoxy substituents unaffected. Pyrrole reactions involving carbanionic reagents are complicated by 1-proton abstraction. Therefore, when necessary, the nitrogen was protected by an *N*-benzyloxymethyl substituent which can be cleaved to the *N*-hydroxymethyl derivative by aluminum chloride or by hydrogenolysis. Subsequent treatment with benzyltrimethylammonium hydroxide gave back the pyrrole.

On a réalisé la synthèse de divers derivés bifonctionnels du pyrrole, y compris celle de l'agent antimitotique 'Verrucarin E', à partir des esters de l'acide pyrroledicarboxylique-3,4 qui furent préparés d'une réaction du type "Diels–Alder". L'hydrolyse partielle des esters a donné les ester-4-acides-3 qui furent alors transformés en de différents composés bifonctionnels et non-symmétriques. La réduction d'un thiolester en présence de nickel de Raney conduit à l'hydroxymethyl correspondant sous des conditions qui n'ont pas touché un groupe acyle ou carboalcoxy. Les réactions de pyrrole avec des réactifs carbanioniques sont compliquées par l'arrachement du proton-1. Alors, selon le besoin, l'azote fut protégé par un substituant benzyloxymethyl-*N* qui peut être scié par traitement avec le chlorure d'aluminium ou par l'hydrogenolyse pour amener a l'hydroxymethyl correspondant. Un traitement ultérieur par l'hydroxide de benzyltrimethylammonium ramène au pyrrole.

Can. J. Chem., **51**, 1089 (1973)

We have recently reported new syntheses of some 3-substituted pyrroles (1, 2) and in continuation of our efforts to devise viable routes to the less accessible pyrroles we have developed syntheses of a variety of 3,4-disubstituted pyrroles. These were of particular interest in view of the recent reassignment of the structure of the antimitotic agent Verrucarin E; originally thought to be 2-hydroxymethyl-4-acetylpyrrole (3), but later revised to 3-acetyl-4-hydroxymethylpyrrole (4). A synthesis of Verrucarin E starting from 2-carbethoxy-3-acetylpyrrole has been described (4), but the yield was very low and the method lacked flexibility.

The introduction of substituents into the two β-positions of the pyrrole nucleus may be accomplished by reaction with acetylenic dienophiles (5–8). Addition across the pyrrole "diene" system **1** gives 7-azanorbornadienes (**2**) which may undergo a retrodiene reaction to either reactants or the substituted pyrrole **3** (see Scheme 1). Although pyrrole itself is known to undergo cycloaddition reactions (9) the formation of 3,4-substituted pyrroles in reasonable yield requires the presence of an electron-withdrawing *N*-substituent. This is said to increase the diene character of the pyrrole system (*cf.* ref. 10) and inhibits attachment of a second molecule of dienophile (11, 12).

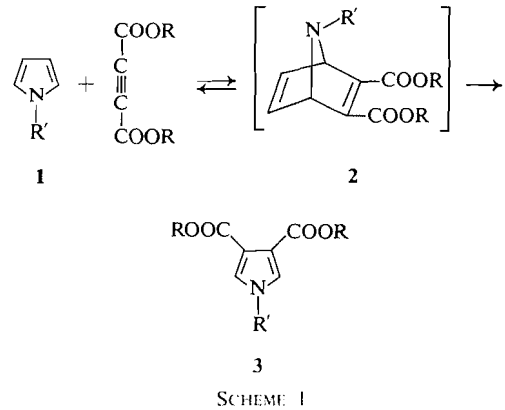

1 **2** **3**

SCHEME 1

Pyrrole *N*-esters have been converted to the triester **3** (R = Me or Et, R′ = COOMe or COOEt) and then selectively hydrolyzed to dialkyl 3,4-pyrroledicarboxylate (**4**, R = Me or Et) (6, 7). *N*-Benzoylpyrrole was found to give higher yields of the 3,4-diesters **3** (R = Me or

[1]Presented in part at the 54th Canadian Chemical Conference of the Chemical Institute of Canada, Halifax, N.S., June, 1971.

Can. J. Chem. Downloaded from www.nrcresearchpress.com by 210.87.254.6 on 09/05/12
For personal use only.

Can. J. Chem. Downloaded from www.nrcresearchpress.com by 210.87.254.6 on 09/05/12
For personal use only.

Et, R′ = COPh) with dimethyl and diethyl acetylenedicarboxylate than did the *N*-esters. Hydrolysis of the trisubstituted pyrroles may be controlled to afford either the diester **4** (R = Me or Et), the monoester **5** (R = Me or Et), or the diacid **6** in very high yield.

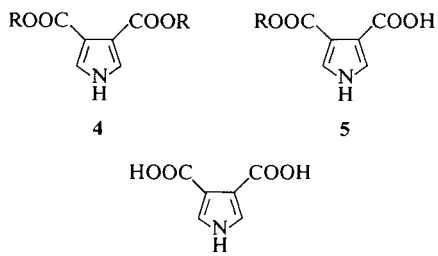

4 **5**

6

The monoester **5** is a potential starting material for the synthesis of 3,4-disubstituted pyrroles. The carboxylic acid group of the monoester **5** (R = Me) was readily converted into an aroyl ketone **8** by a Friedel–Crafts reaction of the acid chloride **7** with benzene or anisole. The anilide **9** and the mixed esters **10** and **11** were obtained by reaction of **7** with aniline, ethanol, and ethanethiol respectively. The conversion of

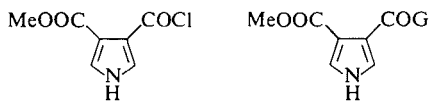

7 **8** G = Ph or anisyl
9 NHPh
10 OEt
11 SEt
14 Et
15 $CH(COO\text{-}t\text{-}Bu)_2$
16 CH_3

an acid derivative to a ketone generally requires a nucleophilic reagent and will be discussed later. 3,4-Pyrroledicarbonyl chloride was found to behave normally with ethanethiol, but Friedel-Crafts acylation using aluminum chloride in benzene was found to give 3,4-dibenzoylpyrrole. This contrasts with 1-*n*-butyl-2,5-dimethyl-3,4-pyrroledicarbonyl chloride which is reported to give an analog of **12** (13) (see Scheme 2).

The reduction of an *N*-unsubstituted carboxylic acid derivative of pyrrole to the corresponding hydroxymethyl compound is often difficult since abstraction of the 1-proton initiates further reduction of the intermediate alcohol to the corresponding alkyl group (14) (Scheme 3). In the case of 3,4-disubstituted pyrroles the problem of reduction is further complicated by the presence of a second reducible group, either ketone or ester. Raney nickel was found to reduce selectively the corresponding ester thiolester **11** to the hydroxymethylpyrrole **13**.

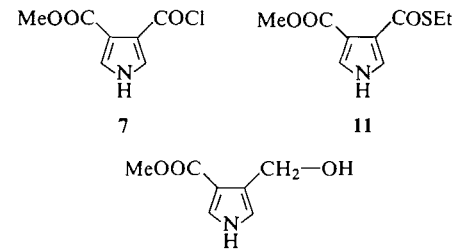

7 **11**

13

The synthesis of Verrucarin E requires the conversion of one of the β-carboxylate substituents into a methyl ketone. Reaction of the acid chloride **7** with excess methylmagnesium bromide or with dimethylcadmium gave only hydrolyzed starting material, while diethylcadmium gave a low yield of the corresponding ethyl ketone **14**. The use of the less basic methylmercuric iodide alone, or catalyzed with aluminum chloride, failed to effect any reaction. Condensation of **7** with sodium di-*tert*-butyl malonate gave only low yields of the ketomalo-

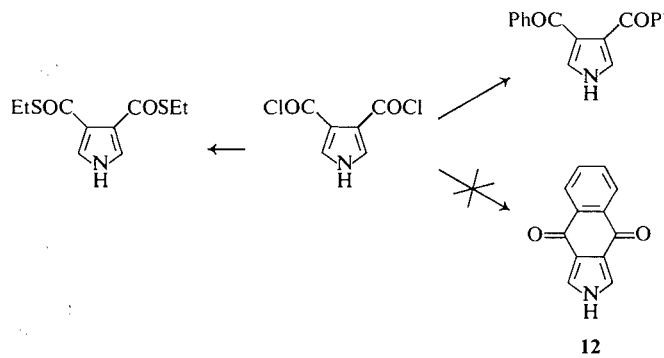

12

SCHEME 2

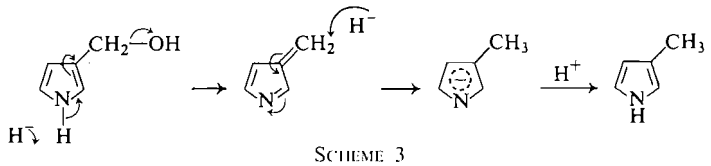

SCHEME 3

nate **15** although subsequent acid-catalyzed conversion to the ketone **16** was successful. Reaction of **7** with diazomethane resulted in *N*-methylation.

Abstraction of the acidic 1-proton by the carbanionic reagent and conjugative transfer of the resulting negative charge to the carbonyl substituents is probably the major factor accounting for the low reactivity of the chlorocarbonyl group in the above reactions.

At this point it was necessary to reconsider the synthetic approach to Verrucarin E. One problem was the very low solubility of pyrroles possessing electron-withdrawing groups in both 3- and 4-positions. This interfered with many of the reactions. For example, a potential ketone synthesis failed when it proved impossible to convert the 3,4-diacid to its cyclic anhydride because of the extreme insolubility of the diacid. The use of the di- and monoethyl esters rather than the methyl ones produced a considerable increase in solubilities and all further reactions involved these compounds.

The second major obstacle was the acidity of the *N*-hydrogen on these compounds as discussed above. This required that a base-stable, removable blocking group be found. Remers and co-workers (15) have examined 1-acetyl, 1-benzyol, 1-benzenesulfonyl, and 1-benzyl substituents for their suitability as protecting groups for the pyrrole nitrogen. Only the 1-benzyl substituent was found to be base-stable and since this is subsequently cleaved by sodium in liquid ammonia, its utility is restricted to compounds compatible with such vigorous reductive cleavage. Catalytic hydrogenolysis of the 1-benzyl substituent has previously been shown to be difficult for compounds in which the pyrrole nucleus bears electron-withdrawing substituents (16). After trials with several other reagents, diethyl 1-benzyloxymethyl-3,4-pyrroledicarboxylate (**17**) was prepared by reaction of the sodium salt of the diester **10** with benzyl chloromethyl ether. This provided an *N*-substituent stable to both acid and base but which could be cleaved by hydrogenolysis (17) or by aluminum chloride to the *N*-hydroxymethyl derivative **18**. On subsequent treatment of **18** with benzyltrimethylammonium hydroxide it rapidly lost formaldehyde to give back the pyrrole. As might be expected, it also increased the generally low solubility of the 3,4-disubstituted compounds.

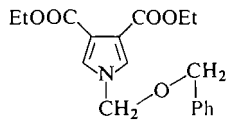

17

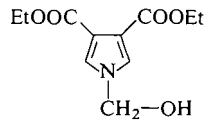

18

Basic hydrolysis of the protected diester **17** gave the corresponding 3,4-diacid **19**. On treatment with dicyclohexylcarbodiimide at 30° the diacid **19** gave an anhydride which was difficult to purify[2] and exhibited only a low reactivity towards dimethylcadmium, methylmagnesium iodide, and methyllithium.

A more satisfactory route to the ketone involves controlled hydrolysis of the diester **17** to the monoester **20**. Subsequent reaction of the corresponding acid chloride **21** with dimethylcadmium afforded the *N*-protected ketone **22** in fair yield, together with some unreacted **21**.

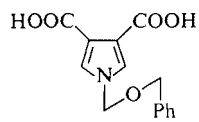

19

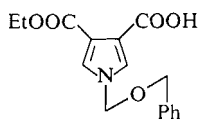

20

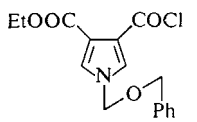

21

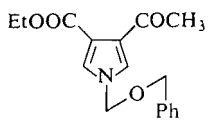

22

Conversion of **22** to Verrucarin E requires the removal of the *N*-protecting group and reduction of the remaining carboxylate substituent into hydroxymethyl via the thiolester. Although selective hydrogenolysis of a benzyl ether in the presence of an aromatic (including pyrrolic) ketone is usually possible (18–20) hydrogenation of **22** under various conditions resulted in either

[2]Physical properties suggested a mixture of monomeric and polymeric species.

Can. J. Chem. Downloaded from www.nrcresearchpress.com by 210.87.254.6 on 09/05/12
For personal use only.

Can. J. Chem. Downloaded from www.nrcresearchpress.com by 210.87.254.6 on 09/05/12
For personal use only.

no reaction or in preferential reduction of the ketone. Whilst cleavage of the benzyl ether occurred subsequent to reduction of the ketone, the p.m.r. of the product showed that concurrent hydrogenolysis of the hydroxyethyl group had occurred. It was then found that the benzyl ether in compound **22** could be readily cleaved to the corresponding 1-hydroxymethyl derivative with aluminum chloride. However, as the *N*-protecting group increased solubilities it was decided to retain it as long as possible. Conversion of the 3-carboxylate substituent to the 3-hydroxymethyl group is the other operation required to complete the synthesis. Hydrolysis of **22** to the acid **23** followed by conversion to the acid chloride and treatment with sodium ethanethioxide, gave an excellent yield of the corresponding thiolcarboxylate **24**. The benzyl ether in compound **24** was cleaved with aluminum chloride to the corresponding *N*-hydroxymethyl derivative **25** which on subsequent treatment with benzyltrimethylammonium hydroxide lost formaldehyde affording ethyl 3-acetyl-4-pyrrolethiolcarboxylate (**26**). The Raney nickel reduction of the thiolester group in compound **26** gave the hydroxymethyl derivative, Verrucarin E (**27**). The m.p. and i.r., u.v., and p.m.r. spectra of the synthetic compound were identical with those of natural Verrucarin E. The R_f values of the synthetic product were in agreement with those of the natural compound in various solvent systems.[3]

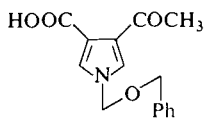

23

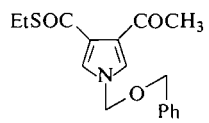

24

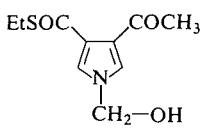

25

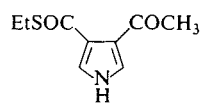

26

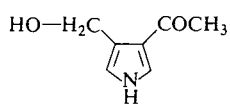

27

[3]The authors are indebted to Prof. Ch. Tamm who kindly provided an authentic specimen of Verrucarin E for comparison.

Confirmation of the proposed product structures is provided by their i.r., n.m.r., and mass spectral data. N.m.r. data for the trisubstituted pyrroles is given in Table 1.

Data for the 3,4-disubstituted pyrroles, given in Table 2, require further comment. Since many of the compounds were of low solubility their spectra were determined in dimethyl sulfoxide-d_6 solution. In this solvent spin–spin coupling between the 1-proton and the α-protons was not apparent, except in those cases where the pyrrole had a CO_2H substituent, because of rapid exchange of the acidic 1-proton with the basic solvent. As a consequence the symmetrical disubstituted compounds exhibited a singlet absorption for the α-protons whilst the unsymmetrical ones gave an AB type quartet. In deuterochloroform solution these absorptions appear as A_2X and ABX respectively.

I.r. data for the compounds are reported in the Experimental. In certain compounds the C=O stretching vibration occurs at an anomalously low frequency, a result which we attribute to intramolecular hydrogen bonding. Compare the values in the Experimental for **4** (R = Me or Et) **16**, **17**, and **22**.

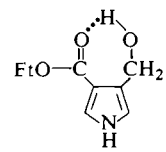

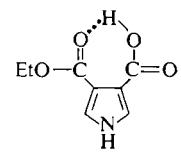

$*\nu_{max}$ 1670 cm^{-1} (Nujol)

1625 (Nujol)

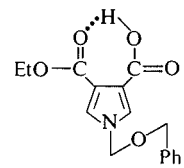

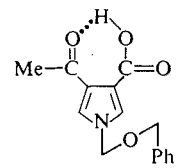

1635 ($CHCl_3$)

1620 ($CHCl_3$)

*Stretching frequency of H-bonded carbonyl group

Most of the compounds reported exhibit an intense u.v. absorption in the 250 nm region. A further maximum below 215 nm was outside the useful range of the instrument used.

The major peaks in the mass spectra of some 2,4-disubstituted pyrroles are reported in Table 3. With the exception of the thiolesters the molecular ions are all of moderate abundance. The major fragmentation of each molecular ion

TABLE 1. N.m.r. data for trisubstituted pyrroles*

Substituent			τ-Value			
1	3	4	1-Substituent	α-H	3-Substituent	4-Substituent
CO_2Me	CO_2Me	CO_2Me	5.90	2.10	6.10	6.10
COPh	CO_2Me	CO_2Me	2.10 (m)	2.18	6.13	6.13
COPh	CO_2Et	CO_2Et	2.10 (m)	2.15	5.62 8.66	5.62 8.66
CH_2OH	CO_2Et	CO_2Et	4.68	2.64	5.72 8.68	5.72 8.68
CH_2OCH_2Ph	CO_2Et	CO_2Et	2.66 (br) 4.77 5.55	2.66	5.71 8.66	5.71 8.66
CH_2OCH_2Ph	CO_2H	CO_2H†	2.58 (br) 4.40 5.38	2.30	—	—
CH_2OCH_2Ph	CO_2Et	CO_2H	2.65 (br) 4.66 5.48	2.46§ 2.20§	5.59 8.62	— —
CH_2OCH_2Ph	CO_2Et	COMe	2.65 (br) 4.75 5.53	2.65 (br)	5.69 8.65	7.45
CH_2OCH_2Ph	CO_2H	COMe‡	2.58 (br) 4.35 5.33	2.30 (m)	—	7.35
CH_2OCH_2Ph	COMe	COSEt	2.63 4.75 5.50	2.63	7.51	6.94 8.65
CH_2OH	COMe	COSEt	4.6 (br)	2.63§ 2.55§	7.60	7.00 8.68
H	COMe	COSEt	—	2.50 (m)	7.51	7.00 8.70
H	COMe	CH_2OH	—	2.6 (q) 3.3 (m)	7.55	5.38

*In $CDCl_3$ except as noted.
†In $(CD_3)_2SO$.
‡In $(CD_3)_2CO$.
§$J_{2,5}$ = 2.6 Hz.

involves acylium ion formation. The subsequent major fragmentation of the ions **28** (R′ = OEt or SEt) appears to involve ejection of ethylene to give an ion to which may be ascribed structure **29***a* or *b* (X = O or S) (21). The corresponding ion **28**(R′ = OMe) undergoes a different fragmentation with the loss of CH_2O, to give the ion $C_6H_4NO_2^+$.

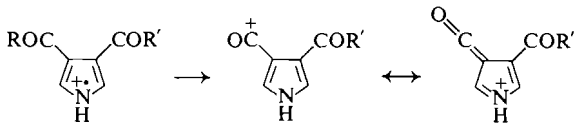

28

SCHEME 4

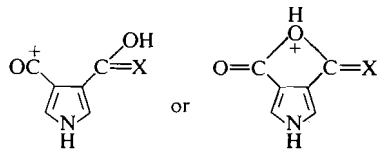

29*a* **29***b*

Experimental

Instruments and conditions were as described in ref. 22 except that i.r. spectra were determined in chloroform solution unless otherwise stated.

General Procedure for Diels–Alder Reactions

Dialkyl acetylenedicarboxylate (1.0 equiv) was added over 30 min to the 1-substituted pyrrole in a flask maintained at 190° and flushed with nitrogen. The reaction

Can. J. Chem. Downloaded from www.nrcresearchpress.com by 210.87.254.6 on 09/05/12
For personal use only.

TABLE 2. N.m.r. data for disubstituted pyrroles*

Substituents		τ-Value		
3	4	α-H	3-Substituent	4-Substituent
CO_2Me	CO_2Me	2.57	6.30	6.30
CO_2Et	CO_2Et	2.64	5.87 8.79	5.87 8.79
COSEt	COSEt	2.35	7.05 8.75	7.05 8.75
COPh	COPh	complex multiplet	2.0–2.7	
CO_2H	CO_2H	2.32 ($J_{1,2}$ = 3.0)	—	—
CO_2Me	CO_2H	2.40 ($J_{1,2}$ = 3.0) ($J_{2,5}$ = 2.2)	6.15	—
CO_2Me	CO_2Et	2.52	6.25	5.79 8.75
CO_2Me	COSEt	2.52	6.40	7.13 8.80
CO_2Me	CONHPh	2.53	6.83	2.1–2.6 (m)
CO_2Me	COC_6H_4OMe	2.42 ($J_{2,5}$ = 2.2)	6.46	6.12 2.18 2.92
CO_2Me	COC_6H_5	2.16 ($J_{2,5}$ = 2.2) 2.69	6.50	2.0–2.7(m)
CO_2Me	COEt	2.50 2.60	6.28	7.15 8.95
CO_2Me	CH_2OH	2.58 ($J_{2,5}$ = 2.3) 3.20	6.30	5.37(J=0.8)

*In $(CD_3)_2SO$.

TABLE 3. Mass spectral data for some disubstituted pyrroles

Substituents		Ion mass and abundance				
3	4					
(COR′)	(COR)	$M\cdot^+$	$(M\text{-}R')^+$	$(M\text{-}R)^+$	**29**	$C_6H_4NO_2^+$
CO_2Me	CO_2Me	183 (38)	152 (100)			122 (69)*
CO_2Et	CO_2Et	211 (22)	166 (40)		138 (100)†	—
COSEt	COSEt	243 (0.02)	182 (100)		154 (76)‡	—
COPh	COPh	275 (93)	198 (100)			—
CO_2Me	CO_2Et	197 (37)	166 (22)	152 (100)	138 (76)†	122 (51)*
CO_2Me	CO_2H	169 (43)	138 (100)	152 (100)		122 (12)*
CO_2Me	CONHPh	244 (39)	213 (4)	152 (100)		122 (53)*
CO_2Me	COSEt	217 (1)	186 (3)	152 (100)		122 (47)*
CO_2Me	COEt	181 (25)	150 (16)	152 (100)		122 (65)*
CO_2Me	COPh	229 (46)	198 (18)	152 (100)		122 (40)*
CO_2Me	COC_6H_4OMe	259 (18)	228 (6)	152 (26)		122 (18)*

M = 98.
†M* = 115.
‡M* = 130.

Can. J. Chem. Downloaded from www.nrcresearchpress.com by 210.87.254.6 on 09/05/12
For personal use only.

Can. J. Chem. Downloaded from www.nrcresearchpress.com by 210.87.254.6 on 09/05/12
For personal use only.

mixture was maintained at this temperature for a further 2 h prior to isolating the product.

Trimethyl 1,3,4-Pyrroletricarboxylate

Reaction of methyl 1-pyrrolecarboxylate (0.05 mol) and dimethyl acetylenedicarboxylate gave a dark oil which crystallized from methanol affording trimethyl 1,3,4-pyrroletricarboxylate, m.p. 67–68° (4.2 g, 35%) (lit. m.p. 69° (6)); ν_{max} 1775, 1745, and 1718 cm^{-1} (C=O); λ_{max} (MeOH) 247 nm (ε 7950).

Dimethyl 1-Benzoyl-3,4-pyrroledicarboxylate

1-Benzoylpyrrole (0.1 mol) and dimethyl acetylenedicarboxylate afforded an oil which was distilled to give recovered 1-benzoylpyrrole (4 g, 23%) and dimethyl 1-benzoyl-3,4-pyrroledicarboxylate (19.2 g, 67%), b.p. 210–212°/0.2 mm, which crystallized as needless, m.p. 115–116° (from MeOH); λ_{max} (MeOH) 229 (ε 17 600) and 253 nm (sh ε 9900).

Anal. Calcd. for $C_{15}H_{13}NO_5$: C, 62.7; H, 4.5. Found: C, 62.8; H, 4.4.

Diethyl 1-Benzoyl-3,4-pyrroledicarboxylate

Diethyl acetylenedicarboxylate similarly gave recovered 1-benzoylpyrrole (2.0 g, 25%) and diethyl 1-benzoyl-3,4-pyrroledicarboxylate b.p. 205–210°/0.2 mm, needles m.p. 65–66° (from petroleum (8.5 g, 54%); ν_{max} 1715 and 1732 sh cm^{-1} (C=O); λ_{max} (EtOH) 227 (ε 11 850) and 242 nm (sh ε 9750).

Anal. Calcd. for $C_{17}H_{17}NO_5$: C, 64.8; H, 5.4. Found: C, 64.9; H, 5.4.

Dimethyl 3,4-Pyrroledicarboxylate

Dimethyl 1-benzoyl-3,4-pyrroledicarboxylate (10.0 g) was added to KOH (1.5 g) in methanol (50 ml) and the mixture stirred at 5° for 3 h. The precipitated dimethyl 3,4-pyrroledicarboxylate was filtered and recrystallized from xylene to give needles (6.0 g, 94%), m.p. 242–243° (lit. m.p. 245° (6)); ν_{max} (Nujol mull) 1710 (C=O) and 3255 (N—H) cm^{-1}; λ_{max} (EtOH) 253 nm (ε 7900).

Diethyl 3,4-Pyrroledicarboxylate

Diethyl 1-benzoyl-3,4-pyrroledicarboxylate (3.15 g) was added to KOH (600 mg) in EtOH (65 ml) and the mixture was stirred at 20° for 2.5 h. The mixture was then cooled to 0° and the precipitated diethyl 3,4-pyrroledicarboxylate was collected by vacuum filtration. Recrystallization (from aqueous EtOH) gave plates, m.p. 151–152° (2.0 g, 95%) (lit. m.p. 153–154° (7)); λ_{max} (EtOH) 252 nm (ε 7500); ν_{max} 1730 and 1705 sh (C=O) and 3448 cm^{-1} (N—H).

3,4-Pyrroledicarboxylic Acid

Dimethyl 3,4-pyrroledicarboxylate (2.0 g), NaOH (20 g), and 50% aqueous MeOH (15 ml) were heated under reflux for 2 h. The resulting solution was poured onto ice and 3,4-pyrroledicarboxylic acid (1.55 g, 91%) was precipitated by addition of 2 *M* HCl. The acid had m.p. >300° (dec.) (lit. m.p. 290–292° dec. (6, 7)); ν_{max} (Nujol mull) 1590 (C=O), 2000–3000 (O—H), and 3160 cm^{-1} (N—H); λ_{max} (MeOH) 240 (ε 7900) and 259 nm (ε 7500).

3,4-Pyrroledicarbonyl Chloride

3,4-Pyrroledicarboxylic acid (155 mg), oxalyl chloride (1 ml), and dimethylformamide (1 drop) were heated under reflux in benzene (25 ml) for 30 min. Excess oxalyl chloride was distilled off leaving a homogenous, faintly yellow solution of pyrrole-3,4-dicarbonyl chloride.

Diethyl 3,4-Pyrroledithiolcarboxylate

The above diacid chloride solution, ethanethiol (1 ml), and pyridine (1 drop) were heated under reflux for 1 h. Cooling to 10° afforded diethyl pyrrole-3,4-dithiolcarboxylate as needles from benzene (160 mg, 66%), m.p. 179–180°; ν_{max} 1650 and 1640 cm^{-1} (C=O); λ_{max} (EtOH) 270 nm (ε 13 300).

Anal. Calcd. for $C_{10}H_{13}NO_2S_2$: C, 49.4; H, 5.4; N, 5.8. Found: C, 49.7; H, 5.2; N, 5.9.

3-Carbomethoxy-4-pyrrolecarboxylic Acid

Dimethyl 3,4-pyrroledicarboxylate (5.0 g) and methanolic KOH (1.53 g in 60 ml) were heated for 40 h on a steam bath. Water was added (10 ml) and the solution was filtered. Acidification of the filtrate afforded 3-carbomethoxy-4-pyrrolecarboxylic acid, m.p. 247–248° (from EtOH) (4.3 g, 93%); ν_{max} 1700 and 1625 (C=O) and 2500–3400 cm^{-1} (O—H); λ_{max} (EtOH) 245 (ε 8000) and 260 nm (ε 7350).

Anal. Calcd. for $C_7H_7NO_4$: C, 49.7; H, 4.2. Found: C, 49.9; H, 4.1.

3-Carbomethoxy-4-pyrrolecarbonyl Chloride

3-Carbomethoxy-4-pyrrolecarboxylic acid (1.0 g), oxalyl chloride (1.1 equiv), dimethylformamide (1 drop), and benzene (25 ml) were maintained at 50° for 2 h prior to cooling and filtering off the crude acid chloride (1.0 g, 90%); ν_{max} 1760 and 1715 cm^{-1} (C=O).

Ethyl 3-Carbomethoxy-4-pyrrolethiolcarboxylate

The above acid chloride (2.7 g), ethanethiol (1 ml), and benzene (30 ml) were heated under reflux for 2 h and then cooled to 10° to afford ethyl 3-carbomethoxy-4-pyrrolethiolcarboxylate, needles from benzene, m.p. 172.5–173° (2.3 g, 75%); ν_{max} 1710 and 1645 cm^{-1} (C=O); λ_{max} (EtOH) 255 (ε 9600) and 272 nm (7800).

Anal. Calcd. for $C_9H_{13}NO_3S$: C, 50.7; H, 5.2; N, 6.6. Found: C, 50.7; H, 5.0; N, 6.7.

3-Carbethoxy-4-carbomethoxypyrrole

The monoacid chloride (100 mg) and EtOH (5 ml) were heated under reflux for 1 h. Removal of excess EtOH afforded 3-carbethoxy-4-carbomethoxypyrrole, m.p. 159–160° (from $CHCl_3$) (97 mg, 92%); ν_{max} 1730 br cm^{-1} (C=O); λ_{max} (EtOH) 252 nm (ε 8500).

Anal. Calcd. for $C_9H_{11}NO_4$: C, 54.9; H, 5.6. Found: C, 54.9; H, 5.8.

3-Carbomethoxy-4-pyrrolecarboxanilide

3-Carbomethoxypyrrole-4-carbonyl chloride (100 mg), aniline (100 mg), and benzene (5 ml) were heated under reflux for 2 h. The mixture was cooled and filtered to afford 3-carbomethoxy-4-pyrrolecarboxanilide (105 mg, 85%). Sublimation (180°/0.1 mm) gave an analytical sample, m.p. 216–217°.

Anal. Calcd. for $C_{13}H_{12}N_2O_3$: C, 64.0; H, 4.9. Found: C, 63.9; H, 4.8.

3-Carbomethoxy-4-hydroxymethylpyrrole

Ethyl 3-carbomethoxy-4-pyrrolethiolcarboxylate (300 mg) in EtOH (75 ml) was cooled to 0° and W5 Raney nickel (2 g) was added. After 40 min in a Parr hydrogenator at 25° and 30 p.s.i. of hydrogen, the catalyst was removed

Can. J. Chem. Downloaded from www.nrcresearchpress.com by 210.87.254.6 on 09/05/12
For personal use only.

by filtration through a Celite pad and washed with EtOH (200 ml). Concentration of the filtrate and washings yielded 3-carbomethoxy-4-hydroxymethylpyrrole, m.p. 94–95° (from EtOH) (148 mg, 68%); ν_{max} 1690 (C=O) and 3450 cm^{-1} (N—H).

Anal. Calcd. for $C_7H_9NO_3$: C, 54.2; H, 5.8. Found: C, 54.1; H, 5.9.

3-Propionyl-4-carbomethoxypyrrole

3-Carbomethoxypyrrole-4-carbonyl chloride (1.0 g) was added to a benzene solution of diethylcadmium (0.15 mol). The mixture was heated under reflux for 4 h and then poured onto ice – 6 *M* H_2SO_4. The benzene layer was separated and the aqueous layer was extracted with ethyl acetate. The organic solutions were washed with $NaHCO_3$ solution and then dried ($MgSO_4$). The solvent was removed and the product was chromatographed on basic alumina (Brockmann activity III). Elution with ethyl acetate gave 3-propionyl-4-carbomethoxypyrrole, m.p. 179–180° (from ethyl acetate) (0.38 g, 36%); ν_{max} 1720 and 1675 (C=O) and 3450 cm^{-1} (N—H); λ_{max} (EtOH) 253 nm (ε 7000).

Anal. Calcd. for $C_9H_{11}NO_3$: C, 59.7; H, 6.1. Found: C, 59.8; H, 6.0.

3-Benzoyl-4-carbomethoxypyrrole

3-Carbomethoxy-4-pyrrolecarboxylic acid (420 mg) was converted to the acid chloride in benzene solution. The flask was flushed with nitrogen, aluminum chloride (700 mg) was added, and the mixture was heated under reflux for 10 h. The product was poured onto ice–HCl, extracted into ethyl acetate, and washed with $NaHCO_3$ solution. Chromatography on neutral alumina (Brockmann activity I), eluting with ethyl acetate afforded 3-benzoyl-4-carbomethoxypyrrole, m.p. 163–164° (130 mg, 23%); ν_{max} 1717 and 1655 (C=O) and 3445 cm^{-1} (N—H).

Anal. Calcd. for $C_{13}H_{11}NO_3$: C, 68.1; H, 4.8. Found: C, 67.9; H, 5.0.

3-p-Anisoyl-4-carbomethoxypyrrole

3-Carbomethoxypyrrole-4-carboxylic acid (420 mg) similarly gave 3-*p*-anisoyl-4-carbomethoxypyrrole, m.p. 179–180° (from ethyl acetate) (306 mg, 47%); ν_{max} 1715, 1645 (C=O) and 3445 cm^{-1} (N—H); λ_{max} (EtOH) 218 (ε 8600) and 283 nm (ε 9000).

Anal. Calcd. for $C_{14}H_{13}NO_4$: C, 64.9; H, 5.0. Found: C, 64.6; H, 5.2.

3,4-Dibenzoylpyrrole

3,4-Pyrroledicarboxylic acid (155 mg) was converted to the diacid chloride in benzene solution (40 ml) as described earlier. Aluminum chloride (260 mg) was added and the mixture was stirred for 18 h at 50°. The product, 3,4-dibenzoylpyrrole m.p. 223–224° (from ethyl acetate) (94 mg, 34%), was isolated as above; ν_{max} 1650 (C=O) and 3445 cm^{-1} (N—H).

Anal. Calcd. for $C_{18}H_{13}NO_2$: C, 78.5; H, 4.7. Found: C, 78.6; H, 4.9.

Diethyl 1-Hydroxymethyl-3,4-pyrroledicarboxylate

Diethyl 3,4-pyrroledicarboxylate (211 mg), aqueous formaldehyde (5 ml of 37%), tetrahydrofuran (5 ml), and benzyltrimethylammonium hydroxide (0.2 ml) were heated under reflux for 5 h. The mixture was poured onto ice and extracted with ethyl acetate, washed with water, and dried ($MgSO_4$). Removal of the solvent afforded diethyl 1-hydroxymethyl-3,4-pyrroledicarboxylate, m.p. 85–86° (from $CHCl_3$–petroleum) (205 mg, 85%); ν_{max} 1725 br (C=O) 3350 br (O—H bonded), and 3560 cm^{-1} (O—H free); λ_{max} (EtOH) 250 nm (ε 6700).

Anal. Calcd. for $C_{11}H_{15}NO_5$: C, 54.7; H, 6.2. Found: C, 54.8; H, 6.1.

Elimination of Formaldehyde from Diethyl 1-Hydroxymethyl-3,4-pyrroledicarboxylate

Diethyl 1-hydroxymethyl-3,4-pyrroledicarboxylate (150 mg), tetrahydrofuran (3 ml), water (10 ml), and benzyltrimethylammonium hydroxide (0.1 ml) were heated under reflux for 3 h. The mixture was diluted with water and the organic material extracted into ethyl acetate and dried ($MgSO_4$). Removal of the solvent gave a product which was shown (i.r. and n.m.r.) to be diethyl 3,4-pyrroledicarboxylate.

Diethyl 1-Benzoyloxymethyl-3,4-pyrroledicarboxylate

Diethyl 3,4-pyrroledicarboxylate (1.05 g) in dry tetrahydrofuran (50 ml) was treated with 1 equiv of sodium hydride. The solution was heated under reflux for 2 h then cooled to 0° and benzyl chloromethyl ether (800 mg) in tetrahydrofuran (10 ml) was added over 15 min. The solution was allowed to reach 25°, stirred overnight, and then heated under reflux for 2 h prior to filtration. The filtrate was concentrated and, after chromatography on neutral alumina, gave diethyl 1-benzyloxymethyl-3,4-pyrroledicarboxylate as a viscous liquid (1.48 g, 90%); ν_{max} 1725 br cm^{-1}.

1-Benzyloxymethyl-3,4-pyrroledicarboxylic Acid

Diethyl 1-benzyloxymethyl-3,4-pyrroledicarboxylate (450 mg) was heated under reflux with aqueous alcoholic potassium hydroxide (12 ml of 10% solution) for 45 min. The mixture was allowed to stand for a further 1 h at 25° prior to acidification with 2 *M* HCl and subsequent extraction into ethyl acetate. Extraction of the organic acid into $NaHCO_3$ solution and re-precipitation afforded 1-benzyloxymethyl-3,4-pyrroledicarboxylic acid, m.p. 143–144° (from 5:1 aqueous-ethanol) (250 mg, 67%); ν_{max} 1720 and 1645 (C=O), 3200–2200 cm^{-1} (O—H); λ_{max} (EtOH) 257 nm (ε 7400).

Anal. Calcd. for $C_{14}H_{13}NO_5$: C, 61.0; H, 4.7; N, 5.1. Found: C, 61.0; H, 4.8; N, 5.2.

1-Benzyloxymethyl-3,4-pyrroledicarboxylic Anhydride

1-Benzyloxymethyl-3,4-pyrroledicarboxylic acid (125 mg) and dicyclohexylcarbodiimide (110 mg) were added to dichloroethane (25 ml). The mixture was heated under reflux for 90 min. The initial suspension became homogeneous prior to precipitation of the dicyclohexylurea. Filtration and concentration of the filtrate afforded a product (95 mg, 81%), m.p. 72–80°; ν_{max} 1785, 1835, and 1855 cm^{-1}, average molecular weight in dichloroethane: 308 (calcd. 257). Attempted recrystallization from various solvents failed to sharpen the melting point.

1-Benzyloxymethyl-3-carbethoxy-4-pyrrolecarboxylic Acid

Diethyl 1-benzyloxymethyl-3,4-pyrroledicarboxylate (6.5 g), potassium hydroxide (1.10 g), and EtOH (50 ml) were heated under reflux for 18 h. The product was poured into water and extracted with ether. The aqueous layer was separated, acidified, and filtered to afford 1-benzyloxymethyl-3-carbethoxy-4-pyrrolecarboxylic acid, m.p. 82–83° (from ether) (4.8 g, 81%); ν_{max} 1712 and

Can. J. Chem. Downloaded from www.nrcresearchpress.com by 210.87.254.6 on 09/05/12
For personal use only.

1635 cm^{-1} (C=O); λ_{max} (EtOH) 247 (ε 7650) and 260 nm (7300).

Anal. Calcd. for $C_{16}H_{17}NO_5$: C, 63.3; H, 5.6. Found: C, 63.5; H, 5.6.

Ethyl 1-Benzyloxymethyl-3-acetyl-4-pyrrolecarboxylate

The above half-acid (1.50 g) was heated under reflux with a benzene solution (80 ml) of oxalyl chloride (0.65 g) and dimethylformamide (1 drop). A solution of dimethylcadmium was prepared from magnesium (0.48 g) and methyl iodide (1.4 ml) to form a Grignard reagent in ether (50 ml), followed by the addition of cadmium chloride (1.83 g). This mixture was heated under reflux for 2 h prior to replacing the ether by benzene (50 ml). The above acid chloride was added to the dimethylcadmium solution over 15 min and the mixture was then heated under reflux for 3.5 h prior to pouring onto ice–HCl. The organic material was extracted into a large volume of ethyl acetate, washed with $NaHCO_3$ solution, dried ($MgSO_4$) and filtered through a short column of activity I basic alumina. Removal of the solvent afforded ethyl 1-benzyloxymethyl-3-acetylpyrrole-4-carboxylate as a viscous liquid (800 mg, 54%), ν_{max} 1710 and 1665 (C=O) cm^{-1}.

1-Benzyloxymethyl-3-acetyl-4-pyrrolecarboxylic Acid

The above keto-ester (200 mg) was heated under reflux for 2.5 h with a solution of KOH (500 mg) in aqueous ethanol (3 ml, 1:1). The solution was poured into water, acidified with 2 *M* HCl, and the resulting 1-benzyloxymethyl-3-acetyl-4-pyrrolecarboxylic acid was filtered off giving a solid m.p. 149–150° (from aqueous EtOH), (140 mg, 78%); ν_{max} 1710 and 1620 cm^{-1} (C=O); λ_{max} (EtOH) 262 nm (ε 10 300).

Anal. Calcd. for $C_{16}H_{17}NO_5$; C, 63.4; H, 5.6. Found: C, 63.5; H, 5.7.

Attempted Hydrogenolysis of the Benzyloxymethyl Substituent in **22**

Uncontrolled hydrogenolysis of ethyl 1-benzyloxymethyl-3-acetyl-4-pyrrolecarboxylate (**22**) (150 mg) in EtOH (20 ml) in the presence of 10% palladium-on-carbon (25 mg) resulted in complete hydrogenolysis of the benzyl group and complete reduction of the acetyl group as shown in the n.m.r. of the product. When hydrogenolysis under these conditions was stopped after the uptake of 1 mol equiv of hydrogen (2.5 h), the n.m.r. of the product showed the absence of acetyl group but retention of a benzyl group. The α-proton resonances occurred as doublets (J = 2.2 Hz) at τ 2.55 and 3.27.

Hydrogenolysis of **22** (100 mg) in tetrahydrofuran (40 ml) in the presence of 10% palladium-on-carbon (35 mg) and triethylamine (1 drop) for 4 h resulted in recovery of a product, the n.m.r. spectrum of which indicated that it was mainly **22** although a little reduction of the acetyl group was apparent in the spectrum.

Hydrogenolysis of **22** (50 mg) in EtOH (6 ml) in the presence of 10% palladium-on-carbon (20 mg) and sulfur–quinoline poison solution (0.1 ml) for 4 h resulted in complete reduction of the acetyl but retention of the benzyl as shown by the n.m.r. spectrum.

Hydrogenolysis of **22** (100 mg) in the presence of W5 Raney nickel (~200 mg) in EtOH (15 ml) under 30 p.s.i. for 1 h resulted in recovery of unchanged **22**.

Ethyl 1-Benzyloxymethyl-3-acetyl-4-pyrrolethiolcarboxylate

1-Benzyloxymethyl-3-acetyl-4-pyrrolecarboxylic acid (275 mg) was heated under reflux for 2 h in a benzene solution (25 ml) of oxalyl chloride (135 mg) and dimethylformamide (1 drop). A solution of sodium ethanthioxide was prepared by adding ethanethiol (65 mg) to 50 mg of 58% sodium hydroxide in 25 ml of benzene. The above acid chloride was then added to the sodium ethanthioxide solution and the mixture was refluxed for 1 h. The reaction mixture was then cooled and the precipitated inorganic salt was removed by filtration and washed with benzene (100 ml). The filtrate was then evaporated *in vacuo*, and the yellow viscous liquid thus obtained was filtered through a short column of neutral alumina (Brockmann activity I) using ether as eluant. Removal of solvent gave ethyl 1-benzyloxymethyl-3-acetyl-4-pyrrolethiolcarboxylate as a pale yellow viscous oil (225 mg, 71%); ν_{max} 1665 and 1660 cm^{-1} (C=O).

Anal. Calcd. for $C_{17}H_{19}NO_3S$: C, 64.4; H, 6.0; N, 4.4. Found: C, 64.2; H, 6.0; N, 4.5.

Ethyl 1-Hydroxymethyl-3-acetyl-4-pyrrolethiocarboxylate

Ethyl 1-benzyloxymethyl-3-acetyl-4-pyrrolethiolcarboxylate (160 mg) in anhydrous benzene (15 ml) was stirred at 40 °C for 30 min with aluminum chloride (140 mg). The solution was then cooled in ice and the excess aluminum chloride was slowly destroyed through addition of ice-cold water. The organic layer was separated, dried ($MgSO_4$) and evaporated *in vacuo*. The benzyl chloride formed was distilled under vacuum, the reddish gum obtained crystallized from ether–petroleum (92 mg, 81%), m.p. 89–91°; ν_{max} 3400 br (O—H), 1665, and 1660 cm^{-1} (C=O).

Anal. Calcd. for $C_{10}H_{13}NO_3S$: C, 52.9; H, 5.7. Found: C, 52.8; H, 5.9.

Ethyl 3-Acetyl-4-pyrrolethiolcarboxylate

Ethyl 1-hydroxymethyl-3-acetyl-4-pyrrolethiolcarboxylate (60 mg) in aqueous tetrahydrofuran (13 ml of 10:3) was heated under reflux with benzyltrimethylammonium hydroxide (0.2 ml). The mixture was then evaporated to half-bulk, diluted with water (20 ml), and extracted twice with ethyl acetate. The organic layer was separated, dried ($MgSO_4$), and evaporated *in vacuo* affording ethyl 3-acetyl-4-pyrrolethiolcarboxylate as a white powder, (44 mg, 85%). Recrystallization from ether – petroleum ether gave an analytical sample, m.p. 118–120°; ν_{max} 3440 (N—H free), 3250 (N—H bonded), 1665 and 1660 cm^{-1} (C=O).

Anal. Calcd. for $C_9H_{11}NO_2S$: C, 54.8; H, 5.8; N, 7.1. Found: C, 54.8; H, 5.6; N, 7.2.

3-Acetyl-4-hydroxymethylpyrrole

Ethyl 3-acetyl-4-pyrrolethiolcarboxylate (30 mg) in absolute methanol (20 ml) was cooled to 0° and W5 Raney nickel (about 800 mg) was added. The mixture was shaken in a Parr hydrogenator for 70 min at 25° and 30 p.s.i. of hydrogen. The catalyst was then removed by collection on a Celite pad and was washed with ethanol (250 ml). The filtrate and washings were combined and removed *in vacuo* affording a pink gum. Preparative t.l.c. (silica gel GF-254 chloroform–methanol, 97:3) of the crude product resulted in the isolation of pure 3-acetyl-4-hydroxymethylpyrrole (15 mg, 71%), m.p. 88–90°

(lit. (3, 4) 90.5–91°). The i.r., u.v., and p.m.r. spectra were identical with those of natural Verrucarin E. The R_f values of the synthetic product were in agreement with those reported for the natural compound using chloroform–methanol, 97:3; or 92:8; as well as ethyl acetate as eluants.

The continued financial support of the National Research Council of Canada and of the Memorial University of Newfoundland is gratefully acknowledged. The authors are indebted to Dr. C. E. Loader for many useful discussions.

1. C. E. LOADER and H. J. ANDERSON. Tetrahedron, **25**, 3879 (1969).
2. J. K. GROVES, H. J. ANDERSON, and H. NAGY. Can. J. Chem. **49**, 2427 (1971).
3. E. FETZ and CH. TAMM. Helv. Chim. Acta, **49**, 349 (1966).
4. P. PFÄFFLI and CH. TAMM. Helv. Chim. Acta, **52**, 1911 (1969).
5. L. MANDELL and W. A. BLANCHARD. J. Am. Chem. Soc. **79**, 6198 (1957).
6. R. M. ACHESON and J. M. VERNON. J. Chem. Soc. 457 (1961).
7. N. W. GABEL. J. Org. Chem. **27**, 301 (1962).
8. R. M. ACHESON and J. M. VERNON. J. Chem. Soc. 1008 (1963).
9. N. G. BARLOW, R. N. HASZELDINE, and R. HUBBARD. Chem. Commun. 301 (1969).
10. R. A. JONES, T. MCSPOTWOOD, and P. CHEUYEHIT. Tetrahedron, **23**, 4467 (1967).
11. R. M. ACHESON, A. R. HANDS, and J. M. VERNON. Proc. Chem. Soc. 164 (1961).
12. R. KITZING, R. FUCHS, M. JOYEUX, and H. PRINZBACH. Helv. Chim. Acta, **51**, 888 (1968).
13. D. V. NIGHTINGALE and J. A. GALLAGHER. J. Org. Chem. **24**, 501 (1959).
14. K. SCHOFIELD. Hetero-aromatic nitrogen compounds. Butterworths, London. 1967. p. 94.
15. W. A. REMERS, R. H. ROTH, G. J. GIBBS, and M. J. WEISS. J. Org. Chem. **36**, 1232 (1971).
16. H. J. ANDERSON and S. J. GRIFFITHS. Can. J. Chem. **45**, 2227 (1967).
17. H. J. ANDERSON and J. K. GROVES. Tetrahedron Lett. 3165 (1971).
18. R. L. AUGUSTINE. Catalytic hydrogenation. Marcel Dekker, Inc., New York. 1965. p. 136.
19. R. N. RYLANDER. Catalytic hydrogenation over platinum metals. Academic Press, New York. 1967. p. 454.
20. P. J. CROOK, A. H. JACKSON, and G. W. KENNER. J. Chem. Soc. (C) 474, (1971).
21. H. BUDZIKIEWICZ, C. DJERASSI, and D. H. WILLIAMS. Mass spectrometry of organic compounds. Holden Day, San Francisco, California. 1967. p. 202.
22. H. J. ANDERSON and H. NAGY. Can. J. Chem. **50**, 1961 (1972).

Can. J. Chem. Downloaded from www.nrcresearchpress.com by 210.87.254.6 on 09/05/12
For personal use only.

A Proton Magnetic Resonance Study of the Effect of 2′-*O*-Methylation on Ribonucleoside Conformation

FRANK E. HRUSKA AND ALAN MAK
Chemistry Department, University of Manitoba, Winnipeg, Manitoba

AND

HARWANT SINGH
Medical Biophysics Branch, Atomic Energy of Canada Ltd., WNRE, Pinawa, Manitoba

AND

DAVID SHUGAR
Department of Biophysics, University of Warsaw, Warsaw, Poland

Received August 28, 1972

The 100- and 220-MHz p.m.r. spectra of uridine, cytidine, and their 2′-*O*-methyl derivatives are obtained in aqueous solution at several temperatures. The experimental chemical shifts and coupling constants are discussed in terms of the overall molecular conformation. The conclusion is reached that 2′-*O*-methylation has little effect upon the three-dimensional structure of a nucleoside at the monomer level in an aqueous environment.

Les spectres r.m.n. à 100 et 220 MHz de l'uridine, de la cytidine, et de leur dérivé *O*-méthyl-2′ ont été obtenus dans des solutions aqueuses à différentes températures. Les déplacements chimiques expérimentaux ainsi que les constantes de couplage sont discutés en fonction de la conformation moléculaire totale. On a conclu que la *O*-méthylation en 2′ a peu d'effet sur la structure tridimentionnelle du nucléoside au niveau monomérique en milieu aqueux. [Traduit par le journal]

Can. J. Chem., **51**, 1099 (1973)

Introduction

It is well established that 2′-*O*-methylation of ribonucleosides is a highly specific enzymatic process which occurs at the polynucleotide level and leads to a characteristic distribution of these methylated residues in tRNA and rRNA of various organisms (1–6). The precise biological significance of this modification is not clear but, as might be anticipated the presence of the 2′-*O*-methyl substituent renders the phosphodiester linkage resistant to both alkali and ribonucleases (1, 2, 6, 7). A number of spectroscopic investigations of the methylated oligo- and polynucleotides have appeared in the literature and the possible role of the 2′-hydroxyl in stabilizing the three-dimensional structure of polyribonucleotides has been critically discussed (8–12). Studies on the various 2′-*O*-methyl polymers have demonstrated that the presence of the 2′-OH is not a prerequisite for the formation of helical structure of polynucleotides (13–15). We present here our initial p.m.r. studies of the effect of 2′-*O*-methylation on nucleoside conformation (16–19) at the monomer level (structural formulae in Fig. 1). Our data demonstrate that 2′-*O*-methylation has no significant effect upon the sugar–base torsion angle, the exocyclic $C_{4'}$—$C_{5'}$ conformation, or the furanose-ring puckering at the mononucleoside level.

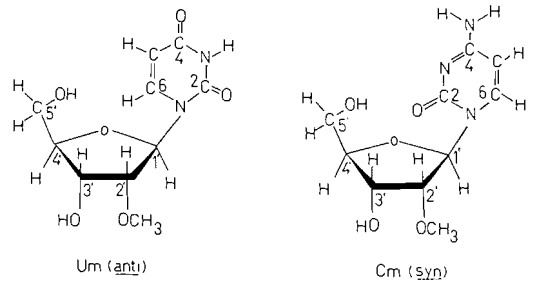

FIG. 1. Structural formulae of 2′-*O*-methyluridine (Um) and 2′-*O*-methylcytidine (Cm). Definition of the *anti*- and *syn*-rotations about the *N*-glycosyl bond of a pyrimidine nucleoside.

Experimental

Uridine (U) and cytidine (C) were obtained from Calbiochem and used without further purification. The 2′-*O*-methyl derivative of C (Cm) was prepared by dimethylsulfate treatment of cytidine in alkaline medium (20). 2′-*O*-methyluridine (Um) was then obtained by bisulfite

AECL No. 4414.

Can. J. Chem. Downloaded from www.nrcresearchpress.com by 210.87.254.5 on 09/05/12
For personal use only.

Can. J. Chem. Downloaded from www.nrcresearchpress.com by 210.87.254.5 on 09/05/12
For personal use only.

deamination of Cm.[1] Both compounds were recrystallized several times from ethanol to ensure elimination of traces of impurity, checked for at high concentrations by paper and thin-layer chromatography. 3-Trimethylsilylpropanesulfonic acid (DSS, E. Merck, Germany) was used as the internal p.m.r. reference. Solutions (0.1 *M*) of each nucleoside containing 0.1 *M* DSS were prepared in D_2O. The p*D* was adjusted to 7.0 ± 0.2 for the U derivatives and 8.0 ± 0.2 for the C derivatives. The samples were freeze-dried three times to reduce the intensity of the HDO resonance. Spectra were obtained on Varian HA-100 D and HR-220 spectrometers by conventional methods. Spectral analyses were carried out using LAME (21).

Results and Discussion

Spectral Assignment

The complete assignment and spectral analysis (for non-exchanging hydrogens) of the 100 and 220 MHz spectra of U in aqueous solution have been discussed in some detail elsewhere (17) and are used as a guide for interpreting the new data reported here for C, Um, and Cm. Recent studies by Narayanan and Iyer (22) of the shielding effect of methylation of the hydroxyl group of secondary alcohols upon the methine hydrogen proved useful for initial assignments of the spectral bonds of the methylated derivatives. The assignments were confirmed by some double resonance experiments and computer-simulated spectra were generated as final tests for the chemical shift and coupling constant data. In Fig. 2*a* we show a sample experimental spectrum (220 MHz) of the ribose region of Cm at 60 °C along with the calculated spectrum. In Fig. 2*b* is shown the 3′-portion of the 100 MHz spectrum of Cm (60 °C). Clearly, with the somewhat better resolution obtainable on 100 MHz spectrometers, additional spacings of 0.30–0.40 Hz become apparent in this region of the Cm (as well as Um) spectra. This spacing was attributed, by spin-decoupling, to a long-range four-bond coupling between $H_{1'}$ and $H_{3'}$ ($^4J_{1'3'}$). The methyl resonance of Um and Cm appeared as a sharp singlet at 3.51–3.54 p.p.m. downfield from DSS.

In Tables 1 and 2 are listed the observed chemical shift and vicinal coupling constant data for U, C, Um, and Cm as well as those for RCA (β-D-ribofuranosylcyanuric acid) taken from ref. 23 for comparison purposes (Fig. 3).

The Sugar–Base Torsion Angle

A conformational problem of considerable interest has been the elucidation of the orientation of the base and sugar moieties as defined by the sugar–base torsion angle about the *N*-glycosyl bond. X-ray diffraction studies are perhaps the most informative in this regard since the accurate bond lengths and bond angles establish unambiguously the favored conformation of the nucleoside in the crystalline state. For solutions o.r.d., c.d., and p.m.r. (24), and recently c.m.r. (25) have provided information, albeit qualitative, for the preference of either the *syn*- or *anti*-ranges of this torsion angle. However, recent applications of the theory of the nuclear Overhauser effect has demonstrated that more quantitative information of conformational distributions can be provided (26).

A preference for the *anti*-conformation of common pyrimidine nucleosides is apparent and generally agreed to be a consequence of unfavorable steric interactions between the 2-keto oxygen of the base and the substituents on the furanose ring which occur when the molecules assume a *syn*-conformation. Recent spectroscopic (27–29) studies point to a preference for the *syn*-conformation of pyrimidine derivatives possessing a bulky substituent (CH_3, COOH) at the 6-position of the base and lend support to the notion that non-bonding interactions between the base substituents at the ortho-positions and the ribose ring are the prime factors determining the favored range of the sugar–base torsion angle. Thus on the basis of purely steric arguments we predict that methylation of the 2′-hydroxyl will have no drastic effect upon the sugar–base torsion angle at the monomer level. In the ensuing discussion a qualitative comparison is made of the p.m.r. data of U, C, Um, and Cm which supports this prediction.

Prestegard and Chan (30) have argued that, because of the proximity of the uracil H_6 proton to the ribose moiety (particularly to the ethereal oxygen) in pyrimidine nucleosides exhibiting the *anti*-form, variations in the relative orientation of the base and sugar should be reflected in the chemical shift of this proton. From the data in Table 1 we see, however, only minor differences (<2 Hz) in the experimental resonant field values of H_6 for each N—Nm pair of nucleosides. These observations are in line with the prediction that no large perturbation of the average sugar–base torsion angle is a consequence of 2′-*O*-methylation.

Information about the favored range of sugar–

[1]J. Kusmierik, J. Giziewicz, and D. Shugar. Acta Biochim. Polon. Submitted for publication.

Can. J. Chem. Downloaded from www.nrcresearchpress.com by 210.87.254.5 on 09/05/12
For personal use only.

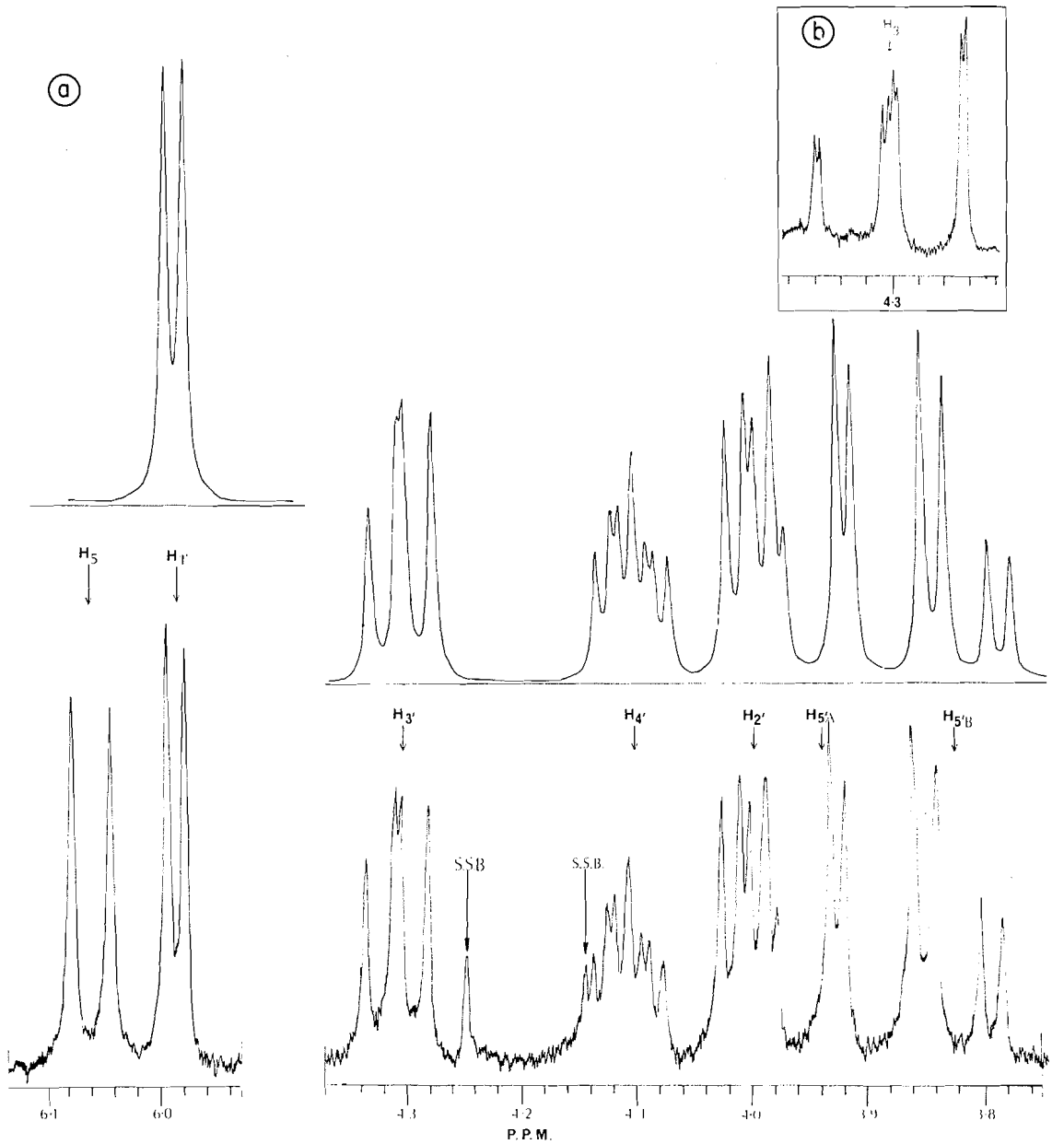

FIG. 2. (*a*) The 220 MHz spectrum of Cm (H_6 not included). Aqueous solution, 23 °C, p*D* 8.0. In p.p.m. relative to internal DSS. S.S.B. = spinning side-band. The computer-simulated spectrum is shown above the experimental. (*b*) 3′-Region of Cm obtained at 100 MHz. Aqueous solution, p*D* 8.0, 60 °C.

base torsion angle of pyrimidine nucleosides has also been obtained from observed long-range coupling ($^5J_{51'}$) interactions between the H_5 hydrogen (or 5-fluoro) of the base and the anomeric hydrogen (31, 32). The stereochemical dependence appears to be such that the largest $^5J_{51'}$ coupling is expected when $C_{1'}$—$H_{1'}$ and the base are coplanar with the molecule in the *anti*-conformation, that is, when $H_{1'}$ and H_5 are connected by an extended zig-zag path. Splittings attributable to $^5J_{51'}$ interactions were readily detected in the 5′ regions of U, Um, and Cm. We are inclined to present these as further evidence that their conformational distributions

TABLE 1. Nucleoside chemical shifts* in aqueous solution

	Um†,§		U‡,‖		Cm†,§		C‡,§		RCA‡,¶	
H	28°	60°	23°	80°	28°	60°	23°	65°	30°	75°
6	7.908	7.861	7.886	7.838	7.869	7.831	7.857	7.824	—	—
5	5.904	5.907	5.883	5.918	6.057	6.067	6.054	6.076	—	—
1′	5.977	5.963	5.901	5.901	5.975	5.969	5.912	5.913	6.10	6.11
2′	4.052	4.047	4.340	4.348	3.997	3.999	4.315	4.324	4.71	4.74
3′	4.342	4.334	4.221	4.222	4.301	4.295	4.215	4.220	4.36	4.36
4′	4.112	4.110	4.127	4.122	4.102	4.099	4.142	4.144	3.95	3.96
5′	3.922	3.913	3.907	3.890	3.938	3.925	3.942	3.933	3.85	3.84
5″	3.813	3.808	3.803	3.798	3.821	3.816	3.828	3.826	3.72	3.74
m	3.509	3.512	—	—	3.535	3.524	—	—	—	—

*Relative to internal DSS.
†100 MHz.
‡220 MHz.
§This work.
‖References 16, 18.
¶Reference 23.

TABLE 2. Nucleoside H–H coupling constants in aqueous solution

	Um*,‡		U†,§		Cm*,‡		C†,‡		RCA†,‖	
J (Hz)	28°	60°	28°	80°	28°	60°	23°	65°	30°	75°
56	8.0	8.1	8.1	8.1	7.5	7.5	7.6	7.6	—	—
51′	—	0.40	—	0.35*	—	0.36	—	—	—	—
1′2′	4.0	4.2	4.8	5.1	3.6	3.8	4.0	4.2	3.9	4.0
2′3′	5.4	5.6	5.2	5.2	5.4	5.5	5.2	5.5	6.4	6.1
3′4′	5.9	5.6	5.4	5.1	6.7	6.3	6.0	5.9	6.6	6.2
4′5′	2.9	3.0	2.9	3.3	2.8	3.0	2.8	3.1	3.2	3.4
4′5″	4.3	4.4	4.4	4.6	4.4	4.6	4.3	4.6	6.2	6.0
5′5″	−12.8	−12.7	−12.7	−12.7	−12.8	−12.9	−12.7	−12.7	−12.4	−12.7
1′3′	0.28	0.35	—	—	0.34	0.36	—	—	—	—

*100 MHz.
†220 MHz.
‡This work.
§References 16, 18.
‖Reference 23.

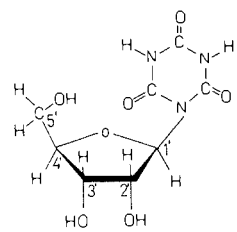

FIG. 3. Structural formula of β-D-ribofuranosylcyanuric acid (RCA).

about the N_1—C_1 bond are similar. However, we have not been able to detect an analogous splitting in the spectrum of C obtained under comparable solution and temperature conditions. For this molecule the H_5 resonances were relatively broad even at elevated temperatures, a feature which would obscure any small coupling. Double resonance experiments were employed to detect line narrowing and hidden spacings in the H_5 region but the experiments were inconclusive. No simple explanations for the H_5 bandwidth differences of C and Cm, other than the presence of paramagnetic impurities in the commercial preparation of C, are apparent.[2]

With recent p.m.r. measurements Schweizer *et al.* (28) and Dugas *et al.* (23) have presented a novel approach to evaluation of the *syn–anti* problem in pyrimidine nucleosides. These authors have noted that the presence of an ortho keto group on the base located over the ribose ring can lead to characteristic perturbations of the ribose hydrogen chemical shifts and coupling

[2]We have taken precautions to ensure that the solution p*H* is in the range where the line broadening effect, due to the presumed tautomeric equilibrium recently discussed by Lee *et al.* (33), should be unimportant.

Can. J. Chem. Downloaded from www.nrcresearchpress.com by 210.87.254.5 on 09/05/12
For personal use only.

Can. J. Chem. Downloaded from www.nrcresearchpress.com by 210.87.254.5 on 09/05/12
For personal use only.

constants. The most complete set of data, for RCA, are included in the tables for comparison purposes. We note that, relative to U, the $H_{2'}$ and $H_{3'}$ resonances in RCA are shifted downfield (by 0.34 and 0.14 p.p.m.) whereas $H_{4'}$, $H_{5'}$, and $H_{5''}$ are shifted upfield (by 0.16, 0.06, and 0.09 p.p.m. respectively), effects which were reasonably traced to the anisotropic shielding effects of the *keto* oxygen located above the furanose moiety. However, the effect of 2′-*O*-methylation is clearly seen to be diamagnetic ($\simeq$0.3 p.p.m.) for $H_{2'}$ (and in line with the work of Narayanan and Iyer (22) but paramagnetic ($\simeq$0.1 p.p.m.) for $H_{1'}$ and $H_{3'}$ and negligible ($<$0.05 p.p.m.) for $H_{4'}$, $H_{5'}$, and $H_{5''}$. The relative magnitudes of these methyl-induced shift changes suggest a (de)shielding mechanism related to separation from the methoxyl group and are not readily treated in terms of any significant *syn–anti* interconversion.

Conformation of the Furanose Ring

Detailed Karplus treatments have recently been carried out for a large number of nucleosides and qualitative models for the three dimensional structure of their furanose moieties have been put forth (16–19). The major conclusion arrived at from these solution studies was that the observed p.m.r. data could be accounted for not in terms of a single conventional puckered mode but if a rapid time-averaged pseudorotational (34) interconversion between several puckered modes was assumed. Suggested (16–17) as particularly attractive for U and β–ψ was a C_2 *endo*-$C_{3'}$ *endo*-equilibrium with significant contributions from each to the overall conformational blend. Rationalization of the *J* data in Table 2 in the manner outlined in ref. 16 leads us to conclude that the equilibrium model is reasonable for 2′-*O*-methyl derivatives and that methylation has no large effect upon either the barrier to the interconversion or upon the conformer weightings in the blend. A slight shift toward the $C_{3'}$ *endo*-mode of puckering may be inferred from the small changes in $J_{1'2'}$ and $J_{3'4'}$ of Um and Cm relative to U and C.

Karplus treatments have been extended (16–19) to the 4′- to 5′(5″)-vicinal couplings to yield estimates of the rotamer populations about the exocyclic $C_{4'}$—$C_{5'}$ bond. Consideration of the data for U in aqueous solution led to the conclusion (17) that the hydroxymethyl group interconverted between the *gauche–gauche*, *gauche–trans*, and *trans–gauche* rotamers with a preference for the *gauche–gauche* (Fig. 4). We may conclude from the similarity in the $J_{4'5'}$ and $J_{4'5''}$ values of U, C, Um, and Cm that 2′-*O*-methylation (or substitution of cytosine for uracil for that matter) has little effect upon rotamer population about the $C_{4'}$—$C_{5'}$ bond. Thus the hydrogen-donor properties of the 2′-hydroxyl seem to be unimportant in so far as mononucleoside conformation in aqueous solution is concerned.

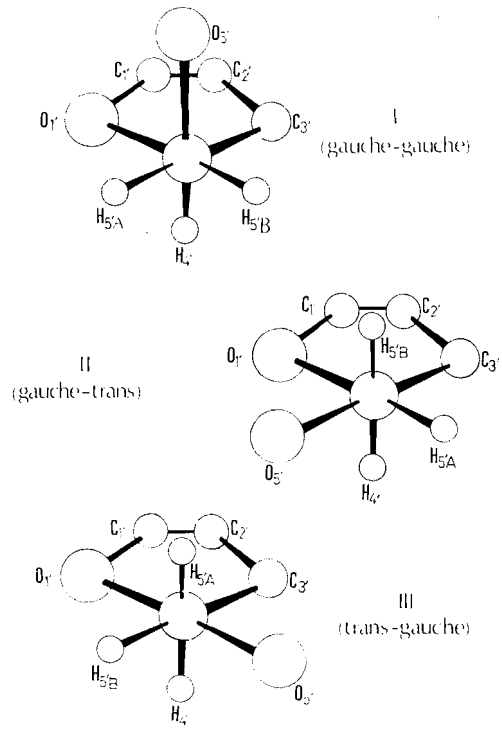

FIG. 4. Conformers about the $C_{4'}-C_{5'}$ bond of a nucleoside.

Mention should be made of the observed long-range coupling between $H_{1'}$ and $H_{3'}$ ($^4J_{1'3'}$) in Um and Cm in view of the strong steric dependence of four bond couplings in H—C—C—C—H propanic fragments and their value in structural problems (35). Splittings of 0.30–0.35 Hz in the 3′-regions, attributable by double resonance experiments to 1′–3′ interactions, were readily resolved in the pair of methyl derivatives (Fig. 2*b*). Analogous splittings were not resolved in either U or C which may indicate absence of $^4J_{1'3'}$ coupling but any 0.3–0.4 Hz splitting could be obscured by virtual coupling which is extensive in tightly-coupled ribose spectra. The presence of the 2′-*O*-methyl group, by virtue of its

shielding effect upon $H_{2'}$ and deshielding effect upon $H_{3'}$, has created a more loosely-coupled spin system in which small couplings have become resolvable, in the 3′-region at least. We are not surprised that the $^4J_{1'3'}$ splitting is not evident in the 1′ regions of Um and Cm in view of our (as well as other (36)) observations (37) that the 1′ hydrogen in furanoid derivatives can exhibit an extensive array of small, and generally unresolvable, long-range interactions which are seen only in the broadening of a proton signal.

It is now generally thought that the favored stereochemistry for four-bond coupling in saturated systems is a planar W path (35), approached, for instance, by 1,3 equatorial:equatorial hydrogens in pyranoid derivatives. $^4J_{e,e}$ couplings of up to 1.5 Hz have been observed in several pyranoses and shown to be positive in sign (38). In these molecules hydrogens connected by paths less favorable for four-bond interaction than the planar W (for instance the 1,3 equatorial:axial pairs of hydrogens), are found coupled with intermediate values of J (0.4–0.7) Hz and to be negative (28). There does not seem to be much evidence for coupling between 1,3 axial:axial hydrogens (37). Experimental data for flexible five-membered systems are scarce and thus far-reaching generalizations regarding the stereochemical dependence of four-bond coupling in furanoses are not permitted. A recent unpublished examination (37) of 2′,2′-anhydroarabinosyluracil (aU, Fig. 5) may be relevant in this regard. Examination of molecular models of aU indicate considerable rigidity in the molecule with the furanose ring locked in an extreme $C_{2'}$ *endo*-like conformation by the two point attachment of the base and arabinose moieties. We see further from models that $H_{2'}$ and $H_{4'}$ assume a quasi-equatorial:quasi-equatorial (qe:qe) relationship while the $H_{1'}$–$H_{3'}$ and $H_{1'}$–$H_{4'}$ pairs assumed a quasi-axial:quasi-equatorial (qa:qe) relationship. The observed values of the coupling constants for the three pairs of hydrogens connected by four-bonds were (aqueous solution, 30 °C): $^4J_{2'4'} = 0.54$, $^4J_{1'3'} = -0.75$, $^4J_{1'4'} = -0.46$ Hz. These data are suggestive of a parallel stereochemical dependence of ^4J in five- and six-membered carbohydrate rings.

The data for aU may seem encouraging in so far as the use of four-bond coupling for conformational assignments of nucleosides is concerned. However, we have obtained to date spectra for a large number of pyrimidine and purine nucleosides and note that resolvable ^4J couplings are the exception rather than the rule. The 2′-*O*-methyl ribosides seem to be special cases in so far as resolvable couplings are concerned, presumably for the reason given above. Even the $^4J_{1'3'}$ couplings of Um and Cm appear to us to be of limited value for conformational assignments. Since $H_{1'}$ and $H_{3'}$ assume a qa:qe orientation in both the $C_{2'}$ *endo*- and $C_{3'}$ *endo*-conformations, we do not expect the magnitude of $^4J_{1'3'}$ to be significantly altered by changes in ring puckering. Thus we do not expect these four-bond couplings to be of any particular value for assessing the position of our assumed equilibrium between $C_{2'}$ and $C_{3'}$ puckered modes.

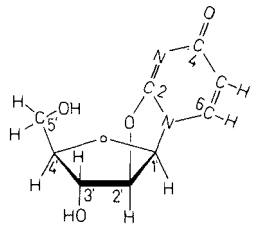

FIG. 5. Structural formula of 2,2′-anhydroarabinosyluracil (aU).

Orientation of the 2′-O-Methyl Group

One conformational problem peculiar to the 2′-*O*-methyl derivatives is the determination of the molecular conformation about the $C_{2'}$—$O_{2'}$ bond which fixes the orientation of the methyl group relative to the furanose ring. Evaluation of the favored orientation of this group is of considerable interest in view of its proximity to the adjacent phosphate and possible influence upon the ribose–phosphate backbone of a polynucleotide. In Fig. 6 are shown the three classically staggered conformations about the $C_{2'}$—$O_{2'}$ bond. In rotamer **I**, C(methyl) and $H_{2'}$ are situated *gauche* and we see in space-filling molecular models the close contact possible between the 2-keto oxygen of the base and the methyl hydrogens. In **II**, C(methyl) and $H_{2'}$ are oriented *gauche* but now close contact between the methyl and 3′-hydroxyl groups arises. In **III**, C(methyl) and $H_{2'}$ are *trans* across $C_{2'}$—$O_{2'}$. In this *trans*-orientation a number of intramolecular contacts are made which severely restrict the rotation of the methyl and the torsional motion of the furanose ring. For this reason we are inclined to think that the *gauche* rotamers will prevail in solution. As yet no spectroscopic evidence has

Can. J. Chem. Downloaded from www.nrcresearchpress.com by 210.87.254.5 on 09/05/12
For personal use only.

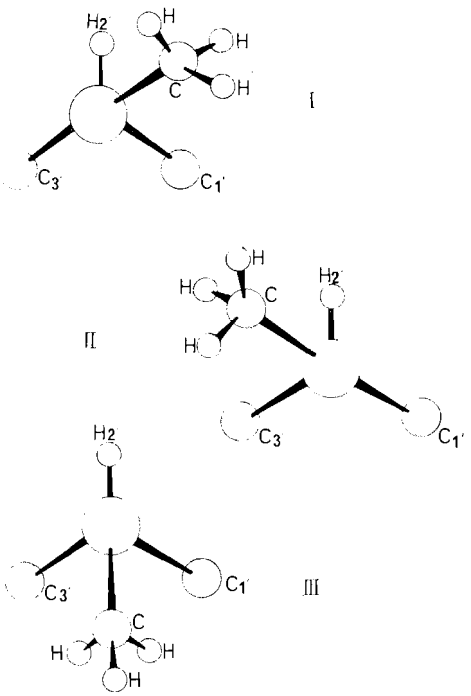

FIG. 6. Possible orientations of the 2′-*O*-methyl group.

appeared in support of either the *gauche* or *trans* possibilities.

Some very qualitative information regarding the methyl group orientation in Um and Cm may be derived from the data in the tables. Certainly the chemical shifts of the methyl hydrogens (which fall in the range observed for *O*-methyl groups in methylated hexoses (39)) are weighted for the relative $C_{2'}$—$O_{2'}$ rotamer populations but in the absence of data for molecules with known structure the favored rotamer cannot be predicted from the methyl–hydrogen shift values in Table 1. The similarity in their shifts, however, suggests that the methyl group experiences similar average environments in Um and Cm while the lack of any significant temperature dependence of the methyl shifts suggests that no large change in the $C_{2'}$—$O_{2'}$ rotamer populations occurs in the temperature interval examined.

The narrow line width (0.3 Hz) of the methyl resonance may give some information on the stereochemistry of the methoxyl group. In the *trans*-conformer **III** a planar zig-zag path between $H_{2'}$ and the methyl hydrogens is encountered during the course of rotation of the methyl group. For this reason a four-bond coupling across the $H_{2'}$—$C_{2'}$—O—C(methyl)—H is not unexpected. However, we may estimate from the line width that any $^4J_{2'm}$ coupling is less than 0.1 Hz. This absence of appreciable ^4J coupling could be a reflection of a low probability of the trans conformer.[3]

Conclusion

P.m.r. data are presented for 2′-*O*-methyl uridine and 2′-*O*-methyl cytidine in aqueous solution and compared with data for uridine and cytidine. The data demonstrate that methylation of the hydroxyl group has little effect on the conformational parameters of the mononucleosides in agreement with conclusion reached from c.d. studies (10). The hydrogen-donating potential of the 2′-hydroxyl group must therefore not be an important factor defining mononucleoside conformation in aqueous solution. The only slight variations in the shift and coupling constant data suggest that the molecular conformations of Um and Cm (as well as U and C) are independent of temperature in the interval from 30–60 °C. The effect, if any, of the 2′-*O*-methyl group on ribose conformation is consequently manifested only at the oligomer and polymer levels, so that its importance must be related to its effect on such properties as base stacking and/or base pairing, and in all probability via modifications in solvation of the molecules.

We are grateful for the financial support of the National Research Council of Canada, the Faculty of Graduate Studies of the University of Manitoba, and the Research Corporation of New York for a Cottrell Grant. We acknowledge Dr. A. A. Grey (Canadian 220 MHz Centre) for obtaining the 220 spectra and the members of the n.m.r. group of the University of Manitoba for valuable discussions. Special thanks are given to Dr. R. Wasylishen for communicating his INDO calculations prior to publication and to thank Dr. K.K. Ogilvie for a sample of aU. We thank Dr. M. Sundaralingam for pointing out a discussion of the effect of 2′-*O*-methylation in a recent work (S. T. Rao, M. Sundaralingam, S. K. Arora, and S. R. Hall. Biochem. Biophys. Res. Commun. **38**, 496 (1970).)

1. H. SINGH and B. G. LANE. Can. J. Biochem. **42**, 87 (1964).
2. H. SINGH and B. G. LANE. Can. J. Biochem. **42**, 1011 (1964).
3. J. L. NICHOLS and B. G. LANE. Can. J. Biochem. **44**, 1633 (1966).

[3]From recent INDO calculations of 4-bond coupling in H—C—O—C—H fragments by Dr. R. Wasylishen we estimate a 0.5–0.6 Hz coupling for the *trans*-conformer.

Can. J. Chem. Downloaded from www.nrcresearchpress.com by 210.87.254.5 on 09/05/12
For personal use only.

4. M. W. GRAY and B. G. LANE. Biochim. Biophys. Acta, **134**, 243 (1967).
5. F. T. TAMOAKI and B. G. LANE. Biochem. **7**, 3431 (1968).
6. L. HUDSON, M. GRAY, and B. G. LANE. Biochem. **4**, 2009 (1965).
7. M. HONJO, Y. KANAI, Y. FURUKAWA, Y. MIZUNO, and Y. SANNO. Biochim. Biophys. Acta, **87**, 698 (1964).
8. (*a*) P. O. P. Ts'O, S. A. RAPAPORT, and F. J. BOLLUM. Biochem. **5**, 4153 (1966). (*b*) J. BRAHMS, J. C. MAURIZOT, and A. M. MICHELSON. J. Mol. Biol. **25**, 481 (1967).
9. B. ZMUDZKA, F. J. BOLLUM, and D. SHUGAR. Biochem. **8**, 3049 (1969).
10. A. RABCZENKO and D. SHUGAR. Acta Biochim. Polon. **18**, 387 (1972); **19**, 89 (1972).
11. M. SINGH and B. HILLIER. Biopolym. **10**, 2445 (1971).
12. M. M. WARSHAW and C. R. CANTOR. Biopolym. **9**, 1079 (1970)m
13. A. M. BOBST, F. ROTTMAN, and P. A. CERUTTI. J. Mol. Biol. **46**, 221 (1969).
14. B. ZMUDZKA, C. JANION, and D. SHUGAR. Biochem. Biophys. Res. Commun. **37**, 895 (1969).
15. B. ZMUDZKA and D. SHUGAR. Acta Biochim. Polon. **18**, 321 (1971).
16. F. E. HRUSKA, A. A. GREY, and I. C. P. SMITH. J. Am. Chem. Soc. **92**, 214, 4088 (1970).
17. B. J. BLACKBURN, A. A. GREY, I. C. P. SMITH, and F. E. HRUSKA. Can. J. Chem. **48**, 2866 (1970).
18. T. SCHLEICH, B. J. BLACKBURN, R. D. LAPPER, and I. C. P. SMITH. Biochem. **11**, 137 (1972).
19. F. E. HRUSKA. *In* Conformations of biological molecules and polymers. Proceedings of the 5th Jerusalem Symposium. F. D. Bergman and B. Pullman, Editors. Academic Press. 1973. In press.
20. J. KUSMIEREK and D. SHUGAR. Acta Biochim. Polon. **18**, 413 (1971).
21. C. W. HAIGH and J. M. WILLIAMS. J. Mol. Spectrosc. **32**, 398 (1969).
22. C. R. NARAYANAN and K. N. IYER. Tetrahedron Lett. 3741 (1965).
23. H. DUGAS, B. J. BLACKBURN, R. DESLAURIERS, R. K. ROBINS, and I. C. P. SMITH. J. Am. Chem. Soc. **93**, 3468 (1971).
24. P. O. P. Ts'O. *In* Fine structure of proteins and nucleic acids. Vol. 4. *Edited by* G. D. Fasman and S. N. Timasheff. Marcel Dekker, Inc., New York. 1970. p. 49.
25. R. U. LEMIEUX, T. L. NAGABHUSAN, and B. PAUL. Can. J. Chem. **50**, 773 (1972).
26. R. E. SHERMER, J. P. DAVIS, J. H. NOGGLE, and P. A. HART. J. Am. Chem. Soc. **94**, 2561 (1972).
27. D. W. MILES, M. J. ROBINS, R. K. ROBINS, M. W. WINLEY, and H. EYRING. J. Am. Chem. Soc. **91**, 831 (1969).
28. M. P. SCHWEIZER, J. I. WITKOWSKI, and R. K. ROBINS. J. Am. Chem. Soc. **93**, 277 (1971).
29. F. E. HRUSKA. J. Am. Chem. Soc. **93**, 1795 (1971).
30. J. H. PRESTEGARD and S. I. CHAN. J. Am. Chem. Soc. **91**, 284 (1969).
31. F. E. HRUSKA. Can. J. Chem. **49**, 2111 (1971).
32. R. J. CUSHLEY, I. WEMPEN, and J. J. FOX. J. Am. Chem. Soc. **90**, 709 (1968).
33. G. C. Y. LEE, J. H. PRESTEGARD, and S. I. CHAN. J. Am. Chem. Soc. **94**, 951 (1972).
34. L. D. HALL, P. R. STEINER, and C. PEDERSEN. Can. J. Chem. **48**, 1155 (1970).
35. M. BARFIELD and B. CHAKRABARTI. Chem. Rev. **69**, 757 (1969).
36. L. D. HALL, J. F. MANVILLE, and A. TRACY. Carbohydr. Res. **4**, 514 (1967).
37. J. G. DALTON. M.Sc. Thesis. University of Manitoba, Winnipeg, Manitoba. 1971.
38. L. D. HALL and J. F. MANVILLE. Carbohydr. Res. **8**, 295 (1968).
39. E. D. GROS, I. O. MASTRONARDI, and A. R. FRASCA. Carbohydr. Res. **16**, 232 (1971).

Can. J. Chem. Downloaded from www.nrcresearchpress.com by 210.87.254.5 on 09/05/12
For personal use only.

A Study of Thermal Motion of Ammine Groups in Carbonatotetramminecobalt(III) Sulfate

B. A. DUNELL, M. D. PACHAL, AND S. E. ULRICH

Department of Chemistry, The University of British Columbia, Vancouver 8, British Columbia

Received August 28, 1972

The results of spin–lattice relaxation measurements are reported for carbonatotetramminecobalt(III) sulfate. The observed T_1 minima and activation energies, 1.9 and 4.3 kcal, for the reorientation of ammine groups are interpreted on the basis of hydrogen bonding effects.

Les résultats obtenus des mesures de la relaxation spin–réseau sont présentés pour le sulfate de carbonatotétraminecobalt(III). Les minima observés T_1 et les énergies d'activation, 1.9 et 4.3 kcal, pour la réorientation des groupes amines sont interprétés en se basant sur les effets causés par les enchaînements par liaison hydrogène. [Traduit par le journal]

Can. J. Chem., 51, 1107 (1973)

Can. J. Chem. Downloaded from www.nrcresearchpress.com by 210.87.254.105 on 09/05/12
For personal use only.

In previous studies (1, 2) of molecular motion in cobalt ammine complexes, two types of motion were observed between 77 and 400 °K. In most complexes studied the ammine groups were reorienting about their Co—N axes even at 77 °K, while whole molecule reorientation occurred for those cations having higher symmetry. In $[Co(NH_3)_4CO_3]Br$ the reorientation frequency of one of the ammine groups was found to become less than the value required to narrow the n.m.r. signal (some 10^4 Hz) at *ca.* 130 °K (3). This paper reports a broadline n.m.r. study of the solid complex $[Co(NH_3)_4CO_3]_2SO_4$ using both continuous wave and pulsed techniques.

Experimental

$[Co(NH_3)_4CO_3]_2SO_4 \cdot H_2O$ was prepared according to Glemser (4). The samples were evacuated at 70 °C for 48 h in order to remove the water of crystallization and to promote desorption of oxygen.

Proton continuous wave spectra were run at 16 MHz as described elsewhere (5). T_1 values were obtained as described previously (6). The free-induction decays were found to be exponential at all temperatures studied.

The calculated points shown in Fig. 1 were computed using a Non-Linear Least Squares program (BMD) written by the Health Sciences Computing Facility of UCLA. The program required a function subroutine, and one was written in which the functional line shape was assumed to be described by the sum of two BPP equations. The calculated curve was fit to the experimental curve by an iterative procedure where there were three variable parameters in each BPP term (6 total parameters). The variable parameters were $P(1)$, determined from the depth of the T_1 minimum, $P(2)$, the pre-exponential term in $A = A_0 \exp(E/RT)$ where $A = \omega_0 t_c = 0.6158$ at the minimum and $A_0 = \omega_0 t_0$, and $P(3)$, the activation energy, estimated from the slope of the experimental curves. The parameter estimates for the other component curve are made in a similar fashion. The calculated output included the computed function, shown in Fig. 1, are refined values of the 6 parameters.

Results and Discussion

The results of the second moment measurements for $[Co(NH_3)_4CO_3]_2SO_4$ are consistent with those found for $[Co(NH_3)_4CO_3]Br$ (3), namely 19 ± 1 G^2 at 77 °K and 10.2 ± 0.75 G^2 at 300 °K. The value at 77 °K corresponds to reorientation of three ammine groups and one rigid group, while the result at 300 °K corresponds to all four ammine groups reorientating.

Figure 1 shows the results of spin–lattice relaxation measurements. The crosses indicate the experimental points (±5%), and the circles are for the calculated values obtained as explained in the experimental section. Two minima are observed in the temperature range 120 to

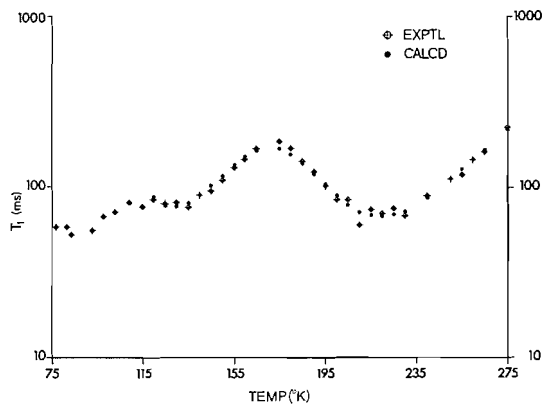

FIG. 1. Spin–lattice relaxation time as a function of temperature for $[Co(NH_3)_4CO_3]_2SO_4$.

Can. J. Chem. Downloaded from www.nrcresearchpress.com by 210.87.254.105 on 09/05/12
For personal use only.

300 °K, one at 125 °K and the other at 215 °K. The calculated depths are 76 and 72 ms, and the pre-exponentials ($\omega_0 t_0$) and activation energies are 2.9×10^{-4} and 3.4×10^{-5}, and 1.9 and 4.3 kcal, respectively. The standard deviation for both activation energies is 0.2 kcal. The magnitude of a T_1 minimum for a particular relaxation mechanism is proportional to the ratio of the total number of resonant spins to the number of spins whose motional correlation frequencies are suitable for producing spin–lattice relaxation, assuming that spin–spin interactions are strong enough to make $T_2 \ll T_1$, and allow spin diffusion to occur (7). Here, where there are two minima of equal magnitude and the expectation of another deeper minimum at a temperature below those accessible to us, we propose that one of the two observed minima represents the motion of one ammine group and the other observed minimum represents the motion of another ammine group. This is substantiated by a calculation, which, using the parameters for the 215 °K minimum, predicts that the midpoint of the second moment transition should occur at 121 °K. The observed midpoint is 120 °K and, as noted earlier, the change in second moment at the transition is appropriate to the motional effect of one ammine group reorienting about its C_3 axis. Below 100 °K the curve decreases toward what we believe to be a minimum representing two ammine groups, as the T_1 at 77 °K is substantially below 70 ms.

Since the second moment curve for $[Co(NH_3)_4CO_3]_2SO_4$ is virtually the same as that for $[Co(NH_3)_4CO_3]Br$ it seems reasonable to assume that the cations do not have greatly dissimilar structures. An X-ray investigation (8) of $[Co(NH_3)_4CO_3]Br$ indicated that there are three N—H···O distances significantly less than non-bonding distances for each cation. Okabe, *et al.* (3), have argued that this accounts for the 2.3 kcal activation energy they found for the rigid ammine group (at 77 °K) in $[Co(NH_3)_4CO_3]Br$. Of the eight hydrogen bonds per molecule reported for $[Co(NH_3)_4CO_3]Br$ five involved bromine atoms. Since hydrogen bonds are stronger to oxygen than to bromine this may account for our observed activation energy of 4.3 kcal in the sulfate as compared with 2.3 kcal for the bromide, assuming the two complexes have similar structures. Since the relative sizes of a sulfate group and a bromine ion are not terribly different, this may be a reasonable assumption.

The fact that there are two long and two short Co—N bonds probably accounts for the multiple minima in the T_1 curve. Two of the ammine groups are thought to have significant hydrogen bonding interactions, though different from one another, thus yielding activation energies of 4.3 and 1.9 kcal. The other two ammine groups have little hydrogen bonding interactions, and low apparent activation energies and they reorient with the same frequencies.

This work has been supported by a grant-in-aid from the National Research Council of Canada.

1. G. R. MURRAY, JR. and J. S. WAUGH. J. Chem. Phys. **29**, 207 (1958).
2. S. S. DHARMATTI, V. SARASURATI, and R. VIJAYARAGHAVAN. Proc. Colloq. Ampere, **XIII**, 133 (1965).
3. M. OKABE, Y. ARATA, A. YAMASAKI, and S. FUJIWARA. J. Phys. Soc. Jap. **28**, 935 (1970).
4. O. GLEMSER. Handbook of preparative inorganic chemistry. Vol. II. *Edited by* G. Brauer. Academic Press, New York. 1965.
5. B. A. DUNELL, C. A. FYFE, C. A. MCDOWELL, and J. RIPMEESTER. Trans. Faraday Soc. **65**, 1153 (1969).
6. S. E. ULRICH and B. A. DUNELL. J. Chem. Soc. Faraday Trans. II, **68**, 680 (1972).
7. J. E. ANDERSON and W. P. SLICHTER. J. Phys. Chem. **69**, 3099 (1965).
8. G. A. BARCLAY and B. F. HOSKINS. J. Chem. Soc. 586 (1962).

Substitution α to the Nitrogen in Dibenzylamine via Carbanion Intermediates

ROBERT R. FRASER, GUY BOUSSARD, I. DAN POSTESCU, JOSEPHINE J. WHITING, AND YUK Y. WIGFIELD

Department of Chemistry, University of Ottawa, Ottawa, Canada K1N 6N5

Received October 12, 1972

A method has been developed for introducing a variety of substituents into the position α to the nitrogen atom of dibenzylamine. Treatment of either the nitroso or the benzoyl derivative of dibenzylamine with lithium diisopropylamide generates a carbanion which reacts with alkyl halides or carbonyl compounds producing α-substitution products in yields of 66–99%. The method also gives good yields of derivatives of *N*-phenyl-*N'*-nitroso-piperazine. Attempts to form the carbanion of *N*-benzoylpiperidine failed.

Une méthode a été developpée pour introduire une série de substituants en position α à l'atome d'azote de la dibenzylamine. Le traitement soit du dérivé nitroso soit du dérivé benzoyle, de la dibenzylamine avec le diisopropylamide de lithium produit un carbanion qui réagit avec les halogénures d'alcoyle ou avec des composés possédant un groupe carbonyle pour produire des composés substitués en α avec des rendements d'environ 66–99% selon le cas. Cette méthode donne aussi de bons rendements en ce qui a trait à la formation de dérivés de la *N*-phényl *N'*-nitroso piperazine. Les tentatives afin de former le carbanion de la *N*-benzoylpiperidine ont échoué. [Traduit par le journal]

Can. J. Chem., **51**, 1109 (1973)

The report of Keefer and Fodor (1) that *N*-nitroso-*N'*-methylpiperazine, (**1**) undergoes base-catalyzed hydrogen–deuterium exchange in D_2O at 100 °C shows that the nitrosamino group exerts a potent stabilizing influence on an adjacent carbanion. The reason for its stabilizing effect was proposed to be the presence of a partial positive charge on the ring nitrogen due to the important resonance interaction **1***a*↔**1***b* in the anion. Subsequently, work in our laboratory (2)

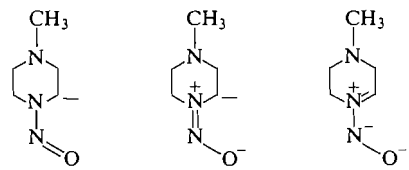

1*a* **1***b* **1***c*

on the stereochemical course of hydrogen–deuterium exchange in the biaryl nitrosamine **2** provided evidence that resonance stabilization of the carbanion by the contributing structure **1***c* is likely of equal or greater importance. Most recently, a report (3) on the use of the α-nitrosamino carbanion for synthetic transformations of secondary amines[1] has appeared. Seebach and Enders showed that the carbanion of dimethylnitrosamine reacts with a variety of electrophiles, giving α derivatives in yields of 70–95%. We wish to describe an investigation of the reactivity of the carbanions derived from **2**, *N*-nitrosodibenzylamine, and *N*-nitroso-*N'*-phenylpiperazine. The results offer further evidence of the utility of this important new reaction In addition, we have discovered a new related type of carbanion, that derived by abstraction of the proton α to nitrogen in *N*-benzoyldibenzylamine. This carbanion appears to be comparable in ease of formation and reactivity to that derived from *N*-nitrosodibenzylamine.

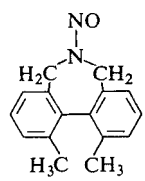

2

Since nitrosamine **2** had been found to undergo proton exchange readily, direct conversion to its carbanion was first examined. Treatment of **2** in tetrahydrofuran (THF) at −78 °C with 1.1 equiv of methyl lithium, followed after 1 min by excess methyl iodide gave, after 30 min reaction

[1]Substitution in the α-position of secondary amines is a novel reaction. We have been informed that Professor Stork has recently described another new method of introducing functional groups into the α-position of secondary amines but the results have not been published (4). Several methods are known for obtaining α-derivatives of primary (5) and tertiary (6) amines.

Can. J. Chem. Downloaded from www.nrcresearchpress.com by 210.87.254.42 on 09/05/12
For personal use only.

Can. J. Chem. Downloaded from www.nrcresearchpress.com by 210.87.254.42 on 09/05/12
For personal use only.

time and work-up, a 98% yield of crude methylated material (**3***a*). Its n.m.r. spectrum taken immediately thereafter indicated it to be solely one of the four possible stereoisomeric products, that in which H_4[2] had been replaced by a methyl group. Since H_4 was exchanged more than 30 times faster than any other proton in **2** the observation of a single methylation product

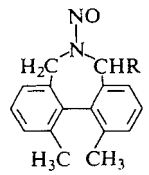

3

a R = CH_3
b R = D
c R = COOH

shows that the most stable carbanion in THF is the same as that observed by the kinetic method in *t*-butanol-*O*-*d*. Reaction of the carbanion derived from **2** with D_2O and with CO_2 gave high yields of **3***b* and *c* (R = D and COOH respectively). Isolation of **3***a–c* in pure form was complicated by the fact that slow but finite rotation about the N—NO bond occurs ($t_{1/2}$ = 0.5–10 h depending on solvent (2)). This caused difficulty in obtaining greater than 50% yields of a single analytically pure isomer.

Reactions of N-Nitrosodibenzylamine

Encouraged by the success in forming and reacting the carbanion of **2**, we then focused our attention on reactions of *N*-nitrosodibenzylamine (**4**). This amine was chosen for study since it is readily available, and it possesses only slight carcinogenicity whereas nitrosamines of lower molecular weight show very significant carcinogenic activity (7). Treatment of **4** in THF at −78° with either methyl lithium or lithium diisopropylamide (LDA) gave a relatively stable carbanion[3] which on reaction with methyl iodide gave, after chromatography, a 91% yield of pure benzyl α-phenethyl nitrosamine **5***a*. The results of the alkylation and condensation reactions of **4** are summarized in Scheme I and Table I. Compounds **5***a*, *b*, *e*, *f* were hydrolyzed to the parent amine and characterized as such. Compounds **5***c* and *d* had been prepared with the aim of achieving cyclization to give the substituted piperidine and azepine rings. Unfortunately the carbanions of **5***c* and *d* failed to cyclize. It would seem that cyclization of **5***c* is impeded by large steric effects. In the transition state leading to the six-membered ring the phenyl *syn* to the oxygen will encounter either $A^{1,3}$ strain if equatorial (8) or the normal 0.3 kcal destabilization if axial (9). Similar problems likely prevent ring closure of **5***d*. To prove their structures, **5***c* and *d* were cleaved to the secondary amines which spontaneously cyclized to the pyrrolidine **6** and the piperidine **7**. Such a sequence of

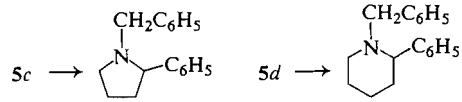

6 **7**

bromoalkylation and ring **6** closure provides a useful route for the synthesis of substituted nitrogen heterocycles.

*Reactions of N-Benzoyldibenzylamine (**8**)*

If the activating influence of the nitroso group results from the presence of a strong resonance interaction between the amine nitrogen and the nitroso group, *i.e.*

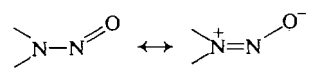

then other groups having the ability to accept the lone pair on nitrogen should similarly stabilize a carbanion α to the nitrogen. The strength of this resonance interaction is revealed by the activation energy for rotation about the partial double bond ($^{\delta+}N{=}N{=}O^{\delta-}$ or in general $^{\delta+}N{=}X{=}Y^{\delta-}$). These activation energies are readily available from n.m.r. studies of a variety of amine derivatives. The highest barriers to rotation are exhibited by nitrosamines, 23 kcal/mol (10, 11) and thioamides, 18–27 kcal/mol (12). Less hindrance to rotation is found in substituted benzamides (15–23 kcal/mol (12)) and aryl triazenes (13–16 kcal/mol (13)). Although the thiobenzoyl group would undoubtedly be of interest as an activating group it suffers from the disadvantage of being less easily introduced than the benzoyl or arylazo groups. We have

[2]The assignment of stereochemistry to the two pairs of diastereotopic protons is described in detail in ref. 2; H_4, the proton whose n.m.r. doublet appears at highest field, was shown to be *syn* to the oxygen atom and "quasi-axial". The n.m.r. of **3***a* lacks absorption in the region of H_4.

[3]The half-life of this carbanion at −78° in THF is approximately 30 min; the nature of the products of the decomposition were not investigated.

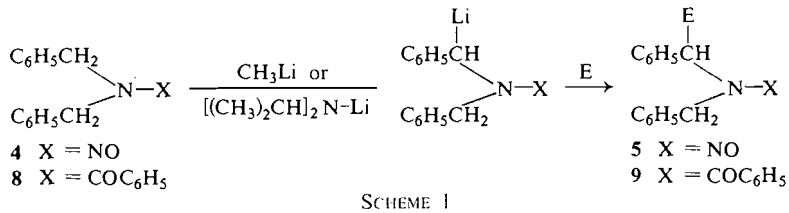

4 X = NO
8 X = COC_6H_5

5 X = NO
9 X = COC_6H_5

SCHEME 1

TABLE 1. Carbanion reactions of *N*-nitrosodibenzylamine (**4**) and *N*-benzoyldibenzylamine (**8**)

Starting material	Electrophile	Product isolated	Yield (%)
4	CH_3I	**5***a* E = CH_3	91
	$CH_3CH_2CH_2I$	*b* E = C_3H_7	85
	$BrCH_2CH_2CH_2Br$	*c* E = $(CH_2)_3Br$	33*
	$Br(CH_2)_4Br$	*d* E = $(CH_2)_4Br$	34*
	CO_2	*e* E = COOH	99
	C_6H_5CHO	*f* E = $CHOHC_6H_5$	62
8	CH_3I	**9***a* E = CH_3	91
	CO_2	*b* E = COOH	98
	CH_3COCH_3	*c* E = $COH(CH_3)_2$	90
	$(CH_3CO)_2O$	*d* E = $COCH_3$	66

*These yields are of pure cyclized products 6 and 7.

examined the activating influence of these latter two groups. Attempts to prepare the carbanion derived from 1-*p*-nitrophenyl-3,3-dibenzyltriazene using methyllithium as base proved unsuccessful. Better results were obtained with *N*-benzoyldibenzylamine (**8**). A 30% yield of product was obtained from reaction of the carbanion generated by methyllithium with methyl iodide. When LDA was used as base, a stable anion was formed[4] which was reacted with four different electrophiles; in each instance the yields of product are listed in Table 1. As in the reactions of **4**, electrophilic substitutions α to the nitrogen of **8** proceed in high yields. There appears to be little to choose between the nitroso or benzoyl groups for the activation of dibenzylamine. Both groups can be introduced and later removed with comparable ease and efficiency. However, use of the benzoyl group is preferable because of the carcinogenicity of nitrosamines.

To our knowledge there is only one similar example of activation of a benzyl group towards carbanion formation. We have recently learned (14) that the *N*-benzyl-β-lactams **10** and **11** on treatment with LDA rearrange to pyrrolidones (12) or azepin-2-ones (13) presumably via carbanion intermediates.

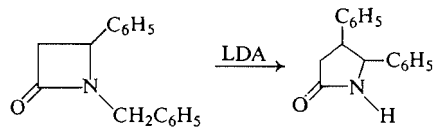

10 **12**

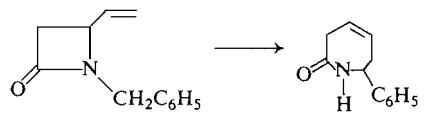

11 **13**

Extension to Less Stable Carbanions

The phenyl groups in **4** and **9** undoubtedly provide appreciable stabilization of the benzylic carbanion. We have examined the reactivity of nitrosamines which lack this beneficial influence and have encountered considerable difficulty in obtaining high yields of substitution product. Alkylation of the carbanion of *N*-phenyl-*N*-nitrosopiperazine, (**14**), has been attempted under a variety of experimental conditions. The nature of the base, effects of added amines, the time for anion formation, and reaction with methyl iodide have all been studied. Under optimum

[4]There was no difference in yield when the interval between carbanion formation and addition of methyl iodide was varied from 2 to 6 min. A difference was found for the anion of **4**, the optimum interval being 4 min.

Can. J. Chem. Downloaded from www.nrcresearchpress.com by 210.87.254.42 on 09/05/12
For personal use only.

conditions only a 46% yield of methylation product could be obtained.[5] Under the same conditions, carboxylation occurred in 73% yield. The poorer yields in the reactions of **14** likely indicate a competition between reaction and decomposition of the intermediate carbanion by the ring opening process **14** → **15**.

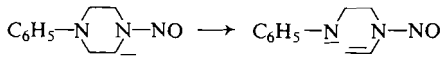

14 **15**

Seebach and Enders (15) have recently described the successful generation and reaction of the nitrosamino carbanions of *N*-nitrosopiperidine, *N*-nitrosopyrrolidine, and many other nitrosamines, including *N*-nitrosodiisopropyl amine. Their results show that nitrosamino carbanions offer great utility in organic synthesis. It would appear that the benzoyl group lacks the potent activating influence of the nitroso group, for we found that treatment of *N*-benzoyl piperidine with LDA followed by either CO_2 or CH_3I gave only unreacted starting material. We are currently investigating the potential activating influence of groups other than nitroso and benzoyl in the hope of finding ones with enhanced stabilizing effects but no adverse pharmacological properties.

Experimental

All melting and boiling points are uncorrected. The n.m.r. spectra were recorded on either a Varian T-60 or HA-100 spectrometer using deuteriochloroform as solvent unless otherwise noted. Chemical shifts are expressed in δ units (p.p.m. downfield from tetramethylsilane). Mass spectra were measured either on a Perkin–Elmer RMU-6D or an AEI, MS 9025, mass spectrometer.

All reactions involving methyllithium were carried out under an atmosphere of dry nitrogen using carefully dried equipment and reagents. Tetrahydrofuran was distilled from lithium aluminum hydride just prior to its use. Methyllithium obtained from Foote Chemical Company as a 5% solution in ether was injected by needle and syringe into the reaction vessel through a rubber septum. Work-up of a reaction refers to the standard operations of extraction, washing, drying, filtration, and removal of solvent by evaporation under vacuum. All chromatographic purifications were done using thin layers of silica gel on 20 × 20 cm glass plates.

Preparation and Nitrosation of N-Nitroso-6,7-dihydro-1,11-dimethyl-5H-dibenz(c,e)azepine, (2)

Reaction of 2,2′-bis-bromomethyl-6,6′-dimethyldiphenyl (16) with benzylamine and hydrogenolysis of the product according to the procedure of Wenner (17) gave the amine hydrochloride in 70% yield for the two steps. The product crystallized from methanol–water and melted from 272–273°; n.m.r.: 2.18 (6H, s), 3.62, and 4.11 (4H, AB q, J = 12 Hz), 7.40 (6H, s).

Anal. Calcd. for $C_{16}H_{18}NCl$: C, 72.91; H, 7.26; N, 5.61. Found: C, 72.69; H, 6.88; N, 5.24.

Nitrosation of this amine with nitrous acid (18) gave **2** in 82% yield. The product was recrystallized from hexane to give pale yellow needles, m.p. 123–123.5°. The n.m.r. spectrum of **2** has been described previously (2).

Anal. Calcd. for $C_{16}H_{16}N_2O$: C, 76.17; H, 6.39; N, 11.10. Found: C, 76.13, H, 6.49; N, 10.92.

Reactions of N-Nitroso-6,7-dihydro-1,11-dimethyl-5H-dibenz(c,e)azepine, (2)

(a) With Methyl Iodide

To a solution of 50 mg (0.2 mmol) of **2** in 15 ml THF at −78° was added with stirring 1.1 equiv of methyllithium and after 1 min, 0.1 ml of methyl iodide. After 30 min, work-up gave 50 mg of solid which was crystallized from *n*-hexane, then twice from methylene chloride – pentane to give a solid, m.p. 109–110°; n.m.r.: 0.70 (3H, d, J = 7 Hz), 2.17 (6H, s), 4.59, 5.45 (2H, ABq, J = 13.5 Hz), 5.69 (1H, q, J = 7 Hz), 7.00–7.40 (6H, m). No absorption due to a second isomer (CH_3 and NO *anti*) was seen until 1 h later.

Anal. Calcd. for $C_{17}H_{18}N_2O$: C, 76.67; H, 6.81; N, 10.52. Found: C, 76.44; H, 7.02; N, 10.48.

After dissolution, an equilibrium of 5:1 *syn*:*anti* was reached after 40 h.

(b) With Carbon Dioxide

Repetition of the above operation except that pieces of solid CO_2 were added in place of methyl iodide gave, after work-up, 58 mg of solid residue. After crystallization from carbon tetrachloride 26 mg, 45%, of a solid was obtained, whose n.m.r. indicated it to be a 2:1 mixture of *syn*:*anti* forms; *syn*-absorption at 2.10 (3H, s), 2.17 (3H, s), 4.51 (1H, d, J = 13 Hz), 5.58 (1H, d, J = 13 Hz), 6.37 (1H, s), 7.1–7.4 (6H, m).

Anal. Calcd. for $C_{17}H_{16}N_2O_3$: C, 68.81; H, 5.44; N, 9.45. Found: C, 68.43; H, 5.33; N, 9.29.

(c) With Deuterium Oxide

Repetition of formation of the carbanion of **2** followed by addition of 0.3 ml of heavy water (99.8%) gave after work-up a solid which was immediately dissolved in *t*-butanol-*O*-*d*: $CDCl_3$ (3:1) (to retard rotation about the N—NO bond (2)). The n.m.r. spectrum of this material was identical to that of **2** except that only 10% of the absorption at δ 3.41 (H_4) remained while 90% of the signal at δ 4.75 (H_3) was observed. The deuterium content at these positions caused the signals for the CH groups at δ 5.41 and 5.45 to appear as broad singlets. After standing for 48 h, the signals for H_3 and H_4 became equal in intensity. No isolation of this product was attempted.

N-Nitrosodibenzylamine, (4)

Nitrosation of dibenzylamine as previously described (19) gave *N*-nitrosodibenzylamine, m.p. 63–63.5° (lit. (19) m.p. 60–61°).

Reactions of N-Nitrosodibenzylamine (4)

(a) With Methyl Iodide

To a solution of 339 mg (1.5 mmol) of **4** in 30 ml of

[5]Details of these reactions are described in the M.Sc. thesis of I.D. Postescu, University of Ottawa, Ottawa, Canada, 1972.

Can. J. Chem. Downloaded from www.nrcresearchpress.com by 210.87.254.42 on 09/05/12
For personal use only.

Can. J. Chem. Downloaded from www.nrcresearchpress.com by 210.87.254.42 on 09/05/12
For personal use only.

THF at −78° was added 0.24 ml (1.65 mmol) of diisopropylamine. When 1.65 mmol of methyllithium was added an immediate red coloration appeared. After 4 min, 0.46 ml (7.5 mmol) of methyl iodide was added and stirring was continued at −78° for 1.5 h. After the solution was warmed to 0°, addition of 15 ml water and work-up gave 417 mg of a yellow liquid. Chromatography using silica gel and elution with ether – petroleum ether (3:7) gave 345 mg (91% yield) of yellow liquid whose n.m.r. showed no significant impurities to be present. Absorptions for the *syn* and *anti* isomers (1:4) could be seen separately;[6] *syn*: 1.17, (3H, d, J = 7.5 Hz), 4.67, 5.25 (2H, ABq, J = 14.3 Hz), 6.18 (1H, q, J = 7.5 Hz), 6.8–7.4 (br m); *anti*: 1.73 (3H, d), 4.07, 4.98 (2H, ABq, J = 14 Hz), 5.35 (1H, q), 6.8–7.4 (br m).

This nitrosamine, **5***a*, was cleaved by the method of Stewart (21) as follows: dry hydrogen chloride was bubbled through a stirred solution of 345 mg **5***a* in 25 ml anhydrous benzene for 30 min. The solution changed from yellow to brown as the bubbling continued. A strong stream of nitrogen was finally passed through the solution for 10 min, during which time it became yellow again. The benzene was concentrated to 4–5 ml. The addition of ether precipitated white crystals (220 mg) on cooling. An additional 75 mg of solid was obtained from the mother liquor after standing overnight. The total yield was 285 mg (76%). Recrystallization from chloroform–ether mixture gave benzyl α-methylbenzylamine hydrochloride which melted at 179–180°, (lit. m.p. 179° (22)); n.m.r.: 1.80 (3H, d, J = 6.4 Hz), 3.40–4.40 (3H, m), 7.50 (10H m), 10.50 (2H, br m).

(b) Methylation of **4** *in Absence of Diisopropyl Amine*

To a solution of 339 mg (1.5 mmol) in 30 ml THF at −75° was added 1.1 equiv. of methyllithium. After 4 min, 0.46 ml methyl iodide was added. The reaction was worked-up as before. The yield, estimated from the n.m.r. spectrum of crude product, was 90%. Cleavage of this crude produce, in anhydrous benzene as above, gave 266 mg (72%) of **4**.

(c) With 1-Iodopropane

Dibenzylnitrosamine, 339 mg (1.5 mmol) was converted with LDA into its anion as in part (*a*). After 4 min, 0.74 ml (5 equiv) of 1-iodopropane was added. The solution was stirred at −75° for 2.5 h, then warmed up to room temperature. Work-up as in (*a*) gave 342 mg of crude **5***b* whose n.m.r. showed absorption for the *anti* isomer at 0.70–2.5 (7H, br m), 4.10, 5.07 (2H, AB q, J = 14 Hz), 5.12 (1H, t, J = 7.5 Hz), 6.80–7.50 (10H m). From the area of the small triplet at δ 6.25 assigned to the methine proton of the *syn* isomer it was found to constitute 15% of the mixture. Other absorptions of the *syn* form were not distinguishable from the predominant *anti* peaks. This material was cleaved as before in benzene (25 ml). After evaporation of solvent the residue was dissolved in ether and 320 mg (77%) of solid was precipitated by the addition of petroleum ether. Recrystallization from ether gave benzyl α-phenylbutylamine hydrochloride, (**5***b*), which melted from 139–140.5°.

Anal. Calcd. for $C_{17}H_{22}NCl$: C, 74.03; H, 8.04; N, 5.08, Cl, 12.85. Found: C, 73.66; H, 8.19; N, 5.47; Cl, 12.82.

This hydrochloride was converted to the free base and distilled (bulb-to-bulb) to produce a yellow oil.

Anal. Calcd. for $C_{17}H_{21}N$: C, 85.30; H, 8.84. Found: C, 85.31; H, 8.98.

(d) With 1,3-Dibromopropane

The same procedure as in (*a*) was followed with the exception that twice the amount of solvent was employed. The crude product after purification by chromatography was shown by n.m.r. to contain a small amount (< 10%) of the *syn* form. The *anti* form showed absorptions at 1.50–2.60 (4H, m), 3.20 (2H, t), 4.05 and 5.15 (2H, AB q, J = 14 Hz), 5.10 (1H, t), 6.85–7.60 (10H, m).

Cleavage of the nitrosamine gave 424 mg of solid amine hydrochloride which was dissolved in 40 ml water. The solution was made alkaline. After 5 min, extraction and work-up gave an oil which was purified by chromatography using petroleum ether – ether (7:3) as solvent. The first eluted material was 117 mg (33%) of solid 1-benzyl-2-phenylpyrrolidine which after recrystallization from acetone had m.p. 44.5–45° (lit. m.p. 43–44° (23)); n.m.r.: 1.50–2.50 (5H, m), 3.03 and 3.90 (2H, AB q, J = 13 Hz), 3.35 (2H m), 7.11–7.60 (10H m). The mass spectrum showed a peak for the molecular ion at m/e 237.

(e) With 1,4-Dibromobutane

As in (*c*) dibenzylnitrosamine was alkylated using a five-fold excess of 1,4-dibromobutane. Work-up and chromatography as above yielded an oil whose n.m.r. again showed the presence of < 10% *syn* isomer. The *anti* form showed peaks at 1.0–2.60 (6H, m), 3.23 (2H, t, J = 7 Hz), 4.08 and 5.10 (2H, AB q, J = 14 Hz), 6.90–7.67 (10H, m). Conversion of this nitrosamine gave the corresponding amine which then cyclized providing, after chromatography, 125 mg (33%) of 1-benzyl-2-phenylpiperidine. After recrystallization from ethanol–water the white solid melted at 90–91° (lit. m.p. 93–93.5° (24)); n.m.r.: 1.10–2.05 (8H, m), 2.76 and 3.78 (2H, AB q, J = 14 Hz), 3.05 (1H, br), 7.1–7.60 (10H, m); mass spectrum shows molecular ion at m/e 251.

(f) With Carbon Dioxide

A solution of 452 mg (2 mmol) of **4** was converted into its carbanion as in (*a*). Dry carbon dioxide gas was bubbled through the solution for 20 min. The temperature was then raised to 25° and the solution concentrated to dryness. Extraction of a solution of the residue in 5% Na_2CO_3 with chloroform yielded 40 mg of unreacted **4**. The aqueous solution was treated with 1 *N* HCl and the liberated acid (**5***e*), after extraction into ether, drying, and solvent removal, weighed 490 mg (99%). Its n.m.r. showed two isomers in the ratio 2:1 with the major one absorbing at 5.63 (1H, s), 4.95 and 5.48 (2H, AB q, J = 15 Hz), 6.75–7.40 (10H m), 12.9 (1H, s). The minor isomer (*syn*) showed absorption at 4.46 and 4.88 (2H, AB q, J = 15 Hz) and 6.30 (1H s). Cleavage as in (*a*) and concentration of the benzene solution gave a semisolid residue which was dissolved in hot acetonitrile. The amino acid, **5***c*, crystallized on cooling to a white solid. The solid was dissolved in hot water, the p*H* was adjusted to 6.8, and on cooling 400 mg of crystals, m.p. 225–227 (lit, m.p.

[6]The n.m.r. assignments for all the derivatives of **4** follow from the works of Karabatsos and Chow (20). In all cases the methine proton of the *syn*-isomer appears at lower field, while a methyl or methylene group in the α position shows the opposite order of shieldings.

Can. J. Chem. Downloaded from www.nrcresearchpress.com by 210.87.254.42 on 09/05/12
For personal use only.

225° (25)) was obtained. This yield is 87% for the two steps, 96% if based on recovery of unreacted **4**.

(g) With Benzaldehyde

Under the standard conditions of (*a*), reaction of the anion of **4** with 1 equiv of benzaldehyde gave a yellow oil which was purified by chromatography. Elution with chloroform developed a band ($R_f = 0.4$) from which a 62% yield of solid condensation product was obtained. Recrystallization gave white crystals, m.p. 120–121°. The n.m.r. spectrum reveals the presence of two isomers both of which likely possess the *anti* configuration. Isomer *a*; 3.80 and 5.06 (2H, AB q, $J = 15$ Hz), 4.84 and 5.64 (2H, AB q, $J = 7$ Hz), isomer *b*; 3.96 and 5.36 (2H, AB q, $J = 15$ Hz), 4.98 and 5.56 (2H, AB q, $J = 8$ Hz), also 2.50 (1H, s), and 6.65–7.4 (15H, m) for both isomers.

Anal. Calcd. for $C_{21}H_{20}N_2O_2$: C, 75.60; H, 6.02; N, 8.25. Found: C, 75.88; H, 6.07; N, 8.43.

N-Benzoyldibenzylamine, (8)

Reaction of benzoyl chloride with dibenzylamine produced **9** in 70% yield. Recrystallization from ethanol (99%) gave white crystals, m.p. 112–113° (lit. m.p. 112° (26)); n.m.r. (at 0° and 100 MHz), 4.40 (2H, s), 4.70 (2H, s), 7.0–7.8 (15H, m); at 37° the two CH_2 peaks coalesce indicating $\Delta G^{\ddagger}$ for rotation equal to 15.6 kcal/mol.

Reactions of N-Benzoyldibenzylamine, (8)

Generation of the Anion

A stirred solution of 300 mg (1 mmol) of *N*-benzoyldibenzylamine in 30 ml of dry THF cooled to −78° was treated with 0.15 ml (1.05 mmol) of diisopropylamine, then 0.7 ml (1.1 mmol) of methyllithium (5% in ether). A red–brown color developed immediately. After 4 min, the electrophile was added.

(a) Reaction with Methyl Iodide. Addition of 0.3 ml (5 mmol) of methyl iodide caused rapid disappearance of color. After 1 h the solution was warmed to room temperature, 15 ml water added, and the mixture was extracted with two 20 ml portions of methylene chloride. The methylene chloride extracts were washed with 5% sodium sulfite and water, then dried. Removal of solvent gave a liquid which crystallized on addition of ether. Recrystallization gave 234 mg of solid, m.p. 110–112°. Another 19 mg was obtained from mother liquors, total yield 253 mg (81%). In a separate experiment the crude product after chromatography on silica gel gave 284 mg (91%) of solid, m.p. 112.5–114 (lit. m.p. 109–111° (27)); n.m.r.: 1.46 (3H, d, $J = 7.5$ Hz), 3.96 and 4.90 (2H, AB q, $J = 16$ Hz), 5.47 (1H q, $J = 7.5$ Hz), 7.10–7.70 (15H m).

(b) With CO_2. A stream of dry CO_2 was bubbled through the solution of the carbanion derived from **8** for 10 min. The cooling was stopped, the solvent was distilled off and the residue dissolved in 5% Na_2CO_3 solution and washed with chloroform. Acidification and work-up gave 313 mg (98%) of a colorless oil which gradually crystallized. Recrystallization from ether gave a white solid, m.p. 124–125°; n.m.r.: 4.35 and 4.81 (2H, AB q, $J = 16$ Hz), 5.57 (1H, s), 7.0–7.5 (15H, m), 12.05 (1H, s).

Anal. Calcd. for $C_{22}H_{19}NO_3$: C, 76.79; H, 5.54; N, 4.05. Found: C, 77.16; H, 5.75; N, 3.79.

(c) With Acetone. After stirring with 0.1 ml (1.25 mmol) of acetone for 1 h, work-up gave 370 mg of a colorless oil which was purified by chromatography on silica gel using chloroform as eluent. The liquid obtained amounted to 320 mg (90%) and gave crystals m.p. 133–133.5° from hexane – ethyl acetate. N.m.r.: 1.0 (3H, s), 1.3 (3H, s), 4.2 (1H, s), 4.40 (2H, AB q, $J = 16$ Hz), 6.4 (1H, br), 7.2–7.4 (15H, m).

Anal. Calcd. for $C_{24}H_{25}NO_2$: C, 80.20; H, 7.01. Found: C, 79.85; H, 6.99.

(d) With Acetic Anhydride. After stirring the solution with 0.11 ml (1.1 mmol) of acetic anhydride for 1 h, work-up gave 365 mg of an oil which was purified by chromatography using chloroform as eluent. The product was an oil weighing 266 mg (66%) which showed n.m.r. 2.15 (3H, s), 4.5 (2H, AB q, $J = 16$ Hz), 5.5 (1H, s), 7.0–7.4 (15H, m); mass spectrum, weak molecular ion, strong peak at *m/e* 300.138 (P − 43). Calcd. for $C_{23}H_{21}NO_2$—CH_3CO: 300.139. This oil thus far has failed to crystallize.

Carboxylation of 1-Nitroso-4-phenylpiperazine

To a solution of 288 mg (1.5 mmol) 1-nitroso-4-phenylpiperazine (28) in 30 ml of THF was added 0.22 ml (1.5 mmol) of diisopropylamine. The mixture was cooled to −75° and 1.1 equiv of methyllithium was injected. After 4 min a stream of carbon dioxide was passed through the stirred solution for 15 min. The stirring was continued at −75° for 0.5 h and then at room temperature for 1 h. Work-up as in the previous carboxylation gave 162 mg (49%) of 1-nitroso-4-phenylpiperazine-2-carboxylic acid; n.m.r.: 2.50–3.80 (4H, m), 4.20 (1H, t), 4.85 (1H, d), 5.63 (1H, d, $J = 10$ Hz), 6.70–7.40 (5H, m), 11.40 (1H, s).

This nitrosamino acid was dissolved in 60 ml of dry benzene and the nitroso group was removed as described previously. The product was filtered to give 139 mg (38%) of pink crystals. Recrystallization from a water–acetone mixture afforded colorless crystals (m.p. 229–230°, dec.) of 4-phenylpiperazine-2-carboxylic acid hydrochloride.

Anal. Calcd. for $C_{11}H_{15}N_2O_2Cl$: C, 54.43; H, 6.23; N, 11.54; Cl, 14.61. Found: C, 54.05; H, 6.25; N, 11.05; Cl, 14.83.

We thank the National Research Council of Canada for the financial support of this work.

1. L. K. KEEFER and C. H. FODOR. J. Am. Chem. Soc. **92**, 5747 (1970).
2. R. R. FRASER and Y. Y. WIGFIELD. Tetrahedron Lett. 2515 (1971).
3. D. SEEBACH and D. ENDERS. Angew. Chem. **84**, 350 (1972).
4. From a lecture presented by G. Stork at the Organic Division, C.I.C. Symposium, Vancouver, B.C., Aug. 1972.
5. U. SCHOLLKOPF. Angew. Chem. **82**, 795 (1970); T. KAUFFMANN, E. KOPPELMANN, and H. BERG. Angew. Chem. **82**, 138 (1970).
6. N. J. LEONARD, L. H. MILLER, and P. D. THOMAS. J. Am. Chem. Soc. **78**, 3463 (1956); A. R. LEPLEY and W. A. KHAN. J. Org. Chem. **35**, 362 (1968).
7. H. DRUCKERY, R. PREUSSMANN, S. IVANKOVIC, and D. SCHMALL. Z. Krebsforsch. **69**, 103 (1967).
8. Y. L. CHOW, C. J. COLON, and J. N. S. TAM. Can. J. Chem. **46**, 2821 (1968); F. JOHNSON and S. K. MALHOTRA. J. Am. Chem. Soc. **87**, 5942 (1965).
9. J. J. HIRSCH. Top. Stereochem. **1**, 207 (1967).
10. C. E. LOONEY, W. D. PHILLIPS, and E. L. REILLY. J. Am. Chem. Soc. **79**, 6136 (1967).

11. R. K. HARRIS and R. A. SPRAGG. Chem. Commun. 362 (1967).
12. I. O. SUTHERLAND. Investigation of kinetics of conformational changes. *In* Ann. Repts. on NMR Spectroscopy. Vol. IV. Academic Press, N.Y. 1971.
13. M. H. AKHTAR, R. S. MCDANIEL, M. FESER, and A. C. OEHLSCHLAGER. Tetrahedron. **24**, 3899 (1968).
14. T. DURST. Private communication.
15. D. SEEBACH and D. ENDERS. Angew. Chem. **84**, 1101 (1972).
16. K. MISLOW, R. GRAEVE, A. J. GORDON, and G. H. WAHL. J. Am. Chem. Soc. **86**, 1733 (1964).
17. W. WENNER. J. Org. Chem. **17**, 1451 (1952).
18. D. F. HEATH and A. R. MATTOCKS. J. Chem. Soc. 4226 (1961).
19. C. G. OVERBERGER, L. C. PALMER, B. S. MARKS, and N. R. BYRD. J. Am. Chem. Soc. **77**, 4100 (1955).
20. Y. L. CHOW and C. J. COLON. Can. J. Chem. **46**, 2827 (1968); G. J. KARABATSOS and R. A. TALLER. J. Am. Chem. Soc. **86**, 4373 (1964); W. LIJINSKI, L. K. KEEFER, and J. LOO. Tetrahedron, **26**, 5137 (1970).
21. F. W. C. STEWART. Austr. J. Chem. **22**, 2451 (1969).
22. A. P. TERENT'EV, E. G. RUKHADZE, V. V. DUNINA, and E. V. DROBYSHEVSKYA. Zh. Obshch. Khim. **38**, 715 (1968); Chem. Abstr. **69**, 51756 (1968).
23. A. V. EL'TSOV, A. C. CHIGAREV, and I. T. STARYKH. Zh. Obshch. Khim. **34**, 3344 (1964); Chem. Abstr. **62**, 3995 (1965).
24. R. A. ABRAMOVITCH, K. S. AHMED, and C. S. GIAM. Can. J. Chem. **41**, 1752 (1963).
25. S. A. HARRIS and C. O. GITTERMAN. U.S. Pat. 3 299 095; Chem. Abstr. **66**, 55376 (1967).
26. H. FRANZEN. Chem. Ber. **42**, 2465 (1909).
27. L. AMOROS-MARIN and R. B. CARLIN. J. Am. Chem. Soc. **81**, 733 (1959).
28. C. H. LOVELL. U.S. Patent 3 287 454; Chem. Abstr. **66**, 65512 (1967).

Can. J. Chem. Downloaded from www.nrcresearchpress.com by 210.87.254.42 on 09/05/12
For personal use only.

Studies of Rhenium β-diketone Complexes. IV. The Synthesis, Properties, and Crystal Structure of Bis(μ-chlorotricarbonyl(1-phenyl-1-hydroxobut-1-ene-3-one)rhenium(I)), a Compound Containing a Monodentate Neutral β-Ketoenol

M. C. FREDETTE AND C. J. L. LOCK[1]

Institute for Materials Research, McMaster University, Hamilton, Ontario

Received August 21, 1972

The title compound, $[Re(CO)_3Cl(C_6H_5 \cdot COH \cdot CH \cdot CO \cdot CH_3)]_2$, is one of a series of compounds obtained by the reaction of chloropentacarbonylrhenium(I) with β-diketones and has been characterized by n.m.r. and infrared spectroscopy and single crystal X-ray diffraction. The crystals are monoclinic with lattice parameters $a = 14.77(2)$, $b = 17.98(2)$, $c = 13.48(2)$ Å, $\beta = 124.34(9)°$; $C2/c$, $Z = 4$. A total of 1293 independent reflections were measured on a single crystal X-ray diffractometer and the structure was refined by full matrix least squares analysis to a weighted R_2 value of 0.0444. The dimeric halves of the molecules are held together by two chlorine atoms symmetrically bridging the rhenium atoms (Re—Cl = 2.511(5) Å). The structure is thus very like that of $[Re(CO)_4Cl]_2$, except that two neutral β-ketoenol molecules replace two carbon monoxide molecules (one on each rhenium) and are bonded through the ketone group (Re—O = 2.16(1) Å). The arrangement of the keto and enol groups is such that hydrogen bonding can occur between them.

Le composé mentionné dans le titre $[Re(CO)_3Cl(C_6H_5 \cdot COH \cdot CH \cdot CO \cdot CH_3)]_2$ appartient à une famille de produits obtenue par réaction du chloropentacarbonylrhénium(I) avec des β-dicétones. Ce produit a été caractérisé par r.m.n., par spectroscopie infrarouge et par diffraction de rayons-X (monocristal). Les cristaux sont du type monoclinique ave les paramètres de mailles qui suivent: $a = 14.77(2)$, $b = 17.98(2)$, $c = 13.48(2)$ Å, $\beta = 124.34(9)°$; $C2/c$, $Z = 4$. Un total de 1293 réflections indépendantes a été mesuré à partir d'un diffractomètre à rayons-X sur un monocristal et la structure a été raffinée par une matrice des moindres carrés jusqu'à une valeur R_2 pondérée de 0.0444. Les moitiés dimériques des molécules sont retenues ensemble par deux atomes de chlore impliquées symétriquement dans un pontage avec ceux de rhenium (Re—Cl = 2.511(5) Å). La structure, par suite, ressemble beaucoup à celle de $[Re(CO)_4Cl]_2$ à l'exception des deux molécules neutres β-cétoenol qui remplacent les deux molécules de monoxyde de carbone (une sur chaque rhénium) et qui sont reliées à l'aide du groupe cétonique (Re—O = 2.16(1) Å). L'arrangement spatial des groupes, cétone et énol, est tel que la formation de ponts hydrogènes peut se produire entre eux.

[Traduit par le journal]

Can. J. Chem., **51**, 1116 (1973)

Introduction

We have investigated the reaction of $Re(CO)_5Cl$ with various β-diketones and have prepared two series of compounds with apparent stoichiometries $Re_2(CO)_6(dik)_2$ and $[Re(CO)_3Cl(dikH)]_2$.[2] The structure of $Re_2(CO)_6(dbm)_2$ has been reported elsewhere (1). The structure of $[Re(CO)_3Cl(bamH)]_2$ was examined by single crystal X-ray diffraction because spectroscopic and magnetic methods of examination gave no detailed information about the structure, and the physical properties (low solubility and general intractibility) were inconsistent with those we expected for a six-coordinate monomeric species. In this paper we discuss these studies and the single crystal X-ray structure determination.

Experiments

Analyses were performed on crystals of the compound for carbon, hydrogen, and chlorine by A.B. Gygli, Toronto, Canada and rhenium and chlorine were determined by neutron activation analysis (2). Infrared spectra were recorded for solid samples ground into a mull with Nujol. The Nujol had been dried by refluxing with phosphorus pentoxide followed by vacuum distillation. The mull samples were mounted between potassium bromide or polyethylene plates and spectra were recorded on Perkin-Elmer 337 and 301 spectrometers. Mass spectra were recorded on a Consolidated Electrodynamics Corp. Mass Spectrometer Model 21-110B. Measurements of magnetic susceptibility were made by the Gouy method. The apparatus used has been described elsewhere (3). Proton n.m.r. spectra were recorded on a Varian Associates HA 100 spectrometer using tetramethylsilane as a standard. All solvents and reagents

[1]To whom correspondence should be addressed.

[2]dik is a β-ketoenolate anion and dikH is the corresponding neutral β-ketoenol or β-diketone, dbm is the anion of dibenzoylmethane, $C_{15}H_{11}O_2^-$, bam is the anion of benzoylacetone, $C_{10}H_9O_2^-$, and acac is the anion of acetylacetone, $C_5H_7O_2^-$.

Can. J. Chem. Downloaded from www.nrcresearchpress.com by 210.87.254.5 on 09/05/12
For personal use only.

Can. J. Chem. Downloaded from www.nrcresearchpress.com by 210.87.254.5 on 09/05/12
For personal use only.

used were reagent grade and were not purified before use.

Bis(μ-chlorotricarbonyl(1-phenyl-1-hydroxobut-1-ene-3-one)rhenium(I))

Choropentacarbonylrhenium(I) (2 g) and benzoylacetone (1.5 g) were refluxed in benzene (~150 ml) for 1 day. The pale yellow solution gradually turned green. The solution was evaporated to near dryness, dichloromethane (20 ml) was added, the solution was filtered, and the filtrate was evaporated to near dryness. A mixture (1 :1 v/v) of dichloromethane and petroleum ether (40–60°) was added and the resulting solution was allowed to evaporate slowly over a few days to give the desired product as a yellow-green powder (yield 45%).

Anal. Calcd. for $C_{26}H_{20}Cl_2O_{10}Re_2$: C, 33.2; H, 2.2; Re, 40; Cl, 7.6. Found: C, 33.4; H, 1.9; Re, 40; Cl, 7.6.

The material was recrystallized from dichloromethane – petroleum ether to give crystals which were usually hexagonal plates or occasionally rhombic needles. The two forms have been shown by single crystal X-ray diffraction to be structurally identical. The product is slightly soluble in benzene, dichloromethane, diethyl ether, chloroform, and benzene and insoluble in petroleum ether (40–60°).

Crystallography

A piece of acicular crystal was sandpapered by hand to a sphere of 0.2 mm diameter. The crystal was shown by precession photographs to be monoclinic, and with proper choice of the *a* and *c* axes, the systematic absences hkl, $h + k = 2n + 1$, $h0l$, $l = 2n + 1$ revealed the space group was $C2/c$ or Cc. The former space group was suggested by the Patterson syntheses which showed rhenium atoms related by a center of symmetry and the choice was confirmed by the successful solution of the structure. Accurate unit cell parameters were obtained by least squares refinement of the output from a Syntex $P\bar{1}$ automatic diffractometer which centered on fifteen moderate angle reflections. The density of a few crystals was measured by flotation in a bromoform–chloroform mixture.

$C_{26}H_{20}Cl_2O_{10}Re_2$ f.w. = 935.2

Monoclinic, $a = 14.77(2)$, $b = 17.98(2)$, $c = 13.48(2)$ Å, $\beta = 124.34(9)°$, $V = 2956$ Å^3, $\rho_0 = 2.15(1)$, $Z = 4$ (dimer units), $\rho_c = 2.07$(20 °C, MoKα, $\lambda = 0.71069$ Å) $C2/c$ (No. 15, C_{2h}^6).

Data were recorded using zirconium-filtered MoKα radiation on a Syntex $P\bar{1}$ diffractometer. The radiation was made monochromatic by using the 002 reflection from highly oriented graphite. Intensities were measured by the θ/2θ scan technique up to a value of $2\theta = 45°$. 2° scans were made over θ, and the background was counted on both sides. Peaks less than 3σ above the background were called unobserved, and peaks less than background were rejected. The intensity of a standard reflection was measured every 50 reflections. It showed a deviation of ±2.6%. The linear absorption coefficient for the compound for MoKα radiation was 92.5 cm^{-1}. The data were corrected for Lorentz, polarization, and absorption errors. Absorption corrections were made assuming the crystal was a sphere of radius 0.1 mm. The data set consisted of 1293 independent reflections of which 1087 were observed.

Solution and Refinement of the Structure

Using Patterson maps for the (100), (010), and (001) zones it was possible to detect the rhenium atoms, which occurred as centrosymmetrically related pairs. Using all the data, refinement of the rhenium atom parameters gave $R_1 = 0.23$.[3] Electron density and difference maps located the chlorine atom and R_1 dropped to 0.18. Subsequent electron density and difference syntheses, with calculations based on known geometries for phenyl rings, revealed all the remaining atoms, except the hydrogen atoms. At this stage, temperature factors, which were isotropic for all atoms in the initial stages of refinement, were made anisotropic for the rhenium atom. Further refinement, using a Cruickshank weighting scheme (4) with the weights set equal to $(75 - 0.8F_o + 0.0029F_o^2 + 6100\ (\sigma/F_o)^2)^{-1}$ for observed reflections and zero weight for unobserved reflections, was terminated at $R_1 = 0.0445$ and $R_2 = 0.0444$.

Refinement of the diffractometer data was done using the full matrix least squares program CUDLS written for the CDC-6400 computer by J. S. Stephens. In all refinement cycles the rhenium and chlorine scattering curves of Cromer (5), including anomalous dispersion corrections (6), were used. The oxygen scattering curve was also that of Cromer and that for carbon was taken from the International Tables (7). No anomalous dispersion corrections were applied to carbon or oxygen.

In the final cycle of refinement no parameter shifted by more than 1/200 of its estimated standard deviation and a series of electron density difference maps through the unit cell showed no residual peaks outside ±0.8 e/Å^3. The final set of atom parameters is given in Table 1 and a comparison of $|F_o|$ and $|F_c|$ is given in Table 2.[4]

Results and Discussion

Selected bond distances and angles are given in Table 3, and the molecule is pictured in Fig. 1. The molecule is dimeric, based on the rhenium atoms, and the two halves are joined by two

[3] $R_1 = \Sigma||F_o| - |F_c||/\Sigma|F_o|$;
$R_2 = (\Sigma\omega(|F_o| - |F_c|)^2/\Sigma\omega F_o^2)^{1/2}$

[4] Table 2 is available, at a nominal charge, from the Depository of Unpublished Data, National Science Library, National Research Council of Canada, Ottawa, Canada K1A 0S2.

TABLE 1. Atomic parameters* for $[Re(CO)_2Cl\ (bamH)]_2 \times 10^3$

Atom	x	y	z	U†
Re	425.14(5)	176.46(4)	327.93(6)	‡
Cl	383.4(3)	188.1(2)	120.4(3)	65(1)
O(1)	441(1)	296(1)	334(1)	67(3)
C(1)	383(1)	355(1)	289(1)	59(4)
C(2)	262(1)	350(1)	199(1)	80(5)
C(3)	435(1)	425(1)	326(1)	54(4)
C(4)	541(1)	434(1)	402(1)	56(4)
O(2)	611(1)	375(1)	453(1)	76(3)
C(5)	606(1)	505(1)	444(1)	57(4)
C(6)	718(1)	506(1)	521(2)	80(5)
C(7)	778(2)	574(1)	557(2)	90(6)
C(8)	718(2)	637(1)	513(2)	93(6)
C(9)	608(2)	640(1)	438(2)	86(6)
C(10)	548(1)	571(1)	399(1)	67(5)
C(11)	429(2)	73(1)	331(2)	100(6)
O(3)	435(1)	8(1)	337(1)	129(5)
C(12)	465(1)	172(1)	486(1)	73(5)
O(4)	492(1)	174(1)	586(1)	91(3)
C(13)	280(1)	167(1)	277(1)	84(5)
O(5)	187(1)	166(1)	244(1)	125(5)

*Estimated standard deviations in parentheses.
†U is in $(Å)^2 \times 10^3$.
‡$U_{11} = 54.7(4)$, $U_{22} = 62.6(5)$, $U_{33} = 59.2(4)$, $U_{12} = 0(10)$, $U_{13} = 27.7(3)$, $U_{23} = 0(4)$.

chlorine bridges which are symmetric. The molecule is thus very like $[Re(CO)_4Cl]_2$ (8) in which two of the carbonyl groups are replaced by neutral β-ketoenol molecules bonded through the ketone groups. Surprisingly, both ketoenol groups are approximately at 90° to each of the Re—Cl bridges and are on the same side of the $ReCl_2Re$ plane. The β-ketoenol molecules are oriented such that the best planes through the two molecules lie roughly along the Re—Cl bonds. The Re—Cl distances are 2.511(5) Å each and are comparable to the distances of 2.465(13) Å found in Re_2Cl_{10} (9). The Re—O (ketone) distance of 2.16(2) Å is identical, within the errors, to the Re—O distances found in $Re_2(CO)_6(dbm)_2$ (2.15(1) Å) (1) but these distances are considerably shorter than the monodentate β-ketoenolate Cu—O distance in bis(1,1,1,5,5,5-hexafluoropentane-2,4-dionato)-bis(*N*,*N*-dimethylenediamine) copper (II) which is 2.76(1) Å (10). The steric requirements of the bridging chlorine atoms require the Cl—Re—Cl angle to be 80.4(1)° (Re_2Cl_{10} = 81.9(4), 80.8(4)°). The Cl—Re—O(1) angle is also less than 90° (84.9(4)°). The three mutually *cis* carbonyl groups are possibly slightly less than 90° apart from each other (87(1), 86(1), and 88.5(9)°) and thus the angles between the carbonyl group and the chlorine and oxygen atoms are opened up from 90° (92(1) to 95(1)°).

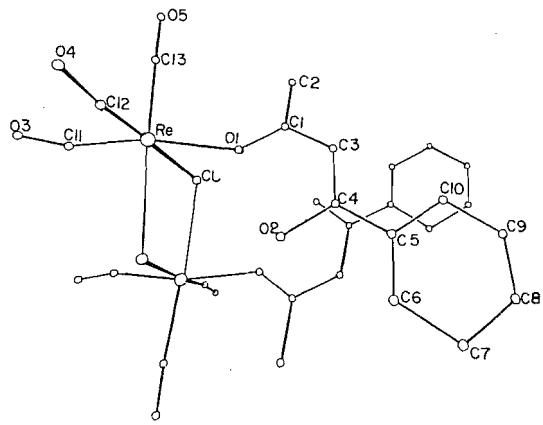

FIG. 1. The molecular structure of $Re_2Cl_2(CO)_6(bamH)_2$. The labelling of the atoms is as in Table 1.

The Re—C≡O systems are essentially linear and the Re—C and C≡O bond lengths are in good agreement with these found previously (1 and references therein). The β-diketone ring is essentially planar (see Table 4) and the two C—O distances in the ring are significantly different at the 95% confidence level and marginally different at the 99% confidence level as are the two ring C—C distances. This suggests that the ligand is in the ketoenol form with very little, if any, delocalization of electrons, in contrast to complexes of β-ketoenolate anions. The planarity

Can. J. Chem. Downloaded from www.nrcresearchpress.com by 210.87.254.5 on 09/05/12
For personal use only.

TABLE 3. Bond distances and angles $Re(CO)_3Cl$ bamH)$_2$*

Bond†	Distance (Å)	Bond	Distance (Å)
Re—Cl	2.511(5)	C(4)—O(2)	1.37(2)
Re—Cl‡	2.511(5)	C(4)—C(5)	1.50(2)
Re—O(1)	2.16(1)	C(5)—C(6)	1.37(2)
Re—C(11)	1.87(2)	C(6)—C(7)	1.44(3)
Re—C(12)	1.86(2)	C(7)—C(8)	1.35(3)
Re—C(13)	1.85(2)	C(8)—C(9)	1.35(3)
O(1)—C(1)	1.29(2)	C(9)—C(10)	1.44(3)
C(1)—C(2)	1.49(2)	C(10)—C(5)	1.40(2)
C(1)—C(3)	1.40(2)	C(11)—O(3)	1.17(3)
C(3)—C(4)	1.32(2)	C(12)—O(4)	1.17(3)
		C(13)—O(5)	1.19(3)

Bond	Angle (deg)	Bond	Angle (deg)
Cl—Re—Cl‡	80.4(1)	O(1)—C(1)—C(2)	120(1)
Cl—Re—O(1)	84.9(4)	O(1)—C(1)—C(3)	119(1)
Cl—Re—C(11)	95.4(9)	C(2)—C(1)—C(3)	121(1)
Cl—Re—C(12)	175.7(6)	C(1)—C(3)—C(4)	124(1)
Cl—Re—C(13)	95.3(7)	C(3)—C(4)—O(2)	122(1)
O(1)—Re—C(11)	173.3(9)	C(3)—C(4)—C(5)	129(1)
O(1)—Re—C(12)	92.3(7)	O(2)—C(4)—C(5)	109(1)
O(1)—Re—C(13)	100.4(7)	C(4)—C(5)—C(10)	117(1)
O(1)—Re—Cl‡	80.0(4)	C(4)—C(5)—C(6)	123(1)
C(11)—Re—C(12)	87(1)	C(10)—C(5)—C(6)	120(1)
C(11)—Re—C(13)	86(1)	C(5)—C(6)—C(7)	121(2)
C(11)—Re—Cl‡	93.5(9)	C(6)—C(7)—C(8)	116(2)
C(12)—Re—C(13)	88.5(9)	C(7)—C(8)—C(9)	125(2)
C(12)—Re—Cl‡	95.9(6)	C(8)—C(9)—C(10)	118(2)
C(13)—Re—Cl‡	175.6(7)	C(5)—C(10)—C(9)	118(1)
Re—Cl—Re‡	98.8(1)	Re—C(11)—O(3)	177.7(6)
Re—O(1)—C(1)	141(1)	Re—C(12)—O(4)	176(2)
		Re—C(13)—O(5)	176(2)

*Estimated standard deviations in parentheses.
†Non-bonded atom distances: Re—Re‡, 3.852(1) Å; Cl—Cl‡, 3.240(5) Å; Cl‡—O(2), 3.52(2) Å; Cl—O(2), 5.02(2) Å; O(1)—O(2), 2.52(2) Å.
‡The double dagger refers to an atom generated by $(-x, y, 1/2 - z)$.

is probably maintained by hydrogen bonding from the enol oxygen atom to the ketone: the oxygen atoms are close enough (2.52(2) Å). The O(OH)—Cl distance of 3.52 Å is too long to allow any hydrogen bonding (11). The least squares planes data in Table 4 also show that the phenyl group is planar, as expected, and is almost coplanar with the β-ketoenol ring (dihedral angle 2.4°).

To our knowledge this is the first case in which it has been clearly shown by an X-ray structure determination that a neutral β-ketoenol molecule can act as a monodentate ligand, although a metal complex containing neutral acetylacetonimine has a very similar metal–ligand geometry (12). In addition, this type of structure has been postulated recently (13) for $Mn(acacH)_2Br_2$. The postulate by Kawaguchi and co-workers based on infrared spectra, that metal–ligand bonding to a neutral β-ketoenolate molecule will be weaker than to the β-ketoenolate anion, and the corresponding observation by Richardson *et al.* that M—O-(ketoenolate) distances are longer than M—O-(ketoenolate-hydrogen bonded) distances are not borne out for the two Re(I) compounds, $Re_2(CO)_6(dbm)_2$ and $Re_2Cl_2(CO)_6(bamH)_2$.

The packing of the molecules in the unit cell is shown in Fig. 2. The molecules are packed in rows in the *a* direction with overlap of the β-ketoenolate and phenyl rings from alternate molecules, which are arranged head to head, like a stack of knifes with blades overlapping, and the handle of each successive knife pointing in the opposite direction to the preceding one. Further contact in the *a* direction is between carbonyl groups in the $ReCl_2Re$ plane. In the *c* direction the chains of phenyl and methyl groups contact the carbonyl groups of the next chain related by the C-centering. In the *b* direction

Can. J. Chem. Downloaded from www.nrcresearchpress.com by 210.87.254.5 on 09/05/12
For personal use only.

TABLE 4. Selected planes* of atoms in $[ReCl(CO)_3(bamH)]_2$

Plane	Atoms	Deviation (Å)	Equation
A	Re	−0.06	−0.07002X + 0.99742Y
	Cl	+0.04	+0.01585Z = 3.01765
	Cl‡	−0.01	
	Re‡	+0.03	
B	O(1)	+0.01	−0.65251X + 0.01914Y
	C(1)	−0.01	+0.75754Z = 0.31492
	C(3)	+0.01	
	C(4)	0.00	
	O(2)	−0.01	
C	C(5)	0.00	−0.62424X + 0.04314Y
	C(6)	+0.01	+0.78004Z = 0.76202
	C(7)	−0.01	
	C(8)	0.00	
	C(9)	+0.01	
	C(10)	−0.01	

*All planes are least squares planes determined by the program PALS written by P. G. Ashmore for the CDC 6400 computer and based on the work of Schomaker *et al.* (16). The program transforms the cell into an orthogonal cell corresponding to the crystallographic *a*, *b*, *c** axes.

FIG. 2. Stereogram (stereoscopic pair of perspective projections) of $Re_2Cl_2(CO)_6(bamH)_2$. The *c* axis is parallel to the top of the page and the *b* axis to the side of the page. The view is approximately along *a**.

the contacts are primarily β-ketoenol–β-ketoenol and carbonyl–carbonyl.

Although the structural features revealed by the X-ray examination are consistent with a complex of rhenium(I) containing a neutral β-ketoenol bonded through the ketone group, it was impossible to find the hydrogen atoms and we have examined the compound by other physical methods to eliminate alternative structures, such as a neutral β-diketone complex of Re(I) or a β-ketoenolate complex of Re(II). Mass spectroscopy of the compound was not very helpful: the compound was relatively involatile and decomposed on heating. The major peak was at *m/e* 162 corresponding to $bamH^+$. The compound is diamagnetic and since there is a quasioctahedral arrangement of ligands around the rhenium atom a d^6 Re(I) system seems more likely than a d^5 Re(II) system. The Re—Re distance of 3.852(1) Å is too long to allow metal–metal bonding, although superexchange might take place through the chlorine atoms. As the compound was diamagnetic at both 23 and −180 °C, any superexchange would have to be very strong.

Chemical and physical evidence considered with the X-ray results shows clearly the presence of a neutral β-diketone or ketoenol: the pure neutral ligand was isolated when our compound was treated with dry CO at 50 atmospheres in the temperature range 90–150 °C. The reaction is

$$[Re(CO)_3Cl(bamH)]_2 + 2CO \rightarrow [Re(CO)_4Cl]_2 + 2bamH$$

At the higher temperature some $Re(CO)_5Cl$ was obtained, probably from the reaction

$$[Re(CO)_4Cl]_2 + 2CO \rightarrow 2Re(CO)_5Cl$$

Proton n.m.r. spectra gave the best evidence for the proposed structure and are consistent only with the ketoenol form. Although spectra showed that some decomposition took place with time, giving free β-ketoenol ligand, fresh solutions showed a peak at −13.8 p.p.m. from

Can. J. Chem. Downloaded from www.nrcresearchpress.com by 210.87.254.5 on 09/05/12
For personal use only.

TABLE 5. Comparison of the analyses of Hieber's compounds with various formulations

Compound	Value				
	C	H	Re	Cl	M.W.
Acetylacetone complex (found)	25.7	1.8	43.5	8.3	429
$(C_5H_8O_2)Re(CO)_3Cl$ (calcd.)	23.68	1.99	45.88	8.74	406
$C_9H_8ClO_5Re$ (calcd.)*	25.87	1.93	44.57	8.49	418
$(C_5H_8O_2)Re(CO)_4Cl$ (calcd.)	25.10	1.85	42.92	8.17	434
Benzoylacetone complex (found)	35.0	2.0	7.4	38.9	469
$(C_{10}H_{10}O_2)Re(CO)_3Cl$ (calcd.)	33.37	2.15	7.58	39.80	468
$C_{14}H_{10}ClO_5Re$ (calcd.)*	35.04	2.10	7.38	38.80	480
$(C_{10}H_{10}O_2)Re(CO)_4Cl$ (calcd.)	33.90	2.03	7.15	37.56	496
Dibenzoylmethane complex (found)	42.0	2.1	6.4	34.2	561
$(C_{15}H_{12}O_2)Re(CO)_3Cl$ (calcd.)	40.79	2.28	6.69	35.14	530
$C_{19}H_{12}ClO_5Re$ (calcd.)*	42.11	2.23	6.54	34.36	542
$(C_{15}H_{12}O_2)Re(CO)_4Cl$ (calcd.)	40.90	2.16	6.35	33.37	558

*These figures are almost identical to the figures calculated by Hieber, but which he claimed applied to the compound given on the previous line.

tetramethylsilane assignable to an enol OH group: this peak had the same area as a peak at −5.55 p.p.m. assignable to the γ C—H. (Similar peaks occur in the free ketoenol at −13.4 and −5.6 p.p.m. relative to tetramethylsilane).

Previously Hieber and Stanner (14) assigned a structure to a complex containing a neutral (but chelated) ketoenol on the basis of a δ-OH band at ~1610 cm^{-1} in the infrared spectrum. Our compound also shows a band at 1610 cm^{-1} as well as two others in the 1500–1600 cm^{-1} region, but we have observed (15) three infrared absorptions in this region for several β-ketoenolate compounds. The highest band for some of these compounds is near 1610 cm^{-1}. Thus, we do not regard this as a useful diagnostic test. We have not reported the infrared spectrum in detail since we have not assigned all the bands. A comparison of the infrared spectrum in the carbonyl stretch region with that of $(C_5H_5N)_2Re(CO)_3Cl$ (8) is interesting. Absorptions for $(C_5H_5N)_2Re(CO)_3Cl$ occur at 2041, 1934, and 1891 cm^{-1}. For $[Re(CO)_3(dikH)Cl]_2$ the absorptions are at 2040(m), 2030(s), 1930(m), 1910(m), 1910(s), and 1895(s) cm^{-1}. The *cis* arrangement of carbonyl groups postulated for the former compound is similar to that in one half of the second compound. The extra bands are consistent with a coupling of the vibrations of the two halves of the molecule to give rise to a doubling of the 2041 cm^{-1} (2040, 2030) and 1934 cm^{-1} (1930, 1910) bands.

The work of Hieber and Stanner (14), referred to above, reported the preparation of the monomeric form of our compound prepared by the reaction

$$[Re(CO)_3Cl]_x + dikH \xrightarrow{\text{heat}} Re(CO)_3Cl(dikH)$$

The structure proposed was

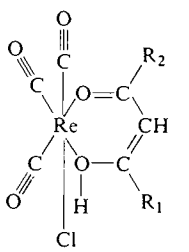

Very little physical evidence was given for this structure, and it seems very unlikely, as we have observed no tendency for our compound to form a monomer. If such a monomer exists, the structure of our compound, in which the enol group is relatively near the bridge position, would easily allow bridge breaking. Relatively little environmental change would take place at the rhenium atom, certainly not sufficient to give rise to a drastic colour change from the pale yellow-green of our compound to the deep red-brown of Hieber's. The final point against the structure proposed by Hieber is that, although the calculated and observed analytical results for Hieber's compounds agree very well, the calculated analyses are in error and fit better a formulation containing an extra carbon atom (see Table 5). Relatively little experimental detail is given of the preparations, but clearly

Can. J. Chem. Downloaded from www.nrcresearchpress.com by 210.87.254.5 on 09/05/12
For personal use only.

this work should be reinvestigated; so far we have been unable to repeat the preparations.

We thank the National Research Council of Canada for financial support of this work.

1. J. C. BARRICK, M. C. FREDETTE, and C. J. L. LOCK. Can. J. Chem. To be published.
2. W. D. COURRIER, A. GUEST, C. J. L. LOCK, and R. H. TOMLINSON. Can. J. Chem. **46**, 2965 (1968).
3. P. W. FRAIS, A. GUEST, and C. J. L. LOCK. Can. J. Chem. **47**, 1069 (1969).
4. D. W. J. CRUICKSHANK, D. E. PILLING, A. BUJOSA, F. M. LOVELL, and M. R. TRUTER. *In* Computing methods and the phase problem in X-ray crystal analysis. *Edited by* R. Pepinsky, J. M. Robertson, and J. C. Speakman. Pergamon Press, New York. 1961.
5. D. T. CROMER and J. T. WABER. Acta Cryst. **18**, 104 (1965).
6. D. T. CROMER. Acta Cryst. **18**, 17 (1965).
7. International tables for X-ray crystallography. Vol. III. Kynoch Press, Birmingham. 1962. (Table 3.3.1A).
8. E. W. ABEL, G. B. HARGREAVES, and G. WILKINSON. J. Chem. Soc. 3149 (1958).
9. K. MUCKER, G. S. SMITH, and Q. JOHNSON. Acta Cryst. **B24**, 874 (1968).
10. M. A. BUSH, D. E. FENTON, R. S. NYHOLM, and M. R. TRUTER. Chem. Commun. 1335 (1970).
11. W. C. HAMILTON and J. A. IBERS. Hydrogen bonding in solids. Benjamin, N.Y. 1968.
12. M. F. RICHARDSON, P. W. R. CORFIELD, D. E. SANDS, and R. E. SIEVERS. Inorg. Chem. **9**, 1632 (1970).
13. Y. NAKAMURA, K. ISOBE, H. MORITA, S. YAMAZAKI, and S. KAWAGUCHI. Inorg. Chem. **11**, 1573 (1972).
14. W. HIEBER and F. STANNER. Chem. Ber. **103**, 2836 (1970).
15. M. C. FREDETTE and C. J. L. LOCK. To be published.
16. V. SCHOMAKER, J. WASER, R. E. MARSH, and G. BERGMAN. Acta Cryst. **12**, 600 (1959).

Can. J. Chem. Downloaded from www.nrcresearchpress.com by 210.87.254.5 on 09/05/12
For personal use only.

Pulse Radiolysis of Nitric Oxide in Aqueous Solution[1]

W. A. SEDDON, J. W. FLETCHER, AND F. C. SOPCHYSHYN

Physical Chemistry Branch, Atomic Energy of Canada Limited, Chalk River Nuclear Laboratories, Chalk River, Ontario

Received October 25, 1972

Transient spectra observed on the pulse radiolysis of aqueous solutions of nitric oxide at p*H* 7.0 have been assigned to the species NO^-, $N_2O_2^-$, and $N_3O_3^-$. In acid solution these species are protonated to form the corresponding acids, HNO, HN_2O_2, and HN_3O_3. Both the basic and acid forms undergo similar reactions, but at different rates, to form the products of radiolysis N_2O and NO_2^-.

$$N_3O_3^- \rightarrow N_2O + NO_2^-$$

$$HN_3O_3 \rightarrow N_2O + HNO_2$$

The basic species decays more slowly than the corresponding acid species but both processes have appreciable activation energies of 15 and 10 kcals/mol, respectively. Computer calculations have been used in conjunction with the experimental data over a wide range of p*H* and NO concentration to deduce a reaction mechanism consistent with the observed results. Reaction rate constants, acid dissociation constants and extinction coefficients for the various species are presented and compared with earlier work.

Les spectres temporaires observés lors de la radiolyse pulsée de solutions aqueuses d'oxyde nitrique à p*H* 7.0 ont été attribués aux espèces NO^-, $N_2O_2^-$, et $N_3O_3^-$. En solution acide ces espèces sont protonées, en formant les acides correspondants, HNO, HN_2O_2, et HN_3O_3. Les formes acides et basiques subissent toutes les deux des réactions similaires mais à des vitesses différentes, en formant des produits de radiolyse N_2O et NO_2^-.

$$N_3O_3^- \rightarrow N_2O + NO_2^-$$

$$HN_3O_3 \rightarrow N_2O + HNO_2$$

L'espèce basique disparait plus lentement que l'espèce acide correspondante mais les deux processus ont des énergies d'activation appréciables de 15 kcal/mol et 10 kcal/mol, respectivement. Des calculs par ordinateur ont été utilisés conjointement avec les données experimentales obtenues dans une grande gamme de pH et de concentration en NO pour en déduire un mécanisme de réaction en accord avec les resultats observés. Les constantes de vitesse des réactions, les constantes de l'equilibre de dissociation des acides, et les coefficients d'extinction pour les différentes espèces sont présentés et comparés avec des travaux antérieurs. [Traduit par le journal]

Can. J. Chem., **51**, 1123 (1973)

Introduction

Earlier studies (1–3), on the γ radiolysis of nitric oxide in aqueous solutions showed that the major products, HNO_2 and N_2O, were explicable by a simple mechanism:

$$H_2O \rightsquigarrow e_{aq}^-, H_3O_{aq}^+, H, OH, H_2, H_2O_2$$

$$e_{aq}^- + NO \rightarrow NO^- \xrightarrow{H^+} HNO$$

$$H + NO \rightarrow HNO$$

$$OH + NO \rightarrow HNO_2$$

$$HNO + 2NO \rightarrow N_2O + HNO_2$$

While the above reaction sequence is stoichiometrically correct a preliminary pulse radiolysis study (4) indicated the detailed mechanism to be much more complex involving the anionic species NO^- and $N_2O_2^-$ and their corresponding protonated forms HNO and HN_2O_2. Subsequent studies (5) confirmed the existence of NO^- and $N_2O_2^-$ together with the formation and eventual decay of a third polymeric anion $N_3O_3^-$. A detailed mechanism involving these species and their corresponding acid forms was proposed to explain the radiolytic reduction of NO in aqueous solutions (5).

Significant differences were noted, however, in acid and neutral solutions in the rates of decay of the species $N_3O_3^-$. For example at p*H* 7.0 the measured half life ranged from 2.1 ms (4) to 8 ms (5). In view of this and the complexity of the reaction kinetics we extended our earlier

[1]AECL No. 4417.

Can. J. Chem. Downloaded from www.nrcresearchpress.com by 210.87.254.5 on 09/05/12
For personal use only.

studies to cover a wider range of NO concentration, pH, and temperature.

Computer calculations have been used in conjunction with the experimental data to check the proposed reaction mechanism, evaluate rate constants and determine pK values for the various equilibria. A large measure of agreement is obtained with the previous work (4, 5), but it is also found that the rate of decay of $N_3O_3^-$ is temperature dependent and additional reactions are required to explain the observations in detail.

Experimental

Nitric oxide solutions contained in 30 ml Pyrex syringes were prepared by the continuous bubbling and dilution techniques described previously (1, 3). Commercially available NO (Matheson Ltd. CP grade 99.8% min) was purified by passing over molecular sieve, type 4A, to remove N_2O and then through the NO flow system (1). The major impurity, NO_2^-, analyzed in the final product was always $< 10\ \mu M$. Triply distilled water was used throughout and glassware cleaned by baking in an air oven at 550 °C overnight.

Detailed descriptions of the pulse radiolysis facilities have been presented elsewhere (6), and only a brief outline is given here. A Van de Graaff accelerator operating at 2.25 MeV with pulse lengths 0.5–2 μs was used as the electron source. Experiments were generally conducted with a 1 μs pulse with currents in the range of 150 mA/pulse and a dose of about 3 krads. Rectangular quartz irradiation cells, having an optical path length of 2 cm, were filled and drained using the sample changer previously described (7). Fresh aliquots of solution were used for each pulse. For the variable temperature experiments the cell was either cooled with a stream of cold nitrogen gas or warmed with an infrared lamp. The temperature was read directly with a Comark electronic thermometer type 1604, using a Cr/Al thermocouple suspended in the solution.

A Hanovia 300 W high pressure xenon arc operated in the DC or pulsed mode, a General Electric 62 W quartz-iodine lamp or a 30/50 W deuterium lamp, were used as sources of analyzing light. Changes in light intensity were monitored with a Bausch and Lomb f 3.5 high intensity monochromator used together with RCA 1P28, or HTV R166 photomultipliers and a Tektronix 556 oscilloscope. Narrow band pass interference filters (Infrared Industries, Inc.) used below 300 nm in conjunction with the monochromator and R166 photomultiplier ensured spectral purity in this region. Using an automatic subtraction unit (8), a single Polaroid photograph (3000 ASA) recorded both the incident light level and the transient absorption signal in the DC coupled mode.

The dose delivered to the sample was determined using 2 mM aerated solutions of SCN^- as dosimeter taking the product of the G value (mol/100 eV) and extinction coefficient ε (M^{-1} cm^{-1}) $G\varepsilon = 2.10 \times 10^4$ for $(SCN)_2^-$ at 475 nm (9–11). Variations in dose/pulse were monitored by integrating the current striking a 1/4 in. aluminum collimating block placed in front of the cell.

Decay curves were digitized using a D-Mac pencil follower (type PF MKIB-Computer Equipment Co.) and analyzed by computer calculation (12).

Results and Discussion

Absorption Spectra

Transient and permanent spectra observed on the pulse radiolysis of aqueous solutions of NO buffered at pH 7.0 are shown in Fig. 1. These are in good agreement with those observed previously and have been assigned to the species NO^-, $N_2O_2^-$, $N_3O_3^-$, and NO_2^- (4, 5). At wavelengths $\leqslant 240$ nm we find, contrary to Grätzel *et al.* (5), that the absorption due to NO_2^- completely masks transient spectra in this region. The original literature should be consulted for additional details but spectral characteristics are summarized and compared with earlier results in Table 1.

The inset in Fig. 1 shows the build up and decay of the transient absorption (monitored at 380 nm) observed at 25 °C in 1.7 mM solutions of NO maintained at pH 7.0 with phosphate buffer (3). The initial absorption, complete on a μs time scale, is due to the formation of $N_2O_2^-$ (4), while the additional slow build up requiring some 250 μs to reach completion is a composite of the formation of $N_3O_3^-$ and concomitant

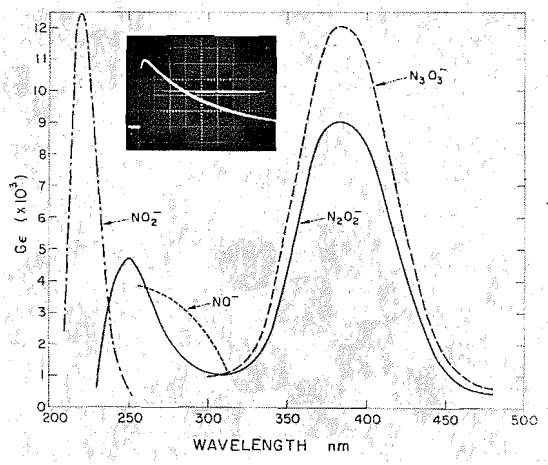

FIG. 1. Absorption spectra of species produced in the pulse radiolysis of NO in aqueous solution at pH 7.0. The NO^- spectrum was obtained in $\sim 10^{-4}$ M NO and the spectra for NO_2^-, $N_2O_2^-$, and $N_3O_3^-$ in $\sim 2 \times 10^{-3}$ M NO. The absorbance of NO^- and $N_2O_2^-$ was recorded immediately after the pulse while that for $N_3O_3^-$ was obtained by extrapolation back to the end of the pulse. The inset shows the formation and decay of the transient absorption at 380 nm and 25 °C in saturated solutions of NO; ordinate, 3.6% absorption/division; abscissa, 1 ms/division, dose/pulse 3.3 krads.

Can. J. Chem. Downloaded from www.nrcresearchpress.com by 210.87.254.5 on 09/05/12
For personal use only.

TABLE 1. Spectral characteristics of species observed on the pulse radiolysis of nitric oxide in aqueous solution. Extinction coefficients calculated assuming $G = G_{e_{aq}^-} + G_H = 3.2$

Species	Absorption maximum (nm)	$G\varepsilon$	Extinction coefficient (M^{-1} cm^{-1}) This work	Reference 5
NO^-	~260	~3750	~1200	1400
$N_2O_2^-$	380	9100	2850±200	3300
$N_3O_3^-$	380	12000	3750±300	4000
NO_2^-	220	12500	4800±400	~5000 (ref. 17)

TABLE 2. Reactions and rate constant data previously determined in the pulse radiolysis of NO solutions

	Reaction	Rate constant	pK (dissociation)	Reference
[1]	$e_{aq}^- + NO \rightarrow NO^-$	$2.3\times10^{10}\ M^{-1}\ s^{-1}$		4
[2]	$e_{aq}^- + H^+ \rightarrow H$	$2.3\times10^{10}\ M^{-1}\ s^{-1}$		14, 15
[3]	$H + NO \rightarrow HNO$	$\sim10^{10}\ M^{-1}\ s^{-1}$		3
[4]	$NO^- + H^+ \underset{r}{\overset{f}{\rightleftharpoons}} HNO$		4.7	5
[5]	$NO + NO^- \underset{r}{\overset{f}{\rightleftharpoons}} N_2O_2^-$	$k_f = 1.7\times10^9\ M^{-1}\ s^{-1}$ $k_f = 3.3\times10^9\ M^{-1}\ s^{-1}$		5 4
[6]	$N_2O_2^- + NO \rightarrow N_3O_3^-$	$4.9\times10^6\ M^{-1}\ s^{-1}$		5
[7]	$N_3O_3^- \rightarrow N_2O + NO_2^-$	$87\ s^{-1}$ $330\ s^{-1}$		5 4
[8]	$N_2O_2^- + H^+ \underset{r}{\overset{f}{\rightleftharpoons}} HN_2O_2$		3.5	5
[9]	$HNO + NO \underset{r}{\overset{f}{\rightleftharpoons}} HN_2O_2$	$k_f = 1.7\times10^9\ M^{-1}\ s^{-1}$		5
[10]	$HN_2O_2 + NO \rightarrow HN_3O_3$	$4.9\times10^6\ M^{-1}\ s^{-1}$		5
[11]	$N_3O_3^- + H^+ \underset{r}{\overset{f}{\rightleftharpoons}} HN_3O_3$		3.1	5
[12]	$HN_3O_3 \rightarrow N_2O + HNO_2$	$4600\ s^{-1}$		5
[13]	$OH + NO \rightarrow HNO_2$	$6.0\times10^9\ M^{-1}\ s^{-1}$		2
[14]	$HNO_2 \underset{r}{\overset{f}{\rightleftharpoons}} H^+ + NO_2^-$		3.5	13

decay of $N_2O_2^-$ (since both absorb at 380 nm but with $\varepsilon_{N_3O_3^-} > \varepsilon_{N_2O_2^-}$). The eventual decay is first order and corresponds to the disappearance of $N_3O_3^-$ (5). It should be noted here that we find the rate of decay of $N_3O_3^-$ to be temperature dependent. This feature will be discussed in more detail later but does explain the large discrepancy in rate constants previously reported for this process (4, 5).

The overall kinetics and yields of NO^-, $N_2O_2^-$, and $N_3O_3^-$ are dependent both on NO concentration and pH. Reactions 1–12 have been proposed to explain their formation and decay and these together with previously measured rate constants are summarized in Table 2. Also included is reaction 13, and the acid–base equilibria [14], since the permanent product HNO_2, pK = 3.5 (13), lowers the pH of unbuffered solutions.

Based on these reactions, we have utilized the

Can. J. Chem. Downloaded from www.nrcresearchpress.com by 210.87.254.5 on 09/05/12
For personal use only.

TABLE 3. Rate constant data, calculated and experimental, obtained from this work on the pulse radiolysis of NO solutions*

Reaction	Rate constant	pK (dissociation)
[5] $NO + NO^- \underset{r}{\overset{f}{\rightleftharpoons}} N_2O_2^-$	$k_f = 1.7\times10^9\ M^{-1}\ s^{-1}$ $k_r = 6.6\times10^4\ s^{-1}$	4.4
[6] $N_2O_2^- + NO \rightarrow N_3O_3^-$	$3.0\times10^6\ M^{-1}\ s^{-1}$	
[7] $N_3O_3^- \rightarrow N_2O + NO_2^-$	$2.35\times10^2\ s^{-1}$ at 23 °C	
[8] $N_2O_2^- + H^+ \underset{r}{\overset{f}{\rightleftharpoons}} HN_2O_2$	$k_r = 5.5\times10^6\ s^{-1}$	3.2_5
[9] $HNO + NO \underset{r}{\overset{f}{\rightleftharpoons}} HN_2O_2$	$k_f = 1.7\times10^9\ M^{-1}\ s^{-1}$ $k_r = 8.0\times10^6\ s^{-1}$	2.3_3
[10] $HN_2O_2 + NO \rightarrow HN_3O_3$	$8.0\times10^6\ M^{-1}\ s^{-1}$	
[12] $HN_3O_3 \rightarrow N_2O + HNO_2$	$1.6\times10^4\ s^{-1}$ at 23 °C	
[13] $OH + NO \rightarrow HNO_2$	$1.0\times10^{10}\ M^{-1}\ s^{-1}$	
[15] $N_2O_2^- \rightarrow N_2O + O^- (\rightarrow OH)$	$3.5\times10^2\ s^{-1}$	

*Other rate constants were found to be the same as in Table 2. Using these values and the extinction coefficients in Table 1, experimental traces such as shown in Figs. 2 and 4 can be accurately reproduced. For all the acid–base equilibria in this table and Table 2 it is assumed that $k_f = 1\times10^{10}\ M^{-1}\ s^{-1}$.

computer programs WR16 and WR20 (16), to calculate the concentrations of all the species taking part in the simultaneous first and second order chemical reactions occurring during and after the pulse. The programs require for input data a list of the species taking part in the chemical reactions, the reaction rate constants, radiation yields of the primary radiolysis products, the initial concentrations of NO and H^+, extinction coefficients of the absorbing species and the dose per pulse. We have therefore sought to check the proposed mechanism by comparing the computed concentrations of the transient species with our experimental data over a wide range of NO concentration and pH.

Solutions of NO Buffered at pH 7.0

The simplest sequence of reactions occurs in saturated ($\sim$2 mM), solutions of NO buffered at pH 7.0. Under these conditions the transient "NO" species exist entirely in their basic form and the equilibrium [5] lies predominantly in favor of $N_2O_2^-$. Preliminary calculations using the previously measured extinction coefficients and rate constants given in Tables 1 and 2 showed that the experimental observations relating to the formation and decay of $N_2O_2^-$ and $N_3O_3^-$ were explicable in terms of reactions 1 and 3 to 7. Note, however the discrepancy in the rate constants given for reaction 7. This we have now shown to be due simply to a temperature effect (see later) and hence for our calculations we chose to use our measured rate constant at 23 °C, *i.e.* $k_7 = 2.35\times10^2\ s^{-1}$.

In solutions of NO there is considerable disagreement with this simple mechanism at concentrations below $5\times10^{-4}\ M$. As a consequence of equilibrium [5], the mechanism predicts that the yield of $N_2O_2^-$ should decrease with decreasing NO concentration and at the same time the rate of formation of $N_3O_3^-$ produced in the pseudo first order reaction 6 should likewise decrease. While the former is observed, no slow build up attributable to $N_3O_3^-$ can be seen in $\sim2\times10^{-4}\ M$ solutions of NO. We suggest, therefore that the species $N_2O_2^-$ must itself decay

[15] $N_2O_2^- \rightarrow N_2O + O^- (\rightarrow OH)$

in competition with reaction 6.

It has been suggested previously that OH radicals might be produced as an intermediate species in the NO system, but competition experiments in the presence of CH_3OH did not support this proposal (2). However such experiments were all conducted in solutions saturated with NO at which concentration our rate constant data (see Table 3) indicate only about 5% of the $N_2O_2^-$ could disappear by [15] in competition

Can. J. Chem. Downloaded from www.nrcresearchpress.com by 210.87.254.5 on 09/05/12
For personal use only.

Can. J. Chem. Downloaded from www.nrcresearchpress.com by 210.87.254.5 on 09/05/12
For personal use only.

with [6]. Such a process would not have been detectable with any reliable accuracy by the standard competition methods employed in ref. 2.

Figure 2 curves A to C show the experimentally observed transient signals as a function of NO concentration. The computed curves (white lines), superimposed on the experimental traces represent the calculated best fit to the data using $G_{e_{aq}^-} = 2.6$, $G_H = 0.56$, $G_{OH} = 2.6$, $G_{H_3O^+} = 2.8$, $G_{OH^-} = 0.2$, $\varepsilon_{N_2O_2^-}$ and $\varepsilon_{N_3O_3^-} = 2850$ and 3750 M^{-1} cm^{-1}, respectively, The dose per pulse used in each case was within $\leqslant 5\%$ of the experimentally monitored dose. Rate constants, where they differ from those in Table 2, are given in Table 3. The overall agreement with previous values obtained at neutral pH is good with the rate constants $k_{5f} = 1.7 \times 10^9\ M^{-1}\ s^{-1}$ and $k_{13} = 1.0 \times 10^{10}\ M^{-1}\ s^{-1}$ being redetermined by observing the pseudo first order formation of $N_2O_2^-$ and NO_2^- at 380 and 220 nm, respectively.

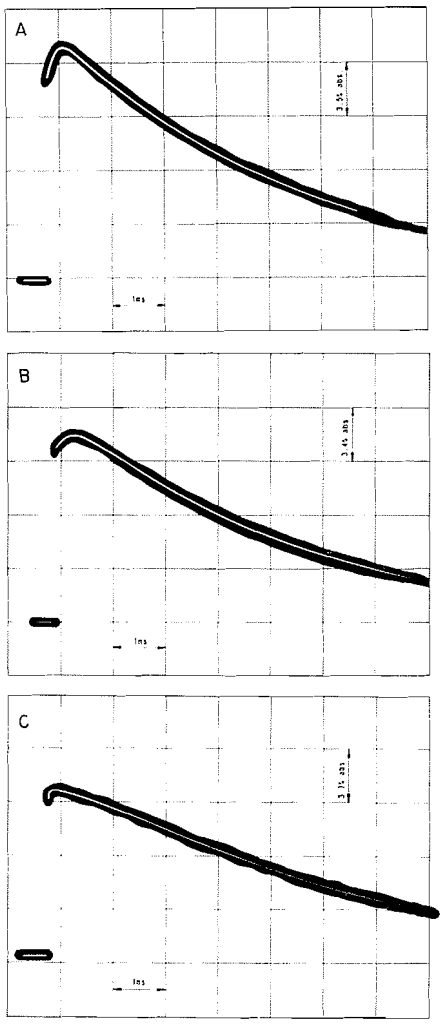

FIG. 2 Oscilloscope traces at 380 nm showing the formation and decay of the transient species $N_2O_2^-$ and $N_3O_3^-$ at pH 7.0 as a function of NO concentration. The computed curves (white lines) are shown superimposed on a reproduction of the experimental traces. Abscissa on all traces: 1 ms/division. Curve A: 2.01 mM NO, 3.4% absorption/division, 3.2 krads/pulse; curve B: 8.7×10^{-4} M NO, 3.4% absorption/division, 2.9 krads/pulse; curve C : 2.03×10^{-4} M NO, 3.6% absorption/division, 3.4 krads/pulse.

Figure 3 shows the change in $N_2O_2^-$ concentration as a function of NO concentration, the open circles being our values and the crosses the normalized results of Grätzel *et al.* (5). The curve drawn through the points represents an equilibrium constant $K_{-5} = 3.9 \times 10^{-5}$ M, *i.e.* $k_{5r} = 6.6 \times 10^4\ s^{-1}$ deduced by computer calculation. This can be compared with the previous value of 3.5×10^{-5} M (5).

Effect of pH

In acid solution the situation becomes much more complex with the yield and rates of formation and decay of NO^-, $N_2O_2^-$, and $N_3O_3^-$ being dependent on pH and NO concentration. Reducing the pH with H_2SO_4 or buffer solutions reduces (*a*) the overall intensity of the transient absorption, (*b*) the time taken to reach the maximum intensity (corresponding to the formation of $N_3O_3^-$), and (*c*) the half life, $t_{1/2}$, for the "first order" decay of $N_3O_3^-$ (Fig. 4*A*).

Reducing the NO concentration at a fixed acid

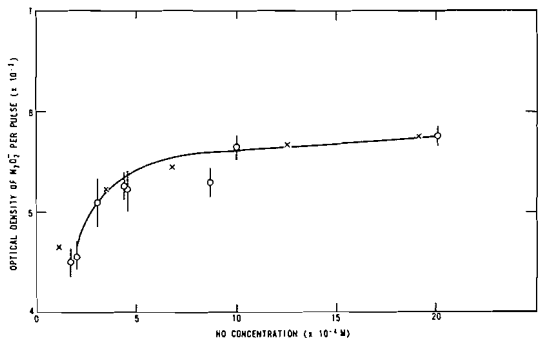

FIG. 3. Change in $N_2O_2^-$ concentration as a function of NO. Open circles, this work, crosses represent normalized data from ref. 5. Curve is calculated using $K_{-5} = 3.9 \times 10^{-5}$ M and the rate constants given in Tables 2 and 3. All data normalized to a dose/pulse of 3.2 krads.

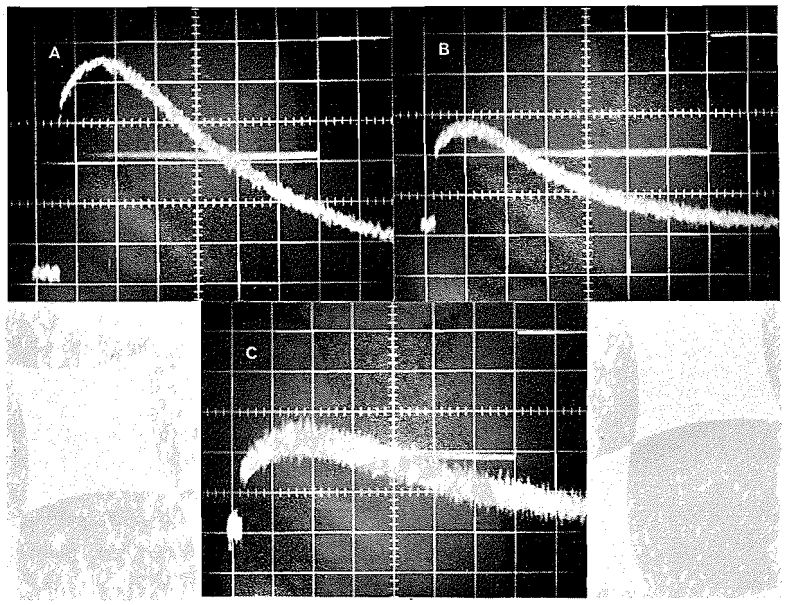

FIG. 4. Oscilloscope traces at 380 nm showing the formation and decay of the transient species $N_2O_2^-$ and $N_3O_3^-$ at pH 3.6_5 as a function of NO concentration. Curve A: 2.11 mM NO, ordinate 1.8% absorption/division, abscissa 100 μs/division, 3.7 krads/pulse; curve B: 1.13 mM NO, ordinate 1.7% absorption/division, abscissa 200 μs/cm, 2.9 krads/pulse; curve C: 4.76×10^{-4} M NO, ordinate 0.9% absorption/division, abscissa 200 μs/cm, 3.0 krads/pulse.

pH reduces the overall signal but increases the time taken to reach the maximum intensity (Fig. 4B and C). Unlike the results obtained at pH 7.0 (Fig. 2), the final rate of decay decreases significantly with decreasing concentration of NO (Fig. 4B and C).

These observations are all consistent with protonation of the basic species to form the corresponding acids HNO, HN_2O_2, and HN_3O_3, reactions 2, 4, 8, and 11 and the existence of equilibrium [9] (5). The extent to which these acids dissociate depends upon their relative acid strengths and since they do not absorb strongly at 380 nm (*i.e.* no transient absorptions are observed at p$H \leqslant 2$), their dissociation constants have been deduced by observing the decrease in concentration of their conjugate bases as a function of pH (5).

Initial computer calculations were again based on the rate constants presented in Table 2 assuming for the acid–base equilibria that the protonation reaction $k_f = 10^{10}\ M^{-1}\ s^{-1}$. Qualitatively, the original data predicted the general features observed in acid solution but, quantitatively, failed to reproduce the experimental traces such as shown in Fig. 4. Principal sources of disagreement were related to the pK for HN_2O_2 and the equilibrium constant for reaction 9 (see below). Having established "best fit" values for these two constants, k_9, k_{10}, and k_{12} were then deduced by matching the observed build up and decays as a function of pH and NO concentration.

Figure 5 shows the change in concentration of the species $N_2O_2^-$ and $N_3O_3^-$ as a function of pH in ~ 2 mM solutions of NO. The open and closed (buffered solution) circles represent our results and the crosses the normalized data of Grätzel *et al.* (5). The curve drawn through the points for $N_2O_2^-$ was calculated using $pK_{HN_2O_2} = 3.25$ and $pK_{HN_3O_3} = 3.1$. These values should be compared with the previous estimates of 3.5 and 3.1, respectively.

By inspection, the data for $N_2O_2^-$ (observed immediately after the pulse) indicate a pK for HN_2O_2 of about 3.7. This latter value is however above the real pK since the points are effectively displaced towards higher pH values as a consequence of equilibrium [9]. In other words the existence of [9] in conjunction with [8] suggests that HN_2O_2 is a weaker acid than is in fact the case.

Reaction 9 is the acid analog of equilibrium [5] and the inset in Fig. 5 shows the decrease in yield of $N_2O_2^-$ as a function of NO concentration at pH's 3.6_5 and 4.2. The curves drawn

Can. J. Chem. Downloaded from www.nrcresearchpress.com by 210.87.254.5 on 09/05/12
For personal use only.

Can. J. Chem. Downloaded from www.nrcresearchpress.com by 210.87.254.5 on 09/05/12
For personal use only.

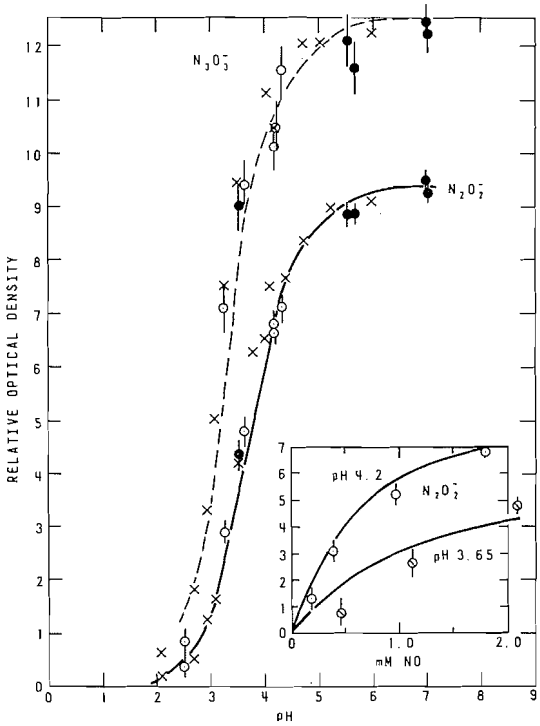

FIG. 5. Change in $N_2O_2^-$ and $N_3O_3^-$ concentration as a function of pH. Circles, this work (closed circles, buffered solution); crosses, normalized data from ref. 5. Inset shows decrease in $N_2O_2^-$ concentration as a function of NO concentration at two different pH's, 3.65 and 4.2. Curves are calculated in all cases (see text).

through the points represent an equilibrium constant $K_{-9} = 4.7 \times 10^{-3}$ M, *i.e.* $k_{9f} = 1.7 \times 10^9$ M^{-1} s^{-1}, and $k_{9r} = 8 \times 10^6$ s^{-1}, a value almost an order of magnitude greater than the previous estimate (5). The "fit" however is not as good as obtained in the analogous neutral case (Fig. 3). Attempts to match this particular aspect more closely were not considered justified in view of the weak absorptions coupled with experimental uncertainties in pH, NO concentration, dose, and temperature. Nevertheless it is clear that the acid species dissociates far more readily than does its conjugate base.

The results representing the change in concentration of $N_3O_3^-$ as a function of pH require further clarification. These points were all obtained by extrapolating the observed decays back to the end of the pulse, since seemingly excellent first order plots were obtained at all pH's. However computed formation and decay curves consistent with the raw data show that as the pH is lowered such extrapolations become a progressively less valid measure of the true $N_3O_3^-$ concentration but rather that of a mixture of $N_2O_2^-$ and $N_3O_3^-$. In the vicinity of the pK the overall decay becomes a composite of the disappearance of $N_2O_2^-$ and the concomitant formation and decay of $N_3O_3^-$. Thus below a pH of about 4.3, ($t_{1/2} \sim 700$ μs at 21 °C), the computed first order plots are in fact non-linear over the first two or three half lives. Since the curvature is within the analytical error such deviations from linearity were not detected experimentally.

The dashed curve in Fig. 5 therefore represents the computed concentrations of "$N_3O_3^-$" obtained by extrapolation to the end of the pulse on a time scale analogous to that of the experimental observations.

Effect of Temperature on the Decay of $N_3O_3^-$

As mentioned previously it was found that the first order decay of $N_3O_3^-$ to give the products of radiolysis N_2O and NO_2^-, reaction 7, was markedly temperature dependent. Figure 6 shows an Arrhenius plot for the decay of $N_3O_3^-$ at pH 5.0. The measured activation energy E_a[1] for this process decreases with pH as shown in Fig. 7. This decrease is due to the fact that the basic species $N_3O_3^-$ decays more slowly than the corresponding acid species HN_3O_3, reactions 7 and 12, but the two are interrelated by the acid–base equilibrium [11]. Based on these three

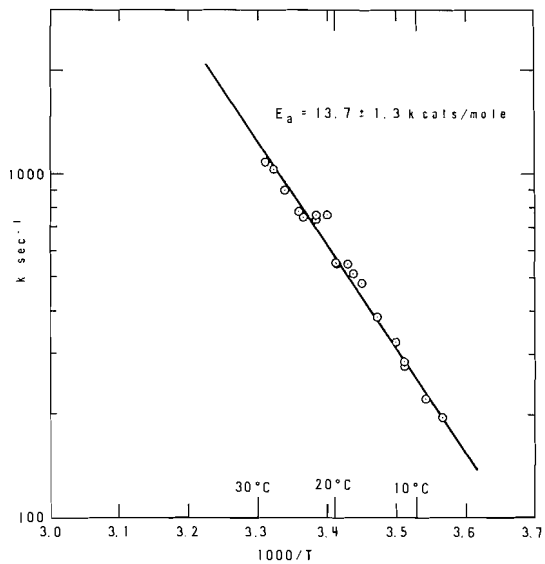

FIG. 6. Arrhenius plot for the first order decay of $N_3O_3^-$ at pH 5.0.

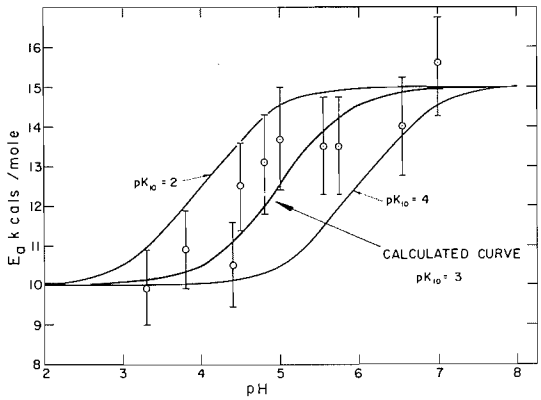

FIG. 7. Activation energy for the first order decay of $N_3O_3^-$ as a function of pH.

reactions one can show that at a given pH, E_a^1 is related to the measured rate constant k_{obs} via the rate constants k_7 and k_{12}, the dissociation constant K_{-11} and the activation energies for the decay of $N_3O_3^-$ and HN_3O_3, $E_a^{N_3O_3^-}$ and $E_a^{HN_3O_3}$, respectively.

The calculated curves in Fig. 7 are based on $E_a^{N_3O_3^-} = 15$ kcals/mol, $E_a^{HN_3O_3} = 10$ kcals/mol and the Arrhenius equation

$$-E_a^1/RT = \ln k_{obs} + C$$

where C is a constant and

$$k_{obs} = \frac{k_7[N_3O_3^-]}{[N_3O_3^-] + [HN_3O_3]} + \frac{k_{12}[HN_3O_3]}{[N_3O_3^-] + [HN_3O_3]}$$

substituting for $[N_3O_3^-]$ and $[HN_3O_3]$ from [11]

$$E_a^1 = \frac{2.303RT_1T_2}{(T_2 - T_1)} \times \log \frac{k_7^{T_2} + k_{12}^{T_2}[H^+]/K_{-11}}{k_7^{T_1} + k_{12}^{T_1}[H^+]/K_{-11}}$$

where $R = 1.987$ cal, T_1 and T_2 the absolute temperatures and $k_7^{296} = 2.35 \times 10^2$ s^{-1}, $k_7^{275} = 33.5$ s^{-1}, $k_{12}^{296} = 1.65 \times 10^4$ s^{-1}, $k_{12}^{275} = 4.5 \times 10^3$ s^{-1}, and pK (HN_3O_3) = 3.0. It is also assumed that both ε and K_{-11} remain independent of temperature over the range of study.

The curves to the left and right of the "best fit" are calculated using p$K_{-11} = 2$ and 4 respectively, showing indirectly the consistency of the rate constants in Table 3 and the value for p$K_{-11} = 3.1$.

In conclusion the results obtained in this work combined with those of Grätzel *et al.* (5), show that the reactions 1–15, and the rate constants presented in Tables 2 and 3 accurately reflect the transient changes observed on the pulse radiolysis of aqueous solutions of NO. In addition we find that the final decay process of $N_3O_3^-$ to form the products of radiolysis has a considerable activation energy which is also pH dependent. This accounts for previous discrepancies in the published rate constants for the decay of $N_3O_3^-$ and also introduces a change in the ratio k_{12}/k_7 with temperature from 135 at 2 °C to 70 at 23 °C.

The authors thank Mr. E. B. Selkirk for the design and construction of the electronics.

1. W. A. SEDDON and H. C. SUTTON. Trans. Faraday Soc. **59**, 2323 (1963).
2. T. W. WOODWARD and H. C. SUTTON. Trans. Faraday Soc. **62**, 70 (1966).
3. R. J. KNIGHT and H. C. SUTTON. Trans. Faraday Soc. **63**, 2628 (1967).
4. W. A. SEDDON and M. J. YOUNG. Can. J. Chem. **48**, 393 (1970).
5. M. GRÄTZEL, S. TANIGUCHI, and A. HENGLEIN. Ber. Bunsen. für physik. Chem. **74**, 1003 (1970).
6. W. A. SEDDON, C. WILLIS, M. J. YOUNG, and E. B. SELKIRK. Atomic Energy of Canada Limited, report AECL-3853.
7. W. A. SEDDON and E. B. SELKIRK. Int. J. Radiat. Phys. Chem. **3**, 447 (1971).
8. E. B. SELKIRK and W. A. SEDDON. Atomic Energy of Canada Limited, Report AECL-4134.
9. G. E. ADAMS, J. W. BOAG, and B. D. MICHAEL. Pulse radiolysis. Academic Press. 1965. p. 117.
10. J. H. BAXENDALE, P. L. T. BEVAN, and D. A. STOTT. Trans. Faraday Soc. **64**, 2389 (1968).
11. E. M. FIELDEN and N. W. HOLM. Manual on radiation dosimetry. *Edited by* N. W. Holm and R. J. Berry. Marcel Dekker Inc. 1970. p. 288.
12. J. W. FLETCHER and N. BURNHAM. Atomic Energy of Canada Limited. Report in preparation.
13. W. L. JOLLY. Inorganic chemistry of nitrogen. W. A. Benjamin Inc. 1964. p. 78.
14. S. GORDON, E. J. HART, M. S. MATHESON, J. RABANI, and J. K. THOMAS. J. Am. Chem. Soc. **85**, 1375 (1963).
15. L. M. DORFMAN and I. A. TAUB. J. Am. Chem. Soc. **85**, 2370 (1963).
16. K. H. SCHMIDT. Argonne National Laboratory, reports ANL-7199 and ANL-7693.
17. H. L. FRIEDMAN. J. Chem. Phys. **21**, 319 (1953).

Can. J. Chem. Downloaded from www.nrcresearchpress.com by 210.87.254.5 on 09/05/12
For personal use only.

Comparisons between Orientation Polarizations and Atom Polarizations among Organomercurials

GEORGE F WRIGHT

Department of Chemistry, University of Toronto, Toronto 181, Ontario

Received September 26, 1972

Although a correlation between orientation and atom polarizations among simple aryl and alkyl mercurials is limited, a definite but inverse correlation is found for 2-oxyorganomercuric salts.

La corrélation qui existe entre l'orientation et la polarisation atomique chez les aryl et alkyl mercuriels simple est limitée; toutefois une corrélation bien définie mais inverse est observée avec les sels organomercuriques hydroxylés en position 2. [Traduit par le journal]

Can. J. Chem., 51, 1131 (1973)

Can. J. Chem. Downloaded from www.nrcresearchpress.com by 210.87.254.42 on 09/05/12
For personal use only.

Because the phenomenon known as atom polarization is not clearly understood it must suffice in this report only to present and compare experimental data for a number of mercurials in which the polarity of the carbon–mercury linkage ought to accentuate structural differences.

The reactance of a substance in the gaseous phase, and to approximations in solution, may be expressed as follows:

$$P_T = P_E + P_A + P_O$$

where the total polarization (P_T) is a composite of the polarization at frequencies greater than $\sim 10^{14}$ Hz (P_E where the electrons can follow the alternating field) plus the polarization between $\sim 10^{12}$ and 10^{14} Hz (P_A) where the atom nuclei react with the field and finally P_O (orientation polarization where the entire molecule can follow the alternating field) at $\nu = \sim 10^6 - 10^8$ Hz if the system is not intrinsically too viscous.

At 10^6 Hz all three polarizations can react reversibly with the alternating electrostatic field to which they are subjected. In order to sort out these three effects we have earlier (1) devised a technique based on measurement of polarization in the solid state where orientation polarization cannot ordinarily occur. In this circumstance

$$P_{(solid)} = P_E + P_A = P_D$$

where P_D is called the distortion polarization.

It must be assumed that this experimentally-determined P_D will have the same magnitude for the substance in the gaseous state or in dilute solution as it displays in the solid state. This assumption is reasonable but it has not been proven. The most that has been shown is identity within experimental error of P_D for one substance in its crystalline and its amorphous state and for the polymorphs of two other substances (1).

Of course the magnitude of P_D will be much less than that of P_O for substances of appreciable dipole moment and P_A ordinarily is less than 20% of P_E. Consequently the magnitude of P_A is of small consequence for substances exceeding 2 D in moment unless high precision is required.

Orientation polarization (P_O) is assumed to be due to the alignment of a fixed dipole in the electric field. If disorientation due to thermal agitation is taken into account according to the Debye relationship (where l is 0.012812 and T is temperature in °K)

$$\mu = l\sqrt{P_O T}$$

then the dipole moment (μ) ought to be a temperature-independent constant for the substance under examination. It has been shown (2) that there are exceptions to this rule, which have been attributed to dipole distortion because of internal molecular energy. In turn it has been postulated (3) that in such instances P_O and P_A are interrelated in respect of temperature dependence. The temperature dependence of P_A has been evaluated theoretically (4) and has been found to be slight.

If there should be a relationship between P_A (due to charge dipole in the molecule) and P_O (orientation of the separated charge of a molecule) this relationship could be of use in evalua-

TABLE 1. Polarizabilities of aryl and alkylmercuric salts where 12.8 cc is atom refraction of mercury and $P_A = P_D - MR_D$ in cc

Mercurial	$d_{22°}$	ε	P_D	MR_D	P_A	μ (D)*
Phenylmercuric chloride (6)	2.883	3.867	53.1	44.0	9.1	2.99
Phenylmercuric cyanide				43.1		4.08–4.09
4-Methoxyphenylmercuric chloride (6)	2.735	3.673	59.2	50.2	9.0	3.65
4-Methoxyphenylmercuric bromide (6)	2.931	3.848	64.4	53.1	11.3	3.85
4-Methoxyphenylmercuric iodide (6)	3.077	4.197	72.9	58.2	14.7	3.55
3-Methoxyphenylmercuric chloride (6)	2.735	3.483	56.9	50.2	6.7	3.35
3-Methoxyphenylmercuric bromide (6)	2.935	3.656	62.0	53.1	8.9	3.49
2-Methoxyphenylmercuric chloride (6)	2.743	3.311	54.5	50.2	4.3	3.84
3-Chlorophenylmercuric chloride (6)	2.950	3.883	57.7	48.8	8.9	2.91
1,4-Dichloromercuridurene (5)	3.015	4.199	103.5	80.1	23.4	—
Methylmercuric iodide	5.130	4.532	35.9	32.4	3.5	2.91–2.94
Methylmercuric chloride (5)	4.238	3.428	26.5	24.5	2.0	3.27–3.24
Ethylmercuric chloride (5)	3.762	3.639	32.8	29.1	3.7	3.64
n-Propylmercuric chloride (5)	3.225	3.157	36.2	33.7	2.5	3.67
n-Butylmercuric chloride (5)	2.891	3.203	42.9	38.3	4.6	3.90
Benzylmercuric chloride	2.780	3.341	51.6	48.6	3.0	
Isopropylmercuric chloride	3.310	3.697	39.9	33.7	6.2	3.43–3.59
Cyclopentylmercuric chloride	2.845	3.312	46.7	40.8	5.9	
Cyclohexylmercuric chloride	2.684	3.280	51.4	45.4	6.0	3.90
α-4-Methylcyclohexylmercuric chloride, m.p. 173–174°	2.521	2.964	52.3	49.8	2.5	3.78
β-4-Methylcyclohexylmercuric chloride, m.p. 150–150.5°	2.519	2.960	52.3	49.8	2.5	4.18
Cyclohexylmercuric cyanide	2.534	3.197	51.5	44.0	7.5	4.69
α-4-Methylcyclohexylmercuric cyanide, m.p. 164–165°	2.374	2.968	54.4	48.9	5.2	4.60
β-4-Methylcyclohexylmercuric cyanide, m.p. 137–138°	2.369	2.961	54.1	48.9	5.1	4.91
Vinylmercuric chloride	3.643	3.522	33.0	28.3	4.7	
Vinylmercuric iodide	4.420	4.350	42.3	34.8	7.5	

*When two values of dipole moment (μ) are given they have been determined at 20 and 40°, respectively.

tion of molecular structure. For example an abnormally high P_A has been found (Table 1) for 1,4-dichloromercuridurene (5) but the P_O and hence the dipole moment of this substance cannot yet be determined because it is non-volatile and is too insoluble in media of low dielectric constant. Consequently we have made a study of comparisons between P_A and P_O (the latter in terms of dipole moment) for a series of candidate substances.

The first series listed in Table 1 includes the arylmercuric halide group (6). There is little correlation between P_O and P_A even in respect of the halogeno–mercuri bond, although it is notable that P_A is unusually high. The values for P_A among the alkylmercuric chlorides is lower than those of the arylmercurials but it is of interest that the dipole moments increase regularly in the homologous series (expected because of the space swept out of the solvent by the alkyl group) whereas the atomic polarizations alternate upward in magnitude, remindful of alternate melting points in other crystalline homologous series among the alkenes. Thus there may be some dependence of P_A on the confinement of the crystal lattice when P_D is measured in the solid state.

More significant are the higher atomic polarizations (P_A) for the secondary alkylmercuric halides over those of the primary analogs.

However it is disturbing to find that substances of supposedly proven structure (7) like the 4-cyclohexylmercuric halides show atom polarizations more of the order of primary rather than secondary alkyl substituents. This discrepancy is consistent for the analogous 4-methylcyclohexylmercuric cyanides which, of course, may be expected to be more polar than the chlorides. In general it may be said that only a limited correlation is found among the items of Table 1.

By contrast we have found a definite correlation among the 2-oxyorganomercurials listed in Table 2, albeit an unexpected one. The so-called α-diastereomers which are obtained by addition (not acid-catalyzed) of the elements of methoxy-

Can. J. Chem. Downloaded from www.nrcresearchpress.com by 210.87.254.42 on 09/05/12
For personal use only.

TABLE 2. Polarizabilities of 1,2-oxyorganomercurials where 12.8 cc is atomic refraction of mercury and $P_A = P_D - MR_D$ in cc

Oxymercurial	$d_{22°}$	ε	P_D	MR_D	P_A	μ (D)
α-2-Iodomercuri-1,8-cineole (8)	2.513	3.128	79.4	71.2	8.2	—
α-2-Bromomercuri-1,8-cineole (8)	2.264	2.806	72.0	66.5	5.5	—
α-2-Chloromercuri-1,8-cineole (8)	2.037	2.826	72.3	63.6	8.7	3.42
β-2-Chloromercuri-1,8-cineole (8)	2.197	2.820	66.9	63.6	3.3	4.82
α-2-Methoxycyclopentylmercuric iodide (9)	3.084	3.708	65.6	54.8	10.8	3.2
α-2-Methoxycyclopentylmercuric bromide (9)	2.922	3.452	58.4	49.8	8.6	3.4
α-2-Methoxycyclopentylmercuric chloride (9)	2.693	3.692	58.9	46.9	12.0	2.9
β-2-Methoxycyclopentylmercuric chloride (9)	2.710	3.088	50.8	46.9	3.9	4.1
β-2-Methoxycyclopentylmercuric bromide	2.908	3.158	54.6	49.8	4.8	4.7
α-2-Methoxycyclohexylmercuric bromide (9)	2.683	2.846	55.9	54.4	1.5	3.7
β-2-Methoxycyclohexylmercuric bromide (9)	2.711	2.859	55.6	54.4	1.2	4.7
α-2-Methoxycyclohexylmercuric chloride (9)	2.498	2.863	53.2	51.5	1.7	3.7
β-2-Methoxycyclohexylmercuric chloride (9)	2.502	2.827	52.8	51.5	1.3	4.9
"α"-1-Chloromercuri-2-methoxy-1,2-diphenylethane from *cis*-stilbene	1.995	2.664	79.6	83.6	−4.0	4.3
"β"-1-Chloromercuri-2-methoxy-1,2-diphenylethane from *trans*-stilbene	2.051	2.795	81.6	83.6	−2.03	3.6
1-Chloromercurimethyl-1,8-nor-cineole	2.558	3.2631	60.7	54.3	6.4	
1-Chloromercuri-1-phenyl-2-methoxy-2-methylpropane	2.118	3.104	77.7	68.6	9.1	
*β-2-Methoxy-3-chloromercuri-[2,2,1]-bicycloheptane, m.p. 126°	2.394	2.950	59.4	54.0	5.4	4.22
*β-2-Hydroxy-3-chloromercuri-[2,2,1]-bicycloheptane, m.p. 131°	2.616	3.522	60.6	49.2	11.4	4.91
*α-2-Hydroxy-3-chloromercuri-[2,2,1]-bicycloheptane, m.p. 120°			63.4	49.2	14.2	3.63

*Orientation polarization determined in benzene at 20 °C.

mercuric acetate to α-Terpineol (8), cyclopentene, and cyclohexane (9) have lower dipole moments but higher atom polarizations than their epimerized β-diastereomers derived by radical-induced isomerization. Likewise the diastereomer which is formed predominately by acid-catalyzed hydroxymercuration of [2,2,1]-bicycloheptene (10) and which has the higher dipole moment (hence is designated as β) has the lower atom polarization by contrast to the less predominant α-diastereomer.

An apparent contradiction of this inverse correlation which is found for the methoxymercuration products of the geoisomeric stilbenes is only nominal. Firstly the apparently absurd (negative) values for P_A listed for these two oxymercurials should be adjusted upwards by 4–5 cc because of the previously demonstrated "phenyl effect" (11). Second, the nomenclature "α" and "β" refers for this pair of diastereomers to their derivation from *cis* and *trans* stilbene respectively (12, 13). With this interpretation it may be seen that the inverse correlation still applies, *i.e.* that the β-diastereomer from *trans*-stilbene has a lower dipole moment but a higher atom polarization (P_A) than does the α-diastereomer from *cis*-stilbene.

It may be of interest in respect of this inverse correlation that the α-diastereomer from *cis*-stilbene is more resistant to deoxymercuration by strong (molecular) hydrochloric acid than is the more slowly-formed β-diastereomer from *trans*-stilbene. This behavior whereby the diastereomer of higher dipole moment and lower atom polarization is more resistant to deoxymercuration by molecular hydrochloric acid also is consistent for the diastereomeric oxymercurials of α-terpineol, cyclopentene, and cyclohexene. It would appear that there is a conformational advantage in deoxymercuration which involves the pivot bond in the methoxydiphenylethane mercurials and which is related to dipole moment and to atom polarization of all these oxymercurials.

In this connection it is of interest to observe the minimal differences of P_A between the α and β diastereomers of 2-methoxycyclohexylmercuric chloride by contrast with those pairs of

Can. J. Chem. Downloaded from www.nrcresearchpress.com by 210.87.254.42 on 09/05/12
For personal use only.

TABLE 3. Far infrared spectral absorption frequencies of some mercurials (Intensities are listed as strong, medium, and weak)

Substance	Absorption peaks in cm^{-1}						
α-Chloromercuricineole	92(s)		126(w)	151(w)			
β-Chloromercuricineole	70(s)	87(s)	124(m)	166.5(m)			
α-Methoxycyclopentylmercuric chloride	56(s)	70(shoulder)	115(w)	207(s)			
β-Methoxycyclopentylmercuric chloride	54(m)		115(w)	203(s)			
α-Methoxycyclohexylmercuric chloride	86(s)	99(s)	126(w)	146(w)	270(w)	319(s)	
β-Methoxycyclohexylmercuric chloride	81(s)	112(s)	160(w)	250(w)	318(s)		
1-Chloromercurimethyl*nor*cineole	105(s)	262(w) 303(s)	307(s) 349(w)	520(w)	530(w)		
Isopropylmercuric chloride in benzene	90(m)	251(m)	300–340(vs)				
Isopropylmercuric chloride in pure wafer	87(s)	251(m)	306(vs)				
n-Butylmercuric chloride	90(s)	113(w)	149(w)	305			
sec-Butylmercuric chloride at −190 °C	66(s) very broad						
sec-Butylmercuric chloride at +40 °C	59.5(m) very broad		202(s)	250(w)			
Tolylmercuric chloride	94(s)	138(s)	185(s)				

oxyorganomercurials from cyclopentene and α-terpineol. In retrospect it would seem that the 2-methoxycyclohexylmercuric chlorides were the poorest candidates to choose for the single-crystal X-ray diffraction studies upon which their diastereomeric configurations were based (12). If heavy substituents can warp a cyclohexane ring out of its traditionally-regular hexagonal geometry then it is a pity that the methoxycyclopentylmercuric halides were not, instead, chosen for single-crystal analysis.

These observations have been made despite doubts about the meaning of atom polarization. It can only be said with reasonable assurance that the involvement of P_A with radiation frequencies above 10^{14} Hz is slight or inconsequential.

It must be realized that only during the past decade have measurements of precision been made for P_A. Previous measurements in the gaseous phase for extrapolation of P_T to infinite temperature are grossly imprecise. In liquids or solutions such extrapolations are absurd. Likewise evaluations of P_A from spectral absorptions lead to absurdities (14).

Indeed spectral absorption in the far infrared region seems to be singularly uniformative about the differences in P_A which have been determined by capacitance measurement. Some frequencies are listed in Table 3. The lack of correlation cannot be attributed to lattice forces in the solid state (in which state most of these spectra must be determined) because in one instance, isopropylmercuric chloride, the frequencies of absorption are similar in solid and solution states.

Perhaps a new conceptual model for P_A is needed. The data of Table 1 might then fall into some order and the inverse correlations of Table 2 might become meaningful.

Experimental

The dielectric constants and the densities of substances in the solid state were determined by methods previously described (1) (15). The orientation polarizations were calculated from the dielectric constants of solutions in benzene at 20° with apparatus previously described (16).

Spectral absorptions have been determined in a Beckman IR-11 Spectrometer using solid dispersions in polypropylene wax (1) except for isopropylmercuric chloride, which was examined both as a 15% solution in benzene (b) or as a very thin wafer of the pure crystalline substance (p). The findings are reported in Table 3.

The author thanks the Defence Research Board and the National Research Council of Canada for grants-in-aid which supported this research. The dielectric constants and densities of the solids were determined for the most part by Mr. H. Huber.

1. M. BEDARD, H. HUBER, J. L. MYERS, and G. F WRIGHT. Can. J. Chem. **40**, 2278 (1962).
2. J. W. SMITH. Electric dipole moments. Butterworths, London. 1955.
3. N. R. DAVIDSON and L. E. SUTTON. J. Chem. Soc. 347 (1939).
4. K. H. ILLINGER and C. P. SMYTH. J. Chem. Phys. **32**, 787 (1960); **35**, 400 (1961).
5. H. SAWATZKY and G. F WRIGHT. Can. J. Chem. **36**, 1555 (1958).
6. J. C. SIPOS, H. SAWATZKY, and G. F WRIGHT. J. Am. Chem. Soc. **77**, 2759 (1955).
7. F. R. JENSEN and L. H. EALE. J. Am. Chem. Soc. **82**, 145 (1960).
8. A. G. BROOK and G. F WRIGHT. J. Org. Chem. **22**, 1314 (1957).

Can. J. Chem. Downloaded from www.nrcresearchpress.com by 210.87.254.42 on 09/05/12
For personal use only.

9. A. G. BROOK, R. DONOVAN, and G. F WRIGHT. Can. J. Chem. **31**, 536 (1953).
10. H. KREHM and G. F WRIGHT. Submitted for publication.
11. H. HUBER and G. F WRIGHT. Can. J. Chem. **42**, 2065 (1964).
12. G. F WRIGHT. Ann. N.Y. Acad. Sci. **65**, 436 (1957).
13. A. G. BROOK and G. F WRIGHT. Acta. Cryst. **4**, 50 (1951).
14. H. HUBER and G. F WRIGHT. Can. J. Chem. **42**, 1446 (1964).
15. M. V. GEORGE and G. F WRIGHT. Can. J. Chem. **36**, 189 (1958).
16. C. C. MEREDITH and G. F WRIGHT. Can. J. Technol. **33**, 182 (1955).

Can. J. Chem. Downloaded from www.nrcresearchpress.com by 210.87.254.42 on 09/05/12
For personal use only.

Can. J. Chem. Downloaded from www.nrcresearchpress.com by 210.87.254.105 on 09/05/12
For personal use only.

Alcohol to Ester Rearrangement. II. Diphenylphosphine and Hexafluoroacetone

ALEXANDER FRANK JANZEN AND OM CHAND VAIDYA
Department of Chemistry, University of Manitoba, Winnipeg, Manitoba R3T 2N2

Received August 17, 1972

The reaction of diphenylphosphine with hexafluoroacetone gives $(C_6H_5)_2PC(OH)(CF_3)_2$ which is readily oxidized to $(C_6H_5)_2P(O)C(OH)(CF_3)_2$ and, in the presence of base catalyst, undergoes rearrangement to the isomeric $(C_6H_5)_2P(O)OCH(CF_3)_2$. Reaction of hexafluoroacetone with diphenylarsine gives $(C_6H_5)_2AsC(OH)(CF_3)_2$ while reaction with diphenyl phosphonate gives $(C_6H_5O)_2P(O)C(OH)(CF_3)_2$ which rearranges to $(C_6H_5O)_2P(O)OCH(CF_3)_2$.

La réaction de la diphénylphosphine sur l'hexafluoroacétone conduit à $(C_6H_5)_2PC(OH)(CF_3)_2$ qui s'oxyde facilement en $(C_6H_5)_2P(O)C(OH)(CF_3)_2$, ce dernier s'isomérise en $(C_6H_5)_2P(O)OCH(CF_3)_2$ selon un réarrangement catalysé par une base. La réaction de l'hexafluoroacétone sur la diphénylarsine conduit à $(C_6H_5)_2AsC(OH)(CF_3)_2$ et sur la diphénylphosphonate fournit $(C_6H_5O)_2P(O)C(OH)(CF_3)_2$ qui se réarrange en $(C_6H_5O)_2P(O)OCH(CF_3)_2$. [Traduit par le journal]

Can. J. Chem., 51, 1136 (1973)

Recently we reported the kinetics and mechanism of the base-catalyzed rearrangement of phosphorus(V) alcohols to the isomeric esters (eq. 1) (1). The alcohols were readily prepared

$$[1]\quad \underset{\text{"Alcohol"}}{(RO)_2\overset{\overset{\displaystyle O}{\|}}{P}\overset{\overset{\displaystyle OH}{|}}{C}(CF_3)_2} \xrightarrow{\text{Base}} \underset{\text{"Ester"}}{(RO)_2\overset{\overset{\displaystyle O}{\|}}{P}O\overset{\overset{\displaystyle H}{|}}{C}(CF_3)_2}$$

$$R = CH_3;\ C_2H_5;\ n\text{-}C_4H_9$$

by the reaction of dialkyl phosphonates with hexafluoroacetone. Whether phosphorus(III) alcohols would behave similarly is of some interest in view of the report that reaction of diphenylphosphine and hexafluoroacetone gives a 1:1 adduct involving trivalent carbon (2). The reaction of hexafluoroacetone with diphenylphosphine was therefore repeated, as well as reaction with diphenylphosphine oxide, diphenyl phosphonate, and diphenylarsine.

Our results from the reaction of diphenylphosphine and hexafluoroacetone are entirely consistent with the initial formation of a phosphorus(III) alcohol of structure **1** (eq. 2).

$$[2]\quad (C_6H_5)_2PH + (CF_3)_2CO \longrightarrow \underset{\mathbf{1}}{(C_6H_5)_2P\overset{\overset{\displaystyle OH}{|}}{C}(CF_3)_2}$$

Compound **1** is a white solid, soluble in tetrahydrofuran (THF) and very susceptible to oxidation. Oxidation prevented satisfactory elemental analysis; however, the oxidized product **2** is stable in air and gave satisfactory elemental analysis.

Rearrangement of alcohol **2** to ester **3** occurred in the presence of a base catalyst such as THF or pyridine, consistent with the alcohol to ester rearrangement described previously (1).

$$[3]\quad \underset{\mathbf{2}}{(C_6H_5)_2\overset{\overset{\displaystyle O}{\|}}{P}\overset{\overset{\displaystyle OH}{|}}{C}(CF_3)_2} \xrightarrow{\text{Base}} \underset{\mathbf{3}}{(C_6H_5)_2\overset{\overset{\displaystyle O}{\|}}{P}O\overset{\overset{\displaystyle H}{|}}{C}(CF_3)_2}$$

The ^{19}F n.m.r. spectra were particularly useful in characterizing compounds **1**, **2**, and **3** and monitoring the rearrangement of **2** to **3**. Figure 1*a* shows a typical ^{19}F n.m.r. spectrum of a mixture of **1**, **2**, and **3** in THF in a sealed n.m.r. tube. The spectrum shown in Fig. 1*b* was recorded 5 h after that shown in Fig. 1*a* and it is evident that concentration of **2** has decreased whereas **3** increased, confirming the alcohol-to-ester rearrangement in THF (eq. 3). The rate of rearrangement may be increased by introducing a stronger base such as pyridine. During the rearrangement, the concentration of **1** remained unchanged, confirming that **1** is stable in THF provided that oxygen and moisture are excluded.

An alternate route to **3**, involving rearrangement of **1** to $(C_6H_5)_2POCH(CF_3)_2$ followed by oxidation to **3** was not observed in our study.

In a separate experiment it was shown that reaction of diphenylphosphine oxide with hexafluoroacetone gave **2** and addition of pyridine catalyzed the rearrangement to **3**. Similarly, reaction of diphenyl phosphonate with hexafluoroacetone gave alcohol **4** and addition of pyridine gave the isomeric ester **5** (eq. 4).

Can. J. Chem. Downloaded from www.nrcresearchpress.com by 210.87.254.105 on 09/05/12
For personal use only.

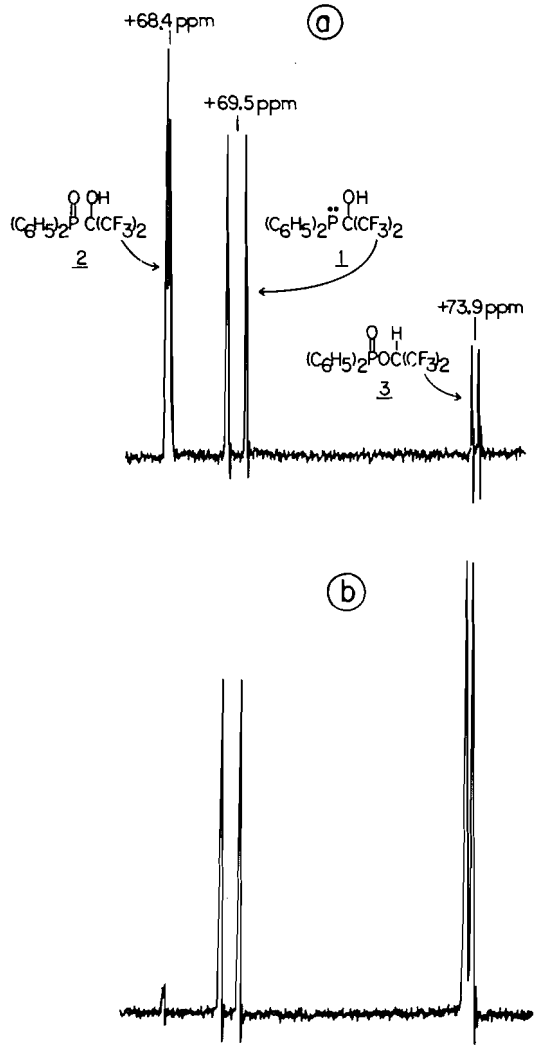

FIG. 1 (*a*) The ^{19}F n.m.r. spectrum of mixture of **1**, **2**, and **3** in tetrahydrofuran. (*b*) After 5 h at 25°. Concentration of **2** decreased, **3** increased while **1** remained unchanged.

[4] $(C_6H_5O)_2P(O)H + (CF_3)_2CO \longrightarrow$

$$(C_6H_5O)_2\overset{\overset{O}{\|}}{P}\overset{\overset{OH}{|}}{C}(CF_3)_2 \xrightarrow{\text{Base}} (C_6H_5O)_2\overset{\overset{O}{\|}}{P}O\overset{\overset{H}{|}}{C}(CF_3)_2$$

4 **5**

The reaction of diphenylarsine with hexafluoroacetone was carried out in an attempt to prepare a stable arsenic(III) alcohol analogous to **1** (eq. 5). Reaction occurred readily to give **6**,

[5] $(C_6H_5)_2AsH + (CF_3)_2CO \longrightarrow (C_6H_5)_2As\overset{\overset{OH}{|}}{C}(CF_3)_2$

6

an oily liquid which was more resistant to oxidation than **1** and gave satisfactory elemental analysis. The reaction of dimethylarsine with hexafluoroacetone to give an arsenic(III) alcohol has been reported by Cullen and Styan (4). Oxidation of **6** with gaseous oxygen gave bis (diphenylarsine) oxide.

Recent investigations have shown that phosphorus(III) derivatives may abstract fluorine attached to a carbon atom (5). During this study it was observed that if **1** was left in the presence of excess hexafluoroacetone, fluorine abstraction

[6] $$\mathbf{1} \xrightarrow[\text{or } XeF_2]{(CF_3)_2CO \text{ excess}} (C_6H_5)_2\overset{\overset{F}{|}}{P}\overset{\overset{OH}{|}}{C}(CF_3)_2$$

7

occurred to give **7** (eq. 6). Addition of a fluorinating agent such as XeF_2 (6) to **1** also gave **7**, which was identified on the basis of its ^{19}F n.m.r. and mass spectra. The ease of fluorination and oxidation is consistent with the structure proposed for **1**.

Experimental

Conventional vacuum line techniques were used for handling volatile materials. Hexafluoroacetone (Matheson of Canada), diphenylphosphine, diphenyl phosphonate (Eastman), diphenylarsine (Alfa), and xenon difluoride (PCR, Gainesville) were used as obtained. Diphenylphosphine oxide was prepared by oxidation of diphenylphosphine (7). The n.m.r. spectra were obtained on a Varian A-56/60A spectrometer using 60 and 56.4 MHz for proton and fluorine, respectively. Chemical shifts are relative to internal tetramethylsilane and trichlorofluoromethane. Mass spectra were obtained on a Finnigan 1015 quadrupole mass spectrometer. Elemental analyses were performed by Alfred Bernhardt, West Germany.

Reaction of Diphenylphosphine with Hexafluoroacetone

Diphenylphosphine (0.56 g, 3.0 mmol) was dissolved in $CFCl_3$ (3 ml) and hexafluoroacetone (0.73 g, 4.4 mmol) condensed onto the solution at −196°. The reaction mixture was allowed to warm to room temperature and stirred for 15 min. Removal of volatile products left a white solid identified as 2-hydroxy-1,1,1,3,3,3-hexafluoroisopropyldiphenylphosphine, $(C_6H_5)_2PC(OH)(CF_3)_2$ (**1**), on the basis of n.m.r., mass spectrometry, and chemical reactions.

The ^{19}F n.m.r. spectrum of **1** showed a doublet, $J_{FCCP} = 17.8$ Hz, at +69.5 p.p.m. and the ^1H n.m.r. showed a singlet (OH) at −3 p.p.m. and phenyl peaks.

1 was found to be very susceptible to oxidation to give **2**, described below, and the difficulty of excluding oxygen from solvents and reaction vessels prevented satisfactory elemental analysis. Rapid hydrolysis and oxidation occurred if **1** was exposed to the atmosphere, the end products being $(C_6H_5)_2P(O)OH$, identified by its mass

Can. J. Chem. Downloaded from www.nrcresearchpress.com by 210.87.254.105 on 09/05/12
For personal use only.

spectrum and m.p. 193° (lit. 192° (8)) and hexafluoroacetone hydrate. A fresh sample of **1** was always prepared when needed.

The mass spectrum of **1** was contaminated by **2**; however, peaks (M = molecular ion) at *m/e* 352(M), 351(M − H), and 313(M − HF_2) may be assigned to **1** since they are not observed in the mass spectrum of purified **2**.

Oxidation of $(C_6H_5)_2PC(OH)(CF_3)_2$ to $(C_6H_5)_2P(O)C(OH)(CF_3)_2$

A slow stream of dry oxygen gas was passed through a suspension of **1** in $CFCl_3$ at −23° for 6 h. Removal of $CFCl_3$ under vacuum left a white solid identified as 2-hydroxy-1,1,1,3,3,3-hexafluoroisopropyldiphenylphosphine oxide $(C_6H_5)_2P(O)C(OH)(CF_3)_2$ (**2**). The ^{19}F n.m.r. spectrum showed a doublet, $J_{FCCP} = 1.5$ Hz, at +68.4 p.p.m. The mass spectrum showed highest mass ions at *m/e* 368(M), 367(M − H), and 348(M − HF).

Anal. Calcd. for $C_{15}H_{11}F_6O_2P$: C, 48.92; H, 3.01; F, 30.96. Found: C, 49.10; H, 3.04; F, 30.64.

Base-catalyzed Rearrangement of $(C_6H_5)_2P(O)C(OH)(CF_3)_2$ (2) to $(C_6H_5)_2P(O)OCH(CF_3)_2$ (3)

The preparation of **3** has been reported previously (2). In this study, a solution of **2** in THF was monitored and found to rearrange to **3**, with an approximate pseudo first-order rate constant $k_1' = 6 \times 10^{-5}$ s^{-1} at 25°. The rate of rearrangement increased on addition of a stronger base catalyst such as pyridine. Compound **2** could be prepared by an alternate route from diphenylphosphine oxide and hexafluoroacetone. Addition of pyridine again catalyzed the rearrangement to **3**.

The ^{19}F n.m.r. of **3** showed a doublet, $J_{FCCH} = 6$ Hz, at +73.9 p.p.m. (lit. +73.0 p.p.m. in dimethylformamide (2)).

Reaction of Diphenyl Phosphonate with Hexafluoroacetone

Diphenyl phosphonate (0.5 g, 2.1 mmol) and hexafluoroacetone (0.8 g, 4.8 mmol) was sealed in an n.m.r. tube and the ^{19}F n.m.r. spectrum recorded after 24 h. Only two doublets were observed. The doublet, $J_{FCCP} = 3$ Hz, at +71.3 p.p.m. is assigned to $(C_6H_5O)_2P(O)C(OH)(CF_3)_2$ (**4**) (46%) while the doublet, $J_{FCCH} = 6$ Hz, at +74.6 p.p.m. is assigned to $(C_6H_5O)_2P(O)OCH(CF_3)_2$ (**5**) (54%), by comparison with the chemical shifts and coupling constants found for $(RO)_2P(O)C(OH)(CF_3)_2$ and $(RO)_2P(O)OCH(CF_3)_2$ (3). Addition of base catalysts such as pyridine, diethylamine, or *n*-butyl lithium resulted in complete rearrangement of **4** to **5**, as monitored by ^{19}F n.m.r.

Reaction of $(C_6H_5)_2PC(OH)(CF_3)_2$ with Excess Hexafluoroacetone or XeF_2

Reaction of diphenylphosphine (0.21 g, 1.1 mmol) with excess hexafluoroacetone (0.71 g, 4.3 mmol) gave a white solid **1** as described above. On standing for 3 days at room temperature the solid dissolved to give a yellow solution. Excess hexafluoroacetone was removed under vacuum and an oily liquid remained, identified as $(C_6H_5)_2PF_2C(OH)(CF_3)_2$ (**7**) on the basis of n.m.r. and mass spectra.

The ^{19}F n.m.r. showed a doublet, $J_{FP} = 806$ Hz, at +38.5 p.p.m. assigned to the PF_2 group and a doublet, $J_{FCCP} = 5.9$ Hz, of triplets, $J_{FCCPF} = 1.5$ Hz, at +74.5 p.p.m. assigned to the trifluoromethyl groups. The mass spectrum showed characteristic ions at *m/e* 390(M), 389(M − H), 371(M − F), 294(M − C_6H_5F), 223($C_{12}H_{10}PF_2$), 204($C_{12}H_{10}PF$).

Compound **7** was also prepared by treating a solution of $(C_6H_5)_2PC(OH)(CF_3)_2$ in $CFCl_3$ with XeF_2 (8% in CH_3CN (6)) at −196°. The mixture was kept at −63° for 2 h and then warmed to −23° for 1 h. Removal of volatile products left behind an oily liquid which gave a ^{19}F n.m.r. spectrum identical to **7** above.

Reaction of Diphenylarsine with Hexafluoroacetone

Diphenylarsine (0.84 g, 3.7 mmol) and hexafluoroacetone (1.54 g, 9.3 mmol) were kept in a sealed tube at 25° for 4 h. Removal of volatile products left behind a viscous liquid, identified as 2-hydroxy-1,1,1,3,3,3-hexafluoroisopropyldiphenylarsine, $(C_6H_5)_2AsC(OH)(CF_3)_2$ (**6**). The ^{19}F n.m.r. spectrum showed a singlet at +69.6 p.p.m. and the ^1H n.m.r. a singlet (OH) at −2.3 p.p.m. and phenyl peaks.

Anal. Calcd. for $C_{15}H_{11}F_6AsO$: C, 45.47; H, 2.80; F, 28.78. Found: C, 45.30; H, 2.95; F, 28.47.

The financial assistance of the National Research Council of Canada is gratefully acknowledged.

1. A. F. JANZEN and T. G. SMYRL. Can. J. Chem. **50**, 1205 (1972).
2. R. F. STOCKEL. Chem. Commun. 1594 (1968).
3. A. F. JANZEN and R. POLLITT. Can. J. Chem. **48**, 1987 (1970).
4. W. R. CULLEN and G. E. STYAN. J. Organomet. Chem. **4**, 151 (1965).
5. F. RAMIREZ, C. P. SMITH, A. S. GULATI, and A. V. PALWARDHAM. Tetrahedron Lett. 2151 (1966); F. RAMIREZ, C. P. SMITH, and S. MEYERSON. Tetrahedron Lett. 3651 (1966); F. RAMIREZ, A. S. GULATI, and C. P. SMITH. J. Am. Chem. Soc. **89**, 6283 (1967); R. A. MITSCH. J. Am. Chem. Soc. **89**, 6297 (1967).
6. J. A. GIBSON and A. F. JANZEN. Can. J. Chem. **49**, 2168 (1971).
7. M. M. RAUHUT and H. A. CURRIER. J. Org. Chem. **26**, 4626 (1961).
8. L. HORNER, P. BECK, and V. G. TOSCANO. Chem. Ber. **94**, 1317 (1961).

Vibrational Spectra and Rotational Isomerism in 2-Mercaptoethanol

S. K. NANDY, D. K. MUKHERJEE, S. B. ROY, AND G. S. KASTHA

Optics Department, Indian Association for the Cultivation of Science, Calcutta 32, India

Received September 18, 1972

From the Raman and i.r. spectra of 2-mercaptoethanol in the liquid state and the temperature variation of the intensity of the Raman lines, it has been concluded that both the *trans*- and *gauche*-isomers are present in the liquid. A tentative analysis of the vibrational frequencies of the isomers has been presented.

D'après les spectres Raman et i.r. du mercapto-2 éthanol à l'état liquide et aussi d'après la variation en fonction de la température de l'intensité des raies du spectre Raman, on peut conclure que les isomères *cis* et *gauche* existent tous les deux dans le liquide. Une analyse provisoire des fréquences de vibration des isomères est présentée. [Traduit par le journal]

Can. J. Chem., **51**, 1139 (1973)

Can. J. Chem. Downloaded from www.nrcresearchpress.com by 210.87.254.6 on 09/05/12
For personal use only.

Introduction

The rotational isomerism in 2-haloethanols was investigated by previous workers (1–4), but complete assignments of their vibrational frequencies were recently made by Buckley *et al.* (5). The molecule of 2-mercaptoethanol is similar to that of 2-haloethanols, so it is expected to show rotational isomerism, which, however, has not yet been reported. It would, therefore, be interesting to study the vibrational spectra of the molecule in relation to its rotational isomerism in the liquid state. With this object, the Raman and the i.r. studies of 2-mercaptoethanol were made in different states and the results of the investigations are discussed in the present paper.

Experimental

A pure sample of 2-mercaptoethanol obtained from Schuchardt (Germany) was distilled under reduced pressure just before use. The Raman spectrum of the compound and the polarization character of the Raman lines in the liquid state were obtained with a Fuess glass spectrograph. The Raman spectrum of the compound in the crystalline state could not be obtained despite numerous attempts, because the substance always yielded a glassy mass whose Raman spectrum was more or less the same as that of the liquid. The i.r. absorption spectrum of the liquid was recorded with a Perkin–Elmer Model 21 i.r. spectrophotometer with rock salt optics. The frequencies of the absorption bands were checked against the i.r. bands of a polystyrene film.

Results

The Raman spectra of the liquid and its glassy mass at -110 °C are shown in Fig. 1. The Raman wave numbers with visually estimated intensity and their polarization character, as well as the wave numbers of i.r. absorption bands are given in Table 1, which also includes the probable assignments of the vibrational frequencies of the molecule.

Discussion

As the Raman spectrum of 2-mercaptoethanol in the crystalline state could not be obtained as mentioned earlier and the Raman spectrum of the glassy mass was found to be more or less the same as that of the liquid, no simplification of the solid state spectrum was available for identification of the lines due to different isomers. However, from a study of the temperature dependence of the Raman spectrum in the liquid state, it was observed that the intensity of some of the prominent Raman lines, *viz.* 295, 668 cm^{-1} increase with increase of temperature, while those of some others such as 400, 763 cm^{-1} decrease with increase of temperature. Evidently, the former lines belong to the high energy form of the molecule, while the latter belong to the low energy form, indicating thereby the existence of at least two isomeric forms in the liquid state.

The assignments given in Table 1 are straightforward with regard to the stretching vibrations of OH, CH, and SH bonds, and the vibrations of the CH_2 group and were made by analogy with similar molecules of 2-haloethanols (5) and the alkanethiols (6, 7). The frequencies arising out of the C—X stretching (X = S or O), C—C stretching, and the skeletal bending vibrations are discussed below.

In alkanethiols (6, 7) the C—S stretching vi-

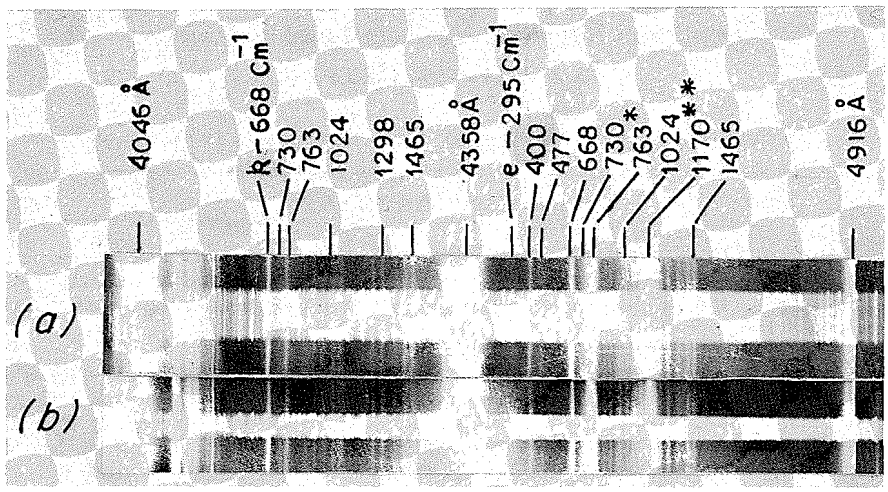

FIG. 1. Raman spectra of 2-mercatoethanol; (*a*) liquid, (*b*) glassy mass (−110 °C). *Overlapped by SH stretching frequency due to 4046 Å. **Overlapped by CH stretching frequency due to 4046 Å.

brations of the two isomers are found in the region 630–730 cm^{-1}. For example, in 1-propanethiol (6) and 2-propanethiol (7) the wave numbers 655 and 670 cm^{-1} respectively, are assigned to the C—S stretching vibration of the *gauche*-isomer, while the similar vibrations of the *trans*-isomer are at 710 cm^{-1} in both the molecules. In the case of 1,2-ethanedithiol (8) the pair of frequencies 639 and 665 cm^{-1} have been assigned to the C—S stretching vibrations of the *gauche*-isomer, while 690 and 718 cm^{-1} represent the similar vibrations of the *trans*-isomer of the molecule. In the present case, there are two Raman lines 668 and 730 cm^{-1} in this region. So in all probability the former line corresponds to a C—S stretching vibration of the *gauche*-isomer and the latter to a similar vibration of the *trans*-isomer. The corresponding i.r. bands are 665 and 735 cm^{-1}. It has already been pointed out that the Raman line 668 cm^{-1} belongs to the high energy form, so it is concluded that the *trans*-isomer of the present molecule in the liquid state is more stable than the *gauche*-isomer. This is unlike the case in 2-chloro- and 2-bromoethanols.

In the present molecule there is a depolarized Raman line of medium intensity at 763 cm^{-1} with a weak i.r. counterpart at 764 cm^{-1}. The C—SH bending vibration in alkanethiols (6–8) has been reported in the region 750–875 cm^{-1}. Therefore, the wave number 763 cm^{-1} probably represents such a vibration of the present molecule. Since this vibration, as already stated, belongs to the low energy form, it follows from the arguments given in the previous paragraph that this frequency arises from the *trans*-isomer. Similar vibration of the *gauche*-isomer is represented by the polarized Raman line 873 cm^{-1}. The corresponding i.r. band is at 875 cm^{-1}.

From Table 1, it can be seen that there are two Raman lines at 477 and 400 cm^{-1} in the spectrum of 2-mercaptoethanol. These lines have been assigned to the CCO bending vibrations of *gauche*- and *trans*-isomers respectively, following Buckley *et al.* (5) in 2-chloroethanol.

By analogy with alkanethiols (6–8) the broad and polarized Raman line, 295 cm^{-1} in the present case, is assigned to C—C—S stretching vibration of both the *trans*- and *gauche*-isomers.

The polarized Raman line 1024 cm^{-1} and the strong i.r. band at 1048 cm^{-1} are assigned to stretching vibration of the C—C bond in the two isomers as in 1,2-disubstituted ethanes.

Following the assignments of C—O stretching vibrations in the 2-haloethanols (5) the two prominent Raman lines 1055 and 1109 cm^{-1} are assigned to the *gauche*- and *trans*-isomers respectively in the present case. Similarly, the two strong i.r. bands 3200 and 3475 cm^{-1} have been assigned to OH stretching vibrations of the *gauche*- and *trans*-conformers respectively. Their low values correspond to free OH— stretching frequencies indicating the presence of intermolecular hydrogen bonding in the liquid state.

Can. J. Chem. Downloaded from www.nrcresearchpress.com by 210.87.254.6 on 09/05/12
For personal use only.

TABLE 1. Raman and i.r. data of 2-mercaptoethanol

Raman wave number, liquid at 30 °C*	Infrared frequency, liquid at 30 °C	Assignment
295 (3b) P		CCS bending (g)
400 (5) P		CCO bending (t)
477 (2b) D		CCO bending (g)
668 (10) P	665 m	C—S stretching (g)
	716 m	O—H torsion ?
730 (2) P	735 wsh	C—S stretching (t)
	748 m	
763 (5) D	764 wsh	CSH bending (t)
873 (3) P	875 wsh	CSH bending (g)
908 (4) P	908 m	CH_2 rocking (t)
	930 w	CH_2 rocking (g)
962 (3) D	975 wsh	
	1010 sh	
1024 (3) P		C—C stretching (t,g)
	1048 vs	
1055 (4b) D	1055 ssh	C—O stretching (g)
1109 (3) P	1090 wsh	C—O stretching (t)
1170 (3) P	1170 m	CH_2 twisting (t)
	1208 wb	OH bending (t) ?
	1228 mb	
1244 (4) D		CH_2 twisting (g)
1298 (5) D	1298 ms	CH_2 wagging
1370 (2) P	1375 mb	OH bending (g)
1422 (6) D	1420 s	CH_2 scissoring (t)
1465 (6) D	1460 ms	CH_2 scissoring (g)
2563 (10b) P	2555 sb	S—H stretching (t,g)
2790 (4)		
	2840 s	
2880 (5) P	2875 s	
	2930 s	C—H stretching
2952 (5) P		
	2968 s	
	3160 ssh	
	3200 s	
	3370 sh	O—H stretching
	3475 vs	

*Parentheses in Raman bands indicate visual relative intensities: P, polarized; D, depolarized; g, gauche; t, trans; s, strong; m, medium; w, weak; b, broad; sh, shoulder.

1. K. W. F. KOHLRAUSCH and G. P. YPSILANTI. Z. Physik. Chem. B 29, 274 (1935).
2. S. MIZUSHIMA, Y. MORINO, and S. NAKAMURA. Sc. Papers. Inst. Phys. Chem. Res. **37**, 205 (1940).
3. S. MIZUSHIMA, T. KUBOTA, and Y. MORINO. Bull. Chem. Soc. Jap. **14**, 15 (1939).
4. L. R. ZUMWALT and R. M. BADGER. J. Am. Chem. Soc. **62**, 305 (1940).
5. PAUL BUCKLEY, PAUL A. GIGUÈRE, and MICHEL SCHNEIDER. Can. J. Chem. **47**, 901 (1969).
6. TORGRIM TORGRIMSEN and PETER KLOEBOE. Acta Chem. Scand. **24**, 1139 (1970).
7. D. W. SCOTT, R. E. PENNINGTON, I. A. HOSSENHOPP, H. L. FINKE, and G. WADDINGTON. J. Am. Chem. Soc. **80**, 56 (1958).
8. M. HAYASHI, Y. SHIRO, T. OSHIMA, and H. MURATA. Bull. Chem. Soc. Jap. **38**, 1734 (1965).

Can. J. Chem. Downloaded from www.nrcresearchpress.com by 210.87.254.6 on 09/05/12
For personal use only.

Synthesis and Nuclear Magnetic Resonance Spectroscopy of some Substituted Aryldiazoalkanephosphonates

N. GURUDATA

Department of Chemistry, Sir George Williams University, Montreal 107, Quebec

AND

C. BENEZRA AND H. COHEN

Department of Chemistry, University of Ottawa, Ottawa 2, Canada

Received October 11, 1972

Six aryl diazoalkanephosphonates have been prepared and their proton and ^{13}C n.m.r. spectra analyzed. The results suggest that the carbon bearing phosphorus (and the diazo-group) is essentially sp^2 hybridized and that the dominant canonical form depends on the substitution of the aryl ring. Evidence is given for double bond character in the C—P bond.

Six diazoalcanephosphonates d'aryle ont été préparés et leurs spectres en r.m.n. du proton et du ^{13}C ont été analysés. Les résultats suggèrent que le carbone porteur du groupe phosphore (et du groupe diazo) possède exclusivement une structure sp^2 hybridée et que la forme canonique dominante dépend de la substitution sur le cycle aryle. Le caractère de double liaison dans le lien C—P a aussi été mis en évidence.

[Traduit par le journal]

Can. J. Chem., 51, 1142 (1973)

Introduction

Diazoalkanephosphonates are versatile reagents which undergo the usual diazoalkane reactions as well as exhibit carbenoid behavior (1,2). They are valuable intermediates in the synthesis of phosphorus substituted pyrazolines (1–3), and cycloalkyl, cycloalkenyl, and cycloalkylidene phosphonates (2). In the present study ^{13}C.m.r. is used to examine the ground state electron distribution of these reagents and its sensitivity to substitution effects.

Materials and Methods

Synthesis of Dimethyl Aryldiazomethylphosphonates

Compounds **1–3** and **6** were prepared according to a general method developed by Seyferth and co-workers (1–3): (*a*) preparation of the corresponding α-ketophosphonate by an Arbuzov reaction between an acylchloride and trimethyl phosphite, (*b*) preparation of the tosylhydrazones, and (*c*) decomposition of those hydrazones with a base (Scheme 1).

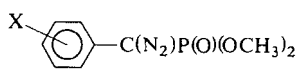

1 X = *p*-CH_3O—
2 X = *p*-CH_3—
3 X = *p*-Br—
4 X = H
5 X = *p*-NO_2
6 X = *o*-CH_3O—

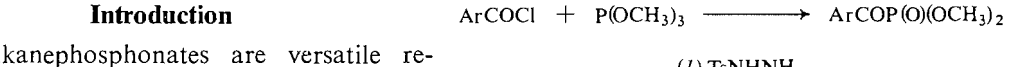

SCHEME 1

The *p*-nitrophenyldiazo compound, **5**, could not be prepared by this general route because $P(OCH_3)_3$ reacts with nitroaromatics to give a number of products (4). We used instead the approach of Regitz *et al.* (5), that is, nitration of dimethyl benzyl phosphonate followed by base exchange with tosyl azide. The reaction of trimethyl phosphite with *p*-nitrobenzoyl chloride is an interesting one, and details will be published elsewhere (6).

Compound **4** has already been prepared (3). All new compounds gave satisfactory elemental analysis and had i.r. data consistent with the proposed structures (see Experimental).

Experimental

General Synthetic Procedures

(a) Ketophosphonates

The starting acid chlorides, RCOCl, were prepared by addition of thionyl chloride (2.5 mol/mol of acid) to a solution of the acid in anhydrous benzene (20–30 ml) to which a few drops of pyridine had been added. Excess $SOCl_2$ was removed by distillation under vacuum (water

Can. J. Chem. Downloaded from www.nrcresearchpress.com by 210.87.254.42 on 09/05/12
For personal use only.

Can. J. Chem. Downloaded from www.nrcresearchpress.com by 210.87.254.42 on 09/05/12
For personal use only.

TABLE 1. α-Ketophosphonates, $ArCOP(O)(OCH_3)_2$

Ar	ArCOCl weight (g)	$ArCOP(O)(OCH_3)_2$ weight (g)*	B.p. (°C) (pressure in Torr)	Analysis		I.r. (cm^{-1}) (C=O, P=O, P—O—C)	N.m.r.‡
				Calcd.	Found		
p-$CH_3O—C_6H_4—$	22.5	24.7	145 (0.2)	C 49.19	49.21	1650	3.90 (*s*,3H,CH_3O—C)
				H 5.37	5.36	1250	3.92 (*d*,6H,P—OCH_3,J_{PH} = 11.0)
				P 12.69	12.45	1050	7.76, 7.67, 7.05, 6.91§ (J_{PCCCH} = 1.25)
p-$CH_3—C_6H_4—$	25	38	130–134†	C 52.63	52.38	1660	2.41 (*s*,3H,CH_3—C)
				H 5.71	5.67	1250	3.92 (*d*,6H,P—O—CH_3,J_{PH} = 10.0)
				P 13.57	13.33	1050	8.20, 8.12, 7.35, 7.26
p-Br—C_6H_4—	22	25	155 (0.2)	C 36.89	36.66	1660	3.92 (*d*,6H,P—O—CH_3,J_{PH} = 11.0)
				H 3.44	3.78	1240	
				P 10.57	10.44	1050	8.16, 8.07, 7.71, 7.62 (J_{PCCCH} = 1.25)
				Br 27.27	26.86		
o-$CH_3O—C_6H_4—$	27	28	165–170†	C 49.19	48.86	1660	3.87 (*d*,6H,P—OCH_3,J_{PH} = 10.75)
				H 5.37	5.29	1250	3.93 (*s*,3H,CH_3O—C)
				P 12.69	12.37	1050	6.8–8.0(*m*-5H,H aromatic)

*Pure, after distillation.
†Atmospheric pressure.
‡Chemical shifts in δ p.p.m., TMS internal standard; coupling constants in Hz.
§AA′BB′ spectrum, positions of the four main peaks given.

TABLE 2. Tosylhydrazones, $ArC(NNHTs)P(O)(OCH_3)_2$

Ar	$ArCOP(O)(OCH_3)_2$ weight (g)	$ArCP(O)(OCH_3)_2$ ‖ NNHTs weight (g)	M.p.* (°C)	Analysis	
				Calcd.	Found
p-CH_3O—C_6H_4—	24	30	115–117	C 49.39	49.38
				H 5.11	5.07
				N 6.77	7.11
				P 7.49	7.45
p-CH_3—C_6H_4—	14	22	157–158	C 51.38	51.21
				H 5.32	5.34
				N 7.05	7.40
				P 7.79	7.77
p-Br—C_6H_4—	20	25	125–127	C 41.56	41.25
				H 3.92	4.02
				N 6.05	6.14
				P 6.70	6.88
				Br 17.30	17.16
o-CH_3O—C_6H_4	20	23	117–118	C 49.39	49.36
				H 5.11	5.12
				N 6.77	7.07
				P 7.49	7.46

*All compounds recrystallized from methanol.

pump). The acid chloride was then distilled under 0.2–0.5 Torr pressure.

Two procedures were followed to prepare the ketophosphonates.

(*i*) *For solid acid chlorides*: Trimethyl phosphite (1.2 mol/mol of acyl halide) was added dropwise to a cooled solution (ice bath) of the acid chloride in anhydrous benzene (20–30 ml). The addition was completed in 1.0–1.5 h. The reaction mixture was allowed to stand for 24 h at room temperature under nitrogen, and then distilled under reduced pressure.

(*ii*) *For liquid or syrupy acid chlorides*: An analogous procedure was followed except that no benzene was used.

The data on the α-ketophosphonates are summarized in Table 1.

(b) Tosylhydrazones

A solution of the ketophonate in methanol (50 ml) was added in small portions to a solution of an equimolar amount of tosylhydrazide in methanol (50–70 ml). After standing for 24 h at room temperature, the resulting solution was reduced in volume under vacuum and the precipitated tosylhydrazone was filtered off and washed with methanol. Table 2 summarizes the results.

(c) Diazo Compounds

The tosylhydrazone was dissolved in 100–150 ml of water to which an equimolar amount of sodium carbonate had been added. The resulting solution was stirred vigorously for 24 h at room temperature and the diazo compound was then obtained by extraction with ether. (More diazo compound could be obtained if extraction from the same solution is repeated after 48h.) Purification was effected by column chromatography on silica gel (Silica Gel 60, Merck, 70-203 mesh ASTM) using ether as the only eluent. Data on the diazo compounds are given in Table 3.

Dimethyl p-nitrophenyldiazomethyl phosphonate (5)

This compound was prepared according to a procedure devised by Regitz and co-workers (5) for preparation of the diethyl analog.

Anal. Calcd. for $C_9H_{10}N_3O_5P$: N, 15.50; P, 11.42. Found: N, 15.80; P, 11.25.

I.r. ($CHCl_3$): 2100 (C=N_2), 1600 (aromatic), 1270 (P=O), 1050 cm^{-1} (P—O—C).

Nuclear Magnetic Resonance Studies

The p.m.r. spectra were obtained in dilute $CDCl_3$ solution on a Varian HA-100 Spectrometer operated in the "frequency sweep" mode. Proton decoupled ^{13}C.m.r. spectra were run at 25.15 MHz using the above spectrometer equipped with a VK-3512-1 Heternuclear Noise Decoupler and a V-3530 wide sweep accessory. A C-1024 Computer of Averaged Transients was used for accumulation. Both "noise decoupled" and "off-resonance decoupled" spectra were obtained from 1 *M* solutions in dioxan.

Results and Discussion

The p.m.r. parameters of the α-ketophosphonates are summarized in Table 1. Proton and C-13 chemical shifts and coupling constants of the aryldiazoalkanephosphonates are listed in Tables 4 and 5. No attempt has been made to analyze the aromatic region of the proton spectra. Both the proton chemical shift (3.80 ± 0.05 p.p.m.) of the methoxyl group bound to phosphorus and the phosphorus–proton coupling constant ($^3J_{POCH}$ = 12.0 ± 0.1 Hz) are insensitive to the substituent on the aromatic ring. These values are similar to

Can. J. Chem. Downloaded from www.nrcresearchpress.com by 210.87.254.42 on 09/05/12
For personal use only.

TABLE 3. Diazophosphonates, $ArC(N_2)P(O)(OCH_3)_2$

Ar	$ArCP(O)(OCH_3)_2$ ‖ NNHTs weight (g)	$ArC(N_2)P(O)(OCH_3)_2$* weight (g) (color)	Analysis		I.r. (cm^{-1}) (C=N_2, P=O, P—O—C)
			Calcd.	Found	
p-CH_3O—C_6H_4—	14	8 (dark red oil)	C 46.70	46.59	2090
			H 5.10	5.36	1245
			N 10.89	10.56	1040
			P 12.04	11.76	
p-CH_3—C_6H_4—	16	8.7 (red oil)	C 49.79	50.12	2080
			H 5.43	5.62	1260
			N 11.61	11.94	1040
			P 12.84	12.70	
p-Br—C_6H_4—	15	7.5 (orange–red oil)	C 35.43	35.66	2090
			H 3.30	3.54	1250
			N 9.18	9.02	1040
			P 10.15	10.33	
			Br 26.19	25.89	
o-CH_3O—C_6H_4—	10	3.7 (yellow oil, solidifies on standing)	C 46.70	47.00	2090
			H 5.10	5.33	1250
			N 10.89	10.57	1040
			P 12.04	12.26	

*Yield after chromatography.

TABLE 4. P.m.r. data of some aryldiazoalkanephosphonates

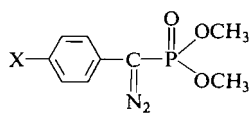

X	δ* OCH_3(P)	δ_X	δ Aromatic	$J_{P-O-C-H}$ (Hz)	J_{CH} (Hz)
OCH_3	3.79_8	3.79_3	6.84–7.16	12.0	148.5 (144.0)
CH_3	3.78_8	2.31_2	6.98–7.25	11.9	148.5
H	3.79_0		7.03–7.45	12.0	148.5
Br	3.80_0		6.95–7.84	12.0	148.5
NO_2	3.85_0		7.20–8.26	12.0	148.5
o-OCH_3	3.77_5	3.85_2	6.79–7.10	12.0	148.0 (144.5)

*P.p.m. from internal TMS; dilute solution in $CDCl_3$.

those obtained in Marmor and Seyferth (2) for alkyl and vinyl dimethyl-phosphono substituted diazoalkanes of general formula $RC(N_2)P(O)(OMe)_2$, and suggest that the substituents have little effect on the nature of the P—O—C—H bonding. This is supported by the constancy of $^1J_{CH}$ for the phosphono methoxyl groups (148.5 Hz for all the para-substituted compounds and 148.0 Hz for the ortho-substituted compound). The values of $^1J_{CH}$ were obtained from ^{13}C satellites in the p.m.r. spectra.

The resonance positions of the aromatic carbon atoms were determined from the multiplicity (in the off-resonance decoupled spectra) and the known substituent effects on the aromatic carbon chemical shifts (7). The signal due to C-7 is readily recognized by the C—P splitting while the methoxyl carbon atoms are at higher field and show a small coupling (5 Hz) to phosphorus.

The range of values for the chemical shift of the benzylic carbon (C-7, 56.9–77.2 p.p.m. from CS_2) is consistent with an sp^2 carbon atom: Feasible canonical forms include **7–10**.

If **9** is a dominant canonical form, the resonance of the benzylic carbon should be at a

Can. J. Chem. Downloaded from www.nrcresearchpress.com by 210.87.254.42 on 09/05/12
For personal use only.

TABLE 5. Carbon-13 chemical shifts* of some aryldiazoalkanephosphonates

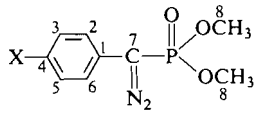

X	C-1	C-2,6	C-3,5	C-4	C-7	C-8	C-X
OCH_3	77.3	67.8	77.3	34.4	74.5	139.9	137.6
CH_3	69.5	69.4	62.7	57.6	68.9	140.0	172.3
H	67.9	69.6	67.4	63.4	65.3	140.0	
Br	60.44	67.83	60.23	61.35	65.95	139.8	
NO_2	62.7	69.9	68.1	47.5	56.9	139.5	
(o-OCH_3)					(77.2)	(140.0)	(137.1)

*P.p.m. from CS_2; 1 M solution in dioxan.

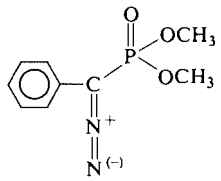

7

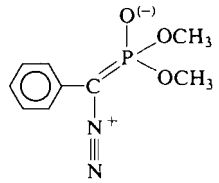

8

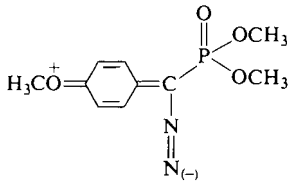

12

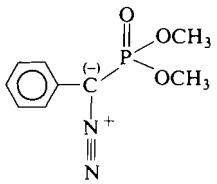

9

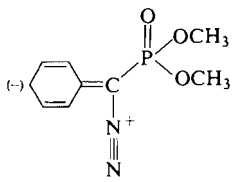

10

much higher field than observed. For example, in benzyl lithium ($C_6H_5CH_2Li$) the benzylic carbon absorbs at 163 p.p.m. upfield from CS_2 (8). The deshielding effect of the p-nitro group can be rationalized in terms of stabilization of **11**, in which the negative charge is distant from the benzylic carbon. The observed shielding effect of the p-methoxy group can be explained in terms of **12**, in which the center of positive charge is removed from the region of C-7. An analogous rationale holds for the shielding effect of the o-methoxy substituent.

Support for some double bond character in

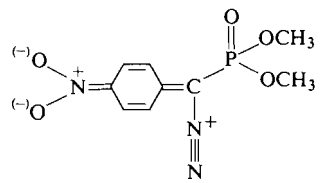

11

the C–aryl bond can be found in the HMO calculations of Schuster and Polansky (9) on phenyl diazomethane. These authors reported (*i*) π-bond contribution to the C–aryl bond, (*ii*) negative charges at both the carbon and nitrogen termini of the diazomethane moiety, and (*iii*) appreciable charge delocalization into the aromatic ring. Further support may be derived from the J_{CH} coupling found by Kaplan and Meloy (10) in compounds **13**. The value of 199 Hz is consistent with an sp^2 carbon adjacent to an electron-withdrawing group. In these

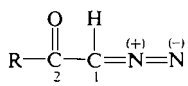

13

cases, the double bond character in the C_1—C_2 bond is enough to account for a rotational barrier of 10 kcal mol^{-1}.

The Nature of the C—P Bond

The ^{13}C–^{31}P coupling constants range from 8.2 Hz for the p-OMe case to 12.3 Hz in the p-NO_2 compound. Although the small magnitude clearly indicates considerable π-character in the C—P bond (11), more detailed interpretations are not feasible. pπ–dπ carbon–phosphorus bonding in phosphonates has been proposed previously by Seyferth *et al.* (1) on the

Can. J. Chem. Downloaded from www.nrcresearchpress.com by 210.87.254.42 on 09/05/12
For personal use only.

basis of i.r. data while Berlin and Burpo (12) drew the same inference from u.v. spectral data of acylphosphonates.

Correlation with Reactivity

Various studies indicate that the behavior of diazoalkanes in cycloaddition to alkenes is predominantly nucleophilic (13) with electron-withdrawing groups reducing the reaction rates. In a recent study (14) the addition of compounds **1**–**6** to norbornadiene has been examined. After 24 h, reactions with **1**–**4** are 90% complete while that with **5** is 75% complete. The only member of the series to show appreciable difference in reaction rate (only 11% after 24 h) is **6**. It seems that, at least for this series of additions, steric factors are more significant than perturbations of electron density caused by substituents on the aromatic ring.

Financial support from the National Research Council of Canada is gratefully acknowledged.

1. D. SEYFERTH, P. HILBERT, and R. S. MARMOR. J. Am. Chem. Soc. **89**, 4811 (1967).
2. R. S. MARMOR and D. SEYFERTH. J. Org. Chem. **36**, 128 (1971).
3. D. SEYFERTH, R. S. MARMOR, and P. HILBERT. J. Org. Chem. **36**, 1379 (1971).
4. J. E. CADOGAN. Quart. Rev. **22**, 222 (1968).
5. M. REGITZ, W. ANSCHUTZ, and A. LIEDHEGENER. Chem. Ber. **101**, 3734 (1968).
6. H. COHEN and C. BENEZRA. In preparation.
7. G. C. LEVY and G. L. NELSON. Carbon-13 nuclear magnetic resonance for organic chemists. Wiley Interscience, New York. 1972.
8. R. WAACK, M. A. DORAN, E.B. BAKER, and G. A. OLAH. J. Am. Chem. Soc. **88**, 1272 (1966).
9. P. SCHUSTER and O. E. POLANSKY. Monatsh. Chem. **96**, 396 (1965).
10. F. KAPLAN and G. K. MELOY. Tetrahedron Lett. 2427 (1964).
11. O. A. GANSOW and B. Y. KIMURA. Chem. Commun. 1621 (1970); GEORGE A. GRAY. J. Am. Chem. Soc. **93**, 2132 (1972).
12. K. D. BERLIN and D. H. BURPO. J. Org. Chem. **31**, 1304 (1966).
13. C. K. INGOLD. Structure and mechanism in organic chemistry. 2nd Ed. Cornell University Press, Ithaca, N.Y. 1969.
14. C. BENEZRA and H. COHEN. J. Org. Chem. Submitted for publication.

Can. J. Chem. Downloaded from www.nrcresearchpress.com by 210.87.254.42 on 09/05/12
For personal use only.

Can. J. Chem. Downloaded from www.nrcresearchpress.com by 210.87.254.6 on 09/05/12
For personal use only.

COMMUNICATIONS

Radical Substitutions of Azo Compounds

HENRY LUI AND JOHN WARKENTIN
Department of Chemistry, McMaster University, Hamilton, Ontario
Received December 20, 1972

Treatment of γ-(*p*-nitrophenylazo)-γ-valerolactone with benzoyl peroxide in benzene at 85°, yields *p*-nitroazobenzene and *p*-nitrobiphenyl. Similarly, α-methyl-α-phenylazotetrahydrofuran yields azobenzene. Radical substitution at azo nitrogen and at N-bearing benzenoid carbon are the suggested mechanisms. Such reactions of aryl azo compounds have not been reported previously.

Le traitement du γ-(*p*-nitrophénylazo)-γ-valérolactone par le peroxyde de benzoyle dans le benzène à 85° conduit au *p*-nitroazobenzène et *p*-nitrobiphényle. De la même manière, l'α-méthyl-α-phényl azotétrahydrofurane conduit à l'azobenzène. La substitution radicalaire sur l'azote de l'azo et sur l'azote porteur du carbone benzénoide a été le mécanisme suggéré. De telles réactions sur les composés azo aryles n'ont pas été rapportées jusqu'à présent.

[Traduit par le journal]

Can. J. Chem., 51, 1148 (1973)

Reactions of radicals with organic, organometallic, and inorganic compounds include substitution at a wide variety of atoms representing many groups of the periodic table (1). Both one step (eq. 1) and two step substitutions (eq. 2) are well known mechanisms.

[1] $A\cdot + D - E \rightarrow AD + E\cdot$

[2] $A\cdot + D - E \rightarrow ADE\cdot \rightarrow AD + E\cdot$

The chemistry of nitrogen compounds does not include one step, radical substitution at that atom (1) (eq. 1, D = N), despite the attractive energetics for displacement at nitrogen of hydrazines (1). Examples of radical substitution at unsaturated nitrogen, by the addition–elimination mechanism (eq. 2), include vapor-phase nitration of methane with nitric acid (1, 2), formation of nitrosomethane dimer from reaction of methyl radicals with nitrites (1, 3–7), and reaction of alkoxy radicals with *C*-nitroso compounds to form alkyl nitrites (1, 8, 9). Some chain reactions of benzoyl azide (10) and phenyl azide (11) with stannanes and of phenyl azide with organosilicon hydrides (12) may also involve such substitution (1), *e.g.*, eq. 3.

[3] $Bu_3Sn\cdot + C_6H_5CO{-}N{=}\overset{+}{N}{=}\overset{-}{N} \rightarrow$

$$C_6H_5CO{-}\underset{\displaystyle SnBu_3}{\underset{|}{N}}{-}\overset{+}{\dot{N}}{=}\underset{-}{N} \rightarrow C_6H_5CO{-}\dot{N}{-}SnBu_3 + N_2$$

Notably absent from the list is substitution at azo nitrogen[1] (eq. 4). Although hyponitrites, sulfonyl azo compounds, and azo thio ethers

[4] $R\cdot + R'{-}N{=}N{-}R'' \rightarrow$

$$\begin{matrix}R'\\R\end{matrix}\!\!>N{-}\dot{N}{-}R'' \rightarrow R'\cdot + R{-}N{=}N{-}R''$$

react rapidly in radical chain processes with trialkyltin hydrides, they do so by radical addition at oxygen or sulfur, not at nitrogen (14–16). In the only reported case of probable radical substitution at azo nitrogen (17), that mechanism was invoked to account for a minor amount (4%) of an azo compound (eq. 4, R = R″ = CH_3, R′ = $CH_2CH{=}CH_2$).

In aryl azo systems, radical aromatic substitution is an additional possibility. Although homolytic displacement of hydrogen and various other aromatic substituents (*e.g.* Cl, Br, I) is known (18), we have not found examples in which the leaving group is an azo function (eq. 5).

[5] $R{-}N{=}N{-}C_6H_4Y + R'\cdot \rightarrow$

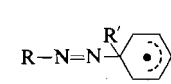

$$R{-}N{=}N{-}\overset{R'}{C_6H_4}{-}Y \rightarrow R\cdot + N_2 + R'C_6H_4Y$$

[1]There is precedent for the first step of eq. 4. Both gas and liquid phase additions to azo compounds, forming substituted hydrazines, have been reported (13).

Can. J. Chem. Downloaded from www.nrcresearchpress.com by 210.87.254.6 on 09/05/12
For personal use only.

We wish to report both types (eqs. 4, 5) of radical substitutions of aryl azo compounds. The experiments described below were undertaken when a minor product from thermolysis of γ-phenylazo-γ-valerolactone (**1**a) was identified as azobenzene (19).

A solution of **1**a (50 mg, 0.25 mmol) and benzoyl peroxide (**2**, 170 mg, 0.70 mmol) in benzene (4 ml) was degassed and heated at 85° in a sealed tube for 17 h. Analysis by g.l.p.c. (S.E. 30, 5%, 5 ft × 1/4 in., 155°) gave: **1**a, 40%; azobenzene, 37% (based on **1**a consumed); and biphenyl. From 1.48 g of **1**a and 5.09 g of **2** in benzene (50 ml) there was isolated, by column chromatography on neutral alumina, 0.41 g, (31%) of azobenzene.

Similarly **1**c (1.25 g, 7.0 mmol) and **2** (5.08 g, 21.0 mmol) in benzene (30 ml) gave, by g.l.p.c. following extraction with bicarbonate solution: **1**c, 57%; azobenzene, 14% (based on **1**c consumed); biphenyl; and phenylbenzoate. In a second run carried to 70% conversion of **1**c, the yield of azobenzene was 12%.

Analogous treatment of **1**b (400 mg, 1.60 mmol) with **2** (1.2 g, 5.0 mmol) in benzene (7 ml) left 10% **1**b unreacted and gave *p*-nitroazobenzene (80 mg, 24%), *p*-nitrobiphenyl (140 mg, 48%), and small amounts of compounds thought to be isomeric nitro terphenyls, on the basis of mass spectra. Qualitative experiments showed that *p*,*p*′-dinitroazobenzene also reacts with phenyl radicals in benzene to produce *p*-nitrobiphenyl.

Control experiments showed that compounds **1** are thermally stable in the reaction conditions. Therefore, the only plausible mechanisms which account for the observed products are those of eqs. 4 and 5. Biphenyl formation from **1**a and c, if it occurs, is obscured by biphenyl formation from benzoyl peroxide.

Recognition of these substitutions as mechanistic possibilities may be important in the further elucidation of the chemistry of azo compounds; the Gomberg–Bachmann reactions, for example. The reactions may be of synthetic value also, for the accessibility of aroyl peroxides and azo substrates (**1**) (20) and the absence of isomeric impurities may make up for the modest yields of unsymmetric diaryl azo compounds and biphenyls.

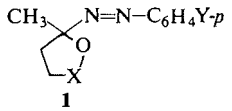

1

a X = CO; Y = H
b X = CO; Y = NO_2
c X = CH_2; Y = H

This work was supported by the National Research Council of Canada.

1. K. U. Ingold and B. P. Roberts. Free-radical substitution reactions. Wiley-Interscience, John Wiley and Sons, New York, N.Y. 1970.
2. T. S. Godfrey, E. D. Hughes, and C. K. Ingold. J. Chem. Soc. 1063 (1965).
3. M. S. Kharasch, T. H. Meltzer, and W. Nudenburg. J. Org. Chem. **22**, 37 (1957).
4. P. Gray. Chem. Ind. (London), 120 (1960).
5. P. Gray and P. Rathbone. Proc. Chem. Soc. 316 (1960).
6. B. Jest and L. Phillips. Proc. Chem. Soc. 73 (1960).
7. B. Bromberger and L. Phillips. J. Chem. Soc. 5302 (1961).
8. A. Mackor, Th. A. J. W. Wajer, Th. J. de Boer, and J. D. W. vanVoorst. Tetrahedron Lett. 385 (1967).
9. A. Mackor, Th. A. J. W. Wajer, and Th. J. de Boer. Tetrahedron, **24**, 1623 (1968).
10. M. Frankel, D. Wagner, D. Gertner, and A. Zilkha. J. Organometal. Chem. **7**, 518 (1967).
11. H. Schumann and S. Ronecker. J. Organometal. Chem. **23**, 451 (1970).
12. F. A. Carey and C. W. Hsu. Tetrahedron Lett. 3885 (1970).
13. (*a*) O. P. Strausz, R. E. Berkeley, and H. E. Gunning. Can. J. Chem. **47**, 3470 (1972). (*b*) M. S. Kharasch, M. Zimmerman, W. Zimmt, and W. Nudenberg. J. Org. Chem. **18**, 1045 (1953). (*c*) O. F. Olaj, J. W. Breitenbach, and I. Hofreiter. Rec. Chem. Prog. **30**, 87 (1969).
14. W. P. Neumann and H. Lind. Angew. Chem. **79**, 52 (1967).
15. W. P. Neumann and H. Lind. Chem. Ber. **101**, 2837 (1968).
16. W. P. Neumann, H. Lind, and G. Alester. Chem. Ber. **101**, 2485 (1968).
17. R. J. Crawford and K. Takagi. J. Am. Chem. Soc. **94**, 7406 (1972).
18. G. Sosnovsky. Free radical reactions in preparative organic chemistry. The Macmillan Co., New York, N.Y. 1964. pp. 308–313.
19. H. Lui and J. Warkentin. Can. J. Chem. **50**, 1767 (1972).
20. G. B. Gubelt and J. Warkentin. Can. J. Chem. **47**, 3983 (1969).

Can. J. Chem. Downloaded from www.nrcresearchpress.com by 210.87.254.40 on 09/05/12
For personal use only.

Canadian Journal of Chemistry

Published by
THE NATIONAL RESEARCH COUNCIL OF CANADA

Journal canadien de chimie

Publié par
LE CONSEIL NATIONAL DE RECHERCHES DU CANADA

Volume 51 Number 8 April 15, 1973

Volume 51 numéro 8 15 avril 1973

On the Bond Order between Atoms in Approximate SCF-MO Theory

R. J. BOYD[1]

Mathematical Institute, Oxford 0X1 3LB, England

Received September 12, 1972

The bond order between two atoms is discussed within the framework of all-valence-electron SCF-MO theories based on the Zero-Differential Overlap Approximation, and a definition of the bond order is proposed which is analogous to the procedure used to extract charge distributions from approximate SCF-MO calculations. Bond orders are calculated for a variety of small molecules and relationships similar to those found in π-electron theory between bond lengths and bond orders are observed. CNDO wave functions are used in this work, although the definition may also be used for calculations based on the INDO and NDDO approximations.

L'ordre de liaison entre deux atomes a été discuté dans le cadre des théories SCF-MO appliquées à tous les électrons de valence et basées sur l'approximation du recouvrement différentiel zéro; une définition de l'ordre de liaison a été proposée semblable au procédé utilisé dans l'extraction des distributions de charge à partir des calculs SCF-MO. Les ordres de liaison ont été calculés pour toute une variété de petites molécules et des relations, semblables à celles tirées de la théorie des électrons π, entre longueurs et ordres de liaisons, ont été observées. Les fonctions d'onde CNDO ont été utilisées dans ce travail bien que notre définition puisse être également appliquée dans les calculs basés sur les approximations INDO et NDDO.
[Traduit par le journal]

Can. J. Chem., 51, 1151 (1973)

The bond order concept has been studied in detail, at several levels of approximation, in the molecular orbital theory of π-electron systems (1). In general, the bond order associated with two atoms varies inversely with the interatomic distance and is regarded as a measure of the strength of a bond. The extensive development of the Hückel molecular orbital theory and the more sophisticated theories of conjugated molecules has established the bond order as a well-known concept of chemistry. Furthermore the formal bond order of the qualitative molecular orbital description of homonuclear diatomic molecules, defined as one half the excess of electrons in bonding orbitals over electrons in antibonding orbitals (2), is consistent with the chemist's view of single, double, and triple bonds. The purpose of this discussion is to propose a definition of the bond order between two atoms in all-valence-electron SCF-MO theories based on the neglect of differential overlap (3).

Definition

In MO theories which treat only the π-electrons explicitly, a single bond order is computed between two atoms which have valence-shell p orbitals available for bonding. Although the π-bond order may be defined in more than one way (4), the situation is much simpler than in all-valence-electron SCF theories. In the latter case, there may be more than a single atomic orbital in the basis set for each of the two atoms of interest, hence there may be many matrix elements in the charge-density and bond-order matrix **P** between the atomic orbitals of the two

[1]Present address: Department of Chemistry, University of British Columbia, Vancouver.

atoms. The **P**, or population, matrix is defined by

$$[1] \qquad P_{kl} = 2 \sum_{i}^{occ} C_{ki}{}^{*} C_{li}$$

where the summation is over occupied molecular orbitals only and C_{ki} is the coefficient of the kth atomic orbital in the ith molecular orbital. The conventional basis set consists of a 1s orbital for hydrogen and valence shell s and p orbitals for the other elements, and therefore if neither of the two atoms is hydrogen, a 4×4 submatrix of the **P** matrix is formed. It is perhaps reasonable to expect that the bond order between the two atoms should be related to the elements of this submatrix. It is not satisfactory, however, to simply sum the P_{kl} for all orbitals k on atom A and l on atom B because the P_{kl} are not necessarily invariant to rotations of the coordinate system. The electronic energy, orbital energies, and charge distributions are, of course, invariant (3) but only the P_{kl} between s orbitals and the trace of the submatrix are invariant.

In order to illustrate the invariance properties of the submatrices of the **P** matrix, it is convenient to consider some CNDO calculations (5) on carbon monoxide. Tables 1 and 2 list the submatrix for two of the many possible choices of coordinates. If the bond order were defined as the sum of the elements of the submatrix, the two orientations would give very different numerical values and, in fact, the bond order could even be negative (Table 2). Clearly the computed bond order should not depend on the orientation of the molecule with respect to the coordinate system. Nor is it reasonable to perform a Mulliken population analysis (6) to obtain the gross overlap population between the two atoms because the overlap of atomic orbitals is not included in the orthonormality condition for the molecular orbitals in SCF-MO theories which invoke the ZDO approximation (3). That is, the Mulliken population analysis is applicable to MO's which satisfy the condition

$$[2] \qquad \mathbf{C}\dagger\mathbf{S}\mathbf{C} = \mathbf{I}$$

but MO's based on the ZDO approximation satisfy the condition

$$[3] \qquad \mathbf{C}\dagger\mathbf{C} = \mathbf{I}$$

where **C**, **S**, and **I** are the coefficient, overlap, and unit matrices, respectively. Wiberg (7) has suggested that the sum of the squares of the P_{kl} for all orbitals k on atom A and l on atom B be used as an index for the character of a bond between atoms A and B. It is easily shown that Wiberg's index does not suffer from the invariance difficulty but it seems rather arbitrary to relate the bond order between two atoms to the squares of the bond orders between the orbitals of the two atoms.

TABLE 1. Submatrix for CO*

	2s(C)	$2p_x$(C)	$2p_y$(C)	$2p_z$(C)
2s(O)	0.2396	0.5137	0.0	0.0
$2p_x$(O)	−0.3211	−0.6885	0.0	0.0
$2p_y$(O)	0.0	0.0	0.8677	0.0
$2p_z$(O)	0.0	0.0	0.0	0.8677

*C at origin and O at (1.128,0,0), r_{CO} = 1.128 Å.

TABLE 2. Submatrix for CO*

	2s(C)	$2p_x$(C)	$2p_y$(C)	$2p_z$(C)
2s(O)	0.2396	0.2966	0.2966	0.2966
$2p_x$(O)	−0.1854	0.3490	−0.5187	−0.5187
$2p_y$(O)	−0.1854	−0.5187	0.3490	−0.5187
$2p_z$(O)	−0.1854	−0.5187	−0.5187	0.3490

*C at origin and O at (a,a,a), $3a^2 = r_{CO}{}^2$.

In view of the above discussion, the following definition is proposed for the bond order between two atoms, neither of which is hydrogen, in all-valence-electron SCF theories. It is suggested that the bond order be defined as the sum of the diagonal elements of the submatrix defined above, subject to the conditions that the submatrix has been block-diagonalized and that the sign of the matrix element between the p orbitals directed along the coordinate axis coincident with the line joining the atoms in the transformed orientation (corresponding to the block-diagonalized submatrix) is changed. The requirement that the submatrix be block-diagonalized eliminates the difficulty of deciding which orientation to choose. In the case of a linear molecule, the submatrix is block-diagonalized if the line joining the atoms lies along, or is parallel with, one of the axes of the coordinate system. Thus the submatrix of CO is block-diagonalized in Table 1 but not in Table 2. The second condition is necessary since the orbital bond order of interest is negative or positive depending on whether the net interaction is bonding or antibonding between the orbitals, as Pople and Segal (8) have noted. The importance of this condition for CO is illustrated by the submatrix in Table 1.

Can. J. Chem. Downloaded from www.nrcresearchpress.com by 210.87.254.40 on 09/05/12
For personal use only.

Can. J. Chem. Downloaded from www.nrcresearchpress.com by 210.87.254.40 on 09/05/12
For personal use only.

A similar situation is found for most molecules and usually the bond orders of σ-bonds are unrealistically small if the second condition of the above definition is ignored.

Calculation of Bond Orders

The submatrix cannot be block-diagonalized directly but rather it is necessary to operate on the entire population matrix. The block-diagonalization may be performed by an appropriate orthogonal transformation of the basis set. Thus if the original basis set is transformed to a new set, the new and original matrices, $\mathbf{P}'$ and $\mathbf{P}$, are related by

$$\mathbf{P}' = \mathbf{OPO}^{-1} \qquad [4]$$

where $\mathbf{O}$ is an orthogonal transformation matrix. Now if we rotate about the x axis by 45° and about the y axis by 54.7°, the $\mathbf{P}$ matrix for carbon monoxide which contains the submatrix of Table 2 will be transformed so that the new submatrix is identical with the one listed in Table 1. This procedure is easily programmed and provides a convenient method for calculating the bond order between two atoms. Complete details and a FORTRAN program are available upon request.

Bond orders calculated by means of the above definition are listed in Table 3 for a variety of molecules. The π and σ components of the bond order between two atoms are denoted by P_π and P_σ and their sum, the total bond order, by P_t. The results are based on some CNDO calculations (5), although it should be stressed that the conclusions of this discussion would not be altered if the INDO or NDDO approximations were used instead of the CNDO approximation. Furthermore the main points of this discussion would not be altered if a different set of parameters were used in the CNDO method, although, of course, the actual numerical values calculated for the bond order will depend on the parameters.

TABLE 3. Bond orders*

Molecule†	P_π	P_σ	P_t
B_2	1.00	0.00	1.00
C_2	2.00	0.00	2.00
N_2	2.00	1.00	3.00
N_2^+	2.00	0.50	2.50
O_2	1.00	1.00	2.00
O_2^+	1.50	1.00	2.50
F_2	0.00	1.00	1.00
F_2^+	0.50	1.00	1.50
CN	1.89	0.49	2.38
BF	0.98	0.67	1.65
CO	1.74	0.93	2.67
CS	1.72	1.00	2.72
NO	1.42	0.99	2.41
SO	1.00	0.96	1.96
ClF	0.00	0.97	0.97
HCN (C—N)	1.96	0.82	2.78
CO_2 (C—O)	1.26	0.83	2.09
NNO (N—N)	1.83	0.83	2.66
NNO (N—O)	0.79	0.78	1.57
OCS (C—O)	1.39	0.90	2.29
OCS (C—S)	1.20	0.79	1.99
BF_3 (B—F)	0.33	0.90	1.23
C_2H_2 (C—C)	2.00	0.86	2.86
C_2H_4 (C—C)	1.00	1.08	2.08
C_2H_6 (C—C)	0.00	1.18	1.18
C_2HO(C—O)	0.94	1.18	2.12

*Calculated with parameter set 1 of ref. 5.
†The bond orders for polyatomic molecules refer to the bonds in parentheses.

Discussion

The total bond orders of homonuclear diatomic molecules and their ions are identical with the values obtained by taking one half of the excess of electrons in bonding orbitals over electrons in antibonding orbitals. This is a consequence of the symmetry constraints imposed on the coefficients of the molecular orbitals in A_2 molecules. The bond orders of heteronuclear diatomic molecules are not constrained by symmetry so that the bond orders for AB molecules are not restricted to integral and half-integral values, although as in the case of the other molecules listed in Table 3 the calculated bond orders seem to be reasonable. Thus, the trends observed for the bond orders of the N_2, CO, and BF isoelectronic sequence and the C_2H_2, C_2H_4, and C_2H_6 hydrocarbon sequence correlate with the experimentally observed trends for bond lengths and force constants. These results are similar to the relationships between bond lengths and bond orders observed in π-electron theory (9). Similar observations can be made for the other bond orders listed in Table 3. As a consequence of such relationships, the bond order concept might be expected to provide a convenient means for the discussion of the lengths and strengths of bonds in large molecules where even with semi-empirical all-valence-electron methods it may not be practical to calculate equilibrium geometries and harmonic force constants.

It is worth noting that if the bond order is computed by means of Wiberg's index (7), the π-bond orders are 0.5, 2.0, 2.0, 0.5, and 0.0 and

the σ-bond orders are 1.15, 1.08, 1.00, 1.00, and 1.00 for B_2, C_2, N_2, O_2, and F_2, respectively. The Wiberg index appears to underestimate π-bonding in some situations and to overestimate σ-bonding in others with the result that the bond order of C_2 is predicted to be comparable to that of N_2. Similarly the Wiberg index suggests that the bond in the C_2 molecule is stronger than the C—C bond in acetylene contrary to the observed harmonic force constants of 12.2 and 16.3 mdyn/A for C_2 (10) and C_2H_2 (11) respectively, although the Wiberg index appears to give reasonable results for the C_2 hydrocarbons (2.94, 2.01, and 1.02 for C_2H_2, C_2H_4, and C_2H_6, see also ref. 12).

The definition of the bond order between two atoms, as proposed in this discussion, does not include the off-diagonal elements of the block-diagonalized submatrix. This may appear to be a serious omission because the interaction of an s orbital on one atom and a p orbital on a second atom can contribute to the formation of a bond between the two atoms provided the overlap of the two orbitals is not zero by symmetry. After allowing for the signs of the interactions, the inclusion of the off-diagonal elements would increase the σ-bond order by about 0.8 in CO (see Table 1) and by amounts ranging from 0.6 in F_2 to 1.5 in B_2 for the homonuclear diatomic molecules. Similarly the σ-bond order of the hydrocarbons in Table 3 would be approximately doubled. Clearly, the effect of including the off-diagonal elements can be quite large. However these terms are omitted here because the definition proposed above leads to bond orders which seem chemically reasonable in view of the preceding discussion. Furthermore the exclusion of the off-diagonal elements is analogous to the procedure commonly used for carving up the charge distribution in approximate SCF-MO theories based on the ZDO approximation. Thus atomic charges are normally obtained from the diagonal elements of the **P** matrix.

And finally it should be mentioned that the definition may be applied to bonds between two atoms where one of the atoms is hydrogen. In this case it is necessary to consider a 1×4 submatrix and the bond order is obtained by adding the elements of the submatrix once it has been reduced to the form $(a\ b\ 0\ 0)$ with the sign of the second element being taken into account. The bond order for through space H–H interactions is simply equal to the invariant P_{kl} matrix element between the 1s orbitals on the H atoms.

The author would like to thank Professor C. A. Coulson, F.R.S., Dr. James P. Snyder, and Dr. M. A. Whitehead for helpful discussions and their interest in this work. The award of a National Research Council of Canada Postdoctorate Fellowship is gratefully acknowledged.

1. L. SALEM. The molecular orbital theory of conjugated systems. Benjamin, New York. 1966.
2. C. A. COULSON. Valence. 2nd ed. Oxford University Press, London. 1962.
3. J. A. POPLE, D. P. SANTRY, and G. A. SEGAL. J. Chem. Phys. **43**, S129 (1965).
4. C. A. COULSON and R. G. A. R. MACLAGEN. Adv. Chem. Phys. **21**, 303 (1971). R. G. A. R. MACLAGEN. Mol. Phys. **22**, 821 (1971).
5. R. J. BOYD and M. A. WHITEHEAD. J. Chem. Soc. Dalton, 73 (1972); 78, (1972); 82 (1972).
6. R. S. MULLIKEN. J. Chem. Phys. **23**, 1833 (1955).
7. K. B. WIBERG. Tetrahedron, **24**, 1083 (1968).
8. J. A. POPLE and G. A. SEGAL. J. Chem. Phys. **43**, S136 (1965).
9. C. A. COULSON. J. Phys. Chem. **56**, 311 (1952).
10. G. HERZBERG. Spectra of diatomic molecules. Van Nostrand, Princeton, N.J. 1950.
11. J. W. NIBLER and G. C. PIMENTEL. J. Mol. Spectrosc. **26**, 294 (1968).
12. J. W. MCIVER, JR., P. COPPENS, and D. NOWAK. Chem. Phys. Lett. **11**, 82 (1971).

Can. J. Chem. Downloaded from www.nrcresearchpress.com by 210.87.254.40 on 09/05/12
For personal use only.

On the Assignment of the Infrared Spectrum of Ethylene Oxide

JOHN E. BERTIE AND DAVID. A. OTHEN[1]

Department of Chemistry, University of Alberta, Edmonton, Alberta

Received September 18, 1972

In the infrared spectrum of gaseous ethylene oxide the A_1 C—H stretching and CH_2 wagging modes are assigned at 3018 and 1148 cm^{-1}, respectively. The previous assignment of the B_1 ring deformation mode at about 890 cm^{-1} is not consistent with the spectrum, but its correct assignment is not clear. The infrared spectrum of ethylene oxide liquid and the frequencies of the fundamental modes in the gas and liquid states are presented.

Dans le spectre infrarouge de l'oxyde d'éthylène gazeux, la bande d'élongation A_1 de C—H et les modes d'oscillation du CH_2 ont été attribués respectivement à 3018 et 1148 cm^{-1}. L'attribution précédente sur la déformation B_1 du cycle à environ 890 cm^{-1} n'est pas compatible avec le spectre mais son attribution exacte n'a été éclaircie. Le spectre infrarouge de l'oxyde d'éthylène liquide et les fréquences de vibrations fondamentales de l'état gazeux et liquide ont été présentés. [Traduit par le journal]

Can. J. Chem., **51**, 1155 (1973)

Introduction

The infrared spectrum of gaseous ethylene oxide has been assigned three times in recent years (1–3). If allowance is made for the unavoidably lower frequency accuracy and resolution of the earlier work (1), the three assignments agree for all modes except the A_1 C—H stretch, the A_1 CH_2 wag, and the B_1 ring deformation. The A_1 C—H stretch has not been identified in the spectrum of the gas and has been assigned by two (2, 3) groups as being coincident with the B_1 C—H stretch. The A_1 CH_2 wag has been assigned only from Raman or infrared spectra of the liquid, while the B_1 ring deformation has been assigned at about 890 cm^{-1} (1, 2) and at 876 cm^{-1} (3). In the course of a study of the infrared spectrum of ethylene oxide clathrate hydrate (4), the spectrum of gaseous ethylene oxide was obtained under higher resolution than appears to have been achieved before. This spectrum has enabled the A_1 C—H stretch and the A_1 CH_2 wag to be assigned, and has shown that the assignment of the B_1 ring deformation at 890 cm^{-1} is not consistent with the spectrum.

The infrared spectrum of liquid ethylene oxide has been partially tabulated in the literature (3) but no spectrum has been published. This paper therefore includes the infrared spectrum of liquid ethylene oxide at 210 ± 5 °K.

[1]Present address: Atlantic Regional Laboratory, National Research Council of Canada, Halifax, Nova Scotia.

Experimental

Matheson 99.7% ethylene oxide was triply distilled in vacuum from −40 °C before use. Gaseous samples were held at ambient temperature in a 10 cm path length, glass, gas cell fitted with cesium iodide windows using glyptal cement. Liquid samples were condensed into an evacuable space between cesium iodide windows held in a metal cryostat of conventional design and were maintained at 210 ± 5 °K. The path length is uncertain but the cesium iodide windows were held apart by a brass or mylar spacer 0.002 or 0.010 in. thick. The spectra were recorded on a Beckman I.R. 12 spectrophotometer, which was calibrated to ±0.5 cm^{-1} below 2000 cm^{-1} and ±1 cm^{-1} above 2000 cm^{-1} using water vapor, ammonia, carbon dioxide, and hydrogen chloride (5). The gaseous samples were studied at 0.5 cm^{-1} resolution, and the liquid samples at 1.5 cm^{-1} resolution.

Results and Discussion

Ethylene oxide belongs (6) to Shimanouchi's (7) type 23, with 100 frequency divisions (7) equalling about 64 cm^{-1}. Thus an A_1 vibration yields a B type band with the two broad Q branches about 12 cm^{-1} apart, a B_1 vibration yields the PQR-structured A type band with the P–R separation equal to about 40 cm^{-1}, and a B_2 vibration yields the PQR-structured C type band with a P–R separation of about 54 cm^{-1} (6, 7). These predictions neglect the variation of the rotational constants with vibrational state, but this is not believed to significantly effect the conclusions drawn in this paper.

Figure 1 shows the infrared spectrum of gaseous ethylene oxide between 2960 and 3160 cm^{-1}. The assignment of the B_2 asymetric CH_2

Can. J. Chem. Downloaded from www.nrcresearchpress.com by 210.87.254.6 on 09/05/12
For personal use only.

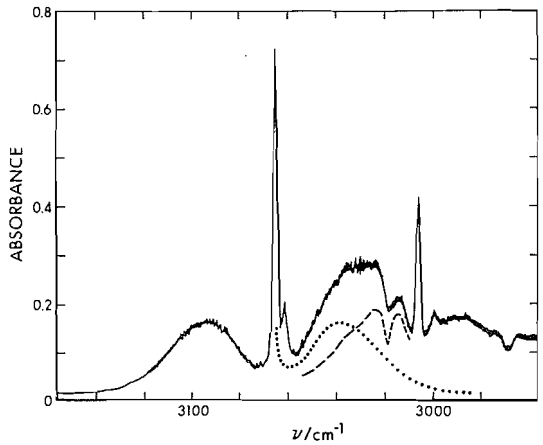

FIG. 1. Solid line, the infrared spectrum of gaseous C_2H_4O at 300 °K; 10 cm path length and 1.7 cm of mercury pressure. Dotted line, the mirror image of the R branch of the 3065.2 cm^{-1} band. Dashed line, the curve obtained by subtracting the dotted line from the observed spectrum, showing the presence of a *B* type band at 3018 cm^{-1}.

stretch at 3065.2 cm^{-1} and the B_1 symmetric CH_2 stretch at 3005.9 cm^{-1} is unambiguous. Subtraction of the P branch, indicated by the dotted line in Fig. 1, which is the mirror image of the R branch of the 3065.2 cm^{-1} band, from the observed spectrum leaves the dashed line shown in Fig. 1. The shape of the dashed line indicates the presence of a *B* type band at 3018 cm^{-1}, which can be immediately assigned to the A_1 symmetric CH_2 stretching mode. The deduction of the presence of this *B* type band does not depend upon the above subtraction. In the spectrum of gaseous ethylene oxide the only feature that causes an increase in absorbance such as is seen just above 3018 cm^{-1} in Fig. 1 is the rise to one of the Q branches of a *B* type band. Further support for this identification is that the two resulting Q branches are about 10 cm^{-1} apart, compared to the 12 cm^{-1} expected for a *B* type band.

The assignment of the A_1 symmetric CH_2 stretch at 3018 cm^{-1} and of the B_1 symmetric CH_2 stretch at 3005.9 cm^{-1} is consistent with the assignment of the corresponding modes in methylene cyclopropane (8) where the A_1 mode is at 2999.3 cm^{-1} and the B_1 is at 2996.0 cm^{-1}. Further support for this assignment comes from the infrared spectra of liquid (Fig. 2) and enclathrated ethylene oxide (4). The liquid shows a strong band at 3003 cm^{-1} which has a slight but definite shoulder at about 3014 cm^{-1} while in ethylene oxide clathrate hydrate at 100 °K distinct lines are resolved at 2998 and 3014 cm^{-1}.

The solid line in Fig. 3 shows the infrared spectrum of ethylene oxide gas in the region of 1150 cm^{-1}. This has been interpreted in terms of one *A* type band and one *C* type band only (1–3). The two features on the high frequency sides of the two strong Q branches strongly suggest the existence of a *B* type band in this region. The dotted line in Fig. 3 represents the *B* type band observed at 1270.3 cm^{-1} drawn with suitable intensity. Subtraction of this dotted curve from the observed spectrum yields the residual band shown as the dashed line in Fig. 3. This residual band can be readily interpreted in terms of an *A* type band at 1150.6 cm^{-1} and a *C* type band at 1142.0 cm^{-1}. The R branches of these two bands overlap to yield the peak at 1170 cm^{-1}, while the P branch of the *A* type band at 1150.6 cm^{-1} causes the peak at 1135 cm^{-1} and the P branch of the *C* type band at 1142.0 cm^{-1} causes the peak at 1117 cm^{-1}. Some distortion is evident in the residual bandshape, but this could well arise from imperfections in the bandshapes assumed. It seems clear that the A_1 CH_2 wag can be assigned to a *B* type band at 1148 cm^{-1} in the spectrum of ethylene oxide gas.

This assignment must rest on the merits of the arguments presented above and on the fact that no other band of significant intensity appears in the spectrum between 900 cm^{-1} and the ring breathing mode at 1270 cm^{-1}. In the Raman spectrum of the liquid this mode is clearly identified by the polarized line at 1122 ± 2 cm^{-1}, with the B_1 and B_2 modes at 1151 cm^{-1} (1, 3). The infrared spectrum of the liquid shows the same bands as the Raman spectrum, while the infrared spectrum of the clathrate shows ethylene oxide absorption at 1123 and 1147 cm^{-1}. Thus, an argument against the assignment of the A_1 CH_2 wag at 1148 cm^{-1} in the infrared spectrum of the gas is the gas-to-liquid frequency shift of about −25 cm^{-1} that it implies. This argument is not compelling, however, because the B_2 CH_2 rock appears to shift by −22 cm^{-1} from 821.2 cm^{-1} in the gas (refs. 1–3 and this work) to 799 cm^{-1} in the liquid (ref. 3 and this work).

Figure 4 shows the infrared spectrum of ethylene oxide gas in the region of 850 cm^{-1}. The A_1 ring deformation is unambiguously assigned to the *B* type band at 876.9 cm^{-1}, and the Q branch of an *A* or *C* type band clearly occurs at

Can. J. Chem. Downloaded from www.nrcresearchpress.com by 210.87.254.6 on 09/05/12
For personal use only.

Can. J. Chem. Downloaded from www.nrcresearchpress.com by 210.87.254.6 on 09/05/12
For personal use only.

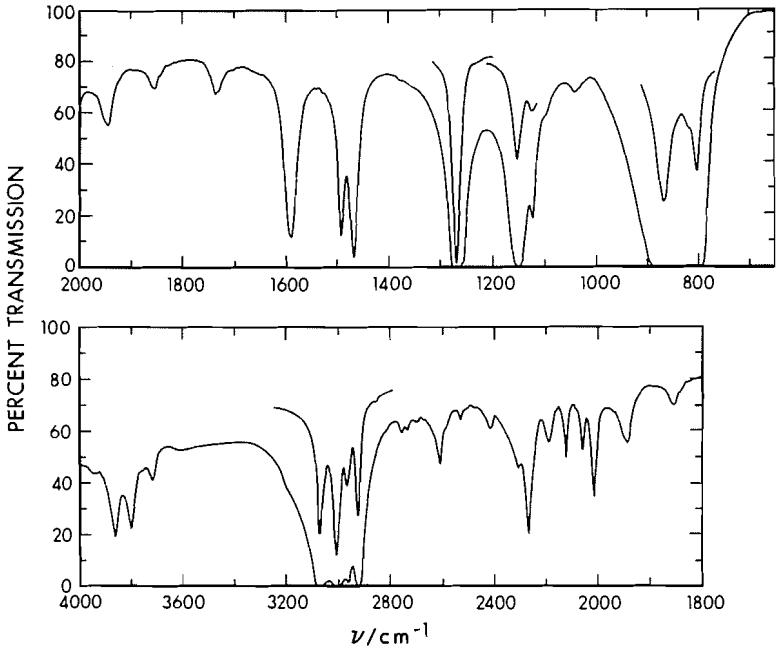

FIG. 2. The infrared spectrum of liquid ethylene oxide at 210 °K.

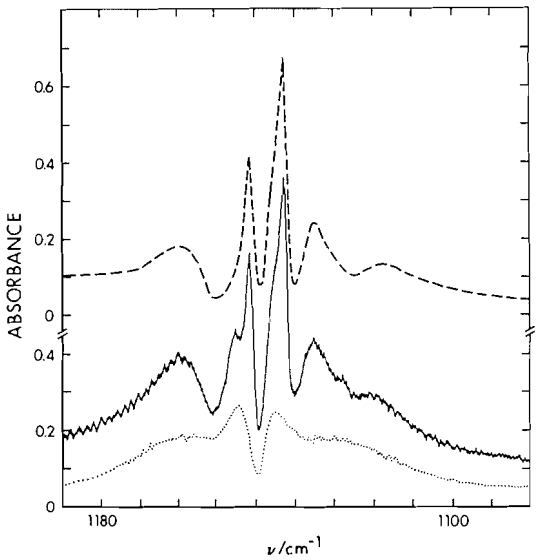

FIG. 3. Solid line, the infrared spectrum of gaseous C_2H_4O at 300 °K; 10 cm path length and 30 cm of mercury pressure. Dotted line, the *B* type band at 1270.3 cm^{-1} drawn with appropriate intensity. Dashed line, the curve obtained by subtracting the dotted curve from the observed spectrum.

821.2 cm^{-1} and has been assigned to the B_2 CH_2 rock (1–3). Earlier authors (1, 2) have assigned the B_1 ring deformation to a feature at about 890 cm^{-1}, but clearly this region contains only the *B* type band. Aleksanyan and co-workers (3) assigned the B_1 ring deformation at 876 cm^{-1} in the infrared spectrum of the solid, and the 867 cm^{-1} Raman line of the liquid is depolarized, suggesting that the B_1 ring deformation is indeed very close to the A_1 ring deformation at this frequency. On this basis the most reasonable assignment for the B_1 ring deformation in the infrared spectrum of the gas is to propose that the Q branch of its *A* type band coincides with the lower frequency Q branch of the *B* type band, at about 872 cm^{-1}. The broad peak at about 855 cm^{-1} is at about the right frequency for the P branch of the *A* type band, but its R branch is not detectable.

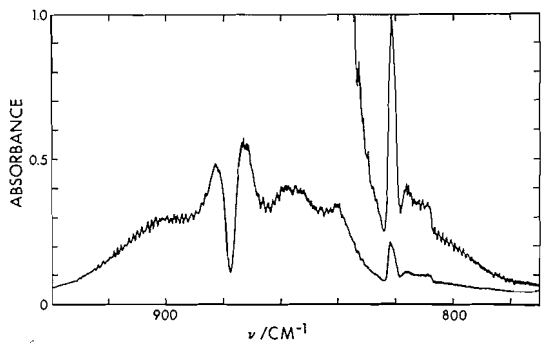

FIG. 4. The infrared spectrum of gaseous C_2H_4O at 300 °K; 10 cm path length and 1.7 and 8.7 cm of mercury pressure.

TABLE 1. The frequencies in cm^{-1} of the fundamental vibrations of ethylene oxide

Assignment			Frequency (cm^{-1}) Gas	Liquid
CH stretch	A_1	ν_1	3018	3014
	A_2	ν_6	—	—
	B_1	ν_9	3005.9	3003
	B_2	ν_{13}	3065.2	3072
CH_2 deformation	A_1	ν_2	1498.4	1492
	B_1	ν_{10}	1471.9	1468
Ring vibration	A_1	ν_3	1270.3	1268
	A_1	ν_5	876.9	864
	B_1	ν_{12}	872	864
CH_2 wag	A_1	ν_4	1148	1124
	B_1	ν_{11}	1150.6	1150
CH_2 rock	A_2	ν_8	—	815
	B_2	ν_{15}	821.2	799
CH_2 twist	A_2	ν_7	—	—
	B_2	ν_{14}	1142.0	1150

Many questions remain to be answered concerning this region of the spectrum. The lowest frequency fundamental is at 821.2 cm^{-1}. Therefore hot bands and difference bands should be exceedingly weak at 300 °K, and it is not at all obvious what transitions could contribute to the spectrum between 780 and 860 cm^{-1} apart from the fundamentals. Yet the spectrum in this region is unexpectedly complicated (Fig. 4), with sharp increases in absorption at about 808 and 818 cm^{-1}, and a weak but definite maximum at 840 cm^{-1}. Further, very weak Q branches occur at 1626, 1636, 1643.1, and 1648 cm^{-1} in the spectra of our samples. Even if the possible frequencies of the A_2 modes is considered no assignment of these frequencies is obvious from the present assignment of the fundamentals.

For convenience, the frequencies obtained in this work for the fundamental modes of ethylene oxide in the gas and liquid states are given in Table 1.

We thank the National Research Council of Canada for their support of this work and for a scholarship to one of us (D.A.O.).

1. R. C. LORD and B. NOLIN. J. Chem. Phys. **24**, 656 (1956).
2. W. J. POTTS. Spectrochim. Acta, **21**, 511 (1965).
3. V. T. ALEKSANYAN, E. R. RAZUMOVA, A. P. KURBAKOVA, and S. M. SHOSTAKOVSKII. Opt. Spectrosc. **31**, 369 (1971).
4. J. E. BERTIE and D. A. OTHEN. Can. J. Chem. This issue.
5. I.U.P.A.C. Tables of Wavenumbers for the Calibration of Infrared Spectrometers. Butterworths Scientific Publications, London. 1961.
6. G. L. CUNNINGHAM JR., A. W. BOYD, R. J. MYERS, W. D. GWINN, and W. I. LEVAN. J. Chem. Phys. **19**, 676 (1951).
7. T. UEDA and T. SHIMANOUCHI. J. Mol. Spectrosc. **28**, 350 (1968).
8. J. E. BERTIE and M. G. NORTON. Can. J. Chem. **48**, 3889 (1970).

Can. J. Chem. Downloaded from www.nrcresearchpress.com by 210.87.254.6 on 09/05/12
For personal use only.

The Infrared Spectrum of Ethylene Oxide Clathrate Hydrate at 100 °K between 4000 and 360 cm^{-1}

JOHN E. BERTIE AND DAVID. A. OTHEN[1]

Department of Chemistry, University of Alberta, Edmonton, Alberta

Received September 18, 1972

The infrared spectra of characterized samples of ethylene oxide hydrate made from 100% H_2O, 99.7% D_2O, and several dilute isotopic solutions, are presented between 4000 and 360 cm^{-1}. The similarity between the absorption by the water molecules in the hydrate and in ice I is discussed. The frequency and halfwidth of the OH and OD stretching modes of isolated HDO molecules in the hydrate are related to those in the disordered ice phases; the frequencies correlate rather well with the weighted-mean hydrogen bond lengths in these phases.

The ethylene oxide vibrations show sharp, single-line absorption. The only exceptions are the ring-breathing mode which appears as a doublet, separated by 2 cm^{-1}, with much weaker absorption about 13 cm^{-1} away on either side, and the ring deformation modes which interact with the $\nu_R(H_2O)$ modes. The possible causes of this behavior are discussed, but no firm conclusions can be drawn. The sharpness of the absorption by enclathrated ethylene oxide, compared to that by liquid ethylene oxide, is briefly discussed in the light of modern theories of bandshapes in liquids.

Les spectres infrarouge des échantillons caractérisés d'hydrate d'oxyde d'éthylène composé de 100% H_2O, 99.7% D_2O et de diverses solutions diluées isotopiques, sont rapportés entre 4000 et 360 cm^{-1}. La similitude de l'absorption par les molécules d'eau dans l'hydrate et dans la glace I a été discutée. La fréquence et la largeur à mi-hauteur des modes d'élongation du OH et OD des molécules isolées de HDO dans l'hydrate ont été reliées à celles des phases désordonnées de la glace ; la corrélation des fréquences est plutôt bonne avec la moyenne pondérée des liaisons hydrogène dans ces phases. Les vibrations de l'oxyde d'éthylène se présentent sous la forme d'une raie simple et fine. Les seules exceptions proviennent des modes d'élongation du cycle qui donnent un doublet séparé de 2 cm^{-1} en plus d'une absorption beaucoup plus faible de part et d'autre de ce doublet dont l'écart est d'environ 13 cm^{-1} ; et, les modes de distorsions qui entrent en interaction avec les modes $\nu_R(H_2O)$. Les causes possibles de ce phénomène ont été discutées mais aucune conclusion ferme n'a pu être tirée. La finesse de l'absorption du clathrate de l'oxyde d'éthylène, comparée à celle de l'oxyde d'éthylène liquide, a été brievement discutée en fonction des théories modernes sur les formes de bandes dans les liquides.

[Traduit par le journal]

Can. J. Chem., **51**, 1159 (1973)

Introduction

The far infrared spectrum of ethylene oxide hydrate at 100 °K has recently been published (1). This paper presents the spectrum of the same compound between 4000 and 360 cm^{-1}. These two papers report the first extensive study of well-characterized samples of a clathrate hydrate. The relevant literature has been summarized previously (1).

Experimental

The experimental methods used in this work have been reported (1). For the present work some samples were prepared by condensing excess ethylene oxide into an evacuated flask containing de-gassed water, and allowing crystallization to proceed to completion at 5 °C, while the remaining samples were prepared by the methods described earlier (1). Method *ii* of ref. 1 was found to yield the purest hydrate samples.

Cesium iodide windows were used in the infrared cells, and the spectra were recorded using a Beckman I.R. 12 spectrophotometer fitted with a fiducial marker. The marks were calibrated to ± 0.4 cm^{-1} below 2000 cm^{-1} and ± 1.0 cm^{-1} above 2000 cm^{-1} using the standard gases (2). The resolution was generally 1.5 cm^{-1} but individual bands were studied at 0.5 cm^{-1} resolution. For many of the spectra the transmission scale was expanded using the Beckman variable scale expansion facility. Propane, propylene, and Freon 13 were used as mulling agents. The sample temperature was very close to the melting point of Freon 13, 92 °K, and is cited as 100 $\pm$ 10 °K to allow for slight heating which was applied to keep the Freon 13 in the liquid state. This temperature is consistent with that measured at the copper block which contained the sample and windows. The X-ray camera was calibrated using sodium chloride at room temperature (3).

Results and Assignment

The X-ray photographs clearly characterized the samples as the structure **1** clathrate hydrate,

[1]Present address: Atlantic Regional Laboratory, National Research Council of Canada, Halifax, Nova Scotia.

Can. J. Chem. Downloaded from www.nrcresearchpress.com by 210.87.254.6 on 09/05/12
For personal use only.

Can. J. Chem. Downloaded from www.nrcresearchpress.com by 210.87.254.6 on 09/05/12
For personal use only.

and gave the unit cell parameter as 11.88 ± 0.03 Å for the hydrate and 11.90 ± 0.03 Å for the deuterate at about 120 °K. The presence of ice or solid ethylene oxide impurity was detected in some samples, enabling the spectral effect of these impurities to be determined, as discussed later.

The infrared spectra of ethylene oxide hydrate and deuterate in the three mulling agents at 100 °K are shown in Figs. 1 and 2, while, for convenience, Fig. 3 shows the spectra of the hydrate and deuterate deduced from these original spectra. The frequencies of the features in the spectra are listed in Table 1, along with their relative intensities and assignments. The frequency accuracy is about ±5 cm^{-1} for the bands due to water, except as noted in the table, ±1 cm^{-1} for the stronger, and ±2 cm^{-1} for the less intense, ethylene oxide bands. The assignment of the features to water or ethylene oxide absorption follows from the isotope shift of the water absorptions.

The detailed assignment of the H_2O and D_2O absorption follows immediately from that for ice I (4). The absorption by the water molecules in the clathrate is extremely similar to that in ice I, as illustrated by the $\nu_{OH}(H_2O)$ and $\nu_{OD}(D_2O)$ bands, which resemble poorly resolved bands of ice I, and the $\nu_R(D_2O)$ band which is almost identical to that in ice I. The $\nu_R(H_2O)$ band in the clathrate is complicated by ethylene oxide absorption at 800 and 860 cm^{-1}. The presence of small amounts of ice I in the samples caused no detectable change in the absorption by H_2O or D_2O, and the same experimental techniques reproduced the published (4) spectra of ice I perfectly, so the similarity between the spectrum of the clathrate and that of ice I does not arise from error. The condensation of water vapor onto the cell windows during assembly is easily eliminated by proper technique, and does not influence the spectra presented. The peak at 3277 cm^{-1} in the spectra of the deuterate (Figs. 2 and 3) is due to $\nu_{OH}(HDO)$ and not to ice.

The detailed assignment of the ethylene oxide absorptions follows in general from that of pure ethylene oxide (5). In the first spectra recorded the only ethylene oxide absorptions clearly seen were the 1268 cm^{-1} band in the hydrate and those at 872, 1268, and about 3000 cm^{-1} in the deuterate. The remaining bands were only detected by repeated study using all three mulling agents and expansion of the transmission scale. Except for the combination bands between 2900 and 2980 cm^{-1} only the fundamental transitions were observed, and the corresponding absorption is shown in Fig. 4. Only the 1268 cm^{-1} band was clearly observable in the spectra of both the hydrate and the deuterate, the remainder being more or less masked by the water absorption in one of the two spectra. It is noteworthy that in spite of this overlap with either the H_2O or the D_2O absorption, only the absorption near to 870 cm^{-1} shows a significant frequency shift or change in shape between the spectra of the hydrate and deuterate. The greatest frequency shift for the other bands is 3 cm^{-1} at 3066 cm^{-1}, and this undoubtedly arises from the difficulty of measuring this band in the hydrate on the side of the intense water absorption.

The authenticity of the absorptions shown in Fig. 4 as bands due to enclathrated ethylene oxide is proved by comparison with the spectra of liquid and solid ethylene oxide (5–7) and of the clathrate hydrate containing solid ethylene oxide impurity. The absorption by the clathrate is sharper than that by liquid ethylene oxide, the halfwidths ranging from 2 to 5 cm^{-1} in general (Fig. 4), and does not show the factor group splitting seen in the spectrum of the solid (6, 7).

The band at 3069 cm^{-1} has a half-width of 10 cm^{-1}, much greater than that of any other ethylene oxide band. This band is assigned to the B_2 C—H stretching mode of ethylene oxide, and it seems probable that the breadth is due to the A_2 mode which is activated by the low site symmetry in this disordered solid. The 1260–1270 cm^{-1} region shows the only fine structure seen in the spectrum. Under 1.5 cm^{-1} resolution this band (Fig. 4) shows a peak and a weak shoulder, but under 0.4 cm^{-1} resolution the doublet shown in Fig. 4 is obtained. At this resolution the noise level is high and, for clarity, the curve presented has been smoothed to show only the reproducible features. Only one fundamental, the ring breathing mode, is expected in this region and, while the 1255 cm^{-1} feature can be assigned to the fundamental of ethylene oxide, $^{13}C^{12}CH_4O$, the origin of three other features, rather than the one expected, is unclear as discussed later. The relative intensities of the various bands in this region were studied for different samples, some of which had the uniform composition $6.7C_2H_4O.46H_2O$ and some of which had the average stoichiometry $6.4C_2H_4O$

Can. J. Chem. Downloaded from www.nrcresearchpress.com by 210.87.254.6 on 09/05/12
For personal use only.

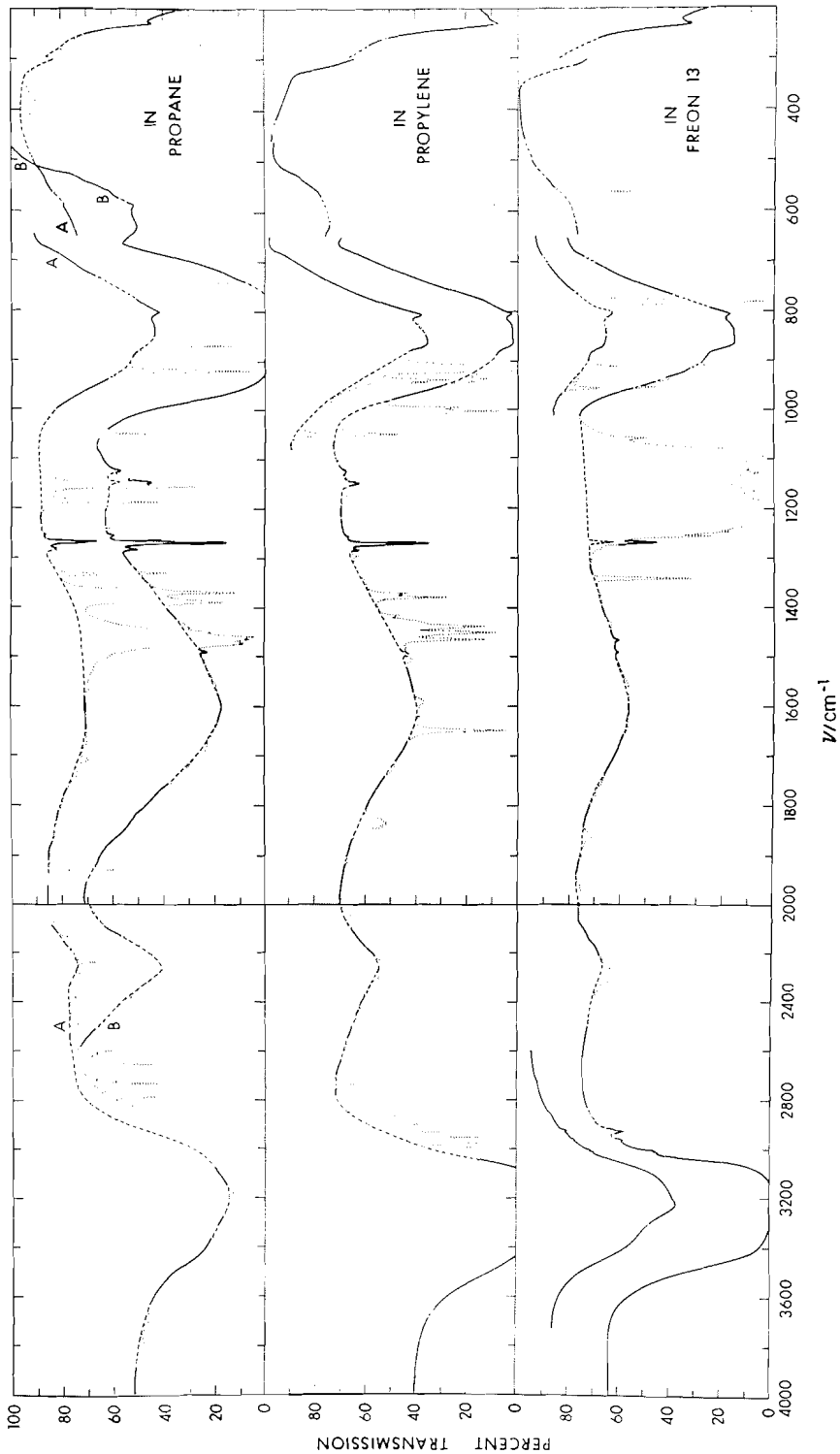

FIG. 1. The infrared spectrum of ethylene oxide hydrate at 100 °K as a mull in propane (upper), propylene (middle), and Freon 13 (lower). The dashed lines show the hydrate absorption deduced in regions where it is obscured by the mulling agent absorption (dotted lines).

Can. J. Chem. Downloaded from www.nrcresearchpress.com by 210.87.254.6 on 09/05/12
For personal use only.

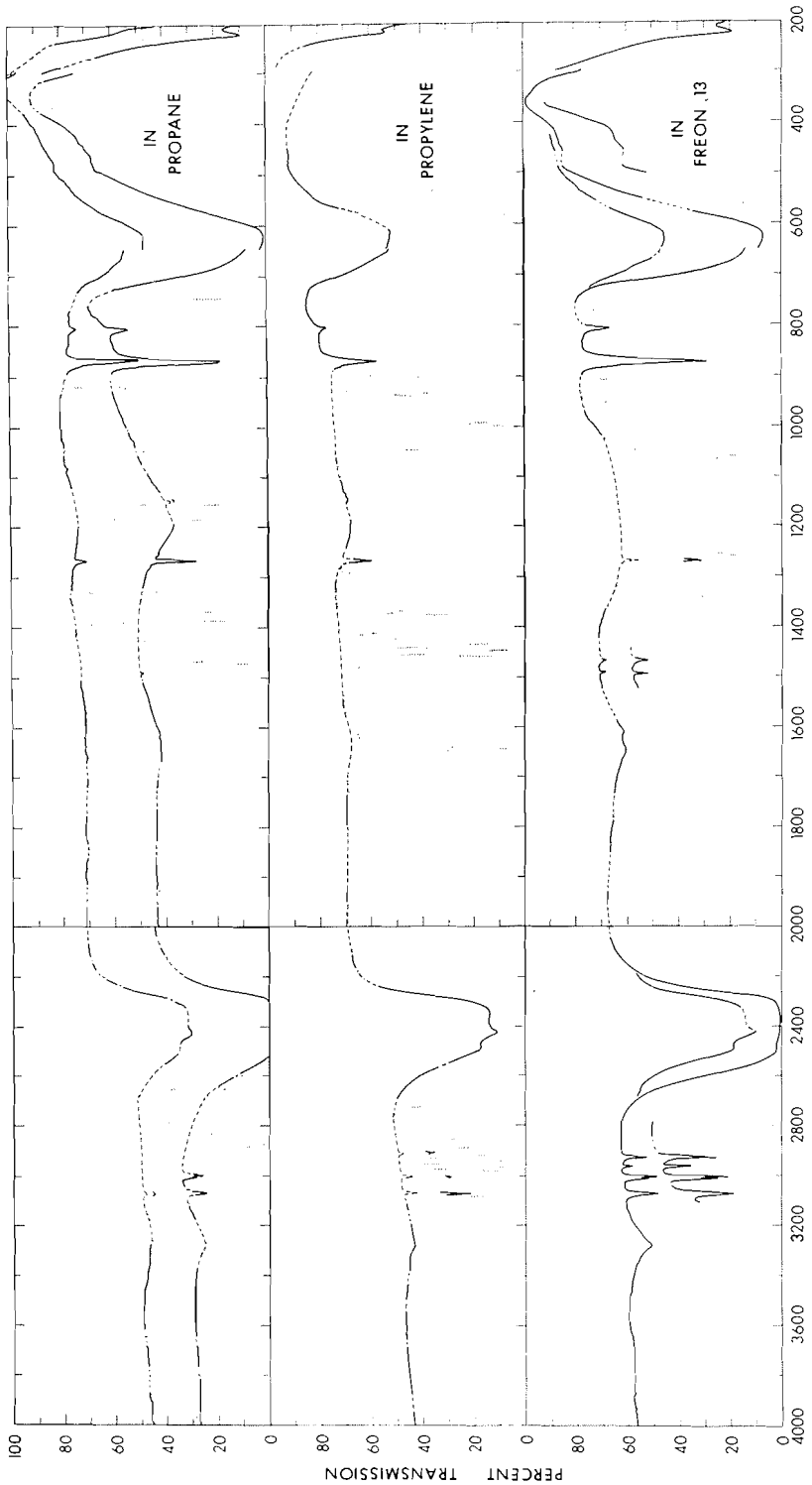

FIG. 2. The infrared spectrum of ethylene oxide deuterate (99.7% D_2O) at 100 °K as a mull in propane (upper), propylene (middle), and Freon 13 (lower). The dashed lines show the deuterate absorption deduced in regions where it is obscured by the mulling agent absorption (dotted lines).

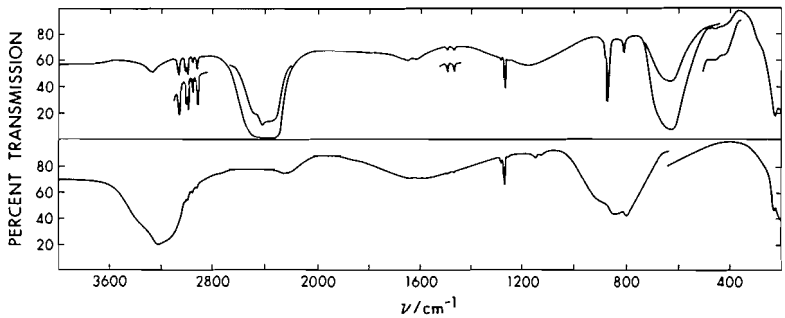

FIG. 3. The infrared spectra of ethylene oxide hydrate (lower) and deuterate (99.7% D_2O, upper), composed from original spectra such as are shown in Figs. 1 and 2.

TABLE 1. Frequencies and assignment of features in the infrared spectra of ethylene oxide hydrate and deuterate at about 100 °K*

Hydrate		Deuterate	
3400 sh 3220 vs br 3100 sh	$\nu_{OH}(H_2O)$	3272 ± 10 br	ν_{OH}(HDO)
3066 w	E.O. ν_{13}, ν_6	3069 m	
3009 w	E.O. ν_1	3008 m	
2998 w	E.O. ν_9	2999 m	
2957 w	E.O. $2\nu_2$	2958 m	
2920 w	E.O. $\nu_2 + \nu_{10}$	2922 m	
2913 vw	E.O. $2\nu_{10}$	2914 w	
2427 br	ν_{OD}(HDO)	2490 br sh 2425 br s 2333 br sh	$\nu_{OD}(D_2O)$
2250 ± 15 v br w	$\nu_2 + \nu_R$ $3\nu_R(H_2O)$		
		1630 ± 15 m br 1610 sh	$\nu_2 + \nu_R$ $3\nu_R(D_2O)$
1605 ± 20 v br m	$\nu_2(H_2O)$		
1489 w	E.O. ν_2	1491 w	
1466 w	E.O. ν_{10}	1467 w	
1282 w	E.O.	1282 w	
1270 m	E.O. ν_3	1270 m	
1268 v s	E.O. ν_3	1268 v s	
1255 v w	E.O.	1255 v w	
		1200 ± 15 w br	$\nu_2(D_2O)$
1147 w	E.O. ν_{11}, ν_{14}	1147 w	
1123 v w	E.O. ν_4	1122 v w	
890 sh	$\nu_R(H_2O)$ + E.O. ν_{12}	881 sh	E.O. ν_{12}
864 i	$\nu_R(H_2O)$ + E.O. ν_5	872 v s	E.O. ν_5
845 s br	$\nu_R(H_2O)$		
808 sh	E.O. ν_8	810 sh	
805 s	E.O. ν_{15}	807 s	
630 w sh 590 w sh? 560 w sh 530 w sh	$\nu_R(H_2O)$	680 sh 620 s br 465 w sh 422 w sh	$\nu_R(D_2O)$

*Frequencies in cm^{-1} units; E.O. = ethylene oxide, v = very, s = strong, br = broad, sh = shoulder, m = medium, w = weak, i = point of inflection.

Can. J. Chem. Downloaded from www.nrcresearchpress.com by 210.87.254.6 on 09/05/12
For personal use only.

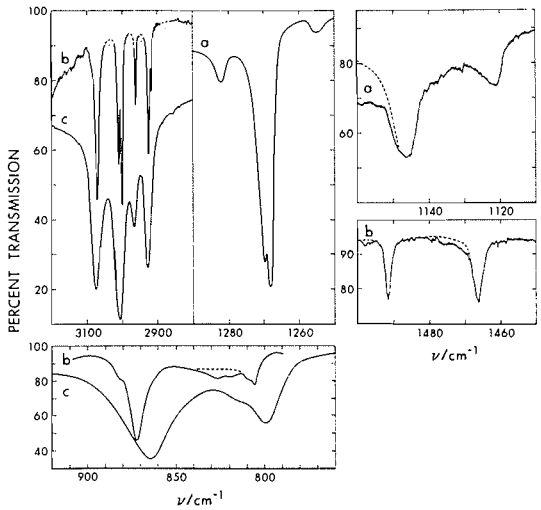

FIG. 4. Absorption by ethylene oxide in: curves (*a*) ethylene oxide hydrate at 100 °K; curves (*b*) ethylene oxide deuterate at 100 °K; curves (*c*) liquid ethylene oxide at 210 °K. The dashed lines indicate the estimated hydrate or deuterate absorption in regions where the mulling agent absorbed.

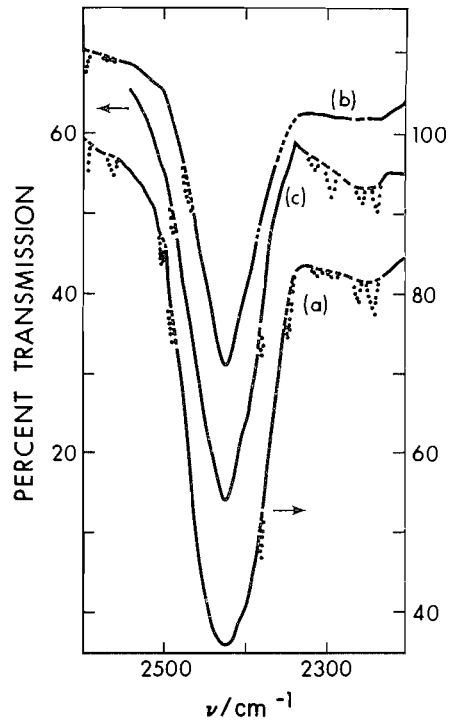

FIG. 5. Absorption by ν_{OD}(HDO) in ethylene oxide hydrate containing 5% D, 95% H. Curve (*a*) an ice-free sample, curve (*b*) a sample containing ice, curve (*c*) the sample used for curve (*a*) after holding it at −2 °C for 12 h and recooling to 100 °K. Curve (*a*) refers to the transmission scale on the right hand side and curves (*b*) and (*c*) to that on the left hand side. Curve (*c*) has been displaced by +25% T. for clarity. The dotted lines indicate mulling agent absorption.

.46H_2O, judging from the conditions of preparation (1, 8). No changes in the relative intensities were observed for different samples, but the experimental difficulties made the sensitivity such that the possibility of observing an effect in the samples available was marginal.

The assignment of the ethylene oxide bands between 800 and 900 cm^{-1} requires some comment. The features at 881, 872, and 807 cm^{-1} are assigned to the B_1 and A_1 ring deformations and the B_2 CH_2 rock, respectively, by analogy with the assignment for gas and liquid ethylene oxide. The shoulder at 810 cm^{-1} appears to be real, although it is slightly masked by mulling agent absorption (Fig. 4), and it can be assigned to the A_2 CH_2 rock. This mode has been assigned at 818 cm^{-1} in the spectrum of the solid and the liquid (7).

The infrared spectra of ethylene oxide hydrate made from dilute solutions of H_2O in D_2O or vice versa are identical to those of the pure hydrate or deuterate, except for the appearance of the ν_{OH}(HDO) or ν_{OD}(HDO) absorption, due to the OH or OD stretching mode of HDO molecules surrounded by D_2O or H_2O molecules, respectively. These absorptions proved to yield the most sensitive test for ice as an impurity in the clathrate. Curve *a* of Fig. 5 shows the ν_{OD}(HDO) band in a sample of pure clathrate formed from 95% H_2O and 5% D_2O, and curve *b* of Fig. 5 shows the same band in a sample of the same isotopic composition but containing some ice, as shown by the X-ray photographs. Curve *a* shows a peak at 2427 ± 3 cm^{-1} with a halfwidth of 80 ± 10 cm^{-1}, while curve *b* shows a more pointed peak at 2419 cm^{-1} with a halfwidth of about 65 cm^{-1}. The assignment of these differences to the influence of ice as an impurity in the clathrate was confirmed by keeping the sample used to obtain curve *a* of Fig. 5 at −2 °C for 12 h in a closed vessel and then re-cooling it to −196 °C. This procedure should have caused some decomposition of the hydrate to ice I*h*. The X-ray pattern of the original sample showed no ice lines, and after the above treatment a very weak but definite indication of the ice lines was obtained. The sample after treatment yielded curve *c* of Fig. 5, clearly proving

Can. J. Chem. Downloaded from www.nrcresearchpress.com by 210.87.254.6 on 09/05/12
For personal use only.

Can. J. Chem. Downloaded from www.nrcresearchpress.com by 210.87.254.6 on 09/05/12
For personal use only.

the assignment. These differences in the $\nu_{OD}(HDO)$ peak shape are accompanied by measureable differences in the relative intensities of the $\nu_{OD}(HDO)$ peak for a 5 atom% D sample and the 1268 cm^{-1} ethylene oxide peak. The ratio of the intensities $\nu_{OD}(HDO)/EO.1268$ is 0.8 to 0.9 for a pure sample and 1.1 for a sample containing enough ice to show clearly on the X-ray pattern, such as that used for curve *b* of Fig. 5. The sample that yielded curve *c* of Fig. 5 showed a ratio of 1.0. Similar effects were noted for the $\nu_{OH}(HDO)$ peak. These peaks in the pure compound are rather flat-topped and broad, and the measurement of their frequency and halfwidth is difficult. From a large number of spectra of samples made from 1, 2, and 5% of D_2O in H_2O the best values of the frequency and halfwidth of the $\nu_{OD}(HDO)$ peak are 2427 $\pm$ 3 cm^{-1} and 80 $\pm$ 10 cm^{-1}, respectively, while from the spectra of samples containing from 0.3 to 5% of H_2O in D_2O the corresponding values for $\nu_{OH}(HDO)$ are 3272 $\pm$ 10 cm^{-1} and 125 $\pm$ 15 cm^{-1}. The samples with the lower percentages of the impurity isotope did not show significantly smaller halfwidths than the 5% samples. The relative intensities of the band in the different samples showed that this was not due to significant uncertainty in the isotopic composition.

Discussion

Absorption by the Water

The water molecules in ethylene oxide hydrate at 100 °K are orientationally disordered and reorient extremely slowly (ref. 1 and references therein). Thus, apart from the inclusion of ethylene oxide molecules in the structure, the clathrate system is similar to ice and the discussion of the vibrational spectrum of the water molecules must parallel that for ice. The comparison of the ethylene oxide absorption frequencies, and bandshapes in so far as they can be determined, in the spectra of the hydrate and deuterate shows that the vibrations of the water molecules do not couple with those of the ethylene oxide molecules, except for the $\nu_R(H_2O)$ band which appears to interact with the ring deformation modes of ethylene oxide at about 870 cm^{-1}.

The water molecule spectrum of the deuterate, and that of the hydrate apart from the $\nu_R(H_2O)$ band, is extremely similar to that of ice I. It is not straightforward to interpret this observation in terms of the structural differences and similarities between these phases, because the detailed assignment of the features in the mid-infrared spectrum of ice I is not known (4). It is clear (4) that all crystal vibrations based on the water molecule vibrations are infrared active, and that the spectra must be related to the density of vibrational states through an intensity distribution function. A comparison of the infrared (4) and Raman (9) spectra of ice I shows that the Raman intensity distribution function is extremely asymmetric with respect to the band of OH stretching frequencies in ice. Further the infrared intensity distribution function is extremely asymmetric with respect to the band of water rotational vibrations (4, 10, 11). However, the atomic displacements that occur at frequencies corresponding to the various peaks and shoulders in the spectrum of ice are quite unknown, other than that they involve OH stretching or rotational vibrations, etc. For the $\nu_{OH}(H_2O)$ and $\nu_{OD}(D_2O)$ bands there is the added complication that the first overtone, $2\nu_2$, of the HOH or DOD angle deformation modes may gain intensity from the stretching modes through Fermi resonance and influence the spectrum significantly. $2\nu_2$ does appear to influence the Raman spectrum of liquid water (12) and the infrared spectra of H_2O dissolved in various organic bases (13), and it seems possible that it also contributes to the spectrum of ice I. However the infrared (4) and Raman (9) spectra of ice I contain many features in the region of the OH or OD stretching modes, and it is clear that an assignment in terms of ν_1, ν_3, and $2\nu_2$ is a gross oversimplification, and that the correct assignment is unknown.

Because of these uncertainties the only discussion that can be given of the spectrum of the water molecules in the clathrate is to point out certain empirical relations between the structure and spectra of the clathrate and ice I. This discussion will be limited to the influence of the different hydrogen bond lengths in the two phases. Even with this simplification the conclusions are limited and there is, therefore, no justification for including a discussion of the influence of the O—O—O angles or the effect of non-nearest neighbors, except to point out that the angles around the oxygen in the hydrate are not all tetrahedral, as they are in ice I, although the weighed mean angle is 109.6° (14).

In ice I*h* all the hydrogen bond lengths are very close to 2.75 Å at 100 °K (ref. 1 and refer-

Can. J. Chem. Downloaded from www.nrcresearchpress.com by 210.87.254.6 on 09/05/12
For personal use only.

ences therein), while in the hydrate at 100 °K 52% of the hydrogen bonds are 2.75 Å long, 26% are 2.79 Å long, and the remainder are either 2.74 or 2.82 Å long (ref. 1 and references therein). The $\nu_{OH}(H_2O)$ and $\nu_{OD}(D_2O)$ bands in the hydrate and in ice I (4) are at the same frequencies and their shapes are very similar, with the band in the hydrate resembling a poorly resolved spectrum of ice I. It is, therefore, reasonable to conclude that the bandshapes and frequencies in the clathrate are primarily determined by the 2.75 Å bonds. The breadth of the features, which causes the appearance of a poorly resolved spectrum of ice I, can then be mainly attributed to the effect of the 2.79 Å bonds with smaller effects due to the 2.74 and 2.82 Å bonds. Phenomenologically the spectra and structure of the hydrate and ice I*h* can be understood in this way, as can the corresponding relations for ice I*h* and ice I*c* (4).

Theoretically this discussion is less satisfactory, because the conclusion must be drawn that the significant differences between the nearest-neighbor distances and long range packing in the hydrate and ice I are not great enough to greatly influence the density of states or the intensity distribution function. However, Shawyer and Dean (10) have shown that the OH stretching modes in ice I*h* are quite localized as a result of the disorder. Therefore, the density of states curve and the intensity distribution curve must represent some average of the effects of the disorder over the whole crystal. It is possible that this reduces the sensitivity of the spectrum to structural changes.

The discussion of the ν_R, ν_2, and the combination bands in the hydrate must follow the above discussion, with the added comment that the $\nu_R(D_2O)$ bands in the hydrate and ice I are almost identical, and therefore the structural differences have even less effect than for the OH and OD stretching bands.

The featureless breadth of the $\nu_{OH}(HDO)$ and $\nu_{OD}(HDO)$ bands in the hydrate provides further evidence of the orientational disorder in the clathrate structure. The ratio of their frequencies is 1.350, which is consistent with the corresponding ratio for the other ices (4, 15, 16) and shows that the anharmonicity of the OH stretching vibrations is similar in all of these phases. Kamb and Prakash (17) have shown that the hydrogen bond length and the $\nu_{OD}(HDO)$ frequency in ice I do not correlate well with the corresponding

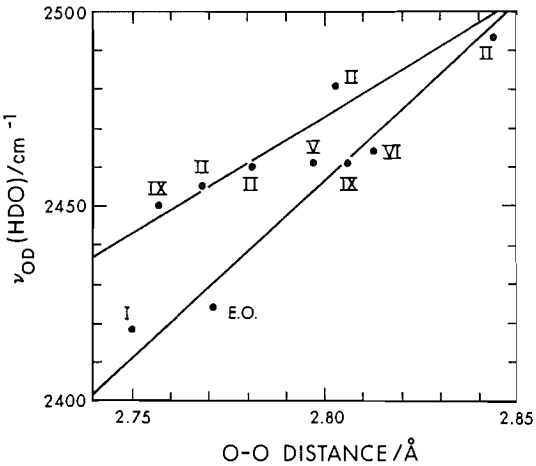

FIG. 6. Graph: $\nu_{OD}(HDO)$ *vs.* O—O distance for ordered phases or weighted-mean O—O distance for disordered phases. The Roman numerals refer to the ice phases and E.O. indicates ethylene oxide hydrate.

parameters in ices II and IX. In Fig. 6 Kamb's data (17, 18) is replotted along with the frequencies of $\nu_{OD}(HDO)$ in ethylene oxide hydrate, ice V (15) and ice VI (16) which are plotted against the weighted mean hydrogen bond length in these phases (1). As Kamb and Prakash showed (17) the four points for ice II and one of the points for ice IX lie close to a line with a slope of 510 cm^{-1} Å^{-1}. The data for ices I*h*, I*c*, V, and VI, and ethylene oxide hydrate, and one of the points for ice IX, lie further from this line, but all lie within 8 cm^{-1} of a second straight line with a slope of 910 cm^{-1} Å^{-1}. Hence a rough correlation does exist for all of the ices and the hydrate, and a rather precise correlation seems to exist for the phases that are predominantly orientationally disordered, but no exact correlation applies to both the ordered and the disordered phases.

The halfwidths of the $\nu_{OD}(HDO)$ absorptions should reflect the range of crystallographically non-equivalent bond lengths in the disordered phases. For ice I the halfwidth of about 20 cm^{-1} (19) has been related (4) to the range of O—O distances that actually exist because of the disorder in the structure, which has only one crystallographically determined hydrogen bond length (1 and references therein). If a similar width is taken to apply for each crystallographically determined bond length in the other disordered phases, then the range of such bond lengths present should be related

Can. J. Chem. Downloaded from www.nrcresearchpress.com by 210.87.254.6 on 09/05/12
For personal use only.

to the observed halfwidth of ν_{OD}(HDO) minus 20 cm^{-1}. These residual halfwidths are 60, 50, and 60 cm^{-1} for ice V (15), ice VI (16), and the hydrate, respectively. Attempts to correlate these residual halfwidths with the actual range of hydrogen bond lengths were unsuccessful, even if the multiplicity of each bond length were taken into account. However, the residual halfwidths are roughly consistent with the weighted mean deviation of the hydrogen bond lengths, which are (1) 0.021, 0.022, and 0.025 Å for ice V, VI, and the hydrate, respectively, although the halfwidth for ice V is somewhat large.

Absorption by the Ethylene Oxide

It was pointed out above that the ethylene oxide vibrations do not appear to interact with those of the water molecules except for the $\nu_R(H_2O)$ modes and the ring deformation modes at 870 cm^{-1}. In the deuterate a strong peak and a shoulder are seen at 872 and 881 cm^{-1}, respectively, while in the hydrate this peak appears to have broadened and merged with the water absorption, indicating that interaction occurs between the two vibrations. The reasons for this interaction are obscure, because no other vibrations show it even though other ethylene oxide modes coincide with strong absorption by the water, which also absorbs quite strongly throughout the entire region of study. From the structural data (14) and the van der Waal's radii of the methylene group and the oxygen atoms (20), the methylene groups are within 0.3 Å and the oxygen atom of the ethylene oxide is within 0.4 Å of being in van der Waal's contact with the water molecules of the cage. Thus a mechanical interaction between the guest and host vibrations is possible, but it is not clear why it would not also affect the other modes, particularly the methylene rocking modes at 810 cm^{-1}. An alternative, and perhaps more likely, interaction mechanism is transition dipole – transition dipole coupling. The magnitude of such coupling is proportional to the magnitude of the transition dipole and, because the 870 cm^{-1} band is the strongest ethylene oxide absorption (Fig. 2) and the $\nu_R(H_2O)$ band is very intense, it is reasonable that these two modes should be the only ones to show such interaction.

The other ethylene oxide ring vibration, the ring breathing mode, also shows complicated behavior in the spectrum of the clathrate (Fig. 4). This is the only mode that shows fine structure, showing a doublet at 1268 and 1270 cm^{-1}, and much weaker side bands at 1255 and 1280 cm^{-1}. These side bands are roughly equidistant from the strongest peak at 1268 cm^{-1}, and the low-frequency band is the weaker of the two, so their assignment as sum and difference bands with a 13 cm^{-1} energy level is possible. The far infrared study (1) did not extend to 13 cm^{-1}, and thus yielded no evidence on this point. Alternatively, the 1255 cm^{-1} band can readily be assigned as the ring breathing mode of $^{13}C^{12}CH_4O$, so the correct assignment of these features is unclear. It seems unlikely that they arise from ethylene oxide molecules in different environments to the majority, because the ring breathing mode is quite insensitive to the molecule's environment, and occurs at 1270.3, 1268, and 1266 cm^{-1} in the spectra of the gas, liquid, and solid, respectively (5).

The main absorption in this region consists of bands at 1268 and 1270 cm^{-1}, each of which must have a halfwidth of less then 2 cm^{-1}. It is clear that they cannot arise from intermolecular coupling effects because the ethylene oxide molecules are far apart, rotate at about 10^{10} c.p.s. at 100 °K (21) and are, therefore, almost certainly disordered. It is possible that they arise from site effects, that is from molecules in non-equivalent positions or orientations in the structure. In discussing this possibility it must be borne in mind that the X-ray data has been interpreted (14) as indicating two non-equivalent orientations of the molecules in the tetrakaidecahedral cages, while the fast reorientation of the molecules at low temperatures (21, 22) and energy calculations (23) both argue that the barrier to reorientation is very low and that more than two orientations are likely to exist. The energy calculations further indicate that a range of different fields exist in the different cages, because of the random orientation of the water molecules, and that the most probable value of these fields is close to the mean value, and no other particularly probable values exist (23). Ethylene oxide molecules situated in these different fields should have different vibration frequencies and one would, thus, expect a single peak to arise from this source. The breadth due to the different fields is presumably included in the halfwidth of each component of the doublet. Then the doublet must indicate

either that two distinct orientations of the guest molecules do exist in the tetrakaidecahedral cages or that the 1268 cm^{-1} peak corresponds to molecules in these cages and the 1270 cm^{-1} peak corresponds to those in the dodecahedral cages. Only about 10% of the guest molecules are believed (8, 14) to be in the dodecahedral cages, and the apparent intensity of this peak appears to argue against this latter possibility, but the argument is not compelling. This interpretation, that site effects are responsible for the doublet, is the most probable one, but if it is correct it is not clear why similar splittings are not seen on other ethylene oxide absorptions, particularly when, for example, the 1491 and 1467 cm^{-1} peaks are extremely sharp (Fig. 4), and the ring breathing mode shows the smallest frequency shift of any mode between the spectra of the gas and the condensed phases of ethylene oxide (5).

It may be significant that only the ethylene oxide ring vibrations show unusual behavior in the spectrum of the clathrate at 100 °K but no clear interpretation of this exists at present.

The halfwidths of the bands due to enclathrated ethylene oxide are much smaller than those of corresponding bands in the liquid. This is shown in Fig. 4 for the C—H stretching region and the ring deformation and methylene rocking region. At 100 °K the ethylene oxide molecules in the clathrate reorient at about 10^{10} s^{-1} (21) which is of the same order as the reorientation rate in liquids. It has been argued that the bandwidths in liquids are due wholly (24) or at least in part (25) to the rapid reorientation of the molecules. It is clear from the present data that either the bandwidth is extremely sensitive to the reorientation rate, and in the hydrate the molecules rotate significantly more slowly than in the liquid, or that molecular reorientation without intermolecular vibrational coupling or collisions of like molecules is an ineffective source of broadening. In order to obtain more evidence on this point, and on the correct assignment of the peaks around 1270 cm^{-1}, studies of the temperature dependence of the spectrum are planned.

We thank the National Research Council of Canada for their continuing support of this work and for the award of a scholarship to one of us (D.A.O.).

1. J. E. Bertie and D. A. Othen. Can. J. Chem. **50**, 3443 (1972).
2. I.U.P.A.C. Tables of wavenumbers for the calibration of infrared spectrophotometers. Butterworth's Scientific Publications, London. 1961.
3. I. Waller and R. W. James. Proc. Roy. Soc. (London), **117A**, 214 (1927).
4. J. E. Bertie and E. Whalley. J. Chem. Phys. **40**, 1637 (1964).
5. J. E. Bertie and D. A. Othen. This issue.
6. J. LeBrumant and D. Maillard. C. R. (Paris), **264B**, 1107 (1967).
7. V. T. Aleksanyan, E. R. Razumova, A. P. Kurbakova, and S. M. Shostakovskii. Opt. Spectrosc. **31**, 369 (1971).
8. D. N. Glew and N. S. Rath. J. Chem. Phys. **44**, 1710 (1966).
9. M. J. Taylor and E. Whalley. J. Chem. Phys. **40**, 1660 (1964).
10. R. E. Shawyer and P. Dean. J. Phys. C, **5**, 1028 (1972).
11. H. J. Prask, S. F. Trevino, J. D. Gault, and K. W. Logan. J. Chem. Phys. **56**, 3217 (1972).
12. W. F. Murphy and H. J. Bernstein. J. Phys. Chem. **76**, 1147 (1972).
13. D. N. Glew and N. S. Rath. Can. J. Chem. **49**, 837 (1971).
14. R. K. McMullan and G. A. Jeffrey. J. Chem. Phys. **42**, 2725 (1965).
15. J. E. Bertie and E. Whalley. J. Chem. Phys. **40**, 1646 (1964).
16. J. E. Bertie, H. J. Labbé, and E. Whalley. J. Chem. Phys. **49**, 2141 (1968).
17. W. B. Kamb and A. Prakash. Acta Cryst. **B24**, 1317 (1968).
18. W. B. Kamb, W. C. Hamilton, S. J. LaPlaca, and A. Prakash. J. Chem. Phys. **55**, 1934 (1971).
19. T. A. Ford and M. Falk. Can. J. Chem. **46**, 3579 (1968).
20. L. Pauling. The nature of the chemical bond. Cornell University Press. 1945. p. 189.
21. M. Davies and K. Williams. Trans. Faraday Soc. **64**, 529 (1968).
22. S. K. Garg, B. Morris, and D. W. Davidson. J. Chem. Soc. Faraday II, **68**, 481 (1972).
23. D. W. Davidson. Can. J. Chem. **46**, 1024 (1968).
24. R. G. Gordon. J. Chem. Phys. **41**, 1819 (1964).
25. F. J. Bartoli and T. A. Litovitz. J. Chem. Phys. **46**, 404 (1972).

Can. J. Chem. Downloaded from www.nrcresearchpress.com by 210.87.254.6 on 09/05/12
For personal use only.

Correlation between the Electrochemical and Spectroscopic Behavior of some Substituted Pyridines[1]

RAFIK O. LOUTFY

Chemistry Division, National Research Council of Canada, Ottawa, Canada, K1A 0R6

AND

RAOUF O. LOUTFY[2]

Department of Chemistry, University of Guelph, Guelph, Ontario

Received October 16, 1972

The n,π^* triplet energies of pyridine, 2-, 3-, 4-cyano, and 2,6-dimethylpyridines were found to correlate linearly with the corresponding half-wave potentials, $E_{1/2}$. Similar relationship was obtained for acetophenone, 2-, 3-, and 4-acetylpyridines as well as for benzophenone, 2-, 3-, and 4-benzoylpyridines. The latter relationships indicated that the n $\rightarrow \pi^*$ transition of the benzoyl and acetylpyridines must involve the n-electron of the carbonyl oxygen.

On montre que les énergies du triplet n,π^* de la pyridine et des cyano-2, -3, -4 diméthyl-2,6 pyridines sont reliées linéairement avec les potentiels de demi-vogue, $E_{1/2}$ correspondants. Une relation semblable a été obtenue pour l'acétophénone et les acétyl-2, -3, et -4 pyridines aussi bien que pour la benzophenone et les benzoyl-2, -3, et -4 pyridines. Cette dernière relation montre que la transition n $\rightarrow \pi^*$ du benzoyle et des acétylpyridines doit impliquer l'électron-n de l'oxygène du groupe carbonyle.

[Traduit par le journal]

Can. J. Chem., 51, 1169 (1973)

Pyridine derivatives are the most fundamental heterocyclic aromatic hydrocarbons in which the —N= group replaces the methine group, —CH=, of the parent π-isoelectronic homocyclic compounds. Nevertheless, until rather recently there have been relatively few studies of the electronic properties of these compounds (1, 2). No correlations, however, between the electronic and physical properties have been investigated. We had previously correlated the n,π^* triplet energy ($^3E_{n,\pi^*}$) and the half-wave reduction potential ($E_{1/2}$) for some benzophenones and thiobenzophenones (3), aliphatic and aromatic ketones and aldehydes (4) and for some aza aromatic compounds (5).

In this report extension of the above relationship to include substituted pyridines is presented and discussed with respect to previous work.

The polarographic reduction of ten aza-heterocyclics, 2-, 3-, 4-cyano and 2,6-dimethylpyridine; 2-, 3- and 4-acetylpyridines; and 2-, 3-, and 4-benzoylpyridine, have been measured under similar condition, parallels to that of the corresponding parent aromatic hydrocarbons being: pyridine, acetophenone, and benzophenone respectively. The molecular structures are shown in Fig. 1. Reduction was carried out in 0.05 *M* TEAP – acetonitrile electrolyte and the experimental procedures were the same as described previously (3). Each of these heteromolecules gave a well characterized a.c. wave with a width at half-height of 90 ± 2 mV, corresponding to one electron process. In all cases, the reduction occurs at a more positive potential compared to the parent aromatic hydrocarbon. The rate of electron transfer, K_{ap}, *i.e.* the degree of reversibility of the reduction process will be discussed elsewhere. However, for this report it is sufficient to report that all reduction processes proceeded reversibly with K_{ap} much greater than 0.01 cm s^{-1}. The half-wave reduction potentials, $E_{1/2}$, are summarized in Table 1 together with the n,π^* triplet energies for compounds investigated.

Relationship between $E_{1/2}$'s and n,π^* Triplet Energies of Pyridine Derivatives

(a) Cyano and Methyl Substituted Pyridine

The activity of aza-heterocyclic compounds toward reduction can primarily be due to the heterocyclic ring, where substitution in the ring would affect the reduction through the σ or π donation of the substituents. The effect of sub-

[1]NRCC No. 12959.

[2]Present address: Department of Chemistry, Colorado State University, Fort Collins, Colorado 80521.

Can. J. Chem. Downloaded from www.nrcresearchpress.com by 210.87.254.6 on 09/05/12
For personal use only.

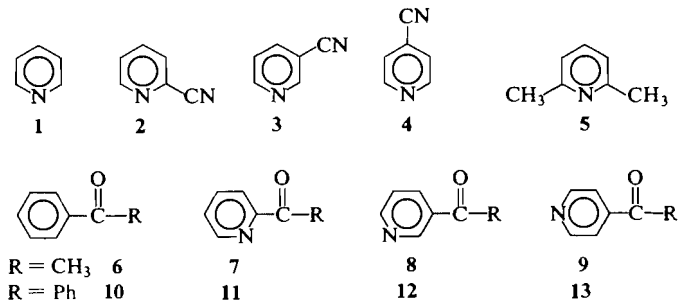

FIG. 1. Molecular structures of the substituted pyridines and the corresponding homocyclic analog and numbering systems.

stituents on the reduction potential of pyridine depends on the position of the substitution and the nature of the substituents. Replacing a hydrogen by cyano group in the pyridine ring, in general, eases the reduction process (reduction potential becomes more positive), while methyl substitution shifts $E_{1/2}$ toward a more negative potential (see Table 1). This behavior is due to the fact that electron-withdrawing substituents lower the energy of the π^*-level and electron-donating groups have the opposite effect. Since, during the reduction process the electron has to be placed in the lowest unoccupied π-molecular orbital, therefore, the $E_{1/2}$ should be related to the energy of this orbital (6). The positions in the pyridine ring are not equivalent, thus the 4-cyanopyridine reduces at a slightly more positive potential than the 2-cyano derivative and both are more positive than the 3-cyanopyridine. This behavior is in general agreement with Volke's concepts (7, 8).

TABLE 1. Electrochemical data and n,π^* triplet energies of the studied compounds

No.	Compound	$-E_{1/2}$ (V)	$^3E_{n,\pi^*}$ (kcal/mol)
1	Pyridine	2.76	80.06*
2	2-Cyanopyridine	2.09	77.0* (75.6)‡
3	3-Cyanopyridine	2.11	77.04* (75.5)‡
4	4-Cyanopyridine	1.912	76.19*
5	2,6-Dimethylpyridine	2.85	80.67*
6	Acetophenone	2.09	73.6†
7	2-Acetylpyridine	1.905	70.0†
8	3-Acetylpyridine	1.944	71.1†
9	4-Acetylpyridine	1.855	69.5†
10	Benzophenone	1.81	68.6†
11	2-Benzoylpyridine	1.655	67.4†
12	3-Benzoylpyridine	1.760	68.4†
13	4-Benzoylpyridine	1.596	67.1†

*Reference 1.
†Reference 10.
‡$^3E_{\pi,\pi^*}$ (kcal/mol).

One basic feature of the aza-heterocyclics, which differs from the aromatic hydrocarbons, is the presence of nitrogen atom with a lone pair of electrons. Therefore, it should be possible to excite one of the electrons to the lowest unoccupied π^*-orbital, Indeed, many pyridine derivatives have lowest n,π^* triplet state. It is, therefore, anticipated that $E_{1/2}$ to correlate with the $^3E_{n,\pi^*}$ of substituted pyridine provided that the energy of the nitrogen lone pair (E_n) is not affected by the substituents. The latter is to be expected due to the orthogonality of the nitrogen n-orbital with respect to the π-system. The correlation between $E_{1/2}$ and $^3E_{n,\pi^*}$ for the cyanopyridines, pyridine, and 2,6-dimethylpyridine is shown in Fig. 2*a*.

(b) Acetyl and Benzoyl Pyridines

The 4-substituted derivative, in both series, reduces at a more positive potential than the 2-substituted pyridine and in turn they are reduced at a more positive potential than 3-substituted pyridine. This behavior is in agreement with the previous results. The acetyl and benzoyl pyridines were also reduced at a more positive potential than the corresponding homocyclic analog. This is because the nitrogen is more electronegative than carbon, therefore, it lowers all energy levels. This energy lowering is a consequence of two factors: (*1*) the $2P_\pi$ orbital of the nitrogen atom has a lower energy and hence, lowers the energy of the π-system in general; (*2*) the inductive effect of the nitrogen atom lowers the $2P_\pi$ energy levels of the carbon atoms, particularly, the vicinal ones and thus produces a smaller and more uniform lowering of all levels (9). The same applies to the π^*-levels. The acetyl and benzoylpyridines, similar to the corresponding homocyclic analog, acetophenone, and benzophenone, respectively, have

Can. J. Chem. Downloaded from www.nrcresearchpress.com by 210.87.254.6 on 09/05/12
For personal use only.

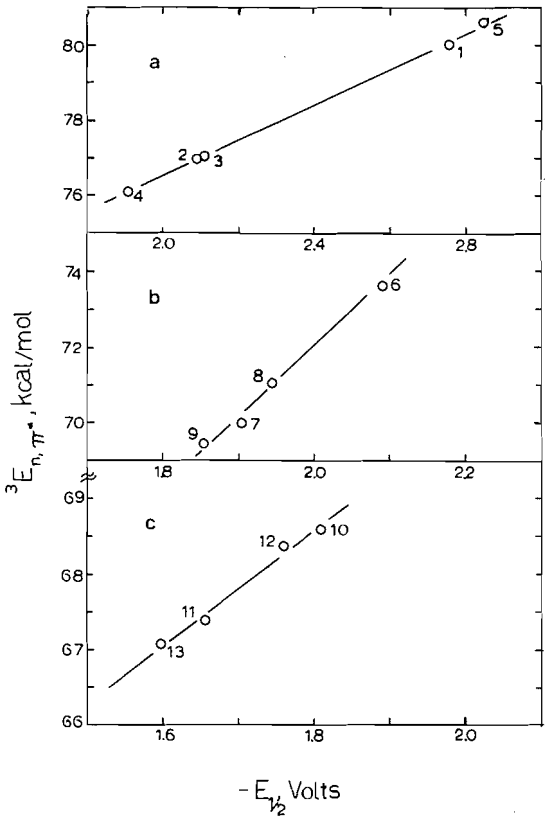

FIG. 2. Half-wave potentials *vs.* n,π* triplet energies of (*a*) cyanopyridines and pyridine; (*b*) acetylpyridines and acetophenone, and (*c*) benzoylpyridines and benzophenone.

triplet states which correspond to $n \rightarrow \pi^*$ transition. However, the energies of these triplet states (67–68 kcal/mol) are much lower than the pyridine (80 kcal/mol) and slightly lower than the corresponding homocyclic analog. Moreover, the $^3E_{n,\pi^*}$ of acetophenone and acetylpyridines correlate linearly with the corresponding $E_{1/2}$ (See Fig. 2*b*). Similar behavior was obtained for the benzophenone and the benzoylpyridines (Fig. 2*c*). The above results indicate that the $n \rightarrow \pi^*$ transition in the acetyl and benzoyl series must involve the n-electron of the carbonyl oxygen rather than that of the nitrogen atom. Arnold (10 and references therein) earlier showed that the triplet energies of acetophenone and acetylpyridines as well as benzophenone and benzoylpyridines correlate linearly with the Hammett's σ constant, which is in accordance with results obtained above.

The existence of a linear relationship between $^3E_{n,\pi^*}$ *vs.* $E_{1/2}$ for acetylpyridines including acetophenone and for benzoylpyridines including benzophenone indicates that the nitrogen in the ring acts as external substituent and changes the π*-level energy depending on its position with respect to the CO group, which is reflected on the $E_{1/2}$'s. It also indicates that the nitrogen in the ring exerts no or relatively small effect on the carbonyl oxygen n-level energy. According to the latter, it would be expected that the slope of the plots shown in Figs. 2*b* and 2*c* (0.54 and 0.33 respectively) to be identical to that of the acetophenones (11) and benzophenones (3) series, respectively. However, the results of comparison indicated that the pyridines series have larger slopes than the corresponding phenones series (0.42 and 0.19 respectively) and obviously they intercept at the parent homocyclic compound. Thus, deviation could be due to solvation energy differences, ΔE_{sol} between the various series (4, 12).

The authors wish to express their sincerest appreciation to Dr. W. R. Fawcett of the Chemistry Department, University of Guelph, Guelph, Ontario for making available the instrumentation used to determine the reduction potentials for all the compounds investigated.

1. R. J. HOOVER and M. KASHA. J. Am. Chem. Soc. **91**, 6508 (1969).
2. E. T. HARRIGAN, T. C. WONG, and N. HIROTA. Chem. Phys. Lett. **14**, 549 (1972).
3. R. O. LOUTFY and R. O. LOUTFY. J. Phys. Chem. **76**, 1650 (1972).
4. R. O. LOUTFY and R. O. LOUTFY. J. Phys. Chem. **77**, 336 (1973).
5. R. O. LOUTFY and R. O. LOUTFY. J. Phys. Chem. To be published.
6. A. MACCOLL. Nature, **163**, 178 (1949).
7. J. HOLUBEK and J. VOLKE. Coll. Czech. Chem. Commun. **27**, 680 (1962).
8. J. VOLKE and V. SKA'LA. J. Electroanal. Chem. **36**, 383 (1972).
9. H. H. JAFFE' and M. ORCHIN. Theory and applications of ultra-violet spectroscopy. John Wiley and Sons Inc., New York. 1962.
10. D. R. ARNOLD. Adv. Photochem. **6**, 302 (1968).
11. R. O. LOUTFY and R. O. LOUTFY. Tetrahedron. Submitted.
12. M. E. PEOVER. Electrochim. Acta, **13**, 1083 (1968).

Can. J. Chem. Downloaded from www.nrcresearchpress.com by 210.87.254.6 on 09/05/12
For personal use only.

Palladium(II), Platinum(II), and Copper(I) *N*-Bonded Complexes with Thiazolidine-2-thione as Ligand

D. De Filippo, F. Devillanova, E. F. Trogu, and G. Verani
Istituto Chimico Policattedra, Università di Cagliari, Italy

C. Preti
Istituto Chimica Generale ed Inorganica, Università di Modena, Italy

AND

P. Viglino
Istituto di Chimica Fisica, Facoltà di Chimica Industriale, Università di Venezia, Italy

Received April 21, 1972

The preparation and characterization of the ($Mttz_nX_2$) complexes (where M = Pd or Pt; *ttz* = thiazolidine-2-thione; n = 2, 3 or 4; X = Cl, Br, I) are reported. By i.r., p.m.r., and u.v.–visible spectra and by magnetic susceptibility and conductivity measurements it appears that in all complexes the ligand is *N*-bonded to the metal and that many equilibria are present in polar solvents. In particular, for ($Mttz_4I_2$)-derivatives there is an equilibrium between a square-planar and a penta-coordinate species. Furthermore, water is competing with the ligands and counterions in the coordination sphere. Our ligand is placed near water in the spectrochemical series. With copper(I) we have obtained complexes of the type ($Cuttz_3X$) (where X = Cl, Br, I, NO_3, ClO_4, and $\frac{1}{2}SO_4$), and in each case the anion is coordinated to the metal. The *ttz* molecule in these complexes behaves as a hard-base.

La préparation et la caractérisation des complexes ($Mttz_nX_2$) (où M = Pd ou Pt; *ttz* = thiazolidine thione-2, n = 2, 3 ou 4; X = Cl, Br, I) sont présentées. D'après les spectres i.r., r.m.n., u.v. et visible et d'après les mesures de la susceptibilité magnétique et de la conductivité, il apparait que dans tous ces complexes, le ligand est lié au métal par l'azote et que beaucoup d'équilibres existent dans les solvants polaires. Par exemple, pour les dérivés ($Mttz_4I_2$) un équilibre se produit entre les espèces carré-plane et penta-coordinée. De plus l'eau entre en compétition avec les ligands et les contre-ions dans la sphère de coordination. Notre ligand est situé près de l'eau dans la série spectrochimique. Avec le Cuivre (I), des complexes du type ($Cuttz_3X$) (où X = Cl, Br, NO_3, ClO_4 et $\frac{1}{2}SO_4$) sont obtenus et dans tous les cas, l'anion est coordiné au métal. Le comportement de la molécule de *ttz* dans ces complexes est celui d'une base dure. [Traduit par le journal]

Can. J. Chem., **51**, 1172 (1973)

Working on the problem of the competition between group VA and VIA donor atoms in the formation of a metal–ligand bond, we have reported in our previous papers (1–9) the characterization of many complexes with heterocyclic ligands. Particularly the thiazolidine-2-thione (*ttz*; $S{=}{}^{2}C{-}{}^{3}NH{-}{}^{4}CH_2{-}{}^{5}CH_2{-}{}^{1}S$) behaves as a soft (9) or a hard (8) base depending on the metal class. In order to extend the study of this ligand we have now prepared the palladium(II), platinum(II), and copper(I) complexes described below.

Palladium(II) and Platinum(II) Complexes

Results

All complexes were obtained from reactions in aqueous solution between K_2MCl_4 (where M = Pd or Pt) and *ttz* in the required stoichiometric ratio, in the presence of a small excess of HX (X = Cl, Br, I), as in the following scheme

$$K_2MCl_4 \xrightarrow[\text{(from 1:1 to 1:4)}ttz]{HX} Mttz_nX_2 \quad \begin{matrix} n = 2,3,4 \\ X = Cl, Br, I \end{matrix}$$

The $Pdttz_4(NO_3)_2$ derivative was obtained starting from $Pd(NO_3)_2$. With a metal:ligand molar ratio of 1:1 only a low yield of the 1:2 derivative was obtained. All compounds are diamagnetic; some of these are soluble in DMSO, DMF, or CH_3CN. Their colors change from yellow to brown, getting darker from chlorides to iodides and lighter from n = 2 to n = 4 (see Table 1). The conductivity values at 25 °C in DMF solutions are strongly concentration-dependent and show that, in very dilute solutions, all complexes seem to behave as 1:2 electrolytes (but the color of the solutions changes on diluting).

Can. J. Chem. Downloaded from www.nrcresearchpress.com by 210.87.254.105 on 09/05/12
For personal use only.

TABLE 1. Analytical data and some physical properties*

Number	Compounds	Color	Decomposition temperature (°C)	Solubility†	Analysis (%) Found M	Found C	Found H	Calcd. M	Calcd. C	Calcd. H
1	$Pd(ttz)_2Br_2$	Red-brown	204–205	A	20.7	14.3	2.1	21.1	14.3	2.0
2	$Pd(ttz)_3Cl_2$	Yellow	—	B	20.6	20.2	2.9	19.9	20.2	2.8
3	$Pd(ttz)_3Br_2$	Dark-yellow	185–186	C	16.9	17.0	2.4	17.1	17.3	2.4
4	$Pd(ttz)_3I_2$	Dark-brown	246–247	C	14.7	15.0	2.0	14.9	15.1	2.1
5	$Pd(ttz)_4Cl_2$	Yellow	179–180	B	16.0	22.1	3.2	16.3	22.0	3.1
6	$Pd(ttz)_4Br_2$	Yellow	183–184	C	14.6	19.3	2.9	14.4	19.4	2.7
7	$Pd(ttz)_4I_2$	Red-brown	142–143	C	12.4	17.5	2.6	12.7	17.2	2.4
8	$Pd(ttz)_4(NO_3)_2$	Yellow	—	A	15.0	20.6	2.6	15.1	20.4	2.9
9	$Pt(ttz)_2Cl_2$	Yellow	—	A	38.8	14.4	1.7	38.7	14.3	2.0
10	$Pt(ttz)_2Br_2$	Dark-yellow	254–255	A	33.4	12.4	1.7	32.9	12.1	1.7
11	$Pt(ttz)_2I_2$	Orange	251–252	A		10.4	1.3	28.4	10.5	1.5
12	$Pt(ttz)_3Cl_2$	Yellow	140–141	C	31.5	17.7	2.7	31.3	17.3	2.4
13	$Pt(ttz)_3Br_2$	Light-yellow	207–208	C	27.1	15.5	2.3	27.4	15.2	2.1
14	$Pt(ttz)_3I_2$	Light-yellow	190–191	C	24.0	13.3	1.7	24.2	13.4	1.9
15	$Pt(ttz)_4Cl_2$	Lemon-yellow	252–253	C	25.9	19.2	3.2	26.3	19.4	2.7
16	$Pt(ttz)_4Br_2$	Dark-yellow	231–232	C	23.1	17.2	2.8	23.5	17.3	2.4
17	$Pt(ttz)_4I_2$	Hazel-brown	197–198	C	21.6	15.9	2.1	21.1	15.6	2.2
18	$[Cu(ttz)_3Cl]$	Pale-yellow	194–195	B	13.6	23.6	3.3	13.9	23.7	3.3
19	$[Cu(ttz)_3Br]$	Pale-yellow	152–153	B	12.5	21.9	3.1	12.7	21.6	3.0
20	$[Cu(ttz)_3I]$	Pale-yellow	125–126	B	11.7	19.6	2.8	11.6	19.7	2.8
21	$[Cu_2(ttz)_6SO_4]$	Orange	108–109	A	13.0	23.2	3.2	13.5	23.0	3.2
22	$[Cu(ttz)_3NO_3]$	Orange	99–100	B	13.4	22.4	3.1	13.5	22.4	3.1
23	$[Cu(ttz)_3ClO_4]$	Yellow	—	A	11.7	20.9	2.9	12.1	20.8	2.9

*Molar conductivity measurements in 10^{-3} *M* DMF solutions: compounds **18**, 36.8; **19**, 36.8; **20**, 34.6; **22**, 6.3 ohm^{-1} cm^2.
†A, Insoluble; B, soluble in DMF; C, soluble in DMF, DMSO.

TABLE 2. Electronic spectra of compounds **3**–**17** in DMF solutions and in solid phase (in parentheses)

Compound	Electronic spectra			
3		29.000	23.250	
4		28.750	23.800	20.400
5		28.750	(24.400)	
6		29.150		
7		29.000	24.400	20.600
10		29.000	23.250	
11	32.250	28.800	(23.250)	
12		28.800		(21.750)
13	31.250	28.750		
14	31.750	28.750		(22.000)
15		28.750	(22.700)	
16	31.750	28.800		
17	31.750	28.750(27.000)	25.000(22.000)	19.600(19.000)

The electronic spectra (see Table 2) of freshly prepared DMF solutions show a shoulder at 28 750–29 150 cm^{-1} and, sometimes, shoulders at 31 250–32 250, and 23 250–25 000 cm^{-1}. Only the iodo-derivatives exhibit another shoulder near 20 000 cm^{-1}, whose molar absorbance is not linear against concentration. The spectra of **7** and **17**, extensively studied (at 20 ± 0.1 °C and with $[7] = [17] = 2 \times 10^{-4}$ *M*, $[ttz] = 0.1$ *M* and $[KI] = 2 \times 10^{-3}$ to $3.6\ 10^{-2}$ *M*), change slowly and become constant after 15 days, showing a shoulder at 20 160 cm^{-1} (**7**) or a peak at 19 610 cm^{-1} (**17**), whose intensities are still non-linear against $[I^-]$ (see Fig. 1). With the continuous variations method it is found that the maximum absorbance value corresponds to a 1:1

Can. J. Chem. Downloaded from www.nrcresearchpress.com by 210.87.254.105 on 09/05/12
For personal use only.

Can. J. Chem. Downloaded from www.nrcresearchpress.com by 210.87.254.105 on 09/05/12
For personal use only.

TABLE 3. Assignments of the most important i.r. bands in the solid phase spectra

Compound	ν(NH)	Thioamide I	ν(C═S) +δ(NCS)	ν(CS) symmetric and antisymmetric	ν(MN)	Other bands
*ttz**	3120s(3400s)†	1490s	1288s	690s, 660vs	—	
1	3240s	1505s	1300ms	690w, 670w	217s	357s, 257vs
2	?	1530s	1305s	690vs, 650w	—	378w, 367m, 303vw, 285s, 262s
3	3220s	1505s	1312s	690w, 660w	234m	357s, 257vs, 217s
4	3210s	1500s	1300s	690w, 660m	227m	357s, 218m
5	3060sh	1520vs	1305s	690s, 645s	224m	368m, 355ms, 202m
6	3240s?	1535s	1310s	685w, 645m	—	367m, 352s
7	3210sh	1510s	1320–1300vs	675vs, 660s	227s	370w, 358m, 350s, 274m, 218m
8‡	—	1530vs	1312s	690m, 650w	—	369s, 303w, 263m; (2330vw, 1745vw, 1380s, 1040s)‡
9	3220s	1520vs	1300s	690m, 650mw	228s	223s
10	—	1520vs	1300s	690w, 660m	236s	374m, 208s
11	3200s	1500vs	1310s	690mw, 660mw	227w	364m, 309s, 203m
12	3310s	1530vs	1310vs	690m, 660s	228m	375m, 214s
13	3340ms	1530vs	1310vs	700w, 660m	226m	374m, 213s
14	3200m	1500vs	1300s	690m, 660m	—	374m, 202m
15	3320s	1530vs	1310vs	700mw, 660m	230m	375m, 214s
16	3340s	1530vs	1310vs	700w, 660mw	227m	374m, 213s
17	—	1510vs	1295vs	700m, 660m	227m	374m, 360w, 212s
18	3120s	1505vs	1305vs	695m, 650m	310m	(1140sh, 1120sh, 1110vs, 615s, 580w, 460w)§ 225s
19	3120s	1505vs	1300vs	685m, 645m	306m	(2320vw, 1750vw, 1580s, 1380vs, 1025s, 740vw)‖
20	3140s	1505vs	1290vs	670m, 640m	312m	
21§	3120s	1505vs	1300vs	690m, 650m	329m	(1140sh, 1120sh, 1110vs, 615s, 580w, 460w)§
22‖	3120s	1505vs	1300vs	695m, 650m	323m, 314s	(2320vw, 1750vw, 1580s, 1420m, 1380vs, 1025s, 760vw, 740vw)‖
23¶	3120s	1500vs	1300vs	690m, 650m	322m, 310s	(1110vs, 1085vs, 630m, 620s)¶

*Data for *ttz* assignments are taken from ref. 11.
†In chloroform solution.
‡Typical bands for a non-bonded NO_3 group.
§Bands for a SO_4 bonded group.
‖Bands for a bonded NO_3 group.
¶Assignments for a bonded ClO_4 group.

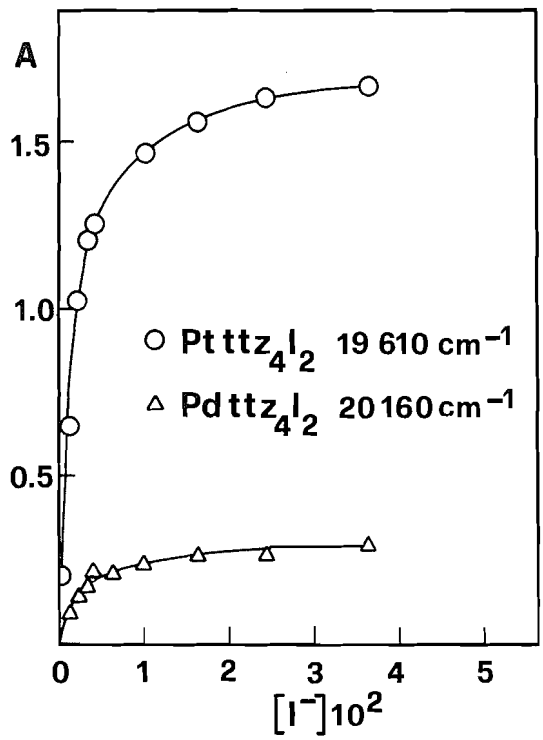

FIG. 1. Absorbance of palladium (7) and platinum (17) derivatives against iodide ion concentration: [7] = [17] = 2×10^{-4} *M*; [*ttz*] = 0.1 *M*; [KI] = $2 \times 10^{-3}/3.6 \times 10^{-2}$ *M*; 20 ± 0.1 °C.

molar ratio between the iodide and the complex.

As far as the i.r. spectra (Table 3) are concerned, the ν(Pd—Br) vibrations occur in the spectra of compounds **1** and **3** at 257 cm^{-1} as a very strong band while in those of compounds **2** and **5** the ν(Pd—Cl) vibrations are found at 368–367 cm^{-1} (medium) and near 303 cm^{-1} (weak), in very good agreement with literature data (3, 10). The ν(N—H) band shows an average shift of about −160 cm^{-1} if compared with the spectrum of a chloroform solution of the free ligand, while the thioamide I band and the absorption attributed to ν(C=S) + δ(NCS) (11) show positive shifts averaging 28 and 18 cm^{-1}, respectively. In the far i.r. region two halide-independent medium–strong bands in the range 370–350 cm^{-1} and near 230 cm^{-1} are present.

The p.m.r. of the free ligand spectrum shows a hyperfine structure in hexadeuterodimethylsulfoxide (DMSO-d_6) similar to that previously characterized (9) in $CDCl_3$ solution. The chemical shift values and the spectral patterns of CH_2(5)- and CH_2(4)-proton resonances of the free ligand in DMSO-d_6 (see Table 4) do not show noticeable modifications with respect to those obtained in $CDCl_3$ solutions (9) whereas the NH-proton resonance shifts by about 2 p.p.m. towards lower field. Further, all the chemical shift values are practically concentration-independent.

On going from the spectrum of the free ligand to those of the palladium derivatives in freshly-prepared DMSO solutions we observe: (*1*) the disappearance of the hyperfine structure of the resonances as a consequence of line broadening and (*2*), a general deshielding effect on the cited resonances increasing in the order $CH_2(5) < CH_2(4) \ll NH$.

In the p.m.r. spectra of the platinum-derivatives we observe a doubling of each ligand resonance, one component maintaining the hyperfine structure and showing the same chemical shift values as the respective free ligand resonance while the other one (assigned to the complexed ligand) showing instead a deshielding effect stronger than that observed for palladium complexes.

Furthermore, we observe that the deshielding effect on the NH-proton resonance decreases in the order chloride > bromide > iodide for both palladium and platinum compounds. In order to obtain a full characterization of these complexes additional p.m.r. experiments have been carried out changing *ttz* or KI concentrations or by adding water and/or by running several spectra many hours after the complexes solutions were prepared. The results of the measurements will be discussed below.

Discussion

The first problem to consider is the identification of the reaction center in the ligand molecule. The negative shift of ν(NH) of about 160 cm^{-1} accompanied by the positive shifts of the thioamide I band for ν(C=S) + δ(NCS) of about 28 and 18 cm^{-1}, respectively, clearly suggest that the nitrogen atom is involved in the coordination bond. In fact, in $Mttz_2X_2$ *N*-bonded compounds (where M = Zn, Cd, or Hg and X = Cl, Br, or I) (8) we have found a negative ν(N—H) shift of about 270 cm^{-1} and positive shifts for the thioamide I band for ν(C=S) + δ(NCS) of 36 and 19 cm^{-1}, respectively. The magnitude and sign of these shifts are typical of *N*-bonded derivatives (11). The hypothesis that the complexes studied here are *N*-bonded is strongly supported

Can. J. Chem. Downloaded from www.nrcresearchpress.com by 210.87.254.105 on 09/05/12
For personal use only.

TABLE 4. Chemical shift values in p.p.m. from TMS, as internal reference

Number	Compound	$\delta_{CH_2(5)}$	$\delta_{CH_2(4)}$	δ_{NH}
	ttz	3.50	3.88	10.05
3	$Pdttz_3Br_2$	3.58	4.03	10.80*
4	$Pdttz_3I_2$	3.58	4.04	10.65*
6	$Pdttz_4Br_2$	3.58	4.01	10.70*
7	$Pdttz_4I_2$	3.58	4.01	10.50*
12	$Pttz_3Cl_2$	3.50–3.63	3.88–4.16	10.05–11.43
13	$Pttz_3Br_2$	3.51–3.63	3.88–4.16	10.05–11.25
14	$Pttz_3I_2$	3.51–3.62	3.88–4.16	10.05–11.12
15	$Pttz_4Cl_2$	3.50–3.63	3.88–4.15	10.05–11.42
16	$Pttz_4Br_2$	3.50–3.63	3.88–4.15	10.05–11.23
17	$Pttz_4I_2$	3.50–3.63	3.88–4.16	10.04–11.16

*Very broad lines.

by the noticeable deshielding effect on the NH-proton resonance observed in the spectra of all examined complexes. In fact, this deshielding effect is ascribed to electron withdrawal by the metal from the nitrogen atom. The electron withdrawal cannot be ascribed to hydrogen bond because in dilute DMSO solution the only possible hydrogen bond is with the solvent. The deshielding effect pointed out here results on comparing the spectra of complexes with those of the free ligand in DMSO solutions. On the other hand, in our previously studied *S*-bonded *ttz*-derivatives (9) the NH-proton resonances show a certain shielding effect. The examination of (CH_2) chemical shift values also leads to the same conclusion. In fact, the $CH_2(4)$ (the one directly bonded to the NH-group) is the most affected CH_2 resonance.

From this set of results we conclude that the ligand is *N*-bonded to the metal in all the complexes. The medium–strong i.r. band near 230 cm^{-1} may by attributed to the ν(M—N) vibration, in very good agreement with literature data (12–15).

According to the previously reported u.v. data (16), the shoulder near 32 000 cm^{-1} could be assigned to the first charge-transfer transition $L \rightarrow M$ while the shoulders near 29 000 cm^{-1} in the spectra of all the compounds could be due to the $\bar{\nu}_1$(d–d) transition of a square-planar chromophore species. In fact, the $\bar{\nu}_1$ transition in $[Pd(H_2O)_4]^{2+}$ occurs at 26 400 cm^{-1} while in thiourea derivatives it occurs at 27 700 cm^{-1}.

The absorption in the range between 25 000 and 19 600 cm^{-1} is generally absent in the spectra of the chloride derivatives but is almost always present in those of the other compounds (see Table 2). Further, on going from bromide to iodide complexes a red shift is also observed in the $Mttz_4X_2$ compounds. The magnitude of the deshielding effect on the NH-proton resonance is also shown to depend on the nature of the halide-atom both in $Mttz_3X_2$ and $Mttz_4X_2$ derivatives, being stronger in the order chloride > bromide > iodide (see Table 4). From both these findings it is clear that the halide atom is involved in the coordination sphere of the metal in $Mttz_4X_2$-type compounds too.

The systems $Mttz_4I_2$ (M = Pt or Pd) with KI have been further studied extensively both by u.v.–visible and p.m.r. techniques. The equilibria between the $Mttz_4^{2+}$ and I^- ions have been studied by the u.v. continuous variation method[1] and the results could be explained in terms of the two following reactions

$$[1] \qquad Mttz_4^{2+} + I^- \rightleftarrows Mttz_3I^+ + ttz$$

$$[2] \qquad Mttz_4^{2+} + I^- \rightleftarrows Mttz_4I^+$$

However, in our spectrophotometric experiments, the presence of a large excess of free-ligand (500:1 to the complex) should prevent reaction 1 occurring to a large extent. Furthermore, the absorptions near 20 000 cm^{-1}, which are a non-linear function of the $[I^-]$ values, cannot be attributed to $Mttz_3I^+$ (or $Mttz_2I_2$) species because these complexes do not absorb in this range, neither in the solid phase nor in DMF solution.[2] However, the shoulder at 20 160

[1]Obviously the method of continuous variations is insufficiently reliable when more than two species are present, as is likely here.

[2]Moreover, the yellow DMF solution obtained by thermal reaction between K_2MCl_4 and a large excess of KI does not absorb at 20 000 cm^{-1}. Thus the presence of this absorption cannot be due to a possible substitution of more than one iodide.

Can. J. Chem. Downloaded from www.nrcresearchpress.com by 210.87.254.105 on 09/05/12
For personal use only.

Can. J. Chem. Downloaded from www.nrcresearchpress.com by 210.87.254.105 on 09/05/12
For personal use only.

cm^{-1} and the peak at 19 610 cm^{-1} for palladium- and platinum-derivatives, respectively, could be assigned to a penta-coordinate species, of the type $Mttz_4I^+$, probably with a square-pyramidal geometry. This stereochemical hypothesis is supported by the high absorbance intensities ($\varepsilon \simeq 8\,300$ after 15 days at 19 160 cm^{-1} in the presence of $Pttz_4I_2$, KI, and *ttz* in 1:180:500 molar ratio), which would be expected to be much lower for trigonal-bipyramidal geometry (16, 17).[3]

On the other hand, it is very likely that the equilibrium reactions between $Mttz_4^{2+}$ and I^- ions above discussed are not the only ones present in polar-solvent solutions. In fact, the p.m.r. spectra of platinum derivatives indicate the presence of free ligand in the solution which might be formed by slow ligand exchange reactions, both in $Pttz_3X_2$ and $Pttz_4X_2$ complexes. In the palladium-derivatives these reactions also seem to occur but with a faster exchange rate. In fact, by adding an excess of *ttz* to the palladium complex solutions we do not obtain the free ligand spectrum but only a shift of all the resonances towards the respective resonance shift of the spectrum of the free ligand, so that the observed chemical shift values would be the weighted averages between those of the free ligand and those of the complexes.

By studying the OH-proton resonance, arising from the water traces present in our DMSO-d_6 solutions, we observe that this resonance moves towards lower fields with time[4] (for example: $Pttz_4Cl_2$: $t = 0$, $\delta_{OH} = 3.46$ p.p.m. from internal TMS; $t = 44$ h, $\delta_{OH} = 3.90$ p.p.m.; $Pttz_4Br_2$: $t = 0$, $\delta_{OH} = 3.51$ p.p.m.; $t = 44$ h, $\delta_{OH} = 3.79$ p.p.m.; $Pttz_4I_2$: $t = 0$, $\delta_{OH} = 3.99$ p.p.m.; $t = 44$ h, $\delta_{OH} = 4.08$ p.p.m.; $Pdttz_4I_2$: $t = 0$, $\delta_{OH} = 4.36$ p.p.m.; $t = 40$ h, $\delta_{OH} = 4.72$ p.p.m.; etc.).

Further, by adding small quantities of water the OH-resonances shift towards higher fields, *i.e.* towards the free water shift value, which may be interpreted as a fast proton exchange between free water and coordinated water.

Both these effects on the OH-resonance can be explained in terms of the water oxygen competing with the nitrogen atom of the ligand and the halide ions in coordinating the metal atom. This interpretation is further confirmed by the up field shift of the OH-resonance on adding a small amount of KI or *ttz*.

However, the complexity of these systems deriving from the possible existence of many ionic species in mutual equilibrium with very fast exchange processes does not allow a quantitative interpretation.

The DMF molar conductivities of dilute solutions tend to values typical of 1:2 electrolytes (Λ ranging between 180 and 200 $ohm^{-1}\,cm^2$). This could be a consequence of the existence in solutions of a number of equilibria involving variously coordinated complexes and complete halide-substitution in the coordination sphere in very dilute solutions. Finally the competition between water and ligand nitrogen atoms demonstrates that in these complexes our ligand should be placed near water in the spectrochemical series. In fact, in the u.v.–visible spectra the $\bar{\nu}_1$(d–d) bands occur in our complexes near 28 kK and in $[Pd(H_2O)_4]^{2+}$ ion at 26 400 cm^{-1}.

Copper Complexes

Pale-yellow, microcrystalline compounds with general formula ($Cuttz_3X$) (where X = Cl, Br, I, NO_3, ClO_4, and $\frac{1}{2}SO_4$) were prepared by various methods (see Experimental section). The conductivity measurements in DMF show that all derivatives behave as non-electrolytes. The magnetic susceptibility measurements demonstrate that the metal is present as copper(I). From the i.r. spectra it is clear that the NO_3^-, ClO_4^-, and SO_4^{2-} groups are always bonded. In fact, in the spectrum of compound **22** the strong band present at 1380 cm^{-1} (due to the ν_3 mode of NO_3) is accompanied by a medium absorption at 1420 cm^{-1} as a consequence of symmetry lowering in the nitrato-group (18). Furthermore, the ν_4 absorption is also split into two very weak bands at 760 and 740 cm^{-1} while a medium–strong band appears at 1580 cm^{-1}, where the ligand does not absorb. As far as the sulfato-derivative (**21**) is concerned, in its spectrum we observe a set of bands at 1140sh, 1120sh, 1110vs, 615s, 580w, and 460w cm^{-1} which could arise from bridging groups (19, 20). In the spectrum of the perchlorate derivative (**23**) the bands present at 630 and 620 cm^{-1} (due to ν_3 and ν_5 modes) and those at 1110 and 1085 cm^{-1} confirm that the group is present as the fragment

[3]No ε values are reported in Table 2 because many species are probably present in the solutions.

[4]The time independent chemical shift value of OH-resonance in the free ligand spectrum is $\delta_{OH} = 3.38$ p.p.m.

—O—ClO_3 of the complex (21, 22). These results are in agreement with those obtained by conductivity measurements. As far as the ligand–metal interaction is concerned, the remarkable shift of ν(NH) band towards lower frequencies (of about 280 cm^{-1}, having as reference the chloroform solution spectrum of the free ligand) clearly shows that the nitrogen atom is involved in the coordination bond. This hypothesis is confirmed by the strong band (independent of anion) present at 306–329 cm^{-1} which could, tentatively, be attributed to a ν(Cu—N) stretch, according to the values reported for morpholine- and imidazol-copper derivatives (23, 24).

Experimental

Preparation of the Compounds

The ligand (supplied by Fluka) was purified by recrystallization from hot water.

Method A: All the palladium(II) and the platinum(II) complexes were obtained by reaction in hot aqueous solution between K_2MCl_4 and *ttz* (in molar ratios from 1:1 to 1:4) in the presence of a small excess of HX; with the molar ratio of 1:1 only low yields of the ($Mttz_2X_2$)-type compounds were separated out. Compound $Cuttz_3I$ was obtained by reaction in hot aqueous solution between 1 mol of $CuSO_4$, 4 mol of *ttz* and an excess of KI in the presence of acetic acid. Compound $Cuttz_3ClO_4$ was obtained starting from $CuCO_3$ by reaction with 4 mol of *ttz* and $HClO_4$.

Method B: The compounds **8**, **18**, **19**, **21**, and **22** were obtained by reactions in aqueous solution between MX_2 and 4 mol of *ttz*.

Infrared Measurements

All compounds were examined in the region 4000–200 cm^{-1} with Perkin–Elmer Model 457 and 225 spectrophotometers on KBr discs and, in the far i.r. region, in Nujol mulls between thin polyethylene sheets.

Magnetic Susceptibility Measurements

These measurements were carried out by Gouy's method. All compounds were diamagnetic.

Conductivity Measurements

These measurements were carried out in 10^{-3} *M* DMF solutions (accuracy ±1%).

Ultraviolet–Visible Measurements

The spectra were recorded with Perkin–Elmer Model 402 and Beckman-DK2A spectrophotometers working in DMF solutions or in the solid phase respectively.

Nuclear Magnetic Resonance Measurements

All p.m.r. spectra were recorded on a Varian 100 MHz spectrometer at room temperature using TMS as internal standard. Only the DMSO-d_6 soluble compounds were studied.

The authors are indebted to the Italian Council of Research (C.N.R.) for financial support.

1. D. De Filippo and C. Preti. Gazz. Chim. Ital. **98**, 64 (1968).
2. C. Preti and D. De Filippo. Annual Meeting of Inorg. Chem. 137 (1968).
3. D. De Filippo and C. Preti. Inorg. Chim. Acta, **3**, 287 (1969).
4. D. De Filippo, F. Devillanova, and C. Preti. Inorg. Chim. Acta, **3**, 341 (1969).
5. C. Preti and D. De Filippo. J. Chem. Soc. (A), 1901 (1970).
6. D. De Filippo and C. Preti. J. Chem. Soc. (A), 1904 (1970).
7. D. De Filippo, F. Devillanova, and C. Preti. Inorg. Chim. Acta, **5**, 103 (1971).
8. D. De Filippo, F. Devillanova, C. Preti, and G. Verani. J. Chem. Soc. (A), 1465 (1971).
9. D. De Filippo, F. Devillanova, C. Preti, E. F. Trogu, and P. Viglino. Inorg. Chim. Acta, **6**(1), 23 (1972).
10. R. J. Clark, G. Natile, U. Belluco, L. Cattalini, and C. Filippini. J. Chem. Soc. (A), 659 (1970).
11. P. P. Singh and R. Rivest. Can. J. Chem. **46**, 2361 (1968).
12. B. Crociani, T. Toschi, R. Pietropaolo, and U. Belluco. J. Chem. Soc. (A), 531 (1970).
13. R. J. H. Clark and C. S. Williams. Chem. and Ind. 1317 (1964).
14. R. J. H. Clark and C. S. Williams. Inorg. Chem. **4**, 350 (1965).
15. M. N. Hughes and R. J. Rutt. J. Chem. Soc. (A), 3015 (1970).
16. T. Tarantelli and C. Furlani. J. Chem. Soc. (A), 1717 (1968); Gazz. Chim. Ital. **100**, 1012 (1970).
17. M. J. Norgett, J. H. M. Thornley, and L. M. Venanzi. J. Chem. Soc. (A), 540 (1967).
18. W. J. Eilbeck, F. Holmes, and A. E. Underhill. J. Chem. Soc. (A), 757 (1967).
19. L. S. Ahuja. Inorg. Chim. Acta **3**, 110 (1969).
20. K. Nakamoto, J. Fujita, S. Tanaka, and M. Kobayshi. J. Am. Chem. Soc. **79**, 4904 (1957).
21. P. S. K. Chia, S. E. Livingstone, and T. N. Lockyer. Aust. J. Chem. **19**, 1391 (1966).
22. R. A. Walton. Inorg. Chem. **5**, 643 (1966).
23. L. S. Ahuja. J. Inorg. Nucl. Chem. **29**, 2091 (1967).
24. B. M. L. Goodgame, M. Goodgame, P. J. Hayward, and J. W. Rayner-Canham. Inorg. Chem. **7**, 2447 (1968).

Can. J. Chem. Downloaded from www.nrcresearchpress.com by 210.87.254.105 on 09/05/12
For personal use only.

Trends in the Spectrochemical Series and ^{31}P Chemical Shifts of Five-coordinated Cyclopentadienylnickel(II) Complexes

J. THOMSON AND M. C. BAIRD

Department of Chemistry, Queen's University, Kingston, Ontario

Received June 14, 1972[1]

The electronic spectra and ^{31}P n.m.r. spectra of the complexes π-$C_5H_5NiPPh_3X$ (X = Cl, Br, I, NCO, NCS, NO_2, CN, $SnCl_3$, $SnPh_3$, $PbPh_3$, alkyl, and aryl) have been obtained and interpreted. The "common" anions form a spectrochemical series which is identical with that reported for many octahedral systems, while the carbon, tin, and lead donors lie relatively high in the series. Currently accepted theory for the chemical shifts of ligand donor atoms fails to satisfactorily rationalize the ^{31}P chemical shifts.

Les spectres électroniques et les spectres de RMN du ^{31}P des complexes π-$C_5H_5NiPPh_3X$ (X = Cl, Br, I, NCO, NCS, NO_2, CN, $SnCl_3$, $SnPh_3$, $PbPh_3$, alkyle, et aryle) ont été obtenus et interprétés. Les anions "courants" forment une série spectrochimique identique à celles rapportées pour plusieurs systèmes octaèdraux tandis que les donneurs carbone, étain et plomb se trouvent à des valeurs relativement élevées dans la série. La théorie couramment acceptée sur les déplacements chimiques des atomes du ligand donneur ne rationalise pas de façon satisfaisante les déplacements chimiques du ^{31}P.

[Traduit par le journal]

Can. J. Chem., 51, 1179 (1973)

Introduction

During the current wave of interest in five-coordinated transition metal complexes (1–3), compounds of nickel(II) have played an important role (4). Both trigonal bipyramidal and square pyramidal complexes are known and have been intensively studied, and it seems to be generally assumed that all five-coordinated nickel(II) complexes are of one or both of these symmetries (or distortions thereof). It is the purpose of this paper to point out that the complexes π-C_5H_5NiLX (L = neutral ligand; X = monoanion) are 18-electron systems and thus may also be considered to be five-coordinated. They have a quite different symmetry from the other nickel(II) systems previously studied, and yet the relative energies of the d–d transitions in their electronic spectra agree very well with the well-known spectrochemical series for octahedral nickel(II) complexes (5).

We also report the ^{31}P chemical shifts for a variety of triphenylphosphine complexes. We have previously reported data for a few of these compounds in an attempt to correlate chemical shifts with electronic spectra in accord with the well-known equation describing the second order paramagnetic term (6). The correlation seemed promising, although the slope of the resulting linear plot had the wrong sign (7). We now realize that the theory of Buckingham and Stephens (8) for the chemical shifts of ligand donor atoms should be much more applicable to this system; unfortunately, in adding more compounds to the series, the linearity of the correlation is lost.

Experimental

The compounds π-$C_5H_5NiPPh_3X$ (X = Me, Et, *n*-Pr, *iso*-Pr, *n*-Bu, *iso*-Bu, *sec*-Bu, Ph, CH_2Ph, CH_2SiMe_3, $CHPhSiMe_3$, $SnPh_3$, $PbPh_3$, $SnCl_3$, CH_2CMe_3, CN, NCO, NO_2, NCS, Cl, Br, I) and $[\pi$-$C_5H_5Ni(PPh_3)_2]^+$-BF_4^- were prepared by the methods outlined previously (9–13).

Visible and Ultraviolet Spectra

The electronic spectra of the complexes were obtained on a Unicam SP800 spectrophotometer. Three absorptions with extinction coefficients of approximately 10^4, 10^3, and 10^2 cm^{-1} mol^{-1} were observed in most cases using 0.015 *M* solutions (prepared under nitrogen) of the complexes in cyclohexane and cells of pathlengths 0.1, 1.0, and 10 cm, respectively. The results are shown in Table 1.

^{31}P Nuclear Magnetic Resonance Spectra

The ^{31}P n.m.r. spectra were run on a Bruker HX60 spectrometer using approximately 0.5 *M* CS_2 solutions in 13 mm tubes. Hexafluorobenzene, which was used as lock, was contained in a coaxial tube, and complete proton decoupling was accomplished by broad-band decoupling at 60 MHz. The chemical shifts are listed in Table 1 referenced to 85% phosphoric acid (downfield shifts negative).

[1]Revision received December 15, 1972.

Can. J. Chem. Downloaded from www.nrcresearchpress.com by 210.87.254.42 on 09/05/12
For personal use only.

TABLE I. Electronic spectra and ^{31}P chemical shifts of the complexes π-$C_5H_5NiPPh_3X$

X	λ (mμ)	(ε)	δ (p.p.m.)	X	λ (mμ)	(ε)	δ (p.p.m.)
Me	296	(10400)	−49.5	$SnPh_3$	347	(6890)	−49.8
	394	(1440)			~405 (Sh)	(~1850)	
	586	(65)			568	(70)	
Et	300	(10000)	−49.0	$PbPh_3$	386	(10850)	−42.7
	406	(1300)			~440 (Sh)	(~3000)	
	575	(80)			568	(80)	
n-Pr	300	(7640)	−49.1	$SnCl_3$*	307 (Sh)	(10000)	−38.9
	405	(1010)			340 (Sh)	(6000)	
	575	(65)			448	(1190)	
					646	(60)	
iso-Pr	306	(7650)	−47.6				
	418	(1190)		*N*CO*	317	(10000)	−27.1
	560	(85)			486	(1230)	
					789	(65)	
n-Bu	301	(9550)	−49.1				
	406	(1280)		*N*CS*	305	(10500)	−27.9
	573	(80)			~347 (Sh)	(~4600)	
					461	(1410)	
iso-Bu	303	(8920)	−47.9		757	(80)	
	413	(1075)					
	589	(70)		CN*	297	(13100)	−39.7
					406	(990)	
sec-Bu	308	(7430)	−47.2		607	(60)	
	420	(1140)					
	572	(70)		NO_2*	~300 (Sh)	(~9500)	−29.4
					~335 (Sh)	(~7700)	
CH_2SiMe_3	309	(10700)	−45.9		461	(1500)	
	421	(1240)			650	(40)	
	639	(85)					
				Cl	331	(8500)	−27.6
CH_2CMe_3	305	(6940)	−46.1		512	(900)	
	424	(800)			835	(31)	
	600	(75)					
				Br	344	(5300)	−32.0
$CHPhSiMe_3$	373	(4700)	−42.3		518	(870)	
	464	(1370)			845	(32)	
	674	(100)					
				I	~350 (Sh)	(4200)	−41.9
Ph	305	(10300)	−41.9		527	(770)	
	408	(1200)			~850 (Sh)	(34)	
	559	(95)					
				PPh_3†	~340 (Sh)	(~7350)	−42.7
CH_2Ph	306	(5650)	−46.7		441	(1300)	
	446	(2030)			553	(100)	
	629	(85)					

*In chloroform.
†$[\pi\text{-}C_5H_5Ni(PPh_3)_2]^+BF_4^-$.

Discussion

Several crystal structure determinations have been carried out (13–16) for complexes of the type discussed here, and it has been shown that generally the PNiX plane is orthogonal to the C_5H_5 ring.

Considering the cyclopentadienyl group as a three-electron pair donor, the nickel is thus five-coordinated. Of the transitions listed in Table 1, the high energy band of extinction coefficient 4200 – 13 100 can generally be attributed to a charge transfer transition associated with the aromatic ligands and will not be considered further. In the cases of X = $CHPhSiMe_3$, $SnPh_3$, $PbPh_3$, and $SnCl_3$, this band is of unusually low energy and may be associated with

Can. J. Chem. Downloaded from www.nrcresearchpress.com by 210.87.254.42 on 09/05/12
For personal use only.

Can. J. Chem. Downloaded from www.nrcresearchpress.com by 210.87.254.42 on 09/05/12
For personal use only.

the anionic ligands; the relative energies of the charge transfer bands of the halide complexes are in the order expected for halide-to-metal charge transfer transitions (17).

The microsymmetry about the nickel in the complexes is very low (C_s, and then only for one orientation of the C_5H_5 ring), and thus there is no center of inversion and the parity selection rule may be expected to be relaxed. Making this assumption, we attribute the two low-energy bands in the spectrum of each compound to transitions between orbitals which are essentially nickel d orbitals in character. On this basis, a spectrochemical series for the "common" anions, X, can be established which parallels exactly that established for octahedral complexes (5), *i.e.*

$$I < Br < Cl < NCS < NO_2 < CN$$

This correlation, which holds for both series of the weaker bands, confirms that the bands can be attributed to d–d transitions. It may be noted also that trigonal bipyramidal and square pyramidal complexes of nickel(II) also often exhibit two d–d transitions in their spectra, although the relative intensities are often reversed (4).

The correlation between the two series is not very good for the IVa donors, although definite trends can be established. The complete spectrochemical series for the stronger and weaker d–d transitions, respectively are: $I < Br < Cl \ll NCO < NCS \ll CHPhSiMe_3 < NO_2 \ll SnCl_3 < CH_2Ph < PPh_3 \sim PbPh_3 \ll CH_2CMe_3 < CH_2SiMe_3 \sim$ *sec*-Bu $<$ *iso*-Pr $<$ *iso*-Bu $< Ph < SnPh_3 =$ *n*-Bu $= Et = CN \sim$ *n*-Pr $< CH_3$; $I < Br < Cl \ll NCO < NCS \ll CHPhSiMe_3 < NO_2 < SnCl_3 < CH_2SiMe_3 < CH_2Ph < CN < CH_2CMe_3 <$ *iso*-Bu $< CH_3 < Et =$ *n*-Pr $<$ *n*-Bu $\sim$ *sec*-Bu $< SnPh_3 = PbPh_3 <$ *iso*-Pr $\sim Ph < PPh_3$.

Although Ciampolini (18) successfully applied a crystal field model to explain the spectra of a number of trigonal bipyramidal and square pyramidal complexes of nickel(II), such an approach should be inappropriate for the complexes discussed here. Unfortunately, a semi-empirical molecular orbital calculation (19) has also proven inadequate to describe the spectra, and thus assignments of the d–d transitions cannot unambiguously be made at this time.

Although the differences in details of the two spectrochemical series cannot be explained, it would seem that some generalizations and comparisons with other systems can be made. First, the carbon donors in both series exhibit very high ligand field strengths, in some cases greater even than cyanide, and in most cases greater than the nitro or trichlorotin groups. These results are to some extent in contrast to the spectrochemical series found for the systems *trans*-$RuXY[C_2H_4(PMe_2)_2]_2$ (X = Y = Cl, Br, I, CN; X = H, Me, Ph, *p*-tolyl, Y = Cl) (20) and $[Rh(NH_3)_5X]^{2+}$ (X = I, Br, Cl, Et, *n*-Pr, *n*-Bu, NH_3, NO_2) (21). In the ruthenium system, the methyl group was found to exhibit a high ligand field strength, although less than that of cyanide. In the rhodium system on the other hand, the alkyl groups were placed below even ammonia and the nitro group. Thus it appears that relative ligand field strengths for strong field ligands may vary between different systems of transition metal complexes.

The triphenyltin and -lead groups are obviously strong field ligands, presumably because of their strong donor abilities, while the trichlorotin group may owe its position above, for instance, the nitro group to its pronounced π-acid properties (22, 23) (the σ-donor properties of this ligand have not yet been satisfactorily established (22, 23)).

The position of the isocyanate group in the spectrochemical series appears not to have been established in many metal systems; the ion lies between chloride and isothiocyanate in the nickel system. The position of triphenylphosphine is highly ambiguous, but this ligand does lie, as expected, high in the spectrochemical series.

The phosphorus chemical shifts were determined in an attempt to clarify some of the confusion in this area (6). By keeping the metal and the phosphine constant and varying only the relatively distant substituents on the nickel, it was hoped that we could avoid, for instance, the variations in the diamagnetic contribution and the substituent effects of the groups bonded to the phosphorus, and the deviations of symmetry about the phosphorus that have plagued other workers (6).

As expected, an attempted correlation of the phosphorus chemical shifts with the electronegativities of the anions was unsatisfactory, suggesting that inductive effects are not important. To test the theory of Buckingham and Stephens (8), we plotted the ^{31}P chemical shifts

vs. the wavelength of the stronger d–d transition, choosing this transition rather than the other on the grounds that its greater intensity suggests that it is probably not of "pure" d–d character, but may involve significant mixing of ligand character into the orbitals involved (24).

Assuming a constant metal–ligand distance and d-orbital exponent (Slater k), the theory, developed originally for transition metal hydrides, predicts that the shielding of the donor nucleus should decrease as the separation between the ground and excited state(s) of the metal increases. The theory appears to apply to about half of the compounds studied in this paper, to our knowledge the first time such a correlation has been made for tertiary phosphine coordination compounds.

Unfortunately the correlation does not hold for the bromo and iodo complexes, which have anomalously low chemical shifts, or for the phenyl, cyano, trichlorotin, nitro, isocyanato, isothiocyanato and triphenylphosphine complexes, which have anomalously high chemical shifts. Interestingly, Buckingham and Stephens (24) noted that the hydride chemical shifts of many hydrido–halide complexes also decrease in the order Cl > Br > I, *i.e.* the reverse of the order expected from the relative ligand field strengths. To explain this apparent anomaly, they suggested an increase in the covalency (change in k) in the order Cl < Br < I, as predicted by the relative positions of these ligands in the nephelauxetic series (25). Such covalency factors may dominate the chemical shifts in many other metal systems (26), and may be considered a result of the strong π-donor abilities of the halide ions, which are expected to increase in the order Cl < Br < I (21).

On this basis, the anomalously high chemical shifts of the phenyl, cyano, trichlorotin, triphenylphosphine and nitro groups may perhaps be a result of the π-acid properties of these ligands. We are aware of no evidence for π-acid properties of the isocyanate and isothiocyanate groups, but both at least have π-antibonding orbitals of the correct symmetry to π-bond to the nickel. At any rate, the presence of π-acidic ligands might be expected to raise the ^{31}P chemical shifts to higher fields.

The ^{31}P chemical shifts of the methyl, benzyl, and phenyltrimethylsilylmethyl derivatives remain anomalous.

We are grateful for financial assistance from the International Nickel Company of Canada and the National Research Council of Canada.

1. C. FURLANI. Coord. Chem. Rev. **3**, 141 (1968).
2. M. CIAMPOLINI. Struct. Bonding, **6**, 52 (1969).
3. B. A. FRENZ and J. A. IBERS. Inorg. Chem. **11**, 1109 (1972) and refs. therein.
4. L. SACCONI. Trans. Met. Chem. **4**, 199 (1968).
5. A. B. P. LEVER. Inorganic electronic spectroscopy. Elsevier, New York. 1968. p. 203.
6. J. F. NIXON and A. PIDCOCK. Ann. Rev. NMR Spectrosc. **2**, 346 (1969).
7. J. THOMSON, D. GROVES, and M. C. BAIRD. J. Mag. Res. **5**, 281 (1971).
8. A. D. BUCKINGHAM and P. J. STEPHENS. J. Chem. Soc. 2747 (1964).
9. H. YAMAZAKI, T. NISHIDO, Y. MATSUMOTO, S. SUMIDA, and N. HAGIHARA. J. Organomet. Chem. **6**, 86 (1966).
10. J. THOMSON and M. C. BAIRD. Can. J. Chem. **48**, 3443 (1970).
11. M. VAN DEN AKKER and F. JELLINEK. J. Organomet. Chem. **10**, P37 (1967).
12. J. THOMSON, W. KEENEY, M. C. BAIRD, and W. F. REYNOLDS. J. Organomet. Chem. **40**, 205 (1972).
13. J. THOMSON and M. C. BAIRD. Inorg. Chim. Acta. In press.
14. M. R. CHURCHILL and T. A. O'BRIEN. J. Chem. Soc. A, 2970 (1968).
15. M. R. CHURCHILL and T. A. O'BRIEN. J. Chem. Soc. A, 161 (1970).
16. F. GLOCKLING, A. MCGREGOR, M. L. SCHNEIDER, and H. M. M. SHEARER. J. Inorg. Nucl. Chem. **32**, 3103 (1970).
17. Reference 5, p. 225.
18. M. CIAMPOLINI. Inorg. Chem. **5**, 35 (1966).
19. R. J. BURNS, G. ELDER, and J. P. COLPA. Unpublished results.
20. J. CHATT and R. H. HAYTER. J. Chem. Soc. 772 (1961).
21. K. THOMAS, J. A. OSBORN, A. R. POWELL, and G. WILKINSON. J. Chem. Soc. A, 1801 (1968).
22. G. W. PARSHALL. J. Am. Chem. Soc. **88**, 704 (1966).
23. K. L. WATTERS, W. M. BUTLER, and W. M. RISEN. Inorg. Chem. **10**, 1970 (1971).
24. Reference 5, p. 136.
25. Reference 5, p. 207.
26. R. R. DEAN and J. C. GREEN. J. Chem. Soc. A, 3047 (1968).

Can. J. Chem. Downloaded from www.nrcresearchpress.com by 210.87.254.42 on 09/05/12
For personal use only.

The Ultracentrifuge as a Pressure-Densitometer

KENNETH S. ROGERS, ROSALIND BURKAT, AND ALFRED J. RICHARD

Departments of Biochemistry and Pharmaceutical Chemistry, Medical College of Virginia, Health Sciences Division of Virginia Commonwealth University, Richmond, Virginia 23219

Received September 18, 1972

The Spinco E analytical ultracentrifuge has been used to determine specific volumes or densities for organic liquids and water at pressure from 1 to 100 bars. Specific volumes calculated from experimental isothermal compressibilities (β_T) were in very close agreement with values from measurements recorded in literature. Bulk modulus ($1/\beta_T$) *vs.* pressure plots indicated that the Lennard–Jones 6-12 potential does not satisfactorily describe the molecular interactions for carbon tetrachloride, benzene, cyclohexane, or water. The organic liquids were reasonably approximated by a 7-28 potential or more exactly by a 6-24 potential. None of the two-term potentials could account for the interaction of water molecules.

L'ultracentrifuge analytique a été utilise pour déterminer le volume spécifique de certains liquides organiques et de l'eau, aux pressions de 1 à 100 bars. Nos résultats sont comparables aved les résultats obtenus par d'autres méthodes. Nos résultats ne sont pas in accord avec le potentiel 6-12 de Lennard-Jones pour les liquides que nous avons étudiés; tétrachlorure de carbone, benzène, cyclohexane, et eau. Les interactions entre les molécules des liquides organiques sont interprétées approximativement par un potentiel 7-28 ou mieux, par un potentiel 6-24. Un potentiel de deux termes n'est pas suffisant pour expliquer les interactions entre les molécules d'eau.

Can. J. Chem., 51, 1183 (1973)

Can. J. Chem. Downloaded from www.nrcresearchpress.com by 210.87.254.5 on 09/05/12
For personal use only.

Introduction

Recently, we have reported additional evidence (1) that the ultracentrifuge may be used (2) to determine isothermal compressibilities

$$[1] \qquad \beta_T = -(1/V)(\mathrm{d}v/\mathrm{d}P)_T$$

for liquids at 1 bar and that β_T was inversely proportional to the cohesive energy of the liquid as measured by its bulk surface tension (1). In this study we wish to report the use of the ultracentrifuge as a pressure-densitometer in that specific volumes ($\bar{v}_p$) of liquids may be calculated directly from the definition (3) of β_T as a function of pressure, P, as follows:

$$[2] \qquad \int_{P=0}^{P=P} \beta_T \, \mathrm{d}P = -\int_{\bar{V}_0}^{\bar{V}_P} \frac{\mathrm{d}\bar{V}}{\bar{V}} = -\ln \frac{\bar{V}_p}{\bar{V}_0} = \ln \frac{\bar{V}_0}{\bar{V}_p}$$

The integral term may be evaluated graphically from a plot of β_T *vs.* P. $\bar{V}_0$ is the specific volume of liquid at 1 bar.

Other methods for determining β_T have required the direct measurement of liquid volume changes as a function of pressure (4, 5). Adiabatic compressibilities (6) have been calculated from the velocity of sound through a compressed liquid. These methods that do not use the ultracentrifuge may be open to some criticism in that (*a*) at low pressures, 0–200 bars, it is difficult to measure accurately the small changes which occur in the volume and (*b*) heat capacity data required for conversion of adiabatic compressibility to β_T may not be readily available. Therefore we have compared the specific volumes of several liquids at various pressures using the ultracentrifuge with those reported by other investigators.

In addition, we have calculated the tangent bulk modulus ($1/\beta_T$) directly from compressibility data. The pressure variation of $1/\beta_T$ is somewhat difficult to obtain from the experimentally observed volume changes of a liquid under pressure (7). Moelwyn-Hughes (3) has shown that $1/\beta_T$ can provide some insight into the molecular events that occur upon compression of a liquid from the following relationship

$$[3] \qquad \frac{\mathrm{d}(1/\beta_T)}{\mathrm{d}P} = (1/3)(y + z + 6)$$

where y and z are the attraction and repulsion exponents, respectively, of the Mie equation. Although it is quite common to assume that the Lennard–Jones potential, $y = 6$ and $z = 12$, may be used to approximate the interaction of organic molecules in the liquid state (3, 8), our data on the compressibility of liquids as a

Can. J. Chem. Downloaded from www.nrcresearchpress.com by 210.87.254.5 on 09/05/12
For personal use only.

function of pressure strongly indicate that such a supposition of the 6-12 potential is in error.

Experimental

The modified (1, 2, 9) procedure of Dayantis for pressure studies was used throughout this work. In addition the camera lens and the cylinder lens were refocussed for each liquid since Richards *et al.* (10) indicated the need for refocussing every time a solution of different refractive index was used. The method of Wiener (11) was used[1] to establish a linear relation between the plane of focus for schlieren optics in the ultracentrifuge cell along the optic axis, and the refractive index of the liquid contained in the cell. Our compressibility experiments were performed with the camera lens focussed on a level of the cell along the optic axis such that the emerging light ray would be recorded on the photograph at its entrance coordinate along the centrifugal axis. The optic and centrifugal axes are at 90° to each other. The linear relationship between the plane of focus measured from the back of a 1.2 cm centrifuge cell, and n the refractive index at 5461 Å, and 25° was

$$[4] \qquad X_{(cm)} = 0.2726\, n + 0.3914$$

From this least squares equation (r, correlation coefficient = 0.999) and known refractive indices of various organic liquids, correct focussing values could be obtained.

An aluminum centerpiece and sapphire windows were used in the centrifuge cell. All organic liquids were purchased CP or of spectroanalyzed grade and were used after drying overnight with pellet KOH or $CaSO_4$. Gases were eliminated by vacuum distillation. Water was double distilled from glass and then vacuum distilled. To keep gas contaminants minimal, it was necessary to fill and to cap the centrifuge cell under a helium atmosphere. Pictures were taken 30 min after reaching the appropriate temperature and speed, *e.g.* 25°, 33 450 r.p.m. and then 25°, 3000 r.p.m. in that order. The base line photograph was taken second to account for slight base line shifts frequently observed due to rearrangements of the cell components subjected to high centrifuge speeds (1). The photographic plates were aligned on their reference lines in a Nikon two dimensional microcomparator and readings of the height of the schlieren pattern above the references were taken every 0.2 cm. Meniscus values were obtained by extrapolation. The height (h) of the schlieren pattern at any speed above the base line pattern (3000 r.p.m.) was proportional to isothermal compressibility, β_T, as demonstrated by the equation of Dayantis (2)

$$[5] \quad (1 + (\beta_T)_p P)(\beta_T)_p = \frac{(h)6n_p \tan\theta}{Lam_1m_2(n_p^2 + 2)(n_p^2 - 1)\rho_0 w^2 r_p}$$

where θ was the schlieren bar angle, 70°; L, the optical lever; a, the cell thickness; m_1m_2, the vertical magnification of the optical system; w, the angular velocity; and r_p, the distance from center of rotation. Densities, ρ_0, of the liquids were literature values (12) and n_p, the refractive index of the liquids under pressure, was calculated as previously reported (9).

[1]L. I. Epstein, P. Nixon, and A. J. Richard. To be published.

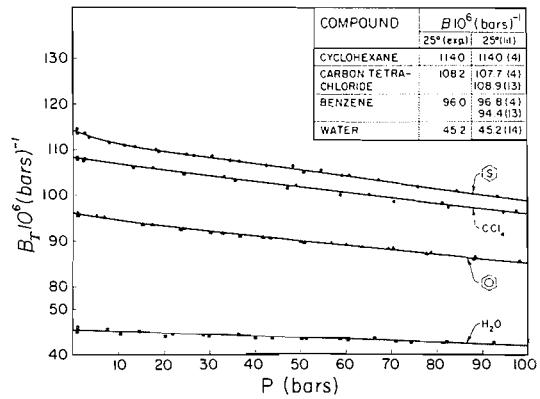

FIG. 1. Compressibilities (β_T) as a function of pressure for cyclohexane, carbon tetrachloride, benzene, and water at 25°.

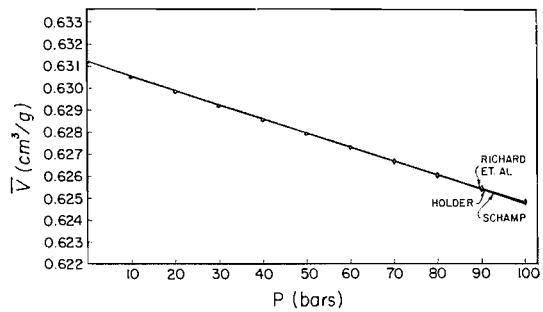

FIG. 2. The effect of pressure on specific volume ($\bar{v}$) of carbon tetrachloride.

Results and Discussion

In Fig. 1 are shown the plots of β_T *vs.* P for the liquids water, benzene, carbon tetrachloride, and cyclohexane at 25 °C. The *insert* compares our experimental β_T values with those in the literature at 1 bar. The specific volume of CCl_4 obtained at 25° from β_T values is plotted in Fig. 2 against pressure, together with curves given by Holder and Whalley (4) and by Schamp *et al.* (13). Excellent agreement may be seen between our work and that of Holder, since a difference at 100 bars of only 10 p.p.m. is observed (Table 1). An equation of state of the form

$$[6] \qquad \bar{V}_p = \bar{V}_0(1 - AP + BP^2 - CP^3)$$

may be used (4) to represent our data for liquids, *e.g.* carbon tetrachloride, benzene, cyclohexane,

TABLE 1. (*a*) Effect of pressure on the specific volumes of carbon tetrachloride, benzene, cyclohexane, and water at 25°

Compound	Equation 6 coefficients and their standard errors		
	A (bar^{-1})	B (bar^{-1})^2	C (bar^{-1})^3
CCl_4			
This work	$108.1 \pm 0.5 \times 10^{-6}$	$76.1 \pm 11 \times 10^{-9}$	$72.4 \pm 73 \times 10^{-12}$
Holder and Whalley (4)	$107.7 \pm 0.09 \times 10^{-6}$	$69.4 \pm 2.2 \times 10^{-9}$	$71 \pm 14 \times 10^{-12}$
Schamp *et al.* (13)	108.9×10^{-6}	68.2×10^{-9}	57×10^{-12}
Benzene			
This work	$95.3 \pm 1.7 \times 10^{-6}$	$61.1 \pm 41 \times 10^{-9}$	$53.5 \pm 26.9 \times 10^{-12}$
Holder and Whalley (4)	$96.8 \pm 0.2 \times 10^{-6}$	$42.9 \pm 3.0 \times 10^{-9}$	$22 \pm 8 \times 10^{-12}$
Schamp *et al.* (13)	94.4×10^{-6}	45.3×10^{-9}	29×10^{-12}
Cyclohexane			
This work	$112.5 \pm 0.9 \times 10^{-6}$	$79.9 \pm 21 \times 10^{-9}$	$48 \pm 140 \times 10^{-12}$
Holder and Whalley (4)	$114 \pm 0.3 \times 10^{-6}$	$81 \pm 5 \times 10^{-9}$	$81 \pm 27 \times 10^{-12}$
Water			
This work	$45.3 \pm 0.77 \times 10^{-6}$	$18.0 \pm 0.74 \times 10^{-9}$	0
Kell and Whalley (14)	45.2×10^{-6}	6.4×10^{-9}	6.2×10^{-12}

(*b*) Calculated $\bar{V}_p$ at 100 bars and 25°

	CCl_4	Benzene	Cyclohexane	Water	
				25°	20°
This work	0.62480	1.13442	1.27892	0.99864	0.99738
Holder and Whalley (4)	0.62479	1.13408	1.27870	—	—
Schamp *et al.* (13)	0.62471	1.13437	—	—	—
Kell and Whalley (14)	—	—	—	0.99853	0.99731

and water at 25°. $\bar{V}_p$ is the specific volume at any pressure, and $\bar{V}_0$ is the specific volume at 1 bar. The constants were evaluated by multiple linear least squares regression analysis; and these constants, A, B, and C, are listed in Table 1. Also given in Table 1 are the $\bar{V}_p$ values at 25 °C and 100 bars for comparison with those from the literature. Thus, it is concluded that the ultracentrifuge may be used to advantage for determining specific volumes or densities of organic liquids as a function of pressure. Errors in such determinations are not greater than one or two parts in ten thousand. The major difficulty in extending the pressure range of the ultracentrifuge above about 100 bars results from bending of the sapphire cell windows (at about 35 000 r.p.m.) for which no corrections can be made at present time.

In addition, it should be noted that the approximation inherent in eq. 5 where the pressure average β of the $(1 + (\beta_T)P)$ term is assumed to be $(\beta_T)P$ will be less satisfactory as pressure increases.

In order to evaluate the repulsion (z) and attraction (y) exponents of the Lennard–Jones type from eq. 3, the tangent bulk modulus $(1/\beta_T)$ was plotted against pressure (Fig. 3). The slopes $d(1/\beta_T)/dP$ for the three organic liquids carbon tetrachloride, benzene, and cyclohexane, range from 11.7–12.0. The slope for water was 18.8. An unexplained downward curvature was noted at low pressures for the three organic liquids. Although the 6-12 potential was successful in representing molecular interactions of the inert gases and mercury (3), the work of Hamann and Lambert (15) and of Gupta and King (16) has shown that 7-28 potential functions were superior in representing the experimental properties of high density gases and fluids of somewhat spherical molecules, *e.g.* CCl_4. Application of 7-28 potential to eq. 3 permits calculations of a $d(1/\beta_T)/dP$ value of 13.6 whereas a 6-12 potential gave a $d(1/\beta_T)/dP$ value of 8. Thus, use of the 7-28 potential approximates our data (Fig. 3) much more closely than use of the 6-12 potential. A 6-24 potential would best describe

Can. J. Chem. Downloaded from www.nrcresearchpress.com by 210.87.254.5 on 09/05/12
For personal use only.

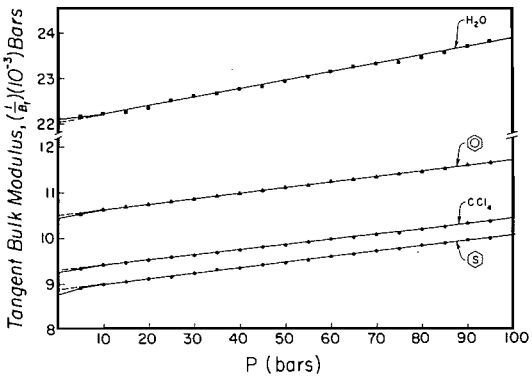

FIG. 3. The effect of pressure on the tangent bulk modulus ($1/\beta_T$) of several liquids.

our data. Water, because of its dipolar nature, behaves differently from the organic liquids and should require at least a three term potential such as the one presented by Rao and Keer (17). There is considerable evidence that liquid water also may contain ice-like clusters at 25° (18) and thus may not behave as a "pure" liquid. Unfortunately, the three term approach leads to an expression for $d(1/\beta_T)/dP$ which is dependent upon the distance between molecules at the potential energy minimum and on the distance between molecules when the potential energy equals zero. Neither of these distances are known experimentally.

1. A J. RICHARD and K. S. ROGERS. Can. J. Chem. **49**, 3956 (1971).
2. J. DAYANTIS. C. R. Acad. Sci. Paris Ser. C, **267**, 223 (1968).
3. E. A. MOELWYN-HUGHES. Physical chemistry. Pergamon Press, New York. 1957. pp. 259, 323.
4. G. A. HOLDER and E. WHALLEY. Trans. Faraday Soc. **58**, 2095 (1962).
5. M. DIAZ PENA and M. L. MCGLASMAN. Trans. Faraday Soc. **57**, 1511 (1961).
6. E. B. FREYER, J. C. HUBBARD, and D. H. ANDREWS. J. Am. Chem. Soc. **51**, 759 (1929).
7. A. T. J. HAYWARD. Brit. J. Appl. Phys. **18**, 965 (1967).
8. J. L. WEBB. Enzyme and metabolic inhibitors. Vol. I. Academic Press, New York. 1963 pp. 229–237.
9. A. J. RICHARD, J. GLICK, and R. BURKAT. Anal. Biochem. **37**, 378 (1970).
10. E. G. RICHARDS, D. TELLER, and H. K. SCHACHMAN. Anal. Biochem. **41**, 189 (1971).
11. O. WIENER. Ann. Phys. Chem. **49**, 105 (1893).
12. Handbook of chemistry and physics. 49th ed. The Chemical Rubber Co., Cleveland, Ohio. 1966. pp. F-12 through F-31.
13. H. W. SCHAMP, J. R. HASTINGS, and S. WEISSMAN. Phys. Fluids, **8**, 8 (1965).
14. G. S. KELL and E. WHALLEY. Phil. Trans. Roy. Soc. Lond. A, **2**, 58, 565 (1965).
15. S. D. HAMANN and J. A. LAMBERT. Aust. J. Chem. **7**, 18 (1954).
16. S. K. GUPTA and A. D. KING. Can. J. Chem. **50**, 660 (1972).
17. R. V. G. RAO and H. V. KEER. Z. Phys. Chem. **119**, 321 (1962).
18. G. NEMETHY and H. A. SCHERAGA. J. Chem. Phys. **36**, 3382 (1962).

Can. J. Chem. Downloaded from www.nrcresearchpress.com by 210.87.254.5 on 09/05/12
For personal use only.

Folded Conformations. IV. Intramolecular Shielding and Intramolecular Charge-Transfer Interaction in Benzyl Phenyl Sulfones and Sulfoxides

(MRS.) RENÉE VAN EST-STAMMER AND JAN B. F. N. ENGBERTS[1]

Department of Organic Chemistry, The University, Zernikelaan, Groningen, The Netherlands

Received September 18, 1972

Proton magnetic resonance spectra of the title compounds (A-SO_2CHR-D) were measured and compared with the spectra of appropriate reference systems containing an alkyl substituent instead of one of the aromatic rings. The observed upfield shifts of the aromatic proton resonances in the title compounds suggest that there is a significant population of folded conformations, which possess a *gauche* orientation of the aromatic rings. This conclusion is supported by the observation of an intramolecular charge-transfer band in the u.v. spectra of the compounds containing an A ring of high electron affinity and a D ring of low ionization potential. Stabilization of the folded forms may be obtained through minimizing the n–π repulsive forces between the sulfonyl oxygen lone pairs and the π-electron system of the D ring.

Les spectres de résonance magnétique nucléaire des composés cités (A-SO_2CHR-D) ont été enregistrés et comparés avec les spectres de référence de systèmes appropriés contenant un substituant alkyle au lieu d'un des cycles aromatiques. Les déplacements observés pour les protons aromatiques vers un champ élevé, laissent penser à l'existence d'une population importante en conformères plissés qui possèdent une orientation *gauche* pour les cycles aromatiques. Cette conclusion a été confirmée par l'observation en u.v. d'une bande de transfert de charge intramoléculaire pour les composés possédant un cycle A d'électroaffinité élevée et un cycle D à faible potentiel d'ionisation. La stabilisation des formes plissées peut être obtenue par minimisation des forces répulsives n–π entre les doublets libres de l'oxygène du groupe sulfonyle et le système électronique π du cycle D. [Traduit par le journal]

Can. J. Chem., **51**, 1187 (1973)

Introduction

During recent years it has been established that in solution a number of relatively simple molecules, possessing many degrees of internal rotational freedom, occur in preferred folded conformations (1–6). In suitably designed structures reliable probes for the detection of these folded conformations are: (*i*) intramolecular (de)shielding effects in n.m.r. spectra and (*ii*) intramolecular charge-transfer (CT) interaction between donor (D) and acceptor (A) groups which are positioned in the vicinity of each other as a result of the folding of the molecule (2, 7–13).

It has been shown by X-ray crystallography that the folded conformation of cyclo-glycyl-L-tyrosyl (14) and of ethyl *N*-methyl-*N*-*p*-tolylsulfonylmethylcarbamate (15) is retained in the solid state. In sharp contrast, 2-methyl-3-*N*-methylanilinomethyl-1,4-naphthoquinone, which shows intramolecular CT interaction in solution (10), adopts an unfolded conformation in the crystal (16).

The causes of the folding of the molecules in question have not been defined clearly. Intramolecular dipole–dipole interactions, dipole-induced dipole interactions, and dispersion forces have all been invoked to explain the conformational preferences (3–5).

Preliminary work (2) has demonstrated the occurrence of folded conformations for benzyl phenyl sulfones (A-SO_2CH_2-D). In continuing these studies, we have now obtained new data that shed some additional light on the factors that help to stabilize the folded forms.

Results and Discussion

In Table 1 chemical shifts are presented of the aromatic protons of systems of the type A-SO_2CHR-D (R = H and —CH_3). In order to check for n.m.r. spectral perturbations due to intramolecular proximity effects, the selection of proper reference compounds is of crucial importance. We have used systems related as closely as possible to the compounds under study, but lacking either the A or D aromatic ring (n.m.r. data also included in Table 1). Unfortunately, for the D part of **6** no reliable reference is available at the moment because of our inability to prepare the corresponding alkane sulfonyl derivative.

[1]To whom correspondence should be addressed.

Can. J. Chem. Downloaded from www.nrcresearchpress.com by 210.87.254.42 on 09/05/12
For personal use only.

TABLE 1. Chemical shifts of the aromatic protons of the D and A groups of the compounds A-SO_2CHR-D (R = —H and —CH_3), A-S(O)CH_2-D, A-SCH_2-D, and of suitable reference compounds (40°)*

Compound	A		D	
	$\delta_{H_{2,6}}$†	$\delta_{H_{3,5}}$†	$\delta_{H_{2,6}}$†	$\delta_{H_{3,5}}$†
1 *p*-$NO_2C_6H_4SO_2CH_2C_6H_4N(CH_3)_2$-*p*	7.77 (23.4)	8.23 (10.8)	6.88 (21.0)	6.54 (10.8)
2 *p*-$NO_2C_6H_4SO_2CH_3$	8.16	8.41		
3 $C_2H_5SO_2CH_2C_6H_4N(CH_3)_2$-*p*			7.23	6.72
4 *p*-$NO_2C_6H_4SO_2CH(CH_3)C_6H_4N(CH_3)_2$-*p*	7.73 (25.8)	8.20 (12.6)	6.96 (18.6)	6.57 (7.8)
5 $C_2H_5SO_2CH(CH_3)C_6H_4N(CH_3)_2$-*p*			7.27	6.70
6 (*p*-$NO_2C_6H_4SO_2CH_2C_6H_4$-*p*)$_2NCH_3$	7.86 (18.0)	8.27 (8.4)	7.01‡	6.86‡
7 *p*-$ClC_6H_4SO_2CH_2C_6H_4OCH_3$-*p*	7.50 (21.6)	7.37 (10.2)	6.97 (21.0)	6.77 (9.6)
8 *p*-$ClC_6H_4SO_2CH_3$	7.86	7.54		
9 *n*-$C_4H_9SO_2CH_2C_6H_4OCH_3$-*p*			7.32	6.93
10 *p*-$ClC_6H_4S(O)CH_2C_6H_4OCH_3$-*p*	7.36 (13.2)	7.26 (8.4)	(22.8) 6.82§	(0.0)
11 *p*-$ClC_6H_4S(O)CH_3$	7.58	7.40		
12 *n*-$C_4H_9S(O)CH_2C_6H_4OCH_3$-*p*			7.20	6.82
13 *p*-$ClC_6H_4SCH_2C_6H_4OCH_3$-*p*	(0.6) 7.17§	(0.6)	7.13 (3.0)	6.78 (0.6)
14 *p*-$ClC_6H_4SCH_3$	7.18§			
15 *n*-$C_4H_9SCH_2C_6H_4OCH_3$-*p*			7.18	6.79

*Chemical shifts in p.p.m. downfield from internal TMS (δ = 0). Concentration 0.2 *M* in $CDCl_3$. Ring carbon attached to SO_2, S(O), S, or CHR is called C_1.
†Upfield shifts ($\Delta\delta_H$) in Hz between parentheses.
‡No suitable reference available.
§Center of broad singlet.

The data given in Table 1 reveal that the aromatic proton resonances of **1**, **4**, **6**, and **7** are shifted to higher field by *ca.* 0.15–0.40 p.p.m. ("$\Delta\delta_H$-values"). Since the effect of dilution (0.1–1.0 *M*) on the chemical shifts is negligible (<0.05 p.p.m.), significant shifts due to intermolecular shielding can be excluded. Therefore, the upfield shifts suggest that these compounds possess significant populations of conformations in which the aromatic rings experience each other's magnetic anisotropy effect.

In the benzyl sulfones a conformation with eclipsed aryl rings will be sterically unfavorable owing to π–π repulsion. Conformations with S=O eclipsed with the D ring will be destabilized by n–π repulsion. However, two *gauche* conformations, which permit mutual shielding of the aromatic ring protons, are easily attainable (Fig. 1). The observed upfield shifts are only slightly smaller than those found for the phenyl

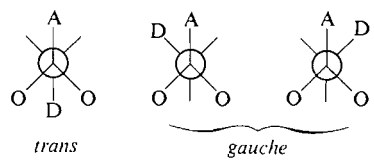

FIG. 1. Newman projections of stable rotamers, that result from rotation about the SO_2—CHR bond in A-SO_2CHR-D.

TABLE 2. Position (λ_{max}) and molar absorptivity (ε_{max}) of the intramolecular CT band of some sulfonyl systems (in $CHCl_3$)

Compound	Color	λ_{max} (nm)	ε_{max} (l mol^{-1} cm^{-1})
1	Orange	364	526
4	Orange	367	590
6	Red	365 (sh)	1740

absorptions of 1,8-diphenylnaphthalene (17) where the phenyl rings assume a preferred face-to-face arrangement.

Additional evidence for folding of the sulfonyl systems is provided by u.v. spectroscopy. Those compounds that contain an A ring of high electron affinity together with a D ring of low ionization potential are colored and they exhibit a broad and structureless long-wavelength absorption band which cannot be attributed to either of the separate chromophores (Table 2 and Fig. 2). The new band obeys Beer's law in the concentration range between at least 10^{-5}–10^{-3} *M*. This strongly suggests that the band should be attributed to intramolecular CT interaction. Since it is reasonable to suppose that the σ and π electrons of the SO_2—CHR bridge are involved to only a minor extent in the CT interaction (18), the transition will be mainly

Can. J. Chem. Downloaded from www.nrcresearchpress.com by 210.87.254.42 on 09/05/12
For personal use only.

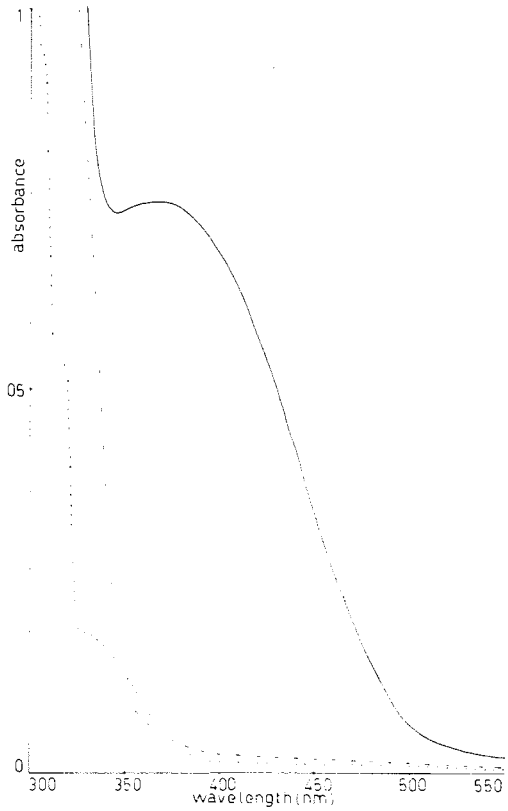

FIG. 2. U.v. spectra of 10^{-3} *M* solutions of **4** (—), **2** (···), and *p*-$CH_3C_6H_4CH_2C_6H_4N(CH_3)_2$-*p* (---) in $CHCl_3$.

the result of excitation of an electron from the highest occupied molecular orbital of the D ring to the lowest vacant orbital of the A ring in a folded conformation. However, there is a considerable difference in orientation of the A and D ring in the folded form of **1** as compared with that in the *inter*molecular complex between *N*,*N*-dimethyl-*p*-toluidine and methyl *p*-nitrophenyl sulfone because in the latter case a CT band is observed at much longer wavelength (2). It is of interest to note that sulfone **6**, which contains two potential donor–acceptor systems, shows a much larger ε_{max} (at 365 nm) than **1**. Apparently both benzyl phenyl sulfone systems are partially folded in solution.

For **1**, **4**, and **7** (and the corresponding reference compounds) the temperature dependence of the n.m.r. and u.v. spectra was examined in the hope of obtaining sufficiently large effects to allow the calculation of the thermodynamic parameters for the equilibrium between folded and unfolded forms. Although at higher temperatures deshielding of the aromatic proton resonances was observed, indicating partial unfolding, the differences were distressingly small (*i.e.* <3 Hz over the range -60 to $+60°$ in $CDCl_3$ or $+40$ to $+180°$ in DMSO-d_6).

However, the temperature effect suggests that there exists a (small) preference for the folded *gauche* conformations. This is in contrast to the situation for (substituted) 1,2-diphenylethanes where the *trans*-form is definitely favored, presumably owing to the repulsive π–π interaction in the *gauche* forms (19).

For **1** an increase in temperature is accompanied by a small hypsochromic shift of the CT maximum (17.8°, λ_{max} 368 nm, ε_{max} 526 l mol^{-1} cm^{-1}; 47.8°, λ_{max} 360 nm, ε_{max} 536 l mol^{-1} cm^{-1}), most likely attributable to a solvent-effect. The limited data presented in Table 3 also suggest that solute–solvent interactions play a role in determining the equilibrium between folded and unfolded forms. More polarizable solvents seem to destabilize the folded conformations of **7** in contrast to the minor effect of solvent polarizability on the folding tendency of some cyclic peptides (4).

The data obtained thus far do not allow definite conclusions regarding all possible mechanisms which may produce the folding tendency of the molecules. It is clear however, that CT interaction does not contribute significantly to the ground state stabilization as demonstrated by the approximately equal $\Delta\delta_H$ values for **1** and **7**.

In order to investigate whether dipolar interactions involving the strongly polarized sulfur–oxygen bonds of the sulfonyl function are effective in producing folded *gauche* conformations, we have prepared the sulfoxide and sulfide analogs of **7**. The data in Table 1 reveal that intramolecular shielding is decreased in the sulfoxide **10** and is negligible in the sulfide **13**, as compared with **7**. These results may be rationalized by assuming that the repulsive interaction between the lone pairs on the sulfonyl oxygen(s) and the π-electron cloud of the D ring (Fig. 1) will at least partially determine the favored dihedral angle defined by the bonds C_1^A—S—CHR—C_1^D and therefore the folding tendency. The known preference (20) of aryl sulfones to adopt conformations in which the ring C_1^A 2*p*-orbital is staggered between the two sulfonyl oxygen atoms ("case II conjugation")

Can. J. Chem. Downloaded from www.nrcresearchpress.com by 210.87.254.42 on 09/05/12
For personal use only.

TABLE 3. Solvent effects on the upfield shifts, $\Delta\delta_H$*, of the aromatic protons of 7 (40°)

Compound	Solvent	A		D	
		$\Delta\delta_{H_{2,6}}$	$\Delta\delta_{H_{3,5}}$	$\Delta\delta_{H_{2,6}}$	$\Delta\delta_{H_{3,5}}$
7	$CDCl_3$	21.6	10.2	21.0	9.6
7	CF_3COOH	~20†	~3	18.6	8.4
7	DMSO-d_6	~16†	~2	15.6	5.4

*$\Delta\delta_H$ in Hz. Concentration of solute: 0.2 *M*.
†Less accurate values because of the broad resonances.

TABLE 4. Chemical shifts of alkyl groups in some sulfones, sulfoxides, and sulfides

Compound	Chemical shift* of		
	CH$_3$	$CH_3CH_2SO_2$—	—*CH*$_2$Ar
16 $CH_3SO_2CH_2C_6H_5$	2.74		4.26
17 $CH_3SO_2CH_3$	2.99		
18 $C_2H_5SO_2CH_2C_6H_5$	1.29	2.83	4.18
19 $C_2H_5SO_2C_2H_5$	1.40	3.02	
20 $C_2H_5SO_2C_6H_4CH_3$-*p*	1.25	3.09	
21 $CH_3SOCH_2C_6H_5$	2.45		4.03
22 CH_3SOCH_3	2.62		
23 $CH_3SCH_2C_6H_5$	1.96		3.64
24 CH_3SCH_3	2.06		

*Chemical shifts in p.p.m. downfield from internal TMS (δ = 0). Concentration 0.2 *M* in $CDCl_3$.

will help to orient the A and D ring parallel to each other.

In an attempt to gain additional evidence for the proposed nonbonded interactions, the chemical shifts were measured of alkyl groups in some sulfones, sulfoxides, and sulfides containing either an aryl or an alkyl moiety in one of the β-positions (Table 4). In **16**, **18**, and **21**, the methyl and ethyl groups clearly experience upfield shifts as compared with **17**, **19**, and **22**, respectively, most likely due to the magnetic anisotropy effect of the β-aryl group.[2,3] Analysis of the intramolecular shielding of the methyl group in the *gauche* conformations of **16**, **21**, and **23** using Johnson and Bovey's isoshielding lines (21) and known bond angles and distances (22–24) reveals that the shielding should be approximately equal in **16** and **23** and appreciably less in **21** (Table 5).[4] The data in Table 4 show however, that intramolecular shielding decreases in the order sulfone > sulfoxide > sulfide, as in the case of the benzyl phenyl sulfones, thereby supporting the proposed n–π repulsive interactions.

TABLE 5. Calculated and observed intramolecular shielding in the *gauche* conformations of **16**, **21**, and **23**

Compound	Shielding (Hz)		Mole fraction of *gauche* conformation*
	Calcd.	Observed	
16	+18	+15	0.83
21	+13	+10	0.77
23	+18	+6	0.33

*These values are presumably slightly too low because of the inductive effect of the β-aryl ring (see text).

Experimental

N.m.r. spectra were recorded on a Varian A-60 D spectrometer equipped with a Varian V 6049 variable temperature controller. The recorder was calibrated with a side band technique using a Hewlett–Packard 200 AB audiooscillator and a Hewlett–Packard 5223 L electronic counter. Chemical shifts are given relative to TMS (δ = 0) as internal reference. If necessary, peak assignments were confirmed through the use of $Eu(DPM)_3$ as a paramagnetic shift reagent. U.v. spectra were taken with a Zeiss PMQ II spectrophotometer using 1 cm cells at

[2]A downfield shift would be expected solely on basis of the inductive effect of the β-aryl ring.

[3]In **20** only the methyl part of the ethyl moiety can be positioned in the shielding region of the aromatic ring.

[4]Calculation of the intramolecular shielding in benzyl phenyl sulfones is less straightforward but it is reasonable to expect that the preference for *gauche* conformations will be decreased due to π–π repulsions.

Can. J. Chem. Downloaded from www.nrcresearchpress.com by 210.87.254.42 on 09/05/12
For personal use only.

TABLE 6. Yields and physical properties of the new compounds

Compound	Yield (%)	M.p. (°C)	Color	Recrystallizing solvent	I.r. of SO or SO_2 (cm^{-1}, KBr)
1	80	200–201	Orange	CH_2Cl_2/MeOH (1:1)	1149, 1345
3	30	114.5–115.5	Colorless	EtOH (96%)	1115, 1300
4	80	166–167	Dark red	CH_2Cl_2/MeOH (1:1)	1140, 1320
5	40	92–93	Colorless	EtOH (96%)	1125, 1300
6	40	207–209	Orange	CH_2Cl_2/MeOH (1:1)	1140, 1305
7	70	151–153	Colorless	EtOH (96%)	1145, 1325
9	70	69–71	"	"	1120, 1300
10	70	141–143	"	"	1040
12	60	93–95	"	"	1020
13	80	71–73	"	EtOH (60%)	—
14	40	*	"	—	—

*B.p. 119°/0.3 mm; n_D^{20} 1.5400.

room temperature and 2 cm cells at variable temperatures in a temperature-controlled cell holder. I.r. spectra were measured on a Perkin–Elmer model 257 or model 125.

Melting points (uncorrected) were determined with a Mettler FP 1 melting point apparatus equipped with a Mettler FP 52 microscope attachment. Elemental analyses were carried out in the Microanalytical Section of our Department (supervisor: Mr. W. M. Hazenberg) and were satisfactory for the new compounds described.

Compounds **2** (25), **8** (26), **11** (27), **14** (28), **16**, **18**, **20**, **21**, and **23** were prepared by literature procedures. The new compounds were prepared as follows: sulfones **1** and **3–6** by condensation of aromatic amine with formaldehyde (or acetaldehyde) and the appropriate sulfinic acid (29); benzyl sulfides **13** and **15** from the corresponding thiols with *p*-methoxybenzylalcohol (29, 30); and sulfoxides **10** and **12** and sulfones **7** and **9** by oxidation of **13** and **15**, respectively, with 30% H_2O_2 in acetic acid (31). Yields and physical data of the new compounds are given in Table 6.

1. R. VAN EST-STAMMER and J. B. F. N. ENGBERTS. Rec. Trav. Chim. **91**, 1298 (1972). (Part III of this series).
2. R. VAN EST-STAMMER and J. B. F. N. ENGBERTS. Tetrahedron Lett. 3215 (1971). (Part II of this series).
3. S. VAN DER WERF and J. B. F. N. ENGBERTS. Rec. Trav. Chim. **89**, 423 (1970) and refs. cited therein.
4. K. D. KOPPLE and D. H. MARR. J. Am. Chem. Soc. **89**, 6193 (1967).
5. K. D. KOPPLE and M. OHNISHI. J. Am. Chem. Soc. **91**, 962 (1969).
6. M. D. BENTLEY and M. J. S. DEWAR. Tetrahedron Lett. 5043 (1967).
7. W. N. WHITE. J. Am. Chem. Soc. **81**, 2912 (1959).
8. E. M. KOSOWER, D. HOFMAN, and K. WALLENFELS. J. Am. Chem. Soc. **84**, 2755 (1962).
9. S. SHIFRIN. Biochim. Biophys. Acta, **96**, 173 (1965).
10. R. CARRUTHERS, F. M. DEAN, L. E. HOUGHTON, and A. LEDWITH. Chem. Commun. 1206 (1967).
11. M. OKI and K. MUTAI. Tetrahedron, **26**, 1181 (1970).
12. H. A. H. CRAENEN, J. W. VERHOEVEN, and TH. J. DE BOER. Rec. Trav. Chim. **91**, 405 (1972).
13. J. C. NNADI, A. W. PETERS, and S. Y. WANG. J. Am. Chem. Soc. **94**, 712 (1972).
14. L. E. WEBB and C. F. LIN. J. Am. Chem. Soc. **93**, 3818 (1971).
15. J. TICKLE and J. B. F. N. ENGBERTS. J.C.S. Perkin II. Submitted for publication.
16. C. K. PROUT and E. E. CASTELLANO. J. Chem. Soc. A, 2775 (1970).
17. H. O. HOUSE, R. W. MAGIN, and H. W. THOMPSON. J. Org. Chem. **28**, 2403 (1963).
18. J. W. VERHOEVEN. Thesis, University of Amsterdam, Amsterdam, The Netherlands. 1969.
19. C. H. BUSHWELLER and W. J. ANDERSON. Tetrahedron Lett. 1811 (1972), and refs. cited therein.
20. G. JEMINET, C. PIGENET, and H. LUMBROSO. Bull. Soc. Chim. Fr. 3631 (1966).
21. C. E. JOHNSON and F. A. BOVEY. J. Chem. Phys. **29**, 1012 (1958). The calculations are tabulated in J. W. Emsley, J. Feeney, and L. H. Sutcliffe. High resolution nuclear magnetic resonance spectroscopy. Pergamon Press, Ltd. Oxford. 1965. pp. 595–604.
22. G. ROBINET, F. CRASMER, J. F. LABARRE, and C. LEIBOVICI. Theor. Chim. Acta Berl. **25**, 259 (1972).
23. G. ROBINET, C. LEIBOVICI, and J. F. LABARRE. Theor. Chim. Acta Berl. **26**, 257 (1972).
24. W. R. BLACKMORE and S. C. ABRAHAMS. Acta Cryst. **8**, 329 (1955).
25. E. FROMM and J. DE SEIXAS PALMA. Chem. Ber. **39**, 3308 (1906).
26. H. R. TODD and R. L. SHRIVER. J. Am. Chem. Soc. **56**, 1382 (1934).
27. H. GILLMANN and F. J. WEBB. J. Am. Chem. Soc. **71**, 4062 (1949).
28. F. G. BORDWELL and B. M. PITT. J. Am. Chem. Soc. **77**, 572 (1955).
29. *Cf.* F. E. POLLAK and G. F. GRILLOT. J. Org. Chem. **32**, 3101 (1967).
30. B. HOLMBERG. J. Prakt. Chem. **141**, 93 (1934).
31. M. NISHIO and T. ITO. Chem. Pharm. Bull. **13**, 1392 (1965).

Can. J. Chem. Downloaded from www.nrcresearchpress.com by 210.87.254.42 on 09/05/12
For personal use only.

On the Mechanism of Ring Inversion in Cycloheptene and Its Derivatives

MAURICE ST-JACQUES AND CAMBYSE VAZIRI
Department of Chemistry, University of Montreal, Montreal, Quebec

Received October 6, 1972

Free energy barriers to ring inversion of 3,3-dimethyl-, 4,4-dimethyl-, and 5,5-dimethylcycloheptene were found to be much smaller than those of corresponding benzocycloheptene derivatives but show the same trend. This observation strongly suggests that the chair conformation of both types of molecules interconverts through the same mechanism. On the other hand, the $\Delta G^{\neq}$ value for 4,4,6,6-tetramethylcycloheptene is about 3 kcal/mol out of line from that expected from a consideration of the behavior of the corresponding benzocycloheptene derivative. An explanation is offered.

Les barrières d'énergie libre pour l'inversion des diméthyl-3,3, diméthyl-4,4 et diméthyl-5,5 cycloheptènes, tout en conservant la même tendance, sont plus faibles que celles qui caractérisent les dérivés correspondants du benzocycloheptène. Cette observation indique que la conformation chaise des deux classes de molécules s'inverse par le même mécanisme. Par contre, la valeur de $\Delta G^{\neq}$ pour le tétraméthyl-4,4,6,6 cycloheptène est environ 3 kcal/mol plus élevée que celle attendue après examen des benzocycloheptènes correspondants. Une explication est présentée.

[Traduit par le journal]

Can. J. Chem., **51**, 1192 (1973)

Can. J. Chem. Downloaded from www.nrcresearchpress.com by 210.87.254.105 on 09/05/12
For personal use only.

Attention has recently been given to the determination of the conformations and conformational mobility of cycloheptene and several of its derivatives (1–4). Most of the published experimental work has been concerned with n.m.r. investigations either of derivatives of benzocycloheptene (1*a*) or of cycloheptene with ring carbons replaced by heteroatoms (1*b*) as it was realized that constraints imposed by such modifications of cycloheptene raised the barrier to inversion sufficiently to enable a complete study of the p.m.r. spectral change occurring at readily accessible low temperatures. Because simple derivatives of the cycloheptene carbocycle have very low $\Delta G^{\neq}$ value (2), relatively few have been investigated until now.

Considerable efforts have also been oriented towards the theoretical prediction of the nature of the most stable conformations of cycloheptene and benzocycloheptene and their interconversion mechanisms. In fact, calculations by force field methods (1*a*, 4) suggest that the chair form is of lowest energy in both cases although there appears to be some disagreement on the nature of the conformation of the transition state for the most likely interconversion pathway. The earlier work (1*a*) on benzocycloheptene predicted a transition state whose conformation contains five carbon atoms essentially coplanar whereas the most recent work (4) predicts a conformation with six coplanar carbon atoms for cycloheptene.

A valuable step towards understanding the effect of the benzo group consists in demonstrating experimentally whether or not the cycloheptene and benzocycloheptene chairs interconvert through the same mechanism, especially since there is a possibility that the large difference in the free energies of activation ($\Delta G^{\neq}$) of 5.7 kcal/mol (1*a*, 2) might be the result of dual mechanisms.

Our approach to this question has been through the study of a particular substituent effect on $\Delta G^{\neq}$ for both systems. For this purpose we prepared the following compounds: 3,3-dimethylcycloheptene (**1**), 4,4-dimethylcycloheptene (**2**), 5,5-dimethyl-1,3,3,7,7-pentadeuteriocycloheptene (**3**), and 4,4,6,6-tetramethylcycloheptene (**4**).

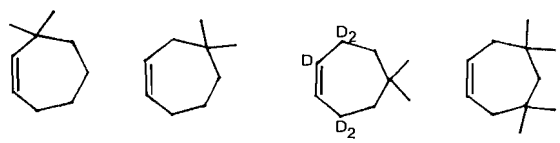

1 **2** **3** **4**

Results

Compounds **1** and **2** were prepared from the same starting material, 2,2-dimethylcyclohexanone, through ring expansion with diazomethane in the presence of boron trifluoride (5) to give a mixture of 2,2-dimethylcycloheptanone and 3,3-

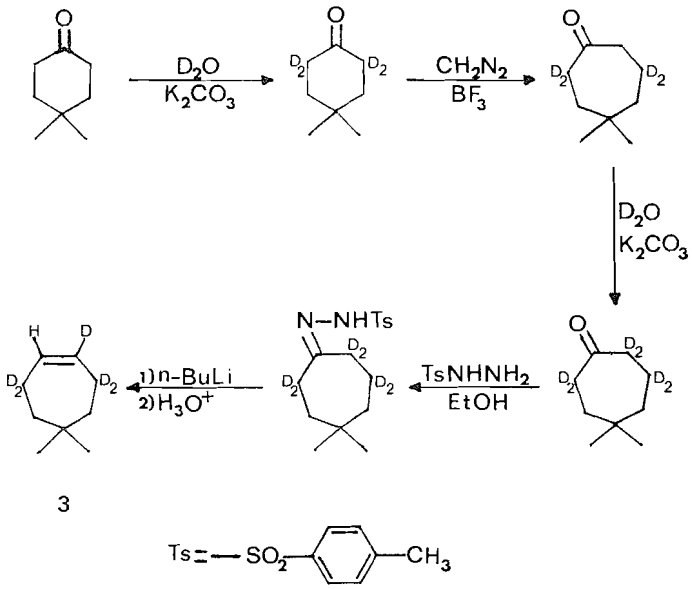

CHART 1

dimethylcycloheptanone (6). Each ketone was obtained pure by preparative v.p.c. and then transformed into the desired cycloheptene derivatives, **1** and **2** respectively, by a procedure utilizing tosylhydrazine and *n*-butyl lithium as recently described (7).

The derivative **4** was prepared from 3,3,5,5-tetramethylcyclohexanone by an analogous route. Compound **3** was also synthesized similarly from 4,4-dimethylcyclohexanone, but since the sequence of reactions involved several deuteration steps, it is illustrated on Chart 1.

The 100 MHz p.m.r. spectrum of **1** at room temperature contains a methyl singlet at δ 1.04 and broad methylene multiplets over the range δ 1.3–2.5. A gradual decrease in temperature down to −170° revealed no spectral change which could be attributed to a slowing down of ring inversion on the n.m.r. time scale. A very slight change in appearance was observed, however; it is due to increased viscosity and small variations in chemical shifts with temperature as indicated clearly from spectra above −120°.

On the other hand, lowering the temperature of a sample of **2** led to a splitting of the methyl singlet (δ 0.91 at +25°) into a doublet separated by 6.5 Hz below −153°, the coalescence temperature (T_c). The free energy of activation characteristic of the underlying process was calculated to be 6.0 ± 0.3 kcal/mol, at T_c, by standard procedures (8) using a transmission coefficient of one half. Consideration of the absence of a spectral change for **1** down to −170° suggests that its corresponding $\Delta G^{\neq}$ must be less than 5 kcal/mol (2, 9).

A preliminary investigation of 5,5-dimethylcycloheptene revealed that its methyl signal remains a singlet down to −170° whereas the broad methylene multiplet centered at δ 1.47 shows an ill-defined spectral change between −130 and −160°. In order to simplify the spectrum and its change, the deuterated derivative **3** was prepared. Figure 1 illustrates the spectral change in the region of the methylene protons (δ 1.47, singlet at +25°) as the temperature is decreased. This behavior is characteristic of the change of an A_2 singlet into an AB pattern. A careful examination of the spectrum at −162° shows a certain degree of asymmetry whereby the right side of the AB pattern is more intense. This deformation appears to be due in part to an overlap with the broad methyl signal. In addition, the small impurity peak, identified with a star in Fig. 1 adds to the asymmetry of the peak in the intermediate region of the spectral change. The analysis of the low temperature AB quartet gives a chemical shift difference of 29.6 Hz and a coupling constant of −13.7 Hz.

Can. J. Chem. Downloaded from www.nrcresearchpress.com by 210.87.254.105 on 09/05/12
For personal use only.

Can. J. Chem. Downloaded from www.nrcresearchpress.com by 210.87.254.105 on 09/05/12
For personal use only.

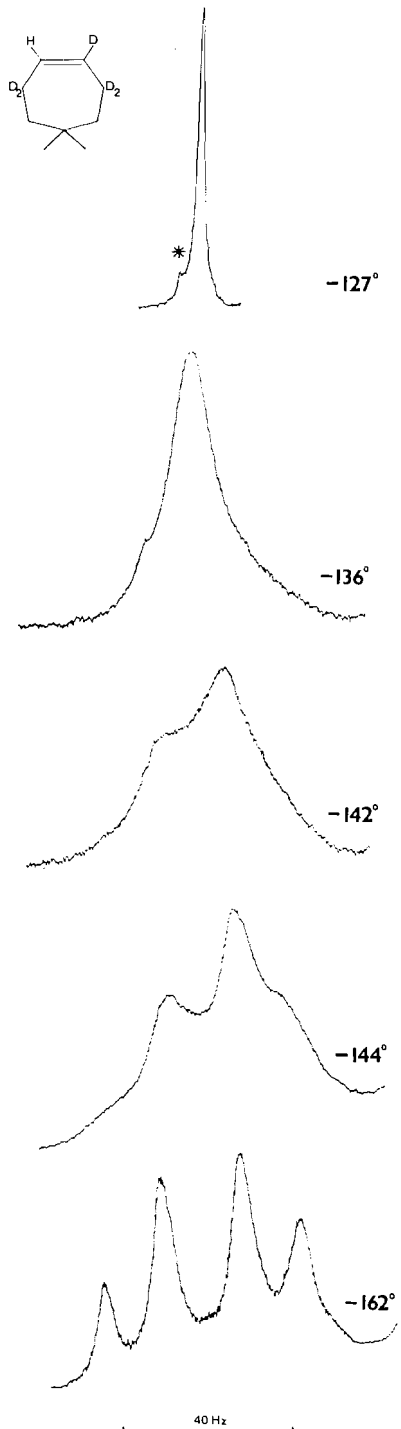

FIG. 1. The 100 MHz p.m.r. deuterium decoupled spectra of the C-4 and -6 methylene protons of **3** at several temperatures.

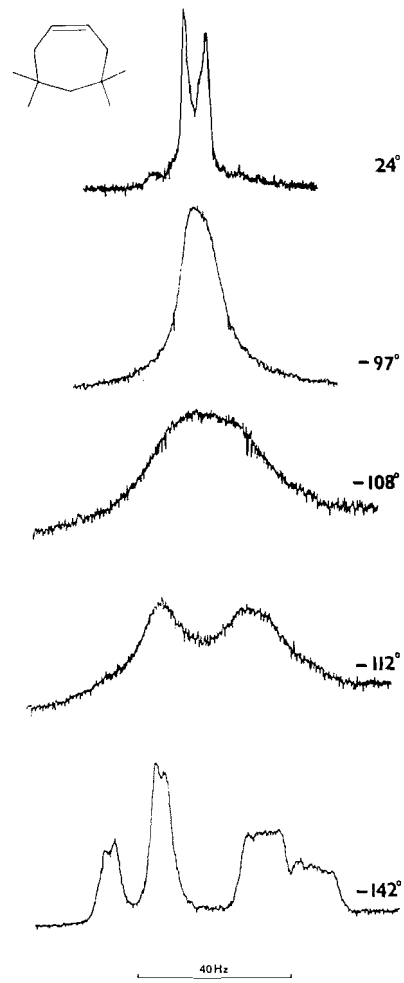

FIG. 2. The 100 MHz p.m.r. spectra of the C-3 and -7 methylene protons of **4** at several temperatures.

T_c is estimated at $-140°$ and a $\Delta G^{\neq}$ value of 6.2 kcal/mol is calculated at this temperature (8).

The 100 MHz, room temperature, p.m.r. spectrum of **4** contains three peaks characteristic of the non-olefinic protons: a singlet at δ 0.94 (four methyl groups), a singlet at 1.48 (C-5 methylene protons), and a doublet at 2.02 (J = 5.5 Hz; C-3 and -7 methylene protons). At low temperature the methyl signal splits into a doublet separated by 10.3 Hz below $-117°$ (T_c) whereas the C-5 methylene peak remains a singlet down to $-170°$. Figure 2 illustrates the change taking place for the signal of the allylic protons. The spectrum at $-142°$ is easily

Can. J. Chem. Downloaded from www.nrcresearchpress.com by 210.87.254.105 on 09/05/12
For personal use only.

recognized as an AB pattern for which the A and B protons are coupled differently to the olefinic protons. Approximate values for these vicinal coupling constants are 2.5 and 8.5 Hz for the low and high field components respectively; the average of these values agrees quite well with the separation of the high temperature doublet.

From the spectral change of the methyl signal of **4**, $\Delta G^{\neq}$ was calculated to be 7.7 kcal/mol at $-117°$. Table 1 contains a summary of the pertinent n.m.r. and thermodynamic parameters for the derivatives of cycloheptene investigated as well as for corresponding derivatives of benzocycloheptene (1*a*) which are identified by adding the letter *a* to the number of the corresponding cycloheptene derivative.

TABLE 1. N.m.r. and thermodynamic parameters for derivatives of cycloheptene and benzocycloheptene

Compounds	Δν (p.p.m.)	T_c (°C)	$\Delta G^{\neq}$
Cycloheptene	0.56[a]	−165	5.0
Benzocycloheptene	0.41[a]	− 57	10.7
1	—	—	<5
1*a*[b]	0.20[c]	− 73	10.3
2	0.065	−153	6.0
2*a*	0.47	− 45	11.3
3	0.296[d]	−140	6.2
3*a*	0.21	− 52	11.8
4	0.103	−117	7.7
4*a*	0.33	− 63	10.4

[a]For these compounds Δν refers to the C-5 protons whereas it refers to the methyl protons for all other compounds except 3; data taken from refs. 1*a* and 2.
[b]The label a in **1a** means that it is the benzo derivative of **1**. Data for these derivatives taken from ref. 1*a*.
[c]The spectra were taken at 60 MHz.
[d]The Δν refers to the C-4 protons.

Discussion

It has recently been demonstrated that benzocycloheptene (3) and some of its methyl derivatives (1*a*) exist in the chair conformation and cycloheptene undoubtedly also does (2, 4, 10). While the low temperature spectra of compounds **1**, **2**, **3** and **4** do not give direct information on the stable conformation, there is no reason to suspect a change in the geometry of the ground state and so we assume that all molecules considered in this work exist as chair conformations.

A careful examination of the results given in Table 1 shows that each class of dimethyl compounds exhibits a similar trend in the variation of $\Delta G^{\neq}$ with respect to the parent compound. The behavior of the tetramethyl derivatives, on the other hand, seems abnormal since the $\Delta G^{\neq}$ of **4** is 2.7 kcal/mol higher than that of cycloheptene whereas that of **4***a* is about 0.3 kcal/mol lower than the value of benzocycloheptene.

Experimental conditions (very low temperature, small Δν values, impossibility to get accurate T_2 in absence of exchange) make meaningful estimates of $\Delta S^{\neq}$ through computer simulation impossible. But since it is known that $\Delta S^{\neq}$ is close to zero for 5,5-difluorocycloheptene (10), symmetry arguments (2) suggest that it will be similar for the compounds of interest to us. It therefore appears that $\Delta H^{\neq} \approx \Delta G^{\neq}$ and that the differences in Table 1 ($\Delta\Delta G^{\neq}$) are fair approximations to $\Delta\Delta H^{\neq}$ for these compounds.

Ring inversion of the cycloheptene chair, responsible for the spectral changes of compounds **1** to **4**, must proceed through several steps (1*a*, 4). The first one consists of the change from the chair to a boat form; it is followed by

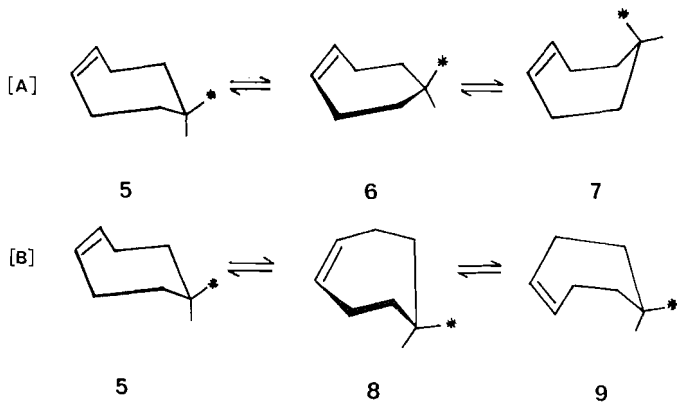

a pseudorotation among the boat forms and then by a conformational change to an inverted chair. While there is agreement on the mechanism for pseudorotation, two different pathways, [A] and [B], have been suggested for the chair to boat interconversion. One possibility [A] involves wagging C-5 of the chair (**5**), through an intermediate (**6**) having five carbon atoms in one plane, into the boat form (**7**) while the other [B] involves wagging the double bond, through a conformation (**8**) having six coplanar carbon atoms, into the boat form (**9**).

Pseudorotation which interconverts boat and twist-boat forms is illustrated below and shown to proceed through the high energy conformations **10** for which C-1, -2, -3, -4, and -7 lie essentially in one plane while C-4, -5, -6, and -7 lie in another (refered to as 1,2-biplanar form; **10′** is an inverted form of **10**).

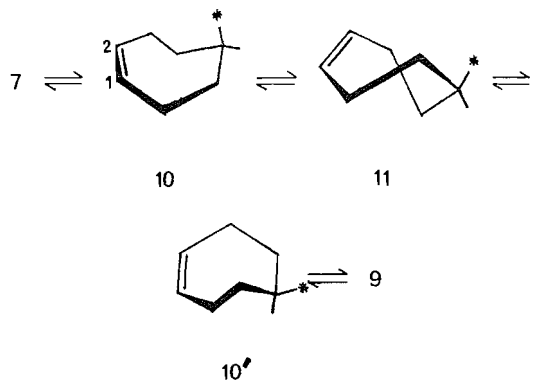

Since the wagging of C-5 or C=C through transition states **6** or **8** involves deformations of different parts of the cycloheptene ring, it follows that substituent effects should depend on the actual mechanism of inversion. The observation (Table 1) of the same trend in $\Delta G^{\neq}$ for dimethyl derivatives of cycloheptene and benzocycloheptene therefore suggests strongly that the chair conformation of both classes of compounds interconverts through the same pathway.

Variations in $\Delta G^{\neq}$ with substitution are normally due to changes in energy of the ground state and/or transition state conformations provided all derivatives follow the same mechanism. It is often difficult to assess quantitatively the various contributions to each, although under favorable circumstances, when substituent effects are very large, it is usually possible to distinguish between two alternatives. Data in Table 1 show that differences are small within each class of dimethyl derivatives whereas the effect of the benzo group is quite large (~5 kcal/mol) for all substitution patterns. Since a unique mechanism is inferred from the results, it seems highly probable that the pathway which best explains the effect of the benzo group is the correct one.

Previous rationalizations of n.m.r. results (2, 10) in terms of transition state **6** were of limited success since they could not account adequately for the large effect of the benzo group. The theoretical prediction by Allinger and Sprague (4) that the cycloheptene conformation should invert through pathway B appears to go against a prediction based on model calculations (1*a*) but the remarkable agreement between the calculated energy barrier of 5.16 kcal/mol and the experimental value of 5.0 kcal/mol (2) supports the contention that models are indeed misleading here. The above agreement together with the results reported in Table 1 indicate that benzocycloheptene derivatives also invert through the same pathway B, the large effect of the benzo group being a consequence of the much lower torsional energy for rotation about the C_1—C_7 and C_2—C_3 bonds of benzocycloheptene than of cycloheptene (4, 11).

A detailed account of the various factors responsible for the trends in $\Delta G^{\neq}$ is virtually impossible since it would require the quantitative evaluation of several interactions both in the ground state and transition state. On the other hand, it is possible to point out some of the most important interactions and assess qualitatively their effect on $\Delta G^{\neq}$. For example, the eclipsing between the C-3 equatorial methyl group and the olefinic proton in structure **12** as well as transannular synaxial CH_3/H interactions between the C-3 axial methyl with the axial protons on C-5 and -7 should lead to a larger relief of torsional and repulsive strain for the inversion of **1** than of cycloheptene. Similar arguments are also valid for **1***a* so that it is not surprising to observe that $\Delta G^{\neq}$ for both **1** and **1***a* are lower than values for the parent compounds.

Methyl interaction with either an aromatic carbon or an olefinic proton should be absent in compounds **2**, **2***a*, **3** and **3***b* as seen in structures **13** and **14** which also reveal serious transannular

Can. J. Chem. Downloaded from www.nrcresearchpress.com by 210.87.254.105 on 09/05/12
For personal use only.

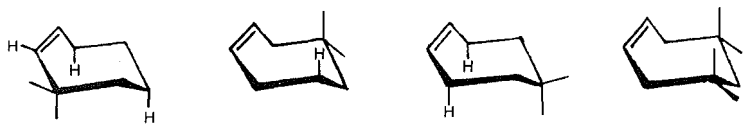

12 13 14 15

syn-axial CH_3/H interactions. The inversion of **2** and **2***a* (4,4-dimethyl derivatives) is characterized by small changes of torsional strain about the C_3—C_4 and C_4—C_5 bonds and an increase in *syn*-axial CH_3/H repulsion since the distance between the groups concerned gets smaller in transition state **8**. The sum of the energies involved could easily account for a large fraction of the increase in $\Delta G^{\neq}$ of **2** and **2***a* over that of cycloheptene and benzocycloheptene. On the other hand, the inversion of **3** and **3***a* (5,5-dimethyl derivatives) is characterized by a relief of transannular interaction and an increase in torsional strain about the C_4—C_5 and C_5—C_6 bonds, the net effect being an increased barrier to ring inversion over that of the parent compounds.

Structure **15** illustrates the strong transannular methyl–methyl repulsion present in the chair form of **4** and **4***a* (4,4,6,6-tetramethyl derivatives). The energy of this interaction is probably comparable to that in 1,1,3,3-tetramethylcyclohexane (about 3.7 kcal/mol (12)) since the methyl–methyl distance is slightly less for the seven-membered ring. The change in torsional strain about the C_3—C_4, C_4—C_5, C_5—C_6, and C_6—C_7 bonds and the small increase in transannular *syn*-axial interaction during inversion through transition state **8** could add up to account for the small decrease in $\Delta G^{\neq}$ for **4***a*. Results for the dimethyl derivatives suggest that the same trend should carry over to **4** provided the energy profile for inversion was such that **8** is the rate determining transition state as is the case for **4***a*. Instead, a very significant departure in trend is observed.

Figure 3*a* illustrates the energy profile for the ring inversion of cycloheptene based on calculations (4) and recent p.m.r. results (2). The effect of the benzo group on the inversion profile of benzocycloheptene is shown qualitatively in Fig. 3*b* where the dominant feature is the large energy difference between the chair form and the transition state of geometry similar to **8**. While

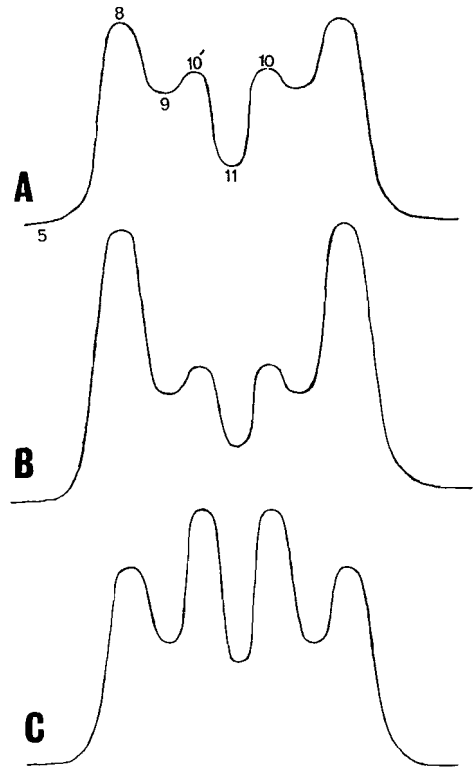

FIG. 3. Possible free energy profiles for the interconversion of chair conformations of (*a*) cycloheptene; (*b*) benzocycloheptene; (*c*) 4,4,6,6-tetramethylcycloheptene (**4**). The prime indicates the inverted form.

profile *b* is able to account for the substituent effect on $\Delta G^{\neq}$ for **1***a*, **2***a*, **3***a*, and **4***a*, profile *a* cannot explain the large increase in $\Delta G^{\neq}$ for 4,4,6,6-tetramethylcycloheptene (**4**).

It therefore appears that a different energy profile must exist for **4** and curve *c* in Fig. 3 is a possibility. This profile supposes that the stable conformation of **4** is a chair by analogy with **4***a* (1*a*) and suggests that the transition state **10** for pseudorotation becomes rate determining. This change is possible for **4** because the two maxima of profile *a* have very close conformational energies as suggested from

Can. J. Chem. Downloaded from www.nrcresearchpress.com by 210.87.254.105 on 09/05/12
For personal use only.

Can. J. Chem. Downloaded from www.nrcresearchpress.com by 210.87.254.105 on 09/05/12
For personal use only.

calculations (4). The examination of a structure of geometry **10** for **4** reveals a large transannular C_4–methyl and C_7–proton interaction as well as increased torsional energy about the C_5—C_6 bond. These factors therefore could be responsible in large part for the very significant increase in the energy barrier to pseudorotation. Alternatively, if the stable conformation of **4** was a twist-boat, implying that the serious *syn*-axial methyl repulsion shown in structure **15** results in a change of conformation for **4** but not **4***a*, then an increased barrier to pseudorotation of twist-boat forms could also explain the $\Delta G^{\neq}$ value of **4**. The p.m.r. spectrum of **4**, unlike that of **4***a* (1*a*), is compatible with a twist-boat conformation since its C-5 methylene group remains a singlet down to lowest temperature attained.

In conclusion, we think that our study has provided sufficient experimental data to justify the comparison of the properties of the seven-membered ring of cycloheptene and benzocycloheptene. Our results strongly suggest that, in spite of the large difference in $\Delta G^{\neq}$ values for ring inversion, simple derivatives of both ring systems have similar conformational properties. For the more substituted derivatives, however, a careful consideration of possible change in energy profile for the cycloheptene derivative is necessary to predict substituent effects.

Experimental

The v.p.c. analyses and separations were carried out as previously reported (2, 3). Mass spectral analyses were performed on an Associated Electrical Industries MS-902 high resolution mass spectrometer operating at 70 and 12 eV. Mass determinations were made by comparison with perfluorotributylamine. Samples for low temperature studies consisted of 5% solutions in chlorodifluoromethane containing a small quantity of TMS, degassed and sealed.

Preparation of 3,3-Dimethylcycloheptene (1) and 4,4-Dimethylcycloheptene (2)

A solution of 1.0 g (0.007 mol) of 2,2-dimethylcyclohexanone in 20 ml of ether containing 1 ml of freshly distilled boron trifluoride etherate was reacted with diazomethane by a procedure described previously (6) until the amount of cycloheptanone was maximized as determined by v.p.c. analysis using a carbowax column at 200 °C. 2,2-Dimethylcycloheptanone (shorter retention time) and 3,3-dimethylcycloheptanone (longer retention time) were obtained in comparable amounts. The products of several reactions were separated and purified by preparative v.p.c. and found to have identical properties to those reported in the literature (13) and used in the next reactions.

3,3-Dimethylcycloheptene (1)

2,2-Dimethylcycloheptanone, 0.20 g (0.0014 mol), and 0.28 g of tosylhydrazine were dissolved in 10 ml of hot absolute ethanol. After 24 h of reflux, the reaction mixture is held at 0° for a few hours. The tosylhydrazone crystallized out and was collected by filtration. Elimination was carried out using a recently described procedure by Shapiro and Heath (7), whereby 10 ml of a 1.6 *M* solution of *n*-butyllithium in *n*-hexane was added dropwise at 0° to the above tosylhydrazone in 7 ml of ether; the reaction mixture was then stirred overnight. After work-up, v.p.c. analysis revealed a major product which was then collected using a silicon fluid DC550 column at 100°. The p.m.r. spectrum (60 MHz) of the product in carbon disulfide is in accord with that expected for 3,3-dimethylcycloheptene (**1**): singlet at δ 1.04 (6H); a broad signal centered at 1.6 (6H); a broad signal at 2.05 (2H), and a multiplet at 5.45 (2H).

Mol. Wt. Calcd. for C_9H_{16}: 124.1252. Found (mass spectrum at 70 eV): 124.1251.

4,4-Dimethylcycloheptene (2)

A quantity of 0.25 g (0.0018 mol) of 3,3-dimethylcycloheptanone from above was reacted similarly with tosylhydrazine followed by elimination with *n*-butyl lithium and purification by v.p.c. The product gave a p.m.r. spectrum in carbon disulfide (60 MHz) characteristic of 4,4-dimethylcycloheptene (**2**): singlet at δ 0.89 (6H); multiplet at 1.50 (4H); multiplet at 2.0 (4H), and a multiplet at 5.50 (2H).

Mol. Wt. Calcd. for C_9H_{16}: 124.1252. Found (mass spectrum at 70 eV): 124.1253.

Preparation of 5,5-Dimethyl-1,3,3,7,7-pentadeuteriocycloheptene (3)

4,4-Dimethylcyclohexanone (13) (6.5 g, 0.051 mol) was refluxed 16 h with 60 ml of deuterium oxide containing 6.0 g of potassium carbonate. The product was extracted with ether, dried, and condensed. A second exchange with 15 ml of deuterium oxide and 1.5 g of potassium carbonate followed by extraction and evaporation of the ether solvent gave 4,4-dimethyl-2,2,6,6-tetradeuteriocyclohexanone with a very high deuterium content as revealed from its p.m.r. spectrum in CCl_4: singlet at δ 1.10 (6H) and a broader singlet at 1.65 (4H).

Ring expansion of 5.0 g (0.038 mol) of the deuterated ketone as previously described gave a mixture of products from which 4,4-dimethyl-2,2,6,6-tetradeuteriocycloheptanone could be isolated by preparative v.p.c. using a UCW-98 column at 180°. A characteristic p.m.r. spectrum (60 MHz) in carbon tetrachloride showed the following peaks: a singlet at δ 0.97 (6H); two partially overlapping singlets at 1.48 and 1.55 (4H), and a singlet at 2.36 (2H).

A quantity of 1.2 g of the above tetradeuterated ketone was further exchanged with deuterium oxide as previously described to give 4,4-dimethyl-2,2,6,6,7,7-hexadeuteriocycloheptanone as revealed from the complete disappearance of the signal at δ 2.36 in the p.m.r. spectrum.

The hexadeuterated cycloheptanone derivative (0.75 g,

Can. J. Chem. Downloaded from www.nrcresearchpress.com by 210.87.254.105 on 09/05/12
For personal use only.

0.0051 mol) was then reacted with tosylhydrazine followed by elimination with *n*-butyl lithium as previously described to give 5,5-dimethyl-1,3,3,7,7-pentadeuteriocycloheptene (**3**) as the predominant product which was purified by preparative v.p.c. using a silicone fluid SF-96 column at 125°. A p.m.r. spectrum (60 MHz) in carbon disulfide is in accord with the proposed structure: a singlet at δ 0.90 (6H); a singlet (4H) at 1.38, and a singlet (1H) at 5.54. A mass spectrum at 12 eV revealed the following isotopic distribution: $d_5 = 86$; $d_4 = 11$; $d_3 = 3\%$.

Preparation of 4,4,6,6-Tetramethylcycloheptene (4)

A solution of 5.0 g of 3,3,5,5-tetramethylcyclohexanone (14) in anhydrous ether containing some boron trifluoride etherate was submitted to a ring expansion reaction with diazomethane as previously described. A v.p.c. analysis using a carbowax column at 200° revealed a relative product distribution cyclohexanone–cycloheptanone–cyclooctanone and higher in the ratio (%) 27:27:46. The 3,3,5,5-tetramethylcycloheptanone was isolated by preparative v.p.c. and characterized by its p.m.r. spectrum in $CDCl_3$ (60 MHz): singlet (6H) at δ 1.00; singlet (6H) at 1.03; singlet (2H) at 1.43; a multiplet centered at 1.6 (2H); a multiplet centered at 2.5 (2H), and a singlet (2H) at 2.47.

Anal. Calcd. for $C_{11}H_{20}O$: C, 78.58; H, 11.90. Found: C, 78.31; H, 11.91.

The above ketone (0.37 g, 0.0022 mol) was dissolved with 0.4 g of tosylhydrazine in 7 ml of hot ethanol. The solution was left standing at 0° overnight during which time the hydrazone crystallized out. The hydrazone (0.44 g) was filtered, dried, and then with 0.74 g of $LiAlH_4$ was refluxed in 30 ml of tetrahydrofuran for 24 h. After hydrolysis with 10% sulfuric acid, the organic product was extracted with petroleum ether, washed with a 5% NaOH solution, water, and then dried over magnesium sulfate. The main product was isolated and purified by v.p.c. using a β,β′-oxydipropionitrile column at 90°. It was then identified by its p.m.r. spectrum (60 MHz) in carbon disulfide to be 4,4,6,6-tetramethylcycloheptene (**4**): a singlet (12H) at δ 0.92; a singlet (2H) at 1.38; a doublet (4H) at 1.96, and a multiplet centered at 5.7 (2H).

Mol. Wt. Calcd. for $C_{11}H_{20}$: 152.1565. Found (mass spectrum at 70 eV): 152.1563.

We wish to acknowledge financial assistance from the National Research Council of Canada and the Quebec Ministry of Education.

1. (*a*) S. KABUSS, H. G. SCHMID, H. FRIEBOLIN, and W. FAISST. Org. Mag. Res. **2**, 19 (1970); (*b*) H. FRIEBOLIN, R. MECKE, S. KABUSS, and A. LÜTTRINGHAUS. Tetrahedron Lett. **29**, 1929 (1964).
2. M. ST-JACQUES and C. VAZIRI. Can. J. Chem. **49**, 1256 (1971).
3. M. ST-JACQUES and C. VAZIRI. Org. Mag. Res. **4**, 77 (1972).
4. N. L. ALLINGER and J. T. SPRAGUE. J. Am. Chem. Soc. **94**, 5734 (1972).
5. F. A. L. ANET, M. ST-JACQUES, and G. SCHMURNY. J. Am. Chem. Soc. **90**, 5243 (1968).
6. J. JACQUES and A. BRUYLANTS. Bull. Cl. Sci. Acad. Roy. Belg. **9**, 1015 (1968).
7. R. H. SHAPIRO and M. J. HEATH. J. Am. Chem. Soc. **89**, 5734 (1967).
8. D. KOST, E. H. CARLSON, and M. RABAN. Chem. Commun. 656 (1971), and refs. cited therein.
9. F. R. JENSEN and B. H. BECK. J. Am. Chem. Soc. **90**, 1066 (1968).
10. E. S. GLAZER, R. KNORR, C. GANTER, and J. D. ROBERTS. J. Am. Chem. Soc. **94**, 6026 (1972).
11. A review of such barriers with references for the sources of individual values is given by J. P. Lowe, Progr. Phys. Org. Chem. **6**, 1 (1968).
12. N. L. ALLINGER and M. A. MILLER. J. Am. Chem. Soc. **83**, 2145 (1961).
13. A. CHAMPAGNE, H. FAVRE, D. VOCELLE, and I. ZBIKOWSKI. Can. J. Chem. **42**, 212 (1964).
14. G. CHIURDOGLU and A. MAQUESTIAU. Bull. Soc. Chim. Belge, **63**, 357 (1954).

Vicinal Electron Pairs and Conformation in Six-membered Rings. Some Evidence from the 1,3,2-Dioxathianes

GORDON WOOD, R. M. SRIVASTAVA, AND B. ADLAM
Department of Chemistry, University of Windsor, Windsor 11, Ontario
Received October 2, 1972

Barriers to ring reversal ($\Delta G^{\ddagger}$) at the n.m.r. coalescence temperature are reported for a series of 1,3,2-dioxathianes. The value for 1,3,2-dioxathiane-4,4,6,6-d_4 of 11.2 kcal/mol is compared with the corresponding values for cyclohexane and various six-membered rings with and without vicinal electron pairs. The 1,3,2-dioxathiane system is suggested as a model for trimethylene sulfites, where the strong preference of the exocyclic oxygen for the axial position interferes with barrier determination by n.m.r. techniques.

Les barrières d'inversion de cycle ($\Delta G^{\ddagger}$) à la température de coalescence r.m.n. sont rapportées pour une série de dioxathianes-1,3,2. La valeur obtenue, 11.2 kcal/mol pour le dioxathiane-1,3,2 d_4-4,4,6,6 est comparée avec les valeurs correspondantes pour le cyclohexane et divers systèmes cycliques à six membres avec ou sans paire d'électrons vicinale. Le système dioxathiane-1,3,2 est proposé comme modèle pour les sulfites de triméthylene, où la préférence marquée de l'oxygène exocyclique pour la position axiale gêne la détermination de la barrière par la technique du r.m.n. [Traduit par le journal]

Can. J. Chem., 51, 1200 (1973)

Introduction

There is now substantial evidence that the conformational properties of six-membered rings with two or more adjacent heteroatoms in the ring are significantly different from those of cyclohexane (1–3). This result is usually attributed to the presence of vicinal electron pairs which appear to increase the barrier to rotation about the connecting bond and at the same time displace, or even reverse (ref. 1*b*, p. 1205), the potential energy minima and maxima associated with rotation. Similar deviations exist in acyclic molecules (4) when ethane is considered the reference substance and their importance in six-membered ring behavior is a direct result of the importance of torsional barriers in determining conformational properties of rings.[1]

The work of Bushweller and co-workers (3) on the *s*-tetrathianes constitutes the most thorough study of this phenomenon to date. In addition to the expected high barriers to ring reversal, these workers have found changes in conformational energies dramatic enough to give rise to non-chair ground states and high barriers to pseudo-rotation between non-chair states.

[1]This relationship is generally accepted (5, 6). However, successful application of this principle to estimate ring reversal barriers requires careful choice of acyclic models, as we will show.

Compounds with three adjacent oxygen and/or sulfur atoms (**1**–**4**) might be expected to demonstrate similar interesting properties. Experimental work on systems of this type has been limited

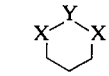

1 X = S; Y = S
2 X = O; Y = S(=O)
3 X = O; Y = S
4 X = O; Y = S(=O)(=O)

so far to a determination of the ring reversal barrier of **1** and its 5,5-dimethyl derivative for which $\Delta G^{\ddagger} = 13.2$ and 14.7 kcal/mol, respectively (7), in addition to rather extensive data collection on trimethylene sulfites (**2**) by such diverse techniques as dipole moments (1*b*, 8, 9), i.r. (9*a*, 10), n.m.r. (1*a*, 2, 10, 11), osmometry (12), and ultrasonic absorption (13). Although all of the data point to some novel conformational properties, uncertainties in interpretation of the more derivative forms of data, especially from ultrasonic absorption (14, 15) and the present lack of a trimethylene sulfite suitably substituted for direct measurement of chair ⇄ chair ring reversal by the n.m.r. technique have thus far prevented the emergence of a generally accepted conformational description for this molecule.

Can. J. Chem. Downloaded from www.nrcresearchpress.com by 210.87.254.6 on 09/05/12
For personal use only.

Can. J. Chem. Downloaded from www.nrcresearchpress.com by 210.87.254.6 on 09/05/12
For personal use only.

This paper expands on our initial communication (16) of the magnitude of the barrier of ring reversal for some 1,3,2-dioxathianes (**3**). This system presents some synthetic difficulty, but its symmetry makes it ideal for n.m.r. study and its close structural resemblance to trimethylene sulfite confers on it some value as a model for the latter. Also, in this connection, **4** represents a closely related structure, the 5,5-dimethyl derivative of which has $\Delta G^{\ddagger} = 8.3$ kcal/mol (17). This result is in conformity with the fact that the ground state of this molecule has its energy increased by the location of a polar bond along the bisector of two electron pairs (4).

Results and Discussion

We here report the synthesis and low temperature n.m.r. data for several 1,3,2-dioxathianes, including the barrier to ring reversal for 1,3,2-dioxathiane-4,4,6,6-d_4, (**3***b*), which probably provides the most reliable value for comparison with cyclohexane and other six-membered ring compounds.

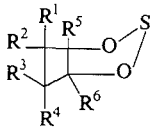

3

a —
b $R^1, R^2, R^5, R^6 = D$
c $R^3, R^4 = CH_3$
d $R^1, R^6 = CH_3$
e $R^1, R^6 = CH_3; R^2, R^3, R^4, R^5, = D$
f $R^2, R^6 = CH_3$
g $R^2, R^6 = CH_3; R^1, R^3, R^4, R^5 = D$

All unspecified R groups = H

Synthesis and Spectra of 1,3,2-Dioxathianes

The compound **3***a* was synthesized from 1,3-propanediol and sulfur dichloride according to the method of Thompson (18). The isolated liquid showed two peaks which could be separated readily by preparative g.l.c. The peak with lower retention time was found to be **3***a*. The retention time of the other liquid was identical to that for authentic trimethylene sulfite.

The i.r. spectrum of **3***a* showed no hydroxyl absorption. The ^1H n.m.r. spectrum at room temperature consisted of a triplet at δ 4.38 and a quintet at 1.98. Had the compound possessed a macrocyclic structure such as **5**, the same n.m.r. spectrum would have been observed. The

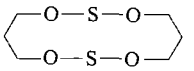

5

mass spectrum showed a peak at *m/e* 106 which was assigned to the molecular ion. No peak at *m/e* 212 or higher was evident, nor was there any evidence of sulfite contamination (*m/e* 122).

In the low temperature n.m.r. experiment, the quintet at δ 1.98 broadened until at −70° two separate signals were obtained: δ 2.0–3.0 (multiplet) and 1.6 (broad doublet). These signals were assigned to axial and equatorial protons respectively. The C-5 proton signals sharpened at −85° and remained unchanged on further cooling. At −80° the doublet at δ 1.6 became a doublet of triplets ($J \simeq 2$ Hz).

These changes in the spectrum were shown to be reversible, and the coalescence temperature obtained was used to estimate the rate constant, k_c, for interconversion of the conformers from the equation

$$k_c = \Pi/\sqrt{2}\sqrt{(\nu_A - \nu_B)^2 + 6J_{AB}^2}$$

which reduces to

$$k_c = \Pi/\sqrt{2}(\nu_A - \nu_B)$$

when the signals are not coupled.[2] The value of $\Delta G^{\ddagger}$ was obtained from the Eyring equation,

$$k_c = k(K_B T/h)e^{-\Delta G^{\ddagger}/RT}$$

taking the transmission coefficient as unity. Both k_c and $\Delta G^{\ddagger}$ for the molecules studied are presented in Table 1.

The above procedure was repeated for 1,3,2-dioxathiane-4,4,6,6-d_4 (**3***b*) synthesized from labelled 1,3-propanediol and di-1-imidazolyl sulfide. The coalescence phenomenon of the simple AB spectrum provided a further check on the ring reversal barrier in this ring system and we consider the latter result of $\Delta G^{\ddagger} = 11.2$ kcal/mol at −42° to be the most reliable measure of ring reversal in 1,3,2-dioxathianes.

[2]A recent comparative study of n.m.r. methods of determining free energies of activation has indicated the conditions under which this approximate method gives satisfactory results (19).

Can. J. Chem. Downloaded from www.nrcresearchpress.com by 210.87.254.6 on 09/05/12
For personal use only.

The 4,6-dimethyl derivatives were synthesized from 2,4-pentanediol (mixed isomers). G.l.c. of the product showed the presence of small amounts of all three 4,6-dimethyltrimethylene sulfites as well as racemic (**3***d*) and meso (**3***f*) 4,6-dimethyl-1,3,2-dioxathiane in a 56:44 ratio. I.r. and n.m.r. spectra for **3***f* were consistent with the assigned structure and the mass spectrum showed a peak at *m/e* 134 corresponding to the molecular ion. Proton n.m.r. spectra recorded in 1:1 CD_2Cl_2:C_2D_5Br showed no temperature dependence between +25 and −100°, a fact consistent with its expected adoption of a single chair conformation with both methyl groups equatorial.

Compound **3***d* produced a peak at *m/e* 134 which was assigned to the molecular ion. A small peak at *m/e* 150 was presumably due to contamination from a related sulfite. The ^1H n.m.r. spectrum consisted of a multiplet at δ 4.60, a triplet at 1.80, and a doublet at 1.43, in agreement with a fast equilibrium between conformations. On cooling, the spectrum underwent the expected broadening with two methyl doublets appearing at −90°. Below −100° these doublets are sharp and no further change occurred to −110°. The coalescence temperature for these signals was estimated to be −83° which gives $\Delta G^{\ddagger} = 9.4$ kcal/mol. The methylene and methine protons in this compound did not give definable coalescence. As a further check on the ring reversal barrier in racemic-4,6-dimethyl-1,3,2-dioxathiane, the labelled derivative **3***e* was found to give $\Delta G^{\ddagger} = 9.75$ kcal/mol based on coalescence of the methyl signal (δ 1.40) at −79.[3]

Interpretation of Nuclear Magnetic Resonance Results and Comparison with Related Systems

The barriers determined in the present work are presented in Fig. 1 along with a variety of other determinations on related molecules.[4] The 1,3,2-dioxathiane barriers, like those for other six-membered ring systems with vicinal electron pairs, are generally higher than the comparable cyclohexane or 1,3-dioxane structure. Generally, the substitution of oxygen for sulfur in the ring appears to lower the barrier (tetramethyldithiane and -dioxane are exceptions). Removal of the vicinal electron pair interaction in 1,3,2-dioxathiane by conversion to trimethylene sulfate lowers the barrier to a value comparable to the similarly substituted 2,2,5,5-tetramethyl-1,3-dioxane.

If the analysis presented here has any relevance for the case of trimethylene sulfite barriers which are not amenable to direct n.m.r. measurement, then these compounds should have ring reversal barriers near those for the 1,3,2-dioxathianes and certainly higher than the trimethylene sulfates. It is unfortunate that the ultrasonic absorption method which appears to detect a barrier to conformational change in the trimethylene sulfite system (13, 21) gives no evidence as to the structure of either the low energy or high energy state which the barrier separates.[5] Clarification of the nature of the ultrasonic process must await comparative n.m.r. and ultrasonic data on representatives of each of the ring systems under discussion. In the meantime, it should be noted that although no experimental value exists for S—O bond rotation, the ring reversal barrier for 1,3,2-dioxathiane is consistent with a high rotation barrier, as has been found for related bond types.[6]

The effect of exocyclic oxygen in the axial position on a trimethylene sulfite in the chair form has often been discussed in terms of interaction with the axial substituents on C-4 and -6. Values of n.m.r. shifts for several 1,3,2-dioxathianes which lack this exocyclic oxygen make it possible to check for evidence of this interaction. When allowance is made for the averaging of n.m.r. signals caused by conformational interconversion in the 1,3,2-dioxathianes,

[3]In spite of strenuous effort, complete purification of this compound was not achieved. Persistent n.m.r. signals appeared at δ 1.70, 1.50, and 1.18 p.p.m.

[4]These comparisons are presented in the format used by Kabuss and co-workers. References 20*a* and *c* contain additional data on six-membered ring reversal barriers.

[5]The difficulty with the low energy state is generally recognized (15) and in favorable cases this structure can be assigned from spectral data. The high energy state presents a much more formidable problem. Attempts to assign this structure and to attribute the measured barrier must of necessity rest on analogy with model compounds. In the case of trimethylene sulfites, lack of appreciation of the importance of vicinal electron pair effects led to inappropriate choice of acyclic models (13, 21) for estimation of the contribution of torsional barriers to the ring inversion barrier (1).

[6]Recent work has established a minimum value for S—S at 7.0 kcal/mol (22).

TABLE 1. Barriers to ring reversal for 1,3,2-dioxathianes

Compound 3	T_c(°C)*	$\Delta\nu_{AB'}$ (Hz)	J_{AB} (Hz)	K_c (s^{-1})	$\Delta G^{\ddagger}$‖ (kcal/mol)
a†	−38	56.1	15.1	147.5	11.3
b‡	−42	53.1	15.5	126.7	11.2
c†	−20	29.3	—	65.0	12.6
	−26	8.7	10.7	61.5	12.3
d§	−83	19.3	7.0	57.3	9.4
e§	−79	18.2	—	40.4	9.8

*Error in temperature measurement is ±2°.
†Measured in CD_2Cl_2 solution.
‡Measured in $CDCl_3$ solution.
§Measured in solution of CD_2Cl_2:C_2D_5Br (1:1).
‖Error estimated to be ±0.2 kcal/mol. Uncertainty in temperature is the major source of error (see ref. 19).

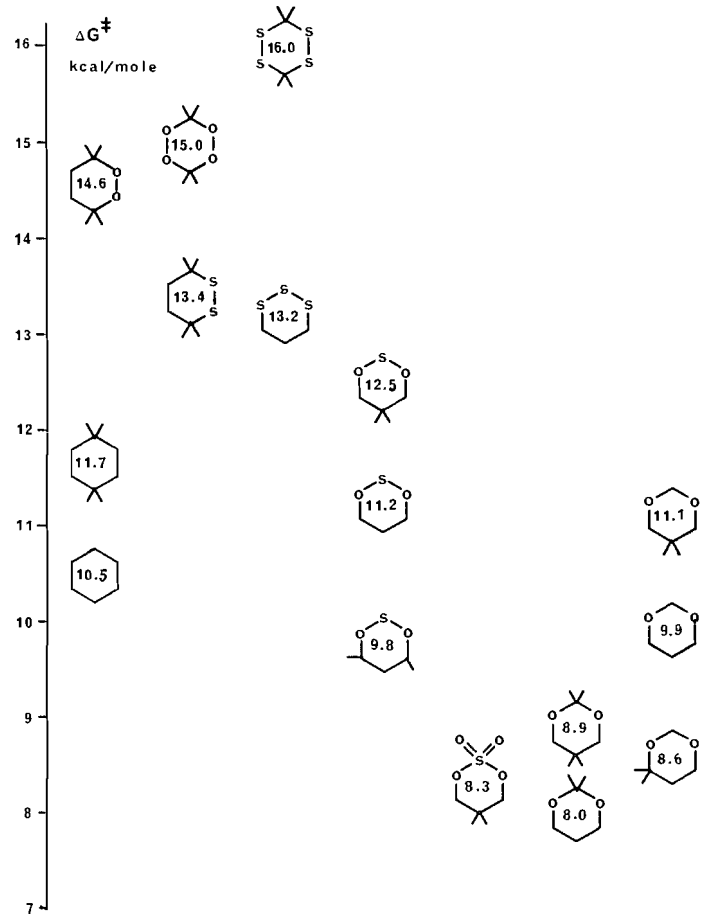

FIG. 1. Barriers to ring reversal ($\Delta G^{\ddagger}$ at T_c) for 1,3,2-dioxathianes and other six-membered rings.

most of the shifts observed for these compounds are within 0.1 p.p.m. of the value for the corresponding trimethylene sulfite (ref. 1*a*, p. 522). The most clear-cut exception arises from the meso-4,6-dimethyl-1,3,2-dioxathiane which, like its sulfite analog, is assumed to be fixed in the chair conformation with methyl groups equatorial. The axial 4,6-protons in the former appear at δ 4.25 p.p.m. which is 0.7 p.p.m. upfield from the corresponding proton in the trimethylene

Can. J. Chem. Downloaded from www.nrcresearchpress.com by 210.87.254.6 on 09/05/12
For personal use only.

Can. J. Chem. Downloaded from www.nrcresearchpress.com by 210.87.254.6 on 09/05/12
For personal use only.

sulfite. This puts a quantitative estimate on the magnitude of S=O axial deshielding.

With the latter effect removed, the difference in chemical shift between axial and equatorial protons at C-4 and -6 in the dioxathianes (estimated from low temperature spectra) becomes smaller than typical cyclohexane values of 0.3–0.5 p.p.m. (*e.g.* $\Delta\nu = 8.7$ Hz for **3***c*, Table 1), but it is not possible from the present data to determine which proton appears at higher field.

The protons at C-5 generally show the same shifts as the corresponding sulfites. The axial proton of the parent compounds (δ 2.5 p.p.m.) is almost 1 p.p.m. toward lower field than the equatorial one, a phenomenon common to 1,3-dioxanes and other compounds with oxygens at positions 1 and 3.

Throughout this paper possible non-chair forms of 1,3,2-dioxathianes have been ignored. The data discussed here appear to be consistent with this assumption, but the evidence is in no sense compelling. The presence of vicinal electron pairs should at least reduce the energy of non-chair forms relative to cyclohexane, for reasons previously discussed (1*b*).

Summary and Conclusions

The synthesis and n.m.r. study of a series of 1,3,2-dioxathianes has extended the available data on six-membered ring compounds with vicinal electron pairs. In conformity with previous findings for systems of this general type, ring reversal barriers are found to be higher than for similar compounds lacking vicinal electron pairs. The results support the general conclusion that electron pairs on adjacent atoms in a ring increase the barrier to rotation about the bond joining them, and in this way increase the barrier to ring reversal.

When the considerable evidence now available to reinforce this generalization is applied to the relatively intractable trimethylene sulfite problem, it becomes apparent that the latter compounds must be in some sense anomalous. Perhaps the chair $\rightleftarrows$ chair interconversion in these molecules occurs across a barrier very much lower than that measured for any other similar ring (to accomodate one interpretation of ultrasonic absorption results). Alternately, the chair $\rightleftarrows$ chair interconversion may have a barrier which is comparable to that for structurally similar molecules, but which is not amenable to n.m.r. measurement because the sulfite ring system is strongly biased toward one chair form. Weighing these possibilities against each other, we find that uncertainties in conformational assignments for the higher energy state in ultrasonic absorption studies remove the necessity for the former interpretation. The latter situation appears to us particularly likely since it can readily incorporate the ultrasonic results on the basis of chair $\rightleftarrows$ non-chair interconversions.

Experimental

Elemental analyses were obtained from Midwest Microlab, Ltd., Indianapolis, Indiana.

Proton n.m.r. spectra were measured on a JEOL C60HL spectrometer using TMS as internal reference.

Mass spectra were taken by Dr. Larry Dusold, Chemistry Department, Wayne State University, Detroit, on an AEI MS902B spectrometer.

G.l.c. analyses were made with an F & M Model 720 instrument using columns packed with 10% diethyleneglycol succinate (LAC728) on chromosorb W and at a flow rate of carrier gas (helium) of 60 ml/min. Analytical work was done on a 1/4 in. × 5 1/2 ft column (70–90°) and collections on a 3/4 in. × 8 ft column (135°). Dioxathianes were prepared essentially by the method of Thompson (18). For the preparation of 4,6-dimethyl-1,3,2-dioxathianes, the reaction was carried out under a nitrogen atmosphere to reduce the formation of sulfites. The deuterated parent compound, **3***b* was prepared in better yield by substituting di-1-imidazolyl sulfide for sulfur dichloride.

1,3,2-Dioxathiane (3a)

From 38.0 g (0.5 mol) of 1,3-propanediol and 51.5 g (0.5 mol) of sulfur dichloride there was obtained an oil which after distillation afforded 4.5 g of light yellow liquid, b.p. 38–48° at 12–13 mm. G.l.c. of this liquid showed two peaks. The component of lower retention time was identified as 1,3,2-dioxathiane by spectral means although the index of refraction, $n_D^{25.5}$ 1.4750, differed from the reported value, n_D^{23} 1.4948 (18).

The i.r. spectrum of the pure liquid showed no hydroxyl absorption. The n.m.r. spectrum in CD_2Cl_2 consisted of a triplet at δ 4.38 p.p.m. ($J = 5.0$ Hz) and a quintet at 1.98 p.p.m. ($J = 5.0$ Hz). The low temperature n.m.r. results have been described. A peak at *m/e* 106 in the mass spectrum was assigned to the molecular ion.

Authentic trimethylene sulfite possessed the same retention time as the second product from the reaction.

1,1,3,3-Tetradeuterio-1,3-propanediol (23)

A solution of 5.0 g of $LiAlD_4$ in 200 ml of anhydrous tetrahydrofuran was placed under a nitrogen atmosphere in a 500 ml three-necked flask equipped with a reflux condenser, dropping funnel, and magnetic stirrer. Dimethyl malonate (13.2 g) diluted to 25 ml with anhydrous tetrahydrofuran was introduced with stirring at a rate sufficient to maintain gentle reflux. The mixture was then heated and stirred under reflux for 20 h. Decom-

Can. J. Chem. Downloaded from www.nrcresearchpress.com by 210.87.254.6 on 09/05/12
For personal use only.

position was accomplished by the careful addition of water (50 ml), 15% NaOH (5.0 ml), and water (150 ml). The mixture was filtered and the precipitate washed with six 50-ml portions of boiling tetrahydrofuran. Evaporation of solvent from the dried ($MgSO_4$) filtrate and washings yielded 4.4 g of a clear, light yellow oil.

I.r. analysis showed the usual hydroxyl absorption as well as C—D stretching at 2100 and 2200 cm^{-1}. A singlet at 1.7 p.p.m. in the n.m.r. spectrum was assigned to C-2 protons and the hydroxyl protons appeared at 3.89 p.p.m.

Di-1-imidazolyl Sulfide

Following the procedure of Walter and Radke (24), 36.0 g of imidazole was reacted with sulfur dichloride (13.5 g) to yield 16.2 g of product, m.p. 78–83° (lit. (24) m.p. 80–85°).

4,4,6,6-Tetradeuterio-1,3,2-dioxathiane

Under a nitrogen atmosphere 8.58 g of di-1-imidazolyl sulfide was dissolved in 250 ml of anhydrous tetrahydrofuran in a 500 ml three-necked flask equipped with an addition funnel and a magnetic stirrer. 1,1,3,3-Tetradeuterio-1,3-propanediol (4.35 g diluted to 15 ml with anhydrous tetrahydrofuran) was introduced rapidly with stirring. After 15 min of stirring, the tetrahydrofuran was removed on the rotary evaporator and the residue vacuum distilled. The product was contained in a fraction (2.24 g) with b.p. 29–33°/0.25 mm.

The peak of lower retention time on preparative g.l.c. (17% of total) was found to be the desired product (**3***b*). The other major peak (83%) had a retention time corresponding to trimethylene sulfite.

*5,5-Dimethyl-1,3,2-dioxathiane (**3***c*)

Reaction of 52 g (0.5 mol) of 2,2-dimethyl-1,3-propanediol with sulfur dichloride gave a brown liquid which was separated by distillation into two fractions: (*i*) 1.65 g, b.p. 26–30°/2.0–2.2 mm and (*ii*). 14.7 g, b.p. 31–40°/1.2 mm. In addition to the desired product, these fractions contained 12 and 37%, respectively, of 5,5-dimethyltrimethylene sulfite.

Spectral results for this compound (**3***c*) have been reported (16).

Anal. Calcd. for $C_5H_{10}O_2S$: C, 44.75; H, 7.51; S, 23.89. Found: C, 45.0; H, 7.6; S, 23.6.

*4,6-Dimethyl-1,3,2-dioxathianes (**3***d and f)*

Sulfur dichloride (26.0 g, 0.25 mol) was reacted with 2,4-pentanediol (26.0 g, 0.25 mol, mixed isomers) under nitrogen to yield a crude oil. Distillation gave two fractions: (*i*) 13.8 g, b.p. 67–74°/13 mm and (*ii*). 4.23 g, b.p. 67–70°/1.25 mm. G.l.c. of fraction *i* showed five peaks, of which the two major peaks had the lowest retention times and n.m.r. spectra corresponding to the desired products.

The *trans*-4,6-dimethyl compound (**3***d*) showed a multiplet at δ 4.60 p.p.m., a triplet at 1.8 p.p.m. (J = 5.3 Hz), and a doublet at 1.43 p.p.m. (J = 6.8 Hz).

Anal. Calcd. for $C_5H_{10}O_2S$: C, 44.75; H, 7.51; S, 23.89. Found: C, 44.7; H, 7.5; S, 23.9.

The *cis*-compound (**3***f*) showed a multiplet at δ 4.25 p.p.m., a five-line signal at 1.5–1.83 p.p.m., and a doublet at 1.33 p.p.m. (J = 6 Hz) in $CDCl_3$ solution.

Anal. Found: C, 44.5; H, 7.6; S, 23.8.

2,3,3,4-Tetradeuterio-2,4-pentanediol

The procedure of Pritchard and Vollmer for synthesis of 2,4-pentanediol (25) was adapted to make the tetradeuterio derivative. Sodium borodeuteride (5.0 g, 0.12 mol) was added to a three-necked 300 ml flask containing 50 ml of D_2O and 0.3 ml of a 40% solution of NaOD in D_2O. The reaction flask was cooled to 10° and 20.0 g (0.20 mol) of 2,4-pentanedione in 60 g of CH_3OD was added during 2 h while the temperature was maintained at 10–15°. Following an additional 2 h of stirring at room temperature, the solvent was removed under vacuum and glycerine (100 ml) was added. Fractional distillation yielded 18.2 g (84.3%) of a colorless liquid, b.p. 50–55°/0.1 mm; n_D^{25} 1.4314.

*4,5,5,6-Tetradeuterio-4,6-dimethyl-1,3,2-dioxathianes (**3***e and g)*

The procedure described for **3***d* and *f* was followed using tetradeuteriodiol, and preparative g.l.c. which provided the dioxathianes as before. The peak of lowest retention time showed an n.m.r. singlet (δ 1.32 p.p.m.) which was unchanged on cooling to −100° and this compound was therefore assigned the *cis*-structure (**3***g*). The second g.l.c. peak also had as the most prominent feature of its n.m.r. spectrum a singlet (δ 1.40 p.p.m.), but cooling caused a broadening of the signal and separation into two singlets (δ 1.25, 1.55 p.p.m.) at −100°. This compound was assigned the *trans*-structure (**3***e*). Weak signals at δ 1.2, 1.5, and 1.7 p.p.m. were also present and are probably due to contamination from the corresponding sulfites, which are also represented by the three smaller peaks of higher retention time in the crude product as before.

The financial assistance of the National Research Council of Canada is gratefully acknowledged.

1. (*a*) G. Wood, G. W. Buchanan, and M. H. Miskow. Can. J. Chem. **50**, 521 (1972). (*b*) G. Wood, J. M. McIntosh, and M. H. Miskow. Can. J. Chem. **49**, 1202 (1971).
2. W. Wucherpfennig. Ann. Chem. **737**, 144 (1970).
3. (*a*) C. H. Bushweller, G. U. Rao, and F. H. Bissett. Int. J. Sulfur Chem. A, **1**, 216 (1971). (*b*) C. H. Bushweller. J. Am. Chem. Soc. **91**, 6019 (1969). (*c*) C. H. Bushweller, J. Golini, G. U. Rao, and J. W. O'Neil. J. Am. Chem. Soc. **92**, 3055 (1970).
4. For a review with leading refs. see S. Wolfe. Acc. Chem. Res. **5**, 102 (1972).
5. J. B. Hendrickson. J. Am. Chem. Soc. **83**, 4537 (1961).
6. R. K. Harris and R. A. Spragg. J. Chem. Soc. 684 (1968).
7. S. Kabuss, A. Luttringhaus, H. Friebolin, and R. Mecke. Z. Naturforsch. **21**b, 320 (1966).
8. G. Wood and M. H. Miskow. Tetrahedron Lett. 1109 (1969).
9. (*a*) H. F. van Woerden and E. Havinga. Rec. Trav. Chim. Pays-Bas, **86**, 341 (1967); (*b*) **86**, 353 (1967).
10. C. H. Green and D. G. Hellier. J. Chem. Soc. Perkin II, 458 (1972).
11. P. Albriktsen. Acta Chem. Scand. **25**, 478 (1971).
12. G. Wood and M. H. Miskow. Tetrahedron Lett. 1775 (1970).

13. G. ECCLESTON, R. A. PETHRICK, E. WYN-JONES, P. C. HAMBLIN, and R. F. M. WHITE. Trans. Faraday Soc. **66**, 310 (1970).
14. E. L. ELIEL, N. L. ALLINGER, S. J. ANGYAL, and G. A. MORRISON. Conformational analysis. Interscience Publishers, John Wiley and Sons Ltd., New York. 1965. p. 185.
15. E. WYN-JONES. Tetrahedron Lett. 907 (1971).
16. G. WOOD and R. M. SRIVASTAVA. Tetrahedron Lett. 2937 (1971).
17. G. WOOD, J. M. MCINTOSH, and M. MISKOW. Tetrahedron Lett. 4895 (1970).
18. Q. E. THOMPSON. J. Org. Chem. **30**, 2703 (1965).
19. D. KOST, E. H. CARLSON, and M. RABAN. Chem. Commun. 656 (1971).
20. (*a*) H. G. SCHMID, A. JAESCHKE, H. FRIEBOLIN, S. KABUSS, and R. MECKE. Org. Mag. Res. **1**, 67 (1969). (*b*) **1**, 163 (1969). (*c*) H. FRIEBOLIN, H. G. SCHMID, S. KABUSS, and W. FAISST. Org. Mag. Res. **1**, 147 (1969).
21. E. WYN-JONES and R. A. PETHRICK. *In* Topics in stereochemistry. Vol. 5, E. L. Eliel and N. L. Allinger, Editors John Wiley and Sons, Inc., New York, N.Y., Interscience Division. 1970. p. 205.
22. R. R. FRASER, G. BROUSSARD, J. K. SAUNDERS, J. B. LAMBERT, and C. E. MIXAN. J. Am. Chem. Soc. **93**, 3822 (1971).
23. J. T. GERIG and R. A. RIMERMAN. J. Am. Chem. Soc. **92**, 1224 (1970).
24. W. WALTER and M. RADKE. Angew. Chem. Intl. Ed. **7**, 302 (1968).
25. J. G. PRITCHARD and R. L. VOLLMER. J. Org. Chem. **28**, 1547 (1963).

Can. J. Chem. Downloaded from www.nrcresearchpress.com by 210.87.254.6 on 09/05/12
For personal use only.

The Mechanism of the HgH $A_2{}^2\Pi_{3/2} \rightarrow X^2\Sigma^+$ Emission in the Hg(6^3P_0) Photosensitization of Hydrogen and the Alkanes

A. C. VIKIS AND D. J. LE ROY

Department of Chemistry, University of Toronto, Toronto 181, Ontario

Received November 10, 1972

The mechanism of the HgH $A_2{}^2\Pi_{3/2} \rightarrow X^2\Sigma^+$ emission detected in the Hg(6^3P_0) photosensitized decomposition of H_2 and some of the lower alkanes, RH, was investigated. It was concluded that ground state HgH was formed in the primary process Hg(6^3P_0) + RH(or H_2) → HgH($X^2\Sigma^+$) + R(or H). The HgH $A_2{}^2\Pi_{3/2} \rightarrow X^2\Sigma^+$ emission and presumably the $A_1{}^2\Pi_{1/2} \rightarrow X^2\Sigma^+$ and $B^2\Sigma^+ \rightarrow X^2\Sigma^+$ emission, also observed in the above systems, result from secondary excitation of ground state HgH on collision with Hg(6^3P_0). Studies of the emission made possible the estimation of relative quantum yields for the above primary process.

Le mécanisme de l'émission HgH $A_2{}^2\Pi_{3/2} \rightarrow X^2\Sigma^+$ détectée dans la décomposition photosensibilisée par Hg(6^3P_0) de H_2 et de quelques un des alcanes inférieurs RH, a été étudie. On a conclu à la formation de HgH fondamental résultant du processus primaire Hg(6^3P_0) + RH (ou H_2) → HgH ($X^2\Sigma^+$) + R (ou H). L'émission de HgH $A_2{}^2\Pi_{3/2} \rightarrow X^2\Sigma^+$ et probablement celles de $A_1{}^2\Pi_{1/2} \rightarrow X^2\Sigma^+$ et $B^2\Sigma^+ \rightarrow X^2\Sigma^+$ également observées pour les systèmes ci dessus, résultent d'une excitation secondaire de HgH fondamental par collision avec Hg(6^3P_0). Les études sur l'émission permettent d'évaluer les rendements quantiques relatifs aux processus primaires décrits ci dessus.

[Traduit par le journal]

Can. J. Chem., 51, 1207 (1973)

Can. J. Chem. Downloaded from www.nrcresearchpress.com by 210.87.254.42 on 09/05/12
For personal use only.

In a recent communication (1) we have reported the detection of HgH by its emission spectrum in the Hg(6^3P_0) photosensitized decomposition of H_2, CH_4, C_2H_6, C_3H_8, and n-C_4H_{10}. We had concluded that our finding was an indication of the long-sought (2–5) evidence for primary HgH formation in the Hg($6^3P_{1,0}$) photosensitized decomposition of

[1] $$Hg(6^3P_{1,0}) + RH \rightarrow HgH(X^2\Sigma^+) + R$$

the alkanes, RH, rather than, or in addition to the alternative primary process,

[2] $$Hg(6^3P_{1,0}) + RH \rightarrow Hg(6^1S_0) + H + R$$

Medium resolution spectra of the HgH emission are shown in Fig. 1, where the main emission bands are identified. The mechanism which we proposed (1) for HgH formation and excitation of the various bands was in accord with previous similar studies in the presence of hydrogen (2, 6, 7),

[3] $$Hg(6^3P_0) + RH \rightarrow HgH(X^2\Sigma^+) + R$$

[4] $$Hg(6^3P_0) + HgH(X^2\Sigma^+) \rightarrow HgH(A_1{}^2\Pi_{1/2}, A_2{}^2\Pi_{3/2}, B^2\Sigma^+) + Hg(6^1S_0)$$

[5] $$HgH(A_1{}^2\Pi_{1/2}, A_2{}^2\Pi_{3/2}, B^2\Sigma^+) \rightarrow HgH(X^2\Sigma^+) + h\nu$$

This mechanism was supported by qualitative evidence and the approximate light intensity dependence of the HgH fluorescence on the intensity of the primary lamps. It was felt necessary, however, to investigate the system in greater detail in order to support our claim that reaction 3 was responsible for the HgH formation and that reactions 4 and 5 were responsible for the emission. The present work supports this mechanism and also makes possible the calculation of relative HgH yields for reaction 3.

Experimental

The flow system used in the present work was described previously (8). Matheson prepurified grade nitrogen (99.997%) was used as the carrier gas at a flow rate of 20 std cc/min. The carrier gas was passed through a 1 ft long (12 mm i.d.) quartz tube packed with activated copper turnings at ~500 °C, in order to eliminate any oxygen impurity. Activation of the copper turnings was accomplished by a number of oxidation–reduction cycles using O_2 and H_2. Two Dry Ice – acetone traps followed the above treatment. The other reagents and their purity were as follows: H_2, Canox grade (99.9%), was passed before use through a catalytic Deoxo unit followed by two liquid nitrogen traps. The hydrocarbons were Phillips research grade; their purity in % by mole was stated by the manufacturer as follows: CH_4 (99.99), C_2H_6 (99.99), C_3H_8 (99.99), n-C_4H_{10} (99.8), i-C_4H_{10} (99.9). The most troublesome impurities in the alkanes were small amounts of olefins which were largely removed by adsorbing the gases on molecular sieve 13X at 77 °K and desorbing them at temperatures giving sufficient vapor pressure for transfer to a separate liquid nitrogen trap. The first fraction to transfer, which was

Can. J. Chem. Downloaded from www.nrcresearchpress.com by 210.87.254.42 on 09/05/12
For personal use only.

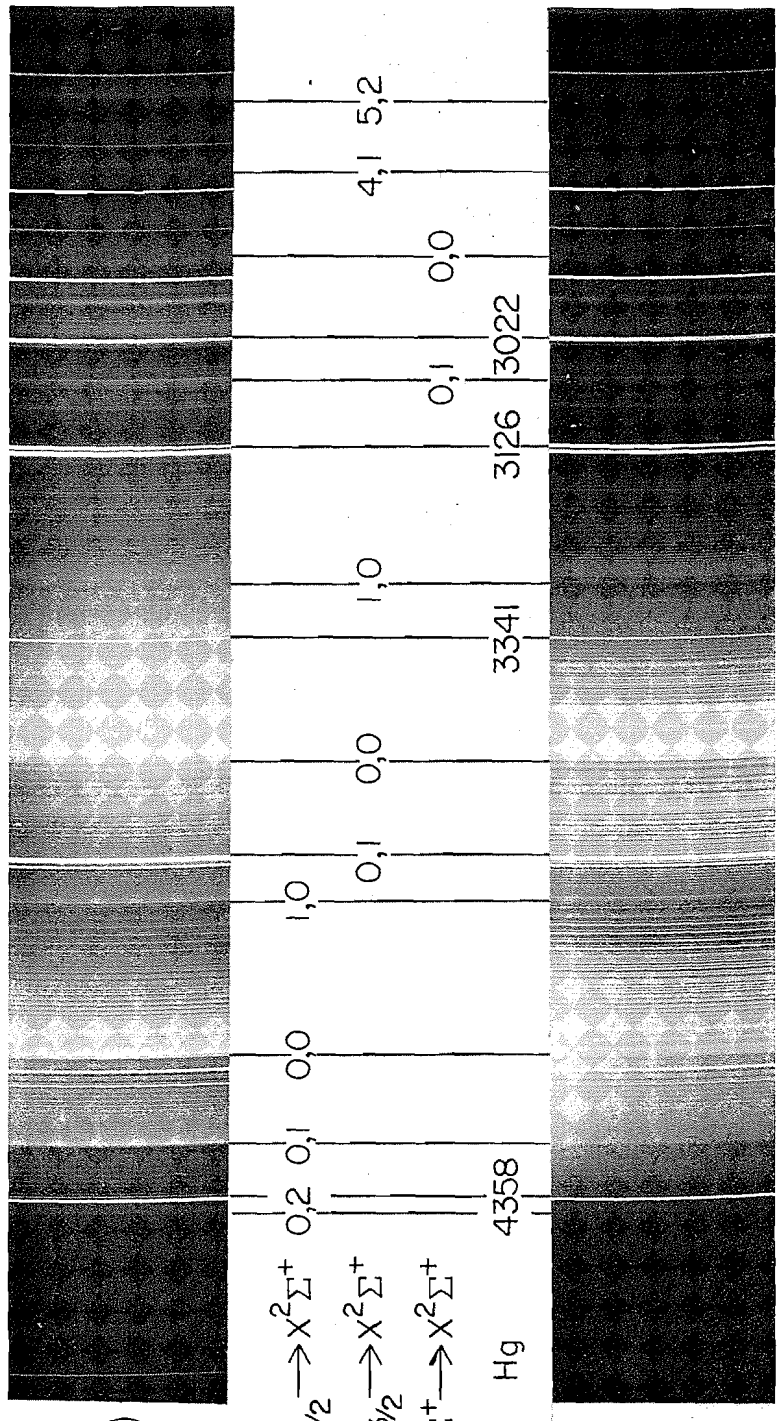

FIG. 1. The HgH emission spectrum excited by $Hg(6^3P_0)$ ((*a*) $P_{N_2} \sim 1$ Torr, $P_{Hg} = 1.2 \times 10^{-3}$ Torr, $P_{H_2} \sim 0.1 \times 10^{-3}$ Torr. (*b*) $P_{N_2} = 20$ Torr, $P_{Hg} = 1.8 \times 10^{-4}$ Torr, $P_{H_2} = 1.5 \times 10^{-3}$ Torr).

Can. J. Chem. Downloaded from www.nrcresearchpress.com by 210.87.254.42 on 09/05/12
For personal use only.

found to be purest with respect to olefins, was used after several freezing, pumping, and thawing cycles which served to remove condensibles.

The optical system used in the present work is shown in Fig. 2. Mercury(6^3P_0) is formed from Hg(6^3P_1) by collisions with N_2. The following elementary steps and their respective rate constants are well known (3).

$$Hg(6^1S_0) + h\nu\,(2537\text{ Å}) \rightarrow Hg(6^3P_1)$$

$$Hg(6^3P_1) \rightarrow Hg(6^1S_0) + h\nu\,(2537\text{ Å})$$

$$Hg(6^3P_1) + N_2 \leftrightarrows Hg(6^3P_0) + N_2$$

$$Hg(6^3P_0) \rightarrow Hg(6^1S_0)$$

The effective Hg(6^3P_1) lifetime with respect to emission, allowing for radiation imprisonment, is 2.06×10^{-7} s for the particular cell and Hg pressure (1.8×10^{-4} Torr) used (8). The overall lifetime of the Hg(6^3P_0) atoms at 20 Torr of N_2 is of the order of 10^{-3} s. The relative Hg(6^3P_0)/Hg(6^3P_1) steady state concentration is of the order of 10^3/l. Under these conditions and at the low partial pressures of H_2 and RH used (10^{-3} to 1 Torr, depending on the quenching efficiency of each gas) all reactions studied are to a good approximation initiated by Hg(6^3P_0).

The Hg(6^3P_0) population was followed by absorption of 4047 Å radiation emitted from a Pen-Ray mercury lamp, L_3, (Type 22 SC-3S). Light emitted from the Pen-Ray lamp was collimated and passed through a Pyrex filter before entering the reaction cell. The path length illuminated by the primary lamps was 18 cm. After passing through the reaction cell the analytical 4047 Å beam was focussed on the slit of a Bausch and Lomb grating monochromator, M (dispersion 33 Å/mm), and detected with an EMI 6255B photomultiplier, P. With the monochromator set at the peak of the 4047 Å line and the slits set at 0.10 mm the calibration graph of Fig. 3 was obtained by varying the intensity of the primary 2537 Å radiation emitted from the two U-shaped low pressure Hg lamps, L_1 and L_2. The absorption-concentration relationship was found to deviate significantly from Beer's law. Relative or absolute Hg(6^3P_0) concentrations were obtained from Fig. 3 according to the method of Ladenburg and Reiche (9, 10).

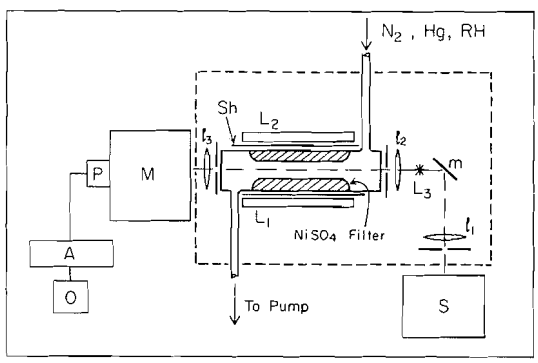

FIG. 2. Optical system and reaction cell assembly.

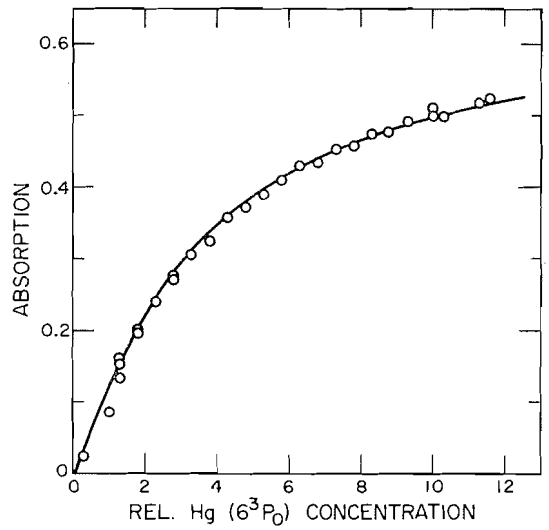

FIG. 3. Absorption of 4047 Å light *vs.* relative Hg(6^3P_0). (The solid line is the calculated absorption with $\alpha = 2.8$ (*cf.* ref. 9) and represents the best fit to the experimental absorption indicated by open circles. The product $k_0 l$[Hg(6^3P_0)] can be obtained by multiplying the abscissa by 0.458; k_0 is 5.90×10^{-12} cm^2/atom (11) and $l = 18.0$ cm.)

In order to eliminate problems associated with fast removal of Hg(6^3P_0) by olefins produced under steady irradiation the photomultiplier signal, after amplification by a Keithley Model 417 picoammeter, A, was displayed and photographed on a Phillips PM3230 oscilloscope, O. This made it possible to determine Hg(6^3P_0) populations at delay times of 0.2 s after exposing the reaction cell to the light from the 2537 Å lamps by the manual removal of a shutter, Sh. Typical oscillographs are shown in Fig. 4. It can be seen that olefin impurities, either initially present in the alkanes or formed during the reaction, are a serious problem and most likely account for the rather large discrepancies in Hg(6^3P_0) quenching cross sections reported by various groups (12–15).

The HgH emission spectra were obtained with the M-P-A-O arrangement, whenever low resolution was desired. For better resolution a Hilger and Watts model E-517 quartz spectrograph, S (82 Å/mm dispersion at 3500 Å) and Kodak 102-O plates were used. A few higher resolution spectra (Fig. 1) were obtained with a Hilger and Watts Model E-498 quartz spectrograph (24 Å/mm dispersion at 3500 Å).

In the kinetic studies the HgH emission, I^*, at the maximum of the $A_2{}^2\Pi_{3/2}$–$X^2\Sigma^+$ 0,0 band (340–350 mμ), was monitored, because this region was the most intense and also free of atomic mercury lines. To eliminate scattered radiation of other wavelengths a Bausch and Lomb 340 mμ (20 mμ half-width) interference filter was placed before the monochromator and the monochromator slits opened to 1.5 mm. This emission signal was displayed on the oscilloscope and monitored at short delay times whenever olefinic impurities were a problem. Typical oscillographs are shown in Fig. 4.

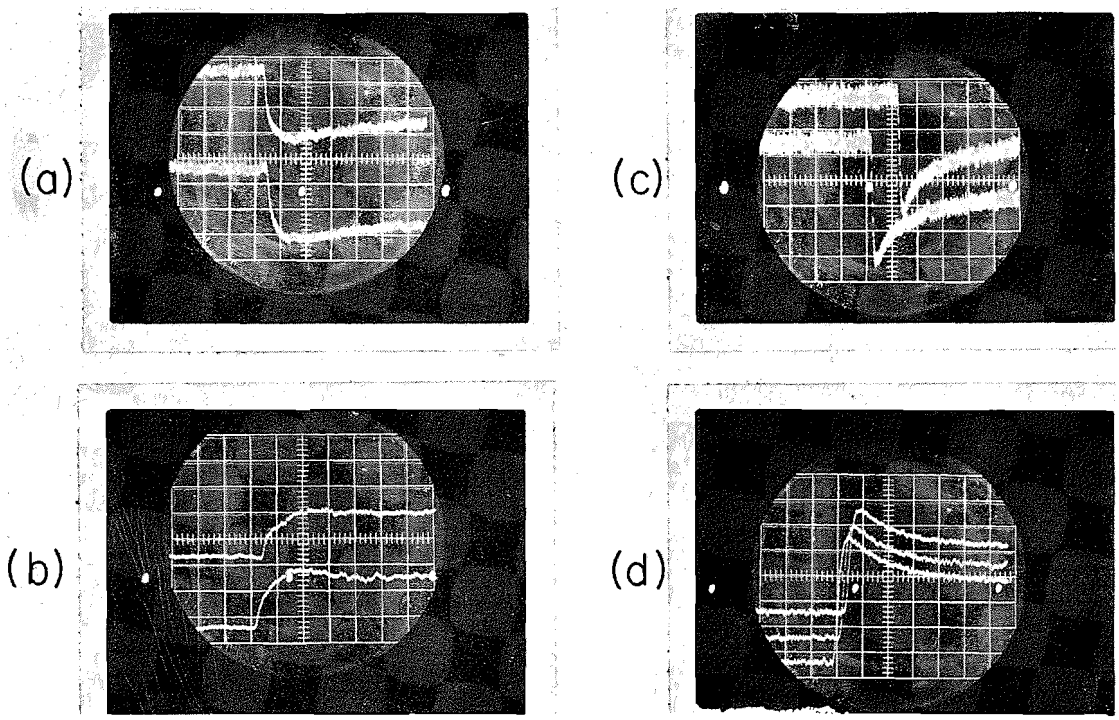

FIG. 4. The variation of $Hg(6^3P_0)$ absorption and HgH emission with irradiation time. The full time axis is 5 s. Oscillographs (*a*) and (*b*) were obtained with untreated research grade C_2H_6; (*c*) and (*d*) with treated C_2H_6. The absorption attenuation setting is the same in (*a*) and (*c*) (dumping control decreased in (*c*)); the same is true for the emission attenuation in (*b*) and (*d*). The C_2H_6 pressures in Torr are: (*a*) both 0.41; (*b*) 0.63 (upper) and 0.35 (lower); (*c*) 0.61 (upper) and 0.46 (lower); (*d*) 0.86 (upper), 0.66 (middle), and 0.42 (lower). The initial increase in absorption or emission in (*a*) and (*b*) occurring in the first second is probably due to removal of ethylene initially present. The subsequent decrease in absorption or emission is due to ethylene built-up as the system achieves steady state.

Results and Discussion

Besides the elementary steps associated with $Hg(6^3P_0)$ formation from $Hg(6^3P_1)$ and decay, already discussed in the experimental section, the reactions that follow were found necessary to explain the data. Other possible mechanisms are also discussed in this section and shown to be inadequate.

[6] $Hg^0 + RH \rightarrow HgH + R$

[7] $Hg^0 + HgH \rightarrow (HgH)^{**} + Hg$

[8] $(HgH)^{**} + M \rightarrow (HgH)^{*} + M$

[9] $(HgH)^{**}, (HgH)^{*} \rightarrow HgH + h\nu$

[10] $HgH\ (+M) \rightarrow Hg + H\ (+M)$

[11] $HgH + R\ (H) \rightarrow Hg + RH\ (H_2)$

where Hg^0 and Hg denote $Hg(6^3P_0)$ and $Hg(6^1S_0)$, respectively; $(HgH)^{**}$ and $(HgH)^{*}$ denote the initial and collisionally altered vibronic populations of the $A_1{}^2\Pi_{1/2}$, $A_2{}^2\Pi_{3/2}$, and $B^2\Sigma^+$ states, and HgH the ground electronic state; M denotes the bath gas, which is mainly N_2. The bimolecular reaction 10 is expected to be the dominant reaction of HgH decay in the absence of reaction 11. Callear and Hedges' (4) HgH decay curves indicate a HgH lifetime of $\sim 10^{-4}$ s at pressures roughly ten times ours. Thus at 20 Torr an upper limit for the HgH decay would be $\sim 10^{-3}$ s. This is approximately ten times higher than the simple collision theory prediction but could be feasible if the rotational degrees of freedom contribute to the dissociation according to the mechanism of Palmer and Hornig (16).

The variation of the peak intensity of the $A_2{}^2\Pi_{3/2} \rightarrow X^2\Sigma^+$, 0,0 band *vs.* the intensity of primary excitation (2537 Å light), is shown in Fig. 5 for various conditions. Earlier studies in this laboratory (1) and others (7), employing spectrographic methods, indicated that the HgH emission intensity was roughly dependent on

Can. J. Chem. Downloaded from www.nrcresearchpress.com by 210.87.254.42 on 09/05/12
For personal use only.

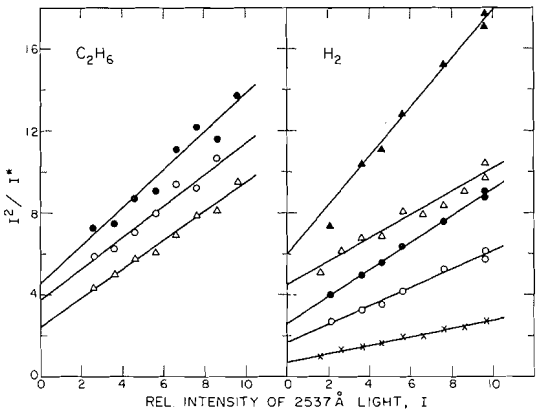

FIG. 5. Variation of HgH emission intensity, I^*, with the primary light intensity, I (C_2H_6: P_{N_2} = 20 Torr, $P_{Hg} = 1.8 \times 10^{-4}$ Torr; ●, 0.153 Torr; ○, 0.098 Torr; △, 0.048 Torr, the ordinate displaced by −3; H_2:P_{N_2} = 20 Torr, $P_{Hg} = 1.8 \times 10^{-4}$ Torr; ▲, 7.9×10^{-3} Torr; ●, 3.1×10^{-3} Torr; ○, 1.90×10^{-3} Torr; H_2:P_{Hg} = 1.8×10^{-3} Torr; △, P_{N_2} = 1 Torr; $P_{H_2} = 2.5 \times 10^{-3}$ Torr; X, P_{N_2} = 4.5 Torr, $P_{H_2} = 2.5 \times 10^{-3}$ Torr).

the second power of the primary radiation, I. This would indicate that two Hg^0 atoms are involved in the overall process, as expected. More precise photoelectric measurements obtained in the present work indicate that the above is true in the limit of low light intensities but that at higher intensities the exponent of I assumes lower values. Since the Hg^0 concentration, which was followed by absorption, was found to be directly proportional to I, it is concluded that, in addition to reaction 10, there must be a competitive process of removal of HgH due to reaction with H atoms and/or alkyl radicals present in the system. The possibility that in the case of the alkane reactions, HgH or $Hg(6^3P_0)$ are consumed in reactions with olefinic products is excluded since the above measurements refer to short delay times (0.2 s) when such products are not significant. The data in Fig. 5 indicate that at the primary light intensities used, corresponding to 9.5 in Fig. 5, reaction 11 is two to five times faster than the combined first and pseudo first order decay of HgH. Reaction 11 is expected to proceed with high efficiency with either H or R (4). The radical concentrations are expected to be of the order of 10^{-4} Torr in our system.

The variation of HgH emission, I^*, with H_2 and RH is shown in Figs. 6 and 7. An equation which describes this dependence and which is also in accord with the given mechanism is

$$[12] \qquad I^* = \frac{C\phi_{RH}k^{0g}_{RH}[RH][Hg^0_{RH}]^2}{k + C'_{RH}k^{0g}_{RH}[RH][Hg^0_{RH}]}$$

where C is a composite constant associated with the formation of Hg^0 and the efficiency of detecting the emission; C'_{RH}, is another composite rate constant associated with the rate constants of reaction 11 and the presumably pseudo-first order decay of H and R. That R decays by a first order process only, *e.g.* wall recombination, is not clear. It is possible, however, that gas phase recombination contributes but that the net rate can be approximated by a first order one; k, is a net first order HgH decay constant; ϕ_{RH} is the yield of HgH per quenching collision; k^{0g}_{RH}, is the $Hg(6^3P_0)$ quenching rate constant

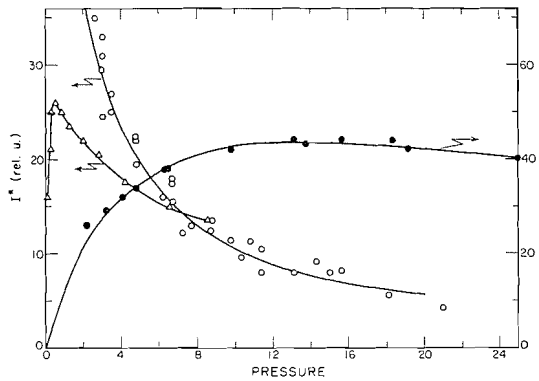

FIG. 6. Variation of HgH emission with quencher pressure (P_{N_2} = 20 Torr, $P_{Hg} = 1.8 \times 10^{-4}$ Torr; ○, H_2 in Torr × 10^3; △, C_2H_6 in Torr × 10; ●, CH_4 in Torr × 10; the solid lines are obtained from the least squares fit to eq. 12).

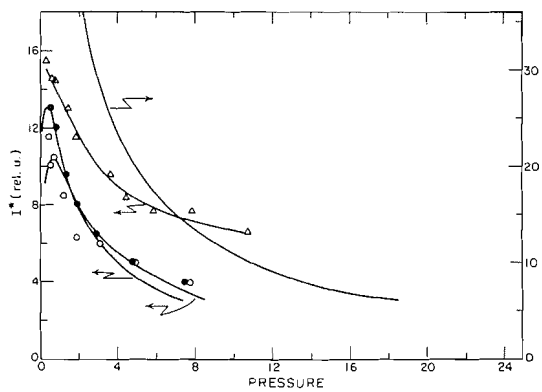

FIG. 7. Variation of HgH emission with quencher pressure. (P_{N_2} = 20 Torr, $P_{Hg} = 1.8 \times 10^{-4}$ Torr; ○, n-C_4H_{10}; ●, i-C_4H_{10}; △, C_3H_8 in Torr × 10^2; the solid lines are obtained from the least squares fit to eq. 12; the solid line with no points is for H_2, Fig. 6).

Can. J. Chem. Downloaded from www.nrcresearchpress.com by 210.87.254.42 on 09/05/12
For personal use only.

TABLE 1. Relative HgH yields

Molecule	$\phi_{RH}k^{0g}_{RH}/\phi_{H_2}k^{0g}_{H_2}$	$k^{0g}_{H_2}/k^{0g}_{RH}$* This work	Reference 13	Reference 12	ϕ_{RH}/ϕ_{H_2}
H_2	1	1	1	1	1
CH_4	$(3.9\pm0.1)\times10^{-5}$	$(0.96\pm0.11)\times10^{4}$	$>1.1\times10^{4}$	0.91×10^{4}	0.4 ± 0.1
C_2H_6†	$(6.2\pm3.2)\times10^{-4}$	$(1.3\ \pm0.4)\times10^{3}$	4.5×10^{2}	$6.0\ \times10^{2}$	0.8 ± 0.5
C_3H_8	$(3.4\pm0.5)\times10^{-3}$	83 ± 8	54	$1.2\ \times10^{2}$	0.3 ± 0.1
n-C_4H_{10}†	$(1.8\pm1.0)\times10^{-2}$	27 ± 8	34	—	0.5 ± 0.3
i-C_4H_{10}	$(3.4\pm0.4)\times10^{-2}$	13 ± 1	11	—	0.4 ± 0.1

*Individual rate constants can be obtained using $k^{0g}_{H_2} = (3.23\pm0.21)\times10^{10}\ M\ s^{-1}$ (12).
†Values for these molecules represent averages of more than one determination.

and $[Hg^0_{RH}]$ is the population of $Hg(6^3P_0)$ in the presence of RH. Quenching or reaction of HgH or any of its excited states by H_2 or RH is not included due to the relatively low partial pressures used.

Other Possible Mechanisms

Mercury hydride emission in the $Hg(6^3P_0)$ photosensitized decomposition of H_2 and alkanes could also arise through other mechanisms than the one proposed here. Three such mechanisms are discussed below and excluded on the basis of experimental evidence.

(a) Mercury hydride formation via the combination of Hg and H, followed by excitation with $Hg(6^3P_0)$

[13] $$Hg + H \rightleftarrows HgH$$

or most likely

[14] $$Hg + H + M \rightleftarrows HgH + M$$

Figure 8 shows the variation of I^* *vs.* $Hg(6^3P_0)$. The $Hg(6^3P_0)$ population was varied in two ways: (*i*) by varying the primary light intensity at fixed Hg pressure, and (*ii*) by varying the Hg pressure at fixed light intensity. All other conditions were kept constant. The variation of I^* in (*ii*) when compared to that in (*i*) shows no evidence of either reactions 13 or 14 occurring to any significant extent, despite the six-fold variation in the Hg pressure. This is due to the fact that at the conditions of our experiments the above equilibria favor the free atoms ($HgH/H \sim 10^{-3}$). Similar experiments were not performed with any of the alkanes but it can be shown that if such a mechanism were correct the quantum yields of HgH determined for the alkanes would be at least two orders of magnitude lower than that of H_2. This is not the case (see Table 1).

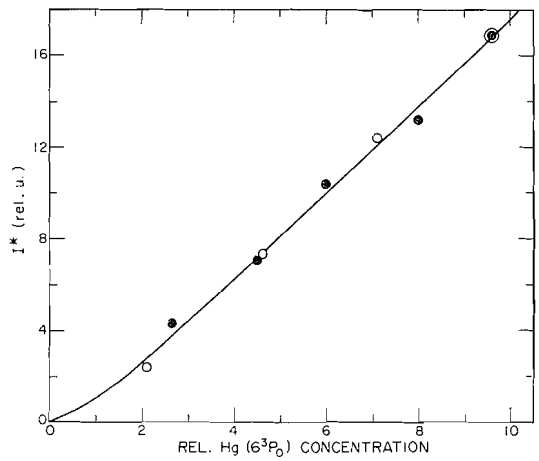

FIG. 8. Variation of HgH emission with $Hg(6^3P_0)$ concentration (○, method (*i*) in text, $P_{Hg} = 1.2 \times 10^{-3}$ Torr; ●, method (*ii*) in text, the Hg pressures in Torr × 10^4 are 1.8, 3.3, 4.9, 7.6, and 12, read on the graph from left to right).

(b) Direct formation of HgH in the excited states via the combination of Hg^0 with H

It is expected that such a combination would proceed on the $A_1{}^2\Pi_{1/2}$ surface because this is the only one that correlates with $Hg(6^3P_0)$ and $H(^2S_{1/2})$ (see Fig. 9). Population of the $A_2{}^2\Pi_{3/2}$ or $B^2\Sigma^+$ state could arise via inverse predissociation (17).

[15] $$Hg(6^3P_0) + H(^2S_{1/2}) \rightleftarrows HgH(A_1{}^2\Pi_{1/2}) \rightarrow HgH(X^2\Sigma^+) + h\nu(\text{continuous})$$

[16] $$HgH(A_1{}^2\Pi_{1/2}) \rightleftarrows HgH(A_2{}^2\Pi_{3/2}, B^2\Sigma^+) \rightarrow HgH(X^2\Sigma^+) + h\nu(\text{discrete})$$

This mechanism is excluded firstly because of the discrete spectra observed and secondly because the observed discrete spectra are due to transitions from much lower energy states than the ones

Can. J. Chem. Downloaded from www.nrcresearchpress.com by 210.87.254.42 on 09/05/12
For personal use only.

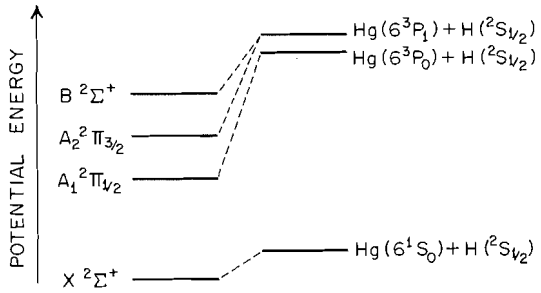

FIG. 9. Relevant energy states of HgH (schematic).

which could be populated by inverse predissociation.[1]

A more feasible mechanism would require a third body, such as

[17] $Hg(6^3P_0) + H(^2S_{1/2}) + M \rightarrow HgH(A_1{}^2\Pi_{1/2}) + M$

[18] $HgH(A_1{}^2\Pi_{1/2}) \rightarrow HgH(A_2{}^2\Pi_{3/2}, B^2\Sigma^+)$

This mechanism, however, can certainly be excluded on the basis of the rather high emission intensities observed. Relative intensity measurements of the $Hg(6^3P_1)$ emission at 2537 Å and the integrated intensity of the $A_2{}^2\Pi_{3/2} \rightarrow X^2\Sigma^+$ 0,0 band, indicate that the emission rate of the latter is $\sim 10^{12}$ quanta $cm^{-3}\ s^{-1}$. A maximum emission rate of 10^8 quanta $cm^{-3}\ s^{-1}$ can be calculated from the termolecular rate $k_r[N_2]\,[Hg^0]\,[H]$ using the fairly generous values of $k_r \sim 10^{10}$ $M^{-2}\ s^{-1}$ and $H \sim 10^{-4}$ Torr (the total H_2 pressure was 2×10^{-3} Torr). The N_2 pressure was 20 Torr and the Hg^0 pressure was 1.3×10^{-7} Torr (measured by absorption). The discrepancy of 10^4 between calculated and observed rates is beyond any uncertainty in estimating these quantities.

(c) Mercury hydride formation via reaction of Hg^0 with H_2 formed in the photosensitized decomposition of the alkanes

[19] $Hg^0 + RH \rightarrow Hg + H + R$

[20] $H \xrightarrow{\text{wall}} \frac{1}{2} H_2$

[21] $H + R\ (\text{or } RH) \rightarrow H_2 + R'(R)$

[22] $Hg^0 + H_2 \rightarrow HgH + H$

This possibility is particularly important in view of earlier failures to detect HgH in the alkanes (2–5). If such a mechanism were applicable, however, one would expect a higher order dependence of the HgH emission on the intensity of the primary radiation, *i.e.*, $2 \leqslant n \leqslant 3$ in the expression $I^* \propto I^n$ rather than $1 \leqslant n \leqslant 2$ as observed.

Furthermore, one should observe an induction period for I^* as the system approaches a steady state. The intensity profile of I^* with time would be characterized by the product $[Hg^0(t)]^n[H_2(t)]$. $Hg^0(t)$ is the variation of $Hg(6^3P_0)$ with reaction time due to olefin formation and can be determined from $Hg(6^3P_0)$ absorption *vs.* time. The variation of H_2 with time, $H_2(t)$, would be of the form $(H_2)_{s.s.}(1 - e^{-t/\tau})$, where τ is the lifetime of H_2 with respect to flowing out of the cell, and $[H_2]_{s.s.}$ is the steady state concentration of H_2. Such intensity profiles are shown in Fig. 10 for $n = 1$, 2, and 3 (curves *A*, *B*, and *C*, respectively) for 0.28 Torr of C_2H_6 and the standard conditions of 20 Torr of N_2 and a flow rate of 20 std cc/min. Curve *D* is the experimental one and should be compared to a curve calculated between *A* and *B*, since $1 \leqslant n \leqslant 2$. The two curves are in disagreement which would indicate that reaction of the

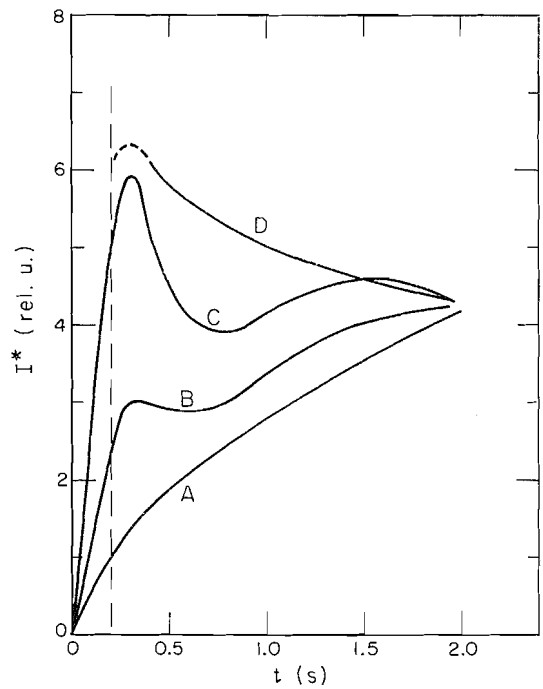

FIG. 10. The variation of HgH emission with reaction time. (The dotted vertical line at 0.25 s delineates the time required for complete removal of the shutter isolating the reaction cell from the lamps.)

[1]In the case of transitions from the upper states of $A_1{}^2\Pi_{1/2}$, $A_2{}^2\Pi_{3/2}$, $B^2\Sigma^+$ to the ground state, $X^2\Sigma^+$, the spectra would be continuous due to the instability of the lower surface.

Can. J. Chem. Downloaded from www.nrcresearchpress.com by 210.87.254.42 on 09/05/12
For personal use only.

product H_2 with $Hg(6^3P_0)$ cannot account for the observed emission.

Relative Quantum Yields of HgH

Relative quantum yields of HgH are obtained from graphs of $[RH][Hg^0_{RH}]^2/I^*$ *vs.* $[RH]$-$[Hg^0_{RH}]$, (*cf.* eq. 12). The intercepts of such plots give $k/C\phi_{RH}k^{0g}_{RH}$. These results are shown in Table 1, where ϕ_{RH}/ϕ_{H_2} is obtained from the ratio of intercepts for H_2 and RH, $\phi_{RH}k^{0g}_{RH}/\phi_{H_2}k^{0g}_{H_2}$, and the ratio of quenching rate constants determined in this work. The latter, with the exception of $k^{0g}_{H_2}/k^{0g}_{C_2H_6}$, compare very well with other literature values (12, 13), which are listed for comparison. The rather large probable errors in ϕ_{RH}/ϕ_{H_2} are the result of a combination of uncertainties in Hg^0_{RH} and k^{0g}_{RH}, as well as in the extrapolation to small intercepts. Callear and McGurk (5) have determined a HgH quantum yield of 1.0 for the reaction of $Hg(6^3P_0)$ with H_2, thus the ratios listed in Table 1 could also represent absolute values.

Conclusions

The present results indicate that the HgH emission in the $Hg(6^3P_0)$ photosensitization of hydrogen and the alkanes is due to direct formation of HgH in the primary quenching process followed by excitation of HgH on collision with another $Hg(6^3P_0)$. Earlier failures (2–5) to detect HgH in the presence of the alkanes may have been the result of rapid accumulation of olefins in these systems and the relatively fast reaction of HgH with H atoms and alkyl radicals.

The quantum yield data, when put on an absolute basis using the result of Callear and McGurk (5) on the $Hg(6^3P_0)$–H_2 system, show that quenching of $Hg(6^3P_0)$ by RH through formation of HgH is a significant process. It could possibly be the major process but, due to the higher exothermicity in the case of the alkanes, a higher proportion of vibrationally and/or rotationally excited HgH is formed and decays before detection.

The relatively high HgH yields detected in the alkanes could be interpreted as an indication that the exothermicity of the reaction does not appear entirely as localized repulsion between the H atom and the alkyl group, as suggested by the relative yields of HgH and HgD in the case of the $Hg(6^3P_{1,0})$–HD system studied by Callear and McGurk (5). Due to the high exothermicities (15 to 26 kcal/mol) and the heavy mass of the alkyl group such an energy release would result in vibrational and rotational excitation of HgH well beyond its dissociation limit ($D_0{}^0 = 8.67$ kcal/mol (17)).

A possible explanation of the observed high HgH yields is that a relatively long-lived complex is formed between $Hg(6^3P_0)$ and the alkane. This would allow equipartitioning of the exothermicity among the various degrees of freedom of the complex. From this point of view it would be desirable to have more precise quantum yield data in order to reveal any correlation between the yield, the exothermicity, and the structure of the alkane. Such correlations were shown to exist in the quenching of $Hg(6^3P_{1,0})$ and in the spin–orbit relaxation process induced by the same molecules (8, 18).

The authors gratefully acknowledge the financial support received from the National Research Council of Canada. The authors are also indebted to Messrs. D. George, P. Moore, and F. Safian for their assistance in this work.

1. A. C. Vikis and D. J. Le Roy. Can. J. Chem. **50**, 595 (1972).
2. C. R. Masson and E. W. R. Steacie. J. Chem. Phys. **18**, 210 (1950).
3. R. J. Cvetanović. Prog. React. Kinet. **2**, 41 (1964).
4. A. B. Callear and R. E. M. Hedges. Trans. Faraday Soc. **66**, 615 (1970).
5. A. B. Callear and J. C. McGurk. J. C. S. Faraday II, **68**, 289 (1972).
6. E. Gaviola and R. W. Wood. Phil. Mag. (7), **6**, 1191 (1928).
7. F. F. Rieke. J. Chem. Phys. **4**, 513 (1936).
8. A. C. Vikis, G. Torrie, and D. J. Le Roy. Can. J. Chem. **50**, 176 (1972).
9. A. C. G. Mitchell and M. W. Zemansky. Resonance radiation and excited atoms. Cambridge University Press, New York. 1961.
10. H. Horiguchi and S. Tsuchiya. Bull. Chem. Soc. Jap. **44**, 1213 (1971).
11. N. P. Penkin. J. Quant. Spectrosc. Radiat. Transfer, **4**, 74 (1964).
12. A. B. Callear and J. C. McGurk. Chem. Phys. Lett. **6**, 417 (1970).
13. A. C. Vikis and H. C. Moser. J. Chem. Phys. **53**, 1491 (1970).
14. J. M. Campbell, S. Penzes, H. S. Sandhu, and O. P. Strausz. Int. J. Chem. Kinet. **3**, 175 (1971).
15. S. Penzes, H. S. Sandhu, and O. P. Strausz. Int. J. Chem. Kinet. **4**, 449 (1972).
16. H. B. Palmer and D. F. Hornig. J. Chem. Phys. **26**, 98 (1957).
17. G. Herzberg. Molecular spectra and molecular structure. Vol. I, 2nd ed. Van Nostrand Reinhold Company, New York. 1950.
18. A. C. Vikis and H. C. Moser. J. Chem. Phys. **53**, 2333 (1970).

Can. J. Chem. Downloaded from www.nrcresearchpress.com by 210.87.254.42 on 09/05/12
For personal use only.

Crystal Structure of β-D, 1 → 4 Xylobiose Hexaacetate

F. LEUNG AND R. H. MARCHESSAULT

Department of Chemistry, University of Montreal, Montreal 101, Quebec

Received August 14, 1972

Three dimensional crystal structure analysis has been carried out on β-D, 1 → 4 xylobiose hexaacetate (**1**)

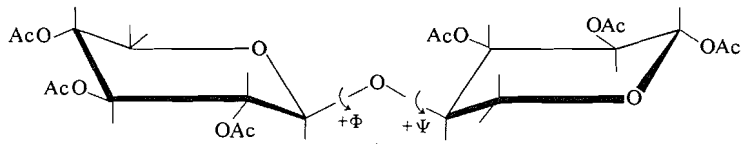

1

The crystal data are: orthorhombic, $P2_12_12_1$, $a = 10.938(2)$, $b = 8.377(4)$, $c = 29.976(7)$ Å. It was found that the bond lengths and angles of the Cl chairs are similar to other carbohydrate structures, the conformational angles $(\Phi,\Psi) = (20.4°, -15.2°)$ and the orientations of the acetate groups are in good agreement with those predicted by stereochemical calculations using Flory functions. The structural resemblance between this molecule and the polymer, xylan diacetate, is discussed.

L'analyse de la structure de la tridimensionelle d'un cristal a été effectué sur la β-D, 1 → 4 hexaacétate de xylobiose (**1**)

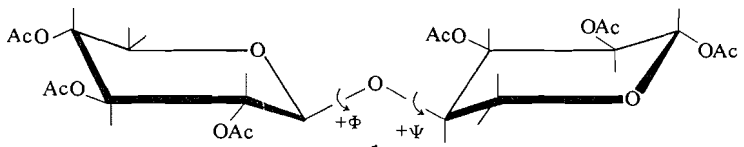

1

Les données cristallines sont: orthorhombique $P2_12_12_1$, $a = 10.938(2)$ $b = 8.377(4)$, $c = 29.976(7)$ Å. Il a été montré que la longueur des liens ainsi que les angles des chaises Cl sont semblables à ce que l'on trouve dans les structures des carbohydrates. Les angles conformationnels $(\Phi,\Psi) = (20.4°, -15.2°)$ et les orientations des groupes acétates sont en accord avec les valeurs prévues par des calculs stéréochimiques impliquant la fonction de Flory. La ressemblance structurale entre cette molécule et le polymère diacetate de xylane est discutée. [Traduit par le journal]

Can. J. Chem., **51**, 1215 (1973)

Introduction

The structure of xylan diacetate has been studied by Gabbay, Sundararajan, and Marchessault (1). By means of conformational analyses, the conformational angles[1] (Φ,Ψ) of the disaccharide unit (Fig. 1) were found to be $(42°, -21°)$ for $\tau = 117.5°$. Their findings were based on the assumption that xylan diacetate has a two-fold axis with a fiber repeat of 10.31 Å. Assuming these (Φ,Ψ) values, the preferred orientations of the acetate groups were established using energy minimization methods in an iterative manner (1). It was found in general that the acetate groups were approximately 20–30° off the positions where the C—H and C(A)—O bonds were eclipsed in the four-atom system H—C—O—C (A) (Fig. 2). Similar results were obtained when electrostatic interactions were considered (2).

Structurally, xylobiose hexaacetate (Fig. 3) closely resembles the xylobiose tetraacetate unit, which is the basis of the stereochemical calculations performed on xylan diacetate. The

[1]Angle Φ is the angle between the planes defined by the atoms C(1), O(1), C′(4) and O(4), C(1), O(1); Ψ is the angle between the planes defined by C(1), O(1), C′(4) and by O′(1), C′(4), O(1). The conformation corresponding to $(\Phi,\Psi) = (0°, 0°)$ has the C(1)—H(1) bond *cis* to O(1)—C′(4) and C′(4)—H′(4) is *cis* to C(1)—O(1). Keeping the unprimed ring fixed and looking along the directed bonds C(1) → O(1) and O(1) → C′(4), the clockwise rotation of the primed ring is considered to be positive. This is the convention adopted by Gabbay *et al.* which is the same as that used by Sundararajan and Rao (1).

Can. J. Chem. Downloaded from www.nrcresearchpress.com by 210.87.254.42 on 09/05/12
For personal use only.

Can. J. Chem. Downloaded from www.nrcresearchpress.com by 210.87.254.42 on 09/05/12
For personal use only.

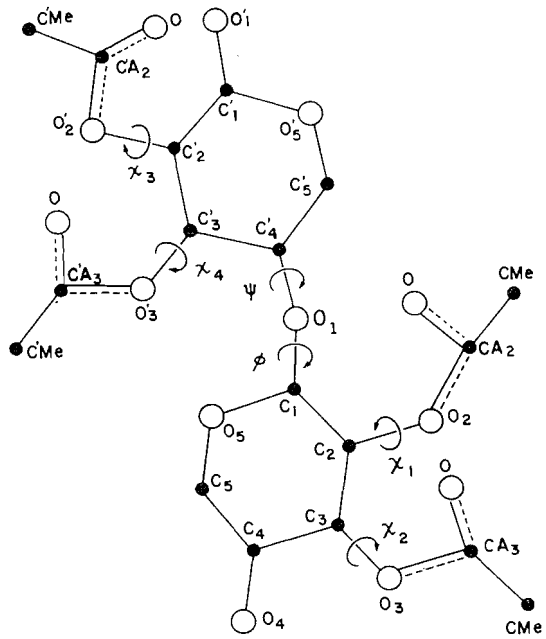

FIG. 1. A schematic diagram of the xylobiose tetraacetate unit. The direction of rotations Φ,Ψ are marked and χ measures the orientation of the acetate group. In this diagram the acetate groups are shown in their positions corresponding to $\chi = 0°$ (ref. 1*a* or Fig. 7).

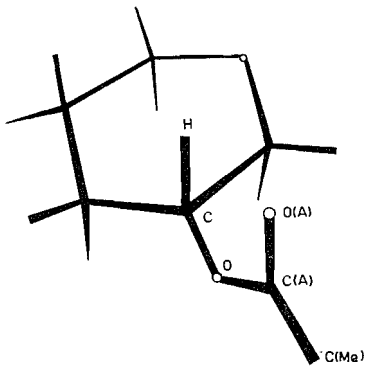

FIG. 2. A diagram showing the orientation of the acetate group with respect to the pyranose ring.

purpose of this work is to compare the structural details of xylobiose hexaacetate with some known carbohydrate structures, and with the structure of xylan diacetate deduced from X-ray and stereochemical studies. Such comparison will add to our understanding of stereochemical calculations which are of paramount importance in structural investigations of polysaccharides. In addition to the backbone conformation, particular interest is placed in comparing the acetate positions from X-ray data with those from the iterative stereochemical approach.

Experimental

Suitable crystals were obtained after recrystallization from 1:1 methanol–water solution of xylobiose hexaacetate. The compound was dissolved in methanol and water, the solution was allowed to stand at room temperature in a small (10 ml) conical flask which was loosely plugged with tissue paper. After a few days, clusters of minute crystals (fine needles) were formed. The clusters of crystals were dispersed by shaking the solution and after about one week, layers of plate-like crystals were obtained.

The unit cell dimensions were determined from diffractometer measurements and refined by a least-squares procedure. The crystal density was determined by flotation in a mixture of hexane and carbon tetrachloride. The crystal data are:

$C_{22}H_{30}O_{15}$ f.w. = 534.1

Orthorhombic, $a = 10.938(2)$, $b = 8.377(4)$, $c = 29.976(7)$, $V = 2746.6$ Å^3, $Z = 4$, $D_c = 1.29$ g/cc, $D_m = 1.30$ g/cc, space group $P_{2_12_12_1}$, $\mu = 9.7$ cm^{-1} (CuKα, $\lambda = 1.5418$ Å).

The intensity data were collected on the FACS-1 automatic diffractometer with 2θ-scan using CuKα (Ni-filtered) radiations. The crystal used for data collection had the dimensions of 0.6 × 0.4 × 0.1 mm and was mounted along the *b*-axis. A total of 2366 independent reflections were measured within the range $0 \leqslant 2\theta \leqslant 120°$, of which 491 have net counts less than 10% of the background. These reflections were considered to be unobserved and were not used in the structure refinement. No absorption correction was made in the data reduction procedure. Normalized structure factors were generated by the K-curve method.

Structure Determination and Refinement

The structure was solved using the multisolution TANFOR program[2] which involves direct application of the tangent formula (3):

$$\tan \phi_h \simeq \frac{\sum_k |E_k E_{h-k}| \sin(\phi_k + \phi_{h-k})}{\sum_k |E_k E_{h-k}| \cos(\phi_k + \phi_{h-k})}$$

Reflections with the initial phases are listed in Table 1. The symbol *b* must be either $-\pi/2$ or $+\pi/2$, but both *a* and *c* can have any value in the range of $-\pi$ to $+\pi$. In the course of tangent formula application, four initial values of $\pm\pi/4$, $\pm 3\pi/4$ were allocated to each of the

[2]A tangent formula program by M. Drew, Lawrence Radiation Laboratory, University of California, Berkeley, California, extensively modified by A. C. Larson and S. Motherwell at Cambridge University, England, K. Fawcett at the University of Toronto, Ontario, further modified and adapted to CDC 6600 computer by F. Leung at the Université de Montréal, Montreal, Quebec.

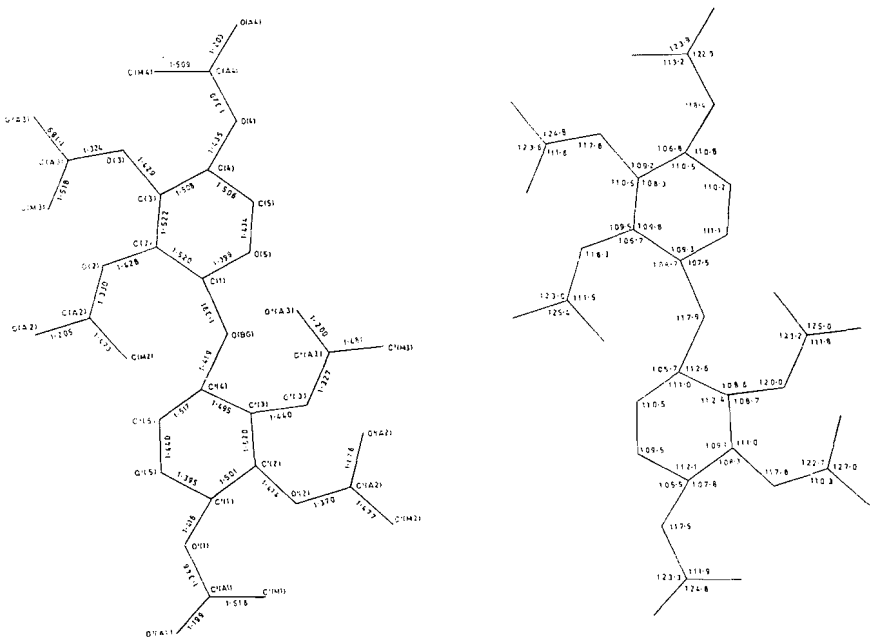

FIG. 3. A schematic diagram of xylobiose hexaacetate with bond lengths and angles.

TABLE 1. Starting phases for tangent formula

h	k	l	$\|E\|$	Phase
1	0	8	2.86	0.0
0	5	1	2.83	$\pi/2$
2	5	0	2.62	0.0
0	5	12	2.24	$\pi/2$
4	6	1	2.98	a
8	0	5	3.13	b
5	7	3	3.18	c

symbols a and c, while $\pm\pi/2$ were given to the symbol b. Consequently a total of 32 different sets of phases were obtained, corresponding to the 32 different combinations of initial phases allocated to the symbols. For the set with the lowest R_{Karle} (0.27), 201 phases ($|E| \geq 1.50$) were determined. R_{Karle} is defined by (3):

$$R_{\text{Karle}} = \sum_{k_r} | |E_h|_{\text{obs}} - |E_h|_{\text{calcd}}| / |\sum_{k_r} |E_h|_{\text{obs}}$$

By further applications of the tangent formula with 201 known phases, an additional 121 phases with $1.30 \leq |E| \leq 1.50$ were determined. The E-map computed using these 312 reflections revealed 31 non-hydrogen atoms. Successive Fourier syntheses revealed all the non-hydrogen atoms of the molecule.

The atomic coordinates estimated from the final Fourier synthesis were refined with individual isotropic thermal parameters by full-matrix least-squares employing unit weights. The refinement converged to an R-factor of 0.14.

$$R = \frac{\sum ||F_o| - |F_c||}{\sum |F_o|}$$

The refinement was continued with anisotropic thermal parameters using block-diagonal matrix. Upon the convergence of anisotropic refinement, all hydrogen atoms were located from successive difference Fourier syntheses. At this stage, the hydrogen atoms were included in the refinement with isotropic temperature factors, and the following weighting function was used

$$\omega = \frac{1}{(1.358 - 0.022|F_o| + 0.003|F_o|^2)^2}$$

This weighting function was deduced from a plot of $|\Delta F|$ *vs.* $|F_o|$. The atomic scattering factors used for the hydrogen and non-hydrogen atoms were taken from Stewart *et al.* (4*a*) and Cromer *et al.* (4*b*) respectively. The least-squares program used was NUCLS.[3] The hydrogen

[3]NUCLS a highly modified version of ORFLS, modified by Doedens at the University of Wisconsin, Madison, Wisconsin, and J. Ibers at Brookhaven National Laboratories, Brookhaven, Philadelphia, further modified for block-diagonal option by J. Sygusch at the Université de Montréal, Montreal, Quebec.

Can. J. Chem. Downloaded from www.nrcresearchpress.com by 210.87.254.42 on 09/05/12
For personal use only.

TABLE 2. Fractional atomic coordinates with standard deviations in parentheses, for β-D, 1 → 4 xylobiose hexaacetate

Atom	x/a	y/b	z/c	Atom	x/a	y/b	z/c
C′(1)	0.2241(6)	−0.0932(8)	0.1198(3)	O(A2)	−0.2705(5)	0.2756(8)	0.0199(2)
C′(2)	0.2470(6)	0.0479(8)	0.1495(2)	O(A3)	−0.1522(5)	0.8498(7)	0.0114(2)
C′(3)	0.1331(6)	0.1518(8)	0.1507(2)	O(A4)	−0.3607(6)	0.8428(7)	0.1766(2)
C′(4)	0.0840(6)	0.1852(8)	0.1051(2)	H′(1)	0.165(5)	−0.182(6)	0.134(1)
C′(5)	0.0752(7)	0.0331(9)	0.0778(3)	H′(2)	0.310(4)	0.114(5)	0.139(1)
C′(A1)	0.3284(7)	−0.3370(9)	0.1090(3)	H′(3)	0.081(4)	0.108(5)	0.170(1)
C′(A2)	0.3716(7)	0.0618(11)	0.2147(3)	H′(4)	0.137(4)	0.260(5)	0.091(1)
C′(A3)	0.1269(9)	0.3308(12)	0.2130(3)	H′(1,5)	0.056(7)	0.058(9)	0.045(2)
C′(M1)	0.4539(7)	−0.4132(11)	0.1064(4)	H′(2,5)	0.016(8)	−0.019(11)	0.010(3)
C′(M2)	0.3922(11)	−0.0174(15)	0.2581(3)	H′(1M1)	0.454(11)	−0.511(15)	0.134(4)
C′(M3)	0.1689(12)	0.4892(13)	0.2288(3)	H′(2M1)	0.506(12)	−0.336(16)	0.127(4)
O′(1)	0.3354(4)	−0.1782(6)	0.1155(2)	H′(3M1)	0.471(9)	−0.451(11)	0.076(3)
O′(2)	0.2763(5)	−0.0091(6)	0.1926(2)	H′(1M2)	0.319(10)	−0.073(12)	0.265(3)
O′(3)	0.1633(4)	0.3014(6)	0.1716(1)	H′(2M2)	0.419(8)	0.034(11)	0.276(3)
O′(5)	0.1915(4)	−0.0475(6)	0.0767(2)	H′(3M2)	0.438(7)	−0.109(10)	0.248(3)
O′(A1)	0.2335(5)	−0.4077(6)	0.1058(2)	H′(1M3)	0.133(11)	0.580(14)	0.213(4)
O′(A2)	0.4285(5)	0.1675(8)	0.1993(2)	H′(2M3)	0.136(13)	0.493(16)	0.256(4)
O′(A3)	0.0668(8)	0.2388(9)	0.2345(2)	H′(3M3)	0.235(10)	0.502(13)	0.232(3)
O(BG)	−0.0360(4)	0.2492(5)	0.1061(2)	H(1)	0.023(4)	0.468(5)	0.098(1)
C(1)	−0.0486(6)	0.4142(8)	0.1086(2)	H(2)	−0.216(4)	0.403(5)	0.085(1)
C(2)	−0.1489(6)	0.4659(8)	0.0766(2)	H(3)	−0.096(4)	0.713(6)	0.070(1)
C(3)	−0.1686(5)	0.6453(7)	0.0802(2)	H(4)	−0.281(5)	0.634(7)	0.140(2)
C(4)	−0.1945(6)	0.6852(8)	0.1283(2)	H(1,5)	−0.022(5)	0.689(6)	0.155(2)
C(5)	−0.0948(7)	0.6212(9)	0.1580(2)	H(2,5)	−0.110(5)	0.627(7)	0.190(2)
C(A2)	−0.1714(7)	0.3240(10)	0.0087(3)	H(1M2)	−0.130(6)	0.192(9)	−0.042(2)
C(A3)	−0.2501(6)	0.8003(8)	0.0217(2)	H(2M2)	−0.121(11)	0.376(14)	−0.053(4)
C(A4)	−0.2911(7)	0.9204(9)	0.1543(3)	H(3M2)	−0.034(7)	0.248(10)	−0.029(2)
C(M2)	−0.1073(8)	0.2802(12)	−0.0328(3)	H(1M3)	−0.421(9)	0.792(14)	0.007(3)
C(M3)	−0.3685(7)	0.8558(11)	0.0003(3)	H(2M3)	−0.359(8)	0.898(10)	−0.034(3)
C(M4)	−0.2970(9)	1.0998(10)	0.1501(4)	H(3M3)	−0.378(9)	0.946(12)	0.014(3)
O(2)	−0.1071(4)	0.4279(5)	0.0327(1)	H(1M4)	−0.286(9)	1.133(11)	0.114(3)
O(3)	−0.2702(4)	0.6936(5)	0.0535(1)	H(2M4)	−0.365(9)	1.144(11)	0.159(3)
O(4)	−0.2009(4)	0.8560(5)	0.1312(2)	H(3M4)	−0.220(10)	1.145(12)	0.164(3)
O(5)	−0.0831(4)	0.4519(6)	0.1522(1)				

atoms and the non-hydrogen atoms were refined isotropically and anisotropically respectively. After several cycles of block-diagonal least-squares refinement, an ultimate R-factor of 0.058 was obtained. Structure factor calculations including the unobserved reflections showed an R-factor of 0.070. The difference Fourier computed subsequently revealed no residual electron density other than background fluctuations. The final positional and thermal parameters are listed in Tables 2 and 3. Final F_o and F_c values have been placed in the Depository for Unpublished Data.[4]

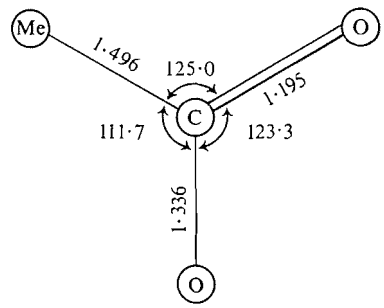

FIG. 4. The average bond-lengths and angles for the acetate groups.

Results and Discussion

As expected from experimental (5, 6) and theoretical (7) investigations, the β-D-xylose unit has a C1 chair conformation. The pyranose rings are joined through β, 1 → 4′ linkages. All acetate groups occupy equatorial positions and are planar within experimental error. The average bond lengths and angles for the acetate groups are shown in Fig. 4; the bond lengths and bond angles of the molecule are given in Fig. 3 and Fig. 5 is a stereoscopic view of the

[4]Complete set of tabular data is available, at a nominal charge, from the Depository of Unpublished Data, National Science Library, National Research Council of Canada, Ottawa, Canada K1A 0S2.

Can. J. Chem. Downloaded from www.nrcresearchpress.com by 210.87.254.42 on 09/05/12
For personal use only.

Can. J. Chem. Downloaded from www.nrcresearchpress.com by 210.87.254.42 on 09/05/12
For personal use only.

TABLE 3

(*a*) Thermal parameters × 10^4, the temperature factor expression is exp $(-(h^2\beta_{11} + k^2\beta_{22} + l^2\beta_{33} + 2hk\beta_{12} + 2hl\beta_{13} + 2kl\beta_{23}))$

Atom	β_{11}	β_{22}	β_{33}	β_{12}	β_{13}	β_{23}
C′(1)	95(7)	180(13)	25(1)	9(9)	−6(3)	3(3)
C′(2)	95(6)	164(11)	17(1)	5(9)	0(2)	14(3)
C′(3)	104(7)	203(13)	14(1)	−23(9)	1(2)	20(3)
C′(4)	86(6)	174(12)	18(1)	−10(8)	1(2)	8(3)
C′(5)	123(8)	202(14)	22(1)	26(10)	−15(3)	−9(4)
C′(A1)	133(8)	226(15)	20(1)	−33(11)	−6(3)	9(4)
C′(A2)	134(9)	320(19)	20(1)	80(12)	−11(3)	−18(4)
C′(A3)	220(13)	341(21)	16(1)	48(16)	−16(3)	9(5)
C′(M1)	104(8)	326(21)	39(2)	68(12)	−9(4)	−31(6)
C′(M2)	308(18)	519(32)	22(2)	151(23)	−28(5)	−13(6)
C′(M3)	360(20)	408(26)	23(2)	120(23)	−38(5)	−37(6)
O′(1)	108(5)	177(8)	30(1)	−16(6)	−6(2)	2(3)
O′(2)	140(6)	242(10)	18(1)	24(7)	−8(2)	21(2)
O′(3)	131(5)	214(9)	15(1)	23(7)	−5(2)	1(2)
O′(5)	131(5)	208(9)	23(1)	5(7)	−11(2)	−8(2)
O′(A1)	132(6)	210(9)	32(1)	−39(7)	−6(2)	9(3)
O′(A2)	144(6)	368(14)	30(1)	−34(9)	−16(2)	−16(4)
O′(A3)	384(14)	444(18)	19(1)	49(16)	21(3)	28(3)
O(BG)	78(4)	167(8)	25(1)	−2(5)	−6(2)	10(2)
C(1)	109(7)	166(12)	12(1)	−21(8)	−1(2)	8(3)
C(2)	76(6)	179(12)	14(1)	−34(8)	−2(2)	10(3)
C(3)	64(5)	154(11)	16(1)	−14(7)	−32(2)	8(3)
C(4)	116(7)	170(12)	14(1)	−4(9)	2(2)	−1(3)
C(5)	123(8)	243(15)	13(1)	−33(10)	−1(2)	−2(3)
C(A2)	106(7)	255(16)	22(1)	29(11)	−10(3)	−3(4)
C(A3)	92(6)	181(12)	16(1)	−3(9)	1(2)	7(3)
C(A4)	121(8)	247(16)	20(1)	−13(10)	10(3)	−16(4)
C(M2)	187(11)	367(23)	24(1)	−81(15)	21(3)	−50(5)
C(M3)	132(9)	303(18)	20(1)	37(12)	−12(3)	10(4)
C(M4)	181(12)	186(15)	40(2)	4(11)	26(4)	−6(5)
O(2)	89(4)	191(8)	17(1)	−11(5)	−8(1)	−10(2)
O(3)	69(4)	193(8)	16(1)	−4(5)	−1(1)	9(2)
O(4)	111(5)	188(8)	20(1)	−14(6)	16(2)	−10(2)
O(5)	124(5)	217(9)	15(1)	−4(6)	−5(2)	16(2)
O(A2)	153(7)	376(15)	34(1)	−79(10)	−9(2)	−36(4)
O(A3)	111(5)	325(12)	26(1)	−13(7)	0(2)	47(3)
O(A4)	187(7)	286(12)	32(1)	0(9)	40(2)	−9(3)

(*b*) Isotropic temperature factors of the hydrogen atoms

Atom	B (Å^2)	Atom	B (Å^2)
H′(1)	4(1)	H(1)	3(1)
H′(2)	3(1)	H(2)	3(1)
H′(3)	3(1)	H(3)	3(1)
H′(4)	2(1)	H(4)	6(2)
H′(1,5)	10(2)	H(1,5)	4(1)
H′(2,5)	14(3)	H(2,5)	6(2)
H′(1M1)	20(4)	H(1M2)	9(2)
H′(2M1)	22(5)	H(2M2)	21(5)
H′(3M1)	14(3)	H(3M2)	11(2)
H′(1M2)	15(3)	H(1M3)	16(3)
H′(2M2)	14(3)	H(2M3)	12(3)
H′(3M2)	11(2)	H(3M3)	16(3)
H′(1M3)	22(5)	H(1M4)	16(3)
H′(2M3)	24(5)	H(2M4)	14(3)
H′(3M3)	18(4)	H(3M4)	17(4)

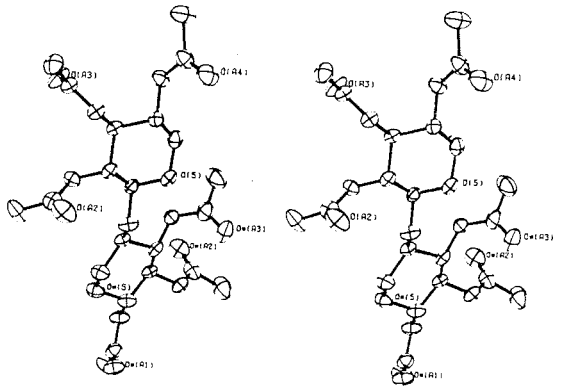

FIG. 5. A stereoscopic view of the molecule looking down the *a*-axis. Atoms in the contiguous residue are marked with an asterisk.

molecule. The average standard deviations of the bond lengths are shown in Table 4 while the average standard deviation for the bond angles is 0.7°. The average carbon–carbon bond-length (1.514 Å) in the unprimed ring is slightly shorter than the average in the primed ring (1.508 Å). Although the difference is less than a standard deviation, a similar difference was also observed for β-cellobioside–methanol and for cellobiose 8. The average ring carbon–O(Ac) bond length is 1.427 Å with a spread of 0.026 Å. In contrast to the case of β-cellobioside–methanol, the two ring carbon–oxygen bonds in both primed and unprimed rings are unequal: C(1)—O(5) = 1.399 Å *vs.* C(5)—O(5) = 1.434 Å, and C′(1)—O′(5) = 1.395 Å *vs.* C′(5)—O′(5) = 1.440 Å. According to Arnott and Scott (9), the average values for C(1)—O(5) and C(5)—O(5) are 1.429 and 1.436 Å respectively, thus the discrepancies here are much more pronounced: 3σ in the unprimed ring and 4σ in the primed ring. Kim and Jeffrey (10) pointed out that similar discrepancies were observed in the case of glycosidic substituted sugars.

The ring carbon–hydrogen bond lengths lie in the range of 0.89–1.07 Å and those of the methyl groups are in the range of 0.73–1.17 Å.

TABLE 4. Average standard deviations of the bond lengths for β-D, 1 → 4 xylobiose hexaacetate

	Length (Å)		
Bond	Rings	Equatorial bonds	Acetate groups
C—C	0.0092		0.0118
C—O	0.0086	0.0078	0.0088
C=O			0.0098

The average interior and exterior ring angles are 110.4° and 108.7°, respectively, similar values were observed in β-cellobioside–methanol. The average angle at the oxygen atom linked to the acetate group is 118.3° with a spread of 2.5°. The angles Me—C(A)—O(Ac) for all acetate groups are 111.7°, much less than 120° as one might expect; the spread was 2.9°. Similar distortion of this bond angle was also observed in 3′-*O*-acetyl-4-thiothymidine (11).

There is neither hydrogen bonding nor obviously short interatomic contacts throughout the crystal structure. The molecular packing is shown in Fig. 6.

Following the convention adopted by Sundararajan and Rao (1*b*) and used by Gabbay, Sundararajan, and Marchessault (1*a*), the conformational angles (Φ,Ψ) as shown in Fig. 1 were calculated to be (20.4°, −15.2°) for the structure in question. These values are somewhat different from those deduced for xylan (42°, −21°) but since the O′(1)...O(4) distance is 10.47 Å as compared with the fiber repeat in xylan diacetate which is reported (1*a*) as 10.31 Å the difference is in the expected direction.

For cellobiose, the conformational angles are (42°, −18°) (8).[5] These results are in excellent agreement with those deduced from conformational analysis of cellulose (40°, −20°) (12, 16). The reason that one gets better agreement between cellobiose and cellulose is perhaps due to the intramolecular hydrogen bonding between O′(3) and O(5) which is present in both compounds. (Polarized infrared spectroscopy provided the evidence for such intramolecular hydrogen bonding in cellulose (13). The O′(3)....O(5) distance in xylobiose hexaacetate is 3.03 Å while in cellobiose it is 2.767 Å (14). If the conformations of a polysaccharide and its chemically related disaccharide are mainly determined by the same factors, *e.g.* an intramolecular hydrogen bond in the case of cellulose and cellobiose, then one would expect that in xylan diacetate and xylobiose hexaacetate the O′(3)...O(5) distance would be the same. In the conformational study by Gabbay, Sundararajan,

[5]The (Φ,Ψ) reported by Ham *et al.* (8) were (−42°, +162°). To transform these values to our convention, the relationships $\Phi = -\Phi_{Rees}$, $\Psi = \Psi_{Rees} + 180$ were used (15).

Can. J. Chem. Downloaded from www.nrcresearchpress.com by 210.87.254.42 on 09/05/12
For personal use only.

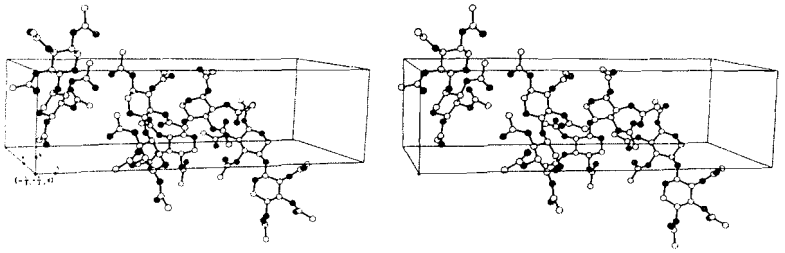

FIG. 6. Molecular packing diagram: oxygen atoms are represented by solid circles and the molecule closest to $(-\frac{1}{2}, -\frac{1}{2}, 0)$ corresponds to the atomic coordinates listed in Table 3.

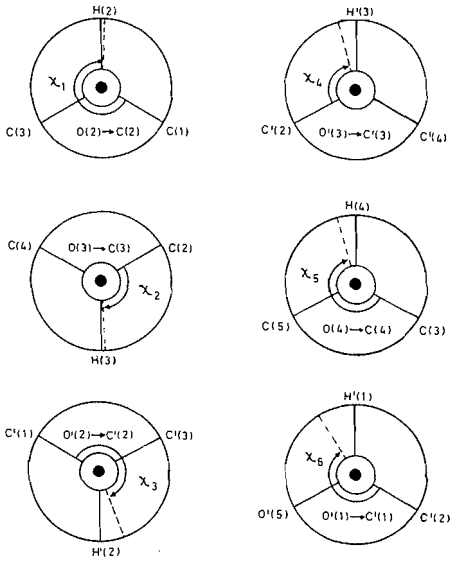

	χ°_1	χ°_2	χ°_3	χ°_4	χ°_5	χ°_6
THIS WORK	242	119	220	105	225	210
XYLAN DIACETATE (FLORY FUNCTIONS)	270	90	210	95		
XYLAN DIACETATE (KITAIGORODSKY FUNCTIONS)	270	150	270	85		

FIG. 7. Orientations of the acetate groups (Newman projections) with angles χ corresponding to observed values. In the table the observed values of χ are compared to those calculated by a semi-empirical approach (1).

and Marchessault (1*a*) the geometry chosen and the observed fiber repeat was such as to lead to a 2.7 Å distance between O'(3)...O(5) in xylan diacetate. The observed Φ,Ψ angles for xylobiose hexaacetate correspond to Φ,Ψ = (20.4°, −15.2°) which is near the helical parameters $n = 2$ and $h = 5.2$ Å, *i.e.*, a two-fold axis and a fiber repeat corresponding to 10.4 Å. The reported fiber repeat for cellulose triacetate is 10.43 Å (17) which is in keeping with this. It would seem that some adjustment either in molecular geometry or in the observed fiber repeat for xylan diacetate is required to bring about agreement between the conformational angles predicted (1*a*) for xylan diacetate and those observed for its disaccharide.

The observed orientations of the acetate groups together with those obtained from stereochemical calculations by Gabbay, Sundararajan, and Marchessault (1) are shown in Fig. 7. In all four cases, the predicted positions of the C(A)—O bonds, measured by the angle χ, are further away from the coplanar position with respect to the C—H bonds than those obtained from X-ray crystallography. It is also evident that the χ values computed using the Flory functions (18) give much better agreement with experiment than those calculated using the Kitaigorodsky functions (19). In spite of the fact that the calculated acetate orientations are based on the conformational angles (42°, −21°) instead of what were actually observed, the agreement between experimental and calculated values (Flory functions) is reasonably good. This seems to indicate that the orientations of the acetate groups are independent of Φ and Ψ. This is being further substantiated by investigating the structures of other acetylated sugars.

The authors wish to thank Dr. F. Brisse and Mr. J. Sygusch for their advice on computing and helpful discussions.

1. (*a*) S. M. GABBAY, P. R. SUNDARARAJAN, and R. H. MARCHESSAULT. Biopolym. **11**, 79 (1972). (*b*) P. R. SUNDARARAJAN and V. S. R. RAO. Biopolym. **8**, 305 (1969).
2. P. R. SUNDARARAJAN and R. H. MARCHESSAULT. Biopolym. **11**, 829 (1972).
3. J. KARLE and I. L. KARLE. Acta Cryst. **21**, 849 (1966).
4. (*a*) R. F. STEWART, E. R. DAVIDSON, and W. T. SIMPSON. J. Chem. Phys. **42**, 3175 (1965). (*b*) D. T.

Can. J. Chem. Downloaded from www.nrcresearchpress.com by 210.87.254.42 on 09/05/12
For personal use only.

CROMER and J. T. WALKER. Acta Cryst. **18**, 104 (1965).
5. V. S. R. RAO, J. F. FOSTER, and R. L. WHISTLER. J. Org. Chem. **28**, 1730 (1963).
6. M. RUNDRUM and D. F. SHAW. J. Chem. Soc. 52 (1965).
7. P. R. SUNDARARAJAN and V. S. R. RAO. Tetrahedron, **24**, 289 (1968).
8. J. T. HAM and D. G. WILLIAMS. Acta Cryst. **B 26**, 1373 (1970).
9. S. ARNOTT and W. E. SCOTT. J. Chem. Soc. Perkin II, 324 (1972).
10. S. H. KIM and G. A. JEFFREY. Acta Cryst. **22**, 537 (1967).
11. W. SAENGER and D. SUCK. Acta Cryst. **B 27**, 2105 (1971).
12. P. R. SUNDARARAJAN. Ph.D. Thesis. University of Madras, India, 1969.
13. C. Y. LIANG and R. H. MARCHESSAULT. J. Polym. Sci. **37**, 385 (1959).
14. S. S. C. CHU and G. A. JEFFREY. Acta Cryst. **B 24**, 830 (1968).
15. M. GIACOMINI, B. PULLMAN, and B. MAIGRET. Theoret. Chim. Acta, Berlin, **19**, 347 (1970).
16. P. R. SUNDARARAJAN and R. H. MARCHESSAULT. Can. J. Chem. **50**, 792 (1972).
17. W. J. DULMAGE. J. Polym. Sci. **26**, 277 (1957).
18. D. A. BRANT and P. J. FLORY. J. Am. Chem. Soc. **87**, 663 2791 (1965).
19. A. I. KITAIGORODSKY. Tetrahedron, **14**, 230 (1961).

Can. J. Chem. Downloaded from www.nrcresearchpress.com by 210.87.254.42 on 09/05/12
For personal use only.

Fungal Steroids. A Stereoselective Synthesis of Isoantheridiol

C. R. POPPLESTONE AND A. M. UNRAU

Department of Chemistry, Simon Fraser University, Burnaby 2, British Columbia

Received October 11, 1972

The synthesis and characteristics of the 23-hydroxy-δ-lactone isomer of antheridiol and (22S,23R) 3β-hydroxy-24-carbethoxymethylene-cholest-5-en-22,23-epoxide are described. The synthesis of the latter compound follows from the highly stereoselective epoxidation of 3β-acetoxy-cholesta-5,22-diene-24-one followed by a Wittig reaction to give (22S,23R) 3β-acetoxy-24-carbethoxymethylene-cholest-5-en-22,23-epoxide which upon treatment with perchloric acid gave exclusively the δ-lactone. Hematoporphyrin-sensitized photooxygenation followed by cupric acetate oxidation gave the required α,β-unsaturated ketonic system in ring B. The 22R,23S stereochemical assignment of the final product is based on circular dichroism spectra.

La synthèse et la caractérisation de l'isomère hydroxy-23 δ-lactone de l'anthéridiol et du (22S,23R) hydroxy-3β carbethoxyméthylène-24 cholestène-5 époxyde-22,23 ont été données. La synthèse de ce dernier passe par l'époxydation hautement stéréosélective de l'acétoxy-3β cholestadiène-5,22 one-24 suivie d'une réaction de Wittig pour conduire au (22S,23R) acétoxy-3β carbethoxyméthylène-24 cholestène-5 époxyde-22,23 qui, après traitement à l'acide perchlorique donne la δ-lactone exclusivement. La photooxygénation sensibilisée de l'hématoporphyrine par l'acétate cuivrique conduit au système cétonique α,β-insaturé requis pour le cycle B. L'attribution stéréochimique 22R,23S du produit final est basée sur les spectres de dichroisme circulaire. [Traduit par le journal]

Can. J. Chem., **51**, 1223 (1973)

Continued refinement of analytical techniques has led to the discovery and characterization of a multitude of intermediate compounds involved in the biosynthetic pathways leading to major end products. Many postulated intermediates have been identified although present in only minute quantities. It is now quite obvious that in the course of the elaboration of the side chains of phytosterols, an extensive array of biogenetic intermediates is involved. The rather highly functionalized side chain of antheridiol (**1**), a mold sex hormone, is an example in which the hydrocarbon side chain of the most probable precursor, fucosterol, has been extensively modified. This steroidal hormone has been isolated, along with the biologically inactive 23-deoxyantheridiol (**2**), from culture liquids of the water mold, *Achlya bisexualis* (1, 2). Both antheridiol (**1**) (in its natural 22S,23R configuration), and 23-deoxyantheridiol (**2**) (in its unnatural 22S configuration) have been chemically synthesized (2, 3). In this communication we describe a relatively efficient synthesis of the 23-hydroxy-δ-lactonic isomer of antheridiol, **3***a*, having the 22R,23S configuration. We also describe the synthesis and characterization of 3β-hydroxy-24-carboxymethylene-cholest-5-en-22,23-epoxide (**7***a*).

Our recent identification of fucosterol as the major sterol in *Achlya bisexualis*, and the occur-

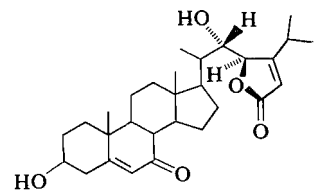

1

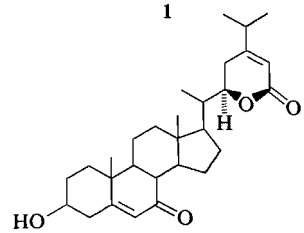

2

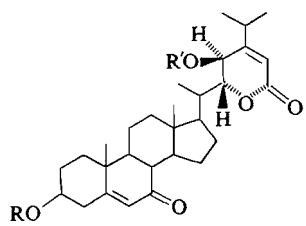

3

a R = R′ = H
b R = Ac; R′ = H
c R = R′ = Ac

Can. J. Chem. Downloaded from www.nrcresearchpress.com by 210.87.254.105 on 09/05/12
For personal use only.

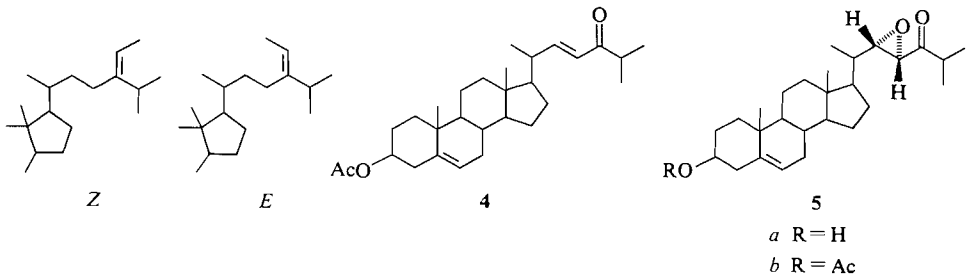

Z *E* **4** **5**

a R = H
b R = Ac

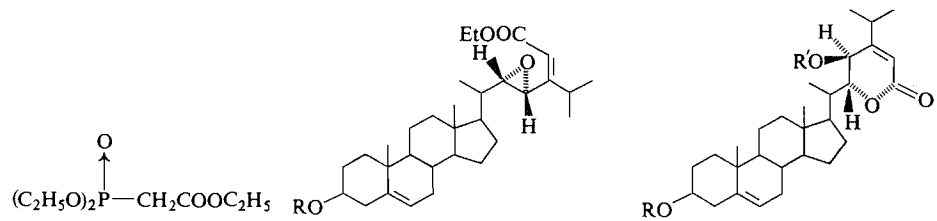

6 **7** **8**

a R = H
b R = Ac

a R = R′ = H
b R = Ac; R′ = H
c R = R′ = Ac

rence of both the γ- and δ-lactone derivatives in this fungal species, thus indicating a common biosynthetic precursor, prompted our attempts to synthesize the 23-hydroxy-δ-lactone isomer.

The starting material for our synthesis was the α,β-unsaturated ketone, **4**, derived from readily available stigmasterol, a sterol which has been extensively used in our laboratory as a chemical precursor for synthesis of biogenetic steroid precursors in yeast (4). Alkaline epoxidation with hydrogen peroxide in methanol gave a mixture of epoxy acetate **5***b* and alcohol **5***a*. This reaction is known to be highly stereoselective giving the 22S,23R isomer (5). Deacetylation of the mixture gave the epoxy alcohol **5***a* in 70% yield.

A Wittig reaction (6) of the carbanion of diethyl carbethoxymethyl phosphonate (**6**) with α,β-unsaturated ketone **5***a*, was used to generate the important intermediate **7***a* in 30% yield. When this reaction was carried out on **5***b*, a mixture of **7***a* and *b* was obtained due to alkaline hydrolysis of the 3β-acetoxy group. Compound **7** can have two possible side chain isomeric forms (7). The *E*-configuration was assigned to **7** based on the following evidence. The *Z*-configuration would require isomerization to *E* as a prerequisite to lactone formation. Such a step would involve protonation at C-28 to give the C-24 carbonium ion and allow free rotation about the C_{24}—C_{28} bond. In the presence of D_2O, the C-28 olefinic proton, in the case of the *Z*-isomer, would be expected to exchange. In the conversion of **7** to **8** in the presence of D_2O, no reduction in the intensity of the C-28 proton signal was observed. This would be expected for the *E*-configuration of **7** in which isomerization of the C_{24}—C_{28} double bond is not required for lactone formation.

Treatment of **7***a* with aqueous perchloric acid in methanol resulted in rapid formation of the highly insoluble δ-lactone **8***a* in quantitative yield. This substance (**8***a*) gave one spot on t.l.c. as did the monoacetate **8***b* and diacetate **8***c*. Since the 22S,23R and 22R,23S isomers of the corresponding γ-lactone have been separated by t.l.c. (3), this indicated the product **8***a* was a single epimer. No formation of the γ-lactone was detected in the reaction. The monoacetate, **8***b* was noticeably more soluble in organic solvents than the corresponding 3β-alcohol, **8***a*. For this reason the n.m.r. spectrum for the monoacetate is recorded in preference to that of **8***a*. It is significant to note that the coupling constant of the C-23 proton (J = 10 Hz) is strongly indicative of *trans* C-22 and -23 hydrogens thus further substantiating the assigned *E*-configuration of **7** and is also supportive of the suggested mechanism of δ-lactone formation.

Compound **8***a* was readily converted into the

Can. J. Chem. Downloaded from www.nrcresearchpress.com by 210.87.254.105 on 09/05/12
For personal use only.

Can. J. Chem. Downloaded from www.nrcresearchpress.com by 210.87.254.105 on 09/05/12
For personal use only.

(22R,23S) 23-hydroxy δ-lactone isomer of antheridiol (**3***a*) by hematoporphyrin-sensitized photooxygenation (8) and oxidative rearrangement (9) in 50% yield.

The stereochemical assignments at C-22 follow from a comparison of the circular dichroism (c.d.) spectra of the δ-lactones **3** and **8** and parasorbic acid **9** in which the methyl group is known from n.m.r. measurements to be equatorial (10). The c.d. curve of **3***a* (in methanol) revealed a strong negative peak at 255 nm ([θ] = −20 460°), as did **8***a* at 260 nm ([θ] = −8440°). Since parasorbic acid exhibits a positive CD curve at 260 nm (11) due to the chirality of the nonplanar enone system, it follows that both the δ-lactones (**3** and **8**) have the opposite stereochemistry to parasorbic acid. Since the C-22 stereochemistry of both jaborosalactone A (**10**) and withaferin A (**11**) have been determined by this method (the assignments were subsequently found to agree with those determined by X-ray measurements (12, 13)), we feel justified in assigning the 22R configuration to the δ-lactones **3** and **8**.

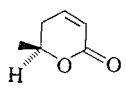

9

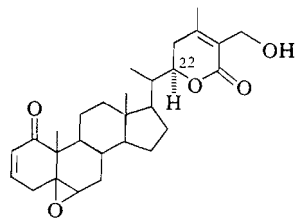

10

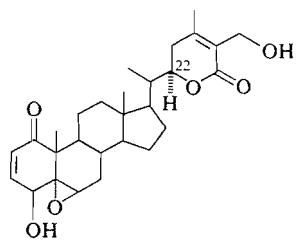

11

The assignment of the R configuration at C-22, and the fact that only the δ-lactone is formed, is based on the n.m.r. evidence for *trans* C-22 and -23 hydrogens (J = 10 Hz). We further interpreted these observations to indicate a relatively concerted epoxide ring opening resulting in the formation of the δ-lactone exclusively. Epoxide ring opening to yield a relatively free carbo-cation (C-22) would be expected to give an R,S configuration at C-22 of the eventual δ-lactone. A plausible route could involve hydrolysis of the α,β-unsaturated ester function with concomitant protonation of the epoxide followed by a concerted epoxide ring opening (nucleophilic attack at C-22) to give the δ-lactone.

The mass spectrum of the 23-hydroxy-δ-lactone (**3***a*) is similar to that reported for antheridiol (14). The molecular ion **a** undergoes a retro-Diels–Alder fragmentation (15) to furnish a very intense peak (*m/e* 344, **b**) and fragment **c**.

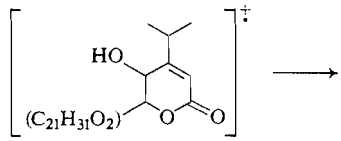

a

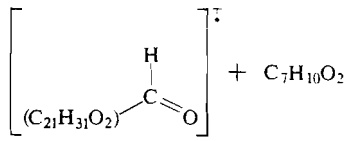

b c

The 23-hydroxy-δ-lactone, **3***a*, is characterized by its m.p. 240–243°, a broad absorption band in the u.v. at 230 nm (ε 16 500), and a strong absorption band in the i.r. at 1685 cm^{-1}. When the ethanolic solution which had been used for the u.v. spectrum was refluxed with hydrochloric acid the u.v. spectrum changed to λ_{max} 216, 279 nm resulting from extended conjugation of the $\Delta^{3,5}$-7-ketone.

The monoacetate **3***b* was also prepared with the expectancy that it would be more soluble in chloroform than the 3β-hydroxy compound **3***a*, but this was not the case. However, the n.m.r. of the monoacetate **3***b* has been included for comparison.

Experimental

Instruments and Materials

Melting points were obtained on a Fisher–Johns m.p. apparatus and are uncorrected. Spectra were obtained on the following instruments: Perkin–Elmer 457 (i.r.), Unicam SP 800 (u.v.), and Varian XL-100 n.m.r. spectrometer. N.m.r. results are reported as δ using TMS as internal standard (δ = 0). Ionizing voltage for mass spectrometry, Perkin–Elmer Hitachi RMU-7, was 80 eV if not specifically mentioned otherwise. Stigmasterol was generously supplied by the Upjohn Company, Kalamazoo, Michigan.

Can. J. Chem. Downloaded from www.nrcresearchpress.com by 210.87.254.105 on 09/05/12
For personal use only.

Preparation of 3β-Acetoxy-24-oxo-cholest-5-en-22, 23-epoxide (5b)

To a solution of **4** (3.0 g, 6.8 mol) in 100 ml acetone and 300 ml methanol, was added 20 ml of 38% hydrogen peroxide. The solution was stirred at room temperature and 4 *N* NaOH (3 ml) added at such a rate as to keep the solution alkaline over a period of 3 h, and the solution was then left to stand at 4 °C for 5 h. Most of the solvent was removed *in vacuo* and water added to the residue. The solution was extracted twice with ether and removal of the solvent *in vacuo* gave a non-crystalline residue, which was shown by t.l.c. (SiO_2, 2% MeOH–$CHCl_3$) to be a mixture of **5***a* and *b*. The mixture was refluxed for ½ h with 100 ml 2% K_2CO_3 in 10% H_2O–MeOH. The solvent was removed (*in vacuo*), water added to the residue, and the product extracted with ether. The ether layer was dried over $MgSO_4$ and removal of the solvent gave a crystalline solid. Recrystallization from methanol gave **5***a*, m.p. 180–181 °C, (70%).

Acetylation of **5***a* with acetic anhydride – pyridine gave **5***b*.

Recrystallization from methanol gave m.p. 125–126 °C; ν_{max} ($CHCl_3$): 2940, 1715, 1250, and 1030 cm^{-1}; n.m.r. ($CDCl_3$): δ 0.65 (CH_3—C_{18}, s), 1.01 (CH_3—C_{19}, s), 1.01, 1.06, (2 × d, J = 7 Hz, $2CH_3$—C_{25}), 2.01 (CH_3OCO—, s), 2.5–2.9 (2H; sept. centered at 2.69, H—C_{25}; m centered at 2.80, H—C_{22}), 3.25 (H—C_{23}, d, J = 2 Hz), 4.4–4.8 (H—C_3, broad m), 5.51 (H—C_6, narrow m).

Anal. Calcd. for $C_{29}H_{44}O_4$ (mol. wt. 456): C, 76.27; H, 9.71. Found (*m/e*, 456): C, 76.23; H, 9.64.

Preparation of (22S,23R) 3β-Acetoxy-24-carbethoxy-methylene-cholest-5-en-22,23-epoxide (7b)

A solution of **6** (2 g, 0.01 mol), prepared from ethyl bromoacetate and triethyl phosphite (16), in THF (10 ml) (distilled over $LiAlH_4$) was added dropwise with stirring to a suspension of sodium amide (0.4 g, 0.01 mol) in dry THF (10 ml) at 20 °C. The solution was then stirred at room temperature under a slow stream of N_2 to sweep out the evolved ammonia. To the resulting yellowish-green solution was added **5***a* (0.8 g, 2 mmol) in THF (10 ml) over a 1 h period at 20–25 °C after which the solution was left for a further period of 1 h. The solvent was removed *in vacuo*, and water added to the residue. The aqueous solution was extracted with ether, the extract dried over $MgSO_4$ and evaporated to give a colorless oil which was purified by chromatography (SiO_2, benzene) to give **7***a* which crystallized as needles from petroleum ether (30:60), m.p. 117–118° (40%).

Mol. Wt. Calcd. for $C_{31}H_{48}O_4$: 484. Found (mass spectrum): 484.

When this Wittig reaction was carried out with acetate (**5***b*) the product was found by t.l.c. (SiO_2, $CHCl_3$) to be a mixture consisting mainly of **7***a* and *b*. Acetylation of **7***a* with acetic anhydride – pyridine gave **7***b* as an oil which crystallized as needles from ethanol, m.p. 117–118°; ν_{max} (KBr) 2970, 1730, 1710, 1630, 1245, 1210, 1172, and 1030 cm^{-1}; λ_{max} (EtOH) 231 nm (ε 14 800); n.m.r. ($CDCl_3$): δ 0.68 (CH_3—C_{18}, s), 1.03 (CH_3—C_{19}, s), 1.06 (H—C_{21}, d, J = 7 Hz), 1.28 (C_2H_5OOC—, t, J = 7 Hz), 4.18 (C_2H_5OOC—, q, J = 7 Hz), 4.32 (H—C_{23}, broad s), 4.3–4.8 (H—C_3, broad m), 5.35 (H—C_6, narrow m), 5.78 (—OOC—CH=, s).

Anal. Calcd. for $C_{33}H_{50}O_5$ (mol. wt. 526): C, 75.29; H, 9.50. Found (*m/e*, 526): C, 75.41; H, 9.64.

Preparation of (22R,23S) 3β,23-Dihydroxy-24-carboxymethylene-cholest-5-en-19,22-lactone (8a)

To **7***a* (500 mg) dissolved in methanol (50 ml), 5 ml 30% perchloric acid was added. After 5 min the solution was concentrated to about half volume *in vacuo* then poured into water and extracted twice with ethyl acetate. The solvent layer was washed with saturated $NaHCO_3$ solution and water, and dried over $MgSO_4$. The ethyl acetate was concentrated *in vacuo* to small volume and left to stand at room temperature for crystallization to give **8***a*, m.p. 267–270° (>90%). ν_{max}(KBr): 3360, 2930, 1685, and 1380, cm^{-1}; λ_{max} EtOH 210 nm (ε 11 800); c.d. (*c*, 0.04, MeOH)$[\theta]_{300}$ ±0, $[\theta]_{285}$ −677, $[\theta]_{280}$ −1360, $[\theta]_{275}$ −2940, $[\theta]_{270}$ −4960, $[\theta]_{265}$ −7210, $[\theta]_{260}$ −8440, $[\theta]_{255}$ −7660, $[\theta]_{250}$ −3160, $[\theta]_{245}$ +3400, $[\theta]_{240}$ +12 000, $[\theta]_{323}$ −18 000, $[\theta]_{225}$ +10 200, $[\theta]_{220}$ −4520°.

Anal. Calcd. for $C_{29}H_{44}O_4$ (mol. wt. 456): C, 76.27: H, 9.71. Found (*m/e*, 456): C, 76.34; H, 9.73.

The monoacetate **8***b*, was prepared in a similar way from **7***b*. Recrystallization from benzene gave m.p. 249–252° (d); n.m.r. ($CDCl_3$): δ 0.72 (CH_3—C_{18}, s), 1.03 (CH_3—C_{19}, s), 1.04 (H—C_{21}, d, J = 6.5 Hz), 1.17 ($2CH_3$—C_{25}, d, J = 7 Hz), 2.02 (CH_3OCO—, s), 2.87 (H—C_{25}, sept., J = 7 Hz), 4.16 (H—C_{22}, d, J = 10 Hz), 4.2–4.8 (2H, m; addition of D_2O gives d at 4.37 J = 10 Hz, H—C_{23} and H—C_3), 5.36 (H—C_6, m), 5.72 (lactone olefinic-H, s).

Mol. wt. Calcd. for $C_{31}H_{46}O_5$: 498. Found (mass spectrum): 498.

Compound **8***b* was also prepared using 60% perchloric acid (2.5 ml) – D_2O (2.5 ml). The n.m.r. ($CDCl_3$) of the product was identical to that reported above, *i.e.* no exchange occurred at C-28.

Acetylation of **8***b* or *a* with acetic anhydride – pyridine gave diacetate **8***c*. Recrystallization from methanol gave m.p. 207–209°.

Mol. Wt. Calcd. for $C_{33}H_{48}O_6$: 540. Found (mass spectrum): 540.

T.l.c. of compounds **8***a*, *b*, and *c* on SiO_2 using 10% EtOAc–C_6H_6 as solvent showed each compound as a single spot.

Preparation of (22R,23S) 3β,23-Dihydroxy-24-carboxymethylene-5-en-7-one-29,22-lactone (3a)

A stirred solution of **8***a* (100 mg) in 20 ml pyridine containing 10 mg hematoporphyrin was irradiated in a water-cooled jacket with seven 15 W fluorescent lamps (General Electric F15T12), during which time O_2 was bubbled through the solution. The reaction was monitored by t.l.c. (SiO_2 – 4% MeOH in $CHCl_3$). After 24 h the mixture was diluted with ether, treated with 20 mg charcoal, filtered through Celite and the ether evaporated. Cupric acetate (70 mg) was added to the pyridine solution and the mixture was stirred for 5 h and diluted with ethyl acetate. The solution was washed with dilute phosphoric acid, dilute $NaHCO_3$ and H_2O, dried over $MgSO_4$, and evaporated to dryness to give **3***a*. Recrystallization twice from ethyl acetate gave m.p. 240–243° (50%); ν_{max}(KBr) 3390, 2940, 1685, 1380, 1270, and 1050 cm^{-1}; λ_{max} EtOH 230 nm (ε 16 500). The solution of **3***a* which had been used for the u.v. spectrum (2 mg in 50 ml EtOH) was treated with a few drops of 6 *N* HCl and refluxed for 4 h. The u.v. spectrum now gave maxima at 279 and 216 nm. Mass spectrum (inlet temperature

270°): *m/e* (relative intensity) 470 (45, M^+), 452 (18), 345 (42), 344 (41), 287 (29), 269 (26), 245 (41), 126 (62), 43 (100); c.d. (*c*, 0.0345, MeOH) $[\theta]_{310} \pm 0$, $[\theta]_{300} -538$, $[\theta]_{295} -1080$, $[\theta]_{290} -2160$, $[\theta]_{285} -2960$, $[\theta]_{280} -4300$, $[\theta]_{280} -4300$, $[\theta]_{275} -7000$, $[\theta]_{270} -10\,000$, $[\theta]_{265} -14\,800$, $[\theta]_{260} -18\,850$, $[\theta]_{255} -20\,460$, $[\theta]_{250} -18\,850$, $[\theta]_{245} -12\,120$, $[\theta]_{240} -4050$, $[\theta]_{235} +810$, $[\theta]_{230} -4050$, $[\theta]_{225} -18\,850$, $[\theta]_{220} -70\,000°$.

Anal. Calcd. for $C_{29}H_{42}O_5$: C, 74.01; H, 8.99. Found: C, 74.21; H, 9.00.

The monoacetate 3*b* was prepared in a similar manner from **8***b*. Recrystallization from benzene gave m.p. 290–295 °C; n.m.r. (pyridine): δ 0.68 (CH_3—C_{18}, s), 1.09 (CH_3—C_{19}, $2CH_3$—C_{25}, d, $J = 7$ Hz), 1.13 (H—C_{21}, d, $J = 6.5$ Hz), 2.03 (CH_3OCO—, s), 3.20 (H—C_{25}, sept., $J = 7$ Hz), 4.44 (H—C_{22}, d, $J = 10$ Hz), 4.5–4.8 (2H, m, 23-H and H—C_3), 5.74 (H—C_6, broad s), 5.90 (lactone olefinic-H, broad s).

Mol Wt. Calcd. for $C_{31}H_{44}O_6$: 512. Found (mass spectrum): 512.

Acetylation of 3*a* or *b* with acetic anhydride – pyridine gave diacetate 3*c*. Recrystallization from methanol gave m.p. 215–216 °C.

Mol. Wt. Calcd. for $C_{33}H_{46}O_7$: 554. Found (mass spectrum): 554.

The authors gratefully acknowledge the many suggestions and constructive criticism offered by Dr. A. C. Oehlschlager and Mr. Mario Fryberg. We are indebted to Dr. L. D. Hayward, Department of Chemistry, University of British Columbia for his kind assistance in obtaining circular dichroism spectra. This work was supported by a National Research Council of Canada operating grant and a University Graduate Studies stipend to C.R.P.

1. T. C. McMorris and A. W. Barksdale. Nature, **215**, 320 (1967).
2. D. M. Green, J. A. Edwards, A. W. Barksdale, and T. C. McMorris. Tetrahedron, **27**, 1199 (1971).
3. J. A. Edwards, J. Sundeen, W. Salmond, T. Iwadare, and J. H. Fried. Tetrahedron Lett. 791 (1972).
4. M. Fryberg, A. C. Oehlschlager, and A. M. Unrau. Tetrahedron, **27**, 1261 (1971).
5. W. Sucrow, B. Schubert, W. Richter, and M. Slopianka. Chem. Ber. **104**, 3689 (1971).
6. H. Takahashi, K. Fujiwara, and M. Ohta. Bull. Chem. Soc. Jap. **35**, 1498 (1962).
7. J. E. Blackwood, C. L. Gladys, K. L. Loening, A. E. Petrarca, and J. E. Rush. J. Am. Chem. Soc. **90**, 509 (1968).
8. A. Nikon and J. F. Bagli. J. Am. Chem. Soc. **83**, 1498 (1961).
9. J. A. Edwards, J. S. Mills, J. Sundeen, and J. H. Fried. J. Am. Chem. Soc. **91**, 1248 (1969).
10. J. A. Elvidge and P. D. Ralph. J. Chem. Soc. (London) B, 243 (1966).
11. G. Snatzke. Angew. Chem. Intl. Ed. Eng. **7**, 14 (1968).
12. R. Tschesche, H. Schwang, H. W. Fehlhaber, and G. Snatzke. Tetrahedron, **22**, 1129 (1966).
13. S. M. Kupchan, W. K. Anderson, P. Bollinger, R. W. Doskotch, R. M. Smith, J. A. Saenz Renauld, H. K. Schnos, A. L. Burlingame, and D. H. Smith. J. Org. Chem. **34**, 3858 (1969).
14. G. P. Arsenault, K. Biemann, A. W. Barksdale, and T. C. Morris. J. Am. Chem. Soc. **90**, 5635 (1968).
15. H. Budzikiewiez, C. Djerassi, and D. H. Williams. Structure elucidation of natural products by mass spectrometry. Vol. II. Holden-Day, Inc., San Francisco, Calif. 1964.
16. G. M. Kosolapoff. Organophosphorus compounds. 1st ed. J. Wiley and Sons, Inc., New York, N.Y. 1950. Chapt. 7.

Can. J. Chem. Downloaded from www.nrcresearchpress.com by 210.87.254.105 on 09/05/12
For personal use only.

The High Dose Rate Radiolysis of H_2S: Sulfur as an Electron Scavenger[1]

A. W. BOYD, C. WILLIS,[2] AND O. A. MILLER

Physical Chemistry Branch, Chalk River Nuclear Laboratories, Atomic Energy of Canada Limited, Chalk River, Ontario

Received October 2, 1972

The radiolysis of gaseous hydrogen sulfide has been studied in the presence of added sulfur at 200–250 °C. At 2×10^{27} eV g^{-1} s^{-1} sulfur reduces the hydrogen yield from $G(H_2) = 12.0 \pm 0.3$ to $G(H_2) = 7.3 \pm 0.3$. This reduction in yield appears to be due to electron attachment by the sulfur thereby suppressing formation of hydrogen from dissociative neutralization. Assuming the sulfur is S_8 we estimate the attachment rate of electrons to sulfur to be about 1×10^{14} M^{-1} s^{-1}.

At 25 °C the reduction in the H_2 yield at 2×10^{27} eV g^{-1} s^{-1} with increasing dose appears to be due to polysulfanes rather than radiolytic sulfur.

Over the range of $10^{26} - 10^{28}$ eV g^{-1} s^{-1} the H_2 yield increases from $G(H_2) = 11$ to $G(H_2) = 13$. Mechanisms to account for this increase are discussed.

La radiolyse du sulfure d'hydrogène gazeux a été étudiée en présence de soufre additionné, à 200–250 °C. Pour des valeurs de 2×10^{27} eV g^{-1} s^{-1}, le soufre diminue le rendement en hydrogène de $G(H_2) = 12.0 \pm 0.3$ à $G(H_2) = 7.3 \pm 0.3$. Cette réduction dans le rendement est imputable, semble-t-il, à l'attachement par le soufre d'un électron ce qui empêche la formation de l'hydrogène à partir de la neutralisation dissociative. En supposant que le soufre est sous forme S_8, on estime que le taux d'attachement d'électrons par le soufre est d'environ 1×10^{14} M^{-1} s^{-1}.

A 25 °C, la réduction dans le rendement en H_2 pour des valeurs de 2×10^{27} eV g^{-1} s^{-1} avec augmentation des doses semble imputable aux polysulfanes plutôt qu'au soufre radiolytique.

Dans l'intervalle $10^{26} - 10^{28}$ eV g^{-1} s^{-1}, le rendement en H_2 augmente de $G(H_2) = 11$ jusqu'a $G(H_2) = 13$. Les mécanismes expliquant cette augmentation sont discutés.

[Traduit par le journal]

Can. J. Chem., 51, 1228 (1973)

Introduction

Rcently several studies of the radiolysis of hydrogen sulfide have been reported (1–14) and we have proposed a mechanism based on our measurements at high dose rates (13). While this mechanism is in general agreement with the observed yields there are problems which need further investigation.

The main experimental results all obtained at room temperature are as follows. At low dose rates ($10^{16} - 10^{18}$ eV g^{-1} s^{-1}) $G(H_2) = 7.0$–9.3 (1–11) with more recent data supporting values at the lower end of this range. Addition of compounds capable of electron attachment, N_2O or SF_6, does not reduce this hydrogen yield. At high dose rates ($10^{26} - 10^{28}$ eV g^{-1} s^{-1}) the yield is much higher $G(H_2) = 11.5$–13.0 (12–14) and appears to increase with dose rate over this range. At 2×10^{27} eV g^{-1} s^{-1} the hydrogen yield $G(H_2) = 12.0 \pm 0.3$ is reduced to $G(H_2) = 7.9 \pm 0.3$ by the addition of SF_6 (13). In multi-pulse irradiation experiments of pure H_2S at a dose rate of 2×10^{27} eV g^{-1} s^{-1} the hydrogen yield decreases with dose to $G(H_2) \approx 8$ above a total dose of ~ 10 Mrads. For H_2S–SF_6 mixtures no similar reduction with dose is observed (13), the hydrogen yield remaining constant at $G(H_2) = 7.9$.

We interpreted these results in terms of changing charge neutralization processes. At high dose rates for single pulse irradiations in pure H_2S, charge neutralization involves the free electron, reaction 1.[3]

[1] $$H_5S_2^+ + e \rightarrow H + 2H_2S$$

On the addition of SF_6, SF_6^- is involved in the neutralization step and the formation of hydrogen atoms, [1], is suppressed.

[2] $$e + SF_6 \rightarrow SF_6^-$$

[3] $$H_5S_2^+ + SF_6^- \rightarrow HF + 2H_2S + SF_5$$

[1] A.E.C.L. No. 4456.

[2] Present address: Chemistry Department, University of the West Indies, Kingston, Jamaica.

[3] As will be discussed, the predominant positive ion is more probably $H_5S_2^+$, rather than H_3S^+ which was assumed in ref. 13.

Can. J. Chem. Downloaded from www.nrcresearchpress.com by 210.87.254.5 on 09/05/12
For personal use only.

Can. J. Chem. Downloaded from www.nrcresearchpress.com by 210.87.254.5 on 09/05/12
For personal use only.

This correspondingly reduces the hydrogen yield from [4].

[4] $$H + H_2S \rightarrow H_2 + SH$$

The decrease in yield with increasing dose can be explained if elemental sulfur, which is formed in a yield equivalent to that of hydrogen, can act in a manner similar to SF_6, reactions 5 and 6.

[5] $$S_n + e \rightarrow S_n^-$$

[6] $$H_5S_2^+ + S_n^- \rightarrow 2H_2S + HS_n$$
or
$$2H_2S + SH + S_{n-1}$$

Clearly, if reactions 5 and 6 can occur, then at low dose rates, because of the much longer lifetime of the electron with respect to neutralization, only very low concentrations of sulfur and hence very low doses will be required to suppress completely production of hydrogen via neutralization.

To test our suggestion that sulfur is acting as an electron scavenger we have irradiated mixtures of H_2S and sulfur at 200 °C. This temperature is required to obtain a sufficient concentration of sulfur in the vapor phase.

There are other points which need further study.

The proposed mechanism does not predict any dose rate effect in the range $10^{27} - 10^{28}$ eV g^{-1} s^{-1}, yet we observed an increase from $G(H_2) = 12.0 \pm 0.5$ to $G(H_2) = 13.1 \pm 0.4$ over this range (13, 14). To study this further we have measured H_2 yields in both pure H_2S and H_2S–SF_6 mixtures from 1×10^{26} eV g^{-1} s^{-1} to 2×10^{28} eV g^{-1} s^{-1} at room temperature.

The equilibrium vapor pressure of sulfur at 25 °C is less than 10^{-5} Torr. If there is vapor–solid equilibrium for the sulfur, formed in multipulse irradiations at room temperature, then the concentration of sulfur in the gas phase is so low that k_5 would have to be improbably high for reaction 5 to compete with reaction 1 and there should be no effect of dose at high dose rates. To determine if the observed fall-off is due to supersaturation of sulfur vapor we have both varied the time between pulses and cooled the cells in liquid nitrogen between pulses.

Experimental

Radiation Sources and Dosimetry

Both Febetron 705 and Febetron 706 accelerators were used. In the 705 irradiations the gas samples were irradiated in quartz cells with a break-seal. These could be heated in a furnace (15) at temperatures up to 250 °C prior to irradiation. In the 706 irradiations the samples were irradiated in aluminum cells (14). The average dose in both types of cells was determined by nitrous oxide dosimetry taking $G(N_2) = 12.4$(14, 16–18). The maximum dose per pulse and average dose rate obtained with the 705 were 1×10^{20} eV g^{-1} and 2×10^{27} eV g^{-1} s^{-1}. These were reduced to 5×10^{18} eV g^{-1} and 1×10^{26} eV g^{-1} s^{-1} by the use of a scattering foil (19). The dose in the aluminum cells with the 706 was 5×10^{19} eV g^{-1} per pulse and the average dose rate 2×10^{28} eV g^{-1} s^{-1}.

Materials and Analyses

The H_2S and SF_6 (Matheson C.P. grade) were purified by eliminating gases non-condensible at 77 °K by several freeze–pump–thaw cycles. The sulfur (Fisher USP) was added to the irradiation cells in solution in CS_2. The CS_2 was removed by use of a vacuum oven followed by pumping on a vacuum line at room temperature. This was shown not to remove any appreciable amount of sulfur. As in ref. 13, the hydrogen was measured using a McLeod gauge and a calibrated mass spectrometer.

Results

H_2S–S Mixtures

The hydrogen yields from single pulse irradiations of H_2S–S mixtures at 200–250 °C are shown in Fig. 1. These yields have not been corrected for the slight increase in total dose due to the addition of sulfur. There appears to be no significant change in the initial yield of hydrogen $G(H_2) = 12.0 \pm 0.5$ (13) from H_2S on increasing the temperature from 25 °C to 200–250 °C.

Two other sets of data are plotted in Fig. 1. Cells containing pure H_2S were irradiated with 6 to 10 pulses at room temperature. These were cooled with liquid nitrogen and the hydrogen formed was removed. The cells were then irradiated at 200 °C. The amount of sulfur formed was calculated assuming the yield to equal that of hydrogen. The effect of the radiolytically produced sulfur appears to be the same

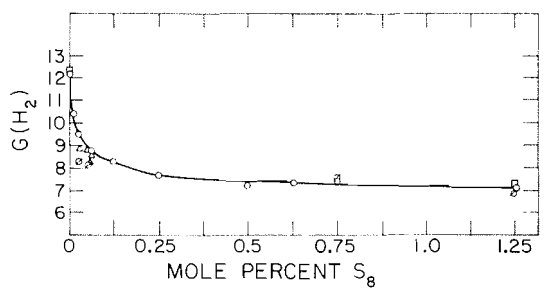

FIG. 1. Hydrogen yields in the radiolysis of H_2S–S mixtures, 2×10^{27} eV g^{-1} s^{-1}, 10^{20} eV g^{-1} 200 °C: ○, 800 Torr; □, 300 Torr; ∅, 800 Torr plus 2 mol % SF_6; △, 800 Torr sulfur formed radiolytically.

Can. J. Chem. Downloaded from www.nrcresearchpress.com by 210.87.254.5 on 09/05/12
For personal use only.

as that of the added sulfur. At room temperature however added sulfur did not significantly reduce the hydrogen yield.

In addition mixtures with H_2S containing 2 mol% SF_6 as well as sulfur were irradiated at 200 °C. The SF_6 has little or no effect on the hydrogen yield except at low sulfur concentrations.

To facilitate comparison between H_2S–SF_6 and H_2S–S mixtures the curve from Fig. 1 is plotted with data for H_2S–SF_6 mixtures in Fig. 2. For reasons of scale the sulfur is assumed to be S_4 rather than S_8 in this figure.

Dose Rate Effects

The hydrogen yields from single pulse irradiations of H_2S and H_2S–SF_6 mixtures at 25 °C at various dose rates are listed in Table 1.

Multipulse Irradiations

The hydrogen yields from H_2S samples following 8 or 10 pulses each at a dose rate of 2×10^{27} eV g^{-1} s^{-1} under different conditions are listed in Table 2.

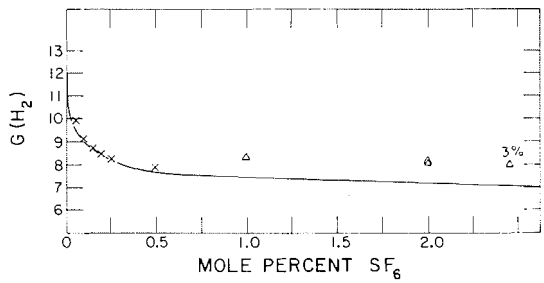

FIG. 2. Hydrogen yields in the radiolysis of H_2S–SF_6 mixtures 800–1000 Torr, 2×10^{27} eV g^{-1} s^{-1}, 10^{20} eV g^{-1} 25 °C: △, this work; ×, from ref. 13; —, from Fig. 1 but with scale doubled so that sulfur is as S_4.

TABLE 1. Hydrogen yields as a function of dose rate in H_2S H_2S–SF_6 mixtures at 25 °C

Average dose rate (eV g^{-1} s^{-1})	$G(H_2)$ H_2S	$G(H_2)$ H_2S – 1 mol % SF_6	Reference
1×10^{26}	11.1±0.2	8.0±0.2	This work
~2×10^{26}*	11.5±0.5	—	12
2×10^{27}	12.0±0.3	7.9±0.3	13
2×10^{28}	13.1±0.4	7.8±0.2	14 and this work

*Estimated from the data given in ref. 12.

TABLE 2. Hydrogen yields from 800 Torr of H_2S irradiated at 25° to a dose of 8–10 × 10^{20} eV g^{-1} (8–10 pulses), average dose rate 2×10^{27} eV g^{-1} s^{-1}

Conditions of samples	$G(H_2)$*
Kept at 25 °C with a wait of 1–2 min between each pulse	8.30† (10 pulses) 9.07† (8 pulses)
Kept at 25 °C with a wait of 8–16 h between each pulse	7.21 (10 pulses) 8.29 (10 pulses)
Cooled to 77 °K after each pulse then warmed to 25° and kept at 25 °C ~5 min before the next pulse	11.91 (10 pulses) 11.79 (8 pulses)
Cooled to 77 °K after each pulse then warmed to 25 °C and kept at 25 °C 8–16 h before the next pulse	7.27 (10 pulses) 7.72 (10 pulses)

*Average yield for total number of pulses.
†These values are in agreement with those obtained under the same conditions in ref. 13.

Discussion

Comparison of H_2S–S and H_2S–SF_6 Mixtures

It is clear that the reduction in the hydrogen yield from H_2S radiolysis at Febetron dose rates by the addition of sulfur vapor is similar to the reduction by the addition of SF_6. It seems almost certain, then, that sulfur is a very efficient electron scavenger. Assuming this to be the case a rate constant for reaction 5 can be derived from the relative reduction in hydrogen yield. The major species in pure sulfur vapor at room temperature is S_8 (20). At 200–250 °C the composition is ~60% S_8, ~25% S_6, and ~15% S_7 but for the present discussion we shall assume that all the sulfur is S_8. Using the computer program of Schmidt (21) and our knowledge of the dose and duration and shape of the electron pulse the reduction in the hydrogen yield can be calculated for various values of k_1 and k_5. The rate of dissociative recombination of H_2S, reaction 1, has not been measured but the value for water vapor is in the range 6–18 × 10^{14} M^{-1} s^{-1} (22). Using these values for k_1 the rate constant for reaction 5 was calculated to be $k_5 = 8$–16×10^{13} M^{-1} s^{-1}. For comparison the rate constant for thermal electron attachment to SF_6 is 1.8×10^{14} M^{-1} s^{-1} (23, 24). As we have discussed (13) the rate constant for attachment of electrons to SF_6 under our conditions appears to be about 10 times smaller. Thus for Febetron conditions sulfur is a more effective electron scavenger than SF_6.

As can be seen in Fig. 2 the plateau values of the hydrogen yield in H_2S–SF_6 and H_2S–S

Can. J. Chem. Downloaded from www.nrcresearchpress.com by 210.87.254.5 on 09/05/12
For personal use only.

mixtures are different. This difference is supported by comparing the reciprocal plot of the yields for H_2S–S and H_2S–SF_6 mixtures shown in Fig. 3. These plots are based on the expression

$$\frac{1}{G(H_2)_0 - G(H_2)_A} = \frac{1}{G(H_2)_0 - G(H_2)} \times \left[\frac{1 + \text{Constant} \times [H_2S]}{K[A]}\right]$$

where A may be S or SF_6. The intercepts at $[H_2S]/[A] = 0$ give values of $G(H_2)_0 - G(H_2) = 4.1$ and 4.7 for SF_6 and S_8, respectively. Obviously the H_2 yield with sulfur may be too low or the yield with SF_6 may be too high.

It is likely that the lower plateau yield of $G(H_2) = 7.3 \pm 0.3$ obtained with sulfur is closer to the true yield in the presence of an electron scavenger. Charge transfer to sulfur from $H_5S_2^+$ would reduce $G(H_2)$ and is exothermic but for this to compete with neutralization of these ions the rate constant would have to be two orders of magnitude greater than that of any observed charge transfer reactions. It is also unlikely that, at a concentration of 1 mol%, sulfur will compete with H_2S for H atoms. The rate constant for reaction 4 at 200 °C is $\sim 1 \times 10^9\ M^{-1}\ s^{-1}$ (25). On the other hand Huyton and Woodward (1) observed an increase in $G(H_2)$ on the addition of SF_6 in the low dose rate radiolysis of H_2S.

Dose Rate Effects at $10^{26} - 10^{28}\ eV\ g^{-1}\ s^{-1}$

The H_2S yields in the H_2S–SF_6 mixtures, Table 1, are the same at the three dose rates

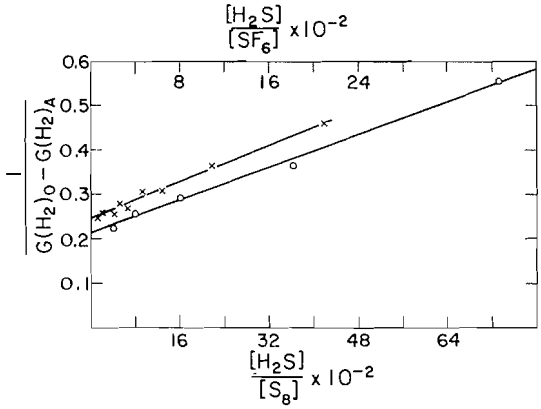

FIG. 3. Reciprocal plot of reduction in hydrogen yield, 2×10^{27} eV g^{-1} s^{-1}, 10^{20} eV g^{-1}; ○, 800 Torr H_2S–S mixtures sulfur 200 °C; ×, 1000 Torr H_2S–SF_6 mixtures 25 °C.

used, therefore the changes in the yields in pure H_2S are presumably due to dose rate dependent changes in ionic processes. The primary positive ions formed in H_2S in a mass spectrometer are H_2S^+ (52%), SH^+ (22%), S^+ (23%), and H^+ (3%) (26). Taking $G(e) = 4.0$ ($W_{H_2S} = 25.3$ eV/ion pair (2)) and assuming that the same relative concentration of primary ions are produced in radiolysis we have

[7] $H_2S \rightsquigarrow H_2S^+ + e$ $G = 2.08$

[8] $H_2S \rightsquigarrow HS^+ + H + e$ $G = 0.88$

[9] $H_2S \rightsquigarrow S^+ + H + H + e$ $G = 0.92$

[10] $H_2S \rightsquigarrow H^+ + SH + e$ $G = 0.12$

The reactions of these ions with H_2S are listed in Table 3. We shall assume that under our conditions the major ion is $H_5S_2^+$ with a yield of $G(H_5S_2^+) = 3.55$. The yields of the other positive ions are relatively small $G(H_2S_3^+) = 0.4$, $G(H_2S_2^+) = 0.04$. It is most unlikely that the yields of these three ions will be reduced by neutralization of the primary ions. To compete with reactions 11–20 the rate constants for neutralization would have to be greater than $10^{17}\ M^{-1}\ s^{-1}$. The highest reported neutralization rate constant is $1.5 \times 10^{16}\ M^{-1}\ s^{-1}$ for neutralization in NH_3 (31).

Neutralization of $H_2S_3^+$ is assumed not to produce H_2

[21] $H_2S_3^+ + e \rightarrow H_2S + S_2$

and the yield of hydrogen that can be affected by the addition of an electron scavenger then arises from the reactions of $H_5S_2^+$.

As discussed the plateau yield of radiolytic H_2 on the addition of an electron scavenger to H_2S corresponding to suppression of the dissociative neutralization of the positive ion is taken to be $G(H_2) = 7.3 \pm 0.3$. Thus the contribution of dissociative neutralization of the positive ion in H_2S to the H_2 yield increases from $G(H_2) = 3.8 \pm 0.3$ to $G(H_2) = 5.8 \pm 0.4$ as the dose rate increases from 10^{26} to 2×10^{28} eV g^{-1} s^{-1}. These values are consistent with a change in number of H atoms formed per neutralization as the dose rate is increased.

There does not appear to be a satisfactory mechanism to account for this change. We have considered mechanisms based on formation of H_2S^- and ion clustering beyond $H_5S_2^+$ but there are objections to each of these. In both cases it was assumed that neutralization of

TABLE 3. Ionic and radical reactions in H_2S

	Reaction	Rate constant ($l\ mol^{-1}\ s^{-1}$)	Reference
[11]	$H_2S^+ + H_2S \rightarrow H_3S^+ + SH$	3.5×10^{11} to 5.5×10^{11}	27, 28 29, 30
[12]	$HS^+ + H_2S \rightarrow H_3S^+ + S$	5.4×10^{11}	30
[13]	$HS^+ + H_2S \rightarrow HS_2^+ + H_2$	1.5×10^{11}	30
[14]	$HS^+ + H_2S \rightarrow H_2S_2^+ + H$	3.7×10^{10}	30
[15]	$HS_2^+ + H_2S \rightarrow S_2 + H_3S^+$	2.6×10^{11}	30
[16]	$S^+ + H_2S \rightarrow H_2S^+ + S$	2.6×10^{11}	30
[17]	$S^+ + H_2S \rightarrow H_2 + S_2^+$	2×10^{11}	30
[18]	$H_3S^+ + 2H_2S \rightarrow H_5S_2^+ + H_2S$	5.5×10^{11}	29, 30
[19]	$S_2^+ + 2H_2S \rightarrow H_2S_3^+ + H_2S$	1.1×10^{11}	29, 30
[20]	$H^+ + H_2S \rightarrow H_3S^+$	10^{11}	Assumed

$H_5S_2^+$ by an electron gives two H atoms as in reaction 22.

[22] $$H_5S_2^+ + e \rightarrow 2H + SH + H_2S$$

Decreasing the dose rate would favor formation of H_2S^- and further clustering of $H_5S_2^+$. The neutralization reactions could then be [23] and [24]

[23] $$H_5S_2^+ + H_2S^- \rightarrow H + 3H_2S$$

[24] $$H_7S_3^+ + e \rightarrow H + 3H_2S$$

The objections to the first of these are that nondissociative electron attachment to H_2S has not been observed and it has been estimated that the lifetime of H_2S^- is $\sim10^{-15}$ s (32). For the second mechanism to be valid clustering reactions subsequent to reaction 18 would have to have rate constants smaller than k_{18} by about two orders of magnitude. This is not likely in view of the rates of clustering reactions in water vapor (33) nor does it seem likely that there should be a difference in the number of H atoms produced in reactions 22 and 24.

A further possibility is that instead of competition between reaction 22 and reactions such as [23] or [24] the observed dose rate dependence is due to trace amounts of an electron scavenger in the H_2S. As will be discussed sulfanes appear to be very efficient electron scavengers.

It is important to note that whatever the reason for the observed dose rate dependence of the yields there must be neutralization reactions in the high dose rate radiolysis of H_2S that produce more than one H atom per ion pair.

Multipulse Irradiations

As stated in the introduction the vapor pressure of sulfur at room temperature is less than 10^{-5} Torr. Using the data tabulated by Yost and Russell (34) a ln p *vs.* $1/T$ plot gives a value of 1×10^{-6} Torr for the vapor pressure of rhombic sulfur at 25 °C. The mole ratio of sulfur to H_2S at this temperature is thus less than 10^{-8}. For sulfur at this concentration to effectively compete with the neutralization of electrons by $H_5S_2^+$ at Febetron dose rates would require a rate constant of electron attachment to sulfur of the order of $10^{18}\ M^{-1}\ s^{-1}$. This is 10^4 times the rate constant derived from the data at 200 °C.

The results in Table 2 show that the observed reductions in the hydrogen yield cannot be attributed to simple supersaturation in the vapor phase. Any supersaturation that does occur must be longer lived than 8–16 h and be capable of being reestablished in 8–16 h after cooling to 77 °K. The most likely explanation of these results and the lack of any effect of added sulfur in 25 °C irradiations is that radiolytically formed sulfur reacts with H_2S at room temperature to form polysulfanes of the form H_2S_n. These polysulfanes, which are sufficiently volatile, then act as very efficient electron scavengers as for example in reaction 25 and suppress dissociative neutralization.

[25] $$H_2S_n + e \rightarrow H_2S + S_{n-1}^-$$

The polysulfanes are thermodynamically unstable with respect to H_2S and S but are metastable at room temperature (35) and presumably are not decomposed by cooling to 77 °K. Clearly if we are to quantitatively explain the reduction

Can. J. Chem. Downloaded from www.nrcresearchpress.com by 210.87.254.5 on 09/05/12
For personal use only.

Can. J. Chem. Downloaded from www.nrcresearchpress.com by 210.87.254.5 on 09/05/12
For personal use only.

of the H_2 yield as a function of dose a relatively large amount of radiolytic sulfur must be able to be vaporized as polysulfanes in 1 atm of H_2S.

It does not seem possible that the sulfanes can exist at 200 °C. For example the rate constant for the decomposition of H_2S_2 at 50 °C is 0.56 h^{-1} (35). The activation energy for decomposition is 25 kcal/mol (35) so that the rate constant for decomposition at 200 °C is 18 s^{-1}. Thus sulfur itself appears to be the electron scavenger at 200–250 °C. This is supported by the results of Febetron irradiations of N_2O–S mixtures at 200 °C (36). We have found that the dependence of the reduction of the N_2 yield in these irradiations on the sulfur concentration is similar to the dependence of $G(H_2)$ on the sulfur concentration in H_2S–S mixtures at 200 °C and to the dependence of $G(N_2)$ on the concentration of SF_6 in N_2O–SF_6 mixtures.

Conclusions

The results in this paper provide strong evidence for our suggestion that sulfur is a very efficient electron scavenger. Assuming that sulfur at 200–250 °C is S_8 the rate constant for electron attachment to sulfur is of the order 1×10^{14} M^{-1} s^{-1}. The limiting yield of hydrogen from Febetron irradiations of H_2S–S mixtures at 200–250 °C $G(H_2) = 7.3 \pm 0.3$ is in good agreement with the most precisely determined value of the hydrogen yield $G(H_2) = 7.0 \pm 0.2$ (2) at low dose rates.

It appears however that the reduction in the hydrogen yield at Febetron dose rates observed at high doses at room temperature is due to polysulfanes. Like sulfur these must be very efficient scavengers. We are unable to quantitatively examine the role of polysulfanes because of the lack of basic information. However for reasons which we have previously discussed (13) H_2S_2 is not an electron scavenger and n must be greater than two for the sulfane H_2S_n to be involved. It should be noted that it cannot be assumed that H_2S as an additive in radiation chemistry will act only as an H atom scavenger.

The reduction in the H_2 yield on the addition of SF_6 at dose rates in the range $10^{26} - 10^{28}$ eV g^{-1} s^{-1} shows that neutralization reactions occurring must give more than one H atom per ion pair.

We are indebted to Professor M. Forys for providing us with his preliminary results on the H_2S system with added sulfur and for much helpful correspondence.

1. D. W. Huyton and T. W. Woodward. Can. J. Chem. **48**, 2300 (1970).
2. D. W. Huyton and T. W. Woodward. Trans. Faraday Soc. **66**, 1648 (1970).
3. D. W. Huyton and T. W. Woodward. Trans. Faraday Soc. **67**, 2989 (1971).
4. D. W. Huyton and T. W. Woodward. J. Chem. Soc. (London), Faraday Trans. II, 1, 144 (1972).
5. G. Meissner and A. Henglein. Z. Naturforsch. **20b**, 1005 (1965).
6. R. M. P. Torrey. Ph.D. Thesis. Syracuse University, Syracuse, N.Y. 1969.
7. M. Forys and K. Jezierska. Radio Chem. Radioanal. Lett. 1, 237 (1969).
8. M. Forys and E. Migdal. Radio Chem. Radioanal. Lett. **3**, 177 (1971).
9. M. Forys and E. Migdal. Radio Chem. Radioanal. Lett. **3**, 181 (1971).
10. K. Jezierska, M. Forys, and M. Tanbe. Khim. Vysokikh Energii, **4**, 280 (1970).
11. B. G. Dzantiev, M. S. Unukovich, and A. V. Shishkov. Khim. Vysokikh Energii, **5**, 172 (1971).
12. D. Perner and T. Franken. Ber. Bunsenges. Phys. Chem. **73**, 897 (1969).
13. C. Willis, A. W. Boyd, and O. A. Miller. Can. J. Chem. **49**, 1677 (1971).
14. C. Willis, A. W. Boyd, and O. A. Miller. Radiation Res. **46**, 428 (1971).
15. C. Willis, A. W. Boyd, and O. A. Miller. Can. J. Chem. **47**, 3007 (1969).
16. C. Willis, O. A. Miller, A. E. Rothwell, and A. W. Boyd. Adv. Chem. Ser. **81**, 539 (1968).
17. A. W. Boyd, C. Willis, and O. A. Miller. Can. J. Chem. **47**, 351 (1969).
18. C. Willis, A. W. Boyd, and D. A. Armstrong. Can. J. Chem. **47**, 3783 (1969).
19. A. W. Boyd, C. Willis, and O. A. Miller. Can. J. Chem. **49**, 2283 (1971).
20. B. Meyer. Elemental sulfur. University of California Lawrence Radiation Laboratory Report UCRL 16700 (1966).
21. K. H. Schmidt. USAEC Res. and Dev. Report ANL-7693 (1970).
22. J. N. Bardsley and M. A. Biondi. Adv. At. Mol. Phys. **6**, 1 (1970).
23. B. H. Mahan and C. E. Young. J. Chem. Phys. **44**, 2192 (1966).
24. R. N. Compton, L. G. Christophorou, G. S. Hurst, and P. W. Reinhart. J. Chem. Phys. **45**, 4634 (1966).
25. M. J. Kurylo, N. C. Peterson, and W. Brown. J. Chem. Phys. **54**, 943 (1971).
26. A. Cornu and R. Massot. Compilation of mass spectral data. Heyden and Sons, London. 1966.
27. A. G. Harrison and J. C. J. Thynne. Trans. Faraday Soc. **62**, 3345 (1966).
28. S. K. Gupta, E. G. Jones, A. G. Harrison, and J. J. Myher. Can. J. Chem. **45**, 3107 (1967).

29. W. E. W. RUSKA and J. L. FRANKLIN. Int. J. Mass Spectrom. Ion Phys. **3**, 221 (1969).
30. A. G. HARRISON. Int. J. Mass Spectrom. Ion Phys. **6**, 297 (1971).
31. D. E. WILSON and D. A. ARMSTRONG. J. Phys. Chem. **75**, 444 (1971).
32. F. FIQUET-FAYARD, J. P. ZIESEL, R. AZRIA, M. TRONC, and J. CHIARI. J. Chem. Phys. **56**, 2540 (1972).
33. A. GOOD, D. A. DURDEN, and P. KEBARLE. J. Chem. Phys. **52**, 222 (1970).
34. D. M. YOST and H. RUSSELL. Systematic inorganic chemistry of the fifth and sixth group nonmetallic elements. Prentice–Hall Inc., New York. 1944.
35. F. FEHER and H. WEBER. Z. Elektrochem. **61**, 285 (1957).
36. A. W. BOYD, C. WILLIS, and O. A. MILLER. Unpublished work.

Can. J. Chem. Downloaded from www.nrcresearchpress.com by 210.87.254.5 on 09/05/12
For personal use only.

Liquid Bismuth Calorimetry: Enthalpies of Solution of Copper, Indium, and Tellurium, and Enthalpies of Formation of Cuprous Selenides

KENNETH GORDON SKEOCH AND ROBERT DONALD HEYDING

Department of Chemistry, Queen's University, Kingston, Ontario

Received September 19, 1972

An isoperibol liquid metal solution calorimeter in which samples are introduced below the surface of the melt is described. Enthalpies of solution in liquid bismuth at *ca.* 625 °K in kcal mol^{-1} were found to be $+0.99 \pm 0.05$ for copper, -1.41 ± 0.08 for indium, and -1.16 ± 0.07 for tellurium.

Enthalpies of formation in kcal mol^{-1} at 625 °K of cubic cuprous selenides are -7.98 ± 0.20 for $Cu_{1.80}Se$; -7.80 ± 0.19 for $Cu_{1.85}Se$; -5.92 ± 0.20 for $Cu_{1.90}Se$; -5.29 ± 0.20 for $Cu_{1.95}Se$; and -5.21 ± 0.14 for $Cu_{2.00}Se$.

Un calorimètre constitué par une solution liquide métal isopéribol, dans lequel les échantillons sont introduits au dessous de la surface de fusion, est décrit. Les enthalpies de solution dans le bismuth liquide vers 625 °K, en kcal mol^{-1}, sont égales à $+0.99 \pm 0.05$ pour le cuivre, -1.41 ± 0.08 pour l'indium, et -1.16 ± 0.07 pour le tellurium.

Les enthalpies de formation à 625 °K, en kcal mol^{-1}, pour les séléniures de cuivre cubiques sont de -7.98 ± 0.20 pour $Cu_{1.80}Se$; -7.80 ± 0.19 pour $Cu_{1.85}Se$; -5.92 ± 0.20 pour $Cu_{1.90}Se$; -5.29 ± 0.20 pour $Cu_{1.95}Se$; et -5.21 ± 0.14 pour $Cu_{2.00}Se$. [Traduit par le journal]

Can. J. Chem., **51**, 1235 (1973)

Can. J. Chem. Downloaded from www.nrcresearchpress.com by 210.87.254.40 on 09/05/12
For personal use only.

Introduction

At 625 °K, a cubic phase exists in the Cu/Se system from *ca.* $Cu_{2.0}Se$ to $Cu_{1.8}Se$ (1). The structure is disordered, with Se forming a face centered cubic sublattice, Cu in half of the tetrahedral holes as in the zinc blende (*B*3) structure, and the remaining copper ions randomly distributed between sites slightly displaced from the centers of the remaining tetrahedral holes (pseudo trigonal sites) and the octahedral holes in the Se lattice (2). Stevels has found that ~2.6 of the 7.2 copper ions in the unit cell in $Cu_{1.8}Se$ occupy trigonal sites while ~0.6 occupy octahedral sites (3). The distribution at other compositions is not known.

Gattow and Schneider obtained enthalpies of formation by bomb (reaction) calorimetry for $Cu_{1.8}Se$ and $Cu_{2.0}Se$ of -13.23 ± 0.02 and -14.17 ± 0.03 kcal mol^{-1}, respectively (4). Rossini *et al.* listed a value of -5.5 kcal mol^{-1} for $Cu_{2.0}Se$ (5).

We have measured ΔH_f for $Cu_{2-x}Se$ in a liquid metal solution calorimeter using bismuth as the solvent. In this paper the calorimeter is described briefly, and enthalpies of solution of Cu, In, Te, and several $Cu_{2-x}Se$ specimens at *ca.* 625 °K are reported and discussed.

Experimental

The Calorimeter

An isoperibol liquid metal solution calorimeter was patterned after the calorimeter described by Orr, Goldberg, and Hultgren (6). In this calorimeter the temperature of the solution cell during the dissolution process is measured relative to a large "isothermal" heat sink in the form of a heavy metal block surrounding the cell. The unique feature of our calorimeter is in the design of the solution cell, in which sample ampoules are broken on demand beneath the surface of the molten metal. The advantage of such an arrangement over the more conventional design in which the sample is dropped into the solvent from a temperature controlled holding zone is significant if the specimen has an appreciable vapor pressure at the temperature of the solvent, or if the density of the specimen is such that it is likely to float on the surface of the solvent. One of the disadvantages is that the calorimeter cannot be calibrated by the addition of a specimen of the solvent itself at the temperature of the holding zone, a common practice in drop calorimeters.

Details of the solution cell are shown in Fig. 1. The cell was machined from a block of 310 stainless steel. The upper section contains six sample wells, in each of which an evacuated thin walled Pyrex sample ampoule is secured by a clip. The dome contains a filling hole by which the final portion of the solvent can be added to the cell following assembly. The upper section fits snugly into the lower. Its orientation is fixed by a small keyway in the rim of the lower section and by a small screw. The shaft of the stirrer enters the cell, from below, through a long housing. Assembled and in operation, this major passage between the cell and the rest of the calorimeter is sealed by the liquid metal between the shaft and the skirt of the stirrer. The lower section of the cell is tapped at six points on its circumference to accept six thermopile junction assemblies.

The cell is supported by three legs which are secured by adjustable feet to the bottom of the heat sink (Fig. 2). Heat transfer via the legs is minimized by mica spacers in the foot assemblies.

The stirrer has two paddles, one of which sweeps the

Can. J. Chem. Downloaded from www.nrcresearchpress.com by 210.87.254.40 on 09/05/12
For personal use only.

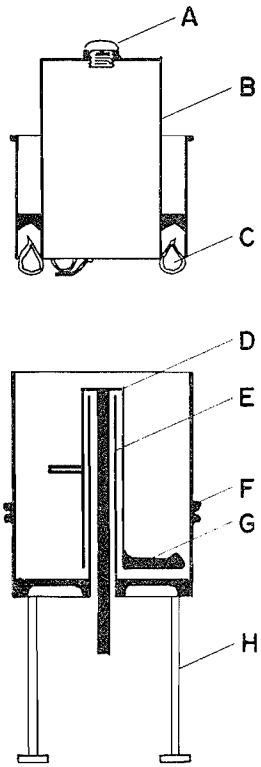

FIG. 1. Detail of calorimeter cell: *A*, filling port; *B*, dome; *C*, sample ampoule (6); *D*, stirrer; *E*, stirrer housing; *F* thermopile junction anchor (6); *G*, hammer/stirrer blade; *H*, leg (3).

surface while the second agitates the bulk of the solution. The second paddle also serves as the hammer which breaks the sample ampoules. This function is obtained by activating solenoids in the body of the calorimeter which lift the stirrer assembly and the stirrer at any one of six points corresponding to the positions of the ampoules in the cell. The position of the paddle is registered by a pointer on the stirring shaft between the rotary vacuum seal and the stirring motor on the bottom external face of the calorimeter.[1]

The cell is surrounded by a copper block weighing 52 kg; a heater with independent top, side, and bottom elements; three molybdenum radiation shields, and a vacuum jacket. In operation the calorimeter is pumped to $< 5.10^{-3}$ Torr. The cell is maintained at 360 °C by a heater input of *ca.* 290 W. The difference in temperature between the cell and the copper block is measured by a twelve junction thermopile, whose signal is amplified by a nanovoltmeter and fed to a strip-chart recorder.

[1]Detail sketches of the calorimeter, including the stirring/ampoule breaking mechanism, are available, at a nominal charge, from the Depository of Unpublished Data, National Research Council of Canada, Ottawa, Canada K1A 0S2.

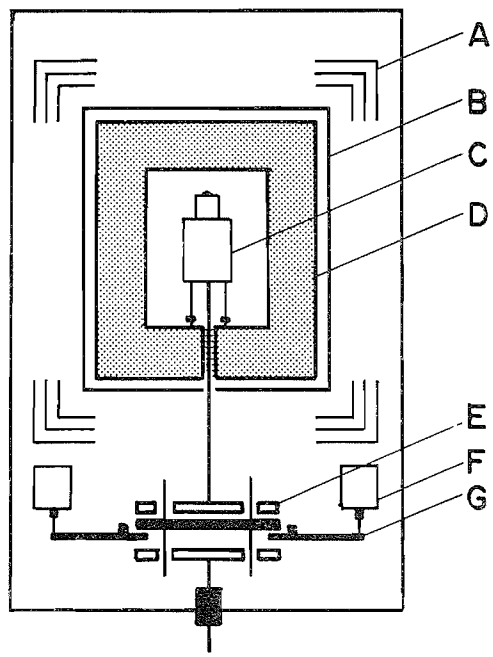

FIG. 2. Calorimeter schematic: *A*, radiation shields; *B*, heater shell; *C*, cell; *D*, heat sink; *E*, drive discs; *F*, solenoids; *G*, lift yoke.

Experimental Procedures

Specimens were prepared using Cominco 69 grade cadmium and zinc; Asarco 69 grade copper, selenium and tellurium; and 59 grade zinc supplied by Alfa Inorganic. The copper selenides $Cu_{2-x}Se$, $0 \leqslant x \leqslant 0.2$, were prepared by reaction between the elements in sealed Pyrex or silica ampoules in the usual manner. The products were identified by X-ray powder diffraction patterns. Diffraction patterns of the cuprous selenides were also obtained in a 19 cm Unicam high temperature camera at the temperature of the calorimeter to confirm the structure of the phase going into solution.

Approximately one-half of total charge of 410 g (1.96 mol) of bismuth (Cominco 59 grade) was premelted *in vacuo* in the lower section of the cell with the stirrer in position. The balance of the charge could then be accommodated in the dome of the upper section following assembly. Since the calorimeter was calibrated by the dissolution of selenium or of copper, at least one of these was included in each set of six solutes in the cell. Each ampoule contained between 2.5 and 5 mmol of solute. At these concentrations the energy associated with breaking the glass of the ampoule is negligible compared with the heat of solution.

Interpretation of Results

The form of the differential signal as a function of time from a calorimeter of this type has been discussed by Orr *et al.* (6) and by Morris and Pratt (7). The two equations used here in the interpretation of the recorder trace are

TABLE 1. Heats of solution in liquid bismuth at 625 °K

Solute	Concentration (mol %)	Other solutes (mol %)	Calibration	ΔH^{625} (kcal mol^{-1}) This work	ΔH^{625} (kcal mol^{-1}) Literature
Cu	0.24	—	Se	+1.03±0.04*	<1.4 (9) (1473 °K)
	0.24	Se (0.12)	Se	+0.96±0.04	
In	0.12	Se (0.12), Te (0.12)	Se	−1.41±0.08	−1.38±0.02 (10)
Te	0.12	Se (0.12)	Se	−1.20±0.07	−1.13±0.02 (10)
	0.24	Se (0.24), In (0.12)	Se	−1.13±0.07	−1.25±0.01 (11)

*Standard error limits are the standard deviations in the analysis of the experimental data using eq. 2.

[1] $$\ln \Delta T = -kt + \text{const}$$

and

[2] $$\Delta T^* = \frac{\Delta H}{C} = \Delta T_f + k\int_{t_0}^{t} \Delta T \mathrm{d}t$$

where ΔT is the difference in temperature between the cell and the heat sink at time t following addition of the solute, provided the solution process is complete; ΔH is the total heat effect due to the solution process and C is the heat capacity of the cell; and ΔT_f is the difference in temperature between cell and sink on completion of the solution process. ΔT^* is the difference in temperature which would have been observed had the solution process been instantaneous. The cooling constant k and ΔT_f are evaluated by plotting the logarithm of ΔT (*i.e.*, recorder pen deflection) against time. The value of the last term in eq. 2 is determined by successive graphical integrations at increasing values of t until a constant value for ΔT^* is obtained.

The calorimeter was calibrated with selenium as the primary standard, using the values for the enthalpy of solution of selenium in liquid bismuth reported by Chaudhari and Bever (8). In some experiments in which the selenium specimen was lost and in those experiments in which selenium was incompatible with the other solutes, copper was used as a secondary standard.

Results and Discussion

The enthalpies of solution of several elements in liquid bismuth at 625 °K are given in Table 1 together with literature values. Selenium is not a suitable calibration standard for experiments with cadmium and zinc, because cadmium and zinc selenides are not soluble in bismuth. Addition of either of these elements to a bismuth solution containing selenium produces a large exothermic signal from the calorimeter due to the formation of the selenides.

The enthalpies of solution of indium and tellurium agree well with values given in the literature.

A mean value for the enthalpy of solution of copper of +0.99 ± 0.05 kcal mol^{-1} was used in those experiments in which copper was the calibrating standard, and in the estimation of enthalpies of formation of the cuprous selenides.

Heats of solution of several $Cu_{2-x}Se$ specimens are given in Table 2. Enthalpies of formation at 625 °K calculated from these data are given in Table 3, assuming enthalpies of solution of copper and selenium of +0.99 ± 0.05 kcal mol^{-1} and −5.96 ± 0.17 kcal mol^{-1} (8), respectively. The Kopp–Neumann rule was assumed to hold in estimating the standard enthalpies of formation, ΔH_f^0, given in this table. With this assumption, the difference in the two enthalpies of formation are due to the fusion of selenium and the difference in heat capacities of solid and liquid selenium:

[3] $$\Delta H_f^0 = \Delta H_f^{625} + \Delta H_{\text{fusion}}^{\text{Se}} + \int_{491}^{625} (C_{p(l)}^{\text{Se}} - C_{p(s)}^{\text{Se}})\mathrm{d}T$$

The difference in heat capacities of liquid and solid selenium is 2.7 cal mol^{-1} deg^{-1} at 491 °K, and the enthalpy of fusion is 1.25 kcal mol^{-1} (11). Values of ΔH_f^0 for $Cu_{2.0}Se$ to $Cu_{1.9}Se$ are given in parentheses in Table 3 to emphasize that the cubic phase does not exist in this composition range at room temperature.

The data in Table 3 can be used to estimate the energy required to remove an electron/copper ion pair from the Cu_2Se lattice:

[4] $$Cu_2{}^{+}Se_{(s)}{}^{2-} \rightleftharpoons Cu_{(2-2x)}Cu_x{}^{2+}\square_x Se_{(s)}{}^{2-} + xe^- + xCu_{(g)}{}^{+} \quad \Delta H_4$$

using the cycle

[5] $$Cu_2{}^{+}Se_{(s)}{}^{2-} \rightleftharpoons Cu_{(2-2x)}Cu_x{}^{2+}\square_x Se_{(s)}{}^{2-} + xCu_{(s)} \quad \Delta H_5$$

Can. J. Chem. Downloaded from www.nrcresearchpress.com by 210.87.254.40 on 09/05/12
For personal use only.

TABLE 2. Heats of solution of cuprous selenides in liquid bismuth at 625 °K

Solute	T (°K)	Concentration (mol %)	Other solutes (mol %)	Calibration	ΔH_{soln}^{625}
$Cu_{1.80}Se$	623	0.12	{Se (0.12) Cu (0.24)}	Cu	+3.79±0.30
	629	0.12	—	Cu	+3.82±0.30
	626	0.12	{Se (0.12) Cu (0.24)}	Se	+3.65±0.15
$Cu_{1.85}Se$	626	0.12	Cu (0.24)	Se	+3.70±0.13
$Cu_{1.90}Se$	625	0.12	Cu (0.24) Se (0.12)	Cu	+1.81±0.09
$Cu_{1.95}Se$	627	0.12	Cu (0.24)	Cu	+1.18±0.09
$Cu_{2.00}Se$	628	0.12	{Se (0.12) Cu (0.24)}	Cu	+1.20±0.09
	622	0.12	{Se (0.12) Cu (0.24)}	Cu	+1.22±0.09
	624	0.12	{Cu (0.24) Se (0.12)}	Se	+1.21±0.06
	624	0.24	{Cu (0.24) Se (0.12)}	Se	+1.20±0.06

TABLE 3. Enthalpies of formation of cuprous selenides (kcal mol^{-1})

Composition	ΔH_f^{625}	ΔH_f^0
$Cu_{1.80}Se$	−7.98±0.20	−6.36±0.25
$Cu_{1.85}Se$	−7.80±0.19	−6.18±0.25
$Cu_{1.90}Se$	−5.92±0.20	(−4.30±0.25)
$Cu_{1.95}Se$	−5.29±0.20	(−3.67±0.25)
$Cu_{2.00}Se$	−5.21±0.14	(−3.59±0.19)

[6] $$x\mathrm{Cu}_{(s)} \rightleftharpoons x\mathrm{Cu}_{(g)} \qquad \Delta H_6$$

[7] $$x\mathrm{Cu}_{(g)} \rightleftharpoons x\mathrm{Cu}_{(g)}^{+} + xe^{-} \qquad \Delta H_7$$

The enthalpy of sublimation of copper at 298 °K is *ca.* 85 kcal mol^{-1} and the first ionization energy is 178.0 kcal mol^{-1} (12). The enthalpy change ΔH_4 associated with the removal of 10% of the copper ions in the Cu_2Se lattice is therefore +50 kcal mol^{-1}, and the average energy required to form a vacancy in this way is +11 eV. The energy required to form a vacancy by removal of a neutral gaseous copper atom (eqs. 5 and 6) is *ca.* +3 eV per vacancy.

One of us (K.G.S.) acknowledges with thanks the award of Graduate Fellowships by the Province of Ontario. This study was supported by operating grants from the National Research Council of Canada.

1. R. D. HEYDING. Can. J. Chem. **44**, 1233 (1966).
2. W. BORCHERT. Z. Krist. **106**, 5 (1945).
3. A. L. N. STEVELS. Philips Res. Rep. Suppl. No. 9, 124 (1969).
4. G. GATTOW and A. SCHNEIDER. Z. Anorg. Allgem. Chem. **286**, 296 (1956).
5. F. D. ROSSINI, D. D. WAGMAN, W. H. EVANS, S. LEVINE, and J. JAFFE. Selected values of chemical thermodynamic properties. National Bureau of Standards, Circular 500, Washington. 1952.
6. R. L. ORR, A. GOLDBERG, and R. HULTGREN. Rev. Sci. Instrum. **28**, 767 (1957).
7. A. W. H. MORRIS and J. N. PRATT. Brit. J. Appl. Phys. **16**, 517 (1965).
8. P. CHAUDHARI and M. B. BEVER. Trans. Met. Soc. AIME, **239**, 501 (1967).
9. C. WAGNER. Thermodynamics of alloys. *Translated by* S. Melgren and J. H. Westbrook. Addison–Wesley, Reading, Mass. 1952.
10. P. M. ROBINSON and J. S. LEACH. Trans. Met. Soc. AIME, **236**, 818 (1966).
11. B. W. HOWLETT, S. MISRA, and M. B. BEVER. Trans. Met. Soc. AIME, **230**, 1367 (1964).
12. D. E. GRAY (*Editor*). American institute of physics handbook. 2nd ed. McGraw-Hill, New York. 1963.

Can. J. Chem. Downloaded from www.nrcresearchpress.com by 210.87.254.40 on 09/05/12
For personal use only.

Solvent Effects on the Position of *cis–trans* Olefin Equilibrations and Additivity of Vicinal Group Pairs in Determining the Equilibrium Position for Trisubstituted Olefins[1]

DONALD EDWARD MCGREER, BRIAN DENIS PAGE, AND DHARAM PAUL KAUSHAL

Department of Chemistry, University of British Columbia, Vancouver 8, British Columbia

Received October 10, 1972

The equilibrium positions reached by a photo-induced bromine-catalyzed reaction for eight disubstituted *cis–trans* isomer pairs have been determined in pentane and carbon tetrachloride at room temperature. Data were collected for these conditions due to the observation that equilibrium positions can be markedly solvent dependent. The data thus obtained were used to calculate the expected equilibrium position for 15 trisubstituted isomer pairs, and comparison between calculated and observed data for the six available isomer pairs was good.

Les positions d'équilibre atteintes par la réaction induite photochimiquement et catalysée par du brome pour huit paires d'isomères *cis–trans* disubstitués ont été déterminées dans le pentane et dans le tétrachlorure de carbone à température de la pièce. Des données furent recueillies pour ces conditions à cause de l'observation selon laquelle les positions d'équilibre peuvent être profondément dépendante du solvant. Les données ainsi obtenues ont été utilisées pour calculer la position d'équilibre prévue pour 15 paires d'isomères trisubstitués, et la comparaison entre les valeurs calculées et observées pour les six paires d'isomères disponibles est satisfaisante. [Traduit par le journal]

Can. J. Chem. **51**, 1239 (1973)

Can. J. Chem. Downloaded from www.nrcresearchpress.com by 210.87.254.40 on 09/05/12
For personal use only.

In an earlier paper (1) we found evidence to suggest that the position of a *cis–trans* equilibrium for a trisubstituted olefin could be estimated by adding the contribution of the isolated vicinal pairs of substituents. Thus by using the fact that the equilibrium position recorded for 3-chloroacrylonitrile is 69% *cis* (2) and for 1-chloropropene is 75.5% *cis* (2) we can estimate that the percentage of the *E* form of 3-chloromethacrylonitrile should be 58% (1) (31/69 × 75.5/24.5 = 58/42). This estimate compares favorably with the 60% value found experimentally (1). The success of such calculations is encouraging; however, we recognized that most literature values of the equilibrium constants are made on neat samples at a variety of temperatures thus introducing unknown solvent and temperature effects on the data.

Our present paper has two objectives. Firstly, to determine when and by how much can solvents affect the position of equilibrium and secondly, to set up standard conditions under which equilibrium constants can be measured to further test the additivity relationship earlier encountered.

We have examined the photo-induced bromine-catalyzed equilibrium position for five *cis–trans* pairs of compounds, neat and as 10% solutions, in a variety of solvents at room temperature (25 °C). The compounds studied were crotononitrile (**1**), 3-bromoacrylonitrile (**2**), 2-bromocrotononitrile (**3**), 1,2-dibromoethene (**4**), and 1,2-dichloroethene (**5**). The measured values for these compounds appear in Table 1.

In order to discuss the trends in Table 1 we have included observed values of the dipole moments of the individual isomers or, where these were not available, calculated values from bond moments. There are many parameters for measuring solvent polarity. We have correlated our results with the E_T values of the pyridinium *N*-phenolbetaine of Reichardt (3).

The proportion of the more polar isomer is enhanced in all cases in the more polar solvent. This corresponds to an increase of the more dominant isomer found under non-polar conditions for **2**, **4**, and **5**, a decrease of the more dominant isomer for **1** and little change for **3** where the calculated dipole moments of the two isomers show little difference. The neat liquid in the case of **1**, **2**, and **3** is clearly a polar solvent whereas in the case of **4** and **5** is of intermediate polarity. The measured value of the equilibrium position for the neat liquid is consistent with this conclusion.

Clearly then solvents do affect the position of

[1]Taken in part from the Ph.D. thesis of B. D. Page, October, 1970.

Can. J. Chem. Downloaded from www.nrcresearchpress.com by 210.87.254.40 on 09/05/12
For personal use only.

TABLE 1. Solvent effects on the equilibrium* of some nitriles and dihaloolefins at 25°

		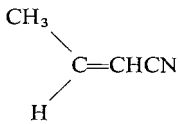 **1**	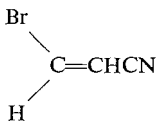 **2**	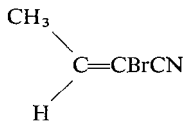 **3**	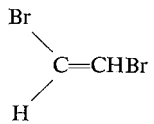 **4**	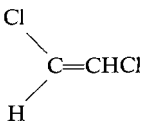 **5**
Dipole moment of *Z*-form		4.08	4.70†	3.88†	1.35	1.91
Dipole moment of *E*-form		4.53	2.48†	3.51†	0.00	0.00
Calculated dipole moment of equilibrium mixture for the neat sample		4.3	4.0	3.8	0.68	0.96
Solvent	E_T (kcal/mol) (25 °C) (ref. 3)					
Neat liquid		56 *Z*	68 *Z*	69 *Z*	61 *Z*	81 *Z*
Pentane	30.9‡	61 *Z*	51 *Z*	67 *Z*	52 *Z*	74 *Z*
Carbontetrachloride	32.5	61 *Z*	55 *Z*			
Benzene	34.5	57 *Z*		69 *Z*	63 *Z*	
Ether	34.6	59 *Z*			60 *Z*	80 *Z*
Benzonitrile	42.0	54 *Z*	65 *Z*	69 *Z*	66 *Z*	84 *Z*
Acetonitrile	46.0	56 *Z*	68 *Z*	69 *Z*	72 *Z*	87 *Z*

*The equilibrium position is given as the percent of the dominant isomer which is identified by *Z* or *E*.
†Calculated dipole moments.
‡This is the value for *n*-hexane.

Can. J. Chem. Downloaded from www.nrcresearchpress.com by 210.87.254.40 on 09/05/12
For personal use only.

the equilibrium and particularly when an isomer pair have a large difference in dipole moment. The presence of a dipole moment in at least one of the isomer pairs will also imply that the equilibrium measured on the neat sample will differ from that measured in a non-polar solvent.

Because of the above observations we have standardized our measurements of *cis–trans* equilibria, where possible; to measurements of 10% solutions in pentane or carbon tetrachloride at 25 °C. An investigation of the effect of concentration of 1,2-dibromoethylene (**4**) in pentane showed no significant change in the range 0.5–10%. In nearly all of our studies equilibrium was achieved by adding 0.5 μl (bout 2 mol %) of a bromine – carbon tetrachloride (1:9 by volume) solution to 100 μl of the olefin solution (10%) and followed by irradiation by sunlight or 310 nm light in a Rayonet apparatus. The bromine was found to be a true catalyst as it permitted equilibration from either isomer and equilibration did not occur in its absence. Data presented involve at least four measurements (two from each isomer) and frequently many more, and were reproducible to ±1%. The percent composition of equilibrium mixtures was determined by n.m.r. spectroscopy and/or v.p.c. for which it was found that no correction was necessary for differences in detector response.

For the present study we have only examined interactions between substituents having symmetric top symmetry Br, Cl, CH_3, and CN. There are ten possible pairings of these groups and the equilibrium positions for eight vicinal pairings are given in Table 2.

These same substituents can be used to form 24 trisubstituted olefins of which 15 make use of a combination of pairs of interactions listed in Table 2. We have experimentally measured many of these and have calculated most of them. These results are listed in Table 3.

It is significant that from Table 2 we can see that the *cis*- or *Z*-isomer is favored at equilibrium in all cases except 2-butene. We do not intend, in this paper, to determine the contributing interactions that lead to the value of a particular equilibrium position; however, if it is a single factor or a combination of factors it is of interest to see whether they might be separated and com-

TABLE 2. Equilibrium positions for vicinal disubstituted olefins

Substituents		Percent of major isomer at 25 °C			
C-1	C-2	CCl_4	Pentane	Neat	Literature
Br	Br		52 *Z*	61 *Z*	
Br	CH_3	75 *Z*	75 *Z*	73 *Z*	68(4)
Br	CN	55 *Z*	51 *Z*	68 *Z*	
Cl	Cl		74 *Z*	81 *Z*	
Cl	CH_3	76 *Z*	70 *Z*	74 *Z*	75.5(2)
Cl	CN	59 *Z*	58 *Z*	69 *Z*	69(2)
CH_3	CH_3	77 *E**	77 *E**		
CH_3	CN	61 *Z*	61 *Z*	56 *Z*	57(2)

*The value used here was determined in the solvent ethylene chloride (17).

TABLE 3. Equilibrium positions found and calculated* for trisubstituted olefins

Substituents		Percent of major isomer at 25 °C found (calcd.)			
C-1	C-2	CCl_4	Pentane	Neat	Literature
Br	Br, CH_3		(74 *E*)	(63 *E*)	65(5)
Br	Br, CN		(51 *Z*)	(58 *E*)	
Br	CH_3, CN	73 *E* (71 *E*)	73 *E* (74 *E*)	60 *E* (56 *E*)	60(1)
Cl	Cl, CH_3		(55 *Z*)	(60 *Z*)	
Cl	Cl, CN		(67 *Z*)	(66 *Z*)	
Cl	CH_3, CN	76 *E* (69 *E*)	75 *E* (63 *E*)	61 *E* (56 *E*)	60(1)
CH_3	Br, Cl	(51 *E*)	(56 *Z*)	(51 *E*)	
CH_3	Br, CH_3	88 *Z* (91 *Z*)	88 *Z* (91 *Z*)	86 *Z* ( )	83(6)
CH_3	Br, CN	(66 *Z*)	67 *Z* (66 *Z*)	69 *Z* (68 *Z*)	
CH_3	Cl, CH_3	(99 *Z*)	89 *Z* (89 *Z*)	86 *Z* ( )	
CH_3	Cl, CN	(63 *Z*)	(60 *Z*)	(69 *Z*)	
CH_3	CH_3, CN	77 *Z* (84 *Z*)	77 *Z* (84 *Z*)	72 *Z* ( )	
CN	Br, Cl	(54 *E*)	(57 *E*)	(51 *E*)	
CN	Br, CH_3	57 *E*† (57 *E*)	58 *E*† (61 *E*)	62 *Z*† (62 *Z*)	
CN	Cl, CH_3	52 *E*† (52 *E*)	53 *E*† (53 *E*)	63 *Z*† (63 *Z*)	

*Calculated values were determined where possible from the data of Table 2 as described in the text.
†The predicted switch of the dominant isomer from *E* to *Z* has been observed.

Can. J. Chem. Downloaded from www.nrcresearchpress.com by 210.87.254.40 on 09/05/12
For personal use only.

bined in a linear free energy sense. Unfortunately we still lack sufficient raw data to properly test such a hypothesis; however, Table 3 shows the results of combining the free energy component of the vicinal pairs in Table 2 to calculate the expected equilibrium position in trisubstituted olefins and compares these with data obtained experimentally. We find this is done most conveniently by converting the percent-terms of Table 2 to free energy differences. Then by adding or subtracting these we find the free energy differences for the trisubstituted olefins and the equilibrium percent can thus be derived. Table 4 provides the conversion of isomer percent to free energy difference and back. The correspondence of isomer percent found *vs.* calculated in Table 3 falls in the range $\pm 7\%$ in all cases except one ($ClCHC(CH_3)CN$ in pentane). This is equivalent to an error in the calculated free energy difference of ± 0.21 kcal.

We feel therefore that the concept of additivity for free energy contributions in the cases listed is very useful and we welcome further experimental data to complete Tables 2 and 3.

TABLE 4. Conversion of isomer percent to free energy differences at 25 °C

%	Ratio	$-\Delta G$	%	Ratio	$-\Delta G$
50	1	0	75	3.00	0.651
51	1.04	0.024	76	3.17	0.683
52	1.08	0.047	77	3.35	0.715
53	1.13	0.071	78	3.55	0.749
54	1.17	0.085	79	3.76	0.785
55	1.22	0.119	80	4.00	0.821
56	1.27	0.143	81	4.26	0.859
57	1.33	0.167	82	4.56	0.899
58	1.38	0.191	83	4.88	0.939
59	1.44	0.216	84	5.25	0.982
60	1.50	0.240	85	5.67	1.027
61	1.56	0.265	86	6.14	1.075
62	1.63	0.290	87	6.69	1.126
63	1.70	0.315	88	7.33	1.180
64	1.78	0.341	89	8.09	1.238
65	1.86	0.367	90	9.00	1.301
66	1.94	0.393	91	10.1	1.37
67	2.03	0.419	92	11.5	1.45
68	2.13	0.446	93	13.3	1.53
69	2.23	0.474	94	15.7	1.63
70	2.33	0.502	95	19.0	1.74
71	2.45	0.530	96	24.0	1.88
72	2.57	0.559	97	32.3	2.06
73	2.70	0.589	98	49.0	2.30
74	2.85	0.619	99	99.0	2.72

Experimental

All of the compounds studied herein were obtained as mixtures of *E* and *Z* forms from commercial suppliers or by literature procedures. These were separated using standard conditions on an Aerograph A90P vapor phase chromatograph. Table 5 lists these compounds with an identifying physical constant to be compared with the literature value in brackets. Boiling points are at 1 atm unless otherwise stated. In addition, all stereochemical assignments were confirmed by n.m.r.

β-Bromoacrylic Acid

Propiolic acid (15.6 g, 0.22 mol) was added dropwise over 0.5 h to 91 ml of 48% hydrobromic acid with stirring at 0 °C. The reaction mixture was allowed to come slowly to room temperature and stirring was continued for 30 h. Filtration of the white solid which had separated gave 2.1 g of β-bromoacrylic acid (*E*), m.p. 115.5–116.5° (lit. (8), m.p. 121°). The filtrate was extracted with six portions of 50 ml of chloroform. The combined extracts were dried and solvent evaporated to yield 27.8 g of β-bromoacrylic acid (*Z*), m.p. 54.5–55° (lit. (8), m.p. 55°). The n.m.r. spectrum indicated that there was 12% of the *E*-isomer present in this sample, however, it was used as such for the next step.

β-Bromoacrylamide

Thionyl chloride (8.4 g) was added to 10.1 g of the β-bromoacrylic acid (*Z*) and the mixture was stirred at room temperature for 18 h. Removal of the thionyl chloride followed by distillation gave 9.05 g of β-bromoacryloyl chloride (*Z*), b.p. 63°/18 mm. The acid chloride thus obtained was added to 50 ml of anhydrous ether and cooled in an ice bath. Anhydrous ammonia was bubbled through the solution with stirring for 30 min. The ether and excess ammonia were evaporated and the solid residue was extracted with ether in a Soxhlet extractor for 66 h. On evaporation of the ether extract there was obtained 8 g of product which was crystallized from methanol–ether to give pure β-bromoacrylamide (*Z*), m.p. 90–90.5° with n.m.r. peaks in acetone at 3.18 and 3.24 τ, $J_{cis} = 8.1$ Hz.

Anal. Calcd. for C_3H_4BrN: C, 24.02; H, 2.69; N, 9.34. Found: C, 24.12; H, 2.90; N, 9.55.

A sample of the *Z*-isomer was converted by irradiation in carbon tetrachloride with a bromine catalyst to the *E*-isomer, m.p. 153–155° (lit. (9) m.p. 155–156°) which had n.m.r. peaks in acetone at 2.56 and 3.28 τ, $J_{trans} = 13.5$ Hz.

β-Bromoacrylonitrile

To 3.8 g of phosphorus pentoxide was added 3.0 g of β-bromoacrylamide (*Z*). From this mixture, which was heated in an oil bath at 75–90°, 2.25 g of β-bromoacrylonitrile (*Z*), b.p. 171/760 mm, was distilled at 40 mm; n_D^{20} 1.5006 with n.m.r. peaks in carbon tetrachloride at 2.72 and 3.68 τ, $J_{cis} = 8.4$ Hz.

Anal. Calcd. for C_3H_2BrN: C, 27.31; H, 1.53. Found: C, 26.96; H, 1.75.

As this product was very sensitive to moisture and light it was stored in a sealed ampoule at −78° in the dark. A sample was converted by irradiation in carbon tetrachloride with a bromine catalyst to a mixture containing

Can. J. Chem. Downloaded from www.nrcresearchpress.com by 210.87.254.40 on 09/05/12
For personal use only.

TABLE 5. Physical properties and source of the compounds used in this study

Compound	Properties		Source or reference for procedure	Reference for literature values of properties
	E	*Z*		
Crotononitrile (**1**)	B.p. 121–122° (118–119°)	B.p. 107° (107.4°)	Eastman	7
β-Bromoacrylonitrile (**2**)	M.p. 58–59° (56–58°)	B.p. 171°*	8, 9	9
α-Bromocrotononitrile (**3**)	B.p. *E*, *Z*-mixture	63–68°/20 mm† (65–74°/40 mm)	10	10
1,2-Dibromoethene (**4**)	B.p. 108.5° (108°)	B.p. 111° (112.5°)	Eastman	7
1,2-Dichloroethene (**5**)	B.p. 49° (48°)	B.p. 60° (60°)	Eastman	7
1-Bromopropene	B.p. 63.8° (63.25°)	B.p. 59° (58–58.8°)	Aldrich	11, 12
1-Chloropropene	B.p. 37.5° (36.7°)	B.p. 32.5° (32°)	K and K	13
β-Chloroacrylonitrile	M.p. 45–46° (45–46°)	B.p. 145–146°	14	9, 14
β-Bromomethacrylonitrile	n_D^{20} 1.4995	n_D^{20} 1.4929	1	1
β-Chloromethacrylonitrile	Vinyl H τ 3.10	Vinyl H τ 3.37	15	1
β-Methylmethacrylonitrile	B.p. 136° (138°)	B.p. 122° (122°)	16‡	7

*The *Z*-isomer is newly prepared in this work. See Experimental.

†For this preparation we used potassium acetate in acetic acid for the dehydrobromination. The isomers were only partially separated on an FFAP column at 153°; however, n.m.r. peaks at 7.94 (CH_3) and 3.22 τ (H) could be assigned to the *E*-isomer having the lower retention time and peaks at 8.05 (CH_3) and 3.02 τ (H) to the *Z*-isomer having the longer retention time due to deshielding of the CH_3 or vinyl H by the CN when oriented *cis*.

‡Dehydration of the cyanohydrin of methyl ethyl ketone (16) using pyridine and thionyl chloride gave a mixture containing α-ethylacrylonitrile, angelonitrile and tiglonitrile in a ratio of 6 :80 :14 which was separated by v.p.c.

30% of the *E*-isomer. Separation by v.p.c. on a FFAP column gave β-bromoacrylonitrile (*E*), m.p. 58–59° (lit. (9), m.p. 56–58°) with n.m.r. peaks in carbon tetrachloride at 2.56 and 3.88 τ, J_{trans} = 14.9 Hz.

Support for this work from the National Research Council of Canada is gratefully acknowledged.

1. D. V. GARDNER and D. E. MCGREER. Can. J. Chem. **48**, 2104 (1970).
2. J. W. CRUMP. J. Org. Chem. **28**, 953 (1963).
3. C. REICHART. Angew. Chem. Intl. Ed. **4**, 29 (1965).
4. K. E. HARWELL and L. T. HATCH. J. Am. Chem. Soc. **77**, 1682 (1955).
5. H. VON RISSEGHEM. Bull. Soc. Chim. Belg. **28**, 376 (1919).
6. A. S. DREIDING and R. J. PRATT. J. Am. Chem. Soc. **76**, 1902 (1954).
7. Dictionary of organic compounds. Eyre and Spottiswoode Ltd. London, 1965.
8. K. ALDER, T. BROCKHAGEN, C. KAISER, and W. ROTH. Ann. **593**, 1 (1955).
9. E. GRYSZKIEWICZ-TROCHIMOWSKI, W. SCHMIDT, and O. GRYSZKIEWICZ-TROCHIMOWSKI. Bull. Soc. Chim. Fr. 593 (1948).
10. L. LECLERCQ and A. BRUYLANTS. Bull. Soc. Chim. Belg. **58**, 5 (1949).
11. G. CHAVANNE. C.R. **158**, 1698 (1914).
12. M. T. ROGERS. J. Am. Chem. Soc. **69**, 1243 (1947).
13. M. S. KHARASCH, H. ENGELMANN, and F. R. MAYO. J. Org. Chem. **2**, 288 (1937).
14. A. N. KURTZ, W. E. BILLUPS, R. B. GREENLEE, H. J. HAMIL, and W. T. PACE. J. Org. Chem. **30**, 3141 (1965).
15. C. D. HURD and C. H. RECTOR, JR. J. Org. Chem. **10**, 441 (1945).
16. J. W. BAILEY, F. E. NAYLOR, and J. J. HEWITT. J. Org. Chem. **22**, 1076 (1957).
17. J. M. CLAYTON and A. M. EASTHAM. J. Chem. Soc. 1636 (1963).

Can. J. Chem. Downloaded from www.nrcresearchpress.com by 210.87.254.40 on 09/05/12
For personal use only.

Studies of the Carbonyl Group in Some Five-membered Ring Compounds by Photoelectron Spectroscopy

A. D. BAIN AND D. C. FROST

Department of Chemistry, University of British Columbia, Vancouver 8, British Columbia

Received October 12, 1972

A study has been made of the ionization potentials (IP) of the carbonyl lone pair orbitals in a series of five-membered carbonyl ring compounds. CNDO/2 and INDO calculations have been performed on these molecules, and correlation of IP shifts with changes in molecular bonding is obtained.

Une étude a porté sur les PI(s) de la paire d'électrons libres du groupe carbonyle dans une série de composés cycliques à cinq membres possédant une fonction carbonyle. Des calculs CNDO/2 et INDO ont été effectués sur ces molécules et la corrélation dans les déplacements des PI(s) en fonction des changements dans les liaisons moléculaires est obtenue. [Traduit par le journal]

Can. J. Chem., **51**, 1245 (1973)

Can. J. Chem. Downloaded from www.nrcresearchpress.com by 210.87.254.6 on 09/05/12
For personal use only.

Introduction

Lone pair orbitals have been amenable to study by photoelectron spectroscopy (PES) (1–3) because their ionization potentials (IP's) are usually lower than other types of orbitals and they can often be easily and unambiguously assigned to a peak in the PE spectrum. Through a series of molecules these lone pairs retain much of their atomic character and so the correlation of IP shifts with changes in bonding is a valid procedure.

An orbital that is well suited to this kind of study is the lone pair of the oxygen atom of the carbonyl group. Some simple carbonyl compounds have already been studied (4–8) but this paper extends this work by presenting the carbonyl oxygen lone pair IP's of a series of five-membered ring carbonyl compounds (**1**–**9**).

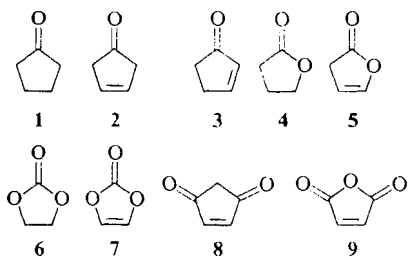

1 **2** **3** **4** **5**

6 **7** **8** **9**

The IP's for cyclopentanone (**1**), cyclopenten-2-one (**3**), and cyclopenten-3-one (**2**) were obtained from previous work (6), but for the rest of the compounds, PE spectra were taken on a spectrometer using a 584 Å light source and a $2\frac{1}{2}$ in. mean radius hemispherical analyzer, with a resolution of 20 meV (9). Also LCAO–MO–SCF calculations were performed, using the CNDO/2 and INDO methods, to help in assigning the spectra and elucidating the composition of the orbitals. The observed vertical IP's of the orbital corresponding to the carbonyl lone pair, along with the calculated IP's (the calculated orbital energy minus a 4 eV "scale factor" (10)) and the calculated charge on the carbonyl oxygen, are given in Table 1.

Discussion

All of these molecules are planar, or approximately so, and from this assumption of planarity there follows a rigorous separation of σ- and π-type orbitals. Since it is symmetric with respect to reflection in the plane of the molecule, the carbonyl oxygen lone pair orbital is of σ-symmetry. The rest of the σ-orbitals are similar in all the molecules in the series but the major difference between each of these molecules is in the π-orbitals.

However, since these π-orbitals are of different symmetry than the carbonyl lone pair, there can be no net overlap between them. This means that changes in the π-structure can only influence the carbonyl lone pair indirectly, for instance by changing the effective nuclear charge of the oxygen atom. Assuming that these indirect effects can be treated as perturbations it was thought that the results of several alterations should simply add together, since first-order perturbations are additive (11).

For example, this hypothesis states that the difference in the carbonyl lone pair IP between ethylene carbonate (**6**) (which has two oxygens

TABLE 1. Ionization potentials of the carbonyl lone pairs (eV)

Compound	Observed IP	ΔIP (relative to **1**)	ΔIP (calcd.)	Calculated IP		Charge on Oxygen	
				CNDO/2	INDO	CNDO/2	INDO
Cyclopentanone (**1**)	9.25	0	0				
Cyclopenten-2-one (**3**)	9.34	0.1	0.21				
Cyclopenten-3-one (**2**)	9.44	0.2	0.21				
α-Butyrolactone (**4**)	10.26	1.0	1.16	8.83	8.03	0.34	0.39
α-Crotonolactone (**5**)	10.70	1.5	1.37	9.74	8.72	0.31	0.36
Ethylene carbonate (**6**)	11.47	2.2	2.32	10.53	9.69	0.32	0.38
Vinylene carbonate (**7**)	11.91	2.7	2.53	10.24	9.35	0.37	0.43
Cyclopentene dione (**8**)	10.25	1.0	1.05	9.85	8.88	0.25	0.30
Maleic anhydride (**9**)	11.45	2.5	2.21	10.30	9.32	0.26	0.31

α to the carbonyl) and cyclopentanone (**1**) should be twice the difference between butyrolactone (**4**) (having only one oxygen α to the carbonyl) and cyclopentanone.

In this series of molecules there are three alterations to be considered. First, there is the substitution of an oxygen for a methylene group α to the carbonyl (the difference between butyrolactone and cyclopentanone). Second, there is the difference between the cyclopentenones (**2** and **3**) and cyclopentanone, a double bond in the ring. However, there are not enough data available here to really distinguish between the two possible positions of the double bond, because changing the position does not affect the carbonyl lone pair IP very much (the difference in this IP between the two cyclopentenones is only 0.1 eV (6)). Finally, there is the effect of a second carbonyl group at the β position in the ring. In the case of these dicarbonyl compounds there are, of course, two carbonyl lone pairs and for the purposes of assigning a shift, the mean of these two IP's was used. Because of this somewhat arbitrary use of the average IP, and also the fact that there are only two dicarbonyl compounds in the series, then the numerical parameter obtained for this case will not be very reliable.

The difference in the lone pair IP, ΔIP, between each compound and cyclopentanone was calculated and these numbers fitted to an equation of the form of eq. 1. The quantities $n_{C=C}$, n_O,

$$[1] \quad \Delta IP = n_{C=C}\,\delta_{C=C} + n_O\,\delta_O + n_{C=O}\,\delta_{C=O}$$

and $n_{C=O}$ are, respectively, the numbers of double bonds, oxygen atoms in the ring, and additional carbonyl groups (for example, vinylene carbonate has $n_{C=C} = 1$, $n_O = 2$, $n_{C=O} = 0$) and the δ's are the effects of each of these groups. The values of the δ's were obtained from a least squares fit and the results were as follows:

$$\delta_{C=C} = 0.21 \text{ eV}, \quad \delta_O = 1.16 \text{ eV}, \quad \delta_{C=O} = 0.84 \text{ eV}$$

In order to see if the dicarbonyl compounds' presence affected the other two parameters, a fit was done with just the six numbers from the monocarbonyl compounds, but the values of the parameter obtained were not significantly different.

Therefore, each of these groups stabilizes the carbonyl lone pair orbital, and for example, an oxygen atom next to the carbonyl group causes the lone pair IP to increase by about 1.2 eV. By inserting these values of the δ's back into eq. 1, calculated values for the ΔIP's were obtained and these are compared with experimental values in Table 1. It can be seen that these all agree within 0.2 eV.

Both the carbonyl group and the oxygen atom in the ring have a strong electron-withdrawing inductive effect, and the replacement of sp^3-hybridized carbons by sp^2-types, which occurs on the creation of a double bond in the ring, also has this kind of effect (6). Although these inductive effects play an important part in the observed stabilization of the carbonyl oxygen lone pair, the parameters obtained cannot be called true inductive parameters. The results of the MO calculations show that there are more subtle influences as well. For instance, the calculations predict that vinylene carbonate (**7**) will have a higher IP than crotonolactone (**5**), in agreement with experiment, but the calculations also show a greater negative charge on the carbonyl oxygen in vinylene carbonate. If the inductive effect were the only influence that caused the IP to shift, then vinylene carbonate

Can. J. Chem. Downloaded from www.nrcresearchpress.com by 210.87.254.6 on 09/05/12
For personal use only.

should have a lower IP. However, the exact nature of these other effects is not well understood at present.

Thanks are due to Dr. L. Weiler for his helpful discussions and to Dr. F. G. Herring for his assistance with the MO calculations. A.D.B. would like to thank the National Research Council of Canada for the award of a scholarship, which body also supported this work with generous financial assistance. We thank Professor C. A. McDowell for his interest in the work.

1. A. KATRIB. Ph.D. Thesis. University of British Columbia, Vancouver, B.C. 1972.
2. J. L. RAGLE, I. A. STENHOUSE, D. C. FROST, and C. A. MCDOWELL. J. Chem. Phys. **53**, 178 (1970).
3. H. BOCK and G. WAGNER. Angew. Chem. **11**, 150 (1972).
4. B. J. COCKSEY, J. H. D. ELAND, and C. J. DANBY. J. Chem. Soc. B, 790 (1971).
5. D. O. COWAN, R. GLEITER, J. A. HASHMALL, and E. HEILBRONNER. Angew. Chem. **10**, 401 (1971).
6. D. CHADWICK, D. C. FROST, and L. WEILER. J. Am. Chem. Soc. **93**, 4320 (1971).
7. D. CHADWICK, D. C. FROST, and L. WEILER. Tetrahedron Lett. 4543 (1971).
8. D. CHADWICK, D. C. FROST, and L. WEILER. J. Am. Chem. Soc. **93**, 4962 (1971).
9. G. R. BRANTON, D. C. FROST, T. MAKITA, C. A. MCDOWELL, and I. A. STENHOUSE. J. Chem. Phys. **52**, 802 (1970).
10. D. W. DAVIES. Chem. Phys. Lett. **2**, 173 (1968).
11. L. PAULING and E. B. WILSON. Introduction to quantum mechanics. McGraw-Hill, New York. 1935.

Can. J. Chem. Downloaded from www.nrcresearchpress.com by 210.87.254.6 on 09/05/12
For personal use only.

Scandium(III) Complexes of 8-Hydroxyquinoline and Derivatives

A. CORSINI, F. TONEGUZZO, AND M. THOMPSON[1]

Department of Chemistry, McMaster University, Hamilton, Ontario

Received September 20, 1972

Under the conditions specified, scandium(III) and 8-hydroxyquinoline react in aqueous solution to give $Sc(C_9H_6NO)_3 \cdot H_2O$ and not the adduct, $Sc(C_9H_6NO)_3 \cdot C_9H_7NO$, as previously reported. The adduct is formed by reaction of the aquo tris chelate in molten 8-hydroxyquinoline and the anyhdrous tris chelate is obtained by thermal decomposition of the adduct. The 2-chloro, 4-chloro, and 5-methyl and 5-nitro derivatives also yield aquo tris chelates from aqueous solution while the 2-methyl and 4-methyl derivatives give adducts.

Placé dans les conditions spécifiées le scandium(III) et l'hydroxy-8 quinoléine réagissent en solution aqueuse pour donner le $Sc(C_9H_6NO)_3 \cdot H_2O$ et non pas le produit d'addition $Sc(C_9H_6NO)_3 \cdot C_9H_7NO$ tel que rapporté antérieurement. Le produit d'addition est formé par réaction du chélate tris aquo dans l'hydroxy-8 quinoléine fondu alors que le chélate tris anhydre est obtenu par décomposition thermique du produit d'addition. Les dérivés, chloro-2, chloro-4, méthyl-5 et nitro-5 donnent aussi des chélates tris aquo à partir de solutions aqueuses alors que les dérivés méthyl-2 et méthyl-4 donnent des produits d'addition. [Traduit par le journal]

Can. J. Chem., 51, 1248 (1973)

Introduction

8-Hydroxyquinoline (QH) forms solid adducts with the general formula $MQ_n \cdot pQH$, where M is a metal ion or central group of charge n^+ (*e.g.*, $UO_2Q_2 \cdot QH$, $ThQ_4 \cdot QH$, $YQ_3 \cdot QH$, SbOQ·2QH, and NaQ·QH (1–5). In aqueous solution, the reaction between Sc(III) and QH has been reported by Pokras and Bernays to give a lemon-yellow precipitate with the formula $ScQ_3 \cdot QH$ (6, 7).

Several investigations have been made to determine the nature of the forces binding the QH molecule. On the basis of cryoscopic experiments in benzene and toluene (8), it was concluded that the QH molecule is bound in the solid merely by lattice forces. This view was favored by Van Tassel *et al.* (9) and is in contrast to recent findings regarding the adducts $UO_2Q_2 \cdot QH$ and $ThQ_4 \cdot QH$, in which X-ray, i.r., and carbon-14 techniques have shown that the QH molecule is a monodentate ligand coordinated to the metal ion through the oxygen atom, with the acidic proton being located on the nitrogen atom and strongly hydrogen-bonded (10–12). In a thermogravimetric and infrared study, Cardwell and Magee were unable to draw clear conclusions regarding the binding of QH in $ScQ_3 \cdot QH$ (13). These workers did report the preparation of two new compounds $[ScQ_3]_2 \cdot QH$ (prepared by precipitation from homogeneous solution using 8-acetoxyquinoline), and $[ScQ_3]_2 \cdot 3QH$ (prepared by a "solid-phase" reaction between $ScQ_3 \cdot QH$ and QH). Numerous attempts to thermally convert $ScQ_3 \cdot QH$ to ScQ_3 have failed (6, 7, 13–16), even though such conversions of the U(VI) and Th(IV) adducts are well-established (*e.g.*, ref. 17). In a careful study (18), Petronio and Ohnesorge reported that the complex prepared according to the procedure of Pokras and Bernays is not an adduct but simply ScQ_3, and that this composition is consistent with the failure of the thermal reaction. Petronio and Ohnesorge further reported that they could not obtain analytical data for % C and % H that were satisfactory for either ScQ_3 or $ScQ_3 \cdot QH$, using the procedure of Pokras and Bernays. Not only were the results for % C significantly lower and those for % H slightly higher than the theoretical values for the normal and adduct complexes, but the reproducibility was poor.

In view of the existing uncertainty regarding this compound, we undertook to re-examine its preparation and composition. In the present work, we confirm the view of Petronio and Ohnesorge that the compound precipitated from aqueous solution is not the adduct $ScQ_3 \cdot HQ$, but neither is it the simple normal chelate ScQ_3; it is $ScQ_3 \cdot H_2O$ (at least under the conditions described), and as discussed below, the presence of water could well account for the analytical

[1]Present address: Department of Chemistry, Loughborough University of Technology, U.K.

Can. J. Chem. Downloaded from www.nrcresearchpress.com by 210.87.254.6 on 09/05/12
For personal use only.

Can. J. Chem. Downloaded from www.nrcresearchpress.com by 210.87.254.6 on 09/05/12
For personal use only.

data obtained by Petronio and Ohnesorge. The adduct $ScQ_3 \cdot QH$ can be prepared by dissolving $ScQ_3 \cdot H_2O$ in molten QH, and ScQ_3 can be prepared by thermal treatment of $ScQ_3 \cdot QH$. Thermal dehydration of $ScQ_3 \cdot H_2O$ results in a slightly sub-stoichiometric ScQ_3 compound.

We also report the new scandium complexes of 2-chloro, 4-chloro, 4-methyl, and 5-methyl-8-hydroxyquinoline, and additional information on the previously known 2-methyl-8-hydroxyquinoline complex (14, 19–22).

Experimental

Materials

Stock solutions of scandium containing 1.57 mg/ml Sc (0.035 mmol/ml) were prepared from $ScCl_3 \cdot 6H_2O$ and standardized by EDTA titration before use (23). Hexachloro-1,3-butadiene for i.r. mulls was vacuum-distilled over BaO and then stored over molecular sieves (Type 4A). Acetic acid-d_4, ammonia-d_3, and D_2O (Stohler Isotope Chemicals) were used as supplied. 8-Hydroxyquinoline and the 2-methyl derivative (obtained commercially) were steam-distilled and recrystallized from aqueous ethanol. 2-Chloro- and 4-chloro-8-hydroxyquinoline were synthesized by the procedures of Rudolph *et al.* (24) and Pinnington (25), respectively. The 4-methyl and 5-methyl derivatives were prepared according to Phillips *et al.* (26) and Hollingshead (27), respectively.

Physical Measurements

I.r. spectra were recorded with a Beckman IR-5 spectrophotometer. Sample mulls were prepared in hexachloro-1,3-butadiene (in a dry-box, where appropriate). All spectra were recorded over the range 5000–630 cm^{-1} using NaCl windows. Thermograms were recorded in air at atmospheric pressure on a Stanton HT-D thermobalance at an initial heating rate of 1 °C/min to approximately 160 °C, and thereafter at 6 °C/min to about 600 °C, where the constant weight-level associated with Sc_2O_3 was attained. Thermal conversions *in vacuo* were done in the apparatus described previously (28). Proton magnetic resonance spectra were recorded with a Varian A-60 spectrometer. X-Ray powder photographs were obtained using CuK_α radiation emitted by a Philips PW1011 generator. Protonation (concentration) constants, $\log K_{NH}$ and $\log K_{OH}$, of the ligands were determined by potentiometric titration in 50% v/v aqueous dioxane, at 25 °C and ionic strength 0.1.

The scandium content of the complexes was determined by wet-oxidation of the sample (~0.1 g) with concentrated nitric acid (20 ml) and subsequently with hot perchloric acid (4 ml), dilution and adjustment of the p*H* to about 2.5, and titration of an aliquot of the resulting solution with EDTA, using xylenol-orange indicator (23). The accuracy was ±0.02 mg Sc. The ligand content of the complexes was determined bromometrically (29), with an accuracy of ±0.1–0.2 mg ligand. Microanalyses (C, H, and N) reported in this work were performed by Alfred Bernhardt, Elbach über Engelskirchen, West Germany.

Preparation of Complexes

$ScQ_3 \cdot H_2O$

From the stock Sc solution, 7.35 ml (0.26 mmol Sc) were diluted with 100 ml of water and warmed to 70–80 °C. Ten ml of QH solution (2.26% w/v in 2 *M* acetic acid) containing 1.56 mmol QH and 45 ml of a buffer solution (30 ml 2 *M* ammonium acetate and 15 ml 2 *M* ammonia) were added, the latter solution by dropwise addition with stirring. The resulting suspension was stirred for 1 h. The lemon-yellow precipitate was filtered hot (p*H* of the cooled filtrate was 7.8–8.0) and washed with 100 ml of water at 70–80 °C. The compound was dried *in vacuo* at 40 °C (overnight) and at 100 °C (14 h). For each drying condition, the analytical data indicated the same composition. The data for 40 °C precede that for 100 °C (in brackets) below.

Anal. Calcd. for $Sc(C_9H_6NO)_3 \cdot H_2O$: C, 65.46; H, 4.07; N, 8.48; Sc, 9.07, $C_9H_6NO^-(Q^-)$, 87.29. Found: C, 65.84 (65.24); H, 4.00 (4.17); N, 8.75 (8.59); Sc, 9.02 ± 0.01 (9.05 ± 0.01); Q^-, 86.8 ± 0.2 (87.2 ± 0.2); Q^-:Sc ratio, 3.00:1 (3.00:1).

The data for Sc and Q^- represent the average of three determinations on three seperate preparations for each drying condition.

The compound was also prepared as above using deuterated reagents and D_2O as solvent. Samples of the nondeuterated and deuterated compounds dried at 100 °C were retained for infrared analysis.

The effect of p*H* on the composition was studied over the p*H* range 5–8 by varying the amount of buffer solution added. The filtered compounds were dried overnight at 100 °C and samples taken for wet-chemical, molecular weight and p.m.r. analysis.

The effect of QH concentration on the composition of the precipitate was also investigated. The above procedure was used except that 10 ml of the Sc solution (0.35 mmol Sc) were taken and 10 ml of a 5.0, 3.5, 3.0, 2.5, and 2.0% w/v solution of QH in 2 *M* acetic acid were added (corresponding to 3.45, 2.41, 2.07, 1.72, and 1.38 mmol of QH, respectively). The procedure with 3.45 mmol of QH closely approximated that used by Pokras and Bernays (7). In a further study, this procedure was modified by precipitating the compound from a mixed aqueous organic solvent in which the final precipitation medium was 10% v/v aqueous acetone. In all cases, the filtered compound was dried overnight at 40 °C *in vacuo*. The analytical data are summarized in Table 1.

$ScQ_3 \cdot QH$

This complex was prepared from molten QH as follows. One hundred mg of $ScQ_3 \cdot H_2O$ (0.20 mmol) were thoroughly mixed with 145 mg of QH (1.00 mmol). The yellow mixture was ground to a fine powder and placed in an air-oven at 90 °C. Near the m.p. of QH (73 °C), the color turned orange. Above 80 °C, a homogeneous melt was obtained. Heating was continued for 30 min at 90 °C. On cooling, an orange glass was obtained which was ground to a fine powder and heated over night *in vacuo* at 100 °C to remove the excess (unbound) QH. The solid was reground and reheated to yield a bright-orange compound.

Anal. Calcd. for $ScQ_3 \cdot QH$: Sc, 7.22; Q^-, 92.62. Found: Sc, 7.05; Q^-, 92.3; Q^-:Sc ratio, 4.08:1.

Similarly, the compound was prepared from $ScQ_3 \cdot D_2O$

TABLE 1. Effect of QH concentration and solvent on the Sc(III)–QH complex

Solvent	QH added* (mmol)	% Q^- found†	% Sc found†	Sum (%)	Q^-:Sc ratio found
Aqueous	3.45	90.1	6.92	97.0	4.06:1‡
Aqueous	2.41	89.7	7.14	96.8	3.91:1
Aqueous	2.07	89.2	7.24	96.4	3.84:1
Aqueous	1.72	87.2	8.79	96.0	3.09:1
Aqueous	1.38	87.4	8.99	96.4	3.04:1
10% v/v aqueous acetone	3.45	87.8	7.95	95.8	3.40:1

*In all preparations, Sc taken was 0.35 mmol.
†Average of a single determination on two different preparations (maximum deviation, ±0.2%).
‡This compound was prepared by the procedure of Pokras and Bernays. Found: C, 67.00; H, 4.09; N, 8.65. Compare with last line, Table 2.

TABLE 2. Calculated percentages of possible Sc(III)–QH complexes

Compound	C (%)	H (%)	N (%)	Sc (%)	Q^- (%)
ScQ_3	67.93	3.80	8.80	9.42	90.58
$ScQ_3 \cdot H_2O$	65.46	4.07	8.48	9.07	87.29
$ScQ_3 \cdot NH_3$	65.59	4.27	11.33	9.09	87.46
$ScQ_3 \cdot QH$	69.45	4.05	9.00	7.22	92.62

TABLE 3. Effect of 2-Me-QH concentration and solvent on the Sc(III)–2-Me-QH complex

Solvent	2-Me-QH added* (mmol)	% 2-Me-Q^- found†	% Sc found†	Sum (%)	2-Me-Q^-:Sc ratio found
Aqueous	3.51	90.0	6.09	96.1	4.20:1
		89.4	6.12	95.5	4.15:1
Aqueous	2.07	88.4	6.26	94.7	4.01:1
		93.1‡	6.65	99.8	3.98:1
Aqueous	1.44	88.3	7.16	95.5	3.50:1
10% v/v aqueous acetone	3.51	88.3	6.28	94.6	3.99:1
		88.5	6.29	94.8	4.00:1

*In all preparations, Sc taken was 0.35 mmol.
†Anal. Calcd. for $Sc(2\text{-Me-}Q)_3$; Sc, 8.65; 2-Me-Q^-, 91.35.
Anal. Calcd. for $Sc(2\text{-Me-}Q)_3 \cdot (2\text{-Me-QH})$: Sc, 6.62; 2-Me-$Q^-$, 93.23.
Anal. Calcd. for $Sc(2\text{-Me-}Q)_3 \cdot (2\text{-Me-QH}) \cdot 2H_2O$: Sc, 6.29; 2-Me-$Q^-$, 88.53.
‡Data in this row for samples dried at 95 °C. All other samples dried at 40 °C.

TABLE 4. Analytical data for Sc(III) complexes of QH derivatives

Formula	Calculated (%)		Found (%)		Sum (%)	Ligand:Sc ratio found
	Ligand anion	Sc	Ligand anion	Sc		
$Sc(4\text{-Me-}Q)_3 \cdot H_2O$	88.28	8.36				
$Sc(4\text{-Me-}Q)_3 \cdot (4\text{-Me-QH})$	93.23	6.62	92.5	6.57	99.1	4.00:1
$Sc(2\text{-Cl-}Q)_3 \cdot H_2O$	89.48	7.51	89.9	7.11	97.0	3.2:1
$Sc(2\text{-Cl-}Q)_3 \cdot (2\text{-Cl-QH})$	93.95	5.91				
$Sc(4\text{-Cl-}Q)_3 \cdot H_2O$	89.48	7.51	88.0	7.43	95.4	3.0:1
$Sc(4\text{-Cl-}Q)_3 \cdot (4\text{-Cl-QH})$	93.95	5.91				
$Sc(5\text{-Me-}Q)_3 \cdot H_2O$	88.28	8.36	89.5	8.07	97.6	3.2:1
$Sc(5\text{-Me-}Q)_3 \cdot (5\text{-Me-QH})$	93.23	6.62				

Can. J. Chem. Downloaded from www.nrcresearchpress.com by 210.87.254.6 on 09/05/12
For personal use only.

Can. J. Chem. Downloaded from www.nrcresearchpress.com by 210.87.254.6 on 09/05/12
For personal use only.

and molten QD. An atmosphere saturated with D_2O was used to minimize deuterium–hydrogen exchange due to moisture.

$Sc(2\text{-}Me\text{-}Q)_3 \cdot (2\text{-}Me\text{-}QH) \cdot 2H_2O$

The compound was prepared as described for $ScQ_3 \cdot H_2O$ except that 10 ml of Sc solution (0.35 mmol Sc) and 10 ml of a 3.3% w/v solution of 2-Me-QH in a 2 *M* acetic acid (2.07 mmol) were taken and the final p*H* was adjusted to 8.3–8.5 with the buffer solution. The bright yellow compound was dried *in vacuo* overnight at 40 °C and then at 95 °C for 1 h. At the latter temperature, the anhydrous compound $Sc(2\text{-}MeQ)_3 \cdot (2\text{-}Me\text{-}QH)$ was obtained. Analytical data are reported in Table 3, together with data for compounds obtained when 3.51 and 1.44 mmol of 2-Me-QH were used, and when the precipitation medium was 10% v/v aqueous acetone.

$Sc(4\text{-}Me\text{-}Q)_3 \cdot (4\text{-}Me\text{-}QH)$

The procedure was identical to that for the 2-Me-QH complex except that the yellow precipitate was dried overnight *in vacuo* at 95 °C. Analytical data are given in Table 4.

$Sc(2\text{-}Cl\text{-}Q)_3 \cdot H_2O$, $Sc(4\text{-}Cl\text{-}Q)_3 \cdot H_2O$, and $Sc(5\text{-}Me\text{-}Q)_3 \cdot H_2O$

To 10 ml of the Sc solution were added 2.79 mmol of 2-Cl-QH (or 3.50 mmol of 4-Cl-QH or 5-Me-QH) dissolved in 18 ml of acetone, 80 ml of water, and 10 ml of 2 *M* acetic acid. The mixture was heated to 60–70 °C and 50 ml of the buffer solution were added dropwise with stirring (p*H* ~ 8.5). After 15 min, the yellow precipitate was filtered hot, washed with 150 ml of warm water and dried for 4–12 h at 95 °C *in vacuo*. Analytical data are given in Table 4.

Determination of Water Content

The water content in all complexes sufficiently soluble in anhydrous methanol was determined by titration with stabilized Karl Fischer reagent. The necessary precautions to exclude atmospheric moisture from the titration assembly and the reaction vessel were taken (30). The KF reagent was standardized prior to each series of titrations with a methanol solution containing a known amount of water (2 mg H_2O/ml CH_3OH). The water content of the essentially anhydrous methanol solvent was determined in a blank titration. The amount of the complexes taken for analysis (150–250 mg) was limited by their solubility in methanol and provided only about 5–8 mg H_2O for determination. The volume of methanol solvent was kept small (usually 25 ml) to limit the magnitude of the blank correction. Each result below is the average of at least two titrations.

% H_2O calculated for $ScQ_3 \cdot H_2O$: 3.64. Found: 3.97.

% H_2O calculated for $Sc(2\text{-}Me\text{-}Q)_3 \cdot (2\text{-}Me\text{-}QH) \cdot 2H_2O$: 5.03. Found: 5.32.

No water was found in the compounds $Sc(2\text{-}Me\text{-}Q)_3 \cdot (2\text{-}Me\text{-}QH)$ and $Sc(4\text{-}Me\text{-}Q)_3 \cdot (4\text{-}Me\text{-}QH)$ prepared and dried as described above. The solubility of $Sc(2\text{-}Cl\text{-}Q)_3 \cdot H_2O$, $Sc(4\text{-}Cl\text{-}Q)_3 \cdot H_2O$ and of $Sc(5\text{-}Me\text{-}Q)_3 \cdot H_2O$ was too low to allow a meaningful titration.

Results and Discussion

The procedure described by Pokras and Bernays for the preparation of $ScQ_3 \cdot QH$ is not clear. In particular, it is uncertain whether 0.03 mmol of scandium were taken as stated (7), or whether ~0.3 mmol were taken as calculated from the amounts of Sc_2O_3 given in Tables 2 and 3 of ref. 7. In an additional report (6), the amount of Sc_2O_3 taken (Table 1) corresponds to ~0.3 mmol. Depending on which figure is used, the molar ratio of QH:Sc taken for the preparation was either 100:1 or 10:1. Since 10:1 is considered more likely, ~0.3 mmol of scandium were used in the present study. The analytical data for the compound obtained by the assumed procedure of Pokras and Bernays are given in Table 1 (first row), together with data for compounds prepared by using smaller amounts of QH or prepared from an aqueous acetone medium. At first glance, the Q^-:Sc ratio (4.06:1) found for Pokras and Bernays' compound suggests support for their proposed composition, $ScQ_3 \cdot QH$. It is noteworthy, however, that the % Q^- and % Sc values are in poor agreement with this composition (compare with last line of Table 2) and that their sum is only 97%. Indeed, when smaller amounts of QH were used, the Q^-:Sc ratio decreased to nearly 3.00:1, and the % Q^- and % Sc values approached good agreement with the composition $ScQ_3 \cdot H_2O$ (compare with the second line of Table 2). Furthermore, when acetone was present in the precipitation medium, the Q^-:Sc ratio was reduced to 3.4:1 and the sum of % Q^- and % Sc was only about 96%. These results suggest that the compound reported by Pokras and Bernays is not $ScQ_3 \cdot QH$ but $ScQ_3 \cdot X$ (where X is a moiety of molecular weight such that the sum of % Sc and Q^- is ~96%) contaminated by QH. This compound could not be heated to constant weight at 105 °C (in air) but continued to lose weight slowly for several days, probably because of slow volatilization of the contaminant.

To reduce the risk of contamination by QH, which has only limited solubility in weakly basic aqueous solution, Pokras and Bernays' procedure was altered by lowering the amount of QH used from 3.45 to 1.56 mmol. The amount of Sc was slightly lowered (to 0.26 mmol) to give a QH:Sc ratio of 6:1. Because the presence of the moiety X was suspected, the drying temperature was lowered from 110 °C to 40 °C. As shown in the Experimental, elemental analysis yielded data that agreed well with the composition $ScQ_3 \cdot H_2O$; furthermore the compound could be safely dried at 100 °C. The presence of H_2O

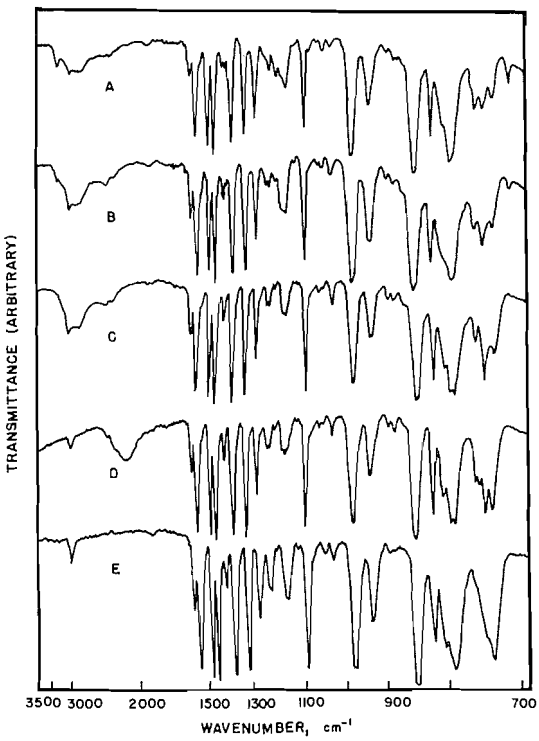

FIG. 1. Infrared spectra of Sc(III) complexes of 8-hydroxyquinoline: (*A*) Pokras and Bernays' compound, (*B*) compound precipitated from 10% v/v aqueous acetone, (*C*) $ScQ_3 \cdot H_2O$, (*D*) $ScQ_3 \cdot D_2O$, and (*E*) thermal product, ScQ_3.

was confirmed by infrared spectra (below) and by heating the complex *in vacuo* at 160 °C and trapping the evolved water in a U-tube. Titration with Karl Fischer reagent confirmed the presence of one water molecule in the complex.

The 3.00:1 ratio found for Q^-:Sc confirms the finding of Petronio and Ohnesorge (18) that the compound is not $ScQ_3 \cdot QH$. These workers reported the compound to be ScQ_3 but pointed out that the results of carbon determinations were appreciably lower and those for hydrogen slightly higher than the calculated values for ScQ_3. However, it is noteworthy that their average values for % C (65.63) and % H (4.16) are in good agreement with the calculated values based on $ScQ_3 \cdot H_2O$ (65.46, 4.07), although this observation may be fortuitous in view of the poor precision of the data. Petronio and Ohnesorge suggested that the poor precision of the data (not only from different samples but also from the same sample) could be reconciled if the compound ScQ_3 is hygroscopic after drying at 110–120 °C. This suggestion is reasonable since we observed that loss of water from $ScQ_3 \cdot H_2O$ begins at about 120 °C. The milder drying conditions used in the present work minimized the loss of water and afforded reproducible data.

The i.r. spectra of Pokras and Bernays' compound, the compound prepared from 10% v/v aqueous acetone, and the proposed complex $ScQ_3 \cdot H_2O$ are shown in Fig. 1, spectra *A*, *B*, and *C* respectively. Two significant features are apparent. Firstly, the three spectra are very similar except that the weak bands at 3330, 1410, and 710 cm^{-1} in spectrum *A* are reduced in intensity in spectrum *B* (relative to other bands in the spectrum), and are absent in spectrum *C*. The bands at 1410 and 710 cm^{-1} are present in the spectrum of pure QH (not shown). The band at 3300 cm^{-1} (ν_{OH}) is shifted from the center (3100 cm^{-1}) of the very broad OH band in the spectrum of QH, probably because of a lower order of intermolecular hydrogen bonding. The decrease in intensity of the three bands is consistent with a decrease in the Q^-:Sc molar ratio from 4.06:1 to 3.00:1. Thus, the bands are likely due to contaminating reagent. Secondly a broad band centered at 2900 cm^{-1} is present in all three spectra. The spectrum *D*, Fig. 1, of the complex precipitated from D_2O solution shows the 2900 cm^{-1} band shifted to 2150 cm^{-1}, proving that the absorption is protonic ($\nu_H/\nu_D = 1.34$). This band is absent (*E*, Fig. 1) after the compound has been heated at 160 °C *in vacuo* to remove the water. (The band at about 3000 cm^{-1} in spectra *D* and *E* is ν_{CH}.) Similar broad bands have been found in the i.r. spectra of the complexes $MgQ_2 \cdot 2H_2O$, $BiQ_3 \cdot H_2O$, $ZnQ_2 \cdot 2H_2O$, $NiQ_2 \cdot 2H_2O$, and $Be_2OQ_2 \cdot 2H_2O$ (31–33). The OH stretching modes of these compounds occur in the range 3300–3600 cm^{-1}. The 2900 cm^{-1} frequency is unusually low by comparison; this is likely the result of stronger hydrogen-bonding (34) and/or stronger coordination of the water molecule to the scandium atom (35).

From the results above, it appears that the extra reagent in Pokras and Bernays' compound is due to contamination of $ScQ_3 \cdot H_2O$ by coprecipitation. The powder diffraction lines of the compound do not contain lines from QH or $ScQ_3 \cdot H_2O$. Therefore, the compound is not a bi-crystalline mixture of the latter two components, and the extra reagent is likely incorporated into the $ScQ_3 \cdot H_2O$ crystal by occlusion.

Can. J. Chem. Downloaded from www.nrcresearchpress.com by 210.87.254.6 on 09/05/12
For personal use only.

Can. J. Chem. Downloaded from www.nrcresearchpress.com by 210.87.254.6 on 09/05/12
For personal use only.

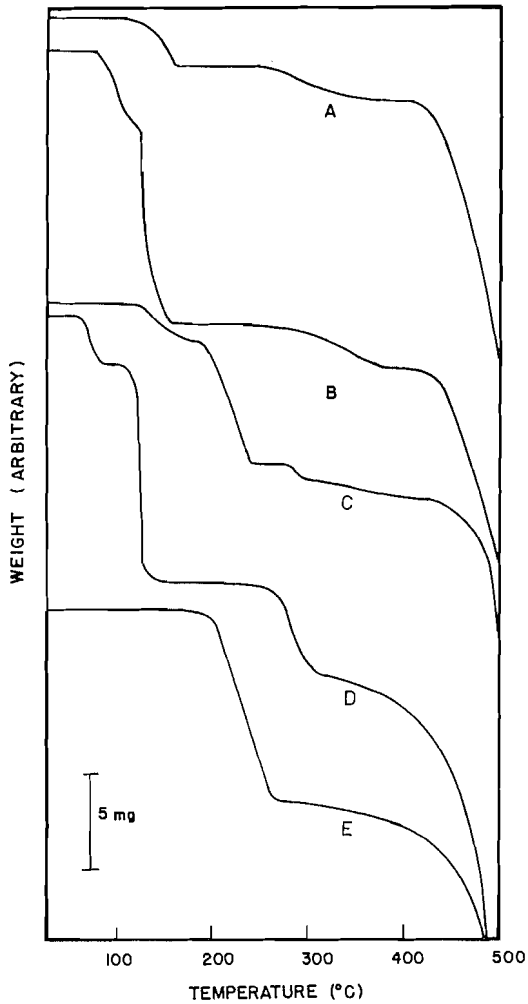

FIG. 2. Thermograms of (*A*) $ScQ_3 \cdot H_2O$ (initial weight, 58.9 mg), (*B*) Pokras and Bernays' compound (58.6 mg), (*C*) melt product $ScQ_3 \cdot QH$ (32.9 mg), (*D*) $Sc(2\text{-Me-Q})_3 \cdot (2\text{-Me-QH}) \cdot 2H_2O$ (55.1 mg), and (*E*) $Sc(4\text{-Me-Q})_3 \cdot (4\text{-Me-QH})$ (45.6 mg).

The thermogram (*A*, Fig. 2) of $ScQ_3 \cdot H_2O$ shows that loss of H_2O occurs over the range 120–160 °C. The constant-weight level associated with ScQ_3 occurs in the range 160–240 °C. Ultimately, the compound decomposes to Sc_2O_3 at approximately 600 °C. Pokras and Bernays' compound (*B*, Fig. 2) loses both the bound water and extra reagent in the range 75–160 °C to yield ScQ_3. Analysis of several samples of $ScQ_3 \cdot H_2O$ heated in the temperature range 160–240 °C *in vacuo* revealed that removal of water results in a slightly substoichiometric compound. In all experiments, a small amount of QH was evolved (1–3 mg from 100 mg of hydrate), and a residue deficient in Q^- (Q^-:Sc ratios in the range 2.86–2.92) remained. The ligand deficiency is likely the result of solid-phase hydrolysis of the hydrate according to the following thermal reactions:

$$ScQ_3 \cdot H_2O \rightarrow ScQ_2 \cdot OH + QH$$

$$ScQ_2 \cdot OH \rightarrow ScQ \cdot O + QH$$

The reaction occurs only to a small extent, the major process being the total removal of water from the hydrate. Similar behavior has been observed for other QH complexes such as $MgQ_2 \cdot 2H_2O$, $BaQ_2 \cdot 4H_2O$, and $Be_2OQ_2 \cdot 2H_2O$ (33, 36), and for the rare-earth acetylacetonates $Ln(acac)_3 \cdot nH_2O$ (37) and dibenzoyl-methides $Ln(dby)_2 \cdot H_2O$ (38). Muetterties and Wright (39) have suggested that the hydrolysis of the rare-earth complexes indicates a significant bonding interaction between the metal atoms and the oxygen atom of the water molecule. The monohydrate phases may well contain hepta-coordinate metal atoms. Therefore, in $ScQ_3 \cdot H_2O$, the water molecule is likely coordinated to the scandium atom, but an X-ray or neutron diffraction structural determination is required to decide this point.

In the preparation of $ScQ_3 \cdot H_2O$, the effect of p*H* on the composition of the precipitate was examined over the p*H* range 5–8, and a marked effect was noted. The compound $ScQ_3 \cdot H_2O$ was obtained only between p*H* 7–8. Between p*H* 5–6.8, the composition could be formulated as $Sc(Q)_{3-x}(OAc)_x$, where OAc^- is acetate and $x = 0.4$ at p*H* 5.0 and 0.2 at p*H* 6.8. The Q^-:Sc ratio of the compounds varied from 2.59:1 to 2.78:1 from p*H* 5.0 to 6.8, respectively. The compound precipitated at p*H* 6.2 (Q^-:Sc = 2.70:1) was taken to be representative and studied in more detail. The p.m.r. spectrum in DMSO exhibited a sharp singlet at 1.72 p.p.m. characteristic of the acetate methyl group; this band is not present in the spectrum of $ScQ_3 \cdot H_2O$. Integration of the spectrum gave 17:1 for the 8-hydroxyquinoline–anion and acetate – anion proton ratio. This ratio compares favorably with the ratio 18:1 for the formula $Sc(Q)_{2.7}(OAc)_{0.3}$ arrived at from the analytical data. These acetate complexes are most likely associated or polymerized in the solid phase. A molecular weight determination of $Sc(Q)_{2.7}(OAc)_{0.3}$ (calculated molecular weight, 452) by vapor-phase osmom-

Can. J. Chem. Downloaded from www.nrcresearchpress.com by 210.87.254.6 on 09/05/12
For personal use only.

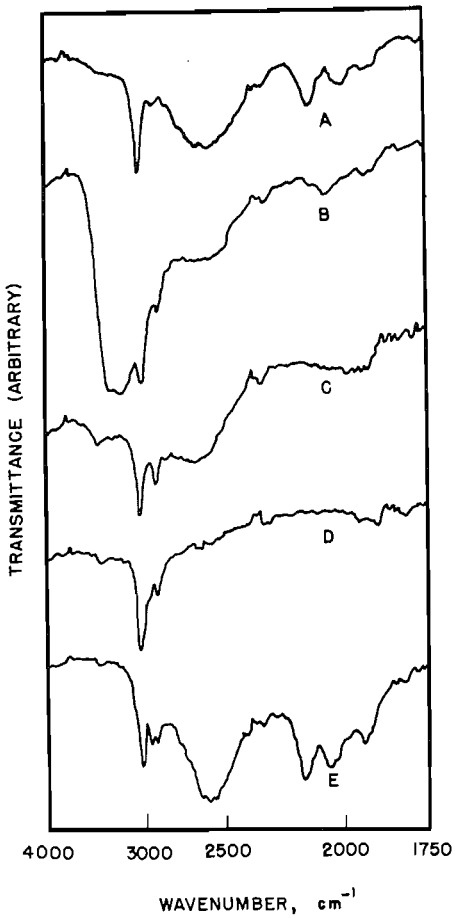

FIG. 3. Infrared spectra of (*A*) melt product $ScQ_3 \cdot QH$, (*B*) $Sc(2\text{-Me-Q})_3 \cdot (2\text{-Me-QH}) \cdot 2H_2O$, (*C*) $Sc(2\text{-Me-Q})_3 \cdot (2\text{-Me-QH})$, (*D*) $Sc(2\text{-Me-Q})_3$, and (*E*) $Sc(4\text{-Me-Q})_3 \cdot (4\text{-Me-QH})$.

etry gave a value of 760, suggestive of some degree of association in benzene solution.

The product, $[ScQ_3]_2 \cdot 3QH$, from the "solid-phase" reaction between $ScQ_3 \cdot QH$ and QH described by Cardwell and Magee (13) was re-examined. It was presumed that $ScQ_3 \cdot H_2O$ was the reactant rather than $ScQ_3 \cdot QH$. The color change from yellow to bright-orange upon formation of the melt suggests that the reaction does not occur in the solid-phase but in molten QH in which $ScQ_3 \cdot H_2O$ dissolves. Analysis showed the bright-orange product to be $ScQ_3 \cdot QH$, replacement of H_2O by QH having occurred.

The i.r. spectrum (*A*, Fig. 3) of $ScQ_3 \cdot QH$ shows bands centered at 2600 and 2100 cm^{-1} that are characteristic of hydrogen-bonded $>\overset{+}{N}H$ (11, 12, 40); the broad water band at 2900 cm^{-1} is absent. The spectrum (not shown) of the product obtained from molten QD showed a significant reduction in intensity at 2600 cm^{-1} and a broadening of the band intensity at 2100 cm^{-1} ($\nu_H/\nu_D = 1.25$), confirming that the vibrations are protonic. The bands are identical to those observed for the QH adducts of U(VI) and Th(IV) (11, 12, 40). As with the U(VI) and Th(IV) adducts, the additional molecule of reagent in the Sc(III) adduct is likely monodentate and bound to the metal atom through the oxygen atom. (The disposition of the water molecule in $ScQ_3 \cdot H_2O$ may well be similar.) If it is assumed that the complex exists as a monomer in the solid-phase, the result suggests that the scandium is hepta-coordinate in the complex. No examples of hepta-coordinate scandium have been reported in the literature, although several examples of hexa-coordination and a few of octa-coordination are documented (41).

The thermogram (*C*, Fig. 2) of $ScQ_3 \cdot QH$ shows the loss of the extra HQ molecule over the temperature range 130–240 °C. The constant weight level associated with lime-green ScQ_3 occurs in the range 240–280 °C. As expected, the i.r. spectrum (not shown) of ScQ_3 shows the disappearance of the $>\overset{+}{N}H$ bands.

Interestingly, and unlike QH, the compound precipitated from aqueous solution by 2-Me-QH is the adduct (Table 3): this result confirms the finding of Phillips *et al.* (19). If the amount of reagent used is too large, contamination occurs, resulting in too high a 2-Me-Q^-:Sc ratio (Table 3). Contamination can be overcome by the presence of acetone in the solvent medium. Too low a concentration of the ligand leads to a substoichiometric product. The composition of the compound is $Sc(2\text{-Me-Q})_3 \cdot (2\text{-Me-QH}) \cdot 2H_2O$ when dried at 40 °C and $Sc(2\text{-Me-Q})_3 \cdot (2\text{-Me-QH})$ when dried at 95 °C (see Table 3 and Karl Fischer titration data in Experimental). Phillips *et al.* (19) reported the composition of the precipitated complex as the anhydrous adduct but the drying temperature used (100 °C) was adequate for the removal of water from the complex.

The infrared spectrum (*B*, Fig. 3) of the compound dried at 40 °C features an intense broad band at 3200 cm^{-1}, which confirms the

Can. J. Chem. Downloaded from www.nrcresearchpress.com by 210.87.254.6 on 09/05/12
For personal use only.

presence of water. The breadth and position of the band indicate water of hydration rather than contaminating moisture. Moisture bands in the i.r. spectra of complexes usually occur at higher frequency (~3400 cm^{-1}) and are considerably less broad and intense. The spectrum also shows broad bands at 2650 and 2070 cm^{-1} characteristic of hydrogen-bonded $\rangle\overset{+}{N}H$, although the band at 2650 cm^{-1} is somewhat overlapped with the broad water band at 3200 cm^{-1}. The sharp peaks at about 3000 and 2900 cm^{-1} represent ν_{CH} (aromatic and aliphatic, respectively).

The thermogram (*D*, Fig. 2) of Sc(2-Me-Q)$_3$·(2-Me-QH)·2H_2O shows a weight loss at 70 °C and then a constant-weight level over the range 80–100 °C. Chemical analysis showed this level to correspond closely to the yellow anhydrous compound Sc(2-Me-Q)$_3$·(2-Me-QH). A further weight loss occurs at 105 °C followed by a constant-weight level over the range 150–240 °C; analysis of the Sc and ligand content (see Experimental) showed this level to be associated with the lime-green complex Sc(2-Me-Q)$_3$. The i.r. spectrum of Sc(2-Me-Q)$_3$·(2-Me-QH) (*C*, Fig. 3) shows the removal of the water band, and that of Sc(2-Me-Q)$_3$ (*D*, Fig. 3) the disappearance of the $\rangle\overset{+}{N}H$ bands. As suggested above from infrared data, X-ray powder diffraction studies indicated that the water in the complex is not likely present as moisture; Sc(2-Me-Q)$_3$·(2-Me-QH) has a different powder pattern (and therefore crystal structure) from that of Sc(2-Me-Q)$_3$·(2-Me-QH)·2H_2O. The thermal removal of moisture would not affect the powder pattern in this manner. The low temperature required for removal of the water suggests, however, that it is not coordinated to the scandium.

The ligand 4-Me-QH also forms an adduct with Sc(III) (Table 4). The adduct is anhydrous (confirmed by Karl Fischer titration) although the higher drying temperature could conceivably have removed water of hydration. The i.r. spectrum (*E*, Fig. 3) of Sc(4-Me-Q)$_3$·(4-Me-QH) shows $\rangle\overset{+}{N}H$ bands at 2650, 2150, and 2050 cm^{-1}. The thermogram of the adduct (*E*, Fig. 2) shows a weight-loss occurring initially at 190 °C, with a discontinuity at 270 °C corresponding to the composition of the lime-green complex Sc(4-Me-Q)$_3$, as shown by elemental analysis of the residue. In the i.r. spectrum of the latter

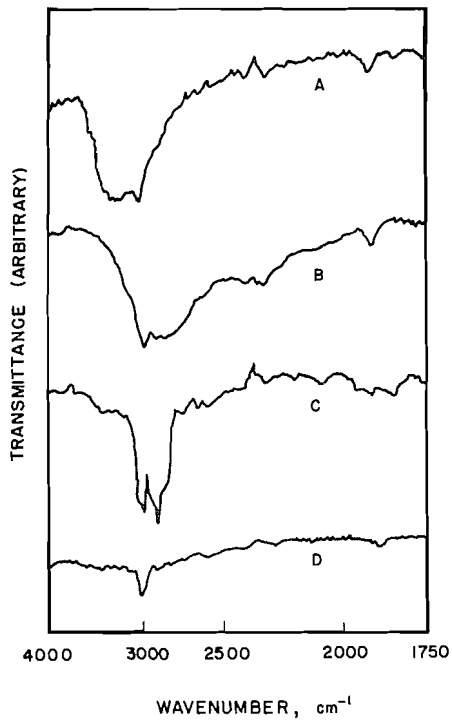

FIG. 4. Infrared spectra of (*A*) Sc(2-Cl-Q)$_3$·H_2O, (*B*) Sc(4-Cl-Q)$_3$·H_2O, (*C*) Sc(5-Me-Q)$_3$·H_2O, and (*D*) Sc(4-Cl-Q)$_3$.

(not shown), the $\rangle\overset{+}{N}H$ bands are not present.

The i.r. spectra of the 2-Cl-QH, 4-Cl-QH, and 5-Me-QH complexes (Fig. 4; *A*, *B*, and *C*, respectively) do not show the presence of $\rangle\overset{+}{N}H$ bands. Broad bands in the region 2900–3200 cm^{-1} suggest the presence of water. Limited analytical data (Table 4) indicate the compositions Sc(2-Cl-Q)$_3$·H_2O, Sc(4-Cl-Q)$_3$·H_2O, and Sc(5-Me-Q)$_3$·H_2O, but the amount of water present could not be confirmed by Karl Fischer titration because of the low solubility of these complexes in methanol. The water could be readily removed from Sc(4-Cl-Q)$_3$·H_2O by heating at 170 °C *in vacuo* to yield Sc(4-Cl-Q)$_3$, as shown by elemental analysis. The water band is absent in the i.r. spectrum (*D*, Fig. 4). Presumably, the other complexes behave similarly. The very low solubility of the ligands in aqueous media increased the risk of contamination of the complexes. In view of this and the limited amount of data, the composition reported for these complexes should be regarded as tentative.

In summary, two main classes of compounds

are formed by reaction between Sc(III) and 8-hydroxyquinoline and derivatives in aqueous solution: aquated tris chelates and adduct complexes. The parent ligand QH, and the 2-chloro, 4-chloro, and 5-methyl derivatives precipitate Sc(III) as the aquo tris chelates, while the 2-methyl and 4-methyl derivatives yield the adducts in which the extra ligand is coordinated as a monodentate (zwitterion) ligand, as in the U(VI) and Th(IV) complexes of QH (12, 40). It appears that there is a competition between the monodentate ligand and water for a coordination site. The competition is well illustrated by the displacement of water in $ScQ_3 \cdot H_2O$ by QH on dissolution of the compound in molten QH. The reason for the difference in behavior between these two groups of ligands in not obvious. Of the properties considered (solubility of the reagents, steric properties of the substituents, and basicity of the ligand nitrogen and oxygen atoms), the only apparent correlation is with nitrogen basicity. The nitrogen protonation constants (log K_{NH}) of 2-Me-QH and 4-Me-QH (4.75 and 4.85, respectively) are appreciably higher, on the whole, than those of the ligands forming tris complexes (2-Cl-QH, 2.0; 4-Cl-QH, 2.83; QH, 4.12; 5-Me-QH, 4.27). Since the tendency for zwitterion formation both in solution and in the complex is increased with increasing nitrogen basicity, it is possible that the formation of the aquo or adduct complex is determined, at least in part, by nitrogen basicity. If this is so, then the pK_{NH} value for QH and 5-Me-QH must be very close to the threshhold pK_{NH} value at which adduct formation is favored.

We wish to thank the National Research Council of Canada for the financial support of this study. One of us (M.T.) is indebted to the International Nickel Company of Canada for a Fellowship.

1. F. HECHT and W. REICH-ROHRWIG. Monatsh. 53–54, 596 (1929).
2. F. J. FRERE. J. Am. Chem. Soc. **55**, 4362 (1933).
3. T. J. CARDWELL and R. J. MAGEE. Anal. Chim. Acta, **43**, 321 (1968).
4. T. J. CARDWELL, F. G. NASOURI, H. H. MCCONNELL, and R. J. MAGEE. Aust. J. Chem. **21**, 359 (1968).
5. A. K. BANERJEE, A. J. LAYTON, R. S. NYHOLM, and M. R. TRUTER. J. Chem. Soc. (A), 2536 (1969).
6. L. POKRAS and P. M. BERNAYS. J. Am. Chem. Soc. **73**, 7 (1951).
7. L. POKRAS and P. M. BERNAYS. Anal. Chem. **23**, 757 (1951).
8. L. POKRAS, M. KILPATRICK, and P. M. BERNAYS. J. Am. Chem. Soc. **75**, 1254 (1953).
9. J. H. VAN TASSEL, W. W. WENDLANDT, and E. STURM. J. Am. Chem. Soc. **83**, 810 (1961).
10. D. HALL, A. D. RAE, and T. N. WATERS. Acta Cryst. **22**, 258 (1967).
11. A. CORSINI, J. ABRAHAM, and M. THOMPSON. Chem. Commun. 1101 (1967).
12. J. ABRAHAM and A. CORSINI. Anal. Chem. **42**, 1528 (1970).
13. T. J. CARDWELL and R. J. MAGEE. Anal. Chim. Acta, **36**, 180 (1966).
14. G. R. HORTON and W. W. WENDLANDT. J. Inorg. Nucl. Chem. **25**, 241 (1963).
15. W. W. WENDLANDT. Anal. Chem. **28**, 499 (1956).
16. G. R. HORTON and W. W. WENDLANDT. Anal. Chem. **34**, 1098 (1962).
17. A. CORSINI and J. ABRAHAM. Can. J. Chem. **47**, 1435 (1969).
18. J. N. PETRONIO and W. E. OHNESORGE. Anal. Chem. **39**, 460 (1967).
19. J. P. PHILLIPS, J. F. EMERY, and H. P. PRICE. Anal. Chem. **24**, 1033 (1952).
20. W. W. WENDLANDT. Anal. Chim. Acta, **17**, 274 (1957).
21. J. H. VAN TASSEL and W. W. WENDLANDT. J. Am. Chem. Soc. **82**, 4821 (1960).
22. G. R. HORTON and W. W. WENDLANDT. J. Inorg. Nucl. Chem. **25**, 247 (1963).
23. R. PRIBIL and V. VESELY. Talanta, **11**, 1545 (1954).
24. T. RUDOLPH, F. PRYSTAL, and J. P. PHILLIPS. J. Med. Pharm. Chem. **10**, 981, 1967.
25. A. R. PINNINGTON. Ph.D. Thesis. Oxford University, Oxford, England. 1954–1955.
26. J. P. PHILLIPS, R. L. ELBINGER, and L. L. MERRITT. J. Am. Chem. Soc. **71**, 3986 (1949).
27. R. G. W. HOLLINGSHEAD. Anal. Chim. Acta, **12**, 201 (1955).
28. A. CORSINI and J. ABRAHAM. Talanta, **15**, 562 (1968).
29. A. CORSINI and R. P. GRAHAM. Anal. Chim. Acta, **28**, 583 (1963).
30. I. M. KOLTHOFF, E. B. SANDELL, E. J. MEEHAN, and S. BRUCKENSTEIN. Quantitative chemical analysis. 4th ed. MacMillan, London. 1969. p. 858.
31. K. G. STONE. J. Am. Chem. Soc. **76**, 4997 (1954).
32. J. P. PHILLIPS and J. F. DEYE. Anal. Chim. Acta, **17**, 231 (1957).
33. M. N. SASTRI and T. P. PRASAD. Talanta, **14**, 481 (1967).
34. W. C. HAMILTON and J. A. IBERS. Hydrogen bonding in solids. W. A. Benjamin, N.Y. 1968. p. 73.
35. G. SARTORI, C. FURLANI, and A. DAMIANI. J. Inorg. Nucl. Chem. **8**, 119 (1958).
36. R. G. CHARLES. J. Inorg. Nucl. Chem. **20**, 211 (1961).
37. G. W. POPE, J. F. STEINBACH, and W. F. WAGNER. J. Inorg. Nucl. Chem. **20**, 304 (1961).
38. R. G. CHARLES and A. PERROTTO. J. Inorg. Nucl. Chem. **26**, 373 (1964).
39. E. L. MUETTERTIES and C. M. WRIGHT. Quart. Rev. **21**, 109 (1967).
40. A. CORSINI, J. ABRAHAM, and M. THOMPSON. Talanta, **18**, 481 (1971).
41. G. A. MELSON and R. W. STOTZ. Coord. Chem. Rev. **7**, 133 (1971).

Can. J. Chem. Downloaded from www.nrcresearchpress.com by 210.87.254.6 on 09/05/12
For personal use only.

The Rate Constants for the Reactions of Ozone with Triphenylphosphite and Triphenylphosphine[1]

STANISLAV DMITRIEVICH RAZUMOVSKII[2] AND GEORGE DAVID MENDENHALL[3]

Division of Chemistry, National Research Council of Canada, Ottawa, Canada K1A 0R9

Received May 29, 1972

The stoichiometry and rate constants for the reaction of triphenylphosphite and triphenylphosphine with ozone were measured at several temperatures. The rate was first order in each reactant, with $k = (3 \pm 1) \times 10^4$ and $(5 \pm 2) \times 10^3$ M^{-1} s^{-1}, respectively, for the reaction of ozone with triphenylphosphine and triphenylphosphite (2,4-dimethylhexane, $-90°$). The reaction of ozone with triphenylphosphite has a low activation energy in carbon tetrachloride. The stoichiometry was 1:1 for both compounds under these conditions.

La stoechiométrie et les constantes de vitesse de la réaction entre le triphénylphosphite et la triphénylphosphine avec l'ozone ont été mesurées à diverses températures. La vitesse est du premier ordre pour chaque réactant avec $k = (3 \pm 1) \times 10^4$ et $(5 \pm 2) \times 10^3$ M^{-1} s^{-1} respectivement pour la triphénylphosphine et le triphénylphosphite (diméthyl-2,4-hexane, $-90°$). La réaction de l'ozone sur le triphénylphosphite possède une faible énergie d'activation dans le tétrachlorure de carbone. La stoechiométrie est de 1:1 pour les deux composés dans ces conditions.

[Traduit par le journal]

Can. J. Chem., 51, 1257 (1973)

The reaction of ozone with heteroatom compounds containing free electron pairs or *d* orbitals has come under increasing study in recent years (1–5). In most cases the final products do not incorporate all three oxygen atoms of the ozone and variously formulated intermediates have been proposed. The relatively stable adduct from triphenylphosphite and ozone (2) has aroused particular interest because it oxidizes organic substrates by at least two mechanisms, one involving singlet molecular oxygen (6).

The reaction of trivalent phosphorus compounds with ozone to give the corresponding R_3PO species [2] may be described by the scheme shown below.

$$[1] \qquad R_3P + O_3 \underset{k_{-1}}{\overset{k_1}{\rightleftharpoons}} R_3PO_3$$

$$[2] \qquad R_3PO_3 \xrightarrow{k_2} R_3PO + {}^1O_2$$

$$[3] \qquad {}^1O_2 + R_3P \xrightarrow{k_3} \text{products}$$

$$[4] \qquad R_3PO_3 + R_3P \xrightarrow{k_4} \text{products}$$

$$[5] \qquad {}^1O_2 \xrightarrow{k_5} {}^3O_2$$

The initial product **1** from triphenylphosphite contains pentacovalent phosphorus (^{31}P n.m.r.) (2) and decomposes slowly at $-70°$, although triphenylphosphine in contrast does not give a stable adduct (2).

We studied the reactions of triphenylphosphine and triphenylphosphite at several temperatures in a flow system described by one of us earlier (7). A 6% O_3–O_2 mixture is bubbled through a dilute solution (isopentane or CCl_4) of the reactant and the appearance of ozone is monitored in the effluent. As the reaction proceeds, the concentration of ozone observed increases and reaches a constant value when the reaction is complete and the solution is saturated with ozone (see Fig. 1). From the shape of the O_3 *vs.* time curve compared to that for pure solvent both rate constants and the stoichiometry of the reaction may be calculated.

As the ozone–oxygen is passed through the solution, equilibrium is rapidly established:

$$[O_3]_g \rightleftharpoons [O_3]_l$$

where α is the solubility coefficient. The dissolved ozone reacts with the substrate:

$$[O_3]_l + s \xrightarrow{k_r} \text{products}$$

Provided that the rate of solution is not the limiting stage, at any time the following equality must hold

$$k_r = w([O_3]_0 - [O_3]_g)/\alpha[RH][O_3]_g \text{ l mol}^{-1} \text{ s}^{-1}$$

[1]N.R.C.C. No. 12978.

[2]Russian Exchange Scientist. Present address: Institute of Chemical Physics, Academy Nauk USSR, 26, Vorobjevskoe Shosse, Moscow 117334, USSR.

[3]National Research Council of Canada Postdoctorate Fellow. Present address: Stanford Research Institute, Menlo Park, Calif. 94025.

Can. J. Chem. Downloaded from www.nrcresearchpress.com by 210.87.254.105 on 09/05/12
For personal use only.

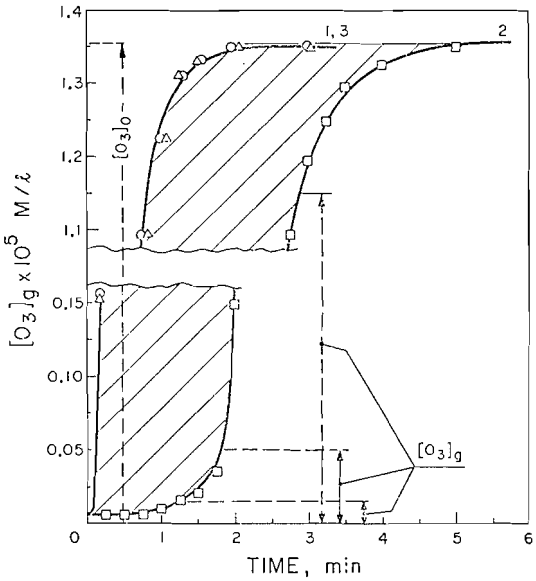

FIG. 1. The dependence of the ozone concentration after the reactor, $[O_3]_g$, on the time of reaction between ozone and triphenylphosphite. Initial concentration $[O_3]_0 = 1.36 \times 10^{-5}$ mol/l. Curve *1*, pure solvent (○); *2*, solution $[(PhO)_3P]_0 = 1.42 \times 10^{-4}$ mol/l (□); *3*, after complete reaction and removing excess of ozone (△).

where w is the specific rate of feed of the gas mixture in s^{-1}; $[O_3]_0$ and $[O_3]_g$ are the ozone concentrations at the reactor inlet and outlet, respectively. The numerator of the equation express the amount of reacted ozone per unit time, the denominator the product of the concentrations of the reactants.

Dilute solutions of both substrates examined showed 1:1 stoichiometry and the reaction was first-order in each component. The stoichiometry observed indicates that the reactions 3 and 4 are not important under these conditions, though Thompson (2) found up to 2.5 atoms of oxygen per ozone molecule appeared in the products at higher concentrations. A spent reaction mixture, flushed free of ozone, showed the same curve on readmitting ozone as did pure solvent, indicating the absence of side reactions with oxidation products. This also follows from the slow rates of reaction of ozone with benzene and with anisole, which roughly simulate the organic portions of our phosphorus compounds. Finally, no ozone reappeared in the effluent when the solution was flushed with O_2 4 h after the initial reaction, indicating that $k_{-1} \ll k_1 + k_2$.

The rate constants derived are listed in Table 1. The constants for both compounds are high (10^4 M^{-1} s^{-1}) and nearly temperature-invariant. If the rate in 2,4-dimethylhexane is included with those in CCl_4, an activation energy of 2 ± 1 kcal can be estimated for the reaction of ozone with triphenylphosphite. Both the high rate and low E_a are consistent with the strength of the P—O bond (84 kcal) (8) presumably formed in the process. It is expected that the phosphine reacts faster with ozone than triphenylphosphite, though the difference is not large. The observed order is common; for instance triphenylphosphine reacts 26 times faster than triethylphosphite toward ethyl iodide (acetonitrile, 60°) (9). The rates of reaction of *t*-butylperoxy radical toward triphenylphosphine and triphenylphosphite are 200 and 260 M^{-1} s^{-1}, respectively (*i*-pentane, −95°) (11). The lower P—O bond order in the species formed from *t*-butylperoxy radical in the latter reactions is consistent with the fact that their rates are orders of magnitude slower than the corresponding ozone reactions.

Our results do not bear directly on the question why triphenyl phosphine ozonide (**1**, R = Ph) is

TABLE 1. Rate constants for the reaction of ozone with triphenylphosphite, triphenylphosphine, and related compounds

Compound	Temperature (°C)	Solvent	$10^5[O_3]_0$* (*M*)	10^5[Substrate]$_0$ (*M*)	10^{-4} k_1 (M^{-1} s^{-1})
1 Triphenyl-phosphite	20	CCl_4	1.49	2.6	7±3
	1	CCl_4	1.36	4.5	3±1
	−20	CCl_4	1.7	3.6	1.8±0.4
	−90	2,4-Dimethylhexane	2.17	6.4	0.5±0.2
2 Triphenyl-phosphine	−90	2,4-Dimethylhexane	1.8	3.7	3±1
3 Anisole	20	CCl_4	1.65	5500	0.00013
4 Benzene	20	CCl_4	1.65	1.1×10^5	0.000006

*Concentration in entering ozone stream.

Can. J. Chem. Downloaded from www.nrcresearchpress.com by 210.87.254.105 on 09/05/12
For personal use only.

not stable, except to show it is not due to a reverse reaction. If the instability results from an enhanced value of k_2 (unimolecular decomposition), we might not detect this process by a change in stoichiometry due to the subsequent reaction 3, because deactivation of $^1O_2$ probably competes effectively at our concentrations.[4]

The large rate constants observed here suggest that phosphites may be a useful class of antiozonants.

1. A. MAGGIOLO and E. BLAIR. Adv. in Chem. Ser. **21**, 200 (1959).
2. Q. E. THOMPSON. J. Am. Chem. Soc. **83**, 845 (1961).
3. YU. A. ALEXSANDROV and N. G. SHEYANOV. Zh. Obsheh Khim **37** (9), 2136 (1967).
4. P. S. BAILEY, J. E. KELLER, and TH. P. CARTER. J. Org. Chem. **35** (8), 2777 (1970). P. S. BAILEY, J. W. WARD, and R. E. HORNISH. J. Am. Chem. Soc. **93**, 3552 (1971).
5. L. SPIALTER, L. PAZDERNIK, S. BERNSTEIN, W. A. SWANSIGER, G. R. BUELL, and M. E. EREEBURGER. J. Am. Chem. Soc. **93**, 5682 (1971).
6. (*a*) R. W. MURRAY and M. L. KAPLAN. J. Am. Chem. Soc. **90**, 537, 4101 (1968); **91**, 5358 (1969). (*b*) P. D. BARTLETT and G. D. MENDENHALL. J. Am. Chem. Soc. **92**, 210 (1970). (*c*) P. D. BARTLETT, G. D. MENDENHALL, and A. P. SCHAAP. Ann. N.Y. Acad. Sci. **171**, 79 (1970); R. W. MURRAY, J. W. LIN, and M. L. KAPLAN. Ann. N.Y. Acad. Sci. **171**, 121 (1970). (*d*) A. P. SCHAAP and P. D. BARTLETT. J. Am. Chem. Soc. **92**, 6055 (1970).
7. S. D. RAZUMOVSKII. Izv. Akad. Nauk SSSR, Ser. Khim (2), 335 (1970).
8. F. A. COTTON and G. WILKINSON. Advanced inorganic chemistry. 2nd ed. John Wiley and Sons, New York, N.Y. 1966.
9. G. AKSNES and D. AKSNES. Acta Chem. Scand. **18**, 38 (1964).
10. P. B. MERKEL and D. R. KEARNS. J. Am. Chem. Soc. **94**, 7244 (1972).
11. E. FURIMSKY and J. A. HOWARD. J. Am. Chem. Soc. **95**, 369 (1973).

[4]This follows if k_5 is 4×10^4 s^{-1} (its value in cyclohexane (10)) and $k_3 \approx 10^8$ M^{-1} s^{-1} for R = Ph (G. D. Mendenhall, unpublished results).

Can. J. Chem. Downloaded from www.nrcresearchpress.com by 210.87.254.105 on 09/05/12
For personal use only.

Some Oxime and Amide Complexes of $NiCl_2$

M. E. STONE[1] AND K. E. JOHNSON[2]

Department of Chemistry, University of Saskatchewan, Regina, Saskatchewan

Received November 23, 1971[3]

$[Ni(Aox)_4Cl_2]$ (Aox = acetaldoxime), $[Ni(Acm)_4(H_2O)_2]Cl_2$ (Acm = acetamide), $Ni(Cy)_3Cl_2$-(Cy = cyclohexanone oxime), and $[Ni(cap)_6]Cl_2$(Cap = caprolactam) have been prepared. Their solution electronic spectra indicate approximately octahedral environments for Ni(II) while solid $Ni(Aox)_4Cl_2$ shows a small tetragonal distortion. The i.r. spectra can be accounted for by oxime bonding to Ni via nitrogen and amide bonding to Ni via oxygen alone.

Les produits, $[Ni(Aox)_4Cl_2]$ (Aox = Acetaldoxime), $[Ni(Acm)_4(H_2O)_2]Cl_2$ (Acm = acétamide), $[Ni(Cy)_3Cl_2]$ (Cy = oxime de cyclohexanone) et $[Ni(Cap)_6]Cl_2$ (Cap = caprolactame) ont été préparés. Leurs spectres électroniques en solution montrent approximativement un environnement octaédrique pour le Ni(II) alors que le $Ni(Aox)_4Cl_2$ solide possède une légère déformation tétragonale. Les spectres i.r. peuvent s'expliquer par la liaison de l'oxime au Ni par l'intermédiaire de l'azote et par la liaison de l'amide au Ni par l'intermédiaire de l'oxygène seulement.

[Traduit par le journal]

Can. J. Chem., **51**, 1260 (1973)

Oxime and amide complexes of nickel(II) are of interest as possible intermediates in Beckman rearrangements catalyzed by Raney nickel or nickel(II) salts (1–3). Acetaldoxime has been reported (4, 5) to form $Ni(Aox)_4Cl_2$ and Ni—N bonding was postulated in this complex. Acetamide, the rearrangement product of acetaldoxime, forms several complexes with Ni(II), *viz.*, $(NiCl_2)_2(Acm)$ (6), $Ni(Acm)_4Cl_2\cdot(H_2O)$ (7), $Ni(Acm)_4Cl_2\cdot 2H_2O$ (8) and $Ni(Acm)_6Cl_2$ (9). Ni—O bonding was suggested for the latter (9) but the one of interest to us, $Ni(Acm)_4Cl_2\cdot 2$-(H_2O) was not studied in detail. In concurrent work (10) we have determined the crystal structures of $Ni(Aox)_4Cl_2$ and $Ni(Acm)_4Cl_2\cdot 2(H_2O)$ and find that Ni(II) is essentially octahedrally coordinated in both: in the former by 4 N at 2.114 Å and 2 Cl at 2.441 Å, and in the latter by 2 amide O at 2.044 Å, 2 amide O at 2.102 Å, and 2 water O at 2.063 Å.

In this paper we wish to compare the i.r. spectra of $[Ni(Aox)_4Cl_2]$ and $[Ni(Acm)_4(H_2O)_2]Cl_2$ with those of the free ligands and to report the electronic spectra of solid $Ni(Aox)_4Cl_2$ and ethanolic solutions of both complexes. In addition, we include i.r. and electronic spectra for the cyclohexanone oxime complex $Ni(Cy)_3Cl_2$ and the caprolactam complex $Ni(Cap)_6Cl_2$, noting that Pd and Pt complexes of cyclohexanone oxime are known (11, 12) and that Madan and Denk (13) have prepared and studied in some detail $Ni(Cap)_6(ClO_4)_2$, $Ni(Cap)_6I_2$, and $Ni(Cap)_2Cl_2$. We were unable to obtain crystals of $Ni(Cy_3)Cl_2$ and $Ni(Cap)_6Cl_2$ suitable for X-ray structure work.

Experimental

Anhydrous $NiCl_2$ (Alfa Inorganics, 99.9% pure) was dissolved in absolute ethanol and excess ligand (Baker Chemical Co.) alone (in the case of Aox) or dissolved in absolute ethanol, was added. The solid products formed after standing for several days were recrystallized from ethanol–methanol (50% v/v). All of them were hygroscopic.

Analyses were carried out by both Chemalytics, Inc., and Galbraith Laboratories, Ltd., as follows:

Anal. Calcd. for $[Ni(Aox)_4Cl_2]$: C, 26.26; H, 5.52; N, 15.31; Cl, 19.38. Found: C, 26.1, 26.2; H, 5.6, 5.4; N, 15.4, 15.3; Cl, 19.1, 19.5.

Anal. Calcd. for $[Ni(Acm)_4(H_2O)_2]Cl_2$: C, 23.91; H, 6.03; N, 13.94; Cl, 17.64. Found: C, 23.8, 23.7; H, 6.1, 6.0; N, 14.0, 13.6; Cl, 17.5, 18.7.

Anal. Calcd. for $Ni(Cy)_3Cl_2$: C, 46.09; H, 7.09; N, 8.96; Cl, 15.12. Found: C, 45.7, 45.9; H, 7.2, 7.3; N, 8.9, 8.9; Cl, 14.9, 15.4.

Anal. Calcd. for $Ni(Cap)_6Cl_2$: C, 53.48; H, 8.28; N, 10.39; Cl, 8.77. Found: C, 54.9, 54.4; H, 8.6, 8.9; N, 10.9, 10.2; Cl, 7.8, 8.4.

It is interesting to note that the acetamide complex was a hydrate, although superficially dry conditions were maintained.

Electronic spectra of 0.02 to 0.3 *M* solutions of the complexes in absolute ethanol in the range 5–33 kK were obtained with a Beckman DK 2A recording spectrophotometer. The spectra were analyzed into their Gaussian

[1]Present address: Ladies College, Cheltenham, England.

[2]On leave at Department of Chemistry, University of California, Riverside, California 92502.

[3]Revision received November 22, 1972.

Can. J. Chem. Downloaded from www.nrcresearchpress.com by 210.87.254.105 on 09/05/12
For personal use only.

components by the method of Chatt (14). The spectrum of a single crystal of $Ni(Aox)_4Cl_2$ was measured by Dr. J. R. Dickinson at the University of Virginia. A Beckman IR 12 spectrometer was used to record infrared spectra of the complexes and pure ligands in the range 200–4000 cm^{-1}; KBr pellets were used for solid compounds while a KBr cell was used for liquid acetaldoxime. Conductances of solutions were measured with a Beckman Model RC-18A bridge and a conventional cell by Dr. J. L. Meyer.

Results and Discussion

The conductances of ethanolic solutions of $[Ni(Aox)_4Cl_2]$ and $[Ni(Acm)_4(H_2O)_2]Cl_2$ indicate that both complexes yield weak electrolytes. The Λ *vs.* $\sqrt{C}$ plots (Λ = equivalent conductance in $ohm^{-1}\,cm^{-1}\,l^{-1}$ equivalents, C = concentration in equivalent l^{-1}) are curved, Λ rising from 1.82 to 35.4 for an acetaldoxime complex concentration change from 0.0385 to 0.00010 and rising from 15.0 to 49.3 for an acetamide complex concentration change from 0.0139 to 0.000028. Calculated maximum values of the degree of dissociation of the most dilute ethanolic solutions used in the spectral studies are 5% for the acetaldoxime complex and 15% for the acetamide complex.

The infrared spectra of $Ni(Aox)_4Cl_2$ and $[Ni(Acm)_4(H_2O)_2]Cl_2$ are consistent with the X-ray results for these compounds. In particular, on complexing the oxime the C=N band shifted from 1675 to 1630 cm^{-1} and decreased in intensity and the 1200–1500 cm^{-1} region was radically changed since only the *syn*-configuration is preserved and the OH is H-bonded to Cl. The amide I band, the C=O stretching frequency, was lowered from 1690 to 1672 cm^{-1} in the acetamide complex and the amide II band, the NH stretch, shifted from 1605 to 1586 cm^{-1}, in line with Ni—O bonding (15) and H-bonding between the NH_2 and Cl (10). The new bands appearing at 504 cm^{-1} in the oxime complex and 385 cm^{-1} in the amide complex might be due to Ni—N and Ni—OH_2 stretches, respectively (*cf.* ν_{Ni-N} at 515 and 480 cm^{-1} in $[Ni(NH_2CH{=}CHNH_2)_2][PtCl_4]$ (16) and ν_{Ni-O} at 405 cm^{-1} in $[Ni(H_2O)_6]SO_4$ (17)) but new bands at 637 cm^{-1} in the oxime complex and 531 cm^{-1} in the amide complex are not readily assigned.

Complexing of cyclohexanone oxime lowered the C=N frequency from 1676 to 1664 cm^{-1} with a shoulder at 1640 cm^{-1} and produced new bands at 607 and 550 cm^{-1} while the C=O stretch of caprolactam changed from 1668 cm^{-1} to bands at 1661 and 1638 cm^{-1} and a new band occurred at 535 cm^{-1}.[4] One can speculate that Ni—O frequencies are at $\sim$535 cm^{-1} for both amides but these bands could easily be combination modes.

The details of the electronic spectra of ethanolic solutions of the complex are given in Table 1 and the peak positions of the unresolved reflectance spectrum of $[Ni(Aox)_4Cl_2]$ are listed in Table 2. The only previously published spectrum for comparison is that by Bright *et al.* (18) of $Ni(Cap)_6(ClO_4)_2$ but although the assignments are the same the details do not agree very well with our results for $Ni(Cap)_6Cl_2$ (Table 3), perhaps because different solvents were used, the ethanol displacing the lactam to some extent for example.

The electronic spectra of all four complexes in solution correspond to octahedrally coordinated Ni(II). This is no surprise for the caprolactam complex. The X-ray data indicate that the 6 coordinating oxygens in $[Ni(Acm)_4(H_2O)_2]Cl_2$ are at virtually equal distances and if we compare the spectrum with that of $[Ni(H_2O)_6]^{2+}$ we see that there is little change beyond a shift of 0.6 to 1.6 kK to lower energy. For $[Ni(Acm)_6]^{2+}$ we can predict a further shift of 0.3 to 0.8 kK in the spectrum. The octahedral coordination in $Ni(Cy)_3Cl_2$ is not easy to rationalize without Cl bridges but apart from the fit of the transition energies to an octahedral structure the intensities of the bands are low for D_{3h} symmetry (19).[5]

Since the solution process involves little dissociation of the entity $[Ni(Aox)_4Cl_2]$ and no rupture of molecular bonds, the Cl atoms being H-bonded to ligands within the same group, it is surprising to find a typical octahedral Ni^{2+} spectrum for the blue solution of this complex in ethanol. However, the spectrum of the solid does exhibit a small tetragonal distortion, resembling that of $[Ni(pyridine)_4Cl_2]$ (20) (Table 2). We note that the solution spectrum of $[Ni(py)_4Cl_2]$ also showed no tetragonal splitting (20).

From the solution spectra, the ligand field strength (Δ), Racah parameters (B and C) and nephelauxetic coefficient (β) were calculated to give the best fit to the observed values using a program described elsewhere (21, 22) based on the Tanabe–Sugano energies for pure octahedral

[4]Ni—N and Ni—O bonding are thereby inferred, respectively, for these two complexes.

[5]The absorption spectrum of Ni(II) in several symmetries is discussed and Fig. 48, ref. 19, in particular is cogent to these arguments.

Can. J. Chem. Downloaded from www.nrcresearchpress.com by 210.87.254.105 on 09/05/12
For personal use only.

TABLE 1. Electronic spectra of the complexes in solution

Compound	$\bar{\nu}$(kK) Observed	$\bar{\nu}$(kK) Calculated	ε (l mol^{-1} cm^{-1})	f	Assignment
$Ni(Aox)_4Cl_2$	8.5	8.6	3.9	6.8×10^{-5}	$^3T_{2g}(F) \leftarrow {}^3A_{2g}(F)$
	12.5	12.4	0.5	1.3×10^{-6}	$^1E(D) \leftarrow$
	14.4	14.2	4.4	7.7×10^{-5}	$^3T_{1g}(F) \leftarrow$
	20.4	20.6	0.7	3.9×10^{-6}	$^1T_2(D), {}^1A_1(G) \leftarrow$
	24.6	24.6	9.9	1.6×10^{-4}	$^3T_{1g}(P) \leftarrow$
$Ni(Acm)_4Cl_2(H_2O)_2$	7.9	7.4	4.4	4.1×10^{-5}	$^3T_{2g}(F) \leftarrow {}^3A_{2g}(F)$
	12.6	12.4	4.7	6.0×10^{-5}	$^3T_{1g}(F) \leftarrow$
	14.8	14.1	1.8	1.4×10^{-5}	$^1E(D) \leftarrow$
	20.4	21.1	1.2	1.2×10^{-5}	$^1T_2(D), {}^1A_1(G) \leftarrow$
	23.7	23.7	13.7	1.7×10^{-4}	$^3T_{1g}(P) \leftarrow$
$Ni(Cy)_3Cl_2$	7.7	7.2	5.9	6.1×10^{-5}	$^3T_{2g}(F) \leftarrow {}^3A_{2g}(F)$
	12.4	12.1	9.3	1.2×10^{-4}	$^3T_{1g}(F) \leftarrow$
	14.6	13.7	3.1	2.3×10^{-5}	$^1E(D) \leftarrow$
	19.6	20.5	3.1	5.9×10^{-5}	$^1T_2(D), {}^1A_1(G) \leftarrow$
	23.2	23.3	24.1	3.5×10^{-4}	$^3T_{1g}(P) \leftarrow$
$Ni(Cap)_6Cl_2$	7.7	7.4	1.5	1.3×10^{-5}	$^3T_{2g}(F) \leftarrow {}^3A_{2g}(F)$
	12.7	12.5	1.5	2.1×10^{-5}	$^3T_{1g}(F) \leftarrow$
	14.6	14.0	0.2	1.1×10^{-6}	$^1E(D) \leftarrow$
	20.4	21.0	0.4	3.5×10^{-6}	$^1T_2(D), {}^1A_1(G) \leftarrow$
	23.5	23.5	4.5	5.4×10^{-5}	$^3T_{1g}(P) \leftarrow$

TABLE 2. Spectra of $Ni(Aox)_4Cl_2$ and $Ni(py)_4Cl_2$*

Excited state	Solids $Ni(py)_4Cl_2$	Solids $Ni(Aox)_4Cl_2$	Solutions $Ni(Aox)_4Cl_2$	Solutions $Ni(py)_4Cl_2$	Excited state
^3E_g	9.04	8.6	8.6	8.65	$^3T_{2g}(F)$
$^3B_{2g}$	11.73	11.3		10.25	
$^1A_{1g}$	12.62	12.7			
			13.5	12.5	$^1E_g(D)$
$^1B_{1g}$	12.80	13.0			
$^3A_{2g}$	14.93	14.3			
			14.2	15.8	$^3T_{1g}(F)$
^3E_g	16.82	16.3			
$^1A_{1g}, {}^1E_g$	21.77	21.1	20.6		$^1T_{2g}(D), {}^1A_{1g}(G)$
$^3A_{2g}, {}^3E_g$	26.76	26.1	24.6	25.4	$^3T_{1g}(P)$

Parameters	Value $Ni(py)_4Cl_2$	Value $Ni(Aox)_4Cl_2$	Value $Ni(Aox)_4Cl_2$	Value $Ni(py)_4Cl_2$	Parameters
Dt	0.31	0.31	8.6	9.4	Δ
Ds	0.38	0.40	0.87	0.84	β

*$Ni(py)_4Cl_2$ spectra taken from ref. 20.

symmetry (23). Comparison of the Δ and β values for the complexes indicates that acetaldoxime gives rise to the strongest field and the greatest covalency and in fact Δ/β is such in $[Ni(Aox)_4Cl_2]$ that the $^3T_1(F)$ state has higher energy than the $^1E(D)$ state and therefore results in a different order of transitions. This is quite consistent with mainly nitrogen coordination as opposed to oxygen coordination in the amides.

A crystal field treatment of solid $Ni(Aox)_4Cl_2$ including configuration interaction between T_{1g} states (24) gave the very reasonable parameters $\Delta_{Aox} = 8.6$ kK, $\Delta_{Cl} = 8.3$ kK, $Dt = 0.31$ kK, and $Ds = 0.38$ kK. Thus the distortion is com-

Can. J. Chem. Downloaded from www.nrcresearchpress.com by 210.87.254.105 on 09/05/12
For personal use only.

TABLE 3. Spectra of $[Ni(Cap)_6]^{2+}$*

$[Ni(Cap)_6]Cl_2$ in EtOH		$[Ni(Cap)_6](ClO_4)_2$ in CH_2Cl_2 (18)		
$\bar{\nu}_{max}$ (kK)	ε_{max} (l mol^{-1} cm^{-1})	$\bar{\nu}_{max}$ (kK)	ε_{max} (l mol^{-1} cm^{-1})	Assignment
7.7	1.6	8.337	9.25	$^3T_{2g}(F) \leftarrow {}^3A_{2g}(F)$
12.6	1.7			
		13.430	5.95	$^3T_{1g}(F) \leftarrow$
14.0	1.1			
23.7	4.7	24.680	18.9	$^3T_{1g}(P) \leftarrow$

*Values given are spectral maxima, not the results of a Gaussian analysis.

TABLE 4. Spectral parameters of Ni complexes in ethanol*

Complex	Δ	B	C	Δ/B	β	λ
$Ni(Aox)_4Cl_2$	8.6	0.87	2.9	9.9	0.84	0.24
$Ni(Acm)_4Cl_2(H_2O)_2$	7.4	0.92	3.7	8.1	0.89	0.31
$Ni(Cy)_3Cl_2$	7.2	0.92	3.5	7.9	0.87	0.32
$Ni(Cap)_6Cl_2$	7.5	0.91	3.7	8.2	0.87	0.30

*All values, except those of β, are in kK.

parable to that found in $Ni(py)_4Cl_2$.

The Tanabe–Sugano expressions for the energies of the ligand field transitions are based on the assumption that there is no spin–orbital coupling. In practice we find not only spin-allowed, parity-forbidden transitions but also spin-forbidden, parity-forbidden transitions. The spin-forbidden transitions involve excited states close in energy to states of the same spin as the ground state (23) and, thus, are a consequence of spin–orbital coupling (25). Fortunately, although it is large enough to make the spin-forbidden transitions observable, it is insufficient to invalidate the Tansabe–Sugano energy expressions and, indeed, an approximate value for the spin–orbital coupling constant is given by (26):

$$\lambda = 2.7 \frac{B^2}{\Delta}$$

It is interesting to note the reasonable values derived for the series of complexes studied here (Table 4): in particular, the value for $Ni(Aox)_4Cl_2$ is distinctly lower than the rest following the trend for β.

We are grateful to the National Research Council for support of this work.

1. R. PAUL. C.R. Acad. Sci., Paris, **204**, 363 (1937).
2. A. BRYSON and F. P. DWYER. J. Proc. Roy. Soc., New South Wales, **74**, 471 (1941).
3. L. FIELD, P. B. HUGHMARK, S. H. SHUMAKER, and W. S. MARSHALL. J. Am. Chem. Soc. **83**, 1983 (1961).
4. W. HIEBER and F. LEUTERT. Chem. Ber. **60B**, 2296 (1927).
5. W. M. PESHKOVA. Trudy Komissii Anal. Khim., Akad. Nauk SSSR, Inst. Geokhim. i Anal. Khim. **8**, 75 (1958).
6. H. V. BAROT, H. KAZI, and C. M. DESAI. Vidya, J. Gujarat Univ. **2**, 73; C.A., **53**, 16789*e* (1959).
7. G. ANDRE. Chem. Ber. **19**, 1303 (1886).
8. G. ANDRE. C.R. Acad. Sci., Paris, **102**, 115 (1886).
9. R. C. PAUL, S. L. CHADHA, and R. DEV. Indian J. Chem. **3**, 364 (1965).
10. M. E. STONE, B. E. ROBERTSON, and E. STANLEY. J. Chem. Soc. A, 3632 (1971).
11. A. V. BABAEVA and M. A. MOSYAGINA. Dokl. Akad. Nauk SSSR, **89**, 293 (1953).
12. T. TAKIGUCHI, K. KUROSAKI, and M. ABE. Kogyo Kagaku Zasshi, **72**, 1549 (1966).
13. S. K. MADAN and H. H. DENK. J. Inorg. Nucl. Chem. **27**, 1049 (1965).
14. J. CHATT, G. A. GAMLEN, and L. E. ORGEL. J. Chem. Soc. 486 (1958).
15. S. C. JAIN and R. RIVEST. Can. J. Chem. **45**, 139 (1967).
16. D. B. POWELL and N. SHEPPARD. Spectrochim. Acta, **17**, 68 (1961).
17. Y. KERMARREC. C.R. Acad. Sci., Paris, **258**, 5836 (1946).
18. J. H. BRIGHT, R. S. DRAGO, D. M. HART, and S. K. MADAN. Inorg. Chem. **4**, 18 (1965).

Can. J. Chem. Downloaded from www.nrcresearchpress.com by 210.87.254.105 on 09/05/12
For personal use only.

19. K. E. JOHNSON and J. R. DICKINSON. *In* Advances in molten salt chemistry. Vol. II. *Edited by* G. P. Smith, G. Mamantov, and J. Braunstein. Plenum Press. In press.
20. D. A. ROWLEY and R. S. DRAGO. Inorg. Chem. **6**, 1092 (1967).
21. L. G. BOXALL, K. W. FUNG, and K. E. JOHNSON. J. Inorg. Nucl. Chem. In press.
22. K. W. FUNG and K. E. JOHNSON. Inorg. Chem. **10**, 1347 (1971).
23. Y. TANABE and S. SUGANO. J. Phys. Soc. Jap. **9**, 753 (1954).
24. A. B. P. LEVER. Coord. Chem. Rev. **3**, 119 (1968).
25. C. K. JORGENSEN. Mol. Phys. **1**, 410 (1958).
26. J. REEDIJK, P. W. N. M. VAN LEEUWEN, and W. L. GROENEVELD. Rec. Trav. Chim. Pays-Bas, **87**, 129 (1968).

Can. J. Chem. Downloaded from www.nrcresearchpress.com by 210.87.254.105 on 09/05/12
For personal use only.

The Reaction of CH_3^+ with D_2

ALEX. G. HARRISON AND BERNARD G. KEYES
Department of Chemistry, University of Toronto, Toronto 181, Ontario

Received December 12, 1972

The exchange reaction between CH_3^+ and D_2 leading to CH_2D^+ and CHD_2^+ is shown to proceed through a collision complex in which the hydrogens and deuteriums become equivalent. The rate coefficient for reaction of CH_3^+ with D_2 is $6.1 \pm 0.1 \times 10^{-10}$ cm^3 molecule^{-1} s^{-1}.

On démontre que la réaction d'échange entre CH_3^+ et D_2 conduisant à CH_2D^+ et CHD_2^+ procède par l'intermédiaire d'un complexe de collision dans lequel les hydrogènes et les deutériums deviennent équivalents. Le coefficient de vitesse pour la réaction de CH_3^+ avec D_2 est de $6.1 \pm 0.1 \times 10^{-10}$ cm^3 molécule^{-1} s^{-1}. [Traduit par le journal]

Can. J. Chem., 51, 1265 (1973)

Two recent ion cyclotron resonance (i.c.r.) studies (1, 2) of isotopic methane–hydrogen systems have shown conclusively that the reaction between methyl ions and D_2 is responsible for at least part of the isotopic exchange observed when methane–deuterium mixture are subjected to high energy irradiation (3). However in the $CH_4(CD_4) - D_2(H_2)$ systems studied a number of other reactions occur which produce the various deuterated methyl ions and consequently these i.c.r. studies have not provided much detail concerning the exchange reaction nor have they established the rate coefficient for the reaction.

In connection with other studies we have examined the reaction of CH_3^+, produced by electron impact ionization of CH_3Cl, with D_2 by the pressure variation technique. This system has proven to be much simpler and permits a more detailed study of the exchange reaction.

The mass spectrometer and experimental techniques employed have been described previously (4, 5). Runs were carried out varying the D_2 pressure at a constant CH_3Cl pressure of 1 μ and repeller fields corresponding to ~1.1 eV ion exit energy. Nominal ionizing electron energies of 16.0 and 17.0 eV were employed, giving D_2^+/CH_3^+ ratios at 1 μ pressure of each component of 0.036 and 0.16, respectively. Identical results were obtained at the two electron energies indicating that reactions originating with D_2^+ did not play a significant role.

Typical results obtained at 16.0 eV electron energy are shown in Fig. 1 as a plot of the relative abundance of the $C(H,D)_3$ ions (% total methyl ions) *vs.* the D_2 pressure. The sequential conversion of CH_3^+ to CD_3^+ by reactions 1 to 3 is clearly established.

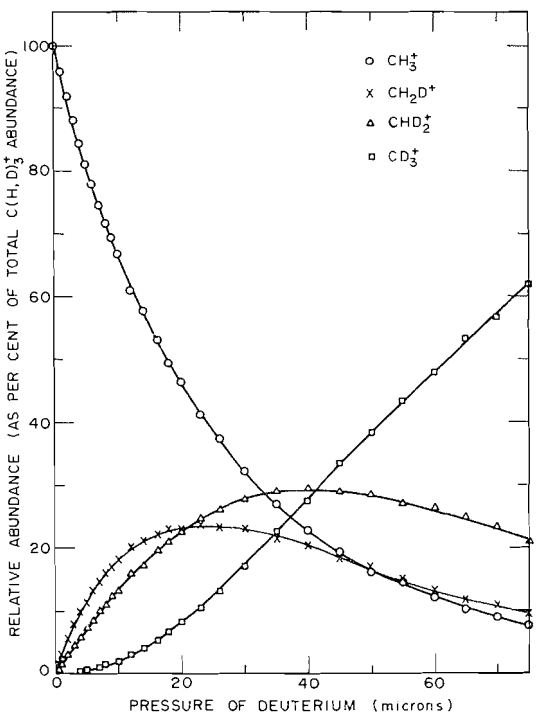

FIG. 1. Normalized $C(H,D)_3^+$ intensities as a function of D_2 pressure.

[1*a*] $CH_3^+ + D_2 \rightarrow CH_2D^+ + HD$

[1*b*] $\rightarrow CHD_2^+ + H_2$

[2*a*] $CH_2D^+ + D_2 \rightarrow CHD_2^+ + HD$

[2*b*] $\rightarrow CD_3^+ + H_2$

[3] $CHD_2^+ + D_2 \rightarrow CD_3^+ + HD$

Can. J. Chem. Downloaded from www.nrcresearchpress.com by 210.87.254.6 on 09/05/12
For personal use only.

At low D_2 pressures (<2 μ), before any CD_3^+ was observed, the ratio CH_2D^+/CHD_2^+ was found to be 2.0 ± 0.4. This value is in excellent agreement with the ratio of 2.0 predicted if the hydrogens and deuteriums in a $CH_3D_2^+$ collision complex become equivalent. This provides strong evidence that a collision complex is formed which has a lifetime sufficient for equilibration of the hydrogens and deuteriums to occur. Presumably the complex has the protonated methane structure which has long been known from ion–molecule reactions (6, 7).

From the semi-logarithmic plot of the normalized CH_3^+ intensity as a function of the D_2 pressure we obtain $k = 5.5 \pm 0.1 \times 10^{-10}$ cm^3 molecule^{-1} s^{-1}. Since the loss of H_2 and HD from the $CH_3D_2^+$ collision complex is statistical, we can assume that ~10% of the complexes will lose D_2 to regenerate CH_3^+. Correcting for this experimentally unobservable reaction, we derive a rate coefficient of 6.1×10^{-10} cm^3 molecule^{-1} s^{-1} for the reaction of CH_3^+ with D_2. This value is approximately one-half the collision rate coefficient of 1.2×10^{-9} cm^3 molecule^{-1} s^{-1} calculated using the ion-induced dipole model (8) indicating that a significant fraction of the collisions do not lead to a complex which survives for a time long enough for isotopic exchange to occur. The present experimental rate coefficient is considerably higher than the value $k_1 = 1.7 \times 10^{-10}$ cm^3 molecule^{-1} s^{-1} reported some years ago (9). However this earlier value was obtained from studies of CH_4–D_2 mixtures and recent work has shown that in these mixtures many reactions occur. It is possible that the earlier work is in error because of unrecognized reactions.

The authors are indebted to the National Research Council of Canada for financial support.

1. M. INOUE and S. WEXLER. J. Am. Chem. Soc. **91**, 5730 (1969).
2. M. T. BOWERS and D. D. ELLEMAN. J. Am. Chem. Soc. **92**, 1847 (1970).
3. T. H. PRATT and R. WOLFGANG. J. Am. Chem. Soc. **83**, 10 (1961).
4. S. K. GUPTA, E. G. JONES, A. G. HARRISON, and J. J. MYHER. Can. J. Chem. **45**, 3107 (1967).
5. A. A. HEROD and A. G. HARRISON. J. Phys. Chem. **73**, 3189 (1969).
6. V. L. TALROZE and A. K. LYUBIMOVA. Dokl. Akad. Nauk. SSSR. **86**, 909 (1952).
7. D. P. STEVENSON and D. O. SCHISSLER. J. Chem. Phys. **23**, 1353 (1955).
8. G. GIOUMOUSIS and D. P. STEVENSON. J. Chem. Phys. **29**, 294 (1958).
9. M. S. B. MUNSON, F. H. FIELD, and J. L. FRANKLIN. J. Am. Chem. Soc. **85**, 3584 (1963).

Can. J. Chem. Downloaded from www.nrcresearchpress.com by 210.87.254.6 on 09/05/12
For personal use only.

Regiospecificity and Stereoselectivity in the Photodimerization of 2,3-Dihydro-2,6-dimethyl-4-pyrone[1]

PETER YATES AND DONALD J. MACGREGOR
Lash Miller Chemical Laboratories, University of Toronto, Toronto 5, Ontario
Received October 6, 1972

Ultraviolet irradiation of 2,3-dihydro-2,6-dimethyl-4-pyrone in aqueous solution leads to the regiospecific and stereoselective formation of three *cis–anti–cis* photodimers of the cyclobutane type, *i.e.*, octahydro-2,7-8*a*,8*b*-tetramethylcyclobuta[1,2-*b*:4,3-*b*']dipyran-4,5-diones, whose structures have been established by chemical and spectroscopic methods, including studies of nuclear Overhauser effects in the proton magnetic spectrum of one of them. The dimers undergo photointerconversion, and it is proposed that this process involves photoreversion to monomer and that the reversibility of the dimerization reaction may be a factor in determining the regiochemistry and stereochemistry of the photodimers. A bisdehydro product prepared from the dimers of the dihydropyrone has been shown to undergo photocleavage to 2,6-dimethyl-4-pyrone, and it is proposed that reversibility may also be a factor affecting the course of the photodimerization of this pyrone.

Si l'on irradie la dihydro-2,3 diméthyl-2,6 pyrone-4 avec de l'ultraviolet en phase aqueuse, on observe la formation régiospécifique et stéréosélective de trois photodimères *cis–anti–cis* du type cyclobutane *i.e* octahydro tétraméthyl-2,7,8*a*, 8*b* cyclobutadipyranne-[1,2-*b*:4,3-*b*'] diones-4,5. Ces structures ont été élucidées à l'aide de méthodes chimiques et spectroscopiques qui incluent des études de l'effet Overhauser nucléaire dans le spectre de résonance magnétique nucléaire du proton pour l'une de ces structures. Les dimères subissent une photointerconversion dont le processus semble impliquer une photoréversion au monomère et que la réversibilité de la dimérisation peut être un facteur déterminant dans la régiochimie et dans la stéréochimie des photodimères. Un produit bisdehydro préparé à partir de dimères de la dihydropyrone semble subir un photoclivage pour donner la diméthyl-2,6 pyrone-4; il est proposé que la réversibilité peut aussi être un facteur influencant le processus de photodimérisation de cette pyrone.
[Traduit par le journal]

Can. J. Chem., **51**, 1267 (1973)

Introduction

The photodimerization of 2,6-dimethyl-4-pyrone (**1**) in the solid state and in solution has been found to give the cage compound **2** (2); an analogous photodimer is formed from 2,6-diethyl-4-pyrone when irradiated as the neat liquid or in solution (3). The formation of **2** from **1** must proceed via the intermediate formation of the head-to-tail *cis–syn–cis seco*-dimer **3** or by a concerted process involving the corresponding orientation of the monomer units. Compound **3** was prepared by pyrolysis of **2** and shown to undergo facile photocyclization to **2**.

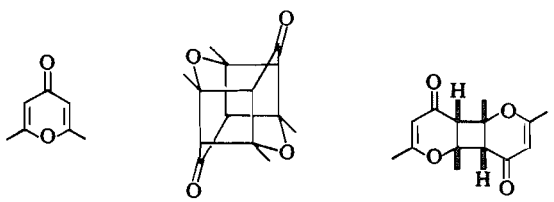

1 **2** **3**

[1]A preliminary report on part of this work has appeared (1).

The apparent regiospecific and stereospecific formation of **2** was of considerable interest in that it contrasted with the photodimerization of 2-cyclohexenones, which either give mixtures of regioisomers or stereoisomers (*e.g.*, 2-cyclohexenone (4), 3-methyl-2-cyclohexenone (5), piperitone (6), isophorone (7)), or proceed regiospecifically and stereospecifically to give *cis–anti–cis* products (*e.g.*, 3-phenyl-2-cyclohexenone (8)). Since **1** differs from 2-cyclohexenones both in the presence of the annular oxygen atom and of a second ethylenic bond, it was considered to be of importance to determine whether the unusual course of the photodimerization of the pyrone could be attributed to one of these structural features individually. To this end, the photodimerization of 2,3-dihydro-2,6-dimethyl-4-pyrone (**4**) has been investigated.

Preparation of 2,3-Dihydro-2,6-dimethyl-4-pyrone and Determination of the Structure of its Photodimers

The dihydropyrone **4** was prepared by hydrogenation of the pyrone **1** over 10% pal-

Can. J. Chem. Downloaded from www.nrcresearchpress.com by 210.87.254.42 on 09/05/12
For personal use only.

TABLE 1. P.m.r. spectra of photodimers of **4**

	A (20)	B (21)	C (22)*
δ ($CDCl_3$) (100 MHz)	1.29 (d, J = 6 Hz, 6 H)	1.25 (d, J = 6 Hz, 3 H) 1.29 (d, J = 6 Hz, 3 H)	1.28 (d, J = 6 Hz, 6 H)
	1.39 (s, 6 H)	1.32 (s, 3 H) 1.35 (s, 3 H)	1.28 (s, 6 H)
	2.15–2.55 (m, 4 H)	2.1–2.6 (m, 4 H)	2.1–2.6 (m, 4 H)
	3.05 (s, 2 H)	2.99 (d, J = 6 Hz, 1 H) 3.15 (d, J = 6 Hz, 1 H)	2.89 (s, 2 H)
	4.15–4.45 (m, 2 H)	3.9–4.5 (m, 2 H)	3.9–4.2 (m, 2 H)
δ (C_6H_6)† (100 MHz)	0.91 (d, J = 6 Hz, 6 H)	0.90 (d, J = 6 Hz, 3 H) 0.95 (d, J = 6 Hz, 3 H)	0.95 (d, J = 6 Hz, 6 H)
	1.25 (s, 6 H)	1.16 (s, 3 H) 1.19 (s, 3 H)	1.18 (s, 6 H)
	1.6–2.1 (m, 4 H)	1.7–2.2 (m, 4 H)	1.7–2.25 (m, 4 H)
	2.94 (s, 2 H)	2.85 (d, J = 6 Hz, 1 H) 3.04 (d, J = 6 Hz, 1 H)	2.88 (s, 2 H)
	3.75–4.1 (m, 2 H)	3.4–3.7 (m, 1 H) 3.8–4.2 (m, 1 H)	3.4–3.8 (m, 2 H)
δ (C_5H_5N)† (60 MHz)	1.22 (d, J = 6 Hz, 6 H)	1.17 (d, J = 6 Hz 3 H) 1.21 (d, J = 6 Hz, 3 H)	1.21 (d, J = 6 Hz, 6 H)
	1.45 (s, 6 H)	1.39 (s, 3 H) 1.42 (s, 3 H)	1.34 (s, 6 H)
	2.1–2.7 (m, 4 H)	2.1–2.75 (m, 4 H)	2.3–2.5 (m, 4 H)
	3.34 (s, 2 H)	3.16 (d, J = 6 Hz, 1 H) 3.32 (d, J = 6 Hz, 1 H)	3.14 (s, 2 H)
	4.2–4.5 (m, 2 H)	3.8–4.5 (m, 2 H)	3.8–4.3 (m, 2 H)

*Extracted from spectra of a 1 : 2.5 : 6.5 mixture of A, B, and C.
†δ-Values are concentration dependent.

ladium – calcium carbonate (9, 10) (see Scheme 1); this gave the tetrahydropyranol **6**[2] in addition to **4** and the tetrahydropyrone **5** (9). Most of the **6** could be removed from the product mixture by extraction of its chloroform solution with 6 *N* hydrochloric acid; fractional distillation then gave **4** in 10–12% yield, contaminated with 1–10% of **6**, which has the same boiling point; the latter could be removed by chromatography on alumina.[3] The u.v. spectrum of **4** showed λ_{max} (EtOH) 263 nm (ε 14 000); while the position of this maximum corresponds with that

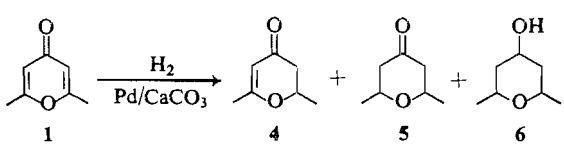

SCHEME 1

[2]This is most probably identical with the product obtained earlier (9) by hydrogenation of **1** over Raney nickel.

[3]It was shown that the presence of **6** did not affect the photochemistry of **4**, and thus the photodimers of **4** could be prepared from samples of **4** that had not been chromatographed.

observed by de Vrieze (9), its intensity is twice that previously reported, and it appears most probable that the product previously obtained in 25% yield was only 50% pure.[4]

Irradiation of a 12% aqueous solution of **4** under nitrogen in Pyrex with a Hanovia 450 W medium pressure lamp for 4 weeks led to the deposition of a crystalline mixture of photodimers. An additional amount of this mixture could be obtained by extraction of the aqueous solution with chloroform; the total yield was 97%. The p.m.r. spectra of the product mixtures in benzene or pyridine (but not in deuteriochloroform) showed that they were composed of three closely related compounds and provided an analytical method for following the difficult fractionation of the product mixture (*cf.* Table 1).

Crystallization of this mixture from polar solvents gave dimer **A**, m.p. 163–164°, and an

[4]An alternative method of formation of **4** by acid treatment of 5,6-dihydrodehydroacetic acid (11) gave a product with λ_{max} (EtOH) 263 nm (ε 10 500); exploratory experiments indicated that the yield of pure **4**, based on dehydroacetic acid, obtained by this route was *ca.* 5%.

Can. J. Chem. Downloaded from www.nrcresearchpress.com by 210.87.254.42 on 09/05/12
For personal use only.

TABLE 2. I.r. and u.v. spectra of photodimers of **4**

	A (20)	B (21)	C (22)*
λ_{max} ($CHCl_3$) μ	5.83, 7.8 (br) 9.29	5.83, 7.8 (br) 9.29	5.83, 7.9 (br) 9.12
λ_{max} (EtOH) mμ (ε)	285 (85)	281 (98)	281 (97)

*Spectra of a 1 : 2.5 : 6.5 mixture of **A**, **B**, and **C**.

eutectic mixture of dimers **A** and **B**, m.p. 130–133°, in a 1:4 ratio. Repeated crystallization of this mixture from hexane gave dimer **B**, m.p. 133–134°. From the combined mother liquors was obtained a crystalline mixture of **A**, **B**, and a third product, dimer **C**. The last was not isolated in pure form, but the mixture was enriched in **C** by countercurrent distribution between water and cyclohexane to give a mixture of **A**, **B**, and **C** in the ratio of 1:2.5:6.5. The ratio of these dimers in the original reaction product mixture was *ca.* 9:15:1.

The gross structure of **A** can be assigned on the basis of its elemental composition, molecular weight, and spectra as a cyclobutane type dimer, **7**. Its i.r. and u.v. spectra (Table 2) are in accord

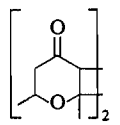

7

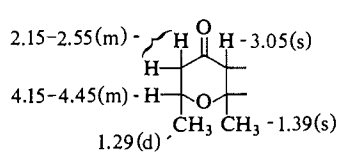

8

with the presence of two carbonyl groups in six-membered rings (*cf.* the cyclobutane-type photodimers of piperitone, whose u.v. spectra show maxima at 302 nm (ε 85) (6)). Its p.m.r. spectrum can readily be interpreted, as shown in **8**, if each of the five types of protons associated with one six-membered ring are chemically equivalent to the corresponding types of protons associated with the other six-membered ring. The p.m.r. spectrum of **A** excludes the possibility that this dimer is of the oxetane type (12).

The relationship of the spectra of **B** to those of **A** shows that it also has the gross structure **7**; its p.m.r. spectrum reveals that in this case the environment of the five types of protons associated with one six-membered ring is different from that of the corresponding types of proton associated with the other six-membered ring. Although **C** was not obtained pure, the spectra of a mixture of **A**, **B**, and **C** containing 70% of **C** showed that it also has the gross structure **7** and that it resembles **A** in having five types of chemically equivalent protons.

The conclusion that **A**, **B**, and **C** all have the gross structure **7** leads to the formulation of each of them as one of the regioisomers **9** or **10**. In the case of **B**, the head-to-head structure **9** can be chosen immediately since the coupling constant, $J = 6$ Hz, of its cyclobutyl protons shows that these must be adjacent (13). In the case of **A** and **C**, because of the chemical equivalence of the cyclobutyl protons, a direct choice between **9** and **10** cannot be made. However, examination of the low field ^{13}C—H satellite of the cyclobutyl proton signal in the 100 MHz p.m.r. spectrum of **A** showed it to be a doublet, $J = 7$ Hz, demonstrating that **A** also has structure **9** (14). This was confirmed by the preparation of the monobromo derivative, **11**, which was not obtained pure, but whose p.m.r. spectrum clearly showed that the cyclobutyl protons have a coupling constant, $J = 7$ Hz, characteristic of vicinal cyclobutyl protons. Dimer **C** was also shown to have structure **9** by its interrelation with **A** and **B** (*vide infra*).

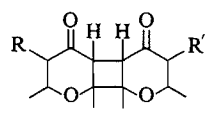

9 R = R′ = H
11 R = Br; R′ = H
15 R = R′ = Br

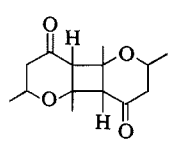

10

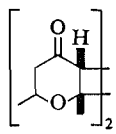

12

That both ring fusions in **A**, **B**, and **C** are *cis*, as in **12**, was shown by the fact that individual treatment of **A**, **B**, and a mixture of **A**, **B**, and **C** with boiling pyridine caused no change in these compounds as shown by their p.m.r. spectra (15). This was confirmed by the observation that chromatography on alumina of a mixture of **A** and **B** or the heating of such a mixture at 200° for 1 h led to no change of its p.m.r. spectrum (15). The possibility that one or both of the ring fusions is *trans*, and that conversion to the *cis* fusion does not occur because of failure of the adjacent carbonyl group(s) to enolize,

Can. J. Chem. Downloaded from www.nrcresearchpress.com by 210.87.254.42 on 09/05/12
For personal use only.

was excluded by the demonstration that treatment of **A** with boiling 10% D_2O – pyridine led to the exchange of six deuterium for hydrogen atoms. The p.m.r. spectrum of the hexadeutero derivative (see Experimental) confirmed the assignments made previously in the p.m.r. spectrum of **A**. The three dimers must therefore have stereostructure **13** or **14**.

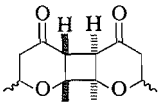

13

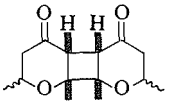

14

Distinction between the *anti* structure **13** and the *syn* structure **14** cannot be made directly on the basis of p.m.r. spectroscopy because of the similarity of the coupling constants between *cis* and *trans* vicinal cyclobutyl protons (13). The choice was made on the following basis. Bromination of **A** with two molar equivalents of bromine gave a dibromo derivative **15**, which on dehydrobromination with boiling pyridine gave **16**; compound **16** could also be obtained directly from **A** by treatment with *N*-bromosuccinimide in carbon tetrachloride. The gross structure of the dibromo compound **15** followed from the relationship of its spectra (see Experimental) to those of **A**; that of the dehydrobromination product **16** was assigned on the basis of a comparison of its spectra with those of **3**, the *seco*-photodimer of **1** (Table 3). Reaction of **B** with *N*-bromosuccinimide under the same conditions also gave **16**, confirming that **A** and **B** are both in the head-to-head series.

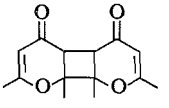

16

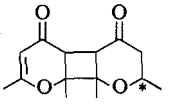

17

The reaction of **A** and **B** with *N*-bromosuccinimide gave in addition to the common bisdehydro product **16** an individual monodehydro side product in each case; these were not fully characterized, but their spectra showed that they are stereoisomeric forms of **17**. Since a single bisdehydro product is formed from both **A** and **B**, the stereoisomers of **17** must differ in relative configuration only at the asterisked carbon atom.

The bisdehydro product **16** from **A** and **B** will have the stereostructure **18** or **19** depending on whether **A** and **B** have the *anti* or *syn* structure, **13** or **14**. U.v. irradiation of the *seco*-photodimer **3**, which has perforce a *syn* disposition of the six-membered rings with respect to the cyclobutane ring, analogous to **19**, has been shown to result in facile reclosure to the cage photodimer **2** (2). Compound **16** was therefore subjected to irradiation to determine whether it underwent a corresponding ring closure. The formation of a cycloaddition reaction product analogous to **2** was not observed, the only product obtained was 2,6-dimethyl-4-pyrone (**1**), formed by fission of the cyclobutane ring.[5] It is therefore concluded that the bisdehydro product from **A** and **B** has the *anti* structure **18** and that **A** and **B** have the *anti* structure **13**. The possibility that the bisdehydro product has the *syn* structure **19**, but that ring closure does not occur because of unfavorable dipolar interaction between the carbonyl groups in the transition state, is contraindicated by the fact that analogous interactions do not inhibit the formation of cage photodimers from *p*-quinones (12). The assignment of the *anti* structure in the case of **B** has been confirmed by a study of nuclear Overhauser effects (n.O.e.) in its p.m.r. spectrum (*vide infra*).

The assignment of structure **13** to **A** and **B** restricts their full stereostructures to **20**, **21**, or **22** (or their respective enantiomorphs). Only in

TABLE 3. Spectra of bisdehydro-**A** (**16** = **18**) and the *seco*-photodimer (**3**)

	16	**3**
λ_{max} ($CHCl_3$)	6.02, 6.20	6.04, 6.18
λ_{max} (EtOH) mμ (ε)	267 (19 500)	266 (22 000)
δ ($CDCl_3$)	1.63 (s, 6H)	1.70 (s, 6H)
	2.00 (s, 6H)	1.93 (s, 6H)
	3.12 (s, 2H)	3.10 (s, 2H)
	5.25 (s, 2H)	5.25 (s, 2H)
δ (C_6H_6)	1.32 (s, 6H)	1.20 (s, 6H)
	1.53 (s, 6H)	1.50 (s, 6H)
	3.08 (s, 2H)	2.70 (s, 2H)
	5.15 (s, 2H)	5.17 (s, 2H)

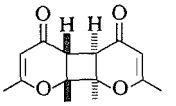

18

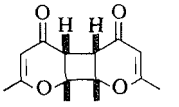

19

[5]The pyrone was shown not to undergo dimerization under the conditions of the irradiation.

Can. J. Chem. Downloaded from www.nrcresearchpress.com by 210.87.254.42 on 09/05/12
For personal use only.

Can. J. Chem. Downloaded from www.nrcresearchpress.com by 210.87.254.42 on 09/05/12
For personal use only.

the case of **21** is the environment of the five types of protons associated with one six-membered ring different from that of the corresponding types of protons associated with the other six-membered ring. This permits the immediate assignment of this structure to **B**.

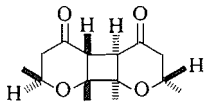

20

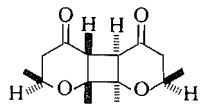

21

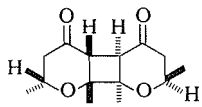

22

Hydrogenation of **18** over palladium–calcium carbonate gave a crystalline product mixture whose p.m.r. spectra in deuteriochloroform and in benzene showed that it consists of **C** and a dihydro product **17**, identical with the dehydro product obtained previously from **B**. The presence of **A** or **B** could not be detected. Examination of molecular models of **18** shows that the less hindered side of each of the six-membered rings is the side remote from the other six-membered ring. Thus hydrogenation is expected to lead to **22**, and this structure can be assigned to **C**; likewise, the dihydro product from **18** can be formulated as **23**. Finally, structure **20** can be assigned to **A** by exclusion of **21** and **22**. The last assignment leads to the assignment of structure **24** to the dehydro product from **A** (**17**); the dehydro product from **B** is then **23**, identical with dihydro **18** as observed.

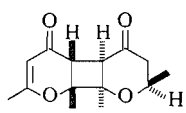

23

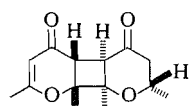

24

The hydrogenation of the *seco*-photodimer **3** was examined as a model for the hydrogenation of **18**. A single tetrahydro product was obtained. Its structure is considered to be **25**, since molecular models of **3** indicate that in this case, too, hydrogen addition will occur from the side of each six-membered ring remote from the other six-membered ring. As expected, the p.m.r. spectrum of this product shows signals attributable to five sets of equivalent protons.

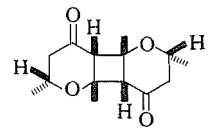

25

A consideration of the conformations of **A** (**20**), **B** (**21**), **C** (**22**) and their dehydro products, **23** and **24**, corroborates the conclusions reached above in respect to the relative configurations of the carbon atoms bearing methyl groups. The cyclobutane rings of these compounds may have planar or puckered conformations (16); however, this does not affect the gross conformations of the six-membered rings, which in either case may be expected to adopt half-chair conformations analogous to the stable conformation of cyclohexene.[6] Methyl groups at C-6 that are *cis* to a methyl group at C-2 (*cf.* **26**) will lead to a strong preference for the conformation **26***a* in which they are equatorial because of the 1,3-diaxial interaction with the C-2 methyl group in the alternative conformation **26***b* (see Scheme 2). The same preference is expected for methyl groups at C-6 that are *trans* to a methyl group at C-2 (*cf.* **27**) in the case of the head-to-head *anti* dimers and their derivatives, because of severe interaction of a C-6 axial methyl group with the C-2′ methyl group of the other six-membered ring, *i.e.*, conformation **27***a* is strongly favored over **27***b*. Thus, the preferred conformations of the three head-to-head *anti*

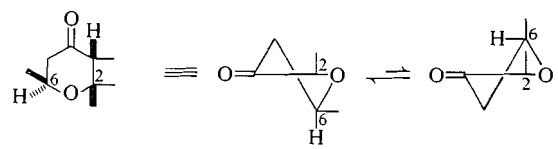

26 **26***a* **26***b*

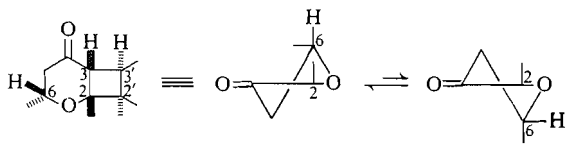

27 **27***a* **27***b*

SCHEME 2

[6]The possibility exists that the six-membered rings may exist in boat conformations, which in the present instance are anticipated to have only slightly higher energies than the half-chair conformations; however, the following considerations are applicable to both types of conformation.

Can. J. Chem. Downloaded from www.nrcresearchpress.com by 210.87.254.42 on 09/05/12
For personal use only.

TABLE 4. Chemical shifts of C-6(6′) protons in the p.m.r. spectra of **A**, **B** and **C** and related compounds

	δ (C_6H_6)*	
A (**20**)	3.8–4.1	—
B (**21**)	3.8–4.2	3.4–3.7
C (**22**)	—	3.4–3.8
Dehydro-**A** (**24**)	3.8–4.1	—
Dehydro-**B** (**23**)	—	3.3–3.8

*Parallel results were obtained in deuteriochloroform.

dimers **A**, **B**, and **C** will correspond to the three possible different combinations of part-structures **26***a* and **27***a*.

The chemical shift values for the C-6(6′) methine protons for compounds **A**, **B**, **C**, dehydro-**A**, and dehydro-**B** fall into two distinct ranges (Table 4). This can be interpreted as due to a shielding of the C-6(6′) proton by the carbon–carbon bond (17) of the methyl group at C-2(2′) in part structure **27***a*, an effect absent in part structure **26***a*. In these terms **A** can be assigned a structure with two part-structures **26***a*, *i.e.*, structure **20** in agreement with the earlier conclusions. The structures previously assigned to **B**, **C**, dehydro-**A**, and dehydro-**B** are similarly corroborated.

The *anti* stereochemistry assigned to the three dimers was also substantiated by studies of n.O.e.'s in the p.m.r. spectra of **B** (**28** = **21**). The maximum n.O.e. enhancements observed on irradiation of the C-2 and -2′ methyl signals are shown in Table 5. The observation of a n.O.e. in only one cyclobutyl proton (H-3(3′)) signal on saturation of an individual CH_3-2(2′) group is consistent with the *anti* stereochemistry: if **B** were *syn*, individual saturation of these methyl signals should give n.O.e.'s in both of the cyclobutyl proton signals. Furthermore, the n.O.e.'s observed for both methine protons at C-6(6′) on irradiation of one but not the other of the CH_3-2(2′) proton signals is in accord only with the assignment to **B** of the structure and stereochemistry depicted in **28**. It may be noted that these n.O.e.'s are the source of the H-3(3′) signal assignments given in Table 5[7]; the assignments of the H-6(6′) signals follow from the conformational analysis above.

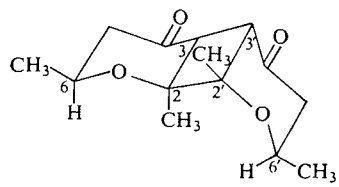

28

It remains to record a further important experimental observation concerning the three photodimers of **4**, *viz.* their photointerconversion. Individual irradiations (Pyrex filter) of dimers **A** and **B** in solution led to mixtures of all three dimers; similar irradiation of a dimer mixture enriched in dimer **C** led to a change in the composition of the dimer mixture (Table 6).

TABLE 5. N.O.e. in the p.m.r. spectrum of **B** (**28**)

Signal irradiated (δ)	Signal integrated (δ)	Maximum n.O.e. (%)
1.16 (Me-2)	2.85 (H-3′)	0 ± 2
	3.04 (H-3)	8 ± 1
	3.55 (H-6)	10 ± 2
	3.95 (H-6′)	9 ± 1
1.29 (Me-2′)	2.85 (H-3′)	8 ± 1
	3.04 (H-3)	0 ± 2
	3.55 (H-6)	0 ± 2
	3.95 (H-6′)	0 ± 2

Discussion

Considerable attention has been paid recently to the photodimerization of α,β-unsaturated carbonyl compounds and to the related photoaddition of such compounds to olefins (18), but the interplay of the factors that influence the regiochemistry and stereochemistry of these reactions remains far from elucidation. Although the present work has not provided a solution to this general problem, it has led to results

TABLE 6. Photochemical interconversion of dimers **A**, **B**, and **C**

Dimer irradiated*	Dimers produced (%)		
	A	**B**	**C**
A	30	60	10
B	15	85	Trace
C†	Trace	50	50

*See Experimental section for conditions.
†Enriched fraction containing A (10%), B (25%), and C (65%).

[7]The measurement of n.O.e.'s in conjunction with monosubstitution of one of the terminal rings promises to be a general method for distinguishing between *syn* and *anti* dimers of the cyclobutane type.

Can. J. Chem. Downloaded from www.nrcresearchpress.com by 210.87.254.42 on 09/05/12
For personal use only.

that should contribute to an eventual clarification.

The investigation had its inception in our interest in the photodimerization of 2,6-dimethyl-4-pyrone (**1**), which gives the cage compound **2**, an unusual *cis–syn–cis* head-to-tail product (see Introduction), and we discuss this process before proceeding to discuss the photodimerization of 2,3-dihydro-2,6-dimethyl-4-pyrone (**4**). The work has shown that it is the second ethylenic bond of **1** in relation to **4** that is the structural factor associated with the unusual stereochemistry of this dimerization. It has also revealed that photoreversibility may well play a crucial role, as suggested earlier (2). This conclusion stems from the observation that the bisdehydrodimer **18** of **4** undergoes photoreversion to the monomeric pyrone **1**. Thus it can be proposed that irradiation of **1** leads initially to a mixture of regioisomeric and stereoisomeric dimers of type **29**, of which only the *cis–syn–cis* head-to-tail compound undergoes photocycloaddition to give the cage compound **2**, which precipitates from solution, and that photoreversion of the other dimers of type **29** followed by redimerization leads to eventual formation of **2** as essentially the only photodimeric product. This view receives considerable support from recent observations of Hammond and MacGregor (19), who have found that irradiation of the pyrone **1** in acetonitrile leads to initial formation of two dimers of type **29**, *viz.* **3** and **18**, in addition to the cage dimer **2** (see Scheme 3).[8]

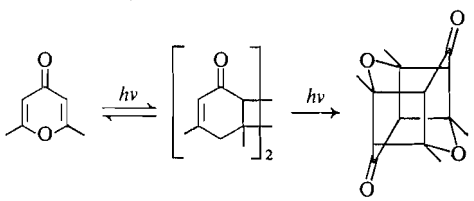

1 **29** **2**

SCHEME 3

The dimerization of **4** proceeds regiospecifically in a variety of solvents to give head-to-head dimers only. Further, although the reaction is stereoselective rather than stereospecific in that three stereoisomers are formed, these isomers differ only in the relative configurations of the C-6(6′) carbon atoms and the reaction is stereospecific with respect to cyclobutane ring formation, giving only *cis–anti–cis* dimers. This combined regiospecificity and stereospecificity is in marked contrast to the cases of the photodimerization of 2-cyclopentenone, 2-cyclohexenone, and alkyl-2-cyclohexenones (4–7, 20). It finds analogy, however, in the cases of 3-phenyl-2-cyclohexenone and 3-*p*-anisyl-2-cyclohexenone, which give only *cis–anti–cis* head-to-head photodimers (8, 21). It is therefore important to consider what features these 3-aryl-2-cyclohexenones possess in common with **4** that distinguish them from 2-cyclopentenone, 2-cyclohexenone, and alkyl-2-cyclohexenones. In terms of factors that have previously been adumbrated (18) as having importance in determining the course of photodimerization reactions, the possibility exists that the substitution of an aryl group or an ether oxygen atom at the β carbon of the α,β-unsaturated carbonyl system leads to a change in the nature of the excited state involved in the dimerization or that these substituents exert their influence by virtue of their stabilizing effect on an intermediate complex or diradical.

More intriguing is a third factor, *viz.*, again the reversibility of the photodimerization reaction (21). The photodimerization of the two 3-aryl-2-cyclohexenones has been shown to be reversible (8, 21), while, as far as we are aware, a similar observation has not been made in the cases of 2-cyclopentenone, 2-cyclohexenone, or alkyl-2-cyclohexenones. We now find that the photodimerization of **4** also is reversible. This conclusion stems from the observation of the photointerconversion of the photodimers of **4**, which can readily be interpreted as involving reversion to the monomer followed by redimerization.[9] Although we cannot offer a rationale to relate reversibility with the formation of *cis–anti–cis* head-to-head dimers[10] nor can we rule

[8]A very minor product from this reaction is considered to be the head-to-head analog of **2**; it cannot be excluded that traces of this compound accompanied **2** in the final reaction product in our original photodimerization experiments.

[9]Other routes for the photointerconversion could involve cleavage and reformation of $C_{6(6')}$—O bonds or exchange of monomer units among dimer molecules, initiated by a small amount of monomer. We know of no analogies for these processes and consider them to be considerably less probable than a process involving reversion to monomer and recombination.

[10]An interpretation in terms of preferential product precipitation cannot be made in the case of **4**, as was made for **1**, since no precipitation occurred during the photointerconversion of its dimers in solution.

Can. J. Chem. Downloaded from www.nrcresearchpress.com by 210.87.254.42 on 09/05/12
For personal use only.

out the possibility that the other photodimerization reactions may in fact also be reversible,[11] we consider that the present results make consideration of this factor important in the eventual formulation of any comprehensive mechanistic scheme.

Finally, we refer to the composition of the mixture of stereoisomeric dimers obtained from **4**, which, as emphasized previously, differ only in the relative configurations at the C-6(6′) carbon atoms. Random regiospecific dimerization of racemic **4** to give *cis*-fused products would lead to a mixture of racemic dimers **A**, **B**, and **C** in a 1:2:1 ratio. The observed ratio from the preparative experiments in water was 9:15:1. This distribution must reflect the interplay of differing rates of formation, differing rates of interconversion, and differing solubilities of the dimers. Although the last factor was inoperative in the photointerconversion studies, where no precipitation occurred, another factor now intervened, the occurrence of side-reactions, and thus no quantitative conclusions can be drawn from the data in Table 6. It is of interest to note that dimerization of a single enantiomorph of **4** should lead to a mixture of single enantiomorphs of dimers **A** and **C**, but no dimer **B**.

Experimental

Melting points were determined in capillary tubes with a Thomas–Hoover apparatus and are uncorrected. Unless otherwise stated, i.r. spectra were recorded in chloroform, u.v. spectra were recorded in 95% ethanol, and p.m.r. spectra were recorded at 60 MHz in deuteriochloroform containing tetramethylsilane (TMS) as internal reference. Mass spectra were recorded at 70 e.V. with an A.E.I. MS-9 spectrometer. Preparative t.l.c. was carried out on 20 × 20 cm glass plates coated with a 0.5 mm thickness of fluorescent silica gel G. Solutions of products in organic solvents were dried over anhydrous magnesium sulfate before removal of the solvent with a rotatory evaporator in conjunction with a water aspirator.

2,3-Dihydro-2,6-dimethyl-4-pyrone (4)

A modification of the method of de Vrieze (9) and Yates and Hand (10) was employed. 2,6-Dimethyl-4-pyrone (**1**) (50 g, 0.40 mol) in 95% ethanol (250 ml) was hydrogenated over 10% palladium – calcium carbonate (Engelhard Type 1, 13 g) at an initial pressure of 28 p.s.i. in a calibrated Parr apparatus; the hydrogen uptake was 0.42 mol during 90 min. The pyrophoric catalyst was removed by filtration (sintered glass), and the combined filtrates from four successive hydrogenations were concentrated to *ca.* 125 ml and cooled to give crude **1** (72 g, 36%), which was collected by filtration and washed with a small amount of petroleum ether (b.p. 90–100°). Analytical g.l.p.c. (6 ft × 1/4 in. 10% DIDP – Chromosorb P, 60 ml He/min, 150°) of the combined filtrate and washings showed the presence of **4**, **5**, and **6**. These were concentrated to an oil which was dissolved in chloroform (100 ml) and washed in turn with 6 *N* hydrochloric acid (2 × 50 ml) and water (4 × 50 ml); removal of the chloroform gave a brown oil (52 g). Fractional distillation (10 mm) of the oil gave crude tetrahydropyrone **5** (b.p. 25–70°; 23 g), a 1:1 mixture of **4** and **5** (b.p. 70–83°; 5.3 g), and **4** (b.p. 83–85°; 20 g (10%)) contaminated with 1–10% of the tetrahydropyranol **6**. The dihydropyrone (**4**) had λ_{max} 6.04 and 6.21 μ; λ_{max} 263 nm (log ε 4.15) (*cf.* de Vrieze (9) λ_{max} 263 nm (log ε 3.84)); δ 1.45 (d, J = 7 Hz, 3H), 1.98 (s, 3H), 2.1–2.5 (m, 2H), 4.5 (m, 1H), 5.28 (s, 1H); *m/e* (relative abundance) 126 (51), 111 (4), 85 (99), 84 (10), 69 (43), 43 (100), 42 (19), 41 (18), 39 (19). The dihydropyrone decomposed slowly on standing, but could be stored for long periods in the frozen state at −20°.

Redistillation of the first fraction above gave pure **5**, b.p. 80–82° (30 mm); $\lambda_{max}(CCl_4)$ 5.81 μ; δ (CCl_4) 1.27 (d, J = 6 Hz, 6H), 2.0–2.2 (m, 4H), 3.6 (m, 2H).

A small amount of tetrahydropyranol **6** was isolated from the crude hydrogenation product by g.l.p.c. and had λ_{max} (CCl_4) 2.75 (m), 2.8–3.0 (w) μ, and no bands in the carbonyl region. In other experiments in which the extraction with hydrochloric acid was omitted, the distillates with b.p. > 70° (10 mm) were chromatographed on alumina (B.D.H. chromatographic grade). Elution with chloroform gave a mixture of **4** and **5**; elution with acetone gave pure **6**, b.p. 102–103° (27 mm); $\lambda_{max}(CCl_4)$ as above; δ (CCl_4) 1.15 (d, J = 6 Hz, 6H), 1.8 (m, 4H), 3.5 (m, 3H), 4.08 (s, 1H).

Irradiation of 2,3-Dihydro-2,6-dimethyl-4-pyrone (4): Preparation of Dimers A (20), B (21), and C (22)

A solution of **4** (18.83 g, 96% pure by g.l.p.c.) in water (150 ml) was purged with a slow stream of nitrogen for 30 min in a Pyrex tube; the stoppered tube was placed 3 in. from the cooling well of a 450 W medium-pressure Hanovia lamp and irradiated for 2 weeks. The precipitated crystalline product (9.15 g) was collected, and the filtrate was irradiated as above to give a second crystalline crop (4.48 g). Extraction of the filtrate with chloroform and evaporation of the extracts gave a resinous yellow solid (4.50 g) which showed in its p.m.r. spectrum in addition to bands attributable to dimers of **4** weak bands due to the tetrahydropyranol **6**. P.m.r. analysis of the total product (18.13 g; 96% yield based on 100% pure **4**) in pyridine showed the presence of dimer **A** (**20**) (36%), dimer **B** (**21**) (60%), and dimer **C** (**22**) (4%). Preliminary qualitative experiments showed that similar product mixtures were obtained by irradiation of neat **4** or its ethanol, benzene, cyclohexane, and aqueous solutions in quartz (254 nm).

The total photoproduct was crystallized from ethanol to give a white crystalline fraction, m.p. 144–150°. Six recrystallizations of this material from polar solvents (ethanol, isopropyl alcohol, 50% aqueous isopropyl

[11]It may be noted that the asymmetric centers at C-6(6′) in the dimers of **4** serve to make evident the photoreversion of these dimers; it is possible that in cases lacking such a marker photoreversion followed by redimerization has gone undetected.

Can. J. Chem. Downloaded from www.nrcresearchpress.com by 210.87.254.42 on 09/05/12
For personal use only.

alcohol) gave dimer **A** (**20**),[12] m.p. 163–164°; molecular weight 244 (osmometric determination in benzene; calcd. 252); *m/e* 127 (56), 126 (26), 85 (100), 84 (8), 82 (8), 69 (13), 56 (4), 43 (38), 42 (16), 41 (8). The p.m.r. spectrum (100 MHz) of **A** in deuteriochloroform showed a doublet (J = 7 Hz) for the low-field satellite of the cyclobutyl protons ($J_{C^{13}-H}$ = 126 Hz).

Anal. Calcd. for $C_{14}H_{20}O_4$: C, 66.67; H, 7.94. Found: C, 66.40; H, 7.94.

Recrystallization (ethanol) of the combined residues obtained from the above mother liquors gave a large fraction, m.p. 130–133°. P.m.r. analysis (pyridine) of this material showed it to be a 1:4 mixture of dimers **A** and ***B***; subsequent construction of an m.p. *vs.* composition diagram for **A** and ***B*** showed a single eutectic point at 20% **A**. Attempts to fractionate this mixture by column chromatography on alumina or silica gel, by analytical t.l.c. on silica gel G or alumina, by preparative t.l.c. (silica gel G), by analytical g.l.p.c. (10% SE-30/Diatoport S, 180°; 10% Fluorosilicone – Diatoport S, temperature programmed from 175° at 3°/min), by zone refining, and by fractional sublimation were all unsuccessful.

Four recrystallizations of the eutectic mixture of dimers **A** and ***B*** (the first two from 100 vol/wt.) from hexane gave pure dimer ***B***[12] (**21**), m.p. 133–134°; *m/e* 127 (67), 126 (40), 85 (100), 84 (11), 82 (15), 69 (18), 56 (7), 43 (59), 42 (10), 41 (13).

Anal. Calcd. for $C_{14}H_{20}O_4$: C, 66.67; H, 7.94. Found: C, 66.93; H, 7.96.

A crystalline mixture (*ca.* 1 g) of dimers **A** (15%), **B** (50%), and **C** (35%), obtained from unsuccessful attempts to isolate dimer **C** by fractional crystallization of the lowest-melting fractions (m.p. *ca.* 115–123°), was dissolved in cyclohexane (100 ml) and subjected to 24 liquid–liquid extractions in a 10-funnel distribution train with 100 ml portions of cyclohexane and water as the stationary and mobile phases, respectively. Small amounts of crystalline material were obtained from all but the first aqueous fraction; the proportion of dimer *C* increased from 35% in the second fraction to 60% in the sixteenth fraction and remained at 60–65% in the next eight fractions. A fraction containing dimer **A** (10%), dimer **B** (25%), and dimer C (65%) was used to record spectra[12]; this fraction had *m/e* 127 (62), 126 (33), 85 (100), 84 (6), 82 (14), 69 (13), 56 (3), 43 (40), 42 (7), 41 (9).

Attempted Isomerization of the Photodimers

The eutectic mixture of dimers **A** and **B** (*ca.* 100 mg) was sealed in a Pyrex tube under a nitrogen atmosphere and heated for 1 h at 200°. No change was observed in the p.m.r. spectra of the mixture.

A solution of dimer *A* (55 mg) in dry pyridine (15 ml) was refluxed for 1 h under a nitrogen atmosphere; no change was observed in the p.m.r. spectra of the residue. Parallel results were obtained on reflux of pyridine solutions of dimer **B** and of a dimer C-enriched fraction of the mixture of photodimers.

Base-catalyzed Deuteriation of Dimer A

A solution of dimer **A** (50 mg) in deuterium oxide (2 ml) and dry pyridine (20 ml) was refluxed for 1 h under a nitrogen atmosphere; removal of the solvent gave a residue whose p.m.r. spectrum showed partial deuteration. This was treated overnight under the same conditions to give crystalline hexadeutero-**A**; λ_{max} 5.84 μ; δ 1.22 (d, J = 6 Hz, 6H), 1.39 (s, 6H), 4.34 (q, J = 6 Hz, 2H); *m/e* 130 (40), 129 (18), 86 (100), 70 (13), 56 (8), 44 (11), 43 (80), 42 (8), 41 (8), 40 (8).

Bromination of Dimer A

*(i) Formation of α-Bromo Ketone **11***

A stirred solution of dimer **A** (109 mg, 0.43 mmol) in chloroform (25 ml) was treated dropwise with a solution of bromine (32 mg, 0.20 mmol) in chloroform (10 ml) at a rate such that the reaction mixture became colorless before each new addition of bromine. The chloroform layer was washed with aqueous 5% sodium carbonate (15 ml) and evaporated to give a crystalline residue (124 mg), which was chromatographed (4% ethanol–benzene) on two t.l.c. plates to give dimer **A** (70 mg) and crude **11** as white crystals (45 mg). The major contaminant in the product was *ca.* 25% of dimer **A**. The crude ketone **11** had λ_{max} 5.82 μ; δ 1.31 (d, J = 6 Hz, 3H), 1.34 (d, J = 6 Hz, 3H), 1.43 (s, 3H), 1.51 (s, 3H), 2.31–2.45 (m, 2H), 3.07 (d, J = 5 Hz, 1H), 3.78 (d, J = 5 Hz, 1H), 4.08 (d, J = 2 Hz, 1H), 4.0–4.5 (m, 2H). It decomposed on standing.

*(ii) Preparation of α,α′-Dibromo Ketone **15***

A stirred solution of dimer **A** (75 mg, 0.30 mmol) in chloroform (3 ml) was treated as above with a solution of bromine (96 mg, 0.60 mmol) in chloroform (5 ml). The chloroform layer was washed with 5% aqueous sodium bicarbonate (10 ml) and evaporated. Recrystallization of the white crystalline residue (123 mg; *ca.* 90% pure by p.m.r. analysis) from hexane (12 ml) gave pure **15** as fine white needles, m.p. 168–170° (dec.); λ_{max} (CCl_4) 5.79 μ; λ_{max} 304 nm (log ε 2.20); δ 1.33 (d, J = 6 Hz, 6H), 1.53 (s, 6H), 3.80 (s, 2H), 4.05 (d, J = 2 Hz, 2H), 4.23 (q of d J_q = 6 Hz, J_d = 2 Hz, 2H); *m/e* 208 (10), 207 (5), 206 (10), 205 (5), 127 (13), 126 (20), 86 (100), 70 (20), 43 (54), 41 (26).

Anal. Calcd. for $C_{14}H_{18}Br_2O_4$: C, 40.99; H, 4.22; Br, 38.97. Found: C, 41.02; H, 4.47; Br. 39.15.

*Preparation of the Bis-enone **18***

*(i) By Dehydrobromination of **15***

Crude α,α′-dibromo ketone **15** (210 mg; *ca.* 90% pure by p.m.r. analysis) was dissolved in dry pyridine (40 ml), and the solution was refluxed with stirring in a nitrogen atmosphere for 5 h and then stirred overnight at ambient temperature. The dark red solution was diluted with ether (75 ml) and water (50 ml) and extracted with chloroform (3 × 10 ml). A black tar (129 mg) was obtained after prolonged drying of the residue from the chloroform extracts over concentrated sulfuric acid *in vacuo*. P.m.r. analysis of the tar showed the presence of the bis-enone **18** with *ca.* 15% of the monomeric pyrone **1** as the only major impurity; the latter was removed by chromatography on silica gel; elution with 2–4% ethanol–chloroform gave spectroscopically pure, but yellow, **18** (106 mg). This was purified by crystallizing it once from 70% aqueous isopropyl alcohol, followed by chromatography on silica gel. The column was developed by slowly changing the mobile phase from 20% chloroform–benzene to 15% benzene–chloroform; the colorless product was eluted with 10–0% benzene–chloroform. After one

[12]The p.m.r. spectra of this dimer are recorded in Table 1 and its u.v. and i.r. spectra in Table 2.

Can. J. Chem. Downloaded from www.nrcresearchpress.com by 210.87.254.42 on 09/05/12
For personal use only.

recrystallization from ethanol, **18** (22 mg, 17%) had m.p. 179–181°; *m/e* 248 (6), 163 (10), 125 (100), 124 (43), 96 (43), 95 (10), 80 (4), 69 (16), 53 (9), 43 (63).[13]

(ii) By Treatment of Dimer A with N-Bromosuccinimide

A mixture of *N*-bromosuccinimide (NBS; 144 mg, 0.81 mmol) and a solution of dimer **A** (102 mg, 0.41 mmol) in carbon tetrachloride (35 ml) was heated to boiling in a flask equipped with a pressure-equalizing addition funnel, a gas delivery tube, and a condenser. A slow stream of nitrogen was passed through the mixture until the first appearance of a pink coloration due to bromine (2–3 min after the commencement of boiling); nitrogen flow was then continued very briskly during the ensuing reaction to assist the rapid removal of bromine by codistillation with carbon tetrachloride. The volume was kept approximately constant by adding carbon tetrachloride from the addition funnel during the distillation (*ca.* 5 min). The rapid distillation cooled the reaction mixture, and the heating – rapid distillation process was continued until no further bromine evolution occurred on reheating the mixture to its boiling point. The precipitated succinimide was removed by filtration after refrigeration, and the yellowish crystalline residue obtained by removal of the solvent was fractionated by preparative t.l.c. on two plates (10% methanol – carbon tetrachloride). In order of increasing R_F values, five fractions were obtained and identified by i.r. spectroscopy: succinimide (8 mg); two mixtures of succinimide and the bis-enone **18** (19 and 4 mg); the enone **24** (47 mg); and dimer **A** (36 mg). The mixtures of succinimide and **18** were separated by extraction of their solutions in carbon tetrachloride with water or by chromatography on silica gel with 50–60% chloroform–benzene. After one recrystallization (−20°) from isopropyl alcohol, bis-enone **18**, m.p. 172–173°, spectroscopically identical with the product obtained in (*i*) above, was obtained.

The crude enone **24** obtained above had λ_{max} 5.83, 6.07, 6.23 μ; δ 1.32 (d, J = 6 Hz, 3H), 1.48 (s, 3H), 1.52 (s, 3H), 1.98 (s, 3H), 2.30–2.45 (m, 2H), 3.07 (d, J = 5 Hz, 1H), 3.17 (d, J = 5 Hz, 1H), 4.05–4.50 (m, 1H), 5.22 (s, 1H).

(iii) By Treatment of Dimer B with N-Bromosuccinimide

Several experiments similar to that described in (*ii*) above were performed with dimer **B**. After aqueous extraction of succinimide, the combined crude products were chromatographed as described in (*i*) above; elution with 0–5% ethanol–chloroform gave the bis-enone **18** (25 mg). One recrystallization (−20°) from ethanol gave an analytical sample, m.p. 181–182°, unchanged on recrystallization from ethanol and spectroscopically identical with the two samples of **18** prepared above. The product had mixed m.p. 179–181° with the product obtained in (*i*) above.

Anal. Calcd. for $C_{14}H_{16}O_4$: C, 67.73; H, 6.50. Found: C, 67.75; H, 6.43.

Preparative t.l.c. of other reaction products of dimer **B** with NBS, as described in (*ii*) above, gave the crude enone **23**: λ_{max} 5.83, 6.04, 6.24 μ; δ 1.28 (d, J = 6 Hz, 3H), 1.38 (s, 3H), 1.47 (s, 3H), 2.02 (s, 3H), 2.32–2.47 (m, 2H), 2.92 (d, J = 5Hz, 1H), 3.15 (d, J = 5 Hz, 1H), 3.9–4.3 (m, 1H), 5.27 (s, 1H).

Acid-catalyzed Cleavage of Cage Photodimer 2: Preparation of the seco-Dimer 3

A suspension of the cage photodimer **2** (5.01 g) in a solution of 2 *N* hydrochloric acid (1.85 l) in methanol (2.5 l) was stirred for 2 days in a nitrogen atmosphere at room temperature. Unconsumed **2** (0.33 g) was removed by filtration, and the filtrate was neutralized with potassium carbonate and distilled (35°/15 mm) to remove the methanol. The concentrated aqueous solution was extracted with chloroform. Evaporation of the combined extracts left an orange paste (3.37 g) from which a white crystalline fraction (1.24 g) was obtained by trituration with ether. This material was chromatographed on silica gel (100 g); prolonged development of the column with chloroform (which was recycled), slowly displaced unconsumed **2** as a turbid band which was subsequently eluted with 0–2% acetone–chloroform. Continued elution of the column with 3–5% acetone–chloroform gave the *seco*-dimer **3** (0.96 g, 21%). One recrystallization from ethanol gave pure **3**, m.p. 223–224° (sealed capillary); *m/e* 248 (3), 126 (9), 125 (100), 124 (45), 96 (31), 80 (29), 79 (9), 69 (12), 43 (37), 39 (7).[13]

Photolysis of the Bis-enone 18

Spectroscopically pure bis-enone **18** (33 mg) dissolved in absolute ethanol (2.5 ml) in a tightly corked Pyrex semi-micro test tube was irradiated for 1 day with the 254 nm light source of a Rayonet Photochemical Reactor. After removal of the solvent, the residue was identified as crude **1** by its i.r., p.m.r., and mass spectra. In a control experiment under identical conditions, most of the *seco*-dimer **3** was converted to cage photodimer **2** in 6 h; a separate control irradiation of the pyrone **1** showed it to be photochemically unreactive under the above conditions for 2 days.

Catalytic Hydrogenation of Bis-enone 18: Formation of Dimer C

Analytically pure bis-enone **18** (28 mg) was dissolved in 95% ethanol (2.5 ml) and hydrogenated at atmospheric pressure in the presence of 10% palladium – calcium carbonate (*ca.* 5 mg) for 4 days.[14] Removal of the catalyst and solvent left a crystalline residue, whose p.m.r. spectra in deuteriochloroform and in benzene identified it as a *ca.* 2:1 mixture of dimer **C** and the enone **23**.

Catalytic Hydrogenation of seco-Dimer 3: Formation of 25

A solution of *seco*-dimer **3** (126 mg) in 95% ethanol (25 ml) containing a suspension of 10% palladium – calcium carbonate (14 mg) was hydrogenated at atmospheric pressure for 10 h. The crystalline residue was chromatographed on silica gel; elution with 25% benzene–chloroform gave a fraction (89 mg) which showed no bands due to **3** in its i.r. spectrum. Two recrystallizations of this product from petroleum ether (b.p. 90–100°) gave a sample, m.p. 113–115°, with a satisfactory microanalysis for **25**, but whose p.m.r. spectrum indicated the presence

[13]Other spectral data for this compound are given in Table 3.

[14]Hydrogenation of **3** on the same scale was also very slow.

of impurity; the major component had δ 1.26 (d, J = 6 Hz, 6H), 1.43 (s, 6H), 2.28–2.44 (m, 4H), 2.58 (s, 2H), 3.7–4.0 (m, 2H); *m/e* 127 (39), 126 (30), 111 (9), 85 (100), 69 (22), 55 (7), 44 (9), 43 (63), 42 (13), 41 (20).

Anal. Calcd. for $C_{14}H_{20}O_4$: C, 66.67; H, 7.94. Found: C, 66.92; H, 8.17.

Intramolecular Nuclear Overhauser Effect Measurements on Dimer B

Measurements were performed with a Varian HA-100 spectrometer operated in the frequency sweep mode at an r.f. attenuation of 20 dB. The saturating r.f. field was provided by a Muirhead-Wigan D-890-A decade oscillator. The instrument was tuned to maximum deflection of an A.C. voltmeter connected to the oscilloscope; in this way field stability could be monitored during the n.O.e. measurements. The effects cited in Table 5 were measured as percentage area increases obtained during irradiation of a given resonance at predetermined optimum external frequency, power level, and phase settings, compared with integrals obtained under identical conditions except for a 100 Hz offset in the position of the saturating field. All integrals were measured at a sweep rate of 2 Hz/s; the pen output was set to give integrals > 50 mm. The results quoted are the average of at least four separate determinations and are precise to at least ±2%.

The samples employed were filtered 5–6% solutions of dimer **B** in hexadeuteriobenzene containing 10% of benzene for a frequency lock signal. Oxygen was removed by passing oxygen-free nitrogen through the solutions (22). A 10% solution of β,β-dimethylacrylic acid in deuteriochloroform containing 10% TMS, prepared by the above method, gave an optimum n.O.e. of 15 ± 2%, in good agreement with the result of Anet and Bourn (23).

Irradiation of Dimers A, B, and C

Solutions of dimers **A**, **B**, and a fraction enriched in dimer C (*ca.* 50 mg each) in absolute ethanol (3 ml) were irradiated simultaneously in Pyrex tubes with the 300 nm source of the Rayonet apparatus for 1 day. Analysis (p.m.r.) of the residues obtained after evaporation of the solvent showed that interconversion of the dimers had occurred concomitant with the formation of an oily, uncharacterized product. The approximate compositions of the dimeric fractions (*ca.* 75% of the product mixtures) are shown in Table 6.

We thank the National Research Council of Canada for support of this work and Dr. S. N. Eğe for preliminary experiments. D.J.M. thanks the Province of Ontario and the Canadian Kodak Co. for financial assistance. The n.O.e. measurements were carried out at the School of Chemistry, University of Bristol, England, by D.J.M. during the tenure of a National Research Council of Canada postdoctoral fellowship; grateful acknowledgement is made to Professor M. C. Whiting for his hospitality and to Dr. R. J. Goodfellow for technical advice.

1. P. YATES and D. J. MacGREGOR. Tetrahedron Lett. 453 (1969).
2. P. YATES and M. J. JORGENSON. J. Am. Chem. Soc. **85**, 2956 (1963).
3. P. YATES, E. S. HAND, P. SINGH, S. K. ROY, and I. W. J. STILL. J. Org. Chem. **34**, 4046 (1969).
4. E. Y. Y. LAM, D. VALENTINE, and G. S. HAMMOND. J. Am. Chem. Soc. **89**, 3482 (1967); P. J. WAGNER and D. J. BUCHECK. J. Am. Chem. Soc. **91**, 5090 (1969).
5. P. GERIKE. Ph.D. Thesis. University of Utah, Salt Lake City, Utah. 1966; W. W. EPSTEIN. Private communication; H. ZIFFER and I. W. LEVIN. J. Org. Chem. **34**, 4056 (1969); H. ZIFFER, H. M. FALES, G. W. A. MILNE, and F. H. FIELD. J. Am. Chem. Soc. **92**, 1597 (1970); H. ZIFFER and B. W. MATTHEWS. Chem. Commun. 294 (1970); D. K. HUI. M.Sc. Thesis. University of Toronto, Toronto, Ontario. 1970.
6. H. ZIFFER, N. E. SHARPLESS, and R. O. KAN. Tetrahedron, **22**, 3011 (1966).
7. D. J. TRECKER, A. A. GRISWOLD, and O. L. CHAPMAN. Abstr. 152nd Nat. Meet. Am. Chem. Soc. New York, N.Y., September, 1966, S 28; O. L. CHAPMAN, P. J. NELSON, R. W. KING, D. J. TRECKER, and A. A. GRISWOLD. Rec. Chem. Progr. **28**, 167 (1967); O. L. CHAPMAN. 20th Nat. Org. Chem. Symp. Burlington, Vermont, June, 1967.
8. P. YATES, S. N. EĞE, G. BÜCHI, and D. KNUTSEN. Can. J. Chem. **45**, 2927 (1967).
9. J. J. DE VRIEZE. Rec. Trav. Chim. Pays-Bas, **78**, 91 (1959).
10. P. YATES and E. S. HAND. J. Am. Chem. Soc. **91**, 4749 (1969).
11. J. R. BARTELS-KEITH and W. B. TURNER. J. Chem. Soc. 3413 (1960).
12. R. C. COOKSON, D. A. COX, and J. HUDEC. J. Chem. Soc. 4499 (1961); R. C. COOKSON, J. J. FRANKEL, and J. HUDEC. Chem. Commun. 16 (1965).
13. I. FLEMING and D. H. WILLIAMS. Tetrahedron, **23**, 2747 (1967).
14. *Cf.* R. ANET. Tetrahedron Lett. 3713 (1965).
15. *Cf.* E. J. COREY, J. D. BASS, R. LEMAHIEU, and R. B. MITRA. J. Am. Chem. Soc. **86**, 5570 (1964).
16. See, for example, T. N. MARGULIS and M. S. FISCHER. J. Am. Chem. Soc. **89**, 223 (1967); T. N. MARGULIS. Acta Cryst. **18**, 742 (1965); N. CAMERMAN, S. C. NYBURG, and D. WEINBLUM. Tetrahedron Lett. 4127 (1967).
17. J. I. MUSHER. J. Chem. Phys. **35**, 1159 (1961).
18. P. E. EATON. Acc. Chem. Res. **1**, 50 (1968); P. DE MAYO. Acc. Chem. Res. **4**, 41 (1971).
19. G. S. HAMMOND and D. J. MacGREGOR. Unpublished results.
20. P. E. EATON. J. Am. Chem. Soc. **84**, 2344 (1962).
21. S. N. EĞE and P. YATES. Can. J. Chem. **45**, 2933 (1967).
22. J. G. COLSON, P. T. LANSBURY, and F. D. SAEVA. J. Am. Chem. Soc. **89**, 4987 (1967).
23. F. A. L. ANET and A. J. R. BOURN. J. Am. Chem. Soc. **87**, 5250 (1965).

Can. J. Chem. Downloaded from www.nrcresearchpress.com by 210.87.254.42 on 09/05/12
For personal use only.

Mechanism of Ozonolysis. The Initial Ozonide. Lack of Evidence for "Unified Concept" Involving Staudinger Molozonide

PHILIP S. BAILEY, THOMAS P. CARTER, JR., CHARLES M. FISCHER, AND JAMES A. THOMPSON

Department of Chemistry, The University of Texas at Austin, Austin, Texas 78712

Received October 30, 1972

Contrary to previous reports cyclohexanone and pinacolone are not oxidized to the corresponding Baeyer–Villiger oxidation products during ozonolysis of ethylidenecyclohexane in their presence. Addition of propionaldehyde to a solution of the 1,2,3-trioxolane initial ozonide of *trans*-1,2-di-*t*-butylethylene resulted in oxidation of the aldehyde to propionic acid and reduction of the 1,2,3-trioxolane to pivaldehyde. Thus, there is no necessity for the four-membered Staudinger molozonide as an ozonolysis intermediate, as recently proposed by Story.

Contrairement aux publications antérieures, la cyclohexanone et la pinacolone ne sont pas oxydées selon un Baeyer–Villiger pendant l'ozonolyse de l'éthylidènecyclohexane en leur présence. L'addition du propionaldéhyde à une solution de trioxolane-1,2,3, ozonide dérivé initial du *trans*-di-*t*-butyl-1,2 éthylène, a pour résultat l'oxydation de l'aldéhyde en acide propionique et la réduction du trioxolane-1,2,3 en pivalaldéhyde. Ainsi, il n'est plus nécessaire d'avoir le monozonide à quatre membres de Staudinger comme intermédiaire d'ozonolyse, comme cela a été proposé recemment par Story.

[Traduit par le journal]

Can. J. Chem., 51, 1278 (1973)

Can. J. Chem. Downloaded from www.nrcresearchpress.com by 210.87.254.5 on 09/05/12
For personal use only.

Story and coworkers (1–3) recently have proposed a so-called "unified concept" (2) for the mechanism of the ozonolysis reaction, in which they invoke the initial formation of a four-membered ring system (**1**, a Staudinger "molozonide") as a precursor to the accepted 1,2,3-trioxolane (*e.g.* **2**) initial ozonide and/or peroxidic and nonperoxidic ozonolysis products. The experimental basis for this proposal is their reported finding that ozonolysis of several olefins in a large excess of propionaldehyde (1), cyclohexanone (1), or pinacolone (3) resulted in reduction of the initial ozonide (to aldehydes and/or ketones) and Baeyer–Villiger oxidation of the added aldehyde or ketone (to propionic acid, 6-hexanolactone, and *t*-butyl acetate, from the above three, respectively). Since it had previously been shown that ozonolysis of an olefin in the presence of only 1 mol of added aldehyde gave cross ozonides (4, 5) and since the earlier Story–Murray mechanism (4) accounts for this via attack of the aldehyde on a 1,2,3-trioxolane (*e.g.* **2**) intermediate, Story (2, 3) felt that some other species, a precursor to the trioxolane and/or ozonolysis products, was the oxidant which was reduced by the excess aldehyde or ketone. As further evidence that this species was the Staudinger molozonide (**1**), Story (3) reported that several olefins yielded the corresponding dioxetane (**3**) upon ozonation in the presence of pinacolone; the dioxetane, of course,

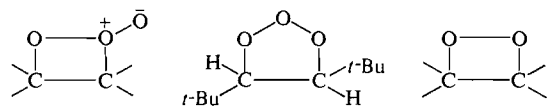

1 **2** **3**

would readily break down to aldehyde and/or ketone moieties.

Because ozone is considered to be one of the most typical 1,3-dipoles (6), it seemed highly unlikely to us that it would react initially with an alkene to form a strained four-membered ring adduct, especially as a precursor to the five-membered 1,2,3-trioxolane ring which has been established in several cases as an ozonolysis intermediate (7, 8).

The purpose of the present paper is to give additional experimental details concerning our earlier low temperature n.m.r. proof of the 1,2,3-trioxolane structure for the initial ozonide (**2**) of *trans*-1,2-di-*t*-butylethylene (7) and to show that there is no experimental basis for the "unified" ozonolysis mechanism of Story and coworkers (1–3). Just as we were finishing this work, Professor K. R. Kopecky kindly sent us a preprint of the paper describing his work (9) which also refutes the Story mechanism.

Our first approach to testing the "unified concept" of Story (2) was to determine whether or not a known 1,2,3-trioxolane would oxidize propionaldehyde, cyclohexanone, etc., to their

TABLE 1. N.m.r. studies of the ozonation of *trans*-1,2-di-*t*-butylethylene and related substances

Experiment	Spectrum taken	Solvent	Temperature (°C)	δ-Values: Methine protons	δ-Values: *t*-Butyl protons
1	Ozonation solution of **2**	$CFCl_3$	−95	4.20[a]	0.97[a]
2	Solution of **2**	$CFCl_3$ + Acetone (1:1)[b]	−95	4.44	0.96
3	Solution of **2**	$CFCl_3$ + Acetone (1:2)[b]	−95	4.50	0.97
4	Ozonation solution of **2**	Acetone[b]	−95	4.67[c]	0.99[d]
5	Ozonation solution	$CFCl_3$	−85	4.29	1.01
6	Ozonation solution	$CFCl_3$	−63	4.28	1.08, 0.99
7	Ozonation solution	$CFCl_3$	−48	9.57, 4.29	1.08, 1.00
8	Ozonation solution	$CFCl_3$	28	9.41[e]	1.05[e]
9	Ozonation solution	Acetone[b]	28	9.46, 4.75	1.05, 0.91
10	Pivaldehyde	$CFCl_3$	28	9.41	1.05
11	Pivaldehyde	Acetone[b]	28	9.46	1.05
12	*cis* true ozonide	$CFCl_3$	28	4.76	0.97
13	*cis* true ozonide	Acetone[b]	28	4.90	0.97
14	*trans* true ozonide	$CFCl_3$	28	4.71	0.97
15	*trans* true ozonide	Acetone[b]	28	4.81	0.97
16	*trans* dtbe[f]	$CFCl_3$	28	5.34	0.99
17	*trans* dtbe[f]	Acetone[b]	28	5.40	0.99
18	*cis* dtbe[f]	$CFCl_3$	28	5.18	1.14
19	Ozonation solution of *cis* dtbe[f]	$CFCl_3$	−103	4.86, 4.80[g]	1.00[g]
20	Ozonation solution	$CFCl_3$	−77	4.86, 4.81	0.99
21	Ozonation solution	$CFCl_3$	−31	4.76, 4.71	0.97

[a]Ratio of approximately 1:9 for methine to *t*-butyl protons.
[b]The acetone was acetone-d_6.
[c]A water peak was also present, varying from around δ 4.3 at low temperatures to 2.8 at room temperature.
[d]Minor peaks due to slight decomposition also were observed, along with a small peak due to H^1 content of acetone-d_6 (2.11).
[e]Addition of pivaldehyde increased these peaks. Also some minor peaks due to ozonides or polymeric peroxides were observed.
[f]Di-*t*-butylethylene.
[g]Addition of *cis*- and *trans*-ozonides increased these peaks.

Baeyer–Villiger oxidation products; if so, there would be no need to invoke the Staudinger molozonide structure (**1**). Such a substance is the initial ozonide (**2**) of *trans*-1,2-di-*t*-butylethylene, which we showed in 1966 by low temperature n.m.r. to have a symmetrical structure and, therefore, to possess a five- (**2**) rather than a four- (**1**) membered ring. Both in acetone-d_6 at −95° and in Freon 11 ($CFCl_3$) at −95° or below only two singlet peaks were observed, one for the *t*-butyl protons and one for the methine protons (Table 1) in the ratio 9:1.

In his first paper on the "unified" mechanism, Story (1) reported that he ozonized *trans*-1,2-di-*t*-butylethylene in pentane, added propionaldehyde to the cold reaction mixture, and found that oxidation of propionaldehyde to propionic acid occurred. However, the initial ozonide is insoluble in pentane and Story (1) assumed that the precipitate was the Staudinger molozonide (**1**) and that the symmetrical trioxolane structure was present only in solution. We, therefore, used very dilute (0.5%) solutions of *trans*-1,2-di-*t*-butylethylene in acetone in order to insure that all of the initial ozonide stayed in solution after the ozonation. The ozonation was carried out at −78° (the initial ozonide does not decompose until −60° or above, see Table 1) in a special two-chambered ozonation vessel (Fig. 1) after which a precooled solution of a large excess of freshly distilled propionaldehyde or cyclohexanone was added as described in the Experimental. The results are shown in Table 2. The propionaldehyde was oxidized to propionic acid and the initial ozonide (**2**) was partially reduced to pivaldehyde. However, no oxidation of cyclohexanone to 6-hexanolactone was observed.

The propionaldehyde experiment shows that it is unnecessary to invoke a Staudinger molozonide (**1**) precursor to account for the oxidation to propionic acid; the oxidation must have been brought about by the trioxolane (**2**), the Criegee carbonyl oxide zwitterion, or some species in between. If it involved the trioxolane or an initial

Can. J. Chem. Downloaded from www.nrcresearchpress.com by 210.87.254.5 on 09/05/12
For personal use only.

TABLE 2. Ozonation of *trans*-1,2-di-*t*-butylethylene followed by addition of excess propionaldehyde or cyclohexanone[a]

Experiment	Dtbe[b] (mmol)	Solvent (ml)	Added substance (mmol)	Propionic acid or 6-hexanolactone[c] (mmol)	Other products (mmol)
1	3.05	100, acetone	84, propionaldehyde[d]	3.05	4.51, pivaldehyde; 0.324, pivalic acid, ozonides, and polymeric peroxides
2	3.21	100, acetone	84, propionaldehyde[d]	1.93	5.56, pivaldehyde; 0.33, pivalic acid, ozonides, and polymeric peroxides
3	3.06	100, acetone	97, cyclohexanone[d]	None	4.54, pivaldehyde[e]; ozonides, polymeric peroxides, pivalic acid (trace)
4	3.19	100 acetone	49, cyclohexanone[d]	None	5.31, pivaldehyde[e], ozonides, polymeric peroxides, pivalic acid (trace)
5	1.0	8 ether	10, cyclohexanone[f]	None	0.93 pivaldehyde, ozonides, polymeric peroxides
6	3.1	100, acetone	None	—	1.2, pivaldehyde[g]

[a]Ozonized at −78° in special ozonation vessel (Fig. 1) and added precooled propionaldehyde or cyclohexanone at −78°.
[b]*trans*-Di-*t*-butylethylene.
[c]Propionic acid from propionaldehyde, 6-hexanolactone from cyclohexanone.
[d]In 25 ml acetone.
[e]The greater than 1 mol equiv of pivaldehyde obtained is probably due to decomposition of polymeric peroxides on the v.p.c. column.
[f]In 5 ml ether.
[g]No other products were looked for.

decomposition product thereof, the difference in the action of propionaldehyde when present to the extent of 1 mol per mole of olefin (to give a cross ozonide) (1) and in large excess (to reduce the initial ozonide) could be explained on the basis that the first reaction is first order with respect to the propionaldehyde whereas the second reaction probably is second order or higher. A possible mechanism is shown in Scheme 1. A similar Baeyer–Villiger oxidation could also be invoked for the carbonyl oxide zwitterion as the oxidant.

In order to determine whether or not the cyclohexanone results favored the Story mechanism, in that some species other than the 1,2,3-trioxolane was needed to oxidize the cyclohexanone to the 6-hexanolactone, *trans*-1,2-di-*t*-butylethylene was ozonized in cyclohexanone as a solvent. Gas chromatographic analysis revealed no 6-hexanolactone. Next, the very experiment reported by Story (1) was performed, namely the ozonation of ethylidenecyclohexane in cyclohexanone solvent. Whereas Story (1) reported a 50% yield of 6-hexanolactone, we found either none or only a trace. This experiment was performed several times, independently, by two different people in our laboratory. It was shown that under our v.p.c. conditions, 6-hexanolactone could easily be determined if present. Similar results were obtained using *trans*-3-hexene. Finally, again following Story's procedure (3), ethylidenecyclohexane was ozonized in pinacolone solvent; no *t*-butyl acetate was observed as a product. This experiment also was performed many times, independently, by three different people in our laboratory, by Kopecky and coworkers (9), in Criegee's laboratory in Karlsruhe,[1] and Fliszar's laboratory in Montreal.[2] Table 3 compares the results of ozonation of ethylidenecyclohexane in pentane and in pinacolone. Ethyli-

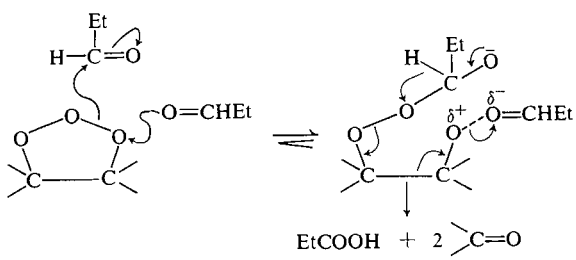

SCHEME 1

[1]Rudolph Criegee. Private communication.
[2]Sandor Fliszár. Private communication.

Can. J. Chem. Downloaded from www.nrcresearchpress.com by 210.87.254.5 on 09/05/12
For personal use only.

TABLE 3. Ozonation of ethylidenecyclohexane[a]

Solvent	O_3[b] (mmol)	Recovered starting material (mmol)	Cyclohexanone		Active oxygen (mmol)	
			mmol	% yield	KI[c]	HI[c]
Pentane	1.8	0.42	0.71	45	0.22	1.21
Pentane	1.9	0.19	0.88	49	0.02	1.17
Pinacolone	1.8	0.43	1.17[d]	75	1.30	1.63
Pinacolone	1.9	0.37	1.17[d]	72	1.22	1.78

[a]2 mmol in 10 ml of solvent was employed.
[b]An ozone–nitrogen stream was used.
[c]The low KI and high HI values in the first two experiments indicate the ozonide which was shown to react only slightly with KI, probably because it was trisubstituted. In the last two experiments the peroxide seems to be polymeric.
[d]The greater than 1 mol equiv of cyclohexanone obtained is probably due to decomposition of polymeric peroxides on the v.p.c. column.

denecyclohexane ozonide was isolated from the pentane experiments, but not from the pinacolone experiments, which appeared to give largely polymeric peroxides. Ozonation of ethylidenecyclohexane in acetone gave dimeric cyclohexanone peroxide and polymeric peroxides.

It is of interest that with the experiments in which cyclohexanone was added to a cold solution of the initial ozonide of *trans*-1,2-di-*t*-butylethylene (Table 2) more than 1 mol of pivaldehyde was obtained per mole of olefin. Likewise, in the ethylidenecyclohexane ozonations, considerably more cyclohexanone was obtained using pinacolone solvent than pentane solvent. This could be interpreted as indicating that reduction of some form of an initial ozonide or some other peroxidic species occurred, as reported by Story (1, 3). However, no oxidation of the solvent or added ketone occurred and only minor amounts of pivalic acid (from di-*t*-butylethylene) and acetic acid (from ethylidenecyclohexane) were obtained. We believe that the excess aldehyde or ketone product in these experiments comes from decomposition on the v.p.c. of polymeric peroxides or polymeric ozonides. There appears to be a solvent effect of cyclohexanone and pinacolone upon the fate of the initial ozonide, causing polymeric peroxidic ozonolysis products rather that ozonides to be produced (Tables 2 and 3).

Like Kopecky and coworkers (9) we found no evidence for the production of a dioxetane upon ozonolysis of ethylidenecyclohexane in pinacolone. Since our work parallels Kopecky's in this respect, we will relegate our results to the Experimental. We also found no evidence for the formation of a dioxetane upon ozonolysis of 2-methyl-2-butene in pinacolone.

These results, therefore, make the recent proposals of Story and coworkers (1–3) both unnecessary and untenable. The best description of the ozonolysis reaction at the present time is that a π complex is initially formed (10) which then is converted to a 1,2,3-trioxolane via 1,3-dipolar cycloaddition. There undoubtedly are several fates possible for the initial ozonide, including that described by the SMY mechanism (4) when a small excess of aldehyde is present. However, the Criegee mechanism, as refined recently (11), still provides the best description of the fate of the initial ozonide under normal conditions.

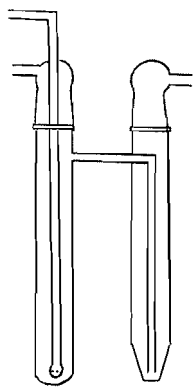

FIG. 1. Two-chambered ozonation vessel.

Experimental

The ozonation equipment and procedures using ozone–oxygen or ozone–nitrogen are described in earlier papers (12). For ozonations involving the addition of a cold solution of a substrate to an ozonized solution, without warming or introduction of oxygen occurring, a special two-chambered vessel shown in Fig. 1 was used. Different sizes were employed, varying from 10 to 125 ml volume in the ozonation chamber. V.p.c. determinations were made either with a Varian Aerograph 1520 B chromatograph or with an F and M 500 chromatograph. The low temperature n.m.r. spectra were recorded with a Varian DP-60 spectrometer using TMS as an internal standard. Other n.m.r. spectra were recorded either with

Can. J. Chem. Downloaded from www.nrcresearchpress.com by 210.87.254.5 on 09/05/12
For personal use only.

Can. J. Chem. Downloaded from www.nrcresearchpress.com by 210.87.254.5 on 09/05/12
For personal use only.

a Varian A-60 or HA-100 spectrometer. *Ethylidenecyclohexane* and *trans-1,2-di-t-butylethylene* were obtained from Chemical Samples Co. and were 99% pure. Other reagents and solvents also were obtained commercially and were checked for purity by v.p.c. The propionaldehyde was redistilled under nitrogen before each use.

Ozonation of trans-1,2-Di-t-butylethylene. N.m.r. Proof of 1,2,3-Trioxolane Structure of the Initial Ozonide

The ozonations were on 1% by weight solutions of *trans*-1,2-di-*t*-butylethylene in 5 ml of acetone-d_6 or Freon 11 ($CFCl_3$) at -95 to $-110°$. In earlier work 2.5–5% solutions were used, but the initial ozonide did not remain completely in solution. The solutions were ozonized with ozone in a nitrogen stream until pale blue, after which the excess ozone was swept out with nitrogen. An aliquot of the reaction mixture was then transferred to a precooled n.m.r. tube by means of a precooled disposable pipette. Tetramethylsilane was added and the n.m.r. spectrum taken in the low temperature probe of the spectrometer. In some cases the temperature was allowed to rise and new spectra taken. Where mixed solvents were employed, cold acetone-d_6 was added to a cold aliquot of the Freon 11 ozonation mixture. The results are shown in Table 1. It can be seen that decomposition of the initial ozonide begins somewhere between -63 and $-48°$ (experiments 6–8). The unusually large shift to lower field for the methine protons of the initial ozonide in going from the less polar Freon 11 to the more polar solvent appears to be only a solvent effect, rather than a difference in structure of the initial ozonide in the two solvents (*cf.* ref. 7), since the change gradually occurs as acetone is added to the Freon 11 solution (experiments 1–4). Ozonation of *cis*-1,2-di-*t*-butylethylene under the same conditions gave only ozonides (experiments 19–21).

Addition of Propionaldehyde or Cyclohexanone to Solution of Initial Ozonide (2) of trans-Di-t-butylethylene

A solution of approximately 0.5% by weight of *trans*-1,2-di-*t*-butylethylene in spectro-quality acetone was placed in the ozonation chamber of a large two-chamber ozonation vessel (Fig. 1). The appropriate amount of propionaldehyde or cyclohexanone in acetone was placed in the other compartment and the entire reaction vessel was cooled to $-78°$ in a Dry Ice – isopropanol bath. An equivalent of ozone in a nitrogen stream was then passed into the olefin solution, after which the reaction mixture was swept with nitrogen for 15 min. At this point the propionaldehyde or cyclohexanone solution was blown over into the ozonation solution with a nitrogen stream, the two solutions were mixed well by means of a nitrogen stream, and the reaction mixture was allowed to interact at $-78°$ for 1 h. Next, it was kept at $-60°$ for $\frac{1}{2}$ h, at $-30°$ for $\frac{1}{2}$ h, and then allowed to warm to room temperature. Benzene was added as an internal standard and pivaldehyde was determined on a 20 ft diisodecyl phthalate on Chromosorb G column at 80° (Aerograph 1520 B). Acetone and other volatiles were removed at room temperature by means of a water aspirator (6-hexanolactone boils at 118–119° at 15 mm) and the residue was taken up in carbon tetrachloride and analyzed by v.p.c. for pivalic acid and propionic acid or 6-hexanolactone. Propionic acid was identified by comparison with an authentic sample on a 5% DEGS, 2% phosphoric acid column (Aerograph 1520 B) and determined on a 5% Dimer Acid – Silicone Oil on Haloport F column at 90° (F and M 500) using the standard solution method. Pivalic acid was then determined on the DEGS–H_3PO_4 column at 90° (Aerograph 1520 B) using propionic acid as the internal standard. In the cyclohexanone experiments, pivalic acid was determined by n.m.r. (singlet at δ 1.22). No evidence for the 6-hexanolactone was obtained by v.p.c. using a 10 ft 30% Silicone Gum Rubber SE-30 on Chromosorb P column at 150° and comparing with an authentic sample. Likewise n.m.r. failed to show any lactone: multiplets at δ 4.20 (2H), 2.65 (2H), and 1.80 (6H). Other identifications also were made by n.m.r.: pivaldehyde, δ 9.42 (singlet), 1.07 (singlet); propionic acid, 1.16 (triplet), 2.35 (quartet); ozonide, 4.80, 4.74, 0.97 (singlets); polymeric peroxide, 5.2–5.0 (multiplet).

Ozonations of trans-Di-t-butylethylene, trans-3-Hexene, and Ethylidenecyclohexane in Cyclohexanone Solvent

These were carried out as described by Story (1). The reaction mixtures were evaporated and analyzed for 6-hexanolactone as described above. In some cases (concentrated solutions, 0.2–3.0 *M*) the undistilled reaction mixture was analyzed for the lactone. In no case was more than a trace (1–3% yield) of lactone obtained. It was shown that significant quantities of 6-hexanolactone could be detected under these conditions.

Ozonation of Ethylidenecyclohexane in Pinacolone Solvent

A solution of 2.5 mmol of ethylidenecyclohexane in 10 ml of pinacolone was ozonized to completion (blue color) at $-45°$ with ozone–nitrogen. The solvent was stripped off in *vacuo* (oil pump) at 0° and collected in a cold trap at $-78°$. V.p.c. analyses for *t*-butyl acetate were made on the original solution, the stripped solvent, and the residue using a 10 ft diethyleneglycol adipate on acid-washed Chromosorb P column at 70° (F and M 500) and a 10 ft 10% Silicone Fluid XF-1150 on Chromosorb P column at 100° (Aerograph 1520 B). No *t*-butyl acetate was found, as shown by comparison to the retention time of an authentic sample. The residue and stripped solvent also were analyzed for acetic acid and cyclohexanone by v.p.c. using a 10 ft 5% Dimer Acid – Silicone Oil on Haloport F column at 70° (F and M 500). Considerable cyclohexanone but only a trace of acetic acid was found.

A small amount of the residue from the above experiment was dissolved in 2 ml of *cis*-decalin and to this solution 50 mg of rubrene was added. The mixture was heated rapidly to boiling (195°). An orange glow which lasted for about 1 min was readily visible in the dark. In a similar experiment without rubrene, no luminescence was observed. In another experiment the ethylidenecyclohexane was ozonized in methylene chloride rather than pinacolone and the solvent was stripped. The rubrene experiment was performed on the residue and luminescence was similarly noted. This, therefore, can not be used as evidence for a dioxetane, as reported by Story (3). Kopecky *et al.* (9) discusses this further.

In another experiment, a sample of the freshly stripped, cold (0°) residue was transferred by means of a precooled pipette to a precooled n.m.r. tube and an n.m.r. spectrum was taken in a low temperature probe at 0°. Of particular

Can. J. Chem. Downloaded from www.nrcresearchpress.com by 210.87.254.5 on 09/05/12
For personal use only.

interest was the methine proton absorption which was a featureless multiplet at δ 4.8, characteristic of polymeric peroxide methine protons. The dioxetane methine absorption is in the form of a quartet at δ 5.09 (9). A similar experiment was carried out with 2-methyl-2-butene; a broad structureless multiplet was observed at δ 4.8 (*cf.* ref. 3).

Lithium aluminum hydride reductions of the residue from the ethylidenecyclohexane ozonation were carried out in the standard fashion. Like Kopecky and coworkers (9) and contrary to the report of Story (3) none of the glycol expected from the dioxetane was obtained. Similar results were obtained with the 2-methyl-2-butene ozonation mixture.

In certain other ozonations, slightly less than 1 equiv of ozone was employed. Analyses for unreacted ethylidenecyclohexane and cyclohexanone were carried out as described in the next experiment. The results are shown in Table 3. The peroxidic residue after the removal of the solvent gave a positive lead tetraacetate test for a hydroperoxide group. Potassium iodide and hydriodic acid determinations for active oxygen were made as described in the following experiment. The nearly identical results (Table 3) appear to indicate a polymeric peroxide. T.l.c. indicated a mixture of products. N.m.r. showed that no ozonide was present (*cf.* following experiment).

Ozonation of Ethylidenecyclohexane in Pentane

A solution similar to the one above, except using pentane rather than pinacolone solvent, was ozonized with slightly less than 1 equiv of ozone at −45°. Determinations of unreacted ethylidenecyclohexane and cyclohexanone were made on a 5% Dimer Acid – Silicone Oil on Haloport F column at 120° (F and M 500). The solvent was evaporated as in the preceding experiment and KI (room temperature) and HI (56% at 60°) determinations for active oxygen were made (titration of released iodine with standard thiosulfate). The results are shown in Table 3. In another experiment the residue was distilled and a fraction collected at 39–40° (5 mm). This was shown to be ethylidenecyclohexane ozonide; n.m.r. in CCl_4: δ 1.33 (doublet, J = 5.3 Hz); 1.62 (broad singlet); 5.20 (quartet, J = 5.3 Hz); ratio of upfield protons to quartet was 13:1. The material gave a strong HI, but weak KI, test.

Anal. Calcd. for $C_8H_{14}O_3$ (mol. wt. 158): C, 60.74; H, 8.93. Found (158 (mass spectra)): C, 59.57; H, 8.96.

Ozonation of Ethylidenecyclohexane in Acetone

This experiment at −78° resulted in the appearance of a white precipitate which was shown to be the dimeric cyclohexanone peroxide by comparison with an authentic sample (13).

This work was supported by grants from the Robert A. Welch Foundation (F-042) and the National Science Foundation (GP 28187). We thank Doctors Edward Nieh and Y. G. Chang for checking some of our experiments.

1. P. R. Story, J. A. Alford, J. R. Burgess, and W. C. Ray. J. Am. Chem. Soc. **93**, 3042 (1971).
2. P. R. Story, J. A. Alford, W. C. Ray, and J. R. Burgess. J. Am. Chem. Soc. **93**, 3044 (1971).
3. P. R. Story, E. A. Whited, and J. A. Alford. J. Am. Chem. Soc. **94**, 2143 (1972).
4. P. R. Story, C. E. Bishop, J. R. Burgess, R. W. Murray, and R. D. Youssefeh. J. Am. Chem. Soc. **90**, 1907 (1968).
5. S. Fliszár, J. Carles, and J. Renard. J. Am. Chem. Soc. **90**, 1364 (1968); S. Fliszár and J. Carles. J. Am. Chem. Soc. **91**, 2637 (1969).
6. R. Huisgen. Angew. Chem. Int. Ed. Engl. **2**, 565, 633 (1963).
7. P. S. Bailey, J. A. Thompson, and B. A. Shoulders. J. Am. Chem. Soc. **88**, 4098 (1966).
8. L. J. Durham and F. L. Greenwood. J. Org. Chem. **33**, 1629 (1968).
9. K. R. Kopecky, P. A. Lockwood, J. E. Filby, and R. W. Reid. Can. J. Chem. **51**, 468 (1973).
10. P. S. Bailey, J. W. Ward, and R. E. Hornish. J. Am. Chem. Soc. **93**, 3552 (1971).
11. N. L. Bauld, J. A. Thompson, C. E. Hudson, and P. S. Bailey. J. Am. Chem. Soc. **90**, 1822 (1968).
12. A. M. Reader, P. S. Bailey, and H. M. White. J. Org. Chem. **30**, 784 (1965) and references therein.
13. R. Criegee and G. Lohaus. Ann. **583**, 6 (1953).

Use of *N*-Carboxyanhydrides in the Synthesis of Dipeptides. Factors Affecting the Yields of Several Alanine and Valine-containing Dipeptides[1]

ERIC M. GROVESTINE,[2] JEAN R. LANGLOIS,[3] AND ROSS E. WILLIAMS[4]

Division of Biological Sciences, National Research Council of Canada, Ottawa, Canada K1A 0R6

Received November 20, 1972

A series of dipeptides having aliphatic side chains have been prepared in aqueous solution from alanine and valine NCA. An organic base was used to establish and maintain the p*H*. After the reaction the amounts of unreacted amino acid nucleophile and the overall yields in the reaction were determined. Our observations have led us to propose that NCA stability, the pK_a of the amino acid nucleophile and the stability of the carbamate all can play an important role in determining synthetic yields during these preparations.

Une série des dipeptides qui possédent les chaînes latérales aliphatiques a été preparée en phase aqueuse avec alanine et valine NCA. Pour établir et maintenir le p*H* on a employé une base organique. Après la réaction nous avons déterminé la quantite du nucléophile non-reagie et le rendement totale du dipeptide. Nous proposons donc que la stabilité du NCA, le pK_a de l'acide aminé et la stabilité du carbamate peut jouer un rôle important dans la détermination de la synthèse du dipeptide.

Can. J. Chem., **51**, 1284 (1973)

Can. J. Chem. Downloaded from www.nrcresearchpress.com by 210.87.254.40 on 09/05/12
For personal use only.

Introduction

Use of *N*-carboxyanhydrides (NCA's) for the synthesis of racemization-free dipeptides under controlled conditions has received attention in recent times (1–4). The original method (1), *i.e.* borate buffer (p*H* 10.2), rapid stirring, has been modified in several ways including the use of 0.2 *M* sodium carbonate solutions containing acetonitrile (no p*H* control exercised) (2) or the use of organic buffers (p*H* control exercized) (3). A further simplifying modification of this latter type involved the use of only a liquid organic base to establish and maintain the p*H* during the reaction (4). In view of the demonstrated utility of this procedure for the large scale preparation of dipeptides we have studied the effect of p*H* on the yields of several peptides derived from the reaction of alanine and valine NCA with amino acids having various sized aliphatic side chains. These studies have allowed us to delineate the factors which control the synthetic yields of this reaction.

Methods and Materials

Amino acids were obtained from Bion Biochemicals. Toronto, Ontario. They were all of the L-configuration. Water was doubly distilled from glass. All other chemicals were of reagent grade and were used as received.

N-Carboxyanhydrides were prepared, using suitable precautions, according to established procedures (5). They were twice precipitated from ethyl acetate with petroleum ether (30–60°) and gave decomposition temperatures in accord with those reported.

A Beckman amino acid analyzer, model 120C, using a standard elution programme on a 69 × 0.9 cm column (resin UR 30, sodium citrate buffers, 0.2 *N* in sodium ion, p*H* 3.25 and 4.30, temperature 55 °C) was employed for determination of the extent of reaction. In order to ensure quantitative conversion of all valine-containing peptides to ninhydrin-positive materials a buffer flow rate of 50 ml/h was used. Amino acid standards were those supplied by Beckman. Dipeptide standards were obtained from commercial sources (Schwarz-Mann, Sigma Chemical, and Fox Chemical. They were dried overnight under vacuum at 60 °C and all gave satisfactory elemental analyses. They contained less than 1% ninhydrin-positive impurities when subjected to amino acid analysis.

Dipeptide syntheses were carried out on an analytical scale (1 m*M* amino acid nucleophile per 10 ml) as previously described (4). In general, a solution (40 ml) containing a known amount of the amino acid to be used as nucleophile was cooled to 2 °C in a jacketed Waring blendor (125 ml capacity). A few drops of cetyl alcohol was added to prevent foaming and the p*H* was adjusted to the desired value with triethylamine. A slight excess of the solid NCA (1.1 mol equiv) was added under conditions of rapid stirring. More triethylamine was added to maintain the p*H*. At cessation of base uptake, as evidenced by stability in the p*H*, the solution was rapidly acidified with formic acid to p*H* 3. The blendor contents were decanted, washed through a glass filter, and made up to 100.0 ml with water. An aliquot (0.100 ml) was applied to the amino acid analyzer to determine the amount of amino acid nucleophile remaining in the solution and the amount of product formed during the reaction.

[1]NRCC No. 13063.

[2]NRCC Summer Student, 1971–1972.

[3]Present address: Station de Recherche, Ministère d'Agriculture, Ste-Foy, Québec.

[4]To whom communications should be addressed.

Can. J. Chem. Downloaded from www.nrcresearchpress.com by 210.87.254.40 on 09/05/12
For personal use only.

All yields were calculated on the basis of the amount of input nucleophile used. Percentages of amino acid nucleophile reacting were calculated as follows:

$$(N_0 - N_f)/N_0 \times 100$$

Overall yields, in percent, were calculated as follows:

$$D_f/N_0 \times 100$$

where N_0 is initial molar concentration of amino acid nucleophile, N_f is final molar concentration of amino acid nucleophile, and D_f is final molar concentration of dipeptide. The yields, presented in graphical form in Figs. 1–4, are based upon the average of triplicate runs at p*H*'s 9.2, 9.8, 10.3, and 11.0. Experimental variation amounted to approximately ±8% in each one of the calculated yields. This variability can be attributed in part to the purity of the NCA used, the rate at which it was added, the variation of the p*H* from that desired during the reaction, as well as the time elapsed before acidification in order to terminate the reaction.

Results and Discussion

In a previous communication (4) it was shown that the use of an organic base to establish and maintain the p*H* during the reaction of an amino acid NCA with another amino acid is adequate for the preparation of dipeptides in yields which are synthetically useful. Product isolation was aided since all the buffer components could be removed prior to isolation of the dipeptide via conventional procedures, such as crystallization or chromatography.

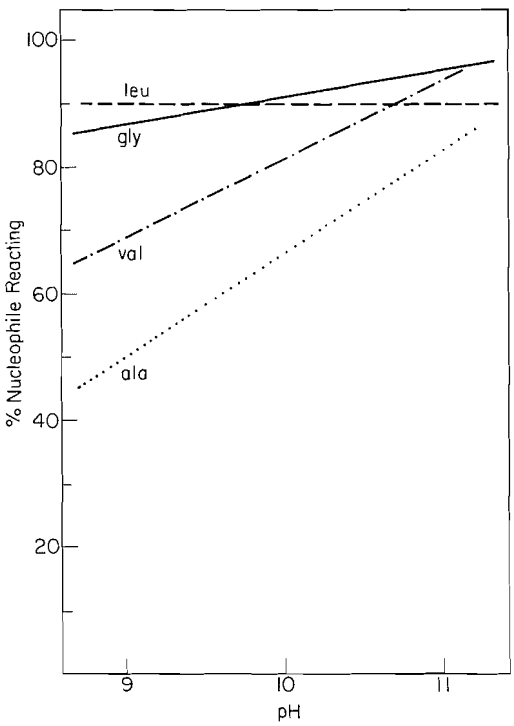

FIG. 1. NCA preparation of alanyl dipeptides from alanine NCA. Variation with p*H* of the percentage of amino acid nucleophile reacted. Glycine (———); alanine (···); valine (-·-·-); and leucine (---).

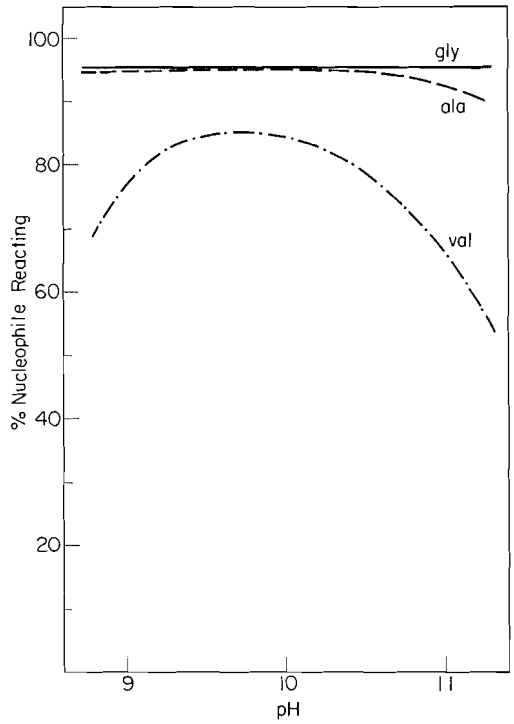

FIG. 2. NCA preparation of valyl dipeptides from valine NCA. Variation with p*H* of the percentage of amino acid nucleophile reacted. Glycine (———); alanine (---); and valine (-·-·-).

Because of the obvious preparative utility of the method we wished to investigate the effects which might control yields in the reaction. By determining both the overall reaction yield and the amount of nucleophile consumed in the reaction of various amino acid nucleophiles with an NCA at different p*H*'s we have been able to investigate the effects that NCA stability, steric interference of the side chains, the amino acid nucleophilicity (related to the amino function's pK_a), and the stability of the intermediate carbamate, have upon the synthesis of a representative group of dipeptides: alanyl-X and valyl-X, where X is an aliphatic amino acid.

Steric control of the nucleophilic attack on the NCA by the amino acid (see Scheme 1) might be important in limiting the synthetic

Can. J. Chem. Downloaded from www.nrcresearchpress.com by 210.87.254.40 on 09/05/12
For personal use only.

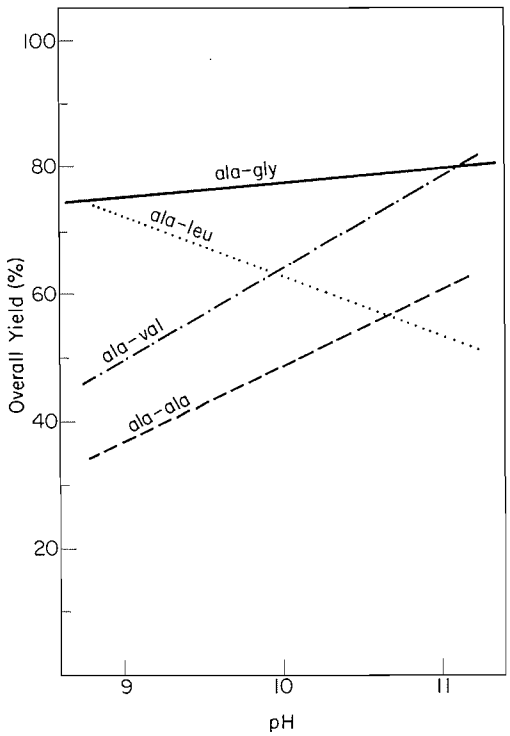

FIG. 3. NCA preparation of alanyl dipeptides from alanine NCA. Variation of the overall yield with p*H*. Alanyl–glycine (———); alanyl–alanine (---); alanyl–valine (-·-·-) and alanyl–leucine (···).

yields. This effect would be primarily reflected in the amount of amino acid nucleophile removed from solution during the reaction since a slower reacting species would allow destruction of the NCA by base hydrolysis. Both alanine NCA and valine NCA were reacted with a series of amino acid nucleophiles to form the respective dipeptides. The percentage of the amino acid nucleophile removed from solution during the reaction is given in Figs. 1 and 2. When alanine NCA was used (Fig. 1) glycine was nearly totally consumed and showed a very slight p*H* dependency (rising at p*H* 11). With leucine as nucleophile, percentages paralleled those observed with glycine. With either alanine or valine as nucleophile the percentages consumed were very much reduced. However, they were in an order opposite to that expected for steric control of attack. The valine being more hindered would be expected to give lower yields. The p*H* effects on the reactions with alanine and valine as nucleophiles show the result of having a larger portion of unprotonated amine as nucleophile in the solution, that is, the amount of unprotonated amine in the solution at the beginning of the reaction controls the extent of the reaction. This is, thus, an effect related to the pK_a of the amino acid involved and shows the ability of hydroxide ion to compete with bulky amino acid nucleophiles for the alanine NCA. This effect seems to be important with these two compounds but nothing of this sort is observed with glycine or leucine.

When valine NCA was used to prepare a similar series of dipeptides, the order of consumption of glycine, alanine, and valine gave a definite indication of steric control (Fig. 2). p*K* effects were only noticeable in the preparation of valyl–valine and did not seem to be as important as those seen with alanyl NCA. This would indicate that the hindered valine NCA is more stable towards hydrolysis than alanine NCA, allowing the nucleophile ample time to attack before the NCA is destroyed. The decreasing consumption seen at high p*H*'s with valine NCA may reflect a decrease in the NCA stability due to attack by hydroxide ion.

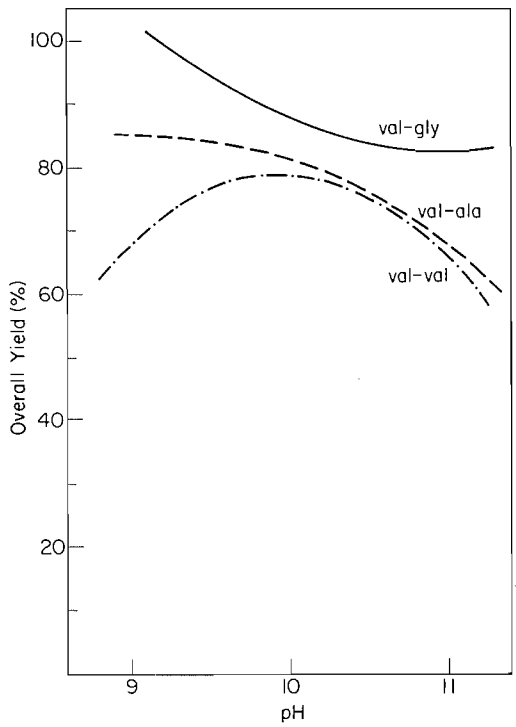

FIG. 4. NCA preparation of valyl dipeptides from valine NCA. Variation of the overall yield with p*H*. Valyl–glycine (———); valyl–alanine (---); and valyl–valine (-·-·-).

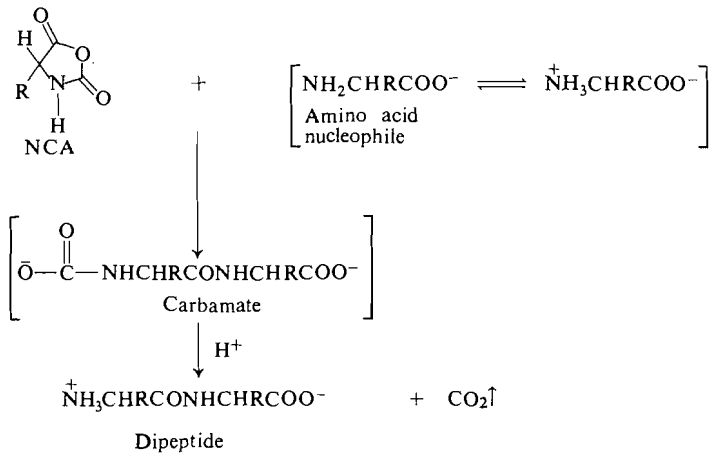

SCHEME I

The overall yields in the alanine series (Fig. 3) present p*H* dependency profiles paralleling that seen for the nucleophile consumption except for one case, that of alanyl–leucine. This parallelism indicates that the stability of the intermediate carbamate is not playing an important role in determining the overall yield of most of the reactions. If carbamate stability were important no such parallelism would be noted since destruction of the carbamate by hydroxide ion would result in overreaction to higher peptides and a lowering of yields at higher p*H*'s. In the case of alanyl–leucine we see a definite case of the carbamate instability affecting the reaction yields. Between the point at which the leucine is removed from the solution and the product formation begins, a reaction occurs, perhaps controlled by the intermediate's conformation, in which the carbamate is destroyed either by hydrolysis yielding a product capable of further reaction to tri- and tetra-peptides, or to ninhydrin-negative materials.

Examination of overall yields in the valine series (Fig. 4), on the other hand, shows the order expected for steric control, *i.e.* the more bulky alanine and valine nucleophiles form product to less of an extent than the less bulky glycine nucleophile. Carbamate stability, in this series, does not seem to play an important role in controlling the synthetic yields.

As can be seen from the above results not only steric effects (the valine series) but also amino acid pK_a's (the alanine series) play an important role in controlling the yields of dipeptides synthesized by this method. Steric effects seem to dominate when the NCA is relatively stable to hydrolysis by hydroxide ion. The pK_a effects become relevant when hydroxide ion can effectively compete with the nucleophile for the NCA. The results with alanyl–leucine suggest that carbamate stability can also play an important role in determining the overall yields in the reaction.

While no definite conclusions may be drawn regarding the interplay of all the various factors influencing the reaction yields our results do provide the necessary information for the successful large scale synthesis of these aliphatic dipeptides. These results also support our previous contention (4) that all large scale syntheses must be preceded by a series of analytical runs in order that the optimum conditions for any new preparation might be determined.

We wish to thank H. Seguin for the elemental analyses and A. E. Castagne for the amino acid analyses. Our thanks are also due to Dr. D. R. Lauren for discussions and reading the manuscript.

1. R. HIRSCHMANN *et al.* J. Org. Chem. **32**, 3415 (1967).
2. Y. IWAKURA, K. UNO, M. OYA, and R. KATAKAI. Biopolym. **9**, 1419 (1970).
3. K. D. KOPPLE, T. SAITO, and M. OHNISHI. J. Org. Chem. **34**, 1631 (1969).
4. R. J. GAIT, J. R. LANGLOIS, and R. E. WILLIAMS. Can. J. Chem. **50**, 299 (1972).
5. J. P. GREENSTEIN and M. WINITZ. Chemistry of the amino acids. Vol. II. J. Wiley and Sons, Inc., New York. 1961; S. M. BLOOM, G. D. FASMAN, C. DE LOZÉ, and E. R. BLOUT. J. Am. Chem. Soc. **84**, 458 (1962); J. L. BAILEY. J. Chem. Soc. 3461 (1961).

Can. J. Chem. Downloaded from www.nrcresearchpress.com by 210.87.254.40 on 09/05/12
For personal use only.

Crystal and Molecular Structure of *B,B*-Diphenylboroxazolidine (2-Aminoethyl Diphenylborinate), $Ph_2BO(CH_2)_2NH_2$

STEVEN J. RETTIG AND JAMES TROTTER

Department of Chemistry, University of British Columbia, Vancouver 8, British Columbia

Received August 18, 1972

Crystals of the title compound are monoclinic, $a = 13.840(1)$, $b = 8.9169(5)$, $c = 10.170(1)$ Å, $\beta = 98.85(1)°$, $Z = 4$, space group $P2_1/n$. The structure was determined by direct methods, and refined by electron-density and full-matrix least-squares procedures to R 0.041 for 1458 observed reflections. The five-membered boroxazolidine ring is in the half-chair conformation. Bond angles in the ring range from 99.7° for OBN to 110.1° for BOC. Bond lengths are as follows: mean B—C, 1.611(2), B—N, 1.653(3), B—O, 1.484(3), C—N, 1.485(3), C—O, 1.413(3), mean C—C (aromatic), 1.383(11), and C—C, 1.505(4) Å. The structure consists of discrete molecules linked by O...H—N hydrogen bonds (2.874(2) Å) to form continuous spirals about the 2_1 axes.

Le composé du titre cristallise dans le système monoclinique, $a = 13.840(1)$, $b = 8.9169(5)$, $c = 10.170(1)$ Å, $\beta = 98.85°$, $Z = 4$, groupe d'espace $P2_1/n$. La structure a été déterminée à partir des methodes directes, et a été affinée par les procédés de la densité électronique et de moindres carrés (matrice complète) jusqu'à un facteur résidual R 0.041 pour 1458 reflexions observées. Le cycle de cinq chaînons est dans la conformation demi-chaise. Les angles des liaisons dans le cycle s'etendent de 99.7° pour OBN à 110.1° pour BOC. Les longuers des liaisons sont: B—C (moyenne), 1.611(2), B—N, 1.653(3), B—O, 1.484(3), C—N, 1.485(3), C—O, 1.413(3), C—C (moyenne aromatique), 1.383 (11), et C—C, 1.505(4) Å. La structure est constituée par les molecules discrètes liées par liaisons hydrogènes (2.874(2) Å) qui forment les spirales continues autour des axes 2_1.

Can. J. Chem., **51**, 1288 (1973)

Introduction

In recent years the boroxazolidines have been extensively studied, the primary concern being the unusual stability of the amino alcohol esters with respect to boron esters of ordinary alcohols. *B,B*-Diphenylboroxazolidine (**1**) was originally

1

prepared by Letsinger and Skoog (1), who correctly proposed the cyclic structure of the ester. The possibility of the N—B dative bond was first proposed by Brown and Fletcher (2) for triethanolamine borate (triptych boroxazolidine) in 1951. The first substantial evidence for the existence of the N—B dative bond in boroxazolidines was the result of detailed kinetic studies of the acid hydrolysis of these compounds by Zimmerman and co-workers, the details of which are the subject of a review article by Zimmerman (3). The X-ray crystallographic study of *B,B*-diphenylboroxazolidine was undertaken to provide conclusive proof of the existence of the boroxazolidine ring.

Experimental

B,B-Diphenylboroxazolidine was prepared as previously described (1, 4). Recrystallization from 1:1 ethanol – carbon tetrachloride gave colorless needles, elongated along *b*, with (100), (001), and (101) variously developed. The crystal chosen for study was mounted with *b* parallel to the goniostat axis and was *ca.* 0.5 mm in length with a cross section of 0.3 × 0.3 mm. Unit-cell and space group data were obtained from film and diffractometer measurements. The unit-cell parameters were refined by a least-squares treatment of $\sin^2\theta$ values for 22 reflections measured on a diffractometer with Cu-Kα radiation. Crystal data are:

$C_{14}H_{16}BNO$ f.w. = 225.1

Monoclinic, $a = 13.840(1)$, $b = 8.9169(5)$, $c = 10.170(1)$ Å, $\beta = 98.85(1)°$, $V = 1240.1(2)$ Å^3, $\rho_o = 1.201(5)$, $Z = 4$, $\rho_c = 1.2055(3)$, $F(000) = 480$ (20 °C, CuKα, $\lambda = 1.5418$ Å, $\mu = 5.9$ cm^{-1}). Absent spectra: $0k0$, $k \neq 2n$ and $h0l$, $h + l \neq 2n$ define uniquely the space group $P2_1/n$ (C_{2h}^5, No. 14).

Intensities were measured on a Datex-automated General Electric XRD 6 diffractometer, with a scintillation counter, CuKα radiation (nickel filter and pulse height analyzer), and a θ–2θ scan at 2° min^{-1} over a range of $(1.80 + 0.86 \tan\theta)$ degrees in 2θ, with 20 s background counts being measured at each end of the scan. Data were measured to $2\theta = 120°$ (minimum interplanar spacing 0.89 Å). A check reflection was monitored every 40 reflections throughout the data collection. The intensity of the check reflexion remained within ±2.5% of its initial value during the data collection, the final

Can. J. Chem. Downloaded from www.nrcresearchpress.com by 210.87.254.42 on 09/05/12
For personal use only.

Can. J. Chem. Downloaded from www.nrcresearchpress.com by 210.87.254.42 on 09/05/12
For personal use only.

value being equal to the initial value. Lorentz and polarization corrections were applied, and the structure amplitudes were derived. No absorption correction was made in view of the low value of μ. Of the 1837 independent reflections measured, 369 had intensities less than $3\sigma(I)$ above background where $\sigma^2(I) = S + B + (0.05\ S)^2$ with S = scan count and B = background count, corrected to time of scan. These reflections were classified as unobserved.

Structure Analysis

The structure was solved by direct methods. Sixteen sets of signs for 254 reflections with normalized structure factor $|E| \geqslant 1.50$ were determined by a computer program which uses Sayre relationships in an iterative procedure (5). The starting set of reflections is given in Table 1. One set of signs was outstanding in that it converged in 5 cycles to a set having the highest consistency index (5) (0.85) with 130 positive signs and 124 negative signs. An E-map was computed using the 254 signed values of E from this set. The 17 non-hydrogen atoms accounted for the highest 17 peaks on the map. A structure factor calculation based on the positions from the E-map gave R 0.211. Two cycles of full-matrix least-squares refinement of the positions and isotropic temperature factors of the boron, nitrogen, oxygen, and carbon atoms reduced R to 0.151. All 16 hydrogen atoms were then located from a difference Fourier. One cycle with the non-hydrogen atoms having anisotropic temperature factors and the hydrogen atoms isotropic resulted in $R = 0.058$. Convergence was reached after two more cycles at $R = 0.041$, for 1458 observed reflections (10 reflections were given zero weight in the final stages of refinement due to suspected extinction errors: 002, 10$\bar{1}$, 200, 111, 31$\bar{1}$, 310, 020, 021, 22$\bar{1}$, and 130).

The least-squares refinement was based on the minimization of $\Sigma w(F_o - F_c)^2$. The scattering factors of ref. 6(*a*) were used for the boron, nitrogen, oxygen, and carbon atoms and those of ref. 6(*b*) for the hydrogen atoms. The anisotropic temperature factors employed in the refinement are U_{ij} in the expression:

$$f = f^0 \exp\,[-2\pi^2(U_{11}h^2a^{*2} + U_{22}k^2b^{*2} + U_{33}l^2c^{*2} + 2U_{12}hka^*b^* + 2U_{13}hla^*c^* + 2U_{23}klb^*c^*)]$$

where f^0 is the tabulated scattering factor and f is that corrected for thermal motion. The weighting scheme: $\sqrt{w} = 1$ if $|F_o| \leqslant 10$; $\sqrt{w} = 10/|F_o|$ if $|F_o| > 10$, and $\sqrt{w} = 0.7$ for the unobserved reflections gave constant average values of $w(F_o - F_c)^2$ over ranges of $|F_o|$, and was employed in the final stages of refinement.

On the final cycle of refinement, no parameter shift was greater than 0.33 σ. The final positional and thermal parameters are given in Tables 2 and 3, respectively. Measured and calculated structure factors have been placed in the Depository of Unpublished Data.[1]

[1]The structure factor table is available, at a nominal charge, from the Depository of Unpublished Data, National Science Library, National Research Council of Canada, Ottawa, Canada K1A 0S2.

TABLE 1. Starting set of reflections for $C_{14}H_{16}BNO$

h	k	l	$\|E\|$	
6	1	−8	4.00	origin determining
3	1	−1	2.25	
0	2	1	2.20	
6	3	0	3.14	
1	2	−4	2.47	
9	3	−1	3.19	
10	3	4	3.21	

TABLE 2. Final positional parameters (fractional × 10^4) with standard deviations in parentheses

Atom	x	y	z
B	7855(2)	2708(2)	3710(2)
O	7244(1)	4083(1)	3574(1)
N	7069(1)	1504(2)	2904(2)
C(1)	6243(2)	3698(3)	3325(3)
C(2)	6182(2)	2385(3)	2386(3)
C(3)	8799(1)	2978(2)	2988(2)
C(4)	8782(2)	2916(3)	1616(2)
C(5)	9594(2)	3304(3)	1032(3)
C(6)	10440(2)	3758(3)	1796(3)
C(7)	10487(2)	3833(3)	3157(3)
C(8)	9678(2)	3449(2)	3730(2)
C(9)	8111(1)	2110(2)	5216(2)
C(10)	8600(2)	759(3)	5526(3)
C(11)	8829(2)	247(3)	6827(3)
C(12)	8591(2)	1086(3)	7858(3)
C(13)	8111(2)	2418(4)	7595(2)
C(14)	7876(2)	2912(3)	6289(2)
H(1)	6010(18)	3454(30)	4199(27)
H(1′)	5853(20)	4484(32)	2942(25)
H(2)	6285(22)	2691(34)	1518(31)
H(2′)	5598(19)	1826(28)	2317(23)
H(N)	6900(20)	776(34)	3565(28)
H(N′)	7276(16)	955(27)	2321(24)
H(4)	8142(19)	2619(28)	1026(25)
H(5)	9514(19)	3250(30)	80(29)
H(6)	11013(19)	3993(28)	1398(25)
H(7)	11087(21)	4149(30)	3742(25)
H(8)	9720(15)	3520(26)	4694(24)
H(10)	8819(18)	226(30)	4837(25)
H(11)	9176(23)	−700(38)	6942(29)
H(12)	8777(21)	744(32)	8783(30)
H(13)	7910(21)	3063(35)	8278(31)
H(14)	7529(17)	3834(27)	6127(21)

Results and Discussion

The X-ray analysis confirms the cyclic structure first proposed for this compound by Letsinger and Skoog (1). Figure 1 shows the molecule viewed down the b axis. Individual bond lengths with their standard deviations are shown in Fig. 2 and mean bond lengths are given in Table 4. Bond angles are in Table 5.

TABLE 3. Final thermal parameters and their estimated standard deviations

(*a*) Anisotropic thermal parameters (U_{ij} (Å^2) × 100)

Atom	U_{11}	U_{22}	U_{33}	U_{12}	U_{13}	U_{23}
B	5.16(13)	3.99(12)	5.67(14)	−0.11(10)	1.06(11)	−0.57(10)
O	3.91(8)	3.30(8)	5.64(9)	0.08(6)	0.93(6)	0.11(6)
N	4.90(11)	3.91(10)	5.56(11)	−0.44(8)	1.06(9)	−0.81(9)
C(1)	3.98(12)	4.83(14)	8.27(18)	0.19(11)	0.78(12)	0.11(13)
C(2)	4.76(15)	5.88(16)	7.83(19)	−0.84(12)	−0.52(13)	−0.39(13)
C(3)	4.27(11)	3.10(10)	4.47(11)	0.30(9)	0.80(9)	−0.03(9)
C(4)	5.32(13)	5.44(14)	4.77(13)	−0.13(11)	1.21(11)	−0.21(11)
C(5)	7.32(17)	6.49(17)	5.23(15)	0.11(13)	2.45(13)	0.22(12)
C(6)	5.67(15)	5.59(15)	8.00(18)	0.26(11)	3.16(14)	1.15(13)
C(7)	4.44(13)	5.72(15)	7.66(17)	−0.40(11)	1.09(12)	0.38(13)
C(8)	4.71(12)	4.96(13)	4.95(13)	−0.20(10)	0.90(10)	−0.05(10)
C(9)	4.03(10)	3.56(11)	4.93(12)	−0.54(9)	1.02(9)	0.14(9)
C(10)	7.30(16)	4.04(13)	6.32(15)	0.39(11)	0.76(13)	0.28(12)
C(11)	7.88(18)	4.68(15)	8.10(20)	−0.43(14)	−0.81(15)	2.05(14)
C(12)	6.69(16)	8.09(20)	5.48(15)	−2.50(15)	−0.09(12)	1.80(15)
C(13)	6.04(15)	8.72(20)	4.69(14)	−0.94(14)	1.27(11)	−0.11(14)
C(14)	4.78(13)	5.51(15)	5.08(13)	0.14(11)	1.19(10)	−0.12(11)

(*b*) Isotropic thermal parameters

Atom	B (Å^2)
H(1)	5.92(61)
H(1′)	5.72(59)
H(2)	7.05(76)
H(2′)	4.98(54)
H(N)	6.84(70)
H(N′)	4.06(53)
H(4)	5.76(58)
H(5)	6.22(63)
H(6)	5.85(60)
H(7)	5.99(61)
H(8)	4.58(50)
H(10)	5.40(59)
H(11)	7.54(74)
H(12)	6.94(67)
H(13)	7.70(77)
H(14)	4.22(49)

TABLE 4. Mean bond distances with r.m.s. deviations in parentheses

Type	Number of individual values*	Distance (Å)
B—C	2	1.611(2)
B—N	1	1.653(3)
B—O	1	1.484(3)
C—C	1	1.505(4)
C—C(ar)	12	1.383(11)
C—N	1	1.485(3)
C—O	1	1.413(3)
C—H	4	0.96(3)
C—H(ar)	10	0.974(25)
N—H	2	0.92(7)

*For single value parameters, the least-squares standard deviation is given in parentheses.

The five-membered boroxazolidine ring is in the half-chair conformation, with C(2) displaced 0.08 Å from the BON plane and C(1) lying 0.50 Å on the opposite side of the BON plane. The dihedral angle C(2)N—BO is 3°. There is considerable strain in the ring as evidenced by the sum of interior angles, 524°, which is 23.5° less than the ideal 547.5° (5 × 109.5). The BOC(1) angle (110.1°) is close to the expected value. The high angular strain at the remaining ring atoms is partially relieved by a shortening of the C(1)—C(2) bond to 1.505 Å from the expected value of 1.537 Å (7) for a C(sp^3)—C(sp^3) bond and a lengthening of the B—N bond to 1.653 Å from the mean value of 1.55 Å (7) for B(sp^3)—N(sp^3) bonds. The iso-

Can. J. Chem. Downloaded from www.nrcresearchpress.com by 210.87.254.42 on 09/05/12
For personal use only.

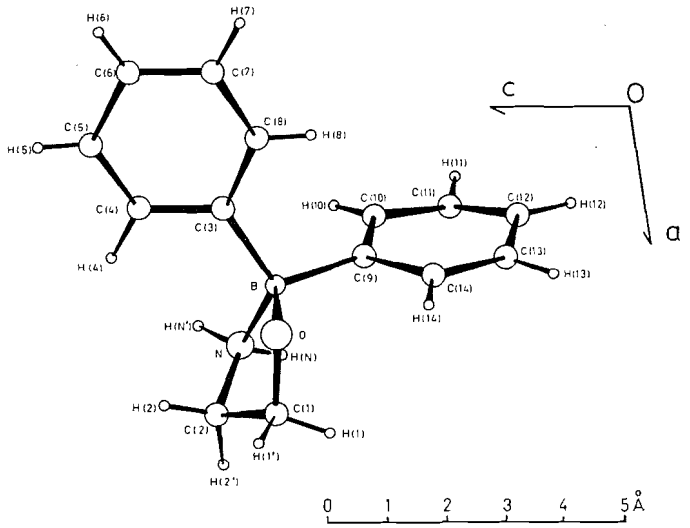

FIG. 1. The molecule viewed down *b*, showing crystallographic numbering scheme.

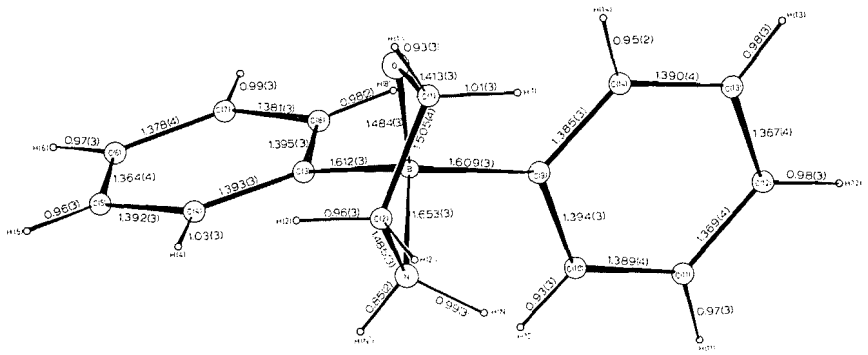

FIG. 2. A general view of the molecule with bond distances (Å) and their standard deviations in parentheses. The C(2)—H(2′) distance is 0.94(3) Å.

electronic N—C (1.485 Å) and O—B (1.484 Å) bonds as well as the C—O bond (1.413 Å) are normal (7).

The two phenyl groups are planar within experimental error (see Table 6). All of the phenyl hydrogen atoms lie in the respective phenyl planes with the exception of H(10) which lies 0.08 Å (3 σ) below the C(9)—C(14) plane. The boron atom deviates significantly from both phenyl planes, being displaced 0.15 Å from the C(3)—C(8) plane and −0.02 Å from the C(9)—C(14) plane representing a slight folding of the two planes away from each other. The angle between phenyl plane normals is 100°. The two rings are not equivalent as the C(3)—C(8) ring is twisted 21° with respect to the BNC(3) plane while the C(9)—C(14) ring lies nearly in the BOC(9) plane, dihedral angle 7°. The C—C (ar) distances range from 1.364 to 1.395 Å with a mean value of 1.383(11) Å. The mean value agrees with the literature mean of 1.394 Å(7). There are, however, significant differences between the individual C—C distances in the phenyl rings. There is a noticeable trend toward shortening of the C—C distances as they are removed from the boron substituent. This is probably due to a combination of electron delocalization, steric, and thermal libration effects (these distances have not been corrected for thermal motion). The boron–carbon distances, mean 1.611(2) Å, are significantly shorter than the B—C distances of 1.631(9)–1.646(8) Å found in the tetraphenyl borate anion (8), in accord with electron delocalization.

The mean bond angles at tetrahedrally and trigonally coordinated atoms are 109.4 and

Can. J. Chem. Downloaded from www.nrcresearchpress.com by 210.87.254.42 on 09/05/12
For personal use only.

TABLE 5. Bond angles with standard deviations in parentheses

Bonds	Angle (deg)	Bonds	Angle (deg)
O—B—C(3)	108.9(2)	C(4)—C(5)—C(6)	120.6(2)
O—B—C(9)	113.7(2)	H(5)—C(5)—C(4)	116.3(16)
O—B—N	99.7(1)	H(5)—C(5)—C(6)	123.1(16)
C(3)—B—C(9)	114.0(2)	C(5)—C(6)—C(7)	119.3(2)
C(3)—B—N	112.9(2)	H(6)—C(6)—C(5)	120.9(15)
C(9)—B—N	106.8(2)	H(6)—C(6)—C(7)	119.7(15)
B—O—C(1)	110.1(2)	C(6)—C(7)—C(8)	119.7(2)
H(N)—N—H(N′)	103.7(23)	H(7)—C(7)—C(6)	121.6(15)
H(N)—N—B	107.2(16)	H(7)—C(7)—C(8)	118.7(15)
H(N)—N—C(2)	108.7(16)	C(7)—C(8)—C(3)	122.9(2)
H(N′)—N—C(2)	113.9(15)	H(8)—C(8)—C(3)	118.3(13)
H(N′)—N—B	116.9(15)	H(8)—C(8)—C(7)	118.8(13)
C(2)—N—B	106.1(2)	B—C(9)—C(10)	122.0(2)
H(1)—C(1)—H(1′)	106.6(21)	B—C(9)—C(14)	122.4(2)
H(1)—C(1)—O	109.3(14)	C(10)—C(9)—C(14)	115.6(2)
H(1)—C(1)—C(2)	113.3(15)	C(9)—C(10)—C(11)	122.1(3)
H(1′)—C(1)—O	112.4(16)	H(10)—C(10)—C(9)	118.1(16)
H(1′)—C(1)—C(2)	110.3(16)	H(10)—C(10)—C(11)	119.6(16)
O—C(1)—C(2)	105.2(2)	C(10)—C(11)—C(12)	120.2(3)
H(2)—C(2)—H(2′)	109.3(23)	H(11)—C(11)—C(10)	115.9(18)
H(2)—C(2)—N	104.2(19)	H(11)—C(11)—C(12)	123.8(18)
H(2)—C(2)—C(1)	111.3(18)	C(11)—C(12)—C(13)	119.5(3)
H(2′)—C(2)—N	113.5(15)	H(12)—C(12)—C(11)	120.3(17)
H(2′)—C(2)—C(1)	115.0(15)	H(12)—C(12)—C(13)	120.2(17)
N—C(2)—C(1)	102.9(2)	C(12)—C(13)—C(14)	119.8(3)
B—C(3)—C(4)	124.1(2)	H(13)—C(13)—C(12)	123.8(18)
B—C(3)—C(8)	120.0(2)	H(13)—C(13)—C(14)	116.4(18)
C(8)—C(3)—C(4)	115.6(2)	C(13)—C(14)—C(9)	122.8(2)
C(3)—C(4)—C(5)	121.8(2)	H(14)—C(14)—C(13)	118.4(13)
H(4)—C(4)—C(3)	118.4(14)	H(14)—C(14)—C(9)	118.9(13)
H(4)—C(4)—C(5)	119.7(14)		

120.0°, respectively. There are a number of significant deviations from these values, resulting from steric and charge delocalization effects. Intramolecular contacts between atom pairs N and C(4), N and C(10), and O and C(14) are responsible for angular distortions at the boron atom, and at carbon atoms C(3) and C(9). Expansion of the angles NBC(3), OBC(9), BC(3)C(4), BC(9)C(4), and BC(9)C(10) (112.9, 113.7, 124.1, 122.4, and 122.0 respectively) allows the distances C(4)...N (3.143 Å), O...C(14) (2.955 Å), and N...C(10) (3.210 Å) to be equal to or slightly greater than the sum of the van der Waals radii. The expansion of OBC(9) and NBC(3) causes a contraction of NBC(9) to 106.8° which is balanced by an expansion of BC(9)C(10) (as above) to allow the N...C(10) contact to be normal. The phenyl C—C—C angles at C(3) and C(9) are both contracted to 115.6° as a result of expansion of B—C—C angles. This, in turn, makes angular adjustments at the remaining phenyl carbon atoms necessary in order to retain the planarity of the phenyl rings. The magnitude of these distortions is also dependent on the electron delocalization in as much as the C—C distances are not all equal.

The angle opposite the small OBN angle (99.7°) is opened to 114.0° and is normal for the angle between two bulky substituents. The interior angles in the boroxazolidine ring, as previously mentioned, are all contracted as are the H—N—H and H—C—H angles opposite them, all of which are less than, but not significantly different from the tetrahedral angle. The remaining angles involving the ring hydrogen atoms are generally greater than the tetrahedral angle. The angles H(N′)—N—C(2) (113.9°) and H(N′)—N—B (116.9°) represent bending of H(N′) toward the oxygen atom to which it is hydrogen bonded.

Bond angles involving the phenyl hydrogen atoms show a trend that when the adjacent C—C distances are different, so are the corresponding H—C—C angles. The H—C—C angle which

Can. J. Chem. Downloaded from www.nrcresearchpress.com by 210.87.254.42 on 09/05/12
For personal use only.

Can. J. Chem. Downloaded from www.nrcresearchpress.com by 210.87.254.42 on 09/05/12
For personal use only.

TABLE 6. Equations of weighted least-squares mean planes*

Plane *1*: C(3)—C(8)			Plane *2*: C(9)—C(14)		
Atom	Δ (Å)	Δ/σ	Atom	Δ (Å)	Δ/σ
C(3)	0.0001	0.04	C(9)	−0.0008	0.42
C(4)	−0.0009	0.39	C(10)	−0.0030	1.15
C(5)	0.0012	0.47	C(11)	0.0069	2.35
C(6)	−0.0003	0.10	C(12)	−0.0041	1.43
C(7)	−0.0008	0.30	C(13)	−0.0014	0.51
C(8)	0.0006	0.28	C(14)	0.0029	1.26
B	0.1502	67.35	B	−0.0246	10.70
H(4)	0.0401	1.58	H(10)	−0.0801	3.14
H(5)	0.0197	0.74	H(11)	−0.0066	0.20
H(6)	−0.0322	1.27	H(12)	−0.0349	1.21
H(7)	−0.0073	0.28	H(13)	0.0064	0.21
H(8)	0.0119	0.52	H(14)	0.0232	1.00

*Plane *1*, $-0.3074X + 0.9482Y - 0.0800Z + 1.3230 = 0$; plane *2*, $-0.8759X - 0.4753Y - 0.0823Z + 10.4443 = 0$. *X*, *Y*, *Z* are orthogonal coordinates in Å w.r.t. axes *a*, *b*, *c**; the dihedral angle between the planes is 100°; Δ is the deviation from planes.

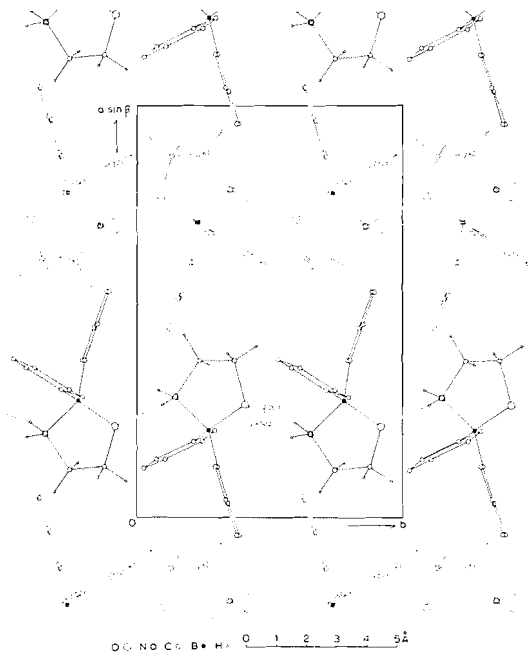

FIG. 3. The structure viewed down *c*; hydrogen bonds are represented by broken lines.

H—C(11)—C(10) (115.9°) and H—C(11)—C(12) (123.8°) differ by more than 4 σ.

The mean C—H, C—H (ar), and N—H bond lengths of 0.96(3), 0.97(3), and 0.92(7) Å, respectively, are as expected. The distances are shorter than those obtained spectroscopically indicating that the hydrogen electron has been pulled toward the atom to which it is bonded.

Figure 3 shows the structure viewed down *c*. The crystal structure consists of discrete molecules of *B*,*B*-diphenylboroxazolidine which are linked by O...H—N hydrogen bonds (2.874 Å) to form continuous spirals about the 2_1 axes along *b*. Details of the hydrogen bonding scheme are given in Table 7 as well as intermolecular

TABLE 7. (*a*) Selected intramolecular and intermolecular contacts less than 3.5 Å

Intramolecular		Intermolecular*	
Atoms	Distance (Å)	Atoms	Distance (Å)
O...C(14)	2.955(3)	N...C(3^{I})	3.437(3)
O...C(8)	3.395(3)	N...C(4^{I})	3.470(3)
O...C(4)	3.299(2)	C(4)...H(N^{II})	2.72(3)
N...C(4)	3.143(3)	C(7)...H(11^{III})	2.84(3)
N...C(10)	3.201(3)	C(11)...H(1′^{IV})	2.87(3)
		C(12)...H(14^{V})	2.83(2)
		C(14)...H(7^{VI})	2.99(3)

(*b*) Hydrogen bond data

Atoms	Distance (Å)	Atoms	Angle (deg.)
O...H(N′^{II})	2.06(3)	C(1)—O...H(N′^{II})	119.5(6)
O...N^{II}	2.874(2)	C(1)—O...N^{II}	118.9(1)
		B—O...H(N′^{II})	119.6(6)
		B—O...N^{II}	116.1(1)
		H(N′^{II})..O..N^{II}	5.8(6)
		H(N′^{II})—N$^{(II)}$..O	14(1)
		H(N^{II})—N^{II}..O	90(2)
		C(2^{II})—N^{II}..O	122.3(2)
		B^{II}—N^{II}...O	120.1(1)
		N^{II}—H(N′^{II})..O	160(2)

*Roman numeral superscripts refer atoms at positions: I, $1\frac{1}{2} - x$, $y - \frac{1}{2}$, $\frac{1}{2} - z$; II, $1\frac{1}{2} - x$, $\frac{1}{2} + y$, $\frac{1}{2} - z$; III, $2 - x$, $-y$, $1 - z$; IV, $\frac{1}{2} + x$, $\frac{1}{2} - y$, $\frac{1}{2} + z$; V, $1\frac{1}{2} - x$, $y - \frac{1}{2}$, $1\frac{1}{2} - z$; VI, $2 - x$, $1 - y$, $1 - z$.

involves the carbon atom nearer the vertex atom is larger than the other H—C—C angle. As the difference between the adjacent C—C distances increases, so does that between the H—C—C angles. An example is C(11), where C(10)—C(11) (1.389 Å) is 5 σ longer than C(11)—C(12) (1.369 Å) and the angles

and intramolecular contacts less than 3.5 Å. There are only two heavy atom intermolecular contacts less than 3.5 Å: N—C(3), 3.437 Å, and N—C(4), 3.470 Å (apart from the hydrogen bond). These, and all other intermolecular contacts correspond to van der Waals interactions.

We thank Dr. Y. Rasiel for suggesting the problem, the National Research Council of Canada for financial support, and the University of British Columbia Computing Centre for assistance.

1. R. L. LETSINGER and I. SKOOG. J. Am. Chem. Soc. **77**, 2491 (1955).
2. H. C. BROWN and E. A. FLETCHER. J. Am. Chem. Soc. **73**, 2808 (1951).
3. H. K. ZIMMERMAN. Adv. Chem. Ser. No. **42**, 23 (1964).
4. Y. RASIEL and S. RETTIG. Unpublished.
5. R. E. LONG. Ph.D. Thesis. University of California at Los Angeles, 1965.
6. (*a*) International tables for X-ray crystallography. Vol. III. Kynoch Press, Birmingham. 1962. (*b*) R. F. STEWART, E. R. DAVIDSON, and W. T. SIMPSON. J. Chem. Phys. **42**, 3175 (1965).
7. Chem. Soc. Special Publ. No. 11, 1958 and No. 18, 1965.
8. R. J. SIME, R. P. DODGE, A. ZALKIN, and D. H. TEMPLETON. Inorg. Chem. **10**, 537 (1971).

Can. J. Chem. Downloaded from www.nrcresearchpress.com by 210.87.254.42 on 09/05/12
For personal use only.

Crystal and Molecular Structure of Hexakis(dimethylamino)cyclotriphosphazene, $[NP(NMe_2)_2]_3$

STEVEN J. RETTIG AND JAMES TROTTER

Department of Chemistry, University of British Columbia, Vancouver 8, British Columbia

Received September 18, 1972

Crystals of the title compound are monoclinic, $a = 15.539(4)$, $b = 9.061(1)$, $c = 16.707(6)$ Å, $\beta = 107.19(5)°$, $Z = 4$, space group $P2_1/c$. The measured and calculated densities are 1.19 and 1.180(1) g cm^{-3}, respectively. The structure was determined by direct methods and refined by electron-density and full-matrix least-squares procedures to $R = 0.047$ for 2503 observed reflections. The six-membered phosphazene ring is slightly, but significantly, non-planar, the conformation being that of a distorted boat. The molecule has approximate D_3 symmetry. The ring P—N bonds are all equal, mean P—N = 1.588(3) Å, and the relatively short exocyclic P—N bonds, mean 1.652(4) Å, indicate the presence of exocyclic π-bonding in the molecule. The N—C bonds range from 1.417(7) to 1.471(5) with a mean of 1.45(2) Å. The mean endocyclic N—P—N and P—N—P angles are 116.7(4) and 123.0(4)°, respectively, while the exocyclic N—P—N angles average 101.5(8)°.

Les cristaux du composé cité dans le titre crystallise dans le système monoclinique, $a = 15.539(4)$, $b = 9.061(1)$, $c = 16.707(6)$ Å, $\beta = 107.19(5)°$, $Z = 4$, groupe spatial $P2_1/c$. Les densités mesurées et calculées sont respectivement 1.19 et 1.180(1) g cm^{-3}. La structure a été déterminée à l'aide de la procédure directe et a été affinée par un calcul de densité électronique et par la méthode de moindres carrés (matrice complète) jusqu'à un indice $R = 0.047$ pour 2503 réflexions observées. Le cycle hexagonal du phosphazène est légèrement, mais d'une manière significative, gauche, sa conformation étant celle d'un bateau déformé. La molécule s'écarte à peine de la symétrie D_3. Les longueurs des liaisons P—N du cycle sont toutes égales à 1.588(3) Å, et les liaisons P—N exocycliques courtes, 1.652(4) Å en moyenne, indiquent la présence de liaisons π exocycliques dans la molécule. Les longueurs des liaisons N—C s'eténdent de 1.417(7) à 1.471(5) Å, ayant la valeur moyenne de 1.45(2) Å. Les angles N—P—N et P—N—P endocycliques sont égaux respectivement à 116.7(4) et 123.0(4)° en moyenne, tandis que les angles N—P—N exocycliques sont égaux à 101.5(8)° en moyenne.

Can. J. Chem., 51, 1295 (1973)

Introduction

The crystal structures of six homogeneously substituted cyclotriphosphazenes have been reported, $[NPX_2]_3$ (X = F, Cl, Br, Ph, $\frac{1}{2}[O_2C_6H_4]$, and OPh) (1–8). The P—N bonding mechanism in cyclophosphazenes (9, 10) is a topic of current interest. The crystal and molecular structure of $[NP(NMe_2)_2]_3$ has now been determined to enhance the understanding of the bonding in this class of compounds, to provide additional information on exocyclic π-bonding between phosphorus and nitrogen atoms (already established by the structures of $[NP(NMe_2)_2]_4$ (11) and $[NP(NMe_2)_2]_6$ (12)), and to provide a starting point for the analysis of the structure of $[(P_3N_3(NMe_2)_6H]_2CoCl_4$ (13).

Experimental

Crystals of $[NP(NMe_2)_2]_3$ are colorless plates elongated along *b*. The specimen chosen for study had dimensions of *ca.* 0.4 × 0.6 × 0.4 mm and was mounted with *b* parallel to the goniostat axis. Unit-cell and space group data were obtained from film and diffractometer measurements. The unit-cell parameters were refined by a least-squares treatment of $\sin^2\theta$ values for 30 reflections measured on a diffractometer with CuKα radiation. Crystal data are:

$C_{12}H_{36}N_9P_3$ f.w. = 399.40

monoclinic, $a = 15.539(4)$, $b = 9.061(1)$, $c = 16.707(6)$ Å, $\beta = 107.19(5)°$, $V = 2247(1)$ Å^3, $\rho_{exp} = 1.19$ (by flotation in KI solution), $Z = 4$, $\rho_{calc} = 1.180(1)$, $F(000) = 864$, (20 °C, CuKα, $\lambda = 1.5418$ Å, $\mu = 24$ cm^{-1}). Absent spectra: $0k0$, $k \neq 2n$ and $h0l$, $l \neq 2n$ define uniquely the space group $P2_1/c$ (C_{2h}^5, No. 14).

Intensities were measured on a Datex-automated General Electric XRD 6 diffractometer, with a scintillation counter, CuKα radiation (nickel filter and pulse height analyzer), and a θ–2θ scan at 2° min^{-1} over a range of (1.80 + 0.86 tan θ) degrees in 2θ, with 20 s background counts being measured at each end of the scan. Data were measured to $2\theta = 120°$ (minimum interplanar spacing 0.89 Å). A check reflection was monitored every 50 reflections throughout the data collection. The intensity of the check reflection had fallen off by 24% of its starting value by the end of the data collection. Lorentz and polarization corrections were applied, and the structure amplitudes derived. No absorption correction was made. Of the 3299 independent reflections measured, 794 had intensities less than $3\sigma(I)$ above background where $\sigma^2(I) = S + B + (0.03S)^2$ with S = scan count and B = background count. These reflections were classified as unobserved.

Structure Analysis

The structure was solved by direct methods. Sixteen sets of signs for 432 reflections with normalized structure factor $|E| \geqslant 1.50$ were determined by a computer program which uses Sayre relationships in an iterative procedure (14). The starting set of reflections is given in Table 1. One set of signs converged in the least number of cycles, 4, and had the highest consistency index (14), 0.97, with 212 positive signs and 220 negative signs. An *E*-map was computed using the 432 signed values of *E* from this set. The three phosphorus atoms accounted for the three highest peaks on the map and the nine nitrogen and eight of the twelve carbons were among the 40 highest peaks. One cycle of isotropic full-matrix least-squares refinement gave *R* 0.213. The four remaining carbon atoms were then located from a difference Fourier. One cycle with the phosphorus and nitrogen atoms anisotropic and the carbon atoms isotropic reduced *R* to 0.109. The carbon atoms were then refined anisotropically for one cycle, giving *R* 0.088. A difference Fourier revealed possible locations for all 36 hydrogen atoms which were then refined isotropically for one cycle, resulting in *R* 0.061. It was noted at this point that two of the hydrogen atoms, one associated with C(3) and the other with C(12), would not refine. Large thermal vibrations of these carbon atoms along *b* indicated possible disorder. An attempt to refine a split-atom disordered model failed. It should be noted that geometrical data involving the C(3) and C(12) methyl groups may be subject to errors arising from a possible slight disordering of the atoms involved. The two bad hydrogen atoms were removed from the list of atoms and a difference Fourier was calculated which revealed the locations of the two hydrogen atoms. All the non-hydrogen atoms were then treated anisotropically and the hydrogen atoms isotropically for four cycles of refinement. Convergence was reached at *R* 0.047 for 2503 observed reflections (2 reflections were given zero weight in the final stages of refinement due to suspected extinction errors: 002 and $20\bar{2}$).

The least-squares refinement was based on the minimization of $\Sigma w(F_o - F_c)^2$. The anisotropic thermal parameters are U_{ij} in the expression:

$$f = f_o \exp[-2\pi^2(U_{11}a^{*2}h^2 + U_{22}b^{*2}k^2 + U_{33}c^{*2}l^2 + 2U_{12}a^*b^*hk + 2U_{13}a^*c^*hl + 2U_{23}b^*c^*kl)]$$

The scattering factors, f_o, of ref. 15 were used for the non-hydrogen atoms and those of ref. 16 for the hydrogen atoms. A standard errors weighting scheme: $w = 1/\sigma^2(F)$, where $\sigma^2(F)$ is derived from the previously defined $\sigma^2(I)$, gave constant average values of $w(F_o - F_c)^2$ over ranges of $|F_o|$ and was employed in the final stages of refinement.

A final difference Fourier was calculated and showed maximum fluctuations of 1.0 e Å^{-3} near the P_3N_3 ring and 0.2 e Å^{-3} elsewhere. On the final cycle of refinement, no parameter shift was greater than 0.6 σ for all non-hydrogen atoms except C(3) and C(12). These carbon atoms, as well as some of the hydrogen atoms, had parameter shifts of up to 1.7 σ. Final atomic positions are given in Table 2 and thermal parameters in Table 3. Measured and calculated structure factors have been placed in the Depository of Unpublished Data.[1]

TABLE 1. Starting set of reflections for $P_3N_3[N(Me)_2]_6$

h	*k*	*l*	*E*	
5	2	−14	3.64	origin determining
1	1	−2	2.09	
1	3	−1	1.65	
3	2	−12	3.24	
3	2	−10	−2.73	
9	4	−10	3.48	
5	2	−12	−3.48	

Results and Discussion

A view of the molecule down *c* is shown in Fig. 1. Individual bond lengths and angles, with standard deviations, are given in Tables 4 and 5 respectively. Some weighted least-squares mean planes appear in Table 6.

The six-membered phosphazene ring is slightly but significantly non-planar, all atoms lying between −0.099 and 0.097 Å from the mean plane (see Table 6). The NP—NP dihedral angles in the ring, given in Table 7, range from −9.5

TABLE 2. Final positional parameters (fractional × 10^4; × 10^5 for phosphorus atoms) and standard deviations

Atom	*x*	*y*	*z*
P(1)	34291(5)	26076(9)	29461(5)
P(2)	15493(5)	25526(9)	23488(5)
P(3)	25439(5)	38(9)	22974(5)
N(1)	2477(2)	3402(3)	2723(1)
N(2)	1617(1)	835(3)	2192(2)
N(3)	3436(2)	942(3)	2645(2)
N(4)	4162(2)	3487(3)	2578(2)
N(5)	3887(2)	2766(3)	3964(2)
N(6)	846(2)	2717(3)	2916(2)
N(7)	990(2)	3460(3)	1494(2)
N(8)	2669(2)	−1465(3)	2911(2)
N(9)	2465(2)	−742(3)	1377(2)
C(1)	4367(4)	5019(6)	2856(4)
C(2)	4120(4)	3275(7)	1704(3)
C(3)	3452(5)	3443(11)	4508(4)
C(4)	4768(4)	2141(8)	4367(4)
C(5)	891(4)	1656(7)	3570(3)
C(6)	635(3)	4216(5)	3139(3)
C(7)	122(4)	2889(8)	1012(4)
C(8)	1454(4)	4255(8)	1004(3)
C(9)	3098(6)	−1325(8)	3799(3)
C(10)	1955(4)	−2573(6)	2701(5)
C(11)	3224(4)	−1599(8)	1279(4)
C(12)	1789(6)	−421(14)	619(4)

[1]The structure factor table is available, at a nominal charge, from the Depository of Unpublished Data, National Science Library, National Research Council of Canada, Ottawa, Canada K1A 0S2.

TABLE 2. (*Concluded*)

Atom	*x*	*y*	*z*
H(11)	4545(27)	5030(49)	3461(29)
H(12)	4844(32)	5388(49)	2754(27)
H(13)	3907(31)	5611(53)	2616(29)
H(21)	3687(27)	4120(49)	1289(26)
H(22)	3974(26)	2297(48)	1599(25)
H(23)	4739(34)	3672(54)	1675(29)
H(31)	2899(33)	4176(55)	4215(28)
H(32)	3964(38)	4220(65)	4933(39)
H(33)	3481(47)	2881(83)	4960(51)
H(41)	4725(34)	1437(66)	4781(37)
H(42)	5041(33)	1919(54)	4011(30)
H(43)	5154(43)	2886(69)	4582(38)
H(51)	346(34)	1626(53)	3729(29)
H(52)	1185(32)	631(61)	3588(31)
H(53)	1435(31)	1862(52)	4129(30)
H(61)	24(26)	4251(39)	3197(21)
H(62)	528(24)	4839(43)	2581(24)
H(63)	1170(24)	4643(42)	3693(23)
H(71)	−235(28)	3524(47)	707(26)
H(72)	199(29)	2224(52)	691(27)
H(73)	−217(42)	2381(71)	1256(38)
H(81)	1962(31)	4670(53)	1344(30)
H(82)	1027(35)	4921(60)	533(36)
H(83)	1653(48)	3802(81)	656(45)
H(91)	2589(35)	−874(62)	4091(33)
H(92)	3387(36)	−2329(65)	3918(35)
H(93)	3582(40)	−640(70)	3963(35)
H(101)	1635(26)	−2541(44)	2156(24)
H(102)	1460(35)	−2360(52)	2915(30)
H(103)	2255(32)	−3379(61)	2874(31)
H(111)	3592(36)	−1990(57)	1936(38)
H(112)	3556(50)	−794(87)	956(46)
H(113)	3062(49)	−2310(84)	1014(49)
H(121)	1275(42)	192(68)	615(34)
H(122)	1487(69)	−1345(130)	392(67)
H(123)	2026(57)	42(95)	476(51)

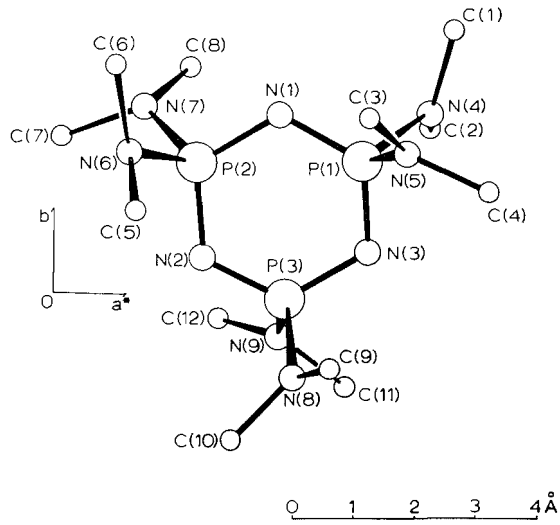

FIG. 1. A view of the molecule down *c* showing crystallographic numbering scheme. Hydrogen atoms have been omitted for clarity.

to 11.4° with a mean amplitude of 6.3°. Atoms P(1) and N(2) lie on one side of the mean plane while the remaining atoms lie on the opposite side so that the conformation of the P_3N_3 ring is that of a distorted boat. Of the other $[NPX_2]_3$ molecules whose structures have been studied, the fluoride (1) has a planar ring, the chloro- (2–4), bromo- (5), and phenyl (6) derivatives have slightly non-planar rings in the chair conformation, and the phenoxy derivative (8) has a slightly folded ring with approximate C_2 symmetry. In $P_3N_3Cl_3(NMe_2)_3$ (17) the P_3N_3 ring also has a distorted boat conformation. These small deviations from planarity have been ascribed to intra- and intermolecular steric effects (2, 5, 6).

The molecule has approximate D_3 symmetry. Bond lengths and angles averaged assuming D_3 symmetry appear in Table 8. The ring nitrogen atoms will be designated N_R and the exocyclic nitrogen atoms N_E. There are two classes of carbon atoms: one set [C(2), C(3), C(5), C(8), C(9), and C(12)], rotated toward the center of the P_3N_3 ring, are designated C_I (for inner) and the other set [C(1), C(4), C(6), C(7), C(10), and C(11)] C_O (for outer).

The P—N_R distances are equal within experimental error. They range from 1.583 to 1.592 Å (σ = 0.002–0.003 Å) with a mean value of 1.588(3) Å which is essentially equal to the mean P—N_R distances of 1.581(13) Å in $P_3N_3Cl_6$ (4) and 1.576(10) Å in $P_3N_3Br_6$ (5). The ring P—N distances in other $[NPX_2]_3$ molecules are: X = F (1), 1.560(10), Ph (6), 1.597(6), $\frac{1}{2}[O_2C_6H_4]$ (7), 1.575(2), and OPh (8), 1.575(2) Å. In $[NP(NMe_2)_2]_n$, where n = 4 (11) and 6 (12), the P—N_R distances average 1.578(10) and 1.563(10) Å, respectively. The close agreement of P—N_R distances in this structure with those in the chloro derivative (4) is in accord with the conclusion that the mean P—N bond length of a P—N—P segment is dependent primarily on the mean electronegativity of the two pairs of substituents on the bordering P atoms of the segment (6). On this basis the P—N_R bonds in the Cl and NMe_2 derivatives are expected to be of equal length since both substituents have an electronegativity of 3.0.

The exocyclic P—N_E bonds are also equal within experimental error. They range from

TABLE 3. Final thermal parameters with standard deviations in parentheses

(*a*) Anisotropic thermal parameters (Å² × 10²)

Atom	U_{11}	U_{22}	U_{33}	U_{12}	U_{13}	U_{23}
P(1)	4.91(5)	5.60(5)	5.60(5)	−0.18(4)	1.17(3)	0.39(4)
P(2)	4.80(5)	5.44(5)	5.37(5)	0.34(4)	1.13(3)	0.39(4)
P(3)	5.53(5)	5.00(5)	6.85(5)	0.27(4)	1.54(4)	0.42(4)
N(1)	5.69(15)	5.24(15)	6.40(15)	0.13(13)	1.39(12)	0.06(13)
N(2)	4.97(14)	5.37(16)	7.93(17)	−0.29(12)	1.49(12)	0.14(13)
N(3)	5.25(15)	5.25(16)	8.07(18)	0.41(12)	1.62(12)	0.08(13)
N(4)	6.57(17)	6.38(19)	8.01(19)	−0.87(14)	2.79(14)	0.43(15)
N(5)	6.22(16)	9.35(22)	5.63(16)	0.31(16)	0.87(13)	0.28(15)
N(6)	6.17(16)	6.72(18)	6.57(16)	0.47(14)	2.23(13)	0.54(14)
N(7)	6.43(17)	7.76(20)	6.04(16)	0.07(15)	0.74(13)	1.10(15)
N(8)	7.43(19)	5.71(19)	9.61(22)	0.07(15)	1.68(16)	2.25(16)
N(9)	7.71(19)	8.01(21)	7.64(20)	0.83(16)	1.59(15)	−1.47(17)
C(1)	9.29(35)	8.03(33)	12.85(47)	−2.51(29)	3.88(33)	0.58(31)
C(2)	10.25(35)	9.77(38)	8.64(31)	0.18(32)	4.71(25)	1.41(29)
C(3)	13.07(47)	22.27(76)	6.38(30)	4.21(53)	1.56(30)	−1.51(43)
C(4)	7.54(30)	12.99(51)	8.62(34)	0.52(32)	−0.36(27)	1.17(35)
C(5)	9.95(35)	11.74(42)	9.15(33)	−0.04(33)	4.47(29)	2.13(30)
C(6)	7.15(27)	9.82(34)	10.62(35)	0.86(24)	3.74(26)	−1.92(28)
C(7)	7.54(29)	10.39(41)	8.54(32)	1.33(30)	−1.51(25)	0.67(33)
C(8)	11.29(40)	13.08(45)	6.88(28)	−0.25(36)	1.89(29)	3.13(31)
C(9)	15.21(57)	10.46(46)	8.95(35)	0.04(46)	1.13(37)	3.69(33)
C(10)	9.76(39)	6.93(33)	15.13(57)	−0.80(30)	3.45(40)	2.44(36)
C(11)	10.71(38)	11.36(44)	11.91(44)	2.43(34)	4.54(34)	−2.63(38)
C(12)	10.58(44)	18.72(81)	8.58(36)	3.89(55)	0.74(31)	−1.78(45)

(*b*) Isotropic thermal parameters

Atom	B (Å²)	Atom	B (Å²)	Atom	B (Å²)
H(11)	8.97(130)	H(51)	11.18(144)	H(91)	12.14(177)
H(12)	9.15(129)	H(52)	11.54(163)	H(92)	12.44(169)
H(13)	10.02(157)	H(53)	10.24(128)	H(93)	14.26(213)
H(21)	9.44(109)	H(61)	7.52(90)	H(101)	6.66(115)
H(22)	7.88(122)	H(62)	7.54(98)	H(102)	10.05(146)
H(23)	11.73(140)	H(63)	8.09(95)	H(103)	10.83(162)
H(31)	10.77(131)	H(71)	7.87(114)	H(111)	12.41(157)
H(32)	13.46(180)	H(72)	8.07(147)	H(112)	18.98(282)
H(33)	13.08(268)	H(73)	14.51(245)	H(113)	16.81(299)
H(41)	13.38(197)	H(81)	9.36(142)	H(121)	12.40(182)
H(42)	8.87(162)	H(82)	12.43(154)	H(122)	27.86(502)
H(43)	14.00(209)	H(83)	15.05(265)	H(123)	19.53(405)

1.645 to 1.656 Å (σ = 0.003 Å) and the mean value of 1.652(4) Å is comparable to the mean P—N_E bond lengths of 1.678 (10) Å in $N_4P_4(NMe_2)_8$ (11), 1.669(10) Å in $N_6P_6(NMe_2)_{12}$ (12), and 1.636 Å in $N_3P_3Cl_3(NMe_2)_3$ (17). The P—N_E distances are considerably shorter than the 1.77 Å expected for a normal P(sp^3)—N(sp^3) bond (18). The shortening of P—N_R and P—N_E bonds in phosphazenes is indicative of some π-character in the bond but is also contributed to by a σ-hybridization effect (10), and can only be discussed in terms of π-bonding after σ-effects have been considered. Using the methods outlined by Craig and Paddock (10), the σ-hybridization adjustments have been made and corrected π-contractions estimated for all the P—N bonds. The observed and σ-adjusted π-contractions appear in Table 9, and show that the π-character of the P—N_R bonds is somewhat greater than in the P—N_E bonds.

The mean N—C distance (corrected for thermal motion) of 1.482(10) Å is close to the expected value of 1.472(5) Å (19). The uncorrected N—C bonds average 1.447(21) Å, 1.453(12) Å

TABLE 4. Bond lengths with standard deviations in parentheses; values in square brackets are corrected for thermal libration

Bond	Length (Å)	Bond	Length (Å)	
P(1)—N(1)	1.588(2)	N(4)—C(1)	1.468(6)	[1.494(6)]
P(1)—N(3)	1.592(3)	N(4)—C(2)	1.455(5)	[1.478(5)]
P(2)—N(2)	1.587(3)	N(5)—C(3)	1.422(6)	[1.488(6)]
P(2)—N(1)	1.590(2)	N(5)—C(4)	1.449(5)	[1.478(5)]
P(3)—N(3)	1.583(3)	N(6)—C(5)	1.442(5)	[1.473(5)]
P(3)—N(2)	1.589(2)	N(6)—C(6)	1.471(5)	[1.493(5)]
Mean	1.588(3)	N(7)—C(7)	1.447(5)	[1.472(5)]
		N(7)—C(8)	1.435(5)	[1.468(6)]
P(1)—N(4)	1.651(3)	N(8)—C(9)	1.442(6)	[1.487(6)]
P(1)—N(5)	1.645(3)	N(8)—C(10)	1.461(6)	[1.487(6)]
P(2)—N(6)	1.652(3)	N(9)—C(11)	1.460(5)	[1.492(6)]
P(2)—N(7)	1.655(3)	N(9)—C(12)	1.417(7)	[1.469(7)]
P(3)—N(8)	1.656(3)	Mean	1.447(21)	[1.482(10)]
P(3)—N(9)	1.652(3)	C—H	0.65(8) – 1.14(6),	
Mean	1.652(4)	Mean	0.96(11)	

TABLE 5. Bond angles with standard deviations in parentheses

Bonds	Angle (deg)	Bonds	Angle (deg)
N(1)—P(1)—N(3)	116.7(1)	P(1)—N(4)—C(1)	116.5(3)
N(1)—P(1)—N(5)	107.0(1)	P(1)—N(4)—C(2)	118.6(3)
N(1)—P(1)—N(4)	113.0(1)	C(1)—N(4)—C(2)	112.6(4)
N(3)—P(1)—N(5)	111.6(1)	P(1)—N(5)—C(3)	123.8(3)
N(3)—P(1)—N(4)	105.7(1)	P(1)—N(5)—C(4)	120.4(3)
N(5)—P(1)—N(4)	102.0(1)	C(3)—N(5)—C(4)	115.7(4)
N(2)—P(2)—N(1)	116.3(1)	P(2)—N(6)—C(5)	118.8(3)
N(2)—P(2)—N(6)	105.7(1)	P(2)—N(6)—C(6)	117.7(3)
N(2)—P(2)—N(7)	112.8(1)	C(5)—N(6)—C(6)	112.9(4)
N(1)—P(2)—N(6)	114.0(1)	P(2)—N(7)—C(7)	117.9(3)
N(1)—P(2)—N(7)	106.4(1)	P(2)—N(7)—C(8)	121.2(3)
N(6)—P(2)—N(7)	100.5(1)	C(7)—N(7)—C(8)	113.9(4)
N(3)—P(3)—N(2)	117.0(1)	P(3)—N(8)—C(9)	120.0(3)
N(3)—P(3)—N(9)	112.2(1)	P(3)—N(8)—C(10)	117.5(3)
N(3)—P(3)—N(8)	105.9(1)	C(9)—N(8)—C(10)	113.2(5)
N(2)—P(3)—N(9)	106.0(1)	P(3)—N(9)—C(11)	118.8(3)
N(2)—P(3)—N(8)	112.7(1)	P(3)—N(9)—C(12)	125.4(4)
N(9)—P(3)—N(8)	102.1(1)	C(11)—N(9)—C(12)	114.8(4)
P(1)—N(1)—P(2)	123.1(2)	N—C—H 96(8)–123(3), mean 110.5(60)	
P(2)—N(2)—P(3)	123.3(2)	H—C—H 84(3)–132(9), mean 108(10)	
P(3)—N(3)—P(1)	122.5(2)		

if C(3) and C(12) are excluded, compared to the value of 1.455 Å for $N_4P_4(NMe_2)_8$ (11), $N_3P_3Cl_3(NMe_2)_3$ (17), and $HNMe_2$ (20). The mean $N—C_I$ bond is shorter than the mean $N—C_O$ bond for both the corrected and uncorrected distances (see Table 8). Table 4 shows that at each N_E the two N—C distances differ by at least 2 σ (for the uncorrected distances). This is due to steric and electronic effects which will be discussed later.

The individual bond angles and dihedral angles (Table 7) show some small but significant deviations from D_3 symmetry. The most notable of these distortions is the inequivalence of the two NMe_2 groups bonded to each P atom. (In view of the possible disorder in C(3) and C(12), associated geometrical parameters may be in error. It is felt, however, that the errors are small enough to retain the validity of the ensuing discussion, supported by data in refs. 11, 12, and 17 and the location of C(3) and C(12) H atoms.) This is due to interaction of the two N_E lone electron

TABLE 6

(*a*) Distances of relevant atoms from mean planes through the molecule (phosphazene ring)

Atom	*d* (Å)	*d*/σ
P(1)	−0.014	17.5
P(2)	0.006	7.4
P(3)	0.002	2.8
N(1)	0.055	23.1
N(2)	−0.099	40.3
N(3)	0.097	38.7

(*b*) Equations of planes: $lX + mY + nZ = p$, where X, Y, and Z are orthogonal coordinates (Å), referred to a, b, and c^*, respectively

Plane*	*l*	*m*	*n*	*p*
(*1*)	0.3196	0.2513	−0.9136	−2.4506
(*2*)	−0.5194	0.8545	−0.0082	−0.0332
(*3*)	−0.3530	−0.8480	−0.3953	−3.8837
(*4*)	−0.9792	−0.0623	−0.1930	−3.4680

*Plane (*1*), phosphazene ring; Plane (*2*), P(1)N(4)N(5); Plane (*3*), P(2)N(6)N(7); Plane (*4*), P(3)N(8)6(9).

(*c*) Angles between the planes

Planes	Angle (deg)
(*1*)–(*2*)	87
(*1*)–(*3*)	88
(*1*)–(*4*)	99

pairs with different d orbitals of the phosphorus atom (10). This causes no noticeable difference between the two P—N_E bond lengths at each phosphorus atom, but manifests itself primarily in the bond angles at the N_E atoms. The sum of bond angles at N_E atoms ranges from 347.7 to 359.9° with a mean value of 353.3° (mean angle at N_E = 117.8°), some 25° greater than expected (3 × 109.45). This is indicative of delocalization of the N_E lone pairs into the ring system in agreement with the estimated π-contractions calculated for the P—N_E bonds. Data in Table 6 show that for each phosphorus atom one of the NMe_2 groups is significantly more planar than the other; in fact the group P(1)N(5)C(3)C(4) is planar within experimental error. Moreover, the more planar NMe_2 groups, N(5), N(7), and N(9), are not all on the same side of the P_3N_3 ring. N(5) which is attached to P(1), the unique P atom in the boat conformation, lies on the opposite side of the ring from the two other more planar NMe_2 groups. The bond angle sums at the various N_E atoms are: N(4), 347.7, N(5), 359.9, N(6), 349.4, N(7), 353.0, N(8), 350.7, and N(9), 359.0°. The mean value for the more planar groups is 357.3° and for the less planar groups 349.3°. Comparable differences between two NMe_2 groups attached to the same phosphorus atom have been noted for other phosphazene derivatives, for example, sums of bond angles about the two classes of N_E atoms average 358.5 and 349.5° in $N_4P_4(NMe_2)_8$ (11), 357.5 and 348.7° in $N_6P_6(NMe_2)_{12}$ (12), and 351.1 and 347.9° in $N_3P_3Cl_3(NMe_2)_3$ (17). Averaged bond lengths and angles treating the more and less planar N_E atoms separately also appear in Table 8. These parameters have better r.m.s. deviations than those calculated assuming D_3 symmetry.

The mean C—N—C angle is 113.9(12)°, each individual value being significantly larger than the 111.8° in $HNMe_2$ (20). Again we note a difference between the more and less planar N_E atoms, the C—N—C angles average 114.8(9) for the former and 112.9(3)° for the latter. Steric interactions between the ring nitrogen atoms and C_I hydrogen atoms are responsible for significant differences between the two PN_EC angles at each N_E atom and the two N_RPN_E angles at each phosphorus atom. Expansion of the PN_EC_I angles to a mean value of 121.3(27), and the corresponding N_EPN_R to a mean of 112.7(8)° combined with corresponding contractions of PN_EC_O to a mean

TABLE 7. Dihedral angles in the molecule

Atoms	Value (deg)	Atoms	Value (deg)
N(3)P(1)—N(1)P(2)	−9.5	N(3)P(1)—N(4)C(1)	−58.6
P(1)N(1)—P(2)N(2)	0.8	N(1)P(1)—N(5)C(4)	−51.1
N(1)P(2)—N(2)P(3)	6.7	N(1)P(2)—N(6)C(6)	−52.6
P(2)N(2)—P(3)N(3)	−4.9	N(2)P(2)—N(7)C(7)	−49.5
N(2)P(3)—N(3)P(1)	−4.6	N(2)P(3)—N(8)C(10)	−54.1
P(3)N(3)—P(1)N(1)	11.4	N(3)P(3)—N(9)C(11)	−51.6
Mean absolute value	6.3	Mean	−53

TABLE. 8. Averaged geometrical parameters

Bond	Length* (Å)					
	Assuming D_3 symmetry		More planar N_E		Less planar N_E	
$P—N_R$	1.588(3)		—		—	
$P—N_E$	1.652(4)		1.651(5)		1.653(3)	
$N_E—C_I$	1.436(14)	[1.477(9)]†	1.425(9)	[1.475(11)]	1.446(8)	[1.479(7)]
$N_E—C_O$	1.460(10)	[1.486(9)]	1.452(6)	[1.481(10)]	1.467(5)	[1.491(4)]

Bonds	Angle (deg)		
	Assuming D_3 symmetry	More planar N_E	Less planar N_E
$N_R—P—N_R$	116.7(4)	—	—
$N_E—P—N_E$	101.5(8)	—	—
$N_R—P—N_E$	106.1(5)	106.5(5)	105.8(1)
$N_R—P—N_E$	112.7(8)	112.2(6)	113.2(7)
$P—N_R—P$	123.0(4)	—	—
$C—N_E—C$	113.9(12)	114.8(9)	112.9(3)
$P—N_E—C_I$	121.3(28)	123.5(21)	119.1(8)
$P—N_E—C_O$	118.1(13)	119.0(13)	117.2(6)

*Numbers in parentheses are r.m.s. deviations from the mean.
†Values in square brackets are corrected for thermal libration.

TABLE 9. P—N bond lengths and π-contractions in $[NP(NMe_2)_2]_3$*

Bond length (Å)	π-contraction	
	Observed	σ-adjusted
	Ring P—N bond	
1.588	0.182	0.140
1.592	0.178	0.140
1.587	0.183	0.143
1.590	0.180	0.137
1.583	0.187	0.148
1.589	0.181	0.140
1.588	0.182	0.141
	Exocyclic P—N bond	
1.651	0.119	0.110
1.645	0.125	0.108
1.652	0.118	0.109
1.655	0.115	0.104
1.656	0.114	0.102
1.652	0.118	0.101
1.652	0.118	0.106

*Both observed and σ-adjusted π-contractions are tabulated (π-contractions are estimated with reference to a P—N single bond length of 1.77 Å). The last value in each column is an average value.

of 118.1(3)° (from an expected 119.7° assuming equality of the two PN_EC angles) and of N_RPN_E to a mean of 106.1(5)° ease the intramolecular contacts $N_R...H(C_I)$ and $N_R...C_I$ which are compiled in Table 10. Each of the listed N...H contacts is less than the van der Waals distance of 2.7 Å, and the N...C contacts are less than the corresponding 3.2 Å. There are again small differences in these angles for the more and less planar N_E atoms listed in Table 8.

The mean angle at each phosphorus atom is 109.3°; the ring angles N_RPN_R average 116.7(4)°, comparable to the $[NPX_2]_3$ molecules (1–8) where the endocyclic NPN angles have mean values ranging from 116.6 to 120.0°. There are

TABLE 10. Selected nonbonded contacts less than 3.5 Å

Intramolecular		Intermolecular	
Atoms	Distance (Å)	Atoms	Distance (Å)
N(1)...H(31)	2.48(4)	N(1)...H(112^{I})	2.96(6)
N(1)...H(81)	2.48(5)	N(2)...H(61^{II})	2.83(4)
N(2)...H(122)	2.62(5)	N(3)...H(12^{III})	2.98(5)
N(2)...H(51)	2.60(6)	C(2)...H(33^{IV})	2.98(8)
N(3)...H(93)	2.58(6)	C(5)...H(62^{II})	2.96(4)
N(3)...H(22)	2.48(4)	H(13)...H(111^{I})	2.43(7)
N(1)...C(3)	2.918(6)	H(32)...H(111^{V})	2.45(10)
N(1)...C(8)	2.945(6)		
N(2)...C(12)	2.943(6)		
N(2)...C(5)	2.948(7)		
N(3)...C(9)	2.969(7)		
N(3)...C(2)	3.010(6)		

*Roman numeral superscripts refer to atoms at positions: I, x, 1 + y, z; II, $-x$, $y - \frac{1}{2}$, $\frac{1}{2} - z$; III, 1 − x, $y - \frac{1}{2}$, $\frac{1}{2} - z$; IV, x, $\frac{1}{2} - y$, $z - \frac{1}{2}$; V, x, $\frac{1}{2} - y$, $\frac{1}{2} + z$.

small but significant deviations between the individual values which range from 116.3(1) to 117.0(1)°, a range of 5σ. The mean P—N_R—P angle is 123.0(4)° which is slightly, but not significantly larger than in the other $[NPX_2]_3$ molecules (1–8), where mean P—N_R—P angles range from 121.3° in the bromo-derivative (5) to 122.5° for $X = \frac{1}{2}[O_2C_6H_4]$ (7). Again there are small but significant differences between the individual values due to inter- and intramolecular steric effects as mentioned earlier.

The angles made by the planes of the ligands (PN_EN_E) with the mean plane of the phosphazene ring are inequivalent, being 87, 88, and 99° at P(1), P(2), and P(3), respectively. The rotations of the NMe_2 groups about the P—N_E bonds (measured by the N_RP—N_EC_O dihedral angles listed in Table 7) range from −49.5 to −58.6°, mean −53(3)°, the angles being smaller (mean −50.7°) at the more planar N_E atoms than at the less planar (mean −55.1°). These values are similar to the values of 50 and 53 in the $\diagdown P(NMe_2)_2 \diagup$ segment of $P_3N_3Cl_3(NMe_2)_3$ (17).

The geometry involving the hydrogen atoms is as expected; C—H bonds range from 0.65 to 1.14 Å, mean 0.96(11) Å. The mean angle at carbon is 109.2°, the N—C—H angles average 110.5° and the H—C—H angles 108.0°, as expected on steric grounds.

The structure viewed down *b* is shown in Fig. 2. There are no N...C or C...C intermolecular contacts less than 3.5 Å. The shortest intermolecular contacts involve hydrogen atoms and are given in Table 10. All of these correspond to normal van der Waals contacts.

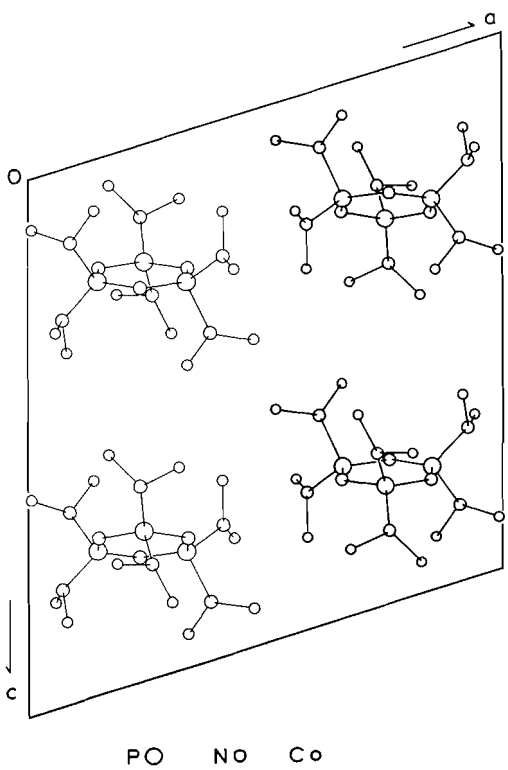

FIG. 2. Projection of the structure down *b*. Hydrogen atoms have been omitted for clarity.

We thank Professor N. L. Paddock and Dr. J. N. Wingfield for the crystals and discussion, the National Research Council of Canada for financial support, and the University of British Columbia Computing Centre for assistance.

1. M. W. DOUGILL. J. Chem. Soc. 3211 (1960).
2. A. WILSON and D. F. CARROLL. J. Chem. Soc. 2548 (1960).
3. E. GIGLIO. Ric. Sci. Suppl. **30**, 721 (1960).
4. G. J. BULLEN. J. Chem. Soc. (A), 1450 (1971).
5. (*a*) E. GIGLIO and R. PULITI. Acta Cryst. **22**, 304 (1967). (*b*) H. ZOER and A. J. WAGNER. Acta Cryst. **B26**, 1812 (1970).
6. F. R. AHMEDJÍ, P. SINGH, and W. H. BARNES. Acta Cryst. **B25**, 316 (1969).
7. L. A. SIEGEL and J. H. VAN DEN HENDE. J. Chem. Soc. (A), 817 (1967).
8. W. C. MARSH and J. TROTTER. J. Chem. Soc. (A), 169 (1971).
9. N. P. PADDOCK. Q. Rev. **18**, 2, 168 (1964).
10. D. P. CRAIG and N. L. PADDOCK. *In* Nonbenzenoid aromatics. Vol. 2. Academic Press, New York. 1971.
11. G. J. BULLEN. J. Chem. Soc. 3193 (1962).
12. A. J. WAGNER and A. VOS. Acta Cryst. **B24**, 1423 (1968).
13. A. L. MACDONALD and J. TROTTER. To be published.
14. R. E. LONG. Ph.D. Thesis. University of California at Los Angeles, Los Angeles, California. 1965.
15. International tables for X-ray crystallography. Vol. III. Kynoch Press, Birmingham. 1962.
16. R. F. STEWART, E. R. DAVIDSON, and W. T. SIMPSON. J. Chem. Phys. **42**, 3175 (1965).
17. F. R. AHMED and D. R. POLLARD. Acta Cryst. **B28**, 513 (1972).
18. E. HOBBS, D. E. C. COBRIDGE, and B. RAISTRICK. Acta Cryst. **6**, 21 (1953); D. W. J. CRUICKSHANK. Acta Cryst. **17**, 671 (1964).
19. Chem. Soc. Special Publ., No. 11, 1958 and No. 18, 1965.
20. B. BEAGLEY and T. G. HEWITT. Trans. Faraday Soc. **64**, 2561 (1968).

Crystal and Molecular Structure of Potassium *trans*-1,2-Diaminocyclohexane-*N*,*N*′-tetraacetatomanganate(III) Monohydrate, K[Mn(DCTA)]·H_2O[1]

STEVEN J. RETTIG AND JAMES TROTTER

Department of Chemistry, University of British Columbia, Vancouver 8, British Columbia

Received September 18, 1972

Crystals of the title compound are triclinic, $a = 15.60(3)$, $b = 8.66(2)$, $c = 7.36(1)$ Å, $\alpha = 103.8(1)$, $\beta = 95.7(1)$, $\gamma = 70.7(3)°$, $Z = 2$, space group $P\bar{1}$. The measured and calculated densities are 1.69(2) and 1.656(6) g cm^{-3}, respectively. The structure was determined by Patterson and Fourier synthesis and refined by full-matrix least-squares procedures to a final R of 0.067 for 2333 observed reflections. The structure is composed of layers of oxygen bridged potassium ions situated between two layers of $[Mn(DCTA)]^-$ anions, thus forming the basic structural unit which repeats along a. The manganese(III) is six-coordinated to the two nitrogen and four oxygen atoms of the hexadentate ligand, the coordination polyhedron being a very distorted octahedron with N—Mn—O and O—Mn—O angles of 77.1(2) and 128.5(2)°, respectively. The anion has approximate C_2 symmetry with two classes of Mn—O bonds, mean bond lengths 1.887(7) and 2.015(22) Å; the mean Mn—N distance is 2.263(5) Å. The water molecule is twofold disordered and is coordinated to the potassium ion in both positions. The potassium ion is eight or nine coordinated to oxygen atoms depending on the position taken by the water molecule. Weak hydrogen bonds involving the water molecule are probably present, O...O distances range from 2.71(3) to 3.18(3) Å, as well as possible C—H...O hydrogen bonds with C...O distances ranging from 3.300(9) to 3.388(8) Å.

Le composé cité dans le titre cristallise dans le système triclinique, $a = 15.60(3)$, $b = 8.662(2)$, $c = 7.36(1)$ Å, $\alpha = 103.8(1)$, $\beta = 95.7(1)$, $\gamma = 70.7(3)°$, $Z = 2$, groupe spatial $P\bar{1}$. Les densités mesurées et calculées valent respectivement 1.69(2) et 1.656(6) g cm^{-3}. La structure a été déterminée à l'aide des synthèses de Patterson et de Fourier, et a été affinée par la méthode de moindres carrés (matrice complète) jusqu'à un indice $R = 0.067$ pour 2333 réflexions observées. L'unité fondamentale de la structure se compose d'une couche d'ions de potassium reliés par des ions d'oxygène, située entre deux couches d'anions $[Mn(DCTA)]^-$, et cette unité se répète le long de l'axe a. L'ion manganese(III) est coordonné aux deux atomes d'azote et aux quatre atomes d'oxygène du ligand hexadenté, le polyèdre de coordination étant un octaèdre très déformé dont les angles N—Mn—O et O—Mn—O sont égaux respectivement à 77.1(2) et 128.5(2)°. L'anion, qui s'écarte à peine de la symétrie C_2, possède deux classes de liaisons Mn—O, dont les longueurs moyennes sont égales à 1.887(7) et 2.015(22) Å, et la longueur moyenne de la liaison Mn—N est égale à 2.263(5) Å. La molécule d'eau est doublement désordonnée et dans chaque position elle est coordonnée à un ion de potassium. L'ion de potassium est coordonné à huit ou neuf atomes d'oxygène selon les positions des molécules d'eau. Il est probable que la molécule d'eau s'engage dans de faibles liaisons hydrogène ; les distances O...O s'étendent de 2.71(3) à 3.18(3) Å. Des liaisons hydrogène C—H...O sont possibles ; les distances C...O s'eténdent de 3.300(9) à 3.388(8) Å.

Can. J. Chem., 51, 1303 (1973)

Introduction

The structure analysis of K[Mn(DCTA)]·H_2O has been undertaken to investigate the possibility of a seven-coordinate Mn(III) complex. Parallel chemical investigations (1 and references therein; 2, 3) have suggested a strong association between the water molecule and the complex ion in solution, and seven-coordination has been found in related complexes (4 and references therein). The present analysis however shows that in the solid state the Mn(III) ion is six-coordinated to the hexadentate ligand. It has been pointed out (4) that the ring constraints are incompatible with a quasi-octahedral configuration except for a relatively small central cation. The apparently strong interaction in solution and the large angular distortions from octahedral geometry in the six-coordinated anion found in the solid state for the present compound imply that the size of the manganese(III) ion is near the upper limit for six-coordination to DCTA.

Experimental

Single crystals of K[Mn(DCTA)]·H_2O, suitable for X-ray analysis were prepared by Poh (2). The recrystallization solvent was a 3:2 mixture of water and methanol.

[1]Here, and elsewhere in this paper, EDTA and DCTA refer to the ethylenediaminetetraacetate and *trans*-1,2-diaminocyclohexane-*N*,*N*′-tetraacetate anions.

Can. J. Chem. Downloaded from www.nrcresearchpress.com by 210.87.254.5 on 09/05/12
For personal use only.

TABLE 1. $|E|$ statistics and distribution

	Observed value	Theoretical value*	
		Centrosymmetric	Noncentrosymmetric
$\langle\|E\|\rangle$	0.780	0.798	0.886
$\langle\|E\|^2\rangle$	0.986	1.000	1.000
$\langle\|E^2 - 1\|\rangle$	0.975	0.968	0.736
$\|E\| \geqslant 3.0$ (%)	0.20	0.30	0.01
$\|E\| \geqslant 2.0$ (%)	4.19	5.00	1.80
$\|E\| \geqslant 1.0$ (%)	32.58	32.00	37.00

*See ref. 5.

The crystals were dark and irregularly developed. The specimen chosen for study was elongated along c and was mounted with c^* along the goniostat axis. The crystal dimensions were *ca.* 0.3 × 0.3 × 0.45 mm. Unit cell and space group data were obtained from film and diffractometer measurements. The unit cell was refined by a least-squares treatment of $\sin^2\theta$ values for 30 reflections measured on a diffractometer with MoKα radiation. The density was measured by flotation in benzene–chloroform. Crystal data are:

$C_{14}H_{20}KMnN_2O_9$ f.w. = 454.0

Triclinic, $a = 15.60(3)$, $b = 8.66(2)$, $c = 7.36(1)$ Å, $\alpha = 103.8(1)$, $\beta = 95.7(1)$, $\gamma = 70.7(3)°$, $V = 910(3)$ Å^3, $\rho_o = 1.69(2)$, $Z = 2$, $\rho_c = 1.656(6)$, $F(000) = 468$ (20 °C, MoKα, $\lambda = 0.71069$ Å, $\mu = 10$ cm^{-1}). Space group $P\bar{1}$(C_i^1, No. 2) from structure analysis.

Intensities were measured on a General Electric XRD 6 diffractometer, with a scintillation counter, MoKα radiation (zirconium filter and pulse height analyzer), and a θ–2θ scan at 2° min^{-1} over a range of (1.80 + 0.86 tan θ) degrees in 2θ, with 20 s background counts being measured at each end of the scan. Data were measured to $2\theta = 52°$ (minimum interplanar spacing 0.81 Å). A check reflection was monitored every 40 reflections throughout the data collection. The intensity of the check reflection had dropped to 63% of its original intensity by the end of the data collection. The intensities of 20 strong reflections which had been measured early in the data collection were remeasured at the end and were found to have the same relative intensities as before. Lorentz and polarization corrections were applied, and structure amplitudes were derived. No absorption correction was made in view of the low value of μ. Of the 3560 independent reflections measured, 1227 had intensities less than $3\sigma(I)$ above background where $\sigma^2(I) = S + B + (0.03\ S)^2$ with S = scan count and B = background count. These reflections were classified as unobserved.

Structure Analysis and Refinement

The $|E|$ statistics are compared with theoretical values (5) for centrosymmetric and noncentrosymmetric structures in Table 1; the former distribution is strongly indicated, confirming the space group as $P\bar{1}$.

The positions of the manganese and potassium atoms were determined from the three-dimensional Patterson function. One cycle of full-matrix least-squares refinement of the positional and isotropic thermal parameters of the heavy atoms gave R 0.320. A difference Fourier synthesis revealed the positions of all the non-hydrogen atoms with the exception of O(9), the water oxygen. The atoms located were refined as follows; two cycles of isotropic refinement of all the atoms followed by one cycle with the carbon atoms isotropic and all the remaining atoms anisotropic, reducing R to 0.109. A second difference Fourier was calculated which revealed a possible location for O(9) as well as 17 of the 20 hydrogen atoms. The carbon atoms were refined anisotropically and O(9) isotropically for one cycle followed by one cycle of isotropic refinement of the hydrogen atoms and O(9), resulting in R 0.074. It was noted that the temperature factor for O(9) was not refining and a difference Fourier was calculated revealing a peak greatly elongated along z for O(9). The remaining non-water hydrogen atom was also located. Positions and site-occupancies were estimated for the twofold disordered O(9) from the difference Fourier and the positional, thermal, and then occupational parameters for the split O(9) were refined over two cycles resulting in R 0.069. Finally the entire structure was refined, all non-hydrogen atoms anisotropically and the hydrogen atoms isotropically for two cycles. Convergence was reached at R 0.067 for 2333 observed reflections.

The least-squares refinement was based on the minimization of $\Sigma w\ (F_o - F_c)^2$. The scattering factors of ref. 6(*a*) were used for the non-hydrogen atoms and those of ref. 6(*b*) for the hydrogens. The weighting scheme: $\sqrt{w} = 1$ if $|F_o| \leqslant 15$, $\sqrt{w} = 15/|F_o|$ if $|F_o| > 15$, and $\sqrt{w} = 0.50$ for the unobserved reflections gave constant average values of $w(F_o - F_c)^2$ over ranges of $|F_o|$, and was employed in the final stages of refinement.

On the final cycle of refinement, no parameter shift was greater than 0.45σ. A final difference Fourier was calculated and showed maximum fluctuations of 0.8 e Å^{-3} in the proximity of the heavy atoms and 0.4 e Å^{-3} elsewhere. The final positional and thermal parameters are given in Tables 2 and 3, respectively. Measured and calculated structure factor amplitudes have been placed in the Depository of Unpublished Data.[2]

[2]The structure factor table is available at a nominal charge from the Depository of Unpublished Data, National Science Library, National Research Council of Canada, Ottawa, Canada K1A 0S2.

Can. J. Chem. Downloaded from www.nrcresearchpress.com by 210.87.254.5 on 09/05/12
For personal use only.

Can. J. Chem. Downloaded from www.nrcresearchpress.com by 210.87.254.5 on 09/05/12
For personal use only.

TABLE 2. Final positional parameters (fractional × 10^4) with standard deviations in parentheses*

Atom	*x*	*y*	*z*
Mn	2006(1)	1933(1)	633(1)
K	−264(1)	2425(2)	−3977(2)
O(1)	1875(3)	4202(5)	2390(7)
O(2)	1826(5)	5434(6)	5420(9)
O(3)	3008(3)	1877(6)	−635(6)
O(4)	4448(3)	1921(6)	−460(8)
O(5)	1040(3)	1810(5)	1901(6)
O(6)	170(3)	320(5)	2273(6)
O(7)	1401(3)	1435(6)	−1852(6)
O(8)	1480(3)	−429(7)	−4563(6)
O(9)	499(15)	−4851(23)	−1753(36)
O(9′)	315(18)	−4862(24)	−3338(51)
N(1)	3072(3)	1285(5)	2883(6)
N(2)	2369(3)	−897(5)	54(6)
C(1)	3230(4)	−485(6)	3023(7)
C(2)	3262(4)	−1602(6)	1032(7)
C(3)	3506(4)	−3474(7)	1036(9)
C(4)	4379(4)	−4063(7)	2195(9)
C(5)	4231(5)	−3046(7)	4224(9)
C(6)	4063(4)	−1184(7)	4268(8)
C(7)	2667(5)	2530(7)	4602(9)
C(8)	2084(5)	4190(7)	4120(10)
C(9)	3863(4)	1609(8)	2259(9)
C(10)	3792(4)	1821(7)	262(9)
C(11)	1579(4)	−1182(7)	722(8)
C(12)	864(3)	405(7)	1700(7)
C(13)	2417(4)	−1385(9)	−1983(8)
C(14)	1715(4)	−44(9)	−2887(8)
H(11)	2658(42)	−407(72)	3629(84)
H(21)	3750(51)	−1466(93)	335(103)
H(31)	2991(51)	−3714(84)	1456(94)
H(32)	3568(58)	−4090(115)	−75(134)
H(41)	4923(43)	−3949(72)	1847(81)
H(42)	4554(44)	−5243(90)	2211(90)
H(51)	3592(72)	−3074(126)	4858(143)
H(52)	4847(52)	−3485(93)	5043(106)
H(61)	3892(46)	−530(87)	5537(103)
H(62)	4586(55)	−1035(94)	3966(103)
H(71)	2297(60)	2127(110)	5213(121)
H(72)	3208(57)	2734(102)	5573(116)
H(91)	3844(52)	2731(104)	3153(112)
H(92)	4468(52)	691(97)	2192(100)
H(111)	1299(52)	−1779(95)	−121(110)
H(112)	1846(51)	−1965(95)	1613(108)
H(131)	3145(44)	−1598(79)	−2514(86)
H(132)	2366(46)	−2415(92)	−2425(96)

*Multiplicities for the positions of the disordered water molecule are O(9), 0.62 and O(9′), 0.38.

Results and Discussion

The Complex Anion $[Mn(DCTA)]^-$

Individual bond lengths and angles in the anion are given in Tables 4 and 5, respectively. The manganese(III) ion is six-coordinated to the two nitrogen and four oxygen atoms of the hexadentate ligand DCTA. The coordination polyhedron of the manganese(III) ion is a very distorted octahedron with N—Mn—O and O—Mn—O angles of 77.1(2) and 128.5(2)°, respectively. The mean Mn—N distance is 2.263 Å and the Mn—O bonds fall into two classes with mean bond lengths of 1.887 and 2.015 Å. The anion, illustrated in Fig. 1, has approximate C_2 symmetry despite its asymmetric environment. The quasi-twofold axis, common in this type of structure (see *e.g.* refs. 4, 7–9), passes through the Mn atom and the midpoints of the C(1)—C(2) and C(4)—C(5) bonds of the cyclohexane ring. The geometrical parameters for the anion, averaged assuming twofold symmetry, appear in Table 6.

Using the terminology of ref. 4, the less strained glycinate rings, MnO(3)C(10)C(9)N(1) and MnO(5)C(12)C(11)N(2), are designated as L, and the more strained, MnO(1)C(8)C(7)N(1) and MnO(7)C(14)C(13)N(2), as M. The cyclohexane and pseudoethylenediamine (MnN(1)-

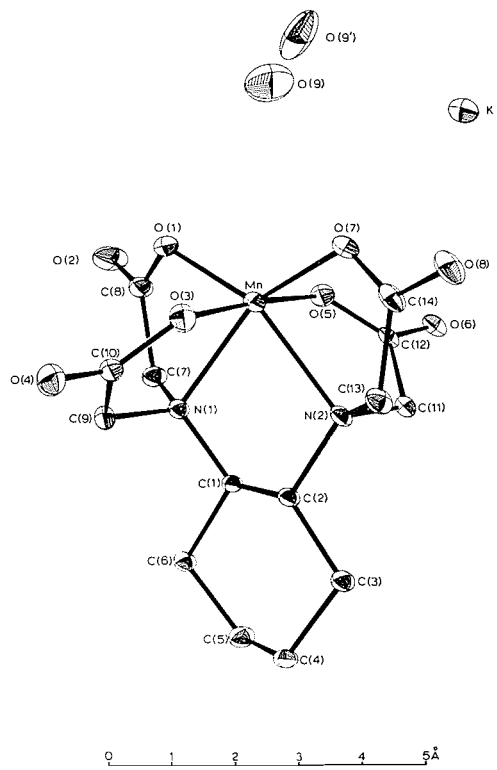

FIG. 1. A view of the anion and the neighboring potassium and disordered water molecule, 50% probability ellipsoids are shown. Hydrogen atoms are omitted for clarity.

TABLE 3. Final thermal parameters* with estimated standard deviations in parentheses

(*a*) Anisotropic thermal parameters (U_{ij} (Å^2) × 100)

Atom	U_{11}	U_{22}	U_{33}	U_{12}	U_{13}	U_{23}
Mn	3.77(5)	3.85(5)	4.51(5)	−1.05(3)	−1.14(4)	1.25(3)
K	5.23(9)	5.28(8)	6.77(10)	−0.82(6)	−1.16(7)	2.02(7)
O(1)	5.78(27)	3.68(21)	7.26(32)	−1.28(19)	−1.85(24)	1.94(20)
O(2)	11.70(51)	3.85(27)	9.96(45)	1.00(28)	−4.27(38)	−1.72(28)
O(3)	5.80(27)	6.42(27)	4.48(24)	−2.75(22)	−0.72(20)	2.23(20)
O(4)	5.29(29)	6.31(30)	8.70(37)	−2.12(24)	0.64(27)	1.61(26)
O(5)	4.54(24)	3.98(21)	5.39(25)	−0.78(18)	0.13(19)	0.62(18)
O(6)	3.72(23)	6.01(26)	3.95(22)	−0.95(19)	−0.82(17)	1.19(18)
O(7)	5.17(25)	5.59(26)	5.38(26)	−1.56(21)	−2.36(20)	2.46(21)
O(8)	6.26(30)	9.89(37)	3.72(23)	−3.42(27)	−1.97(21)	2.67(23)
O(9)	14.15(142)	9.54(112)	23.84(232)	−0.10(90)	−0.99(165)	4.75(147)
O(9′)	10.72(183)	4.12(90)	24.72(322)	−2.04(100)	6.68(213)	−1.36(155)
N(1)	3.66(24)	3.12(21)	3.47(23)	−0.78(18)	−0.83(19)	0.54(17)
N(2)	3.02(22)	4.12(23)	3.21(22)	−0.88(18)	−1.04(18)	0.95(18)
C(1)	3.45(28)	2.75(24)	3.61(28)	−0.41(21)	−0.86(23)	0.78(20)
C(2)	3.30(28)	3.16(25)	3.27(26)	−0.40(21)	−0.85(22)	0.49(20)
C(3)	4.35(34)	3.54(28)	3.93(31)	−0.46(25)	−1.31(26)	0.30(24)
C(4)	3.96(33)	3.08(28)	5.08(34)	−0.01(24)	−1.10(27)	0.72(24)
C(5)	5.96(40)	3.91(31)	4.30(33)	−0.68(28)	−1.62(30)	1.06(25)
C(6)	4.50(34)	3.79(29)	3.66(30)	−0.83(25)	−1.67(26)	0.87(23)
C(7)	5.20(36)	3.40(28)	4.14(31)	−0.44(26)	−0.60(28)	0.20(24)
C(8)	5.25(38)	3.01(30)	7.51(47)	−0.28(26)	−1.69(34)	−0.12(29)
C(9)	3.61(30)	3.81(30)	6.32(40)	−1.41(25)	−0.68(27)	0.56(27)
C(10)	3.74(31)	3.15(27)	5.75(35)	−0.80(23)	−0.51(27)	0.44(24)
C(11)	3.34(28)	4.06(29)	4.22(31)	−1.17(23)	−0.87(24)	1.01(24)
C(12)	2.62(27)	4.84(32)	3.57(28)	−0.75(23)	−0.92(22)	0.97(23)
C(13)	4.74(36)	5.27(37)	3.22(29)	−0.99(28)	−0.81(26)	0.47(25)
C(14)	4.28(32)	7.48(43)	3.03(29)	−2.19(30)	−1.17(25)	2.06(28)

(*b*) Isotropic thermal parameters

Atom	B (Å^2)	Atom	B (Å^2)
H(11)	3.06(119)	H(62)	4.91(176)
H(21)	5.01(175)	H(71)	6.67(220)
H(31)	4.48(155)	H(72)	6.54(193)
H(32)	6.80(217)	H(91)	5.94(180)
H(41)	2.79(127)	H(92)	5.29(165)
H(42)	4.26(144)	H(111)	4.87(170)
H(51)	9.56(273)	H(112)	5.33(168)
H(52)	5.37(167)	H(131)	3.82(135)
H(61)	4.41(152)	H(132)	3.70(154)

*Anisotropic temperature factors are U_{ij} in: $f = f^0 \exp(-2\pi^2(U_{11}h^2a^{*2} + U_{22}k^2b^{*2} + U_{33}l^2c^{*2} + 2U_{12}hka^*b^* + 2U_{13}hla^*c^* + 2U_{23}klb^*c^*))$.

C(1)C(2)N(2)) rings are designated as CH and E, respectively. The carboxylate oxygen atoms are classified as O_c or O_u depending on whether or not they are complexed to the manganese atom. The O_c are the odd numbered carboxylate oxygens and the O_u the even numbered. The hydrogen atoms are identified by the number of the carbon atom to which they are bonded followed by a 1 or 2. For the cyclohexane ring hydrogen atoms, the 1 denotes axial and the 2 equatorial positions; the glycinate hydrogens were arbitrarily numbered 1 or 2.

The cyclohexane ring is in the "chair" form, showing only minor angular strain. The CC—CC dihedral angles range from 47 to 64° in absolute value with a mean magnitude of 55°. The C—C bond lengths in the CH ring range from 1.537–1.551 Å with a mean value of 1.541(7) Å in excellent agreement with the standard 1.54 Å for a C(sp^3)—C(sp^3) bond (10). The C—C—C

Can. J. Chem. Downloaded from www.nrcresearchpress.com by 210.87.254.5 on 09/05/12
For personal use only.

TABLE 4. Individual bond lengths (Å), with standard deviations in parentheses

Bond	Length (Å)	Bond	Length (Å)
Mn—O(3)	1.880(5)	N(1)—C(1)	1.498(7)
Mn—O(5)	1.894(4)	N(1)—C(7)	1.489(8)
Mn—O(1)	2.036(4)	N(1)—C(9)	1.489(7)
Mn—O(7)	1.993(4)	N(2)—C(2)	1.509(7)
Mn—N(1)	2.258(4)	N(2)—C(11)	1.484(8)
Mn—N(2)	2.268(5)	N(2)—C(13)	1.460(7)
C(10)—O(3)	1.324(7)	C(1)—C(2)	1.546(7)
C(12)—O(5)	1.305(7)	C(2)—C(3)	1.538(8)
C(8)—O(1)	1.284(8)	C(3)—C(4)	1.537(7)
C(14)—O(7)	1.287(8)	C(4)—C(5)	1.537(7)
C(10)—O(4)	1.235(8)	C(5)—C(6)	1.538(8)
C(12)—O(6)	1.230(7)	C(6)—C(1)	1.551(7)
C(8)—O(2)	1.239(8)	C(7)—C(8)	1.528(8)
C(14)—O(8)	1.250(7)	C(9)—C(10)	1.512(9)
C—H	0.86–1.18(8), mean 1.00	C(11)—C(12)	1.525(8)
		C(13)—C(14)	1.541(9)

TABLE 5. Bond angles with standard deviations in parentheses

Bonds	Angle (deg)	Bonds	Angle (deg)
N(1)—Mn—O(1)	77.1(2)	C(1)—N(1)—C(7)	112.6(4)
N(1)—Mn—O(3)	82.5(2)	C(2)—N(2)—C(13)	113.3(4)
N(1)—Mn—O(5)	95.6(2)	C(9)—N(1)—C(7)	111.9(5)
N(2)—Mn—O(7)	78.1(2)	C(11)—N(2)—C(13)	111.3(4)
N(2)—Mn—O(5)	81.6(2)	Mn—O(3)—C(10)	120.4(4)
N(2)—Mn—O(3)	94.1(2)	Mn—O(5)—C(12)	121.5(4)
N(1)—Mn—N(2)	78.1(1)	Mn—O(1)—C(8)	116.3(4)
O(1)—Mn—O(3)	95.6(2)	Mn—O(7)—C(14)	117.7(3)
O(1)—Mn—O(5)	87.9(2)	O(3)—C(10)—O(4)	123.1(6)
O(1)—Mn—O(7)	128.5(2)	O(5)—C(12)—O(6)	123.2(5)
O(3)—Mn—O(7)	88.1(2)	O(1)—C(8)—O(2)	123.9(6)
O(5)—Mn—O(7)	91.9(2)	O(7)—C(14)—O(8)	123.3(6)
O(1)—Mn—N(2)	151.9(2)	O(3)—C(10)—C(9)	116.7(5)
O(7)—Mn—N(1)	153.7(2)	O(5)—C(12)—C(11)	116.5(5)
Mn—N(1)—C(1)	109.3(3)	O(1)—C(8)—C(7)	117.9(5)
Mn—N(2)—C(2)	109.0(3)	O(7)—C(14)—C(13)	117.3(5)
Mn—N(1)—C(9)	103.1(3)	O(4)—C(10)—C(9)	120.2(5)
Mn—N(2)—C(11)	104.3(3)	O(6)—C(12)—C(11)	120.2(5)
Mn—N(1)—C(7)	103.5(3)	O(2)—C(8)—C(7)	118.2(6)
Mn—N(2)—C(13)	103.0(4)	O(8)—C(14)—C(13)	119.4(6)
C(1)—N(1)—C(9)	115.2(4)	C(6)—C(1)—C(2)	112.9(4)
C(2)—N(2)—C(11)	114.9(4)	C(1)—C(2)—C(3)	112.8(4)
C(2)—C(3)—C(4)	111.2(5)	N(1)—C(1)—C(2)	109.2(4)
C(3)—C(4)—C(5)	108.9(5)	N(2)—C(2)—C(3)	114.2(4)
C(4)—C(5)—C(6)	109.4(5)	N(1)—C(7)—C(8)	110.6(5)
C(5)—C(6)—C(1)	111.4(5)	N(1)—C(9)—C(10)	114.9(5)
N(1)—C(1)—C(6)	114.2(4)	N(2)—C(11)—C(12)	114.6(5)
N(2)—C(2)—C(1)	107.4(4)	N(2)—C(13)—C(14)	110.8(5)
Angles involving H atoms 99–119(5)			

bond angles in the CH ring range from 108.9(5) to 112.9(4)° and average 111.1°, slightly greater than the tetrahedral angle but in good agreement with the 110.8° average in $[Fe(OH_2)DCTA]^-$ (4). Although there are significant differences between the bond angles in the CH ring, they are in good agreement with the assumed C_2 axis, as can be seen in Table 6.

With the exception of the OCC angles, the bond angles in the L rings are larger than or

Can. J. Chem. Downloaded from www.nrcresearchpress.com by 210.87.254.5 on 09/05/12
For personal use only.

TABLE 6. Geometrical parameters for the anion averaged assuming twofold (C_2) symmetry

Bond type	No. of bonds	Ring type(s)	Mean length (Å)	R.m.s. deviation*
C_1—C_2	1	E,CH	1.546	0.007
C_4—C_5	1	CH	1.537	0.007
C—C	4	CH	1.541	0.007
C—C	4	L,M	1.527	0.008
C—N	6	E,L,M	1.488	0.016
C—O_c	2	L	1.315	0.010
C—O_c	2	M	1.286	0.002
C—O_u	2	L	1.233	0.003
C—O_u	2	M	1.245	0.005
Mn—O	2	L	1.887	0.007
Mn—O	2	M	2.015	0.022
Mn—N	2	E	2.263	0.005

Ring type	Bond angle	Mean value (deg)	R.m.s. deviation
CH	C—C—C(C_1,C_2)	112.9	0.1
	C—C—C(C_3,C_6)	111.0	0.1
	C—C—C(C_4,C_5)	109.2	0.4
E	Mn—N—C	109.2	0.2
	N—C—C	108.3	1.3
	N—Mn—N	78.1	0.1
L	Mn—O—C	121.0	0.8
	O—C—C	116.6	0.1
	C—C—N	114.8	0.2
	C—N—Mn	103.7	0.8
	N—Mn—O	82.1	0.7
	C—C—O_u	120.2	0.1
	O—C—O_u	123.2	0.1
M	Mn—O—C	117.0	1.0
	O—C—C	117.6	0.4
	C—C—N	110.7	0.1
	C—N—Mn	103.3	0.4
	N—Mn—O	77.6	0.7
	C—C—O_u	118.8	0.8
	O—C—O_u	123.6	0.4
E—L†	C—N—C	115.1	0.2
E—M†	C—N—C	113.0	0.5
L—M†	C—N—C	111.6	0.4

*R.m.s. deviation from the mean given when more than one value has been used, for single values the least-squares standard deviation is quoted.
†Angle at the junction of two rings.

equal to those in the M rings. Ring strain in the L, M, and E rings is indicated by the sum of the interior angles in the rings, and by the dihedral angles. The ideal L and M rings should be nearly planar (7), the sum of interior angles then should be 540° and the dihedral angles 0°. The ideal E ring should have a 528° sum of interior angles (90 + 4(109.5)) (7). The sums of interior angles for the L, M, and E rings, respectively, are 538.1(6), 526.2(18), and 513.1°, and the mean magnitudes of the dihedral angles in the L and M rings are 9 and 25°. The larger OCC angle in the M ring (compared to that in the L ring) is compatible with closing the O(1)—Mn—O(7) angle and is a notable difference between this structure and the similar seven-coordinate $[Fe(OH_2)DCTA]^-$ in which the corresponding O—Fe—O angle is 148.9°, and the OCC angle is equal to 115.7° in both L and M rings (4).

The mean C—N bond length of 1.488(16) Å is close to the expected value of 1.479 Å for a N(sp^3)—C(sp^3) bond (10). The C—C(glycinate) distances, mean 1.527(8) Å, are somewhat longer than the 1.510 Å expected for C(sp^3)—C(sp^2) bonds (10), but agree with the values found in similar structures, *e.g.* 1.523 Å in $[Fe(OH_2)DCTA]^-$ (4), 1.523 Å in $[Ni(H_2EDTA)\cdot H_2O]$ (11), and 1.53 Å in $[Co(EDTA)]^-$ (7), all

Can. J. Chem. Downloaded from www.nrcresearchpress.com by 210.87.254.5 on 09/05/12
For personal use only.

Can. J. Chem. Downloaded from www.nrcresearchpress.com by 210.87.254.5 on 09/05/12
For personal use only.

of which have relatively strong M—O interactions. The difference in C—O_u and C—O_c bond lengths is an indication of the strength of the metal–oxygen interaction. In this structure, unlike that of [Fe(OH_2)DCTA]$^-$, there is a difference between the C—O distances for the L and M rings. The C—O_u and C—O_c bond lengths are 1.233 and 1.315 Å for the L rings, and 1.245 and 1.286 Å for the M rings. These can be compared to the mean values for the above structures: C—O_u and C—O_c are 1.233 and 1.273 Å for the Fe compound, and 1.22 and 1.30 Å for the Co compound.

The geometry involving the hydrogen atoms is normal; the C—H bond lengths range from 0.86 to 1.18 Å, mean 1.00(9) Å. The N—C—H, C—C—H and H—C—H bond angles do not differ significantly from the tetrahedral value, ranging from 99–119°, mean 108(5)°.

The two Mn—N bonds are equal, within experimental error, to the mean value of 2.263 Å. These distances are significantly longer than the 2.019 and 2.020 Å "short" and the 2.153 Å "long" Mn—N bonds in (acac)Mn(III)(pati)$_2$ (acetylacetonatobis-(*N*-phenylaminotroponiminato)manganese(III)) (12). The shorter Mn—O distances in the L rings are equal, and their mean, 1.887 Å, agrees well with the mean Mn—O distance of 1.894 Å found for (acac)$_3$Mn(III)-(trisacetylacetonatomanganese(III)) (13 and a refinement of the data given by Davis *et al.*). The Mn—O distances in the M rings, however, differ by a statistically significant 0.042 Å (7σ). These distances, Mn—O(1), 2.036 Å and Mn—O(7), 1.993 Å, are intermediate between the short (1.959 Å) and long (2.134 Å) Mn—O bonds found for (acac)Mn(pati)$_2$ (12). This difference can be ascribed to the effects of the asymmetric environment. The difference between the two sets of Mn—O distances (*ca.* 0.12 Å), the long Mn—N distances, and angular distortions at the manganese atom are due primarily to the stereochemical constraints imposed by the ligand and by the size of the manganese(III) ion. In the similar [Fe(OH_2)DCTA]$^-$ anion (4), the metal–nitrogen bonds were also found to be relatively long. If the Mn—N distances were reduced, the C—N—C angles between the E ring and both the L and M rings would need to be expanded further from their already strained values (E–L, 115.1, E–M, 113.0°) in order to maintain the same Mn—O bond lengths. It is of interest to note that the mean bond distance (of M—O and M—N bonds) in this complex is 2.055 Å, nearly equal to that of (acac)Mn(pati)$_2$, 2.051 Å (12). It is also greater than that of six-coordinate [Co(EDTA)]$^-$, 1.908 Å (7), and shorter than found in the seven-coordinate complexes [Fe(OH_2)DCTA]$^-$ (4), [Fe(OH_2)-EDTA]$^-$ (9), 2.127 and 2.120 Å, respectively. The range of bond distances in [Mn(DCTA)]$^-$ is 0.38 Å (including the Mn—N distances). This is much larger than observed in other six coordinate EDTA complexes, *e.g.* 0.04 Å in [Co(EDTA)]$^-$ (7) and 0.15 Å in [Ni(H_2EDTA) H_2O] (11). The possibility that the pattern of two short and four long bonds is to some degree due to a "Jahn–Teller distortion" for this high-spin Mn(III) complex should not be ruled out. Distortions of both distances and angles are present in (acac)Mn(pati)$_2$ (12).

Statistically significant deviations from C_2 symmetry occur in the inner coordination group. In addition to the difference between the Mn—O bond distances in the M rings, the bond angles at the manganese atom all show small but significant deviations from C_2 symmetry, except the pair O(1)—Mn—O(5) and O(7)—Mn—O(3). The largest of these differences is 3.7° between the angles O(1)—Mn—O(3) and O(7)—Mn—O(5). The edges of the coordination polyhedron show considerable deviation from C_2 symmetry, the significant differences being: 0.109 Å between O(1)—O(3) and O(7)—O(5), 0.040 Å between O(3)—N(2) and O(5)—N(1), and 0.035 Å between O(1)—O(5) and O(7)—O(3). As has been pointed out (8, 9), the strains produced by the asymmetric environment accumulate in the coordination group.

The four carboxylate groups are all planar within experimental error. The carbon atoms of the E ring (C(1), C(2)) lie on opposite sides of the MnNN plane, being displaced 0.34 and 0.42 Å from the plane, respectively. The two L rings are roughly perpendicular to the MnNN plane, the angles between the mean planes of the L rings and the MnNN plane averaging 80.6(8)°. The angle between the C.COO reference planes in the two L rings is 91°. The deviations of the manganese and nitrogen atoms, respectively, from C.COO reference planes in the L rings are −0.18 and 0.17 Å for the ring containing O(5), and 0.32 and 0.05 Å for the ring containing O(3).

The methylene carbon atoms of the M rings (C(7), C(13)) lie 1.0 Å on opposite sides of the

Can. J. Chem. Downloaded from www.nrcresearchpress.com by 210.87.254.5 on 09/05/12
For personal use only.

MnNN plane, as in $[Co(EDTA)]^-$ (7). The Mn—O bonds in the M rings should ideally lie in the MnNN plane, but due to angular strain in the ligand, this is not the case. The M ring oxygen atoms [O(1)1,O(7)] lie 0.46 and 0.38 Å on opposite sides of the MnNN plane. The angle between the reference C.COO planes of the M rings is 12°. All the atoms in the M rings lie to one side of the Mn—O bond, the manganese and nitrogen atoms lie on opposite sides of the C.COO planes, being displaced 0.60 and 0.30 Å in the M ring containing O(1), and 0.32 and 0.46 Å in the ring containing O(7). The C.COO planes make angles of 34 (O(1) ring) and 26° (O(7) ring) with the MnNN plane.

It is apparent from the previous data that the individual L and M rings are not equivalent. The reason for these deviations from C_2 symmetry is asymmetric interaction of the oxygen atoms with the potassium ion and the water molecule. The O_u atoms of both glycinate rings containing N(2) bridge two potassium ions, while for their counterparts O(2) (M ring) is coordinated to a potassium ion and O(4) is involved in, at best, a very weak CH...O hydrogen bond. Both O_c atoms in the M rings interact with potassium ions, but O(7) is more strongly coordinated than is O(1). The L ring O_c atoms (O(3), O(5)) are also different in that O(3) coordinates only the manganese while O(5) is probably hydrogen bonded to the water molecule

Crystal Packing Arrangement

Projections of the structure along *c* and *b* are shown in Figs. 2 and 3, respectively. The structure consists of layers of oxygen bridged potassium ions which form dimers when O(9) is present and polymers with O(9′). The potassium atoms form zig-zag arrays along *b* which lie approximately in the *bc* plane as shown in Fig. 4. The layers of potassium ions are situated between two layers of $[Mn(DCTA)]^-$ anions. These three layers form a basic unit as each potassium ion coordinates oxygen atoms from five different $[Mn(DCTA)]^-$ anions. This basic structural unit repeats along *a*, layers are staggered, thereby minimizing contacts between the cyclohexane rings.

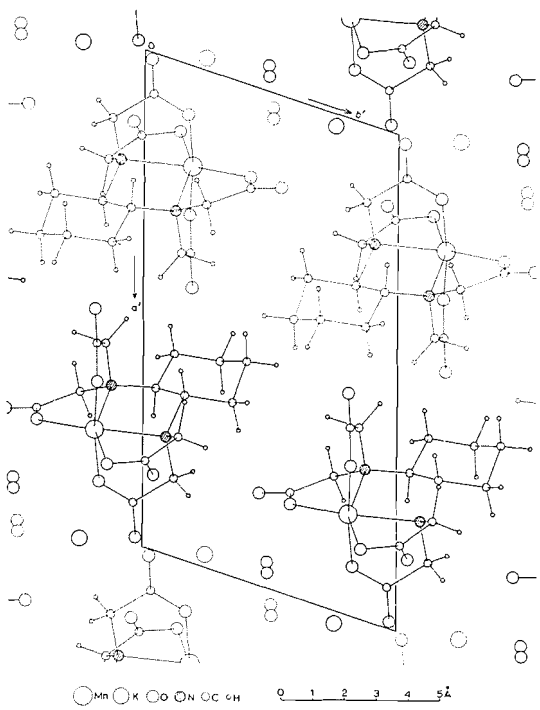

FIG. 2. Projection of the structure down the *c* axis.

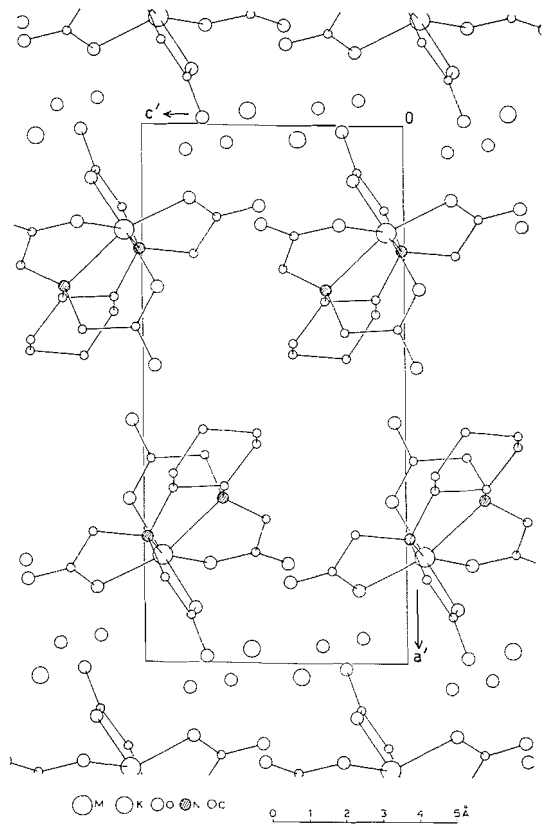

FIG. 3. Projection of the structure down the *b* axis; hydrogen atoms are omitted for clarity.

TABLE 7. Possible hydrogen bonds

	Lengths (Å)		Angles (deg)
A.....H—B	A...H	A...B	A...H—B
O(5)...(H)O(9)	—	2.94(2)	—
O(2)...(H)O(9)	—	3.18(3)	—
O(5)...(H)O(9′)	—	2.83(2)	—
O(2)...(H)O(9′)	—	2.72(3)	—
O(2)...H(132)—C(13)	2.46(7)	3.300(9)	156
O(4)...H(92)—C(9)	2.48(8)	3.388(8)	150
O(8)...H(11)—C(1)	2.38(6)	3.383(8)	151

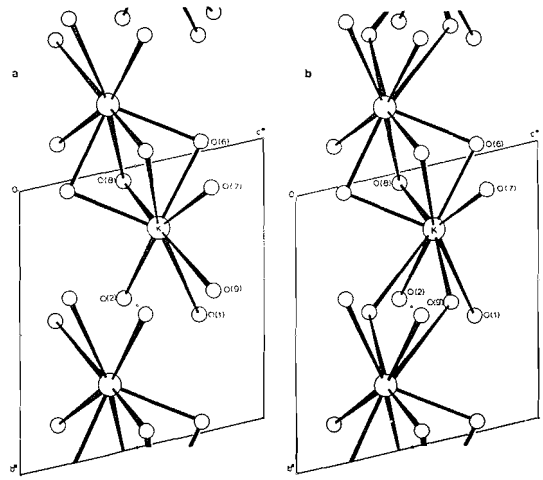

FIG. 4. Views of the arrangement of the potassium and oxygen atoms down *a*; (*a*) water molecule in position O(9), (*b*) water molecule in position O(9′).

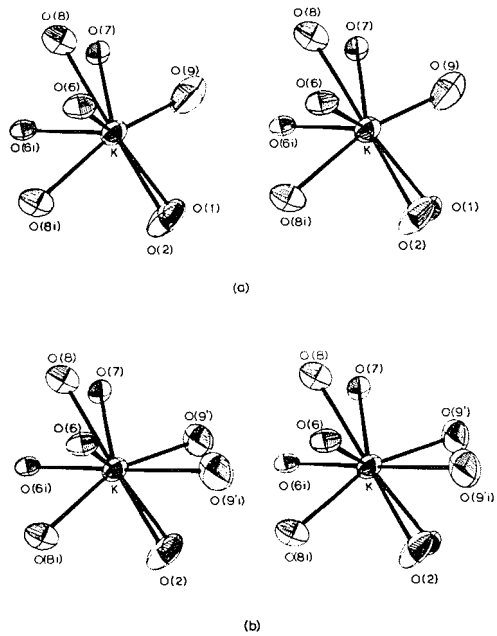

FIG. 5. Stereo views of the coordination group of the potassium ion; (*a*) the eight coordinate structure resulting from occupation of position O(9) by the water molecule, (*b*) the nine coordinate structure resulting from occupation of the position O(9′) by the water molecule.

The nearest neighbors of the potassium ion are eight or nine oxygen atoms from the water molecules and the anions at distances ranging from 2.71 to 3.21 Å. Distances observed in similar structures range from 2.6 to 3.2 Å (14–26). The next nearest neighbor to the potassium atom is C(14) at 3.275 Å. The potassium atoms lie astride centers of symmetry at (0,0,1/2) and (0,1/2,1/2). Oxygen atoms O(6) and O(8) bridge between two potassium atoms related by the center at (0,0,1/2), the water oxygen O(9′) bridges potassium atoms related by the center at (0,1/2,1/2). Oxygen atoms O(1) and O(7) are coordinated to the potassium and form bridges between Mn and K atoms. The coordination sphere is completed by oxygen atoms O(2) and O(9). Stereo views of two of the possible coordination groups of the potassium atom, those involving either O(9) or O(9′) but not both, are shown in Fig. 5. The bridging arrangement involving O(6) and O(8) is quite similar to that found in the structure of K[PhC(O)CH:NOHON:CHC(O)Ph] (14). The coordination polyhedra formed were not found to have any obvious simple geometry (27).

The water molecule is probably involved in hydrogen bonds to O(2) and O(5) (see Table 7 for relevant geometrical data). O(9′) is the more favorable of the two disordered positions for hydrogen bonding; the distances to O(2) and O(5) are 2.72(3) and 2.83(2) Å. O(9) forms weak hydrogen bonds with the same atoms at distances of 3.18(2) and 2.94(2) Å. The distance O(7)...O(9)

Can. J. Chem. Downloaded from www.nrcresearchpress.com by 210.87.254.5 on 09/05/12
For personal use only.

is 3.04 Å, but a hydrogen bond between these atoms was rejected on the basis of geometrical data.

It has been remarked that a good criterion for the existence of the hydrogen bond is that at least two heavy atom – hydrogen distances less than the sum of the van der Waals radii be present (28). There are three independent O...H separations less than the 2.6 Å sum of van der Waals radii present in this structure. The O...H distances range from 2.38–2.48 Å (see Table 7), and involve O_u atoms O(2), O(4), and O(8), and methylene hydrogen atoms H(132), H(92), and H(11). There is a good possibility that these are weak C—H...O hydrogen bonds. The full geometrical data in Table 7 are quite reasonable for hydrogen bonding schemes. The O...C distances, ranging from 3.300 to 3.388 Å, are somewhat longer than the 2.95–3.22 Å reported previously for postulated C—H...O hydrogen bonds (ref. 28, p. 182; 29). All other intermolecular contacts correspond to van der Waals interactions.

We thank Professor R. Stewart and Dr. B.L. Poh for crystals and discussion, the National Research Council of Canada for financial support, and the University of British Columbia Computing Centre for assistance.

1. B. L. Poh and R. Stewart. Can. J. Chem. In press.
2. B. L. Poh. Ph.D. Thesis. University of British Columbia, Vancouver, British Columbia. 1972.
3. B. L. Poh. Private communication.
4. G. H. Cohen and J. L. Hoard. J. Am. Chem. Soc. **88**, 3228 (1966).
5. I. L. Karle, K. S. Dragonette, and S. A. Brenner. Acta Cryst. **19**, 713 (1965).
6. (*a*) International tables for X-ray crystallography. Vol. III. Kynoch Press, Birmingham. 1962; (*b*) R. F. Stewart, E. R. Davidson, and W. T. Simpson. J. Chem. Phys. **42**, 3175 (1965).
7. H. A. Weaklim and J. L. Hoard. J. Am. Chem. Soc. **81**, 549 (1959).
8. S. Richards, B. Pedersen, J. V. Silverton, and J. L. Hoard. Inorg. Chem. **3**, 27 (1964).
9. M. D. Lind, M. J. Hamor, T. A. Hamor, and J. L. Hoard. Inorg. Chem. **3**, 34 (1964).
10. Chem. Soc. Special Publ., No. 11, 1958, and No. 18, 1965.
11. G. S. Smith and J. L. Hoard. J. Am. Chem. Soc. **81**, 556 (1959).
12. M. Bartlett and G. J. Palenik. Chem. Commun. 416 (1970).
13. B. Morosin and J. R. Brathovde. Acta Cryst. **17**, 705 (1964). T. S. Davis, J. P. Fackler, and M. J. Weeks. Inorg. Chem. **7**, 1994 (1968).
14. M. A. Bush, H. Luth, and M. R. Truter. J. Chem. Soc. (A), 740 (1971).
15. M. A. Bush and M. R. Truter. J. Chem. Soc. (A), 745 (1971).
16. D. R. McGregor and J. C. Speakman. J. Chem. Soc. (A), 2106 (1968).
17. J. H. Bryden. Acta Cryst. **12**, 581 (1959).
18. D. J. Sutor, F. J. Llewellyn, and H. S. Maslen. Acta Cryst. **7**, 145 (1954).
19. J. P. G. Richards. Z. Krist. **116**, 468 (1961).
20. H. N. Shrivastava and J. C. Speakman. J. Chem. Soc. 1151 (1961).
21. R. D. Ellison and H. A. Levy. Acta Cryst. **19**, 260 (1965).
22. J. C. Speakman. Chem. Commun. 32 (1967).
23. G. Larsson and I. Nahringbauer. Acta Cryst. **B24**, 666 (1968).
24. H . Ringertz. Acta Cryst. **B24**, 1686 (1968).
25. R. F. Mayers, E. T. Keve, and A. C. Skapski. J. Chem. Soc. (A), 2258 (1968).
26. J. P. Roux and J. C. A. Boeyens. Acta Cryst. **B25**, 2395 (1969).
27. R. B. King. J. Am. Chem. Soc. **91**, 7211 (1969).
28. W. C. Hamilton and J. A. Ibers. *In* Hydrogen bonding in solids. W. A. Benjamin Inc., New York. 1968. p. 14.
29. D. S. Savage, A. F. Cameron, G. Ferguson, C. Hannaway, and I. R. Mackay. J. Chem. Soc. (B), 410 (1971).

Can. J. Chem. Downloaded from www.nrcresearchpress.com by 210.87.254.5 on 09/05/12
For personal use only.

Can. J. Chem. Downloaded from www.nrcresearchpress.com by 210.87.254.5 on 09/05/12
For personal use only.

Canadian Journal of Chemistry

Published by
THE NATIONAL RESEARCH COUNCIL OF CANADA

Journal canadien de chimie

Publié par
LE CONSEIL NATIONAL DE RECHERCHES DU CANADA

Volume 51 Number 9 May 1, 1973

Volume 51 numéro 9 1 mai 1973

Nucleic Acid Related Compounds. 5. The Transformation of Formycin and Tubercidin into 2′- and 3′-Deoxynucleosides[1,2]

MORRIS J. ROBINS,[3] JAMES R. MCCARTHY, JR.,[4] ROGER A. JONES,[3,5] AND RUDOLF MENGEL[3,6]

Department of Chemistry, The University of Alberta, Edmonton, Alberta T6G 2G2 and Department of Chemistry, University of Utah, Salt Lake City, Utah

Received November 7, 1972

Reaction of tubercidin (4-amino-7-β-D-ribofuranosylpyrrolo[2,3-*d*]pyrimidine) (**1**) with α-acetoxyisobutyryl chloride in the presence of excess sodium iodide in acetonitrile gave an acylated iodo intermediate (**2**) which was converted into 3′-deoxytubercidin (**4**) by hydrogenolysis and subsequent saponification.

Analogous treatment of formycin (7-amino-3-β-D-ribofuranosylpyrazolo[4,3-*d*]pyrimidine) (**5**) gave 3′-deoxyformycin (**6**) and 2′-deoxyformycin (**7**) in an approximate ratio of 3:2. These purified nucleosides, **6** and **7** were individually deaminated enzymatically to give 3′-deoxyformycin B (**8**) and 2′-deoxyformycin B (**9**).

Biological rationale, n.m.r., and mass spectra of these antibiotic-derived deoxynucleosides are discussed.

La réaction de la tubercidine (amino-4 β-D-ribofuranosyl-7 pyrrolo pyrimidine [2,3-*d*]) (**1**) avec le chlorure d'α-acétoxyisobutyryle en présence d'un excès d'iodure de sodium dans l'acétonitrile donne un intermédiaire iodo acylé (**2**) qui a été transformé en déoxy-3′ tubercidine (**4**) par hydrogénolyse suivie d'une saponification.

Le traitement identique de la formycine (amino-7 β-D-ribofuranosyl-3 pyrazolo pyrimidine [4,3-*d*]) (**5**) donne la déoxy-3′ formycine (**6**) et la déoxy-2′ formicyne (**7**) dans un rapport approximativement égal à 3:2. Les nucléosides purifiés, **6** et **7**, donnent respectivement la déoxy-3′ formycine B(**8**) et la déoxy-2′ formycine B(**9**) lorsque l'on enlève leur groupement aminé par action enzymatique.

Les caractéristiques biologiques ainsi que les spectres de masse et r.m.n. de ces déoxynucléosides dérivés d'antibiotiques sont discutés. [Traduit par le journal]

Can. J. Chem., **51**, 1313 (1973)

We wish to report the synthesis of 3′-deoxytubercidin (**4**), 3′-deoxyformycin (**6**), and 2′-deoxyformycin (**7**) using the "abnormal" reaction of α-acetoxyisobutyryl halides with diols discovered by Mattocks (1) and first applied to nucleosides by Moffatt and coworkers (2).

The nucleoside antibiotics tubercidin (**1**) and formycin (**5**) have been studied in considerable detail in biological systems and a comprehensive review is available (3). Formycin (**5**) is currently undergoing investigation in molecular biology

[1]This work was supported by Grant Number A5890 from The National Research Council of Canada, Grant Number 9530-108 from the Defence Research Board of Canada, and (in part) by Contract Number PH43-65-1041 with the Cancer Chemotherapy National Service Center, National Cancer Institute, NIH, USPHS.

[2]For previous paper in this series see ref. 23.

[3]The University of Alberta.

[4]University of Utah. Present address, Dow Chemical Company, Midland, Michigan.

[5]University of Alberta Graduate Research Assistantship Awardee, 1971–1972.

[6]University of Alberta Postdoctoral Fellow, 1969–1971.

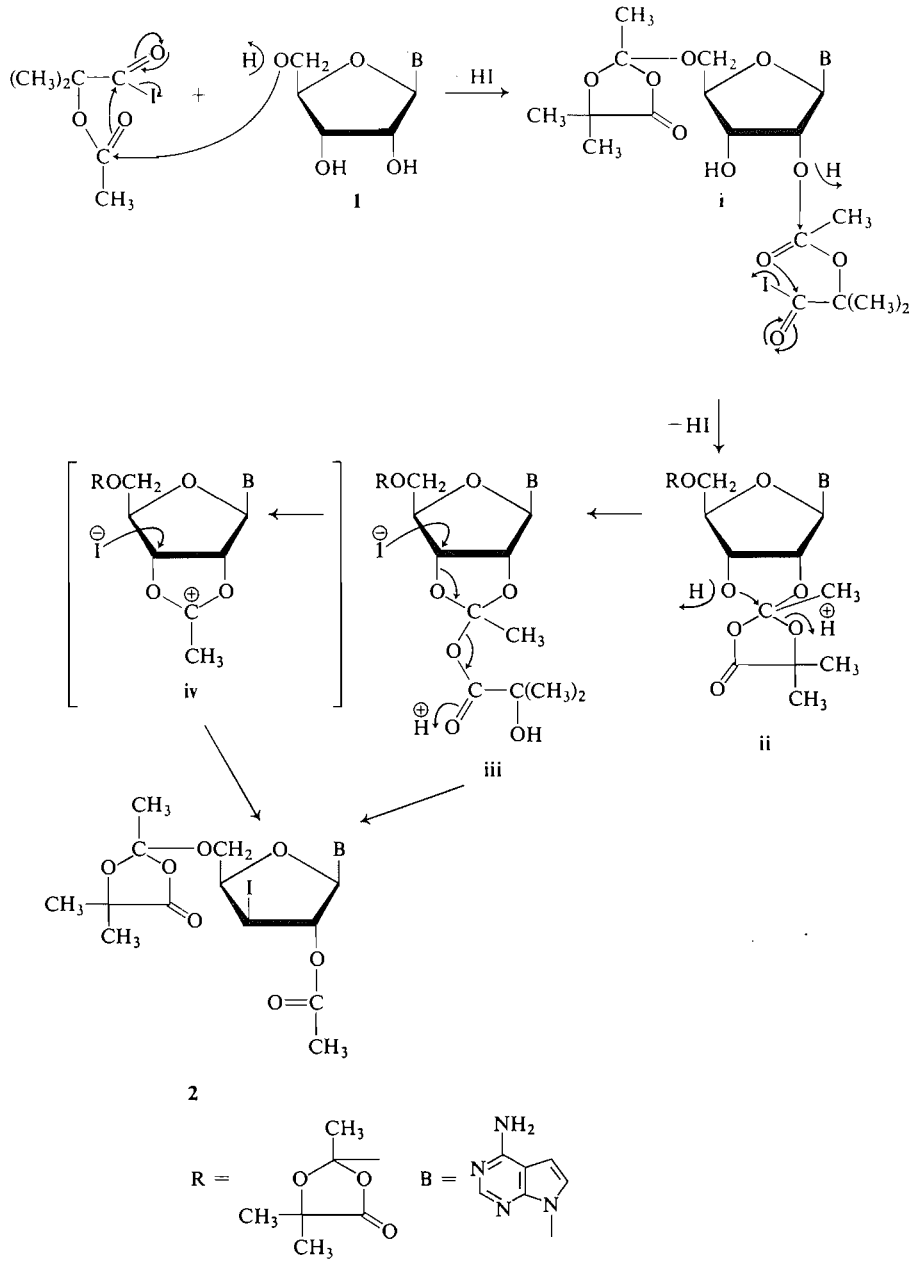

SCHEME I

due to its fluorescent properties which make its observation in polynucleotide and coenzyme systems unique (4), and also due to its *syn*-sugar–base conformation (5). The synthesis and study of deoxypolynucleotides containing 2′-deoxyformycin as well as enzyme-monomer studies of various deoxyformycin phosphates would be of considerable interest. Enzymatic systems can reduce tubercidin (**1**) to a 2′-deoxy derivative in microgram quantities 6), but no chemical syntheses of deoxy analogs of these antibiotics have been reported.

Reaction of tubercidin (**1**) with α-acetoxyisobutyryl chloride (7) in the presence of a threefold molar excess of sodium iodide in acetonitrile (*in situ* formation of α-acetoxyisobutyryl iodide

Can. J. Chem. Downloaded from www.nrcresearchpress.com by 210.87.254.5 on 09/05/12
For personal use only.

Can. J. Chem. Downloaded from www.nrcresearchpress.com by 210.87.254.5 on 09/05/12
For personal use only.

with sodium chloride precipitation from solution) gave the acylated iodo intermediate (**2**) which could arise by the mechanism depicted in Scheme 1. Attack of the 5′-oxygen on the less sterically hindered acetyl carbonyl carbon of α-acetoxyisobutyryl iodide with concurrent attack of the acetyl carbonyl oxygen on the carbonyl iodide and subsequent deprotonation of 5′-*O* would lead to **i** as analogously proposed by Mattocks (1). Corresponding attack of either the 2′- or 3′-hydroxyl oxygen of **i** (illustrated in Scheme 1 with the 2′-isomer) would lead to the 2′,5′-bis-*O*-(2,5,5-trimethyl-1,3-dioxolan-4-on-2-yl)tubercidin intermediate (**ii**). Protonation of the ether-type oxygen of **ii** and attack of the 3′-oxygen on the orthoacetate carbon would lead to the mixed orthoester-anhydride **iii**. This intermediate (**iii**) could be protonated at the carbonyl function of the mixed anhydride and suffer S_N2 attack by iodide concurrently at the 3′-carbon to give 4-amino-7-(2-*O*-acetyl-5-*O*-[2,5,5-trimethyl-1,3-dioxolan-4-on-2-yl]-3-iodo-3-deoxy-β-D-xylofuranosyl)pyrrolo[2,3-*d*]pyrimidine (**2**) directly or lose α-hydroxyisobutyric acid to give the 2′,3′-acetoxonium ion intermediate (**iv**) (2) which could then undergo S_N2 attack by iodide at the 3′-carbon to give **2**.

The *trans*-orientation of substituents at the 2′- and 3′-positions was proven by conversion of **2** to the *ribo*-epoxide by base. The u.v. spectra of **2** indicated no modification of the heterocyclic base since acylation of the amino function causes significant bathochromic shifts.[7] The i.r. spectra of **2** show bands corresponding to the dioxolanone carbonyl at 1796 cm^{-1} (1) and the acetyl carbonyl at 1746 cm^{-1}. The n.m.r. spectrum of **2** is also consistent with the proposed diastereomeric structure with *gem*-dimethyl peaks at δ 1.52 and 1.59, orthoacetate methyl at 1.79, and 2′-*O*-acetyl methyl at 2.12.

Compound **2** was catalytically hydrogenated to give the blocked 3′-deoxy intermediate **3** (see Scheme 2). Treatment of **3** with methanolic ammonia gave 3′-deoxytubercidin (**4**) in 38% overall yield, which was purified by ion-exchange chromatography. The n.m.r. spectrum of **4** exhibited an anomeric proton doublet at δ 5.95, $J_{1'-2'}$ = 2.7 Hz and a two-proton multiplet at δ 1.98 as expected (8, 9) from the 3′-deoxy structure **4**. The mass spectrum of this product was consistent with the assigned structure **4** with peaks at *m/e* 250 (M), 220 (c), 177 (d), 163 (h), 147 (f), 134 (b + H; 100%), and 135 (b + 2H) (peaks are assigned letters as discussed by McCloskey and coworkers (10)). Indeed, the fragmentation pattern down to ion "k" (B + H − HCN, *m/e* 107) was completely parallel to that (11) of 3′-deoxyadenosine (cordycepin) except at one lower mass unit (^{12}C—^{1}H *vs.* ^{14}N at the 7-position — purine numbering).

The same reaction procedure was applied to formycin (**5**). However, it is of considerable interest that in this case 3′-deoxyformycin (**6**) and 2′-deoxyformycin (**7**) were formed in an approximate ratio of 3:2 as estimated by n.m.r. spectroscopy. Since the supply of formycin was limited and the diastereomeric mixtures of 2′- and 3′-acylated intermediates were not resolved in numerous chromatographic systems, the total mixture of intermediates was purified, catalytically hydrogenated, and then deblocked to give **6** and **7** (as the hydrochlorides) in 30% overall yield from **5**.

The separation of **6** and **7** was extremely challenging. The useful Dekker column (12) is, of course, precluded by the acidic pyrazole proton. Of some 15 solvent systems investigated with five types of thin-layer and paper chromatography supports and adsorbants, only the system described in the Experimental gave effective resolution for analytical observation after three developing/drying cycles. Preparative t.l.c. using this system failed to resolve the isomers, however. A clean separation of **6** and **7** was achieved on a Dowex 1-X2 (Cl^-) column using an ammonium chloride – ammonium hydroxide buffer. The 3′-deoxy isomer **6** was eluted before the 2′-deoxy isomer **7**, which is opposite to the behavior of the corresponding deoxy adenosine isomers on an (OH^-) column (12).

The n.m.r. spectrum of **6** exhibited a doublet for the anomeric proton at δ 5.06, $J_{1'-2'}$ = 3.6 Hz and a two-proton multiplet at δ 1.98 for the 3′-protons whereas that of **7** had an ABX "triplet" for the anomeric proton at δ 5.43, $J_{1'-2',2''}$ = 8.1 Hz and a two-proton multiplet at δ 2.24 for the 2′-protons as expected from the respective structures (8, 9, 13). The mass spectral patterns of **6** and **7** were also consistent with the assigned structures. The 3′-deoxy isomer **6** had peaks at *m/e* 251 (M), 221 (c), 178 (d), 164 (h), 148 (f), 135 (b + H), and 136 (b + 2H) whereas 2′-deoxyformycin (**7**) had peaks at *m/e* 251 (M),

[7]M. J. Robins, R. Mengel, and R. A. Jones. To be published.

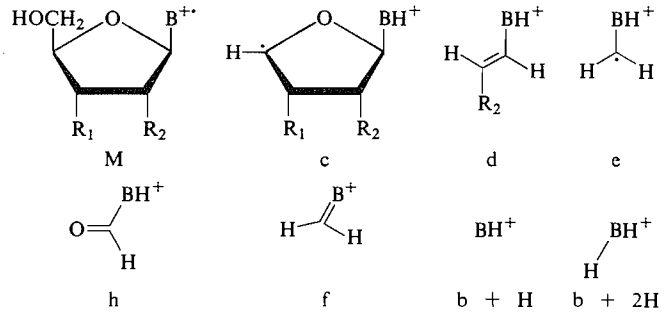

Mass spectral ions (see ref. 10)

221 (c), 162 (d), 164 (h), 148 (f), 135 (b + H), and 136 (b + 2H) with peaks identified as discussed by McCloskey and co-workers (10). In the case of **6**, the mass spectral base peak was at *m/e* 164 (ion "h") as was observed by Townsend and Robins (14) with formycin and other *C*-linked nucleosides. However, the mass spectral base peak for **7** occurred at *m/e* 162 which corresponds to cleavage of the $C_{1'}$—$O_{4'}$ and $C_{2'}$—$C_{3'}$ bonds to give the "2′-substituent-identifying" ion "d" (10). The corresponding ion "h" at *m/e* 164 was of 40.4% relative intensity whereas the heterocycle peak (base + H) at *m/e* 135 was of 12.4% relative intensity. Therefore a *C*-linked nucleoside will *not always* exhibit a mass spectral base peak at heterocyclic base + 30 as suggested earlier by Townsend and Robins (14) on the basis of their studies on unmodified ribosides. Ions "e" and "f" at *m/e* 149 and 148 are 18.8 and 4.8% relative intensity for **7** and 26.6 and 16.5% for **6** which is in accord with observations on nucleosides having a 2′-OH absent or present respectively (10).

Previous studies (15) have shown that formycin is deaminated by adenosine deaminase and it is well-known (16) that 2′- and 3′-deoxyadenosines are effective substrates for this enzyme. Treatment of the anomerically pure deoxyformycins **6** and **7** with calf intestinal adenosine deaminase gave rapid and quantitative conversion to 3′-deoxyformycin B (3-(3-deoxy-β-D-*erythro*-pentofuranosyl)pyrazolo[4,3-*d*]pyrimidin-7-one) (**8**) and 2′-deoxyformycin B (3-(2-deoxy-β-D-*erythro*-pentofuranosyl)pyrazolo[4,3-*d*]pyrimidin-7-one) (**9**) as evaluated by t.l.c.

Again the isomers had n.m.r. spectral properties in agreement with the assigned structures. The 3′-deoxy compound **8** had a peak at δ 4.87, $J_{1'-2'}$ = 3.9 Hz for the 1′-proton and a two-proton multiplet centered at δ 1.97 corresponding to the 3′-protons whereas the 2′-deoxy isomer **9** had the anomeric peak at δ 5.27 as an ABX "quartet" with $J_{1'-2',2''}$ = 6.1 and 10.1 Hz. The large coupling observed is indicative of a quasi *trans* diaxial relation between $H_{1'}$ and $H_{2'}$ and suggests a 1′-*exo*-2′-*endo* sugar conformation. Although the anomeric peak width (16 Hz) is much wider than observed for α-anomers, the ABX "quartet" pattern is not common for β-anomers (13, 17) and again emphasizes the empirical nature of this means of anomeric assignment. A *syn* orientation of the base over the sugar ring of **9** could contribute to an unusual sugar ring pucker.

The 3′-deoxy isomer **8** had characteristic mass spectral peaks at *m/e* 252 (M), 222 (c), 179 (d), 165 (h), 149 (f), 136 (b + H), and 137 (b + 2H) and the 2′-deoxy isomer **9** at *m/e* 252 (M), 222 (c), 163 (d), 165 (h), 149 (f), 136 (b + H) and 137 (b + 2H). Again as in the case of the 7-amino analogs **6** and **7**, the mass spectral base peak (100% relative intensity) for **8** is ion "h" at *m/e* 165 whereas the mass spectral base peak of the 2′-deoxy isomer **9** is ion "d" at *m/e* 163; and ion "f" at *m/e* 149 is about four-fold more intense in the isomer **8** (2′-OH present).

The chemical shifts observed for the 1′- (anomeric) and 4′-protons of these deoxynucleosides are of interest. The anomeric proton peak for 2′-deoxyformycin (**7**) is at δ 5.43 whereas that for the 3′-deoxy isomer **6** occurs at 5.06. The corresponding peak positions for the 2′- and 3′-deoxyformycin B isomers are at δ 5.27 and 4.87, respectively. These Δδ shifts of 0.37 p.p.m. for the formycins and 0.40 p.p.m. for the formycin B isomers are of comparable magnitude to shifts observed between α and β pairs of anomeric nucleosides (18). The peaks arising from

Can. J. Chem. Downloaded from www.nrcresearchpress.com by 210.87.254.5 on 09/05/12
For personal use only.

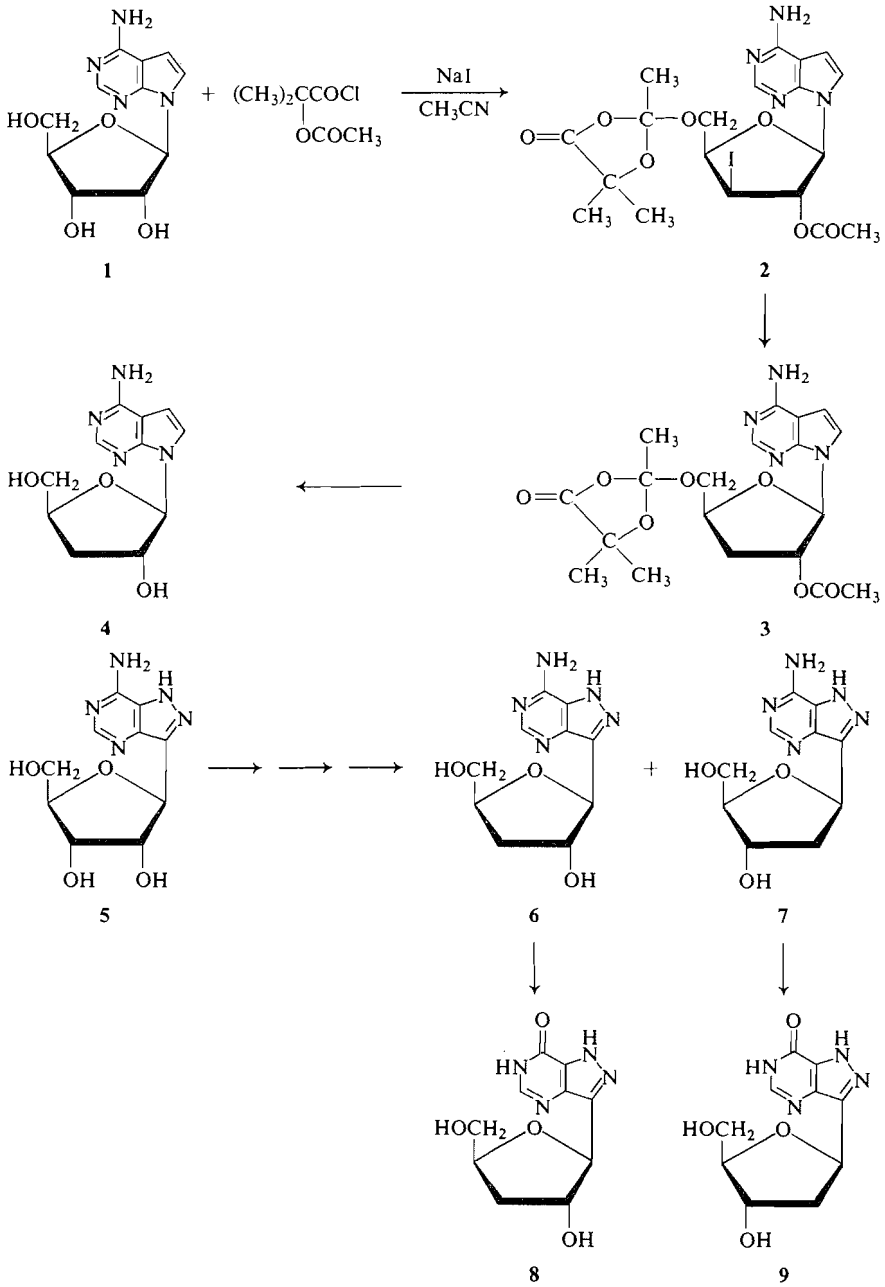

SCHEME 2

the 4′-proton occurred at δ 3.85 for 2′-deoxyformycin (**7**) 4.30 for the 3′-isomer **6** and 3.79 for 2′-deoxyformycin B (**9**) *vs.* δ 4.18 for the 3′-isomer **8**. Again the Δδ shifts of 0.45 p.p.m. for the 4′-protons of the deoxyformycins and 0.39 p.p.m. for the deoxyformycin B isomers correspond to proton shifts observed with *cis–trans* 1′-H to 2′-OH orientations in anomeric nucleoside pairs (18) and suggest a diamagnetic *shielding* effect of a *cis–vicinal* hydroxyl group. This effect has been discussed by Smith and coworkers (19). However, the same authors have referred to this paper (19) to support the *deshielding* effect of a *cis*-hydroxyl group on the $H_{2''}$ resonance of

Can. J. Chem. Downloaded from www.nrcresearchpress.com by 210.87.254.5 on 09/05/12
For personal use only.

Can. J. Chem. Downloaded from www.nrcresearchpress.com by 210.87.254.5 on 09/05/12
For personal use only.

deoxyuridine in a later article (20). Fraser-Reid and Radatus (21) have demonstrated by specific deuteration that the $H_{2''}$-proton *cis* to the 3'-OH is at lower field in deoxycytidine but anisotropy or conformational effects due to the pyrimidine base could also be involved.

The present study exemplifies a convenient route (2) for the modification of nucleoside antibiotics (ribofuranosides) to the biologically interesting 2'- and 3'-deoxy derivatives with retained stereochemistry. A new procedure (22) for access into deoxy and other modified nucleoside structures employing intact nucleosides and a study of factors affecting substitution reactivity of sugar carbons in different nucleosides will be reported separately.

Experimental

Melting points were determined on a Kofler micro melting point apparatus and are uncorrected. N.m.r. spectra were determined on Varian A-60 and HA-100 instruments with sodium, 5,5-dimethyl-5-silapentanesulfonate, or TMS as reference. U.v. spectra were determined on a Cary 14M spectrometer by dissolving the sample in distilled water and then diluting a 1 ml portion of this quantitative stock solution to 10 ml with 0.1 *N* HCl, freshly prepared 0.001 *N* or 0.1 *N* NaOH, or alcohol. Evaporations were accomplished using a Büchler rotating evaporator under reduced pressure (aspirator or vacuum pump) at 40 °C or lower unless otherwise specified. Hydrogenations were effected using a Parr shaking apparatus at specified hydrogen pressure and room temperature. Optical rotations were determined on a Perkin–Elmer model 141 polarimeter using a 1 ml, 10 cm micro cell. Mass spectra were obtained by the Mass Spectroscopy Laboratory at the University of Alberta on AEI MS-2 and MS-9 spectrometers using a direct probe at 70 eV and 200° or higher temperature. The peak intensity values are not completely reproducible under these conditions and somewhat different relative intensity patterns at higher *m/e* ranges have been observed especially with compound **9** which requires 250°. Tubercidin was purchased from The Upjohn Company, Kalamazoo, Michigan. Type II adenosine deaminase was purchased from Sigma Chemical Company, St. Louis, Missouri.

3'-Deoxytubercidin (4-Amino-7-(3-deoxy-β-D-erythro-pentofuranosyl)pyrrolo[2,3-d]pyrimidine) (4)

To a vigorously stirred solution of 15 g (0.10 mol) of dried sodium iodide in 100 ml of anhydrous acetonitrile (distilled from P_2O_5) was added 5.8 g (0.035 mol) of α-acetoxyisobutyryl chloride (7) (separation of a white solid occurred, presumably NaCl) followed immediately by 2.66 g (0.01 mol) of dried (18 h at 100°/15 mm Hg) tubercidin (**1**). The brown reaction mixture was stirred for 1 h at room temperature while protected from moisture and then poured into a stirred solution made by mixing 250 ml of saturated aqueous $NaHCO_3$ and 150 ml of saturated aqueous $Na_2S_2O_3$. A 100 ml portion of $CHCl_3$ was added and the layers were separated. The aqueous layer was extracted with two 50 ml portions of $CHCl_3$ and the combined organic phase was washed with water, dried over Na_2SO_4, filtered, and evaporated to dryness. A small sample of this white solid foam was purified for analysis by chromatography on a column of acid washed charcoal (Barnebey Cheney, AU-4) using MeOH–$CHCl_3$ (1:9) followed by a column of silica gel (Mallinckrodt CC-7) using Me_2CO–$CHCl_3$ (1:1). The amorphous solid obtained in 80% yield from evaporation of the appropriate middle fractions was completely free of trace impurities observed in the crude sample by t.l.c. Pure **2** had u.v. (MeOH) max 268 (ε 13 400), min 238 nm (ε 3100); (0.1 *N* HCl) max 271 (ε 11 700), min 245 nm (ε 4100); (0.1 *N* NaOH) max 270 (ε 12 200), min 245 nm (ε 5200); i.r. ($CHCl_3$) ν 1796 (lactone, C=O), 1746 cm^{-1} (acetate, C=O); n.m.r. ($CDCl_3$) δ 1.52, 1.59 (s, s; 3,3; $(CH_3)_2$-C(O—)CO—), 1.79 (s, 3, CH_3C(O—)(O—)O—), 2.12 (s, 3, CH_3COO—), 3.86 (m, 3, $H_{5',5'',4'}$), 4.25 (m, 1, $H_{3'}$), 5.28 (br, 2, NH_2), 5.79 (m, 1, $H_{2'}$), 6.24 (m, 2, $H_{1'}$, H_5), 7.49 (m, 1, H_6), 8.28 (s, 1, H_2) mass spectra, calcd. for M^+ ($C_{19}H_{23}IN_4O_7$), 546.0611; found *m/e*, 546.0595.

Anal. Calcd. for $C_{19}H_{23}IN_4O_7$: C, 41.77; H, 4.24; I, 23.23; N, 10.26. Found: C, 41.53; H, 4.21; I, 23.01; N, 10.30.

The bulk of the crude white solid foam (**2**) was dissolved in 75 ml of ethanol and 0.83 g (0.011 mol) of NaOAc in 25 ml of water was added. This solution was hydrogenated for 18 h at 50 p.s.i. in the presence of 1.2 g of 10% Pd/C catalyst. The mixture was filtered using a Celite pad and the filtrate was evaporated to dryness. The resulting product was partitioned between $CHCl_3$ and H_2O and the organic phase was washed with water, dried over Na_2SO_4, filtered, and evaporated to dryness. A small sample of this residue which was obtained in 63% yield was chromatographed on silica gel (Mallinckrodt CC-7) using Me_2CO–$CHCl_3$ (1:1). Evaporation of middle fractions which were homogeneous by t.l.c. gave **3** as a white solid foam, u.v. (MeOH) max 270, min 243 nm; (0.1 *N* HCl) max 272, min 246 nm; (0.1 *N* NaOH) max 271, min 242 nm; i.r. ($CHCl_3$) 1795 (lactone, C=O), 1736 cm^{-1} (acetate, C=O); n.m.r. ($CDCl_3$) δ 1.50 (s, 6, $(CH_3)_2$-C(O—)CO—), 1.77 (s, 3, CH_3C(O—)(O—)O—), 2.11 (s, 3, CH_3COO—), 2.16 (m, 1, $H_{3'}$), 2.56 (m, 1, $H_{3''}$), 3.78 (m, 2, $H_{5',5''}$), 4.50 (m, 1, $H_{4'}$), 5.37 (br, 2, NH_2), 5.55 (m, 1, $H_{2'}$), 6.34 (m, 2, $H_{1'}$,H_5), 7.14 (m, 1, H_6), 8.28 (s, 1, H_2); mass spectra, calcd. for M^+ ($C_{19}H_{24}N_4O_7$), 420.1645; found *m/e*, 420.1658.

The bulk of the sample of crude **3** was dissolved in 100 ml of methanol presaturated with ammonia at −5° and allowed to stand at room temperature for 18 h. The solution was evaporated to dryness and the residue was coevaporated several times with ethanol and then dissolved in 5 ml of MeOH–H_2O (5:95). This solution was applied to a column (2.6 × 60 cm; 300 ml) of Dowex 1-X2 (OH^-) (200–400 mesh) packed in 5% aqueous methanol. The column was eluted using 3000 ml of this solvent, and then with 15% methanol in water, 10 ml fractions were collected. Fractions 7–13 (after changing to 15% MeOH) contained **4** contaminated with a slightly

Can. J. Chem. Downloaded from www.nrcresearchpress.com by 210.87.254.5 on 09/05/12
For personal use only.

slower migrating spot on t.l.c. (EtOAc – *n*-PrOH – H_2O, 4:1:2 upper phase; neutral alumina on glass plates). Continuing fractions 15–150 contained chromatographically pure **4** and were combined and evaporated to dryness. The resulting white foam was crystallized from 100 ml of EtOAc to give 0.95 g (38% overall from **1**) of needles of **4**, m.p. 180–181°; $[\alpha]_D^{27}$ −75.1° (*c*, 1, EtOH); u.v. max (0.1 *N* HCl) 270, 227 nm (ε 11 000, 24 700); (0.001 *N* NaOH) 268 nm (ε 12 300); (MeOH) 269 nm (ε 11 700); n.m.r. (DMSO-d_6) δ 8.04 (s, 1, H_2), 7.28 (d, 1, J_{6-5} = 3.8 Hz, H_6), 6.92 (s, 2, 4-NH_2), 6.52 (d, 1, J_{5-6} = 3.8 Hz, H_5), 5.95 (d, 1, $J_{1'-2'}$ = 2.7 Hz, $H_{1'}$), 5.43 (broad s, 1, 5′-*OH*), 4.98 (broad s, 1, 2′-*OH*), 4.34 (m, 1, $H_{2'}$), 4.20 (m, 1, $H_{4'}$), 3.48 (m, 2, $H_{5',5''}$), 1.98 (broad m, 2, $H_{3',3''}$); mass spectra, calcd. for M^+ ($C_{11}H_{14}N_4O_3$), 250.1066; found *m/e*, 250.1082 (and see discussion).

Anal. Calcd. for $C_{11}H_{14}N_4O_3$: C, 52.79; H, 5.64; N, 22.39. Found: C, 53.01; H, 5.92; N, 22.41.

*3′-Deoxyformycin (7-Amino-3-(3-deoxy-β-D-erythro-pentofuranosyl)pyrazolo[4,3-d]pyrimidine) (**6**) and 2′-Deoxyformycin (7-Amino-3-(2-deoxy-β-D-erythro-pentofuranosyl)pyrazolo[4,3-d]pyrimidine) (**7**)*

To a solution of 30 g (0.20 mol) of dried sodium iodide in 200 ml of dry acetonitrile (distilled from P_2O_5) was added 11.6 g (0.070 mol) of α-acetoxyisobutyryl chloride (**7**) and then 5.34 g (0.020 mol) of dry formycin (dried at 100° under aspirator vacuum for 15 h) was added to the vigorously stirred mixture. The resulting dark-colored mixture was stirred for 1 h at room temperature while protected from moisture and was then poured into a solution made by mixing 500 ml of saturated aqueous $NaHCO_3$ and 300 ml of saturated aqueous $Na_2S_2O_3$. Chloroform (200 ml) was added and the phases separated. The aqueous layer was washed with two 100 ml portions of $CHCl_3$. The combined organic phase was washed with H_2O, dried over Na_2SO_4, and evaporated to dryness. The resulting white foam was dissolved in 100 ml of EtOH and this solution was evaporated to dryness. The residue was dissolved in 115 ml of EtOH and 1.7 g (0.021 mol) of sodium acetate dissolved in 35 ml of H_2O was added. This mixture was hydrogenated at 50 p.s.i. for 18 h in the presence of 2.5 g of 10% Pd/C catalyst. The catalyst was removed by filtration using a Celite pad and the filtrate was evaporated to dryness. The resulting solid was partitioned between 200 ml of $CHCl_3$ and 100 ml of H_2O. The $CHCl_3$ layer was washed with 100 ml of H_2O, dried over Na_2SO_4, and evaporated to dryness. The resulting white solid foam was dissolved in 100 ml of methanol presaturated at −5° with ammonia and this solution was allowed to stand for 15 h at room temperature and was then evaporated to dryness. The residue was dissolved in a minimal volume of EtOAc–MeOH (8:2) and applied to a column (2.4 × 105 cm, 400 g) of neutral alumina packed in the same solvent. The column was washed with 600 ml of EtOAc–MeOH (8:2) and this wash was discarded. The column was then developed with the upper phase of EtOAc – *n*-PrOH – H_2O (4:1:2) and 10 ml fractions were collected. Fractions 85–143 were homogeneous on t.l.c. (alumina, glass plates, upper phase of EtOAc – *n*-PrOH – H_2O (4:1:2)) and migrated more slowly than did small quantities of material in earlier fractions. These fractions were combined and evaporated to dryness to yield 1.7 g (34%) of amorphous solid which was a 3:2 mixture of 3′-deoxyformycin (**6**) and 2′-deoxyformycin (**7**), respectively, as estimated by n.m.r. analysis.

A sample of this solid (0.5 g) was dissolved in 30 ml of MeOH and 50 ml of 1% HCl in dry MeOH was added. The solution was evaporated to dryness and the residue was crystallized from absolute EtOH to give 0.5 g (87% recovery) of 2′- and 3′-deoxyformycin hydrochlorides, m.p. 195–215°.

Anal. Calcd. for $C_{10}H_{13}N_5O_3$·HCl: C, 41.74; H, 4.90; N, 24.34; Cl, 12.32. Found: C, 41.52; H, 4.80; N, 24.08; Cl, 12.20.

A solution of 0.6 g of the above amorphous solid in 4 ml of 0.2 *N* NH_4Cl adjusted to p*H* 9.35 with NH_4OH was applied to a column (3.3 × 134 cm) of Dowex 1-X2 (Cl^-) (200–400 mesh packed in the same NH_4Cl–NH_4OH buffer solution). The column was developed with this buffer solution and migration and separation of the bands corresponding to 3′-deoxyformycin and 2′-deoxyformycin could be observed visually using a 2537 Å u.v. hand lamp. The formycin aglycone has strong absorption at 295 nm and blue fluorescent bands can be seen through the Pyrex column in a dark room. The eluate was also monitored with an automatic recording u.v. cell at 2537 Å.

After a fore-run of 10.33 l, 3′-deoxyformycin (**6**) was eluted in the next 5.15 l of buffer solution. There was then a volume of 750 ml which was u.v. transparent at 296 nm followed by a volume of 4.5 l which contained 2′-deoxyformycin (**7**).

The 5.15 l of fractions containing 3′-deoxyformycin (**6**) were combined and stirred for 15 h with 1.5 g of acid-washed activated charcoal (Barnebey-Cheney, AU-4). The charcoal was collected by filtration and washed well with H_2O. The combined aqueous filtrate and washings were u.v. transparent at 296 nm. The charcoal was placed in a Soxhlet thimble and was continuously extracted with EtOH – 28% NH_4OH (7:3) for several days. The combined extracts were evaporated to dryness and the residue was converted (as described earlier for the mixture) to the hydrochloride salt (recrystallized from EtOH) to give 0.39 g (56% recovery) of 3′-deoxyformycin (**6**) hydrochloride, m.p. 214–216°; $[\alpha]_D^{24}$ −31.4° (*c*, 1, H_2O); u.v. (0.1 *N* HCl) max 296, 233 (ε 10 900, 8400), min 267, 223 nm (ε 3700, 7300); (0.1 *N* NaOH) max 303, 233 (ε 8400, 19 400), min 272, 223 nm (ε 3700, 15 500); n.m.r. (DMSO-d_6) δ 8.52 (s, 1, H_5), 5.06 (d, 1, $J_{1'-2'}$ = 3.6 Hz, $H_{1'}$), 4.44 (m, 1, $H_{2'}$), 4.30 (m, 1, $H_{4'}$), 3.61 (m, 2, $H_{5',5''}$), 1.98 (m, 2, $H_{3',3''}$); mass spectra, calcd. for M^+ ($C_{10}H_{13}N_5O_3$), 251.1018; found *m/e* 251.1018.

Anal. Calcd. for $C_{10}H_{13}N_5O_3$·HCl: C, 41.74; H, 4.90; N, 24.34; Cl, 12.32. Found: C, 41.71; H, 5.09; N, 24.14; Cl, 12.36.

Identical treatment of the 4.5 l of combined fractions containing 2′-deoxyformycin (**7**) with 1 g of activated charcoal followed by the above-described isolation procedure gave 0.17 g (25% recovery) of 2′-deoxyformycin hydrochloride, m.p. 200–202°; $[\alpha]_D^{24}$ 19.1° (*c*, 1, H_2O); u.v. (0.1 *N* HCl) max 295, 233, (ε 10 200, 7700), min 265, 222 nm (ε 3400, 6300), (0.1 *N* NaOH) max 303, 234 (ε 8100, 18 000), min 272, 223 nm (ε 3400, 14 000); n.m.r. (DMSO-d_6) δ 8.50 (s, 1, H_5), 5.43 ("t", 1, $J_{1'-2',2''}$ = 8.1 Hz, $H_{1'}$), 4.28 (m, 1, $H_{3'}$), 3.85 (m, 1, $H_{4'}$), 3.55 (m,

2, $H_{5',5''}$), 2.24 (m, 2, $H_{2',2''}$); mass spectra, calcd. for M^+ ($C_{10}H_{13}N_5O_3$), 251.1018; found *m/e*, 251.1010.

Anal. Calcd. for $C_{10}H_{13}N_5O_3 \cdot HCl$: C, 41.74; H, 4.90; N, 24.34; Cl, 12.32. Found: C, 41.46; H, 5.14; N, 24.29; Cl. 12.10.

The deoxyformycins **6** and **7** could be resolved for analytical observation on t.l.c. employing two or three developing–drying cycles using glass plates coated with silica gel (p*H* 7) and the upper phase of freshly prepared *n*-BuOH – H_2O – concentrated NH_4OH (3:1:0.05). The 2′-deoxy isomer **7** migrated slightly faster in this system.

3′-Deoxyformycin B (3-(3-Deoxy-β-D-erythro-pentofuranosyl)pyrazolo[4,3-d]pyrimidin-7-one) (8)

To a solution of 0.40 g (0.0014 mol) of 3′-deoxyformycin (**6**) hydrochloride in 80 ml of water was added 20 mg of adenosine deaminase and the solution was stirred for 3 days at room temperature. A 5 ml portion of Amberlite IRC-50 resin was added and the mixture was stirred. After 0.5 h a precipitate began to separate. The reaction mixture was filtered using a Celite pad and the pad was then washed with 20% aqueous ammonia. The u.v. spectrum of the ammoniacal filtrate indicated the presence of the formycin B chromophore. The filtrates were combined and evaporated to dryness. The resulting solid was crystallized from 25 ml of water to give 0.26 g (74%) of crystalline **8**. Recrystallization of this material from H_2O proceeded readily to give needles of **8**, m.p. 263–264°; $[\alpha]_D^{24}$ −48.3° (*c*, 0.5, H_2O); u.v. (0.1 *N* HCl) max 277, 220 (ε 7370, 13 800), min 243 nm (ε 4150); (distilled H_2O) max 279, 219 (ε 7380, 14 300), min 238 nm (ε 3630); (0.1 *N* NaOH) max 292, 228 (ε 8140, 15 900), min 250 nm (ε 3400); n.m.r. (DMSO-d_6) δ 7.83 (s, 1, H_5), 4.87 (d, 1, $J_{1'-2'}$ = 3.9 Hz, $H_{1'}$), 4.50 (m, 1, $H_{2'}$), 4.18 (m, 1, $H_{4'}$), 3.44 (m, 2, $H_{5',5''}$), 1.97 (broad m, 2, $H_{3',3''}$); mass spectra, calcd. for M^+ ($C_{10}H_{12}N_4O_4$), 252.0859; found *m/e*, 252.0854.

Anal. Calcd. for $C_{10}H_{12}N_4O_4$: C, 47.62; H, 4.80; N, 22.21. Found: C, 47.69; H, 4.64; N, 22.44.

2′-Deoxyformycin B (3-(2-Deoxy-β-D-erythro-pentofuranosyl)pyrazolo[4,3-d]pyrimidin-7-one) (9)

To a solution of 0.138 g (0.00048 mol) of 2′-deoxyformycin (**7**) hydrochloride in 60 ml of distilled water was added 7 mg of adenosine deaminase and the solution was stirred for 24 h at room temperature.

The solution was evaporated to approximately 3 ml and this was applied to a column (0.5 × 5 cm) of Dowex 50W-X8 (30–80 mesh) (H^+). The column was eluted with water and after 400 ml the concentration of **9** in the eluate was minimal. The combined eluant was neutralized with aqueous sodium bicarbonate and then evaporated. The residue was triturated with 30 ml of absolute ethanol which was filtered and the filtrate evaporated to dryness. The solid (100 mg) was dissolved in 2 ml of water and applied to a column (0.8 × 9 cm, 2 g) of acid-washed activated charcoal (Barnebey-Cheney AU-4). This column was washed with water until the eluate gave no precipitate when treated with nitric acid–silver nitrate. Elution with ethanol–concentrated aqueous ammonia (7:3) (approximately 50 ml) and evaporation of this solution gave 80 mg (76%) of a white solid. This product crystallized slowly from methanol to give needles of **9**, m.p. 229–230°; $[\alpha]_D^{24}$ 9.0° (*c*, 0.97, H_2O); u.v. (0.1 *N* HCl) max 277; 220 (ε 6490, 12 500), min 242 nm (ε 3670); (distilled H_2O) max 278; 218 (ε 6620, 12 800), min 238 nm (ε 2910); (0.1 *N* NaOH) max 292, 228 (ε 7150, 14 000), min 250 nm (ε 2970); n.m.r. (DMSO-d_6) δ 7.80 (s, 1, H_5), 5.27 ("q", 1, $J_{1'-2',2''}$ = 10.1 and 6.1 Hz, $H_{1'}$), 4.25 (m, 1, $H_{3'}$), 3.79 (m, 1, $H_{4'}$), 3.43 (m, 2, $H_{5',5''}$), 2.44 and 1.98 (m and m, 1 and 1, $H_{2'}$ and $H_{2''}$); mass spectra calcd. for M^+ ($C_{10}H_{12}N_4O_4$), 252.0859; found *m/e*, 252.0847.

Anal. Calcd. for $C_{10}H_{12}N_4O_4$: C, 47.62; H, 4.80; N, 22.21. Found: C, 47.53; H, 5.01; N, 22.02.

We wish to thank Dr. R. K. Robins for laboratory facilities and the University of Utah Research Fund for the purchase of antibiotics used in early stages of this work. We wish to thank Dr. H. Umezawa and Dr. T. Wakazawa for a gift of formycin to M. J. R.

1. A. R. Mattocks. J. Chem. Soc. 1918 (1964).
2. S. Greenberg and J. G. Moffatt. Abstracts, 155th National Meeting of the American Chemical Society, San Francisco, Calif., March–April 1968, C 054; A. F. Russell, S. Greenberg, and J. G. Moffatt. Abstracts, 158th National Meeting of the American Chemical Society, New York, N.Y., Sept. 1969, CARB 014.
3. R. J. Suhadolnik. Nucleoside antibiotics. John Wiley and Sons, Inc., New York, N.Y. 1970. Chapts. 8 and 9.
4. D. C. Ward, E. Reich, and L. Stryer. J. Biol. Chem. **244**, 1228 (1969); D. C. Ward, A. Cerami, E. Reich, G. Acs, and L. Altwerger. J. Biol. Chem. **244**, 3243 (1969).
5. D. C. Ward and E. Reich. Proc. Natl. Acad. Sci. U.S. **61**, 1494 (1968); D. C. Ward, W. Fuller, and E. Reich . Proc. Natl. Acad. Sci. U.S. **62**, 581 (1969); G. Koyama, K. Maeda, H. Umezawa, and Y. Iitaka. Tetrahedron Lett. 597 (1966).
6. G. Acs, E. Reich, and M. Mori. Proc. Natl. Acad. Sci. U.S. **52**, 493 (1964).
7. E. M. Filachione, J. H. Lengel, and C. H. Fisher. J. Am. Chem. Soc. **68**, 330 (1946).
8. W. W. Lee, A. Benitez, C. D. Anderson, L. Goodman, and B. R. Baker. J. Am. Chem. Soc. **83**, 1906 (1961).
9. E. A. Kaczka, E. L. Dulaney, C. O. Gitterman, H. B. Woodruff, and K. Folkers. Biochem. Biophys. Res. Commun. **14**, 452 (1964).
10. S. J. Shaw, D. M. Desiderio, K. Tsuboyama, and J. A. McCloskey. J. Am. Chem. Soc. **92**, 2510 (1970).
11. S. Hanessian, D. C. DeJongh, and J. A. McCloskey. Biochim. Biophys. Acta, **117**, 480 (1966).
12. C. A. Dekker. J. Am. Chem. Soc. **87**, 4027 (1965).
13. M. J. Robins and R. K. Robins. J. Am. Chem. Soc. **87**, 4934 (1965).
14. L. B. Townsend and R. K. Robins. J. Heterocycl. Chem. **6**, 459 (1969).
15. Y. Fukagawa, T. Sawa, T. Takeuchi, and H. Umezawa. J. Antibiot. (Tokyo), Ser. A, **18**, 191 (1965).
16. See for example: A. Bloch, M. J. Robins, and J. R. McCarthy, Jr. J. Med. Chem. **10**, 908 (1967).

Can. J. Chem. Downloaded from www.nrcresearchpress.com by 210.87.254.5 on 09/05/12
For personal use only.

17. J. ŽEMLIČKA, R. GASSER, J. V. FREISLER, and J. P. HORWITZ. J. Am. Chem. Soc. **94**, 3213 (1972).
18. T. NISHIMURA, B. SHIMIZU, and I. IWAI. Chem. Pharm. Bull. (Tokyo), **12**, 1471 (1964); T. NISHIMURA and B. SHIMIZU. Chem. Pharm. Bull. (Tokyo), **13**, 803 (1965).
19. F. E. HRUSKA, A. A. GREY, and I. C. P. SMITH. J. Am. Chem. Soc. **92**, 4088 (1970).
20. T. SCHLEICH, B. J. BLACKBURN, R. D. LAPPER, and I. C. P. SMITH. Biochemistry, **11**, 137 (1972).
21. B. FRASER-REID and B. RADATUS. J. Am. Chem. Soc. **93**, 6342 (1971).
22. R. MENGEL and M. J. ROBINS. Abstracts, 161st National Meeting of the American Chemical Society, Los Angeles, Calif., March–April, 1971, CARB 002.
23. M. J. ROBINS and S. R. NAIK. Chem. Commun. 18 (1972).

Can. J. Chem. Downloaded from www.nrcresearchpress.com by 210.87.254.5 on 09/05/12
For personal use only.

Constituents of *Solidago* Species. Part III.[1] The Constitution of Diterpenoids from *Solidago juncea* Ait.

M. S. HENDERSON AND R. D. H. MURRAY
Department of Chemistry, University of Glasgow, Glasgow, Scotland

AND

R. MCCRINDLE[2] AND D. MCMASTER
Chemistry Department, University of Guelph, Guelph, Ontario

Received November 27, 1972

The constitution and stereochemistry of five new diterpenoids from *Solidago juncea* Ait., junceic acid (**3***a*), the related epoxide (**6***a*), junceanol W(**4***a*), junceanol X (**4***b*), and junceanol Y (**5***a*), have been assigned on the basis of their chemical and spectroscopic properties. Of key importance in these deductions have been the transformations of **4***b* and **5***a* into the previously described hydrocarbon **19** and of **3***a* into **3***e*. Two known diterpenoids, (−)-hardwickiic acid (**2***a*), which has also been converted into **3***e*, and *ent*-16-kauren-19-oic acid (**1**), are further constituents of *S. juncea*.

La constitution ainsi que la stéréochimie de cinq nouveaux diterpènes issus du *Solidago juncea* Ait., l'acide junceique (**3***a*), l'époxyde parent (**6***a*), le junceanol W(**4***a*), le junceanol X (**4***b*) et le junceanol Y (**5***a*) ont été attribuées en se basant sur les propriétés chimiques et spectroscopiques. Les transformations de **4***b* et **5***a* pour donner l'hydrocarbure **19** décrit antérieurement et de **3***a* en **3***e* ont été de la plus grande importance dans ces déductions. Deux diterpènes connus, l'acide (−) hardwickiique (**2***a*) qui a aussi été transformé en **3***e* et l'acide kauren-16-*ent* oique-19 sont aussi d'autres constituants du *S. juncea*.
[Traduit par le journal]

Can. J. Chem., **51**, 1322 (1973)

Continuing our investigations of the constituents of *Solidago* species we have examined two samples of *S. juncea* Ait. (Early Goldenrod), one collected[3] near New London, Connecticut and the other[4] in Hamilton, Ontario. From ether extracts of the former we have obtained two known diterpenoids, *ent*-16-kauren-19-oic acid (**1**) (2) and (−)-hardwickiic acid (**2***a*) (3), and four new diterpenoids which we have named junceic acid (**3***a*), junceanol W (**4***a*), junceanol X (**4***b*), and junceanol Y (**5***a*). Of these six compounds all but hardwickiic acid were detected in similar extracts of the Hamilton sample, while in this case an additional new diterpenoid, junceic acid epoxide (**6***a*), was isolated. The formulation of these new diterpenoids as shown rests on the evidence which follows.

The ent-Clerodanes

Junceic acid (**3***a*) was isolated as an oil by successive column and preparative t.l.c. over silica gel and its molecular formula established as $C_{20}H_{28}O_3$ by mass spectrometry. The acidic nature of the compound was deduced from its behavior on t.l.c. ("streaking"), the broad absorption band between 3000 and 3400 cm^{-1} in its i.r. spectrum and the strong peak at *m/e* 271 ($M - CO_2H$) in its mass spectrum. The presence of a β-substituted furan moiety in junceic acid, first indicated by its color reaction with Ehrlich's reagent, was readily confirmed by its absorption in the i.r. at 877 cm^{-1} and the three characteristic resonances at τ 2.63, 2.76 (α-furan), and 3.70 (β-furan) in its n.m.r. spectrum. Also clearly evident in the n.m.r. spectra of junceic acid and the derived methyl ester (**3***b*), alcohol (**3***c*), and acetate (**3***d*), m.p. 82–84°, are resonances attributable to an olefinic, a secondary, and a tertiary methyl group, and a vinylic proton. These data were taken to indicate a close structural relationship between junceic and hardwickiic acid and this conclusion was reinforced when the latter (**2***a*) was found to be a minor constituent of *S. juncea*.

Two plausible structures, **3***a* and **7***a*, for junceic acid emerged at this point and that one or other did indeed represent the correct constitution and stereochemistry was shown un-

[1]For Part II see ref. 1.

[2]To whom correspondence should be addressed.

[3]We are indebted to Dr. R. Goodwin, Department of Botany, Connecticut College, for providing this material.

[4]Dr. J. S. Pringle, Royal Botanical Gardens, Hamilton, kindly located this sample.

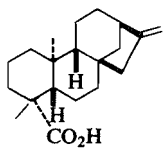

1

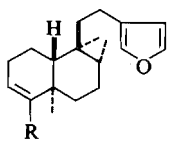

2

a R = CO_2H
b R = CH_2OAC
c R = CH_2OH

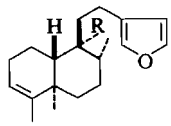

3

a R = CO_2H
b R = CO_2Me
c R = CH_2OH
d R = CH_2OAc
e R = CH_3
f R = CHO
g R = CH_2OTs

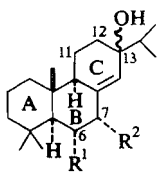

4

a R^1 = OH; R^2 = $OCOC_4H_7$
b R^1 = $OCOC_4H_7$; R^2 = OH
c R^1 = R^2 = OH
d R^1 = R^2 = OAc
e R^1 = OH; R^2 = $OCOC_4H_9$

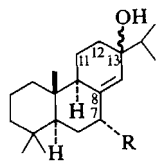

5

a R = OH
b R = OAc

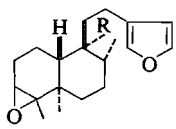

6

a R = CO_2H; α-epoxide
b R = CH_2OAc; β-epoxide
c R = CH_2OAc; α-epoxide
d R = CO_2Me; α-epoxide
e R = CO_2Me; β-epoxide

ambiguously by the conversion of both junceic acid and hardwickiic acid (**2***a*) into the furano-olefin (**3***e*). Methyl junceate (**3***b*) on reduction with lithium aluminum hydride formed the alcohol (**3***c*) which was then converted smoothly into the aldehyde (**3***f*) with the Sarett reagent. Huang–Minlon reduction of this aldehyde under carefully controlled conditions yielded the oily furano-olefin (**3***e*), $[\alpha]_D$ −58°. The transformation of hardwickiic acid (**2***a*) into **3***e* was effected via the acetate (**2***b*). This acetate on hydrogenation in triethylamine–ethanol over palladized charcoal suffered hydrogenolysis of the allylic ester group and produced the furano-olefin (**3***e*), identical in all respects with that synthesized from junceic acid.

The decision that **3***a* rather than **7***a* correctly represented junceic acid was made on the following grounds. First, clerodanes with a furan ring in the side chain often (4) have major fragments at M − 95 in their mass spectra resulting from scission of the C_9—C_{11} bond. However, in the case of junceic acid, the ion of this type is absent and replaced by one at *m/e* 222 (M − 94), which presumably arises by transfer of a hydrogen atom in a process such as that outlined in **8**. Second, in contrast to solidagoic acid A (**9**) (5), junceic acid does not decarboxylate readily. It was, for example, recovered after heating at 290° under nitrogen for 30 min. Such thermal stability would be surprising for a βγ-unsaturated acid as in **7***a*. Finally, certain n.m.r. data indicate the close proximity of the carboxyl and the secondary methyl group. The magnitudes (see Experimental) of the downfield shifts observed in pyridine for the C—CH_3 resonances on going from the methyl ester (**3***b*) to the acid (**3***a*) reveal (6) not only the 1:3 diaxial arrangement of the carboxyl and the tertiary methyl group but also the juxtaposition of the former to the secondary methyl group. In addition, examination of the spectrum of the alcohol (**3***c*) containing progressively increasing concentrations of tris(dipivalomethanato)europium indicates that the tertiary and the secondary methyl group are similar distances (7) from the interacting europium atom (1.2:1 respectively) while the olefinic methyl and vinylic proton are further removed. This evidence accords only with the structure **3***a* for junceic acid. However, with a view to final confirmation of this, efforts were made to establish the steric relationship between the furan ring and the carboxyl group. To this end, the epoxides **6***b*, m.p. 98–101°, and **6***c* were prepared but attempts to convert the former into the acid (**10**) and thence to the lactone (**11**) failed. An examination of the buffered acetolysis of the toluene-*p*-sulfonate (**3***g*) was next undertaken. No acetates were detected in the product mixture which was shown by t.l.c. on silver nitrate–silica gel to consist essentially of one minor and three major components. These were separated by repeated preparative t.l.c. and tentative structures assigned to the major products on the basis of their u.v. and n.m.r. spectra. As anticipated, all three had retained the β-substituted furan ring and the Δ^3-olefinic bond as evidenced by the characteristic signals for the furanic protons and the C-3 olefinic hydrogen and C-4 methyl group. Surprisingly, they also all contain

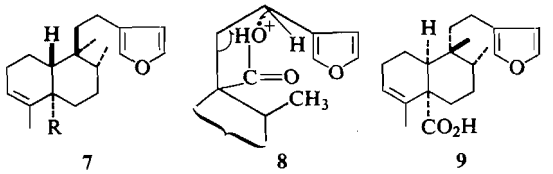

7

a R = CO_2H
b R = CH_2OTs

8

9

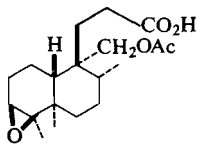

10

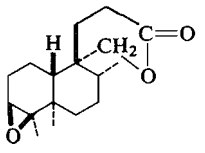

11

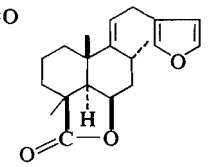

12

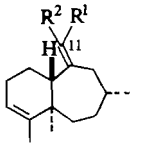

13

R^1 = H; R^2 = CH_2Fu
or
R^1 = CH_2Fu; R^2 = H

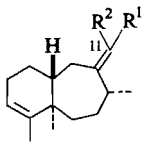

14

R^1 = H; R^2 = CH_2Fu
R^1 = CH_2Fu; R^2 = H

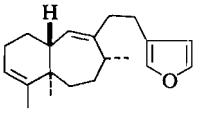

15

a secondary methyl group. Further, none of these compounds exhibits absorption in the u.v. arising from conjugation of the newly introduced olefinic bond with either of the unsaturated systems already present. Easily recognized in the n.m.r. spectrum of the compound of intermediate polarity is a new AX_2 system (τ 4.70, 1H, t; 6.89, 2H, d; J = 7 Hz) of the type encountered (8) in anhydromarrubiin (**12**) and attributed to 1 H-11 and 2 H-12. A compound with this functionality would be expected to arise from the toluene-*p*-sulfonate **3***g* rather than from the alternative **7***b* and thus convincingly proves that junceic acid has the constitution and stereochemistry depicted in **3***a*.[5] Bearing in mind its genesis, the furano-diene could be formulated as **13** or **14**. The latter is preferred since double irradiation experiments show that the secondary methyl is coupled (J = 6 Hz) to a proton which resonates as a broad multiplet at τ 7.34, a shift value attributable to an *allylic* proton. The least polar of these solvolysis products also contains the AX_2 system and may be simply the geometric isomer (at C-11) of the compound discussed above. However, in this case, the structures **13** cannot be ruled out since the resonance of the C-8 proton was located by double irradiation at τ 7.67, a value less readily ascribed to an allylic methine. In the third, most polar, furano-diene a new olefinic proton resonates at τ 4.97 (d, J = 6 Hz). Double irradiation experiments showed that this proton and the secondary methyl group are spin–spin coupled to two *different* allylic methines (τ 7.64 and 7.42 respectively) and thus the structure **15** can be assigned to the compound.

The structure of the other new naturally-occurring *ent*-clerodane was readily established as an epoxyjunceic acid (**6***a*). Its n.m.r. spectrum is similar to that of junceic acid except that the resonances of the olefinic proton and methyl group are replaced by signals attributable to a proton (τ 7.18) and methyl group (τ 8.90) attached to an epoxide ring. This structural assignment was confirmed by the preparation of the corresponding ester (**6***d*) from methyl junceate. Treatment of the latter (**3***b*) with *m*-chloroperbenzoic acid in carbon tetrachloride yielded two epoxides the minor of which (**6***d*) was identical with the methyl ester of the acid

[5]Indeed the compound of structure **7***a*, maingayic acid, has been isolated recently (9) from *Callicarpa maingayi*.

of natural provenance. The C_3—C_4 stereochemistry in these two epoxides can be deduced from the multiplicity of the H-3 resonances. In the major isomer (**6***e*), m.p. 82–86°, H-3 appears as a broadened doublet (J = 3.5 Hz) and in the minor (**6***d*) as a singlet. Examination of models and application of a suitably modified (10) Karplus equation leads to the assignments shown. Indeed a preponderance of **6***e* might be expected from the epoxidation reaction since the β-face appears more open to attack.

The Abietanes

Later fractions from column chromatography of the plant extract over silica gel yielded three additional new diterpenoids, junceanols W (**4***a*), X (**4***b*), and Y (**5***a*). The most polar, junceanol Y, m.p. 136–140°, analyzed for $C_{20}H_{34}O_2$. Inspection of the n.m.r. spectrum of the derived monoacetate (**5***b*) reveals the presence of one isopropyl and three tertiary methyl groups as expected for an abietane (or totarane, **16**) skeleton. Only two resonances are present at low field, one attributable to an olefinic proton (τ 4.17). Thus the molecule contains a trisubstituted double bond and a secondary acetate and these together with a tertiary hydroxyl, which gives rise to a peak at about τ 8.3 in its n.m.r. spectrum (lost on D_2O exchange) and at 3615 cm^{-1} in the i.r., account for all the functionality in a tricyclic system.

Definitive evidence for the skeletal structure and the location of the functional groups was next sought. In an attempt to interrelate the tertiary hydroxyl group and the olefinic bond, the monoacetate (**5***b*) was subjected to a variety of conditions, each aimed at its dehydration. However, of these, only one, treatment with toluene-*p*-sulfonyl chloride in pyridine at 100°, proved successful. Separation of the three major products by preparative t.l.c. on silver nitrate – silica gel afforded a stable (**17**) and an unstable (**18**) triene (λ_{max} 315 and 288 nm respectively) and the known (11) abietatriene (**19**), m.p. 38–43°, $[\theta]_{277}$ −320, $[\theta]_{269}$ −320, $[\theta]_{262}$ −120. The production of this last compound allows the assignment of the abietane skeleton to Y and in addition provides unequivocal proof of the absolute configurations at C-5 and -10 (as in **5***a*).

The following arguments suggest that the functional groups are located as shown in **5***a*. The facile formation of the aromatic hydrocarbon (**19**) *and* the nonaromatic trienes (**17** and

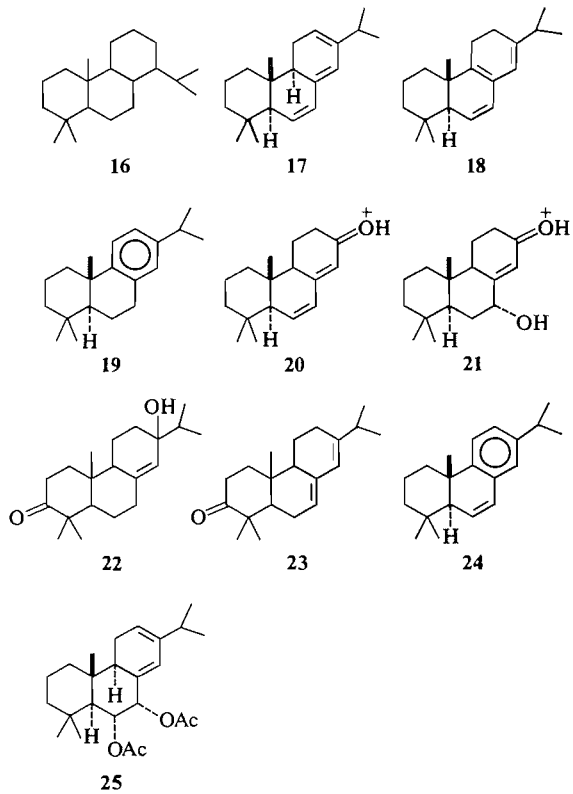

18) from the monoacetate (**5***b*) indicates the probability that two of the functional groups are borne by ring C and the third by ring B. It soon became evident that this indeed is the case. Thus an intense M − 61 peak and an even more intense one for M − 43 in the mass spectrum of Y (**5***a*) were taken as representing the oxonium ions **20** and **21** (or equivalent species) respectively, produced by excision of the isopropyl side chain. This cleavage would be expected (12) for a C-13 tertiary alcohol especially if a $\Delta^{8(14)}$ double bond were also present. This substitution pattern in ring C would also explain the sharpness ($w_{1/2}$ < 3 Hz) of the olefinic proton resonance in Y and its acetate since it would have no vicinal but only long range spin–spin couplings. Confirmation that the olefinic proton and isopropyl group are both in close proximity to the tertiary hydroxyl was obtained by recording the n.m.r. spectrum of the monoacetate (**5***b*) in the presence of tris-(dipivalomethanato)europium. Indeed, the magnitude of the induced shifts (see Experimental) was similar to that obtained for the hydroxyketone (**22**) from *Solidago patula* Muhl. (13) and *S. missouriensis* Nutt. (14). A decision as to

the location and orientation of the acetate group in **5***b* was also forthcoming. As mentioned above, the production of the nonaromatic trienes made it appear likely that this third substituent is attached to ring B. Two distinct pieces of evidence allow its assignment to C-7. First, **5***b* is much more stable than the related **22**, which even on standing in chloroform at 20° slowly formed the diene (**23**). This suggests that C-7 is functionalized in **5***b*. Second, although nuclear magnetic double resonance experiments on the monoacetate (**5***b*) failed[6] to show spin–spin coupling between the two protons responsible for the resonances at low field, they did reveal that the proton assignable to *H*COAc is coupled to two protons of near-identical chemical shift, the value of which indicates that they are probably *not allylic*. Irradiation at τ 8.33 (2 H-6) caused the narrow triplet (J = 2 Hz) at 4.73 to collapse to a sharp singlet. A further experiment located the resonance attributable to H-9, since irradiation at τ 7.96 sharpened the singlet at 4.17 (olefinic proton). The multiplicity of the signal at τ 4.73 (see above) indicates the equatorial nature of the proton involved (H-7) and thus the monoacetate of Y can be assigned the structure and stereochemistry shown in **5***b*. The stereochemistry at C-9 is tentatively assigned on a biogenetic basis, while that at C-13 remains unresolved. The structures of junceanols W (**4***a*) and X (**4***b*) discussed below lend credence to the substitution pattern proposed for Y (**5***a*).

The structural similarity of junceanols W and X, first indicated by the observation that they both gave a characteristic pink color when sulfuric acid was used for spot location after analytical t.l.c., was established by the following chemical and spectroscopic studies. The n.m.r. spectra of the two are markedly similar, each containing resonances attributable to an isopropyl and three tertiary methyl groups, an olefinic proton and two protons of the type *H*—C—O. The signals arising from these two protons appeared to suggest that the two compounds are derived from a single diterpenoid which contains two secondary alcohol groups. In W, one of these groups is esterified, while in X, it is the other. Thus the relevant two protons resonate as a doublet (J = 3.5 Hz) and an ill-resolved quartet (J = 3.5, 12 Hz) at τ 4.63 and 6.07 respectively in W and at τ 5.90 and 4.97 respectively in X. The validity of our conclusions as to the relationship of the two compounds was substantiated in two ways. First, distillation of X *in vacuo* furnished a mixture of **24**, X and W, the last resulting from acyl group migration. Second, X and W on saponification or reduction with lithium aluminum hydride produced the same compound (**4***c*). This product on acetylation formed a diacetate (**4***d*) which still showed stretching absorption in the i.r. attributable to a hydroxyl group at 3618 cm^{-1}. This must be tertiary in nature since the n.m.r. spectrum contains no resonances arising from carbinyl protons. It seemed clear that W and X are related to Y but bear an additional oxygen function at C-6. The vicinal nature of the C-6, -7 substituents was demonstrated by a nuclear magnetic double resonance experiment on X. Irradiation at τ 4.97 (H-6) caused collapse of the doublet at τ 5.90 (H-7) to a sharp singlet. The resonance arising from H-5 was located at τ 8.15 since irradiation at this point reduced the quartet at τ 4.97 to a doublet (J = 3.5 Hz). When the n.m.r. spectrum of the diacetate (**4***d*) was run in the presence of a europium shift reagent, H-5 was clearly seen as a clean doublet (J = 12 Hz). The multiplicity of H-6 convincingly demonstrates the equatorial nature of the functional group at C-6. In the thermal conversion of X (**4***b*) into W (**4***a*), described above, the acyl group, although moving from an equatorial to an axial orientation, escapes a strong steric interaction with the geminal methyl groups at C-4. The assignment of the secondary functional groups to ring B rather than ring C, at C-11 and -12, in W and X can be rationalized by arguments analogous to those applied above to Y. However, in addition, it was noted that dehydration of the diacetate (**4***d*) with toluene-*p*-sulfonyl chloride in pyridine afforded, as the major product, the *homocyclic* diene (**25**), λ_{max} 273 nm. Significantly, in the n.m.r. spectrum of this product, neither resonance from the *H*—C—OAc protons had been shifted to appreciably lower field and presumably therefore has not *become* allylic.

Final confirmation of the structure of X as **4***b*, and consequently of W as **4***a*, was achieved by treating it with hydrochloric acid in chloroform. The resulting styrene (**24**) on catalytic hydrogenation furnished the identical abietatriene (**19**) to that prepared earlier from Y. The abso-

[6]An equatorial proton at C-7 would be expected (15), because of its orientation, to have a minimal coupling to an olefinic proton at C-14.

lute configuration can be assigned with assurance to all centers save C-9 and -13 although the former is tentatively advanced on biogenetic grounds.

Remaining for discussion is the nature of the ester grouping in W and X. An important clue as to its identity was obtained from the n.m.r. spectra of these two compounds which contain three resonances not attributable to the diterpenoid moiety, namely, an olefinic proton at τ 4.31 and two methyl groups attached to an olefinic bond at τ 7.81 and 8.08. This suggested that W and X are senecioates and indeed the corresponding acid was recovered from alkaline hydrolysis of the latter and identified by its n.m.r. and mass spectra.[7]

Experimental

Melting points are uncorrected and were determined on a Kofler hot-stage apparatus. Specific rotations refer to solutions in chloroform unless otherwise stated. For analytical and preparative t.l.c., chromatoplates were spread with Kieselgel G (Merck). G.l.c. was carried out using a Varian Aerograph 1200 gas chromatograph and a stainless steel column ($\frac{1}{8}$ in. × 5 ft packed with 3% SE-30) and nitrogen as carrier gas with a flow rate of 25 ml/min. Light petroleum was of b.p. 60–80°. Microanalyses were by Miss F. Cowan, Glasgow. I.r. solution spectra were recorded in carbon tetrachloride on a Beckmann IR12 or IR5A spectrophotometer, u.v. spectra in ethanol unless otherwise stated on a Unicam S.P.800 spectrophotometer, and circular dichroism curves on a Cary 61 spectropolarimeter. P.m.r. spectra were run on a Varian Associates A-60A or HA 100 spectrometer in carbon tetrachloride, unless otherwise stated, using approximately 0.3 *M* solutions and tetramethylsilane as internal standard. Mass spectra were run on a Varian Associates CH7 instrument.

Isolation Procedure, the Root Extract

(*i*) The ground, dried roots (82 g) of *Solidago juncea* (New London sample) were continuously extracted with ether for 8 h in a Soxhlet apparatus. The extract (4.7 g), which showed one intense and one faint spot on analytical t.l.c. when sprayed with the Ehrlich reagent, was submitted to preparative t.l.c. (ether – light petroleum, 1:4) and four fractions were recovered. Fraction I contained non-polar, essentially non-terpenoid (n.m.r. evidence) material and was not investigated further. Fraction II afforded the major furanoid component, junceic acid (**3***a*, 2.2 g) as an oil, contaminated with a small amount of a second component (n.m.r. evidence), later shown to be *ent*-16-kauren-19-oic acid (**1**). Further purification, by preparative t.l.c. followed by distillation *in vacuo* provided junceic acid (**3***a*) as an oil which had $[\alpha]_D$ −59° (*c*, 0.84); ν_{max} 3400–3000 (br), 1743(w), 1696(s), and 877 cm^{-1} (0.006 *M*); 1743(vw), 1723(s) and 1696(m) cm^{-1} in presence of tetrahydrofuran (0.3 *M*); τ 2.63, 2.76, 3.70 (all m, 1H; furan protons), 4.72 (m, 1 H-3 $w_{1/2}$ = 8 Hz), 8.40 (broad s, 3 H-18), 8.83 (d, 3 H-17, J = 6 Hz), and 9.04 (s, 3 H-19); τ (pyridine) 8.60 (d, 3 H-17, J = 6 Hz) and 8.75 (s, 3 H-19); *m/e* 316 (M; $C_{20}H_{28}O_3$). The corresponding methyl ester (**3***b*) prepared by treatment of the acid with diazomethane in ether, was purified by preparative t.l.c. (ethyl acetate – light petroleum, 1:30) and distillation at 160°/0.4 mm. It had $[\alpha]_D$ −54° (*c*, 1.57); ν_{max} 1735 and 878 cm^{-1}; τ 4.83 (m, 1 H-3, $w_{1/2}$ = 7 Hz), 6.47 (s, 3H, —OCH_3), 8.45 (broad s, 3 H-18; sharpens on irradiation at τ 4.83), 8.88 (d, 3 H-17, J = 6 Hz; s on irradiation at τ 8.34) and 9.20 (s, 3 H-19); τ (pyridine) 8.76 (d, 3 H-17, J = 6 Hz) and 9.06 (s, 3 H-19); *m/e* 330 (M).

Anal. Calcd. for $C_{21}H_{30}O_3$: C, 76.32, H, 9.15. Found: C, 76.58; H, 8.93.

Preparative t.l.c. (acetic acid – ether – light petroleum, 1:2:17) of fraction II (160 mg) afforded the minor component, *ent*-16-kauren-19-oic acid (**1**, 12 mg); **1** was more readily separated as its methyl ester from the mixture resulting from treatment of fraction II with diazomethane. The mixture of esters (250 mg) gave by preparative t.l.c. (ethyl acetate – light petroleum, 1:20; silica gel – silver nitrate, 9:1) the oily methyl ester of **1** (28 mg), which had $[\alpha]_D$ −92° (*c*, 1.55) (lit. (2) $[\alpha]_D$ −104°). Alternatively, reduction of the mixture of esters with lithium aluminum hydride allowed easy separation by preparative t.l.c. (1:15, ethyl acetate – chloroform) of *ent*-16-kauren-19-ol, m.p. 141–143°, $[\alpha]_D$ −85° (*c*, 1.4) (lit. (2) m.p. 143–145°, $[\alpha]_D$ −78°).

Fraction III (190 mg), which contained two furanoid compounds, (t.l.c., Ehrlich stain), was treated with diazomethane. Preparative t.l.c. (ethyl acetate – light petroleum, 1:30, run thrice) afforded in addition to methyl junceate (**3***b*, 28 mg) the more polar (−)-methyl hardwickiate (39 mg), $[\alpha]_D$ −89° (*c*, 1.3) (lit. (3) $[\alpha]_D$ −113.5°), identified by conversion with lithium aluminum hydride into hardwickiol (**2***c*) and comparison (t.l.c., n.m.r.) of this product with an authentic sample (**9***b*).

Fraction IV contained polar compounds which were present (t.l.c.) in greater abundance in an extract of the whole plant and are discussed below.

(*ii*) The ground, dried roots (158 g) of *S. juncea* (Hamilton sample) were extracted as above to give an oil (6.3 g). Preparative t.l.c. (acetic acid – ether – light petroleum, 1:2:17) of this oil (1 g) afforded, in addition to junceic acid (**3***a*, 460 mg), epoxyjunceic acid (**6***a*, 18 mg). This compound (**6***a*) was more conveniently separated as its methyl ester. Preparative t.l.c. (ethyl acetate – light petroleum, 1:10, run twice) of the methylated extract (1 g) afforded the oily epoxyester (**6***d*, 47 mg) which distilled at 160°/0.01 mm and had $[\alpha]_D$ −49° (*c*, 2.1); τ 6.43 (s, 3H, —OCH_3), 7.18 (broad s, 1 H-3), 8.85 (d, 3 H-17, J = 6 Hz), 8.89 (s, 3 H-18) and 9.16 (s, 3 H-19); *m/e* 346 (M).

Anal. Calcd. for $C_{21}H_{30}O_4$: C, 72.80; H, 8.73. Found: C, 72.61; H, 8.85.

[7]These showed the presence of small amounts of isovaleric acid (less than 10%), thus "compound" X is probably a mixture consisting mainly of **4***a* but in addition a small proportion of the corresponding monoisovalerate (**4***e*). Indeed, a small fraction which was isolated from the original plant extract runs just ahead of **4***a* on t.l.c. and appears on n.m.r., i.r., and mass spectral evidence to consist mainly of **4***e*.

Epoxidation of Methyl Junceate (3b)

Methyl junceate (**3b**, 166 mg) in carbon tetrachloride (10 ml) was treated with *m*-chloroperbenzoic acid (120 mg) in the dark at 20° for 16 h. The reaction mixture was eluted through a short alumina column with carbon tetrachloride, the solvent evaporated, and the crude product submitted to preparative t.l.c. (ethyl acetate – light petroleum, 1:12, run four times). Three compounds were recovered, unreacted **3b** (10 mg), the β-epoxyester (**6e**, 66 mg), and the α-epoxyester (**6d**, 20 mg). The less polar epoxyester (**6e**) after crystallization from light petroleum had m.p. 82–86°; τ 6.44 (s, 3H, —OCH_3), 7.21 (m, 1 H-3, $w_{1/2}$ = 5.5 Hz), 8.87 (s, 3 H-18), 8.88 (d, 3 H-17, J = 6 Hz), and 9.13 (s, 3 H-19).

Anal. Calcd. for $C_{21}H_{30}O_4$; C, 72.80; H, 8.73. Found: C, 73.00; H, 8.78.

The minor, more polar epoxyester (**6d**) had $[\alpha]_D$ −43° (*c*, 1.0) and was identical (t.l.c., n.m.r., and mass spectral fragmentation pattern) to the methyl ester of the naturally occurring epoxyacid (**6a**) (see above).

Attempted Decarboxylation of Junceic Acid (3a)

Junceic acid (20 mg) was heated at 290° under nitrogen in a sublimation tube for 30 min and the material was then distilled at the same temperature and 0.2 mm. T.l.c. (ethyl acetate – light petroleum, 1:30 and ethyl acetate – chloroform, 1:15) and its n.m.r. spectrum showed that the distillate was essentially pure starting material.

Reduction of Methyl Junceate (3b) with Lithium Aluminum Hydride

Methyl junceate (**3b**, 460 mg) was treated with excess lithium aluminum hydride in dry refluxing ether for 20 h. Work-up with saturated aqueous sodium sulfate afforded the crude product (416 mg). Preparative t.l.c. (ethyl acetate – chloroform, 1:15) of this material yielded the oily alcohol (**3c**, 365 mg) which after distillation *in vacuo* had $[\alpha]_D$ −49° (*c*, 1.3); ν_{max} 3650, 3460, and 877 cm^{-1}; τ 2.72, 2.80, 3.78 (all m, 1 H, furan protons), 4.84 (m, 1 H-3, $w_{1/2}$ = 7 Hz), 6.33 (s, 2 H-20), 8.42 (broad s, 3 H-18), 8.97 (s, 3 H-19) and 9.08 (d, 3 H-17, J = 6 Hz); with a 0.36 *M* ratio of Eu(DPM)$_3$ to **3c**, τ −2.2 (m, 2 H-20, $w_{1/2}$ = 9 Hz), 2.35, 2.62, 3.17 (all m, 1H, furan protons), 4.20 (m, 1 H-3, $w_{1/2}$ = 8 Hz), 6.23 (broad s, 3 H-17), 7.15 (s, 3 H-19), 7.87 (narrow m, 3 H-18); *m/e* 302 (M; $C_{20}H_{30}O_2$).

Treatment of **3c** with acetic anhydride – pyridine furnished the corresponding acetate (**3d**), which was purified by preparative t.l.c. (ethyl acetate – light petroleum, 1:10) and then crystallization from light petroleum. It had m.p. 82–84°, τ 5.92 (s, 2 H-20), 8.04 (s, 3H, —OCOCH_3), 8.43 (narrow m, 3 H-18), 8.98 (s, 3 H-19), and 9.07 (d, 3 H-17, J = 6 Hz).

Anal. Calcd. for $C_{22}H_{32}O_3$: C, 76.70; H, 9.36. Found: C, 76.79; H, 9.44.

The Aldehyde 3f

Chromium trioxide (295 mg) in pyridine (10 ml) was added to the alcohol (**3c**, 150 mg) in the same solvent (10 ml) and the mixture kept at 20° for 6 h. The solvent was removed by azeotroping with benzene and the reaction product (100 mg) recovered from the residue with ether. Preparative t.l.c. (ethyl acetate – light petroleum, 1:20) of the product afforded the unstable aldehyde (**3f**, 58 mg) as an oil, which had ν_{max} 1715 and 873 cm^{-1}; τ 0.15 (s, 1 H-20), 4.82 (m, 1 H-3), 8.38 (broad s, 3 H-18), 8.92 (d, 3 H-17, J = 6 Hz), and 9.08 (s, 3 H-19); *m/e* 300 (M; $C_{20}H_{28}O_2$).

The Furano-olefin 3e

The aldehyde (**3f**, 58 mg) was heated under nitrogen with 99% hydrazine hydrate (2 ml) in ethylene glycol (2 ml) at 85° for 3 days. Potassium hydroxide pellets (145 mg) were then added and the temperature was raised to 195°, allowing excess hydrazine hydrate to distill out of the mixture. After 8 h at this temperature the mixture was allowed to cool and then diluted with ethyl acetate. This ethyl acetate solution was washed successively with dilute sulfuric acid, saturated aqueous sodium bicarbonate, and brine. Preparative t.l.c. (ethyl acetate – light petroleum, 1:20) of the crude product (66 mg) gave the furano-olefin (**3e**, 37 mg) which had $[\alpha]_D$ −58° (*c*, 1.09); τ 2.73, 2.86, 3.82 (all m, 1H, furan protons), 4.85 (m, 1 H-3), 8.43 (narrow m, 3 H-18), 9.00 (s, 3H, quaternary C—CH_3), 9.14 (d, 3 H-17, J = 6 Hz), and 9.26 (s, 3H, quaternary C—CH_3); with a 0.3 *M* ratio of Eu(DPM)$_3$ to **3e**, practically no change in spectrum except furan protons, now at τ 2.65, 2.77, and 3.78; *m/e* 286 (M; $C_{20}H_{30}O$). **3e** was identical (n.m.r., mass spectrum, t.l.c., g.l.c. and $[\alpha]_D$) to the furano-olefin obtained (**9b**) by hydrogenolysis of hardwickiol acetate (**2b**).

Epoxidation of Acetate 3d

The acetate (**3d**, 68 mg) was reacted with *m*-chloroperbenzoic acid (45 mg) in carbon tetrachloride for 2.5 h in the dark at 20°. The reaction mixture was washed through a short alumina column with ether and the crude product (53 mg) submitted to preparative t.l.c. (ethyl acetate – light petroleum, 1:10, run twice). Three compounds were isolated, the unreacted acetate (**3d**, 6 mg) and the epoxyacetates (**6b**, 32 mg; **6c**, 11 mg). The less polar β-epoxyacetate (**6b**) crystallized from light petroleum and had m.p. 98–101°, τ 5.96 (s, 2 H-20), 7.23 (m, 1 H-3, $w_{1/2}$ = 5 Hz), 8.05 (s, 3H, —OCOCH_3), 8.84 (s, 3 H-18), 8.93 (s, 3 H-19) and 9.10 (broadened d, 3 H-17, J = 6 Hz).

Anal. Calcd. for $C_{22}H_{32}O_4$: C, 73.30; H, 8.95. Found: C, 73.23; H, 8.91.

The minor α-epoxyacetate (**6c**), after distillation *in vacuo*, solidified and had m.p. 85–91°; τ 6.00 (d, 1 H-20, J = 11 Hz), 6.07 (d, 1 H-20, J = 11 Hz), 7.21 (s, 1 H-3, $w_{1/2}$ = 3.5 Hz), 8.03 (s, 3H, —OCOCH_3), 8.88 (s, 3 H-18), 8.97 (s, 3 H-19), and 9.10 (broadened d, 3 H-17, J = 6 Hz).

Anal. Calcd. for $C_{22}H_{32}O_4$: C, 73.30; H, 8.95. Found: C, 73.17; H, 9.16.

Attempted Formation of the Lactone 11

The less polar epoxyacetate (**6b**, 78 mg) was treated with chromium trioxide (85 mg) in an acetic acid (2 ml) – water (0.2 ml) mixture for 4.5 days. The crude product from work-up, from its t.l.c. behavior (ethyl acetate – light petroleum, 3:2) appeared to be a mixture of acids. Treatment with potassium hydroxide in ethanol (to hydrolyze the acetate) followed by attempted lactonization with toluene-*p*-sulfonic acid in refluxing benzene, or dicyclohexylcarbodiimide in pyridine at 100°, afforded very complex mixtures of mainly polar compounds.

The Tosylate 3g

Toluene-*p*-sulfonyl chloride (470 mg) and alcohol **3c** (290 mg) were dissolved separately in pyridine (3 ml

each) and the resulting solutions cooled to 0° and then mixed. After 26 h at 20° the reaction was worked-up (ice-water – ether). The resulting tosylate (**3***g*, 445 mg) ran as one spot on t.l.c. (ethyl acetate – light petroleum, 1:6) and had τ 2.27, 2.67 (benzenoid protons), 2.74, 2.90, 3.83 (all m, 1H, furan protons), 4.86 (m, 1 H-3), 5.97 (s, 2 H-20), 7.54 (s, 3H, Ar—CH_3), 8.44 (narrow m, 3 H-18), 9.08 (s, 3 H-19) and 9.12 (d, 3 H-17, J = 6 Hz).

Solvolysis of the Tosylate 3g

A solution of the tosylate (**3***g*, 675 mg) in acetic acid (41 ml) containing sodium acetate (1 g) was heated under reflux for 8 h. The solvent was removed by azeotroping with benzene and the residue dissolved in ether–water. The ether fraction was washed with brine, saturated aqueous sodium bicarbonate, and again brine. Evaporation of the solvent gave an oil (455 mg) which by t.l.c. over silica gel impregnated with silver nitrate (10%) (ethyl acetate – light petroleum, 1:60, or benzene – light petroleum, 1:7) was shown to contain one minor and three major components. Samples of each of the three major constituents were obtained by repeated preparative t.l.c. using the above conditions (ethyl acetate – light petroleum mixture). The least polar furano-diene (**13** or **14**, 50 mg) after distillation at 125°/0.06 mm had $[\alpha]_D$ −126° (*c*, 1.57); τ 4.75 (m, 1 H-3 and 1 H-11, $w_{1/2}$ = 12 Hz), 6.89 (d, 2 H-12, J = 7 Hz; s on irradiation at τ 4.76), 8.39 (broadened d, 3 H-18, J = 1.5 Hz), 8.94 (d, 3 H-17, J = 6 Hz; s on irradiation at τ 7.67) and 9.12 (s, 3 H-19); *m/e* 284 (M).

Anal. Calcd. for $C_{20}H_{28}O$: C, 84.45; H, 9.92. Found: C, 84.25; H, 9.83.

The furano-diene of intermediate polarity (**14**, 37 mg) was distilled at 120°/0.04 mm and had $[\alpha]_D$ −106° (*c*, 1.8); τ 4.70 (t, 1 H-11, J = 7 Hz; s on irradiation at τ 6.89), 4.83 (m, 1 H-3, $w_{1/2}$ = 8 Hz), 6.89 (d, 2 H-12, J = 7 Hz; s, on irradiation at τ 4.70), 8.41 (broadened d, 3 H-18, J = 1.5 Hz), 9.02 (s, 3 H-19) and 9.04 (d, 3 H-17, J = 6 Hz; s on irradiation at τ 7.34); *m/e* 284 (M).

Anal. Calcd. for $C_{20}H_{28}O$: C, 84.45; H, 9.92. Found: C, 84.47; H, 10.03.

The most polar furano-diene (**15**, 67 mg) was distilled at 120°/0.03 mm and had $[\alpha]_D$ −84° (*c*, 1.12); τ 4.70 (m, 1 H-3, $w_{1/2}$ = 10 Hz; t, J_{obs} = 6 Hz, on irradiation at τ 8.41), 4.97 (d, 1 H-20, J = 6 Hz; s on irradiation at τ 7.64), 8.41 (narrow m, 3 H-18), 8.92 (d, 3 H-17, J = 7 Hz; s on irradiation at τ 7.42) and 9.17 (s, 3 H-19); *m/e* = 284 (M).

Anal. Calcd. for $C_{20}H_{28}O$: C, 84.45; H, 9.92. Found: C, 84.45; H, 9.74.

Isolation Procedure, the Whole Plant Extract

Ground, dried, whole plant (120 g) of *S. juncea* was extracted with ether for 9 h in a Soxhlet apparatus. The crude extract (5.2 g) was chromatographed over silica gel (200 g) using light petroleum – ethyl acetate solvent mixtures. Early fractions contained junceic acid. Later fractions (10–40% ethyl acetate) were submitted to repeated preparative t.l.c. (ethyl acetate – light petroleum, 2:1) and afforded (in order of increasing polarity), junceanol W (**4***a*, 120 mg), junceanol X (**4***b*, 950 mg) and junceanol Y (**5***a*, 375 mg). Junceanol W (**4***a*) was obtained as an oil which decomposed fairly rapidly at 20° (t.l.c. evidence). It had ν_{max} 1720 cm^{-1}; τ 4.07 (broad s, 1 H-14, $w_{1/2}$ = 3 Hz), 4.63 (d, 1 H-7, J = 3.5 Hz), 6.07 (q, 1 H-6, J = 3.5, 12 Hz), 8.88, 8.96, 9.20 (all s, quaternary C—CH_3's), 8.92 and 9.06 (both d, 3 H-16 and 3 H-17, J = 6 Hz). Junceanol X (**4***b*), also an oil, on distillation *in vacuo* suffered extensive decomposition (see below). It was purified by further preparative t.l.c. (taking only a central "cut" from the band) and had $[\alpha]_D$ −11° (*c*, 1.3); ν_{max} (0.0025 *M*) 3615, 3595 (sh), 3530 (w) cm^{-1}; ν_{max} (0.01 *M*) 1737, 1720, and 1652 cm^{-1}; τ 4.29 (broad s, 1 H-14 and olefinic proton of senecioate), 4.97 (q, 1 H-6, J = 3.5, 12 Hz; d, J = 3.5 Hz on irradiation at τ 8.15), 5.90 (d, 1 H-7, J = 3.5 Hz; s on irradiation at τ 4.97), 7.35 (broad s, —O*H*; disappears on D_2O exchange), 7.80, 8.08 (both broad s, senecioate methyls), 8.97 (s, quaternary C—CH_3), 9.07, 9.12 (both d, 3 H-16 and 3 H-17, J = 6 Hz) and 9.13 (s, 6H, quaternary C—CH_3's). Junceanol Y (**5***a*) crystallized from ether – light petroleum and had m.p. 136–140°; $[\alpha]_D$ −34° (*c*, 2.0); ν_{max} 3600 and 3400 cm^{-1}; τ 4.37 (broad s, 1 H-14, $w_{1/2}$ = 3.5 Hz) 5.7 (broad s, 2 —O*H*; disappears on D_2O exchange), 5.82 (broad s, 1 H-7, $w_{1/2}$ = 4 Hz), 9.10 (m, 12H, —CH_3's) and 9.28 (s, quaternary C—CH_3); *m/e* 263 (M-43) and 245 (M-61).

Anal. Calcd. for $C_{20}H_{34}O_2$: C, 78.43; H, 11.11. Found: C, 78.54; H, 11.37.

Hydrolysis of Junceanol X (4b)

Junceanol X (entire t.l.c. band, see above) (**4***b*, 205 mg) was treated with potassium hydroxide (350 mg) in refluxing ethanol (15 ml) for 4 h and the mixture was then diluted with water and extracted with ether. The ether extract was washed with water (the aqueous layer and aqueous washings being retained, see below) and afforded the crude triol (**4***c*, 126 mg). Purification of this material by preparative t.l.c. (ethyl acetate – light petroleum, 2:1) followed by crystallization from moist ether gave **4***c*, m.p. 90–96°; τ 4.30 (broad s, 1 H-14), 5.95 (d, 1 H-7, J = 3.5 Hz), 6.25 (q, 1 H-6, J = 3.5 ,12 Hz), 6.75 (broad s, 2? —O*H*; lost on D_2O exchange), 8.85, 8.96, 9.25 (all s, quaternary C—CH_3's), 9.06 and 9.11 (both d, 3 H-16 and 3 H-17, J = 6 Hz); *m/e* 304 (M − 18), 280 (M − 42), 279 (M − 43) and 261 (M − 61).

Anal. Calcd. for $C_{20}H_{34}O_3.H_2O$: C, 70.59; H, 10.59. Found: C, 70.32; H, 10.83.

The aqueous fractions from the above reaction were combined, evaporated to near dryness *in vacuo* and acidified with the minimum quantity of dilute sulfuric acid. A large amount of anhydrous sodium sulfate was added and the mixture was then extracted with carbon tetrachloride. The n.m.r. of this solution corresponded to that of a mixture (*ca.* 10:1) of authentic samples of senecioic and isovaleric acids. The above reaction was repeated and the mixture of acids recovered this time in ether. This extract was evaporated carefully to small bulk and submitted to mass spectral analysis which showed *m/e* 100 (senecioic; M) and 60 (isovaleric; M − propene).

Conversions of Junceanol W (4a) into Triol 4c

Junceanol W (**4***a*, 10 mg) was treated with excess lithium aluminum hydride in refluxing dry ether (2 ml) for 1 h. Work-up afforded triol **4***c* (8.5 mg).

Junceanol W (9 mg) was heated in refluxing ethanol with potassium hydroxide (80 mg) for 1 h. The mixture was diluted with ether and then washed with brine. Evaporation of the ether layer gave triol **4***c* (8 mg).

These two samples were identical in n.m.r. and t.l.c. (ethyl acetate – light petroleum, 2:1) behavior to the triol prepared (see above) from junceanol X (**4***b*).

The Acetate 5b

Junceanol Y (**5***a*, 110 mg) was treated with acetic anhydride (0.5 ml) and pyridine (0.5 ml) at 20° for 14 h. The mixture was diluted with ether, washed with saturated aqueous sodium bicarbonate and water, and the solvent evaporated. Preparative t.l.c. (ethyl acetate – light petroleum, 2:1) of the residue afforded the oily acetate **5***b* (95 mg) which was distilled at 135–140°/0.02 mm and had $[\alpha]_D$ −26° (*c*, 1.3); ν_{max} 3615 and 1735 cm^{-1}; τ 4.17 (broad s, 1 H-14, $w_{1/2}$ = 4 Hz; sharpens on irradiation at τ 7.96), 4.73 (t, 1 H-7, J_{obs} = 2 Hz; s on irradiation at τ 8.33), 8.03 (s, 3H, —OCOCH_3), 8.3 (broad s, —O*H*, lost on D_2O exchange), 9.12, 9.17 (both d, 3 H-16 and 3 H-17, *J* = 7 Hz), 9.15 (s, 6H, quaternary C—CH_3's), and 9.24 (s, 3H, quaternary C—CH_3); with a 0.46 *M* ratio of Eu(DPM)$_3$ to **5***b*, τ −2.9 (broad s, —O*H*), 0.03 (broad s, 1 H-7), 0.63 (broad s, 1 H-14), 5.32 (s, 3H, —OCOCH_3), 7.73 (was 9.12), and 7.91 (was 9.07) (both d, 3 H-16 and 3 H-17, *J* = 7 Hz), 8.25, 8.45, and 8.77 (all s, quaternary C—CH_3's).

Anal. Calcd. for $C_{22}H_{36}O_3$: C, 75.81; H, 10.41. Found: C, 75.59; H, 10.24.

Eu Shifts in Model Compounds

(*i*) Compound **22** (13, 14) had τ 4.53 (broad s, 1 H-14), 8.97 (s, 6H, quaternary C—CH_3's), 9.00 (s, quaternary C—CH_3), 9.08 and 9.13 (both d, 3 H-16 and 3 H-17, *J* = 6 Hz); with a 0.42 *M* ratio of Eu(DPM)$_3$ to **22**, τ 1.53 (broad s, 1 H-14), 6.83, 7.21, 7.47 (all s, quaternary C—CH_3's), 7.15 and 7.25 (both d, 3 H-16 and 3 H-17, *J* = 6 Hz).

(*ii*) Compound **23** (13, 14) had τ 4.27 (broad s, 1 H-14), 4.60 (broad s, 1 H-7), 8.91 (s, quaternary C—CH_3), 8.98 (s, 6H, quaternary C—CH_3's), and 8.98 (d, 3 H-16 and 3 H-17, *J* = 6 Hz); with a 0.21 *M* ratio of Eu(DPM)$_3$ to **23**, τ 4.16 (broad s, 1 H-14), 4.42 (broad s, 1 H-7), 7.92, 8.12, 8.63 (all s, quaternary C—CH_3's), and 8.93 (d, 3 H-16 and 3 H-17, *J* = 6 Hz).

Treatment of Acetate 5b with Toluene-p-sulfonyl Chloride

The acetate (**5***b*, 165 mg) was heated in pyridine (6 ml) with toluene-*p*-sulfonyl chloride (200 mg) at 100° for 10 h. The reaction mixture was poured into ice-water and extracted with ether. The crude product (124 mg) showed three spots on analytical t.l.c. (ethyl acetate – light petroleum, 1:70) on silica gel impregnated with silver nitrate (10%), and separation of the components was achieved by preparative t.l.c. using the same conditions. The least polar component was the known aromatic hydrocarbon (**19**, 39 mg), m.p. 37–43° (lit. (11) 41–43°); λ_{max} (cyclohexane) 269 (ε 850) and 277 nm (ε 900) (lit. (11) (ethanol) 275 nm (ε 800)); τ 2.93 (d, 1 H-11, *J* = 8 Hz), 3.17 (q, 1 H-12, *J* = 8, 1.5 Hz), 3.23 (broad s, 1 H-14), 8.80 (d, 3 H-16 and 3 H-17, *J* = 6 Hz), 8.83 (s, quaternary C—CH_3), and 9.05 (s, 6H, quaternary C—CH_3's); c.d. (ethanol) $[\theta]_{277}$ −320, $[\theta]_{269}$ −320 and $[\theta]_{262}$ −120; g.l.c. retention time 10.9 min at 175°; identical by g.l.c., t.l.c., n.m.r., and c.d. to an authentic sample[8] of **19**. The second component (27 mg) was the oily triene **17** which had λ_{max} 329, 315, and 304 nm; τ 4.13 (m, 1 H-6, 1 H-7, and 1 H-14), 4.38 (broadened t, 1 H-11, J_{obs} = 6 Hz), 8.80, 8.98 (both d, 3 H-16 and 3 H-17, *J* = 6.5 Hz), 8.86 (s, 6H, quaternary C—CH_3's) and 9.15 (s, quaternary C—CH_3); *m/e* 270 (M). The most polar component (21 mg) was the oily triene **18** which underwent very rapid decomposition (t.l.c.) to more polar material. It had λ_{max} 301 (sh), 288 and 276 nm.

[8]We cordially thank Professor E. Wenkert for supplying this sample.

The Diacetate 4d

The triol **4***c* (126 mg) in pyridine (2 ml) was treated with acetic anhydride (2 ml) at 20° for 15 h. Work-up afforded an oil (156 mg) from which the diacetate **4***d* (125 mg) was recovered by preparative t.l.c. (ethyl acetate – light petroleum, 1:2). After crystallization from light petroleum **4***d* had m.p. 114–118°, $[\alpha]_D$ +31° (*c*, 2.7); ν_{max} (0.005 *M*) 3618 (s), 3588 (vw) and 1745 (s) cm^{-1}; τ 4.20 (s, 1 H-14, $w_{1/2}$ = 3 Hz), 4.65 (d, 1 H-7, *J* = 3.5 Hz), 5.02 (q, 1 H-6, *J* = 12, 3.5 Hz), 8.00, 8.09 (both s, 3 H each, 2—OCOCH_3), 9.00 (s, quaternary C—CH_3), 9.06, 9.11 (both d, 3 H-16 and 3 H-17, *J* = 6 Hz) and 9.13 (s, 6H, quaternary C—CH_3's); with a 0.51 *M* ratio of Eu(DPM)$_3$ to **4***d*, τ 0.55 (broad s, 1 H-14), 1.23 (d, 1 H-7, *J* = 3.5 Hz), 3.05 (q, 1 H-6, *J* = 12, 3.5 Hz), 6.73, 7.42 (both s, 3 H each, 2—OCOCH_3), 6.97 (d, 1 H-5, *J* = 12 Hz), 7.28, 7.43 (both d, 3 H-16 and 3 H-17, *J* = 6 Hz), 8.02, 8.35, and 8.48 (all s, quaternary C—CH_3's).

Anal. Calcd. for $C_{24}H_{38}O_5$: C, 70.90; H, 9.42. Found: C, 70.96; H, 9.66.

Treatment of Junceanol X with Hydrochloric Acid

Concentrated hydrochloric acid (0.1 ml) was added to a solution of junceanol X (**4***b*, 75 mg) in chloroform (1 ml). After *ca.* 2 min, the solution was applied to a preparative t.l.c. plate, heated for *ca.* 1 min with a hair dryer, and the plate then developed with light petroleum in the usual fashion. The major non-polar product was the oily styrene (**24**, 23 mg) which after distillation at 125°/0.1 mm had $[\alpha]_D$ −136° (*c*, 1.55); λ_{max} 266 nm (ε 9000); c.d. (ethanol) $[\theta]_{258}$ +7000; τ 3.06 (d, 2H, aromatic protons, *J* = 1 Hz), 3.21 (narrow m, 1H, aromatic proton), 3.55 (q, 1 H-7, *J* = 10, 3 Hz), 4.07 (q, 1 H-6, *J* = 10, 3 Hz), 7.17 (septet, 1 H-15, *J* = 7 Hz), 7.88 (t, 1 H-5, *J* = 3 Hz), 8.77 (d, 3 H-16 and 3 H-17, *J* = 7 Hz), 8.94, 8.98 and 9.02 (all s, quaternary C—CH_3's); *m/e* 268 (M).

Anal. Calcd. for $C_{20}H_{28}$: C, 89.49; H, 10.51. Found: C, 89.27; H, 10.68.

Catalytic Hydrogenation of the Styrene 24

The styrene (**24**, 25 mg) in ethyl acetate was shaken with hydrogen over palladized charcoal (5%, 25 mg) for 2 h. Removal of catalyst and solvent left an oil (24 mg) which was purified by preparative t.l.c. (light petroleum) and gave the aromatic hydrocarbon **19** (18 mg). This material was identical (t.l.c., g.l.c., n.m.r., u.v., and c.d.) to the sample of **19** prepared from junceanol Y (see above).

Treatment of Diacetate 4d with Toluene-p-sulfonyl Chloride

The diacetate **4***d* (80 mg) was heated with toluene-*p*-sulfonyl chloride (95 mg) in refluxing pyridine (3 ml) for 11 h. Work-up afforded an oil (60 mg) which was subjected to preparative t.l.c. (ethyl acetate – light petroleum,

1:5), two major constituents being obtained. The less polar component (28 mg) was identified as the styrene **24** by its n.m.r. and t.l.c. behavior. The more polar component (24 mg) was the oily diene **25** which had λ_{max} 273 nm; τ 4.12 (broad s, 1 H-14), 4.45 (d, 1 H-7, J = 3.5 Hz), 4.68 (broad s, 1 H-12), 4.91 (q, 1 H-6, J = 12, 3.5 Hz), 7.97. 8.07 (both s, 3 H each, 2—OCOCH_3), 8.95 (s, quaternary C—CH_3), 9.02 (s, 6H, quaternary C—CH_3's) and 9.07 (d, 3 H-16 and 3 H-17, J = 6 Hz); with a 0.48 M ratio of Eu(DPM)$_3$ to **25**, τ 2.6 (d, 1 H-7, J = 3.5 Hz), 3.73 (broad s, 1 H-14), 3.78 (q, 1 H-6, J = 12, 3.5 Hz), 4.30 (broad s, 1 H-12), 7.13, 7.57 (both s, 3H each, 2—OCOCH_3), 8.63, 8.73, 8.81 (all s, quaternary C—CH_3's) and 9.03 (d, 3 H-16 and 3 H-17, J = 6 Hz).

Distillation–Pyrolysis of Junceanol X

(*i*) Junceanol X (51 mg) was heated at 200° under N_2 for 5 min and the product distilled at that temperature and 0.2 mm. The distillate on t.l.c. (ethyl acetate – light petroleum, 1:2) showed a non-polar compound, one of R_F *ca.* 0.5 and polar material but no substrate. Preparative t.l.c. using the same solvent mixture furnished the two less polar compounds. The first of these was identified as the styrene **24** (12 mg) by its n.m.r. and t.l.c. behavior while the second was identified as essentially pure junceanol W (**4***a*, 18 mg) on similar evidence.

(*ii*) Junceanol X (50 mg) was heated at 270° under nitrogen for 3 min and the product then distilled out at the same temperature and 0.1 mm. The distillate contained no detectable amounts of junceanols W or X (t.l.c. evidence). Preparative t.l.c. (light petroleum) afforded the styrene **24** (6 mg) which was again identified by its n.m.r. and t.l.c. behavior.

We thank the Science Research Council of the U.K. for a maintenance award (to M.S.H.), the National Research Council of Canada for an operating grant (to R.McC.), and Mr. Jyoti Chatterji for his assistance in the isolation of junceanols W and X.

1. T. ANTHONSEN, P. H. MCCABE, R. MCCRINDLE, R. D. H. MURRAY, and G. A. R. YOUNG. Tetrahedron, **26**, 3091 (1970).
2. J. ST. PYREK. Tetrahedron, **26**, 5029 (1970).
3. R. MISRA, R. C. PANDEY, and S. DEV. Tetrahedron Lett. 2681 (1968).
4. T. ANTHONSEN and R. MCCRINDLE. Acta Chem. Scand. **23**, 1068 (1969).
5. T. ANTHONSEN, M. S. HENDERSON, A. MARTIN, R. MCCRINDLE, D. MCMASTER, and R. D. H. MURRAY. Can. J. Chem. This issue.
6. C. R. NARAYANAN and K. VENKATASUBRAMANIAN. Tetrahedron Lett. 3639 (1965).
7. O. ACHMATOWICZ, A. EJCHART, J. JURCZAK, L. KOZERSKI, and J. ST. PYREK. Chem. Commun. 98 (1971); D. G. BUCKLEY, G. H. GREEN, E. RITCHIE, and W. C. TAYLOR. Chem. and Ind. 298 (1971); J. W. APSIMON and H. BEIERBECK. J. Chem. Soc. Chem. Commun. 172 (1972) and references therein.
8. J. W. B. FULKE, M. S. HENDERSON, and R. MCCRINDLE. J. Chem. Soc. C, 807 (1968).
9. (*a*) C. NISHINO, K. KAWAZU, and T. MITSUI. Agr. Biol. Chem. **35**, 1921 (1971). (*b*) K. KAWAZU, C. NISHINO, R. MCCRINDLE, and D. MCMASTER. Agr. Biol. Chem. **36**, 1245 (1972).
10. K. TORI, T. KOMENO, and T. NAKAGAWA. J. Org. Chem. **29**, 1136 (1964).
11. E. WENKERT, J. D. MCCHESNEY, and D. J. WATTS. J. Org. Chem. **35**, 2422 (1970) and references therein.
12. J. H. BEYNON, R. A. SAUNDERS, and A. E. WILLIAMS. The mass spectra of organic molecules. Elsevier Publishing Company, Amsterdam. 1968. p. 142.
13. E. NAKAMURA. M.Sc. Thesis. University of Guelph, Guelph, Ontario. 1972.
14. T. ANTHONSEN and GUDRUN BERGLAND. Acta Chem. Scand. **24**, 1499 (1970); Acta Chem. Scand. In press.
15. L. M. JACKMAN and S. STERNHELL. Applications of nuclear magnetic resonance spectroscopy in organic chemistry. Pergamon Press, Oxford. 1969. p. 316.

Constituents of *Solidago* Species. Part IV.[1] Solidagoic Acids A and B, Diterpenoids from *Solidago gigantea* var. *serotina*

T. ANTHONSEN, M. S. HENDERSON, A. MARTIN, AND R. D. H. MURRAY
Department of Chemistry, University of Glasgow, Glasgow, Scotland

AND

R. MCCRINDLE[2] AND D. MCMASTER
Chemistry Department, University of Guelph, Guelph, Ontario

Received November 27, 1972

Solidagoic acids A and B, two new diterpenoids from *Solidago gigantea* Ait. var. *serotina* (Kuntze) Cronqu., are formulated (absolute configuration tentative) as **1***a* and *b* on the basis of chemical, spectroscopic, and optical evidence.

On propose les formules **1***a* et **1***b* pour les acides solidagoïques A et B, deux nouveaux diterpénoides isolés de *Solidago gigantea* Ait. var. *serotina* (Kuntze) Cronqu. Ces structures pour lesquelles les configurations absolues ne sont pas définitives sont attribuées en se basant sur des preuves chimiques spectroscopiques et optiques. [Traduit par le journal]

Can. J. Chem., **51**, 1332 (1973)

In the course of our studies on the constituents of *Solidago* species, we have obtained (1) from the roots of *S. gigantea* Ait. var. *serotina* (Kuntze) Cronqu.[3] several new diterpenoids. In the present paper we discuss the constitution and stereochemistry of two of them, solidagoic acids A (**1***a*) and B (**1***b*).

The chloroform soluble fraction of an ethyl acetate extract of dried root material was examined by t.l.c. and found to contain a large number of furanoid compounds which were detected by their color reaction with Ehrlich's reagent. Column chromatography of this material over alumina and elution with chloroform – light petroleum furnished nine neutral diterpenoids, which form the subject of the following article. Two acidic compounds, solidagoic acids A and B, were then recovered by elution with ethyl acetate – acetic acid and separated by rechromatography, this time over silica gel.

Solidagoic Acid A

The less polar acid, A, m.p. 169–171°, was isolated in approximately 0.6% yield, based on the weight of dried roots. Analytical and mass spectral data indicated that the compound has the molecular formula $C_{20}H_{28}O_3$. Its i.r. absorption at 875 cm^{-1} taken in conjunction with three narrow multiplets at τ 2.75, 2.94, and 3.82 in its n.m.r. spectrum indicated the presence of a β-substituted furan ring. This probably constitutes part of a furano-ethyl side chain since its mass spectrum has a prominent ion at *m/e* 189 (M – 95; cleavage of C_9—C_{11} bond). The broad absorption band between 3100 and 3600 cm^{-1} in the i.r. confirmed that the remaining oxygen atoms are present in a carboxyl group, as had been deduced from its chromatographic behavior. In the n.m.r. spectrum an olefinic proton and a methyl group attached to a double bond give rise to an unresolved multiplet ($w_{1/2}$ = 11 Hz) at τ 4.45 and a broad singlet at 8.48 respectively, while a three proton singlet at τ 9.02 and a doublet at 9.11 (J = 6 Hz) can be attributed to two additional methyl groups, the former tertiary, the latter secondary. The results presented above indicated the possibility that solidagoic acid A has a clerodane-type skeleton (**2**), one of the tertiary methyl groups in **2** being replaced by a carboxyl group. The n.m.r. spectra of several simple derivatives of the acid added support to this proposal. Thus in the alcohol (**1***c*) and the acetate (**1***d*) the —CH_2O— protons appear as AB quartets (J = 11 Hz) centered at τ 6.47 and

[1]For Part III see ref. 4.

[2]To whom correspondence should be addressed.

[3]Dr. C. Jeffrey, Royal Botanic Gardens, Kew, U.K. kindly identified this taxon and has retained the specimens supplied as vouchers. In our preliminary communication this taxon was referred to by the presently unacceptable name, *S. serotina* Ait.

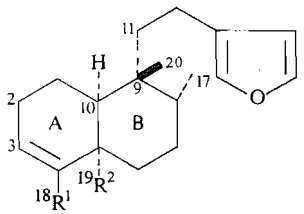

1

a $R^1 = CH_3$; $R^2 = CO_2H$
b $R^1 = CH_2OAng$; $R^2 = CO_2H$
c $R^1 = CH_3$; $R^2 = CH_2OH$
d $R^1 = CH_3$; $R^2 = CH_2OAc$
e $R^1 = CH_3$; $R^2 = CHO$
f $R^1 = R^2 = CH_3$
g $R^1 = CH_3$; $R^2 = CO_2Me$
h $R^1 = R^2 = CH_2OH$
i $R^1 = R^2 = CH_2OAc$
j $R^1 = CH_2OAng$; $R^2 = CO_2Me$
k $R^1 = CH_2OAc$; $R^2 = CH_2OH$
l $R^1 = CH_2OH$; $R^2 = CH_2OAc$

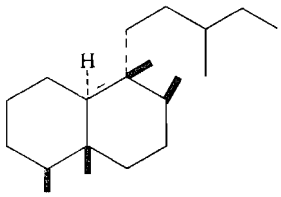

2

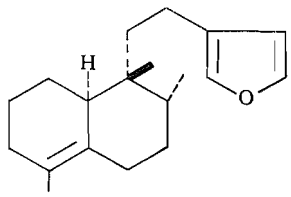

3

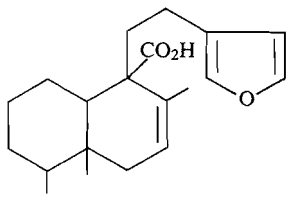

4

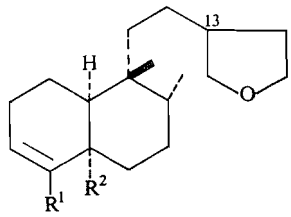

C-13 epimeric mixture

5

a $R^1 = CH_3$; $R^2 = CHO$
b $R^1 = R^2 = CH_3$
c $R^1 = CH_3$; $R^2 = CO_2Me$
d $R^1 = CH_3$; $R^2 = CH_2OAc$
e $R^1 = CH_3$; $R_2 = CH_2OH$
f $R^1 = R^2 = CH_2OH$
g $R^1 = R^2 = CH_2OAc$

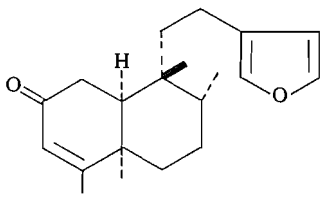

6

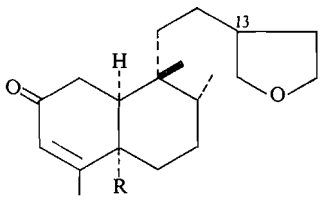

C-13 epimeric mixture

7

a $R = CH_3$
b $R = CO_2Me$
c $R = CHO$

5.96 respectively, while in the related aldehyde (**1***e*) the aldehydic proton resonates as a sharp singlet at τ 0.54. Significantly, none of these protons shows evidence of vicinal spin–spin coupling indicating that these functional groups are indeed attached to a quaternary carbon atom.

Further evidence for a clerodane-type skeleton came from the discovery that the olefinic bond is βγ to the carboxyl group. When acid A (**1***a*) was heated at 270° under N_2 for 20 min, it decarboxylated and furnished the olefin (**3**), which retains a resonance at τ 8.35 attributable to a methyl on a double bond but no resonance from an olefinic proton. Surprisingly, this nor-olefin (**3**) was the only product recovered from treatment of the alcohol (**1***c*) with chloroacetic anhydride in refluxing pyridine. In this case its formation presumably involves a reaction of the retro-Prins type. At this stage acid A could be tentatively assigned either the gross structure **1***a* (no stereochemistry) or the alternative **4**. The latter, which is unlikely on biogenetic grounds, was eliminated from consideration on the basis of the following evidence.

Huang–Minlon reduction of the aldehyde (**1***e*) and of its tetrahydro analog (**5***a*) afforded **1***f* and **5***b* respectively. Oxidation of these and of

the tetrahydro derivative (**5***c*) of methyl solidagoate (**1***g*) with the Sarett reagent slowly produced the enones **6**, **7***a*, and **7***b*, all of which exhibit resonances attributable to a methylene group α to the ketone at about τ 7.5. Significantly, in each case, the multiplets appear to constitute[4] the AB part of an ABX system. Indeed, when the n.m.r. spectrum of the alcohol (**1***c*) was recorded in the presence of tris(dipivalomethanato)europium the resonance of the proton giving rise to the X part in the enones separated out and appeared as a fairly narrow triplet. Therefore this proton (H-10) has probably no further vicinal neighbors. These results, and the observation that catalytic hydrogenation of **7***a* afforded a ketone (**8***a*), the i.r. absorption of which at 1720 cm^{-1} is compatible with its formulation as a cyclohexanone, allows the part structure **9** to be written for acid A with reasonable assurance. Bearing in mind biogenetic considerations and the presence of a β-furanoethyl side chain, a secondary and a tertiary methyl group, this can be expanded to **1***a* (no stereochemistry). The results reported below concerning the stereochemistry of acid A place this assignment of structure beyond reasonable doubt.

Solidagoic Acid B

The more polar acidic component, solidagoic acid B (**1***b*), m.p. 134–135°, analyzed for $C_{25}H_{34}O_5$, although its mass spectrum shows no peak higher than *m/e* 314, which thus probably corresponds to loss of a five carbon unit. An i.r. absorption band at 1695 cm^{-1} and characteristic (2) resonances at τ 3.96 (1H) and between 7.95 and 8.15 (6H) indicated the presence of an angelate ester. The remainder of the n.m.r. spectrum shows a marked similarity to that of acid A, suggesting a close relationship. Thus two methyl groups, one tertiary, the other secondary, give rise to a singlet at τ 8.97 and a doublet at 9.09 (J = 6 Hz) respectively while a multiplet at 4.02 ($w_{1/2}$ = 10 Hz) may be assigned to an olefinic proton. However, the resonance attributed to the olefinic methyl in acid A has been replaced by a two-proton singlet at τ 5.50, suggesting that in acid B this methyl has suffered oxygenation. The latter compound could then be formulated as **1***b* (no stereochemistry).

Certain nuclear magnetic double resonance and chemical experiments added substance to this conclusion. When the broad singlet at τ 5.50 (—CH_2—OAng) was irradiated the resonance of the olefinic proton at τ 4.02 was converted into a triplet (J_{obs} = 4 Hz). Irradiation at τ 7.93 (allylic protons, 2 H-2) also collapsed the multiplet at τ 4.02, this time to a broad singlet ($w_{1/2}$ = 4 Hz) and in addition sharpened ($w_{1/2}$ = 2.5 Hz) the singlet at τ 5.50. These experiments confirmed that the double bond bears on one end a proton and an allylic methylene and on the other a —CH_2—O— group. Moreover, pyrolysis of the acid at 320° in an evacuated tube afforded, in addition to an oily distillate, crystalline angelic acid (**10***a*), m.p. 45°, which was collected separately in a cold trap. Comparison of this material with an authentic sample of angelic acid was achieved by g.l.c. over 20% free fatty acid phase (FFAP) at 125°, the three isomeric acids, senecioic (**10***b*), tiglic (**10***c*), and angelic, being well separated on this free acid phase. The less volatile material from the above pyrolysis was seen from t.l.c. to consist of two compounds of very similar polarity which were separated only by repeated preparative t.l.c. The less polar component, $C_{20}H_{26}O_3$ (**11**), an oil, which was by far the more abundant, shows a strong absorption in the i.r. at 1778 cm^{-1}, indicative of a γ-lactone. The methylene protons in the lactone ring resonate as a pair of doublets at τ 5.31 and 5.60 (J = 12 Hz), the former being markedly broadened by long range coupling. The very minor component, m.p. 145–147°, on i.r. and mass spectral evidence only, is formulated tentatively as the isomeric lactone **12**. The formation of these lactones can be rationalized by suggesting attack of the carboxyl group at, in the former case the methylene group carrying the ester, in the latter C-3 with a concomitant rearrangement of the olefinic bond into the exocyclic position, each process involving expulsion of angelic acid.

A direct correlation of acids A and B was next sought and accomplished in the following manner. Reduction of the methyl ester of B with lithium aluminum hydride furnished the corresponding diol (**1***h*). Hydrogenation of the derived diacetate (**1***i*) in ethanol–triethylamine over 10% palladized charcoal afforded an acetate identical in all respects to that (**1***d*) previously prepared from A. A minor product from the hydrogenation was the tetrahydro derivative (**5***d*) of **1***d*. These experiments demonstrated that the sole difference in the two acids A and B lies in the nature of the function attached at C-4, in the

[4]This n.m.r. system is more fully discussed below under the heading stereochemistry.

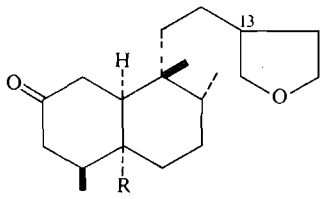

C-13 epimeric mixture

8

a R = CH_3
b R = CO_2Me

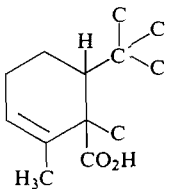

9

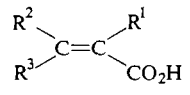

10

a $R^1 = R^3 = CH_3$; $R^2 = H$
b $R^2 = R^3 = CH_3$; $R^1 = H$
c $R^1 = R^2 = CH_3$; $R^3 = H$

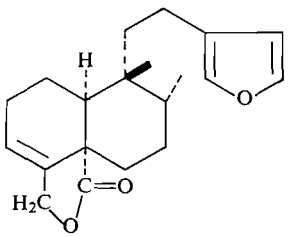

11

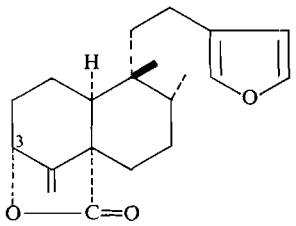

12

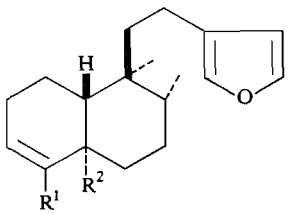

13

a $R^1 = CO_2H$; $R^2 = CH_3$
b $R^1 = CH_3$; $R^2 = CH_3$
c $R^1 = CH_3$; $R^2 = CH_2OH$
d $R^1 = CH_3$; $R^2 = CHO$

former this is a methyl group, in the latter, an allylic primary angelate ester.

Stereochemistry

The constitutions of acids A and B having been established with some certainty the major problem remaining involved the assignment of stereochemistry at the four asymmetric centers, C-5, -8, -9, and -10. At the outset, attempts were made to correlate **1***a* with hardwickiic acid (**13***a*, 3) in which rings A and B are *trans*-fused. With this intention, the furano-olefin (**1***f*) was prepared from acid A as described above and compared with the analogous compound (**13***b*, 4) from hardwickiic acid. Significant differences were observed in their n.m.r. spectra, for example in the chemical shifts of the resonances of the C-5, -8, and -9 methyl groups (τ 8.83, 9.08, and 8.92 respectively in the former and τ 9.00, 9.14, and 9.26 in the latter). If these two olefins have the same gross structure then they must differ in configuration at one or more centers. Indeed, results gradually accumulated which when taken *in toto* pointed unequivocally to the presence of the relatively rare *cis*-AB ring fusion[5] in acid A (**1***a*).

In this context, the first results which arrested our attention came from studies on the catalytic hydrogenation of **1***a*. Treatment with hydrogen in the presence of platinum oxide produced a mixture of products from which the two major constituents, the tetrahydroacids (**14***a* and *b*), were readily separated. The residue after methylation furnished two compounds (**15***a* and *b*) which had suffered hydrogenolytic cleavage of the furan ring. That these are epimers at C-13 rather than C-15/C-16 structural isomers follows (10) from the presence of an ill-resolved doublet ($w_{1/2}$ = 6 Hz) at τ 6.5 in the n.m.r. spectrum of both. The following aspects of this reaction were initially surprising. First, appreciable quantities of material in which the Δ^3 olefinic

[5]At the time the main bulk of this work was carried out only columbin (5) and its congeners were known to have this type of structure. Since then plathyterpol (6), tinophyllone (7), gutierolide (8), cistodiol, and the related diacid (9) have swollen this list.

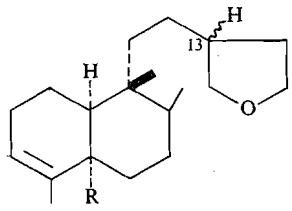

14

a R = CO_2H; 13*S*
b R = CO_2H; 13*R*
c R = CO_2Me; 13*S*
d R = CH_2OH; 13*S*
e R = CO_2Me; 13*R*

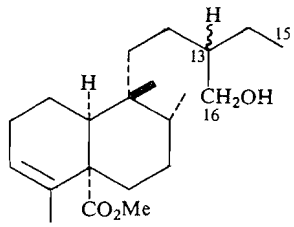

15

a 13*R*
b 13*S*

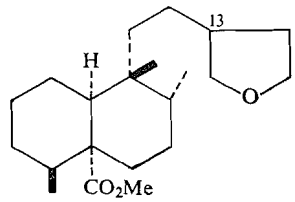

16 13*S*

bond had been saturated were absent. Indeed, the methyl ester **14***c* of the less polar tetrahydro acid (**14***a*) and **15***a* only very slowly gave products (**16** and **17**) of hydrogenation of the double bond under the same conditions. The unreactivity of the olefin in this reaction and towards osmium tetroxide, diborane, and *m*-chloroperbenzoic acid (see Experimental) contrasts with the behavior of related compounds (4, 11). The only configurational and conformational assignment for acid A which seemed to explain this situation is the *cis*-fused system **18***a* (or enantiomer) in which one face of the olefinic bond is shielded by the carboxyl group and the other by either the C-9 methyl or C-9 side chain. Second, **14***a* and *b* were very readily separated by chromatography even though they are simply C-13 epimers. This led us to suspect interaction of the tetrahydrofuran moiety with the carboxyl group in the less polar acid and this was confirmed spectroscopically. At high dilution **14***a* shows two strong carbonyl bands in the i.r. at 1729 (intramolecular hydrogen bond) and 1692 (dimer) cm^{-1} while **14***b* has only one band at 1692 and a weak shoulder at 1729 cm^{-1}. It appeared unlikely that a difference of configuration at C-13 could directly affect the conformations of rings A and/or B and lead to a difference in the tendencies of the carboxylic groups in **14***a* and *b* to hydrogen bond to the olefinic bond. Thus the peaks at 1729 cm^{-1} presumably result from hydrogen bonding of the carboxyl to the ethereal oxygen in the side chain. The ν(CO) is considerably lower than that predicted (12, 13) for species with the carboxylic hydroxyl involved in hydrogen bonding intramolecularly to an oxygen atom other than the carboxylic carbonyl. However, the value observed in the present case is very close to that obtained for ν(CO) when the i.r. spectra of **14***a* and *b* are recorded in carbon tetrachloride in the presence of tetrahydrofuran. In both only one band was observed (1724 cm^{-1}) and attributable to free —C(=O)—OH...O (of THF). By reference to molecular models it is apparent that if this interpretation is correct then the tetrahydroacids must have the relative stereochemistry shown in **14***a* (less polar) and *b* (more polar), the assignments at C-13 being tentative. The hydrogen bonding ring size is fairly large, in fact 11-membered. Presumably, substitution effects reduce the number of favorable conformations and facilitate intramolecular hydrogen bonding. The hydroxy esters **15***a* (less polar) and *b* (more polar) also showed evidence of interaction of the C-5 substituent and the functional group in the side chain. Their hydroxyl and carbonyl stretching absorptions provided firm i.r. evidence for the existence of strong intramolecular hydrogen bonds between the hydroxyl and methoxycarbonyl groups. Both have two bands attributable to free and bonded hydroxyl groups (the latter band being much more intense especially for **15***a*), $\Delta\nu_{OH}$ about 100 cm^{-1}, and peaks in the carbonyl region at 1725 and 1712 (less intense) cm^{-1}. This last absorption can be assigned to a conformer in which the hydroxyl is bonded to the ester carbonyl, a situation in which ν(CO) is known to decrease (13). However, to explain the relative intensities of the hydroxyl and carbonyl bands in even approximate terms the presence of a further hydrogen bonded species, —OH...O—C(=O)—, must be proposed. In this ν(CO) should be similar to that of

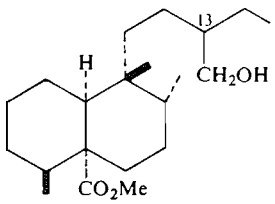

17 13*R*

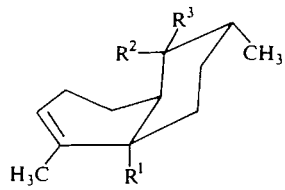

18

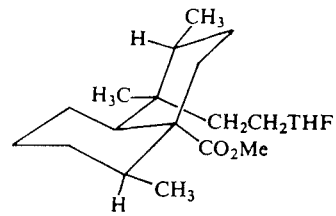

19

a $R^1 = CO_2H$; $R^2 + R^3 = CH_3 + CH_2CH_2Fu$
b $R^1 = CO_2Me$; $R^2 = CH_3$; $R^3 = CH_2CH_2THF$

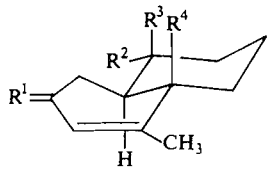

20

a $R^1 = O$

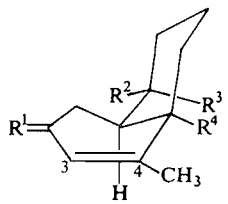

21

a $R^1 = O$
b $R^1 = O$; 3,4-dihydro

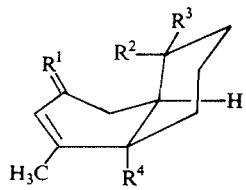

22

a $R^1 = O$
b $R^1 = H_2$

non-bonded conformers (13). The tentative assignment of relative stereochemistry at C-13 to **15***a* and *b* is again based on a study of molecular models. These results appeared to indicate clearly the presence in **1***a* of an A–B *cis*-ring fusion *and* a *cis*-relationship of the carboxyl and furanoethyl side chain.

Further results reinforced these stereochemical conclusions. The acid strength ($pK_{MCS}^* = 8.14$, (14)) of **1***a* corresponds (15) much more closely to that for an angular carboxyl group in a *cis*- rather than a *trans*-fused decalin system. In addition, the relative stereochemistry proposed above would explain the marked difference in reactivity of **14***c* and **16** towards lithium aluminum hydride. Thus in refluxing ether reduction of the former to **14***d* was complete in 4 h while under identical conditions the latter was essentially unchanged. Catalytic hydrogenation of **14***c* in conformation **18***b* would be expected to proceed on the face of the molecule remote from the shielding influence of the C-9 methyl group. The product (**16**) would be expected to flip into the other possible chair–chair conformation (**19**) because of the severe steric interaction between the C-4 and -9 methyl groups. In **18***b* the methoxycarbonyl group is relatively unencumbered and open to attack by lithium aluminum hydride, while in **19** this is not the case.

In the early stages of the investigation it was felt that the n.m.r. spin–spin coupling constants of H-10 to 2 H-1 in derivatives of acid A might serve to distinguish among the various possibilities of mode of A-B ring fusion and ring conformation. With respect to relative stereochemistry three *distinct*[6] possibilities exist, namely, a *trans*-fused decalin (**20**) or a *cis*-fused decalin in either conformation **21** or **22**. In the first two, H-10 is axial to ring A and should show one axial–axial and one axial–equatorial coupling. Recently, as mentioned above, it has been possible in one instance to discern the resonance due to H-10. When spectra of **1***c* were recorded in the presence of gradually increasing concentrations of tris(dipivalomethanato)europium a multiplet separated out downfield from the remaining methylene and methine resonances. In several of these it forms a well-defined, though broadened, triplet presumably because the 2 C-1 protons have become accidentally equivalent. The spacings (5 Hz) observed would then represent an average of the two true coupling constants. Nonetheless, this strongly indicates the stereochemical situation **22***b* for

[6]Related conformations with ring A in flattened chair, boat, or twist-boat conformations will be discussed where appropriate.

this compound, in accord with the conclusions reached above. Our original approach to determine the couplings of H-10 involved a study of the resonances arising from the C-1 protons. Readily available for this purpose was the enone **23**, which was formed from diol **1***h* by catalytic hydrogenation of the furan ring and then oxidation (16) with the Sarett reagent. In **23** the C-2 carbonyl effects a downfield shift of the resonances of the two C-1 protons, while the complicating signals of 2 H-12 are shifted upfield by saturation of the furan ring. In deuterobenzene–deuterochloroform (85:15) the C-1 protons are accidentally equivalent and resonate as a clean doublet (splitting 9 Hz) at τ 7.96 while in deuterobenzene alone they form a multiplet with three strong lines at about τ 8. Analysis of this as the AB part of an ABX system gave values for J_{AX} (3.75 Hz) and J_{BX} (14.25 Hz). The magnitude of these coupling constants revealed that the compound has either the *trans*-AB ring fusion or the *cis*-fusion in conformation **21***a*. Other results suggested choice of the latter, conformation **21***a* being preferred to **22***a* in this case probably because the constraint imposed by closure of the lactone ring is less in the former. To investigate the role, if any, of the lactone ring in determining the conformational preference in **23**, the n.m.r. spectra of the enones **6** and **7***a* were recorded for solutions in carbon tetrachloride, benzene, and various mixtures of these. By this means the resonances attributable to 2 H-1 were located for both. In each, the coupling constants of these two protons (A and B) to H-10 (X) were calculated as $J_{AX} = 8.25$ and $J_{BX} = 0.75$ Hz. These results clearly indicated that the compounds should not be formulated as **20***a* or **21***a*. Left for consideration are the ring A *classical* half-boat analogs of **20***a* and **21***a*, which might have coupling constants of this order of magnitude, and **22***a* or related half-boat or twist analogs. Of these, a situation close to **22***a*, but with ring A in a flattened half-boat, is considered to be the favored conformation[7] on the basis of three pieces of evidence. First, of the various possibilities described above this best explains (17) the magnitude of the coupling constants under discussion, the H-1 equatorial/H-10, H-1 axial/H-10 dihedral angles being *ca.* 75 and 45° respectively. Second, in this

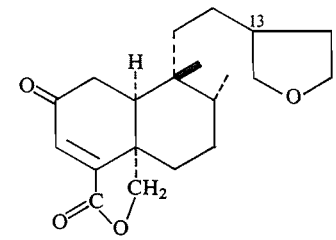

C-13 epimeric mixture

23

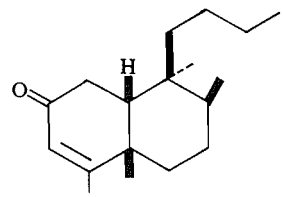

24

conformation the C-9 methyl group now protrudes over the olefinic bond and should be shielded by it (18). Indeed, in other compounds in this series, this methyl typically produces a resonance at about τ 8.95 but in these enones at about 9.15. Third, the magnitudes of the shifts induced by benzene on the C-4, -5, and -9 methyl groups of **6** and **7***a* accord with the values expected (19) for this conformation. At this stage the relative stereochemistry of acid A at C-5, -9, and -10 could be written with confidence as in **1***a*. Further support for this assignment came from a comparison of the n.m.r. spectrum of **6** with plathyterpenone (**24**) the constitution and relative stereochemistry of which have been rigidly defined (20). In either $CDCl_3$ or C_6D_6 the resonances attributed to 2 H-1, H-3, C-4 CH_3, C-5 CH_3, C-8 CH_3, and C-9 CH_3 are nearly identical in shape and value of chemical shift for both compounds.[8] On this basis the stereochemistry at C-8 is assigned as in **1***a*.

The absolute configuration of acids A and B remains for discussion. Since **6** and **24** appear to have the same relative stereochemistry and conformation of the ring system, a comparison was made of their Cotton effects. Both showed negative Cotton effects for the $n \rightarrow \pi^*$ transition, the former in c.d., the latter (20) in o.r.d., measurements. Thus plathyterpenone and acids

[7]This of course may represent an "average" of several contributing forms.

[8]We are grateful to Professor T. J. King for supplying the n.m.r. spectra and o.r.d. curve of plathyterpenone.

A and B have identical stereochemistry at C-5, -8, -9, and -10. The absolute configuration of plathyterpenone has been assigned (20) as in **24** on the basis of o.r.d. measurements. However, if the conformation deduced above for **6** on the basis of n.m.r. results is indeed preferred, then ring A is in a flattened boat and these compounds on the basis of their Cotton effects should be assigned (21) the *opposite* absolute configuration to that presently accepted for plathyterpenone. Since the deduction of absolute configurations from the Cotton effects of αβ-unsaturated ketones is known (21) to be fraught with difficulties, c.d. measurements were performed on **8***a* and *b*, prepared by catalytic hydrogenation of **7***a* and *b*. The relative stereochemistry at C-4 in **8***a* and *b* would be expected to be that shown, on the basis of their mode of formation and arguments analogous to those applied above to **16**.

Conformational analysis of these compounds appears to suggest that they should adopt conformation **21***b*. On this assumption and on the basis of the octant rule (22) the observed positive c.d. would lead to the assignment of absolute configuration *identical* to that published for plathyterpenone. However, precedent (23) warns that in *cis*-2-decalones related twist-forms although of minor abundance may play a decisive role in the Cotton effect. In the present instance a form of the type **25** might well

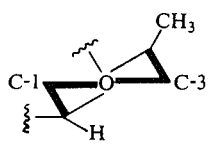

25

contribute to the conformational equilibrium and dictate the sign of the c.d., in which case the absolute configuration is *opposite* to that published for plathyterpenone. In a further attempt to resolve the problem, the two norenones **26** and **27** were prepared (16) by oxidation of **1***c* and maingayol (**13***c*, (14)), a compound of known absolute configuration, respectively. It seems probable that in both, C-10 would retain its original stereochemistry. The negative c.d. observed for **27** accords with that expected (24) for a ring B chair/ring A half-chair conformation, with C-9 pseudo-equatorial to the latter ring. The c.d. measured for **26** was opposite in sign and would appear to indicate that this compound and **27** have opposite configurations at C-10, if ring A has the same conformation in both. It appears unlikely that the difference in relative stereochemistry at C-8 could lead to marked changes in the conformation of ring A especially in the absence of a methyl group at C-10 (24). However, conclusions based on the above type of evidence for the absolute configuration of acids A and B, and by extension plathyterpol, can only be regarded as tentative although on balance it would appear that they should be formulated as shown in **1***a* and *b*.

At various stages in these studies, attempts were made to prepare heavy atom derivatives suitable for X-ray crystallographic examination, originally with the purpose of elucidating the relative stereochemistries, but more recently the absolute configuration. So far no suitable compounds have been obtained. Various heavy metal salts of acid A and the iodoacetate and *p*-iodobenzoate of **1***c* all failed to crystallize satisfactorily. Treatment of acid A with bromine in dioxan produced a complex mixture from which the bromofuran (**28***a*), dibromofuran (**28***b*), and butenolide (**29**) were isolated. The former two, although crystalline, again proved unsuitable for X-ray studies, in one case (**28***a*) because of poor crystalline form, in the other (**28***b*), because the data collected were insufficient and of poor quality.

Experimental

Melting points are uncorrected and were determined on a Kofler hot-stage apparatus. Specific rotations refer to solutions in ethanol unless otherwise stated. Woelm Grade I alumina, deactivated to the appropriate grade according to Brockmann, was used for chromatography. For analytical and preparative t.l.c., chromatoplates were spread with Kieselgel G (Merck). G.l.c. was carried out with a Varian Aerograph 1200 gas chromatograph using a stainless steel column (1/8 in. × 5 ft packed with 3% SE-30) and nitrogen as carrier gas with a flow rate of 25 ml/min except for angelic, senecioic, and tiglic acids. These were separated on a Pye "Argon" gas chromatograph at 125° with a gas flow rate of 60 ml/min using a glass column (1/8 in. × 4 ft) packed with 20% FFAP. Light petroleum was of b.p. 40–60°. Microanalyses were by Miss F. Cowan, Glasgow. High resolution mass spectra were run on an AEI MS 902 instrument equipped with a PDP 8 computer at the N.T.H., Trondheim by one of us (T.A.). I.r. solution spectra were recorded in carbon tetrachloride on a Unicam SP100 Mark II or Perkin–Elmer 225 or 257 or Beckman IR12 spectrophotometer, u.v. spectra in ethanol on a Unicam S.P. 800 spectrophotometer and circular dichroism curves on a Cary 61 spectropolarimeter. P.m.r. spectra were run on a Perkin–Elmer R-10 or Varian Associates A-60A or HA 100

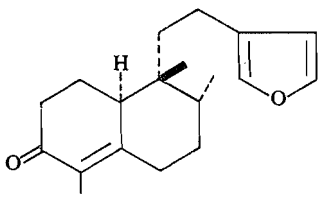

26

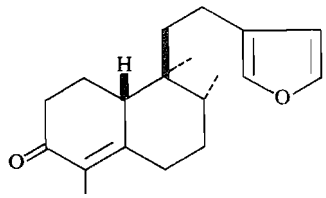

27

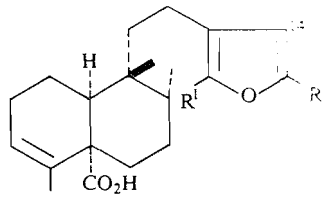

28

a R^1 = Br; R^2 = H
b R^1 = R^2 = Br

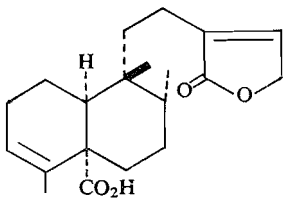

29

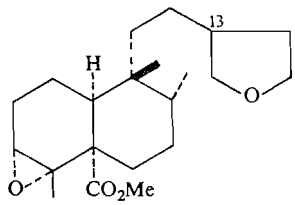

C-13 epimeric mixture

30

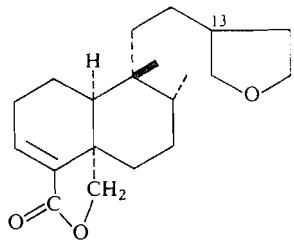

C-13 epimeric mixture

31

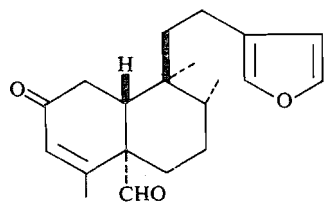

32

spectrometer in carbon tetrachloride, unless otherwise stated, using approximately 0.3 *M* solutions and tetramethylsilane as internal standard. Mass spectra were run on a Varian Associates CH7 or A.E.I. MS9 or MS12 instrument.

Isolation of Solidagoic Acids A and B

Finely ground, dried roots of *Solidago gigantea* var. *serotina* (500 g) were extracted for 24 h with ethyl acetate in a Soxhlet apparatus. Evaporation of the solvent afforded the crude extract (27 g) which on t.l.c. showed 11 major components when sprayed with the Ehrlich reagent. The chloroform soluble portion (24 g) of this extract was chromatographed over alumina (Grade III; neutral; 2 kg) using as eluting solvent light petroleum – chloroform mixtures. Non-acidic constituents were isolated from the various fractions (see Part V, ref. 16). After elution with chloroform–methanol (19:1) the acidic components were recovered with ethyl acetate – acetic acid (4:1). These were separated by column chromatography over silica gel. Elution with ether – light petroleum (1:9) afforded solidagoic acid A (**1***a*, 3.1 g) which crystallized as large plates from ethyl acetate – light petroleum and had m.p. 169–171°; $[\alpha]_D$ −58° (*c*, 0.9); ν_{max} 1743 (w) and 1695 (s) cm^{-1} (0.008 *M*); 1741 (vw), 1722 (s), and 1695 (m) cm^{-1} in presence of tetrahydrofuran (0.3 *M*); τ 4.45 (m, 1 H-3, $w_{1/2}$ = 11 Hz), 8.48 (s, 3 H-18), 9.02 (s, 3 H-20) and 9.11 (d, 3 H-17, *J* = 6 Hz); *m/e* 316 (M).

Anal. Calcd. for $C_{20}H_{28}O_3$: C, 75.91; H, 8.92. Found: C, 75.75; H, 8.58.

Elution with ether – light petroleum (1:4) afforded solidagoic acid B (**1***b*, 371 mg) which on crystallization from ethyl acetate – light petroleum formed needles, m.p. 134–135°; $[\alpha]_D$ −28° (*c*, 0.7; $CHCl_3$); ν_{max} 3600, 3100, 1720, 1695, 875 cm^{-1}; λ_{max} 221 nm (ε 6000); τ 3.96, 7.95–8.15 (1H and 6H respectively; angelate proton and methyl groups), 4.02 (m, 1 H-3), 5.50 (s, 2 H-18), 8.97 (s, 3 H-20) and 9.09 (d, 3 H-17, *J* = 6 Hz); *m/e* 314 (M − 100).

Anal. Calcd. for $C_{25}H_{34}O_5$: C, 72.43, H, 8.27. Found: C, 72.40, H, 8.55.

Methyl Esters of Acids A and B

The methyl esters were prepared by treatment of the acids in ether with ethereal diazomethane for 5 min. Ester A (**1***g*), an oil, after distillation at 100–105°/0.01 mm had $[\alpha]_D$ −67° (*c*, 1.0); ν_{max} 1728 and 878 cm^{-1}; τ 4.51 (m, 1 H-3, $w_{1/2}$ = 9 Hz), 6.47 (s, 3H, —OCH_3), 8.47 (broad s, 3 H-18), 8.97 (s, 3 H-20) and 9.10 (d, 3 H-17, *J* = 6 Hz).

Anal. Calcd. for $C_{21}H_{30}O_3$: C, 76.32; H, 9.15. Found: C, 76.60; H, 9.25.

The oily ester B (**1***j*), purified by preparative t.l.c. (ethyl acetate – light petroleum, 3:17) and then distillation at 110–120°/0.005 mm, had $[\alpha]_D$ −25° (*c*, 0.95; $CHCl_3$); ν_{max} 1728 cm^{-1}; τ 3.97 (m, angelate H), 4.09 (m, 1 H-3), 5.63 (s, 2 H-18), 6.52 (s, 3H, —O*CH*$_3$), 9.05 (s, 3 H-20) and 9.19 (d, 3 H-17, J = 6 Hz); *m/e* 428 (M).

Anal. Calcd. for $C_{26}H_{36}O_5$: C, 72.86; H, 8.47. Found: C, 73.32; H, 8.49.

Reduction of Methyl Ester with Lithium Aluminum Hydride

The methyl ester (**1***g*), (1.58 g) was treated in dry refluxing tetrahydrofuran (50 ml) with excess lithium aluminum hydride for 72 h. Work-up gave the crude alcohol (**1***c*, 1.50 g) which failed to crystallize and was distilled at 115–120°/0.01 mm. The resulting oil had $[\alpha]_D$ −38° (*c*, 1.0); ν_{max} 3630 and 875 cm^{-1}; τ 2.74, 2.82, 3.78 (all m, 1 H each, furan protons), 4.35 (m, 1 H-3), 6.47 (ABq, 2 H-19, J = 11 Hz), 8.33 (broad s, 3 H-18), 8.91 (s, 3 H-20) and 9.10 (d, 3 H-17, J = 6 Hz); with 0.21 *M* ratio of Eu(DPM)$_3$ to **1***c*, τ 1.55 (very broad ABq, 2 H-19, J = 11 Hz), 2.77, 2.90, 3.67 (all m, furan protons), 3.43 (m, 1 H-3), 5.4 (broadened t, 1 H-10, J_{obs} = 5 Hz), 7.32 (broad s, 3 H-18), 8.18 (s, 3 H-20), 8.44 (d, 3 H-17, J = 6 Hz).

Anal. Calcd. for $C_{20}H_{30}O_2$: C, 79.42; H, 10.00. Found: C, 79.57; H, 10.11.

The Acetate **1***d*

The alcohol (**1***c*, 50 mg) in dry pyridine (2 ml) was treated at 20° for 14 h with acetic anhydride (2 ml). The oily acetate obtained on work-up was purified by preparative t.l.c. (benzene) and then distillation *in vacuo*. It had $[\alpha]_D$ −60° (c, 0.8); ν_{max} 1740, 1235, 872 cm^{-1}; τ 4.26 (m, 1 H-3), 5.96 (q, 2 H-19, J = 12 Hz), 8.00 (s, 3 H, —OCO*CH*$_3$), 8.35 (broad s, 3 H-18), 8.91 (s, 3 H-20) and 9.10 (d, 3 H-17, J = 6 Hz); *m/e* 344 (M).

Anal. Calcd. for $C_{22}H_{32}O_3$: C, 76.70, H, 9.36. Found: C, 76.99; H, 9.54.

Decarboxylation of Acid A

Solidagoic acid A (**1***a*, 72 mg) was heated at 270° under N_2 for 20 min and the product distilled out at that temperature *in vacuo*. The resulting oil was redistilled at 110–120°/0.005 mm and afforded the furano–olefin **3** (45 mg) which had $[\alpha]_D$ −33° (*c*, 1.0); τ 8.35 (s, 3 H-18), 8.98 (d, 3 H-17, J = 6 Hz), and 9.1 (s, 3H-20); *m/e* 272 (M).

Anal. Calcd. for $C_{19}H_{28}O$: C, 83.77; H, 10.36. Found: C, 83.57; H, 10.19.

When the alcohol (**1***c*, 125 mg) was treated with excess chloroacetic anhydride in refluxing pyridine for 5 days and the mixture resulting from work-up separated by preparative t.l.c. (light petroleum – ethyl acetate, 19:1) this same furano-olefin (**3**, 24 mg) and substrate (43 mg) were obtained.

Oxidation of Alcohol **1***c*

The alcohol (**1***c*, 725 mg) in dry pyridine (10 ml) was treated at 20° for 14 h with chromium trioxide (800 mg). The crude material obtained (782 mg) consisted of three major components, which were separated by preparative t.l.c. (ethyl acetate – light petroleum, 1:9). The least polar component, the aldehyde (**1***e*) had $[\alpha]_D$ −161° (*c*, 0.85); ν_{max} 2690, 1722 and 872 cm^{-1}; τ 0.54 (s, 1 H-19), 4.28 (m, 1 H-3), 8.57 (d, 3 H-18, J = 2 Hz), 9.00 (s, 3 H-20) and 9.18 (d, 3 H-17, J = 6 Hz); *m/e* 300 (M).

Anal. Calcd. for $C_{20}H_{28}O_2$: C, 79.95; H, 9.39. Found: C, 79.90; H, 9.38.

The compound of intermediate polarity, the nor-enone (**26**, 35 mg) was obtained as an oil and after distillation (160°/0.02 mm) had $[\alpha]_D$ −100° (*c*, 0.7); ν_{max} 1675 and 872 cm^{-1}; λ_{max} (ethanol) 257 nm (ε 13 000); λ_{max} (chloroform) 252 nm (ε 14 500); c.d. (ethanol) $[\theta]_{314}$ +8000 and $[\theta]_{257}$ −37 000; c.d. (chloroform) $[\theta]_{326}$ +7000 and $[\theta]_{250}$ −39 000; τ 8.27 (d, 3 H-18, J = 2 Hz), 8.90 (d, 3 H-17, J = 7 Hz) and 9.06 (s, 3 H-20); *m/e* 286 (M).

Anal. Calcd. for $C_{19}H_{26}O_2$: C, 79.68; H, 9.15. Found: C, 79.58; H, 9.15.

The most polar of the major components was the aldehydo-enone (**7***c*, 25 mg) which was purified further by distillation at 140°/0.03 mm. It had $[\alpha]_D$ −197° (*c*, 0.86); ν_{max} 2700, 1730, 1680 and 873 cm^{-1}; λ_{max} 243 nm (ε 7000); τ 0.43 (s, 1 H-19), 4.09 (s, 1 H-3), 8.29 (s, 3 H-18), 9.04 (s, 3 H-20), and 9.16 (d, 3 H-17, J = 6 Hz); *m/e* 314 (M).

Anal. Calcd. for $C_{20}H_{26}O_3$: C, 76.40; H, 8.34. Found: C, 76.48; H, 8.40.

*Catalytic Hydrogenation of Methyl Ester A (***1***g)*

Methyl ester A (**1***g*, 380 mg) in absolute ethanol (40 ml) was hydrogenated for 25 min over Adams catalyst (200 mg). Removal of the catalyst and solvent afforded an oil (390 mg) consisting (t.l.c.) of one major and several minor components. Separation of these by preparative t.l.c. (ethyl acetate – light petroleum, 1:3) afforded the oily tetrahydro-methyl ester (**5***c*, mixture of epimers at C-13, 215 mg) which was further purified for analysis by distillation at 130°/0.04 mm. It had ν_{max} 1728 cm^{-1}; τ 4.56 (m, 1 H-3) and 6.33 (s, 3H, —O*CH*$_3$).

Anal. Calcd. for $C_{21}H_{34}O_3$: C, 75.40; H, 10.25. Found: C, 75.62; H, 10.47.

The Alcohol **5***e*

Reduction of the tetrahydro-methyl ester (**5***c*, 60 mg) with excess lithium aluminum hydride in refluxing ether for 14 h and work-up afforded the oily alcohol (**5***e*, 57 mg) which after distillation at 140°/0.02 mm had $[\alpha]_D$ −16° (*c*, 1.2, $CHCl_3$); τ 4.42 (m, 1 H-3), 6.56 (q, 2 H-19, J = 12 Hz), 8.36 (broad s, 3 H-18), 8.99 (s, 3 H-20) and 9.14 (d, 3 H-17, J = 6 Hz).

Anal. Calcd. for $C_{20}H_{34}O_2$: C, 78.38; H, 11.18. Found: C, 78.52; H, 11.28.

The Aldehyde **5***a*

The above alcohol (**5***e*, 23 mg) in dry pyridine (2 ml) was treated at 20° for 15 h with chromium trioxide (100 mg). Work-up and preparative t.l.c. (ethyl acetate – light petroleum, 1:4) of the product yielded the aldehyde (**5***a*, 17 mg). Distillation *in vacuo* afforded a colorless oil, $[\alpha]_D$ −88° (*c*, 1.2, $CHCl_3$); ν_{max} 1723 cm^{-1}; τ 0.76 (d, 1 H-19, separation 2 Hz) and 4.36 (m, 1 H-3); *m/e* 304 (M).

Anal. Calcd. for $C_{20}H_{32}O_2$: C, 78.89; H, 10.59. Found: C, 78.92; H, 11.05.

Huang–Minlon Reduction of Aldehydes **1***e and* **5***a*

Aldehyde **1***e* (50 mg) in ethylene glycol (2 ml) was treated at 95° for 48 h with 100% hydrazine hydrate (3 ml).

Potassium hydroxide (100 mg) was added and the temperature of the mixture allowed to rise to 210° and remain there for 13 h under N_2. After cooling, the solution was acidified and then extracted with ethyl acetate. The product was purified by preparative t.l.c. (ethyl acetate – light petroleum, 1:9) and distillation. The resulting furano-olefin (**1***f*, 24 mg) was obtained as an oil and had $[\alpha]_D$ −19° (*c*, 1.0); ν_{max} 872 cm^{-1}; τ 4.67 (m, 1 H-3), 8.36 (broad s, 3 H-18), 8.83 (s, 3 H-19), 8.92 (s, 3 H-20) and 9.08 (d, 3 H-17, J = 6 Hz); *m/e* 286 (M).

Anal. Calcd. for $C_{20}H_{30}O$: C, 83.86; H, 10.56. Found: C, 83.82; H, 10.75.

An identical procedure converted **5***a* (125 mg) into the oily tetrahydrofuran (**5***b*, 58 mg) which had τ (deuterochloroform) 4.70 (m, 1 H-3), 8.36 (broad s, 3 H-18), 8.85 (s, 3 H-19), 9.00 (s, 3 H-20), 9.14 (d, 3 H-17, J = 6 Hz).

Mol. Wt. Calcd. for $C_{20}H_{34}O$: 290.2610. Found: (high resolution mass spectrometry): 290.2609.

Oxidation of the Furano-olefin (1f) with the Chromium Trioxide – Pyridine Complex

The furano-olefin (**1***f*, 68 mg) in pyridine (4 ml) was added to chromium trioxide (75 mg) in pyridine (1 ml), and stirred at 20° for 18 days. The resulting mixture was treated with ethanol (1 ml) for 15 min and then diluted with water (20 ml). Extraction with ethyl acetate, followed by preparative t.l.c. (ethyl acetate – light petroleum) afforded, in addition to unreacted **1***f* (26 mg), the enone **6** (17 mg) which was distilled at 175°/0.2 mm. The resulting low melting solid had ν_{max} 1665 cm^{-1}; λ_{max} 247 nm (ε 7500); τ (carbon tetrachloride) 4.21 (broad s, 1 H-3, $w_{1/2}$ = 4 Hz), 7.45 (3 lines, 2 H-1), 8.05 (d, 3 H-18, J = 1 Hz), 8.73 (s, 3 H-19), 8.98 (d, 3 H-17, J = 7 Hz), and 9.10 (s, 3 H-20); τ (benzene) 4.10 (broad s, 1 H-3), 7.45 (d, 2 H-1, J_{obs} = 4.5 Hz), 8.49 (d, 3 H-18, J = 1 Hz), 9.12 (s, 3 H-19), 8.19 (s, 3 H-20) and 9.25 (d, 3 H-17, J = 7 Hz); c.d. (ethanol) $[\theta]_{328}$ −3000 and $[\theta]_{247}$ +2000; c.d. (chloroform) $[\theta]_{335}$ −2300.

Mol. Wt. Calcd. for $C_{20}H_{28}O_2$: 300.2089. Found (high resolution mass spectrometry): 300.2094.

Oxidation of the Ester (5c) with Chromium Trioxide – Acetic Acid

Chromium trioxide (195 mg) was added to the ester (**5***c*, 252 mg) in acetic acid (20 ml) and water (1 ml). After stirring at 20° for 1 h, ethanol (50 ml) was added and then the solvent removed *in vacuo*. The residue was dissolved in ether–brine and the ether layer washed with saturated aqueous bicarbonate and brine. Evaporation of the solvent gave an oil (265 mg). The two major constituents of this complex mixture were separated by preparative t.l.c. (ethyl acetate – light petroleum, 1:1). The less polar constituent, the epoxy-ester (**30**, 54 mg) was further purified by preparative t.l.c. (ethyl acetate – chloroform, 1:10) and then distillation *in vacuo*. It had ν_{max} (liquid film) 1720 cm^{-1}; τ 6.37 (s, 3H, $-OCH_3$), 7.06 (m, 1 H-3, $w_{1/2}$ = 4 Hz), 8.97 (s, 3 H-18), 9.21 (s, 3 H-20) and 9.22 (d, 3 H-17, J = 6 Hz).

Mol. Wt. Calcd. for $C_{21}H_{34}O_4$: 350.2457. Found (high resolution mass spectrometry): 350.2456.

The more polar component, the enone-ester (**7***b*, 43 mg) was isolated as an oil and gave one peak on g.l.c. (250°, retention time 6 min). After distillation *in vacuo* it had ν_{max} (liquid film) 1725 and 1670 cm^{-1}; λ_{max} 237 nm; τ 4.24 (broad s, 1 H-3, $w_{1/2}$ = 2.5 Hz), 6.30 (s, 3H, $-OCH_3$), 8.27 (d, 3 H-18, J = 1.5 Hz), 9.11 (s, 3 H-20), and 9.13 (d, 3 H-17, J = 7 Hz).

Mol. Wt. Calcd. for $C_{21}H_{32}O_4$: 348.2301. Found (high resolution mass spectrometry): 348.2303.

Oxidation of the Olefin 5b with Chromium Trioxide – Acetic Acid

Oxidation of the tetrahydrofurano-olefin (**5***b*, 275 mg) with chromium trioxide (275 mg) in acetic acid (20 ml) and water (1 ml) as above afforded an oil (200 mg). Separation of the very complex mixture by preparative t.l.c. (ethyl acetate – light petroleum, 1:3, run thrice) furnished the oily enone (**7***a*, 29 mg) which gave one peak on g.l.c. (230°, retention time 7 min) and after distillation *in vacuo* had ν_{max} 246 nm (ε 8500); τ (carbon tetrachloride) 4.20 (broad s, 1 H-3, $w_{1/2}$ = 3 Hz), 7.46 (3 lines, 2 H-1), 8.06 (d, 3 H-18, J = 1.5 Hz), 8.72 (s, 3 H-19), 9.04 (d, 3 H-17, J = 6.5 Hz) and τ 9.17 (s, 3 H-20); τ (carbon tetrachloride – benzene, 1:1) 7.50 (d, 2 H-1, J_{obs} = 4.5 Hz), 8.34 (d, 3 H-18, J = 1.5 Hz), 8.97 (s, 3 H-19), 9.22 (d, 3 H-17, J = 7 Hz), and 9.24 (s, 3 H-20).

Mol. Wt. Calcd. for $C_{20}H_{32}O_2$: 304.2402. Found (high resolution mass spectrometry): 304.2404.

The Keto-ester 8b

The enone-ester (**7***b*, 63 mg) in 95% ethanol (50 ml) was shaken in a low pressure hydrogenator with hydrogen (33 p.s.i.) over palladized charcoal (5%, 80 mg) for 5 h. Removal of catalyst and solvent left an oil which was submitted to preparative t.l.c. (ethyl acetate – light petroleum, 1:3, run four times). The major, and least polar, component of the mixture was the oily keto-ester (**8***b*, 24 mg) which gave one peak on g.l.c. (250°, retention time 5.3 min) and had ν_{max} 1735 cm^{-1}; τ 6.35 (s, 3H, $-OCH_3$) and 9.20 (broad s, 9H, $3CH_3$); c.d. (ethanol) $[\theta]_{305}$ −45 and $[\theta]_{273}$ +190.

Mol. Wt. Calcd. for $C_{21}H_{34}O_4$: 350.2457. Found (high resolution mass spectrometry): 350.2459.

The Ketone 8a

Hydrogenation of the enone (**7***a*, 43 mg) as described immediately above afforded an oil which showed one major product on t.l.c. Preparative t.l.c. (ethyl acetate – light petroleum, 1:10) afforded the ketone (**8***a*, 22 mg) as an oil, which showed one peak on g.l.c. (230°, retention time 7 min) and had ν_{max} 1720 cm^{-1} (liquid film 1715 cm^{-1}); τ (carbon tetrachloride) 8.78 (s, 3 H-19), 9.03 (d, 3 H-18, J = 7 Hz), 9.10 (s, 3 H-20), and 9.13 (d, 3 H-17, J = 6 Hz); τ (benzene – carbon tetrachloride, 1:1) 8.99 (s, 3 H-19), 9.25 (d, 3 H-18, J = 7 Hz), 9.29 (d, 3 H-17, J = 6 Hz) and 9.30 (s, 3 H-20); c.d. (ethanol) $[\theta]_{283}$ +375.

Mol. Wt. Calcd. for $C_{20}H_{34}O_2$: 306.2559. Found (high resolution mass spectrometry): 306.2557.

Pyrolysis of Acid B (1b)

Acid B (**1***b*, 75 mg) was heated at 300° for 5 min in an evacuated tube. A few crystals of angelic acid, m.p. 45° (sealed tube), collected on a cooled part of the tube. This material was identified by g.l.c. over 20% FFAP at 125°, angelic, senecioic, and tiglic acids being well separated under these conditions, having retention times of 26, 28, and 35 min respectively. The less volatile distillate (49 mg) consisted (t.l.c.) of two products and starting material. The unreacted acid B was removed by filtration through

a short column of neutral alumina and the products were then separated by preparative t.l.c. (ethyl acetate – light petroleum, 1:19). The more abundant lactone (**11**, 20 mg) after distillation *in vacuo* had $[\alpha]_D$ −66° (*c*, 1.4); ν_{max} 1778 and 872 cm^{-1}; τ 4.41 (m, 1 H-3), 5.45 (ABq, 2 H-18, J = 12 Hz), 8.96 (s, 3 H-20), and 9.13 (d, 3 H-17, J = 6 Hz).

Anal. Calcd. for $C_{20}H_{26}O_3$: C, 76.40, H, 8.34. Found: C, 76.34; H, 8.48.

The more polar lactone (**12**, 6 mg) crystallized from ethyl acetate – light petroleum and had m.p. 145–147°; ν_{max} 1785 cm^{-1}; *m/e* 314 (M).

*The Diol **1h***

Reduction of methyl ester B (**1***j*, 200 mg) in refluxing ether with lithium aluminum hydride gave the diol (**1***h*, 180 mg) which crystallized from ethyl acetate – light petroleum and had m.p. 61–62°; $[\alpha]_D$ −46° (*c*, 0.7); ν_{max} 3620, 3300, and 875 cm^{-1}; τ 4.11 (m, 1 H-3), 8.96 (s, 3 H-20), and 9.11 (d, 3 H-17, J = 6 Hz); *m/e* 318 (M).

Anal. Calcd. for $C_{20}H_{30}O_3$: C, 75.43; H, 9.50. Found: C, 75.26; H, 9.30.

*Acetylation of Diol **1h***

The diol (**1***h*, 960 mg) in dry pyridine (20 ml) was treated with acetic anhydride (0.35 ml) at 20° for 2 h. Work-up afforded an oil (975 mg) which was separated into its components by preparative t.l.c. (ethyl acetate – light petroleum, 3:7). The least polar component (320 mg) was the oily diacetate (**1***i*) which after distillation *in vacuo* had $[\alpha]_D$ −44° (*c*, 1.7); ν_{max} 1745, 1238, and 875 cm^{-1}; τ 4.06 (m, 1 H-3), 5.43 (s, 2 H-18), 6.01 (s, 2 H-19), 7.98 (s, 6H, 2 —OCOCH_3), 8.93 (s, 3 H-20) and 9.08 (d, 3 H-17, J = 6 Hz); *m/e* 402 (M).

Anal. Calcd. for $C_{24}H_{34}O_5$: C, 71.61; H, 8.51. Found: C, 71.58; H, 8.72.

The next component, the monoacetate (**1***k*, 175 mg), was also an oil. After distillation at 120°/0.01 mm it had $[\alpha]_D$ −54° (*c*, 0.8); ν_{max} 3460, 1740, 1220, and 872 cm^{-1}; τ 4.08 (m, 1 H-3), 5.53 (q, 2 H-18, J = 12 Hz), 6.49 (q, 2 H-19; J = 12 Hz), 8.00 (s, 3H, —OCOCH_3), 8.94 (s, 3 H-20), and 9.12 (d, 3 H-17, J = 6 Hz).

Anal. Calcd. for $C_{22}H_{32}O_4$: C, 73.30; H, 8.95. Found: C, 73.20; H, 8.82.

The next component, the oily monoacetate **1***l* (170 mg), after distillation at 150°/0.01 mm had ν_{max} 3580, 1745, 1230, and 878 cm^{-1}; τ 4.12 (m, 1 H-3), 5.50 (s, 2 H-18), 6.06 (s, 2 H-19), 8.03 (s, 3H, —OCOCH_3), 8.92 (s, 3 H-20) and 9.16 (d, 3 H-17, J = 6 Hz).

Anal. Calcd. for $C_{22}H_{32}O_4$: C, 73.30; H, 8.95. Found: C, 73.32; H, 8.73.

The final component was unreacted diol (**1***h*, 102 mg).

*Hydrogenolysis of Diacetate **1i***

The diacetate **1***i* (60 mg) was hydrogenated in absolute ethanol (30 ml) containing triethylamine (5 ml) over 10% palladized charcoal for 40 min. Removal of catalyst and solvent afforded an oil which consisted (t.l.c.) essentially of two compounds. These were separated by preparative t.l.c. (benzene). The less polar product was the acetate **1***d* (37 mg), identical (i.r., n.m.r., t.l.c., and $[\alpha]_D$) with the acetate prepared from acid A. The other product, the corresponding tetrahydro-acetate (**5***d*, 14 mg) after distillation at 150°/0.04 mm had $[\alpha]_D$ +28° (*c*, 1.2); ν_{max} 1740 and 1235 cm^{-1}; τ 4.50 (m, 1 H-3), 6.05 (s, 2 H-19), 8.01 (s, 3H, —OCOCH_3), 8.36 (broad s, 3 H-18), 8.97 (s, 3 H-20), and 9.12 (d, 3 H-17, J = 6 Hz).

Anal. Calcd. for $C_{22}H_{36}O_3$: C, 75.81; H, 10.41. Found: C, 75.86; H, 10.20.

*Hydrogenation of Acid A (**1a**)*

Acid A (403 mg) in absolute ethanol (20 ml) was shaken with hydrogen over Adams catalyst for 2.5 h. The product (427 mg) was submitted to preparative t.l.c. (chloroform, run thrice) and split into three fractions. The least polar fraction (73 mg) contained the oily tetrahydro-acid **14***a* which distilled at 165–170°/0.02 mm and had ν_{max} 1729 and 1692 cm^{-1} (0.008 *M*); 1724 cm^{-1} in presence of tetrahydrofuran (0.95 *M*); τ 4.58 (m, 1 H-3), 8.47 (broad s, 3 H-18), 9.12 (s, 3 H-20), and 9.20 (broad s, 3 H-17).

Anal. Calcd. for $C_{20}H_{32}O_3$: C, 74.96; H, 10.06. Found: C, 74.75; H, 9.88.

The fraction (148 mg) of intermediate polarity contained the tetrahydro-acid **14***b* which after sublimation at 155–165°/0.04 mm had m.p. 156–159°; ν_{max} 1692 and weak shoulder at 1729 cm^{-1} (0.007 *M*); 1724 cm^{-1} in presence of tetrahydrofuran (0.5 *M*); τ 4.58 (m, 1 H-3), 8.47 (broad s, 3 H-18), and 9.12 (broad s, 6H, 2CH_3).

Anal. Calcd for $C_{20}H_{32}O_3$: C, 74.96; H, 10.06. Found: C, 74.89; H, 10.14.

The final fraction (85 mg) ran as two poorly-resolved spots on t.l.c. (methanol–chloroform 1:9). The mixture was treated with diazomethane and the derived esters separated by preparative t.l.c. (chloroform, run twice). The less polar methyl ester (**15***a*, 52 mg) after distillation at 117–122°/0.05 mm was obtained as an oil ν_{max} 3642, 3554, 1725, and 1712 cm^{-1}; τ 4.58 (m, 1 H-3), 6.33 (s, 3H, —OCH_3), 6.55 (m, 2 H-16, $w_{1/2}$ = 6 Hz), 9.12 (s, 3 H-20) and 9.16 (d, 3 H-17, J = 6 Hz).

Anal. Calcd. for $C_{21}H_{36}O_3$: C, 74.95; H, 10.78. Found: C, 74.79; H, 10.71.

The more polar methyl ester (**15***b*, 15 mg) also was obtained as an oil and after distillation at 125–130°/0.04 mm it had ν_{max} 3644, 3544, 1725, and 1712 cm^{-1}; τ 4.58 (m, 1 H-3), 6.30 (s, 3H, —OCH_3) 6.55 (m, 2 H-16, $w_{1/2}$ = 6 Hz), and 9.15 (broad s, 6H, 2CH_3).

Anal. Calcd. for $C_{21}H_{36}O_3$: C, 74.95; H, 10.78. Found: C, 74.81; H, 10.85.

*Methyl Esters **14c** and **e***

The tetrahydro-acids (**14***a* and *b*) were treated with diazomethane and furnished the corresponding methyl esters. The ester (**14***c*) of the less polar acid (**14***a*) was distilled at 107–113°/0.06 mm. The oil obtained had ν_{max} 1728 cm^{-1}; τ 4.56 (m, 1 H-3), 6.33 (s, 3H, —OCH_3), 9.12 (s, 3 H-20), and 9.23 (d, 3 H-17, J = 6 Hz).

Anal. Calcd. for $C_{21}H_{34}O_3$: C, 75.40; H, 10.25. Found: C, 75.60; H, 10.44.

The ester (**14***e*) of the more polar acid (**14***b*) was also obtained as an oil. After distillation at 110–115°/0.02 mm it had ν_{max} 1728 cm^{-1}; τ 4.56 (m, 1 H-3), 6.32 (s, 3H, —OCH_3), 9.12 (s, 3 H-20), and 9.20 (d, 3 H-17, J = 6 Hz).

Anal. Calcd. for $C_{21}H_{34}O_3$: C, 75.40; H, 10.25. Found: C, 75.31; H, 10.27.

A mixture of **14***c* and *e* ran as one spot on t.l.c. in all eluent mixtures examined.

*The Esters **16** and **17***

Ester **14***c* (70 mg) in absolute ethanol (20 ml) was shaken with hydrogen over Adams catalyst (80 mg) for

28 h. Removal of catalyst and solvent left an oil which was subjected to preparative t.l.c. (ethyl acetate – light petroleum, 1:9, run twice). The less polar major constituent was the oily hexahydro-ester **16** (25 mg) which after distillation at 115–120°/0.1 mm had ν_{max} 1722 cm^{-1}; 6.36 (s, 3H, —OCH_3), 9.18 (s, 6H, 2CH_3), and 9.38 (d, 3H, CH_3, J = 6 Hz).

Anal. Calcd. for $C_{21}H_{36}O_3$: C, 74.95; H, 10.78. Found: C, 75.17; H, 10.77.

The more polar constituent was unreacted **14***c* (34 mg).

Hydroxy-ester **15***a* (23 mg) in absolute ethanol (10 ml) was shaken with hydrogen over Adams catalyst (50 ml) for 24 h. The residual oil after removal of catalyst and solvent was separated into its two major constituents by preparative t.l.c. (ethyl acetate – light petroleum, 1:9, run thrice). The less polar constituent, **17** (9 mg), was distilled at 105–112°/0.005 mm and the resulting oil had ν_{max} 3630, 3520, 1722, and 1710 cm^{-1}; τ 6.37 (s, 3H, —OCH_3), 6.50 (m, 2 H-16, $w_{1/2}$ = 6 Hz), 9.18 (s, 6H, 2CH_3), and 9.38 (d, 3H, CH_3, J = 6 Hz).

Anal. Calcd. for $C_{21}H_{38}O_3$: C, 74.51; H, 11.32. Found: C, 74.79; H, 11.26.

The more polar constituent was unreacted **15***a* (7 mg).

Attempted Hydroxylation, Hydroboration, Epoxidation of ***1a***, ***1d***, ***1g***

Acid A (**1***a*), its methyl ester (**1***g*), and the derived acetate (**1***d*) were recovered from treatment with (*a*) osmium tetroxide in ether for 20 h, (*b*) freshly distilled boron trifluoride etherate and lithium aluminum hydride for 2 h and then work-up with sodium hydroxide – hydrogen peroxide, (*c*) *m*-chloroperbenzoic acid in chloroform for 90 min. In each case extended reaction times led to destruction of the furan ring (n.m.r.).

Reduction of Ester ***14c***

The tetrahydro-ester (**14***c*, 113 mg) in dry refluxing ether was treated with excess lithium aluminum hydride for 4.5 h. Work-up gave the alcohol (**14***d*, 88 mg) as an oil which distilled at 120°/0.01 mm and was nearly identical (t.l.c., $[\alpha]_D$ and n.m.r.) with **5***e*.

The hexahydro-ester (**16**, 12 mg) was recovered essentially unchanged (n.m.r., t.l.c.) from attempted reduction with lithium aluminum hydride as above for 4 h.

Hydrogenation of Diol ***1h***

The diol (**1***h*, 325 mg) in absolute ethanol (35 ml) was hydrogenated over Adams catalyst (300 mg) for 2 h. Removal of catalyst and solvent afforded an oil (320 mg) which was seen from t.l.c. to consist of a complex mixture of compounds none of which contained a furan ring (Ehrlich's test). The major component, the tetrahydro-diol (**5***f*, 175 mg) was obtained by preparative t.l.c. (chloroform–methanol, 17:1). Distillation at 180°/0.035 mm gave an oil, $[\alpha]_D$ −47° (*c*, 0.77); ν_{max} 3620 and 3320 cm^{-1}; τ 4.22 (m, 1 H-3), 9.07 (s, 3 H-20), and 9.18 (d, 3 H-17, J = 6 Hz).

Anal. Calcd. for $C_{20}H_{34}O_3$: C, 74.49; H, 10.63. Found: C, 74.20; H, 10.80.

The corresponding diacetate (**5***g*) was also obtained as an oil by treatment of the diol with acetic anhydride – pyridine. After distillation at 175°/0.04 mm it had ν_{max} 1745 and 1235 cm^{-1}; τ 4.11 (m, 1 H-3), 5.49 (s, 2 H-18), 6.06 (s, 2 H-19), 8.00 (s, 6H, 2 —OCOCH_3), 8.99 (s, 3 H-20) and 9.10 (d, 3 H-17, J = 6 Hz).

Anal. Calcd. for $C_{24}H_{38}O_5$: C, 70.90; H, 9.42. Found: C, 70.66; H, 9.51.

Oxidation of Tetrahydro-diol ***5f***

The tetrahydro-diol (**5***f*, 102 mg) in dry pyridine (2 ml) was treated with chromium trioxide (500 mg) at 20° for 14 h. The products (98 mg) were separated by preparative t.l.c. (ethyl acetate – light petroleum, 3:17, run four times). Two major components were obtained. The less polar was the lactone **31** (27 mg) which on distillation at 155°/0.015 mm afforded an oil, $[\alpha]_D$ +26° (*c*, 1.1), ν_{max} 1775 cm^{-1}; τ 3.41 (t, 1 H-3, J_{obs} = 3 Hz), 9.11 (s, 3 H-20), and 9.18 (d, 3 H-17, J = 6 Hz).

Anal. Calcd. for $C_{20}H_{30}O_3$: C, 75.43; H, 9.50. Found: C, 75.67; H, 9.47.

The more polar component, the oily enone-lactone **23** (43 mg), was distilled *in vacuo* and had $[\alpha]_D$ −4° (*c*, 0.9); ν_{max} 1783 and 1694 cm^{-1}; τ (carbon tetrachloride) 3.64 (s, 1 H-3), 5.57 (d, 1 H-19, J = 8 Hz), 6.12 (d, 1 H-19, J = 8 Hz), 7.72 (m, 2 H-1), 9.16 (s, 3 H-20), and 9.18 (d, 3 H-17, J = 6 Hz); τ (deuterobenzene–deuterochloroform, 85:15), 3.40 (s, 1 H-3), 5.58 (4 lines, 1 H-19), 6.61 (d, 1 H-19, J = 8 Hz), 7.92 and 8.02 (2 lines, 2 H-1), 9.48 (d, 3 H-17, J = 6 Hz), 9.62 (s, 3 H-20); τ (deuterobenzene) 3.36 (s, 1 H-3), 6.01 (4 lines, 1 H-19), 6.65 (d, 1 H-19, J = 8 Hz), 7.94, 8.02, and 8.05 (3 lines, 2 H-1), 9.50 (d, 3 H-17, J = 6 Hz), and 9.67 (s, 3 H-20); *m/e* 332 (M).

Anal. Calcd. for $C_{20}H_{28}O_4$: C, 72.26; H, 8.49. Found: C, 72.03; H, 8.28.

*Oxidation of Maingayic Alcohol (****13c****)*

The alcohol[9] (**13***c*, 193 mg) in pyridine (10 ml) was added to chromium trioxide (415 mg) in pyridine (8 ml) and kept at 20° with stirring for 5 h. The resulting mixture was treated with methanol (1 ml) for 30 min and then diluted with water (20 ml). Extraction with ethyl acetate, followed by preparative t.l.c. (ethyl acetate – light petroleum, 1:7) afforded three compounds, described below in order of increasing polarity. The known (14) aldehyde (**13***d*, 108 mg) was obtained as an oil. The nor-enone (**27**, 25 mg), also an oil, was distilled *in vacuo* and had ν_{max} 1678 cm^{-1}; λ_{max} (ethanol) 257 nm (ε 13 000); c.d. (ethanol) $[\theta]_{314}$ −12 000 and $[\theta]_{257}$ +37 000; c.d. (chloroform) $[\theta]_{325}$ −9000 and $[\theta]_{250}$ +42 000; τ 8.22 (s, 3 H-18) 9.07 (d, 3 H-17, J = 6 Hz), and 9.33 (s, 3 H-20).

Mol. Wt. Calcd. for $C_{19}H_{26}O_2$: 286.1933. Found (high resolution mass spectrometry): 286.1931.

The aldehydo-enone (**32**, 17 mg), also an oil, was distilled *in vacuo* and had ν_{max} 1715 and 1675 cm^{-1}; λ_{max} 244 nm (ε 9500); τ 0.40 (s, 1 H-19), 3.98 (broad s, 1 H-3, $w_{1/2}$ = 2.5 Hz), 8.29 (d, 3 H-18, J = 1 Hz), 9.13 (d, 3 H-17, J = 6 Hz), and 9.27 (s, 3 H-20).

Mol. Wt. Calcd. for $C_{20}H_{26}O_3$: 314.1882. Found (high resolution mass spectrometry): 314.1880.

*Bromination of Acid A (****1a****)*

Acid A (**1***a*, 355 mg) was treated with bromine (0.15 ml) in dioxan (15 ml) at 0° for 3 h. Work-up afforded an oil which was subjected to preparative t.l.c. (light petroleum – ether, 1:3). By this means ten fractions were

[9]Kindly supplied by Dr. K. Kawazu, Okayama University, Japan.

obtained. The three major components were investigated (from bands 2, 3, and 7, numbered in order of increasing polarity). The least polar component of the three, the dibromide (**28***b*, 35 mg), on crystallization from ethyl acetate – light petroleum had m.p. 170–174° (dec.); τ 3.82 (s, 1 H-14), 4.50 (m, 1 H-3), 8.48 (broad s, 3 H-18), 8.98 (s, 3 H-20), and 9.12 (d, 3 H-17, $J = 6$ Hz); *m/e* 472, 474, 476 (M). The component of intermediate polarity, the monobromide (**28***a*, 14 mg), on crystallization from ethyl acetate – light petroleum had m.p. 173–178° (dec.); τ 2.78 (d, 1 H-15, $J = 2$ Hz), 3.80 (d, 1 H-14, $J = 2$ Hz), 4.47 (m, 1 H-3), 8.46 (broad s, 3 H-18), 8.97 (s, 3 H-20), and 9.14 (d, 3 H-17, $J = 6$ Hz); *m/e* 394, 396 (M). The most polar, the butenolide (**29**, 74 mg), was obtained as an oil and had n.m.r. signals at τ 2.83 (broad s, 1 H-14), 4.55 (m, 1 H-3), 5.25 (broad s, 2 H-15), 9.01 (s, 3 H-20), and 9.15 (d, 3 H-17, $J = 6$ Hz). Treatment with diazomethane afforded the oily methyl ester which was distilled *in vacuo* and had ν_{max} 1767 and 1727 cm^{-1}; τ 2.93 (t, 1 H-14, $J_{ob_s} = 1.5$ Hz), 4.58 (m, 1 H-3), 5.27 (m, 2 H-15), 6.51 (s, 3H, $-OCH_3$), 8.50 (broad s, 3 H-18), 9.02 (s, 3 H-20), and 9.16 (d, 3 H-17, $J = 6$ Hz).

Anal. Calcd. for $C_{21}H_{30}O_4$: C, 72.80; H, 8.73. Found: C, 72.70; H, 8.68.

We thank the Science Research Council of the U.K. for maintenance awards (to M.S.H. and A.M.) and the National Research Council of Canada for an operating grant (to R.McC.).

1. T. ANTHONSEN, M. S. HENDERSON, A. MARTIN, R. MCCRINDLE, and R. D. H. MURRAY. Acta Chem. Scand. **22**, 351 (1968).
2. R. R. FRASER. Can. J. Chem. **38**, 549 (1960).
3. R. MISRA, R. C. PANDEY, and S. DEV. Tetrahedron Lett. 2681 (1968).
4. M. S. HENDERSON, R. D. H. MURRAY, R. MCCRINDLE, and D. MCMASTER. Can. J. Chem. This issue. Preceding paper.
5. K. H. OVERTON, N. G. WEIR, and A. WYLIE. Proc. Chem. Soc. 211 (1961).
6. T. J. KING and S. RODRIGO. Chem. Commun. 575 (1967).
7. L. BREHM, T. G. HALSALL, and O. J. R. HODDER. J. Chem. Soc. C, 2529 (1971).
8. A. A. AL-SHAMMA, J. K. BEAL, W. B. T. CRUSE, R. W. DOSKOTCH, and M. N. G. JAMES. Chem. Commun. 1278 (1971).
9. G. BERTI, O. LIVI, and D. SEGNINI. Tetrahedron Lett. 1401 (1970).
10. J. W. B. FULKE, M. S. HENDERSON, and R. MCCRINDLE. J. Chem. Soc. C, 807 (1968).
11. S. KUSUMOTO, T. OKAZAKI, A. OHSUKA, and M. KOTAKE. Bull. Chem. Soc. Jap. **42**, 812 (1969).
12. C. PASCUAL. Ph.D. Thesis. Swiss Federal Institute of Technology, Zurich, Switzerland 1965.
13. W. S. BENNET, G. EGLINTON, J. W. B. FULKE, K. HIRAO, W. SIMON, and A. TAHARA. J. Chem. Soc. B, 211 (1967).
14. C. NISHINO, K. KAWAZU, and T. MITSUI. Agr. Biol. Chem. **35**, 1921 (1971); K. KAWAZU, C. NISHINO, R. MCCRINDLE, and D. MCMASTER. Agr. Biol. Chem. **36**, 1245 (1972).
15. C. PASCUAL and W. SIMON. Helv. Chim. Acta, **47**, 683 (1964); P. F. SOMMER, C. PASCUAL, V. P. ARYA, and W. SIMON. Helv. Chim. Acta, **46**, 1734 (1963).
16. M. S. HENDERSON, R. MCCRINDLE, and D. MCMASTER. Can. J. Chem. This issue. Following paper.
17. L. M. JACKMANN and S. STERNHELL. Applications of nuclear magnetic resonance spectroscopy in organic chemistry. Pergamon Press, Oxford. 1969.
18. K. H. PEGEL, L. P. L. PIACENZA, L. PHILLIPS, and E. S. WAIGHT. Chem. Commun. 1351 (1971); E. WENKERT, P. W. JEFFS, and J. R. MAHAJAN. J. Am. Chem. Soc. **86**, 2218 (1964); P. R. JEFFRIES, R. S. ROSICH, and D. E. WHITE. Tetrahedron Lett. 1793 (1963).
19. J. D. CONNOLLY and R. MCCRINDLE. Chem. and Ind. 379 (1965); N. S. BHACCA and D. H. WILLIAMS. Tetrahedron, **21**, 2021 (1965); C. J. TIMMONS. Chem. Commun. 576 (1965).
20. T. J. KING, S. RODRIGO, and S. C. WALLWORK. Chem. Commun. 683 (1969).
21. G. SNATZKE. Optical rotatory dispersion and circular dichroism in organic chemistry. Heyden, London. 1967. p. 208.
22. W. MOFFITT, R. B. WOODWARD, A. MOSCOWITZ, W. KLYNE, and C. DJERASSI. J. Am. Chem. Soc. **83**, 4013 (1961).
23. C. DJERASSI, J. BURAKEVICH, J. W. CHAMBERLIN, D. ELAD, T. TODA, and G. STORK. J. Am. Chem. Soc. **86**, 465 (1964); W. G. DAUBEN, R. M. COATES, N. D. VIETMEYER, L. J. DURHAM, and C. DJERASSI. Experientia, **21**, 565 (1965).
24. Reference 21. p. 213.

Constituents of *Solidago* Species. Part V.[1] Non-acidic Diterpenoids from *Solidago gigantea* var. *serotina*

M. S. HENDERSON

Department of Chemistry, University of Glasgow, Glasgow, Scotland

AND

R. MCCRINDLE[2] AND D. MCMASTER

Chemistry Department, University of Guelph, Guelph, Ontario

Received November 27, 1972

Eight new furan-containing diterpenoids from *Solidago gigantea* Ait. var. *serotina* (Kuntze) Cronqu., are formulated as **1***c–g*, **2**, **3***a*, and **4***a* on the basis of chemical and spectroscopic evidence and by correlation with solidagoic acid A of previously defined constitution and stereochemistry. The structure (**5***a*) of a ninth related compound is tentatively assigned. The allylic oxidation of some of these new diterpenoids and related compounds with the chromium trioxide – pyridine complex is reported. In the course of this investigation of formal total synthesis of compound Y from *Leonotis leonurus* was achieved.

On propose les formules **1***c–g*, **2**, **3***a* et **4***a* pour huit nouveaux diterpénoïdes contenant du furanne qui ont été isolés de *Soligado gigantea* Ait. var. *serotina* (Kuntze) Cronqu.; ces conclusions sont basées sur des preuves chimiques et spectroscopiques et aussi par corrélation avec l'acid solidagoïque A dont la constitution et la stéréochimie ont été définies précédemment. La structure **5***a* est proposée pour un neuvième composé relié aux précédents. On rapporte aussi les résultats obtenus lors de l'oxydation allylique de quelques-uns de ces diterpénoïdes et composés apparentés par le complexe CrO_3 : pyridine. Au cours de cette étude une synthèse totale formelle du composé Y isolé de Leonotis leonurus a été réussie. [Traduit par le journal]

Can. J. Chem., 51, 1346 (1973)

In the preceding paper (1) we have summarized the evidence which allows the assignment of constitution and relative stereochemistry[3] to solidagoic acids A (**1***a*) and B (**1***b*), constituents of the ethyl acetate soluble extractive of the roots of *Solidago gigantea* Ait. var. *serotina* (Kuntze) Cronqu. The present paper is devoted to nine furan-containing diterpenoids which have been isolated from neutral fractions of the same extract. The complex mixture containing these compounds was separated initially by chromatography over silica gel, final purification of each being achieved by preparative t.l.c. The presence of a β-substituted furan ring in all nine diterpenoids was indicated by their reaction with Ehrlich's reagent and the presence of signals arising from this moiety in their i.r. (ν_{max} near 1500 and 870 cm^{-1}), n.m.r. (near τ 2.65, 2.75, and 3.65; 1H each), and mass (*m/e* 81 and 95) spectra. It thus appeared probable that these compounds and the solidagoic acids have an identical carbon skeleton and indeed it has been possible to interrelate eight of the neutral constituents with the two acids. On this and additional chemical and spectroscopic evidence, firm assignments of constitution and relative stereochemistry can be made for the eight (**1***c–g*, **2**, **3***a*, and **4***a*). A structure (**5***a*) is advanced for the ninth primarily on spectroscopic grounds. The absolute configuration assigned to these compounds rests on their correlation with acid A and is therefore only tentative. The compounds will be discussed in the following order of increasing chromatographic polarity on silica gel (ethyl acetate – light petroleum mixtures as eluant).

Compound I

The least polar constituent was the oily aldehyde **1***c*, $[\alpha]_D$ −164°. Peaks at 2690 and 1722 cm^{-1}, typical of an aldehyde function, are clearly visible in its i.r. spectrum while the —C*H*O proton resonates at τ 0.54 (s). Other resonances which may be readily assigned are those of an olefinic proton (τ 4.28, m) and three methyl groups, one tertiary (τ 9.22, 3H, s), one secondary (τ 9.22, 3H, d, J = 6 Hz), and the

[1]For Part IV see ref. 1 and for the preliminary account of this work ref. 2.

[2]To whom correspondence should be addressed.

[3]The absolute configuration advanced must be viewed as only tentative.

Can. J. Chem. Downloaded from www.nrcresearchpress.com by 210.87.254.40 on 09/05/12
For personal use only.

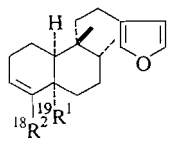

1

a $R^1 = CO_2H$; $R^2 = CH_3$
b $R^1 = CO_2H$; $R^2 = CH_2OAng$
c $R^1 = CHO$; $R^2 = CH_3$
d $R^1 = R^2 = CHO$
e $R^1 = CH_2OH$; $R^2 = CH_3$
f $R^1 = CH_3$; $R^2 = CH_2OH$
g $R^1 = R^2 = CH_2OH$
h $R^1 = R^2 = CH_2OAc$
i $R^1 = CHO$; $R^2 = CH_2OAc$
j $R^1 = CH_3$; $R^2 = CH_2OAc$
k $R^1 = R^2 = CH_3$
l $R^1 = CHDOAc$; $R^2 = CH_2OAc$
m $R^1 = CH_2OH$; $R^2 = CH_2OAc$
n $R^1 = CH_2OAc$; $R^2 = CH_2OH$
o $R^1 = CO_2Me$; $R^2 = CH_3$
p $R^1 = CH_2OAc$; $R^2 = CH_3$
q $R^1 = CH_2OAc$; $R^2 = CHO$
r $R^1 = CHO$; $R^2 = CH_2OAc$

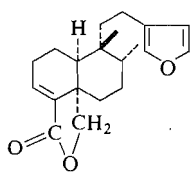

2

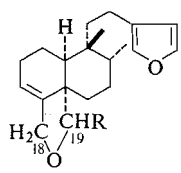

3

a R = OH
b R = OAc
c R = H

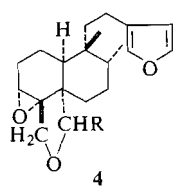

4

a R = OH
b R = OAc

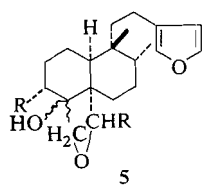

5

a R = OH
b R = OAc

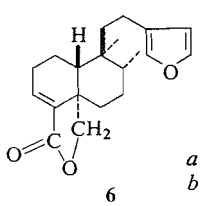

6

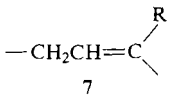

7

a R = CH_2OH
b R = CH_2O—

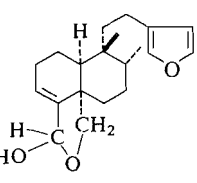

8

other on an olefinic bond (τ 8.58, 3H, d, J = 2 Hz). These data suggested that this compound is identical with the aldehyde prepared (1) from solidagoic acid A (**1***a*) via the alcohol (**1***e*) and this was verified by direct comparison of the two samples.

Compound II

The next constituent (**2**), m.p. 92–95°, $[\alpha]_D$ +12°, could be readily formulated as a γ-lactone because of the strong carbonyl absorption at 1772 cm^{-1} in the i.r. The presence of a double bond in conjugation with the carbonyl group was deduced from the intensity (ε 18 000) of a u.v. maximum at 210 nm and from the chemical shift value and multiplicity of a resonance attributable to an olefinic proton. This proton resonates as a triplet at τ 3.35, showing only vicinal coupling to the C-2 methylene group and significantly no allylic coupling. This was confirmed by a nuclear double resonance experiment in which irradiation of a broad triplet at τ 7.77 (2 H-2) caused that of the olefinic proton to collapse to a sharp singlet. Double irradiation also located H-8, since with H_2 at τ 8.37 the doublet at τ 9.10 (secondary methyl) collapsed to a singlet. Also assignable in the n.m.r. spectrum are resonances arising from a tertiary methyl group (τ 8.97, 3H, s) and the methylene group in the lactone ring (τ 5.56 and 6.20, both 1H, both d, J = 9 Hz), an *isolated* AB system. Assuming this lactone to have the same skeleton as the aldehyde discussed above, these spectroscopic data indicate the formulation **2**. Confirmation of this conclusion was obtained by its reduction with lithium aluminum hydride to the diol **1***g*. This compound and the derived diacetate (**1***h*) were identical with the corresponding samples prepared (1) from solidagoic acid B (**1***b*). It should be noted that although the lactone described here has the same gross structure as that (**6**) isolated (3) from *Dodonaea* species, they differ in stereochemistry at C-9 and -10.

Compound III

The third component, m.p. 103–105°, $[\alpha]_D$ −49°, was readily assigned the structure **1***d*, the presence of two aldehyde groups being immediately recognized from the n.m.r. singlets at τ −0.17 and 0.89. The chemical shift of the former reflects the allylic nature of the proton involved. Support for our conclusions concerning the structure of this compound came from its i.r. absorption at 1720 (isolated aldehyde) and 1690

Can. J. Chem. Downloaded from www.nrcresearchpress.com by 210.87.254.40 on 09/05/12
For personal use only.

Can. J. Chem. Downloaded from www.nrcresearchpress.com by 210.87.254.40 on 09/05/12
For personal use only.

cm^{-1} ($\alpha\beta$-unsaturated aldehyde). Reduction of this dialdehyde with lithium aluminum hydride and then acetylation of the resulting diol added final confirmation of the constitution and stereochemistry (as **1***d*), the products again being identical with those prepared from solidagoic acid B.

Compound IV

The next component, an oil, $[\alpha]_D$ $-38°$, shows hydroxyl absorption in the i.r. at 3630 cm^{-1}, while in its n.m.r. spectrum two carbinyl protons form an AB quartet at τ 6.37 and 6.51 (J = 11 Hz). In addition, a proton and methyl group attached to an olefinic bond give rise to signals at τ 4.29 and 8.33 respectively. These data suggested formulation of the compound as **1***e* and direct comparison with a sample of the primary alcohol derived from solidagoic acid A confirmed this.

Compound V

Compound V, $[\alpha]_D$ $-45°$, also failed to crystallize. Its spectral properties appeared to indicate that it is an isomer of compound IV. In the i.r. it lacks carbonyl absorption but a peak at 3620 cm^{-1} reveals the presence of a hydroxyl group. Resonances in its n.m.r. spectrum at τ 9.15 (d, J = 6 Hz), 8.82 (s) and 8.97 (s) can be assigned to a secondary and two tertiary methyl groups, while a multiplet at τ 4.26 (1H) and broad singlet at τ 5.84 (2H) arise from one olefinic and two carbinyl protons respectively. The chemical shift of this last resonance is indicative of the allylic nature of the primary alcohol group. A tentative assignment of structure, **1***f*, can be made on the basis of the above evidence and it gains support from a series of spin–decoupling experiments. Irradiation at τ 7.95 (2 H-2) caused collapse of the multiplet at τ 4.26 (H-3) to a broad singlet and significant sharpening of the singlet at τ 5.84 (2 H-18). In addition, this last signal appeared as a doublet (J = 1.5 Hz) upon irradiation at the olefinic proton (τ 4.26) and conversely with H_2 at τ 5.84 the multiplet at τ 4.26 simplified to a triplet (J_{obs} = 4 Hz). These results suggest the part structure **7***a* which is accommodated in the postulated structure, **1***f*. Our initial attempts to confirm this structural assignment involved preparation of **1***f* from solidagoic acid B (**1***b*) via the diol (**1***g*) and the derived aldehydo-acetate (**1***i*), but conversion of the aldehyde group into a methyl group could not be effected (see below). Correlation of **1***f* with a compound of known constitution was achieved as follows. The derived acetate (**1***j*) when hydrogenated in ethanol–triethylamine over palladized charcoal (1) afforded the furanoolefin (**1***k*) and its tetrahydro- and hexahydroderivatives. The first of these (**1***k*) was identical with the compound prepared previously (1) from solidagoic acid A.

Compound VI

The n.m.r. spectrum of the next component, an oil, $[\alpha]_D$ $-30°$ shows a marked similarity to those of the less polar compounds discussed above. The resonances at τ 4.52 (1 H, m), 9.03 (3H, s), and 9.15 (3H, d, J = 6 Hz) are assignable to an olefinic proton and two methyl groups, the former tertiary, the latter secondary. The n.m.r. spectrum also reveals the presence of a hemiacetal ring. This gives rise to a multiplet at τ 6.65 (—O*H*) which is lost upon exchange with D_2O and two broad singlets, one from —C*H*(OH)O— at τ 4.58, the other from —CH_2O— at τ 5.79. If one considers only structures related to those discussed above for this compound then two possibilities arise, **3***a* and **8**. Certain double resonance experiments demonstrated that the former formulation is preferable. Upon irradiation in turn at τ 4.52 (H-3) and 7.90 (2 H-2) the broad singlet at 5.79 (2 H-18) collapsed to an ill-resolved doublet ($w_{1/2}$ = 5 Hz) and a clean doublet (J = 3 Hz) respectively. These results lead to the part structure **7***b* and then to **3***a*. The coupling of the hydroxyl proton to H-19 was demonstrated by irradiating at τ 6.65 whereupon the resonance at τ 4.58 became a very sharp singlet.

The presence of a cyclic hemiacetal moiety in compound VI was also indicated chemically. Acetylation of this compound furnished **3***b* from which the parent was readily regenerated by chromatography over neutral alumina. Although all attempts to oxidize **3***a* to the corresponding lactone (**9**) (1) failed, correlation with a known compound was achieved by treating it with sodium borohydride. The resulting diol (**1***g*) and the derived diacetate were identical with those prepared previously. Further confirmation of the orientation of the hemiacetal ring was obtained from an examination of the n.m.r. spectrum of the deuterated diacetate, **1***l*, prepared from **3***a* by reduction with lithium aluminum deuteride and acetylation of the product. This spectrum was nearly identical to that

Can. J. Chem. Downloaded from www.nrcresearchpress.com by 210.87.254.40 on 09/05/12
For personal use only.

of the simple diacetate except that the methylene resonance at *higher field* (τ 6.01) in the latter has been replaced by a signal that integrates for only one proton. An unexpected conversion of the diol (**1***g*) into **3***a* was achieved as follows. In the course of attempts to reduce the aldehyde group in **1***i* to a methyl group, it was treated with hydrazine hydrate in methanol at 20° but none of the desired hydrazone was obtained. However, the only isolable product was identical with the hemiacetal of natural provenance.

Compound VII

Compound VII (**4***a*), $[\alpha]_D$ −47° was isolated as an oil which slowly solidified at −5° but melted at *ca.* 18°. In keeping with its chromatographic polarity it shows evidence of hydroxylic absorption in the i.r. at 3600 and 3400 cm^{-1}. The deduction was made that this group forms part of a hemiacetal ring because of the presence in its n.m.r. spectrum of a singlet at τ 4.49 (H-19) and an AB quartet centered at τ 6.11 (J = 10 Hz, 2 H-18) and since the derived acetate (**4***b*) was readily transformed back to **4***a* by alumina. A structural difference between this compound and those discussed above was clearly evident in its n.m.r. spectrum. Thus, the multiplet at *ca.* τ 4.4 arising from the olefinic proton is absent and replaced by a singlet at τ 6.71, a chemical shift value indicative of a proton attached to an epoxide ring. Treatment of **4***a* with sodium borohydride furnished the diol (**10**) in which the epoxide ring remained intact. It appeared likely that compound VII is the epoxy analog of compound VI, but all attempts to convert the latter into the former with *m*-chloroperbenzoic acid, in various solvents, led either to the recovery of substrate or to non-furanoid products. However, the validity of our structural assignment was demonstrated as follows.

Reduction of **4***a* with lithium aluminum hydride gave the triol **11***a* which was then transformed into the hydroxy-diacetate **11***b*. This compound absorbs in the i.r. at 3590 (hydroxyl) and 1745 (acetate carbonyl) cm^{-1}, while in its n.m.r. spectrum resonances at τ 5.63 (q, J = 13 Hz) and 5.83 (broad s) can be assigned to two functional groups of the type $-CH_2OAc$. The failure of the third hydroxyl group to acetylate and the lack of a resonance attributable to a carbinyl proton in the n.m.r. spectrum of **11***b* was taken to indicate the tertiary nature of the hydroxyl group. Treatment of **11***b* with phosphoryl chloride in pyridine gave mainly one product, the known diacetate **1***h*. These reactions allowed compound VII to be formulated as either **4***a* or **12**. To solve this residual problem the above sequence of reactions (**4***a* → **1***h*) was repeated substituting lithium aluminum deuteride for the corresponding hydride. The mass

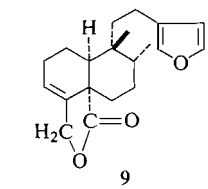

9

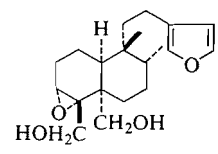

10

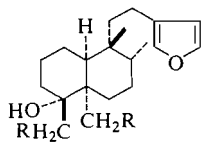

11

a R = OH
b R = OAc

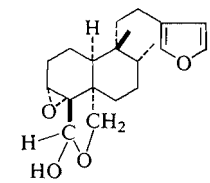

12

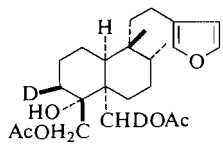

13

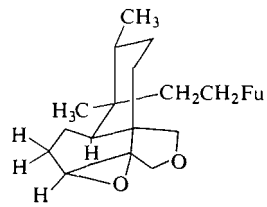

14

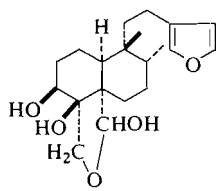

15

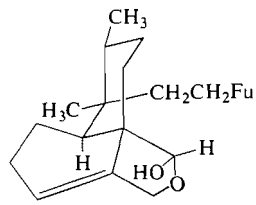

16

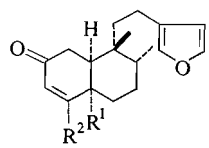

17

a $R^1 = R^2 = CH_3$
b $R^1 = CO_2Me$; $R^2 = CH_3$
c $R^1 = CH_2OAc$; $R^2 = CH_3$
d $R^1 = CHO$; $R^2 = CH_3$
e $R^1 = R^2 = CH_2OAC$

Can. J. Chem. Downloaded from www.nrcresearchpress.com by 210.87.254.40 on 09/05/12
For personal use only.

spectrum of the resulting hydroxy-diacetate (**13**) revealed the presence of two deuterium atoms as anticipated, while in its n.m.r. spectrum the two-proton singlet at τ 5.83 is still present but the quartet centered at τ 5.63 (in **11***b*) has been replaced by a one-proton singlet at τ 5.35. This reflects the stereospecificity of the reductive opening of the hemiacetal ring. Dehydration as described above yielded the monodeutero-diacetate (**1***l*) prepared previously from compound VI, confirming that both compounds have the hemiacetal ring attached in the same fashion. This second reaction sequence also enables assignments to be made for the resonances between τ 5 and 6 in the n.m.r. spectrum of the hydroxy-diacetate **11***b*. The singlet at τ 5.83 derives from the methylene group of the C-18 acetate function, shifting downfield to τ 5.43 on dehydration since it is now allylic, while the quartet at τ 5.63 from the C-19 methylene shifts upfield to 6.01 and becomes a singlet. The epoxide ring is assigned to α-orientation on the following grounds. First, the narrowness ($w_{1/2}$ = 3 Hz) of the signal arising from the proton attached to the epoxide ring in **4***a* suggests (4) the stereochemical situation **14**. Second, *trans*-diaxial opening (5) of the epoxide in **14** with lithium aluminum hydride would lead to a tertiary alcohol, as is observed. Third, **11***a* has been prepared from **1***g* by a route (see below) which would be expected to introduce the tertiary hydroxyl on the α-face of the molecule.

Compound VIII

The neutral compound penultimate in polarity was the diol (**1***g*), m.p. 60–63°, $[\alpha]_D$ −46°, into which several of the compounds discussed above have been converted. The functional groups in **1***g* were readily inferred from its i.r. and n.m.r. data and those of the derived monoacetates (**1***m* and *n*) and diacetate (**1***h*), while chemical transformations clearly defined the spatial relationship of the two primary hydroxyl groups. In the first of these reactions, the diol was converted into a cyclic ether by treatment with *p*-bromobenzenesulfonyl chloride in pyridine (6). Its formulation as **3***c* followed from its very low polarity on t.l.c. and from spectral evidence. In the i.r. it lacks both carbonyl and hydroxyl absorption while its mass spectrum has the molecular ion at *m/e* 300 ($C_{20}H_{28}O_2$). In its n.m.r. spectrum the ethereal methylene groups resonate as two AB quartets, one centered at τ 5.85 (2 H-18) the other at 6.28 (2 H-19). A second important transformation involved the oxidation of the diol with the Sarett reagent. Under mild conditions (see below) the major product was significantly a γ-lactone (ν_{max} 1772 cm^{-1}), thus providing additional confirmation of the disposition of the two hydroxylic groups. This lactone (**2**) m.p. 89–90°, was in fact shown by direct comparison to be identical to compound II. Unambiguous proof of the structure of the diol **1***g* was obtained by hydrogenation (1) of the derived diacetate in ethanol containing triethylamine over palladized charcoal. The resulting monoacetate (**1***p*) was identical with that prepared from solidagoic acid A (1) of well-defined structure.

Compound IX

The most polar of these neutral furanoid compounds (**5***a*), m.p. 135–137°, $[\alpha]_D$ −18° has no resonances attributable to olefinic protons in its n.m.r. spectrum. However, it does have a multiplet at τ 4.50 which can be assigned to HO—C*H*—O— in a hemiacetal ring. Additional lines which form a complex pattern between τ 5.6 and 6.6 although presumably arising from protons of the type >C*H*—O— were of little diagnostic value. However, the n.m.r. spectrum of the derived hydroxy-diacetate (**5***b*) proved more informative. Thus the methine proton (H-19) of the hemiacetal acetate has shifted downfield and appears as a singlet at τ 3.28 while the ethereal methylene protons (2 H-18) are now clearly visible as an AB quartet centered at τ 5.88. A broadened triplet at τ 5.18 (J = 6 Hz) can be assigned to the methine of a secondary acetate group. The multiplicity and value of the observed coupling constant for this proton indicate that if it is attached to a cyclohexane ring, it is probably axial and vicinally related to two protons. Bearing in mind the above spectral evidence and the structures of the other diterpenoids in this plant the plausible structure (**5***a*) can be advanced for compound IX. In an attempt to relate this compound to one of known structure the hemiacetal **3***a* was treated with osmium tetroxide. However, the resulting triol was not identical with the natural product. The formulation of this new triol as **15** rests on the narrowness of the resonance from H-3 ($w_{1/2}$ = 6 Hz, τ 6.33). Presumably the presence of the hemiacetal ring has induced the decalin system

Can. J. Chem. Downloaded from www.nrcresearchpress.com by 210.87.254.40 on 09/05/12
For personal use only.

to adopt the conformation **16** in which, although both faces of the olefinic bond are open to attack, the β would probably be preferred if the C-19 hydroxyl group is α-orientated.

Oxidations with the Chromium Trioxide – Pyridine Complex

Of major importance in our arguments concerning the structure and stereochemistry of solidagoic acids A and B (1), and by extension the related neutral diterpenoids of natural provenance, have been n.m.r. and c.d. studies on the αβ-unsaturated ketones **17***a*, **18***a*, **18***b*, and **19**. A key step in the formation of **17***a* was the introduction of the C-2 ketone using the chromium trioxide – pyridine complex at 20°, conditions which minimize oxidative attack on the furan ring. In the course of our structural studies the reactions of other derivatives of solidagoic acid A and its congeners with this complex were examined and in addition the investigation was extended to related compounds for two reasons. First, compounds containing the enone substitution pattern in **17***a*, but with a *trans*-fused decalin system, were required as models for our n.m.r. work (1). Second, at the time the major portion of the work described in this section was completed[4] (7), only one report of an allylic oxidation with the Sarett reagent existed (9) and the reaction appeared to have enough intrinsic interest to warrant study. It should be noted, that in general, these reactions were carried out using concentrations of chromium trioxide in pyridine of the order of 100 mg/ml.

Oxidation of the methyl ester **1***o* and the acetate **1***p* for 18 days afforded the enones **17***b* and *c* (56 and 50% respectively, based on substrate consumed). The alcohol **1***e* in only 12 h gave (1) the aldehyde **1***c* (67%), the enone-aldehyde **17***d* (3%) and the nor-enone **20** (5%). Maingayol (**21***a*) (10) reacted (1) similarly and furnished **21***b*, **22**, and **23**. The formation of these nor-enones and of **24** from drimenol (**25***a*) (11) might involve a mechanism of the type **26** (arrows) or equivalent intermolecular process. The diacetate **1***h*, as anticipated, was converted into the enone **17***e* (*ca.* 50%) during 17 days. The parent diol (**1***g*) was subjected to oxidation for 14 h under two distinct sets of conditions, namely, with a chromium trioxide – pyridine concentration of first, 250 mg/ml, and second, 2.5 mg/ml. In the former case the major product was the enone-lactone **27** (60%), the minor being the lactone **2** (15%). In the latter oxidation the lactone **2** (74%) was the only isolable product. Our attention was next directed to the two monoacetates **1***m* and *n* (1). The latter with chromium trioxide in pyridine (25 mg/ml) during 14 h smoothly formed the aldehyde **1***q* (74%). The other monoacetate (**1***m*) during 12 h was converted with the complex at a concentration of 2.5 mg chromium trioxide per milliliter of pyridine into the aldehydo-acetate **1***r* (*ca.* 100%)

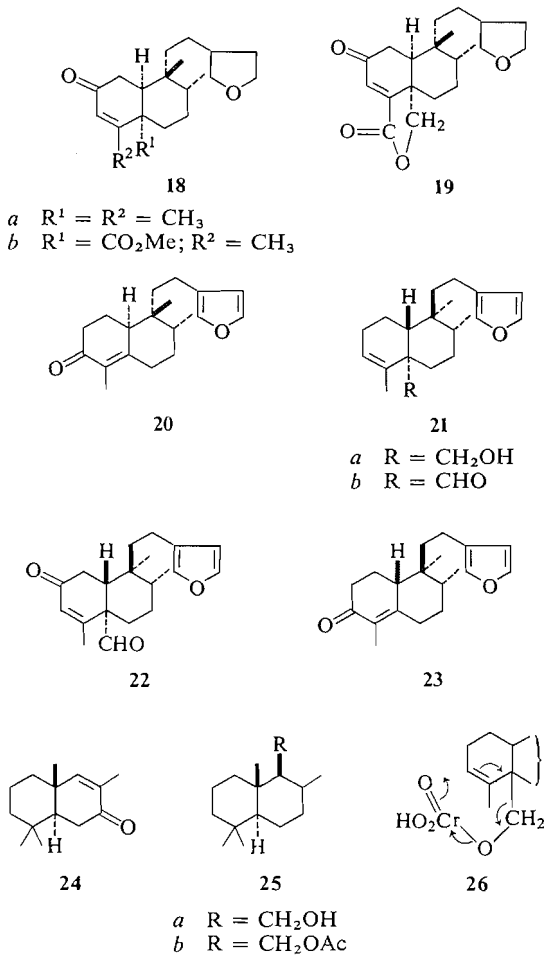

[4]However, soon thereafter a paper was published (8) concerning the oxidation of 17 olefins with the isolated chromium trioxide – pyridine complex in methylene chloride. In this medium similar results to those reported here were obtained, but the reaction times involved were significantly shorter. Probable mechanisms for the reaction are outlined in this paper (8) and no further discussion is required here.

Can. J. Chem. Downloaded from www.nrcresearchpress.com by 210.87.254.40 on 09/05/12
For personal use only.

and unexpectedly at a concentration of 100 mg/ml into the corresponding epoxide **28** (68%). This epoxide on reduction with lithium aluminum hydride furnished the known triol **11***a*. Formation of an epoxide by chromium(VI) oxidation of an alkene, although a well-known (1, 12, 13) reaction under acidic conditions, is a novel reaction in pyridine solution. The orientation of the epoxide ring in **28** is assigned as α for two reasons. First, in the substrate the β-face of the A ring is probably (1) shielded by the C-9 methyl group. Second, it seems likely that even in pyridine solution, the initial step in the reaction would involve formation of the chromate ester of the primary alcohol at C-5 followed by transfer (13) of an oxygen atom from this ester to the double bond, *i.e.* from the α-side.

As models in our n.m.r. and c.d. studies on the stereochemistry of solidagoic acid A (1), we required compounds of the general type **29** or enantiomer. In view of the results reported above, the diacetate **30***a* from confertifolin (**31**) (14) was treated with chromium trioxide in pyridine (100 mg/ml) for 18 days and afforded, as anticipated, the enone **32***a* (81%). For this compound the relevant coupling constants, H-5/H-6 equatorial and H-5/H-6-axial, were calculated as $J = 3.5$ and 13.5 Hz respectively. When the diol **30***b* was oxidized under similar conditions but for a shorter time (14 h), three products were isolated, the β,β′-disubstituted furan (**33**) (40%), confertifolin (**31**, 22%), and isodrimenin (**34** (14), 25%). The reaction can be envisaged as proceeding through the two possible hydroxyaldehydes to the corresponding hemiacetals and thence by dehydration to the furan or oxidation to the lactones. The oxidation of drimenyl acetate (**25***b*) was examined next. In this case the only product isolated was the enone **32***b* (67%) in which the double bond had migrated into the $\Delta^{8,9}$ position. Earlier workers had reported (15) the isolation of the enone-acid **32***c*, albeit in very low yield, from the products of oxidation of drimenol (**25***a*) with the Sarett reagent. A mechanism which would explain the formation of these isomeric enones has been proposed recently (9). Oxidation of the furanoolefin (**35***a*) (16) gave the expected enone (**35***b*) which showed a negative Cotton effect for the $n \rightarrow \pi^*$ transition.

Oxidation of cholesteryl acetate (**36***a*) for 14 days afforded the 7-keto derivative (**36***b*, 33%). It is noteworthy that in this case the yield

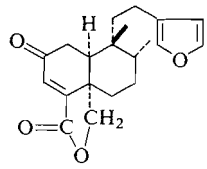

27

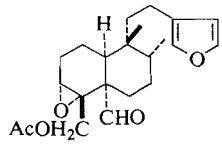

28

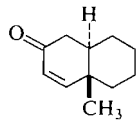

29

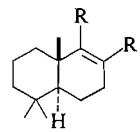

30

a R = CH_2OAc
b R = CH_2OH

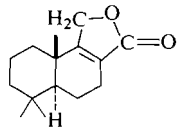

31

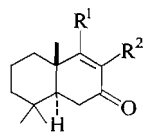

32

a $R^1 = R^2 = CH_2OAc$
b $R^1 = CH_2OAc$; $R^2 = CH_3$
c $R^1 = CO_2H$; $R^2 = CH_3$

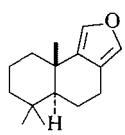

33

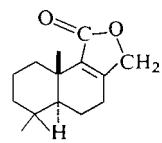

34

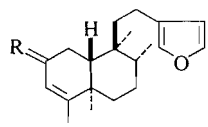

35

a R = H_2
b R = O

is inferior to that from oxidation by either the chromium trioxide – pyridine complex in methylene chloride (74%) (9) or *t*-butylchromate (60%) (17). Finally, the oxidation of two derivatives of marrubiin (18) was studied. The ester **37***a* during 10 days formed the enone **38***a* (81%) while **37***b* in just less than 1 week gave **38***b* (70%) and over 25 days the corresponding product **39** (12%) which has suffered cleavage of the furan ring. Direct comparison showed that the enone **38***b* is identical to compound Y[5] from *Leonotis*

[5]Dr. D. E. A. Rivett kindly supplied a sample of this compound.

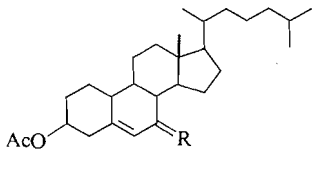

36

a R = H_2
b R = O

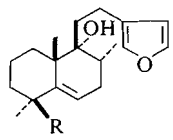

37

a R = CO_2Me
b R = CH_3
c R = CH_2OH
d R = CH_2OAc

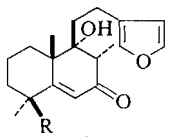

38

a R = CO_2Me
b R = CH_3
c R = CHO

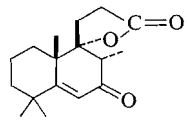

39

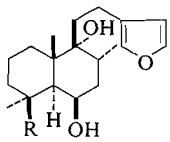

40

a R = CO_2Me
b R = CH_3

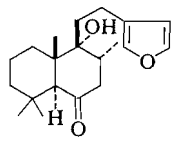

41

leonurus (19). Since marrubiin has been synthesized (20), this conversion of marrubiin into compound Y constitutes a formal total synthesis of the latter.

Experimental

Melting points are uncorrected and were determined on a Kofler hot-stage apparatus. Specific rotations refer to solutions in ethanol unless otherwise stated. Woelm Grade I alumina, deactivated to the appropriate grade according to Brockmann, was used for chromatography. For analytical and preparative t.l.c., chromatoplates were spread with Kieselgel G (Merck). Light petroleum was of b.p. 40–60°. Microanalyses were by Miss F. Cowan, Glasgow. High resolution mass spectra were run at the N.T.H, Trondheim, by Dr. T. Anthonsen. I.r. solution spectra were recorded in carbon tetrachloride on a Perkin–Elmer 225 or 257 or Beckmann I.R.12 spectrophotometer, u.v. spectra in ethanol on a Unicam S.P.800 spectrophotometer and the circular dichroism curve on a Cary 61 spectropolarimeter. P.m.r. spectra were run on a Perkin–Elmer R-10 or Varian Associates A-60A or HA 100 spectrometer in carbon tetrachloride, unless otherwise stated, using approximately 0.3 *M* solutions and tetramethylsilane as internal standard. Mass spectra were run on a Varian Associates CH 7 or A.E.I. MS9 or MS12 instrument.

Isolation Procedure

The chloroform soluble portion (24 g) of an extract (1) of *Solidago gigantea* var. *serotina* was chromatographed over alumina (Grade III; neutral; 2 kg) using as eluting solvent light petroleum – chloroform mixtures. Compounds were isolated from the various fractions by preparative t.l.c. and then either crystallization or distillation *in vacuo*.

Fraction A (4.3g), eluted with chloroform – light petroleum (1:19) was a complex mixture (t.l.c.) of non-polar compounds which was not investigated further. Fraction B (923 mg) was eluted with chloroform – light petroleum (1:9) and contained compound I, the oily aldehyde **1***c* (471 mg) as the major constituent. It had $[\alpha]_D$ −164° (*c*, 0.9) and was identical (i.r., n.m.r., and t.l.c.) to the aldehyde prepared (1) from solidagoic acid A. Fraction C (1.3 g), eluted with chloroform – light petroleum (1:4), furnished compounds II and III. The first of these, the lactone **2** (311 mg) formed needles from light petroleum and had m.p. 92–95°, $[\alpha]_D$ +12° (*c*, 0.65); ν_{max} 1772 and 874 cm^{-1}; λ_{max} 210 nm (ε 18 000); τ 3.35 (t, 1 H-3, J_{obs} = 3 Hz), 5.56 (d, 1 H-19, *J* = 9 Hz), 6.20 (d, 1 H-19, *J* = 9 Hz), 8.97 (s, 3 H-20) and 9.10 (d, 3 H-17, *J* = 6 Hz); *m/e* 314 (M).

Anal. Calcd. for $C_{20}H_{26}O_3$: C, 76.40; H, 8.34. Found: C, 76.44; H, 8.41.

Compound III, the dialdehyde **1***d* (472 mg), crystallized from ethyl acetate – light petroleum as needles, m.p. 103–105°, $[\alpha]_D$ −49° (*c*, 0.7); ν_{max} 1720, 1690 and 878 cm^{-1}; τ −0.17 (s, 1 H-18), 0.89 (s, 1 H-19), 3.16 (t, 1 H-3, J_{obs} = 4 Hz), 9.04 (s, 3 H-20) and 9.15 (d, 3 H-17, *J* = 6 Hz) *m/e* 314 (M).

Anal. Calcd. for $C_{20}H_{26}O_3$: C, 76.40; H, 8.34. Found: C, 76.52; H, 8.43.

Fractions D, E, and F were all eluted with chloroform – light petroleum (1:1). The first of these, fraction D (928 mg), contained two major components. Compound IV, the alcohol **1***e* (38 mg), had $[\alpha]_D$ −38° (*c*, 0.9) and was identical (n.m.r. and t.l.c.) to the alcohol prepared (1) from solidagoic acid A. Compound V, the alcohol **1***f* (671 mg), had $[\alpha]_D$ −45° (*c*, 0.6); ν_{max} 3620, 3400 and 875 cm^{-1}; τ 4.26 (m, 1 H-3; $w_{1/2}$ = 8 Hz), 5.84 (s, 2 H-18), 7.80 (s, —O*H*), 8.82, 8.97 (both s, 3 H-19 and 3 H-20), and 9.15 (d, 3 H-17, *J* = 6 Hz); *m/e* 302 (M).

Anal. Calcd. for $C_{20}H_{30}O_2$: C, 79.42; H, 10.00. Found: C, 79.30; H, 9.94.

Fraction E (4.3 g) contained compound VI, the hemiacetal **3***a* (1.7 g), and a sterol (220 mg) which crystallized from ethyl acetate – light petroleum as needles, m.p. 161–163°; ν_{max} 3600 cm^{-1}; *m/e* 412 ($C_{29}H_{48}O$). The hemiacetal had $[\alpha]_D$ −30° (*c*, 1.1; chloroform); ν_{max} 3600, 3390 and 872 cm^{-1}; τ 4.52 (m, 1 H-3, $w_{1/2}$ = 10 Hz), 4.58 (broad s, 1 H-19), 5.79 (broad s, 2 H-18, $w_{1/2}$ = 7 Hz), 6.65 (m, —O*H*), 9.03 (s, 3 H-20) and 9.15 (d, 3 H-17, *J* = 6 Hz); *m/e* = 316 (M).

Anal. Calcd. for $C_{20}H_{28}O_3$: C, 75.91; H, 8.92. Found: C, 75.91; H, 9.03.

The derived oily acetate (**3***b*), ν_{max} 1740 and 882 cm^{-1}, τ 3.68 (s, 1 H-19), 4.44 (m, 1 H-3) and 5.72 (m, 2 H-18, $w_{1/2}$ = 12 Hz), on chromatography over alumina (Grade III, neutral) was reconverted into the parent hemiacetal. Fraction F (3.2g) furnished compound VII, the epoxy-hemiacetal **4***a* (1.9g), which solidified on cooling and had m.p. *ca.* 18°; $[\alpha]_D$ −47° (*c*, 0.8); ν_{max} 3600, 3400, and 872 cm^{-1}; τ 4.49 (s, 1 H-19), 6.00 (d, 1 H-18, *J* = 10 Hz), 6.22 (d, 1 H-18, *J* = 10 Hz), 6.71 (s, 1 H-3, $w_{1/2}$ = 3 Hz), 7.03 (m, —O*H*), 9.12 (s, 3 H-20), and 9.19 (d, 3 H-17, *J* = 6 Hz); *m/e* 332 (M).

Can. J. Chem. Downloaded from www.nrcresearchpress.com by 210.87.254.40 on 09/05/12
For personal use only.

Can. J. Chem. Downloaded from www.nrcresearchpress.com by 210.87.254.40 on 09/05/12
For personal use only.

Anal. Calcd. for $C_{20}H_{28}O_4$: C, 72.26; H, 8.49. Found: C, 72.33; H, 8.64.

Its acetate (**4***b*), τ 3.62 (s, 1 H-19), 6.10 (d, 1 H-18, J = 10 Hz), 6.18 (d, 1 H-18, J = 10 Hz), 6.71 (s, 1 H-3), 8.17 (s, 3H, —OCOCH_3), 9.13 (s, 3 H-20), and 9.20 (d, 3 H-17, J = 6 Hz), was transformed back to the parent hemiacetal on chromatography over alumina.

Fraction G (2.9 g), eluted with chloroform, afforded compound VIII the diol **1***g* (2.6 g), m.p. 60–63°, $[\alpha]_D$ −46° (*c*, 0.9), which was identical to the diol prepared (1) from solidagoic acid B. Fraction H (509 mg) was eluted with methanol–chloroform (1:19) and yielded compound IX, the dihydroxy-hemiacetal **5***a* (284 mg), which on crystallization from ether – light petroleum had m.p. 135–137°; $[\alpha]_D$ −18° (*c*, 0.95); ν_{max} 3425 and 875 cm^{-1}; τ 4.50 (m, 1 H-19, $w_{1/2}$ = 10 Hz), 9.03 (s, 3 H-20) and 9.15 (d, 3 H-17, J = 6 Hz); *m/e* 350 (M).

Anal. Calcd. for $C_{20}H_{30}O_5$: C, 68.54; H, 8.63. Found: C, 68.42; H, 8.89.

The derived diacetate **5***b* had n.m.r. signals at τ 3.28 (s, 1 H-19), 5.18 (t, 1 H-3, J_{obs} = 6 Hz), 5.74 (d, 1 H-18, J = 10 Hz), 6.03 (d, 1 H-18, J = 10 Hz), 7.89, 8.02 (both s, 2—OCOCH_3), 8.98 (s, 3 H-20) and 9.18 (d, 3 H-17, J = 6 Hz).

Reduction of the Lactone **2** *with Lithium Aluminum Hydride*

The lactone **2** (17 mg) was treated with a very large excess of lithium aluminum hydride in refluxing dry ether for 14 h. Work-up afforded an oil (16 mg) which was submitted to preparative t.l.c. (ethyl acetate – light petroleum, 2:3). The major component (11 mg) on crystallization from ethyl acetate – light petroleum had m.p. 57–61°, $[\alpha]_D$ −50° (*c*, 1.1) and was identical (t.l.c. and n.m.r.) to the diol (**1***g*) of natural provenance (see above).

Reduction of the Dialdehyde **1***d* *with Lithium Aluminum Hydride*

The dialdehyde (24 mg) when reduced for 2 h as above gave on work-up and purification the known diol **1***g* (13 mg), m.p. 58–61°, $[\alpha]_D$ −51° (*c*, 1.3).

Conversion of the Alcohol **1***f* *into the Furano-olefin* **1***k*

The alcohol **1***f* (100 mg) in dry pyridine (2 ml) was treated at 20° for 15 h with acetic anhydride (1 ml). The crude product, the acetate **1***j* (98 mg), was purified by preparative t.l.c. (chloroform) and distillation *in vacuo*. It was obtained as an oil $[\alpha]_D$ −34° (*c*, 1.4); ν_{max} 1740, 1230, and 878 cm^{-1}; τ 4.34 (m, 1 H-3), 5.55 (s, 2 H-18), 8.05 (s, 3H, —OCOCH_3), 8.82, 8.93 (both s, 3 H-19 and 3 H-20), and 9.10 (d, 3 H-17, J = 6 Hz).

Anal. Calcd. for $C_{22}H_{32}O_3$: C, 76.70; H, 9.36. Found: C, 76.95; H, 9.34.

Hydrogenation of this acetate (50 mg) in ethanol (25 ml) containing triethylamine (5 ml) over 10% palladized charcoal for 5 min afforded a mixture (t.l.c.) of two products. These were separated by preparative t.l.c. (light petroleum), the less polar being the major component. This compound was the furano-olefin **1***k* (31 mg) which after distillation *in vacuo* had $[\alpha]_D$ −21° (*c*, 1.1) and was identical (i.r., n.m.r., t.l.c.) to the furano-olefin prepared (1) from solidagoic acid A. The minor component was the tetrahydrofuran-olefin on mass spectrometric evidence, *m/e* 290 (M).

In a separate experiment the above acetate (**1***j*, 45 mg) was hydrogenated in ethanol containing triethylamine over palladized charcoal for 40 min. Work-up gave mainly one compound which was purified by preparative t.l.c. (ethyl acetate – light petroleum, 1:19) and distillation at 100°/0.05 mm. The resulting oil (28 mg) was the hexahydro derivative of **1***k* and had $[\alpha]_D$ −7° (*c*, 0.7, chloroform); *m/e* 292 (M).

Anal. Calcd. for $C_{20}H_{36}O$: C, 82.12; H, 12.40. Found: C, 81.95; H, 12.23.

Reduction of the Hemiacetal **3***a*

(*i*) The hemiacetal **3***a* (60 mg) in absolute ethanol (5 ml) was treated at 20° for 15 h with a large excess of sodium borohydride. The solution was diluted with water and extracted with ethyl acetate. The product was essentially pure (t.l.c.) diol **1***g* (54 mg) which on crystallization from ethyl acetate – light petroleum had m.p. 60–61°; $[\alpha]_D$ −52° (*c*, 1.2).

(*ii*) The hemiacetal **3***a* (50 mg) was heated with excess lithium aluminum deuteride in refluxing dry ether for 14 h. The deuterodiol (47 mg) obtained after work-up was acetylated with acetic anhydride – pyridine and afforded the corresponding deuterodiacetate (**1***l*, 39 mg). In its n.m.r. spectrum it exhibited resonances at τ 4.06 (m, 1 H-3), 5.43 (s, 2 H-18), 6.01 (s, 1 H-19), 7.98 (s, 6H, 2—OCOCH_3), 8.93 (s, 3 H-20), and 9.08 (d, 3 H-17, J = 6 Hz); *m/e* 403 (M).

Hydroxylation of the Hemiacetal **3***a*

The hemiacetal **3***a* (450 mg) was treated with osmium tetroxide (500 mg) in dry ether for 4 days. The reaction was worked-up with hydrogen sulfide gas, precipitated sulfides being filtered off. The crude product (430 mg) consisted (t.l.c.) of two components which were separated by preparative t.l.c. (chloroform–methanol, 19:1). The less polar (350 mg) was unreacted hemiacetal while the more polar, minor, product (40 mg) was the triol **15**, which could not be induced to crystallize. It had ν_{max} 3500 and 880 cm^{-1}; τ 4.51 (m, 1 H-19), 5.18 (m, 1H, —O*H*; lost on D_2O exchange), 5.56 (s, 1 *H*, —O*H*; lost on D_2O exchange), 6.14 (s, 2 H-18), 6.33 (s, 1 H-3, $w_{1/2}$ = 6 Hz after D_2O exchange), 6.82 (m, 1H, —O*H*; lost on D_2O exchange), 9.01 (s, 3 H-20) and 9.18 (d, 3 H-17, J = 6 Hz); *m/e* 350 (M).

Treatment of Acetoxy-aldehyde **1***i* *with Hydrazine Hydrate*

The acetoxy-aldehyde **1***i* (50 mg) in methanol (5 ml) was treated at 20° for 15 h with hydrazine hydrate (3 ml). Work-up afforded an oil (47 mg) from which the major product (32 mg) was recovered by preparative t.l.c. (chloroform). It had $[\alpha]_D$ −74° (*c*, 1.1) and was identical (n.m.r., i.r., and t.l.c.) with the hemiacetal (**3***a*) of natural provenance.

Attempted Epoxidation of the Hemiacetal **3***a*

Reaction of the hemiacetal **3***a* (15 mg) with *m*-chloroperbenzoic acid (20 mg) in chloroform (5 ml) at 20° for 90 min and work-up by filtration through a short column of neutral alumina afforded essentially pure (t.l.c.) starting material (13 mg). The reaction was repeated this time for 15 h. The products were a complex mixture (t.l.c., Ehrlich, and sulfuric acid staining) of non-furanoid compounds and starting material. Similar results were obtained when carbon tetrachloride or benzene was used as solvent.

Can. J. Chem. Downloaded from www.nrcresearchpress.com by 210.87.254.40 on 09/05/12
For personal use only.

Attempted Oxidation of the Hemiacetal 3a

(*i*) The hemiacetal **3***a* (10 mg) in ether was stirred at 20° for 16 h with activated manganese dioxide. Removal of the reagent and solvent afforded pure (t.l.c.) starting material (8 mg). This experiment was repeated using various grades of manganese dioxide but in all cases the result was similar.

(*ii*) Treatment of the hemiacetal (10 mg) at 20° with excess of the Sarett reagent for 6 h also yielded only starting material (10 mg).

Formation of the Epoxy-diol 10

A large excess of sodium borohydride was added to a solution of the epoxy-hemiacetal **4***a* (50 mg) in ethanol (10 ml) and the mixture allowed to remain at 20° for 15 h. Work-up afforded an oil (47 mg) which contained one major component. This compound, the epoxy-diol **10**, was purified by preparative t.l.c. (ethyl acetate – light petroleum, 1:1) and then distillation at 150°/0.04 mm. The resulting oil had $[\alpha]_D$ −6° (*c*, 1.5); ν_{max} 3630, 3380, and 875 cm^{-1}; τ 9.03 (s, 3 H-20) and 9.20 (d, 3 H-17, J = 6 Hz).

Anal. Calcd. for $C_{20}H_{30}O_4$: C, 71.82; H, 9.04. Found: C, 71.89; H, 9.12.

The corresponding acetate had $[\alpha]_D$ −11° (*c*, 0.6); ν_{max} 1745, 1235, and 875 cm^{-1}; τ 5.57 (d, 1 H-18, J = 12 Hz), 5.85 (d, 1 H-19, J = 7 Hz), 5.94 (d, 1 H-19, J = 7 Hz), 6.08 (d, 1 H-18, J = 12 Hz), 6.89 (d, 1 H-3, J = 3 Hz), 7.97, 7.99 (both s, 3H each, 2 —OCOCH_3), 8.97 (s, 3 H-20), and 9.14 (d, 3 H-17, J = 6 Hz).

Anal. Calcd. for $C_{24}H_{34}O_6$: C, 68.86; H, 8.19. Found: C, 69.04; H, 8.39.

Conversion of the Epoxy-hemiacetal 4a into the Diacetates 1h and l

(*i*) Treatment of the epoxy-hemiacetal **4***a* (50 mg) in refluxing dry tetrahydrofuran with excess lithium aluminum hydride for 15 h gave a product (43 mg) which consisted of two components of similar, high, polarity. These were separated by preparative t.l.c. (ethyl acetate – light petroleum, 3:1). The major, less polar component, the triol **11***a* (21 mg) was an oil which after distillation at 180°/0.1 mm had $[\alpha]_D$ −22° (*c*, 0.75); ν_{max} 3420 and 880 cm^{-1}.

Anal. Calcd. for $C_{20}H_{32}O_4$: C, 71.39; H, 9.59. Found: C, 71.33; H, 9.60.

This triol (50 mg) was acetylated and gave the hydroxy-diacetate **11***b* (46 mg), an oil which was distilled at 75°/0.01 mm and had $[\alpha]_D$ −13° (*c*, 1.0); ν_{max} 3590, 3480, 1745, 1240, and 875 cm^{-1}; τ 5.35 (d, 1 H-19, J = 13 Hz), 5.83 (s, 2 H-18), 5.91 (d, 1 H-19, J = 13 Hz), 8.00, 8.13 (both s 3 H each, 2 —OCOCH_3), 9.07 (s, 3 H-20) and 9.18 (d, 3 H-17, J = 6 Hz).

Anal. Calcd. for $C_{24}H_{36}O_6$: C, 68.54; H, 8.63. Found: C, 68.74; H, 8.86.

The hydroxy-diacetate **11***b* (15 mg) was heated at 80° with redistilled phosphoryl chloride (0.5 ml) in dry pyridine (3 ml) for 3 h. The reaction mixture was poured onto crushed ice and extracted with ethyl acetate to afford the crude product (17 mg). This consisted (t.l.c.) of two components which were separated by preparative t.l.c. (ethyl acetate – light petroleum, 1:4). The major, more polar, component (10 mg) was the oily diacetate which had $[\alpha]_D$ −58° (*c*, 1.0) and was identical (n.m.r., t.l.c.) to that obtained previously by acetylation of the diol **1***g*.

(*ii*) The above sequence of reactions was repeated starting with epoxy-hemiacetal (50 mg) but substituting lithium aluminum deuteride for the hydride. The hydroxy-diacetate **13** had n.m.r. resonances at τ 5.35 (s, 1 H-19) and 5.83 (s, 2 H-18); *m/e* 422 (M). The diacetate **1***l* (17 mg) obtained by dehydration was identical (n.m.r., mass spectroscopy) to that prepared from **3***a*.

Formation of the Ether 3c

The diol **1***g* (50 mg) was heated for 15 h with *p*-bromobenzenesulfonyl chloride (150 mg) in refluxing dry pyridine (5 ml). Work-up afforded an oil (46 mg) from which the major product (32 mg) was obtained by preparative t.l.c. (ethyl acetate – light petroleum, 3:17). This ether **3***c* was distilled at 150°/0.03 mm and had $[\alpha]_D$ −30° (*c*, 0.65), ν_{max} 872 cm^{-1}; τ 4.57 (m, 1 H-3), 5.73 (broad d, 1 H-18, J = 11 Hz), 5.84 (d, 1 H-19, J = 8 Hz), 5.98 (broad d, 1 H-18, J = 11 Hz), 6.73 (d, 1 H-19, J = 8 Hz), 9.01 (s, 3 H-20) and 9.16 (d, 3 H-17, J = 6 Hz); *m/e* 300 (M).

Anal. Calcd. for $C_{20}H_{28}O_2$: C, 79.95, H, 9.39. Found: C, 79.88; H, 9.52.

Oxidation of Methyl Ester 1o

Oxidation of the ester **1***o* (152 mg) in dry pyridine (2 ml) with chromium trioxide (500 mg) at 20° for 18 days and work-up afforded an oil (172 mg). The two major components of this oil were obtained by preparative t.l.c. (ethyl acetate – light petroleum, 3:7). The less polar component (48 mg) was unreacted ester while the other was the enone-ester **17***b* (63 mg). It was purified further by distillation *in vacuo* and had ν_{max} 1725, 1675, and 882 cm^{-1}; τ 4.23 (s, 1 H-3), 6.50 (s, 3H, —OCH_3), 8.29 (d, 3 H-18, J = 1 Hz), 9.07 (s, 3 H-20) and 9.07 (d, 3 H-17, J = 6 Hz); *m/e* 344 (M).

Anal. Calcd. for $C_{21}H_{28}O_4$: C, 73.22; H, 8.19. Found: C, 73.26; H, 8.35.

Oxidation of Acetate 1p

The acetate **1***p* (40 mg) in dry pyridine (2 ml) was treated at 20° for 17 days with chromium trioxide (100 mg). The oil (38 mg) obtained on work-up was separated by preparative t.l.c. (ethyl acetate – light petroleum, 2:3) to afford unreacted **1***p* (17 mg) as the less polar component. The other component, the enone-acetate **17***c* (12 mg) was obtained as an oil which distilled at 140°/0.04 mm; $[\alpha]_D$ −88° (*c*, 0.08); ν_{max} 1740, 1670, and 872 cm^{-1}; τ 4.07 (s, 1 H-3), 5.84 (d, 1 H-19, J = 12 Hz), 6.18 (d, 1 H-19, J = 12 Hz), 8.00 (s, 3 H, —OCOCH_3), 8.28 (broad s, 3 H-18), 8.97 (d, 3 H-17, J = 6 Hz), and 9.08 (s, 3 H-20).

Anal. Calcd. for $C_{22}H_{30}O_4$: C, 73.71; H, 8.44. Found: C, 73.83; H, 8.52.

Oxidation of Diacetate 1h

The crude product (51 mg) obtained from oxidation of the diacetate **1***h* (50 mg) with chromium trioxide (120 mg) for 17 days at 20°, was submitted to preparative t.l.c. (ethyl acetate – light petroleum, 2:3). This furnished two components, starting material (18 mg) and the more polar enone-diacetate **17***e* (16 mg). The latter, an oil, after distillation at 150°/0.03 mm had ν_{max} 1753, 1675, 1220, and 875 cm^{-1}; τ 4.05 (s, 1 H-3), 5.28 (narrow m, 2 H-18), 5.86 (d, 1 H-19, J = 11 Hz), 6.13 (d, 1 H-19, J = 11 Hz), 7.91, 8.02 (both s, 3H each, 2 —OCOCH_3), 8.99 (d, 3 H-17, J = 7 Hz), and 9.12 (s, 3 H-20).

Can. J. Chem. Downloaded from www.nrcresearchpress.com by 210.87.254.40 on 09/05/12
For personal use only.

Anal. Calcd. for $C_{24}H_{32}O_6$: C, 69.21; H, 7.74. Found: C, 69.21; H, 7.72.

Oxidation of Diol 1g

(*i*) The diol **1***g* (50 mg) in dry pyridine (20 ml) was treated at 20° for 14 h with chromium trioxide (50 mg). The oily product (55 mg) resulting from work-up was purified by preparative t.l.c. (ethyl acetate – light petroleum, 1:19) and afforded as the sole product the lactone **2** (37 mg) which crystallized from ethyl acetate – light petroleum and had m.p. 89–90°, $[\alpha]_D$ +8° (*c*, 1.5). It was identical (m.p., mixed m.p., n.m.r., i.r., t.l.c.) with a sample of the naturally occurring lactone (see above).

(*ii*) The diol **1***g* (75 mg) in dry pyridine (2 ml) was treated at 20° for 14 h with a large excess of chromium trioxide (500 mg). The product consisted of two components (t.l.c.), the less polar of which corresponded to the lactone (**2**) obtained previously. Separation of the two compounds was effected by preparative t.l.c. and afforded **2** (11 mg) as the minor component. The more polar, major product (47 mg) the enone-lactone **27**, crystallized from ethyl acetate – light petroleum and had m.p. 148–149°; $[\alpha]_D$ −9° (*c*, 1.2); ν_{max} 1779, 1690, and 872 cm^{-1}; τ 3.56 (s, 1 H-3), 5.50 (d, 1 H-19, J = 8 Hz), 6.03 (d, 1 H-19, J = 8 Hz), 9.03 (s, 3 H-20), and 9.10 (d, 3 H-17, J = 6 Hz); *m/e* 328 (M).

Anal. Calcd. for $C_{20}H_{24}O_4$: C, 73.14; H, 7.37. Found: C, 73.11; H, 7.23.

Oxidation of the Monoacetate 1n

The known (1) monoacetate **1***n* (50 mg) was oxidized in dry pyridine (2 ml) with chromium trioxide (50 mg) for 14 h. Work-up gave the crude product (52 mg) which consisted of two compounds (t.l.c.), the more polar being the much more abundant. This component, the acetoxy-aldehyde **1***q* (37 mg) was isolated by preparative t.l.c. (ethyl acetate – light petroleum 1:3). It was an oil which after distillation at 155°/0.025 mm had $[\alpha]_D$ −21° (*c*, 0.88); ν_{max} 2710, 1745, 1695, 1235 and 874 cm^{-1}; τ 0.73 (s, 1H-18), 3.29 (t, 1 H-3, J_{obs} = 4 Hz), 5.51 (d, 1 H-19, J = 12 Hz), 5.77 (d, 1 H-19, J = 12 Hz), 8.14 (s, 3H, —OCOCH_3), 8.97 (s, 3 H-20), and 9.16 (d, 3 H-17, J = 6 Hz); *m/e* 358 (M).

Anal. Calcd. for $C_{22}H_{30}O_4$: C, 73.71; H, 8.44. Found: 73.70; H, 8.42.

Oxidation of Monoacetate 1m

(*i*) Oxidation of the known (I) monoacetate **1***m* (45 mg) with chromium trioxide (50 mg) in dry pyridine (20 ml) at 20° for 12 h and work-up afforded an oil (49 mg) which consisted of essentially one compound (t.l.c.). This compound, the acetoxy-aldehyde **1***r* was purified by preparative t.l.c. (chloroform – light petroleum, 4:1) and then distillation at 160°/0.04 mm. The resulting oil had $[\alpha]_D$ −89° (*c*, 0.8); ν_{max} 2690, 1745, 1725, 1230, and 878 cm^{-1}; τ 0.53 (s, 1 H-19), 4.03 (m, 1 H-3), 5.82 (s, 2 H-18), 8.08 (s, 3H, —OCOCH_3), 9.02 (s, 3 H-20), and 9.23 (d, 3 H-17, J = 6 Hz); *m/e* 358 (M).

Anal. Calcd. for $C_{22}H_{30}O_4$: C, 73.71, H, 8.44. Found: C, 73.86; H, 8.47.

(*ii*) When the monoacetate **1***m* (130 mg) was oxidized in dry pyridine (2 ml) at 20° for 12 h with a large excess of chromium trioxide (500 mg) the only product isolable, by preparative t.l.c. (chloroform – light petroleum, 1:9), was the aldehydo-epoxide **28** (90 mg). This was purified further by distillation at 150°/0.015 mm and the resulting oil had $[\alpha]_D$ +3° (*c*, 1.3); ν_{max} 2710, 1755, 1722, 1230, and 878 cm^{-1}; τ 0.05 (s, 1 H-19), 6.09 (d, 1 H-18, J = 12 Hz), 6.40 (d, 1 H-18, J = 12 Hz), 6.97 (s, 1 H-3, $w_{1/2}$ = 4 Hz), 8.04 (s, 3H, —OCOCH_3), 9.13 (s, 3 H-20), and 9.25 (d, 3 H-17, J = 6 Hz); *m/e* 374 (M).

Anal. Calcd. for $C_{22}H_{30}O_5$: C, 70.56; H, 8.08. Found: C, 70.21; H, 7.89.

Reduction of the Aldehydo-epoxide 28

Reduction of the aldehydo-epoxide **28** (60 mg) with excess lithium aluminum hydride in refluxing dry ether for 14 h afforded an oily mixture (t.l.c.) of products (57 mg) the less polar of which was the more abundant. This compound was isolated by preparative t.l.c. (methanol–chloroform, 3:97) and had $[\alpha]_D$ −27° (*c*, 0.91). It was identical (n.m.r., t.l.c.) with the triol **11***a* prepared from the epoxy-hemiacetal **4***a*. Acetylation furnished the hydroxy-diacetate **11***b* (35 mg), $[\alpha]_D$ −16° (*c*, 1.0) which was identical (t.l.c., n.m.r., i.r.) with a sample prepared from **4***a* (see above).

Oxidation of Diol 30b

Diol **30***b* was prepared by reduction of confertifolin[6] (**31**) (14) with lithium aluminum hydride and a sample (150 mg), m.p. 123°, was then treated with chromium trioxide (200 mg) in dry pyridine (2 ml) at 20° for 14 h. Work-up afforded a crude product which consisted (t.l.c.) essentially of three components. These were separated by preparative t.l.c. (ethyl acetate – light petroleum, 1:19). The major, and least polar, constituent was the furan **33** (57 mg) which after distillation *in vacuo* had ν_{max} 889 cm^{-1}; τ 2.93 (s, 1 H-11 and 1 H-12), 8.81, 9.08, and 9.10 (all s, 3H each, quaternary C—CH_3's).

Anal. Calcd. for $C_{15}H_{22}O$: C, 82.51; H, 10.16. Found: C, 82.40; H, 10.12.

The minor components were of similar polarity. The less polar of the two was isodrimenin (**34** (14), 37 mg), m.p. 125–127°, the identity of which was established by comparison (n.m.r., t.l.c., mixed m.p.) with an authentic sample. The more polar was confertifolin (**31** (14), 34 mg), m.p. 150–152°, the identity of which was also established by comparison (n.m.r., t.l.c., mixed m.p.) with an authentic sample.

Oxidation of Diacetate 30a

Acetylation of diol **30***b* (14) furnished the corresponding diacetate (**30***a*) as an oil which after distillation at 100°/0.05 mm had ν_{max} 1743 and 1225 cm^{-1}; τ 5.37, 5.40 (both s, 2 H-11 and 2 H-12), 7.93, 7.97 (both s, 3H each, 2 —OCOCH_3), 8.97, 9.03, and 9.10 (all s, 3H each quaternary C—CH_3's).

Anal. Calcd. for $C_{19}H_{30}O_4$: C, 70.77; H, 9.38. Found: C, 71.05; H, 9.55.

A portion (80 mg) of this diacetate was treated with chromium trioxide (200 mg) in dry pyridine (2 ml) at 20° for 16 days and afforded an oily product which contained two major components. These were separated by preparative t.l.c. (ethyl acetate – light petroleum, 1:3). The less polar component was substrate (23 mg) and the more polar the enone-diacetate **32***a* (47 mg) which was purified further by distillation *in vacuo*. The resulting oil had ν_{max} 1750, 1685, and 1230 cm^{-1}; τ 5.16 (s, 2 H-11 and 2

[6]We are grateful to Dr. K. H. Overton for suppling samples of confertifolin, isodrimenin, and drimenol.

Can. J. Chem. Downloaded from www.nrcresearchpress.com by 210.87.254.40 on 09/05/12
For personal use only.

H-12), 7.95, 8.00 (both s, 3H each, 2 —OCOCH_3), 8.81, 9.06, and 9.08 (all s, 3H each, quaternary C—CH_3's); *m/e* 336 (M).

Anal. Calcd. for $C_{19}H_{28}O_5$: C, 67.83; H, 8.39. Found: C, 68.26; H, 8.47.

Oxidation of Drimenyl Acetate ***25b***

Drimenyl acetate (**25***b* (15), 70 mg) in dry pyridine (2 ml) was treated at 20° with chromium trioxide (200 mg) for 16 days. The oily product (77 mg) was separated into two components by preparative t.l.c. (ethyl acetate – light petroleum, 3:17). The less polar was starting material (23 mg). The more polar, the enone-acetate **32***b* (33 mg) was obtained as an oil which slowly crystallized at 0° and had m.p. 48–50°; ν_{max} 1745, 1677 and 1228 cm^{-1}; τ 5.27 (d, 1 H-11, J = 13 Hz), 5.29 (d, 1 H-11, J = 13 Hz), 7.97 (s, 3H, —OCOCH_3), 8.24 (s, 3 H-12), 8.91, 9.10, and 9.13 (all s, 3H each, quaternary C—CH_3's).

Anal. Calcd. for $C_{17}H_{26}O_3$: C, 73.34; H, 9.41. Found: C, 73.10; H, 9.40.

Oxidation of the Furano-olefin ***35a***

Treatment of the furano-olefin **35***a* (16, 50 mg) in dry pyridine (4 ml) with chromium trioxide (61 mg) at 20° for 4 weeks afforded an oil (45 mg) on work-up. This oil was separated into two components by preparative t.l.c. (ethyl acetate – light petroleum, 1:4). The less polar was unreacted furano-olefin (**35***a*, 24 mg). The other component was the oily enone **35***b* (16 mg) which was distilled *in vacuo* and had ν_{max} 1665 cm^{-1}; λ_{max} 239 nm (ε 10 500); c.d. in ethanol $[\theta]_{325}$ −4800 and $[\theta]_{241}$ +17 600; c.d. in chloroform $[\theta]_{331}$ −4500; τ 4.37 (q, 1 H-3, J = 1 Hz), 8.13 (d, 3 H-18, J = 1 Hz), 8.87 (s, 3 H-19), 9.12 (d, 3 H-17, J = 6 Hz), and 9.17 (s, 3 H-20).

Mol. Wt. Calcd. for $C_{20}H_{28}O_2$: 300.2089. Found (high resolution mass spectrometry): 300.2094.

Oxidation of Cholesteryl Acetate ***36a***

Cholesteryl acetate (**36***a*, 330 mg) in dry pyridine (10 ml) was treated with chromium trioxide (800 mg) at 20° for 14 days. The product (340 mg) when subjected to preparative t.l.c. (ethyl acetate – light petroleum, 3:17) gave two major fractions. The less polar was starting material (130 mg) and the other, the known (8) enone-acetate **36***b* (68 mg). It crystallized from light petroleum and had m.p. 154° (lit. value 161–163°); ν_{max} 1740 and 1682 cm^{-1}; τ 4.30 (s, 1 H-6) and 5.33 (m, 1 H-3, $w_{1/2}$ = 20 Hz).

Dehydration of Methyl Marrubiate ***40a***

Methyl marrubiate (**40***a*, 421 mg) in dry pyridine was treated at 20° for 7 days with toluene-*p*-sulfonyl chloride according to the method developed (21) by Burn and Rigby for the dehydration of marrubiic acid. Work-up afforded an oil (414 mg) which consisted essentially of only one compound, **37***a*. This was purified by preparative t.l.c. (chloroform) and distillation at 130°/0.02 mm. The resulting oil had ν_{max} 3650, 1772, and 882 cm^{-1}; τ 4.17 (t, 1 H-6, J_{obs} = 3 Hz), 6.37 (s, 3H, —OCH_3), 8.70 (s, 3H, quaternary C—CH_3), 9.00 (d, 3 H-17, J = 6 Hz), and 9.07 (s, 3H, quaternary C—CH_3).

Anal. Calcd. for $C_{21}H_{30}O_4$: C, 72.80; H, 8.73. Found: C, 72.61; H, 8.62.

This compound was further characterized by preparation of the corresponding primary alcohol (**37***c*) which was furnished by reduction of **37***b* with lithium aluminum hydride in refluxing ether. It was obtained as an oil, τ 4.38 (broad s, 1 H-6), 6.43 (d, 1 H-19, J = 11 Hz), 6.75 (d, 1 H-19, J = 11 Hz), 8.88, 8.92, (both s, 3H each, quaternary C—CH_3's) and 8.99 (d, 3 H-17, J = 6 Hz).

Anal. Calcd. for $C_{20}H_{30}O_3$: C, 75.43; H, 9.50. Found: C, 75.13; H, 9.27.

The corresponding acetate **37***d*, also an oil, had τ 4.29 (t, 1 H-6, J_{obs} = 3 Hz), 5.86 (d, 1 H-19, J = 11 Hz), 6.15 (d, 1 H-19, J = 11 Hz), 8.90 (s, 6H, quaternary C—CH_3's) and 9.00 (d, 3 H-17, J = 6 Hz).

Anal. Calcd. for $C_{22}H_{32}O_4$: C, 73.30; H, 8.95. Found: C, 73.15; H, 8.92.

Oxidation of the Olefinic-ester ***37a***

Oxidation of the ester **37***a* (750 mg) in dry pyridine (3 ml) with chromium trioxide (500 mg) at 20° for 10 days afforded an oily product (687 mg). This material was chromatographed over neutral alumina (grade III; 60 g). Early fractions containing unreacted **37***a* (320 mg) were eluted with ethyl acetate – light petroleum (1:19). The enone **38***a* (360 mg) was eluted next (ethyl acetate – light petroleum, 3:17) as an oil which had ν_{max} 1730, 1680, and 878 cm^{-1}; λ_{max} 241 nm (ε 12 000); τ 3.82 (sharp s, 1 H-6), 6.38 (s, 3 H, —OCH_3), 8.61 (s, 3 H quaternary C—CH_3) 8.73 (d, 3 H-17, J = 6 Hz), and 8.86 (s, 3H, quaternary C—CH_3). No satisfactory elemental analysis was obtained for this compound and it was characterized by preparation of **38***c*. Reduction of **38***a* with lithium aluminum hydride in refluxing ether gave a mixture (t.l.c.) of two triols (epimeric at C-7). This mixture was oxidized with the Sarett reagent and afforded **38***c*, an oil, which had ν_{max} 1720, 1670 and 882 cm^{-1}; λ_{max} 240 nm (ε 12 500); τ 0.79 (s, 1 H-19), 3.87 (sharp s, 1 H-6), 8.70 (d, 3 H-17, J = 7 Hz), 8.82 and 8.90 (both s, 3H each, quaternary C—CH_3's).

Anal. Calcd. for $C_{20}H_{26}O_4$: C, 72.70; H, 7.93. Found: C, 72.65; H, 8.01.

Preparation of the Furano-olefin ***37b***

The known (5) ketone **41** (176 mg) was heated with excess lithium aluminum hydride in refluxing dry ether for 18 h. The product (182 mg) was chromatographed over neutral alumina (Grade III; 25 g), the major component, the axial alcohol **40***b* (88 mg), being eluted with ethyl acetate – light petroleum (1:9). This alcohol failed to crystallize and was purified by distillation at 155°/0.05 mm. It had ν_{max} 3610, 3390, and 865 cm^{-1}; τ 5.70 (m, 1 H-6, $w_{1/2}$ = 7 Hz), 8.75, 8.78, 9.02 (all s, 3H each, quaternary C—CH_3's), and 9.05 (d, 3 H-17, J = 6 Hz).

Anal. Calcd. for $C_{20}H_{32}O_3$: C, 74.96; H, 10.06. Found: C, 74.73; H, 10.03.

The diol **40***b* (66 mg) in dry pyridine (2 ml) was treated at 20° for 80 min with methane sulfonyl chloride (1 ml). The oil obtained (72 mg) was subjected to preparative t.l.c. (ethyl acetate – light petroleum, 1:19) and afforded the olefin **37***b* (57 mg) which was distilled *in vacuo*. The resulting oil had ν_{max} 3560 and 878 cm^{-1}; τ 4.36 (t, 1 H-6, J_{obs} = 3 Hz), 8.85, 8.88, and 8.90 (all s, 3H each, quaternary C—CH_3's), and 9.00 (d, 3 H-17, J = 6 Hz).

Mol. Wt. Calcd. for $C_{20}H_{30}O_2$: 302.2246. Found (high resolution mass spectrometry): 302.2250.

This olefin (50 mg) in dry pyridine (3 ml) was treated at 20° with chromium trioxide (100 mg) for 25 days. The crude product was submitted to preparative t.l.c. (chloro-

form) which furnished the only isolable product, the enone-lactone **39** (19), (7 mg). This material solidified after distillation *in vacuo* and had m.p. 128–134° and was identical (t.l.c., i.r., u.v., mass spectra) with a sample of **39** supplied by Dr. Rivett. A further sample (16 mg) of the olefin **37***b* was oxidized in dry pyridine (2 ml) with chromium trioxide (35 mg) for 5 days. The product contained (t.l.c.) essentially only two components. These were separated by preparative t.l.c. (ethyl acetate – light petroleum, 1:1). The less polar was starting material (3 mg) and the other, compound Y (**38***b*, (19), 8.5 mg) which crystallized from ethyl acetate – light petroleum. It had m.p. 110–114°, $[\alpha]_D$ −23° (*c*, 0.8), and was identical (mixed m.p. (110–114°), t.l.c., i.r., u.v.) with a sample of **38***b*, m.p. 112–114°, provided by Dr. Rivett.

We thank the Science Research Council of the U.K. for a maintenance award (to M.S.H.) and the National Research Council of Canada for an operating grant (to R.McC.). We are also indebted to Dr. T. Anthonsen, Trondheim, for the high resolution mass spectra and to Mr. E. Nakamura for performing the experiment which effected conversion of **37***b* into **38***b*.

1. T. ANTHONSEN, M. S. HENDERSON, A. MARTIN, R. D. H. MURRAY, R. MCCRINDLE, and D. MCMASTER. Can. J. Chem. This issue. Preceding paper.
2. T. ANTHONSEN, M. S. HENDERSON, A. MARTIN, R. MCCRINDLE, and R. D. H. MURRAY. Acta Chem. Scand. **22**, 351 (1968).
3. P. R. JEFFERIES and T. G. PAYNE. Tetrahedron Lett. 4777 (1967).
4. K. TORI, T. KOMENO, and T. NAKAGAWA. J. Org. Chem. **29**, 1136 (1964).
5. T. ANTHONSEN, P. H. MCCABE, R. MCCRINDLE, and R. D. H. MURRAY. Tetrahedron, **25**, 2233 (1969).
6. R. A. APPLETON, J. W. B. FULKE, M. S. HENDERSON, and R. MCCRINDLE. J. Chem. Soc. C, 1943 (1967).
7. M. S. HENDERSON. Ph.D. Thesis. University of Glasgow, Glasgow, Scotland. 1969.
8. W. G. DAUBEN, M. LORBER, and D. S. FULLERTON. J. Org. Chem. **34**, 3587 (1969).
9. I. YOSIOKA and T. KIMARA. Chem. Pharm. Bull. **13**, 1430 (1965).
10. C. NISHINO, K. KAWAZU, and T. MITSUI. Agr. Biol. Chem. **35**, 1921 (1971); K. KAWAZU, C. NISHINO, R. MCCRINDLE, and D. MCMASTER. Agr. Biol. Chem. **36**, 1245 (1972).
11. C. J. W. BROOKS, G. LINDSAY, and K. H. OVERTON. J. Chem. Soc. C, 203 (1970).
12. K. B. WIBERG. Oxidation in organic chemistry. Academic Press, New York. 1965.
13. E. GLOTTER, S. GREENFIELD, and D. LAVIE. J. Chem. Soc. C, 1646 (1968).
14. H. H. APPEL, J. D. CONNOLLY, K. H. OVERTON, and R. P. M. BOND. J. Chem. Soc. 4685 (1960).
15. H. H. APPEL, C. J. W. BROOKS, and K. H. OVERTON. J. Chem. Soc. 3322 (1959).
16. M. S. HENDERSON, R. MCCRINDLE, D. MCMASTER, and R. D. H. MURRAY. Can. J. Chem. This issue.
17. K. BLOCH. Helv. Chim. Acta, **36**, 1611 (1953).
18. M. S. HENDERSON and R. MCCRINDLE. J. Chem. Soc. C, 2014 (1969).
19. E. R. KAPLAN and D. E. A. RIVETT. J. Chem. Soc. C, 262 (1968).
20. L. MANGONI, M. ADINOLFI, G. LAONIGRO, and R. CAPUTO. Tetrahedron, **28**, 611 (1972).
21. D. BURN and W. RIGBY. J. Chem. Soc. 2964 (1957).

Can. J. Chem. Downloaded from www.nrcresearchpress.com by 210.87.254.40 on 09/05/12
For personal use only.

Base-catalyzed Degradations of Carbohydrates. V. The Conversion of 3-Deoxyhex-2-enopyranoses into 2-Furoic Esters

G. O. ASPINALL,[1] R. KHAN, R. R. KING, AND ZOFIA PAWLAK[2]

Department of Chemistry, Trent University, Peterborough, Ontario

Received October 30, 1972

Condensation of 2,3,4-tri-*O*-acetyl-α-D-xylopyranosyl bromide and benzyl 2,3,4-tri-*O*-methyl-β-D-glucopyranoside (**2**), followed by removal of protecting groups, affords 2,3,4-tri-*O*-methyl-6-*O*-(β-D-xylopyranosyl)-D-glucopyranose (**5**). Alkaline degradation of the disaccharide **5**, followed by treatment with dilute acid, furnishes 5-β-D-xylopyranosyloxymethyl-2-furaldehyde (**8**), which is converted by oxidation and esterification, followed by acetylation, into methyl 5-(2,3,4-tri-*O*-acetyl-β-D-xylopyranosyloxymethyl)-2-furoate (**11**), whose structure has been confirmed by direct synthesis.

La condensation du bromure de tri-*O*-acétyl-2,3,4 α-D-xylopyranosyle et du benzyl tri-*O*-méthyl-2,3,4 β-D-glucopyranoside (**2**), suivie de l'enlèvement des groupes protecteurs, fournit le tri-*O*-méthyl-2,3,4 *O*-(β-D-xylopyranosyl)-6 D-glucopyranose (**5**). La dégradation alcaline du disaccharide **5** suivie d'un traitement acide dilué, conduit au β-D-xylopyranosyloxyméthyl-5 furaldéhyde-2 (**8**) qui est converti après oxydation, estérification et acétylation, en (tri-*O*-acétyl-2,3,4 β-D-xylopyranosyloxyméthyl)-5 furoate-2 de méthyle (**11**) dont la structure a été confirmée par synthèse directe.

[Traduit par le journal]

Can. J. Chem., **51**, 1359 (1973)

Can. J. Chem. Downloaded from www.nrcresearchpress.com by 210.87.254.6 on 09/05/12
For personal use only.

3-Deoxyhex-2-enopyranoses, which are formed on alkaline degradation of 2,3-di- and higher *O*-substituted hexopyranoses, may be converted into γ-pyrones (kojic acid derivatives) in a series of reactions in which the initial step involves oxidation with *m*-chloroperbenzoic acid (1, 2). The overall yields in these transformations are not high and of the *O*-substituents originally present only that at O-6 remains in the final product. A much simpler transformation with loss of the same *O*-substituents occurs when 3-deoxyhex-2-enopyranoses are treated with dilute acid, as in the conversion of 3-deoxy-2,4,6-tri-*O*-methyl-D-*erythro*-hex-2-enopyranose into 5-methoxymethyl-2-furaldehyde (3). The disaccharide, 2,3,4-tri-*O*-methyl-6-*O*-(β-D-xylopyranosyl)-D-glucopyranose (**5**), has been synthesized as a model compound for regions of branching in polysaccharides in which alkaline degradation would lead to 3-deoxy-6-*O*-glycosylhex-2-enopyranoses, and the reaction sequence, alkaline degradation, treatment with dilute acid, and appropriate derivatization, has been studied.

The synthesis of the disaccharide **5** from benzyl β-D-glucopyranoside was performed in the following stages: (*i*) tritylation and methylation to give benzyl 2,3,4-tri-*O*-methyl-6-*O*-trityl-β-D-glucopyranoside (**1**), (*ii*) detritylation, (*iii*) condensation of the derived benzyl 2,3,4-tri-*O*-methyl-β-D-glucopyranoside (**2**) with 2,3,4-tri-*O*-acetyl-α-D-xylopyranosyl bromide to give the fully-substituted disaccharide derivative **3**, (*iv*) de-*O*-acetylation to afford the benzyl glycoside **4**, and (*v*) catalytic hydrogenolysis. Treatment of the disaccharide **5** with oxygen-free saturated lime-water furnished 3-deoxy-2,4-di-*O*-methyl-

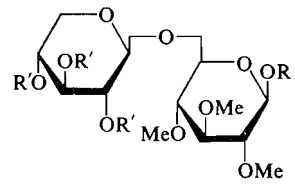

3 R = Bn (benzy), R′ = Ac
4 R = Bn, R′ = H
5 R = R′ = H

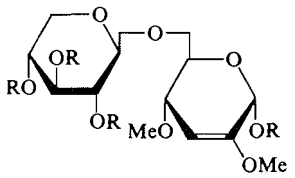

6 R = H
7 R = Ac

[1]Present address to which correspondence should be sent: Department of Chemistry, York University, Downsview, Ontario.

[2]On leave (1969–1970) from the Department of Organic Chemistry, University of Warsaw, Warsaw, Poland.

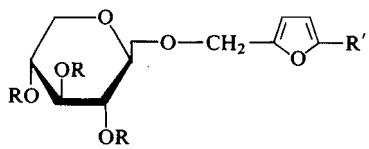

8 R = H; R′ = CHO
10 R = H; R′ = CO_2CH_3
11 R = Ac; R′ = CO_2CH_3

6-*O*-(β-D-xylopyranosyl)-D-*erythro*-hex-2-enopyranose (**6**) which was characterized by conversion into the crystalline 1-*O*-acetyl-3-deoxy-2,4-di-*O*-methyl-6-*O*-(2,3,4-tri-*O*-acetyl-β-D-xylopyranosyl)-α-D-*erythro*-hex-enopyranose (**7**).

Reaction of the hex-2-enopyranose **6** with dilute acid at room temperature furnished the crystalline 5-β-D-xylopyranosyloxymethyl-2-furaldehyde (**8**). In order to obtain more stable furan derivatives which could be synthesized independently and which might serve as reference compounds for polysaccharide degradations, 2-furaldehydes were converted into methyl 2-furoates by the procedure of Corey *et al.* (4). Treatment of 5-hydroxymethyl-2-furaldehyde with activated manganese dioxide in methanol in the presence of sodium cyanide and acetic acid afforded methyl 5-hydroxymethyl 5-hydroxymethyl-2-furoate (**9**), and similar reaction of the 2-furaldehyde derivative **8** furnished methyl 5-(β-D-xylopyranosyloxymethyl)-2-furoate (**10**) which was further converted into the triacetate **11**. Methyl 5-(2,3,4-tri-*O*-acetyl-β-D-xylopyranosyloxymethyl)-2-furoate (**11**), thus obtained, was identical with a sample prepared by condensation of 2,3,4-tri-*O*-acetyl-α-D-xylopyranosyl bromide and methyl 5-hydroxymethyl-2-furoate (**9**). Attempts to de-*O*-acetylate the triacetate **11** with sodium methoxide in methanol were unsuccessful. Since t.l.c. of the reaction products failed to reveal the presence of typical u.v.-absorbing furan derivatives, it is probable that 2-furoic esters, like other furans with strongly electron-withdrawing 2-substituents, *e.g.* 2-nitrofuran (5), undergo ready ring opening in the presence of base. De-*O*-acetylation was satisfactorily achieved with retention of the *O*-glycosyl substituent when methanolic hydrogen chloride was used (6). Base-sensitivity of such furan derivatives probably also accounts for our failure to methylate the sugar residue in **10** using methyl iodide and silver oxide in *N*,*N*-dimethylformamide (7). Repeated treatments of compound **10** with diazomethane – boron trifluoride failed to achieve complete methylation.

Experimental

Unless otherwise stated experimental procedures were as described in Part III (1).

Benzyl 2,3,4-Tri-O-methyl-6-O-trityl-β-D-glucopyranoside (1)

Reaction of benzyl β-D-glucopyranoside (8) (10 g) with chlorotriphenylmethane in pyridine under standard conditions (9) followed by normal work-up and chromatography on silica gel furnished syrupy benzyl 6-*O*-trityl-β-D-glucopyranoside (18 g, 94%). The trityl ether (3.1 g) was methylated with methyl iodide and sodium hydride in *N*,*N*-dimethylformamide (10), and recrystallization of the product from ethanol gave benzyl 2,3,4-tri-*O*-methyl-6-*O*-trityl-β-D-glucopyranoside (**1**) (2.8 g, 83%), m.p. 134–135°, $[\alpha]_D$ −3.2° (*c*, 1.0); n.m.r.: τ 2.40–2.86 (20-proton multiplet, 4 × phenyl), 5.64 (1-proton doublet, $J_{1,2}$ = 7.5 Hz, H-1), 6.38, 6.41, 6.72 (3-proton singlets, 3 × OCH_3).

Anal. Calcd. for $C_{35}H_{38}O_6$: C, 75.83; H, 6.87. Found: C, 75.58; H, 6.81.

Benzyl 2,3,4-Tri-O-methyl-β-D-glucopyranoside (2)

The trityl ether **1** (10 g) in glacial acetic acid (80 ml) was heated to 80°, water was added slowly whilst maintaining complete solution, and the solution was kept at 80° for 1 h and at room temperature overnight. Precipitated tritanol was removed by filtration and washed with cold acetic acid – water (4:1), and the combined filtrate and washings were concentrated during which process further tritanol separated. The syrupy residue was diluted with ethanol and pentane to induce crystallization, and recrystallization from ether–pentane furnished benzyl 2,3,4-tri-*O*-methyl-β-D-glucopyranoside (**2**) (4.8 g, 85%), m.p. 53–54°, $[\alpha]_D$ −46.5° (*c*, 1.0 in CH_2Cl_2); n.m.r.: τ 2.60 (5-proton multiplet, phenyl), 5.64 (1-proton doublet, $J_{1,2}$ = 7.5 Hz, H-1), 6.38, 6.41, 6.49 (3-proton singlets, 3 × OCH_3).

Anal. Calcd. for $C_{16}H_{24}O_6$: C, 61.53; H, 7.68. Found: C, 61.46; H, 7.72.

Benzyl 2,3,4-Tri-O-methyl-6-O-(2,3,4-tri-O-acetyl-β-D-xylopyranosyl)-β-D-glucopyranoside (3)

The benzyl glycoside **2** (4.2 g), silver carbonate (8.3 g), and Drierite (23 g) were stirred in dichloromethane in the dark for 24 h. Iodine (1.4 g) and 2,3,4-tri-*O*-acetyl-α-D-xylopyranosyl bromide (4.1 g) were added and the mixture was stirred at room temperature for 48 h. The inorganic residue was removed by filtration, and the filtrate was concentrated to a syrup which crystallized from ether to give benzyl 2,3,4-tri-*O*-methyl-6-*O*-(2,3,4-tri-*O*-acetyl-β-D-xylopyranosyl)-β-D-glucopyranoside (**3**) (3.5 g, 46%), m.p. 127–129°, $[\alpha]_D$ −75° (*c*, 1.0); n.m.r.: τ 2.64 (5-proton multiplet, phenyl), 6.40 (6-proton singlet, 2 × OCH_3), 6.51 (3-proton singlet, OCH_3), 7.93 (9-proton singlet, 3 × $OCOCH_3$).

Anal. Calcd. for $C_{27}H_{38}O_{13}$: C, 56.80; H, 6.71. Found: C, 56.75; H, 7.17.

Benzyl 2,3,4-Tri-O-methyl-6-O-(β-D-xylopyranosyl)-β-D-glucopyranoside (4)

Methanolic 1.5 *N* barium methoxide (2 ml) was added to the fully-substituted disaccharide **3** (2.39 g) in methanol (100 ml) and the solution was kept at room temperature for 4 h. The solution was deionized by shaking with

Can. J. Chem. Downloaded from www.nrcresearchpress.com by 210.87.254.6 on 09/05/12
For personal use only.

Can. J. Chem. Downloaded from www.nrcresearchpress.com by 210.87.254.6 on 09/05/12
For personal use only.

Amberlite resins IR-120(H) and IR-45(OH) and the filtrate was concentrated to a syrup which crystallized from ether–pentane to give benzyl 2,3,4-tri-*O*-methyl-6-*O*-(β-D-xylopyranosyl)-β-D-glucopyranoside (**4**) as a monohydrate (1.6 g, 86%), m.p. 67–68°, $[\alpha]_D$ −65.2° (*c*, 1.2).

Anal. Calcd. for $C_{21}H_{32}O_{10}.H_2O$: C, 54.54; H, 6.90; OCH_3, 20.10. Found: C, 54.33; H, 7.07; OCH_3, 20.08.

2,3,4-Tri-O-methyl-6-O-(β-D-glucopyranose) (5)

The benzyl glycoside **4** (0.3 g) in ethanol–water (4:1, 10 ml) was shaken in hydrogen at atmospheric pressure over 5% palladium–charcoal for 18 h. Catalyst was removed by filtration and the filtrate was concentrated to a syrup which crystallized from acetone–pentane to give the disaccharide **5** (0.17 g, 71%), m.p. 142°, $[\alpha]_D$ +7° → +22.7° (equil.) (*c*, 1.0 in water).

Anal. Calcd. for $C_{14}H_{26}O_{10}$: C, 47.46; H, 7.31; OCH_3, 25.54. Found: C, 46.93; H, 7.66; OCH_3, 25.54.

1-O-Acetyl-3-deoxy-2,4-di-O-methyl-6-O-(2,3,4-tri-O-acetyl-β-D-xylopyranosyl)-α-D-erythro-hex-2-enopyranose (7)

The disaccharide **5** (0.2 g) was kept in oxygen-free saturated lime-water (20 ml) at 50° for 30 h. The cooled solution was neutralized with carbon dioxide and concentrated. The residue was extracted with acetone and the filtered solution was concentrated to give syrupy 3-deoxy-2,4-di-*O*-methyl-6-*O*-(β-D-xylopyranosyl)-D-erythro-hex-2-enopyranose (**6**); λ_{max} (H_2O) 198 nm; ν_{max} (film) 1660 cm^{-1} (C=C). Treatment of a sample of the hex-2-enopyranose **6** with acetic anhydride and pyridine in the usual way furnished 1-*O*-acetyl-3-deoxy-2,4-di-*O*-methyl-6-*O*-(2,3,4-tri-*O*-acetyl-β-D-xylopyranosyl)-α-D-erythro-hex-2-enopyranose (**7**) which, after crystallization from ether–pentane, had m.p. 137–138°, $[\alpha]_D$ −27.5° (*c*, 1.0); *m/e* 490 (M^+) (1), 430 ($M - CH_3CO_2H$) (11), 43 (100); ν_{max} 1745 (acetate C=O), 1660 cm^{-1} (C=C); n.m.r.: τ 3.96 (1-proton singlet, H-1), 6.41, 6.63 (3-proton singlets, 2 × OCH_3), 7.89, 7.93 (3-proton singlets, 4 × $OCOCH_3$).

Anal. Calcd. for $C_{21}H_{30}O_{13}$: C, 51.41, H, 6.17. Found: C, 51.57; H, 6.58.

5-β-D-Xylopyranosyloxymethyl-2-furaldehyde (8)

The hex-2-enopyranose **6** (140 mg) was kept in 0.1 *N* hydrochloric acid (5 ml) at room temperature for 4 days. The solution was neutralized with silver carbonate, filtered, and concentrated to a syrup. The syrup was purified by preparative layer chromatography (ethyl acetate – ethanol, 10:1) to give 5-β-D-xylopyranosyloxymethyl-2-furaldehyde (**8**) (86 mg) as a syrup which crystallized from ethyl acetate and then had m.p. 124–126°, $[\alpha]_D$ −23° (*c*, 1.0); λ_{max} 282 nm (log ε 3.2); ν_{max} 3410 (OH), 1675 (aromatic aldehyde), 1590, 1540 cm^{-1} (heteroaromatic C=C).

Anal. Calcd. for $C_{11}H_{14}O_7$: C, 51.16; H, 5.47. Found: C, 51.29; H, 5.92.

Methyl 5-β-D-Xylopyranosyloxymethyl-2-furoate (10) and Derived Triacetate (11)

Corey oxidation (4) of 5-hydroxymethyl-2-furaldehyde, as a model compound gave methyl 5-hydroxymethyl-2-furoate (11). In a similar manner the 2-furaldehyde derivative **8** (60 mg) in methanol (10 ml) was stirred with sodium cyanide (80 mg), acetic acid (30 mg), and activated manganese dioxide (570 mg) at room temperature for 4 h. The reaction mixture was worked-up as described above and crystallization of the product from ethyl acetate furnished methyl 5-β-D-xylopyranosyloxymethyl-2-furoate (**10**) (42 mg), m.p. 136–138°, $[\alpha]_D$ −21° (*c*, 1.0); ν_{max} 3410 (OH), 1705 (aryl ester C=O), 1596, 1545 cm^{-1} (heteroaromatic C=C).

Anal. Calcd. for $C_{12}H_{16}O_8$: C, 50.00; H, 5.60. Found: C, 49.48; H, 5.63.

The methyl ester **10** (30 mg) in pyridine (3 ml) and acetic anhydride (2 ml) was kept at 0° for 1 h and at room temperature overnight. The reaction mixture was worked-up in the usual way and crystallization of the product from ether – light petroleum afforded methyl 5-(2,3,4-tri-*O*-acetyl-β-D-xylopyranosyloxymethyl)-2-furoate (**11**) (28 mg), m.p. 165–167°, $[\alpha]_D$ −18° (*c*, 1.0); M^+, 414; ν_{max} 1740 (acetate C=O), 1722 (aryl ester C=O), 1590, 1540 cm^{-1}; n.m.r.: τ 2.95 (1-proton doublet, $J_{3',4'}$ = 3.2 Hz, H-3'), 3.65 (1-proton doublet, $J_{3',4'}$ = 3.2 Hz, H-4'), 6.16 (3-proton singlet, OCH_3), 8.96 (9-proton singlet, 3 × $OCOCH_3$).

Anal. Calcd. for $C_{18}H_{22}O_{11}$: C, 52.17; H, 5.35. Found: C, 51.95; H, 5.41.

Synthesis of Methyl 5-(2,3,4-Tri-O-acetyl-β-D-xylopyranosyloxymethyl)-2-furoate (11)

A mixture of the methyl ester **9** (300 mg), 2,3,4-tri-*O*-acetyl-α-D-xylopyranosyl bromide (1 g), cadmium carbonate (350 mg), and Drierite (2 g) in toluene (30 ml) was heated with stirring on a steam bath for 2 h. The inorganic residue was removed by filtration, the filtrate was concentrated, and the resulting syrup was purified by preparative layer chromatography (ethyl acetate – light petroleum, 1:1) to give the triacetate **11** (235 mg) which, after crystallization from ether – light petroleum, was identical (m.p. and mixed m.p., t.l.c., and i.r. spectrum) to the previously isolated sample. The triacetate **11** (200 mg) was kept in methanol containing concentrated hydrochloric acid (3 drops) for 2.5 days at room temperature. The solution was neutralized with silver carbonate, filtered, and concentrated to a residue which was crystallized from ethyl acetate to give the methyl ester **10** (96 mg), identical (m.p. and mixed m.p., t.l.c., and i.r. spectrum) to the previously isolated sample. Attempted methylation of the methyl ester **10** with methyl iodide and silver oxide in *N*,*N*-dimethylformamide (7) at room temperature caused extensive degradation of the starting material. Repeated treatments of methyl ester **10** with diazomethane – boron trifluoride in ether furnished a product whose i.r. spectrum (ν_{max} 3430 cm^{-1} (OH)) and mass spectrum (peak of highest mass at *m/e* 316) indicated incomplete methylation.

The authors acknowledge financial support from the National Research Council of Canada.

1. G. O. ASPINALL, R. R. KING, and Z. PAWLAK. Can. J. Chem. **51**, 388 (1973).
2. G. O. ASPINALL and R. R. KING. Can. J. Chem. **51**, 394 (1973).
3. A. KLEMER, H. LUKOWSKI, and F. ZERHUSEN. Chem. Ber. **96**, 1515 (1963).

4. E. J. COREY, N. W. GILMAN, and B. E. GANEM. J. Am. Chem. Soc. **90**, 5616 (1968).
5. T. IRIE, E. KUROSAWA, and T. HAMADA. J. Fac. Sci. Hokkaido Univ. Ser. III, **5**, 6 (1957); Chem. Abstr. **52**, 16328 (1958).
6. J. STANEK and J. CERNA. Tetrahedron Lett. 35 (1963).
7. R. KUHN, H. TRISCHMANN, and I. LOW. Angew. Chem. **67**, 32 (1955).
8. K. H. SLOTTA and H. HELLER. Chem. Ber. **68**, 1024 (1930).
9. G. R. BARKER. Meth. Carbohydr. Chem. **1**, 168 (1962).
10. J. S. BRIMACOMBE. Meth. Carbohydr. Chem. **6**, 376 (1972).
11. P. A. FINAN. J. Chem. Soc. 3917 (1963).

Can. J. Chem. Downloaded from www.nrcresearchpress.com by 210.87.254.6 on 09/05/12
For personal use only.

Substituent Effects on the Acetyl Group Conformation and the Carbonyl Frequency in Acetophenones

P. J. KRUEGER

Department of Chemistry, University of Calgary, Calgary, Alberta T2N 1N4

Received November 1, 1972

The fundamental carbonyl stretching frequencies for *o*-, *m*-, and *p*-substituted acetophenones in dilute CCl_4 solution are correlated with the electrophilic substituent constant σ^+ by the expression $\nu_{C=O}$ (cm^{-1}) = 11.53 σ^+ + 1691.5 (n = 27, correlation coefficient = 0.988, standard deviation = 1.2 cm^{-1}). The frequencies of carbonyl groups *trans* to an *o*-substituent follow this correlation, assuming $\sigma_o^+ \approx \sigma_p^+$, while those oriented *cis* to the substituent generally do not. Deviations from this correlation are interpreted in terms of dipole–dipole interactions, steric hindrance to planarity, intramolecular hydrogen bonding, and non-additivity of σ^+ values for some combinations of substituents. The carbonyl frequencies for singly *m*- and *p*-substituted acetophenones are also correlated with the polar and resonance components of σ^+ by the expression $\nu_{C=O}$ (cm^{-1}) = 15.66σ_I + 10.99σ_R^+ + 1689.8 (n = 13, correlation coefficient = 0.981, standard deviation = 0.9 cm^{-1}). Thus the sensitivity of the carbonyl frequency to the polar effect is greater than to the resonance effect. In ω-substituted acetophenones no precise correlation with polar substituent constants is observed.

Les fréquences fondamentales d'élongation du carbonyle des acétophénones *o*, *m*, et *p* substituées, en solution diluée dans le CCl_4, ont été reliées à la constante σ^+ du substituant électrophile par l'expression $\nu_{C=O}$ (cm^{-1}) = 11.53σ^+ + 1691.5 (n = 27, coefficient de correlation = 0.988, déviation standard = 1.2 cm^{-1}). Les fréquences des groupes carbonyles en *trans* par rapport à un substituant en *o* satisfont à cette correlation en assumant que $\sigma_o^+ \approx \sigma_p^+$, tandis que ceux qui sont en *cis* par rapport à ce substituant ne la suivent généralement pas. Les déviations par rapport à cette corrélation ont été interprétées en fonction des interactions dipole-dipole, de l'empêchement stérique à la planéarité, de la liaison hydrogène intramoléculaire et de la non additivité des valeurs σ^+ pour certaines combinaisons de substituants. Les fréquences du carbonyle des acétophénones simplement substituées en *m* et *p*, ont été également reliées aux composantes de polarité et de résonance de σ^+ par l'expression $\nu_{C=O}$ (cm^{-1}) = 15.66σ_I + 10.99σ_R + 1689.8 (n = 13, coefficient de correlation = 0.981, déviation standard = 0.9 cm^{-1}). Ainsi, la fréquence du carbonyle est plus sensible à l'effet de polarité qu'à l'effet de résonance. Pour les acétophénones ω substituées, aucune correlation précise n'a été observée avec les constantes de polarité du substituant. [Traduit par le journal]

Can. J. Chem., 51, 1363 (1973)

Introduction

Linear relationships between i.r. "group frequencies" and the Hammett (1, 2) and Taft σ-type substituent constants (3–7) have been demonstrated for a large number of aromatic and aliphatic systems (8–16). For aromatic compounds with substituents in an ortho-position with respect to the group in which the vibration is localized, it has been shown that the Taft ortho-σ substituent constants (3*a*) correlate these i.r. data along with the Hammett σ relationships for *m*- and *p*-substituted members of the series, provided that specific interactions like intramolecular hydrogen bonds and steric effects are absent (7, 13).

The correlation of the carbonyl stretching frequency in *m*- and *p*-substituted acetophenones with Hammett σ values of substituents has been noted previously (10*a*, 14, 15), and Rao and Venkataraghavan (9) have shown that the correlation with σ^+ for a small number of compounds is equally good.

No previous investigation appears to delineate quantitatively the effect of *cis–trans* isomerism of the acetyl group on the transmission of a substituent effect from an ortho-position to the carbonyl bond. Thus a recent correlation of carbonyl stretching frequencies for a large number of compounds of different structural types with a "new" substituent constant uses only average values for acetophenones in which conformational mobility of the acetyl group leads to a doublet carbonyl band (16).

This paper reports additional measurements on a wider range of ring-substituted acetophenones, including compounds with several substituents, and establishes that the linear dependence of $\nu_{C=O}$ on σ^+ (or its additive equivalent for multi-substituted compounds) includes *o*-substituted compounds, for which it

Can. J. Chem. Downloaded from www.nrcresearchpress.com by 210.87.254.5 on 09/05/12
For personal use only.

TABLE 1. Carbonyl frequencies and substituent constants in ring-substituted acetophenones

Compound	Substituent(s)	σ^{+a}	$\sigma_I{}^b$	$\sigma_R{}^{+c}$	$\nu_{C=O}$ (cm^{-1})[d]
1	2,4-di-OCH_3	−1.556			1673
2	2,4,5-tri-OCH_3	−1.509			1668
3	4-NH_2	−1.3	+0.10	−1.2	1677[e]
4	2-NH_2	−1.3			1653
5	2,4,6-tri-CH_3	−0.933			1705
6	4-OCH_3	−0.778	+0.25	−1.028	1683
7	2-OCH_3	−0.778			1681
8	2,3,5,6-tetra-CH_3	−0.754			1704[e]
9	2,5-di-OCH_3	−0.731			1679
10	2,4,5-tri-CH_3	−0.688			1685
11	2,4-di-CH_3	−0.622			1685
12	3,4-di-CH_3	−0.377			1686
13	2,5-di-CH_3	−0.377			1687
14	4-CH_3	−0.311	0	−0.311	1687[e]
15	2-CH_3	−0.311			1690[e]
16	3-NH_2	−0.16	+0.10	−0.26	1689[e]
17	4-F	−0.073	+0.52	−0.593	1692[e]
18	2-F	−0.073			1692[e]
19	H	0	0	0	1691[e]
20	4-Cl	+0.114	+0.47	−0.356	1692[e]
21	2-Cl	+0.114			1694, 1702[e]
22	4-I	+0.135	+0.38	−0.245	1693[e]
23	4-Br	+0.150	+0.45	−0.480	1693[e]
24	2-Br	+0.150			1692, 1706[e]
25	2,4-di-Cl	+0.228			1692, 1706
26	3-F	+0.352	+0.52	−0.168	1696[e]
27	3-Cl	+0.399	+0.47	−0.071	1696[e]
28	2,5-di-Cl	+0.513			1697, 1709
29	3,4-di-Cl	+0.513			1696
30	3-NO_2	+0.674	+0.63	+0.044	1701[e]
31	4-NO_2	+0.790	+0.63	+0.160	1700[e]
32	2-NO_2	+0.790			1702, 1712[e]

[a]Additivity of substituent constants assumed; σ^+ values from ref. 4, and values for ortho-substituents set equal to those for corresponding para-substituents.
[b]Data from ref. 6, based on aliphatic compounds.
[c]$\sigma_R{}^+ = \sigma^+ - \sigma_I$ for both *m*- and *p*-substituents.
[d]Measurements in dilute CCl_4 solution.
[e]Data from ref. 15.

can be used to assign the conformation of the acetyl group.

The σ_I and σ_R substituent parameters (6) were first used by us some time ago to establish the relative sensitivity of i.r. frequencies (and integrated absorption band intensities) to the polar and resonance effect of substituents (13). The result of this approach to ring-substituted acetophenone carbonyl frequencies is also reported here, and compared with the substituent dependence of carbonyl frequencies in ω-substituted acetophenones.

Experimental

All the compounds used were commercial materials which were purified by standard methods until their physical constants were in acceptable agreement with literature values. A spectroscopic grade of CCl_4 shown to be free of water was used as the solvent for the measurements. Spectra were generally recorded in triplicate, using a pair of standard matched 1 mm cells with KBr windows and a purged Beckman IR-7 i.r. spectrophotometer. The frequency scale of the instrument was calibrated, and the accuracy of carbonyl frequency measurements is ± 1 cm^{-1}, except where precluded by large bandwidths or by overlapped carbonyl doublets.

Results and Discussion

The carbonyl frequencies for ring-substituted acetophenones drawn from the literature and supplemented by additional measurements in our own laboratory are given in Table 1, together with the applicable substituent constants. The known high electron accepting ability of the acetyl group makes the electrophilic substituent constant σ^+ the most reasonable choice (11). Although Taft has devised some ortho-σ values (3*a*) the list is not extensive, and as a first

Can. J. Chem. Downloaded from www.nrcresearchpress.com by 210.87.254.5 on 09/05/12
For personal use only.

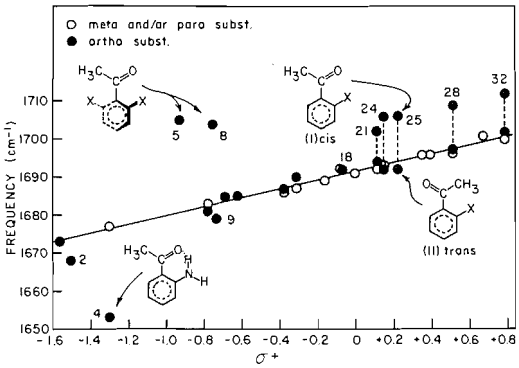

FIG. 1. Dependence of carbonyl frequencies in ring-substituted acetophenones on electrophilic substituent constant σ^+. Numbers refer to compounds listed in Table 1.

approximation it was assumed in this study that $\sigma_o^+ \approx \sigma_p^+$. There is, however, some evidence which indicates that σ values for *o*-substituents are somewhat smaller than those for corresponding *p*-substituents (17). For a full discussion of the "ortho effect" the reader is referred to Charton's recent review (7). For multi-substituted acetophenones additivity of the substituent effects was also assumed (17).

The carbonyl frequencies for compounds **2**, **4**, **5**, **8**, and **9**, and the high frequency components of the doublets observed for compounds **21**, **24**, **25**, **28**, and **32** were found to deviate from the general correlation with σ^+ (Fig. 1) and were removed from the least-squares treatment. The other 27 frequencies are correlated by eq. 1,

$$[1] \qquad \nu_{C=O}\,(cm^{-1}) = 11.53\sigma^+ + 1691.5$$

with a correlation coefficient of 0.988 and a standard deviation of 1.2 cm^{-1}. Frequencies reported for the two components of the carbonyl doublets are undoubtedly not the true band centers because of severe band overlapping, and this may be the cause of some deviations from the straight line. The recent conclusion by Laurence and Wojtkowiak (10*a*) that *m*- and *p*-substituted acetophenones must be treated separately in carbonyl frequency correlations with σ^+ cannot be justified, particularly since eq. 1 includes more compounds and has a higher correlation coefficient.

In **4** intramolecular NH···O hydrogen-bonding is well established (18–20) and $\nu_{C=O}$ is expected to be depressed. In **2** and **9** the additivity of substituent effects is questionable, as the methoxy group in the 5-position may lead to an enhanced electron density at the 2-carbon (with a methoxy substituent) which may be transmitted to the acetyl group. The acetyl group in **5** and **8** is twisted out of planarity with the aromatic ring by the 2,6-methyl groups, thereby increasing the C=O bond order and raising $\nu_{C=O}$ (21).

In ortho-substituted acetophenones where *cis–trans* isomerism can be observed through doublet carbonyl frequencies, Jones *et al.* (15) have previously assigned the high frequency component to the *cis*-conformer (I) (Fig. 1), by analogy with the known increase in $\nu_{C=O}$ in equatorially α-halogenated cyclohexanones where C=O and C—X dipoles are aligned in the same direction. The temperature-dependent equilibrium between I and II was held to depend on the near equivalence of the X···CH_3 repulsive force in I (largely steric) and the X···O repulsive force in II (largely electrostatic).

Figure 1 shows that the carbonyl frequencies for *trans*-isomers in *o*-substituted acetophenones follow the σ^+ correlation as the carbonyl bond is influenced predominantly by the substituent through the aromatic ring.[1] In contrast to *o*-iodo-, *o*-bromo-, and *o*-chloroacetophenone, *o*-fluoroacetophenone (**18**) is thus established to be wholly *trans*. Compounds with an ortho-methoxy group (**1** and **7**) are also in a *trans*-conformation. This correlation is therefore useful in the characterization of conformers in ortho-substituted acetophenones. Relative peak heights and conformer populations support this view, *e.g.* in a comparison of **25** with **28**, both of which have an *o*-Cl substituent, the high frequency *cis* (I) peak of **28** is strongest since the carbonyl dipole has been reduced ($\sigma^+ = 0.513$), whereas in **25** the total electron-withdrawing effect is not as great ($\sigma^+ = +0.228$), the carbonyl dipole is therefore larger, and the low frequency *trans* (II) component dominates (see Fig. 2).

The substituent dependence of $\nu_{C=O}$ can be analyzed further through the use of the σ_I and σ_R^+ substituent parameters (6), where

[1] A direct field effect in the *trans*-form is not ruled out, but it will certainly be small relative to the field effect in the *cis*-form. It should be noted that the term "polar effect" is used to characterize the total influence of an unconjugated remote substituent on the reaction site (here the carbonyl bond). This designation permits the use of the terms inductive and field effect to describe the mechanism of transmission, *i.e.* propagation by the successive polarization of intervening bonds, or by the interaction of bond dipole moments through space according to the classical laws of electrostatics (22).

Can. J. Chem. Downloaded from www.nrcresearchpress.com by 210.87.254.5 on 09/05/12
For personal use only.

TABLE 2. Carbonyl frequencies and substituent constants in ω-substituted acetophenones[a]

Compound	X in C_6H_5COX	σ_X*[b]	$\nu_{C=O}$ (cm^{-1})[c] *cis*	*gauche*
33	$-CH_3$	0.0	1691	
34	$-CH_2C_6H_5$	+0.215	1698	1685
35	$-CH_2OH$	+0.555	1692	
36	$-CH_2I$	+0.85	1701	1683
37	$-CH_2Br$	+1.000	1709	1688
38	$-CH_2Cl$	+1.050	1714	1694
39	$-CH_2CN$	+1.300	1709	
40	$-CHBr_2$	(+1.84)[d]	1707	1682
41	$-CHCl_2$	+1.940	1716	1693
42	$-CBr_3$	(+2.52)[d]	1704	
43	$-CCl_3$	+2.65	1718	

[a]Measurements in dilute CCl_4 solution.
[b]Polar substituent constants from ref. 3.
[c]Data from ref. 24.
[d]Since σ* for $-CH_2Br$ is 5% less than for $-CH_2Cl$, these values were estimated to be 5% less than those for the corresponding chlorinated substituent.

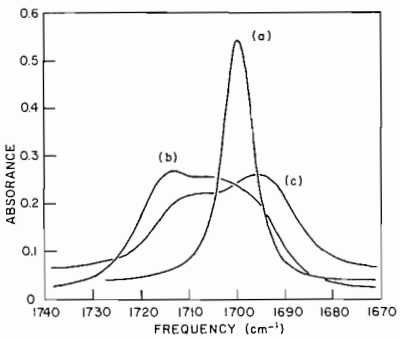

FIG. 2. Carbonyl bands in ring-substituted acetophenones in dilute CCl_4 solution, 1 mm pathlength: (*a*) 3,4-dichloroacetophenone (0.0056 *M*); (*b*) 2,5-dichloroacetophenone (0.0094 *M*); (*c*) 2,4-dichloroacetophenone (0.0080 *M*).

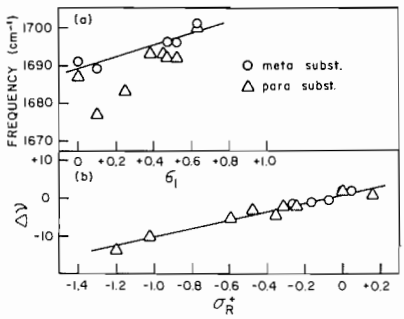

FIG. 3. (*a*) Dependence of carbonyl frequencies on the polar substituent constant σ_I. (*b*) Deviations from linear relationship in (*a*) plotted *vs.* resonance substituent constant σ_R^+. Data from Table 1.

$$[2] \qquad \sigma^+ = \sigma_I + \sigma_R^+$$

for both *m*- and *p*-substituents (23) in an attempt to separate the polar and the resonance effects of substituents. Only compounds with single *m*- or *p*-substituents were selected (**3**, **6**, **14**, **16**, **17**, **19**, **20**, **22**, **23**, **26**, **27**, **30**, and **31**) and $\nu_{C=O}$ plotted against corresponding σ_I values noted in Table 1 (see Fig. 3*a*). After a least-squares fit to the *m*-points, *all* frequency deviations from the straight line were correlated with σ_R^+ (Fig. 3*b*). The 13 carbonyl frequencies, therefore, follow the relationship given by eq. 3

$$[3] \quad \nu_{C=O}\,(cm^{-1}) = 15.66\sigma_I + 10.99\sigma_R^+ + 1689.3$$

with a correlation coefficient of 0.981 and a standard deviation of 0.9 cm^{-1}. The transmission coefficients of σ_I and σ_R^+ indicate that the carbonyl frequency is more susceptible to the polar effect than to the resonance effect in acetophenones. Again, this is a more unified treatment than that reported previously (10*c*).

The effect of ω-substituents on $\nu_{C=O}$ is summarized in Table 2, and the data are presented with respect to σ* of the substituent group (3) in Fig. 4. The frequency behavior of the carbonyl group in aliphatic ketones has been studied extensively, and is generally well understood with respect to *cis–gauche* isomerism and the resulting frequency increase due to field effects in the *cis*-isomer (III) (25). Figure 4 shows that the carbonyl frequencies in both conformations relate to σ* only in terms of broad correlation zones, the carbonyl groups with one (or two) substituents in the *gauche*-position being relative-

Can. J. Chem. Downloaded from www.nrcresearchpress.com by 210.87.254.5 on 09/05/12
For personal use only.

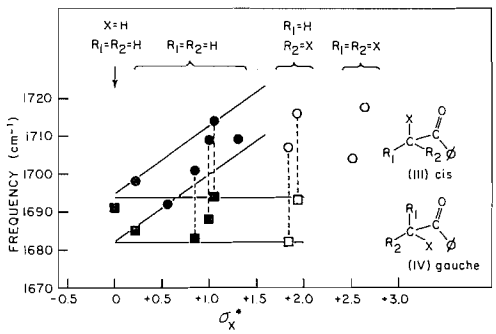

FIG. 4. Carbonyl frequencies in ω-substituted acetophenones *vs.* aliphatic polar substituent constant σ*. Data from Table 2. Closed symbols represent compounds with only a single ω-substituent.

ly insensitive to the substituent effect, whereas carbonyl groups with a polar substituent in the *cis*-orientation show a rise in frequency as σ* increases. The apparent plateau at high σ* values, reflecting the fact that only one substituent can be *cis* to the carbonyl group, emphasizes that the frequency increase in III is due to a direct field effect. Other factors which are hard to assess but which may affect the frequencies in this series are a field effect in IV, and the presence of steric effects leading to conformations not exactly *cis* or *gauche*. The precise correlations in ring-substituted acetophenones clearly relate to the rigidity of that system.

Financial support of the Defence Research Board of Canada under Grant 9530-75 is gratefully acknowledged. The spectra for this work were recorded by Miss Marelle Law.

1. H. H. JAFFE. Chem. Rev. **53**, 191 (1953).
2. D. H. MCDANIEL and H. C. BROWN. J. Org. Chem. **23**, 420 (1958).
3. R. W. TAFT, JR. *In* Steric effects in organic chemistry. *Edited by* M. S. Newman. Wiley, New York. 1956. (*a*) p. 619.
4. H. C. BROWN and Y. OKAMOTO. J. Am. Chem. Soc. **80**, 4979 (1958).
5. S. EHRENSON. *In* Progress in physical organic chemistry. Vol. 2. Interscience, New York. 1964. pp. 195–251.
6. C. D. RITCHIE and W. F. SAGER. *In* Progress in physical organic chemistry. Vol. 2. Interscience, New York. 1964. pp. 323–400.
7. M. CHARTON. *In* Progress in physical organic chemistry. Vol. 8. Interscience, New York. 1971. pp. 235–317.
8. C. N. R. RAO. Chemical applications of infrared spectroscopy. Academic Press, New York. 1963. pp. 568–577.
9. C. N. R. RAO and R. VENKATARAGHAVAN. Can. J. Chem. **39**, 1757 (1961).
10. (*a*) C. LAURENCE and B. WOJTKOWIAK. Bull. Soc. Chim. Fr. 3124 (1971); (*b*) 3833 (1971); (*c*) 3870 (1971); (*d*) 3874 (1971).
11. R. STEWART and K. YATES. J. Am. Chem. Soc. **80**, 6355 (1958).
12. M. LILER. Spectrochim. Acta, **23**A, 139 (1967).
13. P. J. KRUEGER and H. W. THOMPSON. Proc. Roy. Soc. A**250**, 22 (1959).
14. H. W. THOMPSON, R. W. NEEDHAM, and D. JAMESON. Spectrochim. Acta, **9**, 208 (1957).
15. R. N. JONES, W. F. FORBES, and W. A. MUELLER. Can. J. Chem. **35**, 504 (1957).
16. W. A. SETH-PAUL and A. VAN DUYSE. Spectrochim. Acta, **28**A, 211 (1972).
17. P. R. WELLS. Linear free energy relationships. Academic Press, New York. 1968. pp. 32–34.
18. P. J. KRUEGER. Can. J. Chem. **40**, 2300 (1962).
19. A. N. HAMBLY and B. V. O'GRADY. Austral. J. Chem. **16**, 459 (1963).
20. R. WASYLISHEN and T. SCHAEFER. Can. J. Chem. **49**, 3575 (1971).
21. L. L. INGRAHAM. *In* Steric effects in organic chemistry. *Edited by* M. S. Newman. Wiley, New York. 1956. pp. 505–506.
22. See for example F. W. BAKER, R. C. PARISH, and L. M. STOCK. J. Am. Chem. Soc. **89**, 5677 (1967), and refs. cited therein.
23. R. W. TAFT. J. Phys. Chem. **64**, 1805 (1960).
24. R. N. JONES and E. SPINNER. Can. J. Chem. **36**, 1020 (1958).
25. L. J. BELLAMY. Advances in group frequencies. Methuen, London. 1968. pp. 141–159.

Can. J. Chem. Downloaded from www.nrcresearchpress.com by 210.87.254.5 on 09/05/12
For personal use only.

Synthesis of 1,3,4-Dioxazoles from Hydroxamic Acids and Acetylenic Compounds

F. M. F. CHEN AND T. P. FORREST
Chemistry Department, Dalhousie University, Halifax, Nova Scotia
Received October 31, 1972

Hydroxamic acids have been shown to undergo a base-catalyzed reaction with acetylenic compounds containing electron-withdrawing groups, to yield substituted 1,3,4-dioxazoles.

On a démontré que sous l'influence des bases les acides hydroxamiques réagissent avec les composés acétyléniques contenant des groupes électroaffinitaires pour conduire à des dioxazoles-1,3,4 substituées.
[Traduit par le journal]

Can. J. Chem., **51**, 1368 (1973)

Can. J. Chem. Downloaded from www.nrcresearchpress.com by 210.87.254.40 on 09/05/12
For personal use only.

The reaction of aryl hydroxamic acids with ethyl ethynyl ether has been reported (1) to yield isocyanates. Although the intermediate in this reaction had not been characterized, it was assumed to be **1**. However, it was later noted that the reaction of hydroxamic acids with methylene ketene diethyl acetal, ethyl orthopropionate, or diethyl ketals yield isolable 1,3,4-dioxazoles, which decompose at elevated temperatures and also yield isocyanates. The possibility (2) that 1,3,4-dioxazoles may be formed by the addition of hydroxamic acids to acetylenic bonds led us to consider using this type of reaction as a method for the synthesis of this heterocyclic ring system. Since nucleophilic reagents are known (3) to add most readily to triple bonds activated by electron-withdrawing groups, the reaction with hydroxamic acids was attempted on acetylenic compounds of this type.

Benzhydroxamic acid and acetohydroxamic acid were found to react with *o*-nitro-phenylacetylene in dimethylsulfoxide with sodium hydride as a catalyst, yielding **2** and **3** respectively. The spectral data of these compounds (see Table 1) leave no doubt as to the structures of the reaction products. An analogous reaction of these two hydroxamic acids with ethyl propiolate yielded the 1,3,4-dioxazoles **4** and **5**.

It was anticipated that the reaction with dimethyl acetylenedicarboxylate might not yield 1,3,4-dioxazoles because this compound has been reported to react with other bidentate nucleophiles by the addition of one nucleophilic atom to the triple bond and substitution of the other at the ester group. The reaction with 1,2-diamines or aminoalcohols has been utilized (4) as a general method for the synthesis of compounds of type **6**. Substituted imidazolidones (**7**) were obtained when guanidines were used as bidentate nucleophiles in the reaction with dimethyl acetylenedicarboxylate (5). However, the reaction with benzo- and acetohydroxamic acids was found to yield the 1,3,4-dioxazoles (**8** and **9**) derived from the addition of both nucleophilic atoms to the same acetylenic carbon.

The yields of the 1,3,4-dioxazoles reported in Table 1 are not necessarily the optimum yields obtainable, since conditions have not been altered to minimize the side reactions. By-products identified are, for example, 1,3-diphenyl urea which is formed in the reactions employing benzohydroxamic acid, and triethyl trimesoate which is formed when ethyl propiolate is used.

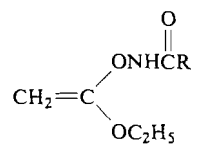

1

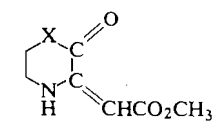

X = O or NH

6

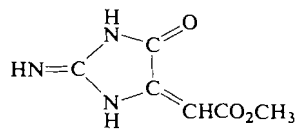

7

Can. J. Chem. Downloaded from www.nrcresearchpress.com by 210.87.254.40 on 09/05/12
For personal use only.

TABLE 1. Physical constants and yields for 1,3,4-dioxazoles

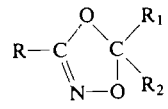

Compound no.	N.m.r. spectra* R	R_1	R_2	M.p. (°C) or b.p. (°C/mm Hg)	I.r. cm^{-1} C=N	Mass spectrum†	Yield (%)
2	$-C_6H_5$ 7.22–8.02(m)	—H 6.40(t) $J = 4.7$	$-CH_2-C_6H_4-NO_2$ 3.54(d) 7.22–8.02(m) $J = 4.7$	102–105	1630	284(2) 148(38) 120(100) 77(92)	50
3	$-CH_3$ 1.97(s)	—H 6.20(t) $J = 4.5$	$-CH_2-C_6H_4-NO_2$ 3.42(d) 7.20–8.02(m) $J = 4.5$	70/0.1	1650	222(8) 148(15) 136(10) 120(60) 86(100)	25
4	$-C_6H_5$ 7.20–7.82(m)	—H 6.43(t) $J = 5.0$	$-CH_2-C(=O)-O-CH_2-CH_3$ 2.91(d) 4.20(q) 1.30(t) $J = 5.0$ $J = 7.0$ $J = 7.0$	96/0.05	1625	235(1) 148(10) 120(35) 105(90) 103(100)	45
5	$-CH_3$ 2.03(s)	—H 6.25(t) $J = 5.2$	$-CH_2-C(=O)-O-CH_2-CH_3$ 2.80(d) 4.19(q) 1.26(t) $J = 5.2$ $J = 7.0$ $J = 7.0$	55/0.1	1645	88(24) 86(100) 71(30) 60(84) 58(72)	15
8	$-C_6H_5$ 7.32–7.82(m)	$-C(=O)-OCH_3$ 3.82(s)	$-CH_2-C(=O)-O-CH_3$ 3.32(AB) 3.70(s) $J_{AB} = 16$ $\nu_{AB} = 12$	120/0.05	1630	279(2) 220(16) 120(10) 101(100) 59(85)	65
9	$-CH_3$ 2.08(s)	$-C(=O)-OCH_3$ 3.83(s)	$-CH_2-C(=O)-O-CH_3$ 3.20(AB) 3.70(s) $J_{AB} = 16$ $\nu_{AB} = 15$	80/0.1	1650	217(1) 158(60) 144(12) 101(100) 69(18)	50

*Recorded at 60 MHz in deuterochloroform with tetramethylsilane as internal standard; chemical shifts in p.p.m. (δ), coupling constants and ν_{AB} in Hz.
†Numbers in parentheses represent percentage of base peak.

Experimental

The following procedure was used in the preparation of all of the 1,3,4-dioxazoles described in Table 1.

The hydroxamic acid (0.003 mol) was dissolved in 3 ml of dry dimethylsulfoxide. A 50% dispersion of sodium hydride and oil (0.0003 mol) was added under nitrogen gas. The acetylenic reactant (0.003 mol) was then added to the mixture in 2 ml of dry dimethyl sulfoxide. After stirring at room temperature for 16 h the mixture was acidified with glacial acetic acid (0.0004 mol). The dimethylsulfoxide was then removed under high vacuum (0.1 mm at 35 °C) and the residue transferred to a silica gel column. The products were eluted with a mixture of chloroform and hexane (1:8). The physical properties and yields of the dioxazoles are given in Table 1.

The financial assistance of the National Research Council of Canada is acknowledged.

1. T. MUKAIYAMA, H. NOHIRA, and S. ASANO. Bull. Chem. Soc. Jap. **35**, 71 (1962).
2. H. NOHIRA, K. INOUE, H. HATTORI, T. OKAWA, and T. MUKAIYAMA. Bull. Chem. Soc. Jap. **40**, 664 (1967).
3. E. WINTERFELD. *In* Newer methods of preparative organic chemistry. *Edited by* W. Foerst. Vol. VI. Verlag Chemie, Weinheim. 1971. p. 243.
4. Y. IWANAMI, Y. KENJO, K. NISHIBE, M. KAJIURA, and S. ISOYAMA. Bull. Chem. Soc. Jap. **37**, 1740 (1964).
5. Y. IWANAMI, H. SAAKI, and H. SAKATA. J. Chem. Soc. Jap. Pure Chem. Sect. (Nippon Kagaku Zassi) **85**, 704 (1964).

Can. J. Chem. Downloaded from www.nrcresearchpress.com by 210.87.254.40 on 09/05/12
For personal use only.

Heterogeneous Isomerization of Ethylene Oxide to Acetaldehyde

O. O. BERNARDINI[1] AND E. A. CHERNIAK[2]

Department of Chemistry, Carleton University, Ottawa, Canada

Received June 13, 1972

Surface catalyzed isomerization of $(CH_2)_2O$ to CH_3CHO occurs in a small, Pyrex reactor containing 15 or 230 Torr $(CH_2)_2O$ at temperatures in the range 339.2 °C to 461.4 °C. $R_0(CH_3CHO)$, the initial rate of formation of CH_3CHO, depends on the number of successive pyrolyses and on the evacuation time between pyrolyses, which is not true of the initial rates of formation of H_2, CO, CH_4, CH_2CO, and C_2H_6. $R_0(CH_3CHO)$ also depends on the reactor S/V and on pretreatment of the reactor with product gases, particularly H_2. The reproducible and limiting values of $R_0(CH_3CHO)$ are independent of the $(CH_2)_2O$ pressures used. Above 385 °C these initial rates exhibit an Arrhenius temperature dependence while below 385 °C they pass through a maximum.

Analysis of the Langmuir–Hinshelwood, low surface coverage mechanism shows that the $T > 385$ °C isomerization is partially or totally controlled by CH_3CHO desorption and that $-\Delta H_{ads} < (55 \pm 10)$ kcal mol^{-1}, for CH_3CHO on this surface.

$E_a = 57$ kcal mol^{-1} for the homogeneous first order decomposition of $(CH_2)_2O$, in the 15 Torr pyrolysis at temperatures in the range 374.0 to 406.7 °C, and any vibrationally excited CH_3CHO, formed in the gas phase at this pressure (and possibly even at 230 Torr), dissociates into chain initiating radicals.

L'isomérisation catalysée superficiellement du $(CH_2)_2O$ en CH_3CHO se produit dans un petit réacteur en Pyrex contenant 15 ou 230 Torr en $(CH_2)_2O$, pour des températures allant de 339.2 à 461.4 °C. La vitesse initiale de formation du CH_3CHO, $R_0(CH_3CHO)$, dépend du nombre successif de pyrolyses et de la durée d'évacuation entre ces pyrolyses; cette vitesse n'est pas réellement celle de la formation de H_2, CO, CH_4, CH_2CO, et C_2H_6. $R_0(CH_3CHO)$ dépend également du rapport S/V et du prétraitement du réacteur en produit gazeux, en particulier H_2. Les valeurs reproductibles et limitatives sur $R_0(CH_3CHO)$ sont indépendantes des pressions en $(CH_2)_2O$ utilisées. Au dessus de 385 °C, les vitesses initiales varient avec la température selon une fonction d'Arrhénius tandis qu'au dessous de 385 °C, elles passent par un maximum.

L'analyse du recouvrement faible de la surface selon Langmuir et Hinshelwood montre que l'isomérisation pour $T > 385$ °C est partiellement ou totalement contrôlée par la désorption de CH_3CHO et que $-\Delta H_{ads} < (55 \pm 10)$ kcal mol^{-1} pour CH_3CHO sur cette surface.

La décomposition homogène du premier ordre de $(CH_2)_2O$ a un $E_a = 57$ kcal mol^{-1} dans la pyrolyse sous 15 Torr et à des températures de 374.0 à 406.7 °C; le méthanal formé en phase gazeuse et vibrationnellement excité se dissocie alors en radicaux initiateurs de réactions en chaîne pour cette pression et peut être même pour la pression de 230 Torr. [Traduit par le journal]

Can. J. Chem., **51**, 1371 (1973)

The chain mechanism, proposed by Benson (1), for the gas phase pyrolysis of ethylene oxide, is initiated by reactions 1 to 3 which involve highly vibrationally excited (CH_3CHO^*) and normal (CH_3CHO) acetaldehyde molecules (1–3).

$$[1] \quad (CH_2)_2O \rightleftarrows \dot{C}H_2CH_2\dot{O} \longrightarrow CH_3CHO^*$$

$$[2] \quad CH_3CHO^* \longrightarrow \dot{C}H_3 + \dot{C}HO$$

$$[3] \quad CH_3CHO^* + M \longrightarrow CH_3CHO + M$$

Subsequent reactions in this chain mechanism resul in chain catalyzed isomerization of $(CH_2)_2O$ to CH_3CHO and chain decompositions of both $(CH_2)_2O$ and CH_3CHO. While the catalyzed isomerization of propylene oxide to propionaldehyde on seasoned Pyrex surfaces (4) and of $(CH_2)_2O$ to CH_3CHO on supported silver surfaces (5) is established and the catalyzed isomerization of $(CH_2)_2O$ to CH_3CHO on Pyrex surfaces is suspected (6), no evidence for the latter surface catalyzed isomerization is available. This study provides such evidence.

Experimental

The pyrolyses were performed in a cylindrical Pyrex reactor (o.d. = 2.5 cm, $V = 26.3$ cc) with $S/V \sim 1$ cm^{-1}. After washing with chromic acid solution and distilled water the reactor was embedded in a large cylindrical aluminum block which formed the core of a thermistor temperature controlled oven of standard design. The reactor, which was connected through two four-way stopcocks to a Perkin–Elmer 154C gas chromatograph, with thermistor thermal conductivity detector, was

[1]Present address: Montecatini Edison S.P.A., Foro Bonaparte 31, Milan, Italy.

[2]Present address: Department of Chemistry, Brock University, St. Catharines, Ontario.

Can. J. Chem. Downloaded from www.nrcresearchpress.com by 210.87.254.6 on 09/05/12
For personal use only.

Can. J. Chem. Downloaded from www.nrcresearchpress.com by 210.87.254.6 on 09/05/12
For personal use only.

evacuated with a mercury diffusion pump, filled with helium and heated continuously, at temperatures in the range 350 to 500 °C. After withdrawing helium from the reactor, ethylene oxide gas was rapidly introduced, with a Töpler pump, to the desired pressure (either 15 or 230 Torr) and at the end of a pyrolysis period carrier gas was introduced into the reactor to sweep its contents to the chromatograph for analysis. Pyrolyses were performed at temperatures in the range 339.2 ± 0.1 °C to 461 ± 1 °C, as determined by an iron–constantan thermocouple which was fixed to the mid-section of the reactor with aluminum foil.

Ethylene oxide (Matheson) was dried over Linde molecular sieves 5A, treated with dry Ascarite, condensed, and degassed *in vacuo* at −196 °C and vacuum distilled. Acetaldehyde (Eastman) was degassed *in vacuo* at −196 °C and vacuum distilled. Hydrogen, carbon monoxide, methane, and ethane (Matheson) were used without further purification. Ketene, prepared by refluxing the vapor of diketene (Aldrich) over electrically heated tungsten wire, was degassed *in vacuo* at −196 °C and vacuum distilled.

Chromatographic calibration curves for all the above compounds were obtained using standard 2 m, 1/4 in. stainless steel columns, 25 cc min^{-1} carrier gas flow rates and temperatures in the range 23 to 29 °C. Column F (tetraethylene glycol dimethyl ether on diatomaceous earth) was used in the analysis of ethylene oxide and acetaldehyde. A 40 ft, 1/4 in. coiled copper column, filled with 10% (w/w) tetraethylene glycol dimethyl ether on 60–80 mesh Chromasorb W, was used in the analysis of small quantities of acetaldehyde in the presence of excess ethylene oxide. Column I (calcium zeolite) was used for H_2 analysis and column J (silica gel) was used for ethane and ketene analysis, after preconditioning at 125 °C for several hours using a helium carrier gas flow rate of 25 cc min^{-1}. Columns I and J were used in series for the analysis of CO and CH_4. Nitrogen was used as the carrier gas for H_2 analysis and helium was used in the analysis of the remaining gases.

To test the effect of the possible adsorption of each gaseous product on the rates of formation of acetaldehyde the reactor was evacuated overnight and then subjected to 15 min contact with a gaseous product at 230 Torr and the appropriate temperature. The usual pyrolysis run was undertaken after removal of the product gas by evacuation for 1 min.

In some experiments the reactor was filled with Pyrex beads, which had been cleaned in the same manner as the reactor. In these experiments the reactor volume was approximately 21 cc and $S/V \sim 5$ cm^{-1}.

Results and Discussion

In the pyrolysis of 15 Torr $(CH_2)_2O$, in the temperature range 348.4 to 406.7 °C, the major products identified, in addition to CH_3CHO, were CO, CH_4, H_2, C_2H_6, and CH_2CO. Methyl ketene dimer was a minor pyrolysis product.[3]

[3]This product, which was analyzed with column J, had the same retention time as methyl ketene dimer produced by the pyrolysis of methyl ethyl ketone in a conventional ketene generator.

A search was made for formaldehyde and ethylene, in th pyrolys s products, and these compounds were not found.

No special precautions needed to be taken to determine the rates of fo mation of CO, CH_4, H_2, C_2H_6, and CH_2CO. However, to obtain reproducible rates of formation of CH_3CHO, it was found necessary to condition the reactor by repeated reaction and to use short evacuation times between successive runs. This was also true for a series of runs perfo med on 230 Torr $(CH_2)_2O$ in the temperature range 339.2 to 461.4 °C. The dependence of CH_3CHO yields on the number of pyrolysis runs, at two evacuation times, is shown in Fig. 1. The first run was made after a 15 h evacuation and the con tant carrier gas flushing t me was 5 min. Not only is the rate of CH_3CHO production depressed by repeated reaction (Fig. 1) but th reproducible, limiting CH_3CHO yield, $[CH_3CHO]_\infty$, obtained after performing a sufficiently large number of runs, is a function of the time of evacuation (Figs. 1 and 2). Complete reactivation of the reactor was not obtained even after 20 h of

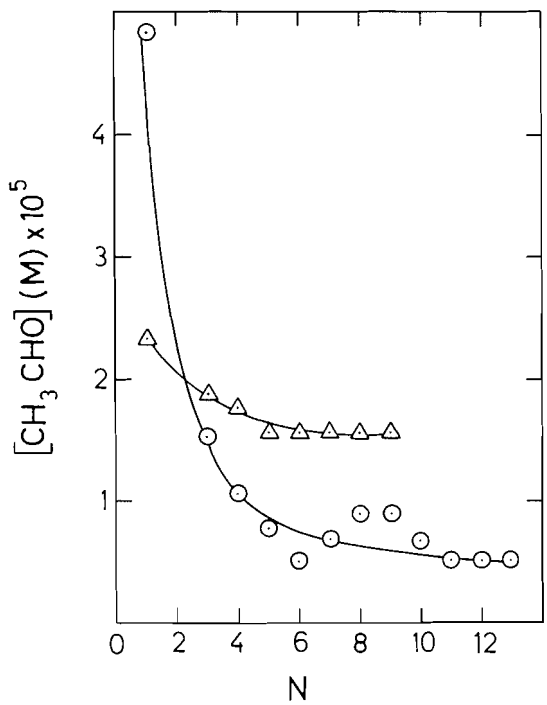

FIG. 1. CH_3CHO yields (mol l^{-1}) as a function of the number (N) of pyrolysis runs in the 40 min pyrolyses of 230 Torr $(CH_2)_2O$ at 374.0 °C. Evacuation times between runs: ○, 1 min; △, 5 min.

TABLE 1. Initial rates of product formation (mol min^{-1}) and C, H, O atom balances in the pyrolysis of ethylene oxide (15 Torr)

T(°C)	$R_0(CH_3CHO)$ $\times 10^9$	$R_0(CH_2CO)$ $\times 10^9$	$R_0(CO)$ $\times 10^9$	$R_0(C_2H_6)$ $\times 10^{11}$	$R_0(CH_4)$ $\times 10^9$	$R_0(H_2)$ $\times 10^{10}$	C	H	O
348.4	5.05	1.41	1.07	4.75	0.70	6.81	1.96	3.66	1
353.2	3.00	4.22	1.74	12.2	1.42	10.6	1.99	3.27	1
359.0	2.26	2.80	4.01	16.3	2.76	14.4	1.90	3.33	1
374.0	$\simeq 0$	3.83	10.3	136	8.11	42.6	2.03	3.72	1
384.8	3.14	12.3	18.7	169	14.7	51.9	1.98	3.96	1
394.4	8.10	15.0	34.4	280	31.0	121	2.04	3.94	1
406.7	37.0	63.0	70.0	650	50.0	234	1.96	3.29	1

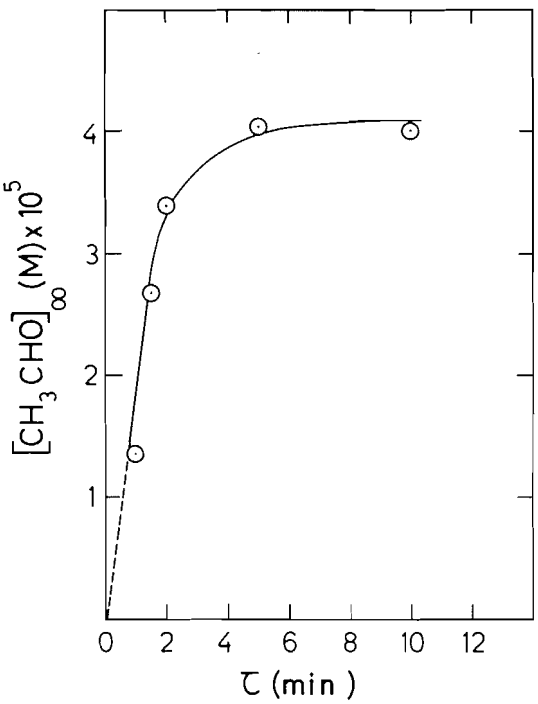

FIG. 2. Reproducible, limiting CH_3CHO yields (mol l^{-1}) as a function of the evacuation time (τ) between 40 min pyrolyses of 230 Torr $(CH_2)_2O$ at 374.0 °C.

evacuation. The CH_3CHO yield, obtained in the first pyrolysis run after 48 h of evacuation, was found to be twice as great as the corresponding yield obtained after 20 h of evacuation. Similar experiments were made at 348.4 and 359.0 °C with analogous results. At 348.4 °C, seven successive runs, separated by 5 min of carrier gas flushing and 1 min of evacuation, reduced the CH_3CHO yield to 1/15th of the yield obtained in the first pyrolysis run.

Initial rates of formation of all major products of the pyrolysis of 15 Torr $(CH_2)O$ in the temperature range 348.4 to 406.7 °C are shown in Table 1. The $R_0(CH_3CHO)$ values represent reproducible, limiting rates obtained after performing a large number of runs with the shortest possible evacuation time (*i.e.* 1 min). Table 1 also shows that in this temperature range good carbon and oxygen atom balances were obtained from the measured initial rates of formation of these products. The oxygen atom balance condition was used to show that the disappearance of $(CH_2)_2O$ (initial pressure = 15 Torr) was first-order at each temperature studied in the range 348.4 to 406.7 °C.[4]

The temperature dependence of ln $R_0(CH_3CHO)$, in the pyrolysis of 230 Torr $(CH_2)_2O$ in the range 339.2 to 461.4 °C and of 15 Torr $(CH_2)_2O$ in the range 348.4 to 406.7 °C, is shown in Fig. 3. This dependence is clearly non-Arrhenius in character in the range 339.2 to 359.0 °C. $R_0(CH_3CHO)$ is also zero order from 348.4 to 406.7 °C, since the reproducible initial rates of formation of CH_3CHO, obtained at initial $(CH_2)_2O$ pressures of 15 and 230 Torr, in this temperature range are the same within the limits of experimental error.

Figure 3 also shows the temperature dependence of ln $R_0(CH_3CHO)$ calculated from the data of Benson (1), Neufeld and Blades (6), and Mueller and Walters (7). The R_0 (CH_3CHO) values of Benson represent initial rates of formation of CH_3CHO in the first order gas phase isomerization of 230 Torr $(CH_2)_2O$ and are given by [4].

[4] $R_0(CH_3CHO) = k_1((CH_2)_2O)_0$ mol min^{-1}

$k_1 = 1.90 \times 10^{16} \exp(-57\,000/RT)$ min^{-1} is the specific rate for the homogeneous formation

[4]Plots of ln $[(CH_2)_2O]$ *vs.* the pyrolysis time t were linear at each temperature studied where $[(CH_2)_2O]_t = [(CH_2)_2O]_0 - [CO]_t - [CH_2CO]_t - [CH_3CHO]_t$ mol l^{-1}.

Can. J. Chem. Downloaded from www.nrcresearchpress.com by 210.87.254.6 on 09/05/12
For personal use only.

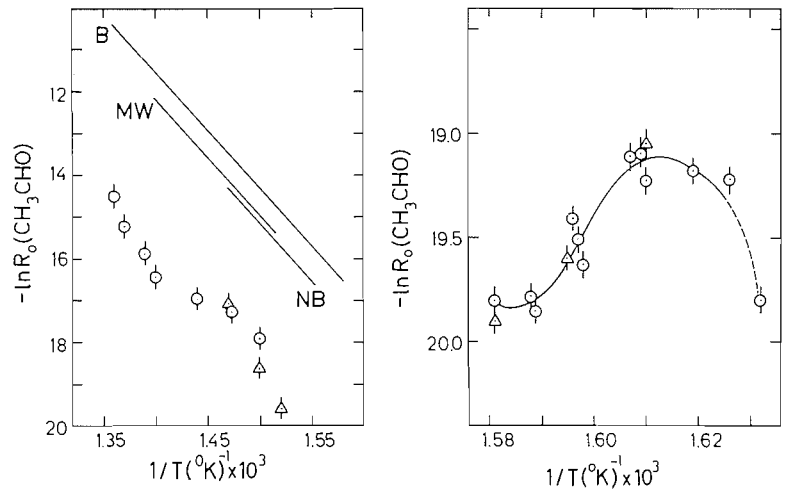

FIG. 3. Temperature dependence of ln $R_0(CH_3CHO)$ in the pyrolysis of 230 Torr ethylene oxide (339.2 to 461.4 °C), ○; and 15 Torr ethylene oxide (348.4 to 406.7 °C, △; B, Benson (1); MW, Mueller and Walters (7); and NB, Neufeld and Blades (6).

of CH_3CHO^* by the overall process [1] and $((CH_2)_2O)_0 = [(CH_2)_2O]_0 \times V/1000 = 0.097/T$ mol. (It is assumed that $k_3(M) \gg k_2$ at a pressure of 230 Torr.) The $R_0(CH_3CHO)$ values of Neufeld and Blades and Meuller and Walters, given by [5] and [6], respectively, represent initial rates of formation of CH_3CHO in the first order gas phase isomerization of 230 Torr $(CH_2)_2O$ in the presence of sufficient propene to provide maximum inhibition.

$$[5]\quad R_0(CH_3CHO) = 9.58 \times 10^{15} \times \exp(-56\,900/RT)((CH_2)_2O)_0 \text{ mol min}^{-1}$$

$$[6]\quad R_0(CH_3CHO) = 1.32 \times 10^{16} \times \exp(-57\,400/RT)((CH_2)_2O)_0 \text{ mol min}^{-1}$$

The $R_0(CH_3CHO)$ values obtained in this study are approximately two orders of magnitude smaller than the $R_0(CH_3CHO)$ values expected for the formation of acetaldehyde in the gas phase, according to Benson, Neufeld and Blades, and Mueller and Walters. Also, the processes responsible for CH_3CHO formation in this study possess an apparent activation energy ($E_A = 55 \pm 10$ kcal mol^{-1}) in the range 384.5 to 461.4 °C.

Not only was the rate of formation of CH_3CHO increased by a factor ~5 when pyrolyses took place in the reactor with $S/V \sim 5$ cm^{-1} but also pretreatment of the reactor (with $S/V \sim 1$ cm^{-1}) with product gases influenced the rate of CH_3CHO production (Table 2). With the possible exception of CH_2CO all product gases inhibit CH_3CHO formation and H_2 is the most powerful inhibitor. One pretreatment with H_2 reduced the CH_3CHO yield to 5-6 μM. For comparison, repeated runs separated by 1 min evacuation and 5 min flushing with carrier gas reduced the CH_3CHO yield from 25 μM in the first run ($N = 1$) to 5–6 μM for $N \geqslant 12$.

TABLE 2. Effect of pretreatment of reactor with product gases on 40 min ($N = 1$) acetaldehyde yields in the pyrolysis of 230 Torr ethylene oxide at 374.0 °C*

Product gas	$[CH_3CHO]$ μM
H_2	5.9
CO	13.5
CH_4	11.3
C_2H_6	21.9
CH_2CO	23.5

*With no pretreatment, $[CH_3CHO] = 25$ μM and $[CH_3CHO]_\infty = 5$–6 μM.

The above observations indicate that in these experiments CH_3CHO is formed by surface catalyzed isomerization of $(CH_2)_2O$. The marked suppression of $R_0(CH_3CHO)$ by preadsorbed H_2 indicates that H_2 and $(CH_2)_2O$ compete for surface active sites; H_2 remains adsorbed while $(CH_2)_2O$ isomerizes to CH_3CHO. If, on evacuation, H_2 does not desorb rapidly enough then repeated runs in the same reactor lead to accumu-

Can. J. Chem. Downloaded from www.nrcresearchpress.com by 210.87.254.6 on 09/05/12
For personal use only.

Can. J. Chem. Downloaded from www.nrcresearchpress.com by 210.87.254.6 on 09/05/12
For personal use only.

lation of H_2 on adsorption sites. Thus CH_3CHO production is suppressed by repeated reaction (with constant evacuation times between runs), is enhanced by prolonged evacuation at sufficiently high temperatures prior to a given run and occurs from surfaces characterized by high H_2 and other product gas coverage (or low $(CH_2)_2O$ coverage) to provide the reproducible, limiting values of $R_0(CH_3CHO)$ measured in this study. While it is not possible to specify the nature of the surface involved in these experiments it may contain some chromium oxides. That H_2 gas was so effectively adsorbed may be due to the fact that the reactor had received a chromic acid washing (8).

In this study, CH_3CHO may be formed entirely by surface catalyzed isomerization of $(CH_2)_2O$. The Arrhenius plot for the first order decomposition of 15 Torr $(CH_2)_2O$, in the temperature range 348.4 to 406.7 °C is shown in Fig. 4 where the results are again compared with those of Benson (1), Neufeld and Blades (6), and Mueller and Walters (7). In the temperature range 374.0 to 406.7 °C Arrhenius behavior is noted with an activation energy (E_a = 57 kcal mol^{-1}) in good agreement with the activation energies reported by the above workers. In the same temperature range $R_0(-(CH_2)_2O)$ values obtained in this work are approximately twice those predicted by Benson (if $k_3(M) \gg k_2$), approximately four times greater than the "propene inhibited" rates measured by Neufeld and Blades and Mueller and Walters and approximately an order of magnitude greater than the $R_0(CH_3CHO)$ values obtained in this work. At P = 15 Torr it is expected that the condition $k_3(M) \ll k_2$ holds (1), *i.e.* at this pressure homogeneous CH_3CHO formation is not occurring for vibrationally excited CH_3CHO molecules become sources of $\cdot CH_3$ and $\cdot CHO$ radicals and these radicals, directly and indirectly, will be responsible for the larger rates of $(CH_2)_2O$ disappearance obtained. The fact that the reproducible limiting CH_3CHO yield may be zero at $\tau = 0$ (Fig. 2) implies that homogeneous CH_3CHO formation is also not occurring in the 230 Torr $(CH_2)_2O$ pyrolyses at 374.0 °C.

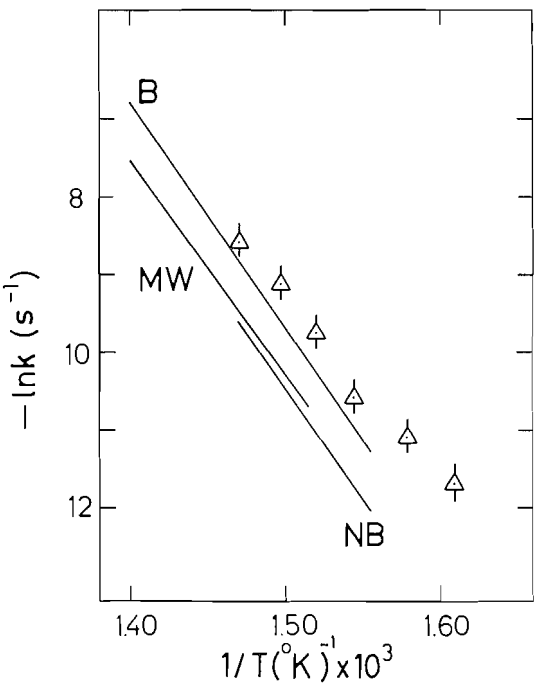

FIG. 4. Temperature dependence of specific rate (k) for first order decomposition of ethylene oxide in the range 348.4 to 406.7 °C. This work, △ (15 Torr ethylene oxide). B, Benson (1); MW, Mueller and Walters (7); and NB, Neufeld and Blades (6).

The Langmuir–Hinshelwood mechanism for the 384.8 to 461.4 °C isomerization is given by reactions 7 to 9, inclusive.[5]

[7] $(CH_2)_2O$ (g) ⇄ $(CH_2)_2O$ (ads)

[8] $(CH_2)_2O$ (ads) ⇄ CH_3CHO (ads)

[9] CH_3CHO (ads) ⇄ CH_3CHO (g)

The adsorption controlled value of $R_0(CH_3CHO)$ is k_7P_0 where P_0 is the initial $(CH_2)_2O$ pressure (11, 12). Adsorption controlled heterogeneous isomerization is not a possibility since $R_0(CH_3CHO)$ has been shown to be independent of P_0 and E_7, the activation energy for the adsorption of $(CH_2)_2O$, is expected to be very much less than $E_A = 55 \pm 10$ kcal mol^{-1}, obtained in this work. The very high and very low $(CH_2)_2O$ coverage, surface reaction controlled values of $R_0(CH_3CHO)$ are k_8 and $K_Ek_8P_0$, respectively, where $K_E = k_7/k_{-7}$, the equilibrium constant for $(CH_2)_2O$ adsorption. If, as assumed above, low $(CH_2)_2O$ coverage exists in this system then surfacereaction controlled heterogeneous isomerization is also not taking place.

[5]Reaction 8 may involve a diradical intermediate. While dioxanes were not searched for in this study large quantities of these products have been found in the pyrolysis of $(CH_2)_2O$ in the presence of magnesia and alumina surfaces (9, 10).

The desorption controlled value of $R_0(CH_3CHO)$ is given by [10].

$$[10] \quad R_0(CH_3CHO) = k_8k_9/(k_8 + k_{-8})$$

For very low $(CH_2)_2O$ coverage, the inequalities, shown in [11], must be satisfied.

$$[11] \quad [1 + (k_8/k_{-8})]^{-1} \ll K_EP_0 \ll 1$$

Now

$$k_8/k_{-8} \simeq \exp(28\,000/RT)$$

since

$$E_{-8} = E_8 - (\Delta H_f^0(CH_3CHO) - \Delta H_f^0((CH_2)_2O))^6 = E_8 + 28 \text{ kcal mol}^{-1}$$

Thus

$$[1 + (k_8/k_{-8})]^{-1} \simeq \exp(-28\,000/RT) \ll 1$$

(at temperatures in the range 384.8 to 461.4 °C) and [11] is very easily satisfied to provide very low $(CH_2)_2O$ coverage. The desorption controlled value of $R_0(CH_3CHO)$, for very low $(CH_2)_2O$ coverage, thus becomes k_9 with $E_9 = E_{-9} - \Delta H_A$ where ΔH_A is the heat of adsorption of CH_3CHO. Desorption-controlled heterogeneous isomerization is thus possible and $-\Delta H_A < (55 \pm 10)$ kcal mol^{-1}. This value is not unreasonable for it is a low CH_3CHO coverage quantity and heats of adsorption values are known to increase with decreasing surface coverage (12).

It is possible for two of the processes [7], [8], and [9] to be slow and rate determining while the third is fast and approaching equilibrium. Of the three possibilities, the one involving slow adsorption and surface reaction steps ([7], [8]) is impossible for k_8/k_{-7} has to be negative in order to provide very low $(CH_2)_2O$ coverage. The adsorption and desorption controlled value of $R_0(CH_3CHO)$ is also given by [10]. For very low $(CH_2)_2O$ coverage, the inequalities shown in [12] must be satisfied. Since

$$k_9/k_{-7} \simeq \exp(\Delta H_A - \Delta H_E)/RT$$

$$[12] \quad (\exp(-28\,000/RT) + k_9/k_{-7}) \ll K_EP_0 \ll 1$$

where ΔH_E is the heat of adsorption of $(CH_2)_2O$. The inequalities shown in [12] can be satisfied only if $\Delta H_A - \Delta H_E$ is negative and a few kcal mol^{-1} in magnitude. For example, if $K_EP_0 = 10^{-3}$ and $(\exp(-28\,000/RT) + k_9/k_{-7}) \simeq 10^{-6}$ then at 384.8 °C, $\Delta H_A = \Delta H_E - 3.4$ kcal mol^{-1}. The surface reaction and desorption controlled value of $R_0(CH_3CHO)$ is given by [13]. For very low surface coverage, the inequalities,

$$[13] \quad R_0(CH_3CHO) = k_8k_9/(k_8 + k_{-8} + k_9)$$

shown in [14] must be satisfied. If $E_9 \sim 55$ kcal mol^{-1} and $E_{-8} \sim 60$ kcal mol^{-1} then $k_9/k_{-8} \simeq \exp(5000/RT)$

$$[14] \quad (1 + k_9/k_{-8})[\exp(28\,000/RT) + k_9/k_{-8}]^{-1} \ll K_EP_0 \ll 1$$

since $k_9/k_{-8} \simeq \exp(E_{-8} - E_9)/RT$. Thus the left term in [14] is again $\simeq \exp(-28\,000/RT) \ll 1$ (at temperatures in the range 384.8 to 461.4 °C) and [14] is again very easily satisfied to provide very low $(CH_2)_2O$ coverage. The surface reaction and desorption controlled value of $R_0(CH_3CHO)$ for very low $(CH_2)_2O$ coverage again becomes k_9.

The above analysis shows that the surface catalyzed isomerization of $(CH_2)_2O$ to CH_3CHO in the temperature range 384.8 to 461.4 °C is partially or totally desorption controlled if the assumption of low $(CH_2)_2O$ coverage is valid. For partial or total desorption controlled heterogeneous isomerization the zero order $R_0(CH_3CHO)$ is predicted to be k_9 from which the upper limit to the low coverage heat of adsorption of CH_3CHO is estimated to be $-(55 \pm 10)$ kcal mol^{-1}.

We thank the National Research Council of Canada for financial support and for providing one of us (O.O.B.) with a National Research Council Bursary. The technical assistance of Messrs. A. Raffler and B. Weston is gratefully acknowledged.

1. S. W. BENSON. J. Chem. Phys. **40**, 105 (1964).
2. D. W. SETSER. J. Phys. Chem. **70**, 826 (1966).
3. W. H. RICHARDSON and H. E. O'NEAL. Comprehensive chemical kinetics. Vol. 5. Elsevier, Amsterdam. 1972.
4. A. T. BLADES. Can. J. Chem. **46**, 3283 (1968).
5. R. E. KENSON and M. LAPKIN. J. Phys. Chem. **74**, 1493 (1970).

[6] $\Delta H_f^0(CH_3CHO) = -37.4$ kcal mol^{-1}, $\Delta H_f^0((CH_2)_2O) = -9.83$ kcal mol^{-1} (13).

Can. J. Chem. Downloaded from www.nrcresearchpress.com by 210.87.254.6 on 09/05/12
For personal use only.

6. M. L. NEUFELD and A. T. BLADES. Can. J. Chem. **41**, 2956 (1963).
7. K. H. MUELLER and W. P. WALTERS. J. Am. Chem. Soc. **73**, 1458 (1951).
8. R. L. BURWELL and H. S. TAYLOR. J. Am. Chem. Soc. **58**, 697 (1936).
9. M. S. MALINOVSKI and S. N. BARANOV. Sbornik Statei pa Obschchei Khimii, **2**, 1674 (1953).
10. Y. K. YURIEV and K. Y. NOVIZKI. Dokl. Akad. Nauk. **63**, 285 (1948).
11. H. L. HUTCHINSON, P. L. BARRICK, and L. F. BROWN. Chem. Eng. Progr. Symp. Ser. **63**, 18 (1967).
12. A. CLARK. The theory of adsorption and catalysis. Academic Press, New York. 1970.
13. F. D. ROSSINI. NBS Circular 500. U.S. Government Printing Office, Washington. 1952.

Can. J. Chem. Downloaded from www.nrcresearchpress.com by 210.87.254.6 on 09/05/12
For personal use only.

Acyl Alkyl Diimides. III. Influence of Structure on Decomposition

THOMAS R. LYNCH, FREDERICK N. MACLACHLAN, AND JOHN L. SUSCHITZKY
Chemistry Department and Scarborough College, University of Toronto, West Hill, Ontario

Received October 16, 1972

Eleven compounds of general structure RCON=NC(CN)R_2', where R = C_6H_5, CH_3, $C_6H_5CH_2$ and R_2' = $(CH_3)_2$, $(CH_2)_4$, $(CH_2)_5$, $(CH_2)_6$, have been found to decompose in a first-order manner in dilute toluene solution in the temperature range 60–100°. The *N*-acetyl compounds decompose *ca.* four times faster than the corresponding *N*-benzoyl cases. Variation in R_2' causes changes in rate parallel to those observed by Overberger for the analogous bis-α-cyanoalkyl diimides but of smaller magnitude. The products are those expected from homolytic cleavage, and intermediate *N*-acylketenimines have been trapped by added water in two cases.

Il a été démontré que les onzes composés de structure générale RCON=NC(CN)R_2', où R = C_6H_5, CH_3, $C_6H_5CH_2$ et R_2' = $(CH_3)_2$, $(CH_2)_4$, $(CH_2)_5$, $(CH_2)_6$, se décomposent selon un mode du premier ordre en solution diluée dans le toluène et ceci dans l'intervalle de température suivant 60–100°. Les composés *N*-acétylés se décomposent *ca.* quatre fois plus rapidement que les produits correspondants *N*-benzoylés. Les changements dans R_2' entraînent des variations dans le taux identiques a celles observées par Overberger pour les diimides bis-α-cyanoalcoyle analogues mais avec une amplitude moins prononcée. Les produits sont ceux prévus à partir d'un clivage homolytique et les intermédiaires *N*-acylcetènenimines ont été isolés par addition d'eau dans les deux cas. [Traduit par le journal]

Can. J. Chem., **51**, 1378 (1973)

In previous papers we have reported on the synthesis and spectra of a number of acyl alkyl diimides (1) and on the kinetics of the thermal decomposition of one example (2). Our continuing interest in this heretofore relatively neglected class of diimides has prompted us to undertake a more extensive investigation of their properties. In this paper we report the results of a study in which the effect of alteration of both acyl and alkyl substituents on decomposition rates has been investigated. We have also performed a product study on two cases, and have measured the cage effect exhibited by one example.

$$\underset{\mathbf{1}}{\text{RCONHNHCR}_2'} \xrightarrow{[O]} \underset{\mathbf{2}}{\text{RCON=NCR}_2'}$$

a R = CH_3; R_2' = $(CH_2)_5$
b R = CH_3; R_2' = $(CH_2)_4$
c R = CH_3; R_2' = $(CH_2)_6$
d R = CH_3; R′ = CH_3
e R = $C_6H_5CH_2$; R_2' = $(CH_2)_5$
f R = C_6H_5; R_2' = $(CH_2)_6$
g R = C_6H_5; R_2' = $(CH_2)_4$
h R = C_6H_5; R′ = CH_3
i R = *p*-$MeOC_6H_4$; R_2' = $(CH_2)_5$
j R = *p*-ClC_6H_4; R_2' = $(CH_2)_5$
k R = *p*-MeC_6H_4; R_2' = $(CH_2)_5$

Accordingly, the benzoyl, acetyl, and phenylacetyl α-cyanoalkyl diimides **2***a–k* were obtained by lead tetraacetate oxidation of the *N′*-α-cyanoalkyl acid hydrazides **1***a–k*, the latter being synthesized by a general route previously described (1). An alternate route to these hydrazides was also explored, *viz.*: by transfer of the elements of hydrogen cyanide from acetone cyanohydrin to an acylhydrazone of a ketone. This method gave the desired α-cyanoalkyl acid hydrazides in yields of 25–80%. However, the first-mentioned route generally resulted in higher yields of purer products and was the method of choice.

The kinetic studies were performed in dilute toluene solution by monitoring the disappearance of the n–π* bands at *ca.* 400 nm (due to product absorption, this method was not applicable in the phenylacetyl case, compound **2***e*; disappearance of **2***e* in chlorobenzene was followed by integration of the $C_6H_5CH_2$— methylene signal in its n.m.r. spectrum). The results are collected in Table 1, and except where noted, are derived from two runs at each temperature. High concentration runs in the benzoyl series (compounds **2***h* and *j*) indicate little, if any, induced decomposition; such substrate concentration increases in the acetyl series (compounds **2***a* and *d*) actually led to slight decreases in rate, a phenomenon not normally associated with the onset of induced decomposition, and may be due to changes in the nature of the medium

Can. J. Chem. Downloaded from www.nrcresearchpress.com by 210.87.254.42 on 09/05/12
For personal use only.

TABLE 1. Rates* and activation energies for the thermal decomposition of RCON=NC(CN)R_2' in toluene

Concentration (mol/l ($\times 10^2$))	Temperature (°C)	k ($\times 10^5$ s^{-1})	E_A†	$\Delta S^{\neq}$†
		2a, $R = CH_3$, $R_2' = (CH_2)_5$		
4.94	82.0	5.21±0.19‡	27.4±0.9	−3.3±2.4
4.92	85.9	8.62±0.39‡		
1.81	89.7	11.00±0.40‡		
3.66	89.8	12.60±0.40‡		
22.00	89.8	10.70±0.60‡		
40.30	89.8	7.13±0.64‡		
4.87	92.8	17.00±0.60‡		
3.66	97.0	25.30±1.20‡		
4.94	100.6	37.40±1.00‡		
		2b, $R = CH_3$ $R_2' = (CH_2)_4$		
3.90	65.6	1.82±0.09	28.7±0.71	2.2±2.1
3.99	70.7	3.33±0.08		
4.00	76.8	7.29±0.3		
3.99	82.8	14.7 ±0.3		
3.95	91.5	36.5 ±4.0‡		
		2c, $R = CH_3$, $R_2' = (CH_2)_6$		
3.45	59.4	4.44±0.09	26.74±0.27	−0.4±0.8
3.45	66.1	9.82±0.33		
3.56	73.1	21.7 ±1.5		
3.79	79.6	45.1 ±2.2		
		2d, $R = CH_3$, $R' = CH_3$		
4.32	60.8	2.46±0.17	26.32±1.9	−3.1±5.5
4.32	68.6	5.45±0.21		
4.32	75.2	13.5 ±0.5		
3.64	75.2	12.9 ±0.5‡		
18.20	75.2	12.5‡		
36.40	75.2	9.8‡		
4.32	82.0	24.9 ±1.6		
		2e, $R = C_6H_5CH_2$, $R' = (CH_2)_5$		
49.0	74.3	3.08±0.13‡	31.96±1.7	10.5±4.8
49.0	79.3	6.63±0.53‡		
45.0	82.9	9.76±0.53‡		
45.0	87.2	16.2 ±1.7‡		
45.0	91.2	27.7 ±2.5‡		
		2f, $R = C_6H_5$, $R_2' = (CH_2)_6$		
1.87	74.6	6.43±0.23	29.30±1.09	4.3±3.7
1.84	78.6	10.59±0.45		
1.89	82.8	17.81±0.73		
1.85	89.2	35.19±1.57		
		2g, $R = C_6H_5$, $R_2' = (CH_2)_4$		
1.95	76.7	1.62±0.08	31.47±0.85	7.5±3.1
1.89	82.0	3.17±0.16		
1.94	92.6	11.64±0.58		
1.92	98.4	22.52±0.97		
		2h, $R = C_6H_5$, $R' = CH_3$		
1.81	69.2	1.31±0.06	30.53±0.76	6.1±3.3
2.25	73.2	2.28±0.10‡		
22.45	73.2	2.34±0.16‡		
2.22	83.2	7.96±0.36		
1.77	90.0	17.44±0.48		

Can. J. Chem. Downloaded from www.nrcresearchpress.com by 210.87.254.42 on 09/05/12
For personal use only.

TABLE 1 (*Concluded*)

		***2i*, $R = p\text{-}CH_3OC_6H_4$, $R' = (CH_2)_5$**		
1.33	80.8	0.71±0.04	34.08±1.05	11.8±2.3
1.32	87.9	1.71±0.08		
1.33	94.0	3.94±0.21		
1.32	101.2	9.73±0.38		
		***2j*, $R = p\text{-}ClC_6H_4$, $R' = (CH_2)_5$**		
1.78	79.1	0.86±0.04	31.68±0.93	5.8±2.2
1.78	86.4	2.01±0.06		
1.77	92.8	4.52±0.15‡		
17.70	92.8	5.05±0.47‡		
1.78	99.7	10.44±0.34		
		***2k*, $R = p\text{-}CH_3C_6H_4$, $R' = (CH_2)_5$**		
2.00	81.4	1.06±0.04	32.00±0.99	6.6±2.3
2.00	87.3	2.20±0.05		
2.00	95.5	6.01±0.20		
2.00	101.9	12.55±0.68		

*Rate constants calculated by least-squares method.
†Errors in E_a and $\Delta S^{\ddagger}$ are estimated.
‡From one run.

TABLE 2. Calculated rate constants for the thermal decomposition of $RCON{=}NC(CN)R_2'$ at 80° in toluene

	$R = CH_3$		$R = C_6H_5$			$R = C_6H_5CH_2$	$(R_2'C(CN)N{=})_2$†
R_2'	k ($\times 10^5$ s^{-1})	k_{rel}*	k ($\times 10^5$ s^{-1})	k_{rel}*	$k_{CH_3CO}/k_{C_6H_5CO}$	k ($\times 10^5$)	k_{rel}*
$(CH_3)_2$	20.76	4.8	5.32	6.1	3.9		24.3
$(CH_2)_4$	10.17	2.4	2.47	2.8	4.1		11.5
$(CH_2)_5$	4.33	1.0	0.88‡	1.0	4.9	6.69	1.0
$(CH_2)_6$	45.53	10.5	12.48	14.2	3.7		193.7

*Relative to the cyclohexyl case.
†References 6 and 7.
‡Reference 2.

(now *ca.* 0.4 *M* in diimide). Here it should be noted that diimide **2***e* gave good first-order kinetics over 2–3 half-lives although the concentration was necessarily high (*ca.* 0.5 *M*).

Table 2 gives the calculated rate constants at 80.0° for the unsubstituted diimides studied here, and for *N*-benzoyl *N'*-α-cyanocyclohexyl diimide, **2***l*, reported on previously. It can be seen (column 6) that the *N*-acetyl diimides decompose approximately four times faster than the *N*-benzoyl analogs having the same alkyl group, perhaps suggestive of some degree of *N*-acyl cleavage in the transition state. The very slight rate enhancement of the phenylacetyl case, **2***e*, over its acetyl relative, compound **2***a*, can be taken to indicate that loss of carbon monoxide is not concerted with formation of nitrogen. This contrasts with the case of *t*-butyl phenylperacetate in which formation of carbon dioxide is considered to be simultaneous with cleavage of the perester O—O bond (3). In addition, it can be seen that the effects of *p*-substituents on the rate of decomposition of benzoyl diimides having a common alkyl group (Table 3, compounds **2***i–l*), is small and that there appears to be no significant contribution from a polar transition state such as 3.[1,2]

TABLE 3. Calculated rate constants for the thermal decomposition of $p\text{-}X\text{-}C_6H_4CON{=}NC(CN)(CH_2)_5$ at 80° in toluene

Compound **2**	X	k ($\times 10^5$ s^{-1})	k_{rel}
l	H	0.88	1.00
i	Me	0.88	1.00
j	Cl	0.94	1.07
k	MeO	0.61	0.69

[1]Polar transition states in the formation of benzoyl radicals have previously been invoked (ref. 4 and refs. therein).

[2]It has been suggested from e.s.r. studies (5) that benzoyl radicals are not stabilized by *p*-Cl or *p*-MeO substituents.

Can. J. Chem. Downloaded from www.nrcresearchpress.com by 210.87.254.42 on 09/05/12
For personal use only.

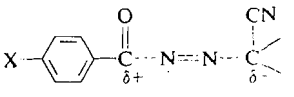

3

As inferred previously, the effect of alkyl group variation on rates is quite similar in both the benzoyl and acetyl series (Table 2) and the relative ordering (cyclohexyl < cyclopentyl < isopropyl < cycloheptyl) is the same as that observed by Overberger (refs. 6 and 7, Table 2, column 8) for the corresponding bis-α-cyanoalkyl diimides, and would seem to establish *N*-alkyl bond cleavage. It should be noted that the rate range observed here (10–14) is much less than for the dialkyl compounds (*ca.* 200) of Overberger, and more closely resembles the range of 5 observed for the related *t*-butylcycloalkyl peresters (8, 9). Whether acyl C—N bond cleavage is also occurring is less clear. This bond is expected to be the stronger, being an sp^2–sp^2 bond rather than sp^2–sp^3, and because of conjugation effects. However, the similarity between the activation energies for our compounds and those of Overberger's may support a two bond cleavage, the faster rate of the acetyl compounds reflecting greater acyl C—N bond cleavage, or a more stable acyl radical.

We have also examined the products from the thermal decomposition of compounds **2***d* and *h*. Decomposition of a degassed 0.1 *M* solution of **2***d* in toluene containing added water,[3] at 80° for 8.5 half-lives gave (average of two runs): α-acetylisobutyronitrile (1.3%), tetramethylsuccinonitrile (4%), isobutyramide (7%), *N*-acetylisobutyramide (12%), isobutyronitrile (22%), acetic acid (25%), acetone (14%) and α-methylacrylonitrile (3%), accounting for 67% of the isobutyronitrile radicals but a more disappointing 38% of the acetyl radicals, together with a number of other products which were not identified but which may arise by attack of radicals on the solvent.[4] Decomposition of **2***h* (0.075 *M* in degassed toluene containing water at 90° for 8.5 half-lives) gave (average of two runs): α-benzoylisobutyronitrile (3%), *N*-benzoylisobutyramide (70%),[5] benzaldehyde (2%), tetramethylsuccinonitrile (4%), benzene (2%),[6] and a trace of bibenzyl, accounting for 77% of the benzoyl radicals and 81% of the isobutyronitrile radicals. Neither isobutyronitrile nor α-methylacrylonitrile were detected.

The most notable feature of the product distributions from **2***d* and *h* is the marked preference for combination of the acyl radicals with the isobutyronitrile radicals on nitrogen, rather than on the more sterically hindered carbon, in agreement with the preference previously observed for the recombination of α-cyanoalkyl radicals themselves (12). The *N*-acylketenimines so formed in the cases reported are then presumed to react with water to give the *N*-acylamides observed as the predominant products. Parenthetically, it might be mentioned that *N*-acylketenimines appear to be a hitherto unreported class of ketenimine (13), and, in the absence of water, thermal decomposition of α-cyanoalkyl acyl diimides is a potential route to their isolation.

To return to the products studies, the significant amounts of isobutyronitrile and acetic acid from the diimide **2***d* can most reasonably be explained by nucleophilic attack of water on the carbonyl group of the diimide (14), whilst the isobutyramide probably arises by hydrolysis of *N*-acetylisobutyramide. The acetone formed may arise by reaction of the isobutyronitrile radicals with residual oxygen, although the solutions were considered to be thoroughly degassed.

In contrast to the thermal results, irradiation ($\lambda > 350$ nm) of an 8×10^{-2} *M* solution of **2***h* in toluene containing water, followed by g.l.c. analysis, gave benzaldehyde (6%), tetramethylsuccinonitrile (9%), α-benzoylisobutyronitrile (14%), *N*-benzoylisobutyramide (3%), benzene (1%), and a number of other unidentified products. Isobutyronitrile and α-methylacrylonitrile were not analyzed for. The low yield of *N*-acylamide under these photochemical conditions may be due to the lower solubility of water in toluene at room temperature, or photochemical decomposition of the *N*-acylketenimine when formed, or a combination of these factors.

The cage effect in the decomposition of **2***h*

[3]The rate of decomposition of **2***l* was unaltered on addition of a small amount of water.

[4]No bibenzyl was detected.

[5]In a subsequent set of runs the amounts of α-benzoylisobutyronitrile and *N*-benzoylisobutyramide were determined to be 9 and 58%, respectively.

[6]The decarbonylation of benzoyl radicals generated from dibenzoyl diimide has been observed previously (10) and more recently studied quantitatively in the system:

$$C_6H_5CHO + I_2 \rightarrow C_6H_5ClO + HI \quad (11)$$

Can. J. Chem. Downloaded from www.nrcresearchpress.com by 210.87.254.42 on 09/05/12
For personal use only.

Can. J. Chem. Downloaded from www.nrcresearchpress.com by 210.87.254.42 on 09/05/12
For personal use only.

in toluene at 90° was measured by the iodine consumption method (15), and found to be 53 ± 3%. Simultaneously, the yield of ketone was measured in the presence of iodine and was observed to fall to 33% of its value in the absence of this scavenger. A similar discrepancy in cage effect determinations by iodine scavenging and product analysis has previously been reported (16).

In conclusion, the work described in this paper establishes that the *N*-benzoyl and *N*-acetyl α-cyanoalkyl diimides examined decompose by first-order kinetics to give radical intermediates. The major mode of recombination leads to *N*-acylketenimines which rapidly react with water present to give *N*-acylamides. *N*-Acetyldiimides decompose more rapidly than the *N*-benzoyl analogs, and variation of the alkyl group affects the rates in a similar, but attenuated, manner to that observed by Overberger, for his bis-α-cyanoalkyldiimides.

Experimental

Instruments used and related information are as reported previously (1, 2). Details of the kinetic method have also been given before (2).

A number of the *N'*-α-cyanoalkyl acid hydrazides and derived diimides have been prepared before; the following are new compounds:

1*b*: yield 50%; m.p. 103–104°; n.m.r.: δ 8.08 (br s, 1H), 4.85 (br s, 1H), 2.02 (s, 3H), 1.55–1.95 p.p.m. (br, 8H).

Anal. Calcd. for $C_8H_{13}N_3O$: C, 57.47; H, 7.84; N, 25.13. Found: C, 57.43; H, 7.82; N, 25.08.

2*b*: yellow oil, yield 92%; λ_{max} (C_6H_{12}) 395 nm (ε 36); n.m.r.: δ 2.30 (s, 3H), 1.8–2.6 p.p.m. (br, 8H).

1*c*: yield 16%; m.p. 94.5°; n.m.r.: δ 8.35 (br s, 1H), 5.02 (br s, 1H), 2.02 (s, 3H), 1.4–2.2 p.p.m. (br, 12H).

Anal. Calcd. for $C_{10}H_{17}N_3O$: C, 61.51; H, 8.78; N, 21.52. Found: C, 61.74; H, 8.82; N, 21.86.

2*c*: yellow oil, yield 91%; λ_{max} (C_6H_{12}) 397 nm (ε 35); n.m.r.: δ 2.35 (s, 3H), 1.8–2.1 p.p.m. (br, 12H).

1*e*: yield 70%; m.p. 98–99°; n.m.r.: δ 7.20 (br d, J = 5 Hz, 1H), 7.25 (s, 5H), 5.0 (br d, J = 5 Hz, 1H), 3.53 (s, 2H), 0.8–2.0 p.p.m. (br, 10H).

Anal. Calcd. for $C_{15}H_{19}N_3O$: C, 70.01; H, 7.44; N, 16.33. Found: C, 69.69; H, 7.29; N, 16.13.

2*e*: yield 86%; m.p. 43°; n.m.r.: δ 7.27 (s, 5H), 3.93 (s, 2H), 1.90 p.p.m. (br, 10H).

Anal. Calcd. for $C_{15}H_{17}N_3O$: C, 70.56; H, 6.71; N, 16.46. Found: C, 70.52; H, 6.73; N, 16.32.

1*f*: yield 87%; m.p. 123–125°; n.m.r.: δ 7.2–8.17 (m, 6H), 5.2 (d, J = 5 Hz, 1 H), 1.2–2.2 p.p.m. (m, 12H).

Anal. Calcd. for $C_{15}H_{19}N_3O$: C, 70.01; H, 7.44; N, 16.33. Found: C, 70.12; H, 7.19; N, 16.39.

2*f*: yield 80%; m.p. 55.5–57°; λ_{max} (C_6H_{12}) 244 (ε 8600), 290 (sh, ε 1400), 321 (sh, ε 275), 408 nm (ε 50); n.m.r.: δ 7.4–8.0 (m, 5H), 1.46–2.4 p.p.m. (m, 12H).

1*g*: yield 50%; m.p. 124.5–126°, n.m.r.: δ 8.1–8.20 (d, J = 7 Hz, 1H), 7.23–7.90 (m, 5H), 5.24 (d, J = 7 Hz, 1H), 1.57–2.30 p.p.m. (br, 8H).

Anal. Calcd. for $C_{13}H_{15}N_3O$: C, 68.10; H, 6.59; N, 18.33. Found: C, 67.93; H, 6.68; N, 18.39.

2*g*: orange oil, yield 79%; λ_{max} (C_6H_{12}) 244 (ε 8600), 289 (sh, ε 1700), 323 (sh, ε 244), 408 nm (ε 46); n.m.r.: δ 7.47–8.0 (m, 5H), 1.67–2.67 p.p.m. (m, 8H).

1*i*: yield 80%; m.p. 144–146.5°, n.m.r.: δ 8.38 (s, 1H), 7.78 (d, J = 8.5 Hz, 2H), 6.87 (d, J = 8.5 Hz, 2H), 5.33 (br s, 1H), 3.81 (s, 3H), 1.1–2.37 p.p.m. (m, 10H).

Anal. Calcd. for $C_{15}H_{19}N_3O_2$: C, 65.91; H, 7.01; N, 15.37. Found: C, 66.15, H, 7.27; N, 15.26.

2*i*: yield 89%; m.p. 108.5–109°, λ_{max} (CH_3CN) 286 (ε 10 850), 406 nm (sh, ε 56), n.m.r.: δ 7.98 (d, J = 9 Hz, 2H), 7.02 (d, J = 9 Hz, 2H), 3.91 (s, 3H), 1.3–2.37 p.p.m. (m, 10H).

1*k*: yield 65%; m.p. 137–139°, n.m.r.: δ 8.36 (s, 1H), 7.70 (d, J = 8 Hz, 2H), 7.18 (d, J = 8 Hz, 2H), 5.27 (br s, 1H) 2.35 (s, 3H), 0.93–2.27 p.p.m. (m, 10H).

Anal. Calcd. for $C_{15}H_{19}N_3O$: C, 70.01; H, 7.44; N, 16.33. Found: C, 70.16; H, 7.19; N, 16.23.

2*k*: yield 79%; m.p. 80.5–81°; λ_{max} (C_6H_{12}) 255 (ε 10 500), 290 (sh, ε 3000), 321 (sh, ε 510), 409 nm (ε 47); n.m.r.: δ 7.83 (d, J = 8 Hz, 2H), 7.28 (d, J = 8 Hz, 2H), 2.43 (s, 3H), 1.53–2.36 p.p.m. (m, 10H).

1*j*: yield 87%; m.p. 160–162°, i.r. (Nujol): 3290 (w), 3225 (s), 1640 cm^{-1} (s); n.m.r.: not obtainable due to insolubility.

2*j*: yield 86%; m.p. 81.5–82.5, λ_{max} (C_6H_{12}) 259 (ε 13 000), 415 nm (ε 57), n.m.r.: δ 7.80 (d, J = 8 Hz, 2H), 7.50 (d, J = 8 Hz, 2H), 1.0–2.3 p.p.m. (br, 10H).

Anal. Calcd. for $C_{14}H_{14}ClN_3O$: C, 60.98; H, 5.12; N, 15.24. Found: C, 61.00; H, 5.13; N, 15.08.

Reaction of acylhydrazones with acetone cyanohydrin: a mixture of the hydrazone (4 mmol), acetone cyanohydrin (3 ml), methanol (7 ml), and either 10% aqueous sodium carbonate solution (0.5 ml) or triethylamine (0.25 ml) was refluxed overnight. The solvent was removed and the desired hydrazide obtained by crystallization (in some cases colored impurities were removed with charcoal).

A typical oxidation of an α-cyanoalkyl acid hydrazide was as follows: a solution of lead tetraacetate (0.92 g, 2.1 mmol) in dichloromethane (15 ml) was added to a solution of the hydrazide (2.0 mmol) in dichloromethane cooled to −20°. The solution was stirred at −20° for 1 h, then decanted from the insoluble lead salts, washed with ice-cold water (2 × 50 ml), cold saturated aqueous sodium bicarbonate solution (2 × 50 ml), ice-cold water (2 × 50 ml), dried, and the solvent was then removed at *ca.* 10°. The benzoyl and phenylacetyl diimides (with the exception of compounds **2***g* and **2***h*) were solids and were recrystallized from pentane. The remaining diimides were orange or yellow oils and were used as obtained; they were pure by n.m.r. and i.r.

α-Benzoyl isobutyronitrile was obtained by methylation of benzoylacetonitrile (17) with methyl iodide. The crude product (b.p. 73–78°/0.25 mm (lit. (18) b.p. 139°/10 mm)) was purified by preparative g.l.c. (Varian Aerograph Model 700) on a 20 ft × 1/4 in. SE-30 column. The pure material was a colorless liquid, λ_{max} (EtOH) 248 (ε 11 000), 282 nm (sh, ε 1100); ν_{max} 1694 cm^{-1}; n.m.r.: δ 1.71 (s, 6H), 7.4–8.4 p.p.m. (m, 5H).

α-Acetyl isobutyronitrile was prepared by methylation of α-acetylpropionitrile (19) with methyl iodide, b.p.

163–166° (lit. (20) b.p. 162–165°), λ_{max} (EtOH): 233 (ε 195), 281 nm (ε 26); ν_{max} 1725 cm^{-1}; n.m.r.: δ 2.43 (s, 3H), 1.53 p.p.m. (s, 6H). *N*-Benzoylisobutyramide, m.p. 155–156° (lit. (21) m.p. 154°) and *N*-acetylisobutyramide, m.p. 68–70° (lit. (22) m.p. 73–74°) were obtained by treatment of benzamide and acetamide, respectively, with isobutyryl chloride. Tetramethylsuccinonitrile was obtained from azoisobutyronitrile (23).

Product identifications were performed on a Varian Model 1740 Gas Chromatograph using the following 5 ft × 1/8 in. columns: 5% DEGSE on acid-washed 80/100 mesh Chromosorb W; 3% SE-30 on 100/120 mesh VarAport 30; 5% Carbowax 20 M on DMCS-treated 80/100 mesh Chromosorb W, and a 10 ft × 1/8 in. 80/100 mesh Chromosorb 103 column. For quantitative analyses, the detector was calibrated using solutions of known concentration of the products. Peak areas were measured with a planimeter.

For measurement of the cage effect, 2 ml aliquots of toluene, 0.037 *M* in **2***h* and 0.074 *M* in iodine were degassed and sealed in tubes, then heated for 8 h at 90°. The iodine concentration before and after was monitored at 498 nm. The cage effect is then given by [(moles diimide at $t = 0$) − (moles I_2 consumed)]/[moles diimide at $t = 0$]. The results given are the average of three determinations.

Photochemical studies were performed on degassed solutions of **2***h* in Pyrex tubes using a Hanovia #901C1 Xenon lamp, and passing the light through a Corning cso 52 filter.

The authors are grateful to Mr. A. Shum for excellent experimental assistance and to the National Research Council of Canada for financial support.

1. T. R. Lynch, F. N. MacLachlan, and Y. K. Siu. Can. J. Chem. **49**, 1598 (1971).
2. T. R. Lynch and F. N. MacLachlan. Can. J. Chem. **50**, 2143 (1972).
3. P. D. Bartlett and R. R. Hiatt. J. Am. Chem. Soc. **80**, 1398 (1958).
4. K. H. Lee. Tetrahedron, **24**, 4793 (1968).
5. U. Schmidt, K. Kabitzke, and K. Markau. Monatsch. Chem. **97**, 1000 (1966).
6. C. G. Overberger, H. Biletch, A. B. Finestone, J. Lilker, and J. Herbert. J. Am. Chem. Soc. **75**, 2078 (1953).
7. C. G. Overberger, M. T. O'Shaughnessy, and H. Shalit. J. Am. Chem. Soc. **71**, 2661 (1949).
8. P. Lorenz, C. Ruchardt, and E. Schacht. Tetrahedron Lett. 2787 (1969).
9. P. D. Bartlett and L. B. Gortler. J. Am. Chem. Soc. **85**, 1864 (1963).
10. D. Mackay, V. F. Marx, and W. A. Waters. J. Chem. Soc. 4793 (1964).
11. R. K. Solly and S. W. Benson. J. Am. Chem. Soc. **93**, 2127 (1971).
12. C.-H. S. Wu, G. S. Hammond, and J. M. Wright. J. Am. Chem. Soc. **82**, 5386 (1960).
13. G. R. Krow. Ang. Chem. Int. Ed. Engl. **10**, 435 (1971).
14. R. W. Hoffmann and K. R. Eicken. Chem. Ber. **100**, 1465 (1967).
15. J. B. Levy and E. J. Lehmann. J. Am. Chem. Soc. **93**, 5790 (1971).
16. P. D. Bartlett and C. Ruchardt. J. Am. Chem. Soc. **82**, 1760 (1960).
17. J. B. Dorsch and S. M. McElvain. J. Am. Chem. Soc. **54**, 2962 (1932).
18. H. Brederick, B. Fohlisch, and R. Franz. Makromol. Chem. **92**, 86 (1966).
19. E. Mohr. J. Prakt. Chem. **90**, 189 (1914).
20. A. Jonsson. Acta. Chem. Scand. **8**, 1391 (1954).
21. W. I. Awad, A. F. M. Fahmy, and A. M. A. Sammour. J. Org. Chem. **30**, 2222 (1965).
22. T. Ogata and R. Goto. Nippon Kagaku Zasshi. **84**, 849 (1963); Chem. Abstr. **60**, 450c (1964).
23. G. S. Hammond, J. N. Sen, and C. E. Boozer. J. Am. Chem. Soc. **77**, 3244 (1955).

Can. J. Chem. Downloaded from www.nrcresearchpress.com by 210.87.254.42 on 09/05/12
For personal use only.

A Study of Solvent Effects on the ^{13}C Nuclear Magnetic Resonance Spectra of Cholesterol, Pyridine, and Uridine[1]

H. H. MANTSCH[2] AND IAN C. P. SMITH[3]

Division of Biological Sciences, National Research Council of Canada, Ottawa, Canada K1A 0R6

Received November 17, 1972

The ^{13}C n.m.r. chemical shifts for cholesterol in five solvents are reported. All carbon atoms were subject to solvent effects of varying sign and magnitude. The chemical shifts in the solvent pair dioxane–chloroform 1:1 could be predicted on an additivity basis. Pyridine was studied in 24 solvents; the chemical shifts of all carbons were solvent-dependent. Solvent effects at positions β and γ were correlated, while those at position α bore no simple relation to those of the other carbons. A small isotope effect was noted on comparing the data for H_2O and ^2H_2O. Coupling between ^{13}C and ^{14}N was observed in some cases; its magnitude was solvent-dependent. Uridine was studied in four solvents. While all carbons were subject to solvent-induced shifts, evidence for specific solvent interaction at C-4, -5, -1′, and -2′ was obtained. An appreciable contribution to the relaxation of carbonyl C-2 and -4 from dipole–dipole interaction with the hydrogen on N-3 was observed. Solvent effects can result in scrambling and misassignment of ^{13}C resonances if care is not taken with choice of solvent.

Les déplacements chimiques du cholesterol en r.m.n. du ^{13}C ont été rapportés pour cinq solvants. Tous les atomes de carbone sont soumis à des effets de solvant d'amplitude et de signe variables. Les déplacements chimiques dans la paire de solvants dioxane:$CHCl_3$ 1:1 peuvent être prévus par additivité. La pyridine a été étudiée dans 24 solvants, les déplacements chimiques de tous les carbones sont fonction du solvant. Les effets du solvant sur les positions β et γ ont été reliés tandis qu'il n'existe aucune relation simple pour la position α. Un faible effet isotopique a été noté en comparant les données sur H_2O et ^2H_2O. Le couplage entre ^{13}C et ^{14}N a été observé dans certains cas, son amplitude dépend du solvant. L'uridine a été étudiée dans quatre solvants. Alors que tous les carbones subissent des déplacements induits par le solvant, une interaction spécifique du solvant a été mise en évidence pour les C-4, -5, -1′, et -2′. On a noté une contribution notable à la relaxation du carbonyle des C-2 et -4, à partir de l'interaction dipole–dipole avec l'hydrogène sur l'azote 3. Les effets de solvant peuvent masquer et conduire à une mauvaise attribution des pics de résonance du ^{13}C si le solvant n'a pas été choisi avec précaution.

[Traduit par le journal]

Can. J. Chem., **51**, 1384 (1973)

^{13}C n.m.r. spectra are in general much more informative than those of ^1H for structural analyses of complex molecules. Although the ^{13}C chemical shifts are most sensitive to structural changes, solvent effects cannot be minimized and those working with ^{13}C spectra should be aware of such effects. Carbon shieldings are apparently more solvent-sensitive than proton shieldings, yet relatively little is known about the dependence. Solvent effects on ^1H spectra have been studied extensively (1).

A few solute–solvent interactions have been investigated by ^{13}C n.m.r., particularly on carbon atoms bearing functional groups (substituents). Maciel and co-workers examined thoroughly the ^{13}C chemical shifts of carbonyl- and hydroxyl-bearing carbon atoms as a function of solvent (2–7). Solvent effects on the ^{13}C resonances of methyl iodide (8, 9), chloroform and carbon tetrachloride (10), acetonitrile and methyl isocyanide (11), and of monosubstituted benzenes (12, 13) have been reported. In general, a shift towards lower field was observed in more acidic solvents, paralleling the tendency of the solvents to form hydrogen bonds. For the carbonyl carbon this solvent shift could be interpreted reasonably in terms of an increased polarization of the C=X bond by hydrogen bonding. The shifts in aprotic solvents are more difficult to rationalize, but major contributions probably arise from polar and van der Waals interactions. For carbonyl-containing compounds, it has been concluded that the shifts in aprotic solvents reflect the carbonyl π-bond polarity (2, 3, 6).

For obtaining a ^{13}C n.m.r. spectrum, one usually attempts to achieve the highest concentration of compound possible, and therefore

[1]NRCC No. 13062.

[2]NRCC Visiting Research Officer, 1971. Present address, Institute of Chemistry, Str. Donath 65, Cluj, Romania.

[3]To whom correspondence should be addressed.

Can. J. Chem. Downloaded from www.nrcresearchpress.com by 210.87.254.40 on 09/05/12
For personal use only.

Can. J. Chem. Downloaded from www.nrcresearchpress.com by 210.87.254.40 on 09/05/12
For personal use only.

turns to the most favorable solvent. A good example of this is the pioneering work of Reich *et al.* (14) on a wide series of sterols; mixtures of dioxane and chloroform of varying proportions had to be used to maximize solubility. Thus, it is vital at this stage in the development of ^{13}C n.m.r. to demonstrate carefully the types of solvent-induced chemical shift changes one can expect. We have done so for three structurally different compounds, cholesterol, pyridine, and uridine, in a wide variety of solvents.

Experimental

The natural abundance ^{13}C n.m.r. spectra were measured on a VARIAN XL-100-15 spectrometer operating in Fourier transform mode at 25.16 MHz with proton noise decoupling (4 KHz bandwidth). Data were accumulated in a VARIAN 620i computer using 5000 Hz spectral widths and 4096 data points (resolution of 0.1 p.p.m.). Data acquisition and pulse delay times were 0.4 and 0.8 s, respectively (cycle time 1.2 s).

Cholesterol (5-cholesten-3β-ol, Steraloids, Pawling, N.Y. recrystallized from methanol) and uridine (1-β-D-ribofuranosyl-uracil, Raylo Chemicals, Edmonton) were studied as 0.3 *M* solutions in spectrograde solvents; dry spectrograde pyridine was studied at 0.17 mol fraction in each solvent. The samples, in 8 mm o.d. inner Pyrex tubes, were studied in concentric 12 mm n.m.r. tubes containing deuterium oxide for the spectrometer field frequency lock. In this way susceptibility corrections were kept constant and the effects of solvent on internal references were avoided. The susceptibility correction between external TMS (D_2O in outer tube) and TMS in $CDCl_3$ is 1.3 p.p.m. (the internal reference resonates at lower field, higher frequency, than the external reference). Sample temperature was 37 °C (with complete proton decoupling). Increasing positive values of chemical shift indicate increasing frequency (decreasing magnetic field).

Results and Discussion

Cholesterol

The choice of the best solvent becomes particularly important if a large number of ^{13}C resonances are closely situated, as is the case for instance with the 27 carbon atoms in the steroid skeleton. Thus, it is unreliable to compare the absolute values of ^{13}C chemical shifts obtained in different solvents, since a scrambling of resonances is possible. This point is well demonstrated by the ^{13}C n.m.r. data for cholesterol. Cholesterol has the advantage for our purpose of possessing polar, nonpolar, and unsaturated carbon atoms, and a tentative assignment of the resonances has been made (14). For a few closely-situated signals alternative assignments are possible. For cholesterol such an ambiguity arises in the case of resonances separated by less than 0.5 p.p.m., namely C-4 and -13; C-16 and -24; C-10 and -22; C-8, -7, and -2; C-12 and -25; C-15 and -23; and C-27 and -26.

We used for this investigation strictly comparable conditions and the following solvents: benzene, pyridine, *p*-dioxane, chloroform, and carbon tetrachloride. The chemical shifts are shown in Table 1: They are also displayed diagrammatically in Fig. 1 for benzene, *p*-dioxane, and chloroform. The total range of the cholesterol spectrum is 130 p.p.m.

The most solvent-sensitive positions are the hydroxyl-bearing C-3 and the unsaturated C-6, both of which are shifted by about 1 p.p.m. to lower field in $CHCl_3$ and CCl_4 as compared to benzene, pyridine, or *p*-dioxane. The chemical shifts in CCl_4 and $CHCl_3$ are nearly identical, *i.e.* the differences are less than 0.1 p.p.m., always with those in $CHCl_3$ to slightly lower field. This difference is more pronounced, but still in the same direction, for C-6 (0.4 p.p.m.) and -3 (0.7 p.p.m.).

Similarly, benzene and pyridine can be grouped together, the differences of the individual chemical shifts (except for C-6, -5, and -3) are less than 0.2 p.p.m., with shifts in pyridine always to slightly lower field. The corresponding resonances in *p*-dioxane are generally intermediate between those in benzene and pyridine.

The saturated hydrocarbon skeleton is also sensitive to medium effects, although to a lesser extent than C-3 and -6. Most affected are the five CH_3 groups (C-18, -19, -21, -26, and -27). They are shifted by 0.7–0.8 p.p.m. to lower field in CCl_4 and $CHCl_3$ as compared to benzene, pyridine, and dioxane. Less affected are the CH_2 groups which in CCl_4 and $CHCl_3$ are also at lower field by 0.5–0.7 p.p.m., while the CH and the quaternary carbons are shifted by 0.3–0.5 p.p.m. to lower field.

In summary, it is clear that all resonances appear at lower field in CCl_4 or $CHCl_3$ as compared to benzene, pyridine, or *p*-dioxane, with quantitative differences for various groups; even the protected quaternary carbons are sensitive to medium effects. These solvent shifts are roughly additive, provided there is no strong interaction between the solvents. The experimental values obtained for a binary 1:1 mixture of chloroform and *p*-dioxane compare well within experimental error with the calculated mean values from chloroform and *p*-dioxane (Table 1).

TABLE 1. ^{13}C chemical shifts* for cholesterol in various solvents†

No. of carbon atom	Benzene	Pyridine	*p*-Dioxane	Chloroform	CCl_4	Dioxane–chloroform (1:1) Obs.	Calcd.
18	12.3	12.5	12.4	13.1	13.1	12.8	12.8
21	19.3	19.5	19.4	20.0	20.0	19.7	19.7
19	19.8	20.1	19.9	20.6	20.6	20.3	20.2
11	21.7	21.9	21.9	22.3	22.3	22.1	22.1
26	23.1	23.1	23.1	23.9	23.9	23.5	23.5
27	23.3	23.5	23.3	24.1	24.1	23.7	23.7
23	24.6	24.7	24.7	25.1	25.1	24.9	24.9
15	24.8	25.0	25.0	25.5	25.4	25.3	25.3
25	28.6	28.7	29.0	29.2	29.1	29.0	29.1
12	28.8	29.0		29.4	29.4	29.2	29.2
2	32.4	32.7	32.7	32.8	32.6	32.7	32.7
7	32.6			33.1	33.1	33.0	32.9
8		33.0					
20	36.5	36.6	36.8	37.0	37.0	36.8	36.9
22	37.0	37.0	37.2	37.4	37.4	37.2	37.3
10		37.4	37.4	37.6	37.6	37.6	37.5
1	38.0	38.4	38.2	38.6	38.6	38.4	38.4
24	40.2	40.2	40.3	40.7	40.7	40.5	40.5
16	40.2	40.6	40.7	41.0	41.0	40.9	40.9
13	43.0	43.0	43.2	43.4	43.3	43.4	43.3
4	43.2	43.8	43.5	43.5	43.5	43.5	43.5
9	50.9	51.0	51.3	51.4	51.4	51.3	51.3
17	56.9	57.0	57.2	57.4	57.4	57.3	57.3
14	57.3	57.4	57.8	58.0	58.0	57.8	57.9
3	71.9	71.6	71.7	72.8	72.1	72.0	72.3
6	121.8	121.5	121.7	122.7	122.3	122.1	122.2
5	141.6	142.4	142.4	142.1	142.1	142.2	142.2

*Expressed relative to external tetramethylsilane.
†The ^{13}C resonances of the individual solvent carbons in these solutions are as follows: C_6H_6: 128.7; C_6H_5N: 150.4 (α); 136.1 (γ) and 124.1 (β); $C_4H_8O_4$: 68.0; $CHCl_3$: 78.5; CCl_4: 97.3.

This shows that solvent mixtures could be used conveniently to separate closely-situated signals.

Pyridine

Pyridine provides a good model for heteroaromatic compounds. The natural abundance ^{13}C n.m.r. spectra were obtained for 1:5 mol fraction solutions of pyridine in 25 different solvents which were inert, highly basic, and very acidic. The ^{13}C chemical shifts were measured under strictly comparative conditions for the α (ortho), β (meta), and γ (para) carbon atoms and are shown in Table 2 for all 25 solvents. Because pyridine self-associates weakly through intermolecular hydrogen bonds, we choose pyridine in cyclohexane as a reference. The chemical shifts of pyridine in cyclohexane are given at the bottom of Table 2. Relative to pyridine in cyclohexane all other solvents produce a downfield shift of the resonances of the γ ($\Delta\delta_\gamma$) and β ($\Delta\delta_\beta$) carbon atoms and almost always a high field shift for the α carbon resonances ($\Delta\delta_\alpha$).

Most solvent-sensitive is C-γ with a maximum observed downfield shift ($\Delta\delta_\gamma$) of 14 p.p.m. in hydrobromic acid. A downfield shift is experienced also by C-β, which is less pronounced (maximum $\Delta\delta_\beta$ is 5.8 p.p.m.) and apparently related to $\Delta\delta_\gamma$ for the same solvent. There is a monotonic, although not strictly linear increase of $\Delta\delta_\beta$ with increasing $\Delta\delta_\gamma$ for most solvents and a nearly linear relationship for the seven protonated cations.

The solvent-induced upfield shifts of the α carbons ($\Delta\delta_\alpha$) (maximum −8.7 p.p.m. in trifluoroacetic acid) cannot be simply related to either $\Delta\delta_\beta$ or $\Delta\delta_\gamma$. The downfield shifts of the γ and β carbons appear to be related to charge polarization (inductive) effects dominated by hydrogen bonding to the lone pair nitrogen while the upfield shift of the α carbon is much

Can. J. Chem. Downloaded from www.nrcresearchpress.com by 210.87.254.40 on 09/05/12
For personal use only.

Can. J. Chem. Downloaded from www.nrcresearchpress.com by 210.87.254.40 on 09/05/12
For personal use only.

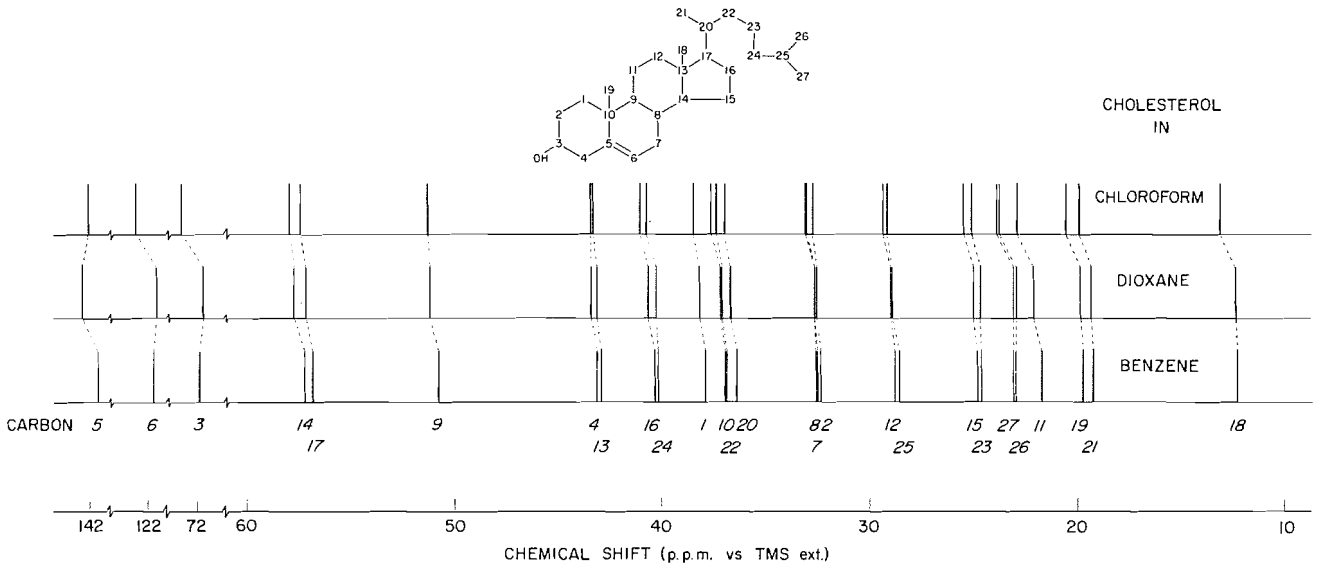

FIG. 1. Schematic representation of the 25.16 MHz ^{13}C n.m.r. spectra of cholesterol 0.3 *M* in chloroform, dioxane, and benzene.

Can. J. Chem. Downloaded from www.nrcresearchpress.com by 210.87.254.40 on 09/05/12
For personal use only.

TABLE 2. ^{13}C chemical shifts* of pyridine as a function of solvent

ortho (α)		meta (β)		para (γ)	
Solvent	$\Delta\delta_\alpha$ (p.p.m.)	Solvent	$\Delta\delta_\beta$ (p.p.m.)	Solvent	$\Delta\delta_\gamma$ (p.p.m.)
Carbon disulfide	0.4	*Cyclohexane*	0.0	*Cyclohexane*	0.0
Dimethylsulfoxide	0.4	Benzene	0.1	Benzene	0.2
Carbon tetrachloride	0.3	*N*-Triethylamine	0.2	*N*-Triethylamine	0.2
Chloroform	0.3	Diethylether	0.3	Diethylether	0.4
1,4-Dioxane	0.2	Neat	0.5	Acetone	0.8
N-Triethylamine	0.1	Acetone	0.5	Carbon tetrachloride	0.8
N,*N*-Dimethylformamide	0.0	Nitromethane	0.6	Nitromethane	0.8
Cyclohexane	0.0	1,4-Dioxane	0.7	Neat	0.8
Benzene	−0.1	Carbon tetrachloride	0.7	1.4-Dioxane	0.9
Neat	−0.1	Carbon disulfide	0.9	Carbon disulfide	0.9
Acetonitrile	−0.1	Acetonitrile	0.9	Acetonitrile	1.3
Diethylether	−0.3	*N*,*N*-Dimethylformamide	1.0	*N*,*N*-Dimethylformamide	1.4
Acetone	−0.3	Methanol	1.1	Chloroform	1.6
Nitromethane	−0.5	Chloroform	1.1	Methanol	2.0
Ammonium hydroxide (30%)	−0.7	Water (H_2O)	1.4	Dimethylsulfoxide	2.0
Methanol	−1.1	Water (^2H_2O)	1.4	Water (H_2O)	2.5
Water (H_2O, p$H \approx 9.1$)	−1.1	Dimethylsulfoxide	1.6	Water (^2H_2O)	2.6
Water (^2H_2O,p$^2H \approx 9.3$)	−1.1	Ammonium hydroxide	1.6	Ammonium hydroxide	2.6
Hydrobromic acid (46%)	−7.8	Acetic acid	2.8	Acetic acid	10.5
Hydrochloric acid (38%)	−8.0	Trifluoroacetic acid	4.6	Trifluoroacetic acid	12.7
o-Phosphoric acid (85%)	−8.0	Nitric acid	4.7	Nitric acid	12.8
Sulfuric acid (99.5%)	−8.2	Sulfuric acid	5.5	Hydrochloric acid	13.8
Acetic acid (99.7%)	−8.4	Hydrochloric acid	5.6	*o*-Phosphoric acid	13.8
Nitric acid (70%)	−8.6	*o*-Phosphoric acid	5.6	Sulfuric acid	13.9
Trifluoroacetic acid (neat)	−8.7	Hydrobromic acid	5.8	Hydrobromic acid	14.1

*Positive values represent downfield shifts and negative values upfield shifts from the corresponding carbon resonances of pyridine in cyclohexane (whose values relative to external TMS are: α, 150.5; β, 123.6; γ, 135.3 p.p.m.).

Can. J. Chem. Downloaded from www.nrcresearchpress.com by 210.87.254.40 on 09/05/12
For personal use only.

more subject to anisotropic magnetic field effects of the solvent as well, making any simple correlation difficult.

To demonstrate this, we could compare chemical shifts in CCl_4 and $CHCl_3$. The γ and β resonances appear in $CHCl_3$ at slightly lower field than in CCl_4 (0.8 and 0.4 p.p.m., respectively); this can be interpreted in terms of the known hydrogen-bonding properties of chloroform. If the effect on the γ and β resonances is only due to hydrogen bonding in a 1:1 complex the α carbon should experience an *upfield* shift of at least 0.5 p.p.m. (*vide infra*, effect of water) while in reality it moves *downfield* by 0.3 p.p.m. from cyclohexane. This suggests that effects other than hydrogen bonding must be considered for the α position.

The values in Table 2 show little correlation with the dipole moments or dielectric constants of the solvent. There is, however, a qualitative relation between the increase of Δδ (relative to the inert solvent cyclohexane) and the ability of the solvent molecules to participate in hydrogen bonding.

It is evident in Table 2 that for each of the α, β, and γ carbon atoms there are two distinct groupings of solvents. For most neutral and basic solvents the medium effects on pyridine are moderate *i.e.* shifts of 2.5 p.p.m. for the more sensitive γ position and about 1.5 p.p.m. for the β and α positions. Much larger shifts occur with acidic solvents which not only form hydrogen bonds to the nitrogen, but protonate the molecule. Although all seven protonating solvents were concentrated acidic solutions, there are individual differences in the magnitude of the corresponding Δδ's, reflecting either a different acidity or effects due to the anions.

Any desired intermediate shift can be obtained by combining two different solvents. Hydration effects, which also can be included here, were investigated by de Jeu on the ^{13}C and ^{17}O resonances of acetone (15) and by Pugmire and Grant on the ^{1}H and ^{13}C chemical shifts in pyridine (16). Increasing the water content from 0 (neat pyridine) to 50 mol % causes the ^{13}C resonances of the γ and β carbons to move downfield by 0.93 and 0.39 p.p.m., respectively, while those of the α carbons move upfield by 0.55 p.p.m. These data correspond to intermediate values between pyridine in cyclohexane and in water at 83 mol %; the shifts in the latter relative to those in the former solvent are 1.67 and 0.91 p.p.m. for the γ and β carbons, respectively, and −0.99 p.p.m. for the α carbon. Hydrogen bonds between water and the nitrogen lone pair electrons have been suggested as the most plausible explanation for the changes in chemical shifts upon dilution in water. The shifts associated with hydration are similar in sign to those of direct protonation, but of smaller magnitude.

It is interesting to notice the slight isotope effect on comparing the data for pyridine in H_2O and D_2O (Table 2). Although the α and β resonances are unaffected, the more sensitive γ resonance moves downfield 0.1 p.p.m. in D_2O. This must be due to the different hydrogen-bonding properties of the two hydrogen isotopes.

Because the resonances for the α and γ carbon atoms in pyridine are only 15.2 p.p.m. apart in cyclohexane solution, and because they vary with protonating power of the solvent ($\Delta\delta_\alpha$ moves upfield by as much as 9 p.p.m. and $\Delta\delta_\gamma$ moves downfield by as much as 14 p.p.m.), at certain solvent compositions there can be a scrambling of the resonances. Besides the differences in intensity in the proton-decoupled spectra, C-α can be distinguished from C-γ by the half band widths of the resonances, the former usually being broader due to coupling to the neighboring nitrogen.

Carbon–Nitrogen Couplings in Pyridine

Variations in $J_{^{13}C,^{1}H}$ due to the nature of the solvent have been observed (17). We report here some preliminary findings on a similar variation of $J_{^{13}C,^{14}N}$ and the relaxation time of the ^{14}N nucleus. Determination of carbon–nitrogen spin–spin couplings is considerably hampered by quadrupole broadening due to ^{14}N. In order to observe ^{13}C–^{14}N couplings, compounds must have nitrogen nuclei with long relaxation times. Such couplings have been observed in tetraalkylammonium ions (18); triplets (1:1:1) were observed in the proton-decoupled spectra of the tetramethyl- (J = 4.15 Hz) and the tetraethylammonium (J = 2.85 Hz) ions. These are in agreement with our data for pyridine in concentrated hydrobromic and hydrochloric acid where corresponding triplets (J = 4–5 Hz) can be observed. If the relaxation time of the nitrogen is shorter, as in most of the other solvents studied, only a broad band is seen for carbons coupled to the nitrogen. Some information is still available from the widths of the ^{13}C resonances. It is interesting to note that in pyridinium salts the magnitude of

TABLE 3. ^{13}C chemical shifts of uridine*

Solvent	C-4	C-2	C-6	C-5	C-1′	C-4′	C-2′	C-3′	C-5′
DMSO	164.6	152.3	142.3	103.3	89.3	86.3	75.1	71.4	62.4
Pyridine	164.6	152.3	141.2	102.5	90.5	86.3	76.0	71.2	61.9
^2H_2O	167.3	152.8	143.0	103.4	90.6	85.5	74.8	70.6	62.0
H_2O	167.4	152.9	143.1	103.5	90.7	85.5	75.0	70.8	62.2

*Measured from 0.3 *M* solutions and expressed in p.p.m. *vs.* external tetramethylsilane.

$J_{^{13}C,^{14}N}$ seems to depend also on the nature of the anion, since the α resonances of pyridine in concentrated H_2SO_4 or concentrated H_3PO_4 have very small half band widths (< 2 Hz) and no coupling with nitrogen can be detected.

Uridine

Uridine is of interest because of its wide diversity of substituents and its biological importance. The ^{13}C chemical shifts of 0.3 *M* uridine in dimethylsulfoxide, pyridine, water, and deuterium oxide are given in Table 3. Some ^{13}C spectra are given in Fig. 2; assignments were made according to earlier studies (19–21).

Comparing the chemical shifts in H_2O and ^2H_2O we find no differences (beyond the limit of experimental accuracy, ±2.5 Hz) for carbons other than those bearing an hydroxyl group. The resonances of C-2′, -3′, and -5′ are shifted upfield by 5 Hz in ^2H_2O relative to H_2O. Thus, a small but detectable isotope effect is manifest.

The spectra of Fig. 2 demonstrate an interesting aspect of the relaxation by carbonyl C-2 and -4. Bearing no hydrogen, they must relax via mechanisms involving spin rotation, chemical shift anisotropy, or dipole–dipole coupling to distant magnetic nuclei. In Fig. 2*a* the resonances of C-2 and -4 are barely distinguishable. Replacement of ^2H_2O by H_2O results in an augmentation of the carbonyl resonances. In dimethylsulfoxide, where the uracil nitrogen at position 3 bears a hydrogen which cannot exchange with the solvent, the carbonyl resonances are much more intense. This demonstrates the importance of dipole–dipole interaction between the carbonyl ^{13}C atoms and the hydrogen on N-3.

On going to the non-aqueous solvents large changes in chemical shift of either sign can occur. Carbonyl C-4 shifts upfield by 2.7 p.p.m. whereas carbonyl C-2 moves upfield by only 0.6 p.p.m. These shifts are indicative of the decreased hydrogen-bonding expected in dimethylsulfoxide and pyridine, but the large differences between the effects on C-2 and -4 are surprising. Special

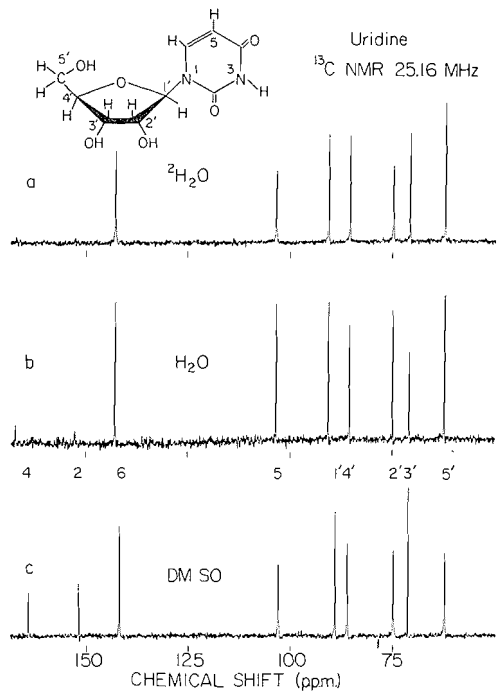

FIG. 2. ^{13}C n.m.r. spectra of 0.3 *M* uridine, pulse angle 90°, data acquisition time 0.4 s, pulse delay 0.8 s, in (*a*) ^2H_2O, p^2H = 7.4, 45 000 accumulations; (*b*) H_2O, p*H* = 7.0, 13 000 accumulations; (*c*) dimethylsulfoxide, 35 000 accumulations.

solvent influences at positions 2 and 4 have already been invoked to explain ^{13}C n.m.r. data (19). Similarly, a dramatic difference in solvent shifts at positions 5 and 6 is apparent. The resonance of C-6 moves −1.9 p.p.m. on going from H_2O (or ^2H_2O) to pyridine, whereas that of C-5 moves only −1.0 p.p.m.; on going to dimethylsulfoxide from H_2O (^2H_2O) the resonance of C-6 moves by −0.7 p.p.m.; and that of C-5 is unchanged. Evidence for specific solvent interactions at C-6 has been obtained earlier from ^1H (22) and ^{13}C (19) n.m.r.

Another surprising effect occurs at C-1′. On going from H_2O (or ^2H_2O) to pyridine a barely

Can. J. Chem. Downloaded from www.nrcresearchpress.com by 210.87.254.40 on 09/05/12
For personal use only.

Can. J. Chem. Downloaded from www.nrcresearchpress.com by 210.87.254.40 on 09/05/12
For personal use only.

detectable upfield shift of the C-1′ resonance occurs. On going to dimethylsulfoxide, however, the C-1′ resonance moves −1.4 p.p.m. A specific interaction between dimethylsulfoxide and this region of the molecule must be present! This underlines the importance which must be attached to choice of solvent, particularly for biological molecules where the conformation under physiological conditions is the principal goal.

Pyridine and dimethylsulfoxide have equal effects on the resonance of C-4′, producing a downfield shift of 0.8 p.p.m. relative to H_2O (or ^2H_2O). In sharp contrast the resonance of C-2′, which bears an hydroxyl group, moves only slightly (+0.2 p.p.m.) in dimethylsulfoxide but substantially (+1.1 p.p.m.) in pyridine. This might at first glance be attributed to hydrogen-bonding of the hydroxyl group to pyridine, but the roughly equal influences of dimethylsulfoxide and pyridine (+0.6 and 0.4 p.p.m., respectively) on C-3′ argue against such a simple interpretation. Further rebuttal of this thesis comes from the opposite small shifts in the resonance of C-5′, which also has a contiguous hydroxyl group, noted for pyridine (−0.3 p.p.m.) and dimethylsulfoxide (+0.2 p.p.m.) relative to H_2O.

Thus, it is clear that the interactions between solvents and the various positions in uridine are very different. If assignments of the resonances of related compounds are to be made by reference to the known assignments, care must be taken to obtain spectra in the same solvent.

Conclusion

Solvent effects may be appreciable on all carbon atoms of a molecule, even at relatively protected positions such as the tertiary carbons of steroids. Specific solvent–solute interactions other than hydrogen bonding may be manifest. The solvent-induced shifts can be of such a character as to scramble resonances and thus alter assignments made in other solvents. In some cases coupling between ^{13}C and ^{14}N can be observed, and its magnitude is strongly solvent-dependent. Relaxation times of carbonyl carbons can be appreciably affected by dipole–dipole coupling to hydrogen attached to a neighboring atom.

1. (*a*) E. M. Engler and P. Laszlo. J. Am. Chem. Soc. **93**, 1317 (1971); (*b*) P. Laszlo. *In* Progress in NMR spectroscopy. Vol. 3. *Edited by* J. W. Emsley, J. Feeney, and L. H. Sutcliffe. Pergamon Press, London. 1967. p. 231; (*c*) J. C. Davis and K. K. Deb. *In* Advances in magnetic resonance. Vol. 4. *Edited by* J. S. Waugh. Academic Press, New York. 1970. p. 201.
2. G. E. Maciel and G. C. Ruben. J. Am. Chem. Soc. **85**, 3903 (1963).
3. G. E. Maciel and R. V. James. J. Am. Chem. Soc. **86**, 3893 (1964).
4. G. E. Maciel and D. D. Traficante. J. Phys. Chem. **69**, 1030 (1965).
5. G. E. Maciel. J. Chem. Phys. **42**, 2746 (1965).
6. G. E. Maciel and J. J. Natterstad. J. Chem. Phys. **42**, 2752 (1965).
7. G. E. Maciel and D. D. Traficante. J. Am. Chem. Soc. **88**, 220 (1966).
8. H. Spiesecke and W. G. Schneider. J. Chem. Phys. **35**, 722 (1961).
9. J. K. Becconsall and P. Hampson. Mol. Phys. **10**, 21 (1965).
10. R. L. Lichter and J. D. Roberts. J. Phys. Chem. **74**, 912 (1970).
11. A. Loewenstein and Y. Margalit. J. Phys. Chem. **69**, 4153 (1965).
12. G. C. Levy, G. L. Nelson, and J. D. Cargioli. Chem. Commun. **1971**, 506.
13. G. L. Nelson, G. C. Levy, and J. D. Cargioli. J. Am. Chem. Soc. **94**, 3089 (1972).
14. H. J. Reich, M. Jautelat, M. T. Messe, F. G. Weigert, and J. D. Roberts. J. Am. Chem. Soc. **91**, 7445 (1969).
15. W. H. de Jeu. Mol. Phys. **18**, 31 (1970).
16. R. J. Pugmire and D. M. Grant. J. Am. Chem. Soc. **90**, 697 (1968).
17. J. B. Stothers. Carbon-13 NMR spectroscopy. Academic Press, New York. 1972.
18. F. T. Weigert. Ph.D. Thesis, California Institute of Technology, Pasadena. 1968.
19. H. H. Mantsch and I. C. P. Smith. Biochem. Biophys. Res. Commun. **46**, 808 (1972).
20. I. C. P. Smith, H. H. Mantsch, R. D. Lapper, R. Deslauriers, and T. Schleich. *In* Conformation of biological molecules and polymers. *Edited by* E. Bergmann and B. Pullman. Academic Press, New York. In press.
21. R. D. Lapper, H. H. Mantsch, and I. C. P. Smith. J. Am. Chem. Soc. **94**, 6243 (1972).
22. I. C. P. Smith, B. J. Blackburn, and T. Yamane. Can. J. Chem. **47**, 513 (1969).

The Solvent Exchange of $Co(CH_3NH_2)_5OH_2^{3+}$

A. G. SHAVER AND M. PARRIS

Department of Chemistry, Carleton University, Ottawa, Canada K1S 5B6

Received November 17, 1972

The rate constant for entry of ^{18}O from solvent water into $Co(CH_3NH_2)_5OH_2^{3+}$ ion was found to be 1.1×10^{-4} s^{-1} at 24.9 °C. The equilibrium constant for the formation of $Co(CH_3NH_2)_5Cl^{2+}$ ion was found to be 7.7 M^{-1}. From these data, the competition ratio between chloride ion and water for a hypothetical intermediate $Co(CH_3NH_2)_5$ was calculated as 2.5, unexpectedly high.

La constante de vitesse pour l'introduction de ^{18}O de l'eau utilisée comme solvant dans l'ion $Co(CH_3NH_2)_5OH_2^{3+}$ est de 1.1×10^{-4} s^{-1} à 24.9 °C. La constante d'équilibre pour la formation de l'ion $Co(CH_3NH_2)_5Cl^{2+}$ est de 7.7 M^{-1}. A partir de ces données, il est possible de déduire le taux de compétition entre l'ion chlorure et l'eau pour l'intermédiaire hypothétique $Co(CH_3NH_2)_5$; la valeur trouvée 2.5 est plus haute que prévue. [Traduit par le journal]

Can. J. Chem., **51**, 1392 (1973)

The acid and base hydrolyses of a series of chloropentakis(alkylamine)cobalt(III) complexes have been found (1) to be much accelerated by comparison with the corresponding ammine complex. Since the bulk of the experimental evidence appears to favor an interchange process of the dissociative type for cobalt(III) complexes' substitution reactions (2) this is not unexpected, and it was the possibility that a ligand-selective or dissociative mode of substitution might ultimately be detected in the case of these sterically-hindered complexes which prompted the present investigation.

Experimental

Chloropentakis(methylamine)cobalt(III) Chloride, $[Co(CH_3NH_2)_5Cl]Cl_2$

This was prepared as previously described (3).

Aquated Solution

Excess of an ice-cold solution 2 M in $AgClO_4$, 1 M in $HClO_4$ was added to 3 g chloropentakis(methylamine)-cobalt(III) chloride. The blue-violet slurry was shaken at 5 °C overnight in the dark, when the supernatant liquid became deep red and the AgCl precipitate corresponded to complete aquation. The excess Ag^+ was removed by potentiometric addition of concentrated HCl using Ag/AgCl and calomel/KNO_3 electrodes. The solution was diluted to 25 ml with $HClO_4/H_2O$, and finally was 0.395 M in $Co(CH_3NH_2)_5OH_2^{3+}$, 0.800 M in $HClO_4$. This, solution A, was subdivided into aliquots which were stored, sealed, frozen.

Aquopentakis(methylamine)cobalt(III) Trichloromercurate, $[Co(CH_3NH_2)_5OH_2]3HgCl_3$

To a small amount (1 ml) of the cold aquated solution (A) was added an equal amount of an ice-cold solution 4 M in HCl, 2 M in $HgCl_2$. Within 30 s red needles began to form and after 2 min the precipitation was virtually complete. The red crystals were air-dried for 15 min. Cobalt was analyzed by decomposing the salt in 10% NaOH, adding solid KI, and acidifying with 1 N HCl followed by thiosulfate titration, standardized with KIO_3. Methylamine was determined by steam distillation from a strongly alkaline solution into a standardized aliquot of H_2SO_4. It appeared from the analytical figures that a relatively rapid decomposition was occurring in the solid, evidenced also by the color change from pale red to the bright purple of the chlorocomplex upon standing at room temperature for 2 days. Carbon, hydrogen, and nitrogen analyses were carried out within 1 h of the sample precipitation by the Analytical Chemistry Research Branch of the Department of Agriculture, National Research Council of Canada, Ottawa.

Anal. Calcd. for $[Co(CH_3NH_2)_5OH_2]3HgCl_3$: C, 5.20; H, 2.34; N, 6.04; CH_3NH_2, 13.5; Co, 5.11. Found: C, 5.19; H, 2.5; N, 6.04; CH_3NH_2, 13.7; Co, 5.13.

Analysis of Isotopic Content in the Coordinated Water

In order to determine the conditions required completely to remove occluded water prior to removing ligated water, the freshly-prepared trichloromercurate (0.15 g) was loaded onto a continuously monitored, thermostatted, evacuable quartz spring balance (Worden Laboratories). After 20–30 min the evacuated sample was heated to 50 °C and the gas evolved condensed at 77 °K. The condensate was redistilled onto a clean sodium mirror at 77 °K and the volume of the non-condensible gas evolved upon warming measured with a Toepler pump. Figure 1 shows the weight record throughout these manoeuvres.

Rates of Exchange

The rate of exchange between solvent and aquo complex was determined as follows. Three stock solutions were used: Solution A: the aquated solution (see above), 0.395 M in $Co(CH_3NH_2)_5OH_2^{3+}$, 0.800 M in $HClO_4$, water of normal isotopic composition. Solution B: oxygen enriched water, nominally 5.29% ^{18}O, 0.07% ^{17}O, normalized H content, purchased from Yeda Research and Development Co., Rehovoth, Israel, batch No. 1857. Solution C: 4.0 M HCl, 2.0 M $HgCl_2$, water of normal isotopic composition.

One ml aliquots of solutions A and B were weighed

Can. J. Chem. Downloaded from www.nrcresearchpress.com by 210.87.254.6 on 09/05/12
For personal use only.

Can. J. Chem. Downloaded from www.nrcresearchpress.com by 210.87.254.6 on 09/05/12
For personal use only.

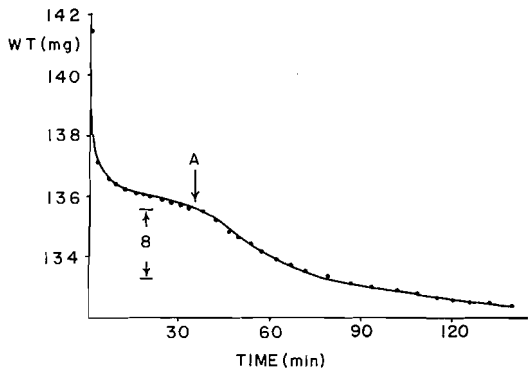

FIG. 1. Quartz spring balance record for $[Co(CH_3NH_2)_5OH_2]3HgCl_3$: *A*, 50 °C water-bath applied to sample compartment; *B*, calculated weight of ligated water.

separately and sealed into ampoules. These were thermostatted (24.9 °C) and at the commencement of exchange crushed together. A small sample (3 drops) of the mixture was taken in order to determine the ^{18}O content of the mixed waters.

To terminate exchange 2.0 ml ice-cold solution C was added and the mixture immediately quenched in ice. The solid was collected after 3 min, washed with a little cold methanol and air-dried for 5–10 min. A portion of the trichloromercurate (30 mg) was dried at room temperature, 3 μ for 30 min. Then the temperature was raised to 50 °C and the water evolved was condensed onto guanidine hydrochloride (B.D.H. 99%, recrystallized from ethanol) contained in a break-seal vial at 77 °K. The vial was sealed off and heated in a furnace at 250 °C for 10 h to convert the water completely to CO_2 (4). The CO_2 was transferred via the break-seal, dried with de-aerated concentrated H_2SO_4, and condensed into a sample bulb at 77 °K. The 3-drop sample of the solvent was similarly treated. The two CO_2 samples were used for mass-spectral analysis, using a Hitachi Perkin–Elmer R.M.U. 6D MS kindly made available by the University of Ottawa. Eight such experiments were performed, with exchange times 0.5, 1, 10, 15, 20, and 30 min.

Equilibrium Constant

The visible spectra of ten solutions, each about 10^{-2} *M* in chloropentakis(methylamine)cobalt(III) chloride, varying HCl ($2 \times 10^{-2} - 2 \times 10^{-1}$ *M*) and constant ionic strength (0.16, adjusted with $NaClO_4$ and $HClO_4$ to p*H* 2), were recorded while being thermostatted (25 °C) for 2–3 days. The absorbances at 363 and 515 mμ were measured using a Gilford 240 spectrophotometer when equilibrium had been attained. The extinction coefficients for the aquospecies were obtained by measuring the absorbance of a solution that had been completely aquated with excess $AgClO_4$ and then filtered.

Results

Figure 1 illustrates the loss of water from the $[Co(CH_3NH_2)_5OH_2]3HgCl_3$ for one typical experiment, where the initial rapid loss of occluded water is accompanied by a continuous slow loss in weight. Under these conditions there is a continuous deposition of $HgCl_2$ upon the walls of the spring balance so that a direct determination of water from the observed weight change is not practicable. For this reason, the indirect determination of water by means of the sodium reaction was undertaken.

TABLE 1. Water determination in $[Co(CH_3NH_2)_5OH_2]3HgCl_3$

	% H_2O	
Expt. No.	Found	Calculated
1	1.6	1.6
2	1.3	1.6
3	1.6	1.6
4	1.4	1.6

Table 1 shows the results obtained for four such water determinations, and it is apparent that the break in the curve of Fig. 1 is caused by complete loss of the ligating water.

In order to determine k, the rate-constant for the exchange reaction,

$$[1]\quad CoL_5{}^{16}OH_2^{3+} + {}^{18}OH_2 \underset{}{\overset{k}{\rightleftharpoons}} CoL_5{}^{18}OH_2^{3+} + {}^{16}OH_2$$

the oxygen isotope effect has been neglected. Considering the complex ions present, the total concentration of aquo species is represented by a and the concentration of aquo species containing the ^{18}O label by x

$$[CoL_5{}^{16}OH_2{}^{3+}] + [CoL_5{}^{18}OH_2{}^{3+}] = a$$

$$[CoL_5{}^{18}OH_2{}^{3+}] = x$$

For the solvent,

$$[{}^{16}OH_2] + [{}^{18}OH_2] = b$$

$$[{}^{18}OH_2] = y$$

The observed rate at which solvent ^{18}O exchanges with ligated ^{16}O is proportional to the fraction of the isotopes in each species

$$\frac{dx}{dt} = k\frac{y}{b}\frac{(a-x)}{a} - k\frac{(b-y)}{b}\frac{x}{a}$$

$$= k\frac{(ay - bx)}{ab}$$

Since

$$y - y_\infty = x_\infty - x$$

TABLE 2. Mass spectrometric ^{18}O assay

Time (min)	$\frac{[\text{mass } 46]}{[\text{mass } 44]}$ (%)	$\frac{[\text{mass } 45]}{[\text{mass } 44]}$ (%)	R_T	R_∞	α (%)	α_∞ (%)
0.5	1.60	1.25	63.3		0.784	
	6.50	1.26		15.6		3.10
1.0	1.79	1.25	56.6		0.876	
	6.53	1.26		15.5		3.12
10.0	3.28	1.20	30.8		1.59	
	5.91	1.25		17.1		2.84
15.0	3.41	1.23	29.7		1.66	
	6.89	1.40		14.7		3.29
20.0	3.56	1.26	28.4		1.73	
	6.56	1.40		15.5		3.12
30.0	4.25	1.25	23.8		2.06	
	6.70	1.31		15.1		3.21

and

$$x_\infty/y_\infty = a/b$$

$$\frac{dx}{dt} = \frac{k(a+b)(x_\infty - x)}{ab}$$

or $$\ln\left(\frac{x_\infty}{x_\infty - x}\right) = k\frac{(a+b)t}{ab}$$

In these exchange experiments $b \simeq 55.5\ M$, $a \simeq 0.2\ M$, that is, $a \ll b$.

$$\therefore \ln\left(\frac{x_\infty}{x_\infty - x}\right) = \frac{kt}{a}$$

Let α be the ^{18}O atom fraction within the aquo species. This was determined from the 44/46 ratio, corrected for the 45/44 ratio

$$R = \frac{[\text{mass } 44]}{[\text{mass } 46]}\left(1 + \frac{[\text{mass } 45]}{[\text{mass } 44]}\right)$$

R values are listed in Table 2.

$$\alpha = \frac{[^{18}OH_2]}{[^{18}OH_2] + [^{16}OH_2]} = \frac{1}{2R+1}$$

Initially, the ^{18}O content in the salt was the normal 0.2%. After complete exchange it is the same as in the solution, *viz.* about 2.5%. $x/a = \alpha$ and in particular $x_\infty/a = \alpha_\infty$

$$\therefore \ln\left(\frac{x_\infty}{x_\infty - x}\right) = -\ln\left(\frac{\alpha_\infty - \alpha}{\alpha_\infty}\right)$$

$$= k_{obs}t$$

where

$$k_{obs} = k/a$$

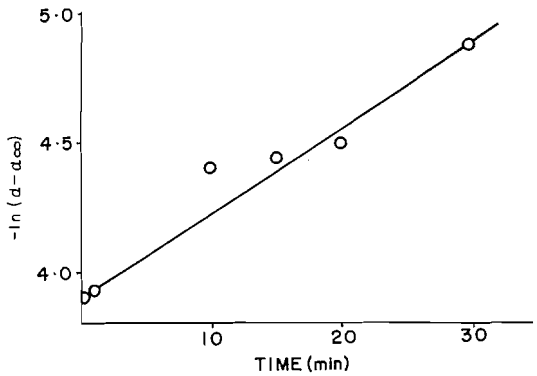

FIG. 2. Exchange of coordinated water for $Co(CH_3NH_2)_5OH_2^{3+}$: $\alpha = {}^{18}O$ atom fraction in $[Co(CH_3NH_2)_5OH_2]3HgCl_3$ precipitate; $\alpha_\infty = {}^{18}O$ atom fraction in solvent.

Figure 2 shows $-\ln(\alpha - \alpha_\infty)$ plotted *vs.* time for 0.20 M solutions, leading to a corrected value of the rate constant $k = 1.1 \times 10^{-4}\ s^{-1}$ at 24.9 °C.

The equilibrium constant for anation

$$[2] \quad CoL_5OH_2^{3+} + Cl^- \overset{K}{\rightleftharpoons} CoL_5Cl^{2+} + OH_2$$

was determined by the Newton–Arcand method (5)

$$K = \frac{1}{[Cl^-]}\frac{\varepsilon - \varepsilon_a}{\varepsilon_c - \varepsilon}$$

where ε = apparent molar extinction coefficient of the complex in the equilibrated solution, and ε_a and ε_c are the extinction coefficients of the aquo and chloro complex respectively. Table 3 contains values of K over a range of $[Cl^-]$. The average K is 7.7 M^{-1}.

Can. J. Chem. Downloaded from www.nrcresearchpress.com by 210.87.254.6 on 09/05/12
For personal use only.

TABLE 3. Equilibrium constant for the anation

$$Co(CH_3NH_2)_5H_2O^{3+} + Cl^- \overset{K}{\rightleftharpoons} Co(CH_3NH_2)_5Cl^{2+} + OH_2$$

Solution No.*	$[Co]_t$ ($\times 10^3$ M)	$[Cl]_t$ ($\times 10^2$ M)	A515 mμ	K† (M^{-1})
1	8.27	2.48	0.507	7.67
2	8.21	3.56	0.500	6.66
3	8.30	4.69	0.499	7.10
4	8.12	5.73	0.481	8.01
5	8.50	6.95	0.500	7.54
6	8.29	7.98	0.484	7.49
7	8.07	9.02	0.465	8.24
8	8.23	10.17	0.469	8.68
9	8.14	11.24	0.462	8.32
10	8.15	13.44	0.462	7.06

*Ionic strength = 0.16, temperature 25 °C.
†Based on $\varepsilon_a = 63.3$, $\varepsilon_c = 47.3$, $K_{calc} = 7.7$ M^{-1}.

Discussion

The values obtained for the solvent exchange and the anation equilibrium constants make it possible to calculate the competition ratio between water and chloride ion for the hypothetical intermediate CoL_5 of reaction 3

$$[3] \qquad CoL_5OH_2^{3+} \underset{k_{+a}}{\overset{k_{-a}}{\rightleftharpoons}} CoL_5 \underset{k_{-c}}{\overset{k_{+c}}{\rightleftharpoons}} CoL_5Cl^{2+}$$

Since

$$\frac{[CoL_5]}{[CoL_5OH_2{}^{3+}]} = \frac{k_{-a}}{k_{+a}}$$

and

$$\frac{[CoL_5Cl^{2+}]}{[CoL_5]} = \frac{k_{+c}}{k_{-c}}[Cl^-]$$

the equilibrium constant for reaction 2

$$K = \frac{k_{-a}}{k_{-c}}\frac{k_{+c}}{k_{+a}}$$

A competition ratio may be defined as

$$c = \frac{k_{+c}}{k_{+a}} = \frac{k_{-c}}{k_{-a}}K$$

Given reaction 3, k_{-c} is the aquation rate constant and equals 3.7×10^{-5} (6, 7), k_{-a} is the oxygen exchange rate constant and equals 1.1×10^{-4}, while K is the anation equilibrium constant and equals 7.7.

The competition ratio c is 2.6, which is a factor of ten larger than those previously measured for similar compounds (8). The values of k_{-c} given in refs. 6 and 7 agree quite closely. It is likely that the k_{-a} obtained presently is an upper limit, for the inclusion of any occluded water in the mass-spectroscopic analysis would produce an apparently faster exchange rate. In any event the ratio k_{-c}/k_{-a} is 0.34 for the methylamine complexes which is almost identical to the ratio 0.31 for the corresponding ammines (9, 10). The high value for c derives mainly from the high value for K. The same constant for the ammine is about 1.25 (8), and it might be expected that K for the methylamine complex should be smaller than this, due to steric crowding. While ion pairing would indeed increase the apparent K, the observed K should now *decrease* with increasing $[Cl^-]$. In fact K, though not particularly reliable, shows a small *increase* with $[Cl^-]$, while ion pairing should be less in the case of the bulkier methylamine complex.

The larger equilibrium constant is consistent with the difficulty of obtaining an aquo salt. It is also consistent with the competition experiments reported in ref. 1. During base hydrolysis of the chlorocomplexes, N_3^- and NCS^- competed more effectively with water for the pentakis(methylamine)cobalt(III) than for the pentaamminecobalt(III) species which may indicate that an intermediate which is longer-lived because of steric interaction is at the same time necessarily more selective in its reactants. The increased steric interaction is also consistent with the rather lower rates of bridged electron transfer between chloropentakis(methylamine)cobalt(III) ion and Fe(II) (11).

Can. J. Chem. Downloaded from www.nrcresearchpress.com by 210.87.254.6 on 09/05/12
For personal use only.

1. D. A. BUCKINGHAM, B. M. FOXMAN, and A. M. SARGESON. Inorg. Chem. **9**, 1790 (1970).
2. C. H. LANGFORD and H. B. GRAY. Ligand substitution processes. W. A. Benjamin, Inc. 1966.
3. R. MITZNER, P. BLANKENBURG, and W. DEPKAT. Z. Chem. **9**, 68 (1969).
4. P. D. BOYER, D. J. GRAVES, C. H. SUELTER, and M. E. DEMPSEY. Anal. Chem. **33**, 1906 (1961).
5. T. W. NEWTON and G. M. J. ARCAND. J. Am. Chem. Soc. **75**, 2449 (1953).
6. S. C. CHAN and K. Y. HUI. Aust. J. Chem. **20**, 2529 (1967).
7. M. PARRIS. J. Chem. Soc. (A), 583 (1967).
8. A. HAIM and H. TAUBE. Inorg. Chem. **2**, 1199 (1963).
9. A. W. ADAMSON and F. BASOLO. Acta Chem. Scand. **9**, 1261 (1955).
10. A. C. RUTENBERG and H. TAUBE. J. Chem. Phys. **20**, 825 (1952).
11. K. OHASHI. Bull. Chem. Soc. Jap. **45**, 947 (1972).

Can. J. Chem. Downloaded from www.nrcresearchpress.com by 210.87.254.6 on 09/05/12
For personal use only.

The Pyrolysis of Trimethylthallium and Evaluation of $D[(CH_3)_2Tl—CH_3]$

S. J. PRICE,[1] J. P. RICHARD,[2] AND R. C. RUMFELDT
Department of Chemistry, University of Windsor, Windsor 11, Ontario

AND

M. G. JACKO
Bendix Corporation, Detroit, Michigan

Received October 12, 1972

The pyrolysis of trimethylthallium has been studied in a mercury free toluene carrier flow system (452–536 °K, total pressure 6.7–39.3 mm, contact time 0.9–5.1 s, 5.4–90.2% decomposition). In a vessel cleaned with boiling concentrated HNO_3 and coated by decomposing 0.1 g $Tl(CH_3)_3$ no heterogeneous reaction could be detected. The extent of reaction measured by product analysis (CH_4, C_2H_6, $C_6H_5C_2H_5$) assuming three CH_3 per $Tl(CH_3)_3$ undergoing reaction 1

[1] $$Tl(CH_3)_3 \rightarrow Tl(CH_3)_2 + CH_3$$

is in agreement with that determined by analysis for undecomposed alkyl. Least squares analysis of the first order rate constants gives

$$\log k_1(s^{-1}) = 15.10 - (36\,400 \pm 600)/2.3RT$$

Under the conditions used the activation energy should be a good approximation to $D[(CH_3)_2Tl—CH_3]$.

Oxidation of Tl on the surface of Tl_2O causes a marked increase in the rate. Omission of the coating step following cleaning has no effect on the rate based on undecomposed alkyl but initially causes a sharp drop in the yield of products, particularly ethane.

La pyrolyse du triméthylthallium a été étudiée dans un système en continu avec du toluène sans mercure comme gaz vecteur (452–536 °K, pression totale 6.7–39.3 mm, durée de contact 0.9–5.1 s, décomposition de 5.4–90.2%). Dans un réacteur lavé à l'acide nitrique concentré et bouillant puis recouvert par la décomposition de 0.1 g de $Tl(CH_3)_3$, aucune réaction hétérogène n'a pu être détectée. Le cours de la réaction suivi par l'analyse des produits (CH_4, C_2H_6, $C_6H_5C_2H_5$) en supposant trois méthyles par $Tl(CH_3)_3$ dans la réaction 1:

[1] $$Tl(CH_3)_3 \rightarrow Tl(CH_3)_2 + CH_3$$

est en accord avec celle déterminée par l'analyse de l'alkyle intact. L'analyse par la méthode des moindres carrés des constantes de vitesse du premier ordre conduit à:

$$\log k_1(s^{-1}) = 15.10 - (36\,400 \pm 600)/2.3RT$$

Dans les conditions utilisées, l'énergie d'activation pourrait être une bonne approximation pour $D[(CH_3)_2Tl—CH_3]$. L'oxydation superficielle de Tl en Tl_2O provoque un accroissement notable dans la vitesse. Si le réacteur n'a pas été traité après lavage acide, aucun effet ne se manifeste sur la vitesse en alkyle non décomposé mais le rendement initial en produits (en particulier l'éthane) subit une chute notable.

[Traduit par le journal]

Can. J. Chem., 51, 1397 (1973)

Introduction

The only previously reported study of the pyrolysis of trimethylthallium was also carried out in a toluene carrier system (1). The reaction was first order and the rate constants were measured in approximately the high pressure limit. The decomposition was shown to be approximately 80% heterogeneous in an untreated vessel and 14–27% heterogeneous in a vessel pretreated with hot 50% HF. Attempts to reduce the observed heterogeneity below this level were unsuccessful. An estimate of the homogeneous reaction in the pretreated vessel was given as

$$\log_{10} k(s^{-1}) = 10.8 - 27\,400/2.3RT$$

The excessively low A-factor suggests that either the extent of the heterogeneous reaction was underestimated or that the reaction measured was not the simple decomposition of $Tl(CH_3)_3$ to give $Tl(CH_3)_2 + CH_3$.

[1]To whom correspondence should be addressed.

[2]Recipient of a National Research Council of Canada Studentship. Present address: Explosives Research Laboratory, Canadian Industries Limited, McMasterville, Quebec.

Can. J. Chem. Downloaded from www.nrcresearchpress.com by 210.87.254.40 on 09/05/12
For personal use only.

Can. J. Chem. Downloaded from www.nrcresearchpress.com by 210.87.254.40 on 09/05/12
For personal use only.

This study was undertaken with the purpose of isolating the homogeneous release of the first CH_3 group in order to arrive at a reliable value for $D[(CH_3)_2Tl{-}CH_3]$.

Experimental

Materials

(*a*) The trimethylthallium used was purchased from Alfa Inorganics Inc. (Catalog No. 78116). After thorough degassing by bulb-to-bulb distillation *in vacuo*, it was stored under its own vapor pressure in tinted glass storage vessels. Vapor pressure data at 0 and 22.8 °C gave 0.67 and 4.19 mm of Hg and a melting point of 38.4 °C all in excellent agreement with previous results (2).

Trimethylthallium was handled and stored in the dark as it is sensitive to light.

(*b*) Toluene from sulfonic acid (Eastman Organic X325) was used. Gas chromatographic analysis detected traces of higher hydrocarbons (xylenes, ethyl benzene). These were reduced to less than 40 p.p.m. by a fractional distillation in which a large tail fraction was discarded. Prior to use, the toluene was dried by refluxing over sodium metal for 24 h and then degassed by bulb-to-bulb distillation.

Apparatus and Procedure

The toluene carrier system used was similar to that previously employed in studying $In(CH_3)_3$ (3). Toluene vapor is allowed to flow over the $Tl(CH_3)_3$ thus utilizing what may be described as a pick-up system. A weighed sample of the alkyl is distilled into a U-tube equipped with a by-pass through which the toluene vapor flows during the pre-run. After a 5 min flow of toluene part of the toluene flow is diverted through the thermostated U-tube and the run is continued until 5 min after the last visible deposit has disappeared. In the majority of runs some toluene condenses on the $Tl(CH_3)_3$ but the extent to which this occurs has no measurable effect on the observed rate constants. Direct injection of the $Tl(CH_3)_3$ vapor into the toluene stream is precluded by the limited thermal stability of this alkyl (appreciable decomposition above 90 °C (4)).

The apparatus was operated in total darkness except for two shielded 2 W lamps which were used to take manometer readings. The reaction vessel had a volume of 135 cc. The tests for surface effects were carried out in a vessel packed with small quartz tubes. This vessel had a volume of 100 cc and a surface to volume ratio 14 times that of the unpacked vessel. Both vessels were treated with hot fuming nitric acid before use.

The residual acid was baked out under vacuum after the vessels were installed in the system. Preconditioning by decomposition of about 0.1 g $Tl(CH_3)_3$ was then carried out.

The gaseous products were analyzed using a Perkin–Elmer model 154 gas chromatograph equipped with a 1/4 in. × 6 ft silica gel column. The column was maintained at 80 °C and a helium flow rate of 20 cm³ per min was used.

The liquid products which condensed along with the toluene in an acetone – Dry Ice trap were analyzed using a Perkin–Elmer model 800 gas chromatograph equipped with a 150 ft × 0.02 in. i.d. open tubular column coated with poly(propylene glycol). (Isothermal operation at 60 °C, nitrogen carrier flow rate 10 cm³ per min.)

Analysis of the undecomposed alkyl, which also condensed in the acetone – Dry Ice trap, could not be performed by gas chromatography due to decomposition of the alkyl within the injection port. The undecomposed alkyl was determined by volumetric analysis as $Tl(CH_3)_2OH$ (4). The procedure involved treating the products in the acetone – Dry Ice trap with several portions of distilled H_2O and titrating the resulting solution of $Tl(CH_3)_2OH$ with standard 0.1 N H_2SO_4. Loss of toluene and liquid products to the aqueous solution due to their solubilities was negligible. This procedure when carried out with known weights of alkyl always gave a recovery of better than 99%.

Results and Discussion

The results obtained from the pyrolysis of $Tl(CH_3)_3$ in a mercury free toluene carrier system are best discussed in the two separate sections.

(*a*) *Results Obtained when a Preconditioned Reaction Vessel is Used and Air is Excluded both During and Between Runs*

Results obtained under these conditions are given in Tables 1–2 and form the basis of the

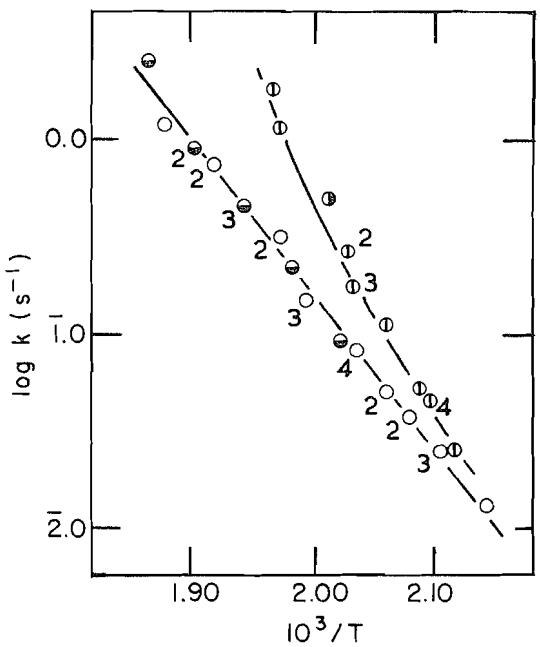

FIG. 1. Arrhenius plots for the pyrolysis of trimethylthallium. Upper curve: Tl_2O on surface. Lower curve: conditioned vessel. Numbers represent the number of runs averaged to obtain the given point. Individual points used to obtain average points for upper curve considerably scattered (see Table 4 obtainable from the Depository of Unpublished Data). Half filled points represent runs in the packed reaction vessel.

TABLE 1. Selected experimental results for the pyrolysis of $Tl(CH_3)_3$

Temperature (°K)	Pressure (mm Hg)	t_c (s)	Concentration: Alkyl (mol $cc^{-1} \times 10^9$)	CH_4 (mol $\times 10^4$)	C_2H_6 (mol $\times 10^4$)	C_6H_5 (mol $\times 10^4$)	C_2H_5 (mol $\times 10^4$)	k_g* (s^{-1})
515.1†	20.5	1.05	4.40	3.03	0.144	1.61	0.102	0.457
515.1†	18.6	0.96	5.93	4.10	0.138	2.02	0.110	0.450
515.1†	18.0	0.72	2.31	1.95	0.091	0.74	0.079	0.458
507.6‡	21.3	2.96	7.65	5.44	0.211	7.85	0.201	1.78
502.0	23.6	3.36	5.07	4.89	0.229	2.63	0.186	0.145
502.0	22.3	3.18	16.56	2.53	0.054	1.36	0.049	0.147
501.9	21.8	3.31	9.92	3.89	0.161	2.07	0.089	0.143
491.9‡	21.0	1.99	10.54	4.29	0.619	0.89	0.052	0.106
491.3	39.3	2.86	9.53	5.13	0.241	1.45	0.149	0.0838
491.3	24.3	3.33	12.19	6.82	0.241	2.26	0.172	0.0828
491.3	23.6	4.03	11.02	4.43	0.172	1.78	0.118	0.0850
491.3	15.3	5.08	13.24	4.01	0.148	2.08	0.077	0.0892
484.6‡	23.1	2.66	8.96	5.72	0.286	2.03	0.098	0.112

*Rate constant based on product analysis.
†Packed vessel work.
‡Runs under catalytic conditions (Tl_2O on surface of reaction zone). Full data are available, at a nominal charge, from the Depository of Unpublished Data, National Science Library, National Research Council of Canada, Ottawa, Canada K1A 0S2.

TABLE 2. Percent decompositions by product analysis and alkyl recovery

T (°K)	Percent decomposition: Product analysis*	Alkyl recovery†
536.6‡	90.2	92.3
526.1‡	76.9	78.8
525.6‡	59.9	59.1
515.1‡	36.7§	39.4§
507.1	24.6	21.8
504.4‡	41.6	44.4
502.0	38.2§	40.7§
494.0‡	18.3	19.9
491.3	22.7	23.2
485.4	16.0§	15.5§
480.8	15.2	16.6
474.5	10.5	10.9

*Based on release of all 3 methyl groups from each molecule undergoing reaction.
†From volumetric analysis of unreacted alkyl which condensed in the acetone–Dry Ice trap along with the toluene and other liquid products.
‡Packed vessel work.
§Average of two runs.

lower curve in Fig. 1. They may be discussed in terms of the following mechanism

[1] $Tl(CH_3)_3 \rightarrow Tl(CH_3)_2 + CH_3$

[2] $Tl(CH_3)_2 \rightarrow TlCH_3 + CH_3$

[3] $Tl\,CH_3 \rightarrow Tl + CH_3$

[3a] $2TlCH_3 \rightarrow Tl(CH_3)_2 + Tl$

[4] $CH_3 + C_6H_5CH_3 \rightarrow CH_4 + C_6H_5CH_2$

[5] $2CH_3 + M \rightarrow C_2H_6 + M$

[6] $CH_3 + C_6H_5CH_2 \rightarrow C_6H_5C_2H_5$

[7] $2\,C_6H_5CH_2 \rightarrow$ Dibenzyl

plus the usual reactions leading to trace quantities of xylenes.

Based on the reported Arrhenius parameters for $\dot{H}$ abstraction by CH_3 from related metal alkyls (11) k_8 should be approximately equal to

[8] $CH_3 + Tl(CH_3)_3 \rightarrow CH_4 + (CH_3)_2TlCH_2$

0.23 to 0.55 k_4 at the temperatures used in the present work. With the toluene-to-alkyl ratio used (>35:1) a maximum of 1.5% of the CH_4 may be attributed to reaction 8 and in general no more than 0.5% should be formed this way. This leads to the conclusion that no more than 0.2% of the alkyl reacts via reaction 8 (in most cases probably less than 0.1%). Reaction 8 is therefore of negligible importance with respect to both alkyl removal and methane formation.

Values of k_1 were calculated from the first order equation

$$k = \frac{2.303}{t_c} \log \frac{1}{1 - x}$$

where t_c is the average residence time in the reaction zone. The fraction decomposed, x, may be calculated in two ways. From product analysis

$$x = \frac{\text{moles } (CH_4 + C_6H_5C_2H_5) + 2 \times \text{moles } C_2H_6}{3 \times \text{moles } (Tl(CH_3)_3 \text{ used})}$$

Can. J. Chem. Downloaded from www.nrcresearchpress.com by 210.87.254.40 on 09/05/12
For personal use only.

From alkyl recovery

$$x = \frac{\text{g of alkyl used} - \text{g of alkyl recovered}}{\text{g of alkyl used}}$$

The product distribution in Table 1 and the agreement shown in Table 2 between the percent decompositions calculated from product analysis and from alkyl recovery, indicate that reaction 1 is the rate controlling step in a sequence of reactions that produces three methyl radicals and free thallium. The simple linear nature of the Arrhenius plot of $k_4/k_5^{1/2}$ shown in Fig. 2 is further supporting evidence (3).

After a number of runs the reaction vessel was removed in a helium atmosphere. A bluish-grey deposit was present in the reaction zone. Samples scraped from the walls and subjected to EDTA analysis (5) showed that the deposit was essentially pure thallium (99.7% Tl found).

All contact times used were such that thermal equilibrium and diffusion problems should not be significant (6).

The negligible effect on k_1 of a variation by a factor of 2.5 in concentration in the packed vessel at 515 °K and by a factor of 3.3 in the unpacked vessel at 502 °K indicates that the decomposition is first order. The agreement in Fig. 1 between the experiments in the packed vessel and those in the unpacked vessel shows that no detectable surface reactions are occurring. Least squares analysis of the points used to obtain this plot gives

$$\log_{10} k_1 = 15.10 - (36\,400 \pm 600)/2.3RT$$

From the runs at 491 °K, it is apparent that above approximately 14 mm of Hg total pressure the values of k_1 are close to the high pressure limiting values. The observed activation energy, 36.4 kcal mol^{-1}, should be a reasonable measure of $D[(CH_3)_2Tl{-}CH_3]$.

No studies on the determination of the heat of formation of trimethylthallium have been reported. From trends in the periodic table, a value of 32 ± 3 kcal mol^{-1} may be estimated for the mean metal–carbon bond dissociation energy in trimethylthallium. Using this value and the same arguments used in the study of similar alkyls (7–9), it appears that methylthallium may decompose via reaction 3*a*. However, if the mean bond energy is taken as 29 kcal mol^{-1} (the lower limit of the estimated value), the same arguments lead to the conclusion that methylthallium could decompose via reaction 3. Obviously no significant conclusion can be drawn until the heat of formation of $Tl(CH_3)_3$ becomes available.

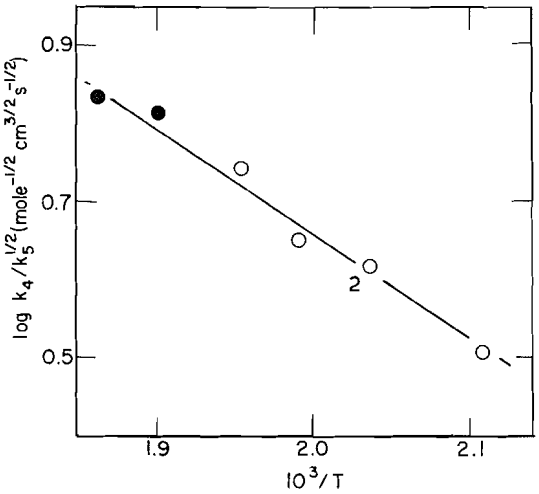

FIG. 2. Arrhenius plot of $k_4/k_5^{1/2}$ for runs at 20–24 mm total pressure. Points shown cover the range 7–90% decomposition. Filled circles: runs in packed reaction vessel.

(b) Results Obtained when Air is Admitted while a Coating of Thallium is Present in the Reaction Zone

The upper curve in Fig. 1 and the results in Table 1 show the behavior observed upon admission of air. It must be emphasized that this catalytic behavior is only observed if thallium metal is present in the reaction zone at the time the air is admitted. The observed effect may be gradually reduced by carrying out further runs while air is carefully excluded. From a practical point of view, however, it is much faster and more economical in terms of alkyl consumption simply to remove the vessel, clean it with boiling concentrated HNO_3, remove the residual acid under vacuum (600 to 700 °K), and precondition by decomposing about 0.1 g of alkyl in the reaction zone. If the preconditioning step is omitted, rate constants based on residual alkyl analysis (k_m) are unaffected. The k_g value is initially very low but increases toward the k_m value over a number of runs. One possible explanation is that a very fast reaction occurs between CH_3 and residual NO on the surface of the reaction zone. This would be consistent with the almost zero yield of C_2H_6 in the first run after cleaning. If such a reaction is occurring the

Can. J. Chem. Downloaded from www.nrcresearchpress.com by 210.87.254.40 on 09/05/12
For personal use only.

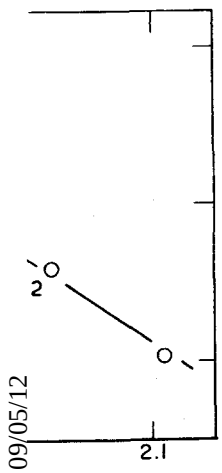

$^{1/2}$ for runs at 20–24
ver the range 7–90%
in packed reaction

se via reaction 3.
nclusion can be
tion of $Tl(CH_3)_3$

Admitted while a
in the Reaction

d the results in
ved upon admis-
asized that this
ved if thallium
zone at the time
ved effect may be
out further runs
From a practical
much faster and
lkyl consumption
an it with boiling
the residual acid
and precondition
f alkyl in the re-
ditioning step is
on residual alkyl
The k_g value is
es toward the k_m
ns. One possible
st reaction occurs
on the surface of
be consistent with
I_6 in the first run
on is occurring the

CH_3NO, whether it exists as such or as the formaldehyde oxime (CH_2:NOH), either remains absorbed on the wall of the reaction zone or reaches the acetone – Dry Ice trap at the outlet of the furnace in a form not detectable by our usual analytical procedures.

As previously mentioned when the reaction vessel is removed in an inert atmosphere following runs in which air has been carefully excluded, a bluish-grey deposit of thallium is found in the reaction zone. Following runs in which catalysis is observed, this deposit is black indicating the probable presence of Tl_2O. The results of solubility tests (10) are in agreement with this.

Finally it is perhaps interesting to note that although the product distribution shown for catalytic runs is not much different from that shown in the homogeneous pyrolysis, comparison of $k_4/k_5^{1/2}$ values shows some enhancement of methane formation in the catalytic system. With the relatively low yields of CH_4 in this work and the extent of scatter in $k_4/k_5^{1/2}$ values it is probably inadvisable to try to draw any formal conclusions. However, it seems possible that over the range of catalytic runs done, some 10–50% of the CH_4 arises from surface reactions with the remainder being formed in the usual way by reaction 4 and associated processes.

This work has been supported by a grant from the National Research Council of Canada.

1. M. G. JACKO and S. J. W. PRICE. Can. J. Chem. **43**, 1961 (1965).
2. S. J. PRICE and M. G. JACKO. Can. J. Chem. **43**, 3481 (1965).
3. M. G. JACKO and S. J. W. PRICE. Can. J. Chem. **42**, 1198 (1964).
4. H. GILMAN and R. G. JONES. J. Am. Chem. Soc. **68**, 517 (1946).
5. J. KINNUMEN and B. WINNESTRAND. Chem. Anal. **46**, 92 (1957).
6. M. F. R. MULCAHY and M. R. PETHARD. Aust. J. Chem. **16**, 527 (1961).
7. S. J. W. PRICE and J. P. RICHARD. Can. J. Chem. **48**, 3209 (1970).
8. S. J. W. PRICE and J. P. RICHARD. Can. J. Chem. **50**, 966 (1972).
9. R. P. JOHNSON and S. J. W. PRICE. Can. J. Chem. **50**, 50 (1972).
10. B. SMITH HOPKINS. Chapters in the chemistry of the less familiar elements. Vol. 1. 1st ed. Stipes Publ. Co., Chicago, Ill. 1939. Chapt. 9. p. 4.
11. (*a*) Tables of bimolecular gas reactions. NSRDS-NBS 9. 1967. p. 111. (*b*) E. TATAJEZAK and A. F. TROTMAN-DICKENSON. Supplementary tables of bimolecular gas reactions. University of Wales Institute of Science and Technology, Cardiff. 1971.

Can. J. Chem. Downloaded from www.nrcresearchpress.com by 210.87.254.40 on 09/05/12
For personal use only.

The Synthesis of Some Analogs of the Hallucinogen 1-(2,5-Dimethoxy-4-methylphenyl)-2-aminopropane (DOM)

RONALD T. COUTTS AND JERRY L. MALICKY

Faculty of Pharmacy and Pharmaceutical Sciences, University of Alberta, Edmonton, Alberta

Received October 31, 1972

The synthesis of a series of 4-substituted 1-(2,5-dimethoxyphenyl)-2-aminopropanes, in which the 4-substituent is Br, Cl, I, NO_2, NH_2, and NHAc, is described. These compounds are analogs of 1-(2,5-dimethoxy-4-methylphenyl)-2-aminopropane (DOM), a known hallucinogen. A synthesis of *N*-(2,5-dimethoxy-4-methylphenethyl)hydroxylamine, the *N*-hydroxy homolog of DOM, is also reported. Brief reference is made to the preliminary pharmacology of these compounds.

La synthèse d'une série de (diméthoxy-2,5 phényl)-1 amino-2 propanes substituées en 4 par Br, Cl, I, NO_2, et NHAc, est décrite. Ces composés sont des analogues de la (diméthoxy-2,5 méthyl-4 phényl)-1 amino-2 propane (DOM), hallucinogène connu. Une synthèse de la *N*-(diméthoxy-2,5 méthyl-4 phénétyl) hydroxylamine, homologue *N*-hydroxyle de la DOM, a été aussi rapportée. Une référence brève a été faite sur la pharmacologie préliminaire de ces composés. [Traduit par le journal]

Can. J. Chem., **51**, 1402 (1973)

Can. J. Chem. Downloaded from www.nrcresearchpress.com by 210.87.254.42 on 09/05/12
For personal use only.

Structure-activity relationship studies of potential psychotomimetic phenethylamines have shown (1–3) that the most potent psychoactive drugs of this chemical class are ring-methoxylated phenylisopropylamines. The compounds possessing greatest psycho-activity are 1-(2,5-dimethoxy-4-substituted-phenyl)-2-aminopropanes (**1**). Five such compounds (**1***a–e*) have been prepared and pharmacologically evaluated (3–7). Of these, the 4-methyl analog (DOM) (**1***c*) has gained wide publicity as the potent major constituent of the 'street hallucinogen', STP. The related compound, 1-(4-bromo-2,5-dimethoxyphenyl)-2-aminopropane (**1***e*) has only recently been evaluated and has been found to induce in humans a mescaline-like action more profound than that of an equal amount of DOM (6). Five other bromo-isomers were also evaluated in this study but all were less active than **1***e*. Ho *et al.* (8) described some compounds which retained the 2,4,5-trisubstituted-phenyl moiety of DOM (*i.e.* **2**; R^1, R^2, and R^3 = H or CH_3) and found that psychoactivity (disruption of rat behavior) was also retained.

The studies just described suggest that a 2,5-dimethoxy-4-substituted-phenyl substituent might be important for psychotomimetic activity. For this reason, the preparation of additional compounds of general structure **1** was undertaken.

The synthetic approach most commonly employed to prepare 1-phenyl-2-aminopropanes involves the synthesis of the corresponding phenylnitropropenes which are then reduced by means of lithium aluminum hydride in ether or tetrahydrofuran (*e.g.* 5, 8) (Scheme 1). For the preparation of compounds **1***e–g* by this method, the aldehydes **3***a–c* were required but none of the various synthetic methods attempted proved satisfactory. Formylation of 1-bromo and 1-chloro-2,5-dimethoxybenzene using phosphorus oxychloride and *N*-methylformanilide (5) did produce the aldehydes **3***a* and *b* but yields were very low and purification proved impossible. The synthetic approach summarized in Scheme 1, therefore, could not be used.

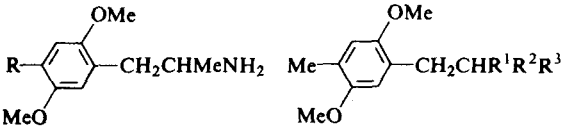

1 **2**

R		R	
a	OMe	*f*	Cl
b	OEt	*g*	I
c	Me	*h*	NO_2
d	Et	*i*	NH_2
e	Br	*j*	NHAc

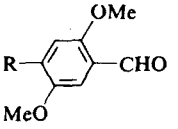

3

R	
a	Br
b	Cl
c	I

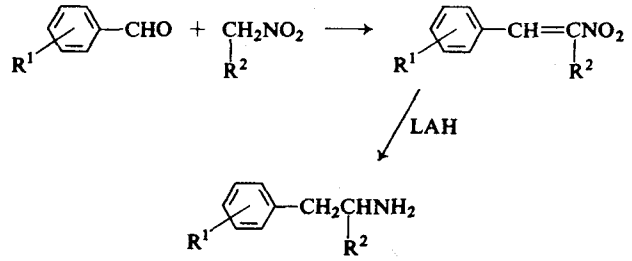

SCHEME 1

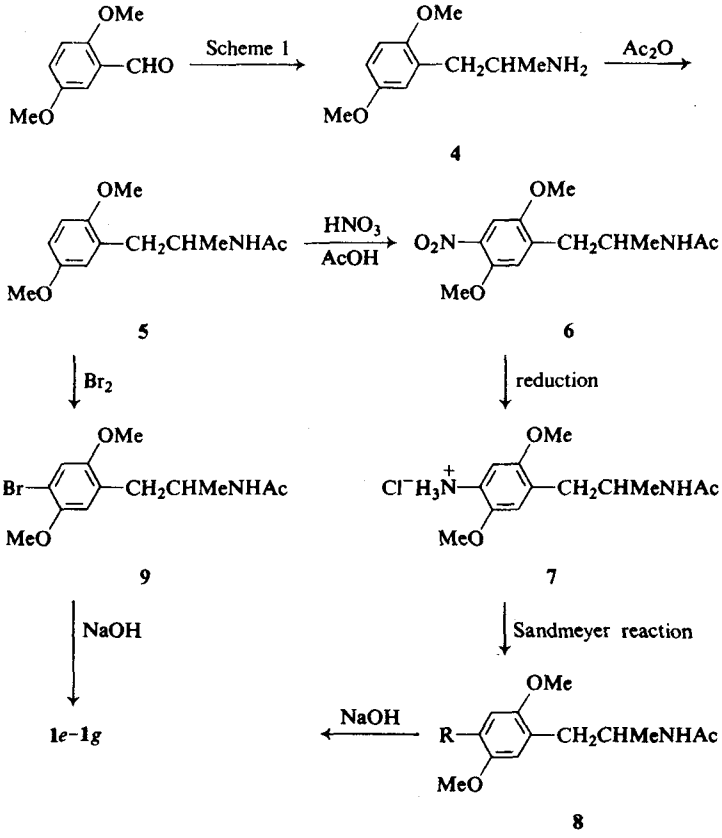

a R = Cl
b R = I

SCHEME 2

The halogenated compounds (**1***e–g*) were prepared successfully from 1-(2,5-dimethoxyphenyl)-2-aminopropane (**4**) which was readily synthesized from 2,5-dimethoxybenzaldehyde using Scheme 1. The reaction sequences employed are summarized in Scheme 2. Acetylation of **4** followed by nitration of the acetate (**5**) gave *N*-acetyl-1-(2,5-dimethoxy-4-nitrophenyl)-2-aminopropane (**6**) in excellent yield. Verification that nitration had occurred at the 4-position was obtained from n.m.r. spectral data. The two aromatic protons came to resonance at δ 6.97 and 7.41 and appeared as singlets, indicative of a para arrangement.

Can. J. Chem. Downloaded from www.nrcresearchpress.com by 210.87.254.42 on 09/05/12
For personal use only.

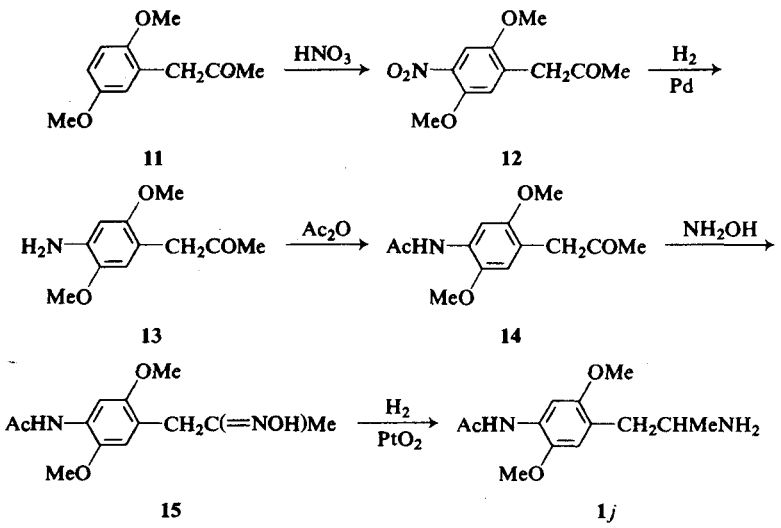

SCHEME 3

The nitro-compound (**6**) when subjected to catalytic hydrogenation readily incorporated hydrogen and *N*-acetyl-1-(4-amino-2,5-dimethoxyphenyl)-2-aminopropane hydrochloride (**7**) was isolated in good yield. *N*-Acetyl-1-(4-chloro-2,5-dimethoxyphenyl)-2-aminopropane (**8***a*) and the related 4-iodo-compound (**8***b*) were successfully prepared by subjecting the amine (**7**) to the Sandmeyer reaction, whereas the 4-bromo-compound (**9**) was obtained by the action of bromine water on *N*-acetyl-(2,5-dimethoxyphenyl)-2-aminopropane (**5**). The aromatic protons again appeared as singlets in the n.m.r. spectrum of **5**, which confirmed that the bromine atom occupied the 4-position in the ring.

A suitable means of hydrolyzing the amide group of compounds **9**, **8***a*, **8***b*, **6** and **7**, thereby completing the syntheses of **1***e–i* respectively, was sought. In most instances, these aliphatic amides proved resistant to hydrolysis by means of hydrochloric acid, sulfuric acid, or aqueous sodium hydroxide. Various reaction temperatures and times were tried and reagent concentrations were altered, but the amines were usually isolated in low yields, if at all. Eventually, a procedure employing ethylene glycol and sodium hydroxide (9) was used and reasonable yields of the 2-aminopropanes **1***e–h* were recovered.

The hydrolysis of *N*-acetyl-1-(4-amino-2,5-dimethoxyphenyl)-2-aminopropane (**7**) was also successful but the product (**1***i*) could not be purified by crystallization. An alternative procedure, in which 1-(2,5-dimethoxy-4-nitrophenyl)-2-aminopropane (**1***h*) was catalytically reduced, produced the pure amine (**1***i*).

After a preliminary pharmacological screening of compounds **1***e–i*, (see below), it became necessary to prepare and evaluate 1-(4-acetamido-2,5-dimethoxyphenyl)-2-aminopropane (**1***j*). The synthetic route summarized in Scheme 2 cannot be used for this compound in view of the severe hydrolytic conditions necessary to cleave the aliphatic amide group. The most obvious alternative synthetic route involved the preparation of 4-acetamido-2,5-dimethoxyphenylacetone oxime (**15**) which would be expected (10) to reduce catalytically to the desired compound. The series of reactions leading to the synthesis of **1***j* is shown in Scheme 3. The starting material, 2,5-dimethoxyphenylacetone (**11**), together with the related oxime (**11***a*) were the products recovered from a catalytic reduction of 1-(2,5-dimethoxyphenyl)-2-nitropropene-1 (**10**) (see eq. 1).

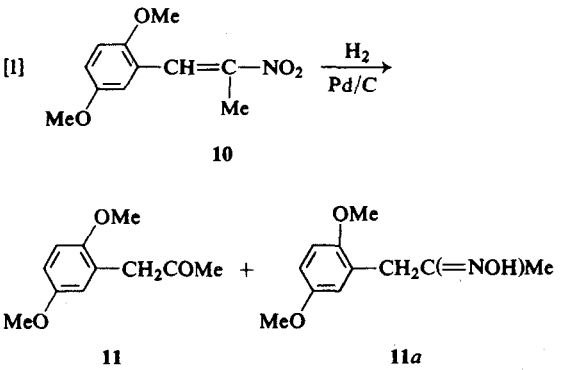

Can. J. Chem. Downloaded from www.nrcresearchpress.com by 210.87.254.42 on 09/05/12
For personal use only.

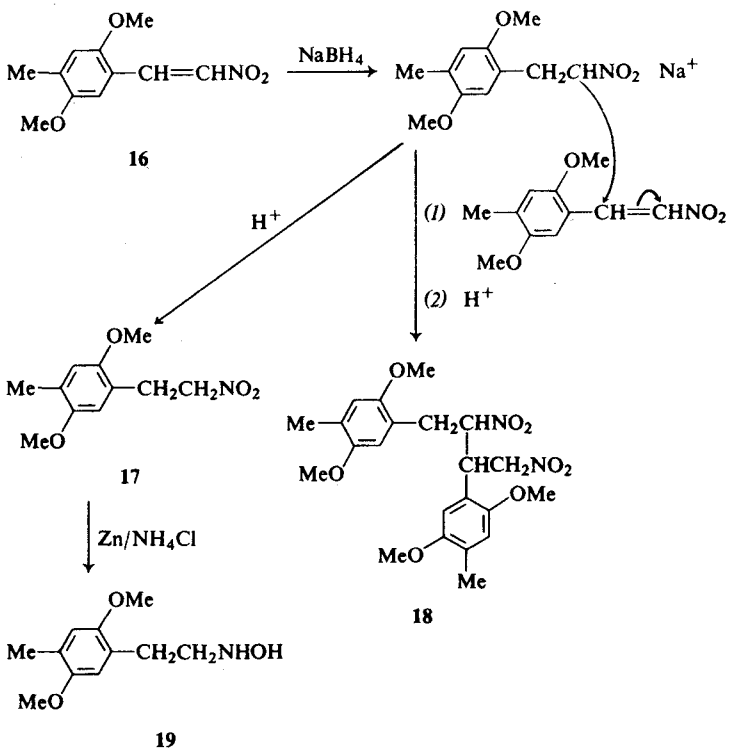

SCHEME 4

Nitration of 2,5-dimethoxyphenylacetone with nitric acid in glacial acetic acid gave the 4-nitro-derivative (**12**). The position at which nitration occurred was again confirmed by n.m.r. spectral data. Catalytic reduction of **12** followed by acetylation gave the intermediates **13** and **14** respectively in good yields. The preparation of the oxime (**15**) was somewhat difficult. Catalytic hydrogenation of this material yielded the desired amine (**1***j*). Each of the compounds illustrated in Scheme 3 was characterized by its elemental analysis and by i.r. spectral data.

One additional compound related to DOM was required in the present study, *i.e.* the *N*-hydroxy-derivative, *N*-(2,5-dimethoxy-4-methylphenethyl)-hydroxylamine (**19**). The method employed in its synthesis is outlined in Scheme 4. 1-(2,5-Dimethoxy-4-methylphenyl)-2-nitroethene (**16**), the starting material, was obtained from the interaction of 2,5-dimethoxy-4-methylbenzaldehyde and nitromethane (see Scheme 1). Reduction of this styrene with sodium borohydride gave two compounds which were easily separated because of differences in their solubilities in ethanol. The ethanol-soluble product, $C_{11}H_{15}NO_4$, gave i.r. and n.m.r. spectra which established its structure as 1-(2,5-dimethoxy-4-methylphenyl)-2-nitroethane (**17**).

Shechter *et al.* (11) found that the sodium borohydride reduction of nitroalkenes was accompanied by a concurrent reaction of the Michael-type in which the primary reduction product, the nitroalkane salt, added to the initial nitroalkene to yield a 1,3-dinitroalkane. The ethanol-insoluble product from the reduction of the nitrostyrene (**16**), therefore, was suspected to be 2,4-di-(2,5-dimethoxy-4-methylphenyl)-1,3-dinitrobutane (**18**). The elemental analysis of the compound and its i.r. spectrum were consistent with this deduction. The molecular ion in its mass spectrum was located at *m/e* 448 which corresponds to the molecular weight of the dinitroalkane (**18**).

An ethanolic solution of 1-(2,5-dimethoxy-4-methylphenyl)-2-nitroethane (**17**) was heated with zinc and ammonium chloride and yielded the required *N*-(2,5-dimethoxy-4-methylphenethyl)-hydroxylamine (**19**).

Can. J. Chem. Downloaded from www.nrcresearchpress.com by 210.87.254.42 on 09/05/12
For personal use only.

Can. J. Chem. Downloaded from www.nrcresearchpress.com by 210.87.254.42 on 09/05/12
For personal use only.

Preliminary Pharmacology

The 2-aminopropanes prepared in this study were subjected to a simple preliminary pharmacological screening to provide some guidelines for the synthesis of other compounds and to select compounds for more detailed pharmacological testing. The effects of an oral dose of each compound on male rats (150–500 g) were compared with those caused by an oral dose of DOM (10 mg/kg) which reliably caused hypersalivation, papillary dilation, retraction of scrotum, loss of orientation reflexes, analgesia, hypomotility, and walking with a slinking gait. This crude test revealed that compounds **1***e*, *f*, and *h* (10 mg/kg) were equipotent with DOM but that compound **1***i* was devoid of activity. Compound **1***g* was not evaluated. The inactivity of **1***i* suggested it, or its active metabolite, was not reaching the brain so the acetamide (**1***j*) was prepared and evaluated. It, too, was devoid of activity. The nature of the substituent at C-4 in the phenyl ring undoubtedly has a profound effect on pharmacological activity.

A 60 mg/kg intraperitoneal dose of compound **19** in male rats caused hypersalivation, pupil dilation, loss of orientation reflex, and a reduction in motility, and caused the rat to crouch and walk backwards following a circular path when objects were placed in front of it.

Experimental

Melting points were determined on a Thomas Hoover capillary melting point apparatus and are uncorrected. I.r. spectra were recorded on a Beckman IR-10 spectrophotometer as Nujol mulls and n.m.r. spectra were taken on a Varian A-60D spectrometer. Tetramethylsilane was used as the internal standard. Mass spectra were recorded by Dr. A. M. Hogg and his associates at the Department of Chemistry, University of Alberta, Edmonton, with an A.E.I. MS-9 or MS-12 mass spectrometer at an ionizing potential of 70 eV using the direct probe technique. Elemental analyses were determined at the Department of Chemistry, and at the Faculty of Pharmacy and Pharmaceutical Sciences (by Mr. W. Dylke), University of Alberta, Edmonton.

1-(2,5-Dimethoxyphenyl)-2-nitropropene-1

A solution of 2,5-dimethoxybenzaldehyde (10.0 g), ammonium acetate (4.0 g), and nitroethane (6.8 g) in glacial acetic acid (50 ml) was heated on a boiling water-bath for 3 h, then the solvent was evaporated. The residue which remained was suspended in water and extracted with chloroform. Evaporation of the chloroform left the title compound (11.2 g). Crystallization from ethanol gave m.p. 73–75°; no lit. (12) m.p. reported; i.r. ν_{max} 1300, 1502 (NO_2), 1645 (C=C) cm^{-1}.

Anal. Calcd. for $C_{11}H_{13}NO_4$: C, 59.18; H, 5.87; N, 6.28. Found: C, 58.99; H, 5.88; N, 5.95.

1-(2,5-Dimethoxyphenyl)-2-aminopropane Hydrochloride (4)

A solution of 1-(2,5-dimethoxyphenyl)-2-nitropropene-1 (17.0 g) in dry ether (500 ml) was added slowly to a stirred suspension of lithium aluminum hydride (12.0 g) in the same solvent (150 ml). When the addition was complete, the mixture was refluxed for 20 h, cooled, and the excess lithium aluminum hydride was decomposed by the careful addition of water. The resulting suspension was filtered and the solid which was removed was washed with ether. The combined ether solutions were dried ($MgSO_4$), then saturated with dry hydrogen chloride. This precipitated the title compound (16.3 g), m.p. 114–116° (from ethanol); lit. (13) m.p. 111.5–112.5°; i.r. ν_{max} 1600; 2000–2550 (weak bands) ($\overset{+}{N}$—H) cm^{-1}.

N-Acetyl-1-(2,5-dimethoxyphenyl)-2-aminopropane (5)

Acetic anhydride (40 ml) was added to a solution of 1-(2,5-dimethoxyphenyl)-2-aminopropane hydrochloride (5.0 g) and sodium acetate (25.0 g) in water (300 ml) and the mixture was shaken vigorously until the exothermic reaction ceased. The cooled solution was filtered and gave the title compound (4.2 g), m.p. 104–105.5° when crystallized from ethanol. The i.r. ν_{max} 1635 (C=O); 3100 (NH) cm^{-1}.

Anal. Calcd. for $C_{13}H_{19}NO_3$: C, 65.80; H, 8.07; N, 5.90. Found: C, 65.75; H, 8.13; N, 5.90.

N-Acetyl-1-(2,5-dimethoxy-4-nitrophenyl)-2-aminopropane (6)

A solution of 70% nitric acid (50 ml) in water (400 ml) was added to a solution of *N*-acetyl-1-(2,5-dimethoxyphenyl)-2-aminopropane (40.0 g) and sodium nitrite (0.5 g) in glacial acetic acid (400 ml). The solution was stirred for 4 h, cooled, then diluted with water (400 ml). The title compound (42.1 g) precipitated and, when crystallized from ethanol, had m.p. 166–168°. The i.r. ν_{max} 1350, 1515 (NO_2); 1640 (C=O); 3310 (NH) cm^{-1}. The n.m.r. ($CDCl_3$) δ 1.16 (d, 3H, J = 7, α-CH_3); 1.88 (s, 3H, $COCH_3$); 2.85 (d, 2H, J = 7, CH_2); 3.85 (s, 3H, OCH_3); 3.90 (s, 3H, OCH_3); 4.0–4.5 (m, 1H, CH); 5.66–5.91 (m, 1H, NH); 6.97 (s, 1H) and 7.41 (s, 1H) (aromatic protons).

Anal. Calcd. for $C_{13}H_{18}N_2O_5$: C, 55.31; H, 6.43; N, 9.92. Found: C, 55.26; H, 6.63; N, 9.92.

N-Acetyl-1-(4-amino-2,5-dimethoxyphenyl)-2-aminopropane Hydrochloride (7)

A solution of *N*-acetyl-1-(2,5-dimethoxy-4-nitrophenyl)-2-aminopropane (39.0 g) in ethanol was hydrogenated over 10% palladium–charcoal (1.0 g) until the theoretical amount of hydrogen was absorbed (3 days). The catalyst was removed and the filtrate evaporated. The residue was suspended in 5% sodium hydroxide solution (100 ml) and extracted with chloroform (3 × 100 ml). The combined chloroform solution was evaporated and the solid which remained was dissolved in dry ether. When dry hydrogen chloride was passed through this solution, the title compound (31.5 g) precipitated. It had m.p. 237–239° when crystallized from ethanol–ether. The i.r. ν_{max} 1635 (C=O); 2450–2600 (weak bands) ($\overset{+}{N}$—H) cm^{-1}.

Anal. Calcd. for $C_{13}H_{21}ClN_2O_3$: C, 54.07; H, 7.33; N, 9.70. Found: C, 54.18; H, 7.40; N, 9.78.

N-Acetyl-1-(4-chloro-2,5-di aminopropane (8a)

A solution of *N*-ace phenyl)-2-aminopropane h chloric acid (15 ml) and w To this stirred solution, s (10 ml) was slowly added w of diazonium salt was ad solution of cuprous chlori (9 ml). The reaction mixt room temperature, then h title compound (2.8 g) pre 152° when crystallized fro (C=O); 3310 (NH) cm^{-1}; J = 7, α-CH_3); 1.85 (s, 3H CH_2), 3.79 (s, 3) and 3. groups); 4.20 (m, 1H, C 6.76 (s, 1H) and 6.90 (s, 1H

Anal. Calcd. for $C_{13}H_{1}$ 5.16. Found: C, 57.35; H,

N-Acetyl-1-(2,5-dimethox aminopropane (8b)

The diazonium salt o described immediately a solution was added grad iodide (8.0 g) in water (10 to warm to room tempera of nitrogen ceased. The which separated was diss the title material (1.97 g) s when crystallized from eth 3310 (NH) cm^{-1}.

Anal. Calcd. for $C_{13}H$ 3.86. Found: C, 43.00; H

N-Acetyl-1-(4-bromo-2,5- aminopropane (9)

A slight excess of bron tion of *N*-acetyl-1-(2,5 pane (3.0 g) in dioxane stirred for 6 h. The solve compound (3.0 g) which and had a m.p. 153–155°. (NH) cm^{-1}; n.m.r. (CD 1.90 (s, 3, $COCH_3$); 4.41 and 3.85 (s, 3) (OCH_3 g 5.91 (broad s, 1H, NH) (aromatic protons.) Ma $^{81}BrNO_3$); 315 (5) (C_1 abundance).

Anal. Calcd. for $C_{13}H$ 4.43. Found: C, 49.38; H

1-(4-Bromo-2,5-dimetho Hydrochloride (1e)

(*a*) A suspension of oxyphenyl)-2-aminoprop (60 ml) and water (60 ml) for 18 h during which tim dissolved. Unreacted sta the filtrate evaporated Crystallization from et pound as a colorless so m.p. 198–199°.

N-Acetyl-1-(4-chloro-2,5-dimethoxyphenyl)-2-aminopropane (8a)

A solution of *N*-acetyl-1-(4-amino-2,5-dimethoxyphenyl)-2-aminopropane hydrochloride (5.0 g) in hydrochloric acid (15 ml) and water (30 ml) was cooled to 0°. To this stirred solution, sodium nitrite (1.4 g) in water (10 ml) was slowly added with cooling. This cold solution of diazonium salt was added slowly with shaking to a solution of cuprous chloride (2.5 g) in hydrochloric acid (9 ml). The reaction mixture was allowed to come to room temperature, then heated to 70° and cooled. The title compound (2.8 g) precipitated. It gave a m.p. 150–152° when crystallized from ethanol. The i.r. ν_{max} 1630 (C=O); 3310 (NH) cm^{-1}; n.m.r. ($CDCl_3$) δ 1.11 (d, 3H, $J = 7$, α-CH_3); 1.85 (s, 3H, $COCH_3$); 4.60 (d, 2H, $J = 7$, CH_2), 3.79 (s, 3) and 3.81 (s, 3) (overlapping OCH_3 groups); 4.20 (m, 1H, CH); 5.96 (broad s, 1H, NH); 6.76 (s, 1H) and 6.90 (s, 1H) (aromatic protons).

Anal. Calcd. for $C_{13}H_{18}ClNO_3$: C, 57.46; H, 6.68; N, 5.16. Found: C, 57.35; H, 6.48; N, 5.33.

N-Acetyl-1-(2,5-dimethoxy-4-iodophenyl)-2-aminopropane (8b)

The diazonium salt of **7** (5.0 g) was prepared as described immediately above and to the cooled (0°) solution was added gradually a solution of potassium iodide (8.0 g) in water (10 ml). The reaction was allowed to warm to room temperature and left until the evolution of nitrogen ceased. The dark brown viscous semi-solid which separated was dissolved in ethanol. On cooling, the title material (1.97 g) separated. It had a m.p. 167–168° when crystallized from ethanol. The i.r. ν_{max} 1645 (C=O); 3310 (NH) cm^{-1}.

Anal. Calcd. for $C_{13}H_{18}INO_3$: C, 42.99; H, 4.99; N, 3.86. Found: C, 43.00; H, 5.01; N, 3.77.

N-Acetyl-1-(4-bromo-2,5-dimethoxyphenyl)-2-aminopropane (9)

A slight excess of bromine water was added to a solution of *N*-acetyl-1-(2,5-dimethoxyphenyl)-2-aminopropane (3.0 g) in dioxane (30 ml), and the solution was stirred for 6 h. The solvent was removed, leaving the title compound (3.0 g) which was crystallized from ethanol and had a m.p. 153–155°. The i.r. ν_{max} 1630 (C=O); 3310 (NH) cm^{-1}; n.m.r. ($CDCl_3$) δ 1.16 (d, 3, $J = 7$, α-CH_3); 1.90 (s, 3, $COCH_3$); 4.41 (d, 2H, $J = 7$, CH_2); 3.81 (s, 3) and 3.85 (s, 3) (OCH_3 groups); 3.91–4.50 (m, 1H, CH); 5.91 (broad s, 1H, NH); 6.80 (s, 1H) and 7.07 (s, 1H) (aromatic protons.) Mass spectrum: 317 (5) ($C_{13}H_{18}{}^{81}BrNO_3$); 315 (5) ($C_{13}H_{18}{}^{79}BrNO_3$) *m/e* (% relative abundance).

Anal. Calcd. for $C_{13}H_{18}BrNO_3$: C, 49.38; H, 5.74; N, 4.43. Found: C, 49.38; H, 5.85; N, 4.29.

1-(4-Bromo-2,5-dimethoxyphenyl)-2-aminopropane Hydrochloride (1e)

(*a*) A suspension of *N*-acetyl-1-(4-bromo-2,5-dimethoxyphenyl)-2-aminopropane (2.5 g) in hydrochloric acid (60 ml) and water (60 ml) was heated at reflux temperature for 18 h during which time most of the *N*-acetyl compound dissolved. Unreacted starting material was removed and the filtrate evaporated to give a yellow solid (1.7 g). Crystallization from ethanol–ether gave the title compound as a colorless solid, m.p. 195–196°. Reported (7) m.p. 198–199°.

(*b*) *N*-Acetyl-1-(4-bromo-2,5-dimethoxyphenyl)-2-aminopropane (1.5 g) was added to a solution of sodium hydroxide (5.0 g) in water (25 ml) and ethylene glycol (50 ml) and the mixture was heated under reflux for 15 h then cooled. The solution was extracted with chloroform and the combined chloroform extracts evaporated. The resulting solid was dissolved in 5% hydrochloric acid (15 ml) and the solution filtered. The title compound (0.85 g) was the product obtained, m.p. 197–198° after crystallization from ethanol–ether. The i.r. ν_{max} 1610, 1980, 2010–2740 ($\overset{+}{N}$—H) cm^{-1}.

Anal. Calcd. for $C_{11}H_{17}BrClNO_2$: C, 42.53; H, 5.52; N, 4.51. Found: C, 42.86; H, 5.72; N, 4.29.

1-(4-Chloro-2,5-dimethoxyphenyl)-2-aminopropane Hydrochloride (1f)

The title compound (0.46 g), m.p. *193–194.5°* (from ethanol–ether) was obtained when *N*-acetyl-1-(4-chloro-2,5-dimethoxyphenyl)-2-aminopropane (1.5 g) was treated as described for the synthesis of **1e**, method *b*. The i.r. ν_{max} 1610, 2010, 2500–2640 ($\overset{+}{N}$—H) cm^{-1}.

Anal. Calcd. for $C_{11}H_{17}Cl_2NO_2$: C, 49.63; H, 6.44; N, 5.44. Found: C, 49.79; H, 6.70; N, 5.44.

1-(2,5-Dimethoxy-4-iodophenyl)-2-aminopropane Hydrochloride (1g)

The title compound (0.75 g), m.p. 198–200° (from ethanol–ether) was prepared from *N*-acetyl-1-(2,5-dimethoxy-4-iodophenyl)-2-aminopropane (1.5 g) using method *b* procedure for the synthesis of compound **1e**. The i.r. ν_{max} 1605, 2000, 2500–2710 ($\overset{+}{N}$—H) cm^{-1}.

Anal. Calcd. for $C_{11}H_{17}ClINO_2$: C, 36.94; H, 4.79; N, 3.93. Found: C, 36.68; H, 4.75; N, 3.98.

1-(2,5-Dimethoxy-4-nitrophenyl)-2-aminopropane Hydrochloride (1h)

Hydrolysis of *N*-acetyl-1-(2,5-dimethoxy-4-nitrophenyl)-2-aminopropane (2.0 g) using procedure *b* for the synthesis of compound **1e** gave the title compound (0.76 g), m.p. 203–204° when crystallized from ethanol–ether. The i.r. ν_{max} 1340, 1520 (NO_2); 1610, 2000, 2500–2690 ($\overset{+}{N}$—H) cm^{-1}.

Anal. Calcd. for $C_{11}H_{17}ClN_2O_4$: C, 47.74; H, 6.19; N, 10.13. Found: C, 47.98; H, 6.33; N, 10.01.

1-(4-Amino-2,5-dimethoxyphenyl)-2-aminopropane Dihydrochloride (1i)

A solution of 1-(2,5-dimethoxy-4-nitrophenyl)-2-aminopropane hydrochloride (1 g) in ethanol (25 ml) and hydrochloric acid (2 ml) was hydrogenated over 10% palladium–charcoal (0.1 g) until the theoretical amount of hydrogen was absorbed. The catalyst was removed and the filtrate evaporated to give a solid (0.92 g) which, when crystallized from ethanol–ether gave the title compound, m.p. 248–250°. The i.r. ν_{max} 1610, 2010, 2500–2610 ($\overset{+}{N}$—H) cm^{-1}.

Anal. Calcd. for $C_{11}H_{20}Cl_2N_2O_2$: C, 46.55; H, 7.12; N, 9.89. Found: C, 46.98; H, 7.36; N, 9.63.

Catalytic Reduction of 1-(2,5-Dimethoxyphenyl)-2-nitropropene-1

A solution of 1-(2,5-dimethoxyphenyl)-2-nitropropene-1 (7.0 g) in ethanol (150 ml) was hydrogenated at room temperature and pressure in the presence of palladium–

Can. J. Chem. Downloaded from www.nrcresearchpress.com by 210.87.254.42 on 09/05/12
For personal use only.

charcoal (0.7 g). After approximately 3 h, the uptake of hydrogen ceased. The mixture was filtered and the solution evaporated, leaving a light yellow oil. A solution of this oil in chloroform (100 ml) was extracted with 5% hydrochloric acid (3 × 50 ml) and the aqueous layer discarded. The oil which remained following evaporation of the chloroform was distilled under reduced pressure and yielded two fractions. The first (2.3 g), b.p. 100° (0.07 mm Hg) was 2,5-dimethoxyphenylacetone (reported (12) b.p. 95° (1.25 mm)). The i.r. ν_{max} 1710 (C=O) cm^{-1}; n.m.r. ($CDCl_3$) δ 1.95 (s, 3H, CH_3); 3.45 (s, 2H, CH_2); 4.25 (s, 6, $(OCH_3)_2$); 6.00–6.62 (m, 3, aromatic protons).

Anal. Calcd. for $C_{11}H_{14}O_3$: C, 68.02; H, 7.26. Found: C, 67.87; H, 7.25.

The second fraction (2.4 g), b.p. 150–170° (0.13–0.15 mm), was dissolved in ether and the solution saturated with dry hydrogen chloride. The resulting precipitate (1.2 g) was crystallized from acetone–ether to yield 2,5-dimethoxyphenylacetone oxime hydrochloride, m.p. 94–97°. The i.r. ν_{max} 2560 ($\overset{+}{N}$—H) cm^{-1}; mass spectrum: 209 (55), $C_{11}H_{15}NO_3$; 178 (100), $C_8H_{10}NO_2$ *m/e* (% relative abundance).

Anal. Calcd. for $C_{11}H_{16}ClNO_3$: C, 53.55; H, 6.96; N, 5.68. Found: C, 53.87; H, 6.75; N, 5.98.

*2,5-Dimethoxy-4-nitrophenylacetone (**12**)*

To a solution of 2,5-dimethoxyphenylacetone (4.0 g) and sodium nitrite (0.03 g) in glacial acetic acid (25 ml), stirred and cooled to 5°, was slowly added a solution of 80% nitric acid (6 ml) in water (15 ml). Stirring for 2 h, then dilution with water (100 ml) caused the precipitation of the title compound (3.71 g) which, when crystallized from ethanol, had m.p. 77–79°. The i.r. ν_{max} 1350, 1515 (NO_2); 1730 (C=O) cm^{-1}; n.m.r. ($CDCl_3$) δ 2.23 (s, 3H, CH_3); 3.80 (s, 2H, CH_2); 3.85 (s, 3H) and 3.92 (s, 3H) (OCH_3 groups); 6.98 (s, 1H) and 7.45 (s, 1H) (aromatic protons).

Anal. Calcd. for $C_{11}H_{13}NO_5$: C, 55.23; H, 5.48; N, 5.86. Found: C, 55.00; H, 5.42; N, 5.93.

*4-Amino-2,5-dimethoxyphenylacetone Hydrochloride (**13**)*

A solution of 2,5-dimethoxy-4-nitrophenylacetone (3.5 g) in ethanol (100 ml) and hydrochloric acid (5 ml) was hydrogenated at room temperature and normal pressure under 10% palladium–charcoal (1.0 g) until the theoretical amount of hydrogen was absorbed. The catalyst was removed and the filtrate evaporated *in vacuo* to give a colorless solid (3.1 g). Crystallization from ethanol–ether afforded the title compound, m.p. 195–198°. The i.r. ν_{max} 1711 (C=O); 1980, 2550 ($\overset{+}{N}$—H) cm^{-1}.

Anal. Calcd. for $C_{11}H_{16}ClNO_3$: C, 53.77; H, 6.55; N, 5.70. Found: C, 53.85; H, 6.40; N, 6.03.

*4-Acetamido-2,5-dimethoxyphenylacetone (**14**)*

This compound (2.4 g) was prepared from the amine (**13**, 3.0 g) by the method described for the preparation of compound **5**. The title compound, when crystallized from ethanol, had m.p. 138–140°. The i.r. ν_{max} 1670 (amide C=O); 1710 (ketone C=O); 3390 (NH) cm^{-1}.

Anal. Calcd. for $C_{13}H_{17}NO_4$: C, 62.13; H, 6.82; N, 5.58. Found: C, 61.81; H, 6.67; N, 5.92.

*4-Acetamido-2,5-dimethoxyphenylacetone Oxime (**15**)*

A solution of 4-acetamido-2,5-dimethoxyphenylacetone (2.0 g) and hydroxylamine hydrochloride (2.0 g) in ethanol (30 ml) and pyridine (5 ml) was heated at 75° for 7 h. The solvent was removed *in vacuo* and water (30 ml) was added to the residue. Extraction with chloroform (3 × 30 ml) followed by evaporation of the chloroform gave a pale yellow oil which solidified (1.4 g) on triturating with ether. Crystallization from ethanol yielded the title compound, m.p. 141–144°. The i.r. ν_{max} 1660 (C=O); 3250 broad peak (OH) cm^{-1}.

Anal. Calcd. for $C_{13}H_{18}N_2O_4$: C, 58.63; H, 6.81; N, 10.52. Found: C, 58.63; H, 7.01; N, 10.29.

*1-(4-Acetamido-2,5-dimethoxyphenyl)-2-aminopropane Hydrochloride (**1j**)*

A solution of 4-acetamido-2,5-dimethoxyphenylacetone oxime (1.0 g) in ethanol (50 ml) and hydrochloric acid (1.0 ml) was hydrogenated at room temperature and 50 p.s.i. pressure in the presence of platinum dioxide (0.1 g) for 14 h (arbitrary). Evaporation of the filtrate gave a solid which, when crystallized from ethanol and ether gave the title compound (0.72 g), m.p. 249–250°. The i.r. ν_{max} 1600, 2500–2700 ($\overset{+}{N}$—H); 1660 (C=O); 3250 (NH) cm^{-1}.

Anal. Calcd. for $C_{13}H_{21}ClN_2O_3$: C, 54.07; H, 7.33; N, 9.70. Found: C, 54.35; H, 7.58; N, 9.64.

Sodium Borohydride Reduction of 1-(2,5-dimethoxy-4-methylphenyl)-2-nitroethene

The title compound (8) (15.0 g, m.p. 116°), dissolved in dioxane, was added to a stirred solution of sodium borohydride (5.0 g) in water (25 ml) and dioxane (25 ml) at such a rate that decolorization occurred between additions. The final pale yellow solution was stirred for 1 h, cooled, and diluted with hydrochloric acid until effervescence ceased. The residue which remained after evaporation of the solvent was suspended in water (100 ml) and extracted with chloroform (100 ml). The chloroform extract was evaporated to give a dark brown oil which solidified (10.5 g) when triturated with cold ethanol. Crystallization from ethanol gave an insoluble product (2.8 g) and an ethanol-soluble compound (5.9 g), m.p. 67–70°. The latter was 1-(2,5-dimethoxy-4-methylphenyl)-2-nitroethane (**17**). The i.r. ν_{max} 1370, 1550 (NO_2) cm^{-1}; n.m.r. ($CDCl_3$) δ 2.21 (s, 3H, CH_3); 4.91 (t, 2H, J = 8, CH_2); 4.58 (t, 2H, J = 8, CH_2); 6.63 (s, 1H) and 6.68 (s, 1H) (aromatic protons).

Anal. Calcd. for $C_{11}H_{15}NO_4$: C, 58.65; H, 6.71; N, 6.22. Found: C, 58.32; H, 7.06; N, 6.10.

The ethanol-insoluble product was recrystallized from dioxane to yield what was assumed to be 2,4-di(2,5-dimethoxy-4-methylphenyl)-1,3-dinitrobutane (**18**), m.p. 167.5–169°. The i.r. ν_{max} 1370, 1550 (NO_2) cm^{-1}; mass spectrum: 448 (27) ($C_{22}H_{28}N_2O_8$) *m/e* (% relative abundance).

Anal. Calcd. for $C_{22}H_{28}N_2O_8$: N, 6.24. Found: N, 6.18.

*N-(2,5-Dimethoxy-4-methylphenethyl)-hydroxylamine (**19**)*

A solution of 1-(2,5-dimethoxy-4-methylphenyl)-2-nitroethane (1.5 g) in ethanol (50 ml) and water (10 ml) was stirred with ammonium chloride (1.5 g) and zinc powder (1.5 g) for 30 min, then heated under reflux for 5 min. The suspension was cooled and filtered and the filtrate basified with 5% sodium bicarbonate solution

(50 ml) then extracted
The combined extract
chloride and evaporate
with water (100 ml) an
with ammonium hydr
chloroform (100 ml). T
with water, saturated
orated to give a solid
from ethanol–ether yi
hydrochloride, m.p. 13
2750 ($\overset{+}{N}$—H) cm^{-1}; m
NO_3) *m/e* (% relative a
Anal. Calcd. for C_1
N, 5.66. Found: C, 53.

The authors thank t
Canada for the award
an operating grant, N
discussions with Dr. D

1. J. R. SMYTHIES, R
BENINGTON, R.
Psychopharmacol.
2. J. R. SMYTHIES, V

Can. J. Chem. Downloaded from www.nrcresearchpress.com by 210.87.254.42 on 09/05/12
For personal use only.

(50 ml) then extracted with chloroform (3 × 100 ml). The combined extract was saturated with dry hydrogen chloride and evaporated. The solid residue was treated with water (100 ml) and filtered. The filtrate was basified with ammonium hydroxide solution and extracted with chloroform (100 ml). The chloroform extract was washed with water, saturated with hydrogen chloride, and evaporated to give a solid (0.52 g) which when crystallized from ethanol–ether yielded the title compound as the hydrochloride, m.p. 137–138°. The i.r. ν_{max} 1610, 2510–2750 ($\overset{+}{N}$—H) cm^{-1}; mass spectrum: 211 (10) ($C_{10}H_{17}NO_3$) *m/e* (% relative abundance).

Anal. Calcd. for $C_{11}H_{18}ClNO_3$: C, 53.33; H, 7.32; N, 5.66. Found: C, 53.18; H, 7.57; N, 5.57.

The authors thank the Medical Research Council of Canada for the award of a studentship (to J. L. M.) and an operating grant, MA-2993 (to R. T. C.). Helpful discussions with Dr. D. F. Biggs are also acknowledged.

1. J. R. SMYTHIES, R. J. BRADLEY, V. S. JOHNSTON, F. BENINGTON, R. D. MORIN, and L. C. CLARK. Psychopharmacol. **10**, 379 (1967).
2. J. R. SMYTHIES, V. S. JOHNSTON, R. J. BRADLEY, F. BENINGTON, R. D. MORIN, and L. C. CLARK. Nature, **216**, 128 (1967).
3. A. T. SHULGIN, T. SARGENT, and C. NARANJO. Nature, **221**, 537 (1969).
4. A. T. SHULGIN. Experientia, **20**, 366 (1964).
5. A. T. SHULGIN. J. Med. Chem. **11**, 186 (1968).
6. A. T. SHULGIN, T. SARGENT, and C. NARANJO. Pharmacol. **5**, 103 (1971).
7. C. F. BARFKNECHT and D. E. NICHOLS. J. Med. Chem. **14**, 370 (1971).
8. B. T. HO, L. W. TANSEY, R. L. BALSTER, R. AN, W. M. MCISAAC, and R. T. HARRIS. J. Med. Chem. **13**, 134 (1970).
9. D. E. PEARSON, J. F. BAXTER, and K. N. CARTER. *In* Organic syntheses, Coll. Vol. 3. *Edited by* E. C. Horning. John Wiley and Sons, Inc., London. 1955. p. 154.
10. F. BENINGTON, R. D. MORIN, and L. C. CLARK. J. Med. Chem. **8**, 100 (1965).
11. H. SHECHTER, D. E. LEY, and E. B. ROBERSON. J. Am. Chem. Soc. **78**, 4984 (1956).
12. French patent 1 496 706 (1962) to Merck and Co., Inc.; Chem. Abstr. 69, 36445n (1968).
13. B. T. HO, W. M. MCISAAC, R. AN, L. W. TANSEY, K. E. WALKER, L. F. ENGLERT, and M. B. NOEL. J. Med. Chem. **13**, 26 (1970).

Can. J. Chem. Downloaded from www.nrcresearchpress.com by 210.87.254.42 on 09/05/12

Reactions of Thiyl Radicals. XI. Further Investigations of Thiol–Disulfide Photolyses in the Liquid Phase[1]

DONNA D. CARLSON AND ARTHUR R. KNIGHT

Department of Chemistry and Chemical Engineering, University of Saskatchewan, Saskatoon, Saskatchewan

Received October 10, 1972

The photolysis of C_2H_5SH liquid at 2537 Å has been shown to give H_2 and $C_2H_5SSC_2H_5$ at equal rates with a quantum yield of 0.25. The photolysis of ethanethiol – methyl disulfide liquid mixtures leads, via a chain reaction involving propagation by attack of thiyl radicals on the disulfide S—S bond, to the formation with high quantum efficiency of CH_3SH, $C_2H_5SSC_2H_5$ and, as an intermediate that is consumed after long exposures, $CH_3SSC_2H_5$. The net result of the sequence of exchange processes is the essentially irreversible conversion of the methyl disulfide into methanethiol. The same overall reaction occurs thermally at room temperature, but the rate is appreciably less than that of the photochemical process. The quantum yields of formation of the unsymmetrical disulfides arising from the photochemically initiated exchange reaction in equimolar mixtures of CH_3SSCH_3 + n-$C_3H_7SSC_3H_7$ and $C_2H_5SSC_2H_5$ + n-$C_3H_7SSC_3H_7$ have been shown to be 6.9 and 4.4, compared to 355 for CH_3SSCH_3 + $C_2H_5SSC_2H_5$ mixtures. In all three types of system examined in this investigation all thiyl radicals can be accounted for stoichiometrically on the basis of exchange and combination reactions alone, indicating negligible disproportionation of these species in condensed phase.

La photolyse de C_2H_5SH liquide à 2537 Å conduit à H_2 et $C_2H_5SSC_2H_5$ à des vitesses égales, avec un rendement quantique de 0.25. La photolyse de mélanges liquides d'éthane thiol et de disulfure de méthyle conduit (via une réaction en chaîne impliquant une propagation par attaque de radicaux thiyles sur la liaison disulfure) à CH_3SH avec un bon rendement quantique et à $C_2H_5SSC_2H_5$, avec comme intermédiaire $CH_3SSC_2H_5$ qui est consommé au bout d'un certain temps. Le résultat net de la séquence des processus d'échange est la conversion essentiellement irréversible du disulfure de méthyle en méthane thiol. La même réaction globale se produit thermiquement à la température ambiante mais avec une vitesse inférieure à celle du processus photochimique. Les rendements quantiques de formation de disulfures dissymétriques issus de l'échange initié photochimiquement, de mélanges équimoléculaires de CH_3SSCH_3 + n-$C_3H_7SSC_3H_7$ et $C_2H_5SSC_2H_5$ + n-$C_3H_7SSC_3H_7$, ont pour valeurs respectives 6.9 et 4.4 comparées à la valeur 355 pour les mélanges CH_3SSCH_3 + $C_2H_5SSC_2H_5$. Dans les trois types de systèmes examinés au cours de cette étude, tous les radicaux thiyles rendent compte de la stoechiométrie des seules réactions d'échange et de combinaison, indiquant une disproportionation négligeable de ces espèces en phase condensée. [Traduit par le journal]

Can. J. Chem., **51**, 1410 (1973)

Introduction

In a previous investigation in this laboratory (1) the liquid phase photolysis of disulfide mixtures was examined and it was shown that these systems are characterized by a rapid exchange reaction involving attack by photochemically produced thiyl radicals on the S—S linkage of the disulfide. A number of investigations of the photolysis of thiols (2–4) have demonstrated that the primary process yields thiyl radicals and hydrogen atoms.

We have studied and report on here three aspects of these systems in the liquid phase: the photolysis of neat C_2H_5SH to determine the effective quantum yield of C_2H_5S radical and H-atom formation in condensed phase, the photolysis of ethanethiol – methyl disulfide mixtures in experiments designed to establish the nature and quantum efficiency of the thiyl radical – disulfide exchange reaction and to determine how this process is influenced by the presence of a labile hydrogen, and the photolysis of methyl disulfide – n-propyl disulfide mixtures and ethyl disulfide – n-propyl disulfide mixtures to demonstrate the influence of steric effects on the efficiency of the exchange process.

Experimental

The photolyses were conducted at 25 °C in a grease and mercury free glass and stainless steel vacuum system. The reaction cell was a demountable quartz tube, 4 mm i.d., with axis parallel to that of the Hanovia 687A45 mercury resonance lamp used as the light source for 2537 Å radiation. The cell was suitably masked so that photolysis was confined to the liquid phase. The light source for the photolysis of the disulfide mixtures was a

[1]From the M.Sc. Thesis of D. D. Carlson, University of Saskatchewan, Saskatoon, Saskatchewan, 1972.

FIG. 1. Yield of h
μmol C_2H_5SH at 253

Hanovia 608A-36 me
7910 filter.

The ethanethiol was
at a fixed temperatu
vacuum system and su
tion cell. In the experir
the required amount
admitted to the deta
Following thorough de
the ethanethiol was ad
used in these experime
of which 8.84% was
were made up directly fi
ly degassed after admis

At the conclusion of
H_2 was removed at −1
vacuum system where i
Because of the desirab
as rapidly as possible
(see below) hydrogen v
The fraction condensa
completely to a trap
acted as the sampling v
g.c. That fraction, con
and the products was ar
on Gas Chrom Z in ¼
not possible to carry o
column. Therefore each
analyzing for CH_3SH
column and for the ren
separated after CH_3SH
a 3 ft column. In som
found that decomposit
ethyl disulfide, sometir
attempted using coppe
not occur with stainless

The photolysate from
was analyzed by flame
determination of two o

Can. J. Chem. Downloaded from www.nrcresearchpress.com by 210.87.254.6 on 09/05/12
For personal use only.

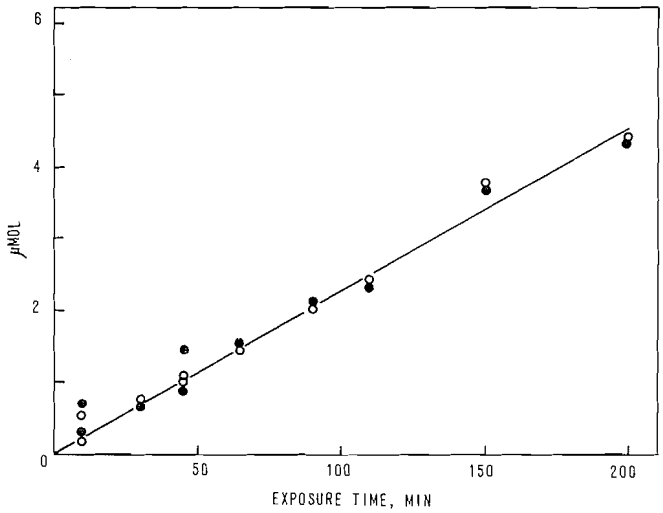

FIG. 1. Yield of hydrogen, ○, and ethyl disulfide, ●, as a function of exposure time for the photolysis of 10^3 μmol C_2H_5SH at 2537 Å and 25 °C in the liquid phase.

Hanovia 608A-36 medium pressure lamp with Vycor 7910 filter.

The ethanethiol was expanded, from a liquid reservoir at a fixed temperature, into a known volume in the vacuum system and subsequently frozen out in the reaction cell. In the experiments with thiol–disulfide mixtures the required amount of liquid CH_3SSCH_3 was first admitted to the detached cell with a micro-syringe. Following thorough degassing of the disulfide in the line, the ethanethiol was admitted as before. The photolysate used in these experiments contained a total of 890 μmol of which 8.84% was CH_3SSCH_3. Disulfide mixtures were made up directly from the pure liquids and thoroughly degassed after admission to the reaction cell.

At the conclusion of each reaction with pure ethanethiol H_2 was removed at −196 °C and transferred to a second vacuum system where it was determined in a gas burette. Because of the desirability of carrying out the analyses as rapidly as possible in the thiol-disulfide experiments (see below) hydrogen was not determined in those runs. The fraction condensable at −196 °C was transferred completely to a trap in the vacuum system that also acted as the sampling volume for the thermal conductivity g.c. That fraction, consisting of all unreacted substrate and the products was analyzed on 15% tricresyl phosphate on Gas Chrom Z in ¼ in. stainless steel columns. It was not possible to carry out a complete analysis on a single column. Therefore each experiment was done in duplicate, analyzing for CH_3SH in one analysis using an 18 ft column and for the remainder of the products, that were separated after CH_3SH and C_2H_5SH eluted together, on a 3 ft column. In some preliminary experiments it was found that decomposition of ethanethiol, principally to ethyl disulfide, sometimes occurred when analysis was attempted using copper g.c. columns; the reaction does not occur with stainless steel.

The photolysate from the disulfide mixture experiments was analyzed by flame ionization gas chromatographic determination of two or three syringe extracted aliquots.

The ethanethiol and methyl disulfide used were American Petroleum Institute standard samples with specified minimum purity of 99.95%. The ethyl disulfide and *n*-propyl disulfide (Eastman) were fractionally distilled at atmospheric or reduced pressure before use.

The absorbed light intensity at 2537 Å in the experiments utilizing the Hg-resonance lamp was determined using the photolysis of mixtures of methyl disulfide and ethyl disulfide. The quantum yield of methyl ethyl disulfide formation in this system, 355 ± 15, is independent of time for small percent conversions and does not vary with light intensity over the range $1–25 \times 10^{-2}$ μeinstein min^{-1} (5). A mixture of the two disulfides, 49.8 mol % CH_3SSCH_3, was photolyzed for periods of 5–30 s and an average initial rate of $CH_3SSC_2H_5$ formation determined. Thermal blanks were run simultaneously to allow correction for the small amount of thermal reaction that also yields methyl ethyl disulfide (1, 5). The value of I_a so determined was $9.4 \pm 0.4 \times 10^{-2}$ μeinstein min^{-1}.

Results and Discussion

Ethanethiol

In the first series of experiments pure liquid C_2H_5SH was photolyzed and the yields of the only products that could be detected, H_2 and $C_2H_5SSC_2H_5$, measured as a function of exposure time. The results are shown in Fig. 1 and indicate that the yields are linearly dependent on time in the range investigated. The average rate gives a value of 0.25 for $\Phi(H_2)$ and $\Phi(C_2H_5SSC_2H_5)$. The fact that the quantum yields for these two products are the same, forms part of a growing body of evidence (6) pointing to a very minor role for disproportionation of alkylthiyl radicals in relation to their

Can. J. Chem. Downloaded from www.nrcresearchpress.com by 210.87.254.6 on 09/05/12
For personal use only.

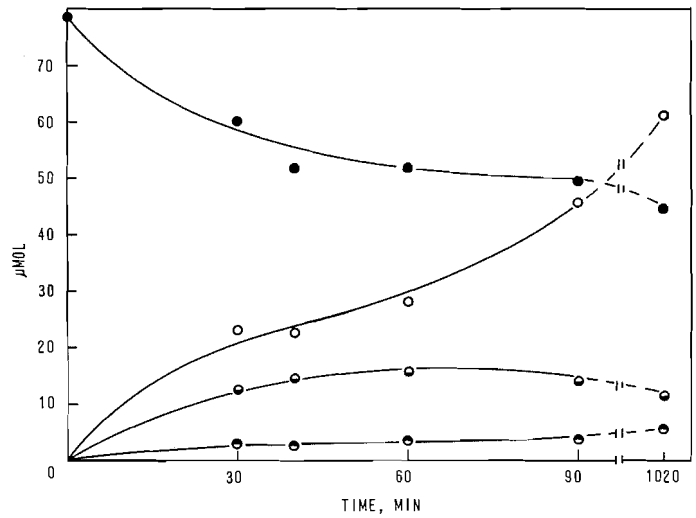

FIG. 2. Yield of CH_3SH, ○, $CH_3SSC_2H_5$, ◒, and $C_2H_5SSC_2H_5$, ◓, and the residual amount of CH_3SSCH_3, ●, as a function of time in the thermal reaction of 78.6 μmol CH_3SSCH_3 with 810 μmol C_2H_5SH at 25 °C.

combination reaction. The observations here are consistent with C_2H_5S radical and H-atom formation in the primary process, followed by abstraction from the substrate giving H_2, and combination of thiyl radicals producing disulfide. It is perhaps suprising, however, that no evidence is found for the C—S bond cleavage that characterizes the gas phase decomposition of thiols (4, 7, 8). This aspect of the system and the fact that the decomposition quantum yield is less than unity indicate the desirability of further investigation of the condensed phase photolysis.

Ethanethiol – Methyl Disulfide Mixtures

When preliminary experiments with C_2H_5SH–CH_3SSCH_3 mixtures were carried out it became apparent that there is some thermally induced thiol–disulfide exchange, leading to the same products anticipated as arising from the photochemical reaction. No reaction can be detected in the thiol or disulfide alone.

Figure 2 shows the total micromoles of products formed and the micromoles of residual disulfide in the thermal reaction. The first 30 min during which no analyses are reported represents the sample "handling-time" in the vacuum line during which the thiol and disulfide are present together at room temperature. As is apparent from the figure the net result of the thermal reaction is the conversion of the disulfide into CH_3SH. The observed yields of products containing the CH_3S group are stoichiometrically consistent within experimental error with the amount of CH_3SSCH_3 consumed. Since 78.8 μmol of disulfide is present initially, $[CH_3S]$, calculated from eq. 1, should remain

$$[1] \quad [CH_3S] = 2\,[CH_3SSCH_3] + [CH_3SH] + [CH_3SSC_2H_5]$$

constant at 157 μmol. The observed concentrations shown in Fig. 2 give $[CH_3S]$ values of 156, 141, 144, 159, and 162 μmol at 30, 40, 60, 90, and 1020 min respectively. The occurrence of the thermal reaction, presumably catalyzed by trace impurities or the container walls, is consistent with the previously reported (1, 5, 9) similar reaction that gives at room temperature in the dark, methyl ethyl disulfide from mixtures of CH_3SSCH_3 and $C_2H_5SSC_2H_5$.

When mixtures of ethanethiol and methyl disulfide are photolyzed there is a very rapid increase in the amount of CH_3SH produced and a concomitant decline in the concentration of CH_3SSCH_3. The yields of CH_3SH, $C_2H_5SSC_2H_5$ and $CH_3SSC_2H_5$ along with the residual amounts of CH_3SSCH_3 are shown as a function of exposure time in Fig. 3. Some fraction of these yields will arise from the thermal reaction, which will occur here principally *after* the exposure, during the 30 min sample processing period. However, since the rate of the thermal reaction initiated by the disulfide will decline as the proportion of CH_3SSCH_3 is reduced, the yields shown in Fig. 2 represent the *maximum* contribution of the thermolysis to the

Can. J. Chem. Downloaded from www.nrcresearchpress.com by 210.87.254.6 on 09/05/12
For personal use only.

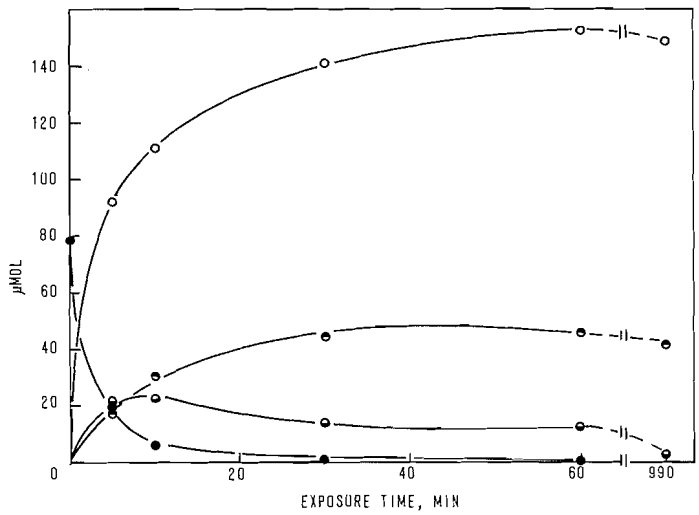

FIG. 3. Yield of CH_3SH, ○, $CH_3SSC_2H_5$, ◒, and $C_2H_5SSC_2H_5$, ◓, and the residual amount of CH_3SSCH_3, ●, as a function of exposure time in the photolysis of 78.6 μmol CH_3SSCH_3 and 810 μmol C_2H_5SH at 2537 Å and 25 °C.

total yields determined in the photolytic experiments. The amounts of the three products formed give a value for $[CH_3S]$ from eq. 1 that is essentially constant and consistent with the initial disulfide concentration. Thus the calculated $[CH_3S]$ values are 151, 147, 159, 165, and 152 μmol for 5, 10, 30, 60, and 990 min exposure time.

In considering the photochemical initiation of the chain processes operative here, the fact that both components of the mixture absorb 2537 Å radiation significantly is important. The absorption coefficient of liquid methyl disulfide at this wavelength is 316 liter mol^{-1} cm^{-1} (5) while that of ethanethiol is 34.2 (10). In the initial mixture, therefore, with 78.6 μmol CH_3SSCH_3 and 810 μmol C_2H_5SH, the ratio of absorbances, $A_{disulfide}/A_{thiol}$, is 0.90. However, after 5 min of exposure the amount of disulfide is reduced to 18.5 μmol and the ratio decreases to 0.22. Therefore, although initially the photolysis of methyl sulfide will be important, absorption and photodecomposition of C_2H_5SH will rapidly become a principal photochemical process. At the same time, however, the two disulfide products, which have absorption coefficients quite close to that of CH_3SSCH_3 (5), will begin to absorb significantly. At the end of 5 min they account together for 26% of the total absorbance in the system. The data in Fig. 3 indicate that their absorption will predominate at longer exposure times.

The observed products and their formation with large quantum efficiencies can be explained on the basis of the mechanism depicted by eqs. 2–11, wherein reactions 4, 5, and 7 are the

[2] $CH_3SSCH_3 + h\nu \rightarrow 2\,CH_3S$

[3] $C_2H_5SH + h\nu \rightarrow C_2H_5S + H$

[4] $C_2H_5S + CH_3SSCH_3 \rightarrow CH_3SSC_2H_5 + CH_3S$

[5] $C_2H_5S + CH_3SSC_2H_5 \rightarrow C_2H_5SSC_2H_5 + CH_3S$

[6] $CH_3S + C_2H_5SH \rightarrow C_2H_5S + CH_3SH$

[7] $H + C_2H_5SH \rightarrow H_2 + C_2H_5S$

[8] $2\,C_2H_5S \rightarrow C_2H_5SSC_2H_5$

[9] $CH_3S + C_2H_5SSC_2H_5 \rightarrow CH_3SSC_2H_5 + C_2H_5S$

[10] $CH_3SSC_2H_5 + h\nu \rightarrow CH_3S + C_2H_5S$

[11] $C_2H_5SSC_2H_5 + h\nu \rightarrow 2\,C_2H_5S$

exchange processes, involving attack by RS radicals on the S—S disulfide linkage, for which evidence has been given previously (1). As indicated above the secondary photolyses represented by reactions 10 and 11 will become important as the reaction proceeds and the disulfide products accumulate.

The key factor in the interpretation of the results in terms of this mechanism and the relative importance of its component steps is the fundamental difference in the possible reactions of CH_3S and C_2H_5S radicals. Ethylthiyl radicals in this system will have an appreciably longer lifetime since they are regenerated via H-atom

Can. J. Chem. Downloaded from www.nrcresearchpress.com by 210.87.254.6 on 09/05/12
For personal use only.

Can. J. Chem. Downloaded from www.nrcresearchpress.com by 210.87.254.6 on 09/05/12
For personal use only.

abstraction from the ethanethiol present in "solvent-like" concentrations, or via the exchange reaction with the ethyl disulfide product. The analogous reactions of CH_3S radicals, on the other hand, leads to consumption of that species, in converting CH_3S to methanethiol in the reaction with C_2H_5SH, reaction 6, or to methyl ethyl disulfide in reaction 9. Because of the relative concentrations, reaction 6 would be expected to be considerably more important.

In the initial stages of the photochemical reaction both reactions 2 and 3 are important. The disulfide photolysis leads to the chain production of methanethiol through the sequence of reactions 2, 6, 4, 5, and 6, while the photodecomposition of ethanethiol yields C_2H_5S radicals through reactions 3 and 7, which species then participate in the chain propagation steps 4 and 5. As the concentration of CH_3SSCH_3 is reduced, reaction 5 becomes the more important exchange process and thus the yield of the methyl ethyl disulfide product passes through the observed maximum after *ca.* 10 min. The concentration of $CH_3SSC_2H_5$ is also influenced by the secondary photolysis in reaction 10. Methylthiyl radicals produced in this reaction will be converted to CH_3SH via process 6, but CH_3S species following this sequence are much less important than those involved in the exchange reactions. The contribution of reaction 11 is essentially that of reducing the net effectiveness of reaction 8. Again the net result is the same whether C_2H_5S radicals are formed in reaction 11 or reaction 3.

The initial rates of formation of the three products indicate that a chain reaction is operative in this system. Utilizing measured amounts after 5 min exposure, and subtracting the amount of each product formed in the thermal reaction in 35 min (Fig. 2), the *minimum* initial quantum yields are $\Phi^0(CH_3SH) = 151$, $\Phi^0(C_2H_5SSC_2H_5) = 31$, and $\Phi^0(CH_3SSC_2H_5) = 15$. A smaller net contribution from the thermal conversion would increase these values. The maximum values that would apply if the thermal reaction were neglected are 196, 37, and 46 for CH_3SH, $C_2H_5SSC_2H_5$, and $CH_3SSC_2H_5$ respectively. Because of this uncertainty, the Φ values for the two disulfides have not been corrected for the fact that in the first 5 min of reaction each of these products themselves absorbs on the average *ca.* 10% of the incident radiation.

The large quantum yields are definitive evidence for the important role of the thiyl radical – disulfide exchange processes proposed, and, as well, suggest that disulfide production via the chain terminating step 8 and its analog for CH_3S radicals is minor. The efficiency of the exchange process is also evidenced by the fact that even after relatively short exposure times there is sufficient consumption of the "intermediate" methyl ethyl sulfide that its concentration is increasing at a rate very much less than that of CH_3SH.

In the thermal reaction the initiating step is most likely thiyl radical formation from the thermal decomposition of the disulfide since reactions of thiyl radicals formed in this way are observed in disulfide mixtures but not for thiols. The observed similarity of the time dependence of the concentrations in both the photochemical and thermal systems, although much less pronounced in the latter, also suggests that the same subsequent reactions characterize both processes. The rate of the thermal reaction will decline as $[CH_3SSCH_3]$ is reduced, while the photochemical system should exhibit a constant initiation rate since the latter is governed by the *total* thiol–disulfide concentration.

In summary then the thermally or photochemically induced thiyl radical–disulfide exchange process that is known to occur in disulfide mixtures takes place with high quantum efficiencies in thiol–disulfide systems as well. Because of the lability of the sulfhydryl hydrogen in the thiol, however, the thiyl radicals originating with the disulfide component of the mixture are essentially irreversibly converted to the corresponding thiol when the disulfide is present initially in solute proportions and thus the establishment of a simple photochemical equilibrium characteristic of the disulfide mixture systems does not occur.

Disulfide Mixtures

Three series of equimolar mixtures of (*a*) methyl disulfide + ethyl disulfide, (*b*) methyl disulfide + *n*-propyl disulfide, and (*c*) ethyl disulfide + *n*-propyl disulfide were photolyzed and the initial rate of appearance of the only detectable product, the unsymmetrical disulfide, was determined as well as the total irradiation time required to bring the system to photochemical equilibrium. Using the known values

TABLE 1. Effect of substrate on the thiyl radical – disulfide exchange reaction*

	System		
	CH_3SSCH_3–$C_2H_5SSC_2H_5$	CH_3SSCH_3–$C_3H_7SSC_3H_7$	$C_2H_5SSC_2H_5$–$C_3H_7SSC_3H_7$
Relative initial rate of formation of the unsymmetrical disulfide	100	1.9	1.2
Initial quantum yield	355†	6.9	4.4
Relative time to attain photochemical equilibrium	1	44	63

*Photolysis at 254 nm of equimolar mixtures at 25 °C.
†Reference 5.

for mixture *a*, the relative initial rates, absolute quantum yields, and relative time required to attain equilibrium were calculated for mixtures *b* and *c*. The results are summarized in Table 1.

The dramatic decrease in the efficiency of the thiyl radical – disulfide exchange in moving from the methyl disulfide – ethyl disulfide system to the methyl disulfide – *n*-propyl disulfide mixtures may indicate that facile re-orientation of the thiyl radicals in the liquid cage immediately following their formation is a necessary prerequisite if interaction with surrounding disulfide molecules is to occur to a significant extent. However, the change from methyl disulfide – *n*-propyl disulfide to ethyl disulfide – *n*-propyl disulfide results in a much smaller alteration in the overall rate, suggesting that the principal effect in these systems may be a reduced susceptibility of *n*-propyl disulfide itself to the exchange.

These results suggest that the exchange reaction will not be important in mixtures of higher molecular weight disulfides in the liquid phase, including those disulfides of biological importance. Whether the exchange reaction will occur if the thiyl radicals are produced by the photolysis of a thiol or sulfide component added to the mixture could be determined only by further investigations of a variety of higher molecular weight systems. The absence of detectable thiol yields in these systems indicates that a minor role for disproportionation is apparently a general characteristic of all lower molecular weight alkylthiyl radicals.

The authors gratefully acknowledge the assistance of Miss H. Walker who carried out the experiments with the disulfide mixtures. This research was supported by the Defence Research Board of Canada, grant number 1675-07 and by the National Research Council of Canada.

1. K. SAYAMOL and A. R. KNIGHT. Can. J. Chem. **46**, 999 (1968).
2. W. A. PRYOR, J. P. STANLEY, and T. H. LIN. Quart. Rev. Sulfur Chem. **5**, 305 (1970).
3. R. P. STEER and A. R. KNIGHT. J. Phys. Chem. **72**, 2145 (1968).
4. R. P. STEER and A. R. KNIGHT. Can. J. Chem. **47**, 1335 (1969).
5. K. SAYAMOL. M.Sc. Thesis, University of Saskatchewan, Saskatoon, Saskatchewan. 1968.
6. D. R. TYCHOLIZ and A. R. KNIGHT. J. Am. Chem. Soc. In press.
7. L. BRIDGES, G. L. HEMPHILL, and J. M. WHITE. J. Phys. Chem. **76**, 2668 (1972).
8. B. G. DZANTIEV, A. V. SHISKOV, and M. S. UNUKOVICH. Khim. Vys. Energ. **3**, 111 (1969).
9. S. F. BIRCH, T. V. CULLUM, and R. A. DEAN. J. Inst. Petrol. **39**, 206 (1953).
10. DMS U.V. Atlas of organic compounds. Vol. IV. Verlag, London. 1968. p. 6.

Can. J. Chem. Downloaded from www.nrcresearchpress.com by 210.87.254.6 on 09/05/12
For personal use only.

Some Observations on the Hydrolysis of the Amides of Primary α-Acetylenic Amines

JOHN NICHOLSON GARDNER

Technical Development Department, Hoffmann-La Roche Inc., Nutley, New Jersey 07110

Received October 11, 1972

Some amides of primary α-acetylenic amines were made from the corresponding α-acetylenic alcohols by the Ritter reaction. Depending upon the other substituents on the carbon atom bearing nitrogen and the ethynyl group, hydrolysis resulted in formation of the α-acetylenic amine or in hydration of the triple bond to yield a ketone.

Quelques amides d'amines primaires α-acétiléniques ont été préparées par la réaction Ritter sur les alcools α-acétyléniques correspondants. Dépendant de la nature des autres substituants portés par l'atome de carbone portant l'azote et le groupe éthynyle, l'hydrolyse des amides conduit soit à l'amine α-acétylénique ou à l'hydratation de la triple liaison fournissant la cétone.

[Traduit par le journal]

Can. J. Chem., 51, 1416 (1973)

The amide **1** ($R_1 = R_2 = CH_3$) undergoes hydration to **2**, via the oxazolinium salt **3**, upon reaction with aqueous hydrochloric acid (1), but the corresponding formamide derivative **1** ($R_1 = CH_3$, $R_2 = H$) yields, under similar conditions,

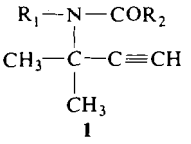

1

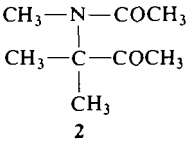

2

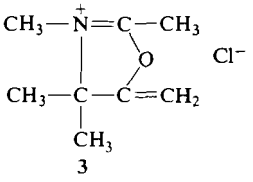

3

the acetylenic amine (1). In contrast the amide **1** ($R_1 = H$, $R_2 = CH_3$) was reported (2) to be insoluble in dilute hydrochloric acid and to yield with the concentrated acid a product in which 3-amino-3-methyl-2-butanone was detected spectroscopically. In the case of **1** ($R_1 = R_2 = H$), almost quantitative hydrolysis to the amine **4** occurs (3) with aqueous mineral acid. Our interest in the efficiency of this last reaction has resulted in observations which extend those already reported.

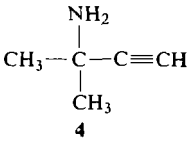

4

We prepared the amide **1** ($R_1 = H$, $R_2 = CH_3$) by the Ritter reaction of acetonitrile with 3-hydroxy-3-methyl-1-butyne, using a modified version of the published procedure (4). We found that upon hydrolysis with sulfuric or hydrochloric acid in aqueous methanol, followed by basification of the reaction mixture and steam distillation, the dihydropyrazine **5** ($R = CH_3$) was formed in good yield. This product was obtained even when the reaction mixture was

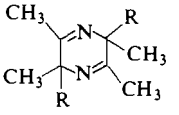

5

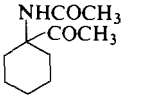

6

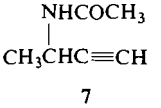

7

carefully adjusted to p*H* 7 prior to the steam distillation, and thus it may be concluded that alkaline conditions are not necessary for its formation. It clearly results from hydration of **1** ($R_1 = H$, $R_2 = CH_3$) to 3-amino-3-methyl-2-butanone and condensation of two molecules of the latter to yield **5** ($R = CH_3$). The formation of dihydropyrazines from α-amino ketones is well documented (5) and conditions for interconversion of these two classes of compound have been recorded (5), so that this reaction sequence provides a convenient route to compounds of these types. A procedure (which has not been optimized) for obtaining **5** ($R = CH_3$) from 3-hydroxy-3-methyl-1-butyne in 54% yield, without isolation of the intermediate amide **1** ($R_1 = H$, $R_2 = CH_3$), is given in the Experimental. The reaction sequence is thus a viable alternative to the recently reported synthesis (5) of **5** ($R = CH_3$), in 37% yield, by

Can. J. Chem. Downloaded from www.nrcresearchpress.com by 210.87.254.105 on 09/05/12
For personal use only.

Can. J. Chem. Downloaded from www.nrcresearchpress.com by 210.87.254.105 on 09/05/12
For personal use only.

reaction of methyl isopropyl ketone with aqueous alkaline potassium ferricyanide. The two procedures are not fully equivalent, however, for although 3-hydroxy-3-methyl-1-pentyne was successfully converted to the dihydropyrazine **5** ($R = C_2H_5$) (isolated as the dihydrochloride), with 1-ethynylcyclohexanol as substrate, the product was the amido ketone **6**. It may be that under more rigorous conditions it would be possible to hydrolyze the amide function in **6** and to obtain the corresponding dihydropyrazine which has been prepared (5) by the reaction of cyclohexyl methyl ketone with ferricyanide.

The conditions for hydrolysis of **1** ($R_1 = H$, $R_2 = CH_3$) which led to **5** ($R = CH_3$) also gave a very minor amount of the amine **4**, which was detected by gas chromatography. It was thus of interest to investigate the hydrolysis of the amide **7** to see whether it yielded the corresponding amine or (through hydration of the triple bond, hydrolysis of the amide, condensation, and autoxidation) 2,3,5,6-tetramethylpyrazine. The product obtained from this reaction was 3-amino-1-butyne hydrochloride. Thus, we may conclude that the behavior of the amides of primary α-acetylenic amines on hydrolysis is critically influenced by alterations in the substituents on nitrogen and on the carbon atom α to the triple bond.

Experimental

2,2,3,5,5,6-Hexamethyl-2,5-dihydropyrazine (5, R = CH_3)

Acetonitrile (500 g) was added with stirring to sulfuric acid (98% w/w, 500 g), while cooling to maintain a temperature of 0–5°. When the addition was complete, the mixture was stirred for 15 min at the same temperature and then 3-hydroxy-3-methyl-1-butyne (250 g) was added slowly while continuing to maintain a temperature of 0–5°. Upon completion of the addition, the solution was brought to 10° and stirred for 2.5 h. Ice (2 kg) was added and the resulting mixture was distilled at atmospheric pressure, using a 20-plate Oldershaw[1] column (reflux ratio 4:2) until the vapor temperature reached 97°. The distillation residue was cooled and, while maintaining < 50° by the addition of ice, sodium hydroxide (50% w/w, 750 ml) was introduced. The resultant alkaline solution was subjected to steam distillation. The dihydropyrazine **5** ($R = CH_3$) (219 g, yield[2] 54%) was isolated from the distillate by filtration, m.p. 88–91° (lit. (5) m.p. 88–89°). The assignment of structure was confirmed by the product's i.r., u.v., n.m.r., and mass spectra.

[1]The column was used as it was desired to recover the excess acetonitrile.

[2]Microanalysis indicated that the material was approximately a hexahydrate, and the yield was calculated on this basis.

N-(3-Methylpent-1-yn-3-yl)acetamide

3-Hydroxy-3-methyl-1-pentyne (75 g) was reacted with sulfuric acid (98% w/w, 150 g) and acetonitrile (150 g) as described for the preparation of **5** ($R = CH_3$). After quenching with ice, the reaction mixture was made alkaline with sodium hydroxide solution (20% w/w), saturated with sodium chloride, and extracted with ether (3 × 600 ml). The extracts were washed with water and brine, then dried (sodium sulfate) and evaporated to dryness. The residue was distilled (b.p. 60–75°/2.0 mm) to yield a distillate (27.5 g) which crystallized. Two recrystallizations from hexane-dichloromethane gave pure *N*-(3-methylpent-1-yn-3-yl)acetamide: m.p. 62–65°; i.r. ($CHCl_3$) 3445, 3300, 1680, and 1500 cm^{-1}; n.m.r. ($CDCl_3$) 0.98 (t, 3, $J = 7$ Hz, CH_3CH_2), 1.60 (s, 3, CH_3C), 1.9 (s, 3, CH_3CO), 2.33 (s, 1, ≡CH), and 5.92 p.p.m. (br, 1, NH).

Anal. Calcd. for $C_8H_{13}NO$: C, 69.03; H, 9.41; N, 10.06. Found: C, 69.16; H, 9.50; N, 9.87.

3,6-Diethyl-2,3,5,6-tetramethyl-3,6-dihydropyrazine Dihydrochloride (5, R = C_2H_5)

The aforegoing amide (5.2 g) in methanol (25 ml) and sulfuric acid (12% w/w, 25 ml) was heated under reflux for 3 h. The mixture was then steam-distilled, 200 ml of distillate being collected. The residue was made alkaline with sodium hydroxide solution (20% w/w, 15 ml) and again steam-distilled, 100 ml of distillate being collected. The distillate was brought to pH 2 by addition of hydrochloric acid (37% w/w) and then evaporated to dryness at reduced pressure. The residue was crystallized from ethanol–ether to yield **5** ($R = C_2H_5$) as a dihydrate (1.9 g): m.p. 196–199°; i.r. (KBr) 1705 and 1570 cm^{-1}; n.m.r. ($CDCl_3$) 1.02 (t, 6, $J = 7$ Hz, CH_3CH_2), 1.68 (s, 6, CH_3C), 2.26 (s, 6, CH_3C=), and 8.86 p.p.m. (br, 6, NH and H_2O).

Anal. Calcd. for $C_{12}H_{24}Cl_2N_2 \cdot 2H_2O$: C, 47.53; H, 9.31; N, 9.24; Cl, 23.38. Found: C, 47.50; H, 9.33; N, 9.20; Cl, 23.68.

N-(1-Acetylcyclohexyl)acetamide 6

N-(1-Ethynylcyclohexyl)acetamide (2, 4) (5.2 g) was heated with sulfuric acid exactly as for the preparation of **5** ($R = C_2H_5$), a reaction time of 15 h being used. The reaction mixture was cooled, diluted with its own volume of water, and made alkaline with sodium hydroxide solution (20% w/w, 25 ml). Extraction with ethyl acetate and crystallization from ethyl acetate – hexane gave **6** (1.9 g): m.p. 140–142° (lit. (2) 133–135°); i.r. ($CHCl_3$) 3445, 1715, 1680, and 1500 cm^{-1}; n.m.r. ($CDCl_3$) 2.02 (s, 3, CH_3CO), and 2.12 p.p.m. (s, 3, CH_3CO).

Anal. Calcd. for $C_{10}H_{17}NO_2$: C, 65.54; H, 9.52; N, 7.64. Found: C, 65.81; H, 9.52; N, 7.65.

N-(But-1-yn-3-yl)acetamide (7)

Acetic anhydride (30 ml) was added slowly to sulfuric acid (98% w/w, 50 ml) while the temperature was held at < 40°. The mixture was cooled and, at 15–25°, but-1-yn-3-ol (14.5 g) in acetonitrile (21 g) was added. The reaction vessel was cooled[3] to hold the temperature at 15–25° and after 7 h at this temperature it was poured onto crushed

[3]The reaction is very slowly exothermic and on one occasion the temperature rose to 175° after the reactants had been mixed and the mixture was thought to be quiescent.

ice (200 g) and, using external cooling, made alkaline with sodium hydroxide solution (50% w/w, 125 ml). The product was isolated by extraction with ether and sublimed at 50–80°/2.0 mm. The sublimate (1.53 g) comprised **7**, sufficiently pure for further reactions. Two recrystallizations from dichloromethane–hexane gave pure **7**: m.p. 94–95°; i.r. ($CHCl_3$) 3450, 3310, 1680, and 1510 cm^{-1}; n.m.r. ($CDCl_3$) 1.23 (d, 3, J = 7 Hz, CH_3CH), 2.00 (s, 3, CH_3CO), and 2.26 p.p.m. (d, 1, J = 2.5 Hz, $\equiv CH$).

Anal. Calcd. for C_6H_9NO: C, 64.84; H, 8.16; N, 12.60. Found: C, 64.87; H, 8.05; N, 12.47.

3-Amino-1-butyne Hydrochloride

Compound **7** (1.17 g) was heated under reflux for 4 h in sulfuric acid (12% w/w, 25 ml). The mixture was cooled to 60°, diluted with water (25 ml), and made alkaline with sodium hydroxide solution (20% w/v, 35 ml). This solution was steam-distilled and the distillate (700 ml) adjusted to pH 3 with hydrochloric acid (37% w/w). The water was evaporated and the residue, dissolved in methanol, was treated with charcoal. The methanol solution was evaporated to dryness and the residue sublimed at 135–140°/0.5 mm. The sublimate was recrystallized from methanol – ethyl acetate to give the amine hydrochloride (370 mg); m.p. 162–165°. Three recrystallizations from the same solvents gave analytically pure material: m.p. 166–169°; i.r. (KBr) 3250 cm^{-1}; n.m.r. (D_2O) 2.02 (d, 3, J = 7 Hz, CH_3CH), and 2.45 p.p.m. (d, 1, J = 2 Hz, $\equiv CH$).

Anal. Calcd. for C_4H_8ClN: C, 45.52; H, 7.64; N, 13.27. Found: C, 45.25; H, 7.39; N, 13.44.

The author is indebted to the staff of the Physical Chemistry Department of Hoffmann-La Roche Inc. for the measurement of spectral data and for microanalyses.

1. N. R. Easton and R. D. Dillard. J. Org. Chem. **28**, 2465 (1963).
2. N. R. Easton, D. R. Cassady, and R. D. Dillard. J. Org. Chem. **30**, 3884 (1965).
3. Belgian Patent 751 189.
4. N. M. Libman and S. G. Kuznetsov. Zh. Org. Khim. **4**, 2122 (1968).
5. D. G. Farnum and G. R. Carlson. Synth. 191 (1972).

Can. J. Chem. Downloaded from www.nrcresearchpress.com by 210.87.254.105 on 09/05/12
For personal use only.

A Facile Reduction of Sulfones to Sulfides

J. N. GARDNER AND S. KAISER
Technical Development Department, Hoffmann-La Roche Inc., Nutley, New Jersey 07110
AND
A. KRUBINER AND H. LUCAS
Chemical Research Department, Hoffmann-La Roche Inc., Nutley, New Jersey 07110
Received October 11, 1972

Diisobutylaluminum hydride is shown to be an effective reagent for the reduction of sulfones to sulfides. Yields as high as 70% are obtained in this normally difficult reduction. A technique for the easy isolation from the reaction mixture of volatile sulfides is described.

Il est montré que l'hydrure de di-iso-butylaluminium est un réactif permettant la réduction facile des sulfones en sulfures. Des rendements aussi hauts que 70% ont été obtenus pour cette réduction qui est normalement difficile. On décrit une technique permettant la récupération facile des sulfures volatiles des mélanges réactionnels. [Traduit par le journal]

Can. J. Chem., **51**, 1419 (1973)

We wish to report that diisobutylaluminum hydride (Dibal-H) is an effective and convenient reagent for the reduction of sulfones to sulfides. Over the past 20 years, only one major paper dealing with conversion of sulfones to sulfides (1) has appeared and, indeed, it is widely recognized that this reduction is a difficult operation. This is unfortunate because sulfones are compounds of potential synthetic utility as a result of the ability of the sulfone moiety to stabilize a negative charge on the carbon atom α to sulfur.

In their paper, Bordwell and McKellin (1) describe the reduction of sulfones with lithium aluminum hydride (LAH) using in most cases 3–9 mol of this reagent per mol of sulfone, which is equivalent to 6–18 times the theoretical amount of active hydrogen. Only in cases of sulfones related to benzothiophene and dibenzothiophene were high yields of the corresponding sulfides obtained when using smaller excesses of the reagent. Furthermore, those sulfides which are relatively volatile (*e.g.*, tetramethylene sulfide) were isolated only as their mercuric chloride complexes.

Our results are presented in Table 1. As may be seen, aliphatic, alicyclic, and aromatic sulfones were reduced using between 2.2 and 5.0 mol of Dibal-H per mol of sulfone. The fact that 2.2 mol of Dibal-H effected almost complete reduction of 1 mol of benzyl methyl sulfone strongly suggests that the stoichiometry of the reaction is as indicated in the equation:

$$R_2SO_2 + 2(C_4H_9)_2AlH \rightarrow R_2S + 2(C_4H_9)_2AlOH$$

This equation implies that the sulfide is formed in a free state and does not require water to liberate it from a complex with the aluminum salts. In agreement with this, we have found that volatile sulfides are conveniently made by reduction of sulfones with Dibal-H in mineral oil, the sulfide being distilled directly from the reaction mixture.

The reactivity of the sulfones with Dibal-H follows a similar order to their reactivity with LAH. Thus, in both cases the alicyclic sulfones with five-membered rings are the most easily reduced, and it is noteworthy that the reaction of Dibal-H with tetramethylene sulfone is quite exothermic. The aliphatic sulfones are the most resistant to reduction, while other compounds listed in Table 1 fall between these two extremes.

None of the reductions reported in Table 1 has been optimized, and in three reactions the products were not isolated. The reduction of 2,5-dihydrothiophene sulfone to 2,5-dihydrothiophene is not a simple reaction as several attempts to improve the yield resulted in none of the desired product. It may be that interaction of the Dibal-H with the double bond occurs under all except carefully defined conditions, and it is interesting to note that Bordwell and McKellin obtained only polymeric material when they attempted to carry out this reduction with LAH. Preparation of 2,5-dihydrothiophene in

Can. J. Chem. Downloaded from www.nrcresearchpress.com by 210.87.254.42 on 09/05/12
For personal use only.

TABLE 1. Reduction of sulfones to the corresponding sulfides

Sulfone	Reaction time (h)	Solvent	Reaction temperature (°C)	Dibal-H mol/mol sulfone	Yield (%)	Footnote
Di-*n*-propyl	72	Toluene	110	4	77	*a, b*
Di-*n*-butyl	72	Toluene	110	3	68	*a, c, d*
Tetramethylene	72	Mineral oil	20–25	3	73	*a, c, e*
2,5-Dihydrothiophene	1.5	Mineral oil	20–25	3	12	*e, f*
Benzyl methyl	18	Toluene	110	2.2	—	*a*
	18	Hexane–Toluene	103	5	61	*a, d, g*
Diphenyl	48	Hexane–Toluene	103	5	57	*a, d, h*
Methyl phenyl	20	Toluene	110	5	61	*a, b*

[a]Identified by g.c. comparison with an authentic sample.
[b]The yield was determined gas chromatographically. A solution containing the authentic product at a concentration similar to its concentration in the reaction product was used as a standard.
[c]Identified by comparison of i.r. spectra.
[d]Product isolated by conventional aqueous procedures.
[e]Product isolated by distillation from the reaction mixture.
[f]See Experimental.
[g]The yield given allows for recovery of 10% of the starting sulfone.
[h]The yield given allows for recovery of 14% of the starting sulfone.

this way may have some synthetic merit if the reaction can be controlled as the normal preparation, by sodium-in-ammonia reduction of thiophene (2), involves the separation of 2,5- and 2,3-dihydrothiophenes.

In contrast to Dibal-H, sodium diethyl aluminum dihydride (OMH-1), which has recently become commercially available, was ineffective in reducing di-*n*-butyl and tetramethylene sulfones under conditions comparable with those under which Dibal-H brought about reduction.

Experimental

Dibal-H was purchased from the Stauffer Chemical Company as an approximately 20% solution in either toluene or hexane. OMH-1 (25% in toluene) was a gift from the Ethyl Corporation, and the attempted reductions with it were carried out in toluene. All the sulfones were commercial materials and were used as received.

Use of Mineral Oil as the Solvent. Tetramethylene Sulfide

Light mineral oil (500 ml) was added to 500 ml of a 23.5% solution of Dibal-H (0.75 mol) in toluene. The mixture was distilled to a residue temperature of 100° at 0.5 mm and then, while this vacuum and temperature were held, nitrogen was passed through the solution for 2 h to remove the last traces of toluene. The mixture was cooled to 20–25° and tetramethylene sulfide 1,1-dioxide (30 g, 0.25 mol) was added slowly while cooling to hold 20–25°. The mixture was stirred for 1.5 h and then distilled to a residue temperature of 125° at 3 mm. The distillate weighed 11.5 g. The reaction mixture was cooled to ambient temperature and again stirred for 72 h.[1] It was then distilled as before to yield a further 10 g of distillate. The combined distillates were redistilled at atmospheric pressure via a 4 in. × 0.5 in. Goodloe column to yield tetramethylene sulfide (16 g, 0.18 mol; 73%); b.p. 121°.

Use of Toluene as the Solvent. Dibutyl Sulfide

A solution of di-*n*-butyl sulfone (44.5 g, 0.25 mol) in toluene (50 ml) was added to 500 ml of a 23.5% solution of Dibal-H (0.75 mol) in toluene. The mixture was heated under reflux for 72 h and cooled to room temperature, and ethanol (50 ml) was cautiously added, followed by water (200 ml), and concentrated hydrochloric acid (100 ml). The organic layer was separated and washed with water (2 × 50 ml). The solvent was distilled off at atmospheric pressure and the residue was distilled through a Vigreux column to yield the sulfide (18 g); b.p. 69°/11 mm. G.c. evaluation of the residue from fractionation of the recovered solvent detected another 6.8 g of sulfide, giving a total yield of 24.8 g (0.17 mol; 68%).

2,5-Dihydrothiophene

A solution of Dibal-H (0.75 mol) in mineral oil (500 ml) was prepared as in the preparation of tetramethylene sulfide. To this at 20° was added slowly 2,5-dihydrothiophene 1,1-dioxide (30 g, 0.25 mol), the mixture being cooled as required. When the addition was

[1]This time was determined purely on the basis of convenience.

Can. J. Chem. Downloaded from www.nrcresearchpress.com by 210.87.254.42 on 09/05/12
For personal use only.

complete, the reaction mixture was stirred for 1.5 h and then distilled to a residue temperature of 150° at 4 mm. The distillate weighed 10 g. Stirring for another 18 h and distillation gave no additional distillate. The distillate was redistilled at atmospheric pressure through a 4 in. × 0.5 in. Goodloe column to yield 2,5-dihydrothiophene (2.7 g, 0.03 mol; 12%) assaying 92.4% by g.c.; b.p. 122°; n_D^{20} 1.5279; n.m.r. ($CDCl_3$) δ 3.73 (s, 4, CH_2) and 5.83 p.p.m. (s, 2, CH=); Raman (neat liquid) 1630 cm^{-1} (C=C); i.r. ($CHCl_3$) 1638 cm^{-1} (C=C) (lit. (2), b.p. 122.3°; n_D^{20} 1.5306).

Anal. Calcd. for C_4H_6S: C, 55.77; H, 7.02; S, 37.22. Found: C, 55.63; H, 7.15; S, 36.92.

1. F. G. BORDWELL and W. H. MCKELLIN. J. Am. Chem. Soc. **73**, 2251 (1951).
2. S. F. BIRCH and D. T. MCALLAN. Nature, **165**, 899 (1950).

Can. J. Chem. Downloaded from www.nrcresearchpress.com by 210.87.254.42 on 09/05/12
For personal use only.

Theory of Molecular Size Distribution in Multichain Polymers: Condensation of $R—A_f$ with $R'—B_{f'}$, and $R—A_f$ with $R'—A_{f'}$ [1]

S. G. WHITEWAY, I. B. SMITH, AND C. R. MASSON

Atlantic Regional Laboratory, National Research Council of Canada, Halifax, Nova Scotia

Received February 7, 1972[2]

Expressions are derived for the mole fractions of various oligomers formed by condensation of the monomer $R—A_f$ with the monomer $R'—B_{f'}$. It is assumed that A groups can react only with B groups and that intramolecular condensation may be neglected. The results, for cases where comparison is possible, agree with those derived previously for the self-condensation of $R—A_f$. In addition, expressions are derived for the condensation of $R—A_f$ with $R'—A_{f'}$, where A groups react with one another.

Des expressions sont déduites en ce qui a trait aux fractions molaires de plusieurs oligomères formés par condensation du monomère $R—A_f$ avec le monomère $R'—B_{f'}$. On suppose que les groupes A peuvent réagir seulement avec les groupes B et que la condensation intra moléculaire peut être négligée. Les résultats, pour les cas où une comparaison est possible, sont en accord avec ceux obtenus antérieurement pour la condensation sur lui-même du monomère $R—A_f$. De plus, des expressions sont déduites pour la condensation de $R—A_f$ avec $R'—A_{f'}$, où les groupes A réagissent les uns avec les autres.

[Traduit par le journal]

Can. J. Chem., 51, 1422 (1973)

In previous publications (1–3) we derived an expression for the molecular size distribution in multichain polymers formed by self-condensation of the monomer $R—A_f$, where A is a functional group. The method is based on probability considerations, and the result is a particular solution of the Bernoulli binomial probability function. In the above publications the method was discussed from a particular point of view, and the first purpose of this paper is to outline the method briefly in alternative terms. To test this expression experimentally we require polymerizing systems whose characteristics resemble closely those assumed for the model. Some inorganic polymers (silicates) fulfill these conditions and thermodynamic data on these systems agree with the size distribution predicted using our expression (4). However, organic polymers are not well suited for the purpose of investigating quantitatively the self-condensation of $R—A_f$ monomers, and conclusive experiments along these lines have never been performed. The second purpose of this communication is to extend the theoretical treatment to models not treated in the previous work, anticipating that the results can be tested by experiments performed on organic as well as inorganic polymers.

Self Condensation of $R—A_f$

When monomers of type $R—A_f$ condense without intramolecular condensation, molecules of the type shown in Fig. 1 are formed for $f = 3$. If N_0 = number of molecules of monomer RA_f at the beginning of self-condensation, N = total number of molecules after condensation, α = fraction of A groups initially present that have reacted to form AA groups and f = functionality of monomers RA_f, then

$$N = N_0\left(1 - \frac{\alpha f}{2}\right) \qquad [1]$$

It is important to note that N is independent of the distribution of molecular sizes.

The method used to determine the most probable distribution may be described as an

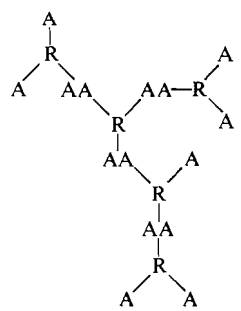

FIG. 1. Polymer formed by self-condensation of the monomer $R—A_3$.

[1]NRCC No. 12998.

[2]Revision received September 8, 1972.

Can. J. Chem. Downloaded from www.nrcresearchpress.com by 210.87.254.6 on 09/05/12
For personal use only.

Can. J. Chem. Downloaded from www.nrcresearchpress.com by 210.87.254.6 on 09/05/12
For personal use only.

imaginary process of cutting the molecules into fragments and reassembling these by a method which simulates the original random condensation. It is understood, of course, that no attempt is made to reassemble the fragments in their original juxtaposition. Repeated assembly will cause any particular A group, if it could be distinguished from the others, to occur in a different location each time; however, if N_0 is large the same distribution of molecular sizes will result each time. The final step is counting the number of molecules of each size. A virtue of the method is that the numbers of molecules of different types are continually kept in the forefront, so that the calculation of mole fractions is direct. The best way of "cutting" the molecules so that there is no ambiguity about how the parts can be reassembled is to allow the R groups to carry the linkages. Thus molecules of the type shown in Fig. 1 are separated into fragments of the types A—R$\langle$, AA—R$\langle$ and A. Except when $f = 1$, each molecule of size x units (an x-mer) has only one fragment of type A—R$(f-1)$—, $(x-1)$ of type

$$\text{AA—R}(f-1)\text{—}$$

and $(fx - 2x + 1)$ of type A. The entire system of N_0 structural units has $N_0(1 - \alpha f/2)$ fragments of the first type, $N_0\alpha f/2$ of the second and $N_0(f - \alpha f/2 - 1)$ of the third type. (For the situation $f = 1$, of course, not all molecules contain fragments of type A—R$(f-1)$—, so that the above expressions do not apply. This situation is discussed later.)

Reassemblage of these fragments into structures whose size distribution resembles the original requires N molecules. The correct way to achieve this is to let each of the

$$NA\text{—R}(f-1)\text{—}$$

fragments start one molecule.[3] The logic of this step is fundamentally important and deserves elaboration here. Each molecule, in terms of size and configuration, may be regarded as an assembly of fragments arranged relative to one datum fragment. A particular x-mer can then be described on the basis of how all other fragments are arranged relative to the chosen one, which, of course, may be any one of the fragments *known* to be in that x-mer. For example, a 5-mer, $f = 3$, contains 1 A—R$\langle$, 4 AA—R$\langle$, and 6 A fragments. Because all are known to exist in that x-mer, any one of those 11 may be chosen as the datum around which the 42 different 5-mer configurations may be developed. However, if the distribution of x-mers is not stipulated in advance, but rather the process of assembling the molecules is begun and allowed to develop in a random way, the principle of equal reactivity requires that no molecule may have any artificial restriction imposed on its development. For example, no structure may be started by an AA—R$(f-1)$— fragment because the final molecule would have no statistical chance of being a monomer. On the other hand, it is certain that every molecule contains a fragment of the type A—R$(f-1)$—, and therefore it is the datum around which any molecule can be developed. The first step, therefore, is to begin construction of the molecules with a fragment whose probability of occurrence in every molecule is unity. (Other cases will be discussed where this fragment differs from A—R$(f-1)$—, but the basic principle remains the same.)

After N fragments of the type A—R$(f-1)$— have been allotted to starting the N structures, the remaining $N_0\alpha f/2$ fragments of the type AA—R$(f-1)$— and $N_0(f - \alpha f/2 - 1)$ of type A together form a pool from which the uncommitted fragments may be drawn in a random fashion in order to develop the structural patterns. The chance, p_{AA}, of selecting a fragment of the type AA—R$(f-1)$— at random from this pool is $\alpha f/2(f-1)$, while that of selecting a fragment of type A is $1 - p_{AA}$. Structures are developed by filling the reactive sites, consecutively, by AA—R$(f-1)$— or A fragments according as they are withdrawn at random from this pool of uncommitted fragments. The mole fractions of the various x-mers follow directly from this scheme, as has been shown in detail in ref. 1, merely by counting the number of the various species.

Self Condensation of R—A

It should be noted that the above scheme cannot be used directly when $f = 1$ because there

[3]It should be reemphasized that these A—R$(f-1)$— fragments, previously named the "committed" groups (1), do not lead a special existence. If the molecules are cut and reassembled repeatedly each A group of the system occasionally becomes part of one of the N A—R$(f-1)$— fragments.

Can. J. Chem. Downloaded from www.nrcresearchpress.com by 210.87.254.6 on 09/05/12
For personal use only.

is no A-containing fragment common to all molecules. (R—A cannot be developed to yield dimer because it is already a stable monomer; R—AA will yield only dimer.) In this case molecules are cut into R—, A, and AA—R. They are reassembled beginning with the N R— fragments, as the probability is unity that every molecule contains at least one R— fragment. All the A and AA—R fragments are in the pool of uncommitted groups, and p_{AA} is $\alpha/2 - \alpha$. The mole fractions of the two possible structures follow directly from this scheme: $N_{monomer} = 2(1 - \alpha)/(2 - \alpha)$; $N_{dimer} = \alpha/(2 - \alpha)$. The correctness of these expressions may, of course, be verified by inspection for this special situation. While this is a trivial case, it is somewhat similar to a more important one which also cannot be treated directly by the method described: this is the condensation of R—A_f and R′—$B_{f'}$ units to yield polymers of which Fig. 2 is an example ($f = 4, f' = 2$).

Condensation of R—A_f with R′—$B_{f'}$

Molecules of the kind shown in Fig. 2 can, in general, be cut into imaginary fragments of the type A—R($f - 1$)—, B—R′($f' - 1$)—, AB—R′($f' - 1$)—, BA—R($f - 1$)—, A and B. However, no single fragment can be associated with every possible molecule: *e.g.* A—R($f - 1$)— cannot be used to start the reassembly of all the molecules as the monomer R′—$B_{f'}$ cannot be constructed; nor can B—R′($f' - 1$)— be used for the corresponding reason.

By an obvious extension of the basic method the way to determine the distribution in these cases is to reassemble the molecules by two schemes starting from two different datum points. Some of the molecules are started with fragments of the type A—R($f - 1$)— while the remainder are started with B—R′($f' - 1$)—. For each of these schemes, as the structures are developed, sites must be filled by either, on one hand, AB—R′($f' - 1$)— or A fragments, or on the other by BA—R($f - 1$)— or B fragments. Thus there must be two separate pools of uncommitted fragments. Some molecules (for example the monomers, as mentioned above) are reassembled by only one of the two schemes. Most molecules will occur in each scheme, and their numbers must be added. It is apparent that the molecular size distribution which will result from operation of such a process is greatly dependent on the relative numbers of molecules started in each scheme. It is important, therefore, that these relative numbers be correctly deduced, in a statistical sense, from α_A and α_B (α_A, α_B = fraction of A or B groups initially present that have reacted, in condensation of RA_f with R′$B_{f'}$), so that no artificial restraint is imposed on the system.

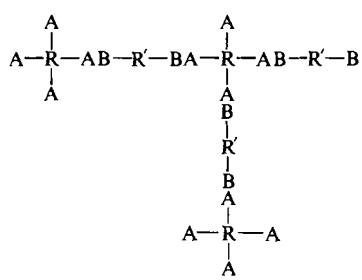

FIG. 2. Polymer formed by condensation of monomer R—A_4 with monomer R′—B_2.

If we define the number of structural units (at the beginning of their condensation) of type R—A_f to be N_A and the number of R′—$B_{f'}$ units to be N_B, and further take $N_B = rN_A$, $f' = qf$, then expressions 2–6 are deduced readily.

$$\alpha_B = \alpha_A/qr \qquad [2]$$

$$\text{Number of molecules} = N = N_A(1 + r - \alpha_A f) \qquad [3]$$

Defining μ_A = fraction of all unreacted groups that are A;

$$\mu_A = \frac{1 - \alpha_A}{1 + qr - 2\alpha_A} \qquad [4]$$

Considering only the stoichiometric range, where α_A and α_B mutually < 1, we have

$$(\alpha_A)_{max} = (1 + r)/f \qquad [5]$$

$$(\alpha_B)_{max} = \left(1 + \frac{1}{r}\right) \Big/ f' \qquad [6]$$

In general we expect X, the fraction of molecules which must be started by fragments of the type A—R($f - 1$)—, to be a function of α_A. The solutions of this function at the lower and upper limits of α_A may be written immediately. When $\alpha_A = 0$, then N_A molecules must be started by fragments of the type A—R($f - 1$)—, and $X = N_A/N = 1/1 + r$. On the other hand if α_A approaches $(\alpha_A)_{max}$ (for conditions where both $(\alpha_A)_{max}$ and $(\alpha_B)_{max} \leqslant 1$) then the system approaches one very large molecule. The fraction of unreacted A groups on this molecule is μ_A, hence at this limit of $\alpha_A = \alpha_{max}$, $X = \mu_A$. As-

Can. J. Chem. Downloaded from www.nrcresearchpress.com by 210.87.254.6 on 09/05/12
For personal use only.

suming that X is a linear function of α_A between these limits, we have

$$[7]\quad X = \frac{1}{1+r} \times \left[1 + f\alpha_A\left(\frac{\alpha_A - r\alpha_A - qr + r}{(1+r)(1+qr-2\alpha_A)}\right)\right]$$

In addition, if Y = the fraction of molecules that must be started by fragments of the type B—R′(f' − 1)—, then

$$[8]\quad Y = 1 - X$$

If the number of molecules started by A—R(f − 1)— and B—R′(f' − 1)— are designated n_A and n_B, then

$$[9]\quad n_A = XN = XN_A(1 + r - \alpha_A f)$$

and

$$[10]\quad n_B = (1 - X)N = YN_A(1 + r - \alpha_A f)$$

All the remaining groups are uncommitted to specific locations in the molecules and must be assigned to these locations at random. All locations, whether in molecules started by fragments of the type

A—R(f − 1)— or B—R′(f' − 1)—,

are of two types: (*1*) those which can be filled only after choosing, in a random fashion, between A and AB—R′(f' − 1)—, and (*2*) those which can be filled after choosing between B and BA—R(f − 1)—. Two pools of fragments must be established, corresponding to these two types of locations. The first pool contains the uncommitted $fN_A(1 - \alpha_A) - n_A$ fragments of type A and $N_B - n_B$ of type AB—R′(f' − 1)—; choosing between these two yields fragments which are chemically correct for filling locations (denoted by ○) of the type ----R○. The second pool contains the uncommitted $f'N_B(1 - \alpha_B) - n_B$ fragments of type B and $N_A - n_A$ of type BA—R(f − 1)—; either may fill locations of the type ----R′○. In the first pool the probability, p_{AB}, of choosing at random a fragment of type AB—R′(f − 1)— is

$$[11]\quad p_{AB} = \frac{N_B - n_B}{N_B - n_B + fN_A(1 - \alpha_A) - n_A} = \frac{r - Y(1 + r - \alpha_A f)}{f - 1}$$

In the second pool the probability, p_{BA}, of choosing a fragment of the type BA—R(f − 1)— is

$$[12]\quad p_{BA} = \frac{N_A - n_A}{N_A - n_A + f'N_B(1 - \alpha_B) - n_B} = \frac{1 - X(1 + r - \alpha_A f)}{r(q f - 1)}$$

The use of these equations may be illustrated for the case where $f = 4$ and $f' = 2$, which yields molecules of the type illustrated in Fig. 2. NX molecules are started, as in Fig. 3, by fragments of type A—R≤ while in Fig. 4 NY molecules are started by B—R′—. (For convenience the R and R′ groups are not shown.) Reactive sites which must be filled by either A or AB—R′— are depicted by circles, while those to be filled

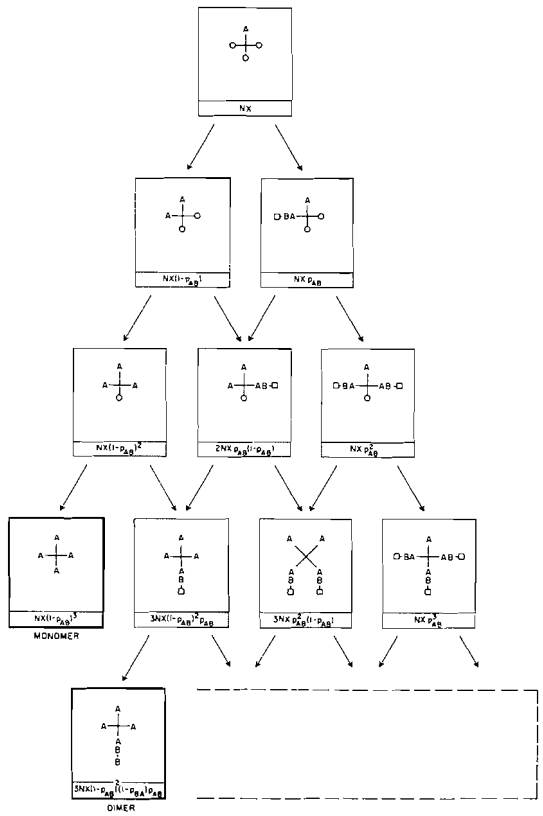

FIG. 3. Derivation of molecular size distribution for polymers started from the fragment A—R≤. Each circle denotes the site of an A or AA—R≤ fragment. Each square denotes the site of a B or BB—R′— fragment. The number in each box is the number of molecules of that structure. For convenience, the R and R′ groups are not shown.

Can. J. Chem. Downloaded from www.nrcresearchpress.com by 210.87.254.6 on 09/05/12
For personal use only.

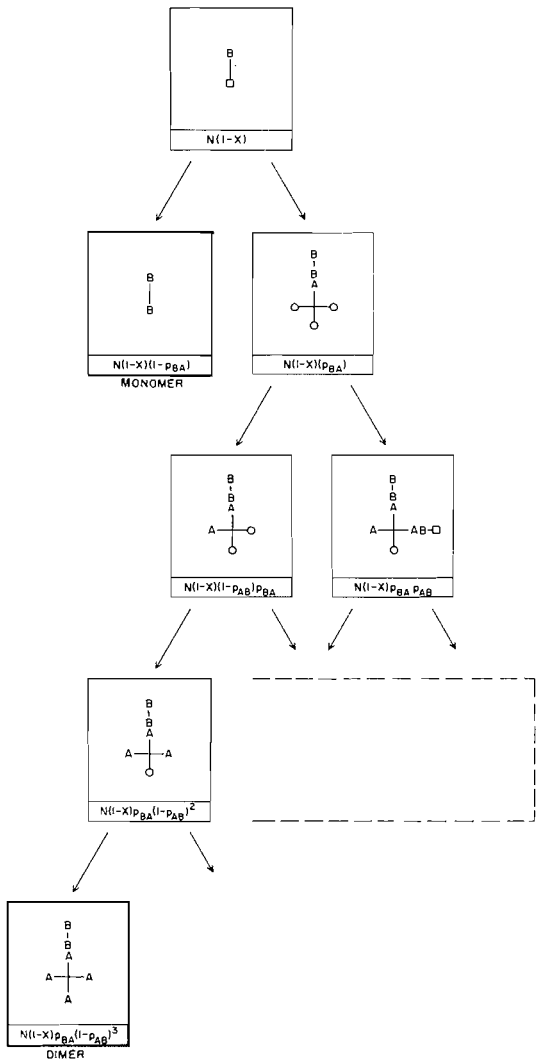

FIG. 4. Derivation of molecular size distribution for polymers started from the fragment B—R′—, with the same symbolism as for Fig. 3.

by either B or BA—R$\lessdot$ are depicted by squares. Sites are filled by removing fragments at random from the appropriate pools; various completed structures, and their number, are shown in the heavily bordered boxes. The mole fractions of these completed structures are obtained from the numbers of molecules in each box, the numbers in Figs. 3 and 4 being added when the same molecule occurs in both. These total numbers are divided by N to obtain the mole fraction. The mole fractions of monomer developed in Figs. 3 and 4, as well as of a few larger molecules,

TABLE 1. Mole fractions of selected oligomers of type $(A_4)_i(B_2)_j$

Molecule	Mole fraction
Monomer A	Xc^3
Monomer B	Yd
Dimer AB	$3Xac^2d + Ybc^3$
Trimer ABB	$3Xa^2cd^2 + 3Yabc^2d$
Trimer AAB	$3Xabc^5$
Tetramer ABBB	$Xa^3d^3 + 3Ya^2bcd^2$
Tetramer AABB	$15Xa^2bc^4d + 3Yab^2c^5$
Pentamer ABBBB	Ya^3bd^3
Pentamer AABBB	$30Xa^3bc^3d^2 + 15Ya^2b^2c^4d$
Pentamer AAABB	$12Xa^2b^2c^7$

are given in Table 1. To simplify, we define $p_{AB} = a$, $p_{BA} = b$, $(1 - p_{AB}) = c$, $(1 - p_{BA}) = d$; a is therefore the probability of selecting an AB—R′(f' − 1)— in a choice between A and AB—R′(f' − 1)—, is the probability of selecting a BA—R(f − 1)— in a choice between B and BA—R(f − 1)—, c is the probability of selecting an A in same choice as for p_{AB}, and d is the probability of selecting a B in same choice as for p_{BA}. Molecules are written as combinations of A and B (*i.e.*, R—A_4 = A, R′—B_2 = B, etc.).

To calculate mole fractions from Table 1, X and Y are calculated from eqs. 7, 8 and a, b, c, d, from eqs. 11 and 12. Figures 5–8 show mole fractions of various species versus α_A for values of r of 1, 1.25, 2, and 3. The values $r = 1$ and $r = 3$ are the limits of the stoichiometric range. At each limit the mole fraction of the appropriate monomer just goes to zero as $\alpha = \alpha_{max}$. For intermediate values of r the mole fraction of each monomer is finite when $\alpha = \alpha_{max}$. The mole fractions of the various polymers are consistent with their relative complexity. For most cases (although this is not universal as for the previous simple case of condensation of R—A_f units (1)) one of the monomers is the most numerous species. Figure 9 is also for the case where $r = 2$, but drawn to a larger scale than Fig. 7 and with the monomers omitted and the trimers, tetramers, and pentamers separated into their main isomers. It is interesting that the theory predicts that at values of α larger than 0.55 the total mole fraction of trimer exceeds that of the dimer.

No attempt is made here to derive a general expression for the mole fraction of an x-mer. In general such an expression would be the combination of two particular solutions of the Bernoulli probability function; Figs. 3 and 4 represent a diagrammatic approach to these solutions.

Can. J. Chem. Downloaded from www.nrcresearchpress.com by 210.87.254.6 on 09/05/12
For personal use only.

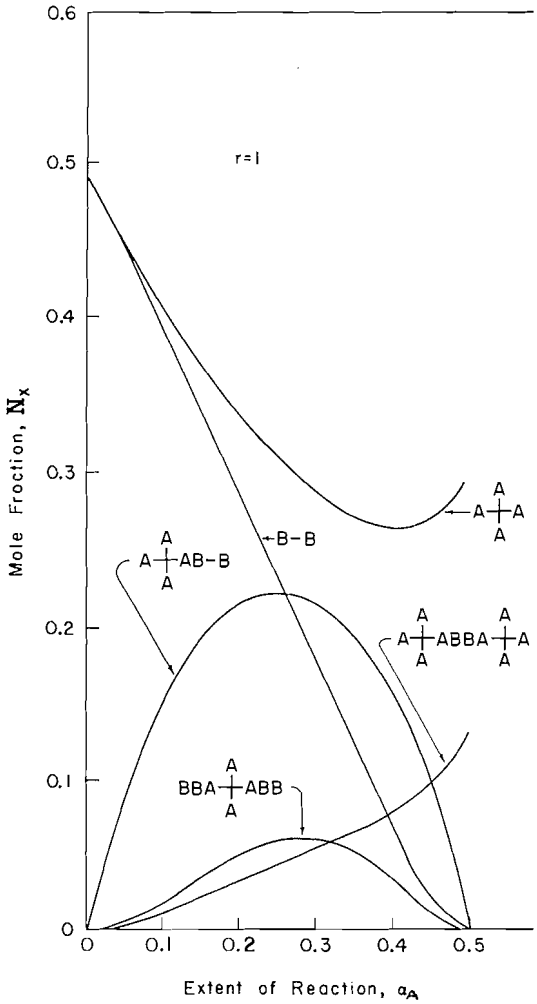

FIG. 5. Mole fractions of various oligomers when r, the ratio of R′—B_2 to R—A_4, is unity.

Distributions for cases where r is outside the stoichiometric range are not given by the above equations, but may be derived readily.

A particularly simple case arises when $r = 1$, $q = 1$, for we begin with equal numbers of equi-functional structural units. When $f = 3$, we have $X = Y = \frac{1}{2}$ and $p_{AB} = p_{BA} = 3\alpha_A/4$. The two schemes for the reassembly of the molecules corresponding to Figs. 3 and 4 are readily constructed, and the mole fractions of the monomers R—A_3 and R′—B_3 each become $\frac{1}{2}(1 - 3\alpha_A/4)^2$. If now we say that the starting units R—A_3 and R′—B_3 are identical we obtain for the mole fraction of monomer $(1 - 3\alpha/4)$, a result identical with that derived directly for the self-condensation of R—A_3. An even more simple case is the one where $f = f' = 2$ and $r = 1$. There $X = Y = \frac{1}{2}$ and $p_{AB} = p_{BA} = \alpha_A$. This equality between α and p occurred before (1) for the condensation of R—A_2.

The expressions given above may be compared with the result of Stockmayer (5) for this system. His p_A, p_B are equivalent to our α_A, α_B and his eq. 2 yields mole fractions when divided by the number of molecules, *e.g.* our eq. 3. For the case considered before, *i.e.*, $f = 4, f' = 2, r = 2$, Stockmayer's expression becomes, in our terminology

$$[13] \quad N_{n,l} = \frac{4[3n]![1 - \alpha_A]^{2+2n}[\alpha_A]^{n+l-1}}{n![3n - l + 1]![l - n + 1]![3 - 4\alpha_A]}$$

where $N_{n,l}$ is the mole fraction of mixed poly-

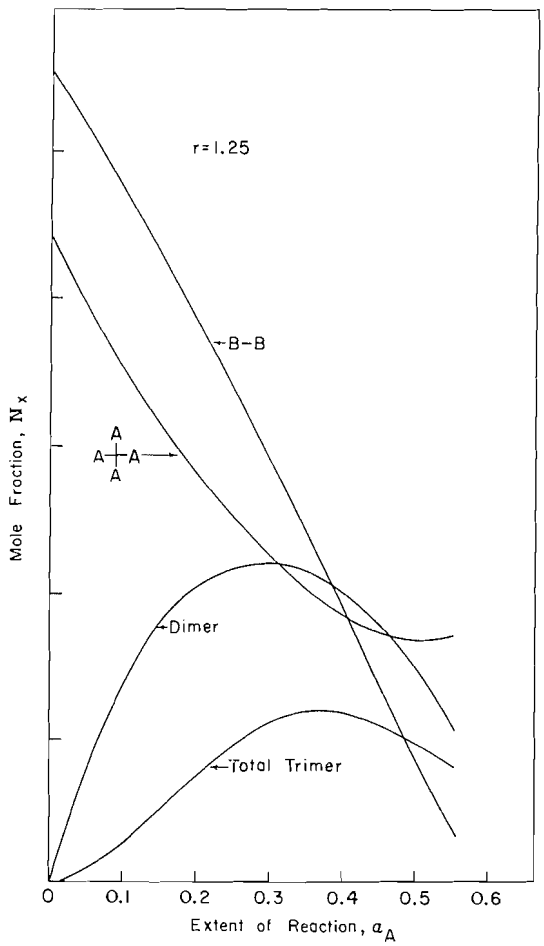

FIG. 6. Mole fractions of various oligomers when $r = 1.25$.

Can. J. Chem. Downloaded from www.nrcresearchpress.com by 210.87.254.6 on 09/05/12
For personal use only.

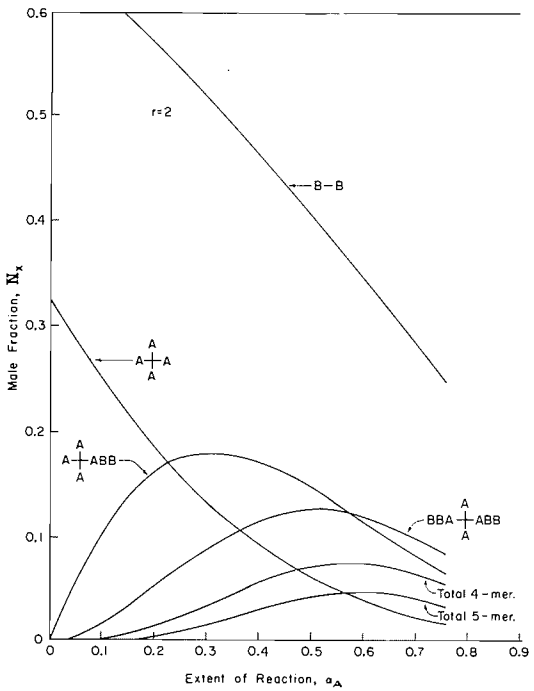

FIG. 7. Mole fractions of various oligomers when $r = 2$.

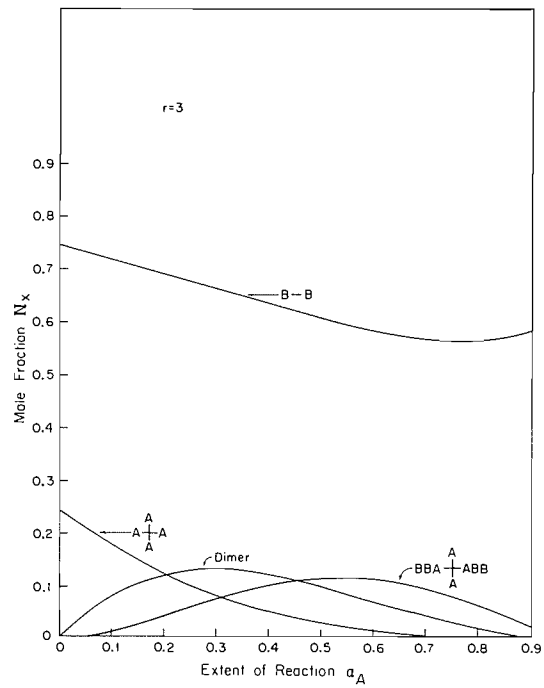

FIG. 8. Mole fractions of various oligomers when $r = 3$.

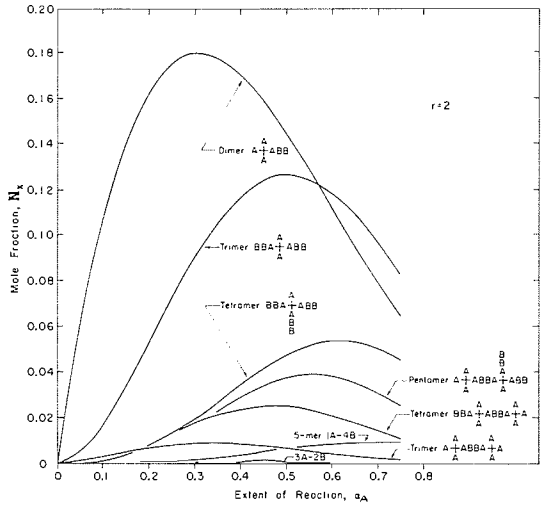

FIG. 9. Mole fractions of dimer, trimer, tetramer and pentamer, showing the various amounts of the isomers.

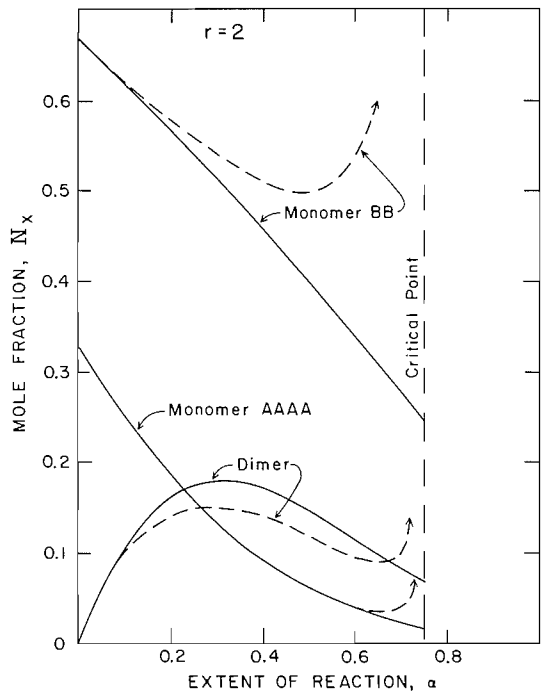

FIG. 10. Mole fractions of various oligomers for $r = 2$. Solid lines, this theory. Dashed lines, theory of Stockmayer.

mer containing nR (tetrafunctional units) and lR (bifunctional units). Figure 10 compares the results of this equation with the present work for the two monomer molecules and the dimer. The main difference is that Stockmayer's equation yields mole fractions which become infinite

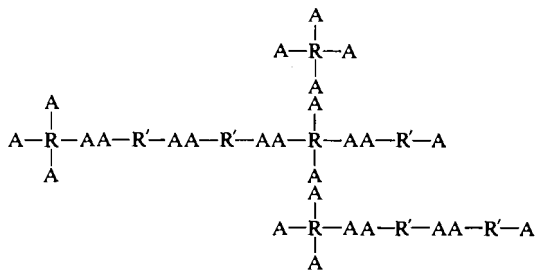

FIG. 11. Polymer formed by condensation of monomer R—A_4 with monomer R′—A_2.

when $\alpha_A = \alpha_{max}$ (0.75 for this system) because the term in the denominator $(3 - 4\alpha_A)$ becomes zero. This is discussed further in the next section.

Condensation of R—A_f with R′—$A_{f'}$

This condensation yields polymers of the type shown in Fig. 11. Expressions derived for this case are important for examining the distributions in silicophosphate and borosilicate glasses.

Molecules of the kind shown in Fig. 11 can, in general, be cut into

$$\text{A—R}(f-1)\text{—},\ \text{A—R}'(f'-1)\text{—},$$

$$\text{AA—R}(f-1)\text{—},\ \text{AA—R}'(f'-1)\text{—},\ \text{and A.}$$

Again no single fragment can be associated with every possible molecule and the molecules must be reassembled by two schemes. We define the number of structural units of type R—A_f to be N_A, the number of type R′—$A_{f'}$ to be M_A, at the beginning of their condensation, and further take $M_A = rN_A, f' = qf$. The following expressions are deduced readily

[14] Number of molecules $= N$

$$= N_A\left[1 + r - \frac{\alpha f}{2}(1 + qr)\right]$$

[15] $$(\alpha_A)_{max} = 2(1 + r)/f(1 + qr)$$

We define X to be the fraction of molecules which must be started by fragments of type A—R$(f-1)$— and Z the remaining fraction which are started by A—R′$(f'-1)$—. As before we determine X as a function of the stoichiometry of the system. When $\alpha_A = 0$ then N_A molecules must be started by these fragments, and $X_{\alpha_A=0} = 1/1 + r$. When α_A approaches $(\alpha_A)_{max}$ the system has condensed to one very large molecule. During this condensation the parts of it composed of R(f)— units exposed $N_A(f-1)$ sites where fragments could be attached while the R′(f')— parts exposed $M_A(f'-1)$ such sites. Therefore the fraction of the A fragments attached to R (and which is also $X_{(\alpha_A=max)}$) is $(f-1)/(f-1+rf'-r)$. Assuming that X is a linear function of α_A between these limits we have

[16] $$X = \frac{1}{1+r} \times \left[1 + \frac{rf^2\alpha(1-q)(1+rq)}{2(1+r)(f-1+rqf-r)}\right]$$

If the number of molecules started by

$$\text{A—R}(f-1)\text{— and A—R}'(f'-1)\text{—}$$

are designated by n_A and m_A, then

[17] $$n_A = XN = XN_A\left[1 + r - \frac{\alpha f}{2}(1 + qr)\right]$$

[18] $$m_A = (1 - X)N = ZN_A \times \left[1 + r - \frac{\alpha f}{2}(1 + qr)\right]$$

None of the remaining fragments has unit probability of being in a specific site relative to the datum site, hence these fragments must be assigned to positions at random. All sites contain AA—R$(f-1)$—, AA—R′$(f'-1)$—, or A, hence the pool of uncommitted fragments must contain all three. In this pool the number of A fragments is the original number minus $n_A + m_A$; expressed as u, this is

[19] $$u = N_A\left[(1-\alpha)(f + f'r) - 1 - r + \frac{\alpha f}{2}(1 + qr)\right]$$

The AA—R$(f-1)$— fragments equal the number of R's remaining after the A—R$(f-1)$— fragments have been committed (eq. 17) and expressing this as v

[20] $$v = N_A - XN$$

Similarly the number of AA—R′$(f'-1)$— fragments in the pool is given by w

[21] $$w = rN_A - ZN$$

Defining the probabilities in the pool of uncommitted fragments as

p_1 = probability of selecting an AA—R$(f-1)$—

Can. J. Chem. Downloaded from www.nrcresearchpress.com by 210.87.254.6 on 09/05/12
For personal use only.

p_2 = probability of selecting an AA—R′(f' − 1)—

p_3 = probability of selecting an A

we may write

[22] $p_1 = v/u + v + w$

[23] $p_2 = w/u + v + w$

[24] $p_3 = u/u + v + w$

As a specific example it is convenient to take as before $f = 4$, $f' = 2$, $r = 2$, $q = 1/2$. The above expressions become

[25] $N = N_A(3 - 4\alpha)$

[26] $X = (15 + 16\alpha)/45$

[27] $Z = (30 - 16\alpha)/45$

[28] $p_1 = [45 - (3 - 4\alpha)(15 + 16\alpha)]/225$

[29] $p_2 = [90 - (3 - 4\alpha)(30 - 16\alpha)]/225$

[30] $p_3 = (5 - 4\alpha)/5$

Two schemes are started, one by XN A—R< fragments, the other by ZN A—R′— fragments. The schemes are developed as in Figs. 3 and 4 but here there are more structures because each gives rise to three other structures. The mole fractions of a few molecules are shown in Table 2, and in Fig. 12. To simplify, molecules are written as combinations of A_4 and A_2. The chief difference between the distribution of this case and that of condensation of RA_4 with $R'B_2$ is the presence of additional molecules such as A_2A_2, A_4A_4 as well as the effect of these molecules upon the mole fraction of monomers, due to the equilibria involved. Thus dimer A_2A_2 is produced chiefly at the expense of monomer A_2, while the relative decrease in dimer A_4A_2 is reflected by the increase in A_4.

TABLE 2. Mole fractions of selected oligomers of type $(A_4)_i(A_2)_j$

Molecule	Mole fraction
Monomer A_4	p_3^3X
Monomer A_2	p_3Z
Dimer A_4A_2	$3p_3^3p_2X + p_1p_3^3Z$
Dimer A_4A_4	$3p_3^5p_1X$
Dimer A_2A_2	p_2p_3Z
Trimer $A_2A_2A_2$	$p_2^2p_3Z$
Trimer $A_4A_4A_4$	$6p_1^2p_3^7X$
Trimer $A_2A_4A_4$	$9p_3^5p_1p_2X + 3p_3^5p_1^2Z$
Trimer $A_2A_4A_2$	$3p_3^3p_2^2X + 2p_1p_3^3p_2Z$
Trimer $A_4A_2A_4$	$3p_3^5p_2p_1X$
Trimer $A_2A_2A_4$	$3p_3^3p_2^2X + 2p_1p_2p_3^3Z$

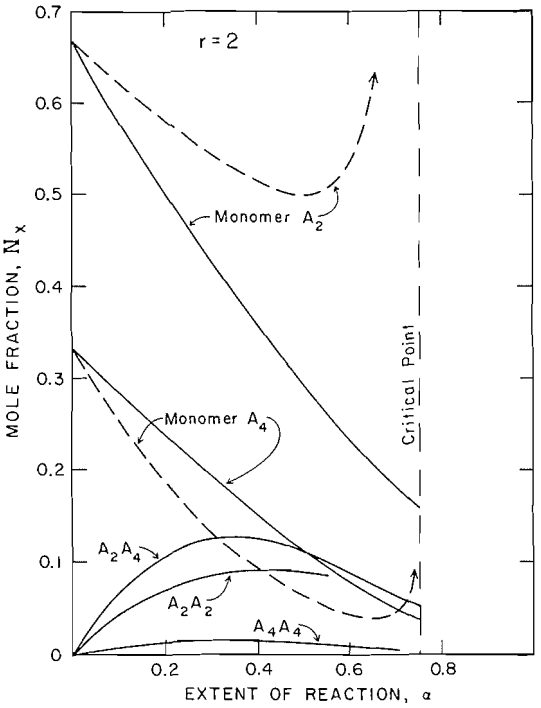

FIG. 12. Mole fractions of various oligomers for $r = 2$ for the condensation of R—A_4 with R′—A_2. Solid lines, this theory. Dashed lines, theory of Flory and Stockmayer.

Stockmayer (6) and Flory (ref. 7, p. 393) give the size distribution for the condensation of R—A_f with R′—A_2. It should be noted that their "p" is equal to our "α", and their ρ is related to our r as follows: $\rho = f/(f + 2r)$. For the example used above their equation becomes:

$$[31]\quad N_{n,l} = \frac{4(l + 3n)!(1 - \alpha)^{2+2n}(\alpha/2)^{n+l-1}}{l!n!(2n + 2)!(3 - 4\alpha)}$$

The results of this expression for the two monomers are shown also in Fig. 12. Again, a major difference between their mole fraction and ours is the behavior as $\alpha \to \alpha_{max}$; our mole fractions remain finite while theirs approach infinity. The reasons for this type of discrepancy, and the errors believed to be inherent in Flory's original derivation, have been discussed before in detail (1, 8) and will not be repeated here.

Further discussion of the molecular size distribution in these systems is given by Gordon and Judd (8) and our reply to their comments (9). The expressions derived in the present work may

Can. J. Chem. Downloaded from www.nrcresearchpress.com by 210.87.254.6 on 09/05/12
For personal use only.

provide a basis for distinguishing experimentally between the two theories. For example, in the condensation of RA_4 with $R'A_2$ when the initial molar ratio $R'A_2/RA_4$ is 2, the Flory–Stockmayer theory predicts that this ratio will increase during polycondensation to a value of 8 at $\alpha = 0.5$, as shown in Fig. 12, whereas our expressions predict that at this conversion the ratio will be 2.7 and will not exceed 4 at all conversions. In view of the simplifying assumptions in both theories, exact agreement with experiment cannot be expected but the differences may be sufficient to permit an experimental test.

It may be useful to reiterate the underlying principle of our method, as it has been applied to the four cases discussed here. Molecules are "cut" into elementary fragments. Where possible, one type of fragment is chosen so that it is common to every molecule. All molecules then can be reassembled by starting with this type. Because we have no other such definite structural information, the remaining fragments can only be distributed at random among the molecules. (Alternatively two fragments, each common to one class of molecules are produced in the initial imaginary cutting step.) The method ensures a complete accounting of the number of fragments at all stages and guarantees that mole fractions sum to unity over the entire range of α applicable to the model.

1. S. G. WHITEWAY, I. B. SMITH, and C. R. MASSON. Can. J. Chem. **48**, 33 (1970).
2. S. G. WHITEWAY. Can. J. Chem. **48**, 1432 (1970).
3. C. R. MASSON, I. B. SMITH, and S. G. WHITEWAY. Can. J. Chem. **48**, 201 (1970).
4. C. R. MASSON, I. B. SMITH, and S. G. WHITEWAY. Can. J. Chem. **48**, 1456 (1970).
5. W. H. STOCKMAYER. J. Polymer. Sci. **9**, 69 (1952).
6. W. H. STOCKMAYER. J. Chem. Phys. **11**, 45 (1943).
7. P. J. FLORY. Principles of polymer chemistry. p. 393. Cornell University Press, Ithaca, New York. 1953.
8. M. GORDON and M. JUDD. Nature, **234**, 96 (1971).
9. C. R. MASSON, I. B. SMITH, and S. G. WHITEWAY. Nature, **234**, 97 (1971).

Can. J. Chem. Downloaded from www.nrcresearchpress.com by 210.87.254.6 on 09/05/12
For personal use only.

A Theoretical Study of the Site of Protonation of Formamide Using Non-empirical LCAO-MO-SCF Calculations

ALAN C. HOPKINSON
Department of Chemistry, York University, Downsview, Ontario
AND
IMRE G. CSIZMADIA
Lash Miller Chemical Laboratories, University of Toronto, Toronto 181, Ontario

Received November 10, 1972

Molecular orbital calculations are used to show that *O-protonated* formamide is more stable than its *N-protonated* tautomer by 6.2 kcal/mol. The computed proton affinity of formamide (assuming *O-protonation*) is computed to be 254.8 kcal/mol.

On a utilisé des calculs impliquant les orbitales moléculaires pour montrer que la formamide protonée sur l'oxygène est plus stable que son tautomère protoné sur l'azote par 6.2 kcal/mol. L'affinité calculée de la formamide pour un proton (en considérant la protonation sur l'oxygène seulement) est égale à 254.8 kcal/mol. [Traduit par le journal]

Can. J. Chem., **51**, 1432 (1973)

Can. J. Chem. Downloaded from www.nrcresearchpress.com by 210.87.254.105 on 09/05/12
For personal use only.

The interpretation of physical measurements on protonated amides has led to differing views on the *site* of protonation. Low temperature n.m.r. studies using fluorosulfuric acid as solvent show that the added proton is different from the amino-protons, indicating the amides to be *oxygen-protonated* (1–3). This was reinforced by kinetic studies on the hydrolysis of benzimidates (4). However, in dilute acid the rotational barrier about the C—N bond is reduced below the level of detection and the amino protons exchange with the solvent (5), both suggesting that the amides are *nitrogen-protonated.* The argument for *N-protonation* is further supported by the failure of amide basicities to correlate with the carbonyl stretching frequency (6).

Recently the problem has been re-examined by Liler (3) who suggests that this apparent discrepancy may be explained by amides being *nitrogen-protonated* in dilute aqueous acids but with the *oxygen-protonated* isomer becoming more stable and eventually being predominant as the water activity is decreased. Martin (7), however, using data from proton exchange rates concludes that *oxygen protonation* occurs in all aqueous mineral acid solutions.

The objective of the present work was to use non-empirical molecular orbital calculations to establish which conjugate acid of formamide is the more stable in the gas phase and, using calculated charge densities for the cation, to estimate which will be the more stable in solution. Similar *ab initio* studies have been successful in predicting the relative stabilities of tautomers of CH_3O^+ (8) and $HCOOH_2^+$ (9).

In earlier molecular orbital studies on protonated formamide (10) energy curves were calculated for the approach of the proton to an *unchanged* formamide molecule. We have used a slightly larger basis set and have adopted a different approach, optimizing (*i*) the conformations of the protons on the OH and NH_3 groups and (*ii*) the C—N and C—O bond lengths in both conjugate acids.

The other bond lengths were taken from a previous theoretical study (11); all the bond angles were taken to be trigonal or tetrahedral. The experimental geometry was used for formamide (12). The basis set consisted of 8^S and 3^P-type Gaussian functions on oxygen, nitrogen, and carbon, and 3^S-type functions on hydrogen (13) contracted to 3^S, 1^P, and 1^S, respectively. All the computations were carried out on an IBM-360-65 using a modified version of IBMOL-IV (14).

As in previous calculations (15, 16) on formamide, the charge densities show the nitrogen atom to carry the largest negative charge (structure **1**) and, using these as a guide to reactivity, predict *nitrogen protonation.*

The initial calculations on the conjugate acids showed (*i*) the *O-protonated* isomer to be planar

TABLE 1. Computed total energies and energy differences (relative to formamide)

Species	Computed total energy (hartree)	Energy difference (kcal/mol)
Formamide (*a*) experimental geometry	−168.1299	—
(*b*) planar	−168.1296	0.2
O-Protonated formamide	−168.5358	−254.8*
N-Protonated formamide	−168.5259	−248.6*

*These values are proton affinities.

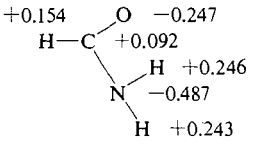

1

with the oxygen proton being *cis* to the hydrogen of the carbon atom (structure **2**) and having a rotational barrier of 12.1 kcal/mol and (*ii*) the rotational barrier about the carbon–nitrogen bond of the *N-protonated* isomer to be 1.3 kcal/mol, with the rotamer in which the in-plane hydrogen is *cis* to the oxygen (structure **3**) being the most stable. This is consistent with other rotational studies in which it has been shown that there is a weak covalent bond between the oxygen of a carbonyl group and an eclipsing hydrogen atom on a neighboring methyl (17) or hydroxy (9) group. The low rotational barrier of the *N-protonated* formamide would result in free rotation about the carbon–nitrogen bond at room temperature, as observed experimentally (5).

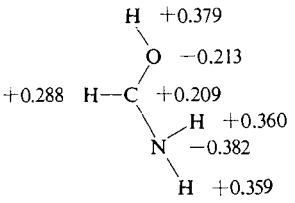

2

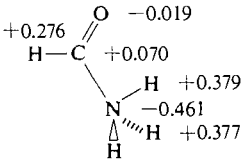

3

Optimization of the geometry of **2** gave C—N and C—O bond lengths of 1.353 and 1.343 Å, respectively; for **3** optimum values of 1.569, and 1.250 Å were obtained for these bonds. The computed total energies are given in Table 1. The energy difference between the two isomers was found to be 6.2 kcal/mol, with the *O-protonated* formamide being the more stable. In general as the size of the basis set is increased, the energy differences converge on the experimental value (18), and these calculations therefore set an upper value on the energy difference between the isomers.

The molecular orbital calculations are for isolated ions in the gas phase at absolute zero, and it is conceivable that solvation of the ions could still reverse the order of stability in solution. Calculations on the fully solvated tautomers of protonated formamide are computationally too expensive to be attempted by the *ab initio* method. Even addition of only one water molecule, which should result in a stabilization of about 30 kcal/mol (19–23) compared with a total free energy of between 60 and 100 kcal/mol (24) for a small ion, requires too many calculations with a very large number of Gaussian functions to be included in the present work. Also experimental gas phase solvation energies for similar ions are unavailable. However *ab initio* calculations (21–23) on $NH_4^+ \cdot NH_3$ and $H_3O^+ \cdot H_2O$ have shown that the stabilization produced by formation of the monosolvated ion is larger for the hydronium ion. In addition Hogg and Kebarle (25) have shown that NH_4^+ is preferentially solvated in its primary solvation shell by ammonia rather than by water, with $NH_4^+ \cdot 4NH_3$ being more stable than $NH_4^+ \cdot 4H_2O$ by about 5 kcal/mol at 25°C. It therefore seems safe to conclude that addition of at least the first water molecule to the hydroxy group of *O-protonated* formamide will be more exothermic than the same addition to the protonated amino group of the other tautomer. This deduction is in keeping with a previous semi-empirical molecular orbital treatment (11) which showed that one water molecule forms a stable hydrogen bond with *O-protonated* formamide but has no appreciable attractive interaction with the *N-protonated* tautomer.

Can. J. Chem. Downloaded from www.nrcresearchpress.com by 210.87.254.105 on 09/05/12
For personal use only.

The molecular orbital calculations place similar positive charges on the amino protons of both the *O-protonated* and *N-protonated* isomers, and it is therefore reasonable to expect addition of a further two molecules of water to these groups in the monosolvated ions to have similar energies.

Equilibrium results from aqueous acid solutions have shown that weak organic bases which produce hydroxy groups on protonation (*e.g.* ketones, aldehydes, and carboxylic acids) (26, 27) have indicator slopes less than unity, when using the primary aniline acidity function (H_0) (28) as reference. This is interpreted as implying that there is a larger increase in solvation on protonation of the carbonyl group than in the protonation of primary amines (29, 30).

Summarizing the arguments on solvation then (*1*) addition of the initial water molecule to the protonated amides should be more exothermic for the *O-protonated* amide; (*2*) the energies associated with addition of the next two water molecules will probably be very similar for both tautomers, and (*3*) solution results suggest that, contrary to Liler's suggestion (3) the *O-protonated* tautomer will probably have the larger primary solvation shell. (The low ionization slopes for amides have been used to predict that the protonated amides have five water molecules in their primary solvation shells (26, 31, 32).) This reasoning suggests then that solvation will *further stabilize* the *O-protonated* formamide relative to its *N-protonated* tautomer.

Finally, the proton affinity of formamide, assuming *oxygen protonation*, was calculated to be 254.8 kcal/mol. No experimental value is known to the present authors but this estimate is again expected to set an upper limit on the proton affinity (18).

The authors wish to thank the National Research Council of Canada for financial support.

1. R. J. GILLESPIE and T. BIRCHALL. Can. J. Chem. **42**, 148 (1963).
2. R. J. GILLESPIE and T. BIRCHALL. Can. J. Chem. **41**, 2642 (1963).
3. M. LILER. J. Chem. Soc. C, 115 (1971).
4. C. R. SMITH and K. YATES. Can. J. Chem. **50**, 771 (1972).
5. A. BERGER, A. LOEWENSTEIN, and S. MEIBOOM. J. Am. Chem. Soc. **81**, 61 (1959).
6. M. LILER. Spectrochim. Acta, **23**A, 139 (1967).
7. R. B. MARTIN. Chem. Commun. 73 (1972).
8. M. A. HANEY, J. C. PATEL, and E. F. HAYES. J. Chem. Phys. **53**, 4105 (1970).
9. A. C. HOPKINSON, K. YATES, and I. G. CSIZMADIA. J. Chem. Phys. **52**, 1784 (1970).
10. R. BONACCORSI, A. PULLMAN, E. SCROCCO, and J. TOMASI. Chem. Phys. Lett. **12**, 622 (1972); B. MÉLY and A. PULLMAN. C.R. Acad. Sc. Paris, **274**B, 1371 (1972).
11. A. C. HOPKINSON, R. A. MCCLELLAND, K. YATES, and I. G. CSIZMADIA. Theoret. Chim. Acta, Berlin, **13**, 65 (1969).
12. C. C. COSTAIN and J. M. DOWLING. J. Chem. Phys. **32**, 158 (1960).
13. M. KLESSINGER. Theoret. Chim. Acta, Berlin, **15**, 353 (1969).
14. A. VEILLARD. IBMOL: computation of wave functions for molecules of general geometry, version 4. IBM Research Laboratory, San Jose, California.
15. M. A. ROBB and I. G. CSIZMADIA. Theoret. Chim. Acta, Berlin, **10**, 269 (1968).
16. D. H. CHRISTENSEN, R. N. KORTZEBORN, B. BAK, and J. J. LED. J. Chem. Phys. **53**, 3912 (1970).
17. L. C. ALLEN and W. L. JORGENSON. J. Am. Chem. Soc. **93**, 567 (1971).
18. A. C. HOPKINSON, N. K. HOLBROOK, K. YATES, and I. G. CSIZMADIA. J. Chem. Phys. **49**, 3596 (1968).
19. R. P. BELL. The proton in chemistry. Ithaca, Cornell University Press. 1959. p. 24.
20. P. KEBARLE, S. K. SEARLES, A. ZOLLA, J. SCARBOROUGH, and M. ARSHADI. J. Am. Chem. Soc. **89**, 6393 (1967).
21. W. P. KRAEMER and G. F. DIERCKSEN. Chem. Phys. Lett. **5**, 463 (1970).
22. P. A. KOLLMAN and L. C. ALLEN. J. Am. Chem. Soc. **92**, 6101 (1970).
23. P. MERLET, S. D. PEYERIMHOFF, and R. J. BUENKER. J. Am. Chem. Soc. **94**, 8301 (1972).
24. D. R. ROSSEINSKY. Chem. Rev. **65**, 467 (1965).
25. A. M. HOGG and P. KEBARLE. J. Chem. Phys. **43**, 449 (1965).
26. K. YATES and H. WAI. Can. J. Chem. **43**, 2131 (1965).
27. A. C. HOPKINSON and P. A. H. WYATT. J. Chem. Soc. B, 1333 (1967).
28. M. J. JORGENSON and D. R. HARTTER. J. Am. Chem. Soc. **85**, 878 (1963).
29. R. W. TAFT. J. Am. Chem. Soc. **82**, 1965 (1960).
30. C. H. ROCHESTER. Acidity functions. Academic Press, London. 1970. Chapt. 3.
31. K. YATES, J. B. STEVENS, and A. R. KATRITZKY. Can. J. Chem. **42**, 1957 (1964).
32. K. YATES and J. B. STEVENS. Can. J. Chem. **43**, 529 (1965).

Can. J. Chem. Downloaded from www.nrcresearchpress.com by 210.87.254.105 on 09/05/12
For personal use only.

Photochemistry of Ketones in Carbon Tetrachloride Solution

J. O. PAVLIK, P. I. PLOOARD, A. C. SOMERSALL, AND J. E. GUILLET
Department of Chemistry, University of Toronto, Toronto, Ontario

Received September 5, 1972

Acetone, chloroacetone, 4-heptanone, 8-pentadecanone, 12-tricosanone, and dimethyl γ-keto pimellate were photolyzed at 3130 Å in carbon tetrachloride solution. The quantum yields of C_2Cl_6 formed, the decrease in Norrish type I and type II products, the copious yields of HCl and the Stern–Volmer quenching of ketone fluorescence by carbon tetrachloride provide definitive evidence for energy transfer which is rationalized by an exciplex mechanism of low efficiency. The excited $[n,\pi^*]^1$ state of the ketone forms a loose complex with the CCl_4 and radiationless energy transfer leads to dissociation of the CCl_4 in the primary chemical step.

L'acétone, la chloroacétone, la pentadécanone-8, la tricosanone-12 et le γ cétopimellate de diméthyle ont été photolysés à 3130 Å en solution dans le tétrachlorure de carbone. Les rendements quantiques en C_2Cl_6 formé, la décroissance des produits selon le Norrish type I et II, les rendements élevés en HCl et l'extinction de la fluorescence de la cétone selon le mécanisme de Stern–Volmer, par la tétrachlorure de carbone, fournissent une preuve définitive du transfert d'énergie expliqué par un complexe excité de fabile efficacité. L'état excité $[n,\pi^*]^1$ de la cétone forme un complexe labile avec le tétrachlorure de carbone et l'énergie de transfert sans radiation conduit à la dissociation du tétrachlorure de carbone durant l'étape chimique primaire. [Traduit par le journal]

Can. J. Chem., 51, 1435 (1973)

Can. J. Chem. Downloaded from www.nrcresearchpress.com by 210.87.254.105 on 09/05/12
For personal use only.

Introduction

The photochemistry of aliphatic ketones has been intensively investigated both in the vapor phase and in solution (1, 2). Photolysis studies of mixtures of ketones and halogenated compounds have revealed several new and interesting aspects of ketone photochemistry. The importance of the $[n,\pi^*]$ singlet state of ketones in organic photochemistry has only recently become generally appreciated. The sensitization of biacetyl fluorescence (3) and other photophysical processes has now been complemented with the observation of a singlet ketone-sensitized chemical process, the photodecomposition of dichlorobutanes (4–6). Several investigators (7–10) have previously suggested that the photosensitized decomposition of CCl_4 may be an important mechanism in the photolysis of ketones in the presence of CCl_4, but no definitive experiments have been reported to substantiate any general conclusion.

Cvetanović *et al.* (8) observed HCl as a product in the gas phase photolysis of mixtures of acetone and CCl_4 in the region where CCl_4 is transparent and Peterson and Mains (10) obtained a similar result in solution. Mettee (11) monitored phosgene as one of the major products of both continuous and flash photolyses of dilute, oxygenated CCl_4 solutions of acetone, benzophenone, and several α,β-unsaturated ketones. HCl was also detected after the photolyses of degassed acetone and of carvone in CCl_4. In an attempt to confirm that photosensitization could occur, Mettee also found that the emission of acetone at 3130 Å was reduced with increasing CCl_4 pressure but concluded that since quenching could occur by mechanisms other than energy transfer the experiment was not definitive. Gregory and Wijnen (12) found C_2Cl_6 as a minor product on irradiating mixtures of diethyl ketone and CCl_4 in the gas phase as well as other recombination and disproportionation reactions involving $CCl_3\cdot$ radicals.

The present study was initiated to elucidate further the photochemistry of aliphatic ketones in CCl_4 solution.

Experimental

Materials

Acetone, cyclohexane, and carbon tetrachloride were of Fisher spectranalyzed quality. 8-Pentadecanone and 12-tricosanone were prepared by the method of Davis and Schultz (13). The other ketones were purified on a Varian Aerograph preparative gas chromatograph. Dimethyl γ-ketopimelate (DMKP) was synthesized from the crude product furylacrylic acid by the method of Lukes *et al.* (14). The white solid was purified by redistillation at 130°/1 mm and checked by gas chromatography, n.m.r., and u.v. spectra.

Photolysis

The source of u.v. light was a 250 W medium pressure mercury arc lamp (A.E.I., M.E/D box type) fitted with

TABLE 1. Quantum yields of photolysis products of ketones in CCl_4 at 3130 Å (30 °C)

Ketone	$\phi_{C_2Cl_6}$ Air	$\phi_{C_2Cl_6}$ Vacuo	ϕ_{HCl} air	Other products (quantum yield)
Acetone	0.049	0.087	1.5	Chloroacetone (0.068)
4-Heptanone	0.20	0.27	2.4	Not identified
8-Pentadecanone (60 °C)	0.14	—	0.95	1-Chloroheptane (0.018) type I Octanoyl chloride (0.013) type I 1-Hexene (0.034) type II
12-Tricosanone	0.13	0.14	0.88	Not identified
Chloroacetone	0.21	—	Detected	Acetone (0.042)
Dimethyl γ-keto pimelate	0.20	—	—	Methyl propanoate (0.03) type I

an interference filter to isolate 3130 Å light. Samples were irradiated in 1 mm and 10 mm path length quartz cells in a temperature block for C_2Cl_6 measurements. Actinometry was done using both uranyl oxalate and ferrioxalate actinometers. Photolysis products were measured on a Perkin–Elmer Model 800 Gas Chromatograph. Some products of irradiation were identified by comparing retention times on the gas chromatograph, others were collected for mass spectrometric analysis and some remained unidentified.

For measurements of HCl yields a 10 mm cell was fitted with a side arm and bulbs in which liberated gas was collected in distilled water. The water and CCl_4 residues were titrated separately with standardized sodium hydroxide using phenolphthalein as indicator. The total titrant volume was reproducible over several measurements and different radiation times, but in general more titrant was required for the water portion with increasing radiation dose.

Fluorescence Measurements

Fluorescence spectra were obtained in 10 mm quartz cells on a Perkin–Elmer Hitachi MPF-2A Fluorescence Spectrophotometer with a 150 W xenon lamp source. Spectra were ratio recorded to correct for any fluctuation in source intensity and at right angle illumination.

Results

Photolysis

Acetone, chloroacetone, 4-heptanone, 12-tricosanone, and dimethyl γ-keto pimelate (DMKP) were photolyzed in CCl_4 solution at 30° using 3130 Å which was not absorbed by the neat solvent. A more detailed analysis of photolysis products was carried out for 8-pentadecanone under similar conditions, but at 60°. The principal products analyzed by gas chromatography and apparent yields of HCl from titration are summarized in Table 1. The estimated errors are less than 10%. The major products of irradiation of ketones in CCl_4 solution were consistently C_2Cl_6 and HCl. No products were detected after extended irradiation of neat CCl_4. In the case of acetone photolysis, chloroacetone was also a major product. Similarly, in the irradiation of chloroacetone, acetone was a major product. Only one Norrish type I product, acetyl chloride, was observed for acetone and with very low quantum yield ($\sim 10^{-5}$ mol/einstein). However, for the larger representative symmetric ketone, 8-pentadecanone, both Norrish type I and II products were obtained. For the keto diester DMKP the yield of type I product was also significant.

HCl yields were determined by titration and confirmed by precipitation with $AgNO_3$. The quantum yields in air are unusually high, but many irradiations of different ketones gave consistent and reproducible results although neat CCl_4 showed no HCl after extended irradiation. The quantum yield for HCl in the absence of air and moisture was obtained by degassing CCl_4 and 4-heptanone through several freeze–thaw cycles. The CCl_4 was then distilled under high vacuum into the cell containing the frozen ketone and the cell was sealed off for photolysis. After the irradiation, the mixture was cooled in liquid nitrogen, water was added, and the liquid solution titrated. Under these reproducible conditions, the quantum yield of HCl was reduced to 0.56 for 4-heptanone.

Fluorescence Measurements

The broad fluorescence band of aliphatic ketones in solution (λ_{max} 4000 Å) has been characterized recently by O'Sullivan and Testa (15). Similar spectra were obtained in this work for all the symmetric ketones measured in solvent mixtures ranging from neat cyclohexane to neat CCl_4. Stern–Volmer plots of the relative fluorescence intensity values, obtained from area integration of the band spectra, against the CCl_4 concentration show a linear dependence

Can. J. Chem. Downloaded from www.nrcresearchpress.com by 210.87.254.105 on 09/05/12
For personal use only.

TABLE 2. Fluorescence lifetimes and quenching constants for ketones in CCl_4

Ketone	$\phi_F \times 10^{3}$*	$\tau_R \times 10^{6}$ s	$\phi_F\tau_R = {}^1\tau \times 10^{9}$ s	$k_q{}^1\tau$	$k_q \times 10^{-7}$	k_q/k_{diff}
Acetone	1.00	2.1	2.1	0.076	3.6	0.004
3-Pentanone	1.49	1.9	2.8	0.38	14.0	0.014
4-Heptanone	1.13	1.6	1.8	0.20	11.0	0.011
5-Nonanone	0.40	1.6	0.6	0.12	20.0	0.020
6-Undecanone	0.35	1.5	0.5	0.12	24.0	0.024
8-Pentadecanone	0.35	1.5	0.5	0.12	24.0	0.024
12-Tricosanone	0.35	1.5	0.5	0.13	26.0	0.026

*Relative to ϕ_F (acetone). The value obtained by O'Sullivan and Testa (ref. 15) of 10^{-3} is assumed as a secondary standard.

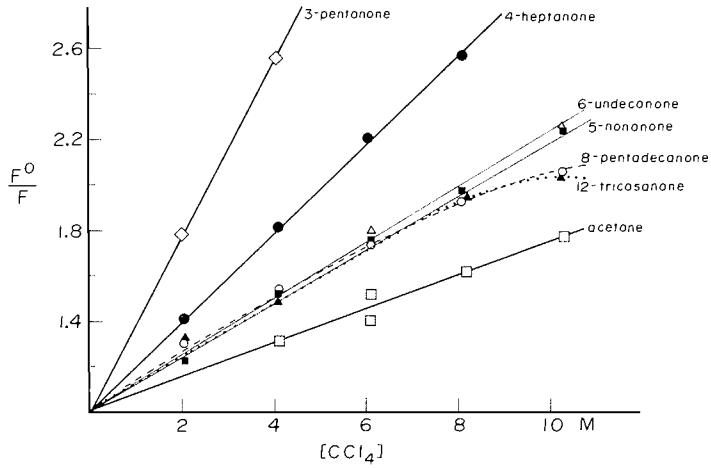

FIG. 1. Stern–Volmer plots for fluorescence quenching of various ketones by CCl_4 at 30 °C in cyclohexane. F^0 is the intensity of fluorescence in absence of quencher, F the intensity in presence of designated concentration of CCl_4.

(Fig. 1). The slopes of these lines give values of $k_q{}^1\tau$ and hence k_q, where ${}^1\tau$ is the singlet lifetime of the ketone and k_q is the rate constant for quenching of the excited ketone singlet by CCl_4. Singlet lifetimes were estimated from the fluorescence quantum yields and integrated absorption spectra following O'Sullivan and Testa (16) and are consistent with values in the literature. Quenching efficiency was estimated from the ratio of the fluorescence quenching constant k_q to the diffusion constant k_{diff} obtained from the equation of Osborne and Porter (17),

$$[1] \qquad k_{diff} = \frac{8RT}{2000\,\eta}$$

where η is the solvent viscosity. The results are summarized in Table 2.

Discussion

The consistent observation of C_2Cl_6 as a photolysis product of ketones in CCl_4 at a wavelength where the solvent is transparent is consistent with radical recombination of $CCl_3^{\cdot}$ formed by sensitized decomposition of CCl_4

$$[2] \qquad CCl_4^* \rightarrow CCl_3^{\cdot} + Cl^{\cdot}$$

The observed increase of the C_2Cl_6 yield in degassed solution probably indicates the removal of $CCl_3^{\cdot}$ radicals by the formation of phosgene in aerated solution. No attempt was made to monitor this latter product. Phosgene, which has been identified in similar work by Mettee (11) in oxygenated solutions would be formed here by the reaction of $CCl_3^{\cdot}$ radicals with oxygen from the dissolved air.

$$[3] \qquad CCl_3^{\cdot} + \tfrac{1}{2}O_2 \rightarrow COCl_2 + Cl^{\cdot}$$

Hartley and Guillet (18) found that for irradiation of 8-pentadecanone at 60° in hydrocarbon solvent, the type II process had a quantum efficiency as high as 0.07 and measured a quantum yield of 0.005 for carbon monoxide. Com-

Can. J. Chem. Downloaded from www.nrcresearchpress.com by 210.87.254.105 on 09/05/12
For personal use only.

Can. J. Chem. Downloaded from www.nrcresearchpress.com by 210.87.254.105 on 09/05/12
For personal use only.

parison with the results in Table 1 indicates that ϕ_{II} is decreased in CCl_4 compared with hydrocarbon solvents, and $\phi_{C_2Cl_6}$ is too high to be explained by any other ketone decomposition pathway. The type I process of DMKP was shown to give a product quantum yield as high as 0.40 in *p*-dioxane (19) compared to 0.03 in CCl_4. The considerable reduction of the quantum yields of ketone reactions in CCl_4 and the consistent formation of C_2Cl_6 is good evidence for energy transfer from the excited ketone to CCl_4 molecules in solution.

Comparison of the fluorescence quenching efficiencies (Table 2) shows that energy transfer from the excited ketone singlet occurs in only a few encounters in every hundred. However, the linear Stern–Volmer plots for various ketones have slopes ($k_q{}^1\tau$) which follow similar trends to the quantum yields of C_2Cl_6 and HCl, which is consistent with sensitization of CCl_4 decomposition as a result of energy transfer.

It is obvious that the observed kinetics cannot imply that the quenching rate is determined by the number of collisions which takes place by the mutual diffusion of the excited molecule and the quenchers. If diffusion were rate-determining, then at high CCl_4 concentration, the probability of a ketone molecule being surrounded by a quencher molecule would be very high, and instantaneous "static" quenching would have caused the lines to curve upwards sharply. This was not observed in CCl_4 even as a neat solvent for the ketones and therefore some factor other than diffusion must be controlling the quenching rate.

Classical electronic transfer by excitation of the acceptor to an *electronic* level above the ground state on collision, as in the Dexter mechanism (20), cannot be important here because the absorption spectrum of neat CCl_4 shows zero absorbance above 300 nm and the ketone fluorescence showed a cut-off at a minimum above 320 nm. There is therefore a negligible overlap in the emission spectrum of the donor and the absorption spectrum of the acceptor which is demanded by any classical electronic transfer mechanism. However, the excited $[n,\pi^*]^1$ state is estimated to be more than 80 kcal/mol above the ground state for aliphatic ketones (2) and the C—Cl bond strength is only 68 kcal/mol so that exothermic transfer by some other mechanism is energetically feasible.

Quenching of singlet states without classical electronic energy transfer has recently been investigated for the quenching of aromatic compounds by quenchers having no lower-lying singlet states (21). The phenomenon has been visualized by Hammond and his co-workers as involving an interaction between the excited state of the donor and the quencher molecule, forming a loosely bound exciplex or an excited dimer which results in an increase in the rates of non-radiative decay processes. Examples of such a mechanism include the quenching of fluorescence of aromatic molecules by dienes (21), methyl chloroacetate, and chloroacetamide (22), the quenching of ketone singlets at high diene concentration (23) and the sensitization of dichlorobutanes by ketones (4–6). The quenching rate is determined by the efficiency of formation of the exciplex during an encounter and this efficiency is rather low.

The results obtained here for ketone fluorescence quenching by carbon tetrachloride, the measurements of the C_2Cl_6 quantum yields, and the formation of copious amounts of HCl are consistent with the following mechanism, where the ketone molecule is designated as KH:

[4] $KH + h\nu_F$

[5] $KH + \text{heat}$

[6] $KH \xrightarrow{h\nu} {}^1KH^* \rightarrow {}^3KH$

[7] Norrish products

[8] $({}^1KH^*.CCl_4)$

[9] $({}^1KH^*\ CCl_4) \rightarrow KH + Cl^{\cdot} + CCl_3^{\cdot}$

[10] $2CCl_3^{\cdot} \rightarrow C_2Cl_6$

[11] $Cl^{\cdot} + KH \rightarrow K^{\cdot} + HCl$

[12] $K^{\cdot} + CCl_4 \rightarrow (K)Cl + CCl_3^{\cdot}$

[13] $K^{\cdot} + Cl^{\cdot} \rightarrow (K)Cl$

[14] $K^{\cdot} + CCl_3^{\cdot} \rightarrow (K)CCl_3$

In the presence of air and moisture the yield of HCl would increase as other reactions become important:

[15] $CCl_3^{\cdot} + \frac{1}{2}O_2 \rightarrow COCl_2 + Cl^{\cdot}$

[16] $COCl_2 + 2H_2O \rightarrow CO(OH)_2 + 2HCl$

[17] $CO(OH)_2 \rightarrow CO_2 + H_2O$

If the mechanism by which CCl_4 quenches the ketone fluorescence in solution leads to the sensitized decomposition of the CCl_4 as in reactions 8 and 9, and if proton abstraction is very

TABLE 3. Comparison of sensitization data

	$k_q{}^1\tau$	$\phi_{C_2Cl_6}$ (air)	ϕ_{HCl} Air Obsd.	ϕ_{HCl} Air Calcd.	ϕ_{HCl} Vacuo Obsd.	ϕ_{HCl} Vacuo Calcd.
Acetone	0.076	0.05	1.5	1.7		
4-Heptanone	0.20	0.20	2.5	2.7	0.56	0.67
8-Pentadecanone	0.12	0.14	0.95			
12-Tricosanone	0.13	0.13	0.88			

efficient, then in the absence of air and moisture the scheme would predict

$$[18] \qquad \phi_{HCl}(vac) \sim \frac{k_Q[CCl_4]}{k_Q[CCl_4] + \frac{1}{{}^1\tau^0}}$$

Equation 18 predicts for 4-heptanone $\phi_{HCl} \sim 0.67$ which is in good agreement with the measured value 0.6. However in the presence of air and moisture, reactions 15 and 16 also lead to the formation of HCl and would suggest that

$$[19] \qquad \phi_{HCl}(air) \sim 4\phi_{HCl}(vac)$$

Again the results for 4-heptanone and for acetone are quite good (Table 3). The larger ketones do not succumb to such simple treatment as the importance of reactions 13 and 14 and other secondary reactions lead to other products as evidenced by the occurrence of unidentified peaks in the gas chromatograms of these irradiated solutions. Thus transfer to excitation energy from a ketone molecule to CCl_4 leads to exothermic cleavage of a C—Cl bond followed by a complex sequence of free radical reactions, some products of which have been characterized.

The existence of the exciplex as some kind of metastable intermediate is not indispensable to the mechanism since the results are consistent with a single-step transfer process

$$[20] \qquad {}^1K^* + CCl_4 \rightarrow K + Cl^{\cdot} + CCl_3^{\cdot}$$

However it is reasonable to suppose that the exciplex does have a finite lifetime during which electronic–vibrational coupling takes place. The nature of the deactivation pathway for the exciplex is probably dependent on the nature of the donor–acceptor interaction which may be of different types including resonance transfer and more probably charge transfer. An explanation based on the increase in intersystem crossing due to the "heavy atom" effect seems unlikely since it has been shown by Kearns and Case (24) that this effect is very small in the case of n–π* transitions.

Results obtained for chloroacetone photolysis in CCl_4 show that energy transfer also takes place in this case, since C_2Cl_6 is observed as a significant product, but the primary step involved cleavage of the C—Cl bond of the substituted ketone as was shown in the gas phase (25). The C—Cl bond in chloroacetone, unlike the C—H bond in acetone, is weak enough for exothermic cleavage following absorption of 3130 Å radiation.

Conclusions

The evidence from photolysis studies of ketones in carbon tetrachloride at 3130 Å suggests that energy transfer occurs from the $[n,\pi^*]^1$ state of the ketone to CCl_4 leading to photosensitized decomposition of the CCl_4 into Cl atoms and $CCl_3^{\cdot}$ radicals. The major chemical products seem to result from subsequent reactions of these fragments with the substrate. Fluorescence studies are consistent with an exciplex mechanism for the energy transfer process.

The authors wish to acknowledge the financial support of Imperial Oil Enterprises Ltd., and the National Research Council of Canada.

1. J. G. CALVERT and J. N. PITTS, JR. Photochemistry. Wiley, New York, N.Y. 1966.
2. J. C. DALTON and N. J. TURRO. Ann. Rev. Phys. Chem. 1970. pp. 499–560.
3. F. WILKINSON. Adv. Photochem. **3**, 241 (1964).
4. M. GOLUB. J. Am. Chem. Soc. **91**, 4925 (1969).
5. M. GOLUB. J. Am. Chem. Soc. **92**, 2615 (1970).
6. M. GOLUB. J. Phys. Chem. **75**, 1168 (1971).
7. H. A. CURME and G. K. ROLLEFSON. J. Am. Chem. Soc. **74**, 28 (1952).
8. R. J. CVETANOVIĆ, F. A. RAAL, and E. W. R. STEACIE. Can. J. Chem. **31**, 171 (1953).
9. R. PIECK and E. W. R. STEACIE. Can. J. Chem. **33**, 1304 (1955).

Can. J. Chem. Downloaded from www.nrcresearchpress.com by 210.87.254.105 on 09/05/12
For personal use only.

10. D. B. PETERSON and G. J. MAINS. J. Am. Chem. Soc. **81**, 3510 (1959).
11. H. D. METTEE. Can. J. Chem. **45**, 339 (1967).
12. J. E. GREGORY and M. H. J. WIJNEN. J. Chem. Phys. **38**, 2925 (1963).
13. R. DAVIS and H. P. SCHULTZ. J. Org. Chem. **27**, 854 (1962).
14. R. M. LUKES, G. I. POOS, and L. H. SARETT. J. Am. Chem. Soc. **74**, 1493 (1952).
15. M. O'SULLIVAN and A. C. TESTA. J. Am. Chem. Soc. **92**, 5842 (1970).
16. M. O'SULLIVAN and A. C. TESTA. J. Am. Chem. Soc. **92**, 258 (1970).
17. A. D. OSBORNE and G. PORTER. Proc. Roy. Soc. (London), **A284**, 9 (1965).
18. G. H. HARTLEY and J. E. GUILLET. Macromolecules, **1**, 413 (1968).
19. P. I. PLOOARD and J. E. GUILLET. Macromolecules. **5**, 405 (1972).
20. D. L. DEXTER. J. Chem. Phys. **21**, 836 (1953).
21. S. MUROV and G. S. HAMMOND. J. Phys. Chem. **72**, 3797 (1968).
22. M. T. MCCALL and G. S. HAMMOND. J. Am. Chem. Soc. **92**, 699 (1970).
23. F. S. WETTACK, A. D. RENKES, M. G. ROCKLEY, N. J. TURRO, and J. C. DALTON. J. Am. Chem. Soc. **92**, 1793 (1970); N. C. YANG, M. H. HUI, and S. A. BELLARD. J. Am. Chem. Soc. **93**, 4056 (1971).
24. D. R. KEARNS and W. A. CASE. J. Am. Chem. Soc. **88**, 5087 (1966).
25. A. N. STRACHAN and F. E. BLACET. J. Am. Chem. Soc. 77, 5354 (1955).

Can. J. Chem. Downloaded from www.nrcresearchpress.com by 210.87.254.105 on 09/05/12
For personal use only.

Low Temperature Infrared Study of Hydrogen Bonding in Acetone Oxime-d_6

THÉRÈSE DI PAOLO AND CAMILLE SANDORFY
Département de Chimie, Université de Montréal, Montréal, Québec
Received November 15, 1972

The infrared spectrum of $(CD_3)_2C{=}N{-}OH$ was measured in solution down to liquid nitrogen temperature. As the temperature is lowered several new "associated bands" appear indicating the presence of species more highly associated than cyclic dimers or trimers.

Le spectre infrarouge de la molécule $(CD_3)_2C{=}N{-}OH$ a été mesuré en solution à des températures différentes jusqu'à celle de l'azote liquide. Plusieurs "bandes associées" nouvelles apparaissent révélant la présence d'espèces plus associées que les dimères et les trimères cycliques.

Can. J. Chem., 51, 1441 (1973)

Can. J. Chem. Downloaded from www.nrcresearchpress.com by 210.87.254.42 on 09/05/12
For personal use only.

Self-association of oximes by hydrogen bonding has been investigated by several authors. Among their works we are mentioning those of Califano and Lüttke (1, 2), Ossart, Sauvaître, and Pineau (3), Hadži and Premru (4), Jackson (5), and Harris and Bush (6). These relate to acetone oxime; for higher oximes we refer to Geiseler and Fruwert (7). All these authors agree that in solution and in the solid state oximes form mainly cyclic dimers and trimers through O—H---N bonds. Cyclic trimers containing O—H---O type bonds were also considered (1). Outside of the free OH band which is near 3610 cm^{-1} in dilute solutions these authors described two associated bands in more concentrated solutions, centered at about 3300 and 3150 cm^{-1}.

We measured the infrared spectrum of acetone oxime in a 1:1 mixture of CCl_3F (Freon-11) and CF_2BrCF_2Br (Freon 114-B-2) (8, 9) (which forms a rigid glass at liquid nitrogen temperature) in order to study the changes in molecular associations over a wide range of temperatures. Since bands affected by hydrogen bond formation appeared in the methyl CH stretching region we studied the deuterated compound $(CD_3)_2C{=}N{-}OH$ instead of the light compound. The isotopic purity of the sample was 99.5%.

Our measurements were made on a Perkin–Elmer model 621 spectrometer. The low temperature techniques used were described earlier (8, 9). $(CD_3)_2C{=}N{-}OH$ was supplied by Merck, Sharp and Dohme of Canada, Ltd.

The spectra obtained at temperatures ranging from 25 to −180 °C are shown in Fig. 1. At room temperature at 0.1 *M* concentration we see the free band, a very broad band centered at 3260 cm^{-1}, a weaker band at about 3100 cm^{-1}, and a band at about 2900 cm^{-1}. (The band at 2675 cm^{-1} is likely to be the first overtone of the free OH bending vibration (2, 6).) As the temperature is lowered the low frequency bands become more intense. At −180 °C we see at least six bands or shoulders located at approximately 3200, 3150, 3075, 3020 sh, 2880, and 2760 cm^{-1}. Although the first overtone of the C=N stretching vibration might be present at about 3300–3250 cm^{-1}, a combination of the C=N stretching and OH bending vibrations may fall into the 3000 cm^{-1} region and may be boosted by Fermi resonance it is plain that we have at least four and possibly more associated species present in the solution. (The OH band falling into the CH_3 stretching region is particularly noteworthy.)

In order to rule out the possibility of the presence of hydrogen bonds involving the bromine atoms of the solvent we measured the spectra in a 1:1 mixture of CCl_3F and fully deuterated methylcyclohexane which also forms a glass at low temperature. The spectra were essentially unchanged.

According to available crystallographic studies (10) the structure of solid acetone oxime consists of sheets of planar trimers having intermolecular O—H---N hydrogen bonds. In the infrared spectrum of the crystal two broad bands are seen in the 3200–3100 cm^{-1} region (2, 6). Thus a comparison with crystal spectra indicates that the bands we have found at lower frequencies must be due to species more highly associated than cyclic dimers and trimers, possibly to hydrogen bonded chainlike structures. Tautom-

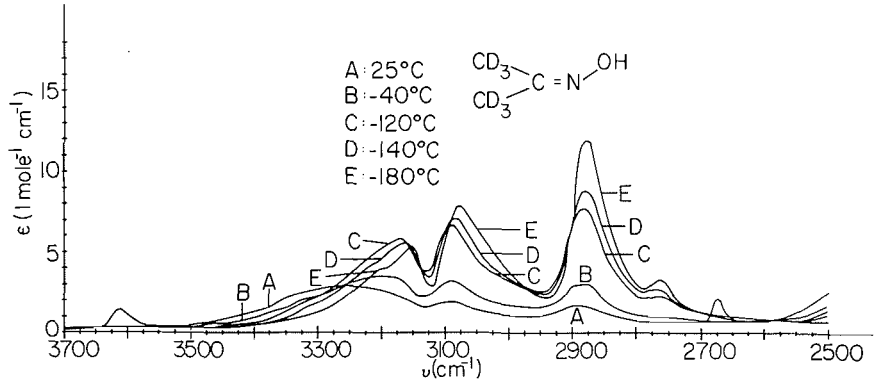

FIG. 1. The infrared spectra of $(CD_3)_2C{=}N{-}OH$ in a 1:1 mixture of CCl_3F and CF_2BrCF_2Br at different temperatures.

erization leading to N—H---O bonds is also a possibility. We cannot go any further.

We acknowledge financial help and a scholarship (T.D.P.) from the National Research Council of Canada.

1. S. CALIFANO and W. LÜTTKE. Z. Phys. Chem. **5**, 240 (1955).
2. S. CALIFANO and W. LÜTTKE. Z. Phys. Chem. **6**, 83 (1956).
3. A. OSSART, H. SAUVAÎTRE, and P. PINEAU. J. Chim. Phys. **64**, 953 (1967).
4. D. HADŽI and L. PREMRU. Spectrochim. Acta, **23A**, 35 (1967).
5. D. S. JACKSON. J. Chem. Soc. (B), 785 (1969).
6. W. C. HARRIS and S. F. BUSH. J. Chem. Phys. **56**, 6147 (1972).
7. G. GEISELER and J. FRUWERT. Z. Phys. Chem. **26**, 111 (1960).
8. G. DUROCHER and C. SANDORFY. J. Mol. Spectrosc. **20**, 410 (1966).
9. M. ASSELIN and C. SANDORFY. J. Mol. Struct. **8**, 145 (1971).
10. T. K. BIERLEIN and E. C. LINGAFELTER. Acta Cryst. **4**, 450 (1951).

Can. J. Chem. Downloaded from www.nrcresearchpress.com by 210.87.254.42 on 09/05/12
For personal use only.

A Low-temperature Infrared Study of Self-association in Thiolic Acids

R. BICCA DE ALENCASTRO[1] AND C. SANDORFY

Département de Chimie, Université de Montréal, Montréal, Québec

Received November 16, 1972

The i.r. spectra of thioloacetic and thiolobenzoic acids were measured in both the fundamental and first overtone regions of the S—H stretching vibration, in a mixture of CCl_3F and $C_2F_4Br_2$, at temperatures ranging from 20 to −190 °C. S—H---O type bonds are formed at low temperatures or at high concentrations of solute. Two different species can be detected. The first is probably an open dimer and the second a cyclic dimer. The S—H anharmonicity constants are of the order of 50–60 cm^{-1}, for both free and associated species, and have about the same value as in aliphatic or aromatic mercaptans. Carbonyl groups have lower anharmonicities. Their value is about 10 cm^{-1} for both free and associated species.

Les spectres i.r. des acides thioloacétique et thiolobenzoïque ont été mesurés au niveau de la fondamentale et de la première harmonique de la vibration de valence S—H dans un mélange de CCl_3F et $C_2F_4Br_2$ à des températures allant de 20 à −190 °C. Sur l'effet de l'abaissement de la température ou de l'augmentation de la concentration des liaisons du type S—H---O sont formées. Deux espèces différentes sont observées. La première est probablement un dimère ouvert et la deuxième un dimère fermé. Les constantes d'anharmonicité pour les vibrateurs S—H libres et associés sont de l'ordre de 50–60 cm^{-1}, c'est-à-dire du même ordre de grandeur que celles des mercaptans. Les constantes d'anharmonicité pour les carbonyles libres et associés sont plus faibles et sont de l'ordre de 10 cm^{-1}.

Can. J. Chem., 51, 1443 (1973)

Introduction

In previous publications (1, 2) we have studied the self-association in thiols and the association of thiols with organic nitrogen bases. We have been able to detect associated S—H---S type species, in the case of the self-association of thiols and, S—H---N type species, in the presence of the strong bases pyridine and triethylamine. In this paper we deal with the interesting case of the self-association of thiolic acids, where the possibility of S—H---O type hydrogen-bonded species occurs.

Some earlier studies of the association of thiolic acids have been made (3–6). Ginzburg and Loginova (3) studied the self-association of thioloacetic and thiolobenzoic acids, in solution in CCl_4 by i.r. spectrometry, and were able to detect changes in the S—H and C=O stretching vibration regions. They suggested that the predominant associated species is, at room temperature, an open dimer of the S—H---O type. The shape of the associated band suggested, furthermore, that another species was present, probably the cyclic dimer.

In the present work we have studied the self-association of thioloacetic and thiolobenzoic acids over a wide temperature range and have measured both the fundamental and first overtone of the S—H and C=O stretching vibrations. The solvent was a 1:1 mixture of CCl_3F (Freon 11) and $C_2Br_2F_4$ (Freon 114-B2), (FR), which becomes a rigid glass at liquid nitrogen temperature. We hoped to follow the changing pattern of self-association from room to −190 °C temperature and to identify the associated species which appeared.

Experimental

The technique and instruments used were fully described elsewhere (1, 2). CCl_3F (Freon 11) and $C_2Br_2F_4$ (Freon 114-B2) were obtained from E.I. Dupont de Nemours Co., and were distilled and kept over phosphorus pentoxide. Spectrograde quality carbon tetrachloride from Anachemia Chems. Ltd., Montreal, was dried on molecular sieves of the type 4A. The thiolic acids were from Aldrich Chem. Co. Inc., and were i.r. and refraction index controlled. The i.r. spectra of these compounds were practically identical with their previously published spectra. They were handled in inert atmosphere to avoid oxidation or moisture adsorption. The solutions were prepared gravimetrically and the concentrations were corrected for solvent contraction. They were used immediately after preparation.

Results

The results we obtained by concentration and temperature studies are very similar for thioloacetic and thiolobenzoic acids and we shall dis-

[1]Brazil–Canada exchange fellow. On leave of absence from Instituto de Química, Universidade Federal do Rio de Janeiro, Rio de Janeiro, Brazil.

Can. J. Chem. Downloaded from www.nrcresearchpress.com by 210.87.254.105 on 09/05/12
For personal use only.

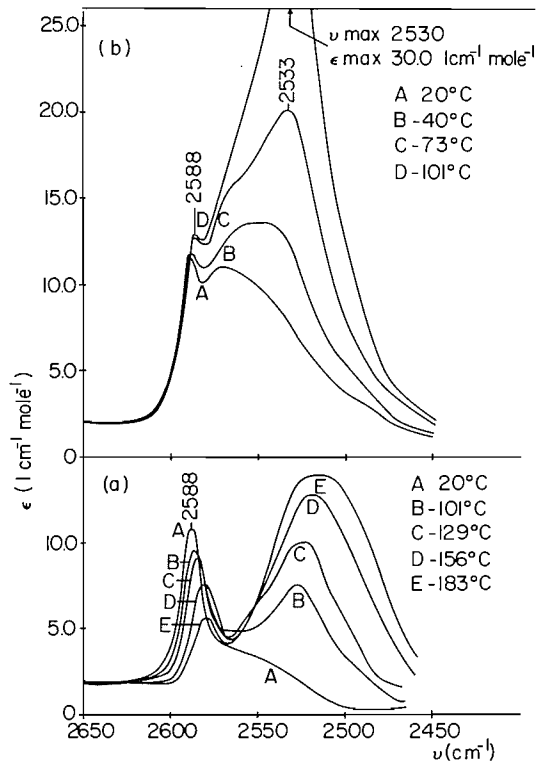

FIG. 1. The i.r. spectra (2450–2650 cm^{-1}) of solutions of thioloacetic acid in FR (*a*) 0.32 *M*; (*b*) 1.55 *M*, at different temperatures.

cuss both cases as a whole (Figs. 1–6). In the case of thiolobenzoic acid our temperature studies were somewhat limited by poor solubility.

(a) The S—H Vibrator

Concentration studies on the S—H stretching region give essentially the same results as those published by Ginzburg and Loginova (3) and, therefore, we shall not reproduce them here. The free band of thioloacetic acid is found to have a half-width of 15 cm^{-1} in a 0.21 *M* solution in CCl_4. Its maximum, located at 2587 cm^{-1}, has an intensity coefficient of about 23.1 cm^{-1} mol^{-1}, which is several times stronger than those we found for the mercaptans (1). In the case of thiolobenzoic acid, the free band has a half-width of 13 cm^{-1} in a 0.31 *M* solution in CCl_4, and its maximum, which is located at 2589 cm^{-1}, has an intensity coefficient of about 28.1 cm^{-1} mol^{-1}. In a solvent less active than CCl_4 (in the present case our solvent FR) the free bands are less intense (about 11.1 cm^{-1} mol^{-1} for both thiolic acids) but have about the same half-widths. The frequency is only slightly changed. These systems seem to behave similarly to the dimethylamine NH stretching band, as described by Wolff and Gamer (7). (For a more elaborate discussion of the effect of "inert" solvents on X—H stretching bands (X = O,N), see ref. 8.)

Upon lowering of the temperature (Figs. 1 and 3), the free band loses intensity and a broad band appears at lower frequencies. In the case of thioloacetic acid, only one large and broad band can be seen in dilute solution (Fig. 1*a*), which has a half-width of 68 cm^{-1}, with maximum near 2515 cm^{-1}, at −183 °C. Temperature studies in a more concentrated solution (Fig. 1*b*) clearly show that this band is actually due to two different species. Naturally, since increasing concentration should favor association, the apparent extinction coefficient of the associated bands is larger in Fig. 1*b* than in Fig. 1*a*, at the same temperature. In dilute solution of thiolobenzoic acid, the lowest temperature we could reach was −129 °C but two bands are also clearly seen (Fig. 3). The frequencies of the associated bands are about the same as for thioloacetic acid.

Concentration and temperature studies on the first overtone of the S—H stretching vibration (Figs. 2 and 4) seem to confirm these observations. Although no new maxima are observable when the concentration of the thiolic acids in CCl_4 is increased, the half-width is greatly increased and the free band loses intensity. In the case of a 0.66 *M* solution of thioloacetic acid in FR, however, two bands are readily seen when temperature is lowered. The case of thiolobenzoic acid in FR is less clear when temperature is lowered, but the associated bands can be seen to appear in the same region. Weaker bands are present near 4915 cm^{-1}, for thioloacetic acid, and 4980 cm^{-1}, for thiolobenzoic acid. Since these bands are found to persist even in very dilute solutions (where the ε_{max} of the free band no longer increases), and the possibility of intramolecular hydrogen bonding is considered unlikely on sterical grounds, these bands are probably combination tones.

(b) The C=O Vibrator

We have studied the C=O stretching region of thioloacetic acid. Thiolobenzoic acid must behave similarly as shown by concentration studies (3).

Figure 5 shows the effect of temperature

Can. J. Chem. Downloaded from www.nrcresearchpress.com by 210.87.254.105 on 09/05/12
For personal use only.

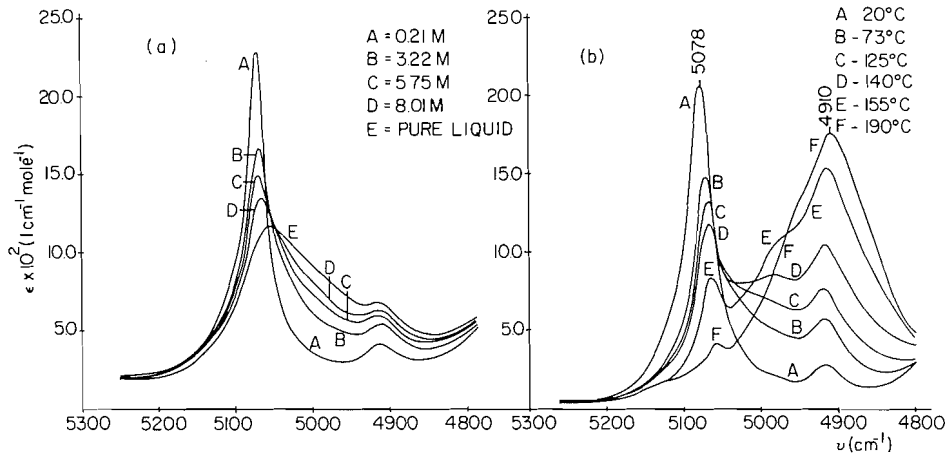

FIG. 2. The i.r. spectra (4800–5300 cm^{-1}) of solutions of thioloacetic acid (*a*) at different concentrations in CCl_4 at 20 °C; (*b*) 0.66 *M* in FR, at different temperatures.

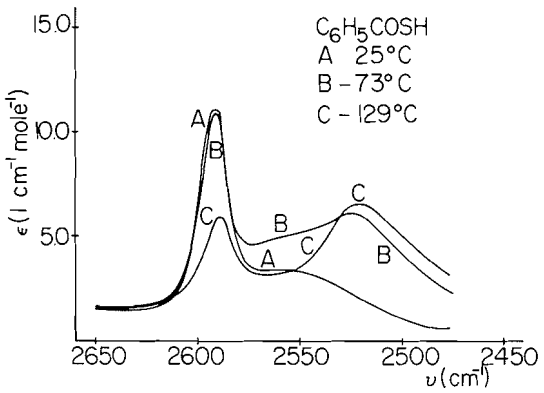

FIG. 3. The i.r. spectra (2450–2650 cm^{-1}) of a 0.59 *M* solution of thiolobenzoic acid in FR at different temperatures.

variation on the frequency of the CO stretching vibration. At room temperature one band is seen in a 0.26 *M* solution of thioloacetic acid in FR, which has its maximum at 1715 cm^{-1}. At −185 °C the band is at 1686 cm^{-1} with a shoulder on the high frequency side. At intermediate temperatures two bands are seen. Concentration studies (3) give, at room temperature, the free carbonyl stretching band at 1710 cm^{-1}, in CCl_4, and the associated carbonyl at 1690 cm^{-1}.

The first overtone of the carbonyl stretching vibration seems to confirm the presence of at least two different carbonyls (Fig. 6), and the maxima shift with temperature in the same way as the fundamental. Concentration studies show no double maxima in CCl_4, but the increase of the half-width and a pronounced asymmetry at the lower frequency side suggests that more than one species are present.

Discussion

Although no spectroscopic evidence is found against the existence of S—H---S hydrogen-bonded species in thiolic acids (these are to be

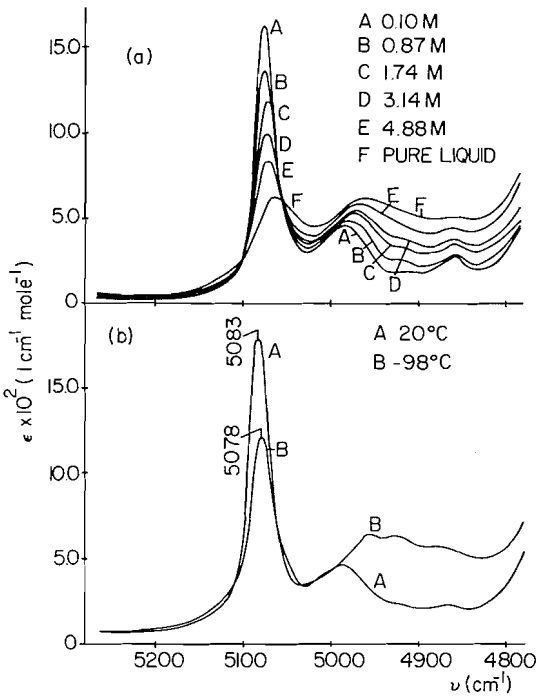

FIG. 4. The i.r. spectra (4800–5300 cm^{-1}) of solutions of thiolobenzoic acid (*a*) at different concentrations in CCl_4, at 20 °C; (*b*) 0.32 *M* in FR, at 20 and −98 °C.

Can. J. Chem. Downloaded from www.nrcresearchpress.com by 210.87.254.105 on 09/05/12
For personal use only.

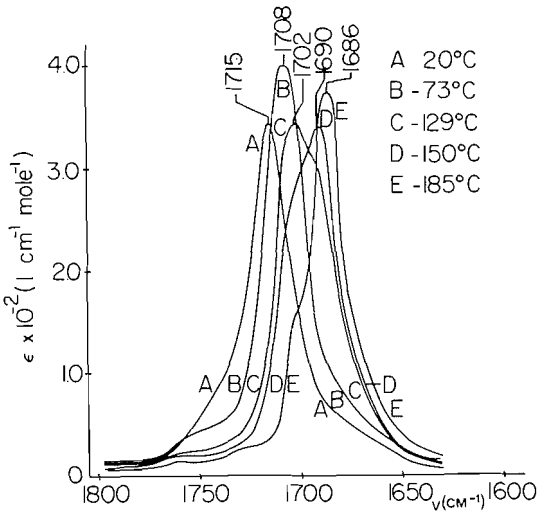

FIG. 5. The i.r. spectra (1600–1800 cm^{-1}) of a 0.26 *M* solution of thioloacetic acid in FR at different temperatures.

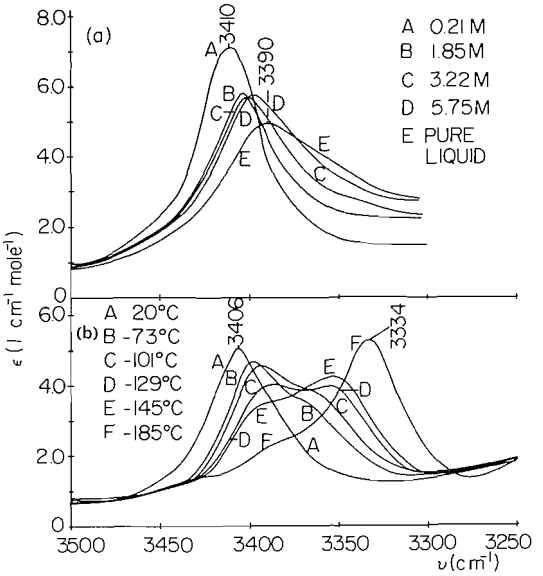

FIG. 6. The i.r. spectra (3250–3500 cm^{-1}) of solutions of thioloacetic acid (*a*) at different concentrations in CCl_4 at 20 °C; (*b*) 0.90 *M* in FR at different temperatures.

found also in the region 2500–2550 cm^{-1} where we have found the association bands), they should be considered unlikely because the oxygen atom is a better acceptor than the sulfur atom. In fact one can see that the carbonyl stretching frequency undergoes changes paralleling those of the S—H band, both upon increases in concentration of the thiolic acids at the same temperature in solution, or upon decreasing the temperature of a dilute solution. It seems, therefore, that S—H---O type bonds are formed, and that the best analogy for the understanding of self-association in thiolic acids is the carboxylic acids, as pointed out by Ginzburg and Loginova (3). On the other hand, since mercaptans are known to associate less than the corresponding alcohols, we must expect to observe the formation of only a few associated species of the S—H---O type. The possible structures are small chain oligomers and small cyclic structures with probably no more than three molecules in each.

Our evidence (the existence of two associated bands in the S—H stretching region and the virtual absence of free S—H and C=O bands at low temperatures) seems to show that only the cyclic structures remain at the lowest temperature but the possibility of having open structures is likely at intermediate temperatures. Acetic acid is known (9) to form cyclic dimers, both in the gas phase and in dilute solutions. In more concentrated solutions or in the pure liquid, open chain oligomers are found. It seems natural to assign the less displaced associated bands to the open dimer **1** which at lower

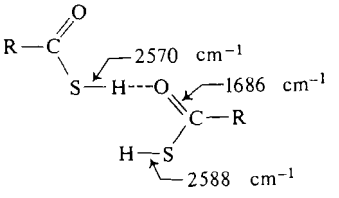

1

temperatures changes into a cyclic structure. Earlier data on thioloacetic acid add support for the existence of the cyclic dimer structure **2** (10). A CSH angle of 105° is sufficient to obtain a structure similar to the acetic acid dimer. No distortion in the obtained structure in the gas phase is required supposing a linear hydrogen bonding (compare with a HSH angle of 92° in H_2S (11) and a CSH angle of 96° 30′ in simple mercaptans (12, 13)).

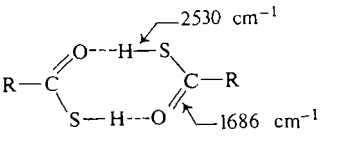

2

Can. J. Chem. Downloaded from www.nrcresearchpress.com by 210.87.254.105 on 09/05/12
For personal use only.

The anharmonicity coefficients computed from

$$W_e X_e = \nu_{01} - \nu_{02}/2$$

are of the order of 50–60 cm^{-1}, for both the free and associated S—H groups which is about the same value we found for mercaptans (1). The values for the C=O stretching vibration are of about 10 cm^{-1} and are not very different from those of free or associated carbonyls.

Conclusions

The above results seem to indicate that thiolic acids are associated by S—H---O bonds. Two species are found when temperature is lowered or concentration raised. The first is probably an open dimer and the second a cyclic dimer. The S—H stretching anharmonicity constants are low and are of the order of 50–60 cm^{-1} for both free and associated species and have about the same values as in aliphatic or aromatic mercaptans. Carbonyl groups have lower anharmonicities. Their values are about 10 cm^{-1} for both free and associated species.

We would like to express our thanks to the National Research Council of Canada for financial help. One of us (RBA) would like also to express his gratitude to the National Research Council of Canada and the Conselho Nacional de Pesquisas, Rio de Janeiro, Brazil, for financial support under the Brazil-Canada Program for Scientific Exchange, and to the Instituto de Química da Universidade Federal do Rio de Janeiro, Rio de Janeiro, Brazil, for a special leave of absence.

1. R. Bicca de Alencastro and C. Sandorfy. Can. J. Chem. **50**, 3594 (1972).
2. R. Bicca de Alencastro and C. Sandorfy. Can. J. Chem. In press.
3. I. M. Ginzburg and L. A. Loginova. Opt. Spectrom. **20**, 130 (1966).
4. A. S. N. Murthy, C. N. R. Rao, B. D. Nageswara Rao, and P. Venkateswarhi. Trans. Faraday Soc. **58**, 855 (1962).
5. R. Mecke and H. Spiesecke. Chem. Ber. **89**, 1110 (1956).
6. G. Allen and R. O. Colclough. J. Chem. Soc. 3912 (1957).
7. H. Wolff and G. Gamer. J. Phys. Chem. **76**, 871 (1972).
8. S. N. Vinogradov and R. H. Linnell. Hydrogen bonding. Van Nostrand Reinhold Co. N.Y. 1971. p. 64.
9. (*a*) M. Haurie. Ph.D. Thesis. Université de Bordeaux. France. 1966. (*b*) M. Haurie and A. Novak. Spectrochim. Acta, **21**, 1217 (1965).
10. W. Gordy. J. Chem. Phys. **14**, 560 (1946).
11. G. Herzberg. Infrared and Raman spectra. Van Nostrand Co., Inc. London. 1945. p. 489.
12. M. Hayashi, H. Imaishi, K. Ohno, and H. Murata. Bull. Chem. Soc. Japan, **43**, 872 (1971).
13. T. Kojima. J. Phys. Soc. Jap. **15**, 1248 (1960).

Can. J. Chem. Downloaded from www.nrcresearchpress.com by 210.87.254.105 on 09/05/12
For personal use only.

Synthesis and Rearrangement Control of Substituted Benzobicycloheptane Aziridines

K. WIESNER, PAK-TSUN HO, R. C. JAIN, S. F. LEE, S. OIDA, AND A. PHILIPP

Natural Products Research Center, University of New Brunswick, Fredericton, New Brunswick

Received December 1, 1972

A general synthesis of various substituted benzonorbornene derivatives is described. Benzenesulfonyl aziridines of these compounds were prepared and their acetolysis was studied. The influence of various substitution patterns on the direction of the aziridine rearrangement is discussed and it is shown that the rearrangements may be used as a convenient approach to the synthesis of ring B bridged diterpene alkaloids. Considerable general synthetic utility of these techniques is anticipated.

Une synthèse générale de plusieurs dérivés du benzonorbornène substitué est décrite. Les aziridines benzènesulphonyles de ces composés ont été préparés et leurs acétolyses furent étudiées. L'influence de plusieurs patrons de substitution sur la direction du réarrangement de l'aziridine est discutée. On a montré que ces réarrangements peuvent être utilisés pour une approche convenable à la synthèse de l'anneau B des diterpènes alcaloides pontés. Une utilité considérable en synthèse générale de ces techniques est envisagée. [Traduit par le journal]

Can. J. Chem., **51**, 1448 (1973)

In connection with studies aimed at the synthesis of ring B bridged diterpene alkaloids, we wished to develop highly efficient regio and stereospecific routes to tricyclic compounds of the type **i** and **ii**.

A simple and efficient synthesis of **i** in which the acetolysis of the aziridine **v** was the key step was worked out (1) and the product converted to the songorine intermediate **iii** (2).

The second target of our synthetic work was compound **ii**, which if available could be developed by the same techniques to the chasmanine intermediate **iv**. It turned out, however, that the aziridine **vi** cannot be used to this end since (not surprisingly) it does not yield compound **ii** on acetolysis. This problem has now been fully solved and the synthesis of **iv** is under way. Since the methods which we have developed for the synthesis and rearrangement-control of benzobicycloheptane aziridines are quite novel and of general synthetic interest, we report them in detail in the present paper.

The derivatives which were found to be most suitable for acetolytic rearrangement were benzenesulfonyl aziridines prepared by the action of benzenesulfonyl azide on the corresponding substituted benzobicycloheptenes (3). Consequently, it was first necessary to devise regiospecific methods for the preparation of these last compounds with varying substitution.

The synthesis of the ester **3** was quite simple (3), since no problem with the orientation of a benzene ring substituent existed in this case. Cyclopentadiene carboxylic ester **1**, freshly prepared by distillation of the dimer, was added to the benzyne precursor **2** which had been previously used by Wittig (4). The oily adduct **3** was isolated in a 30% yield by chromatography.[1]

The synthesis of compound **8** had to be performed in an entirely different manner in order to achieve a regiospecific orientation of the methoxyl. The known keto ester **4** (5) was reduced with sodium borohydride to the alcohol **5** and this compound was dehydrated with a

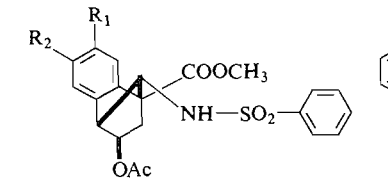

i $R_1 = OCH_3; R_2 = H$
ii $R_1 = H; R_2 = OCH_3$

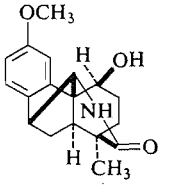

iii

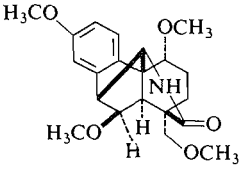

iv

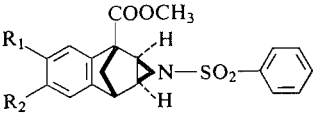

v $R_1 = OCH_3; R_2 = H$
vi $R_1 = H; R_2 = OCH_3$

[1]Full characterization and all spectral data for all compounds may be found in the Experimental.

Can. J. Chem. Downloaded from www.nrcresearchpress.com by 210.87.254.42 on 09/05/12
For personal use only.

Can. J. Chem. Downloaded from www.nrcresearchpress.com by 210.87.254.42 on 09/05/12
For personal use only.

simultaneous double bond shift to the unsaturated ester **6**. Since it was known that indene adds maleic anhydride to yield the anhydride of benzonorbornane dicarboxylic acid (6), it was originally hoped that addition of acetylene or of an acetylene equivalent to **6** would yield directly the desired compound **8**. It turned out however, that while the crystalline adduct with maleic anhydride **7** was formed quantitatively, no other suitable dienophile reacted in an acceptable yield.

After many months of experimentation it was finally discovered that **7** may be bisdecarboxylated to **8** in refluxing diglyme by the action of bistriphenylphosphinenickel dicarbonyl (7) in a yield of 81%. Compound **8** was identical with one of the two products obtained by us previously by the non-regiospecific addition of cyclopentadiene carboxylic ester and methoxy benzyne (8). The entire sequence **4** → **8** was accomplished in a yield of 44% and is consequently quite satisfactory.

The synthesis of compound **16** starting with the ketoester **12** was performed precisely as described above for compound **8**. The ketoester **12** however was not known and it was synthesized as follows. *m*-Methoxyacetophenone

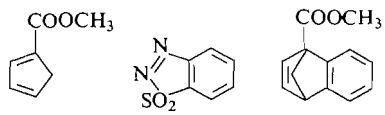

1 **2** **3**

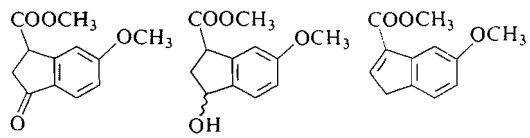

4 **5** **6**

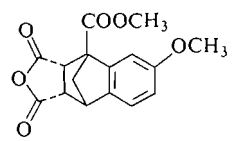

7

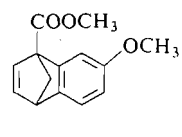

8

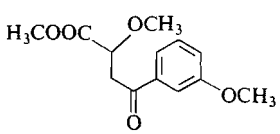

9

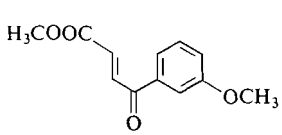

10

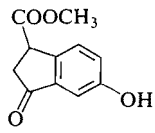

11

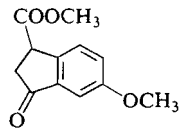

12

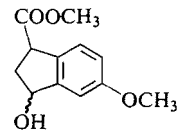

13

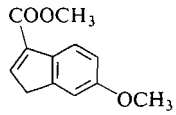

14

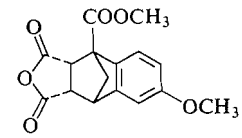

15

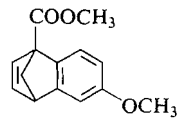

16

was condensed in methanolic sodium hydroxide with glyoxylic acid, freshly generated by periodate cleavage of tartaric acid. The oily mixture of compounds **9** and **10** which was produced almost quantitatively was directly used in the next step. The mixture was cyclized with aluminum chloride at 185 °C for 90 min. The crystalline phenol **11** was obtained in a yield of 46% based on the starting *m*-methoxyacetophenone. Finally, the phenol **11** was methylated with dimethyl sulfate in the presence of anhydrous potassium carbonate in benzene to yield quantitatively the crystalline methoxyester **12**.

The phenol **11** was also mesylated with mesylchloride in pyridine to the mesyloxyketoester **17** and this compound was transformed by the already described route (via **18**, **19**, and **20**) to compound **21**. The yield in the transformation **19** → **20** was only approximately 50% as compared to the quantitative reaction of the methoxy derivatives **6** and **14**. It would appear that the thermal 1,5 hydride shift which presumably precedes the Diels–Alder addition of maleic anhydride is favored by an electron releasing substituent in the benzene ring.

Finally the compound **24** which contains a methoxy group at the bridgehead was required. It was prepared by a simple adaptation of our general indene approach. The ketoester **12** was stirred with trimethyl orthoformate and a small amount of hydrogen chloride in benzene–methanol to give a quantitative yield of the enolether **22**. The addition of maleic anhydride to **22** yielded the adduct **23** and bisdecarboxylation of

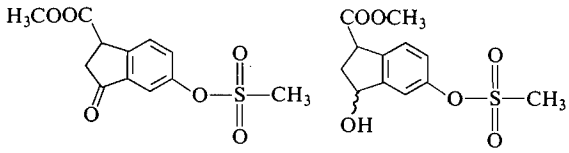

17

18

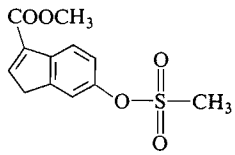

19

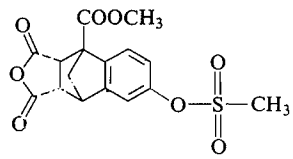

20

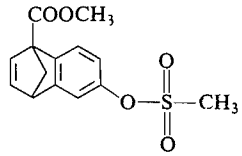

21

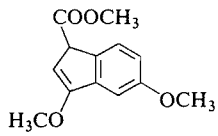

22

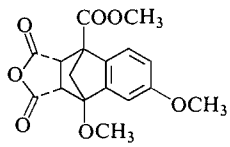

23

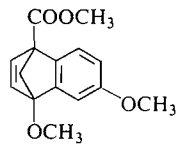

24

this compound gave finally the desired product **24**.

Having described the synthesis of all the desired substituted benzonorbornenes we shall now proceed and discuss the preparation and rearrangements of the corresponding aziridines.

The aziridine **25** (Chart 1) was prepared by treating compound **3** with benzenesulfonyl azide in anhydrous benzene. It was a somewhat unstable oil but gave spectral data (see Experimental) which confirmed its structure and the expected *exo* stereochemistry. In this respect the singlet of the two protons unshielded by the nitrogen (τ 6.65 p.p.m.) in the n.m.r. spectrum was significant. The absence of coupling with the bridgehead proton indicated clearly the *endo* configuration of the protons unshielded by the aziridine.

The acetolysis of the aziridine **25** was performed by heating the compound to 100 °C in glacial acetic acid. Under these conditions the aziridine ring opens with rearrangement and the resulting carbonium ion reacts with acetic acid. This process as portrayed by arrows in formula **25** (Chart 1) leads to the product **26**.

An exactly analogous process initiated by the opening of the second carbon–nitrogen bond yields the product **27**. It was anticipated that the product **26** will greatly predominate, since the formation of compound **27** requires the development of a carbonium ion adjacent to a carbonyl group, a situation known to be energetically very unfavorable.

Thus, we hoped that the ester group shall play a dual role in our projected terpene alkaloid syntheses. It was expected to serve in the annelation of ring A and as a site of a future substituent and at the same time to steer the aziridine rearrangement.

The result of the acetolysis experiment in fact bore out our prediction. The desired acetolysis product **26** predominated over compound **27** in a ratio 94:6. Compound **26** was crystalline and the small amount of **27** remained oily. Spectral data recorded in the Experimental leave no doubt about the assignment of structures to the two compounds. While **26** shows in the n.m.r. spectrum a proton unshielded by acetate (τ 5.33 p.p.m.), compound **27** displays two benzylic bridgehead protons (τ 6.65 p.p.m.) and a methoxy group highly shielded by the benzene ring (τ 7.82 p.p.m.) as a result of the *endo* configuration of the carbomethoxyl.

The songorine intermediate **8** was investigated next. In this case the aziridine formed in benzene by the action of benzenesulfonyl azide proved to be too unstable for isolation and it was acetolyzed at room temperature yielding exclusively the product **28**. The methoxyl located in para position to the migrating carbon–carbon bond greatly accelerates the reaction rate of the rearrangement leading to **28**. At the same time the carbomethoxy group slows down as before the rate of the alternative competing reaction. Thus, complete selectivity and a much faster reaction rate result. Compound **28** was beautifully crystalline and spectral data recorded in the Experimental leave no doubt about its structure. Moreover, the structure of an intermediate derived from **28** on the way to **iii** was corroborated by X-ray crystallography (2).

The unlikely possibility that compound **ii** could be prepared by acetolysis of the benzenesulfonyl aziridine derived from **16** was demolished by a single experiment. The acetolysis proceeded at room temperature and the single amorphous product had clearly the structure **29**. All n.m.r. data obtained for compound **29** were

Can. J. Chem. Downloaded from www.nrcresearchpress.com by 210.87.254.42 on 09/05/12
For personal use only.

Can. J. Chem. Downloaded from www.nrcresearchpress.com by 210.87.254.42 on 09/05/12
For personal use only.

Olefins	Aziridines	Rearranged products		Overall yields from olefins
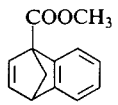 **3**	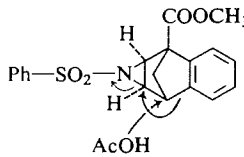 **25**	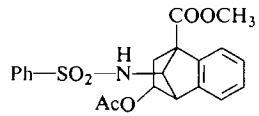 **26** (94%)	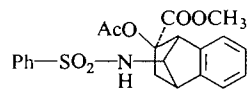 **27** (6%)	66.4%
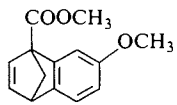 **8**		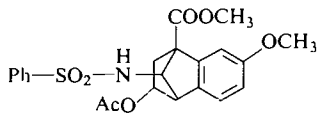 **28** (100%)		75%
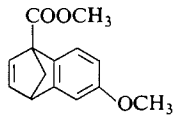 **16**			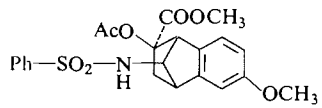 **29** (100%)	74%
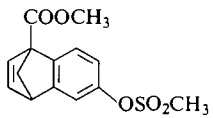 **21**	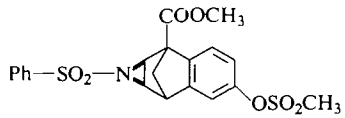 **30**	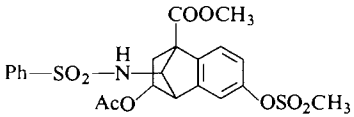 **31** (90%)	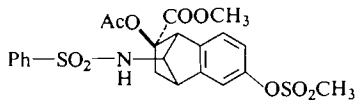 **32** (10%)	52.5%
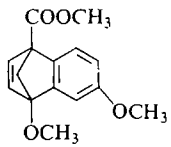 **24**	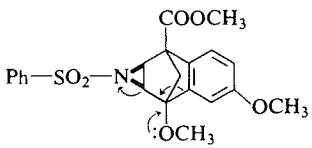 **33**	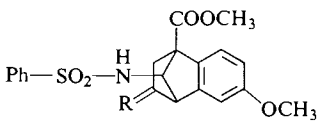 **34** R = O **35** R = (70%)	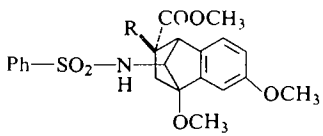 **36** R = OH **37** R = OAc (30%)	86%

CHART I

Can. J. Chem. Downloaded from www.nrcresearchpress.com by 210.87.254.42 on 09/05/12
For personal use only.

comparable to those of compound **27** and excluded the desired structure **ii**.

It was thus clear that the great increase in migratory aptitude of the bond para to the methoxyl overpowered the reaction rate decelerating influence of the carbomethoxyl.

Since a compound of the type **ii** was needed as a chasmanine starting material two devices were tried to steer the corresponding aziridine rearrangement.

First the methoxyl of compound **16** was replaced by a mesyloxy group and the substituted benzonorbornene derivative **21** was synthesized by the method which we have described above. Treatment of this product with benzenesulfonyl azide gave the stable crystalline aziridine **30**.

It was anticipated that the behavior of compound **30** on acetolysis will be similar to the unsubstituted aziridine **25**. We assumed that since the electron-releasing properties of a mesyloxy group are approximately equal to those of a hydrogen the aziridine rearrangement will be dominated by the already discussed influence of the carbomethoxyl.

This expectation was born out by experiment. The acetolysis of **30** was slow and had to be performed at 110 °C, but the ratio of the products **31** and **32** was favorable (9:1). However, the overall yield of the acetolysis was a low 52.5% and a few additional steps would be required to convert compound **31** into **ii**. Consequently we have turned to the examination of a still different possibility of rearrangement control.

As described above we have synthesized compound **24** which featured a methoxy group at the bridgehead. Treatment of **24** with benzenesulfonyl azide in a mixture of benzene and acetic acid presumably gave the unstable aziridine **33**. This compound underwent immediate acetolysis, in which the bridgehead methoxyl cooperated with the carbomethoxyl (as indicated by arrows in **33**) to counteract the influence of the aromatic methoxyl. The overall yield of the reaction was 86%. Of this 70% was the ketone **34** which was isolated after being converted into the crystalline ketal **35**. The alcohol **36** and the corresponding acetate **37** formed 30% of the mixture.

Compound **36** was characterized by conversion into the crystalline acetate **37** by acetic anhydride and pyridine.

The ketal **35** is a very advantageous chasmanine starting material and the synthesis is now underway using this supply route. Our methods of synthesis and rearrangement control of various substituted benzonorbornane aziridines are capable of wide synthetic application and consequently are described in the Experimental in considerable detail.

We shall report in the future on synthetic applications of these techniques in several fields unrelated to diterpene alkaloids.

Experimental

Preparation of the Olefin 3

A dimer of methyl cyclopentadiene carboxylate (9) (25 g) was distilled at 90–120 °C (12 mm Hg) and the monomeric ester **1** was collected in a cold flask (−80 °C). The monomer was dissolved in cold anhydrous tetrahydrofuran (200 ml) and added to freshly prepared crystalline 1,2,3-benzothiadiazol-1,1-dioxide (**2**) (4) at −20 °C. When the reaction mixture reached room temperature, evolution of nitrogen and sulfur dioxide occurred and the mixture was left overnight. Evaporation of solvent gave a crude product which was purified by chromatography on silica gel. Elution with benzene yielded 8.3 g (30%) of oily **3**, homogeneous in t.l.c., b.p. 50 °C (0.1 mm Hg).

Anal. Calcd. for $C_{13}H_{12}O_2$ (mol. wt. 200): C, 77.98; H, 6.04; OMe, 15.50. Found (*m/e* 200): C, 78.07; H, 6.21; OMe, 15.13.

I.r. ($CHCl_3$): 1735 cm^{-1} (ester); n.m.r. ($CDCl_3$): τ 2.77–3.20 (m, 6H, aromatic and vinylic protons), 6.07 (m, 1H, bridgehead proton), 6.17 (s, 3H, $-\overset{\overset{O}{\|}}{C}-O-CH_3$), 7.47 (broad s, 2H, apex protons).

Preparation of Benzenesulfonyl Aziridine 25

A solution of the olefin **3** (1.03 g) and benzenesulfonyl azide (1.60 g) in anhydrous benzene (2 ml) was stirred at room temperature for 17 h and the mixture was chromatographed on silica gel. Elution with benzene – ethyl acetate (97:3) gave 1.52 g (83%) of the aziridine **25** as an oil, homogeneous in t.l.c.

Mol Wt. calcd. for $C_{19}H_{17}O_4NS$: 355. Found (*m/e*): 355.

I.r. ($CHCl_3$): 1730 (ester), 1160 cm^{-1} (aziridine); n.m.r. ($CDCl_3$): τ 6.16 (s, 3H, $-\overset{\overset{O}{\|}}{C}-O-CH_3$), 6.46 (broad s, 1H, bridgehead proton), 6.65 (broad s, 2H, 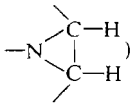), 8.97 (two d, 2H, apex protons).

Acetolysis of the Aziridine 25

A solution of **25** (327 mg) in glacial acetic acid (10 ml) was heated to 100 °C for 2½ h. The mixture was poured into cold aqueous sodium bicarbonate and extracted with chloroform. The chloroform solution was washed with water, dried, and taken to dryness. Analysis of the residue by t.l.c. showed the presence of two products **26** and **27** (ratio, 94:6). The mixture was separated by preparative t.l.c. on silica gel using benzene – ethyl acetate (85:15) to afford 287 mg of **26** (75%) and 16 mg

Can. J. Chem. Downloaded from www.nrcresearchpress.com by 210.87.254.42 on 09/05/12
For personal use only.

(4.8%) of the tertiary acetate **27**. Recrystallization of **26** from chloroform–ether gave white crystals, m.p. 165–166 °C; **27** refused to crystallize in several solvents.

Anal. Calcd. for $C_{21}H_{21}O_6NS$ (secondary acetate **26** mol. wt. 415): C, 60.71; H, 5.10. Found (*m/e* 415): C, 60.51; H, 5.10.

I.r. (KBr pellet): 3300 (NH), 1735 (ester, acetate), 1335, 1170 cm^{-1} (sulfonyl); n.m.r. ($CDCl_3$): τ 4.16 (d, J = 9 Hz, 1H, —NH), 5.33 (m, 1H, proton adjacent to acetate), 6.23 (d, J = 9 Hz, 1H, apex proton), 6.40 (s, 3H, —C(=O)—OCH_3), 6.90 (broad s, 1H, benzylic proton), 7.90 (s, 3H, acetate methyl).

Mol. Wt. Calcd. for $C_{21}H_{21}O_6NS$ (tertiary acetate **27**): 415. Found (*m/e*): 415.

I.r. ($CHCl_3$): 3400 (NH), 1762, 1740 (acetate and ester), 1360, 1162 cm^{-1} (sulfonyl); n.m.r. ($CDCl_3$): τ 4.39 (d, J = 8 Hz, 1H, —NH), 6.40 (d, J = 8 Hz, 1H, apex proton), 6.65 (m, 2H, two benzylic protons), 6.72 (s, 3H, —C(=O)—OCH_3 shielded by aromatic ring), 7.82 (s, 3H, acetate methyl).

*Reduction of **4** to **5***

Sodium borohydride (2.3 g) was added in portions over a period of ½ h at room temperature to a stirred solution of the ketone **4** (5) (31.3 g) in tetrahydrofuran (250 ml) and methanol (250 ml). The mixture was stirred at room temperature for 1 h, diluted with water (1 l), and extracted with chloroform three times. The combined extracts were washed with water and dried over anhydrous magnesium sulfate. Removal of the solvent *in vacuo* gave 30.6 g (97%) of the alcohol **5**. For analysis, **5** was crystallized from benzene–hexane, m.p. 79–80 °C.

Anal. Calcd. for $C_{12}H_{14}O_4$: C, 64.85; H, 6.35. Found: C, 64.79; H, 6.11.

I.r. (CCl_4): 3480 (OH), 1724 cm^{-1} (ester); n.m.r. ($CDCl_3$): τ 6.14 (s, 3H, aromatic methoxyl), 6.20 (s, 3H, —C(=O)—OCH_3), 6.00 (q, 1H, benzylic proton adjacent to —C(=O)—OCH_3), 4.87 (q, 1H, proton adjacent to OH).

*Preparation of the Indene **6***

A solution of the alcohol **5** (30.6 g) in methanol (150 ml) was added dropwise over a period of 1½ h to a refluxing solution of concentrated sulfuric acid (20 ml) in methanol (300 ml) and the mixture was kept at reflux for an additional 2 h. The reaction mixture was cooled, diluted with water (1 l) and extracted with chloroform three times. The extract was washed with a saturated sodium chloride solution and dried over anhydrous magnesium sulfate. After removal of the solvent, the residue was distilled *in vacuo* to give the pure **6** (19.5 g, 67% based on **4**) as an oil homogeneous in t.l.c., b.p. 139 °C (0.3 mm Hg).

Mol. Wt. Calcd. for $C_{12}H_{12}O_3$: 204. Found (*m/e*): 204.

I.r. (CCl_4): 1727 cm^{-1} (ester); n.m.r. ($CDCl_3$): τ 2.47 (t, J = 2 Hz, 1H, vinylic proton), 6.05 (s, 3H, aromatic methoxyl), 6.08 (s, 3H, —C(=O)—OCH_3), 6.52 (d, 2H, benzylic protons).

*Preparation of the Adduct **7***

A mixture of compound **6** (19.5 g), maleic anhydride (9.36 g), and a small amount of hydroquinone (10 mg) was heated under nitrogen at 170 °C (oil bath temperature) for 3 h. The adduct **7** was homogeneous in t.l.c. and the yield was quantitative. Material of this purity was used in the subsequent step. An analytical sample was prepared by crystallization from benzene as white crystals, m.p. 147–148 °C.

Anal. Calcd. for $C_{16}H_{14}O_6$: C, 63.57; H, 4.67. Found: C, 63.45; H, 4.39.

I.r. ($CHCl_3$): 1870, 1790 (anhydride), 1740 cm^{-1} (ester); n.m.r. ($CDCl_3$): τ 6.03 (s, 3H, aromatic methoxyl), 6.15 (broad s, 1H, bridgehead proton), 6.18 (s, 3H, —C(=O)—O—CH_3), 7.67 (m, 2H, apex protons).

*Preparation of the Olefin **8***

The Diels–Alder adduct **7** (16.4 g) was dissolved in anhydrous diglyme (300 ml) to which bistriphenylphosphinenickel dicarbonyl (42 g) was added. The mixture was heated under reflux in a dry nitrogen atmosphere for 6 h. The solvent was distilled off under reduced pressure. The residue was dissolved in chloroform and the black precipitate was removed by filtration. After evaporation of the solvent, the product was isolated by chromatography on silica gel. Elution with benzene gave the crystalline olefin **8** (10.2 g, 81%), homogeneous in t.l.c. The analytical sample had m.p. 63–64 °C after recrystallization from hexane.

Anal. Calcd. for $C_{14}H_{14}O_3$: C, 73.02; H, 6.13. Found: C, 73.05; H, 5.92.

I.r. (CCl_4): 1745 cm^{-1} (ester); n.m.r. ($CDCl_3$): τ 3.17 (broad d, 2H, vinylic protons), 6.10 (broad s, 1H, bridgehead benzylic proton), 6.09 (s, 3H, aromatic methoxyl) 6.21 (s, 3H, —C(=O)—OCH_3), 7.45 (broad s, 2H, apex protons).

*Preparation of Rearranged Sulfamido Acetate **28***

A solution of the olefin **8** (38 g) and benzenesulfonyl azide (80 g) in anhydrous benzene (150 ml) was stirred at room temperature for 3 days. Glacial acetic acid (240 ml) was then added to this stirred solution and the reaction mixture was kept at room temperature for 2 days. After this time, benzene and most of the acetic acid was distilled off *in vacuo*. The residue was then dissolved in benzene–hexane and the product **28** crystallized on standing. Recrystallization of the product from benzene–hexane gave 56.5 g (75%) of **28**, m.p. 137 °C.

Anal. Calcd. for $C_{21}H_{23}O_7NS$ (mol. wt. 445): C, 59.13; H, 5.24; N, 3.14. Found (*m/e* 445): C, 59.23; H, 5.26; N, 3.19.

I.r. ($CHCl_3$): 3300 (NH), 1740 (ester and acetate), 1345, 1170 cm^{-1} (sulfonyl); n.m.r. ($CDCl_3$): τ 4.20 (d, J = 9 Hz, 1H, —NH), 5.24 (broad t, 1H, proton adjacent to acetate), 6.17 (d, J = 9 Hz, 1H, apex proton), 6.24 (s,

Can. J. Chem. Downloaded from www.nrcresearchpress.com by 210.87.254.42 on 09/05/12
For personal use only.

3H, aromatic methoxyl), 6.34 (s, 3H, —C(=O)—OCH_3), 6.70 (s, 1H, bridgehead benzylic proton), 7.84 (s, 3H, acetate methyl).

*Preparation of the Condensed Products (**9**, **10**)*

A solution of *d*-tartaric acid (20 g) in distilled water (30 ml) was added to a cooled suspension of trisodium periodate (para) (30 g) in concentrated sulfuric acid (3 ml) and distilled water (160 ml), and the mixture was stirred at room temperature for ½ h. *m*-Methoxyacetophenone (20 g), sodium hydroxide (20 g) in distilled water (360 ml), and methanol (300 ml) were added in sequence. The reaction mixture was stirred at room temperature overnight. The solution was poured into ice-water, acidified with dilute hydrochloric acid and extracted with ether (3 × 500 ml). The ethereal extract was washed with water and dried over anhydrous sodium sulfate. The volume of the dried ethereal solution was reduced to 200 ml, and treated with diazomethane. The solvent was removed *in vacuo*, the mixture (30 g) was immediately used in the subsequent step.

Analysis by t.l.c. showed that the mixture consisted of two components, **9** and **10** (ratio, 8:1). A portion (121 mg) was separated by preparative t.l.c. Compound **9** (85 mg) was oily; compound **10** (15 mg) was a waxy solid.

Mol. Wt. Calcd. for $C_{13}H_6O_5$ (saturated ketone **9**): 252. Found (*m/e*): 252.

I.r. ($CHCl_3$): 1750 (ester), 1690 cm^{-1} (ketone); n.m.r. ($CDCl_3$): τ 6.17 (s, 3H, aromatic methoxyl), 6.24 (s, 3H, —C(=O)—OCH_3), 6.54 (s, 3H, methoxyl), 6.64 (d, 2H, methylene protons).

Mol. Wt. Calcd. for $C_{12}H_{12}O_4$ (unsaturated ketone **10**): 220. Found (*m/e*): 220.

I.r. ($CHCl_3$): 1725 (ester), 1675 cm^{-1} (conjugated ketone); n.m.r. ($CDCl_3$): τ 2.14 (d, J = 15 Hz, 1H, vinylic proton), 3.15 (d, J = 15 Hz, 1H, vinylic proton), 6.15 (s, 3H, aromatic methoxyl), 6.19 (s, 3H, —C(=O)—OCH_3); u.v. (EtOH): λ_{max} 235 nm (ε 12 000).

*Preparation of the Phenol **11***

A solution of **9** and **10** (30 g) in a small volume of anhydrous dichloromethane (30 ml) was added dropwise over a period of 5 min to a preheated (at 130 °C) mixture of anhydrous aluminum chloride (300 g) and sodium chloride (45 g). The mixture was shaken mechanically and at the same time the temperature was raised to 185 °C (oil bath temperature) and maintained at this temperature for 1½ h. While the mixture was cooled to 100 °C, water and concentrated hydrochloric acid (200 ml) were added slowly in sequence. The product was extracted with ether and the ethereal solution was dried over anhydrous sodium sulfate and evaporated to dryness. The resulting brown residue (20 g) was dissolved in methanolic hydrogen chloride (300 ml) and heated under reflux for 2 h. After removal of the solvent, the residue was chromatographed on silica gel to give 12 g (46%, based on *m*-methoxylacetophenone) of the crystalline phenol **11**. Recrystallization from acetone–ether gave an analytical sample as white crystals, m.p. 141–142 °C.

Anal. Calcd. for $C_{11}H_{10}O_4$: C, 64.07; H, 4.88. Found: C, 64.20; H, 4.88.

I.r. ($CHCl_3$): 3600, 3500 (OH), 1740, 1710 cm^{-1} (ester and ketone); n.m.r. ($CDCl_3$): τ 5.82 (q, 1H, benzylic proton), 6.20 (s, 3H, —C(=O)—OCH_3), 6.99 (t, 2H, methylene).

*Preparation of the Methyl Ether **12***

A mixture of the phenol **11** (1.03 g), benzene (20 ml), anhydrous potassium carbonate (1.42 g), and dimethyl sulfate (1 ml) was refluxed under nitrogen for 8 h and then stirred at room temperature overnight. The precipitate was filtered and washed with dichloromethane. The filtrate was washed with dilute aqueous hydrochloric acid and water, dried over anhydrous sodium sulfate, and evaporated to give the methyl ether **12** (1.10 g, 100%) homogeneous in t.l.c. Recrystallization of **12** from benzene–hexane gave colorless plates, m.p. 73–74 °C.

Anal. Calcd. for $C_{12}H_{12}O_4$ (mol. wt. 220): C, 65.44; H, 5.49. Found (*m/e* 220): C, 65.46; H, 5.55.

I.r. (CCl_4): 1750, 1725 cm^{-1} (ester, ketone); n.m.r. (CCl_4): τ 5.87 (two d, 1H, benzylic proton), 6.17 (s, 3H, aromatic methoxyl), 6.27 (s, 3H, —C(=O)—OCH_3).

*Reduction of **12** to **13***

The ketone **12** (678 mg) was dissolved in methanol (10 ml) and tetrahydrofuran (5 ml), and sodium borohydride (90 mg) was added at 0 °C. The mixture was stirred for 40 min and the same work-up as described above yielded 680 mg (100%) of the alcohol **13** as white crystals. Recrystallization of **13** from chloroform–ether gave crystals, m.p. 93–94 °C.

Anal. Calcd. for $C_{12}H_{14}O_4$: C, 64.85; H, 6.35. Found: C, 64.81; H, 6.10.

I.r. ($CHCl_3$): 3612, 3484 (OH), 1740 cm^{-1} (ester); n.m.r. ($CDCl_3$): τ 4.10 (q, 1H, benzylic proton), 4.97 (m, 1H, proton unshielded by OH), 6.22 (s, 3H, aromatic methoxyl), 6.27 (s, 3H, —C(=O)—OCH_3).

*Dehydration of **13** to **14***

A solution of **13** (324 mg) in 12% methanolic sulfuric acid (15 ml) was heated under reflux for 2 days. The reaction mixture was worked-up in the same way as described above. Recrystallization of the product from ether gave 120 mg (40%) of **14** as colorless needles, m.p. 96 °C.

Anal. Calcd. for $C_{12}H_{12}O_3$ (mol. wt. 204): C, 70.57; H, 5.92. Found (*m/e* 204): C, 70.52; H, 5.84.

I.r. ($CHCl_3$): 1708 cm^{-1} (unsaturated ester); n.m.r. ($CDCl_3$): τ 2.72 (t, 1H, vinylic proton), 6.12 (s, 3H, aromatic methoxyl), 6.20 (s, 3H, —C(=O)—OCH_3), 6.57 (d, 2H, benzylic protons).

*Preparation of the Diels–Alder Adduct **15***

The indene **14** (230 mg) and maleic anhydride (140 mg) were heated to 168 °C for 13 h in a sealed tube. The adduct **15** was recrystallized from acetone–ether to a m.p. of 154–155 °C. The yield was 270 mg (80%).

Anal. Calcd. for $C_{14}H_{14}O_6$ (mol. wt. 302): C, 63.57; H, 4.67. Found (*m/e* 302): C, 63.35; H, 4.66.

Can. J. Chem. Downloaded from www.nrcresearchpress.com by 210.87.254.42 on 09/05/12
For personal use only.

I.r. ($CHCl_3$): 1844, 1792 (anhydride), 1744 cm^{-1} (ester); n.m.r. (acetone-d_6): τ 6.14 (s, 3H, aromatic methoxyl), 6.21 (broad s, 1H, bridgehead proton), 6.25 (s, 3H, —C(=O)—OCH_3), 7.70 (t, 2H, apex protons).

Preparation of the Olefin ***16***

The crude adduct **15** (370 mg) was dissolved in anhydrous diglyme (6 ml) and bistriphenylphosphinenickel dicarbonyl (1.2 g) was added. The mixture was refluxed under nitrogen for 40 min and it was worked-up as described above. The product was isolated by preparative t.l.c. on silica gel to give 126 mg (48% based on **14**) of oily **16**, homogeneous in t.l.c.

Mol. Wt. Calcd. for $C_{14}H_{14}O_3$: 230.0943. Found (*m/e*): 230.0947.

I.r. ($CHCl_3$): 1733 cm^{-1} (ester); n.m.r. ($CDCl_3$): τ 3.20 (m, 2H, vinylic protons), 6.11 (broad s, 1H, bridgehead proton), 6.14 (s, 3H, aromatic methoxyl), 6.25 (s, 3H, —C(=O)—OCH_3), 6.57 (d, 2H, apex protons).

Preparation of the Rearranged Product ***29***

A mixture of **16** (91 mg) and an excess of benzenesulfonyl azide (1 ml) in anhydrous benzene (0.5 ml) was stirred at room temperature for 3 days. Glacial acetic acid (1.5 ml) was added, the solution was stirred for an additional day, and the reaction mixture was worked-up as described above. Examination of the residue by t.l.c. in several solvent systems showed one product only. Preparative t.l.c. on silica gel gave 129 mg (74%) of **29** (homogeneous in t.l.c.) as a foam which refused to crystallize in several solvents.

Mol. Wt. Calcd. for $C_{21}H_{23}O_7NS$: 445.1195. Found (*m/e*): 445.1183.

I.r. ($CHCl_3$): 3400 (NH), 1756, 1740 cm^{-1} (acetate and ester); n.m.r. ($CDCl_3$): τ 4.50 (d, J = 8 Hz, 1H, —NH), 6.26 (s, 3H, aromatic methoxyl), 6.36 (broad s, 1H, benzylic proton), 6.40 (d, J = 8 Hz, 1H, apex proton), 6.67 (s, 3H, —C(=O)—OCH_3 shielded by benzene ring), 6.70 (s, 1H, benzylic proton), 7.84 (s, 3H, acetate methyl).

Preparation of the Mesylate ***17***

The phenol **11** (5.3 g) was dissolved in anhydrous pyridine (35 ml) and methane sulfonyl chloride (3 ml) was added at 0 °C. The reaction mixture was stirred for 5 h at that temperature and worked-up in the usual manner. The product **17** was recrystallized from chloroform to a m.p. 141–142 °C. The yield was 6.6 g (90%).

Anal. Calcd. for $C_{12}H_{12}O_6S$: C, 50.69; H, 4.25. Found: C, 50.66; H, 4.30.

I.r. ($CHCl_3$): 1744, 1725 (ester and ketone), 1375, 1144 cm^{-1} (sulfonyl); n.m.r. ($CDCl_3$): τ 5.67 (q, 1H, benzylic proton), 6.20 (s, 3H, —C(=O)—OCH_3), 6.80 (s, 3H, —OSO_2—CH_3).

Reduction of ***17*** *to the Alcohol* ***18***

The ketone **17** (2.0 g) was dissolved in methanol (30 ml) and tetrahydrofuran (15 ml), and sodium borohydride (250 mg) was added at 0 °C. The mixture was stirred for 20 min and the same work-up as described above yielded 2.0 g (quantitative yield) of the alcohol **18** as a colorless oil, homogeneous in t.l.c.

Mol. Wt. Calcd. for $C_{12}H_{14}O_6S$: 286. Found (*m/e*): 286.

I.r. (film): 3490 (OH), 1735 (ester), 1365, 1125 cm^{-1} (—OSO_2—); n.m.r. ($CDCl_3$): τ 4.90 (q, 1H, proton adjacent to hydroxyl), 6.09 (q, 1H, benzylic proton), 6.25 (s, 3H, —C(=O)—OCH_3), 6.89 (s, 3H, —OSO_2—CH_3), 7.50 (m, 2H, methylene).

Dehydration of ***18*** *to the Indene* ***19***

A mixture of the alcohol **18** (690 mg) and potassium bisulfate (700 mg) in anhydrous benzene (25 ml) was heated under reflux for 20 min with a water separator. The solid was removed by filtration, the filtrate was diluted with benzene (200 ml), washed, dried over anhydrous magnesium sulfate and evaporated to dryness. The residue was recrystallized from ether to give 445 mg (70%) of pure **19**, m.p. 106–107 °C.

Anal. Calcd. for $C_{12}H_{12}O_5S$: C, 53.72; H, 4.51. Found: C, 53.57; H, 4.55.

I.r. ($CHCl_3$): 1719 cm^{-1} (unsaturated ester); n.m.r. ($CDCl_3$): τ 2.54 (t, 1H, vinylic proton), 6.09 (s, 3H, —C(=O)—OCH_3), 6.45 (d, 2H, benzylic protons), 6.85 (s, 3H, —OSO_2—CH_3).

Preparation of the Diels–Alder Adduct ***20***

The indene carboxylic ester **19** (200 mg) and maleic anhydride (90 mg) were heated to 165 °C for 3 h in a sealed tube. The adduct **20** was homogeneous in t.l.c. and was used in the crude form for further work. For analysis it was purified by recrystallization from acetone to a constant, m.p. 223–224 °C.

Anal. Calcd. for $C_{16}H_{14}O_8S$ (mol. wt. 366): C, 52.45; H, 3.85. Found (*m/e* 366): C, 52.39; H, 3.88.

I.r. ($CHCl_3$): 1844, 1792 (anhydride), 1744 cm^{-1} (ester); n.m.r. (acetone-d_6): τ 6.02 (broad s, 1H, bridgehead proton), 6.07 (s, 3H, —C(=O)—OCH_3), 6.67 (s, 3H, —OSO_2—CH_3), 7.57 (t, 2H, apex protons).

Preparation of the Olefin ***21***

The crude adduct **20** (290 mg) was dissolved in anhydrous diglyme (6 ml) and bistriphenylphosphinenickel dicarbonyl (1.1 g) was added. The reaction mixture was refluxed under nitrogen for 2 h and worked-up as described above. Chromatography of the residue on silica gel gave 62 mg (30%, based on the indene **19**) of the pure olefin **21** as an oil homogeneous in t.l.c.

Mol. Wt. Calcd. for $C_{14}H_{14}O_5S$: 294.0562. Found (*m/e*): 294.0568.

I.r. ($CHCl_3$): 1737 cm^{-1} (ester); n.m.r. ($CDCl_3$): τ 3.17 (m, 2H, vinylic protons), 6.03 (broad s, 1H, bridgehead proton), 6.10 (s, 3H, —C(=O)—OCH_3), 6.90 (s, 3H, —OSO_2—CH_3), 7.42 (d, 2H, apex protons).

Preparation of the Aziridine ***30***

A solution of the olefin **21** (210 mg) and benzenesulfonyl azide (1.5 ml) in benzene (1 ml) was stirred at room

Can. J. Chem. Downloaded from www.nrcresearchpress.com by 210.87.254.42 on 09/05/12
For personal use only.

temperature for 2 days. The reaction mixture was purified by preparative t.l.c. on silica gel to yield 223 mg (70%) of the pure aziridine **30** as the only crystalline product. Recrystallization from benzene gave an analytical sample, m.p. 155–156 °C.

Anal. Calcd. for $C_{20}H_{19}O_7NS_2$ (mol. wt. 449): C, 53.44; H, 4.26; N, 3.11. Found (*m/e* 449): C, 53.47; H, 4.41; N, 3.20.

I.r. ($CHCl_3$): 1740 (ester), 1370, 1325 (OSO_2), 1160 cm^{-1} (aziridine); n.m.r. ($CDCl_3$): τ 6.35 (s, 3H, —C(=O)—OCH_3), 6.39 (broad s, 1H, bridgehead proton), 6.67 (broad s, 2H, —CH—CH— (N)), 6.87 (s, 3H, —OSO_2—CH_3), 7.67 (d, J = 9 Hz, 1H, one apex protons), 8.20 (d, J = 9 Hz, 1H, one apex protons).

Acetolysis of the Aziridine 30

A solution of **30** (130 mg) and *p*-toluenesulfonic acid (4 mg) in glacial acetic acid (2.5 ml) was heated to 110 °C for 2 h. After removal of the solvent *in vacuo*, chloroform (150 ml) was added to the residue and the solution was washed with water three times, dried, and evaporated to dryness. Analysis of the residue by t.l.c. showed the presence of two acetates **31** and **32** (ratio 9:1). This mixture was separated by preparative t.l.c. on silica gel to give 97 mg (67%) of crystalline **31** and 11 mg (7.5%) of the tertiary acetate **32** as an oil, homogeneous in t.l.c. Recrystallization of **31** from benzene gave an analytical sample, m.p. 196–197 °C.

Anal. Calcd. for $C_{22}H_{23}O_9NS_2$ (acetate **31** mol. wt. 509): C, 51.85; H, 4.55; N, 2.75. Found (*m/e* 509): C, 51.56; H, 4.67; N, 2.66.

I.r. ($CHCl_3$): 3400 (NH), 1750 cm^{-1} (acetate and ester); n.m.r. ($CDCl_3$): τ 4.20 (d, J = 8.5 Hz, 1H, —NH), 5.24 (m, 1H, proton unshielded by acetate), 6.17 (d, J = 8.5 Hz, 1H, apex proton), 6.30 (s, 3H, —C(=O)—OCH_3), 6.59 (s, 1H, benzylic proton), 6.85 (s, 3H, —OSO_2—CH_3), 7.85 (s, 3H, acetate, methyl).

Mol. Wt. Calcd. for $C_{22}H_{23}O_9NS_2$ (tertiary acetate **32**): 509. Found (*m/e*): 509.

I.r. ($CHCl_3$): 3400 (NH), 1755, 1738 cm^{-1} (acetate and ester); n.m.r. ($CDCl_3$): τ 4.40 (d, J = 8 Hz, 1H, —NH), 6.40 (d, J = 8 Hz, 1H, apex proton), 6.62 (broad s, 1H, benzylic proton), 6.89 (s, 1H, benzylic proton), 6.69 (s, 3H, —C(=O)—OCH_3 shielded by benzene ring), 6.91 (s, 3H, —OSO_2—CH_3), 7.80 (s, 3H, acetate).

Preparation of the Enol Ether 22

Methanol (1 ml), trimethyl orthoformate (1.2 ml), and saturated methanolic hydrogen chloride (10 drops) were added in sequence to a solution of the ketoester **12** (1.13 g) in benzene. The mixture was stirred under nitrogen at room temperature for 24 h after which time it was evaporated to dryness *in vacuo*. The residue was heated under reflux for 20 min in 10 ml of xylene. After evaporation of the solvent *in vacuo*, **22** was obtained quantitatively as an oil homogeneous in t.l.c. and it was used immediately for further work.

Mol. Wt. Calcd. for $C_{13}H_{14}O_4$: 234.0892. Found (*m/e*): 234.0887.

I.r. (CCl_4): 1745, 1625 cm^{-1} (ester, enol ether); n.m.r. (CCl_4): τ 4.75 (d, J = 2 Hz, 1H, vinylic proton), 5.82 (d, J = 2 Hz, 1H, benzylic proton), 6.14 (s, 3H, aromatic methoxyl), 6.34 (s, 3H, —OCH_3); u.v. (EtOH): λ_{max} 237 (log ε 4.06), 257 (log ε 3.66), 293 nm (log ε 3.43).

The Diels–Alder Adduct 23

The enol ether **22** (1.19 g) was dissolved in xylene (5 ml) and maleic anhydride (500 mg) was added. The mixture was heated under nitrogen to 170 °C (oil bath temperature) for 12 h. The solvent was evaporated to give a solid (1.68 g), homogeneous in t.l.c. An analytical sample of **23** was obtained by recrystallization from chloroform as colorless plates, m.p. 206–207 °C.

Anal. Calcd. for $C_{17}H_{16}O_7$ (mol. wt. 332): C, 61.44; H, 4.85. Found (*m/e* 332): C, 61.34; H, 4.78.

I.r. ($CHCl_3$): 1870, 1790 (anhydride), 1740 cm^{-1} (ester); n.m.r. ($CDCl_3$): τ 6.07 (s, 3H, aromatic methoxyl), 6.20 (s, 3H, —C(=O)—OCH_3), 6.40 (s, 3H, bridgehead —OCH_3), 7.54 (d, J = 2 Hz, 2H, apex protons).

Preparation of the Olefin 24

The crude Diels–Alder adduct **23** (1.68 g) was dissolved in anhydrous diglyme (30 ml) and bistriphenylphosphinenickel dicarbonyl (3.84 g) was added. The mixture was heated under nitrogen to 200–210 °C for 7 h and worked-up in the usual manner. The residue was chromatographed on silica gel. Elution with benzene gave 765 mg (58%, based on **22**) of **24** as an oil homogeneous in t.l.c.

Mol. Wt. Calcd. for $C_{15}H_{16}O_4$: 260.1049. Found (*m/e*): 260.1041.

I.r. (CCl_4): 1740 cm^{-1} (ester); n.m.r. (CCl_4): τ 3.33 (m, 2H, vinylic protons), 6.18 (s, 3H, aromatic methoxyl), 6.27 (s, 3H, —C(=O)—OCH_3), 6.50 (s, 3H, bridgehead methoxyl), 7.38 (q, J = 6 Hz, 2H, apex protons).

Preparation of Rearranged Products From 24

The olefin **24** (205 mg) was dissolved in anhydrous benzene (2 ml) to which benzenesulfonyl azide (275 mg), *p*-toluenesulfonic acid (10 mg), and glacial acetic acid (0.4 ml) were added. The solution was stirred under nitrogen at room temperature for 7 days. Removal of the solvent *in vacuo* gave a light brown residue which was chromatographed on silica gel. Elution with ether–benzene (1:9) yielded 336 mg of foam. This material appeared to be homogeneous when examined by t.l.c. on silica gel in several solvent systems. However, its n.m.r. spectrum showed that it consisted of three products, **34**, **36**, and **37** which could not be separated.

The mixture was refluxed with *p*-toluenesulfonic acid (42 mg) and ethylene glycol (1 ml) in dry benzene (50 ml) for 18 h with a water separator. After cooling the solution was diluted with methylene chloride, washed with aqueous sodium bicarbonate and water, dried, and taken to dryness. The residue was chromatographed by preparative t.l.c. on silica gel to yield 213 mg of the crystalline

ketal **35** (60%, based on **24**) and 94 mg of the mixture **36** and **37**. After recrystallization from benzene–ether the pure **35** melted at 149–150 °C.

Anal. Calcd. for $C_{22}H_{23}O_7NS$ (ketal **35**, mol. wt. 445): C, 59.32; H, 5.21; N, 3.14. Found (*m/e* 445): C, 59.20; H, 5.20; N, 3.07.

I.r. ($CHCl_3$): 3340 (NH), 1740 (ester), 1350, 1160 cm^{-1} (sulfonyl); n.m.r. ($CDCl_3$): τ 3.70 (d, J = 10 Hz, 1H, —NH), 5.97 (d, J = 10 Hz, 1H, apex proton), 6.13 (m, 4H, dioxolane), 6.23 (s, 3H, aromatic methoxyl), 6.37 (s, 3H, $-\overset{\overset{O}{\|}}{C}-O-CH_3$), 7.21 (broad s, 1H, bridgehead benzylic proton).

The mixture of **36** and **37** was dissolved in pyridine (3 ml) and acetic anhydride (2 ml) was added. The reaction mixture was heated to 45 °C for 3 h, kept at room temperature for 10 h and worked-up in the usual manner. Preparative t.l.c. (silica gel) of the product followed by recrystallization from chloroform–benzene gave 94 mg (26%, based on **24**) of the tertiary acetate **37**, m.p. 217–218 °C.

Anal. Calcd. for $C_{23}H_{25}O_8NS$ (acetate **39**, mol. wt. 475): C, 58.10; H, 5.30; N, 2.95. Found (*m/e* 475): C, 58.08; H, 5.28; N, 2.83.

I.r. ($CHCl_3$): 3390 (NH), 1755, 1745 (acetate and ester), 1340, 1165 cm^{-1} (sulfonyl); n.m.r. ($CDCl_3$): τ 4.25 (d, J = 9 Hz, 1H, —NH), 6.20 (d, J = 9 Hz, 1H, apex proton), 6.21 (s, 3H, aromatic methoxyl), 6.57 (s, 3H, bridgehead $-OCH_3$), 6.67 (s, 3H, $-\overset{\overset{O}{\|}}{C}-OCH_3$, shielded by aromatic ring), 6.80 (broad s, 1H, bridgehead benzylic proton), 7.83 (s, 3H, acetate methyl).

Deketalization of 35 to 34

A solution of the ketal **35** (96 mg) in 70% aqueous acetic acid (4 ml) was heated to 80 °C for 20 h. After cooling dichloromethane (100 ml) was added and the solution was washed with aqueous sodium carbonate, then with water, dried, and evaporated to dryness. The product **34** was recrystallized from benzene–hexane to a m.p. of 180–181 °C. The yield was 85 mg (98%).

Mol. Wt. Calcd. for $C_{20}H_{19}O_6NS$: 401.0933. Found: (*m/e*): 401.0927.

I.r. ($CHCl_3$): 3350 (NH), 1755, 1730 (ketone and ester), 1330, 1160 cm^{-1} (sulfonyl); n.m.r. ($CDCl_3$): τ 4.13 (d, 1H, —N—H), 6.08 (broad s, 2H, apex and bridgehead protons), 6.13 (s, 3H, aromatic methoxyl), 6.22 (s, 3H, $-\overset{\overset{O}{\|}}{C}-OCH_3$), 7.46 (two d, 2H, methylene).

We thank the National Research Council of Canada and Hoffmann La-Roche, Nutley, New Jersey, for financial support of this work.

1. Pak-tsun Ho, S. Oida, and K. Wiesner. Chem. Commun. 883 (1972).
2. K. Wiesner, Pak-tsun Ho, D. Chang, and J. F. Blount. Experientia, **29**, 766 (1972).
3. K. Wiesner and A. Philipp. Tetrahedron Lett. 1467 (1966).
4. G. Wittig and R. W. Hoffmann. Ber. **95**, 2718 (1962).
5. V. Askam and W. H. Linnel. J. Chem. Soc. 2435 (1954).
6. C. F. Huebner, P. L. Strachan, E. M. Donoghue, N. Cahoon, L. Dorfman, R. Margerison, and E. Wenkert. J. Org. Chem. **32**, 1126 (1967).
7. B. M. Trost and F. Chen. Tetrahedron Lett. 2603 (1971).
8. A. Philipp. Unpublished work at the University of New Brunswick.
9. D. Peters. J. Chem. Soc. 1761 (1959).

Can. J. Chem. Downloaded from www.nrcresearchpress.com by 210.87.254.42 on 09/05/12
For personal use only.

Mass Spectrometry of Some Substituted 2-Benzylidenecyclohexanones and 2,6-bis-Benzylidenecyclohexanones

P. J. SMITH[1]

Department of Chemistry and Chemical Engineering, University of Saskatchewan, Saskatoon, Saskatchewan

AND

J. R. DIMMOCK AND W. A. TURNER[2]

College of Pharmacy, University of Saskatchewan, Saskatoon, Saskatchewan

Received July 4, 1972

The mass spectra of a series of some substituted 2-benzylidenecyclohexanones and a series of substituted 2,6-bis-benzylidenecyclohexanones have been determined at 70 eV. The major fragmentation pathways include an intramolecular aromatic substitution reaction leading to the loss of an ortho-substituent with the formation of a stable benzopyrylium ion, loss of carbon monoxide and ethylene from the parent ion and also further ions derived from subsequent cleavages of the cyclohexanone ring. The structural and electronic factors involved in the aromatic substitution reaction were examined by comparing the M − H/M and M − Cl/M ratios determined from the spectra of the various substrates.

Les spectres de masse d'une série de benzylidène-2 cyclohexanones substituées et d'une série de bis-benzylidène-2,6 cyclohexanones ont été enregistrés à 70 eV. Le processus principal de fragmentation comprend une réaction de substitution aromatique intramoléculaire conduisant à la perte d'un substituant en ortho avec la formation d'un ion benzopyrylium stable, à la perte de monoxyde de carbone et d'éthylène à partir de l'ion parent et aussi à d'autres ions provenant de clivages subséquents de l'anneau de la cyclohexanone. Les facteurs structuraux et électroniques impliqués dans la réaction de substitution aromatique ont été examinés à partir des spectres de plusieurs substrats. [Traduit par le journal]

Can. J. Chem., 51, 1458 (1973)

Introduction

A series of α,β-unsaturated ketones have been synthesized, since these alkylating agents (1, 2) are known to possess anticancer activity.[3] The availability of these compounds led us to examine their mass spectral fragmentation patterns which we compared with the electron-induced fragmentation of a series of acyclic analogs, series 3, which was recently reported (3).

In our earlier paper on the mass spectra of a series of substituted styryl ketones (series 3) (3) we showed that an intramolecular aromatic substitution reaction occurred in the molecular ion to give a benzopyrylium ion. This fragmentation pattern was pronounced when the aromatic ring contained an ortho-chlorine atom and was only of minor significance when the ortho position contained solely hydrogen atoms. We postulated that this substitution reaction required a prior isomerization of the *E* substrates to the *Z* configuration. In addition, an α-cleavage product was obtained as well as the McLafferty rearrangement product. The styryl ketones in series 3 are capable of existing in the *s-cis* and *s-trans*

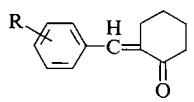

Series 1

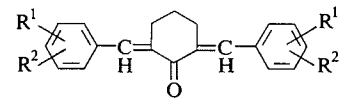

Series 2

1 R = H
2 R = 2-Cl
3 R = 3-Cl
4 R = 4-Cl
5 R = 4-$N(CH_3)_2$

6 $R^1 = R^2 = H$
7 R^1 = 2-Cl; R^2 = 6-Cl
8 R^1 = 2-Cl; R^2 = 4-Cl
9 R^1 = 3-Cl; R^2 = 4-Cl
10 R^1 = 4-$N(CH_3)_2$; $R^2 = H$

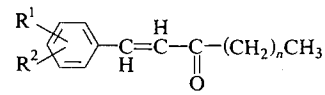

Series 3

$R^1 = R^2$ = H, Cl, or $N(CH_3)_2$
n = 1, 5

[1]Author to whom all correspondence should be addressed.

[2]Holder of a Medical Research Council Studentship, 1968–1972.

[3]The compounds described in this paper (series 1 and 2) are currently being evaluated against several tumors and preliminary results indicate that **1** has a high level of activity against the 9KB tumor *in vitro*, accompanied by low toxicity towards mice (J. R. Dimmock and W. A. Turner. Unpublished data).

Can. J. Chem. Downloaded from www.nrcresearchpress.com by 210.87.254.40 on 09/05/12
For personal use only.

Can. J. Chem. Downloaded from www.nrcresearchpress.com by 210.87.254.40 on 09/05/12
For personal use only.

configuration (4) but the exocyclic α,β-unsaturated cycloalkanones (series 1 and 2) have a fixed *s-cis* configuration of the olefinic group with respect to the carbonyl function. However, both *E* and *Z* isomers are possible in series 1 and 2. In the case of some 2-(4-halobenzylidene)cyclohexanones including **4** and also 2,6-bis-(4-halobenzylidene)cyclohexanones, it has been shown from dipole moment measurements that the compounds exist as the *E* isomers (5). Furthermore, Hassner and Mead (6) have shown that condensation of benzaldehyde with 2-methylcyclohexanone and 2,2-diphenylcyclohexanone gave the *E* isomers (ε 16 000 and 17 000, respectively) which were converted to the *Z* isomers (ε 6700 and 7810, respectively) by u.v. irradiation. The molar absorptivities of our compounds (Table 5) were similar to the *E* isomers prepared by Hassner and Mead. Furthermore, 2-benzylidene derivatives of 1-indanones and a substituted 1-tetralone have been shown from n.m.r. spectroscopy to have the *E* configuration (7). The vinylic proton of these derivatives ranged from δ 7.65–7.71 in the *E* isomers and from 6.63–6.89 in the *Z* isomers which were prepared from the *E* isomers by u.v. irradiations. The n.m.r. spectra of the compounds in series 1 and 2 showed a vinylic proton ranging from δ 7.30–7.85. It was assumed, therefore, that in series 1 and 2 the compounds were the *E* isomers, the shape of which is indicated below.

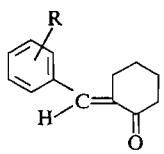

Series 1

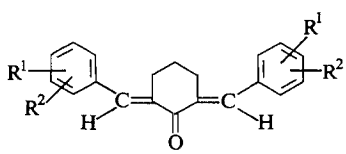

Series 2

Thus, in series 1 and 2, after the prior isomerization from the *E* arrangement to the *Z* configuration, the carbonyl oxygen atom is in close proximity to the ortho substituent of the aromatic ring. Furthermore, in the cyclohexanone series, α-cleavages to the carbonyl and McLafferty rearrangement processes would be inhibited or suppressed thereby allowing the intramolecular substitution reaction to be a major fragmentation pathway. Finally, it was considered of interest to examine the effect of substituents on the aromatic ring on the formation of various benzopyrylium ions in the light of the relative stabilization of these ions compared with the corresponding parent ion.

Results and Discussion

The mass spectral data for the major ions of the compounds in series 1 and 2 are recorded in Tables 1 and 2.[4] Figures 1–4 are bar graphs of the spectra of **1**, **6**, **2**, and **7**, respectively.

Mass Spectrum of 2-Benzylidenecyclohexanone

Figure 1 indicates the mass spectrum of 2-benzylidenecyclohexanone. This spectrum exhibits an intense M − 1 peak at *m/e* 185(*a*), and M − 1/M = 1. This ion presumably has the benzopyrylium structure and is formed by a loss of a hydrogen atom after *E* to *Z* isomerization has occurred. This reaction is favored since in the *Z* isomer the ortho-hydrogen and carbonyl oxygen are in close proximity and loss of a hydrogen atom is favored. The mass spectrum of the *Z* isomer of **1** is virtually identical to that of **1**. At 15 eV the M − 1/M ratio is 0.36, whereas in the case of the unsubstituted styryl ketone in series 3, there is absence of the M − 1 peak at this ionization voltage. In both compounds further fragmentation at 15 eV is negligible. Thus the geometry of the rigid structure in **1** allows a hydrogen to be abstracted more readily than from the corresponding flexible acyclic analog in series 3.

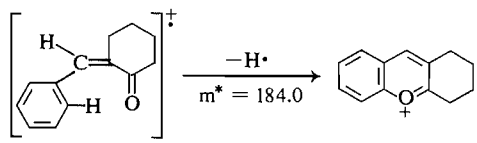

1 (*Z*) *m/e* 186 (*a*) *m/e* 185

The ion at *m/e* 158 (M − 28) can arise from either of two possible α-cleavages of the parent ion to form structures (*b*) and (*c*) with subsequent loss of carbon monoxide or ethylene to give (*d*), (*e*), and (*f*), m/e 158 (Scheme 1). It is of interest to note that (*E*)-2-furfurylidene-9-methyl-1-decalone also loses carbon monoxide by a similar fragmentation pathway (8). It is expected that (*c*) would be more favored than (*b*) for the α-cleavage product due to resonance stabilization. Consequently, the loss of 28 mass units

[4]A complete listing of the mass spectral peaks for all of the compounds in series 1 and 2 down to 3% intensity (except in the cases where the peak represented the parent or M − 1 ion where intensities of less than 3% were recorded) is available from the Depository of Unpublished Data, National Science Library, National Research Council of Canada, Ottawa, Canada K1A 0S2.

Can. J. Chem. Downloaded from www.nrcresearchpress.com by 210.87.254.40 on 09/05/12
For personal use only.

TABLE 1. Relative intensity (r.i.) and *m/e* values of the principal ions observed in the 70 eV mass spectra of compounds in series 1

1	*m/e*	186(M)	185(M − 1)	158(M − 28)	157	143	130	129	128	127	117	115	102	91	77	67
	r.i.	100	100	18	9	11	32	46	27	10	36	60	17	24	12	39
2	*m/e*	220(M)	185(M − Cl)	129	128	127	115	67								
	r.i.	3	100	17	15	9	15	11								
3	*m/e*	220(M)	219(M − 1)	192(M − 28)	185(M − Cl)	164	157	151	129	128	127	116	115	67		
	r.i.	59	35	12	57	4	13	24	47	25	15	12	37	100		
4	*m/e*	220(M)	219(M − 1)	192(M − 28)	185(M − Cl)	164	157	151	129	128	127	116	115	67		
	r.i.	100	52	18	44	9	15	22	44	22	15	10	22	42		
5	*m/e*	229(M)	228(M − 1)	201(M − 28)	173	172	160	158	129	128	115					
	r.i.	100	32	12	23	19	9	13	11	7	11					

TABLE 2. Relative intensity (r.i.) and *m/e* values of the principal ions observed in the 70 eV mass spectra of compounds in series 2*

6	*m/e*	274(M)	273(M − 1)	246(M − 28)	218	217	129	128	115							
	r.i.	100	95	9	10	14	9	11	20							
7	*m/e*	410(M)	375(M − Cl)	152	151	149										
	r.i.	1	100	11	9	10										
8	*m/e*	410(M)	375(M − Cl)	152	151	149										
	r.i.	1	96	8	7	13										
9	*m/e*	410(M)	409(M − 1)	375(M − Cl)	347	312	202	188	185	183	170	160	149	128	127	115
	r.i.	76	36	78	30	40	12	12	12	15	14	30	67	32	31	21
10	*m/e*	360(M)	359(M − 1)	332(M − 28)	331	212	166	134								
	r.i.	100	35	16	17	19	31	14								

*The base peak for compound 8 was at *m/e* 377 and for compound 9 at 412 due to the presence of more than one chlorine atom in the ions. The ions used for discussion will be those with *m/e* values corresponding to the presence of only the ^{35}Cl isotope.

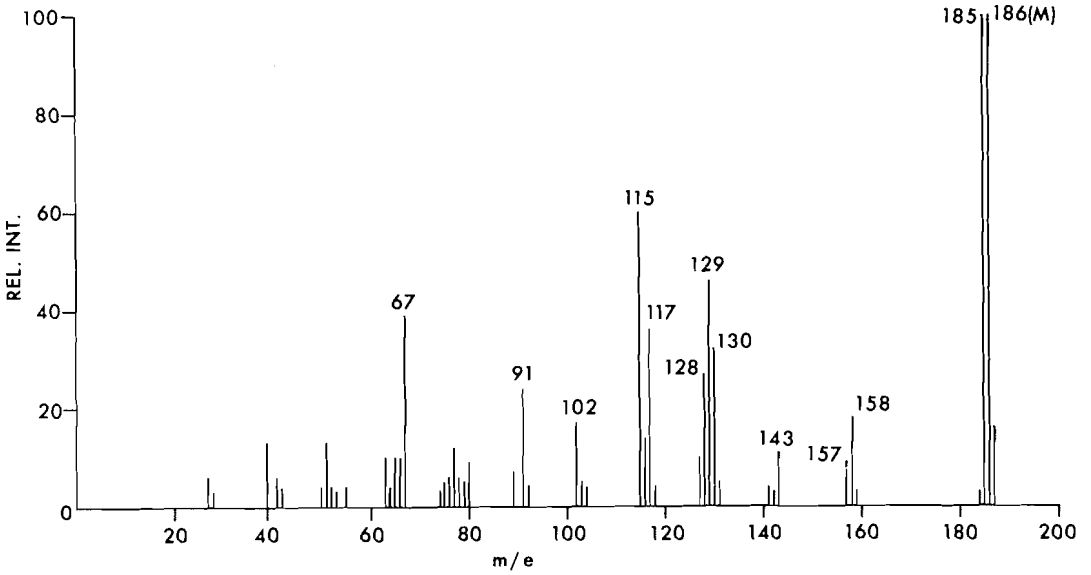

FIG. 1. Mass spectrum (70 eV) of **1**.

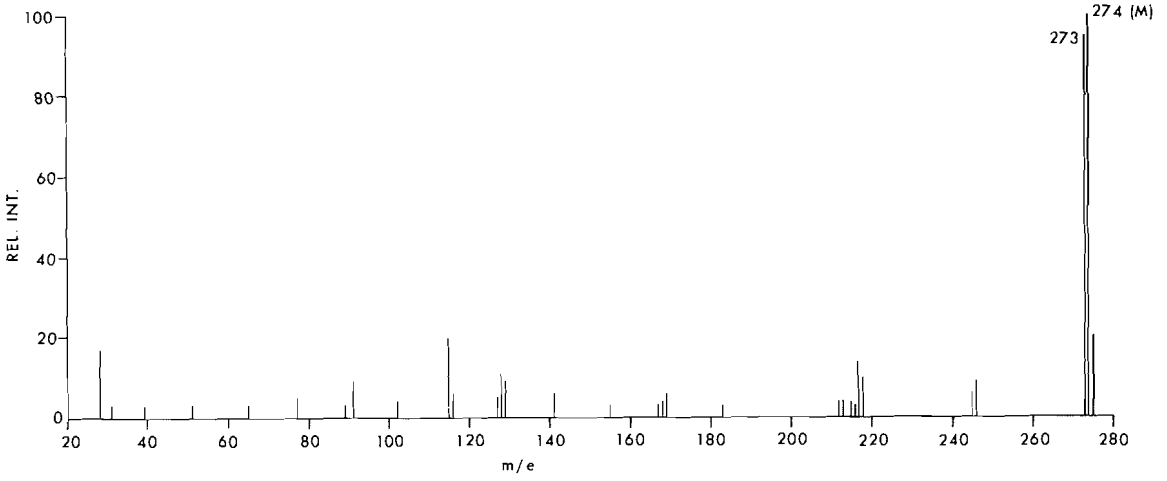

FIG. 2. Mass spectrum (70 eV) of **6**.

from the parent ion would emanate principally from (*c*) to give (*e*) and (*f*). Indeed, when the ion at *m/e* 158 was examined using high resolution mass spectrometry it was found that these ions, $C_{12}H_{14}$ (*e* and possibly *d*) and $C_{11}H_{10}O$ (*f*), were formed in the approximate ratio of 2:1. It should be noted that the usual fragmentation scheme for cyclohexanone (9) to give such ions as $CH_2{=}CH{-}C{\equiv}\overset{+}{O}$ is blocked for structure (*c*). Scheme 2 illustrates possible fragmentation of the ions (*c*), (*e*), and (*f*).

Scheme 3 shows that the precursor of the ion at *m/e* 117 is *m/e* 158 (*e*) as evidenced by a metastable ion at 86.6. Identical processes involving loss of the allyl radical were observed for both the 3-chloro and 4-chloro compounds,

Can. J. Chem. Downloaded from www.nrcresearchpress.com by 210.87.254.40 on 09/05/12
For personal use only.

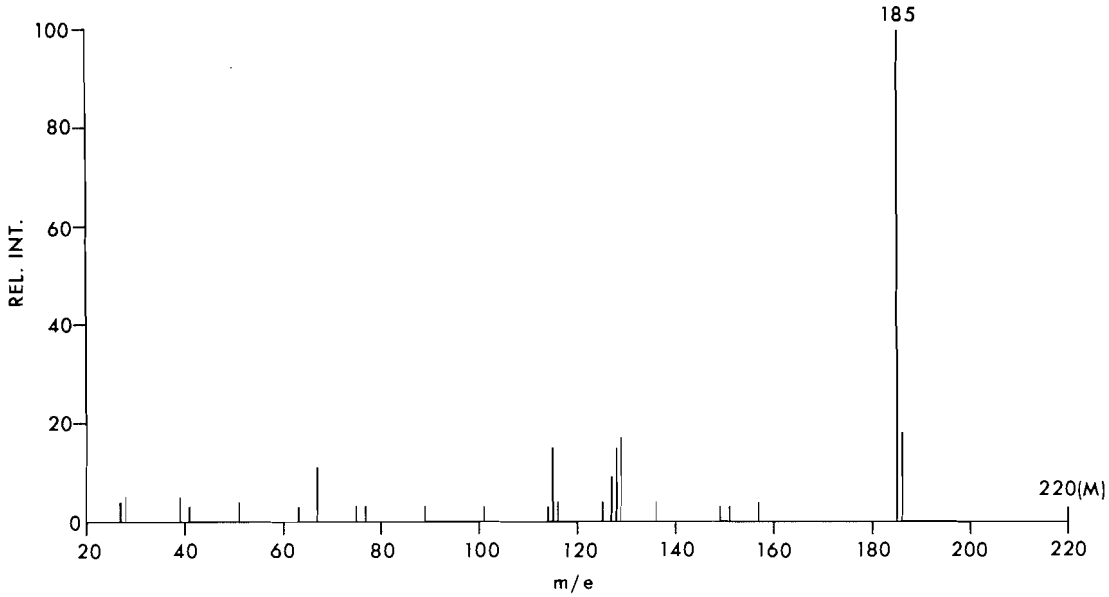

FIG. 3. Mass spectrum (70 eV) of **2**.

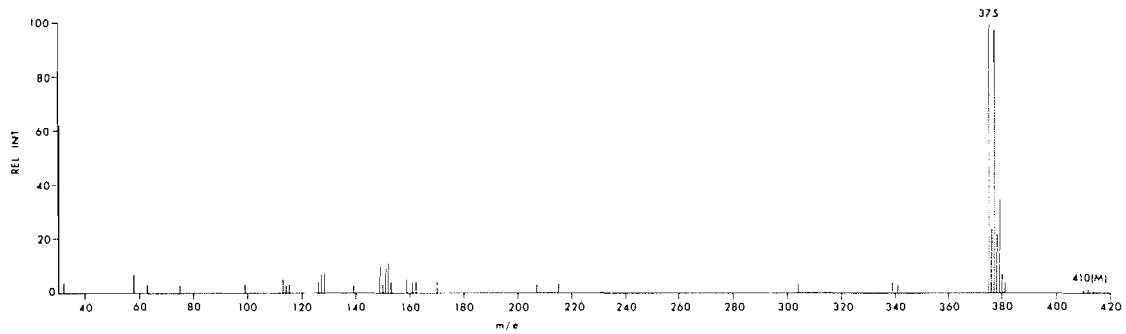

FIG. 4. Mass spectrum (70 eV) of **7**.

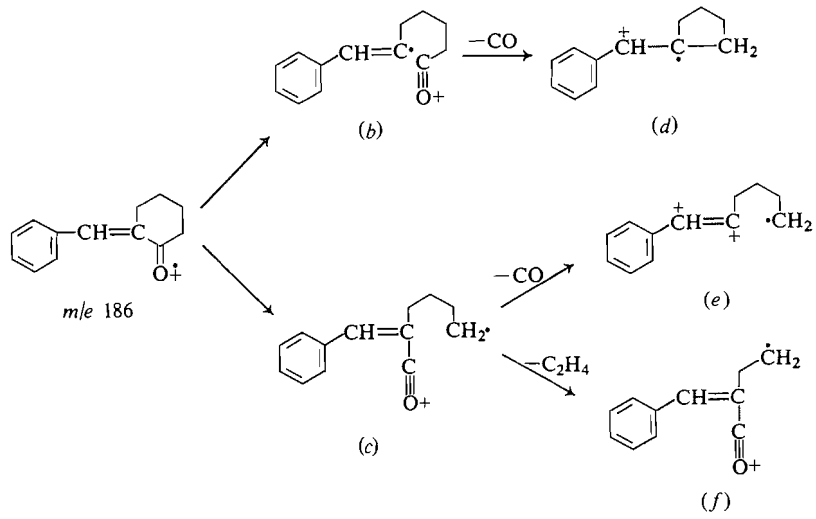

SCHEME 1

Can. J. Chem. Downloaded from www.nrcresearchpress.com by 210.87.254.40 on 09/05/12
For personal use only.

Can. J. Chem. Downloaded from www.nrcresearchpress.com by 210.87.254.40 on 09/05/12
For personal use only.

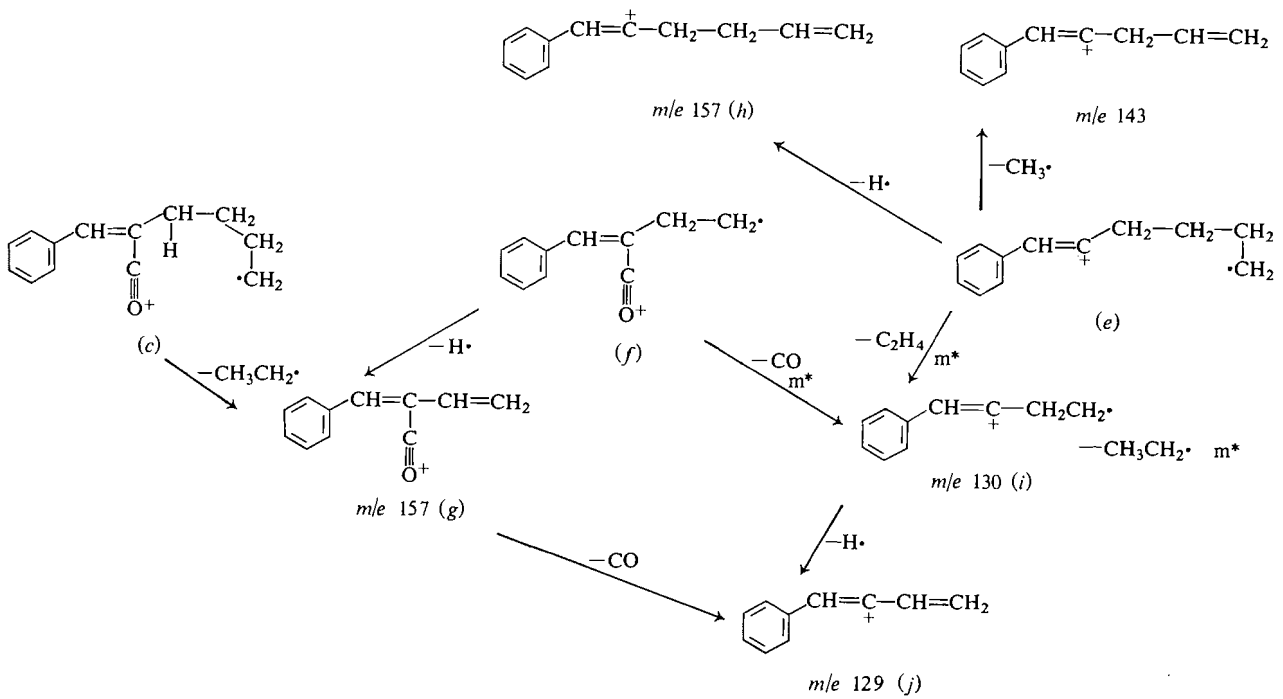

SCHEME 2

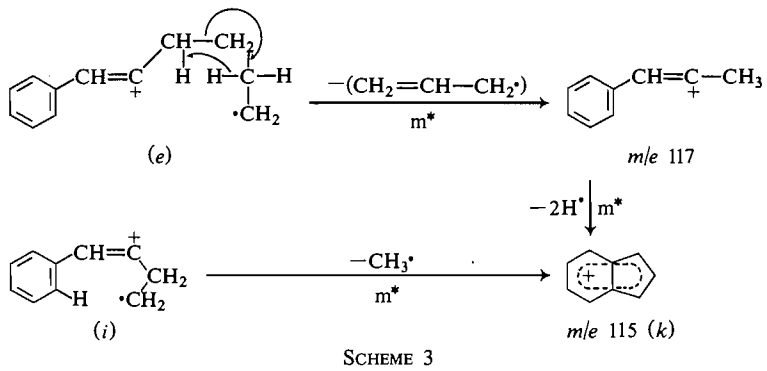

SCHEME 3

TABLE 3. M − 1/M and M − Cl/M ratios at 70 eV for a series of substituted 2-benzylidenecyclohexanones and a series of mono-substituted 1-phenyl-1-nonen-3-ones*

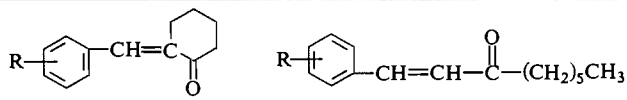

	Series 1		Series 3	
Substituent (R)	M − 1/M	M − Cl/M†	M − 1/M	M − Cl/M†
2-Cl	0.3	33.3	0.1	3.3
3-Cl	0.6	0.69	—	—
4-Cl	0.5	0.35	0.1	0.0
4-H	1.0	—	0.1	—
4-$N(CH_3)_2$	0.3	—	0.1	—

*Data taken from ref. 3.
†The M − Cl/M ratios were calculated using the M − Cl values from both P and P + 2 ions.

3 and **4**, respectively, as indicated by the appropriate metastable peaks. The ion at *m/e* 117 loses two hydrogen atoms to give *m/e* 115 (m* = 113.0). An indenyl structure (*k*) has been proposed for *m/e* 115 (10) and this ion was observed to lose acetylene (m* = 68.9). The indenyl cation is also confirmed to be formed from *m/e* 130 (*i*) by loss of methyl radical (m* = 101.7).

The origin and structure of the ion at *m/e* 67 is of particular interest since this ion appears in the spectra of all the substituted 2-benzylidenecyclohexanones except **5**. In fact, the most intense ion in the spectrum of the 3-chloro substrate (**3**) is at *m/e* 67. High resolution mass spectrometry has shown this ion to have the elemental composition, $C_5H_7^+$. It is noteworthy that *m/e* 67 does not appear in any of the spectra obtained for the bis-substrates (**6**–**10**) which suggests that the origin of the ion is from the cyclohexanone ring. It has been proposed that *m/e* 67 has the structure of the pentadienyl cation, $CH_2{=}CH{-}CH{=}CH{-}CH_2^+$, and a mechanism has been proposed for its formation from cyclohexene (11). As well, 1-pentyne loses a hydrogen atom to give *m/e* 67, the most intense ion in the spectrum (12).

Mass Spectra of Some Substituted 2-Benzylidenecyclohexanones

The effect of substituents on the intramolecular aromatic substitution reaction was investigated for both the loss of a hydrogen atom and a chlorine atom from the parent ion. The results are shown in Table 3.

The loss of a hydrogen atom from the parent ion to give the M − 1 ion was observed for all the substituted 2-benzylidenecyclohexanones. It is seen from Table 3 that the ratio of M − 1/M varies from 1.0 for the unsubstituted compound (**1**) to 0.3 for the 4-dimethylamino substrate (**5**). A comparison with the styryl ketones in series 3 shows that the M − 1/M ratio is considerably

Can. J. Chem. Downloaded from www.nrcresearchpress.com by 210.87.254.40 on 09/05/12
For personal use only.

Can. J. Chem. Downloaded from www.nrcresearchpress.com by 210.87.254.40 on 09/05/12
For personal use only.

less for series 3 than for the 2-benzylidenecyclohexanones, conforming with the view that facile α-cleavage and McLafferty rearrangement mechanisms compete in series 3 and that loss of a hydrogen atom is less favorable in the acyclic compounds than in series 1.

The correlation of substituents with log Z/Z_0 values, where Z is defined as M − fragment/M and Z_0 refers to the unsubstituted compound has received considerable attention in recent years (13–15). Although a Hammett-like correlation is not expected when the fragment retains the charge at high ionization voltages (70 eV), since further fragmentation can be influenced by the substituent, it is of interest to compare the M − 1/M ratios for the substrates under discussion. A comparison of the ratio for **1** and **5** is the most meaningful since these compounds do not have the competing fragmentation mode of the loss of chlorine from the parent ion and, indeed, **5** has as the major fragmentation process the loss of a hydrogen atom. A reasonable explanation for the decrease in the ratio M − 1/M from 1.0 to 0.3 for compounds **1** and **5**, respectively, is that the parent ion[5] receives considerable stabilization from the electron-donating dimethylamino function in **5**, making attack of the carbonyl oxygen on to the aromatic ring less favored. Alternatively, the presence of

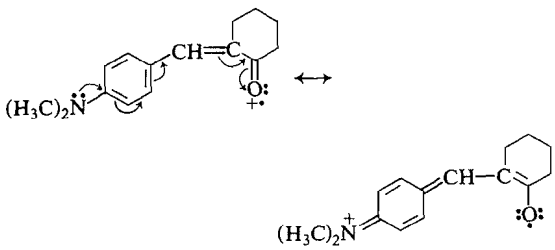

two hetero atoms in **5** allows the possibility of charge localization on either atom which might lead to fewer fragment ions as observed. In fact, the ionization potentials of *N*,*N*-dimethylaniline and cyclohexanone are 7.14 and 9.14 eV, respectively (16), which suggests that the positive charge probably resides mainly on nitrogen. It should be noted that the stabilization of the M − 1 ion is not the prime factor since **A** would be more stable than the corresponding unsubstituted benzopyrylium ion.

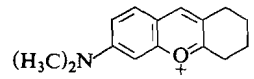

A

A comparison of the M − 1/M ratio for the chloro compounds (**2**–**4**) with the unsubstituted compound (**1**) is difficult due to the competing M − Cl reaction. Indeed, this loss of chlorine leads to the base peak in the spectrum of the 2-chloro compound (**2**) where M has only a relative intensity of 3%.

From Table 3 it may be seen that both the 3-chloro and 4-chloro substrates give M − 1/M ratios considerably less than for the unsubstituted compound. This is reasonable for the 4-chloro compound since the chlorine can stabilize the parent ion by the mesomeric effect as discussed for the dimethylamino substrate. The 3-chloro substituent cannot directly conjugate with the carbonyl function and presumably makes the substitution reaction less favorable than for the unsubstituted compound by withdrawing electron density from the benzene ring. It should be noted that the 3-chloro substituent is lost more readily than the 4-chloro from the parent ion in a competing reaction with the formation of the M − 1 species. This would presumably lead to a relatively higher M − 1/M ratio than observed for the former substrate in the absence of the M → M − Cl · reaction.

The parent ion is destabilized for the 3-chloro derivative relative to the 4-chloro substrate as is shown from the data in Table 1 where it is seen that the parent ion for the 3-chloro substrate (**3**) carries 13% of the total ion current whereas the parent ion for the 4-chloro compound (**4**) carries 24% of the total ion current. The base peak for the 3-chloro compound is at *m/e* 67, $C_5H_7^+$, which further suggests that the chlorine in the 3-position on the ring deactivates the parent ion and fragment ions bearing the substituent, which leads to increased intensity of ions derived from the cyclohexanone ring ($C_5H_7^+$). This is borne out by the data for the 4-dimethylamino compound where the parent ion and subsequent fragment ions bearing the dimethylamino group are stabilized by the electron-donating substituent; no ion at *m/e* 67 was observed (Table 1).

The loss of the chlorine from the 2-chloro compound (**2**), as expected, was considerably more favored than loss from either the 3-chloro (**3**) or 4-chloro (**4**) substrates; *i.e.* M − Cl/M =

[5]It is assumed that ease of isomerization of the *E*-substrates to the *Z*-isomers is independent of substituents on the benzene ring.

TABLE 4. M − 1/M and M − Cl/M ratios at 70 eV for a series of substituted 2,6-bis-benzylidenecyclohexanones and a series of substituted 1-phenyl-1-nonen-3-ones*

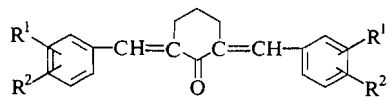

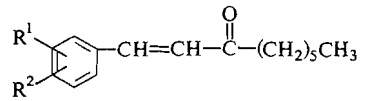

Substituents	Series 2		Series 3	
	M − 1/M	M − Cl/M†	M − 1/M	M − Cl/M†
$R^1 = R^2 = H$	1.0	—	0.1	—
R^1 = 4-$N(CH_3)_2$; $R^2 = H$	0.4	—	0.1	—
R^1 = 3-Cl; R^2 = 4-Cl	0.5	1.0	0.1	0.0
R^1 = 2-Cl; R^2 = 4-Cl	0.3	96.0	0.1	2.5
R^1 = 2-Cl; R^2 = 6-Cl	0.0	100.0	0.0	16.7

*Data taken from ref. 3.
†Ratio was calculated using the peaks corresponding to the parent and the fragment ions containing only the ^{35}Cl isotope. The ion corresponding to the loss of a chlorine atom can also arise from the M + 2 peak with loss of ^{37}Cl.

33.3, 0.69, and 0.35, respectively. The loss of the ortho-chlorine from (**2**) is considerably more favored than loss of the ortho-chloro from 1-(2-chlorophenyl)-1-nonen-3-one; M − Cl/M = 33.3 and 3.3, respectively, Table 3. The trend in ratio is the same as observed for the loss of hydrogen from the unsubstituted substrates of series 1 and 3. It is of interest to note that a large M − Cl ion has also been observed in a number of acyclic chlorophenyl ureas, thioureas, and carbamates in the case of the 2-chloro substituted but not in the 3- and 4-substituted compounds (17).

The fragmentation of both the 3-chloro and 4-chloro compounds is considerably more extensive than for the 2-chloro substrate, Table 1. This is presumably due to the ease of formation of the M − Cl ion (*d*) from the 2-chloro substrate via the intramolecular substitution reaction. Compounds **3** and **4** presumably lose a halogen atom by simple carbon–chlorine bond cleavage as does chlorobenzene (18). From the data in Table 3 it is noted that the ease of loss of a chlorine atom from the 3-position is approximately twice as facile as from the 4-position.

The loss of 28 mass units from the parent ion was noted for compounds **3**, **4**, and **5**, but as expected, the 2-chloro compound did not exhibit such an ion due to the much greater propensity for loss of the ortho-chlorine. It is noteworthy that a metastable ion was observed for the M → M − 28 process only for the 4-dimethylamino substrate (**5**), m* = 176.4 for the transition 229 → 201. In fact, this metastable peak was observed to be broad and have a relatively flat top. These flat top metastable peaks have been attributed to the release of a small amount of kinetic energy during the dissociation process (19). This is consistent with the earlier discussion dealing with substituent effects on the formation of the M − 1 ion for the various substrates since the M—CO ion can be stabilized when a good electron-releasing substituent is in the 4-position, *e.g.* a dimethylamino group.

Mass Spectra of Some Substituted 2,6-bis-Benzylidenecyclohexanones

The spectra of several substituted 2,6-bis-benzylidenecyclohexanones were determined and the major ions with their relative intensities recorded in Table 2. The ratio of M − 1/M and M − Cl/M for these compounds (**6**–**10**) is shown in Table 4 along with ratios obtained in series 3.

It is noted from the data in Table 2 that there is generally considerably less fragmentation at 70 eV for the bis-compounds than in series 1. The only major ions for the bis-unsubstituted compound (**6**) and the 2,6-bis-(4-dimethylaminobenzylidene)cyclohexanone (**10**) are the M and M − 1 ions. The 2,6-bis-(2,6-dichlorobenzylidene)cyclohexanone (**7**) and 2,6-bis-(2,4-dichlorobenzylidene)cyclohexanone (**8**) exhibited essentially only one peak (M − Cl) with the parent ions for both these compounds having a relative intensity of approximately 1.0. The only substrate in the bis-series (Series 2) where significant fragmentation was observed is the 2,6-bis-(3,4-dichlorobenzylidene)cyclohexanone (**9**) and the fragmentation pattern is illustrated in Scheme 4. The formation of the ions down to *m/e* 312 presumably proceeds as described for

Can. J. Chem. Downloaded from www.nrcresearchpress.com by 210.87.254.40 on 09/05/12
For personal use only.

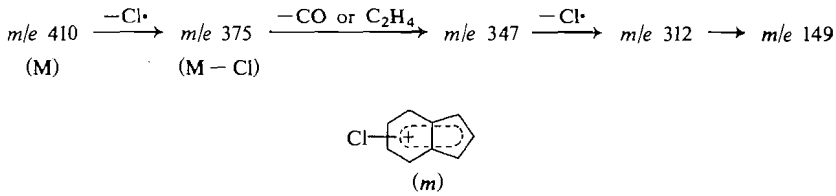

SCHEME 4

the unsubstituted compound in series 1. It is suggested that the ion at *m/e* 149 has the structure (*m*), an analogous structure to *m/e* 115 (*k*) discussed earlier.

The M − l/M ratios for the bis-substrates are approximately the same as found for the compounds of series 1. The ratios for compounds **7** and **8** are not meaningful since the parent ion has only a relative intensity of 1.0 (Table 2).

The loss of a chlorine atom from the bis-3,4-dichloro compound (**9**) occurs with approximately the same ease as from 2-(3-chlorobenzylidene)cyclohexanone (**3**) since both processes involve cleavage of the meta-chlorine atom from the aromatic ring. The M − Cl/M ratio for the 1-(3,4-dichlorophenyl)-1-nonen-3-one as shown in Table 4 is zero as expected since this substrate can fragment by pathways not available in the cyclohexanone series.

The M − Cl ion is the only appreciable ion found in the spectra of both the bis-2,6-dichloro (**7**) and bis-2,4-dichloro (**8**) compounds. The M − Cl/M ratio in both cases is approximately 100 in comparison with a ratio of 33 observed for the 2-(2-chlorobenzylidene)cyclohexanone (**2**). This difference presumably arises from the increased stability of the fragment ion when it retains an electron-donating ortho- or para-substituent. Isomerization at only one double bond of the bis-compounds is necessary for the intramolecular substitution reaction. The second aromatic ring, where the two chlorines are retained, is able to stabilize the benzopyrylium ion, as shown below.

It is of interest to note that the 2,4-dichloro and 2,6-dichloro substrates from series 3 have a M − Cl/M ratio of 2.5 and 16.7, respectively. In this series, where also a prior *E* to *Z* isomerization is necessary before the intramolecular substitution can occur, the low ratio for the 2,4-dichloro compound compared with the 2,6-dichloro compound could reflect in some measure the relative ease of formation of ions (*n*) and (*o*) of which only (*n*) can lose a chlorine atom from the ortho-position (Scheme 5). In the case of the 2,6-dichloro compounds on isomerization it will always have a chlorine atom at an ortho-position.

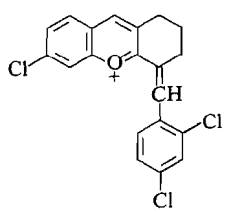

M − Cl ion from **8**

Experimental

Mass spectra were determined by Mr. D. Bain with an MS-12 mass spectrometer operating at 70 eV and an ion source temperature of 100°. The samples were introduced via the direct probe technique. M.p. and b.p. are uncorrected. Microanalyses were performed by Mr. O. Douglas of the College of Pharmacy, University of Saskatchewan, Saskatoon.

N.m.r. spectra were run on a Varian T-60 spectrometer, using deuterochloroform as solvent, with tetramethylsilane as the internal standard. U.v. spectra were obtained on a Beckman DU spectrophotometer in 95% ethanol as solvent. G.l.c. was performed on a Pye Series 104 Gas Chromatograph equipped with a flame ionization detector. The glass column (5 ft × 0.25 in. o.d.) was packed with 4% SE-30 adsorbed onto acid washed Chromosorb W (100/200 mesh). The column temperature was 160–180° and the nitrogen flow rate was 50 ml/min.

*General Procedure for the Preparation of Substituted 2-Benzylidenecyclohexanones (Table 5, **1–4**)*

A mixture containing cyclohexanone (2.0 mol), the appropriate aromatic aldehyde (1.0 mol), sodium hydroxide (1.0 mol), and water (1000 ml) was heated under reflux with stirring for 20 h. After cooling to room temperature, the mixture was extracted with chloroform, the organic extracts were washed with water and dried ($MgSO_4$). The chloroform was evaporated *in vacuo* to give a crude product, purified by vacuum distillation followed by repeated recrystallization from methanol.

*(Z)-2-Benzylidenecyclohexanone (**11**)*

A solution of the *E* isomer (**1**) (20 g) in methanol (300 ml) was irradiated with a Hanovia 450 W u.v. lamp through quartz, the solution being cooled by a water jacket. Aliquot samples were taken at 1 h intervals and the course of the reaction was followed by g.l.c. analysis.

Can. J. Chem. Downloaded from www.nrcresearchpress.com by 210.87.254.40 on 09/05/12
For personal use only.

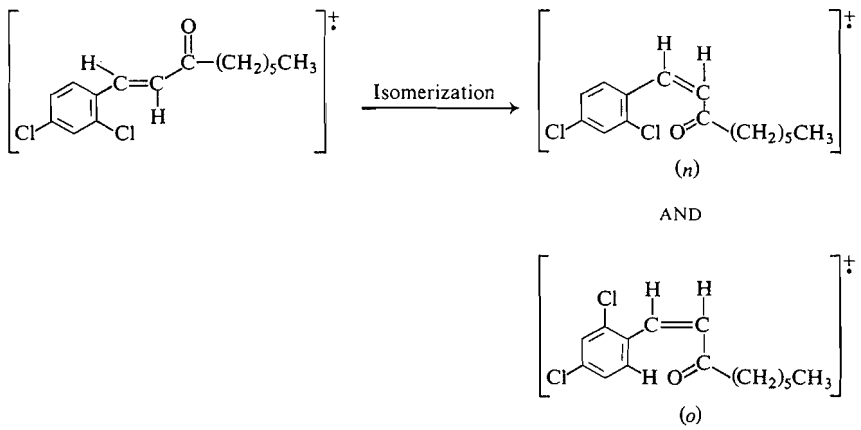

SCHEME 5

TABLE 5. Substituted 2-benzylidenecyclohexanones

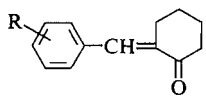

Compound	R	B.p. (°/mm)	M.p. (°C)	Yield (%)	δ (Olefinic proton)	λ_{max}	ε
1	H	122°/1	55(lit. (20) m.p. 55)	74	7.43	290	14 725
2	2-Cl	128°/1	70.0–70.5(lit. (21) m.p. 69.5–70.5)	43	7.50	278	10 940
3	3-Cl	145–150°/0.5	75.0–75.5*	20	7.30	284	12 975
4	4-Cl	140°/1	56.5–57.0(lit. (5) m.p. 57–57.5)	28	7.40	293	16 370
5	4-$N(CH_3)_2$	—	127–128(lit. (22) m.p. 127–127.5)	43	7.51	381	23 700

*Anal. Calcd. for $C_{13}H_{13}ClO$: C, 70.75; H, 5.94. Found: C, 70.65; H 5.85.

After 4 h the *Z–E* ratio was 88:12; unchanged after irradiation for a further 4 h. The solvent was removed under reduced pressure and the residual liquid was distilled, b.p. 122–130°/2 mm, to give a yellow syrup (18.3 g). Crystallization from Skelly F gave pure **11** as colorless crystals (12 g, 60%), m.p. 37–38°; λ_{max} 272 (ε 5575) and 222 mμ (ε 7900); N.m.r.: δ 6.27 (1H, t, J = 2 Hz, C_6H_5—C*H*=).

Anal. Calcd. for $C_{13}H_{14}O$: C, 83.83; H, 7.52. Found: C, 83.90; H, 7.61.

11 reverts to **1** on prolonged heating (120° for 40 h).

*2-(4-Dimethylaminobenzylidene)cyclohexanone (**5**) and 2,6-bis-(4-Dimethylaminobenzylidene)cyclohexanone (**10**)*

The general method used in preparing compounds **1–4** was followed except that after cooling the crude product was removed by filtration and heated under reflux with ethanol. The insoluble material was removed by filtration and **5** deposited from the mother liquor as yellow crystals and purified by repeated recrystallization from ethanol. The residue from filtration was extracted several times with hot alcohol and recrystallization from acetone gave **10** as orange crystals.

*2,6-bis-Benzylidenecyclohexanone (**6**)*

Cyclohexanone (0.05 mol) and benzaldehyde (0.10 mol) were dissolved in ethanol (20 ml) containing aqueous sodium hydroxide solution (3 *N*, 10 ml). The solution was heated for 30 min at 100°. Removal of the ethanol gave a yellow solid which was recrystallized from ethanol to give **6** as bright yellow crystals.

*Preparation of Substituted 2,6-bis-Benzylidenecyclohexanones (Table 6, **7–9**)*

A mixture containing cyclohexanone (0.34 mol), the appropriate aromatic aldehyde (0.085 mol), and aqueous sodium hydroxide solution (1 *N*, 86 ml) was heated at 50° for 12 h. After cooling, the mixture was extracted with chloroform, the organic extracts were washed with water and dried ($MgSO_4$). The chloroform was evaporated *in vacuo* to give a crude product, purified by recrystallization

Can. J. Chem. Downloaded from www.nrcresearchpress.com by 210.87.254.40 on 09/05/12
For personal use only.

Can. J. Chem. Downloaded from www.nrcresearchpress.com by 210.87.254.40 on 09/05/12
For personal use only.

TABLE 6. Substituted 2,6-bis-benzylidenecyclohexanones

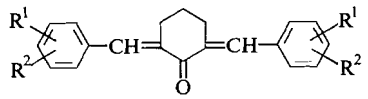

Compound	R^1	R^2	Recrystallization solvent	M.p. (°C)	Yield (%)	δ (Olefinic proton)	λ_{max}	ε
6	H	H	Ethanol	116–117(lit. (23) m.p. 118.5–119)	62	7.30	330	39 880
7	2-Cl	6-Cl	Acetone	183*	54	7.52	289	14 920
8	2-Cl	4-Cl	Dimethylformamide	163(lit. (24) m.p. 162)	37	7.85	318	21 925
9	3-Cl	4-Cl	Ethanol	150(lit. (24) m.p. 147–148)	21	7.65	329	34 725
10	4-$N(CH_3)_2$	H	Acetone	250(lit. (22) m.p. 248–249)	4	7.68	432†	45 170†

*Anal. Calcd. for $C_{20}H_{14}Cl_4O$: C, 58.28; H, 3.42. Found: C, 58.17; H, 3.50.
†Spectrum determined in dichloromethane.

from an appropriate solvent. The substituted 2,6-bis-benzylidenecyclohexanone was the only product isolated from this reaction.

One of the authors (W.A.T.) thanks the Medical Research Council of Canada for providing a studentship. Financial support was also provided by Smith, Kline and French Laboratories of Philadelphia, Pa. for the project. Our thanks are also extended to Mr. M. S. Auyeung of the College of Pharmacy, University of Saskatchewan, Saskatoon, Sask. who prepared some of the compounds described in this work. In addition we are grateful to Mr. D. K. Kowal of the College of Pharmacy who determined some of the u.v. spectra.

1. W. B. GEIGER and J. E. CONN. J. Am. Chem. Soc. **67**, 112 (1945) and references quoted therein.
2. W. C. J. Ross. Biological alkylating agents. Butterworths, London. 1962. p. 17.
3. P. J. SMITH, J. R. DIMMOCK, and W. G. TAYLOR. Can. J. Chem. **50**, 871 (1972).
4. J. R. DIMMOCK, P. L. CARTER, and P. D. RALPH. J. Chem. Soc. B, 698 (1968).
5. A. C. HUITRIC and W. D. KUMLER. J. Am. Chem. Soc. **78**, 614 (1956).
6. A. HASSNER and T. C. MEAD. Tetrahedron, **20**, 2201 (1964).
7. D. N. KEVILL, E. D. WEILER, and N. H. CROMWELL. J. Org. Chem. **29**, 1276 (1964).
8. R. L. N. HARRIS, F. KOMITSKY, JR., and C. DJERASSI. J. Am. Chem. Soc. **89**, 4775 (1967).
9. D. H. WILLIAMS, H. BUDZIKIEWICZ, Z. PELAH, and C. DJERASSI. Monatsh. **95**, 166 (1964).
10. B. WILLHALM and A. F. THOMAS. Org. Mass Spectrom. **1**, 627 (1968).
11. H. BUDZIKIEWICZ, C. DJERASSI, and D. H. WILLIAMS. Mass spectrometry of organic compounds. Holden-Day, San Francisco. 1967. p. 68.
12. Z. DOLEJŠEK, V. HANUŠ, and K. VOKAČ. Advances in mass spectrometry. *Edited by* W. L. Mead. The Institute of Petroleum, London. Vol. 3. 1966. pp. 503–514.
13. M. M. BURSEY and F. W. MCLAFFERTY. J. Am. Chem. Soc. **88**, 29 (1966).
14. M. M. BURSEY. Org. Mass Spectrom. **1**, 31 (1968).
15. I. HOWE, D. H. WILLIAMS, and R. G. COOKE. Org. Mass Spectrom. **2**, 137 (1969).
16. R. W. KISER. Introduction to mass spectrometry and its applications. Prentice-Hall Inc., Englewood Cliffs, N.J. 1965. pp. 312, 310.
17. M. A. BALDWIN, A. G. LONDON, A. MACCOLL, D. SMITH, and A. RIBERA. Chem. Commun. 350 (1967).
18. F. W. MCLAFFERTY. Anal. Chem. **34**, 16 (1962).
19. J. H. BENYON and A. E. FONTAINE. Z. Naturf. **22a**, 334 (1967).
20. G. DURR. C.R. **236**, 1571 (1953).
21. R. D. CAMPBELL and H. M. GILOW. J. Am. Chem. Soc. **82**, 2389 (1960).
22. R. L. SHRINER and W. O. TEETERS. J. Am. Chem. Soc. **60**, 938 (1938).
23. D. WALLACH. Ber. **4*c***, 71 (1907).
24. E. P. DIBELLA. U.S. patent 3 389 986; Chem. Abstr. **69**, 51812*y* (1968).

Can. J. Chem. Downloaded from www.nrcresearchpress.com by 210.87.254.40 on 09/05/12
For personal use only.

Mass Spectrometry of Some Substituted 2-Benzylidenecyclohexanone Oximes

P. J. SMITH[1]

Department of Chemistry and Chemical Engineering, University of Saskatchewan, Saskatoon, Saskatchewan

AND

J. R. DIMMOCK AND W. A. TURNER[2]

College of Pharmacy, University of Saskatchewan, Saskatoon, Saskatchewan

Received July 4, 1972

The mass spectra of several substituted 2-benzylidenecyclohexanone oximes have been determined at 70 eV and at lower ionization voltages. The major fragmentation pathways for the oximes are loss of the ortho substituent from the parent ion as well as loss of hydroxyl radical. The facility of loss of the ortho substituent is compared with a similar process involved in the fragmentation of substituted 2-benzylidenecyclohexanones. In addition, the mass spectrum of the acetate of 2-benzylidenecyclohexanone oxime was determined and showed a M − 1 peak and also a peak corresponding to the parent oxime formed by loss of ketene.

Les spectres de masse de plusieurs oximes substitués de la benzylidène-2 cyclohexanone ont été enregistrés à 70 eV et à des voltages d'ionisation moins élevés. Le processus principal de fragmentation pour les oximes comprend la perte d'un substituant en ortho à partir de l'ion parent ainsi que la perte d'un radical hydroxyle. La facilité impliquée dans la perte du substituant en ortho est comparée à celle d'un processus similaire que l'on retrouve dans la fragmentation des benzylidène-2 cyclohexanones substituées. De plus, le spectre de masse de l'acétate de l'oxime de la benzylidène-2 cyclohexanone a été enregistré et a montré un pic M − 1 et aussi un pic correspondant à l'oxime parent formé par la perte d'un groupe cétène.

[Traduit par le journal]

Can. J. Chem., 51, 1471 (1973)

Can. J. Chem. Downloaded from www.nrcresearchpress.com by 210.87.254.40 on 09/05/12
For personal use only.

Introduction

In our previous work the mass spectra of a series of nuclear substituted styryl ketones (1) and also some substituted 2-benzylidenecyclohexanones and 2,6-bis-benzylidenecyclohexanones (2) were determined. As well, the structural and electronic factors involved in an intramolecular aromatic substitution reaction with loss of an ortho substituent to give an ion with a benzopyrylium structure were examined and discussed using the measured ratios M − H/M and M − Cl/M.

In order to further investigate this aromatic substitution reaction, it was decided to prepare the oximes of several of the mono-substituted 2-benzylidenecyclohexanones. Since oximes have two hetero atoms the possibility of charge localization on either atom exists which might lead to fewer fragment ions emanating from the cyclohexanone ring, favoring the formation of the substitution product. Furthermore, ring closure with nitrogen in the ring rather than oxygen might be expected to be more favorable since the electron in the C=N bond is more available than in the C=O bond due to the difference in electronegativities of the two hetero atoms.

Results and Discussion

The following compounds (**1**–**4**) were prepared in addition to the acetate of **1** (compound **5**). Figures 1–5 are bar graphs of the spectra of compounds **1**–**5**, respectively.

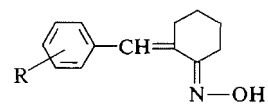

1 R = H
2 R = 4-N(CH$_3$)$_2$
3 R = 4-Cl
4 R = 2-Cl

The parent 2-benzylidenecyclohexanones have the *E* configuration (2) and it has been shown that 2-benzylidenecyclohexanone oxime exists as a single isomer as revealed by n.m.r. spectroscopy and t.l.c. (3). In view of the large steric effect of the 2-benzylidene groups, it is probable

[1]Author to whom all correspondence should be addressed.

[2]Holder of a Medical Research Council Studentship, 1968–1972.

Can. J. Chem. Downloaded from www.nrcresearchpress.com by 210.87.254.40 on 09/05/12
For personal use only.

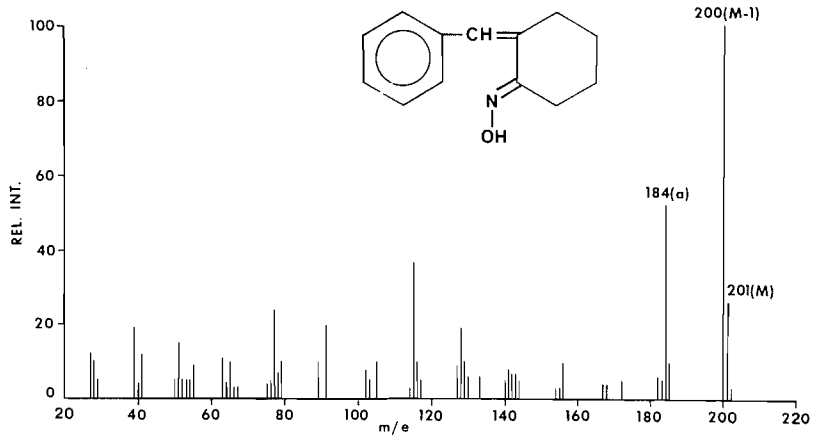

FIG. 1. Mass spectrum (70 eV) of **1**.

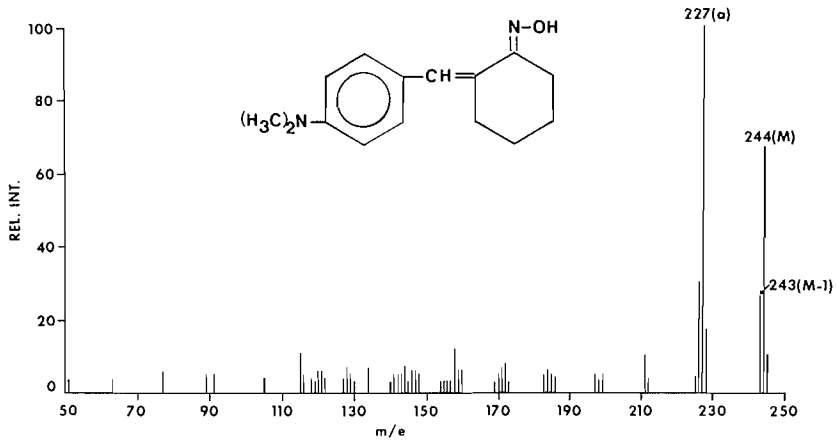

FIG. 2. Mass spectrum (70 eV) of **2**.

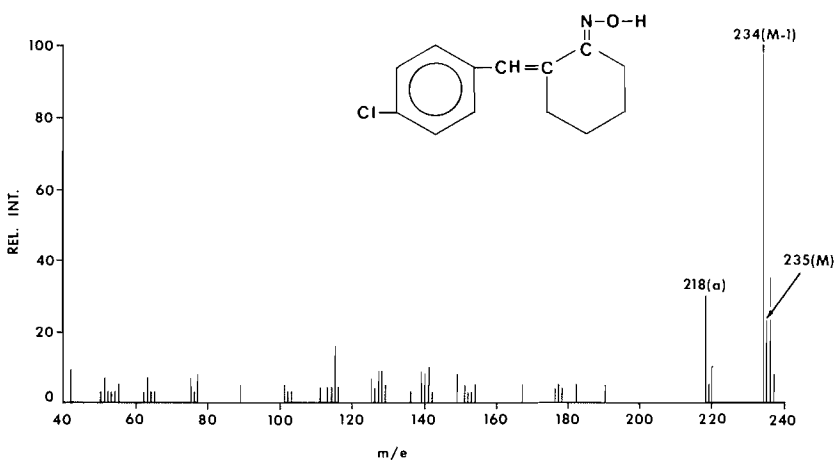

FIG. 3. Mass spectrum (70 eV) of **3**.

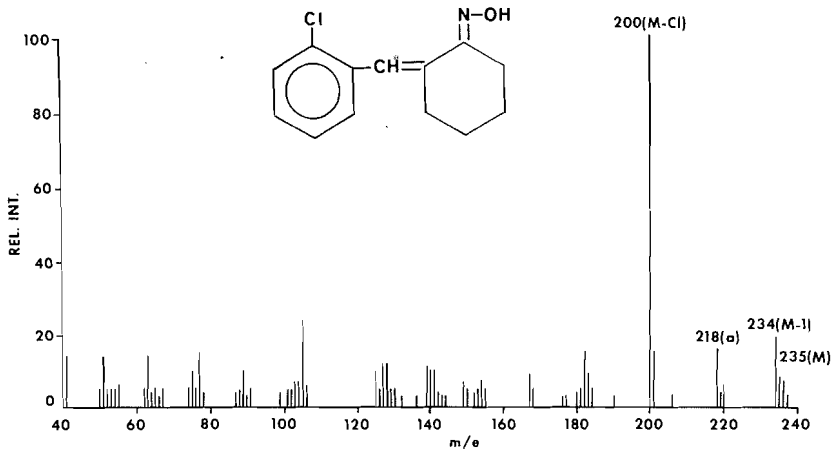

FIG. 4. Mass spectrum (70 eV) of **4**.

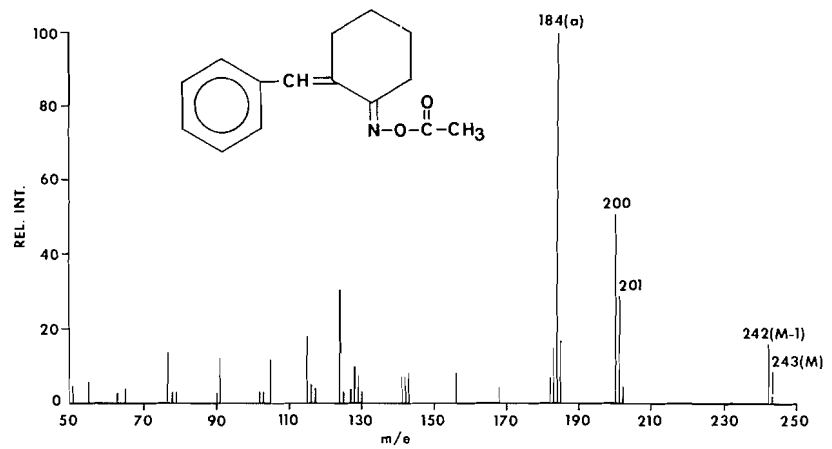

FIG. 5. Mass spectrum (70 eV) of **5**.

that the oximes **1**–**4** have the *E* configuration with respect of the oxime hydroxyl groups to the benzylidene groups and in fact the *E* configuration has been assigned as the most probable structure in several 2-substituted cyclohexanone oximes (4).

A striking feature of the spectra of the four oximes is a large peak at M − 1. In fact this peak is approximately three times more intense than the parent ion peak for all the substrates except the 4-dimethylamino derivative (**2**) where it is only one-third as intense as the parent ion. The spectrum of the acetate of the unsubstituted oxime (**5**) shows an appreciable M − 1 peak indicating that the M − 1 peak in the oximes **1**–**4** is not mainly due to loss of the hydrogen atom from the hydroxyl group. In the light of our recent studies on the intramolecular substitution reaction of 2-benzylidenecyclohexanones leading to the formation of the stable benzopyrylium ion (2), it is reasonable to assume that such a mechanism is operative in the case of the oximes with nitrogen-bonding to the aromatic ring. In all cases a metastable peak was observed for this process (see Scheme 1).

The formation of the M − 1 ion in the oxime series appears to be more favorable than for the substituted 2-benzylidenecyclohexanones as the ratio M − 1/M is greater for the former substrates with the exception of the 4-dimethylamino compound (**2**). Indeed, the M − 1 ion represents the base peak in the spectra of compounds **1** and **3**. This high ratio for M − 1/M is surprising since it is expected that the oxime parent ions would be relatively more stable than the ketone parent ions due to the

Can. J. Chem. Downloaded from www.nrcresearchpress.com by 210.87.254.40 on 09/05/12
For personal use only.

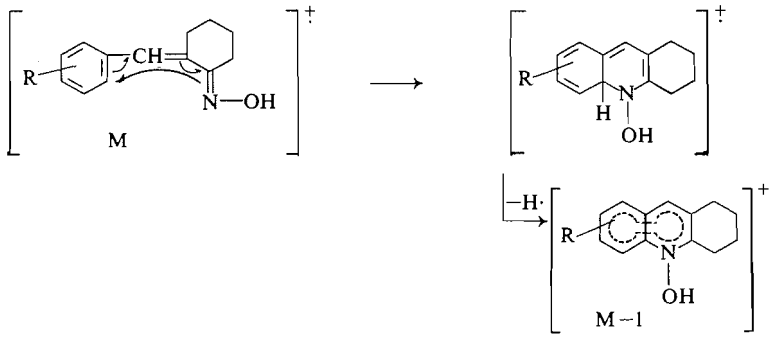

SCHEME 1

presence of the two hetero atoms and less fragmentation would result (5). However, the formation of the even-electron M – 1 ion could be the driving force for the loss of a hydrogen atom from the parent ion (6). As well, it is expected that ring closure using the electron in the C=N rather than in the C=O bond would be more facile due to the decrease in electronegativity of the hetero atom.

It was noted that the M → M – 1 process was considerably less favorable for the 4-dimethylamino substrate (**2**) than for any of the other oximes. Apparently, for this compound the strongly electron-donating para substituent makes the parent ion sufficiently stable due to greater charge delocalization, so that further fragmentation is retarded. The electron-donating substituent influences markedly the mode and ease of fragmentation as shown by the observation of a fairly intense ion resulting from the loss of a hydroxyl radical from the M – 1 ion. Such a process is very minor or non-existent for the other substrates. Presumably, the electron-donating substituent allows the formation of this odd-electron ion while for the other substrates the loss of hydroxyl radical from the M – 1 ion would lead to a relatively more unstable ion.

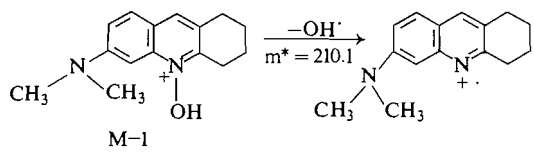

The intramolecular aromatic substitution reaction was further investigated as in the substituted 2-benzylidenecyclohexanone series by preparing the corresponding para- and ortho-chloro oximes, **3** and **4**, respectively. In the oxime series as in the ketone series it is noted that the loss of the ortho-chlorine is extremely facile leading to the most intense peak in the spectrum, M – Cl, Fig. 4. This process is confirmed by the appropriate metastable peak. The loss of the para-chlorine from the parent ion of **3**, however, is not observed for the oxime, Fig. 3, in contrast to the corresponding cyclohexanone where such a loss of chlorine was observed (2). This is consistent with a more facile cyclization process for the oxime and consequently the competing process, loss of chlorine, is not observed.

A major fragmentation pathway observed for oximes **1**–**4** is the loss of a hydroxyl radical from the parent ion to form the even-electron M – OH species, ion (*a*), Figs. 1-4. In fact, ion (*a*) is

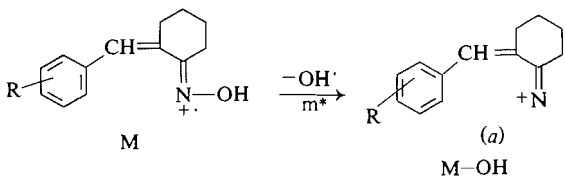

the most intense ion in the spectrum of the 4-dimethylamino substrate (**2**). Such a process has been observed for aliphatic aldoximes and ketoximes as well as alicyclic ketoximes (6) but is of minor importance due to the competing McLafferty rearrangement observed in the aliphatic series. However benzophenone oxime (5) has the M – OH ion as the base peak which suggests that its formation is made favorable by conjugation.

An interesting feature of the mass spectra of aliphatic ketoximes and aromatic ketoximes (5) is the loss of an oxygen atom from the parent ion which is a very rare process. Loss of an oxygen

Can. J. Chem. Downloaded from www.nrcresearchpress.com by 210.87.254.40 on 09/05/12
For personal use only.

TABLE 1. Substituted 2-benzylidenecyclohexanone oximes

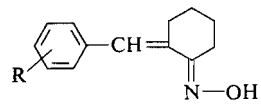

Compound	R	M.p. (°C)	Yield (%)	Found (%)		Calculated (%)	
				C	H	C	H
1	H	125–126 (lit. (7) m.p. 126)	97				
2	2-Cl	169	98	66.09	5.93	66.24	5.99
3	4-Cl	131	94	66.32	6.04	66.24	5.99
4	4-$N(CH_3)_2$	166–168	87	73.46	8.19	73.73	8.25

atom from the oximes studied in the present investigation was not observed.[3]

Experimental

Mass spectra were determined with an MS-12 mass spectrometer operating at 70 eV and lower ionization voltages with an ion source temperature of 100°. The samples were introduced using the direct probe technique. Melting points are uncorrected. Microanalyses were performed by Mr. O. Douglas of the College of Pharmacy, University of Saskatchewan, Saskatoon, Sask.

General Procedure for the Preparation of Substituted 2-Benzylidenecyclohexanone Oximes (Table 1, 1–4)

A mixture of the appropriate ketone (0.087 mol) in 95% ethanol (250 ml), hydroxylamine hydrochloride (0.105 mol) in water (25 ml), and sodium acetate (0.096 mol) in water (20 ml), was heated at 60° for 1 h with stirring. The mixture was diluted with water and cooled. The crude product was removed by filtration, washed with water, and purified by repeated recrystallization from acetone.

2-Benzylidenecyclohexanone Oxime Acetate (5)

A solution of 2-benzylidenecyclohexanone oxime (3.5 g, 0.0175 mol) in freshly distilled acetic anhydride (15 ml) was heated under reflux for 0.5 h. Crushed ice was added to the cooled solution and 10% aqueous sodium carbonate solution was added to decompose the excess acetic anhydride. The gummy yellow precipitate (2.3 g) was removed by filtration and recrystallized from methanol to give pure **5** as colorless needles (1.0 g, 24%), m.p. 105.5°.

Anal. Calcd. for $C_{15}H_{17}NO_2$: C, 74.05; H, 7.04. Found: C, 74.11; H, 7.06.

One of the authors (W.A.T.) thanks the Medical Research Council of Canada for providing a Studentship. Financial support was also provided by Smith, Kline and French Laboratories of Philadelphia, Pa. for the project.

1. P. J. SMITH, J. R. DIMMOCK, and W. G. TAYLOR. Can. J. Chem. **50**, 871 (1972).
2. P. J. SMITH, J. R. DIMMOCK, and W. A. TURNER. This issue.
3. T. SATO, H. WAKATSUKA, and K. AMANO. Tetrahedron, **27**, 5381 (1971).
4. K. K. KELLY and J. S. MATTHEWS. Tetrahedron, **26**, 1555 (1970).
5. H. BUDZIKIEWICZ, C. DJERASSI, and D. H. WILLIAMS. Mass spectrometry of organic compounds. Chapt. 10. Holden-Day, San Francisco. 1967. pp. 367–375.
6. F. W. MCLAFFERTY. Mass spectrometry of organic ions. Academic Press, New York. 1963. p. 318.
7. G. VAVON and J. M. CONIA. C.R. **234**, 526 (1952); Chem. Abstr. **47**, 1618*f* (1953).

[3]A high resolution study of the M − 16 ions for compounds **1** and **2** confirmed this observation.

Can. J. Chem. Downloaded from www.nrcresearchpress.com by 210.87.254.40 on 09/05/12
For personal use only.

Partial Oxidation of Vicinal Hydroxyl Groups of Methyl 4,6-*O*-Benzylidene-α- and β-D-Glucopyranosides with Dimethyl Sulfoxide and Phosphorus Pentoxide[1]

YÔTARO KONDO AND FUJIKAZU TAKAO
Department of Agricultural Chemistry, Kyoto University, Kyoto, Japan
Received October 5, 1972

Oxidation of methyl 4,6-*O*-benzylidene-α-D-glucopyranoside with dimethyl sulfoxide – phosphorus pentoxide gives the corresponding 3-ketone (**3**), the 2,3-*O*-oxidomethylenebenzylidene acetal (**5**), and the 2,3-*O*-oxidodimethylene acetal (**6**). By a similar treatment of methyl 4,6-*O*-benzylidene-β-D-glucopyranoside only starting material was recovered.

L'oxydation du méthyl-*O*-benzylidène-4,6-α-D-glucopyranoside par le pentoxyde de phosphore-diméthylsulfoxyde conduit à la cétone-3 correspondante (**3**), à l'*O*-oxydométhylène benzylidène-2,3 acétal (**5**) et à l'*O*-oxydodiméthylène-2,3 acétal (**6**). Par un traitement similaire, le méthyl-*O*-benzylidène-4,6-β-D-glucopyranoside a été retrouvé inchangé. [Traduit par le journal]

Can. J. Chem., **51**, 1476 (1973)

Introduction

Oxidation of "isolated" secondary hydroxyl groups of carbohydrates to the corresponding keto sugars, which are important intermediates in the synthesis of amino, branched-chain, and rare sugars (1), has been reported by many authors (2). It has been demonstrated that a dimethyl sulfoxide (DMSO) – acid anhydride (acetic anhydride, phosphorus pentoxide (P_2O_5) mixture is useful for oxidation of "isolated" secondary hydroxyl groups of monosaccharides (3, 4) and also for the partial oxidation of "vicinal" hydroxyl groups of polysaccharides (5, 6). However, little is known about the partial oxidation of "vicinal" diols of monosaccharides by these reagents. For the comparative studies of partial oxidation of mono- and polysaccharides, we selected methyl 4,6-*O*-benzylidene-α- and β-D-glucopyranosides (**1** and **2**) and 6-*O*-tritylamylose[2] (7) as the respective models. This communication describes the partial oxidation of **1** and **2** with DMSO–P_2O_5 and also identification of the products obtained by a side reaction of this oxidation.

Results and Discussion

Treatment of compound **1** with DMSO-P_2O_5 for 3 days at 40 °C gave seven compounds as detected by t.l.c. (silica gel G, benzene–ether, 4:1, v/v). The reaction mixture was extracted with chloroform and the extract was evaporated to afford crystalline material which on recrystallization from hot benzene gave methyl 4,6-*O*-benzylidene-α-D-*ribo*-hexopyranosid-3-ulose (**3**). The assigned structure of **3** is based on the p.m.r. and i.r. spectral properties, revealing respectively the signal of H-1 as a one-proton doublet ($J_{1,2}$ = 4.5 Hz) at τ 4.90, which indicates that H-2 remained intact, and characteristic absorptions in the carbonyl region at 1740 cm^{-1} and in the hydroxyl region at 3500 cm^{-1}. Acetylation of **3** with acetic anhydride in pyridine yielded methyl 2-*O*-acetyl-4,6-*O*-benzylidene-α-D-*ribo*-hexopyranosid-3-ulose (**4**)[3] of which analytical data were in good agreement with those of an authentic sample prepared via oxidation of methyl 2-*O*-acetyl-4,6-*O*-benzylidene-α-D-glucopyranoside. These observations suggest that the C-3 hydroxyl of the vicinal diol of **1** is selectively oxidized with DMSO-P_2O_5. Upon silicic acid column chromatography of the mother liquor, from which compound **3** was previously removed, six compounds were isolated (see Experimental). The i.r. spectra of these compounds did not show any absorption of the carbonyl group.

The structures of compounds **5** and **6** isolated chromatographically were determined by elemental analysis, p.m.r., and mass spectrometry. The p.m.r. spectrum (Fig. 1) of **5** showed the signal of H-1 as a one-proton doublet ($J_{1,2}$ =

[1]Presented in part at the 274th Meeting of the Kansai Division of the Agricultural Chemical Society of Japan, October 1971, Kagawa, Japan.

[2]Oxidation of 6-*O*-tritylamylose with DMSO-P_2O_5 gave results similar to those obtained with DMSO – acetic anhydride oxidation (6). The details will be published elsewhere.

[3]It is of particular interest that the p.m.r. spectrum of **4** showed $^4J_{a,a}$ long-range coupling ($J_{2,4}$ = 1.0 Hz).

Can. J. Chem. Downloaded from www.nrcresearchpress.com by 210.87.254.105 on 09/05/12
For personal use only.

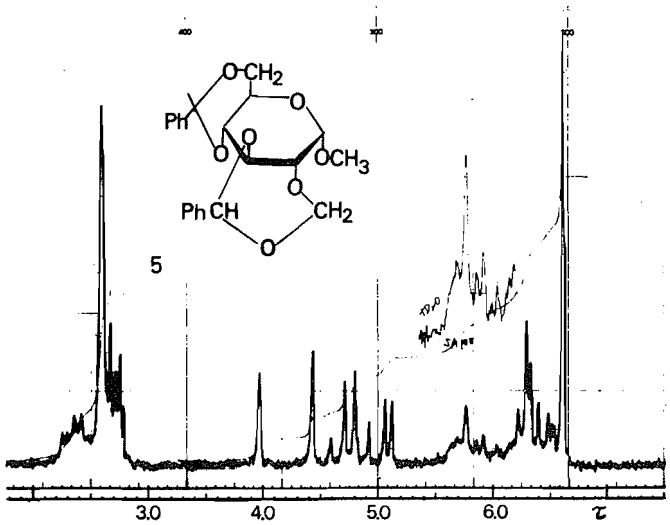

FIG. 1. The 60 MHz p.m.r. spectrum of cyclic acetal **5** ($CDCl_3$).

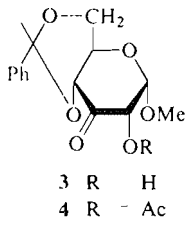

3 R H
4 R Ac

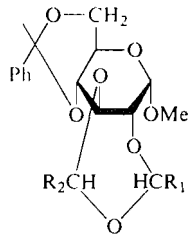

5 R_1 = H; R_2 = Ph
6 R_1 = R_2 = H
7 R_1 = R_2 = Me

3.5 Hz) at τ 5.09, and two singlets at 4.43 and 6.62 corresponding to the 4,6-benzylic proton and the glucosidic methyl proton respectively. Furthermore, new signals appeared as a one-proton singlet at τ 3.97 and as a two-proton quartet (AB system) at 4.76 due to the 2,3-benzylic proton and the methylene portion of the seven-membered 2,3-cyclic acetal, respectively. Compounds **5** and **6** showed a similarity in their p.m.r. spectra, except that the methylene moiety of the 2,3-cyclic acetal of **6** occurred as a four-proton quartet at τ 5.01 which was superimposed upon the signal of H-1 appearing as a one-proton doublet at τ 5.11 ($J_{1,2}$ = 3.6 Hz) (Fig. 2). To provide further structural confirmation for the position of the 2,3-benzylidene group of **5**, the chemical shift of H-1 of compounds **5**, **6**, and methyl 4,6-*O*-benzylidene-2,3-oxidodiethylidene-α-D-glucopyranoside (**7**) which was prepared by the method of Appel *et al.* (8) were compared; the signal of H-1 of **7** appeared at τ 5.17 higher field by 0.06 p.p.m., as compared with that of **6**. Since structures of **6** and **7** are different only in substituted groups (R_1 and R_2), this significant upfield shift of the H-1 signal of **7** may be due to the shielding effect of the methyl moiety of the ethylidene group attached to C-2 in the 2,3-cyclic acetal of **7** provided that the cyclic acetals of **6** and **7** adopt a twist-chair conformation as suggested by Stoddart (9) for methyl 4,6-*O*-ethylidene-2,3-oxidodiethylidene-α-D-glucopyranoside (**9**). If this is the case, a considerable change in the chemical shift of H-1 would be expected for the

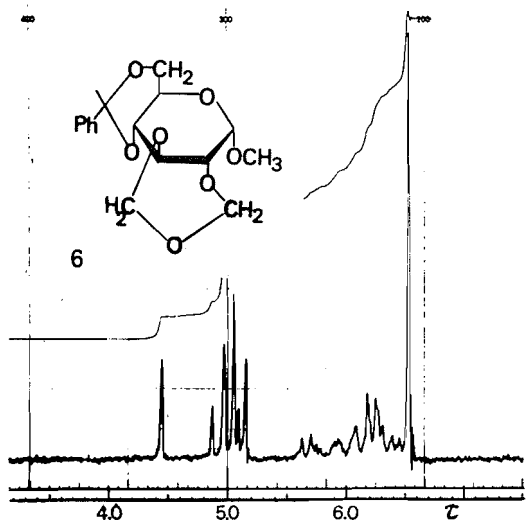

FIG. 2. The 60 MHz p.m.r. spectrum of cyclic acetal **6** ($CDCl_3$).

Can. J. Chem. Downloaded from www.nrcresearchpress.com by 210.87.254.105 on 09/05/12
For personal use only.

Can. J. Chem. Downloaded from www.nrcresearchpress.com by 210.87.254.105 on 09/05/12
For personal use only.

TABLE 1. Mass numbers of the main ions arising from cyclic acetals (**5**, **6**, **7**, and **9**)

	M^+		**10**		**11**		**12**		**13**		**14**		**15**	
Compound	*m/e*	Intensity %	*m/e*	Intensity (%)	*m/e*	Intensity (%)	*m/e*	Intensity (%)	*m/e*	Intensity (%)	*m/e*	Intensity (%)	*m/e*	Intensity (%)
5	400	44.0	370	0.2	149	23.4	251	8.9	221	10.4	178	5.2	148	7.8
			294	0.6					145	20.0			72	46.9
6	324	25.2	294	1.0	149	16.6	175	29.1	145	56.4	102	33.2	72	31.8
7	352	19.5	308	9.4	149	26.9	203	10.1	159	40.0	130	6.5	86	81.2
9	290	1.4	246	0.5	87	31.0	203	19.0	159	44.5	130	5.0	86	100.0

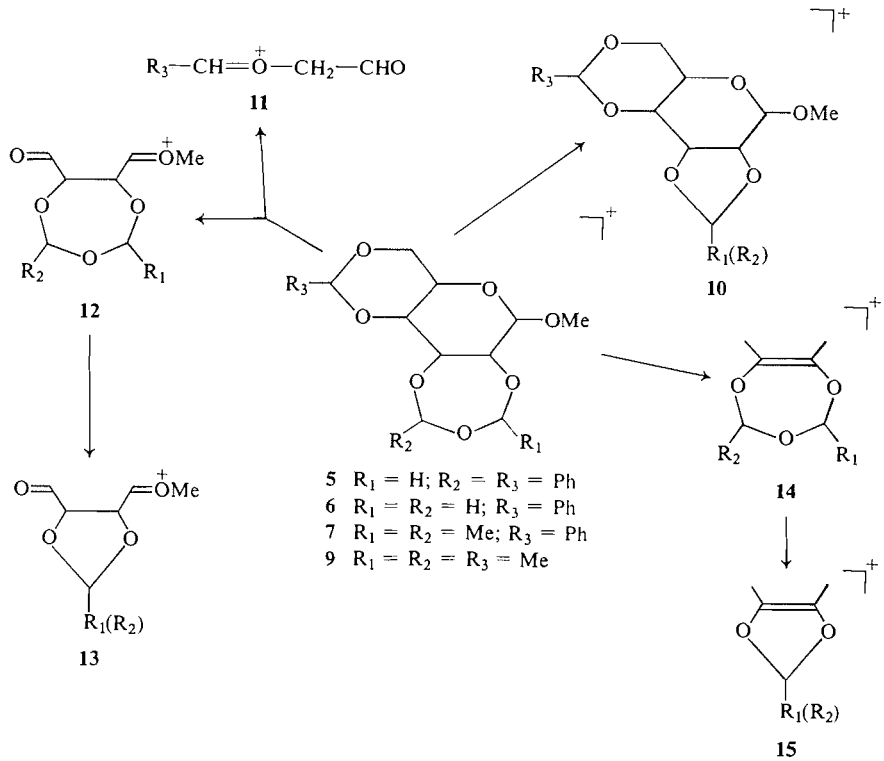

SCHEME 1. Mass spectrometric fragmentation pattern.

acetal analog of **5** with the benzylidene group attached to C-2 rather than to C-3. However, it was found that the H-1 signals of compounds **5** and **6** appeared at nearly the same field at τ 5.09 and 5.11, respectively, suggesting that the benzylidene group of the 2,3-cyclic acetal in compound **5** is attached to the oxygen atom of C-3 as shown in Fig. 1.

The formation of the methyleneoxy linkages of compounds **5** and **6** may be attributed to the reaction of hydroxyl groups of the sugar moiety with formaldehyde derived from DMSO, in view of the fact that treatment of **1** with paraformaldehyde–P_2O_5 in *N*,*N*-dimethylformamide (DMF) for 3 days at 40 °C gave compound **6** as the major product. Furthermore, the 2,3-benzylidene group in compound **5** is presumably derived from benzaldehyde which is liberated by acid degradation of the 4,6-benzylidene group of the starting material.

The low yield of **3** may be explained in terms of a rapid condensation of the diol with formaldehyde, which may occur faster than the formation of the oxidation product, thus giving methyleneoxy acetals as the major product. It is of interest to note that the reaction of **2** with DMSO–P_2O_5 yields neither cyclic acetals nor oxidized products under the same reaction conditions as that described for α-anomer, while treatment of **2** with paraformaldehyde gave methyl 4,6-*O*-benzylidene-2,3-*O*-oxidodimethylene-β-D-glucopyranoside (**8**) as observed with α-anomer.

Finally, the mass spectrometric fragmentation of the 2,3-cyclic acetals of methyl 4,6-*O*-benzylidene-α-D-glucopyranoside (**5**, **6**, **7**, and **9** (8)) was examined (see Scheme 1 and Table 1). All the mass spectra of the above 2,3-cyclic acetals exhibited the peak of molecular ion and the peak characteristic of the fragment **10** in the higher mass range which is formed by the loss of an aldehyde (R-CHO). Fragments **11** and **12** are formed by an elimination similar to "h-rupture" which is one of the characteristic fragmentations to methyl 4,6-*O*-benzylidene-α-D-glucopyranoside (10). The resulting ion **12** further loses an aldehyde leading to fragment **13**, and the cleavage at C-1 and -3 bonds of the molecular ion produces fragment **14**, which upon loss of an aldehyde gives fragment **15**. It appears that the

Can. J. Chem. Downloaded from www.nrcresearchpress.com by 210.87.254.105 on 09/05/12
For personal use only.

fragmentation accompanied by the loss of aldehydes is characteristic of the mass spectrometry of 2,3-cyclic acetals.

Experimental

The t.l.c. was performed on silica gel G (Merck, benzene–ether, 4:1, v/v) and the spots were detected by spraying a solution of 10% sulfuric acid and by heating. Column chromatography was carried out on silicic acid (Mallinkrodt, 100 mesh) by stepwise elution with the solvent systems; benzene–ether, 4:1, 2:1 (v/v), and pure ether. Melting points were determined on a Yanagimoto hot stage microscope and are uncorrected. The optical rotations were measured with a Yanagimoto Model OR-20 direct reading polarimeter and the i.r. spectra were recorded with a Shimazu AR-7 spectrophotometer by the potassium bromide disk method. The p.m.r. spectra were measured on a Varian A-60 spectrometer using tetramethylsilane as an internal reference at the normal operating temperature of the instrument. The mass spectra were taken with a Hitachi RUM-60 at 200 °C and ionizing potential 70 eV.

Reaction of Methyl 4,6-O-Benzylidene-α-D-glucopyranoside with Dimethyl Sulfoxide – Phosphorus Pentoxide

A mixture of methyl 4,6-*O*-benzylidene-α-D-glucopyranoside (**1**, 5 g) and P_2O_5 (2.5 g) in dry DMSO (75 ml) was stirred for 3 days at 40 °C. After dilution with chloroform (250 ml) and water (250 ml) followed by neutralization with aqueous 3 *M* K_2CO_3 solution, the reaction mixture was extracted with chloroform (50 ml × 3). The extract was washed with saturated aqueous NaCl solution (50 ml × 5) and dried over Na_2SO_4. After evaporation to dryness *in vacuo*, the crystalline residue obtained was recrystallized from hot benzene to give methyl 4,6-*O*-benzylidene-α-D-*ribo*-hexopyranosid-3-ulose (**3**, 0.55 g, 11%) which is slightly soluble in common organic solvents, m.p. 190–192 °C; $[\alpha]_D^{23}$ +113.0° (*c*, 1, pyridine) (lit. (11), m.p. 184–186 °C, $[\alpha]_D^{23}$ +128.4° (*c*, 0.48, acetone)); i.r.: ν_{max} 1740 (C=O), 3500 cm^{-1} (OH); p.m.r. (in DMSO-d_6): τ 4.34 (one-proton singlet, benzylic H), 4.90 (one-proton doublet, H-1, $J_{1,2}$ = 4.5 Hz), 6.67 (three-proton singlet, OMe).

Anal. Calcd. for $C_{14}H_{16}O_6$: C, 60.0; H, 5.9. Found: C, 59.96; H, 6.22.

The mother liquor, from which **3** was previously removed, was applied to a silicic acid column (415 × 40 mm) which is subjected to sequential elution. A mixture of benzene and ether (4:1, v/v) first eluted a trace amount of syrupy compound (0.02 g, R_f 0.85), followed by 2,3-oxidomethylenebenzylidene acetal (**5**) (0.24 g, 3.4%, R_f 0.70) and then 2,3-oxidodimethylene acetal (**6**) (0.45 g, 7.5%, R_f 0.50). The syrupy compound was not further investigated because of its low yield.

Methyl 4,6-*O*-benzylidene-2,3-*O*-oxidomethylenebenzylidene-α-D-glucopyranoside (**5**) had m.p. 127–128 °C and $[\alpha]_D^{23}$ +82.0° (*c*, 1, $CHCl_3$); p.m.r. (in $CDCl_3$): τ 3.97 (one-proton singlet, 2,3-benzylic H), 4.43 (one-proton singlet, 4,6-benzylic H), 4.76 (two-proton quartet, $-CH_2-$, J_{gem} = 7.6 Hz), 5.09 (one-proton doublet, H-1, $J_{1,2}$ = 3.5 Hz), 6.62 (three-proton singlet, OMe).

Anal. Calcd. for $C_{22}H_{24}O_7$: C, 65.99; H, 6.04. Found: C, 65.85; H, 6.28.

Methyl 4,6-*O*-benzylidene-2,3-*O*-oxidodimethylene-α-D-glucopyranoside (**6**) had m.p. 133–134 °C and $[\alpha]_D^{23}$ +89.5° (*c*, 1.8, $CHCl_3$); p.m.r. (in $CDCl_3$): τ 4.36 (one-proton singlet, benzylic H), 5.01 (four-proton quartet, $-CH_2-$, J_{gem} = 7.8 Hz), 5.11 (one-proton doublet, H-1, $J_{1,2}$ = 3.6 Hz), 6.75 (three-proton singlet, OMe).

Anal. Calcd. for $C_{16}H_{20}O_7$: C, 59.25; H, 6.22. Found: C, 59.14; H, 6.36.

Further elution of the above column with a mixture of benzene and ether (2:1, v/v) gave crystals (0.45 g, R_f 0.30) having m.p. 272–275 °C, $[\alpha]_D^{23}$ −89.0° (*c*, 1, pyridine), and M^+ 564[4] and then crystals (0.71 g, R_f 0.15) having m.p. 236–238 °C, $[\alpha]_D^{23}$ +76.0° (*c*, 1, pyridine), and M^+ 576.[5] The complexity of their p.m.r. spectra precluded detailed structural elucidation. However, on the basis of the mass spectral data dimeric structures may be suggested. Starting material **1** (0.71 g, R_f 0.08) was eluted with pure ether and had m.p. 169–170 °C, and $[\alpha]_D^{23}$ +110.0° (*c*, 1, $CHCl_3$).

Anal. Calcd. for $C_{14}H_{18}O_6$: C, 59.56; H, 6.43. Found: C, 59.52; H, 6.24.

Methyl 2-O-Acetyl-4,6-O-benzylidene-α-D-ribo-hexopyranosid-3-ulose (4)

Preparation A

A solution of the 3-keto sugar **3** (0.1 g) in dry pyridine (20 ml) and acetic anhydride (20 ml) was stirred overnight at room temperature. The reaction mixture was poured into ice-water and extracted with chloroform (150 ml). The extract was washed successively with aqueous sulfuric acid, saturated aqueous sodium bicarbonate and water, and dried over Na_2SO_4. The residue from evaporation of the solution was recrystallized from ethanol to give title compound **4** (0.12 g) as fine needles, m.p. 190–193 °C, $[\alpha]_D^{23}$ +69.0° (*c*, 1, $CHCl_3$), that was identical with the product of preparation B.

Preparation B

A solution of methyl 2-*O*-acetyl-4,6-*O*-benzylidene-α-D-glucopyranoside (**12**) (0.5 g) in dry DMSO (15 ml) and acetic anhydride (5 ml) was stirred for 4 days at room temperature. The solution was diluted with chloroform and water, and then extracted with chloroform. The extract was washed with saturated sodium bicarbonate solution and water, dried over Na_2SO_4, and evaporated. The syrupy residue was co-distilled with ethanol to give a crystalline mass. Recrystallization yielded the 3-ketone **4** (0.29 g, 60%), m.p. 189–190 °C; $[\alpha]_D^{30}$ +65.0° (*c*, 1, $CHCl_3$); i.r.: ν_{max} 1753 (C=O), 1743 cm^{-1} (C=O, ester); p.m.r. (in $CDCl_3$): τ 4.44 (one-proton singlet, benzylic H), 4.62 (one-proton quartet, H-2, $J_{1,2}$ = 4.3, $J_{2,4}$ = 1.0 Hz), 4.81 (one-proton doublet, H-1, $J_{1,2}$ = 4.3 Hz), 6.57 (three-proton singlet, OMe), 7.80 (three-proton singlet, OAc).

Anal. Calcd. for $C_{16}H_{18}O_7$: C, 59.62; H, 5.63. Found: C, 59.56; H, 5.85.

Reaction of Methyl 4,6-O-Benzylidene-α-D-glucopyranoside with Paraformaldehyde in N,N-Dimethylformamide

Methyl 4,6-*O*-benzylidene-α-D-glucopyranoside (**1**, 0.5 g) was stirred with paraformaldehyde (0.5 g) in DMF (5 ml) containing P_2O_5 (0.25 g) for 3 days at 40 °C. The

[4]The mass spectrum was measured at 320 °C.

[5]The mass spectrum was measured at 350 °C.

Can. J. Chem. Downloaded from www.nrcresearchpress.com by 210.87.254.105 on 09/05/12
For personal use only.

reaction mixture was diluted with chloroform (100 ml) and filtered through Celite to remove the excess paraformaldehyde. The solution was extracted with chloroform (50 ml × 3) and the extract was evaporated to a thin syrup. It was then chromatographed on a silicic acid column to yield a colorless syrup which was crystallized from methanol to give methyl 4,6-*O*-benzylidene-2,3-*O*-oxidodimethylene-α-D-glucopyranoside (**6**) as fine needles (0.11 g, 19%), m.p. 133–134 °C, $[\alpha]_D^{30}$ +91.1° (*c*, 0.5, $CHCl_3$).

Reaction of Methyl 4,6-O-Benzylidene-β-D-glucopyranoside with Paraformaldehyde in N,N-Dimethylformamide

Methyl 4,6-*O*-benzylidene-β-D-glucopyranoside (**2**, 2 g) was added to a mixture of paraformaldehyde (2 g) and P_2O_5 (1 g) in dry DMF (40 ml) and stirred for 3 days at 40 °C. It was worked-up as described for α-anomer to give a crystalline residue which was recrystallized from a mixture of chloroform and petroleum ether to afford methyl 4,6-*O*-benzylidene-2,3-*O*-oxidodimethylene-β-D-glucopyranoside (**8**) as fine needles (0.5 g, 20%), m.p. 205–206 °C; $[\alpha]_D^{23}$ −34.4° (*c*, 1, $CHCl_3$); p.m.r. (in $CDCl_3$): τ 4.36 (one-proton singlet, benzylic H), 5.10 (four-proton quartet, $-CH_2-$, J_{gem} = 6.0 Hz), 5.43 (one-proton doublet, H-1, $J_{1,2}$ = 7.8 Hz), 6.75 (three-proton singlet, OMe).

Anal. Calcd. for $C_{16}H_{20}O_7$: C, 59.25; H, 6.22. Found: C, 59.09; H, 6.16.

The authors thank Professor K. Onodera for his interest and Dr. N. Miyazaki (Research Laboratories, Takeda Chemical Industries, Ltd.) for mass spectrometry measurements.

1. R. F. Butterworth and S. Hanessian. Synth. **2**, 70 (1971).
2. J. S. Brimacombe. Angew. Chem. **81**, 415 (1969).
3. K. E. Pfitzner and J. G. Moffat. J. Am. Chem. Soc. **85**, 3027 (1965).
4. K. Onodera, S. Hirano, and N. Kashimura. J. Am. Chem. Soc. **87**, 4651 (1965).
5. K. Bredereck. Tetrahedron Lett. 695 (1967).
6. M. L. Wolfrom and P. Y. Wong. Carbohydr. Res. **12**, 109 (1970).
7. Y. Kondo. A study on the synthesis of aminated amylose. M.Sc. Thesis, Kyoto University, Kyoto, Japan, 1970.
8. H. Appel, W. N. Haworth, E. G. Cox, and F. J. Llewellyn. J. Chem. Soc. 793 (1938).
9. J. F. Stoddart. Stereochemistry of carbohydrates. John Wiley & Sons, Inc., New York. 1971. p. 219.
10. O. S. Chizhov, L. S. Golovkina, and N. S. Wulfson. Carbohydr. Res. **6**, 138 (1968).
11. G. J. F. Chittenden and R. D. Guthrie. J. Chem. Soc. 695 (1966).
12. R. W. Jeanloz and D. A. Jeanloz. J. Am. Chem. Soc. **79**, 2579 (1957).

Can. J. Chem. Downloaded from www.nrcresearchpress.com by 210.87.254.105 on 09/05/12
For personal use only.

cis Virtual Coupling

G. M. BANCROFT[1] AND E. T. LIBBEY
Department of Chemistry, University of Western Ontario, London, Ontario

Received November 20, 1972

The proton n.m.r. spectra of the new compounds *cis*-$Fe(NCS)_2(PR_3)$ (R = Me, MeO) consist of two identical triplets assignable to *trans* PR_3 and *cis* PR_3 linkages in the same complex.

On observe que les spectres R.M.N. des composés $Fe(NCS)_2(PR_3)_4$ *cis* (R = Me et OMe) sont formés de deux triplets identiques attribuables aux groupes PR_3 *trans* et PR_3 *cis* d'un même complexe.
[Traduit par le journal]

Can. J. Chem., **51**, 1482 (1973)

Can. J. Chem. Downloaded from www.nrcresearchpress.com by 210.87.254.6 on 09/05/12
For personal use only.

The phenomenon of "virtual coupling" has been used extensively in both square planar (1) and octahedral systems (2, 3) to establish the *trans* configuration of ligands in coordination compounds. Using ligands such as $P\phi_2Me$, $P(OMe)_3$, and $P\phi Me_2$, a triplet of apparent $J(PH)$ of about 4–5 Hz was observed, although the width of the central peak often varied markedly. There have been several suggestions in the literature (4, 5) recently that the appearance of a triplet should be interpreted with caution, and at least two recent experimental papers (5, 6) indicate that broadened triplets can be observed for *cis* phosphines or phosphites. Theoretical considerations (7, 8) suggest that a sharp triplet will occur when the ^{31}P–^{31}P coupling is large, and that the central line will broaden and collapse as the ^{31}P–^{31}P coupling decreases. We report here identical "virtual coupling" patterns for both the *trans* PR_3 pair and *cis* PR_3 pair (R = Me, MeO) in two new compounds, *cis*-$Fe(NCS)_2[P(OMe)_3]_4$ and *cis*-$Fe(NCS)_2[P(Me)_3]_4$. Unfortunately, other analogous *cis* compounds containing other halides (or pseudohalides) and simple phosphines or phosphites could not be prepared. Indeed, these are the first two Fe(II) low spin octahedral phosphine or phosphite compounds yet reported which do not contain the powerful ligands H or CO. Thus Booth and Chatt (9) were able to prepare just the tetrahedral ferrous complexes.

Experimental

All reactions were performed under a nitrogen atmosphere using deoxygenated solvents. Trimethyl phosphite was obtained from J. T. Baker Chemical Co. and redistilled prior to use. Trimethyl phosphine was prepared by standard Grignard techniques: phosphorous trichloride was added slowly, with vigorous stirring, to excess MeMgBr in di(*n*-butyl ether) at 0 °C (10). PMe_3 was distilled out in a N_2 stream at ~120 °C and trapped in saturated AgI/KI solution as the $(AgI{\cdot}PMe_3)_n$ complex which was used without further purification.

Preparation of Compounds

cis-Diisothiocyanate Tetrakis(trimethyl Phosphite) Iron(II)

To 1.98 g (1 mmol) of $FeCl_2{\cdot}4H_2O$ and 2.5 g of NH_4NCS (~3 mmol) in 50 cc methanol, 5 cc of $P(OMe)_3$ were added. Crystals of *trans*-$Fe(NCS)_2[P(OMe)_3]_4$ began to form after a few minutes. These were washed with cold methanol and dried under vacuum. Yield 80%.

Anal. Calcd. for *trans*-$Fe(NCS)_2[P(OMe)_3]_4$: C, 25.15; H, 5.38; N, 4.18. Found: C, 25.04; H, 5.76; N, 4.28.

Recrystallization of the *trans* isomer from acetone–ether afforded the *cis* isomer.

Anal. Calcd. for *cis*-$Fe(NCS)_2[P(OMe)_3]_4$: C, 25.15; H, 5.38; N, 4.18. Found: C, 25.53; H, 5.40; N, 3.80.

The *trans* isomer is air stable, but the *cis* isomer is moderately air sensitive.

cis-Diisothiocyanate Tetrakis(trimethyl Phosphine) Iron(II)

0.06 g (0.5 mmol) of anhydrous $FeCl_2$ and 0.12 g (2 mmol) of NH_4NCS were dissolved in 40 cc of absolute ethanol. 2.6 g of $AgI{\cdot}PMe_3$ (~8 mmol of PMe_3) was heated on a wax bath at ~170 °C in a stream of dry nitrogen. At this temperature, the PMe_3 was evolved, and the gases were passed directly into the ethanol solution. After about 15 min ~0.15 g of the desired product slowly formed as a red powder. Attempts at recrystallization resulted in loss of phosphine. The compound is unstable in air and solution. Yield 70%.

Anal. Calcd. for the compound: C, 35.3; H, 7.6; N, 5.9. Found: C, 35.3; H, 7.4; N, 5.9.

Infrared spectra were recorded on a Perkin–Elmer 621 instrument. In the NC stretching region, the *trans*-$P(OMe)_3$ isomer gave a sharp line at 2114 cm^{-1}, while the *cis*-$P(OMe)_3$ isomer gave a broad doublet at 2118 and 2131 cm^{-1}. Similarly, the *cis*-PMe_3 isomer gave a broad line centered at 2100 cm^{-1} with two shoulders at 2120 and 2049 cm^{-1}. The Mössbauer quadrupole splittings confirm

[1]To whom correspondence should be addressed.

Can. J. Chem. Downloaded from www.nrcresearchpress.com by 210.87.254.6 on 09/05/12
For personal use only.

the above structural assignments. Mössbauer spectra, run at 78 °K on an Austin Science Associates Spectrometer showed the expected 2:1 *trans*:*cis* ratio (11) of quadrupole splittings for the $P(OMe)_3$ complexes (*trans* = 0.56 mm s^{-1}; *cis* = 0.30 mm s^{-1}), and the small quadrupole splitting for *cis*-$Fe(NCS)_2[P(Me)_3]_4$ (= 0.31 mm s^{-1}) is also consistent with *cis* geometry. The n.m.r. spectra were recorded on Varian HA 100 and T60 instruments in $CHCl_3$. For the $P(OMe)_3$ compounds, 5% excess phosphite was added. This phosphite slowed down both the rate of isomerism and the rate of ligand exchange which, at ambient temperatures, produced broad unresolved absorptions.

Results and Discussion

The proton n.m.r. spectrum of *trans*-$Fe(NCS)_2[P(OMe)_3]_4$ shows the pentet pattern characteristic of the square planar environment of phosphites (6), $\tau = 6.32$.

The proton n.m.r. spectra of both *cis*-$Fe(NCS)_2[P(OMe)_3]_4$ (Fig. 1) and *cis*-$Fe(NCS)_2[P(Me)_3]_4$ consist of two sharp chemically shifted 1:2:1 triplets which are indistinguishable. For *cis*-$Fe(NCS)_2[P(OMe)_3]_4$, $\tau_1 = 6.25$, $\tau_2 = 6.48$, and $^3J(PH) + {}^5J(PH) = 9.9 \pm 0.2$ Hz. For *cis*-$Fe(NCS)_2[P(Me)_3]_4$, $\tau_1 = 8.50$, $\tau_2 = 8.72$, and $^2J(PH) + {}^4J(PH) = 7.6 \pm 0.4$ Hz.

Selective decoupling experiments on *cis*-$Fe(NCS)_2[P(OMe)_3]_4$ collapsed each triplet independently with no observable change in the other triplet. Although the line widths are a function of both temperature and concentrations, the central lines of each triplet remain of equal width. At 30 °C, all the lines in the *cis*-$Fe(NCS)_2[P(OMe)_3]_4$ spectrum (Fig. 1) have a width of ~0.8 Hz compared to the ligand line width of ~0.5 Hz. All the lines in *cis*-$Fe(NCS)_2[P(Me)_3]_4$ have widths which are somewhat broader (~2 Hz), but all lines in this spectrum are still of very similar width.

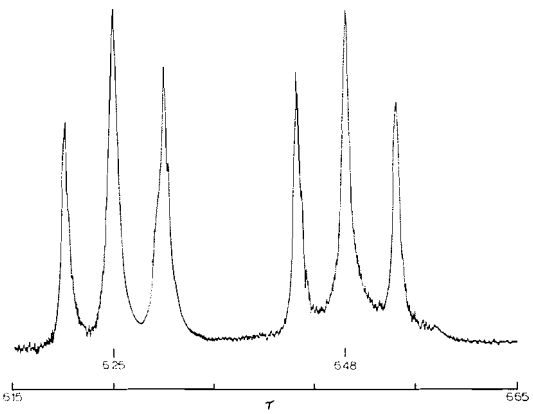

FIG. 1. Proton n.m.r. spectrum of *cis*-$Fe(NCS)_2[P(OMe)_3]_4$ at 30 °C in $CHCl_3$ obtained on a Varian HA 100 instrument. The small peaks due to the *trans*-isomer are not shown.

These spectra represent the first observation of two sharp "virtual coupled" triplets from within one molecule. The only reasonable assignment is: one triplet to the *trans*-PR_3 pair, and the other triplet to the *cis*-PR_3 pair *trans* to the NCS groups. It is apparent then that the ^{31}P–^{31}P coupling between the *trans*-$P(OMe)_3$ pair and the coupling between the *cis*-$P(OMe)_3$ pair are of comparable magnitude, and surprisingly that cross coupling between the two pairs is very small.

The slight asymmetry of the outer lines of the triplets indicates that some protonic cross coupling is occurring (7), but that it is small compared with both the *cis* and *trans* "virtual coupling". Because the low field triplet in the *cis*-$Fe(NCS)_2[P(OMe)_3]_4$ spectrum has a similar chemical shift to *trans*-$P(OMe)_3$ linkages in *trans*-$Fe(NCS)_2[P(OMe)_3]_4$, we assign the low field triplets to the *trans*-PR_3 pairs and the high field triplets to the *cis*-PR_3 pairs.

The simplicity of the "double-triplet" line patterns make a polymeric species highly unlikely; *e.g.* the simple dimer, $[P(OMe)_3]_4Fe(NCS)_2Fe[P(OMe)_3]_4^{2+}$, would have three chemically different phosphites, those *trans* to phosphites, thiocyanate, and isothiocyanate, presumably distinguishable in the n.m.r. spectrum. Similarly, the possibility of two monomeric species is small since the triplets are of equal intensity.

Our results suggest strongly that the appearance of a sharp triplet in the proton n.m.r. need not be characteristic of *trans* phosphines or phosphites (4).

We are grateful to Drs. J. Thompson and I. Pete of the University of Toronto for running the decoupled spectra, Drs. A. G. MacDiarmid and M. L. H. Green for helpful discussions, and the National Research Council of Canada for financial support.

1. J. M. JENKINS and B. L. SHAW. J. Chem. Soc. (A), 770 (1966).
2. R. R. BROOKS and B. L. SHAW. J. Chem. Soc. (A), 1079 (1967).
3. B. L. SHAW and A. C. SMITHIES. J. Chem. Soc. (A), 2784 (1968).

4. R. D. BERTRAND, F. B. OGILVIE, and J. G. VERKADE. J. Am. Chem. Soc. **92**, 1916 (1970).
5. W. J. CULLEN, J. R. SAMS, and J. A. J. THOMPSON. Inorg. Chem. **10**, 843 (1971).
6. L. M. HAINES. Inorg. Chem. **10**, 1685 (1971); **10**, 1693 (1971).
7. R. K. HARRIS. Can. J. Chem. **42**, 2275 (1964).
8. J. P. FACKLER, JR., J. A. FETCHIN, J. MAYHEW, W. D. SEIDEL, T. J. SWIFT, and M. WEEKS. J. Am. Chem. Soc. **91**, 1941 (1969).
9. G. BOOTH and J. CHATT. J. Chem. Soc. 2099 (1962).
10. R. A. ZINGARO and R. E. MCGLOTHLIN. J. Chem. Eng. Data, **8**, 226 (1963).
11. G. M. BANCROFT, M. J. MAYS, and B. E. PRATER. J. Chem. Soc. (A), 956 (1970).

Can. J. Chem. Downloaded from www.nrcresearchpress.com by 210.87.254.6 on 09/05/12
For personal use only.

Can. J. Chem. Downloaded from www.nrcresearchpress.com by 210.87.254.40 on 09/05/12
For personal use only.

Acid-catalyzed Exchange at 250 °C; a Simple and Quantitative Method for the Replacement of Aromatic Protons by Deuterium[1]

NICK H. WERSTIUK AND TONY KADAI

Department of Chemistry, McMaster University, Hamilton, Ontario

Received January 29, 1973

Treatment of benzene (**1**), biphenyl (**2**) and *o*- and *m*-xylene (**3** and **4**) with 4% v/v concentrated HCl (concentrated DCl) in D_2O at 250 °C results in selective deuteration of the aromatic nucleus with excellent isotopic incorporation and quantitative yield.

Le traitement à 250 °C du benzène (**1**), du biphényle (**2**), de l'*o*- et du *m*-xylène (**3** et **4**) avec une solution à 4% v/v de DCl concentré dans D_2O conduit à une deutération sélective du noyau aromatique avec une incorporation isotopique excellente et un rendement quantitatif.

[Traduit par le journal]

Can. J. Chem., **51**, 1485 (1973)

The introduction of one or more deuterium atoms into organic molecules is usually accomplished by one of many possible methods, depending on the nature of the molecule and the extent and stereospecificity of deuteration desired (1). Of the methods available, only metal-catalyzed homogeneous and heterogeneous exchange, base-catalyzed exchange and acid-catalyzed exchange have been used extensively for perdeuteration (1–5). Most, if not all, acid-catalyzed exchange procedures involve highly acidic media (1). Typically, liquid DBr and DCl, D_3PO_4, $DFSO_3$–SbF_5, and 50–80% D_2SO_4 in D_2O may be used to accomplish exchange at moderate temperatures. Many of these systems, however, are unsatisfactory because of cost, complicated apparatus and procedures (2, 3),[2] incomplete or slow exchange (4) and low yields (2–4) (*i.e.* due to sulfonation and decomposition).

In contrast, exchange under the conditions of high temperature and dilute acid has not been explored in any detail (6).

In this communication, we report preliminary results which establish a simple and quantitative one-step procedure for the perdeuteration of the aromatic hydrocarbons. The process utilizes dilute acid and the most inexpensive deuterium source, D_2O. The results are listed in Table 1.

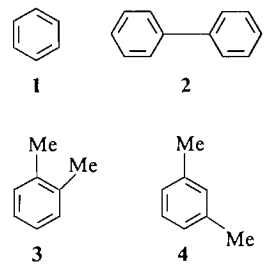

1 **2** **3** **4**

Although aqueous acetic acid is sufficiently acidic to effect slow exchange in dialkyl substituted benzenes (entry 9), benzene and biphenyl require increased acidity (entries 1 and 4). Entries 2, 3, 5, 6, 10, and 11 show that a temperature of at least 250 °C is required to facilitate exchange. Entries 2, 5, 7, and 10 show that *one cycle* results in complete equilibration and maximum exchange as dictated by the deuterium pool. Entries 7 and 8 show that *two cycles only*, using DCl in the final cycle, are required to accomplish at least 98% exchange in 95–100% yield.

In a typical experiment a mixture of *o*-xylene (25 g) and 4% v/v concentrated DCl–D_2O (100 ml) was sealed in each of three glass tubes (10 in. × 2 in. O.D.) after being degassed three times *via* freeze–thaw cycles. The tubes were heated at 250 °C in a 2 l Parr Pressure Apparatus, Model 4914 containing H_2O and *o*-xylene to

[1]Patent pending.

[2]Perdeuteration of benzene in 98% isotopic purity and 72% yield has been accomplished with DCl and $AlCl_3$ at room temperature in 50–60 h using a complicated vacuum apparatus (3).

TABLE 1. Exchange of benzene and its derivatives with dilute hydrochloric acid in D_2O at 250 °C

Entry	Substrate	Conditions* Acid	Temperature (°C)	Time (h)	D/molecule†	% Exchange‡	Position of Deuterium‡	% Recovery
1	**1**	a	250	60	0.0	0	—	—
2	**1**	b	250	48	5.3	88	—	98
3	**1**	b	200	48	1.3	22		98
4	**2**	a	250	48	0.0	0	—	—
5	**2**	b	250	48	9.4	94	—	98
6	**2**	b	200	48	4.0	40		98
7	**3**	c	250	43	3.5	88	ring	99
8§	**3**	c	250	42	3.9	98	3.9 ring 0.1 methyl	100
9	**4**	a	250	48	0.9	24	ring	—
10	**4**	b	250	40	3.8	91	3.6 ring 0.3 methyl	97
11	**4**	b	200	48	3.2	78	3.1 ring‖ 0.2 methyl	97

*a = 10% v/v CH_3COOD–D_2O; b = 4% v/v concentrated HCl–D_2O; c = 4% v/v concentrated DCl–D_2O.
†These values were determined mass spectrometrically.
‡The % exchange is based only on exchange in the aromatic ring as determined by n.m.r. integration analysis. The total deuterium content determined by n.m.r. is slightly greater than that by mass spectrometry.
§The *o*-xylene used was obtained from entry 7.
‖Total equilibration at all the ring positions did not occur. The 5 position contained only 0.3 D.

equalize the internal pressure. After 43 h, the clear, colorless *o*-xylene (74 g) layers were drawn off with the aid of a separatory funnel. The clear D_2O–DCl solution was retained for the first cycle of a subsequent exchange. N.m.r. analysis showed 90% of the aromatic and less than 1% of methyl hydrogens had been exchanged. The *o*-xylene was heated in three tubes in a second cycle with fresh DCl–D_2O solution (75 ml per 25 g) for 42 h. The *o*-xylene (74 g >98% pure by g.l.p.c.) isolated after the second cycle, contained 3.9 deuterium atoms in the aromatic nucleus and 0.1 deuterium atoms in the methyl groups as established by n.m.r. and mass spectrometric analysis.

The dilute acid – high temperature method presents substantial advantages over the other perdeuteration methods (*vide supra*) because of selectivity, simplicity, cost, freedom from steric effects and side reactions, high degree of isotope incorporation, essentially quantitative yields and most importantly its adaptibility to large scale preparations.[3]

At this time, the results are describable on the basis of initial electrophilic attack of D^+ on the aromatic system (7) followed by rearomatization. Interestingly, deprotonation from the methyl group is not competitive with aromatization even at elevated temperatures.

The obvious extensions of these studies to the perdeuteration and/or selective deuteration of substituted aromatics, polynuclear aromatics, bicyclics, and heterocyclics are presently underway.

We thank the National Research Council of Canada for financial support.

[3]Large scale reactions may be carried out directly in a 2 liter Hastelloy B bomb which is inert to HCl.

1. A. F. THOMAS. Deuterium labeling in organic chemistry. Meredith Corp., New York, 1971. Chapt. 3.
2. B. LUNELLI and C. PECILE. Can. J. Chem. **46**, 391 (1968).
3. M. BRULLMANN, H. J. GERBER, and D. MEIER. Helv. Chem. Acta, **41**, 1831 (1958).
4. G. E. CALF, B. D. FISHER, and J. L. GARNETT. Aust. J. Chem. **21**, 947 (1968).
5. M. A. LONG, J. L. GARNETT, R. F. W. VINING, and T. MOLE. J. Am. Chem. Soc. **94**, 5913 (1972) and references therein.
6. N. WERSTIUK and T. KADAI. Chem. Commun. 1349 (1971).
7. C. K. INGOLD, C. G. RAISIN, and C. L. WILSON. J. Chem. Soc. 915 (1936); 1637 (1936).

Can. J. Chem. Downloaded from www.nrcresearchpress.com by 210.87.254.40 on 09/05/12
For personal use only.

Can. J. Chem. Downloaded from www.nrcresearchpress.com by 210.87.254.40 on 09/05/12
For personal use only.

Canadian Journal of Chemistry

Published by
THE NATIONAL RESEARCH COUNCIL OF CANADA

Journal canadien de chimie

Publié par
LE CONSEIL NATIONAL DE RECHERCHES DU CANADA

Volume 51 Number 10 May 15, 1973

Volume 51 numéro 10 15 mai 1973

A Stereochemical and Kinetic Study of the Conversion of Methyl Cyclopropyl Ketones to 4,5-Dihydrofurans[1]

DONALD EDWARD MCGREER AND JAMES WILLIAM MCKINLEY

Department of Chemistry, The University of British Columbia, Vancouver 8, British Columbia

Received December 5, 1972

The thermal and photochemical conversion of (1R*,2R*,3S*), (1S*,2R*,3S*), and (1S*,2R*,3R*)-1-acetyl-1,2-dimethyl-3-phenylcyclopropane (**1**, **2**, and **3**) to *cis*- and *trans*-2,3,4-trimethyl-5-phenyl-4,5-dihydrofurans has been studied. Concurrent with this reaction is an equilibration of **1**, **2**, and **3**, a thermal ring opening of **1** by a 1,5-hydrogen shift, and a cyclopropane-to-propene type reaction under the photochemical conditions. The dihydrofuran from **1** and **2** by the thermal and photochemical conditions is 97% *trans*- and 3% *cis*- corresponding to predominant retention at the migrating carbon. The dihydrofuran formed from **3** by the thermal and photochemical reaction is 85% *cis*- and 15% *trans*- again corresponding to predominant retention. A kinetic study of the rearrangement of 1-acetyl-1-methyl-2-phenylcyclopropane to 1,2-dimethyl-5-phenyl-4,5-dihydrofuran provides E_a of 48.1 kcal/mol and log A of 14.9 for this first order reaction in the temperature range of 255–288 °C.

It is concluded that the thermal and photochemical reactions occur by a non-concerted process through a common 1,3-diradical intermediate in which bond rotation and ring closure steps are competitive.

La transformation thermique et photochimique du (1R*,2R*,3S*), (1S*,2R*,3S*), et (1S*, 2R*, 3R*) acétyl-1 diméthyl-1,2 phényl-3 cyclopropane (**1**, **2**, et **3**) en *cis* et *trans* triméthyl-2,3,4 phényl-5 dihydro-4,5 furanes, a été étudiée. Entrent en compétion avec cette réaction, une équilibration de **1**, **2**, et **3**, une ouverture thermique de cycle de **1** par transfert-1,5 d'hydrogène et une réaction du type cycloprane–propène dans les conditions photochimiques. Le dihydrofurane issu de **1** et **2** dans les conditions thermique et photochimique est à 97% *trans* et 3% *cis* avec rétention prédominante sur le carbone qui migre. Le dihydrofurane formé à partir de **3** par réaction thermique et photochimique est à 85% *cis* et 15% *trans* avec encore rétention prédominante. Une étude cinétique du réarrangement thermique de l'acétyl-1 méthyl-1 phényl-2 cyclopropane en diméthyl-1,2 phényl-5 dihydro-4,5 furane conduit à un E_a de 48.1 kcal/mol et à un log A de 14.9 pour cette réaction de premier ordre dans l'intervalle de température de 255–288 °C.

Il a été conclu que les réactions thermique et photochimique se produisent selon un processus non concerté, par l'intermédiaire d'un diradical-1,3 dans lequel les étapes de rotation autour de la liaison et de fermeture de cycle sont en compétition. [Traduit par le journal]

Can. J. Chem., **51**, 1487 (1973)

The non-catalyzed conversion of cyclopropyl ketones to dihydrofurans formally resembles the conversion of vinylcyclopropanes to cyclopentenes. This latter reaction has been studied extensively by kinetic and stereochemical means; however, the former reaction has been discussed in only a few notes. The thermally induced reaction was first noted by Wilson and Armitage (1, 2) and a photochemically induced reaction has been reported by Dauben and Shaffer (3). The reverse reaction of dihydrofurans to cyclopropanes has also been observed (1, 4–7). In the present paper we examine in more detail the stereochemistry and kinetics of the thermal and

[1]Taken in part from the Ph.D. thesis of J.W.M., University of British Columbia, Vancouver, B.C., May 1972.

Can. J. Chem. Downloaded from www.nrcresearchpress.com by 210.87.254.40 on 09/05/12
For personal use only.

TABLE 1. Product distribution of the thermal and photochemical reaction of 1-acetyl-1,2-dimethyl-3-phenylcyclopropanes **1–3**

Run	Compound	Conditions	Time	Product (%)						
				1	**2**	**3**	**5 + 6**	**7 + 8**	Olefins*	Ratio (**5**:**6**)
1	**1**	285°	75 min	14	6	Trace	37	43	—	97:3
2	**1**	*hν*	1 day	79	1	—	20	—	Trace	97:3
3	**1**	*hν*	7 days	11	3	—	84	—	Trace	97:3
4	**2**	283.5°	15 min	1.1	90.4	6.0	2.5	—	—	95:5
5	**2**	283.5°	1 h	3.0	79.4	12.0	4.7	0.9	—	95:5
6	**2**	283.5°	6 h	3.6	38.4	25.8	29.6	2.6	—	85:15
7	**2**	*hν*	6 h	1	94	—	2.3	—	Trace	97:3
8	**2**	*hν*	6 days	1	16	—	30	—	54	97:3
9	**3**	283.5°	3 min	0.1	1.2	98.5	0.2	—	—	15:85
10	**3**	283.5°	10 min	0.7	5.5	93.1	0.7	—	—	14:86
11	**3**	283.5°	1 h	2.5	20.0	71.5	5.8	—	—	44:56
12	**3**	283.5°	6 h	3.0	27.3	25.3	39.6	4.8	—	70:30
13	**3**	*hν*	3 h	—	3	95	0.6	—	1	15:85
14	**3**	*hν*	6 h	—	9	86	1.6	—	3	31:69
15	**3**	*hν*	6 days	2	14	8	26	—	51	74:26

*The olefins referred to here are a mixture of α,β- and β,γ-unsaturated ketones resulting from a cyclopropane-to-propene type reaction. These olefins have been characterized previously (8).

Can. J. Chem. Downloaded from www.nrcresearchpress.com by 210.87.254.40 on 09/05/12
For personal use only.

photochemical conversion of a series of methyl cyclopropyl ketones to 4,5-dihydrofurans.

Stereochemistry

From an earlier study (8) we have on hand three stereoisomers of 1-acetyl-1,2-dimethyl-3-phenylcyclopropane (**1**–**3**). The fourth possible isomer (**4**) has not been available. These ketones at 300 °C or on irradiation with 310 nm light (Rayonet Reactor) are converted to a variety of products illustrated in eqs. 1–3 by the reaction of **1**.

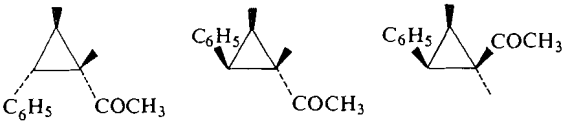

Reaction 1 is the conversion of a cyclopropyl ketone to a dihydrofuran. This reaction is (at least, formally) a 1,3 sigmatropic shift from carbon to oxygen and in this case permits one to evaluate the stereochemistry of the migrating carbon. Reaction 2 is the *cis*:*trans* interconversion of cyclopropane stereoisomers and in this case is expected to occur exclusively through the breaking of the bond between the carbons bearing the phenyl and acetyl groups, since both of these groups would provide major stabilization of the intermediate diradical or transition state. Reaction 3 is a well-known ring opening of a cyclopropyl ketone carrying an alkyl group *cis* to the carbonyl group (9, 10). A further minor reaction encountered in our work results from a hydrogen migration yielding a cyclopropane-to-propene type ring opening.

Typical data that we have collected are presented in Table 1 for the reactions of **1**, **2**, and **3**.

The structures of **1**, **2**, and **3** and the reaction of **1** to form **7** and **8** have been reported earlier (8). A series of dihydrofurans related to **5** and **6** and having a C-4 methyl and a C-5 phenyl have been reported by Scribe and Delepine (11). The stereochemical assignment to them was based on the argument that in the *cis* compounds the C-5 phenyl should shield the C-4 methyl and they reported values of 9.48 for the *cis* C-4 methyl against 8.85 τ for the *trans* C-4 methyl. The major dihydrofuran from **1** and **2** gave a C-4 methyl at 8.88 τ and the major dihydrofuran from **3** (run 9) gave a C-4 methyl at 9.50 τ and thus these compounds can be assigned the *trans*-**5** and *cis*-**6** structures respectively. As additional verification of this assignment we determined the nuclear Overhauser effect (n.O.e.) on the C-5 hydrogen (5.28 τ) in **5** that resulted from irradiation of the C-4 methyl. An enhancement of 23% was observed. The measured distances between these groups in models were 2.8 Å and >3.6 Å for **5** and **6** respectively. Thus the enhancement of 23% is only consistent with structure **5** (12).

The results of Table 1 suggest a reaction scheme such as Scheme 1 involving thermal or photochemical bond-breaking in the cyclopropanes, followed by ring closures to cyclopropane or dihydrofurans competitive with bond rotations at the diradical stage. The only significant amount of bond rotation, however, is in the thermal reaction of **2** or **3**, whereby **2** and **3** are interconverted. This corresponds to the rotation of the terminal carbon of the trimethylene diradical species carrying one substituent (phenyl), in preference to that carrying two substituents. This effect of substituents on bond

[1]

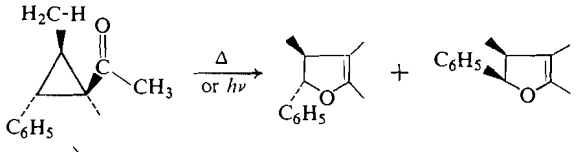

[2]

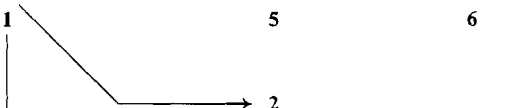

[3]

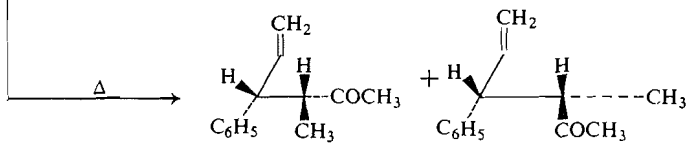

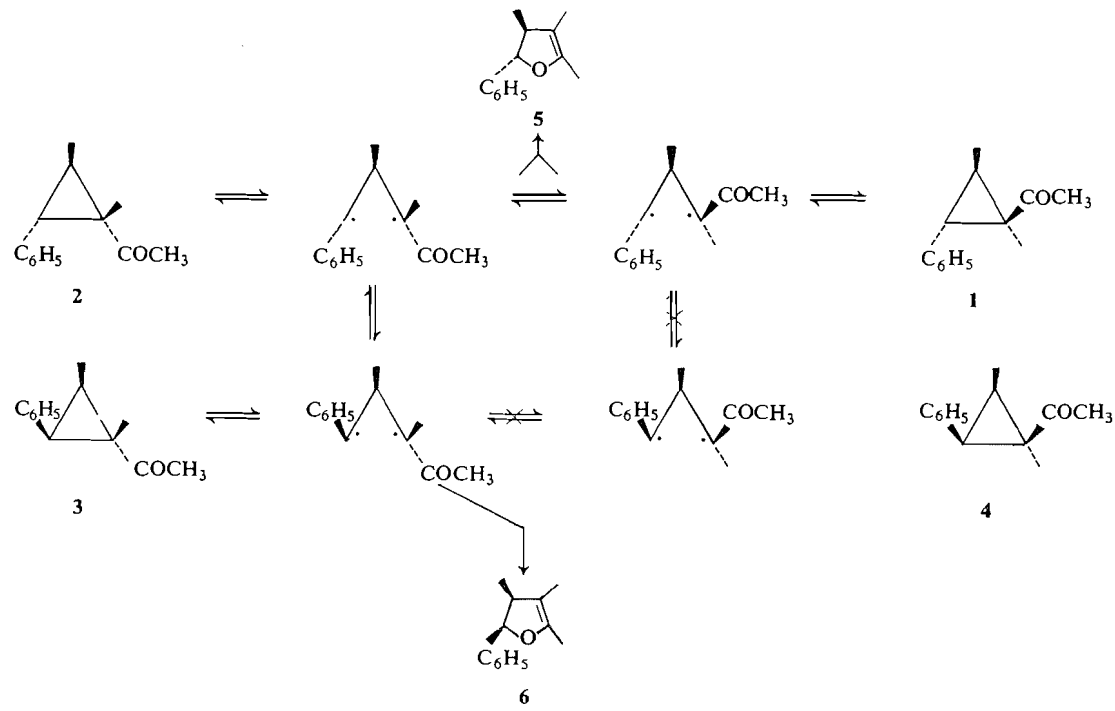

SCHEME 1

rotation rates has previously been noted by Berson *et al.* and has been described as a ponderal effect (13).

A secondary consequence of the interconversion of **2** and **3** is the variation, with degree of reaction, of the ratio of **5**:**6**. The stereochemistry of the cyclopropane to dihydrofuran reaction needs to be determined at as early a stage as possible and when this is done it becomes clear that the cyclopropane to dihydrofuran reaction is not stereospecific. Bond rotation again competes with ring closure and it is significant that a greater degree of bond rotation occurs in the system which would lead to the dihydrofuran having the C-4 methyl and C-5 phenyl *cis*. It is particularly interesting that the photochemical and thermal reactions give the *same* stereoselectivity.

All of the above observations suggest that the cyclopropane to dihydrofuran reaction is not a concerted reaction, although there is some stereoselectivity. Similar conclusions have been made concerning the vinylcyclopropane to cyclopentene reaction where similar stereochemical evidence is available (14). Supporting stereochemical evidence also comes from a study on the degenerate rearrangement of vinylcyclopropane which must pass through a diradical intermediate (15).

Of closer interest to our study is the photochemical conversion of *cis*- and *trans*-5-(1-methylpropenyl)-3,4-dimethyl-4,5-dihydrofuran to 2-(1-methylpropenyl)-1,2-dimethylcyclopropane carboxaldehyde (7). Stereoselectivity was observed favoring retention at the migrating carbon and to almost the same degree as our results for the reverse reaction, with the *cis* isomer giving 80% retention and the *trans* 94%. Scribe and Wiemann (7), because of this selectivity, favored a concerted mechanism. The factor swinging our support to the diradical mechanism is the parallel results found for the thermal and photochemical modes of reaction. The possibility, however, of competitive concerted reactions cannot be overlooked (18).

To obtain a further correlation between our reaction and the vinylcyclopropane to cyclopentene reaction we have made a preliminary kinetic study. Unfortunately the reactions of **1**, **2**, and **3** are just too complicated for such a study and

Can. J. Chem. Downloaded from www.nrcresearchpress.com by 210.87.254.40 on 09/05/12
For personal use only.

Can. J. Chem. Downloaded from www.nrcresearchpress.com by 210.87.254.40 on 09/05/12
For personal use only.

therefore we have looked at the reaction of *cis*- and *trans*-1-acetyl-1-methyl-2-phenylcyclopropane (**9** and **10**).

Kinetics

Addition of phenyl diazomethane to methyl isopropenyl ketone at room temperature gives directly a 1:2 mixture of the isomeric 1-acetyl-1-methyl-2-phenyl cyclopropanes (eq. 4) Pre-

[4] $C_6H_5CHN_2 + CH_2{=}C(CH_3)COCH_3 \rightarrow$

9 **10**

sumably a pyrazoline is formed as an intermediate; however it is not stable at room temperature (16). The cyclopropanes were separated by v.p.c. and identified by their n.m.r. spectra. The major isomer has the acetyl and C-1 methyl at 7.87 and 8.98 τ respectively. The minor isomer has the acetyl methyl and the C-1 methyl at 8.33 and 8.54 τ. Thus based on the shielding effect by the phenyl the major isomer has the C-1 acetyl and the C-2 phenyl groups *trans* as in **10** and the minor isomer has the C-1 acetyl and the C-2 phenyl *cis* as in **9**.

Samples of **9** or **10** when heated in sealed ampoules, such that reaction would take place in the gas phase at 250–290°, led to an initial rapid equilibrium of **9** and **10**, to the value of 15:85 respectively, followed by conversion to 2,3-dimethyl-5-phenyl-4,5-dihydrofuran (**11**). Kinetic runs made use of **9** and **10** close to equilibrium. The dihydrofuran proportion of the total samples rose to a maximum value of about 89%, at which time equilibrium between it and the cyclopropanes **9** and **10** was reached. Clearly there are a number of subtle substituent effects, which determine the position of such an equilibrium under thermal and photochemical conditions, and which as yet are still unclear (1–5, 7). The kinetic data are reported in Table 2 and yield by an Arrhenius plot E_a of 48.1 kcal/mol and log A of 14.9.

These kinetic parameters correlate well with those found for vinylcyclopropanes (17) with some selected values given in Table 3. One might however have anticipated a lower activation energy with both phenyl and acetyl groups capable of stabilizing the transition state. These factors show up in the faster rate of reaction, however, since the rate for **9** and **10** is comparable to vinylcyclopropane at a temperature 60° below that for vinylcyclopropane. Thus the kinetics support the view that the cyclopropyl methyl ketone-to-dihydrofuran rearrangement is of the same mechanistic form as the vinylcyclopropane-to-cyclopentene rearrangement.

TABLE 2. Kinetic data for the reaction

$$\mathbf{9} + \mathbf{10}\ (15{:}85) \underset{k_2}{\overset{k_1}{\rightleftarrows}} \mathbf{11}$$

Temperature (°C)	$(k_1 + k_2) \times 10^5$ (s^{-1})	$k_1:k_2$
287.5	15.2	88.4:11.6
279.6	8.10	88.8:11.2
270.0	3.84	89.1:10.9
262.5	2.00	89.4:10.6
254.9	1.04	89.7:10.3

TABLE 3. Selected activation parameters for the conversion of some vinylcyclopropanes to cyclopentenes (17)

Compound	log A	E_a
Vinylcyclopropane	13.5	49.6
2-Cyclopropylpropene	13.99	50.9
2-(1-Methylcyclopropyl)propene	14.14	50.5

Experimental

The preparation and characterization of cyclopropanes **1**–**3** and products **7** and **8** have been reported earlier along with some general procedures used (8).

cis- and trans-2,3,4-Trimethyl-5-phenyl-4,5-dihydrofuran (6 and 5)

Several ampoules of about 920 μl volume containing 12 mg of **1** were degassed and sealed under vacuum and heated at 338° for 10 min. The separate samples were combined and v.p.c. analysis (20% FFAP at 205°) showed a major peak well separated and to lower retention time than **1**, **2** or **3**, or any possible unsaturated ketone product. The peak was collected and high resolution v.p.c. on a Perkin–Elmer 226 instrument using a Carbowax 20 M 0.01 in. i.d. × 150 ft column at 175° showed it to be a 96:4 mixture of two components. For the major component: i.r. 1700 cm^{-1}, n.m.r. τ (60 MHz, CCl_4) 8.47 and 8.22 (singlets showing long-range coupling) for the C-2 and -3 methyls, 8.88 (doublet, J = 7.0 Hz) for the C-4 methyl, 7.33 (multiplet) for the C-4 hydrogen, 5.28 (doublet, J = 8.0 Hz) for the C-5 hydrogen, and 2.78 for the aromatic hydrogens.

Anal. Calcd. for $C_{13}H_{16}O$: C, 82.93; H, 8.57. Found: C, 82.74; H, 8.34.

To a solution of 36 mg of the above sample in 1.0 ml

Can. J. Chem. Downloaded from www.nrcresearchpress.com by 210.87.254.40 on 09/05/12
For personal use only.

of CCl_4 was added 2.2 mg of *p*-dioxane (internal standard) and 50 μl of *sym*-tetrachloroethane (internal lock). Using an HA100 spectrometer the C-4 methyl peak was irradiated while the peaks for the C-4 and -5 hydrogens were being observed for nuclear Overhauser enhancements. The average enhancement to the C-4 hydrogen was 30% and that to the C-5 hydrogen 23%. Models of **5** and **6** gave the internuclear distances for the hydrogens of the C-4 methyl and the C-5 hydrogen of 2.8 and 3.6–4.0 Å respectively, corresponding to expected enhancements of 21 and < 6% respectively (12). Coupled with the fact that the C-4 methyl appears at 8.88 τ compared to 9.50 in the minor isomer, we have assigned the *trans*-stereochemistry **5** to the major dihydrofuran isomer from **1**.

Photolysis of a sample of 100 mg of **1** in 100 ml of ether for 24 h using 310 nm radiation (Rayonet Reactor) gave a product which contained a peak (65%) at the same v.p.c. retention time as **5** and when isolated was found to have the same n.m.r. spectrum as **5**, with peaks at τ 8.50 and 8.26, 8.90 (doublet), 7.35 (multiplet), 5.32 (doublet) and 2.80.

Several sealed ampoules of **3** were heated at 338° for 10 min. The products were combined and the dihydrofuran peak isolated by v.p.c. Analytical v.p.c. showed this sample to be a 83:17 mixture of **5** and **6** respectively. The n.m.r. spectrum of this mixture showed peaks for *cis*-2,3,4-trimethyl-5-phenyl-4,5-dihydrofuran (**6**) at τ 4.62 (doublet, J = 9.2 Hz) for the C-5 hydrogen and 9.50 (doublet, J = 7.2 Hz) for the C-4 methyl. The other peaks for **6** were not clearly separated from the peaks of **5**.

Experimental Conditions for the Rearrangement Reactions

Samples of about 2.2 mg were degassed and sealed under vacuum in Pyrex tubes (4.2 × 100 mm for the thermal runs and 4.2 × 50 mm for the photochemical runs). For the thermal runs the tubes were placed in a constant-temperature salt ($NaNO_3$–KNO_3) bath and samples removed at appropriate times for analysis. For the photochemical runs the tubes were placed in a Rayonet Reactor fitted with 310 nm lamps. Product distributions were monitored using a P.E. 226 analytical v.p.c. using a column (0.01 in. i.d. × 150 ft) charged with Carbowax 20 M. Typical results are recorded in Table 1.

Samples of the dihydrofurans **5** and **6** as prepared above in the ratio of 96:4 and 83:17 respectively, were heated over 10 half-lives at 285° with no change in the ratio of **5** to **6**. Similar samples were irradiated with 310 nm light for 15.5 h with again no change in the ratio of **5**:**6** being observed, although trace peaks corresponding to **1** and **2** were observable. Although dihydrofurans often readily polymerize (5, 7), control runs indicated that **5** and **6** did not show this tendency under the reaction conditions. They did, however, rapidly deteriorate on exposure to air either due to polymerization or hydration or both.

cis-[2] *and trans-1-Acetyl-1-methyl-2-phenylcyclopropane (**9** and **10**)*

Addition of 8.4 g (0.1 mol) of methyl isopropenyl ketone to a petroleum ether solution of phenyldiazomethane (prepared from 0.1 mol of benzaldehyde hydrazone and 0.1 mol of yellow mercuric oxide (8)) caused immediate evolution of nitrogen. After 2 h, the red color of the diazo compound had completely disappeared. Rotatory evaporation of the solvent followed by vacuum distillation (90–95° at 0.3 mm Hz) yielded 12.6 g of a slightly yellowed solution. The v.p.c. (20% FFAP, 205°, 60 ml/min) indicated two peaks in a 1:2 ratio with respective retention times of 7.7 and 9.3 min. The two peaks were separated and collected by v.p.c. The first peak was identified by n.m.r. as the *cis*-isomer 9 and the second peak as the *trans*-isomer **10**. For the *cis*-cyclopropyl ketone (**9**): i.r. 1695, 1605, 725, and 697 cm^{-1}; n.m.r. τ (60 MHz, CCl_4) 8.33 and 8.54 (singlets) acetyl and C-1 methyls respectively, 7.75 (triplet, J = 7.7 Hz) C-2 hydrogen, 8.09 (doublet of doublets, J = 4.6 and 7.5 Hz) one C-3 hydrogen, 9.04 (doublet of doublets, J = 8.4 and 4.6 Hz) other C-3 hydrogen, and 2.80 (aromatic).

Anal. Calcd. for $C_{12}H_{14}O$: C, 82.76; H, 8.05. Found: C, 83.03; H, 8.25.

For the *trans*-cyclopropyl ketone (**10**): i.r. 1690, 1605, 778 and 698 cm^{-1}; n.m.r. τ (60 MHz, CCl_4) 7.87 and 8.98 (singlets) acetyl and C-1 methyls respectively, 7.34 (doublet of doublets J = 7.0 and 9.0 Hz) C-2 hydrogen, 8.37 (doublet of doublets, J = 4.2 and 9.0 Hz) one C-3 hydrogen, 8.94 (doublet of doublets, J = 4.2 and 7.0 Hz) other C-3 hydrogen, and 2.84 (aromatic).

Anal. Calcd. for $C_{12}H_{14}O$: C, 82.76; H, 8.05. Found: C, 82.54; H, 8.02.

*2,3-Dimethyl-5-phenyl-4,5-dihydrofuran (**11**)*

Six 50 μl samples of a mixture of ketones **9** and **10** were sealed in ampoules (4.2 × 100 mm) and were heated at 335° for 10 min. The slightly charred samples were bulb-to-bulb vacuum distilled (bath temperature of 85–100° at 0.5 mm Hg). V.p.c. of this combined product (20% FFAP column at 205°) showed five peaks: The first of these peaks was the dihydrofuran **11**; i.r. 1701 cm^{-1}, n.m.r. τ (60 MHz, CCl_4) 2.80 (singlet) phenyl hydrogens, 4.70 (doublet of doublets with J = 8.0 and 10.0 Hz) for the C-5 hydrogen, 6.7–7.8 (multiplet) for the C-4 hydrogens, 8.26 and 8.40 (singlets showing long range coupling) for the C-2 and -3 methyls.

Anal. Calcd. for $C_{12}H_{14}O$: C, 82.78; H, 8.05. Found: C, 82.43; H, 8.25.

The remaining peaks in the vapor chromatogram were identified as **9**, **10**, and two unsaturated ketones 3-methyl-5-phenyl-3- and -4-pentene-2-one which were identified by their n.m.r. These olefins were completely absent in the kinetic runs and became particularly noticeable as byproducts when the reaction vials were too small to allow all of the sample to enter the gas phase.

Kinetics

Samples (3.0–3.5 mg) of **9** and **10** near an equilibrium composition were sealed under vacuum after degassing in Pyrex ampoules (4.2 × 100 mm) and were heated in a constant temperature bath (a 50:50 mixture of sodium nitrate and potassium nitrate) equipped with a stirrer and a thermometer calibrated against an N.B.S. calibrated thermometer. The progress of the reaction was monitored by analyzing samples with an Aerograph Model A-90-P3 v.p.c. (20% FFAP, 205°, 120 ml/min helium) equipped with a thermal conductivity detector. A Honeywell Model Electronic 15 recorder having a disc

[2] *cis* refers to the C-1 acetyl and C-2 phenyl.

chart integrator was used to estimate the ratio of products.

Straight line fits were calculated by the method of least squares using a Hewlett Parkard 9100 Calculator equipped with a 9125A Calculator plotter. The results are presented in Table 2. The percent of dihydrofuran **11** at equilibrium varied from 88.4% at 287.5° to 89.7% at 254.9°.

It is estimated that the main source of error is in controlling the bath temperature to ±0.4 °C leading to estimated error limits in E_a of ±5%.

The authors gratefully appreciate the support received for this work from NRCC and from the Committee on Research of the University of British Columbia.

1. C. L. WILSON. J. Am. Chem. Soc. **69**, 3002 (1947).
2. D. M. A. ARMITAGE and C. L. WILSON. J. Am. Chem. Soc. **81**, 2437 (1959).
3. W. G. DAUBEN and G. W. SHAFFER. J. Org. Chem. **34**, 2301 (1969).
4. D. W. BOYKIN, JR. and R. E. LUTZ. J. Am. Chem. Soc. **86**, 5046 (1964).
5. D. E. McGREER, M. G. VINJE, and R. S. McDANIEL. Can. J. Chem. **43**, 1417 (1965).
6. P. SCRIBE, M. R. MONOT, and J. WIEMANN. Tetrahedron Lett. 5157 (1967).
7. P. SCRIBE and J. WIEMANN. Bull. Soc. Chim. Fr. 2268 (1971).
8. D. E. McGREER and J. W. McKINLEY. Can. J. Chem. **49**, 105 (1971).
9. R. M. ROBERTS, R. G. LANDOLT, R. N. GREENE, and E. W. HEYER. J. Am. Chem. Soc. **89**, 1404 (1967).
10. D. E. McGREER and N. W. K. CHIU. Can. J. Chem. **46**, 2217 (1968).
11. P. SCRIBE and M. DELEPINE. C.R. **261**, 160 (1965).
12. R. A. BELL and J. K. SAUNDERS. Can. J. Chem. **48**, 1114 (1970).
13. J. A. BERSON, D. C. THOMPKINS, and S. JONES. J. Am. Chem. Soc. **92**, 5799 (1970).
14. P. H. MAZZOCCHI and H. J. TAMBURIN. J. Am. Chem. Soc. **92**, 7220 (1970).
15. M. R. WILLCOTT and V. H. CARGLE. J. Am. Chem. Soc. **91**, 4311 (1969).
16. D. E. McGREER and Y. Y. WIGFIELD. Can. J. Chem. **47**, 3965 (1969).
17. M. R. WILLCOTT, R. L. CARGILL, and A. B. SEARS. *In* Progress in physical organic chemistry. Vol. 9. *Edited by* A. Streitweiser, Jr. and R. W. Taft. John Wiley and Sons, Inc. New York. 1972.
18. J. A. BERSON. Acc. Chem. Res. **5**, 406 (1972).

Can. J. Chem. Downloaded from www.nrcresearchpress.com by 210.87.254.40 on 09/05/12
For personal use only.

Rearrangement Studies with ^{14}C. XXXVIII. Isotopic Scrambling in the Synthesis of Labeled 2-Phenylethyl Triflate

C. C. LEE AND D. UNGER

Department of Chemistry and Chemical Engineering, University of Saskatchewan, Saskatoon, Saskatchewan

Received November 27, 1972

2-Phenylethyl triflate (**1**-OTf) was synthesized by the reaction of AgOTf with 2-phenylethyl iodide (**1**-I) in cyclohexane as solvent. However, when 1-^{14}C-2-phenylethyl iodide (**1**-I-1-^{14}C) was used as a reactant, the resulting **1**-OTf-^{14}C showed an essentially complete scrambling of the ^{14}C-label over the C-1 and -2 positions. Similar reactions of **1**-I-1-^{14}C with AgOTs and with AgOAc gave **1**-OTs-^{14}C and **1**-OAc-^{14}C with, respectively, about 49 and 11% rearrangement of the label from C-1 and -2.

Le triflate de phényl-2 éthyle (**1**-OTf) a été synthétisé par réaction du AgOTf avec l'iodure de phényl-2 éthyl (**1**-I) dans le cyclohexane comme solvant. Cependant, lorsque l'iodure de ^{14}C-1 phényl-2 éthyl a été utilisé comme réactif, le produit **1**-OTf-^{14}C résultant s'est révélé être un mélange pratiquement complet en ce qui a trait à la distribution du ^{14}C sur les positions C-1 et -2. Des réactions semblables du **1**-I-^{14}C-1 avec du AgOTs et avec du AgOAc ont donné le **1**-OTs-^{14}C et le **1**-OAc-^{14}C avec, respectivement, un réarrangement de la distribution du ^{14}C de C-1 à -2 d'environ 49 et 11%.

[Traduit par le journal]

Can. J. Chem., **51**, 1494 (1973)

The trifluoromethanesulfonate (triflate) anion is a facile leaving group in solvolytic reactions (1). Studies on the kinetics and deuterium isotope effects for the ethyl and propyl systems, however, have led to the conclusion that solvolyses of such primary alkyl triflates and tosylates are mechanistically similar, the reaction of the triflate being no more limiting than the tosylate (2, 3).

Since a great deal of work has been done on the isotopic scrambling that occurs in the solvolyses of 1-^{14}C-2-phenylethyl tosylate (**1**-OTs-1-^{14}C) (4–7), it would be of interest to have another comparison of the behaviors of triflates and tosylates by an investigation on the analogous solvolyses of 1-^{14}C-2-phenylethyl triflate (**1**-OTf-1-^{14}C). Hence attempts were made to synthesize **1**-OTf-1-^{14}C.

1-OTf was prepared from the reaction of 2-phenylethyl iodide (**1**-I) with silver triflate by the method of Gramstad and Haszeldine (8) as used in the synthesis of ethyl triflate, except that cyclohexane instead of ether was employed as solvent. When the reaction was carried out in ether, the product was highly contaminated by ethyl 2-phenylethyl ether and di-2-phenylethyl ether, apparently derived from *O*-alkylation of ethers by the triflate ester (9). When the synthesis was attempted by reacting **1**-I-1-^{14}C with AgOTf, the product obtained, however, showed an essentially complete scrambling of the ^{14}C-label over the C-1 and -2 positions (Table 1). The method thus failed to give the desired **1**-OTf-1-^{14}C.

Alternative syntheses of triflate esters were considered, but they too failed to give the desired result. Schleyer and coworkers (1) prepared a number of triflates of relatively inert systems by treatment of the alcohol with trifluoromethanesulfonic acid anhydride in the presence of pyridine. This method was not attempted in the present work since **1**-OTf was found to react readily with pyridine to give a solid product, presumably the result of *N*-alkylation, giving rise to the pyridinium salt (9, 10). Hansen (11) has prepared a series of 1,1-dihydroperfluoroalkyl triflates by treating the appropriate alcohol with trifluoromethanesulfonyl fluoride in the presence of triethylamine at −30°. When **1**-OH was treated in an analogous way using commercially purchased trifluoromethanesulfonyl chloride, no **1**-OTf could be obtained. A number of phenols have been converted to the corresponding aryl triflates by reaction with trifluoromethanesulfonic imidazolide at 80–90° (12). When the reaction was tried with **1**-OH, extensive decomposition occurred at 80–90°, while at room temperature or 50°, much of the **1**-OH remained unreacted. Thus **1**-OTf was successfully synthesized only by the treatment of **1**-I with AgOTf, and this reaction led to a complete scrambling of the ^{14}C-label when **1**-I-1-^{14}C was used as a reactant.

The isotopic scrambling in the **1**-OTf-^{14}C

Can. J. Chem. Downloaded from www.nrcresearchpress.com by 210.87.254.5 on 09/05/12
For personal use only.

TABLE 1. Data from the reaction of 1-^{14}C-2-phenylethyl iodide (1-I-1-^{14}C) with silver salts

Salt	Compound	Specific activity* (d.p.m./mmol) Run 1	Specific activity* (d.p.m./mmol) Run 2	Rearrangement to C-2(%) Run 1	Rearrangement to C-2(%) Run 2
AgOTf	$PhCH_2CH_2OTf$†	1 290 000	364 000	51.0	50.8
	PhCOOH	659 000	185 000		
AgOTs	$PhCH_2CH_2OTs$	974 000	358 000	48.5	49.2
	PhCOOH	472 000	176 000		
AgOAc	$PhCH_2CH_2OAc$†	481 000	444 000	11.2	10.6
	PhCOOH	54 100	46 900		

*Measured by a liquid scintillation counter.
†Converted to $PhCH_2CH_2OH$ and then assayed as the solid α-naphthylurethane.

could be most reasonably explained by the intervention of the ethylenebenzenium ion[1] (**2**) formed in the reaction of 1-I-1-^{14}C with Ag^+ ion. Support for this interpretation was obtained

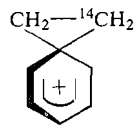

2

from the isotopic scramblings observed when 1-I-1-^{14}C was treated with silver tosylate or silver acetate. As can be seen from Table 1, reaction with AgOTs also gave a product, 1-OTs-^{14}C, with nearly complete scrambling of the label over C-1 and -2, while the 1-OAc-^{14}C from the reaction of 1-I-1-^{14}C with AgOAc showed about 11% rearrangement of the label from C-1 to -2. The lesser amount of scrambling in the 1-OAc-^{14}C could be explained on the basis of concurrent S_N1–S_N2 processes (7). The more nucleophilic acetate ion could take part in a non-scrambling direct displacement and effectively compete with phenyl participation in the formation of **2**, thus giving rise to a net result of 11% rearrangement, much less than the 50% rearrangement expected in a product formed solely via **2**.

Experimental

Reaction of 1-^{14}C-2-Phenylethyl Iodide (1-I-1-^{14}C) with Silver Salts

A solution of 18.6 g (0.08 mol) of 1-I-1-^{14}C, obtained from treatment of 1-OTs-1-^{14}C with NaI in acetone (4), in 50 ml of cyclohexane, was added dropwise to a stirred suspension of 25.7 g (0.10 mol) of AgOTf in 150 ml of cyclohexane. The resulting mixture was stirred at room temperature for 4 h. The AgI was then removed by filtration through Celite and the cyclohexane was distilled off under reduced pressure to give 16.2 g (80%) of residual ^{14}C-2-phenylethyl triflate (1-OTf-^{14}C) as a colorless liquid. (In the second run, the yield of 1-OTf-^{14}C calculated from isotope dilution was 87%). The product so obtained decomposed readily at elevated temperatures, but purification was effected by distillation at 65–70° and 1 Torr using an apparatus with a short condensation column jointed directly to the receiver to minimize any refluxing of the condensate into the distillation flask. The distilled 1-OTf obtained from inactive trials gave the following data.

Anal. Calcd. for $C_9H_9O_3SF_3$: C, 42.52; H, 3.56. Found: C, 42.67; H, 3.51.

N.m.r. (CCl_4) δ 7.2 (m, 5, aromatic H), 4.60 (t, 2, J = 7 Hz, CH_2OTf), 3.08 (t, 2, J = 7 Hz, $PhCH_2$); mass spectrum *m/e* 254 (M^+) and major peaks at *m/e* 105 $(M - OTf)^+$, 104 $(M - HOTf)^+$, 91 ($C_7H_7^+$). The titrimetric rate constant for the acetolysis of 0.5 *M* 1-OTf at 30° was found to be 9.44×10^{-5} s^{-1}. Comparison with data extrapolated from Coke's results (6) indicated that at 30°, the acetolysis of 1-OTf is faster than the acetolysis of 1-OTs by a factor of about $10^{4.9}$.

The reaction of 1-I-1-^{14}C with AgOTs or AgOAc was carried out in a similar way with only minor modifications. In the reaction with AgOTs, the mixture was refluxed for 4 and 10 h in the two runs, giving yields of 1-OTs-^{14}C, based on isotope dilution, of 67 and 90%, respectively. The reaction mixture between 1-I-1-^{14}C and AgOAc was refluxed for 20 h and the yields of 1-OAc-^{14}C, based on isotope dilution, were 94 and 96% for the two runs.

Degradation

1-OTf-^{14}C and 1-OAc-^{14}C were oxidized directly with alkaline $KMnO_4$ to give PhCOOH, while the 1-OTs-^{14}C was converted to 1-I-^{14}C by treatment with NaI in acetone before being oxidized to PhCOOH (4). The ^{14}C activity in the PhCOOH gave the extent of rearrangement of the label from C-1 to -2.

[1]Previously, **2** has been commonly referred to as the ethylenephenonium ion. In accordance with the nomenclature recently suggested by Olah (13), **2** should be named as the ethylenebenzenium ion.

Can. J. Chem. Downloaded from www.nrcresearchpress.com by 210.87.254.5 on 09/05/12
For personal use only.

The financial support given by the National Research Council of Canada is gratefully acknowledged.

1. T. M. Su, W. F. Sliwinski, and P. v. R. Schleyer. J. Am. Chem. Soc. **91**, 5386 (1969).
2. A. Streitwieser, Jr., C. L. Wilkins, and E. Kiehlmann. J. Am. Chem. Soc. **90**, 1598 (1968).
3. G. A. Dafforn and A. Streitwieser, Jr. Tetrahedron Lett. 3159 (1970).
4. C. C. Lee, R. Tkachuk, and G. P. Slater. Tetrahedron, **7**, 206 (1959).
5. J. E. Nordlander and W. G. Deadman. J. Am. Chem. Soc. **90**, 1590 (1968).
6. J. L. Coke, F. E. McFarlane, M. C. Mourning, and M. G. Jones. J. Am. Chem. Soc. **91**, 1154 (1969).
7. C. C. Lee, D. Unger, and S. Vassie. Can. J. Chem. **50**, 1371 (1972).
8. T. Gramstad and R. N. Haszeldine. J. Chem. Soc. 173 (1956).
9. T. Gramstad and R. N. Haszeldine. J. Chem. Soc. 4069 (1957).
10. J. Burdon and V. C. R. McLoughlin. Tetrahedron, **21**, 1 (1965).
11. R. L. Hansen. J. Org. Chem. **30**, 4322 (1965).
12. F. Effenberger and K. E. Mack. Tetrahedron Lett. 3947 (1970).
13. G. A. Olah. J. Am. Chem. Soc. **94**, 804 (1972).

Can. J. Chem. Downloaded from www.nrcresearchpress.com by 210.87.254.5 on 09/05/12
For personal use only.

The Static Dielectric Constants of the Liquified Fluoromethanes[1]

PETER TREMAINE AND MAURICE G. ROBINSON
Chemistry Department, University of Alberta, Edmonton, Alberta, T6G 2G2

Received November 9, 1972

The static dielectric constants of CF_4, CHF_3, CH_2F_2, and CH_3F have been measured at temperatures ranging from their melting points to their normal boiling points. The molar polarization of CF_4 agrees with that of the gas phase to within experimental error. The deviation of the dielectric constants of the polar fluoromethanes from the values predicted by the Onsager equation cannot be fully due to their non-spherical shape.

It is postulated that although a significant parallel dipole correlation may be present in each fluoromethane, the polarization resulting from the liquid lattice vibrations, may account for much, or all, of the effect in CH_3F and CH_2F_2.

Les constantes diélectriques statiques de CF_4, CHF_3, CH_2F_2, et CH_3F ont été mesurées à des températures comprises entre leur température de fusion et d'ebullition normales. La polarization molaire de CF_4 est en accord, dans les limites d'erreurs expérimentales, avec celle en phase gazeuse. Les déviations des constantes diélectriques de ces fluorométhanes polaires par rapport aux valeurs prédites par l'équation d'Onsager ne peuvent être attribuées entièrement à leur forme non-sphérique ou à l'anisotropie de leur polarizabilité.

Bien que pour chaque fluorométhane polaire une corrélation significative de dipole parallèle puisse être présente, il est postulé que la polarization résultant des vibrations du réseau liquide puisse expliquer la plus grande partie si ce n'est la totalité de l'effet présent dans CH_3F et CH_2F_2.

Can. J. Chem., **51**, 1497 (1973)

Introduction

Although the dielectric constants of the other halomethane liquids have been studied exhaustively (1), the dielectric properties of the liquid fluoromethanes have not been reported. The dielectric constants of most chloro, bromo, and iodo methanes have been satisfactorily described by a spheroidal modification to the Onsager equation (2), which took account of the molecular shape, but ignored intermolecular association, the anisotropy of the polarizability, and atomic polarization. Since these latter assumptions should be less valid for the fluoromethanes, it is of interest to attempt to account for their static dielectric constants by an Onsager treatment.

The purpose of this work was to determine the dielectric constants of the liquified fluoromethanes, and to treat this data using the spheroidal Onsager equation.

Experimental

Purification of Materials

Matheson reagent grade CF_4 and CHF_3, and reagent grade CH_2F_2 amd CH_3F from the Columbia Organic Chemicals Co. were introduced into a high vacuum system through a 25 × 2 cm column containing sodium hydroxide pellets and then passed through an 80 × 1.5 cm column of high activity silica gel at room temperature. The silica gel was supplied by the Burrell Corporation and was previously activated by heating at 220 °C for several hours under a pumping vacuum of less than 10^{-5} Torr. The gas was then condensed into a trap at −196 °C. After about 25 ml of the solidified gas had been collected, it was distilled into a flask containing sodium hydroxide pellets, allowed to warm up, and held at −90 °C for 1 h (−130 °C for CF_4). It was then distilled into a cell and electrolized at ~1 kV/cm and −90 °C (−130 °C for CF_4) for 1 h. After this purification stage, the sample was distilled into the previously cooled and evacuated capacitance cell.

To avoid contamination of the samples, the vacuum system was thoroughly evacuated overnight, and the silica gel reactivated between runs. CF_4 was introduced into the system first, followed by CHF_3, CH_2F_2, and lastly, CH_3F. This was the order of increasing sample conductance, and should have minimized the accumulation of ionic impurities in the cell. Sample conductances ranged from $< 1 \times 10^{-10}$ mho/cm for CF_4 to 8.2×10^{-8} mho/cm for CH_3F, as measured at 5 kHz and the warmest temperature to which each sample was taken.

Techniques

Capacitance measurements were carried out in a guarded, 3-terminal dielectric cell which had stainless steel plates set 3 mm apart. The cell constant was determined to be 2.4870 ± 0.0080 pF from room temperature measurements on Eastman spectro-grade cyclohexane, Matheson–Coleman and Bell spectro-grade carbon tetrachloride, and carbon disulfide, from freshly opened bottles. The capacitance of the evacuated cell at low

[1]Supported by the National Research Council of Canada.

Can. J. Chem. Downloaded from www.nrcresearchpress.com by 210.87.254.6 on 09/05/12
For personal use only.

Can. J. Chem. Downloaded from www.nrcresearchpress.com by 210.87.254.6 on 09/05/12
For personal use only.

temperatures was used to determine the temperature dependence of the cell constant, assuming that the lead capacitance did not change from its value of 0.020 pF. Capacitance was measured using a General Radio 1615A bridge in conjunction with a GR 1310B oscillator and a Rhode–Schwartz type UBM null detector. The bridge was calibrated against a GR 1404B 100 pF reference standard capacitor.

Temperature control was achieved by surrounding the cell with an insulated box which was cooled by a controlled stream of cold nitrogen gas. Regulation of the gas stream was effected by feedback from an iron–constantan thermocouple which was placed inside a 25 ml bulb of isopentane. A copper–constantan thermocouple, surrounded by indium for good thermal contact, was glued to the outside of the cell to monitor temperature. The thermocouple was calibrated against a Hewlett–Packard 2801A quartz thermometer which had, in turn, been calibrated against an NBS platinum resistance thermometer. The temperature measurements are considered accurate to ± 0.1 °C at -80 °C and ± 0.3 °C at -160 °C.

Runs were carried out on two samples of each compound. After a sample had been distilled into the cell, it was allowed to reach thermal equilibrium. Capacitance readings were then taken at 5, 10, 20, and 50 kHz before changing the temperature. Although some electrode polarization was observed for CH_3F, the 50 kHz value of the dielectric constant was taken to be correct since it agreed with the values at 20 kHz and 10 kHz to within 0.025% and 0.045% respectively in the worst case. The results obtained for each compound are listed in Table 1 and illustrated in Fig. 1.

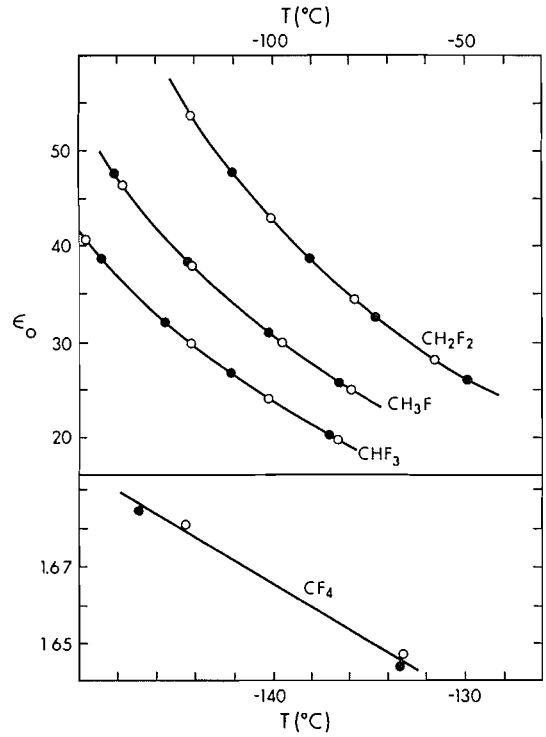

FIG. 1. Static dielectric constants of the liquids CF_4, CHF_3, CH_2F_2, and CH_3F as a function of temperature. Open and closed circles represent measurements on the two samples of each compound.

Results and Discussion

Carbon Tetrafluoride

The listed value of 1.624 g/cm^3 for the density of CF_4 at -131.2 °C (3) allowed the density to be calculated from the dielectric constant at each temperature using the Clausius–Mossotti relationship (4), which should be valid over this small temperature range. It is these calculated values which are listed in Table 1.

From a linear least squares fit of ε *vs.* T, as shown in Fig. 1, $\varepsilon_{CF_4} = 1.644 \pm 0.005$ at -131.2 °C. The error estimate is based on uncertainties in the cell constant and differences in the results of the two runs. The molar polarization, $P = P_a + P_e = [(\varepsilon - 1)/(\varepsilon + 2)](M/d) = 9.58 \pm 0.06$ cm^3, where M is the molecular weight and d is the density in g/cm^3.

This result compares with a value of $P = 9.73$ cm^3 and a maximum error of ± 0.08 cm^3, reported for the gas phase by Tipton *et al.* (5) in the range 20 to 350 °C.

Fluoroform, Difluoromethane, and Methyl Fluoride

The dielectric constants of the polar fluoromethanes are listed in Table 1. The absolute error is estimated to be $\pm 0.8\%$ for all values, with a precision of $\pm 0.3\%$ between the two samples of each compound.

The Onsager equation (6) attempts to describe the behavior of the dielectric constants of liquids by assuming the liquids to be composed of spherical, non-associated, dipolar molecules which possess isotropic polarizabilities. Buckley and Maryott (2) have extended the Onsager equation to include both prolate and oblate spheroidal molecules in which the permanent dipole is aligned along the axis of symmetry.

Their equation takes the form

$$[1]\quad \frac{(\varepsilon_0 - 1)(2\varepsilon_0 + 1)}{9\varepsilon_0}\,\overline{V} = \frac{4}{3}\pi N_0\left[\frac{\alpha k_\alpha}{1 - \frac{\alpha}{v}gk_R} + \frac{\mu_0^2}{3kT\left(1 - \frac{\alpha}{v}gk_R\right)^2}\right]k_c$$

where ε_0 = static dielectric constant, $\overline{V}$ = molar volume, N_0 = Avogadro's number, α = isotropic polarizability, μ_0 = gas phase dipole

Can. J. Chem. Downloaded from www.nrcresearchpress.com by 210.87.254.6 on 09/05/12
For personal use only.

moment, v = the volume of the cavity surrounding each dipole = $\overline{V}/N_0$, $g = (4\pi/3)\ (2\varepsilon_0 - 2)/(2\varepsilon_0 + 1)$. k_α, k_R, and k_c are constants which are calculated (2) from the eccentricity of the molecule, e, where:

$$[2]\quad \begin{cases} e = \sqrt{1 - \left(\frac{b}{a}\right)^2} & \text{for a prolate spheroid} \\ e = \sqrt{1 - \left(\frac{a}{b}\right)^2} & \text{for an oblate spheroid} \end{cases}$$

where a and b are the axes of the spheroid, with a being the dipolar axis.

The calculations of ref. 2 could only be reproduced if, in the prolate case, $k_c = k_R/\beta$ with β defined as in ref. 2, and not $k_c = \beta k_R$ as stated in that reference. For a spherical molecule $k_\alpha = k_c = k_R = 1$ and eq. 1 reduces to the Onsager equation (6). The criterion for a successful fit is to calculate $G = \mu_0^2(\text{calculated})/\mu_0^2$ from eq. 1. If $G = 1$ at many temperatures, then the fit is perfect. Buckley and Maryott found empirically that G values which drifted with temperature often became constant if the cavity volume, v, was fixed at some arbitrary value, rather than being allowed to vary with the density, as in the original Onsager equation.

The values of G listed in Table 1 were calculated from the spheroidal Onsager equation at various levels of sophistication. The data used for all of these calculations is listed in Table 1. The densities of CHF_3 (7), CH_2F_2 (8), and CH_3F (9) were taken from the data of other workers. The densities listed for CF_4, CH_3F, and CHF_3 agree with those of Shinsaka and Freeman (8) to within 0.6%. The gas phase dipole moments were taken to be 1.851 for CH_3F (10), 1.97 for CH_2F_2 (11), and 1.649 for CHF_3 (10). The polarizations, P, were considered interchangeable with the polarizabilities, α, by the Clausius–Mossotti equation (4). The values of the gas phase atomic plus electronic polarizations, $P_a + P_e$, were obtained from ref. 10. Values of the electronic polarizations, P_e, were obtained for CH_3F and CH_2F_2 from the bond polarizabilities (12). The value of P_e for CHF_3 was measured by Bridge and Buckingham (13).

Equation 1 makes no distinction between the polarizability in the direction of the cavity field and that in the direction of the dipolar axis in calculating the reaction field (14, 15). The former may be approximated by the isotropic polarizability of the molecule, while the latter is the anisotropic polarizability along the axis of the dipole moment of the molecule. Both polarizabilities should include the atomic polarization, P_a. In addition, the cavity field polarizability should include the lattice mode polarization, P_{lm}, that is the additional contribution to the atomic polarization caused by the intermolecular lattice vibrations of the liquid state (16). If ε_0 is large, it can be shown (17) that eq. 1 requires the use of the polarization along the dipolar axis unless the cavity field polarization is itself very large. Otherwise a value of P, intermediate between the cavity field and dipolar axis values can be chosen so that eq. 1 still provides a reasonably accurate description of the dielectric data. Buckley and Maryott (2), however, were able to treat many systems successfully using values of P which did not include P_a, P_{lm}, or the anisotropy of the polarization.

Columns 1 and 2 of Table 1 show that the spherical Onsager equation cannot describe these systems well, although the G values were closer to unity when atomic polarization was included. The data for the prolate spheroid, CH_3F, is particularly interesting, since its shape should cause the Onsager value of G to be less than unity (2). The axial ratios, b/a were determined from Fisher–Hirschfelder–Taylor atomic models to be 0.9 for CH_3F, 1.2 for CH_2F_2, and 1.1 for CHF_3. The values of G listed in column 3 of Table 1 were calculated using these axial ratios and the spheroidal modification to Onsager's equation. These results show that the large values of G in columns 1 and 2 cannot be explained by molecular shape alone. In no case was the drift in G improved by assuming a constant arbitrary cavity volume.

By analogy with the treatment of Buckley and Maryott (2), or with the Frohlich–Kirkwood theory (14), these results could be interpreted as indicating a definite tendency for parallel alignment of the molecular dipoles in the liquid. This conclusion must be treated with caution, however, because the treatment has neglected the anisotropy of the molecular polarizability, and the contribution to the polarization from that part of the far infrared absorption which is due to the intermolecular lattice vibrations in the liquid.

The polarization along the dipolar axis of CHF_3 and CH_3F molecules can be crudely estimated by adding the anisotropic P_e (13, 18)

Can. J. Chem. Downloaded from www.nrcresearchpress.com by 210.87.254.6 on 09/05/12
For personal use only.

TABLE 1. The dielectric results for the fluoromethanes in the liquid state

(*a*) CH_3F

			G				
T(°C)	ε_o	Density (g/cm^3)	Column 1 $P=P_e=6.56$ cm^3 $e=0$	Column 2 $P=P_a+P_e=7.49$ cm^3 $e=0$	Column 3 $P=P_a+P_e=7.49$ cm^3 $e=0.436$	Column 4 $P=P_a+P_e$(an)$=9.00$ cm^3 $e=0.436$	Column 5 $P=12.2$ $e=0.436$
−140.4	47.62	1.002	1.46	1.36	1.48	1.33	1.04
−138.4	46.40	0.9982	1.45	1.35	1.47	1.32	1.03
−121.6	38.45	0.9669	1.41	1.32	1.43	1.29	1.02
−120.7	37.98	0.9652	1.41	1.32	1.43	1.29	1.01
−100.9	30.95	0.9269	1.37	1.28	1.38	1.25	1.00
−97.7	29.93	0.9206	1.36	1.27	1.38	1.25	0.99
−82.4	25.77	0.8897	1.33	1.25	1.35	1.22	0.98
−79.5	25.06	0.8837	1.32	1.24	1.34	1.22	0.98

(*b*) CH_2F_2

			G				
T(°C)	ε_o	Density (g/cm^3)	Column 1 $P=P_e=6.68$ cm^3 $e=0$	Column 2* $P=P_a+P_e$ $e=0$	Column 3 $P=P_e=6.68$ cm^3 $e=0.553$	Column 4 $P=P_e$(an)$=6.73$ cm^3 $e=0.553$	Column 5 $P=12.3$ $e=0.553$
−121.0	53.74	1.376	1.94	—	1.69	1.68	1.04
−110.2	47.82	1.350	1.90	—	1.65	1.65	1.03
−100.5	43.00	1.327	1.85	—	1.61	1.61	1.01
−90.2	38.77	1.301	1.81	—	1.59	1.58	1.01
−78.4	34.50	1.270	1.77	—	1.55	1.55	1.00
−72.9	32.65	1.257	1.74	—	1.53	1.53	0.99
−57.4	28.19	1.219	1.68	—	1.49	1.48	0.98
−49.2	26.11	1.199	1.65	—	1.46	1.46	0.97

*P_a not known.

Can. J. Chem. Downloaded from www.nrcresearchpress.com by 210.87.254.6 on 09/05/12
For personal use only.

TABLE 1. (*Concluded*)

(*c*) CHF_3

			G				
T(°C)	ε_o	Density (g/cm³)	Column 1 $P=P_e=7.80$ cm³ $e=0$	Column 2 $P=P_a+P_e=9.01$ cm³ $e=0$	Column 3 $P=P_a+P_e=9.01$ cm³ $e=0.417$	Column 4 $P=P_a+P_e(an)=8.55$ cm³ $e=0.417$	Column 5 $P=14.8$ $e=0.417$
−148.0	40.70	1.679	1.84	1.71	1.58	1.63	1.02
−143.9	38.74	1.665	1.83	1.70	1.57	1.62	1.02
−127.4	32.04	1.609	1.79	1.66	1.54	1.59	1.01
−120.8	29.76	1.587	1.77	1.65	1.53	1.57	1.01
−110.7	26.69	1.553	1.74	1.62	1.51	1.55	1.01
−101.2	24.07	1.521	1.70	1.59	1.48	1.52	1.00
−85.0	20.24	1.466	1.64	1.53	1.43	1.47	0.98
−82.9	19.78	1.459	1.63	1.52	1.42	1.46	0.98

(*d*) CF_4

T(°C)	ε_o	Density (g/cm³)
−146.9	1.685	1.708
−144.5	1.681	1.700
−131.7	1.644	1.624
−131.6	1.647	1.630

Can. J. Chem. Downloaded from www.nrcresearchpress.com by 210.87.254.6 on 09/05/12
For personal use only.

TABLE 2. Values of μ_o^2/I for several halomethanes $I = (I_x + I_y)/2$ where z is the dipolar axis

Halomethane	(μ_o^2/I) $(D^2/g\ cm^2) \times 10^{44}$
CH_3F	1040
CH_3Cl	554
CH_3Br	370
CH_3I	249
CH_2F_2	457
CH_2Cl_2	92
CHF_3	335
$CHCl_3$	38

along that axis, to the isotropic values of P_a. The values are shown in Table 1. Column 4 of Table 1 lists G values calculated from them, using the geometric eccentricities. Column 5 lists values of G which were fitted to unity by using rather large values of P. The large discrepancy between the estimated anisotropic polarization and that required to set G near unity must indicate either a very strong contribution from the lattice vibrations of the liquid to the cavity field polarization, or the presence of intermolecular forces which favor parallel alignment of these dipoles and, hence, values of G greater than unity.

The lattice mode polarization undoubtedly arises primarily from rotational oscillations of the molecules about their equilibrium positions (19). The intensity of the resulting absorption band in the far infrared is, very crudely, proportional to μ_0^2/I, where I is the moment of inertia (16, 19). From the Kramers–Kronig relationship (20), the contribution of this band to the polarization will be highly dependent on its position and shape, but a very rough correlation between μ_0^2/I and Δn, the contribution of the band to the low frequency refractive index, would be expected.

Table 2 lists values of μ_0^2/I for several halomethanes as calculated from values of the rotational constants, B_0 and C_0, obtained from microwave spectra (21). Because the far infrared absorption includes a contribution from the orientational polarization (22) it is not possible to calculate the lattice mode contribution from the far infrared spectrum alone. A Kramers–Kronig treatment of the spectrum of CH_3I (19) indicates, however, that the total absorbance from 20 to 70 cm^{-1} would increase the polarization from the "sodium D" value of 19.3 to 24, and so the contribution of the lattice modes might well be significant. From the relative values of μ_0^2/I, the effect of lattice vibrations on cavity field polarization would follow the order $CH_3F > CH_2F_2 > CHF_3$. Hence, although this effect might account for the high values of the molar polarization required to set $G = 1$ for CH_3F, and possibly for CH_2F_2, the high value of G for CHF_3 must indicate at least in part, that the molecular dipoles tend to align parallel, perhaps due to hydrogen bonding (23–26).

If the lattice vibrations do significantly influence the reaction fields of the fluoromethanes, they might also be expected to influence those of the methyl halides. Using Buckley and Maryott's data (2), that is using the "sodium D" values of the polarizations which should be a lower limit, the spheroidal Onsager equation fits CH_3Cl and CH_3Br quite well with $G = 1$, assuming the gas phase geometries. CH_3I, however, requires a polarization which is 22% smaller than this lower limit (Table 3).

These results can be rationalized using arguments similar to those used above, if the tendency for antiparallel dipole alignment increases in the order $CH_3F < CH_3Cl < CH_3Br < CH_3I$ because, as can be seen in Table 2, the

TABLE 3. The discrepancies between the gas phase molar polarizations and those required to fit the methyl halides to the spheroidal Onsager equation using molecular geometries*

Halomethane	P, the gas phase molar polarization (cm^3)	P', the polarization required to fit the Onsager equation (cm^3)	$\frac{P' - P}{P}$
CH_3F	9.00	12.2	+0.36
CH_3Cl	11.7	12.5	+0.05
CH_3Br	14.6	14.6	+0.00
CH_3I	19.3	14.9	−0.22

*P is the gas phase anisotropic polarization of methyl fluoride and the isotropic "sodium D" polarization in all other cases.

contribution of the lattice vibrations is expected to increase in the reverse order. These two effects may roughly cancel each other for CH_3Br and CH_3Cl and thus enable their static dielectric constants to be fitted to the Onsager equation with $G = 1$.

Conclusion

In the absence of an exact knowledge of the dipolar axis and cavity field polarizations, deviations of G from unity do not necessarily imply liquid structure. The static dielectric constants of the fluoromethanes can be rationalized either by assuming significant parallel dipole correlation in all members of the series or, by assuming a significant lattice mode polarization which follows the order $CH_3F > CH_2F_2 > CHF_3$, and that a degree of parallel dipole correlation is present in CHF_3. An increasing tendency for antiparallel alignment of the methyl halides, with increasing size of the halogen, is consistent with both arguments.

The authors wish to thank Dr. J. E. Bertie and Dr. G. R. Freeman for many invaluable discussions and much assistance. The National Research Council of Canada is thanked for the award of a 1967 Science Scholarship to P.T.

1. A. A. MARYOTT and E. R. SMITH. Tables of dielectric constants of pure liquids. NBS Circ. **514** (1951).
2. F. BUCKLEY and A. A. MARYOTT. J. Res. Natl. Bur. Stand. **53**, 229 (1954).
3. O. RUFF and R. KEIM. Z. Anorg. Chem. **201**, 225 (1931).
4. C. P. SMYTH. Dielectric behavior and structure. McGraw-Hill, New York. 1955. p. 5.
5. A. BAUGH TIPTON, A. P. DEAM, and J. E. BOGGS. J. Chem. Phys. **40**, 1144 (1964).
6. L. ONSAGER. J. Am. Chem. Soc. **58**, 1486 (1936).
7. O. RUFF. Ber. **69**, 302 (1936).
8. K. SHINSAKA and G. R. FREEMAN. Unpublished work.
9. A. V. GROSSE, R. C. WACKHER, and C. B. LINN. J. Phys. Chem. **44**, 278 (1940).
10. H. SUTTER and R. H. COLE. J. Chem. Phys. **52**, 132 (1970).
11. D. R. LIDE, JR. J. Am. Chem. Soc. **74**, 3548 (1952).
12. J. A. BERAN and L. KEVAN. J. Phys. Chem. **73**, 3860 (1969).
13. N. J. BRIDGE and A. D. BUCKINGHAM. Proc. Royal Soc. (London), A**295**, 334 (1966).
14. N. E. HILL, W. E. VAUGHAN, A. H. PRICE, and M. DAVIES. Dielectric properties and molecular behavior. Van Nostrand Reinhold, New York. 1969. p. 24.
15. J. NORTON WILSON. Chem. Rev. **25**, 377 (1939).
16. B. MORRIS and D. W. DAVIDSON. Can. J. Chem. **49**, 1243 (1971).
17. E. WHALLEY. Adv. High Press. Res. **1**, 143 (1966).
18. R. J. W. LEFEVRE. Rev. Pure Appl. Chem. **20**, 67 (1970).
19. S. R. JAIN and S. WALKER. J. Phys. Chem. **75**, 2942 (1971).
20. F. STERN. Solid-State Phys. **15**, 331 (1963); S. MAEDA and P. N. SCHATZ. J. Chem. Phys. **36**, 571 (1962).
21. C. H. TOWNES and A. L. SCHAWLOW. Microwave spectroscopy. McGraw-Hill, New York. 1955. p. 618.
22. G. BIRNBAUM and E. R. COHEN. J. Chem. Phys. **53**, 2885 (1970).
23. C. J. CRESWELL and A. L. ALLRED. J. Am. Chem. Soc. **85**, 1723 (1963).
24. A. ALLERHAND and P. VON RAGUE SCHLEYER. J. Am. Chem. Soc. **85**, 1715 (1963).
25. N. THORP and R. L. SCOTT. J. Phys. Chem. **60**, 1441 (1956).
26. R. J. W. LEFEVRE, G. L. D. RITCHIE, and P. J. STILES. Chem. Commun. **253**, 326 (1966).

Can. J. Chem. Downloaded from www.nrcresearchpress.com by 210.87.254.6 on 09/05/12
For personal use only.

The Reaction of O_3 with CCl_2CH_2 [1]

LESLIE A. HULL,[2] I. C. HISATSUNE, AND JULIAN HEICKLEN

Department of Chemistry and Center for Air Environment Studies, The Pennsylvania State University, University Park, Pa. 16802

Received October 10, 1972

The gas-phase reaction of O_3 with CCl_2CH_2 at 25 °C was studied by monitoring O_3 consumption by ultraviolet absorption and product formation and olefin consumption by infrared absorption. In the absence or presence of excess N_2, and for initial olefin-to-O_3 ratios, $[CCl_2CH_2]_0/[O_3]_0$, in excess of 20 ($[O_3]_0 \sim 1.0$ Torr), the rate law is

$$-d[O_3]/dt = k[CCl_2CH_2][O_3]^2$$

with $k = 2.4 \times 10^6\ M^{-2}\ s^{-1}$. At lower olefin-to-$O_3$ ratios, the rate is initially more rapid than predicted by the above equation, but follows the equation after the reaction has proceeded for some time. In the presence of excess O_2, the rate is markedly reduced, and the rate law becomes

$$-d[O_3]/dt = k'[CCl_2CH_2][O_3]$$

with $k' = 2.2\ M^{-1}\ s^{-1}$.

The products of the reaction are CCl_2O, HCOOH, $CH_2ClCCl(O)$, CO, O_2, HCl, and presumably H_2O. In the absence of O_2, the CCl_2CH_2-to-O_3 consumption ratio approaches 2, but the CCl_2O produced per O_3 consumed is between 0.25 and 0.4. With excess O_2, the latter ratio becomes unity, but the CCl_2CH_2-to-O_3 consumed approaches 5.

The results are interpreted in terms of a chain mechanism with CCl_2O_2 as the chain carrier. The mechanism developed explains the main features of the reaction.

La réaction en phase gazeuse de O_3 sur CCl_2CH_2 à 25 °C a été étudiée en suivant la disparition de O_3 par absorption ultraviolette, formation de produit et disparition de l'oféline par absorption infrarouge. En l'absence ou en présence d'un excès de N_2 et pour des rapports initiaux oléfine sur O_3, $[CCl_2CH_2]_0/[O_3]_0$ de 20 avec ($[O_3]_0 \sim 1.0$ Torr), la loi de vitesse est

$$-d[O_3]/dt = k[CCl_2CH_2][O_3]^2$$

avec $k = 2.4 \times 10^6\ M^{-2}\ s^{-1}$. Pour des rapports oléfine sur O_3 plus faibles, la vitesse initiale est plus rapide que celle qui est prévue par l'équation ci-dessus, mais au bout d'un certain temps la réaction satisfait à cette équation. En présence d'un excès de O_2, la vitesse est réduite de façon appréciable et la loi de vitesse devient

$$-d[O_3]/dt = k'[CCl_2CH_2][O_3]$$

avec $k' = 2.2\ M^{-1}\ s^{-1}$.

Les produits de la réaction sont CCl_2O, HCOOH, $CH_2ClCCl(O)$, CO, O_2, HCl, et vraisemblablement H_2O. En l'absence de O_2, la consommation de CCl_2CH_2/O_3 tend vers deux mais le CCl_2O produit par O_3 consommé, oscille entre 0.25 et 0.4. Avec un excès de O_2, ce dernier rapport vaut un, le CCl_2CH_2 consommé par O_3 tend vers 5.

Les résultats sont interprétés par un mécanisme de réaction en chaîne avec CCl_2O_2 comme initiateur. Le mécanisme évoqué rend compte des principales caractéristiques de la réaction.

[Traduit par le journal]

Can. J. Chem., **51**, 1504 (1973)

Introduction

The gas-phase reaction of O_3 with olefins has been examined in several laboratories in recent years (1–5). Wei and Cvetanović (3) found that the ratio of olefin-to-ozone consumed was 1.0 in the presence of excess N_2, but between 1.4 and 2.0 in the presence of excess O_2. They attributed the increase to secondary attack of some species on the olefin in the latter case. At temperatures below room temperature (−40 to −95 °C), DeMore (5) found the rate of O_3 consumption to be independent of the absence or presence of excess O_2 in the O_3–C_2H_4 reaction.

The products of the reaction have been examined by Vrbaski and Cvetanović (2). While the detailed mechanism has never been fully explained, the products are consistent with addition of O_3 to the olefin followed by cleavage to a carbonyl compound and a zwitterion. For C_2H_4, the reaction steps would be

[1]CAES Report No. 270–72.

[2]Present address: Department of Chemistry, Union College, Schenectady, N.Y. 12309.

Can. J. Chem. Downloaded from www.nrcresearchpress.com by 210.87.254.6 on 09/05/12
For personal use only.

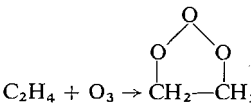

$$C_2H_4 + O_3 \rightarrow CH_2—CH_2 \rightarrow CH_2O + CH_2O_2$$

The CH_2O_2 zwitterion has never been trapped in the gas phase and presumably rearranges quickly to excited formic acid (HCOOH) which can either be stabilized or decompose to CO plus H_2O.

In our laboratory, we have initiated studies of the reaction of O_3 with halogenated ethylenes. The halogen atom migrates less readily (if at all) than the hydrogen atom. Thus stabilization of the zwitterion should be enhanced. In fact oxidation of perhaloolefins has been interpreted in terms of stable (to isomerization) zwitterions (6).

In this paper we report our results on the reaction of O_3 with CCl_2CH_2. The reaction of chlorinated olefins with O_3 in the gas phase has not been reported previously. Williamson and Cvetanović (7) have examined the reaction in CCl_4 solution at 25 °C. For CCl_2CH_2, they found that the ratio of olefin-to-ozone consumption was one, that one $COCl_2$ was formed per O_3 consumed, and that the rate of reaction was first order in both olefin and O_3 concentration. An explosive white solid compound was also found after evaporation of the solvent.

Experimental

The kinetic apparatus has been described previously (8). It consists of two 100 cc bulbs connected by a T-stopcock (one that opens simultaneously in three directions) to a stem adaptor which leads either through a stopcock to the vacuum line or through a stopcock to the optical cell. Silicone grease was used in all the stopcocks. Two optical cells were used. One was a 10.0 cm long quartz cell for following O_3 decay at 2537 Å in a Cary 14 spectrometer. The other cell was 10.3 cm long and had NaCl windows to permit monitoring olefin decay at 1620 cm^{-1} and phosgene – acid chloride appearance at 1830 cm^{-1} by infrared spectroscopy. A Perkin–Elmer 112 infrared spectrometer with a CaF_2 prism was used. All experiments were performed at room temperature, about 25 °C.

Before a run, the kinetic apparatus was evacuated for at least an hour by an oil diffusion pump and then conditioned for 10 min with about 5 Torr of O_3 before final evacuation. The O_3 was prepared from a tesla coil discharge through O_2, the excess O_2 being removed at −196 °C. A desired amount of freshly prepared O_3 was then measured into the cell with a Kel-F oil manometer. The half-life of the O_3 in the cell was about 8 h, which was very much longer than the rest of the procedure. The 1,1-dichloroethylene was obtained from the Fisher Scientific Co. and distilled at −98 °C before use. Mixtures of it and the appropriate diluent gas were prepared in the 100 cc bulbs.

The kinetic apparatus then was removed from the vacuum line and transferred to the appropriate spectrometer with the cell in the optical path. The spectrometer was set at a fixed wavelength, and the reaction was initiated by opening the T-stopcock first and then opening and closing the stopcock to the cell. The reaction was followed continuously for 4 or more half-lives and then intermittently for 3 more to get an infinity point. The initial pressures of the olefin and diluent gas in the cell were calculated using the measured ratio of the volumes of the bulbs to the entire kinetic apparatus. These were 0.485 for the infrared cell and 0.75 for the quartz cell. Kinetic runs in which the O_3 was added to the olefin were performed in a similar manner by reversing the roles of the O_3 and olefin.

Runs for product analysis were performed in the infrared cell in the manner described for the kinetic runs, except that the entire region (4000–600 cm^{-1}) was scanned on a Perkin–Elmer 521 grating infrared spectrometer. HCl was identified from its known band sequence (2750–3050 cm^{-1}), but no quantitative estimates could be made. Quantitative analysis for the olefin, CCl_2O, $CH_2ClCCl(O)$, and CO were made from their respective bands at 1620, 850, 720, and 2050–2200 cm^{-1}. In experiments to measure O_2, the diluent gas was a halocarbon (CCl_4, CH_2Cl_2, or CF_3CFCl_2) that was condensable at −196 °C. The residual pressure of gas noncondensable at −196 °C was considered to be CO plus O_2, and the O_2 computed by difference.

Results

Initially kinetic runs were done in which the rate of disappearance of O_3 was monitored by ultraviolet absorption. Experiments were done in both the absence and presence of excess N_2 and both by adding the olefin to the O_3 and *vice versa*. In the absence of N_2 for O_3 pressures >2 Torr, explosions occurred. Therefore all experiments were done with initial O_3 pressures <2 Torr. Typical runs are shown in Fig. 1 for three different initial olefin pressures, $[CCl_2CH_2]_0$. The data are displayed as second order kinetic plots. At $[CCl_2CH_2]_0/[O_3]_0$ ratios >20, the plots are linear to >90% conversion indicating a rate law second-order in $[O_3]$. At lower initial ratios, the O_3 decay is rapid at first and then becomes second order as the run progresses.

The pseudo second order rate coefficients increase proportionately with the olefin pressure, so that the rate law follows the expression

$$-d[O_3]/dt = k[CCl_2CH_2][O_3]^2$$

For several runs the values of k are listed in Table 1. At low values of $[CCl_2CH_2]_0/[O_3]_0$, the rate coefficients were obtained late in the run, when the O_3 decay became second order. In one case the olefin consumption, rather than the O_3

Can. J. Chem. Downloaded from www.nrcresearchpress.com by 210.87.254.6 on 09/05/12
For personal use only.

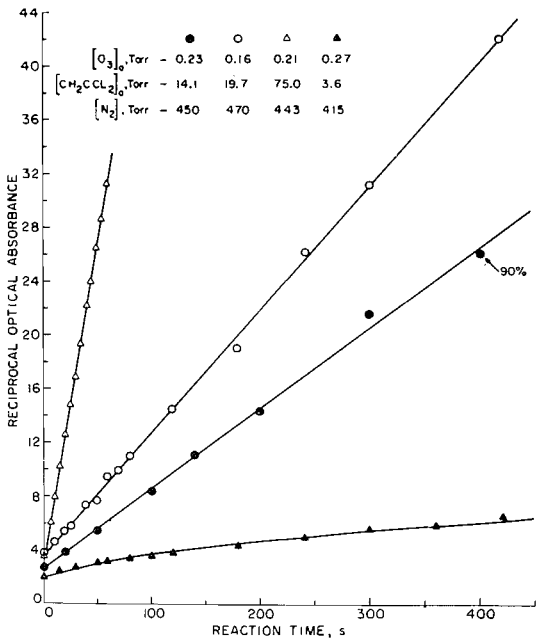

FIG. 1. Plots of reciprocal optical absorbance of O_3 *vs.* reaction time for 4 reactions of O_3 with CH_2Cl_2 in the presence of excess N_2 at 25 °C.

TABLE 1. Rate coefficients for the reaction of O_3 with CCl_2CH_2 at 25 °C

$[CH_2CCl_2]_0$ (Torr)	$[O_3]_0$ (Torr)	$[N_2]$ (Torr)	$10^{-6}k$ (M^{-2} s^{-1})
2.6	0.23	0.0	2.3
3.6	0.27	415	2.2
4.9	0.84	465	1.9
4.9	0.96	365	2.6*
6.5	0.37	270	2.3
7.5	0.11	190	3.5
7.6	0.43	0.0	1.5
7.8	0.25	436	1.7
8.7	0.36	370	1.6
9.3	0.45	350	1.9
10.0	0.13	0.0	3.1
11.1	0.30	0.0	1.8
12.9	0.13	0.0	3.4
13.4	0.10	340	4.0
13.4	0.23	0.0	1.6
14.1	0.23	450	2.3
19.1	0.32	470	2.0
19.7	0.16	470	2.6
19.8	0.09	270	3.7
22.0	0.45	450	2.2
23.0	0.30	0.0	1.7
30.0	0.088	464	2.6
75.0	0.18	443	3.3
			Ave. 2.4 ± 0.6

*Based on CCl_2CH_2 disappearance.

consumption, was monitored by infrared analysis. In this case, the amount of olefin consumed was measured at the end of the run to provide a stoichiometric factor to compute k. In all cases k is approximately the same, there being no discernible trend with $[CCl_2CH_2]$. The average value for k is $(2.4 \pm 0.6) \times 10^6\ M^{-2}\ s^{-1}$.

Next, kinetic runs were done in the presence of excess O_2. The rate of O_3 consumption was markedly reduced for comparable conditions in the presence of N_2. Furthermore the decay law was first order in $[O_3]$ to at least 90% removal at large $[CCl_2CH_2]_0/[O_3]_0$ as shown in Fig. 2. The pseudo first order rate coefficients were approximately proportional to the CH_2CCl_2 pressure, suggesting the rate law

$$-d[O_3]/dt = k'[O_3][CCl_2CH_2]$$

The rate coefficients k' are listed in Table 2. They are independent of the O_2 pressure, for O_2 pressures >43 Torr. However there are two trends. Those coefficients based on olefin consumption or $CCl_2O + CH_2ClCCl(O)$ formation appear somewhat larger than those based on O_3 consumption. Presumably this reflects stoichiometric uncertainties, since it is difficult to explain such a phenomenon otherwise. The second and more meaningful trend is the approximately

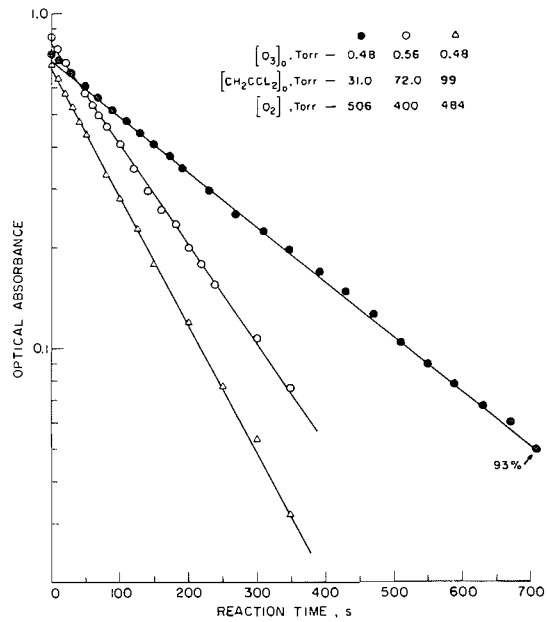

FIG. 2. Semilog plots of O_3 optical absorbance *vs.* reaction time for 3 reactions of O_3 with CH_2Cl_2 in the presence of excess O_2 at 25 °C.

Can. J. Chem. Downloaded from www.nrcresearchpress.com by 210.87.254.6 on 09/05/12
For personal use only.

TABLE 2. Rate coefficients for the reaction of O_3 with CCl_2CH_2 in the presence of O_2 at 25 °C

$[CCl_2CH_2]_0$ (Torr)	$[O_3]_0$ (Torr)	$[O_2]$ (Torr)	k' (M^{-1} s^{-1})
8.1	1.00	253	4.1*
8.3	1.00	250	4.5†
8.5	0.96	250	3.5
8.5	0.97	43	3.7†
9.9	0.56	356	5.0*
11.3	0.26	340	2.8
15.2	0.28	450	2.4
31.0	0.49	450	2.2
72.0	0.14	420	1.9
72.0	0.32	470	1.9
72.0	0.56	400	1.9
76.0	0.30	320	3.3†
76.0	1.00	260	3.7†
99.0	0.48	380	1.7
			Ave. 2.2 ± 0.6‡

*Based on olefin consumption.
†Based on CCl_2O + $CH_2ClCCl(O)$ formation.
‡Based on O_3 consumption only.

factor of 2 drop as the olefin pressure increases from 8.5 to 99 Torr. This suggests that the rate law is slightly less than first order in $[CCl_2CH_2]$. However for simplicity, we shall assume first order kinetics, which leads to an average value of k' of 2.2 ± 0.6 M^{-1} s^{-1}.

As in the absence of O_2, runs in the presence of O_2 at low initial olefin pressures showed an excessive rate initially. As the reaction progressed the rate slowed and became first order in both $[O_3]$ and $[CCl_2CH_2]$.

Finally the products of the reaction were measured. The products were $CH_2ClCCl(O)$, CCl_2O, HCOOH, CO, O_2, and HCl. Presumably H_2O was also produced, but no measurements for it were attempted. (Separate experiments showed that H_2O and CCl_2O are stable in the presence of each other, if the pressure of each is <5 Torr.) Notable for its absence was CH_2O. In all cases $[HCOOH] \lesssim [CCl_2O]$. Quantitative analysis for HCl was too difficult to be reliable and no quantitative results are reported.

In the presence of excess N_2, the olefin-to-ozone consumed was approximately unity at low ratios of $[CCl_2CH_2]_0/[O_3]_0$, but rose towards 2 as the ratio increased to 20. The CCl_2O production to O_3 consumption remained between 0.25 and 0.40 throughout the whole range of $[CCl_2CH_2]_0/[O_3]_0$ ratios.

In the presence of excess O_2, the olefin consumption and CCl_2O formation were about the same as in excess N_2 for low olefin-to-O_3 ratios. However at higher ratios, CCl_2CH_2 consumption approached 5 times the O_3 consumption, and CCl_2O production approached O_3 consumption.

In order to detect the noncondensable products more easily, some runs were done with halocarbon diluents which are condensable at −196 °C. Presumably these diluents act like N_2. In the presence of a relatively small amount of CCl_4 (38 Torr), no HCOOH or $CH_2ClCCl(O)$ was formed, but one O_2 was formed for each O_3 removed. At higher diluent pressures, the O_2 produced to O_3 consumed was about 1/3 at medium $[CCl_2CH_2]_0/[O_3]_0$ ratios, but dropped to 0.09 at an initial ratio of 22. In all cases the CO produced was about 1/4 of the O_3 consumed.

Discussion

It is clear that the gas-phase ozonolysis of CCl_2CH_2 is considerably different than in CCl_4 solution or that for C_2H_4, especially at high olefin to O_3 ratios. At high ratios the rate law is second order in $[O_3]$, the olefin-to-O_3 consumption exceeds unity, and the CCl_2O production is 0.25–0.40 of the O_3 consumption. Furthermore a long chain is involved since the presence of excess O_2 markedly reduces the rate and changes the rate law. Even at low olefin-to-O_3 ratios, differences exist, since CCl_2O production is less than O_3 consumption.

The reaction mechanism must be complex and cannot be elucidated in detail from our studies. However some overall formal mechanistic conclusions can be drawn, even though they must be speculative at this time.

Presumably the initial step is the addition of O_3 across the double bond of the olefin followed by cleavage to form a carbonyl compound and a zwitterion. This can occur in two ways. One possibility is

$$O_3 + CCl_2CH_2 \rightarrow CCl_2O + CH_2O_2$$

The CH_2O_2 zwitterion could then rearrange to HCOOH or decompose to CO + H_2O. If this were the sole reaction, then this reaction should be similar to the ozonolysis of C_2H_4, *i.e.* the rate should be first order in each of the reactants, the olefin-to-O_3 consumption should be unity, the CCl_2O production to O_3 removal should be unity, and the addition of O_2 should have no effect. Of course it is possible that the CH_2O_2 zwitterion could be stabilized long enough to enter into a chain reaction. However in no other

Can. J. Chem. Downloaded from www.nrcresearchpress.com by 210.87.254.6 on 09/05/12
For personal use only.

Can. J. Chem. Downloaded from www.nrcresearchpress.com by 210.87.254.6 on 09/05/12
For personal use only.

TABLE 3. Product formation in the reaction of O_3 and CCl_2CH_2 at 25 °C

$[CH_2CCl_2]_0$ (Torr)	$[O_3]_0$ (Torr)	[X] (Torr)	$[CH_2CCl_2]$* (Torr)	$[COCl_2]$ (Torr)	[HCOOH] (Torr)	$[CH_2ClCCl(O)]$ (Torr)	[CO] (Torr)	$[O_2]$ (Torr)
				X = N_2				
0.3	0.2	230	0.2	0.071	0.042	0.07	—	—
1.1	1.0	300	1.0	0.28	0.15	0.3	—	—
4.9	0.96	365	1.4	—	—	—	—	—
6.3	2.1	200	2.7	0.70	~0.4	1.9	—	—
10.0	1.0	300	1.8	0.42	0.22	0.9	—	—
20.0	1.0	280	1.9	0.40	0.25	1.1	—	—
				X = O_2				
1.0	1.9	300	0.9	0.63	0.51	0.2	—	—
2.2	1.9	300	2.0	1.1	1.0	0.6	—	—
6.1	2.1	300	4.0	1.7	2.0	2.1	0.45	—
8.1	1.0	253	4.5	—	—	—	—	—
9.7	1.0	300	4.9	0.91	~1.0	2.7	—	—
9.9	0.56	356	3.7	—	—	—	—	—
				X = Halocarbon				
14.4	2.0	38†	1.6	0.49	0.0	0.0	0.6	2.0
14.5	2.1	145‡	3.2	0.7	~0.4	—	0.6	0.7
6.3	2.1	200§	—	—	—	—	0.5	0.6
48.5	2.2	180§	—	—	—	—	0.5	0.2

*CH_2CCl_2 consumed.
†CCl_4.
‡CH_2Cl_2.
§CF_3CFCl_2.

Can. J. Chem. Downloaded from www.nrcresearchpress.com by 210.87.254.6 on 09/05/12
For personal use only.

system is such a stabilization known for CH_2O_2, and it is difficult to see why it should occur here.

It seems more likely to us that all or part of the time, the ozonolysis proceeds via the alternate pathway

[1] $O_3 + CCl_2CH_2 \rightarrow CCl_2O_2 + CH_2O$

The CCl_2O_2 zwitterion, which should be stable to isomerization, could then react with either O_3 or CCl_2CH_2

[2] $CCl_2O_2 + O_3 \rightarrow CCl_2O + 2O_2$

[3] $CCl_2O_2 + CCl_2CH_2 \rightarrow A$

where we envision A as a diradical adduct. Actually A could be any fragment that carries the chain to regenerate CCl_2O_2. If A is the adduct it could either add to O_3 or react with it

[4a] $A + O_3 \rightarrow AO_3$

[4b] $\rightarrow CCl_2O_2 + CCl_2O + HCOOH$

Likewise it could undergo similar reactions with O_2

[5a] $A + O_2 \rightarrow AO_2$

[5b] $\rightarrow 2CCl_2O + HCOOH$

or it could decompose via

[6] $A \rightarrow CCl_2O + CH_2ClCCl(O)$

The product $CH_2ClCCl(O)$, which is observed, may be formed through rearrangement of a "hot" epoxide. Presumably it also is formed with excess energy, and if not stabilized by collision can decompose to form HCl and CO among other things. We believe this to be the source of HCl and some of the CO. The absence of $CH_2ClCCl(O)$ at low pressures of diluent gas (*i.e.* at 38 Torr of CCl_4) supports this argument.

No CH_2O was observed under any conditions. This can be attributed to the reaction of CH_2O with O_3 to produce either HCOOH or CO + H_2O

[7] $CH_2O + O_3 \rightarrow O_2 + HCOOH$ (or $CO + H_2O$)

It is known that O_3 reacts readily with aldehydes (9, 10), though the detailed mechanism has not been elucidated. For our purposes reaction 7 should be adequate, though if free radical intermediates are involved, the mechanism will be more complex.

In order to account for the chain nature of the reaction the following reactions (or others mechanistically similar) are needed

[8] $AO_3 + 2CCl_2CH_2 \rightarrow 3CH_2ClCCl(O) + CCl_2O_2$

[9] $AO_2 + CCl_2CH_2 \rightarrow 2CH_2ClCCl(O) + CCl_2O_2$

In the gas phase in the absence of O_2, the mechanism consisting of reactions 1–4 and 6–8 leads to the prediction

$$[10] \quad -d[O_3]/dt = k_1[CCl_2CH_2][O_3] \times \left(2 + \frac{k_2[O_3] + k_3[CCl_2CH_2]}{k_2[O_3] + k_3k_6[CCl_2CH_2]/k_4[O_3]}\right)$$

if $k_6 \ll k_4[O_3]$. Since our results will be shown to be consistent with a value of $k_4/k_6 = 2.1 \times 10^6\ M^{-1}$, the condition is valid over our entire experimental range.

At sufficiently high pressures of CCl_2CH_2 and low pressures of O_3, $k_2[O_3] \ll k_3k_6[CCl_2CH_2]/k_4[O_3]$, and eq. 10 reduces to

$$[11] \quad -d[O_3]/dt = k_1k_4[O_3]^2[CCl_2CH_2]/k_6$$

Thus $k = k_1k_4/k_6 = 2.4 \times 10^6\ M^{-2}\ s^{-1}$.

Under all of our conditions, $k_2[O_3] \ll k_3[CCl_2CH_2]$, but at low CCl_2CH_2 pressures and high O_3 pressures, $k_2[O_3] \gg k_3k_6[CCl_2CH_2]/k_4[O_3]$. Then eq. 11 reduces to

$$[12] \quad -d[O_3]/dt = k_1k_3[CCl_2CH_2]^2/k_2$$

For these conditions, *i.e.* $[O_3] \sim 1.0$ Torr, $[CCl_2CH_2] < 10$ Torr, the rate is higher than predicted by eq. 11 and does not follow the same rate law. At the cross over point $k_2[O_3] = k_3k_6[CCl_2CH_2]/k_4[O_3]$, so that $k_2 \sim 1.9 \times 10^5\ k_3k_6/k_4\ M^{-1}$.

For all conditions of the reaction, the mechanism predicts $d[CCl_2CH_2]/d[O_3] = 1 + 2\ k_{4a}/k_4$ and $-d[CCl_2O]/d[O_3] = k_{4b}/k_4$. The results are consistent with values of $k_{4a}/k_4 = 0.6$ and $k_{4b}/k_4 = 0.4$.

For the kinetic runs in the presence of excess O_2, $k_{5b}[O_2] \gg k_6$, $k_5[O_2] \gg k_4[O_3] + k_6$, and $k_2[O_3] \ll k_{5b}k_3[CCl_2CH_2]/k_5$. Then the mechanism predicts

$$[13] \quad d[CCl_2O]/dt = -d[O_3]/dt = 2k_1[CCl_2CH_2][O_3]$$

Thus $k_1 = k'/2 = 1.1\ M^{-1}\ s^{-1}$. Furthermore $d[CCl_2CH_2]/d[O_3] = 1 + k_{5a}/k_{5b} = 5$, so that $k_{5a}/k_{5b} \sim 4$.

From the values of k_1k_4/k_6 and k_1, the value of k_4/k_6 is computed to be $2.1 \times 10^6\ M^{-1}$. All the rate coefficient ratios obtained in this study are summarized in Table 4.

Finally it is pointed out that if $[CCl_2CH_2]_0/$

TABLE 4. Rate constant ratios

Ratio	Value	Units
k_1k_4/k_6	2.4×10^6	$M^{-2}\ s^{-1}$
k_{4a}/k_4	0.6	None
k_{4b}/k_4	0.4	None
k_2k_4/k_3k_6	$\sim 1.9 \times 10^5$	M^{-1}
k_1	1.1	$M^{-1}\ s^{-1}$
k_{5a}/k_{5b}	4	None
k_4/k_6	2.1×10^6	M^{-1}

$[O_3]_0$ is sufficiently small, as it is in some of the product studies, CCl_2CH_2 will be consumed sufficiently rapidly so that reaction 2 can compete with reaction 3. Then, in the limiting case, $d[CCl_2O]/dt = -d[CCl_2CH_2]/dt = -(1/3)d[O_3]/dt$. Such a limit is being approached in the first entry in the presence of O_2 in Table 3.

A comparison of our results in the absence of excess O_2 to those obtained in CCl_4 solution (7) show marked differences. The gas-phase rate law is second order in $[O_3]$, whereas the liquid phase results are first order in $[O_3]$. A chain mechanism must be involved in the gas phase, since the addition of excess O_2 reduces the rate and gives a second order rate coefficient.

This work was supported by the Office of Air Programs of the Environmental Protection Agency under Grant No. R-800949 for which we are grateful.

1. T. VRBASKI and R. J. CVETANOVIĆ. Can. J. Chem. **38**, 1053 (1960).
2. T. VRBASKI and R. J. CVETANOVIĆ. Can. J. Chem. **38**, 1063 (1960).
3. Y. K. WEI and R. J. CVETANOVIĆ. Can. J. Chem. **41**, 913 (1963).
4. J. J. BUFALINI and A. P. ALTSHULLER. Can. J. Chem. **43**, 2243 (1965).
5. W. B. DEMORE. Int. J. Chem. Kinet. **1**, 209 (1969).
6. J. HEICKLEN. Adv. Photochem. **7**, 57 (1969).
7. D. G. WILLIAMSON and R. J. CVETANOVIĆ. J. Am. Chem. Soc. **90**, 4248 (1968).
8. I. C. HISATSUNE and L. ZAFONTE. J. Phys. Chem. **73**, 2980 (1969).
9. H. M. WHITE and P. S. BAILEY. J. Org. Chem. **30**, 3037 (1965).
10. R. E. ERICKSON, D. BAKALIK, C. RICHARDS, M. SCANLON, and G. HUDDLESTON. J. Org. Chem. **31**, 461 (1966).

Can. J. Chem. Downloaded from www.nrcresearchpress.com by 210.87.254.6 on 09/05/12
For personal use only.

Chemistry of Metal Hydrides. XIV. Insertion Reactions of an Iridium(III) Hydride

H. C. CLARK AND R. K. MITTAL

Department of Chemistry, University of Western Ontario, London, Ontario

Received November 27, 1972

The iridium(III) hydride, $IrHCl_2\{P(C_2H_5)_3\}_3$, gave 1:1 insertion products with perfluoropropene and 3,3,3-trifluoropropyne containing two and three phosphines per iridium respectively. With tetrafluoroethylene, or 1,1-difluoroethylene a simple fluorine – hydridic hydrogen exchange reaction appears to occur. An unusual tricyanovinylic derivative is obtained as a major product of the reaction with tetracyanoethylene, while dimethylacetylene dicarboxylate gave an interesting product containing two acetylene molecules per molecule of hydride. This is formulated as the π-acetylenic complex of the vinylic insertion product. The importance of ligand dissociation in these insertion processes is discussed.

L'hydrure d'iridium(III), $IrHCl_2\{P(C_2H_5)_3\}_3$, a donné avec le perfluoropropène et le trifluoro-3,3,3 propyne un produit d'insertion 1:1 contenant deux et trois groupes phosphines par iridium respectivement. Avec le tétrafluoroéthylène ou avec le difluoro-1,1 éthylène une simple réaction d'échange entre l'hydrogène de l'hydrure et un fluor a semblé se produire. Comme produit majeur de la réaction avec le tétracyanoéthylène, on a obtenu un dérivé tricyanovinylique inhabituel alors que le diméthylacétylène dicarboxylate a donné un produit intéressant contenant deux molécules d'acétylènes par molécules d'hydrure. Ce fait a été formulé comme étant le complexe π-acétylènique du produit d'insertion vinylique. L'importance de la dissociation du coordinat dans ces processus d'insertion est discutée.

[Traduit par le journal]

Can. J. Chem., 51, 1511 (1973)

Introduction

The insertion of unsaturated compounds into transition metal – hydrogen bonds has been widely studied, particularly for square planar d^8 complexes (1, 2) and for metal carbonyl hydrides (3, 4). The mechanism is thought to involve a π-complex as intermediate followed by insertion into the M—H bond, this being a reversible process in some cases (1). Such a process requires either a vacant coordination site on the transition metal for facile formation of the transition state or alternatively at least one labile ligand, exchange of which can facilitate π-complex formation by the unsaturated reactant. In most studies to date, one or other of these requirements has been met, and it seemed desirable to examine the insertion reactions of a hydride with less favorable characteristics.

Iridium(III) forms a large number of stable hydrido complexes in which the neutral ligands are usually tertiary phosphines, arsines, or stibines. These are essentially octahedral in geometry, and so do not contain a coordination site that can be regarded as "vacant"; moreover, iridium(III) complexes with this d^6 configuration are inert towards substitution reactions, so that facile ligand exchange reactions are unlikely to occur. We have therefore examined the behavior of $IrHCl_2\{P(C_2H_5)_3\}_3$ towards a variety of olefins and acetylenes. Here we report on reactions with some fluorinated olefins and acetylenes, these being employed since their insertion reactions with transition metal hydrides are usually not reversible (4, 5) and the products of insertion frequently have considerable stability. We have also investigated some similar reactions with cyanoolefins and with dimethylacetylene dicarboxylate.

Experimental

Standard high vacuum techniques were used throughout. Infrared spectra were recorded on a Beckman IR-10 spectrometer. ^1H and ^{19}F n.m.r. spectra were recorded on a Varian HA-100 spectrometer; chemical shifts are given in p.p.m. relative to TMS or $CFCl_3$ as internal standard. Microanalyses were carried out by Schwarzkopf Microanalytical Laboratory, New York. All reactions with fluoro-olefins were performed in a stainless steel autoclave, and all others in thick-walled Pyrex glass tubes.

Tetrafluoroethylene was obtained from dibromotetrafluoroethane (6) and trifluoropropyne by the method of Finnegan and Norris (7). Other fluoro-olefins and perfluorobut-2-yne were obtained commercially and used without further purification. All solvents were of spectroscopic grade and were dried by standard methods. Tetracyanoethylene, fumaronitrile, acrylonitrile, and cinnamonitrile were all obtained commercially; liquids were purified by distillation and solids by crystallization before use. The starting material $IrHCl_2\{P(C_2H_5)_3\}_3$, **1**, was prepared by the method of Chatt and Shaw (8).

Can. J. Chem. Downloaded from www.nrcresearchpress.com by 210.87.254.40 on 09/05/12
For personal use only.

Can. J. Chem. Downloaded from www.nrcresearchpress.com by 210.87.254.40 on 09/05/12
For personal use only.

In the reactions described below, the following procedure was employed to separate and purify reaction products chromatographically. The reaction mixture was eluted through a small column of silica gel using *n*-hexane, or *n*-hexane-benzene mixtures, in which the products described below were soluble. Purification was usually attempted by crystallization from *n*-hexane–benzene mixtures, but in a number of cases complete separation of products from fluorocarbon oligomers was impossible (see Discussion).

Reaction with Tetrafluoroethylene

This reaction was performed several times in different solvents (cyclohexane, pentane, toluene), at different temperatures (60–120°) and for different reaction times (6–60 h), using Pyrex glass reaction tubes or a stainless steel autoclave. Since all reactions gave similar results, a typical procedure is described. Tetrafluoroethylene (0.44 g, 4.4 mmol) with **1** (0.618 g, 1.0 mmol) was heated in toluene (10 ml) at 100° for 10 h. Removal of solvent left a yellow viscous material which was purified chromatographically. The product then gave an infrared spectrum which displayed no Ir—H stretching absorption (2000–2200 cm^{-1}) but did show absorptions assignable to C—F stretching (1000–1300 cm^{-1}). However, on standing for a few hours this viscous material slowly gave a white crystalline solid, insoluble in benzene, which showed no C—F stretching absorption. From the remaining liquid, a yellow crystalline solid was finally obtained after recrystallizations from benzene–*n*-hexane mixtures. The infrared spectrum of this material also indicated the absence of fluorocarbon groups. Analytical results suggested, but did not clearly establish, that these products were isomers of $IrFCl_2\{P(C_2H_5)_3\}_3$.

Reaction with 1,1-Difluoroethylene

1,1-Difluoroethylene (0.26 g, 4.0 mmol) and **1** (0.618 g, 1.0 mmol) were heated in toluene (10 ml) for 10 h at 100° in the autoclave. Removal of solvent gave a viscous yellow oil, purification of which was attempted chromatographically. The infrared spectrum of the resulting yellow oil showed absorption in the C—F stretching region and the Ir—H stretching absorption was no longer present. On standing for a few hours, a white crystalline solid was deposited and this was washed with benzene. Evaporation of the benzene solution followed by recrystallization from a benzene–*n*-hexane mixture gave a yellow solid whose composition was identical with that of the white material which separated first. Both the white and yellow solids were the same as those obtained in the reactions with C_2F_4.

Reaction with Trifluoroethylene

Trifluoroethylene (0.33 g, 4.0 mmol) and **1** (0.62 g, 1.0 mmol) were heated with toluene (10 ml) in the autoclave for 10 h at 100°. Evaporation of the solvent, followed by chromatographic separation and recrystallization from *n*-hexane–benzene gave a yellow crystalline product. Analytical and spectroscopic results (see Discussion) suggested that this was $IrCl_2(C_2F_3H_2)\{P(C_2H_5)_3\}_3$ contaminated with fluorocarbon polymer.

Reaction with Perfluoropropene

Perfluoropropene (0.60 g, 4 mmol) and **1** (0.62 g, 1 mmol) were heated in toluene (10 ml) at 100° for 10 h. Removal of solvent gave a yellow oil, which was purified chromatographically to give, on crystallization from benzene–*n*-hexane, a yellow crystalline product (0.06 g). This showed no absorption in the infrared spectrum associated with the Ir—H group, but did show strong C—F absorption.

Anal. Calcd. for $IrCl_2F_6P_2C_{15}H_{31}$: C, 27.69; H, 4.80; F, 17.61; P, 9.52. Found: C, 27.25; H, 4.72; F, 17.30; P, 9.81. M.p. 100–101.

Reaction with 1,1,1-Trifluoropropyne

The propyne (0.38 g, 4.0 mmol) and **1** (0.62 g, 1.0 mmol) were heated in dichloromethane in a sealed glass tube at 60° for 2 h. A yellow oil was obtained which was purified chromatographically, and then recrystallized from benzene–*n*-hexane. The yellow crystals so obtained (0.125 g) showed infrared absorption bands due to ν(C—F) and ν(C=C) but not to ν(Ir—H).

Anal. Calcd. for $IrCl_2F_3P_3C_{21}H_{47}$: C, 35.39; H, 6.64; F, 8.00; P, 13.03. Found: C, 34.97; H, 6.52; F, 8.11; P, 13.13. M.p. 120–122.

Reaction with Perfluorobut-2-yne

Perfluorobut-2-yne (0.65 g, 4.0 mmol) and **1** (0.62 g, 1.0 mmol) underwent complete reaction in dichloromethane (10 ml) in 2 h at 60°; the solution changed in color from yellow to red. Removal of solvent gave a red oil which was purified chromatographically to give an orange solid (0.06 g). The infrared spectrum showed no absorption due to Ir—H but an intense absorption at 1550 cm^{-1} ν(C=C) and absorption in the 1000–1200 cm^{-1} region ν(C—F).

Reaction with Tetracyanoethylene

Tetracyanoethylene (0.064 g, 0.5 mmol) and **1** (0.309 g, 0.5 mmol) in 10 ml toluene were heated at 60° for about 2 h during which time the mixture turned dark brown. The solution was decanted off and solvent removed by evaporation to give a brown solid which was purified by dissolving it in ethanol and re-precipitating by addition of methylene dichloride.

Anal. Calcd. for $IrCl_2P_2N_3C_{17}H_{30}$: C, 33.08; H, 5.14; N, 6.97; P, 10.30; Cl, 11.80. Found: C, 33.07; H, 5.44; N, 6.55; P, 10.40; Cl, 11.56.

Reaction with Fumaronitrile

The complex **1** (0.309 g, 0.5 mmol) and fumaronitrile (0.039 g, 0.5 mmol) were heated in toluene (10 ml) at 60° for 4 h with stirring. The solution turned deep violet. The solution was decanted off any solid and the solvent evaporated, to leave a brown compound which was then reprecipitated from a dichloromethane – diethyl ether mixture.

Reaction with $CH_3COOC{\equiv}CCOOCH_3$

The complex **1** (0.62 g, 1.0 mmol) and the acetylene (1 mmol) were heated in toluene for 4 h at 100°. After decantation from a small amount of residue, the solvent was evaporated off, and the solid recrystallized from a dichloromethane – diethyl ether mixture.

Anal. Calcd. for $IrCl_2O_8P_2C_{24}H_{43}$: C, 36.70; H, 5.40; P, 7.80; Cl, 9.00. Found: C, 37.03; H, 5.51; P, 7.84; Cl, 8.80.

Results and Discussion

The iridium(III) hydride, $IrHCl_2\{P(C_2H_5)_3\}_3$, **1**, exists in several isomeric forms; the yellow isomer used here has *trans* choride ligands, and

Can. J. Chem. Downloaded from www.nrcresearchpress.com by 210.87.254.40 on 09/05/12
For personal use only.

hydridic hydrogen *trans* to phosphine. It is not surprising, therefore, that many of its reactions with olefins and acetylenes proceed slowly and give low yields of products.

The reaction of **1** with tetrafluoroethylene was examined under a variety of conditions, but in no case was a fluorocarbon product identified. The only new compound, formed in an impure state, appeared to be a fluorodichloride of iridium(III) which apparently exists in white and yellow isomeric forms. The same product was also obtained from the reaction of **1** with 1,1-difluoroethylene. These simple fluorine – hydridic hydrogen exchange reactions, presumably also leading to trifluoroethylene and ethylene from tetrafluoroethylene and 1,1-difluoroethylene, respectively, perhaps involve formation and decomposition of iridium fluoroalkyl derivatives. Similar exchanges have been observed in reactions of fluoro-olefins with organo-tin hydrides (9).

With trifluoroethylene, at 100°, **1** gave a yellow crystalline product which showed no $\nu_{(Ir-H)}$ stretching absorption in the infrared spectrum at 2100–2250 cm^{-1}, but did show strong C—F absorptions in the 950–1300 cm^{-1} region. Together with the analytical data which showed a very high fluorine content, these results suggest that the product is $IrCl_2(C_2F_3H_2)\{P(C_2H_5)_3\}_3$ contaminated possibly with fluorocarbon polymer. Nor did the ^{19}F n.m.r. spectrum provide definitive structural information.

The compound obtained from **1** and perfluoropropene, after reaction at 100°, had a composition corresponding to a bis(phosphine) product incorporating one unit of the olefin, *i.e.* for $IrCl_2(C_3F_6H)\{P(C_2H_5)_3\}_2$. Again the infrared spectrum showed the loss of Ir—H stretching absorption as well as the appearance of strong absorptions at 950–1300 cm^{-1} associated with fluorocarbon groupings. Unfortunately, the ^{19}F n.m.r. spectrum could not be completely resolved because of low solubility problems, but two resonances were observed at 67.5 and 100 p.p.m., each consisting of a 1:2:1 triplet in which each line was split into a doublet. However, the resonance at 100 p.p.m. was very broad and clearly contained additional unresolved couplings. If the molecule was trigonal bipyramidal with axial phosphines, then assuming that the signal from the single fluorine nucleus is too weak to be resolved, these observations still do not distinguish clearly between an $IrCF(CF_3)CF_2H$ and an $IrCF_2CFH(CF_3)$ structure. The resonance at 67.5 p.p.m. showed couplings of 10 Hz (splitting into 1:2:1 triplet) and 3 Hz (each component split to doublet), consistent with couplings of the CF_3 fluorine nuclei to two equivalent phosphorus nuclei and to the α-fluorine nucleus of an $IrCF(CF_3)CF_2H$ group. The 100 p.p.m. resonance might then arise from a terminal $—CF_2H$ group attached to an asymmetric α-carbon atom, so that the two fluorines are inequivalent. A coupling between these two fluorines of 136 Hz and a further coupling F—H of approximately 30 Hz would be consistent with the observed spectrum. However, no other case has been reported for the formation of an $MCF(CF_3)CF_2H$ group from perfluoropropene and a metal hydride, and further spectroscopic data are needed to confirm this.

The reaction of **1** with trifluoropropyne $CF_3C{\equiv}CH$, was much cleaner and gave a product readily identified by analysis as $IrCl_2\{P(C_2H_5)_3\}_3CH{=}CHCF_3$, thus showing the retention of three phosphines per molecule. The infrared spectrum showed the loss of Ir—H due to the disappearance of the 2110 cm^{-1} band; also, a strong sharp band is observed at 1595 cm^{-1} characteristic of $\nu_{(C=C)}$, while intense absorptions at 1100 and 1035 cm^{-1} are characteristic of a single CF_3 group, although shifted some 40 cm^{-1} to frequencies lower than those usually observed (see, for example, ref. 10). The ^{19}F n.m.r. spectrum consists just of a sharp singlet at 62.4 p.p.m., while the proton spectrum in addition to the expected resonances of the phosphine protons shows two signals at lower field, at $\delta = -8.2$ p.p.m. consisting of a sharp doublet with a splitting of 18 Hz, and a more complex signal at $\delta = -6.80$ p.p.m. showing a coupling of 18 Hz with further smaller couplings apparent. These data are consistent with a geometry $Ir—CH{=}CHCF_3$ with the hydrogens *trans* to each other with $J(H—H) = 18$ Hz. The complexity of the absorption at $\delta = -6.80$ p.p.m. must be due to the H—H coupling together with further couplings to two *cis* and one *trans* phosphorus nuclei. The fact that the product appears to have exclusively the *trans* geometry about the C=C bond is probably not significant since ready isomerization of such compounds is known to occur.

With perfluorobut-2-yne, reaction of **1** again gave an impure product which probably contained polymerized fluorocarbon as well as an iridium-containing product.

Can. J. Chem. Downloaded from www.nrcresearchpress.com by 210.87.254.40 on 09/05/12
For personal use only.

One of the chief reasons for studying reactions of unsaturated fluorocarbons, such as those described above, lies in the enhanced stability of fluorocarbon – transition metal compounds compared with their hydrocarbon analogues. It is also well-known (11 and references therein, 12) that cyano-olefins form more stable complexes with noble metal compounds than do the analogous hydrocarbons, and this presumably also holds for other olefins and acetylenes containing strongly electron-withdrawing substituents. Thus tetracyanoethylene (TCNE) forms 1:1 adducts with *trans*-$PtHCN(PR_3)_2$ (13) and $IrX(CO)(Ph_3E)_2$ where X = halide, etc., and E = P or As (14). Also, 1:1 adducts of the types $IrCl(CO)L_2$ (acetylene) and $RhCl(CO)L_2$ (acetylene) where L = tertiary phosphine, etc., are readily formed (15) by disubstituted acetylenes containing electron-withdrawing substituents. With the five coordinate iridium(I) hydride, $IrH(CO)(Ph_3P)_3$, TCNE, and related compounds such as cinnamonitrile, fumaric acid, dimethyl maleate, etc., give (11) stable complexes of the type $IrH(CO)(Ph_3P)_2$(olefin), in which the olefin has displaced one of the original three phosphine ligands. Moreover, perfluorobut-2-yne and dimethylacetylene dicarboxylate give complexes containing two units of acetylene per iridium formulated as having structure **2**,

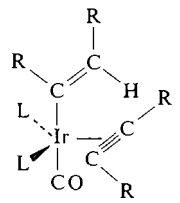

2

in which insertion into the Ir—H bond has occurred, with the other acetylene unit π-bonded to the metal.

With the iridium(III) complex **1**, reaction with tetracyanoethylene occurs fairly readily at 60°, with loss of one phosphine unit. However the product does not contain an Ir—H bond, since neither $\nu_{(Ir-H)}$ nor the Ir—H bending absorption at 880 cm^{-1} is observed in the infrared spectrum, nor is the hydridic resonance observed at high field in the proton n.m.r. spectrum. A strong peak appears in the infrared spectrum at 2200 cm^{-1} and also a broad strong peak at 1600 cm^{-1}. Bearing in mind the analytical data, the product is therefore formulated as $IrCl_2[C_2(CN)_3][P(C_2H_5)_3]_2$, containing a tricyanovinyl group σ-bonded to iridium. Interestingly, a number of tricyanovinylic derivatives have been reported very recently by other workers (16), although not all of them were prepared from tetracyanoethylene; presumably the mechanism leading to this vinyl product involves elimination of HCN from a 1:1 adduct $IrHCl_2[P(C_2H_5)_3]_2$.TCNE. This is very different from the reductive elimination of HX observed, for example, in the reaction of TCNE with *trans*-$PtHX(PR_3)_2$ leading (13) to the formation of $(PR_3)_2Pt$(TCNE).

Although other cyano-olefins such as cinnamonitrile and acrylonitrile (11) are known to form adducts with $IrH(CO)(Ph_3P)_3$ (and indeed acrylonitrile proceeds further to give the insertion product $Ir(CH_2CH_2CN)(CO)(Ph_3P)_2(NCCH{=}CH_2)$), reactions of **1** with a variety of other cyano-olefins were unsuccessful, in that pure products were not obtained. With fumaronitrile, the product had a composition close to that expected for the 1:1 adduct, although the high carbon, hydrogen, and nitrogen contents suggested that some polymeric material was also present. The infrared spectrum showed no $\nu_{(Ir-H)}$ and no $\delta_{(Ir-H)}$ at 880 cm^{-1}. No absorption attributable to C=C was observed although there was an intense band at 2200 cm^{-1} due to $\nu_{(C\equiv N)}$. The proton n.m.r. spectrum showed no high field resonance due to an hydridic hydrogen. It seems likely that insertion of the nitrile C=C bond into Ir—H has occurred, and again it is noticeable that one phosphine molecule has been lost. Neither acrylonitrile nor cinnamonitrile gave identifiable products other than polymeric material.

However, dimethylacetylene dicarboxylate gave a pure crystalline product containing two units of the acetylene per molecule of hydride. Loss of the hydridic hydrogen was apparent from the fact that the infrared spectrum showed no absorption in the 1800–2500 cm^{-1} region, and also that no high field signal was observed in the proton n.m.r. spectrum. The infrared spectrum showed a strong absorption at 1710 cm^{-1} which we assigned to $\nu_{(C\equiv C)}$, lowered in frequency because of coordination to iridium through the triple bond, as well as a strong band at 1535 cm^{-1} assigned to $\nu_{(C=C)}$. The appearance of a medium intensity band at 340 cm^{-1} assigned to $\nu_{(Ir-Cl)}$ is consistent with two *trans* chlorines, rather than with chlorines *trans* to phosphine or

Can. J. Chem. Downloaded from www.nrcresearchpress.com by 210.87.254.40 on 09/05/12
For personal use only.

some other ligand. These data are all consistent with geometry **3** and this is also supported by the proton n.m.r. spectrum.

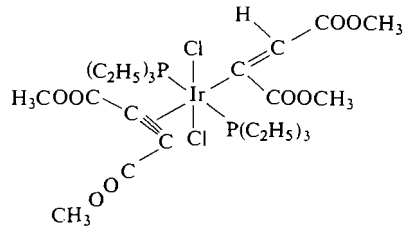

3

The phosphine ethyl protons showed a well-resolved quintet at $\delta = -0.62$ p.p.m. consistent with coupling of the $-CH_3$ protons to methylene protons and to two equivalent *trans* phosphorus nuclei, and also a broad, poorly resolved resonance centered at $\delta = -1.65$ p.p.m. presumably associated with the methylene protons. Additionally, three sharp singlets are observed at $\delta = -3.35$, -3.25, and -3.10 p.p.m., these being in the intensity ratio of 1:2:1. The total integrated intensity of these three resonances with respect to the intensities of the phosphine methylene and $-CH_3$ protons was in the ratio 2:2:3. On the basis of structure **3**, we therefore assign the singlet at -3.25 p.p.m. to the methyl protons of the coordinated acetylene, since the CH_3 groups are equivalent, and the two singlets at -3.35 and -3.10 to the protons of the two methyl groups of the substituted vinylic function.

While the above results are, in general, to be expected, they show several interesting features. In every case in which there is evidence for insertion into the Ir—H bond, with the exception of the reactions with trifluoroethylene and 3,3,3-trifluoropropyne, loss of one phosphine molecule is observed. Not only would such a loss be anticipated as the first step of a reaction with an octahedral complex such as **1**, presumably as an equilibrium

$$IrHCl_2[P(C_2H_5)_3]_3 \rightleftharpoons IrHCl_2[P(C_2H_5)_3]_2 + P(C_2H_5)_3$$

but it is also consistent with the behavior reported by Baddley and Frazer (11) for $IrH(CO)[P(C_6H_5)_3]_3$ with cyano-olefins. In those reactions, displacement of the phosphine by olefin occurs to give hydrido olefin complexes (*e.g.* where the olefin is fumaronitrile) and this is then followed by insertion into Ir—H. For this five coordinate Ir(I) hydride such displacement of phosphine is presumably necessary in order that the effective atomic number of iridium-(I) not be exceeded in the transition state; *i.e.* that the 18-electron configuration not be exceeded.

The fact that the products obtained with 3,3,3-trifluoropropyne and trifluoroethylene contain three phosphines per iridium is difficult to account for. A process consisting of loss of one phosphine, coordination of alkene or alkyne to give a hydrido π-complex, followed by insertion to form the alkyl or vinyl derivative appears possible, but there seems no reason to suppose that for these cases only, this should be followed by recombination of the third phosphine with iridium.

Another point of interest concerns the geometry of the product **3** obtained with dimethylacetylene dicarboxylate. This geometry indicates that the phosphine *trans* to the hydride is lost in the first step, presumably because of the large *trans*-influence of hydride. This may then be followed by coordination of the acetylene in that *trans* position, then by insertion in Ir—H with coordination of the second acetylene unit. Interestingly, this type of mechanism is very similar to that observed (17) for insertion of an olefin into Pt—H in the square planar geometry, *i.e.*, the most important step is displacement of the ligand *trans* to the hydride.

We are grateful for the financial support of this work from the National Research Council of Canada.

1. J. Chatt and B. L. Shaw. J Chem. Soc. 5083 (1962).
2. H. C. Clark and W. S. Tsang. J. Am. Chem. Soc. **89**, 529 (1967).
3. R. F. Heck and D. S. Breslow. J. Am. Chem. Soc. **83**, 4023 (1961).
4. P. M. Treichel, E. Pitcher, and F. G. A. Stone. Inorg. Chem. **1**, 511 (1962).
5. J. B. Wilford and F. G. A. Stone. J. Chem. Soc. 6519 (1965).
6. E. G. Locke, W. R. Brode, and A. L. Henne. J. Am. Chem. Soc. **56**, 1726 (1934).
7. W. G. Finnegan and W. P. Norris. J. Org. Chem. **28**, 1139 (1963).
8. J. Chatt and B. L. Shaw. Chem. Ind. (London), 931 (1961).
9. H. C. Clark, S. G. Furnival, and J. T. Kwon. Can. J. Chem. **41**, 2889 (1963).
10. P. M. Treichel and F. G. A. Stone. *In* Advances in organometallic chemistry. Vol. 1. *Edited by* F. G. A. Stone and R. West. Academic Press, New York, 1964, p. 206.

11. W. H. BADDLEY and M. S. FRASER. J. Am. Chem. Soc. **91**, 3661 (1969).
12. H. C. CLARK and R. J. PUDDEPHATT. Inorg. Chem. **10**, 416 (1971).
13. P. UGUAGLIATTI and W. H. BADDLEY. J. Am. Chem. Soc. **90**, 5446 (1968).
14. W. H. BADDLEY. J. Am. Chem. Soc. **90**, 3705 (1968).
15. J. P. COLLMAN and J. W. KANG. J. Am. Chem. Soc. **89**, 844 (1967).
16. R. B. KING and M. S. SARAN. J. Am. Chem. Soc. **94**, 1784 (1972).
17. H. C. CLARK and H. KUROSAWA. Inorg. Chem. **11**, 1275 (1972).

Can. J. Chem. Downloaded from www.nrcresearchpress.com by 210.87.254.40 on 09/05/12
For personal use only.

Quenching and Trapping of Lyman-α Fluorescence at Large Optical Depths

LEON FRANCIS PHILLIPS

Chemistry Department, University of Canterbury, Christchurch, New Zealand

Received December 18, 1972

Trapping times for 121.6 nm hydrogen resonance radiation in atomic hydrogen gas have been determined by a phase shift method. Rate constants for quenching of H atoms in the $n = 2$ level have been calculated from the measured trapping times together with the slopes of Stern–Volmer plots obtained under steady-state conditions. The results indicated that the trapping times characteristic of fluorescence decay, and of steady-state fluorescence, differed by less than a factor of two. For quenching by O_2, Ar, and He, the values of quenching cross sections obtained (all $\times 10^{-16}$ cm^2) were 30 ± 8, 0.9 ± 0.4, and 0.4 ± 0.2, respectively.

Les temps de piégeage de la radiation de résonance de l'hydrogène à 121.6 nm dans l'hydrogène atomique gazeux, ont été déterminés par la méthode du changement de phase. Les constantes de vitesse d'extinction des atomes H au niveau $n = 2$ ont été calculées à partir des temps de piégeage mesurés et des pentes des courbes de Stern Volmer obtenues à l'état stationnaire. Les résultats indiquent que les temps de captage caractéristiques de la décroissance de fluorescence et de la fluorescence à l'état stationnaire, diffèrent d'un facteur de deux au plus. Dans l'extinction par O_2, Ar, et He, les valeurs obtenues pour des sections droites d'extinction (toutes $\times 10^{-16}$ cm^2) sont respectivement de 30 ± 8, 0.9 ± 0.4 et 0.4 ± 0.2.

[Traduit par le journal]

Can. J. Chem., **51**, 1517 (1973)

Can. J. Chem. Downloaded from www.nrcresearchpress.com by 210.87.254.5 on 09/05/12
For personal use only.

Trapping of resonance radiation by gaseous atoms has been the subject of a number of theoretical and experimental investigations (1–5). For the purpose of the present study the most important conclusions to be drawn from this work are that in the presence of trapping the observed decay of the resonance radiation remains exponential (2, 5) and that when trapping is significant the usual Stern–Volmer expression for fluorescence quenching

$$[1] \qquad I_0/I = \tau_0/\tau = 1 + k\tau_0[Q]$$

has to be replaced by

$$[2] \qquad I_0/I = T_0/T = 1 + kT_0[Q]$$

Here I_0 and I are the fluorescent intensity in the absence of quencher, and in the presence of a quencher whose concentration is [Q], respectively, the lifetimes τ_0 and τ are reciprocals of the observed first order rate constant for decay of fluorescence in the absence and in the presence of quencher, and k is the rate constant of the quenching reaction. When trapping occurs the natural lifetime of the excited state, τ_0, must be replaced by a trapping time T_0, and τ must similarly be replaced by T. The ratio of T_0 to τ_0 may be regarded as a particular kind of average of the number of times a primary emitted photon is reabsorbed and re-emitted before it escapes from the front of the fluorescence cell, and depends on the geometry of the system as well as on the density of absorbers in the cell.

Provided the decay of fluorescence with time t follows a single exponential of the form $\exp(-t/T)$, the use of a modulated exciting beam allows the trapping time T to be determined from the phase-shift δ between the exciting radiation and the fluorescence, by means of the formula

$$[3] \qquad \tan \delta = 2\pi fT$$

where f is the modulation frequency (6). Thus it is possible, in principle, to determine both k and T_0 by measuring the phase and amplitude of a modulated fluorescence signal as a function of [Q]. The calculations of Van Volkenburgh and Carrington (4) have shown that for systems of low or intermediate optical depth the decay of fluorescence does not in general correspond to a single exponential except at long decay times. However, their results appear to indicate that the decay approaches more closely to a single exponential at larger optical depths, so that in such circumstances the phase-shift method should still be applicable to the determination of T_0. A more serious complication is that their calculations also lead to a difference between the trapping time characteristic of the lowest fluorescence decay mode, T_0', and the value T_0 characteristic of a steady-state experiment in which I_0/I is measured. For the case of an infinite slab, with

observation of the face of the slab away from the lamp, T_0' is smaller than T_0, so that rate constants k evaluated on the assumption that $T_0' = T_0$ will be too large. For an experimental system in which observations are made at right angles to the incident beam, the relationship between T_0' and T_0 is expected to depend on the geometry of the particular experiment. For experiments reported here it appears that T_0' is greater than T_0, but the difference is less than a factor of two.

A diagram of the apparatus is given in Fig. 1. Apart from the provision for introducing a steady stream of atoms from a microwave discharge, it is the same as that used in several previous studies (7, 8). The modulating signal (10–100 kHz) for the microwave-powered hydrogen–argon lamp was derived from a Hewlett–Packard audio-frequency oscillator. The reference signal for a PAR model HR-8 lock-in amplifier was obtained from an EMI 9603B particle multiplier which observed the direct radiation transmitted by the cell. The reference signal frequency was monitored with a digital frequency meter. Cell windows (diameter 25 mm) were of magnesium fluoride. The 121.6 nm fluorescence emitted at right angles to the exciting beam was isolated with a McPherson model 218 vacuum monochromator, and detected with an EMR 541G photomultiplier. Gas flows were monitored by calibrated ball-type flowmeters; the pressure in the viewing region was measured with a Texas Instruments quartz spiral gauge. The experiments were performed at room temperature (299 ± 2 K). Hydrogen atoms were produced by discharging a mixture of helium or argon with 1–3% of hydrogen at pressures between 1.5 and 5 Torr. Under the fast-flow conditions which existed in these experiments the H_2 could be expected to be more than 50% dissociated in the viewing region. DC measurements of the Lyman-α signal, using a Keithley picoammeter, showed that trapped radiation from the atom-producing discharge entered the monochromator with almost the same intensity as the fluorescence excited by the lamp, despite the presence of a light trap and two right-angle bends between discharge and cell. The modulation system normally prevented this radiation from contributing to the measured fluorescence.

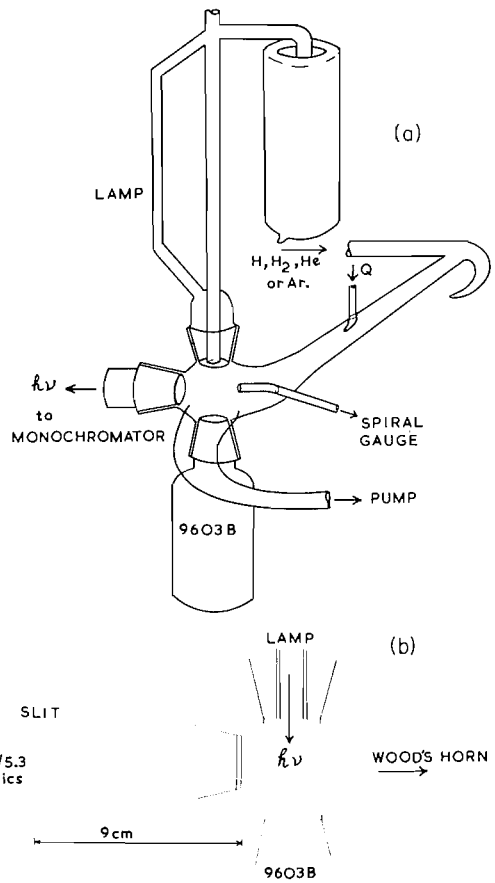

FIG. 1. (*a*) Experimental system. Magnesium fluoride windows are fastened to the glass standard-taper joints with epoxy cement. The taper joints are held together with vacuum wax. (*b*) Geometry of fluorescence cell.

Some representative Stern–Volmer plots for I_0/I, with quenching by O_2, are shown in Fig. 2. These results effectively correspond to steady-state fluorescence, since the measured phase shifts at 75 kHz and 100 kHz were all small (see Fig. 3). Values of the quenching rate constant k can be calculated from the slopes of the lines in Fig. 2 once T_0 is known. To determine T_0' the phase angle φ of the Lyman-α signal was measured, relative to an arbitrary zero phase, as a function of O_2 pressure, and a quantity Δφ was evaluated as the difference between the phase angles observed with and without quencher. If δ_0 is the phase angle corresponding to the trapping time T_0', in terms of eq. 3, then the phase angle corresponding to T' (*i.e.* in the presence of quencher) is given by

$$\delta = \delta_0 - \Delta\varphi \qquad [4]$$

According to eq. 2, and assuming $T_0 \sim T_0'$, we can write

$$\tan \delta_0/\tan (\delta_0 - \Delta\varphi) = 1 + kT_0[Q] \qquad [5]$$

Can. J. Chem. Downloaded from www.nrcresearchpress.com by 210.87.254.5 on 09/05/12
For personal use only.

Can. J. Chem. Downloaded from www.nrcresearchpress.com by 210.87.254.5 on 09/05/12
For personal use only.

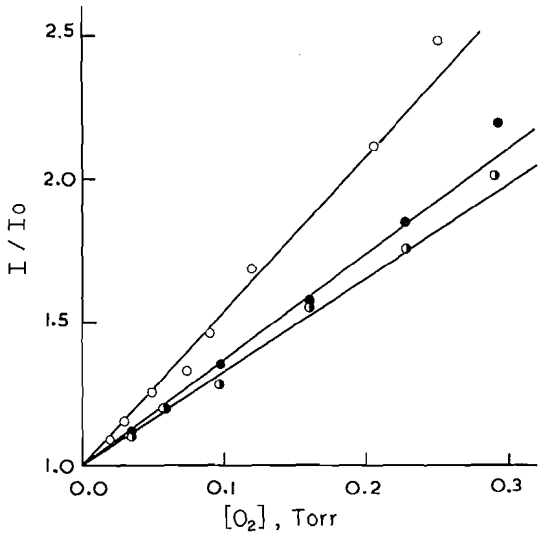

FIG. 2. Stern–Volmer plots for quenching by O_2: ○, He = 1.76 Torr, H_2 + ½H = 0.05 Torr, f = 100 kHz; ●, Ar = 2.22 Torr, H_2 + ½H = 0.06 Torr, f = 75 kHz; ◑, Ar = 3.08 Torr, H_2 + ½H = 0.08 Torr, f = 75 kHz.

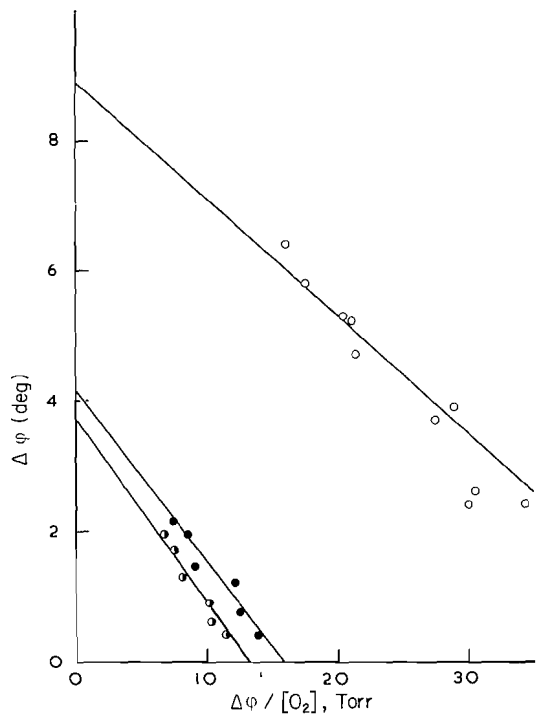

FIG. 3. Test of eq. 6 for experimental data of Fig. 2. ○, 100 kHz, $T_0 = 2.49 \times 10^{-7}$ s; ●, 75 kHz, $T_0 = 1.52 \times 10^{-7}$ s; ◑, 75 kHz, $T_0 = 1.37 \times 10^{-7}$ s.

which for small values of δ_0 reduces to

$$[6] \qquad \delta_0/(\delta_0 - \Delta\varphi) = 1 + kT_0[Q]$$

This can be rearranged to

$$[7] \qquad \Delta\varphi = \delta_0 - \Delta\varphi/(kT_0[Q])$$

Thus a graph of $\Delta\varphi$ *vs.* $\Delta\varphi/[Q]$ should be a straight line of slope $-1/kT_0$. Examples of the use of this result to determine δ_0 are shown in Fig. 3. In each case a line of the required slope (*i.e.* having slope equal to the reciprocal of the slope of the corresponding line in Fig. 2) was drawn to give the best fit with the observed points, and δ_0 was obtained from the intercept at $\Delta\varphi/[O_2] = 0$. Observed trapping times T_0 ranged from 0.8 to 2.5×10^{-7} s (the natural lifetime τ_0 is 1.6×10^{-9} s). At any given pressure the trapping time was longer when the carrier gas was helium than when it was argon. The reasonable fit of the experimental points to the lines of slope $1/kT_0$ in Fig. 3 indicates that T_0 and T_0' are not greatly different from one another. Resulting values of the quenching rate constant k, and corresponding cross-section σ (equal to k divided by $(8RT/\pi\mu)^{\frac{1}{2}}$), are given in Table 1. For argon and helium the

TABLE 1. Rate constants k (cm^3 $molecule^{-1}$ s^{-1}) and cross sections $\sigma(cm^2)$ for quenching of Lyman-α fluorescence

Quencher	$10^{11}k$	$10^{16}\sigma$
O_2	78 ± 20	30 ± 8
Ar	2.3 ± 1.0	0.9 ± 0.4
He	1.2 ± 0.6	0.4 ± 0.2

cross sections were obtained from Stern–Volmer plots for I_0/I (rather than T_0/T) using T_0 values derived from O_2 quenching measurements. The ratio of cross sections for O_2 and Ar is significantly different from the ratio of ~5 obtained previously (10). This demonstrates that the use of relative slopes of Stern–Volmer plots for I_0/I to determine relative quenching cross sections is not a reliable procedure at large optical depths. For all of these quenchers their absorption of Lyman-α radiation could be neglected. Under the conditions of these experiments the 2^2P and 2^2S levels are interconverted very rapidly, so that the rate constants refer to an equilibrium mixture of the two levels. The limits of error shown in Table 1 derive from uncertainties associated with the slopes of Stern–Volmer plots such as those in

Fig. 2, and with the δ_0 values obtained by extrapolation as in Fig. 3. These limits also give an indication of the scatter of the experimental results.

Rate constants for quenching of Lyman-α fluorescence which were previously reported from this laboratory (10) were based on theoretically estimated trapping times, and were found to be anomalously small. Braun and co-workers (11) pointed out that this was due to our having made insufficient allowance for quenching by undissociated H_2, which must have greatly reduced the trapping time from the value T_0. Braun *et al.* measured the quenching of Lyman-α fluorescence in an optically thin system, and used the natural lifetime of the ^2P level to convert the slopes of Stern–Volmer plots into rate constants. The values so obtained were very large; the reported cross sections of 84 and 62 $\times$ 10^{-16} cm^2 for H_2 and N_2, respectively, correspond to rate constant values of 2.5 $\times$ 10^{-9} and 3.6 $\times$ 10^{-9} cm^3 $molecule^{-1}$ s^{-1}, comparable in magnitude with the rates of fast ion–molecule reactions. However, similarly large values have been reported for quenching of the metastable 2^2S level (12–14). In comparison, the present results appear to be low, since O_2 is probably a more efficient quencher than H_2 or N_2 (10). If the Lyman-α emission observed by Braun and coworkers was derived partly from $H(^2S)$, as a result of electrical or other perturbations causing the transition to $H(^2P)$, the effective lifetime could have been significantly longer than τ_0. However, the difference between T_0 and T_0' is clearly the most likely cause of any discrepancy between their work and the present results. More direct observations of the decay time T_0', not dependent on the assumption of a single decay mode, appear to be required.

This work was supported by the New Zealand Universities Research Committee and by Grant AF-AFOSR-71-2134 from the United States Air Force Office of Scientific Research.

1. T. Holstein. Phys. Rev. **72**, 1212 (1947); **83**, 1159 (1951).
2. D. Alpert, A. O. McCoubrey, and T. Holstein. Phys. Rev. **76**, 1257 (1949).
3. P. J. Walsh. Phys. Rev. **116**, 511 (1959).
4. G. Van Volkenburgh and T. Carrington. J. Quant. Spectrosc. Rad. Trans. **11**, 1181 (1971).
5. G. Copley and L. Krause. Can. J. Phys. **47**, 533 (1969).
6. W. S. Metcalf. J. Chem. Soc. London, 3726 (1960).
7. C. G. Freeman, M. J. McEwan, R. F. C. Claridge, and L. F. Phillips. Chem. Phys. Lett. **10**, 530 (1971).
8. C. G. Freeman and L. F. Phillips. Chem. Phys. Lett. In press.
9. L. F. Phillips. Rev. Sci. Instr. **42**, 1058 (1971).
10. T. S. Wauchop, M. J. McEwan, and L. F. Phillips. J. Chem. Phys. **51**, 4227 (1969).
11. W. Braun, C. Carlone, T. Carrington, G. Van Volkenburgh, and R. A. Young. J. Chem. Phys. **53**, 4244 (1970).
12. W. L. Fite, R. T. Brackman, D. G. Hummer, and R. F. Stebbings. Phys. Rev. **116**, 363 (1959); **124**, 2051 (1961).
13. F. J. Comes and U. Wenning. Chem. Phys. Lett. **5**, 199 (1970); Ber. Bunsenges. **73**, 901 (1969); Z. Naturforsch. **24a**, 587 (1969).
14. J. E. Mentall and E. P. Gentieu. J. Chem. Phys. **52**, 5641 (1970).

Can. J. Chem. Downloaded from www.nrcresearchpress.com by 210.87.254.5 on 09/05/12
For personal use only.

Fluoroalicyclic Derivatives of Cobalt Carbonyl

WILLIAM. R. CULLEN AND A. J. T. JULL

Chemistry Department, University of British Columbia, Vancouver 8, British Columbia

Received December 28, 1972

The compounds $(C_6H_5)_3P(CO)_3CoC{=}CCl(CF_2)_nCF_2$ (n = 2, 3) are obtained by reacting the metal carbonyl anion with the appropriate 1,2-dichloro olefin. Similar compounds are not isolated following treatment of cobalt carbonyls with $XC{=}CXCF_2CF_2$ (X = Cl or I). The new bridged complex $(CH_3)_2AsC{=}C[As(CH_3)_2](CF_2)_3CF_2Co_2(CO)_6$ is described.

Les composés $(C_6H_5)_3P(CO)_3CoC{=}CCl(CF_2)_nCF_2$ (n = 2, 3) ont été obtenus en faisant réagir l'anion du dérivé métal carbonyle avec la dichloro-1,2 oléfine appropriée. Des composés similaires n'ont toutefois pas été isolés lors du traitement de dérivés cobalt carbonyles avec $XC{=}CXCF_2CF_2$ (X = Cl ou I). Le nouveau complexe ponté $(CH_3)_2AsC{=}C[As(CH_3)_2](CF_2)_3CF_2Co_2(CO)_6$ est décrit.

[Traduit par le journal]

Can. J. Chem., **51**, 1521 (1973)

Can. J. Chem. Downloaded from www.nrcresearchpress.com by 210.87.254.6 on 09/05/12
For personal use only.

The ditertiary arsine f_4fars,

$$(CH_3)_2AsC{=}CAs(CH_3)_2CF_2CF_2,$$

has a strong tendency to act as a bridging ligand when treated with metal carbonyls (1) and an example is the complex $f_4farsCo_2(CO)_6$, obtained by reaction with dicobalt octacarbonyl (2). The complex has the structure shown in Fig. 1 (3). When a cyclohexane solution of $f_4farsCo_2(CO)_6$ is warmed, one of the products isolated proved to have the structure shown in Fig. 2 (4) in which two cyclobutane rings have condensed to give the bicyclobutenyl moiety following the cleavage of two As—C bonds. It is possible that the molecule contains two hydrogen atoms, one on each of the two carbonyl bridged cobalt atoms. Cleavage of As—C bonds in complexes of this type is now recognized as not being uncommon (1). However, this is the only instance in which the residual cyclobutene moieties have been found to couple together.

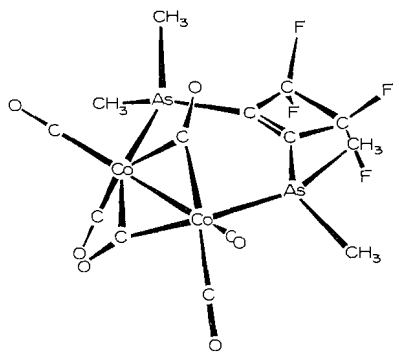

FIG. 1. The structure of $f_4farsCo_2(CO)_6$ (3).

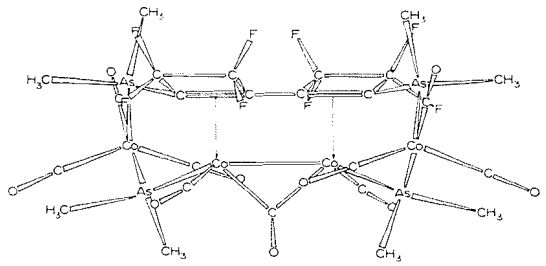

FIG. 2. The structure of $(f_4fars)_2Co_4(CO)_9(2H?)$ (4).

Since metal carbonyls can facilitate the coupling of organic halides with the elimination of metal halides (5) it seemed reasonable to attempt to couple 1,2-dihalotetrafluorocyclobutenes using cobalt carbonyl, since such studies could provide insight into the decomposition of $f_4farsCo_2(CO)_6$.

Park and co-workers (6) have recently synthesized polyhalobicyclobutenyl compounds by coupling reactions using copper bronze.

Experimental

All reactions were carried out under a nitrogen atmosphere. Infrared spectra were recorded on a Perkin–Elmer model 457 spectrophotometer. ^{19}F n.m.r. spectra were obtained using a Varian T-60 instrument, chemical shifts being reported upfield from $CFCl_3$. Mass spectra were recorded on an AEI MS-9 instrument with direct introduction of solid samples. A Mechrolab vapor pressure osmometer was used to obtain solution molecular weights in benzene. Chromatographic separations were carried out using Florisil columns. Microanalyses were performed by P. Borda of this department.

Can. J. Chem. Downloaded from www.nrcresearchpress.com by 210.87.254.6 on 09/05/12
For personal use only.

(1) Reaction of Dicobalt Octacarbonyl with 1,2-Dichlorotetrafluorocyclobutene

(a) Cyclohexane Solution

The carbonyl (2.0 g) and the 1,2-dichlorocyclobutene (1.0 g) were refluxed in cyclohexane (50 ml) for 2 h. A black solid precipitated. The solvent was evaporated and chromatography yielded a small amount of unreacted dicobalt octacarbonyl. The black solid was identified as $Co_4(CO)_{12}$ by means of its infrared spectrum.

(b) Tetrahydrofuran Solution

The carbonyl (3.5 g) and the cyclobutene (2.0 g) were refluxed in 50 ml of THF (3 h). Initial reaction between the solvent and the carbonyl was apparent. Removal of the solvent followed by chromatography gave a very small amount of an orange oil whose infrared spectrum showed bands at 2100(w), 2061(m, sh), 2051(s), 2036(s), 2019(w), 1730(vs), 1600(w), 1580(w), 1380(m), 1270(vs), 1120(s), 1080(s), 1031(m), 1011(m) cm^{-1}. A black band, identified as $Co_4(CO)_{12}$, was also eluted from the column.

(2) Reaction of Dicobalt Octacarbonyl with 1,2-Diiodotetrafluorocyclobutene

The di-iodocyclobutene was prepared following the published procedure by treating the dichloro compound with potassium iodide in dimethylformamide (6). In our hands the method gave a low yield (1.2%) of 1-chloro-2-iodotetrafluorocyclobutene and a 14.5% yield of the di-iodo derivative. The infrared and n.m.r. spectra of the latter compound were as published (6). In addition the mass spectrum showed a parent ion at $m/e = 378$ and intense peaks at 251 and 124 due to loss of iodine.

Dicobalt octacarbonyl (1.0 g) and the di-iodide (1.0 g) were refluxed in 50 ml of THF (3 h). Removal of the solvent yielded a dark solid residue. Extraction of this with cyclohexane gave a small amount of a dark red solid whose mass spectrum showed a peak at $m/e = 622$ and peaks due to the loss of 12 carbonyl groups. The infrared spectrum showed ν(CO) bands at 2087(w), 2061(vs), and 2017(m) cm^{-1}.

The remaining reaction product consisted of $Co_4(CO)_{12}$ (soluble in dichloromethane) and cobalt salts (soluble in acetone).

(3) Preparation of 1-Chlorotetrafluorocyclobuten-2-yltriphenylphosphinetricarbonylcobalt

The sodium salt $NaCo(CO)_3P(C_6H_5)_3$ was prepared by stirring a suspension of 1.5 g of the appropriate dimer in 50 ml of THF over 1% sodium amalgam for 24 h. Excess amalgam was removed in the usual way (7) and 1,2-dichlorotetrafluorocyclobutene (1.0 g) was added. After 2 h the solution was filtered and the solvent removed. Extraction of the residue with ether followed by recrystallization of the residue from petroleum ether/diethyl ether gave 0.82 g (39%) of yellow crystals of 1-chlorotetrafluorocyclobuten-2-yltriphenylphosphinetricarbonylcobalt, m.p. 110–112 °C (dec.).

Anal. Calcd. for $C_{25}H_{15}ClCoF_4O_3P$: C, 53.2; H, 2.66; mol. wt., 564. Found: C, 53.1; H, 2.64; mol. wt. (mass spec.) 564.

^{19}F n.m.r. spectrum: multiplets at 112.0 and 116.0 p.p.m. Infrared spectrum ν(CO): 2078(w), 2009(vs), 2005(vs) cm^{-1}.

In a subsequent preparation of the cyclobutenyl derivative in which the anionic solution was centrifuged to remove suspended mercury prior to addition of the olefin, a total yield of 60.2% was obtained.

(4) Preparation of 1-Chlorohexafluorocyclopenten-2-yltriphenylphosphinetricarbonylcobalt

A THF solution of the sodium salt $NaCo(CO)_3P(C_6H_5)_3$ was prepared as described above and 1,2-dichlorohexafluorocyclopentene (1.0 g) was added. After 2 h the solution was filtered and the solvent removed to leave a dark solid residue. Extraction of this solid with hexane gave a light yellow solution which yielded 0.21 g (9.5%) of light yellow crystals of 1-chlorohexafluorocyclopenten-2-yltriphenylphosphinetricarbonylcobalt, m.p. 100° (dec.) (from petroleum ether/diethyl ether).

Anal. Calcd. for $C_{26}H_{15}ClCoF_6O_3P$: C, 50.8; H, 2.44; mol. wt., 614. Found: C, 52.4; H, 2.90; mol. wt. (osmometer). 590 ± 27.

^{19}F n.m.r. spectrum: multiplets at 101.0, 113.0, 130.6 p.p.m. Infrared spectrum: ν(CO), 2074(w), 2013(vs), 1998(vs) cm^{-1}.

A further 0.19 g (8.4%) of the same compound was obtained by extracting the "hexane insoluble" residue with diethyl ether.

(5) Preparation and Decomposition of $(CH_3)_2AsC{=}C[As(CH_3)_2](CF_2)_3CF_2Co_2(CO)_6$ *[$f_8farsCo_2(CO)_6$]*

The ligand (0.55 g) (8) and dicobalt octacarbonyl (0.40 g) were stirred in 35 ml of hexane at 20 ° (3 h). The solvent was removed and chromatography of the remaining reddish solid gave an orange-brown band which eluted with petroleum ether. On concentration and cooling to −78° this solution gave 0.1 g (14%) of orange-brown crystals of $f_8farsCo_2(CO)_6$, m.p. ~90 ° (dec.).

Anal. Calcd. for $C_{16}H_{12}As_2Co_2F_8O_6$: C, 26.7; H, 1.67; mol. wt., 720. Found: C, 26.4; H, 1.59; mol. wt. (mass spec.), 720.

Infrared spectrum ν(CO): 2059(s), 1997(vs), 1817(w), 1802(m) cm^{-1}.

On warming a solution of $f_8farsCo_2(CO)_6$ (0.08 g) in cyclohexane (15 ml) at 58° the solution turned dark. After 45 min the solvent was evaporated to dryness to give a mixture of white and brown solids. The latter was insoluble in acetone and the former was spectroscopically identified as f_8fars.

Results and Discussion

When 1,2-dichlorotetrafluorocyclobutene is warmed with dicobalt octacarbonyl in a nonbasic solvent the only reaction that is evident is the formation of $Co_4(CO)_{12}$ which is the expected product when the dicobalt species is warmed alone (5). In more basic THF solution where carbonylcobaltates are present as well as $Co_4(CO)_{12}$ (9), reaction with the dichloride yields a small amount of an orange oil which contains Co—CO, C=C, and C—F groups although probably not all associated with one compound. Repetition of the reaction failed to increase yields of the fraction significantly. Since the $[Co(CO)_4]^-$ species was probably present in the initial reaction

Can. J. Chem. Downloaded from www.nrcresearchpress.com by 210.87.254.6 on 09/05/12
For personal use only.

mixture (9) it seemed possible that this could have reacted with the cyclobutene, to give a cyclobutenylcobalt compound (1, 10). Although

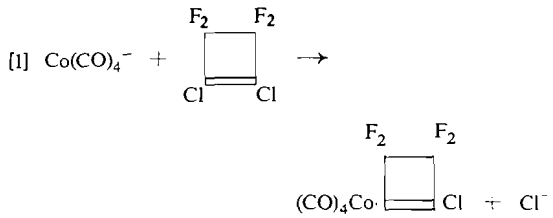

fluoroalicyclic derivatives were known for many elements (1, 11, 12) cobalt complexes had not been isolated so in order to investigate the feasibility of reaction 1 we also studied the reaction of $NaCo(CO)_4$ with 1,2-dichlorotetrafluorocyclobutene, using the deliberately prepared (13) sodium salt. Reaction 1 does not seem to occur, probably because of the low nucleophilicity of the $Co(CO)_4^-$ ion (10, 14). However, when the more nucleophilic triphenylphosphine-containing anion was prepared, reaction proceeded as anticipated, with both 1,2-dichlorotetrafluorocyclobutene and 1,2-dichlorohexafluorocyclopentene (reaction 2).

$$[2]\quad NaCo(CO)_3P(C_6H_5)_3 + ClC{=}CCl(CF_2)_nCF_2 \rightarrow (C_6H_5)_3P(CO)_3CoC{=}CCl(CF_2)_nCF_2 + NaCl \qquad (n = 1, 2)$$

Both new compounds are yellow solids, which is characteristic of simple σ bonded cobalt carbonyl derivatives (15). The cyclopentenyl derivative is not very stable in solution and was not obtained in a pure enough state to give a really satisfactory elemental analysis. However, the carbonyl infrared spectrum of the compound, which is virtually the same as the well characterized cyclobutenyl derivative, and the characteristic ^{19}F n.m.r. spectrum substantiate the formulation (10–12). The mass spectrum of the cyclobutenyl derivative showed a parent ion and peaks due to the progressive loss of three carbonyl groups. The ^{19}F n.m.r. spectrum showed the typical pattern of bands with the expected chemical shifts (10–12). The infrared spectrum is of interest in that it gives a lower limit for the frequencies expected for the product of reaction 1 since triphenylphosphine can be regarded as a poorer π-acceptor than carbon monoxide. A recent relevant example is found in $\pi\text{-}C_5H_5(CO)_2FeC{=}CClCF_2CF_2$ which has ν(CO) at 2056, 2007, and 1997(sh) cm^{-1}. Replacing one carbonyl group by triphenylphosphine lowers the frequencies to 1965(sh), 1961 cm^{-1} (12). Similarly $(CO)_5MnC{=}CF(CF_2)_3CF_2$ has ν(CO) at 2137(w), 2075(vw), 2047(vs), 2020(s) cm^{-1}, the *trans*-triphenylphosphine substituted compound at 2185(w), 2038(w), 1996(s) cm^{-1}, and the *cis*-triphenylphosphine substituted compound at 2088(s), 2015(s), 2010(s), 1970(s) cm^{-1} (16). Thus since the carbonyl infrared frequencies of the orange oil obtained from 1,2-dichlorotetrafluorocyclobutene and cobalt carbonyl in THF solution are only slightly higher than those of the products of reaction 2, 1-chlorotetrafluorocyclobuten-2-yltetracarbonylcobalt (reaction 1) is probably not present.

In an attempt to employ a compound with a better leaving group, 1,2-di-iodotetrafluorocyclobutene was heated with dicobalt octacarbonyl in THF solution. The reaction was difficult to reproduce, but in one attempt a small amount of a dark red solid was isolated whose mass spectrum indicated the formula $CF_2Co_4(CO)_{12}$. Since dicobalt octacarbonyl and tetrafluoroethylene afford the 1:1 "adduct" $(CO)_4CoCF_2CF_2Co(CO)_4$ which on warming decomposes and eventually gives $CF_3CCo_3(CO)_9$ (17, 18), breakdown of the fluorocarbon is not unexpected.

Finally we prepared the complex $f_8farsCo_2(CO)_6$ ($f_8fars = (CH_3)_2AsC{=}CAs(CH_3)_2(CF_2)_3CF_2$) in an attempt to see if the coupling reactions which occur when $f_4farsCo_2(CO)_6$ is warmed, would also occur for this compound. The carbonyl infrared spectrum of the new complex is not like that of the f_4fars derivative. The two bridging carbonyl bands are only 15 cm^{-1} apart, whereas they are 56 cm^{-1} apart in the f_4fars derivative. This is an indication that the structure of $f_8farsCo_2(CO)_6$ is the symmetrically bridged one indicated in **1** (2), where $\widehat{EE}$ represents the ligand,

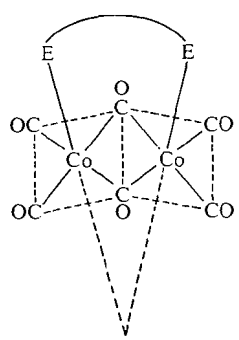

1

and not the asymmetric bridged one of Fig. 1. The symmetrical bridge seems to be favoured by most fluorocarbon-bridged ligands (2, 19). On warming a cyclohexane solution of $f_8farsCo_2(CO)_6$ to 58° slow decomposition took place with liberation of the free ligand.

We thank the National Research Council of Canada for financial assistance.

1. W. R. CULLEN. Adv. Inorg. Chem. Radiochem. **15**, 323 (1972).
2. J. P. CROW and W. R. CULLEN. Inorg. Chem. **10**, 2165 (1971).
3. W. HARRISON and J. TROTTER. J. Chem. Soc. (A), 1542 (1971).
4. F. W. B. EINSTEIN and R. D. G. JONES. J. Chem. Soc. Dalton, 2568 (1972).
5. F. CALDERAZZO, R. ERCOLI, and G. NATTA. *In* Organic syntheses via metal carbonyls. *Edited by* I. Wender and P. Pino. Wiley–Interscience, New York. 1968. p. 1.
6. R. L. SOULEN, B. T. NAKATA, and J. D. PARK. J. Fluorine Chem. **1**, 235 (1971).
7. R. B. KING. Organometallic syntheses. Vol. 1. Academic Press, New York, 1965.
8. L. S. CHIA and W. R. CULLEN. Can. J. Chem. **50**, 1421 (1972).
9. P. CHINI and V. ALBANO. J. Organometal. Chem. **15**, 433 (1968).
10. M. I. BRUCE and F. G. A. STONE. Angew. Chem. Int. Ed. **7**, 747 (1968).
11. W. R. CULLEN. Fluorine Chem. Rev. **4**, 79 (1969).
12. R. B. KING and A. EFRATY. J. Fluorine Chem. **1**, 283 (1971/72).
13. R. B. KING. Advan. Organometal. Chem. **2**, 157 (1964).
14. R. E. DESSY, R. L. POHL, and R. B. KING. J. Am. Chem. Soc. **88**, 5121 (1966).
15. M. I. BRUCE and F. G. A. STONE. *In* Preparative inorganic reactions, Vol. 4. *Edited by* W. L. Jolly. Wiley–Interscience, New York, 1968. p. 177.
16. P. W. JOLLY, M. I. BRUCE, and F. G. A. STONE. J. Chem. Soc. 5830 (1965).
17. A. D. BEVERIDGE and H. C. CLARK. J. Organometal. Chem. **11**, 601 (1968).
18. B. L. BOOTH, R. N. HASZELDINE, P. R. MITCHELL, and J. J. COX. J. Chem. Soc. (A), 691 (1969).
19. L. S. CHIA and W. R. CULLEN. Unpublished results.

Can. J. Chem. Downloaded from www.nrcresearchpress.com by 210.87.254.6 on 09/05/12
For personal use only.

Studies on Hydrogen–Oxygen Systems in the Electrical Discharge. VI. Detection by Laser Raman Spectroscopy of O_2 and O_3 Trapped at 80 °K

JOSÉ L. ARNAU AND PAUL A. GIGUÈRE

Centre de Recherches sur les Atomes et les Molécules, Université Laval, Québec 10, Québec

Received October 20, 1972

Further study by Raman spectroscopy of the condensed products from electrically dissociated water vapor and other related systems has revealed the presence, not only of ozone in appreciable amounts, but also of molecular oxygen in still greater amounts trapped at 80 °K. The concentration of ozone relative to the hydrogen oxides varied somewhat with experimental conditions, and also locally due to some segregation effect in the glassy condensate. The concentration of trapped oxygen showed still wider fluctuations depending particularly on surface effects in the discharge–flow system. On warming up under vacuum the intensity of the O_2 and O_3 bands began to decrease even before the crystallization temperature was reached (about 150 °K), thereby confirming that the gas evolution at that stage is mainly a desorption process. Therefore, the often quoted ratio of total evolved O_2 to residual H_2O_2 could not be a reliable index of the formation of hydrogen polyoxides, H_2O_3 and H_2O_4, in these systems. A mechanism is proposed for the formation *in situ* of the trapped gases and in particular, for a source of oxygen atoms in dissociated water vapor.

The fundamental vibrations of the ozone molecule, $\nu_1 = 1106$, $\nu_2 = 703$, and $\nu_3 = 1036\ cm^{-1}$, were confirmed by polarization and isotope shift measurements.

Continuant l'étude par spectroscopie Raman à laser des produits de la dissociation électrique de la vapeur d'eau et autres systèmes analogues nous avons mis en évidence des quantités appréciables d'ozone, et encore plus d'oxygène moléculaire piégées à environ 80 °K. Les concentrations d'ozone variaient quelque peu avec les conditions expérimentales, et même d'un point à l'autre à cause des effets de ségrégation dans le solide vitreux. Les concentrations d'oxygène piégées variaient encore plus selon l'état des surfaces dans la décharge. En se réchauffant sous vide le dépôt vitreux accusait une diminution graduelle d'intensité des bandes de l'ozone et de l'oxygène avant même que la cristallisation ne s'amorce (vers 150 °K). On doit en conclure que le dégagement gazeux à ce stade provient surtout de la désorption plutôt que d'une réaction de décomposition. Aussi le rapport moléculaire de l'oxygène total dégagé au peroxyde d'hydrogène résiduel, O_2/H_2O_2, souvent cité comme indice de la formation des polyoxydes H_2O_3 et H_2O_4 dans ces systèmes, ne saurait être valide dans ces conditions. Les molécules piégées doivent être formées à la surface froide par réaction entre atomes et radicaux libres. Un mecanisme est proposé à cette fin qui prévoit également une source d'oxygène atomique à partir de la vapeur d'eau dissociée.

Les vibrations fondamentales de la molécule d'ozone, soit $\nu_1 = 1106$, $\nu_2 = 703$, et $\nu_3 = 1036\ cm^{-1}$ ont été confirmées par les décalages isotopiques et des mesures de polarisation.

Can. J. Chem., **51**, 1525 (1973)

Introduction

In the preceding paper of this series (1) we reported on the Raman spectra of the glassy solid formed by trapping in liquid nitrogen the dissociation products from water or hydrogen peroxide vapor and their deuterated analogs. Besides three or four new bands belonging to the polyoxides H_2O_3 and H_2O_4 we observed a weak band at $1025\ cm^{-1}$, and occasionally, a second still weaker one near $1120\ cm^{-1}$. We assigned them tentatively to the ν_3 and ν_1 modes of trapped ozone molecules. However, this required confirmation because the relative intensities were in the wrong order for such an assignment. Furthermore, ozone formation has significant implications for the mechanism of the low temperature reactions in these complex systems. In particular, the evolution of oxygen from the condensed products on warming has often been related quantitatively to the decomposition of H_2O_4 (2).

Experimental

The combined liquid nitrogen trap and laser Raman cell devised previously (1) was modified as shown in Fig. 1. Mainly the flat condensing surface was replaced by a stainless steel block with a concave mirror surface. This made it possible to vary the angle of incidence of the laser beam, from 10° near the bottom to about 30° at the top. In practice the optimum angle was near 15°. The beam was spread slightly by reflection in the glassy deposit, and then deflected upwards. Thus, only the scattered light was focused on the monochromator slit instead of the whole laser beam as before. This reduced considerably the stray light which caused so much noise with the original cell, and was also responsible, incidentally, for the two "ghost" bands erroneously assigned to ozone. In addi-

Can. J. Chem. Downloaded from www.nrcresearchpress.com by 210.87.254.40 on 09/05/12
For personal use only.

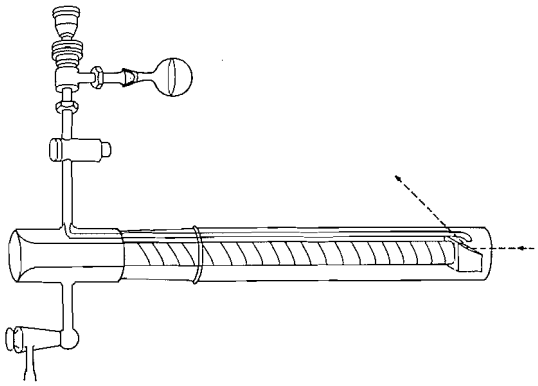

FIG. 1. Modified low-temperature Raman cell (1) for the study of vitreous matrices under laser excitation.

tion, it was now possible to get much closer to the exciting line (about 60 cm^{-1}).

Glass-clear deposits of the right thickness were needed for good quality spectra; that is with low noise level for proper resolution of the bands, and accurate polarization measurements. This required considerable attention and practice. For instance, crystallization invariably resulted from a too rapid deposition rate or the slightest disturbance; such as brief extinction of the electrical discharge, or pressure surge in the system, specks of dust from the coating of the discharge tube, imperfections in the stainless steel surface, etc. Thick deposits tended to develop minute cracks due, no doubt, to temperature gradients and improper heat transfer. To avoid fogging of the glassy deposit, once the reaction was over, it was necessary to prevent condensation of ice in the injector tube and on the coolant well by insulating the latter with tightly wound Teflon tape.

The deposition time was of the order of 4 h with dissociated water or hydrogen peroxide (98%) vapor, and only half as much with mixtures of hydrogen and oxygen gas diluted (3 to 4-fold) in argon. Indeed, with the latter system there was much less tendency of the deposit to crystallize due, probably, to a more exothermic reaction at the cold surface. It was essential to use gases of the highest purity in an absolutely airtight handling system to avoid formation of nitrogen oxides in the discharge. Their presence could easily be detected by the yellow-orange color of the deposit as well as some characteristic Raman bands; particularly in the 1300 and 600 cm^{-1} regions. A few runs were tried with hydrogen alone in the electrical discharge, the other gas being fed through a second injector opening on the other side of the cold surface. In that case, as observed before (3), the attack of the glass surface of the discharge tube was much more pronounced than in presence of oxygen. The whole injector was soon covered with a very fine white powder which greatly impaired the optical quality of the deposit. We intend to investigate this phenomenon further.

With the microwave discharge (4) the Pyrex tube had to be coated with phosphoric acid, as recommended (5), to reduce recombination of hydrogen atoms and secure a better deposit. However, this treatment was unnecessary with a radio-frequency discharge. The latter (6) was of the electrodeless type, some 300 W at 20 MHz, confined in a 100 ml Pyrex bulb. With this the glow of ionized gases extended much further; even down to the cold surface in some instances.

An ionized argon laser (Coherent Radiation, Model 52) was substituted for the helium–neon one used originally. The increased power (600 mW instead of 50 mW) coupled with the greater sensitivity of the photomultiplier cell for the green-blue light (ITT, Model FW-130) resulted in a marked improvement (over 20-fold) in signal-to-noise ratio.

Results

In Fig. 2 we have reproduced the spectrum of the condensed products from ordinary water dissociated in a microwave discharge. The strongest band, as in all cases, is that of H_2O_2 at 880 cm^{-1}. The weak shoulder at about 865 cm^{-1} is now clearly discernible. By means of ^{18}O isotope shift we have confirmed that this band, like the other weak one at 830 cm^{-1}, and the three much stronger ones at 760, 500, and 450 cm^{-1}, all belong to skeleton vibrations of the polyoxide molecules, H_2O_3 and H_2O_4. Detailed description and assignments of these bands based on intensity and polarization data, as well as of the already published infrared bands (7), will be given in a future paper. The broad scattering centered around 1470 cm^{-1} arises from the OOH bending of the various species present in the glassy condensate, as confirmed by the isotope shift on deuteration. Likewise, the much weaker one near 1620–1640 cm^{-1}, which was shifted to 1200 cm^{-1} on deuteration, must belong to the bending mode of H_2O molecules.

The other novel features in our spectra are the three fundamentals of ozone, and, quite unexpectedly, the strong one of molecular oxygen at 1551 cm^{-1}. When this work was done no data were available on the Raman spectra of condensed ozone. Since then Andrews (8) has observed them for the various isotopic species isolated in an argon matrix. The two sets of frequencies agree closely, within reasonable shifts (Table 1). However, our polarization measurements are more accurate due to the absence of scrambling effect in a clear vitreous matrix. A characteristic of these bands of trapped ozone and oxygen was that their intensities (relative, for instance, to that of the H_2O_2 band at 880 cm^{-1}) showed wide variations from one run to another. This was specially true of the oxygen band which varied almost within an order of magnitude. In the case of ozone, part of the intensity fluctuations was traced to segregation effects in the glassy deposit, as confirmed by scanning across

Can. J. Chem. Downloaded from www.nrcresearchpress.com by 210.87.254.40 on 09/05/12
For personal use only.

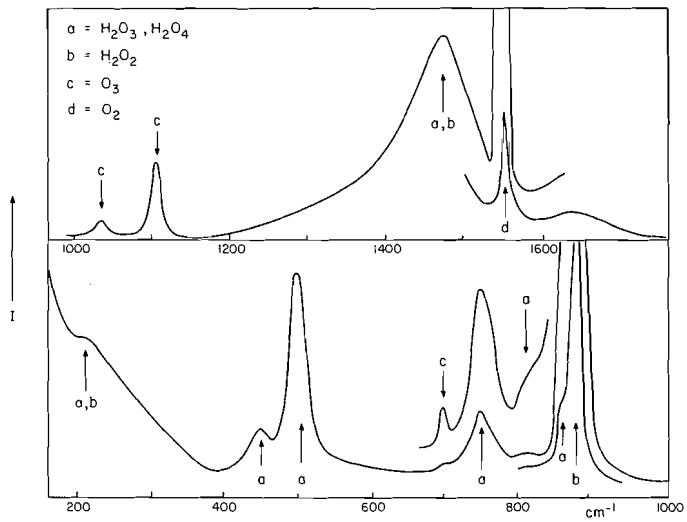

FIG. 2. Raman spectrum of the glassy condensate from electrically dissociated water vapor at 80 °K. The various tracings refer to different slit widths.

TABLE 1. Frequencies (in cm^{-1}) and depolarization ratios of Raman bands of O_2 and O_3

	Free molecule	Trapped in Ar (8)		This work	
	ν	ν	ρ	ν	ρ
Oxygen					
$^{16}O_2$	1554.7 (9)	1553	~0.55	1551.5	~0.115
$^{16/18}O_2$	—	1510		1507.0	
$^{18}O_2$	—	1465		1463.5	
Ozone					
ν_1	1103.3 (10)	1105	~0.64	1106	≤0.155
ν_1*	—	1044		1044	
ν_2	702.1	704.5	~0.78	703	≤0.165
ν_2*	—	664.3		662	
ν_3	—	1040.0	~0.89	1036.5	≥0.75
ν_3*	—	982.8		982	

*For the $^{18}O_3$ molecule.

the latter with the laser beam. In contrast the bands of the various hydrogen oxides showed no such intensity variations.

Generally speaking the amounts of trapped ozone and molecular oxygen seemed particularly sensitive to surface conditions in the discharge-flow system. For instance, one of the best yields (Fig. 2) was achieved by dissociating ordinary water vapor with a microwave discharge in a new, uncoated Pyrex tube. In subsequent runs the yield decreased steadily; eventually a coating of phosphoric acid was required. The composition of the dissociated system had little influence on the concentration of trapped ozone and oxygen, except in the case of an excess (3 to 1) of hydrogen over oxygen, which yielded very little trapped gases. The reaction of dissociated (in the r.f. discharge) oxygen with molecular hydrogen yielded only traces of ozone. The other trapped products, including oxygen, were about in the usual ratios, but the absolute quantities were much smaller (longer deposition time) due, obviously, to the low concentration of oxygen atoms reaching the cold surface.

In one experiment the glassy deposit was allowed to warm slowly, in steps of about 10°, and then cooled back to liquid nitrogen temperature for recording the spectrum. On approaching

Can. J. Chem. Downloaded from www.nrcresearchpress.com by 210.87.254.40 on 09/05/12
For personal use only.

Can. J. Chem. Downloaded from www.nrcresearchpress.com by 210.87.254.40 on 09/05/12
For personal use only.

the maximum workable temperature, near 160 °K, the ozone and oxygen bands decreased noticeably (by roughly 20 to 30% as far as could be ascertained; the increased noise level of the spectra prevented a more accurate estimate). For that reason, and also because the crystallized deposit tended to peal off its support, it was not possible to follow the whole desorption process. The pressure of residual gas in the Raman cell, originally of the order of 10^{-4} Torr, meanwhile rose noticeably. Unfortunately, the experimental arrangement did not allow significant pressure measurements. We intend to develop a different spectroscopic technique for that purpose. Nevertheless, a vague idea of the relative concentrations of the trapped gases may be gained from the over-all intensity of the bands. In the spectra of Fig. 2 the three O—O stretching bands of (*a*) hydrogen peroxide, (*b*) molecular oxygen, and (*c*) ozone (*viz.* ν_1) are approximately in the ratios 60:6:1. As for the hydrogen polyoxides, the H_2O_4 band at 760 cm^{-1} turned out in that particular instance to have about the same intensity as the oxygen fundamental at 1551 cm^{-1}.

Discussion

The outstanding result of this investigation is certainly the confirmation, for the first time, of the trapping of substantial concentrations of molecular oxygen in the products from dissociated water vapor condensed at liquid nitrogen temperature. This had been a much debated question (for a review, *cf.* (2)) ever since the original hypothesis of Willey some forty years ago (11). The suggestion that the oxygen evolved on warming was trapped or occluded in the glassy deposit was opposed vigorously, in particular by the Russian workers, on the basis of various experimental evidence, such as thermal, diffraction, and magnetic measurements. Their results must now be reinterpreted in the light of the present finding. Thermochemical measurements, either by calorimetric (12) or thermographic methods (13) of the first exothermic reaction (beginning around 160 °K) yielded inordinately large, and rather widespread results (61 to 81 kcal/mol) when related to evolved oxygen. Much more reasonable (2.6 kcal/mol) and concordant values were arrived at when the heat effect was related to the amount of residual hydrogen peroxide in the condensate (14, 15). Furthermore, the fair agreement of that quantity with the heat of devitrification of the peroxide glass (16) confirms that a physical transformation is involved at that stage. The decomposition of the hydrogen polyoxides must begin at higher temperature: *viz.* above 200 °K (7).

As for the electron diffraction results (17), they could not provide conclusive evidence in the present case because the diffraction patterns of amorphous solids show only diffuse rings. Therefore, the absence of the characteristic lines of crystalline oxygen and ozone in the glassy deposit does not rule out the occlusion hypothesis. Magnetic susceptibility measurements are better suited to the problem at hand. Here the Russian authors (18) found only a very weak diamagnetism for the condensed product below the crystallization temperature. This seems in direct opposition to the present finding, considering the high paramagnetism of molecular oxygen ($\chi = 106 \times 10^{-6}$ e.m.u.). However, it must be noted that the measurements were made, not on the original condensate, but on the finely ground (under liquid nitrogen) solid. Such a treatment must release most of the trapped gases. In fact the slightly lower diamagnetism observed (-0.1 to -0.2×10^{-6} e.m.u.) compared to that expected for a water – hydrogen peroxide mixture, could be due to a few parts per thousand of residual oxygen.

Another objection often levelled at the occlusion hypothesis was the failure of repeated attempts to trap more than traces of oxygen in a vitreous ice or hydrogen peroxide matrix (19). We have checked this point once again by condensing in our Raman cell the vapor from a sample of concentrated hydrogen peroxide decomposing briskly on a platinum foil. Although the spectrum was of good quality no trace of any scattering by molecular oxygen could be detected under the best conditions: *viz.* with wide slits and high amplifier gain. In an elaborate investigation Ghormley (20) has succeeded in absorbing substantial amounts of oxygen (and also of nitrogen, argon, etc.) in amorphous ice having remarkably high surface area. However, he could absorb much greater amounts of oxygen from dissociated water vapor. Judging from our previous manometric measurements on various systems (3) we believe that the total gas evolved on crystallization could be as large as that from decomposition of the polyoxides.

From all the above it is clear that the trapped gas molecules must be generated *in situ* from

Can. J. Chem. Downloaded from www.nrcresearchpress.com by 210.87.254.40 on 09/05/12
For personal use only.

reactions between atoms and molecules at the cold surface. That this is so in the case of ozone has been proved abundantly (2). Now, the formation of ozone in our system requires a source of atomic oxygen. The latter could not very well be a major component of our water vapor discharges because the lifetime of oxygen atoms is too short to survive under such conditions: *viz.* the long travel (some 40 cm) between the active zone of the microwave discharge and the cold mirror. A more plausible source, on kinetics and thermodynamics grounds (21), is the following sequence of fast reactions:

[1] $$H + HO_2 \rightarrow 2OH$$

[2] $$2OH \rightarrow H_2O + O$$

As for molecular oxygen, it is generated in the recombination reactions

[3] $$2HO_2 \rightarrow H_2O_2 + O_2$$

[4] $$HO + HO_2 \rightarrow H_2O + O_2$$

the latter to a lesser extent in view of the low steady state concentration of OH. In addition, these two reactions afford the possibility of trapping the metastable intermediates H_2O_3 and H_2O_4.

Finally, another obvious conclusion from the present study is the ambiguity of the often quoted ratio of total evolved oxygen to residual hydrogen peroxide (22, 23). That this parameter cannot provide a reliable measure of the formation of hydrogen polyoxides H_2O_3 and H_2O_4 in these systems is now evident, since (*a*) a large portion of the evolved oxygen may have been occluded in the glassy deposit, and (*b*) that portion varies considerably with experimental conditions (especially surface) in the discharge–flow systems. In particular, the contention (24) that the system liquid ozone – atomic hydrogen is much superior to the others in that respect now appears unfounded.

This work was supported by research grants from the National Research Council of Canada, and the Defence Research Board of Canada. The authors are grateful to Messrs. F. Bouchard, glassblower, and G. Marier, mechanic, for the intricate construction of the Raman cell.

1. X. Deglise and P. A. Giguère. Can. J. Chem. **49**, 2242 (1971).
2. M. Venugopalan and R. A. Jones. Chemistry of dissociated water vapor and related systems. Interscience Publishers, John Wiley and Sons, Inc. New York. 1968. Chapt. 3.
3. N. Hata and P. A. Giguère. Can. J. Chem. **44**, 869 (1966).
4. K. Herman and P. A. Giguère. Can. J. Chem. **46**, 2649 (1968).
5. W. V. Smith. J. Chem. Phys. **11**, 110 (1943).
6. P. A. Giguère, E. A. Secco, and R. S. Eaton. Discuss. Faraday Soc. **14**, 104 (1953).
7. P. A. Giguère and K. Herman. Can. J. Chem. **48**, 3473 (1970).
8. L. Andrews and R. C. Spiker, Jr. J. Phys. Chem. **76**, 3208 (1972).
9. G. Herzberg. Molecular spectra and molecular structure, I: diatomic molecules. Van Nostrand, Co. New York. 1950.
10. H. Selig and H. H. Claassen. Isr. J. Chem. **6**, 499 (1968).
11. E. J. B. Willey. Trans. Faraday Soc. **30**, 141 (1934).
12. L. A. Reznitskii, K. G. Khomyakov, L. I. Nekrasov, and I. I. Skorokhodov. Zh. Fiz. Khim. **32**, 87 (1958).
13. I. I. Skorokhodov, L. I. Nekrasov, and N. I. Kobozev. Zh. Fiz. Khim. **35**, 2025 (1961); Russ. J. Phys. Chem. **35**, 994 (1961).
14. M. A. P. Hogg and J. E. Spice. J. Chem. Soc. 3971 (1957).
15. I. I. Skorokhodov, L. I. Nekrasov, L. A. Reznitskii, and K. G. Khomyakov. Zh. Fiz. Khim. **32**, 87 (1958).
16. J. A. Ghormley. J. Chem. Phys. **39**, 3539 (1963).
17. Yu. A. Mal'tsev, I. I. Skorokhodov, and L. I. Nekrasov. Zh. Fiz. Khim. **37**, 2740 (1963); Russ. J. Phys. Chem. **37**, 1480 (1963).
18. I. I. Skorokhodov, L. I. Nekrasov, N. I. Kobozev, and V. B. Evdokimov. Zh. Fiz. Khim. **36**, 274 (1962); Russ. J. Phys. Chem. **36**, 136 (1962).
19. R. A. Ruehrwein, J. S. Hashman, and J. W. Edwards. J. Phys. Chem. **64**, 1317 (1960).
20. J. A. Ghormley. J. Chem. Phys. **46**, 1321 (1967).
21. F. Kaufman. Can. J. Chem. **47**, 1917 (1969).
22. N. I. Kobozev, I. I. Skorokhodov, L. I. Nekrasov, and E. I. Makarova. Zh. Fiz. Khim. **31**, 1843 (1957).
23. J. A. Wojtowicz, F. Martinez, and J. A. Zaslowsky. J. Phys. Chem. **67**, 849 (1963).
24. L. I. Nekrasov, I. I. Skorokhodov, and N. I. Kobozev. Zh. Fiz. Khim. **35**, 691 (1961); Russ. J. Phys. Chem. **35**, 337 (1961).

Determination of the Stoichiometry of the Adducts Formed between some Heterocyclic Bases and Copper(II) Bis(diethyldithiocarbamate) in Various Solvents

J. B. FARMER, F. G. HERRING,[1] AND R. L. TAPPING

Department of Chemistry, University of British Columbia, Vancouver 8, British Columbia

Received October 30, 1972

The stoichiometry of the adducts formed between copper(II) bis(diethyldithiocarbamate) and pyridine in benzene, toluene, and chloroform and between 3-picoline, 4-picoline, and 3,4-lutidine in benzene are shown to be 1:1. The method employed is that of Scatchard using electron paramagnetic resonance studies.

On démontre que la stoichiométrie des composés formés par action d'une part du bis(diéthyldithiocarbamate) de cuivre(II) et d'autre part de la pyridine dans le benzène, le toluène et le chloroforme et de la picoline-3, de la picoline-4, et de la lutidine-3,4 dans le benzène est de 1:1. La méthode utilisée est celle de Scatchard faisant appel à des études de résonance paramagnétique électronique.

[Traduit par le journal]

Can. J. Chem., **51**, 1530 (1973)

Introduction

Recent studies (1–3) of fast Lewis acid–base equilibria between copper(II) bis(dialkyldithiocarbamate) and pyridine in benzene assumed, on the basis of chemical arguments (3), that the formation of a 1:2 adduct is unlikely. Extension of the study of reaction between copper(II) bis(diethyldithiocarbamate), $Cu(DDC)_2$, with pyridine in benzene (3) to reaction in other solvents and with different bases (4) rendered the confirmation of 1:1 adduct formation a necessity in view of the unusual "activation energy" observed in the previous study. Two of the previous studies (1, 3) have observed zero or negative "energies of activation" for the forward reaction, *i.e.* adduct formation.

The determination of adduct stoichiometry, together with the equilibrium, or formation, constant has been the subject of some attention in the past (5–9), with many authors putting undue confidence on unreliable data (6–8). The important work of Person (5) emphasized that the most reliable values for the formation constant are obtained when the concentration of the adduct (or complex) is approximately the same as that of the unbound concentration of the most dilute component. Following Person, and invoking the methods of Weber (10), Deranleau (6) presented a simple graphical method of determining the stoichiometry of simple adducts. Deranleau (6) also discussed the range of Lewis base concentration necessary to obtain both a significant graphical analysis of the experimental data and a reliable value of the formation constant. Deranleau's discussion was detailed for both optical absorption and nuclear magnetic resonance (n.m.r.) measurements, and extension to electron paramagnetic resonance (e.p.r.) follows the discussion for n.m.r. as is now shown.

We assume in the first instance that the adduct formed is simply the result of 1:1 binding between metal chelate ($Cu(DDC)_2$) and Lewis base

$$[1] \qquad A + B \rightleftharpoons AB$$

where A represents the metal chelate and B the Lewis base; then the saturation fraction, S, is defined (5) by

$$[2] \qquad S = [AB]/[A_0]$$

where $[A_0] = [AB] + [A]$. The equilibrium expression is, assuming ideality,

$$[3] \quad K = \frac{[AB]}{[A][B]} = \frac{[AB]}{([A]_0 - [AB])([B_0] - [AB])}$$

where $[B_0] = [B] + [AB]$, *i.e.* total concentration of base. The sensitivity of e.p.r. measurements together with the necessity to avoid spin–spin interactions means that the concentration of the metal complex will be typically 10^{-4} M. The base concentrations employed are 10^{-2} to 10 M so that $[B_0] \gg [A_0]$ whence $[B_0] \gg [AB]$

[1]To whom all correspondence should be addressed.

Can. J. Chem. Downloaded from www.nrcresearchpress.com by 210.87.254.105 on 09/05/12
For personal use only.

Can. J. Chem. Downloaded from www.nrcresearchpress.com by 210.87.254.105 on 09/05/12
For personal use only.

and consequently $K = [AB]/([A_0] - [AB])[B_0]$ to a very good approximation. In addition the fractional populations of A and AB can be written

$$[4] \quad P_A = \frac{1}{1 + K[B_0]} \quad \text{and} \quad P_{AB} = \frac{K[B_0]}{(1 + K[B_0])}$$

In an e.p.r. study of an exchanging two-site system, such as $Cu(DDC)_2$ and pyridines (1–3), the average line position, $\langle\omega\rangle$, can be expressed as the weighted average,

$$[5] \quad \langle\omega\rangle = P_A\omega_A + P_{AB}\omega_{AB}$$

Where ω_A and ω_{AB} are the Larmor frequencies of A and AB, respectively. Following n.m.r. terminology we can define an observed shift δ, such that

$$[6] \quad \delta = \langle\omega\rangle - \omega_A$$

and letting $\delta_0 = \omega_{AB} - \omega_A$ we have

$$[7] \quad \delta = P_{AB}\delta_0 = K[B_0](\delta_0 - \delta)$$

Equation 7 is the basis of the so-called Scatchard (11) plot used by Deranleau (6) in which a linear relationship between $\delta/[B_0]$ *vs.* δ confirms 1:1 adduct formation.

Consider now the conceivable situation that the square planar copper complex forms a 1:2 adduct. The chemical arguments (3) against the formation of 1:2 adducts by square planar copper(II) *bis*(chelate) are very strong but nonetheless the *stepwise* formation of a 1:2 adduct is not impossible. This stepwise formation can be written

$$A + B \rightleftharpoons AB \quad K_1$$
$$AB + B \rightleftharpoons AB_2 \quad K_2$$

and we shall assume that the overall rates of formation and dissociation of the adducts are all in the fast exchange range for the e.p.r. measurements. We emphasize here that if this were not the case *and* two adducts were formed the e.p.r. spectra observed would consist of at least two overlapping spectra, which is not the case (3). The observed average line position in the fast exchange range is (12)

$$[8] \quad \langle\omega\rangle = P_A\omega_A + P_{AB}\omega_{AB} + P_{AB_2}\omega_{AB_2}$$

whence, using detailed balancing,

$$[9] \quad \langle\omega\rangle = \frac{\omega_A + K_1[B_0]\omega_{AB} + K_1K_2[B_0]^2\omega_{AB_2}}{1 + K_1[B_0] + K_1K_2[B_0]^2}$$

and hence

$$[10] \quad \delta = \frac{(\omega_{AB} - \omega_A)K_1[B_0] + (\omega_{AB_2} - \omega_A)K_1K_2[B_0]^2}{1 + K_1[B_0] + K_1K_2[B_0]^2}$$

The behavior of eqs. 7 and 10 will now be discussed.

Discussion

Deranleau pointed out (6) that a graphical presentation of optical absorption, n.m.r., or e.s.r. data is most illuminating when a Scatchard-type (11) plot is used. Such a plot is simply a plot of $\delta/[B_0]$ *vs.* δ over a suitable range of base concentration. Deranleau (6) noted that for meaningful and reliable estimates of K (or K_1 and K_2), the saturation fraction, $S(=\delta/\delta_0)$, must cover the range $0.2 \leq S \leq 0.8$, which in turn means $0.2\delta_0 \leq \delta \leq 0.8\delta_0$. Thus if reliable estimates of ω_A and ω_{AB} can be made then the experiments must be designed so that

$$0.2(\omega_{AB} - \omega_A) \leq (\langle\omega\rangle - \omega_A) \leq 0.8(\omega_{AB} - \omega_A)$$

In many cases (8) the saturation fraction covered by some experimentalists is $0 < S \leq 0.4$ and often $0 < S \leq 0.2$. In the present work on the adducts formed between $Cu(DDC)_2$ with several pyridines in benzene, toluene, and chloroform, S always covers the prescribed range.

An examination of eq. 7 shows that a Scatchard plot will be linear over the entire S range if the 1:1 model is applicable to the exchange system being examined. In order to investigate the effect of two equilibria on a plot of $\delta/[B_0]$ *vs.* δ we chose values of ω_A, ω_{AB}, and ω_{AB_2} that might be expected for CuL_2, CuL_2B, and CuL_2B_2 and then varied K_1 and K_2 to obtain values of δ from eq. 10.

The resultant Scatchard plots are shown in Fig. 1 and correspond to the particular choice $2(\omega_A - \omega_{AB}) = (\omega_A - \omega_{AB_2})$ with the ratio (K_1/K_2) varying from (0.38/0.0) to (0.38/1.0). The curves in Fig. 1 are highly nonlinear except for the special case $K_1 = 4K_2$. That such a situation could obtain was pointed out by Deranleau (6), but it must be emphasized that the linear plot in a two step equilibrium demands that both $K_1 = 4K_2$ *and* $(\omega_A - \omega_{AB_2}) = 2(\omega_A - \omega_{AB})$. These latter conditions are somewhat specialized

Can. J. Chem. Downloaded from www.nrcresearchpress.com by 210.87.254.105 on 09/05/12
For personal use only.

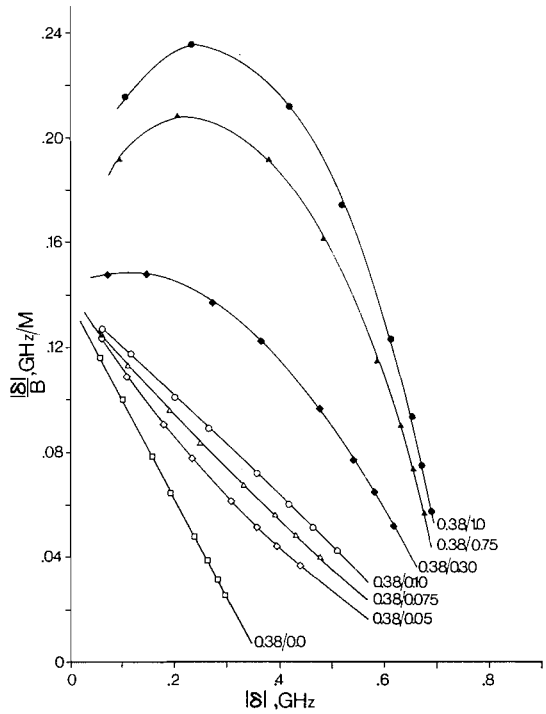

FIG. 1. Scatchard plots for a two equilibrium system. The numbers next to the curves indicate the values of K_1 and K_2 used (K_1/K_2).

and refer to a condition of equivalent and independent binding sites being available. It may be noted that for stepwise complex formation processes, such as that being considered here, the sites represented as AB and AB_2 are neither independent nor equivalent. However should it arise that $K_1 = 4K_2$ and $(\omega_{AB_2} - \omega_A) = 2(\omega_{AB} - \omega_A)$ then, of course, the Scatchard plot will be linear and an ambiguity will exist. In such a circumstance additional data are required to decide between 1:1 stoichiometry or stepwise 1:2 stoichiometry; this point will be discussed later. In passing we note that the special case $(\omega_{AB_2} - \omega_A) = (\omega_{AB} - \omega_A)$ and $K_1 \neq K_2$ will lead to highly non-linear Scatchard plots as might be expected. That this and the previous special case give rise to such slopes can be deduced by making the appropriate substitutions into the equation for the slope

$$-d(\delta/[B_0])/d\delta = \{K_1(\omega_{AB} - \omega_A) - K_2(\omega_{AB_2} - \omega_A) + 2K_1K_2(\omega_{AB} - \omega_A)[B_0] + K_1K_2^2(\omega_{AB_2} - \omega_A)[B_0]^2\}/\{(\omega_{AB} - \omega_A) + 2K_2(\omega_{AB_2} - \omega_A)[B_0] + K_1K_2(\omega_{AB_2} - \omega_{AB})[B_0]^2\}$$

The slope of a Scatchard plot for a 1:1 binding system is equal to $-K$ and the intercept $K\delta$. Thus such plots can be used to determine K and δ_0 provided that the special case outlined above can be ruled out. An alternative procedure, which has been applied previously (3), is to least squares fit eq. 5 in conjunction with eqs. 4 allowing free variation of ω_{AB}, ω_{AB}, and K. This latter method requires that the 1:1 binding model be established and this can be achieved using the Scatchard plot provided that the above ambiguity can be removed (see below).

The Scatchard plot requires a knowledge of ω_A, the Larmor frequency of the free Lewis acid. The procedure that we have adopted to determine this value is to extrapolate the curve of $\langle\omega\rangle$ *vs.* $[B_0]$ to zero base strength. The reason for doing this rather than measuring ω_A in pure solvent is that the curve of $\langle\omega\rangle$ *vs.* $[B_0]$ does not extrapolate smoothly to $[B_0] = 0$; this is illustrated in Fig. 2. We observe that ω_A measured in neat solvent is less than the extrapolated value at zero base concentration. Figure 2 shows that as $[B_0] \leq [A_0]$ the curve of $\langle\omega\rangle$ *vs.* $[B_0]$ turns down toward the value of ω_A measured in pure solvent (benzene was the solvent used in Fig. 2). As is expected the least squares fitting procedure in which $[B_0] > [A_0]$ led to values of ω_A equal to the extrapolated value of ω_A; in addition it was found that the ω_A values obtained from the least squares fitting are independent of solvent to within experimental error. This fact leads us to postulate that the downward turn of $\langle\omega\rangle$ is a manifestation of a change of solvation of the complex on going from the situation when $[B_0] > [A_0]$ to $[B_0] \leq [A_0]$. The ω_A's obtained

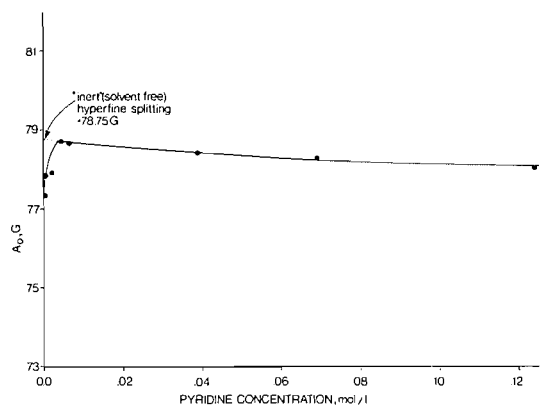

FIG. 2. Variation of the isotropic hyperfine coupling constant of copper(II) bis(diethyldithiocarbamate) with pyridine concentration in benzene.

TABLE 1. Comparison of formation constants obtained from Scatchard plots and least squares analysis of eq. 6

System	Scatchard (mol^{-1})	Least squares (mol^{-1})
$Cu(DDC)_2$ and pyridine in toluene at 280 °K	0.70	0.67
$Cu(DDC)_2$ and pyridine in benzene at 300 °K	0.35	0.38
$Cu(DDC)_2$ and pyridine in chloroform at 320 °K	0.14	0.15
$Cu(DDC)_2$ and 3-picoline in benzene at 310 °K	0.36	0.37
$Cu(DDC)_2$ and 4-picoline in benzene at 310 °K	0.48	0.46
$Cu(DDC)_2$ and 3,4-lutidine in benzene at 310 °K	0.69	0.71

by extrapolation or least squares fitting (3) can in some sense be regarded as solvent-interaction-free parameters and this is borne out experimentally (*e.g.* ω_A is 59.587, 59.578, 59.588 $\times$ 10^9 s^{-1} in benzene, toluene, and chloroform at 300 °K, respectively). We can note here that the formation constants obtained from the Scatchard plots are identical, to within experimental error, to those obtained from the least squares analysis; that this is so is demonstrated by the data in Table 1.

The problem of determining ω_A outlined above does not appear to occur to any appreciable extent in n.m.r. studies. It should also be emphasized that this problem does not invalidate the establishment of stoichiometry since any value of $\langle\omega\rangle$ could be used as an end-point. To illustrate let $\delta' = \langle\omega\rangle - \langle\omega\rangle'$

where $$\langle\omega\rangle' = \omega_A + \alpha$$

then eq. 7 becomes, with $\delta_0' = (\omega_B - \langle\omega\rangle')$

$$\delta' = K[B_0](\delta_0' - \delta')$$

then

$$\delta = K[B_0](\delta_0 - \delta) + \alpha$$

and it is apparent the correction α will not destroy the linearity of the Scatchard plot if the model is 1:1.

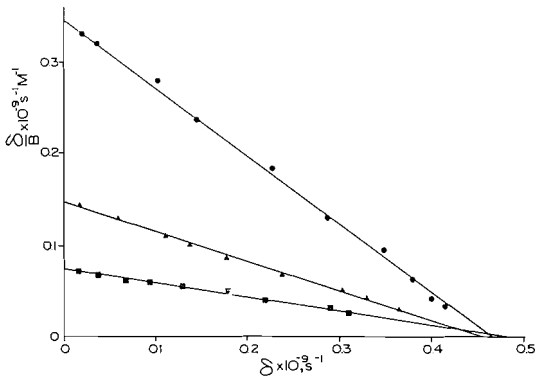

FIG. 3. Scatchard plots for copper(II) bis(diethyldithiocarbamate) and pyridine in benzene (triangles), toluene (circles), and chloroform (squares).

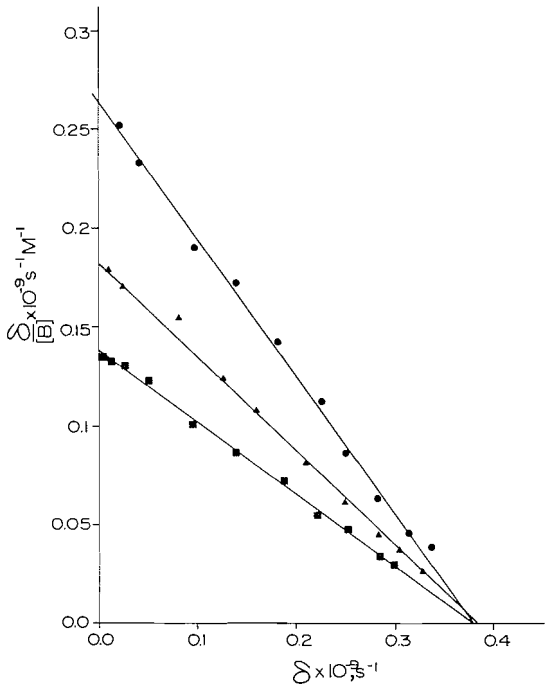

FIG. 4. Scatchard plots for copper(II) bis(diethyldithiocarbamate) and 3,4-lutidine (circles), 4-picoline (squares), and 3-picoline (triangles) in benzene at 310 °K.

The results of carrying out Scatchard plots for the systems $Cu(DDC)_2$ and pyridine in benzene, toluene, and chloroform and $Cu(DDC)_2$ and 3- and 4-picoline, and 3,4-lutidine in benzene are shown in Figs. 3 and 4.

The observed linearity shows that either 1:1 adducts are formed in all cases or that in all cases the special condition that $K_1 = 4K_2$ and $(\omega_{AB_2} - \omega_A) = 2(\omega_{AB} - \omega_A)$ obtains. The latter is very unlikely and can be ruled out on the basis of other e.p.r. evidence.

The rate of chemical exchange is dependent on temperature so that by carrying out experiments

Can. J. Chem. Downloaded from www.nrcresearchpress.com by 210.87.254.105 on 09/05/12
For personal use only.

at suitable low temperatures all sites contributing to the higher temperature fast-exchange-averaged spectrum will be detected. If the particular condition $4K_2 = K_1$ and $(\omega_{AB_2} - \omega_A) = 2(\omega_{AB} - \omega_A)$ occurs then the high sensitivity of the e.p.r. measurements will certainly detect resonances from all three sites, expecially since the line positions should be well separated due to the required conditions on ω_A, ω_{AB}, and ω_{AB_2}. It may be argued that the relative shifts in ω_A, ω_{AB}, and ω_{AB_2} could be so small that only one broad line for each hyperfine component ($I = 3/2$ for both copper isotopes) will be seen; then, of course, the ambiguity will persist. The observation of any separation will obviously rule out this special case. The results of experiments carried out by Corden and Rieger (1), Shklyaev and Anufrienko (2), and in this laboratory (13), however, demonstrate that apparently two sites are resolvable. Thus the special case $(\omega_{AB_2} - \omega_A) = 2(\omega_{AB} - \omega_A)$ can be discounted and so can the situation that $(\omega_{AB_2} - \omega_A) = (\omega_{AB} - \omega_A)$ and all other two step processes since the Scatchard plot would not be linear in such cases (see above). The fact that one of the exchange sites is $Cu(DDC)_2$ is confirmed by the observation that the isotropic hyperfine coupling constant computed from the Larmor frequencies obtained from the least squares analysis is 78.7 ± 0.2 G and that measured from the e.p.r. spectrum of $Cu(DDC)_2$ in the solid state is 81 ± 1.0 G (14).

The above collection of evidence we feel demonstrates convincingly that in all the cases studied here 1:1 adducts are formed exclusively. The "negative activation energy" observed (3) for the forward rate constant cannot, therefore, be due to multiple equilibria of the type considered here.

Experimental

E.p.r. spectra were recorded on a Varian E-4 X-band spectrometer equipped with a Varian V6040 variable temperature accessory. Field and frequency measurements, and temperature calibration, are as detailed previously (3).

Solvents and bases used were spectrograde where possible (Fisher, Eastman–Kodak), and highest available purity otherwise (3,4-lutidine, Eastman–Kodak). N.m.r. and gas chromatographic analysis failed to detect any significant impurities, and all solvents and bases were kept dry after opening. Sample preparation and spectral analysis were as reported earlier (3).

We thank the National Research Council of Canada for financial support.

1. B. J. CORDEN and P. H. RIEGER. Inorg. Chem. **10**, 263 (1971).
2. A. A. SHKLYAEV and V. F. ANUFRIENKO. Zh. Strukt. Khimii, **12**, 601 (1971).
3. J. B. FARMER, F. G. HERRING, and R. L. TAPPING. Can. J. Chem. **50**, 2079 (1972).
4. F. G. HERRING and R. L. TAPPING. To be published.
5. W. B. PERSON. J. Am. Chem. Soc. **87**, 167 (1965).
6. D. A. DERANLEAU. J. Am. Chem. Soc. **91**, 4044, 4050 (1969).
7. M. W. HANNA and D. G. ROSE. J. Am. Chem. Soc. **94**, 2601 (1972).
8. G. R. WILEY and S. I. MILLER. J. Am. Chem. Soc. **94**, 3287 (1972).
9. J. HOMER, M. H. EVERDELL, C. J. JACKSON, and P. M. WHITNEY. Trans. Faraday Soc. **68**, 874 (1972).
10. G. WEBER. *In* Molecular biophysics. *Edited by* B. Pullman and M. Weissbluth. Academic Press, New York. 1965.
11. G. SCATCHARD. Ann. N.Y. Acad. Sci. **51**, 660 (1949).
12. L. H. PIETTE and W. A. ANDERSON. J. Chem. Phys. **30**, 899 (1959).
13. R. L. TAPPING. Ph.D. Thesis. University of British Columbia, Vancouver, British Columbia. 1972.
14. C. P. KEIJZERS, H. J. M. DE VRIES, and A. VAN DER AVOIRD. Inorg. Chem. **11**, 1338 (1972)

Can. J. Chem. Downloaded from www.nrcresearchpress.com by 210.87.254.105 on 09/05/12
For personal use only.

The Molecular Conformation of 1*e*,2*a*,6*e*-Trimethyl-4*e*-phenyl-4*a*-acetoxypiperidine Hydrobomide in the Crystalline State

K. HAYAKAWA AND M. N. G. JAMES

Department of Biochemistry, University of Alberta, Edmonton, Alberta

Received November 2, 1972

The title compound represents one analog of the synthetic 4-phenylpiperidine narcotic analgesics. The crystal structure was determined by the heavy-atom method from data collected on an automated diffractometer. The crystals are monoclinic, space group $P2_1/c$, with unit cell dimensions $a = 11.833$ Å, $b = 11.551$ Å, $c = 14.659$ Å and $\beta = 121° 9'$. The final residual, R, was 0.056. The stereochemistry of the substituents on the piperidine ring as deduced by this structural determination (1*e*,2*a*,6*e*-trimethyl-4*e*-phenyl-4*a*-acetoxypiperidine) confirms the p.m.r. results on the alcohol precursor as *trans* 2-Me/6-Me and *trans* 2-Me/4-Ph. There is a normal length N—H...Br hydrogen bond of 3.234 Å; most intramolecular bond lengths and angles are within the expected ranges but some distortion of the ideal chair conformation of the piperidine ring occurs.

Le composé mentionné dans le titre représente un analogue des analgésiques synthétiques de la série des narcotiques dérivés de la phényl-4 pipéridine. La structure cristalline a été élucidée par la méthode de l'atome lourd à partir de données recueuillies sur un diffractomètre automatique. Les cristaux sont du type monoclinique appartenant au groupe $P2_1$-*c* et possèdent une maille dont les dimensions sont $a = 11.833$ Å, $b = 11.511$ Å, $c = 14.659$ Å et $\beta = 121° 9'$. Le résidu final, R, a été 0.056. La stéréochimie des substituants sur l'anneau pipéridine déduite par l'élucidation de la structure (triméthyl-1*e*,2*a*,6*e* phényl-4*e* acétoxy-4*a* pipéridine) a confirmé les résultats en r.m.n. sur le précurseur alcoolique comme étant *trans* 2-Me/6-Me et *trans* 2-Me/4-Ph. La longueur de la liaison hydrogène N—H...Br est normale et égale à 3.234 Å; la plupart des longueurs de liaison intramoléculaires et des angles se situent à l'intérieur du domaine prévu mais on a noté sur l'anneau pipéridine une certaine déformation comparativement à la conformation du type chaise idéale. [Traduit par le journal]

Can. J. Chem., **51**, 1535 (1973)

Introduction

Various synthetic 4-phenylpiperidine derivatives are in wide clinical use as analgetics; many of these compounds are more potent than the classic analgetic, morphine. The best known and original member of these synthetic analgetics is pethidine (meperidine, **1**), and the crystal structure of its hydrobromide salt has recently been reported (1). A variety of substituents on the piperidine ring and their configurational isomers have been studied with the view to increasing the analgetic potency and at the same time reducing the addiction liability. Little success in the latter direction has been achieved. Replacing the 4-CO_2Et group by 4-OCOEt, giving the so-called reversed esters of pethidine, enhances the analgetic potency in mice by 5–6-fold (2). The positional and configurational isomers of methyl substituents on the piperidine ring have also been widely studied with the view to elucidating the pharmacological determinants of this system. A recent paper by Casy and McErlane (3) presented data relating the pharmacological activity of trimeperidine (γ-promedol, **4**) with the stereochemistry of its other isomers, α and β (**2** and **3** respectively). The most active isomer is the α-promedol (**2**) in the nomenclature suggested by Vlasova and Sheinker (4). Jones *et al.* (5) have corrected the configurational assignments originally described in ref. 3 for the α and β isomers and these have also been confirmed by X-ray structure analysis (6–9) of the α, β, and γ promedol alcohols. Earlier, X-ray studies on alphaprodine (**5**) and betaprodine (**6**) (isomers of 1,3-dimethyl-4-phenyl-4-propionoxypiperidine) showed conclusively that the more potent betaprodine has the 3Me in an axial orientation with a *cis* 3-Me/4-Ph configuration (10,11). This *cis* 3-Me/4-Ph geometry is also observed in the α-promedol (**2**) isomer and suggests it is an important analgetic factor (3). The configuration of the 2-methyl group apparently has little influence on the activity of 4-phenylpiperidine analgetics (3). Although there is little analgetic potency data on the 1,2,6-trimethyl analogs, the details of the stereochem-

Can. J. Chem. Downloaded from www.nrcresearchpress.com by 210.87.254.105 on 09/05/12
For personal use only.

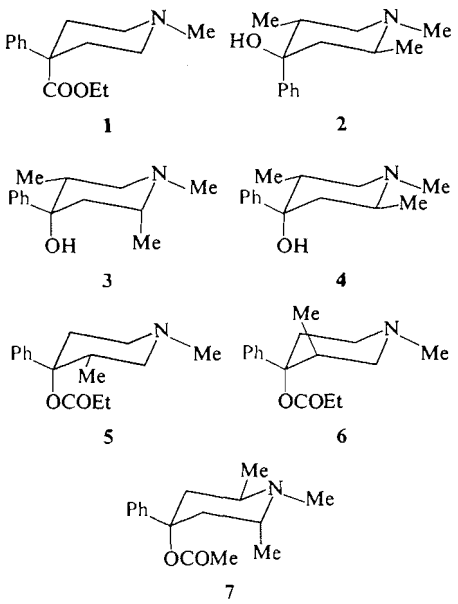

istry of these compounds is unknown. The isomer used in the present study (7) exhibits twice the analgetic potency in mice as does pethidine (12). With the view to carrying out an independent determination of the molecular configuration (unpublished results by Casy suggests *trans* 2-Me/6-Me and *trans* 2-Me/4-Ph) and in addition, supplying details of the molecular geometry, this structural study of one of the isomers of 1,2,6-trimethyl-4-phenyl-4-acetoxypiperidine hydrobromide was carried out.

Experimental

A sample of 1,2,6-trimethyl-4-phenyl-4-acetoxypiperidine hydrobromide was kindly supplied by Dr. A. F. Casy of the Pharmacy Department, University of Alberta. The sample was recrystallized by vapor diffusion of diethyl ether into a solution of the compound in 50% ethanol, 50% methanol. Crystals of a flat needle habit resulted from this recrystallization and preliminary precession photography showed the space group $P2_1/c$. The density was measured by floatation in a mixture of bromobenzene and chlorobenzene. The crystal data are included in Table 1. The measured density, d_m, the cell volume, V, and a cell content of 4 formula units confirms the molecular weight and the fact there was no solvent of crystallization present in these crystals.

The cell dimensions were determined during the initial alignment of the crystal on a FACS-1 automated diffractometer. The accurately centered angles for 12 reflections were used in a least-squares process (13) that simultaneously refined the cell dimensions and the orientation matrix for the reciprocal lattice parameters with respect to the goniostat. The refined cell dimensions are included in Table 1.

TABLE 1. Crystal data for 1,2,6-trimethyl-4-phenyl-4-acetoxypiperidine hydrobromide

Parameter	Value
Formula	$C_{16}H_{24}NO_2Br$
Molecular weight	342.3 daltons
Space group	$P2_1/c$
Cell dimensions	
a	11.833(2) Å
b	11.551(3) Å
c	14.659(3) Å
β	121° 9′
V	1714.2 Å^3
Density	
d_m	1.333 g cm^{-3}
d_c	1.326 g cm^{-3}
Cell content	
Z	4
Absorption coefficient	
μ (MoK$_\alpha$)	25.4 cm^{-1}
F(000)	712 e

The intensity data were collected from a crystal of dimensions 0.5 × 0.4 × 0.2 mm, mounted with the b axis coincident with the phi shaft of the goniostat. The incident X-radiation used was graphite monochromatized MoK$_{\bar{\alpha}}$ (λ = 0.71069 Å) with the tube at 45 kV and 15 mA. A 2θ scan of 2° per min over a range of 1.8° and two 10 s, fixed position background counts on either side of the peak were used in the data collection. Of the 3020 possible unique reflections within the range $3° < 2\theta < 50°$, 2212 (75%) were classified as observed on the basis that the net peak counts for each reflection be numerically larger than 10% of the total background for the reflection. The intensity data were reduced to structure amplitudes by applying $1/Lp$ corrections including the polarization correction for the graphite monochromator. Observational weights were calculated according to the expression $w^{1/2} = 2F_o/[T + (kI)^2 + B]^{1/2}$ (14) where F_o is the derived structure amplitude, T the total peak count in the scan, I the net counts in the peak after background correction, B the total background, and k is a small constant (0.04) included to allow for minor instrumental inaccuracies (15). Since the main objective of this study was to deduce the configuration of the piperidine ring substituents and not to derive a highly accurate structure, no absorption corrections were applied even though the crystal shape warranted it.

Determination and Refinement of the Structure

The bromide ion coordinates were determined from a $1/Lp$ sharpened Patterson map and used to compute structure factors. The residual ($R = \Sigma||F_o| - |F_c||/\Sigma|F_o|$) using an isotropic temperature factor of B = 3.5 Å^2 for the Br^- in this computation was 0.385. The positions of the other 19 non-hydrogen atoms were determined from a Fourier synthesis with all data included and signs derived from the bromide ion coordinates only. Three cycles of block-diagonal least-squares refinement on the positional parameters and isotropic thermal parameters

Can. J. Chem. Downloaded from www.nrcresearchpress.com by 210.87.254.105 on 09/05/12
For personal use only.

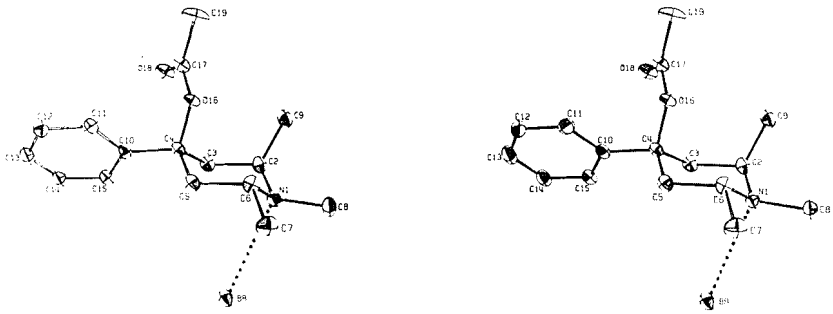

FIG. 1. A stereodrawing of 1,2,6-trimethyl-4-phenyl-4-acetoxypiperidine hydrobromide showing the molecular conformation and the atomic numbering scheme. This drawing and those in Fig. 5(*a*) and 5(*b*) were done using the program ORTEP(25).

of these 20 atoms reduced the *R* factor to 0.119. A difference Fourier synthesis computed at this stage showed positive peaks ranging from 0.3–0.6 e/Å^3 in the regions expected for 21 of the 24 hydrogen atoms in this compound. The three hydrogens of the acetoxy methyl group C(19) (see Fig. 1 for the atom numbering scheme) could not be positioned with certainty. This difference map also indicated anisotropic thermal motion for the majority of atoms.

At this point the bromine scattering curve was corrected for the real and imaginary parts of anomalous dispersion ($\Delta f' = -0.3$ e, $\Delta f'' = -2.7$ e) (16). Least-squares refinement was continued for 6 cycles; the parameters varied were the positional parameters for all atoms and the anisotropic thermal motion parameters for the non hydrogen atoms. The 21 hydrogen atoms were included with isotropic *B* factors of 4.5 Å^2 and these parameters were refined as well. The final *R* factor was 0.056 and the shifts in the parameters were all less than 1/8 of the associated estimated standard deviations. Nine of the most intense low θ reflections showed the effects of secondary extinction and/or absorption and were excluded from these final least-squares cycles. All of the atoms were well behaved during the least-squares refinement, except for one hydrogen atom (H(82)) bonded to C(8). The *B* factor rose to a value of 18.2 Å^2 and positional parameters were shifting by 1/3 of the associated estimated standard deviations. The coordinates for this atom were fixed by an atom positioning program and were not varied in the final cycle. No ordered sites could be found for the hydrogen atoms on C(19) on the final difference Fourier and their coordinates are not reported here.

TABLE 2. Summary of agreement for the observed data only*

Criterion	Number of reflections
$0 < \Delta F/\lvert F_o\rvert < 0.2$	2170
$0.2 < \Delta F/\lvert F_o\rvert < 0.3$	39
$0.3 < \Delta F/\lvert F_o\rvert < 0.4$	3
$0.4 < \Delta F/\lvert F_o\rvert < 0.5$	0

*$\lvert F_o\rvert$, observed structure amplitude; $\lvert F_c\rvert$, calculated structure amplitude based on coordinates in Table 3; ΔF, $\lvert\lvert F_o\rvert - \lvert F_c\rvert\rvert$ differences.

A summary of the agreement for the 2212 observed reflections is included in Table 2; the final atomic coordinates and thermal motion parameters with associated estimated standard deviations are given in Table 3. The scattering factors for the C, N, O, and Br^- atomic species were taken from Cromer (17) and the H curve was that of Mason and Robertson (18). The programs used for this structure analysis were those of Ahmed *et al.* (19) and several programs written in this laboratory for the IBM 360/67. A tabulation of the observed and calculated structure factors for this compound has been submitted to the Depository of Unpublished Data.[1]

Results and Discussion

The molecular conformation and atomic numbering scheme are shown in Fig. 1. The piperidine ring is in the standard chair form with the methyl groups in the following configuration, N(1)—CH_3 equatorial; C(2)—CH_3, axial; C(6)—CH_3, equatorial. The phenyl ring on C(4) is in the equatorial configuration and the reversed acetoxy ester on C(4) is in the axial orientation. This stereochemistry, *trans* 2-Me/6-Me and *trans* 2-Me/4-Ph, confirms the p.m.r. results obtained by Casy (unpublished results) on the 4-OH precursor of the present compound. The configuration of the groups on C(4) is identical to those arrangements in alphaprodine and betaprodine (10, 11) β and γ promedol (6, 7, 9) and pethidine (1). The present compound contains both an axial and an equatorial methyl substituent on the piperidine ring yet exhibits an analgetic potency twice that of pethidine. This indicates that although the enhancement of the activity is small there is some improvement by having these groups present. Unfortunately

[1]Complete set of tabular data is available, at a nominal charge, from the Depository of Unpublished Data, National Science Library, National Research Council of Canada, Ottawa, Canada K1A 0S2.

Can. J. Chem. Downloaded from www.nrcresearchpress.com by 210.87.254.105 on 09/05/12
For personal use only.

Can. J. Chem. Downloaded from www.nrcresearchpress.com by 210.87.254.105 on 09/05/12
For personal use only.

TABLE 3. The positional and thermal parameters for all atoms except the hydrogen atoms on C(19)*

Atom	x/a	y/b	z/c	U_{11}	U_{22}	U_{33}	U_{12}	U_{23}	U_{13}
Br(1)	41787(5)	12424(5)	61508(4)	1202(6)	1179(7)	1070(6)	116(6)	200(6)	749(5)
N(1)	3740(4)	1933(4)	3853(3)	925(45)	998(52)	966(47)	−8(39)	87(41)	603(40)
C(2)	3110(5)	871(4)	3130(4)	1030(59)	853(56)	1163(63)	33(46)	10(49)	698(53)
C(3)	1838(5)	604(4)	3108(4)	1012(54)	680(54)	962(55)	89(44)	109(44)	607(48)
C(4)	851(4)	1600(4)	2763(4)	909(52)	680(50)	756(50)	9(39)	56(39)	523(45)
C(5)	1561(5)	2648(4)	3473(4)	959(54)	737(54)	947(55)	106(44)	31(45)	571(47)
C(6)	2838(5)	2978(4)	3496(4)	1013(57)	640(54)	1044(58)	−22(43)	0(44)	529(50)
C(7)	3510(6)	4007(5)	4264(5)	1376(75)	951(68)	1227(71)	−246(54)	−145(54)	588(62)
C(8)	5088(5)	2179(6)	4018(5)	935(61)	1702(88)	1419(76)	−85(59)	198(67)	758(59)
C(9)	3017(6)	1014(5)	2062(5)	1148(67)	1666(91)	1319(74)	−129(60)	−282(64)	871(62)
C(10)	−370(5)	1339(4)	2819(4)	956(52)	821(54)	811(50)	−20(44)	−135(44)	553(45)
C(11)	−1476(5)	2060(5)	2264(4)	971(59)	1024(64)	955(57)	79(49)	−93(49)	453(50)
C(12)	−2599(5)	1835(6)	2321(4)	870(58)	1597(82)	1135(66)	126(57)	−240(62)	525(53)
C(13)	−2639(6)	945(5)	2906(5)	1177(67)	1678(90)	1425(77)	−468(61)	−587(66)	965(64)
C(14)	−1582(5)	247(5)	3450(4)	1209(66)	1392(76)	1205(68)	−347(57)	−273(59)	881(60)
C(15)	−427(5)	435(4)	3424(4)	1107(60)	879(58)	938(55)	−49(48)	−61(47)	657(50)
O(16)	455(3)	2006(3)	1693(2)	1134(39)	739(36)	776(35)	−20(30)	120(29)	577(32)
C(17)	−286(5)	1296(4)	842(4)	1324(65)	959(60)	934(57)	90(53)	75(50)	720(53)
O(18)	−596(4)	330(3)	915(3)	1735(54)	977(44)	1059(43)	−290(40)	−138(36)	831(42)
C(19)	−644(8)	1914(6)	−175(5)	2698(99)	1451(90)	835(65)	−48(87)	171(63)	849(79)

Atom	x/a	y/b	z/c	B_{iso}	Atom	x/a	y/b	z/c	B_{iso}
H(1)	379(5)	183(5)	445(4)	6.0(1.3)	H(81)	486(5)	268(5)	343(4)	6.4(1.3)
H(2)	377(4)	25(4)	360(4)	4.6(1.0)	H(82)	550†	265†	466†	6.0†
H(31)	198(4)	44(4)	374(3)	3.6(0.9)	H(83)	565(6)	135(5)	426(5)	7.0(1.5)
H(32)	136(5)	−2(4)	256(4)	4.8(1.0)	H(91)	366(5)	87(5)	211(5)	5.9(1.3)
H(51)	96(4)	314(4)	325(4)	4.5(1.0)	H(92)	250(5)	173(5)	169(4)	6.0(1.3)
H(52)	185(4)	241(4)	423(3)	3.7(0.9)	H(93)	246(5)	47(5)	171(4)	5.6(1.2)
H(6)	246(5)	333(5)	263(4)	5.9(1.3)	H(11)	−135(5)	264(5)	174(4)	6.4(1.4)
H(71)	292(5)	465(5)	402(4)	6.3(1.3)	H(12)	−326(5)	225(4)	201(4)	5.0(1.1)
H(72)	434(5)	445(5)	425(4)	6.0(1.3)	H(13)	−337(5)	76(5)	288(4)	5.6(1.2)
H(73)	373(6)	365(5)	488(5)	7.8(1.7)	H(14)	−172(5)	−27(5)	377(4)	6.3(1.3)
					H(15)	23(4)	−6(4)	384(3)	3.4(0.8)

*The positional parameters for Br(1) are $\times 10^5$. The positional parameters for C, N, and O are $\times 10^4$ as are the U_{ij} thermal parameters. The positional parameters for the hydrogen atoms are $\times 10^3$. The U_{ij} are the coefficients in the anisotropic thermal ellipsoid expression $\exp[-2\pi^2(U_{11}h^2a^{*2} + U_{22}k^2b^{*2} + U_{33}l^2c^{*2} + 2U_{12}hka^*b^* + 2U_{23}klb^*c^* + 2U_{13}hla^*c^*)]$. The B_{iso} are given in Å^2.
†This atom was fixed by an atom positioning program and its parameters were not refined.

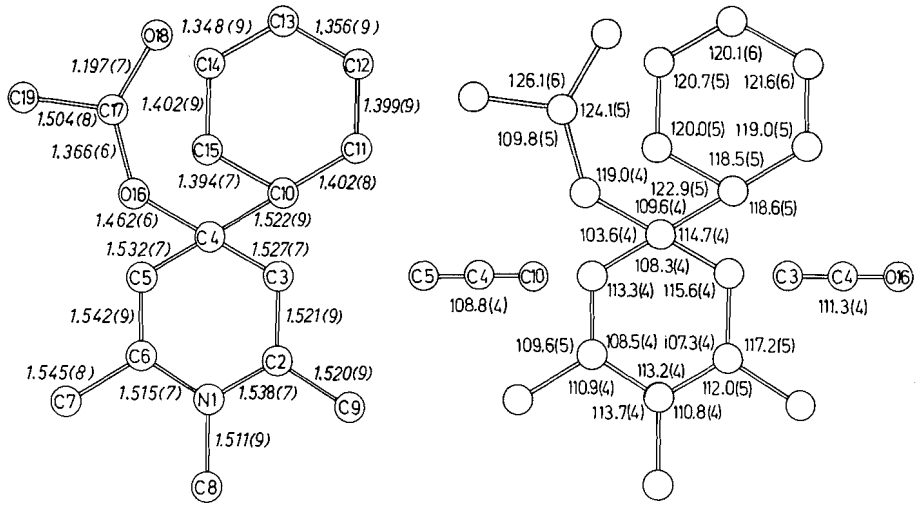

FIG. 2. Schematic drawing of the molecule showing the intramolecular bond lengths (Å) and interbond angles (°) with the e.s.d.'s in parentheses referring to the least significant digit quoted. These molecular parameters have not been corrected for thermal vibration. The C—H bond lengths in this structure fall in the range 0.75 to 1.18 Å.

TABLE 4. Intramolecular distances involving hydrogen atoms*

Bond	Distance (Å)	Bond	Distance (Å)
N(1)—H(1)	0.85(6)	C(8)—H(81)	0.96(6)
C(2)—H(2)	1.02(5)	C(8)—H(82)†	1.05
C(3)—H(31)	0.87(4)	C(8)—H(83)	1.12(6)
C(3)—H(32)	1.00(5)	C(9)—H(91)	0.75(7)
C(5)—H(51)	0.84(5)	C(9)—H(92)	1.01(6)
C(5)—H(52)	1.02(4)	C(9)—H(93)	0.86(6)
C(6)—H(6)	1.18(5)	C(11)—H(11)	1.09(6)
C(7)—H(71)	0.95(6)	C(12)—H(12)	0.83(6)
C(7)—H(72)	1.12(7)	C(13)—H(13)	0.87(7)
C(7)—H(73)	0.89(7)	C(14)—H(14)	0.83(6)
		C(15)—H(15)	0.91(4)

*The estimated standard deviations are in parentheses and refer to the least-significant digit quoted.
†H(82) was positioned and its atomic parameters were not refined.

there is no pharmacological potency data regarding the other congeners of the 1,2,6-trimethyl analgetic and an attempt at drawing conclusions about substitution at the 2 and 6 positions now is premature.

Figure 2 contains the intramolecular bond lengths and bond angles for the non-hydrogen atoms. The bond lengths involving the hydrogen atoms are listed in Table 4. The mean C—C single bond length in the piperidine ring is 1.531 Å and agrees well with the corresponding values found in the similar piperidine rings (7, 8, 10, 11). The three C—N single bond lengths average 1.521 Å and are rather long. The N(1)—C(2) length (1.538(7) Å) is just significantly longer than the other two lengths, a feature that is also observed in the structure of 2-methyl-1-phenethyl-4-phenyl-4-acetoxypiperidine hydrobromide (20). De Camp and Ahmed (7) have noted that protonation of the nitrogen atom of the piperidine ring as occurs in alphaprodine (10) and betaprodine (11), causes an increase in the C—N bond lengths of 0.028 Å from the mean value of 1.471 Å found in the α and γ promedol alcohols. The observed lengthening of these bonds in the present structure is consistent with these observations. The bond lengths in the phenyl group are within the expected limits for aromatic C—C bonds (1.394 Å). The short values for C(12)—C(13) (1.356(9)

Can. J. Chem. Downloaded from www.nrcresearchpress.com by 210.87.254.105 on 09/05/12
For personal use only.

Can. J. Chem. Downloaded from www.nrcresearchpress.com by 210.87.254.105 on 09/05/12
For personal use only.

Å) and C(13)—C(14) (1.348(9) Å) can be attributed to the relatively large thermal motion of C(13) in the crystals, and is not an uncommon feature of phenyl rings in other crystal structure analyses. Correction of these two bonds for riding motion (21) did not significantly increase their lengths. The bond lengths and angles in the acetoxy group are in close agreement with the analogous moieties of pethidine (1), alphaprodine (10) and betaprodine (11) although in these latter three compounds the axial groups are propionoxy.

The mean plane of the phenyl ring is represented by the equation $0.0701x - 0.6019y - 0.7955z + 3.9309 = 0$ where x, y, and z are referred to the a, b, and c^* axes, respectively. The value of χ^2 for this plane is 3.5 and all six atoms are within 0.006 Å of this plane. Atom C(4) of the piperidine ring is 0.015 Å from this plane; this deviation is not significant ($3\sigma = 0.014$ Å). The mean plane of the piperidine ring has the equation $0.2732x + 0.2481y - 0.9294z + 3.2776 = 0$ and all six atoms are approximately 0.23 Å above and below the plane. The best four atom plane for the piperidine ring is that containing atoms C(2), C(3), C(5), and C(6) with atoms N(1) and C(4) displaced −0.68 Å and +0.66 Å respectively from the plane $-0.0240x + 0.1820y - 0.9830z + 3.7040 = 0$ ($\chi^2 = 1.5$). De Camp and Ahmed (7) have defined the dihedral angle made by the mean plane of the phenyl ring and that of the piperidine ring for (±)-γ-promedol alcohol as 73.7°. The corresponding angle in the present study is 52.5°.

Figure 3 shows several Newman projections along the bond C(4) to the phenyl ring for comparative purposes. Only those structures having equatorial phenyl substituents on the piperidine ring have been included. It can be seen from this figure that the dihedral angles between the mean planes of the phenyl rings and the planes comprising C(4), C(10), and O(16) (numbering scheme for this structure) for these several structures range from 16.0° to 65.1°. Examination of these six structures shows that this angle is determined primarily by the orientation of the bulky axial group on C(4); that is, there is a steric effect between the phenyl ring and the acetoxy group (or propionoxy group in the prodines) that determines not only the direction of the dihedral angle but also its magnitude. In γ-promedol where the axial group is an alcoholic OH the angle is the smallest at 16.0°

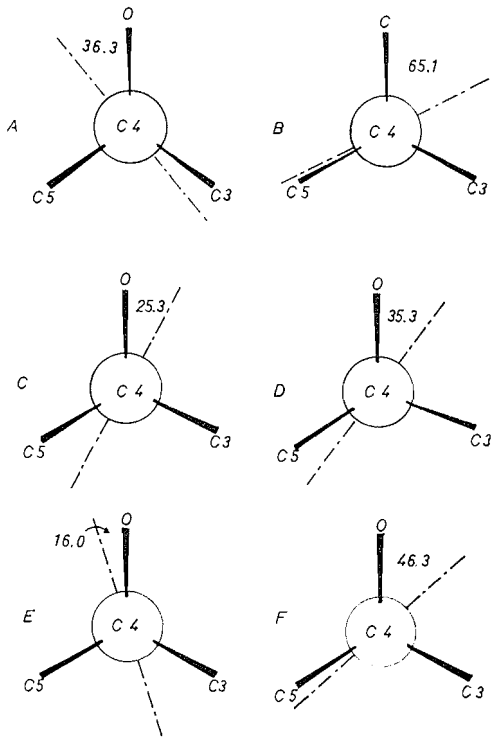

FIG. 3. Newman projection diagrams along the C(4) → phenyl ring bond for the following structures: (*A*) 1,2,6-trimethyl-4-phenyl-4-acetoxypiperidine hydrobromide; (*B*) 1-methyl-4-phenyl-4-carbethoxypiperidine hydrobromide (pethidine) (1); (*C*) 1,3-dimethyl-4-phenyl-4-propionoxypiperidine hydrochloride (*d*, *l*-alphaprodine) (10); (*D*) 1,3-dimethyl-4-phenyl-4-propionoxypiperidine hydrobromide (*d*, *l*-betaprodine) (11); (*E*) 1,2,5-trimethyl-4-phenyl-piperidine-4-ol (γ-promedol) (7); (*F*) 2-methyl-1-phenethyl-4-phenyl-4-acetoxypiperidine hydrobromide (20).

whereas the largest angle, 65.1°, is shown by pethidine which has the propionyl ester in an axial orientation on C(4). This propionyl ester function in pethidine is in the perpendicular orientation (22) thus effecting the largest steric hindrance to the possible position of the phenyl ring. The apparent range of the preferred conformation of the phenyl ring in those compounds with reversed ester groups in the axial position on C(4) is 25° – 46° relative to the axial bond.

The dihedral angles of the piperidine ring are included in Fig. 4. The internal torsion angles in the ring are all less than the perfect chair value of 60° and fall in the range 53.6° to 58.4°. This distortion from ideal chair geometry is a common feature of substituted six-membered pyranose rings (23 and references therein) and

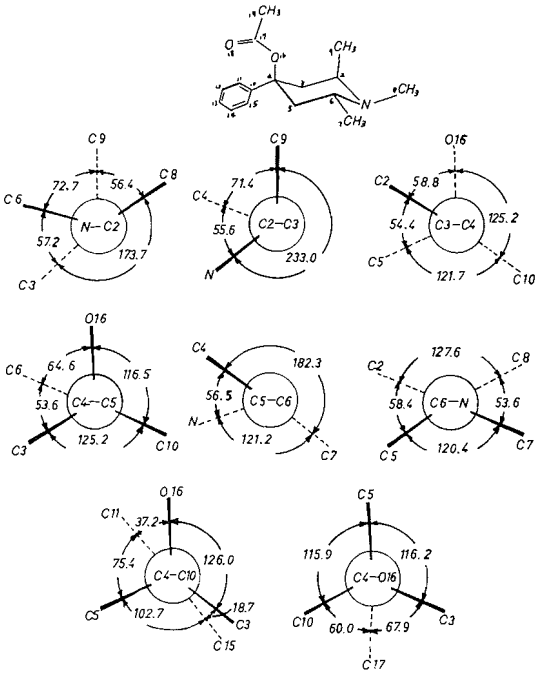

FIG. 4. Torsion angles for 1,2,6-trimethyl-4-phenyl-4-acetoxypiperidine hydrobromide.

cyclohexane rings (24). Several of the external torsion angles also deviate by a large amount from the expected 60.0°. Of particular interest are those angles involving the axial methyl group C(9) which has two torsion angles C(6)—N(1)—C(2)—C(9) = 72.7° and C(9)—C(2)—C(3)—C(4) = 71.4°. These large angles result from the close contact of two axial groups across a six-membered ring, namely C(9) and O(16) of the acetoxy group. The crystal structure of *epi*-inositol (24) has shown that the molecule of inositol containing two axial OH groups on alternate carbon atoms of a cyclohexane ring has comparable exocyclic torsion angles distorted to 65.1 and 69.3°. The internal ring bond angle at the atom bonded to the two carbon atoms containing the axial hydroxyl groups (C(1) in the inositol structure) is distorted to a value of 114.7(2)° (*cf.* the comparable angle at C(3) in the present work of 115.6(4)°). This distortion is also visualized in the two exocyclic bond angles C(3)—C(2)—C(9) = 117.2(4)° and C(3)—C(4)—O(16) = 111.3(4)°. The other external torsion angles which show large deviations from expected values are involved with atom O(16). These deviations result from the bond angle distortion at C(4) from tetrahedral values *viz.* C(3)—C(4)—C(10) = 114.7(4)° and C(5)—C(4)—O(16) = 103.6(4)°. Other piperidine ring bond angles that deviate significantly from the tetrahedral value of 109.5° are C(2)—C(3)—C(4) = 115.6(4)° and C(4)—C(5)—C(6) = 113.3(4)°. These latter two angles are also large in γ-promedol (7), α-promedol (8), and betaprodine (11).

The orientation of the axial acetoxy group on C(4) is seen in the dihedral angle drawing (Fig. 4). The mean plane of the acetoxy group O(16), C(17), O(18), C(19) is given by the equation $-0.9355x + 0.3477y - 0.0622z - 1.3713 = 0$ ($\chi^2 = 0.07$). This plane makes an angle of 3.9° to the plane containing C(4), C(5), O(16) and is *gauche* with respect to both C(3) and C(10). There are two relatively close contacts made to O(18) which could explain the large angle at O(16) of 119.0(4)°. These are C(10)—O(18) = 2.907(7) Å and O(18)—H(32) = 2.36(5) Å. With van der Waals radii of O = 1.40 Å and H = 1.20 Å and the half thickness of a benzene ring of 1.70 Å these distances have expected values of 3.10 Å and 2.60 Å, respectively.

The packing of the molecules in the unit cell is shown in Fig. 5 (*a*) and (*b*). The bromide ion is hydrogen bonded to N(1) and the Br—N(1) distance is 3.234(6) Å. This distance agrees with the corresponding distances in betaprodine hydrobromide (3.209 Å) and pethidine hydrobromide (3.24 Å). The molecules are related across the center of symmetry at the origin by close contact with the acetoxy groups; the distance between O(18) and C(19) across this center is 3.421(9) Å. Contact across the center of symmetry at 1/2,1/2,1/2 brings the methyl groups C(7) bonded to the piperidine ring atom C(6) to a separation of 3.804(8) Å. This is slightly less than 4.0 Å based on a methyl group radius of 2.0 Å. For those molecules related by the *c*-glide plane, there is a close contact between the phenyl ring and the acetoxy methyl carbon atom C(19). The distances from C(19) of the molecule at x, $1/2 - y$, $1/2 + z$ to the atoms of the phenyl ring of the molecule at x, y, z are C(10), 3.715(9) Å; C(11), 3.555(8) Å; C(12), 3.480(8) Å; C(13), 3.568(9) Å; C(14), 3.705(9) Å; C(15), 3.768(9) Å. The contacts to C(11), C(12), and C(13) are therefore approximately 0.2 Å shorter than expected from the van der Waals radii of the groups involved. It is curious that it was the region around C(19) that did not show evi-

Can. J. Chem. Downloaded from www.nrcresearchpress.com by 210.87.254.105 on 09/05/12
For personal use only.

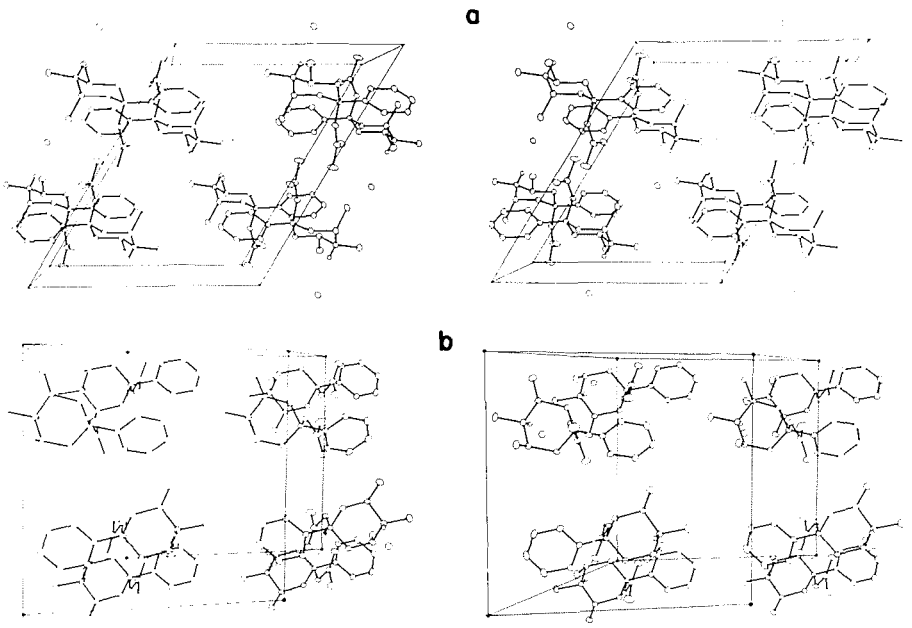

FIG. 5. (*a*) Packing diagram of the molecules in the unit cell as seen along the *b* axis. The *a* axis is horizontal and the *c* axis is down the page. (*b*) Packing diagram of the molecules in the unit cell viewed along the c* axis. The *a* axis is horizontal and the *b* axis is vertical on the page.

dence of the hydrogen atoms on any of the difference maps.

The authors wish to acknowledge the receipt of the crystals of this compound from Dr. A. F. Casy. This work was supported by a grant from the Medical Research Council of Canada (MA-3406) to M.N.G.J.

1. H. VAN KONINGSVELD. Rec. Trav. Chim. Pays Bas, **89**, 375 (1970).
2. P. A. J. JANSSEN and N. B. EDDY. J. Med. Chem. **2**, 31 (1960).
3. A. F. CASY and K. MCERLANE. J. Pharm. Pharmacol. **23**, 68 (1971).
4. T. F. VLASOVA and Y. N. SHEINKER. J. Struct. Chem. USSR, **11**, 640 (1970).
5. A. J. JONES, A. F. CASY, and K. M. J. MCERLANE. Tetrahedron Lett. **17**, 1727 (1972).
6. W. H. DE CAMP and F. R. AHMED. Chem. Commun. 1102 (1971).
7. W. H. DE CAMP and F. R. AHMED. Acta Cryst. **B28**, 1791 (1972) .
8. W. H. DE CAMP and F. R. AHMED. Acta Cryst. **B28**, 1796 (1972).
9. W. H. DE CAMP and F. R. AHMED. Am. Cryst. Assn. Abstr. Winter Meeting. 1972. p. 24.
10. G. KARTHA, F. R. AHMED, and W. H. BARNES. Acta Cryst. **13**, 525 (1960).
11. F. R. AHMED, W. H. BARNES, and L. D. MASIRONI. Acta Cryst. **16**, 237 (1963).
12. A. F. CASY. Private communication.
13. W. R. BUSING and H. A. LEVY. Acta Cryst. **22**, 457 (1967).
14. S. W. PETERSON and H. A. LEVY. Acta Cryst. **10**, 70 (1957).
15. M. N. G. JAMES and G. J. B. WILLIAMS. J. Med. Chem. **14**, 670 (1971).
16. D. T. CROMER. Acta Cryst. **18**, 17 (1965).
17. D. T. CROMER. Acta Cryst. **A24**, 321 (1968).
18. R. MASON and G. B. ROBERTSON. *In* Advances in structure research by diffraction methods. Vol. 2. *Edited by* R. Brill and R. Mason. Interscience, New York, N.Y. 1966. p. 57.
19. F. R. AHMED, S. R. HALL, M. E. PIPPY, and C. P. HUBER. N.R.C. Crystallographic programs for the IBM/360 Systems, *world list of crystallographic computer programs*. 2nd ed. 1966. Appendix p. 52.
20. M. N. G. JAMES and J. MACDONALD. (1972). Unpublished results.
21. W. R. BUSING and H. A. LEVY. Acta Cryst. **17**, 142 (1964).
22. N. L. ALLINGER and M. T. TRIBBLE. Tetrahedron Lett. 3259 (1971).
23. H. M. BERMAN and S. H. KIM. Acta Cryst. **B24**, 897 (1968).
24. G. A. JEFFERY and S. H. KIM. Acta Cryst. **B27**, 1812 (1971).
25. C. K. JOHNSON. ORTEP. Report ORNL-TM3794, Oak Ridge National Laboratory, Oak Ridge, Tennessee. 1965.

Can. J. Chem. Downloaded from www.nrcresearchpress.com by 210.87.254.105 on 09/05/12
For personal use only.

Metal Complexes as Antioxidants. I. The Reaction of Zinc Dialkyldithiophosphates and Related Compounds with Peroxy Radicals[1]

J. A. HOWARD, Y. OHKATSU, J. H. B. CHENIER, AND K. U. INGOLD
Division of Chemistry, National Research Council of Canada, Ottawa, Canada K1A 0R9

Received October 6, 1972

The kinetics of the inhibition of the autoxidation of several hydrocarbons by a number of zinc dialkyldithiophosphates and by zinc isopropylxanthate and zinc diethyldithiocarbamate have been studied at 30° and at 50°. The oxidations were generally auto-retarding but initial rate measurements showed that these compounds trapped peroxy radicals and allowed rate constants for this process to be calculated. Rate constants for the reaction of *t*-butylperoxy radicals with these compounds have been measured by a kinetic e.p.r. method in the temperature range 0° to −90°. Extrapolation of the e.p.r. data to the temperatures of the inhibition studies showed that the various experimental procedures yielded results in satisfactory agreement with one another.

It is suggested that the reaction of peroxy radicals with zinc complexes involves reaction at the metal center either by an electron transfer or an S_H2 process.

Les cinétiques d'inhibition de l'auto-oxydation de plusieurs hydrocarbures par un certain nombre de phosphates de dialkyldithio zinc, d'isopropylxanthate de zinc et de diéthyldithiocarbamate de zinc, ont été étudiées à 30° et à 50°. Les oxydations sont généralement auto-retardées mais les mesures de vitesse initiale montrent que ces composés piègent les radicaux peroxy et permettent ainsi le calcul des constantes de vitesse pour ce processus. Les constantes de vitesse pour la réaction des radicaux *t*-butylperoxy sur ces composés ont été mesurées par une méthode cinétique r.p.e. dans l'intervalle de température de 0° à −90°. L'extrapolation des données r.p.e. aux températures d'étude de l'inhibition montre que tous les divers procédés expérimentaux donnent des résultats en accord satisfaisant.

On a suggéré que la réaction des radicaux peroxy sur les complexes de zinc implique une réaction sur le centre métallique soit par un transfert d'électron soit par un processus S_H2.

[Traduit par le journal]

Can. J. Chem., **51**, 1543 (1973)

Introduction

Zinc dialkyldithiophosphates, $[(RO)_2PS_2]_2Zn$, have been widely used as lubricating oil additives. They combine antioxidant properties with an ability to inhibit corrosion and to function as antiwear and as extreme pressure agents for motor oils and automatic transmission fluids. In spite of numerous investigations the detailed mechanism of their antioxidant activity is still uncertain. These compounds, or their decomposition products, have long been known to catalyze the decomposition of hydroperoxides. At low molar ratios of zinc dialkyldithiophosphate to hydroperoxide the products are identical with those formed in an acid catalyzed decomposition, for example, phenol and acetone are produced from cumene hydroperoxide (1).

$$PhC(CH_3)_2OOH \xrightarrow[\text{in catalytic quantities}]{H^+ \text{ or } [(RO)_2PS_2]_2Zn} PhOH + CH_3COCH_3$$

[1]NRCC No. 13088.

Very recently it has been found that when the dithiophosphate and cumene hydroperoxide are present in approximately equimolar amounts the hydroperoxide is reduced almost quantitatively to α,α-dimethylbenzyl alcohol along with traces of acetophenone and α-methylstyrene (1–3). These products are indicative of either a molecular or free-radical induced decomposition of the hydroperoxide.

$$PhC(CH_3)_2OOH \xrightarrow[\text{equimolar quantity}]{[(RO)_2PS_2]_2Zn \text{ in}} PhC(CH_3)_2OH$$

It has been known for some years that zinc dithiophosphates and related compounds do not owe their entire antioxidant action to their ability to destroy hydroperoxides since they are also able to trap certain free radicals (4–15). Although some kinetic studies of this radical trapping antioxidant process have been undertaken, very little quantitative information has been obtained because simple kinetic laws do not appear to have been obeyed. However, a careful

Can. J. Chem. Downloaded from www.nrcresearchpress.com by 210.87.254.42 on 09/05/12
For personal use only.

Can. J. Chem. Downloaded from www.nrcresearchpress.com by 210.87.254.42 on 09/05/12
For personal use only.

reading of the kinetic papers reveals two important points. In the first place, cumene, tetralin, or ethylbenzene have been employed as the oxidizable substrates. The hydroperoxides derived from these compounds are expected to yield phenols via the catalytic decomposition mentioned above.[2] Since phenols are potent peroxy radical traps, some difficulty in determining the reaction orders and rate constants for the radical–dithiophosphate reaction might be expected. In the second place, in the only detailed kinetic study (6), inhibited oxidation rates were measured under conditions of very short chain lengths ($\nu \sim 1$–3). Meaningful kinetic data on the trapping of the autoxidation chain carrying radicals by the antioxidant cannot be expected to be obtained under such conditions.

The present paper describes a variety of kinetic experiments designed to study the radical trapping antioxidant process for several zinc dialkyldithiophosphates and for a number of related zinc complexes. Rate constants for the peroxy radical – antioxidant reactions have been determined at 50° and at 30° from the rates of inhibited hydrocarbon oxidation and at low temperatures (0° to −90°) by kinetic electron spin resonance spectroscopy. The data obtained by these independent techniques are in satisfactory agreement.

Experimental

Inhibition of Autoxidation

The autoxidation apparatus and general experimental techniques have been adequately described in our earlier papers on inhibition by phenols (16) and amines (17) and on the determination of absolute rate constants for hydrocarbon autoxidation (18). At 50° autoxidations were initiated by the thermal decomposition of α,α′-azo-bis-isobutyronitrile (AIBN) and at 30° they were initiated by the photochemical decomposition of α,α′-azo-bis-cyclohexanecarbonitrile (ACHN). Rates of chain initiation were determined by the usual induction period method (19) using 2,6-di-*t*-butyl-4-methoxyphenol as the inhibitor. The hydrocarbon substrates and the solvents were carefully purified by standard techniques. Adventitious hydroperoxides were the most troublesome impurity and were removed by distillation and/or percolation through basic alumina.

Kinetic E.P.R. Experiments

t-Butylperoxy radicals were generated directly in the cavity of a Varian E-3 e.p.r. spectrometer at temperatures in the range 0° to −90°. The radicals were formed either by the photolysis of 2,2′-azoisobutane (Merck, Sharpe, and Dohme of Canada, Ltd.) in air saturated isopentane,

$$t\text{-BuN=NBu-}t \xrightarrow{h\nu} N_2 + 2t\text{-Bu}^{\cdot} \xrightarrow{O_2} t\text{-BuOO}^{\cdot}$$

or by the photolysis of di-*t*-butyl peroxide in air saturated isobutane.

$$t\text{-BuOOBu-}t \xrightarrow{h\nu} 2t\text{-BuO}^{\cdot} \xrightarrow{t\text{-BuH}} t\text{-Bu}^{\cdot} \xrightarrow{O_2} t\text{-BuOO}^{\cdot}$$

Decays of the radicals upon interruption of the irradiation were followed in the usual way (20). In the absence of a peroxy radical trap *t*-butylperoxy decayed bimolecularly but in the presence of a sufficient concentration of a trap decay was first order. Rate constants for reaction of this peroxy radical with the inhibitor were calculated from the measured rates of radical decay and the concentration of the inhibitor.

Materials

We are indebted to Dr. B. R. Kennedy (Chevron) for generous analytically pure samples of some of the metal complexes used in this work. The few compounds that had to be made in our laboratory were prepared by standard methods and were purified with great care before use.

Results

(a) Kinetics of Inhibited Autoxidations

(1) General

The simplest reaction scheme which can describe the inhibition of the autoxidation of a hydrocarbon, RH, by an antioxidant, A, that traps peroxy radicals can be represented as follows.

Initiation

$$\text{Production of R}^{\cdot} \text{ at a rate} = R_i$$

Propagation

$$R^{\cdot} + O_2 \xrightarrow{\text{fast}} ROO^{\cdot}$$

$$ROO^{\cdot} + RH \xrightarrow{k_p} ROOH + R^{\cdot}$$

(or, for a polymerizable olefin such as styrene (16)

$$ROO^{\cdot} + RH \xrightarrow{k_p} ROO\dot{R}H\ (\equiv R^{\cdot})$$

Termination

$$ROO^{\cdot} + A \xrightarrow{k_{inh}} X$$

$$(n-1)ROO^{\cdot} + X \xrightarrow{\text{fast}} \text{non-radical products}$$

Provided the chain length of the inhibited oxidation, $\nu(= -d[O_2]/dt/R_i)$, is $\geqslant 5$, problems arising from differences in the reactivity of the initiating radical (*i.e.* the radicals from AIBN and ACHN) and the chain propagating radical

[2]Non-alkylaromatic hydrocarbons have, however, been employed in qualitative experiments (4, 5).

TABLE 1. Induction periods and n values for zinc diisopropyldithiophosphate inhibited autoxidations

Substrate	Dithiophosphate concentration $\times$ 10^4 (M)	Induction period $\times$ 10^{-3} (s)	$R_i \times 10^7$ ($M\ s^{-1}$)	n
Thermal initiation at 50°				
Tetralin	1.0	0.38	1.7	0.7
Tetralin	2.0	1.0	1.7	0.9
Tetralin	4.0	3.6	1.7	1.5
Tetralin	8.0	6.8	1.7	1.4
Cyclohexene	5.0	7.5	0.6	0.9
DHA*	1.5	3.1	0.5	1.0
DHA*†	1.5	2.5	0.6	1.0
Photochemical initiation at 30°				
Tetralin	4.0	11	1.2	3.3
Cumene	4.0	10	1.2	3.1
Styrene‡	2.0	7.7	1.1	4.3
Styrene‡§	2.0	7.2	1.2	4.3
Styrene‡‖	2.0	7.5	1.2	4.5
Styrene‡	6.0	32	0.8	4.3

*9,10-Dihydroanthracene, 1.0 M in chlorobenzene.
†With 10^{-3} M 9,10-dihydroanthracene-9-hydroperoxide.
‡1.7 M in chlorobenzene.
§With 10^{-2} M cumene hydroperoxide.
‖With 10^{-2} M t-butyl hydroperoxide.

can be neglected. The initial rate of oxidation (corrected for oxygen absorption by, and nitrogen evolution from, the initiator) according to this scheme will be independent of the oxygen pressure. It is given by

$$\left[\frac{-\mathrm{d}[O_2]}{\mathrm{d}t}\right]_0 = \frac{k_p[RH]_0 R_i}{nk_{inh}[A]_0}$$

where the subscript 0 refers to the initial concentrations, and n is the number of peroxy radicals trapped by each molecule of A. If the antioxidant behaves in this simple manner, then

$$\frac{[RH]_0 R_i}{[A]_0(-\mathrm{d}[O_2]/\mathrm{d}t)_0} = \frac{nk_{inh}}{k_p}$$

We were unable to confirm previous reports (6, 12) that $n \sim 2.0$ for dithiophosphate antioxidants. Using the usual induction period method (19) we obtained $n \sim 1$ for AIBN initiated oxidations at 50° and $n \sim 3$–4 from photochemically initiated oxidations at 30° (see Table 1). The same n values were obtained with zinc isopropylxanthate and zinc diethyldithiocarbamate. However, there are considerable experimental difficulties in determining n for all these compounds because the induction periods are probably influenced by secondary reactions (*e.g.*, reaction between accumulated hydroperoxide and metal complex). For this reason, we have assumed that $n = 2$ in calculating all the values of k_{inh} quoted in this paper (see, however, section (*b*)).

(2) Thermal Initiation (50°)

Although thermally initiated reactions proved satisfactory for unravelling the mechanism and kinetics of the inhibition of hydrocarbon autoxidation by phenols (16) and aromatic amines (17), this method was much less useful for studying the dithiophosphates. The reason is that the oxygen absorption curves were nonlinear and exhibited pronounced curvature even at quite low extents of oxidation (see below). It was therefore necessary to measure initial oxidation rates, which is not particularly easy in a system that may still be approaching thermal equilibrium. However, our initial studies were made in this type of system using styrene, cyclohexene, and tetralin as substrates. The initial rates were sufficiently reproducible to show that the simple kinetic scheme outlined above was at least approximately obeyed with the zinc dialkyldithiophosphates at 50° (see Table 2 and 3 for examples of the data).

Values of the inhibition rate constants, k_{inh}, at 50° for the five zinc dithiophosphates studied are tabulated in Table 4 together with the k_p values used in the calculations. The similarity in the k_{inh} values obtained with different hydro-

Can. J. Chem. Downloaded from www.nrcresearchpress.com by 210.87.254.42 on 09/05/12
For personal use only.

TABLE 2. Inhibition of the AIBN initiated autoxidation of syrene by zinc diisopropyldithiophosphate at 50° and an oxygen pressure of 700 mm Hg

Styrene $[RH]_0$ (M)	Inhibitor $[A]_0 \times 10^4$ (M)	$(-d[O_2]/dt)_0 \times 10^6$ ($M\ s^{-1}$)	$R_i \times 10^7$ ($M\ s^{-1}$)	$\frac{[RH]_0 R_i}{(-d[O_2]/dt)_0[A]_0} \times 10^{-2}$
8.7	5.0	12	1.5	2.0
8.7	10	7.7	1.5	1.7
8.7	20	4.0	1.5	1.6
8.7	40	2.1	1.5	1.5
8.7	80	0.94	1.5	1.7
8.7	100	0.8	1.5	1.6
8.7	40	4.5	3.0	1.4
8.7	40	1.4	0.9	1.4
8.7	40	0.85	0.6	1.5
8.7	40	0.63	0.15	1.0
7.0*	40	1.7	1.5	2.0
5.2*	40	1.1	1.5	1.7
3.5*	40	1.0	1.5	1.3
1.8*	40	0.35	1.5	1.9

*o-Dichlorobenzene as diluent.

TABLE 3. Inhibition of the AIBN initiated autoxidation of cyclohexene by zinc diisobutyldithiophosphate at 50° ($R_i = 1.5 \times 10^{-7}\ M\ s^{-1}$)

Cyclohexene $[RH]_0$ (M)	Inhibitor $[A]_0 \times 10^4$ (M)	$(-d[O_2]/dt)_0$* $\times 10^6$ ($M\ s^{-1}$)	$\frac{[RH]_0 R_i}{(-d[O_2]/dt)_0[A]_0} \times 10^{-2}$
9.9	1.0	13	10.9
9.9	1.0	13†	10.9
9.9	1.0	13‡	10.9
9.9	2.0	7.4	9.9
9.9	3.4	4.0	10.9
9.9	6.0	2.5	9.7
9.9	10	1.5	9.6
9.9	40	0.4	9.1
7.9§	2.0	5.4	10.8
5.5§	2.0	3.5	11.7
4.0§	2.0	2.4	12.4

*At 760 mm O_2 unless otherwise noted.
†At 480 mm O_2.
‡At 330 mm O_2.
§o-Dichlorobenzene as diluent.

TABLE 4. Inhibition rate constants $\times 10^{-3}\ M^{-1}\ s^{-1}$ for zinc dialkyldithiophosphates at 50°

Substrate	k_p ($M^{-1}\ s^{-1}$)	$[(RO)_2PS_2]_2Zn$ for R = $(CH_3)_2CH$	$(CH_3)_2CCH_2$	$CH_3CH_2(CH_3)CH$	n-$C_{16}H_{33}$	$(CH_3)_3C(CH_3)CH$
Styrene	98*	8.0	2.3	3.0	1.4	—
Cyclohexene	12†	7.0	6.4	3.2	7.0	1
Tetralin	13.6‡	3.9	4.4	2.1	5.0	—

*Reference 21.
†Twice the k_p value measured at 30° (ref. 22), *i.e.* calculated assuming $E_p \approx 7.5$ kcal/mol.
‡Reference 22.

Can. J. Chem. Downloaded from www.nrcresearchpress.com by 210.87.254.42 on 09/05/12
For personal use only.

TABLE 5. Inhibition of the photochemically initiated autoxidation of some hydrocarbons by zinc diisopropyldithiophosphate at 30° and an oxygen pressure of 700 mm Hg

Substrate (RH)	$[RH]_0$* (M)	Inhibitor $[A]_0 \times 10^2$ (M)	$(-d[O_2]/dt)_0 \times 10^6$ ($M\ s^{-1}$)	$R_i \times 10^7$ ($M\ s^{-1}$)	$\frac{[RH]_0 R_i}{(-d[O_2]/dt)_0[A]_0}$
Styrene	8.7	1.6	2.3	0.55	13
Styrene	1.8	1.6	1.2	1.8	16
Styrene	8.7	1.6	7.2	1.8	14
Styrene	8.7	2.4	4.0	1.8	16
Styrene	8.7	8.0	2.4	1.8	8
Cyclohexene	9.9	1.6	0.7	1.2	106
Tetralin	7.3	0.8	1.9	1.2	57
Tetralin	7.3	1.6	0.9	1.2	61
Benzaldehyde	0.4	0.8	0.2	0.16	4.0
Benzaldehyde	0.4	0.8	2.3	1.2	2.6
Benzaldehyde	0.4	0.8	1.8	1.2	3.3
Benzaldehyde	0.4	3.2	0.3	0.38	1.5
Benzaldehyde	0.4	1.6	1.6	1.2	1.9
Benzaldehyde	0.4	3.2	1.3	1.2	1.1
Cyclohexa-1,3-diene	0.4	1.6	8.4	1.2	0.36
Cyclohexa-1,4-diene	0.4	1.6	1.2	1.2	2.5
9,10-Dihydroanthracene	0.55	1.6	2.6	1.2	1.6

*The diluent, when used, was chlorobenzene.

TABLE 6. Inhibition of photochemically initiated autoxidations by zinc isopropylxanthate, $[isoPrOCS_2]_2Zn$, at an oxygen pressure of 700 mm Hg at 30°

Substrate (RH)	$[RH]_0$ (M)	Inhibitor $[A]_0 \times 10^3$ (M)	$(-d[O_2]/dt)_0 \times 10^6$ ($M\ s^{-1}$)	$R_i \times 10^7$ ($M\ s^{-1}$)	$\frac{[RH]_0 R_i}{(-d[O_2]/dt)_0[A]_0}$
Styrene	1.8*	2.0	0.62	1.8	260
Styrene	8.7	2.0	3.0	1.8	260
Styrene	8.7	3.0	1.6	1.8	320
Styrene	8.7	4.0	1.5	1.8	260
Styrene	8.7	6.0	0.8	1.8	320
Styrene	8.7	8.0	0.6	1.8	320
Tetralin	7.3	1.0	1.2	1.2	730
Tetralin	7.3	2.0	0.6	1.2	730

*Diluted with chlorobenzene.

carbon substrates provides additional support for the reaction scheme given above. There can be no doubt that these compounds are moderately efficient traps for peroxy radicals. Unfortunately, because of the difficulties involved in initial rate measurements, the variations in k_{inh} from substrate to substrate and from one antioxidant to another are within the probable experimental errors. The mean value for k_{inh} for a zinc dialkyldithiophosphate at 50° is $4.2 \times 10^3\ M^{-1}\ s^{-1}$.

(3) Photochemical Initiation (30°)

The reaction system was allowed to come to thermal equilibrium in the dark before initiating the oxidation photochemically. This allowed initial rates to be determined with much greater accuracy than in the thermally initiated oxidations. In order to reduce the importance of any thermal self-initiation process the photochemically initiated autoxidations were carried out at 30°. Zinc diisopropyldithiophosphate followed the same simple kinetics as at 50° (see Table 5

Can. J. Chem. Downloaded from www.nrcresearchpress.com by 210.87.254.42 on 09/05/12
For personal use only.

TABLE 7. Inhibition of photochemically initiated autoxidations by zinc diethyldithiocarbamate, $[Et_2NCS_2]_2$ Zn, at an oxygen pressure of 700 mm Hg at 30°

Substrate (RH)	$[RH]_0$ (M)	Inhibitor $[A]_0 \times 10^2$ (M)	$(-d[O_2]/dt)_0 \times 10^6$ ($M\,s^{-1}$)	$R_i \times 10^7$ ($M\,s^{-1}$)	$\frac{[RH]_0 R_i}{(-d[O_2]/dt)_0[A]_0}$
Styrene	8.7	0.8	11	0.58	5.8
Styrene	8.7	3.2	2.9	0.58	5.4
Styrene	8.7	3.2	7.0	1.8	7.0
Styrene	8.7	4.8	2.4	0.58	4.4
Styrene	8.7	4.8	5.6	1.8	5.8
Tetralin	7.3	1.5	1.4	1.2	4.2
Tetralin	7.3	3.0	0.8	1.2	3.7

TABLE 8. Inhibition rate constants for some zinc complexes at 30°

Substrate	k_p* ($M^{-1}\,s^{-1}$)	$10^{-2}k_{inh}$ ($M^{-1}\,s^{-1}$)		
		$[(isoPrO)_2PS_2]_2Zn$	$[isoPrOCS_2]_2Zn$	$[Et_2NCS_2]_2Zn$
Styrene	41	2.8	59	8.8
Cyclohexene	5.4	4.3	—	—
Tetralin	6.4	3.0	23	1.3
Benzaldehyde	33000	480	—	—
Cyclohexa-1,3-diene	810	1.5	—	—
Cyclohexa-1,4-diene	1480	28	—	—
9,10-Dihydroanthracene	330	4.0	—	—

*From reference 23.

for representative data). Inhibition by zinc isopropylxanthate (Table 6) and by zinc diethyldithiocarbamate (Table 7) also obeyed the same kinetics. The calculated inhibition rate constants at 30° are summarized in Table 8. For those substrates for which the oxidation chains are carried by alkylperoxy radicals (*i.e.* styrene, cyclohexene, tetralin, cyclohexa-1,3-diene, and 9,10-dihydroanthracene) the mean values of $k_{inh}^{30°}$ are $3.1 \times 10^2\ M^{-1}\ s^{-1}$ for the dithiophosphate, 41×10^2 for the xanthate, and 5.0×10^2 for the carbamate.

(4) Effect of Hydroperoxide on Inhibited Rates

In general, zinc dithiophosphate inhibited autoxidations were strongly autoretarding. Thus, the rates of oxidation of tetralin (Fig. 1, *I*), 9,10-dihydroanthracene (Fig. 2, *I*), and cyclohexa-1,4-diene (Fig. 2, *II*), decreased markedly after the absorption of as little as $3 \times 10^{-4}\ M$ oxygen. The initial, relatively rapid stage in the inhibited oxidation could be eliminated by pre-oxidizing the hydrocarbon (tetralin, for example, to a hydroperoxide concentration of $\sim 7 \times 10^{-4}\ M$). A similar effect was obtained by adding $\sim 5 \times 10^{-4}\ M$ *t*-butyl hydroperoxide, although in this case the autoxidation was not as slow as when the tetralin was pre-oxidized. Auto-retardation was less pronounced with styrene (which yields principally a polyperoxide, Fig. 2, *III*), cyclohexa-1,3-diene (which yields both hydroperoxide and polyperoxide, Fig, 2, *IV*), and cyclohexene (Fig. 2, *V*), than with the three hydrocarbons mentioned above. Auto-retardation of the inhibited autoxidation of benzaldehyde was slight (Fig. 2, *VI*), but the degree of inhibition by the dithiophosphate was much greater than was found with any of the hydrocarbon substrates.

It would appear that zinc dithiophosphates react with hydroperoxides to produce a more active antioxidant.[3] The more pronounced auto-retardation produced by aralkyl hydroperoxides (*i.e.* those from tetralin and dihydroanthracene) compared with alkyl hydroperoxides, suggests that this reaction is, at least in part, ionic. That is, the aralkyl hydroperoxides can yield phenolic antioxidants (for which $k_{inh} \sim 10^4\ M^{-1}\ s^{-1}$ (16)) in addition to any antioxidants produced from the dithiophosphate itself.

[3]The final products formed by reaction of zinc dithiophosphates with 0.25 mole cumene hydroperoxide (*e.g.* $[(RO)_2PS_2]_6Zn_4O$, see ref. 2) are completely ineffective as antioxidants.

Can. J. Chem. Downloaded from www.nrcresearchpress.com by 210.87.254.42 on 09/05/12
For personal use only.

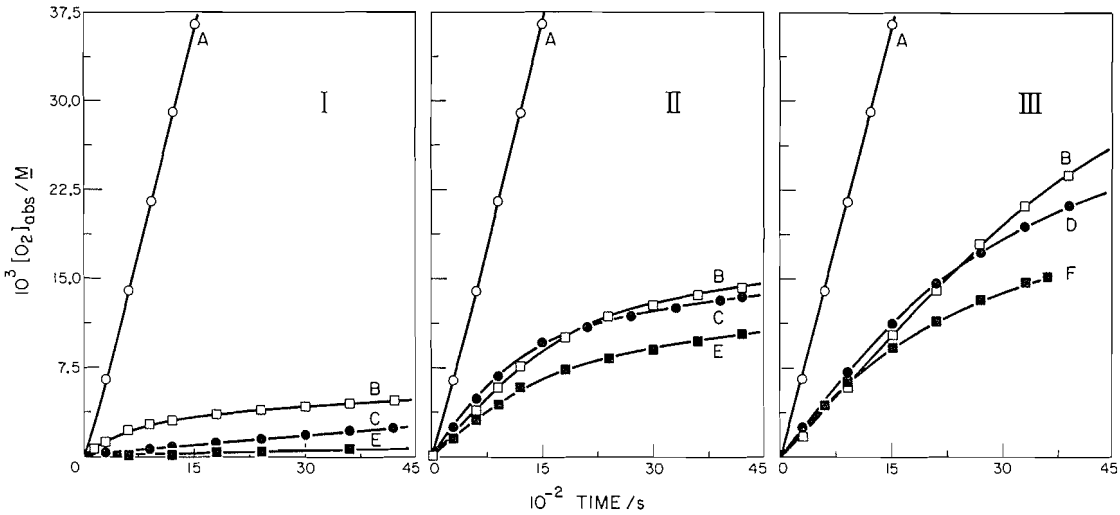

FIG. 1. Oxygen absorption *vs.* time for the photochemically initiated ($R_i = 1.2 \times 10^{-7}$ M s^{-1}) autoxidation of tetralin at 30° inhibited by; *I*, zinc di-isopropyldithiophosphate (0.016M); *II*, zinc isopropylxanthate (0.001 M); and *III*, zinc diethyldithiocarbamate (0.0015 M). *A*, uninhibited; *B*, inhibited, no hydroperoxide present initially; *C*, inhibited, *t*-butyl hydroperoxide (5×10^{-4} M) added; *D*, inhibited, *t*-butyl hydroperoxide (0.01 M) added; *E*, inhibited, tetralin pre-oxidized (to $\sim 7 \times 10^{-4}$ M in hydroperoxide); *F*, inhibited, tetralin hydroperoxide (0.01 M) added.

The effects of hydroperoxides on the initial rates of oxidation of tetralin inhibited by zinc isopropylxanthate (Fig. 1, *II*) and zinc diethyldithiocarbamate (Fig. 1, *III*) are much less than their effects on the dithiophosphate inhibited reaction (Fig. 1, *I*).

It has been reported that zinc dithiophosphates (2, 6, 10) and related compounds (14, 24) *may* exert a pro-oxidant effect on the initial stages of the oxidation of hydrocarbons containing hydroperoxides. We have observed such effects with zinc isopropylxanthate at high hydroperoxide concentrations but not with the dithiophosphate or carbamate. For example, the addition of *t*-butyl hydroperoxide (10^{-2} M) to styrene (7.8 M) containing xanthate (10^{-2} M) that was at thermal equilibrium at 30° caused a rapid, $(-d[O_2]/dt)_0 = 3.7 \times 10^{-7}$ M s^{-1}, but strongly autoretarded absorption of oxygen. No such effect occurred with dithiophosphate or carbamate and, in fact, if *t*-butyl hydroperoxide was added during the course of a dithiophosphate or carbamate inhibited oxidation of styrene, the rate of oxidation was reduced.

(b) Kinetic E.P.R. Spectroscopy

t-Butylperoxy radicals decayed with first order kinetics in the presence of an excess of zinc dialkyldithiophosphates, *i.e.*

$$\frac{-d[t\text{-BuOO}^{\cdot}]}{dt} = nk_{inh}[t\text{-BuOO}^{\cdot}]_0[A]_0$$

The variation with temperature of the k_{inh} values determined by kinetic e.p.r. spectroscopy yielded the Arrhenius parameters listed in Table 9 for the three zinc dialkyldithiophosphates studied in this way. The Arrhenius plot for these inhibitors is shown in Fig. 3 together with the mean k_{inh} values obtained by conventional inhibition studies at 30° and 50°. The agreement in the k_{inh} values obtained by the different methods at different temperatures is satisfactory.

TABLE 9. Arrhenius parameters for the reactions of *t*-butylperoxy radicals with zinc dialkyldithiophosphates and zinc isopropylxanthate as determined by kinetic e.p.r. spectroscopy*

Inhibitor	$\log_{10}(A_{inh}/M^{-1}$ $s^{-1})$	E_{inh} (kcal/mol)
Zinc Dithiophosphates		
Diisopropyl	6.0	4.0
Diisobutyl	6.1	4.1
Di-*s*-butyl	6.0	4.1
Zinc Xanthate		
Isopropyl	7.2	3.8

*Decay constants were measured from 0 to −90 °C.

Can. J. Chem. Downloaded from www.nrcresearchpress.com by 210.87.254.42 on 09/05/12
For personal use only.

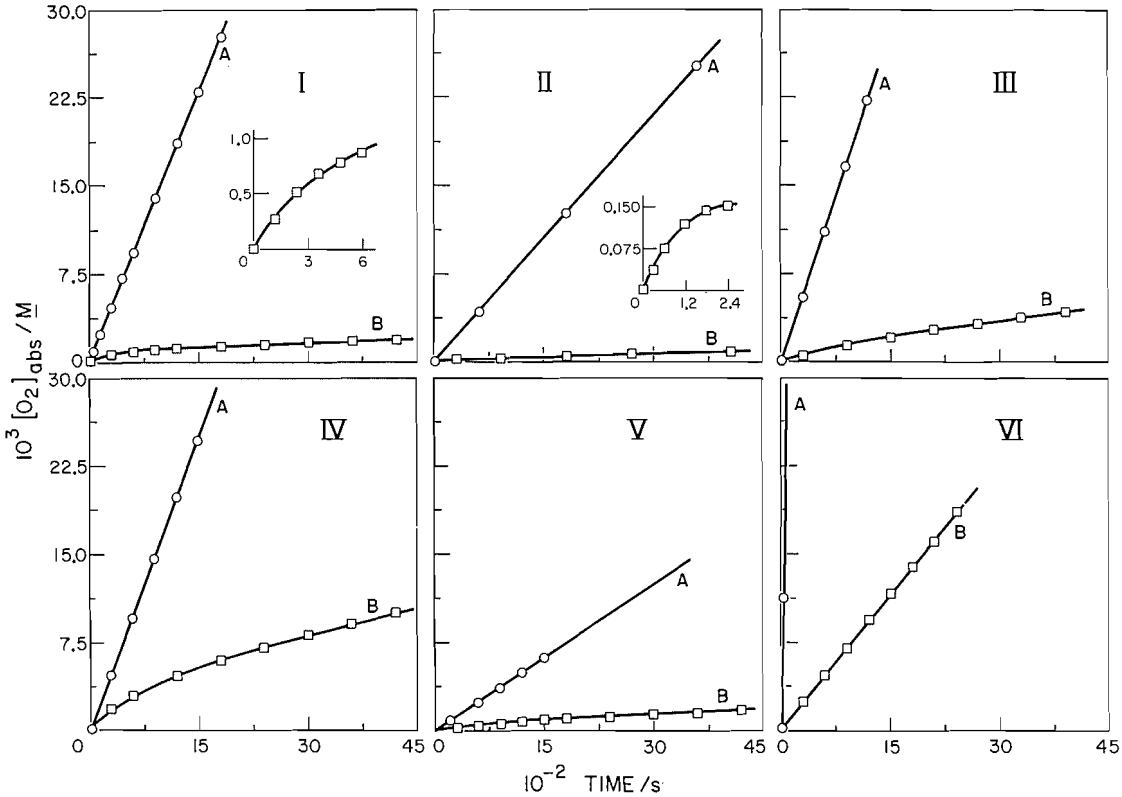

FIG. 2. Oxygen absorption *vs.* time for photochemically initiated ($R_i = 1.2 \times 10^{-7}$ M s^{-1}) autoxidations at 30°; *A*, uninhibited; *B*, inhibited by zinc di-isopropyldithiophosphate (0.016 *M*). *I*, 9,10-dihydroanthracene (0.55 *M* in chlorobenzene); *II*, cyclohexa-1,4-diene (0.42 *M* in chlorobenzene); *III*, styrene (8.7 *M*); *IV*, cyclohexa-1,3-diene (0.42 *M* in chlorobenzene); *V*, cyclohexene (10 *M*); and *VI*, benzaldehyde (0.4 *M* in chlorobenzene).

The decay of *t*-butylperoxy radicals in the presence of zinc isopropylxanthate was also a first order process. The Arrhenius parameters for k_{inh} are listed in Table 9 and the plot is shown in Fig. 3 together with the mean value obtained in the inhibition study at 30°.

Rates of decay of *t*-butylperoxy radicals in the presence of zinc dialkyldithiocarbamates were not reproducible and these experiments were not pursued further.

Discussion

Kinetics of Inhibition

Although several studies have been made of the reactions of peroxy radicals with zinc dialkyldithiophosphates and related compounds (see Introduction), the present work provides the first reliable kinetic data on the inhibition of hydrocarbon oxidation by this process and also the first reliable absolute rate constants for these reactions. The reasonable agreement between the k_{inh} values obtained by conventional inhibition studies and the values calculated by extrapolation of the e.p.r. results provides strong support for the kinetic schemes and for our numerical values of k_{inh}.[4]

The ability of zinc complexes to scavenge peroxy radicals decreases along the series xanthate > dithiophosphate ≥ dithiocarbamate. A similar order in reactivity was obtained from inhibition of the self-initiated oxidation of squalene at 75° (4), for the decomposition of

[4]Ivanov (8) has estimated that for zinc dicyclohexyldithiophosphate k_{inh} is 2.1×10^4 M^{-1} s^{-1} at 80° in ethylbenzene. This value is an order of magnitude greater than our extrapolated e.p.r. data would suggest. A value of k_{inh} which is in better agreement with our work (*viz.* 10^3 M^{-1} s^{-1} at 65°) has been obtained for zinc ditolyldithiophosphate (40).

Can. J. Chem. Downloaded from www.nrcresearchpress.com by 210.87.254.42 on 09/05/12
For personal use only.

Can. J. Chem. Downloaded from www.nrcresearchpress.com by 210.87.254.42 on 09/05/12
For personal use only.

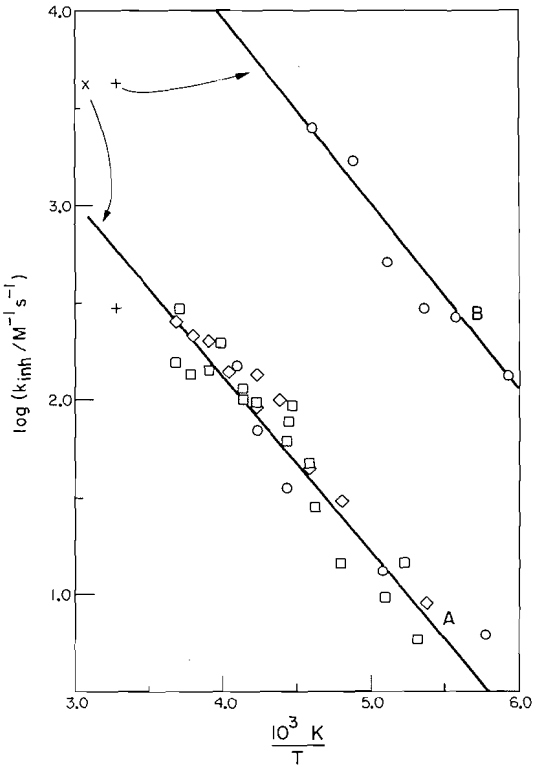

FIG. 3. Plot of log (k_{inh}/M^{-1} s^{-1}) *vs.* the reciprocal of the absolute temperature. The open points refer to values determined by kinetic e.p.r. spectroscopy. The × and + refer to the mean values found by alkylperoxy radicals from oxygen absorption experiments at 50° and 30°, respectively. *A*, reaction with zinc dialkyldithiophosphate (○, diisopropyl-; □, di-*s*-butyl-; and ◇, diisobutyl-). *B*, reaction with zinc isopropylxanthate.

t-butyl hydroperoxide at 20° (4), and (for the first two salts) for the inhibition of the AIBN initiated oxidation of cumene at 60° (5). In contrast, for the inhibition of the AIBN initiated oxidation of squalene at 60°, the order apparently is dithiophosphate > xanthate > dithiocarbamate (4) and for inhibition of the tetralin hydroperoxide catalyzed oxidation of tetralin at 50°, dithiocarbamate > dithiophosphate (24). The difficulties encountered in obtaining reproducible data by conventional methods may be one of the reasons for these conflicting orders in reactivity.

Zinc dithiophosphates are more effective inhibitors in cyclohexa-1,4-diene than in the other hydrocarbons (Table 8). In this compound the oxidation chain is carried by an HOO· radical rather than by an alkylperoxy radical (25). Our results suggest that the HOO· radical is trapped about ten times more readily. Zinc dithiophosphates are even more effective inhibitors in benzaldehyde. The benzoylperoxy radical is known to be between 1000 (26) and 40 000 (27) times as reactive in hydrogen abstraction from hydrocarbons as are alkylperoxy radicals. From the present work it would appear to be about 100 times as reactive towards a dithiophosphate. The high reactivity of benzoylperoxy is because the powerful electron withdrawing carbonyl group immediately adjacent to the peroxy group makes this radical much more electrophilic than an alkylperoxy radical.

Zinc dithiophosphates and related compounds are particularly effective antioxidants for systems subject to autoxidation at temperatures of 150° and above. Under such conditions their principal function is to decompose hydroperoxides. For this reason there is generally a powerful synergistic effect when they are used in conjunction with conventional peroxy radical trapping agents such as phenols[5] and aromatic amines (31, 32). The contribution from peroxy radical trapping to overall inhibition at high temperatures is difficult to estimate. If we take E_{inh} = 4.0 kcal/mol and $A_{inh} = 10^{6.0}$ M^{-1} s^{-1}, then at 150°, $k_{inh} \sim 10^4$ M^{-1} s^{-1}.[6] However, most commercial inhibitors of the zinc dithiophosphate type are unstable above ~150° (28) and it is therefore unlikely that peroxy radical trapping plays as important a role as is implied by the calculated value of k_{inh}.

Mechanism of Inhibition

Three mechanisms have been proposed for the reaction of peroxy radicals with zinc dialkyldithiophosphates (4–13). These are

[5]The conversion of dithiophosphates to acidic products by their oxidation or thermal decomposition (28) may be an important contributing factor to the synergistic effect observed with simple phenols since acids can catalyze the dimerization of certain phenoxy radicals (29). If the phenoxy radicals are not destroyed by dimerization they may continue the oxidation chain (30).

[6]This value is in the general range found for phenolic inhibition at temperatures of 50–80° (16, 23) and expected for phenolic inhibitors at 150° because of the small temperature coefficient for the peroxy radical – phenol reaction (33).

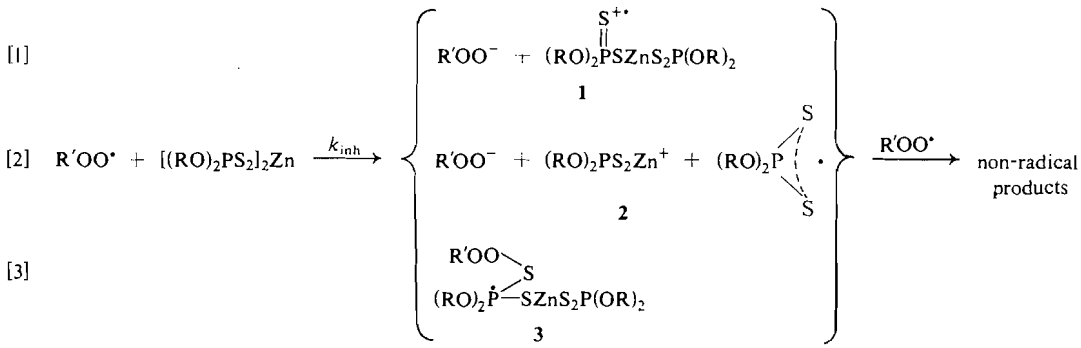

Reactions 1 and 3 have generally been favored in view of Liston, Ingersoll, and Adams (15) work on the *t*-butoxydithiophosphate reaction. These workers reported that photochemically generated *t*-butoxy radicals reacted with zinc dialkyldithiophosphates at 25° to produce a radical with an e.p.r. spectrum that consisted of a simple doublet (a = 24.8–26.7 G, g = 2.0203). The same e.p.r. spectrum was obtained with the diethylammonium salt but no signal was obtained with the free acid. This suggested that the *t*-butoxy radical reacted with the anion and so the observed radical was presumed to be analogous to **1**, or **3**, *i.e.*

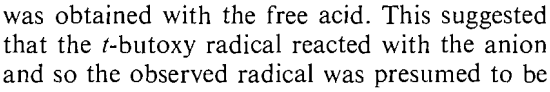

We found, however, that photolysis of both zinc diisopropyldithiophosphate and diisopropyldithiophosphoric acid in the *absence* of di-*t*-butyl peroxide gave doublet e.s.r. spectra with hyperfine interactions of 24.7–24.9 G. The intensity of these spectra did not appear to be influenced to any great extent by the addition of di-*t*-butyl peroxide. Although the radical produced in these systems was most probably $(i\text{-PrO})_2PS_2^{\cdot}$,[7] *i.e.*,

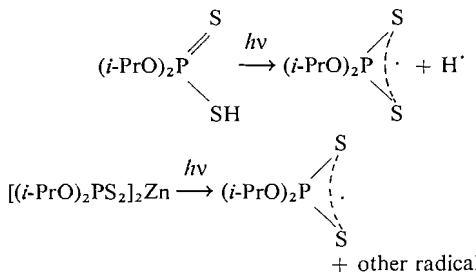

[7]It has been suggested (34) that one of the radical species (a_P = 25.5 G) formed during irradiation of dialkyldithiophosphoric acid glasses has the structure $(RO)_2PS_2^{\cdot}$.

we were unable to prove conclusively that reaction of zinc diisopropyldithiophosphate and diisopropyldithiophosphoric acid with *t*-butoxy radicals (and by analogy with alkylperoxy radicals) produced this radical.

There is no experimental evidence to indicate that peroxy radicals react with organosulfur compounds at the sulfur atom (35). Furthermore, the disulfide, $[(i\text{-PrO})_2PS_2]_2$ (5) or esters of the structure $(RO)_2P(S)SR$, *e.g.*, *O,O'*-diisopropyl-*S*-methylthionophosphate do not inhibit autoxidation or react with *t*-butylperoxy radicals at low temperatures (36). It, therefore, seems most probable that reaction of zinc dialkyldithiophosphates and related zinc complexes with peroxy radicals occurs at the metal center rather than at sulfur. Moreover, the small preexponential factors that we have found for this reaction (Table 9) are consistent with attack at a sterically protected central atom. Such a reaction at zinc could take place either by an electron transfer process analogous to [2] or perhaps by an S_H2 process (37),

[4] $$R'OO^{\cdot} + ZnX_2 \rightarrow R'OOZnX + X^{\cdot}$$

where X is $(RO)_2PS_2$, $ROCS_2$, or R_2NCS_2. Thus zinc diisopropyldithiophosphate may react with peroxy radicals to give the diisopropyldithiophosphate radical. It has been suggested (5) that this radical cannot be involved in inhibition because zinc diisopropyldithiophosphate inhibits the oxidation of olefins. In these substrates the zinc complex might be expected to function simply as a chain transfer agent because of the known ability of dialkyldithiophosphate radicals to add to olefins (38, 39).

It has, however, been reported (15), and we have confirmed (36), that dialkyldithiophosphoric acids inhibit hydrocarbon oxidation. For example, diisopropyl- and diethyl-dithiophosphoric acids inhibit the oxidation of cumene,

Can. J. Chem. Downloaded from www.nrcresearchpress.com by 210.87.254.42 on 09/05/12
For personal use only.

styrene, and cyclohexene. These acids also react with *t*-butylperoxy radicals at $-100°$ with bimolecular rate constants of the order of $5 \times 10^2\ M^{-1}\ s^{-1}$. The most probable mechanism for inhibition by these compounds is abstraction of the hydrogen attached to sulfur by a peroxy radical, *i.e.*,

$$(RO)_2P(S)SH + ROO^{\cdot} \rightarrow (RO)_2PS_2^{\cdot} + ROOH$$

with the dialkyldithiophosphate radical being less reactive than a peroxy radical towards propagation.

Although we are reasonably confident that peroxy radicals react with zinc complexes at the metal center, the experimental results presented in this paper do not enable us to distinguish between a rate controlling electron transfer reaction 2 and a displacement reaction 4. Similarly, zinc isopropylxanthate may be a more efficient scavenger of peroxy radicals than zinc diisopropyldithiophosphate because it can donate an electron more readily to an electrophilic species or because the $ROCS_2$ ligand is less tightly bound to zinc than the $(RO)_2PS_2$ ligand.

We wish to thank the Chevron Research Company for financial support in the form of a Fellowship to one of us (Y.O.).

1. A. J. Burn, R. Cecil, and V. O. Young. J. Inst. Petrol. **57**, 319 (1971).
2. E. Rossi and L. Imparato. Chim. Ind. **53**, 838 (1971).
3. Y. Ohkatsu. Unpublished results.
4. T. Colclough and J. I. Cuneen. J. Chem. Soc. 4790 (1964).
5. A. J. Burn. Tetrahedron, **22**, 2153 (1966).
6. A. J. Burn. Adv. Chem. Ser. **75**, 323 (1968).
7. S. K. Ivanov and D. Shopov. Compt. rend. Acad. Bulg. Sci. **18**, 845 (1965).
8. S. K. Ivanov. Compt. rend. Acad. Bulg. Sci. **20**, 1153 (1967).
9. S. K. Ivanov. Compt. rend. Acad. Bulg. Sci. **20**, 1283 (1967).
10. D. Shopov, S. K. Ivanov, and V. V. Ivanova. Rev. Inst. fr. Pét. **22**, 1520 (1967).
11. D. Shopov and S. K. Ivanov. Int. Oxid. Symp. San Francisco, 1967. Preprints **1**, 675.
12. S. K. Ivanov and I. Kateva. Compt. rend. Acad. Bulg. Sci. **21**, 681 (1968).
13. D. Shopov and S. K. Ivanov. Izv. Otd. Khim. Nauki, Bulg. Akad. Nauk. **2**, 619 (1970); Chem. Abstr. **73**, 44611 m (1970).
14. C. Copping and N. Uri. Discuss. Faraday Soc. **46**, 202 (1968).
15. T. V. Liston, H. G. Ingersoll, Jr., and J. Q. Adams. Am. Chem. Soc. Div. Pet. Chem. Preprints **14**(4), A83 (1969).
16. J. A. Howard and K. U. Ingold. Can. J. Chem. **40**, 1851 (1962); **41**, 1744 (1963); **41**, 2800 (1963); **42**, 2324 (1964); **43**, 2724 (1965).
17. I. T. Brownlie and K. U. Ingold. Can. J. Chem. **44**, 861 (1966); **45**, 2419 (1967); **45**, 2427 (1967).
18. J. A. Howard and K. U. Ingold. Can. J. Chem. **45**, 793 (1967) and subsequent papers in this series.
19. C. E. Boozer, G. S. Hammond, C. E. Hamilton, and J. N. Sen. J. Am. Chem. Soc. **77**, 3233 (1955).
20. K. Adamic, D. F. Bowman, T. Gillan, and K. U. Ingold. J. Am. Chem. Soc. **93**, 902 (1971).
21. J. A. Howard and K. U. Ingold. Can. J. Chem. **43**, 2729 (1965).
22. J. A. Howard and K. U. Ingold. Can. J. Chem. **44**, 1119 (1966).
23. J. A. Howard. Adv. Free Radical Chem. **4**, 49 (1972).
24. J. D. Holdsworth, G. Scott, and D. Williams. J. Chem. Soc. 4692 (1964).
25. J. A. Howard and K. U. Ingold. Can. J. Chem. **45**, 785 (1967).
26. G. E. Zaikov, J. A. Howard, and K. U. Ingold. Can. J. Chem. **47**, 3017 (1969).
27. J. A. Howard and S. Korcek. Can. J. Chem. **48**, 2165 (1970).
28. J. J. Dickert, Jr. and C. N. Rowe. J. Org. Chem. **32**, 647 (1947).
29. L. R. Mahoney and S. A. Weiner. J. Am. Chem. Soc. **94**, 585 (1972).
30. L. R. Mahoney. J. Am. Chem. Soc. **88**, 1895 (1967); Angew. Chem. Int. Ed. Engl. **8**, 547 (1969).
31. G. W. Kennedy and W. L. Patterson. Ind. Eng. Chem. **48**, 1917 (1956).
32. K. U. Ingold. Chem. Rev. **61**, 563 (1961); Adv. Chem. Ser. **75**, 296 (1968).
33. L. R. Mahoney and M. A. DaRooge. J. Am. Chem. Soc. **92**, 4063 (1970).
34. M. Sato, M. Yanagita, Y. Fujita, and T. Kwan. Bull. Chem. Soc. Jap. **44**, 1423 (1971).
35. J. A. Howard and S. Korcek. Can. J. Chem. **49**, 2178 (1971).
36. J. A. Howard. Unpublished results.
37. K. U. Ingold and B. P. Roberts. Free-radical substitution reactions. Wiley, New York, 1971.
38. W. E. Bacon and W. M. Lesuer. J. Am. Chem. Soc. **76**, 640 (1954).
39. S. Oae, A. Nakanishi, and N. Tsujimoto. Tetrahedron, **28**, 2981 (1972).
40. O. L. Harle. Private communication.

Can. J. Chem. Downloaded from www.nrcresearchpress.com by 210.87.254.42 on 09/05/12
For personal use only.

The Chemical Degradation of a Humic Acid[1]

MORRIS SCHNITZER AND MARIA INES ORTIZ DE SERRA[2]
Soil Research Institute, Canada Agriculture, Ottawa, Canada

Received December 1, 1972

A humic acid (HA) extracted from the A_1 horizon of a Brunizem soil was degraded in the unmethylated and methylated form by sequential reaction with oxidants of increasing strength. The HA was first oxidized with alkaline cupric oxide; the products were then further degraded by oxidation with first alkaline $KMnO_4$ and then with H_2O_2 in alkaline solution. Unmethylated HA was also degraded by Na-amalgam reduction. The degradation products were extracted into organic solvents, methylated, and separated by preparative gas chromatography into relatively pure components which were analyzed by mass spectrometry and micro-i.r. spectrophotometry. A matching of the mass and i.r. spectra and gas chromatographic retention times of the isolated components with those of authentic specimens led to their identification.

The experimental data show that the HA contains a relatively easily degradable portion, which comprises guaiacyl and syringyl units and which may be lignin-derived (about 10% of the total weight). This material is degraded by CuO–NaOH oxidation and Na-amalgam reduction. The bulk of the HA structure, however, consists of a more condensed, chemically complex "core", which degrades on more drastic oxidation into complex phenolic and benzenepolycarboxylic acids. It is likely that the "core" originates in part from condensed lignin and in part from products of microbial synthesis. Of the methods investigated, the CuO–NaOH and the $KMnO_4$ oxidation of methylated HA appear most promising for providing information on the chemical structure of the HA.

Un acide humique (HA) extrait du sol de l'horizon A_1 de Brunizem, a été dégradé sous forme non méthylée et méthylée selon une séquence réactionnelle utilisant des oxydants de force croissante. Le HA a d'abord été oxydé par CuO en milieu alcalin; les produits obtenus ont été ensuite degradés par oxydation permanganique et par H_2O_2 en solution alcaline. Le HA non méthylé a été également dégradé par réduction à l'amalgame de Na. Les produits dégradés ont été extraits par des solvants organiques, méthylés puis séparés par chromatographie en phase gazeuse préparative en composés relativement purs qui ont été analysés par spectrométrie de masse et microspectrophotométrie i.r. La comparaison des spectres de masse et i.r. et des temps de rétention de la chromatographie en phase gazeuse des composés isolés avec ceux de specimens authentiques ont suffi à leur identification

Les données expérimentales montrent que le HA comprend une partie relativement facile à degrader qui contient des unités guaiacyle et syringyle, qui peuvent être dérivées de la lignine (environ 10% du poids total). Ce matériel est dégradé par oxydation avec CuO–NaOH et réduction par l'amalgame de Na. Le gros de la structure HA consiste cependant en un noyau plus condensé, chimiquement complexe, qui se dégrade par oxydation plus brutale en phénols complexes et acides benzène polycarboxyliques. Il est probable que ce noyau tire son origine en partie de la lignine condensée et en partie des produits de synthèse microbienne. Parmi les méthodes étudiées, l'oxydation par CuO–NaOH et $KMnO_4$ de HA méthylé est une source d'information pleine de promesse sur la structure chimique de HA.

[Traduit par le journal]

Can. J. Chem., **51**, 1554 (1973)

Introduction

Humic substances are widely distributed in nature and arise from the chemical and biological degradation of plant and animal residues and from synthetic activities of microorganisms. The bulk of the organic matter in most soils and waters consists of humic substances which are amorphous, dark brown or black, hydrophilic, acidic, polydisperse substances of molecular weights ranging from a few hundred to tens of thousands. Based on their solubility in dilute alkali and acid, humic substances are usually subdivided into three main fractions: (*a*) humic acid (HA), which is soluble in dilute alkaline solution but is precipitated by acidification of the alkaline extract; (*b*) fulvic acid (FA), which is that humic fraction which remains in the aqueous acidified solution, *i.e.*, it is soluble in both acid and base; and (*c*) the humic fraction that cannot be extracted by dilute base and acid, which is referred to as humin (1). Important characteristics exhibited by all humic fractions are resistance to microbial degradation, and the ability to form stable water-soluble and water-

[1]Contribution No. 445, Soil Research Institute.

[2]Visiting Scientist from the Universidad Nacional del Sur, Bahia Blanca, Argentina.

Can. J. Chem. Downloaded from www.nrcresearchpress.com by 210.87.254.42 on 09/05/12
For personal use only.

Can. J. Chem. Downloaded from www.nrcresearchpress.com by 210.87.254.42 on 09/05/12
For personal use only.

insoluble salts and complexes with metal ions and hydrous oxides, and to interact with clay minerals and organic chemicals often added by man, which may be toxic pollutants.

Since quantitatively HA is the most important humic fraction, it is not too surprising that a considerable amount of research has been done on this subject. Yet, in spite of the existence of a voluminous literature, going back more than 200 years (1), very little is known about the synthesis and chemical structure of HA's. The relatively recent availability of powerful and sophisticated analytical tools such as the gas chromatographic–mass spectrometric (g.c.–m.s.) system and the g.c.–m.s.-computer system prompted us to take a new look at this problem in the expectation that significant advances in our knowledge of the chemical structure of HA's, a relatively "old" but neglected problem in chemistry, should now be possible.

Thus, we set out to degrade a HA extracted from a Brunizem soil by oxidative methods of increasing strength. The first method that we used was the relatively mild alkaline cupric oxide (CuO–NaOH) oxidation which had been pioneered by Pearl (2) on lignosulfonates and various lignin preparations. In a second series of experiments we methylated the CuO–NaOH oxidation products and then oxidized these again with alkaline $KMnO_4$ solution at p*H* 10. In a third set of experiments we went one step further and oxidized the CuO–NaOH + $KMnO_4$ oxidation products with H_2O_2 at p*H* 10. This approach was similar to that taken recently by Larsson and Miksche (3), who used a sequence of oxidants of increasing strength on birch lignin. A fourth method that we employed was alkaline $KMnO_4$ oxidation which has been used on coal (4), lignin (5), and humic substances (6). Another approach that we investigated was reduction of the HA with Na-amalgam, a relatively mild method that has been used previously on HA with varying degrees of success (7). Finally, we applied each of the oxidative degradation procedures to HA that was methylated prior to oxidation in order to evaluate the effects of methylation on the quality and quantity of products formed. Following each degradation, the products were methylated, extracted into organic solvents, separated by preparative gas chromatography, and identified by matching their mass and micro-i.r. spectra with those of authentic specimens. Our principal objective was to uncover the method or methods that would provide the most meaningful information on the chemical structure of the HA.

Experimental

HA

The soil sample from which the HA was extracted was taken from the A_1 horizon (0–23 cm) of a Brunizem soil (3.84% C; p*H* = 6.0) from a grassland area in the province of Buenos Aires, Argentina. Methods of extraction, fractionation, and purification were analogous to those described previously (8). Elemental analysis (%) of the purified HA (0.73% ash) showed 54.99 C; 4.38 H; 3.29 N; 0.84 S; 36.50 O; and 1.18 OCH_3. One gram of HA contained 4.75 mequiv CO_2H, 2.36 mequiv phenolic OH, 1.99 mequiv alcoholic OH, and 1.37 mequiv C=O. The ratio of optical densities at 465 and 665 nm (E_4/E_6) was 3.92 and the free radical concentration was 11.73×10^{17} spins/g (8).

(I) CuO–NaOH Oxidation

To 500 mg of HA dissolved in 50 ml of 2 *N* NaOH solution in a 300 ml stainless steel autoclave equipped with a magnetic stirrer, 2.5 g of CuO was added. The system was heated to 170 °C with constant stirring over a period of 1 h and then maintained at that temperature for 2 h. Following cooling to room temperature, suspended CuO was removed by centrifugation and washed with distilled H_2O. The supernatant solution plus washings were saturated with NaCl and extracted successively with 3 × 100 ml aliquots of 2:1 (v/v) chloroform–acetone after acidification to p*H* 6 and 2. When the p*H* was lowered to 2, a fraction of the water-soluble oxidation products became insoluble. The insoluble material, (Ii) was removed by filtration and the clear supernatant solution extracted with chloroform–acetone. The two organic extracts were first dried over anhydrous Na_2SO_4 and then taken to dryness in a rotary evaporator, dissolved in a small volume of CH_3OH, and methylated with an ether solution of diazomethane generated from Diazald. Yields of benzene-soluble, methylated extracts were: 32.3 mg for the extract at p*H* 6, and 27.2 mg for the extract at p*H* 2. The two extracts were combined (fraction I, see Fig. 1). The insoluble fraction (Ii) weighed 150 mg, contained 39.3% ash and, on a dry, ash-free basis, analysis (%) showed 61.62 C; 4.56 H; 2.18 N; 0.68 S; 30.96 O; and 1.19 OCH_3. The major components in fraction I were separated by preparative gas chromatography and identified by mass spectrometry and micro-i.r. spectrophotometry as described below.

(II) CuO–NaOH + $KMnO_4$ Oxidation

The CuO–NaOH oxidation of 500 mg of HA was carried out as described under method I. Fractions I and Ii were methylated with diazomethane and then oxidized with aqueous 4% $KMnO_4$ solution (6). The oxidation products were extracted from acidified aqueous solution with ethyl acetate, remethylated with diazomethane, dissolved in benzene, separated by preparative gas chromatography, and identified by mass spectrometry and micro-i.r. spectrophotometry as described below. Yields of methylated, benzene-soluble fractions II*a* (from I) and II*b* (from Ii) were 20.5 and 65.6 mg, respectively.

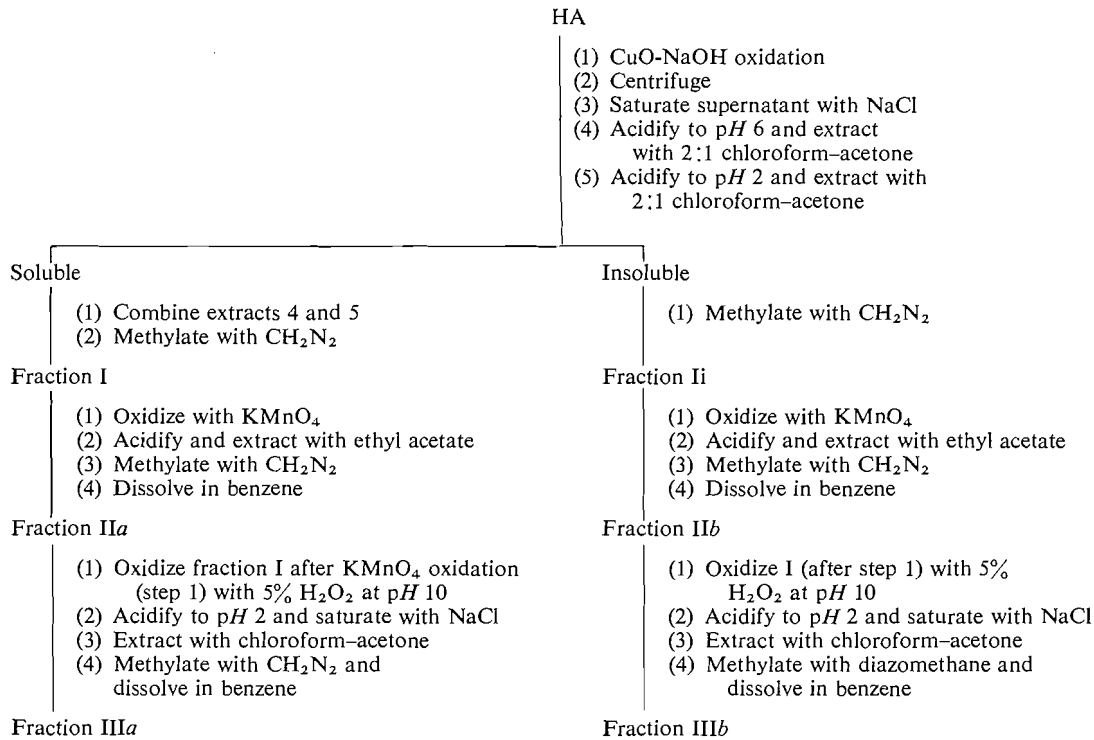

FIG. 1. Oxidation and separation of fractions I, Ii, IIa, IIb, IIIa, and IIIb.

(III) CuO–NaOH + $KMnO_4$ + H_2O_2 Oxidation

Fractions I and Ii were prepared as described above and then oxidized with 4% $KMnO_4$ solution. Water-soluble oxidation products were further oxidized by contact with 5% H_2O_2 solution at p*H* 10 for ½ h at room temperature with intermittent shaking and then warmed briefly to 50 °C. The excess H_2O_2 was destroyed by the addition of a few drops of dilute $KMnO_4$ solution. The resulting solutions were treated briefly with SO_2, acidified to p*H* 2 with 6 *N* H_2SO_4 solution, saturated with NaCl, and extracted three times with 100 ml of 2:1 (v/v) chloroform–acetone. The organic extracts were dried, methylated with diazomethane, dissolved in benzene, and analyzed as described under method I. Yields were as follows: fraction III*a* (from II*a*), 2.1 mg and fraction III*b* (from II*b*), 23.1 mg.

(IV) $KMnO_4$ Oxidation

Five hundred milligrams of HA was refluxed for 8 h with 125 ml of 4% (w/v) aqueous $KMnO_4$ solution (p*H* 10). Following oxidation, the excess $KMnO_4$ was destroyed by careful addition of small volumes of CH_3OH. The insoluble MnO_2 was removed by filtration and washed with small aliquots of hot water. The filtrate plus washings were acidified to p*H* 2, saturated with NaCl, extracted with 3 × 100 ml portions of 2:1 (v/v) chloroform–acetone, dried, methylated, dissolved in benzene, and analyzed as described below. The benzene-soluble, methylated oxidation product (fraction IV) weighed 34.9 mg.

(VI) Na-amalgam reduction

One gram of HA, dissolved in 100 ml of 1% NaOH solution, was refluxed with vigorous stirring under N_2 over 100 g of 5% Na-amalgam (BDH reagent grade) for 3 h. After cooling, the supernatant solution was separated from the insoluble residue by filtration, acidified to p*H* 2, and extracted successively with three 75-ml portions of diethyl ether. The ether extract was dried over anhydrous Na_2SO_4, and then methylated with diazomethane. For additional purification, the methylated reduction products were extracted with three 75-ml portions of benzene to yield fraction VI (39.50 mg). The latter was then separated by preparative gas chromatography and identified as described below.

Oxidation of Methylated HA

Methods I, II, III, and IV were also applied to HA that was methylated with diazomethane (increase in OCH_3 = 14.37%) prior to oxidation. The fractions so obtained are referred to as Im, IIm, IIIm, and IVm (see Table 2 and Fig. 1). Fraction Vm was prepared by oxidizing 500 mg of methylated HA with aqueous 4% $KMnO_4$ solution as described under IV. Water-soluble oxidation products were then further oxidized with 5% H_2O_2 at p*H* 10 as in method III.

Separation and Identification of Degradation Products

Each methylated fraction was first analyzed as a 2.5% solution in benzene by analytical gas chromatography (Hewlett-Packard, Model 402, flame ionization detector,

Can. J. Chem. Downloaded from www.nrcresearchpress.com by 210.87.254.42 on 09/05/12
For personal use only.

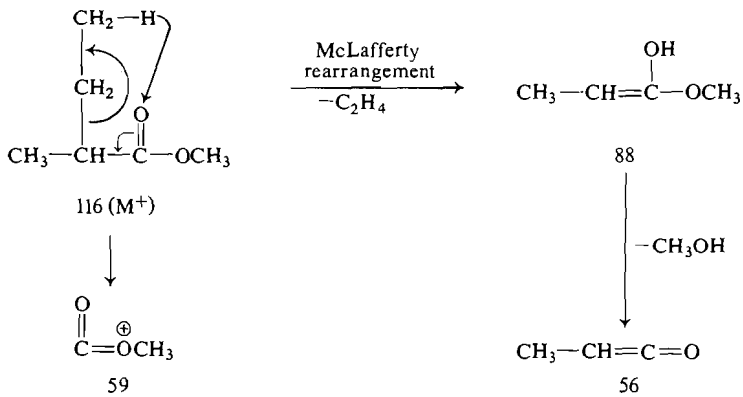

SCHEME 1

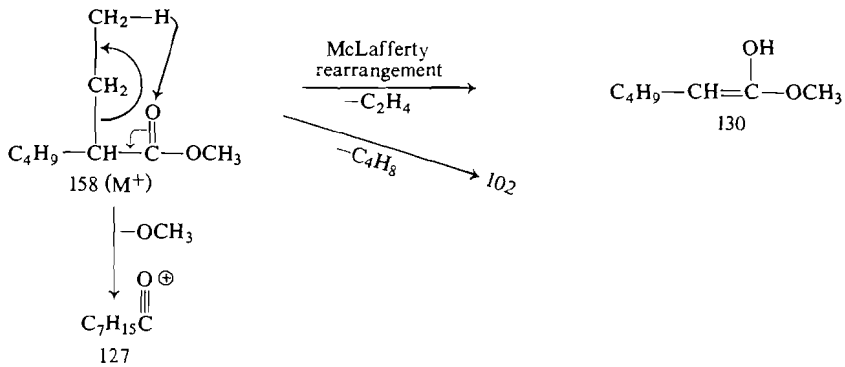

SCHEME 2

1800 × 4 mm glass column packed with 3% OV 17 on Chromosorb W HMDS, 60–80 mesh, programmed from 90–310 °C at a rate of 7.5 °C/min, N_2-flow = 40 ml/min), and then separated as a 10% solution in benzene by preparative gas chromatography under the same conditions. Materials representing the major gas chromatographic peaks were eluted from the gas chromatographic column, collected in capillary tubes, and analyzed by mass spectrometry and by micro-i.r. spectrophotometry as described earlier (9). Mass and i.r. spectra of unknowns were matched with those of standards of known structures. As an additional check, each unknown was co-chromatographed (on the gas chromatograph) with the known compound to which it corresponded. In some instances fractions were analyzed directly on a g.c.–m.s.-computer system. Quantitative estimates of each compound were made by triangulation of peak areas on the gas chromatograms. All solvents were purified by distillation through high-efficiency columns.

The known compounds used as standards for the mass spectrometric and i.r. spectrophotometric identification of the unknowns were either prepared as described earlier (9) or purchased commercially. Each compound was purified by suitable methods. We were unable to obtain appropriate standards for components **27** and **29**, so that the identification of these compounds is tentative only.

Compounds **1** and **5** were identified by g.c.–m.s.-computer (Shrader Analytical and Consulting Laboratories, Detroit, Michigan). The mass spectrum of **1** suggested the fragmentation pattern shown in Scheme 1. The mass spectrum for **5** suggested similarly the fragmentation pattern depicted by Scheme 2. The gas chromatographic separation of fraction Vm is shown in Fig. 2.

Analytical Methods

C and H were determined by dry-combustion, N by the automated Dumas method, S by oxygen-flask combustion, and O was calculated by difference. The OCH_3-content was measured by the Zeisel method.

Results

(A) Degradation of Unmethylated HA

(I) CuO–NaOH Oxidation

Major degradation products resulting from the CuO–NaOH oxidation of the HA are listed in Table 1 under method 1. Since the oxidation products were methylated prior to the gas chromatographic separations, and since the OCH_3-content of the untreated HA was low, it is likely that in the initial HA's the functional group in

Can. J. Chem. Downloaded from www.nrcresearchpress.com by 210.87.254.42 on 09/05/12
For personal use only.

Can. J. Chem. Downloaded from www.nrcresearchpress.com by 210.87.254.42 on 09/05/12
For personal use only.

TABLE 1. Compounds (mg) produced by the degradation of 1 g of unmethylated HA

No.	Compound	Method*								
			II			III				
		I	*a*	*b*	*a* + *b*	*a*	*b*	*a* + *b*	IV	VI
8	1,2-Benzenedicarboxylic acid dimethyl ester	0	1.24	2.55	3.79	0.02	0	0.02	4.12	0
9	1,3-Benzenedicarboxylic acid dimethyl ester	0	0.37	0	0.37	0	0	0	0.68	0
10	3,4-Dimethoxybenzaldehyde	3.82	0	0	0	0	0	0	0	2.50
11	3,4-Dimethoxyacetophenone	4.16	0	0	0	0	0	0	0	0
12	3,4-Dimethoxybenzoic acid methyl ester	1.94	1.77	0	1.77	0	0	0	0	1.72
13	3,5-Dimethoxybenzoic acid methyl ester	0	0	0	0	0	0	0	0	1.50
15	2,3,4-Trimethoxyacetophenone	5.39	0	0	0	0	0	0	0	0
16	3,4,5-Trimethoxybenzaldehyde	4.53	0	0	0	0.13	0	0.13	0	2.00
17	3,4,5-Trimethoxyacetophenone	8.15	0	0	0	0	0	0	0	0.32
18	3,4,5-Trimethoxyphenylacetone	0	0	0	0	0	0.72	0.72	0	2.60
19	3,4,5-Trimethoxybenzoic acid methyl ester	8.65	0.57	0	0.57	0.27	2.16	2.43	0	7.25
20	*N*-Methyl-benzylsulfonamide	7.66	3.49	0	3.49	0.23	0.46	0.69	0	3.25
21	1,2,3-Benzenetricarboxylic acid trimethyl ester	0	5.36	13.35	18.71	0	4.76	4.76	32.52	0
22	1,2,4-Benzenetricarboxylic acid trimethyl ester	0	2.63	12.19	14.81	0.04	3.05	3.09	6.50	0
23	1,3,5-Benzenetricarboxylic acid trimethyl ester	0	0.59	0	0.59	0.67	4.12	4.79	0	0
24	Dibutyl phthalate	32.97	0	0	0	0	0	0	0	0
26	1,2,3,4-Benzenetetracarboxylic acid tetramethyl ester	0	3.59	28.48	32.07	0.33	11.68	12.01	6.45	0
27	1,2,4,5-Benzenetetracarboxylic acid tetramethyl ester	0	0	10.50	10.50	0	0	0	4.99	0
28	1,2,3,5-Benzenetetracarboxylic acid tetramethyl ester	0	0	5.73	5.73	0.25	2.17	2.42	0.11	0
30	Dimethoxy-benzenetetracarboxylic acid tetracarboxylic acid tetramethyl ester	0	1.30	4.16	5.46	0	1.27	1.27	0	0
31	Benzenepentacarboxylic acid pentamethyl ester	0	3.77	26.95	30.72	0.17	6.54	6.71	0.68	0
32	Aceto-benzenepentacarboxylic acid pentamethyl ester	0	0.37	8.79	9.16	0	0	0	0	0
34	Benzenehexacarboxylic acid hexamethyl ester	0	1.75	4.26	6.01	0.15	2.90	3.05	0.27	0
Identified		77.27	26.80	116.96	143.76	2.26	39.83	42.09	56.32	21.14
Total weight of products		119.73	41.00	131.19	172.19	4.07	46.09	50.16	69.85	39.50
% of products identified		65	65	89	83	56	86	84	81	54

*I = CuO–NaOH oxidation.
II = CuO–NaOH + $KMnO_4$ oxidation.
III = CuO–NaOH + $KMnO_4$ + H_2O_2 oxidation.
IV = $KMnO_4$ oxidation.
VI = Na-amalgam reduction.
a = degradation products soluble in organic solvents after CuO–NaOH oxidation.
b = degradation products insoluble at p*H* 2 after CuO–NaOH oxidation.

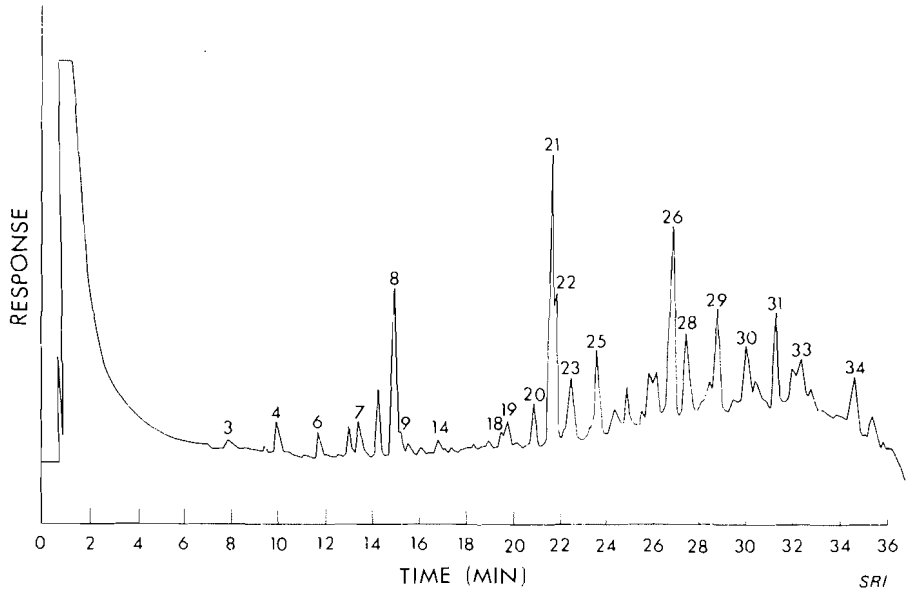

FIG. 2. Gas chromatographic separation of fraction IVm. Numerals above peaks refer to compounds identified in Fig. 3.

the 4-position on the aromatic rings of compounds **10–12** and **15–19** (see Fig. 3) was OH rather than OCH_3. Thus, the major CuO–NaOH oxidation products have guaiacyl and syringyl structures with CHO, $COCH_3$, and CO_2H groups in the 1-position. The weight ratio of guaiacyl (**10–12**) to syringyl (**16–19**) structures was 0.47, indicating a preponderance of syringyl units in the oxidation mixture. Other compounds identified were **20**, which contains both S and N, and about which little is known, and dibutyl phthalate (**24**) which was isolated in relatively large amounts. In view of recent work in this laboratory (10) which showed that HA's can adsorb large amounts of dialkyl phthalates, it is likely that **24** is not a structural HA component but that it is either firmly adsorbed on the HA surface or, less likely, a contaminant.

(II) CuO–NaOH + $KMnO_4$ Oxidation

Further oxidation of methylated fraction I with $KMnO_4$ led to the disappearance of phenolic compounds **10**, **11**, **13**, **15**, **16**, and **17** and to losses of **12** and especially of **19** (Table 1, II*a*). At the same time varying amounts of benzenepolycarboxylic acid methyl esters **8**, **9**, **21–23**, **26**, **30–32**, and **34** were formed, apparently from more complex chemical structures, by the more vigorous oxidation with $KMnO_4$. This was especially so for the CuO–NaOH pretreated material that coagulated at p*H* 2 and that was insoluble in organic solvents. The oxidation ($KMnO_4$) mixture from the latter material (Table 1, II*b*) was free of phenolic compounds but contained relatively large amounts of benzenecarboxylic acid methyl esters, principally the tri-(**21**, **22**), tetra-(**26**) and penta-(**31**) forms. These data indicate the occurrence of more condensed chemical structures in II*b* than in II*a*.

(III) CuO–NaOH + $KMnO_4$ + H_2O_2

Additional oxidation of II*a* with H_2O_2 led to substantial losses of phenolic as well as benzenecarboxylic components (III*a*). In the case of fraction II*b*, H_2O_2 oxidation produced small amounts of C_6C_3-compound **18** and somewhat greater amounts of **19**, but lowered the yields of most benzene – carboxylic acid methyl esters (III*b*, compare with II*b*). It appears that the additional treatment with H_2O_2 in alkaline solution was too drastic.

(IV) $KMnO_4$ Oxidation

The $KMnO_4$ oxidation of the unmethylated HA produced small amounts of benzenecarboxylic acid methyl esters ranging from the di- to the hexa-forms (IV). Especially noteworthy was the formation of relatively large amounts of 1,2,3-benzenetricarboxylic acid trimethyl ester (**21**), accounting for 3.3% of the initial HA. Failure to isolate phenolic compounds under these conditions is not surprising since the pres-

Can. J. Chem. Downloaded from www.nrcresearchpress.com by 210.87.254.42 on 09/05/12
For personal use only.

Can. J. Chem. Downloaded from www.nrcresearchpress.com by 210.87.254.42 on 09/05/12
For personal use only.

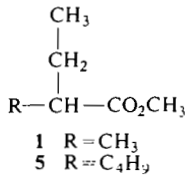

1 $R = CH_3$
5 $R = C_4H_9$

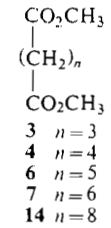

3 $n = 3$
4 $n = 4$
6 $n = 5$
7 $n = 6$
14 $n = 8$

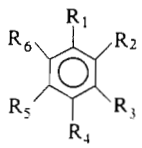

2 $R_1 = CO_2CH_3$; $R_4 = OCH_3$; $R_2 = R_3 = R_5 = R_6 = H$
8 $R_1 = R_2 = CO_2CH_3$; $R_3 = R_4 = R_5 = R_6 = H$
9 $R_1 = R_3 = CO_2CH_3$; $R_2 = R_4 = R_5 = R_6 = H$
10 $R_1 = CHO$; $R_3 = R_4 = OCH_3$; $R_2 = R_5 = R_6 = H$
11 $R_1 = COCH_3$; $R_3 = R_4 = OCH_3$; $R_2 = R_5 = R_6 = H$
12 $R_1 = CO_2CH_3$; $R_3 = R_4 = OCH_3$; $R_2 = R_5 = R_6 = H$
13 $R_1 = CO_2CH_3$; $R_3 = R_5 = OCH_3$; $R_2 = R_4 = R_6 = H$
15 $R_1 = COCH_3$; $R_2 = R_3 = R_4 = OCH_3$; $R_5 = R_6 = H$
16 $R_1 = CHO$; $R_3 = R_4 = R_5 = OCH_3$; $R_2 = R_6 = H$
17 $R_1 = COCH_3$; $R_3 = R_4 = R_5 = OCH_3$; $R_2 = R_6 = H$
18 $R_1 = CH_2COCH_3$; $R_3 = R_4 = R_5 = OCH_3$; $R_2 = R_6 = H$
19 $R_1 = CO_2CH_3$; $R_3 = R_4 = R_5 = OCH_3$; $R_2 = R_6 = H$
20 $R_1 = CH_2SO_2NHCH_3$; $R_2 = R_3 = R_4 = R_5 = R_6 = H$
21 $R_1 = R_2 = R_3 = CO_2CH_3$; $R_4 = R_5 = R_6 = H$
22 $R_1 = R_2 = R_4 = CO_2CH_3$; $R_3 = R_5 = R_6 = H$
23 $R_1 = R_3 = R_5 = CO_2CH_3$; $R_2 = R_4 = R_6 = H$
24 $R_1 = R_2 = CO_2C_4H_9$; $R_3 = R_4 = R_5 = R_6 = H$
25 $R_1 = R_2 = R_4 = CO_2CH_3$; $R_3 = OCH_3$, $R_5 = R_6 = H$
26 $R_1 = R_2 = R_3 = R_4 = CO_2CH_3$; $R_5 = R_6 = H$
27 $R_1 = R_2 = R_4 = R_5 = CO_2CH_3$; $R_3 = R_6 = H$
28 $R_1 = R_2 = R_3 = R_5 = CO_2CH_3$; $R_4 = R_6 = H$
29 $R_1 = R_2 = R_3 = R_4 = CO_2CH_3$; $R_5 = OCH_3$; $R_6 = H$
31 $R_1 = R_2 = R_3 = R_4 = R_5 = CO_2CH_3$; $R_6 = H$
33 $R_1 = OCH_3$; $R_2 = R_3 = R_4 = R_5 = R_6 = OCH_3$
34 $R_1 = R_2 = R_3 = R_4 = R_5 = R_6 = CO_2CH_3$

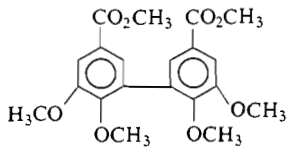

35

FIG. 3. Chemical structures of compounds identified.

Can. J. Chem. Downloaded from www.nrcresearchpress.com by 210.87.254.42 on 09/05/12
For personal use only.

ence of electron-donating OH groups on aromatic rings makes these rings susceptible to attack by electrophilic $KMnO_4$ (4).

(VI) Na-Amalgam Reduction

The major reduction products were phenolic compounds **19**, **18**, and **10** (Table 1, VI). Compound **20** was another major product identified. It was also one of the major components isolated from the mixture resulting from the CuO–NaOH oxidation (I). Thus, the reduction of HA yields both guaiacyl (**10**, **12**) and syringyl (**16–19**) structures, with the latter clearly predominant. Of some interest is the isolation of small amounts of **13**, which is not a "typical" lignin-degradation product.

(B) Degradation of Methylated HA

(Im) CuO–NaOH Oxidation

The CuO–NaOH oxidation of methylated HA (Table 2, Im) yielded the same type of compounds as that of the unmethylated HA (Table 1) but in greater amounts. Again there was a predominance of syringyl (**16–19**) over guaiacyl (**10–12**) moieties. In addition, small amounts of phenolic compound **2** and larger quantities of branched fatty acid methyl esters **1** and **5** were identified in the oxidation mixture. The most abundant products were **20** and **24**. The total weight of oxidation products soluble in organic solvents was about twice that obtained from the CuO–NaOH oxidation of the unmethylated HA. Only about 65% of the oxidation products was identified (Table 2, Im). Most of the compounds that we have so far been unable to identify eluted from the gas chromatographic column at < 200 °C. It is apparent that methylation of the HA prior to CuO–NaOH oxidation increased the yields of oxidation products significantly.

(IIm) CuO–NaOH + $KMnO_4$ Oxidation

Further oxidation with $KMnO_4$ of the products from the CuO–NaOH oxidation that were soluble in chloroform–acetone (IIm*a*) resulted in the virtual disappearance of most of the compounds that eluted at <200 °C and also led to either the disappearance or a reduction in concentration of the phenolic compounds and of **20**. Simultaneously small amounts of benzenecarboxylic acids were formed. The CuO–NaOH pretreated fraction that was insoluble in organic solvents yielded on further oxidation with $KMnO_4$ (IIm*b*), small amounts of aliphatic dicarboxylic acid methyl ester **7**, methylated phenolic acids **12** and **19** and benzenecarboxylic acids, mainly the tetra-**26** and penta-**31** forms.

(IIIm) CuO–NaOH + $KMnO_4$ + H_2O_2

More drastic oxidation of fraction IIm*a* with H_2O_2 produced small amounts of methylated aliphatic dicarboxylic acids (**3**, **4**, **6**, **7**), phenolic compounds (**12**, **18**, and **19**) and benzenecarboxylic acids, some of which contained $OH(OCH_3)$ groups (**25**) (Table 2, IIIm*a*), indicating the occurrence in the HA of complex phenolic structures. Fraction IIIm*b* was similar in composition to IIIm*a*.

(IVm) $KMnO_4$ Oxidation

The permanganate oxidation of methylated HA (Table 2, IVm) yielded small amounts of methylated suberic acid (**7**), complex phenolic acids (**29**, **33**, and **35**) and relatively large amounts of benzenecarboxylic acids, ranging from di- to hexa-types. The most abundant products were the 1,2,3,4-benzenetetra-**26**, the -penta-**31**, and 1,2,4- and 1,2,3-tri-**22** and **-21** benzenecarboxylic acid methyl esters. Of special interest was the isolation of **35**, the only biphenyl compound that we were able to detect.

(Vm) $KMnO_4$ + H_2O_2 Oxidation

Further oxidation of IVm with H_2O_2 yielded fraction Vm which was similar in composition to IVm except that it contained additional small amounts of phenolic compounds **18**, **19**, **25**, **29**, and **30**, aliphatic dicarboxylic acid esters **3**, **4**, **6**, **7**, and **14** but lower concentrations of benzenecarboxylic acid methyl esters. The additional treatment with H_2O_2 appeared to favor, at least to a small extent, the formation of phenolic compounds.

Discussion

The CuO–NaOH oxidation of the unmethylated and methylated HA yields small amounts of guaiacyl and syringyl monomers with up to three C atoms in the aliphatic side chain (Table 1, I; Table 2, Im); in addition, small yields of guaiacyl compounds with a biphenyl structure are obtained by the permanganate oxidation of methylated HA (Table 2, IVm). The CuO–NaOH oxidation of the unmethylated and methylated HA affords phenolic compounds which account for about 3.1 and 6.0% of the weight of the initial HA, respectively. Qualitatively, the compounds identified resemble those isolated by Pearl (2) from products resulting from the CuO–NaOH oxidation of coniferous

Can. J. Chem. Downloaded from www.nrcresearchpress.com by 210.87.254.42 on 09/05/12
For personal use only.

TABLE 2. Compounds (mg) produced by the oxidation of 1 g of methylated HA

No.	Compound	Method*								
		Im	IIm			IIIm			IVm	Vm
			a	*b*	*a* + *b*	*a*	*b*	*a* + *b*		
1	2-Methylbutyric acid methyl ester	13.32	0	0	0	0	0	0	0	0
2	*p*-Methoxybenzoic acid methyl ester	4.24	0	0	0	0	0	0	0	0
3	Dimethyl glutarate	0	0	0	0	0.34	0.07	0.41	0	0.20
4	Dimethyl adipate	0	0	0	0	0.75	0.14	0.89	0	1.00
5	2-Butylbutyric acid methyl ester	9.70	0	0	0	0	0	0	0	0
6	Dimethyl pimelate	0	0	0	0	0.48	0.14	0.62	0	0.70
7	Dimethyl suberate	0	0	1.02	1.02	0.24	2.30	2.54	0.57	1.33
8	1,2-Benzenedicarboxylic acid dimethyl ester	0	0.82	0	0.82	1.10	0.73	1.83	3.47	5.48
9	1,3-Benzenedicarboxylic acid dimethyl ester	0	0	0	0	0.30	0.22	0.52	0.85	0.68
10	3,4-Dimethoxybenzaldehyde	3.42	0	0	0	0	1.67	1.67	0	0
14	Dimethyl sebacate	0	0	0	0	0	0.41	0.41	0	0.53
11	3,4-Dimethoxyacetophenone	8.68	0	0	0	0	0	0	0	0
12	3,4-Dimethoxybenzoic acid methyl ester	12.41	3.65	1.33	4.98	1.96	1.27	3.23	0	0
16	3,4,5-Trimethoxybenzaldehyde	14.08	0	0	0	0	0	0	0	0
18	3,4,5-Trimethoxyphenylacetone	5.12	0.71	0	0.71	0.68		0.68	0	1.38
19	3,4,5-Trimethoxybenzoic acid trimethyl ester	15.56	1.14	0.16	1.30	1.98	3.85	5.83	0	2.53
20	*N*-Methyl-benzylsulfonamide	32.08	13.98	1.73	15.71	1.50	0	1.50	1.42	3.73
21	1,2,3-Benzenetricarboxylic acid trimethyl ester	0	1.45	0	1.45	0.98	3.11	4.09	14.28	11.75
22	1,2,4-Benzenetricarboxylic acid trimethyl ester	0	0.94	0	0.94	0.76	0.92	1.68	15.75	5.38
23	1,3,5-Benzenetricarboxylic acid trimethyl ester	0	1.45	0	1.45	2.50	0.59	3.09	1.55	4.23
24	Dibutyl phthalate	20.20	0	0	0	0	0	0	0	0
25	3-Methoxy-1,2,4-benzenetricarboxylic acid trimethyl ester	0	1.92	0	1.92	8.54	1.40	9.94	0	3.78

Can. J. Chem. Downloaded from www.nrcresearchpress.com by 210.87.254.42 on 09/05/12
For personal use only.

TABLE 2. (*Concluded*)

No.	Compound	Method*								
			IIm			IIIm				
		Im	*a*	*b*	*a* + *b*	*a*	*b*	*a* + *b*	IVm	Vm
26	1,2,3,4-Benzenetetracarboxylic acid tetramethyl ester	0	1.59	8.82	10.41	0	3.86	3.86	36.24	12.93
27	1,2,4,5-Benzenetetracarboxylic acid tetramethyl ester	0	0	0	0	0	0	0	9.03	0
28	1,2,3,5-Benzenetetracarboxylic acid tetramethyl ester	0	0.61	0	0.61	0.28	1.90	2.18	3.39	3.90
29	5-Methoxy-1,2,3,4-benzenetetracarboxylic acid tetramethyl ester	0	0	0	0	0.30	0.85	0.30	4.79	3.10
30	Dimethoxy-benzenetetracarboxylic acid tetramethyl ester	0	0	0	0	0	0.92	0.92	0	3.18
31	Benzenepentacarboxylic acid pentamethyl ester	0	0.61	6.39	7.00	0.74	0.98	1.72	16.25	5.10
32	Aceto-benzenetetracarboxylic acid tetramethyl ester	0	0.45	2.53	2.98	0.06	0.62	0.68	0	0
33	Methoxy-benzenepentacarboxylic acid pentamethyl ester	0	0	0	0	0	0	0	5.02	3.23
34	Benzenehexacarboxylic acid hexamethyl ester	0	0	0.76	0.76	0.18	0	0.18	4.67	4.00
35	Dehydrodiveratric acid dimethyl ester	0	0	0	0	0	0	0	2.12	0
Identified		138.81	29.32	22.74	51.96	23.67	25.95	48.77	119.40	78.14
Total weight of oxidized products		213.22	38.95	26.52	65.47	28.28	28.74	57.02	148.20	90.0
% of products identified		65	75	86	79	84	90	86	81	86

*Im = CuO–NaOH oxidation.
IIm = CuO–NaOH + $KMnO_4$ oxidation.
IIIm = CuO–NaOH + $KMnO_4$ + H_2O_2 oxidation.
IVm = $KMnO_4$ oxidation.
Vm = $KMnO_4$ + H_2O_2 oxidation.
a = oxidation products soluble in organic solvents after CuO–NaOH oxidation.
b = oxidation products insoluble at p*H* 2 after CuO–NaOH oxidation.

Can. J. Chem. Downloaded from www.nrcresearchpress.com by 210.87.254.42 on 09/05/12
For personal use only.

and hardwood lignosulfonates. Quantitatively the amounts of phenolics isolated from the HA are low. For example, Pepper and Karapally (11) found average yields (as % of Klason lignin) of 15.1 for **10**, 3.7 for **11**, and 2.0% for **12** (compared to 0.4, 0.4, and 0.2, and 0.3, 0.9, and 1.2%, respectively, from unmethylated and methylated HA, see Table 1, I and Table 2, Im), when they oxidized spruce potolignin with CuO–NaOH. Chang and Allan (12) report that the CuO–NaOH oxidation of spruce lignin yields 15.90 of **10**, and 3.91% of **11**, while that of aspen lignin produces 7.82 of **10**, 1.96 of **11**, 20.0 of **16**, and 5.34% of **17**. On the other hand Greene and Steelink (13) oxidized two HA's with CuO–NaOH and identified 0.57 and 0.01% of **10**, 0.41 and 0.21% of **12** and 0.05% and a trace of **16**, but failed to detect any of the other compounds listed in Table 1, I. Greene and Steelink (13) identified in addition small amounts of *p*-hydroxybenzaldehyde, *m*- and *p*-hydroxybenzoic acid (**2**), and 3,5-dihydroxybenzoic acid (**13**) for a total of 1.43% phenolics for one HA sample and 0.58% for another HA sample. These amounts are lower than those identified in this investigation although they are of the same general magnitude. Reduction of the HA with Na-amalgam (Table 1, VI) affords 1.8% of phenolic compounds, with syringyl units predominating over guaiacyl moieties. Thus, all experimental data point to the occurrence of lignin or lignin-derived material in the HA. Probably the best indication for the presence of lignin-derived units in the HA is the isolation of 0.2% of dehydrodiveratric acid dimethyl ester (**35**) from products resulting from the $KMnO_4$ oxidation of methylated HA (IVm). According to reports in the literature (12), yields of **35** on permanganate oxidation of a variety of methylated lignins, with and without prior alkaline hydrolysis, range from 0.2 to 4.0%. If we accept an average value of 2.0%, the contribution of lignin-derived units to the total weight of the HA as indicated by the isolation of **35** is about 10%.

An objection to the interpretation advanced above arises from recent work in our laboratory (14) which showed that the Na-amalgam reduction of "HA's" synthesized by fungi grown on a glucose–asparagine medium in the laboratory (and which had never been in contact with lignin) also produced small amounts (0.7%) of guaiacyl structures **10** and **12** and syringyl monomers **16–19**. Thus, the isolation of phenolic compound **10–12** and **16–19** is not an unequivocal proof for the presence of lignin-derived units in the HA. It may be relevant at this point to refer to other work that we have done recently (14) in which we investigated the permanganate oxidation of "HA's" synthesized in the laboratory by *Aspergillus niger*, *Epicoccum nigrum* and *Stachybotrys chartarum* grown on a glucose–asparagine medium. The oxidation products of methylated fungal "HA's" produced practically the same types but, per unit weight, relatively greater amounts of aliphatic acids but smaller amounts of phenolic and benzenecarboxylic compounds than those listed in Table 2 under IVm. The only exception was our failure to detect even traces of dehydrodiveratric acid dimethyl ester (**35**), which the fungi were apparently unable to produce. We believe, therefore, that the isolation of **35** is the most reliable indication of the presence of lignin-derived material in HA.

The permanganate oxidation of unmethylated HA (IV) produces 5.6% benzenecarboxylic acids (as esters) which is higher than the yields of 0.1 to 3.8% obtained by Read and Purves (5) from various lignins under the same experimental conditions. It has been postulated that aromatic rings containing oxygen are destroyed by $KMnO_4$ and that benzenecarboxylic acids originate from rings in which ring-C atoms are bonded to other C atoms but not to O atoms. The suggestion has also been made that in the case of lignin, benzenecarboxylic acids are formed from side chains of condensed units having conidendrin-like structures as a result of dehydrogenation (12) or from cyclolignans (3). Whether and to what extent this applies to the HA remains to be investigated.

Larsson and Miksche (3) have recently shown that the permanganate oxidation of methylated birch lignin that had first been pre-oxidized with CuO–NaOH yielded more than three times as much **12** and nine times as much **19** as that of methylated lignin that had not been so pretreated. They ascribe the increased yields to the degradation of structures bonded via phenolic oxygens to other lignin components in addition to structures with free phenolic OH groups (the latter are apparently degraded by $KMnO_4$ oxidation of methylated lignin). When we used this approach on the HA (Table 1, I and III) we were unable to detect even traces of **12** and the

Can. J. Chem. Downloaded from www.nrcresearchpress.com by 210.87.254.42 on 09/05/12
For personal use only.

yield of **19** was reduced to 25% of that obtained with CuO–NaOH alone. Thus, the HA does not appear to contain many "bonded" phenolic oxygens.

Other oxidation products from the methylated HA are small amounts of *p*-methoxy(OH)-benzoic acid methyl ester (**2**), a typical lignin degradation product (2) and somewhat larger amounts of branched butyric acid methyl esters (**1**, **5**) with CH_3- and C_4H_9-groups in the side chains. In addition, small amounts of aliphatic dicarboxylic acid esters, ranging from glutaric ($n = 3$) to sebacic acids ($n = 8$) are formed. Some of the aliphatic compounds may arise from chains that link aromatic or hydroaromatic rings or from the degradation of saturated ring structures. Furthermore, the oxidation of methylated HA produces a number of methoxy-(OH)-benzenecarboxylic acid esters (**25**, **29**, **33**) which are indicative of the occurrence of complex phenols in the HA. The major oxidation products from methylated HA's, however, are benzenecarboxylic acid methyl esters, ranging from the di- to the hexa-forms. For example, the $KMnO_4$ oxidation of the methylated HA (Table 2, IVm) produces 0.1% aliphatic dicarboxylic acid methyl ester, 1.2% phenolic ethers and esters, but 10.6% benzenecarboxylic acid methyl esters. Of the latter 4% are dicarboxylic, 30% tricarboxylic, 47% tetracarboxylic, 15% pentacarboxylic, and 4% hexacarboxylic. Carbon skeletons of possible precursors of the major oxidation products are shown in Fig. 4.

Relatively large amounts of **20** (up to 3.2% of the initial weight) were isolated from the methylated HA. How **20** fits into the chemical structure of HA is not known at this time. Judging from the N content (3.29%), protein could constitute ±20% of the weight of the HA, although a more realistic figure would be 10% (1). In addition, the HA could also contain a few per cent of carbohydrates. Since recent studies (14) have shown that most of the N-compounds and carbohydrates could be removed by hydrolysis with 6 *N* HCl without causing significant changes in analytical and structural characteristics of HA's, it is likely that proteins and carbohydrates are not structural HA components but are adsorbed on the large HA surfaces.

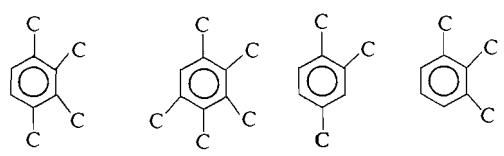

FIG. 4. Carbon skeletons of major products resulting from the $KMnO_4$ oxidation of methylated HA.

The experimental results reported herein show that the HA contains an easily degradable portion which consists of guaiacyl and syringyl units and which may be lignin-derived (about 10% of the total weight). This material is degraded by CuO–NaOH and Na-amalgam. The bulk of the HA-structure, however, consists of a more condensed chemically complex "core" which degrades on more drastic oxidation into complex phenolic and benzenecarboxylic acids. Whether the "core" consists of condensed lignin or whether it is of microbial origin awaits further investigation. It is likely that it is a mixture of the two.

Of the methods that we have examined in this investigation the most promising appear to be: (*a*) the CuO–NaOH oxidation of methylated HA, which produces high yields of products, about half of which elute from the gas chromatographic column at relatively low temperatures (<200 °C), and a substantial portion of which still remains to be identified and (*b*), the permanganate oxidation of methylated HA which provides meaningful information on the chemical structure of the complex "core" of the HA.

We thank S. I. M. Skinner and R. Schaffer of Morgan-Schaffer Corp., Montreal for mass spectrometric analyses, B. Mattson for technical assistance, and G. F. Morris for ultimate analyses.

1. (*a*) M. M. KONONOVA. Soil Org. Mat. Pergamon Press, Oxford. 1966. p. 13. (*b*) M. SCHNITZER and S. U. KHAN. Humic substances in the environment. Marcel Dekker, New York. 1972. pp. 3, 34.
2. I. A. PEARL. The chemistry of lignin. Marcel Dekker, New York. 1967. p. 205.
3. (*a*) S. LARSSON and G. E. MIKSCHE. Acta Chem. Scand. **25**, 647 (1971); (*b*) Acta Chem. Scand. **23**, 3337 (1969).
4. W. A. BONE, L. HORTON, and S. G. WARD. Roy. Soc. Proc. A**127**, 480 (1930).
5. D. E. READ and C. B. PURVES. J. Am. Chem. Soc. **74**, 116 (1952); J. Am. Chem. Soc. **74**, 120 (1952).
6. K. MATSUDA and M. SCHNITZER. Soil Sci. **114**, 185 (1972).
7. (*a*) N. A. BURGES, H. M. HURST, and S. B. WALKDEN. Geochim. Cosmochim. Acta, **28**, 1547 (1964); (*b*) F. J. STEVENSON and J. MENDEZ. Soil Sci. **103**, 383 (1967).
8. (*a*) M. I. ORTIZ DE SERRA and M. SCHNITZER. Can. J. Soil Sci. **52**, 365 (1972); (*b*) Soil Biol. Biochem. In press.

9. (*a*) G. OGNER and M. SCHNITZER. Can. J. Chem. **49**, 1053 (1971); (*b*) S. U. KHAN and M. SCHNITZER. Can. J. Chem. **49**, 2302 (1971).
10. S. U. KHAN and M. SCHNITZER. Geochim. et Cosmochim. Acta, **36**, 745 (1972).
11. J. M. PEPPER and J. C. KARAPALLY. Pulp and Paper Mag. Can. **73**, 88 (1972).
12. H. M. CHANG and G. G. ALLAN. *In* Lignins. *Edited by* K. V. Sarkanen and C. H. Ludwig. Wiley-Interscience, New York. 1971. pp. 447, 453 470.
13. G. GREENE and C. STEELINK. J. Org. Chem. **27**, 170 (1962).
14. (*a*) M. SCHNITZER and M. I. ORTIZ DE SERRA. Geoderma. In press; (*b*) M. SCHNITZER, M. I. ORTIZ DE SERRA, and K. IVARSON. Soil. Sci. Soc. Am. Proc. In press; (*c*) R. RIFFALDI and M. SCHNITZER. Soil Sci. In press.

Can. J. Chem. Downloaded from www.nrcresearchpress.com by 210.87.254.42 on 09/05/12
For personal use only.

Isotopic Studies of the Metal–Ligand Bond. Part III. The Far Infrared Spectra of Some Tetragonal Diamine Complexes of Cobalt(II) and Nickel(II): Studies of the Metal–Nitrogen Bond, as a Function of Metal Ion and of Spin State

A. B. P. LEVER AND ELVIO MANTOVANI

Department of Chemistry, York University, Downsview, Ontario M3J 1P3

Received October 17, 1972

The far infrared spectra of 35 complexes of the formula $M(diamine)_2X_2$ are reported where M = Co(II) and Ni(II), X = Cl^-, Br^-, I^-, NO_3^-, SCN^-, ClO_4^-, and AgI_2^- and the diamine is ethylenediamine or its *N,N*-symmetric or antisymmetrically substituted dimethyl or diethyl derivative. Isotopic substitution studies with ^{62}Ni and with ^2H are carried out with eleven characteristic complexes and assignments for the metal–nitrogen modes in both octahedral and square planar complexes so deduced. In most cases the appropriate number of metal–ligand modes, based on symmetry considerations, are observed. The variations in observed M—N frequencies are discussed in terms of the electronic and geometric factors previously utilized for the corresponding copper(II) complexes. In complexes containing the asymmetric ligands, stretching vibrations arising from the two types of metal–nitrogen bond can be separately identified. Isotopic studies of pairs of complexes containing the same ligand and metal ion but with the latter in alternate spin states are reported here for the first time. All of the cobalt(II) complexes and several of the nickel(II) complexes are reported here for the first time.

Les spectres dand l'infrarouge lointain de 35 complexes de formule M $(diamine)_2X_2$ ont été rapportés, avec M = Co(II) et Ni(II), X = Cl^-, Br^-, I^-, NO_3^-, SCN^-, ClO_4^-, et AgI_2^- et la diamine est l'éthylènediamine ou ses dérivés *N,N*-diméthylés ou *N,N*-diéthylés, symétriquement ou antisymétriquement substitués. Les études de substitution isotopique avec ^{62}Ni et ^2H ont été effectuées sur onze complexes caractéristiques et les attributions sur les modes concernant la liaison métal–azote, à la fois pour les complexes octaédral et carré-plan, ont pu être déduites. Dans la plupart des cas, le nombre approprié de modes relatifs au métal–ligand basé sur des considérations de symétrie, a pu être observé. Les variations dans les fréquences M—N observées ont été discutées par rapport aux facteurs électroniques et géométriques précédemment utilisés pour les complexes de cuivre(II) correspondants. Dans les complexes comprenant des ligands asymétriques, les vibrations d'élongation qui sont dues aux deux types de liaison métal–azote ont pu être séparément identifiées. Les études isotopiques portant sur les paires de complexes contenant le même ligand et le même ion métal, ce dernier se trouvant dans des états de spin alternés, ont été rapportées ici pour la première fois. Tous les complexes de cobalt(II) et plusieurs complexes de nickel(II) ont été décrits ici pour la première fois. [Traduit par le journal]

Can. J. Chem., **51**, 1567 (1973)

Introduction

We recently reported the far infrared and electronic spectra of mono- (1) and bis(diamine) (2) complexes of copper(II) and discussed these data in terms of the electronic and geometric structures of the complexes. Subsequent isotopic substitution data (3) generally confirmed the assignments. Novel correlations were observed between the vibrational and electronic spectra and some useful bonding information so derived. This paper deals with corresponding derivatives of cobalt(II) and nickel(II), whose spectra are fairly closely related both to each other and to the copper derivatives. Many of the nickel complexes have been reported previously, whilst the cobalt derivatives are new. The electronic spectra and magnetism of these cobalt complexes will be the subject of a later paper (4).

Whilst there is little doubt that all the previously discussed (2) copper complexes $Cu(diamine)_2X_2$ have a *trans* octahedral configuration, the complexes $Ni(en)_2Cl_2$ and $Ni(en)_2Br_2$ are *cis* dimeric with halogen bridges (5), whilst the isothiocyanate complex $Ni(en)_2(NCS)_2$ has a *trans* monomeric structure (6).

The Ni(*sym*-$Me_2en)_2X_2$ (X = Br, and NO_3) complexes are also *trans* octahedral (7). (See footnotes to Table 1 for abbreviations.) No other X-ray studies of the paramagnetic members of this series appear to have been reported.

The observation of only one ν(CN) stretching frequency in the thiocyanate complexes $M(diamine)_2(NCS)_2$ (especially if the measurement is carried out at liquid nitrogen temperature) (8) provides strong, though probably not unequivocal, support for a *trans* configuration of these complexes.

The criteria used to assign the far infrared

Can. J. Chem. Downloaded from www.nrcresearchpress.com by 210.87.254.105 on 09/05/12
For personal use only.

TABLE 1. Analytical data and literature references*

Complex†		Composition (%) Carbon	Hydrogen	Nitrogen	Halogen	Metal	Reference
$Ni(en)_2Cl_2$	f.				28.1		5
$C_4H_{16}Cl_2N_4Ni$	r.				28.4		
$Ni(en)_2Br_2$	f.					17.2	5
$C_4H_{16}Br_2N_4Ni$	r.					17.3	
$Ni(en)_2I_2$	f.				13.5		47
$C_4H_{16}I_2N_4Ni$	r.				13.6		
$Ni(en)_2(NCS)_2$	f.				19.7		6, 47
$C_6H_{16}N_4NiS_2$	r.				19.7		
$Ni(en)_2(NO_3)_2$	f.				20.5		48
$C_4H_{16}N_6NiO_6$	r.				20.0		
$Ni(en)_2(AgI_2)_2$	f.					6.3	28, 42
$C_4H_{16}Ag_2I_4N_4Ni$	r.					6.5	
$Ni(sym\text{-}Me_2en)_2(NCS)_2$	f.	34.3	7.0	24.1	33.1		45
$C_{10}H_{24}N_6NiS_2$	r.	34.2	6.9	23.9	33.0		
$Co(sym\text{-}Me_2en)_2(NCS)_2$	f.	34.35	6.7		33.1		This work
$C_{10}H_{24}CoN_6S_2$	r.	34.2	6.9		33.0		
$Ni(sym\text{-}Me_2en)_2(ClO_4)_2$	f.	22.2	5.7	12.7		13.4	46
$C_8H_{24}Cl_2N_4NiO_8$	r.	22.1	5.6	12.9		13.5	
$Ni(sym\text{-}Me_2en)_2Cl_2$	f.	31.1	7.6	18.55	23.1		49
$C_8H_{24}Cl_2N_4Ni$	r.	31.4	7.9	18.3	23.2		
$Co(sym\text{-}Me_2en)_2Cl_2$	f.	31.6	8.05		23.1	19.4	This work
$C_8H_{24}Cl_2CoN_4$	r.	31.4	7.9		23.2	19.3	
$Ni(sym\text{-}Me_2en)_2Br_2$	f.				40.2		49, 7
$C_8H_{24}Br_2N_4Ni$	r.				40.5		
$Co(sym\text{-}Me_2en)_2Br_2$	f.	24.4	6.2		40.3	14.8	This work
$C_8H_{24}Br_2CoN_4$	r.	24.3	6.1		40.5	14.9	
$Ni(sym\text{-}Me_2en)_2I_2$	f.	19.5	5.1	11.4		12.5	This work
$C_8H_{24}I_2N_4Ni$	r.	19.7	4.9	11.45		12.0	
$Co(sym\text{-}Me_2en)_2I_2$	f.	20.0	5.3			12.1	This work
$C_8H_{24}CoI_2N_4$	r.	19.6	4.9			12.05	
$Co(sym\text{-}Me_2en)_2(NO_3)_2$	f.	26.4	7.0			16.1	This work
$C_8H_{24}CoN_6O_6$	r.	26.7	6.7			16.4	
$Ni(asym\text{-}Me_2en)_2(ClO_4)_2$	f.					13.5	44
$C_8H_{24}Cl_2N_4NiO_8$	r.					13.5	
$Co(asym\text{-}Me_2en)_2Cl_2$	f.	31.6	7.7		23.2	19.2	This work
$C_8H_{24}Cl_2CoN_4$	r.	31.4	7.9		23.2	19.2	
$Co(asym\text{-}Me_2en)_2Br_2$	f.	24.5	6.3		40.2	15.1	This work
$C_8H_{24}Br_2CoN_4$	r.	24.3	6.1		40.5	14.9	
$Ni(asym\text{-}Me_2en)_2(NCS)_2$	f.					16.7	44
$C_{10}H_{24}N_6NiS_2$	r.					16.8	
$Co(asym\text{-}Me_2en)_2(NCS)_2$	f.	34.1	6.7		33.2		This work
$C_{10}H_{24}CoN_6S_2$	r.	34.2	6.9		33.0		
$Co(asym\text{-}Me_2en)_2(NO_3)_2$	f.	26.9	6.6			16.2	This work
$C_8H_{24}CoN_6O_6$	r.	26.7	6.7			16.4	
$Ni(sym\text{-}Et_2en)_2(NCS)_2$	f.	41.5	8.0	20.4	28.6		45, 50
$C_{14}H_{32}N_6NiS_2$	r.	41.3	7.9	20.6	28.5		
$Co(sym\text{-}Et_2en)_2(NCS)_2$	f.	41.0	7.85	20.1	28.3	14.65	This work
$C_{14}H_{32}CoN_6S_2$	r.	41.1	7.9	20.6	28.5	14.5	
$Ni(sym\text{-}Et_2en)_2Cl_2$	f.	39.9	9.0	15.6	19.4	16.1	This work
$C_{12}H_{32}Cl_2N_4Ni$	r.	39.8	8.9	15.5	19.6	16.3	
$Co(sym\text{-}Et_2en)_2Cl_2$	f.	40.0	9.0	15.6	19.4		This work
$C_{12}H_{32}Cl_2CoN_4$	r.	39.8	8.8	15.5	19.6		
$Ni(sym\text{-}Et_2en)_2Br_2$	f.				35.8	12.9	This work
$C_{12}H_{32}Br_2N_4Ni$	r.				35.4	13.0	
$Ni(sym\text{-}Et_2en)_2(ClO_4)_2$	f.	29.15	6.7	11.5		12.3	This work
$C_{12}H_{32}Cl_2N_4NiO_8$	r.	29.4	6.6	11.4		12.0	
$Co(sym\text{-}Et_2en)_2(NO_3)_2$	f.	34.9	7.8	20.3		14.2	This work

Can. J. Chem. Downloaded from www.nrcresearchpress.com by 210.87.254.105 on 09/05/12
For personal use only.

TABLE 1. (*Concluded*)

Complex†		Composition (%) Carbon	Hydrogen	Nitrogen	Halogen	Metal	Reference
$C_{12}H_{32}CoN_6O_6$	r.	34.7	7.8	20.2		14.2	
$Ni(asym\text{-}Et_2en)_2Cl_2$	f.					16.5	43
$C_{12}H_{32}Cl_2N_4Ni$	r.					16.2	
$Co(asym\text{-}Et_2en)_2Cl_2$	f.				19.6		This work
$C_{12}H_{32}Cl_2CoN_4$	r.				19.6		
$Ni(asym\text{-}Et_2en)_2Br_2$	f.					12.9	43
$C_{12}H_{32}Br_2N_4Ni$	r.					13.0	
$Ni(asym\text{-}Et_2en)_2I_2$	f.					10.8	43
$C_{12}H_{32}I_2N_4Ni$	r.					10.8	
$Ni(asym\text{-}Et_2en)_2(NCS)_2$	f.				28.8		43
$C_{14}H_{32}N_6NiS_2$	r.				28.5		
$Co(asym\text{-}Et_2en)_2(NCS)_2$	f.	41.1	8.0	20.3	28.8	14.6	This work
$C_{14}H_{32}CoN_6S_2$	r.	41.1	7.9	20.6	28.5	14.5	
$Ni(asym\text{-}Et_2en)_2(ClO_4)_2$	f.					12.0	43
$C_{12}H_{32}Cl_2N_4NiO_8$	r.					12.0	

*Previously characterized complexes have been analyzed for at least one element to ensure purity. Previously uncharacterized complexes have been analyzed for several elements to ensure both purity and identity. The octahedral nickel complexes are pale green or pale blue (Table 2) whilst the square derivatives (Table 3) are yellow or yellow orange. The cobalt complexes are generally pink.

†En = ethylenediamine, *sym*-Me_2en = *sym*-*N*,*N*′-dimethylethylenediamine; *asym*-Me_2en = *asym*-*N*,*N*-dimethylethylenediamine; *sym*-Et_2en = *sym*-*N*,*N*′-diethylethylenediamine; *asym*-Et_2en = *asym*-*N*,*N*-diethylethylenediamine; r = required; f = found.

spectra of complexes of this type have been previously discussed (1–3). In the earlier studies (1, 2) many of the complexes were *N*-deuterated by multiple treatment of the complex with D_2O. The metal–nitrogen band decreased in energy as a consequence of resulting increase in the effective reduced mass of the Cu—N bond. Unfortunately it is difficult to carry out similar studies successfully with the cobalt and nickel complexes. In the majority of such experiments the complexes either hydrolyzed or disproportionated to the $M(ligand)_3^{2+}$ species. However two experiments were successful and are included herein. The isotopic substitution technique (3, 9, 10) provides a more definitive guide to the assignment of metal ligand modes.

It is understood that bands identified as "metal–ligand stretching modes" will in general be coupled with other vibrations of the molecule. The description of a band as arising from such a vibration implies that the potential function describing the vibration is predominantly metal–ligand in origin.

The highest copper–nitrogen stretching frequency in the ethylenediamine derivatives occurs (1–3) in the region 350–420 cm^{-1} depending upon the amine, and the axial interaction. For the octahedral complexes of cobalt(II), nickel(II), and copper(II) of nitrogeneous ligands, previous evidence suggests that the highest energy infrared active metal–nitrogen stretching frequency appears to fall in the sequence ν(Cu—N) > ν(Ni—N) > ν(Co—N). This is supported by consideration of the complexes of ammonia, hydrazine (11), and imidazole (12), *viz.* $Cu(NH_3)_4Cl_2$, 420; $Cu(NH_2.NH_2)_2Cl_2$, 440; $Cu(IMZ)_4Cl_2$, 286; $Ni(NH_3)_6Cl_2$, 334; $Ni(NH_2.NH_2)_2Cl_2$, 409; $Ni(IMZ)_6Cl_2$, 262; $Co(NH_3)_6Cl_2$, 318; $Co(NH_2.NH_2)_2Cl_2$, 388; $Co(IMZ)_6Cl_2$, 240 cm^{-1}.

Pyridine complexes also exhibit this trend (13). Unequivocal confirmation of these nitrogen frequencies using isotopic substitution experiments has been obtained by Nakamoto and co-workers (14, 15) who confirm the sequence, at least for 8-hydroxyquinoline derivatives (14). Further, the Ni—N stretching frequency in $Ni(bipy)_3.2ClO_4.2H_2O$ has been unequivocally identified at 292 cm^{-1} (15). Nakamoto and co-workers (16, 17) have also demonstrated by isotopic experiments that the Ni—N stretching frequency lies between 360 and 400 cm^{-1} in complexes of *asym*-dimethylethylenediamine and some mixed nitrogen sulfur bidentate chelating ligands. Thus the metal–nitrogen modes in the *high spin* octahedral cobalt(II) and nickel(II) complexes under discussion are expected below 400 cm^{-1}, the region where the corresponding copper modes are observed.

Having satisfactorily assigned the copper complexes (1–3), assignments for the cobalt(II)

Can. J. Chem. Downloaded from www.nrcresearchpress.com by 210.87.254.105 on 09/05/12
For personal use only.

Can. J. Chem. Downloaded from www.nrcresearchpress.com by 210.87.254.105 on 09/05/12
For personal use only.

and nickel(II) derivatives should follow readily in those cases where the spectrum of the cobalt or nickel complex is very similar to that of the corresponding copper complex. The intensity of the metal–nitrogen vibration is somewhat variable (18) and whilst it is usually readily identifiable in the copper and nickel spectra, it is frequently very weak in the cobalt spectra. This problem has been partially solved by obtaining low temperature (sample cooled in liquid nitrogen) spectra which are better resolved and in which the band intensities are generally enhanced (19–21).

With weakly coordinating anions, or with sterically bulky amines, nickel(II) commonly forms square planar rather than tetragonal octahedral complexes. These complexes are diamagnetic and will have shorter metal–nitrogen bonds than their octahedral analogs. As a consequence the force constant for the nickel–nitrogen vibration should increase and the absorption frequency is expected to occur at a higher energy than in the octahedral complexes; nickel–nitrogen stretching frequencies in diamagnetic nickel complexes have not been well documented. The data were all recorded in the solid state since the species decompose in solution.

Experimental

The far infrared spectra were obtained with a Beckman IR 12 Spectrometer as Nujol mulls supported on polythene. The isotopic data scanned at 1–2 cm^{-1}/min are accurate to ± 0.2 cm^{-1}. The instrument was calibrated with water vapor, in the far infrared region (22), and with polystyrene in the conventional region. Reproducibility from one sample to another was 0.5 cm^{-1} or better, for the sharper bands. Quoted data are the average of at least three scans. Low temperature spectra were obtained with an evacuated VLT-2 Variable Temperature Cell, equipped with NaCl or polypropylene windows. The cold finger was cooled with liquid nitrogen. Equilibrium was achieved after about 40 min beyond which time there were no further changes in the spectra. The exact temperature achieved is not known but is likely to be within about 20° of −196 °C. The complexes studied are listed in Table 1 together with their analytical data and previous references where relevant. New complexes were prepared by the general method of treating the metal salt with the appropriate ligand in stoichiometric proportions in absolute ethanol. For cobalt complexes it was necessary to add triethylorthoformate to the solvent to remove water and to carry out the reaction under a nitrogen atmosphere to preclude oxidation. Many of the cobalt complexes so obtained decomposed slowly in the solid state in the presence of air. Where possible the complexes were recrystallized from the same solvent. The samples were dried at about 80° under vacuum prior to analysis and spectra determination. The isotopically substituted complexes were prepared from ^{62}Ni obtained in 99% isotopic purity from Oak Ridge National Laboratory. The complexes were obtained on a 5 mg (of Ni) scale through the sequence $^{62}Ni \rightarrow {}^{62}NiX_2 \rightarrow$ complex followed by ignition of the complex to recover the nickel as ^{62}NiO and reconversion to $^{62}NiX_2$. Loss of ^{62}Ni could be maintained below 5% per experiment. Deuterated *asym-N,N*-diethylethylenediamine was prepared *in situ* by multiple treatment of $(C_2H_5)_2NCH_2CH_2NH_2$ with D_2O (99.8% D, Stohler Isotope Chemical Co.) acidified by the addition of a small amount of P_2O_5. The product was extracted with chloroform and the extract dried by several applications of anhydrous sodium sulfate and finally by treatment with a small volume of triethylorthoformate. This solution was then added, in excess, to a solution of anhydrous nickel chloride or bromide in a small volume of dimethyl sulfoxide-d^6. The product separated upon shaking for a short period at room temperature. The identity of these products as the *N*-deuterated Ni(*asym*-$Et_2en)_2X_2$ (X = Cl, Br) was assured by comparison of their electronic spectra with the electronic spectra of the hydrogen analogs. Their vibrational spectra showed a very marked decrease in the intensities of the N—H stretching and NH_2 rocking modes, and the appearance of very strong N—D stretching modes near 2300 cm^{-1}. It was not possible to obtain a sample in which the N—H modes were entirely absent and it may be assumed that the complexes $((C_2H_5)_2NCH_2CH_2ND_2)_2NiX_2$ are probably contaminated with some $((C_2H_5)_2NCH_2CH_2NHD)_2NiX_2$ plus a trace (the NH_2 rocking mode was greatly diminished in intensity) of the NH_2 complex.

Results

The discussion follows that developed for the copper(II) complexes of the same general formula (2, 3). However, whilst the axial bonds in the very strongly tetragonally distorted copper complexes did not in general give rise to metal – axial ligand vibrational absorption above 200 cm^{-1}, this will not necessarily be the case in the cobalt(II) and nickel(II) complexes, where the tetragonal distortion may be less marked. Thus in regular octahedral complexes the Co—Cl and Ni—Cl stretching vibrational frequencies are expected (23, 24) near 240 cm^{-1} and the corresponding thiocyanate frequencies (24–26) from about 240 to 300 cm^{-1}. Metal–nitrate vibrations are the subject of some debate but probably lie in the region 250–350 cm^{-1} (16, 17, 27–29). Metal–bromide and iodide bands lie (23) below 200 cm^{-1} and will not be observed in this study. It is evident from the preceeding discussion that no metal (Co(II) or Ni(II)) ligand bands are expected to occur above 400 cm^{-1} in these complexes (except perhaps in the square nickel complexes) and that bands in the region 400–500 cm^{-1} can therefore be safely assigned to

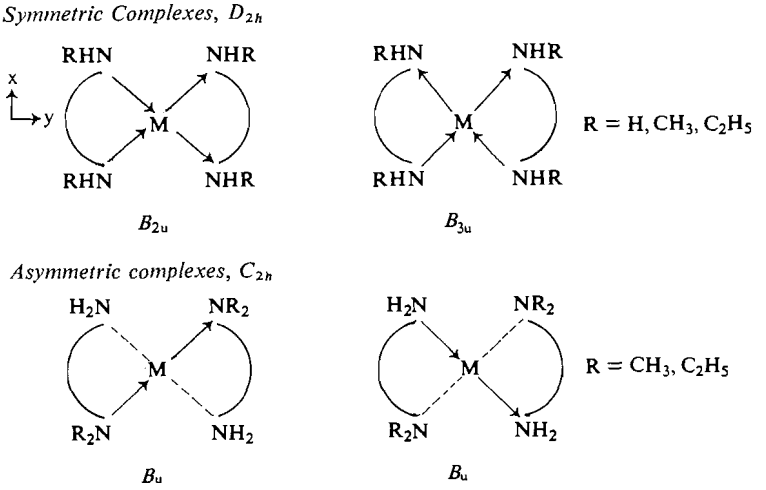

SCHEME 1. Infrared allowed M—N stretching vibrations

ring vibrations (in-plane skeletal vibrations of the ligand back-bone) (1–3). Bending vibrations are unlikely to lie above 225 cm^{-1} (2, 15, 16) in the high spin complexes.

Paramagnetic Complexes

(i) Ethylenediamine derivatives

In view of the *cis* dimeric nature of $Ni(en)_2Cl_2$ and $Ni(en)_2Br_2$ (and on the basis of the similarity of its far infrared spectrum, $Ni(en)_2I_2$), their far infrared spectra differ markedly from the copper complexes of analogous formulation, Since there are no terminal Ni—X bonds, no ν(Ni—X) vibrations will be expected above 200 cm^{-1} (30). The very low symmetry of such complexes should lead to the observation of up to four infrared active metal–nitrogen stretching vibrations. Four bands in the spectrum of natural nickel $Ni(en)_2Cl_2$ shift down by more than 2 cm^{-1} upon substitution with ^{62}Ni. Two strong bands lie at 355.5 and 276 cm^{-1} whilst a weaker double band lies near 300 cm^{-1} (Table 2); these are therefore assigned as ν(Ni—N) vibrations. The bromide and iodide have spectra very similar to each other and to the chloride complex, leading to the facile identification of the four ν(Ni—N) modes in these compounds.

The complex $Ni(en)_2(NCS)_2$, with a *trans* configuration (6), has a very much more simple far infrared spectrum consistent with its higher symmetry. The nitrate $Ni(en)_2(NO_3)_2$ has a similarly simple spectrum and may also be assumed to have a *trans* configuration (note that the ν(NH_2) band is unsplit (31)). Assuming D_{2h} symmetry such complexes should exhibit 2 ν(Ni—N) bands (of B_{2u} and B_{3u} symmetry) and one ν(Ni—X) (B_{1u}) with infrared activity (Scheme 1). In the nitrate complex three bands (at 380, 319, and 292.5 cm^{-1}) shift down in excess of 2 cm^{-1} upon substitution by ^{62}Ni. The band at 380 cm^{-1} is undoubtedly ν(Ni—N). Of the two remaining isotopically sensitive bands that at 319 cm^{-1} is probably ν(Ni—O, NO_3) whilst that at 292.5 cm^{-1} is the remaining ν(Ni—N). This assignment is based on the expected position of ν(Ni—O, NO_3) (16, 17, 27–29), and on its greater sensitivity to isotopic substitution. In the thiocyanate complex, two bands at 305 and 345 cm^{-1} (Table 2) are clearly assignable to ν(Ni—N). Isotopic evidence for some of the substituted thiocyanate complexes presented below suggests that ν(Ni—N, NCS) lies near 240 cm^{-1} in keeping with previous literature (24–26). No such band can be unequivocally identified in this case. Cobalt(II) ethylenediamine complexes are unstable with respect to oxidation and were not studied.

sym-Dimethylethylenediamine Complexes

All these complexes have very similar spectra (Fig. 1) whose gross features are almost independent of change of metal (Co(II), Ni(II), or Cu(II)) or of counter-ion (Cl, Br, I, NCS, or NO_3). The main deviation would appear to be a band observed near 400 cm^{-1} in the copper complexes, probably a ring vibration, which is invariably split into two components in the cobalt and nickel complexes. In these cir-

Can. J. Chem. Downloaded from www.nrcresearchpress.com by 210.87.254.105 on 09/05/12
For personal use only.

Can. J. Chem. Downloaded from www.nrcresearchpress.com by 210.87.254.105 on 09/05/12
For personal use only.

TABLE 2. Vibrational data (500–200 cm^{-1}) for paramagnetic octahedral complexes

Complex*		Vibrational frequencies† (cm^{-1})			
		Ring	M—N	M—X	Other bands
$Ni(en)_2Cl_2$		442w 426.5w	355.5s 308m 302m 276s		240sbr 219m
	[62]	442w 426.5w	353s 304w 299w 272s		239sbr 217m
$Ni(en)_2Br_2$		432m	357s 310m (295) 275s		232s 224m 208m
$Ni(en)_2I_2$		430w 410w	352s (305) 302m 274s		230vs
$Ni(en)_2(NCS)_2$		412m	345s 305s		477s(δNCS) 212s
$Ni(en)_2(NO_3)_2$		449m	380s 292.5m	319s	223s
	[62]	449m	377.5s 290.5m	315s	223s
$Ni(sym\text{-}Me_2en)_2Cl_2$		457.5m 420s 389.5s	353s 284s 251m		(269) 215.5m 197.5m
	[62]	457.5m 420s 389.5s	352s 279s 247.5m		(269) 215.5m 197.5m
$Co(sym\text{-}Me_2en)_2Cl_2$		452m 417s 374s	339s 269s 236s		214m
$Ni(sym\text{-}Me_2en)_2Br_2$		458m 423s 388s	355s 281s 250m		264m 216m
$Co(sym\text{-}Me_2en)_2Br_2$		452m 420s 374s	344s 269s 234s		212m
$Ni(sym\text{-}Me_2en)_2I_2$		451m 425s 387s	362s 282s 245s		305w 261m
$Co(sym\text{-}Me_2en)_2I_2$		453m 420s 374s	345s 267s 230s		257m
$Ni(sym\text{-}Me_2en)_2(NCS)_2$		454m 420s 393s	350s 284s 241s		473s(δNCS) (340) (300) (277)
$Co(sym\text{-}Me_2en)_2(NCS)_2$		450m 416s 376s	338s 267s 235w [247s]		475s(δNCS) (300) 229w
$Co(sym\text{-}Me_2en)_2(NO_3)_2$		455s 428s 380s	350m 283m 266m	303m	228s
$Co(asym\text{-}Me_2en)_2Cl_2$		469s 440m 402s	359w [368m (360)] 240brs‡		(295)
$Co(asym\text{-}Me_2en)_2Br_2$		470s 441s 403s	358w [368m] 340m 240brs‡ [249s 237s]		(295) (262)
$Co(asym\text{-}Me_2en)_2I_2$		475s 445s 416m	356s [360s 342s] 246m‡		289vs 204m
$Co(asym\text{-}Me_2en)_2(NO_3)_2$		486s 442m 421m	372s 268s‡	302m	(298) 228vs (222)
$Ni(asym\text{-}Me_2en)_2(NCS)_2$		(480) 437m 412m	355s 332m 267s‡		470s(δNCS) (285) 218vs
$Co(asym\text{-}Me_2en)_2(NCS)_2$		470s 433m 405s	342s 329m 257s‡		465s(δNCS) 280m 204s
$Ni(sym\text{-}Et_2en)_2Cl_2$		494.5s 434.5s	377s 287.5vs		(277) 212s

Can. J. Chem. Downloaded from www.nrcresearchpress.com by 210.87.254.105 on 09/05/12
For personal use only.

TABLE 2. (*Concluded*)

Complex*		Vibrational frequencies† (cm^{-1})			
		Ring	M—N	M—X	Other bands
	[62]	494s 434.5s	375.5s 282vs		212s
Co(*sym*-$Et_2en)_2Cl_2$		487s 425s	365s 279s		349w (270) 215s
Ni(*sym*-$Et_2en)_2Br_2$		494s 433s	371s 286vs		305w (275)
Co(*sym*-$Et_2en)_2(NO_3)_2$		490m 460m 413m	369brs (279)	305m	(327) 265s (250)
Ni(*sym*-$Et_2en)_2(NCS)_2$		458m 399.5m	363s 281.5s	236s	477s(δNCS) 347w 256s 212s
	[62]	458m 399.5m	363s 279s	234s	477s(δNCS) 347w 256s 212s
Co(*sym*-$Et_2en)_2(NCS)_2$		453s 387m	349s 280s	229s	475s(δNCS) 265w 254s
Ni(*asym*-$Et_2en)_2Cl_2$		505vs 433.5m	401.5s 265.5s		(350) 335s 287.5m 213s
	[62]	505vs 433.5m	399.5s 264s		(350) 335s 287.5m 213s
N-deutero		496vs 489vs 427.5m	390s 259s		352w 333s 277.5m
Co(*asym*-$Et_2en)_2Cl_2$		499vs 419m	390s 254s		348m 332s 285m 215s
Ni(*asym*-$Et_2en)_2(NCS)_2$		503vs 423.5m	388s 284.5w	242vs	482.5s(δNCS) 475s (382) 330.5m (265)
	[62]	503vs 423.5m	386.5s 284w	237vs	482.5s(δNCS) 475s (382) 330.5m (265)
Co(*asym*-$Et_2en)_2(NCS)_2$		493s 418s	379s 280m	240vs	479s(δNCS) 326s

*Nickel complexes prepared with natural nickel except where indicated; [62], complexes prepared with ^{62}Ni.
†Shoulders cited in parentheses. Data in square brackets indicate effect of liquid nitrogen temperature upon band immediately preceding datum. Note that natural nickel contains mainly ^{58}Ni (68%) and ^{60}Ni (26%). Because of the broadening of the absorption due to ^{60}Ni, the isotopic shifts indicated in these tables will be slightly underestimated.
‡See text for discussion of assignment of this band.

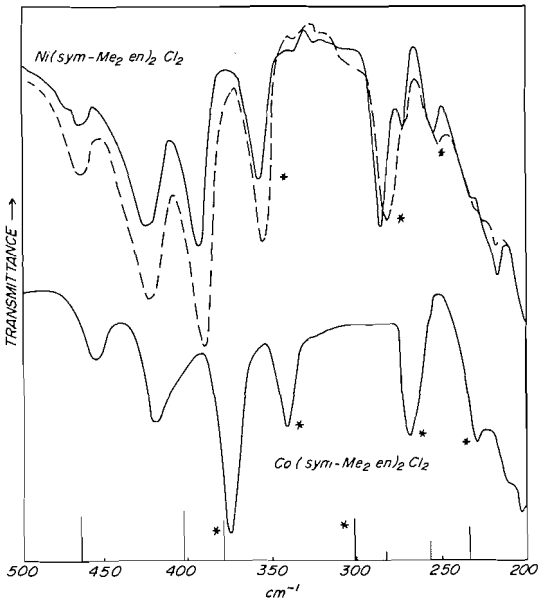

FIG. 1. Representative infrared spectra. Upper: Ni(*sym*-$Me_2en)_2Cl_2$ with natural nickel—, with ^{62}Ni---. Lower: Co(*sym*-$Me_2en)_2Cl_2$. The bars in the bottom of the diagram indicate the positions of the vibrations in Cu(*sym*-$Me_2en)_2Cl_2$ with their height qualitatively proportional to the band intensities.

cumstances a *trans* configuration for all the complexes seems assured. In particular the thiocyanate complexes exhibit a single ν(CN) frequency (at 2104 (Ni) and 2094 (Co) cm^{-1}) which is unsplit when the sample is cooled to −196 °C. Isotopic substitution of Ni(*sym*-$Me_2en)_2Cl_2$ reveals three isotopically sensitive bands at 353, 284, and 251 cm^{-1}. Although in the appropriate region (23, 24) it would be inappropriate to assign the lowest energy band to ν(Ni—Cl) since the band appears in much the same position in all the complexes, *i.e.* is independent of X. In the copper complexes (2, 3) three bands may similarly be identified but the lowest energy band is insensitive to isotopic substitution (3). In the nickel complexes the highest energy band (353 cm^{-1}) is least sensitive. It is probable that these three bands comprise the expected two ν(Ni—N) vibrations plus a ligand vibration of symmetry appropriate for coupling with one of the ν(Ni—N) modes. These three bands are readily picked out in all the complexes of this amine (Table 2); in the case of the cobalt(II) complexes, they are all shifted down, relative to the nickel(II) complexes, by about 15 cm^{-1}. No ν(M—Cl) or ν(M—N, NCS) vibrations can be identified above 200 cm^{-1}. However a band at 303 cm^{-1} in Co(*sym*-$Me_2en)_2(NO_3)_2$ is probably ν(Co—O, NO_3).

asym-Dimethylethylenediamine Complexes

The nickel complexes Ni(*asym*-$Me_2en)_2X_2$ where X = Cl, Br, and NO_3, have been previously discussed by Nakamoto and co-workers (17) with assignments supported by isotopic substitution. These authors assigned a pair of bands near 380 cm^{-1} to ν(Ni—N)(NH_2) and ν(Ni—N)(NMe_2) based on isotopic substitution with ^{62}Ni and ^{2}H. A band near 260 cm^{-1} was assigned to ν(Ni—Cl). Our own data for these complexes were in substantial agreement with this work and are not cited in Table 2. Data for Ni(*asym*-$Me_2en)_2(NCS)_2$ and for some cobalt(II) complexes are however included in Table 2. The spectra are similar to those previously discussed (17) and assignment of the high energy ν(Ni—N) follows readily. However in view of the fairly wide separation of the two ν(Ni—N) vibrations in the copper complexes of this ligand (2, 3), the close spacing of the two ν(Ni—N) modes cited by Nakamoto and co-workers (17) seems anomalous.

Data for *asym*-Et_2en complexes, cited below, suggests that the band at 260 cm^{-1} in Ni(*asym*-$Me_2en)_2Cl_2$ (17) may in fact include *both* ν(Ni—N) and ν(Ni—Cl). Thus the bands near 240 cm^{-1} in the other complexes (indicated in Table 2) may have ν(Ni—N) character, (see discussion below). We note, however, that unlike the symmetric ligand, the spectra of the cobalt and nickel complexes do not bear such a close resemblance to their copper analogs. Moreover broad ν(CN) absorption is noted for the thiocyanate complexes. The possibility of some of these complexes being *cis* rather than *trans* cannot be excluded.

sym-Diethylethylenediamine Complexes

Once again the gross features of the spectra are independent of the metal and of X, providing evidence for a *trans* configuration, and allowing for ease of assignment. The thiocyanate complexes exhibit a single ν(CN) absorption (at 2099 (Ni) and 2090 (Co) cm^{-1}) unsplit at low temperature. Two bands in Ni(*sym*-$Et_2en)_2Cl_2$ at 377 and 287.5 cm^{-1} are sensitive to isotopic substitution and may be assigned as ν(Ni—N) modes. It is inappropriate to assign the 287.5 cm^{-1} band to ν(Ni—Cl) since it is rather too high in energy and a band

Can. J. Chem. Downloaded from www.nrcresearchpress.com by 210.87.254.105 on 09/05/12
For personal use only.

Can. J. Chem. Downloaded from www.nrcresearchpress.com by 210.87.254.105 on 09/05/12
For personal use only.

of similar energy appears in the spectra of the bromide and iodide complexes. No ν(Ni—Cl) band can be identified. The two bands in the spectra of the other halide complexes, and of the cobalt analogs, are readily identified and similarly assigned. The complex Ni(*sym*-$Et_2en)_2(NCS)_2$ was also isotopically substituted. In this case, anomalously, the higher of the two bands did not shift (see below). However a band at 236 cm^{-1} did show sensitivity and is assigned to ν(Ni—N, NCS).

asym-Diethylethylenediamine Complexes

Once again there is a single ν(CN) absorption in the thiocyanate complexes (at 2098 (Ni) and 2090 (Co) cm^{-1}) unsplit at low temperature, suggesting a *trans* configuration. The cobalt and nickel complexes all have similar spectra suggesting all are *trans*. Isotopic substitution of both Ni(*asym*-$Et_2en)_2Cl_2$ and Ni(*asym*-$Et_2en)_2(NCS)_2$ leads to the identification of two metal sensitive modes near 400 and near 265 cm^{-1}, albeit in the thiocyanate case the sensitivity of the lower energy band is slight. In agreement with the observation of two similarly sensitive bands in the analogous copper(II) complexes (3), these are assigned to the expected ν(Ni—N) modes. By analogy with the *asym*-Me_2en complexes (17) the 265.5 cm^{-1} band in the chloride complex may contain both ν(Ni—N) and ν(Ni—Cl). Comparison with the spectrum of the bromide is not possible since this complex is square planar. It is pertinent that the lower energy ν(Ni—N) mode at 284.5 cm^{-1} in the thiocyanate complex is much weaker than in the chloride complex, and that in addition an isotopically sensitive band occurs in the thiocyanate complex at 242 cm^{-1} and is assigned to ν(Ni—N, NCS).

Unlike the case of the *asym*-Me_2en complexes there is no pair of closely spaced isotopically sensitive bands near 400 cm^{-1}. Accordingly the identification (17) of the bands at 378 and 360 cm^{-1} in Ni(*asym*-$Me_2en)_2Cl_2$ as ν(Ni—N)(M—NH_2), and ν(Ni—N)(M—$N(CH_3)_2$ must be considered unproven.

In the spectrum of the *N*-deuterated Ni(*asym*-$Et_2en)_2Cl_2$ both ν(Ni—N) bands are shifted down, the higher energy band being the most affected.

Diamagnetic Square Planar Complexes

The success of the procedures hitherto applied to the study of the far infrared spectra of metal complexes relies on the fact that bands identified as ν(M—L) have a potential distribution dominated by the M—L normal coordinate. In high spin octahedral and tetrahedral first row transition metal complexes this assumption is generally valid because the metal–ligand interaction, *i.e.* force constant, is sufficiently small, that coupling between the metal–ligand modes, and ligand modes of the same symmetry is minimized. However the apparent absence of some of the ν(M—Cl) and ν(M—N, NCS) modes in the above complexes may reflect coupling with other modes to a sufficient degree that isotopic substitution fails to identify them. It seems more likely however that they are obscured by other absorption. The appearance of three ν(M—N) modes in the *sym*-Me_2en complexes would appear to indicate a situation where coupling with one other mode is important leading to isotopic sensitivity for three, rather than two, bands. Alternatively the observation may arise through correlation coupling in the lattice.

With low spin transition metal derivatives, the metal–ligand interaction and force constant will be larger, and the interaction force constants which couple metal–ligand with ligand modes will also be larger. As a consequence it is expected that the metal–ligand normal coordinate will be spread over a greater number of observed vibrations, *i.e.* more vibrations will show isotopic sensitivity. To further complicate the situation, bending modes involving the lighter ligand atoms may now be expected above 200 cm^{-1}.

Ethylenediamine Complexes

The vibrational spectra of square planar ethylenediamine complexes have been of interest for many years (11, 32). The square planar complex $Cu(en)_2(AgI_2)_2$ (33) exhibits only three reasonably intense bands between 200 and 600 cm^{-1}, at 531, 472, and 414.5 cm^{-1}. Only the last of these is isotopically sensitive (3) and is assigned to ν(Cu—N). In particular the band at 472 cm^{-1} does not shift although a recent normal coordinate analysis (32) assigned this band to a ν(Cu—N) vibration in $Cu(en)_2PtCl_4$. Evidently the assignment is incorrect. However some caution should be exercised since conditions could arise in an *impure* M—L mode whereby isotopic substitution fortuitously leads to no observable shift. Such may be the case in the *sym*-Et_2en complex discussed above.

Can. J. Chem. Downloaded from www.nrcresearchpress.com by 210.87.254.105 on 09/05/12
For personal use only.

TABLE 3. Vibrational data (600–200 cm^{-1}) for square planar complexes

Complex*		Vibrational frequencies (cm^{-1}) Ring	ν(M—N)	δ(NMN)	Other bands
$Ni(en)_2(AgI_2)_2$		583s	554 w 525m	485.5s 398.5s 232.5s	508w 317.5w 297w
	[62]	581.5s	551w 521m	482.5s 393.5s 231.5s	317.5w 297w
$Cu(en)_2(AgI_2)_2$†		531vs 472s	414.5s		332 w 309w 197m
	[65]	531vs 472s	412s		197m
$Ni(asym\text{-}Me_2en)_2(ClO_4)_2$		409m	547s 506m	366w (263)	463m(δClO_4) 311m 236m 207w
	[62]	409m	544s 503.5m	363w (260)	463m(δClO_4) 311m 236m 207w
$Ni(asym\text{-}Et_2en)_2(ClO_4)_2$		592.5vs 579vs 440s	515.5s 371.5s	344.5s 265.5vs	465s(δClO_4) 307.5s 233vs
	[62]	592.5vs 579vs 440s	513s 370s	343s 263.5vs	465s(δClO_4) 307.5s 233vs
$Ni(asym\text{-}Et_2en)_2Br_2$		(594) 586vs 445s 435w	516m 380s	340m (262)	318s 240s
N-deutero		593s 563m 544m 537s 437.5m	502.5s 378s	331m 255w	325m 232m
$Ni(asym\text{-}Et_2en)_2I_2$		(591) 580.5vs 440m 400w	518m 375vs	337m 260m	310m 235s

*Footnotes as Table 2.
†See ref. 3.

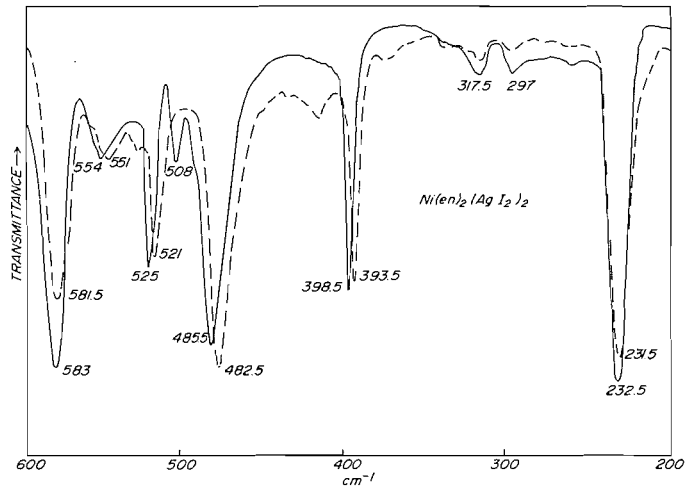

FIG. 2. Vibrational spectrum of $Ni(en)_2(AgI_2)_2$ with natural nickel—, with ^{62}Ni---.

The square planar complex $Ni(en)_2(AgI_2)_2$ (33, 34) on the other hand, has six bands of moderate or high intensity between 230 and 600 cm^{-1} and all are isotopically sensitive (Fig. 2, Table 3). A D_{2h} molecule of this type should have *five* infrared active M—N bending and stretching modes which will all lie above 200 cm^{-1} if the metal–ligand force constant is high enough. Since the Ni—N bond length in a square planar nickel(II) complex, at about 1.8 Å, is about 0.2 Å shorter than in an octahedral nickel(II) amine complex (35), a markedly higher ν(Ni—N) frequency would be expected in the planar ethylenediamine complexes than in the octahedral ones. In this respect the previous assignment (16, 17) of ν(Ni—N) in square planar mercaptoethylamine complexes at frequencies near 380 cm^{-1} comparable to those found in octahedral nickel(II) complexes with ligands of similar type and bulk is anomalous. The ν(Ni—S) vibrations in such square complexes were however assigned at markedly higher frequencies than in the corresponding octahedral complexes. Metal sensitive modes were observed between 500 and 550 cm^{-1} in these square mercaptoethylamine complexes but these were assigned to ring vibrations. In the light of the data presented here, the possibility that these bands contain appreciable ν(Ni—N) character must be considered.

The identification of the 583 cm^{-1} band in $Ni(en)_2(AgI_2)_2$, a band which is almost insensitive to isotopic substitution on a percentage basis, as a ring deformation mode discussed by Omura *et al.* (32) seems secure. Since M—N bending modes are expected to be more intense than stretching modes (16, 17) the weaker bands at 554 and 525 cm^{-1} are tentatively assigned to ν(Ni—N), whilst the stronger bands at 485.5, 398.5, and 232.5 cm^{-1} are tentatively assigned to bending modes (δ(NMN)) coupled with ligand motion. The assignment of the isotopically insensitive 531 cm^{-1} band in the spectrum of $Cu(en)_2(AgI_2)_2$ to a ring vibration must suggest that the bands in the 500–550 cm^{-1} region in the square planar nickel ethylenediamine complexes might also contain some ring vibration coordinate.

asym-Dimethylethylenediamine Complexes

The perchlorate complex has a metal insensitive ring mode at 409 cm^{-1} and four metal sensitive modes at 547, 506, 366, and 263 cm^{-1}. That the two higher energy bands do not differ much in energy from those observed in the ethylenediamine complexes is consistent with their assignment as ν(Ni—N) modes. The apparent decrease in energy of at least two of the bending modes may be a reflection of the increased mass of the ligand. The higher intensity of the stretching vibrations relative to those observed in the unsubstituted ligand probably reflects the lower symmetry of asymmetric ligand.

asym-Diethylethylenediamine Complexes

Further support for these assignments comes from consideration of $Ni(asym\text{-}Et_2en)_2(ClO_4)_2$.

Can. J. Chem. Downloaded from www.nrcresearchpress.com by 210.87.254.105 on 09/05/12
For personal use only.

There is a metal insensitive vibration at 440 cm^{-1} assigned as a ring mode, and four metal sensitive modes at 515.5, 371.5, 344.5, and 265.5 cm^{-1}. By analogy to the previous complexes the first two bands are assigned to ν(Ni—N), and the last two to bending modes. The square Ni(*asym*-Et_2en)$_2Br_2$ has a very similar spectrum and is assigned analogously. In the spectrum of the N-deuterated bromide complex the highest energy ν(Ni—N) band shows greatest sensitivity to isotopic substitution with ^2H, whilst the lower energy ν(Ni—N) band is almost insensitive. The bending modes, which all involve flexing of both —NH_2 (—ND_2) and —$N(C_2H_5)_2$ show moderate sensitivity.

Discussion

Reviewing the data presented, certain general observations may be made, namely:

(*i*) In the octahedral complexes the highest energy ν(M—N) mode falls in the general sequence

I NO_3 > halogens > NCS

as far as dependence upon the counter ion is concerned.

(*ii*) In the octahedral complexes with a given counter ion, the highest energy ν(M—N) mode falls in the general sequence

II *asym*-Et_2en > *sym*-Et_2en ~ *asym*-Me_2en > *sym*-Me_2en > en

(with few exceptions).

(*iii*) The energy separation between the highest and lowest energy ν(M—N) mode in octahedral complexes is variable, but is a maximum for complexes of *asym*-Et_2en.

(*iv*) The above statements are true for both nickel(II) and cobalt(II). In many cases the spectra of the cobalt and nickel complexes are very similar. However the ν(Co—N) frequencies are displaced down about 15 cm^{-1} relative to the corresponding ν(Ni—N) frequencies. Other bands are generally less affected, providing further implicit evidence in support of the (M—N) assignments.

(*v*) In the planar diamagnetic complexes, the highest energy ν(Ni—N) falls in the sequence

III en > *asym*-Me_2en > *asym*-Et_2en

(*vi*) In the planar diamagnetic complexes, the energy separation between the highest and lowest energy ν(Ni—N) mode increases in the sequence III.

Data for the corresponding copper complexes (1–3) were interpreted in terms of an increasing in-plane bond strength as (*i*) the base strength of the amine increased, (*ii*) the bulkiness of the amine increased, (iii) the axial Cu—X interaction decreased. In the copper complexes use of bulky amines together with only weakly coordinating anions, such as BF_4^-, lead to the generation of a continuous series of complexes ranging from almost octahedral to four coordinate square. In the cobalt and nickel complexes, the series is not continuous because of the change in spin state which occurs. Nevertheless there is evidence from electronic spectroscopy that with bulky in-plane ligands such as the asymmetric complexes under discussion, the axial and equatorial interaction in a tetragonal complex is diminished through steric hindrance (36–38). There is an important difference between the copper and nickel (or cobalt) complexes in this respect. In the copper complexes use of a bulky in-plane ligand or of a weakly coordinating counter ion always leads to a strengthened in-plane interaction and a weakened (or zero) axial interaction because of the strong tendency for copper(II) complexes to be tetragonally distorted by virtue of their d^9 configuration. In the nickel complexes no such tendency is operating. The difference between the in-plane and axial ligand interactions must be large before a change in spin state occurs and the complex is square planar. Prior to this, increasing the bulkiness of the in-plane ligand or weakening the coordinating ability of the axial ligand will not lead unambiguously to one result as in the copper case. Instead there will be a choice between weakening the axial interaction and/or the in-plane interaction presumably by bond lengthening, as a means of minimizing the steric interaction. The steric hindrance will be most pronounced in the case of *asym*-Et_2en; indeed with many counter ions, nickel bis complexes with this ligand are square planar. In the specific case of octahedral Ni(*asym*-Et_2en)$_2$-$(NO_2)_2$ for which X-ray data are available (39) the in-plane ligand accomodates the steric hindrance by a marked increase in length of the Ni—$N(Et)_2$— bond (2.219 Å) relative to the Ni—NH_2— bond (2.089 Å).

Speculation concerning band shifts is fraught with difficulties, especially as the low temperature data cited here indicate (Table 2) how complex the spectra can become on cooling. In view

Can. J. Chem. Downloaded from www.nrcresearchpress.com by 210.87.254.105 on 09/05/12
For personal use only.

Can. J. Chem. Downloaded from www.nrcresearchpress.com by 210.87.254.105 on 09/05/12
For personal use only.

of the possibility of vibrational coupling, it would be better to discuss trends in force constants rather than frequencies. Lacking the former, however, and bearing in mind the previous comments, some speculation is admissible if, as we try to show, trends in the spectra of all the cobalt, nickel, and copper complexes, can be reconciled on the basis of one model of tetragonal distortion.

It is proposed that in the asymmetric ligand complexes the higher energy ν(M—N) vibration corresponds to (M—NH_2—) and the lower energy ν(M—N) to (M—NR_2—). These vibrations are depicted in Scheme 1 together with those of the symmetric ligands. The highest symmetry obtainable for the asymmetric ligand complexes is C_{2h} whilst for the symmetric ligands it is D_{2h}. We note, that in the asymmetric ligand case, C_{2h}, there is no symmetry element connecting the two kinds of Ni—N vibration (Ni—N, NH_2 and Ni—N, NR_2) and therefore they should be independently observable. However it is also noted that they both transform as B_u, thus coupling could invalidate this conclusion. The deuteration data (Tables 2, 3) for the Ni(*asym*-Et_2en)$_2X_2$ complexes, especially the bromide, provide substantive evidence for the conclusions that the ν(Ni—N, NH_2) and ν(Ni—N, $N(C_2H_5)_2$) vibrations may be uniquely identified (by their deuteration sensitivity (17)) and that the higher energy vibration is due to ν(Ni—N, NH_2). There is also independent electronic spectroscopic data in support of this (40). Sequence II is now readily explained in terms of (*i*) the increased base strength of the symmetrically substituted ligands causing an increase in the in-plane bond strength reflected by the Ni—N force constant and hence frequency, and (*ii*) a weakening (lengthening) of the M—NR_2 bonds in the asymmetric complexes leading to an inductive increase in the strength of the remaining M—NH_2 bonds. Sequence I is explained on the basis of the amount of electron density supplied to the metal atom by the axial ligand, and parallels the discussion for the copper complexes (1–3). The very electronegative NO_3 oxygen ligand renders the metal(II) ion more positive, relative to the halogens, and causes an increased in-plane interaction. Evidently the thiocyanate ion is able to donate considerable electron density to the metal thereby weakening the in-plane interaction. The reason for this probably stems from the small size of the thiocyanate group relative to a halogen allowing for closer contact with the metal atom even in the presence of bulky in-plane ligands and perhaps from the π-donor characteristic of this ligand (41). Observation (*iii*) is explained if all *asym*-Et_2en complexes parallel the behavior of the nitrite complex in having a long M—$N(Et)_2$— bond. Such a postulate explains the marked energy separation between the two ν(Ni—N) bands in these complexes. Parallel behavior by the *asym*-Me_2en complexes is indicated *if* the ν(Ni—N) assignment for the band near 260 cm^{-1} is accepted. If the previous assignment (17) is assumed valid, then these complexes do not follow the pattern exhibited by the other complexes (see below).

Molecular models of the planar complexes suggest that steric hindrance, except possibly for the *asym*-Et_2en complexes, is minimized. This does however assume a *trans* configuration with respect to the asymmetrically substituted ligands. A *cis* configuration would be very hindered and is unlikely to occur. Thus there is no reason to believe that in the planar complexes, the Ni—NR_2— bond will be longer than Ni—NH_2—; indeed the converse might be expected in view of the difference in base strength between the two residues. In this case the upper frequency (presumed Ni—NH_2—) runs counter to the order shown by the octahedral complexes (sequence III rather than II). Possibly in this case, the increase in electron density supplied to the nickel atom by the strong Ni—NR_2— bond actually results in a slight decrease in the bond strength of Ni—NH_2—.

The above discussion relies heavily on the correct identification of the band near 300 cm^{-1} in most of the complexes as the second ν(M—N) vibration. Since this contradicts a recent isotopic study of certain of the complexes studied here (17) it is worthwhile summarizing the evidence favoring this re-assignment. If the earlier assignment (17) is accepted then this lower energy metal sensitive band must be assigned to a bending mode, to a metal – axial ligand mode or to a ligand mode coupled with motion of the metal. These possibilities seem excluded since in the octahedral complexes bending modes are not expected at such a high frequency (2, 16, 17) and the lower energy band is insensitive to replacement of the axial ligand. Finally this band is isotopically sensitive in *every* copper *and* nickel complex so studied; if the band in question

Can. J. Chem. Downloaded from www.nrcresearchpress.com by 210.87.254.105 on 09/05/12
For personal use only.

is always a ligand mode fortuitously coupled with metal motion, metal sensitivity in every case would not be anticipated. One may further note that if the previous assignment is accepted then the *asym*-Et_2en complexes should exhibit two closely spaced, but certainly well resolved bands near 380 cm^{-1} paralleling thereby the behavior of the *asym*-Me_2en complexes studied previously (17). In fact the high energy ν(M—N) band in the isotopically studied *asym*-Et_2en complexes is quite sharp and symmetric. There is a band to lower energy near 330 cm^{-1} but this is quite insensitive to isotopic substitution. In summary it indeed seems possible to distinguish two separate ν(Ni—N) vibrations of asymmetric ligands such as $(C_2H_5)_2NCH_2CH_2NH_2$. Although this would certainly be anticipated on group theoretical grounds extensive coupling might have invalidated its observation experimentally.

This work presents the first isotopic investigation of the spectra of two complexes containing a given ligand with a metal in alternate spin states, *e.g.*: Ni(*asym*-Et_2en)$_2Cl_2$, $S = 1$, and Ni(*asym*-Et_2en)$_2Br_2$, $S = 0$.

The relevant frequencies are:

Spin state	Configuration	Infrared frequencies (cm^{-1}) ν(Ni—N, NH_2)	ν(Ni—N, $N(C_2H_5)_2$)
$S = 1$	Octahedral	401.5	265.5
$S = 0$	Square planar	516	380

The ratios ν(Ni—N), $S = 1$/ν(Ni—N), $S = 0$, are approximately the same (0.78 and 0.70 respectively). The difference probably reflects the longer Ni—$N(C_2H_5)_2$ bond predicted in the octahedral complexes. The ratio will also be influenced by the ring vibration coordinate contribution to the 516 cm^{-1} band. Similar comparisons may be made with the *asym*-Me_2en data.

In view of the close similarity in behavior of all the cobalt, nickel, and copper complexes in these series, and in view of the fact that the gross changes in metal–nitrogen stretching frequencies can be readily explained in terms of a common argument involving changes in tetragonal distortion, the assignments presented here seem justified.

Note added in proof: Further support for the assumption that there are two markedly unequal metal–nitrogen bond lengths in complexes of the asymmetrically substituted amines arises from an X-ray structural analysis of bis-(1,1,1,5,5,5,-hexafluoropentane-2,4-dionato)bis-(*N*,*N*-dimethylethylenediamine)copper(II) (51). In this complex the Cu—NMe_2 distance is 2.064 Å and the Cu—NH_2 distance is 1.989 Å.

We are indebted to the Consiglio Nazionale delle Richerche, Rome, Italy, and the National Research Council of Canada for financial support. We are also indebted to Mrs. M. Rayner Canham for experimental assistance and to Dr. G. Rayner Canham for useful discussions.

1. A. B. P. Lever and E. Mantovani. Inorg. Chim. Acta, **5**, 429 (1971).
2. A. B. P. Lever and E. Mantovani. Inorg. Chem. **10**, 817 (1971).
3. G. W. Rayner Canham and A. B. P. Lever. Can. J. Chem. **50**, 3866 (1972).
4. B. P. Kennedy, A. B. P. Lever, and E. Mantovani. To be published.
5. A. S. Antsishkina and M. A. Porai-Koshits. Dokl. Akad. Nauk SSSR, **143**, 105 (1962).
6. B. W. Brown and E. C. Lingafelter. Acta Cryst. **16**, 753 (1963).
7. A. Pajunen and E. Luukkonen. Suomen, Kemistilehti, B**42**, 172 (1969).
8. A. B. P. Lever, B. S. Ramaswamy, S. H. Simonsen, and L. K. Thompson. Can. J. Chem. **48**, 3076 (1970).
9. K. Nakamoto, K. Shobatake, and B. Hutchinson. Chem. Commun. 1451 (1969).
10. K. Nakamoto. Angew Chem. Int. Ed. **11**, 666 (1972).
11. D. M. Adams. Metal–ligand and related vibrations. Edward Arnold, London, 1967.
12. W. J. Eilbeck, F. Holmes, C. E. Taylor, and A. E. Underhill. J. Chem. Soc. A, 128 (1968).
13. C. W. Frank and L. B. Rogers. Inorg. Chem. **5**, 615 (1966).
14. N. Ohkaku and K. Nakamoto. Inorg. Chem. **10**, 798 (1971).
15. B. Hutchinson, J. Takemoto, and K. Nakamoto. J. Am. Chem. Soc. **92**, 3335 (1970).
16. C. W. Schläpfer and K. Nakamoto. Inorg. Chim. Acta, **6**, 177 (1972).
17. C. W. Schläpfer, Y. Saito, and K. Nakamoto. Inorg. Chim. Acta, **6**, 284 (1972).
18. J. R. Durig and D. W. Wertz. Appl. Spectrosc. **22**, 627 (1968).
19. A. B. P. Lever and B. S. Ramaswamy. Proc. XIII Internat. Conf. Coordin. Chem., Poland 1970, Abstract No. 66.
20. M. Keeton, A. B. P. Lever, and B. S. Ramaswamy. Spectrochim. Acta, **26**A, 2173 (1970).
21. A. B. P. Lever and B. S. Ramaswamy. Spectrosc. Lett. **6**, 67 (1973).
22. K. Narahari Rao, C. J. Humphreys, and D. H. Rank. Wavelength standards in the infrared. Academic Press, New York. 1966.
23. R. J. H. Clark. Halogen chemistry. Vol. 3. *Edited by* V. Gutman. Academic Press, New York. 1968. p. 85.
24. D. A. Baldwin, A. B. P. Lever, and R. V. Parish. Inorg. Chem. **8**, 107 (1969).

25. D. FORSTER and D. M. L. GOODGAME. Inorg. Chem. **4**, 715 (1965).
26. R. J. H. CLARK and C. S. WILLIAMS. Spectrochim. Acta, **23**A, 1055 (1967); **22**, 1081 (1966).
27. R. H. NUTTALL and D. W. TAYLOR. Chem. Commun. 1417 (1968).
28. J. I. BULLOCK and F. W. PARRETT. Chem. Commun. 157 (1969).
29. D. E. IRISH, A. R. DAVIS, and R. A. PLANE. J. Chem. Phys. **50**, 2262 (1969).
30. C. POSTMUS, J. R. FERRARO, A. QUATTROCHI, K. SHOBATAKE, and K. NAKAMOTO. Inorg. Chem. **8**, 1851 (1969).
31. M. E. BALDWIN. J. Chem. Soc. 4369 (1960); 471 (1961).
32. Y. OMURA, I. NAKAGAWA, and T. SHIMANOUCHI. Spectrochim. Acta, **27**A, 2227 (1971).
33. A. B. P. LEVER, J. LEWIS, and R. S. NYHOLM. J. Chem. Soc. 2552 (1963).
34. R. STOMBERG. Acta Chem. Scand. **23**, 3498 (1969).
35. L. E. Sutton (*Editor*). Chem. Soc. Spec. Publ. No. 11, Interatomic distances. 1958.
36. A. B. P. LEVER. Inorganic electronic spectroscopy. Elsevier Publishing Co., Amsterdam. 1968. Chapt. 9.
37. A. B. P. LEVER. A.C.S. Adv. Chem. Ser. **62**, 430 (1967).
38. A. B. P. LEVER. Coord. Chem. Rev. **3**, 119 (1968).
39. M. G. B. DREW, D. M. L. GOODGAME, M. A. HITCHMAN, and D. ROGERS. Proc. Chem. Soc. 363 (1964).
40. B. P. KENNEDY and A. B. P. LEVER. To be published.
41. B. R. HOLLEBONE. J. Chem. Soc. A, 481 (1971).
42. A. B. P. LEVER, J. LEWIS, and R. S. NYHOLM. J. Chem. Soc. 2552 (1963).
43. D. M. L. GOODGAME and L. M. VENANZI. J. Chem. Soc. 616 (1963).
44. D. M. L. GOODGAME and L. M. VENANZI. J. Chem. Soc. 5909 (1963).
45. M. E. FARAGO and J. M. JAMES. Inorg. Chem. **4**, 1706 (1965).
46. S. F. PAVKOVIC and D. W. MEEK. Inorg. Chem. **4**, 1091 (1965).
47. A. WERNER. Z. anorg. allgem. Chem. **21**, 201 (1899).
48. N. F. CURTIS and Y. M. CURTIS. Inorg. Chem. **4**, 804 (1965).
49. D. A. ROWLEY and R. S. DRAGO. Inorg. Chem. **7**, 795 (1968).
50. D. M. L. GOODGAME and M. A. HITCHMAN. Inorg. Chem. **3**, 1389 (1964).
51. M. A. BUSH and D. E. FENTON. J. Chem. Soc. A, 2446 (1971).

Can. J. Chem. Downloaded from www.nrcresearchpress.com by 210.87.254.105 on 09/05/12
For personal use only.

Isotopic Studies of the Metal–Ligand Bond. Part IV. Variable Temperature and Isotopic Studies of the Metal–Ligand Vibrations in Substituted Pyridine Metal Dihalides. Complexes of Cobalt(II), Nickel(II), and Copper(II)

A. B. P. LEVER AND BARATHAM S. RAMASWAMY

Department of Chemistry, York University, Downsview, Ontario, M3J 1P3

Received November 9, 1972

The far infrared spectra (500–200 cm^{-1}) of a series of picoline and ethylpyridine derivatives of cobalt(II), nickel(II), and copper(II) are reported. Metal–ligand assignments are based on isotopic substitution experiments with ^{65}Cu and ^{62}Ni. Low temperature data are also reported and it is noted that the energies of metal–ligand modes are much more sensitive to temperature than the energies of purely ligand vibrations. This observation is discussed and it is suggested, with some caution, that the low temperature behavior may be used as a guide to band assignment.

Les spectres dans l'infra rouge lointain (500–200 cm^{-1}) d'une série de dérivés de la picoline et de l'éthylpyridine avec le cobalt(II), nickel(II), et cuivre(II) ont été rapportés. Les attributions concernant le métal ligand ont été faites sur la base des expériences de substitution isotopique avec le ^{65}Cu et le ^{62}Ni. Les données à basse température ont été également présentées et on a noté que les énergies relatives aux modes métal-ligand sont beaucoup plus sensibles à la température que les énergies de vibration du ligand pur. Ce fait a été discuté et a amené à suggérer, avec quelque précaution, que le comportement à basse température pouvait servir de guide dans l'attribution des bandes.

[Traduit par le journal]

Can. J. Chem., **51**, 1582 (1973)

Pyridine metal halides were among the first compounds to be studied by far infrared spectroscopy (1–10) and the general regions of absorption of the first row transition metal halide and metal pyridine vibrations are well established. There is however still some controversy over individual assignments. More recently we have demonstrated (11) by means of vibrational spectroscopy that in complexes of substituted pyridines steric and electronic effects influence the metal–ligand vibrational frequencies markedly. Of particular interest was the observation (11) that in the tetrahedral cobalt(II) complexes, CoL_2X_2 where L is a sterically bulky substituted pyridine, the Co—X bond is weakened when X is a halogen, but the Co—L bond is weakened when X is NCS. The isotopic substitution method (12) provides the only procedure for the unequivocal identification of metal–ligand modes; it has not hitherto been applied to these series of complexes. We now report such data. Only data obtained in the solid state are reported. Most of the compounds are either insufficiently soluble, or decompose in solution, to permit solution measurements to be made. Metal-ligand vibrations are not usually "pure" since coupling with ligand modes of the same symmetry will generally occur. As a consequence the identification of metal–ligand modes in a vibrational spectrum, in the absence of isotopic data, is fraught with difficulty. There is evidence (11, 13–15) that metal–ligand vibrations increase in frequency relative to "pure" ligand vibrations, when the sample is cooled. These observations are further investigated to see if they provide an additional reliable procedure for the identification of metal–ligand modes.

Experimental Section

All the complexes which have been previously described were prepared by the literature methods (references in Table 1) and were analytically pure. The isotopically substituted derivatives were prepared using 99+% pure ^{65}Cu and ^{62}Ni as previously described (16, 17). Infrared data were recorded with a Beckman IR 12 spectrophotometer scanning at 1–2 cm^{-1}/min and using Nujol mulls on a polythene support, and low temperature data were recorded with the aid of a Beckman VLT-2 variable temperature cell employing polyethylene windows, as previously described (17). The temperature achieved by use of this cell is believed to be within 20° of −196 °C. The reproducibility of the spectra from one mull to another is good, and there is no evidence to suggest that the rate of cooling influences the final spectrum. Samples for the low temperature data were prepared either as Nujol mulls held tightly between polythene plates or were made into a polythene matrix. In this latter case the sample was mixed with powdered high density polythene and the mixture converted into a thin translucent disc by application of pressure at about 50 °C; a conventional laboratory (KBr disc) press was utilized. For direct

Can. J. Chem. Downloaded from www.nrcresearchpress.com by 210.87.254.5 on 09/05/12
For personal use only.

TABLE 1. Far infrared data*

Complex		Infrared data (cm^{-1}) Ligand bands	M—N	M—X	Reference
$Cu(2\text{-}Pic)_2Cl_2$		481s (442) 434s 398s	254 vs	(305)	1, 4
	Cu-65	481s (442) 434s 398s	251vs	—	
	l.t.	398(0)	257(+3) 229†	305(0)	
$Cu(2\text{-}Pic)_2Br_2$		477.5m 439s (393) 385m 206w	268.5m 261s	233s	1, 4
	Cu-65	477.5m 439s (393) 385m 206w	266.5m 259s	230s	
	l.t.	440(0) 386(+1)	276(+6) 262(0)	236(+3)	
$Cu(3\text{-}Pic)_2Cl_2$		498.5wm 485m 415.5s 360m 213m	267s 236m	294vs	4
	Cu-65	498.5wm 485m 415.5s 360m 212.5m	265.5s 234.5m	292.5vs	
	l.t.	414(0) 362(0) 215(+1)	273(+5) 237(+4)	297(+3) (301)†	
$Cu(3\text{-}Pic)_2Br_2$		498w 485m 415s 360m	270.5m	240vs	33
	Cu-65	498w 485m 415s 360m	268m	237.5vs	
	l.t.	414(0) 362(0)	275(+4)	248(+7)	
$Co(2\text{-}Pic)_2Cl_2$	l.t.	424(+2) 419† 395(+3)	249(+9) 232(+6)	338(+5) 314(+4)	6, 34
$Co(2\text{-}Pic)_2Br_2$	l.t.	423(0) 416(−1) 393(+1)	251(+7) 243†	270(+4)	6, 34
$Co(2\text{-}Pic)_2I_2$	l.t.	423(+2) 393(+2)	258(+8) 234(+2)	222(+4)	34
$Co(3\text{-}Pic)_2Cl_2$	l.t.	416(+2) 408(+2) 366(+3)	250(+5) 246†	348(+3) 309(0)	6, 34
$Co(3\text{-}Pic)_2Br_2$	l.t.	414(+2) (406)† 358(0)	251† 248(+4)	277(+3)	6, 34
$Co(3\text{-}Pic)_2I_2$	l.t.	415(−1) 354(0)	251(+7)	243(+3)	34
$Cu(2\text{-}EtPy)_2Br_2$	l.t.	436(+1) 284(+2) 227(0)	296(+6)	250(0) 255(+1)	1
$Co(2\text{-}EtPy)_2Br_2$	l.t.	427(+2) 423(+2) 401(+1) 395(−1)	257(+11) 236(+1)	268(+4)	11
$Co(3\text{-}EtPy)_2Br_2$	l.t.	421† 414(+2)	261(+7) 254†	280(+5)	11, 35
$Cu(4\text{-}EtPy)_2Cl_2$	l.t.	277(+1) 210†	254(+5)	293.5† 310(+8)	7, 24
$Cu(4\text{-}EtPy)_2Br_2$	l.t.	400(0) 376(+1) 284(+2) 210†	254(+5)	224(+6)	36
$Ni(3\text{-}Pic)_4Cl_2$		475m 417s 364wm	251.5m	243.5s	3, 6
	Ni-62	475m 417s 364wm	249m	238s	
	l.t.	475(0) 415.5(−1.5) 364(0)	260.5(+9)	250.5(+6)	
$Ni(3\text{-}Pic)_4Br_2$		480m 417.5s 359.5s 225m‡	230s	—	3, 6
	Ni-62	480m 417.5s 359.5s	224.5s	—	
	pm.l.t.	415(−2) 362(+3) 230†	241(+11)	—	
$Ni(3\text{-}Pic)_4I_2$	pm.l.t.	420(0) 415† 360(0) 331(+3) 223(0)	256(+7)	—	2

*All data were measured with the natural metal isotope at room temperature except where indicated. Cu-65, data for ^{65}Cu; Ni-62, data for ^{62}Ni; l.t. Nujol mull liquid nitrogen temperature data. The values quoted in parentheses are the shifts from the room temperature data, *e.g.* 424(+2) implies a band observed at 422 cm^{-1} at room temperature and 424 cm^{-1} at liquid nitrogen temperature, *for the same mull*. Slight discrepancies between these data and the data recorded for isotopic comparison may reflect changes in the mull and changes in the operating conditions used to record the spectra; pm.l.t. These data were recorded as polythene matrices.

†Either no band was observed in the room temperature spectrum or it was present only as an ill resolved shoulder.

‡This band is presumably obscured by the Ni—N absorption in the Ni-62 spectrum.

comparison with room temperature Nujol mulls, use of Nujol is preferred. However, the polythene matrix gives a cleaner spectrum. In both cases the mull must be prepared very dilute, since there is a marked apparent increase in intensity on cooling, and the use of a mull of normal strength will cause the recorder pen to go off scale.

Results and Discussion

Isotopic Data

CuL_2X_2 Complexes

Both room temperature and low temperature data for a series of complexes ML_2X_2 with M = Co(II) or Cu(II), X = Cl, Br and L = 2- or 3-methyl or 2-, 3-, or 4-ethyl pyridine are cited in Table 1. Certain of the cobalt data have been published previously (11) but are repeated here for further discussion. In addition ^{65}Cu isotopic studies are reported for a number of copper complexes. Note that the cobalt complexes are pseudo tetrahedral whilst the copper complexes are expected to be *trans* square planar.

These copper complexes generally exhibit two or three isotopically sensitive bands. Data have not been cited above 450 cm^{-1}; the samples were scanned above this wavenumber but no further isotopically sensitive bands were observed, as was anticipated. In square complexes of copper (II), previous data (1–10) suggests that both νCu—Cl and νCu—Br may be expected above 200 cm^{-1}. Such *trans* square planar complexes should exhibit one infrared active νCu–N vibration and one active νCu—X vibration of B_{2u} and B_{3u} symmetry, in the group D_{2h} (assuming the principal axis is z). The experimental observation of more than two

Can. J. Chem. Downloaded from www.nrcresearchpress.com by 210.87.254.5 on 09/05/12
For personal use only.

markedly isotopically sensitive bands is indicative that this simple treatment is inadequate. Note that application of the Teller-Redlich rule (18) suggests shifts of about 3 cm^{-1} should be observed in the metal–ligand vibrations; the observed shifts of 1.5 to 3 cm^{-1} are indicative of a substantial metal–ligand contribution to the absorption bands in question. The additional bands must arise through some kind of intermolecular interaction in the solid. Indeed X-ray studies of both (2-picoline)$_2$CuCl$_2$ (19) and the corresponding bromide (20) reveal that these square planar units are loosely associated into dimeric arrays with intermolecular Cu—X distances of 3.37 Å (Cl) and 3.87 Å (Br). Whilst the symmetry of the dimeric units themselves is very low (C_i) the deviation from C_{2h} is not very great and it is convenient to discuss the $Cu_2N_4X_4$ sub-unit within this point group. Group theoretical analysis reveals that this dimeric sub-unit will exhibit two infrared active vCu—N of symmetry A_u and B_u and two active vCu—X both of symmetry B_u.

Given that the vCu—Br/vCu—Cl frequency ratio is of the order of 0.77 (2) assignments for the Cu—N and Cu—X modes follow logically; they are reported in Table 1. In general only one Cu—X stretching mode may be identified, near 240 cm^{-1} in the bromides and near 300 cm^{-1} in the chlorides. In two cases two Cu—N modes may be identified in the room temperature spectrum. In the low temperature spectra the Cu—Cl band in Cu(3-picoline)$_2$Cl$_2$ is split by 4 cm^{-1}; these may be the two Cu—Cl modes but the splitting may also arise through correlation coupling or isotopic effects. An additional band appears at 229 cm^{-1} in the low temperature spectrum of Cu(2-picoline)$_2$Cl$_2$; this may be the second Cu—N mode. However in view of the coupling between the B_u Cu—X and Cu—N modes it is somewhat artificial to distinguish between them. Band positions and assignments are similar to those previously proposed (1, 4). The assignment for Cu(2-EtPy)$_2$Br$_2$ differs from that previously cited (1) by assigning the band at 290 cm^{-1} to a Cu—N vibration rather than an internal ligand mode (1). This reassignment is based on the considerable temperature sensitivity of this band (see discussion below).

NiL$_4$X$_2$ Complexes

Isotopic data are also cited in Table 1 for Ni(3-picoline)$_4$Cl$_2$ and Ni(3-picoline)$_4$Br$_2$. The electronic spectra of these complexes (3, 21) (*vide infra*) infer that they are *trans* tetragonal octahedral, as are the congeneric pyridine complexes (22, 23). For the purposes of discussion of their metal–ligand vibrational spectra D_{4h} symmetry may be assumed; one vNi—N and one vNi—X infrared active vibration is anticipated. However the Ni—Br band will appear below 200 cm^{-1} outside the range of the instrument used (2). Isotopic substitution leads to the unequivocal assignment shown in Table 1. Of the two bands in the chloride, the lower is assigned to vNi—Cl since it is the more intense.

Unfortunately the non-availability of appropriate non-radioactive isotopes of cobalt prevents similar studies being carried out with the corresponding tetrahedral and octahedral cobalt(II) derivatives. However the close general similarity between the cobalt spectra and the spectra of the copper and nickel analogs, provides very strong circumstantial evidence for the validity of the Co—L assignments previously made (11). Further support comes from consideration of the low temperature data.

Low Temperature Data

Table 1 and Fig. 1 cite low temperature data for the complexes discussed above and also for some cobalt(II) picoline derivatives and copper(II) *n*-ethylpyridine derivatives. The following observations may be made from these data:

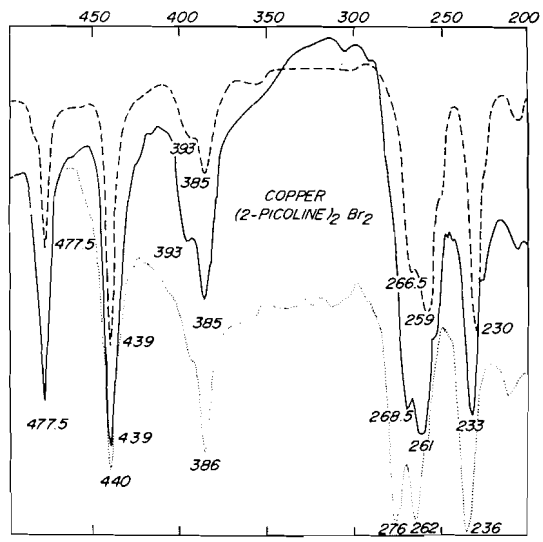

FIG. 1. The vibrational spectrum of Cu(2-Picoline)$_2$-Br$_2$; natural Cu,—; ^{65}Cu,---; natural Cu at liquid nitrogen temperature,....

Can. J. Chem. Downloaded from www.nrcresearchpress.com by 210.87.254.5 on 09/05/12
For personal use only.

Can. J. Chem. Downloaded from www.nrcresearchpress.com by 210.87.254.5 on 09/05/12
For personal use only.

(*i*) Metal–ligand modes generally increase in energy, sometimes by as much as 11 cm^{-1}, upon cooling the sample to liquid nitrogen temperature. Additional components are frequently resolved in the low temperature spectra. This is particularly true, for example, of the two Co—N modes expected in the C_{2v} CoL_2X_2 pseudotetrahedral complexes. Frequently only one is observed in the room temperature spectrum. It is also of interest that the single νCu—Cl band observed in the room temperature spectrum of $Cu(4\text{-}EtPy)_2Cl_2$ is apparently split by some 17 cm^{-1} upon cooling. An X-ray crystal structural analysis of this compound (24) reveals a *trans* square planar structure with non-bonded Cu—Cl′ contacts of 3.21 Å, actually shorter than in the 2-picoline dimeric array referred to above. Correlation coupling may therefore be responsible for this splitting.

(*ii*) Ligand modes are comparatively insensitive to temperature, shifts of from −1 to +3 cm^{-1} generally can be observed, (see Fig. 1 and Table 1).

It therefore appears that it may be possible to distinguish between ligand modes and metal–ligand modes in the region 450–200 cm^{-1} by their temperature behavior. We note that an increase in energy has also been noted for the asymmetric M—O—M vibration when samples of dimeric oxygen bridged porphyrin derivatives are cooled (14, 15).

Care must be taken in exploiting such data. For example the identity of the sample must not change over the temperature range studied; any phase change or structural change could lead to marked shifts in any or all the bands. Moreover at very low energies, usually below 200 cm^{-1}, lattice vibrations appear, and these may be temperature sensitive (25). Where additional bands are resolved in the low temperature spectrum, the interpretation may be ambiguous.

Mechanism of Band Shift

Cooling of a crystal leads to an overall contraction of the lattice which, in principle, may be isotropic or anisotropic. The cooling process is effectively not very different from the application of high pressure at room temperature. Both procedures may be considered to give rise to compression of the unit cell. It is highly relevant therefore that recent studies of the effects of high pressure upon far infrared spectra (26, 27) also revealed frequency shifts, and changes in intensity. In general these workers observed a much greater effect of pressure upon the metal–ligand modes than upon the pure ligand modes, paralleling thereby the temperature data presented here. It should be noted however that the room temperature high pressure experiments led to considerable broadening of the bands, whilst the low temperature experiments discussed here yielded much sharper and highly resolved spectra.

We assume that either cooling, or high pressure, will result in a decrease in the unit cell volume. Some distortion, albeit slight, of the molecular geometry must occur to accommodate this volume decrease. It is clearly much easier to achieve such distortion by a change in metal–ligand bond length or angle, than by changes in the internal normal coordinates of a polyatomic cyclic ligand such as a picoline. The former will surely be much more adaptable to such changes than the latter. The behavior of the picoline metal halides with temperature change can be rationalized readily on this model. However if a chelate ligand, such as an ethylenediamine is involved, similar arguments would suggest that skeletal vibrations, which occur in this low energy region, might also be temperature sensitive. Experiments with such complexes (ref. 28 and unpublished observations) reveal that such skeletal bands are *slightly* more temperature sensitive than the picoline internal ligand modes. Moreover the M—N stretching modes which will necessarily involve motion of the chelate ring in these complexes are *less* temperature sensitive, in general, than the M—N modes involving monodentate ligands such as the picolines.

It is well known that the electronic spectra of transition metal complexes are also temperature sensitive (29). This is due in part, but not *in toto* (32), to lattice contraction, *presumably* causing a decrease in bond length, and hence an increase in the crystal field strength parameter *Dq*. The electronic spectra of the tetragonal nickel complexes cited in Table 1 are temperature sensitive as anticipated, *viz.* Using the admittedly approximate first order analysis (23, eq. 3) the *Dq*. values are seen to increase with cooling of the sample according to $Ni(3\text{-picoline})_4Cl_2$: *Dq* (picoline) from 1130 to 1160, *Dq* (chloride) from 550 to 570 cm^{-1}; $Ni(3\text{-picoline})_4Br_2$. *Dq* (picoline) from 1080 to 1140, *Dq* (bromide) from 430 to 508 cm^{-1}. The very marked increase in the

Nickel complex*	Temperature†	Electronic spectra (cm^{-1}) $^3B_{2g} \leftarrow {}^3B_{1g}$	$^3E_g \leftarrow {}^3B_{1g}$
$Ni(3\text{-picoline})_4Cl_2$	r.t.	11 300	8400
	l.t.	11 600	8650
$Ni(3\text{-picoline})_4Br_2$	r.t.	10 800	7550
	l.t.	11 400	8240

*The iodide complex gave poorly resolved spectra.
†r.t. = room temperature; l.t. = liquid nitrogen temperature.

νNi—N and νNi—Cl frequencies upon cooling is fully consistent with this approach. It is anticipated that the extent to which a particular M—L vibration is sensitive to such thermal compression will also be a function of the symmetry of the vibration, and also upon whether the compression is isotropic or not. Clearly further work is necessary to learn more about this phenomenon. However it is clear that this procedure adds a valuable new technique to the chemists' repertoire and should lead to a deeper understanding of the steric and electronic factors responsible for molecular geometry.

The authors are indebted to Mrs. G. W. Rayner Canham for experimental assistance, and the National Research Council of Canada for financial support.

1. M. GOLDSTEIN, E. F. MOONEY, A. ANDERSON, and H. A. GEBBIE. Spectrochim. Acta, **21**, 105 (1965).
2. R. J. H. CLARK and C. S. WILLIAMS. Inorg. Chem. **4**, 350 (1965).
3. J. R. ALLAN, D. H. BROWN, R. H. NUTTALL, and D. W. A. SHARP. J. Inorg. Nucl. Chem. **27**, 1305 (1965).
4. C. W. FRANK and L. B. ROGERS. Inorg. Chem. **5**, 615 (1956).
5. W. R. MCWHINNIE. J. Inorg. Nucl. Chem. **27**, 2573 (1965).
6. N. S. GILL and H. J. KINGDON. Aust. J. Chem. **19**, 2197 (1966).
7. J. BURGESS. Spectrochim. Acta, **24A**, 277 (1968); **24A**, 1645 (1968).
8. R. J. H. CLARK. Halogen chemistry. Vol. 3. *Edited by* V. Gutman. Academic Press, New York, N.Y. 1968. p. 85.
9. D. E. BILLING. J. Inorg. Nucl. Chem. **31**, 137 (1965).
10. M. KEETON and A. B. P. LEVER. Inorg. Chem. **10**, 47 (1971).
11. M. KEETON, A. B. P. LEVER, and B. S. RAMASWAMY. Spectrochim. Acta, **26A**, 2173 (1970).
12. K. NAKAMOTO, K. SHOBATAKE, and B. HUTCHINSON. Chem. Commun. 1451 (1969); K. NAKAMOTO. Angew. Chem. Int. Ed. **11**, 666 (1972).
13. A. B. P. LEVER and B. S. RAMASWAMY. Proc. XIII I.C.C.C. Poland, 1970. Vol. I. p. 123.
14. H. J. SCHUGAR, G. R. ROSSMAN, C. G. BARRACLOUGH, and H. B. GRAY. J. Am. Chem. Soc. **94**, 2683 (1972).
15. W. M. REIFF, G. J. LONG, and W. A. BAKER, Jr. J. Amer. Chem. Soc. **90**, 6347 (1968).
16. G. W. RAYNER CANHAM and A. B. P. LEVER. Can. J. Chem. **50**, 3866 (1972).
17. A. B. P. LEVER and E. MANTOVANI, Can. J. Chem. This issue.
18. G. HERZBERG. Infrared and Raman spectra of polyatomic molecules. Van Nostrand, N.J. 1945. p. 231.
19. V. F. DUCKWORTH and N. C. STEPHENSON. Acta Cryst. *B***25**, 1795 (1969).
20. P. SINGH, D. Y. JETER, W. E. HATFIELD, and D. J. HODGSON. Inorg. Chem. **11**, 1657 (1972).
21. J. R. ALLAN, D. H. BROWN, R. H. NUTTALL, and D. W. A. SHARP. J. Inorg. Nucl. Chem. **27**, 1529 (1965).
22. D. A. ROWLEY and R. S. DRAGO. Inorg. Chem. **6**, 1092 (1967).
23. A. B. P. LEVER. Coord. Chem. Rev. **3**, 119 (1968).
24. M. LAING and G. CARR. J. Chem. Soc. A, 1141 (1971).
25. I. NAKAGAWA. Coord. Chem. Rev. **4**, 423 (1969).
26. C. POSTMUS, K. NAKAMOTO, and J. R. FERRARO. Inorg. Chem. **6**, 2194 (1967).
27. C. POSTMUS, J. R. FERRARO, A. QUATTROCHI, K. SHOBATAKE, and K. NAKAMOTO. Inorg. Chem. **8**, 1951 (1969).
28. A. B. P. LEVER and B. S. RAMASWAMY. Spectrosc. Lett. **6**, 67 (1973).
29. A. B. P. LEVER. Inorganic electronic spectroscopy. Elsevier, Amsterdam. 1968.
30. J. LEE and A. B. P. LEVER. J. Mol. Spectrosc. **26**, 189 (1968).
31. W. LUDWIG and F. GASSER. Helv. Chim. Acta, **52**, 107 (1969).
32. J. R. ALLAN, D. H. BROWN, R. H. NUTTALL, and D. W. A. SHARP. J. Inorg. Nucl. Chem. **26**, 1895 (1964).
33. G. N. LAMAR. Inorg. Chem. **6**, 1939 (1967).
34. B. K. MOHAPATRA and D. V. RAMANA RAO. Indian J. Chem. **9**, 715 (1971).

Can. J. Chem. Downloaded from www.nrcresearchpress.com by 210.87.254.5 on 09/05/12
For personal use only.

Substituent Interactions in Di- and Tri-acyl Derivatives of *cis*- and *trans*-2-Hydrazinocyclopentanol

J. A. CAMPBELL AND DONALD MACKAY

Department of Chemistry, University of Waterloo, Waterloo, Ontario

Received July 17, 1972

The action of thionyl chloride followed by an alkaline work-up quantitatively isomerizes *trans*-1,2-dibenzoyl-1-(2-hydroxylcyclopentyl)hydrazine (**5**) to *cis*-2-benzoyl-1-(2-benzoyloxycyclopentyl)hydrazine (**3**). One equivalent of tosyl chloride in pyridine converts **5** to an intermediate which can be hydrolyzed to a mixture of **3** and **5** or can be transformed to the *N*-tosyl derivative **13** by tosylation and then hydrolysis. Oxazolidine structures are suggested as intermediates for these reactions.

The alcohol **2** can also be isomerized to **3**, using 0.8 *N* aqueous ethanolic hydrochloric acid, to which **5** is inert. The ester **3** is again the major product in the hydrolysis by this acid mixture of the *cis*-tribenzoyl derivative **17**, the *cis*-N_1-*p*-anisoyl derivative **21***a* and the *cis*-N_1-acetyl derivative **21***b*, the amide group being cleaved much more rapidly than the ester, especially in the case of **21***b*. A mechanism involving ester participation by way of an oxazolidinium cation is proposed for these amide hydrolyses, and this is supported by tracer studies.

The *trans*-esters **24***a* and *b* hydrolyze mainly at the ester group with retention of configuration.

Polymorphism is a common phenomenon among the title compounds.

L'action du chlorure de thionyle suivie d'un traitement alcalin isomérise quantitativement le *trans*-dibenzoyl-1,2 (hydroxyl-2 cyclopentyl)-1 hydrazine (**5**) en *cis* benzoyl-2 (benzoyloxy-2 cyclopentyl)-1 hydrazine (**3**). Un équivalent de chlorure de tosyle dans la pyridine transforme **5** en un intermédiaire qui peut être hydrolysé en un mélange de **3** et **5** ou convertit en dérivé *N*-tosyle **13** par tosylation puis hydrolyse. Les structures oxazolidines ont été suggérées comme intermédiaires réactionnels.

L'isomérisation de l'alcool **2** en **3** est également possible en présence d'une solution aqueuse éthanolique d'acide chlorhydrique 0.8 *N* pour laquelle **5** est inerte. L'ester **3** reste encore le produit majoritaire dans l'hydrolyse par ce mélange acide, du dérivé *cis*-tribenzoyle **17**, du dérivé *cis* N_1-*p*-anisoyle **21***a* et du dérivé cis-N_1-acétyle **21***b*, le groupe amide étant clivé beaucoup plus rapidement que l'ester spécialement dans le cas de **21***b*. Un mécanisme avec participation de l'ester par un cation oxazolidinium a été proposé pour les hydrolyses de ces amides; ce mécanisme a été confirmé par les études par traceur.

Les esters *trans* **24***a* et *b* s'hydrolysent principalement sur le groupe ester avec rétention de configuration. Le polymorphisme est un phénomène commun parmi les composés de cette étude.

[Traduit par le journal]

Can. J. Chem., **51**, 1587 (1973)

In earlier work (1) we used as partial proof of the structure of **1**, the dihydro derivative of the thermal rearrangement product of cyclopentadiene and azodibenzoyl, its ready hydrolysis by acid to *cis*-1,2-dibenzoyl-1-(2-hydroxycyclopentyl)hydrazine (**2**). The alcohol **2** was not itself isolated, but rather its isomer, the ester **3**, and the further hydrolysis product **4**. The intermediacy of **2** was, however, demonstrated by t.l.c., and it was confirmed that under the hydrolysis conditions (0.8 *N* hydrochloric acid in aqueous ethanol) isomerization of **2** to **3** was rapid and efficient. The same ester **3** could also be obtained from the *trans*-isomer **5** of the alcohol **2**, though not under such mild conditions, the use of thionyl chloride or concentrated sulfuric acid being necessary, in which case the yield was quantitative.

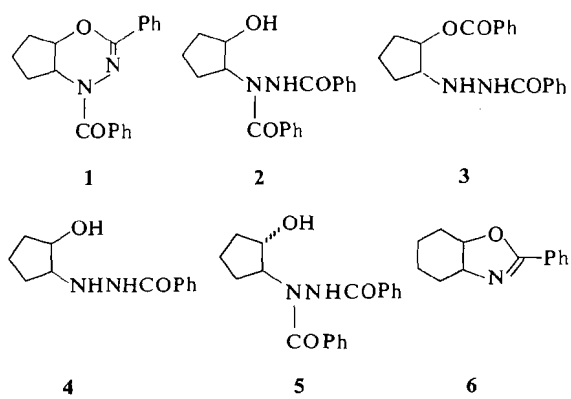

We now wish to discuss in more detail these isomerizations and other acid-catalyzed reactions of related derivatives of *cis*- and *trans*-2-hydrazinocyclopentanol.

Can. J. Chem. Downloaded from www.nrcresearchpress.com by 210.87.254.6 on 09/05/12
For personal use only.

Can. J. Chem. Downloaded from www.nrcresearchpress.com by 210.87.254.6 on 09/05/12
For personal use only.

The conversion of **5** into **3** is in fact an example of a well established reaction type in which an α-acylamino alcohol is transformed by acidic reagents (most frequently thionyl chloride) into a derivative of the amino alcohol with inversion at the carbinol carbon (2–11). The key step is the formation of an oxazolinium cation by S_N2 attack of the acylamino oxygen.[1] In the 2-acylaminocycloalkanol series the process has been achieved only for the *trans*-isomers which lead to *cis*-fused oxazolines. These have been isolated as the free bases, (*e.g.* **6** from *trans*-2-benzoylaminocyclohexanol) which are usually stable, or as their salts (3–5, 7–10). Hydrolysis of the oxazolines by acids gives the *cis*-2-acyloxycycloalkylamines (C—N cleavage, overall N → O migration) (2, 4, 7, 8, 10), or, if prolonged, the *cis*-alcohols themselves (3, 5–8, 10), while hydrolysis by basic reagents appears to give *cis*-2-acylaminocycloalkanols (C—O cleavage) (8, 9).

The formation of a neutral oxazoline like **6** is of course possible only with an acylaminocycloalkanol containing a free NH, and cannot occur with **5** which has a benzamido group on the nitrogen.

We have tried to obtain some insight into the mechanism of the thionyl chloride isomerization of **5** using n.m.r. studies. Addition of 1 equiv of thionyl chloride to a solution of **5** in chloroform-*d* caused replacement of the broad absorptions for the *tert*-hydrogens at 5.5 τ by two separate multiplets at 3.95 and 4.60 τ. A broad low field absorption for two hydrogens also appeared at −1.0 τ. The same absorptions were observed when this solution (or one obtained by reacting **5** with a large excess of thionyl chloride[2]) was evaporated, pumped briefly[3] over sodium hydroxide, and the residue redissolved in chloroform-*d*.

We attribute this spectrum to the quaternary compound **7** (Scheme 1), the absorption at −1.0 τ being that of the (exchanging) protons

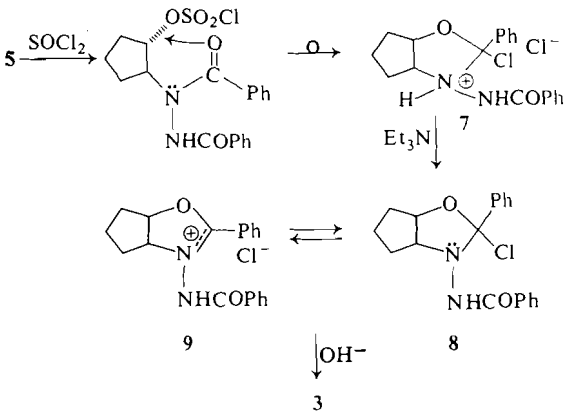

SCHEME 1

on the nitrogens, while that at 3.95 τ is probably due to the C—H adjacent to N^+. Addition of triethylamine (but not of pyridine) caused the two *tert*-hydrogen absorptions to be replaced by a band at 4.7 τ, which must have been due to the *tert*-hydrogens in either the base **8** or the ion **9** (or a mixture of these in equilibrium), since the process was reversed by addition of hydrogen chloride.[4] Neutralization of **7** by alkali gives **3** (1), as expected, and occurs through attack at the electron deficient carbon in **8** or **9**, as in the parallel reaction of the cyclohexane analog (11).

The formulation **7** was also in agreement with the i.r. spectrum, which showed broad absorption for NH^+ between 2900 and 2300 cm^{-1}, but no other absorption in the region down to 1685 cm^{-1}.

Our original objective in using thionyl chloride was to convert **5** into the chloride of the *cis*-alcohol **2**, a potential precursor to the oxadiazine **1**. As an alternative for the synthesis of **2** we tried to make the tosylate **10** in the expectation that its hydrolysis might occur with inversion. Treatment of **5** with 1 equiv of tosyl chloride in pyridine led to the recovery of 78% of **5** on work-up, and the isolation of 7% of a mono-tosyl derivative. This was not the expected *trans*-*O*-tosyl-*N*-benzoyl compound **10** but rather the *cis*-*O*-benzoyl-*N*-tosyl isomer **13**, its identity being confirmed by its synthesis from **3** with 1 equiv of tosyl chloride in pyridine. With 2

[1]Exceptions have been noted, however, in which stereochemistry is retained (7, 12, 13).

[2]The excess of thionyl chloride may have caused reaction of the *sec*-amide group thus: —NHCOPh → —N=C(Cl)Ph (14). This might cause little change in the appearance of the spectrum and would be of no consequence to the final work-up.

[3]Longer pumping caused the gradual appearance of a broad multiplet at 5.4 τ, which was not discharged by addition of thionyl chloride. It was probably a product of loss of hydrogen chloride, but it was not investigated further.

[4]The ion **9** may be destabilized relative to those derived from acylaminocycloalkanols due to the electron-withdrawing effect of the benzamido group. The neutral form **8** may thus be the dominant species here; it must rank in basicity between pyridine and triethylamine, consistent with the fact that its lone pair is localized.

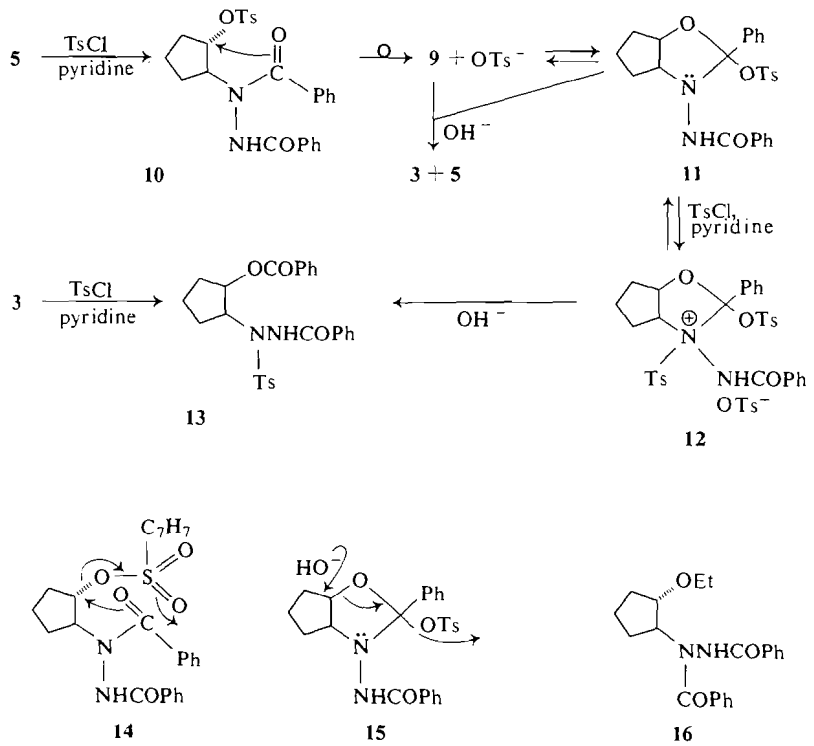

SCHEME 2

equiv of tosyl chloride, however, **5** gave a 90% yield of **13**. On the basis of these results and a study of the reaction by n.m.r. spectroscopy we propose Scheme 2 to account for these unusual results.

The changes in the n.m.r. spectrum were followed when first one and then a second equivalent of tosyl chloride was added to **5** (0.7 *M*) in chloroform-*d* containing 2.5 equiv of pyridine.[5] The broad peak for the *tert*-hydrogens of **5** at 5.5 τ slowly diminished while absorptions grew at lower field, including ones near 4.0 and 4.6 τ; at the same time the methyl peak of *N*-tosylpyridinium chloride at 7.60 τ[6] was replaced by one at 7.73. The spectrum remained unchanged after about 10 h when the peak at 5.5 τ was about half its original area, and the peak at 7.60 τ had almost disappeared. Addition of D_2O to the sample tube at this point caused most of the methyl peak to disappear into the upper aqueous layer, the spectrum now duplicating that of a mixture of the alcohol **5**, and (on the basis of new peaks formed) smaller amounts of the *N*-tosyl derivative **13** and the ester **3**, the latter being distinguishable by its high field C_1—H absorption at 6.7 τ. As the most soluble of the three products it escaped detection in the original work-up.

Addition of the second equivalent of tosyl chloride resulted in the disappearance over a period of 12 h of the peak at 5.5 τ and all the *tert*-hydrogen absorptions except those at 4.0 and 4.6 τ which continued to grow; the corresponding new methyl peaks formed a broadened line at 7.7 τ. The spectrum remained unchanged over a period of days. Addition of D_2O, however, rapidly produced a quite different spectrum, identical with that of **13** in the same solvent mixture, prepared either from an authentic sample of **13**, or by allowing **3** to react (very rapid reaction) with 1 equiv of tosyl chloride in the presence of the same excess of pyridine. Thus neither **3** nor **13** is at any stage present during the reaction of **5** with 1 or 2 equiv of tosyl chloride.

[5]The reaction was faster with larger amounts of pyridine. The changes in the n.m.r. spectrum were, however, the same as those described here (apart from solvent shifts), even when neat pyridine-d_5 was used.

[6]Control experiment.

Can. J. Chem. Downloaded from www.nrcresearchpress.com by 210.87.254.6 on 09/05/12
For personal use only.

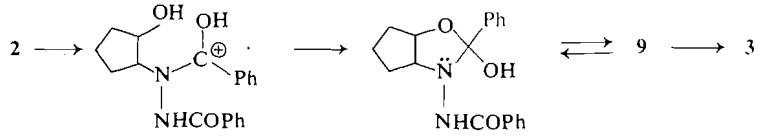

SCHEME 3

The multiplets at 4.0 and 4.6 τ had not only the same chemical shift values as the corresponding ones in **7** but *their splitting patterns were identical* (basically a quartet and a triplet respectively, with added fine structure). We take this as powerful evidence that the intermediate with 2 equiv of tosyl chloride is the quaternary structure **12**. The spectrum after reaction with 1 equiv of tosyl chloride can be interpreted as due to a mixture of a small amount of **12** (the second tosylation step is thus competitive with the first), and the major intermediate, one which is capable both of hydrolysis to **5** and to **3** and of tosylation to **12**. We suggest **11** as the most plausible structure for it.

Two paths to the oxazolidine **11** are possible, either by direct displacement of tosylate to the cation **9** (this has analogy elsewhere (3, 9)), which is neutralized by tosylate anion, or directly, in a concerted mechanism as indicated in **14**. The amounts of **3** formed on work-up are small (n.m.r. analysis indicated 10–15% from the reaction in neat pyridine, but slightly more in chloroform-*d*) and must arise from **11**, in competition with hydrolysis to **5**, or from **9**. We can only speculate on why **11** does not give exclusively **3** by direct displacement of tosylate. Concerted loss of tosylate by attack of hydroxide with inversion at cyclopentyl oxygen, as in **15**, may in this case be sterically preferable. Tosylation of **11** occurs on the ring nitrogen which, like that of **8**, is moderately basic. Alkaline work-up involves attack at the very electrophilic benzylic carbon.

Prolonged evaporation under anhydrous conditions of the solution obtained in the reaction with 1 equiv of tosyl chloride gave a glassy residue. Its n.m.r. spectrum was unchanged, and its i.r. spectrum had NH absorption at 3400 cm^{-1} and a carbonyl doublet at 1685 and 1640 cm^{-1}, reconcilable with structure **11**. The residue was unaffected by treatment with methanol for 12 h at room temperature. Evaporation gave material with the same spectra as before, in particular no trace of methoxy absorption being detectable in the n.m.r. spectrum; work-up gave mainly **5**. Similarly addition of sodium ethoxide in ethanol followed by an aqueous work-up led to **5**. The intervention of the ether **16**, expected by analogy to the hydrolysis to **5**, can be discounted, since an authentic sample of it, prepared from **5** and triethyloxonium fluoroborate, was stable to the work-up conditions.

The ready isomerization of the *cis*-alcohol **2** to the ester **3** under conditions (0.8 *N* acid) to which the *trans*-alcohol was inert, indicated the operation of a different mechanism, probably one in which the alcohol oxygen is retained and adds to the protonated amide to give **9** (Scheme 3). For the *trans*-alcohol this reaction would require formation of the rather strained *trans*-fused isomer of **9**; at the same time the acid concentration is probably too low for protonation of the OH group to an extent favorable for the S_N2 displacement to **9**, similar to that shown in Scheme 1.

To test whether the lability of the benzoyl group on N_1 (the inner nitrogen) under such mild conditions was general for the *cis*-series, or depended specifically on the presence of a free OH group, the *cis*-tribenzoyl derivative **17** was examined. Refluxing of **17** for 19 h and work-up led again to the isolation of the ester **3** (as its hydrochloride) as the major product (36%). The reaction was repeated and monitored by n.m.r. analysis utilizing the areas of the absorptions for C_1—H in both the starting material and the product ester. The ratios of **3**:**17** at 3, 7, and 23 h were 0.18:1, 0.56:1, and 2.3:1 respectively. Further hydrolysis was not extensive, though the monobenzoyl derivative **4** could be detected (C_1—H at 6.78 τ) in the n.m.r. spectrum of the hydrolysate after 23 h. The results can only be reconciled with a rate constant of formation of **3** greater than that of any other product. In a control experiment the ester **3** was recovered in a high yield after refluxing in acid for 17 h.

A more intimate analysis of the reaction path was provided using the *cis*-tribenzoyl derivative ^{14}C labelled at the N_1 carbonyl group, obtained

Can. J. Chem. Downloaded from www.nrcresearchpress.com by 210.87.254.6 on 09/05/12
For personal use only.

Can. J. Chem. Downloaded from www.nrcresearchpress.com by 210.87.254.6 on 09/05/12
For personal use only.

from the ester **3** with ^{14}C-benzoyl chloride in pyridine at 5°. All of the activity was shown to have been incorporated during the benzoylation step,[7] with no further exchange after it, since in a control experiment unlabelled tribenzoyl derivative could not be made active even when refluxed in pyridine with ^{14}C-benzoyl chloride.

Acid hydrolysis of the active tribenzoyl derivative for 21 h followed by work-up and purification gave, as well as unreacted starting material, the expected products **3**, **4**, and benzoic acid.

The percent molar yields[8] and retention of activity of these are shown in Table 1. The ester **3** was isolated as its hydrochloride which was converted into the free base with pyridine and hydrolyzed to the monobenzoyl derivative **4** with alkali. The initially isolated **4**, which was the most troublesome product to purify,[9] was converted with unlabelled benzoyl chloride into the easily purified tribenzoyl derivative. The per cent molar activities of these derivatives are also shown in Table 1.

The ester **3** had only 20% of the molar activity of the starting material and of this about 90% must have been located at the ester carbonyl since the monobenzoyl derivative **4** had only 1.9% retention of activity.

Had the loss of the N_1-benzoyl group occurred exclusively by the sequence of direct ester hydrolysis to **2** followed by benzoyl migration from N → O (Scheme 3) then **3** would have contained all the label. The actual value of 20% cannot be explained in terms of a dilution effect (100 to 20%) through exchange with benzoic acid since the activity of the latter would then have been ⩽20% and not, as observed, much higher.

It thus appears that the hydrolysis of **17** does not go by way of **2** to an extent greater than 20% and that the ratio of tertiary amide cleavage (other than by way of **2**) to ester hydrolysis is at least 0.59 :1 (isolated yield of **3** is 46%; if the remaining 54% undergoes direct ester hydrolysis the ratio is $0.8 \times 0.46 : 0.54 + 0.2 \times 0.46 =$ 0.59 :1). The true value is probably much higher since losses in the work-up of unreacted **17** and **3** would both contribute to lowering the ratio. In addition the previous hydrolysis experiment indicates that loss of tertiary amide (by all mechanisms) is faster than any other process. We conclude, therefore, that amide hydrolysis is faster than ester hydrolysis and presume that it is assisted by the neighboring ester group.[10]

TABLE 1. Hydrolysis of 18 mmol of **17**-^{14}C after 21 h: yields and activities

Compound	Moles	% Yield	Derivative	% Retention of molar activity*
17 (recovered)	6.1			99.6
3 · HCl	5.5	46		19.7
			3	20.2
			4	1.9
4	0.55	4.6		6.3
			12	8.7
$PhCO_2H$	6.6	55		40.8

*Based on starting material with a value of 3.267×10^8 counts min^{-1} mol^{-1}.

Examples have been described of assisted hydrolysis of amides by carboxyl, amide, amine, hydroxyl (15–19) and, more rarely (20), ester functions; in most of these the assisting group has been in the acyl rather than, as here, the amine moiety. We suggest that the protonated ester group of **17** forms the quaternized cyclol **18** by reaction at N_1 (Scheme 4), thus leading to a faster benzoyl cleavage, and one involving loss of label, than normal hydrolysis. A possible mechanism is also shown in Scheme 4 for ester cleavage, which transfers label directly to the ester position by way of **19**, a less important pathway than through **18** since it puts positive charge on oxygen rather than nitrogen. This is an alternative to the transfer of label by initial hydrolysis to

[7]Scambling during benzoylation, *i.e.* to give label at sites other than at N_1, is considered very unlikely.

[8]Rigorous purification of the products to constant activity was carried out at the expense of optimization of yields.

[9]The increase in activity after benzoylation shows that it must have been originally contaminated with inactive material.

[10]Some measure of the stability to hydrolysis of the ester and the amide functions in the absence of neighboring group effects can be judged by the hydrolysis of the monosubstituted derivatives cyclopentyl benzoate and 1,2-dibenzoyl-1-cyclopentylhydrazine. After 7 h the ester was 17% hydrolyzed (determined by g.l.c.) and the hydrazide was ⩾20% hydrolyzed (determined gravimetrically). The results from the hydrolysis of **17**, **21***a*, and **21***b* thus show that participation at once assists hydrolysis of the amide and retards that of the ester. The great stability of **3** to these conditions may indeed be due to protection of it as the neutral cyclic structure of Scheme 4 or as its conjugate acid ($3 \cdot H^+$) by protonation on its basic nitrogen.

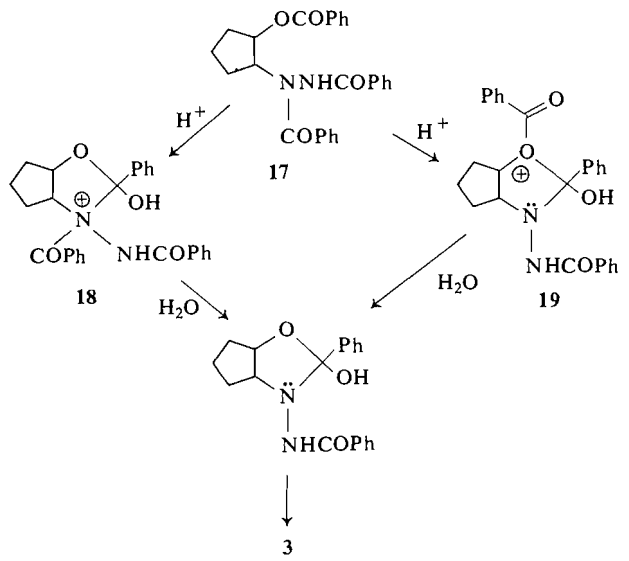

SCHEME 4

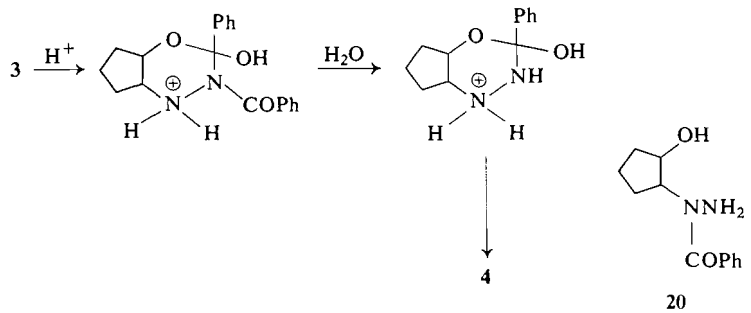

SCHEME 5

the alcohol **2**, followed by the cyclization of Scheme 3. The labelling experiment does not provide a decision between these.

The surprisingly large (~9%) incorporation of label in the isolated monobenzoyl derivative **4** suggests the possibility of acid-catalyzed transfer of benzoyl in **3** from O to N_2 (Scheme 5). We cannot however exclude the possibility that the monobenzoyl derivative **20** is a transient hydrolysis species which isomerizes to **4** and confers activity on it. The isomerization analogous to **20** → **4** in the cyclohexane series has been shown to be efficient in acid, a diaziridine intermediate being proposed to account for it (11).

The hydrolysis of the N_1-*p*-anisoyl derivative **21***a* (Scheme 6) under the same conditions was examined briefly, being followed by n.m.r. analysis, both in the non-acidic hydrolysate by the disappearance of the methoxy singlet relative to the methylene envelope, and in the carboxylic acid fraction by changes in the aromatic region.

After 8 h the products on removal of acid showed a 31% loss of methoxy-containing material (as *p*-anisic acid), the n.m.r. spectrum being readily interpreted through its tertiary proton absorptions as due to starting material, the ester **3**, and probably some **22***a*, with only very little of **23***a*. Work-up of this fraction with cold aqueous methanol gave a 40% recovery of starting material, and by addition of hydrochloric acid to the mother liquor a 33% yield (based on unreacted **21***a*) of the hydrochloride of **3** was isolated. The carboxylic acid fraction had a *p*-anisic – benzoic acid ratio of 2.5 :1. The extent of hydrolysis is thus comparable with that of **17** with cleavage of *tert*-amide again being faster than that of ester.

Hydrolysis of **21***b* was very rapid and occurred

Can. J. Chem. Downloaded from www.nrcresearchpress.com by 210.87.254.6 on 09/05/12
For personal use only.

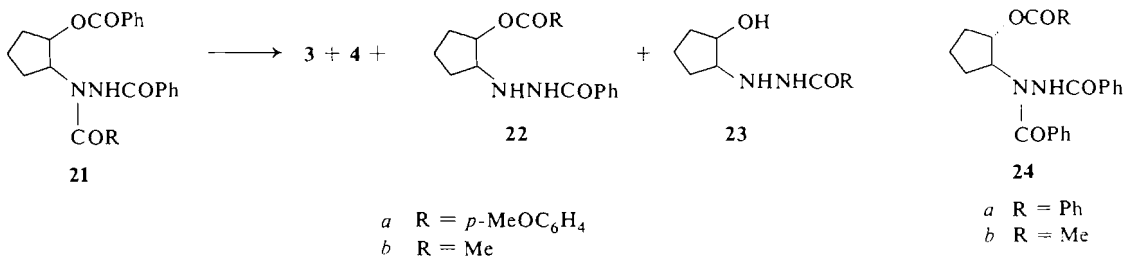

SCHEME 6

almost exclusively at the acetyl group, with 50% hydrolysis after 1 h and 90% after 3.5 h. Work-up at this point led to recovery of 85% of the starting weight after removal of acids. The i.r. and n.m.r. spectra were substantially those of **3** which was isolated pure as its hydrochloride in 50% overall yield. The lability of the acetyl group can be explained if the rate-determining step in amide hydrolysis is typified by the formation of **18** in Scheme 4. The counterpart from **21***b* would be less subject to steric constraints at the quaternized nitrogen than either **18** or the corresponding ion from **21***a*.

The behavior of the *trans*-esters **24***a* and *b* on hydrolysis was examined briefly and found to be more straightforward. The benzoate **24***a* was 40% hydrolyzed in 7 h and 70% in 24 h, the main product being the *trans*-alcohol **5**, identified by t.l.c. At least one minor product was present which was neither the ester **3** nor the alcohol **4** (from the n.m.r. spectrum), the products of inverted stereochemistry. The acetate **24***b* was hydrolyzed much more rapidly, (the differences may be simply steric), again at the ester group, which was completely removed in 7 h. The product was slightly impure **5** (80%). It thus appears that assistance of amide hydrolysis is confined to the *cis*-series.

A number of the di- and tri-substituted *cis*- and *trans*-hydrazinocyclopentanols discussed above showed polymorphism. The *trans*-benzoate **24***a* was typical. From benzene – petroleum ether (b.p. 60–80°) it gave rosettes which melted at 139–139.5°, without prior change in the appearance of the crystals. From aqueous ethanol it gave prisms, the metastable form, which on heating slowly changed appearance; the final m.p. was again 139–139.5°. The i.r. spectra were of course identical in solution but showed differences in the crystalline state, especially so in the NH and CO regions. The stable form had in Nujol NH absorption at 3230 cm^{-1} and CO absorptions at 1715, 1670, and 1652 cm^{-1}. The metastable form had corresponding absorptions at 3320, 1685, and 1664 cm^{-1}. If a sample of the latter was kept at 100° for 10 h, its spectrum changed completely to that of the stable form.

The compounds showing polymorphism are listed in Table 2, polymorph I in each case being the stable form. Included are the solvent from which each polymorph was obtained, and the i.r. absorptions in the OH/NH and CO regions.

The i.r. differences are strongly indicative of differences in hydrogen-bonding types. Models of any of these compounds readily show that free rotation round the sigma bonds of the ester and hydrazine substituents leads to a large number of conformational possibilities with five- or six-membered rings containing hydrogen bonds. The polymorphic pairs presumably correspond to two of these.

Experimental

I.r. spectra were obtained on a Beckman IR 10 spectrophotometer. For the n.m.r. analyses a JEOL C60 or a Varian T60, were used, the τ values quoted being against tetramethylsilane as internal standard.

Thionyl chloride was purified as described by Rigby (21).

The synthesis of compounds **2–5**, **24***a*, and **17** has been described previously (1).

*cis-1-Acetyl-2-benzoyl-1-(2-benzoyloxycyclopentyl)-hydrazine (**21***b*)

A solution of acetyl chloride (1.0 g) and the hydrochloride of **3** (2.0 g, 5.5 mmol) in pyridine (7 ml) was set aside at room temperature for ½ h. Addition of water (100 ml) caused an oil to separate which crystallized overnight (54%). Recrystallization from benzene – petroleum ether (b.p. 60–80°) gave the *N*-acetyl derivative of m.p. 117–118°; ν(CCl_4) 3450, 3380 (NH), 1730, 1707 and 1685 cm^{-1} (ester, *sec*-amide and *tert*-amide C=O); τ($CDCl_3$) 1.5 (NH), 1.9–2.8 (10 phenyl H), 4.50 (C_2—H), 4.90 (C_1—H), 8.00 (Me), 7.3–8.5 p.p.m. (6 methylene H).

Anal. Calcd. for $C_{21}H_{22}N_2O_4$: N, 7.65. Found: N, 7.58.

Can. J. Chem. Downloaded from www.nrcresearchpress.com by 210.87.254.6 on 09/05/12
For personal use only.

TABLE 2. Polymorphic derivatives of *cis*- and *trans*-2-hydrazinocyclopentanol

Compound		M.p. (°C)	Solvent of crystallization	ν(Nujol) NH/OH	ν(Nujol) C=O		
5	I	177.5–178	aqueous MeOH	3325	1672	1656	
	II		C_6H_6	3230	1682	1628	
17	I	177.5–178.5	aqueous MeOH	3310	1702	1678	1666
	II		C_6H_6	3240	1722	1672	1628
24*a*	I	139 –139.5	C_6H_6–P.E.*	3330	1688	1667	
	II		aqueous EtOH	3240	1715	1670	1652
21*a*	I	183 –184	aqueous MeOH	3325	1690	1678	1655
	II		C_6H_6	3220	1715	1670	1621
21*b*	I	117 –118	C_6H_6–P.E.*	3350	1720	1685	1660
	II		aqueous EtOH	3380,3280	1710	1665	1655

*Petroleum ether (b.p. 60–80°).

*trans-1,2-Dibenzoyl-1-(2-acetoxycyclopentyl)hydrazine (**24b**)*

A solution of the *trans*-alcohol **5** (100 mg, 0.30 mmol) and acetic anhydride (0.3 ml) in pyridine (3 ml) was refluxed for ½ h and evaporated to a small volume. Crystallization occurred on addition of water (5 ml), and the acetate (95%) was recrystallized from aqueous ethanol as prisms, m.p. 168.5–169°; ν(CCl_4) 3370 (NH), 1721, 1698 and 1673 cm^{-1} (ester, *sec*-amide and *tert*-amide C=O); τ($CDCl_3$) 1.93 (NH), 2.3–3.1 (10 phenyl H), 4.5–5.7 (2 *tert*-H, overlapping), 7.88 (Me), 7.5–8.7 p.p.m. (6 methylene H).

Anal. Calcd. for $C_{21}H_{22}N_2O_4$: C, 68.84; H, 6.05; N, 7.65. Found: C, 68.59; H, 5.90; N, 7.42.

*cis-1-p-Anisoyl-2-benzoyl-1-(2-benzoyloxycyclopentyl)-hydrazine (**21a**)*

A solution of the hydrochloride of **3** (2.6 g, 7.2 mmol) and *p*-anisoyl chloride (1.0 ml, 7.2 mmol) in pyridine (20 ml) was refluxed for 15 min and then kept at room temperature for 10 h. Addition of water (100 ml) caused precipitation of **21***a* (94%) which after two crystallizations from aqueous methanol had m.p. 182–184°; ν(CCl_4) 3320 (NH), 1728, 1700 and 1670 cm^{-1} (ester, *sec*-amide and *tert*-amide C=O; τ($CDCl_3$) 1.85 (NH), 2.10 (2 methoxyphenyl H, d), 2.3–3.0 (10 phenyl H), 3.30 (2 methoxyphenyl H, d), 4.40 (C_2—H), 5.10 (C_1—H), 6.27 (Me), 7.5–8.9. p.p.m. (6 methylene H).

Anal. Calcd. for $C_{27}H_{26}O_5N_2$: C, 70.73; H, 5.72; N, 6.11. Found: C, 70.43; H, 5.73; N, 6.10.

*trans-1,2-Dibenzoyl-1-(2-ethoxycyclopentyl)hydrazine (**16**)*

The alcohol **5** (0.50 g, 1.6 mmol) was refluxed for 6 h in methylene chloride (10 ml) containing a slight excess of triethyloxonium fluoroborate. The solution was shaken out with aqueous sodium hydrogen carbonate and the organic layer was dried and evaporated, leaving a crystalline residue of high purity (i.r.). Two crystallizations from aqueous methanol gave prisms, m.p. 182–183°; ν(Nujol) 3285 (NH), 1685, 1615 cm^{-1} (*sec*-amide and *tert*-amide C=O); τ($CDCl_3$) 1.3 (NH), 2.2–2.9 (10 phenyl H), 5.60 (C_1—H), 6.00 (C_2—H), 6.53 (OCH_2, J = 8 Hz), 7.8–8.7 (6 methylene H), 8.83 p.p.m. (CH_3).

Anal. Calcd. for $C_{21}H_{24}N_2O_3$: C, 71.57; H, 6.86; N, 7.95. Found: C, 71.91; H, 6.88; N, 8.21.

In a control experiment the ether (20 mg) was kept in a 1 *N*-sodium hydroxide solution of water–ethanol (3:1, 5 ml) for 5 min. The solution was neutralized with acetic acid, the volume reduced, and water added to induce crystallization. The product was analytically pure starting material.

Thionyl Chloride Reactions

*(a) Formation of cis-Ester **3***

Thionyl chloride (50 μl, 0.70 mmol) was added to a suspension of the alcohol (3 ml) at room temperature. The alcohol rapidly dissolved, sulfur dioxide being evolved. After 5 min a solution of sodium hydrogen carbonate (250 mg, 3.0 mmol) in water (10 ml) was added, and the whole was shaken and warmed in a stream of nitrogen to remove the solvent. The gummy residue rapidly crystallized on cooling and scratching (190 mg, 95%), and had the i.r. spectrum and m.p., 86–87.5°, of analytically pure ester without further crystallization.

(b) Nuclear Magnetic Resonance Reactions

Thionyl chloride was added dropwise to a suspension of **5** (100 mg) in chloroform-*d* (0.3 ml) in the sample tube till a clear solution was obtained. The spectrum showed a trace of a broad band at 5.5 τ due to unreacted **5** (C_1— and C_2—H), since it could be intensified by addition of more **5** or removed by addition of more thionyl chloride. The product had τ −1.1 (2H, broad, NH and NH^+), 1.4–2.9 (10 phenyl H), 3.95 (C_1—H, quartet), 4.60 (C_2—H, triplet, the intensities suggesting its origin from two superimposed doublets), 7.0–8.8 p.p.m. (6 methylene H).

Identical spectral patterns were observed for the product with an excess of thionyl chloride, or if thionyl chloride was used as the solvent. In the latter case there were considerable downfield shifts of all absorptions, but the splittings of and the shift between the *tert*-hydrogens were the same.

When the sample from addition of 1 equiv of thionyl chloride was treated with an excess of pyridine there was no effect on the non-aromatic region of the spectrum. Dropwise addition of triethylamine, however, caused

Can. J. Chem. Downloaded from www.nrcresearchpress.com by 210.87.254.6 on 09/05/12
For personal use only.

Can. J. Chem. Downloaded from www.nrcresearchpress.com by 210.87.254.6 on 09/05/12
For personal use only.

disappearance of the *tert*-hydrogen absorptions and formation of a broad band at 4.7 τ. Passage of dry hydrogen chloride regenerated the original spectrum.

(c) Examination of Product

A sample of the product prepared as above from 1 equiv of thionyl chloride had ν($CDCl_3$) 2900–2300 (NH and $NH^{\oplus}$), 1685 cm^{-1} (*sec*-amide C=O).

When a solution prepared from an excess of thionyl chloride in dry methylene chloride (as in section *a*), or in neat thionyl chloride, was evaporated in a stream of dry nitrogen and then pumped over sodium hydroxide (liquid nitrogen trap) the residue frothed but did not crystallize. Redissolved in chloroform-*d* it had the spectrum described above. On prolonged pumping there was a gradual loss of weight from about 1.2 to 1.1 times that of the original alcohol over a period of 3 days. The n.m.r. spectrum of the residue showed a new broad multiplet at 5.4 τ, formed at the expense of the original *tert*-hydrogens. This product was not examined further.

Reactions with p-Toluenesulfonyl Chloride

(a) On cis-Ester 3

The ester (0.20 g, 0.62 mmol) was allowed to react with tosyl chloride (0.12 g, 0.62 mmol) at 5° for 1 day in pyridine (5 ml). Addition of water gave crystalline *cis-1-p-toluenesulfonyl-2-benzoyl-1-(2-benzoyloxycyclopentyl)hydrazine* (**13**) which formed dense prisms (86%), m.p. 153.5–154°, from aqueous methanol; ν(CCl_4) 3410 (NH), 1730, 1708 cm^{-1} (ester, *sec*-amide C=O); τ($CDCl_3$) 1.9–3.0 (14 aromatic H and one H exchangeable with D_2O), 4.45 (C_2—H), 5.45 (C_1—H), 7.68 (Me), 7.4–8.5 p.p.m. (6-methylene H).

Anal. Calcd. for $C_{26}H_{26}N_2O_5S$: N, 5.85. Found: N, 5.93.

(b) On trans-Alcohol 5

The alcohol (0.32 g, 1 mmol) was treated with tosyl chloride (0.19 g, 1 mmol) in pyridine (15 ml) for 17 h at room temperature. Addition of water caused precipitation of a small amount (7%) of the *N*-tosyl derivative **13**. Evaporation of the filtrate and crystallization from aqueous methanol gave the starting alcohol (78%).

Repetition of this reaction on the same scale, but with *2* equiv of tosyl chloride, followed by addition of water gave the *N*-tosyl derivative **13** in 90% yield. Its identity was confirmed by mixed m.p. with the product in section *a*.

(c) Nuclear Magnetic Resonance Reactions

The alcohol **5** (115 mg, 0.35 mmol) was dissolved in chloroform-*d* (5 ml) containing pyridine (0.10 ml, *ca.* 2.5 equiv), and tosyl chloride (67 mg, 0.35 mmol) was added. The volume was reduced to about 0.5 ml by evaporation under dry nitrogen and the solution (0.7 *M*) transferred to a sample tube. The changes in the spectrum till reaction was complete, and thereafter when a second equiv of tosyl chloride was added, are described in the discussion.

The reactions with 1 and 2 equiv of tosyl chloride were also monitored in pyridine-d_5. No significant differences were observed other than solvent shifts.

Addition of D_2O at either stage in the above reactions led to rapid changes in the spectra. The major product from the first stage was the starting alcohol **5** with smaller amounts of the *N*-tosyl derivative **13** and the ester **3**. The yield of the latter from the reaction in pyridine was estimated as 12% by comparison of the area of its C_1—H with that of the total methylene envelope. In the chloroform-*d* reaction the yield appeared to be slightly greater. From the second stage of the reaction the addition of D_2O indicated that **13** was the exclusive product.

Control experiments. To interpret the assignments in the tosylation reactions the spectra of the following compounds or mixtures of reagents were required in chloroform-*d* containing appropriate amounts of pyridine or in pyridine itself: (*i*) tosyl chloride; (*ii*) the ester **3**, alone and with 1 equiv of tosyl chloride; (*iii*) the *N*-tosyl derivative **13**; (*iv*) the alcohol **5**.

(d) Reaction with Methanol and with Sodium Ethoxide

The solution prepared from the alcohol and tosyl chloride (0.50 mmol each) in pyridine (2 ml) was kept for 36 h and then evaporated under reduced pressure (liquid nitrogen trap). The glassy residue was found to have an n.m.r. spectrum the same as that described before; its i.r. spectrum had ν($CDCl_3$) 3400 (NH), 1685 and 1640 cm^{-1} (C=O). The main portion was dissolved in methanol (0.5 ml), kept for 12 h, and pumped down as before. The n.m.r. and i.r. spectra were unchanged. Treatment with aqueous methanol gave a crystalline solid whose i.r. spectrum showed it to be mainly **5**.

To a solution of the complex from 0.30 mmol each of alcohol and tosyl chloride, prepared in pyridine (1.5 ml) and kept 11 h at room temperature, was added a solution of sodium ethoxide (1.0 mmol) in ethanol (1 ml). A flocculent precipitate formed and the whole was briefly warmed to 80° which made it yellow. It was quenched with ice and neutralized with acetic acid. Extraction with methylene chloride gave a residue which crystallized on trituration with a few drops of methanol. The product (80%) was washed with much water and identified as almost pure **5**.

Hydrolysis Reactions

General

The acid solution was prepared by mixing 2 l ethanol, 1 l water, and 200 ml 12 *N* hydrochloric acid. There was a 2.5% shrinkage making the final solution 0.770 *N* in acid. All hydrolyses were done on a scale of 1 mmol in 19.5 ml acid at reflux temperature.

Aliquots were withdrawn at intervals, basified with sodium hydrogen carbonate, evaporated, and shaken with water and methylene chloride. The methylene chloride extraction was repeated four times. The dried extracts were evaporated and the residue analyzed as necessary by i.r. or n.m.r. spectrometry.

Quantitative determinations on the n.m.r. absorptions of protons were carried out at 1 Hz s^{-1} sweep rates in both directions at r.f. power levels low enough to prevent saturation. The traces were photocopied, cut out, and weighed. The absorptions used in individual experiments, the scale and other details follow.

(a) cis-Tribenzoyl Derivative 17 (4 mmol)

C_2—H at 4.3 τ in **17** and C_2—H at 4.7 τ in the product ester **3** were used; they overlapped slightly. In the late stages of the reaction the peak for C_1—H at 6.8 τ in the alcohol **4** was detectable. Ratios of **3**:**17** were, at 3, 7, and 23 h, 0.18:1, 0.56:1, and 2.3:1 respectively.

In a separate experiment **17** (2.3 mmol) was hydrolyzed for 19 h. The residue from the reaction was treated with

Can. J. Chem. Downloaded from www.nrcresearchpress.com by 210.87.254.6 on 09/05/12
For personal use only.

ethanol containing a little hydrochloric acid which precipitated the pure hydrochloride of **3** (36%).

In a control experiment **3** (0.12 mmol) was refluxed for 17 h. On work-up **3** was recovered, contaminated only with a small amount of **4**; it was isolated and identified as its hydrochloride.

*(b) p-Anisoyl Derivative **21a** (4 mmol)*

The area ratio of the methylene envelope to the methoxy singlet was measured in pure **21***a* and its value of 2.35 used in determining the loss of the *p*-anisoyl group during hydrolysis. The sodium hydrogen carbonate solution was acidified and the mixed carboxylic acids extracted with methylene chloride (5 times). Their ratios were determined by n.m.r. analysis by comparing the two high field *p*-anisoyl protons (H_3 and H_5) with the three high field benzoic acid ones (meta and para). At 3, 8, and 19 h the loss of methoxy signal in the non-acidic fraction was 7, 31, and 71% and the ratios of *p*-anisic to benzoic acid at the same times were 2.5:1, 2.5:1, and 0.5:1.

In a separate experiment (1.02 mmol) the hydrolysate was freed from carboxylic acids after 8 h and the non-acidic fraction was crystallized from aqueous methanol. The crystalline product (186 mg, 40%) was identified as starting material. The mother liquor was evaporated and methanolic hydrochloric acid added. An initial crop of crystals was removed, and the soluble fraction worked-up similarly to give a second crop (68 mg in all, 33% based on unrecovered **21***a*); these were combined and identified as the hydrochloride of **3** (superimposable i.r. spectrum). Recrystallization from methanolic hydrochloric acid gave prisms, m.p. 162–164°.

*(c) Acetyl Derivative **21b** (8 mmol)*

The overlapping C_2—H in **21***b* and C_2—H in the product **3** at 4.5 τ were compared with C_1—H in **3** at 6.5 τ. After 1 and 3.5 h the ratios of **3**:**21***b* were 1:1 and 9:1.

After removal of acid, the residue from the reaction (85% by weight of starting material, equivalent to 95% of **3**) had an i.r. spectrum almost identical with that of **3**. Addition of methanol containing 3 *N* hydrochloric acid gave the hydrochloride (50%), m.p. 163–166°, alone or in admixture with an authentic sample.

*(d) trans-Tribenzoyl Derivative **24a** (2 mmol)*

The overlapping C_1—H and C_2—H of **7***d*, between 4.3–5.3 τ, were compared with the sum of the overlapping C_1—H and C_2—H of the product alcohol **5**, between 5.4—6.2τ, and a smaller peak from another product at 6.4 τ. These gave ratios of products: **24***a* of 0.4:1 at 7 h and 1.5:1 at 24 h. T.l.c. on silica gel plates from benzene–ether showed two main spots only, for **24***a* and **5**.

*(e) trans-Acetate **24b** (2 mmol)*

After hydrolysis for 7 h the residue, on removal of acid, was free of an acetyl peak in its n.m.r. spectrum and corresponded to 71% by weight of the starting weight, or a maximum yield of 80% of the *trans*-alcohol **5**. The i.r. spectrum was that of slightly impure alcohol. One crystallization from aqueous methanol gave material of m.p., and mixed m.p. 174–176°.

^{14}C Labeling Experiment

The activity of all compounds was obtained by dissolving a known weight (*ca.* 150 mg) in 20 ml of scintillation fluid and measuring the counts min^{-1} in a Tri-Carb Liquid Scintillation Spectrometer, background count being subtracted. Four determinations were made for each sample. The scintillation fluid consisted of 2,3-diphenyloxazole (PPO, 2.8 g), *p*-bis-[2-(4-methyl-5-phenyloxazolyl)] benzene (dimethyl POPOP, 0.7 g) and Cab-O-Sil (30 g) dissolved in toluene (700 ml) and absolute ethanol (300 ml).

Benzoyl chloride (35 g, 0.25 mol) was made ^{14}C active by heating it at 100° for 2 h with a sample of benzoic acid containing 100 μCi of ^{14}C in the carbonyl group.

The ester **3** as its hydrochloride was converted into the N_1-benzoyl-^{14}C derivative (**17**-^{14}C) with benzoyl chloride-^{14}C in pyridine as described for the synthesis of the unlabelled compound (1). It was crystallized to a constant activity of 3.267×10^8 counts min^{-1} mol^{-1}.

In a control experiment inactive **17** could not be made ^{14}C-active by treatment with benzoyl chloride-^{14}C in refluxing pyridine.

The active ester (18.0 mmol) was hydrolyzed for 21 h. On cooling unreacted ester (6.1 mmol) crystallized out. Concentration of the mother liquor and addition of 3 *N* hydrochloric acid gave the hydrochloride of **3** (5.5 mmol). The remainder of the work-up, as described for the hydrolysis of **1** (1), gave the alcohol **4** (0.37 mmol) and benzoic acid (6.6 mmol).

A portion of the hydochloride of **3** was converted into the free base with pyridine and the remainder was hydrolyzed by heating it at reflux for 3 min in 0.8 *N* sodium hydroxide in aqueous ethanol (1:1). The chilled solution was then extracted thoroughly with ether to give the alcohol **4**.

A portion of the alcohol **4** from the original work-up was converted into the tribenzoyl derivative by treatment with 2 equiv of benzoyl chloride in pyridine at 5° (1).

The percent molar activities of all compounds, based on that of the starting material, are given in Table 1.

We thank the Province of Ontario for a Graduate Fellowship (to J.A.C.) and the National Research Council of Canada for support of this work and for a Scholarship (to J.A.C.).

1. D. MACKAY, J. A. CAMPBELL, and C. P. R. JENNISON. Can. J. Chem. **48**, 81 (1970).
2. A. P. PHILLIPS and R. BALTZLY. J. Am. Chem. Soc. **69**, 200 (1947).
3. J. ATTENBURROW, D. F. ELLIOTT, and G. F. PENNY. J. Chem. Soc. 310 (1948).
4. E. M. FRY. J. Org. Chem. **14**, 887 (1949).
5. K. PFISTER, C. A. ROBINSON, A. C. SHABICA, and M. TISHLER. J. Am. Chem. Soc. **71**, 1101 (1949).
6. J. WEIJLAND, K. PFISTER, E. F. SWANEZY, C. A. ROBINSON, and M. TISHLER. J. Am. Chem. Soc. **73**, 1216 (1951).
7. W. S. JOHNSON and E. N. SCHUBERT. J. Am. Chem. Soc. **72**, 2187 (1950).
8. G. E. MCCASLAND and D. A. SMITH. J. Am. Chem. Soc. **72**, 2190 (1950).
9. S. WINSTEIN and R. BOSCHAN. J. Am. Chem. Soc. **72**, 4669 (1950).
10. R. A. B. BANNARD, N. C. C. GIBSON, and J. H. PARKKARI. Can. J. Chem. **49**, 2064 (1971).
11. T. TAGUCHI, J. ISHIBASHI, T. MATSUO, and M. KOJIMA. J. Org. Chem. **29**, 1097 (1964).

12. G. FODOR and J. KISS. Nature, **164**, 917 (1949).
13. L. H. WELSH. J. Am. Chem. Soc. **71**, 3500 (1949).
14. J. V. BRAUN and W. PINKERNELLE. Chem. Ber. **67B**, 1218 (1934).
15. B. C. CHALLIS and J. A. CHALLIS. *In* The chemistry of amides. *Edited by* J. Zabicky. Interscience Publ., New York. 1970. Chapt. 13 and refs. therein.
16. A. SIGNOR and E. BORDIGNON. J. Org. Chem. **30**, 3447 (1965).
17. G. I. GLOVER, R. B. SMITH, and H. RAPOPORT. J. Am. Chem. Soc. **87**, 2003 (1965).
18. T. A. DOBSON, M. A. DAVIS, A.-M. HARTUNG, and J. M. MANSON. Can. J. Chem. **46**, 2843 (1968).
19. T. COHEN and W. F. GRAY. J. Org. Chem. **37**, 741 (1972).
20. K. STITCH and H. G. LEEMAN. Helv. Chim. Acta, **46**, 1151 (1963).
21. W. RIGBY. Chem. Ind. 1508 (1969).

Can. J. Chem. Downloaded from www.nrcresearchpress.com by 210.87.254.6 on 09/05/12
For personal use only.

ortho Diquaternary Aromatic Compounds. IV. Acid-catalyzed Rearrangements of Polyalkyltetralones and Related Ketones

LAWRENCE ROSS COATES BARCLAY, ROBERT HAYWORTH YOUNG, KEIR LEIGH ADAMS, AND HELEN MARY FOOTE

Department of Chemistry, Mount Allison University, Sackville, New Brunswick

Received September 6, 1972

The ketones 1,1,4,4-tetramethyl-2-tetralone (**1***a*), 1,1,4,4,7-pentamethyl-2-tetralone (**1***b*), and 1,1,4,4,6-pentamethyl-2-tetralone (**1***c*) undergo rearrangement on heating with aluminum chloride or ferric chloride in tetrachloroethane or nitromethane into mixtures of their respective isomeric ketones, 1-acetyl-1,3,3-trimethylindane (**2***a*) and 2,2,4,4-tetramethyl-1-tetralone (**3***a*) from **1***a*, 1-acetyl-1,3,3,6-tetramethylindane (**2***b*) and 2,2,4,4,7-pentamethyl-1-tetralone (**3***b*) from **1***b*, and 1-acetyl-1,3,3,5-tetramethylindane (**2***c*) and 2,2,4,4,6-pentamethyl-1-tetralone (**3***c*) from **1***c*. A quantitative study using g.l.c. of the distribution of the ketones with time shows that the sequence of the rearrangement is: $\mathbf{1} \rightleftarrows \mathbf{2} \rightarrow \mathbf{3}$. A methyl group homologously para to the carbonyl (**1***c*) accelerates the rearrangement. The same kind of rearrangement takes place during Friedel–Crafts cyclialkylation with 2,2,5,5-tetramethyltetrahydrofuranone. A unifying reaction mechanism is postulated to account for the rearrangements. This mechanism also accounts for the rearrangement and fragmentation products from treatment of 1,1,4,4-tetramethyl-2,3-dioxotetralin (**9**) with aluminum chloride or sulfuric–acetic acids. The products from **9** include 1-acetyl-1,3,3-trimethyl-2-indanone, 1,1,3-trimethyl-2-indanone, and, from the aluminum chloride – catalyzed rearrangement, 5(or 6)-acetyl-1,1,3-trimethyl-2-indanone.

Les cétones tétraméthyl-1,1,4,4 tétralone-2 (**1***a*) pentaméthyl-1,1,4,4,7 tétralone-2 (**1***b*) et pentaméthyl-1,1,4,4,6 tétralone-2 (**1***c*) se réarrangement par chauffage en présence de chlorure d'aluminium ou chlorure ferrique dans le tétrachloroéthane ou nitrométhane, en mélange de leurs cétones isomères respectivement acétyl-1 triméthyl-1,3,3 indane (**2***a*) et tétraméthyl-2,2,4,4 tétralone-1 (**3***a*) à partir de **1***a*; acétyl-1 tétraméthyl-1,3,3,6 indane (**2***b*) et pentaméthyl-2,2,4,4,7 tétralone-1 (**3***b*) à partir de **1***b* et acétyl-1 tétraméthyl-1,3,3,5 indane (**2***c*) et pentaméthyl-2,2,4,4,6 tétralone-1 (**3***c*) à partir de **1***c*. Une étude quantitative par c.g.l. de la distribution des cétones en fonction du temps, montre que la séquence du réarrangement est: $\mathbf{1} \rightleftarrows \mathbf{2} \rightarrow \mathbf{3}$. Un groupe méthyle homologue en para du carbonyl (**1***c*) accélère le réarrangement. Le même type de réarrangement a lieu lors de la cycloalkylation selon Friedel et Crafts de la tétraméthyl-2, 2,5,5 tétrahydrofuranone. Un mécanisme réactionnel a été postulé pour expliquer ces réarrangements. Ce mécanisme tient compte également des produits de réarrangement et de fragmentation lors du traitement de la tétraméthyl-1,1,4,4 dioxo-2,3 tétraline (**9**) par la chlorure d'aluminium ou le mélange d'acides sulfurique–acétique. Les produits issus de **9** comprennent l'acétyl-1 triméthyl-1,3,3 indanone-2, la triméthyl-1,1,3 indanone-2 et, à partir du réarrangement catalysé par $AlCl_3$, l'acétyl-5 (ou 6) triméthyl-1,1,3 indanone-2. [Traduit par le journal]

Can. J. Chem., **51**, 1598 (1973)

Introduction

The Friedel–Crafts cyclialkylation of aromatic compounds with 2,2,5,5-tetramethyltetrahydrofuranone is an important synthetic reaction. Since its discovery by Bruson and co-workers in 1958 (1), the reaction has provided intermediates for the synthesis of ortho-di-*t*-butyl-derivatives of benzene (2, 3) and of naphthalene (4). As well as producing the ortho-diquaternary ketone, 1,1,4,4-tetramethyltetralone (**1***a*) this reaction yields isomeric ketones, such as 1-acetyl-1,3,3-trimethylindane (**2***a*) (5) (Scheme 1).

The formation of isomeric ketones, such as **2***a*, placed definite limitations on this cyclialkylation method to produce ortho-di-*t*-butyl-aromatics (6). However, the pathway for formation of **2***a* was not well understood. In view of this and because of our interest in rearrangements of branched condensed ring systems (7), we undertook a study of the acid-catalyzed rearrangements of ketones such as **1***a* and **2***a*. In particular it was desirable to know if rearrangements leading to **2***a* took place before ring closure as was proposed by Grant and coworkers (5) or if rearrangements took place through **1***a*.

Results and Discussion

(1) Rearrangements of 1,1,4,4-Tetramethyltetralone (1a) and 1-Acetyl-1,3,3-trimethylindane (2a)

Initial rearrangement studies carried out on 1,1,4,4-tetramethyltetralone (**1***a*) under various

Can. J. Chem. Downloaded from www.nrcresearchpress.com by 210.87.254.40 on 09/05/12
For personal use only.

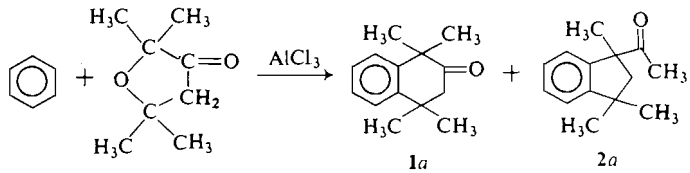

SCHEME 1

conditions are summarized in Table 1. The results show that **1***a* rearranges with different catalysts (aluminum chloride, ferric chloride, hydrogen fluoride) at least partially into 1-acetyl-1,3,3-trimethylindane (**2***a*). A new ketone (**3***a*) was identified in each of the rearrangement experiments. The mass spectrum of **3***a* indicated it to be isomeric with **2***a* and **1***a*. The i.r. and u.v. spectra showed **3***a* to be a conjugated ketone. From these results and its n.m.r. spectrum, the conjugated ketone is assigned the structure 2,2,4,4-tetramethyl-1-tetralone (**3***a*). Results from treatment of 1-acetyl-1,3,3-trimethylindane (**2***a*) with acids (Table 1, nos. 5, 6, and 7) indicate that **3***a* forms from **2***a* (Scheme 2).

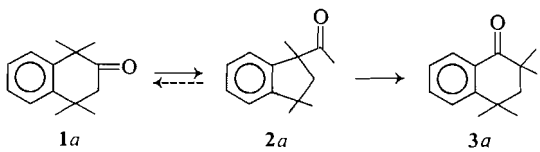

SCHEME 2

(2) Studies of Product Distribution with Time in Rearrangements of Polyalkyltetralones

In order to corroborate the evidence that the sequence of the rearrangement is **1** → **2** → **3**, comparative rearrangements were carried out on **1***a*, 1,1,4,4,7-pentamethyl-2-tetralone (**1***b*), and 1,1,4,4,6-pentamethyl-2-tetralone (**1***c*) by measuring the distribution of products with time using gas chromatographic analyses on aliquots from the reactions.

In the rearrangement of **1***a* by aluminum chloride in tetrachloroethane (Table 2, Fig. 1), there was an initial rapid decrease in per cent of **1***a* with a concomitant rapid build up of the primary rearrangement product, **2***a*. The amount of **2***a* then decreased slowly as the new ketone (**3***a*) slowly formed, and after an extended time became the major component present. The formation of **2***a* from **1***a* could also be detected by direct n.m.r. observations of the signal due to the aluminum chloride-complexed methyl keto function. This method gave a less precise indication of the amount of **2***a* but it does show the same trend as found by v.p.c. analysis of aliquots and the n.m.r. method gives direct corroborative evidence for the formation of **2***a* (Fig. 1).

The rearrangement of **1***a* with aluminum chloride in nitromethane (Table 2, Fig. 2) was faster than in tetrachloroethane. In nitromethane the conversion of **1***a* was more complete and the rate of formation of the conjugated ketone (**3***a*) was at least double that observed in tetrachloroethane. This result is surprising in view of the usual mitigating effect of nitromethane on Friedel–Crafts rearrangements. It might be due to the fact that the aluminum chloride – ketone complexes did not appear to be completely soluble in tetrachloroethane, whereas solutions were more readily obtained in nitromethane.

The results for rearrangement of 1,1,4,4,7-pentamethyl-2-tetralone (**1***b*) are summarized in Table 3 (nos. 1–3). This rearrangement yielded 1-acetyl-1,3,3,6-tetramethylindane (**2***b*) and 2,2,4,4,7-pentamethyl-1-tetralone (**3***b*). The data for **1***b* (nos. 1 and 2) are very similar to that observed for rearrangement of **1***a* under comparable conditions (Table 2). In addition the plots of detailed data points for these rearrangements of **1***b* very closely followed the results shown in Figs. 1 and 2 for **1***a*. There was a slight acceleration amounting to 3–4% after 100 min in the formation of the conjugated ketone (**3***b*) compared to **3***a*. Thus a methyl group situated meta[1] with respect to the site of the rearrangement has a slight accelerating effect on the rearrangement. The ketone **1***b* also underwent rearrangement by treatment with ferric chloride in nitromethane (Table 3, no. 3), analogous to the reaction in aluminum chloride – nitromethane.

The rearrangement of ketone **1***c* is of interest because this ketone has an activating methyl group in a position homologously para to the carbonyl group. The results for rearrangement

[1]The methyl groups at position-7 in **1***b* and -6 in **1***c* will be referred to as homologously meta and para respectively to the carbonyl group.

Can. J. Chem. Downloaded from www.nrcresearchpress.com by 210.87.254.40 on 09/05/12
For personal use only.

Can. J. Chem. Downloaded from www.nrcresearchpress.com by 210.87.254.40 on 09/05/12
For personal use only.

TABLE 1. Rearrangements of 1,1,4,4-tetramethyltetralone (**1***a*) and 1-acetyl-1,3,3-trimethylindane (**2***a*)

Number	Ketone (mmol)	Catalyst (mmol)	Solvent	Temperature (°C)	Time (h)	Products (%)
1	**1***a* (12.5)	$AlCl_3$ (37)	$CHCl_2CHCl_2$	95	4½	**2***a* (20), 2,2,4,4-tetramethyl-1-tetralone (**3***a*) (80)
2	**1***a* (4.95)	$FeCl_3$ (12.4)	$CHCl_2CHCl_2$	90	4	**1***a* (32), **2***a* (26), **3***a* (32)
3	**1***a* (4.95)	$FeCl_3$ (12.4)	CH_3NO_2	90	4	**1***a* (75), **2***a* (19), **3***a* (6)
4	**1***a* (4.00)	HF (500)	CCl_4	20	17	**1***a* (0.6), **2***a* (14), **3***a* (35), unknown (50)
5	**2***a* (24.3)	$AlCl_3$ (49.5)	$CHCl_2CHCl_2$	100	2½	**1***a* (14), **2***a* (58), **3***a* (28)
6	**2***a* (4.95)	$AlCl_3$ (15)	$CHCl_2CHCl_2$	105	5	**3***a* (89)
7	**2***a* (4.95)	HF (500)	CCl_4	20	23	**1***a* (27), **2***a* (37), **3***a* (7) plus unknown compounds
8	1-acetyl-1,3,3,6-tetramethylindane (**2***b*) (4.64)	$AlCl_3$ (15)	C_6H_6	80	4	1,1,4,4,7-pentamethyltetralone (**1***b*) (9), (**2***b*) (70), 2,2,4,4,7-tetramethyl-1-tetralone (**3***b*) (16)

TABLE 2. Rearrangements of 1,1,4,4-tetramethyl-2-tetralone (**1***a*)

Ketone (mmol)	Catalyst (mmol)	Solvent	Temperature (°C)	Time (min)	Products (%)*		
					1*a*	1-Acetyl-1,3,3-trimethylindane (**2***a*)	2,2,4,4-Tetramethyl-1-tetralone (**3***a*)
1*a* (15)	$AlCl_3$ (30)	$CHCl_2CHCl_2$	100	25	42	51	7
				50	16	72	12
				100	11	71	18
				200	10	70	20
				400	10	66	23
1*a* (5.0)	$AlCl_3$ (10)	CH_3NO_2	90	25	52	32	16
				50	13	52	32
				100	6	54	40
				200	5	45	50
				400	5	39	56

*Some representative values are shown for comparative purposes. These percentages were estimated from plots of more detailed data illustrated in Figs.1 and 2.

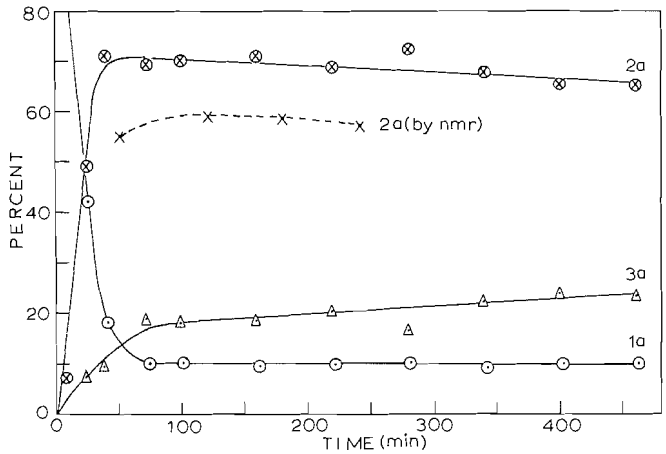

FIG. 1. Progress of rearrangement of 1,1,4,4-tetramethyl-2-tetralone (**1***a*), ⊙, into 1-acetyl-1,3,3-trimethylindane (**2***a*), ⊗ or × (by n.m.r. studies) and 2,2,4,4-tetramethyl-1-tetralone (**3***a*), △, with aluminum chloride in tetrachloroethane (100°).

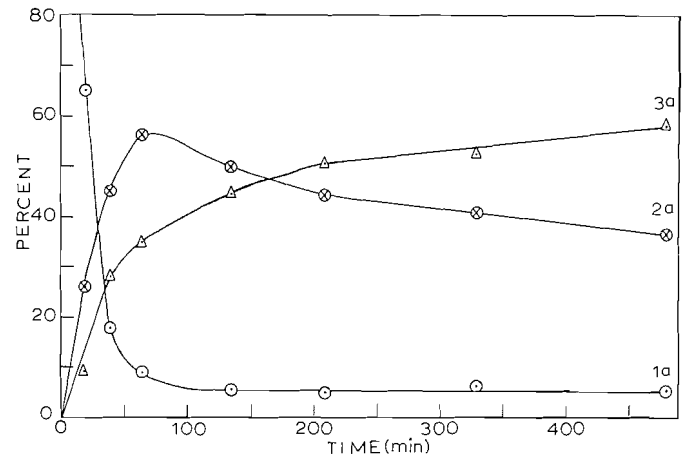

FIG. 2. Progress of rearrangement of 1,1,4,4-tetramethyl-2-tetralone (**1***a*), ⊙, into 1-acetyl-1,3,3-trimethylindane (**2***a*), ⊗, and 2,2,4,4-tetramethyl-1-tetralone (**3***a*), △, with aluminum chloride in nitromethane (90°).

of **1***c* with aluminum chloride in nitromethane are summarized in Table 3 (no. 4) and illustrated in Fig. 3. The methyl group in **1***c* accelerated its rearrangement markedly relative to ketone **1***a* (Fig. 2) or **1***b*. This is especially noticeable in the more rapid formation of the conjugated ketone 2,2,4,4,6-pentamethyl-1-tetralone (**3***c*) with a concomitant rapid decrease in the amount of methyl ketone (**2***c*).

*(3) Rearrangement of 1,1,4,4-Tetramethyl-2,3-dioxotetralin (**9**)*

It was of interest to study the acid-catalyzed rearrangement of the α-diketone **9** under similar conditions to those used for the polyalkyltetralones. The diketone **9** was found to rearrange very rapidly with aluminum chloride. However, by lowering the temperature to 65°, it was possible to follow the course of the rearrangement by v.p.c. analysis of aliquots in the usual way (Table 4 and Fig. 4). The primary product of this rearrangement, 1-acetyl-1,3,3-trimethyl-2-indanone (**10**), formed very rapidly from **9**. The new diketone (**10**) is the result of the same kind of skeletal rearrangement as was observed for the polyalkyltetralones. On the other hand, two other products from the reaction of **9** do not have analogs from previous

Can. J. Chem. Downloaded from www.nrcresearchpress.com by 210.87.254.40 on 09/05/12
For personal use only.

Can. J. Chem. Downloaded from www.nrcresearchpress.com by 210.87.254.40 on 09/05/12
For personal use only.

TABLE 3. Rearrangements of 1,1,4,4,7-pentamethyl-2-tetralone (**1***b*) and 1,1,4,4,6-pentamethyl-2-tetralone (**1***c*)

No.	Ketone (mmol)	Catalyst (mmol)	Solvent	Temperature (°C)	Time (min)	Products (%)*		
						1*b*	1-Acetyl-1,3,3,6-tetramethylindane (**2***b*)	2,2,4,4,7-Pentamethyl-1-tetralone (**3***b*)
1	**1***b* (14)	$AlCl_3$ (28)	$CHCl_2CHCl_2$	100	25	54	40	6
					50	20	67	13
					100	13	65	22
					200	13	63	23
					400	14	59	26
2	**1***b* (5.0)	$AlCl_3$ (10)	CH_3NO_2	90	25	28	57	15
					50	15	59	25
					100	7	53	40
					200	6	41	54
					400	6	32	62
3	**1***b* (9.0)	$FeCl_3$ (19)	CH_3NO_2	90	25	23	53	24
					50	16	44	40
					100	14	33	53
					200	13	32	55
					400	13	30	57
						1*c*	1-Acetyl-1,3,3,5-tetramethylindane (**2***c*)	2,2,4,4,6-Pentamethyl-1-tetralone (**3***c*)
4	**1***c* (4.0)	$AlCl_3$ (8.0)	CH_3NO_2	90	25	28	36	36
					50	3	37	60
					100	2	28	70
					200	3	16	82
					400	2	8	90

*Percentages are representative values estimated from plots of more detailed data.

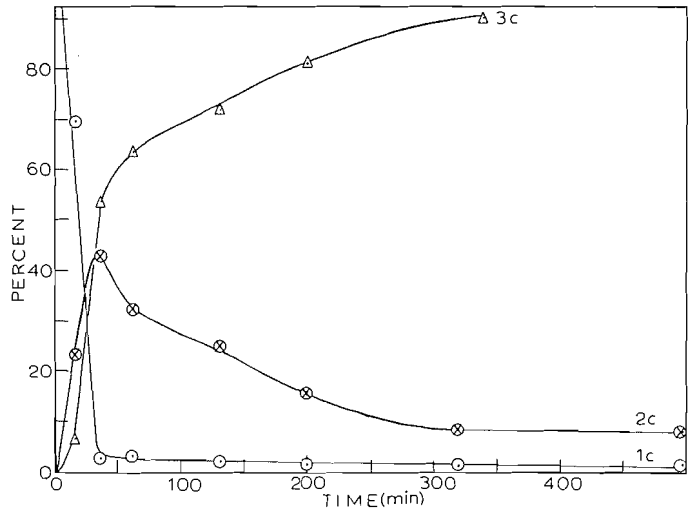

FIG. 3. Progress of rearrangement of 1,1,4,4,6-pentamethyl-2-tetralone (**1***c*), ⊙, into 1-acetyl-1,3,3,5-tetramethylindane (**2***c*), ⊗, and 2,2,4,4,6-pentamethyl-1-tetralone (**3***c*), △, with aluminum chloride in nitromethane (90°).

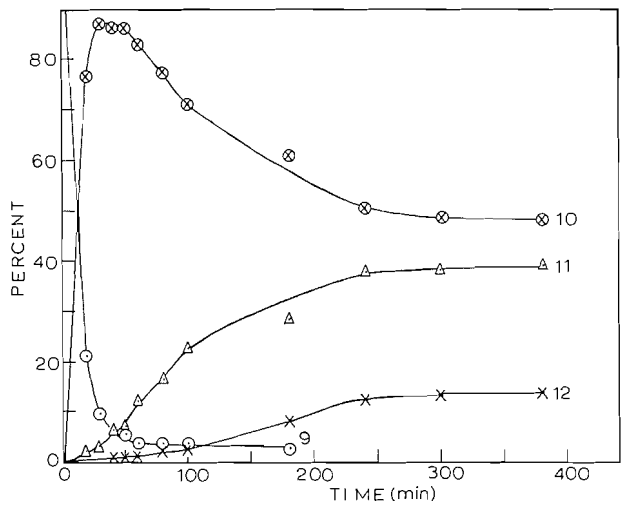

FIG. 4. Progress of rearrangement of 1,1,4,4-tetramethyl-2,3-dioxotetralin (**9**), ⊙, into 1-acetyl-1,3,3-trimethyl-2 indanone (**10**), ⊗, 1,1,3-trimethyl-2-indanone (**11**), △, and 5(or 6)-acetyl-1,1,3-trimethyl-2-indanone (**12**), ×, with aluminum chloride in tetrachloroethane (65°).

rearrangements. One of these was formed in sufficient quantity to be identified as 1,1,3-trimethyl-2-indanone (**11**). The other was formed in later stages of the reaction in relatively small quantities. It is tentatively assigned the structure 5(or 6)-acetyl-1,1,3-trimethyl-2-indanone (**12**) on the basis of spectral evidence.

1,1,4,4-Tetramethyl-2,3-dioxotetralin (**9**) also underwent rearrangement into the diketone **10** and 1,1,3-trimethyl-2-indanone (**11**) on heating with sulfuric acid in acetic acid at 100° (Table 4). There was no evidence of compound **12** from this reaction. The transformation was much slower than the aluminum chloride – catalyzed rearrangement. For example, after 1 h at 100° in the protic acid medium, there remained 80% of the starting diketone (**9**). On the other hand, the aluminum chloride treatment at 65° had transformed all but 4% of **9** in 1 h.

(4) Rearrangements During Cyclialkylation with 2,2,5,5-Tetramethyltetrahydrofuranone

It seemed probable that the sequence of rearrangements **1** ⇄ **2** → **3** would also occur during the Friedel–Crafts cyclialkylations with 2,2,5,5-tetramethyltetrahydrofuranone. This was

Can. J. Chem. Downloaded from www.nrcresearchpress.com by 210.87.254.40 on 09/05/12
For personal use only.

Can. J. Chem. Downloaded from www.nrcresearchpress.com by 210.87.254.40 on 09/05/12
For personal use only.

TABLE 4. Rearrangements of 1,1,4,4-tetramethyl-2,3-dioxotetralin (**9**)

Ketone (mmol)	Catalyst (mmol)	Solvent	Temperature (°C)	Time (min)	Products (%)*			
					9	1-Acetyl-1,3,3-trimethyl-2-indanone (**10**)	1,1,3-Trimethyl-2-indanone (**11**)	5 (or 6)-Acetyl-1,1,3-trimethyl-2-indanone (**12**)
9 (4.63)	$AlCl_3$ (9.26)	$CHCl_2CHCl_2$	65	25	13	84	3	—
				50	6	87	7	1
				100	4	71	23	3
				200	2	56	34	9
				400	—	47	38	14
9 (4.63)	H_2SO_4 (4.63)	CH_3COOH	100	25	84	10	5	
				50	82	12	6	
				100	72	20	7	
				200	57	29	14	
				400	44	30	23	

*Percentages are representative values estimated from plots of more detailed data as shown in Fig. 4.

TABLE 5. Cyclialkylation of toluene with 2,2,5,5-tetramethyltetrahydrofuranone* (100°)

Time (min)	1,1,4,4,7-Pentamethyl-2-tetralone (%)	1-Acetyl-1,3,3,6-tetramethylindane (%)	2,2,4,4,7-Pentamethyl-1-tetralone (%)
10	70.0	21.0	2.1
20	62.0	27.5	3.1
41	47.3	39.2	6.4
60	40.0	47.0	7.7
92	33.7	55.5	8.1
137	27.8	54.5	11.4
255	16.7	56.6	18.9
1125	13.8	52.7	25.5

*Initial amounts of reagents were toluene (21.1 mmol), 2,2,5,5-tetramethyltetrahydrofuranone (35.2 mmol), and aluminum chloride (70.4 mmol). In addition to the compounds listed, a small amount of a fourth ketone (2–4%) was detected but not identified. Percentages are from v.p.c. analyses of aliquots.

confirmed by a study of the product distribution with time for the cyclialkylation of toluene (Table 5). The results show that there was very rapid cyclialkylation of toluene, under the reaction conditions, to form 1,1,4,4,7-pentamethyl-2-tetralone (**1***b*) as the major compound. Then ketone **1***b* underwent rearrangement into 1-acetyl-1,3,3,6-tetramethylindane (**2***b*) and 2,2,4,4,7-pentamethyl-1-tetralone (**3***b*) in a manner similar to the previous rearrangements.

A knowledge of the course of these rearrangements is very useful in preparative reactions with 2,2,5,5-tetramethyltetrahydrofuranone. For example, by quenching the reaction after 10 min, we were able to prepare the ketone **1***b* in 70% yield by cyclialkylation of toluene (6) in the presence of aluminum chloride.

(5) A Reaction Mechanism for the Rearrangements

The rearrangement studies clearly show that the methyl ketones (**2***a–c*) result directly from rearrangement of the polyalkyltetralones (**1***a–c*), either when the latter are initially present in the reaction mixture or when they are formed under cyclialkylation conditions with 2,2,5,5-tetramethyltetrahydrofuranone. These results refute the proposal by Bruson and co-workers (1), supported by Grant and co-workers (5), that the methyl ketone (**2***a*) formed independent of the formation of the tetramethyltetralone (**1***a*), by a pinacol–pinacolone type of rearrangement on the α-ketol-$C_6H_5C(CH_3)_2CH_2COC(CH_3)_2OH$ to form $C_6H_5C(CH_3)_2CH_2COH(CH_3)COCH_3$ followed by ring closure of the latter compound.

The proposed reaction mechanism also has to account for the conversion of the methyl ketones (**2***a–c*) into the conjugated ketones (**3***a–c*). In addition the marked accelerating effect of a methyl group at position-6 (homologously para to the carbonyl group) but not at position-7 must be explained. The various observations can readily be accommodated for by the reaction pathways outlined in Scheme 3. Aluminum chloride forms a complex (**4**) with the carbonyl oxygen. This increases the electron deficiency of the carbonyl carbon. Direct evidence of this was shown in the n.m.r. spectrum of the complex which showed a downfield shift of the adjacent methylene hydrogens of up to 0.7 τ when the ratio of aluminum chloride to **1***a* approached equimolar in tetrachloroethane. A 1,2-methyl shift[2] in **4** yields a carbonium ion **5**, the latter being favored by resonance stabilization with the aromatic ring. Ring contraction by a 1,2-shift in **5** forms **6** which is the complexed form of the methyl ketones (**2**). Eventually the methylketones are irreversibly converted into the conjugated ketones (**3***a–c*). This can be explained by a 1,2-aryl shift in **6** forming the tertiary β-carbonium ion **7**. A 1,2-methyl shift in **7** leads to **8** which is the complexed form of the ketone **3**. A methyl group at position-6 (R_2) is expected to accelerate the rearrangement as observed. This group would stabilize the carbonium ion intermediates **5** and **8**, and presumably the transition states leading to them, and

[2]As pointed out by a referee, this is contrary to the usual trend for an aryl to migrate in preference to a methyl. An initial aryl migration could proceed via

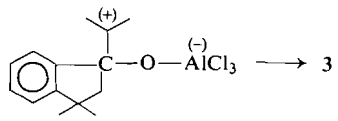

but this is not in agreement with our observation of **2** as an intermediate. In **2** the aryl migration does proceed in preference to a methyl migration.

Can. J. Chem. Downloaded from www.nrcresearchpress.com by 210.87.254.40 on 09/05/12
For personal use only.

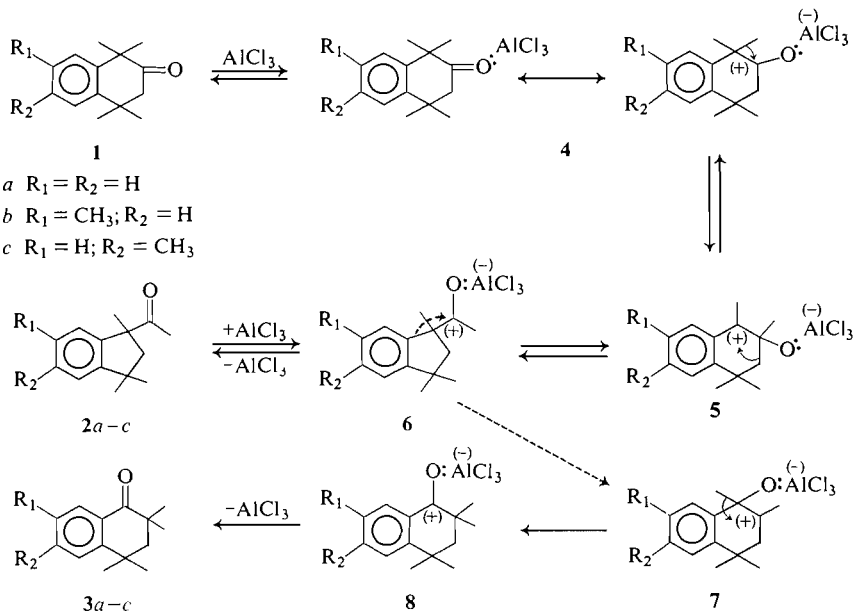

SCHEME 3

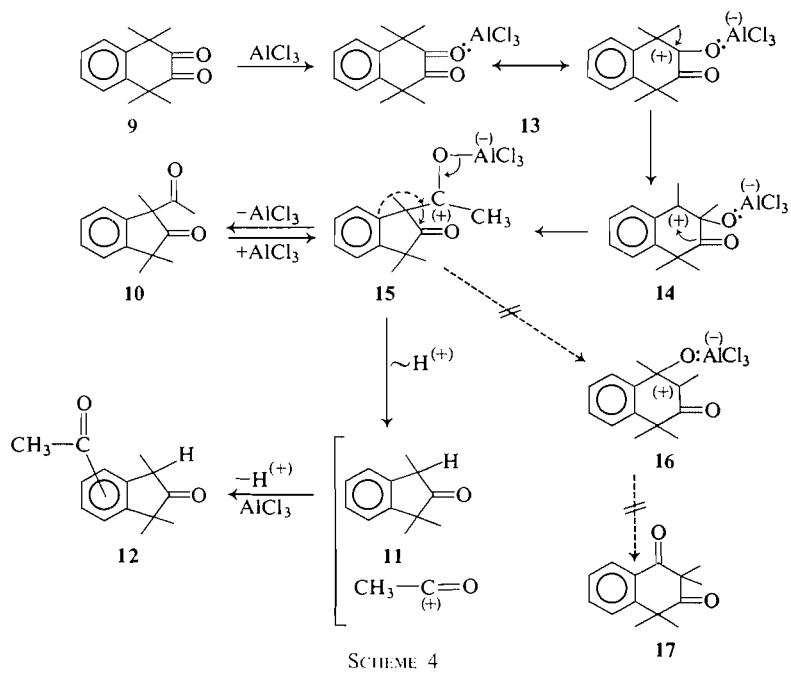

SCHEME 4

therefore promote the rearrangements. The reaction pathways are shown by a series of discreet intermediates for convenience in this discussion. It is possible that the 1,2-migrations may take place in concerted mechanisms. Analogous rearrangements have been reported in the literature for acyclic carbonyl compounds. For example, 2-phenyl-2-methylpropanal undergoes acid-catalyzed rearrangement to form 3-phenyl-2-butanone by a 1,2-methyl shift and isobutyrophenone by a 1,2-phenyl shift (8).

The reaction pathways formulated to account for rearrangements of ketones **1** and **2** can readily be adapted to explain the rearrangement

Can. J. Chem. Downloaded from www.nrcresearchpress.com by 210.87.254.40 on 09/05/12
For personal use only.

Can. J. Chem. Downloaded from www.nrcresearchpress.com by 210.87.254.40 on 09/05/12
For personal use only.

of the α-diketone (**9**) (Scheme 4). Thus a 1,2-methyl shift in the complexed ketone (**13**) leads to **14** and ring contraction of **14** results in **15** and the β-diketone (**10**). In this rearrangement, there was no evidence for the formation of a conjugated ketone (**17**) analogous to the final product from rearrangements on the polyalkyltetralones **1***a–c*. The lack of formation of **17** is probably due to the fact that the necessary precursor-carbonium ion **16** is very unfavorable, having the positive charge adjacent to the second electropositive carbonyl group. Alternative reactions take place in this system. Thus cleavage of the β-diketone (**10**) occurs (presumably through an intermediate such as **15**) resulting in 1,1,3-trimethyl-2-indanone (**11**). The acylium ion also produced apparently acylates **11** in the presence of aluminum chloride to form some substitution product **12**. The rearrangement product **10** and fragmentation product **11** can be similarly accounted for from the protic acid treatment of **9** in sulfuric–acetic acids. Under these conditions, the β-diketone (**10**) also undergoes cleavage to **11** but no Friedel–Crafts type acylation of **11** would take place; thus ketone **12** is not formed.

Experimental

G.l.c. analyses were determined by means of an F & M model 500 programmed temperature gas chromatograph equipped with a dual column attachment. The columns were 12 ft × 1/4 in., packed with Apiezon grease (30%) on Chromosorb W. The n.m.r. spectra were recorded on a Varian A-60 NMR Spectrometer using carbon tetrachloride solvent containing tetramethylsilane as internal standard. The i.r. spectra were recorded on a Perkin–Elmer model 337 Grating Spectrophotometer, using potassium bromide pellets for solids and films for liquids. U.v. spectra were recorded on a Beckmann DK-2 Spectrophotometer using spectro-grade cyclohexane as solvent. Melting points were determined on a Thomas Hoover capillary m.p. apparatus and are uncorrected. Elemental analyses were determined by Dr. E. Thommen, Basel, Switzerland and by Dr. C. Daesslé, Montreal, Quebec.

(a) Procedure for Rearrangement Studies

The syntheses and properties of the ketones 1,1,4,4-tetramethyl-2-tetralone (**1***a*), 1,1,4,4,7-pentamethyl-2-tetralone (**1***b*), 1,1,4,4,6-pentamethyl-2-tetralone (**1***c*), and 1,1,4,4-tetramethyl-2,3-dioxotetralone (**9**) were described previously (6, 2). 1-Acetyl-1,3,3-trimethylindane (**2***a*) and 1-acetyl-1,3,3,6-tetramethylindane (**2***b*) were obtained for rearrangement studies by separation and identification from the products of rearrangement of the ketones **1***a* and *b* respectively as described below. The following general procedure was used for rearrangements catalyzed by aluminum chloride in tetrachloroethane or by ferric chloride in nitromethane. The ketone was dissolved in freshly dried and distilled solvent, using 5 ml of solvent per 1 g of ketone. The anhydrous catalyst was added and the reaction mixture heated in a silicone oil bath maintained at the temperature indicated (±0.5°). The reaction was quenched in ice-water and the organic layer extracted with ethyl ether. The ether extracts were washed with water, dried with anhydrous sodium sulfate, and the ether distilled. Gas chromatographic analyses were then made on the residue. Reactions with hydrogen fluoride were carried out in a stainless steel tube (Autoclave Engineers Inc., Testtube Reactor). Otherwise the procedure was the same as before. The results of these rearrangement studies are summarized in Table 1. The procedure for studies of product distributions with time was similar to that outlined above. In these cases, small aliquots were removed from the reaction mixtures with a syringe and worked up for g.l.c. analysis. The results of these studies are given in Tables 2–5. The order of elution of the various isomeric ketones on the g.l.c. Apiezon (30%) columns used was: methyl ketones (**2***a–c*) first, polyalkyltetralones (**1***a–c*) second, and conjugated ketones (**3***a–c*) last. Samples of these ketones for spectral and analytical purposes were obtained by collection of samples from the gas chromatograph. Larger samples of 1-acetyl-1,3,3-trimethylindane (**2***a*) and 1-acetyl-1,3,3,6-tetramethylindane (**2***b*) were obtained in this way and further purified for rearrangement studies through their semicarbazones.

(b) Direct Observations by Nuclear Magnetic Resonance Studies

The interaction of anhydrous aluminum chloride with 1,1,4,4-tetramethyl-2-tetralone (**1***a*) was first studied at the ambient temperature of the n.m.r. probe (approximately 40°). Separate samples of 0.20 g (1.0 mmol) of **1***a* in five n.m.r. tubes containing 0.5 ml of tetrachloroethane were treated with anhydrous aluminum chloride in the amounts: 0.10, 0.35, 0.60, 0.80, and 1.0 mmol. The effect on the chemical shift of the methylene hydrogens of **1***a* is summarized in Table 6.

A plot of the chemical shifts (Δτ) of the methylene hydrogens *vs.* moles of catalyst (from Table 6) showed a linear relationship. The aluminum chloride did not dissolve completely when attempts were made to make measurements with more than 1 mmol present. No rearrangement was observed under these conditions. The acetyl methyl group of 1-acetyl-1,3,3-trimethylindane (**2***a*) underwent a similar downfield chemical shift (Δτ =

TABLE 6. Effect of aluminum chloride complexing with 1,1,4,4-tetramethyl-2-tetralone (**1***a*) on the n.m.r. chemical shift of methylene hydrogens

Ketone (**1***a*) (mmol)	Aluminum chloride (mmol)	Δτ*
1.0	0.10	0.05
1.0	0.35	0.22
1.0	0.60	0.37
1.0	0.80	0.54
1.0	1.0	0.70

*The chemical shift downfield from the methylene hydrogens of **1***a*.

Can. J. Chem. Downloaded from www.nrcresearchpress.com by 210.87.254.40 on 09/05/12
For personal use only.

0.60) when **2***a* was treated with an equimolar amount of anhydrous aluminum chloride in tetrachloroethane.

The direct n.m.r. observation of the rearrangement of **1***a* was carried out by heating **1***a* (0.20 g, 1.0 mmol) with anhydrous aluminum chloride (0.264 g, 2.0 mmol) at 100° in 0.5 ml tetrachloroethane in an n.m.r. tube. The n.m.r. spectrum of the reaction mixture was scanned at various intervals. Formation of 1-acetyl-1,3,3-trimethylindane (**2***a*) was evident from the appearance of a new peak at 7.23 τ assigned to the complexed acetyl methyl group. The amount of **2***a* was estimated by integration of this methyl signal. The results were not very satisfactory because of the complexity of the spectra and the fact that the signal of this methyl group appeared in the same region of the spectrum as part of the quartet due to the methylene hydrogens. The results for the estimation of **2***a* are included in Fig. 1 of the Discussion.

(c) Separation and Identification of New Compounds

1-Acetyl-1,3,3-trimethylindane (2a)

Ketone **2***a* has been described earlier (1, 5). The n.m.r. spectrum of **2***a* also confirmed the structure assigned. This spectrum showed bands at 8.76 and 8.69 (singlets), 8.58 (singlet), 7.84 (quartet, J = 13.5 Hz), 8.05 (singlet), and 2.90 τ (singlet) in the ratio 6:3:3:2:4 and assigned to the $(CH_3)_2C$, the CH_3 at position-1, the acetyl methyl, the methylene group, and the aromatic hydrogens, respectively. The i.r. spectrum showed a strong band at 1710 cm^{-1} (carbonyl) and a strong band at 760 cm^{-1} assigned to an *o*-disubstituted benzene ring. The u.v. spectrum of **2***a* showed bands at 273 (ε 1090), 266.3 (ε 1050) and 261.2 nm (shoulder, ε 753).

1-Acetyl-1,3,3,6-tetramethylindane (2b)

Ketone **2***b* was separated as a colorless liquid by collection from the gas chromatograph as the first component in the mixture from the rearrangement of 1,1,4,4,7-tetramethyl-2-tetralone (**1***b*). The semicarbazone of **2***b* was formed by reaction with an equimolar amount of semicarbazide hydrochloride and sodium acetate in aqueous ethanol. The crystalline product was recrystallized from ethanol followed by sublimation under reduced pressure. The analytical sample melted at 220–225° with some decomposition.

Anal. Calcd. for $C_{16}H_{23}ON_3$: C, 70.29; H, 8.48; N, 15.37. Found: C, 70.36; H, 8.45; N, 15.32.

It was also convenient to separate ketone **2***b* from the other isomeric ketones (**1***b*, **3***b*) due to the fact that ketone **2***b* readily formed a crystalline semicarbazone while the other ketones remained unreacted in solution. The free ketone (**2***b*) was recovered from its semicarbazone by hydrolysis with 1:1 hydrochloric acid – water on the steam cone. The ketone obtained distilled at 74–76°/0.6 mm. It showed a strong i.r. band at 1700 cm^{-1} (carbonyl) and a strong band at 820 cm^{-1} attributed to a 1,2,4-trisubstituted benzene ring. The u.v. spectrum had bands at 278.3 (ε 1410), 271.5 (ε 1274), and 264.2 nm (shoulder, ε 940). N.m.r. bands for **2***b* appeared at 8.77 and 8.73 (singlets), 8.62 (singlet), 8.06 (singlet), 7.87 (quartet, J = 13.5 Hz), 7.72 (singlet), and 3.07 τ (multiplet) in the ratio 6:3:3:2:3:4, assigned to the $(CH_3)_2C$, the CH_3 at position-1, the acetyl methyl, the methylene group, the aryl methyl (position-6), and the aromatic hydrogens, respectively.

1-Acetyl-1,3,3,5-tetramethylindane (2c)

Samples of ketone **2***c* (colorless liquid) for analyses were obtained by collecting the first component from the gas chromatographic separation of the rearrangement products from 1,1,4,4,6-tetramethyl-2-tetralone (**1***c*). The n.m.r. spectrum of **2***c* showed bands at 8.77 and 8.70 (singlets), 8.60 (singlet), 8.06 (singlet), 7.84 (quartet, J = 13.5 Hz), 7.73 (singlet), and 3.03 τ (singlet) in the ratio 6:3:3:2:3:4, assigned to the $(CH_3)_2C$, the CH_3 at position-1, the acetyl methyl, the methylene group, the aryl methyl (position-5), and the aromatic hydrogens, respectively. The u.v. spectrum showed bands at 278.2 (ε 1450) and 271 nm (ε 1255) and a shoulder at 266 nm (ε 870). The mass spectrum of **2***c* indicated a parent mass of 216 (its formula $C_{15}H_{20}O$ requires 216). The base peak appeared at 173 corresponding to the loss of CH_3CO from the parent.

Anal. Calcd. for $C_{15}H_{20}O$: C, 83.29; H, 9.32. Found: C, 82.53; H, 9.15.

2,2,4,4-Tetramethyl-1-tetralone (3a)

Samples of ketone **3***a* were obtained as a colorless liquid for analysis by collecting the third component from the gas chromatographic separation of the rearrangement products of 1,1,4,4-tetramethyl-2-tetralone (**1***a*). The n.m.r. spectrum of **3***a* showed bands at 8.83 (singlet), 8.62 (singlet), 8.11 (singlet), and 2.68–1.98 τ (multiplet and doublet) in the ratio of 6:6:2:4 and assigned to the $(CH_3)_2C$ at position-4, $(CH_3)_2$ at position-2, the methylene hydrogens, and the aromatic hydrogens, respectively. The i.r. spectrum showed strong bands at 1670 (conjugated carbonyl) and 768 cm^{-1} (*o*-disubstituted benzene). The u.v. spectrum showed bands at 286.4 (ε 1630), 241.4 (ε 9440), and 225.4 nm (ε 11 730).

Anal. Calcd. for $C_{14}H_{18}O$ (mol. wt. 202): C, 83.14; H, 8.95. Found (202 (mass spectrum)): C, 83.28; H, 9.01.

The base peak in the mass spectrum appeared at fragment mass 146, attributed to loss of $(CH_3)_2C(\diagup)—CH_2—(\diagdown)$ from the parent ion.

2,2,4,4,7-Pentamethyl-1-tetralone (3b)

Ketone **3***b* was obtained as a colorless liquid from the third component of the gas chromatographic separation of the rearrangement products from 1,1,4,4,7-pentamethyl-2-tetralone (**2***b*). The n.m.r. spectrum of **3***b* showed bands at 8.72 (singlet), 8.65 (singlet), 8.12 (singlet), 7.68 (singlet) and three groups of bands in the aromatic region at 2.82, 2.64, and 2.31 τ, in the ratio 6:6:2:3:3 and assigned to the $(CH_3)_2C$ at position-4, the $(CH_3)_2C$ at position-2, the methylene hydrogens, the aryl methyl (position-7), and the aromatic hydrogens, respectively. The i.r. spectrum of **3***b* showed a strong band at 1680 cm^{-1} (conjugated carbonyl). The u.v. spectrum showed broad bands at 393 (ε 1191) and 248 nm (ε 6050).

Anal. Calcd. for $C_{15}H_{20}O$: C, 83.28; H, 9.32. Found: C, 83.39; H, 9.32.

2,2,4,4,6-Pentamethyl-1-tetralone (3c)

Ketone **3***c* was isolated as a colorless liquid from the gas chromatographic separation of the rearrangement products of 1,1,4,4,6-pentamethyl-2-tetralone (**1***c*) by collecting the third peak. Compound **3***c* showed n.m.r.

bands at 8.85 (singlet), 8.68 (singlet, 8.16 (singlet), 7.66 (singlet), 3.17 (doublet, J = 4 Hz), 2.94 (singlet), 2.25 (doublet, J = 4 Hz) in the ratio 6:6:2:3:1:1:1 and assigned to the $(CH_3)_2C$ at position-4, $(CH_3)_2C$ at position-2, the methylene hydrogens, the aryl methyl at position-6, aryl hydrogen-7, aryl hydrogen-5, aryl hydrogen-8, respectively. (Aryl hydrogens-7,8 absorbed as an AB quartet.)

The u.v. spectrum of **3***c* was typical of a conjugated aromatic ketone, with bands at 293 nm (shoulder, ε 603), 282.5 nm (ε 873) and 250 nm (ε 9000). The mass spectrum of **3***c* showed the expected parent mass of 216. The base peak appeared at fragment mass 160 attributed to loss of $(CH_3)_2\text{—}\overset{|}{\underset{|}{C}}\text{—}CH_2\text{—}$ from the parent ion as in the mass spectrum of **3***a* (above).

Anal. Calcd. for $C_{15}H_{20}O$: C, 83.28; H, 9.32. Found: C, 82.60; H, 9.17.

*1-Acetyl-1,3,3-trimethyl-2-indanone (**10**)*

Ketone **10** was obtained as a colorless liquid by collecting the second component appearing in the gas chromatographic separation of the compounds from rearrangement of 1,1,4,4-tetramethyl-2,3-dioxotetralin (**9**). The n.m.r. spectrum of **10** showed bands at 8.65 and 8.60 (singlets), 8.49 (singlet), 8.07 (singlet) and 2.73 τ (multiplet) in the ratio 6:3:3:4 and assigned to the $(CH_3)_2C$, the methyl at position-1, the acetyl methyl, and the aromatic hydrogens, respectively. The i.r. spectrum of **10** showed bands at 1750 (carbonyl in five-membered ring) and 1715 cm^{-1} (carbonyl in CH_3CO). The u.v. spectrum of **10** had bands at 275 (ε 1054), 268 (ε 1116), 262 (ε 686), and 262.5 nm (shoulder, ε 686).

The semicarbazone derivative of **10** was prepared by treating a 1:1 ethanol–water solution of it with an equimolar amount of semicarbazide hydrochloride in the presence of sodium acetate. The solution was warmed on the steam cone for 5 min, then cooled. Colorless crystals separated. On recrystallization from ethanol the melting point was 209–210°. The carbonyl band in the i.r. at 1750 cm^{-1} for the group in the five-membered ring remained. This showed that the semicarbazone formed only at the acetyl carbonyl.

Anal. Calcd. for $C_{15}H_{19}N_3O_2$: C, 65.93; H, 6.96; N, 15.39. Found: C, 65.49; H, 7.00; N, 15.35.

*1,1,3-Trimethyl-2-indanone (**11**)*

Ketone **11** was collected from the first peak in the gas chromatographic separation of the rearrangement products of **9** as a colorless liquid. The n.m.r. spectrum of **11** had bands at 8.71 (singlet), 8.61 (doublet, J = 7.5 Hz), 6.54 (quartet, J = 7.5 Hz), and 2.81 τ (singlet) in the ratio 6:3:1:4 and assigned to the $(CH_3)_2C$ group, the CH_3— at position-3, the C—H at position-3, and the aromatic hydrogens respectively. The i.r. spectrum of **11** had a strong band at 1750 cm^{-1} due to the carbonyl group in a five-membered ring. The u.v. spectrum of **11** had benzenoid bands at 274, 267, and 261 nm similar to those observed for **10**. The semicarbazone derivative of **11** (prepared as that derivative from **10**) melted at 209–210°.

Anal. Calcd. for $C_{13}H_{17}N_3O$: C, 67.50; H, 7.41. Found: C, 67.73; H, 7.72.

*5(or 6)-Acetyl-1,1,3-trimethyl-2-indanone (**12**)*

Ketone **12** was separated in small quantity as the fourth peak in the gas chromatographic analysis of the rearrangement products from ketone **9**, as a pale yellow solid, m.p. 78–80°. The n.m.r. spectrum of **12** showed bands at 8.69 (singlet) overlapping with a doublet at 8.63 (J = 7.5 Hz), 7.49 (singlet), 6.49 (quartet, J = 7.5 Hz) and an ABC-type multiplet at 2.67 and 2.19 τ. The coupling constants in this multiplet were J_{AB}(ortho) = 8.4, J_{BC}(meta) = 1.8, and J_{AC}(para) = 1.0 Hz. The ratio of peaks was in the order 9:3:1:3 and they were assigned to the $(CH_3)_2C$ at position-1 plus the CH_3— at position-3, the acetyl methyl, the C—H at position-3, and the aromatic hydrogens, respectively. The i.r. spectrum of **12** showed a carbonyl group absorption band at 1750 (five-membered ring) and one at 1680 cm^{-1} (conjugated). The u.v. absorption spectrum was similar to a conjugated aromatic ketone (*e.g.* acetophenone). It showed bands at 292.5 (ε 1967), 282.8 (ε 2417), 274.4 (shoulder, ε 1856), 248 nm (ε 16 611).

The authors are grateful to the National Research Council of Canada for financial support of this research.

1. H. A. BRUSON, F. W. GRANT, and E. BOBKO. J. Am. Chem. Soc. **80**, 3633 (1958); U.S. Pat. 2 857 433 (1958).
2. L. R. C. BARCLAY, C. E. MILLIGAN, and N. D. HALL. Can. J. Chem. **40**, 1664 (1962).
3. A. W. BURGSTAHLER and M. O. ABDEL-RAHMAN. J. Am. Chem. Soc. **85**, 173 (1963).
4. L. R. C. BARCLAY, G. R. NIXON, H. M. FOOTE, and S. L. BARCLAY. Can. J. Chem. **47**, 4313 (1969).
5. L. AMES, E. CHAITMAN, and F. GRANT. J. Org. Chem. **26**, 1299 (1961).
6. L. R. C. BARCLAY, K. L. ADAMS, H. M. FOOTE, E. C. SANFORD, and R. H. YOUNG. Can. J. Chem. **48**, 2763 (1970).
7. L. R. C. BARCLAY, A. H. GRAY, and C. E. MILLIGAN. Can. J. Chem. **39**, 870 (1961).
8. J. W. HUFFMAN and L. E. BROWDER. J. Org. Chem. **27**, 3208 (1962).

Can. J. Chem. Downloaded from www.nrcresearchpress.com by 210.87.254.40 on 09/05/12
For personal use only.

Can. J. Chem. Downloaded from www.nrcresearchpress.com by 210.87.254.6 on 09/05/12
For personal use only.

Ring–Chain Tautomerism of 5-Oxo-3,5-seco-A-norcholestan-3-ol

JOHN T. EDWARD, MORRIS KAUFMAN, AND RICHARD K. WOJTOWSKI
Department of Chemistry, McGill University, Montreal, Quebec

AND

DESMOND M. S. WHEELER AND THOMAS M. BARRETT
Department of Chemistry, University of Nebraska, Lincoln, Nebraska

Received July 26, 1972

5-Oxo-3,5-*seco*-A-norcholestan-3-ol (**4**) was prepared in four steps from Windaus' keto-acid (**1**; R = H), and found to exist almost completely in the tautomeric hemiketal form **5**. With ethanol and a trace of acid this affords the ethyl ketals **6***a*, **6***b*; under equilibrium conditions the ratio of **6***a*:**6***b* is about 4:1.

Le 5-oxo-3,5-*seco*-A-norcholestan-3-ol (**4**) a été preparé en quatre étapes à partir du céto-acide **1** (R = H) de Windaus, et se présente presque entièrement sous les formes tautomeres **5***a* et *b*. Ces dernières fournissent avec l'éthanol, en presence d'une trace d'acide, les cétals **6***a* et *b*, dans le rapport 4:1 a l'equilibre.

Can. J. Chem., **51**, 1610 (1973)

In organic solvents 1-hydroxy-5-hexanone exists to the extent of about 50% as the cylic hemiketal tautomer, but in aqueous-organic solvents the equilibrium is displaced back toward the chain tautomer (1). The latter can exist in many more conformations than the ring tautomer, and hence it can be expected that cyclization will be opposed by unfavorable entropy effects. By comparison, the number of conformations available to the steroidal hydroxyketone **4** (obtained in connection with the synthesis of *gem*-methyl carboxyl compounds (2)) is much reduced, and so would be expected to favor formation of the cyclic hemiketal tautomers (**5***a*, **5***b*). As shown below, this proved to be correct, and in this respect δ-hydroxyketones resemble δ-hydroxyaldehydes previously studied (3).

The hydroxyketone **4** was obtained by the route outlined in Scheme 1 (*cf.* ref. 4). The methyl ester (**1**; R=Me) (5) was converted to the ketal **2**, which was reduced with lithium aluminum hydride to the hydroxy-ketal **3**, and this was hydrolyzed in aqueous dioxane to the hydroxyketone **4**. Attempts to obtain **4** by direct reduction of Windaus' keto-acid **1** (R=H) (6) with diborane (*cf.* ref. 7) gave an intractable mixture.

The hydroxy ketone **4** was obtained as an oil which set to a waxy solid, probably composed mostly of **5***a*/**5***b* (as shown below), which melted unsharply at temperatures slightly above room temperature. This compound appeared homogeneous by t.l.c.,[1] and gave the mass spectrum expected for **4**/**5** with a small peak for the parent ion at 390, and prominent peaks at 372 and 357 mass units, perhaps because of the fission sequence depicted in eq. 2.

[1] **4**/**5** ⇄ 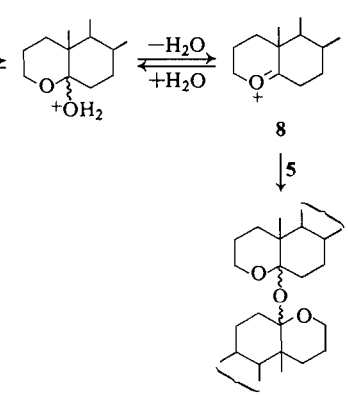

[1]An attempt to purify a sample for analysis by distillation at 2 μ and a temperature of 140–150 °C gave a product which appeared from elemental analysis to contain **9** (see eq. 1). The formation of such compound(s) under apparently neutral conditions would find analogy in the formation of a similar ether from a steroidal hydroxy-aldehyde (8), and is probably explained by the presence of acids in ordinary "neutral" solvents or glassware. The extreme facility of such reactions reflects the ease of formation of oxocarbonium intermediates such as **8** which unlike similar intermediates in carbohydrate chemistry are stabilized by inductive effects.

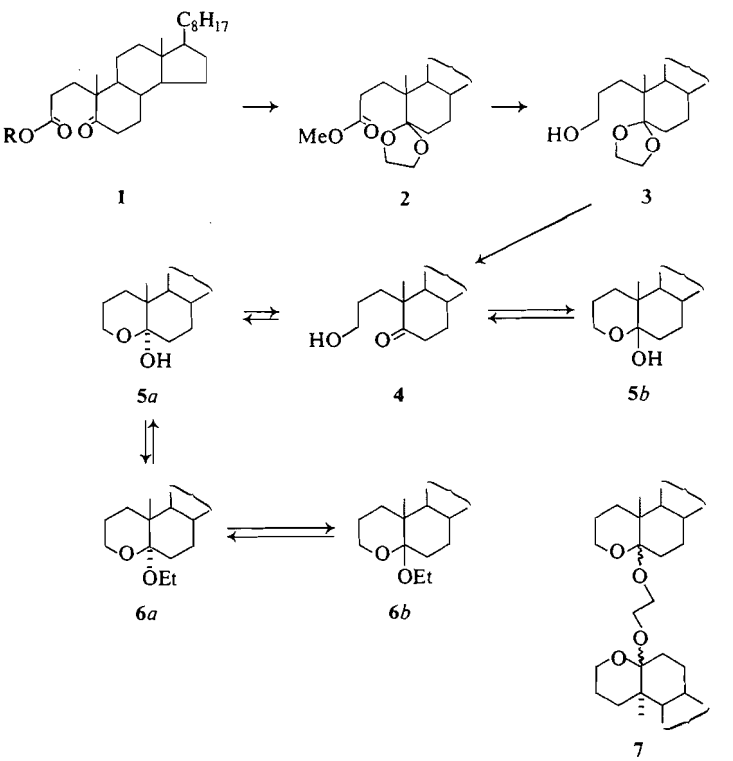

SCHEME 1

[2]

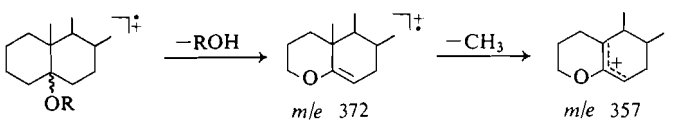

5 R = H
6 R = Et

Because of difficulties in handling the oily **4**/**5**, it was produced *in situ* in hexane solution by hydrolysis of the crystalline ethoxy compound **6***a* (described below) with a few drops of aqueous hydrochloric acid. It was possible to follow the reaction to its completion by t.l.c. This hexane solution showed no u.v. absorption peak at 285 nm, as was shown by 2-methylcyclohexanone (ε 17), which was taken as a reasonable model for **4**. The sensitivity of this method is such that it would have indicated more than 1–2% of **4** in the tautomeric mixture **4**/**5**. The relative absence of **4** in hexane solution was apparent also from the absence of a peak in the circular-dichroism spectrum.

In carbon tetrachloride or chloroform solution the presence of a small amount of the tautomer **4** became apparent from overlapping peaks at 1730 (C=O) and 1700 cm^{-1} (C=O...H—O); the i.r. spectrum also showed a sharp peak at about 3600 (O—H) and a broad peak at 3410 cm^{-1} (bonded O—H). A comparison of the relative areas of the C=O and O—H bands indicates the mixture of **5**/**4** to contain about 8% of **4**, in either solvent, if the intensities of the C=O and O—H bands of **10** and of its 9,11-dihydro derivative (9) in carbon tetrachloride and in chloroform

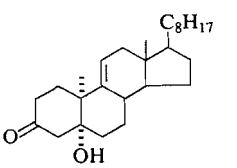

10

Can. J. Chem. Downloaded from www.nrcresearchpress.com by 210.87.254.6 on 09/05/12
For personal use only.

Can. J. Chem. Downloaded from www.nrcresearchpress.com by 210.87.254.6 on 09/05/12
For personal use only.

are accepted as standards. Obviously too many assumptions are involved for much weight to be given to the exact numerical results, but the accumulation of evidence indicates that in organic solvents the tautomeric mixture is more than 90% in the cyclic form **5**. Furthermore, it seems likely, for reasons which will become apparent later, that the cyclic form is made up of the two epimers, **5***a* and *b*, with the former predominating.

In spite of the very great predominance of **5**, the tautomeric mixture reacted with trichloroacetyl isocyanate in deuterochloroform to give a mixture of carbamates containing about 70% of the carbamate derived from **4**, and only about 20% of a carbamate derived from **5** (tentatively assumed to be **5***a*), and 10% of another carbamate derived from **5** (tentatively assumed to be **5***b*). The proportions were deduced from the n.m.r. spectrum of the mixture formed (10). The C-3 protons of the carbamate of **4** would be expected, like the C-3 protons of the carbamate of **3** (2H, at 4.20 δ), to give rise to a triplet, and indeed a triplet (70% of 2H) is observed at 4.24 δ. On the other hand, the C-3 protons of the carbamates of **5***a* and *b* would be expected, like the C-3 protons of **6***a* (2H, at 3.47 δ) and *b* (2H, at 3.49 δ), to give rise to a broad multiplet because of coupling to axial and equatorial protons at C-2, and a broad multiplet (30% of 2H) is observed at 3.71 δ. Singlet N—H peaks are observed at 8.50 δ (70% of 1H, carbamate of **4**), 11.84 δ (20% of 1H, carbamate of **5***a*), and 10.48 δ (10% of 1H, carbamate of **5***b*).

These results require the equilibrium **4** ⇄ **5** in deuterochloroform to be quickly established, perhaps because the trace of DCl resulting from oxidation of deuterochloroform will catalyze both forward and backward reactions (11). The unhindered **4** would then be expected to react with trichloroacetyl isocyanate more rapidly than the hindered **5***a* or *b*, and hence to account for the major part of the trichloroacetyl carbamate formed. As a further example of this effect, chlorosulfonyl isocyanate reacted with the tautomeric mixture **4**/**5** in deuterochloroform to give only the chlorosulfonyl carbamate of **4** (NH singlet, 1H, 9.61 δ; C-3 H_2 triplet, 2H, at 4.27 δ). It seems likely that in this case a trace of chlorosulfonic acid impurity is acting as catalyst, and that the reaction **4** ⇄ **5** has become very fast.

Reaction of the tautomeric mixture **4**/**5** with ethanol containing a trace of hydrogen chloride would be expected to yield the two ethoxy derivatives **6***a* and *b*. Furthermore, because of the presence of angular groups at *both* carbon atoms involved in ring fusion, the two derivatives might be expected to have about the same enthalpy (12), and to be present at equilibrium in roughly equal amounts. In the event, **4**/**5** reacted with acidic ethanol to give a product which appeared from t.l.c. to contain two compounds, but in the proportions of about 4:1. However, crystallization of the product from absolute ethanol gave only one compound, even on further concentration of the other liquors. The structure **6***a* or *b* for this compound (the major product) was supported by elemental analysis, i.r. and n.m.r. spectra, and particularly by its mass spectrum, which showed, beside the peak for the parent ion, prominent peaks at 372 and 357 mass units (see eq. 2). Further analysis of the n.m.r. spectrum (discussed below) indicated the compound to be **6***a*.

The minor compound formed in the reaction is the epimeric **6***b*; the failure to isolate it by concentration of the mother liquors arises from the extraordinary facility of the epimerization **6***b* ⇄ **6***a* (via **8**) in ethanol, and the fact that **6***a* has the smaller solubility and hence crystallizes out first. Similarly, when an attempt was made to crystallize **6***a* from anhydrous methanol, its methoxy analogue (**6***a*; Me in place of Et) was obtained. The later could be obtained readily in a pure state by treatment of **6***a*, **4**/**5**, or **7**A with methanol containing a trace of hydrogen chloride.[2]

The epimerization **6***a* ⇄ **6***b*, and the conversion of **6***a* into its methoxy analog, belong to classes of reactions known to be acid-catalyzed (11), and evidently occur with such facility that they are catalyzed by traces of acids present in ordinary ethanol or methanol. When ethanol was made weakly alkaline with a trace of diethylamine, the interconversion **6***a* ⇄ **6***b* was stopped, and it proved possible to separate **6***a* and **6***b* by chromatography on silica gel which had been made weakly alkaline by exposure to a dilute solution of diethylamine in hexane–benzene.[3]

---

[2]The structure **6***a* (Me in place of Et) is suggested by its rotation ($[\alpha]_D^{25}$ + 55° in ethanol containing a trace of diethylamine), which is the same as that of **6***a*. No attempt was made to isolate **6***b* (Me in place of Et), presumably the minor reaction product.

[3]Chromatography on Merck silica gel which had not been treated with diethylamine resulted in the hydrolysis of **6***a*, **6***b*, or **7**A to **4**/**5**. Very convenient hydrolytic procedures based on this fact are given in the experimental section.

Can. J. Chem. Downloaded from www.nrcresearchpress.com by 210.87.254.6 on 09/05/12
For personal use only.

The structure **6***b* for the second reaction product was indicated by its elemental analysis, its i.r. and mass spectra (which were very similar to those of **6***a*), and, in particular, by its n.m.r. spectrum. Methyl peaks due to the 18-angular methyl group and to the methyl groups of the side chain were observed with about the same chemical shifts as the corresponding methyls of cholestane (13). However, the signal for the 19-methyl group of **6***a* and *b* could be expected to be shifted downfield by the proximity of two oxygen atoms, and furthermore it would be expected that this signal should appear at lower field for **6***b* than for **6***a* (13). In the 220-MHz spectra of the two compounds in carbon tetrachloride, the 19-methyl peak of the predominant epimer appeared at δ 0.83 and of the minor epimer at δ 1.04, so that these are assigned the structures **6***a* and *b* respectively.[4]

At room temperature in untreated ethanol solution both **6***a* and *b* slowly reverted to a mixture of **6***a* and *b*, as could be shown by t.l.c. In the presence of a trace of hydrogen chloride this epimerization became effectively instantaneous, and the rotation of the equilibrium solution ($[\alpha]_D^{25}$ + 45°) was the same whether the starting material was **6***a* ($[\alpha]_D^{25}$ + 55°) or **6***b* ($[\alpha]_D^{25}$ + 5°). This indicates a proportion of 4 : 1 for **6***a* : **6***b* at equilibrium. Approximately the same proportions were obtained by chromatographic separation of **6***a* and *b* from the reaction mixture after interconversion had been quenched by the addition of diethylamine.

Evidently the simple conformational analysis of **6***a* and *b* in terms of *gauche* interactions (12), which indicates structures of equal stability, is in error; it is known that the cyclohexane rings of steroids are somewhat flattened from ideal chair shapes (14). If the *trans* **6***a* is favored over the *cis* **6***b*, it is likely that the *trans* **5***a* is similarly favored over the *cis* **5***b*, and this would explain the unequal formation of the two trichloroacetyl carbamates based on **5**.

While the hydrolysis of the dioxalane **3** was accomplished without difficulty in dioxane–water 2/1 (v/v), unexpected complications were encountered in dioxane–water 98/2 (v/v). The reaction product was shown by t.l.c. to be a mixture, which in hexane solution deposited a small amount of crystalline compound A ($C_{54}H_{94}O_4$). Column chromatography, using hexane–diethyl ether as elutant, gave an isomeric compound B ($C_{54}H_{94}O_4$) as well as 5α-ethoxy-4-oxacholestane (**6***a*), the latter presumably from reaction of **4**/**5** with ethanol, known to be an impurity in the diethyl ether. The structure **7** for both A and B follows from their combustion analyses, molecular weights, and n.m.r. and mass spectra. The high-resolution spectrum of A showed no parent peak, but peaks at 434.376066 ($C_{28}H_{50}O_3$) and 372.339199 mass units ($C_{26}H_{44}O$), as well as a peak at 357 mass units (eq. 3; *cf.* eq. 2). These results indicate the dangers of

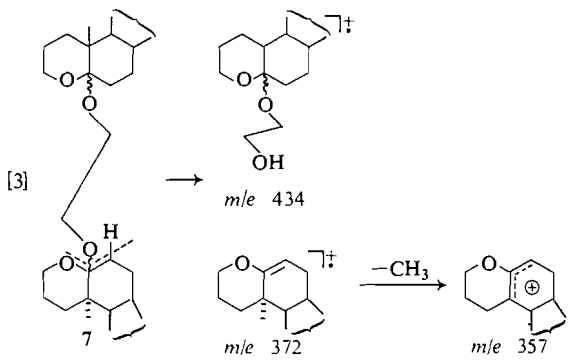

hydrolyzing some ketals (such as **3**) in solutions containing too little water. Under these conditions ketal interchange (**3** → **11**) will predominate over hydrolysis, and this can then be expected to result in formation of the epimers **7***a*, *b*, and *c* (Scheme 2) in proportions depending on the relative stabilities of *trans* and *cis* fusions of the B rings of these compounds. The isolation of **7**A and B in the proportions of about 3 : 1 would indicate the structure **7***a* for **7**A, **7***b* for **7**B,[5] and a 6 : 1 preference for *trans* over *cis* fusion in this series of compounds.[6] This latter figure can only be approximate, because **7**A and B were isolated from a reaction mixture in which reaction had not been quenched by the addition of base.

[4]The 220-MHz spectrum of **6***a* in carbon tetrachloride showed a well-defined CH_3 triplet (δ 1.16) and CH_2 quartet (δ 3.33; J = 7 Hz) due to the ethoxy group. However, the spectrum of **6***b* showed a well-defined triplet (δ 1.19; J = 7 Hz) but a 10-line multiplet for CH_2 centered at δ 3.30. In deuterobenzene at ordinary temperatures the methylene signals of **6***a* showed a similar splitting, and a clean quartet was obtained only when the temperature reached 70°. These effects are being studied further.

[5]As pointed out by a referee, the configurations of **7**A and B should be available from the 220 MHz n.m.r. spectra of the compounds. We hope to confirm these configurations later.

[6]Such a preference would result in the formation of only about 2% of **7***c* in the equilibrium mixture.

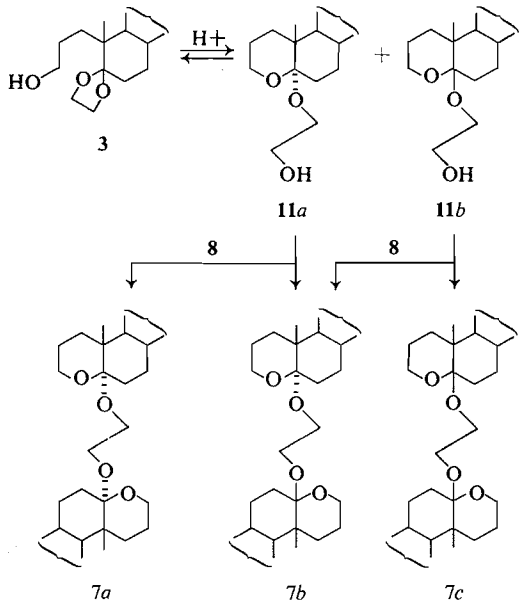

SCHEME 2

Experimental

Unless otherwise specified i.r. spectra were run on Perkin–Elmer Instruments 21, 237, and 137 in CH_2Cl_2 solutions; n.m.r. spectra on Varian spectrometers A-60 and T-60 in $CDCl_3$ solution using TMS as an internal reference. Analyses were by Bernhardt, Micro-Tech Laboratories (Skokie, Illinois), and C. Daesslé (Montreal, Quebec).

*5-Oxo-3,5-seco-A-norcholestan-3-oic acid methyl ester (**1**; R=Me)*

The methyl ester (**1**, R=Me), previously obtained (5) by the action of diazomethane on the acid **1** (R=H), was obtained by refluxing a solution of **1** (R=H) in methanol and concentrated sulfuric acid. The ester had b.p. 110–115° at 15 mm, ν_{max} 1783 (s) (ester C=O) and 1703 (s) cm^{-1} (ketone C=O); n.m.r. peaks at δ 3.59 (s, 3, $COOCH_3$) and singlets at 1.05, 0.86, and 0.68 and a doublet at 0.79.

*5,5-Ethylenedioxy-A-nor-3,5-secocholestan-3-oic acid methyl ester (**2**)*

A stirred mixture of A-nor-3,5-secocholestan-5-one-3-oic acid methyl ester (5.70 g), dry benzene (250 ml), ethylene glycol (100 ml), and *p*-toluenesulfonic acid (2.0 g, 11.6 mmol) was refluxed for 40 h in a flask equipped with a reflux condenser and Dean–Stark water separator. When the reaction mixture had cooled to room temperature it was diluted with water (100 ml). The benzene separated, and the aqueous layer was washed with benzene (2 × 75 ml); the combined benzene layers were dried. Evaporation of the solvent gave 5,5-ethylenedioxy-A-nor-3,5-secocholestan-3-oic acid methyl ester as an oil (6.16 g, 97.8%) having b.p. 170–180° at 7 mm: ν_{max} 1735 (s) cm^{-1}; δ 3.92 (s, 4H, OCH_2CH_2O), 3.64 (s, 3H, OCH_3).

Anal. Calcd. for $C_{29}H_{50}O_4$: C, 75.3; H, 10.9; O, 13.8. Found: C, 75.5; H, 11.0; O, 13.7.

*5,5-Ethylenedioxy-A-nor-3,5-secocholestan-3-ol (**3**)*

A solution of 5,5-ethylenedioxy-A-nor-3,4-secocholestan-3-oic acid methyl ester (558 mg, 1.21 mmol) in anhydrous ethyl ether (15 ml) was added over 5 min to a stirred solution of lithium aluminum hydride (366 mg, 9.7 mmol) in ether (5 ml). The reaction mixture was stirred at room temperature for 9 h, poured onto ice, and acidified with hydrochloric acid (20 ml, 5%), and the acidified solution was extracted with ether (3 × 25 ml). The combined ethereal extracts were washed with saturated aqueous sodium chloride (1 × 25 ml), dried, and concentrated under reduced pressure to yield 5,5-ethylenedioxy-A-nor-3,5-secocholestan-3-ol as an oil (534 mg, 1.23 mmol, 100%) having b.p. 160–170° at 15 mm; ν_{max} 3605 cm^{-1}; δ 3.95 (s, 4, OCH_2CH_2O), 3.68–3.37 (m, 2, CH_2O at C-3), 2.99 (s, 1, OH). After addition of trichloroacetyl isocyanate, δ 8.46 (s, 1, NH), 4.0–4.3 (m, 2H, CH_2O at C-3), 3.94 (s, 4H, $O—CH_2CH_2—O$).

*5-Oxo-3,5-seco-A-norcholestan-3-ol (**4**)*

After a mixture of 5,5-ethylenedioxy-A-nor-3,5-secocholestan-3-ol (920 mg, 2.12 mmol), dioxane (20 ml), water (10 ml), and concentrated sulfuric acid (2 ml) had been refluxed 11 h, the solvents were removed under reduced pressure, and the residue was taken-up in acetone. The solution was steam distilled to remove ethylene glycol (600 ml water distilled) and then extracted with ether (2 × 35 ml). The combined ethereal extracts were dried and evaporated under reduced pressure to give an oil (821 mg, 2.11 mmol, 99.5%) having b.p. 140–150° at 2 μ; δ 3.75–3.25 (3, broad, $—CH_2OH$), and indicated by analysis as being an approximately 1:1 mixture of **4** and **9**.

Anal. Calcd. for 50% $C_{26}H_{46}O_2$ + 50% $C_{52}H_{90}O_3$: C, 80.8; H, 11.9; O, 7.2. Found: C, 81.1; H, 11.7; O, 7.6.

1,2-Di(4-oxa-5ξ-cholestanyloxy)ethane (7A and B)

A solution of the hydroxyketal **3** (5.5 g) in purified dioxane (100 ml) containing 7.9% aqueous sulfuric acid (2 ml) was stirred for 2 h at room temperature. The solvent was then removed by rotatory evaporation at 15 mm and the oily residue was extracted with ethyl ether. The ether solution was washed with aqueous bicarbonate and with water, and dried over magnesium sulfate. Evaporation of the ether left an oil (5.2 g) which dissolved in hot hexane. On cooling the hexane solution deposited hexagonal plates (600 mg) of compound A, m.p. 193–195°, δ 3.56 (s, 4H, OCH_2CH_2O), 3.58–3.98 (m, 2H, CH_2O at C-3).

Anal. Calcd. for $C_{54}H_{94}O_4$: (mol. wt. 806) C, 80.3; H, 11.7; O, 7.9. Found: (771 (vapor phase osmometry of CCl_4 solution)) C, 80.5; H, 11.3; O, 8.1.

Chromatographic separation of a portion (2.18 g) of the original oily reaction product on neutral alumina, grade I (500 g), eluting with 4 l of solvent of composition changing by linear gradient from hexane–ether 9:1 to hexane–ether 8:2, yielded the following products: *5α-ethoxy-4-oxacholestane* (**6***a*) (945 mg), a white solid which crystallized from methanol–ethyl ether as glistening flakes, m.p. 96–97°, identical (m.p. and i.r.) with the compound described below.

1,2-Di(4-oxa-5ξ-cholestanyloxy)ethane A (**7**) (319 mg) identical with the material described above; and *1,2-di(4-oxa-5ξ-cholestanyloxy)ethane B* (**7**) (198 mg), crystallizing from methanol–ethyl ether as needles, m.p. 166–167°, δ 3.48–3.90 (m, $—OCH_2CH_2O—$ and CH_2O at C-3).

Can. J. Chem. Downloaded from www.nrcresearchpress.com by 210.87.254.6 on 09/05/12
For personal use only.

Can. J. Chem. Downloaded from www.nrcresearchpress.com by 210.87.254.6 on 09/05/12
For personal use only.

Anal. Calcd. for $C_{54}H_{94}O_4$ (mol. wt. 806): C, 80.3; H, 11.7; O, 7.9. Found: (734 (vapor phase osmometry of CCl_4 solution)): C, 80.2; H, 11.6; O, 8.1.

Hydrolysis of 1,2-Di(4-oxa-5ξ-cholestanyloxy)ethane A with Silica Gel

Silica gel (20 g) was added to a solution of 7A (1.04 g) which had been dissolved in hexane (100 ml) by warming. The mixture was left at room temperature for 3 days. The silica was removed by filtration and washed with ether (2 × 50 ml). Evaporation of the ether extracts left an oil (924 mg) which solidified on standing, and which was identified as the hydroxyketone **4** by its n.m.r. spectrum (including the changes effected by tricholoroacetyl isocyanate and chlorosulfonyl isocyanate).

5α-Ethoxy-4-oxacholestane (6a)

(a) From 5-Oxo-3,5-seco-A-norcholestan-3-ol (4)

Ethanol containing a trace of hydrogen chloride was prepared by adding 10 drops of acetyl chloride to absolute ethanol (100 ml). In this was dissolved 5-oxo-3,5-*seco*-A-norcholestan-3-ol (70 mg). The solution was left at room temperature overnight, and the ethanol was then removed by evaporation. The residue in hexane was chromatographed on alumina (grade 3) and afforded, after evaporation of the solvent, white crystals of 5α-ethoxy-4-oxacholestane (**6a**) (49 mg, 67%), m.p. 95–96° after one crystallization from ethanol; $[\alpha]_D^{25}$ + 54.6° (in EtOH); n.m.r. δ 3.53 (m, 2H, C-3H_2), 3.41 (q, 2H, —O—CH_2—CH$_3$), 0.62 (s, 3H, C-18H_3).

Anal. Calcd. for $C_{28}H_{50}O_2$ (mol. wt. 418): C, 80.4; H, 11.9; O, 7.6. Found: (426 (vapor phase osmometry in CCl_4)): C, 80.2; H, 11.9; O, 7.6.

Silica gel (10 g) was added to a solution of 5α-ethoxy-4-oxacholestane (100 mg) in hexane (100 ml) and the mixture allowed to stand at room temperature for four days. The silica gel was removed by filtration and extracted by several washings with ethyl ether. Removal of the solvent gave an oil (90 mg), identified by its n.m.r. spectrum as the hydroxyketone **4**.

(b) From 1,2-Di(4-oxa-5ξ-cholestanyloxy)ethane (7A)

Compound 7A (400 mg) was dissolved in ethanol (50 ml) containing a trace of hydrogen chloride by boiling under reflux, and the solution was left overnight at room temperature. It was then worked-up as above to give a 5α-ethoxy-4-oxacholestane (200 mg), identical (m.p., mixture m.p., and i.r.) with the compound described above.

5β-Ethoxy-4-oxacholestance (6b)

(a) From 5α-Ethoxy-4-oxacholestane (6a)

Alkaline silica gel was prepared by adding dropwise 5 ml of freshly-distilled diethylamine in benzene–hexane 1:1 (50 ml) to a stirred suspension of chromatographic silica gel (Merck) (100 g) in benzene–hexane 1:1 (200 ml). The mixture was then stirred for a further 1 h before being transferred to a chromatographic column.

Compound **6a** (590 mg) was dissolved by heating in ethanol (50 ml) containing a trace of hydrogen chloride, and the solution allowed to stand for 30 min. It was then made alkaline with freshly-distilled diethylamine (0.5 ml), and the ethanol removed by evaporation at reduced pressure. The residue in benzene–hexane 1:1 was chromatographed on alkaline silica (60 g). The column was eluted with benzene–hexane 1:1 containing a trace of diethylamine (10 drops/l), and yielded first crystalline 5α-ethoxy-4-oxacholestane (**6a**) (401 mg, 68%), m.p. 95–96°, and then impure 5β-ethoxy-4-oxacholestane (**6b**) (169 mg, 29%), an oil which after some days in the refrigerator solidified to crystals, m.p. 85–87°. These were shown by t.l.c. to be contaminated by small amounts of **6a** and were purified by recrystallization from absolute ethanol containing a trace of diethylamine, followed by a second rapid crystallization (1 h in refrigerator) from absolute ethanol: colorless needless, melting sharply at 89° (m.p. depressed by admixture with **6a**).

Anal. Calcd. for $C_{28}H_{50}O_2$: C, 80.4; H, 11.9. Found: C, 80.5; H, 12.0.

The compound in ethanol solution slowly isomerized to **6a**, as shown by t.l.c.

(b) From 1,2-Di(4-oxa-5ξ-cholestanyloxy)ethane (7A)

Compound 7A (200 mg) was dissolved in hot ethanol (30 ml) containing a trace of hydrogen chloride and the solution left overnight at room temperature. It was then worked-up by the procedure above to give **6a** (120 mg, 67%) and *b* (41 mg, 23%).

(c) From 5-Oxo-3,5-seco-A-norcholestan-3-ol (4)

The tautomeric mixture **4/5** (50 mg) in ethanol (60 ml) containing a trace of hydrogen chloride gave **6a** (35 mg, 70%) and *b* (12 mg, 25%).

5α-Methoxy-4-oxacholestane (6a; Me in place of Et)

(a) From 1,2-Di(4-oxa-5ξ-cholestanyloxy)ethane (7A)

Compound 7A (100 mg) was dissolved by refluxing in anhydrous methanol (60 ml) containing a trace of hydrogen chloride, and the solution left overnight at room temperature. It was concentrated to 5 ml at reduced pressure, and kept in the refrigerator for 48 h. A crystalline solid was removed by filtration and purified by chromatography in hexane on alumina, yielding **6a** (R=Me in place of Et) (75 mg), m.p. 79–82° after crystallization from methanol; $[\alpha]_D^{25}$ + 54.8° (in EtOH with trace of diethylamine), δ 3.23 (s, OCH_3), 3.66 (m, CH_2O at C-3), mass spectral peaks at *m/e* 404 (M^+), 372, and 357.

Anal. Calcd. for $C_{27}H_{48}O_2 \cdot \frac{1}{2}H_2O$: C, 78.4; H, 11.9. Found: C, 78.2; H, 11.9.

(b) From 5-Oxo-3,5-seco-A-norcholestan-3-ol (4)

The hydroxyketone **4** (50 mg), after being boiled for 1 h in anhydrous methanol (40 ml) containing a trace of hydrogen chloride, was worked-up as above to give **6a** (R=Me in place of Et) (30 mg).

We are grateful to Professor P. F. Morand for the hospitality of his laboratory (to M.K.), to Professor A. S. Perlin for n.m.r. measurements and their interpretation, and to the National Research Council of Canada, the Research Council of the University of Nebraska, and the National Cancer Institute (Grant CAO 5796) for financial support.

1. J. E. WHITING and J. T. EDWARD. Can. J. Chem. **49**, 3799 (1971).
2. A. KRÖNIGER and D. M. S. WHEELER. Tetrahedron, **28**, 255 (1972). T. M. BARRETT. Ph.D. Thesis. University of Nebraska, Lincoln, Nebraska, 1970.
3. C. D. HURD and W. H. SAUNDERS. J. Am. Chem. Soc. **74**, 5323 (1952). J. T. EDWARD, P. F. MORAND, and I. PUSKAS. Can. J. Chem. **39**, 2069 (1961).

4. D. J. COLLINS, J. J. HOBBS, and R. J. RAWSON. Aust. J. Chem. **22**, 627 (1969).
5. E. C. PESTERFIELD and D. M. S. WHEELER. J. Org. Chem. **30**, 1513 (1965).
6. J. T. EDWARD, D. HOLDER, W. H. LUNN, and I. PUSKAS. Can. J. Chem. **39**, 599 (1961).
7. H. C. BROWN and B. C. SUBBA RAO. J. Am. Chem. Soc. **82**, 681 (1960). H. C. BROWN and W. KORYTNYK. J. Am. Chem. Soc. **82**, 3866 (1960). H. C. BROWN and D. B. BIGLEY. J. Am. Chem. Soc. **83**, 486 (1961).
8. J. T. EDWARD and I. PUSKAS. Can. J. Chem. **90**, 376 (1962).
9. J. T. EDWARD and N. E. LAWSON. J. Org. Chem. **35**, 1426 (1970).
10. I. R. TREHAN, C. MONDER, and A. K. BOSE. Tetrahedron Lett. 67 (1968).
11. R. BRESLOW. Organic reaction mechanisms. W. A. Benjamin, Inc. New York. 1965. p. 171. E. S. GOULD. Mechanism and structure in organic chemistry. Holt-Dryden. New York. 1959. p. 542. L. P. HAMMETT. Physical organic chemistry. 2nd ed. McGraw-Hill, New York. 1970. p. 115. M. L. BENDER. Mechanisms of homogeneous catalysis from protons to proteins. Wiley-Interscience, New York. 1971. pp. 123, 127.
12. E. L. ELIEL, N. L. ALLINGER, S. J. ANGYAL, and G. A. MORRISON. Conformational analysis. Interscience, New York. 1965. p. 231.
13. N. S. BHACCA and D. H. WILLIAMS. Applications of NMR spectroscopy in organic chemistry. Holden-Day, San Francisco. 1964. pp. 16, 34.
14. H. J. GEISE, C. ALTONA, and C. ROMERS. Tetrahedron, **23**, 439 (1967).

Can. J. Chem. Downloaded from www.nrcresearchpress.com by 210.87.254.6 on 09/05/12
For personal use only.

Scytalone (3,6,8-Trihydroxytetralone), a Metabolite from a *Scytalidium* Species

J. A. FINDLAY AND D. KWAN

Department of Chemistry, University of New Brunswick, Fredericton, New Brunswick

Received November 17, 1972

A metabolite from culture filtrates of a *Scytalidium* strain is shown by spectroscopic and chemical means to have structure **1***a*. The oxygenation pattern is as anticipated from a polyketide precursor.

La structure **1***a* a été proposée pour un métabolite issu de filtrats de culture de *scytalidium*, par les méthodes spectroscopiques et chimiques. Le modèle d'oxygénation est celui attendu pour un précurseur polycétide. [Traduit par le journal]

Can. J. Chem., **51**, 1617 (1973)

Can. J. Chem. Downloaded from www.nrcresearchpress.com by 210.87.254.6 on 09/05/12
For personal use only.

In a recent paper Strunz *et al.* (1) reported the isolation of several metabolites from a species of *Scytalidium* FY strain. The structure of one of these was shown to be related to the nonadrides. We wish to report the structure of a new metabolite, scytalone, from the same source.

The high resolution mass spectrum of scytalone displays a molecular ion at *m/e* 194.0575 corresponding to $C_{10}H_{10}O_4$. The i.r. spectrum (KBr) shows a broad absorption in the hydroxyl region and a strong band at 1640 cm^{-1} indicative of an α,β-unsaturated β-hydroxy ketone system (2) while the u.v. spectrum (λ_{max} (C_2H_5OH, 95%) 222, 232, 284, 322 nm (log ε 4.18, 3.81, 4.11, 3.83) compares favorably with that of 2,4-dihydroxyacetophenone (3). The 60 MHz n.m.r. spectrum (acetone-d_6) of scytalone shows a sharp one-proton, D_2O exchangeable signal at δ 12.8 p.p.m. ascribed to an intramolecularly bonded proton of an ortho hydroxyphenone system (4). Signals at δ 6.3 (1H, dd, $J = 2$, $J = 1$ Hz) and 6.15 (1H, d, $J = 2$ Hz) p.p.m. are assigned to aromatic protons in a meta relationship (5), one of which is additionally long-range coupled. A complex multiplet at δ 4.3 (2H) p.p.m. which collapses to a simpler one-proton signal after addition of D_2O and complex multiplets δ 3.2–2.7 (4H) p.p.m. are the remaining features of the n.m.r. spectrum.

2,4-Dihydroxybenzoylpropionic acid (**2***a*) was prepared by Friedel–Crafts reaction between resorcinol and succinic anhydride. It displayed similar i.r. (1640 cm^{-1}) and u.v. (λ_{max} (C_2H_5OH, 95%) 213, 231, 276, 313 (log ε 4.18, 3.81, 4.11, 3.83) nm) characteristics to the metabolite. Scytalone and the synthetic compound **2***a* show parallel shifts of all u.v. maxima in basic media. Furthermore the n.m.r. spectrum ($CDCl_3$) of **2***a*

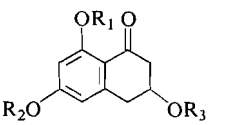

1

a $R_1R_2R_3 = H$
b $R_1R_3 = H$; $R_2 = CH_3$
c $R_1 = H$; $R_2 = CH_3$; $R_3 = Ac$

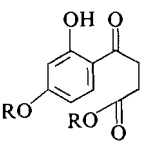

2

a $R = H$
b $R = CH_3$

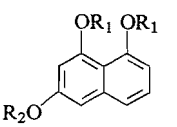

3

a $R_1 = Ac$; $R_2 = CH_3$
b $R_1R_2 = Ac$

displays a sharp singlet at δ 12.6 p.p.m. (1H) and aromatic proton signals at δ 6.45 (1H, dd, $J = 8$, $J = 3$ Hz) and 6.35 (1H, d, $J = 3$ Hz) p.p.m. in close correspondance with the features of scytalone. An additional aromatic proton signal δ 7.85 (1H, d, $J = 8$ Hz) p.p.m. in the spectrum of **2***a* confirms the 1,2,4-substitution pattern (5).

Both scytalone and **2***a* were readily converted into monomethyl ethers by treatment with ethereal diazomethane and in both cases n.m.r. data attest to the survival of the intramolecularly-bonded hydroxyl group. Accordingly structure **2***b* is assigned to the product from **2***a*.

Thus the nature of the chromophoric system in scytalone is established as a 2,4-dihydroxyphenone additionally substituted at position-6.

Treatment of scytalone monomethyl ether with acetic anhydride pyridine at 0 °C afforded an impure, labile monomethyl ethermono-

Can. J. Chem. Downloaded from www.nrcresearchpress.com by 210.87.254.6 on 09/05/12
For personal use only.

acetate whose 60 MHz n.m.r. spectrum ($CDCl_3$) shows a pentuplet at δ 5.4 (1H) p.p.m. indicative of the presence of a secondary oxygen in the acetate and hence in scytalone. Attempts to purify this acetate by preparative t.l.c. and other means led to decomposition and n.m.r. inspection of recovered material indicated diminution of the acetate methyl signal and appearance of signals in the aromatic region.

By refluxing scytalone monomethyl ether with acetic anhydride – pyridine at 76% yield conversion into a monomethoxynaphthalene diacetate was achieved. The 220 MHz n.m.r. spectrum revealed the existence of either a 1,3,8- or a 1,3,6-substitution pattern (5) in accord with formulation **3***a* for this product. That the product is 1,8-diacetoxy-3-methoxynaphthalene follows from consideration of the established oxygenation pattern of the precursor methyl scytalone and the reasonable assumption that the secondary oxygen is eliminated during the reaction. From scytalone we obtained 1,3,8-triacetoxynaphthalene (**3***b*) in 93% yield by similar acetylation procedure.

Clarification of the remaining structural features of scytalone came from 220 MHz nuclear magnetic double resonance (n.m.d.r.) experiments on methyl scytalone. Irradiation of the multiplet at δ 4.3 p.p.m. caused collapse of the AB part of an ABX pattern δ 2.60 (1H, dd, J = 17, J = 7 Hz), 3.14 (1H, dd, J = 17, J = 3 Hz) p.p.m. to a simple AB system 2.60 (1H, d, J = 17 Hz), 3.14 (1H, d, J = 17 Hz) while a more complex signal centered near δ 2.9 (2H) p.p.m. was substantially decoupled at the same time. Irradiation in the regions δ 2.6, 2.9, or 3.1 p.p.m. caused substantial decoupling in the signal at δ 4.3 p.p.m. Thus the non-D_2O exchangeable portion of the δ 4.3 p.p.m. signal is assigned to a secondary hydroxyl having two α methylene groups. Only structures **1***a*, *b*, and *c*, for scytalone, methyl scytalone, and methyl scytalone acetate respectively are in accord with these results.

Corroboration of these assignments is afforded by the high resolution mass spectra of scytalone **1***a* and scytalone methyl ether **1***b* both of which display base peaks corresponding to loss of C_2H_4O, explained by the fragmentation **4** → **5** + **6**.

It is worthy to note that the oxygenation pattern of scytalone corresponds precisely to that anticipated by cyclization of a polyketide

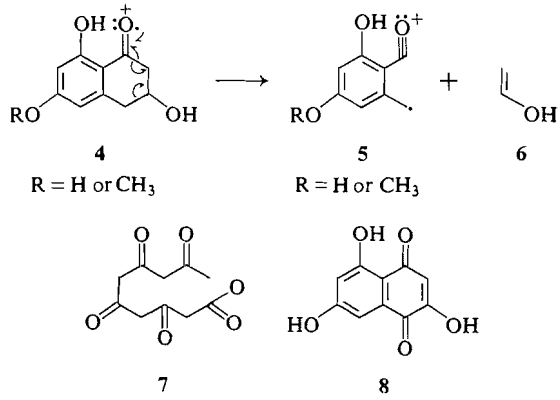

4 **5** **6** **7** **8**

system such as **7** which has been postulated (6) as a biogenetic precursor for structurally related metabolites such as flaviolin **8**.

Experimental

The i.r. spectra were recorded on a Perkin–Elmer model 237B instrument. High resolution mass spectra were obtained from the Mass Spec Lab, University of Alberta, Edmonton, Alberta. Low resolution mass spectra were obtained with an Hitachi Perkin–Elmer RMU-6D spectrometer. The u.v. spectra were determined on a Perkin–Elmer model 467 spectrophotometer. The 60 MHz n.m.r. spectra were recorded with a Varian T-60 instrument employing tetramethylsilane as internal standard. The 220 MHz spectra were obtained from a Varian HR 220 instrument at the Canadian 220 MHz NMR Centre, Ontario Research Foundation. A Kofler hot stage apparatus was employed to determine melting points which are uncorrected.

Scytalone ***1a***

Culture filtrate medium which had supported growth of *Scytalidium* sp FY strain (1) was washed with chloroform (to remove scytalidin) and subjected to continuous extraction with ether The dried ($MgSO_4$) ether extract yielded a dark brown viscous mass on evaporation. A portion (0.5 g) of this material was chromatographed on a silica gel column. Using 20% ether-in-benzene as eluant, scytalone (0.24 g) was recovered and was recrystallized from ether–benzene giving ivory crystals, homogeneous on t.l.c., m.p. 160–168°, ν_{max} (KBr) 3500 (broad), 1640, 1590 cm^{-1}; λ_{max} (95% ethanol) 222, 232, 284, 322 nm (log ε 4.18, 3.81, 4.11, 3 83); λ_{max} (95% ethanol + OH^-) 210, 253, 334 nm (log ε 4.33, 3.73, 4.5); δ 60 MHz (acetone-d_6) 2.7–3.2 (4H, m), 4.3 (2H, m), 6.15 (1H, d, J = 2 Hz), 6.3 (1H, dd, J = 2, J = 1 Hz), 12.8 (1H, s) p.p.m.; δ 60 MHz (acetone-d_6 + D_2O) 2.7–3.2 (4H, m), 4.3 (1H, m), 6.15 (1H, d, J = 2 Hz), 6.3 (1H, dd, J = 2, J = 1 Hz); *m/e* 194.0575 (M^+), $C_{10}H_{10}O_4$ requires 194.0579; 176.0472, $C_{10}H_8O_3$ requires 176.0474; 150.0312, $C_8H_6O_3$ requires 150.0317

*Scytalone Monomethyl Ether (****1b****)*

Scytalone (0.24 g) in ether was treated with excess ethereal diazomethane for 5 h with stirring at room temperature after which time t.l.c. indicated complete reaction. The solution was filtered and evaporated yielding

Can. J. Chem. Downloaded from www.nrcresearchpress.com by 210.87.254.6 on 09/05/12
For personal use only.

the product **1***b* (0.21 g, 82%) which was recrystallized from benzene yielding white crystals, homogeneous on t.l.c., m.p. 76–84°, ν_{max} ($CHCl_3$) 3500 (broad), 1626, 1580 cm^{-1}; λ_{max} (95%, ethanol) 222, 231, 237, 281, 316 nm (log ε 3.82, 3.77, 3.69, 3.84, 3.43); λ_{max} (95% ethanol + OH^-) 218, 238, 281, 347 nm (log ε 3.91, 3.93, 3.58, 3.38); δ 60 MHz ($CDCl_3$) 2.7–3.2 (4H, m), 3.8 (3H, s), 4.3 (2H, m), 6.3 (2H, bs), 12.7 (1H, s); *m/e* 208.0741 (M^+), $C_{11}H_{12}O_4$ requires 208.0736; 190 ($M^+ - H_2O$); 164.0483, $C_9H_8O_3$ requires 164.0474.

Methyl Scytalone Acetate (1c)

A mixture of methyl scytalone **1***b* (0.02 g), pyridine (0.4 ml), and acetic anhydride (0.6 ml) was stirred at 0° for 3 h and then evaporated in high vacuum at room temperature. The residual brown viscous liquid (0.024 g) showed δ 60 MHz 2.0 (3H, s), 2.8 (2H, m), 3.1 (2H, m), 3.8 (3H, s), 5.4 (1H, m), 6.35 (2H, s), 12.6 (1H, s). Attempts to purify the material for further characterization led to decomposition.

2,4-Dihydroxybenzoylpropionic Acid (2a)

A mixture of *m*-resorcinol (8.1 g) and succinic anhydride (7.5 g) in nitrobenzene (48.2 ml) was treated with aluminum chloride (18.8 g) for 48 h at room temperature. The resulting green gelatinous mass was treated with ice (75 g) and concentrated HCl (38 ml) and the mixture steam distilled for 4 h. The p*H* of the residue was adjusted to ~8 by addition of solid NaOH and steam distillation continued for 2 h. The residual yellow suspension was filtered, acidified with concentrated HCl, and cooled whence yellow crystalline **2***a* (1.72 g, 11.1%) was obtained, m.p. 196–200, ν_{max} (KBr) 3350 (broad), 1725, 1640, 1620 cm^{-1}; λ_{max} (95% ethanol) 213, 231, 276, 313 nm (log ε 4.18, 3.81, 4.11, 3.83); λ_{max} (95% ethanol + OH^-) 215, 252, 334 nm (log ε 4.1, 3.72, 4.41); δ 60 MHz (acetone-d_6) 2.7 (2H, t, J = 7 Hz), 3.3 (2H, t, J = 7 Hz), 6.35 (1H, d, J = 3 Hz), 6.45 (1H, dd, J = 8, J = 3 Hz), 7.85 (1H, d, J = 8 Hz), 12.6 (1H, s); *m/e* 210 (M^+, $C_{10}H_{10}O_5^+$), 192, 165, 147, 137, 109.

Methyl-(2-hydroxy-4-methoxybenzoyl)propionate (2b)

A solution of 2,4-dihydroxybenzoyl propionate (0.39 g) in ether (10 ml) was treated with excess ethereal diazomethane for 2 h. Evaporation afforded white crystalline **2***b* (0.442 g, 100%), m.p. 73–76°, ν_{max} (KBr) 3400 (broad), 1736, 1640, 1620 cm^{-1}; λ_{max} (95% ethanol) 217, 229, 236 (s), 275, 315 nm (log ε 4.29, 4.10, 4.04, 4.25, 4.00); λ_{max} (95% ethanol + OH^-) 218, 230, 242, 275, 350 nm (log ε 4.22, 4.23, 4.20, 3.94, 4.04); δ 60 MHz ($CDCl_3$) 2.75 (2H, t, 6 Hz), 3.3 (2H, t, J = 6 Hz), 3.7 (3H, s), 3.9 (3H, s), 6.45 (1H, d, J = 3 Hz), 6.5 (1H, dd, J = 10, J = 3 Hz), 7.7 (1H, d, J = 10 Hz), 12.5 (1H, s); *m/e* 238 (M^+, $C_{12}H_{14}O_5^+$), 207, 179, 151, 137, 108, 95.

1,8-Diacetoxy-3-methoxynaphthalene (3a)

A mixture of methyl scytalone (0.044 g), pyridine (0.8 ml), and acetic anhydride (1.2 ml) was refluxed for 2 h and then evaporated in high vacuum yielding a brown solid (0.063 g) which was chromatographed on a silica gel column. Elution with 2% ether in benzene afforded **3***a* (0.044 g, 76%) m.p. 99–101°, ν_{max} 1770, 1635, 1610 cm^{-1}; λ_{max} (ethanol) 212 (s), 231, 267, 279, 290, 319, 333 nm (log ε 4.22, 4.67, 3.52, 3.62, 3.55, 3.12, 3.45); δ 220 MHz (acetone-d_6) 2.94 (3H, s), 2.96 (3H, s), 3.94 (3H, s), 7.0 (1H, d, J = 2.5 Hz), 7.12 (1H, dd, J = 8, J = 1 Hz), 7.39 (1H, d, J = 2.5 Hz), 7.54 (1H, t, J = 8 Hz), 7.84 (1H, dd, J = 8, J = 1 Hz); *m/e* 274 (M^+, $C_{15}H_{14}O_5^+$), 232, 190.

Anal. Calcd. for $C_{15}H_{14}O_5$: C, 65.69; H, 5.11; O, 29.21. Found: C, 65.23; H, 5.28; O, 28.98.

1,3,8-Triacetoxynaphthalene (3b) from Scytalone

A mixture of scytalone (0.065 g), pyridine (0.8 ml), and acetic anhydride (1.2 ml) was refluxed for 2 h and then evaporated *in vacuo* yielding a pinkish brown crystalline solid **3***b* (0.93 g, 93%), m.p. 120–123°, ν_{max} (KBr) 1760 cm^{-1}, λ_{max} (ethanol) 210, 226, 283 (log ε 4.39, 4.81, 3.70); δ (acetone-d_6) 2.3 (3H, s), 2.4 (6H, s), 7.1 (1H, d, J = 2 Hz), 7.2 (1H, dd, J = 8, J = 2 Hz), 7.51 (1H, t, J = 8 Hz), 7.64 (1H, d, J = 2 Hz), 7.82 (1H, dd, J = 8, J = 2 Hz); *m/e* 302 (M^+, $C_{16}H_{14}O_6^+$) 284, 260, 218, 176.

The authors are indebted to G. M. Strunz, M. A. Stillwell, and M. Kakushima, Canadian Forestry Service, Fredericton, N.B. for providing material for this study.

1. G. M. Strunz, M. Kakushima, and M. A. Stillwell. J. Chem. Soc. Perkin I, 2280 (1972).
2. L. J. Bellamy. The infra-red spectra of complex molecules. Methuen and Co. Ltd., London. 1958. p. 143.
3. N. A. Valyashko and Y. S. Rozum. Zhur. Obschchei Khim. **17**, 783 (1947).
4. M. S. Bhacca, L. F. Johnson, and J. M. Shoolery. NMR spectra catalogue. Spectrum No. 259, National Press, Palo Alto, Calif., 1962.
5. M. Zanger. Org. Mag. Res. **4**, 1 (1972).
6. A. J. Birch and F. W. Donovan. Aust. J. Chem. **6**, 360 (1953); A. J. Birch and F. W. Donovan. Chem. Ind. (London) 1047 (1954).

A Determination of σ^+ Values for the Pyridine Aza Group

TREVOR JAMES BROXTON, GRAEME LYLE BUTT, LESLIE WILLIAM DEADY,[1]
SWEE HIN TOH, AND RONALD DAVID TOPSOM
Department of Organic Chemistry, La Trobe University, Bundoora, Victoria 3083, Australia

AND

ALFRED FISCHER[1] AND MICHAEL WOODFORD MORGAN
Department of Chemistry, University of Victoria, Victoria, British Columbia

Received September 5, 1972

From the solvolysis of the pyridyldimethylcarbinyl chlorides in acetone–water and in methanol, σ^+ values of 0.73, 0.57, 1.13 and 0.72, 0.45, 1.14, respectively, are derived for the 2-, 3-, and 4-aza groups.

En se basant sur les vitesses de solvolyse des chloro-2 pyridyl-2 propanes dans l'acétone–eau et le méthanol, on établit à 0.73, 0.57, 1.13 et 0.72, 0.45, 1.14 respectivement les valeurs σ^+ des groupes aza-2, -3, et -4. [Traduit par le journal]

Can. J. Chem., **51**, 1620 (1973)

Can. J. Chem. Downloaded from www.nrcresearchpress.com by 210.87.254.40 on 09/05/12
For personal use only.

Introduction

The quantitative investigation of the behavior of the pyridine aza group as an aromatic substituent is of current interest. Thus, aza σ values have been obtained for a number of side-chain reactions (1) and these studies have extended to determination of σ_R^0 (2) and σ^0 (3) values, and to the effect of solvent on the aza substituent effect (4). In such reactivity studies it is usual to include the 2-aza substituent since steric effects should be minimal in this case. Because of the similarity between many qualitative aspects of the chemistry of pyridine and nitrobenzene it has been of interest throughout to compare the quantitative effects of the aza and nitro substituents.

As an extension of this investigation to another reaction type, we report here the solvolysis of pyridyldimethylcarbinyl chlorides, and derivation of σ^+ values for the aza substituent. Taylor (5) has previously determined these values from gas phase pyrolysis of pyridylethylacetates and it was of interest to compare his values with those obtained in a reaction where the aza group would be solvated.

Results and Discussion

The kinetics of the solvolysis, in basic conditions, of the three pyridyldimethylcarbinyl chlorides and some other representative carbinyl chlorides were studied both in acetone–water and in methanol solvents. In acetone–water, measurements were made at 25.5° in various solvent compositions, and at 40° in 45% (wt.) acetone–water; reactions in methanol were carried out over the range 0–80°. Non-linear rate plots were encountered with the high temperature runs in methanol with methoxide as base. This trouble was eliminated when triethylamine was used instead and in lower temperature reactions the rates were shown to be independent of the nature of the base. In both solvent systems, the first order rate constants were independent of base concentration.

The kinetic results are listed in Tables 1 and 2. The aza σ^+ values were derived from these results by using the ρ value (−4.82) derived by Brown and co-workers (6) for reaction in methanol at 25°, or from the relative rates of the *m*-bromo and *p*-nitro substituted compounds at 25.5° in 55% acetone–water and 40° in 45% acetone–water. These values and those from the gas phase pyrolysis data of Taylor (5) together with σ values obtained from ester hydrolysis (7) are listed in Table 3.

There is excellent agreement between the σ^+ values of both the 2- and 4-aza substituents for the solvolysis studies in the two different solvent systems, but for the 3-aza substituent the difference between the σ^+ values obtained in the different solvents is greater than would be expected from the precision of the rate constants. For the 3- and 4-aza substituents the σ^+ values obtained in the solvolysis studies are markedly

[1]Enquiries may be sent to either author.

TABLE 1. Rate constants ($10^5\ k_1$(s)) for the solvolysis of some substituted phenyldimethylcarbinyl chlorides in acetone–water

	Weight (% acetone)				
Substituent	20*	35*	45*	55*	45†
3-Br	—	—	—	79.7	983
4-NO_2	—	—	—	1.24	26.7
2-Aza	—	29.0	8.37	2.27	43.9
3-Aza	—	—	—	36.7	588
4-Aza	2.85	0.45	—	0.011‡	0.82

*25.5°.
†40°.
‡Extrapolated value.

TABLE 2. Solvolysis of some substituted phenyldimethylcarbinyl chlorides in methanol

Substituent	T(°C)	Base	$10^5\ k_1$ (s^{-1})
H	10*	—	85.0
	10	MeO^-	85.7
3-Br	25*	—	8.11
	25	MeO^-	7.85
	25	NEt_3	8.12
2-Aza†	25	MeO^-	0.155
	40	"	1.30
	55	"	8.45
3-Aza‡	25	"	0.953
	40	"	8.42
	55	"	58.7
4-Aza§	25	NEt_3	0.00182‖
	55	"	0.0865
	65	"	0.264
	80	"	1.55

*Reference 6.
†E_a = 108, $\Delta H_{298}^{\ddagger}$ = 106, $T\Delta S_{298}^{\ddagger}$ = 0 (kJ/mol)
‡E_a = 110, $\Delta H_{298}^{\ddagger}$ = 108, $T\Delta S_{298}^{\ddagger}$ = 6 (kJ/mol)
§E_a = 108, $\Delta H_{298}^{\ddagger}$ = 106, $T\Delta S_{298}^{\ddagger}$ = −11 (kJ/mol)
‖By extrapolation of Arrhenius plot.

greater than Taylor's gas-phase values; a difference of 0.2 in σ^+ corresponds to a rate ratio, for solvolysis, of greater than 6. A plausible explanation of this difference in σ^+ values is solvation of the nitrogen in the hydrogen-bonding solvents used. Such solvation would enhance the electron-withdrawing character of the aza substituent, relative to that exhibited in the gas phase. It is surprising, however, that the 2-aza values do not show the same trend since the evidence suggests (4) that this ortho substituent effect is the most sensitive to solvent change.[2]

Like the nitro substituent the aza substituent exhibits electron-withdrawing polar and resonance effects. For such substituents σ^+ and σ values are normally not significantly different and Table 3 shows that this is indeed so for the 2-aza substituent. However for the 4-aza substituent, σ^+ is significantly greater than σ determined from ester hydrolysis. The aza substituent cannot be said to be well-behaved, a conclusion which reinforces the observation of Jaffé and Jones (1) that "the picture (for the application of the Hammett equation to pyridine reactivities) is quite discouraging." The variability of the substituent constants for the aza group is attributable, at least in part, to variation in the extent of its solvation in different reactions.

The enthalpies and entropies of activation point to the importance of solvation in the solvolysis reaction. While variation in ester hydrolysis rates among the pyridyl compounds is primarily enthalpy controlled (9), the thermodynamic parameters in Table 2 indicate that in the solvolysis reaction entropy differences are responsible for the rate differences. Thus the least stable transition state (that for the 4-pyridyl compound) is most heavily solvated because this reduces the electron demand on the pyridyl system. The greater solvation of the transition state for solvolysis of the 4-pyridyl compound is also indicated by the slopes of plots of $-\log k$ for solvolysis in acetone–water at 25.5° against the reciprocal of the dielectric constant of the solvent: 228 for 2-, 158 for 3- and 333 for 4-pyridyldimethylcarbinyl chlorides (reciprocal Debye units). The transition state for solvolysis of the 4-pyridyl compound is evidently the most sensitive to solvent change and that for the 3-pyridyl compound the least sensitive. It is consistent with the expected greater solvation of the pyridyl compounds that all of the above slopes are greater than those calculated from Okamoto and Brown's (10) data for solvolysis of

[2]From the rate of deuteration of 4-aminopyridazine, Katritzky and Pojarlieff (8) have estimated for 4-aza σ^+ = 0.67. This cannot be considered a reliable value.

Can. J. Chem. Downloaded from www.nrcresearchpress.com by 210.87.254.40 on 09/05/12
For personal use only.

TABLE 3. σ-Values for aza substituents

	Reaction conditions	Substituent position 2	3	4	Reference
σ^+	MeOH, 25°	0.73	0.57	1.13	*
σ^+	55% acetone, 25.5°	0.72	0.47	1.2	*
σ^+	45% acetone, 40°	0.72	0.45	1.14	*
σ^+	Pyrolysis	0.78	0.30	0.87	5
σ	Ester hydrolysis	0.75	0.65	0.96	7

*This work.

3-iodo, 3-fluoro, and 4-fluorophenyldimethylcarbinyl chlorides: 134, 143, and 132, respectively.

Experimental

N.m.r. spectra were determined on Varian HA-60-IL and Perkin–Elmer R12A spectrometers with tetramethylsilane as internal standard. Coupling constants and chemical shifts were refined using the computer program UEAITR (11). Mass spectra were determined on a Perkin–Elmer Hitachi RMU-7 spectrometer. Microanalyses were by Microanalysis Laboratories Limited, Toronto 5, Ontario. The p*H*-stat consisted of a Radiometer pH Meter 26, Titrator 11, and Autoburette ABU 11. Melting points are uncorrected.

Pyridyldimethylcarbinyl Chlorides

The three pyridyldimethylcarbinols were prepared by established methods (12).

A solution of thionyl chloride (3 ml) in methylene chloride (30 ml) was added dropwise to a solution of the appropriate pyridyldimethyl carbinol (5 g) in methylene chloride (50 ml) at ambient temperature. The mixture was stirred for 1 h, the solvent and excess thionyl chloride were evaporated under reduced pressure at 40°, and the residue taken up in ethanol (100 ml). Excess anhydrous potassium bicarbonate was added, the mixture filtered, and the solvent evaporated at 40°. The residue was dissolved in methylene chloride (100 ml), the solution dried over magnesium sulfate and the solvent evaporated after filtration. The crude product (4–4.6 g) was a mixture of the desired chloride (26–53%) and the isopropenylpyridine. The olefin and chloride were separated by chromatography on silica at −20° with elution by pentane and ether–pentane mixtures.

2-Pyridyldimethylcarbinyl chloride (1.4 g, 24%) was eluted with 1% ether–pentane; n.m.r. (CCl_4) τ 1.54 (m, 1, 6-*H*), 2.24 (m, 1, 3-*H*), 2.39 (m, 1, 4-*H*), 2.91 (m, 1, 5-*H*), 8.07 p.p.m. (s, 6, CH_3), J_{34} 7.86, J_{35} 1.08, J_{36} 0.89, J_{45} 7.30, J_{46} 1.80, J_{56} 4.66 Hz; mass spectrum (70 eV) *m/e* (relative intensity) 140 (1.4, M − CH_3), 120 (100, M − Cl), 104 (11), 92 (21), 79 (11), 78 (15), 77 (5). 2-Pyridyldimethylcarbinyl chloride hydrochloride had m.p. 75–76°.

Anal. Calcd. for $C_8H_{11}NCl_2$: C, 50.02; H, 5.77; N, 7.29. Found: C, 50.05; H, 6.03; N, 7.13.

3-Pyridyldimethylcarbinyl chloride (2.2 g, 39%) was eluted with 10% ether–pentane; n.m.r. (CCl_4) τ 1.26 (m, 1, 2-*H*), 1.54 (m, 1, 6-*H*), 2.13 (m, 1, 4-*H*), 2.76 (m, 1, 5-*H*), 8.03 p.p.m. (s, 6, CH_3), J_{24} 2.41, J_{25} 0.81, J_{26} 0.3, J_{45} 7.88, J_{46} 1.50, J_{56} 4.65 Hz; mass spectrum (70 eV) *m/e* (relative intensity) 155 (12, M_r ($C_8H_{10}NCl$) = 155), 140 (4.5), 120 (100), 104 (16), 92 (47), 78 (13), 77 (11). 3-Pyridyldimethylcarbinyl chloride hydrochloride had m.p. 126–127°.

Anal. Calcd. for $C_8H_{11}NCl_2$: C, 50.02; H, 5.77; N, 7.29. Found: C, 49.92; H, 5.99; N, 7.38.

4-Pyridyldimethylcarbinyl chloride (1.2 g, 21%) was eluted with 10% ether–pentane; n.m.r. (CCl_4) τ 1.49 (m, 2, 2-*H* and 6-*H*), 2.61 (m, 2, 3-*H* and 5-*H*), 8.10 p.p.m. (s, 6, CH_3), J_{23} and J_{56} 5.2, J_{25} and J_{36} 0.6, J_{26} 0.3, J_{35} 2.0 Hz; mass spectrum (70 eV) *m/e* (relative intensity) 155 (26, M_r ($C_8H_{10}NCl$) = 155), 140 (7), 120 (100), 104 (8), 92 (35), 78 (8), 77 (8). 4-Pyridyldimethylcarbinyl chloride hydrochloride had m.p. 160–161°.

Anal. Calcd. for $C_8H_{11}NCl_2$: C, 50.02; H, 5.77; N, 7.29. Found: C, 50.16; H, 5.91; N, 7.35.

3-Bromophenyldimethylcarbinyl chloride (13) and 4-nitrophenyldimethylcarbinyl chloride (10) were prepared from the corresponding carbinol and styrene, respectively.

Kinetics Studies

Acetone–water

Reactions were followed using a p*H*-stat to maintain the p*H* at 8 as the reaction, which liberated hydrogen chloride, proceeded. The pyridyldimethylcarbinyl chloride (0.015 ml) was added to the acetone–water solvent (100 ml) in a jacketed cell containing a glass and calomel combination electrode and the solution titrated to p*H* 8 with sodium hydroxide solution (0.05 *M*). Water from a thermostatted water bath was circulated through the cell jacket. Carbon dioxide was excluded from the reaction vessel by venting through a solution of concentrated sodium hydroxide. At suitable time intervals the volume of sodium hydroxide which had been added by the autoburette was recorded. The product was shown in each case to be the corresponding pyridyldimethylcarbinol by n.m.r.; no olefin was formed.

Methanol

The carbinylchloride (*ca.* 0.5 ml) was added to basic methanol (100 ml, 0.05 *M* in NaOH or NEt_3) at the appropriate temperature, and under air-free conditions. At appropriate times, 5 ml aliquots were quenched in 50 ml acetone at 0° and titrated immediately with 0.025 *M* hydrochloric acid using methyl red – thymol blue indicator. For the higher temperature reactions the initial mixing was carried out at 0° and 5 ml samples were sealed in tubes before initiating reaction.

First-order rate-constants were evaluated by a least squares fit of the exponential form of the first order rate equation to the titer values. Each data point was given

Can. J. Chem. Downloaded from www.nrcresearchpress.com by 210.87.254.40 on 09/05/12
For personal use only.

unit weighting. Mean rate constants (2–4 runs) are estimated to be precise to ±5%. No variation of rate constant was found in the example of 4-pyridyldimethylcarbinyl chloride, over the p*H* range 6.3–10 in 20% acetone at 40° or with 0.3–0.5 *M* NEt_3 in methanol at 65°.

The precision of 5% in the rate constants results in a precision of better than ±0.02 in the σ^+ values, even in the least favorable cases such as when the latter were obtained using the rates of the *m*-bromo and *p*-nitrophenyldimethylcarbinyl chlorides to determine (in effect) the ρ value. This favorable result is a consequence of the large magnitude of ρ. However, for the rate constants determined at 25.5° the value for 4-pyridyldimethylcarbinyl chloride in 55% acetone–water was obtained by extrapolation from the measured values in 20 and 35% acetone–water assuming [3] a linear relationship between log *k* and D^{-1}. The extrapolation reduces the precision by a factor of five, *i.e.*, the derived rate constant is precise to ±25% and the derived σ^+ value to ±0.1.

[3]Okamoto and Brown (10) showed that for the solvolysis of three halophenyldimethylcarbinyl chlorides in acetone–water log *k* is a linear function of $(D - 1)/(2D + 1)$. However, for the range of dielectric constants of acetone–water mixtures the latter function is linear in D^{-1}, within a precision better than that of the rate constants. Within this same precision *D* is linear in wt. % of the acetone (14). We correlated *D* with wt. % acetone (*w*) over the range 20–70% and found $D = 79.74 - 0.63\ w$ and then correlated log *k* with $(79.74 - 0.63\ w)^{-1}$ to extrapolate the rate constant.

1. H. H. JAFFÉ and H. L. JONES. Adv. Heterocycl. Chem. **3**, 209 (1964); J. H. BLANCH. J. Chem. Soc. B, 937 (1966).
2. A. R. KATRITZKY, C. R. PALMER, T. T. TIDWELL, and R. D. TOPSOM. J. Am. Chem. Soc. **91**, 636 (1969).
3. L. W. DEADY and R. A. SHANKS. Aust. J. Chem. **25**, 431 (1972).
4. L. W. DEADY and R. A. SHANKS. Aust. J. Chem. **25**, 2363 (1972).
5. R. TAYLOR. J. Chem. Soc. 2382 (1971).
6. Y. OKAMOTO, T. INUKAI, and H. C. BROWN. J. Am. Chem. Soc. **80**, 4972 (1958).
7. A. D. CAMPBELL, S. Y. CHOOI, L. W. DEADY, and R. A. SHANKS. Aust. J. Chem. **23**, 203 (1970).
8. A. R. KATRITZKY and I. POJARLIEFF. J. Chem. Soc. B, 873 (1968).
9. R. A. SHANKS. Ph.D. Thesis. La Trobe University, Bundoora, Australia. 1972.
10. Y. OKAMOTO and H. C. BROWN. J. Am. Chem. Soc. **79**, 1909 (1957).
11. R. B. JOHANNESEN, J. A. FERRETTI, and R. K. HARRIS. J. Mag. Res. **3**, 84 (1970).
12. G. B. BACHMAN and D. D. MICUCCI. J. Am. Chem. Soc. **70**, 2381 (1948); G. R. CLEMO and E. HOGGARTH. J. Chem. Soc. 41 (1941).
13. H. C. BROWN, Y. OKAMOTO, and G. HAM. J. Am. Chem. Soc. **79**, 1906 (1957).
14. G. ÄKERLÖF. J. Am. Chem. Soc. **54**, 4125 (1932).

Can. J. Chem. Downloaded from www.nrcresearchpress.com by 210.87.254.40 on 09/05/12
For personal use only.

Flash Photolysis Studies of Solute Triplets: an Anomalous Heavy Atom Effect of Xenon[1,2]

DAVID ALAN HEAD,[3] AJIT SINGH,[4] MARGARET GRACE COOK, AND MICHAEL JOHN QUINN

Research Chemistry Branch, Whiteshell Nuclear Research Establishment, Atomic Energy of Canada Limited, Pinawa, Manitoba, R0E 1L0

Received November 15, 1972

Flash photolysis studies show that in solutions of naphthalene in methylcyclohexane the apparent yield of the naphthalene triplet is enhanced ~6% by added krypton and ~50% by added xenon. The effect of xenon on the decay rate of the naphthalene triplet is anomalous; the decay rate decreases instead of increasing. This is attributed to complex formation between singlet excited naphthalene and xenon. We have also investigated the heavy atom effect in solutions of naphthalene in other solvents and in solutions of other solutes. It is anomalous in some of these solutions but to a lesser extent.

Les études par photolyse flash montrent que pour les solutions de naphtalène dans le méthylcyclohexane, le rendement apparent en naphtalène triplet est augmenté de ~6% par addition de krypton et de ~50% par addition de xenon. L'effet du xénon sur la vitesse d'extinction du naphtalène triplet est anormal, celle-ci décroit au lieu de croître. Ce phénomène a été attribué à la formation d'un complexe entre le naphtalène singulet excité et le xenon. L'effet d'un atome lourd dans des solutions de naphtalène avec d'autres solvants et en solution avec d'autres solutés a été également étudié. L'anomalie a été également constatée avec certaines de ces solutions mais à un degré moindre. [Traduit par le journal]

Can. J. Chem., 51, 1624 (1973)

Introduction

Enhancement of forbidden singlet to triplet electronic transitions by the presence of atoms of high atomic number, called the heavy atom effect (h.a.e.) was elegantly demonstrated by Kasha (1). Mixing of the two colorless liquids, ethyl iodide and α-chloronaphthalene, produced a yellow color although no chemical reaction occurred. The observation of an intramolecular h.a.e. in several systems (2–4) prompted Kasha (1) to attribute this yellow color to enhanced ground state singlet to excited triplet electronic transition of α-chloronaphthalene by spin–orbit coupling induced by the external heavy atom (iodine of ethyl iodide). Since then both the theoretical and the experimental aspects of the h.a.e. have been widely studied (5–16).

The h.a.e. results in (10, 13): (*i*) enhanced singlet to triplet absorption, ($S_0 \rightarrow T_1$); (*ii*) enhanced intersystem crossing ($S_1 \rightarrow T_1$); and (*iii*) increased triplet decay rate ($T_1 \rightarrow S_0$). Halogenated solvents have often been used in h.a.e. studies (1, 4, 13). However, halogenated compounds are susceptible to photochemical decomposition (17), particularly those containing bromine or iodine. The overlap of their absorption spectra (18) with that of many of the solutes of interest (aromatic compounds, ketones, etc.) also restricts their usefulness. On the other hand, xenon causes a measurable h.a.e. and although it does undergo photochemical reactions (19–22), its lowest energy level is at 1.332 aJ (8.315 eV, 149 nm), which means that for all practical purposes xenon should be inert in organic solution photochemistry. Hence, xenon has found increasing use in h.a.e. studies (23–27), since it would seem to be an ideal heavy atom (28).

According to one report (12) the magnitude of the heavy atom effect of krypton was about half that of xenon. This investigation was therefore originally undertaken to evaluate the usefulness of krypton as a heavy atom in flash photolysis studies, and to compare it to xenon. At that time krypton was significantly cheaper than xenon (29). However, contrary to expectations, preliminary experiments showed that xenon decreased the decay rate of the naphthalene triplet. The scope of the investigation was then enlarged in an attempt to explain this anomaly.

[1]AECL No. 4419.

[2]Presented, in part, at the Chemical Institute of Canada Pulse Radiolysis Symposium at Pinawa, Manitoba, October, 1971.

[3]National Research Council Postdoctoral Fellow, 1969–1971.

[4]To whom all correspondence should be addressed.

Can. J. Chem. Downloaded from www.nrcresearchpress.com by 210.87.254.5 on 09/05/12
For personal use only.

Can. J. Chem. Downloaded from www.nrcresearchpress.com by 210.87.254.5 on 09/05/12
For personal use only.

Our detailed results of the flash photolysis of naphthalene solutions, along with the results of brief investigations of other systems, are reported here. Brief comments are also made on possible h.a.e. in radiolysis and photosensitization studies where xenon or other heavy atoms are present in the system.

Experimental

Chemicals

The following chemicals were used without further purification: camphorquinone (Eastman; white label); anthracene, biphenyl, 9,10-dimethylanthracene, naphthalene, and phenanthrene (James Hinton; zone refined); acetonitrile, benzene, 2-propanol, and methylcyclohexane (Matheson, Coleman, and Bell; Spectroquality); Freon E_4 fluorinated ether, $C_{14}F_{29}HO_4$ (DuPont); and argon and krypton (Matheson, research grade).

Xenon (Matheson, research grade) was stored on a vacuum line in a Pyrex vessel; it was degassed by the freeze–pump–thaw method (at 77 K) before use. The only detectable impurity found by the mass spectroscopic analysis of samples of this xenon gas was air; the gas was 99.85 ± 0.15% Xe, and O_2 was 0.007 ± 0.004 mol%. Water was triply distilled before use (30).

Apparatus and Techniques

The apparatus and techniques have been described previously (31). Additional details and relevant modifications are now reported. The introduction of a Tobe Deutschmann trigger switch (SBG-5) to discharge the capacitors resulted in a light flash width at half-height of 6, 9, and 12 μs with 4.5, 8, and 15 μF capacitors, respectively. The light flash widths at the 90% decay level are about twice these values. Three different tubing materials were used as filters around the Vycor flash lamps: Plexiglass (~380 nm), cellulose acetate butyrate (~310 nm) and Pyrex (~280 nm); the figures in parentheses indicate their low wavelength cut-offs. The photomultipliers used were the Hamamatsu R 166 (260–320 nm), the RCA 7200 and 1P 28 (310–650 nm), and the RCA 7102 and Philips 150 CVP (600–1100 nm).

Solutions to be flash photolyzed were degassed under vacuum in a mercury free system (31). Pressures of added gases (13.3 mPa to 133 kPa [10^{-4} to 1000 Torr]) were measured with an NRC Alphatron gauge mounted on the vacuum line.

Two different samples of xenon, obtained at different times, were used with the same results. Most of the solutions were flash photolyzed by more than one of the experimenters with similar results. After each flash the solutions were shaken and allowed to stand for a short time (~5 min) before being flash photolyzed again. All solutions were flash photolyzed at room temperature (22 °C).

Results

Effect of the Noble Gases

The h.a.e. of argon, krypton, and xenon on the transient absorption, observed on flash photolysis of 10^{-3} mol l^{-1} solutions of naphthalene in methylcyclohexane, was examined. The enhancement of the transient absorption by these gases was: (*i*) $\leq 10^{-2}$ mol l^{-1} Ar: <2%; (*ii*) ~5×10^{-2} mol l^{-1} Kr: ~6%; (*iii*) ~5×10^{-2} mol l^{-1} Xe: ~50%. The only transient observed by absorption spectroscopy in the absence of these gases was the naphthalene triplet. The concentrations of added noble gases were based upon data in refs. 19 and 32. The decay rate of the transient absorption was found to be:

(*i*) unchanged by Ar, (*ii*) slightly decreased (~6%) by Kr, and (*iii*) markedly decreased (≫6%, see later in Table 1 and Fig. 2) by Xe. Since the h.a.e. of both argon and krypton was much smaller than that of xenon, only xenon was used in further work.

Effect of Xenon on Various Solutions

In degassed solutions of the various solutes (Table 1), the solute triplets were the only transients produced, as observed by absorption spectroscopy. The triplet spectra of these solutes are known (31, 33, 34). The observed h.a.e. of xenon on the transient formation in solutions of these solutes is summarized in Table 1. In most of the cases, the results were as one might have predicted on the basis of the intersystem crossing efficiencies, *i.e.* the higher the intersystem crossing efficiency the lower the h.a.e. However, anomalous behavior was observed in a number of instances. In most of the naphthalene solutions, the transient decay rates in the presence of xenon were lower than those in the degassed solutions. The same effect was observed in solutions of phenanthrene in methylcyclohexane. The transient decay rates in biphenyl solutions seemed unaffected by xenon as were those in solutions of phenanthrene in 2-propanol.

In most of the cases, the decay of the triplets was found to follow first order kinetics over the first three half-lives. The decays of the naphthalene triplet in 2-propanol, acetonitrile, the fluoroether, and water, and of the biphenyl triplet in methylcyclohexane showed some deviation from first order kinetics. However, since enhanced second order effects, *i.e.* triplet–triplet annihilation, would enhance decay rates rather than decrease them, and so tend to mask the anomalous behavior, these deviations from first order kinetics do not affect the conclusions being drawn in this paper. Data from a typical experiment, plotted in both a first order and a second order manner, are given in Fig. 1. The

Can. J. Chem. Downloaded from www.nrcresearchpress.com by 210.87.254.5 on 09/05/12
For personal use only.

TABLE 1. Effect of xenon on flash photolysis of various solutions

Solute	Solvent[a]	Relative yield[b]	Relative half-life[b,c]	E^d Triplet kJ	E^d Triplet kcal/mol	E^d Singlet kJ	E^d Singlet kcal/mol	ϕ_{ISC}[d]	Xenon pressure[e] kPa	Xenon pressure[e] Torr
Naphthalene (1×10^{-3} mol l^{-1})	Methylcyclohexane (~2)	1.5	1.8 (21)	255	60.9	379	90.4	~0.8	54	405
	2-Propanol (20)	1.4	1.1 (58)						160	1200
	Acetonitrile (37)	1.2	0.8 (38)						180	1350
	E-4 fluoroether (2.5)	1.2	1.2 (400)[f]						67	500
	Water (78)	1.2	1.1 (80)						160	1200
Phenanthrene (1.4×10^{-3} mol l^{-1})	Methylcyclohexane	1.2_5	1.2 (53)	260	62.2	344	82.1	~0.8	62	463
	2-Propanol	1.1	1 (76)						160	1200
Phenanthrene + Naphthalene (1.4×10^{-3} mol l^{-1})(1×10^{-4} mol l^{-1})	Methylcyclohexane	1.2	0.9_5[g]						84	626
Anthracene (5×10^{-5} mol l^{-1})	Methylcyclohexane	1.4	0.9_5 (400)[f]	178	42.5	317	75.8	~0.7	63	475
	E-4 fluoroether	1.2	0.8 (840)[f]						64	480
9,10-Dimethylanthracene (3×10^{-4} mol l^{-1})	Methylcyclohexane	1.3	0.9_5 (370)[f]	176	42.0	297	70.9	~0.1	96	720
Camphorquinone (1.2×10^{-2} mol l^{-1})	Benzene	1	0.9_7 (38)	209	50	242	58	~1	67	500
Acetophenone (1×10^{-3} mol l^{-1})	Benzene	1	0.9_5 (<10)[h]	309	73.8	329	78.6	1	67	500
Biphenyl (1.5×10^{-2} mol l^{-1})	Methylcyclohexane	1.1	1 (41)	277	66.2	415	99.0	~0.8	107	800
	2-Propanol	1.3	1 (86)						187	1400

[a]The dielectric constants of the solvents (55–57) are given in parentheses after each solvent.
[b]"Relative" means (the value with Xe/the value without Xe).
[c]Values in parentheses are the initial half-lives (μs) of the solute triplets in degassed solutions.
[d]Data from references 31, 40, 58–59.
[e]53 kPa (400 Torr) pressure in methylcyclohexane solutions = 4×10^{-2} mol^{-1}.
[f]These solutions were investigated at our old flash photolysis apparatus (30) using 13.5 μF capacitors. The results obtained were similar at the old and the modified apparatus.
[g]The effect of xenon on the transient decay rate was the same in 10^{-4} and 10^{-3} solutions of naphthalene.
[h]Exact value not available now.

Can. J. Chem. Downloaded from www.nrcresearchpress.com by 210.87.254.5 on 09/05/12
For personal use only.

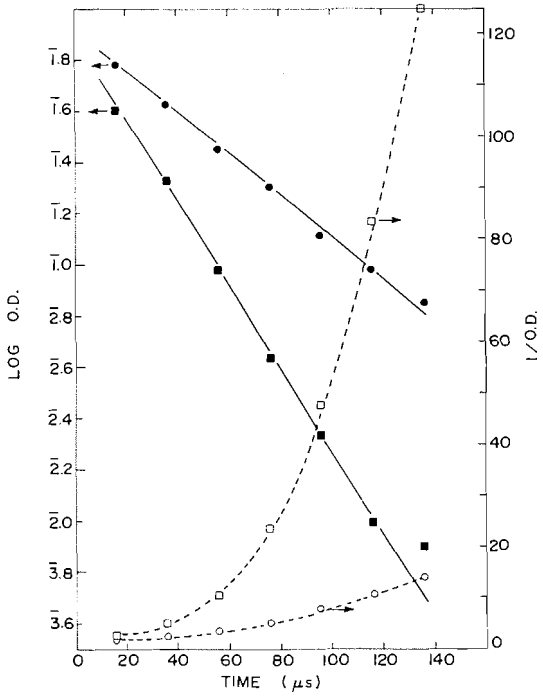

FIG. 1. Decay of transient absorption in a solution of 10^{-3} mol l^{-1} naphthalene in methylcyclohexane (412 nm). Zero time is the start of the flash: □, no xenon present; ○, 0.13 mol l^{-1} xenon.

data show the transient decay to be first order in the presence and in the absence of xenon, in methylcyclohexane solutions.

Since the magnitude of the h.a.e. of xenon was largest and usually anomalous for the naphthalene solutions, these solutions were more thoroughly investigated.

Naphthalene Solutions

(a) Methylcyclohexane Solutions

The effect of xenon concentration on the transient yield and its half-life for 10^{-3} mol l^{-1} solutions of naphthalene in methylcyclohexane is shown in Fig. 2. The data in Fig. 2 represent averages of from four to six determinations, and an estimate of the error in each point is given. Above ~0.04 mol l^{-1} the h.a.e. seems to be independent of the xenon concentration.

The relative transient yields and half-lives were the same whether a 4.5 or a 15 μF capacitor was used. Thus two photon or other bimolecular effects do not contribute to the observed slower transient decay rate in the naphthalene solutions. Changing the analyzing light level by a factor of ~20, by the insertion of neutral density filters in the path of the analyzing beam of light, had no effect on the transient yields or half-lives. Hence the observed effects were not due to photolysis by the analyzing beam of light.

All the above-mentioned results relate to measurements made at the wavelengths of the absorption maxima of the naphthalene triplet. The entire spectral region from 300–1000 nm was also investigated. The observed spectra were in good agreement with the known naphthalene triplet spectrum (33). The shape of the spectral envelope was independent of the presence of xenon through-out this spectral region, with the exception of a very small additional absorption at 380 nm.

To assess the possible role of the naphthalene excimer formation in the h.a.e. of xenon, the relative yield and half-life of the naphthalene triplet in 0.1 mol l^{-1} and 0.4 mol l^{-1} naphthalene solutions were also investigated. In these

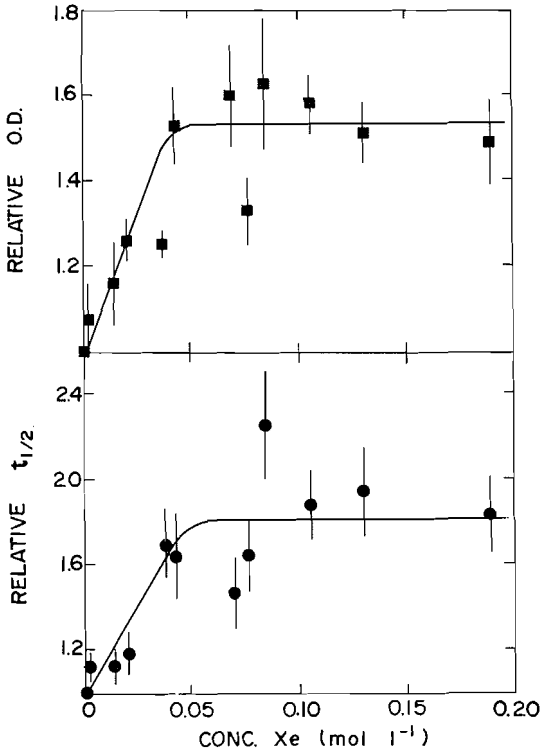

FIG. 2. Effect of xenon on transient yield and half-life in a solution of 10^{-3} mol l^{-1} naphthalene in methylcyclohexane (412 nm). "Relative" indicates the value in the presence of xenon divided by the value in the absence of xenon. Measured at 15 μs after the start of the flash.

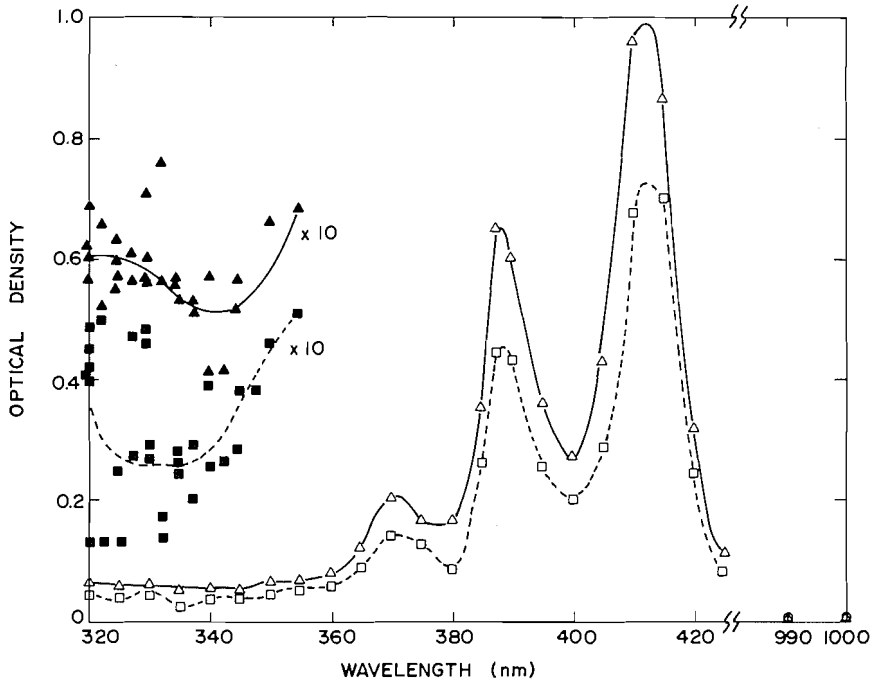

FIG. 3. The transient absorption spectra of a solution of 10^{-3} mol l^{-1} naphthalene in 2-propanol. Measured at 30 μs after the start of the flash: □, no xenon present; △, 160 kPa (1200 Torr) xenon added.

solutions the addition of 0.13 mol l^{-1} xenon enhanced the transient yield by ~20% and increased the half-life by ~15%. Thus, the h.a.e. of xenon was lower at higher naphthalene concentrations.

To determine whether the observed h.a.e. in the naphthalene solutions was due mainly to the interaction of xenon with (*i*) the naphthalene excited singlet, or (*ii*) the naphthalene excited triplet, flash photolysis of solutions containing both phenanthrene and naphthalene was studied, using 310 nm cut-off filters so that phenanthrene would be preferentially excited. The energy level of the lowest excited singlet of phenanthrene is lower than that of naphthalene whereas its triplet energy is greater (Table 1). Therefore only triplet energy transfer from phenanthrene to naphthalene would be expected. This expectation was experimentally substantiated, and it was found that in the presence of xenon the decay rate of the transient so produced, with absorption spectrum indistinguishable from that of the naphthalene triplet, was slightly faster as compared to its decay rate in the absence of xenon (Table 1). This result is in sharp contrast to that obtained by direct flash photolysis of solutions of naphthalene.

Flash photolysis of a solution of xenon in methylcyclohexane and 2-propanol showed no transient absorption.

(b) Other Solutions

In an effort to determine whether ionic transients of naphthalene were involved in the observed h.a.e. of xenon, solutions of naphthalene in solvents with a variety of dielectric constants were flash photolyzed (Table 1). The h.a.e. of xenon was not so marked in the polar solvents. Use of the fluoroether as a solvent (with dielectric constant and viscosity similar to those of methylcyclohexane) also reduced the magnitude of the h.a.e. of xenon.

Transient spectra were measured in solutions of naphthalene in 2-propanol (Fig. 3), acetonitrile (Fig. 4), and water. In general the spectral envelope when xenon was present was indistinguishable from that in the absence of xenon at wavelengths >350 nm. An additional absorption was seen in the 320–340 nm region in the solutions in 2-propanol. The reproducibility of the data was not good in this region due to problems with the equipment. However, each run showed that the absorption in both the presence and the absence of xenon was different in this region. In

Can. J. Chem. Downloaded from www.nrcresearchpress.com by 210.87.254.5 on 09/05/12
For personal use only.

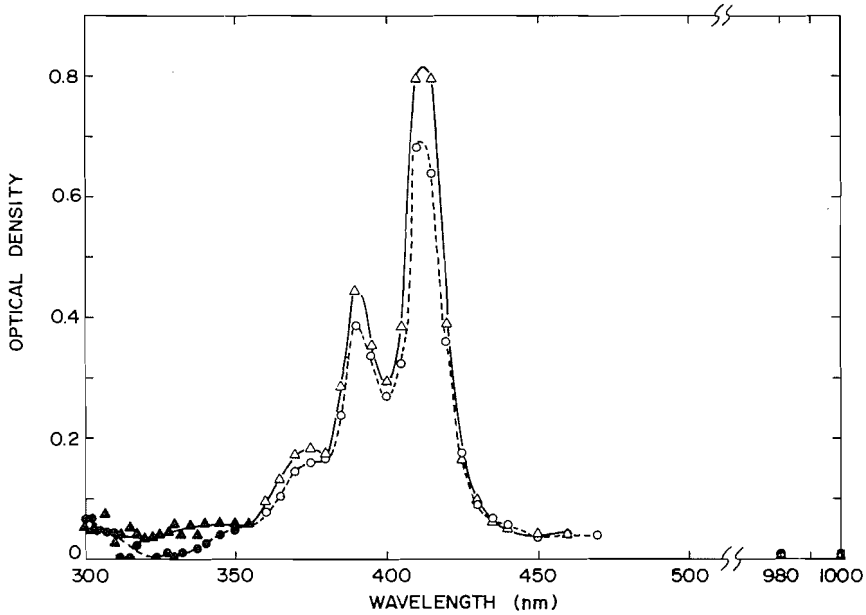

FIG. 4. The transient absorption spectra of a solution of 10^{-3} mol l^{-1} naphthalene in acetonitrile. Measured at 30 μs after the start of the flash (○, △) and 50 μs after the start of the flash (●, ▲): ○, ●, no xenon present; △, ▲, 180 kPa (1350 Torr) xenon added.

acetonitrile solutions, an additional absorption centered at ~325 nm was seen. Within the accuracy of the measurements, no additional absorption was seen in the water solutions. However, no absorption measurements below 370 nm could be made at short times after the flash due to an intense emission. At 80 μs after the start of the flash, no additional absorption was seen in the 300–370 nm region.

To investigate the possibility of the participation of free radicals in the observed h.a.e. of xenon, ethylene was added to 2-propanol solutions of naphthalene in 2-propanol since it is a free radical scavenger (35). Addition of ethylene to a free radical leads to another free radical. Therefore, addition of ethylene would affect the observed results only if the combined effect, due to possible changes in lifetimes and reaction rates, of the new free radicals, and their spectra were different than those of the original ones. Added ethylene (2×10^{-3} mol l^{-1}) had no effect upon the transient life-time or yield in solutions with and without xenon present.

Emission due to fluorescence of naphthalene was found to decrease on the addition of xenon, as expected (5–8, 24).

The effect of varying xenon concentration on the enhancement of the 9,10-dimethylanthracene triplet yield, in solution in methylcyclohexane, was also briefly investigated. The triplet yield was found to increase with the concentration of xenon (≤ 0.13 mol l^{-1}) without reaching a plateau, in contrast to that in the case of naphthalene.

Discussion

Naphthalene Solutions

(a) Heavy Atom Effect on Transient Decay Rate

The observed decrease in the transient decay rate, in the presence of xenon, was totally unexpected. Solute triplet decay rates have not been reported in most of the earlier flash photolysis studies using xenon for h.a.e. (10, 16, 23, 24, 28) although the possibility of increased triplet decay rate as a consequence of h.a.e. has been recognized (10, 11, 28). Indeed, xenon has been found to act as a solute triplet quencher in solutions of benzene and naphthalene at low temperatures (5–8, 11). The decrease in the decay rate of the transient in our studies suggests that either (*i*) a quencher is present in the naphthalene solutions which is rendered ineffective by xenon, or, (*ii*) another transient is formed in solutions containing xenon.

The possibility that the observed decreased

Can. J. Chem. Downloaded from www.nrcresearchpress.com by 210.87.254.5 on 09/05/12
For personal use only.

Can. J. Chem. Downloaded from www.nrcresearchpress.com by 210.87.254.5 on 09/05/12
For personal use only.

decay rate could be an artifact due to continuous formation of the naphthalene triplet by light absorption from the analyzing beam of light (reaction 1; the superscript prefixes 1 and 3 in this and the subsequent reactions denote the lowest excited singlet and triplet states, respectively) may be discounted, since changes in the

[1] $$N + Xe + h\nu \rightarrow {}^3N + Xe$$

intensity of the analyzing light beam, by insertion of neutral density filters, did not affect the triplet decay rate.

It is possible that the naphthalene solutions contained traces of oxygen or some organic impurities which would quench the naphthalene triplet. Since xenon does not react photochemically with oxygen or with organic compounds at the energies available in our experiments ($\lambda > 280$ nm), (19–22, 36), the removal of these impurities by xenon is most unlikely. Therefore, the change in the transient decay rate does not seem to be related to the presence of impurities.

Free radicals are known to quench triplet excited states (37). If free radicals were to be formed from the naphthalene excited singlet then, on the addition of xenon the yield of the free

[2] $$N + h\nu \rightarrow {}^1N$$

[3] $${}^1N \rightarrow \text{Free radicals}$$

radicals should decrease because of the enhanced intersystem crossing of the naphthalene singlet.

[4] $${}^1N + Xe \rightarrow {}^3N + Xe$$

Thus the observed changes in the transient decay rates will be consistent with quenching by free radicals. However, the energy of the naphthalene singlet is not enough to break any of the bonds in the naphthalene molecule (17) and it is recognized that where free radicals are formed on photolysis of aromatic solutes, the phenomenon is attributable to two photon effects (38) (reactions 2 and 5). In our case, assuming the

[5] $${}^1N + h\nu \rightarrow \text{Free radicals}$$

quenching rate constant for the free radicals to be $\sim 10^{-9}$–10^{10} l mol^{-1} s^{-1} (37), a concentration of free radicals of $\sim 10^{-6}$–10^{-5} mol l^{-1} would be necessary to account for the change in decay rates of the transient. The concentration of the triplet formed, on the basis of the known extinction coefficients (39), is $\sim 3 \times 10^{-6}$ mol l^{-1}. Since the quantum yield for intersystem crossing for naphthalene is ~ 0.8 (40), the yield of the excited singlet would only be $\sim 4 \times 10^{-6}$ mol l^{-1}. Therefore, it is difficult to see how a free radical yield of $\sim 10^{-5}$–10^{-6} mol l^{-1} can be produced from the naphthalene excited singlet by two photon effects. Further, the more commonly accepted mechanism for the formation of free radicals is via photon absorption by the triplet (38). In this case, then, the effect of addition of

[6] $${}^3N + h\nu \rightarrow \text{Free radicals}$$

xenon should be just the opposite, *i.e.* increased decay rate of the transient, since the triplet yield would be increased by added xenon (reaction 4). Thus, the observed decrease in the decay rate of the naphthalene triplet is not attributable to free radicals. This interpretation is also consistent with the observed lack of two photon effect and lack of any effect by added ethylene.

Therefore, the observed decrease in the transient decay rate is most probably due to the formation of transient(s) other than free radicals.

(b) New Transient

The lowest excitation potential of xenon is at 1.332 aJ (8.315 eV, 149 nm) (19). Filters around our flashlamps did not allow the passage of light with $\lambda < 280$ nm, so, direct excitation of xenon in the solutions was most unlikely. The lack of observation of any transient absorption on flash photolysis of solutions of xenon is consistent with this expectation.

The non-involvement of excimer formation and decay in the observed decrease in the transient decay rate was shown by the results in the concentrated solutions of naphthalene. In 0.1 and 0.4 mol l^{-1} solutions of naphthalene the observed h.a.e. was lower than that in 10^{-3} mol l^{-1} solutions. This is reasonable, since in the more concentrated solutions there will be competition between the reaction of the naphthalene excited singlet with xenon (reaction 4), and with naphthalene.

[7] $${}^1N + N \rightarrow {}^1N_2$$

The spectra of ionic transients derived from naphthalene are known (41), and the ionization potentials of both naphthalene and xenon are much higher (42) than the energies of photons available from our flash lamps. Therefore, the formation of ionic transients would not be expected. In the 300–1000 nm region, there was no indication of a spectrum of any charged transient.

Can. J. Chem. Downloaded from www.nrcresearchpress.com by 210.87.254.5 on 09/05/12
For personal use only.

It would then appear that another transient (X) is formed in the solutions containing xenon. It must meet one of the following criteria: (*i*) the transient X has no absorption bands in the 350–1000 nm region, but decays (on μs timescale) to triplet naphthalene; (*ii*) it has an absorption spectrum indistinguishable from that of the naphthalene triplet in the 350–1000 nm region, but decays (on μs timescale) faster than the naphthalene triplet to give the naphthalene triplet; (*iii*) it has an absorption spectrum indistinguishable from that of the naphthalene triplet and decays more slowly than the naphthalene triplet. Each of these criteria leads to an overall half-life of the transient to be greater than that of the naphthalene triplet.

If either (*i*) or (*ii*) were correct, one would expect to see a non-exponential decay of the transient absorption; however, the decay is exponential for more than three half-lives in methylcyclohexane solutions (Fig. 1). We therefore favor the possibility (*iii*) and suggest that the transient absorption in solutions of naphthalene, in the presence of xenon, is predominantly due to a complex formed between excited naphthalene and xenon.

It should be pointed out that complex formation involving noble gases has been suggested before in several systems: (*i*) xenon–benzene and xenon–naphthalene complex formation in low temperature spectroscopic studies (5–9, 11); (*ii*) Xe–CO* complex formation in xenon sensitized fluorescence of CO (43); (*iii*) (Xe–Kr)* complexes in luminescence of their condensed solutions (44), and (*iv*) $Xe–H_2$ and $Xe–D_2$ complex formation in photosensitized exchange studies (45). Complex formation between xenon and an excited aromatic compound in liquid solutions has not been recognized before.

(c) Precursor and Nature of the Complex

Our results show that the transient decay rate is decreased, and the complex is formed, when solutions of naphthalene containing xenon are flash photolyzed. However, when the solutions also contain phenanthrene the naphthalene triplet is formed by energy transfer from the phenanthrene triplet and no naphthalene singlet is formed; in this case the rate of decay of the naphthalene triplet is slightly increased by xenon. These results suggest that it is the naphthalene excited singlet, and not the naphthalene triplet, which enters into a complex with xenon (reaction 8). The half-lives of the known lowest

[8] $$^1N + Xe \rightarrow {}^1NXe$$

excited singlets are <1 μs (40, 46). The half-life of the complex is ~40 μs. It is highly unlikely, therefore, that the complex is in excited singlet state. We suggest that the singlet excited complex undergoes rapid intersystem crossing ($t_{\frac{1}{2}} < 1$ μs) to its triplet, and then decays, radiatively and

[9] $$^1NXe \rightarrow {}^3NXe$$

non-radiatively, to ground state naphthalene and xenon. Siegel and Judeikis (11) observed phosphorescence from such complexes (reaction 10).

[10] $$^3NXe \rightarrow N + Xe + h\nu$$

[11] $$^3NXe \rightarrow N + Xe$$

Their xenon–naphthalene complex may also have been formed from the naphthalene excited singlet (reactions 8 and 9.) In these (11) and other low temperature studies (5–8) the rate of decay of the naphthalene phosphorescence was found to increase in the presence of xenon. However, our results on the decay rates are not directly comparable to theirs (5–8, 11) since (*i*) they used much higher concentrations of xenon (≥ 0.9 *M*) and (*ii*) the h.a.e. of xenon on the radiative transitions of triplets should be greater than on the non-radiative transitions. Triplet decay in liquids is mainly due to the non-radiative transitions.

Since the main bands in the absorption spectra of the naphthalene triplet and the complex are indistinguishable from each other, it appears that xenon perturbs the relevant electronic energy levels of the naphthalene triplet to the same extent. Earlier work by Siegel and Judeikis (11) showed lack of a significant perturbation of the naphthalene triplet phosphorescence by xenon; the phosphorescence spectra of the naphthalene–xenon complexes were very similar to that of the naphthalene triplet. Since xenon does not seem to affect the lowest excited triplet level of naphthalene (11), it is probably reasonable to assume that it does not affect the higher triplet levels either; hence the similarity between the main absorption bands of the naphthalene triplet and the complex is not as surprising as it might seem at first sight. Weak new transient absorption in the 300–350 nm region in solutions in acetonitrile (Fig. 4) and 2-propanol (Fig. 3) might also be attributable to the excited naphthalene–xenon complex. The effect of xenon concentration on the transient yield and half-life

Can. J. Chem. Downloaded from www.nrcresearchpress.com by 210.87.254.5 on 09/05/12
For personal use only.

(Fig. 2) is not inconsistent with the complex formation. The small decrease in the decay rate of the transient, in solutions of naphthalene, in the presence of krypton is probably also due to complex formation between excited naphthalene and krypton.

(d) Solvent Effect on Heavy Atom Effect

The h.a.e. appears to decrease as the polarity of the solvent increases (Table 1). Molecules in their excited states are more polarizable than in their ground state (40); therefore, as the solvent polarity increases the solvation of the solute excited states would increase (40). Increased solvation is most likely to inhibit h.a.e. of xenon since a solvent layer would tend to reduce complex formation between the solute excited molecule and xenon. Polarity of solvents has no clearly defined effect on the intersystem crossing efficiency of singlet excited states (46), so the solvent effect cannot be attributed to this. Increasing the polarity of solvents tends to increase the fluorescence lifetime of excited molecules (46); this effect would tend to enhance the h.a.e. Other factors which may contribute to the observed solvent effects, but whose contribution in our system is not known, are solvent viscosity and the solubility of xenon. Increasing solvent polarity seems to affect the yield of the complex and its half-life to different extents (Table 1). This suggests that the solvent polarity affects complex formation (reaction 8) more than the xenon enhanced intersystem crossing (reaction 4) and hence possible differences in the solubility of xenon probably play only a minor role in the observed solvent effects.

Heavy Atom Effect in Other Solutions

It is not certain whether the complex formation is peculiar to excited naphthalene or whether it is a more general phenomenon for polyatomic systems. If an increase in the half-life of the triplet in the presence of xenon, or, lack of quenching by xenon (*i.e.* anomalous h.a.e.) were the criteria of complex formation, then it occurs in solutions of phenanthrene and biphenyl as well. Data in Table 1 show that there is no correlation between the solute triplet energies and the lack of increase of transient decay rates in their solutions by added xenon. However, the energies of the singlet states of the three solutes showing anomalous h.a.e. of xenon are the highest among the solutes studied (Table 1). Perhaps there is a dependence of the complex formation on solute singlet energy. This is consistent with the earlier conclusion that xenon is complexing with the naphthalene excited singlet. It also suggests that the interaction between excited solute and xenon might have a charge transfer character, in accordance with previous suggestions on the nature of h.a.e. (6, 7, 13). The excited singlet energy of biphenyl is greater than that of naphthalene. However, the effect of xenon on the rate of the biphenyl triplet decay is smaller than that on the naphthalene triplet, suggesting that other factors, particularly stereochemistry of the excited molecules, also influence the complex formation.

Heavy Atom Effect in Radiolysis and Photosensitization

The h.a.e. of added xenon has been used to aid in determining the roles of solute excited singlet and triplet states (including those of naphthalene) in the pulse radiolysis of liquid solutions (47, 48). No decrease in solute triplet decay rates, in the presence of xenon, has been observed in these studies (47, 48). While this would seem to be at variance with our results, in radiolysis a larger number and variety of transient species are formed (49, 50). The triplet decay rates observed in pulse radiolysis studies are much faster than those in flash photolysis studies (50), due to quenching by these additional transients. We feel that the presence of these other transients in pulse radiolysis probably interferes with the observation of the complex formation. Xenon and other rare gases have also been used as solvents in many radiolysis studies (*e.g.* 51, 52). The h.a.e. of xenon and krypton on the excited molecules formed in these systems seems to have been overlooked (51, 52). In mercury photosensitization studies, also, the h.a.e. on the excited states formed seems to have been overlooked. It has been pointed out that in energy transfer from excited mercury atoms, the overall spin angular momentum should remain unaltered (53, 54). However, if the energy transfer takes place on collision with an acceptor, the h.a.e. might well alter the overall spin angular momentum. For example, on energy transfer from $Hg(6^3P_1)$ to naphthalene, both the naphthalene triplet and the naphthalene excited singlet could result. Observation of acceptor excited singlet states does not seem to have been attempted in mercury photosensitization studies.

Helpful discussions with Dr. B. Henry, Dr. L. Stein, and Mr. M. Tomlinson are gratefully acknowledged. We

should also like to thank Mr. D. Owens and Mr. P. deSouza for technical help with some of the experiments, Mr. D. Bell for the mass spectral analyses of xenon, and Mr. E. E. Wuschke for modifying the flash photolysis system. Award of a post doctoral fellowship by the National Research Council of Canada to one of us (D.A.H.) is gratefully acknowledged.

1. M. KASHA. J. Chem. Phys. **20**, 71 (1952).
2. D. S. MCCLURE. J. Chem. Phys. **17**, 905 (1949).
3. P. YUSTER and S. I. WEISSMAN. J. Chem. Phys. **17**, 1182 (1949).
4. M. KASHA. Discuss. Faraday Soc. **9**, 14 (1950).
5. M. R. WRIGHT, R. P. FROSCH, and G. W. ROBINSON. J. Chem. Phys. **33**, 934 (1960).
6. G. W. ROBINSON. J. Mol. Spectrosc. **6**, 58 (1961).
7. G. W. ROBINSON and R. P. FROSCH. J. Chem. Phys. **38**, 1187 (1963).
8. C. E. THOMPSON. J. Opt. Soc. Am. **55**, 1184 (1965).
9. G. W. ROBINSON. J. Chem. Phys. **46**, 572 (1967).
10. A. KEARVELL and F. WILKINSON. Mol. Cryst. **4**, 69 (1968).
11. S. SIEGEL and H. S. JUDEIKIS. J. Chem. Phys. **48**, 1613 (1968).
12. C. S. BURTON and W. A. NOYES, JR. J. Chem. Phys. **49**, 1705 (1968).
13. S. P. MCGLYNN, T. AZUMI, and M. KINOSHITA. Molecular spectroscopy of the triplet state. Prentice–Hall, Inc. Englewood Cliffs, New Jersey, 1969.
14. S. H. LIN and D. TWEED. Int. J. Quantum Chem. Symp. **3**, 315 (1969).
15. G. G. GIACHINO and D. R. KEARNS. J. Chem. Phys. **52**, 2964 (1970).
16. A. KEARVELL and F. WILKINSON. Chem. Phys. Lett. **11**, 472 (1971).
17. J. G. CALVERT and J. N. PITTS, JR. Photochemistry. John Wiley and Sons, Inc. New York, 1967.
18. U.V. atlas of organic compounds. Butterworths, London, 1966.
19. G. A. Cook (*Editor*). Argon, helium and the rare gases. Vol. 1. Interscience Publishers, New York, 1961.
20. H. H. HYMAN. *In* Physical chemistry: an advanced treatise, Vol. 5. *Edited by* H. Eyring, D. Henderson, and W. Jost. Academic Press, New York, 1970. p. 589.
21. B. BROCKLEHURST. Q. Rev. **22**, 147 (1968).
22. B. BROCKLEHURST. Radiat. Res. Rev. **1**, 223 (1968).
23. A. R. HORROCKS, T. MEDINGER, and F. WILKINSON. Photochem. Photobiol. **6**, 21 (1967).
24. A. R. HORROCKS, A. KEARVELL, K. TICKLE, and F. WILKINSON. Trans. Faraday Soc. **62**, 3393 (1966).
25. R. B. CUNDALL and A. J. R. VOSS. Chem. Commun. 902 (1968).
26. A. W. JACKSON and A. J. YARWOOD. Can. J. Chem. **48**, 3763 (1970).
27. M. E. MACBEATH and I. UNGER. Can. J. Chem. **49**, 594 (1971).
28. A. KEARVELL and F. WILKINSON. *In* Transfer and storage of energy by molecules. Vol. 1. *Edited by* G. M. Burnett and A. M. North. Wiley–Interscience, London, 1969. p. 94.
29. Matheson of Canada Limited, Whitby, Ontario, Catalogues 27C and 30.
30. I. G. DRAGANIĆ and Z. D. DRAGANIĆ. The radiation chemistry of water. Academic Press, New York. 1971. p. 203.
31. A. SINGH, A. R. SCOTT, and F. SOPCHYSHYN. J. Phys. Chem. **73**, 2633 (1969).
32. H. L. CLEVER, J. H. SAYLOR, and P. M. GROSS. J. Phys. Chem. **62**, 89 (1958).
33. G. PORTER and M. W. WINDSOR. Proc. R. Soc. London, A, **245**, 238 (1958).
34. T. J. KEMP and J. P. ROBERTS. Trans. Faraday Soc. **65**, 725 (1969).
35. W. A. PRYOR. Free radicals. McGraw-Hill Book Co. New York, 1966.
36. J. L. WEEKS and M. S. MATHESON. *In* Noble gas compounds. *Edited by* H. H. Hyman. The University of Chicago Press, Chicago, 1963. p. 89.
37. R. B. CUNDALL, G. B. EVANS, and E. J. LAND. J. Phys. Chem. **73**, 3982 (1969).
38. J. JOUSSOT-DUBIEN and R. LESCLAUX. Isr. J. Chem. **8**, 181 (1970).
39. E. J. LAND. Proc. R. Soc. London, A, **305**, 457 (1968).
40. C. A. PARKER. Photoluminescence of solutions. Elsevier, Amsterdam, 1968.
41. A. HABERSBERGEROVÁ, I. JANOVSKÝ, and J. TEPLÝ. Radiat. Res. Rev. **1**, 109 (1968).
42. L. G. CHRISTOPHOROU. Atomic and molecular radiation physics. Wiley–Interscience, New York, 1971.
43. T. G. SLANGER. J. Chem. Phys. **48**, 586 (1968).
44. N. G. BASOV, E. M. BALASHOV, O. V. BOGDANKEVITCH, V. A. DANILYCHEV, G. N. KASHNIKOV, N. P. LANTZOV, and D. D. KHODKEVITCH. J. Lumin. **1**, 834 (1970).
45. G. VON BÜNAU and R. N. SCHINDLER. Ber. Bunsenges. Phys. Chem. **72**, 142 (1968).
46. J. B. BIRKS. Photophysics of aromatic molecules. Wiley–Interscience. London, 1970.
47. R. COOPER and J. K. THOMAS. J. Chem. Phys. **48**, 5097 (1968).
48. F. DAINTON, T. MORROW, G. A. SALMON, and G. F. THOMPSON. Proc. R. Soc. London, A, **328**, 481 (1972).
49. P. AUSLOOS. *Ed.* Fundamental processes in radiation chemistry. Interscience, New York, 1968.
50. A. SINGH. Radiat. Res. Rev. **4**, 1 (1972).
51. R. D. KOOB and L. KEVAN. J. Phys. Chem. **72**, 3808 (1968).
52. Y. YAMAMOTO, S. TAKAMUKU, and H. SAKURAI. Bull. Chem. Soc. Jap. **44**, 2104 (1971).
53. H. E. GUNNING and O. P. STRAUSZ. *In* Advances in photochemistry. Vol. 1. *Edited by* W. A. Noyes, Jr., G. S. Hammond, and J. N. Pitts, Jr. Interscience, New York, 1963. p. 209.
54. R. J. CVETANOVIĆ. *In* Progress in reaction kinetics. Vol. 2. *Edited by* G. Porter. Macmillan, New York, 1964. p. 39.
55. F. BUCKLEY and A. A. MARYOTT. Tables of dilectric dispersion data for pure liquids and dilute solutions. National Bureau of Standards Circular 589 (1958).
56. E. HAYON. J. Chem. Phys. **53**, 2353 (1970).
57. Freon Product Information, Circular EL-8B (DuPont).
58. R. S. BECKER. Theory and interpretation of fluorescence and phosphorescence. Wiley–Interscience, New York, 1969.
59. A. A. LAMOLA and N. J. TURRO. Energy transfer and organic photochemistry. Interscience, New York, 1969.

Can. J. Chem. Downloaded from www.nrcresearchpress.com by 210.87.254.5 on 09/05/12
For personal use only.

Mechanistic Studies of Isomerization Reactions of Tetragonal Planar Tertiary Phosphine Complexes of Palladium(II)[1]

DAVID G. COOPER AND JOHN POWELL

Lash Miller Chemical Laboratories, University of Toronto, Toronto 181, Ontario

Received October 19, 1972

The complexes $[PdCl_2(Me_2RP)_2]$ (R = *o*-tolyl; α-napthyl) may be isolated in both *cis* and *trans* forms. In $CHCl_3$ solution *cis–trans* isomerization processes for these complexes are slow and this is ascribed to steric hindrance by the bulky R groups. The *cis–trans* isomerization is catalyzed by a variety of added ligands L. These isomerization processes have been extensively studied for the complexes *cis*- and *trans*-$[PdCl_2(Me_2o\text{-tolylP})_2]$ in $CHCl_3$ solution. The results of variable temperature n.m.r. and u.v. kinetic studies are fully consistent with a consecutive displacement mechanism with an ionic species of the type $[PdCl(Me_2o\text{-tolylP})_2L]^+Cl^-$ as an intermediate. The kinetic characteristics are determined by the nature and relative stability of this ionic intermediate. For L = Me_2o-tolylP the rate of isomerization is zero order in complex and second order in added phosphine concentration. (At 38° $k_{cis\rightarrow trans}$ = 6.2×10^3 l mol^{-1} s^{-1}, $k_{trans\rightarrow cis} = 6.3 \times 10^3$ l mol^{-1} s^{-1}.) For L = PPh_3 the rate of isomerization is considerably slower and first order in both complex and added PPh_3 concentrations ($k_{cis\rightarrow trans}$ = 6.3×10 l mol^{-1} s^{-1}, $k_{trans\rightarrow cis} = 6.7 \times 10$ l mol^{-1} s^{-1}). Isomerization is also effected in neat methanol and the rate is first order in complex concentration. N.m.r. studies of mixtures of *trans*-$[PdI_2(Me_2o\text{-tolylP})_2]$ and *cis*-$[PdCl_2(Me_2o\text{-tolylP})_2]$ in $CHCl_3$ solution show halogen exchange to occur more rapidly than isomerization. However a *cis*-diiodo complex is not observed and instead isomerization to the *trans*-diiodo complex is observed to occur.

Les complexes $[PdCl_2(Me_2RP)_2]$ (R = *o*-tolyl, α-naphtyl) peuvent être isolés sous forme *cis* et *trans*. En solution dans le $CHCl_3$, les processus d'isomérisation *cis–trans* pour ces complexes sont lents et ceci est dû à l'empêchement stérique des groupes R volumineux. L'isomérisation *cis–trans* est catalysée par divers ligands L ajoutés. Les processus d'isomérisation ont été intensivement étudiés pour les complexes $[PdCl_2(Me_2o\text{-tolylP})_2]$ en solution dans le $CHCl_3$. Les résultats des études RMN à température variable et des études cinétiques par l'u.v. sont pleinement compatibles avec un mécanisme de déplacement consécutif avec comme intermédiaire, une espèce ionique du type $[PdCl(Me_2o\text{-tolylP})_2L]^+Cl^-$. Les caractéristiques cinétiques ont été déterminées par la nature et la stabilité relative de l'intermédiaire ionique. Pour L = Me_2o-tolylP, la vitesse d'isomérisation est d'ordre zéro pour le complexe et d'ordre deux pour la concentration de phosphine ajoutée. (à 38°, $k_{cis\rightarrow trans} = 6.2 \times 10^3$ l mol^{-1} s^{-1}, $k_{trans\rightarrow cis} = 6.3 \times 10^3$ l mol^{-1} s^{-1}). Pour L = PPh_3, la vitesse d'isomérisation est beaucoup plus lente et d'ordre un pour le complexe et pour les concentrations en PPh_3 ajouté. ($k_{cis\rightarrow trans}$ = 6.3×10 l mol^{-1} s^{-1}, $k_{trans\rightarrow cis} = 6.7 \times 10$ l mol^{-1} s^{-1}). L'isomérisation a été également effectuée dans le méthanol seul et la vitesse est d'ordre un par rapport au complexe. Les études RMN des mélanges de $[PdI_2(Me_2o\text{-tolylP})_2]$ *trans* et $[PdCl_2(Me_2o\text{-tolylP})_2]$ *cis* en solution dans le $CHCl_3$ montrent un échange d'halogène plus rapide que l'isomérisation. Cependant, le complexe *cis*-diiodo n'a pas été observé, à la place une isomérisation en complexe *trans*-diiodo s'est produite.

[Traduit par le journal]

Can. J. Chem., **51**, 1634 (1973)

Introduction

Whilst *cis-trans* isomerization processes in tetragonal planar nickel(II) complexes have been studied in detail (ref. 1 and references cited therein) the mechanism of *cis-trans* isomerization in tetragonal planar complexes of palladium(II) and platinum(II) have received only limited attention. Dichloro-bis(*t*-phosphine)platinum(II) complexes are generally rather inert to *cis–trans* isomerization. However addition of traces of a tertiary phosphine to such a system catalyzes *cis–trans* isomerization. A consecutive displacement mechanism (2) and a mechanism involving pseudo-rotation of a five coordinate intermediate (3) have been proposed to explain the tertiary phosphine catalyzed isomerization. Recently we obtained ^1H n.m.r. and kinetic evidence from studies of *cis–trans* $[PtI_2(Me_2PhP)_2]$/Me_2PhP systems which favored the consecutive displacement mechanism (*e.g.* eq. 1) (4). A consecutive displacement mechanism has been previously proposed for the amine (am) catalyzed

[1]During the preparation of this manuscript Shaw and co-workers described briefly the preparation of *cis*- and *trans*-$[PdCl_2(Me_2o\text{-tolylP})_2]$ (8).

Can. J. Chem. Downloaded from www.nrcresearchpress.com by 210.87.254.42 on 09/05/12
For personal use only.

cis–trans isomerization of the palladium complexes $[PdX_2(am)_2]$. (5) We now report the results of a kinetic study of the tertiary phosphine catalyzed *cis–trans* isomerization of $[PdCl_2(Me_2o\text{-tolylP})_2]$ in chloroform solution. The data obtained fully support a consecutive displacement mechanism analogous to that proposed for the $[PtI_2(Me_2PhP)_2]/Me_2PhP$ system (4).

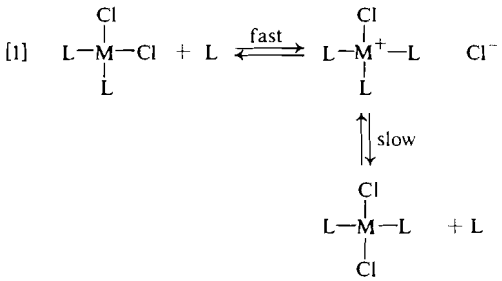

Results and Discussion

The Isolation and Characterization of cis- and trans-$[PdCl_2(Me_2o\text{-tolylP})_2]$ and Related Complexes

The product obtained from the reaction of two Me_2o-tolylP ligands with Li_2PdCl_4 in EtOH consists of a mixture of *cis*- and *trans*-$[PdCl_2Me_2o\text{-tolylP})_2]$. The *cis* isomer may be obtained in a pure form by extraction of the mixture with refluxing ethanol. Extraction of the mixture with refluxing benzene gave the *trans* isomer. The stereochemistry of the *cis* and *trans* isomers in the solid state was confirmed by far infrared and Raman spectroscopy. The *cis* isomer exhibited two νPd—Cl absorptions at 289 and 311 cm^{-1} active in both the i.r. and Raman, whereas the *trans* isomer exhibited one i.r. active and one Raman active νPd—Cl absorption (See Table 1). These stereochemistries are confirmed by n.m.r. studies of the complexes in $CDCl_3$ solution. The ^1H n.m.r. and proton decoupled ^{13}C n.m.r. spectra of the methyl groups of the *trans*-isomer consist of a singlet resonance assignable to the tolyl methyl, together with a 1:2:1 triplet assignable to the phosphine methyls (virtual coupling of two *trans* ^{31}P nuclei (6, 7) (see Table 1). The phosphine methyl resonances of the *cis*-isomer consist of a 1:1 doublet.[1] Slow isomerization of the *cis* isomer or the *trans* isomer to a *ca.* 2:1 *cis–trans* equilibrium occurs in chloroform solution over a period of *ca.* 1–5 d (*e.g.* see Fig. 1*f*). However on addition of a trace amount of a tertiary phosphine (*e.g.* Me_2o-tolylP, Me_2PhP, *n*-Bu_3P, Ph_3P) isomerization is rapid and equilibrium is reached in *ca.* 20 min (34°). The non-lability of $[PdCl_2(Me_2o\text{-tolylP})_2]$ towards *cis–trans* isomerization contrasts markedly with previous studies of dichlorobis(*t*-phosphine)palladium(II) complexes where isomerization has been shown to be extremely facile. (6) Thus for example whilst $[PdCl_2(Me_2PhP)_2]$ may be isolated as the *cis*-isomer in the solid state (9) it very rapidly isomerizes to a *ca.* 2:1 *cis–trans* equilibrium mixture in $CHCl_3$ at *ca.* 34° (6). The Me_2o-tolylP platinum(II) complexes *cis*- and *trans*-$[PtI_2(Me_2o\text{-tolylP})_2]$ are also considerably less labile to ligand substitution and isomerization than their Me_2PhP analogues. As the electronic factors associated with the Me_2o-tolylP and Me_2PhP ligands are very similar, the marked difference in the kinetic lability of these complexes is probably due to a steric effect of the ortho-methyl group of the Me_2o-tolylP ligand. Molecular models indicate that the ortho-methyl group and/or the ortho-hydrogen will tend to impede the approach of a nucleophile along the *z*-axis and hence inhibit S_N2 reactions.

The complex $[PdCl_2(Me_2\alpha\text{-napthylP})_2]$ may also be isolated as *cis* and *trans* isomers which are also non-labile to *cis–trans* isomerization, presumably for similar reasons. However attempts to prepare *cis*-dibromo or *cis*-diiodo derivatives of these complexes by metathetical replacement failed, only the *trans* isomers being isolated.

An unusual feature of the ^1H n.m.r. spectrum of *cis*-$[PdCl_2(Me_2o\text{-tolylP})_2]$ is a high field quartet resonance of relative intensity one (per Me_2o-tolylP) at 6.52δ assignable to an aromatic proton. No anomalous high field aromatic absorptions are observed for the free ligand (Me_2o-tolylP), *trans*-$[PdX_2(Me_2o\text{-tolylP})_2]$ (X = Cl, Br, I), nor *cis*/*trans*-$[PdCl_2(Me_2PhP)_2]$. However the cationic complex $[PdCl(Me_2o\text{-tolylP})_3]^+PF_6^-$ does exhibit a high field aromatic proton resonance of relative intensity one (per Pd atom). It is anticipated that this high field aromatic proton resonance is due to the ortho-hydrogen on the tolyl ring. A 220 MHz ^1H n.m.r. spectrum of *cis*-$[PdCl_2(o\text{-tolyl}Me_2P)_2]$ supported this assignment. Close proximity of the ortho-hydrogen of an aryl phosphine ligand to the central metal atom has been observed in the X-ray diffraction study of *trans*-$[PdI_2(Me_2PhP)_2]$

Can. J. Chem. Downloaded from www.nrcresearchpress.com by 210.87.254.42 on 09/05/12
For personal use only.

Can. J. Chem. Downloaded from www.nrcresearchpress.com by 210.87.254.42 on 09/05/12
For personal use only.

TABLE 1. Spectroscopic data for some palladium(II) halide complexes containing Me_2*o*-tolylP or $Me_2\alpha$-napthylP ligands

Complex	^{1}H data† P—Me δ	J_p	*o*-tolylMe δ	Aromatic H's δ	^{13}C data† P—Me δ	J_p	νPd—X(± 1 cm^{-1}): polarizable (p) I.r. Nujol mull	I.r. $CHCl_3$	Raman Solid	Raman $CHCl_3$	U.v. data for $CHCl_3$ solutions (38°) λ_{max} ± 0.2 mμ (ε l mol^{-1} cm^{-1} × 10^{-2})
trans-[$PdCl_2(Me_2$*o*-tolylP$)_2$]*	1.73(t,6)	3.0	2.83(s,3)	7.1–7.5(m,4)	11.54(t)	16.2	354	357	304	300(p)	267sh(2.44); 327.5(21.7)
cis-[$PdCl_2(Me_2$*o*-tolylP$)_2$]*	1.60(d,6)	10.9	2.82(s,3)	6.52(q,1) 6.9–7.6(m,3)	14.27(d)	38.8	289 311	288 311	290 312	294(p) 312(p)	267(19.4); 327.5sh(3.99)
trans-[$PdBr_2(Me_2$*o*-tolylP$)_2$]*	1.84(t,6)	3.5	2.78(s,3)	7.1–7.5(m,4)			272	277	190	189(p)	281(9.60); 346.5(12.8)
trans-[$PdI_2(Me_2$*o*-tolylP$)_2$]*	2.08(t,6)	3.3	2.65(s,3)	7.1–7.4(m,4)			208		142	137	274(15.0); 312(14.0); 395(4.36)
trans-[$PdCl_2(Me_2\alpha$-napthylP$)_2$]	1.63(t,6)	3.4		7.2–8.9(m,7)	11.54(t)	17.0	358		309		283(7.48); 339.5(9.13)
cis-[$PdCl_2(Me_2\alpha$-napthylP$)_2$]	1.69(d,6)	11.4		6.31(q,1); 6.93(t,1) 7.1–9.0(m,5)	15.57(d)	38.6	286 308		298 320		281(11.5); 224sh(11.0)
trans-[$PdBr_2(Me_2\alpha$-napthylP$)_2$]	1.93(t,6)	3.3		7.0–8.9(m,7)			278		190		282(15.7); 351(12.6)
trans-[$PdI_2(Me_2\alpha$-napthylP$)_2$]	2.20(t,6)	3.4		7.0–8.8(m,7)			207		150		251.5(26.8); 279.5(24.0) 340(13.3); 396(5.03)
[$PdCl(Me_2$*o*-tolylP$)_3$]Cl‡	1.26(d,3) 1.76(t,6)	10 3	2.90(s,9)	6.6(q,1) 6.9–7.7(m,11)				309			
§	1.15(d,3) 1.75(t,6)	11.0 3.6	2.87(s,9)	6.64(q,1) 7.0–7.6(m,11)							
[$PdCl(Me_2$*o*-tolylP$)_3$]PF_6	1.04(d,3) 1.69(t,6)	9.5 3.6	2.81(s,9)	6.5(q,1) 6.9–7.7(m,11)			298	309		300(p)	
[$Pd_2Cl_2(Me_2$*o*-tolylP$)_4$]$(BF_4)_2$											280(276)
[PdCl(MeOH)$(Me_2$*o*-tolylP$)_2$]BF_4‖											275(12.7); 327(3.99); 511(0.31)

*These complexes were recently reported by Shaw and co-workers (8).
†^{1}H and ^{13}C n.m.r. data in $CDCl_3$ (34°). δH ± 0.01 and δ^{13}C ± 0.05 p.p.m. (downfield from TMS); J_{31P} ± 0.2 Hz. Multiplicity and relative intensity given in parentheses, (*m*, *I*); s = singlet, d = doublet, t = triplet, q = quartet, m = multiplet.
‡^{1}H n.m.r. spectrum recorded at −40°.
§^{1}H n.m.r. spectrum recorded in MeOH at 34°.
‖Obtained on dissolving [$Pd_2Cl_2(Me_2$*o*-tolylP$)_4$]$(BF_4)_2$ *in* MeOH, or by addition of $AgBF_4$ (one mol. per Pd) to [$PdCl_2(Me_2$*o*-tolylP$)_2$] in MeOH.

Can. J. Chem. Downloaded from www.nrcresearchpress.com by 210.87.254.42 on 09/05/12
For personal use only.

(10). The only common feature to account for the high field aromatic proton resonances in *cis*-$[PdCl_2(Me_2o\text{-tolylP})_2]$ and $[PdCl(Me_2o\text{-tolylP})_3]^+PF_6^-$ (one high field proton only) is that in both cases the phosphine giving rise to the high field aromatic resonances is *trans* to a chloride ligand. It is anticipated that a P—Pd bond *trans* to Cl will be shorter than one *trans* to P (see ref. 9 and references therein). If the observed high field shift is due to paramagnetic shielding by the d-electrons of the Pd atom, one would expect such shielding to be very sensitive to the Pd–ortho-proton separation and the orientation of the proton relative to the coordination plane (11). An upfield shift would be anticipated if the ortho-proton has a preferred conformation in, or close to the coordination plane. This explanation is not very satisfactory as it implies that the tolyl methyl protons should have a preferred conformation close to the *z*-axis above the coordination plane for which a paramagnetic downfield shift is predicted (11). No downfield shift of the tolyl methyl proton resonances in *cis*-$[PdCl_2(Me_2o\text{-tolylP})_2]$ or $[PdCl(Me_2o\text{-tolylP})_3]^+PF_6^-$ relative to *trans*-$[PdCl_2(Me_2o\text{-tolylP})_2]$ is observed.

The Tertiary Phosphine Catalyzed cis–trans Isomerization of $[PdCl_2(Me_2o\text{-tolylP})_2]$

Because of its relative non-lability we have utilized the complex $[PdCl_2(Me_2o\text{-tolylP})_2]$ to study the mechanism of the tertiary phosphine catalyzed *cis–trans* isomerization of tetragonal planar complexes of palladium(II).[2] The approach used is similar to that previously used to study phosphine catalyzed *cis–trans* isomerization in analogous platinum(II) complexes (4).

^1H *n.m.r. Studies*

Addition of one Me_2o-tolylP per Pd atom to a $CDCl_3$ solution of $[PdCl_2(Me_2o\text{-tolylP})_2]$ (0.2 *M*) at *ca.* $-10°$ gives a proton n.m.r. spectrum containing a broad 1:2:1 triplet resonance (excluding tolyl methyl protons) assignable to two *trans*-Me_2o-tolylP ligands and a doublet resonance assignable to a *cis*-Me_2o-tolylP ligand (see Table 1 and Fig. 1*a*). No resonances assignable to free Me_2o-tolylP are observed. A similar but better resolved pattern is obtained at 34° in MeOH solution (Fig. 1*b*). The spectra are consistent with the solution species being $[PdCl(Me_2o\text{-tolylP})_3]^+Cl^-$ and on addition of NH_4PF_6 to such solutions the salt $[PdCl(Me_2o\text{-tolylP})_3]^+PF_6^-$ is readily isolated and structurally characterized (see Table 1 for n.m.r. data). The far infrared spectrum of a 0.1 *M* chloroform solution of $[PdCl_2(Me_2o\text{-tolylP})_2]$ in the presence of one Me_2o-tolylP per Pd further confirms the formation of $[PdCl(Me_2o\text{-tolylP})_3]^+Cl^-$ (**1**) (see Table 1). In the range 500–250 cm^{-1} the spectrum contains only one absorption assignable to a νPd—Cl band and is identical to the far infrared spectrum of $[PdCl(Me_2o\text{-tolylP})_3]^+PF_6^-$. Thus in $CDCl_3$ solution in the temperature range $-10°$ to 31° equation 2 lies well to the right hand side.

[2] $[PdCl_2(Me_2o\text{-tolylP})_2] + PMe_2o\text{-tolylP} \underset{\text{equilibrium in } CDCl_3}{\overset{\text{fast}}{\rightleftharpoons}} [PdCl(Me_2o\text{-tolylP})_3]^+Cl^-$

The species $[PdCl(Me_2o\text{-tolylP})_3]^+Cl^-$ may exist either as a contact ion pair with a square pyramidal geometry (**1** in Scheme 1) or alternatively as a completely solvated species (*e.g.* **2**$(MeOH)_2$ in Scheme 1). The relative concentrations of such species will be a function of solvent, salt concentration, and temperature. The completely dissociated ionic species (*e.g.* **2**$(MeOH)_2$) will be favored by polar solvents, low concentrations, and low temperatures.

On addition of Me_2o-tolylP (*ca.* 20% per Pd) to a $CDCl_3$ solution of $[PdCl_2(Me_2o\text{-tolylP})_2]$ at $-20°$ the phosphine methyl (P—Me) ^1H n.m.r. spectrum consists of a broad 1:2:1 triplet and a broad 1:1 doublet assignable to $[PdCl(Me_2o\text{-tolylP})_3]^+Cl^-$ (20%) together with a sharp 1:1 doublet assignable to *cis*-$[PdCl_2(Me_2o\text{-tolylP})_2]$ (80%) (see Fig. 1*c*). (The equilibrium *cis–trans* isomer ratio is temperature dependent (12) and at $-20°$ is >95% *cis*.) The broadness of the salt resonances relative to those of the *cis* complex suggest that intramolecular exchange of *cis* and *trans* phosphines in the salt is faster than intermolecular salt–*cis*-phosphine exchange (13). This is borne out by studies using 1:1 salt – *cis* ratios. On raising the temperature of the system (80% $[PdCl_2(Me_2o\text{-tolylP})_2]$ + 20% $[PdCl(Me_2o\text{-tolylP})_3]^+Cl^-$) to 10° the "P—Me" proton resonances of the salt and *cis* isomer coalesce whilst the 1:2:1 "P—Me" triplet of

[2] $[PdCl_2(Me_2o\text{-tolylP})_2]$ was chosen for this study rather than $[PdCl_2(Me_2\alpha\text{-napthylP})_2]$ as the *cis* and *trans* isomers of the latter are less distinguishable by u.v. spectroscopy, see Table 1.

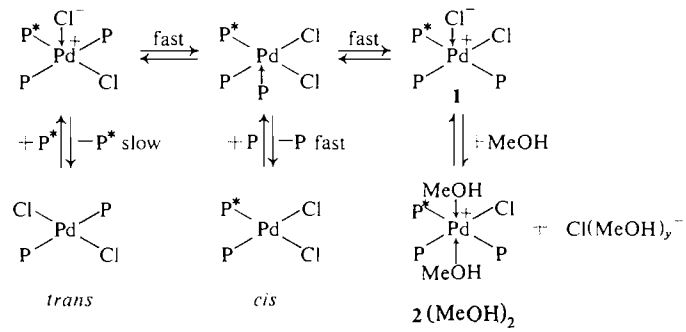

SCHEME 1. Mechanism proposed to account for rapid intramolecular exchange of P* in salt, and rapid salt–*cis* intermolecular exchange of P*. Axially solvating $CHCl_3$ molecules have been omitted for the sake of simplicity. Each ligand substitution is considered to proceed through a trigonal bipyramidal five coordinate intermediate and thus involves loss of a solvating $CHCl_3$ molecule. P = Me_2*o*-tolylP.

the *trans* isomer remains sharp and well resolved (% *trans* at 10° = *ca.* 10%) (see Fig. 1*d*). This indicates that intermolecular Me_2*o*-tolylP exchange between the salt and the *cis* isomer is *fast* on the n.m.r. time scale whereas *cis–trans* isomerization is *slow* on the n.m.r. time scale. This is more obviously so in Fig. 1*e* where the amount of added Me_2*o*-tolylP has been reduced to 5%. If 20% $[PdCl(Me_2o\text{-tolylP})_3]^+PF_6^-$ is added to $[PdCl_2(Me_2o\text{-tolylP})_2]$ in $CDCl_3$ at 34° no collapse of "P—Me" resonances is observed. Thus the ionic chloride ligand of $[PdCl(Me_2o\text{-tolylP})_3]Cl$ must be involved in the mechanism of Me_2*o*-tolylP exchange. The above observations suggest the mechanism shown in Scheme 1 for Me_2*o*-tolylP exchange in the salt–*cis* system. Addition of methanol to a 1:1 mixture of $[PdCl_2(Me_2o\text{-tolylP})_2]$ and Me_2*o*-tolylP in $CDCl_3$ at 34° slows the ligand exchange. In neat methanol no collapse of the phosphine methyl resonances is observed and the spectrum is consistent with *cis*-$[PdCl_2(Me_2o\text{-tolylP})_2]$ and $[PdCl(Me_2o\text{-tolylP})_3]^+(MeOH)_x$, $Cl^-(MeOH)_y$ being the solution species (*i.e.* solvation of the contact ion pair **1** by MeOH removes the Cl^- ligand from the axial position in **1** and thereby inhibits Me_2*o*-tolylP exchange. See Scheme 1.) These observations parallel the previous studies on $[PtI_2(Me_2PhP)_2]$ + Me_2PhP systems (4) and are consistent with the consecutive displacement mechanism for phosphine ligand exchange shown in Scheme 1.

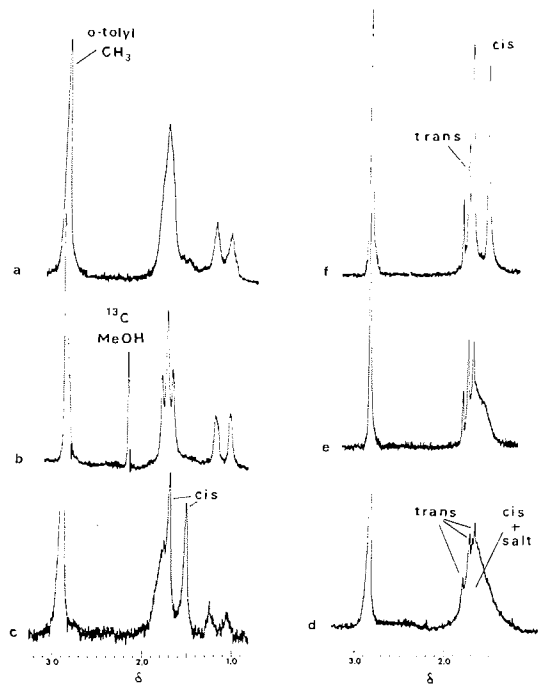

FIG. 1. ^1H n.m.r. spectrum of methylprotons of $[PdCl(Me_2o\text{-tolylP})_3]Cl$ (*a*) in $CDCl_3$ at −10°; (*b*) in MeOH at 34°; (*c,d*) the methyl proton resonance of a *ca* 4:1 mixture of $[PdCl_2(Me_2o\text{-tolylP})_2]$ and $[PdCl(Me_2o\text{-tolylP})_3]Cl$ in $CDCl_3$ solution at −20° (*c*), and +10° (*d*); (*e*) the methyl proton resonance of a *ca.* 19:1 mixture of $[PdCl_2(Me_2o\text{-tolylP})_2]$ and $[PdCl(Me_2o\text{-tolylP})_3]Cl$ in $CDCl_3$ solution at 34°; (*f*) the methyl proton resonance of an equilibrium *cis–trans* mixture of $[PdCl_2(Me_2o\text{-tolylP})_2]$ in $CDCl_3$ at 34°.

Addition of L = Me_2PhP, *n*-Bu_3P, or Me_2-PhAs also collapses the methyl proton resonances of *cis*-$[PdCl_2(Me_2o\text{-tolylP})_2]$ at 34°. At lower temperatures resonances assignable to species of the type $[PdCl(Me_2o\text{-tolylP})_2L]Cl$ similar to **1** are observed. However, whilst collapse of the methyl proton resonances and *cis–trans* isomerization are also promoted by Ph_3P the n.m.r. spectrum of $[PdCl_2(Me_2o\text{-tolylP})_2]$ in $CDCl_3$ in the presence of *ca.* 4 PPh_3 per Pd at −20° exhibits resonances assignable to *cis* (plus a very

Can. J. Chem. Downloaded from www.nrcresearchpress.com by 210.87.254.42 on 09/05/12
For personal use only.

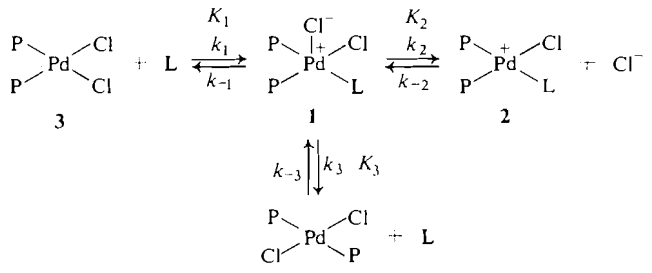

SCHEME 2. Consecutive displacement mechanism of *cis–trans* isomerization for L = P. For L ≠ P the ion-paired species (**1**) (*cis*-[PdClP$_2$L]Cl) must undergo rearrangement to *trans*-[PdClP$_2$L]Cl (of the type shown for P* in Scheme 1) before step 3. Axially solvating $CHCl_3$ molecules have been omitted for the sake of simplicity. Each ligand substitution is considered to proceed through a trigonal bipyramidal five coordinate intermediate and thus involves loss of a solvating $CHCl_3$ molecule.

small amount of *trans*) [PdCl$_2$(Me$_2$*o*-tolylP)$_2$] and free PPh_3. No resonances assignable to a species such as [PdCl(Me$_2$*o*-tolylP)$_2$(PPh_3)]Cl are observed. The relative instability of such a species is further confirmed by far infrared studies. In contrast to the [PdCl$_2$(Me$_2$*o*-tolylP)$_2$] + Me$_2$*o*-tolylP system (see above) the far infrared spectrum (400–250 cm^{-1}) of [PdCl$_2$(Me$_2$*o*-tolylP)$_2$] in the presence of 4 PPh_3 per Pd is the same as that of the equilibrium *cis–trans* mixture.

Ultraviolet Kinetic Studies

The close analogy between the above n.m.r. studies and those previously observed for [PtI$_2$(Me$_2$PhP)$_2$]–Me$_2$PhP systems (4) suggested that the kinetics of the PR_3 catalyzed *cis–trans* isomerization of [PdCl$_2$(Me$_2$*o*-tolylP)$_2$] would probably be similar to those found for the platinum(II) system. Thus the consecutive displacement mechanism shown in Scheme 2 is proposed to account for these isomerization processes. To obtain the fullest consistency with the above n.m.r. data it was decided to test the proposed mechanism by means of a kinetic study of both *cis*-to-*trans* and *trans*-to-*cis* tertiary phosphine catalyzed isomerizations of [PdCl$_2$(Me$_2$*o*-tolylP)$_2$] in chloroform solution at 38°. The above n.m.r. studies and known *trans* effect data indicate that the equilibria K_1 and K_2, involving the *cis* complex **3** (see Scheme 2), L (=PR_3 catalyst), and the ionic species **1** and **2**, are rapidly established and that the interconversion of **1** and the *trans* complex **4** will be rate determining. A *ca.* 10^{-4} *M* solution of [PdCl$_2$(Me$_2$*o*-tolylP)$_2$] in the presence of a *ca.* 5×10^{-6} *M* concentration of added Me$_2$*o*-tolylP catalyst will generate a *ca.* 5×10^{-6} *M* concentration of the ionic species [PdCl(Me$_2$*o*-tolylP)$_3$]$^+$Cl$^-$ which will most probably be in the fully solvated form **2** (*i.e.* [**2**] ≫ [**1**] and [**2**] ≈ [L$_0$] = concentration of L at the instant of addition, prior to formation of **2**).

For *cis* (**3**) to *trans* (**4**) isomerization the rate is represented by eq. 3:

$$[3] \quad \text{Rate} = -\frac{d[\mathbf{3}]}{dt} = \frac{d[\mathbf{4}]}{dt} = k_3[\mathbf{1}] - k_{-3}[\mathbf{4}][L]$$

Assuming the pre-equilibrium approximation and remembering that [**2**] = [Cl$^-$] ≈ [L$_0$] and that [L] ≈ 0 then it follows that

$$[4] \quad K_2 = \frac{[\mathbf{2}][Cl^-]}{[\mathbf{1}]} \approx \frac{[L_0]^2}{[\mathbf{1}]}$$

Initially [**4**] = 0. Substituting eq. 4 into eq. 3 for [**1**] gives the expression:

$$[5] \quad \text{Initial rate } (c \rightarrow t) = \frac{k_3[L_0]^2}{K_2} = k_0[L_0]^2$$

(k_0 = observable second order rate constant.)

For Me$_2$*o*-tolylP catalyzed *trans*-to-*cis* isomerization, the initial rate of formation of **3** is given by

$$[6] \quad \text{Initial rate} = \frac{d[\mathbf{3}]}{dt} = k_{-1}[\mathbf{1}]$$

As equilibria K_1 and K_2 are rapidly established the steady state approximation may be applied, *i.e.*

$$[7] \quad \frac{d[\mathbf{1}]}{dt} = k_1[\mathbf{3}][L] + k_{-2}[\mathbf{2}][Cl^-] + k_{-3}[\mathbf{4}][L] - (k_{-1} + k_2 + k_3)[\mathbf{1}] = 0$$

For conditions applicable to initial stages of reaction, eq. 7 simplifies to

Can. J. Chem. Downloaded from www.nrcresearchpress.com by 210.87.254.42 on 09/05/12
For personal use only.

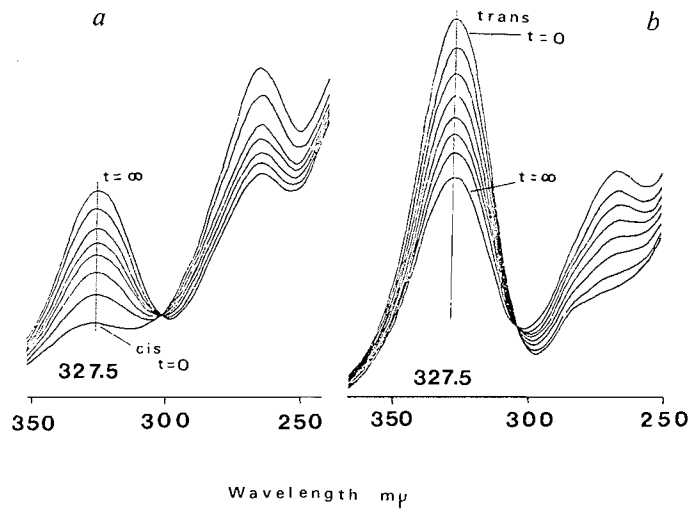

FIG. 2. U.v. spectral changes for PMe_2o-tolyl catalyzed *cis–trans* isomerization of $[PdCl_2(Me_2o\text{-tolylP})_2]$ in $CHCl_3$ at 38°: (*a*) *cis* to equilibrium; (*b*) *trans* to equilibrium.

$$[8] \qquad [\mathbf{1}] = \frac{k_{-2}[L_0]^2}{k_{-1} + k_2 + k_3}$$

Substituting eq. 8 into eq. 6 gives

$$[9] \quad \text{Initial rate } (t \rightarrow c) = \frac{k_{-1}k_{-2}[L_0]^2}{k_{-1} + k_2 + k_3} = k_0[L_0]^2$$

Although K_1 and K_2 are rapidly established it must be remembered that substitution of Cl in **4** by L is the rate determining step. As such an induction period prior to steady state conditions is anticipated for the L catalyzed *trans*-to-*cis* isomerization thereby making the observation of initial rates more difficult (*i.e.* at mixing most of added L is present as free phosphine and has to react with the *trans* isomer to form the salt). On the basis of eqs. 5 and 9, which incorporate the restrictions inferred by the n.m.r. studies, the consecutive displacement mechanism (Scheme 2) predicts that the initial rates of Me_2o-tolylP catalyzed *cis*-to-*trans* and *trans*-to-*cis* (steady state conditions) isomerization will be zero order in complex and second order in the concentration of added Me_2o-tolylP ($[L_0]^2$).

Figure 2 shows the observed changes in the u.v. spectra for *cis* to equilibrium (Fig. 2*a*) and *trans* to equilibrium (Fig. 2*b*) processes studied in 96% chloroform – 4% cyclohexane (by volume) at 38°. The 4% cyclohexane was necessitated by the fact that tertiary phosphines react very slowly with chloroform (14). As a precaution, therefore, standard solutions of the phosphine catalyst were made up in cyclohexane. Using a fixed amount of added Me_2o-tolylP pseudo zero order initial rate plots were obtained, the "initial zeroth order" approximation holding good for *ca.* 50% completion and for a 3-fold range of complex concentration.[3] Plots of the observed pseudo zero order initial rate constants for different concentrations of added Me_2o-tolylP *vs.* the square of the concentration of added Me_2o-tolylP ($[L_0]^2$) gave the linear correlations shown in Fig. 3. The slopes of these plots give the experimentally observed second order rate constants k_0 (see eqs. 5 and 9). Thus the observed kinetics are consistent with the above ^1H n.m.r. studies and the consecutive displacement mechanism when the added phosphine is one that readily generates an ionic species. To further verify the mechanism shown in Scheme 2 we decided to examine the chloride ion dependence of the rate by studying *trans*-to-*cis* isomerization at a fixed Me_2o-tolylP catalyst

[3]For the *trans*-to-*cis* isomerization process an induction period of *ca.* 1 min (during which *trans*-to-*cis* isomerization was rapid) was observed prior to steady state conditions.

The range of complex concentration is limited by experimental difficulties, a particular one being the problem of preparing very dilute ($> 10^{-7}$ *M*) standard solutions of the tertiary phosphine catalyst.

Can. J. Chem. Downloaded from www.nrcresearchpress.com by 210.87.254.42 on 09/05/12
For personal use only.

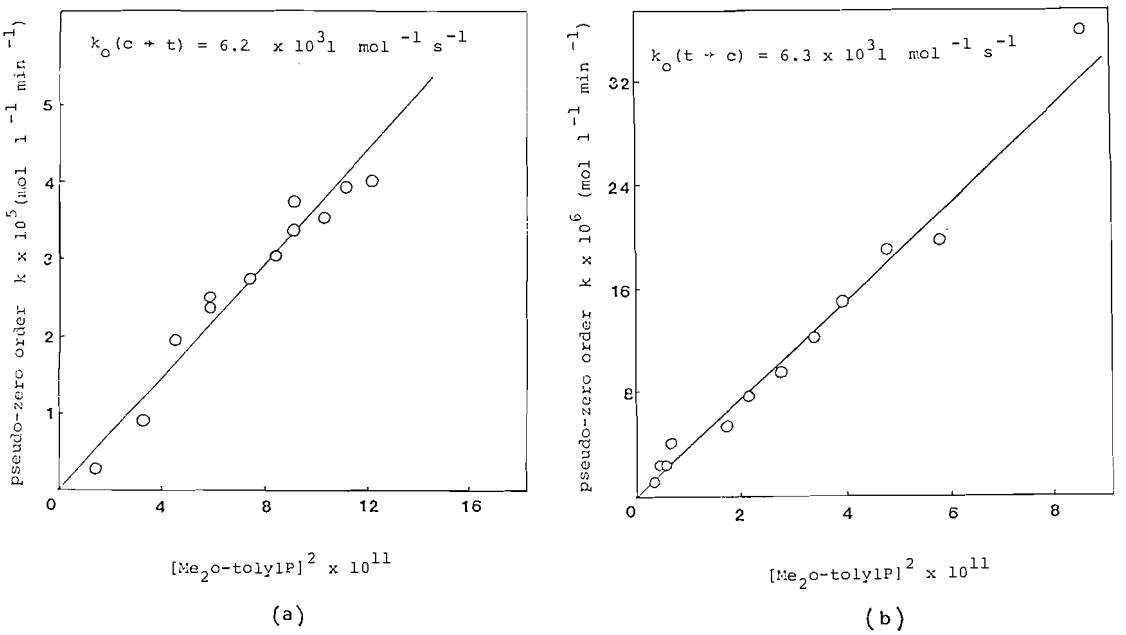

FIG. 3. Plots of the observed pseudo-zero order initial rate constants k *vs.* the square of the concentration of added Me_2o-tolyl catalyst for (*a*) *cis*-to-*trans*, and (*b*) *trans*-to-*cis* isomerization of $[PdCl_2(Me_2o\text{-tolylP})_2]$ in 96% $CHCl_3$ – 4% cyclohexane at 38°. Slope = k_o.

concentration but at varying chloride ion concentrations. Chloride ions were added in the form $[Et_4N]^+Cl^-$. In the presence of a fixed amount of added chloride ion (*ca.* 10^{-2} *M*) a pseudo-zero order reaction was still observed. The observed pseudo zero-order rate constants, although dependent on $[Cl^-]$ did not give a simple first order correlation as initially anticipated. This was found to be due to the fact that the *trans*/*cis* equilibrium constant, $K_{t/c}$, is quite sensitive to the concentration of added $[Et_4N]Cl$ decreasing from 1.06 (38°, no $[Et_4N]Cl$) to 0.56 (38°, 6.9×10^{-2} *M* in $[Et_4N]Cl$). As such we studied the *trans*-to-*cis* isomerization at a fixed concentration of added $[Et_4N]Cl$ (6.9×10^{-2} *M*) and varied the concentration of added Me_2o-tolylP. For the situation where $[Cl^-] \gg [L_0]$ eq. 9 is modified such that

$$\text{Initial rate}_{(t\rightarrow c)} = \frac{k_{-1}k_{-2}[L_0][Cl^-]}{k_{-1} + k_2 + k_3}$$

For fixed concentration of excess "added chloride" a first order dependence on the concentration of added Me_2o-tolylP should be observed. This was indeed found to be the case.

Since ^1H n.m.r. and far infrared studies of the system $[PdCl_2(Me_2o\text{-tolylP})_2] + PPh_3$ have shown that PPh_3 has little tendency to generate an ionic species we decided to carry out a kinetic study of this system in order to see whether or not a consecutive displacement mechanism is still applicable. To be consistent with the mechanism outlined in Scheme 2 and the n.m.r. data, PPh_3 catalyzed isomerization should be slower (more difficult to generate the ionic intermediate). One would also anticipate the following kinetic characteristics:

For L = PPh_3 the n.m.r. data indicates that $[L] \gg [\mathbf{1}]$ and that $[L] \approx [L_0]$. Thus the initial rate of *cis*-to-*trans* isomerization is given by

$$[10] \quad \text{Initial rate}_{(c\rightarrow t)} = k_3[\mathbf{1}] = k_3K_1[\mathbf{3}][L] \approx k_0'\,[\mathbf{3}][L_0]$$

For *trans*-to-*cis* isomerization the initial rate is given by

$$[11] \quad \text{Initial rate}_{(t\rightarrow c)} = k_{-3}\,[\mathbf{4}][L] \approx k_0'\,[\mathbf{4}][L_0]$$

Using a fixed concentration of added PPh_3 (and studying the isomerization in 96% $CHCl_3$ – 4% cyclohexane at 38°) a first order dependence on complex concentration for the initial rates of *cis*-to-*trans* and *trans*-to-*cis* isomerization was observed. A plot of the pseudo first order rate constants *vs.* the concentration of added PPh_3 gave the linear correlations shown in Fig. 4

Can. J. Chem. Downloaded from www.nrcresearchpress.com by 210.87.254.42 on 09/05/12
For personal use only.

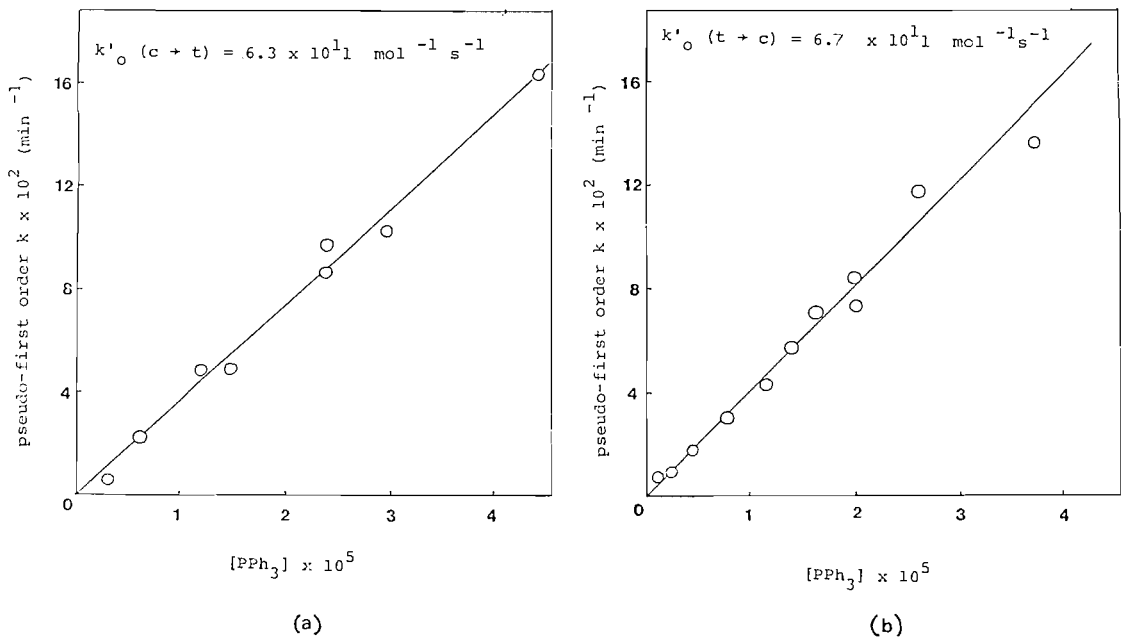

FIG. 4. Plots of the observed pseudo-first order initial rate constants *k vs.* the concentration of added Ph_3P catalyst for (*a*) *cis*-to-*trans*, and (*b*) *trans*-to-*cis* isomerization of $[PdCl_2(Me_2o\text{-tolylP})_2]$ in 96% $CHCl_3$ – 4% cyclohexane at 38°. Slope = k_o'.

from which values of the second order rate constants k_0' are obtained. From eqs. 10 and 11 the ratio $k_0'_{(c\rightarrow t)}/k_0'_{(t\rightarrow c)} = k_3K_1/k_{-3} = K_1K_3 = K_{t/c} = 0.95$. This is in very good agreement with the observed value of the *trans–cis* equilibrium constant, $K_{t/c}$, of 1.06 ± 0.03 ($K_{t/c}$ was calculated from the u.v. spectra of a *ca.* 10^{-4} *M* solution of complex + trace of Me_2o-tolylP, the equilibrium data being obtained after at least $20 \times t_{1/2}$). The experimentally observed kinetics for PPh_3 catalyzed isomerization are clearly consistent with the consecutive displacement. Furthermore, as expected, PPh_3 is a considerably poorer catalyst than Me_2o-tolylP.

The low temperature ^1H n.m.r. spectrum (−20°) of a 1:1 mixture of $[PdCl_2(Me_2o\text{-tolylP})_2]$ and $Me(o\text{-tolyl})_2P$ in $CDCl_3$ exhibits resonances assignable to *at least* two types of ionic species (*ca.* 20%) together with resonances due to *cis*-$[PdCl_2(Me_2o\text{-tolylP})_2]$ (*ca.* 80%) and free $Me(o\text{-tolyl})_2P$. Consistent with this observation, which indicates a situation intermediate between the Me_2o-tolylP and PPh_3 systems, initial rate studies did *not* give linear correlations for plots of the type shown in Figs. 3 and 4. The overall efficiency of tertiary phosphines to promote *cis–trans* isomerization decreases in the order $Me_2PhP \sim {}^nBu_3P \gtrsim Me_2o$-tolylP $\gg$ $Me(o\text{-tolyl})_2P > Ph_3P$.

Methanol Catalyzed trans–cis Isomerization

When *trans*-$[PdCl_2(Me_2o\text{-tolylP})_2]$ is dissolved in methanol complete isomerization to the *cis* isomer is observed at a rate much faster than the spontaneous isomerization observed in chloroform. The kinetics of this isomerization were studied by addition of a solution of the *trans* isomer in 4 parts chloroform to 96 parts methanol at 38°. At a complex concentration of *ca.* 5×10^{-4} *M* reproducible first order kinetics (in complex concentration) were observed which gave a pseudo first order rate constant, $k = 1.7 \times 10^{-4}$ s^{-1}. In more dilute solutions (*ca.* 5×10^{-5} *M*) a competing reaction obscures the kinetics. A new species with a u.v. band at 511 mμ is generated at a rate comparable to isomerization and the color of the solution turns from pale yellow to pink. A large excess of chloride ion (*e.g.* LiCl or $AsPh_4Cl$) eliminates the pink species. Addition of 1 mol of $AgPF_6$ per Pd to $[PdCl_2(Me_2o\text{-tolylP})_2]$ in methanol generates a deep red color (λ_{max} = 511 mμ). Likewise if the dimeric salt $[Pd_2Cl_2(Me_2o\text{-tolylP})_4]^{2+}2BF_4^-$ (pale yellow) is dissolved in methanol; the

Can. J. Chem. Downloaded from www.nrcresearchpress.com by 210.87.254.42 on 09/05/12
For personal use only.

Can. J. Chem. Downloaded from www.nrcresearchpress.com by 210.87.254.42 on 09/05/12
For personal use only.

solution turns red within 10 min (λ_{max} = 511 mμ). Although we have been unable to isolate the red species all the above data are consistent with formation of a salt [PdCl(MeOH)(Me_2o-tolylP)$_2$]$^+Cl^-$. It seems likely therefore that the methanol catalyzed *trans*-to-*cis* isomerization also proceeds via the consecutive displacement mechanism (Scheme 2, L = MeOH; concentrations of **1** and **2** are very small).

The role of solvent molecules on the equilibrium energetics of *cis–trans* isomerization for planar palladium(II)–phosphine complexes and their probable role in the isomerization process has been recently discussed by Redfield and Nelson (15).

trans-$PdI_2(Me_2o$-tolylP$)_2$ Catalyzed *cis–trans* Isomerization of $PdCl_2(Me_2o$-tolylP$)_2$

On mixing *trans*-[$PdCl_2(Me_2o$-tolylP$)_2$] with an equimolar quantity of *trans*-[$PdI_2(Me_2o$-tolylP$)_2$] in $CDCl_3$ a statistical equilibrium between the dichloro, the diiodo, and the *trans* chloro-iodo mixed species was observed immediately (<2 min) (*i.e.* Cl_2:ClI:I_2 = 1:2:1).

In another experiment *ca.* 5% *trans*-[PdI_2-(Me_2o-tolylP$)_2$] was added to a 0.2 *M* solution of *trans*-[$PdCl_2(Me_2o$-tolylP$)_2$] in chloroform. Within 1 h resonances assignable to *cis*-[$PdCl_2$-(Me_2o-tolylP$)_2$] were observed and an equilibrium situation was reached in *ca.* 24 h (22°). A control solution initally containing *trans*-[$PdCl_2$-(Me_2o-tolylP$)_2$] only isomerized very slowly and did not reach equilibrium with the *cis* isomer within 5 d. In neither experiments were n.m.r. resonances assignable to the *cis* isomers of [$PdI_2(Me_2o$-tolylP$)_2$] and [PdClI(Me_2o-tolylP$)_2$] observed.

Similar studies were done with solutions of *cis*-[$PdCl_2(Me_2o$-tolylP$)_2$] and *trans*-[$PdI_2(Me_2o$-tolylP$)_2$]. Again no peaks due to *cis*-[$PdI_2(Me_2o$-tolylP$)_2$] or *cis*-[PdClI(Me_2o-tolylP$)_2$] were observed. Again a rapid statistical equilibration between the reactant *trans*-diiodo, *cis*-dichloro complexes and the *trans*-dichloro and mixed *trans*-iodo-chloro products occurred. Likewise the *trans*-diiodo complex catalyzed the *cis–trans* isomerization of the *cis*-dichloro complex. When *ca.* 5% *trans*-[$PdI_2(Me_2o$-tolylP$)_2$] was mixed with *cis*-[$PdCl_2(Me_2o$-tolylP$)_2$] (22°) in chloroform *cis–trans* equilibrium was reached within 4 h (22°). A control sample took more than 24 h to reach equilibrium.

It seems likely that replacement of chloride by the bulkier iodide ligand in the *cis* isomer (and to a lesser extent the *trans* isomer) will introduce considerable steric strain into the molecule. This will facilitate solvolysis of an iodide to give an ionic intermediate such as [$PdI(Me_2o$-tolylP$)_2$-($CHCl_3$)]$^+I^-$ which rapidly rearranges to the *trans* diodide. Rapid Cl–I exchange then gives the *trans* isomer of the dichloride.

Experimental

The Preparation of Compounds

cis- and *trans*-[$PdCl_2(Me_2RP)_2$] (R = *o*-tolyl, α-napthyl) were prepared from Me_2RP and Li_2PdCl_4 using the general method described by Jenkins and Shaw (6). The *trans*-dibromo and *trans*-diiodo complexes were prepared from the corresponding dichloro complex (either *cis* or *trans*) via the method of metathetical replacement. The *cis* or *trans* stereochemistry of the complexes was determined on the basis of ^1H and ^{13}C n.m.r. and vibrational spectroscopy studies (see Table 1 and discussion section). The following new complexes were isolated:

Dichloro-bis(dimethyl-o-tolylphosphine)palladium(II) was obtained initially as a mixture of *cis* and *trans* isomers (yield 60%).

Anal. Calcd. for $C_{18}H_{26}Cl_2P_2Pd$: C, 44.98; H, 5.43. Found: C, 44.9; H, 5.5.

Extraction of the *cis–trans* mixture with refluxing benzene followed by filtration of the combined extracts and evaporation of the filtrate to dryness gave a yellow solid. Recrystallization from chloroform–cyclohexane gave *trans*-dichlorobis(dimethyl-*o*-tolylphosphine)palladium(II) as yellow needles (41%), m.p. 174–191°. (The large melting point range is due to *trans*-to-*cis* isomerization in the melt.)

Extraction of the *cis–trans* mixture with refluxing ethanol followed by a similar work up of the extracts gave a very pale yellow solid. Recrystallization from chloroform–cyclohexane gave *cis*-dichlorobis(dimethyl-*o*-tolylphosphine)palladium(II) as pale yellow plates (60%), m.p. 186–190°.

trans-Dibromobis(dimethyl-o-tolylphosphine)palladium-(II) was isolated as orange prisms (55%), m.p. 205–210°.

Anal. Calcd. for $C_{18}H_{26}Br_2P_2Pd$: C, 37.89; H, 4.56. Found: C, 37.8; H, 4.65.

trans-Diiodobis(dimethyl-o-tolylphosphine)palladium-(II) was isolated as orange-red prisms (60%), m.p. 215–220°.

Anal. Calcd. for $C_{18}H_{26}I_2P_2Pd$: C, 32.53; H, 3.95. Found: C, 32.4; H, 3.9.

Dichlorobis(dimethyl-α-napthylphosphine)palladium(II) was isolated from the reaction of $2Me_2$NapthylP with Li_2PdCl_4 as a mixture of *cis* and *trans* isomers (80%).

Anal. Calcd. for $C_{24}H_{26}Cl_2P_2Pd$: C, 52.05; H, 4.74. Found: C, 52.2; H, 4.8.

Extraction with benzene gave the *trans* isomer as yellow prisms (20%), m.p. 190–195° (melts and recrystallizes as the *cis* isomer which then melts at 230–235°).

Extraction of the *cis–trans* mixture with ethanol gave the *cis* isomer as pale yellow needles (73%), m.p. 231–235°.

trans-Dibromobis(dimethyl-α-napthylphosphine)palladium(II) was isolated as orange prisms (50%), m.p. 205–210°.

Anal. Calcd. for $C_{24}H_{26}Br_2P_2Pd$: C, 44.85; H, 4.09. Found: C, 44.9; H, 4.1.

trans-Diiodobis(dimethyl-α-napthylphosphine)palladium(II) was isolated as red prisms (60%), m.p. 230–235°.

Anal. Calcd. for $C_{24}H_{26}I_2P_2Pd$: C, 39.13; H, 3.56. Found: C, 39.1; H, 3.4.

Chloro-tris(dimethyl-o-tolylphosphine)palladium(II) Hexafluorophosphate. A solution of dichlorobis(dimethyl-*o*-tolylphosphine)palladium(II) (0.53 g) and dimethyl-*o*-tolylphosphine (0.17 g) in dichloromethane (30 ml) was shaken with excess ammonium hexafluorophosphate (0.51 g) for 2 d. Filtration of the reaction mixture and evaporation of the filtrate to dryness gave a yellow solid. Recrystallization from dichloromethane–cyclohexane gave the required product as pale yellow microprisms (60%), m.p. 194–197°.

Anal. Calcd. for $C_{27}H_{39}ClF_6P_4Pd$: C, 43.37; H, 5.29. Found: C, 43.46; H, 5.56.

μ-Dichloro-tetrakis(dimethyl-o-tolylphosphine)dipalladium(II) Bis(tetrafluoroborate). Silver tetrafluoroborate (0.53 g) in acetone (20 ml) was added to a solution of dichlorobis(dimethyl-*o*-tolylphosphine)palladium(II) (0.11 g) in dichloromethane (5 ml). The reaction mixture was filtered to remove AgCl and the filtrate evaporated to dryness under reduced pressure. The resultant solid was recrystallized from dichloromethane–hexane to yield the required product as pale yellow microprisms (80%), decomp. > 160°.

Anal. Calcd. for $C_{36}H_{52}B_2Cl_2F_8P_4Pd_2$: C, 40.18; H, 4.88. Found: C, 40.2; H, 5.1.

Physical Measurements

^1H and ^{13}C n.m.r. spectra were recorded on Varian A56-60D and XL-100 spectrometers respectively. Far-infrared spectra were recorded on a Perkin–Elmer 180 instrument whilst Raman spectra were recorded on a Spex 1401 spectrometer. Ultraviolet spectra were recorded on a Bausch and Lomb spectronic 505 spectrometer.

All u.v. kinetic studies were carried out at $+38° \pm 0.1°$, using A.C.S. grade solvents which had been previously purged with "O_2-free" dry nitrogen for 1–3 h. The *cis* and *trans* isomers of dichloro-bis(dimethyl-*o*-tolylphosphine)palladium(II) were recrystallized three times from dichloromethane–hexane prior to use. Phosphines used as catalysts were handled under nitrogen and distilled (or recrystallized) immediately prior to use. The rates of *cis–trans* isomerization of dichloro-bis(dimethyl-*o*-tolylphosphine)palladium(II) were monitored at 327.5 mμ and a sharp isobestic point at 303 mμ was always observed. Kinetic runs were carried out in chloroform–cyclohexane with chloroform as the bulk solvent. The phosphine catalyst in 1 part cyclohexane at 38° was added to the palladium complex in 19 parts chloroform at 38°. This procedure was adopted as the phosphines used react very slowly with the chloroform.

The authors wish to thank the National Research Council of Canada for financial support of this investigation and one of us (D.G.C.) wishes to thank the Ontario Government for an Ontario Graduate Fellowship.

1. R. H. HOLM. Acc. of Chem. Res. **2**, 307 (1969).
2. (*a*) F. BASOLO and R. G. PEARSON. Mechanisms of inorganic reactions. 2nd ed. Wiley, New York, N.Y. 1967. p. 426. (*b*) C. H. LANGFORD and H. B. GRAY. Ligand substitution processes. W. A. Benjamin, New York. N.Y. 1966.
3. P. HAAKE and R. M. PFEIFFER. Chem. Commun. 1330 (1969); J. Am. Chem. Soc. **92**, 4996 (1970); **92**, 5243 (1970).
4. D. G. COOPER and J. POWELL. J. Am. Chem. Soc. **95**, 1102 (1973).
5. L. CATTALINI and M. MARTELLI. J. Am. Chem. Soc. **91**, 312 (1969).
6. J. M. JENKINS and B. L. SHAW. J. Chem. Soc. (A), 770 (1966).
7. B. C. MANN, B. L. SHAW, R. C. STAINBANK. Chem. Commun. 151 (1972).
8. A. J. CHENEY, B. C. MANN, B. L. SHAW, and R. M. SLADE. J. Chem. Soc. (A), 3833 (1971).
9. L. L. MARTIN and R. A. JACOBSEN. Inorg. Chem. **10**, 1795 (1971).
10. N. A. BAILEY and R. MASON. J. Chem. Soc. (A), 2594 (1968).
11. A. D. BUCKINGHAM and P. J. STEVENS. J. Chem. Soc. 4583 (1964).
12. J. CHATT and R. G. WILKINS. J. Chem. Soc. 525 (1956).
13. (*a*) J. P. FACKLER, JR., J. A. FETCHIN, J. MAYHER, W. C. SEIDEL, T. J. SWIFT, and M. WEEKS. J. Am. Chem. Soc. **91**, 1941 (1969). (*b*) A. J. DEEMING and B. L. SHAW. J. Chem. Soc. (A), 597 (1969); 2705 (1970). (*c*) J. P. FACKLER. Inorg. Chem. **9**, 2625 (1970).
14. A. J. BURN and J. I. G. CADOGAN. J. Chem. Soc. 5788 (1963).
15. D. A. REDFIELD and J. H. NELSON. Inorg. Chem. **12**, 15 (1973).

Can. J. Chem. Downloaded from www.nrcresearchpress.com by 210.87.254.42 on 09/05/12
For personal use only.

Bimolecular Reactions of Trapped Ions. VI. Ion–Molecule Reactions Involving CH_5^+ and $C_2H_5^+$ [1]

A. S. BLAIR AND A. G. HARRISON

Department of Chemistry, University of Toronto, Toronto 181, Ontario

Received December 8, 1972

The ion–molecule reactions in mixtures of methane with the polar molecules dimethyl-d_6 ether, ethylene-d_4 oxide, acetaldehyde-d_4, acetone, and acetonitrile have been studied using the trapped-ion technique. The CH_5^+ and $C_2H_5^+$ ions produced by ion–molecule reactions in methane react rapidly (predominantly by proton transfer) with the polar molecules; the rate coefficients range from 1.98×10^{-9} cm^3 molecule^{-1} s^{-1} ($C_2H_5^+ + C_2D_4O$) to 5.26×10^{-9} cm^3 molecule^{-1} s^{-1} ($CH_5^+ + (CH_3)_2CO$). The rate coefficients are much larger than those predicted from ion – induced dipole interactions only indicating that ion–dipole interactions play a large role in the collision process.

Rate coefficients for reaction of CH_3^+ and CH_4^+ with the polar molecules also have been measured. Most of these also are larger than predicted from ion – induced dipole interactions indicating in this case as well substantial effects due to ion–dipole interactions.

Les réactions ion–molécule dans des mélanges de méthane avec des molécules polaires du type diméthyléther-d_6, oxyde d'éthylène-d_4, acétone et acétonitrile, ont été étudiées par la technique de captage ionique. Les ions CH_5^+ et $C_2H_5^+$ issus des réactions ion–molécule dans le méthane réagissent rapidement (surtout par transfert de proton) avec les molécules polaires; l'intervalle des coefficients de vitesse va de 1.98×10^{-9} cm^3 molécule^{-1} s^{-1} ($C_2H_5^+ + C_2D_4O$) à 5.26×10^{-9} cm^3 molécule^{-1} s^{-1} ($CH_5^+ + (CH_3)_2CO$). Les coefficients de vitesse sont beaucoup plus grands que ceux prévus à partir des interactions ion-dipôle induit indiquant que les interactions ion–dipôle jouent un grand rôle dans le processus de collisions.

Les coefficients de vitesse pour la réaction de CH_3^+ et CH_4^+ avec les molécules polaires ont été aussi mesurés. La plupart d'entre eux sont également plus élevés que ceux prévus par les interactions ion–dipôle induit montrant aussi bien dans ce cas, des effets substantiels dûs aux interactions ion–dipôle.

[Traduit par le journal]

Can. J. Chem., 51, 1645 (1973)

Introduction

Since the pioneering work of Field and Munson (1) chemical ionization mass spectrometry (2) has become an important tool in the identification and structure elucidation of organic molecules. In this technique the ionization of interest results from ion–molecule reactions between the ions produced in the reactant gas at high pressures ($\sim$ 1 Torr) and the neutral additive present at low concentration. The most commonly used reactant gas has been methane, in which at high pressures the dominant ions are CH_5^+ and $C_2H_5^+$. Consequently, there is a large body of information available concerning the products formed when CH_5^+ and $C_2H_5^+$ react with organic molecules (2–4).

On the other hand there is very little quantitative data concerning the rates of reaction of CH_5^+ and $C_2H_5^+$ with polar organic molecules and what data exist often is contradictory (5, 6). The measurement of rate coefficients requires a knowledge of the ion source residence times of the reactant ions, which, at the high pressures used, are determined by ion mobilities and cannot be calculated simply from source dimensions and applied fields. Rather they must be calculated from mobility theory (5–9)[2] and it is known (9) that such calculated values can be substantially in error even for apparently ideal conditions.

The ion-trapping technique developed recently in this laboratory (11) permits variation of the ion source residence times in a known fashion over a wide range. The technique has proven (12, 13) to be particularly suited to the quantitative study of sequential ion–molecule reactions such as those producing and consuming CH_5^+

[1]Presented, in part, at the 20th Annual Conference on Mass Spectrometry, Dallas, Texas, June 1972. The work reported here will constitute part of the Ph.D. Thesis to be submitted to the University of Toronto by A. S. Blair.

[2]An alternative approach is to measure the residence times directly. Such measurements using a pulsed high pressure source have been reported recently by Meisels and co-workers (10).

Can. J. Chem. Downloaded from www.nrcresearchpress.com by 210.87.254.40 on 09/05/12
For personal use only.

Can. J. Chem. Downloaded from www.nrcresearchpress.com by 210.87.254.40 on 09/05/12
For personal use only.

and $C_2H_5^+$ in mixtures with methane. The present work reports the study of the ionic reactions occurring in mixtures of methane with the polar molecules acetaldehyde-d_4, ethylene-d_4 oxide, dimethyl-d_6 ether, acetone, and acetonitrile.[3] We have obtained rate coefficients and approximate product yields for reaction of CH_5^+ and $C_2H_5^+$ with the organic neutral and, in addition, rate coefficients for reaction of CH_3^+ and CH_4^+ with the organic neutral. With the exception of CH_3CN, the ion–molecule reactions occurring in the one-component polar molecule systems have been studied previously (13) using the ion-trapping technique.

Experimental

All experimental work was carried out using the mass spectrometer and ion trapping technique described previously (11). In this technique ions produced during a short pulse (~ 1 μs) of ionizing electrons of suitable energy are trapped in the negative space charge associated with a continuous electron beam of energy insufficient to cause ionization. A known and variable time after ion formation a positive voltage pulse is applied to the repeller electrode in the ion source to remove the ions for mass analysis. Delay times between the ionizing and withdrawal pulses (and, hence, reaction times) of up to 3.2 ms were used in the present work.

Figure 1 illustrates the results obtained with pure methane at ionizing electron energies sufficient to produce only CH_3^+ and CH_4^+ primary ions. The CH_3^+ and CH_4^+ ions react rapidly with methane to form $C_2H_5^+$ and CH_5^+ respectively (reactions 1 and 2).

[1] $$CH_3^+ + CH_4 \rightarrow C_2H_5^+ + H_2$$

[2] $$CH_4^+ + CH_4 \rightarrow CH_5^+ + CH_3$$

In agreement with previous studies (11, 14, 15) we find that these products do not react further with methane; consequently their relative intensities remain constant from 0.6 to 3.2 ms. When a small amount of a reactive additive is mixed with the methane the CH_5^+ and $C_2H_5^+$ intensities initially increase (reactions 1 and 2); however, they pass through a maximum and then decrease due to reaction with the additive (see, for example, Fig. 2). From the linear portions of the semi-logarithmic plots for the CH_5^+ and $C_2H_5^+$ ions the rate coefficients for reaction with the additive can be determined.

In the present work runs were carried out using CH_4 to additive concentration ratios ranging from 5:1 to 10:1 at approximately 0.5 to 1.0 $\times 10^{13}$ molecule cm^{-3} total source concentration for determination of the rate coefficients. Mixtures were made up accurately by pressure and at least three different mixtures were used to determine the rate data. The error limits quoted represent the mean deviation of the experimental results. Source pressures were not measured directly but were related to the inlet pressure through observation of the rate of reaction 2 in pure methane. All rate data are therefore relative to the established value (16) $k_2 = 1.20 \times 10^{-9}$ cm^3 molecule^{-1} s^{-1}. At the inlet and source pressures used the gas flow from the inlet system to the ion source and the gas flow out of the ion source both are molecular with the result that the gas composition in the ion source is the same as that in the inlet system.

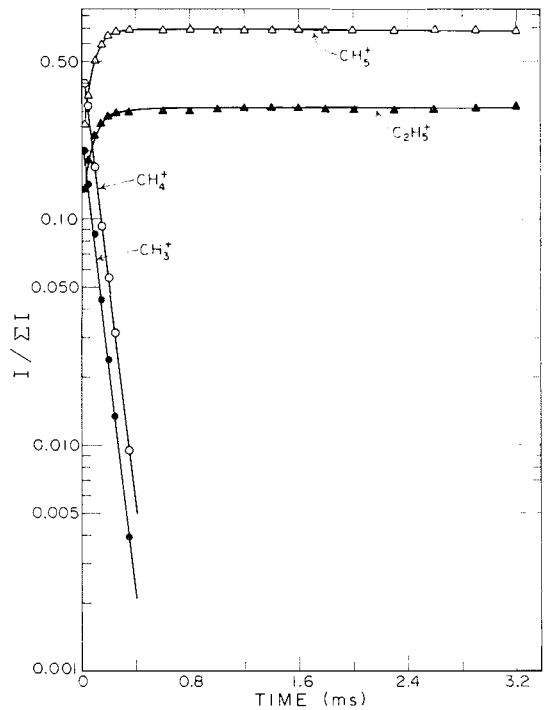

FIG. 1. Methane system $[CH_4] = 9.80 \times 10^{12}$ molecules cm^{-3}.

Additional runs were carried out using approximately 100:1 mixtures at low ionizing energies (CH_4^+ only significant primary ion from methane) to estimate the products formed by reaction of CH_5^+ with the additive. The approximate fractional yields were estimated from the slopes of the plots of the product ion intensities *vs.* $\Delta I_{CH_5^+}$, the CH_5^+ which had reacted, covering the experimental time range beyond 0.5 ms, *i.e.* after the primary methane ions had reacted completely. The yields from reaction of $C_2H_5^+$ were estimated in a similar fashion from runs at higher electron energy after substraction of the CH_5^+ yields.

In the mixtures CH_3^+ and CH_4^+ ions disappear not only by reactions 1 and 2 respectively, but also by reaction with the additive M. Considering reactions 1 and 3 for CH_3^+ we may derive equation 4 for the time dependence of $I_{CH_3^+}$.

[3] $$CH_3^+ + M \rightarrow \text{Products}$$

[4] $$\log I_{CH_3^+} = \frac{-(k_1[CH_4] + k_3[M])t}{2.303} + \text{constant}$$

[3]The deuterated compounds were used in the first three cases to avoid complications due to the $C_2H_5^+$–CHO^+ doublet at *m/e* 29.

TABLE 1. Rate coefficients for reaction of CH_5^+ and $C_2H_5^+$*

M	Dipole moment (Debye)	k			
		$CH_5^+ + M$		$C_2H_5^+ + M$	
		Experimental	Calculated†	Experimental	Calculated†
$(CD_3)_2O$	1.30	2.97 ± 0.24	2.36	2.14 ± 0.19	2.03
CD_2CD_2O	1.90	3.11 ± 0.13	2.66	1.98 ± 0.14	2.31
CD_3CDO	2.72	4.20 ± 0.35	3.27	3.37 ± 0.42	2.86
$(CH_3)_2CO$	2.88	5.26 ± 0.18	3.51	3.99 ± 0.18	3.01
CH_3CN	3.96	4.90 ± 0.24	4.23	3.46 ± 0.12	3.79

*All rate coefficients cm^3 $molecule^{-1}$ s^{-1} × 10^9.
†See text.

From the slope of the plot of log $I_{CH_3^+}$ *vs.* t at constant source concentration we may estimate k_3 since k_1, $[CH_4]$, and [M] are known. A similar equation can be derived for the time dependence of $I_{CH_4^+}$ permitting evaluation of the rate coefficient for reaction of CH_4^+ with M. The value $k_1 = 1.15 \times 10^{-9}$ cm^3 $molecule^{-1}$ s^{-1} (11) was used. In the mixtures used approximately 10–30% of the CH_3^+ or CH_4^+ reacted with the additive, the remainder reacting with methane. Consequently larger errors are possible in the reported rate coefficients for reaction of CH_3^+ and CH_4^+.

All ion intensities in the following are reported as a fraction of the total recorded ion current.

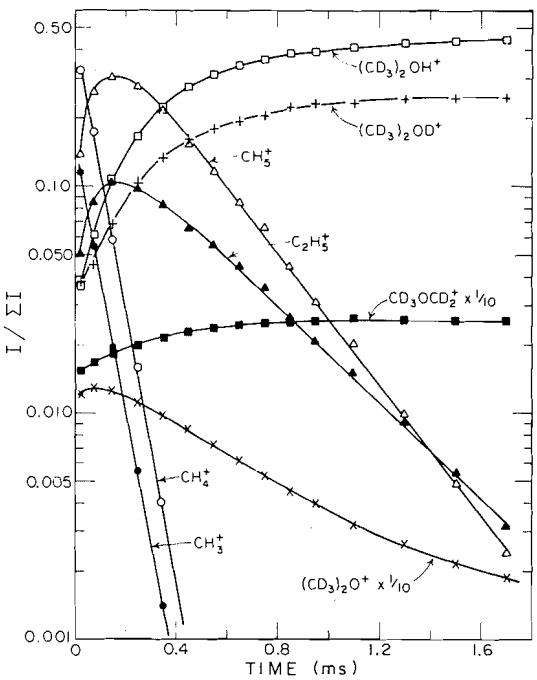

FIG. 2. Methane – dimethyl-d_6 ether system $[CH_4]$ = 9.77 × 10^{12} molecules cm^{-3}, $[(CD_3)_2O]$ = 1.01 × 10^{12} molecules cm^{-3}.

The methane used was Matheson Research grade. Acetaldehyde-d_4, ethylene-d_4 oxide, and dimethyl-d_6 ether were from Merck, Sharp and Dohme, Montreal. Acetonitrile and acetone were commercial samples of high purity. None of the samples showed detectable impurities in their mass spectra.

Results and Discussion

Methane – Dimethyl-d_6 Ether

Typical results obtained in a 9.68:1.00 CH_4–$(CD_3)_2O$ mixture are shown in Fig. 2. The non-linear semi-logarithmic plot for $(CD_3)_2O^+$ at longer times may not be real since this low intensity peak was slightly masked by the large $(CD_3)_2OH^+$ peak, making accurate intensity measurements difficult. Good linear plots for CH_5^+ and $C_2H_5^+$ are observed leading to the average rate coefficients for reaction with $(CD_3)_2O$ recorded in Table 1. The CH_5^+ datum is the average of ten determinations while the $C_2H_5^+$ datum is the average of eight determinations. Five different mixtures were used ranging from 10.21:1.00 to 4.48:1.00 CH_4:$(CD_3)_2O$.

The rate coefficients obtained for reaction of CH_3^+ and CH_4^+ with $(CD_3)_2O$ are presented in Table 2; the former is the average of eight determinations while the latter is the average of thirteen determinations. The previous ion-trapping study (13) of the reactions in $(CH_3)_2O$ has established the reaction

[5] $CH_3^+ + (CH_3)_2O \rightarrow CH_3OCH_2^+ + CH_4$

with a rate coefficient of 2.0 ± 0.3 × 10^{-9} cm^3 $molecule^{-1}$ s^{-1}. The present value for the rate coefficient for the $CH_3^+ + (CD_3)_2O$ reaction is in agreement within the combined experimental error. The increase in $CD_3OCD_2^+$ appears too great to be attributed entirely to reaction of

Can. J. Chem. Downloaded from www.nrcresearchpress.com by 210.87.254.40 on 09/05/12
For personal use only.

TABLE 2. Rate coefficients for reaction of CH_3^+ and CH_4^+ with M*

	k			
	$CH_3^+ + M$		$CH_4^+ + M$	
M	Experimental	Calculated†	Experimental	Calculated†
$(CD_3)_2O$	2.58 ± 0.31	2.47	2.24 ± 0.35	2.42
CD_2CD_2O	1.68 ± 0.13	2.83	2.29 ± 0.27	2.72
CD_3CDO	3.10 ± 0.3	3.48	3.68 ± 0.46	3.33
$(CH_3)_2CO$	4.85 ± 0.31	3.66	4.08 ± 0.45	3.58
CH_3CN	1.63 ± 0.05	4.35	3.92 ± 0.15	4.27

*All rate coefficients: cm^3 molecule^{-1} s^{-1} × 10^9.
†See text.

CH_3^+ and it appears likely that CH_4^+ produces this ion as well as $(CD_3)_2O^+$, which increases at short reaction times, by charge transfer.[4] Proton transfer from CH_4^+ to $(CD_3)_2O$ may also occur. These reactions are all thermochemically permitted,[5] however it is not possible to establish their relative importance.

Figure 3*a* shows the variation of ion intensities with time in a 107:1.0 CH_4–$(CD_3)_2O$ mixture at low ionizing energies (CH_4^+ only primary ion from methane) covering the time range from 0.5 to 2.5 ms. Figure 3*b* shows the product ion intensities plotted *vs.* $\Delta I_{CH_5^+}$, the CH_5^+ which has reacted. $\Delta I_{CH_5^+} = I_{CH_5^+}\ (t = 0.5\text{ ms}) - I_{CH_5^+}\ (t)$. From the slopes of the linear plots in Fig. 3*b* we estimate that 84% of the CH_5^+ reaction produces $(CD_3)_2OH^+$, 7% produces $CD_3OCD_2^+$, and 9% produces $(CD_3)_2O^+$ or some other species which subsequently forms $(CD_3)_2OD^+$.

The first two products presumably are formed by the reaction sequence[6]

[6] $$CH_5^+ + (CD_3)_2O \rightarrow (CD_3)_2OH^+ + CH_4 \qquad \Delta H = -59\text{ kcal mol}^{-1}$$

[7] $$(CD_3)_2OH^+ \rightarrow CD_3OCD_2^+ + HD \qquad \Delta H = +19\text{ kcal mol}^{-1}$$

[4]In the pure ether $CD_3OCD_2^+$ is neither produced nor does it react to a significant extent at the electron energy employed (13).

[5]Thermochemical data are taken from ref. 17 unless otherwise noted. Heats of formation of deuterium containing species are assumed to be identical to the species containing the lighter isotope.

[6]Thermochemical calculations employ $\Delta H_f((CH_3)_2OH^+) = 136$ kcal mol^{-1}, derived from the proton affinity, *PA* ($(CH_3)_2O = 186$ kcal mol^{-1} (18)), $\Delta H_f(CH_3OCH_2^+) = 155$ kcal mol^{-1} (19), and $\Delta H_f(CH_5^+) = 221$ kcal mol^{-1} (20), ($PA(CH_4) = 127$ kcal mol^{-1}).

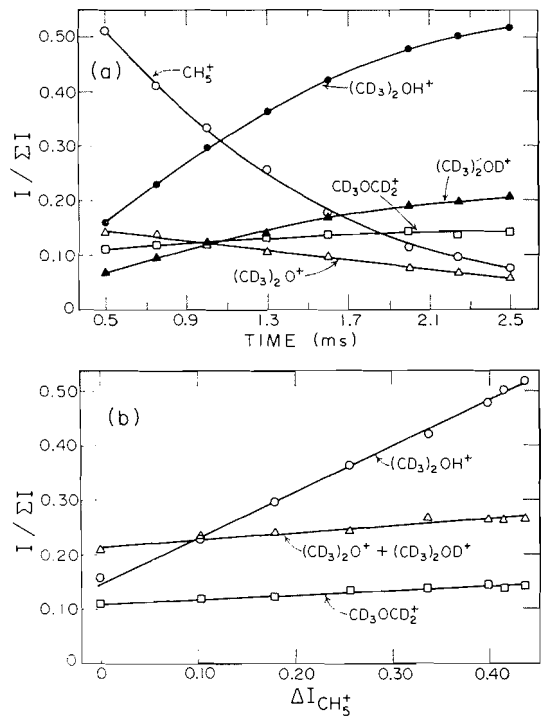

FIG. 3. Methane – dimethyl-d_6 ether system [CH_4]:[$(CD_3)_2O$] = 107:1.0, total source concentration ~2.5 × 10^{13} molecules cm^{-3}. (*a*) Ion intensities *vs.* time. (*b*) Product ion intensities *vs.* $\Delta I_{CH_5^+}$.

The low yield of $CD_3OCD_2^+$ suggests that little of the exothermicity of reaction 6 is retained as internal excitation of the product ion to assist in surmounting the energy barrier for reaction 7.

The increase in the sum $(CD_3)_2O^+ + (CD_3)_2OD^+$, which experimentally is an increase in $(CD_3)_2OD^+$, indicates the formation of a precursor to this ion which must be either $(CD_3)_2O^+$ or CDO^+ (13). Formation of

Can. J. Chem. Downloaded from www.nrcresearchpress.com by 210.87.254.40 on 09/05/12
For personal use only.

$(CD_3)_2O^+$, reaction 8, is quite endothermic and it is probable that at least part of the reaction of CH_5^+ produces CDO^+ by the exothermic reaction 6 followed by reaction 9.

[8] $CH_5^+ + (CD_3)_2O \rightarrow (CD_3)_2O^+ + CH_4 + H$
$\Delta H = +43$ kcal mol^{-1}

[9] $(CD_3)_2OH^+ \rightarrow CDO^+ + HD + CD_4$
$\Delta H = +43$ kcal mol^{-1} [7]

The $C_2H_5^+$ ion reacted with the ether entirely (>95%) by proton transfer at the pressures used in our experiments.

Methane – Ethylene-d_4 Oxide

Figure 4 shows typical results obtained in a 4.84:1.00 CH_4–C_2D_4O mixture. The rate coefficients for reaction of CH_5^+ and $C_2H_5^+$ with the oxide, calculated from the linear portions of the semi-logarithmic plots, are given in Table 1. Each value is the average of five determinations in three different mixtures.

The average rate coefficients determined for reaction of CH_3^+ (four determinations) and CH_4^+ (seven determinations) are summarized in Table 2. The products of the reactions are not clearly established, however $C_2D_3O^+$ and $C_2D_4O^+$ show substantial initial increases in intensity showing that they are products of ion–molecule reactions. Similarly the plot for CDO^+ shows an initial slight increase and curvature consistent with its formation in low yield. It is probable that CH_3^+ reacts with C_2D_4O predominantly by D^- abstraction to produce $C_2D_3O^+$ while CH_4^+ reacts by charge transfer to produce CDO^+ and $C_2D_4O^+$; CH_4^+ may also proton transfer to C_2D_4O. All these reactions are thermochemically permitted.

Figure 5*a* shows the variation of ion intensities with time from 0.5 to 2.0 ms in a 116:1.0 CH_4–C_2D_4O mixture under conditions where CH_4^+ was the only significant primary ion from methane. The plot of product ion intensities *vs.* $\Delta I_{CH_5^+}$ derived from 5*a* is shown in Fig. 5*b*. There is a small but definite increase[8] in $C_2D_4O^+$

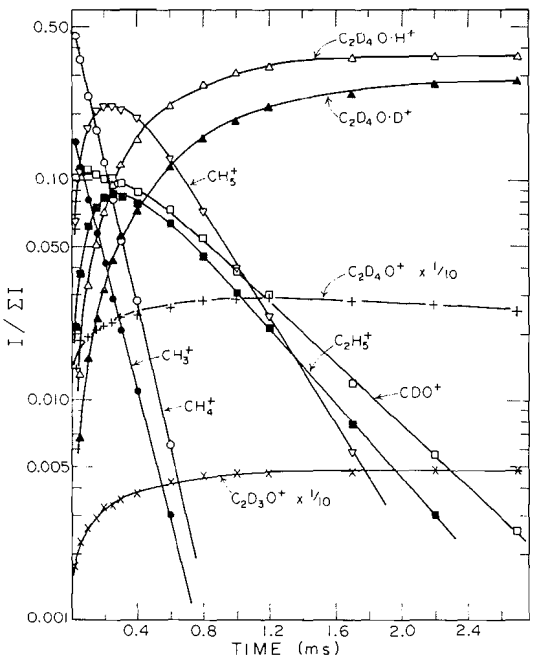

FIG. 4. Methane – ethylene-d_4 oxide system $[CH_4] = 4.50 \times 10^{12}$ molecules cm^{-3}, $[C_2D_4O] = 0.93 \times 10^{12}$ molecules cm^{-3}.

[7]Calculated using $\Delta H_f(CDO^+) = 197$ kcal mol^{-1} (21).

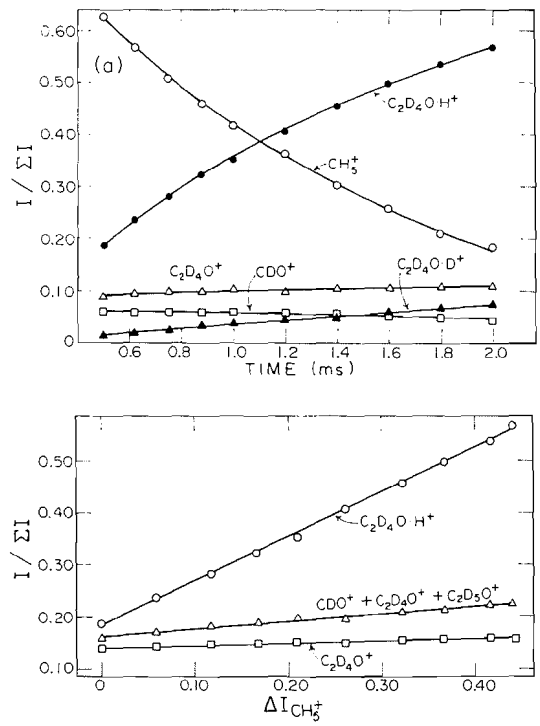

FIG. 5. Methane – ethylene-d_4 oxide system $[CH_4]$: $[C_2D_4O] = 116:1.0$, total source concentration ~2.5 × 10^{13} molecules cm^{-3}. (*a*) Ion intensities *vs* time. (*b*) Product ion intensities *vs.* $\Delta I_{CH_5^+}$.

[8]The increase is detectable because $C_2D_4O^+$ reacts only very slowly with C_2D_4O (13) and, apparently, is unreactive with methane.

Can. J. Chem. Downloaded from www.nrcresearchpress.com by 210.87.254.40 on 09/05/12
For personal use only.

Can. J. Chem. Downloaded from www.nrcresearchpress.com by 210.87.254.40 on 09/05/12
For personal use only.

(~0.05 fractional yield) even though reaction 10 is strongly endothermic.

[10] $CH_5^+ + C_2D_4O \rightarrow C_2D_4O^+ + CH_4 + H$
$\Delta H = +57$ kcal mol^{-1}

The increase cannot be due to formation of other ions which subsequently react to form $C_2D_4O^+$ since no such reactions were detected in the study of the ionic reactions in ethylene oxide (13). The major product is $C_2D_4O{\cdot}H^+$ (~0.84 fractional yield) with a smaller yield (~0.11 fractional yield) of CDO^+ which reacts rapidly (13) to produce $C_2D_4OD^+$. The $C_2D_4O{\cdot}H^+$ and CDO^+ products are formed by the reaction sequence[9]

[11] $CH_5^+ + C_2D_4O \rightarrow C_2D_4OH^+ + CH_4$
$\Delta H = -56$ kcal mol^{-1}

[12] $C_2D_4OH^+ \rightarrow CDO^+ + CD_3H$
$\Delta H = +9$ kcal mol^{-1}

The $C_2H_5^+$ ion reacts entirely (>95%) by proton transfer under our experimental conditions.

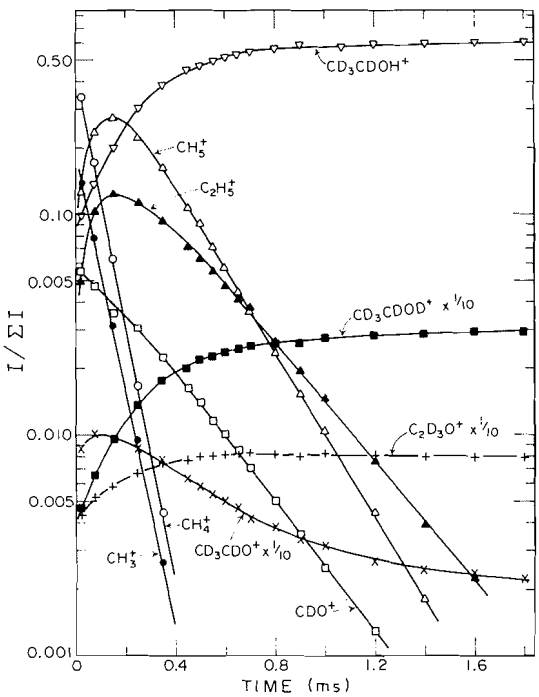

FIG. 6. Methane – acetaldehyde-d_4 system [CH_4] = 9.15×10^{12} molecules cm^{-3}, [CD_3CDO] = 0.99×10^{12} molecules cm^{-3}.

[9]Thermochemical calculations employ $\Delta H_f(C_2H_4O{\cdot}H^+) = 170$ kcal mol^{-1} (18).

Methane – Acetaldehyde-d_4

Typical results obtained in a 9.26:1.00 CH_4–CD_3CDO mixture are shown in Fig. 6. The non-linear semi-logarithmic plot for CD_3CDO^+ at longer reaction times may be an experimental artifact arising from an incorrect estimation of the overlap with the large CD_3CDOH^+ ion signal. Five different mixtures were studied leading to the average rate constants (nine determinations in each case) recorded in Table 1.

The rate coefficients derived for the reactions of CH_3^+ and CH_4^+ with CD_3CDO are recorded in Table 2. The former is the average of three determinations while the latter is the average of eight determinations, each in three different mixtures. Previous trapped-ion experiments (13) have shown that CH_3^+ reacts with CH_3CHO with a rate coefficient of $2.49 \pm 0.05 \times 10^{-9}$ cm^3 molecule^{-1} s^{-1}, predominantly by reaction 13.

[13] $CH_3^+ + CH_3CHO \rightarrow C_2H_3O^+ + CH_4$

The present result for the reaction $CH_3^+ + CD_3CDO$, $k = 3.10 \pm 0.3 \times 10^{-9}$ cm^3 molecule^{-1} s^{-1} is slightly larger but has a large error associated with it. The reaction of CH_4^+ with CD_3CDO produces both CD_3CDO^+ (reaction 14) and possibly CDO^+ (reaction 15) as shown by the initial curved regions of the semi-logarithmic plots for these ions. Proton transfer (reaction 16) is also possible.

[14] $CH_4^+ + CD_3CDO \rightarrow CD_3CDO^+ + CH_4$
$\Delta H = -56$ kcal mol^{-1}

[15] $CH_4^+ + CD_3CDO \rightarrow CDO^+ + CD_3 + CH_4$
$\Delta H = -22$ kcal mol^{-1}

[16] $CH_4^+ + CD_3CDO \rightarrow CD_3CDOH^+ + CH_3$
$\Delta H = -57$ kcal mol^{-1}

Figure 7*a* shows the variation of ion intensities over the time range 0.5 to 2.0 ms in a 125:1.0 CH_4–CD_3CDO mixture at an ionizing electron energy such that CH_3^+ production from methane was negligible. The derived plots of ion intensities *vs.* $\Delta I_{CH_5^+}$ are shown in Fig. 7*b*. From these plots we estimate as fractional yields from the reaction $CH_5^+ + CD_3CDO$: CD_3CDOH^+, 0.94; $C_2D_3O^+$, 0.02_5; CDO^+ or CD_3CDO^+, 0.03_5. (The latter two cannot be distinguished since both react to form CD_3CDOD^+.)

The CD_3CDOH^+ and $C_2D_3O^+$ products probably originate from the reaction sequence

Can. J. Chem. Downloaded from www.nrcresearchpress.com by 210.87.254.40 on 09/05/12
For personal use only.

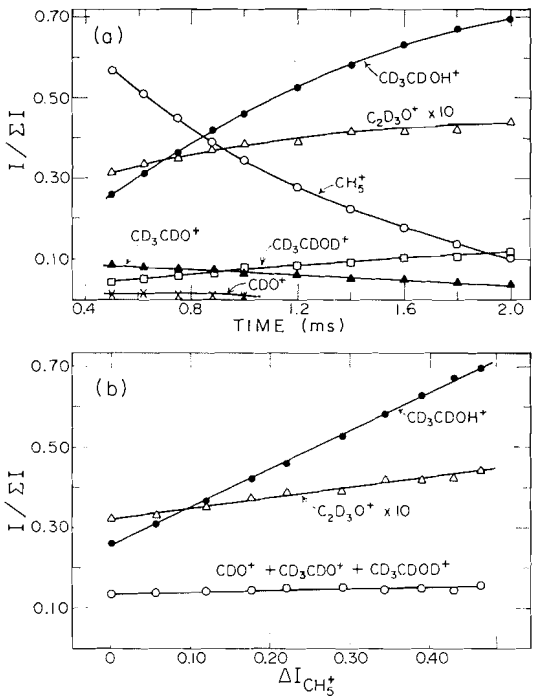

FIG. 7. Methane–acetaldehyde-d_4 system, $[CH_4]$: $[CD_3CDO] = 125:1.0$, total source concentration $\sim 2.5 \times 10^{13}$ molecules cm^{-3}. (*a*) Ion intensities *vs.* time. (*b*) Product ion intensities *vs.* $\Delta I_{CH_5^+}$.

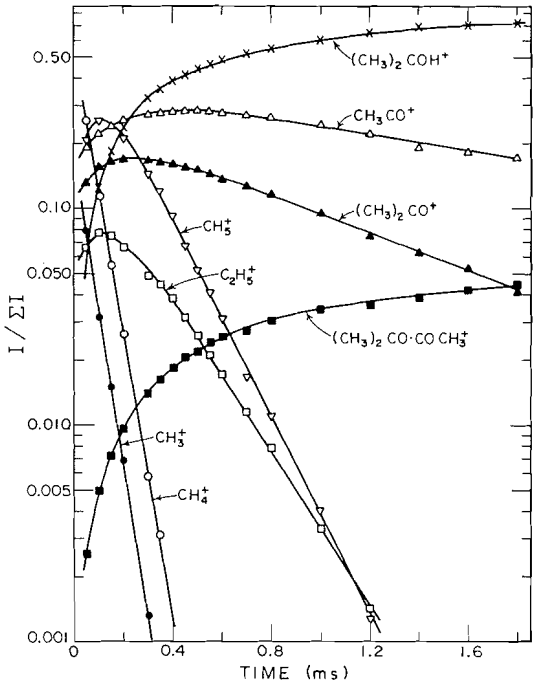

FIG. 8. Methane–acetone system, $[CH_4] = 9.72 \times 10^{12}$ molecules cm^{-3}, $[(CH_3)_2CO] = 1.00 \times 10^{12}$ molecules cm^{-3}.

[17] $CH_5^+ + CD_3CDO \rightarrow CD_3CDOH^+ + CH_4$
$\Delta H = -56$ kcal mol^{-1}

[18] $CD_3CDOH^+ \rightarrow CD_3CO^+ + HD$
$\Delta H = +9$ kcal mol^{-1}

The low yield of $C_2D_3O^+$ again suggests that the ionic product of the proton transfer reaction contains little of the exothermicity of the reaction as internal excitation.

Production of CD_3CDO^+ and CDO^+ cannot be separated since both react rapidly with CD_3CDO to form CD_3CDOD^+ (13).[10] Formation of CD_3CDO^+ by the charge transfer reaction 19 is quite endothermic while formation of CDO^+ by the exothermic reaction 17 followed by reaction 20 is thermochemically possible.

[19] $CH_5^+ + CD_3CDO \rightarrow CD_3CDO^+ + CH_4 + H$
$\Delta H = +49$ kcal mol^{-1}

[20] $CD_3CDOH^+ \rightarrow CDO^+ + CD_3H$
$\Delta H = +36$ kcal mol^{-1}

The $C_2H_5^+$ ion reacts essentially completely (>95%) by proton transfer to CD_3CDO.

Methane–Acetone

Figure 8 illustrates typical results obtained in a 9.72:1.00 CH_4–$(CH_3)_2CO$ mixture. The rate coefficients for reaction of CH_5^+ and $C_2H_5^+$ with acetone determined from the linear portions of the semi-logarithmic plots are recorded in Table 1. Each value is the average of five determinations in three different mixtures.

The rate coefficients estimated for reaction of CH_3^+ and CH_4^+ with acetone are recorded in Table 2. The CH_3^+ result is the average of four determinations while the CH_4^+ result is the average of six determinations both employing three different mixtures. The plots of the CH_3CO^+ and $(CH_3)_2CO^+$ ion intensities both show initial increases indicating that these ions are produced by reaction of CH_3^+ and CH_4^+ while $(CH_3)_2COH^+$ production by proton transfer from CH_4^+ is also possible. The thermochemically permitted reactions are[11]

[10]On the other hand CD_3CO^+ is unreactive with CD_3CDO (13).

[11]Thermochemical calculation employs $\Delta H_f((CH_3)_2COH^+) = 125$ kcal mol^{-1} (22, 23). A value of 111 kcal mol^{-1} has also been reported (24).

Can. J. Chem. Downloaded from www.nrcresearchpress.com by 210.87.254.40 on 09/05/12
For personal use only.

[21] $CH_3^+ + (CH_3)_2CO \rightarrow (CH_3)_2CO^+ + CH_3$
$\Delta H = -4$ kcal mol^{-1}

[22] $CH_4^+ + (CH_3)_2CO \rightarrow (CH_3)_2CO^+ + CH_4$
$\Delta H = -69$ kcal mol^{-1}

[23] $CH_4^+ + (CH_3)_2CO \rightarrow CH_3CO^+ + CH_3 + CH_4$
$\Delta H = -55$ kcal mol^{-1}

[24] $CH_4^+ + (CH_3)_2CO \rightarrow (CH_3)_2COH^+ + CH_3$
$\Delta H = -64$ kcal mol^{-1}

Figure 9*a* shows the variation of ion intensities with time between 0.5 and 2.0 ms in a 157:1.0 CH_4–$(CH_3)_2CO$ mixture where CH_5^+ is the only reactant ion produced from methane. Figure 9*b* shows the plot of product ion intensities *vs.* $\Delta I_{CH_5^+}$ derived from this data. The $(CH_3)_2COH^+$ product accounts for ~98% of the reaction of CH_5^+ while CH_3CO^+ accounts for ~2% of the reaction; in addition there may be a very small yield of $(CH_3)_2CO^+$. The yields of CH_3CO^+ and $(CH_3)_2CO^+$ are lower limits while that for $(CH_3)_2COH^+$ is an upper limit since both $(CH_3)_2CO^+$ and CH_3CO^+ react with acetone to form $(CH_3)_2COH^+$.[12] The reactions definitely occurring are

[25] $CH_5^+ + (CH_3)_2CO \rightarrow (CH_3)_2COH^+ + CH_4$
$\Delta H = -62$ kcal mol^{-1}

[26] $(CH_3)_2COH^+ \rightarrow CH_3CO^+ + CH_4$
$\Delta H = +10$ kcal mol^{-1}

The $C_2H_5^+$ ion reacts with acetone entirely (>95%) by proton transfer at the pressures we have used.

Methane–Acetonitrile

Figure 10 shows typical results obtained in a 9.78:1.00 CH_4–CH_3CN mixture. The rate coefficients for reaction of CH_5^+ and $C_2H_5^+$ derived from the linear portions of the semi-logarithmic plots are given in Table 1. Each value is the average of four determinations in three different mixtures. The only product detected from reaction of either CH_5^+ or $C_2H_5^+$ was protonated acetonitrile, CH_3CNH^+. Since the proton affinity of CH_3CN is 186 kcal mol^{-1} (23) while the proton affinities of CH_4 and C_2H_4 are 127 and 160 kcal mol^{-1}, respectively, these reactions are to be expected.

The rate coefficients determined for reaction of CH_3^+ and CH_4^+ with CH_3CN are given in Table 2. The CH_3^+ result is the average of four determinations while the CH_4^+ result is the average of eight determinations. The only products clearly identified by initial ion intensity increases are CH_2CN^+ and CH_3CNH^+. The former is probably formed by the hydride-transfer reaction 27.

[27] $CH_3^+ + CH_3CN \rightarrow CH_2CN^+ + CH_4$
$\Delta H = -1$ kcal mol^{-1}

There is no initial increase in the CH_3CN^+ intensity and we conclude that this ion cannot be formed to any significant extent by charge transfer from CH_4^+ even though the charge transfer is exothermic. It appears that CH_4^+ reacts entirely by proton transfer to form CH_3CNH^+. The CH_3CN^+ disappears in the mixtures more rapidly than can be accounted for[13] by reaction with CH_3CN and we estimate

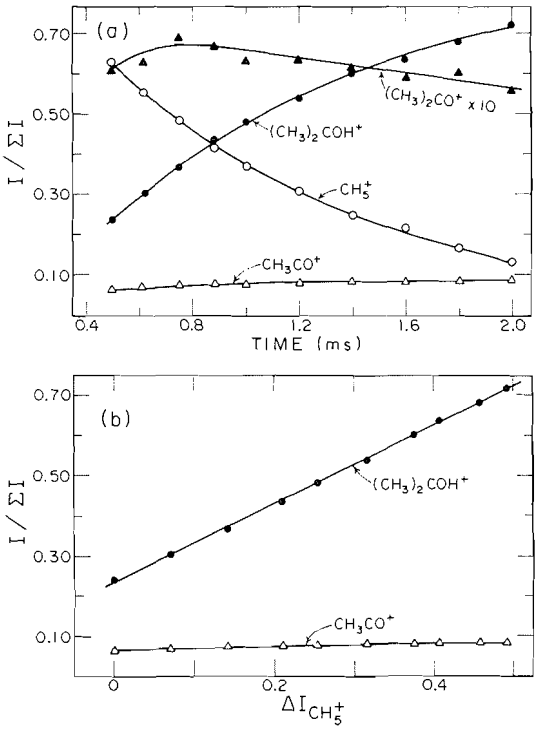

FIG. 9. Methane–acetone system, $[CH_4]:[(CH_3)_2CO] = 157:1.0$, total source concentration ~2.5×10^{13} molecules cm^{-3}. (*a*) Ion intensities *vs.* time. (*b*) Product ion intensities *vs* $\Delta I_{CH_5^+}$.

[12] $(CH_3)_2CO^+$ also reacts (13) with acetone to produce $(CH_3)_2CO{\cdot}COCH_3^+$ which is shown as a product ion in Fig. 8.

[13] In pure CH_3CN we find that CH_3CN^+ reacts with a total rate constant of $1.77 \pm 0.1 \times 10^{-9}$ cm^3 molecule^{-1} s^{-1} predominantly to form CH_3CNH^+. The rate constant is in reasonable agreement with previous values of $1.9_6 \times 10^{-9}$ cm^3 molecule^{-1} s^{-1} (16) and $2.0_1 \times 10^{-9}$ cm^3 molecule^{-1} s^{-1} (25).

Can. J. Chem. Downloaded from www.nrcresearchpress.com by 210.87.254.40 on 09/05/12
For personal use only.

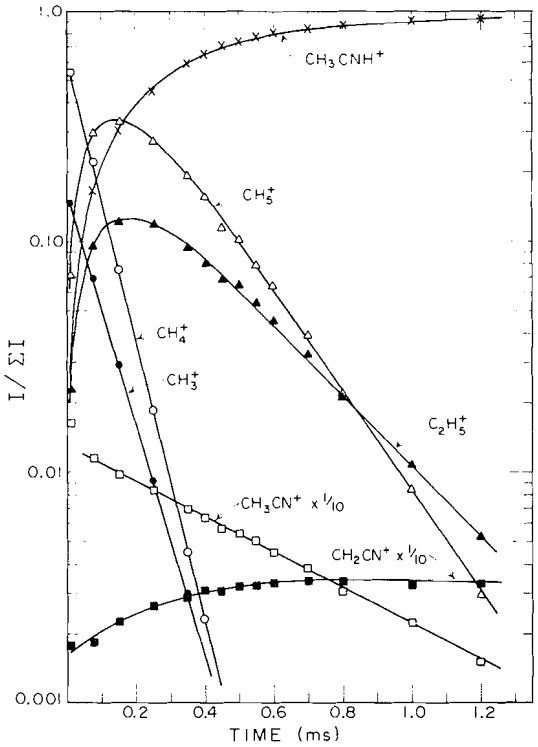

FIG. 10. Methane–acetonitrile system $[CH_4] = 9.59 \times 10^{12}$ molecules cm^{-3}, $[CH_3CN] = 0.98 \times 10^{12}$ molecules cm^{-3}.

for the reaction

[28] $CH_3CN^+ + CH_4 \rightarrow CH_3CNH^+ + CH_3$
$\Delta H = -51$ kcal mol^{-1}

a rate coefficient of $0.3_4 \pm 0.1 \times 10^{-9}$ cm^3 $molecule^{-1}$ s^{-1}.

Comparison of Experiment with Theory

The experimental rate coefficients tabulated in Tables 1 and 2 are, with few exceptions, much larger (at least a factor of two) than the rate coefficients calculated from a collision model which assumes only ion-induced dipole interactions (26). The most noticeable exceptions are the reactions of CH_3^+ with ethylene-d_4 oxide and with acetaldehyde where the experimental results are in reasonable agreement with the values, 1.44×10^{-9} and 1.48×10^{-9} cm^3 $molecule^{-1}$ s^{-1}, respectively, calculated from the ion-induced dipole model.

For the remaining reactions it is clear that ion–dipole interactions must play an important role. This is particularly evident for the proton-transfer results in Table 1 where there is an established trend for the rate coefficient to increase with the dipole moment of the neutral molecule. We have therefore calculated rate coefficients from a model which includes ion–dipole interactions. It has been shown previously (16) that if the dipole "locks-in" as the positive charge approaches the microscopic rate constant $k(g)$ as a function of the relative velocity, g, of the colliding pair is given by

$$[29] \qquad k(g) = 2\pi e\left(\frac{\alpha}{\mu}\right)^{1/2} + \frac{2\pi e\rho}{g\mu}$$

where e is the electronic charge, α the polarizability of the neutral, ρ the dipole moment of the neutral molecule, and μ the reduced mass of the colliding pair. From 29 we may derive (27), for the rate constant $k(E)$ at a relative kinetic energy of the two reactants, E, the expression

$$[30] \qquad k(E) = 2\pi e\left(\frac{\alpha}{\mu}\right)^{1/2} + \pi e\rho\left(\frac{2}{E\mu}\right)^{1/2}$$

Previous experiments (11) have shown that in the ion trapping technique the reactant ions have an average kinetic energy of 0.3 to 0.5 eV (lab scale). This corresponds to an approximate relative kinetic energy (center of mass) of 0.2 eV. Accordingly we have calculated from equation 30 rate coefficients for this value of E. These are listed in Tables 1 and 2 under the heading k(calcd). The calculated values are a factor of two to three higher than those obtained including the ion-induced dipole term only and are, in most cases, in moderately good agreement with the experimental values.

For two reasons this agreement cannot be taken to indicate anything more than the fact that ion–dipole forces are important. First the calculated values depend strongly on E which is not known accurately. Second, the calculations are based on a "locked-in" dipole model which is known (28–30) from trajectory calculations to be a highly simplified and naive model. However, the trajectory calculations have shown that even if the dipole does not "lock-in" ion–dipole interactions can cause a significant increase in the rate coefficients.

Conclusions

The present work has shown that the CH_5^+ and $C_2H_5^+$ ions produced by ion–molecule reactions in methane rapidly proton-transfer to polar organic molecules. The rapidity of these reactions is undoubtedly one of the reasons why chemical ionization mass spectrometry using

methane has been so successful since the rapid reactions will result in a high sensitivity for the technique. The rates of the proton transfer reactions depend on ion–dipole interactions with respect to both the magnitude of the rate constant and the trend among a series of polar molecules.

The above observations concerning ion–dipole effects are in contrast to the conclusions reached by Hellner and Sieck (24). They observed that proton-transfer reactions from $t\text{-}C_4H_9^+$ (produced by photoionization of neopentane) to acetone, ammonia, and various methyl amines all had rate coefficients which could be explained by ion-induced dipole interactions only and they concluded that ion–dipole effects were unimportant. There are a number of differences between our experiments and their's which may be important. Their reactant ions are produced by low energy photons and have thermal kinetic energies, while our reactant ions are produced by exothermic ion–molecule reactions and have $\sim$0.4 eV kinetic energy. In addition the reactions studied by Hellner and Sieck are approximately thermoneutral while those we have studied are strongly exothermic. We are continuing our studies in an effort to elucidate the effects of internal energy, kinetic energy, and reaction exothermicity on the rates of proton transfer reactions involving polar molecules.

The authors are indebted to the National Research Council of Canada for financial support and for the award of studentships (1968–1971) to A.S.B.

1. M. S. B. MUNSON and F. H. FIELD. J. Am. Chem. Soc. **88**, 2621 (1966).
2. (*a*) F. H. FIELD. Acc. Chem. Res. **1**, 42 (1968). (*b*) B. MUNSON. Anal. Chem. **43**, 28A (1971).
3. H. M. FALES. *In* Mass spectrometry techniques and applications. *Edited by* G. W. A. Milne. J. Wiley and Sons, New York, 1971. p. 179.
4. G. P. ARSENAULT. *In* Biochemical applications of mass spectrometry. *Edited by* G. R. Waller. J. Wiley and Sons, New York, 1972. p. 817.
5. F. H. FIELD. J. Am. Chem. Soc. **91**, 2827 (1969).
6. S. VREDENBURG, L. WOJCIK, and J. H. FUTRELL. J. Phys. Chem. **75**, 590 (1971).
7. S. L. CHONG and J. L. FRANKLIN. J. Chem. Phys. **54**, 1487 (1971).
8. J. J. SOLOMON and R. F. PORTER. J. Am. Chem. Soc. **94**, 1443 (1972).
9. E. W. MCDANIEL. Collision phenomena in ionized gases. J. Wiley and Sons, New York, 1967. Chapt. 9.
10. G. SROKA, C. CHANG, and G. G. MEISELS. J. Am. Chem. Soc. **94**, 1052 (1972).
11. A. A. HEROD and A. G. HARRISON. Int. J. Mass Spectrom. Ion Phys. **4**, 415 (1970).
12. A. S. BLAIR, E. J. HESLIN, and A. G. HARRISON. J. Am. Chem. Soc. **94**, 2935 (1972).
13. A. S. BLAIR and A. G. HARRISON. Can. J. Chem. **51**, 703 (1973).
14. F. H. FIELD and M. S. B. MUNSON. J. Am. Chem. Soc. **87**, 3289 (1965).
15. S. WEXLER, A. LIFSHITZ, and A. QUATTROCHI. Adv. Chem. Ser. **58**, 193 (1966).
16. S. K. GUPTA, E. G. JONES, A. G. HARRISON, and J. J. MYHER. Can. J. Chem. **45**, 3107 (1967).
17. Ionization Potentials, Appearance Potentials, and Heats of Formation of Gaseous Positive Ions. NSRDS-NBS 26. Washington, D.C. 1969.
18. J. L. BEAUCHAMP and R. C. DUNBAR. J. Am. Chem. Soc. **92**, 1477 (1970).
19. C. D. FINNEY and A. G. HARRISON. Int. J. Mass Spectrom. Ion Phys. **9**, 221 (1972).
20. W. A. CHUPKA and J. A. BERKOWITZ. J. Chem. Phys. **54**, 4256 (1971).
21. C. S. MATHEWS and P. WARNECK. J. Chem. Phys. **51**, 854 (1969).
22. A. G. HARRISON, A. IVKO, and D. VAN RAALTE. Can. J. Chem. **46**, 1625 (1966).
23. J. L. BEAUCHAMP. Annu. Rev. Phys. Chem. **22**, 527 (1971).
24. L. HELLNER and L. W. SIECK. J. Res. Natl. Bur. Stand. **75A**, 487 (1971).
25. J. L. FRANKLIN, Y. WADA, P. NATALIS, and P. M. HIERL. J. Phys. Chem. **70**, 2353 (1966).
26. G. GIOUMOUSIS and D. P. STEVENSON. J. Chem. Phys. **29**, 294 (1958).
27. S. E. BUTRILL, JR. Paper presented at 19th Annual Conference on Mass Spectrometry, Atlanta, Georgia, May, 1971.
28. J. V. DUGAN and J. L. MAGEE. National Aeronautics and Space Administration Report TN-D-3229. February, 1966.
29. J. V. DUGAN and J. L. MAGEE. J. Chem. Phys. **47**, 3103 (1967).
30. J. V. DUGAN and R. B. CANWRIGHT. J. Chem. Phys. **56**, 3623 (1972).

Can. J. Chem. Downloaded from www.nrcresearchpress.com by 210.87.254.40 on 09/05/12
For personal use only.

The Photolysis of 3,3,3-Trifluoropropyne

D. F. HOWARTH AND A. G. SHERWOOD

Department of Chemistry, Simon Fraser University, Burnaby 2, British Columbia

Received July 13, 1971[1]

The photolysis of 3,3,3-trifluoropropyne has been studied in the 190 nm wavelength region. The primary process is the dissociation of the compound to give ethynyl and trifluoromethyl radicals. In the presence of propane, these radicals undergo abstraction reactions to give fluoroform and acetylene. The presence of nitric oxide also results in the trapping of the CF_3 radical as CF_3NO. Ethynyl radicals are not trapped by NO.

La photolyse du trifluoro-3,3,3 propyne a été étudiée dans la zone de longueur d'onde 190 nm. Le processus primaire est la dissociation du composé en radicaux éthynyle et trifluorométhyle. En présence de propane, ces radicaux arrachent l'hydrogène et conduisent à l'acéthylène et au fluoroforme. La présence de nitroxyde a pour résultat également de piéger le radical CF_3 en CF_3NO. Les radicaux éthynyles ne sont pas piégés par NO. [Traduit par le journal]

Can. J. Chem., 51, 1655 (1973)

Introduction

Investigations of the gas phase photochemistry of alkynes have been almost inclusively confined to studies of acetylene and propyne. It has been suggested that, in the quartz-u.v. region, there are two primary processes, the formation of excited molecules and, as well, the formation of ethynyl radicals and H-atoms (1, 2). The mercury photosensitized decomposition of acetylene has also been studied (3–11) and the same primary products have been suggested although there is some disagreement about the extent of involvement of excited acetylene molecules.

Propyne has been photolyzed at wavelengths near the long wavelength limit of its u.v. absorption (12, 13) and at 147 nm (14). In the former case, propargyl radicals were observed by e.s.r. techniques suggesting the primary process

[1] $$CH_3\text{-}C{\equiv}CH + h\nu \rightarrow H\cdot + \cdot CH_2\text{-}C{\equiv}CH$$

At the shorter wavelength some elimination of molecular hydrogen is indicated.

The mercury photosensitization of propyne was studied by Kebarle (7). The primary product was suggested to be an excited molecule which decomposed to give a propargyl radical and an H-atom as in [1].

There was no indication in either the photosensitized reaction or in the direct photolyses of C—C bond cleavage to give methyl and ethynyl radicals, *i.e.*

[2] $$CH_3{-}C{\equiv}CH \xrightarrow{h\nu \text{ or } Hg(6^3P_1)} \cdot CH_3 + \cdot C{\equiv}CH$$

A study of the photolysis of 3,3,3-trifluoropropyne in the vapor phase was undertaken in order to determine if this type of reaction would take place when the methyl hydrogen atoms were replaced by far less labile fluorine atoms.

Experimental

Materials

Trifluoropropyne, obtained from Peninsular Chemresearch Co., was purified by gas chromatography before use. Nitric oxide, from Matheson of Canada Limited, was distilled prior to use to remove higher oxides of nitrogen. Propane, also from Matheson, was used without further purification. Butadiyne was prepared according to the method of Georgieff and Richard (15). Other chemicals required for calibration of the gas chromatograph were obtained from commercial suppliers.

Apparatus

Irradiations were carried out at 25 ± 2 °C in a Suprasil quartz cell, 10 cm long and 5 cm in diameter. The light source was an unfiltered Hanovia Model 30620 medium pressure mercury arc. Manipulations of reactants and products were done in a conventional high vacuum apparatus. Analysis was done by temperature programmed gas chromatography using a 6 ft × 3/10 in. I.D. Poropak Q column. The chromatograph was fitted with a trapping system so that peaks could be trapped for identification by i.r., n.m.r., and mass spectrometry.

Results and Discussion

Photolysis of Trifluoropropyne

Trifluoropropyne does not absorb at wavelengths greater than about 220 nm. Below this

[1]Revision received January 15, 1973.

Can. J. Chem. Downloaded from www.nrcresearchpress.com by 210.87.254.6 on 09/05/12
For personal use only.

[3] 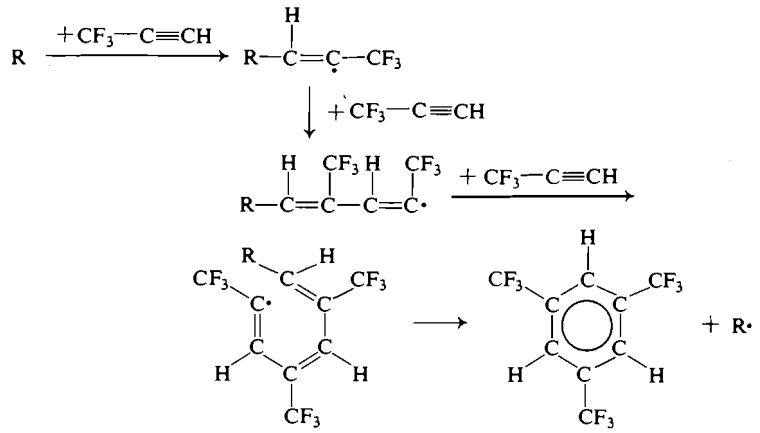

the effective absorption increases to the transmission limit of the cell at about 180 nm. Examination of the emission spectrum of the lamp indicates that the radiation responsible for photolysis is a pair of low intensity lines at 195 and 197 nm. The main product of this reaction is an involatile solid polymer. The only volatile product observed was identified by n.m.r. and by mass spectrometry as the trimer of trifluoropropyne 1,3,5-tris(trifluoromethyl)-benzene. In the absence of an authentic sample of this material, it was not determined quantitatively but the gas chromatographic peak areas indicated that the rates of formation dropped with extent of reaction presumably because of a decrease in the absorbed light intensity as the polymer deposited on the cell.

The origin of this compound is probably the type of reaction which was originally suggested by Cashion and LeRoy (4), *i.e.*, the successive addition of three propyne molecules to a radical followed by cyclization and elimination of the radical (see eq. 3).

The 1,3,5-isomer will be formed whether the initial attack is at the C-1 or -2 position provided only that subsequent attacks are the same as the first one. There was no indication of the formation of other isomers of the benzene so the attack must have been specific in this sense. These observations give no clue to the identity of the initiating radical so the reaction was conducted in the presence of propane as a source of abstractable hydrogen atoms in order to identify the radicals present.

Photolysis of CF_3—C≡CH with Added Propane

A pressure of 2.61 Torr of substrate was photolyzed for 1 h with various pressures of added propane. The propane had the effect of reducing the yield of the benzene while new products, CF_3H, C_2H_2, C_2HF, and 1,1,1,4,4,4-hexafluoro-2-butene were formed.

These results are shown graphically in Fig. 1. Fluoroacetylene is not indicated as its yield is very nearly constant at 0.29 μmol over the pressure of propane used (2). The yield of the trimer is given relative to the yield in the absence of propane.

The CF_3H and C_2H_2 indicate the presence of $CF_3\cdot$ and $C_2H\cdot$ radicals and the following primary process is suggested.

[4] $$CF_3 - C{\equiv}CH + h\nu \rightarrow CF_3\cdot + C_2H\cdot$$

followed by abstraction reactions.

[5] $$CF_3\cdot + C_3H_8 \rightarrow CF_3H + C_3H_7\cdot$$

[6] $$C_2H\cdot + C_3H_8 \rightarrow C_2H_2 + C_3H_7\cdot$$

The decrease in the benzene yield suggests that one of these radicals initiates reaction 3.

The hexafluorobutene must arise from the reaction of CF_3 radicals with substrate to form substituted vinyl radicals which subsequently abstract hydrogen from the propane (eqs. 7 and 8). The CF_3 radical thus adds, in the expected

[7] 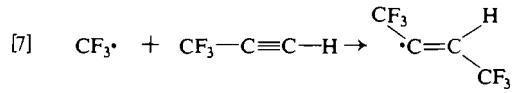

[8] 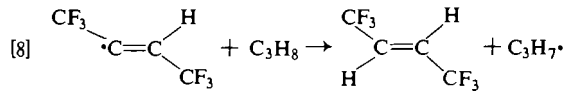

anti-Markovnikov fashion, to give a 2-butenyl radical. The product of the subsequent abstraction reaction was shown to be exclusively the

Can. J. Chem. Downloaded from www.nrcresearchpress.com by 210.87.254.6 on 09/05/12
For personal use only.

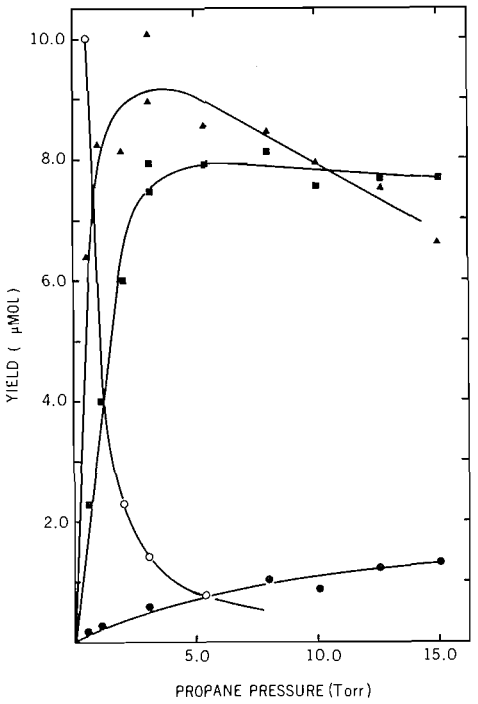

FIG. 1. Product yields as a function of propane pressure: ▲, hexafluoro-2-butene; ●, CF_3H; ■, C_2H_2; ○, 1,3,5-tris(trifluoromethyl) benzene. Pressure of CF_3—C≡CH = 2.61 Torr.

trans-isomer by comparison of its i.r. spectrum with that published by Henne and Nager (16) and by A.P.I. (17). As pointed out by Singer (18), this observation may not be interpreted unambiguously. It may indicate a *trans*-addition of the trifluoromethyl radical followed by abstraction before inversion of the vinyl radical could take place. The other possibility is that the butenyl radical rapidly assumes the more stable *trans*-isomeric form before abstraction takes place.

At pressures of propane greater than 5 Torr, most ethynyl radicals abstract hydrogen to give acetylene while few CF_3 radicals abstract to give CF_3H. Most CF_3 radicals add to substrate to eventually give the hexafluorobutene. This fact makes it possible to calculate a very approximate value of k_5/k_7 from the yields of CF_3H and the butene at low propane pressures. The value obtained is 0.1. Unfortunately there are no values in the literature with which to compare this approximation.

These pressures of propane depress the yield of the trimer to a very small value which suggests that the species which initiates reaction 3 to form the trimer is the ethynyl radical.

The fact that the yield of C_2H_2 is less than the yield of CF_3H + CF_3—CH=CH—CF_3 at intermediate propane pressures suggests that, under those conditions, some low-yield product of ethynyl radical reactions had escaped detection.

Photolysis of CF_3—C≡CH in the Presence of NO

The presence of NO inhibits the formation of the trimer and results in new products: CF_3NO, CF_3CN, butadiyne, and smaller amounts of C_2HF, C_2H_2, N_2O, CO_2, and an unidentified nitroso compound. Yields as a function of NO pressure are indicated in Figs. 2 and 3.

Comparison of emission spectrum of the lamp with the absorption spectrum of NO indicates that photoexcitation of NO had not occurred under the conditions of the experiment. The effect of NO must therefore be explained in terms of its reactions with reactive intermediates. The CF_3NO suggests the presence of CF_3 radicals.

[9] $$CF_3 + NO \rightarrow CF_3NO$$

The yield of this product, identified by its i.r.

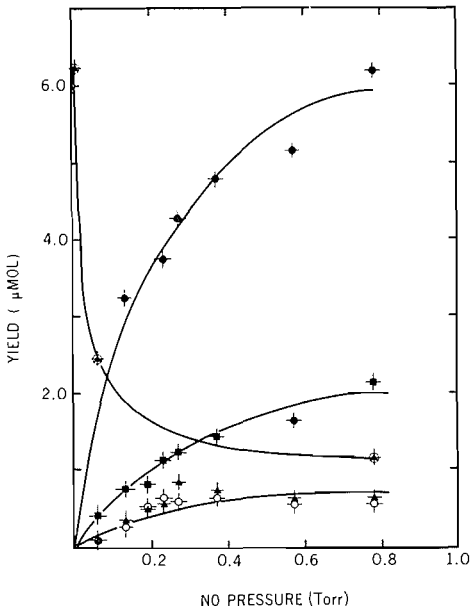

FIG. 2. Product yields as a function of NO pressure: ●, C_4H_2; ◬, 1,3,5-tris(trifluoromethyl) benzene; ■, CF_3CN; ▲, C_2HF; ○, C_2H_2. Pressure of CF_3—C≡CH = 2.61 Torr.

Can. J. Chem. Downloaded from www.nrcresearchpress.com by 210.87.254.6 on 09/05/12
For personal use only.

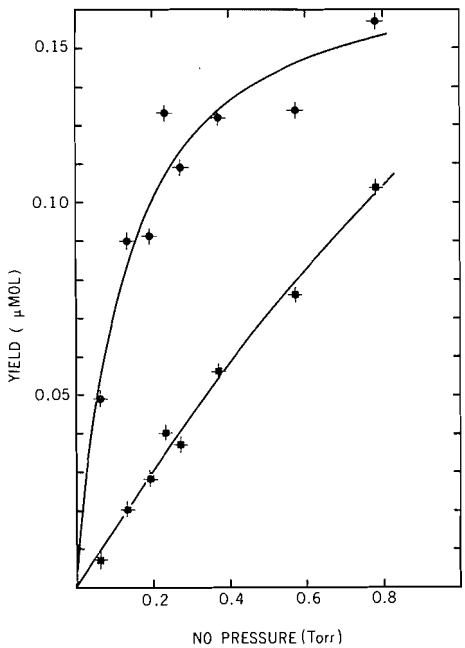

FIG. 3. Product yields as a function of NO pressure: ●, CO_2; ■, N_2O. Pressure of CF_3—C≡CH = 2.61 Torr.

and mass spectra, could not be determined quantitatively by gas chromatography. This difficulty has been encountered previously (19) and is no doubt associated with the formation of the CF_3NO dimer followed by its decomposition which has been shown (20) to yield N_2O and CO_2 which are also products of this reaction.

The vinyl radical formed in reaction 7 is no doubt the source of the nitrile by its reaction with NO in the manner indicated by Sherwood and Gunning (21) (see eq. 10).

[10] 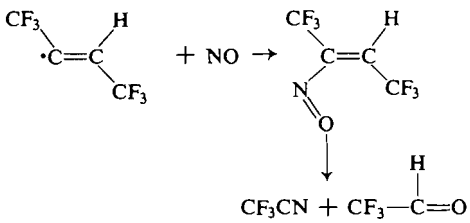

The fluoral, which would be expected from reaction 10 was not found and tests with an authentic sample indicated that it would not have survived the analytical procedures.

The formation of butadiyne by the reaction of ethynyl radicals with acetylenes in the presence of nitric oxide has been observed previously (21, 22). The absence of butadiyne among the

[11] $HC{\equiv}C\cdot + CF_3{-}C{\equiv}CH \rightarrow HC{\equiv}C{-}C{\equiv}CH + CF_3\cdot$

products of the uninhibited reaction, also observed previously in similar systems (21, 22), may be due to consumption of this product by free radicals or to actual participation of NO in its formation. This aspect of the problem requires further work as does the problem of the origins of the C_2HF and C_2H_2.

In summary, the main primary process seems to be the dissociation of the molecule into ethynyl and trifluoromethyl radicals, each of which initiates polymerization reactions. The propyne trimer has been shown to be a product of a free radical initiated reaction.

We thank Drs. O. P. Strausz and R. M. McDaniel of the University of Alberta for emission spectra of the light sources and we acknowledge the financial support of the National Research Council of Canada.

1. M. ZELIKOFF and L. M. ASCHENBRAND. J. Chem. Phys. **24**, 1034 (1956).
2. M. TSUKADA and S. SHIDA. Bull. Chem. Soc. Jap. **43**, 3621 (1970).
3. D. J. LEROY and E. W. R. STEACIE. J. Chem. Phys. **12**, 117 (1944).
4. J. K. CASHION and D. J. LEROY. Can. J. Chem. **32**, 906 (1954).
5. S. SHIDA, Z. KURI, and T. FURUOYA. J. Chem. Phys. **28**, 131 (1958).
6. A. SHERWOOD and H. E. GUNNING. Can. J. Chem. **38**, 466 (1960).
7. P. KEBARLE. J. Chem. Phys. **39**, 2218 (1963).
8. A. G. SHERWOOD and H. E. GUNNING. J. Phys. Chem. **69**, 1732 (1965).
9. M. TSUKUDA and S. SHIDA. J. Chem. Phys. **44**, 3133 (1966).
10. D. J. LEROY. J. Chem. Phys. **45**, 3482 (1966).
11. S. SHIDA, M. TSUKUDA, and T. OKA. J. Chem. Phys. **45**, 3483 (1966).
12. C. P. POOLE, JR. and P. S. ANDERSON. J. Chem. Phys. **31**, 346 (1959).
13. D. A. RAMSAY and P. THISTLETHWAITE. Can. J. Phys. **44**, 1381 (1966).
14. L. J. STIEF, V. J. DECARLO, and W. A. PAYNE. J. Chem. Phys. **54**, 1913 (1971).
15. K. K. GEORGIEFF and Y. RICHARD. Can. J. Chem. **36**, 1280 (1958).
16. A. L. HENNE and M. NAGER. J. Am. Chem. Soc. **73**, 5527 (1951).
17. A.P.I. Research Project 44, Infrared Spectra Data. Thermodynamic Research Center, Texas A and M University, College Station, Texas.
18. L. A. SINGER. Intra-Science Chem. Rep. **4**, 139 (1970).
19. J. HEICKLEN. J. Phys. Chem. **70**, 112 (1966).
20. J. MASON. J. Chem. Soc. 4531 (1963).
21. A. G. SHERWOOD and H. E. GUNNING. J. Am. Chem. Soc. **85**, 3506 (1963).
22. A. M. TARR, Q. P. STRAUSZ, and H. E. GUNNING. Trans. Faraday Soc. **61**, 1946 (1965); **62**, 1221 (1966).

Can. J. Chem. Downloaded from www.nrcresearchpress.com by 210.87.254.6 on 09/05/12
For personal use only.

Aromatic Substitutions with Carbanion Nucleophiles. II. The Kinetics and Mechanism of the Reaction of 1-Fluoro-2,4-dinitrobenzene with the Diethyl Malonate Anion[1,2]

KENNETH T. LEFFEK AND PAUL H. TREMAINE[3]

Department of Chemistry, Dalhousie University, Halifax, Nova Scotia

Received November 14, 1972

The reaction of fluoro-2,4-dinitrobenzene with the sodium salt of diethyl malonate to form diethyl (2,4-dinitrophenyl)malonate is fast in dimethyl sulfoxide solvent. The stable red color of the reaction solution is due to the anion of the product, although the initially formed unstable intermediate between the substrate and the anion nucleophile is also red and can be observed at times less than 200 ms after mixing.

The rate constants for all the steps in the reaction have been measured and the activation parameters for the three processes involved in the nucleophile substitution have been calculated.

La réaction du fluoro dinitro-2,4 benzène avec le sel de sodium du malonate d'éthyle est rapide dans le diméthyl sulfoxyde et conduit au (dinitro-2,4 phényl) malonate du diéthyle. Quoique l'intermédiaire instable formé initialement entre le substrat et l'anion soit rouge et qu'on puisse l'observé jusqu'à 200 ms après le mélange des réactifs, la couleur rouge stable de la solution réactionnelle est attribuée à l'anion du produit.

Les constantes de vitesse pour chacune des étapes de la réaction ont été mesurées et les paramètres d'activation pour chacun des trois processus impliqués dans une substitution nucléophile ont été calculés.

[Traduit par le journal]

Can. J. Chem., **51**, 1659 (1973)

Introduction

In the reaction of 1-fluoro-2,4-dinitrobenzene with diethyl malonate in the presence of triethylamine, Baudet reported (1) the observation of a stable intermediate **1** as a red material in DMSO solution. Leffek and Tremaine (2) compared this reaction with that of the sodium salt of diethylmalonate on the same substrate and re-interpreted Baudet's observation, assigning the red coloration to the anion of the final product diethyl (2,4-dinitrophenyl)malonate. In addition, Shein and Ivanova (3) disputed Baudet's interpretation and showed by fluorine n.m.r. spectroscopy that the stable red material contained no covalently bound fluorine.

This paper presents a spectrophotometric and kinetic study of the reaction between the diethyl malonate anion and 1-fluoro-2,4-dinitrobenzene in DMSO, which is believed to react as in eq. 1 under the experimental conditions in which the malonate anion is present in large excess.

[1]Reference 2 is considered to be Part I.

[2]Presented at the 54th Annual Canadian Chemical Conference of the Chemical Institute of Canada, Halifax, Nova Scotia June 1971.

[3]NRCC Postdoctorate Fellow, 1970–1971. Present address Vanier College St. Laurent, Montreal 379, P.Q.

Results and Discussion

On mixing 1-fluoro-2,4-dinitrobenzene and the sodium salt of diethyl malonate in DMSO, a stable purple color (λ_{max} 520 nm, $\varepsilon_{apparent}$ 24 000 l mol^{-1} cm^{-1}) was produced immediately. A solution of identical λ_{max} and ε was obtained when the same anion was mixed with 2,4-dinitrophenyl malonate **2** in DMSO. With the concentration of **2** equal to 6×10^{-5} *M* and the anion concentration varying between 1.5×10^{-3} and 1.5×10^{-2} *M*, the absorbance at 520 nm remained approximately constant; thus, this third step of the reaction appears to be in equilibrium predominantly on the side of the deprotonated product **3**. This result is as expected, since the acidity of 2,4-dinitrophenyl malonate **2** is obviously very much greater than that of the sodium salt of diethyl malonate. Also, since the third step is a proton transfer from a moderately strong carbon acid, k_3 should be larger than the other rate constants in the reaction scheme.

A series of kinetic experiments were carried out to determine the pseudo first-order rate constants by light absorption at 520 nm with the anion concentration in large excess over that of the substrate. These rate constants are shown

Can. J. Chem. Downloaded from www.nrcresearchpress.com by 210.87.254.42 on 09/05/12
For personal use only.

[1]

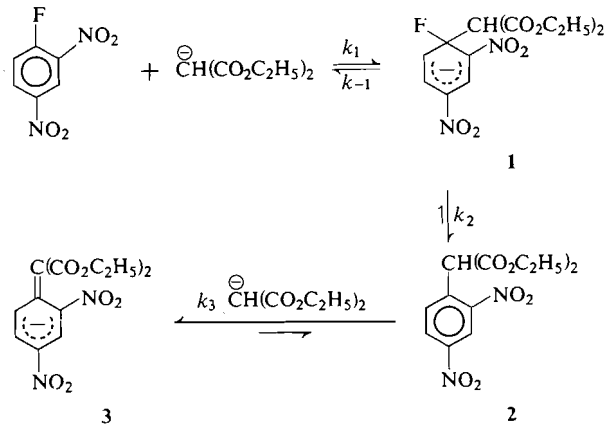

TABLE 1. Pseudo first-order rate constants for the reaction of diethyldinitrophenyl malonate with the sodium salt of diethylmalonate in DMSO at 23.0 °C. Initial concentration of substrate = 5.0×10^{-5} mol l^{-1}

Initial concentration anion $\times 10^3$ (M)	No. of runs	k (s^{-1}) ± std. dev.
1.31	2	32.8 ± 0.3
2.63	5	50.0 ± 1.5
3.94	3	60.5 ± 3.0
4.46	3	69.4 ± 0.4
5.25	3	78.1 ± 0.8
6.56	7	93.3 ± 2.0

in Table 1. Guggenheim plots for these runs had good correlation coefficients, ranging between 0.9950 and 0.9999. A plot of the first-order rate constant against anion concentration has a slope equal to the second order rate constant k_3. The results of Table 1 give a numerical value of 11 500 l mol^{-1} s^{-1} for k_3.

If this step of the reaction in eq. 1 is faster than the two earlier steps, it is possible to use the appearance of this color to study the reaction. Simple kinetics would ensue if the initial attack of the anion on the substrate molecule was the slowest step. However, this does not appear to be the case since the rate of appearance of the purple color from 1-fluoro-2,4-dinitrobenzene and sodiodiethylmalonate, at 520 nm, did not give good first-order rate constants which varied linearly with the anion concentration. There appeared to be an initial rapid reaction which was followed by a slower reaction. If there are two reactions which each give rise to a colored species (*i.e.* **1** and **3**), the absorption spectrum of the reaction mixture should show this, unless these two products have absorption peaks at identical wavelengths. Therefore, a series of absorption scans of the visible spectrum of the reaction mixture was composed at different elapsed times from the time of mixing, using a stopped-flow spectrophotometer. Since the moment of mixing cannot be precisely known, it was arbitrarily set at the origin of the oscilloscope sweep at 2 ms per division of timebase. The absorbance *vs.* time scans were then photographed for a series of different "time-after-mixing" values. In this way visible absorption spectra were obtained for the system at 15 different times-after-mixing, varying between 1 and 2000 ms. Eight of these spectra are shown in Fig. 1, from which it can be seen that there is an initial rapid formation of a peak at 540 nm which is essentially complete after 200 ms, then a slower formation of the product (λ_{max} 520 nm).

The 520 nm peak has been positively identified (2) as the product **3** so the 540 nm peak is assumed to be the intermediate **1**. The only other possibilities are the corresponding intermediates where the diethyl malonate anion is attached at the C-3 or -5 positions. Such intermediates have been postulated for hydrolysis reactions of similar substrates (4) and also have been observed spectroscopically for reactions of methoxide ion with substituted anisoles (5–8). These C-3 and -5 intermediates have been observed to be kinetically favored relative to the C-1 intermediate, but thermodynamically less stable. However, in the present system, it is clear that the intermediate **1** is formed, since the corresponding product is obtained and the u.v. spectra in Fig. 1. show a clear isosbestic point, which indicates the presence of only one species

Can. J. Chem. Downloaded from www.nrcresearchpress.com by 210.87.254.42 on 09/05/12
For personal use only.

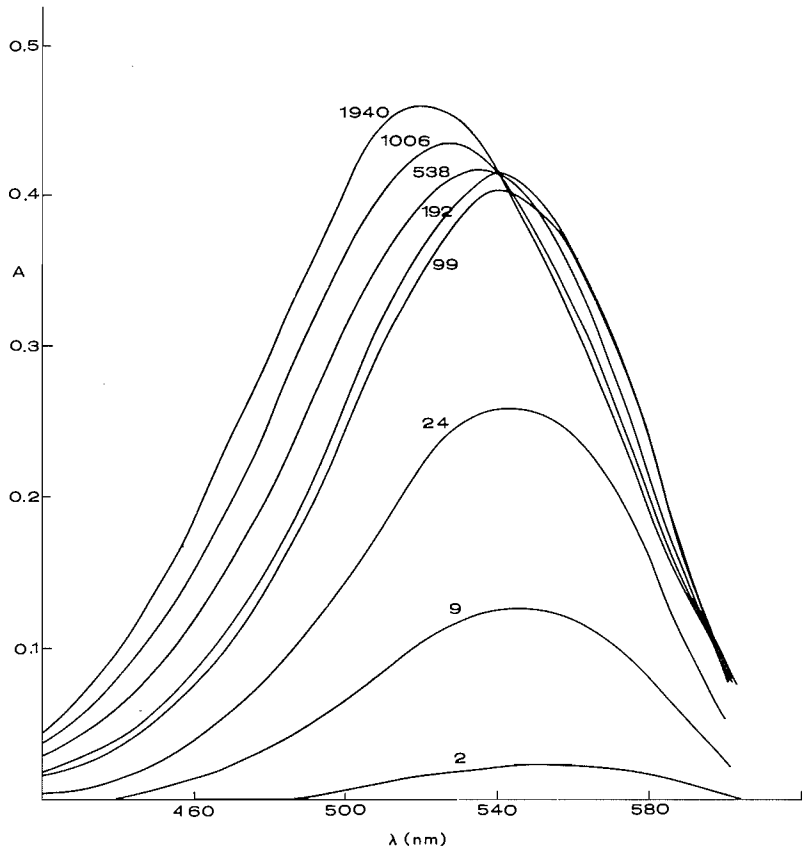

FIG. 1. Visible absorption spectra for the reaction of 1-fluoro-2,4-dinitrobenzene and diethylmalonate anion. The number adjacent to each curve is the "time-after-mixing" in ms.

other than the product. It is concluded, therefore, that if the C-3 or -5 intermediates are formed, they are not kinetically significant.

The kinetic situation is that of a consecutive reaction, for which, if the two steps are sufficiently separated in rate, reasonable approximations to the rate constants might be obtained by carrying out measurements at appropriate wavelengths and time scales. Examples of this type of study of aromatic nucleophilic substitutions have appeared in the literature recently (9, 10).

The first rapid step of the reaction was measured using the wavelength of the isosbestic point. This wavelength varied slightly with reagent concentration; for the conditions under which the kinetic runs were made it was usually higher than 550 nm. If this first step is assumed to be an equilibrium as shown in eq. 1 with the malonate anion in large excess, the kinetic eq. 2 may be derived (11) where x_e and x are the concentrations of the intermediate **1** at equilibrium and at time t, k_1 and k_{-1} are second- and first-order rate constants shown in eq. 1, and b is the concentration of malonate anion. Equation 2 is of the first-order form for which the observed first-order rate constant is equal to $(k_1b + k_{-1})$. The k_{obs} values shown in Table 2 were plotted against anion concentration b and the values of k_1 and k_{-1} thus obtained are shown in Table 3.

$$[2] \quad (x_e - x)/x_e = \exp[-(k_1b + k_{-1})t]$$

The slower second step of the reaction was studied at a lower wavelength, ignoring the first 200 ms of the reaction. This should give a reasonable approximation to k_2, provided k_3 is sufficiently greater than k_2. A series of pseudo first-order rate constants measured at 510 nm at various temperatures are collected in Table 2, from which it can be seen that k_2 is indeed very much less than k_3.

Can. J. Chem. Downloaded from www.nrcresearchpress.com by 210.87.254.42 on 09/05/12
For personal use only.

TABLE 2. Pseudo first-order rate constants for the reaction of 1-fluoro-2,4-dinitrobenzene with the sodium salt of diethyl malonate in DMSO

Temperature (°C)	Substrate concentration × 10^5 (M)	Anion concentration × 10^3 (M)	$k_{obs}(s^{-1})$ at isosbestic point	$k_2(s^{-1})$ at 510 nm
20.5	4.6	1.43	22.8	0.89
		2.86	29.9	1.02
		4.30	38.8	1.10
		4.87	40.4	1.10
		5.73	43.6	1.12
		7.16	49.8	1.14
25.0	6.2	0.63	24.5	0.89
		1.26	29.6	1.16
		1.89	35.0	1.38
		2.52	37.3	1.28
		3.15	41.3	1.30
30.0	2.8	0.81	35.3	1.42
		1.61	43.4	1.80
		2.42	49.6	2.01
		3.22	56.4	2.10
		4.03	61.6	2.24
35.0	4.9	1.86	58.0	2.57
		3.72	79.2	2.91
		5.57	90	3.33
		6.32	99	3.44
		7.43	105	3.66
		9.29	115	3.56
40.0	5.3	1.69	71.0	3.46
		3.37	97	4.13
		5.06	111	4.43
		5.73	122	4.68
		6.75	119	4.76
		8.44	136	4.82

TABLE 3. Forward and reverse rate constants for the reaction of 1-fluoro-2,4-dinitrobenzene with malonate anion to form a σ-bonded complex in DMSO

Temperature (°C)	$k_1(l\ mol^{-1}\ s^{-1})$	$k_{-1}(s^{-1})$
20.5	4680	17.0
25.0	6200	21.8
30.0	8240	29.1
35.0	8690	42.5
40.0	10750	55.4

Thus, from these three sets of values for k_1, k_{-1}, and k_2 at the five temperatures, the activation parameters for this nucleophilic substitution reaction may be calculated. The values of k_2 in Table 2 do not remain constant with reagent concentration but appear to be subject to some catalysis, therefore the k_2 figures used to calculate the activation parameters were those obtained by extrapolation to zero anion concentration. The values of the activation parameters, calculated by the least squares method are given in Table 4. The quoted errors are standard deviations which contain only the random errors of the method. These are rather large, but still do not include systematic errors resulting from the consecutive reaction sequence. Some computations have been made for consecutive reactions with rate constants of the same order of magnitude which have been found in these experiments and it appears that systematic errors in the rate constants as we have derived them are of the order of 5–10%. These result from the assumption in our rate constant calculations that neither step in the reaction sequence interferes with the other. Since the random experimental errors arising in the determination of the rate constants are probably of the same magnitude, these systematic errors are presently acceptable.

Can. J. Chem. Downloaded from www.nrcresearchpress.com by 210.87.254.42 on 09/05/12
For personal use only.

TABLE 4. Activation parameters for the nucleophilic substitution of 1-fluoro-2,4-dinitrobenzene by malonate anion in DMSO

Reaction	$\Delta H^{\ddagger}$ ± std. dev. (kcal mol^{-1})	$\Delta S^{\ddagger}$ ± std. dev. (cal mol^{-1} deg^{-1})	$\Delta G^{\ddagger}_{300\,°K}$ (kcal mol^{-1})
Formation of complex (Step 1)	6.9 ± 0.9	−18.2 ± 3.0	12.3
Decomposition of complex to starting materials (Step −1)	10.7 ± 0.4	−16.5 ± 1.4	15.6
Decomposition of complex to substituted products (Step 2)	12.6 ± 0.8	−16.0 ± 2.7	17.4

At 25 °C our rate constants have the values $k_1 = 6200$ l mol^{-1} s^{-1}, $k_{-1} = 22$ s^{-1}, and $k_2 = 1.0$ s^{-1} which may be compared to the corresponding values of 9.01 mol^{-1} s^{-1}, 6.0 s^{-1}, and 0.12 s^{-1} for the attack of hydroxide ion on 1-chloro-2,4,6-trinitrobenzene obtained by Gaboriaud and Schaal (9).

The magnitudes of the activation parameters seem to be reasonable except for the fact that the entropies of activation for the three steps of the reactions are the same within experimental error and are all negative. It was expected that the decomposition of the intermediate to give either reactants or products would have a positive entropy of activation or at least a much less negative one. However, this result is not without precedent, for Bernasconi (12) found negative entropies of activation for the decomposition of the Meisenheimer adduct of methoxide ion and 2,4-dinitroanisole as well as for its formation. Bernasconi interpreted this result in terms of the concentration of negative change on the incipient methoxide ion in the transition state of the decomposition, which enhanced the solvation of the transition state relative to the initial state. A similar explanation may be advanced in the present case with the negative charge concentrating either on the carbon atom of the incipient malonate anion, or on the incipient fluoride ion for decomposition to reactants and products respectively. At present there are insufficient experimental results to develop a detailed theory, but it is clear that the entropies of activation can only be rationalized if solvation changes are making substantial contributions to this parameter.

It has been assumed in the kinetic analysis that the reaction is that shown in eq. 1 with no other side reactions taking place. However, it is possible that an intermediate could be formed from a reaction between the substrate and the anion of DMSO, if that were present in solution. The dimsyl anion is well known (13, 14) and its adduct with 1,3,5-trinitrobenzene has been observed (15). It is known to be formed in DMSO–alkoxide mixtures (16) and is believed to be the active reagent in some proton transfer reactions in such solutions (17).

The dimsyl anion was prepared from sodium hydride and DMSO and reacted with 1-fluoro-2,4-dinitrobenzene. This yielded rapidly two absorption peaks at 431 and 372 nm, clearly different from the absorption spectrum observed with the malonate anion. It is concluded, therefore, that there is no significant amount of attack by dimsyl anion, which probably means that this ion is formed only in very small concentration in solutions of malonate anion in DMSO.

In summary, the activation parameters for each step of this reaction, while not determined with great precision, give the reaction profile quite clearly. It should be possible to find a number of other aromatic nucleophilic substitutions for which the kinetics and activation parameters for the individual steps can be determined.

Experimental

Materials

The sodium salt of diethyl malonate was prepared from sodium hydride and diethyl malonate. Sodium hydride in oil was washed with several portions of dry petroleum ether and then mixed with an equimolar amount of diethyl malonate in petroleum ether solvent. After 1 h the precipitated salt was filtered and washed with petroleum ether, then dried under vacuum at room temperature for 2 h. On a 0.05 mol scale the yield of this reaction is about 90%. The product was assayed by potentiometric titration against standard perchloric acid in isopropyl alcohol which indicated 98 ± 0.5% purity.

Dimethyl sulfoxide solvent was dried over calcium hydride, then fractionally distilled from fresh calcium hydride under nitrogen.

Can. J. Chem. Downloaded from www.nrcresearchpress.com by 210.87.254.42 on 09/05/12
For personal use only.

Kinetic Procedure

The rate measurements, and the absorption spectra at times less than 2 s after mixing, were determined with a Durrum stopped-flow spectrophotometer fitted with a 2 mm light-path optical cell. The bath in which the drive syringes of the apparatus were immersed was maintained at the quoted temperatures to ± 0.03 °C. This bath fluid was circulated around the mixing jet and optical cell.

Each run consisted of three consecutive trials, for which the transmittance vs. time traces were superimposed on the Tektronix 564 storage oscilloscope screen. The transmittance readings were read from the photograph of the composite trace, converted to absorbance, and the first-order rate constants were computed by the least squares method using the Guggenheim treatment. Correlation coefficients and standard error calculations were included in the program. Two runs, sometimes more, were carried out for each set of concentrations and temperature at different oscilloscope time bases.

The authors are grateful for financial assistance from the National Research Council of Canada.

1. P. BAUDET. Helv. Chim. Acta, **49**, 545 (1966).
2. K. T. LEFFEK and P. H. TREMAINE. Can. J. Chem. **49**, 1979 (1971).
3. S. M. SHEIN and T. M. IVANOVA. J. Org. Chem. USSR **5**, 1763 (1969). (Z. Org. Kmim. **5**, 1816 (1969)).
4. K. BOWDEN and R. S. COOK. J. Chem. Soc. B, 1771 (1971).
5. F. MILLOT and F. TERRIER. Bull. Soc. Chim. Fr. 2692 (1969).
6. F. TERRIER and F. MILLOT. Bull. Soc. Chim. Fr. 1743 (1970).
7. F. TERRIER and M-P. SIMONNIN. Bull. Soc. Chim. Fr. 677 (1971).
8. J. H. FENDLER, E. J. FENDLER, and C. E. GRIFFIN. J. Org. Chem. **34**, 689 (1969).
9. R. GABORIAUD and R. SCHAAL. Bull. Soc. Chim. Fr. 2683 (1969).
10. J. A. ORVIK and J. F. BUNNETT. J. Am. Chem. Soc. **92**, 2417 (1970).
11. E. F. CALDIN, A. JARCZEWSKI, and K. T. LEFFEK. Trans. Faraday Soc. **67**, 110 (1971).
12. C. F. BERNASCONI. J. Am. Chem. Soc. **90**, 4982 (1968).
13. E. J. COREY and M. CHAYKOVSKI. J. Am. Chem. Soc. **84**, 866 (1962).
14. L. F. FIESER and M. FIESER. Reagents for organic synthesis. J. Wiley and Sons, New York. 1967. p. 310.
15. C. A. FYFE, M. I. FOREMAN, and R. FOSTER. Tetrahedron Lett. 1521 (1969).
16. H-D. BECKER, G. J. MIKOL, and G. A. RUSSELL. J. Am. Chem. Soc. **85**, 3410 (1963).
17. C. D. RITCHIE *In* Solute-solvent interactions. *Edited by* J. F. Coetzee and C. D. Ritchie. Marcel Dekker, New York. 1969. p. 266.

Can. J. Chem. Downloaded from www.nrcresearchpress.com by 210.87.254.42 on 09/05/12
For personal use only.

Can. J. Chem. Downloaded from www.nrcresearchpress.com by 210.87.254.6 on 09/05/12
For personal use only.

The Importance of Conformation of the Tetrahedral Intermediate in the Hydrolysis of Amides. Selective Cleavage of the Tetrahedral Intermediate Controlled by Orbital Orientation[1]

PIERRE DESLONGCHAMPS,[2] CLAUDE LEBREUX, AND ROLAND TAILLEFER

Laboratoire de Synthèse organique, Département de chimie, Université de Sherbrooke, Sherbrooke, Québec

Received January 24, 1973

The basic hydrolysis of *N*-disubstituted imidate salts proceeds via a hemi-orthoamide tetrahedral intermediate which can in principle give amide–alcohol or ester–amine products. Experimental evidence has been obtained which shows that the specific conformation of the tetrahedral intermediate determines products formation and it is further suggested that the orientation of the lone pair orbitals of the heteroatoms governs this remarkable selective decomposition.

L'hydrolyse basique des sels d'imidate *N*-disubstitués passe par la formation d'un intermédiaire tétrahédrique du type hémi-orthoamide qui peut conduire soit aux produits amide–alcool ou ester–amine. Les résultats expérimentaux obtenus démontrent que la conformation précise de l'intermédiaire tétrahédrique détermine la formation des produits. Il est de plus avancé que l'orientation des orbitales d'électrons non-liés des hétéroatomes contrôle la décomposition sélective de l'intermédiaire tétrahédrique.

Can. J. Chem., **51**, 1665 (1973)

We have recently demonstrated the importance of the conformation of the tetrahedral intermediate (hemi-orthoester) during the hydrolysis or the transesterification of esters (1).

We now wish to report that the conformation of the tetrahedral intermediate (hemi-orthoamide) formed during the hydrolysis of amide and related functions is equally important; specific cleavage of a carbon–oxygen or a carbon–nitrogen bond being allowed only if the other two heteroatoms (oxygen or nitrogen) of the tetrahedral intermediate have each an orbital oriented antiperiplanar to the leaving *O*-alkyl or *N*-alkyl group. In order to verify this stereoelectronic theory, we have selected for study the basic hydrolysis of the *N*-disubstituted imidate salts **1** (2) (Scheme 1), expecting that such salts would react very fast with hydroxide ion to yield a tetrahedral intermediate **2** which can give in principle the amide-alcohol products **3** or the ester–amine products **4**.[3] If the reaction gives the amide-alcohol products **3** via a kinetically controlled reaction, no information on the orbital assisted decomposition of the tetrahedral intermediate can be obtained since the amide–alcohol products **3** are also the thermodynamically favored products of the reaction. However, the formation of the ester–amine products **4** can give useful information on the decomposition of the tetrahedral intermediate **2** since they are clearly the result of a kinetically controlled reaction. Thus, if products **4** are preferentially observed it means that the transition state leading to those products is of lower energy than the one leading to the formation of the much more stable amide-alcohol products **3**. We disclose here experimental evidence which clearly establishes that the preferential formation of the ester–amine products **4** is possible in basic medium and proposed that whenever such products are formed, the low energy transition state is due to the formation of a specific conformation of the tetrahedral intermediate **2** in which the lone pair orbitals of the oxygens are properly oriented to permit the specific cleavage of the carbon–nitrogen bond.

Imidate salts can exist into two different planar conformations, the *anti* (**1***a*) or the *syn* (**1***b*) form. If the *anti* form **1***a* reacts with hydroxide ion (Scheme 2), it should give specifically

[1]Support for this work by the National Research Council of Canada and by the "Ministère de l'Education" Québec, is gratefully acknowledged.

[2]A. P. Sloan Fellow 1970–1972. To whom inquiries should be addressed.

[3]Study of the decomposition in a basic medium is important in order to prevent the protonation of the basic nitrogen of the intermediate **2**.

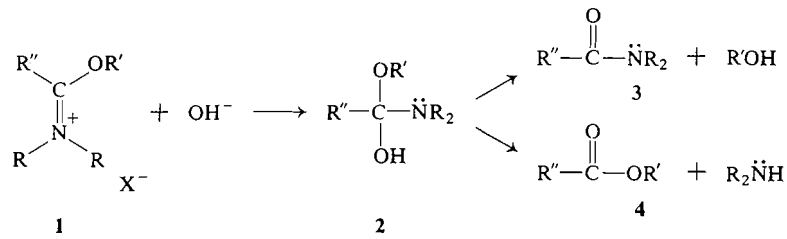

1 2 3 4

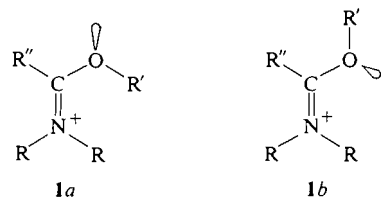

1*a* 1*b*

SCHEME 1

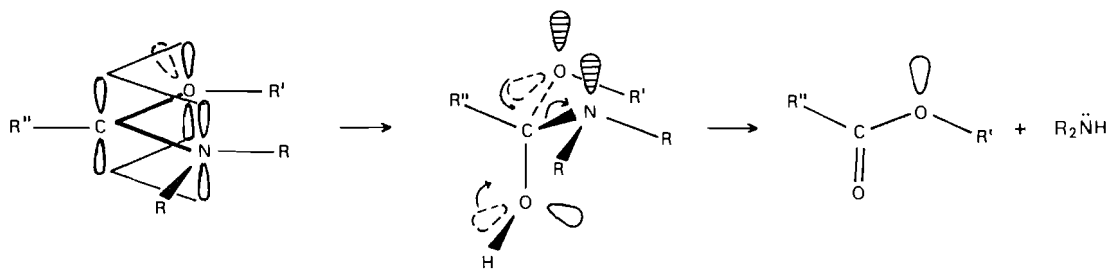

1a 2a 4

SCHEME 2

the conformer **2***a* in which the two new lone-pair orbitals on the oxygen of the OR′ group and the nitrogen are both oriented antiperiplanar to the C—OH bond (1). In this tetrahedral intermediate, the oxygens of the OH and the OR′ group each possess an orbital oriented antiperiplanar to the C—N bond so the cleavage of the C—N bond is possible by an orbital assisted mechanism yielding an ester and a secondary amine.[4] The nitrogen atom does not possess an orbital oriented antiperiplanar to the C—OR′ bond, the cleavage of the C—OR′ bond will therefore be a much higher energy process and should not be observed. Thus *anti* imidate salt **1***a* should give specifically the conformer **2***a* which will immediately decompose in one specific direction giving the ester–amine products **4**.

Reaction of hydroxide ion on the *syn* form **1***b* of the imidate (Scheme 3) should give specifically the conformer **2***b*. In conformer **2***b*, the nitrogen does not possess an orbital oriented antiperiplanar to the C—OR′ bond and similarly the OR′ oxygen does not possess an orbital antiperiplanar to the C—N bond. Therefore, we propose that intermediate **2***b* will not decompose before it undergoes rotational changes to give new intermediates such as **2***a* or *c* for example. In conformer **2***c*, the nitrogen atom and the oxygen of the OH group have each an orbital oriented antiperiplanar to the C—OR′ bond, thus **2***c*, once formed should give immediately the amide–alcohol products **3**. Consequently,

[4]The breakdown of the tetrahedral intermediate is certainly subject to complex general acid–base catalysis (3) which implies that the nitrogen will not be ejected as an amide ion but as a secondary amine.

Can. J. Chem. Downloaded from www.nrcresearchpress.com by 210.87.254.6 on 09/05/12
For personal use only.

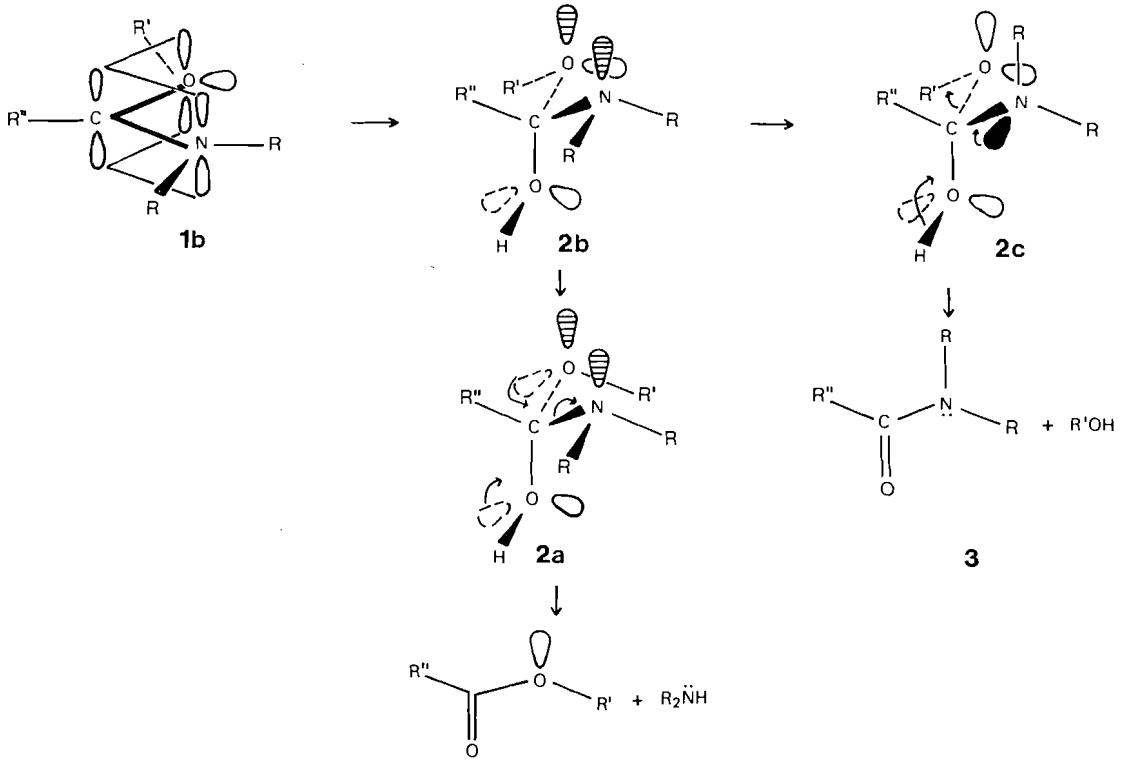

SCHEME 3

basic hydrolysis of *syn* imidate salt **1***b* can in principle give both types of products **3** and/or **4** depending on the new conformers that will be formed by bond rotation of conformer **2***b*.

Hydrolysis[5] of **5**[6] (CD_3CN–D_2O, NaOH, 2 equiv) at room temperature for 2 min gave ≃95% of ester–amine **6** and ≃5% of amide–alcohol **7**. After 30 min, the reaction mixture consisted of **7**[7] only, indicating that **6** is first formed and then converted into **7** under those conditions. Treatment[5] of the ammonium salt **8**[8] under identical basic conditions gave also the ester–amine **6** (≃95% after 2 min) which was completely converted into the amide–alcohol **7**[7] after 30 min. Hydrolysis[5] of **5** utilizing excess sodium carbonate (CD_3CN–D_2O) gave exclusively the ester–amine **6**[9] which was not converted into **7** under these conditions. Similarly, hydrolysis[5] of **9**[10] with sodium carbonate gave exclusively the ester–amine **10**.[9] Hydrolysis of **9** with sodium hydroxide (≃2 min) gave exclusively the amide-alcohol **11**.[7] However, treatment of the ammonium salts **12**[5,8] under similar conditions with sodium hydroxide also gave only the amide–alcohol **11**.[7] This result shows that the transformation of the ester–amine **10** into the amide–alcohol **11** is a very fast reaction in presence of sodium hydroxide. Hydrolysis[5] of **13**[11] with sodium carbonate gave after ≃10 min the ester–amine **14**[9] which is then transformed completely into the amide–alcohol **15**[7] after standing for 1.5 h at room temperature.

It has been reported (8) that the salts **16**, **17**,

[5]This reaction was followed by p.m.r. spectroscopy.

[6]Prepared by alkylation of the corresponding 5,6-dihydro-1,3-4*H*-oxazine (4) with $(CH_3)_3O^+$ BF_4^- (5).

[7]This product was isolated as its acetate derivative (Ac_2O/pyridine) which was identified by comparison with an authentic sample.

[8]Prepared by reaction of the corresponding imidate salts with H_2O (6).

[9]This product was isolated as its acetamide derivative (Ac_2O/pyridine) which was identified by comparison with an authentic sample.

[10]Prepared by alkylation of the corresponding 2-oxazoline (7) with $(CH_3)_3O^+$ BF_4^-.

[11]Prepared by alkylation of the corresponding 2-oxazoline with iodomethane.

Can. J. Chem. Downloaded from www.nrcresearchpress.com by 210.87.254.6 on 09/05/12
For personal use only.

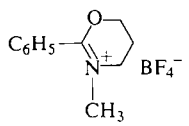

5

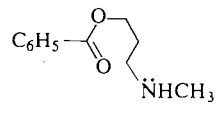

6

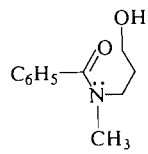

7

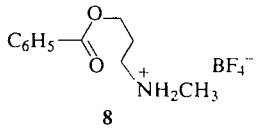

8

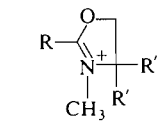

9 R = C_6H_5; R′ = H
13 R = CH_3; R′ = H
16 R = CH_3; R′ = CH_3
17 R = $(CH_3)_3C$; R′ = CH_3
18 R = C_6H_5; R′ = CH_3

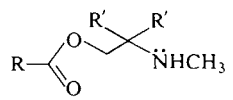

10 R = C_6H_5; R′ = H
14 R = CH_3; R′ = H
19 R = CH_3; R′ = CH_3
20 R = $(CH_3)_3C$; R′ = CH_3
21 R = C_6H_5; R′ = CH_3

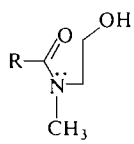

11 R = C_6H_5
15 R = CH_3

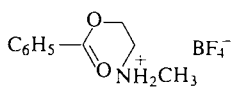

12

18 gave the corresponding ester–amine **19**, **20**, and **21** on basic hydrolysis. Reaction of **22** with water has also been reported recently (9) and the ester–amine **23** was the only product isolated. In those cases (**16**, **17**, **18**, and **22**) two factors direct the specific cleavage of the carbon–nitrogen bond as shown in the intermediate **24**: the orbital orientation factor and a 1,3-diaxial type interaction between the OH group and the pseudo axial methyl group. The importance of this steric compression factor was verified in the following way. Ozonolysis (10, 11) of the acetal **25** gave exclusively the primary ester **26**.[12] During this reaction the intermediate **27** is formed and the orientation of the orbitals favors the opening in both directions equally but the interaction between the OH group and the pseudo axial methyl group in **27** is strong enough to allow a specific cleavage in one direction. The preceding study was carried out with rigid *anti* imidate salts and the experimental results clearly demonstrate that in such case, the ester–amine products are the only products observed under kinetically controlled condition.

We have also studied the basic hydrolysis of the imidate salts **28**[13] (R = H, CH_3, C_6H_{11} (cyclohexyl), $(CH_3)_3C$ and C_6H_5). Such salts can exist in principle in the *anti* (**28***a*) or the *syn* (**28***b*) form. The extent of the electronic interactions in either of these two forms is as yet unknown. There is however a steric repulsion between the R group and the ethyl group in the *syn* form **28***b*. There is also a steric interaction between the ethyl and the methyl groups in the *anti* form **28***a*. Therefore, when R is a small

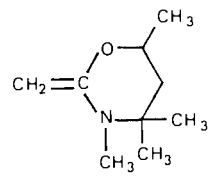

22

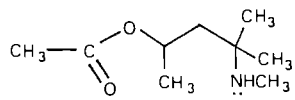

23

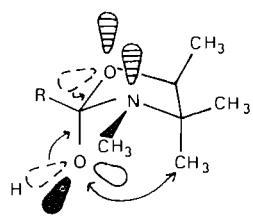

24

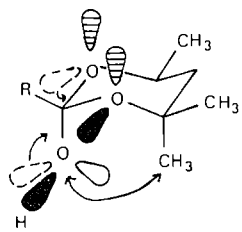

27

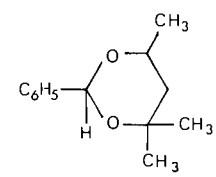

25

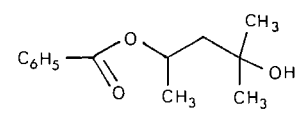

26

[12]Unpublished result, R. Chênevert, this laboratory.

[13]These salts were prepared from the corresponding amide and $(C_2H_5)_3O^+BF_4^-$ (12).

Can. J. Chem. Downloaded from www.nrcresearchpress.com by 210.87.254.6 on 09/05/12
For personal use only.

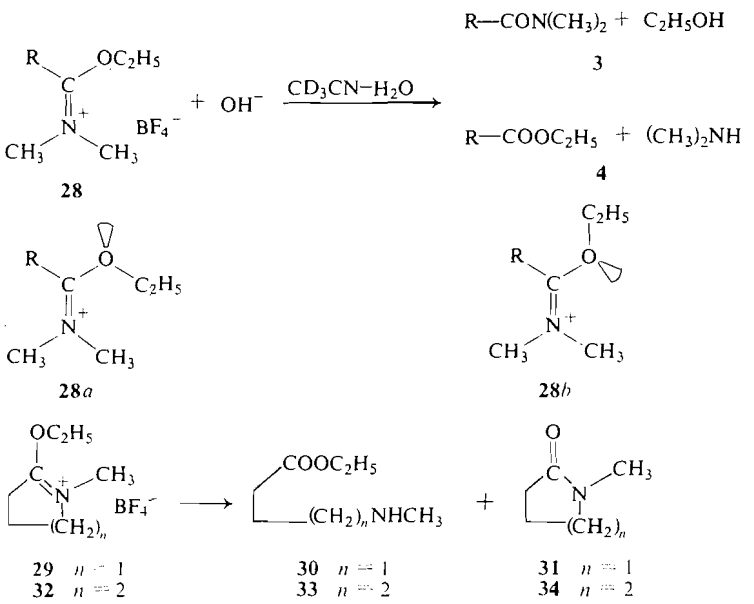

TABLE 1. Basic hydrolysis of imidate salts **28**

R	% ester*	% amide*
H	50	50
CH_3	81	19
C_6H_{11}	50†	50†
$(CH_3)_3C$	>98	—
C_6H_5	>98	—

*Yields were estimated by p.m.r. spectroscopy analysis.
†Yields were estimated by v.p.c. analysis.

group, one can postulate that the *syn* form **28***b* might be favored and when R is a large group (*t*-butyl and planar C_6H_5), the *anti* form **28***a* would predominate. If this assumption is correct, the stereoelectronic theory predicts that basic hydrolysis of **28** should give a mixture of products **3** and **4** when R is a small group and it should give mainly the ester amine products **4** when R is a large group. Table 1 described results which are in accord with the preceding discussion.

Basic hydrolysis of the cyclic imidate salts **29**[13] and **32**[13] was also studied. Treatment of a solution of **29** in dichloromethane with a large excess of aqueous sodium carbonate at 0 °C for ≃15 s (rapid mixing) gave a mixture of ester–amine **30**[9] (65%) and lactam **31** (35%). A similar experiment with **32** gave also a mixture of ester–amine **33**[9] (83%) and lactam **34** (17%).

Work is now in progress to complete this study with various types of *N*-dialkylated imidate salts.

1. P. DESLONGCHAMPS, P. ATLANI, D. FRÉHEL, and A. MALAVAL. Can. J. chem. **50**, 3405 (1972).
2. R. ROGER and D. G. NEILSON. Chem. Rev. **60**, 179 (1960).
3. W. P. JENCKS. Chem. Rev. **72**, 705 (1972).
4. W. SEELIGER, E. AUFDERHAAR, W. DIEPERS, R. FEINAUER, R. NEHRING, W. THIER, and H. HELLMAN. Angew. Chem. Int. Ed. **5**, 875 (1966) and refs. therein.
5. H. MEERWEIN. Org. Synth. **46**, 120 (1966).
6. S. WINSTEIN and R. BOSCHAN. J. Am. Chem. Soc. **72**, 4669 (1950).
7. J. A. FRUMP. Chem. Rev. **71**, 483 (1971).
8. P. ALLEN and J. GINOS. J. Org. Chem. **28**, 2759 (1963).
9. A. I. MEYERS and N. NAZARENKO. J. Am. Chem. Soc. **94**, 3243 (1972).
10. P. DESLONGCHAMPS and C. MOREAU. Can. J. Chem. **49**, 2465 (1971).
11. P. DESLONGCHAMPS, C. MOREAU, D. FRÉHEL, and P. ATLANI. Can. J. Chem. **20**, 3402 (1972).
12. H. MEERWEIN, W. FLORIAN, N. SCHÖN, and G. STOPP. Ann. Chem. **641**, 1 (1961).

Can. J. Chem. Downloaded from www.nrcresearchpress.com by 210.87.254.6 on 09/05/12
For personal use only.

The Surface Analysis of Nickel Chromia Catalysts by X-Ray Photoelectron Spectroscopy[1]

NORMAN STEWART MCINTYRE, NORMAN HENRY SAGERT, AND RITA MARY LOUISE POUTEAU

Chemistry and Materials Science Division, Atomic Energy of Canada Limited, Whiteshell Nuclear Research Establishment, Pinawa, Manitoba R0E 1L0

AND

WARREN GEORGE PROCTOR

Physical Measurements Applications Instrument Division, Varian Associates, 611 Hansen Way, Palo Alto, California 94303

Received January 25, 1973

The surface composition of a series of nickel–chromia catalysts has been examined by X-ray photoelectron spectroscopy. Correlation of the amount of available surface nickel with the activity of the particular catalyst for hydrogen water deuterium isotope exchange is very good. No significant alterations are observed in the valence band spectra as the surface composition changes.

La composition de la surface d'une série de catalyseurs nickel-chrome a été examinée par spectroscopie photoélectronique obtenue par rayon X. La corrélation de la surface de nickel disponible avec l'activité du catalyseur concernant l'échange isotopique hydrogène–deutérium pour l'eau, est très bonne. Il n'y a pas de changements notables dans les spectres de bande de valence avec les changements de composition de la surface. [Traduit par le journal]

Can. J. Chem., **51**, 1670 (1973)

The use of photoelectron spectroscopy (XPS) for catalyst characterization has been recently reviewed (1). From this, it is clear that the ability of XPS measurements to probe the chemical nature as well as the composition of the first few atomic surface layers is potentially very useful in catalyst research. A number of studies (2–4) have already reported chemical shifts in elemental binding energies and changes in line shapes between "active" and "non-active" catalyst samples. This investigation has concentrated on the XPS of a number of "nickel–chromia" catalysts which are known to catalyze the deuterium isotope exchange between hydrogen and water vapor (5, 6). This particular system was chosen because there is a reasonably well defined optimum concentration of nickel (95%) for which catalytic activity reaches a maximum. It was expected that changes in photoelectron line shapes and intensities would be observable in the region of this maximum.

Catalysts with [Ni]/([Ni] + [Cr]) = 100, 99, 98, 97, 95, 90 and 81% w/w were prepared from 2 *M* solutions of the mixed nickel and chromium nitrates. The carbonates were precipitated by slow addition of $(NH_4)_2CO_3$ and were filtered, dried, crushed, and sieved to 40–60 mesh. The samples were then reduced in purified hydrogen at 300 °C and were stored under high purity nitrogen. Chromium and nickel concentrations were determined by atomic absorption spectrophotometric analysis of the dissolved carbonates.

Core and valence electron spectra of the catalysts were studied using a Varian VIEE-15 electron spectrometer fitted with a high intensity MgKα X-ray source (1253.6 eV). Samples were attached to the probe by cellophane tape and were transferred to the spectrometer, under a nitrogen atmosphere. Energy values reported are those directly obtained from the spectrometer which had been calibrated using the core $4f_{7/2}$ level of deposited gold and a secondary voltage standard. The sample surface charging was noted by measuring the shift of the C (1s) impurity line.

When the intensities of the Ni(3d) and (3s) bands are plotted against bulk nickel composition (see Fig. 1) a maximum occurs at 95% nickel catalyst composition. The Cr(3p) intensity also rises sharply up to the 95% sample, past which little further variation is observed.

The increasing nickel intensity in the composition range 99–95% probably results from the decrease in nickel particle size and the resultant increase in nickel surface area known to occur in

[1]AECL No. 4413.

Can. J. Chem. Downloaded from www.nrcresearchpress.com by 210.87.254.40 on 09/05/12
For personal use only.

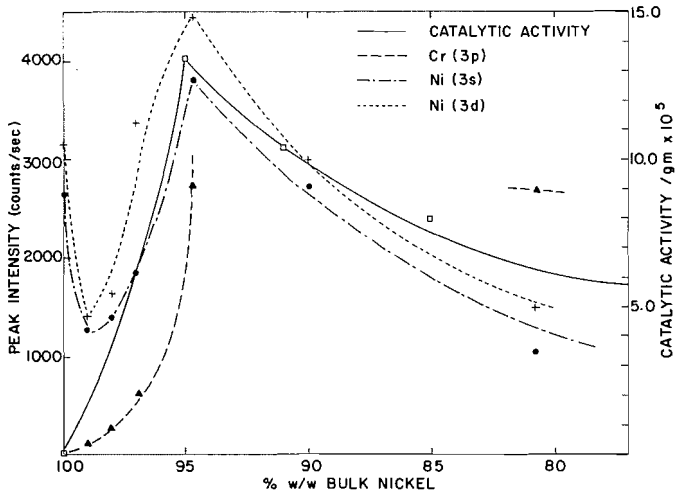

FIG. 1. Elemental surface concentrations and catalytic activity as a function of bulk nickel concentration; □ catalytic activity (see ref. 6); ▲, Cr(3p) line intensity; ● Ni(3s) line intensity; +, Ni(3d) line intensity.

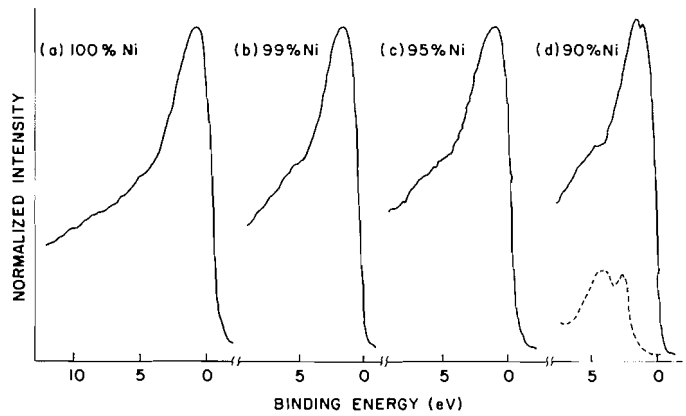

FIG. 2. Nickel valence band shape as a function of bulk nickel composition. Dashed line in (d) indicates the position and shape of the Cr_2O_3 bands.

this composition range (6). It was previously proposed (6) that as chromia is added to the system, it is first deposited in a very thin layer, or possibly a Ni–Cr compound of undetermined structure gives way to a bulk chromia phase at a composition of around 95% nickel. These suggestions are supported by our observation of an initial drop in nickel line intensity at the 99% composition as chromia is first introduced to the system, and by the constant value of the Cr(3p) intensity at compositions lower than 95% nickel.

Catalytic activities for hydrogen–water deuterium exchange are taken from Tarina *et al.* (6). They represent moles of HD formed per g-s at 130 °C. The parallel variation of the Ni(3p) and (3d) line intensities with the reported catalytic activity in the nickel composition range 95–80% suggests that the exchange rate in this range may depend mainly on the availability of surface nickel and is consequently a function of the physical structure. Conclusions regarding a similar correspondence in the composition range 100–95% require further kinetic data for intermediate points in this area.

The Ni(3d) band shapes for four catalyst compositions are shown in Fig. 2. In the pure nickel sample (a), the band maximum occurs at a binding energy 1.4 eV higher than the Fermi level compared with the 1.0 eV found by previous authors (7). This difference and the slightly

Can. J. Chem. Downloaded from www.nrcresearchpress.com by 210.87.254.40 on 09/05/12
For personal use only.

broader band may be due to the powdered nature of our samples. Superimposed on the pure nickel band shape, two new features gradually appear at binding energies of 0.7 and 4.0 eV above the original band maximum as the chromia content increases. A spectrum of pure Cr_2O_3 in the same energy region (see Fig. 2(*d*)) has two d electron bands whose positions closely match those appearing in the catalyst spectrum using the O(2s) peak as energy reference. Thus the observed changes occurring in the catalyst valence spectra probably result from the presence of Cr_2O_3.

Examination of the $Ni(2p_{3/2})$ line for this catalyst series suggests that some oxygen contamination of the surface occurred during sample transfer. However, the $Ni(3p_{3/2, 1/2})$ line for those samples low in Cr_2O_3 is a clean gaussian singlet with only a small shoulder on the high binding energy side indicating that only a very small fraction of the nickel is present as oxide. The apparent difference in surface composition suggested by the two nickel lines is explained by the fact that escaping Ni(3p) electrons have a kinetic energy of about 1200 eV while those from the 2p level have only an energy of about 400 eV. Recent studies of electron escape depths (8) suggest that 1200 eV electrons have at least twice the escape depth of 400 eV electrons. The Ni(3p) line is thus less sensitive to contamination of the very outermost surface since it samples a somewhat greater depth than the 2p line.

A clear correlation between XPS peak intensity and catalytic activity is shown in the present study, but no indication of electronic promotion is seen in the valence band spectra. It is not clear, at present, whether catalytically significant changes in valence band structure can be resolved by current XPS techniques. However, such interaction obviously does occur, since the available surface nickel in the 100% nickel catalyst (Fig. 1) is almost as great as that in the 95% catalyst yet the former is completely inactive. Electronic differences may be occurring in unoccupied nickel orbitals and thus may be observable in the "shake-up" electron spectrum associated with the Ni(2p) lines (9).

1. W. N. DELGASS, T. R. HUGHES, and C. S. FADLEY. Catal. Rev. **4**, 179 (1970).
2. A. W. MILLER, W. ATKINSON, M. BARBER, and P. SWIFT. J. Catal. **22**, 140 (1971).
3. D. A. WHAN, M. BARBER, and P. SWIFT. J.C.S. Chem. Commun. 198 (1972).
4. J. S. BRINEN and A. MELERA. J. Phys. Chem. **76**, 2525 (1972).
5. P. MARGINEANU and A. OLARIU. J. Catal. **8**, 359 (1967).
6. D. TARINA, E. WEISSMANN and D. BARB. J. Catal. **11**, 348 (1968).
7. Y. BAER, P. F. HEDEN, J. HEDMAN, M. KLASSON, C. NORDLING, and K. SIEGBAHN. Physica Scripta, **1**, 55 (1970).
8. M. KLASSON, J. HEDMAN, A. BERDTSSON, R. NILSSON, C. NORDLING, and P. NELICK. Uppsala University, Institute of Physics, Rept. UUIP-757 (1972).
9. T. NOVAKOV. Phys. Rev. N, **3**, 2693 (1971); T. NOVAKOV and R. PRINS. *In* Electron spectroscopy. *Edited by* D. A. Shirley. North-Holland, London. 1972.

Can. J. Chem. Downloaded from www.nrcresearchpress.com by 210.87.254.40 on 09/05/12
For personal use only.

Can. J. Chem. Downloaded from www.nrcresearchpress.com by 210.87.254.105 on 09/05/12
For personal use only.

Canadian Journal of Chemistry

Published by
THE NATIONAL RESEARCH COUNCIL OF CANADA

Journal canadien de chimie

Publié par
LE CONSEIL NATIONAL DE RECHERCHES DU CANADA

Volume 51 Number 11 June 1, 1973

Volume 51 numéro 11 1 juin 1973

Base-catalyzed Isotopic Exchange of Molecular Hydrogen. II.[1] Rate Dependence on Basicity in the Dimethyl Sulfoxide–Water System[2]

E. ALLAN SYMONS[3] AND ERWIN BUNCEL

Department of Chemistry, Queen's University, Kingston, Ontario

Received November 27, 1972

Isotopic exchange of D_2 has been determined in mixtures of dimethyl sulfoxide and water under catalysis by hydroxide ion. The rate of exchange increases by *ca.* 10^4 as the medium composition is changed from 0% DMSO to 99.6% DMSO at 65 °C. The unusually low sensitivity to medium basicity is reflected in abnormally low slope values for the plots of log k_{obs} *vs.* H_- or J_-. When [Me_4NOH] is varied at a given medium composition, the apparent order with respect to [Me_4NOH] is greater than unity.

These results are discussed in terms of (*1*) rate determining proton transfer from D_2 to OH^- with formation of hydride ion; (*2*) a concerted reaction of OH^-, D_2, and H_2O; (*3*) addition of OH^- to D_2 to yield an intermediate adduct, $[HODD]^-$; (*4*) a 6-centered process involving cation participation and electrophilic assistance by H_2O in the reaction of OH^- with D_2.

L'échange isotopique de D_2 a été étudié dans des mélanges de sulfoxyde de diméthyle et d'eau sous l'effet d'une catalyse par l'ion hydroxyle. Le taux d'échange augmente d'environ 10^4 alors que la composition du milieu change de 0% en DMSO à 99.6% en DMSO à 65 °C. La sensitivité anormalement faible à la basicité du milieu est réflétée par des valeurs anormalement faibles de la pente dans les graphiques du log k_{obs} *vs.* H_- ou J_-. Quand la concentration de Me_4NOH est changée pour une composition donnée du milieu, l'ordre apparent en ce qui a trait à la [Me_4NOH] est plus élevé que l'unité.

On discute de ces résultats en fonction du (*1*) transfert de proton responsable du taux d'échange de D_2 à OH^- avec la formation d'un hydrure; (*2*) d'une réaction concertée de OH, D_2 et H_2O; (*3*) d'addition de OH^- à D_2 pour donner un produit d'addition intermédiaire $[HODD]^-$; (*4*) d'un processus à 6 membres impliquant une participation cationique et une assistance électrophile de l'eau dans la réaction de OH^- avec D_2.

[Traduit par le journal]

Can. J. Chem., 51, 1673 (1973)

Wirtz and Bonhoeffer reported in 1936 (1) the observation of proton exchange between hydrogen gas and deuterium oxide in the presence of potassium hydroxide. Since then several groups of workers have studied various aspects of this base-catalyzed reaction in aqueous solution (2–10). It has been determined that the hydroxide ion-catalyzed exchange occurs homogeneously in the liquid phase, the rate being approximately proportional to the base concentration up to 1 *M* (3, 6), and to the hydrogen pressure up to at least 100 atm (6). Acids are not effective as catalysts (3–5), while catalysis by water is extremely slow even at several hundred degrees Centigrade (6). Activation energies of 24, 24 ± 2, 29 ± 3 kcal/mol have been reported for the reaction in the region of 100° (3), 115° (6), and 150° (4), respectively.

Isotope exchange results from heterolytic

[1]Part 1: ref. 17.

[2]Presented in part at the First IUPAC Conference on Physical Organic Chemistry, Crans sur Sierre, Switzerland, 1972. Abstracts p. 88.

[3]Present address: Physical Chemistry Branch, Chalk River Nuclear Laboratories, Atomic Energy of Canada Limited, Chalk River, Ontario.

cleavage of the D—D bond in protic medium. Wilmarth and co-workers (3, 5) suggested that the rate-limiting step involved either transfer of deuterium to OH^-, leaving temporarily a deuteride ion (reaction 1*a*), to be followed by its rapid discharge (reaction 1*b*), or else simultaneous reaction of the D_2, OH^-, and H_2O species (reaction 2) to yield the final products of the exchange, namely HD and DOH. However it was believed that the absence of acid catalysis tends to rule out this latter possibility (3, 5).

$$[1a] \quad HO^- + D{-}D \xrightarrow{\text{slow}} HOD + D^-$$

$$[1b] \quad D^- + HOH \xrightarrow{\text{fast}} DH + OH^-$$

$$[2] \quad HO^- + D{-}D + HOH \rightarrow HOD + DH + OH^-$$

Formation of a free hydride ion (reaction 1*a*) with an appreciable life-time was considered unlikely by Schindewolf (6), since no base-catalyzed reductions or hydrogenations could be detected under the conditions of the exchange measurements. The preferred mechanism (6) was one in which polarization of the hydrogen molecule by hydroxide ion occurred simultaneously with attack by a water molecule:

$$[3] \quad HO^- \cdots \overset{\delta+\ \delta-}{D{-}D} + HOH \rightarrow HO{-}D + D{-}H + OH^-$$

The process in reaction 3, though akin to that given in reaction 2, bears some resemblance to the mechanism discussed below in which association between HO^- and D—D is considered to be complete in an initial stage.

In a theoretical approach to the problem, Ritchie and King (9, 10) have performed non-empirical *ab initio* (l.c.a.o.–m.o.–s.c.f.) calculations of the potential energy surface for the gas phase reaction of water molecule with hydride ion to produce hydroxide ion and hydrogen molecule. These computations point to the formation of an addition complex, $[HODD]^-$, which is stable relative to the reactants and products. Thus a classical activation energy barrier is shown to be absent for the gas phase process. Hence the magnitude of the experimental activation energy for isotopic exchange in solution was ascribed almost entirely to the necessary partial desolvation of the hydroxide ion before it can take part in reaction. On this basis isotopic exchange in solution will take place by the mechanism of reactions 4*a* and 4*b*.

$$[4a] \quad \begin{matrix} HOH{-}{-}{-}O^- \\ \quad\quad\quad | \\ \quad\quad\quad H \end{matrix} + D{-}D \xrightarrow{\text{slow}} HOH + [HO{-}D{-}D]^-$$

$$[4b] \quad [HO{-}D{-}D]^- + HOH \xrightarrow{\text{fast}} HOD + D{-}H + OH^-$$

Somewhat conflicting evidence regarding such an intermediate has appeared recently. Through mass spectrometric measurements, Bohme and co-workers (11) have reported kinetic data for the reaction $H^- + H_2O \rightleftarrows H_2 + OH^-$ in the gas phase at thermal energies. There was no indication of a stable species like $HHOH^-$, though collisional stabilization of transient $HHOH^-$ species would be difficult at the low pressures employed.

The hydroxide ion-catalyzed reaction between D_2 and H_2O is too slow to be of commercial value in an industrial process for the production of heavy water from a hydrogen or water source, despite a favorable separation factor (12). However, it is well known that many base-catalyzed reactions, including those involving proton transfer from carbon, are greatly accelerated when the solvent contains an aprotic component (see for example, refs. 13–16).

The present research was undertaken to examine the effect of adding dimethyl sulfoxide (DMSO) to the aqueous D_2 exchange system. Preliminary exchange rate data measured with tetramethylammonium hydroxide as a function of medium composition from 20.2 to 99.6 mol% DMSO have already been reported (17). We now present the detailed results for the dependence of exchange rate on medium basicity and base concentration. In addition, as part of this work, some solubility data for D_2 have been determined, supplementary to the complete H_2 solubility study recently reported (18).

Experimental

Reagents

Procedures for purification and storage of DMSO and tetramethylammonium hydroxide have been presented previously (18). Deionized distilled water was used throughout the work.

Deuterium gas (Matheson, technical grade) was conveniently stored and purified (removal of traces of O_2) via the uranium deuteride in a narrow cylindrical steel pressure vessel containing uranium turnings (19). The temperature in a furnace surrounding the vessel was raised to 225 °C whenever the latter required recharging, and to 450 °C for gas withdrawal. Some of the later runs in this study were carried out employing C.P. grade

Can. J. Chem. Downloaded from www.nrcresearchpress.com by 210.87.254.105 on 09/05/12
For personal use only.

TABLE 1. Solubilities of H_2 and D_2 in DMSO and water (mol/l at 25.0 °C)

	H_2		D_2	
Solvent	This work*	Literature	This work†	Literature
Water	8.0×10^{-4} 8.0×10^{-4}	7.9×10^{-4}‡	8.3×10^{-4}	—
DMSO	1.05×10^{-3} 1.08×10^{-3}	1.08×10^{-3}§	1.13×10^{-3}	1.13×10^{-3}§

*From ref. 18, estimated error, ±2%.
†±2%.
‡From ref. 21, converted from mole fraction (18).
§From ref. 20, converted from mole fraction (18).

Matheson gas drawn directly from a small cylinder. A comparison of runs under otherwise identical conditions, but performed with the two D_2 sources, indicated no difference in rate constants within experimental error.

Conversion of the experimental vapor phase exchange rate constants to in-solution data required knowledge of the solubility of deuterium gas in the various media studied. Since such data were found to be available only for pure DMSO and only at 25 °C (20), it was necessary to measure the gas solubility in the H_2O–DMSO mixed solvent system.

A gas chromatographic method was chosen (18) because the procedure is simple and fast (21). Since D_2 reacts fairly rapidly in the alkaline media under study, a time-dependent mixture of D_2, HD, and H_2 is always present in solution. Because the thermal conductivities of D_2 and H_2 are quite different (22), consistent solubility results based on D_2 would not be possible by this method. Therefore pure H_2 was employed for most of the solubility measurements, and the data from this investigation have already been reported (18). The conversion to the D_2 data required for the exchange study was accomplished by comparing the D_2 and H_2 solubilities in pure DMSO and water at 25 °C. These D_2 solubilities at 25 °C were determined in the same manner as for H_2 (18).

The solubility results are presented in Table 1, with the corresponding literature data where available. The present data are believed to be accurate within ±2% (18). From the data in Table 1 a factor of 1.05 ± 0.03 is calculated for conversion from H_2 to D_2 solubilities in these media. It has been assumed that this factor is independent of solvent composition and temperature, within the experimental error. It is known that the relative solubilities of H_2 and D_2 do change slightly with temperature in nonpolar solvents (23), but the variation is within the above error limit.

Exchange Run Procedure

The reaction vessel was the same as that employed for the gas solubility measurements (18). Only Pyrex glass and Teflon came into contact with the solutions.

Exchange runs were carried out in the following manner. Stock DMSO was withdrawn under dry nitrogen by calibrated 25 ml volumetric pipet and transferred to the reaction vessel, which was being flushed with nitrogen. The vessel was then stoppered, placed in ice-cold water to chill the DMSO and finally evacuated for several minutes to facilitate degassing. D_2 was admitted to an ambient-temperature pressure so as to yield a partial pressure of one atm at operating temperature. Allowance was made for the change in pressure resulting from subsequent addition of the base solution, and also for the extra water where necessary. The addition of water, when required, was done at this point by syringe. The final solvent composition was calculated from the quantities of DMSO and water used.

The vessel was submerged in a constant temperature bath controlled to better than ± 0.05 °C, and the solution was stirred for 5 min to allow both gas–liquid and temperature equilibration before the base was introduced by syringe. A stirring rate of 700–800 r.p.m. was used, since, within experimental error, the observed rate constant was independent of stirring rate in the range 300–950 r.p.m. for a test series of runs under conditions approaching the fastest exchange rates encountered.

Periodically, 0.5 cc gas samples were withdrawn from the vapor space by means of a 5 cc Becton–Dickinson Plastipak syringe equipped with a two-way valve and 6 in. needle. Normally a total of six or seven such samples, comprising a maximum of 3% of the initial D_2 charge, were taken per run. The samples were transferred to individual evacuated storage tubes constructed from two 2 mm bore stopcocks joined together. One outer end of each tube was fitted with a rubber serum cap, the other end with a ground glass joint for connection to a vacuum rack. Internal volume was approximately 0.8 cc.

The D_2–HD–H_2 molar composition of the samples was determined by mass spectral analysis on a Consolidated Electrodynamics Corporation model 21-130 mass spectrometer connected to a Varian data computer. Accuracy is believed to be ±0.5% absolute and ±0.2% relative per set for the mol% D_2 figures.

Kinetic Analysis

The exchange data were plotted as $\log_{10}$ (mol% D_2) *vs* time, with the best line through the points being obtained by means of least squares computer calculation. For most solvent compositions these first order plots exhibited excellent linearity, whether the particular run was followed for 80 or for just a few percent reaction. The correlation coefficients were consistently 0.998 or better. However in media of compositions above 95 mol% DMSO the exchange rate usually decreased slowly with time, so that only initial rates were measured. The solution color had become pale yellow by the end of these runs, and a strong amine odor could be detected.

It is probable that the tetramethylammonium cation is undergoing hydrolysis under such strongly basic condi-

Can. J. Chem. Downloaded from www.nrcresearchpress.com by 210.87.254.105 on 09/05/12
For personal use only.

Can. J. Chem. Downloaded from www.nrcresearchpress.com by 210.87.254.105 on 09/05/12
For personal use only.

TABLE 2. Dependence of the first order, in-solution rate constants for D_2 exchange on [Me_4NOH] in DMSO–water media at 65.0°

20.2 mol% DMSO		40.1 mol% DMSO		59.0 mol% DMSO		77.9 mol% DMSO		87.5 mol% DMSO		96.9 mol% DMSO	
[Me_4NOH] (M)	$10^4 k_{obs}$ (s^{-1})	[Me_4NOH] (M)	$10^4 k_{obs}$ (s^{-1})	[Me_4NOH] (M)	$10^4 k_{obs}$ (s^{-1})	[Me_4NOH] (M)	$10^4 k_{obs}$ (s^{-1})	[Me_4NOH] (M)	$10^4 k_{obs}$ (s^{-1})	[Me_4NOH] (M)	$10^4 k_{obs}$ (s^{-1})
0.092	0.570	0.080	1.58	0.057	2.86	0.041	7.41	0.014	5.72	0.0055	14.3
0.460	3.78	0.200	4.40	0.104	6.39	0.062	10.1	0.027	12.1	0.0077	23.0
		0.361	11.4	0.208	14.7	0.093	16.7	0.048	20.1	0.011	30.0
				0.415	42.0	0.134	32.2 33.9	0.070	32.8	0.0165	52.2
						0.186	51.7	0.085	46.7	0.022	83.0 90.8
								0.096	57.5		

Can. J. Chem. Downloaded from www.nrcresearchpress.com by 210.87.254.105 on 09/05/12
For personal use only.

tions, since quaternary ammonium cations tend to be fairly unstable in basic media (24). The tetramethyl form appears to be the least reactive, but stability decreases when the water content of the solvent is lowered (24). Trimethylamine has been reported (25) as a decomposition product of the pyrolysis of the solid tetramethylammonium hydroxide.

The rate constants measured by the procedure outlined above apply to the vapor phase rate of change of D_2–HD–H_2 composition. In order to obtain the in-solution first order rate constants, which are necessary to assess the true medium effect on the exchange reaction, the vapor phase values must be multiplied by a factor representing the distribution of D_2 between the two phases. This factor is given by: (total moles D_2 in the system)/(moles D_2 dissolved in the liquid phase) (5). The term in the denominator was calculated by combining the H_2 solubilities in the various exchange media at each temperature (18) with the H_2-to-D_2 conversion factor of 1.05 (see above). The term in the numerator was obtained from a knowledge of the partial pressure of the D_2 at ambient temperature, and the internal volume of the reaction vessel, corrected for solution volume. The net rate correction factor ranged between 95 and 180, being greater the lower the temperature. The main contribution arises from the strong dependence of gas solubility on temperature for most of the media. The in-solution rate constants are believed to be accurate within ±5% in the solvent composition range 20–97 mol% DMSO. However, reproducibility was poorer in solvents richer in DMSO, presumably because of a slight variation in water content from one run to the next.

The ratio of exchangeable H to D atoms, arising respectively from the water and DMSO (26, 27) and from the total D_2 in the system, was always greater than 225. Also, a comparison was made between the rate of D_2 exchange, under conditions of both the fastest and slowest rate measured, and the rate of H/D transfer for DMSO–water mixtures as calculated from the data of Stewart and Jones (26). For example, while the rates are comparable in 20 mol% DMSO at 35 °C, in 78 mol% DMSO at this temperature the DMSO–water exchange is estimated to be approximately 1000 times faster. This means that *if*, in media rich in DMSO, formation of HD can arise only through transfer of H from a water molecule, the DMSO protons would be readily available in that form, because of the rapid DMSO–water exchange.

To ensure that catalysis of the D_2 exchange reaction by water was unimportant in these media, runs were performed without added base in 77.9 mol% DMSO at 65 °C and in 96.9 mol% DMSO at 80 °C. In both cases there was negligible reaction after several hours, in comparison to 35 and 90% exchange under the basic conditions normally employed (0.134 and 0.022 *M* base, respectively).

Results and Discussion

Rate Dependence on Medium Composition: Qualitative Observations

The kinetic results of this investigation, as given in Tables 2 and 3, show that the rate of the hydroxide ion catalyzed exchange of D_2 increases markedly as the DMSO content of the medium is increased. This is shown explicitly in Table 3 where the rate data have been reduced to a common hydroxide ion concentration (0.011 *M*) by extrapolation. The overall increase in rate as one proceeds from purely aqueous medium to 99.6 mol% DMSO is thus of the order of 10^4. This rate enhancement, though appreciable in absolute terms, is less than would have been expected relative to other systems (*vide infra*), and is insufficient from the viewpoint of adoption in a technical process for D_2O production (12). It appears likely that the observed rate behavior is tied in some fashion to the mechanism of the exchange process and it is therefore pertinent to consider in some detail the mechanistic implications of the present results.

TABLE 3. Medium dependence of the first order, in-solution rate constants for D_2 exchange at constant [Me_4NOH], (0.011 *M*), at 65.0°*

Mol% DMSO	$10^4 k_{obs}$ (s^{-1})
0.0	0.018
20.2	0.070
40.1	0.20
59.0	0.55
77.9	1.9
87.5	4.3
96.9	30
98.5	81
99.2	83
99.6	147

*Data for the solvent compositions 20.2–96.9 mol% DMSO have been obtained from Table 2 by extrapolation to a common hydroxide concentration, 0.011 *M*. The results for 98.5, 99.2, and 99.6 mol% DMSO are separate measurements carried out at the single value of [Me_4NOH]. The value for 0% DMSO has been calculated from ref. 5. The estimated error on the data is ±10%.

Rate Dependence on Acidity Functions

Useful information concerning reaction mechanism of base catalyzed processes may often be derived from consideration of rate dependence on solution basicity (28). For binary solvent systems consisting of dipolar aprotic–protic solvent mixtures, such as the DMSO–water case of the present study, the medium basicity at constant stoichiometric hydroxide ion concentration does not remain constant but increases dramatically as the proportion of the protic component decreases (29, 30). The increased basicity is generally ascribed (29–32) largely to the progressive desolvation of hydroxide ion as the

Can. J. Chem. Downloaded from www.nrcresearchpress.com by 210.87.254.105 on 09/05/12
For personal use only.

hydroxylic component is replaced by the poorly hydrogen-bonding DMSO.

The acidity functions, first introduced by Hammett (33), provide quantitative measure of the basicity of such solvent systems. Thus the H_- function is applicable to base-induced ionization of a neutral weakly acidic indicator ($HA + OH^- \rightleftarrows A^- + H_2O$) and is defined as $H_- = -\log a_{H^+} f_{A^-}/f_{HA}$ where a_{H^+} is the hydrogen ion activity and f_{A^-}, f_{HA} are activity coefficient terms. J_- is applicable to addition of hydroxide ion to a neutral indicator ($R + OH^- \rightleftarrows ROH^-$) and is given by $J_- = -\log a_{H^+} f_{ROH^-}/a_{H_2O} f_R$. It is seen that the two functions are related by the expression:

$$[5] \quad J_- = H_- + \log a_{H_2O} + \log \frac{f_R f_{A^-}}{f_{ROH^-} f_{HA}}$$

Correlations of reaction rates with acidity functions are theoretically based on a number of assumptions (28, 34) whose validity may be difficult to ascertain in practice. However such correlations often provide an empirical criterion of reaction mechanism, through classification and comparison with reactions of known mechanistic types.

A number of rate–acidity function correlations have been recorded for base-induced reactions over the past few years (28–30, 34–37). The log (rate) *vs.* H_- plots are generally found to be linear, with slopes in the region 0.5–1.0. Similar relationships have been found for the J_- function. The linearity of such plots is usually taken as indicative of constancy of mechanism over the basicity range considered. The magnitude of the slopes of such plots has been interpreted as signifying the degree of proton transfer between substrate and base in the case of H_- correlations (by analogy with Brønsted β values), or with the extent of bond formation between substrate and base for J_- correlations. For example, in the case of proton exchange in the CH_3SOCH_3–OH^-–H_2O system the observed slope of 0.93 in the log (rate) *vs.* H_- plot was interpreted on the basis of essentially complete transfer of the proton from the carbon acid to OH^- in the rate-determining transition state (38). However it has been pointed out (ref. 39 and others cited therein) that the experimentally observed slope of a Brønsted plot may not be an accurate indication of the transition state structure.

The problem at hand is whether it is feasible to differentiate between the alternative mechanisms for the D_2–OH^- exchange via the acidity function approach. From reaction 1 it is seen that the hydride ion mechanism involves essentially rate-limiting proton transfer from D—D to OH^-, so that a rate correlation with H_- may be expected to apply. Now since D_2 is a much weaker acid than H_2O one would predict that in the transition state for reaction 1*a* the proton would be virtually completely transferred to OH^-, as the weaker base compared to D^-.[4] Hence the slope of the log (rate) *vs.* H_- plot would be expected to be near unity. The actual plot of the data (Table 3) is shown in Fig. 1. As is seen, not only is the plot non-linear, but the slopes are considerably below unity. The observed slope values of the curved plot, ranging from 0.23 in near aqueous medium to 0.36 at the DMSO-rich end, appear to be the lowest yet recorded in the literature and are contrary to expectations for the proton transfer mechanism. The concerted type mechanisms given by reactions 2 and 3 would presumably be expected to show similar dependence of rate on medium basicity, *i.e.* a near unit slope in the log (rate) – H_- plot, since the rate limiting proton transfer aspect is retained in these pathways.

The addition complex mechanism (reaction 4) does not involve proton transfer in the rate-limiting transition state, so that one would predict a low sensitivity of rate to medium

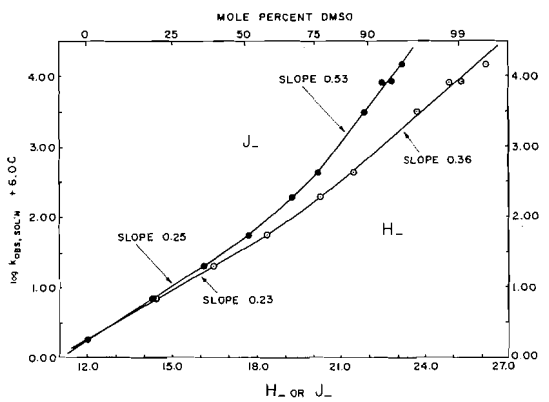

FIG. 1. Plots showing the medium dependence of the first order, in-solution rate constants for D_2 exchange at 65° (s^{-1}) on the H_- and J_- acidity functions.

[4]The pK_a of H_2 is not known with certainty, estimates ranging between 29 and 38 for the value in aqueous medium (40). The pK_a of H_2O (15.7 in aqueous medium) is known to increase in DMSO-containing media (*vide supra* for discussion of solvation of OH^-), reaching the value 26 in 93 mol% DMSO (41).

basicity and hence a small value of the slope in the log k_{obs} – H_- plot, as is in fact observed. On the other hand the slow formation of $DDOH^-$ might have been expected to lead to a satisfactory correlation with the J_- function. As seen in Fig. 1 this plot is also curved and the slopes are still considerably less than unity, though larger than in the H_- plot.[5]

It should be pointed out that quantitative interpretation of the nature of the H_- and J_- plots in the case of D_2 will be tenuous. The necessary condition of similarity in structure between the substrate used in the reaction and the indicators employed to set up the acidity functions, as required for valid interpretation of the rate-acidity function correlations, is probably less well met with D_2 than with any other substrate under investigation. The major problem is that the character of the hydride ion in solution is not known. Intuitively one would have expected H^- to be susceptible to extremely strong solvation by water molecules. However Pearson *et al.* (40) classify it as a *soft* (albeit strong) base and Cotton and Wilkinson (43) consider H^- to be a rather diffuse ion. On the other hand hydroxide ion is generally regarded to be hard. Hence interaction of H^- with the *aprotic* component of the solvent system may in fact be *more extensive*, while solvation by water molecules may be less effective, than occurs with OH^-.

Rate Dependence on Concentration of Tetramethylammonium Hydroxide

The isotopic exchange of D_2 is characterized by an unusual dependence of rate on the concentration of tetramethylammonium hydroxide, as shown by the data in Table 2. Thus for a given DMSO–water medium the plot of the rate constant for exchange (k_{obs}) *vs.* [Me_4NOH] generally exhibits an upward curvature, with slopes greater than unity in the log–log plot at the higher base concentrations. An example is shown in Fig. 2, corresponding to the data for 87.5 mol% DMSO. It appears therefore that the rate of reaction is not simply dependent on the hydroxide ion concentration as in a first order process.

In considering reasons for the apparent deviation from first order dependence on [Me_4NOH], one possibility is that it is caused by deviant H_- behavior, *i.e.* that H_- rises more rapidly than log [OH^-] in a given DMSO–water medium. Unfortunately, literature data on the variation of H_- with [Me_4NOH] are not available for these systems. In principle this factor cannot be excluded, though it would be surprising if such deviation were important for base concentrations of the order of 0.1–0.2 *M*. Significantly, Wilmarth *et al.* (3) observed a similar curvature for D_2 exchange in purely aqueous medium in a region of base concentration where a linear relationship is maintained between H_- and log [OH^-]. It is probable therefore that some other factor(s) are at play in these processes.

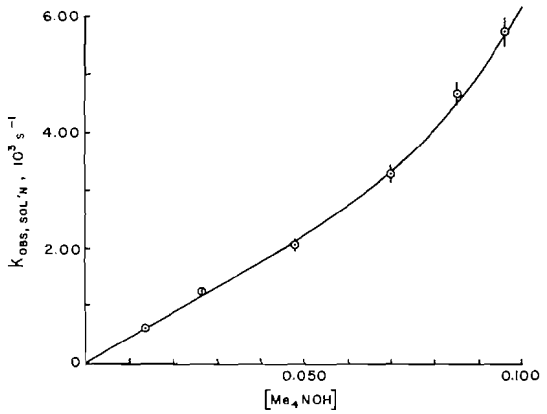

FIG. 2. Illustrative plot to show non-linear dependence of the first order, in-solution rate constants for D_2 exchange at 65° on [Me_4NOH], using the data for 87.5 mol% DMSO.

One general explanation for such behavior was proposed by Prue and co-workers (44), in considering the results of a study of the hydrolysis of diacetone alcohol by various tetraalkylammonium hydroxides. They pointed out that the rate expression will contain the concentrations of substrate and hydroxide ion, multiplied by an activity coefficient factor, $f_A f_{OH^-}/f_{(AOH)^-}{}^{\ddagger}$, where the terms in the numerator refer to reactants and the denominator to the transition state. An increase in the catalytic rate constant would then most likely arise from an increase in the ratio $f_{OH^-}/f_{(AOH)^-}{}^{\ddagger}$, which would be caused by specific short-range interaction of hydroxide ion and/or the transition state with an oppositely charged tetraalkylammonium ion. Similarly, an apparent second order dependence on hydroxide ion concentration was recently ascribed by

[5]The function plotted is $J_- = H_- + \log a_{H_2O}$ according to eq. 5, on the assumption that the activity coefficient ratio cancels (28–30). The a_{H_2O} data for the DMSO–H_2O system are taken from ref. 42.

Can. J. Chem. Downloaded from www.nrcresearchpress.com by 210.87.254.105 on 09/05/12
For personal use only.

Edwards and co-workers (45) to the operation of a salt effect (see also ref. 46).

A mechanistic explanation has been given by Kollmeyer and Cram (35) for the observed non-linear dependence of rate on base concentration for hydrogen exchange involving some carbon acids in a medium of DMSO–MeOH containing MeOK. The experimental data were fitted to the following rate equation

$$[6] \qquad \text{rate} = k_2[RH][B] + k_3[RH][B]^2$$

The term second order in base was then ascribed to a pathway involving participation by methoxide ion and potassium ion (via the ion-pairs) in the rate-determining step, as indicated in the structure **1**. In the present system, one may

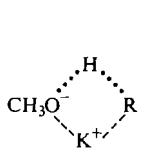

1

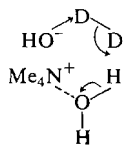

2

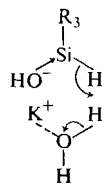

3

tentatively propose a reaction route also involving cation participation. The 6-centered process shown in **2** involves participation by the cation as well as by a solvent molecule; the role of the latter would be to provide electrophilic assistance and thereby eliminate the necessity for free hydride ion formation. Sommer *et al.* (47) have put forward an analogous mechanism, shown in **3**, for base induced displacement of hydride from silicon.

It is difficult at the present time to draw definite conclusions concerning the mechanism of the D_2 exchange process. Such caution is dictated by the unusual nature of some of the results recorded here. Further studies on this problem are in progress.

The authors wish to thank Atomic Energy of Canada Ltd. for a research contract and also for a postdoctoral fellowship to E.A.S., 1969–1971. Sincere appreciation is extended to the staff of the Analytical Branch of the Whiteshell Nuclear Research Establishment at Pinawa, Manitoba, for the mass spectral analyses. Discussions with G. G. Strathdee, N. H. Sagert, and M. Tomlinson are gratefully acknowledged.

1. K. Wirtz and K. F. Bonhoeffer. Z. Phys. Chem. **177**A, 1 (1936).
2. S. Abe. Sci. Pap. Inst. Phys. Chem. Res. (Tokyo) **38**, 287 (1941).
3. W. K. Wilmarth, J. C. Dayton, and J. M. Flournoy. J. Am. Chem. Soc. **75**, 4549 (1953).
4. S. L. Miller and D. Rittenberg. J. Am. Chem. Soc. **80**, 64 (1958).
5. J. M. Flournoy and W. K. Wilmarth. J. Am. Chem. Soc. **83**, 2257 (1961).
6. U. Schindewolf. J. Chim. Phys. **60**, 124 (1963).
7. T. Ishida and M. Benedict. Massachusetts Institute of Technology report MIT-2249-1. 1964.
8. C. Lin. J. Res. Inst. Catal. **15**, 218 (1967).
9. C. D. Ritchie and H. F. King. J. Am. Chem. Soc. **90**, 833 (1968).
10. C. D. Ritchie. *In* Solute–solvent interactions. *Edited by* J. F. Coetzee and C. D. Ritchie. Marcel Dekker, Inc. New York, 1969. pp. 262–264.
11. L. B. Young, E. Lee-Ruff, and D. K. Bohme. Can. J. Chem. **49**, 979 (1971).
12. H. K. Rae. Chemical exchange processes for heavy water. Atomic Energy of Canada Ltd. Report AECL-2555. 1966.
13. A. J. Parker. Q. Rev. **16**, 163 (1962); Chem. Rev. **69**, 1 (1969).
14. R. Alexander, E. C. F. Ko, A. J. Parker, and T. J. Broxton. J. Am. Chem. Soc. **90**, 5049 (1968).
15. D. J. Cram. Fundamentals of carbanion chemistry. Academic Press, New York, 1965.
16. D. Martin, A. Weise, and H.-J. Niclas. Angew. Chem. Int. Ed. **6**, 318 (1967).
17. E. A. Symons and E. Buncel. J. Am. Chem. Soc. **94**, 3641 (1972).
18. E. A. Symons. Can. J. Chem. **49**, 3940 (1971).
19. F. H. Spedding, A. S. Newton, J. C. Warf, O. Johnson, R. W. Nottorf, I. B. Johns, and A. H. Daane. Nucleonics **4**, 4 (1949).
20. J. H. Dymond. J. Phys. Chem. **71**, 1829 (1967).
21. S. K. Shoor, R. D. Walker, Jr., and K. E. Gubbins. J. Phys. Chem. **73**, 312 (1969).
22. The handbook of chemistry and physics, 49th ed. The Chemical Rubber Company, Cleveland, Ohio, 1968.
23. M. W. Cook, D. N. Hanson, and B. J. Alder. J. Chem. Phys. **26**, 748 (1957).
24. G. A. Harlow. Anal. Chem. **34**, 1487 (1962).
25. W. K. Musker. J. Am. Chem. Soc. **86**, 960 (1964).
26. R. Stewart and J. R. Jones. J. Am. Chem. Soc. **89**, 5069 (1967).
27. E. Buncel, E. A. Symons, and A. W. Zabel. Chem. Commun. 173 (1965).
28. J. R. Jones. Prog. Phys. Org. Chem. **9**, 241 (1972).
29. K. Bowden. Chem. Rev. **66**, 119 (1966).
30. C. H. Rochester. Acidity functions. Academic Press, 1970. Chapt. 7.
31. D. Dolman and R. Stewart. Can. J. Chem. **45**, 911 (1967).
32. E. Buncel, E. A. Symons, D. Dolman, and R. Stewart. Can. J. Chem. **48**, 3354 (1970).
33. L. P. Hammett. Physical organic chemistry. McGraw-Hill, New York, 1940. Chapt. 9.
34. R. A. More O'Ferrall. J.C.S. Perkin II, 976 (1972).
35. W. D. Kollmeyer and D. J. Cram. J. Am. Chem. Soc. **90**, 1784 (1968).
36. A. Streitwieser, Jr., C. J. Chang, and A. T. Young. J. Am. Chem. Soc. **94**, 4888 (1972).
37. K. Bowden and R. S. Cook. J. Chem. Soc. (B), 1765 (1971); J.C.S. Perkin II, 1407 (1972).

Can. J. Chem. Downloaded from www.nrcresearchpress.com by 210.87.254.105 on 09/05/12
For personal use only.

38. A. ALBAGLI, R. STEWART, and J. R. JONES. J. Chem. Soc. (B), 1509 (1970).
39. J. R. MURDOCH. J. Am. Chem. Soc. **94**, 4410 (1972); F. G. BORDWELL and W. J. BOYLE, JR. J. Am. Chem. Soc. **94**, 3907 (1972).
40. R. G. PEARSON and J. SONGSTAD. J. Am. Chem. Soc. **89**, 1827 (1967); K. O'DONNELL, R. BACON, K. L. CHELLAPPA, R. L. SCHOWEN, and J. K. LEE. J. Am. Chem. Soc. **94**, 2500 (1972).
41. R. GOTEIN and T. C. BRUICE. J. Phys. Chem. **76**, 432 (1972).
42. J. KENTAMAA and J. J. LINDBERG. Suom. Kem. B**33**, 98 (1960).
43. F. A. COTTON and G. WILKINSON. Advanced inorganic chemistry. 3rd ed. Interscience, 1972. p. 184.
44. E. S. HALBERSTADT and J. E. PRUE. J. Chem. Soc. 2234 (1952); J. E. PRUE, A. J. READ, and G. ROMEO. Trans. Faraday Soc. **67**, 420 (1971).
45. E. J. BEHRMAN, M. J. BIALLAS, H. J. BRASS, J. O. EDWARDS, and M. ISAKS. J. Org. Chem. **35**, 3063 (1970).
46. J. H. SMITH, T. INOUE, and E. T. KAISER. J. Am. Chem. Soc. **94**, 3098 (1972).
47. L. H. SOMMER, W. D. KORTE, and C. L. FRYE. J. Am. Chem. Soc. **94**, 3463 (1972).

Can. J. Chem. Downloaded from www.nrcresearchpress.com by 210.87.254.105 on 09/05/12
For personal use only.

Photooxidation and Reduction of Ascorbic Acid Studied by E.S.R.

ROBERT D. MCALPINE,[1] MICHAEL COCIVERA, AND HOLGER CHEN
Department of Chemistry, University of Guelph, Guelph, Ontario

Received May 16, 1972[2]

The photooxidation of ascorbic acid in water at p*H* 4.5–11.6 was studied using electron spin resonance spectroscopy. In the presence of oxygen, only one radical is detected and its resonance lines are broad. In the absence of O_2, better resolution is obtained and a second radical is observed. When N_2O or H_2O_2 is added, the second radical disappears while the concentration of first radical is increased. These results are consistent with a primary photochemical step involving ejection of an electron from the monoanion of ascorbic acid to form the ascorbate. The second radical appears to be formed by addition of a hydrated electron to the monoanion of ascorbic acid.

La photooxydation de l'acide ascorbique dans l'eau à des p*H* 4.5–11.6 a été étudiée en utilisant la spectroscopie de résonance du spin électronique. En présence d'oxygène, on a détecté un seul radical et ses bandes de résonance sont larges. En absence d'oxygène, on a obtenu une meilleure résolution en même temps qu'un second radical fut détecté. Lorsque l'on a ajouté du N_2O ou du H_2O_2, le second radical est disparu alors que la concentration du premier radical a augmenté. Ces résultats sont donc compatibles avec la première étape photochimique qui implique l'expulsion d'un électron à partir du monoanion de l'acide ascorbique pour former l'ascorbate. Le second radical semble donc être formé par addition d'un électron hydraté au monoanion de l'acide ascorbique.

[Traduit par le journal]

Can. J. Chem., **51**, 1682 (1973)

Introduction

Oxidation–reduction reactions among ascorbic acid, monodehydroascorbic acid radical, and dehydroascorbic acid are believed to play a very important role in a number of biologically essential redox systems (1). Yamazaki, Mason, and Piette (2–4), using electron spin resonance spectroscopy (e.s.r.), have studied the oxidation of ascorbic acid by H_2O_2 and peroxidase. They observed a two line spectrum (one proton with a hyperfine splitting constant of 1.7 G) which they attribute to the monodehydroascorbic acid radical.

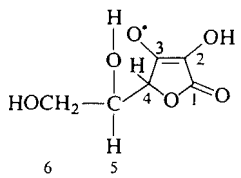

I

Later, Förster, Weis, and Staudinger (5) observed the same spectrum under conditions which yielded greater resolution of the fine details of the spectrum. This spectrum, obtained in water solution by mixing ascorbic acid and dehydroascorbic acid, showed six lines which could be interpreted in terms of one proton with a hyperfine constant of 1.7 G (doublet) and two equivalent protons with hyperfine constant of 0.32 G (triplet). As with Yamazaki, Mason, and Piette (2–4), the hyperfine of 1.7 G was assigned to the lone hydrogen on C_4 of the monodehydroascorbic acid radical (5). The triplet splitting due to two magnetically equivalent protons was not specifically assigned other than to suggest that it was due to hydrogens located on the aliphatic side chain.

We have studied the photochemical oxidation of aqueous ascorbic acid, by e.s.r. spectroscopy, in both oxygen saturated and anaerobic solutions. In both cases we observed the same radical detected by previous workers (1–5). For oxygen saturated solutions, the observed linewidths were about the same as those observed by Yamazaki, Mason, and Piette. However the resolution obtained for deoxygenated solutions was better than that obtained by Förster, Weis, and Staudinger. In addition a new radical was observed. Our results are consistent with the formation of the monodehydroascorbic acid radical via electron ejection from an excited state of the monoanion of ascorbic acid. The second radical appears to be formed by the addition of the hydrated electron to the monoanion.

[1]Present address: Atomic Energy of Canada Ltd., Chalk River, Ontario.

[2]Revision received January 19, 1973.

Can. J. Chem. Downloaded from www.nrcresearchpress.com by 210.87.254.6 on 09/05/12
For personal use only.

Can. J. Chem. Downloaded from www.nrcresearchpress.com by 210.87.254.6 on 09/05/12
For personal use only.

Experimental

Solutions of 10^{-2} *M* L-ascorbic acid (obtained from B.D.H., reagent grade, and Nutritional Biochemical Corporation and used without further purification) were studied at various p*H* values between 4.5 and 11.6 in a continuous closed flow system. A description of this system has been given previously (6). Irradiation was carried out in the microwave cavity of a Varian E-12 e.s.r. spectrometer using the full spectrum (quartz optics) of a 1000 W high pressure Hanovia mercury–xenon lamp. Usually nitrogen gas was bubbled through the solutions. Several experiments were performed with H_2O_2 (Fisher Scientific) added or with N_2O (Canox) replacing the nitrogen gas. In addition a few experiments were carried out using oxygen (Canox) saturated solutions.

5,6-*o*-Isopropylidene-L-ascorbic acid was prepared as reported by Vargha (7). A mixture of 500 ml of acetone, 50 g of $CuSO_4$, and 12 g of L-ascorbic acid was stirred for 24 h. After filtering, the solution was concentrated to one third its volume, and petroleum ether was added to precipitate a white crystalline material. After recrystallization several times and drying, this material melted sharply at 218 °C (uncorrected) compared to 176 °C for ascorbic acid. Mass spectroscopy of this compound showed a strong parent peak at mass 216 whereas a peak due to ascorbic acid could not be detected. The n.m.r. spectrum at 60 MHz indicated a compound containing two methyl groups having a different chemical shift than acetone. Acetone could not be detected.

The Photochemical Oxidation of Ascorbic Acid

The e.s.r. spectrum of an oxygen saturated water solution of ascorbic acid during irradiation is given in Fig. 1*A*. This spectrum (obtained at p*H* 6.3 and ambient temperature) consists of two broad lines (bandwith ~ 0.9 G) about $g = 2.0052$, and is nearly identical to the one obtained by Yamazaki, Mason, and Piette for the enzymatic oxidation of ascorbic acid in water (2–4). When the solution is deoxygenated, the resolution of the spectrum is improved significantly as can be seen from Fig. 1*B*, which was obtained at p*H* 11. Thus, the greater linewidth observed in the presence of molecular oxygen indicates that the oxygen probably is increasing the spin relaxation rate for the radical (**1**). The sweepwidth is the same for Figs. 1*A* and 1*B*; however the linewidth in 1*B* is narrow enough to observe an additional triplet splitting. In addition, the weaker spectrum of another radical (hereafter referred to as **2**) is observed with $g = 2.0045$; this radical has not been reported by previous workers. The spectrum of **2** can be analyzed in terms of two inequivalent hydrogens with hyperfine coupling constants 13.8 and 0.74 G. Regions of the spectrum of **1** and **2** were studied in more detail under conditions of improved instrument resolution (sweepwidth of 4 G, modulation amplitude of 0.02 to 0.06 G and 2 mW of microwave power). The spectrum of **2** showed no further structure (see Fig. 2*A*); however a total of twelve lines was observed in the spectrum of **1** (see Fig. 2*B*). These twelve lines can be ascribed to 4 hydrogens in equivalent sets 2:1:1 with hyperfine coupling constants 0.17, 0.06, and 1.75 G, respectively. To ensure that the 0.06 G splitting is real and not an artifact due to the 100 kHz modulation, the experiment was re-

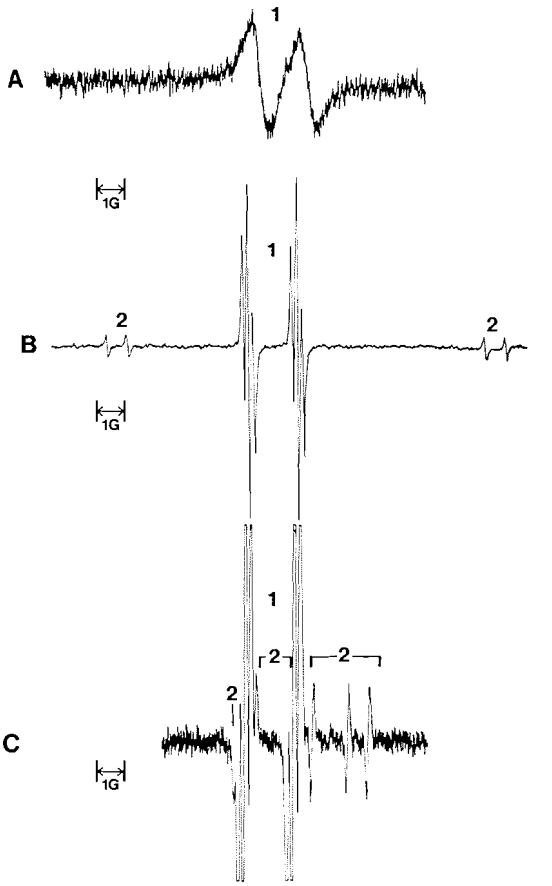

FIG. 1. (*A*) The e.s.r. spectrum of 10^{-2} *M* L-ascorbic acid irradiated in an oxygen saturated aqueous solution at p*H* 6.3. Radical **1** is observed as two broad lines (bandwidth ~ 0.9 G); but radical **2** is not observed. (*B*) The e.s.r. spectrum of a 10^{-2} *M* solution of L-ascorbic acid irradiated in an oxygen free solution of p*H* 11. Radical **1** is seen to sharpen considerably, while a new radical (**2**) is observed with two hyperfine coupling constants of 13.8 and 0.74 G. (*C*) The e.s.r. spectrum of 10^{-2} *M* L-ascorbic acid in D_2O under oxygen-free conditions. Radical **1** is unchanged; however the proton responsible for the 13.8 G splitting in **2** is replaced by a deuterium, yielding a 6 line spectrum for radical **2** with a hydrogen hyperfine of 0.74 G and a deuterium hyperfine of 2.05 G.

Can. J. Chem. Downloaded from www.nrcresearchpress.com by 210.87.254.6 on 09/05/12
For personal use only.

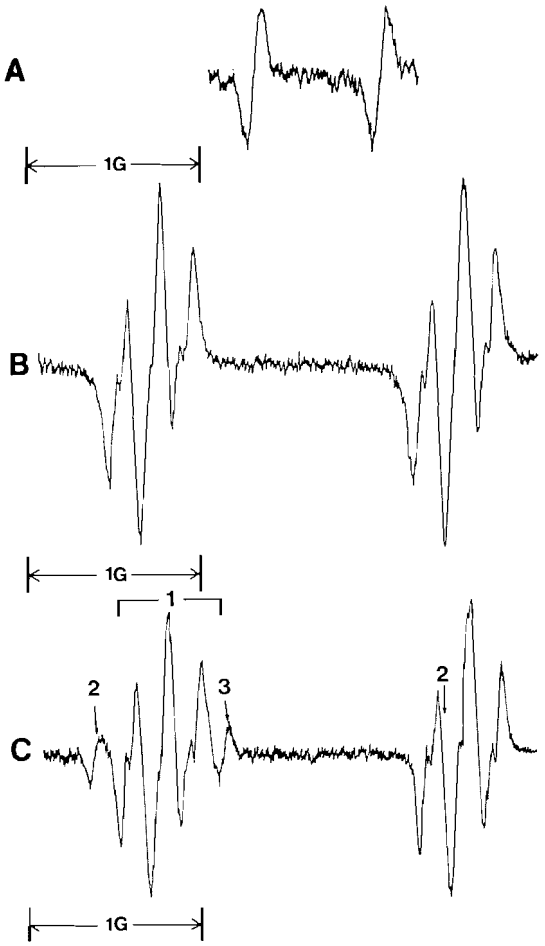

FIG. 2. (*A*) A portion of the e.s.r. spectrum of radical **2** under conditions of high resolution. (*B*) The e.s.r. spectrum of radical **1** under conditions of high resolution. It is evident that radical **1** is a 12 line spectrum which can be ascribed to 4 hydrogens in equivalent sets 2:1:1. The hyperfine coupling constants are 0.17, 0.06, and 1.75 G, respectively. (*C*) The high resolution e.s.r. spectrum of radicals **1** and **2** generated in a D_2O solution. The spectrum of radical **1** is unchanged except for the overlapping of new deuterium lines which arise from radical **2**.

peated using 10 kHz modulation. Under these conditions, the small splitting did not disappear, but on the contrary was somewhat better resolved. Because of the overlap of these lines, a computer simulation was used in this analysis.[3]

In the absence of radiation, radical **1** can still be detected in basic solution but not in acid solution. However, its concentration is about a factor 10 lower than the concentration obtained during irradiation with our light source. Radical **2** is not observed under these conditions. The observation of a small amount of radical **1** in the absence of radiation indicates that a small amount of dehydroascorbic acid is present in the ascorbic acid since radical **1** can be generated in a solution containing ascorbic acid and dehydroascorbic acid (5). The absence of radical **2** under these conditions will be discussed below.

The experiment was repeated using D_2O as a solvent (see Figs. 1*C* and 2*C*). In this case the hydrogen having the coupling constant of 13.8 G in **2** is replaced by a deuterium. This results in the doublet with the 13.8 G splitting becoming a triplet of three equal intensity lines with a splitting of 2.05 G. On the other hand, none of the hydrogens of radical **1** are replaced by deuterium when D_2O is used as a solvent. In Fig. 1*C*, it can be seen clearly that the spectrum of **1** is unchanged except for overlap by the new lines of spectrum **2**. Thus, none of the hydrogens which interact with the unpaired electron of **1** appear to exchange easily with D_2O under basic conditions.

N.m.r. studies (8, 9) indicate that OH-protons of alcohols and acids exchange rapidly in basic media. To determine if any of the CH-protons can readily exchange at the p*H* values employed in the present study, a solution of ascorbic acid in D_2O at p*H* 12 was allowed to sit for several hours at room temperature. Since ascorbic acid decomposes at high p*H* when O_2 is present, the solution was evacuated to 2 μ Hg. Under these conditions, the n.m.r. spectrum obtained indicated that none of the CH-protons had been replaced by deuterium and that no decomposition had occurred. Thus the hydrogen responsible for the 13.8 G coupling constant in **2** probably is hydroxylic in nature, and all of the hydrogens responsible for the observed hyperfine structure in **1** must be attached to carbon atoms.

Structure and Mechanism

The structure of radical **1** has been suggested to be the monodehydroascorbic acid radical (structure **1**) (2–5). Our results are consistent with this structure if the hyperfine coupling constants are assigned as follows: C_4-proton, 1.75 G; C_5-proton, 0.06 G; and C_6-protons, 0.17 G. This assignment requires that the C_6-protons have a somewhat larger electron spin density than the C_5-proton. Since the values are small it is not

[3]Program written by C. S. Johnson, modified by P. J. Black and T. J. Debyer.

Can. J. Chem. Downloaded from www.nrcresearchpress.com by 210.87.254.6 on 09/05/12
For personal use only.

impossible that conformational effects might account for this order. However to check the possibility that the spectrum might be due to a different radical having a second ring formed by bonding the C_6-oxygen to C_3, we have obtained the e.p.r. spectrum of an aqueous solution of 5,6-isopropylidene-L-ascorbic acid under the same conditions. Since the C_5 and C_6 oxygens are blocked in this compound, ring formation involving the aliphatic side chain is unlikely. For this compound, the observed spectrum is the same as the one observed for radical **1**. Consequently, this result does not support a two ring structure for radical **1**, and structure **1** seems more reasonable.

(Note added in proof: Recently, the same e.s.r. spectrum has been observed as a result of reaction of OH with ascorbic acid in H_2O, and the same structure has been proposed (17).)

Radical **2** appears to be formed by the addition of the hydrated electron to the monoanion of ascorbic acid. This conclusion is based on the following evidence. This radical is formed only during irradiation, *i.e.* in the absence of irradiation, radical **2** is not detected even though radical **1** can be detected. Under these equilibrium conditions, one would not expect the formation of radical **2** if the hydrated electron is involved. Furthermore, during irradiation in the presence of N_2O, **2** cannot be detected whereas the concentration of **1** is increased by a factor of two. This increase is prevented by the addition of methanol. Since N_2O reacts with the hydrated electron to form the hydroxy radical (10), this result supports the hypothesis that N_2O prevents the formation of **2** by reacting faster with the hydrated electron than does the monoanion of ascorbic acid.

Furthermore, the increase in the concentration of **1** can be explained by a reaction of the hydroxy radical (formed by the reaction of N_2O with the hydrated electron) with the monoanion of ascorbic acid. The effect of H_2O_2 on the concentrations of **1** and **2** is consistent with this conclusion. In the absence of radiation, the concentration of radical **1** is approximately doubled when 3% H_2O_2 is added to a deoxygenated solution of 0.01 *M* ascorbic acid at p*H* 8. Radical **2** is not detected. However during irradiation of solutions containing 0.3 to 3% H_2O_2 at p*H* values between 4.5 and 11.6, the concentration of radical **1** increases by up to a factor of 25, *i.e.* about 5 times larger than the concentration of **1** obtained during irradiation in the absence of H_2O_2. Radical **2** cannot be detected. Addition of methanol at a concentration equal to that for H_2O_2 decreases the intensity of **1** to the value obtained in the absence of H_2O_2, and radical **2** cannot be detected.[4] Some further quenching is observed if more methanol is added. The effect of methanol is consistent with the suggestion that OH is present since methanol scavenges OH (12). Thus, the effect of N_2O on the concentration of **1** is consistent with the suggestion that the hydrated electron is formed during the irradiation of an aqueous solution of ascorbic acid. We suggest the following mechanism. The monoanion of ascorbic acid absorbs light and subsequently forms radical **1** by ejecting an electron while in an excited electronic state. The hydrated electron formed in this manner adds to another ascorbic acid anion in its ground state to form **2**.

The reduction potential of ascorbic acid indicates that the addition of an electron to the monoanion is a possibility. The reduction potentials for ascorbic acid and cinnamic acid are -2.06 and -1.93 V, respectively. These potentials were measured in solution in acetonitrile on a Hg electrode with an Ag/AgCl reference electrode. Cinnamic acid was chosen for comparison because it is somewhat similar in structure to ascorbic acid and its anion reacts with the hydrated electron at a nearly diffusion controlled rate (13). Unfortunately, it was not possible to measure the reduction potentials for the anions of the acids because the reduction could not be performed with water as the solvent. At any rate, the close similarity in the reduction potentials for these acids indicates that the addition of an electron to the monoanion of ascorbic acid probably is not unreasonable.

The structure of **2** cannot be specified with any certainty at this time. The e.p.r. results using D_2O indicate that the hydrogen having the hyperfine coupling constant of 13.8 G exchanges easily. The n.m.r. study using D_2O indicates that the hydrogens bonded to carbon atoms in ascorbic acid do not exchange easily. Consequently it would appear that the exchangeable hydrogen is attached to an oxygen atom. Furthermore, the hydrated electron most likely would add to the carbonyl group at position 1.

[4]Radical **2** might disappear by reacting with H_2O_2; or H_2O_2 could prevent the formation of **2** by reacting with the hydrated electron (11).

By analogy, the hydrated electron appears to add to the CO_2^- group of tyrosine (14). These results would suggest structure **2** with the

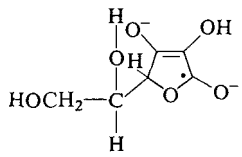

2

coupling constants 13.8 and 0.74 G assigned to the OH in position 2 and the CH in position 4, respectively. However, the coupling constant as large as 13.8 G for an OH-proton in liquid solutions is unprecedented. Usually it is much smaller, although values of 12 and 13.9 G have been observed in the solid state (15, 16). Therefore, structure **2** must be regarded as tentative.

The authors wish to thank Dr. R. O. Loutfy for measuring the reduction potentials, and Professor M. Fujimoto for his generosity in making his e.s.r. facilities available to us. This work has been supported in part by DUA grant #64061, DRB grant #953096, and by PRF grant #PR4904.

1. L. W. MAPSON. *In* The vitamins. Vol. I. *Edited by* W. H. Sebrell and R. S. Harris. Academic Press, New York, 1967. pp. 386–398.
2. I. YAMAZAKI, H. S. MASON, and L. PIETTE. Biochem. Biophys. Res. Commun. **1**, 336 (1959).
3. I. YAMAZAKI, H. S. MASON, and L. PIETTE. J. Biol. Chem. **235**, 2444 (1960).
4. I. YAMAZAKI and L. H. PIETTE. Biochim. Biophys. Acta, **50**, 62 (1961).
5. G. V. FÖRSTER, W. WEIS, and H. STAUDINGER. Justus Leibigs Ann. Chem. **690**, 166 (1965).
6. M. COCIVERA, M. TOMKIEWICZ, and A. GROEN. J. Am. Chem. Soc. **94**, 6598 (1972).
7. L. V. VARGHA. Nat. **130**, 846 (1932).
8. Z. LUZ and S. MEIBOOM. J. Am. Chem. Soc. **86**, 4766 (1964).
9. E. GRUNWALD, C. JUMPER, and S. MEIBOOM. J. Am. Chem. Soc. **84**, 4664 (1962).
10. M. ANBAR and P. NETA. Int. J. Radiat. Isot. **16**, 229 (1965).
11. E. HART and E. FIELDEN. Advan. in Chem. Ser. No. 50. *Edited by* R. Gould. American Chemical Society, Washington D.C. 1965. p. 253.
12. G. ADAMS, J. BOAG, and B. MICHAEL. Trans. Faraday Soc. **61**, 1417 (1965).
13. A. SZUTKA, J. THOMAS, S. GORDON, and E. HART. J. Phys. Chem. **69**, 289 (1965).
14. M. TOMKIEWICZ, R. D. MCALPINE, and M. COCIVERA. Can. J. Chem. **50**, 3849 (1972).
15. D. POOLEY and D. H. WHIFFEN. Trans. Faraday Soc. **57**, 1445 (1961).
16. I. MIYAGAWA and W. GORDY. J. Am. Chem. Soc. **83**, 1036 (1961).
17. G. LAROFF, R. FESSENDEN, and R. SCHULER. J. Am. Chem. Soc. **94**, 9062 (1972).

Can. J. Chem. Downloaded from www.nrcresearchpress.com by 210.87.254.6 on 09/05/12
For personal use only.

Temperature Dependence of Activation Volumes of Solvolysis Reactions in Light and Heavy Water

CLAUDE S. DAVIS[1] AND J. B. HYNE
Department of Chemistry, University of Calgary, Calgary, Alberta

Received October 23, 1972

The pressure dependence of the solvolysis rates for benzyl chloride, isopropyl bromide, and methanesulfonyl chloride in H_2O and D_2O have been measured. The temperature dependence of the activation volumes appears to be indicative of the mechanism of solvolyses and the differences in the temperature dependence of the activation volumes for the two solvents are consistent with D_2O being the more structured. The more extensive data in the case of methanesulfonyl chloride deuterolysis indicates extremum behavior in ΔV^* as a function of temperature in the 5–25 °C range.

La relation entre la pression et le taux de solvolyse du chlorure de benzyle, du bromure d'isopropyle et du chlorure de méthane sulfonyle dans l'H_2O et dans le D_2O a été évaluée. La relation entre la température et les volumes d'activation semble être caractéristique du mécanisme des solvolyses. De plus, les différences dans la relation des volumes d'activation et la température pour les deux solvants sont en accord avec le fait selon lequel le D_2O est le mieux structuré. Les données les plus complètes en ce qui a trait à la deutérolyse du chlorure de méthanesulfonyle montrent un comportement extrême du ΔV^* en fonction de la température dans l'intervalle de 5 à 25 °C. [Traduit par le journal]

Can. J. Chem., 51, 1687 (1973)

Introduction

The temperature dependence of the volumes of activation, $d\Delta V^*/dT$, for solvolysis reactions in H_2O have been reported previously (1–7) and for some reactions $d\Delta V^*/dT$ has been dissected into initial and ground state components (1). The behavior of these parameters has been discussed in terms of the differences in polarity of the initial and transition states. It is well known that aqueous binary solvents significantly alter activation parameters (4, 8). This variation in the activation parameters has been discussed largely in terms of the effect that the addition of cosolvent has on the structure of water as well as in terms of the change in polarity of the substrate in the activation process. In view of the analogous structural properties of H_2O and D_2O and the influence temperature has on them, this investigation deals with the temperature dependence of the activation volume in H_2O and D_2O.

Although there is a large amount of kinetic data for solvolysis reactions in heavy water (9, 10) no data have been obtained at pressures other than atmospheric. The present study was undertaken to determine whether or not the difference in structural properties of D_2O and H_2O are significant enough to be reflected in the temperature dependence of the volume of activation for these solvolyses.

Experimental

Materials

Water

House distilled water was passed through a deionizing resin. The specific conductance of the water used was no greater than $8 \times 10^{-7}\ \Omega^{-1}\ cm^{-1}$ at 25 °C.

Heavy Water

99.8 mol% D_2O from Bio-Rad Laboratories was used. The D_2O was redistilled before use. The H_2O content which was checked by n.m.r. never exceeded 0.4 mol%.

Methanesulfonyl Chloride, Benzyl Chloride, and Isopropyl Bromide

These compounds were each twice distilled under reduced pressure and the middle fractions were collected each time. Analysis by gas–liquid chromatography showed less than 0.02% impurity.

Kinetics

The rates of solvolysis of isopropyl bromide and benzyl chloride in H_2O and D_2O were studied at 40.00 and 60.00 °C.

The rates for methanesulfonyl chloride in H_2O were measured at 0.50 and 13.00 °C. The rates in D_2O were determined at 5.00, 8.17, 11.48, 16.20, 21.00 and 26.00 °C. Rates were usually measured over the pressure range 1 to 3402 atm. Temperature control was ±0.01 °C or better and the pressure was maintained within ±14 atm. The reactions were monitored conductimetrically. Details of the high pressure system, conductance bridge and timer have been described previously (11, 12). Graphical analysis of the conductance–time data by the Guggenheim method (13) yielded pseudo first order rate constants.

[1]Present Address: Department of Chemistry, University of the West Indies, Kingston, Jamaica.

Can. J. Chem. Downloaded from www.nrcresearchpress.com by 210.87.254.105 on 09/05/12
For personal use only.

TABLE 1. Solvolysis rate constants in D_2O

Pressure (atm)	Benzyl chloride 40.00 °C $k \times 10^5$ (s^{-1})	Benzyl chloride 60.50 °C $k \times 10^4$ (s^{-1})	Isopropyl bromide 40.00 °C $k \times 10^5$ (s^{-1})	Isopropyl bromide 60.00 °C $k \times 10^4$ (s^{-1})
1	5.912±0.032	4.611±0.022	2.384±0.006	2.790±0.013
340	6.639±0.040	5.400±0.037	2.702±0.017	3.195±0.041
681	7.497±0.040	6.305±0.044	3.022±0.010	3.667±0.006
1021	8.360±0.020	7.398±0.016	3.379±0.015	4.191±0.020
1361	9.285±0.028	8.610±0.030	3.791±0.011	4.750±0.017
1701	—	9.892±0.090	—	5.361±0.036
2041	11.61 ±0.04	—	4.702±0.019	—

Results

Solvolytic rate constants obtained as a function of pressure for benzyl chloride and isopropyl bromide are shown in Tables 1 and 2. The errors indicated are average deviations of at least three replicate rate determinations.

The pressure dependence of the solvolysis rate of isopropyl bromide in H_2O has been reported previously (2), but in view of the surprising results obtained, the data were redetermined in these laboratories. Although, as indicated in Table 2, the rate constants at atmospheric pressure compare favorably with the previously reported values (2, 14), the complex rate constant-pressure behavior reported previously (2) was not evident.

The pressure dependence of the rate of solvolysis of methanesulfonyl chloride in both heavy and light water was determined in considerable detail as indicated in Tables 3 and 4. Values at six temperatures were obtained in D_2O and the earlier data of Mackinnon and Hyne (1) in H_2O at two temperatures were expanded to give more complete coverage of the low temperature range.

TABLE 2. Rate constants for the solvolysis of isopropyl bromide in H_2O at 40.00 and 60.00 °C at various pressures

Pressure (atm)	$k \times 10^5$ (s^{-1}) 40.00 °C	$k \times 10^5$ (s^{-1}) 60.00 °C
0	3.179±0.023	35.16±0.14
	(3.170)*	(35.56)*
	(3.132)†	(34.98)†
340	3.604±0.019	40.33±0.10
681	4.085±0.020	46.27±0.15
1021	4.574±0.011	52.54±0.20
1361	5.100±0.015	60.27±0.24
2041	6.321±0.024	—

*Reference 2.
†Reference 14.

The rate–pressure data reported in Tables 1–4 were fitted to the equation

$$[1] \qquad \ln k = A + Bp + Cp^2$$

The constants A, B, and C were derived by the least mean squares method using a computer. The volumes of activation and their pressure dependence were calculated using the following relationships (4).

$$[2] \qquad \Delta V^* = -RTB$$

$$[3] \qquad \frac{\partial \Delta V^*}{\partial p} = -2RTC$$

Table 5 lists the values of ΔV^* and $\partial \Delta V^*/\Delta p$ as calculated from the rate–pressure data in Tables 1–4 together with previously published values for light water solvolyses of benzyl chloride (4), and for methanesulfonyl chloride at 5 and 21 °C (1). The activation parameter values presented in Table 5 represent the essential data to be discussed in this paper.

Discussion

Comparison of Hydrolyses

It is interesting to note in Table 5 that at the same temperature there can be small but significant differences in activation volumes for solvolyses reactions in light and heavy water. However, in view of the fact that the structures of H_2O and D_2O vary to different extents as the temperature is altered, we feel that the meaningful parameter to compare is $d\Delta V^*/dT$ in each solvent. Table 6 lists values for $d\Delta V^*/dT$ for the three solvolyses in H_2O and D_2O determined from temperature dependence data in Table 5. In the case of methanesulfonyl chloride the value of 0.00 ± 0.03 merely indicates that the temperature dependence of the volume of activation in this system is small compared with the other

Can. J. Chem. Downloaded from www.nrcresearchpress.com by 210.87.254.105 on 09/05/12
For personal use only.

TABLE 3. Rate constants for the solvolysis of methanesulfonyl chloride in D_2O at various temperatures and pressures

Pressure (atm)	$k \times 10^5$ (s^{-1})					
	5.00 °C	8.183 °C	11.480 °C	16.20 °C	21.00 °C	25.995 °C
0	0.9298±0.0005	1.466±0.005	2.295±0.007	4.284±0.004	7.665±0.008	13.88±0.015
340	1.076 ±0.002	1.684±0.016	2.641±0.020	4.873±0.007	8.766±0.03	15.71±0.10
681	1.238 ±0.004	1.932±0.006	2.995±0.010	5.549±0.014	10.01 ±0.02	18.15±0.01
1021	1.438 ±0.002	2.215±0.001	3.456±0.006	6.368±0.016	11.40 ±0.06	20.74±0.06
1361	1.655 ±0.008	2.554±0.004	3.969±0.004	7.264±0.020	12.96 ±0.06	23.63±0.04
1701	1.922 ±0.008	—	4.522±0.009	—	14.82 ±0.06	—
2041	2.226 ±0.010	3.269±0.008	5.212±0.009	9.486±0.023	16.85 ±0.09	—

TABLE 4. Rate constants for the solvolysis of methanesulfonyl chloride in H_2O as a function of pressure at various temperatures

Pressure (atm)	$k \times 10^5$ (s^{-1})			
	0.500 °C	5.00 °C*	13.00 °C	21.00 °C*
1	0.8012±0.0012	1.463±0.020	4.448±0.007	23.77±0.12
340	0.9187±0.0070	1.569±0.014	5.084±0.005	—
681	1.073 ±0.002	1.680±0.013	5.850±0.009	27.48±0.34
1021	1.252 ±0.001	1.785±0.008	6.708±0.009	29.42±0.37
1361	1.455 ±0.001	1.909±0.011	7.711±0.005	30.82±0.20
1701	1.697 ±0.001	—	8.843±0.022	—
2041	—	2.181±0.020	—	32.43±0.04

*Data from ref. 1.

TABLE 5. Activation parameters for benzyl chloride, isopropyl bromide, and methanesulfonyl chloride in light and heavy water

Compound	Temperature (°C)	$-\Delta V^*$ (ml mol^{-1})	
		H_2O	D_2O
Benzyl chloride	40.00	9.09±0.01*	8.89±0.25
	60.50	10.3 ±0.2*	13.0 ±0.4
Isopropyl bromide	40.00	9.65±0.33	9.07±0.14
	60.00	11.02±0.39	11.42±0.40
Methanesulfonyl chloride	0.50	9.58±0.24	—
	5.00	9.65±0.32†	9.67±0.11
	8.18	—	9.39±0.29
	11.48	—	9.25±0.23
	13.00	9.43±0.26	—
	16.20	—	9.12±0.11
	21.00	10.15±0.01†	9.43±0.08
	26.00	—	9.60±0.22

*Reference 4.
†Reference 1.

solvolyses. The detailed nature of the temperature dependence of ΔV^* for the sulfonyl chloride will be discussed at a later point in the analysis.

The temperature dependence of the volume of activation can be discussed in terms of its component parts, the temperature dependences of the partial molal volumes of the initial and transition states. The more negative $d\Delta V^*/dT$ values for the

$$\frac{d\Delta V^*}{dT} = \frac{d\bar{V}^t}{dT} - \frac{d\bar{V}^g}{dT} \quad [4]$$

benzyl and isopropyl halide solvolyses in D_2O

Can. J. Chem. Downloaded from www.nrcresearchpress.com by 210.87.254.105 on 09/05/12
For personal use only.

TABLE 6. Activation parameters for solvolyses in H_2O and D_2O

Compound	$d\Delta V^*/dT$ ml mol^{-1} deg^{-1}		$-\Delta C_p^*$ cal deg^{-1} mol^{-1}	
	H_2O	D_2O	H_2O	D_2O
Isopropyl bromide	-0.07 ± 0.04	-0.12 ± 0.03	59 ± 2*	66 ± 2*
Benzyl chloride	-0.06 ± 0.01	-0.20 ± 0.03	—	—
Methanesulfonyl chloride	0.00 ± 0.03	0.00 ± 0.03	53 ± 1†	53 ± 1†

*Reference 15.
†Reference 16.

compared with H_2O indicates that the difference in the temperature dependence of the volume of the two states is greater in D_2O than in H_2O. Why should the volumes of the ground and/or transition states in D_2O be relatively more temperature sensitive than in H_2O? The volumes being discussed here are the volumes of the kinetically significant entities which include not only the substrate molecule, but its kinetically important solvent environment. D_2O is known to possess more inherent "structuredness" than H_2O and hence it is reasonable to conclude that a state incorporating the more structured D_2O will in turn have a volume that is more sensitive to thermal disruption. Until some estimate of the values for the thermal expansivity of one or other of the component states are available a more specific analysis of the volume temperature dependence in terms of structure is precluded.

The difference in activation volume temperature dependence between D_2O and H_2O is very significantly less for methanesulfonyl chloride compared with the two alkyl halides. There seems little doubt that the interaction of a highly polar substrate such as methanesulfonyl chloride with a water environment will be significantly different from that in the case of the more hydrophobic and less polar alkyl halides. *The difference* in solute–solvent interaction both between initial and transition states and between light and heavy water will thus be masked in the methanesulfonyl chloride cases and this in turn will be reflected in the greater similarity of the temperature dependences of the volumes. The equal and small $d\Delta V^*/dT$ values (0.00 ± 0.03) for methanesulfonyl chloride support this interpretation.

Available heat capacities of activation in both light and heavy water shown in Table 6 provide further supportive evidence. ΔC_p^* values for methanesulfonyl chloride in the two waters are identical within experimental error in keeping with the postulate that the *difference* between the solute–solvent interaction of both states in both solvents is negligible. On the other hand there is a significant difference between ΔC_p^* values in light and heavy water for isopropyl bromide solvolysis paralleling the behavior observed for the temperature dependence of the activation volume.

The redetermined value of $d\Delta V^*/dT$ for isopropyl bromide hydrolysis deserves comment as it relates to the earlier analysis of Mackinnon and Hyne using the literature rate values (2). Dissection of $d\Delta V^*/dT$ values by these authors for a series of hydrolyses indicated that the $d\bar{V}^t/dT$ component increased in the order:

$$pMe\phi CH_2Cl < MeSO_2Cl < \phi CH_2Cl < \text{allyl Cl} < n\text{BuBr} < \text{isoPrBr}$$

The apparently anomalous position of isopropyl bromide in this sequence required an earlier rationalization based on differences in solvent accessibility to the reaction site. The redetermined $d\Delta V^*/dT$ value for isopropyl bromide *reverses* the order of the two alkyl bromides which is in keeping with the expected larger degree of charge development in the activation process for the secondary halide.

Special Case of Methanesulfonyl Chloride

The gross changes in ΔV^* as a function of temperature for the three solvolyses in light and heavy water have already been discussed. The more extensive data for methanesulfonyl chloride, however, warrant further examination. It must be recognized that the temperature dependence of the volume of activation is a second order derivative of the experimentally measured rate and the inherent uncertainties in such a parameter are expected to be sizeable. Nonetheless, dogmatism excluded, it is considered justifiable to examine the apparent trends in the temperature dependence in both H_2O and D_2O.

The temperature variation of the measured

Can. J. Chem. Downloaded from www.nrcresearchpress.com by 210.87.254.105 on 09/05/12
For personal use only.

Can. J. Chem. Downloaded from www.nrcresearchpress.com by 210.87.254.105 on 09/05/12
For personal use only.

volumes of activation for the solvolyses of methanesulfonyl chloride in light and heavy water are presented graphically in Fig. 1. The error bars shown indicate the uncertainties in ΔV^* as obtained from the least mean squares fit of the rate–pressure data to eq. [1].

An obvious reason for examining the dependence of the volume of activation on temperature in both light and heavy water in this particular temperature range (0–25 °C) was that both solvents exhibit maximum density behavior in this same range. Since this behavior is known to be related to structural phenomena in the liquids is there a reflection of this solvent structural variation in the volume of activation parameter? Having specifically sought such evidence it will be obvious why care was taken to comment on errors and significance in the preceding paragraph! Despite the error limits, the data in Fig. 1 are considered to indicate such a kinetic reflection of solvent structural variation in the case of D_2O. The same cannot be claimed for the H_2O data. In the latter case, however, it should be recalled that the overall "structuredness" of light water is less than heavy water (17) and hence there will be less overall water structure variation to be reflected in the kinetic parameters. Furthermore, the extremum in the density and hence structural behavior is at 3.984 °C (compare 11.185 °C for D_2O (18)), very close to the lower temperature limit dictated by the freezing point. Hence, in light water, a kinetic manifestation of the density extremum would have to be detected at one end of the accessible temperature range compared with the mid-point location in the D_2O case. Clearly the Fig. 1 data for light water does not provide a definitive answer to this question.

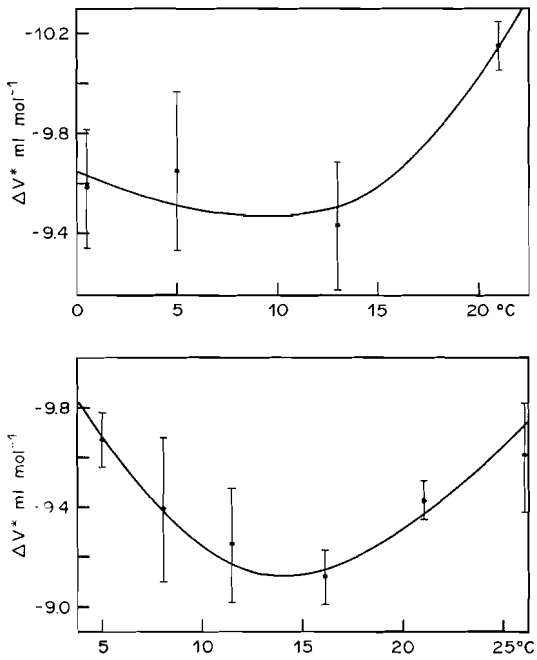

FIG. 1. Variation of volumes of activation for the solvolysis of methanesulfonyl chloride in H_2O and D_2O as a function of temperature.

The heavy water case does suggest an extremum in the temperature dependence of the volume of activation in the 10–20 °C temperature range. Extrema of this kind are commonplace in the dependence of volume of activation on solvent composition for solvolyses in aqueous binary systems, and have been rationalized in terms of the effect of the non-aqueous component on water structure (8). The extremum behavior in ΔV^* for methanesulfonyl chloride in D_2O as a function of temperature can also be rationalized in an analogous manner. The volume of activation for methanesulfonyl chloride is least negative at the extremum. As the temperature is decreased, ΔV^* becomes more negative. This decrease in ΔV^* occurs in the temperature range where the solvent D_2O is becoming increasingly structured. Analogous decreases in ΔV^* are also observed for hydrolyses in aqueous alcohol systems when alcohol is initially added to pure water (8). The effect of the addition of small quantities of alcohol has been asserted to increase the structuredness of the solvent system (19, 20). The extremum in the case of the temperature dependence of ΔV^* for deuterolysis of methanesulfonyl chloride can therefore be due to analogous structural changes induced thermally rather than by adding cosolvent. The extremum is not as marked as in the binary solvent system, but the thermal structural changes in the case of D_2O are likely to be smaller.

The authors acknowledge with thanks general financial support from the National Research Council of Canada and the University of Calgary for a Postdoctoral Teaching Fellowship to C.S.D.

1. MOYRA J. MACKINNON and J. B. HYNE. Can. J. Chem. **49**, 3480 (1971).
2. B. T. BALIGA and E. WHALLEY. J. Phys. Chem. **73**, 654 (1969).
3. A. B. LATEEF and J. B. HYNE. Can. J. Cfem. **47**, 1369 (1969).
4. S. J. DICKSON and J. B. HYNE. Can. J. Chem. **49**, 2394 (1971).

5. K. J. LAIDLER. Discuss. Faraday Soc. **22**, 88 (1956).
6. J. KOSKIKALLIO and E. WHALLEY. Can. J. Chem. **37**, 783 (1959).
7. C. WALLING and H. J. SHUJAR. J. Am. Chem. Soc. **85**, 607 (1963).
8. J. B. HYNE. *In* Hydrogen bonded solvent systems. Taylor and Francis Ltd.
9. P. M. LAUGHTON and R. E. ROBERTSON. *In* Solute–solvent interactions. Marcel and Decker, New York and London. 1969.
10. Isotope effect in chemical reactions. Taylor and Francis Ltd., Van Nostrand Reinhold Co. 1970. Chapt. 2.
11. J. B. HYNE, H. S. GOLINKIN, and W. G. LAIDLAW. J. Am. Chem. Soc. **88**, 2104 (1966).
12. MOYRA J. MACKINNON, A. B. LATEEF, and J. B. HYNE. Can. J. Chem. **48**, 2025 (1970).
13. E. A. GUGGENHEIM. Phil. Mag. (7) **2**, 538 (1926).
14. R. L. HEPPOLETTE and R. E. ROBERTSON. Can. J. Chem. **44**, 677 (1966).
15. L. TREINDL, R. E. ROBERTSON, and S. E. SUGAMORI. Can. J. Chem. **47**, 3397 (1969).
16. R. E. ROBERTSON, B. ROSSALL, S. E. SUGAMORI, and L. TREINDL. Can. J. Chem. **47**, 4199 (1969).
17. G. NEMETHY and H. A. SCHERAGA. J. Phys. Chem. **41**, 680 (1964).
18. G. S. KELL. J. Chem. Eng. Data, **12**, 66 (1967).
19. F. FRANKS and D. J. G. IVES. Quart. Rev. London, **20**, 1 (1966).
20. E. M. ARNETT, W. G. BENTRUDE, J. J. Burke, and P. M. DUGGLEBY. J. Am. Chem. Soc. **87**, 1541 (1965).

Can. J. Chem. Downloaded from www.nrcresearchpress.com by 210.87.254.105 on 09/05/12
For personal use only.

Thallium and Tin Electrode Potentials in Fused LiCl–KCl Eutectic

JOSEPH M. SHAFIR AND JAMES A. PLAMBECK
Department of Chemistry, University of Alberta, Edmonton, Alberta
Received December 11, 1973

Electrode potentials of thallium and tin couples were measured in dilute solutions of the ionic species in fused LiCl–KCl eutectic, at 450 °C. Standard molar electrode potentials of the Tl(III)/Tl(I) and Sn(IV)/Sn(II) couples are +0.155 and −0.310 V against a standard molar platinum reference electrode (s.m.p.e.). The standard potentials of the Tl(III)/Tl(0) and Sn(IV)/Sn(0) couples were calculated to be −0.385 and −0.964 V, respectively, *vs.* the s.m.p.e.

Les potentiels d'électrode des couples thallium et étain ont été mesurés en solutions diluées sur les espèces ionisées dans l'eutectique en fusion LiCl–KCl, à 450 °C. Les potentiels d'électrode standard molaire des couples Tl(III)/Tl(I) et Sn(IV)/Sn(II) sont de +0.155 et −0.310 V par rapport à l'électrode standard molaire de référence de platine. Les potentiels standards des couples Tl(III)/Tl(0) et Sn(IV)/Sn(0) ont été calculés et valent −0.385 et −0.964 V respectivement, par rapport à l'électrode standard molaire de platine. [Traduit par le journal]

Can. J. Chem., **51**, 1693 (1973)

Can. J. Chem. Downloaded from www.nrcresearchpress.com by 210.87.254.105 on 09/05/12
For personal use only.

Introduction

The standard potentials of the Tl(I)/Tl(0) and Sn(II)/Sn(0) couples have been previously measured in the fused LiCl–KCl eutectic at 450 °C (1). Delarue (2), in a voltammetric study of thallium in the LiCl–KCl eutectic melt, has reported the oxidation of thallium(I) to thallium(III) at a graphite electrode; the half-wave potential of this process was given as +0.2 V. Delarue (2) also carried out the voltammetric oxidation of Sn(II) to Sn(IV) at a graphite electrode and reported the half-wave potential of this process as 0.0 V. In the course of a continuing program of measurement of standard potentials in this solvent (3) it appeared desirable to make equilibrium potential measurements of the Tl(III)/Tl(I) and Sn(IV)/Sn(II) couples.

Experimental

The LiCl–KCl eutectic melt (59 mol % LiCl, (4)) was prepared as previously described (3). Thallium (99.9999%, shot) and tin (99.9999%, wire) were obtained from Alfa Inorganics, Beverly, Massachusetts.

The apparatus and procedure employed have been described (3). The reference electrode employed was the s.m.p.e., as described by Laitinen and Liu (1). Thallium metal as obtained from the manufacturer was covered with a brown-black layer of Tl_2O. Since this compound is soluble in the melt (2), the oxide-coated metal was allowed to remain in contact with the bulk melt for 18 h prior to the commencement of experimental work. This resulted in the dissolution of all oxide and the formation of a bright thallium pool for the coulometric oxidizations. The thallium pool electrode was then transferred into an isolation compartment as previously described (4). The thermoelectric potential between platinum and graphite was found to be 0.004 V (graphite positive), and that between platinum and tungsten was found to be 0.005 V (tungsten positive), both at 450 °C. These thermoelectric potentials were appropriately subtracted from the experimental potentials.

Voltammetric curves were obtained, at slow scan rates, with a Metrohm–Polarecord E261 polarograph; a two-electrode system was employed. Solute concentrations were calculated using 1.648 g/ml as the density of the fused LiCl–KCl eutectic at 450 °C (5).

Results and Discussion

Thallium

For the determination of the standard potential of the Tl(III)/Tl(I) redox couple, a solution of Tl(I) was generated by coulometrically oxidizing a liquid thallium pool. In the course of this generation, ten concentration–potential data points were collected in order to obtain a value of the Tl(I)/Tl(0) standard potential, and to compare it with the value obtained by Laitinen and Liu (1) who electrolytically reduced Tl(I) (added to the melt as anhydrous thallium(I) chloride) at a tungsten electrode. The current density employed in the anodization of the thallium pool was 20 mA/cm^2, and the concentration range of Tl(I) over which data was collected was 2.08×10^{-2} to 0.148 *M*. A plot of the cell electromotive force against the logarithm of Tl(I) concentration was linear and had a slope of 0.140 ± 0.002 V/log unit, in agreement with the theoretical value of 0.143 V/log unit for a one-electron process at 450 °C. The standard molar potential of the Tl(I)/Tl(0) redox couple was calculated to be −1.465 ± 0.002 V. This value, corrected for the

Can. J. Chem. Downloaded from www.nrcresearchpress.com by 210.87.254.105 on 09/05/12
For personal use only.

thermoelectric potential between platinum and tungsten, confirms the value of -1.476 ± 0.002 V determined by Laitinen and Liu (1).

Thallium(I), produced by the coulometric oxidation of elemental thallium, was further oxidized at a graphite electrode after the thallium metal had been removed. The current density employed was 0.6 mA/cm^2. A total of thirty concentration–potential points were taken in two separate experiments in which the concentration ratio of Tl(I)/Tl(III) ranged from 27.57 to 1.222. The solution of Tl(I) was colorless, but turned light green when Tl(III) was generated. A plot of the cell electromotive force as a function of log [Tl(I)]/[Tl(III)] was linear (Fig. 1) and had a slope of 0.074 ± 0.002 V/log unit, in agreement with the theoretical value of 0.072 V/log unit for a two-electron process at 450 °C. The standard potential of the Tl(III)/Tl(I) redox couple was calculated to be 0.155 ± 0.002 V. This value is corrected for the thermoelectric potential between graphite and platinum.

From the standard potentials of the Tl(I)/Tl(0) and Tl(III)/Tl(I) redox couples measured in this study, the standard potential of the Tl(III)/Tl(0) redox couple is calculated to be -0.385 ± 0.003 V, and the equilibrium constant for the reaction $3Tl(I) \rightleftarrows Tl(III) + 2Tl(0)$ is calculated to be 2.55×10^{-23} l^2 mol^{-2}. Thus, thallium metal will quantitatively reduce Tl(III) to Tl(I).

Tin

A liquid tin pool was anodized to prepare a solution of Sn(II) for use in the determination of the standard potential of the Sn(IV)/Sn(II) redox couple. In the course of this anodization, eight concentration–potential data points were collected so that a comparison of the value of the Sn(II)/Sn(0) standard potential could be made against the value (1) obtained by electrolytic reduction of Sn(II) (added to the melt as anhydrous Sn(II) chloride). The current density was approximately 40 mA/cm^2. The concentration range of Sn(II) employed was 1.68×10^{-2} to 0.194 *M*. A plot of log [Sn(II)] against the cell potential had a slope of 0.071 ± 0.002 V/log unit, in agreement with the theoretical value of 0.072 V/log unit for a two-electron process at 450 °C. The standard potential determined for the Sn(II)/Sn(0) couple was -1.079 V, with a standard deviation of less than 1 mV. This value (corrected for the thermoelectric potential between platinum and tungsten) confirms the value of -1.082 ± 0.002 V determined by the procedure of Laitinen and Liu (1).

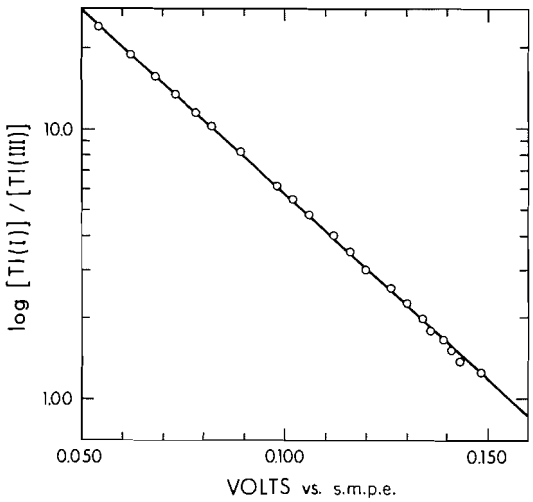

FIG. 1. Nernst plot for the Tl(III)/Tl(I) couple. Potential is corrected for the thermoelectric potential of 0.004 V between graphite and platinum.

The Sn(II) solution was further oxidized to Sn(IV) at a graphite electrode after the tin metal had been removed. The current density was approximately 0.6 mA/cm^2. Few points could be taken in any one experiment because, as the anodization proceeded, the polarization potential steadily drifted to more positive values. In order to maintain the polarization potential below chlorine evolution ($\sim +0.3$ V), the experiment had to be interrupted repeatedly, whereupon the graphite anode was shaken in the melt. This did not completely eliminate the problem, as the amount of current which could be passed between interruptions became steadily smaller; eventually it became impractical to continue the experiment. Careful observation of the graphite electrode did not reveal tin tetrachloride gas evolution. Agitation of the graphite electrode during electrolysis did not reduce the increasing polarization potential, which therefore cannot be attributed solely to concentration polarization of the anode, that is, to depletion of Sn(II) at the surface of the graphite electrode. Although the polarization potential increased, it did not stop at chlorine evolution but went several hundred mV beyond that potential. Normally, anodization of a graphite electrode in the fused LiCl–KCl eutectic results in chlorine evolution, and at low current densities this process occurs at a constant potential of about

TABLE 1. Standard potentials of thallium and tin couples at 450 °C

Couple	E_M^0	E_m^0	E_X^0	Standard deviation
Tl(I)/Tl(0)	−1.465	−1.449	−1.359	0.002
Tl(I)/Tl(0)*	−1.476	−1.460	−1.370	0.002
Tl(III)/Tl(I)	+0.155	+0.139	+0.049	0.002
Tl(III)/Tl(0)†	−0.385	−0.390	−0.420	0.003
Sn(II)/Sn(0)	−1.079	−1.079	−1.079	<0.001
Sn(II)/Sn(0)*	−1.082	−1.082	−1.082	0.002
Sn(IV)/Sn(II)	−0.310	−0.326	−0.416	0.003
Sn(IV)/Sn(0)†	−0.694	−0.702	−0.747	0.003

*Reference 1.
†Calculated from experimental free energies.

+0.3 V. These observations can be explained on the basis that the $SnCl_4(g)$ formed in the anodization of Sn(II) is absorbed onto or into the graphite electrode; it is nonconductive so that a greater potential is required. After current cessation, stirring of the graphite anode resulted in the return of its potential to a steady value well within the potential range of the melt. The $SnCl_4(g)$ adsorbed onto or into the graphite anode during Sn(II) oxidation must dissolve in the melt during this time. Fourteen data points were thus collected in three separate experiments; the concentration ratio of Sn(II)/Sn(IV) varied from 6.86 to 3.58. A plot of log [Sn(II)]/[Sn(IV)] against the observed cell potential was linear and had a slope of 0.063 ± 0.005 V/log unit, in fair agreement with the theoretical value of 0.072 V/log unit for a two-electron process at 450 °C. It is not surprising that the slope of the Nernst plot is low, as Sn(IV) volatilized slowly from the solution as $SnCl_4(g)$. This was evidenced by the slight presence of white fumes when the tin compartment was exposed to the atmosphere at the end of the experiment. Loss of Sn(IV) by volatilization of $SnCl_4(g)$ was not serious, as the potential of the graphite electrode remained constant (maximum drift 4 mV/30 min) after cessation of Sn(IV) generation and stirring. The standard state of Sn(IV) was taken as Sn(IV) in solution. The standard potential of the Sn(IV)/Sn(II) redox couple was determined to be −0.310 ± 0.003 V; this value has been corrected for the thermoelectric potential of +0.004 V between platinum and graphite at 450 °C. In view of the adsorption of $SnCl_4(g)$ onto the graphite electrode, and the possibility that not all $SnCl_4(g)$ was desorbed, the standard deviation of ±0.003 V must be taken to represent only the lower limit of uncertainty in the standard potential of the Sn(IV)/Sn(II) couple.

Delarue (2) reported the half-wave potential of 0.0 V for the voltammetric oxidation of Sn(II) to Sn(IV) at a graphite electrode. Because his half-wave potential value does not correspond to the standard potential determined in this work, the voltammetric study was repeated. A sharpened graphite rod dipping 1–2 mm into the melt was used as the indicating electrode. Scanning anodically, only one wave was observed, and the half-wave potential of this wave was found to be −0.31 V, in excellent agreement with the standard potential of the Sn(IV)/Sn(II) redox couple determined in the present study. Reduction of Sn(II) at the graphite microelectrode gave rise to large, ill-defined waves as expected, due to the large concentration of Sn(II) present. The voltammetric wave crossed the zero current axis at −1.1 V, in good agreement with the standard potential of the Sn(II)/Sn(0) couple. The difference between Delarue's value (2) of the half-wave potential for the oxidation of Sn(II) to Sn(IV) and that obtained in this study can be explained as follows. If Delarue employed large current densities in the oxidation of Sn(II) to Sn(IV), then absorption of $SnCl_4(g)$ into the graphite anode would have taken place and a significant shift of the half-wave potential in the positive direction would have occurred. Also, Delarue (2) did not purify his melt, nor was his cell kept under an inert atmosphere, so contamination by traces of water may also account for the discrepancy.

Reversibility of the Sn(IV)/Sn(II) couple was determined by a micropolarization technique. Small amounts of current were passed in either direction through the graphite electrode and it

Can. J. Chem. Downloaded from www.nrcresearchpress.com by 210.87.254.105 on 09/05/12
For personal use only.

was observed that the open circuit potential recovered its initial value within 30 s after current cessation.

From the standard potentials of the Sn(II)/Sn(0) and Sn(IV)/Sn(II) redox couples measured in this study, the standard potential of the Sn(IV)/Sn(0) couple is calculated to be -0.694 ± 0.003 V, and the equilibrium constant for the reaction $2Sn(II) \rightleftarrows Sn(0) + Sn(IV)$ is calculated to be 1.88×10^{-11} l mol^{-1}. Thus Sn(0) and Sn(IV) will react quantitatively to produce Sn(II).

The standard potentials of thallium and tin are reported in Table 1 on the molar (M), molal (m), and mole fraction (X) concentration scales.

Conclusion

The stable oxidation states of thallium in the LiCl–KCl eutectic melt are Tl(0), Tl(I), and Tl(III), and those of tin are Sn(0), Sn(II), and Sn(IV). The standard potentials of the redox couples between these states have been determined.

The authors are grateful to the National Research Council of Canada for support of this research through an Operating Grant (to J.A.P.) and a NRCC Scholarship (to J.M.S.). The paper is taken in part from the thesis of one of the authors (J.M.S.) submitted to the Faculty of Graduate Studies and Research, University of Alberta, Edmonton, Alberta, in partial fulfillment of the requirements for the Ph.D. degree.

1. H. A. LAITINEN and C. H. LIU. J. Am. Chem. Soc. **80**, 1015 (1958).
2. G. DELARUE. J. Electroanal. Chem. **1**, 285 (1959).
3. J. M. SHAFIR and J. A. PLAMBECK. Can. J. Chem. **48**, 2131 (1970).
4. H. A. LAITINEN, W. S. FERGUSON, and R. A. OSTERYOUNG. J. Electrochem. Soc. **104**, 516 (1957).
5. E. R. VAN ARTSDALEN and I. S. YAFFE. J. Phys. Chem. **59**, 118 (1955).

Can. J. Chem. Downloaded from www.nrcresearchpress.com by 210.87.254.105 on 09/05/12
For personal use only.

Models for the Interaction of Nitrogen with Transition Metals. Part III. Preparation and Properties of some Cationic Arylazo Complexes of Iron[1]

D. R. FISHER AND D. SUTTON[2]

Department of Chemistry, Simon Fraser University, Burnaby 2, British Columbia

Received November 10, 1972

$Fe(CO)_3(PPh_3)_2$ reacts with *p*-substituted aryl diazonium tetrafluoroborates to yield the compounds $[Fe(CO)_2(PPh_3)_2(N_2C_6H_4X)]BF_4$ (where X = F, Cl, Br, H, NO_2, OCH_3, and OH but not NEt_2). The complex cation displays properties consistent with replacement of an equatorial CO ligand in $Fe(CO)_3(PPh_3)_2$ by the more effective π-acceptor ligand $[N_2C_6H_4X]^+$ analogous to NO^+. A very strong band at *ca.* 1720 cm^{-1} in the i.r. spectrum due to $\nu(N_2)$ has been identified by ^{15}N isotopic substitution. This value is much higher than for most other arylazo complexes yet prepared and the azo group resists catalytic hydrogenation. A number of spectroscopic measurements are reported, including unusually small quadrupole splitting effects in the Mössbauer spectra.

Le $Fe(CO)_3(PPh_3)_2$ réagit avec des tétrafluoroborates de diazonium aryle substitué en position para pour donner des composés du type $[Fe(CO)_2(PPh_3)_2(N_2C_6H_4X)]BF_4$ (où X = F, Cl, Br, H, NO_2, OCH_3, et OH mais jamais NEt_2). Le cation du complexe révèle des propriétés en accord avec la substitution du coordinat CO équatorial dans $Fe(CO)_3(PPh_3)_2$ par le coordinat meilleur accepteur d'électrons $[N_2C_6H_4X]^+$ analogue à NO^+. Une bande très forte à environ 1720 cm^{-1} en infra rouge causée par le $\nu(N_2)$ a été identifiée à l'aide d'une substitution isotopique (^{15}N). Cette valeur est de beaucoup supérieure à celle obtenue avec d'autres complexes arylazo déjà obtenus, de plus le groupe azo résiste à l'hydrogénation catalytique. Un grand nombre de mesures spectroscopiques sont rapportées en incluant des effets de dédoublement quadrupolaire faibles de façon inhabituelle dans les spectres Mössbauer.

[Traduit par le journal]

Can. J. Chem., 51, 1697 (1973)

Can. J. Chem. Downloaded from www.nrcresearchpress.com by 210.87.254.40 on 09/05/12
For personal use only.

Introduction

The chemistry governing the interaction of unsaturated nitrogen ligands such as the diazonium ion $Ar—N\equiv N^+$ with the metals iron and molybdenum is largely unexplored. Yet it is potentially a rich area for study, since these metals are present in the nitrogen fixing enzyme *nitrogenase* and either (or both) have been implicated as sites for binding dinitrogen during the fixation process (1). Both metals have been shown capable of forming synthetic dinitrogen complexes. Of the two, only molybdenum has, till now, been found to complex with the diazonium ion (2–6). This paper reports the first arylazo complexes of iron, a series of cationic complexes $[Fe(CO)_2(PPh_3)_2(N_2C_6H_4X)]^+$. Previous attempts by King to prepare arylazo derivatives of $NaFe(C_5H_5)(CO)_2$ were unsuccessful (2).

Results and Discussion

A benzene solution of $Fe(CO)_3(PPh_3)_2$ reacts with acetone solutions of a range of *p*-substituted diazonium salts to give products containing the complex carbonyl cation $[Fe(CO)_2(PPh_3)_2(N_2C_6H_4X)]^+$ according to the reaction

$$p\text{-}XC_6H_4N_2BF_4 + Fe(CO)_3(PPh_3)_2 \rightarrow [Fe(CO)_2(PPh_3)_2(N_2C_6H_4X)]BF_4 + CO$$

The quantitative evolution of the one mole of carbon monoxide per mole of $Fe(CO)_3(PPh_3)_2$ consumed was confirmed volumetrically. Analytical data are listed in Table 1. The molar electrical conductance values obtained (Table 1) are similar to those expected for 1:1 electrolytes. Molecular weight determinations carried out on a 10^{-2} *M* acetone solution of the *p*-bromo compound (having an expected molecular weight of 907) gave an apparent molecular weight of 498 $\pm$ 3 consistent with 82% dissociation as a 1:1 electrolyte at this concentration. The compounds are stable in air, soluble in polar organic solvents such as alcohols, acetone, acetonitrile, nitromethane, dichloromethane, and chloroform, but are insoluble in water and common non-polar solvents.

The stereochemistry of the complex cation is expected to be closely related to that of $Fe(CO)_3(PPh_3)_2$, that is, to possess approximately trigonal bipyramidal geometry, with apical

[1]For Part II of this work see ref. 18.

[2]To whom correspondence should be addressed.

Can. J. Chem. Downloaded from www.nrcresearchpress.com by 210.87.254.40 on 09/05/12
For personal use only.

TABLE 1. Analytical data for $[Fe(CO)_2(PPh_3)_2N_2C_6H_4X]^+BF_4^-$

X	Color and % yield*	Melting point (°C)	% Found					% Calcd					
			C	H	N	Fe	X	C	H	N	Fe	X	Λ_M†
p-F	Orange-brown (50)	204 d§	62.4	4.15	3.50	6.84	—	62.3	4.02	3.31	6.60	—	129
p-Cl	Orange-brown (60)	132 d	61.0	4.09	3.08	6.60	—	61.2	3.94	3.25	6.47	—	127
p-Br	Orange-brown (70)	160 d	58.3	3.89	3.11	6.54	8.58	58.3	3.75	3.08	6.16	8.82	129
p-OH	Yellow-brown (35)	203 d	62.3	4.31	3.19	6.40	—	62.5	4.15	3.32	6.62	—	144
p-NO_2	Orange-brown (45)	184 d	60.3	3.86	4.84	6.23	—	60.4	3.89	4.82	6.39	—	103 (75.7‡)
p-OCH_3	Brown (35)	128 d	62.8	4.20	3.22	5.94	—	62.9	4.31	3.26	6.52	—	117

*After recrystallization.
†10^{-4} *M* solution in acetone.
‡10^{-4} *M* solution in nitromethane.
§d = decomposed at the m.p.

TABLE 2. Vibrational and electronic absorption bands for $[Fe(CO)_2(PPh_3)_2(N_2C_6H_4X)]BF_4$

X	Infrared (cm^{-1}) ν(CO)		ν(N_2)	Raman (cm^{-1}) ν(N_2)	ν/ν_0*	Electronic λ_{max} (nm)† ($\varepsilon_{max} \times 10^{-3}$ in parentheses)		
p-NO_2	2040s	1982vs	1715vs	—	0.743	211(20.9)	242(15.4)	305(9.7)
p-F	2035s	1979vs	1718vs	1714w	0.747	206(14.0)	230sh(7.9)	298(7.1)
p-Cl	2022s	1970vs	1715vs	1715w	0.749	210(16.9)	230(11.1)	301(10.2)
H	2038s	1978vs	1724vs	—	0.750	—	—	—
p-Br	2029s	1968vs	1721vs‡	1714w‡	0.752	209(17.7)	231(11.7)	303(10.8)
p-OMe	2020s	1958vs	1722vs	1724w	0.763	209(32.3)	226sh(23.8)	295sh 317(11.3)
p-OH	2022s	1957vs	1725vs	1719w	0.767	210(20.2)	227sh(15.8)	293sh 322(11.6)

*Ratio ν(N_2) complex/ν(N_2) diazonium ion (see ref. 9). Values for ν(N_2) diazonium ion have been tabulated in ref. 9; other values are 2248 (*p*-OH) and 2289 (*p*-Cl). ν/ν_0 for the complex $[Fe(CO)_2(PPh_3)_2NO]BF_4$ is 0.785 (ref. 10).
†Solutions in ethanol: $Fe(CO)_3(PPh_3)_2$, 204 (12.5), 225sh (4.9) 251 (3.9).
‡Bands are shifted to 1691vs (i.r.) and 1690 cm^{-1} (Raman) in $[Fe(CO)_2(PPh_3)_2{}^{15}N{=}{}^{14}NC_6H_4Br]BF_4$.

phosphine ligands and one of the three equatorial sites occupied by the coordinated diazonium group as in **1**.[3]

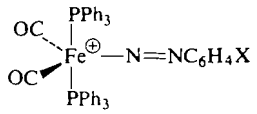

1

All compounds exhibit infrared spectra in which two bands appear in the ν(CO) region (Table 2) consistent with *cis*-carbonyl groups; further, the relative intensities are in agreement with results for other dicarbonyl complexes having two equatorial carbonyl groups in a trigonal bipyramidal geometry (7). A further very strong i.r. band occurs at ~1720 cm^{-1} which we initially suspected from its position to be due to bridging CO, but which was subsequently identified by isotopic substitution as ν(N_2).

The ^1H n.m.r. spectrum of the methyl protons in $[Fe(CO)_2(PPh_2Me)_2(N_2C_6H_4Cl)]BF_4$ (acetone-d_6 solution) appears as a 1:1 doublet of separation 8.9 Hz centered at 7.42 τ separated by a broad unresolved resonance having approximately the same integrated intensity as the outer doublet. Thus, the spectrum is typical of intermediate phosphorus–phosphorus coupling (8) and $|J_{P-H} + J'_{P'-H}| = 8.9$ Hz. No firm stereochemical information may be drawn from this result alone, but it should be noted that $Fe(CO)_3(PPh_2Me)_2$ gives an exactly similar spectrum. We were unable to observe ^{31}P spectra for comparison owing to low solubility in appropriate solvents.

A major feature of interest in the complex cation is the mode of coordination of the diazonium group and the effect of ligation upon the stretching frequency of the N—N bond. Coupled with this is the question of what changes in the geometry of the diazonium are brought about by coordination. Rather little structural or spectroscopic information is available on coordinated diazonium groups and only a few examples are carbonyl complexes. The X-ray structure of hydrotris(1-pyrazolyl) boratobenzenediazodicarbonyl molybdenum ($HB(pz)_3Mo(CO)_2(N_2C_6H_5)$) shows that, in this molecule, coordination of the diazonium group results in a near linear Mo—N—N configuration, but that the N—N—C angle is close to 121°, suggesting the presence of a lone-pair of electrons on the uncoordinated nitrogen (6). This, coupled with the bond lengths Mo—N (1.825(4) Å) and N—N (1.211(6) Å) indicates considerable π-bonding between molybdenum and the coordinating nitrogen atom, which may be described in conventional terms either by back-bonding from molybdenum filled 4d orbitals into the π* system of $[N_2C_6H_5]^+$ or by the valence-bond formalism **2**.

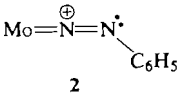

2

Trofimenko assigned a band at 1620 cm^{-1} in these compounds either to ν(N_2) or to an aromatic mode, and in general ν(N_2) has been weak and difficult to assign in those few known

[3]This stereochemistry has now been established by X-ray crystallography by B. J. Haymore and J. A. Ibers (private communication).

Can. J. Chem. Downloaded from www.nrcresearchpress.com by 210.87.254.40 on 09/05/12
For personal use only.

Can. J. Chem. Downloaded from www.nrcresearchpress.com by 210.87.254.40 on 09/05/12
For personal use only.

carbonylazo compounds. Where assignments have been attempted, $\nu(N_2)$ has generally been placed in the region of 1440–1620 cm^{-1} in these compounds (2–4, 11).

The complexes presently described, then, are remarkable in that $\nu(N_2)$ occurs unambiguously as a very strong band at a much higher frequency, in the region of 1720 cm^{-1} (Table 2). Its intensity is similar to that of the stronger ν(CO) bands.[4] However, $\nu(N_2)$ gives only very weak Raman emission, in distinct contrast to $Rh(N_2Ar)Cl_2(PPh_3)_2$ complexes (9) where $\nu(N_2)$ is a prominent feature of the Raman spectrum.

The assignment of $\nu(N_2)$ was confirmed by ^{15}N substitution; for example, it occurs at 1721 cm^{-1} in $[Fe(CO)_2(PPh_3)_2(^{14}N{=}^{14}NC_6H_4Br)]BF_4$ but shifts to 1691 cm^{-1} in $[Fe(CO)_2(PPh_3)_2(^{15}N{=}^{14}NC_6H_4Br)]BF_4$. The high $\nu(N_2)$ values may be partly accounted for by the fact that the complex is a cation. If it is assumed that the metal atom is largely the site of positive charge this would result in a lower degree of back bonding to the diazonium group compared with the neutral compounds. In agreement, ν(CO) occurs 40–60 cm^{-1} higher than in the neutral complexes $LMo(CO)_2(N_2Ar)$ (L = $HB(pz)_3$ or C_5H_5) (2,4) and generally, higher than in a range of isostructural neutral complexes, $Fe(CO)_2(PR_3)_3$ (7). A somewhat parallel situation exists in the related isostructural nitrosyl complex $[Fe(CO)_2(PPh_3)_2(NO)]^+$ where it is observed (10) that both the ν(CO) and ν(NO) are up to 100 cm^{-1} higher than in the isoelectronic neutral complex $Mn(CO)_2(NO)(PPh_3)_2$.

When the cations $[Fe(CO)_2(PPh_3)_2NO]^+$ and $[Fe(CO)_2(PPh_3)_2(N_2C_6H_4X)]^+$ are compared it is seen that ν(CO) bands are both about 20 cm^{-1} lower in the azo complex, and $\nu(N_2)$ about 70 cm^{-1} lower than ν(NO). However, the general similarity of the spectra suggests that the coordination of the diazonium and nitrosyl groups toward iron in these compounds is closely similar and that in the azo compound the diazonium group may be considered formally to be either a 3-electron donor toward Fe^I or coordinated to Fe^0 as the 2-electron donor cation $XC_6H_4N{\equiv}N^+$. The latter view seems to be particularly consistent with $\nu(N_2)$ values. The actual values appear to be almost independent of X or to show, at best, a small decrease as the electron withdrawing properties of X increase. When compared with $\nu(N_2)$ for the free diazonium ion in each case the ratios (ν/ν_0 in Table 2) decrease in the order OH, OCH_3 > Br > H, Cl > F > NO_2 as expected if the diazonium group withdraws electrons from the iron atom by acting as a π-acceptor. This may be contrasted with the constant values of ν/ν_0 observed for the complexes $Rh(N_2C_6H_4X)Cl_2(PPh_3)_2$ (9). In accordance, ν(CO) values increase in the reverse sequence indicating that the diazonium group competes effectively with CO ligands for metal d_π-electrons. Further, a comparison of (ν/ν_0) for these compounds with ν/ν_0 for $[Fe(CO)_2(PPh_3)_2NO]BF_4$ (Table 2) shows that in all cases the relative lowering of $\nu(N_2)$ is greater than that of ν(NO) (from 2280 cm^{-1} to 1790 cm^{-1}), consistent with the diazonium group acting as a rather better π-acceptor than nitrosyl.[5]

The behavior of many arylazo complexes toward hydrogenation under mild conditions has been studied in relation to the use of such complexes as models for the nitrogen-reducing enzyme *nitrogenase* (11). In several cases where $\nu(N_2)$ appears in the region of 1500 cm^{-1} the azo function is hydrogenated at atmospheric pressure and room temperature using an appropriate catalyst (*e.g.* $Pd/BaSO_4$). It is therefore extremely interesting that all of these iron complexes were recovered unchanged after attempts to reduce them catalytically with hydrogen even under more severe conditions.[6] The Mo and W complexes reported by Trofimenko (4) are also resistant to hydrogenation, and we intend to examine further the apparently critical relationship of $\nu(N_2)$ with ease of hydrogenation. In this regard it is perhaps relevant that despite the fact that $\nu(N_2)$ in metal dinitrogen complexes may be lowered as far as 1630 cm^{-1} by attachment of an acceptor atom M′ to the terminal nitrogen atom to form a polynuclear M—N=N—M′ bridge, such compounds have not been found to undergo reduction of the azo-function (12, 13).

The colors of the complexes are orange to

[4] $\nu(N_2)$ has been quoted to occur at *ca.* 1700 cm^{-1} in the arylazo complexes $[Ru(N_2Ar)_2(PPh_3)_2Cl]BF_4$, but no details confirming the assignment were given; ref. 19.

[5] However, ν(CO) values for the nitrosyl complex are consistently higher than ν(CO) for the arylazo complexes, consistent with the opposite view.

[6] The compounds are, however, reduced by $NaBH_4$ in ethanol with apparently cleavage of the N—N bond and the formation of products as yet unidentified.

Can. J. Chem. Downloaded from www.nrcresearchpress.com by 210.87.254.40 on 09/05/12
For personal use only.

brown compared with the yellow color of $Fe(CO)_3(PPh_3)_2$. The electronic spectra of solutions in ethanol at room temperature exhibit three main broad bands of high extinction coefficient in the regions 205, 230, and 300 nm respectively (Table 2). The origin of these bands is difficult to assign with the presently available evidence, since charge transfer transitions, as well as transitions in the aromatic, carbonyl, and azo chromophores may all contribute, and it is probable that the spectrum is a feature of the complex as a whole rather than generally assignable to discrete chromophores. Again, the observed band contours may well envelope several composite absorption bands. In an analysis of $Fe(CO)_5$, intense bands at 200 and 240 nm were assigned to M → L charge transfer (14). The assignment of the bands at 204 and 251 nm in $Fe(CO)_3(PPh_3)_2$ and those at about 205 and 230 nm in this series of cations may be similar. The somewhat shorter wavelength for the second band in the cationic complexes is in accord with this, and the relative positions of this band for the *p*-NO_2 and *p*-OMe complexes follow the anticipated shift to longer wavelength in the case of a π-electron withdrawing substituent on L. The band at 300 nm is absent in $Fe(CO)_5$ and $Fe(CO)_3(PPh_3)_2$ and therefore seems to be a feature of the metal–azo group. However, it exhibits shifts contrary to those expected for M → L charge transfer and we tentatively assign it to a $\pi^* \leftarrow \pi$ transition of the azo chromophore.

The ^1H n.m.r. spectra of all $[Fe(CO)_2(PPh_3)_2(N_2C_6H_4X)]^+$ exhibited broad complex absorptions in the aromatic region together with expected absorptions due to any protons on the *p*-substituents. For example, the *p*-Br complex exhibited two main aromatic multiplets at τ 2.62 and τ 2.38 in a 10:24 approximate ratio, possibly due to the six 4-*H* protons of the triphenyl phosphine groups accidentally absorbing at the same frequency as the four protons of the azophenyl group. The ability to observe n.m.r. spectra at first seemed to be consistent with the absence of paramagnetism, as expected in view of the observation that the cation obeys the 18-electron rule. However, measurements of the magnetic susceptibility by the Faraday technique indicate all the compounds to be paramagnetic with magnetic moments ranging from 0.5–2.5 B.M. Consequently, the magnetism in solution was checked by the proton resonance shift method of Evans (15) and good agreement with the solid state values was observed. On the other hand the complexes do not exhibit e.p.r. spectra, or show line broadening of the ^1H n.m.r. spectra. The observed paramagnetism is presumably due to second-order Zeeman effects ("temperature independent paramagnetism"), but some of the values of μ_{eff} seem to be remarkably large.[7] Paramagnetism was also observed for $[Fe(CO)_2(PPh_3)_2NO]BF_4$, $\mu_{eff} = 0.8$ B.M. but $Fe(CO)_3(PPh_3)_2$ was found to be diamagnetic.

The ^{57}Fe Mössbauer spectra of these complexes exhibit interesting features. We find the parent compound $Fe(CO)_3(PPh_3)_2$ to have Mössbauer parameters $\delta = +0.15$ (± 0.01) with respect to sodium nitroprusside and $\Delta = 2.75$ (± 0.01) mm s^{-1} in good agreement with reported values (16), consistent with trigonal bipyramidal Fe^0 stereochemistry. However, $[Fe(CO)_2(PPh_3)_2NO^+]BF_4^-$ ($\delta = +0.17 \pm 0.01$) displays a considerably smaller quadrupole splitting value of $\Delta = 1.85$ mm s^{-1}. The quadrupole splitting is decreased still further in $[Fe(CO)_2(PPh_3)_2(N_2C_6H_4Br)^+]$ where $\delta = +0.18$ (± 0.01) $\Delta = 0.94$ (± 0.01) mm s^{-1}. Other members of the series are similar. Such a Δ-value is highly atypical of most trigonal bipyramidal Fe^0 complexes. The large Δ-values these normally display are due to a considerable electric field gradient which results from the asymmetric (*i.e.*, non-cubic) environment of the metal in these complexes. The replacement of CO by NO^+ and $N_2C_6H_4X^+$ therefore appears to reduce the electric field gradient despite the fact that the ligand environment of the iron atom is rendered more asymmetric by the removal of trigonal symmetry. There is no evidence to support coordination of a sixth ligand (such as would produce a pseudo-octahedral complex) either by BF_4^- coordination, *o*-metallation of an aromatic ring, or by close contact of an *o*-hydrogen atom with the metal. It therefore seems that the explanation for this effect must lie in the electronic properties of the coordinated nitrosyl and arylazo ligands, and may arise from the increased π-acceptor character of these ligands

[7]NOTE ADDED IN PROOF: We have since been informed by J. A. Ibers and B. J. Haymore that they have succeeded in removing paramagnetism from their preparation by careful recrystallisation. While we have observed paramagnetism despite recrystallisation, the magnetic results must nevertheless be viewed with caution.

in comparison to that of the carbonyl group as evidenced in the i.r. data discussed above.

Experimental

$Fe(CO)_3(PPh_3)_2$ and $Fe(CO)_3(PPh_2Me)_2$ were prepared by the reaction of $Fe_3(CO)_{12}$ with the phosphine as described elsewhere (17). Aryldiazonium tetrafluoroborates were prepared by diazotization of the corresponding anilinium tetrafluoroborate. Purity of these starting materials was checked by i.r. spectroscopy and elemental analysis.

Preparation of $[Fe(CO)_2(PR_3)_2(N_2C_6H_4X)]BF_4$

Details are given for $[Fe(CO)_2(PPh_3)_2(N_2C_6H_4Br)]BF_4$; other derivatives were generally prepared similarly. Reactions were carried out under dry, oxygen-free nitrogen using dry, degassed solvents. An almost saturated solution of $BrC_6H_4N_2BF_4$ (1 mmol) in acetone was added dropwise to a stirred, yellow solution of $Fe(CO)_3(PPh_3)_2$ (1 mmol) in benzene (20 ml) at room temperature. Almost immediately the color of the solution became orange, gas was evolved, and an orange precipitate formed. The precipitate was removed after 2 h and recrystallized from acetone–ether (70% yield). Yields of other recrystallized products are listed in Table 1. The amount of CO evolved was determined in the *p*-Br case by performing the reaction *in vacuo*, transferring the evolved gases by Toepler pump into a known volume, and measuring the pressure. A sample was then identified as carbon monoxide by high resolution mass spectrometry. No nitrogen was present. In the typical run 0.10 mmol of $Fe(CO)_3(PPh_3)_2$ produced 0.10 mmol of CO. Confirmation of the presence of two CO groups in the prepared complexes was obtained by oxygen analysis on $[Fe(CO)_2(PPh_3)_2N_2C_6H_4Br]I$ prepared by metathesis from the tetrafluoroborate and NaI in acetone.

Anal. Calcd. O, 3.39. Found: O, 3.61.

Attempts to synthesize complexes with X = *p*-NEt_2 failed. Instead, intensely red crystals resulted of a compound whose analysis corresponded to $[Et_2NC_6H_4N_2PPh_3]^+BF_4^-$. Details of the synthesis and properties of this compound will follow separately. Isotopic substitution by ^{15}N adjacent to iron was achieved (for examination of i.r. and Raman spectral shifts) by repeating the synthesis with $BrC_6H_4{}^{14}N{\equiv}{}^{15}N^+BF_4^-$ prepared by diazotisation of the corresponding anilinium tetrafluoroborate with $Na^{15}NO_2$ (95% ^{15}N) available from Isomet Corporation, New York.

Infrared spectra were recorded on samples pressed in KBr using Perkin–Elmer 457 and Beckman I.R. 12 spectrometers. Raman spectra on solid samples at room temperature were recorded using a Cary 81 spectrometer with unfocussed He–Ne laser excitation from a Spectra-Physics Model 125 laser producing 70 mW at source. Samples decomposed in a focussed beam. Proton n.m.r. spectra were recorded at 60 and 100 MHz using Varian A-60 and HA-100 spectrometers; τ values are relative to $(CH_3)_4Si$ (τ = 10.0) as internal standard. Mössbauer spectra were recorded (by Dr. C. H. W. Jones of this Department) with the absorbers at 80 ± 1 °K and a ^{57}Co/Pd source (New England Nuclear, 10 mCi) at room temperature. A Technical Measurement Corporation constant acceleration spectrometer was used, providing 2 × 200 channel spectra. The spectrometer was calibrated using a N.B.S. Standard absorber; $Na_2[Fe(CN)_5NO]2H_2O$ (Δ = 1.172 mm s^{-1}, $\delta(^{57}Co/Pd)$ = −0.442 mm s^{-1}). Magnetic susceptibility measurements were made at room temperature on a Faraday apparatus calibrated against $HgCo(NCS)_4$, and yielded the following values of μ_{eff} (corrected for diamagnetism) for the series $[Fe(CO)_2(PPh_3)_2(N_2C_6H_4X)]BF_4$: X = *p*-$NO_2$, 2.30, 2.32, 2.16; *p*-OMe, 2.46, 2.09 (±0.10); *p*-F, 0.76, 0.52 (±0.06); *p*-Cl, 1.21, 1.22, 1.28[8] (±0.08); *p*-Br, 0.84, 0.92 (±0.09); *p*-OH, 2.01, 1.83 (±0.10) B.M. The value obtained for $[Fe(CO)_2(PPh_3)_2NO]BF_4$ was 0.84 (±0.09) B.M. The susceptibility for the *p*-NO_2 compound was also determined over the temperature range 85–281 °K using the automatic variable temperature Faraday balance at York University, Ontario. The values of χ_M^{corr} increased (and μ_{eff} decreased) steadily from 2863 × 10^6 c.g.s. (2.54 B.M.) at 281 °K to 6105 × 10^6 (2.04 B.M.) at 85 °K. Finally, the magnetic susceptibilities of solutions of the *p*-Cl and *p*-NO_2 complexes in acetone were determined from the n.m.r. downfield contact shift of the methyl resonance of added *t*-butanol using the method of Evans (15). The observed shifts gave μ_{eff} = 2.09 (±0.10) B.M. for *p*-NO_2 and 1.39 (±0.10) B.M. for *p*-Cl in reasonable agreement with the Faraday method.

Molecular weights were determined from osmometric measurement on acetone solutions using a Perkin–Elmer Hitachi Model 115 calibrated with benzil. Electrical conductances were determined at room temperature for 10^{-4} *M* solutions in acetone and nitromethane using a standard conductivity meter. Elemental analyses for non-metal content were determined by the SFU Microanalytical Laboratory and by A. Bernhard, Germany. Iron was determined by atomic absorption spectroscopy using a Perkin–Elmer Model 305.

Support of this work was through a National Research Council of Canada Operating Grant. We wish to thank Professor J. A. Ibers and B. J. Haymore for communicating the results of their X-ray study before publication, Dr. C. H. W. Jones for making the Mössbauer measurements, Dr. F. G. Herring for e.p.r., and Dr. K. I. Thé for CO determinations. We are also grateful to Dr. G. W. Rayner Canham for variable-temperature magnetic measurements and to Dr. A. B. P. Lever for making this facility available.

1. J. R. Postgate (*Editor*). The chemistry and biochemistry of nitrogen fixation. Plenum Press, London. 1971.
2. R. B. King and M. B. Bisnette. J. Am. Chem. Soc. **86**, 5694 (1964); Inorg. Chem. **5**, 300 (1966).
3. F. J. Lalor and P. L. Pauson. J. Organomet. Chem. **25**, C51 (1970).
4. S. Trofimenko. Inorg. Chem. **8**, 2675 (1969).
5. D. Cashman and F. J. Lalor. J. Organomet. Chem. **24**, C29 (1970).
6. G. Avitabile, P. Ganis, and M. Nemiroff. Acta Cryst. **B27**, 725 (1971).
7. A. Reckziegel and M. Bigorgne. J. Organomet. Chem. **3**, 341 (1965).

[8]When synthesized from a reaction in acetone alone, this being the method used in the synthesis of the crystals used for the X-ray analysis by B. J. Haymore and J. A. Ibers (private communication).

Can. J. Chem. Downloaded from www.nrcresearchpress.com by 210.87.254.40 on 09/05/12
For personal use only.

8. R. K. HARRIS. Inorg. Chem. **4**, 701 (1966); Can. J. Chem. **42**, 2275 (1964).
9. G. W. RAYNER-CANHAM and D. SUTTON. Can. J. Chem. **49**, 3394 (1971).
10. G. R. CROOKES and B. F. G. JOHNSON. J. Chem. Soc. A, 1238 (1968). B. F. G. JOHNSON and J. A. SEGAL. J. Chem. Soc. (Dalton), 1268 (1972).
11. G. W. PARSHALL. J. Am. Chem. Soc. **89**, 1822 (1967).
12. J. CHATT, J. R. DILWORTH, G. J. LEIGH, and R. L. RICHARDS. Chem. Commun. 955 (1970).
13. J. CHATT, J. R. DILWORTH, R. L. RICHARDS, and J. R. SAUNDERS. Nature, **224**, 1201 (1969).
14. M. DARTIGUENAVE, Y. DARTIGEUNAVE, and H. B. GRAY. Bull. Soc. Chim. Fr. 4223 (1969).
15. D. F. EVANS. J. Chem. Soc. 2003 (1959).
16. N. N. GREENWOOD and T. C. GIBB. Mössbauer spectroscopy. Chapman and Hall Ltd., London. 1971. pp. 221–238.
17. A. F. CLIFFORD and A. K. MUKHERJEE. Inorg. Chem. **2**, 151 (1963).
18. F. W. B. EINSTEIN and D. SUTTON. J. Chem. Soc. (Dalton), 434 (1973).
19. J. A. MCCLEVERTY and R. N. WHITELEY. Chem. Commun. 1159 (1971).

Can. J. Chem. Downloaded from www.nrcresearchpress.com by 210.87.254.40 on 09/05/12
For personal use only.

Neighboring Group Participation in the Halogenation of Sulfoxides

T. DURST, K.-C. TIN, AND M. J. V. MARCIL
Department of Chemistry, University of Ottawa, Ottawa, Canada K1N 6N5

Received October 5, 1972

$PhS(O)(CH_2)_nCH_2OH$(n = 1–3) react with sulfuryl chloride at −78° or 0° in methylene chloride to give the corresponding $PhSO_2(CH_2)_nCH_2Cl$. Evidence is presented that cyclic alkoxyoxosulfonium salts are intermediates in these transformations. When n = 4 only chlorination α to the sulfoxide function was observed. The sulfinyl carboxylic acids $PhS(O)(CH_2)_nCO_2H$ (n = 1–3) and amides $PhS(O)(CH_2)_n$-$CONH_2$ (n = 1–3) were also reacted with SO_2Cl_2. α-Chlorination was observed for both compounds when n = 1 or 3. When n = 2 the products were the 3-phenylsulfonylpropionyl chloride and 3-phenylsulfonylpropionitrile respectively.

Le $PhS(O)(CH_2)_nCH_2OH$ (n = 1–3) réagit avec le chlorure de sulfuryle à −78° ou à 0° dans le dichlorométhane pour donner le produit correspondant $PhSO_2(CH_2)_nCH_2Cl$. On a prouvé que les sels cycliques d'alkoxyoxosulfonium sont des intermédiaires dans ces transformations. Quand n = 4 on a observé que seulement la chloration en α du sulfoxyde s'effectuait. Les acides carboxyliques sulfinylés $PhS(O)(CH_2)_nCO_2H$ (n = 1–3) ainsi que les amides $PhS(O)(CH_2)_nCONH_2$ (n = 1–3) ont aussi été mis en réaction avec le SO_2Cl_2. La chloration en α a été observée pour les deux composés quand n égalait 1 ou 3. Quand n égalait 2, les produits furent le chlorure de phényl-3 sulfonylpropionyle et le phényl-3 sulfonylpropionitrile respectivement. [Traduit par le journal]

Can. J. Chem., 51, 1704 (1973)

As part of a study of the mechanism of the halogenation of sulfoxides we recently reported some preliminary results of our investigation of the reaction of several β, γ, and δ-hydroxy sulfoxides with sulfuryl chloride (1). In these reactions we observed no α-chorination (2–5) but obtained in high yield the corresponding β, γ, and δ-chloro sulfones. The formation of these products was rationalized as occurring via ring opening of a cyclic alkoxyoxosulfonium ion **2** which was generated by an intramolecular displacement of chloride ion from the initially formed chloro-oxosulfonium chloride **1** (Scheme 1). We would now like to present further results in this area and also an extension of the work to the chlorination of sulfoxides bearing other remote nucleophilic groups such as $—CO_2H$ and $—CONH_2$.

The mechanism of the chlorination of sulfoxides with various chlorinating agents *e.g.* SO_2Cl_2 (2, 3), $PhICl_2$ (4), and *t*-BuOCl (5) is in all likelihood as shown in Scheme 2. A point of disagreement which remains is the manner in which the initially formed chloro-oxosulfonium salt **3** is converted to the α-chlorosulfoxide **5**. Two routes have been suggested: (*a*) Formation of the ylid **4**, followed by intramolecular rearrangement to **5** (4) and (*b*) loss of HCl from **3** to give the oxosulfenium ion **6** which rapidly readds Cl^- to give **5** (1, 6, 7).

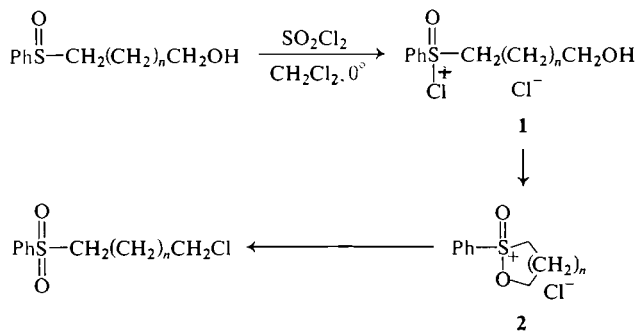

n = 0, 1, 2

SCHEME 1

Can. J. Chem. Downloaded from www.nrcresearchpress.com by 210.87.254.42 on 09/05/12
For personal use only.

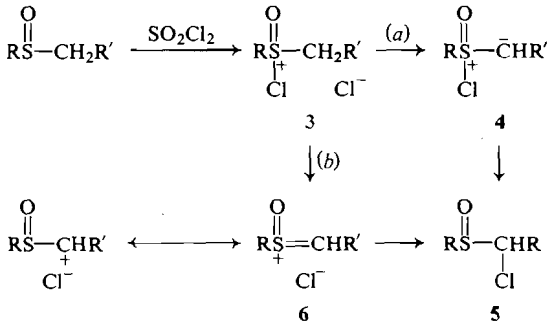

SCHEME 2

Mechanism (*b*) is supported by the observation that unsymmetrical sulfoxides are chlorinated preferentially at the more highly substituted carbon (1, 6, 7). An ylid intermediate, mechanism (*a*), would be expected to lead to substitution at the less substituted carbon whereas a positively charged intermediate should give product arising from substitution at the more substituted carbon (Scheme 3).

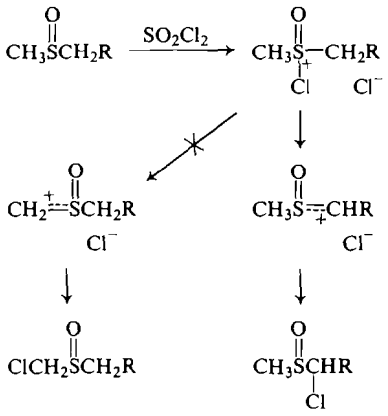

SCHEME 3

Also supporting mechanism (*b*) are the results obtained by Marquet and co-workers (7) in the chlorination of *cis* and *trans*-4-*t*-butyl-thiane-*S*-oxides. Both isomers gave the same mixture of products **8** and **9**. Their formation was rationalized as a "*trans*" addition of Cl^- (Cl^- and sulfur lone pair are *trans*) to the intermediate oxosulfenium ion **7**, the major product **8** being the result of the preferred *trans*-diaxial addition (Scheme 4).

The chlorination of sulfoxides bearing nucleophilic groups in position β, γ... etc. to the sulfoxide function was undertaken with the hope of observing a reaction between these groups and some of the intermediates suggested in Scheme 2. Depending on the position and nature of the nucleophilic group we observed either α-chlorination, or the interaction of the functional group with the chloro-oxosulfonium ion resulting in the formation of a cyclic intermediate from which substituted sulfones were obtained. We have as yet been unable to trap the oxosulfenium ion **6**.

Hydroxy Sulfoxides

Hydroxy sulfoxides bearing the hydroxyl group in the β, γ, or δ position were converted in high yield to the corresponding chlorosulfones. In contrast, those having the OH at a more remote position gave only α-chloro-ω-hydroxy sulfoxides (eq. 1).

The yield of the chlorosulfones was generally over 75% regardless of whether the hydroxyl group was primary, secondary, or tertiary and β, γ, or δ to the sulfoxide (Table 1).

In the preliminary communication (1) we presented strong evidence which supported the intermediacy of cyclic alkoxyoxosulfonium salts in the conversion of **10** (n = 0–2) to **11**. For example, the formation of the *cis*-chloro sulfone

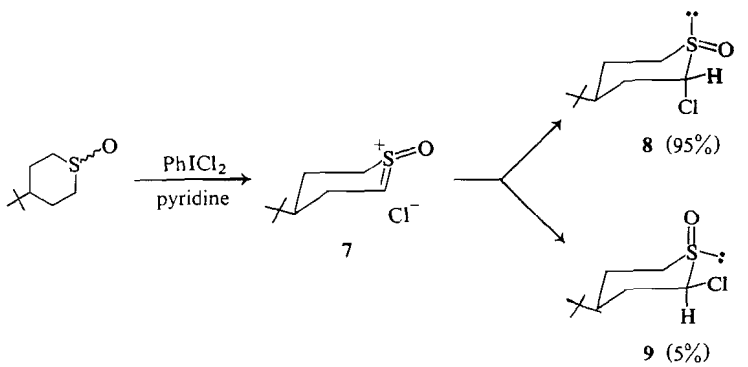

SCHEME 4

Can. J. Chem. Downloaded from www.nrcresearchpress.com by 210.87.254.42 on 09/05/12
For personal use only.

TABLE 1. Reaction of hydroxy sulfoxides with SO_2Cl_2

Hydroxy sulfoxide	Product	Yield (%)
10 ($n = 0$)	$PhSO_2(CH_2)_2Cl$	95
10 ($n = 1$)	$PhSO_2(CH_2)_3Cl$	96
10 ($n = 2$)	$PhSO_2(CH_2)_4Cl$	88
10 ($n = 3$)	$PhS(O)CH(CH_2)_4OH$ (Cl)	>90*
10 ($n = 4$)	$PhS(O)CH(CH_2)_5OH$ (Cl)	~100*
$PhS(O)CH_2CHPh$ (OH) **(28)**	$PhSO_2CH_2CHPh$ (Cl) **(29)**	78
$PhS(O)CH_2C(CH_2)_5$ (OH) **(30)**	$PhSO_2CH_2C(CH_2)_5$ (Cl) **(31)**	73
$PhS(O)CH_2C(CH_3)_2$ (OH) **(32)**	$PhSO_2CH_2C(CH_3)_2$ (Cl) **(33)**	41
	$PhSO_2CH_2C{=}CH_2$ (CH_3) **(34)**	34
$PhS(O)CH_2CPh_2$ (OH) **(35)**	$PhSO_2CH{=}CPh_2$ **(36)**	89
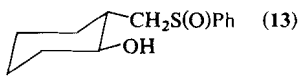 **(13)**	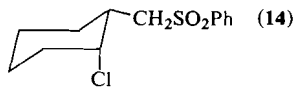 **(14)**	77

*Crude yield.

[1] $PhSCH_2(CH_2)_nCH_2OH$ (O) **10** ($n = 0$–4) $\xrightarrow{SO_2Cl_2}$ $PhSO_2CH_2(CH_2)_nCH_2Cl$ **11** ($n = 0$–2); $PhSCH(CH_2)_nCH_2OH$ (O, Cl) **12** ($n = 3, 4$)

14 from the *trans*-hydroxy sulfoxide **13** verified the required inversion of configuration at the carbon originally bearing the hydroxyl group.

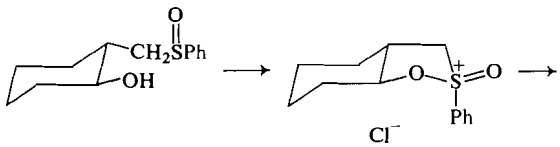

13 **13a**

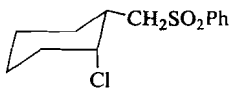

14

In contrast to **13**, the chlorination of the *trans* sulfoxide **15** gave a complicated mixture of products which we have not been able to separate. Very little, if any, of the *cis*-chloro sulfone **16** appeared to have been formed as determined by examination of the n.m.r. spectrum of the crude product. This result was not unexpected since the formation of **16** would require the intermediacy of **17**, a highly strained *trans* 6,4-ring system.

When bromination of **10** ($n = 1$) with Br_2 was carried out in pyridine, both the bromo sulfone **18** and the pyridinium perbromide sulfone **19** were obtained; these products are probably the

Can. J. Chem. Downloaded from www.nrcresearchpress.com by 210.87.254.42 on 09/05/12
For personal use only.

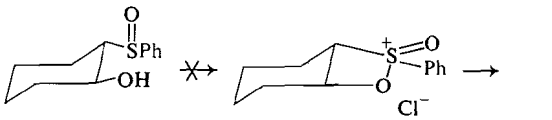

15 17

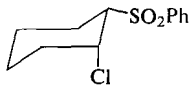

16

result of ring opening of the intermediate **20** by Br^- and pyridine respectively.

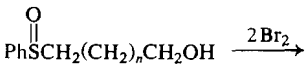

10 ($n = 1$)

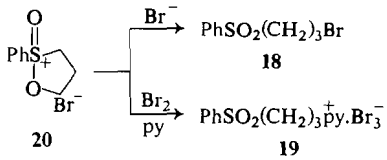

20 **18** **19**

The failure of **10** ($n = 3,4$) to give chloro sulfones is understandable in terms of Scheme 1 since the formation of such products in these cases would require the intermediacy of 7- and 8-membered ring alkoxyoxosulfonium salts respectively.

Among the more interesting facets of the above reactions is the ease with which the displacement of Cl^- from the chloro-oxosulfonium ion occurs. Simple sulfoxides, such as phenyl ethyl sulfoxides, are converted in excellent yield to α-chloro derivatives within 5 min at −78° or 0° upon exposure to SO_2Cl_2 (2). The replacement of a β-hydrogen by an OH group however completely suppresses the rapid chlorination reaction by interception of the chloro-oxosulfonion ion intermediate, despite the fact that such a reaction leads to the formation of a 4-membered ring intermediate. Indeed, chloro-oxosulfonium ions can be effectively intercepted by external nucleophiles such as water or methanol; in these cases sulfones are produced (2).

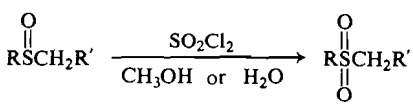

Alkoxyoxosulfonium salts, which can be considered as *O*-alkylated sulfones, have not been previously isolated, presumably because of the ease with which the C—O bond is broken, the cleavage being facilitated by the excellent leaving group characteristics of the $-\overset{+}{O}S(O)R$ function.[1] Particularly impressive, in this connection, is the displacement of the $-\overset{+}{O}S(O)R$ group in **13***a* by Cl^- which occurred in CH_2Cl_2 within minutes at −78°. The closely related aryloxy-oxosulfonium ions, *e.g.* **21**, have been isolated by Whiting and co-workers (8) from the thermal decomposition of aryl diazonium salts in the presence of sulfones. Carbon–oxygen bond cleavage in these species either via an S_N2 or S_N1 process, is not as favorable as for the alkoxyoxosulfonium salts.

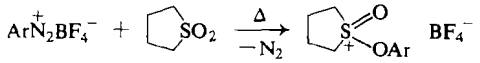

21

We had hoped that the reaction of the hydroxy sulfoxides **10** ($n = 3,4$) might provide conclusive evidence that the conversion of the chloro-oxosulfonium ions to α-chloro sulfoxides occurs via an elimination addition sequence, *i.e.* via oxosulfenium ions such as **6**. In the case of **10** ($n = 3$) such an ion could have been trapped intramolecularly by the OH group to produce the tetrahydropyran derivatives **22** (Eq. 2). However no evidence for the formation of **22** could be obtained. We are presently continuing our efforts to prove the intermediacy of oxosulfenium ions in the migration of chlorine from sulfur to carbon.

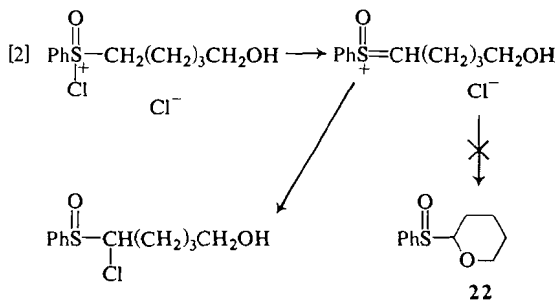

[2]

22

Sulfinyl Carboxyl Acids and Amides

In the reaction of the acid and amide sulfoxides **23** and **24** with SO_2Cl_2 in CH_2Cl_2, the interception of the intermediate chloro-oxosulfonium salt by the acid or amide function occurred only when a 5-membered ring inter-

[1]Sulfones show extremely low nucleophilicity and are only partially protonated by concentrated sulfuric acid. The pK_a of protonated sulfones is estimated to be about −12 (14, 15).

Can. J. Chem. Downloaded from www.nrcresearchpress.com by 210.87.254.42 on 09/05/12
For personal use only.

TABLE 2. Reaction of sulfinyl carboxylic acids with SO_2Cl_2

Sulfinyl carboxylic acid	Product	Yield (%)
$PhS(O)CH_2CO_2H$	$PhS(O)CHCO_2H$ Cl	97
$PhS(O)(CH_2)_2CO_2H$	$PhSO_2(CH_2)_2COCl$	83
$PhS(O)(CH_2)_3CO_2H$	$PhS(O)CH(CH_2)_2CO_2H$ Cl	83
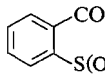	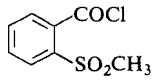	100

TABLE 3. Reaction of sulfinyl carboxamides with SO_2Cl_2

Amide	Product	Yield (%)
$PhS(O)CH_2CONH_2$	$PhS(O)CHCONH_2$ Cl	89
$PhS(O)(CH_2)_2CONH_2$	$PhSO_2(CH_2)_2C{\equiv}N$	95
$PhS(O)(CH_2)_3CONH_2$	$PhS(O)CH(CH_2)_2CONH_2$ Cl	73

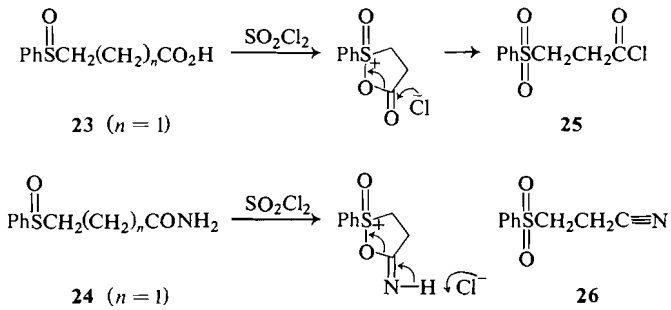

23 ($n = 1$) **25**

24 ($n = 1$) **26**

mediate was formed, the products being the acid chloride sulfone **25** (83%) and the nitrile sulfone **26** (95%), respectively. Chlorination of ortho-methylsulfinyl benzoic acid gave a quantitative yield of ortho-methylsulfonyl benzoyl chloride. Again in this example a five-membered ring acyloxyoxosulfonium ion can be formed as an intermediate.

In the compounds **23** and **24** when $n = 0$ or 2 the only isolable products were the α-chloro sulfoxides (Tables 2 and 3). The failure to form four-membered ring intermediates in the reaction of **23** ($n = 0$) and **24** ($n = 0$) may be that such intermediates contain additional angle strain when compared to the analogs derived from the hydroxy sulfoxides due to the presence of an sp^2 hydridized carbon in the 4-membered ring; **27** *vs.* **2** ($n = 0$). The failure to form 6-membered ring intermediates from **23** ($n = 2$) and **24** ($n = 2$) was unexpected.

Experimental

Melting points were determined on a Thomas Hoover apparatus and are not corrected. Infrared spectra were obtained in chloroform solution on a Beckman IR-20 Spectrophotometer. N.m.r. spectra, $CDCl_3$ solution, were obtained using Varian HA-100 or T-60 Spectrometers, peak positions are reported in δ units. Usual workup refers to separation of the mixture into CH_2Cl_2 and water soluble portions, drying the CH_2Cl_2 layer over anhydrous magnesium sulfate and evaporating the solvent

Can. J. Chem. Downloaded from www.nrcresearchpress.com by 210.87.254.42 on 09/05/12
For personal use only.

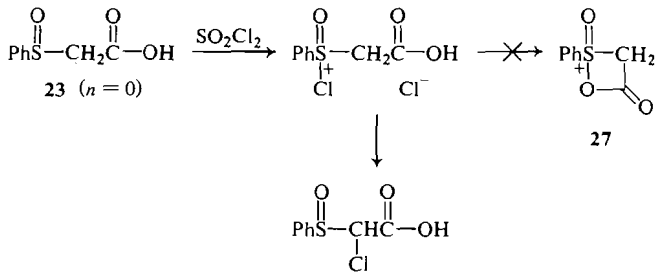

on a rotor evaporator. Unless otherwise stated, yields are based on purified products.

Preparation of β-Hydroxy Sulfoxides by Reaction of Ketones, Aldehydes, and Epoxides with $PhS(O)CH_2Li$

General Procedure

To a solution of methyl phenyl sulfoxide in THF at −78° under N_2 was added 1.2 equivalents of CH_3Li (1.5 *M* in ether, Foote Mineral Co.). The clear yellow solution was stirred for 15 min at −78° and then treated with the appropriate electrophile, neat if liquid, or as a THF solution if solid. The reaction mixture was stirred for several minutes then quenched with water. The usual workup gave the crude products which were generally recrystallized from methylene chloride – pentane. The yields refer to purified products and are given in Table 4. Analytic and n.m.r. data are also given in Table 4.

Reaction of Sulfoxides with SO_2Cl_2

General Procedure

The sulfoxide was dissolved in methylene chloride (approx. 1 g/30 ml) and the reaction mixture was cooled to 0° or −78°. The reaction mixture was protected from moisture. Sulfuryl chloride (1.1–1.2 equiv.) was then introduced and the reaction mixture was stirred for up to 30 min. It was then poured into water and the layers were separated. The aqueous phase was extracted once more with methylene chloride. The methylene chloride fractions were dried and the solvent evaporated. Yields, unless otherwise specified, refer to purified products.

*2-Phenylsulfinylethanol (**10**, n = 0)*

The above sulfoxide (978 mg) and sulfuryl chloride (1.03 g) were allowed to react in 25 ml of CH_2Cl_2 at −78°. The yield of 2-chloroethyl phenyl sulfone, m.p. 54–55°, was 1.14 g (95%). Lit. m.p. 54–55° (9).

*3-Phenylsulfinylpropanol (**10**, n = 1)*

Sulfuryl chloride (810 mg) and sulfoxide (905 mg) in 25 ml of CH_2Cl_2 at −78° gave 1.03 g (96%) of 3-chloropropyl phenyl sulfone (10).

*4-Phenylsulfinylbutanol (**10**, n = 2)*

Reaction of sulfoxide (996 mg) with 810 mg of SO_2Cl_2 at −78° gave 1.01 g (88%) of 4-chlorobutyl phenyl sulfone, m.p. 56° (10).

*5-Phenylsulfinylpentanol (**10**, n = 3)*

Sulfuryl chloride (3.0 mmol) was added to a solution of 565 mg (2.7 mmol) of hydroxy sulfoxide in 20 ml of CH_2Cl_2 at −78°. Workup gave 600 mg of α-chloro-ω-hydroxy sulfoxide **12** (*n* = 3) as a colorless oil. The crude yield was greater than 90%. The spectroscopic properties of this material were: n.m.r. 1.0–2.6 (m, 6H), 3.0 (s, 1H exchangeable with D_2O), 3.4–3.8 (m, 2H), 4.4–4.8 (m, 1H), and 7.3–7.7 (m, 5H); i.r. ($CHCl_3$), 3430 (broad), 1140 (s), 1090 (s), and 1050 (s) cm^{-1}; mass spectrum, M^+ = 246 and 248 (ratio 3:1). The material decomposed slowly at room temperature and was not further purified or analyzed.

*6-Phenylsulfinylhexanol (**10**, n = 4)*

Sulfuryl chloride (9 mmol) was added to a solution of 1.70 g (7.5 mmol) of hydroxy sulfoxide in 25 ml of CH_2Cl_2 at 0°. The yield of crude α-chloro-ω-hydroxy sulfoxide **12** (*n* = 4) was essentially quantitative. The product was purified by silica gel column chromatography using 1:1 ether–pentane as eluent. The n.m.r. spectrum showed peaks from 0.8–2.4 (m, 8H), 2.3 (1H, exchangeable with D_2O), 3.4–3.8 (m, 2H), 4.4–4.7 (m, 1H), and 7.4–7.8 (m, 5H). Infrared bands ($CHCl_3$) occurred at 3440 (broad), 1080 (s) and 1042 (s) cm^{-1}. The mass spectrum showed M^+ at 260 and 262, isotope ratio 3:1. The compound could not be distilled without decomposition.

*β-Hydroxy Sulfoxide **28***

Sulfuryl chloride (470 mg) was added to a solution of 723 mg of **28** in 45 ml of CH_2Cl_2 at −78°. The yield of recrystallized product **29**, m.p. 86°, was 642 mg. The n.m.r. spectrum had peaks at 3.94 (d, *J* = 7.0 Hz, 2H), 5.37 (t, *J* = 7.0 Hz, 1H), 7.25 (s, 5H) and 7.4–7.9 (m, 5H). The sulfone bands occurred at 1320 and 1150 cm^{-1} in the infrared.

Anal. Calcd. for $C_{14}H_{13}ClO_2S$: C, 59.68; H, 4.61. Found: C, 59.97; H, 4.75.

*β-Hydroxy Sulfoxide **30***

Sulfuryl chloride (255 mg) and 375 mg of **30** in 10 ml of CH_2Cl_2 at −78° gave 310 mg (73%) of the β-chloro sulfone **31** m.p. 95–97° (ether–pentane), *m/e* = 272 and 274 (ratio 3:1). The n.m.r. spectrum had peaks at 1.2–2.4 (m, 10H), 3.65 (s, 2H), and 7.5–8.1 (m, 5H). The sulfone bands occurred at 1320 and 1150 cm^{-1}.

The β-chloro sulfone was dehydrochlorinated by passing it through a basic alumina column. The β,γ-unsaturated sulfone thus obtained had m.p. 73–74° and n.m.r. bands at 1.3–2.3 (m, 8H), 3.62 (s, 2H), 5.4 (m, 1H), and 7.4–8.0 (m, 5H).

Anal. Calcd. for $C_{13}H_{16}O_2S$: C, 66.08; H, 6.83. Found: C, 65.68; H, 6.74.

In a second experiment the crude product obtained from the reaction of **30** with SO_2Cl_2 was chromatographed directly. The yield of unsaturated sulfone was 92%.

*β-Hydroxy Sulfoxide **32***

Sulfuryl chloride (400 mg) was added to 350 mg of sulfoxide **32** in 15 ml of CH_2Cl_2. The crude product was separated by preparative t.l.c. The yield of chloro sulfone

Can. J. Chem. Downloaded from www.nrcresearchpress.com by 210.87.254.42 on 09/05/12
For personal use only.

TABLE 4. Preparation of sulfoxides

Sulfoxide	Yield (%)	Method	M.p. (°C)	Found C	Found H	N.m.r. data (δ)
$PhS(O)(CH_2)_2OH$	78	A*	—	56.96	5.88	2.8–3.2 (m, 2H), 3.9–4.3 (m, 3H, including OH) 7.4–7.7 (m, 5H)
$PhS(O)(CH_2)_3OH$	83	B†	—	58.19	6.60	1.5–2.2 (m, 4H), 3.65 (t, J = 6.2 Hz, 2H), 3.76 (OH), 7.3–7.75 (m, 5H)
$PhS(O)(CH_2)_4OH$	88	B	—	58.98	7.01	1.4–2.1 (m, 4H), 2.65–3.05 (m, 2H), 3.78 (OH), 3.4–3.7 (m, 2H), 7.4–7.8 (m, 5H)
$PhS(O)(CH_2)_5OH$	82	A	—	62.04	7.62	1.2–2.0 (m, 6H), 2.5 (OH) 2.65–3.0 (m, 2H), 3.4–3.8 (m, 2H), 7.3–7.7 (m, 5H)
$PhS(O)(CH_2)_6OH$	94	A	—	63.57	8.02	1.2–2.1 (m, 9H, including OH), 2.6–3.0 (m, 2H), 3.4–3.8 (m, 2H), 7.4–7.8 (m, 5H)
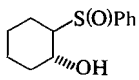	67	B	155–156	64.18	7.15	0.9–2.4 (m, 8H), 2.5–3.1 (m, 1H), 3.4–4.3 (m, 1H), 5.0 (OH), 7.4–7.8 (m, 5H)
$PhS(O)CH_2C(CH_3)_2$§ | OH	71	C‡	116–117	—	—	1.40 (s, 3H), 1.60 (s, 3H), 2.81 (d, J = 14.0 Hz, 1H), 3.03 (d, J = 14.0, 1H), 3.8 (OH), 7.4–7.8 (m, 5H)
$PhS(O)CH_2C(CH_2)_5$ | OH	77	C	95	65.29	7.60 S = 13.49	1.0–2.2 (m, 10H), 2.80 (d, J = 14.0, 1H), (3.02 d, J = 14.0, 1H), 2.94 (OH), 7.4–7.8 (m, 5H)
$PhS(O)CH_2CPh_2$ | OH	61	C	144–146			3.62 (s, 2H), 7.1–7.4 (m, 5H)
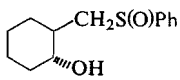	7	C	95–96	65.79	7.36 S = 13.52	0.9–2.3 (m, 9H), 2.6–3.7 (m, 3H), 3.75 (OH), 7.4–7.8 (m, 5H)
$PhS(O)CH_2CHPh$ | OH	65	C	110–125	67.77	5.72	2.7–3.5 (m, 2H), 4.5 (OH), 5.2–5.5 (m, 1H), 7.30 (s, 5H), 7.4–7.8 (m, 5H)
$PhS(O)CH_2CO_2H$‖	81	A	118	—	—	3.82 (s, 2H), 7.4–7.8 (m, 5H), 9.5 (s, 1H)
$PhS(O)(CH_2)_2CO_2H$¶	90	A	98	—	—	2.2–3.0 (m, 2H), 3.0–3.6 (m, 2H), 7.4–7.8 (m, 5H), 10.92 (s, 1H)
$PhS(O)(CH_2)_3CO_2H$	79	A	122–124	56.39	5.70	1.7–2.3 (m, 2H), 2.3–2.7 (m, 2H), 2.92 (t, J = 7.5, 2H), 7.3–7.7 (m, 5H), 9.35 (s, 1H)
** 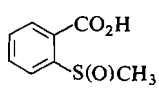	48	A	173–174	—	—	2.94 (s, 3H), 7.4–8.4 (m, 4H)

Can. J. Chem. Downloaded from www.nrcresearchpress.com by 210.87.254.42 on 09/05/12
For personal use only.

TABLE 4 (*Concluded*)

Sulfoxide	Yield (%)	Method	M.p. (°C)	Found C	Found H	N.m.r. data (δ)
$PhS(O)CH_2CONH_2$	54	B	131–133	52.78	4.71	3.45 (d, J = 13.0 Hz, 1H), 3.73 (d, J = 13.0 Hz, 1H), 7 (broad s, 2H), 7.4–7.7 (m, 5H)
$PhS(O)(CH_2)_2CONH_2$	13	B	132–133	54.56	5.55	2.1–3.5 (m, 4H), 5.4–6.5 (NH_2), 7.3–7.7 (m, 5H)
$PhS(O)(CH_2)_3CONH_2$	50	B	124–125	56.61	6.26	1.7–2.6 (m, 4H), 2.7–3.1 (t, 2H), 6.1–6.7 (NH_2), 7.4–7.8 (m, 5H)

*Method A refers to oxidation of the corresponding sulfide, prepared by standard procedures, with $NaIO_4$ in aqueous methanol.
†Method B involved oxidation of the sulfide with meta-chloroperbenzoic acid in CH_2Cl_2.
‡Method C refers to reaction of $PhS(O)CH_2Li$ in tetrahydrofuran with the appropriate ketone (see Experimental).
§Reference 11.
‖Reference 16.
¶Reference 12.
**Reference 17.

33, m.p. 45° (lit. m.p. 44–45° (11)), was 168 mg (41%). In addition, 115 mg (34%) of the unsaturated sulfone **34** (M^+ = 196) was obtained as a colorless oil. N.m.r. peaks occurred at 1.85 (s, 3H), 3.8 (s, 2H), 4.75 (s, 1H), 5.50 (m, 1H), and 7.4–8.1 (m, 5H).

In a second experiment the crude product was chromatographed and gave **34** in 81% yield.

β-Hydroxy Sulfoxide 35

Sulfuryl chloride (230 mg) and sulfoxide **35** (470 mg) in 25 ml of CH_2Cl_2 at −78° gave 417 mg (89%) of the α,β-unsaturated sulfone **36**, m.p. 105–107°; i.r. bands 1320, 1164, and 1150 cm^{-1}; n.m.r. peaks at 6.84 (s, 1H) and 6.9–7.6 (m, 15H).

trans-Hydroxy Sulfoxide 13

(a) Preparation

To a solution of 15.7 mmol of $PhS(O)CH_2Li$ in tetrahydrofuran at −78° was added 1.5 g (15.6 mmol) of cyclohexene oxide. The reaction mixture was warmed to room temperature and then refluxed for 30 min. The usual work-up followed by purification by preparative t.l.c. gave 265 mg (7%) of **13** as colorless needles, m.p. 95–96° (Table 4).

(b) Reaction with SO_2Cl_2

Hydroxy sulfoxide **13** (250 mg) and SO_2Cl_2 (165 mg) were allowed to react in 20 ml of CH_2Cl_2 at −78° for 30 min. The crude product was purified by preparative t.l.c. and gave 224 mg (77%) of the *cis*-chloro sulfone **14** as a colorless oil. The n.m.r. spectrum had peaks at 1.0–2.2 (m, 8H), 2.2–2.7 (m, 1H), 2.8–3.6 (8 line multiplet, J_{gem} = 14.0 Hz, J_{vic} = 5.8 and 6.0 Hz, 2H), 4.53 (m, width at half-height = 7 Hz, 1H) and 7.5–8.1 (m, 5H). The i.r. spectrum had bands at 1150 and 1307 cm^{-1}. The mass spectrum showed the parent ions at m/e = 274 and 272 (ratio 1:3).

Anal. Calcd. for $C_{13}H_{17}ClO_2S$: C, 57.25; H, 6.28. Found: C, 57.39; H, 6.26.

Reaction of Sulfinyl Carboxylic Acids with SO_2Cl_2

Phenylsulfinylacetic Acid

Sulfuryl chloride (470 mg) was added to 595 mg of a suspension of acid sulfoxide in 25 ml of CH_2Cl_2 at −78°. The reaction was complete after 30 min as indicated by the formation of a fine powder. The solvent was evaporated under reduced pressure. The yield of α-chloro-α-phenylsulfinylacetic acid, obtained as a mixture of diastereomers was 670 mg (97%). The n.m.r. spectrum of the mixture showed 2 singlets at 5.20 and 5.34 (2:1 ratio, 1H), a singlet at 9.20 (1H) and a multiplet from 7.45–7.95 (5H); i.r. bands occurred at 3500–2300 (broad), 1735, 1200, 1080, and 1032 cm^{-1}.

Anal. Calcd. for $C_8H_7ClO_3S$: C, 43.96; H, 3.20. Found: C, 44.61; H, 3.63.

3-Phenylsulfinylpropionic Acid

Sulfuryl chloride (670 mg) was added to a solution of 905 mg of the above acid in 20 ml of methylene chloride at −78°. The solvent was evaporated after 20 min and the residue recrystallized from ether–pentane to give 882 mg (83%) of 3-phenylsulfonylpropionyl chloride; i.r. 1782, 1312, and 1146 cm^{-1}. Hydrolysis gave 3-phenylsulfonylpropionic acid, m.p. 124–126°. Lit. m.p. 125.5–127° (11).

4-Phenylsulfinylbutyric Acid

To a solution of 610 mg of acid sulfoxide in 20 ml of methylene chloride at −78° was added 475 mg of SO_2Cl_2. The reaction mixture was allowed to warm to room temperature during 30 min. The solvent was evaporated and the product recrystallized from CH_2Cl_2–ether–pentane. The yield of 4-chloro-4-phenylsulfinylbutyric acid, m.p. 111°, was 587 mg (83%). The n.m.r. spectrum showed multiplets from 1.7–2.9 (m, 4H), 4.65–5.0 (m, 1H), 7.4–7.8 (m, 5H) and a singlet at 10.34 (1H); i.r. peaks occurred at 3400–2500 (broad), 1720 (s), and 1040 (s) cm^{-1}.

Anal. Calcd. for $C_{10}H_{11}ClO_3S$: C, 48.68; H, 4.49; Cl, 14.38; S, 12.90. Found: C, 48.49; H, 4.52; Cl, 14.54; S, 12.90.

2-Methylsulfinylbenzoic Acid

Sulfuryl chloride (730 mg) was added to a suspension of 827 mg of acid sulfoxide in 25 ml of CH_2Cl_2 at 25°. The solid "dissolved" within an hour. The solvent was evaporated and gave a quantitative yield of 2-methylsulfonylbenzoyl chloride, m.p. 60°; i.r. 1785, 1320, and

Can. J. Chem. Downloaded from www.nrcresearchpress.com by 210.87.254.42 on 09/05/12
For personal use only.

1150 cm^{-1}; n.m.r. 3.28 (s, 3H) and 7.6–8.3 (m, 4H). Hydrolysis gave 2-methylsulfonylbenzoic acid, m.p. 130–132° (13).

Phenylsulfinylacetamide

To a solution of 250 mg of sulfoxide in 10 ml of CH_2Cl_2 at −78° was added 200 mg of SO_2Cl_2. The reaction mixture was stirred for 2 h. The solvent was evaporated to yield 258 mg of crude product which solidified upon standing. After three recrystallizations ($CHCl_3$–hexane) 2-chloro-2-phenylsulfinylacetamide had m.p. 138–139°. The n.m.r. spectrum (DMSO-d_6) showed 2 singlets at 5.51 and 5.55 in addition to the amide and aromatic hydrogens. The relative ratio of the singlets due to two diastereomeric sulfoxides was about 1:1.

Anal. Calcd. for $C_8H_8ClNO_2S$: C, 44.11, H, 3.71; Cl, 16.28; S, 14.70. Found: C, 44.20; H, 3.71; Cl, 16.52; S, 14.68.

3-Phenylsulfinylpropionamide

To a suspension of 318 mg of amide sulfoxide in 20 ml of CH_2Cl_2 at −78° was added 257 mg of SO_2Cl_2. The reaction mixture was stirred for 2 h and then worked up to give 298 mg (95%) of 3-phenylsulfonylpropionitrile, m.p. 92° (methylene chloride – pentane). N.m.r., 2.6–3.0 (m, 2H), 3.30–3.6 (m, 2H) 7.5–8.1 (m, 5H); i.r., 2230, 1325, and 1145 cm^{-1}.

Anal. Calcd. for $C_9H_9NO_2S$: C, 55.38; H, 4.60. Found: C, 55.19, H, 4.64.

4-Phenylsulfinylbutyramide

Sulfoxide (211 mg) and SO_2Cl_2 (150 mg) were allowed to react in 20 ml of methylene chloride as above. The yield of 4-chloro-4-phenylsulfinylbutyramide was 178 mg (73%). Recrystallization from $CHCl_3$–hexane gave a colorless powder, m.p. 137.5–139.5°.

Anal. Calcd. for $C_{10}H_{12}ClNO_2S$: C, 48.84; H, 4.92; S, 13.05. Found: C, 48.44; H, 4.85; S, 13.23.

Reaction of 3-Phenylsulfinylpropanol with Br_2/Pyridine

Bromine (8.8 mmol) was added to a solution of 1.38 g (7.5 mmol) of sulfoxide and 1.5 g pyridine in 40 ml of carbon tetrachloride at 0°. The reaction mixture was yellow and a considerable amount of precipitate formed within 1 h. After 2 h the precipitate was filtered to give 2.32 g (62%) of the perbromide salt, yellow flakes, m.p. 137° (CH_3OH–H_2O). N.m.r., (DMSO-d_6) 2.1–2.4 (m, 2H), 3.4–3.6 (m, 2H), 4.68 (t, J = 7 Hz, 2H) and 7.6–9.1 (m, 10H).

Anal. Calcd. for $C_{14}H_{16}Br_3NO_2S$: C, 33.48; H, 3.21; N, 2.79; S, 6.49; Br, 47.75. Found: C, 33.46; H, 3.19; N, 2.80; S, 6.51; Br, 47.71.

The filtrate was washed with dilute acid solution and the organic layer was dried and evaporated to give 315 mg (16%) of 3-phenylsulfonylpropyl bromide **18**, m/e = 262 and 264 (1:1 ratio). The n.m.r. and i.r. spectra were as expected.

Financial support by the National Research Council of Canada is gratefully acknowledged. The authors would like to thank Dr. F. Jung for some technical assistance.

1. T. Durst and K.-C. Tin. Can. J. Chem. **49**, 2374 (1971).
2. K.-C. Tin and T. Durst. Tetrahedron Lett. 4643 (1970).
3. G. Tsuchihashi, K. Ogura, S. Iriuchijima, and S. Tomisawa. Synth. 89 (1971).
4. M. Cinquini, S. Colonna, and F. Montanari. Chem. Commun. 607 (1969).
5. S. Iriuchijima and G. Tsuchihashi. Tetrahedron Lett. 5259 (1969).
6. K.-C. Tin. Ph.D. Thesis University of Ottawa, Ottawa, Canada. 1972.
7. S. Bory, R. Lett, B. Moreau, and A. Marquet. Paper presented at V International Symposium on Organic Sulfur Chemistry, Lund, Sweden. June 5–9, 1972.
8. G. R. Chalkley, D. J. Snodin, G. Stevens, and M. C. Whiting. J. Chem. Soc. **C**, 682 (1970).
9. J. Heyna and W. Riemenschneider. Ger. 887, 505 (1953); C.A. **48**, 12803 (1954).
10. F. G. Bordwell and W. T. Brannen, Jr. J. Am. Chem. Soc. **86**, 4645 (1964).
11. F. Montanari. Tetrahedron Lett. 2685 (1964).
12. B. Holmberg and E. Schjanberg. Arkiv. Kemi, Mineral. Geol. **A15**, 14 (1942); C.A. **38**, 2943 (1944).
13. F. G. Bordwell and G. D. Cooper. J. Am. Chem. Soc. **79**, 916 (1957).
14. J. K. Hall and E. A. Robinson. Can. J. Chem. **42**, 113 (1964).
15. E. M. Arnett and C. Douty. J. Am. Chem. Soc. **86**, 409 (1964).
16. N. J. Leonard and C. R. Johnson. J. Org. Chem. **27**, 282 (1962).
17. G. Barbeieri, V. Davoli, I. Moretti, F. Montanari, and G. Torre. J. Chem. Soc. **C**, 731 (1969).

Can. J. Chem. Downloaded from www.nrcresearchpress.com by 210.87.254.42 on 09/05/12
For personal use only.

The Infrared Spectrum of the Hydrogen-Bonded Molecule Dimethyl Ether ... Hydrogen Chloride in the Gas Phase[1]

JOHN E. BERTIE AND M. VICTOR FALK

Department of Chemistry, University of Alberta, Edmonton

Received November 20, 1972

A detailed study of the infrared spectra of $(CH_3)_2O...HCl$ and its isotopic modifications is presented. The hydrogen-bond stretching mode occurs at $119 \pm 4\ cm^{-1}$ in $(CH_3)_2O...HCl$, $(CD_3)_2O...HCl$, and $(CH_3)_2O...DCl$. The O...H—Cl deformation modes yield a band centered at $470\ cm^{-1}$, which is broad and complex. It is interpreted in terms of sum and difference transitions involving the HCl rocking modes, which are deduced to be at about $50\ cm^{-1}$. The O...D—Cl deformation band is centered at $360\ cm^{-1}$. A band at $790\ cm^{-1}$ in $(CH_3)_2O...HCl$ and $600\ cm^{-1}$ in $(CH_3)_2O...DCl$ is assigned to the overtone of the deformation modes. The shapes of the bands due to the ethereal modes in the molecule can not indicate the molecular geometry and do not agree with the shapes calculated from reasonable moments of inertia. The temperature dependence of the band due to the HCl stretching mode indicates that the fundamental transition is at $2480\ cm^{-1}$, not at $2574\ cm^{-1}$ as previously postulated. The DCl stretching band in $(CH_3)_2O...DCl$ has a different shape to that in $(CD_3)_2O...DCl$. The differences are attributed to combination transitions involving the ethereal modes. It is suggested that the DCl and HCl stretching modes interact with the DCl or HCl rocking modes, thus causing shoulders $50\ cm^{-1}$ away from the DCl stretching fundamental, and contributing to the general diffuseness of the HCl stretching band. The relative intensities of the bands due to $(CH_3)_2O...HCl$ are presented.

Une étude détaillée des spectres infra rouge de $(CH_3)_2O...HCl$ et de ses modifications isotopiques a été présentée. L'élongation de la liaison hydrogène est à $119 \pm 4\ cm^{-1}$ dans $(CH_3)_2O...HCl$, $(CD_3)_2O...HCl$, $(CH_3)_2O...DCl$. Les déformations de O...HCl donnent une bande centrée à $470\ cm^{-1}$, large et complexe, interprétée comme étant la somme et la différence des transitions comprenant les modes de balancement de HCl à environ $50\ cm^{-1}$. La bande de déformation O...DCl est centrée à 360 cm^{-1}, la bande à $790\ cm^{-1}$ dans $(CH_3)_2O...HCl$ et à $600\ cm^{-1}$ dans $(CH_3)_2O...DCl$ ont été attribuées aux harmoniques des vibrations de déformation. Les formes des bandes dues aux vibrations de l'éther dans la molécule ne sont ni une indication de la géométrie moléculaire ni compatibles avec les formes calculées à partir des moments d'inertie raisonnablement choisis. La dépendance de la température de la bande due à l'élongation de HCl indique que la transition fondamentale est à $2480\ cm^{-1}$ et non à 2574 cm^{-1} comme il a été postulé antérieurement. L'élongation DCl dans $(CH_3)_2O...DCl$ a une forme différente de celle dans $(CD_3)_2O...DCl$, les différences ont été attribuées à la combinaison des transitions comprenant celles de l'éther. Il a été suggéré que les modes d'élongation de DCl et HCl sont en interaction avec les modes de balancement de DCl et HCl causant ainsi des épaulements de $50\ cm^{-1}$ de part et d'autre de la fréquence fondamentale d'élongation de DCl et explique l'aspect général diffus de la bande d'élongation de HCl. Les intensités relatives des bandes dues à $(CH_3)_2O...HCl$ ont été présentées.

[Traduit par le journal]

Can. J. Chem., 51, 1713 (1973)

Introduction

The molecule dimethyl ether...hydrogen chloride is one of the simplest hydrogen-bonded molecules that can be studied in the gaseous state. It is, therefore, important that the vibrational spectrum of this molecule be known in as much detail as possible, in order to test the theories of the origins of the vibrational spectra of hydrogen-bonded molecules. This paper presents the results of a detailed study of the infrared spectrum of dimethyl ether...hydrogen chloride, and its isotopically-substituted derivatives, between +35 and −30 °C.

The molecule $(CH_3)_2O...HCl$ has 21 vibrations which are derived from those of the pure ether, plus 6 vibrations of the O---H—Cl part of the molecule which are shown in Fig. 1 along with their designation. The symbols ν_s, ν_b, ν_β, etc. correspond to those of Pimentel and McClellan (1) as closely as possible. It should be noted that in $(CH_3)_2O...HCl$ there are two non-equivalent ν_β modes and that ν_b and ν_t would both correspond to pure rotations of the HCl molecule in the absence of the hydrogen bond, whereas in ref. 1 ν_b would remain the in-plane RAH

[1]This work was presented in part at the International Conference on Hydrogen Bonding, Ottawa, August, 1972.

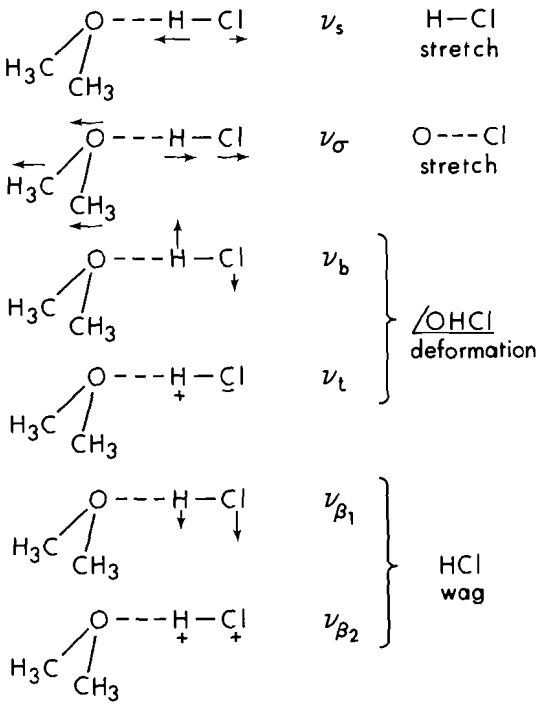

FIG. 1. The six vibrations of the O...H—Cl unit in $(CH_3)_2O$...HCl. The symbols follow those of ref. 1.

bending mode in the absence of the hydrogen bond.

At room temperature the H—Cl stretching mode in $(CH_3)_2O$...HCl yields an absorption at 2574 cm^{-1} which has a halfwidth of about 250 cm^{-1} and consists of a peak and three shoulders separated by 90 to 100 cm^{-1} (2). These main features of the band are quite insensitive to replacement of $(CH_3)_2O$ by some other ether and, in particular, are unchanged if $(CD_3)_2O$ is used (2). Hence they must arise from the O---H—Cl unit and they have been assigned to ν_s and to $\nu_s \pm n\nu_\sigma$, where n is integral (2). The band due to the DCl stretching mode in $(CH_3)_2O$...DCl has been interpreted in the same way and the lower relative intensity of the shoulders in this case has been rationalized (3). One purpose of the present work was to study the temperature dependence of the shape of these bands to test the proposed influence of the difference bands.

The only other mode of Fig. 1 that has been detected is ν_σ which has been reported at 117 ± 3 cm^{-1} in $(CH_3)_2O$...HCl, with some evidence from experiments using a 4:1 HCl:DCl mixture that the isotope shift is small (4). The halfwidth of the band due to ν_σ is about 30 cm^{-1}, which is of the order expected for the rotational envelope in this molecule (2) and found (5) for the bands due to the C—O stretching and methyl rocking modes. A second aim of the present work was to confirm the isotope shift of the 117 cm^{-1} band. Further aims were to locate ν_b, ν_t, and ν_β, and to extend the work of ref. 5 to determine the shapes of the remaining bands due to modes of the ethereal part of $(CH_3)_2O$...HCl.

Experimental

The infrared instrumentation has been described previously (6, 7). The gases were contained in a cylindrical cell with 10 cm pathlength, 1 in. internal diameter and a coaxial cooling jacket. The cylinder containing the gases was made of copper to maximize heat transfer. The cell was capable of holding at least 10 atm pressure and was cooled with cold nitrogen gas. The temperature was controlled to ±1 °C. and was measured to ±1 °C by a calibrated thermometer resting on the copper cell wall in the cooling chamber. The cell windows were potassium chloride, high-density polyethylene, or, for the 300 to 500 cm^{-1} region, cesium iodide coated with a thin layer of paraffin wax to protect it from attack by the hydrogen chloride.

Dimethyl ether-h_6 (Matheson of Canada, Ltd.), dimethyl ether-d_6 and deuterium chloride (Merck, Sharp and Dohme, Montreal), and hydrogen chloride (Matheson of Canada, Ltd., or prepared in vacuum from phosphorus pentachloride and water) were dried in vacuum by repeated distillation from −80 °C. No impurities were detected except for carbon dioxide in some samples, and hydrogen chloride in the deuterium chloride. In spite of extensive pre-deuteration of the vacuum lines and cells, there always was 10 to 20% of HCl in the DCl used. The high-pressure samples were handled in a stainless steel vacuum manifold, and the pressures were measured to ±30 Torr by a monel Bourdon Gauge. Pressures below atmospheric were measured by a mercury manometer to ±1 Torr. All gas pressures quoted were measured at room temperature (22 °C).

Results and Discussion

The ν_σ, ν_β, ν_b, *and* ν_t *Modes*

The far infrared spectra of mixtures of 325 Torr of ether and of acid showed that a band due to the hydrogen-bonded molecule occurs at about 120 cm^{-1}, not only for $(CH_3)_2O$...HCl (4), but also for $(CH_3)_2O$...DCl and $(CD_3)_2O$...HCl. $(CD_3)_2O$...DCl was not studied in this region. The band grows in intensity as the temperature is lowered to the onset of condensation, is independent of whether ether or the acid is in excess and has a halfwidth of about 30 cm^{-1}. The maximum of the band was not clearly observed, due to an overlapping

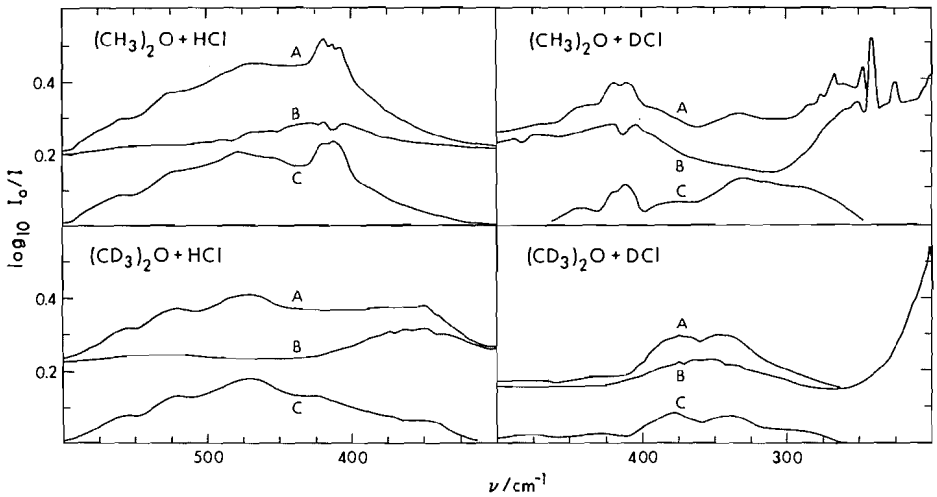

FIG. 2. Curves *A*: infrared absorption by mixtures of 110 Torr of $(CH_3)_2O$ or $(CD_3)_2O$ plus 880 Torr of HCl or DCl, as indicated, at −30 °C. Curves *B*: infrared absorption by 110 Torr of $(CH_3)_2O$ or $(CD_3)_2O$ at −30 °C. 10 cm pathlength. In each box curve *C* was obtained by subtracting curve *B* from curve *A*, and represents the absorption by the appropriate isotopic modification of $(CH_3)_2O...HCl$.

HCl or DCl line, but unless the band is grossly asymmetric the maximum is at 119 ± 4 cm^{-1} in all cases. The isotope shift of this band is consistent with its assignment to ν_σ or to one or both of the ν_β modes. Evidence is given below to suggest that ν_β lies at about 50 cm^{-1}, so the band at 119 cm^{-1} is assigned to ν_σ, in agreement with ref. 4.

Figure 2 shows the absorption by $(CH_3)_2O...HCl$ and $(CD_3)_2O...HCl$ between 300 and 600 cm^{-1} and that by $(CH_3)_2O...DCl$ and $(CD_3)_2O...DCl$ between 200 and 500 cm^{-1}. In each case curve *C* shows the absorption by the hydrogen-bonded molecule, obtained by subtracting that due to the same pressure of pure ether as was put into the mixture (curve *B*) from the spectrum of the mixture (curve *A*). In all cases where the absorption by the free ether was subtracted (Figs. 2, 5, and 6), it was shown that the ether absorption is unaffected by pressure-broadening by nitrogen or argon, and is unchanged by cooling from +35 to −30 °C. There is, however, an uncertainty in how much absorption to subtract (either manually or by putting a cell containing ether in the reference beam of the spectrometer). Three effects of this uncertainty are fairly obvious in Fig. 2: the doublet character of the peak between 410 and 420 cm^{-1} in the spectra of the $(CH_3)_2O$ complexes may not be real, and for $(CH_3)_2O...HCl$ the frequency of the peak at 480 cm^{-1} is slightly higher than it should be, and the weak feature at 450 cm^{-1} is probably spurious. Less obvious is some uncertainty in the correct shape of the band below 300 cm^{-1} for the DCl complexes and in the existence of the shoulder at 425 cm^{-1} for $(CD_3)_2O...HCl$.

The absorption attributed to the hydrogen-bonded molecule increased in intensity as the temperature was lowered to the condensation point, and no changes in the relative intensities of its various features were detected between +30 and −30 °C, or when the ether:acid ratio was changed from 1:2 to 1:8. Therefore it can be assigned to the 1:1 hydrogen-bonded complex, and is clearly due to one, or both, of ν_b and ν_t, and to the C—O—C deformation mode in the complex. For the HCl complexes it is clear that the features at about 570, 525, and 470 cm^{-1} are due to the O...H—Cl part of the molecule, while that between 420 and 410 cm^{-1} in the spectrum of $(CH_3)_2O...HCl$ is due to the C—O—C deformation mode. For $(CD_3)_2O...HCl$, the feature at 425 cm^{-1} can be assigned to the O...H—Cl part of the molecule while that at about 340 cm^{-1} is probably due to the C—O—C deformation mode. The situation is less clear for the DCl complexes. In the spectrum of $(CH_3)_2O...DCl$ the feature between 410 and 420 cm^{-1} is clearly due to the C—O—C deformation mode, and other features occur at 440, 375, 330, and, probably, 280 cm^{-1}. For

$(CD_3)_2O...DCl$ the relative intensities are quite different but features occur at 430, 380, 340, and, probably 290 cm^{-1}, very nearly coincident with those in $(CH_3)_2O...DCl$. We therefore conclude that all of these features in the spectrum of $(CD_3)_2O...DCl$ are due to the O...D—Cl part of the molecule, but the ethereal modes clearly influence their relative intensities and, to a lesser extent, their frequencies.

From the general assignment presented above, the bands due to the O---H—Cl and O---DCl deformation modes, ν_b and/or ν_t, have many of the characteristics of those due to the H—Cl and D—Cl stretching modes. The bands are broad, with a halfwidth of about 150 cm^{-1} for the HCl complexes, and complex, with four features observed for each case. By analogy with the interaction between ν_s and ν_σ (2), it is probable that the breadth and complexity of these bands arise from interaction of ν_b and/or ν_t with the appropriate ν_β, HCl rocking mode. The observed features are assigned, therefore, to transitions of the type ν_b, or ν_t, $\pm n\nu_\beta$, where n is zero or integral. From the separation of the features the fundamental frequency of the ν_β modes must be about 50 cm^{-1}. The observed constancy of the bandshape with temperature was not sufficiently precise to contradict this assignment provided that the difference transitions originate in energy levels that are less than about 100 cm^{-1} above the ground state.

Before the assignment of these features is discussed in more detail, the spectra shown in Fig. 3 must be presented. A weak absorption occurs at 790 cm^{-1} in $(CH_3)_2O...HCl$. Its intensity increases, reversibly, as the temperature is lowered, and is the same for $(CH_3)_2O$:HCl ratios of 1:2 and 2:1 (curves *A* and *B*). The integrated intensity of this absorption is about one sixth of that of the absorption centered at 470 cm^{-1}. The band is not present in $(CH_3)_2$-O...DCl (the weak feature seen in curve *C* undoubtedly arises from the HCl impurity in the DCl used) or in the spectra of pure ether (curve *D*) or HCl (curve *E*). This band could not be studied in $(CD_3)_2O...HCl$ because the symmetric CO stretching mode overlaps this region. In the spectra of $(CH_3)_2O...DCl$ a very weak absorption was detected between 550 and 630 cm^{-1}. This absorption was reproduceable but very near to our detection limit, and rapid formation of methyl chloride prevented the use of higher gas pressures to improve its observation. We tentatively conclude that the 790 cm^{-1} feature does shift to about 600 cm^{-1} in the DCl complex. Only two assignments appear to be possible for this feature. Either it is due to the second O...H—Cl (or O...D—Cl) deformation mode, ν_b or ν_t, or to the first overtone of ν_b or ν_t. Intuitively it seems improbable that one of the deformation modes would be near to 470 cm^{-1} while the other is at 790 cm^{-1} and that one would absorb six times more strongly than the other one; their proposed relative frequencies and intensities in $(CH_3)_2O...HF$ (8) seem far more reasonable. Therefore we assign this feature to the first overtone of ν_b or ν_t.

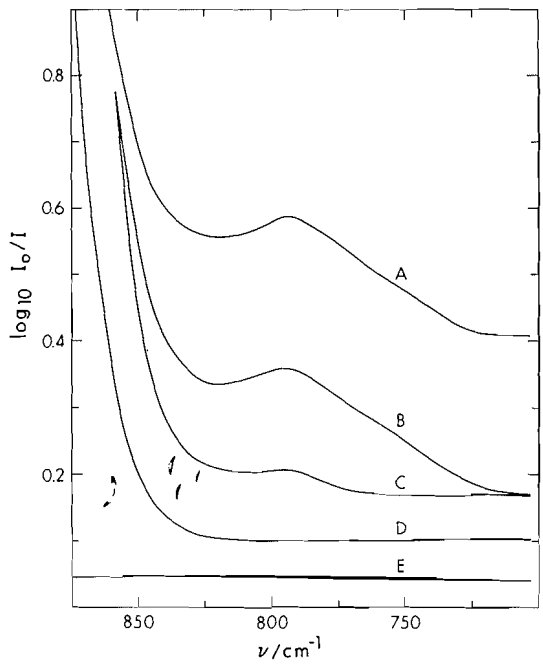

FIG. 3. Infrared absorption in 10 cm pathlength at +35 °C by: *A*, 1 atm of $(CH_3)_2O$ mixed with 2 atm of HCl; *B*, 2 atm of $(CH_3)_2O$ mixed with 1 atm of HCl; *C*, 2 atm of $(CH_3)_2O$ mixed with 1 atm of DCl; *D*, 1 atm of $(CH_3)_2O$; *E*, 1 atm of HCl. The curves have been offset for clarity, but *B* is positioned relative to *C* as observed.

The ν_b and ν_t fundamentals can not be assigned definitively from this evidence. They were assigned at 750 and 660 cm^{-1} for $(CH_3)_2O...HF$ and at 550 and 490 cm^{-1} for $(CH_3)_2O...DF$ (8), although it is not known whether ν_b or ν_t has the higher frequency. If the ratio ν_b/ν_t is the same for the HCl and DCl complexes as for the HF and DF ones, respectively, then ν_b and ν_t must be separated by about

60 cm^{-1} near to 500 cm^{-1} and by about 40 cm^{-1} near to 360 cm^{-1}. Thus ν_b and ν_t can be assigned at 340 and 380 cm^{-1} for the DCl complexes, and their assignment at 470 and 525 cm^{-1} for the HCl complexes yields an isotopic ratio of 1.38 for both bands, compared to 1.40 under the harmonic approximation, if it is assumed that ν_b is higher (or lower) than ν_t in both isotopic molecules. However this assignment suggests that 790 cm^{-1} is a very low frequency for the first overtone. It is possible that the 790 cm^{-1} feature is at the low-frequency end of a broad overtone absorption, most of which is hidden by the much stronger band above 850 cm^{-1}. It is also possible that, because of the vibrational Franck–Condon effect (9), the most intense transition in the overtone band is not the overtone of the most intense transition in the fundamental band. An alternative assignment which uses this feature is to assign ν_b and ν_t at 470 and 420 cm^{-1} in the HCl complexes and at 340 and 290 cm^{-1} in the DCl complexes. The ratio 470/340 = 1.38 is satisfactory, but the ratio 420/290 = 1.45 is somewhat large.

It is helpful to use these frequencies to calculate ω_e and $\omega_e x_e$, where $\omega_e(v + 1/2) - \omega_e x_e(v + 1/2)^2$ is the assumed vibrational term (10). ω_e and $\omega_e x_e$ for the DCl complex can be obtained from those of the HCl complex by multiplying by ρ and ρ^2, respectively (10), where $\rho^2 = G_D/G_H$, where G_D and G_H are the **G** matrix elements (11) for the O...D—Cl and O...H—Cl deformation coordinates, respectively. If the first assignment above is taken, and 790 cm^{-1} is taken to be the first overtone of 470 cm^{-1}, then ω_e = 620 cm^{-1} and $\omega_e x_e$ = 75 cm^{-1} for $(CH_3)_2O$...HCl and the corresponding frequencies in the DCl complex are calculated to be 660 and 370 cm^{-1}. The weak feature observed in the DCl complexes was definitely to low frequency of 660 cm^{-1}, and the pairing of 470 and 370 cm^{-1} indicates that 520 and 340 cm^{-1} must correspond to the same vibration. Thus, this assignment requires that the anharmonicities be very large indeed, and does not agree well with the overtone frequency for $(CH_3)_2O$...DCl. The second assignment, in which 790 cm^{-1} is taken to be the first overtone of 420 cm^{-1}, yields ω_e = 470 cm^{-1} and $\omega_e x_e$ = 25 cm^{-1} for the HCl complex and predicts the corresponding frequencies for the DCl complex to be 595 and 310 cm^{-1}. 595 cm^{-1} agrees well with the observed overtone absorption in the DCl complex, but 310 cm^{-1} does not correspond to any obvious feature in the observed spectra. Thus, with the present data no unique assignment can be made, although of the two discussed the second one is to be preferred on the basis of the smaller anharmonicity that it implies for this mode.

The Band Contours for the Ethereal Modes, and the Molecular Shape

Figure 4 shows the changes that occur in the bands due to the ethereal modes between 800 and 1500 cm^{-1} when the $(CH_3)_2O$...HCl molecule is formed. The results for the CO stretching and methyl rocking modes, between 900 and 1200 cm^{-1} (12), agree with those of Lascombe and co-workers (5), except that the shoulder at 920 cm^{-1} is less pronounced in our spectra.

The shape of the band at 912 cm^{-1} (Fig. 4) has been used (13) as evidence that the hydrogen chloride bonds to one of the two lone pairs of electrons on the ether, creating a molecule with C_s symmetry, rather than bonding symmetrically between them and creating one with C_{2v} sym-

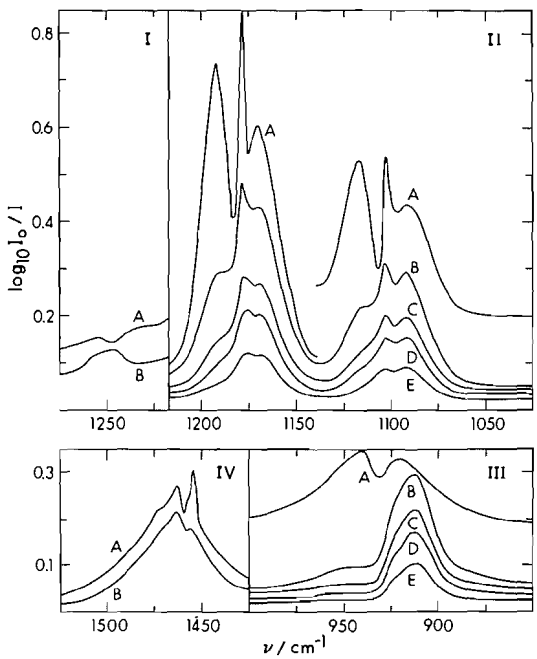

FIG. 4. Infrared absorption in 10 cm pathlength of mixtures of: boxes I and IV, 20 Torr of $(CH_3)_2O$ plus 6000 Torr of Ar (curve *A*) or plus 6000 Torr of HCl (curve *B*), at 0 °C; boxes II and III, 10 Torr of $(CH_3)_2O$ plus 6000 Torr of Ar at +35 °C (curve *A*) or plus 6000 Torr of HCl at +35 °C (*B*), +10 °C (*C*), 0 °C (*D*) or −10 °C (*E*).

metry. This conclusion seems intuitively correct but calculations based on an O---Cl distance of 3.1 Å, reasonable geometry for the ether, and the work of Ueda and Shimanouchi (14), predicted an A–C hybrid band of type 18 (14) for the C_s model and an A-type band of type 8 (14) for the C_{2v} model, with a halfwidth of about 30 cm^{-1} in each case. The halfwidths agree with the observed one, but both predicted bands show pronounced PQR structure which does not agree with the observed bandshape (Fig. 4) nor, therefore, indicate a preference for either model. The failure to predict the observed band shape must be influenced by the high population of excited states of the ν_β and ν_σ modes at −10 °C if, as is probable, rather large deviations from the equilibrium molecular geometry exist in these states.

Because the calculated and observed bandshapes disagree, the frequencies of the vibrational transitions can not be reported accurately. The centers of intensities of the bands in $(CH_3)_2O$...HCl are at 912, 1097, 1171, 1248, and 1465 cm^{-1}. Bands due to ethereal modes in $(CD_3)_2O$...HCl are centered at 815, 920, 1055, and 1150 cm^{-1}.

The ν_s Mode

The absorption by the H—Cl stretching mode, ν_s, in $(CD_3)_2O$...HCl at +34 and −30 °C is shown in Fig. 5. The spectra shown are corrected for the absorption by free ether (2). At the lower temperature the peak is 8 cm^{-1} lower in frequency, the feature at 2475 cm^{-1} is resolved as a peak and is more intense relative to the maximum, and the entire high-frequency side of the band has lower intensity relative to the maximum, than at +34 °C. These results prove that the feature at 2480 cm^{-1} does not arise from $\nu_s - \nu_\sigma$ (the transition [$\nu_s = 0 \rightarrow 1$, $\nu_\sigma = 1 \rightarrow 0$]) as previously postulated (2), but do not allow a unique reassignment to be made.

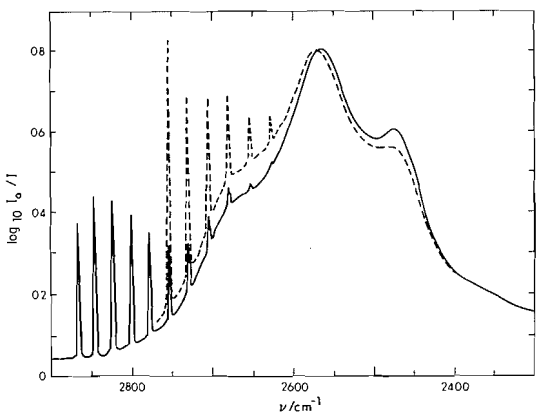

FIG. 5. Infrared absorption in 10 cm pathlength by 250 Torr of $(CD_3)_2O$ mixed with 250 Torr of HCl at +34 °C (dashed line) and by 100 Torr of $(CD_3)_2O$ mixed with 100 Torr of HCl at −30 °C (solid line). In each case the reference beam contained 250 or 100 Torr, as appropriate, of $(CD_3)_2O$ in a 10 cm cell at +34 °C.

The band due to ν_s in $(CH_3)_2O$...HCl was also studied between +34 and −30 °C, and shows the same temperature dependence as that in $(CD_3)_2O$...HCl. The only differences between the two bands are that for $(CH_3)_2O$...HCl the central peak is slightly broader and the 2475 cm^{-1} peak is slightly less well resolved at −30 °C. Lassegues, Huong, and Lascombe (15, 16) have studied the ν_s band of $(CH_3)_2O$...HCl quantitatively between −50 and +90 °C (these workers have also seen the band due to the O..H—Cl deformation mode in $(CH_3)_2O$...HCl (15).) Their results agree with ours between +30 and −30 °C but their spectra above +30 °C showed that $\nu_s - \nu_\sigma$ can be assigned to the shoulder at 2360 cm^{-1}, although the transition [$v_s = 0 \rightarrow 1$, $v_\sigma = 2 \rightarrow 1$] appears to be stronger than [$v_s = 0 \rightarrow 1$, $v_\sigma = 1 \rightarrow 0$]. This allows ν_s to be assigned at 2480 cm^{-1} and $\nu_s + \nu_\sigma$ (the transition [$v_s = 0 \rightarrow 1$, $v_\sigma = 0 \rightarrow 1$]) at 2574 cm^{-1} (at +30 °C). The shoulder at 2680 cm^{-1} is assigned to $\nu_s + 2\nu_\sigma$ and the decrease in intensity on cooling is explained by postulating (15, 16), that, because of the vibrational Franck–Condon effect (9), the transition [$v_s = 0 \rightarrow 1$, $v_\sigma = 2 \rightarrow 4$] is more intense than [$v_s = 0 \rightarrow 1$, $v_\sigma = 0 \rightarrow 2$].

This assignment indicates that the difference between the $v_\sigma = 1$ and $v_\sigma = 0$ states is 95 ± 5 cm^{-1} when $v_s = 1$, compared with 119 cm^{-1} when $v_s = 0$. This implies that although the curve of energy *vs.* O...Cl distance must have a deeper minimum for the $v_s = 1$ state than for the $v_s = 0$ state (9), the minimum must be broader, so that the curvature is smaller, for the $v_s = 1$ state.

This assignment can clearly be applied to the ν_s band of $(CD_3)_2O$...HCl, but it also seems clear that these transitions (16) alone can not account for the entire band unless some special mechanism, such as an abnormally large effect of centrifugal distortion (15), broadens the rotational envelope. Any such effect can only be operative in the $v_s = 1$ state, because the

30 cm^{-1} halfwidth of the bands due to the ethereal modes, for which $v_s = 0$, can be explained without invoking it. It seems probable that hot bands from excited states of ν_β, as well as from ν_σ (16), contribute to the ν_s band and, in view of the results for the deuterium-bonded molecules, it is probable that combination bands between ν_s and ν_β also contribute.

The temperature dependence of the bands due to the DCl stretching mode, ν_s, in $(CH_3)_2O$...DCl and $(CD_3)_2O$...DCl is shown in Fig. 6. The absorption by the free ether has been subtracted from that of the mixture to yield the curves shown. In each case the entire band sharpens as the temperature is lowered and, if allowance is made for the frequency shift of about 5 cm^{-1} between +30 and −30 °C, all features decrease in intensity relative to the peak at 1850 cm^{-1}. The only exception is the shoulder at 1870 cm^{-1} in $(CD_3)_2O$...DCl, which is discussed below.

It has been noted that the ν_s bands of several ether..DCl molecules are similar to those of ether...HCl, with the side bands due to $\nu_s \pm n\nu_\sigma$ weaker for the deuterated acid (3). However, the details of the bands of $(CH_3)_2O$...DCl and $(CD_3)_2O$...DCl can not be entirely explained in this way, and there are differences between these two bands which must be explained. The feature at 1870 cm^{-1} in the spectrum of $(CD_3)_2O$...DCl

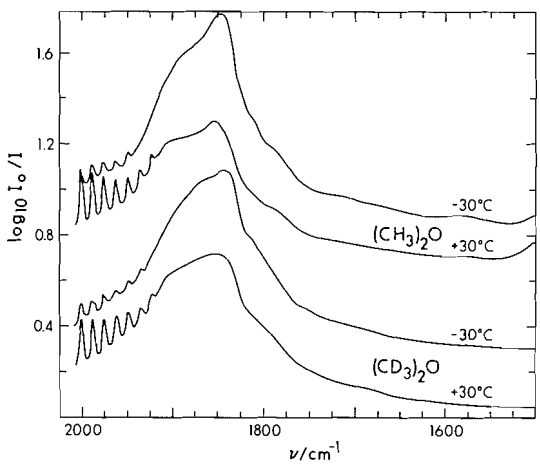

FIG. 6. Infrared absorption in 10 cm pathlength by mixtures of $(CH_3)_2O$ + DCl (upper two curves) and of $(CD_3)_2O$ + DCl (lower two curves). For each pair of curves, the upper one was obtained using 100 Torr of each gas cooled to −30 °C and the lower one required 250 Torr of each gas at +30 °C. In each case the reference beam contained 100 or 250 Torr, as appropriate, of the ether in 10 cm pathlength.

at −30 °C is attributed to the combination transition due to the symmetric CO stretching and CD_3 deformation modes, 815 plus 1055 cm^{-1}. The shoulder at 1800 cm^{-1} in $(CD_3)_2$-O...DCl appears to be a single feature, while in $(CH_3)_2O$...DCl features can be identified at about 1785 and 1810 cm^{-1}, and the additional feature is attributed to the overtone of the symmetric CO stretching mode, 2 × 912 cm^{-1}. The weak feature at 1585 cm^{-1} in the spectrum of $(CH_3)_2O$...DCl is present in that of $(CH_3)_2$-O...HCl and undoubtedly corresponds to a weak feature at this frequency in the pure ether. These features appear to be more intense in the hydrogen-bonded molecules than in the pure ether, in which case they must gain intensity through Fermi resonance with the ν_s mode.

The most prominent features that are common to the ν_s bands of both deuterium-bonded molecules are the central peak at 1850 cm^{-1}, shoulders 50 cm^{-1} away to either side, and much weaker features further away whose frequencies can not be well identified. In view of the deduction that the HCl rocking modes, ν_β, occur at about 50 cm^{-1}, it is logical to assign the fundamental, ν_s, to the peak at 1850 cm^{-1}, and to assign the shoulders 50 cm^{-1} away from the peak to the sum and difference bands $\nu_s + \nu_\beta$, and $\nu_s - \nu_\beta$.

The ratio of the fundamental, ν_s, frequencies for HCl and DCl is 2480/1850 = 1.340, which indicates that the anharmonicity of these modes is greater than that of the OH stretching mode in ice, where the ratio is 1.354 (17), but is not extraordinarily large.

Relative Intensities

In Table 1 the frequencies and approximate relative integrated intensities of the various bands in the spectrum of $(CH_3)_2O$...HCl are presented. The relative intensities of the bands above 850 cm^{-1} should be quite reliable because they were all measured from a single spectrum of a mixture of 20 Torr of $(CH_3)_2O$ plus 8 atm of HCl at 10 °C. The relative intensities of the bands below 850 cm^{-1} must be regarded as approximate. They were determined using an equilibrium constant at 0 °C of 1.13, standard state 1 atm, which was calculated from the mean enthalpy and entropy of formation reported by Govil, Clague, and Bernstein (18). The mean enthalpy of formation was used to determine the temperature dependence of the

TABLE 1. Frequencies and relative intensities of absorption bands in $(CH_3)_2O...HCl$

ν/cm^{-1}	Assignment	Intensity (Arbitrary units)
2675 2574 2480 ~2360	HCl stretch, ν_s	1000
1465	CH_3 deformation	58
1248	CH_3 rock	5
1171 1097	CH_3 rock + asymmetric CO stretch	180 130
912	Symmetric CO stretch	100
790	$2\nu_b$, $2\nu_t$	5
570 525 470	O...H—Cl deformation ν_b, ν_t	30*
415	C—O—C deformation	
119	O---H stretch ν_σ	2.5

*The intensity was measured for $(CD_3)_2O...HCl$.

equilibrium constant. However, the errors on the values of the enthalpy and entropy of formation (18) allow the equilibrium constant at 0 °C to lie between 0.15 and 9.5, standard state 1 atm. Thus the relative intensities quoted may be considerably in error, because widely differing pressures of the component gases were required for the different bands and the intensities obtained markedly reflect the value of the equilibrium constant that was used. It should also be noted that the relative intensity of the O...H—Cl deformation modes was determined for $(CD_3)_2$-O...HCl. The limited part of the band that was observable in $(CH_3)_2O...HCl$ indicated that the intensity was approximately the same in the two systems.

We thank the National Research Council of Canada for their support of this work and the award of a bursary to M.V.F.

1. GEORGE C. PIMENTEL and A. L. MCCLELLAN. The hydrogen bond. W. H. Freeman and Co., San Francisco, 1960. p. 68.
2. J. E. BERTIE and D. J. MILLEN. J. Chem. Soc. 497 (1965).
3. J. E. BERTIE and D. J. MILLEN. J. Chem. Soc. 514 (1965).
4. L. P. BELOZERSKAYA and D. N. SHCHEPKIN. Opt. Spectrosc. Suppl. **3**, 146 (1968).
5. J. LECALVÉ, PIERRE GRANGE, and JEAN LASCOMBE. C. R. (Paris), **261**, 2075 (1965).
6. J. E. BERTIE and M. G. NORTON. Can. J. Chem. **48**, 3889 (1970).
7. J. E. BERTIE and D. A. OTHEN. Can. J. Chem. **50**, 3443 (1972).
8. J. LE CALVÉ, P. GRANGE, and J. LASCOMBE. C. R. (Paris), **260**, 6065 (1965).
9. N. SHEPPARD. *In* Hydrogen bonding. *Edited by* D. Hadzi. Pergamon Press, 1958.
10. G. HERZBERG. Infrared and Raman spectra. D. Van Nostrand Co. Inc., New Jersey, 1959.
11. E. B. WILSON, J. C. DECIUS, and P. C. CROSS. Molecular vibrations. McGraw-Hill, New York, 1955.
12. JEAN-PIERRE PERCHARD, MARIE-THÉRÈSE FOREL, and MARIE-LOUISE JOSIEN. J. Chim. Phys. **61**, 632 (1964).
13. D. N. SHCHEPKIN and L. P. BELOZERSKAYA. Opt. Spectrosc. Suppl. **3**, 101 (1968).
14. T. UEDA and T. SHIMANOUCHI. J. Mol. Spectrosc. **28**, 350 (1968).
15. J. C. LASSEGUES, P. V. HUONG, and J. LASCOMBE. Presented at the International Conference on Hydrogen Bonding, Ottawa, August, 1972.
16. J. C. LASSEGUES and P. V. HUONG. Chem. Phys. Lett. **17**, 444 (1972).
17. J. E. BERTIE and E. WHALLEY. J. Chem. Phys. **40**, 1646 (1964).
18. G. GOVIL, A. D. H. CLAGUE, and H. J. BERNSTEIN. J. Chem. Phys. **49**, 2821 (1968).

Studies on Lactoperoxidase. VI. Kinetics of the Oxidation of *p*-Cresol by Compound II[1]

R. James Maguire and H. Brian Dunford
Department of Chemistry, University of Alberta, Edmonton 7, Alberta
Received February 1, 1972[2]

The kinetics of the oxidation of *p*-cresol by compound II of lactoperoxidase have been studied over the p*H* range 2.1–11.2 by the stopped-flow technique. The reaction is kinetically first-order with respect to *p*-cresol over the entire p*H* range. Use is made of the diffusion-controlled limit that can be placed on a bimolecular rate constant to show that *p*-cresol reacts in the unionized form. The complexity of the p*H*-rate profile is discussed in terms of acid dissociation constants of groups in the enzyme and the ionization of the substrate.

Les cinétiques de l'oxydation du *p*-crésol par le composé II de la lactoperoxydase ont été étudiées dans l'intervalle de p*H* de 2.1–11.2, par la technique du "flow stop". La réaction est d'ordre un par rapport au *p*-crésol dans tout ce domaine de p*H*. On a utilisé la diffusion contrôlée limite qui peut être inclus dans une constante de vitesse bimoléculaire pour montrer que le *p*-crésol réagit sous forme non ionisée. La complexité du profil de vitesse en fonction du p*H* a été discutée en fonction des constantes de dissociation acide des groupes de l'enzyme et de l'ionisation du substrat. [Traduit par le journal]

Can. J. Chem., 51, 1721 (1973)

Studies on the enzyme lactoperoxidase from this laboratory have been directed toward the elucidation of the structure–activity relationship of the active site of the native enzyme and its compounds formed by reaction with hydrogen peroxide (1–4) and simulation of the action of thyroid peroxidase in the thyroid gland, which is involved in the production of thyroxine through coupling of iodinated tyrosine residues (5). The present study was undertaken with a view of determining the effect of a neutral molecule on the reduction of compound II to the native enzyme. *p*-Cresol was chosen because of the remarkable efficiency of oxidation of phenols by peroxidase systems, and because of its resemblance to the amino acid tyrosine, while having fewer acid–base groups.

Experimental

Lactoperoxidase (LP) was obtained and purified as described previously (5). Practical grade *p*-cresol was obtained from Eastman Organic Chemicals and was purified by sublimation.[3] All other substances were of reagent grade and were used without further purification. Kinetic investigations were carried out using a stopped-flow apparatus described previously (5, 6), with the formation of compound II accomplished as described in the investigation of the kinetics of the reaction between compound II and iodide ion (5). All measurements were made at 25° on solutions of total ionic strength 0.05. The acid dissociation constant of *p*-cresol at this value of ionic strength was determined spectrophotometrically to be 10.11 ± 0.01, in agreement with the value 10.10 obtained by the use of Davies' equation (7) together with the value at zero ionic strength found by Chen and Laidler (8).

The experimental conditions were such that there was a large excess of *p*-cresol over compound II. Thus pseudo first-order conditions were obtained, and the value of the second-order rate constant of the reaction was obtained by dividing the value of the pseudo first-order rate constant by the concentration of *p*-cresol. At p*H* values below 2 and above 11.3, the enzyme denatured. Overlapping buffer systems were used to check for buffer effects on the value of the second-order rate constant, k, but no buffer effects were observed.

Results and Discussion

Values of the apparent second-order rate constant, k, obtained at different p*H* values are shown in Fig. 1. By the use of Dixon's rules of p*H* effects in enzyme kinetics (9), which demonstrate that inflections in such curves are the result of kinetically important ionizations occurring in the reacting species, it is seen that the variation of k with p*H* depends on the acid dissociation of the substrate at p*H* 10 and the ionization of three kinetically important enzyme groups having pK_a values of around 2, 6, and 9.5. The minimum reaction scheme consistent with the data is given by Scheme 1, in which P-II, HP-II, H_2P-II, and H_3P-II are the four

[1]This work was supported by the National Research Council of Canada.
[2]Revision received January 16, 1973.
[3]We are grateful to Dr. M. K. Evett for this purification.

Can. J. Chem. Downloaded from www.nrcresearchpress.com by 210.87.254.6 on 09/05/12
For personal use only.

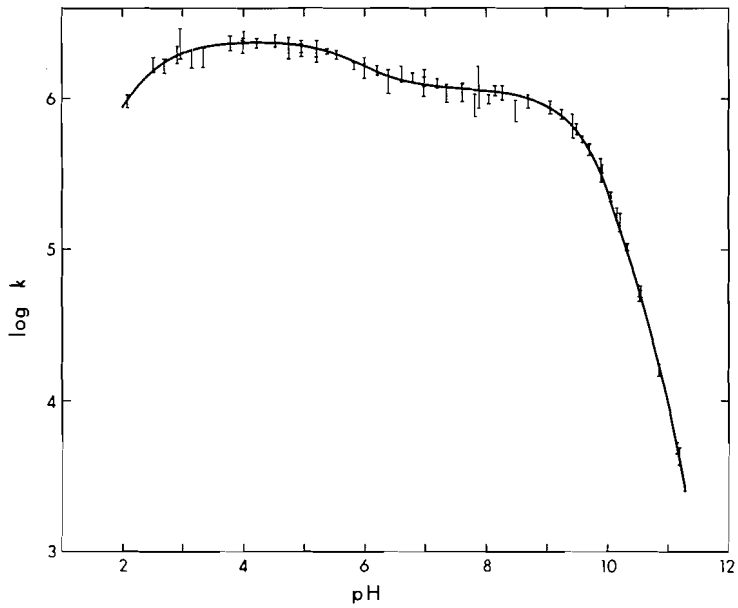

FIG. 1. A plot of log k *vs.* pH for the reaction between LP-II and *p*-cresol. The solid line is a curve calculated by computer for the fitting of the data to eq. 1. The error bars represent standard deviations of the rate constant k, which has units of M^{-1} s^{-1}.

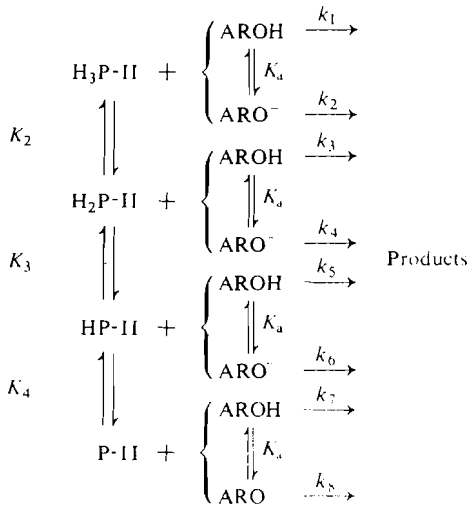

SCHEME 1

kinetically distinct states of protonation of compound II, the K's are molecular or macroscopic acid dissociation constants, and the k's are bimolecular rate constants.

The corresponding kinetic expression is given by eq. 1. The smooth curve in Fig. 1 shows the best fit to eq. 1, and is defined by the parameters of a least squares fit in Table 1. The value of pK_a obtained in this way is different from the spectrophotometric results; however, a second kinetic analysis with a fixed value of pK_a = 10.11 produced only small changes in the other parameters, and a good fit to the experimental data, so that the difference in pK_a values may not be significant.

It is possible to arrive at a conclusion regarding the nature of the reactive form of *p*-cresol. In order to decide which of the kinetically equivalent pathways included in each of the two non-zero rate terms in eq. 1 given in Table 1 is responsible for the reaction rate, it is necessary to make use of the maximum value that can be placed on the rate constant of a bimolecular process, about 10^{10} M^{-1} s^{-1}. Since $K_a/K_2 = 10^{-8}$ and $K_a/K_3 = 3 \times 10^{-5}$, it follows that in order to account for the observed rate the values of k_2 and k_4 would have to exceed 10^{10} M^{-1} s^{-1}, and therefore the predominant pathways are not those denoted by the rate constants k_2 and k_4, but by k_3 and k_5. Thus the protonated forms of lactoperoxidase compound II appear to react with the neutral form of *p*-cresol.

This work can be compared to the reaction between LP-II and iodide ion, in which the second-order rate constant varies with unit

Can. J. Chem. Downloaded from www.nrcresearchpress.com by 210.87.254.6 on 09/05/12
For personal use only.

$$[1]\quad k = \frac{\frac{k_1[H^+]^4}{K_aK_2K_3K_4} + \left(k_3 + \frac{k_2K_a}{K_2}\right)\frac{[H^+]^3}{K_aK_3K_4} + \left(k_5 + \frac{k_4K_a}{K_3}\right)\frac{[H^+]^2}{K_aK_4} + \left(k_7 + \frac{k_6K_a}{K_4}\right)\frac{[H^+]}{K_a} + k_8}{\left(1 + \frac{[H^+]}{K_4} + \frac{[H^+]^2}{K_3K_4} + \frac{[H^+]^3}{K_2K_3K_4}\right)\left(1 + \frac{[H^+]}{K_a}\right)}$$

TABLE 1. Parameter values* and standard deviations for the variation of k with pH, obtained by non-linear least squares fit of data to eq. 1

k_1	0†
$k_3 + \frac{k_2K_a}{K_2}$	$(2.30 \pm 0.05) \times 10^6$
$k_5 + \frac{k_4K_a}{K_3}$	$(1.09 \pm 0.03) \times 10^6$
$k_7 + \frac{k_6K}{K_4}$	0†
k_8	0†
pK_2	2.3 ± 0.1
pK_3	5.8 ± 0.1
pK_4	9.7 ± 0.1
pK_a	10.3 ± 0.1

*Rate constants in units of M^{-1} s^{-1}.
†Zero within experimental error.

negative slope over the experimental pH range, from 4.2×10^6 M^{-1} s^{-1} at pH 2.9 to 2.6×10^{-1} M^{-1} s^{-1} at pH 10.1 (5). The second-order rate constant for *p*-cresol oxidation by LP-II is appreciably greater than the rate constant for iodide oxidation over most of the pH range, except for the low pH region. The radical difference in the pH-rate profiles for these two substrates (three enzyme pK_a's observed in *p*-cresol oxidation, none in the range 2.9–10.1 for iodide oxidation) may be a result of the lack of steric interactions between iodide ion and LP-II, or the result of the operation of a different mechanism. Since *p*-cresol reacts in its unionized form, electrostatic interactions are not a factor in its oxidation.

A comparison with the pH-rate profile of the reaction of compound II of horseradish peroxidase with *p*-cresol shows several differences in detail (10). The analogous comparisons between lacto- and horseradish peroxidases with respect to (*a*) the compound II reactions with iodide (5, 11) and (*b*) cyanide and fluoride binding to the native enzymes (1, 2, 12) also show marked differences, indicating that generalizations about properties of various peroxidases must be made with caution.

1. D. DOLMAN, H. B. DUNFORD, D. M. CHOWDHURY, and M. MORRISON. Biochem. **7**, 3991 (1968).
2. R. SEGAL, H. B. DUNFORD, and M. MORRISON. Can. J. Biochem. **46**, 1471 (1968).
3. R. J. MAGUIRE and H. B. DUNFORD. Can. J. Biochem. **49**, 666 (1971).
4. R. J. MAGUIRE, H. B. DUNFORD, and M. MORRISON. Can. J. Biochem. **49**, 1165 (1971).
5. R. J. MAGUIRE and H. B. DUNFORD. Biochem. **11**, 937 (1972).
6. B. B. HASINOFF and H. B. DUNFORD. Biochem. **9**, 4930 (1970).
7. C. W. DAVIES. J. Chem. Soc. 2093 (1938).
8. D. T. Y. CHEN and K. J. LAIDLER. Trans. Faraday Soc. **58**, 480 (1962).
9. M. DIXON and E. C. WEBB. *In* Enzymes. 2nd ed. Longmans, Green, and Co., London. 1964. pp. 116–145.
10. J. E. CRITCHLOW and H. B. DUNFORD. J. Biol. Chem. **247**, 3703 (1972).
11. R. ROMAN, H. B. DUNFORD, and M. EVETT. Can. J. Chem. **49**, 3059 (1971).
12. W. D. ELLIS and H. B. DUNFORD. Biochem. **7**, 2054 (1968).

Can. J. Chem. Downloaded from www.nrcresearchpress.com by 210.87.254.6 on 09/05/12
For personal use only.

The Synthesis of a 5,6-Dihydropyridazine[1,2]

P. DE MAYO AND M. C. USSELMAN

Photochemistry Unit, Department of Chemistry, The University of Western Ontario, London, Ontario

Received October 10, 1972

The synthesis of 3,6-dimethyl-6-*n*-butyl-5,6-dihydropyridazine, the first 5,6-dihydropyridazine, is described. On heating it undergoes a [1,5] sigmatropic hydrogen rearrangement to give the corresponding 1,6-dihydropyridazine.

On décrit la première synthèse d'une dihydro-5,6 pyridazine, la diméthyl-3,6 butyl-6. Par chauffage, elle se transforme en dihydro-1,6 pyridazine par un réarrangement sigmatropique [1,5] d'hydrogène.
[Traduit par le journal]

Can. J. Chem., 51, 1724 (1973)

Can. J. Chem. Downloaded from www.nrcresearchpress.com by 210.87.254.40 on 09/05/12
For personal use only.

Introduction

In connection with our studies on the mechanism of photoannelation, specifically the addition of cyclic enones to acetylenes (for a general discussion, see ref. 1) we required a 5,6-dihydropyridazine. This paper describes the first synthesis of a member of this class: 3,6-dimethyl-6-*n*-butyl-5,6-dihydropyridazine (**1**); its photochemical properties are discussed in the following paper (17).

At the outset of our investigations the only 5,6-dihydropyridazine mentioned in the literature (2) was a substance tentatively assigned structure **2**. This was prepared by the action of cyclopropene on diphenyldiazomethane. The main basis for the structural designation was the u.v. spectrum (λ_{max} 334 nm) but, as will be seen, this criterion actually eliminates **2** from consideration as a possible structure. The alternative **3**, also considered by the authors, seems at present the more likely candidate. Recently Gorse and Binkley (3) have postulated a member

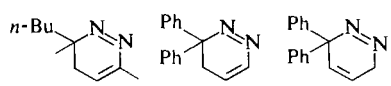

1 **2** **3**

of the related system, 1,9-dihydrophthalazine, as an intermediate in a complex sequence following the photolysis of benzophenone azine. Thus, although dihydropyridazines with the saturated centers at other than the 5,6 positions were well known there appeared to be no authenticated derivative available for our photochemical study, and a direct synthesis was therefore undertaken.

Gillis and Hagarty (4) have developed a convenient route to α,β-unsaturated azo compounds, but their method is not directly applicable to the synthesis of cyclic analogs. The methods used by Closs and Heyn (5) for the synthesis of the 3*H*-pyrazole system appeared more promising. The sequence depicted in Scheme 1 is illustrative, and consists of the bromination of a 2-pyrazoline followed by base-induced dehydrobromination. The product was a mixture of 3*H*-pyrazoles. In an alternative procedure the 1-*p*-toluenesulfonyl derivative of the pyrazoline on treatment with alkoxide ion eliminated the elements of *p*-toluenesulfonic acid to give essentially the same pyrazole mixture.

The dihydropyridazine selected as the object of synthesis was **1**. With the substitution–elimination procedures outlined in mind the tetrahydropyridazine (**7**) then became the immediate objective. This could be obtained from easily available starting materials.

Condensation of acetonylacetone with hydrazine has been shown to give, instead of the expected dihydropyridazine, a dimeric product **6** (6). Under alkylating or arylating conditions, this substance behaves as would be expected of the monomer (6) indicating a ready reversibility. By the method used (7) for the 6-phenyl substituted analog, but employing lithium butyl (2 equiv), **7** was obtained in 50% yield. The stoichiometry of the reaction suggests that the lithium butyl is instrumental in effecting the dissociation of the dimeric **6**.

[1]Dedicated to Professor E. Lederer on the occasion of his 65th birthday.

[2]Publication No. 62 from the Photochemistry Unit, The University of Western Ontario, London, Ontario. Photochemical Synthesis, Pt. 48.

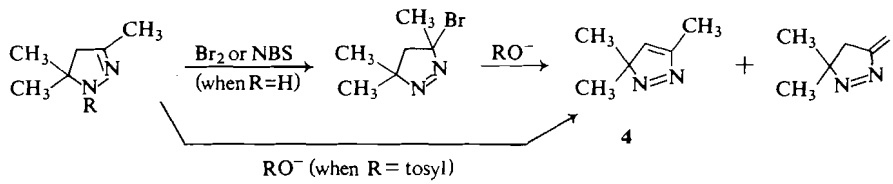

SCHEME 1

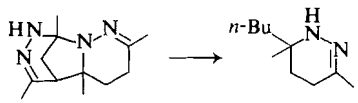

6 7

With the tetrahydro derivative **7** available, a number of direct dehydrogenation procedures were attempted. Mild reagents (mercuric oxide, phenanthraquinone at room temperature) led to essentially unchanged starting material, whilst more powerful conditions (chloranil, phenanthraquinone at 150°) led to intractable and uninspiring tars. An attempt to prepare the *N*-tosyl derivative by the method of Closs and Heyn (5) was similarly discouraging, and attention was then turned to the halogenation–dehydrohalogenation procedure.

Halogenation at the 3-position of 2-pyrazolines was achieved by Closs and Heyn (5) using bromine or *N*-bromosuccinimide. For the present reaction the hypohalites proved to be superior reagents. The tetrahydropyridazine (**7**) in benzene solution reacted very rapidly with *tert*-butylhypochlorite to give the two diastereoisomers of 6-*n*-butyl-3-chloro-3,6-dimethyl-3,4-5,6-tetrahydropyridazine (**5***a*). These could be separated by chromatography. The structures of the diastereoisomers (excluding stereochemical assignments) followed from the n.m.r. data. Further, the u.v. absorption spectrum excluded alternative isomeric possibilities, such as **8**, since an azo grouping was clearly present (λ_{max} 390 nm).

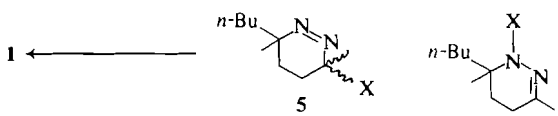

5

a X = Cl
b X = Br
c X = OMe

8

The chloro-compounds were solvolytically stable since the n.m.r. of the less polar diastereoisomers in deuteriochloroform solution showed no change after 48 h at 80°, thus precluding the interconversion of the diastereoisomers. Further, the substances were resistant to dehydrochlorination when treated with an equimolar amount of sodium methoxide in refluxing methanol. The base did not induce interconversion of the diastereoisomers when a pure diastereoisomer was used.

The lack of reactivity of **5***a* to mild dehydrohalogenating conditions suggested the preparation of **5***b*. This was readily achieved under similar conditions using *tert*-butyl hypobromite. The reaction was facile and the spectral properties of the isolated **5***b* closely resembled those of **5***a*. There was, however, a marked difference in stability, and the mixture decomposed rapidly in air. For this reason it was always prepared immediately before use.

A number of dehydrohalogenating agents were used without success (silver oxide in pyridine, sodium hydride, potassium *tert*-butoxide in dimethylsulfoxide) and a study of the complex mixture obtained showed no initial accumulation of any one substance, and adumbrated the instability of **1**. Dehydrohalogenating agents which could also act as nucleophiles led to overall substitution. For instance, reaction of **5***b* with sodium methoxide in refluxing methanol gave **5***c* in good yield,[3] whilst silver acetate in benzene gave a mixture in which the acetate moiety had been incorporated.

Conversion of **5***b* to **1** was ultimately achieved in reasonable yield (15–20%) using 1,5-diazabicyclononene (DABN). Reaction in an excess (1.3 mol) of DABN in tetrahydrofuran at room temperature gave **1** as the only major initial product, but the yield was strongly dependent on reaction time. A maximum was reached after 8–10 h under these conditions, after which the yield declined. At maximum yield some 30% of the starting material remained unchanged. The absence of the exomethylene isomer of **1** is

[3]The substance appeared to be homogeneous, but may well have been the expected mixture of diastereoisomers having closely similar physical properties.

Can. J. Chem. Downloaded from www.nrcresearchpress.com by 210.87.254.40 on 09/05/12
For personal use only.

Can. J. Chem. Downloaded from www.nrcresearchpress.com by 210.87.254.40 on 09/05/12
For personal use only.

surprising, but may be due to its further reaction and transformation to intractable material.

The n.m.r. spectrum of **1** in deuteriochloroform showed a high field methyl signal at 1.18 p.p.m. There was also a three-proton signal for a vinyl methyl group (2.27 p.p.m.) and a single vinyl proton at 5.2 p.p.m. Double irradiation revealed that the vinyl proton and the vinyl methyl protons were both coupled to the two allylic protons as well as to each other. The mass spectrum showed the expected molecular ion, but the spectrum could only be interpreted in terms of the thermal rearrangement described below, and so only indirectly supported the structural allocation.

The u.v. spectrum justifies a brief discussion. The absorption maximum of what is presumably the $\pi \rightarrow \pi^*$ transition at 268 nm is of the same intensity and of slightly lower energy than the corresponding transition in **4** (257 nm). Analogy with the carbocyclic equivalents would have led, perhaps, to the expectation of a somewhat larger shift in the same direction. The $n \rightarrow \pi^*$ transition at 447 nm, however, appears at much longer wavelength than the apparently corresponding transition in **4** which is at 350 nm. Both these values are to be compared with that found (386 nm) for the open-chain substance **9** (4). In fact the only relevant azo substance known to us absorbing at such long wavelengths is *cis*-azo-

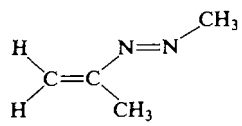

9

10

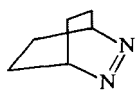

11

2-methyl-2-propane (8) which has a low intensity absorption band at 447 nm. Since *cis*-azomethane absorbs at 353 nm (9) and **10** and **11** have λ_{max} at 342 (10) and 378 nm (11), respectively, the difference in the case of the first substance for lack of a better interpretation would seem to be attributed to the distortion from planarity induced by the bulky groups. It is difficult to see any relevance of this phenomenon to our present problem since both **1** and **4** should be close to planar. Little change can be expected in the energy of the non-bonding electrons and such change as occurs should surely be lowered in the geometry defined by **1** rather than **4** by something like 0.75 eV.[4]

An alternative possiblity is that the bands do not represent the same transition, and that relevant bands may be submerged under the other absorption, or be of very low intensity.[5] The observation by Arnold and his co-workers (13) in a study of five-, six- and seven-membered cyclic 1,4-diaza-1,3-dienes of abnormal spectral changes may be relevant. They found that the long wavelength absorption maximum (normally attributed to an $n \rightarrow \pi^*$ transition) of 2,3-diphenyl-5,6-dihydropyrazine (**12**) to be at significantly longer wavelength than either of the related five- or seven-membered equivalents.

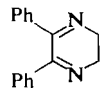

12

These authors have attributed this long wavelength absorption not to an $n \rightarrow \pi^*$ transition, but to a transition between the ground state 5,6-dihydropyrazine and an electronic excited state of the ring-opened enediimine, a transition not available to the other ring systems.

Thermal Rearrangement

When **1** is dissolved in benzene or *n*-hexane, the solution degassed by the freeze–pump–thaw cycle, and heated to 125°, it undergoes a smooth sigmatropic rearrangement to give **13** quantita-

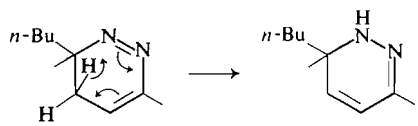

1 **13**

tively. This substance, a 1,6-dihydropyridazine is also unstable to air and the structure assigned to it rests essentially on spectroscopic data and on its presumed mode of genesis.

The n.m.r. spectrum shows absorption for the

[4]Subsequent to the submission of this paper, calculations by Baird *et al.* have established a correlation between the angle subtended by an azo group and the energy of the $^1(n,\pi^*)$ transition (18). On the basis of this correlation, the "anomalous" long wavelength absorptions of **1** and *cis*-azo-2-methyl-2-propane may be attributed, not to out-of-plane distortion, but to in-plane distortion, and a consistent pattern of $n \rightarrow \pi^*$ azo transitions results.

[5]For a discussion of $n \rightarrow \pi^*$ transitions in the azo group, see ref. 12.

Can. J. Chem. Downloaded from www.nrcresearchpress.com by 210.87.254.40 on 09/05/12
For personal use only.

protons of a vinyl methyl group at 2.0 p.p.m. Two vinyl protons were observed at 5.6 and 5.8 p.p.m. with a coupling constant of 10 Hz. The vinyl methyl protons did not appear to be coupled with either of the vinyl protons and appeared as a sharp singlet. The presence of the *cisoid* ethylene moiety implies the transfer of one hydrogen from the allylic methylene group in **1**, and the terminus for its transfer should be the nitrogen in the β position. Indeed NH absorption was visible in the n.m.r. spectrum at approximately 5.7 p.p.m. (broad). In agreement the i.r. spectrum showed strong NH stretching absorption near 3250 cm^{-1} (broad). The character of the u.v. absorption was completely changed, the resolved $\pi \rightarrow \pi^*$ and $n \rightarrow \pi^*$ bands of **1** being replaced by general absorption from 225 nm (ε 2000) extending beyond 350 (ε 50) to 400 nm.

The sigmatropic [1,5] suprafacial hydrogen shift leading from **1** to **13** is thermally allowed and has ample general analogy (14). Rearrangements in six-membered rings appear to be rare, but a [1,5] methyl shift has recently been reported (15).

In the determination of the mass spectrum of **1** it appears that rearrangement, at least in good proportion, must precede fragmentation. The elimination of nitrogen appears to be a minor process as in the formation of methyl acetylene. On the other hand acetonitrile and acetylene formation would seem to be important, as does the formation of valeronitrile (and its further fragmentation products (16)). Cleavage of the C_4 side chain also occurs, and the only significant peak not susceptible to ready interpretation is that at *m/e* 115.

Experimental

Proton spectra were obtained with Varian T-60 and HA-100 spectrometers. I.r. spectra were run on Beckman IR 10 and 20A spectrometers and a Carey 14 was used for obtention of the u.v. spectra. Mass spectra were obtained with a Varian M66 spectrometer.

Unless otherwise stated, all solvents were Fischer Spectranalyzed grade, and were used without further purification.

3,6-Dimethyl-6-n-butyl-2,3,4,5-tetrahydropyridazine (7)

The compound was prepared as previously described (6). It is stable for prolonged periods when stored at 0° under nitrogen. After repeated brief exposures to the atmosphere for withdrawal of samples, the compound assumes a pale yellow color which can be removed by careful redistillation. Upon appearance of the yellow color, the compound is no longer suitable for reaction with the *tert*-butylhypohalites because dark colored impurities are formed. These catalyze the decomposition of the halo products, and make their isolation in pure form exceedingly difficult. The attempted preparation of the *p*-toluenesulfonate derivative by the method of Closs and Heyn (5) gave a complex mixture of products.

3-Chloro-3,6-dimethyl-6-n-butyl-3,4,5,6-tetrahydropyridazine (5a)

To 7 (1.17 g) in benzene (5 ml) at 10° was added dropwise *tert*-butyl hypochlorite (0.77 g, Frinton Laboratories). The solution immediately became bright yellow. After allowing to warm to room temperature the solvent was removed under reduced pressure and the residual mixture separated by chromatography on silica gel (60–120 mesh; 60 g) and elution with ether–benzene (1:19). Two fast-running yellow substances were collected; the first (**A**) in 49% yield (0.7 g) and the second (**B**) in order of elution in 42% (0.6 g) yield. Both gave a positive Beilstein test. The substances were further purified by bulb-to-bulb distillation at 50°/0.2 mm. The substance **A** had ν_{max} ($CHCl_3$) 2960, 2940, 2865, 1460, 1380, and 868 cm^{-1}; δ ($CDCl_3$) 1.90 (3H, s), 1.32 (3H, s), 0.94 (3H, m), 2.20–1.20 (10H, complex); λ_{max} (C_6H_{12}) 385 nm (ε 75).

The substance **B** had ν_{max} ($CHCl_3$) 2970, 2940, 2870, 1450, 1385, and 865 cm^{-1}; δ ($CDCl_3$) 1.98 (3H, s), 1.22 (3H, s), 0.94 (3H, m), 2.20–1.20 (10H, complex); λ_{max} (C_6H_{12}) 390 nm (ε 80).

Anal. mixture of isomers **A** and **B**. Anal. Calcd. for $C_{10}H_{19}N_2Cl$: C, 59.22; H, 9.47; N, 13.81; Cl, 17.50. Found: C, 59.48; H, 9.60; N, 13.82; Cl, 17.40.

The substance **B** was recovered essentially unchanged when refluxed in methanol solution containing 1 equiv of sodium methoxide for 30 min under nitrogen.

3-Bromo-3,6-dimethyl-6-n-butyl-3,4,5,6-tetrahydropyridazine (5b)

The procedure followed was that employed for the chloro-isomers with the substitution of *tert*-butyl hypobromite for the hypochlorite. The combined yield of stereoisomers was 60–70% after bulb-to-bulb distillation, the lower yield being attributed to the greatly increased instability of the bromine-substituted diastereoisomers which precluded the obtention of analytical data.

The faster-running isomer had ν_{max} ($CHCl_3$) 2955, 2935, 2865, 1445, 1380, and 865 cm^{-1}; δ ($CDCl_3$) 2.17 (3H, s), 1.34 (3H, s), 0.94 (3H, m), 2.4–1.2 (10H, complex). The slower-running isomer had ν_{max} ($CHCl_3$) 2955, 2925, 2855, 1440, 1370, and 860 cm^{-1}; δ ($CDCl_3$) 2.19 (3H, s), 1.19 (3H, s), 0.94 (3H, m), 2.4–1.2 (10H, complex).

3,6-Dimethyl-3-methoxy-6-n-butyl-3,4,5,6-tetrahydropyridazine (5c)

To the freshly-prepared slower-running isomer of **5***b* (70 mg) was added an equimolar quantity of sodium methoxide (20 mg) in methanol (2 ml) and the mixture was heated to reflux under nitrogen for 5 h. T.l.c. showed one major product running slower than **5***b* (eluent: ether–benzene, 1:9). On preparative t.l.c. the product was isolated in 60% yield (eluent: ether–benzene, 1:9). It had δ ($CDCl_3$) 3.52 (3H, s), 1.40 (3H, s), 1.27 (3H, s), 0.94 (3H, m), 2.0–1.2 (10H, complex). Under the same conditions the faster-running isomer gave the same product as identified by n.m.r.

The diastereoisomeric mixture when treated with silver acetate in benzene at 45° for 48 h gave three products in poor yield. Two of these contained acetyl groups, as judged by the n.m.r. spectra. They were not further studied.

*3,6-Dimethyl-6-n-butyl-5,6-dihydropyridazine (**1**)*

To a freshly-prepared diastereoisomeric mixture of **5***b* (200 mg) in 2 ml tetrahydrofuran, which had been freshly distilled from sodium borohydride, was added 1,5-diazabicyclononene (200 mg; 1.3 mol equiv) in 2 ml tetrahydrofuran. The mixture was allowed to stand under nitrogen for 10 h during which time the base hydrobromide separated as long needles. The tetrahydrofuran was removed under reduced pressure, the product taken up in benzene and separated by preparative t.l.c. (eluent: ether–benzene, 1:9). In larger scale preparations the product could be isolated by column chromatography on silica gel (60–120 mesh; 60:1) using ether–benzene (1:19) as eluent. The yields after bulb-to-bulb distillation of the product (50°/0.1 mm) were 15–20%. The product had ν_{max} ($CHCl_3$) 2980, 2960, 2885, 1675, 1470, and 1390 cm^{-1}; δ ($CDCl_3$) 5.2 (1H, m), 2.27 (3H, m), 2.0–1.6 (2H, m), 1.6–1.2 (6H, complex), 1.18 (3H, s), 0.94 (3H, m); λ_{max} (C_6H_{12}) 268 nm (ε 2100), 447 nm (ε 150); *m/e* (70 eV) 166 (mol ion) (8.6%), 125 (48), 115 (44), 58 (87), 57 (58), 56 (97), 55 (63), 43 (100), 41 (75), 39 (45).

Anal. Calcd. for $C_{10}H_{18}N_2$: C, 72.24; H, 10.91. Found: C, 72.26; H, 10.96.

*3,6-Dimethyl-6-n-butyl-1,6-dihydropyridazine (**13**)*

The 5,6-dihydropyridazine (30 mg) in C_6D_6 (0.4 ml) with hexamethyldisiloxane as reference was sealed in an n.m.r. tube after degassing. A solution (1 mg/ml) in cyclohexane or hexadecane was similarly sealed in a u.v. cell. The solutions were heated to 125° in the dark for 12 h, at the end of which time conversion to the 1,6-dihydro compound appeared complete. The spectroscopic details are given in the discussion. The compound decomposed rapidly when exposed to the atmosphere, thus precluding analysis.

1. P. DE MAYO. Acc. Chem. Res. 41 (1971).
2. K. B. WIBERG and W. J. BRADLEY. J. Am. Chem. Soc. **82**, 6375 (1960).
3. J. GORSE and R. W. BINKLEY. J. Org. Chem. **37**, 575 (1972).
4. B. T. GILLIS and J. D. HAGARTY. J. Am. Chem. Soc. **87**, 4576 (1965).
5. G. L. CLOSS and H. HEYN. Tetrahedron, **22**, 463 (1966).
6. P. DE MAYO, J. B. STOTHERS, and M. C. USSELMAN. Can. J. Chem. **50**, 612 (1972).
7. C. G. OVERBERGER and G. KESSLIN. J. Org. Chem. **27**, 3898 (1962).
8. T. MILL and R. S. STRINGHAM. Tetrahedron Lett. 1853 (1969).
9. R. F. HUTTON and C. STEEL. J. Am. Chem. Soc. **86**, 745 (1964).
10. S. G. COHEN, R. ZAND, and C. STEEL. J. Am. Chem. Soc. **83**, 2895 (1961).
11. S. G. COHEN and R. ZAND. J. Am. Chem. Soc. **84**, 586 (1962).
12. R. DITCHFIELD, J. E. DEL BENE, and J. A. POPLE. J. Am. Chem. Soc. **94**, 703 (1972).
13. D. R. ARNOLD, V. Y. ABRAITYS, and D. MCLEOD. Can. J. Chem. **49**, 923 (1971).
14. R. B. WOODWARD and R. HOFFMAN. The conservation of orbital symmetry. Academic Press, Germany, 1970.
15. C. W. SPANGLER and D. L. BOLES. J. Org. Chem. **37**, 1020 (1972).
16. Index of Mass Spectral Data. Am. Soc. Test. Materials. 1969.
17. P. DE MAYO and M. C. USSELMAN. Can. J. Chem. This issue.
18. N. C. BAIRD, P. DE MAYO, J. R. SWENSON, and M. C. USSELMAN. Chem. Commun. In press.

Can. J. Chem. Downloaded from www.nrcresearchpress.com by 210.87.254.40 on 09/05/12
For personal use only.

The Photochemistry of a Dihydropyridazine[1]

P. DE MAYO AND M. C. USSELMAN

Photochemistry Unit, Department of Chemistry, The University of Western Ontario, London, Ontario

Received October 10, 1972

Irradiation of a 5,6-dihydropyridazine in either the n → π* or π → π* absorption bands results in ring-opening to the two isomeric diazatrienes expected of a concerted, electrocyclic process. Population of the triplet state of the dihydropyridazine by sensitization also results in ring-opening, but much less efficiently. The quantum yields of the two processes were found to be 0.40 ± 0.04 and 0.07 ± 0.01, respectively. The primary photoproducts, *cis,cis*- and *cis,trans*-4,5-diazatriene, isomerize thermally at temperatures greater than 20° to the *trans,cis* and *trans,trans* isomers.

L'irradiation de la dihydro-5,6 pyridazine selon les bandes d'absorption n → π* ou π → π* conduit par ouverture du cycle aux deux diazatriènes isomériques prévus par un processus électrocyclique et concerté. La population de l'état triplet de la dihydro-5,6 pyridazine par sensibilisation conduit aussi à l'ouverture du cycle mais avec une efficacité de beaucoup inférieure. Les rendements quantiques des deux processus sont égaux à 0.40 ± 0.04 et 0.07 ± 0.01, respectivement. Les photoproduits primaires, *cis,cis*- et *cis,trans*-diazatriènes-4,5 s'isomérisent thermiquement à des températures plus élevés que 20° pour donner des isomères *trans,cis* et *trans,trans*. [Traduit par le journal]

Can. J. Chem. 51, 1729 (1973)

Can. J. Chem. Downloaded from www.nrcresearchpress.com by 210.87.254.105 on 09/05/12
For personal use only.

Introduction

A 1,4-biradical (tetramethylene) has frequently been invoked as an intermediate in cyclobutane formation and rupture. In particular it is believed that the addition of triplet enones to olefins involves such an intermediate (for a general discussion, see ref. 1). Indirect information about the fate of such tetramethylenes, formed by photochemical addition, may be obtained from quantum yield data for product formation in systems where such species are believed transients (1–5, and refs. cited therein).

Interpretations drawn from such indirect information rely heavily upon analogy with systems in which tetramethylenes, singlet and triplet, are studied directly. In the case of tetramethylenes, O'Neal and Benson (6) have calculated that cyclization and cleavage (to two ethylene molecules) are approximately isoenergetic. These calculations are supported by both direct (*e.g.* ref. 7) and indirect (4) experiments.

Through studies of the photoannelation of cyclic enones with acetylenes (8) the conclusion was arrived at that a 1,4-biradical possessing a terminal π-bond does not behave significantly differently in its chemistry from a tetramethylene despite hybridization and obvious stereochemical differences. In an effort to obtain more direct information about the behavior of such a biradical we have synthesized a member of the previously unknown 5,6-dihydropyridazine series, specifically 3,6-dimethyl-6-*n*-butyl-5,6-dihydropyridazine (**1**) (9) in the hope that it would, on irradiation or thermolysis, eliminate nitrogen to generate the biradical (**2**).[2] Under none of the conditions employed was this the case however: thermally the molecule underwent a sigmatropic [1,5] hydrogen migration (9) and photochemically it rearranged. The photochemistry of this substance is described in this paper.

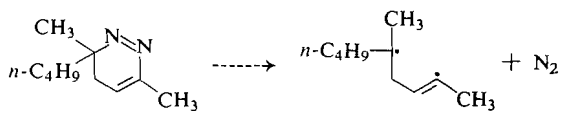

1 **2**

Results and Discussion

On direct irradiation into the n → π* band (435 nm), the dihydropyridazine rearranged to form the two aliphatic diazatrienes **3** and **4** which would be the products expected of a concerted electrocyclic process. Irradiation into the higher energy π → π* envelope (λ_{max} 267 nm) gave the same products at approximately the same rate.

[1]Publication No. 61 from the Photochemistry Unit, The University of Western Ontario, London, Ontario. Photochemical Synthesis, Part 46.

[2]Recently, the irradiation of a series of 1*H*-2,3-benzodiazepines has been reported (39). No nitrogen elimination was observed; rather, each of the diazepines was converted quantitatively to its tricyclic valence tantomer.

TABLE 1. N.m.r. data* for the 4,5-diazatrienes (3–6)

Proton†	*cis,trans* (3)	*cis,cis* (4)	*trans,trans* (5)	*trans,cis* (6)
C_6—CH_3	1.76	1.96	1.74	1.98
C_3—CH_3	2.09	2.08	1.88	1.89
C_2—H	6.85	6.87	6.51	6.50
C_1—H_c	5.39 or 5.40	5.40 or 5.39	5.40	5.40
C_1—H_t	5.55 or 5.54	5.54 or 5.55	5.57	5.57
$J_{H_{cis}}$	= 11.0 Hz			
$J_{H_{trans}}$	= 18.0 Hz			
$J_{H_{gem}}$	= 1.0 Hz			

*Chemical shifts (δ) are given in p.p.m. relative to hexamethyldisiloxane, which absorbs 6.38 Hz downfield from TMS.
†C_n refers to the carbon to which the absorbing species is attached. H_c refers to the hydrogen on C_1 which is *cis* to the hydrogen on C_2 and H_t refers to the hydrogen on C_1 *trans* to that on C_2.

The diazatrienes **3** and **4** were produced (435 nm) when any of benzene, chloroform, or cyclohexane was used as the solvent. These trienes, although stable in degassed solutions at temperatures below 20°, on exposure to atmospheric oxygen were rapidly destroyed. Consequently their structural determinations rest largely on spectroscopic data.

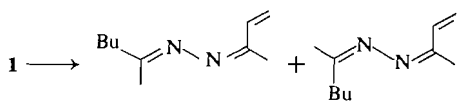

3 **4**

At temperatures above 20° isomerization occurred about the imine functions to give the two further isomers **5** and **6**. At equilibrium one isomer constituted more than 90% of the triene mixture. The assignments of stereochemistry rest

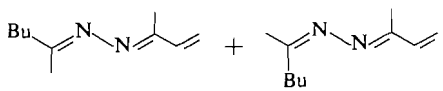

5 **6**

on the assumption that the *trans,trans* isomer is the most stable and is that favored in the equilibrium mixture. The 100 MHz n.m.r. data are summarized in Table 1.

Isomers **3** and **4** have absorptions for the C-2 proton at considerably lower fields than those for the isomers **5** and **6** which contain the central unsaturation in the *trans* configuration. The C-2 proton is deshielded by the terminal imine, an effect which has analogy in the related shift of the γ proton in α,β-unsaturated esters. However, the allylic methyl protons do not show a net deshielding due to a proximate imine, but appear at higher field when attached to a *cis* imine. Thus the C-6 methyl signals in **3** and **5** occur at about 0.2 p.p.m. to higher field than in **4** and **6** and the C-3 methyl is at higher field in **5** and **6** than in **3** and **4**. Similar chemical shift changes have been observed by Baldwin and Krueger (11) in their determination of stereochemistry of the four isomeric 3-methyl-7-isopropylhexatrienes.[3,4]

The coupling constants between the protons of the vinyl group are consistent with those expected of such a grouping (12) and are identical for all four isomers.

The n.m.r. data are consonant with the gross structures and define the stereochemistry. The gross structure is also supported by such u.v. absorption data as were obtained in the following way.

A solution of **1** in cyclohexane was irradiated in a sealed degassed quartz cell under conditions where complete conversion to **3** and **4** occurs. The mixture then showed intense end absorption with a shoulder at 235 nm (ε 12 000), and tailing to 375 nm. Thermal conversion to **6** resulted in only minor modification of the spectrum. Although a model is not available, acetone azine has absorption at 205 (ε 18 000) and 287 nm (ε 105). Addition of a *transoid* ethylenic linkage to many dienic systems frequently leads to a red shift of some 30 nm of the main ($\pi \rightarrow \pi^*$) absorption in agreement with the shift here observed with respect to the azine. The effect on a component of the $n \rightarrow \pi^*$ transition is harder to assess, and the $n \rightarrow \pi^*$ transition here,

[3]We are grateful to Professor Baldwin for copies of his spectra of these trienes.

[4]The absorptions of these vinyl methyls are unlike those observed in β,β-dimethylmethacrylate in which the methyl *cis* to the carbonyl group (10) is deshielded.

Can. J. Chem. Downloaded from www.nrcresearchpress.com by 210.87.254.105 on 09/05/12
For personal use only.

Can. J. Chem. Downloaded from www.nrcresearchpress.com by 210.87.254.105 on 09/05/12
For personal use only.

although not resolved, is probably contributing to the long wavelength absorption.

Evidently the most satisfactory proof of gross structure would be by synthesis, but attempts in this direction were unsuccessful. It was, however, possible to substantiate the gross structure of the diazatrienes chemically, as follows.

2,4-Dinitrophenylhydrazine in diglyme was added anaerobically to a solution of **3** and **4** and the mixture heated. From this reaction mixture it was then possible to isolate, and in high yield, the 2,4-dinitrophenylhydrazone of 2-hexanone.[5] It was, unfortunately, not possible to identify the other product of exchange, but we take the accumulated chemical and physical evidence for the structural designations as conclusive.

The photochemically-induced ring opening of substituted cyclohexadienes is a long-known and well-studied reaction in large part because of its occurrence in vitamin D photochemistry. The stereochemistry of ring opening in simple substituted cyclohexadienes has recently been studied by Baldwin and Krueger (11) and by Spangler and Hennis (13), and the reaction has been extended to 5,6-dihydropyrazines such as **7**.

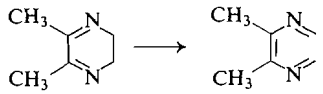

7

The photochemical behavior of the latter chromophore has recently been summarized by Arnold *et al.* (14). Such dienes are predicted by symmetry considerations (and in historical fact were the stimulus for such considerations) to open photochemically in a concerted conrotatory process. A molecule such as α-phellandrene should provide only two of the four possible isomers, and Baldwin and Krueger (11) have shown this to be true: the remaining pair was formed later by secondary absorption. By lowering the temperature to −196°, **8** became favored over **9** (29:1 low temperature; 3:1 room temperature) and it was postulated that the photochemical product ratios reflected the ground state conformation populations of α-phellandrene. We shall return to this point later.

Irradiation of **1** ($n \rightarrow \pi^*$) at 10° gave a ratio of **3**:**4** of 2.6:1.0. Since the products do not

[5]Model studies had previously shown the hydrazone exchange procedure to be applicable to an azine.

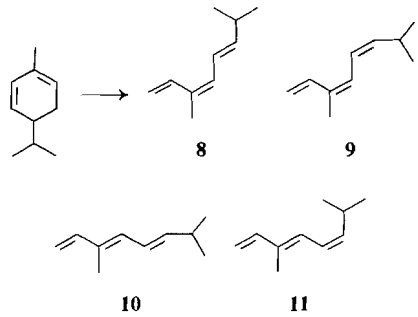

8 **9**

10 **11**

absorb at 435 nm the final product ratio should represent the initial product ratio unless energy may be transferred to **3** and **4** by some other excited molecule. The constancy of this ratio during reaction shows that this process is not occurring. No change in the obtained ratio was observed when the reaction temperature was lowered to −45°, and indeed if the Baldwin view be correct, none should be observed since conformational population changes should be small. The product ratio of *cis,trans* to *cis,cis* observed is intermediate to that obtained by Spangler and Hennis (13) for methyl- and isopropyl-5-substituted cyclohexadienes. Since an *n*-butyl group may be expected to be intermediate in its steric demand between those of a methyl and isopropyl group, a consistent pattern is obtained.

It is not necessarily true, however, that the ratio of conrotatory opening processes reflects directly the ground state conformational equilibrium. Such a conclusion is valid only if ring opening occurs from the geometry produced in the excited state by the Franck–Condon transition, *i.e.* before any vibrational relaxation by collision with solvent molecules. If this be not so, there will then be vibrational cascade to the lowest vibrational levels of the excited state. The energy surface of the excited state should exhibit two minima corresponding to two different conformations. The energy difference between the excited state conformations should be equal to or less than that of the ground state conformers (since steric demands of substituents should be equal or less) and the conformational population in the excited state would be temperature dependent. Thus the conformational population of that state need not necessarily parallel that of the ground state.

Ring opening could follow immediately upon Franck–Condon excitation if the energy surfaces of the excited diene and product triene intersect.

Can. J. Chem. Downloaded from www.nrcresearchpress.com by 210.87.254.105 on 09/05/12
For personal use only.

It has been suggested by Arnold *et al.* (14) in connection with the u.v. absorption spectrum of the dihydropyrazines that the excited state of the dienes actually lies on the same surface as the spectroscopic transition from the triene: that is, the excited state of the diene *is* the excited state of the triene at an appropriate vibrational level. Such seems essentially to have been the view of Woodward when rationalizing the difference in λ_{max} between homoannular dienes contained in five-, six-, and seven-membered rings (15).

The electrocyclic opening of homoannular conjugated dienes is normally understood to proceed in a stereospecific manner because, with the retention of a C_2 axis of symmetry, the first singly excited state of the diene correlates with the first singly excited state of the triene (for discussions in general and also with regards the route to ground state products, see ref. 16–19). In the present case the situation is more complex, since the excited state engendered is one not present in the carbocyclic series. It was shown, in fact, that irradiation into the shorter wavelength absorption band gave the same products at about the same rate when corrected for light intensity as irradiation into the longer wavelength absorption band, strongly suggesting that internal conversion to the n,π^* manifold competes successfully with reaction in the π,π^* state. However, with but one substituted center only analogy suggests that the ring opening be a concerted singlet process at all. Experiments were therefore undertaken to ascertain whether there could be reaction from the triplet if generated, and whether under the conditions of direct irradiation it was the singlet which was reacting.

Firstly, attempts were made to quench the direct reaction. A problem immediately arises in that no experimental evidence exists to indicate the triplet energy of such a molecule. A crude assessment may be made in the following way. If we take the onset of the n,π^* absorption band as the O–O singlet energy of **1** a value of about 53 kcal/mol is obtained. In non-conjugated azo compounds the singlet–triplet splitting has been assessed as being of the order of 15–20 kcal/mol (20, 21) whilst experimental values determined (from emission data) for diazabicycloheptene (22) and diazabicyclooctene (23, 24) indicate a splitting of near 20 kcal/mol. Such values suggest that the triplet energy of **1** may be of the order of 35 kcal/mol. A suitable quencher must have an energy at or below this value and, further, have a singlet energy above 53 kcal/mol to prevent singlet energy transfer. In addition since the lifetime of the triplet may be expected to be short, the quencher must have adequate solubility and exceedingly low absorption in the region of excitation of **1** (~435 nm). As a further requirement, the substance should not have signals in the n.m.r. which would prevent the monitoring of the reaction progress or which decompose to do this. The quencher selected was cyclooctatetraene (COT) despite the fact that its triplet energy, though low, appears not to be known. Present evidence indicates that it is below 40 kcal/mol (25). The result obtained therefore has still an element of doubt. It was found that with concentrations of COT ranging up to 0.19 *M* the rate of conversion, up to 100% conversion, for all samples was the same, nor was there any evidence of extraneous product formation. Since some quenching, even if not diffusion controlled, would have been expected even with 2 kcal/mol endothermicity we conclude that either COT has a triplet energy between 38–40 kcal, or that the triplet of **1**, if formed, has a lifetime too short for detectable quenching at the concentration of COT used. The second alternative requires a triplet lifetime of below 10^{-9} s.

But we are inclined to interpret this evidence as, in fact, indicating that reaction is proceeding through the singlet. Our argument is as follows. If the triplet of **1** were generated the diazatrienes would then exist in the presence of triplet **1**. Since, clearly, the triplet energies of the trienes must be below that of the dienes diffusion controlled quenching would be expected. It has been observed that azo compounds in the triplet state isomerize (26, 27), and such behavior is, of course, well established for dienes, trienes, and higher polyenes (28, 29). Under such circumstances, variation of the composition of the irradiation mixture with time would be expected, and the appearance of the second pair of isomers, **5**, and **6**; such was not the case. Furthermore the generation of triplet **1** by direct irradiation, *i.e.* intersystem crossing, would be a phenomenon that so far has not received support in the literature (23, 30), and, in fact, Allred and Smith (31) have observed a spin-correlation effect in the direct and sensitized decomposition of 5-methoxydiazabicycloheptene. The slowness of intersystem crossing in trienes is well-known,

Can. J. Chem. Downloaded from www.nrcresearchpress.com by 210.87.254.105 on 09/05/12
For personal use only.

but is not acceptable as a model because of the absence of any n,π* state, and, in fact, the question of intersystem crossing in azo compounds cannot be regarded as completely clarified.

The discussion presented above raised the question of what in fact would occur if the triplet of **1** were generated. Unlike aliphatic azo compounds, which either isomerize or decay to the ground state, cyclic compounds such as diazabicycloheptene and diazobicyclooctene (32, 23) when excited to the triplet state (by sensitization) decompose with the evolution of nitrogen.

The generation of triplet **1** was undertaken using benzophenone (E_T 69 kcal/mol) and Michler's ketone (E_T 61 kcal/mol). Both absorb at 366 nm where **1** has a very low extinction coefficient. Both have high intersystem crossing rates, such that quenching of their singlets has not been observed in solution under normal conditions. When a sample of **1** was irradiated in deuteriobenzene in the presence of benzophenone such that the benzophenone absorbed more than 94% of the incident light, a mixture of **3**–**6** was obtained, wherein most probably **5** and **6** arose from **3** and **4** by isomerization. A similar result was obtained when Michler's ketone was used such that the ketone absorbed more than 99.5% of the incident light.

At this stage quantum yields were not available, and though the sensitized reaction appeared to be slow the degree was uncertain, and it was possible that the reaction was induced by the small amount of light absorbed directly. The experiments were then repeated with samples in which the concentration of Michler's ketone was such as to absorb 98.0 and 99.5% of the incident light. The rate of isomerization, measured by n.m.r., was the same for both samples despite the factor of four in the amount of light absorbed directly.

Since exchange singlet energy transfer may be discounted there remain but three possibilities. These are resonance singlet energy transfer, reaction from the triplet, and reaction from a high vibrational level of the ground state generated by intersystem crossing from the triplet.

Although the singlet emission spectrum (not visible) of the ketone would overlap with the absorption n,π* band of the azo compound, the intensities of these transitions are too low for efficient transfer, and we therefore discount resonance transfer as a possibility. We have noted that **1** quenches the room temperature phosphorescence of benzophenone in carbon tetrachloride at or near a diffusion controlled rate but have not been able to measure lifetimes.

We are presently unable to distinguish between the other two processes for the reaction pathway, although the generally high rapidity of vibrational quenching in solutions leads us to prefer the first.

The fact that both a singlet and a triplet mechanism leading to the same type of products appeared to be available made the determination of quantum yields of some importance, since, if the reaction even on direct irradiation, proceeded via the triplet, then the latter pathway should proceed in higher quantum yield.

The only method of analysis available was that employing n.m.r., and so resort was had to irradiation in transparent n.m.r. tubes. The accuracy of such determinations is thus limited. For this purpose we have employed the Jasco spectroirradiator Model CRM-FA which has a holder well-adapted for holding such tubes. The light intensity may be calibrated using a ferrioxalate actinomer, but errors due to reflection may be large.

In an effort to estimate this error, the quantum yield of the ferrioxalate actinometer was determined in a clear n.m.r. tube at 278 (a quartz tube), 362, and 404 nm. Although the values obtained at each individual wavelength were reproducible to within 5%, the percentage of light reflected from the cylindrical tubes varied from 51 to 59% over the three wavelengths. Thus rates and quantum yields determined by this method must contain a similar error, *i.e.* ±5%. Since proton integration as a measure of product yield could contribute a further ±5% error (which we feel is a maximum), we have set error limits of ±10% for the quantum yields reported below.

By this method we were able to determine the approximate quantum yields of diazatriene formation both at 278 and 447 nm as being 0.40 ± 0.04. Using Michler's ketone as sensitizer and assuming efficient energy transfer, the quantum yield is 0.07 ± 0.01. The diazatriene also competes with **1** for the ketone triplet, but at maximum conversion (20%) **1** is still in excess by a factor of four, and both quenching processes are presumably proceeding at the same rate. It would thus seem that making all allow-

Can. J. Chem. Downloaded from www.nrcresearchpress.com by 210.87.254.105 on 09/05/12
For personal use only.

ances the quantum yield of the triplet reaction is significantly lower than that of the singlet and appears to indicate that there are two pathways to the same product.

The systems under discussion may not be treated by the consideration of state correlation diagrams since the involvement of the n,π* state removes significant symmetry.

Fukui (33, 34) has considered the reaction of α,β-unsaturated ketones as taking place with the conversion of an n,π* triplet to a π,π* triplet. Such a process does not appear energetically available to the singlet. It may be relevant, however, that of the two important interactions considered by Fukui, SO–LU and SO′–HO, the former exists in the present system, whilst the latter is nil since in the azo compounds the n and π orbitals are orthogonal. When, however, the molecule begins to react, twisting will occur about the π-bonds, and the resultant modification of orbitals is not predictable in the absence of detailed calculations. It may be that the SO–LU interaction dominates the course of the reaction, and so a concerted electrocyclic process may be simulated, even in the case of the triplet.

Experimental

General procedures are as described in the preceding paper.

All sensitization and quenching studies, relative rate and quantum yield determinations, are the average, at least, of two determinations, and agreement of individual determinations within ±5%.

The JASCO Spectroirradiator Model CRM-FA used for rate measurements and quantum yields consists essentially of a 2000 W Xenon lamp whose emitted light is passed through a grating and dispersed onto a curved cell holder. The wavelength of the light incident upon the cell holder varies from 689 to 222 nm with a dispersion of 1.5 nm/mm. Openings in the cell holder are spaced 18 mm apart and may be varied from 1 to 10 mm in width. The radiant energy incident upon one cell may be accumulated with a thermopile and calibrated against the integrated value of light of 850 nm as collected and totalled with a connected integrator. The instrument enables one to irradiate simultaneously a number of samples at different wavelengths, and to calculate the amount of incident light on each cell.

Irradiation of Dihydropyridazine (1): General Procedure

Freshly prepared pure **1** was dissolved in the appropriate solvent (deuteriobenzene or deuteriochloroform for the longer wavelengths and deuteriocyclohexane for the shorter wavelengths) and placed in a vessel to which a clear quartz or Pyrex n.m.r. tube had been attached, hexamethyldisiloxane (HMDS) being used as an internal reference. The solutions (0.3 *M*) were degassed with the solution in the main receptacle to a pressure of 5×10^{-5} mm by the freeze–pump–thaw method. The degassed solution was then run into the attached n.m.r. tube which was sealed off and detached.

For the irradiation at 10° the sample was immersed in a water-bath held at that temperature by a water-cooled copper coil. For the experiment at −45° the sample was immersed in a chlorobenzene – Dry Ice bath.

Irradiations at 435 nm were performed using the relevant line of a Hanovia 450 W lamp isolated by passage of the light through Corning filters 3–73 and 7–59. Corning filters 7–60 and 0–52 were used to isolate the 366 nm line. The irradiations in the 278 nm region were performed on a JASCO Spectroirradiator Model CRM-FA with the entrance slit at 2 nm and the cell slits at 4 mm. Rate measurements were also performed on this apparatus. For quantum yields the radiation counter in the apparatus was calibrated at 850 nm against the ferrioxalate actinometer. The relative intensities at 447, 362, and 278 ± 3 nm were then determined with a thermopile supplied with the instrument. The samples were held at 10° by placing the n.m.r. tubes during the irradiation in a water-cooled block.

Preparation of the Isomeric Diazatrienes (3–6)

A solution of **1** (0.3 *M*) in deuteriobenzene was irradiated at 435 nm and at 10° until the nmr spectrum showed the complete disappearance of starting material (2–3 h). Two products (**3** and **4**) in a ratio of 2.1:1.0 accounted for all the signals in the spectrum. Upon warming to 45° for 0.5 h the two initial sets of signals decreased and two new sets, assigned to **5** and **6**, appeared in a ratio of 4:1, respectively. After 12 h at 45° the signals attributed to **5** outweighed the combined signals of the other three isomers by 10:1, as determined by proton integration, and continued heating, even to 80°, brought about no further change in the spectrum. Irradiation in $CDCl_3$ at 10° and at −45° gave product mixtures identical with those obtained in C_6D_6 at 10°.

For the obtention of the u.v. spectrum of the products **1** was irradiated in a quartz u.v. cell in cyclohexane (6×10^{-5} *M*) at 10° until continued irradiation produced no further changes in the spectrum. After the recording of the u.v. spectrum the solution was heated to 60° for 12 h, and the absorption spectrum redetermined.

The Reaction of Diazatrienes 3 and 4 with 2,4-Dinitrophenylhydrazine

Into one bulb of a reaction vessel to which two bulbs and a clear n.m.r. tube had been attached was placed 5 ml (10^{-3} mol) of Shine's reagent (35). Into the attached n.m.r. tube was added 63 mg (4×10^{-4} mol) of the dihydropyridazine **1** in 0.5 ml benzene. The two solutions were then degassed, and that containing the dihydropyridazine irradiated for 12 h at 435 nm. This time was more than three times longer than that generally required for complete conversion of **1**. The solutions were then mixed in the second bulb which was sealed and detached. The contents were heated at 60° for 10 h after which the container was opened and the solvent removed under reduced pressure. The residue was analyzed by t.l.c. (solvent: ether–benzene, 1:4). A spot was detected with R_F corresponding to that shown by the 2,4-dinitrophenylhydrazone of 2-hexanone, but none was visible where expected for the derivative of methyl vinyl ketone. The substance responsible for the spot in the position of the 2-hexanone

Can. J. Chem. Downloaded from www.nrcresearchpress.com by 210.87.254.105 on 09/05/12
For personal use only.

derivative was isolated by preparative t.l.c., the crude product (87 mg, 82%) then being crystallized from ethanol when it had m.p. 105–106°, which was undepressed on admixture with an authentic specimen of the 2-hexanone derivative of the same m.p.

Attempted Quenching of the Phototransformation of **1**

Into each of the four n.m.r. tubes was placed 0.4 ml. of a 0.3 *M* solution of **1** in $CDCl_3$. Cyclooctatetraene was added to three tubes so as to achieve the concentrations 0.00, 0.048, 0.096, and 0.192 *M*, respectively. The solutions were degassed, sealed and placed side by side in a bath held at 10°. They were then simultaneously irradiated at 435 nm. The reaction progress was monitored by n.m.r. Product formation proceeded at an equal rate in all four samples up to 100% conversion.

Irradiation near 278 nm

Identical samples of **1** were prepared, one with $CDCl_3$ solvent in a clear n.m.r. tube, and the other with C_6D_{12} as solvent in a clear quartz nmr tube. Both samples were irradiated in the spectroirradiator, one at 447 nm and the C_6D_{12} solution at 278 nm. The concentrations of **1** were such that all incident light was absorbed at both wavelengths ($A > 20$ in a path length of 4 mm). The rate of product formation was followed to 30% conversion and, after correction for differences in light intensity, were found to be identical within the accuracy of proton integration (±5%).

Sensitized Phototransformation of Dihydropyridazine **1**

To one of three identical solutions of **1** in C_6D_6 (0.3 *M*) was added sufficient benzophenone (28 mg) so as to absorb >94% (calculated at the incident wavelength) of the incident light at 366 nm. To a second was added Michler's ketone (0.5 mg) so as to absorb >98% of the light, and to the third Michler's ketone (4.1 mg) so as to absorb >99.5% of the light. The samples, placed side-by-side in a water-cooled bath, were simultaneously irradiated (366 nm; 10°) with a 450 W medium pressure mercury lamp and the transformation followed by n.m.r. spectroscopy. The rates of the reactions appeared to be identical within ±5% up to complete conversion. A mixture of all four stereoisomers (**3–6**) was obtained in all cases.

Phosphorescence Quenching of Benzophenone by Dihydropyridazine **1**

A solution of benzophenone (8.0×10^{-4} *M*) in carbon tetrachloride containing the pyridazine **1** (1.0×10^{-4} *M*) was prepared and the room-temperature phosphorescence compared with an identical solution not containing **1**. The concentration of the quencher **1** was chosen such that, under the assumptions of diffusion controlled quenching and a room-temperature triplet lifetime of benzophenone in carbon tetrachloride as 10^{-4} s (36) *ca.* 98% of the emission would be quenched. The emission of both samples was recorded, under identical conditions, on a spectrophosphorimeter (37).

The intensity of the emission of the solution containing the quencher was reduced by 88 ± 10% as compared with that which did not. The partially-quenched emission was not shifted nor altered in shape from that of the unquenched emission.

Quantum Yields

After calibration of the JASCO Spectroirradiator apparatus against the ferrioxalate actinometer it was found that equivalent irradiation in an n.m.r. tube resulted in large light losses by reflection. Irradiation of a 0.15 *M* solution of ferrioxalate actinometer in an n.m.r. tube yielded quantum yields of 0.64 ± .03, 0.50 ± .01 and 0.50 ± .02 at 278, 362 and 404 nm, respectively. The accepted values (38) at these wavelengths are 1.25, 1.22, and 1.14, which represent corresponding light losses of 51, 59, and 56%. Thus, quantum yields of product formation so obtained are subject to a high error even when corrected.

A solution of **1** in C_6D_{12} in a quartz n.m.r. tube (0.3 *M*) was irradiated near 278 nm simultaneously with irradiation of similar solutions in $CDCl_3$ near 446 nm and in C_6D_6 near 362 nm, the latter containing sufficient Michler's ketone (0.044M) to absorb >99.6% (calculated by integration of the absorption curves of the absorbing species over the band width of the incident light) of the incident light. The samples were irradiated to 20% conversion and the transformation measured by integration of the nmr spectrum. The quantum yields obtained were, respectively, 0.40 ± .04, 0.40 ± .04, and 0.07 ± 0.01.

1. P. DE MAYO. Acc. Chem. Res. 41 (1971).
2. P. J. WAGNER and H. N. SCHOTT. J. Am. Chem. Soc. **91**, 5383 (1969).
3. L. M. STEPHENSON, P. R. CAVIGLI, and J. L. PARLETT. J. Am. Chem. Soc. **93**, 1984 (1971).
4. R. O. LOUTFY, P. DE MAYO, and M. F. TCHIR. J. Am. Chem. Soc. **91**, 3984 (1969).
5. R. O. LOUTFY and P. DE MAYO. Can. J. Chem. **50**, 3465 (1972).
6. H. E. O'NEAL and S. W. BENSON. J. Phys. Chem. **72**, 1866 (1968).
7. P. D. BARTLETT and N. A. PORTER. J. Am. Chem. Soc. **90**, 5317 (1968).
8. P. DE MAYO and M. C. USSELMAN. Anal. Quim. **68**, 779 (1972).
9. P. DE MAYO and M. C. USSELMAN. Can. J. Chem. This issue.
10. L. M. JACKMAN and R. H. WILEY. J. Chem. Soc. 2881 (1960).
11. J. E. BALDWIN and S. M. KRUEGER. J. Am. Chem. Soc. **91**, 6444 (1969).
12. S. CASTELLANO and J. S. WAUGH. J. Chem. Phys. **37**, 1951 (1962).
13. C. W. SPANGLER and R. P. HENNIS. Chem. Commun. 42 (1972).
14. D. R. ARNOLD, V. Y. ABRAITYS, and D. MCLEOD, JR. Can. J. Chem. **49**, 923 (1971).
15. R. B. WOODWARD. J. Am. Chem. Soc. **64**, 72 (1942).
16. R. B. WOODWARD and R. HOFFMANN. The Conservation of orbital symmetry. Academic Press, Germany, 1970.
17. N. T. ANH. Les regles de Woodward Hoffmann. Ediscience, Paris, 1970.
18. W. TH. A. M. VAN DER LUGT and L. J. OOSTERHOFF. Chem. Commun. 1235 (1968).
19. J. MICHL. Mol. Photochem. **4**, 287 (1972).
20. J. R. FOX and G. S. HAMMOND. J. Am. Chem. Soc. **86**, 4031 (1964).
21. D. R. KEARNS. J. Phys. Chem. **69**, 1062 (1965).

22. P. S. ENGEL. J. Am. Chem. Soc. **89**, 5731 (1967).
23. B. S. SOLOMAN, T. F. THOMAS, and C. STEEL. J. Am. Chem. Soc. **90**, 2249 (1968).
24. W. D. K. CLARK and C. STEEL. J. Am. Chem. Soc. **93**, 6347 (1971).
25. R. O. LOUTFY. Ph.D. Thesis. The University of Western Ontario, London, Ontario. 1972.
26. P. S. ENGEL and P. D. BARTLETT. J. Am. Chem. Soc. **92**, 5883 (1970).
27. R. ARNAUD, J. RONAYETT, and J. LEMAIRE. CR Ac. Sci. C. **274**, 2144 (1972).
28. J. SALTIEL, L. METTS, and M. WRIGHTON. J. Am. Chem. Soc. **91**, 5684 (1969).
29. N. C. BAIRD. Mol. Photochem. **2**, 53 (1970).
30. P. S. ENGEL. J. Am. Chem. Soc. **91**, 6903 (1969).
31. E. L. ALLRED and R. L. SMITH. J. Am. Chem. Soc. **91**, 6766 (1969).
32. P. D. BARTLETT and P. S. ENGEL. J. Am. Chem. Soc. **90**, 2960 (1968).
33. K. FUKUI. Acc. Chem. Res. **4**, 57 (1971).
34. K. FUKUI. *In* Mechanism of molecular migration. Vol. 2. Interscience Publishing Company, 1969. p. 117.
35. H. J. SHINE. J. Org. Chem. **24**, 252 (1959).
36. J. SALTIEL, H. C. CURTIS, L. METTS, J. W. MILEY, J. WINTERLE, and M. WRIGHTON. J. Am. Chem. Soc. **92**, 410 (1970).
37. D. S. L. BLACKWELL, C. C. LIAO, R. O. LOUTFY, P. DE MAYO, and S. PASZYC. Mol. Photochem. **4**, 171 (1972).
38. C. G. HATCHARD and C. A. PARKER. Proc. Roy. Soc. London Ser. A. **235**, 518 (1956).
39. A. A. REID, J. T. SHARP, and S. J. MURRAY. Chem. Commun. 827 (1972).

Can. J. Chem. Downloaded from www.nrcresearchpress.com by 210.87.254.105 on 09/05/12
For personal use only.

Iridoids of *Mentzelia decapetala* (Pursh). II. Decaloside[1]

TERRY JOHN DANIELSON AND EDWARD MILES HAWES
College of Pharmacy, University of Saskatchewan, Saskatoon, Saskatchewan

AND

CARMAN ARTHUR BLISS
College of Pharmacy, University of New Mexico, Albuquerque, New Mexico

Received July 31, 1972

Decaloside (**1**), a minor component of *Mentzelia decapetala* (Loasaceae) has been isolated and characterized as *1S,4aS,5R,7aR*-1-*O*-β-D-glucosyl-5-hydroxy-1,4*a*,5,7*a*-tetrahydro-4-hydroxymethylcyclopenta(*c*)pyran.

Le décaloside (**1**), un composé mineur de la *Mentzelia decapetala* (Loasaceae) a été isolé et caractérisé comme étant le β-D-glucosyl-1-*O* hydroxy-5 tétrahydro-1,4*a*,5,7*a* hydroxyméthyl-4 cyclopenta(*c*) pyranne-*1S,4aS,5R,7aR*. [Traduit par le journal]

Can. J. Chem., **51**, 1737 (1973)

A previous study (1) on *Mentzelia decapetala* reported the isolation and elucidation of the relative stereochemistry of an iridoid, mentzeloside (**2**). We report here the determination of the absolute stereochemistry of a second isolated iridoid, decaloside (**1**). **1** was isolated by column

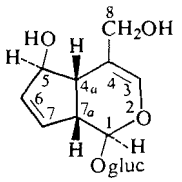

1

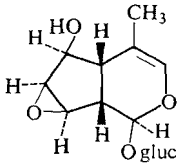

2

chromatography of the methanolic extract of *M. decapetala* after elution of **2**. The optically active product was unstable and a satisfactory elemental analysis could not be obtained. Its mass spectrum showed a weak molecular ion at *m/e* 346, and a relatively strong $(M - 162)^+$ ion at *m/e* 184 indicated loss of glucose. This fragmentation of an unstable glycoside to produce a stable aglycone molecular ion has been found to be a prominent feature of the spectra of iridoids (2). A molecular formula of $C_{15}H_{22}O_9$ was indicated.

The iridoid character of **1** was also indicated by formation of a black polymer on acid hydrolysis, and the enol ether function by a peak of 1658 cm^{-1} in the i.r. spectrum. A band at 204 nm in the u.v. spectrum was attributed to a $\pi \rightarrow \pi^*$ transition of an enol ether double bond in which the β-carbon does not bear a carbonyl substituent. These assignments were confirmed by the 100 MHz (^1H) n.m.r. spectrum. A broadened one-proton signal at 6.34 p.p.m. was designated as the α-proton of an enol ether, and the lack of any large coupling indicated that C-4 was substituted.

Examination of the n.m.r. spectrum was hampered by its complex nature, but a few other features were informative. A slightly broadened two-proton singlet at 5.83 p.p.m. was assigned to two olefinic protons on the basis of chemical shift comparisons (3) with olefinic protons in similar systems such as aucubin (**3**). The lack of any visible couplings between these olefinic protons can be attributed to an A_2 system as $\Delta\nu/J \rightarrow 0$ (4). Two one-proton doublets at 4.50 and 4.62 p.p.m. were assigned to the acetal protons on C-1′ of the sugar moiety and C-1 of the aglycone respectively. The magnitude of the coupling of the former with C-2′ ($J = 7$ Hz) indicated a β-glucoside linkage as in **2** (1). The coupling of the C-1 proton with the C-7*a* proton at 2.72 p.p.m. ($J = 7$ Hz) was suggestive of a *trans*-interaction between these protons. No signal comparable to the allylic methyl of **2** was present so a hydroxymethyl group at C-4 was suspected, although poor resolution did not permit an actual assignment at this stage.

Enzymatic hydrolysis of **1** with emulsin yielded an aglycone and glucose as demonstrated by paper chromatography. The use of various spray reagents indicated the reducing properties of the aglycone. All attempts to isolate or prepare aglycone derivatives failed.

[1]Abstracted in part from the University of Saskatchewan Ph.D. Thesis of T.J.D. (1972).

Can. J. Chem. Downloaded from www.nrcresearchpress.com by 210.87.254.40 on 09/05/12
For personal use only.

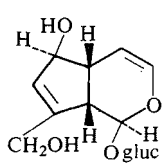

3

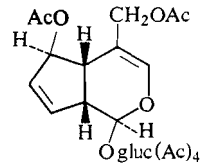

4

When decaloside was allowed to react with acetic anhydride a crystalline hexaacetate (**4**) was obtained. The i.r. and n.m.r. spectra did not display any bands assignable to hydroxyl functions, thereby eliminating the possibility of tertiary alcohol protons in the starting material. All nine oxygen atoms of **1** could now be assigned. Six must be present as primary or secondary alcohol functions, four in the glucose moiety and two in the aglycone, while the remaining three could be assigned as the ethereal and acetal oxygens about C-1 and -1′.

The 100 MHz n.m.r. spectrum of **4** (Fig. 1) was well resolved and enabled assignment of the hitherto undetermined features of **1**. A low-field one-proton multiplet at 6.37 p.p.m. was assigned to the proton on C-3. This displayed long-range coupling into two one-proton quartets at 4.69 (J = 0.5 Hz) and 4.33 (J = 0.5 Hz) p.p.m. These latter protons were presumed to be geminally coupled methylene protons (J = 12 Hz) of an acetylated primary alcohol at C-4. These assignments were substantiated by deoxydodidrovaltrate, an iridoid with a C-4 methylene group. Here the proton on C-3 is reported to appear at 6.42 p.p.m. while the allylic methylene protons at C-4 resonate at 4.63 and 4.39 (J = 12 Hz) p.p.m. (5).

The bridgehead protons on C-4*a* and -7*a* appeared as complex signals at 2.79 and 3.07 p.p.m. respectively. The interaction between these protons (J = 8 Hz) was similar to that observed in **2** (J = 7.5 Hz) (1) and indicated a similar *cis*-ring fusion. The proton on C-7*a* was also coupled with a downfield proton, which was hidden beneath the broad glucosyl proton signal at 5.58–4.75 p.p.m. This hidden signal was assigned to the C-1 acetal proton. The magnitude of the coupling (J = 7 Hz) was suggestive of a *trans*-interaction between the protons on C-1 and -7*a*. Comparison with aucubin (J = 7.5 Hz) confirmed this steric assignment (3).

Two vicinally coupled olefinic protons appeared as a quartet at 6.02 and as an octet at 5.89 p.p.m. The magnitude of the coupling constant (J = 6 Hz) was suggestive of a *cis*-olefinic coupling in a five-membered ring (4). This olefinic function could be assigned as either a Δ^5 or Δ^6 bond. In Δ^5-iridoids the olefinic proton on C-5 appears between 6.1 and 6.3 while the C-6 proton appears between 5.6 and 5.7 p.p.m. (6, 7). In Δ^6-iridoids the C-6 proton appears close to 5.90 p.p.m., as for example, aucubin 5.87 (3), scandoside 5.85 (8), and melittoside 5.91 p.p.m. (3). Although the validity of this comparison is open to question due to the model compounds having substituents on C-7, a Δ^6-iridoid assignment for **1** is indicated. No chemical shift comparisons are possible for the proton on C-7 as no Δ^6-iridoids without a C-7 substituent are reported in the literature.

This assignment was confirmed by mass spectrometry. A prominent feature in the spectra of Δ^5-iridoids involves cleavage of the C_1—C_2 and C_{4a}—C_{7a} bonds, via a retro-Diels–Alder reaction, followed by cleavage of the C_6—C_7 bond. In the mass spectrum of **1** these expected ions at *m/e* 111 and 73 were of low intensity. This feature is compatible with a Δ^6 bond (2).

In view of the Δ^6-iridoid assignment a multiplet at 5.53 p.p.m. was attributed to an allylic acetate methine at C-5. The C-4*a* proton displayed coupling (J = 4 Hz) with this signal. Steyn and Sable (9) reported that in substituted cyclopentenes couplings are in the range 2–5.5 Hz for *trans*- and 6.2–7.4 Hz for *cis*-vicinal protons, while Stevens and Fletcher (10) noted that a coupling of less than about 4 Hz was indicative of a *trans*-vicinal interaction in cyclopentane systems. Thus a *trans*-interaction between protons on C-4*a* and -5 in **4**, and by analogy in **1**, is indicated.

The absolute configuration of **1**, and by similar techniques **4**, may be assigned by measurement of their optical rotatory powers. Mills (11) showed that cyclohexyl allylic alcohols derived from structural unit **5** were more laevorotatory than those derived from the epimeric unit **6**, and that these differences were greatly enhanced by esterification. Brewster (12) also demonstrated that cyclopenten-3-ols corresponding to **5** were laevorotatory while those corresponding to **6** were dextrorotatory.

These principles (11, 12) should be applicable

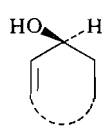

5

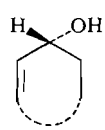

6

Can. J. Chem. Downloaded from www.nrcresearchpress.com by 210.87.254.40 on 09/05/12
For personal use only.

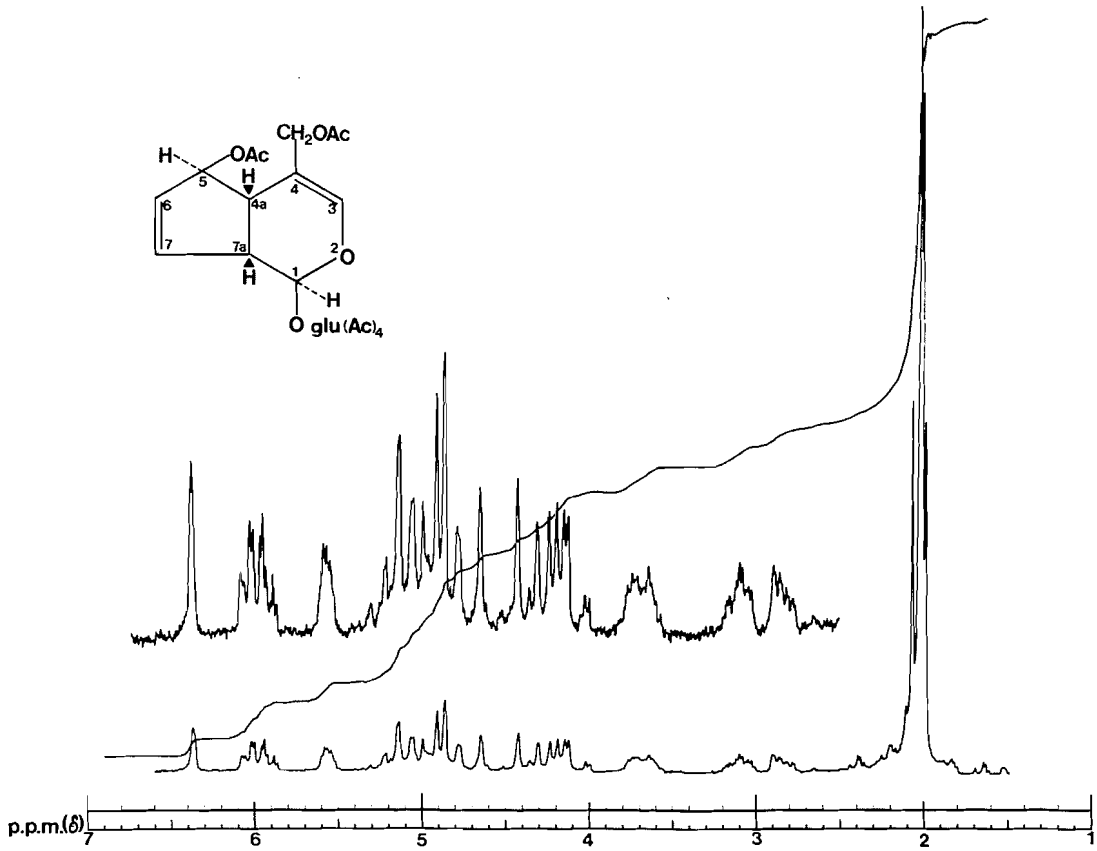

FIG. 1. The 100 MHz [^{1}H] n.m.r. spectrum of decaloside hexaacetate, solvent $CDCl_3$; TMS internal standard.

TABLE 1. Optical rotations of selected iridoid compounds

Compound	Formula number	$[\alpha]_D°$	$[M]_D°$
Decaloside	**1**	−138 (CH_3OH)	−477
Decaloside hexaacetate	**4**	−128 ($CHCl_3$)	−766
Aucubin*	**3**	−162 (H_2O)	−550
Aucubin hexaacetate*		−156 ($CHCl_3$)	−943
Daphylloside†		+20 (H_2O)	+89
Daphylloside hexaacetate†		+51 (EtOH)	+335

*Reference 14.
†Reference 15.

to iridoid glucosides since it has been shown that acetylation of α- or β-methyl-D-glucosides does not significantly alter their molecular rotations (13). Values for **1** and its acetate derivative, and for reference compounds are recorded in Table 1.

Compound **3** (14) which contains structural unit **5** displays laevorotatory powers, while daphylloside (15) which contains **6** displays dextrorotatory powers. **1** was found to become more laevorotatory upon acetylation, and thus the absolute stereochemistry about C-5 must be the same as in **3**. This allows only two possible structures, varying only in the absolute stereochemistry of the dihydropyran ring. **1** must be as shown on the basis of three features. Firstly, this structure contains a *trans*-relationship between protons on C-4*a* and -5, as indicated by the n.m.r. of **4**. Secondly, the C-5 hydroxyl group possesses the same relative stereochemistry as the analogous C-5 hydroxyl in **2**. Finally, the assign-

Can. J. Chem. Downloaded from www.nrcresearchpress.com by 210.87.254.40 on 09/05/12
For personal use only.

ment as shown is the same as that found for all other iridoids for which absolute stereochemistries have been determined.

Experimental

The general experimental procedures were as previously described (1). Paper chromatograms were run on Whatman No. 1 filter paper using a *n*-butanol, acetic acid, and water (63:10:27) solvent system. R_f values were measured to the front of the compound spots. Compounds were detected with either vanillin (1 g) and concentrated hydrochloric acid (3 ml) in methanol (150 ml) and heating for 2 min at 100 °C or with Tollen's ammoniacal silver nitrate reagent.

Extraction and Isolation of Decaloside (1)

The preparation of the crude iridoid fraction and its preliminary separation on a Florisil column was described earlier (1). The crude mentzeloside (**2**) fraction was followed on further elution with benzene–methanol (3:1) by a second iridoid containing fraction (1900–3000 ml). Repeated chromatography of this fraction on Florisil with benzene–methanol (3:1) and crystallization from ethyl acetate yielded decaloside (**1**) as colorless crystals (0.300 g): m.p. 193°; R_f 0.37 (red with vanillin reagent, negative with Tollen's); $[\alpha]_D^{23}$ −137.9° (*c* 0.475, CH_3OH); u.v. max 204 nm (log ε 3.68); i.r. 1658 (C=C—O) and 3390 cm^{-1} (O—H); n.m.r. (DMSO-d_6) δ 6.34 (m, 1, C_3—*H*), 5.83 (S*, 2, C_6—*H* and C_7—*H*), 4.62 (d, 1, $J_{1,7a}$ = 7 Hz, C_1—*H*), 4.50 (d, 1, $J_{1',2'}$ = 7 Hz, glucose), and 2.72 p.p.m. (ddd*, 1, $J_{7a,1}$ = 7 and $J_{7a,4a}$ = 8 Hz, C_{7a}—*H*); mass spectrum *m/e* (relative intensity) 346 (0.2), 184 (8), 120 (42), 91 (42), 45 (45) and 43 (100).

Anal. Calcd. for $C_{15}H_{22}O_9$: C, 52.02; H, 6.40. Found: C, 51.10; H, 6.10.

Enzymatic Hydrolysis of Decaloside

To a solution of decaloside (0.013 g) in water (3 ml) was added β-glucosidase (0.010 g). After 12 h at room temperature the mixture was examined by paper chromatography. Three compounds were shown to be present: the aglycone, R_f 0.68 (red with vanillin reagent, black with Tollen's); decaloside, R_f 0.37 (reference 0.37) (red with vanillin reagent, negative with Tollen's); and glucose R_f 0.17 (reference 0.17–0.18) (negative with vanillin reagent, black with Tollen's). All attempts to isolate the aglycone gave only intractable tars.

Decaloside Hexaacetate (4)

To a solution of **1** (0.025 g) in pyridine (5 ml) was added acetic anhydride (0.5 ml). After heating under reflux (2 h) the reaction mixture was poured into cold water and filtered. Crystallization from ethanol yielded **4** (0.030 g, 70%) as colorless crystals: m.p. 162–164°; $[\alpha]_D^{24}$ −127.62 (*c* 1.144, $CHCl_3$); i.r. 1661 (C=C—O) and 1740 cm^{-1} (ester C=O); n.m.r. ($CDCl_3$) δ 6.37 (m, 1, $J_{3,8}$ = 0.5 Hz, C_3—*H*), 6.02 (dd, 1, *J* = 6 and 2 Hz, C_6—*H* or C_7—*H*), 5.89 (ddd, 1, *J* = 6, 2 and 1.5 Hz, C_6—*H* or C_7—*H*), 5.53 (m, 1, C_5—*H*), 5.58–4.75 (c, 5, C_1—*H*, and glucose 4*H*), 4.69 (dd, 1, $J_{8,8'}$ = 12 and $J_{8,3}$ = 0.5 Hz, C_8—*H*), 4.33 (dd, 1, $J_{8',8}$ = 12 and $J_{8',3}$ = 0.5 Hz, C_8—*H'*), 4.13 (c, 2, glucose 2*H*), 3.65 (m, 1, glucose 1*H*), 3.07 (ddd, 1, $J_{7a,1}$ = 7, $J_{7a,4a}$ = 8, and J_x = 2 Hz, C_{7a}—*H*), 2.79 (ddd, 1, $J_{4a,7a}$ = 8, $J_{4a,5}$ = 4, and $J_{4a,3}$ = 0.5 Hz, C_{4a}—*H*), and 1.98 p.p.m. (c, 18, 6 CH_3COO—).

Anal. Calcd. for $C_{27}H_{34}O_{15}$: C, 54.18; H, 5.69. Found: C, 54.04; H, 5.78.

The financial assistance given by the Medical Research Council of Canada (Grant No. MA-3802) is gratefully acknowledged.

1. T. J. Danielson, E. M. Hawes, and C. A. Bliss. Can. J. Chem. **51**, 760 (1973). Part I.
2. T. W. Bentley, R. A. W. Johnstone, and J. Grimshaw. J. Chem. Soc. C, 2234 (1967).
3. M. L. Scarpati and P. Esposito. Gazz. Chim. Ital. **97**, 1209 (1967).
4. L. M. Jackman and S. Sternhell. Applications of nuclear magnetic resonance spectroscopy. 2nd ed. Pergamon Press, Oxford. 1969.
5. P. W. Thies. Tetrahedron, **24**, 313 (1968).
6. G. Albers-Schönberg and H. Schmid. Helv. Chim. Acta, **44**, 1447 (1961).
7. J. M. Bobbitt, K. V. Rao, and D. E. Kiely. Chem. Ind. 931 (1964).
8. H. Inouye, S. Inouye, N. Shimokawa, and M. Okigawa. Tetrahedron Lett. 683 (1968).
9. R. Steyn and H. Z. Sable. Tetrahedron, **27**, 4429 (1971).
10. J. D. Stevens and H. G. Fletcher, Jr. J. Org. Chem. **33**, 1799 (1968).
11. J. A. Mills. J. Chem. Soc. 4976 (1952).
12. J. H. Brewster. J. Am. Chem. Soc. **81**, 5493 (1959).
13. O. Halpern and H. Schmid. Helv. Chim. Acta, **41**, 1109 (1958).
14. P. Karrer and H. Schmid. Helv. Chim. Acta, **29**, 525 (1946).
15. H. Inouye, S. Ueda, M. Hirabayashi, and N. Shimokawa. Yakagaku Zasshi, **86**, 943 (1966).

Can. J. Chem. Downloaded from www.nrcresearchpress.com by 210.87.254.40 on 09/05/12
For personal use only.

Isothiazolopyridines. I. Synthesis and Spectra of Isothiazolo[3,4-*b*]-, 3-Aminoisothiazolo[4,3-*b*]-, Isothiazolo[5,4-*b*]-, and 3-Methylisothiazolo[5,4-*c*]pyridines. Preparation and Spectra of Some 2,3- and 3,4-Disubstituted Pyridines[1]

ALFRED TAURINS AND VIRGINIA TAN KHOUW[2]

Department of Chemistry, McGill University, Montreal, Quebec

Received September 20, 1972

Isothiazolo[3,4-*b*]pyridine was synthesized from 2-aminonicotinonitrile in three steps: by the reaction with ammonia and hydrogen sulfide to produce 2-aminothionicotinamide; oxidative cyclization with hydrogen peroxide to give 3-aminoisothiazolo[3,4-*b*]pyridine, followed by diazotization and reduction with hypophosphorous acid. 3-Aminoisothiazolo[4,3-*b*]pyridine was prepared in a similar way from 3-aminopicolinonitrile via 3-aminothiopicolinamide. Isothiazolo[5,4-*b*]pyridine was synthesized from 2-chloronicotinonitrile in three steps: by the reduction with formic acid in the presence of Raney nickel to obtain 2-chloronicotinaldehyde; transformation of the latter into 2-thiocyanonicotinaldehyde; and finally cyclization with ammonia to obtain isothiazolo[5,4-*b*]pyridine. 3-Methylisothiazolo[5,4-*c*]pyridine was prepared by cyclization of 4-acetyl-3-thiocyanopyridine with ammonia. N.m.r. and u.v. spectra of the isothiazolopyridines, their derivatives, and the pyridine intermediates were recorded and interpreted.

L'isothiazolo pyridine-[3,4-*b*] a été synthétisée à partir de l'amino-2 nicotinonitrile en trois étapes: par la réaction avec de l'ammoniac et de l'hydrogène sulfuré pour donner l'amino-2 thionicotinamide: par la cyclisation par voie oxydante avec de l'eau oxygénée pour donner l'amino-3 isothiazolo pyridine-[3,4-*b*] suivie par une diazotisation et par une réduction avec de l'acide hypophosphoreux. L'amino-3 isothiazolo pyridine-[4,3-*b*] a été préparée en suivant un procédé similaire à partir de l'amino-3 picolinonitrile en passant par l'amino-3 thiopicolinamide. L'isothiazolo pyridine-[5,4-*b*] a été synthétisée à partir du chloro-2 nicotinonitrile en trois étapes: par réduction avec l'acide formique en présence de nickel de Raney pour obtenir la chloro-2 nicotinaldehyde; par la transformation de ce dernier produit en thiocyano-2 nicotinaldehyde; et finalement par la cyclisation en présence d'ammoniac pour obtenir l'isothiazolo pyridine-[5,4-*b*]. La méthyl-3 isothiazolo pyridine-[5,4-*c*] a été préparée par cyclisation de l'acétyl-4 thiocyano-3 pyridine avec de l'ammoniac. Les spectres r.m.n. et u.v. des isothiazolo pyridines, de leurs dérivés ainsi que des intermédiaires des pyridines ont été enregistrés et interprétés.

[Traduit par le journal]

Can. J. Chem., 51, 1741 (1973)

Introduction

Isothiazolopyridines (**1**–**8**) form a new class of heteroaromatic compounds, four of which possess ortho-quinoid structures (**1**–**4**) while the other four, benzenoid (**5**–**8**). Since isothiazolopyridines have remained hitherto an unknown class of compounds, it seemed to be of significance to synthesize and study them and their derivatives. In this work the preparation and spectra of isothiazolo[3,4-*b*]-, -[4,3-*b*]-, -[5,4-*b*]-, and -[5,4-*c*]pyridines were investigated.

Discussion

The first derivatives of isothiazolo[3,4-*b*]- (**1**) and -[4,3-*b*]pyridine (**2**) prepared were the 3-amino compounds **11** and **18**, respectively

Isothiazolopyridines

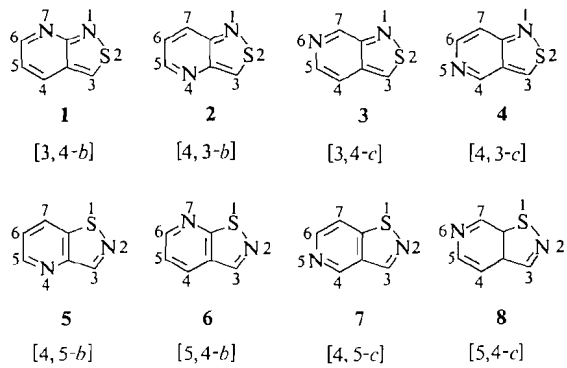

(Schemes 1 and 2). They were obtained by a general method involving the oxidative cyclization of the appropriate pyridine *o*-aminothiocarboxamides. The precursor of 3-aminoisothiazolo[3,4-*b*]pyridine (**11**) was 2-aminonicotinonitrile (**9**) (1) which was transformed into 2-aminothionicotinamide (**10**) by the addition of

[1]This work received financial assistance from the National Research Council of Canada, Ottawa, Canada. Taken from a portion of the Ph.D. Thesis of Virginia Tan Khouw.

[2]Holder of an NRCC Studentship, 1967–1971.

Can. J. Chem. Downloaded from www.nrcresearchpress.com by 210.87.254.6 on 09/05/12
For personal use only.

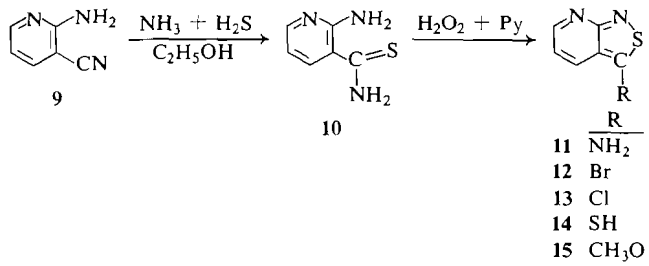

SCHEME 1

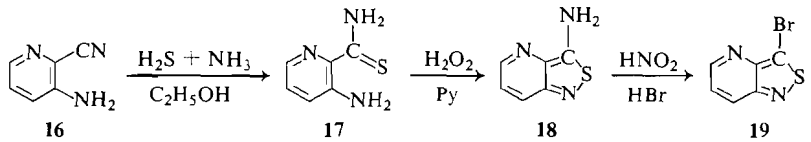

SCHEME 2

hydrogen sulfide to the cyano group. Oxidation of 2-aminothionicotinamide (**10**) with 30% hydrogen peroxide in pyridine produced 3-aminoisothiazolo[3,4-*b*]pyridine (**11**) (Scheme 1).

The mechanism of the oxidative cyclization of the aromatic and heterocyclic thioamides with hydrogen peroxide in pyridine is not known. However, it has been suggested by Davis (2) that the intermediates in such reactions could be *S*-oxides, in analogy to the *S*-oxides formed from aliphatic thioamides and hydrogen peroxide (3).

3-Aminoisothiazolo[3,4-*b*]pyridine (**11**) was diazotized in a mixture of 70% nitric and 85% orthophosphoric acid (1:4) and the diazonium salt reduced with 30% hypophosphorous acid to obtain the new parent compound, isothiazolo-[3,4-*b*]pyridine (**1**).

3-Bromiosothiazolo[3,4-*b*]pyridine (**12**) was prepared by the diazotization of **11** in 48% fuming hydrobromic acid.

3-Chloroisothiazolo[3,4-*b*]pyridine (**13**) was obtained by the Gattermann reaction of **11**. 3-Mercapto- (**14**) and 3-methoxyisothiazolo-[3,4-*b*]pyridine (**15**) were prepared by a nucleophilic substitution of the chlorine atom in **13** (Scheme 1). The red color of the compound **14** indicates that its dominating tautomeric form may be a thione.

In the isothiazolo[4,3-*b*]pyridine series, the starting material was 3-aminopicolinonitrile (**16**) which was transformed into 3-aminopicolinonitrile (**17**) with hydrogen sulfide. 3-Aminoisothiazolo[4,3-*b*]pyridine (**18**) was obtained by the oxidative cyclization of **17** with 30% hydrogen peroxide in pyridine solution (Scheme 2). The presence of the amino group in the 3-position in **18** was proved by the i.r. spectrum and replacement of the amino group by a bromo atom when **18** was diazotized in 48% hydrobromic acid. The efforts to deaminate **18** in order to obtain unsubstituted isothiazolo[4,3-*b*]pyridine (**2**) were unsuccessful.

The general method for the synthesis of isothiazolo[5,4-*b*]pyridine (**6**) (Scheme 3) and 3-

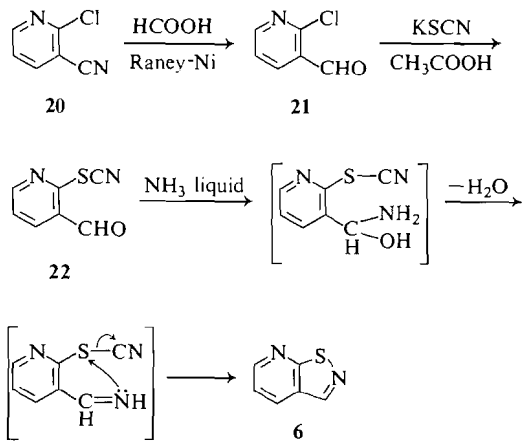

SCHEME 3

methylisothiazolo[5,4-*c*]pyridine (**25**), a derivative of **8**, (Scheme 4) was based on the reaction of *o*-thiocyano-formyl- or *o*-thiocyano-acetyl-pyridine with ammonia. The starting material for the preparation of **6** was 2-chloronicotinonitrile (**20**) (1) which was reduced with formic acid – Raney nickel to obtain 2-chloronicotinaldehyde (**21**). 2-Thiocyanonicotinaldehyde (**22**) was prepared by the treatment of **21** with potassium thio-

Can. J. Chem. Downloaded from www.nrcresearchpress.com by 210.87.254.6 on 09/05/12
For personal use only.

TABLE 1. N.m.r. spectra of 2,3- and 3,4-disubstituted pyridines

No.	Compound	Chemical shifts, δ (p.p.m.) H-2	H-4	H-5	H-6	Other	Coupling constants (Hz) $J_{4,5}$	$J_{4,6}$	$J_{5,6}$
10	2-Aminothionicotinamide*	—	7.57	6.59	8.03	$CSNH_2$ 9.73, 9.43; NH_2 6.82	7.5	2	5
17	3-Aminothiopicolinamide†	—			7.94	$CSNH_2$ 9.5, 9.22		2	4
21	2-Chloronicotinaldehyde‡	—	8.25	7.43	8.62	*CHO* 10.45	8.5	2	4
22	2-Thiocyanonicotinaldehyde*	—	8.52	7.65	8.63	*CHO* 10.15	8	2	5
23	4-Acetyl-3-aminopyridine‡	8.22	—	7.41	7.91	NH_2 6.34; CH_3 2.29	—	—	5
24	4-Acetyl-3-thiocyanopyridine‡	9.13	—	7.87	8.81	CH_3 2.36	—	—	5

*Solvent: DMSO-d_6 + $CDCl_3$ (3:1).
†Solvent: DMSO-d_6.
‡Solvent: $CDCl_3$.

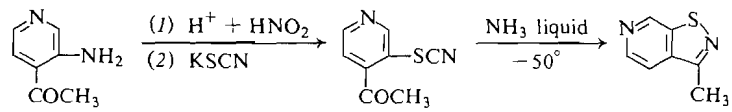

23 **24** **25**

SCHEME 4

cyanate in glacial acetic acid in nitrogen atmosphere. Cyclization of 2-thiocyanonicotinaldehyde (**22**) with a large excess of liquid ammonia at −50° for 4 h produced isothiazolo[5,4-*b*]pyridine (**6**).

The synthesis of 3-methylisothiazolo[5,4-*c*]-pyridine (**25**) was based on a principle similar to one applied in the case of **6** (Scheme 4). 4-Acetyl-3-aminopyridine (**23**) was diazotized and the diazonium salt was treated with potassium thiocyanate to obtain 4-acetyl-3-thiocyanopyridine (**24**) which was cyclized into **25** either with liquid ammonia at −50° for 5 h, or with ammonia in a pressure bomb at about 130° for 15 h.

Spectra

Nuclear Magnetic Resonance Spectra

The n.m.r. spectra of the 2,3-disubstituted pyridines (Table 1) **10**, **17**, **21**, and **22** display three sets of well resolved quartets of the AMX type (protons 3, 4, and 6). The three coupling constants $J_{4,5}$, $J_{4,6}$, and $J_{5,6}$ can be measured directly from the spectra. The spectra of the 3,4-disubstituted pyridines **23** and **24** exhibit a singlet for H-2 and a pair of doublets for H-5 and -6, consequently, there is no observable coupling between H-2 and other ring protons.

The three pyridine ring protons of isothiazolo-[3,4-*b*]pyridine (**1**) and its derivatives **11**–**15**, isothiazolo[5,4-*b*]pyridine (**6**), and 3-aminoisothiazolo[4,3-*b*]pyridine (**18**) also show three sets of quartets of the AMX type (Table 2). If we compare the chemical shifts of protons 2, 3, and 4 in 1,5- and 1,6-naphthyridine (4) (Scheme 5), we notice a similarity between **1** and **6** on one hand, and the two naphthyridines on the other hand.

Ultraviolet Spectra

The u.v. absorption data of 2,3- (**10**, **17**, **21**, **22**, and **26**) and 3,4-disubstituted pyridines (**23** and **24**) are given in Table 3. All of these compounds show three main bands designated as the α-, p- and β-bands (5). In the 2,3-substituted amino-

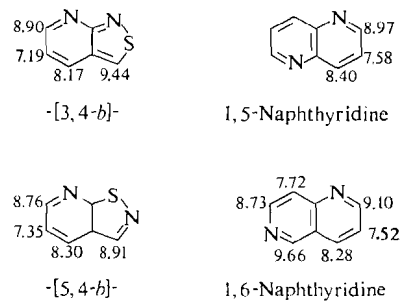

SCHEME 5. Chemical shifts (δ) of isothiazolo[3,4-*b*]-, -[5,4-*b*]pyridine, 1,5- and 1,6-naphthyridine.

Can. J. Chem. Downloaded from www.nrcresearchpress.com by 210.87.254.6 on 09/05/12
For personal use only.

TABLE 2. N.m.r. spectra of isothiazolopyridines

No.	Compound	Chemical shifts, δ (p.p.m.) H-3	H-4	H-5	H-6	H-7	Other	Coupling constants (Hz) $J_{4,6}$	$J_{5,6}$	$J_{4,5}$	$J_{5,7}$
1	Isothiazolo[3,4-*b*]pyridine*	9.44	8.17	7.19	8.90	—	—	2	4	8.8	—
11	3-Amino-†	—	8.27	6.77	8.55	—	NH_2 8.05	1.8	4	8.5	—
12	3-Bromo-†	—	8.17	7.44	8.96	—	—	1.8	4	8.5	—
13	3-Chloro-*	—	8.04	7.23	8.91	—	—	1.8	4	8.5	—
14	3-Mercapto-‡	—	8.49	7.07	8.64	—	—	1.8	5.5	7.5	—
15	3-Methoxy-†	—	8.10	7.09	8.77	—	OCH_3 4.30	2	4	8.5	—
6	Isothiazolo[5,4-*b*]pyridine*	8.91	8.30	7.35	8.76	—	—	1.5	4.8	8	—
18	3-Aminoisothiazolo[4,3-*b*]pyridine*	—	7.72	7.25	8.30	—	NH_2 7.81	1.8	3.8	8.9	—
25	3-Methylisothiazolo[5,4-*c*]pyridine*	—	7.76	8.60	—	9.31	CH_3 2.75			5.5	1.0

*Solvent: $CDCl_3$.
†Solvent: DMSO-d_6 + $CDCl_3$ (3:1).
‡Solvent: DMSO-d_6.

TABLE 3. The u.v. absorption maxima and log ε values of some disubstituted pyridines

No.	Compound	α-Band λ_{max} (nm)	α-Band log ε	p-Band λ_{max} (nm)	p-Band log ε	β-Band λ_{max} (nm)	β-Band log ε
10	2-Aminothionicotinamide*	345	3.65	268	3.83	217	4.25
		299	3.72				
17	3-Aminothiopicolinamide*	372	3.87	311	3.75	223	4.30
				264	3.89		
26	4-Aminothionicotinamide*	335sh		257	3.87	228	4.19
		294	3.67				
21	2-Chloronicotinaldehyde*	290sh	2.44	272	3.01	238	2.97
				265	3.09	210	3.52
22	2-Thiocyanonicotinaldehyde†	302sh	3.07	266	3.61	226	4.01
23	4-Acetyl-3-aminopyridine*	373	3.69	252	3.68	223	4.20
24	4-Acetyl-3-thiocyanopyridine*	320	3.66	247	3.74	224	4.20

*Solvent: 95% ethanol.
†Solvent: absolute methanol.

pyridinethioamides **10** and **17**, the bathochromic shift of the α-band is considerably larger than in the 3,4-substituted isomer, 4-aminothionicotinamide (**26**). This is in conformity with the u.v. absorption of the three isomeric aminopyridines: 2- and 3-aminopyridines absorb at 287 and 288 nm, respectively, as compared with the absorption by 4-aminopyridine at 268(sh) nm (6). In the u.v. spectrum of 4-acetyl-3-thiocyanopyridine (**23**) the α-band is displaced more toward the longer wavelength than in the spectrum of 4-acetyl-3-thiocyanopyridine (**24**) due to the conjugation of acetyl and amino groups.

The u.v. spectra of isothiazolo[3,4-*b*]- (**1**) (Table 4) and -[5,4-*b*]pyridine (**6**) (Table 5) consist of only two absorption bands each. The long wavelength bands at 296 and 298 nm, respectively, actually are not pure α-bands, but are overlapping with the p-bands due to the large bathochromic shift of the latter. The u.v. bands of **1** and **6** at 213 and 228 nm, respectively, are the β-bands, comparable to those present in the spectra of thiazolo[4,4-*c*]pyridine (7) and benzo[*b*]thiophene (8) at 216 and 227 nm, respectively. The u.v. spectra of **1** and **6** are also similar to those of 1,6- and 1,7-naphthyridine (9), but not to any other naphthyridines. The spectra of the halogen derivatives **12**, **13**, and **19**, and of 3-methylisothiazolo[5,4-*c*]pyridine (**25**) display only two bands.

Experimental

The melting points were determined on a Gallenkamp melting point apparatus and are corrected. N.m.r. spectra were obtained on a Varian high resolution n.m.r. model HA-100 spectrometer. Solvents used were deuterio-

Can. J. Chem. Downloaded from www.nrcresearchpress.com by 210.87.254.6 on 09/05/12
For personal use only.

TABLE 4. The u.v. absorption maxima and log ε values of isothiazolo[3,4-*b*]pyridine and its derivatives

No.	Compound*	α-Band		p-Band		β-Band	
		λ_{max} (nm)	log ε	λ_{max} (nm)	log ε	λ_{max} (nm)	log ε
1	Isothiazolo(3,4-*b*)pyridine	296	3.86			213	4.03
11	3-Amino-	400	3.98	302	3.89	245	4.45
				293	3.93	228	4.52
12	3-Bromo-	330	3.86			213	4.29
		303	4.00				
13	3-Chloro-	328sh	3.67			216	4.06
		303	3.83				
14	3-Mercapto-	314	3.56	248sh	3.38	211	3.79
		306	3.59				
15	3-Methoxy-	352	3.58	297sh	3.62	219	4.18
				289	3.66		

*Solvent: 95% ethanol.

TABLE 5. The u.v. absorption maxima and their log ε values of some isothiazolopyridine derivatives

No.	Compound*	α-Band		p-Band		β-Band	
		λ_{max} (nm)	log ε	λ_{max} (nm)	log ε	λ_{max} (nm)	log ε
18	3-Aminoisothiazolo[4,3-*b*]pyridine	390	3.54	307	3.38	245	4.09
				297	3.47	226	4.08
19	3-Bromoisothiazolo[4,3-*b*]pyridine	324	4.00			213	4.29
		306	4.14				
6	Isothiazolo[5,4-*b*]pyridine	307sh	3.40			228	4.19
		298	3.46				
25	3-Methylisothiazolo[5,4-*c*]pyridine	326sh	3.69			224sh	4.01
		313	3.74			209	4.15

*Solvent: 95% ethanol.

chloroform and dimethyl sulfoxide-d_6 and concentrations of solutions were 10–40 mg of solute per 0.5 ml of solvent. Tetramethylsilane was used as an internal reference. The u.v. spectra were recorded on a Unicam model SP-800 spectrophotometer and absolute ethanol and methanol were used as solvents. The i.r. spectra were taken in potassium bromide pellets on a Perkin–Elmer model 521 grating spectrometer. The mass spectra were obtained on an AEI-MS-902 double focusing mass spectrometer. The low resolution mass spectra were used to check the purity of compounds. The high resolution mass spectra served the purpose to prove the empirical formulas of unstable compounds, or when a small amount of material was available.

The elemental analyses were carried out by Dr. C. Daesslé, Montreal, and by A. Bernhardt, Germany.

*2-Aminothionicotinamide (**10**)*

Alcoholic ammonia (65 ml) containing 5 g of NH_3 (five-fold excess) was added to 2-aminonicotinonitrile (**9**) (7.0 g, 58.8 mmol) dissolved in absolute ethanol (16 ml) and triethylamine (5.9 g, 58.8 mmol). The reaction mixture was stirred magnetically and saturated with hydrogen sulfide for 1½–2 h. A yellow crystalline compound precipitated in less than an hour. The flask was loosely stoppered and allowed to stand at room temperature for 2 days to complete the reaction. Then the solution was poured onto crushed ice and the yellow substance was collected by suction filtration and dried at 60–70°. By this procedure 6.9 g of 2-aminothionicotinamide (**10**) was obtained. A further 0.6 g of the product was recovered by concentrating the filtrate under reduced pressure, pouring the solution on crushed ice, and filtering. 2-Aminothionicotinamide (**10**) was obtained in a nearly pure form (yield 7.5 g, 83%). Recrystallization from benzene gave yellow prisms, m.p. 132–133°. I.r. (KBr): 3420, 3310, 3180 cm^{-1} (NH_2).

Anal. Calcd. for $C_6H_7N_3S$ (mol. wt. 153.15): C, 47.0; H, 4.6; N, 27.4; S, 20.9. Found: C, 47.1; H, 4.7; N, 27.5; S, 20.8. *M/e*: 153 (P); 155 (P + 2).

*3-Aminoisothiazolo(3,4-b)pyridine (**11**)*

2-Aminothionicotinamide (**10**) (4.6 g, 0.03 mol) was dissolved in pyridine (10 ml) and warmed at 35° with stirring. Hydrogen peroxide (30%) (3.6 ml) was added very slowly to the reaction mixture. After the addition was completed, a yellow solid precipitated. The solution was further stirred at 35° for 10 min and let stand at room temperature for 16 h. The resulting precipitate was filtered off, washed with water, and dried. Crystallization

Can. J. Chem. Downloaded from www.nrcresearchpress.com by 210.87.254.6 on 09/05/12
For personal use only.

Can. J. Chem. Downloaded from www.nrcresearchpress.com by 210.87.254.6 on 09/05/12
For personal use only.

from ethanol gave 3.67 g (80% yield) of fine needles of 3-aminoisothiazolo(3,4-*b*)pyridine, m.p. 203.5–204.5°. I.r. (KBr): 1620, 3297–3258 (broad), 3100 cm^{-1} (NH_2).

Anal. Calcd. for $C_6H_5N_3S$ (mol. wt. 151.13): C, 47.7; H, 3.3; N, 27.8; S, 21.2. Found: C, 47.8; H, 3.2; N, 27.8; S, 21.3. *M/e*: 151 (P); 153 (P + 2).

*Isothiazolo[3,4-b]pyridine (**1**)*

3-Aminoisothiazolo[3,4-*b*]pyridine (**11**) (2.7 g, 17.9 mmol) was dissolved in 85% phosphoric acid (120 ml) and 70% nitric acid (30 ml) was added. The resulting solution was cooled to −5 to −2° and sodium nitrite (1.32 g, 19.1 mmol) in water (12 ml) was added with stirring over a period of 30 min. The reaction mixture was stirred for another 10 min at this temperature and then was added in portions to a stirred 30% hypophosphorous acid (50 ml) at 25–35°, to which a small amount of cuprous oxide has been added. The reaction mixture was stirred for 1 h at room temperature. It was then made alkaline with 20% sodium hydroxide solution with cooling. The mixture was extracted thrice with 400 ml portions of ether. The ethereal extract was washed with water, dried over sodium sulfate, and evaporated to dryness under reduced pressure. Crystallization from *n*-hexane produced 0.59 g (24% yield) of pure isothiazolo[3,4-*b*]pyridine (**1**) as short colorless needles, m.p. 58.5°.

M/e: 136 (P); 138 (P + 2). Calcd. mass from the exact mass measurement: 136.008933. Calcd. mass for $C_6H_4N_2S$: 136.009519. Delta mass: 0.000585.

*3-Bromoisothiazolo[3,4-b]pyridine (**12**)*

3-Aminoisothiazolo[3,4-*b*]pyridine (**11**) (0.97 g, 6.4 mmol) was suspended in 48% fuming hydrobromic acid (25 ml). Sodium nitrite (0.7 g, 10 mmol) was added in small portions over a period of 20 min with stirring. The temperature of the mixture was kept at −4° to −20°. When the addition was completed, the mixture was stirred at 0° for a further 30 min and let stand overnight at room temperature. It was poured slowly onto 200 g of crushed ice and made strongly alkaline with 20% sodium hydroxide. The solution was extracted thrice with 150 ml portions of ether and the combined ethereal extract was dried over sodium sulfate. The solvent was evaporated under reduced pressure leaving 0.84 g of a crude yellow substance. Chromatography followed by crystallization from ethyl acetate gave 0.52 g (38% yield) of pure 3-bromoisothiazolo[3,4-*b*]pyridine (**12**) as yellow prisms m.p. 158–159°.

Anal. Calcd. for $C_6H_3N_2SBr$ (mol. wt. 215.12): C, 33.5; H, 1.4; N, 13.0; S, 14.9; Br, 37.2. Found: C, 33.4; H, 1.6; N, 13.3; S, 14.8; Br, 37.5. *M/e*: 214 (P); 216 (P + 2).

*3-Chloroisothiazolo[3,4-b]pyridine (**13**)*

Cuprous chloride was prepared from 3.0 g of cupric sulfate, 0.66 g of sodium chloride, 0.5 g of sodium hydrogen sulfite, and 0.36 g of sodium hydroxide and was dissolved in 10 ml of concentrated hydrochloric acid.

3-Aminoisothiazolo[3,4-*b*]pyridine (**11**) (0.9 g, 6 mmol) was dissolved in a mixture of 40 ml of 80% phosphoric acid and 10 ml of 70% nitric acid. The acid mixture was cooled to −5 to −2° (acetone – Dry Ice bath) and stirred magnetically. Sodium nitrite (0.44 g, 6.5 mmol) in water (4.0 ml) was added dropwise to the cooled stirred solution. The resulting diazonium solution was stirred for another 20 min at −5° and subsequently added slowly with stirring to the pre-cooled cuprous chloride solution at −5 to −2°. The reaction mixture was stirred at this temperature for 20 min and at room temperature for another hour. It was then made alkaline with 20% sodium hydroxide solution. The mixture was extracted with three 150 ml portions of ether. The combined ethereal extract was washed with water, dried over sodium sulfate, and evaporated to dryness under reduced pressure leaving 0.71 g of a crude yellow solid. Crystallization from *n*-hexane gave 0.46 g (45% yield) of pure 3-chloroisothiazolo[3,4-*b*]pyridine (**13**) as pale yellow needles, m.p. 96–97°. I.r. (KBr): 1003 cm^{-1} (strong) (Cl).

Anal. Calcd. for $C_6H_3N_2SCl$ (mol. wt. 170.56): C, 42.4; H, 1.8; N, 16.4; S, 18.8; Cl, 20.8. Found: C, 42.3; H, 1.6; S, 18.9; Cl, 20.7. *M/e*: 170 (P); 172 (P + 2).

*3-Mercaptoisothiazolo[3,4-b]pyridine (**14**)*

A solution of 3-chloroisothiazolo[3,4-*b*]pyridine (0.3 g, 1.8 mmol) and thiourea (0.2 g, 2.6 mmol) in 20 ml of absolute ethanol was refluxed for 3 h. The crystalline precipitate was dissolved in 40 ml of 1 *N* sodium hydroxide solution and filtered. Acidification of the filtrate with acetic acid produced a flocculent precipitate which was filtered off, washed with water, and dried to obtain 0.16 g (56% yield) of 3-mercaptoisothiazolo[3,4-*b*]pyridine (**14**). Crystallization from ethanol produced **14** in the form of fine dark purple needles, m.p. 188–189°.

M/e: 168 (P); 170 (P + 2). Calcd. mass from the exact mass measurement: 167.981477. Calcd. mass for $C_6H_4N_2S_2$: 167.981592. Delta mass: 0.000114.

*3-Methoxyisothiazolo[3,4-b]pyridine (**15**)*

3-Chloroisothiazolo[3,4-*b*]pyridine (0.3 g, 1.8 mmol) was dissolved in 30 ml of absolute methanol and a solution of sodium methoxide, prepared from 0.1 g of sodium and 5 ml of methanol, was added. The yellow solution was neutralized with dilute acetic acid and diluted with 50 ml of water. The precipite was filtered off, washed with water and dried. Chromatography and crystallization from methanol gave 0.12 g (41% yield) of **15**, m.p. 104–105°.

M/e: 166 (P); 168 (P + 2). Calcd. mass from the exact mass measurement: 166.027814. Calcd. mass for $C_7H_6N_2SO$: 166.021082. Delta mass: 0.006732.

*3-Aminothiopicolinamide (**17**)*

Alcoholic ammonia (58 ml) was added to 3-aminopicolinonitrile (**16**) (6.3 g, 0.54 mol) dissolved in a mixture of 14.5 ml of absolute ethanol and 53.1 g (0.054 mol) of triethylamine. The solution was stirred and saturated with hydrogen sulfide for 90 min; a yellow substance precipitated. The flask was loosely stoppered and let stand at room temperature for 2 days. The solution was poured onto crushed ice and the yellow product filtered off. Crystallization from benzene gave 2.95 g (36% yield) of 3-aminothiopicolinamide (**17**), m.p. 161–162°.

Anal. Calcd. for $C_6H_7N_3S$ (mol. wt. 153.15): C, 47.0; H, 4.6; N, 27.4; S, 20.93. Found: C, 47.0; H, 4.8; N, 27.6; S, 20.8. *M/e*: 153 (P); 155 (P + 2).

*3-Aminoisothiazolo[4,3-b]pyridine (**18**)*

3-Aminothiopicolinamide (**17**) (0.42 g, 2.7 mmol) was dissolved in 1.7 ml of pyridine by heating at 35° with stirring. Hydrogen peroxide (30%, 1.0 ml) was added dropwise to the reaction mixture to maintain the temperature below 35°. The flask was stoppered and let stand at room temperature for 16 h. It was then poured onto a

Can. J. Chem. Downloaded from www.nrcresearchpress.com by 210.87.254.6 on 09/05/12
For personal use only.

small amount of crushed ice and the yellow product filtered off. Crystallization from benzene produced 0.124 g (30% yield) of 3-aminoisothiazolo[4,3-*b*]pyridine (**18**) as fine yellow needles, m.p. 195–196°. I.r. (KBr): 1652, 3310, 3250, 3080 cm^{-1} (NH_2).

Anal. Calcd. for $C_6H_5N_3S$ (mol. wt. 151.13): C, 47.7; H, 3.3; N, 27.8; S, 21.2. Found: C, 47.4; H, 3.4; N, 28.0; S, 21.0. *M/e*: 151 (P); 153 (P + 2).

*3-Bromoisothiazolo[4,3-b]pyridine (**19**)*

3-Aminoisothiazolo[4,3-*b*]pyridine (**18**) (90 mg, 0.59 mmol) was suspended in 5 ml of 48% hydrobromic acid. Sodium nitrite (70 mg, 1.0 mmol) was added in small portions over a period of 3 min with constant stirring at −4 to 0°. The mixture was stirred for 30 min at 0° and let stand at room temperature overnight. Crushed ice was added and the solution was made strongly alkaline with 20% sodium hydroxide solution. The mixture was extracted continuously with ether in liquid–liquid extractor. The ethereal extract was dried over sodium sulfate and the solvent evaporated to dryness leaving 53 mg of a brown substance. Chromatography and crystallization from benzene gave 28 mg (21% yield) of 3-bromoisothiazolo[4,3-*b*]pyridine (**19**) as yellow needles, m.p. 145–156°.

M/e: 214 (P); 216 (P + 2). Calcd. mass from the exact mass measurement: 215.916945. Calcd. mass for $C_6H_3z_2SBr$: 215.916411. Delta mass: 0.000543.

*2-Chloronicotinaldehyde (**21**)*

Raney nickel alloy (50–50; 30 g) was stirred with 3 l of 2 *N* sodium hydroxide solution for 30–40 min, the temperature being allowed to rise. The alkaline solution was decanted and the Raney nickel was washed twice with distilled water. A solution of 2-chloronicotinonitrile (**20**) (20.0 g, 0.141 mol) in 300 ml of 98% formic acid was added to the moist Raney nickel catalyst and the mixture was stirred for 30 min at 45–80°. The mixture was diluted with 280 ml of ethanol–water (2:1, v/v), filtered, and the catalyst washed twice with 50 ml of warm ethanol. The filtrate together with the ethanol washings was diluted with water and extracted several times with ether. The ethereal extract was washed with dilute sodium bicarbonate solution and water, and dried over sodium sulfate. The solvent was evaporated leaving 14.5 g of an oily brown substance which on distillation at 66–70°/5 mm Hg produced 11.8 g (58% yield) of a colorless oil which solidified immediately on cooling. Crystallization from ether–chloroform gave a pure 2-chloronicotinaldehyde (**21**) as colorless needles, m.p. 42–43°. I.r. (KBr): 2280 (—C*H*O) and 1688 cm^{-1} (—CH*O*).

M/e: 141 (P); 143 (P + 2). Calcd. mass from the exact mass measurement: 140.998452. Calcd. mass for C_6H_4NOCl: 140.998139. Delta mass: 0.000313.

*2-Thiocyanonicotinaldehyde (**22**)*

Potassium thiocyanate (7.4 g, 0.0754 mol) was added to 2-chloronicotinaldehyde (**21**) (6.0 g, 0.0427 mol) in glacial acetic acid (60 ml). The reaction mixture was stirred at room temperature and was kept under nitrogen atmosphere overnight. The solution was poured onto crushed ice and the yellow precipitate was collected by suction after a few hours. Crystallization from ethyl acetate yielded 4.6 g (65%) of 2-thiocyanonicotinaldehyde (**22**) as long yellow needles m.p. 143–144°. I.r. (KBr): 2163 cm^{-1} (SCN).

M/e: 164 (P); 166 (P + 2). Calcd. mass from the exact mass measurement: 164.004568. Calcd. mass for $C_7H_4N_2OS$: 164.004433. Delta mass: −0.000135.

*Isothiazolo[5,4-b]pyridine (**6**)*

Liquid ammonia in a large excess was added over a 3 h period to 2-thiocyanonicotinaldehyde (**22**) (4.1 g, 0.025 mol) placed in a 300 ml two-necked flask equipped with a magnetic stirrer and immersed in an ethanol – Dry Ice bath kept below 50°. The mixture was kept at this temperature with constant stirring for 5 h. Ammonia was allowed to evaporate slowly at room temperature leaving 3.06 g of a tan solid. Crystallization from *n*-hexane gave 1.3 g (38% yield) of isothiazolo[5,4-*b*]pyridine (**6**) in the form of fine colorless needles, m.p. 54.5–55.5°.

M/e: 136 (P); 138 (P + 2). Calcd. mass from the exact mass measurement: 136.009204. Calcd. mass for $C_6H_4N_2S$: 136.009519. Delta mass: 0.000315.

*4-Acetyl-3-thiocyanopyridine (**24**)*

4-Acetyl-3-aminopyridine (**23**) (1.08 g, 7.2 mmol) was dissolved in concentrated sulfuric acid (2.5 g) and water (5 ml), cooled to −4 to −2°, and diazotized with a solution of 0.58 g (8.2 mmol) of sodium nitrite in 2.5 ml of water. The resulting diazonium salt solution was stirred at this temperature for 10 min and then added dropwise with stirring to a solution of 0.88 g of potassium thiocyanate (9.0 mmol) in 2.5 ml of aqueous cuprous thiocyanate (prepared from 0.2 g of cupric sulfate, 0.88 g of potassium thiocyanate and 0.35 g of ferrous sulfate) was added to the mixture which was further stirred at room temperature for another hour. The reaction mixture was poured onto a small amount of crushed ice and neutralized with solid sodium bicarbonate. The brown precipitate was filtered off, dried, and crystallized from *n*-hexane to obtain 0.86 g (45% yield) of a pure 4-acetyl-3-thiocyanopyridine (**24**) as long colorless needles, m.p. 83–84°. I.r. (KBr): 2158 cm^{-1} (SCN).

M/e: 178 (P); 180 (P + 2).

Anal. Calcd. for $C_8H_6N_2SO$: C, 53.9; H, 3.4; N, 15.7; S, 17.99. Found: C, 53.2; H, 3.6; N, 15.6; S, 18.1.

*(a) Cyclization of 4-Acetyl-3-thiocyanopyridine (**24**) with Ammonium Hydroxide Under High Pressure*

A mixture of 1.78 g (0.01 mol) of 4-acetyl-3-thiocyanopyridine (**24**) and 100 ml of concentrated ammonium hydroxide was placed in a glass-liner within a stainless steel pressure bomb equipped with a magnetic stirrer and heated in a silicon oil bath at 130° for 5 h. The reaction mixture was evaporated to dryness leaving a brown solid substance. Chromatography and crystallization of the product from *n*-hexane gave 0.31 g (20% yield) of 3-methylisothiozolo[5,4-*c*]pyridine (**25**) as pale orange prisms, m.p. 57–58°.

M/e: 150 (P); 152 (P + 2); mol. wt. 150.13. Calcd. mass from the exact mass measurement M: 150.02448. Delta mass: 0.00042. Calcd. mass for $C_7H_6N_2S$: M 150.0249. Delta mass: 0.00042.

*(b) Cyclization of 4-Acetyl-3-thiocyanopyridine (**24**) with Liquid Ammonia*

Liquid ammonia was added in a large excess over a 3 h period to 1.0 g (6.7 mmol) of 4-acetyl-3-thiocyanopyridine (**24**) placed in a 200 ml two-neck flask equipped with a magnetic stirrer and immersed in an ethanol – Dry Ice bath kept below −50°. The reaction mixture was further stirred for another 5 h and then ammonia was allowed to

evaporate slowly at room temperature leaving a brown solid substance. Crystallization of the product from *n*-hexane gave 0.185 g (22% yield) of 3-methylisothiozolo-[5,4-*c*]pyridine (**25**), m.p. 57–58°.

The n.m.r. and mass spectra of this compound were exactly the same as for **25** prepared by the procedure *a*.

*4-Aminothionicotinamide (**26**)*

This compound was prepared from 4-aminonicotinonitrile (**27**) by the procedure used in preparing 2-aminothionicotinamide (**10**). From 0.7 g (5.9 mmol) of **27**, 0.56 g (62% yield) of **26** was obtained as fine pale yellow needles, m.p. 157–158°.

Anal. Calcd. for $C_6H_7N_3S$ (mol. wt. 153.15): C, 47.0; H, 4.6; N, 27.4; S, 20.9. Found: C, 47.4; H, 4.5; N, 27.7; S, 20.6. *M/e*: 153 (P); 155 (P + 2).

1. E. C. TAYLOR and A. J. CROVETTI. J. Org. Chem. **19**, 1636 (1954).
2. M. DAVIS. *In* Advances in heterocyclic chemistry. *Edited by* A. R. Katritzky and A. J. Boulton. Vol. 14. Academic Press, Inc., New York and London. 1972. p. 65.
3. W. WALTER. *In* Organosulfur chemistry. *Edited by* M. J. JANSSEN. Interscience – J. Wiley and Sons, New York, N.Y. 1967. p. 241.
4. W. W. PAUDLER and T. J. KRESS. The naphthyridines. *In* Advances in heterocyclic chemistry. *Edited by* A. R. Katritzky and A. J. Boulton. Vol. 11. Academic Press, New York and London. 1970. p. 132.
5. E. CLAR. Aromatische Kohlenwasserstoffe. 2nd Ed. Springer, Berlin. 1952.
6. S. F. MASON. J. Chem. Soc. 219 (1960).
7. T. TAKAHASHI, K. UEDA, and T. ICHIMOTO. Pharm. Bull. (Jap.). **4**, 220 (1956).
8. G. M. BADGER and J. J. CHRISTIE. J. Chem. Soc. 3438 (1956).
9. A. ALBERT. J. Chem. Soc. 1790 (1960).

Can. J. Chem. Downloaded from www.nrcresearchpress.com by 210.87.254.6 on 09/05/12
For personal use only.

The Vibrational Analysis of Cyclopentanone[1]

V. B. KARTHA,[2] H. H. MANTSCH,[3] AND R. N. JONES

Division of Chemistry, National Research Council of Canada, Ottawa, Canada K1A 0R6

Received May 2, 1972[4]

The infrared and Raman spectra of cyclopentanone, $\alpha\alpha\alpha'\alpha'$-$d_4$-cyclopentanone, $\beta\beta\beta'\beta'$-d_4-cyclopentanone and d_8-cyclopentanone have been measured and a normal co-ordinate analysis performed based on a twisted C_2 conformation. The 36 normal vibrations were computed using a selective valence force field comprising 16 diagonal and 16 off-diagonal force constants. The 4 isotopic species provided 144 frequencies to refine 15 diagonal force constants. The initial values of the constants were transferred from a force field for cyclohexanone computed in this laboratory. The infrared and Raman spectra were analyzed in terms of the potential energy distribution coefficients categorized as group frequencies, zone frequencies, and delocalized frequencies.

Les spectres infrarouge et Raman de la cyclopentanone, de la cyclopentanone $\alpha\alpha\alpha'\alpha'$-$d_4$, de la cyclopentanone $\beta\beta\beta'\beta'$-d_4 et de la cyclopentanone-d_8 ont été étudiés et une analyse (en coordonnées normales) a été effectuée en se basant sur une conformation C_2 croisée. Les 36 vibrations normales ont été evaluées en utilisant un champ de force valentielle sélectif qui comprend 16 constantes de force diagonales et 16 autres non-diagonales. Les 4 espèces isotopiques ont engendré 144 fréquences qui ont aidé à déterminer 15 constantes de force diagonales. Les valeurs initiales des constantes ont été obtenues d'un champ de force pour la cyclohexanone calculé dans ce laboratoire. Les spectres infrarouge et Raman ont été analysés en fonction des coefficients de distribution d'énergie potentielle classés selon des fréquences de groupe, des fréquences de zone et des fréquences délocalisées.

[Traduit par le journal]

Can. J. Chem., 51, 1749 (1973)

Introduction

This paper is concerned with a vibrational analysis of cyclopentanone and three deuterium substituted species (**1**–**4**); it supplements earlier work on cyclohexanone (1). These studies are being made to assess the capabilities and limitations of a simplified normal co-ordinate treatment to aid in the interpretation of the vibrational spectra of molecules of low symmetry related to natural products with particular reference to steroids.

Several conformations varying from planar (C_{2v}) to lower symmetries (C_2, C_s, C_1) have been

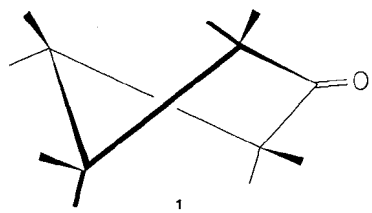

1

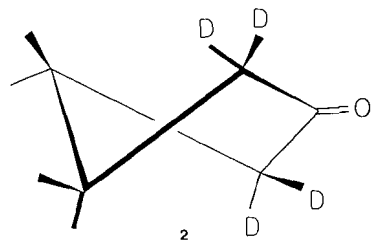

2

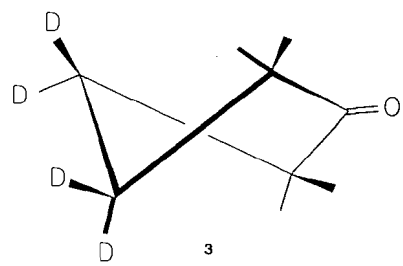

3

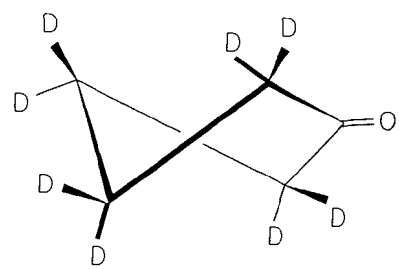

4

[1]NRCC No. 13046. Presented in part at a joint session of the Physical Chemistry and Organic Chemistry Divisions of the Chemical Institute of Canada, Halifax, Nova Scotia, May 1971.

[2]NRCC Postdoctorate Fellow, 1967–1969.

[3]NRCC Postdoctorate Fellow, 1969–1971.

[4]Revision received December 29, 1972.

Can. J. Chem. Downloaded from www.nrcresearchpress.com by 210.87.254.40 on 09/05/12
For personal use only.

proposed for cyclopentanone; they have been reviewed by Howard-Lock and King (2). The ground state geometry assumed in this work (Fig. 1) is based on a least squares fit of the bond parameters (Table 1) to the rotational constants of **1**, **2**, **4**, and two conformers of α-*d*-cyclopentanone (**5**, **6**). The rotational constants were taken from microwave data in the literature (3–7). Calculations were performed with the twisted C_2 and the bent C_3 structures.[5] All 9 parameters were allowed to adjust until the sum of the squares of the differences between the reported and computed rotational constants was minimal. The only restraint was that the C_2—C_3 and C_3—C_4 bond

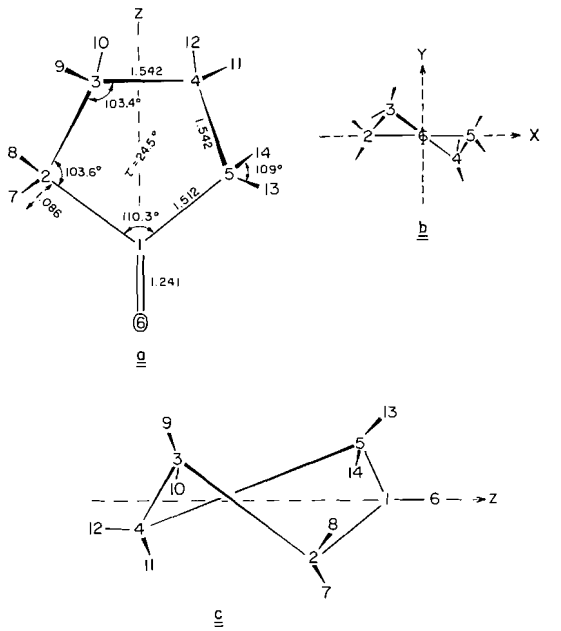

FIG. 1. Atom numeration and geometric parameters in the skew configuration.

TABLE 1. Molecular parameters for cyclopentanone derived from microwave measurements

No.	Parameter	Refined value
1	C_1—C_2	1.512 Å
2	C_2—C_3; C_3—C_4	1.542 Å
3	C=O	1.241 Å
4	C—H	1.086 Å
5	$\angle C_5C_1C_2$	110.283°
6	$\angle C_1C_2C_3$	103.576°
7	$\angle C_2C_3C_4$	103.443°
8	∠HCH	108.999°
9	Twist angle	24.519°

[5]See Fig. 2 of ref. 2.

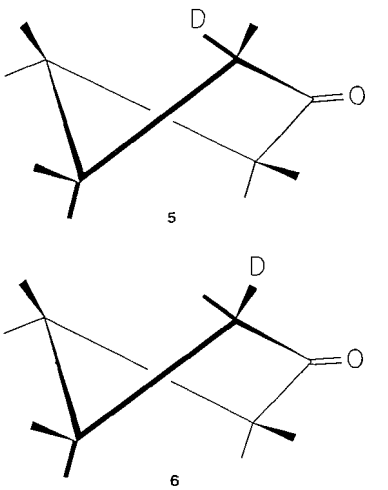

lengths remained equal and the calculations were considered self-consistant when the variations in the bond lengths were less than 0.001 Å.[6] The C_2 conformation in which the ring is twisted in a skew configuration gave much the better fit. Such a C_2 ground state is consistent with similar calculations[7] of Kim and Gwinn (7) and Howard-Lock and King (2) and with more recent far infrared studies of Ikeda and Lord (8), and electron diffraction measurements of Geise and Mijlhoff (9).

The Cartesian co-ordinates of the equilibrium positions of the atoms were computed with respect to an origin centered at the mid-point of the C_2—C_5 axis (Table 2). The 47 selected internal valance co-ordinates are identified[8] in Figs. 2 and 3. Under C_2 symmetry the 36 normal vibrations divide into 18 type A (Raman polarized) and 18 type B (Raman depolarized), and all are infrared and Raman active. The 47 internal co-ordinates were combined into 47 non-normalized symmetry co-ordinates (Table 3). As there are 36 normal modes 11 symmetry co-ordinates are redundant. The local redun-

[6]All molecular dimensions are reported in Å (1 Å = 10^{-10} m).

[7]The refined bond parameters in Table 1 differ slightly from those reported in refs. 2 and 7. Our twist angle (24.5°) is close to that of Kim and Gwinn (24°) but Howard-Lock and King obtained 33°. Our differences from Kim and Gwinn's bond lengths are probably due to the fact that they held the C—H and C=O bond lengths and the CH_2 angles fixed during refinement while we allowed them to adjust.

[8]Figure 1 exhibits the true projections of the non-planar ring but the projection diagrams appearing elsewhere have been distorted to permit more space to portray the bond and angle motions within the ring.

Can. J. Chem. Downloaded from www.nrcresearchpress.com by 210.87.254.40 on 09/05/12
For personal use only.

TABLE 2. Cartesian co-ordinates of cyclopentanone in the C_2 skew conformation

Atom No.*	Co-ordinates (Å)	Atom No.	Co-ordinates (Å)
1(C)	$x = 0.0$, $y = 0.0$, $z = 0.864448$	8(H)	$x = -1.945792$, $y = 0.758048$, $z = 0.329162$
2(C)	$x = -1.241065$, $y = 0.0$, $z = 0.0$	9(H)	$x = -0.641546$, $y = 1.392274$, $z = -1.569303$
3(C)	$x = -0.701264$, $y = 0.319867$, $z = -1.408063$	10(H)	$x = -1.330775$, $y = -0.118765$, $z = -2.176788$
4(C)	$x = 0.701264$, $y = -0.319867$, $z = -1.408063$	11(H)	$x = 0.641546$, $y = -1.392274$, $z = -1.569303$
5(C)	$x = 1.241065$, $y = 0.0$, $z = 0.0$	12(H)	$x = 1.330775$, $y = 0.118765$, $z = -2.176788$
6(O)	$x = 0.0$, $y = 0.0$, $z = 2.105452$	13(H)	$x = 1.730035$, $y = 0.969616$, $z = 0.019405$
7(H)	$x = -1.730035$, $y = -0.969616$, $z = 0.019405$	14(H)	$x = 1.945792$, $y = -0.758048$, $z = 0.329162$

*For numbering of atoms see Fig. 1.

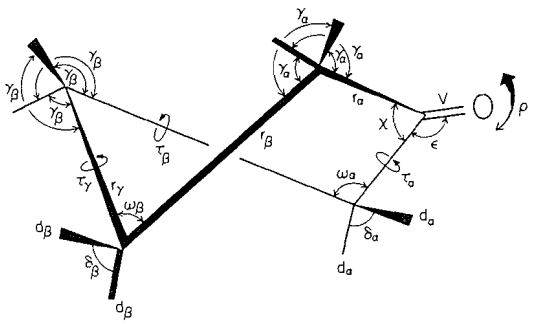

FIG. 2. Internal valence co-ordinates.

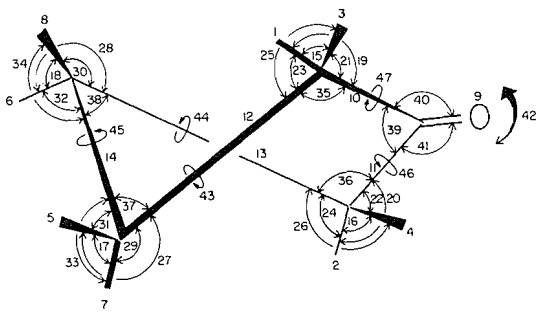

FIG. 3. Numerical identification of the internal valence co-ordinates.

dancies at the 5 carbon atoms are easily recognized and the remaining 6 are eliminated during normalization by the GMAT program (1, 10).

Experimental

1 and **4** are commercially available compounds while **2** and **3** were prepared by exchange reactions at the active α positions.

Cyclopentanone (1)

An Eastman Organic Chemical reagent grade sample was distilled under reduced pressure in a Nester–Faust spinning band column.

αα′α′-d_4-Cyclopentanone (2)

Cyclopentanone (30 ml), purified as above, was stirred with D_2O (99.7%, 60 ml) and Na_2CO_3 (600 mg) at room temperature for 24 h in a sealed glass tube. The product was extracted with ether, dried ($MgSO_4$), the ether removed, and the residue distilled under reduced pressure (55–60 Torr). The product was twice recycled under the same conditions. In the final distillation the first fraction (3.5 ml) was discarded and the next 5 ml collected. The infrared spectrum showed negligible H_2O or D_2O absorption and indicated almost complete α-deuteration. Mass spectrum analysis, when extrapolated to zero ionization voltage, indicate a d_4 content in excess of 90%.

ββ′β′-d_3-Cyclopentanone (3)

d_8-Cyclopentanone (1 ml) was stirred with H_2O (3 ml) and Na_2CO_3 (30 mg) in an all-glass system for 24 h at room temperature. The product was extracted with ether, the ether removed by evaporation at room temperature, and the residue again treated for 24 h with H_2O (2 ml)

Can. J. Chem. Downloaded from www.nrcresearchpress.com by 210.87.254.40 on 09/05/12
For personal use only.

Can. J. Chem. Downloaded from www.nrcresearchpress.com by 210.87.254.40 on 09/05/12
For personal use only.

TABLE 3. Symmetry co-ordinates of cyclopentanone in the C_2 skew configuration (not normalized)

Internal co-ordinates involved*	Approximate description†
Type A	
$S_1 = d_1+d_2-d_3-d_4$	asym α CH stretch
$S_2 = d_5+d_6-d_7-d_8$	asym β CH stretch
$S_3 = d_1+d_2+d_3+d_4$	sym α CH stretch
$S_4 = d_5+d_6+d_7+d_8$	sym β CH stretch
$S_5 = v_9$	C=O stretch
$S_6 = r_{10}+r_{11}$	α C—C stretch
$S_7 = r_{12}+r_{13}$	β C—C stretch
$S_8 = r_{14}$	γ C—C stretch
$S_9 = \delta_{15}+\delta_{16}$	α CH_2 scissor
$S_{10} = \delta_{17}+\delta_{18}$	β CH_2 scissor
$S_{11} = \gamma_{19}+\gamma_{20}+\gamma_{21}+\gamma_{22}-\gamma_{23}-\gamma_{24}-\gamma_{25}-\gamma_{26}$	α CH_2 wag
$S_{12} = \gamma_{27}+\gamma_{28}+\gamma_{29}+\gamma_{30}-\gamma_{31}-\gamma_{32}-\gamma_{33}-\gamma_{34}$	β CH_2 wag
$S_{13} = \gamma_{19}+\gamma_{20}-\gamma_{21}-\gamma_{22}-\gamma_{23}-\gamma_{24}+\gamma_{25}+\gamma_{26}$	α CH_2 twist
$S_{14} = \gamma_{27}+\gamma_{28}-\gamma_{29}-\gamma_{30}-\gamma_{31}-\gamma_{32}+\gamma_{33}+\gamma_{34}$	β CH_2 twist
$S_{15} = \gamma_{19}+\gamma_{20}-\gamma_{21}-\gamma_{22}+\gamma_{23}+\gamma_{24}-\gamma_{25}-\gamma_{26}$	α CH_2 rock
$S_{16} = \gamma_{27}+\gamma_{28}-\gamma_{29}-\gamma_{30}+\gamma_{31}+\gamma_{32}-\gamma_{33}-\gamma_{34}$	β CH_2 rock
$S_{17} = \gamma_{19}+\gamma_{20}+\gamma_{21}+\gamma_{22}+\gamma_{23}+\gamma_{24}+\gamma_{25}+\gamma_{26}$	Redundant
$S_{18} = \gamma_{27}+\gamma_{28}+\gamma_{29}+\gamma_{30}+\gamma_{31}+\gamma_{32}+\gamma_{33}+\gamma_{34}$	Redundant
$S_{19} = \omega_{35}+\omega_{36}$	α-CCC bend
$S_{20} = \omega_{37}+\omega_{38}$	β-CCC bend
$S_{21} = \chi_{39}-\varepsilon_{40}-\varepsilon_{41}$	C_α—CO—C_α bend
$S_{22} = \chi_{39}+\varepsilon_{40}+\varepsilon_{41}$	Redundant
$S_{23} = \tau_{43}+\tau_{44}$	$C_\alpha C_\beta$ torsion
$S_{24} = \tau_{45}$	$C_\beta C_\beta$ torsion
$S_{25} = \tau_{46}+\tau_{47}$	C_αC(O) torsion
Type B	
$S_{26} = d_1-d_2-d_3+d_4$	asym α CH stretch
$S_{27} = d_5-d_6-d_7+d_8$	asym β CH stretch
$S_{28} = d_1-d_2+d_3-d_4$	sym α CH stretch
$S_{29} = d_5-d_6+d_7-d_8$	sym β CH stretch
$S_{30} = r_{10}-r_{11}$	α C—C stretch
$S_{31} = -r_{12}+r_{13}$	β C—C stretch
$S_{32} = \delta_{15}-\delta_{16}$	α CH_2 scissor
$S_{33} = \delta_{17}-\delta_{18}$	β CH_2 scissor
$S_{34} = \gamma_{19}-\gamma_{20}+\gamma_{21}-\gamma_{22}-\gamma_{23}+\gamma_{24}-\gamma_{25}+\gamma_{26}$	α CH_2 wag
$S_{35} = \gamma_{27}-\gamma_{28}+\gamma_{29}-\gamma_{30}-\gamma_{31}+\gamma_{32}-\gamma_{33}+\gamma_{34}$	β CH_2 wag
$S_{36} = \gamma_{19}-\gamma_{20}-\gamma_{21}+\gamma_{22}-\gamma_{23}+\gamma_{24}+\gamma_{25}-\gamma_{26}$	α CH_2 twist
$S_{37} = \gamma_{27}-\gamma_{28}-\gamma_{29}+\gamma_{30}-\gamma_{31}+\gamma_{32}+\gamma_{33}-\gamma_{34}$	β CH_2 twist
$S_{38} = \gamma_{19}-\gamma_{20}-\gamma_{21}+\gamma_{22}+\gamma_{23}-\gamma_{24}-\gamma_{25}+\gamma_{26}$	α CH_2 rock
$S_{39} = \gamma_{27}-\gamma_{28}-\gamma_{29}+\gamma_{30}+\gamma_{31}-\gamma_{32}-\gamma_{33}+\gamma_{34}$	β CH_2 rock
$S_{40} = \gamma_{19}-\gamma_{20}+\gamma_{21}-\gamma_{22}+\gamma_{23}-\gamma_{24}+\gamma_{25}-\gamma_{26}$	Redundant
$S_{41} = \gamma_{27}-\gamma_{28}+\gamma_{29}-\gamma_{30}+\gamma_{31}-\gamma_{32}+\gamma_{33}-\gamma_{34}$	Redundant
$S_{42} = \omega_{35}-\omega_{36}$	α CCC bend
$S_{43} = -\omega_{37}+\omega_{38}$	β CCC bend
$S_{44} = \varepsilon_{40}-\varepsilon_{41}$	C=O bend in-plane
$S_{45} = \rho_{42}$	C=O bend out-of-plane
$S_{46} = \tau_{43}-\tau_{44}$	$C_\alpha C_\beta$ torsion
$S_{47} = \tau_{46}-\tau_{47}$	C_αC(O) torsion

*The + and − signs respectively identify an increase or decrease of the bond length or bond angle during the vibration.

†All symmetry co-ordinates involving combinations of symmetric internal co-ordinates yield in-phase (Type A) and out-of-phase (Type B) vibrations for which the same description is used. Asym (antisymmetric) and sym (symmetric) refer to the local site symmetry not to the symmetry axis of the molecule.

Can. J. Chem. Downloaded from www.nrcresearchpress.com by 210.87.254.40 on 09/05/12
For personal use only.

and Na_2CO_3 (200 mg). The product was extracted three times with 4 ml portions of ether and the bulked extracts dried with freshly regenerated molecular sieve type 4A. The ether was removed by distillation and the residue distilled under reduced pressure for the infrared and Raman measurements.

d_8-Cyclopentanone (4)

This material was purchased from Merck, Sharpe, and Dohme (Canada) Ltd. and used as received.

The infrared spectra of the pure liquids and solutions were measured in a Perkin–Elmer Model 521 infrared spectrophotometer. The digitally recorded spectra were processed as described elsewhere (1, 11). The same operating conditions, spectral slit widths, and solvent ranges were used as for cyclohexanone (1).

The Raman spectra were obtained with the 4880 Å excitation of a Spectra-Physics induction ion laser and a Spex 1400 recording spectrometer. The samples were distilled into quartz capillary tubes and sealed under helium at a pressure of 100–200 Torr. Under these conditions good Raman spectra could be obtained and reliable polarization measurements could be made.[9] The infrared spectra are shown in Fig. 4, and the Raman spectra in Fig. 5. The positions of the peaks of both the infrared and Raman bands are listed in Table 4*a–d*. Averaged values of the infrared and Raman peak positions were used in the computations except for the C=O stretch bands for which infrared values were employed.

Discussion

Factors influencing the choice of the initial set of force constants have been discussed in connection with cyclohexanone (1). Theoretically there are 1128 quadratic force constants. An initial set of 16 diagonal and 60 off-diagonal constants was used. During the refinement many of the interaction constants were eliminated and a satisfactory force field was achieved with the 16 diagonal and 16 off-axis constants listed in Table 5. Initially the starting constants were transferred from literature data for acetone and the generalized alicyclic hydrocarbon as was done for cyclohexanone (1). Subsequently the refined values obtained for cyclohexanone were used as starting values for cyclopentanone. Both computations converged to a similar force field but convergence from the cyclohexanone input data was much faster and only these values will be reported.[10]

The same systematic trend towards the differentiation of the force constants associated with the α and β carbon atoms was observed as with cyclohexanone *viz*:

$$K_{d(\alpha)} > K_{d(\beta)}$$
$$K_{r(\alpha)} > K_{r(\beta,\gamma)}$$
$$H_{\gamma(\alpha)} < H_{\gamma(\beta)}$$
$$H_{\omega(\alpha)} > H_{\omega(\beta)}$$
$$H_{\delta(\alpha)} < H_{\delta(\beta)}$$
$$H_{\chi} > H_{\iota}$$
$$H_{\tau(\alpha)} < H_{(\beta,\gamma)}$$

The stretch constant ($K_{r(\beta,\gamma)}$) and the corresponding C—C torsion ($H_{\tau(\beta,\gamma)}$) (internal coordinates 14, 45) were kept fixed in the sense that values for the β and γ positions were not allowed to differ. All the interaction constants were kept fixed during the refinement. A total of 144 experimental frequencies, derived from the four isotopic species, were used to refine 15 adjustable diagonal force constants. The force constants associated with the alicyclic part of the molecule are all well determined, but force constant No. 12 (H_χ) proved to be strongly correlated with force constant No. 3 (K_ν) and had to be kept fixed during the refinement.

The analysis of the 36 normal modes is based on the potential energy distribution coefficients (E_p) and the normal vibrations are classified as GF, ZF, or DF (1). These are listed in Table 4*a–d* together with the observed and calculated frequency data. Only the four largest E_p coefficients are listed, and these only if they exceed unity. In the vibrational diagrams only motions associated with $E_p > 10$ are indicated.

The C—C—C Skeletal Vibrations

The six normal modes below 600 cm^{-1} are listed in Table 6; they can be traced through the isotopic series by the E_p coefficients. The lowest band is a ring pucker (τ_α, τ_β); it has been described as a pseudo-rotation of the ring (2, 12) and has been recently investigated in detail by Ikeda and Lord (8). We observe it in the Raman spectra of **1** and **2**. The next higher fundamental at 239 cm^{-1} in **1** is an out-of-plane ring distortion with symmetric twists of the β and γ C—C bonds (τ_β, τ_γ) and closure of the β CCC angles (ω_β). Bands III and IV of Table 6 involve deformations of the C_α—CO—C_α group (ρ, ε) and will be discussed with the carbonyl vibrations.

The two in-plane ring vibrations V and VI

[9]We wish to thank Dr. W. F. Murphy for making these measurements for us.

[10]The detailed numerical calculations for the refinement from the cyclohexanone input data will be found in ref. 10 where they are used as illustrative examples in the description of the computer programs.

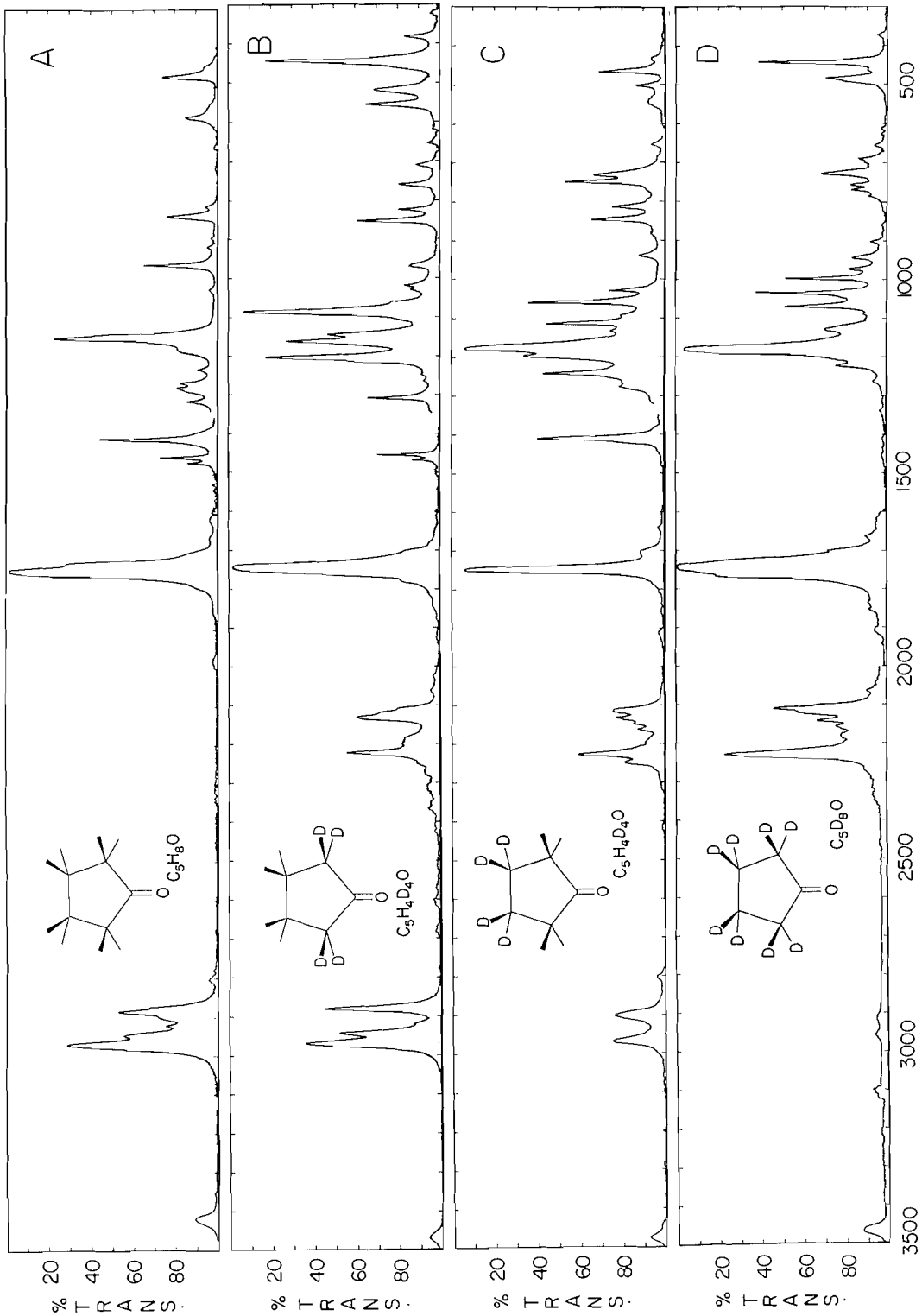

FIG. 4. Infrared spectra in solution. Solvent CCl_4 (4000–1380/630–240 cm^{-1}); CS_2 (1380–630 cm^{-1}). Path length 1 mm.

Can. J. Chem. Downloaded from www.nrcresearchpress.com by 210.87.254.40 on 09/05/12
For personal use only.

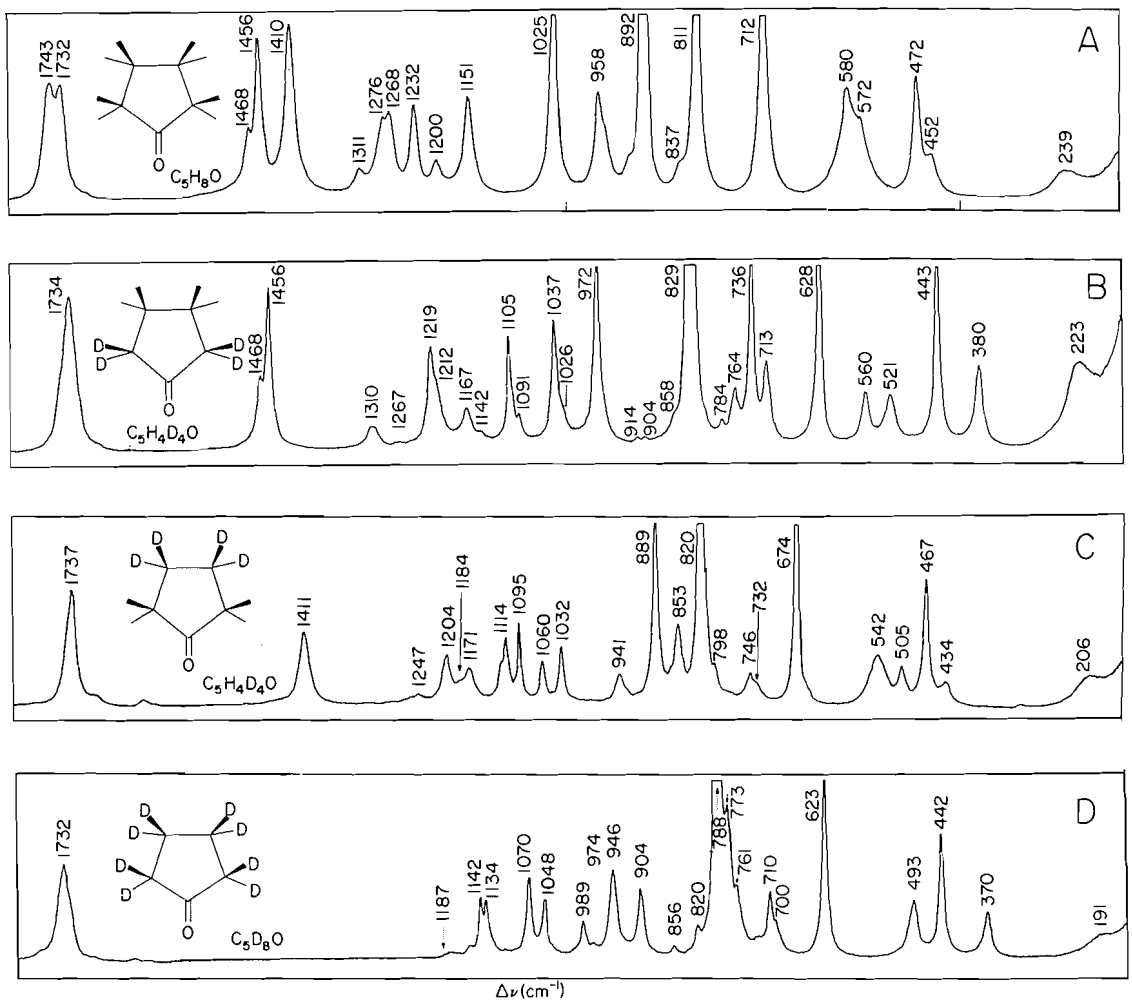

FIG. 5. Raman spectra of the pure liquids measured without polarizers; excitation with 4880 Å argon ion source. The region $\Delta\nu$ = 4600–1800 cm^{-1} is not shown, but the peak positions are listed in Table 12.

overlap near 570 cm^{-1} in **1** and near 490 cm^{-1} in **4**; they are well separated in **2** and **3**. The C_α—CO—C_α angle (χ) and the α C—C—C angle (ω_α) participate in V which is sensitive to α-deuteration. Both V and VI are highly delocalized. Mode VI emphasizes the effect of deuterium substitution on the mixing of the internal co-ordinates (Table 7*a*); on β-deuteration a large contribution to the energy of this mode is injected from the β D—C—C angle bend (γ_β). Above 600 cm^{-1} contributions from H—C—C and D—C—C bend motions predominate and the C—C stretch motions in this region are discussed with the C—H and C—D deformations.

The Carbonyl Group

Linear stretch of the C=O bond (ν) contributes only about 80% to the mode energy of the "C=O stretching group vibration" (Table 8) and the remaining energy is localized mainly in the α C—C stretch (r_α) and the C_α—CO—C_α bend (χ). In **1** the position of the C=O stretch vibration is strongly affected by Fermi resonance.[11] This has not been considered in these calculations since the displacement effect is small, especially for the pure liquid. Of potentially greater significance is the large downward shift in the C=O stretch frequency in passing from

[11]See ref. 13 and other references cited therein.

Can. J. Chem. Downloaded from www.nrcresearchpress.com by 210.87.254.40 on 09/05/12
For personal use only.

TABLE 4. Vibrational analysis

(*a*) Cyclopentanone (**1**)

Band No.	Symmetry type	Wavenumber (cm^{-1}) Calculated	Observed Infrared	Observed Raman	Raman polarization	Potential energy distribution (E_p)				Mode type*
1	B	106	(105)†	95	—	37(τ_α)	35(τ_β)	12(ρ)	8(ω_α)	ZF
2	A	239	(240 w)†	239 w	0.76	51($\tau_{\beta,\gamma}$)	26(ω_β)	10(ω_α)	5(γ_β)	ZF
3	B	440	450 m‡	452 m	0.79	75(ρ)	10(γ_α)	4(τ_α)	4($\tau_{\beta,\gamma}$)	GF
4	B	478	471 vs	472 vs	0.83	75(ε)	7(r_β)	6(r_α)	2(ω_α)	GF
5	A	545	564 m‡	572 s	0.30	27(χ)	25(ω_α)	11($r_{\beta,\gamma}$)	11(ε)	DF
6	B	573	580 s	580 s	0.83	47(ω_β)	20(ω_α)	13(γ_β)	5(r_α)	DF
7	A	771	706 w	712 vs	0.03	66(r_α)	11(γ_α)	6(γ_β)	6(ω_α)	GF
8	A	832	806 m	811 vvs	0.07	61(γ_α)	13(γ_β)	10(r_α)	10($r_{\beta,\gamma}$)	ZF
9	B	832	831 s	837 w	d.p.	61(γ_β)	21(γ_α)	5(r_β)	4(r_α)	ZF
10	A	894	889 w	892 vvs	0.03	79($r_{\beta,\gamma}$)	7(γ_β)	7(γ_α)	3(ω_β)	GF
11	B	954	—	—	—	55(r_β)	22(γ_α)	6(γ_β)	6(ε)	ZF
12	B	974	958 vs	958 s	0.80	49(γ_α)	29(γ_β)	8(r_β)	3(ρ)	ZF
13	A	1038	1021 m	1025 vs	0.59	35(γ_α)	28($r_{\beta,\gamma}$)	24(γ_β)	2(ω_β)	DF
14	A	1066	—	—	—	41(γ_β)	32($r_{\beta,\gamma}$)	11(γ_α)	4(ω_α)	ZF
15	A	1149	1148 vvs	1151 s	0.70	66(γ_α)	30(γ_β)	5($r_{\beta,\gamma}$)	—	GF
16	B	1154	—	—	—	49(γ_α)	42(r_α)	7(ε)	3(r_β)	ZF
17	B	1174	1176 s	—	—	45(γ_α)	40(r_α)	9(ε)	8(γ_b)	ZF
18	A	1184	—	1200 m	0.6	68(γ_α)	26(γ_β)	19($r_{\beta,\gamma}$)	2(r_α)	GF
19	B	1211	1227 m	1232 s	0.79	84(γ_α)	21(r_β)	11(γ_β)	3(ε)	GF
20	B	1231	1262 s	1268 s	—	79(γ_β)	12(γ_α)	10(r_α)	1(r_β)	GF
21	A	1232	—	—	—	71(γ_β)	21(γ_α)	9($r_{\beta,\gamma}$)	2(r_α)	GF
22	A	1280	1274 s	1276 s	—	79(γ_β)	21($r_{\beta,\gamma}$)	18(γ_α)	2(δ_β)	GF
23	B	1327	1311 s	1311 m	0.77	91(γ_β)	8(γ_α)	6(r_β)	4(δ_α)	GF
24	A	1412	1409 vs	1410 vs	0.70	74(δ_α)	25(γ_α)	2(γ_β)	2(δ_β)	GF
25	B	1418	—	—	—	70(δ_α)	25(γ_α)	4(γ_β)	—	GF
26	A	1460	1454 vs	1456 vs	0.74	72(δ_β)	28(γ_β)	1(δ_α)	—	GF
27	B	1467	1469 s	1468 m	—	73(δ_β)	27(γ_β)	—	—	GF
28	A	1745	1748 vvs	1732 vs 1743 vs	0.3 0.4 §	78(υ)	13(r_α)	5(χ)	2(ε)	GF
29	B	2884	2873 s	—	—	99(d_β)	—	—	—	GF
30	A	2885	2885 vs	2886 vs	—	99(d_β)	—	—	—	GF
31	B	2899	2898 s	2905 vs	—	99(d_α)	—	—	—	GF
32	A	2901	—	—	—	99(d_α)	—	—	—	GF
33	B	2952	2946 s	—	—	97(d_β)	3(d_α)	—	—	GF
34	A	2958	—	—	—	89(d_β)	11(d_α)	—	—	GF
35	B	2970	2969 vs	2972 vs	—	97(d_α)	3(d_β)	—	—	GF
36	A	2971	—	—	—	89(d_α)	11(d_β)	—	—	GF

*GF, group frequency; ZF, zone frequency; DF, delocalized frequency.
†These are new measurements on a Perkin–Elmer Model 180 spectrophotometer made after completion of the numerical analysis.
‡Inflection.
§Fermi resonance doublet.

(*b*) $\alpha\alpha\alpha'\alpha'$-$d_4$-Cyclopentanone (**2**)

Band No.	Symmetry type	Wavenumber (cm^{-1}) Calculated	Observed Infrared	Observed Raman	Raman polarization	Potential energy distribution (E_p)				Mode type*
1	B	96	(98)†	89	—	38(τ_α)	36(τ_β)	10(ρ)	8(ω_α)	ZF
2	A	222	—	223 m	—	50($\tau_{\beta,\gamma}$)	26(ω_β)	9(ω_α)	5(γ_β)	ZF
3	B	387	378 m	380 s	0.75	69(ρ)	21(γ_α)	3(ω_β)	2(τ_α)	GF
4	B	456	442 vs	443 vs	0.75	74(ε)	6(γ_α)	6(r_β)	5(γ_α)	GF
5	A	530	519 s	521 m	0.26	26(χ)	25(ω_α)	11(γ_α)	11(ε)	DF
6	B	560	557 s	560 m	0.73	43(ω_β)	20(ω_α)	13(γ_β)	6(γ_α)	DF

Can. J. Chem. Downloaded from www.nrcresearchpress.com by 210.87.254.40 on 09/05/12
For personal use only.

TABLE 4. (*Continued*)

(*b*) αααα′α′-d_4-Cyclopentanone (**2**)

Band No.	Symmetry type	Wavenumber (cm^{-1}) Calculated	Observed Infrared	Observed Raman	Raman polarization	Potential energy distribution (E_p)				Mode type*
7	A	666	624 vw	628 vvs	0.03	67(γ_α)	13(r_α)	8(γ_β)	3($r_{\beta,\gamma}$)	GF
8	A	704	710 s	713 s	0.58	38(γ_α)	35(r_α)	5(ω_α)	4(ω_β)	ZF
9	B	743	760 s	764 m	0.76	62(γ_α)	16(γ_β)	5(ρ)	5(ω_β)	ZF
10	A	787	—	736 s	0.16	80(γ_α)	13($r_{\beta,\gamma}$)	2(r_α)	—	GF
11	A	811	825 s	829 vvs	0.04	37(γ_α)	35($r_{\beta,\gamma}$)	12(r_α)	6(γ_β)	ZF
12	B	825	853 vs	858 w‡	—	57(γ_α)	27(r_β)	3(ω_β)	3(γ_β)	ZF
13	B	873	—	—	—	76(γ_α)	13(γ_β)	5(ρ)	1(r_α)	GF
14	B	901	—	904 vw	—	57(γ_β)	29(γ_α)	5(ρ)	2(r_β)	ZF
15	A	992	970 s	972 vs	0.60	45($r_{\beta,\gamma}$)	32(γ_α)	12(γ_β)	9(r_α)	ZF
16	B	1023	1020 s	1026 m*	—	78(δ_α)	23(γ_α)	5(r_β)	2(ω_α)	GF
17	A	1029	1031 s	1037 vs	0.49	62(δ_α)	21(γ_α)	11(γ_β)	4(r_α)	ZF
18	B	1063	1087 vvs	1091 m	—	40(r_β)	36(γ_α)	20(ε)	8(r_α)	ZF
19	A	1067	—	1105 vs	0.38	64(γ_β)	10($r_{\beta,\gamma}$)	10(γ_α)	10(δ_α)	ZF
20	A	1092	1145 vs	1142 w	—	67($r_{\beta,\gamma}$)	25(γ_α)	8(γ_β)	5(r_α)	GF
21	B	1166	1163 vvs	1167 m	0.83	77(r_α)	16(r_β)	9(γ_β)	9(γ_α)	GF
22	A	1219	1218 w‡	1219 vs	0.64	91(γ_β)	4($r_{\beta,\gamma}$)	3(γ_α)	2(r_α)	GF
23	B	1222	1204 vvs	1212 s‡	0.80	88(γ_β)	8(r_α)	2(γ_α)	—	GF
24	A	1269	1269 w	1267 vw	—	97(γ_β)	26($r_{\beta,\gamma}$)	2(δ_β)	1(ω_α)	GF
25§	B	1325	1309 s	1310 m	0.68	99(γ_b)	8(r_β)	1(δ_β)	1(r_α)	GF
26	A	1458	1454 s	1456 vs	—	74(δ_β)	29(γ_β)	—	—	GF
27	B	1467	1469 m	1468 s	0.80	73(δ_β)	27(γ_β)	—	—	GF
28	A	1743	1744 vvs	1734 vs	0.3	78(v)	13(r_α)	5(χ)	2(ε)	GF
29	B	2120	—	2126 s‡	—	97(d_α)	1(r_α)	—	—	GF
30	A	2124	2130 vs	2130 vs	—	97(d_α)	1($r_{\beta,\gamma}$)	—	—	GF
31	A	2215	—	2210 s‡	—	98(d_α)	1(γ_α)	—	—	GF
32	B	2217	2223 vs	2221 s	—	98(d_α)	1(γ_α)	—	—	GF
33	B	2884	2881 vs	2879 vs	—	99(d_β)	—	—	—	GF
34	A	2885	—	—	—	99(d_β)	—	—	—	GF
35	B	2952	2944 vs	2946 m‡	—	100(d_β)	—	—	—	GF
36	A	2959	2964 vs	2969 s	—	99(d_β)	—	—	—	GF

*GF, group frequency; ZF, zone frequency; DF, delocalized frequency.
†These are new measurements on a Perkin–Elmer Model 180 spectrophotometer made after completion of the numerical analysis.
‡Inflection.
§We have taken note of the anomaly in the Type B assignment of the Raman Band 25 which appears to be polarized.

(*c*) ββββ′β-d_4-Cyclopentanone (**3**)

Band No.	Symmetry type	Wavenumber (cm^{-1}) Calculated	Observed Infrared	Observed Raman	Raman polarization	Potential energy distribution (E_p)				Mode type*
1	B	101	—	—	—	37(τ_α)	35(τ_β)	12(ρ)	8(ω_α)	ZF
2	A	203	—	206 m	—	50($\tau_{\beta,\gamma}$)	25(ω_β)	10(ω_α)	8(γ_β)	ZF
3	B	438	—	434 m	0.76	71(ρ)	10(γ_α)	5(ω_β)	4(τ_α)	GF
4	B	468	—	467 vs	0.73	71(ε)	8(r_β)	6(r_α)	2(ω_α)	GF
5	B	515	—	505 m	0.78	34(ω_β)	34(γ_β)	14(ω_α)	6(ρ)	ZF
6	A	532	—	542 m	0.19	26(χ)	23(ω_α)	12($r_{\beta,\gamma}$)	11(ε)	DF
7	B	688	731 s	732 w	d.p.	63(γ_β)	13(ω_β)	7(ω_α)	5(r_α)	ZF
8	A	716	—	674 vvs	0.04	43(γ_β)	25(r_α)	22(γ_α)	3(ω_β)	ZF
9	A	775	748 vs	746 m	0.40	56(γ_β)	15($r_{\beta,\gamma}$)	12(r_α)	5(ω_α)	ZF
10	A	807	813 s	820 vvs	0.06	33(r_α)	27($r_{\beta,\gamma}$)	15(γ_α)	10(γ_β)	DF
11	B	831	—	—	—	72(γ_β)	16(γ_α)	4(r_β)	2(ε)	GF
12	B	857	847 vs	853 s	0.80	42(γ_β)	27(r_β)	12(γ_α)	7(ε)	ZF

Can. J. Chem. Downloaded from www.nrcresearchpress.com by 210.87.254.40 on 09/05/12
For personal use only.

TABLE 4. (*Continued*)

(*c*) ββββ′β-d_4-Cyclopentanone (**3**)

Band No.	Symmetry type	Wavenumber (cm^{-1}) Calculated	Observed Infrared	Observed Raman	Raman polarization	Potential energy distribution (E_p)				Mode type*
13	A	877	883 w	889 vs	0.16	72(γ_β)	14($r_{\beta,\gamma}$)	2(χ)	2(γ_α)	GF
14	A	910	—	—	—	42(γ_β)	27($r_{\beta,\gamma}$)	15(γ_α)	6(r_α)	ZF
15	A	967	940 m	941 m	0.8	51(γ_α)	30(γ_β)	9($r_{\beta,\gamma}$)	3(ω_β)	ZF
16	B	994	1028 s	1032 s	0.86	58(γ_α)	25(γ_β)	5(ρ)	3(r_β)	ZF
17	A	1056	1058 vvs	1060 s	0.78	74(δ_β)	26(γ_β)	11($r_{\beta,\gamma}$)	3(γ_α)	GF
18	B	1063	—	—	—	74(δ_β)	23(γ_β)	6(r_β)	4(ω_β)	GF
19	B	1124	1113 vs	1114 s	0.84	57(γ_b)	45(r_β)	11(γ_α)	2(ω_β)	ZF
20	A	1130	1092 m	1095 vs	0.09	57(γ_α)	29($r_{\beta,\gamma}$)	16(γ_β)	3(δ_β)	ZF
21	B	1158	1177 vvs	1184 w	d.p.	53(r_α)	36(γ_α)	11(ε)	7(ω_α)	ZF
22	A	1172	—	1171 m	—	60($r_{\beta,\gamma}$)	42(γ_α)	18(γ_β)	2(ω_α)	ZF
23	B	1179	1196 vs	1204 s	0.83	50(γ_α)	40(r_α)	8(ε)	3(γ_β)	ZF
24	A	1217	—	—	—	86(γ_α)	10($r_{\beta,\gamma}$)	9(γ_β)	5(r_α)	GF
25	B	1218	1241 s	1247 vw	d.p.	100(γ_α)	9($r_{\beta,\gamma}$)	3(r_α)	1(ε)	GF
26	A	1412	1408 vs	1411 s	—	77(δ_α)	25(γ_α)	—	—	GF
27	B	1416	—	—	—	74(δ_α)	25(γ_α)	—	—	GF
28	A	1745	1744 vvs	1737 vs	—	78(v)	13(r_α)	5(χ)	2(ε)	GF
29	B	2107	2114 s	2111 vs	—	98(d_β)	1(r_β)	—	—	GF
30	A	2112	2131 s	2137 vs	—	97(d_β)	2($r_{\beta,\gamma}$)	—	—	GF
31	B	2200	2225 vs	2225 s	—	99(d_β)	1(γ_β)	—	—	GF
32	A	2218	2247 s	2252 m	—	97(d_β)	2(γ_β)	—	—	GF
33	B	2899	2901 s	2904 vs	—	99(d_α)	—	—	—	GF
34	A	2900	—	—	—	99(d_α)	—	—	—	GF
35	A	2969	2967 s	2968 s	—	100(d_α)	—	—	—	GF
36	B	2970	—	—	—	100(d_α)	—	—	—	GF

*GF, group frequency; ZF, zone frequency; DF, delocalized frequency.

(*d*) d_8-Cyclopentanone (**4**)

Band No.	Symmetry type	Wavenumber Calculated	Observed Infrared	Observed Raman	Raman polarization	Potential energy distribution (E_p)				Mode type*
1	B	93	—	—	—	38(τ_α)	36(τ_β)	10(ρ)	8(ω_α)	ZF
2	A	189	—	191 m	—	50($\tau_{\beta,\gamma}$)	25(ω_β)	9(ω_α)	8(γ_β)	ZF
3	B	384	368 m	370 s	0.74	65(ρ)	22(γ_α)	4(ω_β)	3(τ_α)	GF
4	B	450	438 vs	442 vs	0.70	72(ε)	7(r_β)	5(r_α)	5(γ_α)	GF
5	B	503	481 s	—	—	33(γ_β)	31(ω_β)	14(ω_α)	8(ρ)	DF
6	A	518	493 s†	493 s	0.55	25(χ)	24(ω_α)	12(γ_α)	10(ε)	DF
7	A	629	618 w	623 vs	0.04	55(γ_α)	23(γ_β)	9(r_α)	4($r_{\beta,\gamma}$)	ZF
8	B	668	689 m	700 m	—	47(γ_β)	16(γ_α)	15(ω_β)	7(ω_α)	DF
9	A	697	706 m†	710 s	0.33	38(r_α)	31(γ_α)	5(ω_α)	5(γ_β)	ZF
10	B	758	727 vs	—	d.p.	41(γ_α)	24(γ_β)	21($r_{\beta,\gamma}$)	2(ω_β)	ZF
11	B	766	756 s	761 m†	—	45(γ_β)	44(γ_α)	4(ρ)	1(r_β)	ZF
12	A	774	769 s	773 vs	—	45($r_{\beta,\gamma}$)	23(γ_α)	9(γ_β)	9(r_α)	ZF
13	A	781	785 m	788 vvs	0.04	68(γ_α)	12(γ_β)	6($r_{\beta,\gamma}$)	3(r_α)	GF
14	A	798	—	—	—	58(γ_β)	28(γ_α)	4($r_{\beta,\gamma}$)	2(r_α)	ZF
15	A	864	856 vw	856 w	p.	80(γ_β)	8(γ_α)	4($r_{\beta,\gamma}$)	1(δ_α)	GF
16	B	870	902 m	904 s	0.80	76(γ_α)	12(γ_β)	5(ρ)	—	GF
17	B	919	972 s	974 w	d.p.	56(γ_β)	29(γ_α)	5(ρ)	1(d_α)	ZF
18	A	945	942 s	946 vs	0.76	56(γ_β)	24(γ_α)	6($r_{\beta,\gamma}$)	3($\tau_{\beta,\gamma}$)	ZF
19	B	1019	996 vs	989 m	—	50(γ_α)	24(γ_β)	11(δ_α)	10(ε)	ZF
20	B	1024	1033 vs	—	—	66(δ_α)	26(γ_α)	12(r_β)	3(ε)	GF

Can. J. Chem. Downloaded from www.nrcresearchpress.com by 210.87.254.40 on 09/05/12
For personal use only.

TABLE 4 (*Concluded*)

(*d*) d_8-Cyclopentanone (**4**)

Band No.	Symmetry type	Wavenumber Calculated	Observed Infrared	Observed Raman	Raman polarization	Potential energy distribution (E_p)				Mode type*
21	A	1036	1044 s†	1048 s	0.54	71(δ_α)	23(γ_α)	10(r_α)	2(ω_α)	GF
22	B	1060	1067 vs	1070 vs	0.46	70(δ_β)	25(γ_β)	22($r_{\beta,\gamma}$)	4(γ_α)	GF
23	B	1066	—	—	—	73(δ_β)	23(γ_β)	4(ω_β)	4(r_β)	GF
24	A	1071	—	—	—	46(γ_α)	28($r_{\beta,\gamma}$)	12(r_α)	10(γ_β)	ZF
25	B	1129	1127 s	1134 s	—	57(γ_β)	45(r_β)	5(ε)	4(r_α)	ZF
26	A	1157	—	1142 s	p.	86($r_{\beta,\gamma}$)	41(γ_β)	3(ω_α)	1(γ_α)	GF
27	B	1167	1181 vvs	1187 vw	d.p.	90(r_α)	11(r_β)	11(ε)	8(γ_α)	GF
28	A	1743	1742 vs	1732 vs	—	78(υ)	13(r_α)	5(χ)	2(ε)	GF
29	B	2107	2110 vs	2099 m	—	97(d_β)	1(r_β)	—	—	GF
30	A	2111	—	—	—	90(d_β)	7(d_α)	2($r_{\beta,\gamma}$)	—	GF
31	B	2119	2119 s†	2120	—	97(d_α)	1(r_α)	—	—	GF
32	A	2125	—	—	—	90(d_α)	7(d_β)	1($r_{\beta,\gamma}$)	—	GF
33	B	2198	2181 s	2181 m	—	87(d_β)	12(d_α)	—	—	GF
34	A	2206	—	—	—	56(d_α)	43(d_β)	—	—	ZF
35	B	2219	2229 vs	2231 vs	—	86(d_α)	12(d_β)	1(γ_α)	—	GF
36	A	2227	—	—	—	54(d_β)	43(d_α)	2(γ_β)	1(γ_α)	ZF

*GF, group frequency; ZF, zone frequency; DF, delocalized frequency.
†Inflection.

the vapor to the liquid state (~30 cm^{-1}). The liquid state values were used in this work.[12]

The in-plane C=O deformation (ε) is easily identified as a strong band in both the infrared and Raman spectra at 471, 456, 467, and 442 cm^{-1} in **1**–**4** respectively. It is highly localized with E_p 71–75. The out-of-plane C=O vibration (ρ) is the lowest of the three carbonyl frequencies at 451, 379, 434, 369 cm^{-1}; it is a medium-strong depolarized Raman band, strongly affected by α-deuteration, and in all four isotopic species accounts for 65–75% of the mode energy. This contrasts with cyclohexanone in which it is highly delocalized.

Bending Vibrations Involving CH and CD Bonds

There are 21 normal vibrations between 600 and 1500 cm^{-1} that involve HCH, HCC, DCD, and DCC angle deformations. Rigorous classification of these as methylene wag, twist, or rock vibrations is impractical since the normal modes are too complex and many couple strongly with C—C stretch co-ordinates.

The CH_2 scissors motions are all good group frequencies (E_p 70–77) with the residual energy localized mainly in the rock/twist motions on the same carbon atom. For the CD_2 scissor the E_p range is 62–74 which brings one of them down into the marginal group frequency range ($E_p < 66$).[13] At each of the C_α and C_β atoms the scissors motion may be in-phase or out-of-phase with its partner across the ring. The calculated wavenumber differences between such pairs are in the range 4–12 cm^{-1} but not all are separated in the measured spectra (Table 9). The empirically well known displacement of the C_α methylene motion to lower wavenumber is confirmed by the calculations. The corresponding effect on the $H_{\gamma(\alpha)}$ force constant has been noted (see Discussion section). Only a few of the other methylene deformation motions can be clearly identified as rocks, wags, or twists[14] (Table 10).

[12]In one computation the observed "carbonyl stretch" frequency was changed to a vapor phase value of 1771 cm^{-1} for all four species with all other experimental frequencies and all input force constants unchanged. Only three of the refined force constants were altered (Table 5), and these were marginal except for the C=O stretch; there were no significant changes in the E_p coefficients (Table 8). It follows that the vibrational modes are not substantially affected by the use of the condensed state experimental frequencies and even less so by the much smaller Fermi resonance displacement in **1**.

[13]This is band 17 in **2** (Fig. 4*b*).

[14]The differentiation between a wag and a twist or between a scissor and a rock depends on the relative signs of the appropriate eigenvectors. These are not included in Table 4*a*–*d* but are recorded in the eigenvector matrices which are listed in ref. 10.

Can. J. Chem. Downloaded from www.nrcresearchpress.com by 210.87.254.40 on 09/05/12
For personal use only.

TABLE 5. Valence force constants*

No.	Symbolic description*	Co-ordinates involved	Common atoms	Starting value†	Refined value‡
		Stretch			
1	$K_{d(\alpha)}$	C—H	—	4.685	4.694
2	$K_{d(\beta)}$	C—H	—	4.610	4.645
3	K_{v}	C=O	—	9.652	10.149 (10.546)
4	$K_{r(\alpha)}$	C—C	—	4.564	4.252
5	$K_{r(\beta,\gamma)}$	C—C	—	4.186	4.144
		Bend			
6	$H_{\delta(\alpha)}$	∠HCH	—	0.554	0.495
7	$H_{\delta(\beta)}$	∠HCH	—	0.567	0.520
8	$H_{\gamma(\alpha)}$	∠HCC	—	0.628	0.601
9	$H_{\gamma(\beta)}$	∠HCC	—	0.657	0.677
10	$H_{\omega(\alpha)}$	∠CCC	—	1.068	1.012 (1.000)
11	$H_{\omega(\beta)}$	∠CCC	—	1.024	0.878 (0.882)
12	H_{χ}	∠CCC	—	1.111	1.111
13	H_{ε}	∠CCO	—	0.919	0.905
14	H_{ρ}	∠C—CO—C	—	0.534	0.341
15	$H_{\tau(\alpha)}$	∠CC—CC	—	0.008	0.032
16	$H_{\tau(\beta,\gamma)}$	∠CC—CC	—	0.093	0.089
		Interaction Constants *Stretch–Stretch*			
17	$F_{d,d}$	C—H, C—H	C	0.006	0.006
18	$F_{v,r(\alpha)}$	C=O, C—C	C	0.0	0.0
19	$F_{r,r}$	C—C, C—C	C	0.101	0.101
		Stretch–Bend			
20	$F_{v,\chi}$	C=O, ∠CCC	C	0.0	0.0
21	$F_{r,\gamma}$	C—C, ∠HCC	C—C	0.328	0.328
22	$F_{r,\gamma}$	C—C, ∠HCC	C	0.079	0.079
23	$F_{r,\omega}$	C—C, ∠CCC	C—C	0.417	0.417
24	$F_{r(\alpha),\chi}$	C—C, ∠CCC	C—C	0.417	0.417
25	$F_{r(\alpha),\varepsilon}$	C—C, ∠CCO	C—C	0.417	0.417
		Bend–Bend			
26	$F_{\gamma,\gamma}$	∠HCC, ∠HCC	C—C	−0.021	−0.021
27	$F_{\gamma,\omega}$	∠HCC, ∠CCC	C—C	−0.031	−0.031
28	$F_{\gamma,\gamma}^{qt}$	∠HCC, ∠HCC	C—C	0.0	0.0
29	$F_{\gamma,\gamma}^{qg}$	∠HCC, ∠HCC	C—C	0.0	0.0
30	$F_{\gamma,\gamma}^{qc}$	∠HCC, ∠HCC	C—C	0.0	0.0
31	$F_{\omega,\omega}$	∠CCC, ∠CCC	C—C	0.0	0.0
32	$F_{\omega,\chi}$	∠CCC, ∠CCC	C—C	0.0	0.0

*The force constant units and symbolism are described in ref. 1. The superscripts on the bend–bend interaction constants are qt (quasi *trans*), qg (quasi *gauche*), qc (quasi *cis*).
†The initial values for the force constants were taken from the refined force field established for cyclohexanone (see Table 3 of ref. 1).
‡The values in parentheses are obtained if an observed C=O stretch frequency of 1771 cm^{-1} is used, corresponding to a vapor state measurement. No other force constants change significantly.

C—C Stretch Vibrations

The bands identifiable as C—C in-plane stretch group frequencies are listed in Table 11. Most notable are the 1166 cm^{-1} (calcd) band in **2** and the bands at 1167 and 1157 cm^{-1} (calcd) in **4**. These motions are illustrated in **7–9** respectively. The intense band at 891 cm^{-1} in **1** is strongly polarized in the Raman spectrum and has been attributed to a ring breathing motion (2) and the E_ρ coefficients support this (Table 7*b*). However, in the deuterated species the "corresponding" bands as judged by the Raman intensity and polarization are readily assigned at 827, 817, 787 cm^{-1} in **2–4** respectively, but the E_ρ data in Table 7*b* suggest that with α-deuteration the energy in the $r_{\beta,\gamma}$ co-ordinate is greatly reduced and much of it transferred to the γ_α and γ_β angle bends. If this is so these modes can no longer be classified as ring breathing motions in **3** and **4** where the $r_{\beta,\gamma}$

Can. J. Chem. Downloaded from www.nrcresearchpress.com by 210.87.254.40 on 09/05/12
For personal use only.

TABLE 6. Vibrational modes below 600 cm^{-1}*

Ring vibration	Symmetry type	Isotopic species 1	2	3	4	Approximate description
I	B	106 (95)	96 (89)	101 (—)	93 (—)	Pseudo-rotation
II	A	239 (239)	222 (223)	203 (206)	189 (191)	Ring torsion
III	B	440 (451)	387 (379)	438 (434)	384 (369)	C=O out of-plane bend
IV	B	478 (472)	456 (443)	468 (467)	450 (440)	C=O in-plane bend
V	A	545 (568)	530 (520)	532 (542)	518 (493)	Sym. ring mode
VI	B	573 (580)	560 (559)	515 (505)	503 (481)	Asym. ring mode

*ν_{calcd} is given first followed by ν_{obs} in parentheses; the observed postions are the mean of the infrared and Raman measurements. Ring vibrations are as follows:

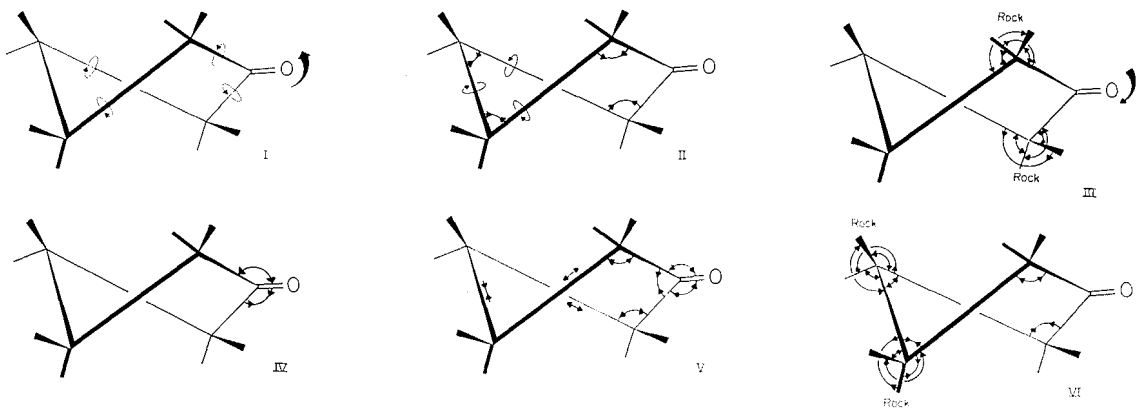

co-ordinates contribute less than 30% of the mode energy. One must bear in mind however that it is in this 800–1100 cm^{-1} region that the computations are most sensitive to small changes in the force field and over-simplified normal co-ordinate analyses are most prone to error.

C—H and C—D Stretch Vibrations

There are 8 calculated frequencies for each isotopic species in the C—H, C—D stretching region (Table 12). The wavenumber differences (1–8 cm^{-1}) calculated for the pairs of in-phase and out-of-phase motions at the C_α and C_β positions correlate with bands in the observed spectra and are reflected in the corresponding force constants. The C—H stretch modes are all good group frequencies with over 90% of the potential energy localized in the C—H bonds. This is true also of most of the corresponding C—D modes except for the symmetric C—D

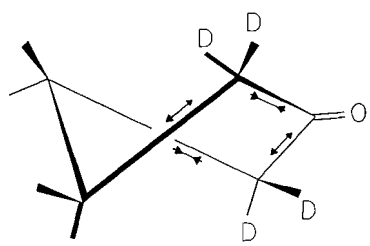

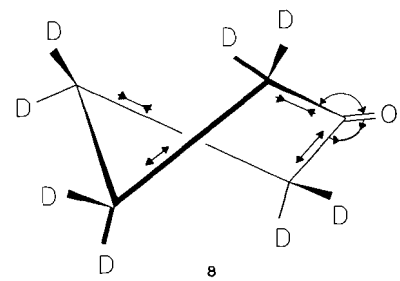

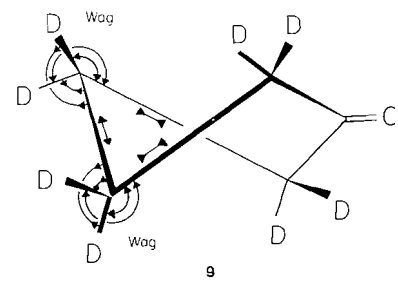

Can. J. Chem. Downloaded from www.nrcresearchpress.com by 210.87.254.40 on 09/05/12
For personal use only.

TABLE 7. Effect of isotopic substitution on the potential energy distribution

(*a*) In-plane ring mode (VI of Table 6)

Structure	Observed Raman wavenumber (cm^{-1})	Depolarization ratio	Potential energy distribution (E_p)		
			(ω_β)	(ω_α)	(γ_β)
1	580	0.83	47	20	13
2	560	0.73	43	20	13
3	505	0.78	34	14	34
4	481*	—	31	14	33

*Infrared band position.

(*b*) "Ring breathing" mode*

Structure†	Observed Raman wavenumber (cm^{-1})	Depolarization ratio	Potential energy distribution (E_p)			
			($r_{\beta,\gamma}$)	(γ_β)	(γ_α)	(r_α)
1	892	0.03	79	7	7	1
2	829	0.04	35	6	37	12
3	820	0.06	27	10	15	33
4	788	0.04	6	12	68	3

*Only motions associated with internal co-ordinates for which $E_p \geq 10$ are shown in the diagrams. The terms "Ψ-wag" etc. indicate that the eigenvectors associated with some of the C—D deformations are near zero; these are indicated as ## in the diagrams. This may not be significant within the error limits of the calculations.

†Ring vibrations as follows:

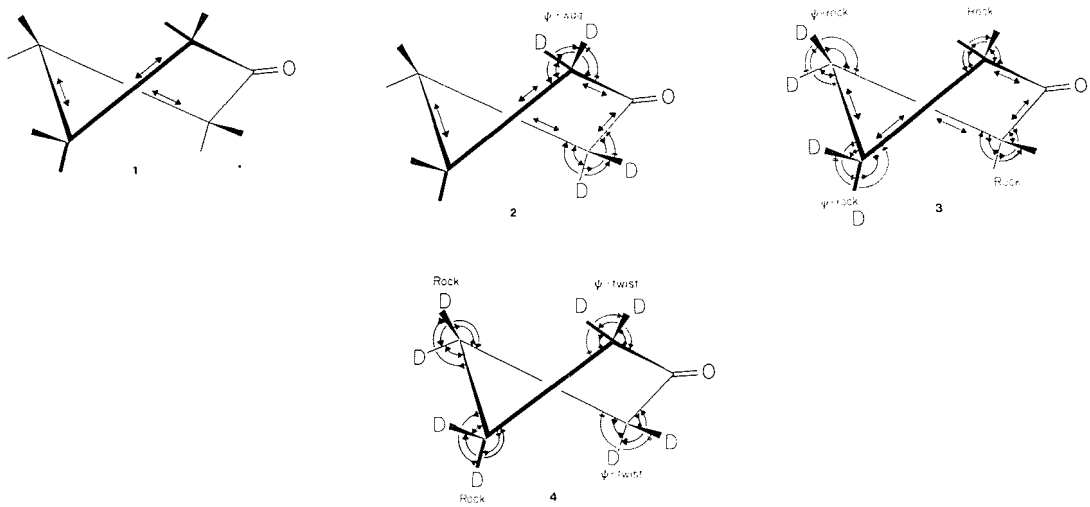

stretch in **4** where there is appreciable coupling between the C_α and C_β atoms.

Concluding Remarks

One may anticipate that these empirical force fields for cyclohexanone and cyclopentanone should aid in setting up similar computations on more complex molecules such as the β-decalones (with and without methyl substituents at the ring junctions) and the corresponding hydrindanones which would be closer analogs of steroids and other cyclic terpenoids. The replacement of C=O by N—H would open a route via piperidine and pyrrolidine to a set of potentially transferable force field parameters applicable to related *N*-heterocyclic systems. As a wider variety of molecular structures is investigated one may expect that a body of practical lore will evolve based on the co-ordination of the work of the various investigators who are taking this approach (14–16). At an earlier period most of the characteristic vibrational group frequencies of complex mole-

Can. J. Chem. Downloaded from www.nrcresearchpress.com by 210.87.254.40 on 09/05/12
For personal use only.

TABLE 8. Potential energy distributions associated with "C=O stretch" mode

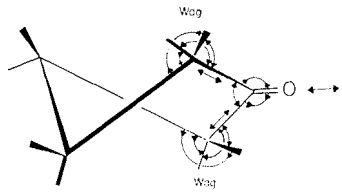

Phase	Structure	Infrared frequency (cm^{-1}) Calcd	Observed	Potential energy distribution (E_p) (ν)	(γ_α)	(χ)	(γ_α)	(ε)
Liquid	**1**	1745	1748	78	13	5	5	2
	2	1743	1744					
	3	1745	1744					
	4	1743	1742					
Vapor*	**1**	1771	1771	79	12	5	2	2
	2							
	3							
	4							

*The vapor phase computations were obtained by using the measured vapor phase band position of **1** for all four isotopic species; no other observed band positions were changed. The same starting values for all the force constants were used (Table 5, column v). The following differences were observed in the refined force constants (*cf.* Table 5, column vi): K_ν 10.546, $H_{\omega(\alpha)}$ 1.000, $H_{\omega(\beta)}$ 0.878 (mdyn Å^{-1}).

TABLE 9. Methylene scissor modes*

Structure	Wavenumber (cm^{-1}) asym C_β	sym C_β	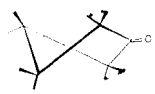 asym C_α	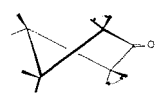 sym C_α
1	1467 (1468)	1460 (1455)	1418 (1410)	1412 (1410)
2	1467 (1468)	1458 (1455)	1023 (1023)	1029 (1034)
3	1063 (1059)	1056 (1059)	1416 (1410)	1412 (1410)
4	1066 (1068)	1060 (1068)	1024 (1033)	1036 (1046)

*ν_{calcd} is given first followed by ν_{obs} averaged for infrared and Raman in parentheses.

cules were established in just such a fashion and, in many cases, it was only later that these were rationalized in terms of more formal vibrational theory. In retrospect the sequence of these events tends to be forgotten.

Molecular spectroscopists who are conditioned to the elegant vibrational analysis that can be made for small molecules of high symmetry may be disconcerted by such drastic simplification of the force fields, but this situation is not uncommon when theoretical concepts developed on the basis of simpler model systems are extended to a more general body of scientific data. The caution which must be exercised in applying normal co-ordinate analysis to polymers has been aptly summarized in eight aphorisms by Zerbi[15] and these are also relevant to molecules of the type considered here.

[15]See ref. 16, pp. 223–224.

Can. J. Chem. Downloaded from www.nrcresearchpress.com by 210.87.254.40 on 09/05/12
For personal use only.

TABLE 10. Vibrational modes assignable as methylene rock, wag, or twist group frequencies (cm^{-1})*

Structure	ν_{calcd}	ν_{obs}†	E_p	Approximate description‡
1	1327	1311	91(γ_β)	β CH_2 wag (o.o.p.)
	1280	1275	79(γ_β)	β CH_2 wag (i.p.)
	1232	1265	71(γ_β)	β CH_2 twist (i.p.)
	1231		79(γ_β)	β CH_2 twist (o.o.p.)
	1211	1232	84(γ_α)	α CH_2 wag (o.o.p.)
2	1325	1310	99(γ_β)	β CH_2 wag (o.o.p.)
	1269	1268	97(γ_β)	β CH_2 wag (i.p.)
	1222	1208	88(γ_β)	β CH_2 twist (o.o.p.)
	1219	1219	91(γ_β)	β CH_2 twist (i.p.)
	873	853	76(γ_α)	α CD_2 twist (o.o.p.)
	787	736	80(γ_α)	α CD_2 twist (i.p.)
	666	626	67(γ_α)	α CD_2 rock (i.p.)
3	1218	1244	100(γ_α)	α CD_2 wag (o.o.p.)
	877	886	72(γ_β)	β CD_2 twist (i.p.)
	831	849	72(γ_β)	β CD_2 twist (o.o.p.)
4	870	903	76(γ_α)	α CD_2 twist (o.o.p.)
	864	856	80(γ_β)	β CD_2 twist (i.p.)

*By our definition a group frequency must have at least 66% of the potential energy localized in the assigned internal co-ordinates (ref. 2).
†Average of the infrared and Raman band positions.
‡o.o.p. = out-of-phase; i.p. = in-phase.

TABLE 11. In-plane C—C stretch modes

Structure	ν_{calcd}	ν_{obs}(i.r.)	Potential energy distribution				ΣE_p
1	894*	889	79($r_{\beta,\gamma}$)	7(γ_β)	7(γ_α)	3(ω_β)	96
	771	706	66(r_α)	11(γ_α)	6(γ_β)	6(ω_α)	89
2	1166†	1163	77(r_α)	16($r_{\beta,\gamma}$)	9(γ_β)	9(γ_α)	111
	1092	1145	67($r_{\beta,\gamma}$)	25(γ_α)	8(γ_β)	5(r_α)	105
3	—	—					
4	1167†	1181	90(r_α)	11($r_{\beta,\gamma}$)	11(ε)	8(γ_α)	120
	1157†	1142‡	86($r_{\beta,\gamma}$)	41(γ_β)	11(ε)	8(γ_α)	145

*For diagram of this vibration see Table 7.
†Note that for these bands ΣE_p is appreciably greater than 100. This must be taken into account in assessing the relevance of the vibrational analysis.
‡This is the Raman peak position; the band was not observed in the infrared spectrum.

Can. J. Chem. Downloaded from www.nrcresearchpress.com by 210.87.254.40 on 09/05/12
For personal use only.

Can. J. Chem. Downloaded from www.nrcresearchpress.com by 210.87.254.40 on 09/05/12
For personal use only.

TABLE 12. C—H and C—D stretch group frequencies*

	Wavenumber (cm^{-1})							
	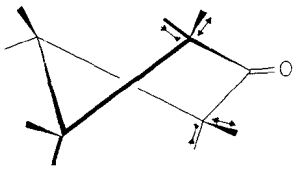 asym C_α i.p.		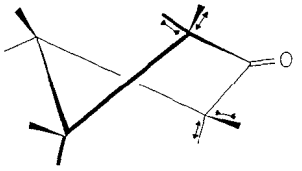 asym C_α o.o.p.		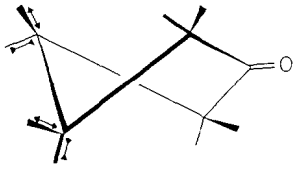 asym C_β i.p.		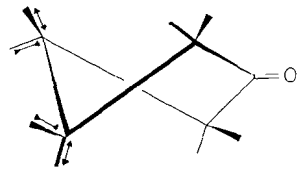 asym C_β o.o.p.	
Structure	Calcd.	Obsd.	Calcd.	Obsd.	Calcd.	Obsd.	Calcd.	Obsd.
1	2971	2971	2970	2971	2958	2946	2952	2946
2	2215	2210	2217	2222	2959	2966	2952	2945
3	2969	2968	2970	2968	2218	2249	2200	2225
4	2206	2181†	2219	2230	2227	2230†	2198	2181
	Wavenumber (cm^{-1})							
	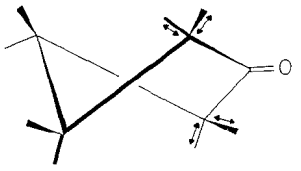 sym C_α i.p.		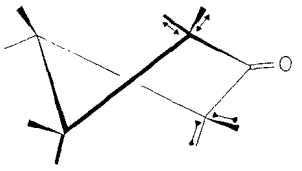 sym C_α o.o.p.		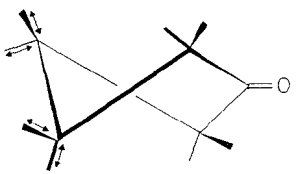 sym C_β i.p.		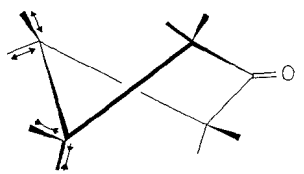 sym C_β o.o.p.	
Structure	Calcd.	Obsd.	Calcd.	Obsd.	Calcd.	Obsd.	Calcd.	Obsd.
1	2901	2901	2899	2901	2885	2886	2884	2873
2	2124	2130	2120	2126	2885	2880	2884	2880
3	2901	2902	2899	2902	2112	2134	2107	2110
4	2125	2120	2120	2120	2111	2110	2107	2110

*The observed positions are the mean of the infrared and Raman measurements. Asym (antisymmetric) and sym (symmetric) refer to the local site symmetry. o.o.p. = out-of-phase; i.p. = in-phase.
†These two modes are appreciably coupled.

We wish to thank Dr. L. C. Leitch for advice and assistance with the preparation of the deuterated compounds, and Dr. K. G. Kidd for comment and discussion during the preparation of the manuscript. We are also indebted to Professor G. W. King and Dr. H. E. Howard-Lock of McMaster University who provided us with an advanced copy of their publication and with whom we exchanged information during the course of the work. Our thanks are also due to Mrs. M. A. MacKenzie and Mr. A. Nadeau for their skilful technical help with the measurement of the spectra.

1. H. FUHRER, V. B. KARTHA, P. J. KRUEGER, H. H. MANTSCH, and R. N. JONES. Chem. Rev. **72**, 439 (1972).
2. H. E. HOWARD-LOCK and G. W. KING. J. Mol. Spectrosc. **35**, 393 (1970).
3. G. ERLANDSSON. J. Chem. Phys. **22**, 563 (1954).
4. J. H. BURKHALTER. J. Chem. Phys. **23**, 1172 (1955).
5. G. ERLANDSSON. Arkiv för Fysik, **9**, 399 (1955).
6. P. G. KÖKERITZ and H. SELÉN. Arkiv för Fysik, **16**, 197 (1959).
7. H. KIM and W. D. GWINN. J. Chem. Phys. **51**, 1815 (1969).
8. T. IKEDA and R. C. LORD. J. Chem. Phys. **56**, 4450 (1972).
9. H. J. GEISE and F. C. MIJLHOFF. Rec. Trav. Chim. Pays. Bas. **90**, 577 (1971).
10. H. FUHRER, V. B. KARTHA, K. G. KIDD, H. H. MANTSCH, and R. N. JONES. NRCC Bulletin No. 15. In preparation.
11. R. N. JONES. Pure and Appl. Chem. **18**, 303 (1969).
12. L. A. CARRIERA and R. C. LORD. J. Chem. Phys. **51**, 1815 (1969).
13. R. CATALIOTTI and R. N. JONES. Spectrochim. Acta, **27A**, 2011 (1971).
14. S. CALIFANO. Pure and Appl. Chem. **18**, 353 (1969).
15. T. SHIMANOUCHI. *In* Physical chemistry, an advanced treatise. Vol. IV. *Edited by* H. Eyring, D. Henderson, and W. Jost. Academic Press, New York. 1970. Chapt. 6.
16. G. ZERBI. Appl. Spectrosc. Rev. **2**, 193 (1969).

Can. J. Chem. Downloaded from www.nrcresearchpress.com by 210.87.254.40 on 09/05/12
For personal use only.

Reductive Cleavage of Carbohydrate *p*-Toluenesulfonates with Sodium Naphthalene

H. C. JARRELL, R. G. S. RITCHIE, W. A. SZAREK, AND J. K. N. JONES

Department of Chemistry, Queen's University, Kingston, Ontario

Received December 8, 1972

Carbohydrate *p*-toluenesulfonates are desulfonylated rapidly and in high yield, by treatment with sodium naphthalene in tetrahydrofuran, to regenerate the original hydroxyl groups. The method has been applied to carbohydrates containing up to three *p*-toluenesulfonate groups, to unsaturated sugars, and to a nucleoside derivative.

Les carbohydrates *p*-toluènesulfonés sont désulfonés rapidement et avec un bon rendement, par traitement avec le naphtalène sodium dans le tétrahydrofurane pour régénérer les groupes hydroxyles originaux. La méthode a été appliquée aux carbohydrates contenant jusqu'à trois groupes *p*-toluènesulfonates, aux sucres insaturés et au dérivé nucléoside. [Traduit par le journal]

Can. J. Chem., **51**, 1767 (1973)

Can. J. Chem. Downloaded from www.nrcresearchpress.com by 210.87.254.40 on 09/05/12
For personal use only.

The importance of *p*-toluenesulfonic esters of carbohydrates in sugar synthesis has been well established (1, 2). Not only are the *p*-toluenesulfonates useful substrates for a wide variety of nucleophilic displacement reactions, but also the sulfonyl group has been extensively employed as a protecting group. Removal of an *O*-*p*-tolylsulfonyl group, without inversion, to regenerate the original sugar or sugar derivative can be effected in several ways. Reductive desulfonylation has been achieved by the use of sodium amalgam (3), Raney nickel (4), lithium aluminum hydride (5), or sodium in liquid ammonia (6). However, in the reaction with sodium amalgam or Raney nickel, anhydride formation has been observed to be a competing reaction if an unsubstituted hydroxyl group is sterically available. Lithium aluminum hydride operates, on secondary sulfonates, principally by oxygen–sulfur fission, but, on primary sulfonates, with carbon–oxygen fission; thus, with the latter derivatives, reduction mainly to the hydrocarbon stage occurs. The sulfonic esters of carbohydrates are also removable, with retention of configuration, by bases (7); however, anhydro-ring formation, if possible, frequently occurs. Moreover, alkaline conditions can occasionally lead to ring-contracted products (8) or unsaturated derivatives (9, 10). An effective, mild procedure for removal of *O*-*p*-tolylsulfonyl groups is by photolysis of the ester in methanolic solution, in the presence of an equimolar proportion of sodium methoxide (11). The present report describes a new method for reductive desulfonylation of carbohydrate *p*-toluenesulfonates, namely, with sodium naphthalene.

Closson *et al.* (12) have reported previously the use of sodium naphthalene anion radical in tetrahydrofuran solution for the conversion of alkyl mono-*p*-toluenesulfonates into the corresponding alcohols (S—O bond cleavage). The method has been applied to several carbohydrate derivatives; the results are summarized in Table 1. The reactions were performed in a Dry Ice – acetone bath, and the products were isolated at room temperature. In all cases the structures of the products were confirmed by comparison of their t.l.c. mobilities, optical rotations, and melting points (where applicable) with those of authentic samples. It appears that a variety of functional groups (benzylidene and isopropylidene acetals, hydroxyl, alkenyl, and aglycon) in sugar molecules are compatible with the reaction conditions. Moreover, the method is applicable to derivatives containing "isolated" or "non-isolated", primary or secondary *p*-tolylsulfonyloxy groups. The desulfonylation of methyl 4,6-*O*-benzylidene-2-*O*-*p*-tolylsulfonyl-α-D-glucopyranoside is particularly noteworthy, since treatment, with alkaline reagents, of a derivative having an hydroxyl group adjacent and configurationally *trans* to a sulfonyloxy group usually results in the formation of an epoxide ring. The desulfonylation, with retention of configuration, of the compounds having contiguous *p*-tolylsulfonyloxy groups is also significant. With each of the substrates listed in Table 1, t.l.c. examination of the reaction mixture

revealed the formation of only one carbohydrate component; usually, reaction times of 10 min were employed. A disadvantage of the method is that, with large-scale reactions, technical difficulties may be encountered, as regards the separation of a pure product alcohol from the naphthalene and other hydrocarbons which may be formed by the reaction (22) of naphthalene anion radical with water during processing of the reaction mixture.

Experimental

General Method

An approximately 0.5 *M* solution of sodium naphthalene in tetrahydrofuran was prepared by stirring (using a glass-covered stirring bar) a mixture of sodium (2.88 g, 0.125 mol) and naphthalene (17.00 g, 0.133 mol) in dry tetrahydrofuran (250 ml) under an atmosphere of nitrogen for approximately 2.5 h at room temperature. The dark green solution was "standardized"[1] by adding a measured aliquot to water and titrating the aqueous mixture with hydrochloric acid using phenolphthalein as the indicator.

TABLE 1. Desulfonylation of carbohydrate *p*-toluenesulfonates with sodium naphthalene

Substrate	Reference	Equivalents of sodium naphthalene	Method of isolation*	Product	Isolated yield (%)
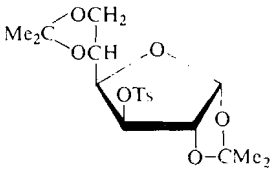	13	3	A	1,2:5,6-Di-*O*-isopropylidene-α-D-glucofuranose	78
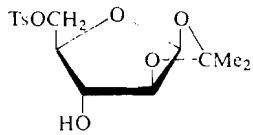	14	3	B	1,2-*O*-Isopropylidene-β-D-arabinofuranose	80
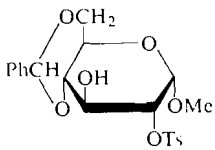	15	3	A	Methyl 4,6-*O*-benzylidene-α-D-glucopyranoside	65
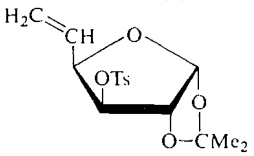	16	3	A	5,6-Dideoxy-1,2-*O*-isopropylidene-α-D-*xylo*-hex-5-enose	67
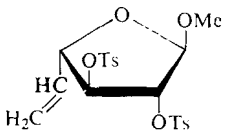	17	6	B	Methyl 5,6-dideoxy-α-L-*arabino*-hex-5-enoside	87
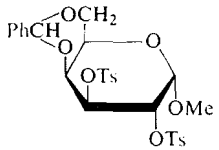	18	6	A	Methyl 4,6-*O*-benzylidene-α-D-galactopyranoside	50
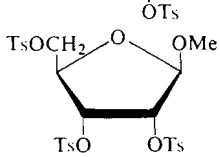	19	12	C	Methyl β-D-ribofuranoside	66

[1]For an alternate and more rigorous method for standardization of anion radical solutions, see ref. 23.

Can. J. Chem. Downloaded from www.nrcresearchpress.com by 210.87.254.40 on 09/05/12
For personal use only.

TABLE 1. (*Concluded*)

Substrate	Reference	Equivalents of sodium naphthalene	Method of isolation*	Product	Isolated yield (%)
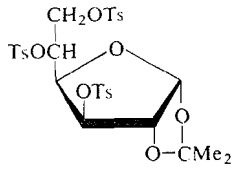	20	9	B	1,2-*O*-Isopropylidene-α-D-glucofuranose	50
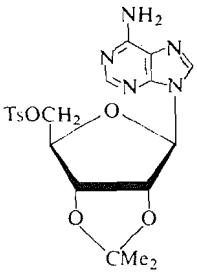	21	3	A	2′,3′-*O*-Isopropylideneadenosine	50

*See Experimental.

A solution of the *p*-toluenesulfonate (1–3g) in a minimum volume of dry tetrahydrofuran was added rapidly to a stirred reagent solution (diluted with tetrahydrofuran to approximately 0.3 *M*), containing usually 3 equiv of sodium naphthalene per *p*-tolylsulfonyloxy group, under nitrogen in a Dry Ice – acetone bath. The progress of the reaction was monitored by t.l.c.; usually, reaction times of 10 min were employed. A few drops of water were added to the reaction mixture, and the product was isolated at room temperature by an appropriate procedure.

Isolation of Desulfonylated Products

(A) Chloroform-soluble Alcohols

The reaction mixture was neutralized with Rexyn-101 (H form) resin and then filtered, and the filtrate was evaporated to dryness. The residue was partitioned between chloroform and water, and the chloroform solution was dried (sodium sulfate), decolorized with charcoal, and then evaporated. The residue was fractionated on alumina, with petroleum ether (b.p. 60–80°) as the first eluant to remove the hydrocarbons, followed by methanol to obtain the product alcohol. The product was further purified by standard procedures.

(B) Chloroform- and Water-soluble Alcohols

The reaction mixture was neutralized and evaporated as in isolation procedure A. The residue was partitioned between chloroform and water to remove the hydrocarbons. The aqueous solution was saturated with sodium chloride and then extracted continuously with chloroform until the presence of the product alcohol in the aqueous solution could no longer be detected by t.l.c. The dried (sodium sulfate) chloroform solution was decolorized with charcoal and then evaporated to give the product, which was further purified.

(C) Water-soluble Alcohols

The reaction mixture was deionized with cation and anion exchange resins and then filtered, and the filtrate was evaporated to dryness. The residue was partitioned between chloroform and water. The aqueous solution was evaporated to give the product alcohol, which was further purified.

The authors are grateful to the National Research Council of Canada for their generous financial support of this work.

1. R. S. TIPSON. Adv. Carbohydr. Chem. **8**, 107 (1953).
2. D. H. BALL and F. W. PARRISH. Adv. Carbohydr. Chem. **23**, 233 (1968); Adv. Carbohydr. Chem. Biochem. **24**, 139 (1969).
3. K. FREUDENBERG and F. BRAUNS. Ber. **55**, 3233 (1922); R. S. TIPSON. Meth. Carbohydr. Chem. **2**, 250 (1963).
4. G. W. KENNER and M. A. MURRAY. J. Chem. Soc. S178 (1949).
5. H . SCHMID and P. KARRER. Helv. Chim. Acta, **32**, 1371 (1949); H. R. BOLLIGER and P. ULRICH. Helv. Chim. Acta, **35**, 93 (1952).
6. M. A. MILJKOVIĆ, M. PEŠIĆ, A. JOKIĆ, and E. A. DAVIDSON. Carbohydr. Res. **15**, 162 (1970); J. KOVÁR. Can. J. Chem. **48**, 2383 (1970).
7. R. S. TIPSON. Adv. Carbohydr. Chem. **8**, 168 (1953).
8. C. L. STEVENS, R. P. GLINSKI, K. G. TAYLOR, P. BLUMBERGS, and F. SIROKMAN. J. Am. Chem. Soc. **88**, 2073 (1966).
9. I. E. MUSKAT. J. Am. Chem. Soc. **56**, 2653 (1934); **57**, 778 (1935).
10. H. AZOUMANIAN, E. M. ACTON, and L. GOODMAN. J. Am. Chem. Soc. **86**, 76 (1964).
11. S. ZEN, S. TASHIMA, and S. KOTO. Bull. Chem. Soc. Jap. **41**, 3025 (1968); A. D. BARFORD, A. B. FOSTER, and J. H. WESTWOOD. Carbohydr. Res. **13**, 189 (1970).
12. W. D. CLOSSON, P. WRIEDE, and S. BANK. J. Am. Chem. Soc. **88**, 1581 (1966).

Can. J. Chem. Downloaded from www.nrcresearchpress.com by 210.87.254.40 on 09/05/12
For personal use only.

13. H. ZINNER, G. WULF, and R. HEINATZ. Chem. Ber. **97**, 3536 (1964).
14. P. A. LEVENE and J. COMPTON. J. Biol. Chem. **116**, 189 (1936).
15. G. J. ROBERTS and C. F. GRIFFITH. J. Chem. Soc. 1193 (1935).
16. J. K. N. JONES and J. L. THOMPSON. Can. J. Chem. **35**, 955 (1957); R. G. S. RITCHIE and W. A. SZAREK. To be published.
17. D. H. BALL, A. E. FLOOD, and J. K. N. JONES. Can. J. Chem. **37**, 1018 (1959).
18. E. SORKIN and T. REICHSTEIN. Helv. Chim. Acta, **28**, 1 (1945).
19. T. KANAZAWA, M. ÔTANI, and T. SATÔ. Nippon Kagaku Zasshi, **80**, 517 (1959); Chem. Abstr. **55**, 6386 (1961); J. CLEOPHAX, J. HILDESHEIM, and S. D. GERO. Bull. Soc. Chim. Fr. 4111 (1967).
20. W. P. SHYLUK, J. HONEYMAN, and T. E. TIMELL. Can. J. Chem. **33**, 1202 (1955).
21. W. SAKAMI. Biochem. Prep. **8**, 5 (1961).
22. S. BANK and W. D. CLOSSON. Tetrahedron Lett. 1349 (1965).
23. W. D. CLOSSON, S. JI, and S. SCHULENBERG. J. Am. Chem. Soc. **92**, 650 (1970).

Can. J. Chem. Downloaded from www.nrcresearchpress.com by 210.87.254.40 on 09/05/12
For personal use only.

Chemisorption of Ammonia on Silica

G. A. BLOMFIELD AND L. H. LITTLE

Department of Physical and Inorganic Chemistry, The University of Western Australia, Nedlands, Western Australia, 6009

Received August 31, 1972

The interaction of ammonia with silicas prepared by a variety of methods was studied to resolve conflicting reports of the mode of ammonia adsorption and to determine the role of chlorine impurities (present in the silica) in the adsorption process. Results for the adsorption of water on silica assisted in making band assignments and competition between ammonia and water for silica adsorption sites was observed. It was concluded that dehydroxylated silicas contain sites which dissociate ammonia to form Si—NH_2 groups having infrared bands at 3540, 3450, and 1550 cm^{-1} (the surface amine groups are not displaced by added water). The presence of chlorine in the silica is not a prerequisite for chemisorption of ammonia.

L'interaction de l'ammoniac avec des silices préparées selon plusieurs méthodes a été étudiée afin d'élucider les problèmes issus du mode d'adsorption de l'ammoniac et afin de déterminer le rôle des impuretés du type chlore (présentes dans la silice) dans le processus d'adsorption. Les résultats obtenus lors de l'adsorption de l'eau sur la silice ont contribué à l'attribution des bandes et la compétition entre l'adsorption de l'eau et celle de l'ammoniac sur les sites de la silice a été étudiée. Il a été conclu que les silices déhydroxylées contiennent des sites susceptibles de dissocier l'ammoniac ce qui entrainent la formation de groupes Si—NH_2 possédant en infra-rouge des bandes à 3540, 3450, et 1550 cm^{-1} (les groupes amines en surface ne sont pas déplacés lorsque l'on additionne de l'eau). La présence du chlore dans la silice n'est pas une condition nécessaire à la chémisorption de l'ammoniac. [Traduit par le journal]

Can. J. Chem., 51, 1771 (1973)

Mapes and Eischens (1) reported that ammonia was only physically adsorbed to pure silica and that no chemisorption occurred. Later reports for silicas evacuated at temperatures of 200–800 °C confirmed these results (2–6). Bands which appear at 3400, 3320, and 1625 cm^{-1} in the infrared spectrum have been assigned to ammonia hydrogen bonded to hydroxyl groups on the silica surface (2, 4, 6).

More recently, extra bands at approximately 3525, 3440, and 1555 cm^{-1} have been reported in the spectrum of ammonia adsorbed on silica and these have been assigned to vibrations of a Si—NH_2 group formed by chemisorption of ammonia to the silica (8–10). However, other workers using similar samples and similar pretreatment temperatures still found no evidence for chemisorption (6, 11, 12).

In one case for which chemisorption was reported (8), the silica was prepared by a method involving the use of hydrochloric acid solution and it was found that the band intensities of chemisorbed groups were enhanced by pretreatment of the silica with chlorine or carbon tetrachloride vapors. The other reports of chemisorption considered adsorption onto Cab-O-Sil (10) or Aerosil (9) silicas and we have found that these powders contain traces of chlorine or chloride impurities. Folman (13) had previously reported the formation of Si—NH_2 groups when ammonia was adsorbed on chlorinated porous silica glass. It is possible that the presence of chlorine in silica samples is necessary for chemisorption of ammonia. The formation of Si—NH_2 groups has been reported for ammonia adsorbed on unchlorinated porous silica glass (14) but the existence of such groups was questioned (15) in view of the many reports which suggest that ammonia is not chemisorbed to silica.

In order to resolve the question of chemisorption of ammonia on silica and the role of chlorine and to distinguish between primary amine and secondary amine groups for ammonia adsorbed on porous silica glass (14, 16), the adsorption of ammonia onto silicas prepared by a variety of methods was investigated using infrared spectroscopy. It was concluded that dehydroxylated silicas contain sites which dissociate ammonia to form Si—NH_2 groups. The presence of chlorine in the silicas is not a prerequisite for chemisorption of ammonia.

Experimental

A variety of silica powders was studied. Cab-O-Sil HS-5 and Cab-O-Sil M-5 silicas were supplied by Godfrey L. Cabot Corporation, Boston, Massachusetts. Aerosil silica is manufactured by Degussa, Frankfurt am

Can. J. Chem. Downloaded from www.nrcresearchpress.com by 210.87.254.40 on 09/05/12
For personal use only.

Can. J. Chem. Downloaded from www.nrcresearchpress.com by 210.87.254.40 on 09/05/12
For personal use only.

Main, Germany. These silicas are prepared by the flame hydrolysis of silicon tetrachloride. A silica powder prepared by precipitation from sodium silicate was obtained (17).

Ludox SM silica was supplied by Dupont, Wilmington, Delaware, as an aqueous sol. Freeze-drying this suspension (initially diluted ten times with distilled, de-ionized water) produced a fluffy white powder. A modified silica was prepared by adding dilute hydrochloric acid to the sol before freeze-drying. The resulting flocculation led to a decrease in the surface area of the chlorinated powder so obtained.

A silica powder was prepared by the hydrolysis of ethyl ortho-silicate. Approximately 10 g of ethyl ortho-silicate was added to 250 ml of distilled, de-ionized water in a polythene beaker and the solution was stirred continuously for 4 days at 20 °C. The resulting silica suspension was freeze-dried.

A chloride-free (as determined by X-ray fluorescence spectroscopy) silica powder was prepared by refluxing approximately 3 g of Cab-O-Sil HS-5 silica for 6 h in concentrated nitric acid. This silica was then washed repeatedly in distilled, de-ionized water, dried at 100 °C and crushed to a fine powder.

Each of these powders was compressed under a pressure of 10 tons/sq in. to form rectangular pellets of 10–35 mg/cm^2. Samples were heated to 400 °C in oxygen before use to remove hydrocarbon impurities.

Pellets of Aerosil silica were suspended in refluxing thionyl chloride for 7 days to induce the exchange of hydroxyl groups on the silica surface by chloride groups. A similar method has been used to chlorinate porous silica glass (13).

The possible effect of iron impurities introduced onto the silica through compression in the steel pellet presses was investigated. Samples of silica – ferric oxide were prepared by soaking pellets of Cab-O-Sil HS-5 silica in a solution of 0.1 *M* ferric chloride in 2 *M* hydrochloric acid. These were then heated in flowing oxygen at 400 °C for 10–12 h to decompose the ferric chloride.

For adsorption onto all samples, anhydrous ammonia obtained from Matheson Company Inc., was used. Surface areas were determined by the B.E.T. method using nitrogen as the adsorbate. The relative chlorine concentrations in each type of silica was determined by X-ray fluorescence spectroscopy using a "Geigerflex X-ray Spectrometer" model KG – 3/5 manufactured by Rigaku–Denki Company Ltd., Tokyo, Japan.

Infrared spectra were recorded on a Perkin–Elmer 521 spectrophotometer in the region 4000 to 1300 cm^{-1}. The spectral slit width was approximately 4 at 3800 cm^{-1} and approximately 2 cm^{-1} in the 1600 cm^{-1} region. A modified windlass cell (16) with a Kanthal wound, silica furnace section permitted evacuation of samples at temperatures up to 900 °C. All spectra were recorded at room temperature and usually a second silica pellet was placed in the reference beam of the spectrometer to compensate for absorption bands due to Si—O vibrations in spectra below 2000 cm^{-1}. Weak bands in the region 3800–3600 cm^{-1} and 1800–1500 cm^{-1} are due to uncompensated water vapor.

Results and Discussion

Spectra of a typical sample of Cab-O-Sil HS-5 silica recorded before and after the addition of ammonia are shown in Fig. 1. Approximately 5 Torr of ammonia was admitted to a sample which had been evacuated at 450 °C (Fig. 1*a*) and bands appeared in the spectrum at 3400, 3320, 3250, 2980, 1625, and 1550 cm^{-1} (Fig. 1*b*). The bands at 3400, 3320, and 1625 cm^{-1} have been assigned to the N—H vibrations of ammonia hydrogen bonded to surface hydroxyl groups (2, 4), and the band at 2980 cm^{-1} is due to the O—H stretching vibration of these hydrogen bonded groups (4). A broad weak band at 3250 cm^{-1} (Fig. 1*b*) is probably due to the first overtone of the N—H deformation fundamental at 1625 cm^{-1}.

Condensing the gas into a liquid air cooled side-arm on the cell removes all the bands due to this hydrogen bonded ammonia from the spectrum and only bands at 3450 and 1550 cm^{-1} remain (Fig. 1*c*). If a larger pressure of gas is admitted to the sample and then condensed the intensities of these bands increase and an additional band appears at 3520 cm^{-1} (Fig. 1*d*). The thickness of samples used in this study was greater than for previous studies in which these bands were undetected (4). These three bands remain in the spectrum of the sample after evacuation at 450 °C and must be produced by one or more species which are chemisorbed to the silica. Folman (13) assigned bands at 3520 and 3540 cm^{-1} to Si—NH_2 groups when ammonia was adsorbed on chlorinated porous silica glass and others have found similar bands for ammonia on dehydroxylated silicas (8–10). All previous reports of ammonia adsorbed on pure silica evacuated at temperatures below 600 °C have concluded that only physical adsorption occurs but the results above indicate that chemisorbed groups are formed as well. It is likely that the smaller gas pressures, the thinner samples, and shorter times of standing used in these former studies produced only low concentrations of chemisorbed species and these were not detected.

The spectrum of Cab-O-Sil HS-5 silica after evacuation at 850 °C (Fig. 1*e*) contains a very sharp peak at 3747 cm^{-1} due to the isolated hydroxyl groups on the silica surface. Admission of approximately 5 Torr of ammonia to this sample produces the spectrum shown in Fig. 1*f*. The bands at 3420, 3337, 3320, 3050, and 1625 cm^{-1} which disappear when the gas is condensed (Fig. 1*g*) are similar to those for ammonia physically adsorbed to Cab-O-Sil evacuated at 450 °C (Fig. 1*b*) except that the band corre-

Can. J. Chem. Downloaded from www.nrcresearchpress.com by 210.87.254.40 on 09/05/12
For personal use only.

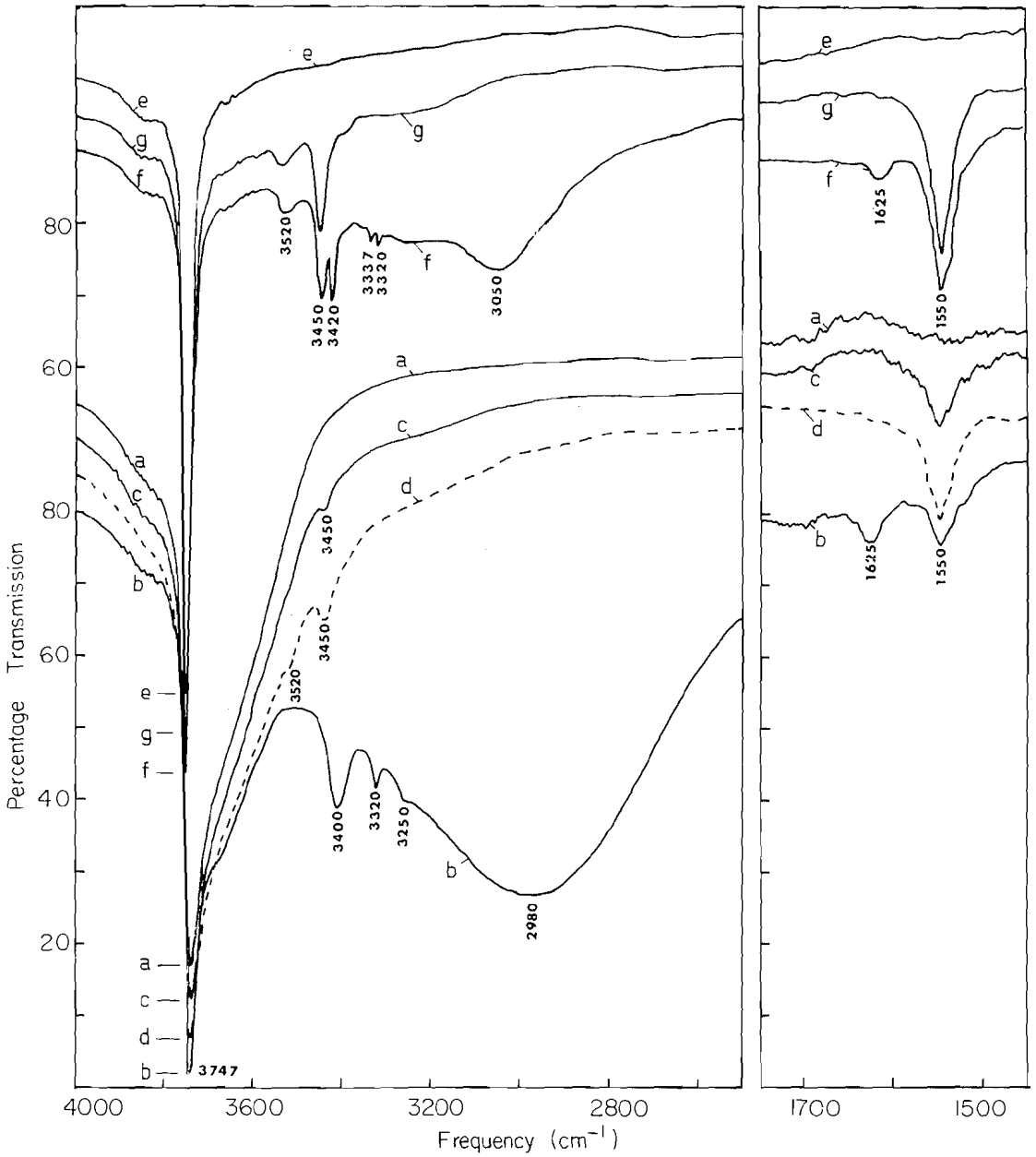

FIG. 1. The infrared spectrum of a sample of Cab-O-Sil HS-5 silica: *a*, after evacuation for 3 h at 450 °C; *b*, after the addition of approximately 5 Torr of ammonia; *c*, after condensing the gas; *d*, after adding 150 Torr of ammonia and condensing the gas; *e*, after evacuation for 5 h at 850 °C; *f*, after adding approximately 5 Torr of ammonia; *g*, after condensing the gas.

sponding to the asymmetric N—H stretching vibration of these hydrogen bonded ammonia molecules has shifted from 3400 to 3420 cm^{-1} and the half-width has decreased. This band is now very sharp suggesting that, unlike the case for Cab-O-Sil evacuated at 450 °C (Fig. 1*b*), the ammonia molecules, hydrogen bonded to single isolated hydroxyl groups are also isolated from one another and from nearby hydroxyl groups and there is no interaction between adjacent groups. Similar sharpening of bands of co-ordinated ammonia were reported on high temperature

Can. J. Chem. Downloaded from www.nrcresearchpress.com by 210.87.254.40 on 09/05/12
For personal use only.

evacuated porous glass (16). The O—H stretching vibration of these $OH\cdots NH_3$ groups has shifted from 2980 cm^{-1} (Fig. 1*b*) to 3050 cm^{-1} (Fig. 1*f*) indicating that the hydrogen bonds between the ammonia and the hydroxyl groups are weaker for ammonia adsorbed on the more dehydrated sample. The band at 3337 cm^{-1} is due to the symmetric N—H stretching vibration of gaseous ammonia.

The bands at 3520, 3450, and 1550 cm^{-1} which remain in the spectrum after the gas has been condensed (Fig. 1*g*) are similar to those found by other workers (8–10). The bands at 3450 and 1550 cm^{-1} arise from the symmetric stretching and the asymmetric deformation modes respectively of the species Si—NH_2. It will be shown later that the asymmetric stretching mode of this group has a band at 3540 cm^{-1} and that the three bands at 3540, 3450, and 1550 cm^{-1} arise from a single Si—NH_2 species which remains on the sample after evacuation at 400 °C or above. These assignments are confirmed by deuteration studies with ND_3 adsorbed on deuterated silica. The corresponding Si—ND_2 stretching bands occur at 2630 and 2526 cm^{-1}. It is possible that a hydroxyl species formed during the reaction of ammonia with the silica, has a band at 3520 cm^{-1} which overlaps this 3540 cm^{-1} band for spectra of samples after the gas is condensed (Fig. 1*g*).

In addition, a weak shoulder at 3400 cm^{-1} which was not reported in previous studies (8–10) was present in the spectrum of ammonia chemisorbed to dehydrated silica (Fig. 1*g*), and this band disappears after evacuation of the sample at 100–150 °C. The assignment of this band to strongly physically adsorbed ammonia will be considered in a later section.

Similar results were obtained for ammonia chemisorbed to Cab-O-Sil M-5 and Aerosil silicas, although the concentration of chemisorbed species was less than for Cab-O-Sil HS-5 which has a larger surface area. Samples were dehydrated at either 450, 650, or 800 °C before admission of ammonia and for each type of silica, the concentration of the chemisorbed species was greatest for samples which had been evacuated at 800 °C. The intensities of these amine bands also increased if larger ammonia gas pressures were admitted, if the sample was left to stand in the gas for longer periods (12 h) or if the sample was heated in the gas. No further increase was observed when the evacuated sample was immersed in liquid ammonia.

Pellets prepared from the Ludox silica did not transmit infrared radiation as readily as the other silicas and their spectra have a steeply sloping background due to scattering losses. When 100 Torr of ammonia was admitted to a sample which has been evacuated at 450 °C, bands appeared in the spectrum at 3450, 3400, 3320, and 1550 cm^{-1} after the gas was condensed. Heating the sample at 450 °C in ammonia gas increased the concentration of the chemisorbed species and a band appeared at 3520 cm^{-1}. The bands at 3400 and 3320 cm^{-1} were not affected by the heat treatment and remain after evacuation at 20 °C but disappear after evacuation at 150 °C.

The concentration of the chemisorbed species formed on the Ludox sample evacuated at 600 °C after treatment with ammonia is greater than after the 450 °C evacuation. However a similar concentration of Si—NH_2 groups results from heating the sample in the gas. The bands at 3400 and 3320 cm^{-1} are present and disappear after evacuation at 150 °C. Gross sintering of the Ludox silica occurs after evacuation at 800 °C and no chemisorption of ammonia was detected then.

Samples of the silica prepared from sodium silicate (17) were more transparent to infrared radiation than the Ludox silica. Similar spectra were obtained after admission and evacuation of ammonia to pellets dehydrated at 450 or 800 °C. As well as bands due to Si—NH_2 groups, the infrared spectrum contained bands at 3400 and 3320 cm^{-1} which could be removed by evacuating the sample at 150 °C.

For the Cab-O-Sil and Aerosil silicas, admission of ammonia after evacuation at 600–800 °C produced a band at 3400 cm^{-1} in the spectrum and this remained after evacuation of the sample at 20 °C (Fig. 1*g*) but disappeared after evacuation at 150–200 °C. This band was not present in the spectra of samples which had been dehydrated at only 450 °C before ammonia was added (Fig. 1*d*). It is probable that a second band at 3320 cm^{-1} accompanies this 3400 cm^{-1} band but it is very weak and its presence is often difficult to detect. No band at 1625 cm^{-1} was found after evacuation of the ammonia at 20 °C for any of the silicas studied.

It appears that some residual ammonia physically adsorbed to the silica remains after evacuation at 20 °C to produce the bands at 3400 and 3320 cm^{-1}. The Ludox silica and the silica precipitated from sodium silicate (both

TABLE 1. Relative chlorine contents and surface areas of various silicas

Silica	Relative chlorine content (X-ray fluoresence analysis) c.p.s.	Surface area after evacuation at 450 °C m^2/g	Surface area after evacuation at 800 °C m^2/g
Cab-O-Sil HS-5	28	278	260
Cab-O-Sil M-5	0	165	152
Aerosil	52	157	140
Silica precipitated from sodium silicate (17)	68	224	170
Dried Ludox	70	240	—
Dried Ludox + HCl solution	152	187	—
Hydrolyzed ethyl-ortho silicate	66		
Cab-O-Sil nitric acid leached	0	227	200
Aerosil treated with thionyl chloride	470		
Standard silicate rock (U.S. Geological Survey reference G-2 (20)) containing 108 p.p.m. chlorine	30		

prepared from solution) will probably consist of particles containing fine pores in which hydrogen bonded ammonia molecules might be more strongly held. For the Cab-O-Sil and Aerosil silicas (prepared at over 1000 °C) it is only after evacuation at temperatures above 600 °C with some loss of surface area, that sufficient ammonia remains after evacuation at 20 °C to produce weak bands at 3400 and 3320 cm^{-1} in the spectrum. The fact that the band due to the asymmetric stretching vibration of these ammonia molecules appears at 3400 cm^{-1} and not 3420 cm^{-1} (Fig. 1*f*, *g*) suggests that these molecules exist in a more perturbing environment.

Griffiths *et al.* (18) reported bands at 3350 and 3280 cm^{-1} when ammonia was adsorbed on silica-supported platinum or on pure silica samples. They assign these bands to ammonia chemisorbed to platinum sites (Pt—NH_3 groups) in the first instance and ammonia bound to siloxane groups $\left(NH_3—O\begin{matrix}Si\\Si\end{matrix}\right)$ in the second. They did not evacuate the gaseous ammonia from the samples to verify that these chemisorbed ammonia groups were in fact chemically bound to the adsorbent.

In the present investigation, much higher resolution of bands could be obtained and no bands at these frequencies were observed for any of the ammonia–silica systems we have studied. Bands at 3360 and 3260 cm^{-1} were observed for ammonia on silica supported oxides in the presence of gaseous ammonia (19). These bands were ascribed to physically adsorbed ammonia molecules. In view of the poor resolution for the spectra in the study of Griffiths *et al.* (18) and the lack of corroborative evidence to support their assignments (1–6, 8–16) it seems unlikely that chemically bound NH_3 groups are adsorbed onto silica adsorbents. However, the assignment of bands to Pt—NH_3 groups may still apply.

Pellets of silica prepared from ethyl orthosilicate were very opaque and infrared transmission was less than 2% at 4000 cm^{-1}, even for very thin pellets. However, after attenuation of the reference beam, infrared spectra could be recorded. Bands at 3450 and 1550 cm^{-1} were present in the spectra of samples dehydrated at 450 and 800 °C after adsorption and subsequent evacuation of ammonia. It appears that this silica chemisorbs ammonia to form Si—NH_2 groups.

Analysis of a pellet of Cab-O-Sil HS-5 by X-ray fluorescence spectroscopy revealed that for the elemental range sodium to tungsten, small concentrations of iron and chlorine atoms were present as well as the silicon atoms. The iron impurity possibly resulted from the steel press used to prepare the pellets, while the chlorine impurity was possibly derived from the silicon tetrachloride used in the manufacture of the Cab-O-Sil, although pellets of Cab-O-Sil M-5 contained no detectable chlorine. Each type of silica was analyzed for chlorine and the results are shown in Table 1. The result for a standard silicate rock (U.S. Geological Survey, ref. G-2 (20)) containing 108 p.p.m. chlorine, is included for comparison.

Cab-O-Sil M-5 silica containing no detectable chlorine will form Si—NH_2 groups after reac-

[1] $\geq Si—Cl + NH_3 \longrightarrow \geq Si—NH_2 + H—Cl$

Can. J. Chem. Downloaded from www.nrcresearchpress.com by 210.87.254.40 on 09/05/12
For personal use only.

Can. J. Chem. Downloaded from www.nrcresearchpress.com by 210.87.254.40 on 09/05/12
For personal use only.

tion with ammonia. It appears therefore that the chemisorption of ammonia on silica does not depend upon the presence of chlorine in the silica. The possibility still exists that chlorine impurities will react according to the following equation to produce more Si—NH_2 groups as postulated by Folman (13).

To test this possibility, a sample of Cab-O-Sil HS-5 powder was treated with nitric acid to remove chlorine (Table 1). This chlorine-free silica still reacted with ammonia and in spite of a slight reduction in surface area (Table 1), the intensities of the Si—NH_2 bands in the spectrum of the sample were similar to those for ammonia adsorbed on untreated Cab-O-Sil HS-5. It appears that surface chlorine does not play a prominent role in the production of surface amine groups for the silicas studied.

Several pellets of Aerosil silica were treated with thionyl chloride to exchange the surface hydroxyl groups by chlorine. Only partial chlorination of these samples was achieved since their spectra still contained a strong band due to SiOH groups. Folman (13) reported the exchange of 90% of the hydroxyls on porous silica glass for samples which had been treated with thionyl chloride for 14 days. Boehm (21) has found it was possible to react only 50% of the hydroxyls on Aerosil with thionyl chloride.

After evacuation of these chlorinated samples at 450 or 800 °C, ammonia was admitted to the cell. In each case the intensities of Si—NH_2 bands produced by reaction with the ammonia were no greater than for those formed on untreated Aerosil. Weak bands at 3150, 3050, and 2805 cm^{-1} due to NH_4Cl (13) were formed but there seemed to be no relationship between the concentration of NH_4Cl produced and the intensity of the Si—NH_2 bands. A side reaction 1 between ammonia and adsorbed chlorine atoms may have occurred but this was not the major reaction for the formation of Si—NH_2 groups. Analysis of one of these chlorinated pellets indicated a marked increase in chlorine content (Table 1).

Presumably these chlorine groups, replacing hydroxyls on the Aerosil pellets, were covalently bound to silicon atoms. A sample of Ludox silica which had been treated with hydrochloric acid solution before drying also contained an increased concentration of chlorine (Table 1), probably in an ionic form on the silica surface. In this case, results for reaction with ammonia were identical with those results obtained using the untreated Ludox silica. Thus it can be seen that the ability for silica to chemisorb ammonia is independent of the presence of chlorine or chloride and is a property of the silica itself.

It is possible that traces of iron introduced into the silica samples during compression in the steel pellet press and detected by X-ray fluorescence analysis, may have affected the adsorption of ammonia onto the silica. Any iron in the silica samples would most likely be present as ferric oxide since the pellets were heated in oxygen before they were placed in the spectral cell. Consequently the adsorption of ammonia onto samples of ferric oxide supported in Cab-O-Sil was investigated and these results have been presented elsewhere (22). After admission of ammonia, bands at 3450 and 1550 cm^{-1} were present in the spectra of the silica–ferric oxide samples and more intense bands (assigned to Fe—NH_3 groups) appeared at 3380, 3290, and 1605 cm^{-1}. If the bands at 3520, 3450, and 1550 cm^{-1} observed in the spectra of ammonia chemisorbed to silica (Fig. 1) were due to ammonia chemisorbed to iron impurities, additional (and more intense) bands due to Fe—NH_3 groups should also have been detected. This was not the case and it appears that the possible iron impurities in the silica samples were not responsible for the chemisorption of ammonia to produce bands in the spectrum at 3520, 3450, and 1550 cm^{-1} (Fig. 1).

It has been proposed that the Si—NH_2 groups on the silica surface are formed by the reaction of ammonia with "highly strained" or ionic siloxane bridges (8).

$$[2] \qquad \overset{\diagup\ \text{O}\ \diagdown}{\text{Si}\qquad\text{Si}} + NH_3 \rightarrow \text{Si—}NH_2 + \text{SiOH}$$

When ammonia is adsorbed on almost completely dehydroxylated porous silica glass, bands at 3747 and 3704 cm^{-1} due to isolated SiOH and BOH groups respectively, appear at the same time as bands due to amine groups (16). Ammonia reacts with the B—O—B sites on the porous glass more readily than with the siloxane sites.

Attempts to completely dehydroxylate a silica pellet were not successful. A pellet of Cab-O-Sil which has been evacuated for 5 d at 800 °C retained 75% of the free hydroxyl groups that were present after only 8 h evacuation at 800 °C (measured by comparison of the optical densities

Can. J. Chem. Downloaded from www.nrcresearchpress.com by 210.87.254.40 on 09/05/12
For personal use only.

of the band at 3747 cm^{-1}). When ammonia was added to this sample, bands due to Si—NH_2 groups appeared in the spectrum but no apparent increase in the intensity of the hydroxyl band was observed.

If the strained siloxane sites on dehydrated silica can abstract a hydrogen from ammonia by the mechanism above, it is possible that an adjacent site might react with the Si—NH_2 groups formed and a secondary amine group would result. By comparison with spectra of various silazanes and disilazanes, such groups should have an N—H stretching vibration in the region 3350—3370 cm^{-1} (23) although it is possible that this vibration may occur at a higher frequency and overlap one of the bands due to the Si—NH_2 groups. Low *et al.* (14) reported that a band at 3455 cm^{-1} (which has been assigned to a secondary B—NH—B group on porous glass (14, 15)) was obscured by the Si—NH_2 band at 3459 cm^{-1}. In order to investigate the possible formation of secondary amine groups when ammonia is added to silica, a careful study was made of the desorption of chemisorbed ammonia. Samples of Cab-O-Sil HS-5 silica evacuated at 800 °C were exposed to 250 Torr of ammonia gas and evacuated for 2 h periods at 100 °C intervals. After each evacuation, a spectrum of the sample plus adsorbed species was recorded. The intensity changes of the N—H vibrations were similar for all the samples studied and a typical sequence of spectra is shown in Fig. 2. After evacuation at 100 °C (Fig. 2*a*) the band due to the asymmetric N—H stretching vibration is broad and is centered at 3520–3540 cm^{-1}. After evacuation at 300 °C (Fig. 2*b*), this band has become quite sharp and is now centered at 3540 cm^{-1}. For evacuation at temperatures up to 400 °C, the optical density of this band decreases more rapidly than the optical densities of the bands at 3450 and 1550 cm^{-1} but above this temperature all three bands decrease at similar rates.

These observations suggest that as well as Si—NH_2 groups, a species having a band at 3520 cm^{-1} is formed by the chemisorption of ammonia onto silica and this is removed after evacuation at 300 °C. The bands due to the NH_2 groups are relatively stable at this temperature and it would be expected that a secondary amine group should be equally stable. Therefore it is unlikely that the species producing the 3520 cm^{-1} band is an amine group.

It has been shown (19) that one of the perturbed hydroxyl groups which exist on mildly evacuated silica and rehydrated silica has a band at 3520 cm^{-1} which disappears from the spectrum of the sample after evacuation at 300 °C. It is possible that the SiOH groups formed by the reaction of ammonia with the silica surface (reaction 2) will be in a strongly perturbed environment such that their O—H stretching frequency occurs at 3520 cm^{-1}. These groups are removed by evacuation at 300 °C. The rigorously dehydrated porous silica glass sample investigated previously (16) contained no surface groups before the admission of ammonia and the majority of the hydroxyl groups formed by reaction with ammonia would exist in an unperturbed environment and given rise to the 3747 cm^{-1} band rather than the 3520 cm^{-1} band discussed above. For the band to occur at 3747 cm^{-1}, there must be no hydrogen bonding between the OH and NH_2 groups shown in eq. 2.

An alternative explanation for the high rate of decrease of the 3520–3540 cm^{-1} band with evacuation at temperatures up to 400 °C may be provided by the observation that often species at very low coverages show an abnormally low intensity for the band due to the asymmetric stretching vibration compared to that for the symmetric stretch. Only at higher coverages does the asymmetric stretching band become appreciably intense. This phenomenon has been observed for many systems: *e.g.* ethylene polymers on Ziegler type catalysts where the band due to the asymmetric CH_2 stretching vibration is weak compared to the symmetric stretch at low coverage (24); also for the asymmetric stretching vibration of co-ordinated ammonia on silica – boric oxide and porous silica glass (16). No explanation can be given for these unusual intensity changes, although it must be appreciated that the band due to the asymmetric stretching vibration of gaseous ammonia is weak and only becomes appreciable when intermolecular interactions occur in condensed states.

For desorption of the chemisorbed species from silica at temperatures above 400 °C, the three bands at 3540, 3450, and 1550 cm^{-1} decrease at approximately equal rates suggesting that a single species produces all three bands. Consequently these bands are assigned to the asymmetric stretching, the symmetric stretching, and the asymmetric deformation modes, respec-

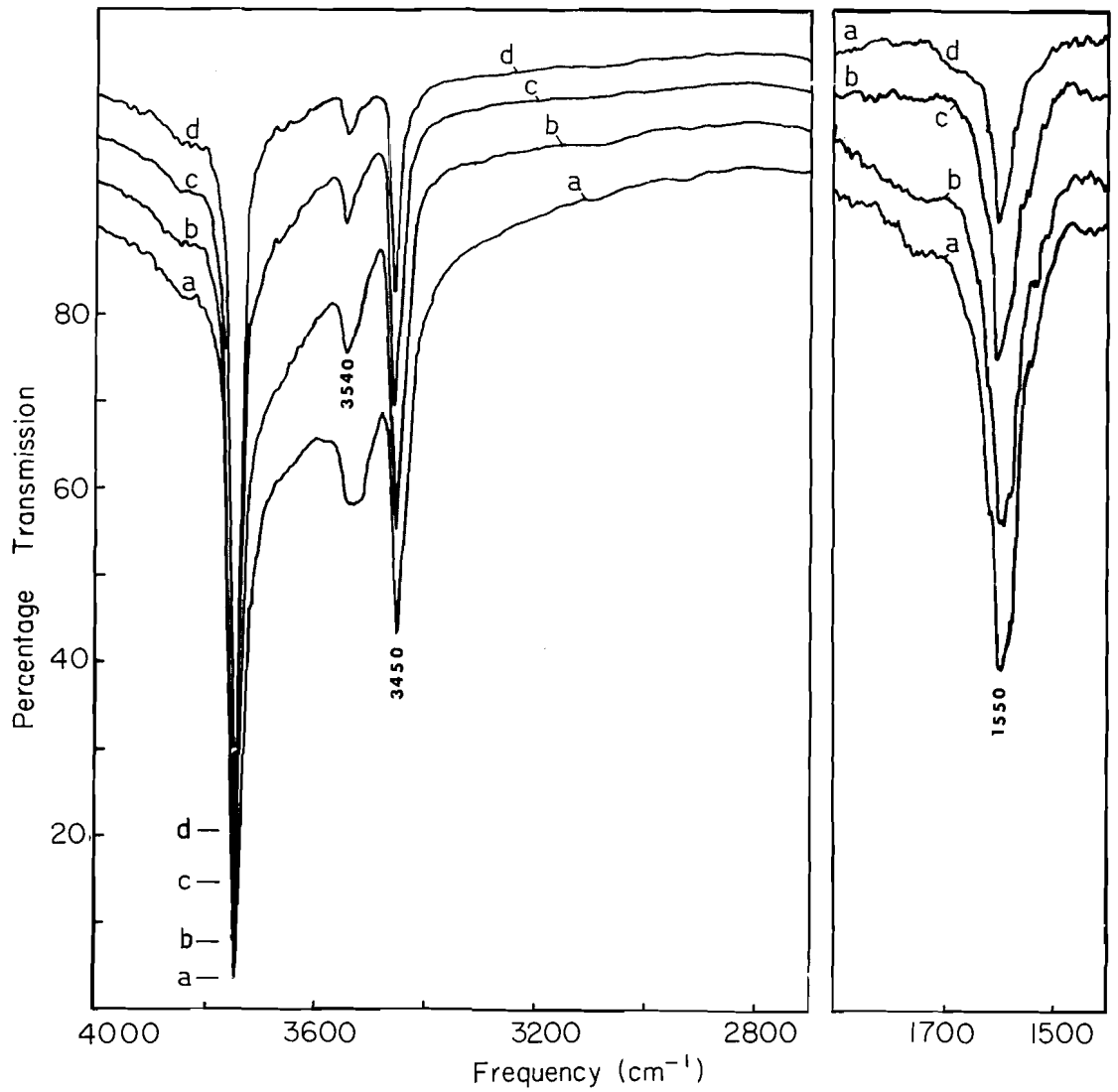

FIG. 2. A sample of Cab-O-Sil HS-5 was evacuated for 10 h at 800 °C and after cooling, 250 Torr of ammonia was admitted. Spectra were recorded: *a*, after subsequent evacuation for 2 h at 100 °C; *b*, after evacuation for 2 h at 300 °C; *c*, after evacuation for 2 h at 500 °C; *d*, after evacuation for 2 h at 700 °C.

tively, of the N—H vibrations of Si—NH_2 groups. These stretching frequencies are approximately 50 cm^{-1} higher than the corresponding frequencies for aminosilanes (23) but the deformation frequency at 1550 cm^{-1} agrees very closely.

It appears that no secondary amine groups are formed by the chemisorption of ammonia on silica. It has been proposed (14, 15) that the band at 3450–3455 cm^{-1} which appears in the spectrum of ammonia chemisorbed to porous silica glass is due to a secondary $\rangle$B—NH— species and this is overlapped by the bands due to the Si—NH_2 groups (14). For the Si—NH_2 groups discussed above, the intensity of the band at 3540 cm^{-1} is less than one-fifth of the intensity of the band at 3450 cm^{-1}. Therefore it is probable that the band at 3450–3455 cm^{-1} reported in the porous silica glass studies (14, 15) is in fact the symmetric stretching vibration of Si—NH_2 groups. The accompanying band at

Can. J. Chem. Downloaded from www.nrcresearchpress.com by 210.87.254.40 on 09/05/12
For personal use only.

Can. J. Chem. Downloaded from www.nrcresearchpress.com by 210.87.254.40 on 09/05/12
For personal use only.

3540 cm^{-1} is very weak and cannot be distinguished from the 3568 cm^{-1} band due to B—NH_2 groups. Thus it seems doubtful whether secondary amine groups exist on either ammonia – porous glass or ammonia–silica systems.

For each type of silica examined, no chemisorption of ammonia was found until the sample had been evacuated at a temperature of 400 °C or higher. The concentration of the Si—NH_2 groups produced by reaction with ammonia increased as the temperature of dehydration was increased above this temperature. A sample of Cab-O-Sil M-5 silica was evacuated at successively higher temperatures and after each evacuation, 70 Torr of ammonia was admitted. Spectra for this sample after evacuation at 200, 400, 600, and 750 °C are shown in Fig. 3. Fine structure due to gaseous ammonia was evident in the spectra when ammonia was standing over the sample.

After evacuation at 200 °C (Fig. 3*a*) the sample retained most of the weakly hydrogen bonded hydroxyls (having an infrared band at 3650 cm^{-1} (7)) and possibly some of the strongly hydrogen bonded groups having a band at 3520 cm^{-1} (7). This sample did not chemically react with ammonia since no N—H bands remained after evacuation of gaseous ammonia (Fig. 3*c*). After evacuation at 400 °C, only groups having a band at 3747 cm^{-1} with a shoulder at approximately 3650 cm^{-1} remained (Fig. 3*d*). A weak band now appeared at 3450 cm^{-1} in the spectrum of the sample after treatment with ammonia (Fig. 3*f*). Evacuation at 600 °C removed most of the hydrogen bonded hydroxyls from the silica and the band at 3650 cm^{-1} had almost disappeared (Fig. 3*g*). Bands due to Si—NH_2 groups formed by reaction with ammonia were now quite strong (Fig. 3*i*). The concentration of these chemisorbed groups was greater still (Fig. 3*l*) on a sample which had been evacuated at 750 °C before treatment with ammonia (Fig. 3*j*).

It appears that the ammonia chemisorption sites are formed when those hydroxyl groups which produce a band at 3650 cm^{-1} in the infrared spectrum are removed by evacuation at 400 °C and above. The greater the dehydroxylation of the silica surface, the greater the number of chemisorption sites that are formed.

It is considered that ammonia is physically adsorbed to the free hydroxyl groups on the silica surface in preference to hydroxyl groups which are hydrogen bonded to one another (4).

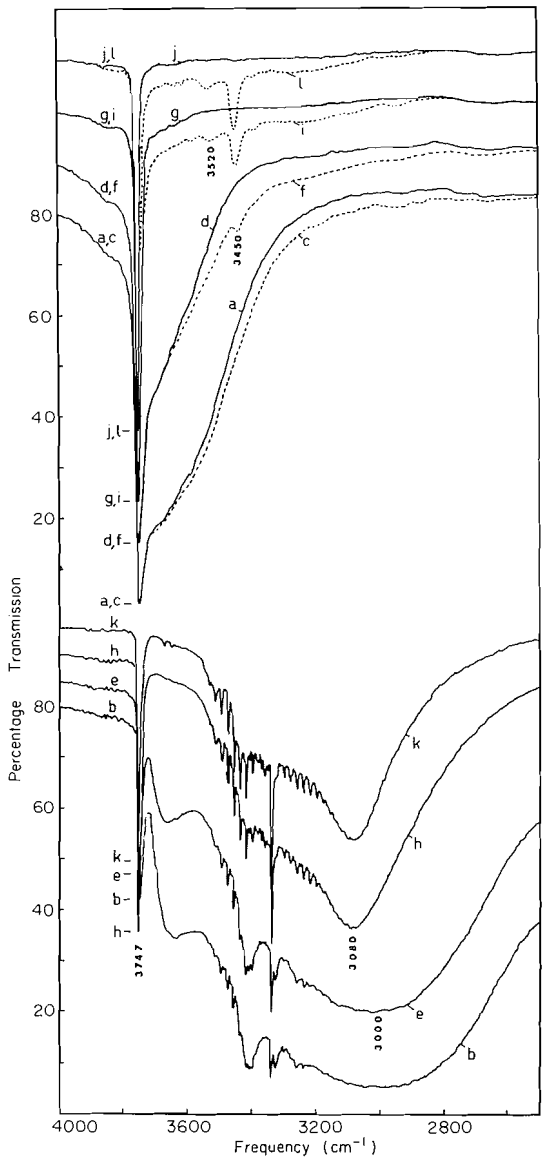

FIG. 3. The infrared spectrum of Cab-O-Sil M-5 silica: *a*, evacuated at 200 °C; *b*, after the addition of 70 Torr of ammonia; *c*, after evacuation at 20 °C; *d*, sample evacuated at 400 °C; *e*, after addition of 70 Torr of ammonia; *f*, after evacuation at 20 °C; *g*, sample evacuated at 600 °C; *h*, after addition of 70 Torr of ammonia; *i*, after evacuation at 20 °C; *j*, sample evacuated at 750 °C; *k*, after addition of 70 Torr of ammonia; *l*, after evacuation at 20 °C.

For temperatures of evacuation up to 600 °C, the intensity of the band at 3747 cm^{-1} in the spectrum of a silica sample is almost constant (Fig. 3*a*, *d*, *g*) suggesting that the number of sites for physical adsorption of ammonia mole-

Can. J. Chem. Downloaded from www.nrcresearchpress.com by 210.87.254.40 on 09/05/12
For personal use only.

cules should be approximately the same after evacuation at any temperature in this range. However, when 70 Torr of ammonia was admitted to a sample of silica which had been dried at 200, 400, or 600 °C (Fig. 3*b*, *e*, *h*), the concentration of physically adsorbed ammonia decreased as the evacuation pre-treatment temperature increased. On a sample evacuated at 200 °C (Fig. 3*b*) bands at 3400 and 3320 cm^{-1} due to N—H vibrations and at approximately 2980 cm^{-1} due to O—H vibrations of the O—H···NH_3 groups are very intense. The corresponding decrease in the intensity of the isolated hydroxyl band is also large. The low frequency of the O—H stretching band at 2980 cm^{-1} suggests that the average strength of hydrogen bonds which are formed is large.

There was less adsorption when 70 Torr of ammonia was admitted to the same sample after evacuation at 400 °C and the hydrogen bonded O—H stretching frequency increased to 3000 cm^{-1}. After evacuation at 600 °C, the sample physically adsorbed even less ammonia (Fig. 3*h*) and these adsorbed molecules were less strongly held (the O—H stretching frequency shifted to 3080 cm^{-1}). The band at 3747 cm^{-1}, due to free hydroxyls not interacting with ammonia, was greater than after ammonia adsorption on the sample evacuated at lower temperatures. Many of the hydroxyl groups which adsorbed ammonia molecules in these previous cases will no longer act as physical adsorption sites. The adsorption of ammonia on the sample after evacuation at 750 °C (Fig. 3*k*) was even less but the initial concentration of free hydroxyl groups had also decreased (Fig. 3*j*).

These results suggest that the preferred site for the physical adsorption of ammonia is the hydroxyl group which is illustrated in **1**. A similar conclusion has been reached previously (24).

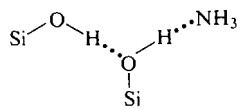

1

This is a group which is free to bond to ammonia molecules but is also involved in bonding to adjacent groups. The O—H bond will vibrate freely so will have a stretching frequency at approximately 3747 cm^{-1} but the oxygen of the group is bound to an adjacent hydroxyl group (which would have an O—H stretching frequency at 3650 cm^{-1}). The free hydrogen on this group may be expected to be somewhat more electropositive than that on a completely isolated hydroxyl group. The adjacent hydrogen bond (**1**) would induce the removal of electron density from the free hydrogen, although possibly not sufficiently to greatly alter the O—H stretching frequency (McDonald reported that a weakly perturbed hydroxyl having a stretching frequency at 3740 cm^{-1} existed on the surface of evacuated Cab-O-Sil). Ammonia molecules adsorbed to such a hydrogen would be somewhat more strongly held than molecules on completely isolated hydroxyls.

The concentration of these electropositive groups is reduced as the temperature of evacuation of the silica is increased and very few of these groups exist after evacuation at 600 °C (the shoulder at 3650 cm^{-1} is very weak for the spectrum of silica evacuated at this temperature (Fig. 3*g*)). The only hydroxyl adsorption site which remains is one which is completely isolated from its neighbors and not subject to perturbation by adjacent hydroxyl groups. Ammonia adsorbed to such a group will be less strongly bound and the O—H stretching frequency for the O—H···NH_3 group shifts to 3080 cm^{-1}.

The intensity changes of the band due to the free hydroxyl groups which remain at 3747 cm^{-1} after adsorption of ammonia (compare Figs. 3*b*, *e*, and *h*) suggests that less of the free hydroxyls on the silica act as adsorption sites when the sample has been evacuated at 600 °C than after evacuation at 400 °C and 200 °C when many of these groups would have been weakly perturbed, existing as hydroxyl pairs (**1**).

To a sample of silica evacuated at 800 °C, 20 Torr of water vapor was added and then evacuated at 20 °C. When ammonia was admitted to this sample, the gas was physically adsorbed to the surface hydroxyl groups but could be all removed by evacuation at 20 °C and the spectrum returned to its original contour. The rehydroxylated silica surface no longer contained sites which could chemisorb ammonia. However, when water vapor was added to a sample of silica having Si—NH_2 groups on its surface (Fig. 1*g*), the water was chemisorbed to form the hydroxyl groups with bands at 3720 and 3520 cm^{-1} and the adsorbed water did not displace any of the Si—NH_2 groups. Evacuation at 300 °C removed most of the newly

formed hydroxyl groups, leaving in the spectrum a band due to the weakly hydrogen bonded hydroxyls at 3650 cm^{-1} as well as bands due to Si—NH_2 groups and isolated hydroxyl groups. Thus the adsorption of water can still take place in the presence of amine groups on the silica surface whereas chemisorption of ammonia as Si—NH_2 groups is blocked by pre-adsorption of water vapor. It is probable that both water and ammonia react with the same type of sites of dehydroxylated silica but water can also react with sites which are not involved in chemisorption of ammonia.

Thanks are due to Mr. P. Bannister of the Department of Geology for the X-ray fluorescence analyses. Financial assistance from the Australian Research Grants Committee is gratefully acknowledged.

1. J. E. Mapes and R. P. Eischens. J. Phys. Chem. **58**, 1059 (1954).
2. A. V. Kiselev, V. I. Lygin, and T. I. Titova. Russ. J. Phys. Chem. **38**, 1487 (1964).
3. T. W. Boyle, W. J. Gaw, and R. A. Ross. J. Chem. Soc. 240 (1965).
4. N. W. Cant and L. H. Little. Can. J. Chem. **43**, 1252 (1965).
5. V. Lorenzelli and F. Gesmundo. Ann. Chim. (Rome), **55**, 628 (1965).
6. I. D. Chapman and M. L. Hair. Trans. Faraday Soc. **61**, 1507 (1965).
7. R. S. McDonald. J. Phys. Chem. **62**, 1168 (1958).
8. J. B. Peri. J. Phys. Chem. **70**, 2937 (1966).
9. B. Camara, H. Dunken, and P. Fink. Z. Chem. **8**, 155 (1968).
10. L. Abrams and J. W. Sutherland. J. Phys. Chem. **73**, 3160 (1969).
11. P. Pichat, M.-V. Mathieu, and B. Imelik. J. Chim. Phys. **66**, 845 (1969).
12. M. L. Hair and W. Hertl. J. Phys. Chem. **73**, 4269 (1969).
13. M. Folman. Trans. Faraday Soc. **57**, 2000 (1961).
14. M. J. D. Low, N. Ramasubramanian, and V. V. Subba Rao. J. Phys. Chem. **71**, 1726 (1967).
15. N. W. Cant and L. H. Little. J. Catal. **12**, 134 (1968).
16. G. A. Blomfield and L. H. Little. J. Catal. **21**, 149 (1971).
17. A. F. Sirianni and I. E. Puddington. Can. J. Chem. **33**, 391 (1955).
18. D. W. L. Griffiths, H. E. Hallam and W. J. Thomas. Trans. Faraday Soc. **64**, 3361 (1968).
19. G. A. Blomfield and L. H. Little. To be published.
20. F. J. Flanagan. Geochim. Cosmochim. Acta, **31**, 289 (1967).
21. H.-P. Boehm. Angew Chem. Int. Ed. Engl. **5**, 533 (1966).
22. G. A. Blomfield and L. H. Little. J. Catal. In press.
23. A. Marchand, M.-T. Forel, F. Metras, and J. Valade. J. Chim. Phys. **61**, 343 (1964).
24. N. W. Cant and L. H. Little. Unpublished results.

Can. J. Chem. Downloaded from www.nrcresearchpress.com by 210.87.254.40 on 09/05/12
For personal use only.

Carbon-13 Magnetic Resonance: the Stereochemistry of 1,2- and 1,3-Dimethyl-4-phenylpiperidine Derivatives

ALAN J. JONES[1]

Department of Chemistry, University of Alberta, Edmonton, Alberta T6G 2G2

AND

A. F. CASY[2] AND K. M. J. MCERLANE

Faculty of Pharmacy and Pharmaceutical Sciences, University of Alberta, Edmonton, Alberta T6G 2G2

Received October 23, 1972

The carbon-13 magnetic resonance spectra of the diastereoisomers of 1,2-dimethyl- (**1**) and 1,3-dimethyl-4-phenylpiperidin-4-ol (**2**), their esters and corresponding hydrochlorides have been determined. The observed chemical shifts can be ascribed to charge polarization or steric effects. The latter is particularly important in establishing the *axial* configuration of the 4-phenyl group and 3-methyl group in the preferred conformations of α-**1** and β-**2**, respectively, and consequently the stereochemistry of these systems. Substituent additivity effects are similar to those in the piperidones and cyclohexanes. Solvent effects on ^{13}C resonances remove the ambiguities of conformational change suggested in earlier proton studies.

Le spectres de résonance magnétique du ^{13}C sur les diastéréoisomères du diméthyl-1,2 (**1**) et diméthyl-1,3 phényl-4 pipéridinol-4 (**2**), leurs esters et les chlorhydrates correspondants ont été mesurés. Les déplacements chimiques observés peuvent être imputés à la polarisation de charge et aux effets stériques. Ce dernier est particulièrement important dans l'attribution de la configuration *axiale* du groupe phényl-4 et du groupe méthyl-3 des conformations préférentielles de l'α-**1** et β-**2** respectivement et par conséquent, de la stéréochimie de ces systèmes. Les effets d'additivité des substituants sont semblables à ceux des pipéridones et cyclohexanes. Les effets de solvant sur les résonances du ^{13}C lèvent les ambiguités sur le changement conformationel suggéré par les études antérieures concernant le proton.

[Traduit par le journal]

Can. J. Chem., **51**, 1782 (1973)

Several recent studies (1–7) have demonstrated the value of carbon-13 magnetic resonance (c.m.r.) as a tool in conformational analysis. The empirical substituent parameters derived in carbocyclic (1, 2) and heterocyclic (3–7) systems provide a mechanism to study not only substitution effects but also details of stereochemistry. In the present work the emphasis is placed on the application of the c.m.r. method in the structural analysis of a series of 4-phenyl-piperidine derivatives, some of which are pharmacologically active.

The potential of the c.m.r. method for stereochemical analysis of pharmacologically active molecules has been outlined in a study of synthetic precursors, the *N*-alkyl-4-piperidones (6). The derivatives, 1,2-dimethyl-4-phenyl-piperidin-4-ol (**1**) and 1,3-dimethyl-4-phenylpiperidin-4-ol (the prodinols, **2***a*) and their corresponding propionate esters (the prodines **2***b*) are the subject of the present work. There are two racemic diastereoisomers of **1** and **2**, which have been designated α- and β-isomers.[3] The stereochemistry of the alcohols **1** (8) and **2**a (9) and corresponding propionate esters (8, 10) has been the subject of considerable investigation and is well established (8–10). The present carbon-13 results confirm the assigned stereochemistry in most cases, though there are interesting discrepancies where solvent effects are considered. From the data it is possible

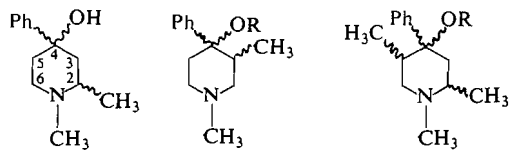

1 **2** **3**

a R = H *a* R = H
b R = COEt *b* R = COEt or $COCH_3$

[1]Author to whom correspondence should be addressed.

[2]Present address: School of Pharmacy, Liverpool Polytechnic, Byrom Street, Liverpool, L33AF, U.K.

[3]It should be emphasized that the Greek letter notations used to designate isomers are merely a convenience for the initial investigator and bear no definite interrelationship.

Can. J. Chem. Downloaded from www.nrcresearchpress.com by 210.87.254.5 on 09/05/12
For personal use only.

Can. J. Chem. Downloaded from www.nrcresearchpress.com by 210.87.254.5 on 09/05/12
For personal use only.

to derive fundamental parameters relating to conformation, configuration, and solvation effects. Further applications of these data in the trimeperidine (or promedol, **3**) series are described in the paper to follow.

Experimental

Carbon-13 spectra were determined at 22.63 MHz in the Fourier mode using a Bruker HFX-90 spectrometer in conjunction with a Nicolet-1085, 20K memory, computer. The spectrometer features a deuterium lock system, a BSV-2 random noise (800 Hz bandwidth) proton decoupler, and a BSV-2 pulse-generator-amplifier. The majority of compounds studied were freshly prepared by methods previously described (8–10). Spectra of all the bases and their corresponding hydrochlorides were determined for solutions in deuterochloroform (which also provided the lock signal) with 2–5% TMS added as internal reference. In the study of solvent effects or where solubility inhibited the use of $CDCl_3$, dimethylsulfoxide-d_6 and/or heavy water were used as solvents. In these cases a mixture containing dioxane and TMS was added as reference. All samples were contained in precision ground 10 mm, o.d., tubes (Wilmad Glass Co.). The spectrometer was used in the cross-coil configuration. On average a 30 μs pulse, corresponding to an approximate tilt angle of 45°, was employed. For the average spectral width of 5000 Hz the delay between pulses was 70 μs. Acquisition times averaged 1–2 h over 8K data points for concentrations of the order of 0.1–0.5 *M*. For off-resonance or coupled spectra this time was approximately doubled.

Results

The conventional labelling system for the piperidine ring (see **1**) is employed throughout this work. Carbon atoms in substituents are identified by a prime symbol on the number appropriate to the position of substitution on the piperidine ring. Phenyl ring carbons are labelled C-q, -*o*, -*m*, and -*p* to indicate the positions C-1, -2,6, -3,5, and -4 on the phenyl ring, respectively. The carbon-13 shifts of the series of α- and β-isomers and their hydrochlorides are given in Tables 1 and 2, respectively. Supporting data on 1-methyl-, 1-methyl-4-phenylpiperidine, 1-methyl-4-phenyl- and 1,2,6-trimethyl-4-phenylpiperidin-4-ol are given in Table 3. The procedure for assigning individual resonances to the appropriate carbon atom has been described in detail elsewhere (6, 11). In most cases assignments were made in a relatively routine and straightforward manner, though ambiguities do remain in the distinction between the ortho- and meta-carbons in all cases. The constant trends observed in the carbon-13 resonances on protonation (6) also served to confirm some of the piperidine ring carbon assignments.

Discussion

It is well established that most simple piperidines undergo rapid chair-to-chair interconversion involving nitrogen inversion (12). The carbon-13 chemical shifts must, therefore, be recognized as weighted averages of these interconverting forms. It is probable that the relatively bulky 4-phenyl substituent in most of the compounds studied in the present work will provide a barrier to this interconversion. We are, therefore, primarily concerned with the measurement of the carbon-13 shifts of the predominant conformer. Previous p.m.r. studies (9, 10) on some of the 4-phenylpiperidine derivatives considered here have suggested that the solvent may induce changes not only in the equilibrium of the interconversion but also give rise to conformational change. We have also investigated these solvent effects. For convenience we first consider the chemical shift effects induced by changes in substituents and their configuration and later the solvent effects.

Chemical Shift Additivity

Figure 1 summarizes schematically the carbon-13 chemical shifts of the piperidine ring carbon atoms in some of the bases studied for solutions in deuterochloroform. Substituent parameters for the directly bonded carbon atom C_α and subsequent carbons C_β, C_γ are summarized in Table 4. As shown in the studies on the *N*-alkyl-4-piperidones (6) these parameters are attenuated relative to those of the cyclohexanes (1, 2). Differences in the effects of equatorial compared with axial substituents are similar to those noted in the cyclohexanes (1, 2). The significance of the γ-parameter is clearly important in cases where 1,3-*syn*-axial interactions occur, otherwise most of the effects can be ascribed to charge polarization (13). The γ-effect at C-5 (7.9 p.p.m. upfield) in the β-1,3-dimethyl isomer (β-prodinol) establishes its configuration compared with the α-form. In contrast, the lower field shift of the C-3′ methyl resonances in the β-isomers (16 p.p.m., compared with 12 p.p.m. in the α-isomers) is attributed to the deshielding effect of the nitrogen lone pair or that of the hydroxyl group (compare the oxygen effect for an axial C-5 substituent in the 1,3-dioxanes (4)) which overides the γ-effect with C-5.

In 1,2,6 - trimethyl - 4 - phenylpiperidin - 4 - ol (Table 3) either the 2- or 6-methyl group must be axial. There is a sharp contrast between the equatorial (19.9 p.p.m.) and axial (13.5 p.p.m.)

Can. J. Chem. Downloaded from www.nrcresearchpress.com by 210.87.254.5 on 09/05/12
For personal use only.

TABLE 1. The carbon-13 chemical shifts in the α-isomers of 1,2- and 1,3-dimethyl-4-phenylpiperidin-4-ol derivatives and their corresponding hydrochlorides

		Carbon position*										
Compound	Solvent	C-2	C-3	C-4	C-5	C-6	C-1′	C-2′ or C-3′	C-q	C-*o*	C-*m*	C-*p*
1,2-Dimethyl-4-phenyl-piperidin-4-ol	$CDCl_3$	56.0_6	42.0_8	71.8_7	38.2_5	52.8_2	46.1_3	19.4_8	145.0_8	128.2_5	126.3_6	127.1_7
Hydrochloride†	$CDCl_3$	(56.0_1) (59.5_1)	39.8_2 (42.4_1)	69.9_3 (69.9_3)	35.2_9 (34.5_3)	(45.7_0) (52.8_8)	(40.3_6) (40.3_6)	13.4_9 17.7_5	146.7_6 142.0_1	128.4_0 129.1_1	125.0_1 126.0_4	127.3_3 *ca.* 127
1,3-Dimethyl-4-phenyl-piperidin-4-ol	$CDCl_3$ $DMSO/D_2O$‡	59.0_8 57.7_9	40.7_9 —	73.3_8 72.4_6	39.4_4 —	51.6_9 50.6_6	46.2_9 45.2_7	12.3_0 12.1_9	147.4_6 147.8_6	128.2_5 127.9_5	124.9_1 125.0_7	126.5_8 126.2_8
Hydrochloride	$CDCl_3$ D_2O	56.3_8 56.0_6	37.8_2 37.7_1	71.4_4 71.8_7	37.1_7 37.3_3	50.8_8 50.6_6	43.4_9 43.4_3	11.8_7 11.1_7	145.0_0 144.8_7	128.4_1 128.9_0	125.1_2 125.0_7	127.1_7 127.7_1
1,3-Dimethyl-4-(*o*-tolyl)piperidin-4-ol	$CDCl_3$§	59.0_3	38.2_5	74.7_3	37.3_9	51.5_8	46.2_4	12.5_7	144.3_3	—	—	—
Hydrochloride	$CDCl_3$	56.1_7	35.8_8	72.9_5	35.1_2	50.6_1	43.4_3	12.1_4	142.0_6	—	—	—
1-Ethyl-3-methyl-4-(*p*-tolyl)piperidin-4-ol	$CDCl_3$‖	56.5_4	40.7_9	73.8_1	39.2_8	52.4_4	$\binom{49.1_0}{12.0_3}$	12.3_6	144.6_0	128.8_4	124.8_0	135.8_6
Hydrochloride	$CDCl_3$	53.9_5	37.7_1	71.7_6	36.9_6	52.1_7	$\binom{48.4_0}{9.3_3}$	11.9_2	142.3_3	128.8_4	125.0_7	136.2_9
1,3-Dimethyl-4-phenyl-piperidine-4-propionate	$CDCl_3$¶ + 10% DMSO $CDCl_3$	56.6_5 56.6_5 56.4_9	40.3_6 40.3_6 40.2_0	81.5_3 81.5_3 81.3_1	30.4_8 30.4_8 30.3_2	50.5_6 50.5_6 50.6_6	43.6_0 43.6_0 43.4_9	11.9_8 11.9_8 11.9_8	139.5_3 139.5_3 139.0_4	128.3_6 128.3_6 128.4_7	125.0_7 125.0_7 125.1_2	127.5_5 127.5_5 127.7_7
(α-Prodine) hydrochloride	$CDCl_3$ + 10% DMSO‡,¶	55.9_0	—	80.8_8	30.0_0	50.0_2	—	11.7_1	139.4_7	128.2_0	125.0_1	127.3_9

*Given in p.p.m. downfield relative to TMS.

†Studied as an approximately 2:1 mixture of epimers. The relative shifts of the methyl- and phenyl-substituents are consistent with an epimeric mixture corresponding to the major isomer having the equatorial (C-q, 146.8 p.p.m.) and the minor isomer the axial phenyl configuration (C-q, 142.0 p.p.m.). Shifts in parentheses are not definitively assigned.

‡Insufficient solubility in D_2O or $CDCl_3$, the absence of a shift value at C-3 or -5 arises from probable masking by the DMSO-d_6 septet.

§Aromatic carbons at 135.3_2 (C-2), 132.9_4, 126.6_9, 125.7, and 22.9_3 (CH_3) p.p.m. in the base and 135.1_6, 133.1_1, 127.3_3, 126.8_5, 126.0_4, and 23.1_5 (CH_3) p.p.m. in the hydrochloride.

‖Prepared according to the procedure of Casy *et al.* (15). Aromatic methyl carbons at 20.8_8 and 23.1_5 p.p.m. in the base and hydrochloride, respectively. Parentheses indicate ethyl group carbons.

¶OCOEt carbons at 172.60 (C=O), 9.2_8 (CH_3), 28.4_9 (CH_2) in base 172.6_6, 9.35, 28.5_4 in hydrochloride for $CDCl_3$ + 10% DMSO solution.

Can. J. Chem. Downloaded from www.nrcresearchpress.com by 210.87.254.5 on 09/05/12
For personal use only.

TABLE 2. The carbon-13 chemical shifts in the β-isomers of 1,2- and 1,3-dimethyl-4-phenylpiperidin-4-ol-derivatives and their corresponding hydrochlorides

		Carbon position*										
Compound	Solvent	C-2	C-3	C-4	C-5	C-6	C-1′	C-2′ or C-3′	C-q	C-*o*	C-*m*	C-*p*
1,2-Dimethyl-4-phenyl-piperidin-4-ol	$CDCl_3$	54.6_6	42.7_9	71.9_2	38.3_6	52.6_6	47.3_7	20.3_4	148.9_2	128.3_0	124.5_8	126.9_0
Hydrochloride	$CDCl_3$	57.5_2	40.4_1	69.9_8	35.3_9	52.3_9	43.9_2	17.2_1	146.7_0	128.3_6	124.8_5	127.3_9
1,3-Dimethyl-4-phenyl-piperidin-4-ol	$CDCl_3$	58.1_4	40.2_3	72.7_0	31.5_0	51.5_6	46.4_9	16.2_9	147.2_4	128.0_4	125.6_6	126.9_6
	DMSO/D_2O†	57.6_8	—	72.5_1	30.3_4	51.0_9	45.9_7	16.1_8	147.4_0	128.4_1	125.9_0	127.1_7
Hydrochloride	$CDCl_3$	56.1_7	39.5_0	71.2_2	28.7_0	50.6_1	44.4_6	15.5_4	144.6_5	128.6_8	125.3_4	128.1_4
	DMSO/D_2O†	56.1_6	—	70.8_9	27.8_9	50.6_6	43.9_7	14.4_0	144.6_5	128.9_0	125.6_0	128.1_4
1,3-Dimethyl-4-phenyl-piperidin-4-propionate	$CDCl_3$‡	57.4_7	39.8_9	82.1_7	26.0_0	51.2_1	45.9_3	14.4_3	142.9_0	127.5_8	124.4_5	126.5_0
	DMSO†‡	56.9_8	—	81.9_6	25.2_5	50.9_3	45.6_5	14.6_2	143.3_6	128.2_0	125.0_7	127.0_6
Hydrochloride	$CDCl_3$‡	56.1_1	39.8_3	80.7_7	24.1_7	50.8_8	44.7_3	14.5_7	140.6_1	128.9_0	124.9_6	128.4_1
	DMSO/D_2O‡	56.0_0	38.7_4	80.7_1	23.8_5	50.4_5	43.9_2	13.0_0	140.9_3	129.0_0	125.1_7	128.4_1

*Given in p.p.m. downfield relative to TMS.
†Insufficient solubility in D_2O, the absence of a shift value at C-3 arises from probable masking by the DMSO-d_6 septet.
‡OCOEt carbons at:
172.3_7 (C=O), 9.1_7 (CH_3), 28.1_3 (CH_2) for $CDCl_3$ solution } base
171.7_9 (C=O), 9.0_6 (CH_3), 28.0_6 (CH_2) for DMSO solution }
172.2_8 (C=O), 9.1_2 (CH_3), 28.0_5 (CH_2) for $CDCl_3$ solution } hydrochloride
175.4_1 (C=O), 8.6_3 (CH_3), 28.4_9 (CH_2) for D_2O solution }

Can. J. Chem. Downloaded from www.nrcresearchpress.com by 210.87.254.5 on 09/05/12
For personal use only.

TABLE 3. Supplementary carbon-13 data on 4-phenylpiperidines and their corresponding hydrochlorides

Compound	Carbon position*										
	C-2	C-3	C-4	C-5	C-6	C-1′	C-2′ or C-6′	C-q	C-*o*	C-*m*	C-*p*
N-Methylpiperidine†	56.7_3	26.2_4	24.3_2	26.2_4	56.7_3	46.8_7	—	—	—	—	—
Hydrochloride	55.2_7	23.7_9	21.8_7	23.7_9	55.2_7	44.2_9	—	—	—	—	—
1-Methyl-4-phenylpiperidine	56.3_9	32.9_3	42.0_0	32.9_3	56.3_9	46.3_9	—	146.5_4	128.5_2	127.1_5	126.5_0
Hydrochloride	54.9_3	30.4_8	39.5_5	30.4_8	54.9_3	43.8_1	—	143.2_5	128.9_5	126.8_5	127.0_0
1-Methyl-4-phenylpiperidin-4-ol	51.6_9	38.3_6	70.0_9	38.3_6	51.6_9	46.2_9	—	149.0_2	128.2_5	124.7_4	126.8_5
Hydrochloride	50.6_1	35.0_1	67.9_8	35.0_1	50.6_1	43.1_1	—	146.3_2	128.0_3	124.4_7	127.0_1
1,2,6-Trimethyl-4-phenylpiperidin-4-ol‡	54.8_9	(43.6_5)	73.4_3	(39.0_6)	47.3_2	(46.8_3)	C-2′ 13.4_9 (a) C-6′ 19.8_6 (e)	149.3_5	128.2_5	124.5_8	126.7_9
Hydrochloride	58.2_2	44.4_6	71.3_8	40.4_1	51.0_4	37.8_8	13.7_0 17.1_6	147.4_6	128.2_5	124.9_1	127.0_6

*Given in p.p.m. downfield relative to TMS deuterochloroform solvent.
†Taken from the literature.
‡A. F. Casy unpublished synthesis.

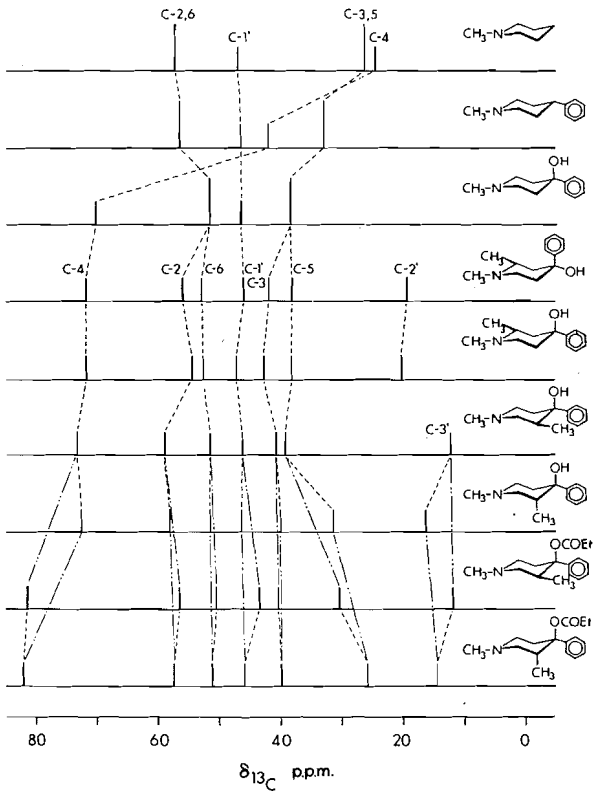

FIG. 1. Carbon-13 chemical shift correlations showing structural variations and assignments in a series of 4-phenylpiperidine derivatives.

TABLE 4. Empirical substituent parameters observed in the 4-phenylpiperidine derivatives

Substituent	Substituent parameter (p.p.m.)* α	β	γ
Ph_e†	17.7	6.7	−0.3
OH_a‡	28.1	5.4	−4.7
2-CH_{3e}§	3.7	4.1	1.8
3-CH_{3e}§	2.4	7.4‖	1.1
3-CH_{3a}§	1.9	6.5‖	−7.9
RNH^+¶	−1.6	−2.5	−2.1

*All determined from data on deuterochloroform solutions. Negative sign indicates upfield shift.
†Measured relative to *N*-methylpiperidine.
‡Measured relative to *N*-methyl-4-phenylpiperidine.
§Measured relative to *N*-methyl-4-phenylpiperidin-4-ol.
‖Determined only at the C-2 carbon atom.
¶Averaged over data in Tables 1–3 neglecting 2-substituted derivatives.

methyl shifts in this compound. Further, the γ-effect of the axial C-2′ methyl group is evidenced at C-6 (upfield 4.4 p.p.m.). There is, however, a surprising downfield shift (3.3 p.p.m.) at C-4, compared with 1-methyl-4-phenylpiperidin-4-ol. In the 1,2-dimethyl- α- and β-compounds, relatively small shift differences are observed. In particular, the C-2′ methyl shifts (19.5 and 20.3 p.p.m.) indicate this group is equatorial in both isomers. Further, the shifts at the γ-positions C-4 and -6 are relatively unchanged. These observations suggest that the configurational differences between the 1,2-dimethyl isomers must occur at C-4. The high field shift of the phenyl ring carbon C-q in the α-isomer (upfield 3.8 p.p.m. relative to the β-isomer) is taken as indicative of the axial configuration for the phenyl group. The absence of appreciable γ-shifts at C-2 or -6 in the α-, compared to the β-isomer, suggests distortion of the ring to accommodate the bulky phenyl group at the C-4 position. These results are in agreement with the conformations determined from p.m.r. measurements (8). The importance of steric effects are also evidenced in the ortho-tolyl derivative (Table 1) in which the ring carbons C-3,5 are shifted upfield (2.3 p.p.m.) compared with α-1,3-dimethyl-4-phenylpiperidin-4-ol or the corresponding *p*-tolyl derivative (Table 1).

Can. J. Chem. Downloaded from www.nrcresearchpress.com by 210.87.254.5 on 09/05/12
For personal use only.

Can. J. Chem. Downloaded from www.nrcresearchpress.com by 210.87.254.5 on 09/05/12
For personal use only.

As indicated in Fig. 1 the steric effects at C-5 in the active analgesic β-prodine (Table 2) are similar (upfield 10.2 p.p.m. compared with 1-methyl-4-phenylpiperidin-4-ol) to those in the corresponding alcohol (7.9 p.p.m.). However, the contrast at C-5 between the α- and β-isomer is still evident, though less marked, in the esters since the ester function does induce a significant upfield shift (8.9 p.p.m.) at this position in α-prodine, compared with α-prodinol. From inspection of Dreiding models it is apparent that the shift at C-5 will be determined by the orientation of the ester and phenyl groups in these systems. In the α-ester the carbonyl double bond orientation is most favored when this group is equidistant from C-5 and -q, which corresponds to a shielding zone for these carbon atoms. The phenyl ring is also at an approximate right angle to the plane of the piperidine ring. In the β-ester an alternative orientation of the ester and phenyl groups is indicated since the steric interaction of the phenyl ring with the C-3 methyl group is removed thus permitting rotation of the phenyl ring into the plane of the piperidine system. That the upfield shifts at C-5 and -q are not steric in origin is indicated by the similar shift of the carbonyl groups (172.3 and 172.6 p.p.m.) in the α- and β-ester isomers, respectively. With the exception of C-4 (β-substituent effect downfield 9.7 p.p.m., compared with the corresponding alcohols) all other ring carbons shift upfield in the esters. The magnitude of these shifts is, in general, larger in the α- than in the β-isomer, a feature which is tentatively attributed to greater steric interactions or shielding effects arising from the C-4 substituent groups and the ring carbons in the less flexible α-isomer.

The shifts induced on protonation of the nitrogen correlate reasonably well with those expected on the basis of additivity effects (6). Average α-, β-, and γ-protonation parameters derived for deuterochloroform solutions are given in Table 4. An additional parameter, which we designate $RNH_{C-\delta}{}^{+}$, was derived from the upfield shift at C-q in the phenyl ring and has a value 2.5 p.p.m. It is assumed this shift may be attributed to an electric field contribution analogous to that at C-4 (6), though its magnitude is larger than expected on the basis of a simple r^{-3} dependence.[4]

[4]NOTE ADDED IN PROOF: The recent report of Morishima *et al.* (16) leads us to suggest that C—C or C—H bond polarization might account for these long-range protonation effects.

Solvent Effects

Earlier p.m.r. studies (9, 10) on the α- and β-1,3-dimethyl-4-phenylpiperidin-4-ols, their esters and corresponding hydrochlorides indicated that the solvent could determine the conformational preference of the axial 3-methyl conformer in the β-hydrochlorides. High skew-boat populations were postulated for the β-hydrochlorides in polar media in order that the 1,3-*syn*-axial interactions between the $CH_3—\overset{\oplus}{N}—H$ and 3-methyl group be minimized (9, 10). The carbon-13 shifts determined under similar conditions are insufficiently consistent to enable generalizations concerning induced solvent shifts to be made. However, it is reasonably clear that the more polar solvent does induce some ring distortion in β-prodinol hydrochloride but the shifts do not appear to demand contributions from skew-boat conformations.[5]

The shifts induced on changing solvent from deuterochloroform to one more polar are significantly upfield (*ca.* 1.0 p.p.m.) at C-2, -4, -6, and -1′ in α-prodinol, at C-5 in β-prodinol, at C-5 and -3′ in β-prodinol hydrochloride, and at C-3 and -3′ in β-prodine hydrochloride. All other shifts do not change substantially outside the usually accepted solvent effect limit (0.5 p.p.m.) (4, 6). It is probable that the shifts in α-prodinol may be accounted for in terms of a collision complex of the type **4**, which is stabilized by hydrogen-bonding with the solvent (6, 14). The increased steric bulk of the group about C-4 will

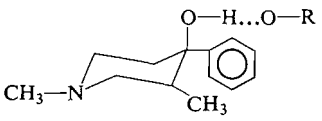

4

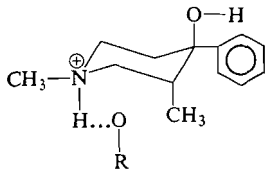

5

[5]It is anticipated that skew-boat or boat conformations would induce upfield shifts, in particular at C-1′ and -4, the consequence of "flagpole" interactions. To the authors' knowledge no parameter for this effect has been determined but it is intuitively expected to be of similar order to that of the 1,3-*syn*-axial term.

result in greater steric-compression at C-2 and -6. It is not clear why a similar effect is not observed in β-prodinol, but in the α-ester derivatives this type (**4**) of H-bonding is not possible. The shifts observed in the β-isomers, however, may be explained by a change in the center of solvation as indicated in **5**. The increased steric-bulk of the solvent-associated nitrogen center increases the steric-compression at C-3, -3′, and -5 and consequently upfield shifts are observed at these sites. Similarly, in the α-hydrochloride we suggest the nitrogen atom as the center of solvation, thus removing the C-4 effects noted for the bases.

We hesitate to draw generalizations based on the above evidence. However, we do suggest, in contrast with the proton data, that in the β-hydrochlorides some distortions from the regular chair conformations (in $CDCl_3$) are probable in polar media but that contributions from skew-boat conformers are negligible.

Conclusions

The empirical substituent parameters derived in the present work add to the generalization that carbon-13 substituent shifts are reasonably transferable from the cyclohexanes to other more complex systems. The determination of stereochemistry is clearly within the reach of carbon-13 magnetic resonance measurements even where solvent effects may induce distortions in the regular conformation.

We thank the National Research Council of Canada for support.

1. D. K. DALLING and D. M. GRANT. J. Am. Chem. Soc. **89**, 6612 (1967); J. Am. Chem. Soc. **94**, 5318 (1972); D. K. DALLING, D. M. GRANT, and L. F. JOHNSON. J. Am. Chem. Soc. **93**, 3678 (1971).
2. G. W. BUCHANAN, J. B. STOTHERS, and SIU-TZYY WU. Can. J. Chem. **47**, 3113 (1969); GURUDATA and J. B. STOTHERS. Can. J. Chem. **47**, 3601 (1969).
3. D. E. DORMAN, S. J. ANGYAL, and J. D. ROBERTS. J. Am. Chem. Soc. **92**, 1351 (1970); D. E. DORMAN and J. D. ROBERTS. J. Am. Chem. Soc. **92**, 1355 (1970).
4. A. J. JONES, E. L. ELIEL, D. M. GRANT, SR. M. C. KNOEBER, and W. G. BAILEY. J. Am. Chem. Soc. **93**, 4772 (1971); F. G. RIDDELL. J. Chem. Soc. B, 331 (1970); G. M. KELLIE and F. G. RIDDELL. J. Chem. Soc. B, 1030 (1971).
5. W. G. BENTRUDE, K. C. YEE, R. D. BERTRAND, and D. M. GRANT. J. Am. Chem. Soc. **93**, 797 (1971).
6. A. J. JONES and M. M. A. HASSAN. J. Org. Chem. **37**, 2332 (1972).
7. G. ELLIS and R. G. JONES. J. Chemm Soc. Perkin II, 437 Z1o7w)m
8. A. F. CASY and K. M. J. MCERLANE. J. Chem. Soc. Perkin I, 726 (1972).
9. A. F. CASY. Tetrahedron, **22**, 2711 (1966) and refs. therein.
10. A. F. CASY. J. Med. Chem. **11**, 188 (1968) and refs. therein.
11. A. J. JONES and M. H. BENN. Can. J. Chem. **51**, 486 (1973).
12. R. A. Y. JONES, A. R. KATRITZKY, A. C. RICHARDS, and R. J. WYATT. J. Chem. Soc. B, 1222 (1970); R. A. Y. JONES, A. R. KATRITZKY, A. C. RICHARDS, R. J. WYATT, R. J. BISHOP, and L. E. SUTTON. J. Chem. Soc. B, 127 (1970).
13. B. V. CHENEY and D. M. GRANT. J. Am. Chem. Soc. **89**, 5319 (1967).
14. A. F. CASY. Pmr spectroscopy in medicinal and biological chemistry. Academic Press, London. 1971. p. 388.
15. A. F. CASY, A. H. BECKETT, M. A. IORIO, and H. Z. YOUSSEF. Tetrahedron, **21**, 3387 (1965).
16. I. MORISHIMA, K. YOSHIKAWA, K. OKADA, T. YONEZAWA, and K. GOTO. J. Am. Chem. Soc. **95**, 165 (1973).

Can. J. Chem. Downloaded from www.nrcresearchpress.com by 210.87.254.5 on 09/05/12
For personal use only.

Carbon-13 Magnetic Resonance: the Stereochemistry of Pharmacologically Active 1,2,5-Trimethyl-4-phenyl-piperidine Derivatives

ALAN J. JONES[1] AND C. P. BEEMAN

Department of Chemistry, University of Alberta, Edmonton, Alberta T6G 2G2

AND

A. F. CASY[2] AND K. M. J. MCERLANE

Faculty of Pharmacy and Pharmaceutical Sciences, University of Alberta, Edmonton, Alberta T6G 2G2

Received November 22, 1972

The carbon-13 magnetic resonance spectra of three diastereoisomers of 1,2,5-trimethyl-4-phenylpiperidin-4-ol and their esters and corresponding hydrochlorides have been determined in deuterochloroform and/or dimethylsulfoxide-d_6. Chemical shifts observed support the configurations *t*-2-Me, *c*-5-Me (γ), *c*-2-Me, *t*-5-Me (β), and *c*-2-Me, *c*-5-Me, *r*-4-OH (α) for the isomers specified in parentheses. Chair conformations are preferred for γ (eq-Ph) and β (ax-Ph) piperidinols while the α-form favors a skew-boat. Evidence is presented for conformational changes in the α- and β-forms after *N*-protonation. The γ- and β-esters have conformations similar to the parent 4-piperidinols while the α-acetate base and hydrochloride prefer chair conformations but with different 4-phenyl orientations (base ax-Ph, HCl eq-Ph).

On a déterminé dans le deutérochloroforme et/ou dans le sulfoxyde de diméthyle les spectres en résonance magnétique du carbone-13 de trois diastéréoisomères du triméthyl-1,2,5, phényl-4 piperidinol-4 ainsi que les esters et les chlorhydrates correspondants. Les déplacements chimiques observés ont confirmé les configurations Me-2-*t*, Me-5-*c* (γ), Me-2-*c*, Me-5-*t* (β), et Me-2-*c*, Me-5-*c*, OH-4-*r* (α) pour les isomères indiqués entre les parenthèses. Les pipéridinols γ (Ph-eq) et β (Ph-ax) possèdent préférentiellement une conformation du type chaise alors que la forme α possède une conformation du type bateau-croisé. Les changements conformationnels dans les formes α et β après protonation de l'azote ont été mis en évidence. Les esters γ et β possèdent des conformations similaires aux pipéridinols-4 parents alors que la base et le chlorhydrate de l'α-acétate préfèrent une conformation du type chaise mais avec des orientations différentes du groupe phényl-4 (base Ph-ax, HCl Ph-eq).

[Traduit par le journal]

Can. J. Chem., **51**, 1790 (1973)

Stereochemical studies on narcotic analgesics have been primarily concerned with the determination of stereostructural–activity relationships in order to provide greater insight into the nature of analgesic–receptor interaction. (1) In previous papers (2–4) we have illustrated the potential of the carbon-13 magnetic resonance technique as a tool in the determination of stereochemistry in analgesics. Empirical substituent parameters have been derived from carbon-13 studies of a series of substituted 4-piperidones (2) and 4-phenylpiperidines (3, 4) of pharmacological interest. The parameters have been related to charge polarization (5) or steric (6) effects and correlate reasonably well with the known stereochemistry of the systems. The most valuable of these fundamental parameters is that arising from the steric compression caused by 1,3-*syn*-axial interactions (the γ-effect) (6). In the prodinols (**1***a*) and prodines (**1***b*) this factor was particularly evident in the observed upfield shift of C-5 in the β-isomers in which the C-3′ methyl group is axial, and enabled confirmation of the stereochemistry of these systems suggested by other techniques (7).

Conflicting evidence about the stereochemistry of the narcotic analgesic trimeperidine (promedol **2***a*) and its isomers, in addition to their precursor 1,2,5-trimethyl-4-phenylpiperidin-4-ols (**2***b*) (8–13) prompted the present study.[3] A preliminary account of some of the results has been presented (3). However, in the present paper we describe a modified stereochemistry for the α-alcohol isomer which enables total reconciliation with earlier p.m.r. studies (12). In addi-

[1]Author to whom correspondence should be addressed.

[2]Present address: School of Pharmacy, Liverpool Polytechnic, Byrom Street, Liverpool, L33Af, U.K.

[3]The α and β-isomers **2***a* are difficult to distinguish by m.p. data and it is now known that our α- and β-samples correspond with β- and α-forms respectively, of the Russian literature (9, 11).

Can. J. Chem. Downloaded from www.nrcresearchpress.com by 210.87.254.42 on 09/05/12
For personal use only.

TABLE 1. Carbon-13 chemical shifts in the diastereoisomers of 1,2,5-trimethyl-4-phenylpiperidin-4-ol and their corresponding hydrochlorides

Isomer	Carbon position*											
	C-2	C-3	C-4	C-5	C-6	C-1′	C-2′	C-5′	C-q	C-*o*	C-*m*	C-*p*
γ	54.8_0	42.8_2	74.7_5	39.4_8	60.0_8	49.6_2	20.1_7	11.9_7	147.2_4	128.2_5	124.9_1	126.6_3
γ-hydrochloride	57.6_0	40.6_7	72.9_2	37.7_5	57.6_0	45.5_4	16.9_4	11.5_4	144.6_5	128.3_6	124.9_1	127.1_7
β	57.2_5	42.5_7	74.9_4	42.5_7	60.4_8	47.3_2	20.6_6	14.4_6	144.9_2	127.6_6	127.3_3	126.8_5
β-hydrochloride†	60.1_1	40.7_4	72.7_9	40.3_0	59.0_8	47.0_5	17.9_7	12.8_4	142.1_7	128.3_6	127.1_7	127.5_5
	56.0_1	39.5_5	72.7_9	38.5_2	59.0_8	34.9_6	15.0_5	14.3_0	145.1_4	128.3_6	125.6_6	127.1_7
α	54.4_9	42.3_5	74.7_8	38.5_8	54.4_9	45.5_9	13.0_0	15.0_0	147.4_6	128.0_9	125.2_8	126.4_7
α-hydrochloride	56.1_1	40.4_7	72.5_7	38.0_4	50.6_1	41.8_7	13.0_6	11.5_5	145.6_8	128.1_4	125.2_8	126.8_5

*Given in p.p.m. downfield from TMS. In all cases deuterochloroform was used as solvent.
†Studied as a 1:1 mixture of epimers. Assignments were determined by changing composition of mixture 9:1 in DMSO solvent.

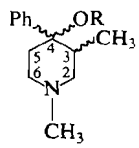

1

a R = H
b R = COEt

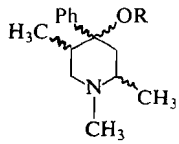

2

a R = COEt or $COCH_3$
b R = H

tion, the carbon-13 shifts of the stereoisomeric esters are described.

Experimental

Carbon-13 spectra were determined in the Fourier mode using a Bruker HFX-90 spectrometer as described in the preceding paper (4). All compounds were prepared and purified by methods previously described (12, 13), and were dissolved in deuterochloroform. Tetramethylsilane was used as internal reference. For the epimeric hydrochlorides the solvent was changed to dimethylsulfoxide-d_6 in which dioxane–TMS was used as reference.

Results

The numbering system employed and assignment techniques have been described previously (4). Table 1 provides a summary of the carbon-13 chemical shifts of the promedol alcohol isomers (**2***b*) and their hydrochlorides. Similar data for their corresponding esters (promedols, **2***a*) is given in Table 2. For the α-isomer of the latter both the propionate and acetate esters were studied. The difference in shifts induced by these substituents was negligible except at the position of substitution and consequently acetate and propionate esters are compared together. Figure 1 summarizes these data.

It should be noted that the hydrochlorides of the β-isomers provide an epimeric mixture. These mixtures were investigated by changing solvent and temperature conditions in order to resolve an appropriate assignment as given in the tables.

Discussion

Evidence of configuration and solute conformation of the isomers (**2**) is based upon an analysis of their carbon-13 spectra aided by data from the previously studied 3-methyl analogs (**1**) of established stereochemistry (4). Thus, since it has been shown that the piperidine ring adopts a chair conformation with the 4-phenyl substituent equatorial in α- and β-prodinol (**1**) (4), we initially adopt this configuration in the promedol series (**2**). Similarly the characteristic carbon-13 shifts determined for equatorial and axial C-2′ (19.9 and 13.5 p.p.m., respectively) (4) and C-3′ (or C-5′) (12.3 and 16.3 p.p.m., respectively) (4) methyl carbons may be used to help determine the orientation of the methyl substituents in the present compounds. It is convenient to analyze the present data for (*a*) the alcohols (**2***b*), Table 1; (*b*) the corresponding esters (**2***a*), Table 2; and (*c*) their salts, Tables 1 and 2.

(a) The Alcohols

In the most abundant γ-isomer of 1,2,5-trimethyl-4-phenylpiperidin-4-ol (γ-**2***b*), the methyl carbon shifts (20.2 and 12.0 p.p.m.) are characteristic of equatorial methyl groups at C-2 and -5 respectively. The phenyl ring carbon shifts, in particular at C-q and -4, are characteristic of a C-3 (or C-5) substituted piperidine ring with the phenyl group equatorial (compare α-prodinol) (4). All other carbon shifts in this isomer agree with the configuration *t*-2-Me, *c*-5-Me, *r*-4-OH,

Can. J. Chem. Downloaded from www.nrcresearchpress.com by 210.87.254.42 on 09/05/12
For personal use only.

Can. J. Chem. Downloaded from www.nrcresearchpress.com by 210.87.254.42 on 09/05/12
For personal use only.

TABLE 2. Carbon-13 chemical shifts in the diastereoisomers of trimeperidine (promedol) and their corresponding hydrochlorides

Isomer	Carbon position*											
	C-2	C-3	C-4	C-5	C-6	C-1′	C-2′	C-5′	C-q	C-*o*	C-*m*	C-*p*
γ-promedol†	54.4_4	42.5_7	84.6_0	41.2_8	60.4_3	43.1_1	20.1_8	12.1_9	141.9_0	127.9_3	124.8_5	126.5_8
γ-promedol hydrochloride†	57.6_0	40.2_0	82.6_6	38.4_7	57.2_5	40.4_7	17.0_5	11.6_0	139.1_0	128.4_1	125.0_1	127.6_6
β-promedol (acetate)‡	58.1_6	(40.9_5)	81.4_7	(36.8_5)	54.6_6	39.1_2	15.6_5	14.0_3	139.4_7	128.4_1	126.0_9	127.2_8
β-promedol (acetate) hydrochloride‡	60.8_1	40.9_0	81.4_7	42.0_8	54.9_8	40.9_0	18.0_2	12.0_9	141.3_6	128.7_9	——	124.7_4
	57.0_1	39.2_3	80.6_6	38.5_2	50.8_3	29.2_4	14.6_2	13.4_9	137.5_3	128.7_9	——	124.7_4
α-promedol (acetate)§	55.5_2	(40.6_8)	81.6_3	(35.0_7)	51.7_4	39.4_9	(12.5_7)	(12.1_4)	139.6_9	128.4_1	125.5_0	127.6_0
α-promedol (acetate) hydrochloride§	54.9_3	40.3_0	81.5_3	34.4_2	50.2_9	40.3_0	11.3_3	11.3_3	139.4_2	128.3_6	125.2_3	127.5_0

*Given in p.p.m. downfield relative to TMS. Parentheses indicate some uncertainty in assignment.
†OCOEt carbons at 172.6_0 (C=O), 9.3_3 (CH_3), 28.7_6 (CH_2) p.p.m. in the base. 172.8_2 (C=O), 9.3_3 (CH_3), 28.7_0 (CH_2) p.p.m. in hydrochloride.
‡$OCOCH_3$ carbons at 169.5_3 (C=O) and 22.2_3 (CH_3) p.p.m. in base, 169.5_8 (C=O) and 22.5_5 (CH_3) p.p.m. and 169.3_6 (C=O) and 22.0_1 (CH_3) p.p.m. in the hydrochlorides.
§$OCOCH_3$ carbons at 169.9_6 (C=O) and 22.3_9 (CH_3) p.p.m. in the base and 169.9_0 (C=O) and 22.3_4 (CH_3) p.p.m. in the hydrochloride.

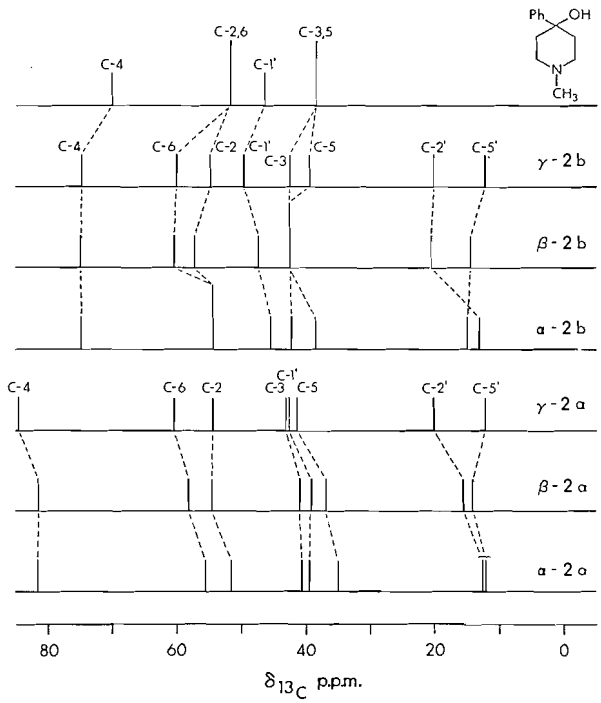

FIG. 1. Carbon-13 chemical shift correlations showing shifts and assignments in the isomers **2***b* and *a* compared with 4-phenylpiperidin-4-ol.

and the preferred conformation (**3**) for the solution of γ-**2***b* in deuterochloroform, also assigned on the basis of the p.m.r. results (12). The same stereochemistry has been shown to be true for γ-**2***b* in the solid state (14).

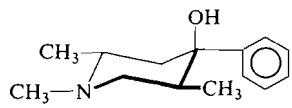

3

The methyl carbon shifts in the spectrum of the β-**2***b* isomer (20.7 and 14.5 p.p.m.) might lead to the suggestion that C-2′ is equatorial and C-5′ axial (or near axial, compare the characteristic C-3′ axial shift 16.3 p.p.m.) (4). However, no concomitant γ-effects are noted at sites across the piperidine ring at C-3. The carbon shifts at C-3 (42.6 p.p.m.) and -6 (60.5 p.p.m.) are very similar to those noted in the γ-**2***b* isomer (42.8 and 60.1 p.p.m.) and suggest that both the C-2 and -5 methyl groups are equatorial in β-**2***b*. Consequently it is the orientation of the phenyl ring which must change. The shift at C-q (144.9 p.p.m.) in β-**2***b* is similar to that in the α-isomer of 1,2-dimethyl-4-phenylpiperidin-4-ol (145.1 p.p.m.) in which the phenyl group is established as having the axial configuration (4). This shift is also upfield (2.4 p.p.m.), compared to that in the γ- or α-**2***b* isomers. The absence of appreciable 1,3-*syn*-axial effects at C-2 and -6 in β-**2***b* was also noted in the α-isomer of 1,2-dimethyl-4-phenylpiperidin-4-ol (4). These observations emphasize that the steric interaction of the axial phenyl group is minimal at C-2 and -6 (15). It is probable that the orientation of the axial phenyl group determines the deshielding shifts at C-5 and -5′, (*ca.* 3 p.p.m.) compared with those in the γ-isomer. Similar deshielding effects at the 5′-methyl group are apparent in the p.m.r. spectrum of β-**2***b* (12). The conformation **4** is thus preferred by the β-**2***b* isomer in deuterochloroform solution. This stereochemistry is also found in the solid state (14).

The assignment of the preferred conformation in the α-**2***b* isomer rests primarily on the presence

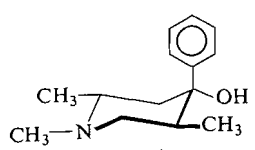

4

Can. J. Chem. Downloaded from www.nrcresearchpress.com by 210.87.254.42 on 09/05/12
For personal use only.

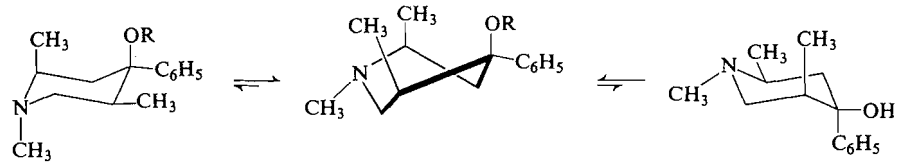

5 6 7

or absence of upfield shifts induced by potential 1,3-*syn*-axial interactions. The proton and carbon-13 data must be reconciled in this case. The methyl resonances in α-**2***b* are observed at 13.0 and 15.0 p.p.m. The higher field line of this pair must be assigned to an axial methyl group at C-2, since not only is the shift similar to that of the analogous carbon in 1,2,6-trimethyl-4-phenylpiperidin-4-ol (13.5 p.p.m.) (4), but also a concomitant *syn*-axial effect is observed at C-6 (upfield 5.5 p.p.m.), compared with the γ-**2***b* isomer. Surprisingly no major *syn*-axial effect is observed at C-4. In contrast, the equatorial configuration may be tentatively assigned to the methyl group at C-5 since no appreciable *syn*-axial effects are evidenced at C-3. The low field shift of this carbon (15.0 p.p.m.) does suggest a deshielding effect similar to that for the analogous position in β-**2***b*. The similarity in shifts for the phenyl ring carbons in γ- and α-**2***b* provides evidence for the equatorial configuration of the phenyl group in these isomers. Most significant is the upfield shift of the *N*-methyl group C-1′ (4.0 p.p.m.), compared with γ-**2***b*. It is possible to account for this upfield shift if the *N*-methyl group adopts the axial configuration, though no appreciable 1,3-*syn*-axial effects are noted at C-3 or -5.[4] The above data suggest that a contributing form to the structure of α-**2***b* is that shown in **5** (R = H). However, this structure does not account for the deshielding effect noted at C-5′ in the carbon-13 spectrum or the larger of the two $^3J_{HH}$ coupling constants of the 3-methylene protons (4.5 and 6.0 Hz, $CDCl_3$) (12). The conformation that best accommodates these data is the skew-boat **6** (R = H). The C-5′ methyl group in this case would be deshielded by the nitrogen lone pair, while the $^3J_{HH}$ value is appropriately increased from the low value expected in the perfect chair conformer **5**. A third conformation **7** (R = H) cannot be excluded as a contributor to this equilibrium, though the carbon-13 data do suggest that the preferred conformation of α-**2***b* in deuterochloroform solution is **6** (R = H) with high contributions from the form **5** (R = H). It should be noted that the carbon-13 data on the hydrochloride of α-**2***b* suggest the chair conformer **5** (protonated) as the most preferred, the C-q and -5′ shifts being typical of equatorial and the C-2′ shift being typical of axial environments. The high field C-1′ shift (41.9 p.p.m.) supports contributions from the axial configuration of this group.

(b) The Esters

The introduction of the relatively bulky ester function to the C-4 position of the piperidine ring might be expected to alter the relative proportions of the two major contributing chair conformations in the esters, compared with their precursor alcohols. However, if it is assumed that the free energy values for the OH and OCOR groups in the present systems are similar (16) then it is expected that the esters will adopt the same preferred conformation as that of the corresponding alcohol. The validity of this assumption was verified for the propionate esters of α- and β-prodinol described in the preceding paper (4). It was noted (4) that the ring carbon shifts in the esters were strongly influenced by the orientation of the ester and phenyl functions. Thus the complexity of possible factors contributing to the carbon-13 shifts of the esters make it extremely difficult to analyze the data in detail. However, the shifts apparently confirm the general premise that the esters adopt similar preferred conformations to those of the corresponding alcohols.

As in the case of the α- and β-prodines (4) substantial changes are noted at most carbon sites in the esters (**2***a*) compared with their corresponding alcohols (**2***b*). The downfield shift at C-4 in all the esters, compared with the alcohols, is attributed to the β-ester substituent effect (9.7 p.p.m. for propionate (4) and 6.7 p.p.m. for acetate). Comparison of acetates and pro-

[4]Inversion at the nitrogen center is usually considered to remove the possibility of the axial configuration in *N*-alkyl piperidines. However, similar high field shifts of *N*-methyl carbons are noted for the axial *N*-methyl group in the frozen conformation of tropinone (−100°) (A. J. Jones, to be published).

Can. J. Chem. Downloaded from www.nrcresearchpress.com by 210.87.254.42 on 09/05/12
For personal use only.

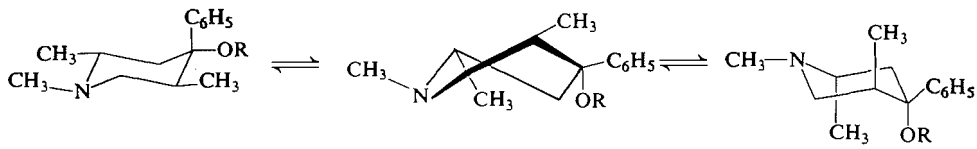

8

pionates in all other respects is considered reasonable since shifts in these esters of α-**2***a* are within 0.1 to 0.3 p.p.m. at all ring carbons sites. Based on earlier p.m.r. studies (13) a structural analogy is expected between the ester γ-**2***a* and α-prodine (**1***b*) (4). With the exception of C-5 (upfield 1.8 p.p.m.) the shifts in γ-**2***a* and α-**1***b*, compared with their corresponding alcohols, are of the same order though they differ in magnitude. It seems probable that the complex shielding contributions at C-5 in α-**1***b* (4) could change to deshielding by simple rotations of the groups at C-4 in γ-**2***a*. However, that these shift effects are induced by the equatorial 2-methyl substituent in γ-**2***a*, compared with α-**1***b* is difficult to reconcile. The lower magnitude of the shift at C-q (upfield 5.3 p.p.m.) in γ-**2***a*, compared with α-**1***b* (upfield 8.0 p.p.m.) might be the result of a rotation of the carbonyl function away from C-q towards C-5, thus changing the position of C-5 from a shielded to a deshielded zone. Further studies are necessary to establish these effects.

The ester β-**2***a* also exhibits some unexpected shifts. The high field shift at C-q (139.5 p.p.m.) in β-**2***a*, compared with γ-**2***a* (C-q 141.9 p.p.m.), suggests retention of the axial configuration for the phenyl group on esterification. The ester function, therefore, is equatorial. Similar ester induced shielding effects to those in α-prodine (4) are observed at C-q (upfield 5.4 p.p.m.) and -3 (analogous to C-5) (upfield 1.6 p.p.m. at C-3 or 5.7 at C-5) in β-**2***a*, compared to β-**2***b*. However, it is apparent that in order to reconcile the upfield shifts at C-2′ (5.0 p.p.m.) and -6 (5.8 p.p.m.) contributions from the alternative chair or skew-boat conformers as in **8** (R = COMe) must be considered. That is, an analogy with the effects observed in the α-**2***b* alcohol is expected. It seems probable, therefore, that the preferred conformation of the β-ester (**2***a*) is best represented by the equilibrium shown in **8**, which is weighted towards the left hand side and, therefore, has a similar conformational equilibrium to that of the corresponding alcohol.

Introduction of the bulky ester substituent to the alcohol α-**2***b* might be expected to shift the equilibrium represented by **5**, **6**, and **7** towards **7** (R = COMe), in order to avoid the steric interaction between the axial C-2 methyl and C-4 ester groups in **5**. The similarity in the quaternary carbon shift in α-**2***a* and that in β-**2***a* is indicative of contributions from an axial phenyl configuration. In addition, the upfield shift of the methyl resonance attributable to C-5′ (3.0 p.p.m., compared with the alcohol) suggests contributions from an axial configuration for this group. Thus, the preferred conformation of the α-**2***a* ester is most satisfactorily represented by an average of the conformers **6** and **7** (R = COMe), weighted towards the conformer **7**, as also suggested by the p.m.r. data (13).

Detailed analysis of the carbon-13 shifts in the ester (**2***a*) derivatives is clearly marred by the difficulty in abstracting the effects induced by substitution of the ester function. A knowledge of the conformation of the precursor alcohols can clearly assist in the interpretation of data for the esters. In addition, the similarities observed on protonation (Section *c* to follow) of the alcohols and the esters provides further indication of conformational similarities. However, the assumption that the free energy values for OH and OCOR groups are similar is not completely valid in the present cases. Clearly, further studies of the complex shielding contributions to carbon-13 chemical shifts induced by such anisotropic groups as the ester function are desirable.

(c) The Hydrochlorides

Protonation of the nitrogen atom in the alcohols and esters (Tables 1 and 2) results in upfield shifts at all piperidine ring carbons with the exception of C-2 which as predicted (2) shifts downfield. Average α-, β-, γ-, and δ- (4) protonation parameters are reasonably close to those observed in earlier studies (2, 4). Of particular significance is the fact that the β-isomers produce epimeric mixtures. The shifts of the epimers were assigned from studies of the compositional changes induced on changing the solvent from deuterochloroform to dimethylsulfoxide-d_6. The structures **9** and **10** are suggested for the major and minor β-epimers in

Can. J. Chem. Downloaded from www.nrcresearchpress.com by 210.87.254.42 on 09/05/12
For personal use only.

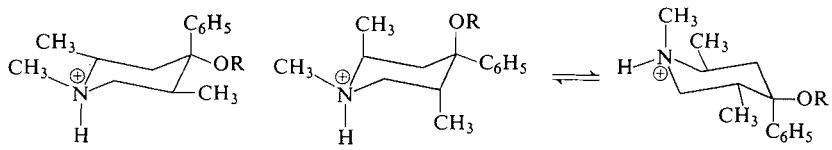

9 10*a* 10*b*

DMSO-d_6 solvent, respectively. The structure of the major epimer **9** is established by the expected upfield shifts induced by protonation of the β-alcohol and ester bases. The equilibrium suggested in **10** is required for the minor isomer in order to account for the typical equatorial phenyl C-q shift 145.1 p.p.m., compared with 145 p.p.m. in the γ- and α-**2***b* hydrochlorides. The large upfield shift at C-1′ (12.3 p.p.m.) in the minor isomer, compared with the base, is attributed to 1,3-*syn*-axial contributions in the conformer **10***b*. Further, the additional upfield shift at C-2′ in the minor epimer, compared to the major, must arise from the 1,3-*syn*-axial interaction with C-6 in **10***a*, while the downfield shift (1.5 p.p.m.) at C-5′ in the minor isomer must be the result of possible deshielding by the phenyl ring in **10***b* (*cf.* α-**2***b*). Similar shift effects are observed in the epimeric hydrochlorides of the β-ester (**2***a*) thus confirming the conformational similarity of this isomer with that of the corresponding alcohol.

It is particularly noteworthy that the conformations of the alcohols and esters which we have established as having an axial phenyl group, including α-1,2-dimethyl-4-phenylpiperidin-4-ol (4), produce an epimeric mixture on protonation. This observation suggests that the conformational strain induced by the axial phenyl substituent is such that a conformational change is readily induced on protonation. The formation of an epimeric mixture of hydrochlorides might, therefore, be considered indicative of the axial phenyl configuration in the preferred conformation of the basic forms of piperidine derivatives.

From the p.m.r. studies (12, 13) there is clear evidence that the ester α-**2***a* changes its preferred conformation on protonation. The carbon-13 data similarly reflect a change in the equilibrium suggested in **5**, **6**, and **7** (R = COMe). In particular, the shifts at the phenyl ring carbon C-q (139.4 p.p.m.) and the C-5′ methyl group (11.3 p.p.m.) are also identical with those in the γ-**2***a* hydrochloride, 139.1 and 11.6 p.p.m., respectively. The equatorial configuration is, therefore, favored for these two groups. Consequently the weighting of the conformation (**5**) is highly favored in the hydrochloride of α-**2***a*.

In conclusion, the carbon-13 chemical shifts have provided an excellent mechanism for determining details of structure in this series of relatively complex stereoisomers in solution. It is clear that the analysis of stereostructural–activity relationship in analgesics will gain much from the use of this spectroscopic technique.

We thank the National and Medical Research Councils of Canada for support.

1. P. S. PORTOGHESE. J. Pharm. Sci. **55**, 865 (1966); R. A. HARDY and M. G. HOWELL. *In* Analgetics. Vol. 5. *Edited by* G. deStevens. Medicinal Chemistry Monographs. Academic Press. 1965; A. F. CASY. *In* Drugs and molecules — a guide to modern pharmacology. *Edited by* R. M. Featherstone. Marcel Dekker, New York. In press.
2. A. J. JONES and M. M. A. HASSAN. J. Org. Chem. **37**, 2332 (1972).
3. A. J. JONES, A. F. CASY, and K. M. J. MCERLANE. Tetrahedron Lett. 1727 (1972).
4. A. J. JONES, A. F. CASY, and K. M. J. MCERLANE. Can. J. Chem. This issue.
5. D. K. DALLING and D. M. GRANT. J. Am. Chem. Soc. **89**, 6612 (1967); B. V. CHENEY and D. M. GRANT. J. Am. Chem. Soc. **89**, 5319 (1967).
6. D. K. DALLING and D. M. GRANT. J. Am. Chem. Soc. **94**, 5318 (1972).
7. A. F. CASY. Tetrahedron, **22**, 2711 (1966); J. Med. Chem. **11**, 188 (1968).
8. N. S. PROSTAKOV and N. N. MIKHEEVA. Russ. Chem. Rev. **31**, 556 (1962).
9. N. S. PROSTAKOV, B. E. ZAITSEV, N. M. MIKHAILOVA, and N. N. MIKHEEVA. Zh. Obshch. Khim. **34**, 234 (1964).
10. N. I. SHVETSOV and V. F. KUCHEROV. Dokl. Akad. Nauk. USSR. **126**, 1017 (1959).
11. T. F. VLASOVA and YU. N. SHEINER. Zh. Strukt. Khim. **11**, 640 (1970).
12. A. F. CASY and K. M. J. MCERLANE. J. Chem. Soc. Perkin I, 334 (1972).
13. A. F. CASY and K. M. J. MCERLANE. J. Chem. Soc. Perkin I, 339 (1972).
14. W. H. DECAMP and F. R. AHMED. Chem. Commun. 1102 (1971).
15. N. L. ALLINGER and M. T. TRIBBLE. Tetrahedron Lett. 3259 (1971).
16. E. L. ELIEL, N. L. ALLINGER, S. J. ANGYAL, and G. A. MORRISON. Conformational analysis. Wiley and Sons, New York. 1965.

Can. J. Chem. Downloaded from www.nrcresearchpress.com by 210.87.254.42 on 09/05/12
For personal use only.

^1H and ^{13}C Nuclear Magnetic Resonance Spectroscopy of Some Derivatives of Nitro Sugars

N. GURUDATA AND F. J. M. RAJABALEE[1]

Department of Chemistry, Sir George Williams University, Montreal 107, Quebec

Received November 27, 1972

Eight 2,3-dideoxy-2-amino-3-nitrosugar derivatives have been obtained by an elimination–addition reaction on the α and β anomers of methyl-4,6-*O*-benzylidene-3-deoxy-3-nitro-glucopyranoside-2-acetate. P.m.r. is used to show that the compounds exist in the CE conformation. ^{13}C.m.r. data are presented for three anomeric pairs. Trends in the C-13 chemical shifts are found to be similar to those reported in other studies of carbohydrates. Exceptions in direction and magnitude of chemical shift differences are discussed.

Huit dérivés de didéoxy-2,3 amino-2 nitro-3 sucres ont été obtenus par une réaction d'addition-élimination sur les anomères α et β de l'*O*-benzylidène-4,6 déoxy-3 nitro-3 glucopyranoside acétate-2 de méthyle. La r.m.n. a été utilisée pour montrer que les composés existent sous la conformation CE. Les données de la r.m.n. du ^{13}C ont été présentées pour trois couples d'anomères. Les tendances dans les déplacements chimiques du ^{13}C ont été trouvées comparables à celles rapportées par les autres études sur les hydrates de carbone. Les exceptions sur le sens et l'amplitude des différences dans les déplacements chimiques ont été discutées. [Traduit par le journal]

Can. J. Chem., 51, 1797 (1973)

Introduction

While direct interest in nitro sugars has intensified since the discovery of evernitrose (1), much of the investigation of these compounds has centered on their value as synthetic intermediates (2). In the present study, a number of 2,3-dideoxy-2-amino-3-nitrosugar derivatives have been obtained by a modification of the procedure reported by Baer and coworkers (3). First-order analysis of the p.m.r. parameters of the compounds is used to establish their configurations and conformations and trends in the C-13 spectral data are discussed.

Experimental

Compounds **2**–**5** and **7**–**10** were obtained by an elimination–addition reaction on the corresponding nitroacetates **1** and **6**. The procedure followed and the physical properties of the compounds are given elsewhere (4).

Nuclear Magnetic Resonance Spectroscopy

Proton n.m.r. spectra were obtained from 0.2 *M* solutions in $CDCl_3$ using a Varian HA-100 spectrometer in the "frequency sweep" mode. Carbon-13 spectra were obtained from 0.5 *M* solutions in $CDCl_3$ using a Varian XL-100 spectrometer in the FT mode with an external deuterium lock (D_2O) and with tetramethylsilane as internal reference. Spectra were obtained both in the "noise-decoupled" and "off-resonance decoupled" modes. Values for the ^{13}C chemical shifts are derived from the "noise-decoupled" spectra and the precision is estimated to be better than ±0.05 p.p.m.

[1]Present address: Department of National Health and Welfare, Health Effects Division, Environmental Health Centre, Tunney's Pasture, Ottawa, Canada, K1A 0K9.

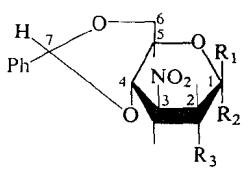

α-Series	β-Series
R_1=H	R_1=OCH_3
R_2=OCH_3	R_2=H

	R_3	
1	OAc	**6**
2	NHC_2H_5	**7**
3		**8**
4		**9**
5		**10**

Results and Discussion

Table I summarizes the first order p.m.r. data for the compounds. The size of the H-1, H-2 splitting in the α-series (2.90–3.75 Hz) shows that H-2 must be axial since H-1 is equatorial (5). The range 7.75–8.00 Hz for $J_{1,2}$ in the β-series is also consistent with H-2 (and H-1) in an axial orientation (6). The ratio of the axial–axial to the axial–equatorial splitting is in the

Can. J. Chem. Downloaded from www.nrcresearchpress.com by 210.87.254.105 on 09/05/12
For personal use only.

TABLE 1. First-order p.m.r. parameters of the title compounds

Compound	Chemical shifts (p.p.m. from TMS)						Coupling constants* (Hz)		
	C_6H_5	C_6H_5CH	OCH_3	H-1	H-3	H-4	$J_{1,2}$	$J_{2,3}$	$J_{3,4}$
2	7.35	5.52	3.43	4.85	4.60	n.a.†	3.75	10.25	10.25
7	7.35	5.52	3.54	4.32	4.64	4.12	7.75	10.60	10.00
3	7.35	5.52	3.40	4.90	5.17	n.a.	3.25	11.06	9.56
8	7.34	5.51	3.49	4.43	4.82	4.10	8.15	10.35	10.00
4	7.34	5.52	3.38	4.87	5.16	n.a.	3.00	11.50	9.75
9	7.33	5.40	3.53	4.55	4.79	4.08	8.25	11.25	10.12
5	7.34	5.52	3.41	4.91	5.14	n.a.	2.88	11.50	9.75
10	7.35	5.51	3.53	4.50	4.77	4.09	8.50	11.00	10.50

*± 0.05 Hz.
†n.a. = not assigned.

range 2–3 expected for a chair conformation. Both $J_{2,3}$ (10.25–11.60 Hz) and $J_{3,4}$ (9.56–10.50 Hz) are of the magnitude characteristic of axial–axial couplings and show that H-3 and -4 are axial. (In the α-series, $J_{2,3}$ and $J_{3,4}$ have been assigned on the basis that little change is expected on anomerization. For example, in the β-anomer, **10**, $J_{2,3}$ = 11.00 and $J_{3,4}$ = 10.50 Hz; for the α-anomer, values of 11.50 and 9.75 Hz are obtained. Since the former is closer to 11.00, it is assigned to $J_{2,3}$; $J_{3,4}$ is then 9.75 Hz. It should be noted that any ambiguity in the assignment of $J_{2,3}$ and $J_{3,4}$ does not affect the arguments presented.)

Taken together, the data indicate that the nitrosugar derivatives have the *gluco* configuration at C-2 and -3 and that the pyranose ring is in the CE conformation. This is consistent with the previous report (5) that the pyranoid part of methyl-4,6-*O*-benzylidene-α-D-aldopyranosides exists exclusively in the C1(D) conformation.

The absorption of the aromatic protons (δ = 7.33–7.35) appears insensitive to both changes of the substituent at C-2 and anomerization at C-1. With the exception of that of the β piperidinyl compound, **9**, all the benzylidene proton resonances lie in the range 5.51–5.52 p.p.m. from TMS. According to the recent observations of Baer and Rank (7), this is good evidence that there is no change of configuration at C-2 and -3 in the series of compounds examined. The deviation seen in **9** may be due to conformational changes necessitated by the steric requirements of the piperidine ring.

Axial *O*-methyl groups (δ = 3.38–3.43) absorb at higher field than the corresponding equatorial groups (δ = 3.49–3.54). The chemical shift difference shows some dependence on the C-2 substituent, being 0.09 p.p.m. for the pyrrolidinyl compounds and 0.15 p.p.m. for the piperidinyl analogues. Contributions to these substituent effects may arise from conformational changes (8) caused by the spatial requirements of the substituent as well as from direct intramolecular screening (magnetic, electrical, and van der Waals shieldings) (9). The relative shifts of the anomeric protons also depend on the C-2 substituent, Δδ varying from 0.32 to 0.53 p.p.m.

Assignment of C-13 Resonances

The aromatic quaternary carbon atom, C-1′, is easily recognized since it appears at lowest field (136.27–136.43 p.p.m. from TMS; see Table 2) and is a singlet in both the noise decoupled and off-resonance decoupled spectra. The other aromatic resonances are assigned on the basis of well established substituent shifts (10). Examination of the data reveals little sensitivity to either anomerization or to the substituent at C-2.

Comparison with literature data (11) for the parent amines allows assignment of the signals for the C-2 substituents (Table 3). Anomerization has little effect on these resonances.

Of the "sugar" resonances (Table 4), those of the methoxyl groups appear as quartets in the off-resonance decoupled spectra. In all cases, the axial OMe carbon absorbs at higher field. The chemical shift difference between the axial and equatorial groups at C-1 depends on the substituent at C-2. It is largest for the secondary amine group (**2**, **7**) while being of similar size for the two tertiary amine groups (**3**, **8**; **4**, **9**) examined.

Can. J. Chem. Downloaded from www.nrcresearchpress.com by 210.87.254.105 on 09/05/12
For personal use only.

TABLE 2. Carbon-13 chemical shifts of the aromatic carbon atoms (p.p.m. from TMS)

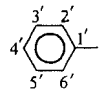

Compound	C-1′	C-2′,6′	C-3′,5′	C-4′
2	136.27	128.97	128.02	125.87
3	136.35	128.97	128.02	125.95
4	136.43	128.97	128.02	125.95
7	136.27	129.05	128.10	125.87
8	136.27	128.97	128.02	125.87
9	136.27	128.97	128.02	125.87

TABLE 3. Carbon-13 chemical shifts of C-2 substituents (p.p.m. from TMS)

2 15.63 41.59

CH_3—CH_2—NH—

7 15.56 41.27

3		**8**		**4**		**9**
48.33		48.17		50.87		57.03
24.05		23.97		26.90		26.75
				24.68		24.52

TABLE 4. Carbon-13 chemical shifts of carbon atoms in the "sugar" region (p.p.m. from TMS)

Compound	C-1	C-2	C-3	C-4	C-5	C-6	C-7	OCH_3
2	98.25	60.08	87.70	78.41	62.06	68.89	101.35	55.48
7	104.52	61.43	89.13	77.94	66.35	68.57	101.27	59.29
3	99.52	61.98	84.52	79.05	61.98	68.97	101.43	54.76
8	102.62	62.30	87.14	78.33	66.27	68.65	101.11	56.51
4	98.97	66.98	83.65	79.29	62.14	69.05	101.43	54.68
9	102.78	67.78	86.59	78.33	66.35	68.65	101.19	56.51

Perlin and co-workers (12) found that, in methyl-D-glucopyranosides, the C-6 carbon of the α anomer absorbs at 0.2 p.p.m. *higher* field than that of the β anomer. In the present data, $\Delta\delta_{ae}$[2] is in the range 0.32–0.40 p.p.m. with the resonance for the α anomer consistently at *lower* field.

Evaluation of substituent effects in the cyclohexane system (13) showed that replacement of a hydroxyl group by a nitro group deshields the attached carbon atom by 14.6 p.p.m. Combining this with a chemical shift of 75.75 p.p.m. for C-3 in methyl-α-D-glucopyranoside (14) gives the basis for assigning the signals in the region of 90 p.p.m. to C-3 of the nitrosugar derivatives. Differences from the predicted value reflect the effects of the acetal ring and the C-2 substituent. The magnitude of $\Delta\delta_{ae}$ (1.43–2.94 p.p.m.) is similar to that obtained for the simple glycopyranosides (12). There is a clear dependence on the C-2 substituent since the observed value (12) for methyl-D-glucopyranosides is 1.6 p.p.m. with C-3 of the α anomer absorbing at higher field.

Neither the chemical shift values for C-5 (Table 4) nor the effect of anomerization (4.21–4.29 p.p.m. with the signal for the α anomer at higher field) shows much dependence on the C-2

[2]$\Delta\delta_{ae}$ is the difference between the chemical shifts of a particular carbon atom in two anomeric compounds.

Can. J. Chem. Downloaded from www.nrcresearchpress.com by 210.87.254.105 on 09/05/12
For personal use only.

substituent. The size of $\Delta\delta_{ae}$ is similar to that obtained (12) for methyl-D-glucopyranoside.

Jones and co-workers (15) found that in *cis*-2-phenyl-4,6-dimethyl-1,3-dioxan, C-4 absorbs at 72.83 p.p.m. An oxygen substituent on the adjacent carbon (C-5) is expected to deshield C-4 by about 5 p.p.m. (13). These considerations lead to the assignment of the C-4 resonances given in Table 4. While previous work (12) showed no systematic anomerization effect at C-4, the present data show that the resonance of the β anomer is consistently at higher field.

Since C-1 and -7 are each attached to two oxygen atoms, the lowest field non-aromatic resonances are attributed to these carbon atoms. The assignments shown in Table 4 are consistent with earlier reports (11, 12, 14, 16) on C-13 chemical shifts of carbohydrates. They are also in accord with present (Table 1) and previous (3) p.m.r. data which indicate that the benzylidene proton is insensitive to the configuration at C-1. In addition, the magnitude of $\Delta\delta_{ae}$ follows the same trend as that of the carbon resonances of the methoxyl group, being largest (6.27 p.p.m.) with the secondary amino group at C-2 and smaller (3.12 and 3.81 p.p.m.) when the C-2 substituent has a tertiary amino group. Alternative assignments of the low field non-aromatic resonances are in principle possible, but suggest anomerization effects at C-7 which are of the same size as those at C-1. These alternatives are, therefore, unlikely.

The authors thank Professor J. B. Stothers of the University of Western Ontario for C-13 spectra on a Varian XL-100 system.

Financial support by the National Research Council of Canada is gratefully acknowledged.

1. A. K. Ganguly, O. Z. Sarre, and H. Reimann. J. Am. Chem. Soc. **90**, 7129 (1968).
2. H. H. Baer. Adv. Carbohydr. Chem. and Biochem. **24**, 67 (1969) and refs. therein.
3. H. H. Baer, T. Nielson, and W. Rank. Can. J. Chem. **45**, 991 (1967).
4. F. J. M. Rajabalee. Carbohydr. Chem. To be published.
5. B. Coxon. Tetrahedron, **21**, 3481 (1965).
6. R. U. Lemieux, R. K. Kullnig, H. J. Bernstein, and W. G. Schneider. J. Am. Chem. Soc. **80**, 6098 (1958).
7. H. H. Baer and W. Rank. Can. J. Chem. **50**, 1216 (1972).
8. T. D. Inch. *In* Annual reviews of NMR spectroscopy. Vol. 2. *Edited by* E. F. Mooney. Academic Press, London and New York. 1969. pp. 35–82.
9. (*a*) R. F. Zurcher. *In* Progress in nuclear magnetic resonance spectroscopy. Vol. 2. *Edited by* J. W. Emsley, J. Feeney, and L. H. Sutcliffe. Pergamon Press, New York, N.Y. 1967. Chap. 5. pp. 205–257; (*b*) M. T. Tribble, M. A. Miller, and N. L. Allinger. J. Am. Chem. Soc. **93**, 3894 (1971).
10. P. Lazzeretti and F. Taddei. Org. Mag. Res. **3**, 283 (1971) and refs. cited therein.
11. G. C. Levy and G. L. Nelson. *In* Carbon-13 nuclear magnetic resonance for organic chemists. Wiley-Interscience, New York. 1972 and refs. cited therein.
12. A. S. Perlin, B. Casu, and H. J. Koch. Can. J. Chem. **48**, 2596 (1970).
13. T. Pehk and E. Lipmaa. Org. Mag. Res. **3**, 679 (1971).
14. E. Breitmaier, W. Voelter, G. Jung, and C. Tanzer. Chem. Ber. **104**, 1147 (1971).
15. A. J. Jones, E. L. Eliel, D. M. Grant, M. C. Knoeber, and W. F. Bailey. J. Am. Chem. Soc. **93**, 4772 (1971).
16. A.-M. Sepulchre, G. Luckacs, G. Vass, and S. D. Gero. Angew. Chem. Int. Ed. Engl. **148** (1972).

Can. J. Chem. Downloaded from www.nrcresearchpress.com by 210.87.254.105 on 09/05/12
For personal use only.

Cyclizations of Dialdehydes with Nitromethane. XV. Synthesis of Four Stereoisomeric Deoxynitroinositol Monomethyl Ethers[1]

JAN KOVÁŘ AND HANS H. BAER

Department of Chemistry, University of Ottawa, Ottawa, Canada K1N 6N5

Received January 4, 1973

Methylation of 1,2:5,6-di-*O*-isopropylidene-α-D-glucofuranose (**1**) followed by hydrolysis of the 5,6-ketal group and periodate oxidation gave 1,2-*O*-isopropylidene-3-*O*-methyl-α-D-*xylo*-pentodialdo-1,4-furanose (**4**). Addition of nitromethane to **4** afforded a mixture of 6-deoxy-1,2-*O*-isopropylidene-3-*O*-methyl-6-nitro-α-D-glucofuranose (**5**) and -β-L-idofuranose (**6**). Removal of the 1,2-ketal group led to a mixture of 6-deoxy-3-*O*-methyl-6-nitro-D-glucose (**7**) and -L-idose (**8**) from which the crystalline β-anomer of **7** could be isolated. Cyclization of the nitro hexoses by internal Henry reaction furnished four stereoisomeric deoxynitroinositol monomethyl ethers which were obtained in crystalline condition, in part directly and in part via acetone and acetyl derivatives. The *scyllo* (**9**), DL-*myo*-1 (**10**), *muco*-3 (**14**), and *epi*-3 (**16**) configurations were assigned to the products by n.m.r. spectroscopy.

La méthylation du di-*O*-isopropylidène-1,2:5,6-α-D-glucofuranose (**1**) suivie de l'hydrolyse du groupe cétal-5,6 et de l'oxydation périodique, conduit à l'*O*-isopropylidène-1,2-*O*-méthyl-3-α-D-*xylo*-pentodialdofuranose-1,4 (**4**). L'addition de nitrométhane à **4** conduit à un mélange de déoxy-6-*O*-isopropylidène-1,2-*O*-méthyl-3 nitro-6-α-D-glucofuranose (**5**) et de -β-L-idofuranose (**6**). L'enlèvement du groupe cétal-1,2 conduit au mélange de déoxy-6-*O*-méthyl-3 nitro-6-D-glucose (**7**) et de -L-idose (**8**) à partir duquel l'anomère β cristallin de **7** a pu être isolé. La cyclisation des nitrohexoses par une réaction de Henry interne fournit quatre éthers déoxynitroinositolmonométhylés diastéréoisomères qui ont été obtenus cristallisés soit par voie directe, soit par les dérivés acétone et acétyle. Les configurations *scyllo* (**9**), DL-*myo*-1 (**10**), *muco*-3 (**14**), et *épi*-3 (**16**) ont été attribuées aux produits par spectroscopie r.m.n.

[Traduit par le journal]

Can. J. Chem., 51, 1801 (1973)

Several recent articles from this laboratory dealt with non-bonded interactions between hydroxyl groups and nitro groups in vicinal position on pyranoside rings, with special reference to the formation and stability of glycoside nitronates. Conformational preferences and configurational equilibrations in such glycosides were correlated with such interactions, and the studies led to new insights into chemical reactivities and mechanisms in this field (2–5). It became desirable to seek, along similar lines, a better understanding of certain aspects of the formation and mutual interconversion of stereoisomeric deoxynitroinositols (6–10), and it now seemed profitable to apply the newly developed concepts and methods of study to this related group of compounds.

It was reasoned that the planned investigations might be facilitated if there were available a number of stereoisomeric deoxynitroinositols that carry an *O*-methyl group in opposition to the nitro function. The methyl group, it was hoped, should render the isomers more readily distinguishable by n.m.r. spectroscopy and thus aid in the analysis of product mixtures while at the same time this functionality would be distant from, and not interfere with, the nitrodiol moiety whose chemistry was to be examined. Consequently we synthesized such methyl ethers as will be reported here, and studied mechanistic aspects of their formation and epimerization as will be communicated elsewhere (11).

The synthesis was to be patterned after the Fischer–Grosheintz nitroinositol synthesis (6, 12) which involves a stepwise nitromethane cyclization of a partially blocked pentodialdose. It was therefore necessary, first, to synthesize 1,2-*O*-isopropylidene-3-*O*-methyl-α-D-*xylo*-pentodialdo-1,4-furanose (**4**) and thence 6-deoxy-3-*O*-methyl-6-nitro-D-glucose (**7**) and (or) its L-*ido* isomer (**8**). The pathway that led to the crystalline β-anomer of **7**, and also to a mixture of **7** and **8** which could not be separated, is delineated in Scheme 1. 1,2:5,6-Di-*O*-isopropylidene-α-D-glucofuranose (**1**) was methylated by the Kuhn method (13), which proved simple and furnished the 3-*O*-methyl derivative **2** in 83% yield. Partial hydrolysis to give 1,2-*O*-isopropylidene-3-*O*-methyl-α-D-glucofuranose (**3**) was readily achieved with 90% acetic acid. The product

[1]For part XIV in this series see ref. 1.

Can. J. Chem. Downloaded from www.nrcresearchpress.com by 210.87.254.5 on 09/05/12
For personal use only.

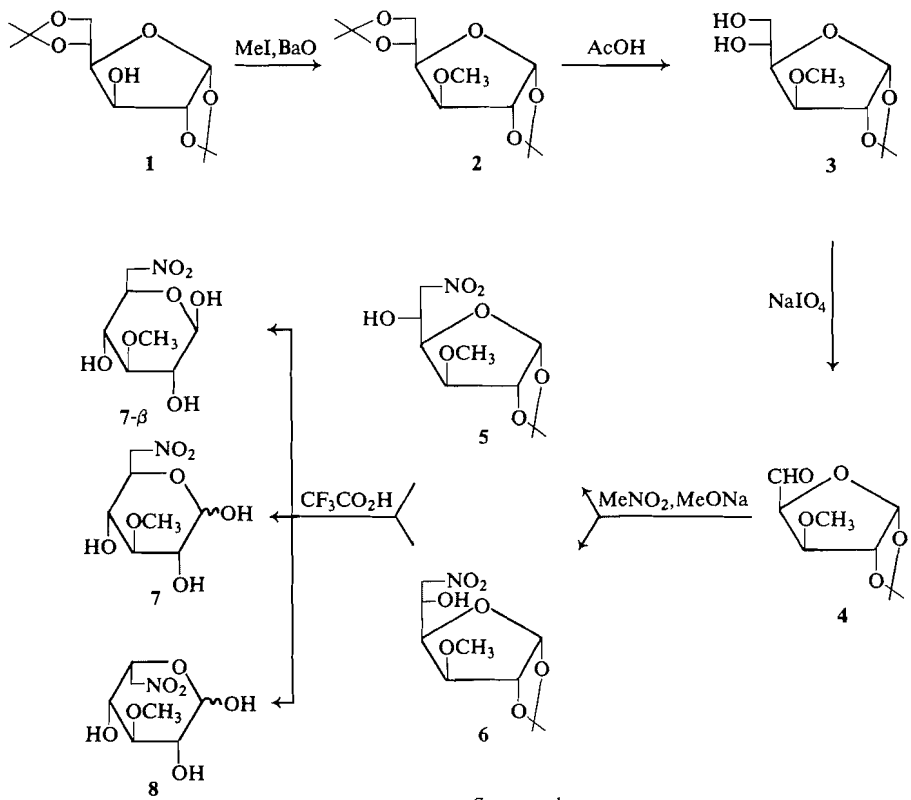

SCHEME 1

could be purified with advantage by chromatography on silica gel instead of distillation as was practiced earlier (14). However, crude **3** was satisfactory for immediate use in the subsequent step. Its periodate oxidation smoothly afforded the partially blocked dialdose **4** as a chloroform-soluble syrup. Because of its apparent sensitivity, purification of **4** for elemental analysis was not pursued, but the n.m.r. spectrum proved its structure beyond doubt. The data (see Experimental) also gave an indication of the conformation of **4** and its precursors **2** and **3**. At 1000 Hz sweep width the signals of H-2 and -3 appeared as doublets due to coupling with H-1 and -4, respectively; the observed splittings were 2.5–4 Hz, and coupling between H-2 and -3 was too small to be observable. These features showed that the furanose ring in these compounds exhibits the same conformational preference as that in 1,2-*O*-isopropylidene-α-D-glucofuranose and related derivatives (15–17). Originally the $^3T_2$ twist conformation had been proposed (15) for this system, but more recent studies indicate (17) that it may better be described by the segment $^3T_4 \rightleftarrows E_4 \rightleftarrows {}^0T_4$ of the cycle of furanose conformers. Another noteworthy signal in the spectrum of **4** was a low-field doublet (δ 9.66, J = 1.5 Hz) whose intensity corresponded to 80% of one proton and tended to decrease when attempts were made to purify the product by repeated distribution between chloroform and water. The signal was assigned to the aldehydic H-5, and the implication is that the compound as prepared under our conditions exists largely as the free aldehyde depicted (**4**) but is prone to undergo hydration and perhaps dimerization. The 3-*O*-benzyl analog of **4** has been regarded as a free aldehyde, whereas the 3-hydroxy analog is known to form, reversibly, a dimeric product (18–20).

The aldehyde **4** was combined with nitromethane in the presence of sodium methoxide in the usual manner. After acidification, the addition product was purified chromatographically to give analytically pure nitro sugar as a syrup which, although exhibiting a single spot on t.l.c., was revealed by its n.m.r. spectrum to be a 2:1 mixture of two components (**5** and **6**). In the

Can. J. Chem. Downloaded from www.nrcresearchpress.com by 210.87.254.5 on 09/05/12
For personal use only.

Can. J. Chem. Downloaded from www.nrcresearchpress.com by 210.87.254.5 on 09/05/12
For personal use only.

expected resonance position of H-1 a slightly asymmetric, apparent triplet consisting of two partially overlapping doublets was found (δ 5.79 and 5.90; $J_{1,2}$ = 4–5 Hz). The outer lines had an intensity ratio 2:1, and the stronger signal could be attributed to 6-deoxy-1,2-*O*-isopropylidene-3-*O*-methyl-6-nitro-α-D-glucofuranose (**5**) when, at a later stage, pure **5** became available for comparison. The second component was judged to be the β-L-*ido* isomer (**6**). The configurational assignments were supported by circular dichroism data (see later).

The preponderance of the D-*gluco* epimer **5** in the expected formation of two epimers from **4** deserves comment since the 3-*O*-benzyl analog of **4** has been shown to react with Grignard reagents to give preponderantly L-*ido* derivatives, with the degree of stereoselectivity being influenced by the solvent (19, 20). It has been suggested that the transition state in those Grignard reactions may involve coordination between the magnesium and the carbonyl and ring oxygen atoms (21). It can be seen in a molecular model that such a cyclic complex requires the aldehyde group to be so oriented as to expose its *si* face to the less hindered, rear side of the molecule, and attack from that direction will generate the *S* configuration at C-5 and therefore produce L-*ido* derivatives. In our reaction, which is characterized by methanenitronate ion preferentially attacking the *re* face to produce the *R* configuration at C-5, the rotameric orientation of the aldehyde group is not constrained by complexing. A preferred arrangement of the carbonyl double bond antiperiplanar to the C_4—O bond, plausible on grounds of dipole considerations, would be able to account for the result.

The mixture of **5** and **6** was hydrolyzed with 90% trifluoroacetic acid for removal of the isopropylidene group. One of the products was obtained in crystalline form in 49% yield. It exhibited a negative Cotton effect, indicative of the *R* configuration at C-5, the asymmetric carbon atom next to the nitromethyl group (22), and was thereby revealed to be the D-*gluco* derivative **7**. The crystalline substance (termed **7**-β) was assigned the β-anomeric configuration as it exhibited upward mutarotation. The mother liquor of the reaction yielded an additional 32% of product as a non-mutarotating syrup which showed a positive Cotton effect such as would accord with a mixture containing preponderantly the L-*ido* isomer **8** along with some **7**. The syrup could be used in the subsequent reactions so that the practical, over-all yield in nitro sugars based on **1** was about 45%.

When crystalline **7**-β was reacetonated, syrupy but analytically pure **5** was obtained. It showed the n.m.r. doublet for H-1 at δ 5.90 and exhibited a negative Cotton effect. Similar reacetonation of the mother liquor mixture **8** + **7** gave a mixture of **5** and **6** similar to that described above, except that the intensity ratio of the H-1 doublets was reversed, indicating a 2:1 preponderance of **6**. This mixture showed a positive Cotton effect.

Cyclization of the nitro hexoses **7** and **8** to furnish inositol derivatives was performed in a manner similar to the cyclization of the non-methylated analogs (6). Two procedures were used, namely, reaction in aqueous barium hydroxide solution, and reaction in a mixture of methanol and nitromethane in the presence of sodium methoxide. The first-mentioned procedure gave better yields and was more convenient in work-up; the results shown in Scheme 2 and to be discussed in detail first refer to it. The results of the second procedure, to be mentioned briefly afterwards, were qualitatively similar although there were some minor differences.

When amorphous mixtures of **7** and **8**[2] were employed for cyclization, a partly crystalline mixture of isomeric inositols arose. The smaller, crystalline part (21–30%) of the product melted above 200°, was sparingly soluble in ethanol, and was shown by chromatography to consist of of two compounds (**9** and **10**). They could not be separated directly but gave separable tetraacetates (**11** and **12**) whose acid-catalyzed methanolysis then furnished pure **9** and **10**. The tetraacetates arose in yields of, for instance, 58 (**11**) and 32% (**12**), and presumably **9** and **10** had constituted the crystalline part of that particular cyclization mixture in a similar ratio. The *scyllo* and *myo*-1 configurations were assigned to these isomers on evidence to be given below. The larger, non-crystalline part (36–56%) of the cyclization mixture contained, besides colored impurities, very little of **9** or **10** but consisted chiefly of at least one other isomer.

[2]This refers to both the mother liquor material (richer in **8**) remaining after isolation of crystalline **7**-β, and to the total mixture (richer in **7**) as obtained prior to such isolation.

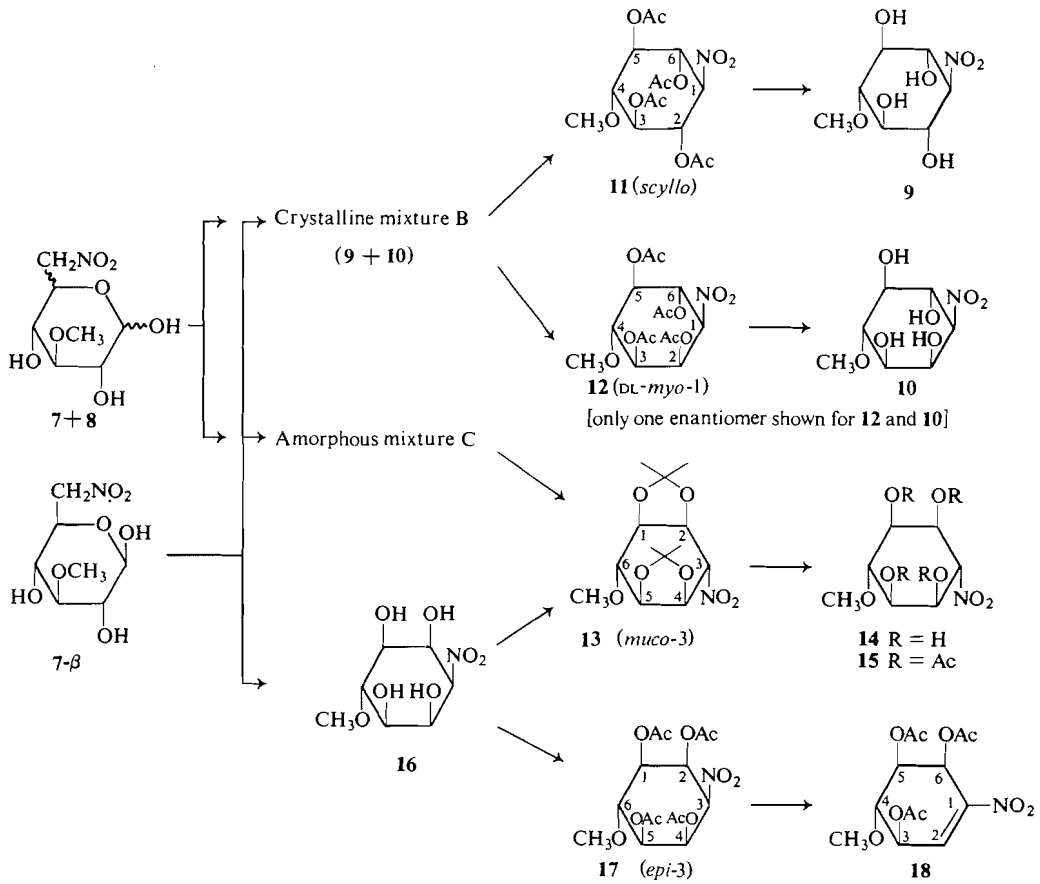

SCHEME 2

Acetonation of this part led to a di-*O*-isopropylidene derivative (**13**) whose deacetonation afforded the crystalline *muco*-3 isomer **14**. For further characterization, **14** was acetylated to its tetraacetate **15**. From the isolated amount of diacetone derivative **13**, one might have concluded that the mixture subjected to acetonation had contained at least 31% of **14**. This was not the case, however. Compound **14** can be distinguished readily by n.m.r. spectroscopy (see later), and it was found that only small proportions of **14** (never more than 10%) were present in the mixture prior to acetonation. The bulk of **13** must therefore have originated from a secondary reaction, the nature of which will be disclosed later on.

Use of crystalline **7**-β in the barium hydroxide-induced cyclization again furnished a partly crystalline product. However, fractional recrystallization of the crystalline portion not only yielded mixtures of **9** and **10** as before, though in somewhat smaller amounts (18–19%), but gave in addition a fourth isomer (m.p. 165–167°) as the chief component (27–45%). The amorphous portion of the reaction product (29–41%) had similar characteristics as in the previous experiment; although it contained little, if any, of the *muco*-3 isomer **14**, it was acetonated to produce the diacetone derivative **13**. The crystalline, fourth nitroinositol isomer just mentioned was allocated the *epi*-3 configuration (**16**). Acetylation gave a crystalline tetraacetate (**17**) that was characterized by n.m.r. spectroscopy but proved too unstable for purification for elemental analysis. In attempted recrystallization from ethanol a sample deteriorated due to dehydroacetylation. This became evident by the appearance of a low-field n.m.r. signal (δ 7.25) attributable to an olefinic proton, and eventually a small amount of the nitroolefin [3,5,6/4]-3,5,6-

Can. J. Chem. Downloaded from www.nrcresearchpress.com by 210.87.254.5 on 09/05/12
For personal use only.

Can. J. Chem. Downloaded from www.nrcresearchpress.com by 210.87.254.5 on 09/05/12
For personal use only.

triacetoxy-4-methoxy-1-nitrocyclohexene (**18**) was isolated.[3]

An unexpected observation was made when the *epi*-3 isomer **16** was acetonated. A di-*O*-isopropylidene derivative was formed, but the isolated product (yield, 36%) evidently had undergone epimerization during work-up or chromatography on silica gel and proved identical with **13**. This was verified by acid-catalyzed methanolysis which did not regenerate **16** but gave **14** instead. The epimerization is reminiscent of the facile conversion of 3-deoxy-1,2:5,6-di-*O*-isopropylidene-3-nitro-α-D-glucofuranose into its D-*allo* isomer (16).

Cyclization of crystalline **7**-β in a methanol–nitromethane solvent containing sodium methoxide furnished a crystalline mixture of **9** and **10** (16%), crystalline **14** (8%), and an amorphous material (61%) that appeared similar in composition to that obtained in the barium hydroxide-promoted reactions.

Configurational Assignments

In the cyclization of the 6-deoxy-6-nitrohexoses considered here, two centers of prochirality (C-1 and -6) are directly involved in producing two new chiral centers in the products. A third chiral center affecting the number of possible epimers stems from chiral C-5 in the hexoses. Due to possibilities of over-all symmetry, however, only six stereoisomeric deoxynitroinositols can thus arise, namely, four meso forms (with the *scyllo*, *myo*-2, *muco*-3, and *epi*-3 configurations) and two racemic forms (with the *myo*-1 and *chiro*-1 configurations). Of these, the *myo*-2 (**19**) and *chiro*-1 (**20**) isomers seemed unlikely to arise under the present conditions because of conformational energy considerations, and the remaining four have all been encountered in this work.

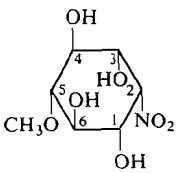

19 (*myo*-2)

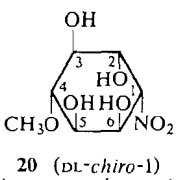

20 (DL-*chiro*-1)
[only one enantiomer shown]

[3]It is interesting to note in this connection that the stereoisomeric tetraacetates **11** and **15** were completely stable, whereas **12** was somewhat prone to decomposition if much less so than **17**.

The two isomers that gave a diisopropylidene derivative (in a non-forcing procedure of acetonation) must each possess two *cis*-glycol groupings, a condition met only by **14** and **16**. The fact that the diisopropylidene derivative of one isomer was converted during work-up into that of the other isomer, shows that they were epimeric at the carbon bearing the nitro group where epimerization through the common nitronate ion can occur. Confirming this, the n.m.r. spectra given by **14** and **16** in the presence of excess sodium deuteroxide in D_2O were identical, in accord with the existence of one common nitronate (**21**).

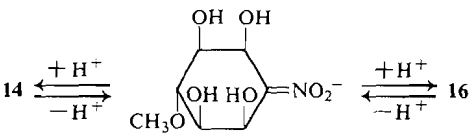

21

Finally, unambiguous allocation of formulas **14** and **16**, and of **9** and **10** to the other two isomers, was possible by analysis of n.m.r. spectra of their tetraacetates in chloroform-*d* (Table 1).[4] The *muco*-3 and *epi*-3 tetraacetates (**15** and **17**) each exhibited in order of decreasing field a one-proton signal for H-6, a one-proton signal for H-3, and two two-proton signals for the enantiotopic pairs H-1, H-5 and H-2, H-4. Two pairs of enantiotopic acetyl groups gave two 6-proton singlets in each compound, and the methoxy group gave a three-proton singlet. Compound **17** showed large coupling in the triplet for H-6 ($J_{1,6} = J_{5,6} = 10$ Hz), indicating a 1,6,5-triaxial proton arrangement and therefore equatorial substituents in these positions. The coupling $J_{1,2}$ ($= J_{4,5}$) was small, requiring the substituents at C-2 and -4 to be axial and hence *cis* to those at C-1 and -5, in accord with the chemical evidence of facile acetonation. The triplet for H-3 showed small coupling (3 Hz), but this feature, even though it was consistent with an equatorial nitro group flanked by two axial acetoxyls as depicted in Table 1, did not disprove an axial nitro group. The *epi*-3 configuration could nevertheless be allocated to **17** with certainty since inversion at C-3 would result in the *muco*-3 configuration which, it was found, must be reserved for compound **15** for the

[4]The spectra of the free nitroinositols in aqueous trifluoroacetic acid were in complete agreement; see Experimental.

Can. J. Chem. Downloaded from www.nrcresearchpress.com by 210.87.254.5 on 09/05/12
For personal use only.

TABLE 1. Nuclear magnetic resonance data of acetates in $CDCl_3$

Compound*	Chemical shifts (δ, from TMS)								Couplings (Hz)					
	H-1	H-2	H-3	H-4	H-5	H-6	CH_3O	CH_3CO_2	$J_{1,2}$	$J_{2,3}$	$J_{3,4}$	$J_{4,5}$	$J_{5,6}$	$J_{6,1}$
11	4.80	5.58	5.14	3.55	5.14	5.58	3.45	2.06, 2.00	10.5	10	9.5	9.5	10	10.5
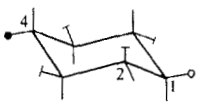 **12**	4.76	5.96	4.95	3.70	5.07	5.90	3.45	2.10, 2.07, 2.03, 1.97	3	2	10	10	10	11
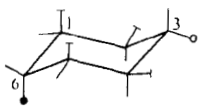 **15**	5.52	5.65	5.16	5.65	5.52	3.68	3.54	2.09, 1.97	3	11	11	3	3	3
17	5.02	6.30	4.82	6.30	5.02	3.85	3.48	2.13, 2.09	3	3	3	3	10	10
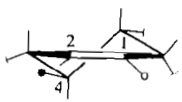 **18**		7.25	5.59	3.82	5.13	6.40	3.51	2.17, 2.11, 2.06		3	8	11	4	

*Symbols: ⚲ OMe, ⊤ OAc, ⚲ NO_2, | H.

Can. J. Chem. Downloaded from www.nrcresearchpress.com by 210.87.254.5 on 09/05/12
For personal use only.

following reason. Compound **15** exhibited large splitting in its triplet of H-3 ($J_{2,3} = J_{3,4} = 11$ Hz), clearly requiring a 2,3,4-triequatorial substituent arrangement. This condition is realized only in one conformer, namely that of the *muco*-3 epimer shown in Table 1. The remaining coupling constants, all small, were in harmony with substituent orientations as depicted. It is noteworthy that the non-acetylated *muco*-3 isomer **14** in aqueous solution also adopts the same conformation, with an equatorial nitro group and an axial methoxyl group, as was revealed by analogous n.m.r. data (see Experimental). Evidently when **21**, the nitronate common to **14** and **16**, is protonated, the rule of equatorial nitro group preference (2) is obeyed for both products. In **14**, the methoxyl proton signal is found markedly upfield (by 0.15–0.2 p.p.m.) from the corresponding signals of its three isomers, rendering **14** easily recognizable.

Assignment of the *scyllo* and *myo*-1 configurations to the tetraacetates **11** and **12**, respectively, was straightforward. Thus **11** (and also its parent compound **9**) revealed molecular symmetry by the presence of two pairs of enantiotopic hydrogen atoms (H-2, H-6 and H-3, H-5) which each gave rise to a two-proton signal. All the coupling constants were large (9.5–10.5 Hz), indicating the all-*trans* substituent orientation. By contrast compound **12** and its parent **10**, which lack molecular symmetry, exhibited six individual one-proton signals for their ring hydrogen atoms. The observed multiplicities and splittings demanded the formula depicted. The data of Table 1 also rule out the *myo*-2 (**19**) and *chiro*-1 (**20**) configurations for any of the products obtained.

Experimental

Melting points were determined in capillaries in an electrically heated aluminum block. The n.m.r. data (100 MHz) were obtained on a Varian HA-100 instrument. Optical rotations were measured at room temperature in a Perkin–Elmer automatic polarimeter, Model 141. Circular dichroism was determined with a Jasco ORD/UV-5 instrument. I.r. spectra of new nitro compounds were compatible with the assigned structures.

1,2:5,6-Di-O-isopropylidene-3-O-methyl-α-D-glucofuranose (2)

A mixture of diacetone glucose **1** (8.0 g), methyl iodide (11.4 g), barium oxide (10.0 g) and *N,N*-dimethylformamide (80 ml) in a stoppered flask was vigorously shaken for 67 h at ambient temperature (29°). The mixture was filtered with suction through a layer of Celite and the residue washed successively with ether (100 ml) and water (125 ml). The phases of the filtrate were separated and the water layer was extracted twice with ether which was combined with the organic phase. The latter was washed twice with water, dried ($MgSO_4$), and evaporated to furnish a pale yellow oil (8.2 g; $[\alpha]_D$ −32° in ethanol). The oil was distilled *in vacuo*; following a forerun (0.4 g) the main fraction was collected at 85° (bath temperature) and 0.1 Torr. Compound **2** was thus obtained as a colorless oil (7.0 g, 83%); $[\alpha]_D$ −33° (*c*, 0.4 in ethanol); lit. (23), b.p. (0.3 Torr) 105°, $[\alpha]_D$ −34° in ethanol.

The n.m.r. data (in $CDCl_3$; TMS): δ 5.88 (1H d, H-1, $J_{1,2} = 4$ Hz), 4.57 (1H d, H-2, $J_{1,2} = 4$ Hz), 3.9–4.3 (4H m, H-4, -5, -6, -6′), 3.78 (1H d, H-3, $J_{3,4} = 2.5$ Hz), 3.47 (3H s, OCH_3), 1.50, 1.43, 1.37, 1.33 (four 3H s, isopropylidene methyl groups). The undistilled crude product gave virtually the same spectrum, with additional weak signals due to DMF (δ 2.80, 2.72).

1,2-O-Isopropylidene-3-O-methyl-α-D-glucofuranose (3)

A solution of **2** (7.0 g) in acetic acid (70 ml) and water (7 ml) was kept at 40° for 1.5 h and then evaporated under reduced pressure. Added toluene and benzene were successively evaporated from the residue which was a colorless, viscous oil. The material contained some unreacted **2** (*ca.* 1.1 g) which was removed by two extractions with ether (25 and 10 ml) from an aqueous solution (25 ml) of the crude **3**. The aqueous solution then contained about 5.0 g of **3** and could be used directly for the preparation of **4**.

A sample of crude **3** (553 mg, from a similar experiment) was purified by column chromatography on silica gel (E. Merck AG., 15 g, with 10% of water added). Elution with benzene (180 ml) and benzene containing 2% of ethanol (150 ml) gave a material (45 mg) that was discarded, and further elution with benzene containing 5% of ethanol (120 ml) then gave pure **3** (466 mg, 84%), $[\alpha]_D$ −52.4° (*c*, 0.4 in chloroform); lit. (24) $[\alpha]_D$ −54° (*c*, 3.1 in chloroform). The n.m.r. data (in $CDCl_3$; TMS): δ 5.93 (1H d, H-1, $J_{1,2} = 4$ Hz), 4.62 (1H d, H-2, $J_{1,2} = 4$ Hz), 3.7–4.1 (5H m), 3.49 (3H s, OCH_3), 1.50, 1.33 (two 3H s, isopropylidene methyl groups). The hydroxyl protons were removed by deuterium exchange.

1,2-O-Isopropylidene-3-O-methyl-α-D-xylo-pentodialdo-1,4-furanose (4)

To a cooled (0°) solution of **3** (463 mg) in water (2.7 ml) was added sodium metaperiodate (463 mg) in two portions with a 20-min interval. After 2 h, a few drops of ethylene glycol were added and the reaction mixture was filtered. The filter residue was washed with chloroform and the aqueous filtrate was extracted with the same solvent. The combined chloroform solution was dried ($MgSO_4$) and evaporated to furnish a pale yellow oil which was dried *in vacuo*. The yield was 333 mg (83%); $[\alpha]_D$ −139° (*c*, 0.3 in $CHCl_3$). The n.m.r. data (in $CDCl_3$; TMS): δ 9.66 (1H d, $J_{4,5} = 1.5$ Hz, H-5); 6.10 (1H d, $J_{1,2} = 3.8$ Hz, H-1); 4.67 (1H d, $J_{1,2} = 3.8$ Hz, H-2); 4.57 (1H q, $J_{3,4} = 4$ and $J_{4,5} = 1.5$ Hz, H-4); 4.17 (1H d, $J_{3,4} = 4$ Hz, H-3); 3.37 (3H s, OCH_3); 1.47, 1.33 (two 3H s, $C(CH_3)_2$).

For use in subsequent experiments it was practical to prepare compound **4** as an alcoholic solution on a larger scale. Thus, a solution of **3** (5.62 g, 24 mmol) in water (35 ml) was stirred with ice cooling, and sodium metaperiodate (6.0 g, 28 mmol) was added in portions during

Can. J. Chem. Downloaded from www.nrcresearchpress.com by 210.87.254.5 on 09/05/12
For personal use only.

½ h, the temperature of the reaction mixture being maintained at 8–11°. Stirring was continued without cooling for another 90 min whereby the temperature gradually rose to 25°. The mixture was then cooled again and 0.2 ml of ethylene glycol followed by 25 ml of ethanol were added. The inorganic precipitate was filtered off and washed thoroughly with ethanol. The filtrate was evaporated to dryness and the residue was taken up in ethanol (10 ml). The solution was filtered from undissolved material which was washed with ethanol (5 ml). The filtrate so obtained (15 ml) was used directly for reaction with nitromethane.

6-Deoxy-1,2-O-isopropylidene-3-O-methyl-6-nitro-α-D-glucofuranose (5) and -β-L-idofuranose (6)

(a) Mixture of 5 and 6 from 4

A solution of oily aldehyde **4** (2.94 g) in nitromethane (4 ml) and methanol (8 ml) was rendered alkaline by the addition of 2.7 *N* sodium methoxide in methanol (6 ml) and stored for 18 h at room temperature, in a pure nitrogen atmosphere. The mixture was then cooled with Dry Ice, glacial acetic acid (1 ml) was added with stirring, and after removal from the cold bath it was shaken briefly with added chloroform (10 ml) and water (10 ml). Upon phase separation the aqueous layer was extracted twice with chloroform, which was combined with the organic layer. The latter was washed five times with 5 ml of water, dried over anhydrous $MgSO_4$, and evaporated to give a brown oil (3.70 g). The oil was chromatographed on silica gel (E. Merck AG; with 10% of water added). The column was eluted first with benzene (500 ml) and then with benzene containing 2% ethanol (900 ml). The last third of the second eluant produced a colorless syrup (3.27 g) of **5** and **6** in a yield of 85%. The t.l.c. with ethyl acetate – chloroform (1:1) showed a single spot, R_f 0.67. Optical rotations: $[\alpha]_{578}$ −48.8, $[\alpha]_{536}$ −56.2, $[\alpha]_{436}$ −102, $[\alpha]_{365}$ −213° (*c*, 0.6, methanol). The n.m.r. spectrum ($CDCl_3$) showed two overlapping H-1 doublets (an apparent triplet), δ 5.98 and 5.90 (J = 4–5 Hz), with an intensity ratio 1:2, indicating that **5** preponderated. The remaining part of the spectrum was identical with that of pure **5** (see below).

Alternatively, an ethanolic solution of **4** (obtained without isolation from 24 mmol of **3**, see earlier) was mixed under nitrogen with nitromethane (7.5 ml) and 3.25 *N* sodium methoxide in methanol (8.25 ml). After 18 h the mixture was cooled, neutralized with glacial acetic acid (1.65 ml, to p*H* 6), and worked-up by dilution with chloroform (25 ml) and addition of water (75 ml). The water layer was extracted four times with chloroform and the combined chloroform extracts were washed four times with 10 ml of water, each water portion being extracted again with chloroform. Drying of the combined chloroform solution ($MgSO_4$) and evaporation furnished a reddish-brown oil (6.62 g) which, according to t.l.c. and n.m.r. analysis, appeared to consist largely of **5** and **6**. Part of the oil (5.1 g) was chromatographed on silica gel as described and gave 4.1 g (84% based on **3**) of a colorless, n.m.r. spectroscopically pure mixture of **5** and **6**.

(b) Pure 5 from 7-β

Crystalline nitro sugar **7-β** (84 mg) was dissolved with Dry-Ice cooling in acetone (4 ml) containing concentrated sulfuric acid (0.08 ml) and then stirred with anhydrous cupric sulfate (0.2 g) for 2 h without further cooling. The mixture was thereafter cooled again, neutralized by addition of concentrated aqueous ammonia (0.33 ml), and filtered through a layer of Dowex 1 × 2 (acetate form; prewashed with acetone) and through a layer of Celite. The filtrate was evaporated to a residue which was taken up in chloroform. The filtered, dried ($MgSO_4$), and evaporated chloroform solution furnished **5** in quantitative yield (100 mg) as a colorless syrup (uniform on t.l.c., R_F 0.67 as in *a* above); $[\alpha]_D$ −34.0, $[\alpha]_{578}$ −35.9, $[\alpha]_{546}$ −41.5, $[\alpha]_{436}$ −88.5, $[\alpha]_{365}$ −256° (in methanol, *c*, 0.7). Circular dichroism (*c*, 0.5 in methanol): $[\theta]_{281}$ −1885. The n.m.r. data (in $CDCl_3$): δ 5.90 (1H d, H-1, $J_{1,2}$ = 4 Hz), 4.4–4.8 (4H m, H-2, -6, -6′, -4 or -5), 4.0–4.2 (1H m, H-4 or -5), 3.88 (d, H-3, J = 3.5 Hz), δ 3.49 (3H s, OCH_3), 1.48 and 1.33 (two 3H s, $C(CH_3)_2$).

Anal. Calcd. for $C_{10}H_{17}NO_7$ (mol. wt. 263.2): C, 45.62; H, 6.51; N, 5.32. Found: C, 45.44; H, 6.38; N, 5.24.

(c) Mixture of 5 and 6 from 7 and 8

An amorphous mixture of **7** and **8** (from which crystalline **7-β** had been collected, see later) was acetonated as described under section *b*. The syrupy product (yield, 87%) gave an n.m.r. spectrum identical with that of the product described under section *a* except that the intensity ratio of the H-1 doublets at δ 5.98 and 5.90 was 3:2, indicating that **6** preponderated. Circular dichroism (*c*, 0.5 in methanol): $[\theta]_{310}$ +260. Assuming a 3:2 ratio for **6** and **5**, and using the [θ] value for pure **5**, the value for **6** may be extrapolated to +1700.

6-Deoxy-3-O-methyl-6-nitrohexoses 7 and 8

(a) Crystalline β-D-gluco Isomer (7-β)

A chromatographically purified mixture of isopropylidene derivatives **5** and **6** (1.56 g, ratio approximately 2:1) was dissolved in trifluoroacetic acid (5.5 ml), water (0.5 ml) was slowly added, and the reaction mixture was stirred for 45 min at room temperature and then evaporated *in vacuo*. From the syrupy residue a few milliliters of added water and subsequently some ethyl acetate were evaporated. The dried syrup (1.7 g) was then triturated with fresh ethyl acetate whereby it partially crystallized on scratching. The crystals (607 mg, 46%) were collected and washed with chloroform; m.p. 149–152°. An analytical sample was recrystallized from ethyl acetate – chloroform; m.p. 152–154°; homogeneous on t.l.c. in ethyl acetate (R_F 0.4) or 2:1 acetone–chloroform (R_F 0.65). The product exhibited upward mutarotation: $[\alpha]_D$ −4 (2 min) → +46° (24 h, final), $[\alpha]_{578}$ −4.3 → +47°, $[\alpha]_{546}$ −5.3 → +51°, $[\alpha]_{436}$ −31 → +61°, $[\alpha]_{365}$ −190 → −48°, in methanol; $[\alpha]_D$ and $[\alpha]_{578}$ +7 (2 min) → +40° (4 h, final), $[\alpha]_{546}$ +6 → +41°, $[\alpha]_{436}$ −10 → +49°, $[\alpha]_{365}$ −141 → −40°, in water.

Circular dichroism (*c*, 0.25 in 2.5 × 10^{-3} *N* acetic acid at anomeric equilibrium): $[\theta]_{319}$ −830, $[\theta]_{275}$ −2050.

The n.m.r. data (in 2 *N* CF_3CO_2D–D_2O with acetone reference): δ 3.0–1.8 (4H m), 1.43 (3H s, OCH_3), 1.4–1.1 (3H m).

Anal. Calcd. for $C_7H_{13}NO_7$ (mol. wt. 223.2): C, 37.66; H, 5.87; N, 6.28. Found: C, 37.90; H, 5.91; N, 6.23.

(b) Mixture of the D-gluco (7) and L-ido (8) Isomers

The ethyl acetate mother liquor obtained upon collection of crude **7-β** was concentrated and deposited an additional 53 mg of less pure **7-β**, which was removed.

Can. J. Chem. Downloaded from www.nrcresearchpress.com by 210.87.254.5 on 09/05/12
For personal use only.

Further evaporation gave a syrup (634 mg) which was partitioned between chloroform and water. The chloroform phase yielded a small amount of what appeared on t.l.c. to be impure starting material; it was discarded. The aqueous phase was decolorized by treatment with 0.5 ml of Dowex 1 × 2 (acetate) and evaporated. The remaining colorless syrup (420 mg, dried *in vacuo*) was a mixture of **7** and **8** (yield, 32%), R_F 0.4, 0.6 and 0.65, 0.8 (t.l.c. as described under section *a*). The material showed no mutarotation; $[\alpha]_{578}$ +9.7, $[\alpha]_{546}$ +11.3, $[\alpha]_{436}$ +23.3, $[\alpha]_{365}$ +68 (*c*, 0.52 in methanol); $[\alpha]_{578}$ +0.6, $[\alpha]_{546}$ +3.0, $[\alpha]_{436}$ +12, $[\alpha]_{365}$ +75° (*c*, 0.2 in water).

Circular dichroism (as for pure **7**): $[\theta]_{319}$ +170, $[\theta]_{272}$ −400. Assuming 40% **7** in the mixture, the ellipticities of **8** may be extrapolated to $[\theta]_{319}$ +840, $[\theta]_{272}$ +700.

The complex n.m.r. spectrum of the mixture showed prominent OCH_3 signals at δ 1.43 and 1.32.

Cyclization of Nitro Hexoses with Aqueous Barium Hydroxide

A suspension of crystalline **7**-β (1.76 g, 7.88 mmol) in 0.0025 *N* acetic acid (8 ml) was stirred in an ice water bath in a nitrogen atmosphere, and a saturated solution of barium hydroxide (16 ml, approximately 0.5 *N*) was added in rapid flow. The mixture was stirred at 0° for 2.5 h and then kept at ambient temperature for 18 h. The dark solution was cooled again and acidified to p*H* 4–5 by dropwise introduction into ice cold, *N* acetic acid (20 ml). It was then passed sequentially through columns containing 5 ml of Dowex 1 × 2 (acetate) and 20 ml of Rexyn 101 (H^+), respectively, each column being washed with water (18 ml). Evaporation of the colorless effluent and drying of the residue *in vacuo* gave the nitroinositol mixture as a white semicrystalline mass (1.78 g).

Reactions using noncrystalline mixtures[3] of **7** and **8** were performed in the same fashion.

The reaction product (1.78 g, from **7**-β) was triturated with absolute ethanol (5 ml). Upon storing overnight at 0°, a crop of crystals (1.30 g, m.p. 156–158°) was isolated. This material was not homogeneous but furnished, upon recrystallizations (once from methanol and three times from 95% ethanol), a pure product designated A (95 mg, m.p. 165–167°). Systematic fractional crystallization of the mother liquor materials gave another 145 mg of pure A and 234 mg of less pure A (m.p. 160–167°), the total yield being 27%. In addition, the procedure yielded 333 mg (19%) of a high-melting material designated B, (m.p. 185–205°, dec.), 97 mg (6%) of a mixture which melted in between (at 173–175°) and was dealt with no further, and finally there remained 731 mg (41%) of an amorphous foam designated C. It will be noted that a total of 904 mg of crystals was eventually isolated and the amount of noncrystallizable material remaining after the various recrystallizations was larger than the amount that did not crystallize in the first place. The relative amounts of products depended upon the number of recrystallizations performed, with amorphous C increasing with that number. Thus, an identical cyclization experiment furnished 45% of A (m.p. 165–166°), 18% of B (m.p. 209–215°), and 29% of C.

The semicrystalline reaction product (3.21 g) obtained from a mixture (3.89 g) of **7** and **8** was triturated with cold ethanol (7 ml) to give inhomogeneous crystals (1.77 g, m.p. 199–205° dec.) and an amorphous material (1.32 g). After fractional crystallizations using methanol and ethanol there was obtained 1.18 g (30%) of B (m.p. 205–222°), a total of 0.43 g (11%) of unresolved mixtures melting anywhere between 100 and 175°, and 1.40 g (36%) of amorphous C. No pure A could be isolated. A similar experiment yielded 21% of B and 56% of C.

*3-Deoxy-6-O-methyl-3-nitro-epi-inositol (**16**)*

The crystalline product A, m.p. 165–167° (see above) represented compound **16**. The n.m.r. data (in 2.1 *N* CF_3CO_2D–D_2O with acetone standard): δ 2.62–2.57 (2H m, H-2, -4), 2.47 (1H t, J = 3 Hz, H-3), 1.47–1.44 (3H m, H-1, -5, -6), 1.42 (3H s, OCH_3).

Anal. Calcd. for $C_7H_{13}NO_7$ (mol. wt. 223.2): C, 37.66; H, 5.87; N, 6.28. Found: C, 37.55; H, 5.71; N, 6.40.

*1,2,4,5-Tetra-O-acetyl-3-deoxy-6-O-methyl-3-nitro-epi-inositol (**17**) and (3,5,6/4)-3,5,6-Triacetoxy-4-methoxy-1-nitrocyclohexene (**18**)*

An ice-cooled suspension of **16** (126 mg) in acetic anhydride (1.3 ml) was stirred for 6 h after addition of 2 drops of boron trifluoride etherate. The inositol dissolved when the catalyst was added, and crystalline **17** began to precipitate soon afterwards. It was collected and washed with ethanol (3 × 0.2 ml); yield, 104 mg; m.p. 172–182°. For the n.m.r. data see Table 1.

The product decomposed on attempted recrystallization from ethanol, becoming extremely soluble in the solvent and developing a low-field, olefinic proton signal which was not present in its original n.m.r. spectrum. A small amount of the nitroalkene **18**, m.p. 120–122°, was eventually isolated by crystallization from ether and ether–ligroin. For the n.m.r. data see Table 1.

Anal. Calcd. for $C_{13}H_{17}NO_9$ (mol. wt. 331.3): C, 47.13; H, 5.17; N, 4.23. Found: C, 47.31; H, 5.32; N, 4.18.

*2,3,5,6-Tetra-O-acetyl-1-deoxy-4-O-methyl-1-nitro-scyllo-inositol (**11**)*

The high-melting crystalline cyclization products previously designated B represented mixtures of the *scyllo* and *myo*-1 isomers **9** and **10**. Such a mixture (0.85 g) was acetylated with acetic anhydride (8.5 ml) in the presence of BF_3 etherate (12 drops) by stirring for 10 h at 0° and another 10 h at room temperature. The reaction mixture was then cooled again (0°) and filtered through sintered glass. The crystals (**11**) were washed with 5 ml of cold ethanol in three portions and dried *in vacuo*, and the combined filtrates containing isomeric acetate **12** were set aside. The crystals (0.87 g, 58.5%) were pure according to their n.m.r. spectrum (Table 1). The m.p. of 257–258° observed at this stage did not appear to be reproducible, as higher (270–272°) or lower (230–232°) values were found on occasion in similar preparations which exhibited, nevertheless, exactly the same well-defined n.m.r. spectrum. Recrystallization of a sample (0.47 g) from glacial acetic acid (3 ml) containing acetic anhydride (0.15 ml) gave translucent prisms (0.43 g) of m.p. 220–222°, whereas recrystallization from methanol (44 mg in 4 ml) gave long needles (35 mg) of m.p. 214–216°. The recrystallized samples gave n.m.r. spectra superimposable on those of the original product, and both gave correct microanalyses.

Anal. Calcd. for $C_{15}H_{21}NO_{11}$ (mol. wt. 391.3): C, 46.03; H, 5.41; N, 3.58. Found: C, 45.90; H, 5.46; N, 3.59. C, 45.92; H, 5.47; N, 3.73.

Can. J. Chem. Downloaded from www.nrcresearchpress.com by 210.87.254.5 on 09/05/12
For personal use only.

*2,3,5,6-Tetra-O-acetyl-1-deoxy-4-O-methyl-1-nitro-*D,L*-myo-inositol (**12**)*

To the filtrate of the acetylation mixture, from which crystalline **11** had been collected (see preceding section), was added excess ethanol; after decomposition of the remaining acetic anhydride the solution was evaporated, and two portions of added ethanol were evaporated from the residue which after drying weighed 0.64 g and consisted of at least 80% of **12** (n.m.r.). After two crystallizations from small volumes of hot ethanol (performed rapidly without prolonged heating, lest losses due to formation of low-melting, unsaturated products occurred), 475 mg (32%) of the tetraacetate **12** was obtained, m.p. 139–140°. Further recrystallization did not change the n.m.r. spectrum (Table 1) although variations in m.p. from 135–136° to 140–142° were observed.

Anal. Calcd. for $C_{15}H_{21}NO_{11}$ (mol. wt. 391.3): C, 46.03; H, 5.41; N, 3.58. Found: C, 45.95; H, 5.44; N, 3.67.

*1-Deoxy-4-O-methyl-1-nitro-scyllo-inositol (**9**)*

A suspension of tetraacetate **11** (430 mg) in anhydrous methanol (25 ml) containing methyl *p*-toluenesulfonate (0.5 ml) was boiled in a flask fitted with a Vigreux column. Distillation was maintained at a slow rate so that 15 ml of distillate was collected in 5 h. Fresh methanol was introduced during the operation so as to approximately maintain the original volume. The solid gradually dissolved, and the resulting solution was subsequently refluxed for another 20 h and then evaporated. Trituration of the residue with ethanol produced a white powder (277 mg) which was recrystallized from 90% ethanol (7 ml) to give **9** (202 mg, 83%) as needles, m.p. 258–260° (dec.). Recrystallization of a sample from water gave large grains that melted with decomposition at 248–249° (with apparent change in crystal structure from 220°). The n.m.r. data (in 2.1 *N* CF_3CO_2D–D_2O, with acetone as reference): δ 2.39 (1H t, H-1, J = 10.5 Hz), 1.81 (2H t, H-2 and -6, J = 10.5 Hz), 1.41 (3H s, OCH_3), 1.35 (2H t, H-3 and -5, J = 9.5 Hz), 1.02 (1H t, H-4, J = 9.5 Hz).

Anal. Calcd. for $C_7H_{13}NO_7$ (mol. wt. 223.2): C, 37.66; H, 5.87; N, 6.28. Found: C, 37.58; H, 5.82; N, 6.44.

*1-Deoxy-4-O-methyl-1-nitro-*D,L*-myo-inositol (**10**)*

The tetraacetate **12** (315 mg) was methanolyzed as described for **11**. The residue obtained upon evaporation of the reaction solution was dissolved in 1–2 ml of ethanol, and addition of benzene caused crystallization of **10** (178 mg, 99%) which was collected and washed with benzene; m.p. 198–203°. Recrystallization from ethanol–benzene gave very fine needles (150 mg, 83%), m.p. 203–205°. The n.m.r. data (in 2.1 *N* CF_3CO_2D–D_2O, with acetone reference): δ 2.49 (1H q, H-1, $J_{1,2}$ = 2.5, $J_{1,6}$ = 10 Hz), 2.30 (1H t, H-2, J = 2.5 Hz), 2.13 (1H, quartet of narrow doublets, H-6, $J_{1,6}$ = 10, $J_{5,6}$ = 9 Hz, and a 1.5 Hz splitting, presumably due to long-range coupling), 1.6–1.2 (3H m, H-3, -4, -5), 1.39 (3H s, OCH_3).

Anal. Calcd. for $C_7H_{13}NO_7$ (mol. wt. 223.2): C, 37.66; H, 5.87; N, 6.28. Found: C, 37.56; H, 5.85; N, 6.34.

*3-Deoxy-1,2;4,5-di-O-isopropylidene-6-O-methyl-3-nitro-muco-inositol (**13**)*

(a) From Amorphous Cyclization Product C

A sample (372 mg) of the product C (see a previous section) was dissolved in acetone (10 ml) containing concentrated sulfuric acid (0.2 ml). (The reagent was freshly prepared under cooling with Dry Ice.) The mixture was stirred with anhydrous cupric sulfate (120 mg) for 2.5 h at room temperature, then cooled with Dry Ice and neutralized by adding concentrated aqueous ammonia (0.6 ml). The voluminous inorganic precipitate was filtered off and the solution passed through small columns of acetone – prewashed ion exchange resins (1 ml each) Dowex 1 × 2 (acetate) and Amberlite IR-120 (H^+). The columns were rinsed with acetone and methanol (10 ml each). Evaporation of the filtrate gave a syrup (387 mg) which upon extraction with chloroform (3.8 ml) left behind a dark mass (85 mg). The extract was chromatographed on Merck silica gel (10 g, with 1 ml of water added), whereby elution with chloroform furnished a crop (119 mg, 24%) of crystalline **13**, m.p. 160–162°, in the second 10 ml fraction. Further elution with chloroform (50 ml) followed by acetone (30 ml) produced syrups that were combined with the aforementioned insoluble material and acetonated again as described. In this way, a second crop of **13** (36 mg) was obtained (total yield, 31%). Recrystallization from ligroin raised the m.p. to 169–170°. The n.m.r. data (in $CDCl_3$, with TMS): δ 4.6–4.5 (3H m, H-2, -3, -4), 4.24 (2H q, H-1 and -5, $J_{1,6} = J_{5,6}$ = 8, $J_{1,2} = J_{4,5}$ = 5.5 Hz), 3.58 (3H s, OCH_3), 3.41 (1H t, H-6, $J_{5,6} = J_{1,6}$ = 8 Hz), 1.54 and 1.34 (two 6H s, for two isopropylidene groups).

Anal. Calcd. for $C_{13}H_{21}NO_7$ (mol. wt. 303.3): C, 51.48; H, 6.98; N, 4.62. Found: C, 51.34; H, 6.79; N, 4.74.

*(b) From the epi-3 Isomer **16***

A 268-mg sample of pure **16** (free from isomers according to n.m.r. spectrum) was acetonated by the method described in section *a*. By chromatography on silica gel 131 mg (36%) of pure **13**, m.p. 168.5–169.5°, was obtained. Its spectrum was superimposable on that of the previous product.

*3-Deoxy-6-O-methyl-3-nitro-muco-inositol (**14**)*

The compound **13** (93 mg) was deacetonated by treatment with trifluoroacetic acid (0.30 ml) containing water (1 drop) for 30 min at room temperature. Evaporation of the solution followed by crystallization of the residue from ethyl acetate gave **14** (66 mg, 96%) as large colorless prisms or flat rectangular plates, m.p. 161–163°. The n.m.r. data (in 2.1 *N* CF_3CO_2D–D_2O, with acetone as reference): δ 2.75 (1H t, H-3, $J_{2,3} = J_{3,4}$ = 10 Hz), 2.07 (2H q, H-2 and -4, $J_{2,3} = J_{3,4}$ = 10, $J_{1,2} = J_{4,5}$ = 3 Hz), 2.01 (2H t, H-1 and -5, $J_{1,2} = J_{1,6} = J_{4,5} = J_{5,6}$ = 3 Hz), 1.58 (1H t, H-6, $J_{1,6} = J_{5,6}$ = 3 Hz), 1.25 (3H s, OCH_3).

Anal. Calcd. for $C_7H_{13}NO_7$ (mol. wt. 223.2): C, 37.66; H, 5.87; N, 6.28. Found: C, 37.54; H, 6.00; N, 6.47.

*1,2,4,5-Tetra-O-acetyl-3-deoxy-6-O-methyl-3-nitro-muco-inositol (**15**)*

Compound **14** (66 mg) was treated with acetic anhydride (0.66 ml) and 1 drop of BF_3–etherate for 1 h at 0°. Ethanol (0.4 ml) was then added, and the tetraacetate **15** (101 mg, 88%) crystallized in part directly and in part upon evaporation of the solution. It was washed with a small amount of ethanol and melted at 187–188°. Recrystallization lowered the melting point: 170–172° (from ethanol), 175–176° (from ethyl acetate – ligroin). How-

ever, the n.m.r. spectra of the crude and recrystallized samples were indistinguishable (data see Table 1).

Anal. Calcd. for $C_{15}H_{21}NO_{11}$ (mol. wt. 391.3): C, 46.03; H, 5.41; N, 3.58. Found: C, 46.18; H, 5.54; N, 3.70.

Cyclization of Nitro Hexoses with Sodium Methoxide

To a suspension of crystalline 7-β (645 mg) in methanol (2 ml) and nitromethane (2.9 ml) was added 0.96 ml of a 3.25 *N* solution of sodium methoxide in methanol. The addition, which was performed at room temperature under nitrogen, caused 7-β to dissolve, and a new solid began to precipitate immediately afterwards. The reaction mixture was allowed to stand in a closed vessel for 4 days, then cooled with Dry Ice, and acidified with glacial acetic acid (0.3 ml). The solution was passed consecutively through short columns containing 5 ml of Dowex 1 × 2 (acetate) and 10 ml of Rexyn 101 (H^+), respectively. The columns were rinsed with methanol and then with water, the former eluant furnishing upon evaporation 418 mg of a brown syrup, and the latter, 246 mg of a yellow semicrystalline mass. Trituration of the products with ethanol and fractional crystallization gave 102 mg (16%) of a mixture of **9** and **10** (m.p. 190–210°), 52 mg (8%) of what according to an n.m.r. spectrum consisted mainly of **14** (although it melted over the range 102–145° and therefore was not pure), and 395 mg (61%) of an amorphous foam similar in composition to the amorphous material C encountered in the barium hydroxide-induced cyclizations.

A similar experiment starting with a noncrystalline mixture (670 mg) of **7** and **8** furnished, after a reaction time of 1 day, 173 mg (26%) of **9** + **10** (m.p. 200–220°) and 429 mg (64%) of amorphous material.

The amorphous products obtained from these cyclizations were acetonated and yielded pure **13** in yields of 30–35%.

Support of this work by the National Research Council of Canada is gratefully acknowledged.

1. H. H. Baer and K. Čapek. Can. J. Chem. **47**, 99 (1969).
2. H. H. Baer and J. Kovář. Can. J. Chem. **49**, 1940 (1971).
3. H. H. Baer and W. Rank. Can. J. Chem. **49**, 3197 (1971).
4. J. Kovář, K. Čapek, and H. H. Baer. Can. J. Chem. **49**, 3960 (1971).
5. H. H. Baer and W. Rank. Can. J. Chem. **50**, 1216 (1972).
6. J. M. Grosheintz and H. O. L. Fischer. J. Am. Chem. Soc. **70**, 1479 (1948).
7. V. Brocca and A. Dansi. Ann. Chim. (Rome) **44**, 120 (1954).
8. F. W. Lichtenthaler. Chem. Ber. **94**, 3071 (1961).
9. F. W. Lichtenthaler. Angew. Chem. Int. Ed. **1**, 662 (1962).
10. H. H. Baer and W. Rank. Can. J. Chem. **43**, 3330, 3462 (1965).
11. J. Kovář and H. H. Baer. Can. J. Chem. This issue.
12. J. M. Grosheintz and H. O. L. Fischer. J. Am. Chem. Soc. **70**, 1476 (1948).
13. R. Kuhn, H. H. Baer, and A. Seeliger. Ann. **611**, 236 (1958).
14. K. Freudenberg. Ber. **61**, 1735 (1928).
15. R. J. Abraham, L. D. Hall, L. Hough, and W. A. McLauchlan. J. Chem. Soc. 3699 (1962).
16. J. Kovář and H. H. Baer. Can. J. Chem. **49**, 3203 (1971).
17. L. D. Hall, S. A. Black, K. N. Slessor, and A. S. Tracey. Can. J. Chem. **50**, 1912 (1972).
18. R. Schaffer and H. S. Isbell. J. Am. Chem. Soc. **79**, 3864 (1957).
19. M. L. Wolfrom and S. Hanessian. J. Org. Chem. **27**, 1800 (1962).
20. T. D. Inch. Carbohydr. Res. **5**, 45, 53 (1967).
21. L. Hough and A. C. Richardson. *In* Rodd's chemistry of carbon compounds. Vol. IF. Elsevier Publishing Co., Amsterdam. 1967. p. 504.
22. C. Satoh, A. Kiyomoto, and T. Okuda. Carbohydr. Res. **5**, 140 (1967).
23. R. S. Tipson. *In* Methods in carbohydrate chemistry. Vol. II. *Edited by* R. L. Whistler and M. L. Wolfrom. Academic Press Inc., New York, N.Y. 1963. p. 155.
24. R. B. Duff and E. G. V. Percival. J. Chem. Soc. 1675 (1947).

Can. J. Chem. Downloaded from www.nrcresearchpress.com by 210.87.254.5 on 09/05/12
For personal use only.

The Synthesis of Nitro and Dimeric Nitroso Sugars by Peracid Oxidation of Amino Sugars[1]

HANS H. BAER AND SHUET-HING LEE CHIU

Department of Chemistry, University of Ottawa, Ottawa, Canada K1N 6N5

Received January 19, 1973

A number of methyl 3-amino-3-deoxyaldopyranosides were oxidized with *m*-chloroperbenzoic acid. The reaction, which had been previously applied to steroidal amines (6), has provided a new route to nitro sugars and at the same time furnished hitherto unknown nitroso sugar derivatives, namely, dimeric methyl 3-deoxy-3-nitrosoaldopyranosides. Oxidation of a model compound, *trans*-2-aminocyclohexanol, likewise gave the corresponding nitro and dimeric nitroso alcohols. The combined yields of oxidation products ranged from 40 to 95%.

Plusieurs méthyl amino-3 déoxy-3 aldopyranosides ont été oxydés en utilisant l'acide *m*-chloroperbenzoique. Ayant déjà été appliquée aux amines stéroïdales (6), la réaction a ainsi permis une nouvelle approche pour l'obtention de sucres comportant des groupes nitro et ainsi fournir des dérivés de sucres comportant des groupes nitroso jusqu'alors inconnus, à savoir des méthyl deoxy-3 nitroso-3 aldopyranosides dimériques. L'oxydation d'un composé modèle, le *trans*-amino-2 cyclohexanol, a produit tel qu'envisagé les alcools correspondants possèdant un groupe nitro et un groupe nitroso typique du composé dimérique. Les rendements combinés des produits d'oxydation se situent dans l'intervalle de 40 à 95%.
[Traduit par le journal]

Can. J. Chem., 51, 1812 (1973)

In order to complement existing methods for the synthesis of nitro sugars (1), we considered the possibility of oxidizing amino sugar derivatives. Whereas permanganate oxidation is limited to tertiary carbinamines (2) and therefore is not apt to become a general method for the purpose stated, peracid oxidation offered itself as a potential alternative. Aliphatic amines have been oxidized to the corresponding nitro compounds by means of peracetic acid (3, 4), perbenzoic acid (5), and *m*-chloroperbenzoic acid (6). Trifluoroperacetic acid has been stated (3) to be unsuitable for oxidation of amines although it is capable of converting oximes to nitro compounds (7, 8); applications to carbohydrate oximes were reported (9) while the present work was in progress. Of the reagents mentioned, *m*-chloroperbenzoic acid appeared to promise the most convenient and hazard-free use. This stable, commercially available compound is widely employed for various oxidative processes even though use for amine oxidation has been made infrequently.

We now report that certain amino glycosides can indeed be converted into nitro glycosides by treatment with *m*-chloroperbenzoic acid. The reaction proved complicated, however, by the formation of varying proportions of nitroso derivatives along with the desired nitro compounds. Similar observations have been made in previous peracid oxidations (6, 10). The nitroso compounds arise as intermediates and, depending on circumstances, tend to form stable dimers that are oxidized no further. In fact, a dimeric nitroso compound may occasionally be the sole product as was the case in one of our examples and, earlier, in the oxidation of cyclohexylamine with peracetic acid (10). Table I shows the results obtained with five amino glycosides and with *trans*-2-aminocyclohexanol which was included as a model compound. In general, the reactions proceeded quite smoothly in mixtures of chloroform and methanol at reflux temperature, and the combined yields of oxidation products were good.

Even though the original purpose of this enterprise was the search for an alternative route to nitro sugars, the isolation of nitroso carbohydrates was actually of equal interest since very few accounts of such derivatives exist in the literature. Serfontein and coworkers (11) obtained 2-nitrosoglycosyl chlorides by the action of nitrosyl chloride upon glycals. Lemieux and his associates (12) studied the same reaction,

[1]Abstracted from the Ph.D. thesis of S. H. Lee Chiu, University of Ottawa, Ottawa, Canada, 1971, and reported at the 8th International Symposium on the Chemistry of Natural Products (IUPAC), New Delhi, India, February, 1972.

Can. J. Chem. Downloaded from www.nrcresearchpress.com by 210.87.254.42 on 09/05/12
For personal use only.

TABLE 1. Yields of oxidation products (%)

Amine	Products	
	Nitro compound	Nitroso dimer
trans-2-Aminocyclohexanol	16	28
Methyl 3-amino-3,6-dideoxy-2,4-di-*O*-methyl-α-L-glucopyranoside	53	0
α-D-glucopyranoside	44*	43*
	51†	33†
	26‡	69‡
	0§	75§
Methyl 3-amino-3-deoxy-β-D-galactopyranoside	28	47
α-D-mannopyranoside	38	32
β-D-xylopyranoside	0	40

*Amine added to oxidant (6.67 mol equiv) over period of 30 min, with final medium being approximately 3:1 chloroform–methanol (v/v); see Experimental.
†Similar to *, with 2:1 chloroform–methanol as final medium.
‡Similar to *, with addition period of 7 min.
§Amine added to oxidant (3 mol equiv) at once, with medium consisting of chloroform only; reaction time, 1 h at reflux temperature.

extended it to include the use of dinitrogentetraoxide which afforded 2-nitrosoglycosyl nitrates, established the dimeric structure of these nitroso sugars, and subjected them to some reactions of mechanistic interest and synthetic promise. But apart from these important studies nothing is known about nitroso sugars, and their availability by simple oxidation of amino sugars should stimulate further exploration of their properties and potential usefulness.

Oxidation of *trans*-2-aminocyclohexanol produced known (13) *trans*-2-nitrocyclohexanol together with dimeric *trans*-2-nitrosocyclohexanol (**1**) which apparently has not yet been described. Its structure followed from spectral data. The compound displayed intense u.v. absorption with λ_{max} 296 nm resembling that reported (10) for dimeric nitrosocyclohexane, λ_{max} 290 nm. Broad i.r. absorption in the 3400 cm^{-1} region indicated hydrogen-bonded hydroxyl, and a strong band near 1200 cm^{-1} was due to the N → O stretching vibration of the dimeric nitroso moiety. Complete lack of absorption between 2800 and 1500 cm^{-1} revealed absence of carbonyl, nitro, amino, and (monomeric) nitroso groups. Similar u.v. and i.r. data were found for our dimeric nitroso glycosides, and according to the literature (14) they suggest *trans*-geometry of the azodioxy bridge. Of further interest were the n.m.r. spectra of **1** and 2-nitrocyclohexanol. In the nitro alcohol, the nitromethine and carbinol protons had similar chemical shifts causing overlapping multiplets near δ 4.2. In **1**, only the carbinol proton (H-1) resonated in that region while H-2 was shifted downfield to δ 5.2 (in $CDCl_3$). The strong deshielding effect of the azodioxy group has been noted previously (12, 15).

Independent work in this laboratory (16) had furnished methyl 3,6-dideoxy-2,4-di-*O*-methyl-3-nitro-α-L-glucopyranoside (**2**) and, by catalytic hydrogenation, the corresponding amino glycoside (**3**). The latter has now been reconverted to the former by oxidation. No nitroso derivative was found in this one case.[2]

When methyl 3-amino-3,6-dideoxy-α-D-glucopyranoside (**4**) was oxidized for 1 h with 3 mol equiv of oxidant in refluxing chloroform, the nitroso dimer **5** was isolated in 75% yield as the sole product, although complete absence of nitro compound **6** was not ascertained. An increased amount of oxidant (4.25 mol equiv) gave rise to a mixture of **5** and **6** in which, according to an estimate from the n.m.r. spectrum, the nitroso

[2]It will be noted (Table 1) that **3** was the only amine thus far examined that does not bear a free hydroxyl group vicinal to the nitrogen. Perhaps this feature favors further oxidation of the nitroso intermediate whose dimer, lacking internal hydrogen bond stabilization, would in this case be less stable than in the others. However, in order to validate such an explanation one ought to reexamine the oxidation of cyclohexylamine (10) under our conditions. An alternative explanation might be steric hindrance to dimerization of the nitroso intermediate. Although a strain-free model of the dimer can be constructed, the two methoxyl groups in positions 2 and 4 could nevertheless have a retarding effect upon the rate of dimerization.

Can. J. Chem. Downloaded from www.nrcresearchpress.com by 210.87.254.42 on 09/05/12
For personal use only.

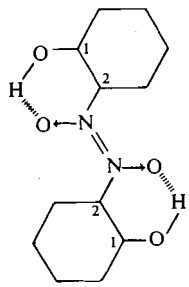

1

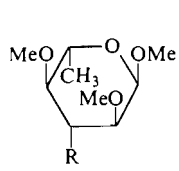

2 R = NO_2
3 R = NH_3Cl

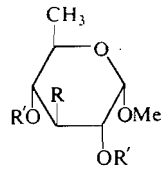

4 R = NH_2; R′ = H
6 R = NO_2; R′ = H
7 R = NO_2; R′ = Ac

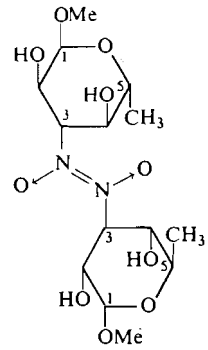

5

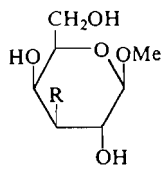

8 R = NH_2
9 R = NO_2

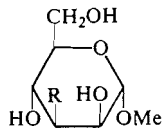

11 R = NH_2
12 R = NO_2

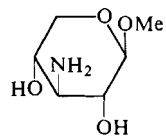

14

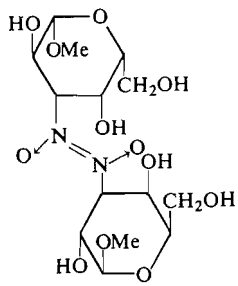

10

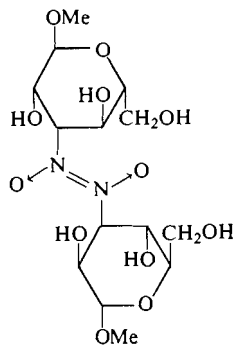

13

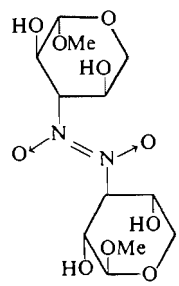

15

compound still preponderated about 1.5-fold. Best results in terms of oxidation to the nitro stage were achieved when the amine was added gradually to a larger excess (6–7 equiv) of oxidant in refluxing chloroform–methanol mixtures. While relatively rapid addition gave predominantly **5**, slow addition changed the product ratio in favor of **6**. An increase in methanol concentration in the reaction medium likewise operated in this direction (Table 1). One may probably conclude from these observations that rapid oxidation of the amine to monomeric nitroso intermediate is followed by slow oxidation of the latter to the nitro compound in competition with dimerization. Thus, if the concentration of the monomeric nitroso derivative is allowed to build up due to a high initial amine concentration and the presence of only a moderate excess of oxidant, dimerization and hence protection from further oxidation is favored. But when the nitroso monomer concentration is kept low by slow introduction of the amine into the reaction medium, and when a larger excess of oxidant is available, then complete oxidation

Can. J. Chem. Downloaded from www.nrcresearchpress.com by 210.87.254.42 on 09/05/12
For personal use only.

Can. J. Chem. Downloaded from www.nrcresearchpress.com by 210.87.254.42 on 09/05/12
For personal use only.

wins over dimerization. The effect of added methanol may consist of opposing dimerization by increasing solvation of the monomer and (or) interfering with internal hydrogen bond stabilization in the dimer.

The nitro glycoside **6**, whose 2,4-diacetate **7** was also prepared for further characterization, was identified by comparison with its known L-enantiomer (17, 18). The nitroso dimer **5** showed spectral characteristics similar to **1**, namely, a high-intensity u.v. band with λ_{max} 298 nm and a strong i.r. band at 1190 cm^{-1}. The n.m.r. spectra of **5** and **6** were similar to each other in most respects (see Experimental) but differed significantly by a downfield shift experienced by the H-3 signal of **5**. Its chemical shift of *ca.* δ 6.0 compared well with data recorded (12) for protons at carbon bearing the azodioxy bridge in dimeric nitroso sugars (δ 5.38–5.53).

Oxidation of methyl 3-amino-3-deoxy-β-D-galactopyranoside (**8**) and its α-D-*manno* isomer (**11**) afforded the corresponding nitro glycosides **9** and **12** as well as the dimeric nitroso glycosides **10** and **13**. Like the preceding products the nitro sugars were identified by comparison with authentic samples, and the new nitroso derivatives were structurally elucidated through their spectral properties. Limited attempts to change the product ratios from those listed in Table 1 were to no avail.

The course of oxidation of methyl 3-amino-3-deoxy-β-D-xylopyranoside (**14**) differed from the aforedescribed experiments insofar as a crystalline product separated directly from the reaction medium during the reflux period. It was sparingly soluble in all solvents tried, including water and dimethyl sulfoxide. For this reason no n.m.r. spectrum could be obtained. The product was different from known (19) methyl 3-deoxy-3-nitro-β-D-xylopyranoside, and its u.v. and i.r. data suggested that it was the nitroso dimer **15**. It seems that the high degree of insolubility of the dimer caused the monomer to be removed from solution so rapidly that it failed to be oxidized to the nitro stage.

Experimental

All reactions were monitored by t.l.c. on 7.5-cm silica gel G plates. The spots were made visible by use of 1% ceric sulfate in 10% sulfuric acid as a spray reagent, and heating. Column chromatography was performed with silica gel 7734 (0.05–0.20 mm) of E. Merck AG, Darmstadt, Germany. I.r. spectra were taken on a Beckman IR-20 spectrometer and refer to Nujol mulls unless otherwise stated; only the most prominent bands are listed for characterization of compounds. Optical rotations were measured with a Perkin–Elmer Model 141 automatic polarimeter at room temperature. Chemical shifts in n.m.r. spectra taken in $CDCl_3$ refer to the tetramethylsilane signal, and in those taken in D_2O, to the DOH signal. U.v. spectra were recorded on a Perkin–Elmer Model 202 spectrophotometer.

Materials

trans-2-Aminocyclohexanol

The amino alcohol was prepared according to Brunnel (20) by reaction of cyclohexene oxide (5.3 ml) in methanol (50 ml) with liquid ammonia (40 ml) in a sealed tube for 2 h at 80° and 12 h at room temperature. The product was purified by sublimation at 45° and 2 Torr. It was obtained as colorless needles, m.p. 67–69°, in 63% yield; lit. (20), m.p. 67–68°. I.r. and n.m.r. spectra were in agreement with the structure. Treatment with ethanolic hydrochloric acid furnished the *hydrochloride* which upon recrystallization from 95% ethanol melted at 178.5–180°; lit. (20), m.p. 175°, 176–177°.

*Amino Glycosides **3**, **4**, **8**, and **14***

The known compounds **8** (21, 22) and **14** (23, 24) were on hand from earlier work in this laboratory. Compound **3** (dec. 263–265°, $[\alpha]_D$ −133° in chloroform) was kindly provided by Dr. Chung-Wai Chiu who had synthesized it from known, crystalline methyl 3,6-dideoxy-3-nitro-α-L-glucopyranoside (25, 17) by an unpublished procedure (16). The known compound **4** (26) was obtained by a new synthesis to be described elsewhere (27).

*Methyl 3-Amino-3-deoxy-α-D-mannopyranoside (**11**)*

The free amino glycoside **11**, which has not been described previously, was made from its known hydrochloride (28). A solution of the latter (0.33 g) in 95% ethanol (25 ml) was passed through a column containing 10 g of dry Dowex 1X2 (OH^-) anion exchange resin. The effluent was evaporated to give **11** which was recrystallized from ethanol; m.p. 160–162°, $[\alpha]_D$ +70 (*c*, 1 in H_2O) and +91° (*c*, 1 in methanol). The yield was 0.24 g (86%).

Anal. Calcd. for $C_7H_{15}NO_5$ (mol. wt. 193.2): C, 43.51; H, 7.83; N, 7.25. Found: C, 43.48; H, 7.80; N, 7.21.

Oxidations with m-Chloroperbenzoic Acid. General Procedure

m-Chloroperbenzoic acid (MCPA) was supplied by Aldrich Chemical Co. According to specifications its degree of purity was 85%; the amounts given in the following have been calculated to represent pure MCPA. A solution of the reagent in chloroform (unless otherwise indicated) was heated to reflux, with efficient magnetic stirring, in a vessel equipped with condenser and dropping funnel. A solution (or partial suspension) of the amine to be oxidized, in chloroform or chloroform–methanol mixture as indicated, was admitted slowly over the period of time stated in parentheses. Refluxing was then continued for another period of time, and the reaction mixture was subsequently cooled and worked-up as described.

Oxidation of trans-2-Aminocyclohexanol

trans-2-Nitrocyclohexanol

The amino alcohol (100 mg, 0.865 mmol) in chloroform (8 ml) was added (5 min) to MCPA (450 mg, 2.6

Can. J. Chem. Downloaded from www.nrcresearchpress.com by 210.87.254.42 on 09/05/12
For personal use only.

mmol) in chloroform (5 ml). The reaction was stopped after 1 h, at which time t.l.c. (10% ethyl acetate in benzene) showed two new spots, R_f 0.6 and 0.3. The solution was cooled in a refrigerator, filtered, washed with ice cold sodium bicarbonate solution, dried (Na_2SO_4), and evaporated. The semi-solid material so obtained was chromatographed on a column of silica gel (5 g). Elution was performed with benzene containing, respectively, 5% ethyl acetate (20 ml), 10 and 25% of the same (20 ml each), and 20% ethyl acetate plus 10% ethanol (40 ml). The faster-moving product, isolated from early fractions that showed a single spot on t.l.c., was a yellow oil which crystallized on trituration with benzene–pentane and cooling. The needles (20 mg, 16%) melted at 46–47°. Recorded (13) for *trans*-2-nitrocyclohexanol, m.p. 46–48°. I.r. absorption was at 3340 (broad; OH), 2930, 2860, 1545, 1450, 1370, 1065, 970, 860, and 735 cm^{-1} (from liquid film). N.m.r. (100 MHz, $CDCl_3$): 2-proton multiplet centered near δ 4.2 (H-1 and -2); 2.74 (s, 1H, exchangeable with D_2O; hydroxy proton); 2.50–0.9 (unresolved, intensity 8H; methylene protons).

*trans-2-Nitrosocyclohexanol Dimer (**1**)*

The fractions containing the slow-moving product from the column mentioned above were evaporated to give a white solid, m.p. 118–122°. Recrystallization from ethyl acetate – petroleum ether (b.p. 60–80°) afforded **1** (31 mg, 28%) as fine needles, m.p. 130–132°. U.v. absorption in methanol: λ_{max} 296 nm (ε 7500). I.r. bands: 3400 (broad), 1195, 1175, 1065, 690 cm^{-1}. N.m.r. (60 MHz, $CDCl_3$): δ 5.2 (m, 1H, H-2); 4.1 (m, 1H, H-1); 3.43 (hydroxyl proton); 2.5–1.0 (unresolved, intensity 8H; methylene protons).

Anal. Calcd. for $C_{12}H_{22}N_2O_4$ (mol. wt. 258.3): C, 55.79; H, 8.59; O, 24.78. Found: C, 55.54; H, 8.38; O, 24.95.

Oxidation of *trans*-2-aminocyclohexanol hydrochloride gave similar results.

*Methyl 3,6-Dideoxy-2,4-di-O-methyl-3-nitro-α-L-glucopyranoside (**2**)*

The amino glycoside hydrochloride **3** (50 mg, 0.21 mmol) in methanol (3 ml) and chloroform (8 ml) was added (20 min) to MCPA (312 mg, 1.81 mmol) in chloroform (10 ml). Although only a trace of **3** remained 5 min later, boiling was continued for another 20 min. One major product spot (R_f 0.70) and a faint shadow just above the baseline were then seen on t.l.c. (15% ethyl acetate in benzene). The reaction mixture was evaporated to dryness and the residue was carefully triturated with chloroform (10 ml) to give a suspension which was strongly cooled (−19°) for some time and then filtered. The filtrate on evaporation gave a material which was chromatographed on silica gel (17 g) using 15% ethyl acetate in benzene (150 ml) as the eluant. The fractions containing the major reaction product yielded a semi-solid mixture of **2** and aromatic acid. Passage of this mixture through a small column (1.5 × 2.0 cm) of aluminum oxide (Woelm, neutral), with benzene as eluant, gave pure **2** as a syrup (26 mg, 53%) from early fractions. The product showed $[\alpha]_D$ −144.3° (*c*, 0.6 in $CHCl_3$), and its spectral data were in agreement with those of an independently synthesized sample (16) which showed $[\alpha]_D$ −141.3° (*c*, 1.6 in $CHCl_3$). Liquid film i.r. absorptions were at 2930, 2840, 1560, 1100, 1050, and 995 cm^{-1}. N.m.r. (60 MHz in $CDCl_3$): δ 4.9–4.8 (2H, d and t overlapping; H-1 and -3 with $J_{1,2} = 3.5$ and $J_{2,3} = J_{3,4} = 10.5$ Hz); 3.82 (1H, q, H-2, with $J_{1,2} = 3.5$ and $J_{2,3} = 10.5$ Hz); 3.65–3.25 (overlapping signals of H-4 and -5, and prominent singlets at 3.47 and 3.42 due to three OCH_3 groups; total intensity 11 H); 1.31 (3H, d, $J_{5,6} = 6$ Hz; C—CH_3).

*Oxidation of Methyl 3-Amino-3,6-dideoxy-α-D-glucopyranoside (**4**)*

The typical procedure described yielded approximately equal amounts of **5** and **6**. Reactions performed in the same general fashion but with variations as specified in Table 1 led to the different yields there recorded.

*Methyl 3,6-Dideoxy-3-nitroso-α-D-glucopyranoside Dimer (**5**)*

Compound **4** (169 mg, 0.95 mmol) in a mixture of methanol (7 ml) and chloroform (10 ml) was added (30 min) to MCPA (1.35 g, 6.67 mmol) in chloroform (12 ml). Ten minutes after the addition, **4** had completely disappeared and two products (R_f 0.23 and 0.1) were formed according to t.l.c. with 5% ethanol in benzene. Another 45 min of refluxing was allowed before the solvent was evaporated. The residue was extracted with water (4 × 5 ml). The material that remained undissolved was mainly aromatic acid and was discarded. Evaporation of the aqueous extract gave a solid (212 mg after drying) which by means of chloroform containing 5% of methanol was passed through a column of 5 g of aluminum oxide (Woelm, neutral, activity grade III). The effluent furnished the nitrogenous sugars still contaminated with aromatic acid. Good separation was then achieved by chromatography on silica gel (9 g) by use of 8 and 10% ethanol in benzene (120 and 50 ml, respectively). The product eluted first (R_f 0.23) was the nitro sugar **6** (see the next section). The fractions that contained the more slowly moving product only were evaporated to give colorless crystals of **5** (78 mg, 43%), m.p. 148–152°. Recrystallization from a small amount of ethyl acetate containing a few drops of absolute ethanol was achieved by adding a few drops of petroleum ether and cooling overnight. The fine prisms then melted at 154–156°, with the melt turning red and decomposing at 165°; $[\alpha]_D$ +152° (*c*, 0.4 in water). U.v. absorption in water, λ_{max} 298 nm (ε 7600). I.r. bands: 3440–3360 (broad), 1295, 1193, 1130, 1095, 1053, 1035, and 960 cm^{-1}. N.m.r. (60 MHz, D_2O): downfield from DOH, 1.25 (t, 1H, $J_{2,3} = J_{3,4} = 10$ Hz; H-3) and 0.20 p.p.m. (d, 1H, $J_{1,2} = 3.7$ Hz; H-1); upfield from DOH, 0.55 p.p.m. (q, 1H, $J_{1,2} = 3.7$, $J_{2,3} = 10$ Hz; H-2); 0.8–1.1 (m, 2H; H-4 and -5); 1.18 (s, 3H; OCH_3); 3.36 (d, 3H, $J_{5,6} = 6$ Hz; C—CH_3).

Anal. Calcd. for $C_{14}H_{26}N_2O_{10}$ (mol. wt. 382.4): C, 43.97; H, 6.85; O, 41.85. Found: C, 43.85; H, 6.70; O, 41.87.

*Methyl 3,6-Dideoxy-3-nitro-α-D-glucopyranoside (**6**)*

The chromatographic fractions containing the faster-moving product (see the preceding section) were evaporated to give a syrup which crystallized on drying *in vacuo* (87 mg, 44%). Recrystallization from chloroform – petroleum ether (b.p. 60–80°) afforded **6** as long needles, m.p. 140–141° and $[\alpha]_D$ +160° (*c*, 1 in water). Data reported (17) for the L-enantiomer: m.p. 136–139°, 141–143°, 142–145°; $[\alpha]_D$ −164.5°, −162°. Compound **6** gave an i.r. spectrum superimposable on that of the enantiomer, and its n.m.r. data agreed completely with those published (25) for the enantiomer.

Can. J. Chem. Downloaded from www.nrcresearchpress.com by 210.87.254.42 on 09/05/12
For personal use only.

Methyl 2,4-Di-O-acetyl-3,6-dideoxy-3-nitro-α-D-glucopyranoside (7)

A sample of **6** (35 mg) was acetylated (0°, 30 min) with acetic anhydride (1 ml) and ethereal boron trifluoride (2 drops). Excess anhydride was decomposed with ice-water and the product extracted with chloroform from which, on evaporation with added toluene, a dry syrup was obtained. The syrup crystallized on trituration with petroleum ether, and recrystallization from ethyl acetate – petroleum ether gave colorless needles (40 mg, 81%) showing m.p. 108–110° and $[\alpha]_D$ +154° (*c*, 0.3 in $CHCl_3$). Reported for the L-enantiomer: m.p. 109–110° and $[\alpha]_D$ −154° (18); m.p. 113–113.5° and $[\alpha]_D$ −155.3° (16). I.r. spectra of **7** and its enantiomer were identical.

Oxidation of Methyl 3-Amino-3-deoxy-β-D-galactopyranoside (8)

Methyl 3-Deoxy-3-nitro-β-D-galactopyranoside (9)

The amino glycoside **8** (193 mg, 1.0 mmol) in a 1:1 methanol–chloroform mixture (8 ml) was added (20 min) to MCPA (1.28 g, 6.32 mmol) in the same solvent (19 ml). Refluxing was continued for another 20 min. Complete consumption of **8** and formation of two products, R_f 0.5 and 0.25, was revealed by t.l.c. (20% methanol in chloroform). The white residue obtained upon evaporation of the reaction mixture was extracted with ether (2 × 10 ml). The part that remained undissolved was dealt with as described later on. The ether extract, which contained part of **9** and aromatic acid, was washed with water (3 × 5 ml) which upon evaporation gave a semi-solid material (89 mg). Passage of this material by means of chloroform containing 5% of methanol through a small silica gel column (5 g) yielded syrupy **9** that crystallized from acetone–chloroform. The colorless product (36 mg) exhibited $[\alpha]_D$ +32.5° (*c*, 0.5 in water) and melted at 80–82° (air dried) and at 125–128° (dried for 12 h *in vacuo* at 56°); lit. (21): $[\alpha]_D$ +32.6°; m.p. 87–89 and 131–132°, respectively. Identity of the product with previously prepared **9** (21) was confirmed by i.r. spectra. The n.m.r. spectrum (100 MHz in D_2O) was in accord with the β-D-*galacto* configuration: downfield from DOH, 0.22 p.p.m. (q, 1H, $J_{2,3}$ = 10, $J_{3,4}$ = 3.5 Hz; H-3); upfield from DOH, 0.21 (d, 1H, $J_{1,2}$ = 8 Hz; H-1), 0.55 (q, 1H, $J_{1,2}$ = 8, $J_{2,3}$ = 10 Hz; H-2), 1.07 p.p.m. (s, 3H; OCH_3).

The ether-insoluble residue mentioned above was suspended in methanol (5 ml) whereby it partly dissolved, leaving behind 80 mg of chromatographically pure nitroso dimer **10** (see the next section). The methanolic solution contained both **9** and **10** (t.l.c.). Evaporation followed by chromatography on silica gel (8 g) with chloroform containing increasing amounts of methanol furnished 26 mg of **9** and 17 mg of **10**, thus raising the total yields to 62 (28%) and 97 mg (47%), respectively.

Methyl 3-Deoxy-3-nitroso-β-D-galactopyranoside Dimer (10)

Compound **10** isolated as just described was recrystallized from methanol–water to form colorless needles; m.p. 141–143°, $[\alpha]_D$ +165° (*c*, 0.6 in water); λ_{max} 295 nm (ε 7500, in water). I.r. bands were at 3300 (broad), 1190, 1160, 1130, 1055, 1020, and 980 cm^{-1}. Most of the n.m.r. signals (60 MHz, D_2O) were poorly resolved, but the signal at lowest field (0.69 p.p.m. downfield from DOH) was a clear quartet assignable to H-3 ($J_{2,3}$ = 10, $J_{3,4}$ = 3 Hz). The OCH_3 singlet occurred 1.08 p.p.m. upfield from DOH.

Anal. Calcd. for $C_{14}H_{26}N_2O_{10}$ (mol. wt. 414.4): C, 40.58; H, 6.42; O, 46.34. Found: C, 40.64; H, 6.42; O, 46.26; mol. wt., 423 (osmometrically in water).

Oxidation of Methyl 3-Amino-3-deoxy-α-D-mannopyranoside (11)

Methyl 3-Deoxy-3-nitro-α-D-mannopyranoside (12)

The amino glycoside **11** (110 mg, 0.57 mmol) in a mixture of methanol (9 ml) and chloroform (4 ml) was added (20 min) to MCPA (800 mg, 3.94 mmol) in chloroform (8 ml). After continued refluxing for another 20 min all **11** had been consumed and two products (R_f 0.6 and 0.23, with 3:1 benzene–ethanol) were seen. The residue obtained on solvent evaporation was extracted with ether (4 × 10 ml) and set aside for further use (see below). The ethereal extract was shaken four times with 5 ml of 50% aqueous tetrahydrofuran. The water phase that separated contained part of **12** along with some aromatic acid. The latter could be removed by chromatography of the solute on silica gel (5 g) using chloroform with increasing proportions of methanol (0, 5, 10, 15%) as eluant. The colorless syrup of **12** obtained from the eluate crystallized from ethyl acetate and petroleum ether after prolonged cooling, forming rosettes of large crystals (23 mg), m.p. 120–120.5° $[\alpha]_D$ +37.2° (*c*, 0.6 in water). The i.r. spectrum was identical with that of authentic **12**; lit. (29): m.p. 113–115° (from tetrahydrofuran–ether); $[\alpha]_D$ + 44.5°.

The crude reaction residue that had been extracted with ether (see above) was fractionated on a silica gel column (8 g) with chloroform–methanol as described. An additional 26 mg of the faster-moving nitro sugar **12** was thereby obtained in crystalline form, raising its yield to 49 mg (38.5%). Later fractions contained the nitroso dimer **13**.

Methyl 3-Deoxy-3-nitroso-α-D-mannopyranoside Dimer (13)

Evaporations of the fractions just mentioned gave **13** as a foam which was dried *in vacuo* to a white, hygroscopic powder (40 mg, 34%) melting at 93–96° and exhibiting $[\alpha]_D$ −14° (*c*, 0.2, in water). All attempts at recrystallization failed. The product showed λ_{max} 293 nm (ε 4000, in water) and i.r. bands at 3300 (broad), 1195, 1140, 1060 (broad), and 975 cm^{-1}. Most of the n.m.r. signals (100 MHz in D_2O) were poorly resolved, but the signal at lowest-field (0.69 p.p.m. downfield from DOH) was a well-separated quartet assignable to H-3 ($J_{2,3}$ = 3, $J_{3,4}$ = 10.5 Hz). The OCH_3 singlet occurred at 1.29 p.p.m. upfield from DOH.

Oxidation of Methyl 3-Amino-3-deoxy-β-D-xylopyranoside (14)

A solution of amino glycoside **14** (26.5 mg, 0.16 mmol) in methanol (2 ml) and chloroform (4 ml) was added (10 min) to MCPA (200 mg, 1.16 mmol) in chloroform (6 ml). The initially clear reaction mixture became turbid during this period due to the separation of crystals, and this condition persisted even when more methanol was added. It was seen on t.l.c. that all the starting glycoside had reacted shortly after its introduction, and only one new spot was detected (R_f 0.27). The crystals (11 mg) were collected after cooling of the solution and recrystallized from hot methanol–water. The fine colorless needles melted at 168–170°, turning dark red in the process. The product was assumed to be methyl 3-deoxy-3-nitroso-β-D-

xylopyranoside dimer (**15**) on grounds of its spectral data, low R_f-value, and poor solubility even in water and DMSO. It displayed λ_{max} 300 nm (ε 7000 in water) and i.r. bands at 3400 (broad), 1295, 1215, 1195, 1150, 1120, 1090, 1060, 1020, 985, and 875 cm^{-1}. No NO_2 vibration was present in the 1550 cm^{-1} region. The product was clearly different in all these characteristics from known methyl 3-deoxy-3-nitro-β-D-xylopyranoside (19) which melts at 186–187°, shows greater solubility, and gives a nitro band in the i.r. but no high-intensity u.v. absorption in the 300 nm region.

Support of this work by the Defence Research Board of Canada is gratefully acknowledged.

1. H. H. BAER. Adv. Carbohydr. Chem. Biochem. **24**, 67 (1969).
2. N. KORNBLUM, R. J. CLUTTER, and W. J. JONES. J. Am. Chem. Soc. **78**, 4003 (1956).
3. W. D. EMMONS. J. Am. Chem. Soc. **79**, 5528 (1957).
4. E. H. MASSEY, H. E. SMITH, and A. W. GORDON. J. Org. Chem. **31**, 684 (1966).
5. L. N. NYSTED and R. R. BURTNER. J. Org. Chem. **27**, 3175 (1962).
6. C. H. ROBINSON, L. MILEWICH, and P. HOFER. J. Org. Chem. **31**, 524 (1966).
7. W. D. EMMONS and A. S. PAGANO. J. Am. Chem. Soc. **77**, 4557 (1955).
8. H. H. BAER and S. R. NAIK. J. Org. Chem. **35**, 2927 (1970).
9. T. TAKAMOTO, R. SUDOH, and T. NAKAGAWA. Tetrahedron Lett. 2053 (1971).
10. W. D. EMMONS, J. Am. Chem. Soc. **79**, 6522 (1957).
11. W. J. SERFONTEIN, J. M. JORDAAN, and J. WHITE. Tetrahedron Lett. 1069 (1964).
12. R. U. LEMIEUX, T. L. NAGABHUSHAN, and I. K. O'NEILL. Tetrahedron Lett. 1909 (1964); Can. J. Chem. **46**, 413 (1968). R. U. LEMIEUX, T. L. NAGABHUSHAN, and S. W. GUNNER. Can. J. Chem. **46**, 405 (1968).
13. T. E. STEVENS and W. D. EMMONS. J. Am. Chem. Soc. **79**, 6008 (1957). H. BALDOCK, N. LEVY, and C. W. SCAIFE. J. Chem. Soc. 2627 (1949).
14. B. G. GOWENLOCK and J. TROTMAN. J. Chem. Soc. 1670 (1956). B. G. GOWENLOCK and W. LÜTTKE. Quart. Rev. (London), **12**, 321 (1958). B. G. GOWENLOCK, H. SPEDDING, J. TROTMAN, and D. H. WHIFFEN. J. Chem. Soc. 3927 (1957).
15. J. P. FREEMAN. J. Org. Chem. **28**, 2508 (1963).
16. C. W. CHIU. Ph.D. thesis. University of Ottawa, Ottawa, Canada. 1971.
17. K. ČAPEK, J. ŠTEFFKOVÁ, and J. JARÝ. Coll. Czech. Chem. Commun. **31**, 1854 (1966). H. H. BAER and K. ČAPEK. Can. J. Chem. **47**, 99 (1969).
18. F. W. LICHTENTHALER and W. FISCHER. Chem. Commun. 1081 (1970).
19. H. H. BAER and J. KOVÁŘ. Can. J. Chem. **49**, 1940 (1971).
20. L. BRUNNEL. Ann. Chim. [8] **6**, 253 (1905). See also G. E. MCCASLAND, R. N. CLARK, and H. E. CARTER. J. Am. Chem. Soc. **71**, 637 (1949).
21. H. H. BAER and F. KIENZLE. Can. J. Chem. **41**, 1606 (1963).
22. F. W. LICHTENTHALER. *In* Methods in carbohydrate chemistry. Vol. VI. *Edited by* R. L. Whistler and J. N. BeMiller. Academic Press, Inc. New York, N.Y. 1972. p. 250.
23. R. E. SCHAUB and M. J. WEISS. J. Am. Chem. Soc. **80**, 4683 (1958). C. D. ANDERSON, L. GOODMAN, and B. R. BAKER. J. Am. Chem. Soc. **80**, 5247 (1958).
24. H. H. BAER and H. O. L. FISCHER. J. Am. Chem. Soc. **81**, 5184 (1959).
25. J. KOVÁŘ, K. ČAPEK, and H. H. BAER. Can. J. Chem. **49**, 3960 (1971).
26. A. C. RICHARDSON. J. Chem. Soc. 2758 (1962).
27. H. H. BAER and S. H. LEE CHIU. Carbohydr. Res. In press.
28. H. H. BAER and H. O. L. FISCHER. J. Am. Chem. Soc. **82**, 3709 (1960). H. H. BAER. J. Am. Chem. Soc. **84**, 83 (1962).
29. H. H. BAER and W. RANK. Can. J. Chem. **50**, 1216 (1972).

Can. J. Chem. Downloaded from www.nrcresearchpress.com by 210.87.254.42 on 09/05/12
For personal use only.

Can. J. Chem. Downloaded from www.nrcresearchpress.com by 210.87.254.42 on 09/05/12
For personal use only.

The Structure of the Capsular Polysaccharide of Klebsiella K-type 24

YUEN-MIN CHOY, GUY G. S. DUTTON, AND ALBERTO M. ZANLUNGO[1]
Department of Chemistry, The University of British Columbia, Vancouver, British Columbia
Received December 11, 1972

Methylation, periodate oxidation, and partial hydrolysis studies on the capsular polysaccharide, and on the carboxyl reduced polymer, of *Klebsiella* K24 show the structure to consist of a repeating unit

$$\begin{array}{l} \underline{\quad 2 \quad}\ \text{D-GlcA}p\ \frac{1\ 3}{\alpha}\ \text{D-Man}p\ \frac{1\ 2}{\alpha}\ \text{D-Man}p\ \frac{1\ 3}{\alpha}\ \text{D-Glc}p\ \frac{1}{\beta} \\ \qquad\quad \beta\Big|\begin{matrix}4\\1\end{matrix} \\ \qquad\quad \text{D-Man}p \end{array}$$

The anomeric linkages were determined in isolated oligosaccharides by p.m.r. spectroscopy which also showed the presence in the polysaccharide of one *O*-acetyl group per seven or eight sugar residues. The *O*-acetyl is tentatively assigned to one of the D-mannose units.

Les méthodes de méthylation, oxydation periodique, et hydrolyse partielle portées au polysaccharide capsulaire, et au polymère avec le groupe carboxyle réduit, de *Klebsiella* K24 ont démontré que la structure se compose d'une unité qui se répéte.

$$\begin{array}{l} \underline{\quad 2 \quad}\ \text{D-GlcA}p\ \frac{1\ 3}{\alpha}\ \text{D-Man}p\ \frac{1\ 2}{\alpha}\ \text{D-Man}p\ \frac{1\ 3}{\alpha}\ \text{D-Glc}p\ \frac{1}{\beta} \\ \qquad\quad \beta\Big|\begin{matrix}4\\1\end{matrix} \\ \qquad\quad \text{D-Man}p \end{array}$$

Les liaisons anomères ont été distinguées chez des oligosaccharides par la spectroscopie r.m.n. qui a aussi mis en évidence dans le polysaccharide la présence d'un groupe *O*-acétyl par rapport à sept ou huit sucres. On pense que le groupe *O*-acétyle est lié à un des restes de D-mannose.

Can. J. Chem., 51, 1819 (1973)

Qualitative analyses of the capsular polysaccharides of the 80 serotypes of *Klebsiella* bacteria have been provided by Nimmich (1, 2). In continuation of our work (3) on the structure of these materials, we now report studies on the capsular polysaccharide from *Klebsiella* K-type 24.

The polysaccharide, purified by precipitation with Cetavlon, moved as a single band on electrophoresis on cellulose acetate and had $[\alpha]_D^{27}$ +79° and an equivalent weight (by titration) of 786. The p.m.r. spectrum of a 2% solution of the sodium salt of the polysaccharide in D_2O run at 95° showed a sharp singlet at τ 7.8 characteristic of *O*-acetyl and the absence of pyruvate (4, 5). The anomeric region of the spectrum suggested that the repeat unit consists of five sugar units of which three are linked by α-D- and two by β-D-glycosidic bonds (5). Integration of the anomeric and acetate signals indicated one acetyl group to seven or eight sugar units. The presence of *O*-acetyl groups was also confirmed by formation of the hydroxamic ester (6).

Acid hydrolysis of the polysaccharide showed the rapid liberation of D-mannose and after 4 h D-mannose and D-glucose were proved to be the only neutral sugars present, in the ratio of 2.7:1. This analysis was carried out on the derived alditol acetates, samples of which were collected by g.l.c., and measurement of their c.d. spectra confirmed the assignment of the D-configuration to both sugars (7).

Partial hydrolysis of the polysaccharide gave a series of acidic oligosaccharides which were separated from the neutral sugars by ion-exchange resins and individual components were obtained by paper chromatography. These were shown to be an aldobiouronic acid together with related aldotri- and aldotetra-uronic acids. The structures of these oligosaccharides (as their alditols) are given in Table 1 together with the chemical shift of the anomeric proton(s) which

[1]On leave from Universidad Technica del Estado, Santiago, Chile.

TABLE 1. P.m.r. data on *Klebsiella* K24 capsular polysaccharide and derived oligosaccharides

Repeating unit of compound	τ-Value* (coupling constant, Hz)	Ratio of integrals	Proton assignment (all sugars have D-configuration)
GlcA $\frac{1\ 3}{\alpha}$ Mannitol	4.85 (3.5)	1	α-GlcA $\frac{1\ 3}{}$ Mannitol
GlcA $\frac{1\ 3}{\alpha}$ Man $\frac{1\ 2}{\alpha}$ Mannitol	4.7 (3.5)	1	α-GlcA $\frac{1\ 3}{}$ Man
	5.0 (1.5)	1	α-Man $\frac{1\ 2}{}$ Mannitol
GlcA $\frac{1\ 3}{\alpha}$ Man $\frac{1\ 2}{\alpha}$ Man $\frac{1\ 3}{\alpha}$ Glucitol	4.7 + 4.73	2	α-GlcA $\frac{1\ 3}{}$ Man and α-Man $\frac{1\ 3}{}$ Glucitol
	4.95 (1.5)	1	α-Man $\frac{1\ 2}{}$ Man
$\frac{2}{}$ GlcA $\frac{1\ 3}{\alpha}$ Man $\frac{1\ 2}{\alpha}$ Man $\frac{1\ 3}{\alpha}$ Glc $\frac{1}{\beta}$ (β|4, β|1 Man)	4.6	2	α-GlcA $\frac{1\ 3}{}$ Man and α-Man $\frac{1\ 3}{}$ Glc
	4.95 (1.5)	1	α-Man $\frac{1\ 2}{}$ Man
	5.27 (1.0)	1	β-Man $\frac{1\ 4}{}$ GlcA
	5.31 (6.0)	1	β-Glc $\frac{1\ 2}{}$ GlcA

*Spectra run in D_2O with external tetramethylsilane (τ = 10) at 100 MHz.

enables the nature of the glycosidic linkages to be determined. The structures given were determined by (*a*) hydrolysis after conversion to the alditol, (*b*) hydrolysis after carboxyl reduction, and (*c*) methylation, as described in the Experimental. The aldobiouronic acid 3-*O*-(α-D-glucopyranosyluronic acid)-D-mannose has been found in *Klebsiella* K2 and K21 and elsewhere (3).

When a sample of the fully methylated (8, 9) polysaccharide was hydrolyzed and the neutral sugars were examined 2,3,4,6-tetra- and 3,4,6-tri-*O*-methyl-D-mannose and 2,4,6-tri-*O*-methyl-D-glucose were found together with a small quantity of 2,4,6-tri-*O*-methyl-D-mannose. An attempt to analyze this mixture quantitatively as alditol acetates was not satisfactory since on columns of ECNSS-M and butanediol succinate the 2,4,6- and 3,4,6-trimethylhexoses were not resolved. On a column of OS 138 these components gave two major peaks poorly resolved and a minor one (*ca.* 9% of the trimethyl fraction) which was identified by its retention time and mass spec rum as 2,4,6-tri-*O*-methyl-D-mannose. A good separation of the main components was obtained by chromatographing the trimethylsilyl derivatives (10) of the methylated sugars. This was done using three different columns and authentic standards as shown in Table 2. Under these conditions 2,3,4,6-tetra-*O*-methyl-D-mannose was clearly distinguished from the D-glucose isomer but it was not possible to estimate accurately the small amount of 2,4,6-tri-*O*-methyl-D-mannose. The ratio of 2,3,4,6-tetra-*O*-methyl-D-mannose : 3,4,6-tri-*O*-methyl-D-mannose : 2,4,6-tri-*O*-methyl-D-glucose was 1.1 : 1 : 1.

Alternatively it has been found (11) that methylated sugars may be separated conveniently as their acetates. When this method was employed here three main groups of peaks (A; B_1, B_2; C_1, C_2) in approximately equal proportions were obtained; B_2 was present in very small amount and was not examined further. Samples were collected of the other components, deacetylated, and examined on paper. Further samples were reduced, acetylated, and examined by g.l.c.–m.s. and each of the main components thus obtained was demethylated and converted to the hexitol peracetate. All of these results were

Can. J. Chem. Downloaded from www.nrcresearchpress.com by 210.87.254.42 on 09/05/12
For personal use only.

TABLE 2. Per(trimethylsilyl) derivatives of methylated sugars from *Klebsiella* K24 capsular polysaccharide

Compounds	Retention time (min) for columns: (a) ECNSS-M	(b) BDS	(c) SE-52
Methylated aldoses of K24	14.4 19.8 21.4	4.6 7.8 11.3	17.6 24.1 16.6
3,4,6-Me_3-Man	14.4	4.6	17.6
2,4,6-Me_3-Glc	19.8	7.8	24.1
2,3,4,6-Me_4-Man	21.4	11.3	16.6
2,3,4,6-Me_4-Glc	15.4 (20%) 17.0 (80%)	7.4 (15%) 8.2 (85%)	

consistent with the assignment of peaks A, B, and C as 2,3,4,6-tetra-*O*-methyl-D-mannose (A), 3,4,6-tri-*O*-methyl-D-mannose (B_1), and 2,4,6-tri-*O*-methyl-D-glucose (C_1 and C_2). The methylated alditol acetate obtained from B_1 showed an additional minor peak whereas both components C_1 and C_2 gave the same single alditol acetate. This indicates that C_1 and C_2 are the two anomers of the trimethylglucose and suggests that the small amount of 2,4,6-tri-*O*-methyl-D-mannose has a similar retention time to the 3,4,6-isomer. It may be noted that in this instance the mannose ethers have shorter retention times than the glucose compound but for the 2,3,6-tri-*O*-methyl derivatives the situation is reversed (11).

These results show the presence of a D-mannose unit substituted at position 2 and a D-glucose unit substituted at position 3 together with a D-mannose residue present as a side chain. The small amount of 2,4,6-tri-*O*-methyl-D-mannose undoubtedly arose by partial cleavage of the aldobiouronic acid linkage.

Another sample of the fully methylated polysaccharide was reduced with lithium borohydride and hydrolyzed. In addition to the methylated sugars described above a new component having the mobility on paper of 3- or 4-*O*-methyl-D-glucose was obtained. The mixture of methylated sugars was reduced with sodium borodeuteride (12) and the new component was isolated by g.l.c. of the alditol acetates. The mass spectrum clearly identified this component as a 3-*O*-methyl hexitol. Furthermore the c.d. spectrum of the alditol acetate was identical in sign (negative) with that obtained from authentic 3-*O*-methyl-D-glucose. This establishes the D-configuration of the glucuronic acid in this polysaccharide (7).

In order to determine the position of attachment of the pendant D-mannose units to the main chain, a sample of the original polysaccharide was subjected to mild hydrolysis and the recovered polymeric material was methylated, reduced with lithium borohydride, and hydrolyzed. Examination of the hydrolyzate by paper chromatography showed, in addition to the compounds previously obtained, a component having the mobility of 3,4-di-*O*-methyl-D-glucose. This was confirmed by g.l.c. separation of the alditol acetates and mass spectrometry of the dimethyl fraction together with demethylation and acetylation to give D-glucitol hexaacetate. The ratio of the tri- to dimethyl fraction was 3.2:1. This indicates that the D-mannose side chains are joined to position 4 of D-glucuronic acid which, in turn, must be linked through position 2 in the main chain.

The methylation data in conjunction with the results of analysis of the acidic oligosaccharides enable the repeat unit of *Klebsiella* K24 capsular polysaccharide to be written thus:

$$\begin{array}{l} \overset{2}{\text{—}}\ \text{D-GlcA}p\ \overset{1\,3}{\alpha}\ \text{D-Man}p\ \overset{1\,2}{\alpha}\ \text{D-Man}p\ \overset{1\,3}{\alpha}\ \text{D-Glc}p\ \overset{1}{\beta} \\ \qquad\quad \beta\Big|{}^{4}_{1} \\ \qquad\quad \text{D-Man}p \end{array}$$

Confirmation of this structure was sought by the Smith degradation procedure (13). Deacetylated polysaccharide was oxidized with periodate when 0.66 mol per hexose unit was consumed. After reduction, the derived polyalcohol was partially hydrolyzed by trifluoroacetic acid at room temperature to give a mixture of glycerol and an oligosaccharide which was then reduced with sodium borohydride. The latter compound

Can. J. Chem. Downloaded from www.nrcresearchpress.com by 210.87.254.42 on 09/05/12
For personal use only.

Can. J. Chem. Downloaded from www.nrcresearchpress.com by 210.87.254.42 on 09/05/12
For personal use only.

was methylated, reduced, and hydrolyzed to give 2,3,4,6-tetra- and 3,4-di-*O*-methyl-D-glucose and 2,4,6-tri-*O*-methyl-D-mannose as expected from the proposed structure; the methylated glycerol derivative was not sought.

An attempt was made to locate the position of the *O*-acetyl group using the procedure of de Belder and Norrman (14). The polysaccharide was dissolved in methyl sulfoxide and reacted overnight with methyl vinyl ether. Excess ether was removed *in vacuo* and the polysaccharide was treated directly with dimethsulfinyl anion and methyl iodide. When the product was hydrolyzed and the components were examined by paper chromatography a major spot for monosaccharide was obtained together with a faint spot with an R_f greater than all monomethylglucose derivatives and which was therefore assumed to be a monomethylmannose. Analysis by g.l.c. of the hydrolyzate, as alditol acetates, suggested that there might be two monomethyl mannoses present. Even if the experiment was to be repeated on a larger scale to allow characterization of the monomethyl sugars their identification as mannose derivatives would still not permit any deduction as to which of the three structurally different mannose residues was acetylated in the original polysaccharide. For this reason and because of the low yields obtained, this aspect of the structure was not pursued further. The use of methyl vinyl ether as a reagent in locating *O*-acetyl groups has been applied successfully to lipopolysaccharides (15) which appear to have lower molecular weights than the capsular polysaccharides of *Klebsiella* (mol. wt. $5–9 \times 10^5$). This difference in molecular weight may account for the low yield obtained in the present instance; similar difficulties have been experienced with other capsular polysaccharides from *Klebsiella* (16). There is good evidence that these capsular polysaccharides have a true repeating unit and also that where a sugar residue is in the form of a pyruvic acid ketal (1-carboxyethylidene derivative) this feature similarly repeats regularly (5). In the case of partial acetylation the substitution pattern appears to be less well defined.

The evidence presented shows clearly that the structure of the capsular polysaccharide of *Klebsiella* K-type 24 is as given above with the tentative assignment of some *O*-acetyl groups on certain of the mannose residues.

Experimental

General methods are as previously described (3).

Isolation and Properties of K24 Capsular Polysaccharide

Klebsiella K24 was grown in the medium (3) as for K21 and the harvested capsular polysaccharide and cells (1½ l) were diluted five-fold and centrifuged at 27 000 r.p.m. at 20° for 45 min. The supernatant was collected and freeze-dried. A 1% aqueous solution of the product (1 vol) was added with stirring to ethanol (6–7 vol). The polysaccharide was collected, washed with acetone, and air dried; yield *ca.* 12 g. The crude product was purified through precipitation with Cetavlon, giving 7 g of pure acidic polysaccharide having $[\alpha]_D^{25}$ +90° (*c* 0.54, water) as Na^+ salt; $[\alpha]_D^{27}$ +79° (*c* 0.68, water) after deionization with Amberlite IR 120. Equivalent weight by titration with 0.03 *N* sodium hydroxide (phenolphthalein) was 786. Addition of excess sodium hydroxide and back titration with hydrochloric acid after stirring under nitrogen for 50 min showed the presence of *ca.* 4% *O*-acetyl. Electrophoresis at p*H* 3 and 8.8 showed the polysaccharide moved as a single component.

Anal.: N, 0; ash, 0%.

A sample of polysaccharide was exactly neutralized and the solution was lyophilized. The residue was dissolved in D_2O and exchanged twice by lyophilization. The p.m.r. spectrum of the solution (*ca.* 2% in D_2O) was run at 95° and showed a sharp peak at τ 7.8 and five protons in the range τ 4.5–5.5 (see Table 1).

The presence of acetate was also confirmed by methanolysis of the polysaccharide and identification of methyl acetate using the hydroxylamine – ferric chloride reagent (6, 16, 17).

Hydrolysis of the Polysaccharide

Polysaccharide (25 mg) was dissolved in sulfuric acid (2.5 ml, *N*) at room temperature (30 min) and the solution was heated on a steam bath for 4 h. The solution was neutralized ($BaCO_3$) and the filtrate was evaporated. On paper chromatography in solvents A and B spots corresponding to D-glucose, D-mannose, and D-glucuronic acid were observed. The hydrolyzate was separated into neutral and acidic fractions using ion-exchange resins and the neutral fraction was found to contain D-mannose and D-glucose in an approximate ratio of 2.7:1 as determined by the g.l.c. of the alditol acetates (column a); D-mannitol hexaacetate had m.p. and mixed m.p. 121.5–122° and D-glucitol hexaacetate had m.p. and mixed m.p. 98.5–99°.

Partial Hydrolysis of the Polysaccharide

The polysaccharide (1.0 g) was dissolved in trifluoroacetic acid (TFA, 100 ml, 2 *M*) and the solution was heated on a steam bath for 4 h. The solution was evaporated, dissolved in 5 ml of water, and evaporated again. The resulting syrup was separated by ion-exchange resins into neutral and acidic (eluted with 4 *M* HOAc) fractions.

The latter was concentrated (300 mg) and chromatography in solvent A showed four components: (*a*) D-glucuronic acid, (*b*) aldobiouronic acid ($R_{glucose}$ 0.43), (*c*) aldotriouronic acid ($R_{glucose}$ 0.13), and (*d*) aldotetrauronic acid ($R_{glucose}$ 0.04). The syrup was separated by preparative paper chromatography on Whatman 3 MM paper in solvent C for 80 h. Yields: (*a*) aldobiouronic

Can. J. Chem. Downloaded from www.nrcresearchpress.com by 210.87.254.42 on 09/05/12
For personal use only.

acid, 130 mg; (*b*) aldotriouronic acid 50 mg; (*c*) aldotetrauronic acid 25 mg.

Structural Analysis of Aldobiouronic Acid

(a) Anomeric Linkage

A sample of aldobiouronic acid (25 mg) was dissolved in water (1 ml) and reduced with sodium borohydride (25 mg) for 8 h. After work-up and removal of borate, the syrup was dissolved in D_2O (2 ml) and freeze-dried. P.m.r. of this product (in D_2O) showed a doublet at τ 4.85, $J \sim 3.5$ Hz, indicating an α-linkage in the disaccharide.

(b) Reducing End

A portion of the above reduced aldobiouronic acid was hydrolyzed with trifluoroacetic acid (2 *M*) at 100° for 1 h. Uronic acids were removed with anion exchange resin and the neutral fraction was concentrated and acetylated. G.l.c. (column a) gave mannitol hexaacetate m.p. 122°.

(c) Carboxyl Reduction and Hydrolysis of the Disaccharide

Aldobiouronic acid (20 mg) was dissolved in anhydrous methanol (15 ml) containing 1% hydrogen chloride and the solution was left 12 h at room temperature. The solution was neutralized (Ag_2CO_3), centrifuged, and evaporated. The resulting syrup was dissolved in the minimum amount of water, followed by the addition of methanol and the solution was added dropwise over 1 h to a stirred solution of sodium borohydride (25 mg) in a mixture of water (0.5 ml) and methanol (2 ml). The solution was left 12 h at room temperature and was then carefully neutralized and stirred with Amberlite IR-120 (H^+) resin until the solution was free of Na^+. A portion of the syrup, after removal of borate, was hydrolyzed with trifluoroacetic acid (2 *M*) at 100° for 1 h and was shown (solvent A) to give D-glucose and D-mannose.

(d) Methylation

Aldobiouronic acid (12 mg) was methylated according to the procedure of Hakomori and was hydrolyzed (HCl, 3.5 *N*) to give 2,4,6-tri-*O*-methyl-D-mannose (R_f 0.55, solvent D) and 2,3,4-tri-*O*-methyl-D-glucuronic acid (R_f 0.22, solvent E). The former compound was also confirmed by g.l.c.–m.s. of the alditol acetate.

Structure of Aldotriouronic Acid

(a) Anomeric Linkage

A sample of aldotriouronic acid (20 mg) was reduced and dissolved in D_2O. The signals at τ 4.7, $J = 3.5$ Hz (from D-glucuronic acid) and τ 5.0, $J = 1.5$ Hz indicate α-linkages (Table 1).

(b) Reducing End

Hydrolysis of the reduced aldotriouronic acid showed D-mannitol (paper, solvent B and g.l.c.) and the same aldobiouronic acid (paper, solvents A and C).

(c) Methylation

The methyl ester methylglycoside (10 mg) was methylated and on hydrolysis showed (solvent D) two overlapping spots corresponding to 3,4,6- and 2,4,6-tri-*O*-methyl-D-mannose (R_f 0.58 and 0.55, respectively). G.l.c. of the trimethylsilyl derivatives on column a at 135° and on column b at 120° confirmed these assignments and showed them to be present in approximately equimolecular amounts.

Structure of Aldotetrauronic Acid

(a) Anomeric Linkage

A portion of the aldotetrauronic acid (15 mg) was reduced as for the aldobiouronic acid. The p.m.r. spectrum in D_2O showed the following signals: τ 4.70, $J = 3.5$ Hz and τ 4.73, $J = 3.0$ Hz (2H); τ 4.95, $J = 1.5$ Hz (1H).

(b) Reducing End

A portion of the reduced aldotetrauronic acid was hydrolyzed and paper chromatography (solvent B) showed D-glucitol, confirmed by g.l.c. of the alditol acetate. Also produced were the same aldobi- and aldotriouronic acids (solvent C) described above.

Methylation

Dry polysaccharide (1.7 g) was dissolved in anhydrous methyl sulfoxide (300 ml) under nitrogen (8, 9). To this solution methyl sulfoxide anion (26 ml, 2 *M*) was added and the mixture was stirred for 9 h under nitrogen. Methyl iodide (15 ml) was added at such a rate to keep the temperature below 20° and the resulting clear solution was stirred for 10 h. The solution was dialyzed against running water for 2 days and concentrated to a syrup which was methylated eight times with Purdie's reagents to give a product showing no absorption at 3600 cm^{-1}, $[\alpha]_D^{20}$ +64.5° (*c* 1.2, chloroform), OMe, 43.2%. Purification on a silica gel column using chloroform–methanol (95:5) raised the methoxyl content to 44.3%.

Methylated polysaccharide (60 mg) was dissolved in trifluoroacetic acid (2 *M*) and the solution was refluxed for 5 h. Separation on ion-exchange resins gave a neutral fraction which showed on paper chromatography (solvent D) three major components corresponding to 2,3,4,6-tetra- and 3,4,6-tri-*O*-methyl-D-mannose, 2,4,6-tri-*O*-methyl-D-glucose (R_f values 0.80, 0.58, and 0.50) and a minor component 2,4,6-tri-*O*-methyl-D-mannose (R_f 0.55). A portion (10 mg) of the neutral fraction was reduced, acetylated, and examined on column a programmed from 170–194° at 2°/min. Two peaks in the ratio of 1:1.8 were observed at 25.1 and 36.6 min. The faster component was tentatively identified by its retention time and mass spectrum as 2,3,4,6-tetra-*O*-methyl-D-mannose. The mass spectrum of the slower material showed it to be a mixture of 2,4,6- and 3,4,6-trimethylhexoses which also did not resolve on column b. On a column of OS-138 15% on Gas Chrom Q, operated isothermally at 240°, the slower moving fraction was shown to contain one minor and two major components. The minor component crystallized, m.p. 63–66° (3), and was further identified as 2,4,6-tri-*O*-methyl-D-mannitol triacetate by mass spectrometry; the main peaks were not sufficiently well resolved to permit identification.

Resolution of the trimethylhexose fraction was obtained when the trimethylsilyl derivatives of the neutral sugars were run on columns a, b, and c (samples injected in hexane, see Table 2).

When a portion (40 mg) of the neutral methylated sugars was acetylated (pyridine – acetic anhydride 1:1, 100°, 15 min), extracted with chloroform, and injected onto column a at 170° the following peaks were obtained: A (5.8 min); B_1 (8.8), B_2 (10.5); C_1 (16.2), C_2 (17.6). The component B_2 was present in only small amount and this, together with a minor component with a retention time of 7.5 min, was not examined further. Individual fractions

Can. J. Chem. Downloaded from www.nrcresearchpress.com by 210.87.254.42 on 09/05/12
For personal use only.

were deacetylated (NaOMe, 1 *N* in MeOH, 25°, 30 min), deionized, and examined on paper in solvent D. Components A, B_1, C_1, and C_2 had R_f values of 0.79, 0.57, 0.49, and 0.49. Samples of the individual fractions were also reduced with sodium borohydride, acetylated, and examined on column b at 175°. Components A′, B_1′, C_1′, and C_2′ were eluted at 7.8, 14.6, 15.8, and 15.8 min, each was examined by mass spectrometry and each was demethylated and the product acetylated. D-Mannitol hexaacetate m.p. 120–122° was obtained from A′ and B_1′ while C_1′ and C_2′ yielded D-glucitol hexaacetate m.p. 96–97°.

Reduced Methylated Polysaccharide

Part (100 mg) of the fully methylated polysaccharide was reduced overnight with lithium borohydride in tetrahydrofuran and the product was hydrolyzed by refluxing for 2 h with trifluoroacetic acid (2 *M*). Paper chromatography in solvent D revealed the presence of an extra sugar having the mobility (R_f 0.08) of a monomethylhexose which was shown in solvent E to have the same characteristics as 3- or 4-*O*-methyl-D-glucose. A portion (30 mg) of the hydrolyzate was reduced with sodium borodeuteride, acetylated, and separated on column b. Mass spectrometry of the component having a retention time of 38 min showed it to be a 3-*O*-methylhexitol and the c.d. spectrum was identical with that from 3-*O*-methyl-D-glucitol pentaacetate ($\Delta\varepsilon_{213}^{MeCN} - 0.29$).

Methylated Degraded Polysaccharide

Capsular polysaccharide (1 g) was hydrolyzed overnight at 95° with trifluoroacetic acid (0.4 *M*) using the apparatus of Galanos and co-workers (18). The recovered polysaccharide (200 mg) was methylated, reduced ($LiBH_4$) and hydrolyzed (TFA, 2 *M*). Paper chromatography showed the presence of a new sugar having the mobility of 3,4-di-*O*-methyl-D-glucose (R_f 0.26, solvent D; 0.51, solvent E). This was confirmed by the mass spectrum of the dimethyl fraction, separated as alditol acetates on column a, and by conversion of this fraction to D-glucitol hexaacetate m.p. 98°. The c.d. curve of 3,4-di-*O*-methyl-D-glucitol tetraacetate is weakly negative.

Smith Degradation

Capsular polysaccharide was deacetylated with aqueous sodium hydroxide, dialyzed, and lyophilized. The product (130 mg) was dissolved in sodium metaperiodate (20 ml, 0.05 *M*) and after 3 days in the dark at 4° 0.66 mol of periodate had been consumed per sugar unit. Following the addition of ethylene glycol, dialysis, reduction with sodium borohydride, dialysis, deionization, lyophilization and removal of borate the product was hydrolyzed (TFA, 0.5 *M*) at room temperature for 8 h. Paper chromatography in solvent A showed mainly glycerol and an oligosaccharide with traces of glucose. A part of the hydrolyzate was acetylated and gave a peak corresponding to glycerol triacetate (4 min) on column b at 150°. The majority of the hydrolyzate was reduced ($NaBH_4$) and paper chromatography (solvent A) showed one component having $R_{galactose}$ 0.37 and glycerol.

The mixture containing the oligosaccharide was methylated (8, 9), reduced and hydrolyzed to give (solvent D) components equivalent to 2,3,4,6-tetra- and 3,4-di-*O*-methyl-D-glucose (R_f 0.80, 0.28) and 2,4,6-tri-*O*-methyl-D-mannose (R_f 0.56). This result was confirmed by g.l.c.–m.s. of the alditol acetates (column a, 160-200° at 2°/min) which had retention times of 14.5, 30, and 21 min, respectively.

Attempted Location of O-Acetyl Group

Capsular polysaccharide (80 mg) was dissolved in methyl sulfoxide (20 ml) and anhydrous *p*-toluene sulfonic acid (*ca.* 20 mg) was added. Methyl vinyl ether was passed into the solution until it turned yellow and the reaction was left overnight. Excess methyl vinyl ether was removed on a rotary evaporator and methyl sulfoxide anion was added directly without isolation of the polysaccharide. The solution was shaken for 20 h, methyl iodide (5 ml) was added and the shaking continued for 3 h. The solution was dialyzed against running water, polymeric material formed from methyl vinyl ether was extracted with chloroform, and the aqueous portion was lyophilyzed. Hydrolysis (TFA, 2 *M*, 100°) showed (solvent E) a major spot for monosaccharides together with a faint spot moving faster than all monomethylglucose derivatives (R_f 0.35). G.l.c. of the alditol acetates gave two small peaks at 21 and 23 min (column b, 190°) in addition to hexitol acetates.

We are indebted to Dr. I. Ørskov, Copenhagen, for the gift of an authentic culture of *Klebsiella* K24 (1680/49), to Dr. P. J. Salisbury of this Department for growing the bacteria, to Dr. J. J. R. Campbell and Dr. J. B. Hudson of the Department of Microbiology, University of British Columbia, for the use of their centrifuges, and to Dr. C. T. Bishop for an authentic sample of 3,4,6-tri-*O*-methyl-D-mannose.

The financial support of the National Research Council of Canada and the award of a Killam Fellowship to Y.M.C. are gratefully acknowledged.

1. W. NIMMICH. Z. Med. Mikrobiol. Immunol. **154**, 117 (1968).
2. W. NIMMICH. Acta biol. med. germ. **26**, 397 (1971).
3. Y. M. CHOY and G. G. S. DUTTON. Can. J. Chem. **51**, 198 (1973).
4. Y. M. CHOY, G. G. S. DUTTON, A. M. STEPHEN, and M. T. YANG. Anal. Lett. **5**, 675 (1972).
5. G. M. BEBAULT, Y. M. CHOY, G. G. S. DUTTON, N. FUNNELL, A. M. STEPHEN, and M. T. YANG. J. Bacteriol. **113**, 1345 (1973).
6. M. ABDEL-AKER and F. SMITH. J. Am. Chem. Soc. **73**, 5859 (1951).
7. G. M. BEBAULT, J. M. BERRY, Y. M. CHOY, G. G. S. DUTTON, N. FUNNELL, L. D. HAYWARD and A. M. STEPHEN. Can. J. Chem. **51**, 324 (1973).
8. S. HAKOMORI. J. Biochem. (Tokyo), **55**, 205 (1964).
9. P. A. SANDFORD and H. E. CONRAD. Biochem. **5**, 1508 (1966).
10. C. C. SWEELEY, R. BENTLEY, M. MAKITA, and W. W. WELLS. J. Am. Chem. Soc. **85**, 2497 (1963).
11. G. M. BEBAULT, G. G. S. DUTTON, and R. H. WALKER. Carbohydr. Res. **23**, 430 (1972).
12. H. BJÖRNDAL, C. G. HELLERQVIST, B. LINDBERG, and S. SVENSSON. Angew. Chem. Int. Ed. **9**, 610 (1970).

13. I. J. GOLDSTEIN, G. W. HAY, B. A. LEWIS, and F. SMITH. Meth. Carbohydr. Chem. **5**, 361 (1965).
14. A. N. DE BELDER and B. NORRMAN. Carbohydr. Res. **8**, 1 (1968).
15. C. G. HELLERQVIST, B. LINDBERG, K. SAMUELSON, and R. R. BRUBAKER. Acta Chem. Scand. **26**, 1389 (1972).
16. G. G. S. DUTTON and M. T. YANG. Can. J. Chem. This issue.
17. J. H. SLONEKER and A. JEANES. Can. J. Chem. **40**, 2066 (1962).
18. C. GALANOS, O. LÜDERITZ, and K. HIMMELSPACH. Eur. J. Biochem. **8**, 332 (1969).

Can. J. Chem. Downloaded from www.nrcresearchpress.com by 210.87.254.42 on 09/05/12
For personal use only.

The Structure of the Capsular Polysaccharide of *Klebsiella* K-type 5

GUY G. S. DUTTON AND MO-TAI YANG

Department of Chemistry, The University of British Columbia, Vancouver, British Columbia

Received December 18, 1972

Methylation, periodate oxidation and partial hydrolysis studies on the capsular polysaccharide, and on the carboxyl reduced polymer of *Klebsiella* K5 show the structure to consist of a repeating unit:

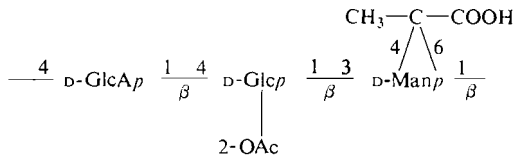

The polysaccharide has a molecular weight (by gel filtration) of 9×10^5 and is the first *Klebsiella* capsule to be found lacking a carbohydrate side chain. The proportion of *O*-acetyl and pyruvate groups was determined by p.m.r. spectroscopy.

Les méthodes de méthylation, oxydation periodique, et hydrolyse partielle portées au polysaccharide capsulaire, et au polymère avec le groupe carboxyle réduit, de *Klebsiella* K5 ont démontré que la structure se compose d'une unité qui se répète.

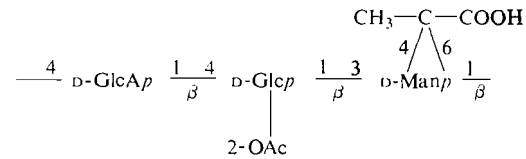

Le polyoside possède un poids moléculaire (par chromatographie sur gel) de 9×10^5 et cette capsule de *Klebsiella* est la première d'être trouvée sans une chaîne latérale de sucre. Le rapport entre les groupes *O*-acétyles, pyruviques et sucres a été dosé par spectroscopie r.m.n.

Can. J. Chem., **51**, 1826 (1973)

Bacteria of the genus *Klebsiella* elaborate a capsular polysaccharide which is antigenic. Approximately 80 different serotypes are recognized and Nimmich (1, 2) has provided qualitative analyses of these capsular materials. In continuation of our studies (3, 4) on the structure of these polysaccharides we now report on the capsule from *Klebsiella* K-type 5. This polysaccharide differs from those previously described in this genus by lacking any carbohydrate side chain. The polysaccharide is also unusual in affording the first example of a 4,6-*O*-(1-carboxyethylidene)-D-mannose unit in a natural product. This aspect of the structure has been discussed briefly (5).

The crude polysaccharide from *Klebsiella* K5 (E5051) was extremely viscous and it was convenient to purify the material by centrifugation and precipitation with Cetavlon only in small batches. Purified material migrated as a single band on electrophoresis on cellulose acetate and had $[\alpha]_D$ −45.2°, an equivalent weight of 233, and a molecular weight, by gel filtration, of 9×10^5. Acid hydrolysis of the polysaccharide gave D-glucose, D-mannose, D-glucurone, and acidic components. The first two compounds were identified as their crystalline alditol hexaacetates and found to be present in the ratio of 3:5. When a portion of the hydrolyzate was saponified to hydrolyze any lactone, reduced, rehydrolyzed, and processed to avoid contamination of the neutral sugars by lactones, D-glucose and D-mannose were found in the ratio of 1:1. In the case of a sample of the polysaccharide which was methanolyzed, the uronic ester was reduced and the product was hydrolyzed to give D-glucose and D-mannose in the ratio of 2:1.

The glucose and mannose were shown to be of D-configuration by the circular dichroism (c.d.) curve of the alditol acetates; D-glucuronic acid was similarly authenticated by the c.d. of glucurone and of 2,3-di-*O*-methylglucitol acetate

Can. J. Chem. Downloaded from www.nrcresearchpress.com by 210.87.254.6 on 09/05/12
For personal use only.

Can. J. Chem. Downloaded from www.nrcresearchpress.com by 210.87.254.6 on 09/05/12
For personal use only.

obtained in the methylation study (6). The presence of pyruvic acid in the acid hydrolyzates was demonstrated by paper chromatography (7) and by preparation of the 2,4-dinitrophenylhydrazone (8). When the polysaccharide was subjected to methanolysis both acetate and pyruvate were detected on paper by the ferric chloride–hydroxamic ester test (9). The presence of these two groups was clearly demonstrated by the p.m.r. spectrum of the polysaccharide (10, 11) run in D_2O at 90°. The chemical shift of the anomeric protons indicated three sugars each β-linked in the repeat unit (3) and the integrals showed one acetyl and one pyruvic acid group per repeat unit.

The p.m.r. spectrum of the fully methylated polysaccharide showed the absence of acetate but confirmed the presence of pyruvate in the ratio of one per three sugars. The neutral crystalline sugars obtained on hydrolysis were identified as 2,3,6-tri-*O*-methyl-D-glucose (12) and 2-*O*-methyl-D-mannose (13) and were present in approximately equal amounts. The acidic component on reduction and hydrolysis gave 2,3-di- and 2,3,6-tri-*O*-methyl-D-glucose. These results were confirmed by reduction of the methylated polysaccharide before hydrolysis.

Autohydrolysis of the original capsular polysaccharide removed the pyruvic acid ketal and methylation of the recovered polymeric material followed by hydrolysis gave 2,4,6-tri-*O*-methyl-D-mannose in place of the 2-methyl ether thus demonstrating the linkage of pyruvic acid to positions 4 and 6 of mannose.

Partial hydrolysis of the original polysaccharide yielded a neutral oligosaccharide (N_3) and a series of acidic oligosaccharides (A_{1-6}). The compound N_3 crystallized and was identified as 3-*O*-(β-D-glucopyranosyl)-D-mannose by hydrolysis of the corresponding alditol and by methylation. The compound A_1 was found by titration to be an aldobiouronic acid and was shown to be cellobiouronic acid. Compound A_2 analyzed as an aldotriouronic acid which was characterized as 3-*O*-(β-D-cellobiosyluronic acid)-D-mannose. The higher acidic oligosaccharides were not examined but were assumed to be aldotetra-, penta-, and hexauronic acids.

Periodate oxidation of the original capsular polysaccharide resulted in the consumption of 0.35 mol of periodate per sugar residue and the derived polyalcohol gave D-glucose on hydrolysis. Oxidation of de-*O*-acetylated capsular polysaccharide resulted in the initial uptake of 0.35 mol of periodate per sugar residue but when the polyaldehyde was reduced and the product was again treated with periodate further reaction took place to give a total consumption of 0.65 mol of periodate per sugar residue. Oxidation of carboxyl-reduced and de-*O*-acetylated polysaccharide consumed 0.60 mol of periodate per sugar unit. Hydrolysis of the last two polyalcohols failed to reveal the presence of D-glucose. The results are readily interpreted in the light of work by Painter and colleagues (14, 15). These authors have shown that in polysaccharides containing 1,4-linkages inter-residue hemiacetal linkages may be formed readily. Such linkages inhibit the consumption of the theoretical amount of periodate until they are destroyed by reduction. In all oxidized polysaccharides an equilibrium exists between the acyclic aldehyde and the cyclic hemiacetal (14). In the present example the presence of the uronic acid appears to favor the cyclic structure whereas in the reduced polysaccharide oxidation is not inhibited. Sloneker and co-workers (16) have also commented on similar anomalous oxidations.

The polyaldehyde arising from the complete oxidation of de-*O*-acetylated polysaccharide was reduced and hydrolyzed. Paper chromatography in solvent *A* indicated the presence of components having the mobilities of D-mannose, erythritol, D-erythronolactone, and pyruvic acid. The material having the mobility of erythritol was eluted (fraction 3) and appeared homogeneous in solvent *A*. However, when this fraction was chromatographed in solvent *B* prior to development in solvent *A* two components were detected one of which moved slower than erythritol and gave a positive response for lactone (9) while the other appeared to be erythritol. Hydrolysis of fraction 3 gave D-mannose, erythritol, L-erythronolactone, and pyruvic acid. These results indicate that this fraction contains 3-*O*-[4,6-*O*-(1-carboxyethylidene)-D-mannopyranosyl]-L-erythronolactone which, coincidentally, has the same mobility as erythritol in solvent *A*. The formation of this lactone is to be expected on periodate oxidation of a polysaccharide having the structure proposed below.

The results of methylation, partial hydrolysis, and periodate oxidation are consistent with the proposed repeating unit and the only feature not yet accounted for is the position of the *O*-acetyl group. This was located using the methyl vinyl

ether method of de Belder and Norrman (17). Methylation and hydrolysis of the substituted polysaccharide showed on paper chromatography a small spot corresponding to monomethyl hexose in addition to a large quantity of D-glucose and D-mannose. G.l.c. of the hydrolyzate in the form of alditol acetates gave a monomethyl fraction which crystallized and which was identified as 2-*O*-methyl-D-glucitol pentaacetate by mixed m.p. with an authentic sample (6). Low yields of methylated sugars have been obtained using this method on other capsular polysaccharides (4) presumably on account of their high molecular weight.

The structure of the capsular polysaccharide of *Klebsiella* K5 may therefore be represented by the repeat unit:

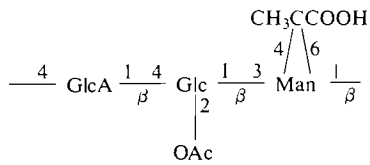

The characteristic p.m.r. signal at about τ 8.5 of the CH_3—C of the pyruvate ketal and its derivatives persists with only slight change in chemical shift through the typical transformations of methylation, carboxyl reduction, and periodate oxidation and is thus a convenient means of checking that no inadvertent loss of this group occurs at any stage during the structural investigation of the polysaccharide.

The presence of a cellobiouronic acid residue in the structure of K5 polysaccharide suggests that there should be a cross reaction with pneumococcal III and VIII antisera (18) and such reactions have been found (19). The reaction is stronger with anti-III than with anti-VIII consistent with the cellobiouronic acid being linked to position three of the next residue in *Pneumococcus* type III rather than to position four as in *Pneumococcus* type VIII (18).

Experimental

General Methods

These were as previously described (3) except as noted. The columns used for g.l.c. were (*a*) 3% ECNSS-M on Gas Chrom Q (4 ft × 3/16 in.), (*b*) 5% butanediol succinate on Diatoport S (4 ft × 1/4 in.), (*c*) 20% SF-96 on Diatoport S (8 ft × 1/4 in.). An additional solvent for paper chromatography was (*F*) phenol–water (4:1). Melting points were recorded on a Fisher–Johns apparatus and are uncorrected. I.r. spectra were recorded on a Perkin–Elmer model 457 spectrophotometer.

Preparation and Properties of K5 Capsular Polysaccharide

A culture of *Klebsiella* K5 (E5051) was obtained from Dr. I. Ørskov, Copenhagen, and grown on 3% sucrose – yeast-extract agar (30 g sucrose, 2 g Bacto yeast-extract, 15 g agar, 1 l H_2O, 2 g NaCl, 1 g KH_2PO_4, 0.25 g $MgSO_4 \cdot 7H_2O$, and 0.5 g $CaSO_4$) at room temperature for 3–4 days. The growth was scraped off the plates to give 600 ml of slime from 1 l of agar medium. The slime was worked-up in portions in the following manner: each 50 ml portion of the slime was diluted six-fold with water containing 1% phenol, then centrifuged at 65 000 × gravity for 1 h to obtain a clear, slightly yellow solution which was freeze-dried for storage or to which was added 45 ml of 3% hexadecyltrimethylammonium bromide (Cetavlon). The acidic polysaccharide which precipitated was dissolved in sodium chloride (35 ml, 2 *N*) and precipitated with five volumes of ethanol. The precipitate, collected by centrifugation, was dissolved in water, treated with Amberlite resin IR-120 (H^+), dialyzed against distilled water for 24 h, then freeze-dried to give 0.65 g of capsular polysaccharide per 50 ml of slime. This material had $[\alpha]_D$ −45.2° (*c* 0.44, water), an equivalent weight of 233, a molecular weight of 9×10^5, and migrated 3.8 cm on electrophoresis for 30 min at p*H* 8.8 and 300 V. Ash content nil; nitrogen nil.

The supernatant from the precipitation of the acidic polysaccharide with hexadecyltrimethylammonium bromide was dialyzed against tap water for 48 h and freeze-dried, yield 0.1 g. This material was not further examined.

To a portion of the Cetavlon purified acidic polysaccharide (0.89 g) in water (50 ml) was added sodium hydroxide (50 ml, 2 *N*) and the solution was allowed to stand at room temperature for 24 h. The alkaline solution was dialyzed against tap water for 24 h, passed through Amberlite resin IR-120 (H^+), dialyzed against distilled water, and freeze-dried, to give deacetylated polysaccharide (0.8 g).

Total Hydrolysis of the Acidic Polysaccharide

The polysaccharide was heated in sulfuric acid (1 *N*) at 98° for 8 h (or with trifluoroacetic acid, 2 *N*, 98°, 10 h). The cooled solution was neutralized ($BaCO_3$), centrifuged, and decationized. Paper chromatography using solvent *B* (8 h), then solvent *A* (10 h) revealed two major spots for D-mannose and D-glucose, along with a small fast moving spot with the same mobility as D-glucuronolactone and two small slow moving spots corresponding to D-glucuronic acid and an aldobiouronic acid.

Acidic components were removed by passage through a column of Duolite A-4 (OH^-) anion exchange resin and the filtrate was concentrated and reduced with sodium borohydride. Borate was removed by passage through Amberlite IR-120 (H^+) and distillation with methanol.

The alditols were dissolved in a 1:1 mixture of acetic anhydride and pyridine and heated at 100° for 20 min. The acetylation reagents were evaporated with the addition of several portions of ethanol. The alditol acetates, injected in chloroform onto column *a* programmed from 185–210° at 1°/min, with a helium flow rate of 60 ml/min, gave peaks identical to authentic standards of the hexaacetates of D-mannitol (20 min) and D-glucitol (24 min) in a ratio of 5:3. Samples were collected and the m.p. and mixed m.p. of D-mannitol hexaacetate was 121–123°, and that of D-glucitol hexaacetate was 93–95°. The c.d. curves of both hexaacetates were positive (6).

Can. J. Chem. Downloaded from www.nrcresearchpress.com by 210.87.254.6 on 09/05/12
For personal use only.

Can. J. Chem. Downloaded from www.nrcresearchpress.com by 210.87.254.6 on 09/05/12
For personal use only.

The glucuronic acid from several hydrolyzates was separated on paper and evaporated with the addition of hydrochloric acid. The c.d. curves of authentic D-glucurone and the isolated material were both positive.

In a second experiment the hydrolyzate was processed to obtain complete hydrolysis of the aldobiouronic acid and to avoid contamination of the neutral sugars by D-glucurone. The hydrolyzate was treated with sodium hydroxide (0.5 *N*) then with sodium borohydride. The reaction mixture was allowed to stand at room temperature for 1 h then hydrochloric acid was added to a concentration of 2 *N* and the solution was heated at 100° for 4 h. The hydrolyzate was evaporated to dryness, distilled three times with methanol, made alkaline with sodium hydroxide (0.5 *N*), and reduced with sodium borohydride. The solution was passed successively through columns of Amberlite IR-120 (H^+) and Duolite A-4 (OH^-) to remove the sodium ion and the L-gulonic acid. The neutral effluent was evaporated to dryness, acidified with acetic acid, and distilled with methanol. The ratio of D-mannitol to D-glucitol as hexaacetates was found to be 1:1.

K5 polysaccharide (10 mg) was heated in a sealed test tube with methanolic hydrogen chloride (4%, 1 ml) for 10 h. After neutralization with silver carbonate and centrifugation, the clear supernatant was treated with sodium borohydride (10 mg) for 24 h. Borate was removed and the residue was hydrolyzed with trifluoroacetic acid (2 *N*) at 100° for 8 h. Analysis gave the ratio of D-mannitol hexaacetate (m.p. and mixed m.p. 120–122°) to D-glucitol hexaacetate (m.p. and mixed m.p. 93–95°) as 1:2.

Characterization of Pyruvic and Acetic Acids

Polysaccharide (30 mg) was hydrolyzed with hydrochloric acid (2 ml, 1 *N*) and paper chromatography (solvent *A*) showed a spot with the mobility of pyruvic acid (R_f 0.7) and having the characteristic fluorescence under u.v. (7). The hydrolyzate was extracted with ether (3 × 15 ml), the extract was neutralized with sodium hydroxide and evaporated to dryness. The 2,4-dinitrophenylhydrazone prepared from the residue had the same mobility (R_f 0.41) on t.l.c. (toluene – acetic acid – water, 4:3:1) as that from authentic pyruvic acid.

Polysaccharide (20 mg) was refluxed for 2 h with methanolic hydrogen chloride (1 ml, 4%), the solution was neutralized (Ag_2CO_3), concentrated, and treated with methanolic hydroxylamine hydrochloride (1.5 ml, 1 *N*) and methanolic sodium hydroxide (1.5 ml, 1 *N*). After centrifugation the supernatant was concentrated to 25% of the volume and examined by paper chromatography in 1-butanol – acetic acid – water (4:1:5). The chromatogram was sprayed with 1% ferric chloride and showed the presence of acetic acid (R_f 0.56), pyruvic acid (0.61 and 0.74), and D-glucurone (0.16 and 0.22) by comparison with standards (acetate from D-glucose pentaacetate).

Proton Magnetic Resonance Spectra of Original and De-O-acetylated Polysaccharides

Capsular polysaccharide (*ca.* 20 mg) was dissolved in D_2O and freeze-dried. After two further treatments, the 100 MHz spectrum (10, 11) was run at 90° and showed sharp singlets at τ 8.50 (pyruvate) and 7.93 (acetate) together with signals at τ 5.15 (1H) and 5.50 (2H). The spectrum of deacetylated material was similar with the absence of the peak at τ 7.93.

Methylation of Original Capsular Polysaccharide

Vacuum-dried polysaccharide (400 mg) was methylated by the method of Hakomori and the product was dialyzed against running water for 24 h. Extraction with chloroform (2 × 30 ml) gave 100 mg of material showing no hydroxyl absorption in the i.r. The aqueous layer was lyophilized and subjected to three methylations with Purdie's reagents to give a fully methylated product which was combined with the chloroform extract. The p.m.r. spectrum ($CDCl_3$) showed τ 8.5 (3H), 6–7 (40 H, calcd. 43H), and 5.44 and 5.55 (3H).

Methylated polysaccharide (300 mg) was dissolved in sulfuric acid (3 ml, 72%) and after 2 h at 0° the solution was diluted with water (24 ml) and refluxed for 4 h. Neutralization ($BaCO_3$) and separation on ion exchange resins gave an acidic fraction (60 mg, eluted with 10% formic acid) and neutral sugars (178 mg). The latter showed two components, one (R_f 0.55, solvent D) corresponding to a trimethylhexose and a second (R_f 0.07) equivalent to a monomethyl hexose. Elution of the paper yielded 2,3,6-tri-*O*-methyl-D-glucose (58 mg), m.p. and mixed m.p. 117–119° (from ethyl ether (12)), and 2-*O*-methyl-D-mannose (40 mg), m.p. and mixed m.p. 138–140° (from ethanol (13)). Examination of a portion of the neutral sugars as alditol acetates on column *a* at 180° gave a peak at 6.4 min corresponding to that obtained from authentic 2,3,6-tri-*O*-methyl-D-glucose and a second peak at 18 min. The two peaks were in the ratio of 1:1.2 and the mass spectra of the two compounds were consistent with 2,3,6-tri- and 2-*O*-methyl hexitol acetates. C.d. for 2,3,6-tri-*O*-methyl-D-glucitol acetate $\Delta\varepsilon_{213}^{CH_3CN}$ +0.3 and for 2-*O*-methyl-D-mannitol acetate +0.42.

A portion (5 mg) of the acidic fraction was methanolyzed and examined on column *b* at 170° and gave peaks corresponding to methyl 2,3,6-tri-*O*-methyl-D-glucopyranoside (4.4 min (m), 6.0 min (s)) and methyl 2,3-di-*O*-methyl-D-glucuronic acid methyl ester (11.5 min (m) and 13.5 min (s)).

A second portion (5 mg) was methanolyzed, reduced, and hydrolyzed to show on paper (solvent *D*) components corresponding to 2,3,6-tri-*O*-methyl-D-glucose (R_f 0.56) and 2,3-di-*O*-methyl-D-glucose (0.28). This was confirmed by g.l.c. of the alditol acetates on column *a* at 200° to give two components eluting at 6.1 and 11.9 min and by their mass spectra. The c.d. curves of the isolated 2,3-di-*O*-methyl-D-glucitol tetraacetate and that of a standard (20) were positive ($\Delta\varepsilon_{213}^{CH_3CN}$ +0.1 and +0.08, respectively).

Reduced Methylated Polysaccharide

Fully methylated polysaccharide (170 mg) in tetrahydrofuran (20 ml) was reduced with lithium aluminum hydride (300 mg) in tetrahydrofuran (30 ml) for 18 h. The reduced product (130 mg) showed ($CDCl_3$) a sharp peak at τ 8.6 (CH_3 of hydroxyisopropylidene) and the absence of two peaks in the range τ 6.2–6.4 assumed due to methyl esters.

A part (56 mg) of the reduced product was hydrolyzed (TFA, 6 ml, 2 *N*) and on paper chromatography (solvent *D*) showed three components with R_f values of 0.10, 0.30, and 0.58. The majority of the hydrolyzate (36 mg) was separated on paper to yield 2-*O*-methyl-D-mannose (6 mg), m.p. and mixed m.p. 137–139° (ethanol), and 2,3,6-tri-*O*-methyl-D-glucose (10 mg), m.p. and mixed m.p. 113–115° (ether). The fraction (10 mg) with R_f 0.30 was indis-

Can. J. Chem. Downloaded from www.nrcresearchpress.com by 210.87.254.6 on 09/05/12
For personal use only.

tinguishable from 2,3-di-*O*-methyl-D-glucose but could not be obtained crystalline. The rest of the hydrolyzate (10 mg) was reduced, acetylated, and examined on column *a* programmed from 160–190° at 2°/min. Three peaks were obtained at 16.0, 22.4, and 26.1 min corresponding to 2,3,6-tri-, 2,3-di-*O*-methyl-D-glucose, and 2-*O*-methyl-D-mannose, each of which was present in equivalent amounts.

Methylation of Polysaccharide Recovered from Autohydrolysis

Capsular polysaccharide (0.5 g) dissolved in water (60 ml, initial p*H* 2.5) was heated on a steam bath for 20 h. The solution was dialyzed and the polysaccharide (0.25 g) was recovered by freeze drying. This sample did not show a p.m.r. signal at τ 8.5. Degraded polysaccharide (200 mg) was methylated and the product (170 mg) was subjected to two treatments with Purdie's reagents. A portion (30 mg) was hydrolyzed (TFA, 8 ml, 2 *N*) and the neutral sugars showed (solvent *D*) a major spot (R_f 0.55) corresponding to trimethylhexoses and a faint spot at R_f 0.78. The sugar having R_f 0.10 was absent. The hydrolyzate was reduced, acetylated, and examined on column *a* programmed from 170–200° at 2°/min. A minor peak at 9.3 min (2,3,4,6-tetra-*O*-methyl-D-glucose) was followed by two strong peaks at 16.1 and 18.8 min corresponding to 2,4,6-tri-*O*-methyl-D-mannose and 2,3,6-tri-*O*-methyl-D-glucose. The 1,3,5-tri-*O*-acetyl-2,4,6-tri-*O*-methyl-D-mannitol was recrystallized from petroleum ether (30–60°) and had m.p. and mixed m.p. 64–66° (21).

Partial Hydrolysis of Capsular Polysaccharide

Acidic polysaccharide (3.5 g) was dissolved in water (300 ml, initial p*H* 2.7), heated on a steam bath for 12 h, and the solution was dialyzed against distilled water (2 × 600 ml). The non-dialyzable material was rehydrolyzed and the dialyzates were combined and concentrated. Only a small amount of product was obtained and chromatography in solvent *A* revealed pyruvic acid (R_f 0.7), D-glucose, D-mannose, and two components having R_{Man} 1.2 and 1.7 with traces of other compounds.

The solution containing the non-dialyzable material was concentrated to 150 ml, heated on the steam bath for 24 h, and dialyzed against distilled water (2 × 500 ml). The process was repeated for a total of 148 h heating with periodic concentration to keep the volume below 300 ml. The dialyzates were combined, concentrated, and passed successively through cation and anion exchange resins. The neutral components were fractionated on paper in solvent *B* to give N_1, N_2, and N_3 and the acidic components (eluted with 10% formic acid) were separated in solvent *C* to give A_1–A_6.

The neutral compounds N_1 and N_2 were chromatographically identical to D-mannose and D-glucose and were not further examined. Compound N_3 crystallized from water and had m.p. 164–166°, $[\alpha]_D$ −7.3° (*c* 2.18, water) which agrees with the value (m.p. 165°) given for 3-*O*-β-D-glucopyranosyl-D-mannose (22). Hydrolysis of N_3 gave D-glucose and D-mannose (solvent *B*) and of reduced N_3 gave D-glucose and D-mannitol (solvent *F*). Methylation of N_3 and examination of the hydrolyzate in solvent *D* showed components equivalent to 2,3,4,6-tetra-*O*-methyl-D-glucose (R_f 0.78) and 2,4,6-tri-*O*-methyl-D-mannose (0.56). The alditol acetates gave, on column *a* at 185°, peaks at 6.5 and 13.1 min in agreement with this assignment. The p.m.r. spectrum of the original N_3 in D_2O showed signals at τ 5.46, ($J_{1,2}$ = 6.0 Hz, 1H), τ 5.16 (0.3H) and 4.81, ($J_{1,2}$ = 1 Hz, 0.7H).

Compound A_1 (58 mg, R_{Glc} 0.23, solvent *A*) had an equivalent weight of 394 and $[\alpha]_D$ +9.1° (*c* 0.8, water) in agreement with the value given (23) for cellobiouronic acid of $[\alpha]_D$ +7° (*c* 2.0, water). Hydrolysis of A_1 gave D-glucose and D-glucuronic acid (solvent *A*). Compound A_1 (6 mg) was dissolved in methanol (1 ml), esterified with diazomethane, reduced with sodium borohydride in methanol, and hydrolyzed. Examination in solvent *F* showed D-glucose and D-glucitol which was confirmed by g.l.c. of the trimethylsilyl derivatives on column *c* programmed from 160–220° at 1°/min (D-glucose 23.3 min (w), 27.6 min (s) and D-glucitol (25.6 min)). Methylation and methanolysis of A_1 showed (column *b*, 150°) peaks characteristic of methyl 2,3,6-tri-*O*-methyl-D-glucopyranosides (10.3 min (w), 13.8 min (s)) and methyl 2,3,4-tri-*O*-methyl-D-glucuronic acid methyl ester (15.2 min (w), 21.2 min (s)). Reduction of the methyl glycosides in methanol followed by hydrolysis and examination in solvent *D* showed components corresponding to 2,3,4- and 2,3,6-tri-*O*-methyl-D-glucose (R_f 0.51 and 0.58 respectively).

Compound A_1 (22 mg) was dissolved in methanol (5 ml) and esterified with diazomethane. The syrupy product was dissolved in acetic anhydride (3.5 ml) containing zinc chloride (0.2 g) and the solution held at 60° for 90 min. The crude product was purified on paper (solvent *D*) and hepta-*O*-acetyl-(β-D-glucopyranosyluronic acid methyl ester)-α-D-glucopyranose recrystallized from ethanol had m.p. 248°, $[\alpha]_D$ +31.5° (*c* 0.1, chloroform), lit. (24) m.p. 252°, $[\alpha]_D$ +44° (*c* 1.2, chloroform). The p.m.r. spectrum of A_1 in D_2O showed τ 5.44, ($J_{1,2}$ = 7.5 Hz, 1H), 5.31, ($J_{1,2}$ = 7.9 Hz) and 4.78, ($J_{1,2}$ = 3.3 Hz, 1H combined).

Compound A_2 had an equivalent weight of 559 and $[\alpha]_D$ −24.2° (*c* 3.1, water). Development of a paper chromatogram of a hydrolyzate for 8 h in solvent *B* followed by 28 h in solvent *A* showed D-mannose, D-glucose, D-glucuronic acid and A_1. When A_2 was reduced and hydrolyzed development in solvent *F* showed (ether wash before dipping) cellobiouronic acid (R_{Glc} 0.34), D-glucuronic acid (0.45), D-glucose, and D-mannitol (1.2). Methylation of A_2 (8 mg) showed by paper chromatography of the hydrolyzate (solvent *D*) an acidic compound at the origin and one spot at R_f 0.57 since this solvent does not resolve 2,3,6-tri-*O*-methyl-D-glucose and 2,4,6-tri-*O*-methyl-D-mannose. Reduction of the hydrolyzate and separation of the neutral compounds as alditol acetates on column *a* showed the presence of these two components and their mass spectra were consistent with this assignment. The p.m.r. spectrum of A_2 in D_2O showed signals at τ 4.88 ($J_{1,2}$ = 1.7 Hz, 0.6H), 5.23 ($J_{1,2}$ = 1.2 Hz, 0.4H), 5.43 ($J_{1,2}$ = 7.5 Hz, 1H), 5.47 ($J_{1,2}$ = 7.3 Hz, 1H).

Carboxyl Reduction of K5 Polysaccharide

Polysaccharide (0.8 g) was converted in turn to the propionate (0.83 g), methyl ester (0.89 g) and reduced as previously described (25) to give the carboxyl reduced polysaccharide (0.4 g). The p.m.r. spectrum showed a peak at τ 8.60 but the integral suggested that some of the ketal grouping had been lost during reduction. Hydrolysis

Can. J. Chem. Downloaded from www.nrcresearchpress.com by 210.87.254.6 on 09/05/12
For personal use only.

gave D-glucose and D-mannose confirmed by separation of the alditol acetates on column *a* programmed from 180–220° at 1°/min; D-glucitol hexaacetate (37.5 min) m.p. and mixed m.p. 93–95° and D-mannitol hexaacctate (31.4 min) m.p. and mixed m.p. 119–121°, ratio 2:1.

Methylation and hydrolysis of reduced polysaccharide gave, as alditol acetates on column *a* programmed from 160–190° at 2°/min, 2,3,6-tri-*O*-methyl-D-glucose (16 min) and 2-*O*-methyl-D-mannose (26 min) in the ratio 2:1.

Periodate Oxidation

Capsular polysaccharide (0.12 g) was oxidized in the dark at 1° with sodium metaperiodate (40 ml, 0.05 *M*) and the consumption, measured spectrophotometrically, became constant at 0.35 mol of periodate per hexose residue after 288 h. Addition of ethylene glycol, dialysis and reduction with sodium borohydride gave the polyalcohol (92 mg). The p.m.r. spectrum in D_2O showed the presence of one pyruvate group to 18 sugar protons, excluding anomeric (theory 3:20). Total hydrolysis of the polyalcohol showed (solvent *A*) components corresponding to D-mannose, D-glucose, erythritol (R_{Man} 2.0), and D-erythronolactone (R_{Man} 3.3; standard obtained from D-glucose by lead tetraacetate oxidation); pyruvic acid was not sought. The lactone was distinguished by the hydroxylamine – ferric chloride spray (9). Reduction and acetylation of the hydrolyzate gave (column *a* programmed from 170–220° at 1°/min) the peracetates of erythritol (7.6 min), D-mannitol (36.1 min), and D-glucitol (40.9 min) in the ratio of 2:2.7:1. Each fraction crystallized and yielded erythritol tetraacetate, m.p. 81–83°, D-mannitol hexaacetate, m.p. 119–121°, and D-glucitol hexaacetate, m.p. 93–95°, undepressed by authentic samples.

Capsular polysaccharide which had been de-*O*-acetylated (0.665 g) was oxidized at 1° in the dark with sodium metaperiodate (200 ml, 0.05 *M*) with a constant uptake of 0.35 mol of periodate per sugar unit after 288 h. After the addition of ethylene glycol, dialysis, borohydride reduction, deionization and removal of boric acid the polyalcohol was recovered by lyophilization. This material was dissolved in sodium metaperiodate solution (100 ml, 0.05 *M*) and consumed a further 0.3 mol of periodate per sugar residue in 120 h. The polyalcohol (0.45 g) was isolated and a portion was hydrolyzed (HCl, 2 *N*, 4 h) to give (solvent *A*) mannose, erythritol, erythronolactone, and a faint spot for pyruvic acid (R_{Man} 4.6). Examination by g.l.c. as before showed the peracetates of erythritol and D-mannitol.

The majority of the polyalcohol (*ca.* 0.4 g) was examined (without hydrolysis) in solvent *C* and showed three main fractions: 1 ($R_{erythritol}$ 1.4), 36.7 mg; 2 ($R_{erythritol}$ 1.2), 23 mg; 3 ($R_{erythritol}$ 1.0), 72 mg. Although fraction 3 had the same mobility as erythritol it gave a pink color with the hydroxylamine – ferric chloride spray. This fraction was therefore examined by running duplicate papers for 8 h in solvent *B* followed by 8 h in solvent *A*. Development of one paper with silver nitrate showed a component with the mobility of erythritol and a slower moving component which streaked somewhat. Development of the duplicate paper with the lactone spray revealed only the slower moving component. *A* portion of fraction 3 was therefore hydrolyzed (HCl, 2 *N*, 4 h) and examined in solvent *A*. Components with the mobilities of D-mannose, erythritol, D-erythronolactone, and pyruvic acid were detected. The p.m.r. spectrum of fraction 3 showed clearly the pyruvate signal at τ 8.5, the anomeric proton at 5.12, and that they were present in the ratio of 3H:1H.

Carboxyl reduced polysaccharide (11.2 mg) consumed 0.60 mol of periodate per sugar residue in 40 h at 1°. Total hydrolysis of the polyalcohol and examination in solvent *A* showed two major components with the mobilities of D-mannose and erythritol with only traces of D-glucose. Partial hydrolysis (H_2SO_4, 1 *N*, 20°) of the polyalcohol for either 4 or 26 h showed (solvent *A*) erythritol and a non-reducing compound with R_{Man} 0.48 assumed to be 2-*O*-β-D-mannopyranosyl-D-erythritol.

Location of O-Acetyl Group

Capsular polysaccharide (30 mg) in methyl sulfoxide (5 ml) was reacted with methyl vinyl ether (5 g) and *p*-toluenesulfonic acid at a temperature not exceeding 20° for 40 min. The reaction mixture was poured into dry acetone (200 ml) and left overnight. The white precipitate was collected by centrifugation and the supernatant was concentrated and added to a column (3 × 22 cm) of Sephadex LH 20 which was eluted with dry acetone. The acetalated polysaccharide was methylated and hydrolyzed. A chromatogram in solvent *B* showed much D-glucose and D-mannose with a small amount of faster moving material. G.l.c. of the reduced hydrolyzate (as column *a* but 8 ft × 1/4 in. at 210°) gave a component which crystallized and had m.p. 54–55° undepressed with an authentic sample (6) of 2-*O*-methyl-D-glucitol pentaacetate m.p. 56–57°

We are indebted to Dr. I. Ørskov, Copenhagen, for a sample of *Klebsiella* K5 (E5051), to Dr. P. J. Salisbury for growing the bacteria, and to Dr. G. H. N. Towers for the use of his centrifuge. We thank Dr. S. C. Churms for the gel chromatography and Dr. E. G. Gros for a sample of 2-*O*-methyl-D-mannose.

The continued financial support of the National Research Council of Canada is gratefully acknowledged.

1. W. NIMMICH. Z. Med. Mikrobiol. Immunol. **154**, 117 (1968).
2. W. NIMMICH. Acta biol. med. germ. **26**, 397 (1971).
3. Y. M. CHOY and G. G. S. DUTTON. Can. J. Chem. **51**, 198 (1973).
4. Y. M. CHOY, G. G. S. DUTTON, and A. M. ZANLUNGO. Can. J. Chem. This issue.
5. G. G. S. DUTTON and M. T. YANG. Can. J. Chem. **50**, 2382 (1972).
6. G. M. BEBAULT, J. M. BERRY, Y. M. CHOY, G. G. S. DUTTON, N. FUNNELL, L. D. HAYWARD, and A. M. STEPHEN. Can. J. Chem. **51**, 324 (1973).
7. M. DUCKWORTH and W. YAPHE. Chem. Ind. (London), 747 (1970).
8. J. H. SLONEKER and A. JEANES. Can. J. Chem. **40**, 2066 (1962).
9. M. ABDEL-AKER and F. SMITH. J. Am. Chem. Soc. **73**, 5859 (1951).
10. Y. M. CHOY, G. G. S. DUTTON, A. M. STEPHEN, and M. T. YANG. Anal. Lett. **5**, 675 (1972).
11. G. M. BEBAULT, Y. M. CHOY, G. G. S. DUTTON, N. FUNNELL, A. M. STEPHEN, and M. T. YANG. J. Bacteriol. **113**, 1345 (1973).

12. E. J. BOURNE and S. PEAT. Adv. Carbohydr. Chem. **5**, 145 (1950).
13. J. O. DEFERRARI, E. G. GROS, and I. O. MASTRONARDI. Carbohydr. Res. **4**, 432 (1967).
14. T. J. PAINTER and B. LARSEN. Acta Chem. Scand. **24**, 813 (1970).
15. M. F. ISHAK and T. J. PAINTER. Acta Chem. Scand. **28**, 3875 (1971).
16. J. H. SLONEKER, D. G. ORENTAS, C. A. KNUTSON, P. R. WATSON, and A. JEANES. Can. J. Chem. **46**, 3353 (1968).
17. A. N. DE BELDER and B. NORRMAN. Carbohydr. Res. **8**, 1 (1968).
18. M. J. HOW, J. S. BRIMACOMBE, and M. STACEY. Adv. Carbohydr. Chem. **19**, 303 (1964).
19. M. HEIDELBERGER and G. G. S. DUTTON. J. Immunol. In press.
20. G. G. S. DUTTON, K. B. GIBNEY, and P. E. REID. Can. J. Chem. **47**, 2494 (1969).
21. Y. M. CHOY and A. M. UNRAU. Carbohydr. Res. **17**, 439 (1971).
22. R. W. BAILEY. Oligosaccharides. Pergamon, Oxford. 1965. p. 99.
23. J. K. N. JONES and M. B. PERRY. J. Am. Chem. Soc. **79**, 2787 (1957).
24. B. LINDBERG and L. SELLEBY. Acta Chem. Scand. **14**, 1051 (1960).
25. G. G. S. DUTTON and S. KABIR. Anal. Lett. **4**, 95 (1971).

Can. J. Chem. Downloaded from www.nrcresearchpress.com by 210.87.254.6 on 09/05/12
For personal use only.

Acenaphthene III. Coupling Reactions. The Preparation of 4,4′-Dinaphthalic Anhydride and 4′,1-Naphthylnaphthalic Anhydride[1]

LOUIS A. JONES[2] AND RONALD WATSON
Department of Chemistry, North Carolina State University, Raleigh, N.C. 27607

Received October 31, 1972

The syntheses of the previously unknown 4,4′-dinaphthalic anhydride (**4**) and 4′,1-naphthylnaphthalic anhydride (**5**) is reported. The vinylic bromination of 5-(1,-3,4-dihydronaphthyl)acenaphthene (**11**) is also described.

On décrit la synthèse des anhydrides dinaphtalique-4,4′(**4**) et (naphtyl-1)-4 naphtalique (**5**) inconnus jusqu'à maintenant. On rapporte aussi les résultats obtenus lors de la bromination vinylique du (dihydro-3,4 naphtyl-1)-5 acénaphtène (**11**). [Traduit par le journal]

Can. J. Chem., **51**, 1833 (1973)

Can. J. Chem. Downloaded from www.nrcresearchpress.com by 210.87.254.42 on 09/05/12
For personal use only.

Recent investigations (1, 2) have resulted in the preparation of 4,5-diaminonaphthalic anhydride (**1**) and 3,4-diaminonaphthalic anhydride (**2**). As part of a continuing study in the chemistry of acenaphthene (**3**) and its derivatives, we now report the syntheses of 4,4′-dinaphthalic anhydride (**4**) and 4′,1-naphthylnaphthalic anhydride (**5**).

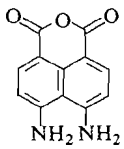

1

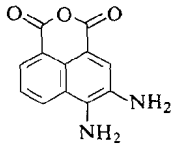

2

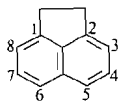

3

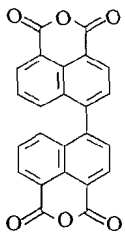

4

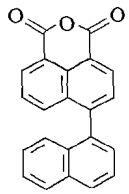

5

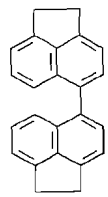

6

Thallium bromide (**1**) has been used as a reagent for the syntheses of biaryls from aromatic Grignard reagents (3). Consequently, 5-acenaphthyl magnesium bromide, prepared from 5-bromoacenaphthene (4), was treated with thallium bromide to give 5,5′-diacenaphthene (**6**) in low yield. Alternatively it was found that the same product could be obtained in far better yield by utilizing the coupling technique of Kharasch and Fields (5) in which cobalt chloride is used as a catalyst. The fact that coupling has indeed taken place in the *peri*-position was established from consideration of its n.m.r. spectrum. The bridgehead protons gave a sharp singlet at τ 6.57 as did the aromatic protons 6,6′, 7,7′, and 8,8′ at τ 2.74. The remaining protons exhibited an AB quartet with a *J* value of 7.3 Hz. Oxidation to the dianhydride **4** was achieved by treatment of the product with sodium dichromate in glacial acetic acid.

Garvey and his co-workers (6) have previously reported the synthesis of 5,5′-diacenaphthene by a different procedure, but no experimental details or spectral data were given.

When the dimer **6** was treated with 2,3-dichloro-5,6-dicyano-1,4-benzoquinone (DDQ) dehydrogenation took place to give 5,5′-diacenaphthylene (**7**) which readily consumed 2 mol of bromine to give the tetrabromo-compound **8**. Also, oxidation with sodium dichromate again gave the dianhydride **4**.

When the Grignard reagent from 5-bromoacenaphthene was treated with α-tetralone in tetrahydrofuran, the expected coupled product **9** was only obtained in low yield. Rather, we obtained acenaphthene and the aldol condensation product **10** of α-tetralone which was identified by its elemental analysis and by preparation of its 2,4-dinitrophenylhydrazone. This same product has previously been isolated (7) from the reaction of α-tetralone with cyclohexyl magnesium bromide. Consequently, treatment of α-tetralone with 5-lithio-acenaphthene (from 5-

[1]The financial support from NASA grant NGR-34-002-125 is gratefully acknowledged.

[2]Author to whom correspondence should be addressed.

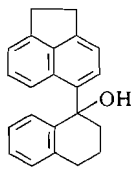

9

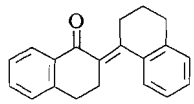

10

bromo acenaphthene and *n*-butyl-lithium) resulted in the isolation of the hydroxy compound **9** in far better yield. Dehydration to 5-(1,-3,4-dihydronaphthyl)acenaphthene (**11**) was readily effected by treatment with polyphosphoric acid. This product was subsequently dehydrogenated by 10% palladium-on-charcoal to 5′,1-naphthylacenaphthene (**12**) or by DDQ which gave 5′,1-naphthylacenaphthylene acenaphthylene (**13**). Treatment of either compound **12** or **13** with sodium dichromate in glacial acetic acid resulted in oxidation to 4′,1-naphthylnaphthalic anhydride (**5**).

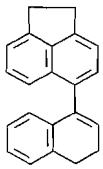

11

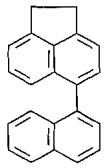

12

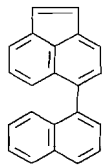

13

Nitration of this anhydride resulted in the isolation of a yellow solid. Consideration of its elemental analysis and mass spectrum indicated the presence of two nitro-groups. Although the positions of these nitro-groups have not as yet been unambiguously assigned, previous experience (8) in this laboratory has shown that, in the case of nitration of 1,1′-binaphthyl the *peri*-positions are more susceptible to nitration. Consequently we propose that this dinitro-compound has the structure **14**. Further, its n.m.r. spectrum exhibits two aromatic multiplets in the ratio of 4:6 which is the pattern one would expect for this structure.

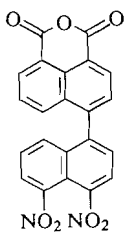

14

The possibility of introducing a bromine atom in the 3′-position of the system **11** and then dehydrobromination as an alternate route to naphthyl acenaphthene (**12**) led us to attempt allylic bromination utilizing *N*-bromosuccinimide (NBS) in carbon tetrachloride as the brominating media (9). This resulted in an inseparable mixture of isomers. When dimethylformamide (DMF) was used as solvent, the reaction proceeded smoothly to give a good yield of a mono-brominated product. This product, however, did not appear to be the required allylically brominated system **15** since it gave no precipitate with alcoholic silver nitrate at room temperature. Consideration of its n.m.r. spectrum revealed that bromination had in fact taken place in the vinyl-2′-position to give compound **16**, the main feature of the spectrum being the disappearance of the triplet at τ 4.0 in the starting material and the appearance of a singlet for the 3′ and 4′-protons. The structure has been unambiguously confirmed by a single crystal X-ray analysis (10).

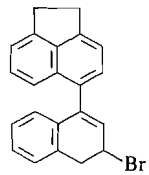

15

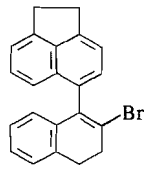

16

Although rare, instances of vinylic bromination in NBS reactions are not altogether unique (11, 12). Pines and his co-workers (13) found that bromination of α-methylstyrene with NBS in carbon tetrachloride gave, as well as the expected 2-phenylallyl bromide (**17**), 1-methyl-1-phenylvinyl bromide (**18**), in a ratio of 3:1. In an earlier study, Roberts and Trumbell (14) found that the reaction of camphene with NBS in carbon tetrachloride gave a 35% yield of mono-brominated

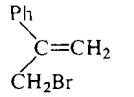

17

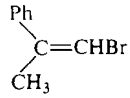

18

products, of which 65% proved to be the vinylic substituted product 8-bromocamphene. In each case a free radical mechanism is proposed.

In our hands, the reaction of α-methylstyrene with NBS in DMF gave 56% of mono-brominated products. From g.l.c. studies of the crude

Can. J. Chem. Downloaded from www.nrcresearchpress.com by 210.87.254.42 on 09/05/12
For personal use only.

Can. J. Chem. Downloaded from www.nrcresearchpress.com by 210.87.254.42 on 09/05/12
For personal use only.

mixture and the pure isomers it was shown that the mixture consisted of 80% of **17** and 29% of **18**. The same proportions were obtained from consideration of the n.m.r. spectra of both the crude mixture and the pure compounds. It had previously been reported (*9b*) that NBS was inactive towards styrene and that no monobrominated products were obtained. However, reaction of styrene with NBS in DMF as the solvent was found to produce a 30% yield of dibromostyrene. This would seem to indicate, therefore, that in DMF the addition of bromine to the double bond takes preference over substitution, although in the case of α-methylstyrene, no dibromo-substituted products were detected. This was confirmed by the fact that when the reaction of compound **11** with NBS in DMF was carried out in the dark, the same product, **16**, was obtained in identical yield as had been obtained previously. Further, addition of bromine to the dihydro system **11** again gave the vinylic brominated product **16**, also in the same yield. The mechanism for the formation of **16** therefore, evidently involves an initial addition of bromine to the double bond to form a dibromo-intermediate, which then spontaneously dehydrobrominates to give the product **16**.

This is consistent with the findings of Horner and Winkelmann (*9d*) that with increasing polarity of the solvent used in the bromination reaction of NBS the allylic bromination activity disappears and the addition of bromine to the double bond becomes the main reaction.

Experimental[3]

5,5'-Diacenaphthene (6)

5-Bromoacenaphthene (10.0 g) in anhydrous tetrahydrofuran (100 ml) was added to magnesium turnings (1.98 g) in tetrahydrofuran (100 ml) and the mixture heated to reflux under nitrogen for 16 h. The resulting solution of 5-acenaphthyl magnesium bromide was added to 5-bromoacenaphthene (10.08 g) and anhydrous cobalt chloride (9.5 g) in anhydrous tetrahydrofuran (100 ml) and the mixture heated to reflux for a further 16 h. The mixture was then poured on ice, acidified (diluted HCl), and extracted with methylene chloride. The organic layer was separated, washed, dried, and evaporated to leave a brown semi-solid which was chromatographed on alumina. Elution with hexane gave unreacted bromoacenaphthene and some acenaphthene followed by the product **6** (3.2 g, 49%) which was recrystallized from methylene chloride – hexane to give pale yellow needles, m.p. 176–178°, $\nu_{C=C}$ 1610 cm^{-1} (Nujol); τ ($CDCl_3$) 2.46–2.72 (4H, AB quartet, J = 7.3 Hz, Ar), 2.74 (6H, s, Ar), and 6.57 (8H, s, CH_2).

Anal. Calcd. for $C_{24}H_{18}$: C, 94.1; H, 5.8. Found: C, 94.2; H, 5.9.

4,4-Dinaphthalic Anhydride (4)

Diacenaphthene (3.3 g), sodium dichromate (27 g), and glacial acetic acid (500 ml) were refluxed overnight, cooled, and added to water (600 ml). The precipitated solid was collected and recrystallized from dimethylformamide to give **4** (3.2 g, 71%) as a yellow amorphous solid m.p. 362° (dec.), ν_{max} (Nujol) 1780, 1730 (C=O) and 1595 cm^{-1} (C=C).

Anal. Calcd. for $C_{24}H_{10}O_6$: C, 73.10; H, 3.45%. Found: C, 72.85; H, 3.15.

5,5'-Diacenaphthylene (7)

Diacenaphthene (1.73 g), DDQ (3.12 g), and benzene (40 ml) were heated at reflux overnight; the mixture was cooled, diluted with hexane (200 ml) and the hydroquinone, which had formed during the reaction, was removed by filtration. The filtrate was chromatographed on alumina. Hexane eluted **7** (1.17 g, 70%), yellow plates, m.p. 164–165% (from ethanol), τ ($CDCl_3$) 2.34–2.76 (10H, m, Ar), and 3.02 (4H, s, methine).

Anal. Calcd. for $C_{24}H_{14}$: C, 95.35; H, 4.65. Found: C, 95.25; H, 4.5.

1,1',2,2'-Tetrabromo-5,5'-diacenaphthene (8)

To diacenaphthylene (1.5 g) in hexane (130 ml), a solution of bromine (1.6 g) in hexane (20 ml) was added dropwise and the mixture stirred for 8 h at 20%. The mixture was concentrated and the precipitated solid separated by filtration and recrystallized to give **8** (1.64 g, 50%), as a yellow amorphous solid, m.p. 218–219° (dec.) (from benzene).

Anal. Calcd. for $C_{24}H_{14}Br_4$: C, 46.3; H, 2.25; Br, 51.45. Found: C, 46.45; H, 2.10; Br, 51.35.

Reaction of 5-Acenaphthyl Magnesium Bromide with α-Tetralone

A solution of α-tetralone (6 g) in anhydrous tetrahydrofuran (50 ml) was added to the Grignard solution obtained from 5-bromoacenaphthene (10 g), magnesium turnings (1.08 g), and anhydrous tetrahydrofuran (100 ml) and the mixture refluxed under nitrogen for 3 days; it was then poured onto ice, acidified (dilute HCl), and extracted with methylene chloride. The extract was washed ($NaHCO_3$ then water) and dried (Na_2SO_4), to give a residue which was chromatographed on Florisil. Hexane eluted acenaphthene (3 g, 45%) and further elution with ether gave a brown gum. Trituration of this gum with ether gave **10** (1.9 g, 32%), pale yellow crystals, m.p. 132–133° (from methylene chloride – hexane) (lit. (7) m.p. 132–133°). Evaporation of the filtrate gave the required product **9** (2.5 g, 19%) as a pale brown amorphous solid, m.p. 112–114° (from methylene chloride – hexane), ν_{max} (Nujol) 3450 (OH), 1612 cm^{-1} (C=C).

Anal. Calcd. for C, 88.0; H, 6.65. Found: C, 88.25; H, 6.5.

[3]Melting points were determined on a Thomas–Hoover capillary melting point apparatus and elemental analyses performed by Galbraith Laboratories, Inc., Knoxville, Tennessee. I.r. spectra were measured on a Beckman I.R.-33 i.r. spectrophotometer and n.m.r. spectra were obtained from a Varian HA-100 spectrometer.

Can. J. Chem. Downloaded from www.nrcresearchpress.com by 210.87.254.42 on 09/05/12
For personal use only.

*1-Hydroxy-1,2,3,4-tetrahydro-5',1-naphthylacenaphthene (**9**)*

5-Bromoacenaphthene (50 g) in ether (300 ml) and a hexane solution of *n*-butyl-lithium were mixed at 20° and stirred at this temperature under nitrogen for 20 min. α-Tetralone (31 g) in ether (150 ml) was then added and the mixture was stirred for a further 15 h at 20°. The mixture was then poured onto ice and acidified (dilute HCl). The ether layer was separated off, washed, dried, and evaporated to leave a light brown semi-solid. This was triturated with hexane and the residue crystallized from methylene chloride–hexane. The product **9** (40 g 63%) formed a fawn-colored semi-crystalline solid, m.p. 112–114°.

*5-(1,-3,4-Dihydronaphthyl)acenaphthene (**11**)*

The preceding product (30 g) was added with stirring to polyphosphoric acid (500 g) and the mixture was stirred at 60° for 5 h; it was then poured into ice-cold water (1000 ml) and extracted with ether. The extract was washed with aqueous sodium bicarbonate solution and then with water, dried (Na_2SO_4), and evaporated. The dehydrated product **11** (27 g, 95%) formed light brown crystals, m.p. 112° (from methylene chloride–hexane), $\nu_{C=C}$ (Nujol) 1595 and 1610 cm^{-1}; τ ($CDCl_3$) 2.64–3.50 (9H, m, Ar), 4.0 (1H, t, 2'-H), 6.76 (4H, s, 1-H and 2-H), 7.04–7.32 (2H, m, CH_2), and 7.5–7.8 (2H, m, CH_2).

Anal. Calcd. for $C_{22}H_{18}$: C, 93.6; H, 6.4. Found: C, 93.4; H, 6.2.

*5',1-Naphthylacenaphthene (**12**)*

The dihydro-compound **11** (16.5 g) and 10% palladium-on-charcoal (5 g) in α-methylnaphthalene (250 ml) were heated to reflux under nitrogen for 25 h; the mixture was cooled, filtered, the α-methylnaphthalene distilled off under reduced pressure, and the residue chromatographed on alumina. Hexane–benzene (1:1) eluted the product (14.5 g, 89%) as pale yellow crystals, m.p. 103–104° (from hexane), τ ($CDCl_3$) 2.02–2.84 (12H, m, Ar), and 6.59 (4H, s, 1-H and 2-H).

Anal. Calcd. for $C_{22}H_{16}$: C, 94.3; H, 5.7. Found: C, 94.1; H, 5.8.

*5',1-Naphthylacenaphthylene (**13**)*

The dihydro-compound **11** (22 g), DDQ (37 g), and benzene (300 ml) were heated to reflux overnight and then worked-up as for diacenaphthylene. The dehydrogenated product (12 g, 55%) afforded yellow crystals, m.p. 112–114° (from ethanol), τ ($CDCl_3$) 2.1–2.9 (12H, m, Ar), and 3.0 (2H, s, 1-H and 2-H).

Anal. Calcd. for $C_{22}H_{14}$: C, 94.95; H, 5.05. Found: C, 94.7; H, 5.1.

*4',1-Naphthylnaphthalic Anhydride (**5**)*

The preceding product (11.7 g), sodium dichromate (40 g) and glacial acetic acid (500 ml) were heated to reflux overnight, cooled, and added to water (1000 ml). The precipitated solid was collected and recrystallized to give **5** (10 g, 74%) as dark yellow crystals, m.p. 250–252° (from aqueous acetic acid), ν_{CO} (Nujol) 1770, 1730 cm^{-1}; τ ($CDCl_3$) 1.24–1.47 (2H, m, Ar), and 1.95–2.84 (10H, m, Ar).

Anal. Calcd. for $C_{22}H_{12}O_3$: C, 81.5; H, 3.75. Found: C, 81.25; H, 3.75.

Nitration of 4',1-Naphthylnaphthalic Anhydride

To a stirred solution of compound **5** (1.4 g) in methylene dichloride (150 ml), 90% nitric acid (15 ml) was added dropwise and the mixture heated to reflux for 60 h; it was then poured into water (300 ml), the organic layer separated, washed ($NaHCO_3$, then water), dried ($MgSO_4$), and evaporated to give a pale yellow solid. This was dissolved in methylene dichloride and addition of hexane gave the product **14** (0.6 g, 32%) as an amorphous yellow solid, (*m/e* 413) m.p. 280° (dec.) (from acetic acid), ν_{max} (Nujol) 1775, 1730 $\nu_{C=O}$, 1530, and 1355 cm^{-1} (NO_2); τ ($(CD_3)_2SO$) 1.15–1.56 (4H, m, Ar), and 1.69–2.26 (6H, m, Ar).

Anal. Calcd. for $C_{22}H_{10}N_2O_7$: C, 63.75, H, 2.4; N, 6.75. Found: C, 63.75; H, 2.3; N, 6.65.

*2-Bromo-3,4-dihydro-5',1-naphthylacenaphthene (**16**)*

(*a*) To compound **11** (3 g) in dimethylformamide (100 ml) a solution of NBS (1.89 g) also in dimethylformamide (50 ml) was added and the mixture stirred overnight at 20°; it was then poured into water (700 ml) and extracted with ether. The extract was washed with water, dried ($MgSO_4$), and evaporated to give a pale yellow gum which was chromatographed on Florisil. Hexane eluted the product **16** (2 g, 55%), which gave yellow crystals, m.p. 150–152° (from methylene chloride–hexane), $\nu_{C=C}$ (Nujol) 1604, 1585 cm^{-1}; τ ($CDCl_3$) 2.68–3.66 (9H, m, Ar), 6.74 (4H, s, 1-H and 2-H), and 7.07 (4H, s, 3'-H and 4'-H).

Anal. Calcd. for $C_{22}H_{17}Br$: C, 73.15; H, 4.7; Br, 22.15. Found: C, 72.95; H, 4.5; Br, 22.3.

(*b*) To compound **11** (6 g) in carbon tetrachloride (100 ml) a solution of bromine (3.5 g) in carbon tetrachloride (20 ml) was added dropwise and the mixture stirred at room temperature for 30 min; evaporation of the solvent gave **16** (4.3 g, 56%) as light brown crystals, m.p. 150–152° (from methylene chloride–hexane).

Styrene with N-Bromo Succinimide

A solution of NBS (50 g) in dimethylformamide (80 ml) was added to styrene (100 ml) in dimethylformamide (20 ml). After the initial exothermic reaction had subsided, the mixture was stirred overnight at 20°. The solvent and excess styrene were removed under reduced pressure and the residue chromatographed on silicic acid. Hexane eluted dibromostyrene (21.3 g, 30%) as white needles m.p. 70–72° (lit. (15) 72–73°) (from aqueous ethanol).

α-Methylstyrene with N-Bromosuccinimide

A solution of NBS (100 g) in dimethylformamide (250 ml) was added to α-methylstyrene (200 ml). After the initial exothermic reaction had subsided the mixture was stirred overnight at room temperature, poured into water, and extracted with methylene chloride. The extract was washed with water, dried ($MgSO_4$), and evaporated to give a dark brown liquid. Excess α-methylstyrene was removed under reduced pressure and vacuum distillation of the residue gave the mono-brominated products (61.6 g, 56%), b.p. 95–105°/11 mm, a yellow liquid containing a mixture of isomers. The mixture (13 g) was chromatographed on silicic acid and eluted with hexane. The first fractions were composed of pure 1-methyl-1-phenylvinyl bromide (**18**) while the end fractions were composed

of pure 2-phenylallyl bromide (17) (11). From g.l.c. studies of the pure isomers it was calculated that the crude mixture of bromides was composed of 80% of **17**, τ ($CDCl_3$) 2.4–2.76 (5H, m, Ar), 4.49 (1H, s, vinyl-H), 4.56 (1H, s, vinyl-H) and 5.68 (2H, s, CH_2); and 20% of **18** τ ($CDCl_3$) 2.69 (5H, s, Ar), 3.57 (1H, m, vinyl-H), and 7.83 (3H, s, CH_3).

1. L. A. JONES, C. T. JOYNER, H. K. KIM, and R. A. KYFF. Can. J. Chem. **48**, 3132 (1970).
2. L. A. JONES, H. K. KIM, and R. WATSON. J. Chem. Soc. C, 3891 (1971).
3. A. MCKILLOP, L. F. ELSOM, and E. C. TAYLOR. J. Am. Chem. Soc. **90**, 2423 (1968).
4. S. D. ROSS, M. FINKLESTEIN, and R. C. PATERSON. J. Am. Chem. Soc. **80**, 4327 (1958).
5. M. S. KHARASCH and E. K. FIELDS. J. Am. Chem. Soc. **63**, 2316 (1941).
6. B. S. GARVEY, L. F. HALLEY, and C. F. H. ALLEN. J. Am. Chem. Soc. **59**, 1827 (1937).
7. J. N. COOK and C. A. LAWRENCE. J. Chem. Soc. 1431 (1936).
8. L. A. JONES and C. T. JOYNER. J. Chem. Eng. Data, In press.
9. (*a*) K. ZEIGLER, A. SPÄETH, W. SCHUMANN, and E. WINKELMANN. Ann. **551**, 80 (1948); (*b*) C. DJERASSI. Chem. Rev. **48**, 271 (1948); (*c*) R. FILLER. Chem. Rev. **63**, 21 (1963); (*d*) L. HORNER and E. H. WINKELMANN. Newer methods of preparative organic chemistry. Vol. 3. Academic Press. 1964. p. 151.
10. J. BORDNER, R. L. GREENE, L. A. JONES, and R. WATSON. Cryst. Struct. Commun. **1**, 393 (1972).
11. P. L. SOUTHWICK, L. A. PURGLOVE, and P. NUMEROF. J. Am. Chem. Soc. **72**, 1600 (1950).
12. K. H. DUDLEY and H. W. MILLER. Tetrahedron Lett. 571 (1968).
13. H. PINES, H. ALUL, and M. KOLOBIELSKI. J. Org. Chem. **22**, 1113 (1957).
14. J. O. ROBERTS and E. R. TRUMBELL. J. Am. Chem. Soc. **71**, 1630 (1949).
15. H. ZINCKE. Ann. **216**, 288 (1883).

Can. J. Chem. Downloaded from www.nrcresearchpress.com by 210.87.254.42 on 09/05/12
For personal use only.

Sur la conformation des *tert*-butylcyclohexanes substitués en position 2

JEAN CLAUDE RICHER ET CHRISTIAN FREPPEL
Département de Chimie, Université de Montréal, B.P. 6128, Montréal, Québec
ET
ALAIN TCHAPLA ET ZOLTAN WELVART
Groupe de Laboratoires du CNRS, 94320 Thiais, France
Reçu le 2 juin 1971[1]

L'examen des pK (dans le méthyl-cellosolve à 80%: pK_{MCS}) d'aminoalcools et d'amines dérivés du *tert*-butylcyclohexane montre que l'introduction d'un groupement *tert*-butyle en position 2 d'un groupement hydroxyle provoque par rapport au cyclohexanol non substitué un aplatissement de cette partie du cycle lorsque l'hydroxyle et le *tert*-butyle sont *trans*; elle provoque un redressement lorsque ces groupements sont *cis*.

Examination of the pK_{MCS} (80% methylcellosolve) of amino alcohols and amines derived from *tert*-butylcyclohexane shows that introduction of a tertiary butyl group in the adjacent position to a hydroxyl leads, by comparison to the non-substituted cyclohexanol, to a flattening of this portion of the ring when the hydroxyl and *tert*-butyl groups are *trans*; when the groups are *cis* a straightening occurs.

Can. J. Chem., **51**, 1838 (1973)

Introduction

Il est admis (1) que l'introduction d'un groupement *tert*-butyle équatorial ne modifie que peu la géométrie d'un noyau cyclohexanique. L'influence de ce groupe est cependant inattendue dans le cas des *tert*-butyl-2 cyclohexanols où l'isomère *trans* (diéquatorial) est moins stable que l'isomère *cis* (axial-équatorial) (2). Cette anomalie n'a toutefois pas été attribuée à la déformation acceptée précédemment (3) dans le cas de la *tert*-butyl-2 cyclohexanone[2] mais plutôt à la conformation de rotation du groupement *tert*-butyle (2, 4). Cette rotation de 17° du groupement *tert*-butyle par rapport à la position parfaitement décalée qui avait été proposée à la suite d'un calcul (4) a été confirmée récemment (5) lors de la détermination par rayons-X de la structure du toluènesulfonate du di-*tert*-butyl-2,5 cyclohexanol-*cis*, *trans*. Cette étude a démontré de plus que la géométrie du cycle est relativement peu affectée malgré l'asymétrie introduite dans le cycle par la rotation du groupement *tert*-butyle qui rend différent les angles de torsion des deux côtés du cycle (4, 5). Il est à noter toutefois que la déformation asymétrique du cycle n'apparait pas pour le *p*-bromobenzoate du *tert*-butyl-4 cyclohexanol-*trans* dont l'étude aux rayons-X a montré que le cycle est légèrement redressé par rapport au cyclohexane non substitué (6).[3]

Il apparait donc que l'influence du groupement *tert*-butyle sur la géométrie d'un noyau cyclohexanique est généralement faible et qu'elle dépende en partie de la nature et de la position des autres substituants. Afin de vérifier si le groupement *tert*-butyle modifie suffisamment la flexibilité du noyau cyclohexanique pour influencer les diverses propriétés de composés cyclohexaniques (7) nous avons fait appel à la détermination des pK (8) de diverses *tert*-butylcyclohexylamines ainsi que d'amino-alcools correspondants; le choix de cette dernière classe de composés est justifié par le fait que des liaisons hydrogènes peuvent s'établir de façon intramoléculaire (9) et que de telles liaisons peuvent amener une déformation supplémentaire du noyau cyclohexanique.

Resultat et Discussion

L'étude des pK_{MCS} est une méthode qui permet de préciser la géométrie relative des substituants des différents isomères d'aminoalcools. Cette

[1]Revision reçue le 27 novembre 1972.

[2]Un calcul d'Allinger effectué dans ce cas montre que la répulsion entre l'oxygène de la cétone et le groupement *tert*-butyle voisin est suffisamment importante pour que cette cyclohexanone adopte une conformation croisée.

[3]Voir cependant le travail de Berti et coll. (17).

Can. J. Chem. Downloaded from www.nrcresearchpress.com by 210.87.254.5 on 09/05/12
For personal use only.

TABLEAU 1. pK_{MCS} de divers *tert*-butylcyclohexylamines et aminoalcools*

Stéréochimie	Isomère					
	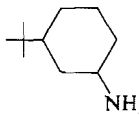	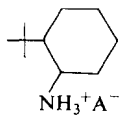	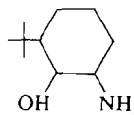		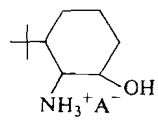	
$NH_3^+A^-$ axial	9.37	8.68	OH_a	8.45	OH_a	7.82
			OH_e	8.85	OH_e	8.00
$NH_3^+A^-$ équatorial	9.54	9.01	OH_a	9.04	OH_a	8.66
			OH_e	8.96	OH_e	8.34

*Valeurs déterminées à 25.0 ± 0.5 °C avec une précision de ±0.01 unité de pK. A^- = picrates; dans tous les autres cas A^- = Cl^-.

méthode proposée par Sicher et coll. (8) consiste à examiner le ΔpK, c'est à dire la différence entre les pK_{MCS} de l'aminoalcool considéré et de l'amine correspondante.

On sait que l'introduction d'un groupement OH vicinal diminue notablement la basicité d'une fonction amine par effet inductif (10). Cependant l'abaissement de la basicité peut être compensé lorsque l'angle dièdre entre les deux fonction diminue, c'est à dire lorsque celles-ci deviennent de plus en plus coplanaires: le ΔpK passe de 0.90 pour un aminoalcool cyclohexanique où les substituants sont diaxiaux (angle dièdre de 180°) à 0.18 pour l'aminoalcool ayant ses deux fonctions dans une conformation *cis* bateau (angle dièdre de 0°) (8).

Ainsi, bien que la signification énergétique précise du ΔpK soit complexe[4] sa diminution peut signifier l'aplatissement du noyau cyclohexanique de l'aminoalcool par rapport au noyau de la cyclohexylamine correspondante.

[4]Le ΔpK est en fait la différence de deux différences d'énergies libres:

$$[\Delta E_{(\text{ammonium—amine})} - \Delta E_{(\text{ammonium alcool—amino alcool})}]$$

Nous pouvons penser que divers facteurs conformationnels importants pour une molécule isolée (par exemple le nombre différent de conformations de rotation d'une fonction axiale ou équatoriale) n'ont dans notre cas que peu d'importance pour la molécule en solution dans un solvant hydroxylé. En effet les fonctions amine et hydroxyle adoptent, dans l'amine libre comme dans l'ammonium, la conformation la plus favorable pour la solvatation. D'après le modèle de Prélog et Hafliger (11) qui est le plus conforme aux divers résultats observés jusqu'à maintenant, une stabilisation de l'ion ammonium interviendrait par l'intermédiaire d'une molécule d'eau et au moyen d'une liaison hydrogène avec le groupement hydroxyle. C'est cette stabilisation qui déterminerait la valeur observée pour le ΔpK.

Dans le tableau 1 nous rapportons le pK_{MCS} (12) de quelques amines et aminoalcools dérivés du *tert*-butylcyclohexane dont la synthèse a déjà été décrite (13). La méthode de mesure employée est celle décrite précédemment par Svoboda et coll. (14).

Dans le tableau 2 sont consignés dans les deux premières colonnes les ΔpK déterminés par Sicher et coll. (8) pour les quatre aminoalcools isomères de chaque série **1** et **2** et dans les troisième et quatrième colonnes les ΔpK calculés à partir des résultats du tableau 1. Considérant d'une part que nous avons dosé les sels d'ammonium par l'hydroxyde de tétraméthylammonium alors que Sicher (8) a dosé les bases libres et d'autre part que les différences de ΔpK obtenues sont faibles, nous nous sommes assurés avec plusieurs amines de référence que nos résultats étaient comparables à ceux de Sicher; nous avons obtenu sensiblement les mêmes résultats à 0.01 unité de pK_{MCS} près. Dans le seul cas de la *tert*-butyl-3 cyclohexylamine nous avons un écart maximum de 0.05 unité.

L'examen du tableau 2 conduit aux considérations suivantes pour les isomères de position **1**, **2**, et **3** (le cas des isomères **4** sera discuté à part).

(*1*) Lorsque les deux substituants NH_2 et OH sont axiaux (premier cas) on observe une valeur moyenne de ΔpK de 0.90 ce qui correspond d'après Sicher et coll. (8) à l'abaissement du pK par l'effet inductif.

(*2*) Lorsque l'hydroxyle est équatorial et le groupement amine soit axial soit équatorial (deuxième cas) les valeurs de pK trouvées sont comprises entre 0.65 et 0.68. Le fait que le ΔpK soit plus petit que celui noté précédemment est en faveur d'une diminution de l'angle dièdre entre les deux fonctions. Mais la constance du

Can. J. Chem. Downloaded from www.nrcresearchpress.com by 210.87.254.5 on 09/05/12
For personal use only.

TABLEAU 2. ΔpK des divers amino-alcools

Stéréochimie relative		Isomère 1* 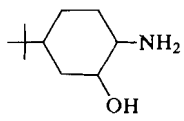	Isomère 2* 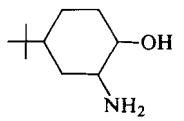	Isomère 3 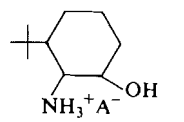	Isomère 4 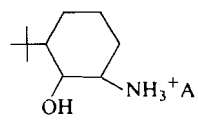
1° cas	NH_{2_a} OH_a	0.88	0.90	0.86	0.92
2° cas	NH_{2_a} OH_e	0.65	0.67	0.68	0.52
	NH_{2_e} OH_e	0.67	0.66	0.67	0.58
3° cas	NH_{2_e} OH_a	0.43	0.40	0.35	0.50

*Sicher et coll. (8).

ΔpK pour ces deux types de composés montre que l'introduction d'un groupement OH équatorial ne doit pas modifier sensiblement la géométrie du cycle de la cyclohexylamine correspondante et ce quelle que soit sa configuration initiale (axiale ou équatoriale).

(*3*) Lorsque l'hydroxyde est axial et le groupement amine équatorial (troisième cas) les valeurs de ΔpK sont nettement plus faibles environ 0.40 ce qui signifie une diminution de l'angle dièdre entre les deux fonctions voisines (aplatissement du cycle). Ceci est en bon accord avec les résultats précédents qui montrent qu'un seul groupement OH axial peut déjà déformer le noyau cyclohexanique (15) substitué par un *tert*-butyle.[5]

(*4*) La position du groupement amine intervient également. En effet la comparaison des valeurs des pK de **1** et **3** (ΔpK = 0.43 et 0.35) montre que l'aplatissement provoqué par l'introduction d'un OH axial est plus important lorsque la fonction amine est en position 2 que lorsqu'elle est en position 4. On voit donc que la répulsion vicinale NH_2-équatorial/*tert*-butyl-équatorial facilite l'aplatissement des carbones 1 et 2 du cycle.

(*5*) Dans les isomères de la série **4** on constate (sauf pour le premier cas) que les valeurs de ΔpK sont différentes de celles des isomères des séries **1**, **2**, ou **3** correspondantes. Ainsi un hydroxyle équatorial en position 2 (deuxième cas) favorise l'aplatissement du cycle puisque les ΔpK sont respectivement de 0.58 et 0.52 au lieu de la valeur moyenne de 0.67 trouvée pour les isomères des séries **1**, **2**, et **3**. Par ailleurs un hydroxyle axial en position 2 (troisième cas) tend à redresser le cycle puisque dans ce cas le ΔpK est de 0.50 au lieu de 0.40 pour les isomères correspondants des séries **1**, **2**, et **3**.

On peut enfin mentionner qu'il est probable que les interactions NH_2 *tert*-butyle provoquent des déformations de cycle semblables à celles dues aux interactions OH/*tert*-butyle; toutefois le pK des amines nous servant de référence, nous ne pouvons les mettre en évidence.

En admettant que la déformation observée par la mesure de ΔpK n'est pas liés à la présence de la fonction amine, mais dépend principalement de la flexibilité du système cyclohexanique, nous pouvons raisonner uniquement sur le motif du *tert*-butyle 2 cyclohexanol. Les figures du schéma I montrent que, lorsque le groupment *tert*-butyle est parfaitement décalé, et que la conformation du cycle est chaise, l'énergie d'interaction *tert*-butyle/OH est la même pour l'isomère *cis* que pour l'isomère *trans*. Or, pour les aminoalcools nos résultats suggèrent l'existence d'un aplatissement du cycle lorsque l'hydroxyle est équatorial et un redressement lorsqu'il est axial. Nous pouvons donc penser que la minimisation de l'énergie d'interaction *tert*-butyle/OH résulte non seulement de la rotation du groupement *tert*-butyle (1, 4, et 5) et d'un resserrement du "parapluie" sur lui même (6 et 16), mais aussi de la modification différente de la géométrie du cycle pour les deux isomères. L'observation des

[5]Un des arbitres nous a demandé de préciser la signification de la déformation: comme la différence entre les valeurs extrêmes des ΔpK est faible (0.72 unité correspond à un changement d'angle dièdre H_2N—C—OH de 180° (8)) une diminution de 0.25 à 0.30 unité de ΔpK indique un changement notable de cet angle dièdre. Or, il nous parait évident que ce n'est possible que si les autres angles dièdres et notamment les angles dièdres correspondants à l'intérieur du cycle (C_1—C_2—C_3 et C_2—C_3—C_4) changent également.

Can. J. Chem. Downloaded from www.nrcresearchpress.com by 210.87.254.5 on 09/05/12
For personal use only.

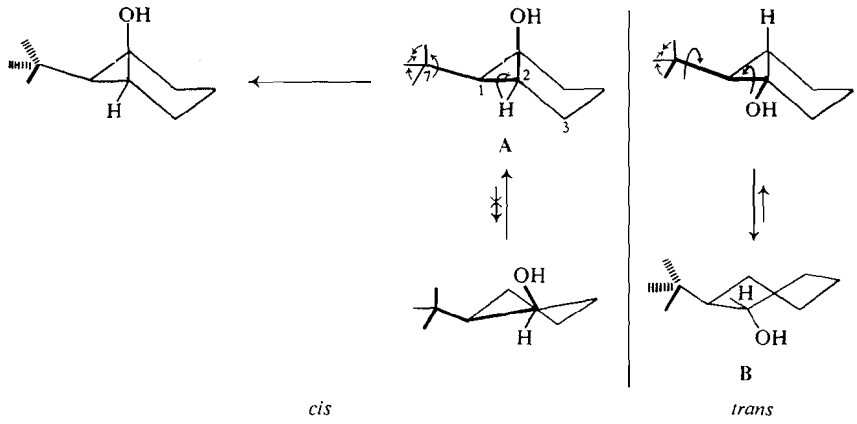

SCHÉMA 1

modèles montre que les interactions OH/*tert*-butyle peuvent se minimiser aussi par la rotation autour de la liaison C_1—C_2. Pour que cette rotation éloigne le groupement hydroxyle du groupement *tert*-butyle, elle doit provoquer pour l'isomère *cis* un redressement et pour l'isomère *trans* un aplatissement du cycle.[6]

Une autre explication a été suggérée par un des arbitres. L'effet stérique proposé par Pasto et Rao (2) permettrait d'expliquer seul l'ensemble des résultats: à savoir que le groupement *tert*-butyle pousse ensemble les groupements fonctionnels, davantage lorsque le groupement fixé en 2 est équatorial que lorsqu'il est axial. De ce fait la liaison hydrogène est favorisée, ce qui diminue le ΔpK. Il ne fait pas de doute que ce facteur intervient, mais il ne peut pas expliquer la différence de ΔpK entre le composé **4** (OH axial – NH_2 équatorial, $\Delta pK = 0.50$) et les composés **3** (OH axial – NH_2 équatorial $\Delta pK = 0.35$ et OH équatorial – NH_2 équatorial $\Delta pK = 0.67$). Or, si le changement de ΔpK est dû à une modification de la géométrie du cycle, il n'est pas étonnant que ces ΔpK deviennent différents.

Finalement, le présent travail montre en outre que la mesure de pK méthode extrêmement simple introduite par Sicher et coll. (14) pour l'étude de la géométrie des cycles permet de mettre en évidence des changements géométriques correspondants même à des faibles variations énergétiques.

[6]Pour l'isomère *trans* la déformation du cyclohexane chaise en conformation croisée (indiquée par les flèches) éloigne l'hydroxyle du *tert*-butyle d'une manière semblable à celle proposée par Allinger et coll. (3) pour la *tert*-butyl-2 cyclohexanone. Il y a diminution notable des interactions pour cette conformation. Pour l'isomère *cis* le passage de la forme chaise à la forme croisée amène l'hydroxyle entre deux méthyles du groupement *tert*-butyle. La diminution des interactions avec un des méthyles est compensée par l'augmentation des interactions avec l'autre méthyle. Les interactions sont donc peu modifiées par cette déformation du cycle. Nous sommes donc amenés à concevoir que la diminution des interactions se fait par la rotation du groupement *tert*-butyle et une rotation autour de la liaison C_1—C_2.

En comparant ces résultats à ceux des divers calculs (3 et 4) et des études au rayons-X (5 et 6) effectués sur divers composés cyclohexaniques substitués par un groupement *tert*-butyle nous pouvons conclure que l'énergie d'interaction du groupement *tert*-butyle avec les substituants du noyau cyclohexanique peut se minimiser de diverses manières. De ce fait les modifications géométriques peuvent être différentes dans l'état cristallin et en solution.

Partie expérimentale

Les pK_{MCS} ont été déterminés en utilisant un ensemble de titration automatique "Radiometer". Les titrages ont été effectués dans les conditions définies par Simon et coll. (12). Les valeurs indiquées dans les tableaux 1 et 2 sont, selon les produits, la moyenne arithmétique de 4 à 7 courbes de titrage indépendante. La méthode des moindres carrés appliquée aux déviations

$$\sqrt{\frac{\sum \Delta^2}{n(n-1)}}$$

est plus petite que 0.018 en unité de pK_{MCS} dans tous les cas considérés.

Nous remercions vivement les Professeurs Altona (Leiden) et Kagan (Orsay) pour leurs diverses remarques sur ce travail, et d'avoir bien voulu faire part de leurs résultats avant leur publication.

Nous remercions également un des arbitres pour ses critiques constructives.

Les auteurs remercient aussi le CNRS et le CNRC pour l'aide financière apportée sous forme d'octrois et de bourses.

Can. J. Chem. Downloaded from www.nrcresearchpress.com by 210.87.254.5 on 09/05/12
For personal use only.

1. R. CORNUBERT. Bull. Soc. Chim. Fr. 996 (1956).
2. (*a*) D. J. PASTO et R. D. RAO. J. Am. Chem. Soc. **91**, 2790 (1969). (*b*) D. J. PASTO et R. D. RAO. J. Am. Chem. Soc. **92**, 5151 (1970).
3. N. L. ALLINGER, H. M. BLATTER, L. A. FREIBERG, et F. M. KARKOWSKI. J. Am. Chem. Soc. **88**, 2999 (1966).
4. C. ALTONA et M. SUNDARALINGAM. Tetrahedron, **26**, 925 (1970). C. ALTONA et M. SUNDARALINGAM. J. Am. Chem. Soc. **92**, 1995 (1970).
5. D. H. FABER et C. ALTONA. Chem. Commun. 1210 (1971).
6. R. PARTHASARATHY, H. B. KAGAN, et J. C. FIAUD. Tetrahedron, **28**, 1529 (1972).
7. F. SHAH MALAK et J. H. P. UTLEY. Chem. Commun., 69 (1967). G. E. HAWKES et J. H. P. UTLEY. Chem. Commun. 1033 (1969). J. P. COLEMAN, F. SHAH MALAK, et J. H. P. UTLEY. J. Chem. Soc. B, 666 (1970).
8. J. SICHER, M. TICHY, F. SIPOS, M. SVOBODA, et J. JONAS. Coll. Czech. Chem. Commun. **29**, 1561 (1964).
9. R. D. STOLOW. J. Am. Chem. Soc. **83**, 2592 (1961). R. D. STOLOW. J. Am. Chem. Soc. **86**, 2170 (1964). R. D. STOLOW et M. M. BONAVENTURA. J. Am. Chem. Soc. **85**, 3636 (1963). R. D. STOLOW, P. M. MCDONAGH, et M. M. BONAVENTURA. J. Am. Chem. Soc. **86**, 2165 (1964). R. D. STOLOW et J. L. MARINI. Tetrahedron Lett. 1449 (1971).
10. D. D. PERRIN et J. CLARK. Quart. Rev. XVIII, 295 (1964).
11. V. PRELOG et O. HAFLIGER. Helv. Chim. Acta, **33**, 2021 (1950).
12. W. SIMON, G. H. LISSY, A. MORIKOFFER, et E. HEILBRONNER. Scheinbare Dissoziationskontanten, Juris Verlag Zurich, 1959.
13. J. C. RICHER et C. FREPPEL. Revista Latinoamericana de Quimica, 125 (1971).
14. M. SVOBODA, J. JONAS, et J. SICHER. Coll. Czech. Chem. Commun. **23**, 1551 (1958).
15. E. L. ELIEL, S. H. SCHROETER, T. J. BRETT, F. J. BIROS, et J. C. RICHER. J. Am. Chem. Soc. **88**, 3327 (1966). E. L. ELIEL et F. J. BIROS. J. Am. Chem. Soc. **88**, 3334 (1966).
16. D. C. BEST, GARY UNDERWOOD, et C. A. KINGSBURY. Chem. Commun. 627 (1969).
17. G. BERTI, B. MACCHIA, F. MACCHIA, S. MERLINO, et U. MUCCINI. Tetrahedron Lett. 3205 (1971).

Can. J. Chem. Downloaded from www.nrcresearchpress.com by 210.87.254.5 on 09/05/12
For personal use only.

The Conformation of Pyridine Nucleotides Studied by ^{31}P and ^{1}H Fast Fourier Transform Nuclear Magnetic Resonance Spectroscopy. II. The Backbone Conformation of Dinucleotides[1]

RAMASWAMY H. SARMA AND RICHARD J. MYNOTT

Department of Chemistry, State University of New York at Albany, 1400 Washington Avenue, Albany, New York 12222

AND

FRANK E. HRUSKA AND DONALD J. WOOD

Department of Chemistry, University of Manitoba, Winnipeg, Manitoba, R3T 2N2

Received December 7, 1972

Using parameters derived from the component mononucleotides, β-NMN, 5′-AMP, and 5′-ADP, the ^{31}P n.m.r. spectra of oxidized pyridine coenzymes, recorded in the presence of coupling from the ribose protons, are analyzed with the use of extensive computer simulations. It is shown that the spectra are compatible only with *gauche–gauche* conformation about the $C_{5'}$—$O_{5'}$ bonds on both the adenine and nicotinamide ends of oxidized pyridine coenzymes. The ^{1}H and ^{1}H–{^{31}P} Fourier transformed 16K n.m.r. spectra of 5′-AMP and 5′-ADP are reported and their full analysis given, and it is shown that the nucleotides exist predominantly in the *gauche–gauche* conformation about the $C_{4'}$—$C_{5'}$ and $C_{5'}$—$O_{5'}$ bonds.

Les spectres r.m.n. ^{31}P des coenzymes oxydées de la pyridine, enregistrés en présence de couplage provenant des protons de la ribose, ont été analysés en utilisant des paramètres obtenus des mononucléotides qui les composent et avec l'aide de nombreuses simulations opérées par l'ordinateur. Il a été montré que les spectres sont seulement en accord avec une conformation *gauche–gauche*, en ce qui a trait aux liens $C_{5'}$—$O_{5'}$ des deux terminaisons adénine et nicotinamide des coenzymes oxydées de la pyridine. Les transformées de Fourier ^{1}H et ^{1}H–{^{31}P} des spectres 16K r.m.n. du 5′-AMP et du 5′-ADP sont décrites ainsi que leurs analyses complètes; il a aussi été montré que les nucléotides existent préférentiellement dans une conformation *gauche–gauche* en ce qui a trait aux liens $C_{4'}$—$C_{5'}$ et $C_{5'}$—$O_{5'}$.

[Traduit par le journal]

Can. J. Chem., **51**, 1843 (1973)

Introduction

An important question about the stereochemistry of pyridine coenzymes **1–4** is the geometric orientation of the pyrophosphate backbone. The three-bond coupling constant data involving ^{31}P nuclei and the 5′-hydrogens ($^{3}J_{PH}$) should provide some information regarding its geometry. Hall and Malcolm (1) demonstrated a

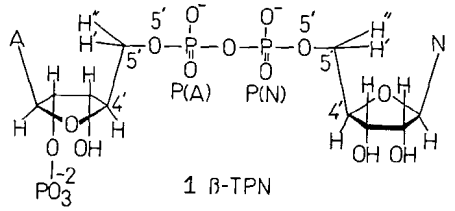

1 β-TPN

2 = TPNH (where N in **1** above is dihydronicotinamide)
3 = DPN (where the PO_3^{2-} in **1** above is OH)
4 = DPNH (where the N in **3** is dihydronicotinamide)

strong stereochemical dependence of vicinal $^{3}J_{PH}$ in H—C—O—P fragments. This was subsequently confirmed by other investigators (2–5). *The gauche $^{3}J_{PH}$ in H—C—O—P fragments have been found to be small and in the range 3 ± 2 Hz whereas the trans $^{3}J_{PH}$ lie in the range of 25 ± 3 Hz.* This information has been used by Schleich *et al.* (6) to determine the conformation of 3′-phosphate in 3′-UMP, by Schweizer and Robins (7) to determine the phosphate conformation of 5′,3′-cyclic AMP and by Sarma and Mynott (8, 9) to determine the preferred conformation constrained to the $C_{5'}$—$O_{5'}$ bonds in β-NMN and β-NMNH.

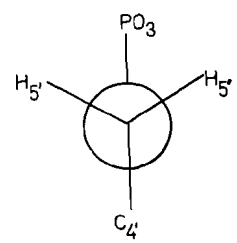

(GAUCHE-GAUCHE)′
gg′
5

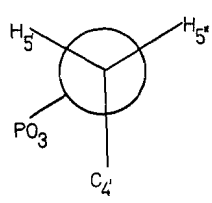

(GAUCHE-TRANS)′
gt′
6

[1]For Part I of this series, see ref. 9.

Can. J. Chem. Downloaded from www.nrcresearchpress.com by 210.87.254.42 on 09/05/12
For personal use only.

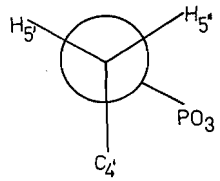

(TRANS - GAUCHE)'
tg'

7

The determination of the conformation (**5**–**7**) about the $C_{5'}$—$O_{5'}$ bonds of the pyridine dinucleotides is complicated by the presence of two phosphate groups, each carrying a ribose unit, making it necessary to define the stereochemistry about two $C_{5'}$—$O_{5'}$ bonds. An obvious way to investigate this problem is to carry out ^1H and ^{31}P n.m.r. studies to determine the four coupling constants, $J_{P(A)5'(A)}$, $J_{P(A)5''(A)}$, $J_{P(N)5'(N)}$, $J_{P(N)5''(N)}$, the letters A and N standing for the adenine and nicotinamide ends of the dinucleotide respectively, and analyze these as for the mononucleotides (8, 9). Unfortunately one cannot obtain these coupling constants *directly* from the ^1H or from the ^{31}P spectra of pyridine coenzymes. In the present investigations, we have examined the ^{31}P n.m.r. spectra of pyridine coenzymes in the presence of coupling from ribose protons at 40.5 MHz and wish to report here that *while the exact* J_{POCH} *coupling constants cannot be determined, the spectrum is consistent only with all the* $^3J_{POCH}$ *coupling constants being in the range for gauche coupling, indicating that the structure is predominantly gauche–gauche about the* $C_{5'}$—$O_{5'}$ *bonds.* Since n.m.r. data from the corresponding mononucleotides were employed during the computer simulations, we have also recorded and fully analysed ^1H n.m.r. spectra of 5′-AMP and 5′-ADP.

Experimental

Instrumentation

The n.m.r. spectra were recorded on a Varian HA-100D spectrometer interfaced to a Digilab FTS-3 NMR-3 Fourier transform data system. The frequencies for the fluorine (lock) channel and proton and phosphorus frequencies (observing or decoupling) were derived from a Digilab 10-94 frequency synthesizer. Hexafluorobenzene in a 1 mm capillary provided the ^{19}F lock signal. The sample temperature was 30.5°, unless otherwise stated. A Digilab 400-2 pulser with a 410-H plug-in unit supplied the proton frequency pulses (100 MHz). Those spectra where the phosphorus nuclei were decoupled were recorded with irradiation derived from a Digilab 50-80 PD plug-in amplifier. The ^{31}P spectra were recorded at 40.48 MHz. The radiofrequency pulses for the observing channel were obtained from a Digilab 400-2 pulser with a 410-P plug-in unit. No internal reference was used for the ^{31}P spectra since the chemical shifts relative to 85% H_3PO_4 had already been determined under similar conditions in the continuous-wave mode in which proton decoupling had been used (10, 11).

Materials

The nucleotides and coenzymes were commercial preparations. The samples were lyophilized three times from 99.8% D_2O and the ^1H spectra were taken in commercial "100%" D_2O. A typical concentration of the internal standard $(CH_3)_4NCl$ was 0.004 *M* for 0.1 *M* solutions. The p*H* values reported are p*H* meter readings from a Leeds and Northrop or a Fischer Accument model 320 p*H* meter. ^{31}P measurements were made in H_2O solutions containing 0.001 *M* EDTA. For solvent perturbation studies, 0.1 *M* sodium salt of the coenzyme (p*H* 8.0 in H_2O) was made up in 50% (v/v) methanol/water mixture.

Results and Discussion

(1) ^1H Fast Fourier Transformed Nuclear Magnetic Resonance Spectra of 5′-AMP and 5′-ADP

In order to determine approximate values of $J_{P(A)5'(A)}$ and $J_{P(A)5''(A)}$ for the dinucleotides we have completely analyzed the ribose region of 5′-AMP and 5′-ADP. The p*H* of the medium was selected such that 5′-AMP would remain as the monophosphate dianion and 5′-ADP as the diphosphate dianion. This situation is most nearly compatible with the ionic state of the phosphates in the pyridine dinucleotides at biological p*H* values. Figure 1*a* shows the ribose region of the ^1H n.m.r. spectrum of 5′-AMP taken in the Fourier mode using a 16K transform. We are primarily interested in the coupling between the ^{31}P nuclei and the 5′-geminal protons. To determine these coupling constants as accurately as possible we have also recorded the ^1H–$\{^{31}P\}$ spectrum of 5′-AMP (Fig. 1*c*). The ribose region of the ^1H and ^1H–$\{^{31}P\}$ n.m.r.[2] spectra of 5′-AMP and 5′-ADP was analyzed with the aid of the computer program LAME. The computer simulated spectra are shown in Fig. 1 and the data are summarized in Table 1.

At this point, it is appropriate to draw some conclusions regarding the favored conformations of 5′-AMP and 5′-ADP from the data in Table 1. The observed sum, $J_{P5'} + J_{P5''}$, strongly suggests (12, 13) that the rotamer constrained to

[2] ^{31}P–$\{^1H\}$ n.m.r. stands for ^{31}P n.m.r. measurements taken under conditions in which the protons are decoupled.

Can. J. Chem. Downloaded from www.nrcresearchpress.com by 210.87.254.42 on 09/05/12
For personal use only.

Can. J. Chem. Downloaded from www.nrcresearchpress.com by 210.87.254.42 on 09/05/12
For personal use only.

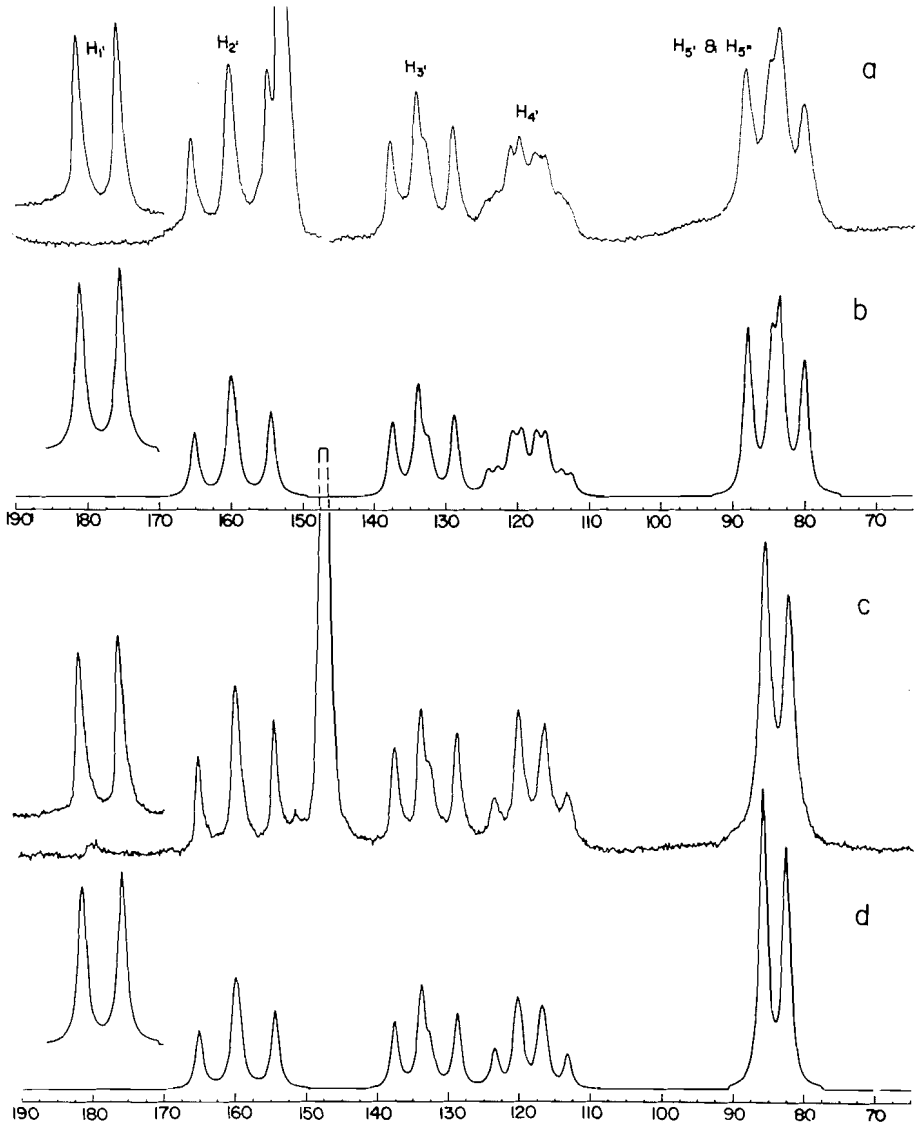

FIG. 1. (*a*), Fourier transformed ^{1}H n.m.r. spectrum of a 0.1 *M* solution of 5′-AMP in 10^{-3} *M* EDTA in 100% D_2O. p*H* = 8.2; number of pulses = 500; pulse width = 50 μs; sampling frequency = 2000 Hz; number of input points = 16 384; delay time = 0.0 s. The scale for (*a*), (*b*), (*c*), and (*d*) is in Hz downfield from internal tetramethylammonium chloride (TMA). (*b*), Simulated spectrum of Fig. 1*a*. Data are given in Table 1. (*c*), Fourier transformed ^{1}H n.m.r. spectrum of the sample as in Fig. 1*a*, but with decoupling of the phosphorus atom. All the parameters are the same as for (*a*), except that the number of pulses = 400. The decoupling caused slight warming up of the sample as is evidenced from the position of the HDO peak. No cooling by N_2 was used because the movement of the HDO resonance was used to uncover the peaks due to 2′ which were partially obscured in (*a*). The slight change in temperature did not affect the chemical shifts or coupling constants to any significant extent. (*d*), Simulated spectrum for the spectrum in Fig. 1*c*.

the $C_{5'}$—$O_{5'}$ is predominantly *gauche–gauche* **5** in both 5′-AMP and 5′-ADP (both 0.1 *M*) at p*H* values 8.2 and 5.2, respectively. Approximate calculations of rotamer populations, using the equations developed in refs. 14 and 15 show that the rotamers constrained to the $C_{4'}$—$C_{5'}$ linkage (**8**–**10**) in 5′-AMP (0.1 *M*) and 5′-ADP (0.1 *M*) at p*H* values 8.2 and 5.2 respectively, are predominantly *gauche–gauche* (**8**), *i.e.* over 65%. We have examined the ^{1}H and ^{1}H–$\{^{31}P\}$ spectra

TABLE 1. ^{1}H chemical shifts and coupling constants of 5′-AMP (pH = 8.2) and 5′-ADP (pH = 5.2), concentrations 0.1 M, temperature 30.5°. Chemical shifts are in p.p.m. downfield from tetramethylammonium chloride

Nucleotide	Proton designation	Chemical shift (p.p.m.)	Coupling constant (Hz)
5′-AMP	1′	2.91	$J_{1'2'} = 5.7$
	2′	1.60	$J_{2'3'} = 5.1$
	3′	1.33	$J_{3'4'} = 3.7$
	4′	1.18	$J_{4'5'} + J_{4'5''} = 6.8$†
	5′	0.85*	
	5″	0.83*	$J_{4'P} = \pm 1.4$
			$J_{5'P} + J_{5''P} = 9.0$†
			$J_{5'5''} = -10.0$‡
5′-ADP	1′	2.91	$J_{1'2'} = 5.6$
	2′	1.55	$J_{2'3'} = 5.1$
	3′	1.37	$J_{3'4'} = 3.8$
	4′	1.22	$J_{4'5'} + J_{4'5''} = 6.3$†
	5′	1.07	
	5″	1.06	$J_{4'P\alpha} = \pm 1.2$
			$J_{4'P\beta} = \pm 1.0$
			$J_{5'P\alpha} + J_{5''P\alpha} = 10.4$†
			$J_{5'P\beta} \simeq 1$
			$J_{5''P\beta} \simeq 1$
			$J_{5'5''} = -10.0$‡
			$J_{P(\alpha)P(\beta)} = +20.0$

*Only the mean value of the chemical shifts of 5′ and 5″ is obtained from the analysis.
†Only the sum significant. (14, 15).
‡This is an arbitrary value. The experimentally observed values for 5′ UMP and 6-*aza*-5′-UMP are −13.5 and −11.3 Hz. In dUMP, the 2′ and 2″ were strongly coupled and no experimental value could be obtained. In fact, during simulations we have used values from −10 to −13; no change in spectrum appearance was observed.

of 5′-AMP, pH 8.2, in the concentration range of 0.4–0.001 M and have been unable to detect any significant change in the value of $J_{4'5'} + J_{4'5''}$ and $J_{POCH(5')} + J_{POCH(5'')}$ with dilution, indicating that in 5′AMP the predominant rotamer constrained to the $C_{4'}$—$C_{5'}$ and $C_{5'}$—$O_{5'}$ bonds are both *gauche–gauche* (**5** and **8**) in the whole of the concentration range presently accessible. The observed four-bond coupling (16) $^4J_{P4'}$ of about 1.4 Hz (Table 1) may be further evidence for an all-*trans* (W) spatial relationship between phosphorus and the 4′-hydrogen encountered when the molecule is oriented *gauche–gauche* about both $C_{4'}$—$C_{5'}$ and $C_{5'}$—$O_{5'}$ bonds (**11**). Hall and coworkers (1) have presented clear evidence that H–P coupling in H—C—

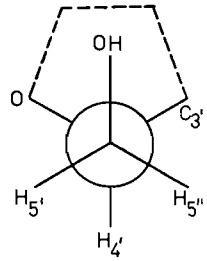

GAUCHE-GAUCHE
gg
8

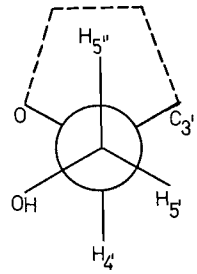

GAUCHE-TRANS
gt
9

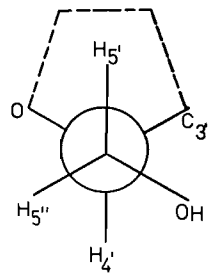

TRANS-GAUCHE
tg
10

C—O—P fragments is maximal (*ca.* 2.5 Hz) when the all-*trans* arrangement is assumed and decreases (probably to zero) for less favorable arrangements.

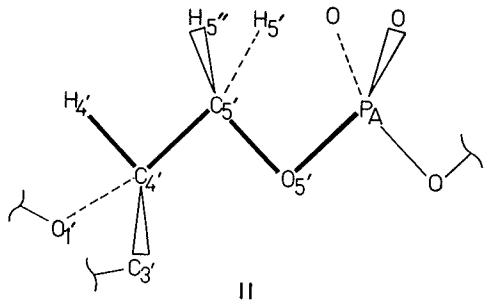

11

Detailed discussion of the use of Karplus equation for elucidating the nature of the furanose ring pucker has appeared in the literature (9, 13, 15). In this work we attempt no indepth analysis of the ribose vicinal $J_{1'2'}$, $J_{2'3'}$, and $J_{3'4'}$ coupling constants. We deem it necessary to indicate that the observed data for 5′-AMP and 5′-ADP (Table 1) are consistent with a flexible ring system undergoing pseudorotational motion proposed by Kilpatrick *et al.* (17)

Can. J. Chem. Downloaded from www.nrcresearchpress.com by 210.87.254.42 on 09/05/12
For personal use only.

Can. J. Chem. Downloaded from www.nrcresearchpress.com by 210.87.254.42 on 09/05/12
For personal use only.

for cyclopentane, and by Hall *et al.* (18) and Sundaralingam (19) for the ribofuranose ring.[3]

(2) ^{31}P Pulsed Fast Fourier Transformed Nuclear Magnetic Resonance Spectra of Oxidized Pyridine Dinocleotides

^{31}P–{^{1}H} spectra of oxidized pyridine dinucleotides (11, 20) show that the two ^{31}P nuclei of the pyrophosphate backbone appear as a *well resolved* AB quartet, $|^{2}J_{POP}|$ being 20.3 Hz and $\nu_0\delta \simeq$ 0.3 p.p.m. Figure 2 shows the ^{31}P fast Fourier transformed 40.48 MHz spectrum of β-TPN, *in which the ribose protons were not decoupled* (β-DPN also gave a similar spectrum). Only the pyrophosphate region is shown. The conditions under which the spectrum was taken are detailed in the caption of Fig. 2. This spectrum has no fine features, and appears as a broad central peak flanked by broad satellites. The 89 MHz ^{31}P n.m.r. spectrum of oxidized pyridine coenzymes (20) also consists of broad resonances in which the central peaks are resolved but there are few defined features. The difference in appearance between the ^{31}P and ^{31}P–{^{1}H} n.m.r. spectra must be due to the coupling of the two ^{31}P nuclei with the neighboring protons (5′, 5″, 4′) of the backbone, but clearly these coupling constants, required to delineate the backbone geometry, cannot be obtained *directly* from either the ^{1}H or the ^{31}P spectrum. However, *it can be shown easily that these coupling constants must fall into the range of gauche* $^{3}J_{POCH}$ *coupling to be able to produce the observed spectrum.*

(3) Computer Simulation of ^{31}P Nuclear Magnetic Resonance Spectra for Possible Backbone Geometries

The observed ^{31}P spectrum of the dinucleotide may arise from any of the nine cases presented in Table 2 or weighted averages of several cases.

[3]X-ray data on a large number of nucleosides and nucleotides indicate that the ribose moiety exists either in the C-3′ *endo* or in the C-2′ *endo* mode. The present n.m.r. data is consistent with a situation in which ribose exist as an equilibrium mixture of the above modes undergoing rapid interconversion. It has been reported (22–24) that the value of $J_{1'2'}$ for 5′-AMP increases slightly as the concentration is reduced. We have examined the H^{1}–{^{31}P} spectra of 5′-AMP in the range 0.4–0.001 *M* and have also observed this increase in $J_{1'2'}$ with dilution; in addition $J_{3'4'}$ shows a corresponding decrease with dilution. These data are consistent with the view that in these concentration ranges 5′-AMP exists as a dynamic equilibrium of 2′-*endo* ⇌ 3′-*endo* with a small shift in population towards 2′-*endo* at lower concentrations.

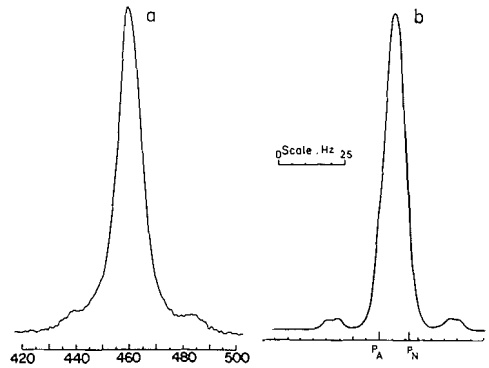

FIG. 2. (*a*) Fourier transformed ^{31}P n.m.r. spectrum of 0.25 *M* aqueous solution of β-TPN in 3×10^{-3} *M* EDTA, p*H* = 7.8. Number of pulses = 15 030; pulse width = 30 μs; sampling frequency = 2000 Hz; number of input points = 2048; delay time = 0.0 s. Scales are given in Hz upfield from external 85% orthophosphoric acid. Observing channel frequency = 40.48 MHz. The spectra illustrated were computed using triangular apodization; the envelope width at half height = 10.5 Hz. Spectra computed from the same FID without apodization were practically identical in shape and had an envelope width at half height of 10.3 Hz. (*b*) Case 1 simulation after refinement and adjustment of parameters. The data used were as follows: *chemical shifts*: P(A) = 11.2; P(N) = 11.5 (both in p.p.m. upfield from external 85% orthophosphoric acid): 4′(A) = 1.20; 5′(A) = 1.07; 5″(A) = 1.07; 4′(N) = 1.20; 5′(N) = 1.01; 5″ (N) = 0.84 (all in p.p.m. downfield from internal TMA). *coupling constants* (in Hz): $J_{P(A)P(N)} = 20.3$; $J_{P(A)4'(N)} = 0.8$; $J_{P(A)4'(A)} = 1.4$; $J_{P(A)5'(A)} = 4.7$; $J_{P(N)4'(N)} = 1.4$; $J_{P(N)4'(A)} = 0.8$; $J_{P(N)5'(N)} = 4.3$; $J_{P(N)5''(N)} = 4.5$; $J_{4'(N)5''(N)} = 2.0$; $J_{4'(N)5'(N)} = 2.6$; $J_{4'(A)5'(A)} = 2.6$; $J_{4'(A)5''(A)} = 2.0$; $J_{5'(A)5''(A)} = 12.1$; $J_{5'(N)5''(N)} = 12.1$.

TABLE 2. Theoretical possibilities of the nine classical torsional diastereomers constrained to the $C_{5'}$—$O_{5'}$ bonds of pyridine dinucleotides

	Adenine component of pyridine dinucleotide		Nicotinamide component of pyridine dinucleotide	
Case no.	5′	5″	5′	5″
1	g*	g	g	g
2	g	g	g	t†
3	g	g	t	g
4	g	t	g	g
5	t	g	g	g
6	g	t	g	t
7	t	g	g	t
8	g	t	t	g
9	t	g	t	g

*g = *gauche* with respect to the ^{31}P nucleus.
†t = *trans* with respect to the ^{31}P nucleus.

TABLE 3. Parameters used for the initial simulations of the ^{31}P n.m.r. spectra of various cases listed in Table 2*

Coupling constants (Hz)		Chemical shift (p.p.m.)
$J_{P(A)5'(A)} = 5.0$ (*gauche*);	$J_{P(A)5''(A)} = 5.0$ (*gauche*)	P(A) = 11.19†
$J_{P(A)5'(N)} = 0.0$	$J_{P(A)5''(N)} = 0.0$	P(N) = 11.53
$J_{P(N)5'(A)} = 0.0$	$J_{P(N)5''(A)} = 0.0$	
$J_{P(N)5'(N)} = 4.2$ (*gauche*);	$J_{P(N)5''(N)} = 4.4$ (*gauche*)	5'(A) = 1.07‡
$J_{5'(A)5'(N)} = 0.0$	$J_{5'(A)5''(N)} = 0.0$	5''(A) = 1.07‡
$J_{5''(A)5'(N)} = 0.0$	$J_{5''(A)5''(N)} = 0.0$	5'(N) = 1.01
$J_{5'(A)5''(A)} = -10.0$	$J_{5'(N)5''(N)} = -12.1$	5''(N) = 0.84
$J_{P(A)P(N)} = 20.3$	$J_{P(N)5'(N)} = \pm 25.0$ (*trans*)	
$J_{P(N)5''(N)} = \pm 25.0$(*trans*);	$J_{P(A)5'(A)} = \pm 25.0$ (*trans*)	
$J_{P(A)5''(A)} = \pm 25.0$(*trans*)		

*The letters (A) and (N) stand for the adenine and nicotinamide ends of the pyridine dinucleotide respectively. The line width at half height used for the lineshape program was 2.3 Hz; this was a representative value from $^{31}P-\{^1H\}$ spectra of the same compound.
†In p.p.m. to higher field than external 85% H_3PO_4.
‡In p.p.m. to lower field than internal tetramethylammonium chloride.

As a starting point in the simulations, we have assumed that one can use the $^3J_{POCH}$ values from the ^1H n.m.r. data of the component mononucleotides, *viz.*, β-NMN, 5'-AMP, and 5'ADP. Data for the last two compounds were taken from Table 1; data for β-NMN were taken from the analysis of spectra recorded at p*H* 8.0 in the Fourier mode by Sarma and Mynott (8, 9). The parameters selected to carry out the simulations of the nine cases are given in Table 3. An absolute spectral assignment of the 5'-, 5''-hydrogens cannot be made at present and thus a distinction between the *gauche–trans* and *trans–gauche* rotamers (about $C_{4'}—C_{5'}$ or $C_{5'}—O_{5'}$ of a particular mononucleotide moiety) should not be made. Thus the nine cases (Table 2), with this limitation, must be grouped into four types: (*a*) the all-*gauche* conformation (case 1); (*b*) the adenine component is *gauche–gauche*, the nicotinamide component *gauche* and *trans* (cases 2 and 3); (*c*) the adenine component *gauche* and *trans*, nicotinamide *gauche–gauche* (cases 4 and 5); (*d*) adenine and nicotinamide components both *gauche* and *trans* (cases 6–9). The approach is thus limited to an evaluation of the contribution from the *gauche–gauche* and the *combined contribution* from the *gauche–trans* and *trans–gauche* conformations of the individual mononucleotides. Representative cases (1, 2, 4, 6) were chosen from each type. The computer simulated spectra, using the parameters in Table 3, are shown in Fig. 3. Also illustrated in the simulations for case 2 is the spectrum to be expected if $^3J_{POCH}$ (*trans*) has the opposite sign from $^3J_{POCH}$ (*gauche*). These preliminary calculations show that *only case 1* or a rapidly exchanging mixture, predominantly of case 1, could possibly give the observed ^{31}P n.m.r. spectrum (compare Fig. 2*a* with case 1 in Fig. 3*a*). The final calculated spectrum for case 1 is shown in Fig. 2*b*, and the line width is 9 Hz. In the experimental spectrum, the band width was found to be 10.3 Hz. The agreement between the calculated (Fig. 2*b*) and experimental (Fig. 2*a*) spectra is reasonable. The various final parameters are listed in the legend for Fig. 2*b*.

(4) Effect of Inter- and Intra-molecular Interactions on the Conformation Constrained to $C_{5'}—O_{5'}$ Bonds

Recent studies (24, 25) have shown that the *chemical shifts* of the adenine and certain ribose protons of pyridine coenzymes show concentration dependence indicating the formation of dimers in which the adenine moieties interact. It is therefore relevant to consider to what extent the conclusions of the previous sections may be invalidated by intermolecular interactions, especially since the concentration employed for recording the ^{31}P n.m.r. spectra (protons not decoupled) were rather high, in order to obtain the wings of the spectral envelope within a reasonable time. Previous studies have shown that intermolecular interactions are much weaker at concentrations of 0.05 *M* (25) and therefore the undecoupled ^{31}P n.m.r. spectra were also examined at this concentration; no significant change in envelope form or width was detected. A concentration below 0.05 *M* was not employed because the compounds are too unstable to last the time required for data collection in the ^{31}P mode. The conclusion about the geometry

Can. J. Chem. Downloaded from www.nrcresearchpress.com by 210.87.254.42 on 09/05/12
For personal use only.

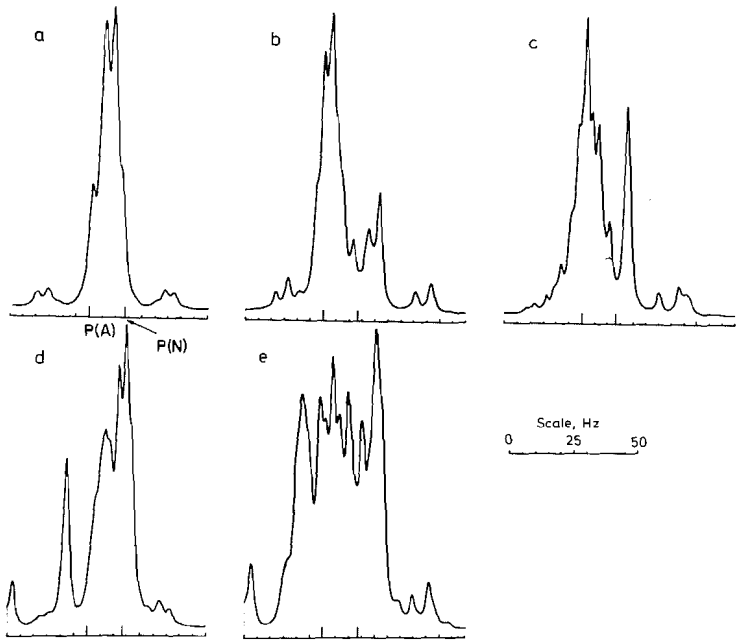

FIG. 3. Simulated ^{31}P n.m.r. spectrum of cases 1, 2, 4, and 6 from Table 1. The parameters used are given in Table 3. (*a*), Case 1; A-$C_{5'}$—$O_{5'}$ *gauche–gauche*-N-$C_{5'}$—$O_{5'}$ *gauche–gauche*. (*b*), Case 2A. A-$C_{5'}$—$O_{5'}$ *gauche–gauche*-N-$C_{5'}$—$O_{5'}$ *gauche–trans*. (*c*), Case 2B. As for (*b*) except that $J_{P(A)5'(A)}$ has been given the opposite sign. (*d*), Case 4. A-$C_{5'}$—$O_{5'}$ *gauche–trans*-N-$C_{5'}$—$O_{5'}$ *gauche–gauche*. (*e*) Case 6. A-$C_{5'}$—$O_{5'}$ *gauche–trans*-N-$C_{5'}$—$O_{5'}$ *gauche–trans*.

constrained to the $C_{5'}$—$O_{5'}$ bonds therefore appears valid in the presence of intermolecular attractions. We have also previously examined the ^{1}H n.m.r. spectra of oxidized pyridine coenzymes in the concentration range 0.4–0.001 *M*. While we have not attempted a full analysis of the ribose proton region, it is clear that there is no significant change in the coupling constants of the ribose region, although there are some minor changes in the spectrum attributable to changes in chemical shift resulting from intermolecular stacking; most certainly a concentration-dependent change in conformation about either $C_{5'}$—$O_{5'}$ bond and introduction of a $^{3}J_{POCH}$ *trans* coupling (25 Hz) would be revealed by a large change in the spectrum in this region.

There is considerable spectrocopic evidence, recently reviewed (10), to show that at biological p*H* and temperature in D_2O or H_2O solutions, pyridine coenzymes exist, on a time-average, in a folded conformation. Sarma and Mynott (25) have shown that the preferred geometry of the folded species is probably an internally stacked right-handed helix. It has not been established whether the system undergoes a dynamic exchange between a folded, several partially folded, and extended forms (21, 24) or whether there is a simple two-state equilibrium (26, 27). However, it is generally agreed that as the temperature is raised, or when organic solvents such as methanol are introduced, the coenzyme becomes more extended (26, 28, 29).

To examine whether unfolding the coenzyme would affect the $C_{5'}$—$O_{5'}$ rotamers, we have studied the effect of temperature on the undecoupled ^{31}P spectrum of oxidized pyridine coenzymes. The range of temperature employed was 8–50°. The concentration of 0.25 *M* enabled the simultaneous monitoring of the effect of both inter- and intramolecular destacking on the backbone geometry. A temperature-induced change in the $C_{5'}$—$O_{5'}$ rotamer population would definitely be manifested in the ^{31}P n.m.r. spectrum, but no such change was observed.[4] In fact, no significant change in the spectrum envelope and width at half height was observed at 8 or 50°, indicating that J_{POCH} was insensi-

[4]Examination of the ^{31}P-{^{1}H} spectra as a function of temperature (8–50°) showed the following results. $^{2}J_{POP}$ was independent of temperature. The difference in chemical shifts between the two ^{31}P nuclei remained the same. However, the center of the AB quartet, as well as the two individual ^{31}P chemical shifts moved to higher fields by 5 Hz (H_3PO_4, 85%, external reference).

Can. J. Chem. Downloaded from www.nrcresearchpress.com by 210.87.254.42 on 09/05/12
For personal use only.

Can. J. Chem. Downloaded from www.nrcresearchpress.com by 210.87.254.42 on 09/05/12
For personal use only.

tive to temperature-induced perturbations. We have also examined the undecoupled ^{31}P n.m.r. spectrum of a 0.1 *M* solution of β-TPN in a 1:1 methanol–water mixture. As expected from temperature studies, the general form of the spectrum envelope was unchanged; however there was a slight narrowing of the central band, which, from $^{31}P-\{^1H\}$ spectrum, is accounted for by a small reduction in $\nu_0\delta$.

(5) Possible Limitations in the Present Approach

The protons of the ribose region and the phosphorus nuclei of the backbone strictly constitute a 14-spin system, but our analysis has been simplified to that of an 8-spin system. This is entirely reasonable since the possibility of virtual coupling of the 1′-, 2′-, or 3′-protons on either ribose to the ^{31}P nuclei cannot be significant. The $^{31}P-\{^1H\}$ n.m.r. spectra of oxidized pyridine coenzymes are strongly coupled AB quartets at 40.5 MHz ($J/\nu_0\delta = 1.7$) and it would be advantageous to record the undecoupled ^{31}P spectra (in order to extract the J_{POCH} couplings) at *very much* higher fields to produce first order spectra. Nevertheless, we feel that the ^{31}P n.m.r. spectra at 40.5 MHz are sensitive enough to variations of $^3J_{POCH}$ to be able to come to reasonable conclusions about the backbone geometry. This is simply because $^3J_{POCH(gauche)} = 3 \pm 2$ and $^3J_{POCH(trans)} = 25 \pm 3$ Hz. The spectra are strongly second order at 89 MHz ($J/\nu_0\delta = 0.78$ for β-TPN, but they can be a useful check of the conclusions reported here. We have compared the published ^{31}P n.m.r. spectrum of β-DPN at 89 MHz (20) with a simulation carried out by us in the way described previously (only changing $\nu_0\delta$) and found this to be consistent with an all *gauche* conformation for the backbone. It could be argued that it is not reasonable to use $^3J_{POCH}$ (*i.e.* $J_{P5'}$) coupling constants from the mononucleotides (to computer-simulate the ^{31}P spectra of dinucleotides) since this is in effect assumes that the mononucleotides can be considered as *entirely gauche–gauche* about the $C_{5'}—O_{5'}$ bonds. However, we have no more reasonable estimates for the *gauche* couplings, and these still fall within the observed range of 3 ± 2 Hz for $^3J_{POCH(gauche)}$ (1–5). One may argue that we cannot assume that the relative chemical shifts of 4′-, 5′-, and 5″-protons of the nicotinamide and adenine ends of the dinucleotide as identical to those of the mononucleotides, as we have done in our simulations. However, examination of the ^1H 220 MHz and the $^1H-\{^{31}P\}$ 100 MHz spectra of the dinucleotides indicates that these chemical shifts fall in the range we have used, though the complex overlap of the transitions does not allow us to determine them exactly. One may further notice that we have attempted to simulate an envelope comprised of hundreds of closely spaced lines (this is especially so in the case of the backbone when both $C_{5'}—O_{5'}$ bonds are *gauche–gauche*) and that we may not be able to obtain the exact values of $^3J_{POCH}$. Similar types of envelope simulations have been successfully done by Chan and Krieshman (30) who obtained the approximate *J* values for the ribose–phosphate backbone in poly U. In the present paper *we wish to make it clear that we have attempted to obtain* the approximate magnitudes of $^3J_{POCH}$ to see whether any of $J_{P(A)5'(A)}$, $J_{P(A)5''(A)}$, $J_{P(N)5'(N)}$ and $J_{P(N)5''(N)}$ can lie in the range for *trans* coupling (*i.e.* 25 Hz). The important conclusion that emerges from the present study is that the rotamers constrained to the $C_{5'}—O_{5'}$ bonds of both the adenine and nicotinamide ends of oxidized pyridine coenzymes are predominantly *gauche–gauche* (**5**) and that this conclusion is valid irrespective of inter- or intra-molecular interactions.

Our conclusion that the favored conformation about both the $C_{5'}–O_{5'}$ bonds of the backbone of oxidized pyridine coenzymes is *gauche–gauche* is consistent with the observation for nucleotides in the solid state. Thus *gauche–gauche* conformation appears overwhelmingly favored for 5′-mononucleotides (31), appears in the dimers UpA (32) as well as in poly A, RNA, and DNA (33, 34).

This research was supported in part by grants from the National Cancer Institute of NIH (CA 12462-01 and CA 12462-02) and the National Science Foundation (GB 28015), the National Research Council of Canada (CI1544, A6434) and the Research Corporation of New York. The Faculty of Graduate Studies of the University of Manitoba are thanked for a postdoctoral fellowship to D.J.W. The fast Fourier transform system was bought by funds kindly furnished by the National Science Foundation (GP28061) and the State University of New York. The authors are greatly indebted to all these agencies for their support of basic research.

1. L. D. HALL and R. B. MALCOLM. Chem. Ind. (Lond). 92, (1968); Can. J. Chem. **50**, 2092, 2102, (1972); B. DONALDSON and L. D. HALL. Can. J. Chem. **50**, 2111 (1972).
2. M. KAINOSHO, A. NAKAMURA, and M. TSUBOI. Bull. Chem. Soc. Jap. **42**, 1713 (1969).

3. M. TSUBOI, M. KAINOSHO, and A. NAKAMURA. *In* Recent developments of magnetic resonance in biological systems. *Edited by* S. Fujiwara and L. H. Piette. Hirokawa Publishing Co., Tokyo. 1969. p. 43.
4. M. TSUBOI, S. TAKAHASHI, Y. KYOGKU, H. HAYATSU, T. UKITA, and M. KAINOSHO. Science, **166**, 1504 (1969).
5. I. C. P. SMITH, H. H. MANTSCH, R. D. LAPPER, R. DESLAURIERS, and T. SCHLEICH. Proceedings international symposium on the conformation of biological molecules and polymers, symposia on quantum chemistry and biochemistry. Vol. V. *Edited by* B. Pullman and E. D. Bergmann. Academic Press. In press.
6. T. SCHLEICH, B. J. BLACKBURN, R. D. LAPPER, and I. C. P. SMITH. Biochem. **11**, 137 (1972).
7. M. P. SCHWEIZER and R. K. ROBINS. Proceedings international symposium on the conformation of biological molecules and polymers, symposia on quantum chemistry and biochemistry. Vol. V. *Edited by* B. Pullman and E. D. Bergmann. Academic Press. In press.
8. R. H. SARMA and R. J. MYNOTT. Chem. Commun. 975 (1972).
9. R. H. SARMA and R. J. MYNOTT. J. Am. Chem. Soc. **95**, 1641 (1973).
10. R. H. SARMA and R. J. MYNOTT. Proceedings international symposium on the conformation of biological molecules and polymers, symposia on quantum chemistry and biochemistry. Vol. V. *Edited by* B. Pullman and E. D. Bergmann. Academic Press. In press.
11. R. H. SARMA and R. J. MYNOTT. Org. Magn. Res. **4**, 577 (1972).
12. F. E. HRUSKA, A. A. Smith, and J. G. DALTON. J. Am. Chem. Soc. **93**, 4334 (1971).
13. F. E. HRUSKA. Proceedings international symposium on the conformation of biological molecules and polymers, symposia on quantum chemistry and biochemistry. Vol. V. *Edited by* B. Pullman and E. D. Bergmann. Academic Press. In press.
14. F. E. HRUSKA, A. A. GREY, and I. C. P. SMITH. J. Am. Chem. Soc. **92**, 4088 (1970).
15. B. J. BLACKBURN, A. A. GREY, I. C. P. SMITH, and F. E. HRUSKA. Can. J. Chem. **48**, 2866 (1970).
16. M. BARFIELD and B. CHAKRABARTI. Chem. Rev. **69**, 751 (1969).
17. J. E. KILPATRICK, K. S. PITZER, and R. SPITZER. J. Am. Chem. Soc. **69**, 2483 (1947).
18. L. D. HALL, P. R. STEINER, and C. PEDERSEN. Can. J. Chem. **48**, 1155 (1970).
19. M. SUNDARALINGAM. Proceedings international symposium on the conformation of biological molecules and polymers, symposia on quantum chemistry and biochemistry. Vol. V. *Edited by* B. Pullman and E. D. Bergmann. Academic Press. In press.
20. M. BLUMENSTEIN and M. A. RAFTERY. Biochem. **11**, 1643 (1972).
21. S. I. CHAN and J. H. NELSON. J. Am. Chem. Soc. **91**, 168 (1969).
22. P. O. P. Ts'O, N. S. KONDO, M. P. SCHWEIZER, and D. P. HOLLIS. Biochem. **8**, 997 (1969).
23. S. S. DANYLUK and F. E. HRUSKA. Biochem. **7**, 1038 (1968).
24. G. MCDONALD, B. BROWN, D. P. HOLLIS, and C. WALTER. Biochem. **11**, 1920 (1972).
25. R. H. SARMA and R. J. MYNOTT. Chem. Commun. 975 (1972).
26. O. JARDETSKY and N. G. WADE-JARDETZKY. J. Biol. Chem. **241**, 85 (1966).
27. N. J. OPPENHEIMER, L. J. ARNOLD, and N. O. KAPLAN. Proc. Natl. Acad. Sci. USA, **68**, 3200 (1971).
28. R. H. SARMA, V. Ross, and N. O. KAPLAN. Biochem. **7**, 3052 (1968).
29. W. A. CATTERALL, D. P. HOLLIS, and C. F. WALTER. Biochem. **8**, 4032 (1969).
30. S. I. CHAN and G. P. KRIESHMAN. J. Am. Chem. Soc. **92**, 1102 (1970).
31. M. SUNDARALINGAM. Biopolym. **7**, 821 (1969).
32. J. RUBIN, T. BRENNAN, and M. SUNDARALINGAM. Biochem. **11**, 3112 (1972).
33. A. RICH, D. R. DAVIES, F. H. C. CRICK, and J. D. WATSON. J. Mol. Biol. **3**, 71 (1961).
34. S. ARNOTT, S. D. DOVER, and A. J. WONACOTT. Acta Cryst. B**25**, 2192 (1969).

Can. J. Chem. Downloaded from www.nrcresearchpress.com by 210.87.254.42 on 09/05/12
For personal use only.

The Synthesis of Specifically Deuterated Anthracenes

J. L. CHARLTON AND R. AGAGNIER

Department of Chemistry, University of Manitoba, Winnipeg, Manitoba

Received December 5, 1972

Synthetic methods for preparation of anthracene-1,2,3,4-d_4, 1,4,5,8-d_4, 2,3,6,7-d_4, 2,3-d_2, 1,4-d_2, and 9,10-d_2 are described.

On décrit des méthodes spécifiques de synthèse pour la préparation de l'anthracène-1,2,3,4-d_4, -1,4,5,8-d_4, 2,3,6,7-d_4, -2,3-d_2, -1,4-d_2 et 9,10-d_2. [Traduit par le journal]

Can. J. Chem., **51**, 1852 (1973)

Can. J. Chem. Downloaded from www.nrcresearchpress.com by 210.87.254.42 on 09/05/12
For personal use only.

Recently, there has been considerable theoretical interest in the mechanism of radiationless transitions in aromatic molecules and, in particular, the effect of various substituent groups on the rate of these transitions (1). In this regard, it has been popular to determine experimentally the triplet lifetimes of specifically deuterated compounds and to correlate the results with theoretically calculated values. In particular, we wished to carry out such a study utilizing the deuterated derivatives of anthracene listed in Table 1.

Of the derivatives listed, only anthracene-9,10-d_2 (**1**) has been mentioned previously in the literature. It was first synthesized by treating anthracene with D_2SO_4. However, the procedure also gave mono and other polydeuterated products from which **1** was inseparable (2). **1** can be synthesized specifically by hydrolyzing the corresponding dimagnesium derivative with D_2O (99.8%) but preparation of the Grignard is difficult (3, 4). The most successful synthetic method involves preparation of the dilithio derivative followed by hydrolysis with D_2O. Using this method, Petukhov *et al.* originally reported synthesizing **1** in 72% isotopic purity (5). However, Pawliczek and Günther reported isotopic purities of greater than 97% using essentially the same method (6).

Two main synthetic routes are possible for the remaining derivatives in Table 1. Either the deuterium can be introduced after the carbon skeleton is constructed or the molecule can be prepared from suitably deuterated precursors. In the former method metalation and D_2O hydrolysis of the aromatic halides has been one of the more popular methods of approach. However, problems are often encountered in preparing the organometallic derivatives and the isotopic purity of the product is variable (3).

TABLE 1. Isotopic composition of deuterated anthracenes synthesized

Anthracene	Purity (%)*		
9,10-d_2 (**1**)	7.0 d_1†	85.0 d_2	7.0 d_3
	11.6 d_1‡	88.0 d_2	
2,3-d_2 (**2**)	4.2 d_0	9.5 d_1	86.0 d_2
1,4-d_2 (**3**)	5.1 d_0	3.8 d_1	91.2 d_2
1,4,5,8-d_4 (**4**)	1.1 d_2	3.6 d_3	95.3 d_4
2,3,6,7-d_4 (**5**)	7.6 d_2	17.0 d_3	74.0 d_4
1,2,3,4-d_4 (**6**)	3.7 d_0	7.0 d_3	88.0 d_4

*Mol. % isotopic composition. Values are precise to only ±2%.
†Method *b*; see Experimental.
‡Method *a*; see Experimental.

The best published method for the preparation of perdeuterated anthracene is that of Dinh-Nguyên and Stenhagen (7) using D_2O_2 and a catalyst. The perdeutero compound can also be prepared by base or acid catalyzed deuterium exchange and the latter method is also suitable for specific deuteration if the rates of exchange are sufficiently position dependent. (8, 9, 2). Synthesis of the deuterated aromatics from deuterated precursors can be successful if a high yield procedure, which utilizes relatively simple starting materials, is available.

Results and Discussion

Anthracene-9,10-d_2 was synthesized both by the method of Petukhov *et al.* (5) and by acid-catalyzed deuterium–hydrogen exchange. The former method involved treating 9,10-dibromoanthracene with *n*-butyl lithium in benzene to prepare the 9,10-dilithioanthracene. This was subsequently hydrolyzed with D_2O yielding the dideutero derivative. This reaction was carried out several times and the isotopic purity (mol % dideutero) was never higher than 90% (the remaining 10% being monodeutero). As an alternative procedure we considered a mild

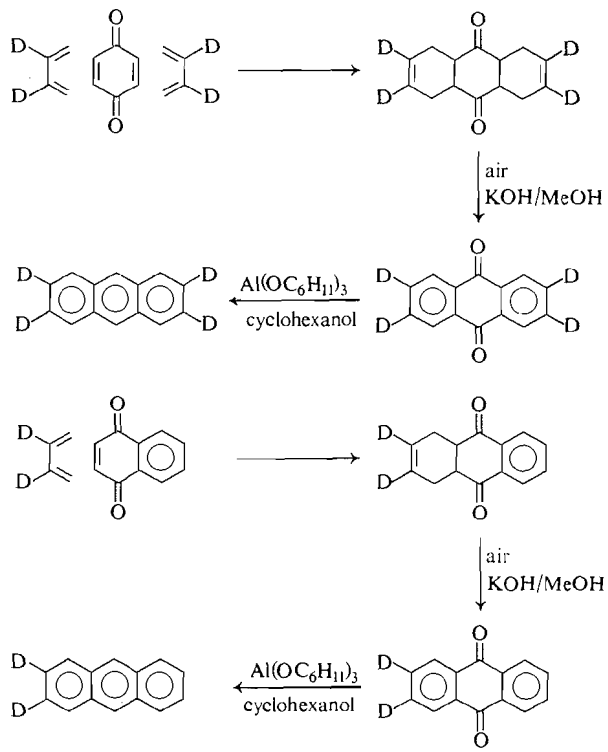

SCHEME 1

acid-catalyzed exchange reaction as the 9,10 positions in anthracene should exchange more rapidly. Since it had already been reported that D_2SO_4 gave a mixture of both mono and polydeuterated material a weaker acid was sought. *p*-Toluenesulfonic acid-*d* was chosen both because of its higher pK_a and its solubility in organic solvents. The acid was prepared *in situ* by adding D_2O to a mixture of anthracene and *p*-toluenesulfonyl chloride in benzene. The exchange occurred rapidly in refluxing benzene after an induction period of up to 48 h. This led us to believe that the hydrolysis of the acid chloride was rate limiting and probably autocatalytic. Although the method used was satisfactory it would probably be more expedient to hydrolyze the sulfonylchloride in a separate step. The product was isolated by stirring the mixture with saturated aqueous bicarbonate overnight and extracting with benzene. The isotopic composition was 85% d_2, 7% d_3, and 7% d_1 (mol %).

After considering the various possibilities for synthesis of the remaining anthracene derivatives we concluded that a scheme based on the Diels–Alder adducts of deuterated butadienes with *p*-benzoquinone or 1,4-naphthoquinone was best. Two representative examples are illustrated in Scheme 1. The basic procedure had been successfully carried out on the nondeuterated analogs by Alder and Stein (10) and by Diels and Alder (11).

In order to utilize the diene synthesis it was necessary to prepare specifically deuterated butadienes. These were prepared using known literature procedures or modifications of these procedures. Perdeutero-1,3-butadiene was synthesized from perchlorobutadiene using zinc and D_2O as described by Craig and Fowler (12). The yields varied from run to run but were generally around 50%. The syntheses of 1,3-butadiene-1,1,4,4-d_4 and -2,3-d_2 are outlined in Scheme 2.

The 3-sulfolenes were prepared from the corresponding butadienes and SO_2 by the method of Grummitt *et al.* (13) and the base-catalyzed exchange accomplished as described by Cope *et al.* (14). The deuterated butadienes were subsequently recovered by pyrolyzing the sulfolenes at 130–160 °C under a slow stream of nitrogen. The Diels–Alder adducts of the

Can. J. Chem. Downloaded from www.nrcresearchpress.com by 210.87.254.42 on 09/05/12
For personal use only.

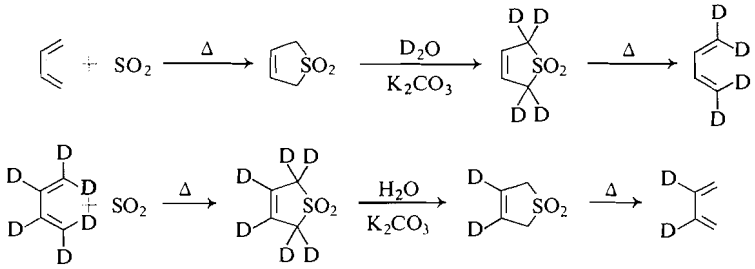

SCHEME 2

deuterated butadienes and *p*-benzoquinone (or 1,4-naphthoquinone) were formed by heating the quinone in an excess of the butadiene at 125 °C for 24 h in a sealed evacuated tube. The yields were quantitative in most cases.

The method of Alder and Stein was also used for the oxidation of the octahydroanthraquinones to the quinones (10). However, it was noted that this base-catalyzed oxidation (air and ethanolic KOH) led to some isotope exchange, especially in the 2,3,6,7-d_4 derivative. This was probably due to a base-catalyzed exchange in the partially oxidized material although it was surprising that it was more severe in the 2,3,6,7-d_4 derivative than in the 1,4,5,8-d_4 derivative. Presumably an alternate oxidation method would eliminate this problem but no other method was attempted in this study.

The reduction of the anthraquinone was achieved using aluminum tricyclohexyloxide in cyclohexanol (15). Although the yields of purified anthracene were very low, this generally reflects extensive purification by chromatography and recrystallization rather than inefficiency in the reduction step.

Table 1 lists the anthracenes synthesized and their isotopic purities as determined by low voltage mass spectrometry (8 eV).

Experimental

Mass spectra were recorded on a Finnigan 1015 mass spectrometer at an ionization energy of 8 eV. Mass ratios were calculated from peak heights and are precise only to ±2%. N.m.r. spectra were recorded on a Varian A56-60 spectrometer and chemical shifts are recorded in p.p.m. downfield from tetramethylsilane. $CDCl_3$ was the solvent used unless otherwise specified.

*Anthracene-9,10-d_2 (**1**)*

(*a*) Butyl lithium (0.01 mol in 3 ml benzene) was added to a solution of 9,10-dibromoanthracene (1.0 g, 0.003 mol) in benzene (35 ml) under nitrogen.

After refluxing 40 min and cooling, D_2O (2 ml) was added and the solution stirred 5 min. The benzene was then washed three times with water, dried ($MgSO_4$) and evaporated to leave a yellow crystalline residue. Ten recrystallizations from chloroform followed by treatment with Norit in chloroform gave 50 mg of blue fluorescent plates.

Mass spectrum: *m/e* (relative intensity) 178(4.9), 180(32), 181(5.0).

(*b*) Anthracene (0.78 g, Baker sensitizer grade) was refluxed in benzene (100 ml) containing *p*-toluene sulfonyl chloride (10 g) and D_2O (2 ml). Progress of the exchange reaction was followed by mass spectrometry. After 30 h the reaction mixture was diluted with benzene (100 ml) and extracted with aqueous sodium bicarbonate (5%). The benzene fraction was evaporated to dryness and the residue heated on a steam bath for 15 h with 100 ml of saturated aqueous sodium bicarbonate. Extraction with $CHCl_3$, drying ($MgSO_4$), and evaporation yielded the crude anthracene-9,10-d_2. This was recrystallized from $CHCl_3$, with treatment with charcoal, to yield blue fluorescent crystals.

Mass spectrum: *m/e* (relative intensity) 179(3.5), 180(42), 181(10.1). N.m.r.: δ 7.46 (m, 4H), 8.03 (m, 4H).

1,3-Butadiene-d_6

The method of Craig and Fowler (12) was used with slight modification. Zinc dust (98 g) and anhydrous dioxane (114 g) were placed in a 500 ml round-bottomed flask fitted with a nitrogen inlet, dropping funnel, condenser, and stirrer. The condenser was connected to a Dry Ice trap. After flushing with nitrogen, NaI (0.8 g), anhydrous CuCl (4.8 g) and D_2O (26.4 g) were added. The mixture was refluxed with stirring and hexachlorobutadiene (52 g) was added over 1 h. The yield of crude product was 7.25 ml (44%).

Mass spectrum: *m/e* (relative intensity) 59(8.7), 60(59.9), 61(3.1).

3-Sulfolene-d_6

The method of Grummitt *et al.* (13) was used with slight modification. 1,3-Butadiene-d_6 (12 ml), sulfur dioxide (13.5 ml), and hydroquinone (0.10 g) were sealed in a thick-walled glass tube after evacuation at −79 °C to 10^{-2} mm Hg. The mixture was heated at 100 °C for 12 h. The crude reaction mixture was dissolved in water and filtered. Evaporation of the water *in vacuo* and recrystallization from methanol gave 15.8 g of yellowish-white crystals (84%).

Mass spectrum: *m/e* (relative intensity) 59(11.0), 60(89.2), 61(4.2).

3-Sulfolene-2,2,5,5-d_4

The method of Cope *et al.* (14) was used with slight modification. 3-Sulfolene (10.0 g), potassium carbonate

Can. J. Chem. Downloaded from www.nrcresearchpress.com by 210.87.254.42 on 09/05/12
For personal use only.

Can. J. Chem. Downloaded from www.nrcresearchpress.com by 210.87.254.42 on 09/05/12
For personal use only.

(0.11 g), D_2O (10 g), and anhydrous dioxane (10 ml) were stirred at room temperature for 48 h. The solvents were removed *in vacuo* at room temperature, fresh D_2O and dioxane added, and the solution again stirred 48 h. This procedure was repeated seven times and the residue was dried at room temperature under high vacuum. The product was used in the next step without purification.

Mass spectrum: *m/e* (relative intensity) 57(3.9), 58(31.9), 59(1.8).

1,3-Butadiene-1,1,4,4-d_4

The dried sulfolene-d_4 sample from above was placed in a round-bottomed flask fitted with a nitrogen inlet and connected in series through two gas absorption traps (each containing 25 ml of 20% aqueous NaOH) and a drying tube (Drierite) to a Dry Ice trap. Nitrogen gas was slowly passed through the system and the sample heated to 130–160 °C for 1.5 h. Five milliliters (79%) of butadiene was collected.

3-Sulfolene-3,4-d_2

The perdeutero-3-sulfolene (7.12 g) was treated with H_2O in a manner analogous to the treatment of perhydro-3-sulfolene with D_2O (described above) yielding 6.0 g of the 3-sulfolene-3,4-d_2 (87%) (some insoluble material formed during the exchange and was filtered off).

Mass spectrum: *m/e* (relative intensity) 55(2.8), 56(70.0), 57(3.9).

1,3-Butadiene-2,3-d_2

The 3-sulfolene-3,4-d_2 was pyrolyzed as described previously (for 3-sulfolene-2,2,5,5-d_4) to yield 2.2 ml of 1,3-butadiene-2,3-d_2 (59%).

1,3-Butadiene-1,1,4,4-d_4-p-benzoquinone Adduct

The procedure was generally similar to that of Alder and Stein (10). 1,3-Butadiene-1,1,4,4-d_4 (2.0 g) was distilled into a thick-walled glass tube containing *p*-benzoquinone (1.0 g) and benzene (2 ml). The tube was degassed by three freeze–thaw cycles with evacuation to 10^{-2} mm Hg, then sealed and heated at 120 °C for 24 h. After cooling the product separated as white crystals and, after evaporation of the benzene, was used without further purification. Yield was 2.0 g (100%).

Anthraquinone-1,4,5,8-d_4

The anthraquinone was prepared from the octahydroanthraquinone using the method of Alder and Stein (10). The adduct from above (2.0 g) was refluxed in 5% ethanolic KOH (50 ml) with a stream of air passing through the mixture for 1 h. The mixture was diluted with water, neutralized with 1 *N* HCl, and the quinone extracted with $CHCl_3$. The combined extracts were dried ($MgSO_4$) and evaporated to dryness to yield 1.89 g (98%) which was used without further purification.

Anthracene-1,4,5,8-d_4 (4)

Anthraquinone-1,4,5,8-d_4 from above (1.0 g), aluminum tricyclohexyloxide solution (10 ml, see preparation below), and cyclohexanol (5 ml) were refluxed 48 h. The solution was poured into water (50 ml), benzene added (50 ml), and the mixture filtered, washing the residue well with hot benzene. The benzene and water were separated and the water extracted with benzene. The benzene solutions and extracts were combined and evaporated *in vacuo*. The residual cyclohexanol was removed as an azeotrope with water and benzene. The anthracene was chromatographed on alumina (Woelm, GrI; eluant benzene) and recrystallized five times from chloroform. Yield of blue fluorescent crystals, 0.173 g (21%).

Mass spectrum: *m/e* (relative intensity) 181(2.9), 182(91.8), 183(15.3).

N.m.r.: δ 7.46 (s, 2H), 8.42 (s, 4H).

Aluminum Tricyclohexyloxide Solution

Aluminum wire (5 g), cyclohexanol (100 ml, distilled from CaO), mercuric chloride (25 mg), and CCl_4 (1 ml) were refluxed overnight. The solution was used without further treatment.

1,3-Butadiene-1,1,4,4-d_4-1,4-naphthoquinone Adduct

1,3-Butadiene-1,1,4,4-d_4 (5 ml), 1,4-naphthoquinone (11.0 g), and ethanol (5 ml) were heated in an evacuated, sealed heavy-walled glass tube at 100 °C for 3 h. The solvent was removed *in vacuo* and the product used without further purification.

Anthraquinone-1,4-d_2

The crude adduct from above (6.2 g) was oxidized in 5% ethanolic KOH (*ca.* 50 ml) with air as previously described to yield 2.55 g of crude anthraquinone-1,4-d_2.

Anthracene-1,4-d_2 (3)

The crude anthraquinone-1,4-d_2 (2.0 g) was reduced as previously described with aluminum tricyclohexyl oxide (20 ml of prepared solution) to give, after purification, 84.5 mg of anthracene-1,4-d_2 (5%).

Mass spectrum: *m/e* (relative intensity) 178(4.5), 179(3.8), 180(80.0), 181(13.0).

N.m.r.: δ 7.45 (m, 4H), 8.00 (m, 2H), 8.40 (m, 4H).

1,3-Butadiene-2,3-d_2-p-benzoquinone Adduct

1,3-Butadiene-2,3-d_2 (2.2 ml), *p*-benzoquinone (0.65 g), and benzene (2.5 ml) were sealed in an evacuated thick-walled tube and heated to 120 °C for 24 h. The slightly yellow crystalline product (1.17 g) was used without further purification.

Anthraquinone-2,3,6,7-d_4

The adduct from above (1.17 g) was air-oxidized in 5% methanolic KOH (*ca.* 50 ml) as previously described to yield 0.67 (71%) of crude anthraquinone which was not further purified.

Anthracene-2,3,6,7-d_4 (5)

Anthraquinone-2,3,6,7-d_4 (0.64 g) was reduced with aluminum tricyclohexyloxide (12 ml of prepared solution) as previously described to yield 81 mg of purified anthracene-2,3,6,7-d_4 (14.5%).

Mass spectrum: *m/e* (relative intensity) 180(7.4), 181(17.0), 182(72.2), 183(13.8).

N.m.r.: δ 8.01 (s, 2H), 8.44 (s, 2H).

1,3-Butadiene-2,3-d_2-1,4-naphthoquinone Adduct

The adduct was prepared as described above from 1,3-butadiene-2,3-d_2 (0.42 ml) and 1,4-naphthoquinone (1.2 g) in 2 ml ethanol. The crude product (1.56 g, 97%) was used without further purification.

Anthraquinone-2,3-d_2

The adduct from above (1.56 g) was air-oxidized in 5% ethanolic KOH (*ca.* 30 ml) yielding 1.13 g (72%) of the anthraquinone after work-up (see above).

Anthracene-2,3-d_2 (2)

The crude anthraquinone-2,3-d_2 (1.13 g) was reduced with aluminum tricyclohexyloxide (6 ml of prepared solution) in the previously described manner to yield 0.167 g of anthracene-2,3-d_2 (17.2%) after purification.

Mass spectrum: *m/e* (relative intensity) 178(4.0), 179(9.3), 180(8.3), 181(14.1).

N.m.r.: δ 7.46 (m, 2H), 7.98 (m, 4H), 8.43 (s, 2H).

1,3-Butadiene-d_6-1,4-naphthoquinone Adduct

The adduct was prepared, as previously described, from butadiene-d_6 (8 ml) and 1,4-naphthoquinone in 15 ml of ethanol. Work-up yielded 14.2 g (89%) of the crude adduct used without purification.

Anthraquinone-1,2,3,4-d_4

The adduct above (14.2 g) was air-oxidized in 5% ethanolic KOH (*ca.* 100 ml) to yield 13.8 g (100%) of crude anthraquinone-1,2,3,4-d_4.

Anthracene-1,2,3,4-d_4 (6)

The anthraquinone-1,2,3,4-d_4 (5.0 g) was reduced with tricyclohexyloxide (25 ml of the prepared solution) to yield 0.11 g of purified anthracene-1,2,3,4-d_4 (3%)

Mass spectrum: *m/e* (relative intensity) 181(8.3), 182(111.5), 183(17.6).

N.m.r.: δ 7.46 (s, 2H), 8.02 (m, 2H), 8.42 (s, 2H).

The financial assistance of the National Research Council of Canada and the Graduate Research Fund, University of Manitoba, are gratefully acknowledged. The technical assistance of R. Tennenhouse and M. Arneson were also appreciated.

1. B. R. Henry and W. Siebrand. J. Chem. Phys. **54**, 1072 (1971).
2. V. Gold and F. A. Long. J. Am. Chem. Soc. **75**, 4543 (1953).
3. H. Bouas-Laurent, R. Calas, and M. Josien. C.R. **252**, 285 (1961).
4. P. Brown and R. C. Cookson. Tetrahedron, **21**, 1993 (1965).
5. G. G. Petukhov, N. U. Likhovidova, and R. F. Galiulina. Tr. po Khim, i Khim, Tekhol. **4**, 682 (1961); Chem. Abstr. **58**, 489 (1963).
6. J. B. Pawliczek and H. Günther. Tetrahedron, **26**, 1755 (1970).
7. Ng. Dinh-Nguyên and E. Stenhagen. *In* Deuterium labelling in organic chemistry. A. F. Thomas (*Editor*). Appleton-Century-Croft. 1971. p. 297.
8. S. Califano. J. Chem. Phys. **36**, 903 (1962).
9. W. C. Ripka and D. E. Applequist. J. Am. Chem. Soc. **89**, 4035 (1967).
10. K. Alder and G. Stein. Ann. **501**, 247 (1933).
11. O. Diels and K. Alder. Ann. **460**, 98 (1928).
12. D. Craig and R. B. Fowler. J. Org. Chem. **26**, 713 (1961).
13. O. Grummitt, A. E. Ardis, and J. Fick. J. Am. Chem. Soc. **72**, 5167 (1950).
14. A. C. Cope, G. A. Berchtold, and D. L. Ross. J. Am. Chem. Soc. **83**, 3859 (1961).
15. S. Coffey and V. Boyd. J. Chem. Soc. 2468 (1954).

Can. J. Chem. Downloaded from www.nrcresearchpress.com by 210.87.254.42 on 09/05/12
For personal use only.

An Investigation into the Nature of π-Inductive Effects: π Polarization Effects in Phenylalkanes with Polar or Charged Substituents[1]

W. F. REYNOLDS[2] AND I. R. PEAT[3]

Department of Chemistry, University of Toronto, Toronto 181, Ontario

AND

M. H. FREEDMAN AND J. R. LYERLA, JR.

Faculty of Pharmacy, University of Toronto, Toronto 181, Ontario

Received August 23, 1972

p*H* dependent ^{13}C chemical shifts for phenylglycine, phenylalanine, and phenylalanyl derivatives demonstrate that the electronic distribution of the phenyl group depends upon the distance of charged groups from the phenyl ring. The pattern of chemical shifts and the results of CNDO/2 MO calculations indicate that this is due to polarization of the phenyl π electron system. ^{13}C chemical shifts and CNDO/2 calculations for α- and β-substituted phenylalkanes (substituent = NH_3^+, Cl or Br) provide further evidence for a π polarization effect.

Les déplacements chimiques en ^{13}C reliés au p*H* de la phénylglycine, de la phénylalanine, et des dérivés de la phénylalanine, ont démontré que la distribution électronique du groupe phényle est fonction de la distance entre les groupes chargés et l'anneau phényle. L'arrangement des déplacements chimiques ainsi que les résultats obtenus par des calculs CNDO/2 MO montrent que cette relation est causée par la polarisation du système d'électrons π du phényle. Les déplacements chimiques en ^{13}C et les calculs CNDO/2 pour des phénylalcanes α et β substitués (substituant = NH_3^+, Cl, ou Br) montrent des caractéristiques jouant en faveur de cet effet de polarisation π. [Traduit par le journal]

Can. J. Chem., **51**, 1857 (1973)

Introduction

The nature of π inductive effects is controversial (1). The root of the controversy is largely a question of semantics as the term "π inductive effect" carries different connotations for different groups of investigators. In a recent survey of substituent effects in phenyl derivatives (1), Katritzky and Topsom point out three substituent effects (their effects labeled 4, 5, 6) to which the name π inductive effect has been applied. Effect 4 refers to the redistribution of π electron density as a result of repulsive interactions between a filled orbital on a substituent and the phenyl π electron system (2) (orbital repulsion effect). This effect is illustrated schematically in **1**.

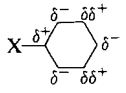

1

Effect 5 is polarization of the π electron system by a polar or charged substituent (3) (π polarization effect) while effect 6 represents changes in the π electron density induced by polarization of the σ electron system (inducto-electromeric effect (4)). These authors point out that theoretical chemists generally consider effects 4 and 5 to be π inductive effects while organic chemists consider effects 5 and 6 to be π inductive effects. Effect 5 is generally considered to be unimportant by both groups of investigators.

We became interested in π inductive effects during an investigation of ^1H and ^{13}C chemical shifts of 4-substituted styrenes (5). Comparison of chemical shifts and valence electron densities estimated by CNDO/2 MO calculations suggested that the phenyl and vinyl π electron systems were polarized by the polar C—X bond. However, a directly bonded substituent can interact with a phenyl group by a variety of mechanisms, making it difficult to separate π polarization effects from other electronic effects. Consequently, since our conclusions were contrary to previous conclusions concerning the importance of π polarization effects (1), it was decided to carry out further investigations of phenyl derivatives. Phenylalkanes with polar or charged substituents in α or β positions were chosen for these investigations. Insulation of the substituent

[1]Taken in part from the Ph.D. Thesis of I. R. Peat, University of Toronto, 1972.

[2]To whom correspondence should be addressed.

[3]Gulf Oil Fellowship Holder, 1971–1972.

Can. J. Chem. Downloaded from www.nrcresearchpress.com by 210.87.254.105 on 09/05/12
For personal use only.

Can. J. Chem. Downloaded from www.nrcresearchpress.com by 210.87.254.105 on 09/05/12
For personal use only.

from the phenyl group by an aliphatic linkage should facilitate the isolation of π polarization effects by minimizing effects which depend upon direct interaction of the substituent with the phenyl ring.

^{13}C chemical shifts were used to monitor changes in the electronic distributions of the phenyl groups. In addition, these electronic distributions were also estimated using all-valence electron (CNDO/2) molecular orbital calculations.

Experimental

^{13}C n.m.r. spectra were determined using a Varian XL-100-15 n.m.r. spectrometer operating in pulsed Fourier transform mode with proton noise-decoupling at 25.16 MHz. Fourier transformations were carried out using a 620 i computer (16 K memory) with standard Varian software. Dioxane was used as an internal ^{13}C reference for aqueous and CF_3COOH solutions while tetramethylsilane was used as a reference for CCl_4 and CD_3OD solutions. Chemical shifts were then expressed relative to $^{13}C_6H_6$ by determining the ^{13}C chemical shift of benzene in the same solvent under the same conditions. D_2O in a concentric tube was used as a lock signal in each case. Repeated measurements under different conditions suggested that chemical shifts were reproducible to 0.04 p.p.m. However, because of low solubility, the chemical shifts of the zwitterionic forms of amino acids and dipeptides as well as the phenylalanyl chemical shifts in polypeptides are probably less accurate (*ca.* 0.10 p.p.m.). Similarly, in some of the phenylalkane derivatives, C-2,6 and -3,5 peaks overlapped, introducing an uncertainty of similar magnitude.

Amino acids, dipeptides and phenylalkane derivatives were obtained commercially and were used without further purification. Commercial bacitracin (Sigma Chemical Co.) was purified by preparative liquid isoelectric focusing (6), using carrier ampholytes covering the range p*H* 5–8. The *15%* uniformly ^{13}C enriched L-phenylalanine was a gift from Dr. J. S. Cohen, the synthetic amino-terminal linear 1–15 peptide of ribonuclease was provided by Dr. I. M. Chaiken, synthetic lysine-vasopressin in the acetate form was obtained from Dr. D. A. J. Ives, while crystalline glucagon was provided by Dr. R. M. Epand. Spectra of these polypeptides were measured in aqueous solution in the p*H* range 5–6 (phenylalanyl chemical shifts were independent of p*H*).

CNDO/2 calculations were carried out on an IBM 370 computer using a standard program (program 141 from the Quantum Chemistry Program Exchange). Bond lengths and angles for CO_2H and CO_2^- groups were identical to those used by Csizmadia and co-workers (7) while standard bond lengths and angles (8) were used for other groups. Conformations used in the calculations are outlined in the Discussion.

Results

^{13}C chemical shifts for L-phenylalanine, DL-phenylglycine, and two dipeptides of phenylalanine are given in Table 1. C-1 and -4 were assigned by intensity measurements and proton-coupled spectra. C-2,6 and -3,5 for phenylalanine were assigned by an observed AB pattern due to direct ^{13}C–^{13}C coupling (*ca.* 56 Hz) between C-4 and -3,5 in a sample of phenylalanine uniformly ^{13}C enriched to 15%. C-2,6 and -3,5 in phenylalanyl derivatives were assigned by analogy to phenylalanine. For phenylglycine, these carbons were assigned by assuming that the titration shifts would be similar in pattern to those for the benzylammonium ion.

^{13}C chemical shifts for phenylalkanes and α and β derivatives of phenylalkanes are given in Table 2. Wherever possible, C-2,6 and -3,5 were assigned by comparing chemical shifts for the compound in question with those for its 4-bromo or chloro derivative. Assuming chemical shift additivity, C-2,6 and -3,5 could then be assigned by comparing the observed shifts with those for 4-halobenzenes relative to benzene (9).

Results of CNDO/2 MO calculations are summarized in Tables 3–7. Only phenyl carbon charge densities are given.

Discussion

(a) Consideration of the Validity of Using ^{13}C Chemical Shifts as a Monitor of Ground State Electronic Distributions in Phenyl groups

The shielding constant for a nucleus can be divided into two terms (10)

$$\sigma = \sigma_d + \sigma_p$$

where σ_d and σ_p respectively represent diamagnetic and paramagnetic contributions to the screening constant. These terms are sometimes further divided into local diamagnetic and paramagnetic contributions and contributions from other atoms (11). It is generally assumed that ^{13}C chemical shift differences are primarily due to changes in σ_p (12) (although it has recently been suggested that variations in σ_d may be larger than previously realized (13)). The magnitude of σ_p depends upon the extent of mixing between ground and excited states and consequently upon the electronic distributions and symmetries of these states as well as the energy separations between the ground state and the various excited states (10). Therefore, it is at first glance surprising that there should be a linear relationship between ^{13}C chemical shifts induced by remote substituents and the ground state charge density of the carbon in question. However, there is

TABLE 1. ^{13}C chemical shifts for phenyl carbons of phenylalanine, phenylglycine, and phenylalanyl derivatives at different pH values (in p.p.m. relative to $^{13}C_6H_6$, low field shifts positive)

Carbon-	Cation*	ΔC†	Zwitterion*	ΔA†	Anion*
			L-Phenylalanine		
1	+5.45	−1.29	+6.74	+3.22	+9.96
2,6	+1.04	+0.07	+0.97	−0.09	+0.88
3,5	+0.96	+0.26	+0.70	−0.49	+0.21
4	−0.36	+0.35	−0.71	−1.08	−1.79
			DL-Phenylglycine		
1	+2.75	−3.25	+6.00	+7.94	+13.94
2,6	+1.25	+0.25	+1.00	−0.55	+0.45
3,5	−0.34	+0.18	−0.52	−1.07	−1.59
4	+1.93	+0.93	+1.00	−1.87	−0.87
			L-Phenylalanylglycine		
1	+5.24	−0.30	+5.54	+3.32	+8.86
2,6	+1.07	0.00	+1.07	−0.10	+0.97
3,5	+0.70	−0.05	+0.75	−0.49	+0.26
4	−0.46	0.00	−0.46	−1.05	−1.51
			L-Glycylphenylalanine		
1	+7.94	−1.30	+9.24	+0.07	+9.31
2,6	+0.82	+0.09	+0.71	+0.12	+0.83
3,5	+0.34	+0.19	+0.15	+0.04	+0.19
4	−1.21	+0.42	−1.63	−0.03	−1.60

	Phenylalanyl residues in polypeptides			
	Bacitracin	Lysine-vasopressin	1–15 Peptide of ribonuclease	Glucagon
1	+7.80	+7.68	+7.67	+7.67
2,6	+0.54	+0.54	+0.62	+0.68
3,5	+0.25	+0.32	+0.18	+0.17
4	−1.32	−1.33	−1.42	−1.42

*Cation chemical shift values at pH = 0.3, zwitterion at pH = 6.2 and anion at pH = 11.0.
†ΔC = cation chemical shift − zwitterion chemical shift, ΔA = anion chemical shift − zwitterion chemical shift.

ample experimental evidence for an empirical relationship of this type for aromatic derivatives (5, 9, 14).

Pugmire and Grant have provided a reasonable explanation for this apparent anomaly (15). They showed that the local paramagnetic term, $\sigma_p^{(1)}$, should vary linearly with charge density over a considerable range of charge densities. This relationship arises from changes in the effective nuclear charge parameter and consequent changes in $\langle r^{-3} \rangle$ (where r is the electron-nucleus separation) with charge density. Karplus and Pople also concluded, on the basis of a simpler theoretical treatment, that $\sigma_p^{(1)}$ should vary linearly with charge density (12). Changes in excitation energy and bond orders to adjacent atoms also contribute to σ_p (15). However, these changes should be small for remote substituents, particularly when the substituent is insulated from conjugation with the ring by an aliphatic linkage.

We had originally hoped to compare experimental and calculated substituent-induced ^{13}C chemical shifts in order to determine the factors contributing to these shifts. Consequently the CNDO/2 program was modified to calculate ^{13}C chemical shifts by two previously described methods; σ_p was calculated by both the average energy approximation as formulated by Pugmire and Grant (15) and by the sum-over-states method (16) in which σ_p is summed over all filled and unfilled (corresponding to excited states) molecular orbitals. σ_p was summed over all atoms other than hydrogen. σ_d was evaluated from local charge densities (17).

^{13}C chemical shifts were calculated for several amino acid, phenylalkane, and styrene derivatives using both approaches. Initial results were

Can. J. Chem. Downloaded from www.nrcresearchpress.com by 210.87.254.105 on 09/05/12
For personal use only.

TABLE 2. Phenyl carbon ^{13}C chemical shifts for phenylalkanes and ammonio, chloro, and bromo derivatives

Solvent	Carbon-	Chemical shifts					
CF_3COOH			$C_6H_5CH_2CH_3$	$C_6H_5CH_2NH_3^+$	Δ*		
	1		+16.84	+2.27	−14.57		
	2,6		−0.41	+0.49	+0.90		
	3,5		0.00	+1.32	+1.32		
	4		−2.88	+2.13	+5.01		
CCl_4		$C_6H_5CH_2CH_3$	$C_6H_5CH_2Cl$	$C_6H_5CH_2Br$	ΔCl*	ΔBr*	
	1	+15.41	+9.28	+9.53	−6.13	−5.88	
	2,6	−0.49	+0.29	+0.80†	+0.78	+1.29†	
	3,5	+0.03	+0.29	+0.39†	+0.26	+0.36†	
	4	−2.61	−0.06	−0.02	+2.55	+2.57	
CF_3COOH			$C_6H_5(CH_2)_2CH_3$	$C_6H_5(CH_2)_2NH_3^+$	Δ		
	1		+15.20	+6.05	−9.15		
	2,6		−0.10†	+0.25	+0.35†		
	3,5		+0.25†	+1.14	+0.89†		
	4		−2.84	−0.15	+2.69		
CCl_4		$C_6H_5(CH_2)_2CH_3$	$C_6H_5(CH_2)_2Cl$	$C_6H_5(CH_2)_2Br$		ΔCl	ΔBr
	1	+13.81	+9.73	+10.58		−4.08	−3.23
	2,6	−0.07†	+0.46†	+0.33		+0.53†	+0.40†
	3,5	+0.13†	+0.33†	+0.33		+0.20†	+0.20†
	4	−2.58	−1.38	−1.34		+1.20	+1.24
CCl_4			$C_6H_5(CH_2)_2CH_3$	$C_6H_5(CH_2)_3Br$		Δ‡	
	1		+13.81	+11.95		−1.86	
	2,6		−0.07†	+0.26		+0.33†	
	3,5		+0.13†	+0.26		+0.13†	
	4		−2.58	−2.02		+0.56	
CCl_4			$C_6H_5C(CH_3)_3$	$C_6H_5CCl_3$		Δ	
	1		+22.14	+16.33		−5.81	
	2,6		−3.20	−1.65		+1.55	
	3,5		−0.21	−0.05		+0.16	
	4		−2.82	+1.81		+4.63	

*Chemical shift difference between NH_3^+, or Cl, or Br derivative and CH_3 derivative.
†Assignment of C-2,6 and -3,5 not confirmed.
‡Comparison made with phenylpropane rather than phenylbutane. This should introduce negligible error since it involves the δ effect due to a methyl group.

promising since the calculations closely reproduced the p*H*-dependent chemical shifts of the imidazole ring of histidine (*18*) and of the phenyl group in phenylalanine (with an r.m.s. difference of 0.4 p.p.m. between calculated and experimental titration shifts for phenyl carbons). However, while the calculated chemical shifts for phenylalkanes and styrenes were very similar in pattern to the experimental chemical shifts, the former were underestimated by a factor of three to four. Similar discrepancies were noted for the series $C_5H_5^-$, C_6H_6, and $C_7H_7^+$. We suspect that the calculations underestimate the sensitivity of $\sigma_p^{(1)}$ to charge density changes and that the agreement for phenylalanine is fortuitous, *i.e.*, that in this case the above-mentioned error is compensated by an overestimation of the calculated charge densities (see below, part (*c*)).

Recently Ellis *et al.* have formulated an approach to ^{13}C chemical shift calculations based on finite perturbation theory applied to INDO MO wave functions (*19*). These calculations closely reproduce gross chemical shift differences (*e.g.*, CH_4 *vs.* C_2H_4). However, they may also underestimate remote substituent effects since the calculated C-4 chemical shift for toluene (−0.3 p.p.m. relative to benzene) is significantly smaller than the experimental value (−2.9 p.p.m. in CCl_4 (*9*)).

The observations outlined above lead us to conclude that existing models for ^{13}C chemical shift calculations are too imprecise to justify any attempt to give a quantitative account of substituent-induced ^{13}C chemical shifts in terms of variations in σ_d, σ_p, excitation energies, etc. Consequently we prefer at present to discuss ^{13}C

Can. J. Chem. Downloaded from www.nrcresearchpress.com by 210.87.254.105 on 09/05/12
For personal use only.

TABLE 3. Calculated charge densities (× 10^3)* and (in brackets) π charge density (× 10^3)† for phenyl carbons of three conformational isomers of phenylalanine shown in Fig. 2

Species	C-1	C-2,6	C-3,5	C-4
		Conformation **A**		
Cation	+11* (−21)†	−13 (−26)	+22 (+27)	+14 (+18)
ΔC‡	−21 (−41)	+2 (+1)	+6 (+11)	+16 (+29)
Zwitterion	+32 (+20)	−15 (−27)	+16 (+16)	−2 (−11)
ΔA§	+30 (+52)	−1 (−4)	−8 (−13)	−19 (−35)
Anion	+62 (+72)	−16 (−31)	+8 (+3)	−21 (−46)
		Conformation **B**		
Cation	+25 (−26)	−5 (−18)	+19 (+22)	+15 (+18)
ΔC	−23 (−42)	+2 (+3)	+6 (+11)	+16 (+29)
Zwitterion	+48 (+16)	−7 (−21)	+13 (+11)	−1 (−11)
ΔA	+11 (+57)	−10 (−12)	−5 (−6)	−21 (−37)
Anion	+59 (+73)	−17 (−33)	+8 (+5)	−22 (−48)
		Conformation **C**		
Cation	+11 (−20)	−13 (−25)	+20 (+27)	+13 (+17)
ΔC	−12 (−50)	+8 (+10)	+5 (+8)	+14 (+32)
Zwitterion	+23 (+30)	−21 (−35)	+15 (+19)	−1 (−15)
ΔA	+29 (+52)	−2 (−6)	−7 (−12)	−24 (−37)
Anion	+52 (+82)	−23 (−41)	+8 (+7)	−25 (−52)

*$(4 - q) \times 10^3$ where q = total valence electron density.
†$(1 - q_\pi) \times 10^3$ where q_π = π electron density.
‡Charge density for cation − charge density for zwitterion.
§Charge density for anion − charge density for zwitterion.

TABLE 4. Calculated total charge density (× 10^3)* and (in brackets) π charge density (× 10^3)† for phenyl carbons of phenylalanine and phenylglycine

Species	C-1	C-2,6	C-3,5	C-4
		Phenylalanine		
Cation	+16* (−22)†	−10 (−23)	+20 (+25)	+14 (+18)
ΔC‡	−18 (−44)	+4 (+5)	+6 (+10)	+16 (+30)
Zwitterion	+34 (+22)	−14 (−28)	+14 (+15)	−2 (−12)
ΔA§	+24 (+54)	−5 (−7)	−6 (−10)	−21 (−37)
Anion	+58 (+76)	−19 (−35)	+8 (+5)	−23 (−49)
Neutral	+40 (+31)	−14 (−31)	+14 (+15)	−6 (−18)
		Phenylglycine		
Cation	+6 (−67)	+5 (−6)	+21 (+24)	+27 (+41)
ΔC	−30 (−69)	+10 (+11)	+7 (+10)	+23 (+42)
Zwitterion	+36 (+2)	−5 (−17)	+14 (+14)	+4 (−1)
ΔA	+32 (+87)	−8 (−23)	−8 (−10)	−33 (−58)
Anion	+68 (+89)	−13 (−40)	+6 (+4)	−29 (−59)
Neutral	+39 (+18)	−11 (−24)	+13 (+14)	−2 (−11)

*$(4 - q) \times 10^3$ where q = total valence electron density.
†$(1 - q_\pi) \times 10^3$ where q_π = π electron density.
‡Charge density for cation − charge density for zwitterion.
§Charge density for anion − charge density for zwitterion.

chemical shifts induced by remote substituents in terms of changes in ground state charge densities. There appears to be ample experimental justification as well as some theoretical justification for this approach. It also facilitates a discussion of electronic substituent effects.

The relationship between ^{13}C chemical shifts and electronic substituent effects is more complex when the substituent is three or fewer bonds removed from the carbon of interest. Grant and Paul noted respective chemical shift contributions of +9.1, +9.4, and −2.5 p.p.m. due to α, β, and γ methyl groups in linear alkanes (δ and ε effects were negligible) (20). Similar parameters have been derived for other substituents (21). While the exact origins of these contributions are

Can. J. Chem. Downloaded from www.nrcresearchpress.com by 210.87.254.105 on 09/05/12
For personal use only.

TABLE 5. Calculated charge densities ($\times 10^3$)* and π charge densities ($\times 10^3$)† for phenyl carbons of phenylalkanes and α- and β-substituted phenylalkanes

Compound	C-1	C-2,6	C-3,5	C-4
$C_6H_5CH_2CH_3$	+44* (+39)†	−18 (−35)	+14 (+15)	−8 (−22)
$C_6H_5CH_2Cl$	+26 (+10)	−2 (−13)	+9 (+9)	+3 (−3)
$C_6H_5CH_2NH_3^+$	−9 (−74)	+11 (+6)	+17 (+19)	+32 (+48)
ΔCl‡	−18 (−29)	+16 (+22)	−5 (−6)	+11 (+19)
$\Delta(NH_3^+)$	−53 (−113)	+29 (+41)	+3 (+4)	+40 (+70)
$C_6H_5(CH_2)_2CH_3$	+42 (+38)	−17 (−34)	+13 (+14)	−8 (−22)
$C_6H_5(CH_2)_2Cl$	+44 (+30)	−15 (−31)	+14 (+15)	−5 (−18)
$C_6H_5(CH_2)_2NH_3^+$	+19 (−22)	−12 (−24)	+20 (+26)	+13 (+17)
ΔCl	+2 (−8)	+2 (+3)	+1 (+1)	+3 (+5)
ΔNH_3^+	−23 (−60)	+5 (+10)	+7 (+12)	+21 (+39)

*$(4 - q) \times 10^3$ where q = total valence electron density.
†$(1 - q_\pi) \times 10^3$ where $q_\pi = \pi$ electron density.
‡Δ = charge density for Cl or NH_3^+ derivative − charge density for CH_3 derivative.

TABLE 6. Calculated charge densities ($\times 10^3$) benzene-ammonium ion pairs with ammonium ion at same position as in benzylammonium and phenethylammonium ions

C-1	C-2,6	C-3,5	C-4
(*a*) Benzylammonium ion geometry			
−33* (−53)†	+10 (+6)	+17 (+16)	+29 (+43)
(*b*) Phenethylammonium ion geometry			
0 (−36)	−8 (−2)	+12 (+10)	+16 (+20)

*Total charge density ($\times 10^3$).
†π Charge density ($\times 10^3$).

TABLE 7. Phenyl carbon chemical shifts and calculated charge densities for NR_3^+ and CR_3 phenyl derivatives (R = H or CH_3)

Substituent	Solvent	C-1	C-2,6	C-3,5	C-4
(*a*) Chemical shifts (in p.p.m. relative to $^{13}C_6H_6$, low field shifts positive)					
CH_3	CF_3COOH	+10.26	+0.73	−0.05	−3.09
NH_3^+	CF_3COOH	+0.14	−5.82	+2.19	+2.19
Δ		−10.12	−6.55	+2.24	+5.28
$C(CH_3)_3$	CD_3OD	+22.76	−3.18	−0.28	−2.93
$N(CH_3)_3^+$	CD_3OD	+19.18	−8.16	+2.29	+2.29
Δ		−3.58	−4.98	+2.47	+5.22
(*b*) Total charge density ($\times 10^3$)* and π charge density ($\times 10^3$)† for phenyl carbons of NR_3^+ and CR_3 derivatives					
CH_3		+43* (+30)†	−12 (−25)	+11 (+12)	−5 (−16)
NH_3^+		+80 (−120)	+5 (0)	+32 (+28)	+36 (+57)
Δ		+37 (−150)	+17 (+25)	+21 (+16)	+31 (+73)
$C(CH_3)_3$		+38 (+34)	−20 (−33)	+13 (+15)	−8 (−21)
$N(CH_3)_3^+$		+86 (−72)	−15 (−24)	+32 (+28)	+22 (+34)
Δ		+48 (−106)	+5 (+9)	+19 (+13)	+30 (+55)

*$(4 - q) \times 10^3$ where q = total valence electron density.
†$(1 - q_\pi) \times 10^3$ where $q_\pi = \pi$ electron density.

still unclear (22), it appears improbable that they will be more than partially reflected by changes in ground state charge density for the carbon of interest. For example, there can be contributions to the two-center paramagnetic term $\sigma_p^{(2)}$ (see eq. 7 of ref. 15), due to replacement of hydrogen by an α substituent. There may also be a contribution to σ_d arising from the electron distribution on the α substituent (13). While the origins of the β effect are uncertain (22), there is good experimental evidence, at least for the methyl group, that the γ effect arises from *gauche* steric

Can. J. Chem. Downloaded from www.nrcresearchpress.com by 210.87.254.105 on 09/05/12
For personal use only.

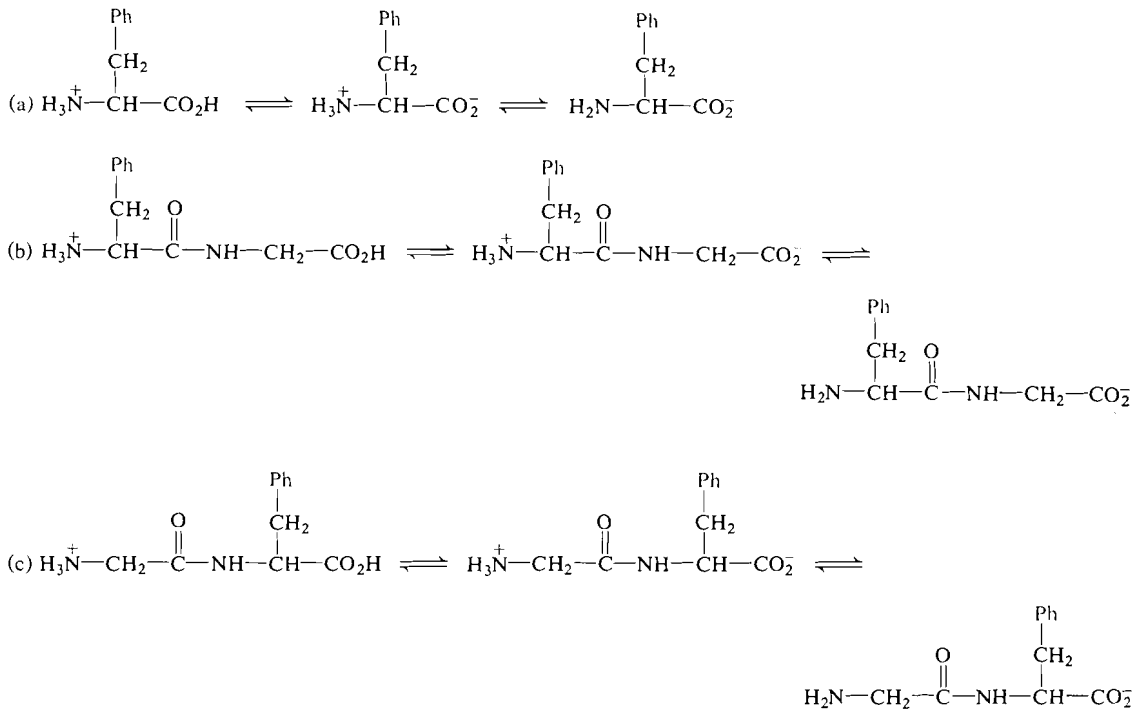

FIG. 1. Structures of ionic forms of (*a*) phenylalanine, (*b*) phenylalanylglycine, and (*c*) glycylphenylalanine.

interactions (17, 22, 23). Substituent-induced changes in excitation energies could also be important, particularly for α or β substituents. Because of α, β, and γ effects, it is essential to choose an appropriate reference compound if one wishes to use ^{13}C chemical shifts to monitor charge density changes due to proximate substituents. This point is further discussed in the following section.

(b) ^{13}C Chemical Shifts of α- and β-Substituted Phenylalkane Derivatives

The first compounds chosen for investigation were the amino acid L-phenylalanine, $C_6H_5CH_2CH(NH_2)CO_2H$, the dipeptides L-glycylphenylalanine (Gly-Phe), and L-phenylalanylglycine (Phe-Gly) (see Fig. 1 for structures), and DL-phenylglycine. These compounds were chosen because it was anticipated that the p*H*-dependent ^{13}C chemical shifts of the phenyl carbons would provide information about changes in the electronic distribution of the phenyl group as the charge on the amino acid function was altered and as the distance of charged functions from the ring was altered.

Two clear trends are apparent from the data presented in Table 1. Firstly, there is a consistent pattern of phenyl carbon chemical shifts on going from the zwitterionic form to either the cationic form (carboxyl titration) or the anionic form (amino titration). In the former case, C-1 shifts to high field with a smaller low field shift for C-4 and very small low field shifts for C-2,6 and -3,5. The ^{13}C chemical shifts associated with the amino titration are similar in pattern but opposite in sign.

Secondly, the magnitudes of the p*H* dependent chemical shifts appear to be closely related to the distance of the charged functions from the ring. For example, if one compares the results for phenylglycine and phenylalanine, the largest shifts are noted for the amino titration of phenylglycine, the shifts for the carboxyl titration of phenylglycine and the amino titration of phenylalanine are almost identical in magnitude while the smallest shift is noted for the carboxyl titration of phenylalanine. These results are exactly what one would expect if the magnitudes of the shifts depend upon the distance of charged functions from the ring since the four titrations

Can. J. Chem. Downloaded from www.nrcresearchpress.com by 210.87.254.105 on 09/05/12
For personal use only.

Can. J. Chem. Downloaded from www.nrcresearchpress.com by 210.87.254.105 on 09/05/12
For personal use only.

involve gain or loss of protons which are respectively two, three, three, and four bonds removed from the phenyl ring (see Fig. 1).[4]

The distance dependence is even more pronounced in the case of the dipeptides. In Phe-Gly the amino titration shifts (zwitterion to anion) are nearly identical to those for phenylalanine while the carboxyl titration shifts are negligibly small. This pattern is reversed in the case of Gly-Phe. In each case, the group which causes a negligible titration shift is three bonds further removed from the phenyl ring than in phenylalanine, (see Fig. 1) apparently far enough away to have a negligible effect. Similar patterns of p*H*-dependent ^{13}C chemical shifts of phenyl carbons of dipeptides and tripeptides incorporating phenylalanine can be observed in the results of Christl and Roberts (24).

Further information is provided by the chemical shifts of the individual ionic species. In terms of distances of charged groups from the phenyl ring, both cationic and zwitterionic forms of Phe-Gly should resemble the cation of phenylalanine, both the anion of Phe-Gly and the cation of Gly-Phe should resemble neutral phenylalanine while the zwitterion and anion of Gly-Phe should resemble anionic phenylalanine. Neutral phenylalanine does not exist to any extent in aqueous solution. However, incorporation of phenylalanine in the middle of a long chain polypeptide should provide a reasonable electronic facsimile of the neutral species, assuming that the peptide linkages resemble neutral amino and carboxyl functions. Using phenylalanyl residues in polypeptides as models for neutral phenylalanine, the chemical shift data in Table 1 are in good agreement with the predictions outlined above. The chemical shift data in Table 1 also indicate that the C-1 and -4 chemical shifts for the zwitterionic form are intermediate between those for the cationic form and the neutral form (as approximated by phenylalanyl residues).

In view of the consistent pattern of results obtained from the p*H*-dependent ^{13}C chemical shifts of amino acids and dipeptides, it was decided to expand the investigation to include other α- and β-substituted phenylalkanes in non-aqueous solvents to see if the same pattern of results was observed. Derivatives chosen contained either charged, *e.g.* ammonio group or polar, *e.g.* chlorine and bromine, substituents. As mentioned in section (*a*), the choice of proper reference compounds is critical. This can be clearly seen from a consideration of the ^{13}C chemical shift data for phenylalkanes given in Table 2 (similar data have recently been reported by Maciel and co-workers (25)). Both C-4 and -3,5 show similar shifts for all of the phenylalkanes. This is not surprising since the different alkyl groups should have similar electronic effects. However, there are large differences for C-1 and, to a lesser extent, for C-2,6. These chemical shift differences appear to reflect effects similar to the α and β effects for aliphatic derivatives (20) (the γ effect upon C-3,5 should be small since the alkyl group and C-3,5 are *trans* to one another and the γ effect reflects *gauche* interactions (17, 22, 23)). For example, on going from benzene to *n*-propylbenzene, C-1 chemical shifts are +9.0, +6.4, and −1.6 p.p.m. for addition of each succeeding methyl group. These are similar to the α, β, and γ effects for methyl groups in aliphatic derivatives (see section (*a*)).[5]

To the extent that α, β, and γ effects reflect either steric interactions or diamagnetic and paramagnetic contributions associated with the electron distribution on the substituent (see section (*a*)), the best reference substituent for comparison with a polar or charged substituent should be similar in size and isoelectronic with the latter substituent. On this basis, the best reference compound for an ammonio derivative is the corresponding methyl derivative, since the latter is isoelectronic to the ammonio group and similar in size. Since a remote methyl group will have little electronic effect, the chemical shift differences should reflect the effect of the positive charge on the NH_3^+ group. There are no ideal non-polar reference compounds for the halo

[4]The proximity of charged or polar groups to the phenyl ring is discussed in terms of the number of intervening bonds rather than the actual distance, since the latter parameter is difficult to define in a conformationally mobile system. We concede that there are possible conformations where, for example, a β substituent can be as close to the ring as an α substituent. However, inspection of molecular models indicates that these are usually sterically hindered conformations and are unlikely to be significantly populated. Consequently, the weight average distance of a β substituent from the ring should be greater than that for an α substituent, etc.

[5]The phenyl carbons of phenylalanine and related compounds also reflect these effects (particularly C-1). However, gain or loss of a proton during titration should at most cause a small change in the γ effect at C-1. Consequently, comparison of chemical shift differences between different ionic species is justified in these systems.

Can. J. Chem. Downloaded from www.nrcresearchpress.com by 210.87.254.105 on 09/05/12
For personal use only.

derivatives. However, the methyl derivatives are probably also the best available references for these compounds. The methyl group is similar in size (van der Waals' radius ≈ 2.0 Å) to chlorine (1.80 Å) and bromine (1.95 Å) and should therefore have similar steric effects. There is unlikely to be a complete cancellation of contributions due to the electronic distribution on the substituent since the methyl group is only crudely similar in electronic structure to the halogens (three σ bonds in lieu of three lone pairs of electrons). This is reflected by gross differences in α effects (respectively +31.2 (21), +20.0 (21), and +9.1 p.p.m. (20) for Cl, Br, and CH_3 groups). However, the β effects (respectively +10.3, +10.6, and +9.4 p.p.m.) and γ effects (−4.6, −3.1, and −2.5 p.p.m.) are similar for the three substituents (the larger γ effect for halogens may reflect the tendency of halopropanes to favor *gauche* conformations (26) while *n*-butane favors the *anti* conformation (27)). Since in the derivatives we have investigated, halogens are either β or γ to the phenyl group, the above discussion suggests that the methyl group is an adequate reference compound for the halo derivatives in these cases.

When ^{13}C chemical shifts of NH_3^+, Cl, or Br derivatives are compared to the chemical shifts for the corresponding methyl derivatives in the same solvent (Table 2), it is seen that there is a consistent pattern of chemical shift changes which is identical to the pattern observed on going from the zwitterionic to the cationic forms of phenylalanine and phenylglycine, *i.e.*, a large negative (high field) chemical shift for C-1, a smaller positive shift for C-4 and very small positive shifts for C-2,6 and -3,5. Furthermore, a similar distance dependence is again noticed since the C-4 chemical shifts decrease regularly (by approximately a factor of two) on going from β to γ to δ substituents. Finally, the magnitudes of the induced chemical shifts by an NH_3^+ group are approximately twice those due to either a Cl or Br substituent for the same phenylalkane. In general, the consistency of the chemical shift patterns in both Table 1 and Table 2 provides further justification for the use of CH_3 derivatives as reference compounds for NH_3^+, Cl, and Br derivatives since it is difficult to believe that such close agreement could be fortuitous.

As can be seen from the above discussion, all of the compounds investigated show very similar patterns of phenyl carbon chemical shifts with the magnitudes of the induced shifts apparently determined by the distance of the substituents from the phenyl groups. Therefore, we felt that it should be possible to account for this consistent pattern of results by a single explanation. It appears highly improbable that it could be accounted for by solvent effects since there is no apparent reason why an effect of this type should depend strongly upon the distance of a substituent from the phenyl group nor why the pattern should be similar for D_2O, CCl_4, and CF_3COOH. The pattern of phenyl carbon chemical shifts is completely inconsistent with a σ inductive effect. Similarly it is inconsistent with a dominant orbital repulsion effect (effect 4, see **1** in Introduction) because in that case C-2,6 should have similar shifts to C-4, with C-3,5 of opposite sign. However, assuming that the ^{13}C chemical shifts are reflecting changes in carbon electron density, the pattern of results is entirely consistent with a π polarization effect in which the phenyl π electrons are polarized towards a positive charge, **2**, and away from a negative charge, **3**. The size of this effect should depend on the distance of the charged function from the ring. A polar $\overset{\delta+}{C}—\overset{\delta-}{X}$ bond should have a similar, but smaller effect, **4**, to a positively charged group.

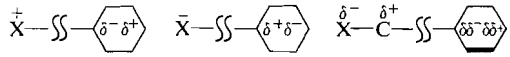

2 **3** **4**

The field substituent parameter, *F*, of Swain and Lupton (28) should provide a reasonable measure of the polarizing ability of a substituent since it measures the through space field effect of the substituent. In fact the ratio of *F* for $N(CH_3)_3^+$ (which should be similar to NH_3^+) to *F* for the halogens (1.46 to *ca.* 0.70) is almost identical to the ratio of shifts induced by NH_3^+ and the halogens. This explanation can even account for more subtle differences. For example, the zwitterionic form of phenylalanine should show a small π polarization effect similar to **2** since the positive charge is one bond closer to the ring than the negative charge. As pointed out above, the chemical shifts of zwitterionic phenylalanine are intermediate between cationic and neutral phenylalanine. Thus all of the results outlined above can be accounted for in terms of π polarization effects. The only result which is not wholly consistent with this explanation is the observation that there tends to be a larger positive shift for C-2,6 than C-3,5 in the α-halo-

Can. J. Chem. Downloaded from www.nrcresearchpress.com by 210.87.254.105 on 09/05/12
For personal use only.

toluenes. This may indicate the presence of a direct (hyperconjugative) interaction. However, even in these cases, C-4 chemical shifts are substantially larger than C-2,6 chemical shifts, indicating that the π polarization effect is dominant.

(c) CNDO/2 MO Calculations and Phenyl Carbon Charge Densities

While the pattern of substituent-induced ^{13}C chemical shifts can be explained in terms of π polarization effects, this assumes that changes in ^{13}C chemical shifts are paralleled by changes in carbon charge density. Consequently, we carried out all-valence electron (CNDO/2) molecular orbital calculations for many of the phenylalkane derivatives in an attempt to determine whether the pattern of charge density changes was similar to the pattern of chemical shift changes.

All of the compounds included in this investigation can exist in more than one conformational isomer. Conformations of phenylalanine for which calculations were performed are illustrated in Fig. 2. Calculated phenyl carbon charge densities are given in Table 3. There are differences between charge densities for the same ionic species in different conformations, particularly for C-1. However, the pattern of charge densities is consistent from conformation to conformation. Furthermore, there is a consistent pattern of changes in charge densities between different ionic species. Although the calculations suggest that conformation B is least stable, all conformations were equally weighted to arrive at average charge densities (Table 4) since the experimental evidence concerning the conformational preference of phenylalanine in solution is ambiguous (29).

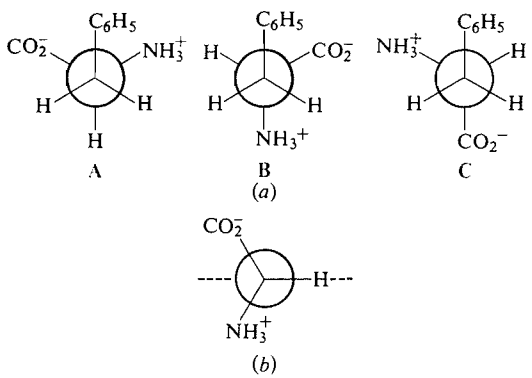

FIG. 2. (*a*) Conformations of phenylalanine used in CNDO/2 calculations (plane of phenyl ring at right angles to C_α—C_β bond). (*b*) Conformation of phenylglycine used in CNDO/2 calculations (dotted line shows the plane of the phenyl ring).

Charge densities for phenylalanine and phenylglycine are summarized in Table 4. The patterns of charge densities for the individual ionic species are not identical to the chemical shift patterns, although the agreement is better for total charge density than for π charge density. The discrepancies may, at least in part, be due to the α, β, and γ effects of the side chain atoms. However, there is much better agreement when chemical shift changes with p*H* are compared with charge density changes. This is not surprising since protonation or deprotonation should at most cause small changes in the γ effect (see footnote 5). In this case, chemical shift trends are almost equally well predicted by total charge density and π charge density,[6] since there are parallel changes in the two parameters, with the π charge densities consistently larger. This apparently arises because changes in π charge density induce smaller changes of opposite sign in σ charge density (a similar phenomenon has been noted in the case of styrene (5) and fluorobenzene (30) derivatives). Consequently, we conclude that changes in total charge density are dominated by changes in π charge density and that the substituent effect primarily involves the π electron system.

These observations are completely inconsistent with an inducto-electromeric effect in which changes in π electron density are induced by changes in σ electron density. However, they are completely consistent with π polarization effects similar to those in **2** and **3**. Furthermore, all of the experimental trends for the two compounds (the signs and relative magnitudes of the chemical shift changes for the different carbons, the relative magnitudes of amino (ΔA) and carboxyl (ΔC) titration shifts, and the relative magnitudes of phenylalanine and phenylglycine shifts) are reflected by corresponding trends in π charge density. The calculations even predict that the chemical shifts for neutral phenylalanine should be intermediate between those for the

[6]Correlation of cation to anion shifts for phenylalanine and phenylglycine with corresponding charge density changes gave a correlation coefficient 0.936 for total charge density and 0.959 for π charge density.

Can. J. Chem. Downloaded from www.nrcresearchpress.com by 210.87.254.105 on 09/05/12
For personal use only.

zwitterionic and anionic forms, as observed for C-1 and -4 (Table 1).

CNDO/2 calculations were also carried out for all compounds from Table 2 except the bromo derivatives (the program does not handle third row elements) with results given in Table 5. Calculations for the benzyl derivatives were carried out for a conformation in which the CH_2—CH_3, CH_2—Cl, or CH_2—NH_3^+ bond was at right angles to the plane of the phenyl group. In the case of phenethyl derivatives, calculations were performed for *gauche* and *anti* conformations. The charge densities in Table 4 are averaged (allowing for the two equivalent *gauche* conformations). If charge densities for NH_3^+ or Cl derivatives are compared with those for CH_3 derivatives, the pattern of chemical shift differences is reasonably well reproduced (particularly for phenethyl derivatives) and the distance dependence of the substituent effect is also predicted.

Calculations were also performed for benzene–ammonium ion pairs with the NH_4^+ group in identical positions to the NH_3^+ group in the benzylammonium and phenethylammonium ions. Results are given in Table 6. These calculations were performed in an attempt to determine the mode of transmission of the π polarization effect from the substituent to the phenyl ring. The calculated π electron densities are very similar in pattern to the experimental chemical shift values. However, the electron density changes (relative to benzene) are approximately 40% less than the corresponding electron density changes for the ammonio derivatives of phenylalkanes. This may either reflect enhanced transmission of field effects through the molecular framework of the phenylalkane[7] or partial transmission through the σ electron system. In either case, the calculations suggest that the π polarization effect is predominantly transmitted through space.

While the ^{13}C chemical shift trends are generally well reproduced by the charge density calculations, there are discrepancies in some cases. For example, the calculations for the benzyl derivatives (particularly the chloro derivative) apparently overestimate hyperconjugative effects since C-2,6 and -4 show similar changes in charge density. This discrepancy may be due to the choice of geometry for the calculations. The chosen geometry (with CH_2—X bonds at right angles to the plane of the phenyl group) should maximize direct (hyperconjugative) interactions with the phenyl π system. In actual fact, it is likely that a significant range of conformations is populated. Agreement is much better for the phenethyl derivatives where direct interactions should be much less important.

A more serious discrepancy is revealed by a comparison of the ratio of chemical shifts and charge densities for the different series of compounds. For example, for the C-4 carbon, this ratio is *ca.* 25 p.p.m./π electron for phenylalanine and phenylglycine, *ca.* 60 p.p.m./π electron for the ammonio derivatives of phenylalkanes, and *ca.* 180 p.p.m./π electron for the α- and β-chloro derivatives. Only the latter values are in good agreement with previously accepted values of 160–200 p.p.m./π electron (14*a*, *b*). The discrepancies may partly arise because the calculations correspond to the molecule in the gas phase while chemical shifts are measured in solution. Amino acids were measured in aqueous solutions where the charged groups should be strongly solvated. This should substantially neutralize these charges and consequently reduce π polarization. Ammonio derivatives were measured in CF_3COOH. While the extent of solvation on an NH_3^+ group by CF_3COOH should be small, some ion pairing may occur between the trifluoroacetate counter ion and the NH_3^+ group, causing a decrease in π polarization. There should be much smaller solvation effects for the halo derivatives in CCl_4. However, the differences in scaling factors appear to be too large to be wholly accounted for by this explanation and it is possible that the CNDO/2 calculations inherently overestimate effects of charged groups.

In spite of these apparent quantitative failures of the CNDO/2 calculations, the overall pattern of agreement between chemical shifts and π charge densities provides further strong support for the suggestion that the consistent pattern of p*H*-dependent or substituent-induced chemical shifts noted for the compounds in this investigation arises from π polarization effects.

(d) Consideration of Other Evidence for π Polarization Effects

In addition to the results outlined above, ^1H

[7]CNDO/2 calculations for styrenes and related compounds (5) and for bicyclo[2.2.2]octanecarboxylic acids (31) indicate an enhancement of the field effect of substituents when transmitted through a molecular framework as opposed to through vacuum.

Can. J. Chem. Downloaded from www.nrcresearchpress.com by 210.87.254.105 on 09/05/12
For personal use only.

and ^{13}C chemical shifts and charge densities for 4-substituted styrenes have provided evidence for polarization of both phenyl and vinyl π electron, systems by a polar C—X σ bond (5). In addition, it has recently been reported that ^{13}C chemical shift data and π charge densities for *trans*-1-substituted 1,3-butadienes provide evidence for a similar effect in these compounds (32). This raises the obvious question of why these effects have not previously been considered to be important. As discussed in the Introduction, when a substituent is directly bonded to a phenyl group, any π polarization effect could be masked by other substituent effects (particularly conjugative interactions). However, careful inspection of charge densities for phenyl derivatives (30) provides evidence for the existence of a π polarization effect in these systems. The π charge density for C-4 should be sensitive to any π polarization effects as well as resonance effects. However, the total π charge density, $\sum C_\pi$, only reflects resonance effects (30). Taking $N(CH_3)_2$ as an example of a group with a strong resonance effect and a small field effect (5), the ratio $C\text{-}4_\pi/\sum C_\pi = 0.59$ (30). Other groups with dominant resonance effects show similar ratios. However, the nitro group, which has a dominant field effect (28), has a ratio $C\text{-}4_\pi/\sum C_\pi = 1.75$ (30). Since the field and resonance effects of NO_2 have the same sign (28), any π polarization effect due to the polar C—NO_2 σ bond system (as in **4**) should reinforce the resonance-induced π charge density at C-4. Thus the large ratio $C\text{-}4_\pi/\sum C_\pi$ for NO_2 is consistent with a π polarization effect. Other groups with large *F* effects show similar trends.

In the light of the above results, we decided to attempt to find experimental evidence for π polarization due to a substituent directly bonded to a phenyl group. $N(CH_3)_3^+$ and NH_3^+ are the best substituents for this purpose. $N(CH_3)_3^+$ is isoelectronic with $C(CH_3)_3$, similar in size and is also believed to have a similar (electron-releasing) resonance or mesomeric effect (33). The same relationship should exist between NH_3^+ and CH_3. Consequently, differences in chemical shifts between pairs of compounds in the same solvent should reflect σ and π inductive effects. ^{13}C chemical shifts for *N,N,N*-trimethylanilinium iodide and *t*-butyl benzene in CD_3OD and anilinium trifluoroacetate and toluene in CF_3COOH are given in Table 7, along with results of CNDO/2 MO calculations for these compounds. The chemical shift differences are clearly consistent with π polarization effects, although the magnitudes of C-1 and -2,6 chemical shifts suggest an imperfect cancellation of α and β structural effects. Somewhat surprisingly, C-4 shifts are almost identical to that for the benzylammonium ion. The CNDO/2 calculations for the anilinium and trimethylanilinium ions show clear evidence for π polarization effects, although this trend is partially obscured when comparisons are made between $-NR_3^+$ and $-CR_3$. They also indicate that the change in C-4 charge density for the anilinium ion is nearly identical to that for the benzylammonium ion. Having the substituent directly bonded to the ring may alter the nature of the π polarization effect, accounting for this apparent discrepancy.

Thus a consideration of available evidence leads us to conclude that π polarization similar to that illustrated in **2**, **3**, and **4** is a significant mechanism of transmission of electronic substituent effects in phenyl derivatives and may be the dominant effect in systems where the substituent is insulated from direct conjugative interaction with the phenyl group.

Note added in proof

Taft and co-workers (34) have recently reported the results of ^{19}F measurements for a series of derivatives of the type X—C_6H_4—G—C_6H_4F where G is a variety of linking groups. Correlations of ^{19}F chemical shifts with σ_I and σ_R indicated a substantial π inductive effect which increased when G was a conjugative linkage. We believe that these results are consistent with a π polarization effect of the type discussed above and in ref. 5.

Financial support from the National (W.F.R.) and Medical Research Councils of Canada and the Ontario Cancer Treatment and Research Foundation is gratefully acknowledged (M.H.F.). I. R. Peat thanks Gulf Oil Canada Ltd. for a fellowship. We thank J. S. Cohen, I. M. Chaiken, D. A. J. Ives, and R. M. Epand for providing compounds used in this investigation.

1. A. R. Katritzky and R. O. Topsom. J. Chem. Ed. **48**, 427 (1971).
2. (*a*) D. T. Clark, J. N. Murrell, and J. M. Tedder. J. Chem. Soc. 1250 (1963). (*b*) D. P. Craig and G. Doggett. Mol. Phys. **8**, 485 (1964).
3. K. B. Everard and L. E. Sutton. J. Chem. Soc. 2821 (1951).
4. M. J. S. Dewar and P. J. Grisdale. J. Am. Chem. Soc. **84**, 3539 (1962).

5. G. K. HAMER, I. R. PEAT, and W. F. REYNOLDS. Can. J. Chem. **51**, 897, 915 (1973).
6. M. H. FREEDMAN. J. Immunol. Meth. **1**, 177 (1972).
7. A. C. HOPKINSON, K. YATES, and I. G. CSIZMADIA. J. Chem. Phys. **52**, 1784 (1970).
8. J. A. POPLE and D. L. BEVERIDGE. Approximate molecular orbital theory. McGraw-Hill, New York. 1970.
9. G. L. NELSON, G. C. LEVY, and J. D. CARGIOLI. J. Am. Chem. Soc. **94**, 3089 (1972).
10. J. A. POPLE, W. G. SCHNEIDER, and H. J. BERNSTEIN. High resolution NMR spectroscopy. McGraw-Hill, New York. 1958. Chapt. 7.
11. A. SAIKA and C. P. SLICHTER. J. Chem. Phys. **22**, 26 (1954).
12. M. KARPLUS and J. A. POPLE. J. Chem. Phys. **38**, 2803 (1963).
13. J. MASON. J. Chem. Soc. A, 1038 (1971).
14. (*a*) P. C. LAUTERBUR. J. Am. Chem. Soc. **83**, 1838 (1961); (*b*) H. SPIESECKE and W. G. SCHNEIDER. Tetrahedron Lett. 468 (1961); (*c*) T. K. WU and B. P. DAILEY. J. Chem. Phys. **41**, 2796 (1964); (*d*) J. E. BLOOR and D. L. BREEN. J. Phys. Chem. **72**, 716 (1968); (*e*) P. LAZZERETTI and F. TADDEI. J. Org. Mag. Res. **3**, 283 (1971); (*f*) G. J. RAY, R. J. KURLAND, and A. K. COLTER. Tetrahedron, **27**, 735 (1971); (*g*) G. C. LEVY and G. L. NELSON. Carbon-13 nuclear magnetic resonance for organic chemists. J. Wiley & Sons, Inc., New York. 1972. Chapt. 4.
15. R. J. PUGMIRE and D. M. GRANT. J. Am. Chem. Soc. **90**, 687 (1968).
16. A. B. STRONG. Ph.D. Thesis. University of Utah, Salt Lake City, Utah, 1971.
17. B. V. CHENEY and D. M. GRANT. J. Am. Chem. Soc. **89**, 5319 (1967).
18. W. F. REYNOLDS, I. R. PEAT, M. H. FREEDMAN, and J. R. LYERLA, JR. J. Am. Chem. Soc. **95**, 328 (1973).
19. P. D. ELLIS, G. E. MACIEL, and J. W. MCIVER, JR. J. Am. Chem. Soc. **94**, 4069 (1972).
20. D. M. GRANT and E. G. PAUL. J. Am. Chem. Soc. **86**, 2984 (1964).
21. T. D. BROWN. Ph.D. Thesis. University of Utah, Salt Lake City, Utah, 1967.
22. D. K. DALLING and D. M. GRANT. J. Am. Chem. Soc. **94**, 5318 (1972).
23. D. K. DALLING and D. M. GRANT. J. Am. Chem. Soc. **89**, 6612 (1967).
24. M. CHRISTL and J. D. ROBERTS. J. Am. Chem. Soc. **94**, 4565 (1972).
25. D. LAUER, E. L. MOTELL, D. D. TRAFICANTE, and G. E. MACIEL. J. Am. Chem. Soc. **94**, 5335 (1972).
26. J. P. LOWE. Progr. Phys. Org. Chem. **6**, 1 (1969).
27. P. B. WOLLER and E. W. GARBISCH. J. Am. Chem. Soc. **94**, 5310 (1972).
28. C. G. SWAIN and E. C. LUPTON. J. Am. Chem. Soc. **90**, 4328 (1968).
29. (*a*) J. R. CAVANAUGH. J. Am. Chem. Soc. **89**, 1558 (1967); (*b*) J. R. CAVANAUGH. J. Am. Chem. Soc. **90**, 4533 (1968).
30. R. T. C. BROWNLEE and R. W. TAFT. J. Am. Chem. Soc. **92**, 7007 (1970).
31. R. B. HERMANN. J. Am. Chem. Soc. **91**, 3152 (1969).
32. O. KAJIMOTO and T. FUENO. Tetrahedron Lett. 3329 (1972).
33. R. T. C. BROWNLEE, R. E. J. HUTCHISON, A. R. KATRITZKY, T. T. TIDWELL, and R. D. TOPSOM. J. Am. Chem. Soc. **90**, 1767 (1968).
34. S. K. DAYAL, S. EHRENSON, and R. W. TAFT. J. Am. Chem. Soc. **94**, 9113 (1972).

Can. J. Chem. Downloaded from www.nrcresearchpress.com by 210.87.254.105 on 09/05/12
For personal use only.

Thiyl Radical Abstraction. A Mechanism for the Free Radical Substitution Reactions of Pentachlorobenzenesulfenyl Chloride

DENNIS D. TANNER, NAOTO WADA,[1] AND BRIAN G. BROWNLEE[2]

Department of Chemistry, University of Alberta, Edmonton, Alberta

Received December 20, 1972

The substitution reactions of pentachlorobenzenesulfenyl chloride with saturated alkanes were found to proceed by a free radical chain mechanism where the pentachlorobenzenethiyl radical is the predominant chain-carrying species. The selectivity of this radical could be determined by the investigation of the photoinitiated reactions of bispentachlorophenyl disulfide with a number of alkanes.

Il a été démontré que les réactions de substitution du chlorure de pentachlorobenzène-sulfényle avec des alcanes saturés se déroulent, selon un mécanisme radicalaire en chaîne où le radical pentachlorobenzène thiyle est l'agent principal de propagation de chaîne. La sélectivité de ce radical peut être déterminée par une étude des réactions de photoinitiées des bisulfures de bis-pentachlorophényle avec plusieurs alcanes.

Can. J. Chem., **51**, 1870 (1973)

Introduction

Homolytic substitution reactions of a number of sulfenyl chlorides (1–5) have been proposed to take place by free radical chain mechanisms where the chain-carrying species could involve the chlorine atom, the thiyl radical, or a mixture of these processes. The choice of the abstracting radical for a particular reagent can be decided on the basis of results obtained from the comparison of the reaction of the reagent with those of the chlorine atom. Product isomer distributions, relative reactivities between substrates (including deuterium isotope effect) and primary:secondary:tertiary (P:S:T) hydrogen selectivities have been used in these comparisons. However, the usefulness of the methods described depends upon the irreversibility of the abstraction (product determining) reaction. The possibility of extensive reversal of thiols formed by thiyl radical abstraction (eq. 1) makes the information obtained from the product studies of these reactions of limited use, since the reversibility of the reaction will mask any kinetically meaningful information that can be obtained.[3]

[1] $$RH + YS\cdot \rightleftarrows R\cdot + YSH$$

If the reactivity of the reagent is different from that of molecular chlorine then one is most likely dealing with a thiyl radical or a mixed chain reaction. It is difficult, however, to determine the true selectivity of the thiyl radical using these methods since the production of thiol which is potentially capable of reversal cannot be ignored.

A typical sulfenyl chloride, pentachlorobenzenesulfenyl chloride (PBSC), was first prepared by Putnam and Sharkey (7). Kharasch and Ariyan found that the reagent underwent reaction with cyclohexane in diffuse sunlight to yield a mixture of products which were qualitatively identified as cyclohexyl chloride, cyclohexyl pentachlorophenyl sulfide, hydrogen chloride, and bispentachlorophenyl disulfide (8). The mechanism of the reaction can potentially yield products via thiyl radical or chlorine atom abstraction or, alternatively, by a mixed chain involving both of these reactive intermediates.

Results

The Photolysis of PBSC with Cyclohexane

The reaction of PBSC with cyclohexane was shown to be a moderately long-chain process since, although not inhibited by *sym*-trinitrobenzene or molecular oxygen, 90% of the material was consumed by initiation with 2 mol % of AIBN (Table 1).

The major products of the photoinitiated reaction of a carbon tetrachloride solution of cyclohexane and PBSC were those which were previously reported. In addition to these four products, hydrogen chloride, bispentachlorophenyl disulfide (**1**), cyclohexyl chloride (**2**), and

[1]University of Alberta, Postdoctoral fellow, 1972.

[2]Taken in part from the M.Sc. dissertation in Chemistry of B. G. Brownlee, University of Alberta, Edmonton, Alberta, 1968.

[3]The kinetic distribution of the radicals initially formed is determined by the selectivity or reactivity of the abstracting radical; however, if a reversible abstraction process is involved in the reaction sequence the rates of reversal of the initially formed radicals will not be necessarily the same as their relative rates of formation. The analysis of the final product distribution of such a sequence of reactions will only give an apparent relative reactivity or selectivity for the abstraction species. For a more detailed discussion of the problem see ref. 6.

Can. J. Chem. Downloaded from www.nrcresearchpress.com by 210.87.254.6 on 09/05/12
For personal use only.

Can. J. Chem. Downloaded from www.nrcresearchpress.com by 210.87.254.6 on 09/05/12
For personal use only.

TABLE 1. The effects of free radical initiators and inhibitors on the reaction between PBSC and cyclohexane[a]

Conditions	Time, (h)	% reaction[e]
Degassed, 40°, *hν*	1.0	87
Degassed, 40°, *hν*	1.0	81
plus *sym*-trinitrobenzene[b]		82
Not degassed, 40°, *hν*	1.0	78
		80
	2.0	91
		93
Degassed, 40°, dark	333	4
		6
Degassed, 40°, dark	98	86
plus AIBN (10 mol %)[c,d]	333	98
		98
Degassed, 71°, dark	25	5
		4
Degassed, 71°, dark	25	90
plus AIBN (2 mol %)[d]		89

[a]Carbon tetrachloride solutions of PBSC (0.3 *M*), cyclohexane (3.7 *M*) run under the defined conditions.
[b]Saturated solution, ≤ 5 mol % of PBSC.
[c]At 40°, AIBN has a $t_{1/2}$ > 800 h and less than 3% of the AIBN had decomposed (16).
[d]Mole % of PBSC.
[e]Percent reaction of PBSC.

cyclohexyl pentachlorophenyl sulfide (**3**), traces of pentachlorothiophenol were found as well as a small amount of hexachlorobenzene. The yields of these materials for reactions run at 40 and 80° constitute a material balance for these reactions and are listed in Table 2. When the photolysis was carried out to 29–100% completion the ratio of the products formed remained unchanged (Table 2, runs 3–7 and 10–12). Reactions run with added pentachlorothiophenol (Table 2, runs 8–9) gave increased yields of **1** and decreased yields of **3**.

The reaction of PBSC (0.32 *M*) with a 1:1 mixture of cyclohexane (1.8 *M*) and perdeuteriocyclohexane (1.8 *M*) was run to completion. The unreacted mixture of cyclohexane and perdeuteriocyclohexane was reisolated by g.l.p.c. and the mixture was subjected to mass spectral analysis. Neither incorporation (< 1%) of deuterium into the cyclohexane nor incorporation of hydrogen into the perdeuteriocyclohexane could be observed.

Photolysis of PBSC with n-Butane and Isobutane

The reactions of these isomeric butanes each gave mixtures of two chlorides and two aryl sulfides. A quantitative determination of the products from each of these reactions is listed in Table 3. Traces (<0.5%) of pentachlorothiophenol were produced in these reactions. From the combination of the yields of the corresponding chloride and sulfide for each of the reactions a relative selectivity/H could be calculated for the reagent of (P:S:T) 1:8:25 at 40°.

The Selectivity of Complexed Molecular Chlorine

The possibility existed that the selectivity observed with the reagent was due to the abstraction reaction of chlorine atoms which had been stabilized by complex formation with PBSC or one of the products of the reaction.

Butane and isobutane were each separately photochlorinated with molecular chlorine at 40° in the presence of 0.1 *M* *n*-butyl pentachlorophenyl sulfide. The P:S:T selectivities calculated from the results of these photochlorinations were 1:2.7:3.5. The results were identical, within experimental error, to the value of 1:2.5:3.2 obtained for chlorination with molecular chlorine alone. Thus the presence of low concentrations of alkyl pentachlorophenyl sulfides did not enhance the selectivity of chlorine atoms. In these photochlorination reactions in the presence of added sulfide the yields of alkyl chlorides were in the order of 50–60% of that expected from the amount of chlorine present. Recovery of the sulfide and analysis by n.m.r. spectroscopy showed that the sulfide itself had undergone substantial chlorination, especially in the α-position. Approximate values for the reactivity of *n*-butyl pentachlorophenyl sulfide relative to the reactivity of butane and isobutane toward chlorine atoms were 17:1 and 27:1 respectively.

PBSC itself was tested as a possible complexing agent by treating isobutane with approximately equimolar amounts of PBSC and molecular chlorine. Reaction conditions and analyses were the same as those used for the PBSC–isobutane reactions. Product yields are quoted in Table 4 along with the selectivities calculated from these yields. The selectivity of the PBSC–chlorine mixture was calculated from the combined yields of the primary chloride and sulfide compared to the yield of the corresponding tertiary substitution products. The values obtained, 1:11 (P:T), can be compared to those predicted, 1:15, for the reaction if the two halogenating reagents reacted independently. Therefore, PBSC could also be eliminated as a complexing agent.

The Abstraction Reactions of Pentachlorophenyl Thiyl Radicals

The photoinitiated reactions of bispenta-

TABLE 2. Product yields of the reactions of PBSC with cyclohexane

	Yield, mol/mol PBSC[d]				
Run[a]	HCl	ArSSAr (1)	$C_6H_{11}Cl$ (2)	$C_6H_{11}SAr$ (3)	C_6Cl_6
1–2	0.74±0.01				
3–7		0.190±0.004	0.174±0.008	0.630±0.008	0.030±0.002
8–9[b]		0.30 ±0.00	0.16 ±0.00	0.525±0.005	0.02 ±0.00
10[c]			0.19	0.61	0.01
11			0.182	0.591	
12			0.178	0.501	

[a]All runs were at 40°, except runs 6 and 7 at 80°; all runs were 0.3 *M* in PBSC; runs 3–10 were 0.12 *M* in Freon 112.
[b]Runs 8 and 9 were 0.04 *M* in pentachlorothiophenol.
[c]Run 10 was carried to 75% completion, analyzed after iodometric titration, and the yields were corrected to 100% reaction. Run 11 was carried out to 29% and run 12 to 65% reaction.
[d]The errors reported are average deviations from the mean.

TABLE 3. Product yields in the photoinitiated reaction of PBSC with normal butane and with isobutane at 40°

	Mol product/mol of PBSC				
	Butane		Isobutane		
	Run 13	Run 14	Run 15	Run 16	
n-C_4H_9Cl	0.003	0.003	0.01	0.01	*iso*-C_4H_9Cl
sec-C_4H_9Cl	0.10	0.10	0.15	0.16	*t*-C_4H_9Cl
n-$C_4H_9SC_6Cl_5$ (7)	0.13	0.13	0.19	0.18	*iso*-$C_4H_9SC_6Cl_5$ (5)
sec-$C_4H_9SC_6Cl_5$(6)	0.58	0.58	0.39	0.39	*t*-$C_4H_9SC_6Cl_5$ (4)
C_6Cl_6	0.03	0.03	0.04	0.03	C_6Cl_6
$(C_6Cl_5S)_2$	0.15	0.16	0.20	0.20	$(C_6Cl_5S)_2$
Primary:secondary selectivity	1:7.7	1:7.7	1:24.3	1:26.1	Primary:tertiary selectivity

TABLE 4. Product yields in the photoinitiated reaction of isobutane with mixtures of PBSC and molecular chlorine at 40°[a]

	Mol/mol PBSC + Cl_2	
	Run 17[b]	Run 18[b]
iso-C_4H_9Cl	0.22	0.21
t-C_4H_9Cl	0.22	0.22
5	0.16	0.16
4	0.23	0.22
C_6Cl_6	0.02	0.02
$(C_6Cl_5S)_2$	0.07	0.07
Primary:tertiary selectivity	1:10.6	1:10.7

[a]Reaction mixtures contained 50 mmol of isobutane in 10 ml of carbon tetrachloride and 1.00 mmol of Freon 112 as internal standard.
[b]Run 17 was with 1.69 mmol (55 mol %) of PBSC and 1.37 mmol (45 mol %) of chlorine. Run 18 was with 1.60 mmol (54 mol % of PBSC and 1.37 mmol (46 mol %) of chlorine.

chlorophenyl disulfide were carried out with butane and with isobutane and yielded a mixture of the corresponding primary and secondary, or primary and tertiary aryl alkyl sulfides and pentachlorothiophenol. The reaction of the disulfide with isobutane (80°, 50 h with incandescent light, 2 × 200 W) yielded pentachlorothiophenol (80%), *t*-butyl pentachlorophenyl sulfide (**4**) (90%), and *iso*-butyl pentachlorophenyl sulfide (**5**) (2–2.5%). The photoinitiated reaction of butane with bispentachlorophenyl disulfide yielded only pentachlorothiophenol, *sec*-butyl pentachlorophenyl sulfide (**6**), and *n*-butyl pentachlorophenyl sulfide (**7**).

Only apparent selectivities (P:S:T) could be calculated from product ratios obtained in this manner since abstraction reactions which take place in the presence of high concentrations of thiophenols lead to reversal of the abstraction processes. At low conversion of the reactants to products when [ArSH] approaches zero the true selectivities could be estimated. Plots of the ratio of products obtained *vs.* the percentage conversion for the reaction of isobutane and butane are given in Figs. 1 and 2.

When small amounts of pentachlorothiophenol (12 mol %) were added to the mixture of the disulfide and the hydrocarbon, the photolysis, even at low percentage reactions, gave high ratios of secondary/primary (butane) product, 93/7, and tertiary/primary (isobutane) product, 97/3.

Can. J. Chem. Downloaded from www.nrcresearchpress.com by 210.87.254.6 on 09/05/12
For personal use only.

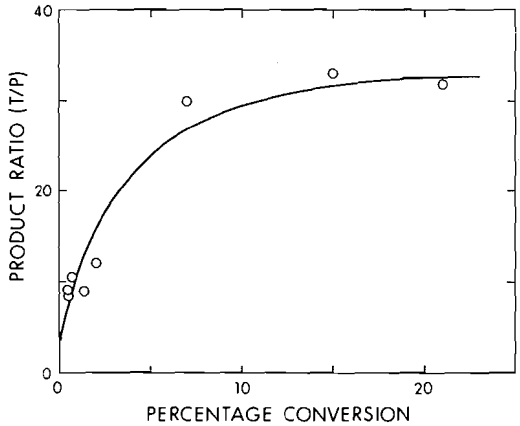

FIG. 1. The ratio of tertiary to primary sulfide formed in the reaction of bispentachlorophenyl disulfide with isobutane *vs.* the % conversion.

The Photolysis of PBSC

The photolysis of PBSC was reported to give bispentachlorophenyl disulfide (8); however, under our reaction conditions (24 h irradiation in carbon tetrachloride) 17% of hexachlorobenzene is obtained (68% of the active halogen, determined by iodometric titration, remained as volatile and nonvolatile products).

Discussion

Several mechanistic schemes can be proposed to rationalize the formation of the products produced in the initiated substitution reactions of PBSC. The observation that the reaction was initiated by small amounts (2%) of AIBN implies a radical chain substitution process of a moderately long chain length (22–45).

Following the initiation step in the light-catalyzed reaction (eq. 2), the chain may be propagated by two distinct and distinguishable sequences of ractions involving abstraction by chlorine atoms or thiyl radicals.

$$\text{[2]} \qquad \text{ArSCl} \xrightarrow{h\nu} \text{ArS}\cdot + \text{Cl}\cdot$$

In order to determine the abstracting species in the chain sequence several control experiments were carried out. If thiyl radical abstraction is proposed as the chain-carrying step in the substitution reaction, and if thiol is only found in trace amounts at the end of the reaction, an efficient reaction is necessary to remove thiol as a reaction product and to produce disulfide in its stead. The reaction of pentachlorothiophenol and PBSC was shown to meet these requirements, eq. 3, since a mixture of these reagents resulted in a very rapid reaction ($k_2 \simeq 2 \times 10^{-2}$ l mol^{-1} s^{-1}) and gave a quantitative yield of bisaryl disulfide. A mixture of hydrogen chloride and

$$\text{[3]} \qquad \text{ArSH} + \text{ArSCl} \xrightarrow{k_2} \text{ArSSAr} + \text{HCl}$$

PBSC was not reactive under the reaction conditions. The third control experiment that allows a determination of the abstracting species in the substitution reaction was one which demonstrates that a reversible abstraction reaction was not involved in the formation of the products. If thiyl radical abstraction is involved in the chain propagation step then the formation of the transfer reagent, ArSH, could lead to reversible abstraction (eq. 4) and to observed radical selectivities which were not the results of the

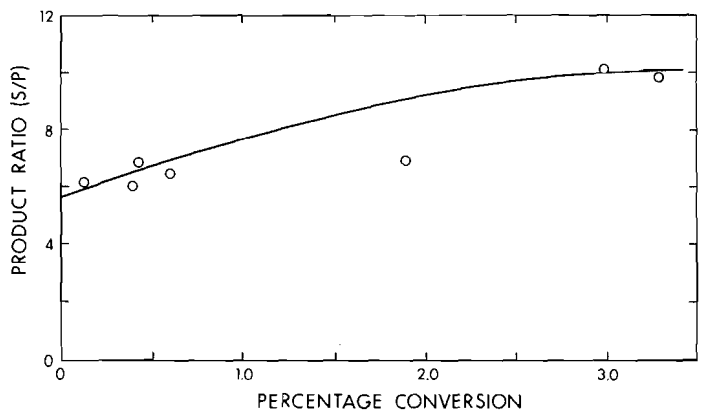

FIG. 2. The ratio of secondary to primary sulfide formed in the reaction of bispentachlorophenyl disulfide with butane *vs.* the % conversion.

Can. J. Chem. Downloaded from www.nrcresearchpress.com by 210.87.254.6 on 09/05/12
For personal use only.

Can. J. Chem. Downloaded from www.nrcresearchpress.com by 210.87.254.6 on 09/05/12
For personal use only.

kinetically determined distribution of the radicals involved.

[4] $ArS\cdot + RH \rightleftarrows ArSH + R\cdot$

The failure to observe any detectable scrambling of protium and deuterium during the reactions of cyclohexane and perdeuteriocyclohexane with PBSC eliminates the possibility that the observed selectivity of the reagent was only an artifact of a combination of abstraction and reversal steps (eq. 4). The absence of this reversal reaction, eq. −4, does not, however, eliminate the possibility that thiol is present during the reaction (traces of this product are found at the completion of the reaction), since the rapid reaction of PBSC with thiol ($k_2 \simeq 2 \times 10^{-2}$ l mol^{-1} s^{-1}, a rate constant which is not incompatible with this suggestion under the concentration conditions of the reaction) could make transfer of an alkyl radical with this reagent a noncompetitive process. The two processes, thiyl radical abstraction and chlorine atom abstraction, are presented in Schemes 1*a* or *b* and 2.

(*a*)

[4] $ArS\cdot + RH \rightarrow ArSH + R\cdot$

[5] $R\cdot + ArSCl \rightarrow RCl + ArS\cdot$

[6] $R\cdot + ArSSAr \rightarrow ArSR + ArS\cdot$

[3] $ArSH + ArSCl \rightarrow HCl + ArSSAr$

AND/OR

(*b*)

[7] $R\cdot + ArSCl \rightarrow RSAr + Cl\cdot$

[8] $Cl\cdot + ArSSAr \rightarrow ArSCl + ArS\cdot$

SCHEME 1

[9] $Cl\cdot + RH \rightarrow HCl + R\cdot$

[5] $R\cdot + ArSCl \rightarrow RCl + ArS\cdot$

[7] $R\cdot + ArSCl \rightarrow ArSR + Cl\cdot$

[6] $R\cdot + ArSSAr \rightarrow ArSR + ArS\cdot$

[9] $ArS\cdot + ArSCl \rightarrow ArSSAr + Cl\cdot$

SCHEME 2

The reagent, PBSC, demonstrated a primary:secondary:tertiary selectivity/H of 1:8:25 at 40°. Since the selectivity/H of chlorine atoms, under the reaction conditions, was found to be 1:2.7:3.5 the process depicted by Scheme 2 could not be the sole mechanistic pathway for the formation of the reaction products. The chain process depicted by Scheme 1*a* and *b* or a mixture of the chain reactions, Schemes 1 and 2, could determine the mechanistic course of the reaction. A choice between these two alternatives could be made if the selectivity of the thiyl radical were known. The selectivity of the pentachlorophenylthiyl radicals can be estimated from the plots of the isomer distribution of products *vs.* the percent conversion for the photoinitiated substitution reaction of the aryldisulfide with butane and isobutane (Scheme 3).

$$Ar{-}S{-}S{-}Ar \overset{h\nu}{\rightleftarrows} 2ArS\cdot$$

$$ArS\cdot + RH \rightleftarrows R\cdot + ArSH$$

$$R\cdot + Ar{-}S{-}S{-}Ar \rightleftarrows R{-}S{-}Ar + ArS\cdot$$

$$R\cdot + ArS\cdot \rightarrow R{-}S{-}Ar$$

$$ArS = C_6Cl_5S$$

SCHEME 3

The true selectivity of the thiyl radical will be its selectivity in the absence of reversible abstraction, *i.e.* the selectivity obtained at 0% reaction. The extrapolated values of the selectivity obtained for the thiyl radical in the absence of thiol, 0% reaction, were estimated to be 1:8.5:31. These values are not significantly different from the values (1:8:25) obtained from the reaction of PBSC with the same substrates. An interpretation of this observation infers that the radical chain substitution processes of PBSC proceed via a mechanism involving thiyl radical abstraction as the dominant chain carrying step (Scheme 1).

The absence of appreciable numbers of chlorine atoms during the PBSC reaction was attested to by the absence in the reaction mixture of the chlorination products of arylalkyl sulfides. It would be expected that chlorine atoms would favor abstraction from the sulfides rather than the hydrocarbons since the relative reactivity of the sulfides to the hydrocarbons butane and isobutane was found to be from 20–30 in the photochlorination reactions of these substrates with molecular chlorine.

The mechanism of formation of the major substitution product, the sulfide, has been the subject of some speculation for the reaction of a number of sulfenyl chlorides (1–5). A choice between a displacement on the sulfur of the

Can. J. Chem. Downloaded from www.nrcresearchpress.com by 210.87.254.6 on 09/05/12
For personal use only.

secondary product, disulfide, or on the sulfenyl chloride itself should, in principle, be able to be made. Since reaction 7 produces a

[6] $R\cdot + ArSSAr \rightarrow ArSR + ArS\cdot$

[7] $R\cdot + ArSCl \rightarrow ArSR + Cl\cdot$

chlorine atom, it would be inconsistent with both the selectivity observed with the reagent and with the absence, as secondary products, of chlorinated arylalkyl sulfide, unless a chlorine destroying process, [8], were also involved. An attempt was made to ascertain the importance of [7] as a major path for the production of sulfide by comparing the ratios of [RCl]/[RSAr] at various percentages of conversion (see Table 2, runs 3–7, 10–12). As the reaction proceeds the sulfenyl chloride to disulfide ratio decreases, and if reactions 7 and 5 are the important product-forming reactions the ratio of [RCl]/[RSAr] should be independent of the percentage of reaction, while if reactions 5 and 6 were the major paths the ratio of products should decrease. The product ratio was found to be, within experimental error, constant; however, it was also observed that at concentrations equivalent to approximately 50% reaction the disulfide began to precipitate from solution. Since the ratio of [ArSCl]/[ArSSAr] would not change as fast under these conditions, no clear choice of reactions could be made for the sulfide-forming reaction.

Hexachlorobenzene was observed as a minor reaction product (1–4% based on PBSC) in all of the reactions run with PBSC. One explanation considered for this was a displacement reaction analogous to that observed by Miller and Walling for displacement of bromine atoms from bromobenzene by chlorine atoms (9), and by Tanner and Van Bostelen for displacement of iodine from iodobenzene by chlorine atoms (10). The yield of hexachlorobenzene did not increase in the reactions using mixtures of chlorine and PBSC, thus discounting the feasibility of proposing a displacement reaction on PBSC by chlorine atoms. A precedent for obtaining hexachlorobenzene as a product during free radical reactions of PBSC was that thermolysis of benzenesulfenyl chloride gave chlorobenzene (60%) plus diphenyl disulfide and sulfur monochloride (11). By analogy a similar mechanism can be suggested for the formation of hexachlorobenzene from the photoinitiated decomposition reaction of PBSC (Scheme 4).

$$ArSCl \xrightarrow{h\nu} ArS\cdot + Cl\cdot$$

$$ArS\cdot \rightarrow Ar\cdot + S$$

$$Ar\cdot + ArSCl \rightarrow ArCl + ArS\cdot$$

SCHEME 4

Experimental

Materials

Pentachlorobenzenesulfenyl chloride was prepared by the method of Putnam and Sharkey (7), m.p. 103–104° (lit. (7) m.p. 103–104°).

Anal. Calcd. for C_6Cl_6S: Cl, 67.14. Found: Cl, 67.55.

Iodometric titration showed the material to contain 99.1 ± 0.4% of the theoretically calculated active halogen.

Cyclohexane, butane, and isobutane were Phillips research grade materials and were used without further purification.

Pentachlorothiophenol (Aldrich Chemical Co., technical grade) was purified by crystallization from benzene – carbon tetrachloride, m.p. 238–240° (sealed tube), lit. (12) m.p. 243°.

Fisher spectranalyzed reagent grade carbon tetrachloride was checked for purity by g.l.p.c. prior to use; purified benzene was prepared for analytical work by twice crystallizing reagent grade material and was free from impurities by g.l.p.c. and n.m.r.

Freon 112 (1,2-difluoro-1,1,2,2-tetrachloroethane) was distilled through a 3 ft helices-packed column and had b.p. 89.5–90.0° (700 mm). No impurities were detected by g.l.p.c.

Perdeuteriocyclohexane (99%) was obtained from Merck, Sharp and Dohme (Canada) Ltd.

Bispentachlorophenyl disulfide was prepared by the reaction (80°, 15 min) of a carbon tetrachloride mixture of pentachlorothiophenol (0.25 *M*) and PBSC (0.25 *M*). The disulfide was recrystallized from benzene several times, m.p. 235.5–237° (lit. (8) m.p. 235–236°).

G.l.p.c. Analysis

Analyses were carried out in triplicate. Peak areas were measured by multiplying peak height times peak width at one-half peak height. Calibration curves were used to convert the area ratios of the alkyl chlorides relative to Freon 112 as internal standard or area ratios of the alkyl sulfides relative to added hexachlorobenzene, into molar ratios. Precision of g.l.p.c. analyses was generally 1–3%. Where quoted, the experimental uncertainties are standard deviations from the mean. Retention time comparison and peak enhancement refer to addition of authentic material to a portion of the sample and reanalysis by g.l.p.c.

Initiation and Inhibition Reactions of PBSC with Cyclohexane

Carbon tetrachloride solutions 0.3 *M* in PBSC and 3.7 *M* in hydrocarbon were allowed to react under the conditions indicated in Table 1. The photochemical and AIBN-initiated reactions did not differ in product composition.

Reaction of PBSC with Cyclohexane (Reactions 1–12)

Between 0.47 and 0.50 g of PBSC (1.48–1.56 mmol) was accurately weighed into an ampoule containing

Can. J. Chem. Downloaded from www.nrcresearchpress.com by 210.87.254.6 on 09/05/12
For personal use only.

3.00 ml of carbon tetrachloride (0.200 *M* in Freon 112 for runs 3–12) and 2.00 ml of cyclohexane. Runs 8 and 9 contained 0.060 g (0.21 mmol) of pentachlorothiophenol. The ampoules were degassed in the absence of light, sealed under vacuum, wrapped in aluminum foil and equilibrated in a water bath at the desired temperature. The foil was then removed and the ampoules irradiated with 2 × 200 W incandescent lamps. At first the reaction mixtures were orange in color. After about 1 h the color had faded to a light yellow and orange solid (**1**) began to crystallize out (except for the 80° runs). After 5–10 h, the reaction mixtures were colorless and crystallization of the solid had apparently been completed. In the reactions containing added pentachlorothiophenol, solid began to crystallize out after 10–15 min.

For the determination of hydrogen chloride (runs 1–2) the ampoules were frozen in liquid nitrogen and broken open under 50–100 ml of water in a stoppered flask. The flask was shaken for 10–15 min. The hydrogen chloride was titrated as iodine liberated after addition of excess potassium iodate and potassium iodide (13).

For the determination of the organic products, the reaction mixtures were first analyzed by g.l.p.c. for cyclohexyl chloride using a 10 ft × 1/4 in. SF-96 column programmed from 75–150°. The material was identified by its isolation and the comparison of retention time and i.r. spectrum with that of an authentic sample. After g.l.p.c. analysis of the supernatant solutions the solid precipitate of orange crystals, bispentachlorophenyl disulfide, was collected by filtration and weighed, m.p. 235–237°. A mixture melting point and i.r. spectrum (Nujol) were identical with those of an authentic sample. The filtrate was evaporated and gave a white solid, m.p. 109.5–112°. The weighed solid was analyzed by g.l.p.c. (5 ft × 1/4 in. SE-30, 15% on 60/80 Chromosorb W at 240°) and showed two components in the ratio 3:97 by area. The first was identical to hexachlorobenzene in retention time, and the mass spectrum of a collected sample was identical to the mass spectrum of an authentic sample of hexachlorobenzene (parent ions at *m/e* 282, 284, 286, and 288 were present with the intensities expected for a molecule containing six chlorine atoms, and were the most intense peaks in the spectrum).

The second component of the mixture was isolated and identified by dissolving the mixture in acetone, filtering the insoluble traces of disulfide and hexachlorobenzene, and crystallizing the soluble portion of the product which consisted of pure cyclohexyl pentachlorophenyl sulfide, m.p. 115–116°, (lit. (8) m.p. 116°); n.m.r. (CCl_4) τ 6.4–7.0 (m, 1H), 7.8–9.0 (m, 10H); i.r. (CS_2) 2935, 2855 (C—H); 1331, 1327, 1309, 1303 (aromatic C=—C) and 687 cm^{-1} (C—Cl). The molar amounts of the sulfide and the hexachlorobenzene determined by isolation were confirmed by the addition of a standard to the admixed material and analysis by g.l.p.c.

The analysis for trace amounts of pentachlorothiophenol was made by acetylation of a portion of the crude reaction mixture, after filtration. The analysis by g.l.p.c. of pentachlorophenyl thiolacetate formed was compared to the amount of hexachlorobenzene (independently calibrated) in the solution. By addition of known amounts of the thiol to the reaction mixture and carrying out the acetylation and analysis an upper limit of 0.2% could be placed on the amount of thiol present in the reaction.

Pentachlorophenyl Thiolacetate

The acetylation was carried out by heating to reflux a carbon tetrachloride solution of the pentachlorothiophenol (0.001–1.0 mmol) with excess acetyl chloride (500 mg, 6.4 mmol). Pyridine (0.5 ml, 6.3 mmol) in 5 ml of carbon tetrachloride was added in small portions through the reflux condenser. After 0.5 h the reaction mixture was cooled and poured onto ice. The carbon tetrachloride layer was separated and washed with ice-cold 3 *N* hydrochloric acid (2 × 30 ml). After drying over anhydrous calcium chloride the solvent was removed to give a >94% yield of pentachlorophenyl thiolacetate, m.p. 116–118° (lit. (14) m.p. 118–119°); i.r. (CS_2) 1722, 1708 (thiolester carbonyl), and 690 cm^{-1} (C—Cl).

The Reaction of PBSC with Cyclohexane and Perdeuteriocyclohexane

A mixture of pentachlorobenzenesulfenyl chloride (0.25 g, 7.9×10^{-4} mol), cyclohexane (0.39 g, 4.5×10^{-3} mol), perdeuteriocyclohexane (0.44 g, 4.6×10^{-3} mol), and carbon tetrachloride (2.4 g) was degassed and sealed in a Pyrex ampoule. The ampoule was irradiated with 2 × 200 W tungsten lamps at 40° for 20 h. Iodometric titration carried out after the irradiation showed the absence of any active halogen. Product analysis carried out in the previously described manner showed the presence of the following: H(D)Cl (74%), chlorocyclohexane (22%), bispentachlorophenyl disulfide (20%), cyclohexyl pentachlorophenyl sulfide (49%), hexachlorobenzene (2%), and pentachlorobenzenethiol (trace).

Mass-spectral analysis of the recovered cyclohexane and perdeuteriocyclohexane was undertaken to compare the ratios of the *m/e* 85 ($C_6H_{11}D$) to 84 (C_6H_{12}), and 95 (C_6HD_{11}) to 96 (C_6D_{12}) intensities with those of the starting mixture of cyclohexane and perdeuteriocyclohexane. The intensity ratios of the *m/e* 85/84 and 95/96 peaks obtained from the analysis were the same, within experimental error $< \pm 1\%$, as those observed from the starting mixture.

A similar experiment without solvent carbon tetrachloride gave the same results.

Synthesis of the Isomeric Butyl Pentachlorophenyl Sulfides, 4–7

The sulfides were prepared by alkylating the sodium salt of pentachlorothiophenol with the appropriate alkyl halide in boiling ethanol (25 ml, 1 h). Compounds **4–7** were isolated by pouring the reaction mixtures onto 100 g of ice. Sulfides **7** and **5** were collected as solids which were crystallized from acetone–ethanol; m.p. of **7** was 38° from methanol–ethanol (lit. (15) m.p. 39–40°). Compound **6** was obtained as a colorless oil which was extracted into benzene. To obtain the *t*-butyl isomer (**4**) free from starting material, the solvent was evaporated and the residue treated with excess 5% sodium hydroxide. The solid remaining was filtered off and crystallized from acetone–ethanol. Analytical samples of **5** and **4** were prepared by sublimation at 110–120° (0.01 mm); m.p. of **5** was 37.5–38°, m.p. of **4** was 122.5–123°. The entire crude yield of **6** was distilled, b.p. 135–145° (0.01 mm), n_D^{20} 1.6124. The analysis was obtained on this material. Table 5 summarizes the details.

The i.r. spectra (CS_2) of all four isomers contained bands for C—H stretching between 2860 and 2980 cm^{-1}. The aromatic C=C stretching appeared as two strong

TABLE 5. The isomeric butyl pentachlorophenyl sulfides **4**–**7**

	C_6Cl_5SH (mmol)	NaOH (mmol)	Alkylating agent (mmol)	Yield (%)	Analysis C	H	Cl
4	10	20	*t*-C_4H_9Cl (20)	9	35.83	2.87	52.57
5	10	12	*iso*-C_4H_9Br (20)	60	35.45	2.79	52.36
6	10	20	*sec*-C_4H_9Br (20)	83	35.54	2.61	52.17
7	10	12	*n*-C_4H_9Br (20)	80	—	—	—
				Calcd. for $C_{10}H_9Cl_5S$:	35.48	2.70	52.37

TABLE 6. Nuclear magnetic resonance data of the isomeric butyl pentachlorophenyl sulfides (CCl_4)

	Group assignment	τ value (multiplicity[a], *J* Hz)
7	ArS—CH_2—[b]	7.12 (t, 6.5)
	—CH_2—CH_2—	8.5 (m, —)
	—CH_3	9.1 (m, —)
6	ArS—C(H)—	6.66 (m, —)
	—CH_2—	8.45 (m, —)
	ArS—C(CH_3)—	8.77 (d, 6.5)
	—CH_3	8.97 (t, 7)
5	ArS—CH_2—	7.26 (d, 6.5)
	—C(H)—	8.32 (m, —)
	H_3C—C(CH_3)—	8.99 (d, 6)
4	ArS—C(CH_3)—CH_3	8.61 (s, —)

[a]s, singlet; d, doublet; t, triplet; m, multiplet.
[b]Ar = C_6Cl_5 group.

bands (split in **7** and **5**) at 1300–1305 and 1325–1335 cm^{-1}. The C—Cl stretching bands for all four isomers was a strong band between 683 and 686 cm^{-1}.

The n.m.r. data of the four isomers are shown in Table 6.

Reaction of PBSC with Normal Butane (Runs 13 and 14) and Isobutane (Runs 15 and 16)

The reaction mixtures consisted of *ca.* 3 mmol of PBSC (0.95–1.0 g), *ca.* 50 mmol of hydrocarbon (5 ml at −80°), 2.00 mmol of Freon 112, and 10 ml of carbon tetrachloride.

The reaction mixtures were degassed and irradiated at 40° in the same way as the cyclohexane reactions (runs 1–12). Irradiation times of 7–10 h were required for complete reaction as shown by complete disappearance of the orange color of PBSC, and crystallization of the disulfide.

The ampoules were frozen in liquid nitrogen, broken open, and analyzed for alkyl chlorides by g.l.p.c. (20 ft × 1/8 in. SF-96 column 5% on 80/100 Chromosorb W, AW-DMCS at 50°). The chlorides were identified by a comparison of their retention times on two columns with those of authentic samples (20 ft SF-96 and 25 ft × 1/8 in. UCON POLAR, 5% on 80/100 Chromosorb W at 50°).

The disulfide was collected by filtration and was found to be identical with authentic material in mixture m.p. The yield and m.p. of the disulfide obtained in these four runs were: run 13, 0.257 g, m.p. 234–236°; run 14, 0.268 g, m.p. 232–235°; run 15, 0.341 g; run 16, 0.352 g, m.p. 234–236°.

Evaporation of the filtrates gave the crude sulfides. Run 13, 0.775 g; run 14, 0.751 g; run 15, 0.640 g; run 16, 0.664 g.

The isomer ratios were determined by n.m.r. By comparing the ArS—C—H signal of **6** (τ 6.65 multiplet) to the ArS—CH_2— signal of **7** (τ 7.12, triplet) in CCl_4 solvent, the ratio of **6**/**7** was found to be 4.5 for run 13 and 4.1 for run 14. Similarly by comparing the *t*-butyl singlet of **4** (τ 8.82) to the *gem*-dimethyl doublet of **5** (τ 9.14) in benzene solvent, the ratio of **4**/**5** was found to be 2.1 for run 15 and 2.2 for run 16.

The product butyl pentachlorophenyl sulfide had an identical n.m.r. spectrum to that of an authentic sample. Further identification was accomplished by g.l.p.c. retention time comparison with authentic samples of **4**, **5**, **6**, and **7** (5 ft × 1/4 in. SE-30 column at 220–240°). The area ratios were in agreement with the ratios determined from the n.m.r. spectra. Samples were collected by preparative g.l.p.c. for comparison of i.r. spectra and were found to be identical to authentic materials in this respect. Mass spectra were obtained for each of the sulfides collected by g.l.p.c. Each spectrum had a set of parent peaks at *m/e* 336, 338, 340, and 342 in the expected ratios for five chlorine atoms ($C_6{}^{35}Cl_5C_4H_9$ = 336). The base peak for each of the isomers was at *m/e* 57 (C_4H_9).

Hexachlorobenzene (identified by g.l.p.c. retention time and by the mass spectrum of a collected sample) was also present in the mixtures. It comprised about 4% (by peak area) for runs 13 and 14, and 5% for runs 15 and 16.

Pentachlorothiophenol was estimated by the acetylation method previously described. For both run 14 and run 16 none of the thiolacetate could be detected by g.l.p.c. Under the analytical conditions employed the upper limit for the yield of pentachlorothiophenol was

Can. J. Chem. Downloaded from www.nrcresearchpress.com by 210.87.254.6 on 09/05/12
For personal use only.

Can. J. Chem. Downloaded from www.nrcresearchpress.com by 210.87.254.6 on 09/05/12
For personal use only.

0.5%. Run 14 could be analyzed under the g.l.p.c. conditions as used before. Run 16 was analyzed using a 5 ft × 1/8 in. QF-1 column at 200°. A summary of the results for runs 13–16 is listed in Table 3.

Photochlorination of Normal Butane and Isobutane

Butane (2 ml, *ca.* 20 mmol) was photochlorinated at 40° with 2.0 mmol of chlorine in sealed, degassed ampoules with 4.0 ml of carbon tetrachloride as solvent.

Analysis by g.l.p.c. (20 ft × 1/8 in. SF-96 column) gave, for three reactions, *sec*-C_4H_9Cl/*n*-C_4H_9Cl = 1.65 ± 0.07 for a primary:secondary selectivity/H of 1:2.5 ± 0.1.

Similarly photochlorination of 20 mmol of isobutane with 1.7 mmol of chlorine in 4.0 ml of carbon tetrachloride gave, for two reactions, *t*-C_4H_9Cl / *iso*-C_4H_9Cl = 0.358 ± 0.016 for a primary:tertiary ratio of 1:3.2 ± 0.15.

Reaction of Isobutane with PBSC–Chlorine (Runs 17 and 19)

Two reactions were run at 40°. Each reaction mixture consisted of isobutane (5 ml, *ca.* 50 mmol), PBSC (run 17, 0.536 g, 1.69 mmol; run 18, 0.507 g, 1.60 mmol), chlorine (1.37 mmol), Freon 112 (1.00 mmol) and carbon tetrachloride (10.0 ml). Irradiation times of 8–9 h were required for completion of reaction.

The alkyl chlorides were quantitated by g.l.p.c. as before (runs 15 and 16).

The yield, melting point, and mixture melting point (with authentic material) of the disulfide (**1**) were: run 17, 0.116 g, 234–236, 235–237°; run 16, 0.113 g, 235–237°, none.

The yield of crude sulfide was 0.423 g (1.25 mmol) for run 17 and 0.399 g (1.18 mmol) for run 18.

The n.m.r. spectra (CCl_4) of the sulfides were qualitatively identical to those previously obtained for the sulfides from runs 15 and 16. Since the spectra did not contain any signals below τ 7.1 it was concluded that no chlorination of the sulfides had occurred. The ratio (n.m.r.) of **4**/**5** was 1.44 for run 17 and 1.41 for run 18.

Hexachlorobenzene was estimated by g.l.p.c. analysis as before and found to comprise 4–5% (by peak area) of the crude sulfide mixtures. The peak area ratio (g.l.p.c.) of **4**/**5** was about 1.3/1 for both runs.

Photochlorination of Normal Butane (Runs 19 and 20) and Isobutane (Runs 21 and 22) in the Presence of n-Butyl Pentachlorophenyl Sulfide (7)

Each reaction mixture contained 2 ml (20 mmol) of hydrocarbon (3.3 *M*), 1.20 mmol of chlorine (0.20 *M*), 0.60 mmol of **7** (0.10 *M*), 2.00 mmol of Freon 112, and 4.0 ml of carbon tetrachloride. The chlorinations were carried out at 40° and required about 0.25 h of irradiation. The alkyl chlorides were analyzed by g.l.p.c. as before. For runs 19 and 20, the molar ratio *sec*-C_4H_9Cl/*n*-C_4H_9Cl was 1.78 ± 0.06 for a primary:secondary selectivity/H of 1:2.7 ± 0.1. The total yield of alkyl chlorides was 0.72 mmol or about 60% of the theoretical, based on chlorine.

The reaction mixtures from runs 19 and 20 were combined and the solvent removed to give 0.454 g of colorless oil. When the n.m.r. spectrum of this oil was obtained in carbon tetrachloride solution it showed that the sulfide had undergone chlorination. The signal at τ 4.6 (triplet) was assigned to the α-chlorinated product, and the signal at 5.8 was assigned to the β-chlorinated product. The ratio of α-chlorination to β-chlorination was about 2:1. From a comparison of the integrated intensities of the chlorinated sulfides and the unchlorinated starting material it was estimated that about 40% of the sulfide had been chlorinated. Because the α,α-dichlorosulfide could not be observed by n.m.r., it was not known for certain if any dichlorosulfide was produced in the reaction.

Runs 21 and 22 were analyzed in the same way. The ratio *t*-C_4H_9Cl/*iso*-C_4H_9Cl was 0.388 ± 0.023 for a primary:tertiary ratio of 1:3.5 ± 0.2. The total yield of chlorides was 0.60 mmol, about 50% of theoretical. The combined yield of (chlorinated) sulfides was 0.450 g. The n.m.r. spectrum was qualitatively identical to that obtained from the chlorinated sulfides in runs 19 and 20. Again the ratio of α-chlorination to β-chlorination was 2:1. About 50% of the sulfide had been chlorinated.

*Photolysis of Bispentachlorophenyl Disulfide, **1**, in Isobutane – Carbon Tetrachloride*

Mixtures of 0.17 g (3.02×10^{-4} mol) of bispentachlorophenyl disulfide, 3 ml (3.0×10^{-2} mol) of isobutane, and 5 ml of carbon tetrachloride were degassed and sealed in Pyrex ampoules. The ampoules were placed in a thermostat at 80 °C and irradiated with a 200 W tungsten lamp for the appropriate times (0.5–32 h). The ampoules were cooled in liquid nitrogen, opened, and the reaction mixtures were filtrated by suction to remove unreacted bispentachlorophenyl disulfide. Analysis of the filtrates by g.l.p.c. (SE 30, 230°) showed three products which were collected and identified by a comparison of their i.r. spectra with those of authentic samples. The compounds were shown to be pentachlorobenzenethiol, *t*-butyl pentachlorophenyl sulfide, and isobutyl pentachlorophenyl sulfide. The reactions were quantitated by adding known amounts of hexachlorobenzene and determining the yields of the products by the use of standard calibration curves constructed for the products and the standard. Product ratios of *t*-butyl pentachlorophenyl sulfide to isobutyl pentachlorophenyl sulfide were determined by comparison of the corresponding peak areas. Results are given in Fig. 1. In typical runs the products were isolated by g.l.p.c. and the structures were determined by their i.r. and n.m.r. spectra. A control experiment carried out without irradiation resulted in complete recovery of the starting disulfide after 24 h.

The photolysis of bispentachlorophenyl disulfide in isobutane – carbon tetrachloride was carried out with added pentachlorobenzenethiol (12 mol %). The reactions were carried out to 0.1, 2.7, 3.3, and 20.2% conversion and were analyzed in the usual manner. The ratio of **4**/**5** was 96.5 ± 0.5/4 ± 0.5 for these four independent reactions.

Photolysis of Bispentachlorophenyl Disulfide in n-Butane – Carbon Tetrachloride

Mixtures of 0.17 g (3.02×10^{-4} mol) of bispentachlorophenyl disulfide, 3 ml (3.0×10^{-2} mol) of *n*-butane, and 5 ml of carbon tetrachloride were degassed and sealed in Pyrex ampoules. The ampoules were placed in a thermostat at 80° and preheated before irradiation for 3 h. Irradiation with a 200 W tungsten bulb was continued for the appropriate times (1–115 h). G.l.p.c. analysis (SE 30, 230°) of the reaction mixtures showed

three products identified by retention times as pentachlorobenzenethiol, *sec*-butyl pentachlorophenyl sulfide, and *n*-butyl pentachlorophenyl sulfide in the order of elution. In some typical cases products were isolated and their structures determined by comparison of their i.r. (CS_2) and n.m.r. spectra with those of authentic samples. Percent conversion of the disulfide into sulfides and the ratio of *sec*-butyl to *n*-butyl derivatives in each ampoule were determined by g.l.p.c. using calibration curves (standard/hexachlorobenzene). The results of these experiments are given in Fig. 2. A control experiment carried out without irradiation resulted in complete recovery of the starting disulfide.

Photolysis of bispentachlorophenyl disulfide in *n*-butane – carbon tetrachloride was carried out with added pentachlorobenzenethiol (12 mol %). The reactions were carried out and analyzed in the usual manner. Reactions run to 0.7, 1.0, and 2.4% conversion showed ratios of **6**/7 of 93.3 ± 0.3/6.7 ± 0.3.

Photolysis of PBSC in Carbon Tetrachloride

PBSC (0.487 g, 1.54 mmol) was photolyzed at 40° for 24 h in a sealed, degassed ampoule using 5 ml of carbon tetrachloride as solvent. The volatile components were removed by vacuum transfer at room temperature and 0.05 mm. By iodometric titration, 0.10 mmol of active halogen was found in the distillate, and 0.94 mmol was found in the residue. After titration, the organic layer was removed and evaporated leaving a pale yellow solid. Analysis of this solid by g.l.p.c. (SE-30 at 200°) showed hexachlorobenzene as the sole volatile product. By sublimation at 150° and 15 mm, 0.075 g (17%) of hexachlorobenzene was obtained, m.p. 223–226° (sealed tube). After one crystallization from carbon tetrachloride it had m.p. 228–229° (sealed tube) and mixture m.p. with authentic material 228–229° (sealed tube). The i.r. spectrum (Nujol mull) was identical to that of authentic material.

The Rate of the Reaction Between Pentachlorobenzenesulfenyl Chloride and Pentachlorobenzenethiol

The solutions of pentachlorobenzenesulfenyl chloride (1.316 g, 0.052 *M*) in 80 ml of carbon tetrachloride – cyclohexane mixture (5:3 in volume) and pentachlorobenzenethiol (1.174 g, 0.052 *M*) in 80 ml of the same mixture were separately equilibrated at 40° for 10 min and then were mixed together in the dark. The pentachlorobenzenesulfenyl chloride remaining in the solution was monitored by withdrawing aliquot portions of the solution and subjecting them to iodometric titration with standard sodium thiosulfate solution. A second order rate constant of $1.8 \pm 0.2 \times 10^{-2}$ l mol^{-1} s^{-1} was obtained.

The authors wish to thank the National Research Council of Canada and the University of Alberta for their generous support of this work.

1. H. KLOOSTERZIEL. Rec. trav. chim. **82**, 497 (1963).
2. V. PREY, E. GUTSCHIK, and H. BERBALK. Monatsh. Chem. **91**, 556 (1960).
3. (*a*) R. G. R. BACON and R. G. GUY. J. Chem. Soc. 2428 (1961). (*b*) R. G. R. BACON, R. G. GUY, and R. S. IRWIN. J. Chem. Soc. 2436 (1961).
4. E. GUTSCHIK and V. PREY. Monatsh. Chem. **92**, 827 (1961).
5. J. F. HARRIS. JR. J. Org. Chem. **31**, 931 (1966).
6. D. D. TANNER and N. J. BUNCE. J. Am. Chem. Soc. **91**, 3028 (1969).
7. R. E. PUTNAM and W. H. SHARKEY. J. Am. Chem. Soc. **79**, 6526 (1957).
8. N. KHARASCH and Z. S. ARIYAN. Chem. and Ind. 929 (1964).
9. B. MILLER and C. WALLING. J. Am. Chem. Soc. **79**, 4187 (1957).
10. D. D. TANNER and P. B. VAN BOSTELEN. J. Org. Chem. **32**, 1517 (1967).
11. R. MAYER and H. J. FREY. Angew. Chem. Int. Ed. **3**, 705 (1964).
12. U.S. Patent 2 765 345. Chem. Abstr. **51**, 5828*i* (1957).
13. G. H. CADY. Inorg. Synth. **5**, 156 (1957).
14. G. SUMRELL, M. ZIEF, E. J. HUBER, G. E. HAM, and C. H. SCHRAMM. J. Am. Chem. Soc. **81**, 4313 (1959).
15. R. PONCI, A. BARUFFINI, F. GIALDI, and P. BORGNA. Farmaco (Pavia), Ed. Sci. **19**, 489 (1964); Chem. Abstr. **61**, 8217g (1964).
16. C. WALLING. *In* Free radicals in solution. John Wiley and Sons, Inc., New York. 1957. pp. 469.

Can. J. Chem. Downloaded from www.nrcresearchpress.com by 210.87.254.6 on 09/05/12
For personal use only.

Erratum: ^{13}C Chemical Shifts of Highly Substituted Bicyclo[2.2.1]heptanes

N. H. WERSTIUK, R. TAILLEFER, R. A. BELL, AND B. G. SAYER
Department of Chemistry, McMaster University, Hamilton, Ontario

Received February 8, 1973
(Ref.: Can. J. Chem. **50**, 2146 (1972))

The chemical shift data for **4** should be corrected as follows:

Compound	C-1	C-2	C-3	C-4	C-5	C-6	C-7	C-8	C-9
4	35.9	44.0*	35.6	61.7	216.0	43.8*	36.7	29.4	27.7

*Assignments may be interchanged.

Can. J. Chem., **51**, 1880 (1973)

Can. J. Chem. Downloaded from www.nrcresearchpress.com by 210.87.254.5 on 09/05/12
For personal use only.

Can. J. Chem. Downloaded from www.nrcresearchpress.com by 210.87.254.42 on 09/05/12
For personal use only.

The Triplet State of Ketones in Solution: The Role of the Charge Transfer State in the Quenching of Triplet Acetone by Aromatic Molecules[1]

R. O. LOUTFY[2] AND R. W. YIP

Division of Chemistry, National Research Council of Canada, Ottawa, Canada K1A 0R6

Received March 2, 1973

The rate constants for quenching of triplet acetone by a series of halobenzenes have been determined by flash emission technique. Quenching was found to be approximately a hundred times faster than that for triplet benzophenone. For both triplet ketones, quenching did not decrease with the increase in triplet energy difference between ketone and quencher (as expected for normal endothermic triplet energy transfer) and did not correlate with the i.p. of all of the quenchers studied. All of the qualitative features of the quenching results can be simply interpreted in terms of enhanced coupling of the locally excited triplet ketone and quencher states as a result of interaction with the charge transfer state.

Les constantes de vitesse de la désactivation de l'état triplet de l'acétone par une série d'halo-benzenes ont été determinées par la technique de la photolyse éclaire en émission. La désactivation est environ cent fois plus rapide que celle de l'état triplet de la benzophénone. Dans les deux cas (benzophénone et acétone) la vitesse de désactivation ne diminue pas quand la différence entre les énergies triplet de la cétone et du désactivateur augmente (comme attendu dans le cas d'un transfert endothermique d'énergie triplet) et la corrélation entre la vitesse de désactivation et le potentiel d'ionisation du désactivateur n'est pas observée dans tous les cas étudiés. Tous les résultats obtenus peuvent être interprétés qualitativement en postulant une augmentation du couplage entre l'état triplet localement excité de la cétone et les états énergétiques du désactivateur, augmentation dûe à une interaction avec l'état de transfert de charge.

Can. J. Chem., 51, 1881 (1973)

The formation of complexes between triplet excited and ground state molecules (triplet exciplexes) has been of current interest, particularly in connection with the quenching of triplet ketones by amines (1), olefins (2), and substituted benzenes (3, 4). In the case of quenching by amines, both thermodynamic calculations, and a correlation between the quenching rate constants (k_q) and the ionization potentials (i.p.) of the amines, provided substantial evidence for the intermediacy of a charge-transfer (c.t.) complex, (A^-B^+), in which charge is transferred from the quencher (B) to the ketone (A) (1). Apparently such a c.t. complex is not formed in the quenching of triplet benzophenones by electron deficient benzenes. It was reported that k_q did not decrease with increasing i.p. of the quencher as expected for the c.t. complex (A^-B^+) but instead tended to increase with i.p. (4).

As part of our study of triplet ketone reactivity in solution (1, 5–8) by various pulsed techniques (1, 6, 9, 10), we have measured rate constants for the quenching of triplet acetone (6) in order to obtain further information on the interaction between triplet ketones and aromatic molecules.

The decay of triplet acetone in degassed acetonitrile solutions was measured by the flash emission technique described earlier (6). The rate constants for quenching of triplet acetone by a series of aryl halides[3] along with relevant values for quenching of triplet benzophenone[4] (4) are recorded in Table 1. Available triplet energies (E_T) ionization potentials (i.p.), electron

[1]N.R.C.C. No. 13183.

[2]N.R.C.C. Postdoctorate Fellow, 1971 to present.

[3]Spectroscopic grade except for the polyfluorobenzenes, which were reagent grade. All quenchers were fractionally distilled.

[4]Substituted benzenes were used as solvents.

TABLE 1. Quenching rate constants of acetone and benzophenone triplet by substituted benzenes; ionization potentials, electron affinities, half-wave reduction potentials, and triplet energies of the compounds studied

Compound	E_T[a] (eV)	Ionization potential[b] (eV)	Electron affinity[c] (E_A) (eV)	$-E_{1/2}^{red}$	Sensitizer: Acetone k_q (M^{-1} s^{-1})	Sensitizer: Benzophenone[d] k_q (M^{-1} s^{-1})
1, C_6H_6	3.65	9.245	−0.40	2.80[e]	2.8×10^6	9.6×10^3
2, C_6H_5N	3.50	9.26	−0.67	2.76	—	9.3×10^3
3, C_6H_5F	3.66	9.20	−0.19	2.69	6.7×10^6	1.0×10^4
4, C_6H_5Cl	3.56	9.07	0.02	2.58	1.8×10^7	1.6×10^4
5, C_6H_5Br	3.56	8.98	0.28	2.32	2.5×10^7	4.8×10^4
6, m-$C_6H_4F_2$		9.40	—	2.64[f]	4.8×10^6	2.2×10^4
7, $C_6H_5CF_3$	3.62[k]	9.68	—	2.54[g]	5.4×10^6	(3.4×10^4)[j]
8, 1,2,4,5-$C_6H_2F_4$	3.49[k]	9.39	—	2.40[h]	(9.9×10^6)[j]	6.2×10^4
9, C_6HF_5	3.31[k]	9.84	>0.2	2.35[h]	1.4×10^7	7.5×10^4
10, C_6F_6	3.22[k]	9.97	>0.2	2.11[g]	2.3×10^7	2.0×10^5
11, C_6H_5CN	3.37	9.70	0.55	2.20	—	2.1×10^5
12, CH_3COCH_3	3.36	9.70	0.29	2.30[i]		
13, $C_6H_5COC_6H_5$	2.99	9.45	0.55	1.84[i]		

[a]Reference 14.
[b]Photoionization values taken from ref. 15.
[c]Calculated using the equation $E_{1/2}^{red} = E_A - E_{solv} + C$, see ref. 16. E_{solv} not known very accurately for compounds 6–10.
[d]Reference 4.
[e]Reference 14.
[f]Reference 18.
[g]The authors are indebted to Dr. Raouf O. Loutfy, Colorado State University, for supplying us with these data.
[h]Reference 19.
[i]Reference 20.
[j]Values in parentheses are predicted from the correlation given in Fig. 2.
[k]Reference 21.

affinities (E_A), and half-wave reduction potentials ($E_{1/2}^{red}$) of the ketones and quenchers are also given. The i.p. values[5] used were those determined by the photoionization method (p.i.).[6]

We note from the results that (*a*) k_q does not decrease with ΔE_T as required by the commonly accepted triplet energy transfer mechanism as applied to endothermic transfer (11); (*b*) contrary to that previously reported for triplet benzophenone (4), we find for both ketones, log k_q does not correlate with the i.p. of all of the quenchers; and (*c*) $k_q^{acetone} > k_q^{benzophenone}$ by ~100 times, in sharp contrast with the amine quenching results where $k_q^{benzophenone} > k_q^{acetone}$ by ~10 times.

Let us consider the possibility of c.t. complex formation in light of the quenching results (*vide supra* point (*b*)) and with regards to the direction of charge transfer. The energy of the zero order (in intermolecular orbital overlap) c.t. state, E(c.t.), is given by

$$[1] \qquad E(\text{c.t.}) = \text{i.p.} - E_A - J$$

where J is the Coulomb integral (12). If it is assumed that J does not differ much for the two possible donor–acceptor pairs, then we have as condition for the pair with the lowest energy, the inequality

$$[2] \qquad (\text{i.p.} + E_A)_{acceptor} > (\text{i.p.} + E_A)_{donor}$$

Calculations based on the relative energies of the zero order c.t. state as applied to both triplet acetone and triplet benzophenone (equation 2) show that the direction of transfer depends very much on the particular substituted benzene. For this reason, we do not expect (nor did we find) that log k_q should correlate with the i.p. of all of the quenchers. Instead, correlations were obtained between log k_q and i.p. for the benzenes forming A^-B^+ complexes (see Fig. 1) and log k_q and $E_{1/2}^{red}$ for the other (more electron-deficient) benzenes (Fig. 2). We note that although the E_A of difluoro- and trifluorobenzene are not known, their $E_{1/2}^{red}$ tend to suggest that these quenchers should act as donors (rather

[5]We thank Dr. F. P. Lossing for valuable discussion in the critical evaluation of i.p. data.

[6]Those determined by electron-impact (e.i.) are consistently higher than the p.i. (~"adiabatic") values. In addition, many earlier e.i. values are now known to be unreliable. Discrepancies of the order of 1 eV can be found. Therefore, from the point of view of reliability and consistency, only p.i. values were used.

Can. J. Chem. Downloaded from www.nrcresearchpress.com by 210.87.254.42 on 09/05/12
For personal use only.

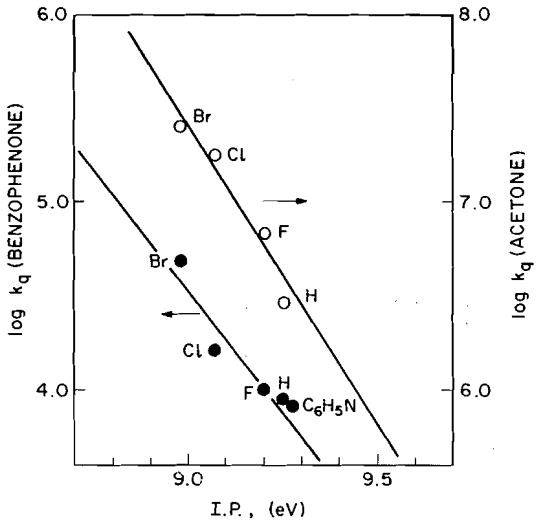

FIG. 1. Plot of log k_q of ketone triplet against the ionization potential of the substituted benzene quenchers. Triplet acetone ○, and triplet benzophenone ●.

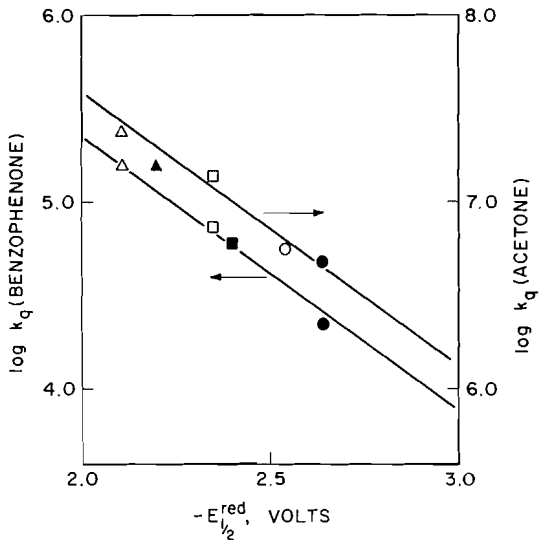

FIG. 2. Plot of log k_q for acetone and benzophenone triplets against the half-wave reduction potential of the quenchers; *m*-$C_6H_4F_2$, ●; $C_6H_5CF_3$, ○; 1,2,4,5-$C_6H_2F_4$, ■; C_6HF_5, □; C_6F_6, △; and C_6H_5CN, ▲.

than acceptors) contrary to experimental results. We believe that for borderline cases like these, the rough guide provided by the energies of the zero order c.t. state is inadequate to explain the direction of charge transfer. When intermolecular overlap is considered, the singlet and triplet c.t. states will be split such that they differ by twice the exchange integral. The possibly larger overlap[7] for $^3(A^+B^-)$ as compared to $^3(A^-B^+)$ could provide the extra stabilization energy needed to alter the direction of charge transfer.

We can view the triplet quenching process in terms of E(c.t.) and its relationship with the energies of the locally excited states ^{3}(*AB) and ^{3}(AB*). Three alternatives exist: (*i*) E(c.t.) > E^3(AB*) > E^3(*AB), (*ii*) E^3(AB*) > E(c.t.) > E^3(*AB), and (*iii*) E^3(AB*) > E^3(*AB) > E(c.t.). Calculations of E(c.t.) using eq. 1, assuming a $J \sim 4$ eV,[8] leads us to favor alternative (*i*). In this case, the main configuration interactions (c.i.) would be (c.t.) $\leftrightarrow\!\!\rightarrow$ ^{3}(AB*) for the benzophenone–benzene complexes, and (c.t.) $\leftrightarrow\!\!\rightarrow$ ^{3}(AB*) > (c.t.) $\leftrightarrow\!\!\rightarrow$ ^{3}(*AB) for the acetone–benzene complexes. As a result of c.i., the ΔE between the locally excited triplet states are reduced, thereby increasing the exchange interactions between these two states and hence the rate of quenching. Since the extent of c.i. depends, in part, on the energy difference between the interacting states, k_q should depend on the energy of the c.t. state, particularly in the case of a closely related series of quenchers. We calculated a decrease in the energy gap between the two locally excited triplets from c.i. with the c.t. states of the order of 0.2–0.3 eV and 0.01–0.08 eV, respectively, for the benzophenone and acetone would account for the observed quenching results. Differences in E(c.t.) between the acetone and the corresponding benzophenone complexes are consistent with larger energy shifts for the benzophenone complexes.

In conclusion, all of the qualitative features of the quenching of triplet acetone (and benzophenone) by substituted benzenes can be simply interpreted in terms of enhanced coupling of the locally excited triplet ketone and quencher states as a result of interaction with the c.t. state. The interpretation neither requires nor

[7]For (A^+B^-) we have overlap of the carbonyl π^* orbital with the π^* orbital of the aromatic ring. For the complex (A^-B^+), the overlap is between the carbonyl n-orbital and the aromatic π orbital (see ref. 13, p. 166).

[8]The value of J taken for the carbonyl–benzene complex is intermediate between the larger naphthalene excimer (3–3.8 eV [12]) and the maximum value assumed by two point charges (4.1–4.8 eV) at similar intermolecular distances. Within the arguments based on the energy of the zero-order c.t. state, our qualitative conclusions are not sensitive to the precise value of J chosen unless the unrealistic assumption is made that J can be represented by two point charges separated by an intermolecular distance $\lesssim$2.8 Å.

Can. J. Chem. Downloaded from www.nrcresearchpress.com by 210.87.254.42 on 09/05/12
For personal use only.

excludes the possibility that $E_{binding} > RT$ for the complex.

We wish to thank our colleagues Drs. J. M. Morris and D. F. Williams for discussing with us aspects of charge transfer and for excercising their critical faculties on our manuscript.

1. R. W. YIP, R. O. LOUTFY, Y. L. CHOW, and L. K. MAGDZINSKI. Can. J. Chem. **50**, 3426 (1972) and references cited.
2. I. H. KOCHEVAR and P. J. WAGNER. J. Am. Chem. Soc. **92**, 5742 (1970).
3. P. J. WAGNER and R. A. LEAVITT. J. Am. Chem. Soc. **92**, 5806 (1970).
4. D. I. SCHUSTER, T. M. WEIL, and A. M. HALPERN. J. Am. Chem. Soc. **94**, 8248 (1972).
5. G. PORTER, R. W. YIP, S. K. DOGRA, R. O. LOUTFY, and S. E. SUGAMORI. To be published.
6. G. PORTER, R. W. YIP, J. M. DUNSTON, A. J. CESSNA, and S. E. SUGAMORI. Trans. Faraday Soc. **67**, 3149 (1971).
7. R. W. YIP and W. SIEBRAND. Chem. Phys. Lett. **13**, 209 (1972).
8. R. W. YIP, A. G. SZABO, and P. K. TOLG. J. Am. Chem. Soc. In press.
9. R. W. YIP. Rev. Sci. Instr. **40**, 1035 (1969).
10. R. W. YIP, W. D. RIDDELL, and A. G. SZABO. Can. J. Chem. **48**, 987 (1970).
11. N. J. TURRO. Molecular photochemistry. W. A. Benjamin, New York. 1967.
12. J. N. MURRELL and J. TANAKA. Mol. Phys. **4**, 363 (1964).
13. J. N. MURRELL. The theory of the electronic spectra of organic molecules. J. Wiley, New York. 1963.
14. S. P. MCGLYNN, T. AZUMI, and M. KINOSHITA. Molecular spectroscopy of the triplet state. Prentice-Hall, New Jersey. 1969. p. 286.
15. L. G. CHRISTOPHOROU. Atomic and molecular radiation physics. *Edited by* J. B. Birks and S. P. McGlynn. Willey Interscience. 1971.
16. M. E. PEOVER. Electroanalytical chemistry. Vol. II. *Edited by* A. J. Bard. Dekker, New York. 1967. Chapt. 1.
17. C. K. MANN and K. K. BARNES. Electrochemical reactions in non-aqueous systems. Mercel Dekker, Inc. New York. 1971.
18. G. G. YAKOBSON and V. P. PETROV. Siberian Chem. J. **2**, 75 (1965).
19. B. H. CAMPBELL. Analytical chemistry. **44**, 1659 (1972).
20. R. O. LOUTFY and R. O. LOUTFY. J. Phys. Chem. **77**, 336 (1973).
21. D. PHILLIPS. J. Photochem. **1**, 97 (1972).

Can. J. Chem. Downloaded from www.nrcresearchpress.com by 210.87.254.42 on 09/05/12
For personal use only.

Can. J. Chem. Downloaded from www.nrcresearchpress.com by 210.87.254.42 on 09/05/12
For personal use only.

Canadian Journal of Chemistry

Published by
THE NATIONAL RESEARCH COUNCIL OF CANADA

Journal canadien de chimie

Publié par
LE CONSEIL NATIONAL DE RECHERCHES DU CANADA

Volume 51 Number 12 June 15, 1973

Volume 51 numéro 12 15 juin 1973

Thermal Anomaly in the Temperature Dependence of the Energy–Volume Coefficient of Aqueous KCl Solutions

IKCHOON LEE[1,2] AND J. B. HYNE

Department of Chemistry, University of Calgary, Calgary, Alberta

Received November 3, 1972

The temperature dependence of the energy–volume coefficient of pure water and of aqueous potassium chloride solutions as a function of concentration over the temperature range 10–50 °C has been determined by direct measurement of constant volume thermal–pressure coefficient. The results show that a thermal anomaly exists in the energy–volume coefficient of aqueous solution in the temperature range 30–40 °C and becomes more pronounced as the concentration of solute is increased.

La relation entre la température et le coefficient énergie–volume de l'eau pure et de solutions de chlorure de potassium aqueuses en fonction de la concentration a été déterminée pour l'intervalle de 10–50 °C par la mesure directe du coefficient reliant le volume thermique constant et la pression. Les résultats ont montré qu'il existe une anomalie d'origine thermique dans le coefficient energie–volume de solutions aqueuses pour l'intervalle de 30–40 °C et que cet effet devient plus important à mesure que la concentration en soluté augmente. [Traduit par le journal]

Can. J. Chem. **51**, 1885 (1973)

Introduction

The energy–volume coefficient, $(\partial U/\partial V)_T$, exhibits marked variation as a function of aqueous solution composition (1). These variations have been interpreted in terms of corresponding changes in the intermolecular interactions within the liquid system, commonly, although somewhat imprecisely, called "structural changes" (2). These previous studies have shown that the energy–volume coefficient can be a useful parameter for investigating the structural properties and intercomponent interactions in liquid mixtures.

The structural properties of water have been investigated extensively (3). One recurring phenomenon is the apparent discontinuity in various properties of water as a function of temperature (4–7). Although there is considerable controversy (8) over such discontinuities, the one postulated in the region of 35 °C has been well established in several reports in the literature (4–7). There is a continued interest in the 30–40 °C discontinuity since this could have important biological implications being near body temperature of man. We have used the energy–volume coefficient as a probe and determined the temperature dependence of this quantity for aqueous potassium chloride solutions as well as for pure water over the temperature range 10–50 °C by direct measurement of the constant volume thermal–pressure coefficient, $\gamma_V = (\partial P/\partial T)_V$, of the solution; γ_V is related to the energy–volume coefficient by

$$[1] \qquad (\partial U/\partial V)_T = T\gamma_V - P \simeq T\gamma_V$$

where P is the external pressure and at 1 atm can be neglected.

[1]Present address: Department of Applied Chemistry, College of Engineering, Seoul National University, Seoul, Korea.

[2]CIDA–NRC Research Associate 1970–1972.

Can. J. Chem. Downloaded from www.nrcresearchpress.com by 210.87.254.42 on 09/05/12
For personal use only.

Experimental

Details of experimental procedure have been reported elsewhere (2). The accuracy claimed for the reported γ_V values is better than $\pm 1\%$. It was found essential for the claimed accuracy to maintain the pressure to within ± 0.5 atm of the contact pressure for over 1 h to permit complete thermal equilibration. The procedure adopted was to maintain the pressure within this limit until the two consecutive readings of the pressure taken at 20 min intervals gave a consistent value.

Aqueous KCl solutions were prepared by dissolving weighed amounts of AR grade KCl in 1 kg of double distilled water at 20.0 °C.

Because of the controversy surrounding the reality of these temperature discontinuities it is particularly important to establish that our observations are not merely experimental artifacts. The temperature dependence of the energy–volume coefficient for pure water has been carefully established by earlier workers and the best values (9) are represented by the curve shown in Fig. 1. The experimental values obtained with the apparatus employed in this work (Table 1) are clearly in excellent agreement with the best literature values providing convincing evidence that the discontinuities observed with the aqueous KCl solutions are not experimental artifacts.

TABLE 1. Measured pressure–thermal and energy–volume coefficients for water

Temperature (°C)	γ_V (atm deg^{-1})	$(\partial U/\partial V)_T$ (atm)
8.50	1.39	392
9.00	1.42	401
10.00	1.82	515
11.00	2.00	568
12.00	2.31	659
13.00	2.56	733
14.00	2.94	844
15.00	3.21	925
19.00	4.21	1230
20.00	4.52	1325
22.00	5.07	1496
25.00	5.71	1702
27.00	6.03	1810
30.00	6.70	2031
34.00	7.61	2337
35.50	7.90	2438
37.50	8.25	2563
38.00	8.31	2586
39.50	8.67	2711
45.00	9.55	3038
50.00	10.40	3361

Results and Discussion

Plots of applied pressure (P) against temperature (T) in each determination were linear. The linearity was particularly good if the temperature range was small. The normal range of temperature employed in determination of the gradient, the observed thermal–pressure coefficient, γ_{obs}, was 1 °C. Each γ_{obs} value was then corrected for the finite thermal expansion and compression of the glass vessel containing the aqueous solution. This correction was made using eq. 2

$$[2] \qquad \gamma_V = \gamma_{obs}\left(\frac{\alpha_s}{\gamma_{obs}\beta_g + \alpha_s - \alpha_g}\right)$$

where α_g and β_g are the coefficients of thermal expansion and compressibility of Pyrex glass and α_s is the coefficient of expansion of the liquid under investigation. Instead of taking average values of α_g and β_g for the temperature range studied (10 to 50 °C) (2), we have used interpolated literature values (10, 11) for each temperature. This procedure gave values of γ_V occasionally differing by as much as 1%, from those obtained assuming a single average temperature independent α_g or β_g value.

The α_s values used were similarly determined (12). Results of the thermal–pressure and energy–volume coefficients are summarized in Table 1 for pure water, and in Table 2 for aqueous KCl solutions. These data are presented in graphical form in Fig. 2. Within the temperature range studied, $(\partial U/\partial V)_T$ for pure water increases in a smooth curvilinear manner with temperature. This behavior is opposite to that of non-polar aprotic liquids, *e.g.* methane and carbon tetrachloride (9), and is considered to be characteristic of the highly hydrogen bonded water structure. While the observed behavior for potassium

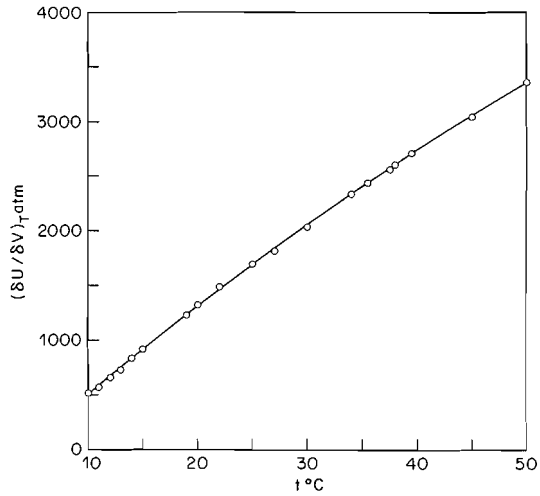

FIG. 1. Energy–volume coefficient as a function of temperature for pure water: — best literature values (ref. 9); ○ this work.

Can. J. Chem. Downloaded from www.nrcresearchpress.com by 210.87.254.42 on 09/05/12
For personal use only.

TABLE 2. Measured pressure-thermal and energy–volume coefficients for aqueous KCl solutions

[KCl] (m)	Temperature (°C)	γ_V (atm deg^{-1})	$(\partial U/\partial V)_T$ (atm)
0.0847	13.50	3.05	874
	17.50	4.14	1203
	23.77	5.56	1651
	28.27	6.43	1938
	30.50	6.80	2065
	35.56	7.81	2411
	36.50	7.99	2474
	42.65	9.24	2918
	47.50	10.07	3229
0.284	13.00	3.15	901
	17.50	4.35	1264
	21.50	5.36	1579
	23.50	5.98	1774
	28.25	6.93	2089
	34.61	8.25	2539
	39.95	9.80	3069
	46.36	10.84	3464
	51.96	11.44	3719
0.552	12.00	3.81	1086
	17.00	5.03	1460
	22.50	6.47	1913
	25.50	7.01	2094
	31.69	7.88	2402
	36.56	9.17	2840
	40.24	10.18	3190
	44.58	11.00	2495
	50.74	11.75	3806
1.038	15.00	5.62	1619
	19.00	6.51	1902
	21.77	7.10	2094
	26.54	7.97	2389
	30.00	8.26	2504
	32.83	8.67	2653
	35.00	9.11	2807
	35.94	9.32	2881
	38.50	9.89	3082
	41.96	10.75	3388
	44.81	11.24	3574
	49.80	11.86	3830

chloride solutions at various concentrations is generally similar to that for pure water, the smooth curvilinear dependence of $(\partial U/\partial V)_T$ on temperature no longer is observed. Inflections are noted between 30 and 40 °C and these become more marked as concentration of the salt increases. In the case of 1.038 m KCl, curve E, the inflection while still spanning a sizeable temperature range is clearly greater than could be accounted for by experimental error. In this system the inflection, at its deepest point, represents a deviation of some 5% from a smoothed

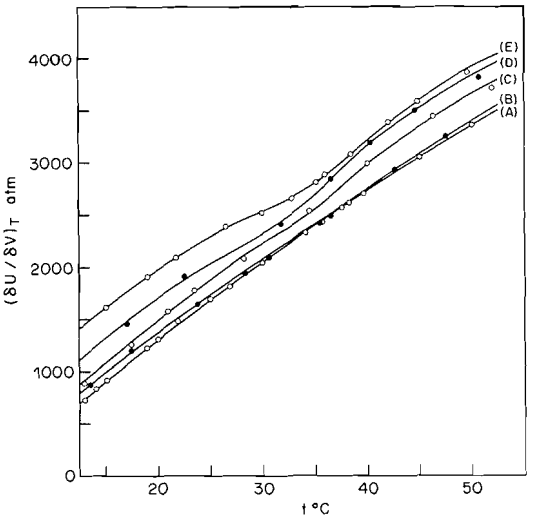

FIG. 2. Plots of the energy–volume coefficient as a function of temperature: (A) pure water; (B) 0.0847 m KCl; (C) 0.284 m KCl; (D) 0.552 m KCl; (E) 1.038 m KCl.

curve of $(\partial U/\partial V)_T$ *vs.* temperature. This deviation is approximately 5 times the experimental error.

In Fig. 3 the interpolated $(\partial U/\partial V)_T$ values from Fig. 2 are presented as a function of concentration. It is interesting to note that at temperatures below 35 °C a straight line correlation holds between $(\partial U/\partial T)_T$ and concentration, while at high temperatures curvilinear behavior is observed.[3] While the somewhat random behavior suggested by the form of presentation in Fig. 2 might lead to a suspicion that the anomalies observed between 30 and 40 °C are experimental artifacts (8), the clearly systematic change in the form of $(\partial U/\partial V)_T$ dependence on concentration as temperature is increased, as shown in Fig. 3, is not likely to be the result of experimental inaccuracies.

The anomalous behavior shown by $(\partial U/\partial V)_T$ at about 35 °C is not unprecedented. Compressibility (4), surface tension (5), viscosity (6), and other (7) properties of water have been reported to exhibit similar behavior in the temperature range 30 to 40 °C. This type of thermal anomaly has been reported both in the properties of aqueous solutions (13) and pure water, and it has been known to be much easier to demonstrate

[3]While statistically tests for linearity or the lack of it are possible the fact that the points in Fig. 3 are interpolated from Fig. 2 data and the limited (five) number of points makes the value of such an analysis arguable.

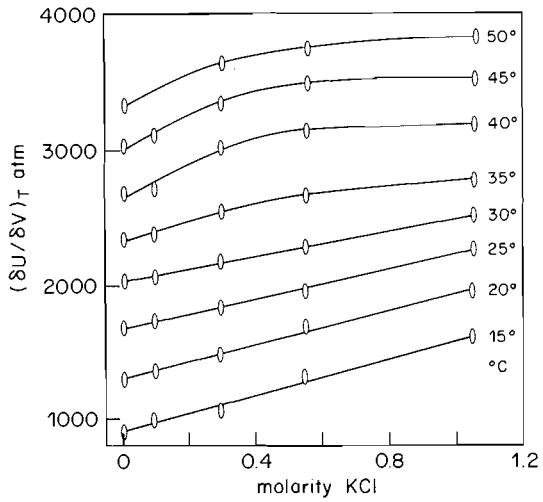

FIG. 3. Plot of the energy–volume coefficient as a function of concentration (*m* KCl).

such an anomaly in solutions than in pure water (13).

Results of the present investigation clearly establish that the thermal anomaly also exists in the energy–volume coefficient of aqueous salt solutions and becomes more pronounced as the concentration of solute is increased.

As noted above the increasing positive $(\partial U/\partial V)_T$ values with temperature are peculiar to extensively hydrogen bonded liquids and in the particular case of water this temperature dependence passes through a maximum at approximately 150 °C (9). The data in Fig. 3 also indicate that increasing concentrations of salt likewise bring about enhancement of $(\partial U/\partial V)_T$ values particularly at lower temperatures. It is tempting to suggest that since increasing temperature and increasing salt concentration both lead to higher energy–volume coefficient values, which have upper limiting values, the reason for the levelling off of $(\partial U/\partial V)_T$ values as a function of salt concentration at high temperatures is that the combined effect of temperature and salt concentration has reached a maximum. Higher temperatures and higher KCl concentrations are both considered to result in water structure disruption and this may well be the phenomenon which is being reflected in the curvature noted in Fig. 3.

The authors are grateful for support of this work by the National Research Council of Canada and in particular for a CIDA-NRC Research Associateship for I.L.

1. D. D. MACDONALD, J. B. HYNE, and F. L. SWINTON. J. Am. Chem. Soc. **92**, 6355 (1970).
2. D. D. MACDONALD and J. B. HYNE. Can. J. Chem. **49**, 611 (1971).
3. (*a*) D. EISENBERG and W. KAUZMAN. The structure and properties of water. Oxford University Press. 1969. (*b*) O. D. BONNER. Rec. Chem. Prog. **32**, 1 (1971).
4. G. TAMMAN. Z. Anorg. Allg. Chem. **235**, 49 (1937).
5. W. DROST-HANSEN. Ind. Eng. Chem. **57** (4), 18 (1965).
6. E. FORSLIND. Acta Polytech. Scand. Chem. Met. Ser. 115 (1966).
7. (*a*) C. SALAMA and D. A. I. GORING. J. Phys. Chem. **70**, 3838 (1966). (*b*) M. J. BLANDAMER, M. F. FOX, and M. C. R. SYMONS. Nature, **214**, 163 (1967). (*c*) W. DROST-HANSEN and H. W. NEILL. Phys. Rev. **100**, 1800 (1955).
8. M. FALK and G. S. KELL. Science, **154**, 1013 (1966).
9. J. S. ROWLINSON. Liquids and liquid mixtures. 2nd ed. Butterworths, London. 1969. p. 55.
10. R. M. BUFFINGTON and W. M. LATIMER. J. Am. Chem. Soc. **48**, 2305 (1926).
11. P. W. BRIDGMAN. Am. J. Sci. **5**, 210 (1925).
12. J. TIMMERMANS. The Physico-chemical constants of binary systems in concentrated solutions. Vol. 3. Interscience, New York. 1960.
13. (*a*) W. DROST-HANSEN. Adv. Chem. Ser. **66**, 70 (1967). (*b*) D. J. G. IVES and T. H. LEMON. Roy. Inst. Chem. Rev. **1**, 62 (1968).

Can. J. Chem. Downloaded from www.nrcresearchpress.com by 210.87.254.42 on 09/05/12
For personal use only.

Oligoribonucleotide Synthesis. VI.[1] Selective Deblocking of the 5′-*O*-Triphenylmethoxyacetyl Grouping in Protected Dinucleotides

EVA S. WERSTIUK AND THOMAS NEILSON
Department of Biochemistry, McMaster University, Hamilton, Ontario

Received November 15, 1972

Synthesis and 5′-deblocking of the triphenylmethoxyacetyl grouping in *N*-benzamido-dinucleotide derivatives, UpA, UpC, GpG, GpC, ApU, ApC, CpA, UpAp, and ApUp, are described. Alkaline cleavage behavior of the majority correlated well with the data found for similarly protected parent nucleosides. Those containing adenine residues adjacent to cytosine showed slow de-*O*-esterification and accelerated de-*N*-benzoylation, while those containing 3′-monophosphates showed enhanced de-*O*-esterification.

La synthèse et le déblocage du groupe triphénylméthoxyacétyle en 5′ dans les dérivés du *N*-benzamido-dinucléotide UpA, UpC, GpG, GpC, ApU, ApC, CpA, UpAp, et ApUp, ont été décrits. Le comportement du clivage alcalin de la plupart de ces dérivés correspond bien avec les données trouvées pour les nucléosides parents protégés de la même façon. Ceux qui contiennent des résidus adénine adjacent à la cytosine subissent une *O*-déestérification lente et une *N*-débenzoylation accélérée, tandis que ceux qui ont un groupe monophosphate en 3′ exhibent une *O*-déesterification accélérée.

[Traduit par le journal]

Can. J. Chem., **51**, 1889 (1973)

Indirect synthesis of intact transfer RNAs by transcription from synthetic genes consisting of two complementary oligodeoxyribonucleotides is in progress (2). However, to explore specific binding interactions involving transfer RNA, for example aminoacyl synthetase recognition sites, a convenient synthesis of series of oligoribonucleotides of predetermined sequence, say with single nucleotide changes, would be advantageous.

Introduction of a prototype for the first general block synthesis for oligoribonucleotides (3) guaranteed that direct synthesis of biologically interesting fragments of native ribonucleic acids could now be realized. Mononucleotides as their 2′-*O*-tetrahydropyranyl-*N*-benzamides were stepwise coupled together using 3′–5′-phosphotriester linkages (4) to give short protected sequences which in their turn, were coupled together to give much longer sequences, subsequent deblocking of which gave the required free oligoribonucleotides.

The crux of such a synthesis lies in appropriate protection of the 5′-hydroxyl of 5′-terminal nucleotide of each short sequence. Specific deblocking of this 5′-protection is necessary for block synthesis to be realized. The triphenylmethoxyacetyl (trac) (3) grouping was chosen for this important function because of its easy removal by very mild alkaline treatment and its simple detection by ceric sulfate. Successful participation was demonstrated in the synthesis of protected UpApUpA from protected UpA units.

In this communication we describe the synthesis of several representative 5′-triphenylmethoxyacetyl dinucleotide derivatives and discuss comparative specific 5′-deblocking studies of these dinucleotides with those of their parent nucleosides.

Simple selective 5′-esterification of *N*-benzamido-2′-*O*-tetrahydropyranylnucleosides (**1**) by a mixed anhydride method using sodium triphenylmethoxyacetate and triisopropylbenzenesulfonyl chloride (TPS) in pyridine gave the corresponding 5′-triphenylmethoxyacetates (**2**) as crystalline derivatives in >70% yield. Some accompanying disubstituted material was also obtained. Protected nucleosides (**2**) where X = U (3), G^{bz} (1), and A^{bz} (5) have been reported. Preparation of **2** (X = C^{bz}) is described in the Experimental.

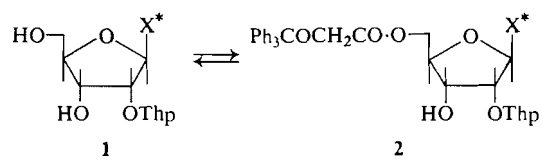

1 **2**

where X* = U, A^{bz}, C^{bz}, or G^{bz}

[1]For part V, see ref. 1.

Syntheses of protected dinucleotide monophosphates, UpA (3), GpG (1), and GpC (1) have already been reported. A summary in the general case is outlined: Phosphorylation of **2** using the pyridinium salt of β,β,β-trichloroethylphosphate (6) and TPS, and subsequent coupling with the higher R_F diastereoisomer of **1** (1, 7, 8) gives the protected dinucleotide XpY[2] (**3**) in yields >50% except when G is involved (*ca.* 30%). "Back tritylation" (4) is routinely carried out to convert any excess nucleoside derivative (**1**) to its more lipophilic 5′-methoxytrityl derivative *and* to convert any 3′–3′ dinucleotide derivative which could arise during coupling, to its more lipophilic 5′-*p*-methoxytrityl derivative. The presence of *p*-methoxytrityl derivatives is easily detected by ceric sulfate spray as an orange coloration on t.l.c. Increase in lipophilicity allows simple chromatographic separation. A typical procedure is illustrated by the synthesis of **3** (X = C^{bz}; Y = A^{bz}) (see Scheme 1). Careful t.l.c. analysis of each XpY derivative (**3**) showed them to be diastereoisomeric mixtures (*ca.* 1 : 1) resulting from phosphotriester chirality (3). In some cases two distinct spots were obtained; however, one elongated spot was more usual. Syntheses of protected dinucleotide diphosphates, UpAp (3), and ApUp (5) have already been reported. Data on all new protected XpY (**3**) and XpYp (**4**) derivatives are summarized in the Experimental. Complete deblocking (4) of **3** and **4** to give free dinucleotides was accomplished in >80% yield. Enzymic analysis (4) of the products confirmed the correct ratio of nucleoside components and checked the fidelity of the 3′–5′ diphosphate linkage.

Comparative studies of the selective deblocking of the 5′-triphenylmethoxyacetyl esters of the four parent nucleosides (**2**) were carried out using dilute methanolic ammonia (0.15 and 0.075 *N*) at room temperature. Conditions of 0.15 *N* smoothly regenerated the 5′-hydroxyl group in *ca.* 2 h in each case. No significant debenzoylation occurred before 2 h. Less concentrated conditions only prolonged the treatment. Stability of *N*-benzamide on heterocyclic bases was found to be C > A > G (Table 1).

Comparative studies of the selective deblocking

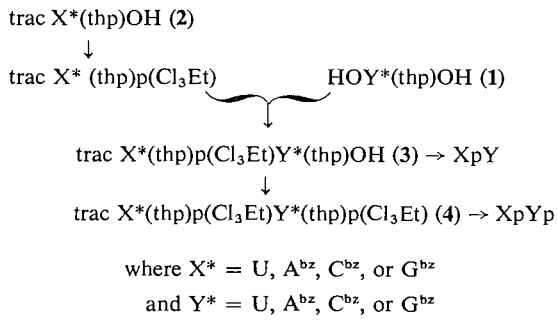

SCHEME 1

of the 5′-triphenylmethoxyacetyl esters of protected dinucleotides (**3** and **4**) were also carried out using the same conditions. Data obtained for protected UpA, GpG, GpC, ApU using 0.15 *N* methanolic ammonia showed reasonable correlation with the behavior of their parents. Protected UpC was best deblocked using the milder 0.075 *N* conditions.

Data on alkaline cleavage of protected ApC and CpA were more complex. Apparently the rate of triphenylmethoxyacetyl removal in **3** (X = A^{bz}, Y = C^{bz}) was slower than that for the parent (**2**; X = A^{bz}) and the de-*O*-benzoylation rate was considerably accelerated, so much so, that both rates were almost similar. In the case of **3** (X = C^{bz}, Y = A^{bz}) triphenylmethoxyacetyl removal was slightly faster than the parent (**2**; X = C^{bz}) but de-*N*-benzoylation was again enhanced. Molecular geometry of both protected dinucleotides must be such that, somehow, triphenylmethoxyacetyl cleavage is sterically hindered, and the debenzoylation of the adenine residue is anchimerically assisted (possibly by carbonyl participation from the neighboring heterocyclic base).

Alkaline cleavage rate of the triphenylmethoxyacetyl group in the protected dinucleotide diphosphate derivatives (**4**) showed considerable enhancement over those of the parents (**2**; X = U and X = A^{bz}). Apparently the charged phosphodiester grouping functions as an intra- or intermolecular catalyst.

The above studies indicated that cleavage conditions suitable for protected parent nucleosides (**2**) could not be extended directly to dinucleotide derivatives (**3** and **4**). Chemical operations performed on these sterically crowded multi-functional molecules were subject to unforeseen accelerations and retardations, especially when an adenosine residue was adjacent to a cytidine. Caution would have to be

[2]To condense the large structural formulae necessary to describe protected dinucleotides shown in Scheme 1, a shorthand method suggested by the IUPAC–IUB Commission on Biochemical Nomenclature is adopted (9).

TABLE 1. Time (h) for completion of de-*O*-acylation and appearance of de-*N*-benzoylation of various protected nucleosides and dinucleotides

Compound	0.15 *N*			0.075 *N*		
	Complete removal of trac	De-*N*-benzoylation		Complete removal of trac	De-*N*-benzoylation	
		trace	*ca.* 5%		trace	*ca.* 5%
2; X = U (3)	1.5	—	—	4.0	—	—
2; X = A^{bz} (5)	2.5	2.0	3.5	4.0	2.5	4.0
2; X = C^{bz}	2.0	1.0	4.0	3.0	2.0	5.0
2; X = G^{bz} (1)	2.0	1.0	2.0	4.0	2.0	3.5
3; X = U, Y = A^{bz} (3)	1.0	2.5	6.0	1.5	4.0	6.0
3; X = U, Y = C^{bz}	1.0	0.5	1.0	2.0	1.5	4.0
3; X = Y = G^{bz} (1)	3.0	2.0	3.5	4.0	3.0	4.0
3; X = G^{bz}, Y = C^{bz} (1)	3.5	2.5	4.0	4.0	2.5	5.0
3; X = A^{bz}, Y = U (5)	3.5	1.0	3.5	6.0	2.0	4.0
3; X = A^{bz}, Y = C^{bz}	6.0	0.5	1.0	12.0	1.0	2.0
3; X = C^{bz}, Y = A^{bz}	1.0	0.3	0.5	1.5	0.5	1.0
4; X = U, Y = A^{bz} (3)	—	—	—	0.1	1.0	—
4; X = A^{bz}, Y = U (5)	—	—	—	0.1	1.0	—

exercised in each case. Further studies on other protected dinucleotides and the use of other hydrolytic conditions would be necessary to rationalize these results.

Prospects for convenient specific 5′-deblocking of protected trinucleotides and longer material consequently are not so bright as once anticipated. Specific 5′-deblocking of protected dinucleotides was accomplished quantitatively in many cases; however, these containing adenine located in the 5′-terminal required chromatographic separation of products and yields for the desired products were around 50% at the best. Perhaps other cleavage conditions may restore selective deblocking.

These present studies *do* show, however, that chemical reactivity of an adenosine residue varies quite markedly depending on its position in a sequence. The biological implications of this discovery are under investigation.

Experimental

The p.m.r. spectra were recorded on a Varian T60 or Varian HA-100 spectrometer in 10–15% (w/v) DMSO-d_6 – D_2O solutions, and line positions are reported in p.p.m. from the reference (TMS).

Silica gel (Baker Analyzed Reagent) was used for column chromatography; and Analtech prescored silica gel plates were employed for t.l.c. The plates were usually developed in 5 or 10% methanol in methylene chloride mixtures. The t.l.c. detection was carried out using a ceric sulfate spray (1 g $H_4Ce(SO_4)_4$ in 10% aqueous sulfuric acid solution) and followed by heating the plates at 300–400 °C. Compounds containing a trityl group develop as yellow spots, while others appear as brown colorations.

Paper chromatography was performed using the descending technique on Whatman No. 1 or 3 MM paper. Analtech pre-coated cellulose plates (Avicel F) were used for t.l.c. of deblocked nucleotides. The solvent systems employed for paper chromatography and t.l.c. on cellulose were ethanol – 1 *M* ammonium acetate, p*H* 7.5 (7:3, v/v), (A); 1-BuOH – glacial HOAc – H_2O (5:3:2, v/v), (B); 2-PrOH – concentrated NH_4OH – H_2O (7:1:2, v/v). (C). A short wave u.v. lamp was used for detection.

It was essential that moisture be excluded from all coupling reactions. After evaporation *in vacuo* of the pyridine solution, normal pressure was restored with dry nitrogen and *not* atmospheric air. All such evaporations were carried out in the temperature range of 30–40 °C.

Emulsion, frequently obtained during methylene chloride extractions of aqueous pyridine solutions, was broken by the addition of a few milliliters of saturated sodium chloride solution.

*N^4-Benzoyl-2′-O-tetrahydropyranyl-5′-O-triphenylmethoxyacetylcytidine (**2**; X = C^{bz})*

Esterification of the low R_F diastereoisomer of N^4-benzoyl-2′-*O*-tetrahydropyranylcytidine (**1**; X = C^{bz}) (7) (0.431 g, 1.0 mmol; R_F 0.52 in 10% CH_3OH–CH_2Cl_2) with sodium triphenylmethoxyacetate (0.674 g, 2.0 mmol) and TPS (0.335 g, 1.1 mmol) (as described earlier for the preparation of **2** (X = U) (3)) gave the desired product (0.520 g, R_F: 0.68 in 10% CH_3OH–CH_2Cl_2) in 72% yield.

An analytically pure sample of **2** (X = C^{bz}) had m.p. 108–110° dec. (from methylene chloride – petroleum ether (30–40°). Its p.m.r. spectrum showed signals (δ TMS) at 8.05–7.75 (4H, multiplet; 6- and 5-protons of C, and *o*-C_6H_5CO protons); 7.6–7.38 (18H, multiplet, trityl aromatic protons, and other C_6H_5CO protons); 5.9 (1H, doublet; $J \simeq 4$ Hz, 1′-anomeric proton); 5.40 (1H, multiplet; 2′-sugar proton); 4.8 (1H, singlet, acetal proton of thp); 3.8 (2H, singlet; —OCH_2CO protons); and 1.6 p.p.m. (6H, broad multiplet; thp protons).

Anal. Calcd. for $C_{42}H_{41}N_3O_9$ (mol. wt. 731.8): N, 5.74. Found: N, 5.61.

N^4-Benzoyl-2′-O-tetrahydropyranyl-5′-O-triphenylmethoxyacetylcytidylyl (3′-β,β,β-trichloroethyl-5′)N^6-benzoyl-2′-O-tetrahydropyranyladenosine (3; X = C^{bz}, Y = A^{bz})

Phosphorylation of the blocked cytidine derivative (as described earlier for blocked uridylate (3)) (**2**; X = C^{bz}) (180 mg, 2.5 mmol; 1 equiv; R_F 0.68 in 10% CH_3OH–CH_2Cl_2) and subsequent coupling with the low R_F diastereoisomer of N^6-benzoyl-2′-O-tetrahydropyranyladenosine (**1**; X = A^{bz}) (7) (172 mg, 3.75 mmol; 1.5 equiv; R_F 0.48 in 10% CH_3OH–CH_2Cl_2) gave the desired product (281 mg, R_F 0.76 and 0.68 in 10% CH_3OH–CH_2Cl_2) in 81% yield as a *ca.* 1:5 mixture of diastereoisomers.

The p.m.r. spectrum of this sample showed signals (δ TMS) at 8.80 and 8.75 (2H, singlets, 2- and 8-protons of A); 8.30–7.20 (27H, multiplet; C_6H_5CO and trityl aromatic protons, and 6- and 5-protons of C); 6.25 and 6.10 (2H, two doublets; superimposed 1′-anomeric protons); 3.80 (2H, singlet; —OCH_2CO protons); and a broad peak centered at *ca.* 1.55 p.p.m. (12H, multiplet; thp protons).

Complete deblocking by the three-step procedure described before (4) gave CpA in 80% yield. (R_{Up} 1.18 in system A, and 1.02 in system C both using paper chromatography, Whatman No. 1). CpA was completely digested by snake venom diesterase to C + pA, and by spleen diesterase to Cp + A. These products were identified with authentic markers using same paper chromatographic systems.

N^6-Benzoyl-2′-O-tetrahydropyranyl-5′-O-triphenylmethoxyacetyladenylyl (3′-β,β,β-trichloroethyl-5′)N^4-benzoyl-2′-O-tetrahydropyranylcytidine (3; X = A^{bz}, Y = C^{bz})

Phosphorylation of the blocked adenosine derivative (5) (**2**; X = A^{bz}) (610 mg, 0.8 mmol; 1 equiv; R_F 0.72 in 10% CH_3OH–CH_2Cl_2) and subsequent coupling with the high R_F diastereoisomer of N^4-benzoyl-2′-O-tetrahydropyranylcytidine (7) (**1**; X = C^{bz}) (520 mg, 1.2 mmol; 1.5 equiv; R_F 0.62 in 10% CH_3OH–CH_2Cl_2) gave the desired product (780 mg, R_F 0.86 and 0.80 in 10% CH_3OH–CH_2Cl_2) in 70% yield as a *ca.* 1:1 mixture of diastereoisomers.

The p.m.r. spectrum showed signals (δ TMS) at 8.65 (2H, broad singlet; 2- and 8-protons of A); 8.25–7.15 (27H, multiplet; C_6H_5CO and trityl aromatic protons and 6- and 5-protons of C); 6.25 and 5.9 (2H, two doublets superimposed; 1′-anomeric protons); 3.8 (2H, singlet; —OCH_2CO protons); and a broad peak centered at *ca.* 1.60 p.p.m. (12H, multiplet; thp protons).

Complete deblocking (4) gave ApC in 86% yield. (R_{Up} 1.24 in system A, and 1.02 in system C both using paper chromatography, Whatman No. 1). ApC was completely digested by snake venom diesterase, to A + pC, and by spleen diesterase to Ap + C. These products were identified with authentic markers using same paper chromatographic systems.

2′-O-Tetrahydropyranyl-5′-O-triphenylmethoxyacetyluridylyl (3′-β,β,β-trichloroethyl-5′)N^4-benzoyl-2′-O-tetrahydropyranylcytidine (3; X = U, Y = C^{bz})

Phosphorylation of the blocked uridine derivative (3) (**2**; X = U) (500 mg, 0.85 mmol; 1 equiv; R_F 0.82 in 10% CH_3OH–CH_2Cl_2) and subsequent coupling with the high R_F diastereoisomer of N^4-benzoyl-2′-O-tetrahydropyranyl-cytidine (7) (**1**; X = C^{bz}) (555 mg, 1.3 mmol; 1.5 equiv; R_F 0.62 in 10% CH_3OH–CH_2Cl_2) gave the desired product (727 mg, R_F 0.40 and 0.31 in 5% CH_3OH–CH_2Cl_2) in 68% yield as a *ca.* 1:1 mixture of diastereoisomers. The p.m.r. spectrum showed signals (δ TMS) at 8.15–7.05 (23H, multiplet C_6H_5CO and trityl aromatic protons; 6- and 5-protons of C, and 6-proton of U); 5.95 and 5.70 (2H, two doublets superimposed; 1′-anomeric protons); 5.45 (1H, doublet, $J \simeq 7$ Hz; 5-proton of U); 3.75 (2H, singlet; —OCH_2CO protons), and a broad peak centered at *ca.* 1.6 p.p.m. (12H, multiplet, thp protons).

Complete deblocking (4) gave UpC in 73% yield. (R_{Up} 1.52 in system A, and 1.1 in system C both using paper chromatography Whatman No. 1). UpC was completely digested by snake venom diesterase, to U + pC; and by spleen diesterase to Up + C. These products were identified with authentic markers using same paper chromatographic systems.

General Method for the Preparation of Protected Dinucleotide Diphosphates (4)

Phosphorylation of protected dinucleotide (**3**) (1 equiv) with the mixed anhydride complex, prepared from the bis-pyridinium salt of mono-β,β,β-trichloroethylphosphate (2 equiv) and TPS (4 equiv), gave desired products (**4**) in *ca.* 80% yield. **4** could be isolated as pyridinium salts from silica gel chromatography on elution with 5–7% methanol – methylene chloride.

Preparation of protected UpAp (**4**; X = U, Y = A^{bz}) using the above method has been reported (3).

*Selective 5′-de-O-Triphenylmethoxyacetylation of **2**, **3**, and **4***

Substrates **2**, **3**, and **4**, (5 mg) were dissolved in methanolic ammonia (0.5 ml) prepared by a 100-fold (0.15 *N*) or 200-fold (0.075 *N*) dilution of concentrated ammonia with methanol. Solutions were sealed and stirred at room temperature. Reaction progress was monitored by t.l.c. in 10% methanol – methylene chloride. Time in hours for disappearance of reactants and appearance of side-products was determined (Table 1).

A large scale experiment of this nature (for protected UpA) has been described (3).

Financial assistance from the Medical Research Council of Canada is gratefully acknowledged.

1. T. Neilson, E. V. Wastrodowski, and E. S. Werstiuk. Can. J. Chem. **51**, 1068 (1973).
2. H. G. Khorana and co-authors. Nature, **227**, 27 (1970).
3. E. S. Werstiuk and T. Neilson. Can. J. Chem. **50**, 1283 (1972).
4. T. Neilson and E. S. Werstiuk. Can. J. Chem. **49**, 3004 (1971).
5. K. V. Deugau. Personal communication.
6. F. Eckstein. Chem. Ber. **100**, 2228 (1967).
7. T. Neilson and E. S. Werstiuk. Can. J. Chem. **49**, 493 (1971).
8. B. E. Griffin, M. Jarman, and C. B. Reese. Tetrahedron, **24**, 639 (1968).
9. Biochem. **9**, 4022 (1970).

Photoelectron Spectra of Sulfuryl and Thionyl Halides

D. CHADWICK, D. C. FROST, F. G. HERRING, A. KATRIB, C. A. MCDOWELL, AND R. A. N. MCLEAN

Department of Chemistry, The University of British Columbia, Vancouver 8, British Columbia

Received November 30, 1972

The HeI photoelectron spectra of some sulfuryl and thionyl halides have been found, and an attempt has been made to relate the results to the bonding in these molecules.

Le spectre photoélectronique HeI de quelques halogénures de sulfuryle et de thionile a été établi et un essai a été fait pour trouver une corrélation entre les résultats et les liens de ces molécules.

[Traduit par le journal]

Can. J. Chem., **51**, 1893 (1973)

Can. J. Chem. Downloaded from www.nrcresearchpress.com by 210.87.254.42 on 09/05/12
For personal use only.

Introduction

There has been considerable interest (*e.g.* 1–5) in the bonding in inorganic sulfur compounds, particularly where the sulfur atom has a formal valence state higher than two and a tendency to form multiple bonds with other atoms. Some of the physical properties of this type of compound, especially bond lengths (2, 3) and vibrational frequencies (6), have been correlated with changes in the π bond orders. As there are a large number of compounds containing sulfur–oxygen bonds available, most of those studies have been carried out on these species.

Photoelectron spectroscopy (p.e.s.) is a direct method for obtaining the orbital energies of molecules and thereby can yield information on multiple bonding involving second row atoms (*e.g.* the halosilanes (7)). However, apart from SO_2 (8) and SO (9) no photoelectron spectra have been published of sulfur–oxygen compounds. In these species considerable changes in molecular structure and properties (particularly S—O stretching vibrations) occur on changing the atom(s) bonded to the sulfur atom, and it is of interest to see if the molecular energy levels obtained from the p.e. spectra reflect these effects. Sulfuryl halides (SO_2X_2) and thionyl halides (SOX_2) are typical examples which show these effects to a large degree. In SO_2F_2, the S—F bond length is reduced only slightly from 1.56 Å in SF_5OF (10) to 1.53 Å in SO_2F_2 (11) whereas the S—O bond length is reduced considerably from 1.64 Å in SF_5OF to 1.405 Å in SO_2F_2. Obviously there must be a considerable increase in the bonding interaction, presumably mainly π bonding (12), in the S—O bond compared to the S—F bond in the latter molecule. This may also be the explanation for the difference in the bond angles. The greater π electron density in the S—O bonds causes greater mutual repulsion than is the case with the S—F bonds, and consequently the OSO angle (124°) is greater than the FŜF angle (96°). A satisfactory bond order – bond length relationship is obtained for S—O bonds in tetra-coordinate sulfur compounds by considering that π bonding involves 2pπ orbitals on the oxygen atoms and only the two d orbitals on the sulfur (2). The shorter SO bond length and wider OSO angle for SO_2F_2 compared to SO_2Cl_2 (1.409 Å and 123° respectively (13)) and SO_2 (1.432 Å and 119° (14)) is most likely caused by the greater contraction of the sulfur d orbitals and hence greater π overlap with the oxygen produced by the more electronegative fluorine atoms. However, it is also possible in this case that the chlorine atoms are more involved in π bonding than the fluorine atoms and this seems to be borne out by the large Cl—S—Cl angle of 100°. It was hoped that the p.e. spectra would give some indication as to the correctness of these views.

Both the p.e. spectrum (8), and recent good SCF calculations (15) on SO_2 indicate that there is a large stabilization of the oxygen pπ orbitals involved in extensive π bonding (a_1, b_1) compared to the other orbitals (a_2, b_2). The corresponding levels in SO_2F_2 may be expected to give evidence for the even stronger π bonding in this molecule.

The bonding in the thionyl halides is complicated by the sulfur "lone pair" electrons, but despite this the X—Ŝ—O and X—Ŝ—X angles are fairly close to those for the analogous sulfuryl compound, *e.g.* in F_2SO, F—Ŝ—O = 107,

Can. J. Chem. Downloaded from www.nrcresearchpress.com by 210.87.254.42 on 09/05/12
For personal use only.

F—Ŝ—F = 93° (16) and in Cl_2SO, Cl—Ŝ—O = 106 and Cl—Ŝ—Cl = 114° (13). All the bond lengths are just significantly longer *e.g.* in F_2SO r(S—F) = 1.585, r(S—O) = 1.412 Å and in Cl_2SO r(S—Cl) = 2.07, r(S—O) = 1.45 Å. As in the sulfuryl compounds, the trends in the thionyl halides have been explained on the basis of a simple LCAO MO treatment (14).

The p.e. spectra of SO_2F_2, SO_2Cl_2, SOF_2, and $SOCl_2$ have been measured and are found to be complex. Despite this the assignment of i.p.'s arising from the mainly halogen "lone pair" orbitals may be made by comparison with the p.e. spectra of a number of the dihalo compounds (17). As we see below, however, the low molecular symmetry in the thionyl compounds makes the interpretation of their p.e. spectra more difficult.

Experimental

The p.e. spectra were recorded using the 584 Å HeI resonance line excited by 2450 MHz microwave discharge. The spectrometer employs a 4 in. radius hemispherical electrostatic analyzer (18) and the resolution (f.w.h.m.) as measured by the argon doublet was 15 mV. The working resolution varied between 20 and 30 mV. Calibration of the spectra was effected by flowing a small quantity of argon or xenon through the spectrometer simultaneously with the sample gas, and because of the reactive nature of these sulfuryl and thionyl halides, the initial spectra were recorded with calibrant present.

The SO_2F_2 sample was obtained from the Matheson Co. and SOF_2 from the Pierce Chemical Co. SO_2Cl_2 and $SOCl_2$ were obtained from B.D.H. Ltd. The purity of the samples was established by i.r. and mass spectrometry.

Some difficulty was experienced in obtaining the p.e. spectra of SO_2Cl_2 and $SOCl_2$ due to sample decomposition. In the case of SO_2Cl_2, the initial few runs produced spectra contaminated with that of SO_2. However, this gradually diminished and finally the spectrum of SO_2Cl_2 was obtained almost completely free of SO_2. In Fig. 2*b*, the strong third band in the spectrum of SO_2 at 16.5 eV is barely visible above the noise level. With $SOCl_2$ the reverse behavior was observed. A quick scan through the spectrum showed that no SO_2 was present. A very slow scan through the spectrum was made, but midway through the scan (~16 eV) the third band in the p.e. spectrum of SO_2 at 16.5–17.0 eV was evident, indicating that now a significant amount of SO_2 was present. It is this spectrum that is reproduced in Fig. 5*b*, though the region above 16 eV is not shown. That very little SO_2 is present in the spectrum below 16 eV can be seen by comparing Fig. 1 with Fig. 5*b*. In particular, the broad second band of SO_2 extends to 14 eV whereas the fifth band in Fig. 5*b* is much sharper and is in the range 13–13.5 eV. Subsequent spectra showed large amounts of SO_2 were present, and finally the spectrum of SO_2 only was observed. After "dosing" the spectrometer with fairly high pressures of $SOCl_2$ the same result was obtained. A glass inlet system was tried without success.

Results and Discussion

The HeI p.e. spectra of SO_2, SO_2F_2, SO_2Cl_2, SOF_2, and $SOCl_2$ are shown in Figs. 1, 2*a* and *b*, 5*a* and *b* respectively. Individual p.e. bands which exhibit resolved vibrational structure are reproduced in Figs. 3, 4 ,and 6 for SO_2F_2, SO_2Cl_2, and SOF_2. Measured vertical ionization potentials (i.p.'s) and vibrational frequencies are given in Tables 1–3. Adiabatic i.p.'s, where appropriate, are reported in the text. The p.e. spectrum of each molecule studied is discussed separately below. For convenience the symmetry elements in the SO_2, SO_2F_2, and SO_2Cl_2 molecules are defined with respect to the SO_2 moiety, which is considered to lie in the *zy* plane. Finally, some general implications concerning the bonding in these molecules are considered.

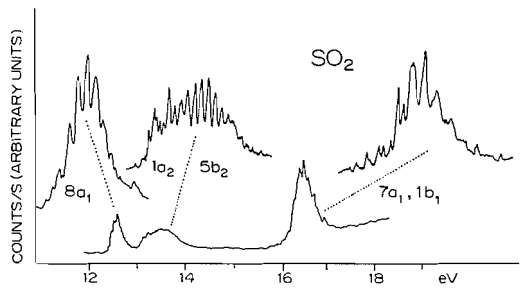

FIG. 1. The HeI photoelectron spectrum of sulfur dioxide.

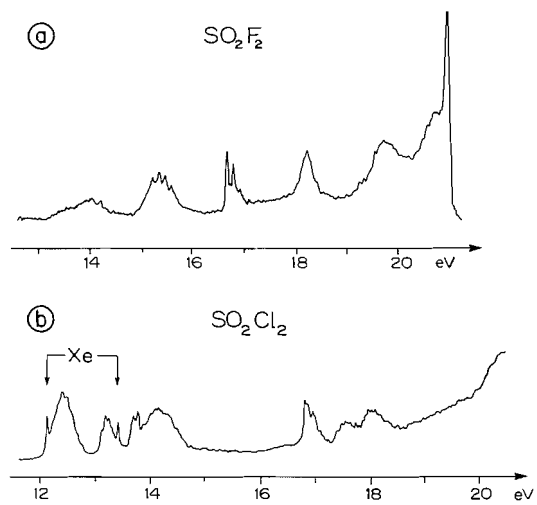

FIG. 2. The HeI photoelectron spectra of (*a*) sulfuryl fluoride and (*b*) sulfuryl chloride.

Can. J. Chem. Downloaded from www.nrcresearchpress.com by 210.87.254.42 on 09/05/12
For personal use only.

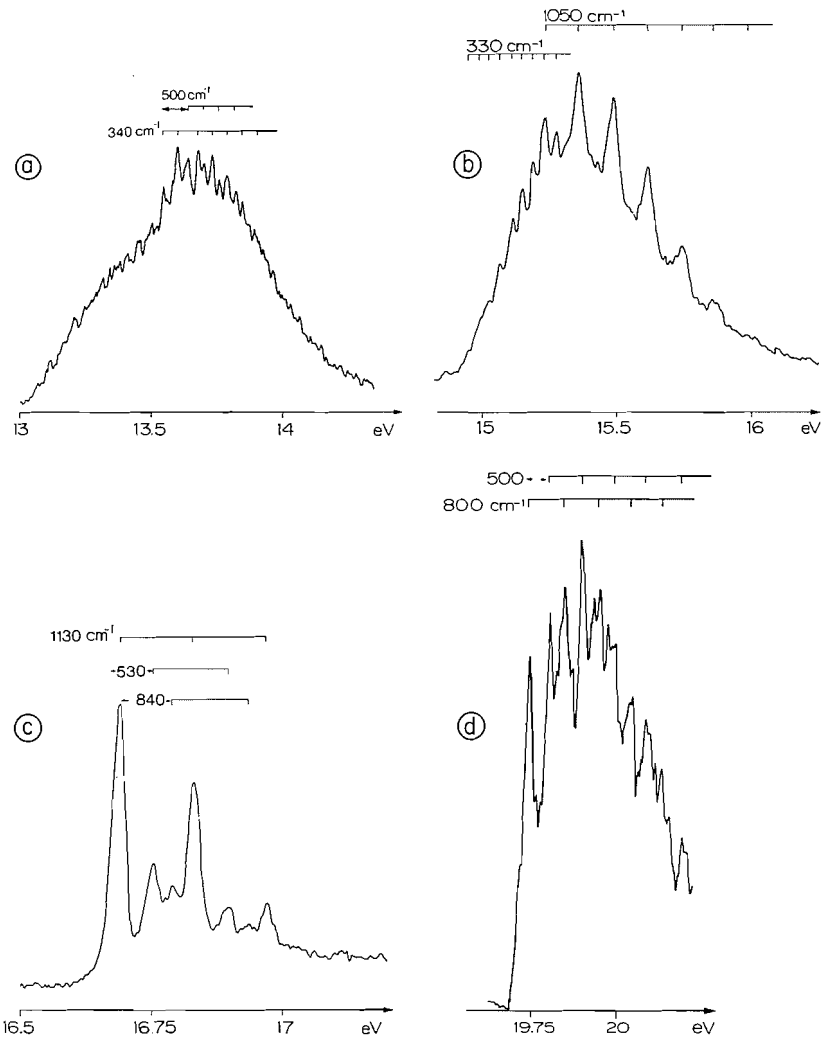

FIG. 3. Individual bands in the HeI photoelectron spectrum of SO_2F_2.

Sulfur Dioxide (SO_2)

To aid the assignment of the sulfuryl species in particular, we first discuss the p.e. spectrum of SO_2 (Fig. 1). The three bands observed below 21 eV have been assigned as follows (8):

(*a*) 12.50 eV band, ionization from the $8a_1$ sulfur "lone pair" orbital.

(*b*) 13–14 eV band, two i.p.'s arising from in-plane ($5b_2$) and out-of-plane ($1a_2$) oxygen non-bonding orbitals.

(*c*) 16–17.5 eV band, at least two ionization processes involving the $7a_1$ and $2b_1$ S—O π bonding orbitals, which may also be regarded as the bonding combinations of oxygen "lone pairs". Possibly a third ionization, from the $4b_2$ S—O σ bonding orbital, occurs in this region.

Recent MO calculations on SO_2 confirm this general pattern, and the separation between the three groups (15). For comparison with the sulfuryl compounds we are particularly interested in the order of the components in the second and third bands. The calculations estimate the separation of the two components of the second band to be 0.6 (15*a*) and 0.9 eV (15*b*) (experimental 0.3 eV) with the a_2 orbital at highest orbital energy. In most species of C_{2v} symmetry containing two equivalent atoms with "lone pairs" the b_2 orbital is at higher energy than the a_2 orbital (16) and, as overlap with sulfur d orbitals would cause greater stabilization of the a_2 orbital (7*b*, 12), this order is surprising. However, a close examination of the band between 13 and 14 eV seems

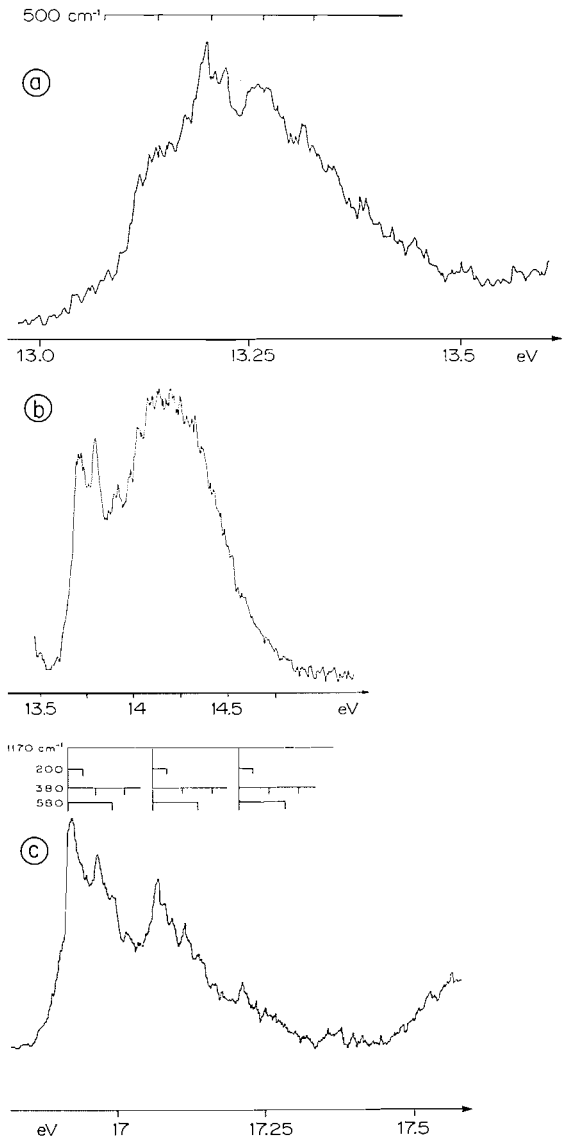

FIG. 4. Individual bands in the HeI photoelectron spectrum of SO_2Cl_2.

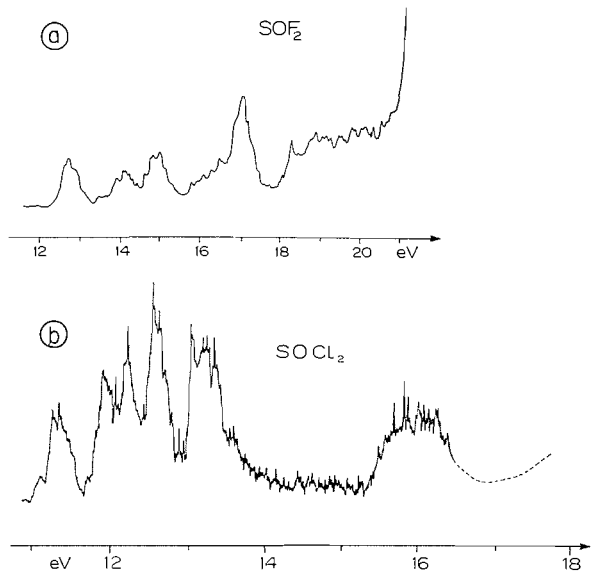

FIG. 5. The HeI photoelectron spectra of (*a*) thionyl fluoride and (*b*) thionyl chloride.

to indicate agreement with the order obtained in the calculations. Our spectrum and analysis of the band is almost identical to that of Eland and Danby (8). It is noted that the first component with adiabatic i.p. 13.01 ± 0.05 eV is narrower in our spectrum and has a vertical i.p. of 13.24 eV. The second component has a vertical i.p. of 13.47 eV but the adiabatic value is not obvious. Eland and Danby prefer to place this at about the same energy as the vertical of the first component (~13.25 eV), but we believe that it may be at least one and possibly up to three vibrational intervals (ν_2) below this. Vibrational analysis of the first component indicated excitation of both the stretching (1100 cm^{-1}) and bending vibrations (~400 cm^{-1}) and of the second, only the bending vibration (~480 cm^{-1}). The following analysis can be made, taking into consideration the oxygen–oxygen antibonding nature of both orbitals involved. The b_2 orbital is a σ type orbital and thus will have considerably more oxygen–oxygen overlap than the a_2 orbital. Therefore, it is likely to cause a larger angle change on ionization and hence a longer progression in the bending vibration. This has been confirmed by calculation (15*b*) and fits well with the b_2 orbital being responsible for the second component of the band. Although normally a decrease in a stretching frequency on ionization indicates a bonding electron has been removed, a decrease in the bending frequency does not necessarily mean this. In other bent triatomics, *e.g.* NO_2 (19) there is always a decrease in the bending vibration on ionization from these orbitals. In NO_2, which has one electron missing from the highest a_1 orbital compared to SO_2 and a bond angle of 134°, the $^3B_2$ and $^1B_2$ states produce similar p.e. bands to the second component referred to above. The decreases in the vibrational spacing from the neutral molecules and the length of the progressions are also simi-

Can. J. Chem. Downloaded from www.nrcresearchpress.com by 210.87.254.42 on 09/05/12
For personal use only.

TABLE 1. Ionization data for SO_2F_2

Band*	Vertical i.p. (in eV)	Vibrational frequencies† (cm^{-1}) ν_1	ν_2	ν_3	ν_4	Ionic* state
(*i*)	13.55	—	—	—	—	$^2B_2$
	13.81	—	—	500	340	$^2A_2$
(*ii*)	15.18	—	—	—	330	$^2B_1$
	15.35	1050	(1050)	—	—	$^2A_2$
(*iii*)	16.68	1130	840	530	—	$^2A_2$
(*iv*)	18.34	—	—	—	—	$^2B_1$
(*v*)	19.89	—	800	500	—	$^2B_2$
(*vi*)	20.5					$^2A_1$
		1269	848	544	384	Neutral molecule‡

*See text.
† ± 40 cm^{-1} at best.
‡Reference 11*c*.

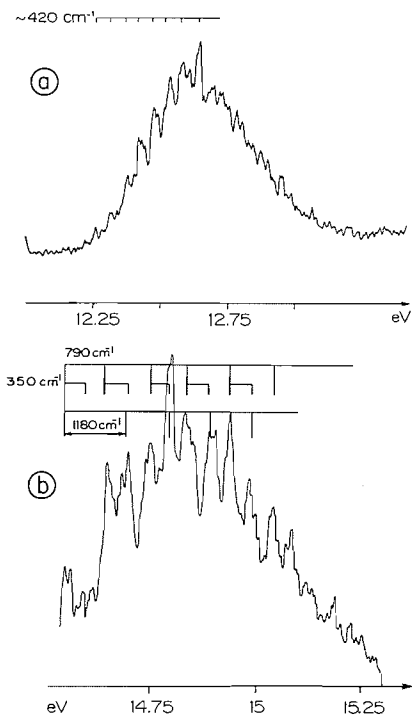

FIG. 6. The first and third bands in the HeI photoelectron spectrum of SOF_2.

lar, indicating that the b_2 orbital is involved in both NO_2 and SO_2. The narrower contour of the first component suggests the more nonbonding a_2 orbital. The excitation of the stretching vibration is consistent with the three times greater p_π–d_π overlap for the a_2 orbital than the b_2. However, similar structure is observed in the $^3A_2$ band of NO_2 where this cannot be the explanation.

In contrast to SO_2 where the b_2 orbital is the third highest in energy, O_3, with the same molecular structure, has the b_2 orbital at highest energy at about the same energy as the a_1 orbital (18, 19). This would indicate a larger "lone pair-lone pair" interaction for the in-plane b_2 orbital probably due to the smaller non-bonded O—O distance. The observed vibrational structure on these states in O_3 is compatible with our assignment of the second band in SO_2, as the i.p. from the b_2 orbital has only a progression on the bending vibration but that arising from the a_2 has progressions involving both the stretching and the bending vibration.

The third band of SO_2 also presents problems in assignment as, although originally it was (8) postulated that there were three components, it has been suggested that only two ionization processes are involved. In fact, Brundle *et al.* (19) assign the ionization from the b_2 σ SO orbital as being at 20.6 eV. Our p.e. spectrum of SO_2, like that of other workers, does not show any obvious structure which could be considered to belong to a third component. The observed structure is well interpreted as belonging to two processes with adiabatic i.p.'s of 15.99 and 16.33 eV and vibrational spacings of 800 and 950 cm^{-1} respectively. If we assign these two components to the $^2A_1$ and $^2B_1$ states of SO_2^+, the order is not obvious. Comparison with the SO_2X_2 species indicates that the $7a_1$ orbital may produce a sharper p.e. band. Therefore, we prefer to assign the higher i.p. (16.33 eV) to the $^2A_1$ state and the

Can. J. Chem. Downloaded from www.nrcresearchpress.com by 210.87.254.42 on 09/05/12
For personal use only.

TABLE 2. Vibrational structure on photoelectron bands of SO_2Cl_2

Band*	Vertical i.p. (in eV)	Vibrational frequencies† (cm^{-1}) ν_1	ν_2	ν_3	ν_4
i	12.4*	—	—	—	—
ii	13.20	—	500	(500)	—
iii	13.74	—	—	640	—
iv	14.1*	—	—	—	—
v	16.93	1170	380	580	200
vi	17.61	—	—	—	—
vii	18.12	—	—	—	—
Neutral molecule‡		1182			

*See text.
†±40 cm^{-1}.
‡Reference 6*b*.

TABLE 3. Ionization data for SOF_2

Band*	Vertical i.p. (eV)	Vibrational frequencies† (cm^{-1}) 1	2	3	4	Ionic* state
i	12.60	—	—	(420)	420	$^2A'$
ii	14.14	(~1000)	—	—	—	$^2A''$
iii	14.8	1180	790	—	350	$^2A''$
iv	16.6	—	—	—	—	$^2A''$
	17.0	—	—	—	—	$^2A'$
Neutral molecule‡		1308	806	530	326	

*See text.
†±40 cm^{-1}.
‡Reference 6*b*.

lower (15.99 eV) to the $^2B_1$ state. This is in agreement with the calculated order (15). However, the calculations place the $7a_1$, $2b_1$, and $4b_2$ orbitals close together and in one case (15*b*) the $4b_2$ orbital is predicted to be above the $2b_1$. In our spectrum the third band does appear to be much stronger than the other two, which may be taken as an indication of three components. In this event the 20.6 eV band would correspond to the $6a_1$ orbital.

Sulfuryl Fluoride (SO_2F_2)

By comparison with SO_2 and difluorocompounds, *e.g.* OF_2, CH_2F_2, and SiH_2F_2 (17), one would expect at least eight i.p.'s in the region below 21 eV, corresponding roughly to the four oxygen and four fluorine "lone pair" orbitals. Some of these, of course, will have considerable bonding contributions but the description suffices for the moment. We expect two low i.p.'s from mainly oxygen non-bonding orbitals (a_2, b_2) together at 13–14 eV as in SO_2 (since there will be little interaction of these orbitals with the fluorines) and two higher i.p.'s from sulfur–oxygen π bonding orbitals (a_1, b_1). Similarly, by comparison with F_2O, CH_2F_2, and SiH_2F_2 (17), the two non-bonding fluorine "lone pair" i.p.'s (a_2, b_1) are expected at about 16 eV and there will also be two higher binding energy fluorine "lone pair" i.p.'s (a_1, b_2) which have considerable σ bonding character.

Turning to the p.e. spectrum of SO_2F_2 (Fig. 2*a*) it is noted that there are six distinct bands at (*i*) 13–14 eV; (*ii*) 15–16 eV; (*iii*) 16.7–17 eV; (*iv*) 18–18.5 eV; (*v*) 19.7–20.1 eV; (*vi*) 20.80 eV. The first two bands have an integrated intensity about twice that of the next two and the band contours and vibrational fine structure (see below) indicate the presence of two components in both cases. Bands (*i*) and (*ii*) are then assigned to the non-bonding oxygen and fluorine "lone pairs" respectively in agreement with the above

Can. J. Chem. Downloaded from www.nrcresearchpress.com by 210.87.254.42 on 09/05/12
For personal use only.

Can. J. Chem. Downloaded from www.nrcresearchpress.com by 210.87.254.42 on 09/05/12
For personal use only.

argument. We now discuss each band separately. The vertical i.p.'s and any resolved ionic vibrational spacings are given in Table 1.

Band (i)

Clearly, this band (Fig. 3*a*) has two components. The first is broad with adiabatic i.p. at *ca.* 13.0 eV and vertical i.p. at *ca.* 13.55 eV. The lack of vibrational structure may indicate the short lifetime of the ion in this state. The second component is much narrower and overlaps the center of the band, and has an adiabatic i.p. apparently at 13.55 eV and a vertical i.p. of 13.61 eV with visible but complex vibrational structure. We tentatively postulate that the principal progression (340 cm^{-1}) is on ν_4 (which is at 384 cm^{-1} in neutral SO_2F_2) and there is another on ν_4 displaced by 500 cm^{-1}, one quantum of ν_3.

The assignment of which of these two components arises from the $2a_2$ (or $6b_2$), mainly oxygen non-bonding orbital is not straightforward. In the second band of SO_2 the higher binding energy component was broader with a progression on the bending frequency but in this case the lower binding energy component is broader and a progression on the OSO bend is not observed. There is little similarity between the vibrational structure on the $^2A_2$ state in SO_2^+ and the second component of this first band in SO_2F_2. Therefore, although on the basis of band shapes it is possible that the assignment of the "non-bonding" oxygen orbitals is reversed compared to SO_2, there is no further confirmation from the observed structure. From qualitative overlap considerations and comparison with other similar "lone pairs" the order should be $6b_2 > 2a_2$, especially if there is considerable d orbital interaction which will be three times as great for the a_2 orbital. This is the order we prefer, as a_2 bands are normally sharper even if there is some d orbital participation (*e.g.* in SiH_2Cl_2 (7)). Also, as the inner a_2 orbital, which is mainly fluorine–fluorine anti-bonding, will be closer than the next highest b_2 orbital, which is fluorine–fluorine bonding, more fluorine character is expected in the $2a_2$ orbital than the $6b_2$ orbital. Thus, excitation of ν_4 is more likely on ionization from the $2a_2$ orbital. However, the order of these two states must remain somewhat speculative.

Band (ii)

This band is plainly made up of two overlapping components each with one main vibrational progression (Fig. 3*b*). The first component has an adiabatic i.p. at 14.89 eV and a regular progression of at least 11 peaks with separation 330 ± 50 cm^{-1}, the tenth peak coinciding with the first peak of the second component. The vibration which is excited must be ν_4, which is 384 cm^{-1} in the neutral species. Using Turner's relationship (20)

$$\text{i.p. (vertical)} - \text{i.p. (adiabatic)} = 1.2\,(\omega_{\text{neutral}}/\omega_{\text{ion}} - 1)$$

and assuming $\omega_{\text{ion}} = 320$ cm^{-1}, the vertical i.p. is at 15.18 eV, which is the most distinct peak. The second component appears to commence at 15.23 eV, *i.e.* coincident with peak 7 of the first component, although it is conceivable that the true adiabatic i.p. is lower at 15.10 eV. Comparing the intensity of the two series we prefer 15.23 eV as the adiabatic value. There is a regular progression of at least seven peaks with a spacing of 1050 ± 50 cm^{-1} which may correspond to ν_1, the symmetric SO stretch, at 1269 cm^{-1} or to ν_2, the symmetric SF stretch at 848 cm^{-1} in neutral SO_2F_2. There is also an indication of weak peaks between the peaks of the main progression, which would correspond to the addition of one quantum of ν_3 (546 cm^{-1} in SO_2F_2). For the second component of this band Turner's relationship gives the vertical i.p. at 15.44 eV, if it is assumed that ν_1 is the excited vibration. This value is between the two peaks at 15.35 eV and 15.48 eV, both of which could be considered as the vertical i.p. for the process; we prefer the value of 15.35 eV.

The progression on ν_4 in the first component of this band is consistent with ionization from a fluorine "lone pair" orbital. This vibrational structure could point to either the $1a_2$ or the $6b_1$ orbital, both of which are antibonding between the two fluorine atoms. There is no obvious preference, however we prefer the assignment $1a_2$ for the following reasons. First, this fits better the assignment of the p.e. spectra of other difluoro-compounds studied (17) and secondly there would be another a_2 orbital fairly close but at higher energy. Finally the F—F σ overlap of the $6b_1$ orbital is more likely to result in extensive excitation of the bending vibration (in the first component) compared to the π overlap of the $1a_2$ orbital.

Band (iii)

This band with an adiabatic i.p. of 16.68 eV

Can. J. Chem. Downloaded from www.nrcresearchpress.com by 210.87.254.42 on 09/05/12
For personal use only.

is shown in Fig. 3*c* and the observed structure is interpreted in terms of the excitation of three vibrational modes. The principal progression consists of three quanta with spacing 1130 cm^{-1} and corresponds to ν_1, the S—O stretching vibration. One quantum of ν_3 (520 cm^{-1}) and of ν_2 (840 cm^{-1}) is observed. Only ν_1 is significantly decreased from the value in the neutral species (see Table 1). The relative strength of the O—O transition indicates the removal of a non-bonding or weakly bonding electron. The major excitation of the SO stretching vibration and weak excitation of the OSO bending vibration together with the bands in this region in the p.e. spectrum of SO_2 suggest that a sulfur–oxygen π electron is involved. This is further confirmed by the p.e. spectrum of SO_2Cl_2 which has a band with very similar vibrational structure at similar binding energy. By comparison with SO_2 there are two possible assignments corresponding to ionization from either the $11a_1$ or $5b_1$ SO π orbitals. For various reasons we prefer the former. First, there are no a_1 orbitals at higher energy, whereas the mainly fluorine "lone pair" $6b_1$ orbital is just over one eV higher in energy. Secondly, the $5b_1$ orbital is expected to be more strongly S—O π bonding; this occurs at higher binding energy and gives rise to a broader p.e. band than the $11a_1$. The structure on this band certainly does not correspond to that of the fourth i.p. of SO_2, but there are similarities with the fifth i.p. band. The assignment of this i.p. in SO_2 to ionization from the $7a_1$ orbital is in agreement with the calculated order (15). In both SO_2 and SO_2F_2 this orbital will contribute less to SO π bonding than the b_1 SO π orbital because of the difference in the overlap contributions.

Band (iv)

This band has a vertical i.p. at 18.36 eV and adiabatic i.p. apparently at 17.89 eV. We believe that this ionization is most likely to arise from the SO π bonding $5b_1$ orbital. The orbital is then about 2 eV lower in energy than in SO_2 and must be stabilized by the effect of the higher energy F "lone pair" orbital, and by the inductive effect, and probably contributes considerably to producing a stronger SO bond in SO_2F_2 than in SO_2 as discussed in the introduction to this paper.

Band (v)

The first four peaks of this band are well resolved, while the remaining bands are broader and very asymmetric (Fig. 3*d*). This may be due to the instability of these vibrational states, but there is also the possibility that a second ionization process occurs. If the band is assumed to result from only one ionization process, the adiabatic i.p. is 19.70 eV and the vertical i.p. 19.89 eV. The observed structure may be interpreted in terms of a progression with a spacing of 800 cm^{-1} which corresponds to ν_2, the S—F stretching vibration (848 cm^{-1} in neutral SO_2F_2), and a second progression involving ν_2 displaced by 500 cm^{-1}, corresponding to one quantum of ν_3, the OSO bending vibration (544 cm^{-1} in SO_2F_2). In view of the vibrational structure and previous assignments this ionization must be from an orbital with considerable fluorine character. We postulate that this is the $5b_2$ fluorine orbital which will also have some S—O_2 σ bonding character. The $4b_2$ SO σ bonding orbital in SO_2 is thought to be close in energy to the $2b_1$ and $7a_1$ SO_2 π orbitals. It would be expected that the two fluorine atoms would have a greater stabilizing influence on the σ orbital than on the π orbital (perfluoro effect), and we can say that the b_2, SO_2 σ orbital may be stabilized by at least 2 eV from SO_2 to SO_2F_2.

Band (vi)

This band, whose vertical i.p. may not be observed in our spectrum, probably arises from ionization from the $10a_1$ orbital. Summarizing our assignments, the orbital configuration of SO_2F_2 is

$$(6b_2)^2\ (2a_2)^2\ (6b_1)^2\ (1a_2)^2\ (11a_1)^2\ (5b_1)^2\ (5b_2)^2\ (10a_1)^2$$

Sulfuryl Chloride (SO_2Cl_2)

Below 15 eV, in addition to ionization from the two essentially oxygen "lone pair" orbitals (a_2, b_2), we expect i.p.'s arising from the four chlorine "lone pair" orbitals to be in the order b_1, a_2, b_2, a_1 on simple considerations of the overlap contribution; the a_1 orbital is thought to occur at higher binding energy and probably arises from the S—Cl σ bonding orbitals (a_1, b_1). It appears, by comparison with the other Cl_2X species, SO_2 and SO_2F_2, that neglecting any mutual interaction these outer "lone pair" orbitals would be close together. Above 15 eV we anticipate there will be two S—O σ orbitals.

Seven distinct bands are observed in the p.e. spectrum (Fig. 2*b*) and it is likely that an eighth

Can. J. Chem. Downloaded from www.nrcresearchpress.com by 210.87.254.42 on 09/05/12
For personal use only.

occurs at about 20.1 eV. Only four bands below 15 eV are apparent, but the cross-sections of the first at 12.41 eV and the fourth at 14.2 eV are approximately three times those of the second and third bands. This indicates that the first and fourth bands contain at least two, and possibly three, components. The seventh band at 17.61 eV may also contain two components. We shall now discuss the bands individually.

Band (i)

The experimental intensity ratios quoted above and the fact that we expect at least 11 states below 21.2 eV indicate that this band probably arises from ionization of three orbitals. However, it was not possible to resolve them, thus we place all the vertical i.p.'s at 12.41 eV, the band maximum. The onset of the band is at 12.05 eV.

Assignment of the three possible components requires consideration of all the "lone pair" ionization processes possible in this region. In the unperturbed state, the a_2 and b_2 oxygen "lone pairs" (*e.g.* in SO_2) are at only slightly higher binding energy (13.5 eV) than the chlorine "lone pairs" in other dichloro compounds (*e.g.* 12.8 eV in Cl_2O, 13.2 eV in Cl_2CO (17)). Thus the interaction between the two a_2 orbitals and the two b_2 orbitals is likely to be such that the resultant molecular orbitals would be of intermediate character between pure oxygen or chlorine lone pairs. In addition, this interaction would destabilize one set of the a_2 and b_2 orbitals so that they are of comparable energy to the lowest binding energy chlorine "lone pair" (b_1) orbital. Thus, we believe that the three states in this band are the $^2A_2$, $^2B_2$ and $^2B_1$.

Band (ii)

This band has an adiabatic i.p. of 13.0 eV and a vertical i.p. of 13.20 eV. There is a poorly resolved progression of broad peaks separated by *ca.* 500 cm^{-1} (Fig. 4*a*), which may correspond to either ν_3, the OSO bend, or to ν_2, the S—Cl stretch, at 560 cm^{-1} and 405 cm^{-1} respectively in the neutral molecule (6*b*). In SO_2 and SO_2F_2 the a_2 and b_2 oxygen "lone pair" orbitals occur in this binding energy region. However, in view of the above discussion concerning the first band we expect these orbitals to be stabilized in SO_2Cl_2 by mixing with the corresponding chlorine "lone pair" orbitals. Therefore, we assign this band to ionization from the a_1 chlorine "lone pair" orbital, however, ionization from the inner a_2 (or b_2) orbital remains a possibility.

Bands (iii) and (iv)

These two bands, shown in Fig. 4*b*, overlap in the region 13.5–14.5 eV. The third band has a vertical i.p. of 13.74 eV and consists of two peaks separated by 640 cm^{-1}, any other peaks being obscured by the strong fourth band. The 640 cm^{-1} spacing is assigned to ν_3, the OSO bend which occurs at 560 cm^{-1} in the neutral molecule. This third band probably corresponds to the removal of an electron from either the a_2 or b_2 oxygen "lone pair" orbitals, though we suggest that these may have substantial chlorine character (see above). The increase in ν_3 in the ion points to the b_2 orbital which is more O—O antibonding than the a_2. In this event the b_2 orbital has been stabilized slightly relative to SO_2 and SO_2F_2.

The broad fourth band, because of its high relative intensity, probably contains three components. We attribute these to ionization from the a_2 oxygen "lone pair" and the a_1 and b_1 S—Cl σ bonding orbitals. It was not possible to obtain vertical i.p.'s for any of these processes. The band maximum is 14.2 eV.

Band (v)

The vibrational structure of this band (Fig. 4*c*) with an adiabatic i.p. of 16.93 eV, is very similar to that observed in the 16.68 eV band in SO_2F_2 (Fig. 3*c*). However, in this case all four symmetric vibrations appear to be excited. Excitation of ν_1 at 1170 cm^{-1} and ν_2 at 380 cm^{-1} is beyond doubt. However, the assignment of single quantum excitation of ν_3 (580 cm^{-1}) and ν_4 (200 cm^{-1}) is slightly more speculative. ν_4 does appear to be excited, but the peaks corresponding to ν_3 could be attributed to multiple excitation of ν_4, which may occur as well as excitation of ν_3 thereby causing the poor resolution. The measured vibrational spacings are insignificantly different from the groundstate values (see Table 2). In contrast, in SO_2F_2 there is a significant decrease in ν_1 (from 1269 cm^{-1} to 1130 cm^{-1} in the ion) and this may be an indication of stronger S—O π bonding in this molecule. Another indication of this may be obtained indirectly by considering the greater excitation of halogen-involved vibrations for SO_2Cl_2. This is shown by excitation of the Cl—S—Cl bend whereas excitation of the F—S—F bend is lacking in the corresponding band in SO_2F_2 and, also, by the increased population of levels involving the S—X stretch (ν_2). It follows that if there is more elec-

Can. J. Chem. Downloaded from www.nrcresearchpress.com by 210.87.254.42 on 09/05/12
For personal use only.

tron density in the S—Cl bonds there must be less in the S—O bonds. Despite this, it is interesting to note that this band is at higher binding energy in SO_2Cl_2 than in SO_2F_2. However, this seems to be further support for the assignment to ionization from the a_1 π SO orbital. In SO_2F_2 there are no higher energy a_1 orbitals but there are two a_1 orbitals just lower in energy (the F "lone pair" and a σ bonding orbital). However in SO_2Cl_2 we assign the Cl "lone pair" and σ S—Cl orbitals to be at higher energy. Obviously the opposite influence of these interactions could place the orbital at higher energy in SO_2F_2. The shape of the band for both molecules makes it clear that the a_1 π SO orbital is very much the less bonding of the two SO π orbitals.

Bands (vi) and (vii)

These bands, which have no vibrational structure, have maxima at 17.61 and 18.12 eV, and are assigned to ionization from the b_1 π SO orbital and b_2 σ SO orbital respectively. The order could be reversed but we prefer to have the π orbital higher than the σ orbital. The b_1 orbital is considerably stabilized compared to that in SO_2 (16.5 eV) and as the other b_1 orbitals in SO_2Cl_2 are at much higher energy, it seems that this is caused by greater π interaction between the sulfur and oxygen atoms. The interaction must be even greater in SO_2F_2 as the b_1 orbital moves at least to -18.34 eV.

Thionyl Fluoride (SOF_2)

By comparison with SO_2F_2 and SO_2, at least seven i.p.'s should be expected for SOF_2 below 21.2 eV, corresponding roughly to ionization from the sulfur lone pair, oxygen lone pair, two fluorine lone pairs, sulfur–oxygen π orbital, and two sulfur–fluorine π orbitals in order of increasing binding energy. It is possible that the sulfur–oxygen σ bonding level is above 21 eV.

Unfortunately it was not easy to obtain a good p.e. spectrum of SOF_2 but five ionization processes are clearly visible below 17 eV (Fig. 5*a*) and in the broad band extending from 18 to 20.5 eV there is likely to be more than one component.

Band (i)

This band with an adiabatic i.p. of 12.25 eV and vertical i.p. of 12.60 eV, has a clear vibrational structure up to the position of the vertical i.p. (Fig. 6*a*). The peaks are irregular and there is the possibility of a double progression. The average spacing of the eight peaks is 420 cm^{-1}, with a decrease through the progression except between the seventh and eighth peaks. This vibrational frequency could correspond to two frequencies in the neutral species, the bending of the SO bond relative to the F—S—F plane (326 cm^{-1}) or the F—S—F bending vibration (526 cm^{-1}). Judging from the width of the peaks it is possible that progressions involving both frequencies are present. The loss of structure just above the vertical transition may be due to dissociation of the ion, or to the ion becoming planar. The ionization process producing this band must involve an a′ orbital localized mainly on the sulfur atom (*i.e.* the sulfur "lone pair"). The corresponding vertical i.p. in SO_2, to which SOF_2 can be compared, is 12.50 eV. The CNDO/2 calculations which we have carried out on SOF_2 agree with this assignment. This a′ orbital will almost certainly be antibonding with respect to the oxygen and fluorine atoms, though the larger interaction should be with the next higher a′ orbital which has mostly π S—O character (see below). This suggests that on ionization the S—O wagging vibration is excited, which requires an increase from 326 cm^{-1} in the neutral species to 420 cm^{-1} in the ion. This would only be possible if there was a strong antibonding interaction between sulfur and oxygen. Although the ionic frequency is closer to the F—S—F bending vibration of the neutral (526 cm^{-1}), there seems no ready mechanism for exciting this vibration. Accepting the first assignment, the decrease in the vibrational spacing through the series and the loss of structure could be explained in a similar manner to the corresponding effect in the $^2A_1$ ionic state of H_2S^+ (21). If the ion becomes planar as the energy increases, the vibrational–rotational energy levels would be doubled, which would reduce the spacing between levels to *ca.* 200 cm^{-1}, which was just beyond the resolution of the spectrometer in this case.

Band (ii)

The adiabatic i.p. of the second band is *ca.* 13.4 eV and the vertical i.p. 14.14 eV. There is an indication of a progression of peaks with a separation of *ca.* 1000 cm^{-1}. By comparison with the p.e. spectra of SO_2 and SO_2F_2 we assign this band to ionization from the "non-bonding" oxygen a″ orbital and thus excitation of the S—O stretching frequency (1308 cm^{-1} in SOF_2) is probably involved. It is interesting that, al-

Can. J. Chem. Downloaded from www.nrcresearchpress.com by 210.87.254.42 on 09/05/12
For personal use only.

though the highest energy orbitals in SO_2 and SOF_2 (sulfur "lone pairs") are at the same energy, the oxygen "lone pair" in SOF_2 is stabilized. This is due to the lower symmetry of SOF_2 allowing more SO π character in the oxygen lone pair orbital, as well as the orbital contraction effect mentioned above. It also partly accounts for the stronger SO bond in SOF_2 compared to SO_2.

Band (iii)

The complex structure of the third p.e. band can be seen in Fig. 6*b*. Both the adiabatic (14.55 eV) and vertical (14.80 eV) i.p.'s are well-defined, though the assignments of ionic vibrational frequencies are clearly dependent on the interpretation of the fine structure. Clearly, two or more normal modes are excited in the ion. We suggest that the principal structure is due to strong excitation of an ionic mode of frequency 790 cm^{-1} as shown in Fig. 6*b*. The additional peaks are attributed to weak excitation of ionic modes of frequency 1180 and 350 cm^{-1}. The 1180 cm^{-1} spacing must correspond to ν_1, the S—O stretch, slightly reduced from its value of 1308 cm^{-1} in the ground state molecule. The 790 and 350 cm^{-1} vibrations correspond to ν_2, the S—F stretch, and ν_4 respectively, which are both insignificantly different from the ground state values. The excitation of several ionic modes is not surprising in a molecule with low symmetry since the orbitals are not well-defined. The similarity of the frequencies in the ion and the neutral species indicates that the parent orbital is essentially non-bonding.

By comparison with a number of other difluoro compounds (17), we assign this band to an a″ fluorine "lone pair" orbital. These have the a_2 and b_2 (in C_{2v} symmetry) orbitals (which are antisymmetric with respect to the plane bisecting the F—S—F angle) around 15 eV. In the C_{2v} molecules the a_2 and b_2 orbitals are fairly close in energy (normally within 0.5 eV). In C_s symmetry both of these become a″ orbitals and interaction between these should cause a much larger separation than that between the a_2 and b_2 orbitals in C_{2v} symmetry. No matter which of the next two i.p.'s involves ionization from the other fluorine lone pair a″ orbital, it is seen that the fluorine orbitals are split apart relative to the other difluoro species.

Band (iv)

This band stretching from 15.5 to 17.5 eV has two structureless components. One is extremely broad and its vertical i.p. is difficult to determine but is probably about 16.6 eV. The other has a half width of *ca.* 0.6 eV, is sharper and has a vertical i.p. of 17.0 eV. By comparison with SO_2 and in line with the discussion of the third band above, the orbitals involved must be (*a*) mainly a″ fluorine "lone pair" and (*b*) mainly a′ π S—O. As the band in this region in $SOCl_2$ (see below) is broad, it could be inferred that the first component is the a′ orbital. There could however be other ionizations present in this band in $SOCl_2$ and the corresponding bands in SO_2, SO_2F_2, and SO_2Cl_2 are quite sharp. None of the evidence is conclusive as neither of these orbitals would be expected to produce such a broad band. In contrast to our earlier suggestion, we now prefer to assign the sharp band to the a′ orbital.

There are obviously other bands between 18 and 21 eV but the rising background prevents us from distinguishing them.

Thionyl Chloride

By comparison with the other species ten i.p.'s should be observed for this molecule below 21.2 eV, corresponding roughly to the following orbitals; sulfur "lone pair", four chlorine "lone pairs", oxygen "lone pair", two sulfur–chlorine σ orbitals, a sulfur–oxygen π orbital, and sulfur–oxygen σ. As it was extremely difficult to obtain a spectrum of $SOCl_2$ free of SO_2, no vibrational structure was observed on any of the bands. Therefore, we shall discuss the spectrum as a whole and not the individual bands.

The observed spectrum below 17 eV (Fig. 5*a*) consists of six well-defined bands with maxima 11.3, 11.9, 12.21, 12.55, 13.04, and 16 eV. The intensity of the last three bands could be enhanced by some SO_2 impurity, but this effect is probably small. The most interesting point about the spectrum is the lack of spread of the lower bands. As the symmetry of the molecule is low (C_s) with only two irreducible representations (a′, a″), it might have been thought that there would be some fairly large interactions between orbitals of the same symmetry. The spectrum indicates that assignments of higher symmetry species on the basis of strong interactions between orbitals of the same symmetry may be erroneous.

The first i.p.'s of thionyl fluoride and dimethylsulfoxide at 12.6 and 9.3 eV respectively are both assigned to the removal of electrons from

Can. J. Chem. Downloaded from www.nrcresearchpress.com by 210.87.254.42 on 09/05/12
For personal use only.

sulfur "lone pair" orbitals. The ionization arising from the corresponding orbital in $SOCl_2$ should fall between these two values, and there are three bands which fit this criterion at 11.3, 11.9, and 12.21 eV. Since the inductive effect of fluorine is considerably greater than that of chlorine, we attribute the first band at 11.3 eV to ionization from an essentially sulfur "lone pair" orbital (a′). Additional evidence for this assignment may be drawn from the fact that ionizations arising from chlorine "lone pair" orbitals are normally in the range 11.5–13 eV and in SO_2Cl_2 the lowest binding energy chlorine i.p. is 12.41 eV.

In $SOCl_2$ it is likely that the main oxygen "lone pair" (a″) orbital will be at higher binding energy than the four chlorine "lone pairs", as SO_2 has its second i.p. in the 13–14 eV range. Simply relating the symmetry of the chlorine "lone pair" orbitals to C_{2v} molecules, the order in $SOCl_2$ should be a″, a″, a′, a′, the in-plane S—Cl_2 a″ orbital being at the lowest binding energy and also having the largest interaction with the oxygen a″ "lone pair". On this basis, we tentatively assign the 11.9 eV band to the in-plane a″ chlorine "lone pair". The intensity of the 12.55 and 13.04 eV bands strongly suggests that they consist of more than one component, and such overlapping of i.p.'s was a feature of the SO_2Cl_2 p.e. spectrum (Fig. 2*b*). The out-of-plane a″ chlorine "lone pair", which corresponds to a_2 in C_{2v} symmetry, should possibly produce a sharp p.e. band and so we assign this to the sharp component of the 12.55 eV band. This corresponds well with the sharpest band in the SO_2Cl_2 spectrum at 12.4 eV. The other component of the 12.55 eV band is then assigned as one of the chlorine "lone pair" a′ orbitals (probably in-plane C—S—Cl) and the other i.p. at 12.21 eV is then assigned to the remaining a′ lone pair orbital. These assignments would fit with most other simple di-chloro compounds. The 13.04 eV band must then have the mainly oxygen "lone pair" orbital (a″) and both sulfur–chlorine σ bonding orbitals. These latter would then be very high in energy. This is not, however, unreasonable when it is considered that the corresponding orbitals in SO_2Cl_2 were assigned at 14.1 eV and the S—Cl bond in SO_2Cl_2 is somewhat stronger on the basis of S—Cl bond lengths: $SOCl_2$, r(S—Cl) = 2.07; SO_2Cl_2, r(S—Cl) = 1.00 Å. The oxygen "lone pair" orbital is almost at the same energy as the non-bonding "lone pairs" in SO_2 (13.3, 13.6 eV) and intermediate between those of $(CH_3)_2SO$ (10.43 eV) and F_2SO (14.14 eV). In dimethylsulfoxide the oxygen "lone pair" is destabilized because of the lower overall charge and the lack of interaction with orbitals on the sulfur atom. The 16 eV band must be assigned to ionization from the a′ SO π orbital. This orbital is the least stable of all the SO π orbitals in the molecules studied here.

Bonding in Sulfuryl and Thionyl Halides

In the introduction we presented the argument, based on π bonding changes, used to explain various properties of the SO bonds in these compounds. Many of these properties have been compared (6) for a large series of sulfur–oxygen compounds and the relevant data for the five compounds studied in this paper are given in Table 4. These data indicate that the SO bond order decreases in the order $SO_2F_2 > SOF_2 > SO_2Cl_2 > SO_2 > SOCl_2$. We now examine the i.p.'s for correlations based mainly on the SO orbitals. Table 5 lists some pertinent average i.p.'s for (A) all the mainly oxygen "π type" orbitals both "lone pair" and SO π, (B) the SO π orbitals, and (C) the low binding energy oxygen "lone pair" orbitals. The energy of the b_1 π SO orbital is also given for the di-oxygen species.

Although none of the averages show exactly the above trend, the overall average of the "π"

TABLE 4. Some properties of the SO bond

Compound	r_{SO}(Å)	ν_{SO}(cm^{-1})	$k \times 10^5$
SO_2F_2	1.405±0.003	1385*	12.05†
SO_2Cl_2	1.409±0.02	1298	10.75
SO_2	1.432±0.002	1259	9.96
SOF_2	1.412±0.001	1308	10.95
$SOCl_2$	1.45±0.02	1229	9.49

*Average SO stretching frequency.
†SO force constant in mdyn/Å.

TABLE 5. Some average ionization energies (in eV) for π orbitals involving the oxygen atom

	A*	B†	C‡	b_1 π SO
SO_2F_2	15.55	17.51	13.58	18.34
SO_2Cl_2	15.37	17.27	13.47	17.61
SO_2	14.99	16.60	13.36	16.60
SOF_2	15.57	17.00	14.14	—
$SOCl_2$	14.7	16.00	13.40	—

*A = average of all orbitals derived from oxygen "lone pairs"; SO_2 species and two for the SO species.
†B = average of the SO π bonding orbitals.
‡C = average of the low binding energy oxygen "lone pair" orbitals.

levels (A) is fairly close to it, *i.e.* $SO_2F_2 \approx SOF_2 > SO_2Cl_2 > SO_2 > SOCl_2$. The range of the average SO π levels (B) is 1.5 eV, whereas the range of the oxygen "lone pair" levels (C) is only 0.8 eV and omitting SOF_2 it is only 0.2 eV. It seems reasonable to suppose that a π bonding orbital would be more influenced by effective charge than the virtually non-bonding orbitals on the oxygen atoms. Current bonding theory would, however, indicate that the a_2 and b_2 oxygen lone pair orbitals have some interaction with the sulfur d orbitals and that this should increase with the charge on the sulfur atoms (1). From SO_2 to SO_2F_2 the "lone pairs" (a_2, b_2) are stabilized on the average by only 0.22 eV whereas the π orbitals (a_1, b_1) are stabilized on an average by 0.9 eV. On symmetry grounds, the d orbitals should affect both those averages by about the same amount. This may be taken as an indication that the major contribution to any increased π bonding in SO_2F_2 is not the increased sulfur d orbital contribution, but the increased sulfur orbital contribution. This is especially noticeable in the b_1 π SO orbital which moves from 16.6 eV in SO_2 to 18.34 eV in SO_2F_2.

It must be borne in mind, however, that the assignments of some bands in the p.e. spectra reported here, with the exception of SO_2 and possibly SO_2F_2 are tentative and, therefore, any conclusions concerning bonding in these molecules based on ionization energies are necessarily of a speculative nature.

We thank the National Research Council of Canada for generous financial support. The awards of a N.A.T.O. Fellowship (to D.C.) from the Science Research Council of Great Britain and a Killam Fellowship (to R.A.N.M.) from the University of British Columbia are gratefully acknowledged.

1. D. W. J. CRUICKSHANK and B. C. WEBSTER. *In* Inorganic sulphur chemistry. *Edited by* G. Nickless. Chapt. 2.
2. D. W. J. CRUICKSHANK. J. Chem. Soc. 5486 (1961).
3. L. S. BARTELL, L. S. SU, and H. YOW. Inorg. Chem. **9**, 1903 (1970) and refs. therein.
4. I. H. HILLIER and V. R. SAUNDERS. Int. J. Quant. Chem. **IV**, 203 (1970).
5. D. S. URCH. J. Chem. Soc. A, 3026 (1969).
6. (*a*) R. J. GILLESPIE and E. A. ROBINSON. Can. J. Chem. **41**, 2074 (1963); (*b*) Can. J. Chem. **39**, 2171 (1961).
7. D. C. FROST, F. G. HERRING, A. KATRIB, R. A. N. MCLEAN, J. E. DRAKE, and N. P. C. WESTWOOD. (*a*) Chem. Phys. Lett. **10**, 347 (1971); (*b*) Can. J. Chem. **49**, 4033 (1971).
8. J. H. D. ELAND and C. J. DANBY. Int. J. Mass. Spectr. Ion Phys. **1**, 111 (1968).
9. M. JONATHAN, D. J. SMITH, and K. J. ROSS. Chem. Phys. Lett. **9**, 217 (1971).
10. H. LYNTON and M. R. TRUTER. J. Chem. Soc. 5112 (1960).
11. (*a*) R. M. FRISTROM. J. Chem. Phys. **20**, 1 (1952); (*b*) D. R. LIDE, D. E. MANN, and R. M. FRISTROM. J. Chem. Phys. **26**, 736 (1957); (*c*) D. R. LIDE, D. E. MANN, and J. J. COMEFORD. Spect. Acta, **21**, 497 (1965).
12. W. MOFFITT. Proc. Roy. Soc. A, **200**, 409 (1949).
13. I. HARGITTAI. Acta Chim. Acad. Sci. Hung. **57**, 403 (1968).
14. D. KIVELSON. J. Chem. Phys. **22**, 904 (1954).
15. (*a*) S. ROTHENBURG and H. F. SCHAEFER. J. Chem. Phys. **53**, 3014 (1970); (*b*) I. H. HILLIER and V. R. SAUNDERS. Mol. Phys. **22**, 193 (1971).
16. R. C. FERGUSON. J. Am. Chem. Soc. **76**, 850 (1965).
17. D. CHADWICK, A. B. CORNFORD, D. C. FROST, F. G. HERRING, A. KATRIB, C. A. MCDOWELL, and R. A. N. MCLEAN. *In* Electron spectroscopy. *Edited by* D. A. Shirley. North Holland Publishing Co., Amsterdam, 1972.
18. D. C. FROST and C. A. MCDOWELL. To be published.
19. C. R. BRUNDLE, D. NEUMANN, W. C. PRICE, D. EVANS, A. W. POTTS, and D. G. STREETS. J. Chem. Phys. **53**, 705 (1970).
20. D. W. TURNER. Phil. Trans. Roy. Soc. **268**, 7 (1970).
21. D. C. FROST, A. KATRIB, C. A. MCDOWELL, and R. A. N. MCLEAN. Int. J. Mass Spectr. Ion Phys. **7**, 485 (1971).

Can. J. Chem. Downloaded from www.nrcresearchpress.com by 210.87.254.42 on 09/05/12
For personal use only.

Electric Dipole Moments and Conformations of ortho-, meta-, and para-Fluoroacetophenones and of ortho-, meta-, and para-Trifluoromethylacetophenones

ERNST BOCK, ROBERT WASYLISHEN,[1] AND BERNARD E. GABOURY
Parker Chemistry Laboratory, University of Manitoba, Winnipeg, Manitoba

AND

EDWARD TOMCHUK
Department of Physics, University of Winnipeg, Winnipeg, Manitoba

Received June 30, 1972[2]

The dipole moments of ortho-, meta-, and para-fluoroacetophenone and of ortho-, meta-, and para-trifluoromethylacetophenone were determined in dilute benzene and carbon tetrachloride solutions at 25 °C. In addition the dipole moments and the total energies of the above molecules and of acetophenone, fluorobenzene, and trifluoromethylbenzene were computed for different molecular conformations by the INDO molecular orbital approximation. In some cases there is quantitative agreement between the experimental dipole moments and the INDO computed dipole moments. The most probable conformation for different fluoroacetophenone and trifluoromethylacetophenone molecules is suggested.

Les moments dipolaires de l'ortho-, méta-, et para-fluoroacétophénone et de l'ortho-, méta-, et para-trifluorométhylacétaphénone ont été évalués à 25 °C dans des solutions diluées de tétrachlorure de carbone et de benzène. En plus, les moments dipolaires et les énergies totales de molécules mentionnées et de l'acétophénone, du fluorobenzène, et du trifluorométhylbenzène ont été calculés pour différentes conformations moléculaires par l'approximation des orbitales moléculaires INDO. Dans certains cas, on a noté un accord quantitatif entre les moments dipolaires expérimentaux et les moments dipolaires calculés (INDO). L'on suggère la conformation la plus probable pour différentes molécules de fluoroacétophénone et de trifluorométhylacétophénone. [Traduit par le journal]

Can. J. Chem., 51, 1906 (1973)

Introduction

In a recent publication (1), we reported on the electric dipole moments and conformations of *o*-, *m*-, and *p*-fluorobenzaldehydes. It was shown there that the dipole moment values computed using the INDO molecular orbital approximation (2) were in remarkably good agreement with the experimental dipole values. We thought it interesting to see whether the same close agreement between theory and experiment would prevail in the case of more complicated molecules. To this end, we computed (using the INDO molecular orbital approximation) and measured (in dilute benzene and carbon tetrachloride solution at 25 °C) the electric dipole moments of ortho-, meta-, and para-fluoroacetophenone and ortho-, meta-, and para-trifluoromethylacetophenone, and of acetophenone, fluorobenzene, and trifluoromethylbenzene.

[1]Holder of an NRCC Scholarship, 1971–1972.

[2]Revision received February 23, 1973.

Experimental

Solvent

Fisher certified reagent benzene and Fisher certified reagent carbon tetrachloride were used as solvents. The solvents were dried by repeated shaking with Linde molecular sieve 4A prior to their use.

Solute

The solute molecules were obtained from the PCR Incorporated Chemical Co. and were used without further purification. However, the purity of the solutes was checked by gas chromatography and n.m.r. In all cases the impurities amounted to less than 1 mol %.

Experimental Procedure

The dipole moment apparatus and experimental procedure have been described elsewhere (3). The experimental error in the dipole moment values is estimated to be ± 0.05 D.

The INDO computations were carried out on an IBM 360/65 computer system, using "standard" molecular geometries (2). In each case less than 25 cycles in the self-consistent-fitting procedure were required to obtain convergence in the electronic energy to within 10^{-6} a.u. = 0.6 cal/mol.

Can. J. Chem. Downloaded from www.nrcresearchpress.com by 210.87.254.42 on 09/05/12
For personal use only.

TABLE 1. Summary of Smith's polarization factors α and ν for different molecules

Solute	Solvent: C_6H_6		Solvent: CCl_4	
	α	ν	α	ν
o-Fluoroacetophenone	6.09	0.00	10.64	0.00
m-Fluoroacetophenone	6.43	0.00	12.37	0.23
p-Fluoroacetophenone	4.17	0.00	7.61	0.28
o-Trifluoromethylacetophenone	9.95	−0.13	16.94	0.00
m-Trifluoromethylacetophenone	5.11	−0.13	9.45	0.00
p:Trifluoromethylacetophenone	3.47	−0.13	6.35	0.00
Acetophenone	7.96	0.00		
Trifluoromethylbenzene	4.59	−0.26		
Fluorobenzene	2.28	0.00		

TABLE 2. Fluoroacetophenones: Experimental and calculated dipole moments of *o*-, *m*-, and *p*-fluoroacetophenones and the energy difference, ΔE, between the *O-cis* and *O-trans* conformers

Compound	μ(INDO) D	μ(Group) D	ΔE(kcal)	μ(eq) D	μ(fr) D	μ_{exp} (C_6H_6) D	μ_{exp} (CCl_4) D
ortho (*O-cis*)	4.52	4.36	1.35	2.99	3.67	2.78	2.76
ortho (*O-trans*)*	2.90	2.81					
meta (*O-cis*)	3.85	3.70	0.13	2.83	2.84	2.86	2.95
meta (*O-trans*)*	1.16	1.58					
para	2.28	2.32		2.32	2.32	2.30	2.29

*The more stable conformer.

Results and Discussion

The solution dipole moments were calculated after the method of Smith (4).

$$[1] \qquad \mu^2 = \frac{27kT}{4\pi N} \frac{M_2}{d_1(\varepsilon_1 + 2)^2} (\alpha - \nu)$$

where μ is the dipole moment of the solute molecule, k the Boltzmann constant, N the Avogadro number, M_2 molecular weight of the solute, d_1 and ε_1 the density and dielectric constant of the pure solvent, α the slope of the curve $\varepsilon_{12} = \varepsilon_1 + \alpha w_2$, where ε_{12} is the dielectric constant of the solution, and w_2 the weight fraction of the solute in solution, and ν is the slope of the curve $n_{12}^2 = n_1^2 + \nu w_2$ where n_{12} and n_1 is the refractive index of the solution and solvent respectively.

The experimental results are presented in Table 1 in terms of α and ν. The dipole moments derived from these data are summarized in Tables 2, 3, and 4. Included in these Tables are the moment values calculated from group moments and using the INDO calculation for different molecular conformations, the energy difference, ΔE, of the various molecular conformations relative to the most stable conformation calculated using the INDO approximation, the mean equilibrium dipole moment, $\mu_{(eq)}$, calculated on the assumption that the two conformers are in equilibrium, and the dipole moment value, $\mu_{(fr)}$, which would result from a free rotation of the acetyl group about the C_1—C_2 bond (see Figs. 1 and 2). The mean equilibrium dipole moment was calculated using the expression shown in eq. 2 (5). Here $\mu_{(cis)}$ and $\mu_{(trans)}$ is

$$[2] \qquad \frac{\mu^2_{(trans)} + \mu^2_{(cis)}\, e^{(\Delta E/-RT)}}{1 + e^{(\Delta E/-RT)}} = \mu_{(eq)}^2$$

the dipole moment of the *O-cis* and *O-trans* conformer respectively estimated from group moments. The latter were obtained from the experimental dipole moments of acetophenone, fluorobenzene, and trifluoromethylbenzene respectively. The angle between the dipole moment and the C_1—C_2 bond direction in

Can. J. Chem. Downloaded from www.nrcresearchpress.com by 210.87.254.42 on 09/05/12
For personal use only.

TABLE 3. Trifluoromethylacetophenones: Experimental and calculated dipole moments of *o*-, *m*-, and *p*-trifluoromethylacetophenones and the energy difference, ΔE, between different conformers

Compound or conformer	μ(INDO) D	μ(Group) D	ΔE (kcal)	μ(eq) D	μ(fr) D	μ_{exp} (C_6H_6) D	μ_{exp} (CCl_4) D
ortho (*O-cis*)	5.51	5.49	1.39				
θ = 45°	5.22	5.22	1.16				
θ = 90°	4.45	4.48	0.00				
θ = 97.5°	4.29	4.34	0.16			4.18	4.07
θ = 105°	4.12	4.18	1.13				
θ = 112.5°	3.96	4.03	4.15				
θ = 135°	3.57	3.61	23.79				
ortho (*O-trans*)	3.12	3.17	309.37				
meta (*O-cis*)	4.72	4.52	0.14	3.03	3.23	3.01	3.04
meta (*O-trans*)*	0.39	0.63					
para	2.52	2.36			2.36	2.50	2.49

*The more stable conformer.

TABLE 4. Experimental and calculated dipole moments of fluorobenzene, acetophenone, and trifluoromethylbenzene

Compound	μ (INDO) D	μ_{exp} (C_6H_6) D
Fluorobenzene	1.73	1.42
	1.67*	1.39–1.54†
Acetophenone	2.93	2.96
		2.8 –2.99†
Trifluoromethylbenzene	2.69	2.55
	2.73*	2.54–2.60†

*Reference 11.
†Reference 12.

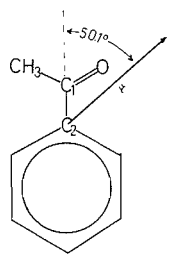

FIG. 1. Direction of the electric dipole moment of acetophenone as calculated by INDO.

acetophenone was computed using the INDO approximation. The angle turned out to be 50.1°. This value is intermediate between the values for this angle given by Smyth (6) and Minkin *et al.* (7); *viz.* 57° and 48° respectively. The values of $\mu_{(fr)}$ resulting from a free rotation of the acetyl group about the C_1—C_2 bond direction were calculated after the method of Fuchs (8).

Fluoroacetophenones

From the entries in Table 2 it is apparent that

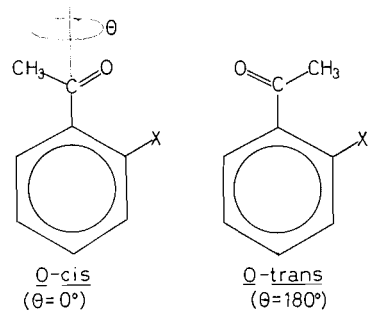

FIG. 2. *O-cis* and *O-trans* conformation of substituted acetophenones. X = F for fluoroacetophenones and X = CF_3 for trifluoromethylacetophenone.

in the case of *o*-fluoroacetophenone the *O-trans* conformer is the more stable conformer. Moreover, it would appear that the energy barrier to free rotation of the acetyl group is at least 1.35 kcal/mol and is high enough to prevent the free rotation of the acetyl group; *o*-fluoroacetophenone exists as an equilibrium mixture of two conformers in the ratio of 9/1 with the *O-trans* conformer predominating. In the case of *m*-fluoroacetophenone the *cis–trans* energy barrier is at least 0.13 kcal/mol and is evidently not high enough to prevent a free rotation of the acetyl group. Thus the dipole moment calculated assuming free rotation, 2.84 D, is in good agreement with the experimental dipole moment measured in dilute benzene solution, *viz.* 2.86 D. It should be noted in this connection that the group moments used in the calculation of $\mu_{(fr)}$ were derived from measurements in benzene solution. These conclusions are not in harmony with the work of Miller *et al.* (9) who investigated

Can. J. Chem. Downloaded from www.nrcresearchpress.com by 210.87.254.42 on 09/05/12
For personal use only.

Can. J. Chem. Downloaded from www.nrcresearchpress.com by 210.87.254.42 on 09/05/12
For personal use only.

the vapor-phase far i.r. spectra of *o*-, *m*-, and *p*-fluoroacetophenone. These workers found that the *cis–trans* energy barrier for *m*-fluoroacetophenone was >3.5 kcal/mol and was higher than the *cis–trans* energy barrier for *o*-fluoroacetophenone, *viz.* ~3.0 kcal/mol. On the other hand our conclusions are in complete agreement with findings of Smith *et al.* (10) who carried out an n.m.r. study of a number of substituted acetophenones, and with the results of our own n.m.r. studies on *o*-, *m*-, and *p*-trifluoromethylacetophenone.[3] Smith *et al.* found that the coupling constant between the methyl and fluorine in *o*-fluoroacetophenone was unusually large (5.1 Hz at room temperature, we found a value of 4.72 ± 0.02 Hz) and exhibited a marked temperature dependence, decreasing with increase in temperature. Moreover, neither the above authors, nor we, could detect any methyl–fluorine coupling in the case of *m*- and *p*-fluoroacetophenone. Smith *et al.* concluded that the large coupling in the case of *o*-fluoroacetophenone resulted from a "through space" coupling mechanism; *i.e.*, the molecule existed in solution mainly in the *O-trans* conformation. Another remarkable feature of Table 2 is the virtually quantitative agreement between the INDO computed dipole moments and the experimental dipole moments in all those cases in which the molecule can exist in one conformation only in solution.

Trifluoromethylacetophenones

From Table 3 it is apparent that the most stable conformation of *o*-trifluoromethylacetophenone is the one in which the acetyl group is at right angles to the plane of the benzene ring. The INDO calculated dipole moment for the 90°-out-of-the-plane conformation is in remarkably good agreement with the experimentally measured dipole moment. The INDO calculations also suggest that the acetyl group executes a rocking motion of some 20° of arc about the 90°-out-of-the-plane position. The above conclusions are supported by the n.m.r. studies of Smith *et al.* (10) who in contrast to *o*-fluoroacetophenone did not detect any methyl-fluorine coupling in *o*-trifluoromethylacetophenone.[4]

In the case of *m*-trifluoromethylacetophenone it is evident that the molecule in solution exists in two conformations of roughly equal proportion and/or there is free rotation of the acetyl group.

Again we note the remarkable agreement between the INDO calculated dipole moment and the experimental dipole moment in the case of *p*-trifluoromethylacetophenone. In this connection it should be noted that the INDO calculations presumably yield gas-phase dipole moment values. Now it is well known that the solution dipole moment values may differ from the gas-phase values by as much as 10% due to the so-called solvent effect (6, 7).

The financial assistance of the National Research Council of Canada and of the Faculty of Graduate Studies and Research of the University of Manitoba are very much appreciated. We thank Dr. T. Schaefer for helpful discussions and the use of the n.m.r. spectrometer.

1. E. Bock and E. Tomchuk. Can. J. Chem. **50**, 2890 (1972).
2. D. L. Beveridge and J. A. Pople. Approximate molelcular orbital theory. McGraw-Hill Book Co., New York, N.Y. 1970.
3. E. Bock and E. F. Dojack. Can. J. Chem. **45**, 1097 (1967).
4. J. W. Smith. Trans. Faraday Soc. **46**, 394 (1950).
5. S. I. Mizushima. Structure of molecules and internal rotation. Academic Press Inc., New York, N.Y. 1954. p. 34.
6. C. P. Smyth. Dielectric behavior and structure. McGraw-Hill Book Co. Inc., New York, N.Y. 1955. p. 253.
7. V. I. Minkin, O. A. Osipov, and Y. A. Zhdanov. Dipole moments in organic chemistry. Plenum Press, New York-London. 1970. p. 91.
8. O. Fuchs. Z. Phys. Chem. B**14**, 399 (1931).
9. F. A. Miller, W. G. Fateley, and R. E. Witkowski. Spectrochim. Acta, **23A**, 891 (1967).
10. W. B. Smith, D. L. Deavenport, and A. M. Ihrig. J. Am. Chem. Soc. **94**, 1959 (1972).
11. J. E. Bloor and D. L. Breen. J. Phys. Chem. **72**, 716 (1968).
12. A. L. McClellan. Tables of experimental dipole moments. W. H. Freeman and Co., San Francisco and London. 1963.

[3]We were anticipated in publishing our results by several weeks by the paper of Smith *et al.* (10).

[4]We found a small coupling of ~0.4 Hz at room temperature between the methyl protons and the fluorines of the trifluoromethyl group.

Synthesis of Tritium Labelled [8-Arginine]-vasopressin[1]

H. Hutch Holton,[2] Luis A. Branda,[3] and Barbara M. Ferrier
Department of Biochemistry, Division of Health Sciences, McMaster University, Hamilton, Ontario
Received January 2, 1973

Ring tritiated phenylalanine has been incorporated into [8-arginine]-vasopressin synthesized by the solid phase method. The peptide produced has levels of biological activities in agreement with those of the highly purified natural hormone.

La phénylalanine tritiée sur le cycle a été incorporée dans l'(Arg-8) vasopressine, synthétisée selon la méthode de la phase solide. Le peptide obtenu possède des degrés d'activité biologique comparables à ceux de l'hormone naturelle hautement purifiée. [Traduit par le journal]

Can. J. Chem., **51**, 1910 (1973)

Can. J. Chem. Downloaded from www.nrcresearchpress.com by 210.87.254.6 on 09/05/12
For personal use only.

[8-Arginine]-vasopressin, the antidiuretic hormone of man and most mammals, acts on the kidney. This organ in rats has been shown to bind [8-arginine]-vasopressin (1) and it was suggested that the mechanism of the hormone's action involved an exchange between the peptide disulfide and a membrane thiol group. It is now apparent that this is not an exclusive mechanism of action, since synthetic analogs of [8-arginine]-vasopressin which lack a disulfide group have been shown to retain biological activity (2).

There is considerable evidence that polypeptide hormones bind to sites on the outer surface of their target cell membranes (3), and in order to study the binding properties of [8-arginine]-vasopressin to kidney cell membranes we have found it convenient to synthesize radioactive [8-arginine]-vasopressin by incorporating ring-tritiated phenylalanine in position 3 of the peptide chain (Fig. 1). Tritium, rather than radioactive iodine was chosen as the radioisotope, since it was thought that iodination of [8-arginine]-vasopressin could result in a derivative with significantly altered binding properties. This opinion has recently received support by the demonstration that radio-iodinated oxytocin shows no specific binding to kidney or uterine tissue (4).

The solid phase method of synthesis of [8-arginine]-vasopressin described by Meienhofer and coworkers (5) was used for the synthesis of the required protected nonapeptide precursor to the hormone (Fig. 2). Some modifications were

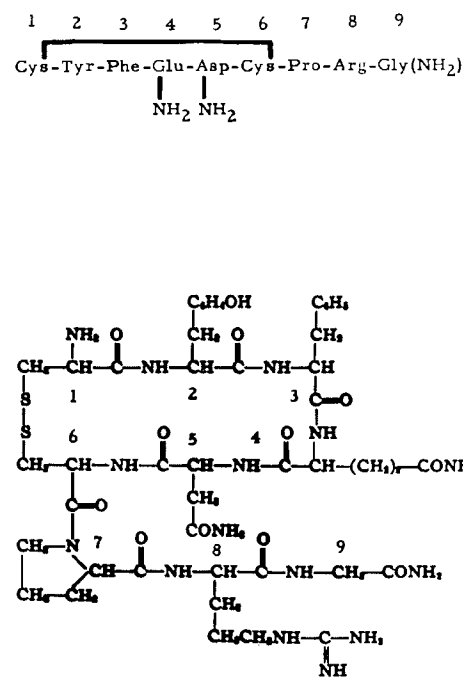

FIG. 1. Structure of [8-arginine]-vasopressin. Numbers indicate amino acid residues.

made in the preparation of the protected amino acids used in the synthesis. The protected nonapeptide derivative was purified by exclusion chromatography on Sephadex LH-20 in *N,N*-dimethylformamide. The protecting groups were removed from the peptide derivative by sodium in liquid ammonia solution and the resultant dithiol compound was oxidatively cyclized using hydrogen peroxide. The [8-arginine]-vasopressin so formed was isolated by sequential exclusion chromatography on Sephadex G-15 in 50% acetic acid, then on Sephadex G-25 in 0.2 *N*

[1]This work was supported by M.R.C. grant MA-3502 to Luis A. Branda.
[2]Medical Research Council Fellow.
[3]Medical Research Council Associate and author to whom correspondence should be addressed.

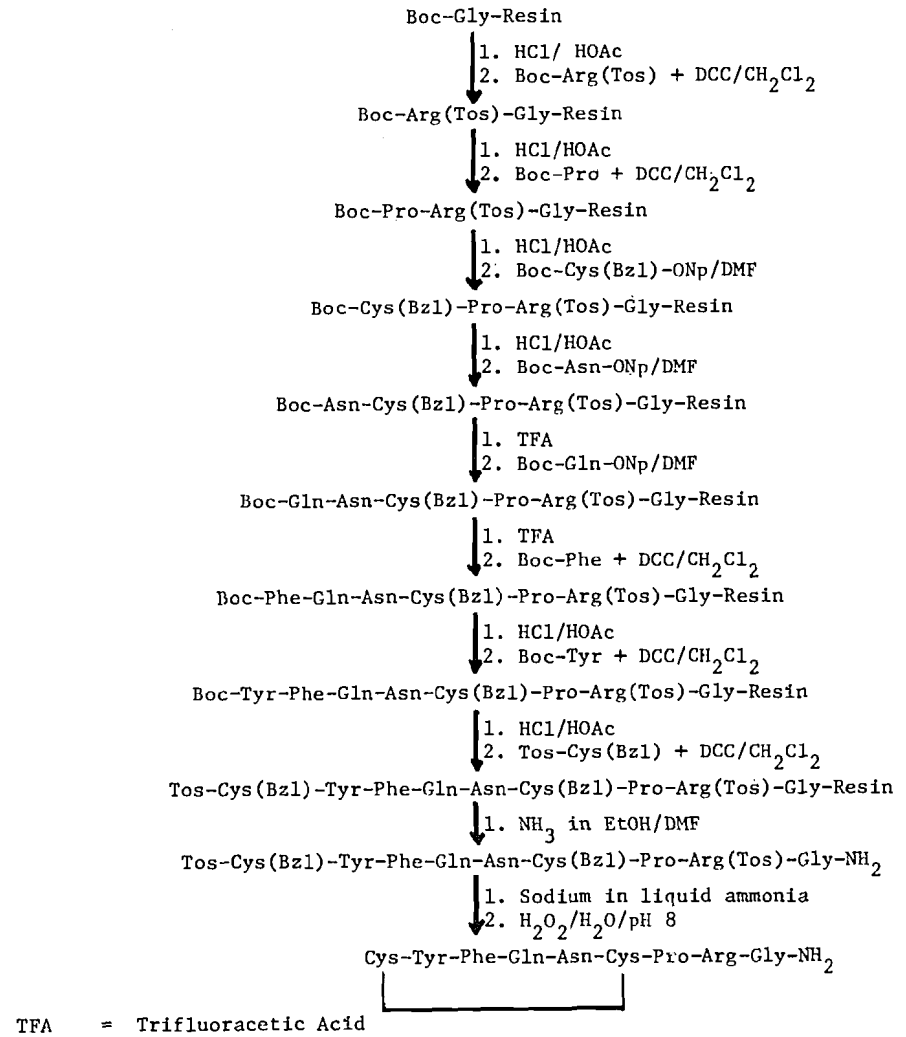

TFA = Trifluoracetic Acid

Boc = tertiary-butyloxycarbonyl protecting group

Resin = Merrifield Resin for solid phase peptide synthesis

HOAc = Acetic Acid

DCC = N,N¹-dicyclohexylcarbodiimide

DMF = N,N-dimethylformamide

EtOH = Ethyl Alcohol

ONp = para-Nitrophenyl ester

FIG. 2. Diagram showing the steps in the solid phase synthesis of [8-arginine]-vasopressin.

Can. J. Chem. Downloaded from www.nrcresearchpress.com by 210.87.254.6 on 09/05/12
For personal use only.

Can. J. Chem. Downloaded from www.nrcresearchpress.com by 210.87.254.6 on 09/05/12
For personal use only.

acetic acid. This yielded 11% (based on the starting glycine content) of the peptide, which was found to have 470 ± 50 units per mg of rat antidiuretic activity (6), 24 ± 6 units per mg of "milk-ejecting-like" activity measured on an isolated strip of lactating mouse mammary gland (7) and 2.0×10^6 c.p.m. per mg in dioxane-based scintillation fluid. Amino acid analysis was in agreement with the structure of [8-arginine]-vasopressin.

Before the radioactive amino acid was incorporated, a portion of the protected hexapeptidyl-resin was used to complete the synthesis of cold [8-arginine]-vasopressin. This allowed more accurate estimation of the amount of radioactive amino acid needed, and the yield of radioactive hormone which could be expected. Position 3 was chosen as the one to have the radioactive residue since it was the last position to be filled in a protected heptapeptide intermediate to several projected radioactive analogs of [8-arginine]-vasopressin with modifications in the amino acid residues at positions 1 and 2.

The radioactive [8-arginine]-vasopressin prepared is currently being used in studies on its binding to isolated kidney cell membranes.

Experimental

Materials and Methods

The physical properties of the protected amino acids prepared correspond with those reported by Bayer *et al.* (8). All the protected amino acids were homogenous to t.l.c. (Silica Gel G) in the solvent systems, acetone – acetic acid, 98:2, and chloroform–methanol – acetic acid, 85:10:5. The Merrifield resin was obtained from Schwartz/Mann (Orangeburg, New York), and prepared with a substitution level of 1.0 mmol *tert*-butyloxycarbonyl-glycine (Boc–glycine) per gram of resin according to the procedure of Merrifield (9). Ring tritiated phenylalanine was obtained from Schwartz–Mann (Picker Nuclear Canada, Downsview, Ontario).

Exclusion chromatography was carried out in 1.5 × 90 cm columns (Pharmacia Canada Ltd.), monitored by u.v. absorption at 280 nm using a Beckman DB-GT recording spectrophotometer with a Beckman flow cell. A flow rate of 5 ml/h was used and 1 ml fractions were collected. Peptide materials were collected by pooling fractions corresponding to absorption peaks, concentrating *in vacuo*, and lyophilizing. Scintillation counting was carried out in a dioxane-based cocktail (1000 ml dioxane, 100 g naphthalene, 5 g 2,5-diphenyloxazole) in a Beckman LS-233 scintillation counter. All solvents and reagents were the highest purity commercially available and were used without further purification. Amino acid analyses were carried out using a Beckman 120C amino acid analyzer.

All couplings and washings in the synthesis of the peptide were carried out according to the procedure of Meienhofer *et al.* (5).

Assays for antidiuretic activity were performed on anesthetized, hydrated Sprague–Dawley male rats according to the procedure of Sturmer (6). Milk-ejecting like activity was measured using isolated strips of lactating mouse mammary gland according to the procedure of Fielitz *et al.* (7).

tert-Butyloxycarbonyl Amino Acids

The N^{α}-*tert*-butyloxycarbonyl (Boc) derivatives of glycine, proline, glutamine, and phenylalanine were prepared according to the procedure of Schwyzer *et al.* (10) with the modification that reaction times were extended from 20 to 48 h, the first 24 h at 40–50 °C, the remaining 24 h at 25 °C.

The N^{α}-Boc derivatives of cysteine, asparagine, and tyrosine were prepared according to the same procedure with the modifications that a dioxane–water ratio of 1:1 rather than 2:1 was employed and reaction times were extended to a minimum of 48 h at 40–50 °C.

N^{α}-Boc-arginine

Arginine (3.5 g, 20 mmol) was dissolved in dioxane–water, 1:1, (100 ml) and magnesium oxide (1.6 g, 40 mmol) was added. Boc-azide was then added dropwise (4.3 g, 30 mmol) with stirring. The resultant mixture was stirred 24 h at 45 °C. The suspension was filtered, washed twice with water (50 ml), and extracted three times with diethyl ether (50 ml portions). The aqueous phase was cooled to 0° and the p*H* was adjusted to 2 with 2 *N* hydrochloric acid. The solution was warmed to 25° and saturated with sodium chloride. This produced a fine white precipitate which was recovered by decantation (from excess sodium chloride) and filtration. After drying for 24 h over phosphorous pentoxide *in vacuo*, the product (6.16 g, 99% yield based on Boc-arginine·HCl) melted at 113–115 °C, and was homogenous to t.l.c. on silica gel G (R_f 0.70 using butanol – acetic acid – water, 4:1:5). This material was used without further purification.

N^{α}-Boc-N^{G}-tosyl-arginine

N^{α}-Boc-arginine·HCl (3.12 g, 10 mmol) was dissolved in acetone (50 ml) and water (15 ml), the solution was cooled to 0 °C, the p*H* adjusted to 12.5 with 4 *N* sodium hydroxide, and the suspension was stirred until homogenous (1 h). Tosyl chloride (4.75 g, 25 mmol) in acetone (10 ml) was added dropwise with stirring and sodium hydroxide (4 *N*) was added simultaneously to maintain the p*H* in the range 12.0–12.5. Once the addition was complete the solution was stirred at 0 °C for an additional 3 h, maintaining p*H* 12.5. The p*H* was then adjusted to 7.0 with 1 *N* hydrochloric acid at 0 °C, the acetone was removed *in vacuo*, the solution volume was doubled by the addition of water and the solution was extracted three times with diethyl ether (25 ml portions). The aqueous layer was cooled to 0 °C and the p*H* adjusted to 3.0 with 6 *N* hydrochloric acid. The resultant emulsion was saturated with sodium chloride and extracted 3 times with ethyl acetate (50 ml portions). The organic phase was washed three times with 0.1 *N* hydrochloric acid (15 ml portions), then with water (25 ml portions) until neutral, dried (Na_2SO_4), filtered, and concentrated *in vacuo* to yield 2.8 g (60%) of a white glassy material exhibiting a softening point in the range 95–100 °C. T.l.c. (Silica Gel G, acetone – acetic acid, 98:2) showed the

Can. J. Chem. Downloaded from www.nrcresearchpress.com by 210.87.254.6 on 09/05/12
For personal use only.

majority of the material to have an R_f of 0.42 with minor components at R_f 0.1 and 0.8. These latter components were removable by extraction with diethyl ether and then 0.1 *N* hydrochloric acid. The optical rotation of the purified material, $[\alpha]_D^{25}$ −3.3° (*c* = 4, DMF) corresponds to that reported by Ramachandran and Li (11).

Tritiated N$^{\alpha}$-tert-Butyloxycarbonyl-phenylalanine

A mixture of ring tritiated L-phenylalanine (17 000 mCi/mmol, 2 mCi total) and unlabelled phenylalanine (0.42 mmol) was protected according to the method of Schwyzer *et al.* (10). The resultant ^{3}H-Boc-phenylalanine was found to be greater than 99% pure by radiochromatography on silica gel G using acetone – acetic acid, 98:2.

p-Nitrophenyl Esters

The *p*-nitrophenyl ester of N$^{\alpha}$-Boc-*S*-Bzl-cysteine was prepared according to the procedure of Beyerman *et al.* (12). N$^{\alpha}$-Boc-asparagine *p*-nitrophenyl ester was prepared according to the procedure of Schröder and Klieger (13). N$^{\alpha}$-Boc-glutamine *p*-nitrophenyl ester was prepared according to the procedure of Bodanszky and du Vigneaud (14).

N$^{\alpha}$-Tosyl-S-Bzl-cysteine

N$^{\alpha}$-Tosyl-*S*-Bzl-cysteine was prepared from *S*-Bzl-cysteine (15) according to the procedure of du Vigneaud *et al.* (16).

N$^{\alpha}$-tert-Butyloxycarbonyl-L-glutaminyl-L-asparaginyl-S-benzyl-L-cysteinyl-L-prolyl-N^{G}-tosyl-L-argininyl-glycyl-resin

This Boc-hexapeptide-resin was prepared according to the stepwise procedure of Meienhofer *et al.* (5) from 1.25 g Boc-glycyl-resin (1.25 mmol Boc-glycine) which yielded 2.12 g (88%).

N$^{\alpha}$-Tosyl-S-benzyl-L-cysteinyl-L-tyrosyl-[^{3}H]-L-phenylalanyl-L-glutaminyl-L-asparaginyl-S-benzyl-L-cysteinyl-L-prolyl-N^{G}-tosyl-L-arginylglycyl-resin

This material was prepared from the Boc-hexapeptide resin (0.37 g, 0.21 mmol based on starting Boc-glycine content) by the stepwise procedure according to Meienhofer *et al.* (5), with the exception that ^{3}H-Boc-phenylalanine was incorporated using only a two-fold excess (0.42 mmol). The protected nonapeptide-resin was recovered by filtration after thorough washing with ethanol and ether, which yielded 0.43 g (81%) material.

[8-Arginine]-vasopressin

The protected nonapeptide, *S*-benzyl-N$^{\alpha}$-tosyl-L-cysteinyl-L-tyrosyl-[^{3}H]-phenylalanyl-L-glutaminyl-L-asparaginyl-*S*-benzyl-L-cysteinyl-L-prolyl-N^{G}-tosyl-L-arginyl-glycinamide was separated from the resin by ammonolysis of the peptide resin according to the procedure of Meienhofer *et al.* (5). The oil obtained was purified by chromatography on a column of Sephadex LH-20 (0.9 × 55 cm) in dimethylformamide. The absorbance reading at 280 nm was plotted against the elution volume and the peptide material in the fractions corresponding to the main peak of absorbance (elution volume: 32 ml) was recovered by evaporation *in vacuo*. The oil so obtained was converted to a solid by trituration with ethanol and drying *in vacuo*. This yielded 118 mg (32%) pale yellow powder, optical rotation $[\alpha]_D^{22}$ −26.3° (*c* = 1, DMF).

The solid protected nonapeptide derivative (58 mg) was dissolved in liquid ammonia (100 ml) which had been distilled from sodium. Sodium was added in small quantities to the boiling ammonia solution until a permanent blue color remained for 30 s. The blue color was removed by addition of glacial acetic acid (2 drops) and the ammonia was removed *in vacuo*. The solid product was dissolved in 0.2 *N* acetic acid (150 ml) and the p*H* of the solution adjusted to 8 with concentrated ammonium hydroxide solution, and then hydrogen peroxide solution (30%, 0.5 ml) was added. The solution was stirred for 5 min, then the p*H* was adjusted to 5 with glacial acetic acid, the volume reduced to 50 ml by evaporation *in vacuo*, and evaporation was completed by lyophilization. The resultant solid product was dissolved in 50% acetic acid (4 ml) and purified by chromatography on a column of Sephadex G-15 (1.5 × 90 cm) in 50% acetic acid. The eluent was monitored both by measurement of its u.v. absorption (at 280 nm) and by liquid scintillation counting. A main peak (elution volume: 60 ml) followed by two minor peaks was detected by u.v. absorption measurement while only the main peak was detected by liquid scintillation counting. The fractions corresponding to the leading half and the trailing half of the main peak were pooled and concentrated *in vacuo* to volumes of about 5 ml each, diluted to 50 ml with water and lyophilized to dryness. The material from the trailing half of the main peak was dissolved in 0.2 *N* acetic acid (2.0 ml) and purified by chromatography on a column of Sephadex G-25 superfine (1.5 × 90 cm) in 0.2 *N* acetic acid. The eluent was monitored by u.v. absorption measurement and liquid scintillation counting. The leading and trailing edges of the single peak were discarded and the center portion (elution volume: 123 ml) was concentrated *in vacuo* to a volume of 25 ml and lyophilized to yield 14 mg (11% based on starting glycine) of a solid, white, fluffy material, optical rotation $[\alpha]_D^{22}$ −26.6° (*c* = 0.20, 1 *N* HOAc). The material possessed 470 ± 50 units/mg rat antidiuretic activity, 24 ± 6 units/mg milk-ejecting like activity and 2.0 × 10^6 c.p.m./mg. On re-chromatography on a column of Bio-Rex 70 (0.9 × 60 cm) in 0.5 *M* ammonium acetate, p*H* 6.4, the material was eluted as a single component (elution volume: 20 ml) when monitored by u.v. absorption, scintillation counting and biological assay (milk-ejecting like activity). No change in biological activity and specific radioactivity of the recovered material was observed.

1. C. T. O. Fong, L. Silver, D. R. Christman, and I. L. Schwartz. Proc. Natl. Acad. Sci. **46**, 1273 (1960).
2. J. Rudinger and K. Jošt. Experientia, **20**, 570 (1964).
3. (*a*) R. Levine. Fed. Proc. **24**, 1071 (1965). (*b*) P. Cuatrecasas. Diabetes, **21**, supp. 2, 396 (1972).
4. E. E. Thompson, P. Freychet, and J. Roth. Endocrinology, **91**, 1199 (1972).
5. J. Meienhofer, A. Trzeciak, R. T. Havran, and R. Walter. J. Am. Chem. Soc. **92**, 7199 (1970).
6. E. Sturmer. *In* Handbook of experimental pharmakologie. Vol. 23. *Edited by* B. Berde. Springer-Verlag, Berlin. 1968. pp. 174–179.
7. C. Fielitz, R. Roca, A. Mattei, S. Melander, E. Garófalo, M. N. Gioia de Coch, and J. A. Coch. Proc. Soc. Exp. Biol. Med. **133**, 1155 (1970).

8. E. BAYER, G. JUNG, and H. HAGENMAIER. Tetrahedron, **24**, 4853 (1968).
9. R. B. MERRIFIELD. J. Am. Chem. Soc. **86**, 304 (1964).
10. R. SCHWYZER, P. SIEBER, and H. KAPPELER. Helv. Chim. Acta, **42**, 2622 (1959).
11. J. RAMACHANDRAN and C. H. LI. J. Org. Chem. **27**, 4006 (1962).
12. H. C. BEYERMAN, C. A. M. BOERS-BOONEKAMP, and H. MAASEN VAN DEN BRINK-ZIMMERMANNOVA. Rec. Tran. Chim. **87**, 257 (1968).
13. E. SCHRÖDER and E. KLIEGER. Ann. Chem. **673**, 208 (1964).
14. M. BODANSZKY and V. DU VIGNEAUD. J. Am. Chem. Soc. **81**, 5688 (1959).
15. J. L. WOOD and V. DU VIGNEAUD. J. Biol. Chem. **130**, 109 (1939).
16. V. DU VIGNEAUD, M. F. BARTLETT, and A. JOHL. J. Am. Chem. Soc. **79**, 5572 (1959).

Can. J. Chem. Downloaded from www.nrcresearchpress.com by 210.87.254.6 on 09/05/12
For personal use only.

N-Methylamino Acids in Peptide Synthesis. II. A New Synthesis of *N*-Benzyloxycarbonyl,*N*-Methylamino Acids[1]

JOHN R. MCDERMOTT AND N. LEO BENOITON

Department of Biochemistry, University of Ottawa, Ottawa, Canada K1N 6N5

Received December 19, 1972

Reaction of *N*-benzyloxycarbonyl derivatives of aliphatic amino acids, and threonine, aspartic, and glutamic acids whose side-chains were protected with the *t*-butyl group, gave the corresponding *N*-methylamino acid derivatives in good yields. The methionine derivative could be obtained by using only one mol of methyl iodide. Derivatives of threonine, and aspartic and glutamic acids whose side-chains were not protected could not be methylated. Analysis of the crude products of methylation in three cases showed that they contained 0–1% of racemized material.

La réaction des dérivés *N*-benzyloxycarbonyle d'acides aminés aliphatiques, de la thréonine, et des acides aspartique et glutamique dont les chaînes latérales furent bloquées avec le groupe *t*-butyle, a conduit aux dérivés *N*-méthylés correspondants des acides aminés avec d'excellents rendements. Le dérivé de la méthionine a pu être obtenu en utilisant seulement une mole d'iodure de méthyle. Les dérivés de la thréonine et des acides aspartique et glutamique dont les chaînes latérales ne sont pas protégées, n'ont pu être méthylés. L'analyse des produits bruts de la méthylation a montré que dans trois cas, ceux-ci contenaient de 0 à 1% de produits racémisés. [Traduit par le journal]

Can. J. Chem., **51**, 1915 (1973)

The methylation of various *N*-protected amino acids using sodium hydride – methyl iodide in tetrahydrofuran (THF)–dimethylformamide (10:1) under reflux gives the *N*-methylated, methyl ester (1). Similar products have been obtained using silver oxide – methyl iodide in dimethylformamide at room temperature (2). Other methods of *N*-methylation (3–5) used for the permethylation of peptides for sequence analysis by mass spectrometry invariably give methyl esters of the carboxyl functions.

In order to obtain a derivative suitable for peptide synthesis by this approach, it is necessary either to saponify the methyl ester (1, 2) or to remove the amino protecting group (1). It has been shown in this laboratory that saponification of methyl esters of *N*-benzyloxycarbonyl,*N*-methylamino acids or peptides can cause racemization (6). For example, saponification of Z-MeIle-OMe[2] gave 12% of the *allo*-isomer, and saponification of Z-Ala-MeLeu-OMe gave 11% of the L,D-isomer. To circumvent this problem, the methylation step should not esterify the carboxyl group.

In a continuing investigation of the conditions for *N*-methylation, it was found that *N*-benzyloxycarbonylamino acids could be selectively *N*-methylated using sodium hydride (3 mol) and methyl iodide (8 mol) in neat THF at room temperature, without ester formation (8).[3] This observation is supported by the fact that the sodium salt of Z-Ala was esterified only very slowly under these conditions (33% ester formation in 5 days). *N*-Methylation is virtually complete in 24 h; for the sterically hindered Z-*a*lle, only 0.7% of the unreacted amino acid was detected on analysis of the crude product of methylation.

We have prepared several *N*-benzyloxycarbonyl,*N*-methylamino acids by this method. The properties of the crystalline derivatives obtained are given in Table 1. Z-MeAsp and Z-MeGlu were obtained by methylation of the ω-*t*-butyl esters followed by treatment with trifluoroacetic acid since it was found that Z-Asp and Z-Glu were completely resistant to methylation (the reaction was incomplete even

[1]Supported by a grant from the Medical Research Council of Canada. N.L.B. is an Associate of the M.R.C.C., J.R.M. was a Fellow of the M.R.C.C. For the first paper in this series, see ref. 1*b*

[2]The abbreviations for the amino-acid and peptide derivatives are those recommended by the IUPAC–IUB Commission on Biochemical Nomenclature (7). The amino-acid symbols represent the L-isomer.

[3]It was found, in addition, that methylation of Z-Tyr or Z-Tyr(Z) under these conditions gave Z-MeTyr(Me), and that MeTyr could be obtained by methylation of Z-Tyr(Bzl) followed by hydrogenation (8*a*).

Can. J. Chem. Downloaded from www.nrcresearchpress.com by 210.87.254.40 on 09/05/12
For personal use only.

TABLE 1. Properties of *N*-benzyloxycarbonyl,*N*-methylamino acids*

Amino acid	Yield (%)	M.p. (°C)	$[\alpha]_D^{27}$† (°)	Analysis						
				Formula	Calculated C	Calculated H	Calculated N	Found C	Found H	Found N
Leu‡	77	73–74	−23.0	$C_{15}H_{21}NO_4$	64.5	7.6	5.0	64.5	7.5	5.3
Val§	90	68–69	−84.8	$C_{14}H_{19}NO_4$	63.4	7.2	5.3	63.3	7.0	5.4
Ile‖	83	55–56	−68.1	$C_{15}H_{21}NO_5$	64.5	7.6	5.0	64.7	7.7	5.2
D-*a*Ile¶	80	86–88	+68.0	$C_{15}H_{21}NO_5$	64.5	7.6	5.0	64.6	7.9	5.3
Asp	59	127–129	−36.6	$C_{13}H_{15}NO_6$	55.5	5.4	5.0	55.9	5.4	4.9
Glu	43	79–80	−25.7	$C_{14}H_{17}NO_6$	56.9	5.8	4.7	56.7	5.5	4.9

*Compounds crystallized by trituration with light petroleum, and recrystallized from ether – light petroleum; Z-MeAsp, crystallized from water and then ether – light petroleum; Z-MeGlu, crystallized twice from water.
†*c*, 1 in ethanol.
‡Literature m.p. 73–74°, $[\alpha]_D^{25}$ −26.0° (*c*, 2 in dimethylformamide) (1*b*).
§Literature m.p. 69–70°, $[\alpha]_D^{24}$ −85.8° (9).
‖Literature m.p. 63–64°, $[\alpha]_D^{26}$ −72.4° (10). Analysis of a sample, deprotected by hydrogenation in 80% aqueous acetic acid before crystallization, showed a 1.1% content of MeaIle.
¶Analysis of a sample as above showed no MeIle and a 0.7% content of *a*Ile.

in dimethylformamide). The products obtained from the di-*t*-butyl esters were also pure, but they had lower optical rotations, indicating that partial racemization had occurred. We suggest that the α-carboxyl group when ionized provides some protection against racemization by preventing ionization at the α-carbon atom. Z-Asp(OMe)-OMe after methylation and saponification gave a product with an even lower rotation, probably due to racemization taking place during saponification (6).

Methylation of Z-Thr gave a mixture of *N*-methylated (~60%) and *O*-methylated (~25%) products, together with some unchanged starting material. Z-Thr(Bu^t), however, gave the oily *N*-methylated derivative in good yield, which on hydrogenation gave crystalline MeThr(Bu^t). Methylation of Z-Met gave a water-soluble product, probably the dimethylsulfonium iodide derivative. However, by restricting the amount of methyl iodide to 1 mol (11, 12) it was possible to methylate without sulfonium salt formation, giving Z-MeMet as an oil. Removal of the benzyloxycarbonyl group with hydrogen bromide in acetic acid gave a product containing 3.4% of methionine. Z-Trp gave on methylation the α-*N*,ω-*N*-dimethyl derivative as an oil.

Attempts to crystallize Z-MeAsp(OBu^t), Z-MeGlu(OBu^t), and Z-MeThr(Bu^t) as their dicyclohexylamine salts revealed that these were soluble in light petroleum. This property enabled the removal of small amounts of unreacted benzyloxycarbonylamino acid derivatives from the reaction products as the dicyclohexylamine salts which are insoluble in this solvent. Thus benzyloxycarbonylamino acids with suitably protected carboxylic acid and hydroxyl side-chains can also be *N*-methylated to give directly a derivative suitable for peptide synthesis.

A possible strategy for the synthesis of *N*-methylated peptides is methylation of the *N*-protected peptide (1*a*). The methylation of Z-Ala-Leu gave a 58% yield (by weight) of an oil, whose n.m.r. spectrum showed no peaks for the benzyl group. Formation of the hydantoin **1**

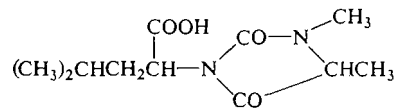

1

would explain this result. This could have arisen from prior ionization of the amide nitrogen followed by cyclization and loss of benzyl alcohol. That this had occurred is supported by the fact that Z-Ala-MeLeu on methylation yielded the *N*,*N*′-dimethyl derivative in good yield.

The method introduced in this laboratory (13) for determination of the optical purity of *N*-methylamino acids has been shown to be invalid, the error having been due to misassignment of the peaks of the amino acid analysis. It transpires that under the conditions described, the L-alanine *N*-carboxyanhydride not only reacts poorly with the *N*-methylleucine but also gives a dipeptide with an unusually low ninhydrin color yield (4.6% of that for alanine, 6.4%

Can. J. Chem. Downloaded from www.nrcresearchpress.com by 210.87.254.40 on 09/05/12
For personal use only.

Can. J. Chem. Downloaded from www.nrcresearchpress.com by 210.87.254.40 on 09/05/12
For personal use only.

of that for Ala-Leu) making it very difficult to identify the Ala-MeLeu peak among the by-product peaks. A direct test for racemization was possible, however, for the isoleucines. Analysis (after hydrogenation) of the crude products of methylation indicated that Z-MeIle and Z-D-Me*a*Ile contained, respectively, 1.1 and 0.0% of the diastereomer. In an indirect racemization test, *N*-methylleucine from the room-temperature methylation was converted to the benzyl ester *p*-toluenesulfonate (14) and the crude ester was coupled to Z-Ala by the mixed-anhydride method. The neutral product of the coupling was hydrogenated and the resulting dipeptide shown to contain 0.6% of the L,D-diastereomer.[4] Using the same method, it was shown that *N*-methylleucine, prepared by the saponification and subsequent hydrogenation of Z-MeLeu-OMe (1*b*) contained 9.6% of the D-isomer. *N*-Methylthreonine obtained from the crude *t*-butyl derivative had, before recrystallization, an optical rotation close to that reported in the literature. Also, crude MeThr(Bu^t) was homogeneous on t.l.c. and amino-acid analysis, indicating that little racemization had occurred.

It might be expected that amino acids with alkyl side-chains would be less prone to racemize during methylation than amino acids with electron-withdrawing side-chains. The optical integrity of products obtained by the methylation of amino acids of the latter type remains to be established by an unambiguous method.

In view of the racemization occurring during the saponification of *N*-benzyloxycarbonyl,*N*-methylamino-acid esters (6), this method of room temperature methylation should have wide applicability for the preparation of *N*-benzyloxycarbonyl,*N*-methylamino-acid derivatives for peptide synthesis.

Experimental

Materials and Methods

Sodium hydride was obtained from Fluka AG, Buchs, Switzerland, and J. T. Baker Chemical Company, Phillipsburg, New Jersey as 55 and 57% dispersions in oil respectively. Analysis showed the presence of 2–3% by weight of NaOH (15). Methyl iodide and tetrahydrofuran (THF) were products from Fisher Scientific Company, Pittsburgh, Pennsylvania. The THF was purified by distillation from KOH and then from sodium hydride. Amino acids were obtained from General Biochemicals, Chagrin Falls, Ohio, except for D-*allo*-isoleucine which was from ICN Nutritional Biochemicals, Cleveland, Ohio. Benzyloxycarbonylamino acids were prepared by the original procedure as described by Greenstein and Winitz (16). Z-Asp(OBu^t) and Z-Thr(Bu^t) were obtained as their dicyclohexylamine salts and were converted to the free acid using aqueous citric acid. Z-Glu(OBu^t) was obtained from Schwarz-Mann, Orangeburg, New York. Z-Asp-(OBu^t)-OBu^t and Z-Glu(OBu^t)-OBu^t were prepared by the isobutylene method of Anderson and Callahan (17). Z-Asp(OMe)-OMe was the neutral product isolated from the reaction of Z-Asp with diazomethane. Hydrogenations were done in the presence of 10% palladium-on-charcoal catalyst at atmospheric pressure. Light petroleum refers to the 30–60° fraction, from Fisher Scientific Co.

Optical rotations were measured with a Perkin–Elmer model 141 polarimeter using a 1-dm tube. Melting points were taken by the capillary method, and are uncorrected. Elemental analyses were done by Organic Microanalyses, Montreal, on the compounds dried under *vacuo* over P_2O_5. Amino-acid analyses were carried out with a Beckman model 120B amino-acid analyzer with the eluting buffer at half flow rate to allow detection of the *N*-methylamino acids (13).

Proton n.m.r. (Varian T-60) and i.r. (Unicam SP 200) analyses were used routinely to check the product of methylation, using the *N*-methyl singlet at τ 7.0 and the >*N*—H stretch and amide II bands at 3280 and 1520 cm^{-1}, respectively. All products had spectra which were consistent with the assigned structures.

General Methylation Procedure

N-Benzyloxycarbonylamino acid or *t*-butyl derivative (10 mmol) and methyl iodide (5 ml; 80 mmol) were dissolved in THF (30 ml) and the solution was cooled to 0 °C in a flask protected from moisture. Sodium hydride dispersion (1.32 g; 30 mmol) was added cautiously with gentle stirring. The suspension was stirred at room temperature for 24 h. Ethyl acetate (50 ml) was then added (to consume the sodium hydride formed from the excess sodium hydride), followed by water, dropwise, to destroy the excess sodium hydride. The solution was evaporated to dryness, and the oily residue partitioned between ether (30 ml) and water (100 ml). The ether layer was washed with aqueous $NaHCO_3$ (50 ml), and the combined aqueous extracts acidified to p*H* 2 with 5 *N* HCl (for *t*-butyl derivatives, aqueous citric acid was used to p*H* 3). The product was extracted into ethyl acetate (2 × 50 ml), the extract was washed with water (2 × 50 ml), 5% aqueous sodium thiosulfate (2 × 50 ml; to remove iodine), and water (50 ml), dried over $MgSO_4$ and evaporated to give a pale yellow oil.

Z-MeAsp and Z-MeGlu

Z-MeAsp(OBu^t) and Z-MeGlu(OBu^t) were obtained as oils from the corresponding *t*-butyl derivative by the general procedure. The oils were dissolved in ether – light petroleum (1:1), dicyclohexylamine (1 ml) was added, the solutions were left overnight at 0 °C, and the precipitates were filtered off. The filtrates were washed with 5% aqueous citric acid (2×) and water (4×), dried ($MgSO_4$), and evaporated. The purified Z-MeAsp(OBu^t) (86%) and Z-MeGlu(OBu^t) (70%) were left in trifluoroacetic acid (5 ml/g) for 1 h and the solutions were evaporated.

[4]The synthesis of reference compounds and the chromatographic data for the analysis of the various diastereomers will be described in a subsequent paper (6*b*).

Can. J. Chem. Downloaded from www.nrcresearchpress.com by 210.87.254.40 on 09/05/12
For personal use only.

MeThr(Bu^t)

Z-MeThr(Bu^t) (0.79 g; 90%) was obtained from Z-Thr(Bu^t) as described for the other *t*-butyl derivatives, including purification through the dicyclohexylamine salt, and was hydrogenated in 65% aqueous ethanol (15 ml) for 4 h. Evaporation of the solution yielded a crystalline product (100% yield) which gave a single peak on amino-acid analysis (long column, p*H* 3.28 buffer). A sample crystallized from water–acetone sublimed at 269–271°, had $[\alpha]_D^{27}$ −53.1° (*c*, 1 in H_2O), and gave only one spot on analysis by t.l.c. The MeThr(Bu^t) was converted to MeThr using trifluoroacetic acid at room temperature for 2 h. The solution was evaporated, the residue dissolved in 1 *N* HCl, and the solution evaporated again. The residue was dissolved in water (5 ml), the solution was stirred with Dowex 50 (H^+ form) resin, and the resin was filtered off and washed with water until the filtrate contained no chloride ions. The product was eluted from the resin with 10 *N* NH_4OH (100 ml), the solution evaporated and the crystalline residue dried over P_2O_5. The product, m.p. 228–236°, $[\alpha]_D^{26}$ −32.0° (*c*, 1 in H_2O), had m.p. 238–240° after recrystallization from methanol, lit. m.p. 244–246°, $[\alpha]_D^{20}$ −35.9° (*c*, 2.3 in H_2O) (18).

Methylation of Z-Asp(OBu^t)-OBu^t, Z-Glu(OBu^t)-OBu^t and Z-Asp(OMe)-OMe

Methylations were carried out by the usual procedure, using 1.5 mol of sodium hydride and 4 mol of methyl iodide. The neutral product was isolated in ether from the ether–water partition, the ether solution was dried ($MgSO_4$) and evaporated to give an oil. N.m.r. and i.r. analyses indicated that complete *N*-methylation had occurred in each case. Deprotection of the *t*-butyl derivatives with trifluoroacetic acid for 2 h gave Z-MeAsp (64% yield, recrystallized) with $[\alpha]_D^{27}$ −21.6° (*c*, 1 in EtOH) and Z-MeGlu (61% yield, recrystallized) with $[\alpha]_D^{27}$ −13.8° (*c*, 1 in EtOH). Saponification of Z-MeAsp-(OMe)-OMe (1.0 g) with 2 *N* NaOH (10 ml) in methanol (10 ml) for 2 h gave Z-MeAsp (0.43 g) with $[\alpha]_D^{26}$ −5.4° (*c*, 1 in EtOH).

Attempted Methylation of Z-Asp, Z-Glu, and Z-Thr

After methylation using 4.5 mol of sodium hydride and 12 mol of methyl iodide, n.m.r. and i.r. analyses of the acidic products indicated that no *N*-methylation of Z-Asp and Z-Glu had taken place. For Z-Thr, n.m.r. analysis showed the presence of *N*-methyl (τ 7.0) and *O*-methyl (τ 6.7) groups with integral values corresponding to 60% *N*-methyl and 25% *O*-methyl. I.r. analysis showed that some >*N*—H was still present.

Methylation of Z-Met

(*a*) When the general procedure was used, the product was lost during the isolation due to its solubility in water.

(*b*) Z-Met (1.34 g; 5 mmol), methyl iodide (0.31 ml; 5 mmol), and sodium hydride dispersion (0.60 g; 15 mmol) were stirred in THF for 18 h. The acidic product was isolated by the general procedure as a pale yellow oil (1.05 g; 71%). N.m.r. and i.r. analyses indicated virtually complete methylation. Analysis of a weighed sample, after deprotection with 2 *N* HBr in acetic acid for 2 h, showed that the sample contained about 3.4% of Z-Met.

Methylation of Z-Trp

N.m.r. analysis of the oily product showed singlets at τ 6.3 and 7.1 in a 1:1 ratio.

Methylation of Z-Ala-Leu

Z-Ala-Leu (19) was methylated by the general procedure using 4.5 mol of sodium hydride and 12 mol of methyl iodide. The acidic product (yield 58% by weight) was an oil whose n.m.r. spectrum showed a singlet at τ 7.0 and no peaks at 2.7 and 4.9 for the benzyl protons. The equivalent weight determined by titration was 294. Required for the hydantoin **1**, 274.

Methylation of Z-Ala-MeLeu

Methylation of Z-Ala-MeLeu[4] by the general procedure gave an oil, 100% yield, with $[\alpha]_D^{19}$ −67.2° (*c*, 2 in EtOH), whose i.r. spectrum showed that no >*N*—H remained.

Racemization Tests

Z-MeLeu was hydrogenated in 80% acetic acid for 4 h and the solution was evaporated giving a white crystalline solid. This compound (0.47 g) was dissolved in benzyl alcohol (20 ml) and benzene (10 ml) containing *p*-toluenesulfonic acid (0.63 g), and the mixture was heated under reflux, the water formed being trapped in a Dean-Stark tube. The benzene was removed by evaporation, the product precipitated with a large volume of ether, and collected by filtration (0.82 g). This MeLeu-OBzl·TosOH (0.106 g) was dissolved in ethyl acetate (1 ml) containing triethylamine (0.035 ml) and the solution was added to the mixed anhydride formed from Z-Ala (0.056 g) and ethyl chloroformate (0.024 ml) in THF (1 ml) at 0 °C by the addition of triethylamine (0.035 ml). The mixture was stirred at 0° for 1 h and at room temperature for 1 h. After removal of the solvent, the total neutral fraction was extracted into ethyl acetate, the solution was dried and evaporated, and the residual oil was hydrogenated in acetic acid containing 2 *N* HCl (0.2 ml) for 8 h to give the free dipeptide. Analysis[4] showed the product to contain 0.6% of the L,D-isomer. A similar experiment using Z-MeLeu prepared by saponification of Z-MeLeu-OMe gave a product containing 9.6% of the L,D-isomer.

1. (*a*) N. L. Benoiton and J. R. Coggins. *In* Progress in peptide research. Vol. 2. Proc. of the 2nd American Peptide Symposium, Cleveland, 1970. S. Lande, editor. Gordon and Breach, New York, N.Y. 1972. p. 145; (*b*) J. R. Coggins and N. L. Benoiton. Can. J. Chem. **49**, 1968 (1971).
2. R. K. Olsen. J. Org. Chem. **35**, 1912 (1970).
3. D. W. Thomas. Biochem. Biophys. Res. Commun. **33**, 483 (1968).
4. K. L. Agarwal, G. W. Kenner, and R. C. Sheppard. J. Am. Chem. Soc. **91**, 3096 (1969).
5. G. Marino, L. Valente, R. A. W. Johnstone, F. Mohammedi-Tabrizi, and G. C. Sodini. Chem. Commun. 357 (1972).
6. (*a*) J. R. McDermott and N. L. Benoiton. *In* Chemistry and biology of peptides. Proc. of the 3rd American Peptide Symposium, Boston, 1972. J. Meienhofer, editor. Ann Arbor Publishers, Ann Arbor, Mich. 1972. p. 369. (*b*) J. R. McDermott and N. L. Benoiton. Can. J. Chem. In press.
7. IUPAC-IUB Commission on Biochemical Nomenclature. J. Biol. Chem. **247**, 977 (1972).
8. (*a*) B. A. Stoochnoff. M.Sc. thesis, University of Ottawa, Ottawa, Canada, 1972. (*b*) B. A.

STOOCHNOFF and N. L. BENOITON. Tetrahedron Lett. 21 (1973).
9. P. A. PLATTNER, K. VOGLER, R. O. STUDER, P. QUITT, and W. KELLER-SCHLIERLEIN. Helv. Chim. Acta, **46**, 927 (1963).
10. P. QUITT, R. O. STUDER, and K. VOGLER. Helv. Chim. Acta, **46**, 1715 (1963).
11. M. L. POLAN, W. J. MCMURRAY, S. R. LIPSKY, and S. LANDE. Biochem. Biophys. Res. Commun. **38**, 1127 (1970).
12. P. A. LECLERCQ and D. M. DESIDERIO. Biochem. Biophys. Res. Commun. **45**, 308 (1971).
13. J. R. COGGINS and N. L. BENOITON. J. Chromatogr. **52**, 251 (1970).
14. J. D. CIPERA and R. V. V. NICHOLLS. Chem. Ind. 16 (1955).
15. J. R. MCDERMOTT and N. L. BENOITON. Chem. Ind. 169 (1972).
16. J. P. GREENSTEIN and M. WINITZ. Chemistry of the amino acids. John Wiley and Sons, New York. N.Y. 1962. p. 891.
17. G. W. ANDERSON and F. M. CALLAHAN. J. Am. Chem. Soc. **82**, 3359 (1960).
18. N. IZUMIYA. J. Chem. Soc. Japan, **71**, 500 (1950).
19. E. KLIEGER, E. SCHRÖDER, and H. GIBIAN. Ann. **640**, 157 (1961).

Can. J. Chem. Downloaded from www.nrcresearchpress.com by 210.87.254.40 on 09/05/12
For personal use only.

Reaction of the Hydrated Electron with HS^-

R. L. EAGER, V. KABACHIA, W. L. WALTZ, R. J. WOODS, AND K. J. MCCALLUM

Department of Chemistry and Chemical Engineering and the Saskatchewan Accelerator Laboratory, University of Saskatchewan, Saskatoon, Saskatchewan

Received December 18, 1972

Evidence is presented to show that the hydrated electron reacts with monohydrogen sulfide ion with a rate constant of $(3.0 \pm 0.4) \times 10^7 M^{-1} s^{-1}$ in contrast to an earlier report that this substrate was unreactive. A comparison of the electron reactivity towards hydrogen sulfides and selenides suggests that the reactivity reflects the ability of the substrate to accommodate the electron as opposed to its ability to donate a proton to the electron.

La réaction de l'électron hydraté sur l'ion hydrogène sulfure a été prouvée et se fait avec une constante de vitesse de $(3.0 \pm 0.4) \times 10^7 M^{-1} s^{-1}$ contrairement à une communication antérieure rapportant la non réactivité de ce substrat. Une comparaison de la réactivité de l'électron avec les sulfures et séléniures d'hydrogène suggère que cette réactivité reflète la capacité du substrat à accepter l'électron opposée à son pouvoir de céder un proton à l'électron. [Traduit par le journal]

Can. J. Chem., 51, 1920 (1973)

Can. J. Chem. Downloaded from www.nrcresearchpress.com by 210.87.254.5 on 09/05/12
For personal use only.

Introduction

An earlier report (1) on the behavior of the hydrated electron, e_{aq}^-, towards H_2S and HS^- indicated that HS^- was unreactive while H_2S was found to be highly reactive ($k_e = 1.1 \times 10^{10} M^{-1} s^{-1}$). In the course of studying the reactions of e_{aq}^- with various sulfur containing materials by pulse radiolysis, we had occasion to observe the behavior of e_{aq}^- in alkaline media in the presence of high concentrations of HS^-. Under these circumstances the disappearance of e_{aq}^- is much more rapid than that of e_{aq}^- in the alkaline matrix itself.

We wish to report here the results of this study which indicate that HS^- can react with e_{aq}^-. These results in conjunction with those reported by others (1–3) on the electron reactivity towards H_2S, H_2Se, and HSe^- lend further credence to the suggestion (4, 5) that electron rate constants for protonic acids reflect the ability of the substrate to incorporate the electron. This situation, shown in reaction 1, is in contrast to a mechanism involving proton transfer, reaction 2. This latter

[1] $$e_{aq}^- + H_nX \rightarrow H_nX^-$$

[2] $$e_{aq}^- + H_nX \rightarrow H_{n-1}X^- + H$$

mechanism has been proposed (6, 7) on the basis that an apparent Bronsted general acid catalysis law has been found to correlate values of k_e for a number of protonic acids with their acid dissociation constants.

Experimental

The pulse radiolysis technique used here is similar to that described elsewhere (8). Deaerated solutions were irradiated in a cyclindrical suprasil quartz cell of 4-cm path length with feeble pulses of *ca.* 17 MeV electrons from the Saskatchewan Linear Accelerator, The behavior of e_{aq}^- was monitored spectrophotometrically at 578 nm using a 200W quartz-tungsten–iodine lamp (GE Q6.6A/T4/CL) as the monitoring light source, a grating monochromator (Bausch-Lomb, 33-86-26-07), and a RCA 931A photomultiplier tube (5 dynodes used). The resulting signals were displayed on a Tektronix oscilloscope (Type 581A) in conjunction with a Type W differential comparator and were photographed on Polaroid Type 107 film. Care was taken to insure that the band width of the electronic circuitry was adequate to display the transient signals.

Triply-distilled water was used to prepare all solutions. Hydrogen sulfide gas (Matheson) was bubbled through saturated Na_2S solutions and then through triply-distilled water. The scrubbed H_2S gas was next passed into water, and the resulting solution diluted to yield solutions of the desired concentrations. The sulfide concentration was determined by standard iodiometric titration. Reagent NaOH was used to adjust the p*H*. The preparation and handling of the deaerated solutions was similar to that described elsewhere (ref. 9 and references therein). All other materials were of reagent quality.

Results and Discussion

The decay of the absorption of e_{aq}^- was measured at 578 nm for both the sodium hydroxide matrices and H_2S solutions in the p*H* range of 10.9 to 12.7 where the total sulfide concentration was greatly in excess of that for e_{aq}^-. The dis-

TABLE 1. Rate constants* for e_{aq}^- decay in H_2S solutions

Total sulfide concentration, M	$k_e \times 10^{-7}$ (M^{-1} s^{-1}) at pH =				
	10.9	11.4	11.8	12.4	12.6–12.7
1.0×10^{-2}	3.2(2)	2.4(2)	2.6	3.5(2)	3.2(3)†
1.5×10^{-2}	—	—	—	—	3.2(2)‡
3.0×10^{-2}	—	—	—	—	3.1(2)‡
Average value of $k_e = (3.0 \pm 0.4) \times 10^7$ M^{-1} s^{-1}					

*The values cited for the various pH's represent averages, the number in parenthesis representing the number of different determinations.
†pH of 12.7.
‡pH of 12.6.

appearance of e_{aq}^- both in the sulfide solutions and matrices obeyed first order kinetics as shown in Fig. 1. No transitory or stable products were observed under these conditions of low dose.[1] The apparent first order rate constants, k_{obs}, can be expressed by eq. 3

$$[3] \qquad k_{obs} = k_e[S] + k_m$$

where k_e is the second order rate constant for e_{aq}^- reaction with solute and k_m is the first order rate constant for e_{aq}^- decay in the matrix itself. The values of k_e calculated from eq. 3 are shown in Table 1: the corrections for k_m ranged between 5 and 20% of k_{obs}. Clearly the disappearance of e_{aq}^- is first order in total sulfide concentration and essentially independent of pH. The average value for k_e of $(3.0 \pm 0.4) \times 10^7$ M^{-1} s^{-1} obtained using H_2S compares favorably with the value of $(2.6 \pm 1.4) \times 10^7$ M^{-1} s^{-1} obtained in preliminary experiments at pH 11.4 using $Na_2S{\cdot}10H_2O$. Such agreement between different starting materials indicates that the disappearance of e_{aq}^- is not due to its reaction with possible impurities present in the starting materials.

Three species, H_2S, HS^-, and S^{2-}, can exist in aqueous media: the prevailing species depends upon the pH. Under the foregoing pH conditions, the major species is HS^-, and thus we ascribe the disappearance of e_{aq}^- primarily to its reaction with HS^-. It is however important to inquire as to the potential contributions of S^{2-} and H_2S, particularly as the latter reacts rapidly with e_{aq}^- ($k_e = 1.1 \times 10^{10}$ M^{-1} s^{-1}) (1). The amount of unionized H_2S present is determined by the first ionization constant of H_2S which is 9.0×10^{-8} (10). At the lowest pH used (10.9), the concentration of unionized H_2S is calculated to be 1.1×10^{-6} M for a 0.01 M sulfide solution. Approximately 4% of e_{aq}^- will be scavenged by unionized H_2S, and the values of k_e in Table 1 will be about 4% too large, an amount within experimental

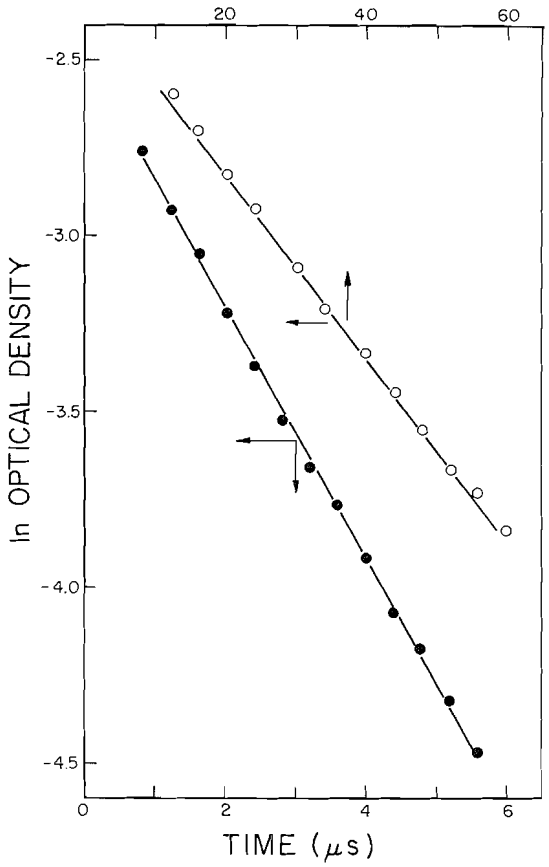

FIG. 1. ln optical density at 578 nm *vs.* time in μs: ○ matrix at pH of 12.6, ●, 0.01 M H_2S at pH of 12.7.

[1]At much higher doses, both intermediates and stable materials were observed at shorter wavelengths; however, so far it has not been possible to positively identify them as to their origin or to their nature.

Can. J. Chem. Downloaded from www.nrcresearchpress.com by 210.87.254.5 on 09/05/12
For personal use only.

error. Unionized H_2S will be of even less significance at higher pH's; however, these solutions will now possibly contain S^{2-} in sufficient quantities to affect the calculated k_e values. The amount of S^{2-} present depends upon the second ionization constant of H_2S. While reported values for this constant range from 10^{-12} to 10^{-14} (10), a recent critical examination of these values has been made (11), and it appears that a value of 1×10^{-14} is appropriate for the present work. For 0.01 M sulfide solutions, the percentage of S^{2-} is calculated to be about 5% at pH 12.6. As HS^- is much less reactive than H_2S, the reactivity of e_{aq}^- towards S^{2-} is anticipated to be less than that of HS^-, and thus the contribution of S^{2-} is expected to be small or negligible. These conclusions appear to be borne out by the independence of k_e on pH, and indicate that e_{aq}^- does react with HS^-. Two situations, as portrayed in reactions 4 and 5

[4] $$e_{aq}^- + HS^- \rightarrow HS^{2-} \rightarrow H + S^{2-}$$

[5] $$e_{aq}^- + HS^- \rightarrow H + S^{2-}$$

can be envisioned as it is likely that H atom is formed by either mechanism (2, 5). Implied in reaction 4 is that k_e reflects the ability of the substrate to accommodate an electron whereas in reaction 5, it reflects proton donation by the substrate. In deciding between these two mechanisms, it is instructive to compare the behavior of the sulfur systems with the analogous selenium systems. The values of k_e for H_2Se and HSe^- are reported (3) to be 1.1×10^{10} and 4.8×10^7 M^{-1} s^{-1} respectively; these are almost identical to those of H_2S and HS^-.

The proton donation mechanism, eq. 5, suggests a relationship between the values of k_e and the appropriate acid dissociation constants. This type of mechanism has found early support in an apparent linear free energy relationship (in the form of a Bronsted Law for general acid catalysis) between k_e for a number of protonic acids and their dissociation constants (6, 7). Such a relationship does not hold for the sulfur and selenium systems as H_2Se and HSe^- are much stronger acids (3) than the corresponding sulfur species (10, 11) yet the similar species react at essentially the same rates. Anbar (4) and Hart and Anbar (5) have also noted additional cases where such a LFER is not fulfilled, and they have suggested that the reactivity of e_{aq}^- with not only protonic acids but also other materials reflects the availability of vacant orbitals on the substrate to accommodate an electron as implied in reaction 4. In this context, the close behavior of sulfur and selenium is understandable in terms of their nearly identical electronegativities (12). The correlation of reactivity and electronegativities probably reflects similar *orbital* electronegativities for the corresponding sulfur and selenium species. This type of explanation also appears consistent with the fact that the dihydrogen forms are much more reactive than the monohydrogen species: the former would be expected to have higher orbital electronegativities than the latter. While differences in overall electrostatic charge may contribute to such disparities in reactivity, it is highly unlikely that they could account for such large differences, as electrostatic effects appear to play a minor role in hydrated electron reactions (4, 5).

We thank the National Research Council of Canada for financial assistance and Messrs. D. Jennings and E. Kozar for technical assistance in operating the linear accelerator.

1. W. KARMANN, G. MEISSNER, and A. HENGLEIN. Z. Naturforsch. B, **22**, 273 (1967).
2. G. MEISSNER and A. HENGLEIN. Berl. Bunsenges. Phys. Chem. **69**, 3 (1965).
3. M. SCHÖNESHÖFER, W. KARMANN, and A. HENGLEIN. Int. J. Radiat. Phys. Chem. **1**, 407 (1969).
4. M. ANBAR. ACS Adv. Chem. **50**, 55 (1965).
5. E. J. HART and M. ANBAR. The hydrated electron. Wiley–Interscience, New York. 1970. pp. 94–96.
6. J. JORTNER, M. OTTOLENGHI, J. RABANI, and G. STEIN. J. Chem. Phys. **37**, 2488 (1962).
7. J. RABANI. ACS Adv. Chem. **50**, 242 (1965).
8. M. S. MATHESON and L. M. DORFMAN. Pulse radiolysis. The M.I.T. Press, Cambridge, Mass. 1969. pp. 29–36.
9. W. L. WALTZ and R. G. PEARSON. J. Phys. Chem. **73**, 1941 (1969).
10. A. SILLÉN and A. E. MARTELL (*Editors*). Stability constants of metal–ion complexes. The Chemical Society, London. Special Publication No. 17, 1964. p. 215.
11. H. P. STEPHENS and J. W. COBBLE. Inorg. Chem. **10**, 619 (1971).
12. L. PAULING. The nature of the chemical bond. 3rd ed. Cornell University Press, New York. 1960. p. 93.

Can. J. Chem. Downloaded from www.nrcresearchpress.com by 210.87.254.5 on 09/05/12
For personal use only.

The Master Equation for the Dissociation of a Dilute Diatomic Gas IX. Rotation–Vibration Relaxation Times

E. KAMARATOS AND H. O. PRITCHARD[1]

Centre for Research in Experimental Space Science, York University, Downsview, Ontario

Received October 25, 1972

The relationships between individual rotational or vibrational transition probabilities and the eigenvalues of the 172nd order relaxation matrix describing the rotation–vibration–dissociation coupling of ortho-hydrogen are explored numerically. The simple proportionality between certain transition probabilities and certain eigenvalues, which was found previously in the vibration–dissociation coupling case, breaks down. However, it is shown that at 2000 °K the second smallest eigenvalue of the relaxation matrix (d_{n-2}), hitherto regarded as determining the "vibrational" relaxation time, is related more to the transition probability assigned to the *largest rotational gap* which lies in the first ($v = 0 \leftrightarrow v = 1$) vibrational gap, *i.e.* to the transition $v = 0, J = 5 \leftrightarrow v = 0, J = 7$, than to anything else; this clearly supports an earlier suggestion that the transient which immediately precedes dissociation in a shock wave has to be regarded as a rotation–vibration relaxation time rather than a vibrational relaxation time. It is suggested that the Lambert–Salter relationships can be rationalized on this assumption.

An analysis is then made of the energy uptake associated with each eigenvalue at three temperatures. At 500 °K, the greatest energy increment is associated with two eigenvalues (d_{n-13} and d_{n-24}) and can be characterized as *essentially* a rotational relaxation: the calculations confirm that the observed rotational relaxation time should first decrease and then increase with increasing temperature, as was recently found to be the case experimentally. At 2000 °K, large energy increments are associated with several eigenvalues between d_{n-2} and d_{n-14}, and at 5000 °K, with most of the eigenvalues d_{n-2} to d_{n-23}; thus, the higher the temperature, the more complex is the (T–VR) rotation–vibration relaxation. Further, relaxation times for the same temperature measured by ultrasonic and shock-wave techniques need not agree.

Les relations entre les probabilités de transition rotationnelle ou vibrationnelle et les valeurs propres d'ordre 172 de la matrice de relaxation décrivant la rotation, vibration, dissociation et couplage de l'hydrogène ortho, ont été explorées par voie numérique. La proportionnalité entre certaines probabilités de transition et certaines valeurs propres qui a été trouvée précédemment pour le cas de la vibration, dissociation et le couplage est rejetée: cependant, on a montré qu'à 2000 °K la seconde valeur propre la plus petite de la matrice de relaxation (d_{n-2}), jusqu'ici considérée comme déterminant le temps de relaxation vibrationnelle, est plus reliée à la probabilité de transition entre l'écart rotationnel le plus grand correspondant à la première intervalle vibrationnelle ($v = 0 \leftrightarrow v = 1$) et la transition $v = 0, J = 5 \leftrightarrow v = 0, J = 7$, qu'a autre chose; ceci confirme de façon claire une suggestion précédente selon laquelle la transition qui précède immédiatement la dissociation dans un choc d'onde, doit être considérée comme un temps de relaxation rotation–vibration plutôt que celui d'une relaxation vibrationnelle. On pense que les relations de Lambert–Salter peuvent être rationnalisées selon cette hypothèse. Une analyse a été ainsi faite sur la dissipation d'énergie associée à chaque valeur propre pour trois températures. A 500 °K, l'incrément d'énergie le plus élevé est associé à deux valeurs propres (d_{n-13} et d_{n-24}) et peut être essentiellement caractérisé par une relaxation rotationnelle: les calculs confirment le fait que le temps de relaxation rotationnelle pourrait décroître dans un premier temps puis croître avec la température comme l'a montré une expérience récente. A 2000 °K, les grands incréments d'énergie sont associés à plusieurs valeurs propres entre d_{n-2} et d_{n-14}; et à 5000 °K, à la plupart des valeurs propres de d_{n-2} à d_{n-23}; ainsi, plus la température croît et plus la relaxation rotation–vibration devient complexe. De plus, les temps de relaxation pour une même température mesurés par les techniques de l'ultra son et du choc d'onde, ne concordent pas nécessairement. [Traduit par le journal]

Can. J. Chem., 51, 1923 (1973)

In the preceding paper in this series,[2] it was found that the second smallest eigenvalue d_{n-2} of the relaxation matrix describing the rotational and vibrational dissociation of hydrogen in the presence of a large excess of inert gas was changed markedly when only *rotational* transition probabilities were altered (1), thus implying that the last transient which immediately precedes the dissociation reaction has a lot of rotational character; hitherto, it had always been tacitly assumed that the last transient was a vibrational relaxation (2, 3). At a macroscopic level, there is strong experimental evidence (3) that at low tempera-

[1]Nuffield Foundation Fellow, Physical Chemistry Laboratory, University of Oxford; Visiting Professor, Chemistry Department, U.M.I.S.T., Manchester, 1972–1973.

[2]Equations taken from other papers in this series and used in the present paper are prefixed with the part numbers in Roman numerals.

Can. J. Chem. Downloaded from www.nrcresearchpress.com by 210.87.254.5 on 09/05/12
For personal use only.

Can. J. Chem. Downloaded from www.nrcresearchpress.com by 210.87.254.5 on 09/05/12
For personal use only.

tures, diatomics (especially hydrogen) exhibit relaxations which can be identified clearly as rotational whereas at higher temperatures, a much slower relaxation is found which is "obviously" vibrational in character; recently however, these well established assumptions have been challenged by Dove, Jones, and Teitelbaum (4) who find that they can only explain their shock-wave results for H_2 in the temperature range 1350–3000 °K on the hypothesis that the relaxation is not purely vibrational in character, but is a coupled relaxation involving both rotational and vibrational degrees of freedom. On the other hand, at a microscopic level, detailed studies of individual rotation–vibration levels have now become possible, and it has been found that in the relaxation of the carbon dioxide molecule, in the 500–2000 °K range, each rotational state has its own characteristic vibrational relaxation time (5), showing that one cannot really regard vibrational and rotational relaxation times as separable. The first part of this paper therefore describes the results of some numerical experiments designed to try to find out to which transition probabilities certain key eigenvalues were sensitive. The later part of the paper is concerned with the problem, which arises when the eigenvalue d_{n-2} is not dominant in the sense that $|d_{n-2}{}^{-1}|$ "ordinarily corresponds to the experimental relaxation time" (6), of how does the disturbance (*i.e.* sound wave or shock wave) "know" which eigenvalue to select out of the rather evenly spaced spectrum of eigenvalues?

Numerical Experiments

It was found in our earlier work, in which only vibration–dissociation coupling for H_2 was considered (2), that if the assumed transition probabilities P_{01} and P_{10} were scaled, the eigenvalue d_{n-2} was scaled by exactly the same amount: further, that at temperatures near 2000 °K, the vibrational relaxation time calculated from P_{01} was in fact close to $|d_{n-2}{}^{-1}|$ (the coincidence becoming less marked at higher temperatures because of the obviously increasing complexity of the vibrational relaxation (3)). This direct scaling was surprising, but has been satisfactorily analyzed and explained by Boyd (7), who predicted that this one-to-one relationship would cease to exist if the relaxing levels were too close together and therefore connected by relatively large transition probabilities; this is exactly what we find if we repeat these calculations for molecules having many more bound vibrational states than does H_2.

First, however, an illustration of the kind of difficulties one can encounter using a truncated set of levels to explore the internal relaxation: ortho-hydrogen has 172 rotation–vibration levels (1), so in order to conserve computer time we thought it would surely be satisfactory to examine the relaxation amongst the bottom-most 40 or 50 levels; the disposition of these levels is shown in Fig. 1. No dissociation was allowed so that particles are strictly conserved: therefore the smallest eigenvalue d_{n-1} is identically zero (2) and the required relaxation time is (6) the inverse of $|d_{n-2}|$, which is now the smallest non-zero eigenvalue. Using the set of T–VR transition probabilities prescribed by[2] eq. VIII(16*a*), it was found that at 2000 °K d_{n-2} was, as we had expected, most affected by changes in the transition probability $v = 0, J = 5 \leftrightarrow v = 0, J = 7$, but there was no longer the strict proportionality that we had found in our previous calculations (2, 7): this was true for several truncated sets of levels, with 44, 49, and 50 members in the set; generally, d_{n-2} was scaled by about 20% of the factor used to scale the pair of transition probabilities. Equation VIII(16*a*) assigns the transition probabilities solely on the basis of the energy gap between the two levels involved in the transition (1). However, using eq. VIII(16) which discriminates against larger changes than $\Delta J = 2$, it was found that for the 44-member set d_{n-2} was perturbed the most strongly by changes to the probability for the $v = 0, J = 19 \leftrightarrow v = 0, J = 21$ transition! If a different truncated set was used, *e.g.* the lowest 49 levels, d_{n-2} was most sensitive to the transition probability for $v = 0, J = 5 \leftrightarrow v = 0, J = 7$, and if the lowest 50 levels were used the key transition remained $v = 0, J = 5 \leftrightarrow v = 0, J = 7$. Clearly what is happening (referring now to our 44-level truncated set) is that when large changes in J are penalized and the chain of levels $v = 1, J = 19$; $v = 2, J = 17$; and $v = 3, J = 15$ is deleted, the transitions from $v = 0, J = 21$ to $v = 1, J = 17$ or $v = 2, J = 15$ have quite small probabilities, and therefore relaxation to equilibrium of the $v = 0, J = 21$ state must take place principally through the transition $v = 0, J = 21 \leftrightarrow v = 0, J = 19$ which is slow and rate determining. One can imagine a set of points forming a network, in which most of the points are connected to several other points,

Can. J. Chem. Downloaded from www.nrcresearchpress.com by 210.87.254.5 on 09/05/12
For personal use only.

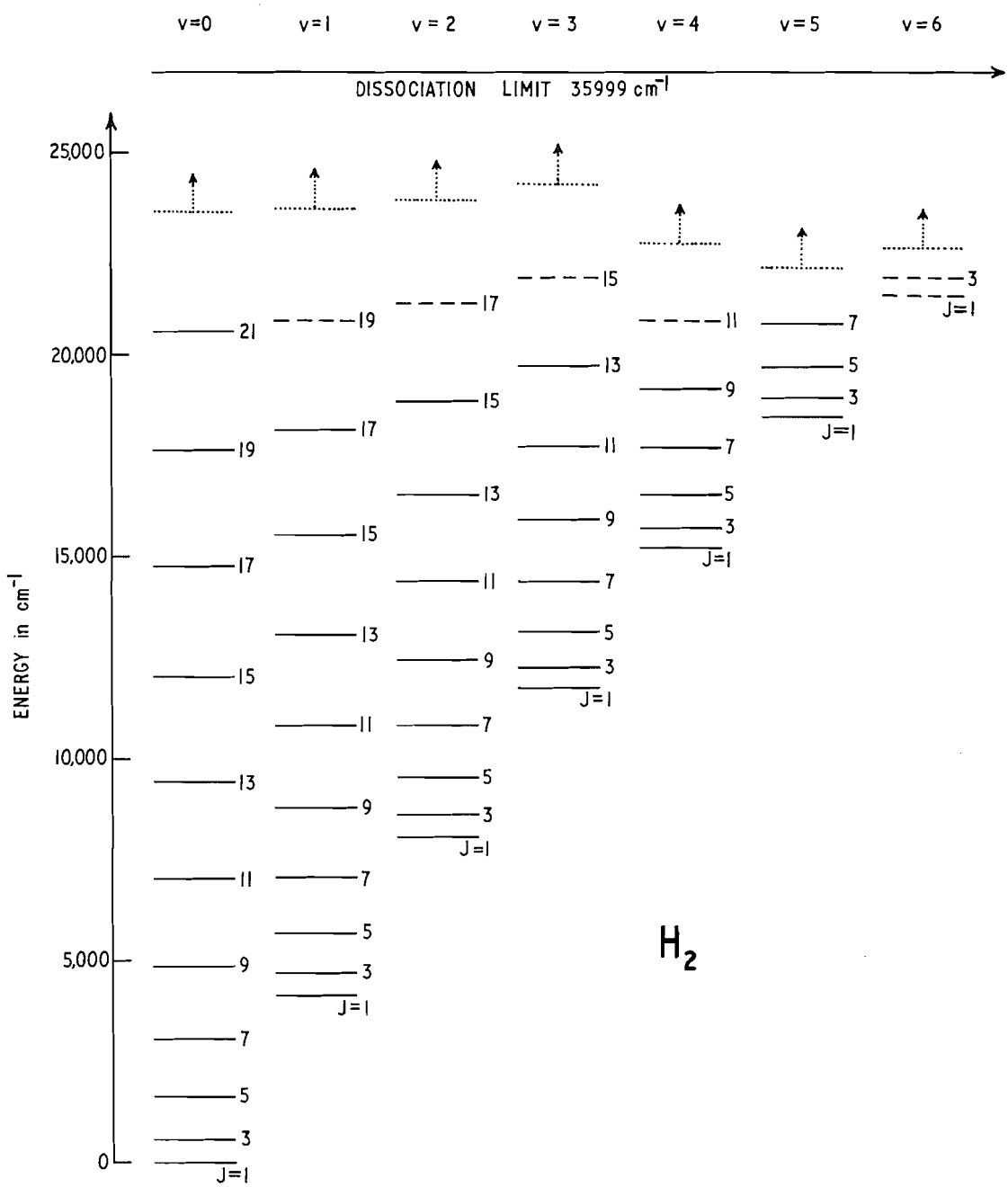

FIG. 1. Energy-level diagram for the 50 lowest rotation–vibration states of ortho-hydrogen: the lowest 44 levels are represented by solid lines, and the remaining 6 levels by dashed lines; progression to higher energies is depicted by dotted lines.

Can. J. Chem. Downloaded from www.nrcresearchpress.com by 210.87.254.5 on 09/05/12
For personal use only.

but in which a few of the outlying points lie on branches, each only connected to the main network by a single line passing through all the points on the branch: under these conditions the overall relaxation time will be determined mainly by the characteristic time of the slowest relaxation of any of the branches.[3] This idea was supported by the fact that when, using the 44-member set, the top-most J-sublevels for each v were connected to each other with higher transition probabilities ($\sim 10^{-3}$ per collision), d_{n-2} became most sensitive to the $v = 0$, $J = 5 \leftrightarrow v = 0$, $J = 7$ transition probability with the ΔJ-restricted set of probabilities VIII(16) also, but not to the same extent as with the probabilities VIII(16a) which are solely dependent on the energy gap. Thus, one can regard a dissociating diatomic molecule (as we have suggested previously (1, 8)) as being analogous to a densely interconnected network, and there is only one branch, which in this case is the sequence of levels $v = 0, J = 1$; $v = 0, J = 3$; $v = 0$, $J = 5$; and $v = 0$, $J = 7$ which can then connect either to $v = 0$, $J = 9$ or $v = 1$, $J = 1$. In the energy-dependent case, the latter transition is easy, and so the relaxation time is principally determined by the $J = 5$ to 7 transition of $v = 0$, with $J = 3$ to 5 of $v = 0$ being of lesser importance: in the ΔJ-dependent case however, the sideways transition from $v = 0$, $J = 7$ to $v = 1$, $J = 1$ is much less favorable, and the relaxation becomes sensitive to the probabilities of several of the transitions in this region.

We remark in passing that it is common to perform relaxation calculations using truncated sets of levels; this has probably not led to any spurious conclusions so far, but as calculations become more sophisticated in the future, it will become more important to examine the network properties of the truncated sets of levels and their associated sets of transition probabilities.

So far, we have confined ourselves to the problem of trying to find which single pair of transition probabilities correlates the best with d_{n-2}, the eigenvalue which has previously been identified with the inverse of the observable relaxation time (2, 3, 6). The question then arises, are there any particular eigenvalues in the spectrum which can be identified as being associated with a purely vibrational, or a purely rotational relaxation time, and which are consistent with experimental experience? At 2000 °K (for a mixture consisting of 3.5×10^{19} He atoms per cc and 3.5×10^{16} H_2 molecules per cc), the eigenvalue spectrum[4] for ortho-hydrogen consists of d_{n-1} at about 6×10^{-1} s^{-1} followed by a series of 171 eigenvalues, well spaced, between $d_{n-2} \approx 9 \times 10^6$ s^{-1} and $d_{n-172} \approx 1 \times 10^{11}$ s^{-1}, using the set of probabilities described by eq. VIII(16), and without tunnelling (1); the inclusion of tunnelling only perturbs the larger eigenvalues, which do not concern us here, and the use of the alternative set of transition probabilities, eq. VIII(16a) does not alter any of the qualitative conclusions described in the remainder of this paper. In the first of two experiments, the probability of *every* $J = 1 \leftrightarrow J = 3$ transition, for *all* v, was multiplied by an arbitrary factor of 100, and the eigenvalues compared with the standard set: most of the largest eigenvalues ($10^{10} - 10^{11}$ s^{-1}) remained unchanged down as far as the fourth, fifth, or even sixth decimal place, but most of the smaller ones, from d_{n-2} (d_{170}) $\approx 9 \times 10^6$ s^{-1} to d_{n-44} (d_{128}) $\approx 5 \times 10^8$ s^{-1} were changed by small amounts; it was also possible to identify a few eigenvalues in this group which had been selectively multiplied by larger factors, sometimes approaching 100. Thus at 2000 °K, one cannot identify any single eigenvalue with rotational relaxation; it appears that many eigenvalues, even up to those characterizing the very longest relaxation, have significant rotational character. Incidentally, if *only* the $J = 1 \leftrightarrow J = 3$ transition of $v = 0$ is changed at this temperature, the eigenvalue d_{n-40} (d_{132}) $\approx 4.3 \times 10^8$ s^{-1} is most affected (to the extent of about 20% of the applied perturbation). In the second experiment, *every* $v = 0 \leftrightarrow v = 1$ transition probability, for *all* J, was scaled by a factor of 100, with the result that many eigenvalues changed somewhat, but none of them was obviously scaled by a large amount; likewise,

[3]We would like to thank a referee for pointing out that this statement could be deceptive: starting with a non-equilibrium state in which all the molecules are present in low-lying energy levels, then (as described later in this paper) the amount of energy associated with raising a relatively small number of molecules into the $v = 0$, $J = 21$ state would not be detectable in any macroscopic experiment, and the observed relaxation time would relate to some other process having more energy associated with it; however, if a large fraction of the molecules were initially present in the $v = 0$, $J = 21$ state, the statement would be strictly true.

[4]Note that *all* the eigenvalues are *negative*: however, since no confusion will arise, the minus sign will be dropped, for convenience, from the numerical values of eigenvalues quoted in the descriptive sections of this paper.

Can. J. Chem. Downloaded from www.nrcresearchpress.com by 210.87.254.5 on 09/05/12
For personal use only.

when only the $v = 0 \leftrightarrow v = 1$ transition probability for $J = 0$ was scaled, some eigenvalues increased, but no clearly defined effect showed up.

The relaxation effects at 2000 °K are obviously very complex: however, vibrational relaxation should be unimportant at 500 °K, and the rotational relaxation effects at this temperature should therefore be easier to resolve. Again, following the same procedure, individual pairs of transition probabilities P_{ij} and P_{ji} were multiplied by an arbitrary factor of 100, and the results for 500 °K were broadly as follows:

(*a*) When the probability $v = 0, J = 1 \leftrightarrow v = 0, J = 3$ was scaled, eigenvalue d_{119} was scaled by a factor of 98, d_{148} was slightly perturbed (factor of 1.03), and the remainder were virtually unchanged.

(*b*) For higher J-levels, the principal scaling factor was of the order of 30 to 50, with the affected eigenvalues being

$$v = 0, J = 3 \leftrightarrow v = 0, J = 5 \qquad \{d_{148}, d_{119}\}$$
$$v = 0, J = 5 \leftrightarrow v = 0, J = 7 \qquad \{d_{159}, d_{148}\}$$
$$v = 0, J = 7 \leftrightarrow v = 0, J = 9 \qquad \{d_{161}, d_{159}\}$$
$$v = 0, J = 9 \leftrightarrow v = 0, J = 11 \qquad \{d_{164}, d_{161}\}$$

(*c*) Thereafter, more eigenvalues were perturbed by smaller amounts, until at very high J values, there was only a small but still noticeable effect on a single eigenvalue, the remaining change in the trace being dissipated in very small perturbations to other eigenvalues.

(*d*) More interestingly, if for $v = 0$, the probabilities for all the first three transitions $J = 1 \leftrightarrow J = 3$, $J = 3 \leftrightarrow J = 5$, and $J = 5 \leftrightarrow J = 7$ were simultaneously scaled by a factor of 100, then eigenvalues d_{119}, d_{148}, and d_{159} were all scaled by factors between 99.5 and 99.95, with very little other discernible effect on the spectrum. Thus, these three eigenvalues are obviously the principal components of a rotational subset (the vestiges of which still persist in the 2000 °K calculation described above).

(*e*) For transitions among the J-sublevels of $v = 1$, the affected eigenvalues were not the same ones as were changed in (*a*) and (*b*) above for $v = 0$.

(*f*) At 500 °K, unlike the 2000 °K case, d_{170} (d_{n-2}) was sensitive to changes in the probabilities $v = 0, J = 1 \leftrightarrow v = 1, J = 1$, and to a lesser extent $v = 0, J = 3 \leftrightarrow v = 1, J = 3$ (40% and 20% respectively of the imposed perturbation factor); however, at 500 °K, vibrational excitation in H_2 is unimportant.

These calculations therefore suggest that whilst it is possible to define, and presumably observe, a rotational relaxation time at moderately low temperatures, it is not possible to define a vibrational relaxation time, nor observe one, and that the observable quantity that has hitherto been thought to be a vibrational relaxation time possesses considerable rotational character. These conslusions are examined in much more detail later in the paper.[5] The concept is not a foreign one (after all, it is possible to observe pure rotational spectra of molecules, but one cannot observe pure vibrational spectra without superposition of rotational effects). It arises in the present context because whenever vibrational excitation occurs, it has to be arrived at through a whole network of transitions, a few of which may be purely vibrational, some purely rotational together with one rotation–vibration (T–VR) transition, but by far the most of them mixed rotation–vibration transitions. Significantly, the $v = 0, J = 1$ to $v = 0, J = 7$ sequence of levels forms essentially a linear branch (transitions from points on the branch to other points in the network are possible but not probable), and it is the rate-determining properties of this single branch that are the most important factors in

[5]It is well known (3) that if the ultrasonic relaxation times for the halomethanes are plotted against the lowest vibration frequencies of the molecules, the experimental data fall fairly well on two straight lines: molecules with two or more hydrogen atoms fall near one line, and molecules with one or no hydrogen atom near the other; this behavior is usually called the Lambert–Salter relationship. Realizing that a vibrational relaxation time *per se* may have no meaning, and that every observable "vibrational relaxation time" could have a substantial rotational component, we believe that it might be possible to rationalize these data into a single plot, and have made a brief examination of the problem. As far as possible with the data available we have tabulated the rotation–vibrational energy-level spectrum for a number of these molecules, and have looked at two possibilities: one, that the ultrasonic relaxation time will be related to the energy of the largest rotation–vibration spacing in the system, and two, that it will be related to the number of rotational gaps in the lowest vibrational gap; the latter approach seems the more promising at this time. Note that the rotational component implied by this description of the vibrational relaxation process is not the same as that proposed recently by Lambert (15); the same difficulties will arise however in respect of the magnitude of the measured ultrasonic velocity dispersion.

Can. J. Chem. Downloaded from www.nrcresearchpress.com by 210.87.254.5 on 09/05/12
For personal use only.

determining the observable relaxation properties of the molecule, at any temperature.

The Mixed Character of Relaxation Times

As we have just seen, there is no single eigenvalue in the spectrum at 2000 °K which can be identified with either a purely rotational or a purely vibrational relaxation time, especially so in the latter case. On the other hand, molecules *do* exhibit well defined and experimentally measureable relaxation times, although in some cases there appear to be double relaxations for more complicated molecules (3). Clearly then, the molecular gas must present to the sound wave or shock wave the appearance of only possessing a few important eigenvalues, and it is obvious that these will be those eigenvalues with which are associated the greatest contributions to the instantaneous heat capacity at the temperature in question. Thus, we now extend our previous analysis to the calculation of the quantity $\Delta\bar{E}(j)$, the amount of energy associated with the jth eigenvalue d_j and which is taken up in the period $|d_j^{-1}|$, *i.e.* the jth relaxation time, given an arbitrary initial distribution: we will in fact only consider the quantity $\Delta\bar{E}_0(j)$ which refers to an initial distribution in which all molecules are in the lowest possible energy level. The following analysis is limited to short times, before any appreciable dissociation takes place (*i.e.* at temperatures where $|d_{n-1}| \ll |d_{n-2}|, |d_{n-3}|$ etc.) and therefore to initial states consisting of only low-lying rotation–vibration states. Thus, eq. III(4) can be approximated to

$$[1] \qquad \dot{\xi} = \mathbf{A}\xi$$

where $\mathbf{A}$ is the transition matrix, ξ is a vector of $n_i/\tilde{n}_i$ (n_i being the instantaneous population of the ith level and $\tilde{n}_i$ being its equilibrium value) and $\dot{\xi}$ is the derivative of ξ with respect to time: the reader is referred to papers I and III of this series (2, 9) for amplification of the precise meaning of symbols, and for clarification of the following derivation. The matrix $\mathbf{A}$, can be symmetrized to a new matrix $\mathbf{B}$ by the transformation $\mathbf{B} = \mathbf{E}\,\mathbf{A}\,\mathbf{E}^{-1}$, and the matrix $\mathbf{B}$ can be diagonalized by the transformation $\mathbf{D} = \tilde{\mathbf{S}}\,\mathbf{B}\,\mathbf{S}$: thus, combining the simplified eqs. III(8a) with III(10), one gets

$$[2] \qquad \tilde{\mathbf{S}}\,\mathbf{E}\,\dot{\xi} = \mathbf{D}\,\tilde{\mathbf{S}}\,\mathbf{E}\,\xi$$

c.f. also ref. 9, eq. I(28). On integration, this becomes

$$[3] \qquad \xi(t) = \mathbf{E}^{-1}\mathbf{S}\,e^{\mathbf{D}t}\,\tilde{\mathbf{S}}\,\mathbf{E}\,\xi(0)$$

whence, writing $\xi = \mathbf{E}^{-2}\mathbf{n}$

$$[4] \qquad \mathbf{n}(t) = \mathbf{E}\,\mathbf{S}\,e^{\mathbf{D}t}\,\tilde{\mathbf{S}}\,\mathbf{E}^{-1}\,\mathbf{n}(0)$$

or, in expanded form, since $(\tilde{\mathbf{S}})_{jk} = (\mathbf{S})_{kj}$, the lth element of the population vector at time t is

$$[4'] \quad n_l(t) = \tilde{n}_l^{1/2} \sum_j S_{lj}\, e^{d_j t} \sum_k S_{kj} \tilde{n}_k^{-1/2} n_k(0)$$

We now abstract from [4'] the component associated with only the jth eigenvalue, yielding

$$[5] \quad n_l(j, t) = \tilde{n}_l^{1/2} S_{lj}\, e^{d_j t} \sum_k S_{kj} \tilde{n}_k^{-1/2} n_k(0)$$

which describes the growth in the population of the lth state which can be ascribed to the jth eigenvalue, from a starting distribution given by $\boldsymbol{n}(0)$; the amount of energy associated with this growth in population is

$$[5e] \quad \varepsilon_l(j, t) = \tilde{n}_l^{1/2} S_{lj}\, e^{d_j t} \sum_k S_{kj} \tilde{n}_k^{-1/2} n_k(0)[\varepsilon_l - \varepsilon_k]$$

where ε_l, ε_k are energy levels. Summation over all l yields the quantity $\Delta E(j, t)$, the total energy increment in the time t associated with the jth relaxation and a given initial distribution. However, the majority of our calculations assumed that all molecules were initially present in the lowest available state ($v = 0, J = 1$), since it was found that the use of two other low-lying initial states ($v = 0$, $J = 3$ or $v = 0$, $J = 5$) gave qualitatively similar results. Thus, apart from a numerical constant, $\boldsymbol{n}(0)$ becomes the vector {1,0,0.....} and we get

$$[6] \quad \Delta E_0(j, t) = \text{constant} \times \sum_l (2J_l+1)^{1/2} \varepsilon_l\, e^{-\varepsilon_l/2kT} S_{lj} S_{0j}\, e^{d_j t}$$

The experimentally important quantity, of course, is the total energy increment associated with the jth relaxation, which is simply

$$[7] \quad \Delta\bar{E}_0(j) = \text{constant} \times S_{0j} \sum_l (2J_l + 1)^{1/2} \varepsilon_l\, e^{-\varepsilon_l/2kT} S_{lj}$$

Alternatively [7] can be regarded as the energy increment taking place in the characteristic period of the relaxation $t = |d_j^{-1}|$.

Use of any of the eqs. 4 to 7 requires the knowledge of the eigenvectors $\mathbf{S}$ of (for ortho-hydrogen) the 172nd order relaxation matrix, and with the

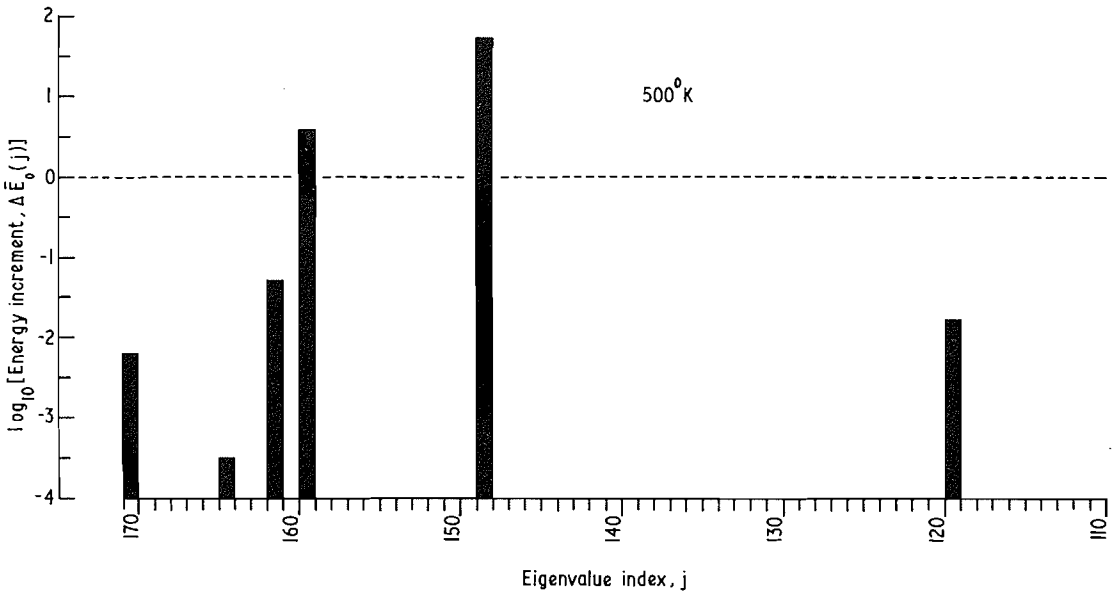

FIG. 2. Logarithmic plot of energy increment $\Delta\bar{E}_0(j)$ against eigenvalue index j for $T = 500\,^{\circ}\mathrm{K}$; the units of $\Delta\bar{E}_0(j)$ are arbitrary.

recent availability of quadruple-length arithmetic on the IBM 370 series of machines, we have been able to calculate most of the vectors of such matrices by existing techniques (9, 10). The eigenvectors we have been unable to find, either because of cancellation or because of overflow difficulties (1), have been those associated with the reaction eigenvalue itself, *i.e.* d_{n-1} especially so at the lower temperatures, and with some of the very large eigenvalues, of the order of 10^{11} s^{-1}: these very rapid processes correspond to equilibrations amongst very highly excited levels, or between these levels and the continuum; hence, it was for these reasons that our derivation and discussion are confined to initial states consisting only of low-lying levels, and to times short compared with the characteristic reaction time.

(i) Rotational Relaxation at 500 °K

It is known that at 500 °K, hydrogen exhibits relaxation properties which can be described with confidence as being rotational in character (3). Thus, in view of the conclusions from the numerical experiments described above, it would seem that one could expect to find the application of eq. 7 to be fairly uncomplicated at this temperature. The energy increment associated with each eigenvalue in its characteristic relaxation time was calculated using the standard set of transition probabilities through eq. 7, and the results are shown graphically in Fig. 2. It can be seen that apart from the three eigenvalues d_{119}, d_{148}, and d_{159}, there is very little other contribution to the energy increment, and taken together with the results of the numerical experiment (*d*) described in the preceding section, clearly identifies these three eigenvalues as being the ones associated with the rotational relaxation at this temperature. Only d_{161}, d_{164}, and d_{170} make any other discernible contribution: d_{161} is closely related to the $v = 0, J = 7 \leftrightarrow v = 0, J = 9$ transition, d_{164} likewise to $v = 0, J = 9 \leftrightarrow v = 0, J = 11$; and d_{170} is related principally to the $v = 0, J = 1 \leftrightarrow v = 1, J = 1$ transition *i.e.* the pure vibrational transition, which is not significantly excited at this temperature.

Then, as a final check on the close connection of the three eigenvalues d_{119}, d_{148}, and d_{159} with the transitions $J = 1 \leftrightarrow J = 3$, $J = 3 \leftrightarrow J = 5$, and $J = 5 \leftrightarrow J = 7$, respectively, of $v = 0$ and their association with an observable relaxation phenomenon, each of these transition probabilities was scaled, in turn, by a small amount (a factor of 2, so as not to upset the relaxation pattern very seriously), and it was found in each case that a large energy increment continued to be associated with the eigenvalue which was moved by this perturbation.

Can. J. Chem. Downloaded from www.nrcresearchpress.com by 210.87.254.5 on 09/05/12
For personal use only.

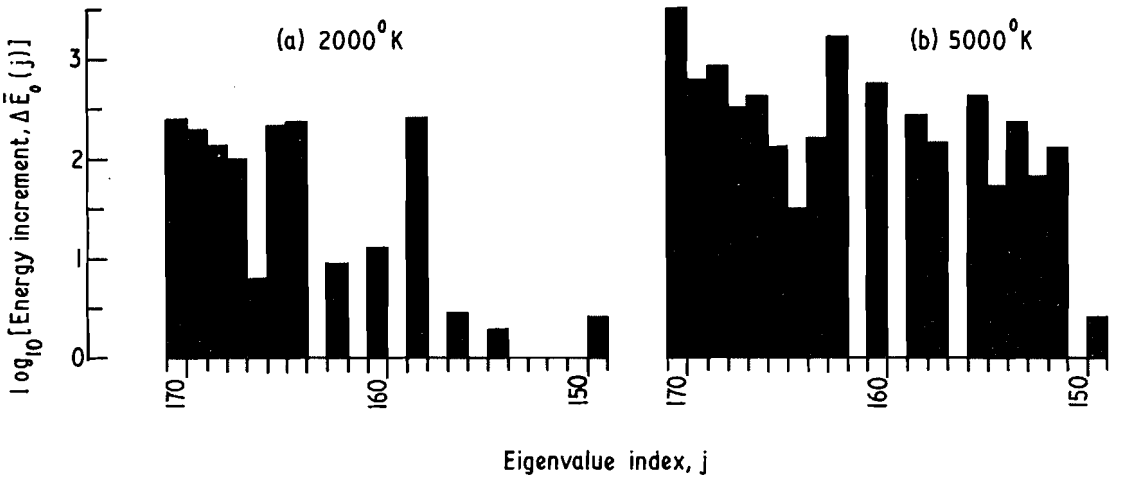

FIG. 3. Logarithmic plot of energy increment $\Delta\bar{E}_0(j)$ against eigenvalue index j: (*a*) for $T = 2000$ °K; (*b*) for $T = 5000$ °K. Note that the units of $\Delta\bar{E}_0(j)$ are arbitrary, but that the constant in eq. 7 is comparable between Figs. 2, 3*a* and 3*b*; thus, only the portion of Fig. 2 above the dotted line is to be compared with Figs. 3*a* and 3*b*.

(ii) Mixed Relaxations at 2000 and 5000 °K

As we noted earlier in the paper, it was not possible to deduce any close connection between individual vibrational transition probabilities and certain eigenvalues for the temperature 2000 °K. Many eigenvalues changed by small amounts as the result of changing one pair of transition probabilities, as expected from the analysis of Boyd (7), and at 5000 °K, the perturbations of the eigenvalues resulting from a single perturbation in a pair of transition probabilities were even more diffuse. Thus, the only analysis of the situation we could perform was an examination of the energy increment associated with each eigenvalue according to eq. 7; only 22 eigenvalues were examined in detail, and the results are shown in Fig. 3. At 2000 °K, about a dozen eigenvalues are associated with significant energy increments, with d_{170}, d_{169}, d_{168}, d_{167}, d_{165}, d_{164}, and d_{158} dominating; the corresponding relaxation times are 10.9, 5.9, 3.8, 2.9, 2.0, 1.7, and 0.7×10^{-8} s, respectively. This implies that the last transient preceding chemical reaction is not a simple relaxation determined by the eigenvalue d_{n-2} (d_{170}), but is rather a complex one which will only approach to a simple exponential decay at the tail end of the relaxation: it would probably be very difficult experimentally to resolve such a complex relaxation into its components (6), but there have been suggestions that, both in N_2 and H_2, the approach to equilibrium is not a pure exponential (11, 12); on the other hand, at low temperatures, one could hope that either ultrasonic or shock-wave relaxation experiments would resolve the kind of behavior depicted in Fig. 2 where the important eigenvalues are very well spaced out in time. At 5000 °K, almost every one of the first 22 eigenvalues makes a significant contribution to the instantaneous heat capacity, as also do several others beyond the 22nd: however, since the interpretation of Fig. 3 can only be extremely qualitative in nature at the present time, we do not reproduce these unnecessary data. It should be noticed that the results depicted in Fig. 3 are *quantitatively* quite sensitive to the assumed sets of transition probabilities. The ones shown were calculated using the ΔJ-dependent probabilities, eq. VIII(16); use of the probabilities eq. VIII(16a) which allow large changes in J to take place if the energy separation is small, appears to simplify the relaxation slightly, in the sense that rather fewer eigenvalues have associated large energy increments; this is consistent with the results found in the numerical experiments described earlier in the paper, but again, we do not reproduce this data since its importance is only qualitative.

Conclusions

The following picture of the relaxation properties of a diatomic gas in a large excess of inert diluent emerges from these calculations; these statements are made in the context of our calcula-

Can. J. Chem. Downloaded from www.nrcresearchpress.com by 210.87.254.5 on 09/05/12
For personal use only.

Can. J. Chem. Downloaded from www.nrcresearchpress.com by 210.87.254.5 on 09/05/12
For personal use only.

tion using ortho-hydrogen which only possesses odd rotational levels, but are clearly extendable to the general case of a molecule having both odd and even levels (with due regard for the size of the rotational spacings compared with kT). At very low temperatures, say 300 °K, so low that only the $v = 0, J = 1 \leftrightarrow v = 0, J = 3$ transition can be significantly excited, the molecule will exhibit a fairly simple rotational relaxation. Because of computational difficulties (1) we have not been able to locate which eigenvalue this is, but in view of the earlier work on this problem (2, 7), this is certain to be the case; since our assumed transition probabilities increase slowly with increasing temperature, the eigenvalue in question at 300 °K will be close to, but slightly lower (*i.e.* slower) than, the corresponding eigenvalue d_{119} at 500 °K which is 1.1×10^8 s^{-1} *i.e.* $\tau \approx 9.4 \times 10^{-9}$ s. As the temperature increases, this relaxation will speed up slightly because the $J = 1 \leftrightarrow J = 3$ transition probability increases with temperature. However, by 500 °K, three eigenvalues and three processes are important. These are d_{119} (1.1×10^8 s^{-1}), d_{148} (3.3×10^7 s^{-1}), and d_{159} (1.4×10^7 s^{-1}), with the latter two having larger contributions to the energy increment than does the simple $J = 1 \leftrightarrow J = 3$ relaxation with which d_{119} is principally associated. Thus, although the relaxation is still essentially rotational, this increasing complexity brings with it a *lengthening* of the relaxation time, in our case to somewhere of the order of 5×10^{-8} s. It is precisely the beginning of this behavior that has been observed recently in shock-wave measurements of the rotational relaxation times for hydrogen (12); that our predicted effect is more severe than the observed one is almost certainly attributable to imperfections in our assumed set of transition probabilities (1). At this temperature also, it is possible to identify *theoretically* a vibrational relaxation time, but its associated instantaneous heat capacity is negligible and the relaxation would not be observable in any coarse-grained experiment. Then as the temperature increases, the vibrational character of the excitation becomes more important, and the relaxation time will continue to increase rather slowly until at 2000 °K, Fig. 3*a* would suggest a value close to $|d_{n-2}{}^{-1}|$ (1.1×10^{-7} s) or $|d_{n-3}{}^{-1}|$ (5.9×10^{-8} s), probably around 1×10^{-7} s. Further increase in temperature then increases the complexity of the relaxation still further, but the dominant factor is the general increase in transition probabilities with increasing temperature, leading to a gradual *shortening* of the relaxation time again, to about 3 or 4×10^{-8} s at 5000 °K in our calculation: as we have noted before the actual times and temperatures are quoted for illustrative purposes only, the precise magnitudes being dependent on the initial choice of the set of transition probabilities (1); it could be that the apparent turning point in the "vibrational" relaxation time of NO near 500 °K is an example of this (13, 14), although there are alternative satisfactory explanations.

Thus there are basically four regimes in the internal relaxation of the gaseous molecule, as shown schematically in Fig. 4: (*a*) at low temperature, there is the almost pure $J = 1 \leftrightarrow J = 3$ (more generally $J = 0 \leftrightarrow J = 1$ for most molecules) rotational relaxation (T–R); (*b*) then at intermediate temperatures, there is a mixed rotational relaxation, of somewhat longer duration because of the participation of additional excited rotational levels in the equilibration process (T–*n*R); (*c*) then, at somewhat higher temperatures, this merges into a mixed rotation–vibration relaxation (T–VR), which (*d*) becomes more and more complex in nature (T–*n*VR) with increasing temperature, and whose duration is determined by the network properties of the

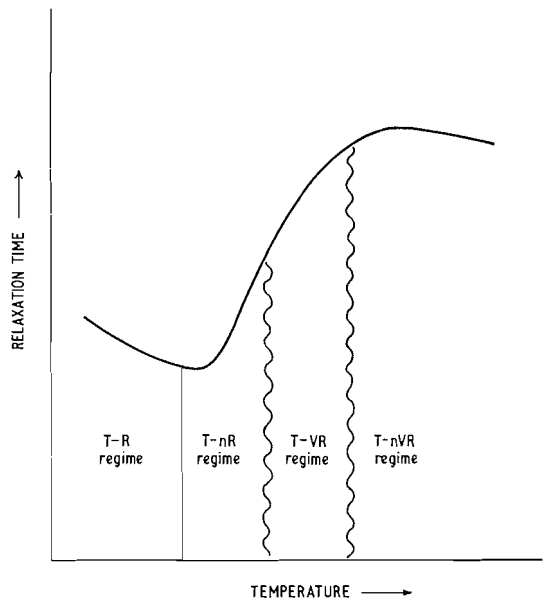

FIG. 4. Schematic diagram of the variation of internal relaxation time with temperature.

larger rotational gaps which interleave the lowest steps on the vibrational ladder.

Thus, whilst to a fair degree of approximation, one can define a rotational relaxation time, it would appear that there is no such thing as a vibrational relaxation time, only a rotation–vibration (T–VR) relaxation time. One should also note that the eigenvalues having large associated energy increments may be dependent on the initial population distribution (*c.f.* eq. 5*e*); thus, it does not necessarily follow that the relaxation time measured for H_2 at 1000 °K in an ultrasonic dispersion experiment needs to be the same as that measured in a shock-wave experiment where the initial temperature is 300 °K and the final temperature is 1000 °K (*c.f.* Fig. 3 of ref. 12).

We would like to express our thanks to Sean McElwain for many helpful discussions, and to Tom Ashton and Gail McCart for programming advice and assistance respectively.

1. T. ASHTON, D. L. S. MCELWAIN, and H. O. PRITCHARD. Can. J. Chem. **51**, 237 (1973). Part VIII.
2. D. L. S. MCELWAIN and H. O. PRITCHARD. Thirteenth Symposium (International) on Combustion. The Combustion Institute, Pittsburgh, 1971. p. 37. Part III.
3. T. L. COTTRELL and J. C. MCCOUBREY. Molecular energy transfer in gases. Butterworths, London, 1961.
4. J. E. DOVE, D. G. JONES, and H. TEITLEBAUM. Fourteenth Symposium (International) on Combustion. 1973. In press.
5. D. J. ECKSTROM and D. BERSHADER. J. Chem. Phys. **53**, 2978 (1970); **55**, 5842 (1971); **57**, 632 (1972).
6. T. CARRINGTON. J. Chem. Phys. **43**, 473 (1965).
7. R. K. BOYD. Can. J. Chem. **50**, 3104 (1972).
8. E. KAMARATOS and H. O. PRITCHARD. Can. J. Chem. **49**, 2617 (1971). Part IV.
9. V. A. LODATO, D. L. S. MCELWAIN and H. O. PRITCHARD. J. Am. Chem. Soc. **91**, 7688 (1969). Part I.
10. D. L. S. MCELWAIN, A. WALLIS and H. O. PRITCHARD. Int. J. Quant. Chem. **3**, 711 (1969).
11. R. K. HANSON and D. BAGANOFF. J. Chem. Phys. **53**, 4401 (1970).
12. C. A. BOITNOTT and R. C. WARDER. Phys. Fluids, **14**, 2312 (1971).
13. J. BILLINGSLEY and A. B. CALLEAR. Nature, **221**, 1136 (1969).
14. W. D. BRESHEARS and P. F. BIRD. Nature, **224**, 268 (1969).
15. J. D. LAMBERT. J. Chem. Soc. Faraday II, **68**, 364 (1972).

Can. J. Chem. Downloaded from www.nrcresearchpress.com by 210.87.254.5 on 09/05/12
For personal use only.

Aqueous Nonelectrolyte Solutions. Part XII. Enthalpies of Mixing of Water and Deuterium Oxide with Tetrahydrofuran[1]

DAVID N. GLEW AND HARRY WATTS

Exploratory Research Laboratory, Dow Chemical of Canada, Limited, Sarnia, Ontario

Received July 21, 1972

Calorimetric enthalpies of mixing have been measured over the whole composition range for the water–tetrahydrofuran and the deuterium oxide – tetrahydrofuran systems at 10.00 and 25.00 °C. The experimental S-shaped, enthalpy of mixing – composition curves are interpreted in terms of changes of the water hydrogen bonding in solution. At low tetrahydrofuran mole fractions the deuterium oxide systems are more exothermal and at high tetrahydrofuran mole fractions more endothermal than the corresponding water systems. A good correlation is found between the enthalpy of mixing and the water proton magnetic resonance chemical shift for solutions with greater than 0.55 mole fraction of tetrahydrofuran.

Les enthalpies calorimétriques de mélange ont été mesurées pour tout l'intervalle de composition des systèmes eau–tétrahydrofuranne et oxyde de deutérium-tétrahydrofuranne à 10.00 et 25.00 °C. Les courbes expérimentales en forme de S, enthalpie de mélange – composition, sont interprétées en fonction des changements dans l'enchainement par liaison hydrogène de l'eau dans la solution. Pour des fractions molaires faibles en tétrahydrofuranne, les systèmes contenant de l'oxyde de deutérium sont plus exothermiques que les systèmes contenant de l'eau similaires; de même pour des fractions molaires élevées en tétrahydrofuranne, les systèmes contenant de l'oxyde de deutérium sont plus endothermiques. On a pu établir une bonne relation entre les enthalpies de mélange et le déplacement chimique en résonance magnétique du proton de l'eau, pour des solutions ayant des fractions molaires en tétrahydrofuranne supérieures à 0.55. [Traduit par le journal]

Can J. Chem., 51, 1933 (1973)

Introduction

Recently we reported measurements of the enthalpies of mixing of water and deuterium oxide with ethylene oxide, EO (1). In that study the S-shaped, enthalpy of mixing – composition curves were interpreted in terms of solution H-bonding changes, with particular reference to the H-bonding of water. We found a good correlation between the enthalpy of mixing and the water proton magnetic resonance (p.m.r.) chemical shift for solutions with mole fraction of EO greater than 0.55. Now we report a continuation of that study in which the enthalpies of mixing of water and deuterium oxide with tetrahydrofuran (THF) have been measured. The behavior of these systems is similar to those containing EO, hence the introduction to that work, and the general comments on the nature of liquid water and aqueous solutions should be read in conjunction with this paper.

Some measurements of the enthalpy of mixing of water with THF at 15 and 25 °C have been reported graphically by Erva (2). However, his study was not so complete as ours.

[1]Contribution No. 196.

Experimental

Materials

The water and deuterium oxide were as used previously (1). Fisher certified grade tetrahydrofuran (THF) was refluxed over lithium aluminum hydride overnight under dry nitrogen and distilled. The distillate was transferred immediately, under an atmosphere of nitrogen, to the calorimeter filling system and freeze-outgassed.

Calorimetry

The calorimeter and its operation have been fully described previously (1, 3). The first system studied with this calorimeter was *n*-hexane–cyclohexane (3), and these measurements have, with others, become embodied in the recommendation that this system be regarded as a standard for testing mixing calorimeters (4). Hence no further comment on the accuracy of the calorimeter is required. All measurements on the water–THF systems were made at 1 atm total pressure.

Results

Enthalpy of mixing measurements at 10.0 and 25.0 °C were made over the complete composition range for both the H_2O–THF and D_2O–THF systems. Tables 1–4 record the weight of H_2O or D_2O and of THF taken in each experiment, together with the temperature of the experiment and the observed heat change. The fifth and sixth columns give the water mole frac-

Can. J. Chem. Downloaded from www.nrcresearchpress.com by 210.87.254.40 on 09/05/12
For personal use only.

TABLE 1. Enthalpy of mixing of water and tetrahydrofuran at 10.00 °C

Weight (g)		Heat change	Temperature	Mole fraction H_2O	$\Delta_m h$	δ
H_2O	C_4H_8O	(J)	(°C)	x_1	(J/mol)	(J/mol)
4.9836	0.1591	37.41	10.013	0.99178	−139.4	−0.3
4.9264	0.4121	90.31	10.005	0.97953	−323.5	−0.2
4.9624	0.6634	134.50	10.013	0.96768	−472.6	−0.4
4.9642	0.8399	160.05	10.009	0.95940	−557.3	1.7
4.9778	1.0914	191.11	10.016	0.94807	−655.9	0.8
4.9560	1.3003	212.65	10.011	0.93848	−725.6	−3.6
4.9547	1.5222	228.69	10.010	0.92871	−772.4	2.1
4.9727	1.7226	242.94	10.007	0.92035	−810.1	−0.2
5.0185	2.6685	281.74	10.014	0.88280	−893.0	−1.0
5.0186	3.5104	295.32	10.023	0.85156	−903.0	2.5
4.9291	4.4035	299.66	10.017	0.81753	−895.6	−1.5
4.0559	4.4543	248.92	10.018	0.78448	−867.6	−0.8
2.9698	4.4150	179.24	10.017	0.72917	−793.0	1.4
1.9976	4.4358	110.93	10.019	0.64318	−643.6	−0.8
1.1771	4.4686	48.88	10.014	0.51198	−385.1	0.5
0.7377	4.4106	17.46	10.026	0.40100	−171.3	−0.5
0.4647	4.4148	−3.01	10.021	0.29642	34.5	0.5
0.3052	4.3282	−12.92	10.007	0.22011	167.8	−0.4
0.2332	4.3976	−16.10	10.003	0.17509	217.7	−0.1
0.1828	4.3942	−16.77	10.008	0.14274	235.9	−0.1
0.1507	4.4267	−16.76	9.998	0.11992	240.3	−0.7
0.1027	4.4484	−15.17	9.996	0.08459	225.2	−0.6
0.0536	4.4466	−10.50	9.998	0.04602	162.4	−0.2
						$\sigma(\Delta_m h) = 1.8$

tion, x_1, and the enthalpy change per mole of mixture formed, $\Delta_m h$, corrected to the reference temperature of the table.

The experimental results for each system were fitted by the method of least squares to the equation

$$[1] \quad \Delta_m h(\text{J/mol}) = x_1(1 - x_1) \sum_{k=0}^{k=m} B_k(1 - 2x_1)^k$$

with regression coefficients B_k. To fit the S-shaped distribution of results adequately for these systems required up to twelve regression coefficients. When the exothermal and endothermal results were fitted separately the number of regression coefficients was six for each region. The final column in Tables 1–4 gives the residual, $\delta(\Delta_m h(\text{obs}) - \Delta_m h(\text{calc}))$, between the observed enthalpy of mixing and the value calculated from [1]. At the bottom of each table $\sigma(\Delta_m h)$ gives the standard error on a single enthalpy of mixing measurement, assessed from the fit of [1]. Over all measurements $\sigma(\Delta_m h)$ has a value of 4.4 J/mol; when the exothermal results alone are fitted $\sigma(\Delta_m h)$ is increased to 5.0, while the endothermal results alone show $\sigma(\Delta_m h)$ significantly reduced to 2.3 J/mol. This properly reflects the greater calorimetric accuracy of the endothermal measurements, as found previously for the EO systems.

Table 5 gives smoothed $\Delta_m h$ values with standard errors σ evaluated from [1] at regular mole fraction intervals.[2] Values of the regression coefficients for [1] for the four sets of measurements are given in Table 6. In Fig. 1 are shown typical S-shaped enthalpy of mixing curves for the H_2O–THF system at 10.00 and 25.00 °C. Increase of temperature leads to increase in $\Delta_m h$ at all compositions. This is consistent with what is commonly observed in aqueous systems in which strong interaction occurs between the components being mixed (5–7).

In Fig. 2 are shown the enthalpy of mixing curves for the H_2O–THF and D_2O–THF systems at 25.00 °C. At low THF concentrations $\Delta_m h$ values with D_2O lie below those with H_2O but at high THF concentrations they lie above, as previously reported for H_2O with EO (1).

[2]Tables 5 and 6 are available, at a nominal charge, from the Depository of Unpublished Data, National Science Library, National Research Council of Canada, Ottawa, Canada K1A 0S2.

Can. J. Chem. Downloaded from www.nrcresearchpress.com by 210.87.254.40 on 09/05/12
For personal use only.

TABLE 2. Enthalpy of mixing of water and tetrahydrofuran at 25.00 °C

Weight (g)		Heat change	Temperature	Mole fraction H_2O	$\Delta_m h$	δ
H_2O	C_4H_8O	(J)	(°C)	x_1	(J/mol)	(J/mol)
4.9882	0.0776	16.08	25.004	0.99613	−57.83	2.6
4.9944	0.1657	33.03	25.019	0.99178	−118.2	5.4
4.9959	0.3588	67.95	25.018	0.98229	−242.0	3.8
4.9682	0.5724	97.99	25.009	0.97202	−345.4	1.1
5.0127	0.6820	119.39	25.014	0.96713	−415.0	−1.3
4.9961	0.8754	135.75	25.008	0.95806	−469.0	6.1
4.9638	1.0593	156.24	25.013	0.94938	−538.5	−4.7
4.8747	1.2161	168.22	25.020	0.94133	−585.4	−6.3
4.9894	1.4255	181.93	25.013	0.93337	−613.2	3.2
4.9820	1.5599	192.74	25.022	0.92745	−646.6	−6.6
5.0405	1.7607	203.00	25.007	0.91973	−667.4	−1.6
4.9871	2.2391	217.67	25.027	0.89927	−707.4	4.3
4.9826	2.5908	225.98	25.012	0.88503	−723.4	5.4
4.9791	3.5766	239.15	24.986	0.84784	−733.5	2.3
4.9897	4.3607	242.30	24.985	0.82079	−716.9	3.3
4.0231	4.4306	197.35	25.000	0.78422	−693.0	−7.4
2.9307	4.4378	138.12	25.005	0.72549	−616.0	−2.6
2.0215	4.4760	84.62	24.996	0.64383	−485.5	3.7
1.4822	4.3715	51.64	25.103	0.57575	−362.4	1.6
0.9051	4.3732	12.98	25.013	0.45307	−117.2	−2.9
0.5647	4.4043	−9.12	25.011	0.33915	98.6	0.5
0.4728	4.3664	−13.54	25.007	0.30236	155.9	−1.6
0.3826	4.4707	−18.95	25.013	0.25514	227.5	2.4
0.3101	4.5182	−21.68	25.012	0.21551	271.3	−0.1
0.2568	4.3386	−22.17	25.013	0.19154	297.8	5.1
0.2047	4.3808	−22.11	25.004	0.15149	306.6	−5.0
0.1683	4.4231	−21.67	25.024	0.13217	306.5	−4.3
0.0947	3.5658	−15.77	25.003	0.09609	288.3	2.7
0.0810	4.3249	−15.79	25.029	0.06973	244.8	1.8
0.0494	4.4385	−11.11	25.020	0.04265	172.8	−0.1
						$\sigma(\Delta_m h) = 5.7$

Discussion

Interpretation of the Enthalpy of Mixing Curves

The S-shaped composition dependence curve for $\Delta_m h$, shown in Figs. 1 and 2, is similar to that observed for many aqueous nonelectrolyte systems (5–9) and in particular to those we observed recently with water and EO (1). As before, we divide our discussion into three sections.

Water-rich Region (100–80% Water)

A qualitative explanation only of the effects observed in this region can be offered. As before (1), we envisage the exothermal mixing of small amounts of THF with water as being due partly to H-bond formation between THF and the small amount of non-H-bonded O—H groups present, partly to the reorientation of water molecules around the template of a THF molecule, and partly to the central van der Waals attractive forces between THF and adjacent water (1, 10–13). The water reorientation relieves strain in the bent H-bonded water network, allowing the water–water–water H-bonds to assume angles closer to the regular tetrahedral angle (10, 13) with consequent strengthening of the H-bonds (11) and lowering of the enthalpy. The central attractive forces between THF and its adjacent water further lower the enthalpy and enhance the water reorientation; the enthalpy is lowered because water interactions with second-nearest water neighbors over the solid angle π are replaced by stronger van der Waals interactions with the closer THF. As more THF is added competition of the THF oxygen atoms for H-bond formation leads to replacement of network water–water H-bonds by water–THF H-bonds with increase of enthalpy, which is responsible for the observed minimum.

The behavior of the H_2O–THF and D_2O–THF systems is similar. However, reference to the smoothed data in Table 5 and to Fig. 2 shows

Can. J. Chem. Downloaded from www.nrcresearchpress.com by 210.87.254.40 on 09/05/12
For personal use only.

TABLE 3. Enthalpy of mixing of deuterium oxide with tetrahydrofuran at 10.00 °C

Weight (g)		Heat change	Temperature	Mole fraction D_2O	$\Delta_m h$	δ
D_2O	C_4H_8O	(J)	(°C)	x_1	(J/mol)	(J/mol)
5.8035	0.1467	36.83	10.026	0.99303	−126.2	5.4
5.5423	0.3646	84.83	10.030	0.98206	−301.0	7.0
5.4661	0.6365	136.27	10.031	0.96868	−483.7	−4.0
5.4528	0.8826	168.35	10.024	0.95699	−591.7	5.0
5.4603	1.1477	203.16	10.043	0.94486	−704.2	−1.3
5.6914	1.4436	227.73	10.023	0.93420	−748.6	7.1
5.5194	1.6554	242.50	10.023	0.92313	−812.3	−5.0
5.5237	2.6366	279.20	10.019	0.88297	−893.8	5.6
5.5166	3.5830	295.35	10.020	0.84721	−908.4	−2.0
5.5349	4.4480	298.23	10.019	0.81757	−882.2	3.1
3.2813	3.5286	176.91	10.017	0.77006	−831.4	−3.9
2.2139	4.4361	105.55	10.017	0.64252	−613.5	1.7
1.3025	4.4159	45.17	10.020	0.51510	−357.9	−0.9
0.8032	4.4094	11.20	10.020	0.39614	−110.8	0.3
0.4865	4.3659	−7.86	10.019	0.28638	92.6	0.0
0.3253	4.4228	−15.93	10.016	0.20941	205.3	−0.2
0.2265	4.5546	−19.07	10.015	0.15190	256.0	0.4
0.1749	4.3806	−18.29	10.022	0.12571	262.2	0.2
0.1585	5.0027	−19.69	10.011	0.10241	254.8	−1.1
0.1003	4.3912	−15.29	10.015	0.07600	231.9	0.7
0.0535	4.4134	−10.39	10.017	0.04183	162.7	−0.1
						$\sigma(\Delta_m h) = 5.7$

TABLE 4. Enthalpy of mixing of deuterium oxide with tetrahydrofuran at 25.00 °C

Weight (g)		Heat change	Temperature	Mole fraction D_2O	$\Delta_m h$	δ
D_2O	C_4H_8O	(J)	(°C)	x_1	(J/mol)	(J/mol)
5.4284	0.2403	27.91	25.015	0.98771	−193.5	−2.7
5.4088	0.3649	73.08	25.021	0.98161	−265.6	3.8
5.6140	0.8074	136.56	25.008	0.96160	−468.5	−1.1
5.2876	1.7152	207.73	24.995	0.91737	−684.4	−0.4
5.4580	2.5533	226.09	25.002	0.88504	−734.1	−0.6
5.5354	3.5651	241.46	25.001	0.84830	−740.9	−1.6
4.5738	4.4230	200.05	25.016	0.78832	−690.5	1.2
3.2204	4.4548	134.97	25.002	0.72249	−606.3	−2.5
2.3064	4.3734	86.25	24.991	0.65509	−490.4	1.4
0.9991	4.4220	10.21	24.998	0.44864	−91.8	−0.4
0.5542	4.4813	−15.11	25.000	0.30815	168.2	0.0
0.3803	3.7768	−16.75	25.025	0.26613	234.4	1.6
0.3745	4.3772	−21.31	24.972	0.23554	268.5	−4.2
0.3683	4.4487	−22.31	25.017	0.22968	282.2	2.8
0.2544	4.3997	−23.86	25.021	0.17234	323.5	−1.9
0.2535	4.4526	−24.41	24.994	0.17015	328.1	1.9
0.1624	4.2998	−21.98	25.021	0.11974	324.4	3.1
0.1640	4.4293	−22.01	24.970	0.11766	316.2	−3.7
0.1023	4.3377	−17.68	24.979	0.07828	271.0	1.0
0.0412	4.0863	−8.96	24.967	0.03504	152.6	−0.6
						$\sigma(\Delta_m h) = 2.9$

Can. J. Chem. Downloaded from www.nrcresearchpress.com by 210.87.254.40 on 09/05/12
For personal use only.

Can. J. Chem. Downloaded from www.nrcresearchpress.com by 210.87.254.40 on 09/05/12
For personal use only.

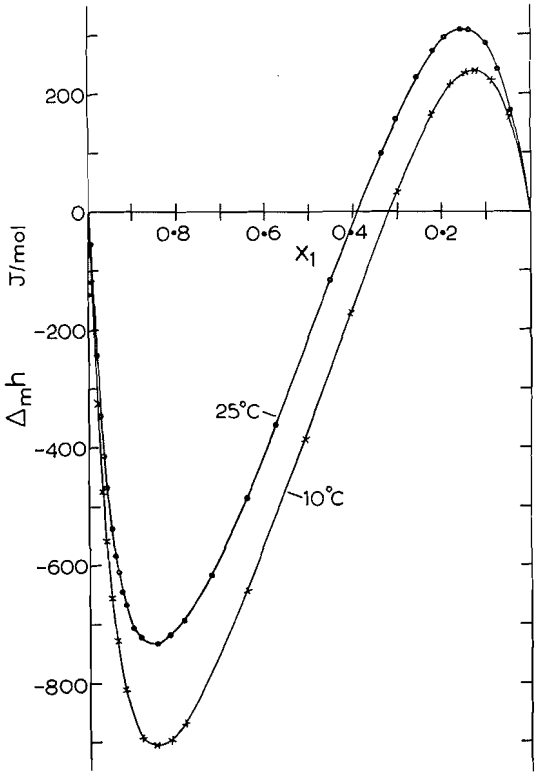

FIG. 1. Molar enthalpy of mixing $\Delta_m h$ dependence on water mole fraction x_1 for the H_2O–THF system at 10.00 and 25.00 °C.

that the D_2O curve lies below the H_2O curve at THF mole fractions less than 0.15 and 0.20 at 10.00 and 25.00 °C, respectively. At higher THF mole fractions the D_2O curve lies above the H_2O curve. A similar effect was observed with EO with the cross-over occurring at lower mole fractions (1). This implies greater strengthening of the three-dimensionally bonded network in D_2O solution than in H_2O solution, and/or stronger THF bonds with D_2O.

The observed minima with THF occur at larger $-\Delta_m h$ values than with EO. This means that THF acts as a better attractive template for reorientation of water molecules than does EO. This is consistent with both the larger downfield water p.m.r. chemical shift observed with THF and the larger excess partial molar volume for water in solution with THF (10) than observed with EO (12).

Intermediate Region (80–20% Water)

A linear dependence of $\Delta_m h$ with composition is observed in the range 0.4–0.7 mole fraction THF. We envisage this as being due to replacement of H-bonds between water molecules by H-bonds between water and THF. This replacement must occur in a perfectly regular manner to cause this long linear region, which has been observed in other aqueous systems (1, 2, 5–9). The water p.m.r. chemical shifts (15) in this linear region show a nearly constant number of water–THF H-bonds per mole of solution with the number of water–water H-bonds decreasing linearly with x_1. This means that the linear increase of $\Delta_m h$ with THF mole fraction directly reflects the linear decrease of the number of water–water H-bonds per mole of solution.

A linear composition dependence of $\Delta_m h$ is also observed with D_2O, but $\Delta_m h$ increases slightly more rapidly for the D_2O systems (Table 5). This implies that the enthalpy difference between a D-bond with D_2O and a D-bond with THF is greater than the corresponding difference for the H_2O–THF system. Thus the breakdown of stronger bonds in the D_2O system leads to larger endothermal enthalpies in this composition region.

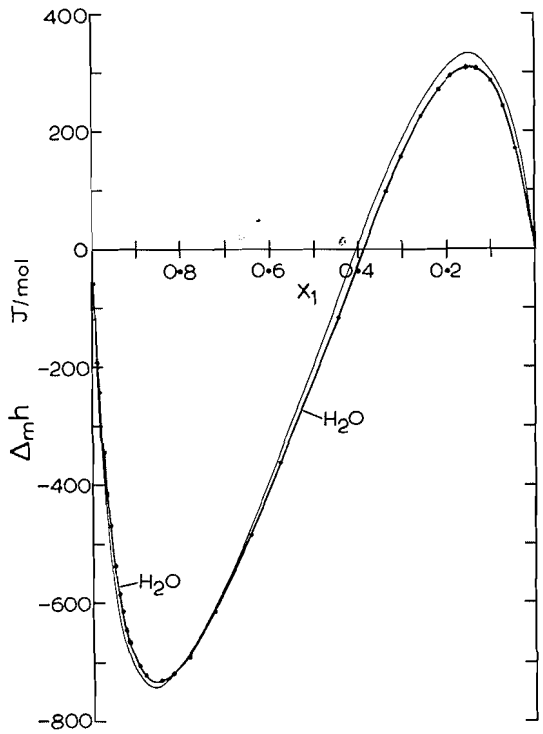

FIG. 2. Comparison of enthalpy of mixing for THF with water (heavy curve showing data points) and with deuterium oxide (fine curve) at 25.00 °C.

Can. J. Chem. Downloaded from www.nrcresearchpress.com by 210.87.254.40 on 09/05/12
For personal use only.

The difference between $\Delta_m h$ values of THF in D_2O and H_2O is smaller than the corresponding difference for EO in D_2O and H_2O over the linear region. Moreover, this difference remains the same within experimental error for the THF systems but decreases with decreasing D_2O (H_2O) mole fraction for the EO systems.

Correlation of Enthalpy of Mixing with Water Proton Magnetic Resonance Chemical Shift

In solutions richer than 0.55 mole fraction THF it is found again that the enthalpy of mixing can be accurately related to the proton magnetic resonance (p.m.r.) chemical shift of the water protons, as found for the aqueous EO systems (1). All symbols are as defined in that earlier work. Due to the relatively large excess of oxygen bonding sites (ether oxygen atoms and water lone pairs) over the water protons we can safely assume that all water protons are H-bonded either to THF oxygen atoms or to water lone pairs, with a negligible fraction as unbonded O—H groups. The lack of detectable unbonded O—H groups for dilute water in THF has already been shown in infrared studies at 0 and 30 °C (10, 14). Thus the water p.m.r. chemical shift in this THF-rich region gives a direct measure of the fraction f_1 of water protons H-bonded to water and of the fraction $(1 - f_1)$ H-bonded to THF (1, 12).

The p.m.r. chemical shifts at 60 MHz have been determined for aqueous THF over the whole composition range at 0 and 25 °C and will be reported elsewhere (15). Some results have already been shown for the water-rich region of aqueous THF at 0 °C (10, 11). The water protons chemical shift relative to the THF α-protons at 25 °C gives $\nu_1 = 60.6$ Hz in pure water (water signal to low field of α-protons signal is defined as positive, and to high field negative) and $\nu_2 = -70.6$ Hz in pure THF. Corresponding linearly interpolated values for 10 °C are $\nu_1 = 69.7$ Hz and $\nu_2 = -65.0$ Hz. In solutions with ideal averaging f_1 values would be expected to be equal to x_1, but in all H_2O–THF solutions measured the f_1 value invariably exceeded x_1, showing that the water protons always formed more than the ideal fraction of H-bonds with water lone pairs and fewer than the ideal fraction with the ether oxygen atom of THF. This was to be expected since water H-bonds with water are on the average stronger, using p.m.r. chemical shift and infrared spectral shift (14) as criteria, than those with THF.

For both the H_2O–THF and D_2O–THF systems at 10.00 and 25.00 °C at THF mole fractions greater than 0.55 the $\Delta_m h$ values were fitted by the two-constant equation

$$[2] \quad \Delta_m h = x_1(1 - x_1)f_1 b_{11} + x_1(1 - x_1)(1 - f_1)b_{12}$$

using the method of least squares, assuming constant enthalpy errors and error-free x_1 and f_1. The f_1 values were interpolated from the p.m.r. chemical shifts for the H_2O–THF system (15). Table 7 shows typical results for the representation of $\Delta_m h$ measurements for H_2O–THF at 25.00 °C by [2] with $b_{11} = -2892$ J/mol and $b_{12} = 5021$ J/mol. The standard error on a single enthalpy determination $\sigma(\Delta_m h)$, assessed from the fit of [2], is 5.1 J/mol, which is larger than that 3.3 J/mol assessed from the fit of the endothermal results by [1] with six regression coefficients.

Table 8 presents the best b_{11} and b_{12} parameters with their standard errors derived from the fit of [2] for the THF-rich regions of the H_2O–THF and D_2O–THF systems. The final column gives the $\sigma(\Delta_m h)$ values assessed from the fits.

The b_{12} values show that the molar transfer of pure water or deuterium oxide to infinite dilution in THF is attended by an enthalpy increase of about 5000 J/mol, with values becoming larger at higher temperatures. This means that the two water H-bonds with THF are each about 2500 J/mol weaker, using enthalpy as a criterion, than the two water H-bonds to water in pure

TABLE 7. Comparison of $\Delta_m h$ for H_2O–THF at 25.00 °C with values from eq. 2

		$\Delta_m h$ (J/mol)		
x_1	f_1	Observed	Calculated	δ (J/mol)
0.04265	0.1067	172.8	170.5	2.3
0.06973	0.1671	244.8	239.9	4.9
0.09609	0.2214	288.3	283.9	4.4
0.13217	0.2912	306.5	311.6	−5.1
0.15149	0.3257	306.6	314.0	−7.4
0.19154	0.3919	297.8	297.2	0.6
0.21551	0.4283	271.3	275.8	−4.5
0.25514	0.4836	227.5	226.8	0.7
0.30236	0.5416	155.9	155.0	0.9
0.33915	0.5833	98.6	90.8	7.8
0.45307	0.6919	−117.2	−112.6	−4.6
			$\sigma(\Delta_m h) = 5.1$	

TABLE 8. Regression coefficients for eq. 2

System	Temperature (°C)	b_{11} (J/mol)	b_{12} (J/mol)	$\sigma(\Delta_m h)$ (J/mol)
H_2O–C_4H_8O	10.00	-3426 ± 62	4652 ± 38	4.7
H_2O–C_4H_8O	25.00	-2892 ± 35	5021 ± 30	5.1
D_2O–C_4H_8O	10.00	-3336 ± 55	4885 ± 31	3.8
D_2O–C_4H_8O	25.00	-2887 ± 22	5219 ± 18	3.0

water. Further, the increase of b_{12} values with temperature shows that the water H-bonds with THF weaken more rapidly at higher temperature than do those in liquid water.

The b_{12} values for the D_2O–THF system are significantly larger than those for the H_2O–THF system at the same temperature, the differences with standard errors are 233 ± 49 J/mol at 10.00 °C and 198 ± 35 J/mol at 25.00 °C; these differences at each temperature are the same within experimental error. If it is assumed that THF bonds with D_2O at infinite dilution are not weaker than THF bonds with H_2O, it is found that D-bonds in liquid D_2O are on a minimum estimate at least 108 J/mol stronger than H-bonds in liquid H_2O over the 10–25 °C range.

The b_{12} values for the H_2O–EO system (1) are considerably larger than those for the H_2O–THF system at the same temperature, the differences with standard errors are 2208 ± 60 J/mol at 10.00 °C and 2259 ± 55 J/mol at 25.00 °C; these differences at each temperature are the same within experimental error. This means that water H-bonds with THF are as a maximum estimate 1117 J/mol stronger than water H-bonds with EO at the same temperature. However, this value is an upper limit because in the definition of b_{12} (1) it also includes enthalpies from changes of the non-H-bonded van der Waals interactions. Such van der Waals interactions are expected to be stronger between H_2O and THF than between H_2O and EO, both on general theoretical grounds (16) and from the 10 000 J/mol enthalpy change calculated for water transfer from liquid heptane (17) to the lower molecular weight liquid propane (18). Thus the real enthalpy difference between the water H-bonds to THF and to EO will be some value smaller than 1117 J/mol.

Similarly the difference of b_{12} values for the D_2O–EO and D_2O–THF systems are 2335 ± 61 J/mol at 10.00 °C and 2448 ± 88 J/mol at 25.00 °C, which values are insignificantly different and show that D-bonds to THF could be up to 1196 ± 38 J/mol stronger than D-bonds to EO at the same temperature. Again the enthalpy difference due to non-D-bonded van der Waals interactions will reduce that between the D-bonds alone to some value smaller than 1196 J/mol.

The negative b_{11} values between -3400 and -2900 J/mol imply that water H-bonds with water at infinite dilution in THF are on the average some 1600 J/mol stronger, lower in enthalpy, than water H-bonds in pure water. However, this value is again an upper limit since our model (1) defines b_{11} to include enthalpy changes from non-H-bonded interactions together with those from the water–water H-bonding changes. These negative b_{11} values in THF solutions with $x_1 < 0.25$ are consistent with the formation of strongly H-bonded, unbranched water chains, with THF forming weaker H-bonds with those protons not bonded to water along the chains. As x_1 increases from 0.25 to 0.5 the one-dimensional water chains progressively cross-link to form two-dimensional water surfaces. The temperature coefficients of b_{11} show that the enthalpy difference between water–water H-bonds in THF and in pure water is reduced at higher temperatures.

The b_{11} value at 10.00 °C for the H_2O–EO system (1) is 2130 ± 69 J/mol larger than for the H_2O–THF system and mainly reflects the larger attractive van der Waals interactions between the water chains and the THF medium.

This work was supported in part by a grant under the National Research Council of Canada Industrial Research Assistance Program, 1966.

1. D. N. GLEW and H. WATTS. Can. J. Chem. **49**, 1830 (1971).
2. J. ERVA. Suom. Kemistil. **B28**, 131 (1955).
3. H. WATTS, E. C. W. CLARKE, and D. N. GLEW. Can. J. Chem. **46**, 815 (1968).
4. M. L. MCGLASHAN and H. F. STOECKLI. J. Chem. Thermodyn. **1**, 589 (1969).
5. D. E. NICHOLSON. J. Chem. Eng. Data, **5**, 309 (1960).
6. J. KENTTAMAA, E. TOMMILA, and M. MARTTI. Ann. Acad. Sci. Fenn. Ser. **A11**, 93 (1959).

Can. J. Chem. Downloaded from www.nrcresearchpress.com by 210.87.254.40 on 09/05/12
For personal use only.

7. V. P. BELOUSOV and V. PONNER. Vest. Leningr. Univ. **3**, 142 (1969).
8. K. W. MORCOM and R. W. SMITH. Trans. Faraday Soc. **66**, 1073 (1970).
9. J. R. GOATES and R. J. SULLIVAN. J. Phys. Chem. **62**, 188 (1958).
10. D. N. GLEW, H. D. MAK, and N. S. RATH. *In* Hydrogen-bonded solvent systems. Taylor and Francis Ltd., London. 1968.
11. D. N. GLEW, H. D. MAK, and N. S. RATH. Chem. Commun. 264 (1968).
12. D. N. GLEW, H. D. MAK, and N. S. RATH. Can. J. Chem. **45**, 3059 (1967).
13. D. N. GLEW. J. Phys. Chem. **66**, 605 (1962).
14. D. N. GLEW and N. S. RATH. Can. J. Chem. **49**, 837 (1971).
15. D. N. GLEW, H. D. MAK, and N. S. RATH. Unpublished work.
16. J. O. HIRSCHFELDER, C. F. CURTISS, and R. B. BIRD. Molecular theory of gases and liquids. John Wiley and Sons, Inc., New York. 1954.
17. C. BLACK, G. G. JORIS, and H. S. TAYLOR. J. Chem. Phys. **16**, 537 (1948).
18. R. KOBAYASHI and D. L. KATZ. Ind. Eng. Chem. **45**, 440 (1953).

Can. J. Chem. Downloaded from www.nrcresearchpress.com by 210.87.254.40 on 09/05/12
For personal use only.

Acid Ionizations of Nitroalkanes in Aqueous Solution

TAKEKI MATSUI AND LOREN G. HEPLER
Department of Chemistry, University of Lethbridge, Lethbridge, Alberta

Received November 20, 1972

Calorimetric measurements have led to ΔH^0 values for ionization of nitromethane, nitroethane, 1-nitropropane, and 2-nitropropane in aqueous solution at 298 °K. Combinations of these enthalpies with free energies from equilibrium constants for ionization have led to ΔS^0 values for the ionization reactions. It is noted that the trend toward decreasing pK with methyl substitution in nitroalkanes is unusual compared to phenols and carboxylic acids. Similarly, correlations of ΔS^0 with ΔG^0 and ΔH^0 are different for nitroalkanes than for other acids.

Les mesures calorimétriques ont conduit à des valeurs ΔH^0 pour l'ionisation du nitrométhane, nitroéthane, nitro-1 propane et nitro-2 propane en solution aqueuse à 298 °K. Les combinaisons de ces enthalpies avec les énergies libres obtenus à partir des constantes d'équilibre pour l'ionisation, ont fourni des valeurs ΔS^0 pour les réactions d'ionisation. Il est à remarquer que l'évolution avec le pK décroissant par la substitution du méthyle dans les nitroalcanes est inhabituelle comparée aux phénols et aux acides carboxyliques. De même les corrélations de ΔS^0 avec ΔG^0 et ΔH^0 sont différentes pour les nitroalcanes comparées aux autres acides. [Traduit par le journal]

Can. J. Chem., 51, 1941 (1973)

Can. J. Chem. Downloaded from www.nrcresearchpress.com by 210.87.254.5 on 09/05/12
For personal use only.

Introduction

The nitroalkanes are interesting acids for several reasons. First, they are "carbon acids" rather than the more usual —O—H and —N—H acids that have been extensively investigated. Further, the nitroalkanes have a variety of unusual acid–base properties as described below.

Several recent investigations (1–5) of nitroalkanes have been concerned with the related problems of equilibrium and rate constants for proton transfer reactions (acid ionizations) and acid–base catalysis, in part because of Bronsted coefficients that are outside the "normal" range of zero to unity. Although not specifically concerned with the particular compounds of interest in our investigations reported here, the recent work of Rose and Stuehr (6) shows that enthalpy and entropy data can provide useful additions to the understanding gained from considerations of free energies in the form of equilibrium and rate constants.

Much of the earlier interest in the nitroalkanes centers on the aci-nitro tautomerism, as reviewed thoroughly by Nielsen (7). As a result, we now have K values for the tautomeric equilibria, which we will refer to later.

Possibly because of concentration of interest in the areas mentioned above, little attention has been paid to the fact that the pK values for ionization of aqueous nitroalkanes show unusual trends. On the basis of ionization constants for a large number of acids (8), we know that replacement of hydrogen by a methyl group generally leads to a *small* change in pK, almost always a small increase. Thus we might expect nitroethane to be a very slightly weaker acid than nitromethane. Further, the statistical effect of having only two ionizable protons in nitroethane as compared to three in nitromethane should make nitroethane a weaker acid by $\Delta pK = 0.2$. But we have $pK = 10.2$ for nitromethane and $pK = 8.2$ for nitroethane. Thus nitroethane is a considerably stronger acid than nitromethane, rather than a somewhat weaker acid as might have been expected. A 2-nitropropane with $pK = 7.7$ is an even stronger acid.

We have undertaken calorimetric measurement of the enthalpies of ionization of nitromethane, nitroethane, 1-nitropropane, and 2-nitropropane with the intention of obtaining some understanding of the unusual acidities of these compounds and the longer range hope of providing data (6) that will prove useful in connection with the relationship between equilibrium and rate constants commonly expressed in terms of the Bronsted coefficient.

Experimental

Calorimetric measurements were made with an LKB 8700 Precision Calorimetry System used as an ampoule calorimeter. All measurements refer to 25.00 ± 0.05 °C, with results reported in terms of the defined calorie (1 cal = 4.1840 J). Concentrations of nitroalkanes and of sodium hydroxide ranged from 0.015 to 0.030 M and 0.03 to 0.05 M, respectively.

TABLE 1. Enthalpies of solution and ionization of nitroalkanes*

Acid	ΔH_1 (kcal mol^{-1})	ΔH_2 (kcal mol^{-1})	ΔH^0_{ioniz} (kcal mol^{-1})
Nitromethane	0.76±0.04	−6.65±0.06	5.93
Nitroethane	0.17±0.01	−10.75±0.01	2.42
1-Nitropropane	0.10±0.02	−10.68±0.03	2.56
2-Nitropropane	0.00±0.01	−13.20±0.15	0.14

*All ± values indicate standard deviations.

Reagent grade nitromethane from Fisher Scientific Company was purified by fractional distillation at 100 mm Hg pressure, followed by two fractional freezings in which two thirds of the sample was discarded as liquid. The resulting material was dried over Drierite and then fractionally distilled again. Practical grade nitroethane, 1-nitropropane, and 2-nitropropane from Baker Chemical Company were purified by three careful fractional distillations at 100 mm Hg. Vapor–liquid chromatography with a silicone column showed that all purified nitroalkanes were at least 99.5 mol% pure. Consistent calorimetric results were obtained with samples prepared at different times as described here. Carbonate free sodium hydroxide solutions were prepared and standardized by usual methods, and water was distilled from alkaline permanganate shortly before each calorimetric measurement.

Results and Discussion

Results of our calorimetric determinations of heats of solution of liquid nitroalkanes in water and in an excess of aqueous sodium hydroxide are summarized in Table 1. The calorimetric reactions are represented by

[1] $R_1R_2CHNO_2(liq) = R_1R_2CHNO_2(aq) \quad \Delta H_1$

and

[2] $R_1R_2CHNO_2(liq) + OH^-(aq) = R_1R_2CNO_2^-(aq) + H_2O(liq) \quad \Delta H_2$

Because solutions used were very dilute, we take these enthalpies to be equal to the desired standard state quantities represented by ΔH_1^0 and ΔH_2^0.

The enthalpies of ionization of aqueous nitroalkanes that are represented by

[3] $R_1R_2CHNO_2(aq) = H^+(aq) + R_1R_2CNO_2^-(aq) \quad \Delta H^0_{ioniz}$

have been obtained from ΔH_1^0 and ΔH_2^0 by way of

[4] $\Delta H^0_{ioniz} = \Delta H_w^0 - \Delta H_1^0 + \Delta H_2^0$

in which $\Delta H_w^0 = 13.34$ kcal mol^{-1} is the standard enthalpy of ionization of water (8).

We have also determined the enthalpies of reaction of aqueous nitroalkanes with aqueous hydroxide. For these measurements an ampoule containing a small excess of concentrated sodium hydroxide was broken in the calorimeter reaction vessel, which contained a weighed amount of dissolved nitroalkane. The calorimetric reaction is represented by

[5] $R_1R_2CHNO_2(aq) + OH^-(conc) = R_1R_2CNO_2^-(aq) + H_2O(liq)$

Separate determination of the enthalpy of dilution of the concentrated sodium hydroxide permitted evaluation of the enthalpy of neutralization of nitroalkane by dilute hydroxide that is represented by

[6] $R_1R_2CHNO_2(aq) + OH^-(aq) = R_1R_2CNO_2^-(aq) + H_2O(liq) \quad \Delta H_6$

Because solutions appropriate to reaction 6 were very dilute, our ΔH_6 values in Table 2 are taken to be equal to the standard state values for this reaction. The enthalpies of ionization of the aqueous nitroalkanes have been calculated as

[7] $\Delta H^0_{ioniz} = \Delta H_w^0 + \Delta H_6^0$

with results that are also listed in Table 2.

The ionization reaction represented by eq. 3 refers to ionization of the equilibrium mixture of *aci* and nitro forms of the weakly acidic compounds under consideration. Our ΔH^0_{ioniz} values are therefore the enthalpies of ionization of one mole of equilibrium mixture of nitro and aci

TABLE 2. Enthalpies of neutralization and ionization of nitroalkanes*

Acid	ΔH_6 (kcal mol^{-1})	ΔH^0_{ioniz} (kcal mol^{-1})
Nitromethane	−7.42±0.08	5.92
Nitroethane	−11.01±0.12	2.33
1-Nitropropane	−10.70±0.10	2.64
2-Nitropropane	−13.33±0.15	0.01

*All ± values indicate standard deviations.

Can. J. Chem. Downloaded from www.nrcresearchpress.com by 210.87.254.5 on 09/05/12
For personal use only.

TABLE 3. Thermodynamics of ionization of aqueous nitroalkanes

Acid	pK	ΔG^0_{ioniz} (kcal mol^{-1})	ΔH^0_{ioniz} (kcal mol^{-1})	ΔS^0_{ioniz} (cal deg^{-1} mol^{-1})
Nitromethane	10.2_2	13.9_4	5.9_3	$-26._9$
Nitroethane	8.5_3	11.6_3	2.4_0	$-31._0$
2-Nitropropane	8.9_8	12.2_5	2.5_8	$-32._4$
1-Nitropropane	7.7	10.5	0.0_8	$-35._1$

forms. The corresponding "apparent" equilibrium constant is

$$[8] \qquad K_{app} = \frac{[H^+][anion]}{[aci] + [nitro]}$$

We have used pK_{app} values (9, 10) to calculate corresponding ΔG^0_{ioniz} values. Combination of these ΔG^0_{ioniz} values with our "best" ΔH^0_{ioniz} values (derived as weighted averages of our calorimetric results already listed in Tables 1 and 2) leads to ΔS^0_{ioniz} values, which also refer to ionization of one mole of equilibrium mixture of the two forms of neutral nitroalkane. All of these quantities are listed in Table 3.

We first note that Turnbull and Maron (9) reported pK values (their estimated uncertainties $\sim \pm 0.02$) based on glass electrode measurements at three temperatures and were thus able to calculate $\Delta H^0_{ioniz} = 6.2$, 1.7, and 3.4 kcal mol^{-1} for nitromethane, nitroethane, and 2-nitropropane, respectively. The reported uncertainties in pK values are of little consequence with respect to ΔG^0_{ioniz} values, but our application of King's (11) method of analysis shows that uncertainties in derived ΔH^0_{ioniz} values are at least $\sim \pm 1$ kcal mol^{-1}. Thus the agreement between the $\Delta H^0_{ioniz} = 6.2$ kcal mol^{-1} from Turnbull and Maron (9) and our calorimetric $\Delta H^0_{ioniz} = 5.9_3$ kcal mol^{-1} is remarkably good and the agreement for nitroethane (1.7 *vs.* 2.4_0 kcal mol^{-1}) is as good as can be expected. We believe that the large discrepancy (3.4 *vs.* 0.0_8 kcal mol^{-1}) for 2-nitropropane can be mostly attributed to errors in the d ln K/dT values from Turnbull and Maron (9).

Now we briefly consider some pK values for some other acids. Methyl substitution in phenol to form cresols, xylenols, and trimethylphenols leads to increases in pK ranging from 0.15 for *m*-cresol to 0.92 for 2,4,6-trimethylphenol, all at 298 °K. Similarly, acetic acid is a weaker acid than is formic acid, and propionic acid is weaker than acetic acid. Both *m*-toluic acid and *p*-toluic acid have larger pK values than does acetic acid, but *o*-toluic acid is stronger (Δp$K = 0.29$) than benzoic acid in aqueous solution at 298 °K.

Christensen, Izatt, and Hansen (12) have noted a general linear relationship between ΔG^0 and ΔS^0 values for ionization of carboxylic acids in aqueous solution, and we find a generally similar relationship for phenol and substituted phenols. In both cases there is a trend toward less negative ΔS^0 of ionization as ΔG° becomes smaller. But the trend for the nitroalkanes is in the opposite direction, with ΔS^0 becoming more negative as ΔG^0 becomes smaller. Similarly, the lines in graphs of ΔH^0 against ΔS^0 have opposite slopes for phenols and nitroalkanes. We also note that the entropies of ionization of the nitroalkanes are more negative than entropies of ionization of most carboxylic acids and phenols.

As already mentioned, Turnbull and Maron (9) have determined equilibrium constants for the aci–nitro equilibria. Their results show that these nitroalkanes are very largely in the nitro form in aqueous solution. It therefore follows that the pK, ΔG^0, ΔH^0, and ΔS^0 values for ionization reported here (Table 3) refer almost entirely to the nitro forms of these acids.

Wheland and Farr (10) have suggested that 2-nitropropane is a stronger acid than nitromethane because in the former compound the lines of force between the large dipole moments of the nitro group and the proton pass largely through the (low dielectric constant) methyl group, while in nitromethane the corresponding lines of force pass mostly through the (high dielectric constant) water. They have also extended this argument to nitroethane and 1-nitropropane. This kind of explanation, partly involving differences in solute–solvent interactions, suggests that there might be something "unusual" in the ΔH^0 and ΔS^0 values for ionization of these acids. As noted above, the ΔH^0 and ΔS^0 values we have found (Table 3) are "unusual", but we have no satisfactory explanation beyond that already offered by Wheland and Farr (10).

We are grateful to Dr. Douglas Dolman for helpful discussions and the National Research Council of Canada for support of this research.

1. F. G. BORDWELL and W. J. BOYLE, JR. J. Am. Chem. Soc. **94**, 3907 (1972).
2. A. J. KRESGE. J. Am. Chem. Soc. **92**, 3210 (1970).

Can. J. Chem. Downloaded from www.nrcresearchpress.com by 210.87.254.5 on 09/05/12
For personal use only.

3. M. FUKUYAMA, P. W. K. FLANAGAN, F. T. WILLIAMS, JR., L. FRAINIER, S. A. MILLER, and H. SHECHTER. J. Am. Chem. Soc. **92**, 4689 (1970).
4. F. G. BORDWELL, W. J. BOYLE, JR., J. A. HAUTALA, and K. C. YEE. J. Am. Chem. Soc. **91**, 4002 (1969).
5. R. A. MARCUS. J. Am. Chem. Soc. **91**, 7224 (1969).
6. M. C. ROSE and J. E. STUEHR. J. Am. Chem. Soc. **94**, 5532 (1972).
7. A. T. NIELSEN. *In* The chemistry of the nitro and nitroso groups (Part 1). *Edited by* H. Feuer. John Wiley and Sons, New York, N.Y. 1969.
8. J. W. LARSON and L. G. HEPLER. *In* Solute–solvent interactions. *Edited by* J. F. Coetzee and C. D. Ritchie. Marcel Dekker, Inc., New York, N.Y. 1969.
9. D. TURNBULL and S. H. MARON. J. Am. Chem. Soc. **65**, 212 (1943).
10. G. W. WHELAND and J. FARR. J. Am. Chem. Soc. **65**, 1433 (1943).
11. E. J. KING. Acid–base equilibria. Pergamon Press, Inc., Oxford, England. 1965.
12. J. J. CHRISTENSEN, R. M. IZATT, and L. D. HANSEN. J. Am. Chem. Soc. **89**, 213 (1967).

Can. J. Chem. Downloaded from www.nrcresearchpress.com by 210.87.254.5 on 09/05/12
For personal use only.

Fragmentation and Rearrangement Processes in the Mass Spectra of Perhalogenoaromatic Compounds. Part IX.[1] Pentafluorophenol and Pentafluorothiophenol Derivatives of Group IV

G. F. LANTHIER[2] AND J. M. MILLER[3]

Department of Chemistry, Brock University, St. Catharines, Ontario

AND

A. J. OLIVER

Department of Chemistry, York University, Downsview, Ontario

Received November 3, 1972

The mass spectra of $R_3MSC_6F_5$ and $R_3MOC_6F_5$ (R = CH_3 or C_6H_5; M = Si, Ge, Sn) are reported and compared with the corresponding pentafluorophenyl derivatives. The sulfur and oxygen compounds show fewer rearrangements leading to the formation of metal fluorides than do simple C_6F_5 derivatives. The ions R_3M^+ are usually observed as the base peaks. Ions containing Sn—S appear more stable than Sn—O species, while the reverse seems true for silicon.

Les spectres de masse du $R_3MSC_6F_5$ et du $R_3MOC_6F_5$ (R = CH_3 ou C_6H_5; M = Si, Ge, Sn) sont décrits et comparés avec les dérivés pentafluorophényles correspondants. Les composés comportant un soufre ou un oxygène subissent moins de réarrangements conduisant à la formation de fluorures métalliques qu'en subissent les dérivés C_6F_5 simples. Les ions R_3M^+ sont habituellement observés et représentés comme pics de base. Les ions contenant les espèces Sn—S semblant être plus stables que ceux contenant les espèces Sn—O, alors que la relation inverse semble être vérifiée dans le cas du silicium.
[Traduit par le journal]

Can. J. Chem., **51**, 1945 (1973)

Introduction

We have previously studied the mass spectra of perfluoroaromatic derivatives of Group IV (1–4) and Group VI (1, 5) and noted extensive fluorine transfer from carbon to the central atom of the former but not the latter. We now report on a series of Group IV derivatives containing either the M—O—C_6F_5 or M—S—C_6F_5 groups and compare the fluorine transfer reactions of these compounds with the simple metal–pentafluorophenyl derivatives.

Experimental

The compounds in this study were prepared as described previously (6). Mass spectra were obtained at Brock University on an A.E.I. MS 30 double beam, double focusing mass spectrometer at 70 eV with a 4 kV accelerating voltage using a 300 μA trap current and a source temperature of 200°. Samples were admitted to beam 1 via the all glass heated inlet system at temperatures between 100° and 200°. PFK was admitted into beam 2 via a gas/liquid probe to serve as a chemical mass marker, recorded simultaneously, but not interfering, with the system under investigation. No problems of metal deposition in the source were noted. Samples were also checked for purity by passing them through a Pye 104 gas chromatograph (3% SE-30, 5 ft glass column) directly into the beam 2 of the MS 30 via a membrane separator. The spectrum recorded for the g.c. effluent corresponded directly with those obtained by batch insertion. Metastable ions and overlapping isotopic peaks were analyzed by computer techniques as described previously (1).

Results and Discussion

The partial mass spectra of the $(C_6H_5)_3MEC_6F_5$ (M = Si, Ge, Sn; E = O, S) are reported in Table 1 while the corresponding trimethyl derivatives are shown in Table 2. The metastable-ion supported fragmentations are shown in partial fragmentation Schemes 1–4, where solid lines indicate a metastable supported transition for at least one metal while dotted lines show ions formed by undetermined routes.

Fragmentation of the Parent Ions

The parent ion abundances are low for the triphenyl derivatives of germanium and tin but reasonably strong in all other cases. All parent ions lose a $C_6F_5O^\cdot$ or $C_6F_5S^\cdot$ unit to give the very abundant (14–60% of the total ion current)

[1]Presented in part at the 164th A.C.S. Meeting, N.Y. 1972. For Part VIII see ref. 1.

[2]Present address: Department of Chemistry, Sir John Abbott College, Montreal, Quebec, Canada.

[3]To whom correspondence should be addressed.

Can. J. Chem. Downloaded from www.nrcresearchpress.com by 210.87.254.105 on 09/05/12
For personal use only.

TABLE 1. Partial* mass spectra of $(C_6H_5)_3MEC_6F_5$ (M = Si, Ge, or Sn; E = O or S)

	Ion intensities as percent of total positive ion current					
	Si		Ge		Sn	
Ion$^+$	O	S	O	S	O	S
Metal-containing ions						
$C_{18}H_{15}MEC_6F_5^{\cdot}$	3.9	0.1	—	—	0.3	0.1
$C_{18}H_{14}MEC_6F_4^{\cdot}$	1.4	—	—	—	—	—
$C_{12}H_{10}MEC_6F_5$	0.7	—	—	—	0.1	0.6
$C_{12}H_9MEC_6F_5$	3.6	—	—	—	—	—
$C_{12}H_9MEC_6F_4$	—	—	—	—	—	2.4
$C_{18}H_{15}MF^{\cdot}$	1.1	2.6	—	—	0.1	—
$C_{18}H_{15}M$	23.6	16.9	47.5	60.3	25.9	25.5
$C_{18}H_{13}M$	1.4	1.5	—	—	—	—
$C_{15}H_9M$	—	3.9	—	—	6.5	3.5
$C_{12}H_{10}MEF$	—	—	1.4	—	—	—
$C_{12}H_{10}MF$	1.2	—	1.8	3.5	3.9	3.0
$C_{12}H_{10}M^{\cdot}$	—	—	—	—	3.5	2.6
$C_{12}H_9M$	5.0	5.6	4.3	6.9	—	—
$C_{12}H_8M^{\cdot}$	1.0	1.2	1.6	2.7	—	—
$C_{12}H_7M$	—	2.8	—	—	—	—
C_6H_5M	4.1	2.3	13.5	0.6	8.9	9.9
C_6H_3M	1.0	—	—	—	—	—
F_3MH	0.6	—	—	—	—	—
$FMEH^{\cdot}$	—	—	—	—	2.0	—
MF	1.7	0.7	0.7	1.0	3.3	3.6
$M^{\cdot}$	—	—	—	—	8.4	7.9
Other ions						
$C_6F_5EH^{\cdot}$	—	8.6	3.0	1.4	5.2	4.4
C_6F_5E	—	3.7	0.8	1.9	0.3	1.7
C_6F_5H	—	1.9	—	0.4	—	1.2
C_5F_5	2.5	—	1.6	1.1	3.3	—
C_5F_4	—	—	3.3	—	—	—
C_5F_3	1.1	1.7	2.1	0.3	1.8	—
$C_{12}H_{10}^{\cdot}$	1.8	4.7	—	—	4.2	4.4
$C_{12}H_8^{\cdot}$	1.2	1.2	—	—	—	0.7
$C_6H_6^{\cdot}$	1.3	1.0	—	0.5	—	5.2
C_6H_5	6.5	1.2	1.5	1.5	—	2.9
CF_2H/C_4H_3	5.2	1.0	1.9	1.6	3.3	2.5

*Ions less than 1% of the base peak and low mass hydrocarbon ions are omitted, unless necessary for comparisons and unless verified for metal containing ions by the appropriate isotopic abundances.

R_3M^+ ion (R = C_6H_5 or CH_3) which forms the base peak except in the case of $(CH_3)_3SiOC_6F_5$ which has as its base peak the $(CH_3)_2SiF^+$ ion, and for its sulfur analog in which a $H_2SiC_5F_3^+$ ion is of equal abundance to $(CH_3)_3Si^+$. This is consistent with the normal tetra-alkyl and aryl derivatives of Group IV which usually have the R_3M^+ ion as the base peak (7), although this is not the case for R = C_6F_5 (3).

An alternate route to the trisubstituted metal involves the loss of either a $C_6H_5^{\cdot}$ or $CH_3^{\cdot}$ radical, the M—O or M—S bond remaining intact. Although no metastables are observed for these transitions in the case of the methyl derivatives loss of a $CH_3^{\cdot}$ group is common, but if phenyl groups are present loss of $C_6F_5O^{\cdot}$ or $C_6F_5S^{\cdot}$ is much preferred. This may be indicative of some interaction of the phenyl π-system with the metal, strengthening the M—C bond.

Other observed species formed from the parent ions involve loss of HF in the case of $(C_6H_5)_3SiOC_6F_5$ and loss of $C_6F_4O^{\cdot}$ or $C_6F_4S^{\cdot}$ to yield $(C_6H_5)_3MF^+$ ions.

Fragmentation of R_3M^+ and $R_2MEC_6F_5^+$

The behavior of the R_3M^+ ions closely parallels that of the equivalent ions formed in the analogous R_4M or $R_3MC_6F_5$ cases (4, 7). Contrary to previous observations (3), the germanes now have the weakest parent ions, and

Can. J. Chem. Downloaded from www.nrcresearchpress.com by 210.87.254.105 on 09/05/12
For personal use only.

TABLE 2. Partial mass spectra of $(CH_3)_3MEC_6F_5$ (M = Si, Ge, Pb, Sn; E = O or S)

	Ion intensities as percent of total positive ion current					
	Si		Ge		Sn	
Ion$^+$	O	S	O	S	O	S
Metal-containing ions						
$C_3H_9MEC_6F_5^{\cdot}$	10.1	3.0	4.7	2.7	0.1	4.7
$C_2H_6MEC_6F_5$	2.7	1.1	3.3	4.8	—	12.6
$C_2H_5GeSC_6F_5$	—	—	—	1.1	—	—
$CH_3MEC_6F_5^{\cdot}$	0.2	0.1	—	2.5	—	4.2
MEC_6F_5	—	—	—	1.2	0.1	8.2
$H_2MC_5F_3$	2.4	15.4	—	—	—	—
MC_5F_3	0.8	0.4	—	—	—	—
$C_2H_6MEC_6F_5^{+\cdot *}$	1.4	—	0.7	0.4	—	0.6
C_2H_6MF	17.8	7.8	11.5	9.1	—	—
CH_3MF_2	5.0	1.2	—	—	—	—
C_3H_9M	14.6	15.4	49.0	42.3	19.0	27.0
$MF_2^{\cdot}$	—	1.4	—	—	—	—
H_2MF	2.9	1.1	—	—	—	—
$C_2H_6M^{\cdot}$	—	—	2.4	2.6	4.4	4.7
MF	4.1	1.2	6.8	4.8	0.3	10.7
CH_3M	2.1	1.8	5.7	6.6	14.6	9.5
$M^{\cdot}$	—	—	1.3	0.7	11.0	3.7
Other ions						
$C_6F_5ECH_3$	—	—	—	—	2.5	—
C_6F_5EH	—	8.2	2.9	3.0	8.3	0.9
C_6F_5E	—	2.8	0.4	1.2	2.2	0.4
C_6F_4E	—	1.0	—	0.4	0.2	0.4
C_6F_5H	—	2.0	0.1	1.0	—	—
$C_6F_4CH_3$	6.3	—	0.3	0.4	—	—
C_5F_5	—	2.3	0.9	1.2	2.7	—
C_5F_3EH	—	0.9	0.3	0.4	—	—
C_6F_4H	—	1.3	—	—	—	—
C_5F_4	—	0.9	2.7	0.4	6.1	—
C_5FE	—	1.3	—	0.9	—	—
C_3F_3	0.4	1.5	—	0.6	0.9	0.6

*Doubly charged ion.

the highest abundance of the R_3M^+ species. In this study only two metastable supported transitions from the R_3M^+ ion are observed when R = C_6H_5; namely the loss of either a molecule of benzene or a molecule of hydrogen. After the loss of benzene the resulting $C_{12}H_9M^+$ ions eliminate a molecule of acetylene, characteristic of phenylated organometallic compounds. $(CH_3)_3M^+$ ions are of lower abundance than the analogous $(C_6H_5)_3M^+$ species, and the only observed metastable transition from the trimethyl-metal ion is loss of a molecule of ethane, yielding CH_3M^+, a species of increasing stability as the metal becomes heavier. A similar trend is not so pronounced for the phenyl derivatives. In their case C_6H_5M may be the neutral species eliminated, leaving a stable biphenyl ion $(C_6H_5)_2^{+\cdot}$ as the charged species, which is observed for silicon and tin, but not for the germanium derivative.

Just as the loss of C_6F_4 was observed from various three coordinate tin ions containing the C_6F_5 group (4) we here observe a metastable for loss of OC_6F_4 from $(CH_3)_2GeOC_6F_5^+$ yielding the $(CH_3)_2GeF^+$ ion. Analogous reactions presumably account for the formation of $C_{12}H_{10}MF^+$ and $(CH_3)_2MF^+$ ions observed for most of the compounds studied.

The formation of the ion $C_2H_5GeSC_6F_4^+$ by the metastable supported loss of HF from $(CH_3)_2GeSC_6F_5^+$ is unique in that the analogous daughter ions (1.1% for the germane derivative) are not observed for any of the other compounds studied as part of this investigation. Loss of

Can. J. Chem. Downloaded from www.nrcresearchpress.com by 210.87.254.105 on 09/05/12
For personal use only.

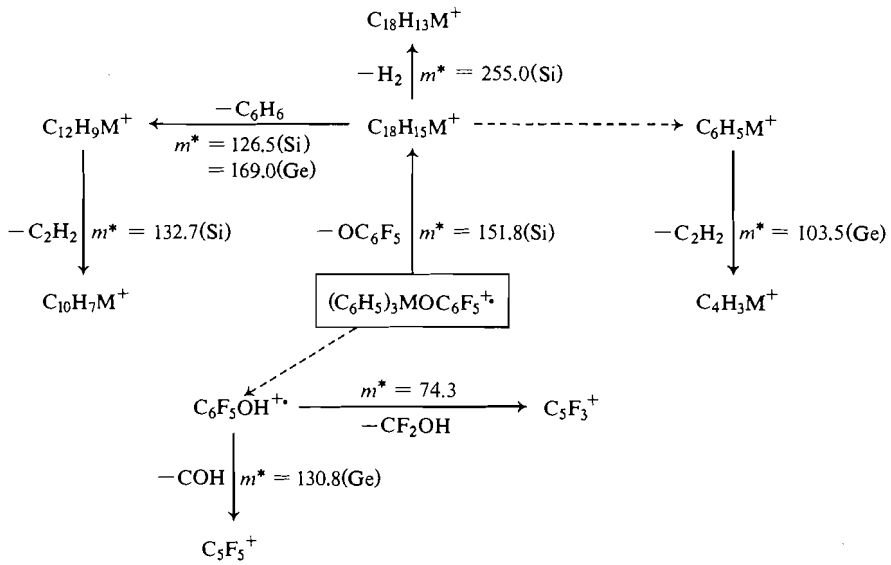

SCHEME 1. Fragmentation of $(C_6H_5)_3MOC_6F_5$

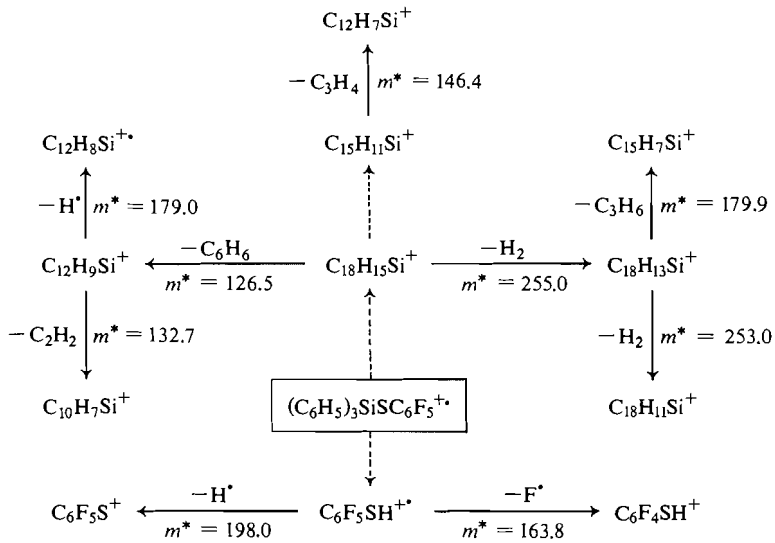

SCHEME 2. Fragmentation of $(C_6H_5)_3SiSC_6F_5$

another $CH_3^\cdot$ is observed from $(CH_3)_2GeSC_6F_5^+$, the resulting $CH_3MSC_6F_5^{+\cdot}$ not having an abundant analog in the spectra of either the oxygen containing systems or the phenylated derivatives. Interestingly, the only abundant doubly charged ions correspond to $(CH_3)_2ME C_6F_5^{2+\cdot}$ (E = O or S), and are not observed for the phenyl derivatives.

Other Metastable Supported Transitions

Metastable ions are observed for various other transitions involving either phenyl–M or methyl–M containing ions, but these are entirely in accord with those reported previously (4, 7). The phenyl derivatives also show several metastable supported transitions which involve fragmentation based on either $C_6F_5OH^{+\cdot}$ or

Can. J. Chem. Downloaded from www.nrcresearchpress.com by 210.87.254.105 on 09/05/12
For personal use only.

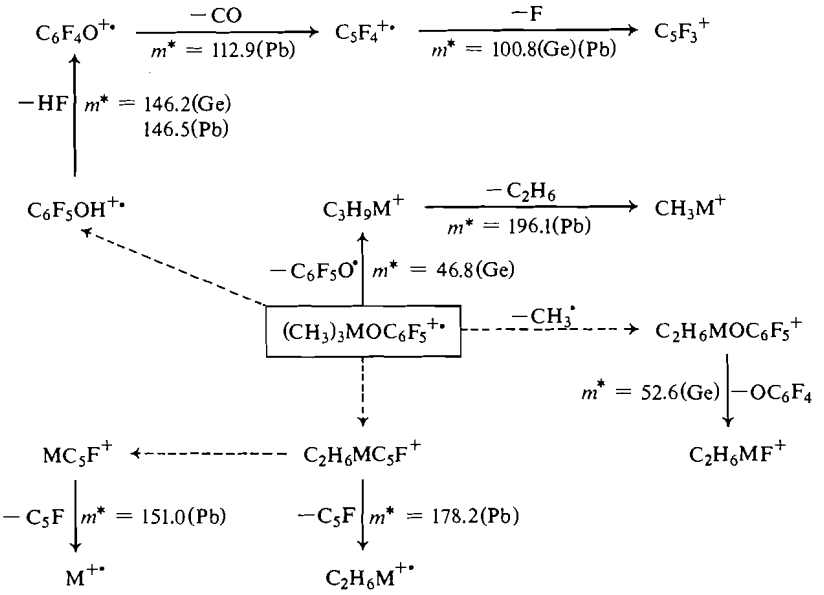

SCHEME 3. Fragmentation of $(CH_3)_3MOC_6F_5$

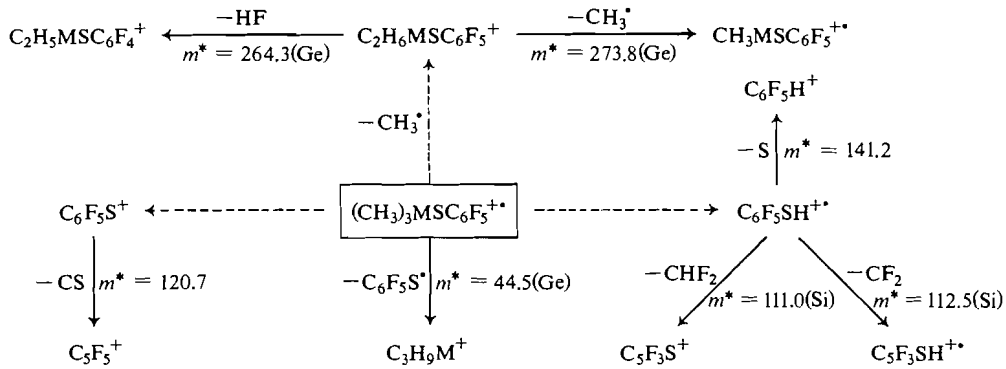

SCHEME 4. Fragmentation of $(CH_3)_3MSC_6F_5$

$C_6F_5SH^+$. Whereas in the spectrum of pentafluorophenol, Smithson *et al.* (8) report metastables for the loss of CFOH from the parent, followed by loss of F$^{\cdot}$, we observed, from the $C_6F_5OH^{+\cdot}$ ion formed in the spectra of $(C_6H_5)_3MOC_6F_5$, the metastable supported loss of $CF_2OH^{\cdot}$, or $COH^{\cdot}$, indicative of either different energetics or structure for our $C_6F_5OH^{+\cdot}$ ions. We plan to follow up this difference using recently developed metastable "defocussing" techniques (9). Similarly, where loss of S and CSH from $C_6F_5SH^{+\cdot}$ has been reported for the pure thiophenol (8), we observe metastables only for the loss of H$^{\cdot}$ or F$^{\cdot}$ A different pattern is followed by our trimethyl derivatives. We now observe metastables for the loss of HF from $C_6F_5OH^{+\cdot}$, followed by loss from the resulting $C_6F_4O^{+\cdot}$ of a molecule of CO, followed by loss of F$^{\cdot}$, *i.e.* differing in terms of observed metastables from both the spectrum of pure C_6F_5OH and that of $C_6F_5OH^{+\cdot}$ formed by electron impact on $(C_6H_5)_3MOC_6F_5$ derivatives. If we look at $(CH_3)_3MSC_6F_5$ (Scheme 4), differences are again observed, loss of either S, CF_2, or CHF_2 neutrals being shown from the $C_6F_5SH^{+\cdot}$ present in the spectrum. These observed differences indicate that the pentafluorophenol and pentafluorothiophenol ions are formed by a re-

Can. J. Chem. Downloaded from www.nrcresearchpress.com by 210.87.254.105 on 09/05/12
For personal use only.

Can. J. Chem. Downloaded from www.nrcresearchpress.com by 210.87.254.105 on 09/05/12
For personal use only.

arrangement involving a hydrogen abstraction, rather than arising from either impurities or simple decomposition of the organometallic compounds under study. In almost every case the $C_6F_5OH^{+\cdot}$ and $C_6F_5SH^{+\cdot}$ ions were more abundant than the expected $C_6F_5O^+$ and $C_6F_5S^+$ species.

Hydrocarbon Ions

Phenyl ions were usually observed for the compounds studied as were biphenyl (with the exception of the Ge derivatives) ions, the latter being more abundant than the former. This was also the case for $(C_6H_5)_3SnC_6F_5$ (4), although for $(C_6F_5)_4M$ compounds the perfluorobiphenyl ions were not as abundant as the $C_6F_5^+$ ions. There was no evidence from the spectra of either the phenyl or methyl series for rearrangements involving the transfer of oxygen or sulfur atoms to either neutral or ionic hydrocarbon species. The only mixing of substituents that took place at all was the previously discussed loss of HF, the formation of $C_6F_5EH^{+\cdot}$ ions and the formation of $C_6F_5H^{+\cdot}$. The latter are quite common in spectra of hydrocarbon/pentafluorophenyl organometallics.

Other Considerations

In Table 3 we show the percent of the total positive ion current which is carried by metal-containing ions.

As has been previously observed (3), silicon derivatives usually have the lowest abundance of metal-containing ions, perhaps due to the low abundance of silicon and silicon fluoride ions. These appear to prefer elimination as neutral species, leaving hydrocarbons or fluorocarbons as the charge-carrying species. Oxygen or sulfur have much less influence than do methyl or phenyl. In the case of the tin derivatives the abundances observed are very similar to those which we have reported for $(CH_3)_3SnC_6F_5$ (93%) and $(C_6H_5)_3SnC_6F_5$ (62%).

TABLE 3. Percentage of metal-containing ions

	% for M =			
Compound	Si	Ge	Sn	Pb
$(CH_3)_3MOC_6F_5$	69.7	78.0	—	57.5
$(CH_3)_3MSC_6F_5$	51.9	79.3	85.8	—
$(C_6H_5)_3MOC_6F_5$	50.5	72.5	63.0	—
$(C_6H_5)_3MSC_6F_5$	42.4	76.9	59.7	—

TABLE 4. Percentage of metal–fluoride containing ions

	% for M =			
Compound	Si	Ge	Sn	Pb
$(CH_3)_3MOC_6F_5$	29.8	18.3	—	0.3
$(CH_3)_3MSC_6F_5$	12.7	13.9	10.7	—
$(C_6H_5)_3MOC_6F_5$	4.6	3.9	9.3	—
$(C_6H_5)_3MSC_6F_5$	3.3	4.5	6.6	—

TABLE 5. M—O *vs.* M—S containing ions

	M =			
Compound	Si	Ge	Sn	Pb
$(CH_3)_3MOC_6F_5$	14.4	8.7	—	2.2
$(CH_3)_3MSC_6F_5$	5.7	11.6	30.3	—
$(C_6H_5)_3MOC_6F_5$	9.6	1.4	0.5	—
$(C_6H_5)_3MSC_6F_5$	0.1	0.0	3.1	—

Table 4 summarizes the abundances of ions which appear to contain fluorine that has migrated to the metal atoms. Metal fluoride species are more common in the spectra of the methyl derivatives compared to their phenyl analogs, perhaps as a result of interaction of the aromatic ring electrons with vacant "d" orbitals on the metals. We had previously postulated (1, 3) the necessity of vacant orbitals on the metal atom if rearrangements leading to the formation of metal fluorides are to be observed. Another apparent trend for the oxygen containing compounds is a decrease in metal–fluoride ion abundance as we go to heavier metals for the methyl derivatives, compared to a corresponding increase for the phenyl compounds. This may again result from more effective p_π–d_π interaction between phenyl and silicon than between phenyl and tin.

A similar reversal is observed as we change from the pentafluorophenol to the thiophenol derivatives. As we compare the abundance of M—O *vs.* M—S containing ions (Table 5), we find the metal–sulfur species increasing in abundance as we go to heavier metals, while the reverse is observed for metal–oxygen containing ions. The tin–oxygen bonds are cleaved more readily than those of tin–sulfur, while silicon–oxygen bonds are retained to a greater extent than silicon–sulfur bonds. Germanium is anomalous, in that the $(C_6H_5)_3MEC_6F_5$ (E = O or S) compounds very readily lost C_6F_5O— or C_6F_5S— so there were therefore few sulfur or

oxygen containing species observed. Again the abundances are lower for the phenyl derivatives than for the methyls, due to the greater stability of the R_3M^+ ions when R = phenyl than when R = methyl, presumably as a result of some form of π interaction, and similarly the greater stability of the oxygen and sulfur containing ions for the methyl derivatives where there is no back donation competition from phenyls.

We can thus summarize our results by characterizing these spectra as typical of R_3MX compounds, and the behavior of X = $-SC_6F_5$ or $-OC_6F_5$ is not radically different from the case where X = C_6F_5. Methyl or phenyl substitution is responsible for far greater differences in fragmentation.

The authors wish to thank the National Research Council of Canada for financial support.

1. G. F. LANTHIER, J. M. MILLER, S. C. COHEN, and A. G. MASSEY. In press.
2. J. M. MILLER. J. Chem. Soc. **A**, 828 (1967).
3. J. M. MILLER. Can. J. Chem. **47**, 1613 (1969).
4. T. CHIVERS, G. F. LANTHIER, and J. M. MILLER. J. Chem. Soc. **A**, 2556 (1971).
5. S. C. COHEN, A. G. MASSEY, G. F. LANTHIER, and J. M. MILLER. Org. Mass Spectrom. **6**, 373 (1972).
6. A. J. OLIVER and W. A. G. GRAHAM. J. Organomet. Chem. **19**, 17 (1969).
7. D. B. CHAMBERS, F. GLOCKLING, and M. WESTON. J. Chem. Soc. **A**, 1759 (1967).
8. L. D. SMITHSON, A. K. BHATTACHARYA, and C. TAMBORSKI. Org. Mass Spectrom. **4**, 1 (1970).
9. J. M. MILLER, J. ROSS, J. RUSTENBURG, and G. WILSON. Anal. Chem. **45**, 627 (1973).

Can. J. Chem. Downloaded from www.nrcresearchpress.com by 210.87.254.105 on 09/05/12
For personal use only.

Crystal and Molecular Structure of tetrakis(4-Methylpyridine)nickel(II)perchlorate, $[Ni(II)(C_6H_7N)_4][ClO_4]_2$

N. Bose and H. Lynton

Department of Chemistry, University of New Brunswick, Fredericton, New Brunswick

Received November 20, 1972

Crystals of tetrakis(4-methylpyridine)nickel(II)perchlorate, $Ni(C_6H_7N)_4(ClO_4)_2$, are monoclinic, space group $C2/c$, with $a = 18.38(1)$, $b = 10.71(1)$, $c = 15.58(1)$ Å, $\beta = 109.83(5)°$, and four molecules in the unit cell. The final atomic parameters were obtained from a block-diagonal least squares refinement using anisotropic thermal parameters. The hydrogen atom positions were established but the parameters were not refined. The final agreement residual for 1199 observed reflections is $R = 0.049$. The structure consists of discrete $Ni(C_6H_7N)_4^{2+}$ and ClO_4^- groups. The perchlorate ion is disordered. The 4-methylpyridine rings are in a square planar arrangement about the nickel atom.

Les cristaux du perchlorate nickel(II) tétrakis (méthyl-4 pyridine) $Ni(C_6H_7N)_4(ClO_4)^2$ sont du type monoclinique appartenant au groupe $C2/c$ avec les paramètres $a = 18.38(1)$, $b = 10.71(1)$, $c = 15.58(1)$ Å, $\beta = 109.83\ (5)°$ et possèdent quatre molécules par maille unitaire. Les derniers paramètres atomiques furent obtenus à l'aide d'un raffinement des moindres carrés (matrice bloc-diagonale), en utilisant des paramètres thermiques anisotropiques. Les positions des atomes d'hydrogène furent établies mais les paramètres ne furent pas raffinés. Le résidu final en accord avec les 1199 réflections observées est $R = 0.049$. La structure se compose donc des groupes $Ni(C_6H_7N)_4^{2+}$ et ClO_4^- séparés. L'ion perchlorate est désordonné. Les cycles méthyl-4 pyridine se trouvent dans un arrangement carré-plan autour de l'atome de nickel. [Traduit par le journal]

Can. J. Chem., **51**, 1952 (1973)

Introduction

Magnetic and spectroscopic data on $Ni(C_6H_7N)_4(ClO_4)_2$ were interpreted by Brewer and co-worker (1). They showed that this yellow compound has square planar geometry with the perchlorate ions not coordinated to the nickel atom. We are now reporting an X-ray structure analysis which supports the previous conclusions.

Experimental

Crystals were grown by slow evaporation of solvent, methyl chloride, from a solution of the compound supplied by M. S. Sun. A single crystal was sealed inside a thin-walled Lindeman glass capillary for protection from the atmosphere.

Crystal data were observed as follows:

$Ni(C_6H_7N_4)_4(ClO_4)_2$ f.w. = 630.00

Monoclinic, $a = 18.38(1)$, $b = 10.71(1)$, $c = 15.58(1)$ Å, $\beta = 109.83(5)°$, $z = 4$, $\rho_o = 1.44(2)$, $\rho_c = 1.44$, $v = 2885.1$ Å^3 (20 °C, MoKα, $\lambda = 0.71069$ Å).

The unit cell dimensions and their estimated standard deviations (in parentheses) were obtained from a least squares evaluation of positions of 12 independent reflections. The space group is either $C2/c$ (C_{2h}^6) or Cc (C_s^4), No. 15 or 9 in International tables for X-ray crystallography. Vol. 1(2).

The intensity data were collected on a Picker computer-controlled four angle diffractometer using a $\theta/2\theta$ scan with β-filtered MoKα radiation and a scintillation detector. The two octants, hkl and $\bar{h}kl$, were explored to a maximum 2θ of 45°. There were 1908 accessible reflections in this region of which 1199 were considered observed. The threshold was taken as $0.10 \times$ backgound count or 25 counts, whichever was greater. The specimen was a needle-shaped crystal with dimensions $0.48 \times 0.20 \times 0.24$ mm, the needle direction being parallel to c-axis. The c-axis of the crystal was mounted along the ϕ direction of the diffractometer. The linear absorption coefficient for MoKα radiation is $\mu = 9.1$ cm^{-1}. No absorption or extinction corrections were applied.

Structure Analysis

The positions of the nickel and chlorine atoms were established from a three-dimensional Patterson synthesis. All of the other non-hydrogen atoms were then located from a three-dimensional Fourier synthesis based on the phases determined by the nickel and chlorine atoms.

The nickel atom was found in special position $4a$; all other atoms were found in general positions $8f$ of the space group $C2/c$.

The method of refinement was by successive cycles of block-diagonal least squares, using 3×3 matrices for the positional parameters and 6×6 matrices for the anisotropic thermal parameters of each atom. The quantity mini-

Can. J. Chem. Downloaded from www.nrcresearchpress.com by 210.87.254.105 on 09/05/12
For personal use only.

Can. J. Chem. Downloaded from www.nrcresearchpress.com by 210.87.254.105 on 09/05/12
For personal use only.

TABLE 1. Final parameters (estimated standard deviations in parentheses), ($x,y,z \times 10^4$, $U_{ij} \times 10^3$) t.f. = exp $[-2\pi^2(a^{*2}h^2U_{11} + \ldots + 2b^*c^*klU_{23} + \ldots)]$

Atom	x	y	z	U_{11}	U_{22}	U_{33}	U_{23}	U_{13}	U_{12}	Occupation factor
Ni^{2+}	0	0	0	75(3)	93(1)	78(1)	5(1)	40(1)	8(1)	—
Cl(1)	1326(1)	3369(2)	1303(1)	149(3)	95(2)	128(2)	−3(2)	28(2)	−31(2)	—
O(1)	1029(7)	4136(10)	0551(7)	325(25)	153(16)	176(17)	37(12)	−17(14)	−45(14)	0.6840
O(2)	1142(5)	2129(6)	1299(6)	334(17)	105(9)	313(16)	−25(9)	173(13)	−59(9)	1.0100
O(3)	1830(6)	3890(8)	2056(5)	357(20)	208(13)	177(12)	−3(9)	−46(10)	−54(12)	1.0000
O(4)	0641(9)	3782(12)	1479(16)	292(28)	199(22)	936(71)	−95(29)	303(36)	16(18)	0.7400
O(5)	1784(13)	3226(17)	0743(12)	636(55)	474(41)	463(40)	−154(32)	423(40)	−324(39)	0.7340
N(1)	4613(0)	3938(5)	3967(3)	75(6)	89(6)	77(6)	8(5)	27(5)	−3(5)	—
N(2)	4175(2)	5522(5)	0385(3)	60(6)	87(6)	80(6)	−7(5)	33(5)	1(4)	—
C(1)	4138(5)	4357(7)	3162(5)	143(11)	101(9)	90(9)	8(7)	37(8)	12(8)	—
C(2)	3816(5)	3583(4)	2438(4)	170(12)	115(10)	78(8)	5(7)	21(8)	−14(9)	—
C(3)	3967(4)	2325(7)	2505(4)	113(9)	125(10)	88(8)	−17(7)	53(7)	−41(8)	—
C(4)	4452(5)	1894(7)	3332(5)	136(10)	100(9)	126(10)	−11(8)	62(8)	−12(8)	—
C(5)	4763(4)	2718(7)	4031(5)	86(8)	106(9)	101(9)	7(7)	19(7)	6(7)	—
C(6)	3575(7)	1465(10)	1726(6)	260(18)	191(15)	125(11)	−65(11)	79(11)	−106(14)	—
C(7)	3479(4)	5003(7)	0044(4)	106(8)	107(8)	96(7)	−17(8)	49(6)	−14(8)	—
C(8)	2860(4)	5379(7)	0290(5)	92(8)	105(9)	108(8)	−5(7)	46(7)	−2(6)	—
C(9)	2946(4)	6334(6)	0907(4)	90(8)	88(8)	118(9)	39(7)	67(7)	30(7)	—
C(10)	3666(4)	6886(7)	1242(5)	108(9)	119(10)	114(9)	−21(7)	60(8)	6(7)	—
C(11)	4263(4)	6461(7)	0984(4)	111(9)	115(9)	96(8)	−19(8)	45(7)	−14(8)	—
C(12)	2288(5)	6753(8)	1214(6)	131(10)	135(11)	162(11)	29(9)	105(9)	26(9)	—

TABLE 2. Parameters for the hydrogen atoms × 10^3
t.f. = exp $[-8\pi^2 U(\sin\theta/\lambda)^2]$

Atom		x	y	z	U (Å^2)
C(1)	H(1)	600	527	183	168
C(2)	H(2)	659	397	312	190
C(4)	H(4)	535	106	157	163
C(5)	H(5)	483	250	048	141
C(6)	H(61)	653	178	384	248
	H(62)	673	100	318	248
	H(63)	609	074	330	248
C(7)	H(7)	342	430	−035	157
C(8)	H(8)	232	501	002	148
C(10)	H(10)	375	762	166	159
C(11)	H(11)	477	692	130	159
C(12)	H(71)	214	760	106	172
	H(72)	213	617	158	172
	H(73)	191	693	058	172

mized was $\sum w(|F_o| - |F_c|)^2$ for observed reflections only, using the weighting function

$$w = \frac{1}{1 + [(|F_o| - P_2)/P_1]^4}$$

where $P_1 = 35.00$ and $P_2 = 45.00$. Scattering factor curves for Ni, Cl, O, N, C, and H were used as given in ref. 3, Table 3.3.1.A. Real and imaginary dispersion corrections were applied to the scattering curves of nickel (3, see Table 3.3.2.C.). The final agreement residual $R = \sum(|F_o| - |F_c|)/\sum|F_o|$ for all atoms was 0.049.

During the early stages of the refinement the relatively high thermal parameters and large coordinate shifts of the two oxygen atoms O(1) and O(4) suggested further investigation of the perchlorate group would be necessary. Fourier and difference syntheses showed the presence of a fifth peak within bonding distance of the chlorine at about half the electron density expected for an oxygen atom. The electron densities of two of the established oxygen positions were also low. It was decided to include all five oxygen atoms and refine the individual occupation factors; final values for these are shown in Table 1. The final agreement residual for all atoms other than hydrogen was 0.062.

A difference synthesis revealed all hydrogen atoms as peaks of electron density 0.4 to 0.6 e Å^{-3}, and no other residual electron density greater than 0.3 e Å^{-3}. The hydrogen atoms were assigned isotropic thermal parameters equal to the carbon atoms to which they are attached. The positions and the thermal parameters for the hydrogen atoms were not refined during the subsequent least squares cycles. In the last cycle no parameter shift exceeded 0.1 times the estimated standard deviation. The final agreement residual for the observed reflections for all atoms with the space group $C2/c$ was $R = 0.049$. The decrease in the residual R obtained by inclusion of the hydrogen atoms is significant by Hamilton's test (4) at the 0.005 (0.5%) level.

The structure was also refined in the other possible space group Cc and a residual of 0.057 obtained for all atoms other than hydrogen. Hamilton's test shows that the decrease in the residual obtained by assuming space group Cc is not significant. This is supported by examination of the normalized structure factor table (Table 4) which shows that the structure is nearer to centrosymmetric.

A set of structure factors for the final parameters given in Tables 1 and 2 has been placed in the Depository of Unpublished Data.[1]

Discussion

The intramolecular bond distances and angles are given in Table 3. The stereochemistry of the molecule and the numbering scheme is shown in Fig. 1.

The perchlorate ions are not bonded to the nickel atom, the shortest nickel–oxygen distance, Ni—O(2), being 3.290(8) Å. The Ni(4-methylpyridine)$_4^{2+}$ ion exhibits square-planar coordination of the ligands. Within experimental

[1]Photocopies are available at a nominal charge from the Depository of Unpublished Data, National Science Library, National Research Council of Canada, Ottawa, Canada, K1A 0S2.

Can. J. Chem. Downloaded from www.nrcresearchpress.com by 210.87.254.105 on 09/05/12
For personal use only.

TABLE 3. Intramolecular distances and angles (estimated standard deviations in parentheses)

Bond		Distance (Å)	Bonds	Angles (deg)
Ni—N(1)		1.900(5)	N(1)—Ni—N(2)	88.9(2)
Ni—N(2)		1.895(5)	Ni—N(1)—C(1)	122.0(5)
N(1)—C(1)		1.340(9)	Ni—N(1)—C(5)	121.0(5)
N(1)—C(5)		1.332(9)	Ni—N(2)—C(7)	121.0(5)
N(2)—C(7)		1.328(9)	Ni—N(2)—C(11)	121.3(5)
N(2)—C(11)		1.343(9)	C(1)—N(1)—C(5)	116.8(6)
C(1)—C(2)	side	1.362(10)	C(7)—N(2)—C(11)	117.6(6)
C(4)—C(5)	side	1.367(11)	N(1)—C(1)—C(2)	122.2(7)
C(7)—C(8)	side	1.378(11)	N(2)—C(7)—C(8)	122.6(6)
C(10)—C(11)	side	1.367(12)	N(1)—C(5)—C(4)	123.5(5)
C(2)—C(3)	top	1.372(11)	N(2)—C(11)—C(10)	122.2(7)
C(3)—C(4)	top	1.374(11)	C(1)—C(2)—C(3)	120.9(7)
C(8)—C(9)	top	1.376(10)	C(7)—C(8)—C(9)	120.1(7)
C(9)—C(10)	top	1.381(11)	C(2)—C(3)—C(4)	116.7(7)
C(3)—C(6)		1.500(12)	C(8)—C(9)—C(10)	116.6(6)
C(9)—C(12)		1.511(12)	C(3)—C(4)—C(5)	119.5(7)
Cl—O(1)		1.382(11)	C(9)—C(10)—C(11)	120.5(7)
Cl—O(2)		1.370(7)	O(1)—Cl—O(2)	123.1(6)
Cl—O(3)		1.344(9)	O(1)—Cl—O(3)	116.7(6)
Cl—O(4)		1.447(18)	O(1)—Cl—O(4)	81.9(9)
Cl—O(5)		1.411(23)	O(1)—Cl—O(5)	71.7(10)
			O(2)—Cl—O(3)	120.1(5)
			O(2)—Cl—O(4)	93.8(8)
			O(2)—Cl—O(5)	95.2(9)
			O(3)—Cl—O(4)	95.3(9)
			O(3)—Cl—O(5)	101.9(9)
			O(4)—Cl—O(5)	153.0(11)

TABLE 4. The distribution and statistics of the normalized structure factors $|E|$

	Theoretical values		
Parameter	Centric	Non-centric	Observed values
$\langle\|E\|\rangle$	0.798	0.886	0.820
$\langle\|E\|^2\rangle$	1.000	1.000	0.999
$\langle\|E^2-1\|\rangle$	0.968	0.736	0.949
$\|E\|>1.0$	31.73%	36.79%	33.18%
$\|E\|>1.2$	23.01%	23.69%	24.37%
$\|E\|>1.4$	16.15%	14.09%	16.56%
$\|E\|>1.6$	10.96%	7.73%	10.80%
$\|E\|>1.8$	7.19%	3.92%	7.18%
$\|E\|>2.0$	4.55%	1.83%	3.77%
$\|E\|>2.5$	1.24%	0.19%	0.79%
$\|E\|>3.0$	0.27%	0.01%	0.21%

error, the 4-methylpyridine rings are planar (Table 5) with the rings making angles of 117.5 and 73.1° with the plane of the nitrogens.

The sum of the occupation factors for the five oxygen positions is 4.168 with the O(2) and O(3) positions fully occupied. From this it seems that the nature of the disorder of the perchlorate ions is quite complex. Cl—O(1) and Cl—O(2) are not significantly different and neither are Cl—O(4) and Cl—O(5) but the mean values for these pairs are significantly different from each other (t = 3.5) and from Cl—O(3) (t = 3.0 and 5.1).

The overall mean Cl—O distance 1.391 Å and the range of O—Cl—O angles 7.17 to 153.0° are compared with some recent results for dis-

Can. J. Chem. Downloaded from www.nrcresearchpress.com by 210.87.254.105 on 09/05/12
For personal use only.

TABLE 5. Best mean plane through the rings (estimated standard deviations in parentheses)

Atom	Distance from plane (Å)
Ring 1	
Equation: $(0.9419)x + (-0.1469)y + (-0.3022)z - (8.0057) = 0$[a]	
N(1)	−0.002(6)
C(1)	−0.001(9)
C(2)	0.001(9)
C(3)	0.002(8)
C(4)	−0.005(9)
C(5)	0.005(8)
Ring 2	
Equation: $(-0.0003)x + (0.6578)y + (-0.7532)z - (3.4678) = 0$[a]	
N(2)	−0.004(5)
C(7)	0.006(7)
C(8)	0.0 (7)
C(9)	−0.008(7)
C(10)	0.010(7)
C(11)	−0.004(7)

[a]Refers to an orthogonal set of axes, x along a, y along b, and z along c^*.

TABLE 6. Intramolecular distances and angles for some disordered perchlorates

Compound	Mean Cl—O distance (Å)	Range of O—Cl—O angles (deg)	Reference
Tetrakis(4-methylpyridine)Ni(II)perchlorate	1.391	71.7–153.0	
Tetrakis(1,8-naphthyridine)Fe(II)perchlorate	1.387	101–118	5
Tetrakis(3,4-dimethylpyridine)Ni(II)perchlorate	1.316	74–125	6
Bis(cyclohexylbenzene)Ag(I)perchlorate	1.390	100–122	7
Racemic 5,7,12,12,14-hexamethyl-1,4,8,11-tetra-azacyclotetradeca-4,14-dieneNi(II)perchlorate	1.370	105–112	8
Bis[1,2-bis(diphenylphosphino)ethane]Rh(I)perchlorate	1.387	107–116	9
Tetrakis(3,5 dimethylpyridineNi(II)perchlorate	1.356	102–119	10

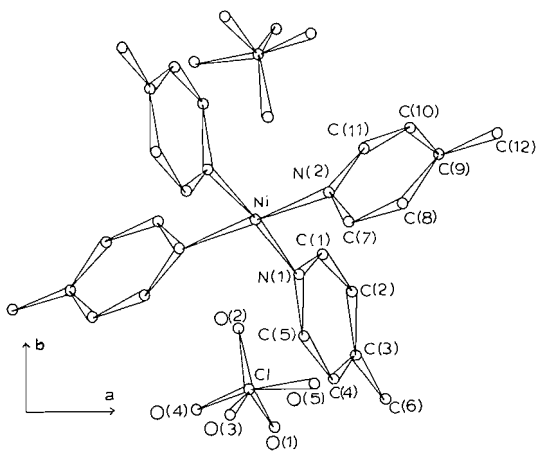

FIG. 1. Structure projected along the c^*-axis. Nickel atom at $\frac{1}{2},\frac{1}{2},\frac{1}{2}$.

ordered perchlorates in Table 6. A recently determined structure, (4-cyanopyridine)Hg(I)perchlorate (11), with an ordered perchlorate ion gives Cl—O distances of 1.45(4), 1.47(4), 1.46(3), and 1.42(4) Å with a range of bond angles 107(2)–113(2)°. Volume III of International tables for X-ray crystallography, p. 273 quotes the range 1.41–1.48(±6) Å for perchlorate ions. The disordered structures show a significantly shorter Cl—O distance which is associated with libration of the group. (5, 8, 9). A correction for riding motion raises the mean Cl—O distance to 1.453 Å in good agreement with the length found in ordered structures.

The Ni—N distances of 1.900(5) and 1.895(5) Å agree very well with 1.897(3) Å in tetrakis(3,4-dimethylpyridine)Ni(II)perchlorate (6), 2.093(2)

Can. J. Chem. Downloaded from www.nrcresearchpress.com by 210.87.254.105 on 09/05/12
For personal use only.

Can. J. Chem. Downloaded from www.nrcresearchpress.com by 210.87.254.105 on 09/05/12
For personal use only.

TABLE 7. Mean bond lengths (Å) and mean bond angles in pyridine and substituted pyridines (ref.12)

	Bond length (Å)				Bond angle (deg)			
		C—C					C—C—C	
Compound	C—N	Side	Top	$C—CH_3$	C—N—C	N—C—C	Side	Top
$Ni(4\text{-}CH_3Py)_4(ClO_4)_2$	1.336	1.369	1.376	1.505	117.2	122.6	120.3	116.7
$Zn(4\text{-}CH_3Py)_2Cl_2$	1.339	1.383	1.368	1.504	117.3	122.5	120.3	117.5
Pyridine (microwave)	1.3402	1.3945	1.3944		116.8	121.3	118.5	118.5
$Zn(Py)_2Cl_2$	1.35	1.39	1.34		119.5	118.0	125.0	114.0
$Ni(3,5\text{-dimethylPy})_4(ClO_4)_2$	1.341	1.370		1.513	117.5	123.4	118.9	
$Ni(3,4\text{-dimethylPy})_4(ClO_4)_2$[a]	1.345	1.379		1.500	118.5	121.7	120.1	
$[HBrB(4\text{-}CH_3Py)N(CH_3)_3][PF_6]$	1.36	1.36	1.39	1.51	117.3	122.1	120.9	116.3

[a]Reference 6.

Å in tetrakis(3,5-dimethylpyridine)Ni(II)perchlorate (10) and 1.891(6), 1.927(6) Å in racemic 5,7,7,12,12,14-hexamethyl-1,4,8,11-tetra-azacyclotetradeca-4,14-dieneNi(II)perchlorate (8). The shorter bond length in the planar complexes indicates the existance of stronger π-bonding.

The mean bond distances C—N 1.336 Å, C—C (side) 1.369 Å, C—C (top) 1.376 Å and mean bond angles C—N—C 117.2°, N—C—C 122.6°, C—C—C (side) 120.3°, C—C—C (top) 116.7° are compared with some other results given in refs. 12 and 6, in Table 7.

There are no intermolecular distances below 3.5 Å.

We wish to thank Dr. D. G. Brewer for suggesting the problem, Mr. M. S. Sun for a sample of the compound, Dr. F. R. Ahmed of the Biochemistry Laboratory, National Research Council of Canada for use of his computer programs, the National Research Council of Canada and the University of New Brunswick for financial support.

1. M. S. Sun and D. G. Brewer. Can. J. Chem. **49**, 1502 (1971).
2. International Tables for X-ray Crystallography. Vol. 1. The Kynoch Press, Birmingham, England, 1962.
3. International Tables for X-ray Crystallography. Vol. III. The Kynoch Press, Birmingham, England, 1962.
4. W. C. Hamilton. Acta Cryst. **18**, 502 (1965).
5. P. Singh, A. Clearfield, and Ivan Bernal. J. Coord. Chem. **1**, 29 (1971).
6. F. Madaule-Aubury and G. M. Brown. Acta Cryst. **B24**, 754 (1968).
7. E. A. Hall Griffith and E. L. Amma. J. Am. Chem. Soc. **93**, 3167 (1971).
8. B. T. Kilbourn, R. R. Ryan, and J. D. Dunitz. J. Chem. Soc. (A), 2409 (1969).
9. Maureen C. Hall, B. T. Kilbourn, and K. A. Taylor. J. Chem. Soc. (A), 2539 (1970).
10. F. Madaule-Aubrey and G. M. Brown. Acta Cryst. **B24**, 745 (1968).
11. D. L. Kepert, D. Taylor, and A. H. White. Inorg. Chem. **11**, 1639 (1972).
12. H. Lynton and M. C. Sears. Can. J. Chem. **49**, 3422 (1971).

Can. J. Chem. Downloaded from www.nrcresearchpress.com by 210.87.254.105 on 09/05/12
For personal use only.

Micellar Effects upon *p-n*-Butylaniline Catalyzed Decarboxylation of Oxalacetic Acid

LEO KA-MING LAM AND DONALD E. SCHMIDT, JR.
Department of Chemistry, University of Windsor, Windsor, Ontario
Received November 27, 1972

p-n-Butylaniline ([nBA] = 1×10^{-3} *M*) incorporated in cationic micelles of cetyltrimethylammonium bromide ([CTABr] = 6×10^{-3}*M*) was found to enhance the rate of decarboxylation of oxalacetic acid (OAA) 45-fold while nBA alone only increases the rate six-fold as compared to the rate of spontaneous decarboxylation at the same p*H*. Anionic micelles of sodium dodecyl sulfate ([SDS] = 6×10^{-3} *M*) completely inhibited the catalytic effect of nBA. Together with the effects of added salts and the change of p*H* on the rate of the reaction the role of micelles in the decarboxylation of OAA is discussed.

La *p-n*-butylaniline ([nBA] = 1×10^{-3} *M*) incorporée dans les micelles cationiques de bromure de cétyltriméthylammonium ([CTABr] = 6×10^{-3} *M*) augmente la vitesse de décarboxylation de l'acide oxaloacétique (OAA) de 45 fois tandis que la nBA seule n'accroît cette vitesse que de six fois comparée à la vitesse de décarboxylation spontanée au même p*H*. Les micelles anioniques de sulfate de sodium dodécyle ([SDS] = 6×10^{-3} *M*) inhibent complètement l'effet catalytique de la nBA. Les effets de sels ajoutés, l'influence du p*H* sur la vitesse de la réaction et le rôle des micelles dans la décarboxylation de l'OAA ont été discutés. [Traduit par le journal]

Can. J. Chem., 51, 1959 (1973)

Can. J. Chem. Downloaded from www.nrcresearchpress.com by 210.87.254.6 on 09/05/12
For personal use only.

Introduction

Decarboxylation of oxalacetic acid is accelerated in the presence of primary amines. Aniline is a particularly effective catalyst (1). The formation of a Schiff's base between the anilinium ion and the keto-acid has been suggested as the rate-determining step for this reaction in acidic medium (1). Westheimer *et al.* (2, 3) proposed that a hydrogen-bonded Schiff's base rather than the conjugate acid was the reactive intermediate. A later investigator (4) felt that the carbinolamine formation rather than Schiff's base formation was the rate-determining step but this conclusion has been criticized by others (5, 6). There seems little doubt that the amine-catalyzed decarboxylation of oxalacetic acid involves at some step the nucleophilic attack of the amine upon the carbonyl carbon of the acid.

The mechanism of amine-catalyzed decarboxylation of β-keto acids has received considerable attention because of its importance as a model system for enzymatic decarboxylation (7). For this same reason the catalytic effects of various metal cations (8–15), amines (1, 4, 16–18), and amino acids (19, 20) upon the decarboxylation have been investigated.

We feel that the catalytic effects of amines upon the decarboxylation of oxalacetic acid may be further enhanced in the presence of micelles whose structure is known to be in general similar to that of proteins (21). Substrate specificity and rate enhancement in micellar solution, as in the case of enzyme-catalyzed reactions, have been observed (22–29). Towards this end we have chosen to form a micelle from cetyltrimethylammonium bromide (CTABr). Micelles of CTABr are reported to strongly enhance the decarboxylation of 6-nitrobenzisoxazole-3-carboxylate (28, 30). To further facilitate the decarboxylation, we have chosen *p-n*-butylaniline as the catalytic amine. N.m.r. studies indicate that the nucleophilic amino group would be favorably situated on the positively charged surface of the micelle (31) where the substrate oxalacetate ion is likely to be found.

Experimental

Materials

Oxalacetic acid (OAA) was obtained from Sigma Chemical Company (St. Louis, Mo.) and was used without further purification. A 1×10^{-3} *M* aqueous solution of OAA was freshly prepared daily.

p-n-Butylaniline, 97% (nBA) was obtained from Aldrich Chemical Co. The compound was purified by vacuum distillation through a 3-in. Vigreux column (b.p. 120–121° at 15 mm). The compound rapidly turned yellow at room temperature. The distilled material was kept under an atmosphere of helium in sealed tubes and was refrigerated when it was not in use. Solutions of 1.25×10^{-2} *M* of nBA in 0.02 *M* buffers (sodium acetate – acetic acid from p*H* 4–5.5; sodium monochloroacetate – monochloroacetic acid from p*H* 4–2.5) were prepared. At

TABLE 1. Rate constants for the decarboxylation of oxalacetic acid*

Reaction	Additions	Concentration (M)	k_{obs} (min^{-1})†
1			0.0052
2	CTABr	6×10^{-3}	0.015
3	nBA	1×10^{-3}	0.030
4	CTABr	6×10^{-3}	
	nBA	1×10^{-3}	0.24
5	CTABr	6×10^{-3}	
	Aniline	1×10^{-3}	0.065

*In 0.02 M sodium acetate – acetic acid buffer of pH 4.13 at 30°.
†Average values of duplicate runs.

pH values greater than 5 the solubility of nBA decreases considerably. To effect a solution of nBA in these cases, the amine was dissolved directly in a buffer containing the desired amount of cetyltrimethylammonium bromide (CTABr). Thus nBA was incorporated into the micelles and the system became homogeneous.

Cetyltrimethylammonium bromide (CTABr) was obtained from Eastman Organic Chemicals and was purified by the method of Duynstee and Grunwald (32). Solutions of CTABr at $1 \times 10^{-3} - 8 \times 10^{-3}$ M were prepared in 0.02 M buffers of pH 2.5–5.5.

Sodium dodecylsulfate (SDS) was obtained from Fisher Chemical Company and was recrystallized before use (32). Solutions of SDS at $1 \times 10^{-3} - 8 \times 10^{-3}$ M in 0.02 M buffers at pH 4.13, were prepared.

Aniline (B.D.H.) was distilled over zinc dust and used immediately in kinetic determinations.

Kinetic Studies

The decarboxylation of OAA at 30° was followed spectrophotometrically by the method of Kosicki and Lipovac (13). Kinetic data were obtained on a Gilford Model 2000 absorbance recorder attached to a Beckman DU monochromator equipped with a water-jacketed cell compartment. Buffered solutions of CTABr and nBA were mixed to the desired molar ratio and placed in a 30° temperature bath for at least 30 min prior to use. Into each cuvette were pipetted 2.90 ml of CTABr–nBA solution and 0.10 ml of OAA solution. The reaction mixture was mixed and placed in the cell compartment. In several parallel measurements using a Gilson differential respirometer, the rate of evolution of carbon dioxide was found to parallel the rate of disappearance of the enol form of OAA as determined spectrophotometrically. In each case the reaction was pseudo first-order in OAA and excellent first-order plots were obtained. The reaction was first order with respect to nBA over the concentration range of $5 \times 10^{-5} - 1 \times 10^{-3}$ M when nBA is incorporated into the micelle of [CTABr]/[nBA] = 6.

The pH values of all the solutions were measured on a Radiometer model 26 pH meter. These pH values were obtained in the presence of the detergent.

Results and Discussion

Micelles formed in a solution of CTABr (6×10^{-3} M) and nBA (1×10^{-3} M) at pH 4.13 enhance the decarboxylation of OAA about 45-fold (Table 1). At the same pH, CTABr (6×10^{-3} M) alone enhances the decarboxylation only three-fold while nBA (1×10^{-3} M) enhances the reaction about six-fold. Incorporation of the hydrophobic portion of the *p-n*-butylaniline molecule into the hydrophobic region of the micelle apparently leaves the amino function exposed on or near the positively charged micelle surface such that effective interaction with OAA results. When aniline (1×10^{-3} M) was incorporated into a CTABr (6×10^{-3} M) micelle, the rate of decarboxylation was enhanced about 11-fold. Incorporation of aniline into a micelle seems to make this amine a less effective catalyst than the free amine. The second-order rate constant for decarboxylation with aniline in a micelle is 65 M^{-1} min^{-1} at 30° while for the free amine this increases to 79 M^{-1} min^{-1} (4) at 25°. Assuming the nucleophilicity difference between aniline and nBA is negligible, this result seems to indicate the importance of an orienting effect of the hydrophobic *n*-alkyl chain in nBA so as to place the amine in an optimal position for interaction with OAA.

The variation of the first-order rate constant, k, with an increasing [CTABr]/[nBA] ratio at fixed nBA concentration exhibits the typical kinetic form of a micelle-catalyzed reaction (Fig. 1); that is, k increases to a plateau value, and then remains constant over a fairly wide range (26, 28, 33, 34). The reaction rate reaches a maximum value of 2.36×10^{-1} min^{-1} at [CTABr]/[nBA] = 3 and remains constant at least up to [CTABr]/[nBA] = 8. This represents an increase of 8-fold over the reaction catalyzed by nBA alone ($k = 3.0 \times 10^{-2}$ min^{-1}) at pH 4.13. This initial increase in the rate of the decarboxylation for [CTABr]/[nBA] ratio from 0 to 3 followed by a constant rate of decarboxylation for [CTABr]/[nBA] ratios from 3 to 8 was found at pH values of 2.26, 3.50, 4.35, 4.72, and 5.50.

Can. J. Chem. Downloaded from www.nrcresearchpress.com by 210.87.254.6 on 09/05/12
For personal use only.

Can. J. Chem. Downloaded from www.nrcresearchpress.com by 210.87.254.6 on 09/05/12
For personal use only.

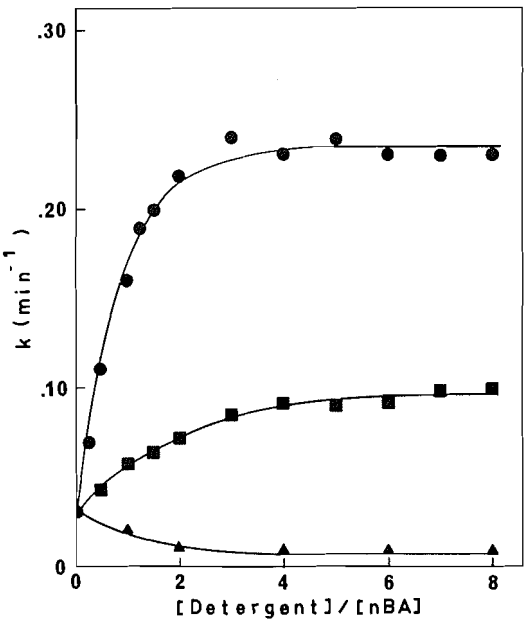

FIG. 1. Rate of oxalacetic acid decarboxylation at increasing ratios of detergent to *p-n*-butylaniline. All rate constants were obtained at 30°, pH = 4.13, and 1 × 10^{-3} M nBA. Concentration of the detergent is as noted.-●-, CTABr in 0.02 M sodium acetate – acetic acid buffer; -■-, CTABr in 0.02 M sodium acetate – acetic acid buffer with 0.5 M sodium bromide added; -▲-, SDS in 0.02 M sodium acetate – acetic acid buffer.

The catalytic effect of micelles is often interpreted in terms of their ability to bring together the reactants. The equilibrium concentration of OAA ion at the micelle–water interface (the Goug–Chapman double layer) (21) is higher than that in the bulk solution. When nBA molecules are incorporated in the micelles, the *n*-butyl chain is preferentially solubilized in the hydrocarbon core of the micelle (31). This leaves the aromatic part with the nucleophilic amino group in the Stern layer. Thus the amino group is brought into close approximation with the OAA ion. This simple picture of electrostatic attraction may be only partly responsible for the rate enhancement.

Added 0.05 M sodium bromide decreases the rate of decarboxylation, but the catalytic effect of the mixed CTABr–nBA micelles upon the reaction is still evident. A plot of first-order rate constants (Fig. 1) of decarboxylation in the presence of 0.05 M sodium bromide against [CTABr]/[nBA] ratio from 0 to 8 gives a curve qualitatively similar to that found in the absence of added salt. According to the hypothesis that the steepness of the k *vs.* micelle concentration plot is related to the strength of micelle–substrate interaction (28), oxalacetate ions appear to be adsorbed less strongly to the micelle surface in the presence of added bromide ions. Reduction in the electrostatic attraction of substrate ions to the area of the nucleophilic amine decreases the overall rate. Other inorganic salts also decrease the rate (Table 2). As observed by others, several additional anions, iodide and perchlorate, could not be examined as inhibitors since they yielded insoluble material in the presence of detergent (29). Increasing concentrations of both sodium fluoride and sodium bromide progressively decrease the decarboxylation rate in the presence of micelles to a value near that of the reaction catalyzed by nBA alone (Table 3). Increasing concentrations of the sodium acetate – acetic acid buffer do not seem to have much effect upon the rate of micellar-catalyzed decarboxylation at pH 4.13. This result is rather surprising as acetate has been reported to promote the catalysis of OAA by aniline (14).

In contrast to the enhancement of the rate of nBA-catalyzed decarboxylation of OAA by cationic micelles, anionic micelles of SDS and nBA markedly inhibit the rate of decarboxylation (Fig. 1). At a ratio of [SDS]/[nBA] of 8 the anionic micelle effectively alleviates the catalysis of nBA on the reaction to such an extent that the rate falls to that of a spontaneous decarboxylation at pH 4.13. SDS (1 × 10^{-3} M) at pH 4.13 in 0.02 M acetate buffer does not retard the decarboxylation of OAA (k = 0.0050 min^{-1}). Anionic micelles would repel the oxalacetate ion

TABLE 2. Inhibition of decarboxylation of OAA by various sodium salts at concentration of 0.05 M in solutions of [CTABr]/[nBA] = 6 in 0.02 M sodium acetate – acetic acid buffer of pH = 4.13 at 30°

Salts	k(min^{-1})
HOAc/NaOAc	0.245
Sulfate	0.230
Fluoride	0.190
Perchlorate	0.190
Formate	0.184
Citrate	0.173
Chloride	0.168
Bromide	0.090
Nitrate	0.086

TABLE 3. Inhibition of decarboxylation of OAA by increasing concentrations of sodium fluoride, sodium bromide, and sodium acetate – acetic acid in micelle solutions of [CTABr]/[nBA] = 6 and pH = 4.13

	Concentration (M)	k(min^{-1})
Sodium fluoride	0.020	0.190
	0.050	0.190
	0.075	0.146
	0.100	0.116
	0.125	0.084
	0.150	0.071
	0.200	0.069
	0.225	0.054
	0.250	0.054
Sodium bromide	0.020	0.170
	0.050	0.095
	0.075	0.072
	0.100	0.054
	0.125	0.045
	0.150	0.041
	0.200	0.033
	0.225	0.032
	0.250	0.030
Sodium acetate – acetic acid*	0.020	0.23
	0.100	0.24
	0.150	0.24
	0.175	0.23

*Total concentration of sodium acetate + acetic acid.

TABLE 4. Spectral shifts of nBA in CATBr cationic micelles in 0.02 M sodium acetate – acetic acid buffer at pH 4.13*

[CTABr]/[nBA]†	λ_{max} (nm)	$\Delta\lambda_{max}$‡ (nm)	$\Delta\varepsilon$ (M^{-1} cm^{-1})
0	286.8	0	0
0.5	288.1	+1.3	20
1	289.4	+2.6	120
1.5	290.6	+3.8	240
2	290.6	+3.8	260
3	292.5	+5.7	350
4	293.0	+6.2	370
5	293.8	+7.0	400
6	294.4	+7.6	430
7	294.4	+7.6	440
8	294.4	+7.6	460

*The pH of the buffer changed by less than 0.03 units upon the addition of nBA and the detergent.
†[nBA] = 1 × 10^{-3} M.
‡Relative to λ_{max} ([CTABr]/[nBA] = 0) = 286.8 nm.

from the nBA molecules which are incorporated into the micelle.

The nBA molecules are incorporated into both the CTABr micelles (Table 4) and the SDS micelles (Table 5). Both the λ_{max} and the extinction coefficient change as the ratio of detergent to nBA increases. The aniline portion of nBA must be near the charged surface of both types of micelle since in the CTABr micelle the extinction coefficient increases with increasing CTABr, while in the SDS micelle it decreases with increasing SDS. If the nBA were incorporated entirely in the hydrocarbon portion of the micelle, common to both types of micelle, one would expect the extinction coefficient to change in only one direction.

Can. J. Chem. Downloaded from www.nrcresearchpress.com by 210.87.254.6 on 09/05/12
For personal use only.

TABLE 5. Spectral shifts of nBA in SDS anionic micelles in 0.02 *M* sodium acetate – acetic acid buffer at p*H* 4.13*

[SDS]/[nBA]†	λ_{max} (nm)	$\Delta\lambda_{max}$‡ (nm)	$\Delta\varepsilon$ (M^{-1} cm^{-1})
0	286.8	0	0
0.5	287.5	+0.7	0
1.0	288.1	+1.3	0
1.25	288.9	+1.0	0
1.5	288.7	+2.0	0
2	288.8	+2.0	−20
3	§		−80
4	§		−100
5	§		−130
6	§		−150
7	§		−140

*The p*H* of the buffer changed by less than 0.03 units upon the addition of nBA and the detergent.
†[nBA] = 1×10^{-3} *M*.
‡Relative to λ_{max} ([SDS]/[nBA] = 0) = 286.8 nm.
§No measurable λ_{max}.

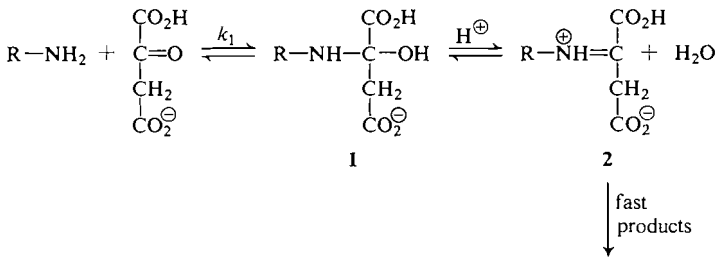

SCHEME 1

It has also been suggested that the catalytic effect of micelles is due to their ability to stabilize the rate-determining transition state (29). The transition state in the amine-catalyzed decarboxylation of OAA has not been clearly established (1–4, 6). Furthermore, the rate-determining step of the reaction is both p*H* and solvent dependent (4). The generally accepted mechanism is an initial nucleophilic attack of the amine on the OAA to form carbinolamine **1** (Scheme 1). Compound **1** reversibly forms the protonated Schiff's base **2** which rapidly decarboxylates (4). Both **1** and **2** have been proposed as the reactive intermediates of the reaction (4, 1). The p*H* rate profile for the micellar-catalyzed decarboxylation of OAA at [CTABr]/[nBA] = 6 is a typical bell-shape curve (Fig. 2). The p*H*–rate profile for aniline-catalyzed decarboxylation (4), nBA-catalyzed decarboxylation, and spontaneous decarboxylation (14) are bell-shape. The p*H* maxima are, respectively, 3.9, 4.2, and 3.5.

For the micelle-catalyzed decarboxylation the decrease in rate from p*H* 3.9 to 2.5 may be due to the decreased rate of formation of carbinolamine as the *p-n*-butylaniline is removed as *p-n*-butylanilinium ion. From p*H* 3.9 to 5.5 the rate decreases as less hydrogen ion is available for conversion of **1** to **2**. One might suggest that the micelle catalyzes the reaction by increasing the absolute value of k_1. This might be due to the greater polarizability of the carbonyl group in the presence of the positively charged micelle surface. Since the absolute value of k_1 is a factor for k_{obs} at both extremes of p*H*, any factor which will enhance the rate of attack of amine on OAA will speed the entire reaction. Increase in counter ion concentration or formation of an anionic micelle would retard the reaction as both

Can. J. Chem. Downloaded from www.nrcresearchpress.com by 210.87.254.6 on 09/05/12
For personal use only.

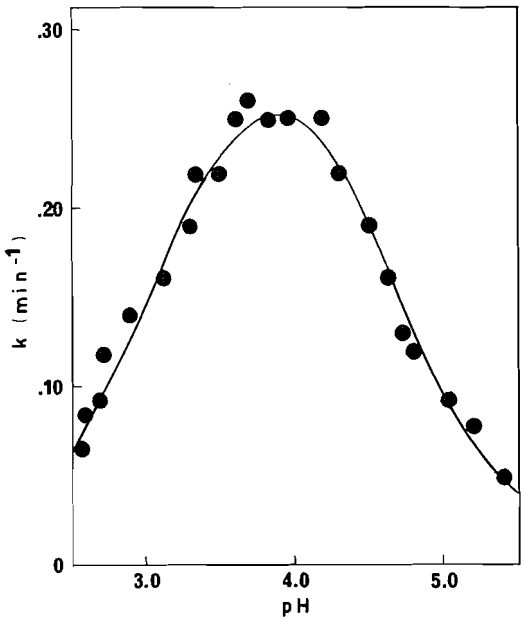

FIG. 2. p*H*-Rate profile for the decarboxylation of oxalacetic acid by mixed micelles of *p-n*-butylaniline and cetyltrimethylammonium bromide.

Experiments conducted at 30° with [nBA] = 1×10^{-3} *M* and [CTABr] = 6×10^{-3} *M*. Sodium acetate – acetic acid was used as a buffer for p*H* values of 4.1–5.4. Sodium monochloroacetate – monochloroacetic acid was used as a buffer for p*H* values of 2.5–4.0. The points are experimental, whereas the curve is calculated by computer best-fit from an equation for bell shaped curves (35):

$$k = \frac{k_o}{1 + \frac{[H^+]}{K_1} + \frac{K_2}{[H^+]}}$$

where $K_1 = 7.53 \times 10^{-4}$ *M*, $K_2 = 2.52 \times 10^{-5}$ *M*, and $k_o = 0.349$ min^{-1}.

effects would essentially decrease the cationic character around the carbonyl group and make it less polarizable.

We thank the National Research Council of Canada for financial support.

1. K. J. PEDERSEN. Acta Chem. Scand. **8**, 710 (1954).
2. F. H. WESTHEIMER. Ann. N.Y. Acad. Sci. 401 (1940).
3. F. H. WESTHEIMER and W. A. JONES. J. Am. Chem. Soc. **63**, 3283 (1941).
4. R. W. HAY. Aust. J. Chem. **18**, 337 (1965).
5. W. P. JENCKS. Prog. Phys. Org. Chem. **2**, 63 (1964).
6. J. P. GUTHRIE. Ph.D. thesis. Harvard University, Cambridge, Mass. 1968. pp. 84–86.
7. F. H. WESTHEIMER. Proc. Chem. Soc. 1963, 253.
8. A. KORNBERG, S. OCHOA, and A. H. MEHLER. J. Biol. Chem. **74**, 159 (1948).
9. R. STEINBERGER and F. H. WESTHEIMER. J. Am. Chem. Soc. **73**, 429 (1951).
10. E. GELLES. J. Chem. Soc. 4736 (1956).
11. E. GELLES and J. P. CALYTON. Trans. Faraday Soc. **52**, 353 (1956).
12. E. J. GELLES. Inorg. Nucl. Chem. **8**, 625 (1958).
13. G. W. KOSICKI and S. N. LIPOVAC. Can. J. Chem. **42**, 403 (1964).
14. C. S. TSAI. Can. J. Chem. **45**, 873 (1966).
15. P. R. BONTCHEV and V. MICHAYLOVA. J. Inorg. Nucl. Chem. **29**, 2945 (1967).
16. B. R. BROWN. Quart. Rev. 131 (1951).
17. A. WOHL and C. OESTERLIU. Ber. dt. Chem. Ges. **34**, 1139 (1901).
18. S. J. KANEKO. Biochem. (Jap.), **28**, 1 (1938).
19. S. P. BESSMAN and E. C. LAYNE. Arch. Biochem. **26**, 25 (1950).
20. D. L. ROHLFING. Arch. Biochem. Biophys. **118**, 468 (1967).
21. E. J. FENDLER and J. H. FENDLER. Adv. Phys. Org. Chem. **8**, 271 (1971).
22. M. T. A. BEHME and E. H. CORDES. J. Am. Chem. Soc. **87**, 260 (1965).
23. F. M. MENGER and C. E. PORTNOY. J. Am. Chem. Soc. **89**, 4634 (1967).
24. T. C. BRUICE, J. KATZHENDLER, and L. R. FEDOR. J. Phys. Chem. **71**, 1961 (1967).
25. T. C. BRUICE, J. KATZHENDLER, and L. R. FEDOR. J. Am. Chem. Soc. **90**, 1333 (1968).
26. C. A. BUNTON and L. ROBINSON. J. Am. Chem. Soc. **90**, 5972 (1968).
27. C. A. BUNTON and L. ROBINSON. J. Am. Chem. Soc. **92**, 356 (1970).
28. C. A. BUNTON, A. KAMEGO, and M. J. MINCH. J. Org. Chem. **37**, 1388 (1972).
29. L. R. ROMSTED and E. H. CORDES. J. Am. Chem. Soc. **90**, 4404 (1968).
30. C. A. BUNTON and M. J. MINCH. Tetrahedron Lett. 3881 (1970).
31. J. C. ERIKSSEN and G. GILBERG. Acta Chem. Scand. **20**, 2019 (1966).
32. E. F. J. DUYNSTEE and E. GRUNWALD. J. Am. Chem. Soc. **81**, 4540 (1959).
33. C. A. BUNTON, E. J. FENDLER, L. SEPULVEDA, and K. U. YANG. J. Am. Chem. Soc. **90**, 5512 (1968).
34. G. J. BUIST, C. A. BUNTON, L. ROBINSON, L. SEPULVEDA, and M. F. STAM. J. Am. Chem. Soc. **92**, 4072 (1970).
35. M. DIXON and E. C. WEBB. Enzymes. 2nd ed. Academic Press Inc. New York, N.Y. p. 129.

Can. J. Chem. Downloaded from www.nrcresearchpress.com by 210.87.254.6 on 09/05/12
For personal use only.

Quaternary Nitrogen Heterocycles. II. Kinetics of Reversible Pseudobase Formation from *N*-Methyl Heterocyclic Cations[1]

JOHN W. BUNTING AND WILLIAM G. MEATHREL

Department of Chemistry, University of Toronto, Toronto, Ontario M5S 1A1

Received January 24, 1973

The kinetics of the formation and decomposition of the pseudobases from the 2-methyl-4-nitroisoquinolinium, 10-methylacridinium, and 10-methyl-9-phenylacridinium ions have been studied. The p*H*–rate profiles of these reactions indicate that for each of these ions, pseudobase formation may kinetically involve either attack of a water molecule or of hydroxide ion on the heterocyclic cation depending upon the p*H* of the reaction. Pseudobase decomposition to the cation may occur through either the neutral or protonated pseudobase species or their kinetic equivalents. The temperature dependences of the equilibrium and kinetics are reported for each ion, and deuterium isotope effects for the reactions of the 2-methyl-4-nitroisoquinolinium ion have been measured. Possible mechanisms for the reactions are discussed on the basis of the observed activation parameters and isotope effects and are compared with related reactions.

Les cinétiques de formation et de décomposition des pseudobases à partir des ions du méthyl-2 nitro-4 isoquinolinium, méthyl-10 acridinium et méthyl-10 phényl-9 acridinium ont été étudiées. Les profils de vitesse en fonction du p*H* de ces réactions indiquent que pour chacun de ces ions, la formation de la pseudobase fait intervenir cinétiquement, soit l'attaque d'une molécule d'eau soit un ion hydroxyde sur le cation hétérocyclique selon le p*H* de la réaction. La décomposition de la pseudobase en cation pourrait se produire soit par l'intermédiaire de la pseudobase sous forme neutre ou protonée ou encore leurs équivalents cinétiques. Les équilibres et les cinétiques en fonction de la température ont été rapportés pour chaque ion; les effets isotopiques du deutérium pour les réactions de l'ion méthyl-2 nitro-4 isoquinolinium ont été mesurés. Les mécanismes possibles de ces réactions ont été discutés à partir des paramètres d'activation observés et des effets isotopiques, puis comparés aux réactions apparentées.

[Traduit par le journal]

Can. J. Chem., **51**, 1965 (1973)

Recently, we reported (1) the structures of the pseudobases (QOH) formed by the addition of hydroxide ion to various aromatic *N*-methyl heterocyclic cations (Q^+), and also equilibrium constants for pseudobase formation (eq. 2; K_w is the ionic product of water). We have now

[1] $$Q^+ + OH^- \rightleftharpoons QOH$$

[2] $$K_{ROH} = \frac{[H^+][QOH]}{[Q^+]} = K_w \cdot \frac{[QOH]}{[Q^+][OH^-]} = K_w \cdot K$$

carried out a comprehensive study of the kinetics of pseudobase formation and decomposition for three such quaternary heterocyclic cations: the 10-methylacridinium[2] (**1**; R = H), 10-methyl-9-phenylacridinium (**1**; R = Ph), and 2-methyl-4-nitroisoquinolinium (**3**) ions. The p*H*–rate profiles and temperature dependences

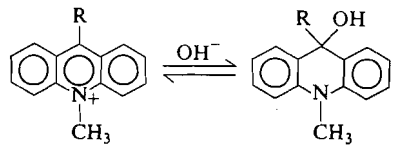

1 **2**

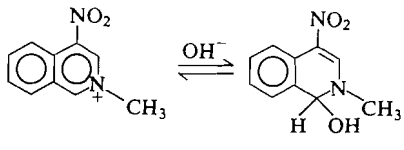

3 **4**

of these reactions have been determined and have been used to interpret the reaction mechanisms. In addition, hydrogen isotope effects have been measured for the reactions of **3** and **4** and preliminary measurements of the catalytic effects of buffer species have been made.

We have been unable, at the present time, to carry out a complete investigation of the dependence of the rates of these reactions on the structure of the heterocyclic cation, because for

[1]For Part I, see ref. 1.

[2]We previously referred to this cation as the 9-methylacridinium ion (1). In the IUPAC systematic nomenclature this is the 10-methylacridinium ion (2).

Can. J. Chem. Downloaded from www.nrcresearchpress.com by 210.87.254.105 on 09/05/12
For personal use only.

Can. J. Chem. Downloaded from www.nrcresearchpress.com by 210.87.254.105 on 09/05/12
For personal use only.

most of the cations considered previously (1), the equilibrium of eq. 1 is established too rapidly to allow study by the stopped-flow technique.

Results

The observed pseudo first-order rate constants, k_{obs}, for the combined formation and decomposition of the pseudobase of the 10-methyl-9-phenylacridinium ion (**1**; R = Ph) are plotted in Fig. 1 as a function of the pH at four temperatures. In general, k_{obs} is the sum of the pseudo first-order rate constants, k_f and k_d respectively, for the formation and decomposition of the pseudobase. Thus

$$k_{obs} = k_f + k_d$$

At equilibrium

$$k_f[Q^+] = k_d[QOH]$$

and hence

$$\frac{k_f}{k_d} = \frac{[QOH]}{[Q^+]} = \frac{K_{ROH}}{[H^+]}$$

Therefore,

[3] $$k_f = \frac{k_{obs}}{1 + [H^+]/K_{ROH}}$$

and

[4] $$k_d = \frac{k_{obs}}{1 + K_{ROH}/[H^+]}$$

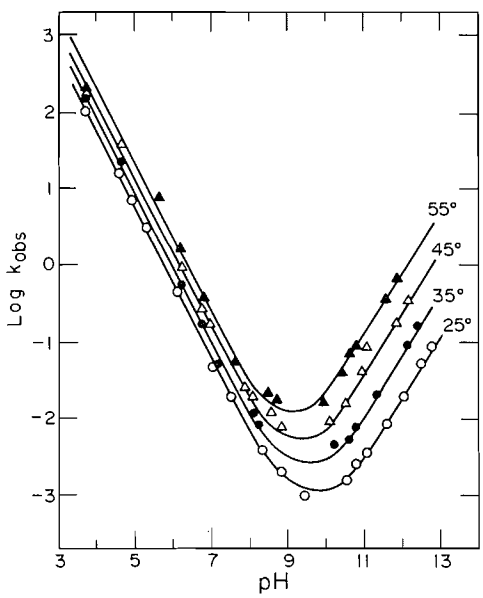

FIG. 1. The pH and temperature dependence of k_{obs} (s^{-1}) for the formation and decomposition of the pseudobase of the 10-methyl-9-phenylacridinium cation. Ionic strength of buffers = 0.1.

Typical values of k_f and k_d calculated from eqs. 3 and 4 are given in Table 1. The appropriate pK_{ROH} values at each temperature are collected in Table 2. Complete pH profiles for k_f and k_d at each temperature are given in Fig. 2 for the interconversion of **1** and **2** (R = Ph). Similar plots of k_{obs}, k_f, and k_d for the 10-methylacridinium ion are given in Fig. 3, and for the 2-methyl-4-nitroisoquinolinium ion in Fig. 4, at

TABLE 1. Rate constants for formation and decomposition of the pseudobase from the 10-methyl-9-phenylacridinium ion at 25°, ionic strength 0.1

pH	k_{obs} (s^{-1})	k_f (s^{-1})	k_d (s^{-1})
3.85	84.7	5.60×10^{-6}	84.7
4.64	13.1	5.33×10^{-6}	13.1
4.98	5.90	5.31×10^{-6}	5.90
5.34	2.54	5.17×10^{-6}	2.54
6.14	0.386	5.26×10^{-6}	0.386
7.04	0.0372	3.85×10^{-6}	0.0372
7.53	0.0153	4.84×10^{-6}	0.0153
8.34	3.22×10^{-3}	6.56×10^{-6}	3.21×10^{-3}
8.85	1.67×10^{-3}	1.10×10^{-5}	1.66×10^{-3}
9.90	1.28×10^{-3}	8.90×10^{-5}	1.19×10^{-3}
10.54	1.26×10^{-3}	3.08×10^{-4}	9.50×10^{-4}
10.87	2.08×10^{-3}	8.54×10^{-4}	1.13×10^{-3}
11.05	2.92×10^{-3}	1.49×10^{-3}	1.43×10^{-3}
11.59	6.89×10^{-3}	4.57×10^{-3}	2.32×10^{-3}
12.07	0.0173	0.0159	1.45×10^{-3}
12.50	0.0436	0.0424	1.42×10^{-3}
12.75	0.0724	0.0710	1.35×10^{-3}

TABLE 2. Variation of pK_{ROH} with temperature at ionic strength 0.1

Temperature (°C)	pK_{ROH}	pK_w*	log K†
	(i) 2-Methyl-4-nitroisoquinolinium ion		
15	5.15 ± 0.05	14.35	9.20
25	5.11 ± 0.01	14.00	8.89
35	5.08 ± 0.02	13.69	8.61
45	5.04 ± 0.02	13.41	8.37
55	4.97 ± 0.03	13.14	8.17
	(ii) 10-Methylacridinium ion		
15	10.20 ± 0.08	14.35	4.15
25	10.01 ± 0.05	14.00	3.99
35	9.77 ± 0.09	13.69	3.92
45	9.50 ± 0.08	13.41	3.91
55	9.35 ± 0.1	13.14	3.79
	(iii) 10-Methyl-9-phenylacridinium ion		
25	11.03 ± 0.04	14.00	2.97
35	10.69 ± 0.07	13.69	3.00
45	10.42 ± 0.07	13.41	2.99
55	10.25 ± 0.08	13.14	2.89

*From ref. 3.
†$\log K = pK_w - pK_{ROH}$ (from eq. 2).

Can. J. Chem. Downloaded from www.nrcresearchpress.com by 210.87.254.105 on 09/05/12
For personal use only.

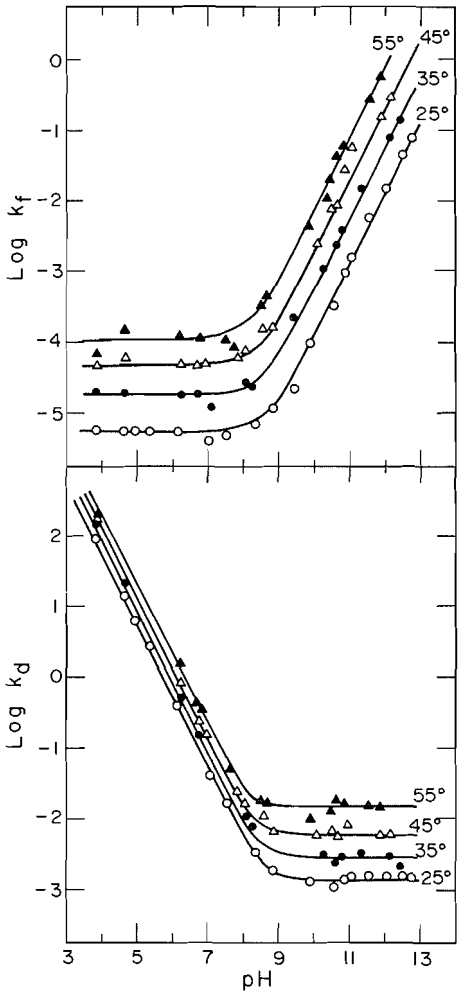

FIG. 2. The pH and temperature dependence of $k_f(s^{-1})$ and $k_d(s^{-1})$ for the formation and decomposition of the pseudobase of the 10-methyl-9-phenylacridinium ion. Ionic strength of buffers = 0.1.

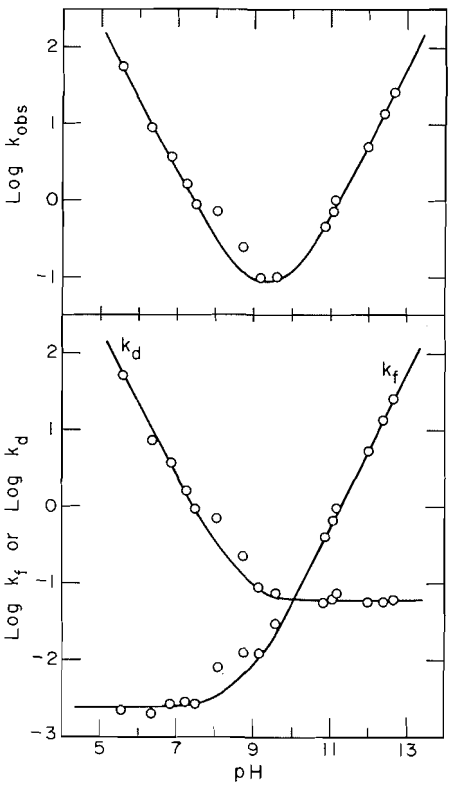

FIG. 3. The pH dependence of (*a*) k_{obs}, (*b*) k_i and k_d for the formation and decomposition of the pseudobase of the 10-methylacridinium cation at 25°. Ionic strength of buffers = 0.1; all rate constants in s^{-1}.

25°. Similar data were also obtained for these two ions at 15, 35, 45, and 55°.

The pH profiles of k_{obs}, k_f, and k_d are similar in shape for all three cations, but are displaced on the pH scale owing to the difference in the pK_{ROH} values of these ions. The pH profiles at each temperature can be fitted by equations of the form:

$$[5] \qquad k_d = k_1[H^+] + k_2$$

$$[6] \qquad k_f = k_3[OH^-] + k_4$$

The rate constants, k_1, k_2, k_3, and k_4, are formally defined by the equations:

$$[7] \qquad Q^+ + H_2O \underset{k_1}{\overset{k_4}{\rightleftharpoons}} QOH + H^+ \qquad K_{ROH} = k_4/k_1$$

$$[8] \qquad Q^+ + OH^- \underset{k_2}{\overset{k_3}{\rightleftharpoons}} QOH \qquad K = k_3/k_2$$

Values of k_1, k_2, k_3, and k_4 are collected in Table 3. Activation parameters calculated from Arrhenius plots for each of these four rate constants are given in Table 4.

In Fig. 4, the rates of formation and decomposition of the pseudobase from the 2-methyl-4-nitroisoquinolinium cation in H_2O and D_2O are compared at 25°. Equilibrium and kinetic constants in D_2O and H_2O are compared in Table 5, and the isotope effects are tabulated.

The results of a limited investigation of buffer catalysis of the reactions of **3** and **4** are indicated in Fig. 5 and Table 6. The buffer catalytic rate constant, k_B is defined in terms of the total con-

TABLE 3. Kinetic parameters* for reversible pseudobase formation

Temperature (°C)	k_1 (M^{-1} s^{-1})	k_2 (s^{-1})	k_3 (M^{-1} s^{-1})	k_4 (s^{-1})	k_1/k_2	k_3/k_4
			(i) 2-Methyl-4-nitroisoquinolinium ion			
15	7.3×10^4	5.0×10^{-3}	6.5×10^6	0.53	1.5×10^7	1.2×10^7
25	1.3×10^5	1.1×10^{-2}	8.8×10^6	1.04	1.2×10^7	8.8×10^6
35	2.3×10^5	3.0×10^{-2}	1.1×10^7	1.9	7.8×10^6	5.8×10^6
45	3.7×10^5	5.4×10^{-2}	1.4×10^7	3.4	6.8×10^6	4.1×10^6
55	6.2×10^5	0.13	1.7×10^7	6.8	4.9×10^6	2.5×10^6
			(ii) 10-Methylacridinium ion			
15	1.8×10^7	1.8×10^{-2}	2.8×10^2	1.2×10^{-3}	1.0×10^9	2.4×10^5
25	2.4×10^7	5.8×10^{-2}	5.5×10^2	2.4×10^{-3}	4.2×10^8	2.3×10^5
35	4.4×10^7	9.1×10^{-2}	7.9×10^2	6.4×10^{-3}	4.9×10^8	1.2×10^5
45	5.6×10^7	0.15	1.2×10^3	1.9×10^{-2}	3.7×10^8	6.3×10^4
55	7.9×10^7	0.34	2.1×10^3	3.9×10^{-2}	2.3×10^8	5.4×10^4
			(iii) 10-Methyl-9-phenylacridinium ion			
25	5.7×10^5	1.4×10^{-3}	1.3	5.3×10^{-6}	4.0×10^8	2.5×10^5
35	8.9×10^5	2.7×10^{-3}	2.6	1.8×10^{-5}	3.3×10^8	1.4×10^5
45	1.1×10^6	5.7×10^{-3}	5.8	4.4×10^{-5}	1.9×10^8	1.3×10^5
55	1.8×10^6	1.5×10^{-2}	12	9.5×10^{-5}	1.2×10^8	1.3×10^5

*For eqs. 5 and 6.

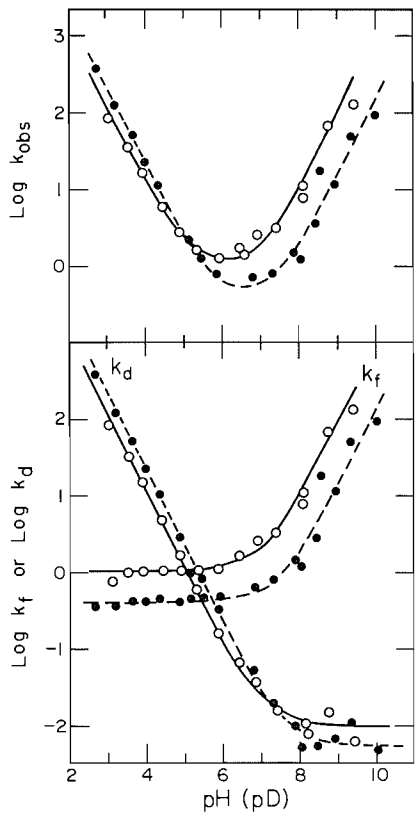

FIG. 4. The pH dependence of (*a*) k_{obs}, (*b*) k_f and k_d for the formation and decomposition of the pseudobase of the 2-methyl-4-nitroisoquinolinium cation at 25°. Ionic strength of buffers = 0.1; all rate constants in s^{-1}. —○—○— H_2O; ---●---●--- D_2O.

TABLE 4. Activation parameters for pseudobase formation and decomposition

Rate constant	$\Delta H^{\ddagger}$ (kcal/mol)[a]	$\Delta S^{\ddagger}$ (e.u.)[b]	r[c]
	(i) 2-Methyl-4-nitroisoquinolinium ion		
k_1	9.8	0	0.999
k_2	15.2	−14	0.998
k_3	4.1	−11	0.997
k_4	11.8	−17	0.999
	(ii) 10-Methylacridinium ion		
k_1	6.6	−2	0.992
k_2	12.8	−22	0.997
k_3	8.5	−17	0.996
k_4	16.5	−15	0.997
	(iii) 10-Methyl-9-phenylacridinium ion		
k_1	6.5	−10	0.991
k_2	14.0	−24	0.993
k_3	13.8	−12	0.999
k_4	18.2	−21	0.997

[a] ± 0.5 kcal/mol.
[b] ± 2 e.u.
[c] Correlation coefficient for Arrhenius plot.

centration of acidic and basic buffer species, *i.e.* $B_T = [B] + [BH^+]$.

Attempts to measure the rates of pseudobase formation and decomposition with many other *N*-methyl heterocyclic cations were unsuccessful. Since it appears from Figs. 1, 2, and 3 that minima in the k_{obs}–pH profiles occur at pH values in the vicinity of pK_{ROH}, attempts to observe those reactions were made over a pH region spanning several pH units on either side

Can. J. Chem. Downloaded from www.nrcresearchpress.com by 210.87.254.105 on 09/05/12
For personal use only.

Can. J. Chem. Downloaded from www.nrcresearchpress.com by 210.87.254.105 on 09/05/12
For personal use only.

TABLE 5. Deuterium isotope effects on the kinetics and equilibrium for pseudobase formation from the 2-methyl-4-nitroisoquinolinium ion at 25°, ionic strength 0.1

Constant	H_2O	D_2O	k_H/k_D	K_H/K_D
k_1	1.33×10^5	2.18×10^5	0.61	
k_2	0.011	5.47×10^{-3}	2.0	
k_3	8.80×10^6	1.02×10^7	0.9	
k_4	1.04	0.405	2.6	
pK_{ROH}	5.11	5.73		
K	7.8×10^8	1.4×10^9		0.56

TABLE 6. Buffer catalysis of reversible pseudobase formation from the 2-methyl-4-nitroisoquinolinium ion

Buffer	pH	k_B* (M^{-1} s^{-1})
Tris†	7.76	7.8
	7.96	11.7
	8.28	13.2
	8.52	11.1
Formate	2.99	7.4
	3.64	14.5
	4.20	9.8

*Based on total buffer concentration (*i.e.* [B] + [BH$^+$]).
†Tris(hydroxymethyl)aminomethane — k_B is the slope of the lines in Fig. 5.

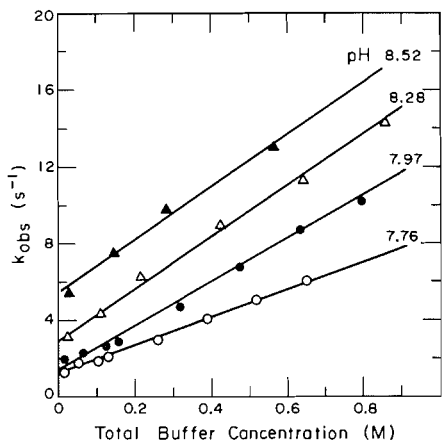

FIG. 5. Influence of buffer concentration and pH on formation (tris(hydroxymethyl)aminomethane buffer) of the pseudobase of the 2-methyl-4-nitroisoquinolinium ion. Temperature 25°; ionic strength 0.5 (neutral salt KCl).

of pK_{ROH}. Reactions of the following cations were too fast to allow study by the stopped-flow technique: 1-methyl-1,5-naphthyridinium; 6-methyl-1,6-naphthyridinium; 7-methyl-1,7-naphthyridinium; 1-methyl-1,8-naphthyridinium; 1-methyl-x-nitroquinolinium (x = 5, 6, 7, 8); 2-methyl-5-nitroisoquinolinium; 2-methylphthalazinium; and 1-methylquinoxalinium. Thus, although the 2-methyl-4-nitroisoquinolinium ion (pK_{ROH} = 5.0) is much more susceptible to hydroxide addition than any of the above cations (pK_{ROH} = 8.6–13 (1)), it is the only ion of this type amenable to investigation by the stopped-flow kinetic technique. Although the second-order rate constant for hydroxide attack on **3** is presumably greater than for the other cations listed above, the low pK_{ROH} value allows the investigation of pseudobase formation at pH values where the pseudo first-order rate constant for hydroxide attack (*i.e.* $k_3[OH^-]$) is relatively small.

Discussion

The temperature dependence of the pK_{ROH} values for pseudobase formation from the three heterocyclic cations in Table 2 suggests that the stability of the cation relative to its pseudobase decreases as the temperature increases. However, these pK_{ROH} values include a contribution from the ionic product of water, K_w. Correction for the temperature dependence of K_w (3), shows that the association constant, K, actually decreases with increasing temperature for the 2-methyl-4-nitroisoquinolinium and 10-methylacridinium cations (see Table 2). Thus despite the temperature dependence of the pK_{ROH} values, these cations are in fact stabilized relative to the corresponding pseudobases by an increase in temperature. The equilibrium constant, K, for the 10-methyl-9-phenyl-acridinium cation appears to be almost temperature independent over the range 25–55°. Furthermore, although the pK_{ROH} values suggest the pseudobase–cation equilibrium is more temperature-dependent in the acridine systems than for the 2-methyl-4-nitroisoquinolinium cation, this is again an artifact resulting from the contribution of pK_w to the pK_{ROH} values. From the association constants, K, it is clear that the temperature dependence of the equilibrium is much greater for the 2-methyl-4-nitroisoquinolinium ion than for either of the two acridinium ions.

A van't Hoff plot of the equilibrium data is shown in Fig. 6 for the two systems having temperature-dependent equilibria. In each case the plot is apparently linear, and we have derived values of $\Delta H^0 = -10.8$ kcal/mol and $\Delta S^0 = +4.5$ e.u. for pseudobase formation from the 2-methyl-4-nitroisoquinolinium cation

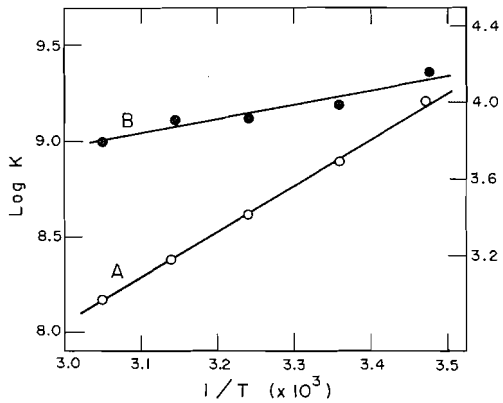

FIG. 6. Dependence of log K on temperature for the 2-methyl-4-nitroisoquinolinium (A, left hand ordinate) and 10-methylacridinium (B, right hand ordinate) ions.

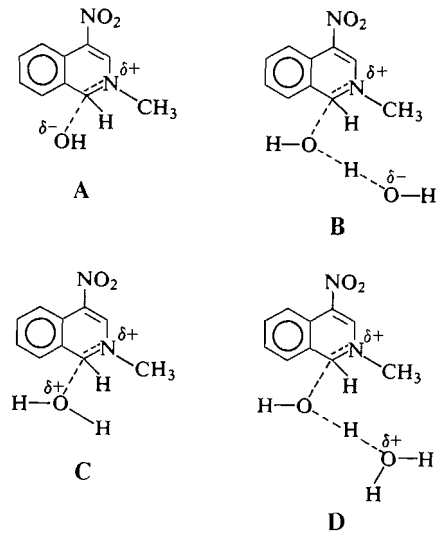

and $\Delta H^0 = -2.9$ kcal/mol and $\Delta S^0 = +8.7$ e.u. for the 10-methylacridinium ion.

It is clear from the representative data in Fig. 5 that the reversible formation of pseudobases from these heterocyclic cations is subject to catalysis by buffer species. However, the pH-dependence of the catalysis by any given buffer is complex, and we have been unable to assign the catalysis as being of a simple general-acid or general-base type. A complete definition of these catalytic effects will require a further extensive study. Despite the complexity of this buffer catalysis, a smooth pH–rate profile is obtained for each reaction (Figs. 1–4) when the buffer solutions are made up so as to give a total ionic strength 0.1 from the buffer species alone without any added neutral salt. This is true despite the fact that eight different buffers of widely varying chemical type were used over the pH range covered by these experiments.

The empirical eqs. 5 and 6 suggest that two kinetically distinguishable pathways are available for each of pseudobase formation and decomposition in the pH ranges that we have studied. For each cation, the rate of pseudobase formation is pH-independent (k_4 in eq. 6) at the lower pH values in the range that was amenable to our experimental techniques. This term is interpretable either as a rate-determining attack of a water molecule on the heterocyclic cation followed by a rapid deprotonation (transition state **C**) or alternatively as the general-base catalyzed attack (by another water molecule) of a molecule of water on the heterocyclic cation (transition state **D**). In more basic solutions, this mechanism becomes unimportant compared with the direct attack of hydroxide ion ($k_3[OH^-]$) on the heterocyclic cation (transition state **A**), or alternatively the kinetically equivalent hydroxide ion catalyzed attack (as a general-base) of a water molecule on the cation (transition state **B**).

The mechanistic significance of the terms in eq. 5 for pseudobase decomposition must, of course, be the microscopic reverse of the interpretations given above for the pseudobase formation reactions. Thus, $k_1[H^+]$ is the microscopic reverse of the k_4 term, and may be formally interpreted as either the spontaneous loss of a molecule of water from the O-protonated pseudobase (*i.e.* specific-acid catalysis; transition state **C**) or alternatively as elimination of hydroxide ion from the neutral pseudobase molecule with the aid of H_3O^+ as a general-acid catalyst (transition state **D**). The k_2 term is the microscopic reverse of $k_3[OH^-]$, and so formally represents either the spontaneous decomposition of the pseudobase to heterocyclic cation and hydroxide ion (transition state **A**) or the kinetically equivalent general-acid catalysis of this reaction by a water molecule (transition state **B**).

The observed kinetic isotope effect $k_4^H/k_4^D = 2.6$ with the 2-methyl-4-nitroisoquinolinium ion seems to be too large to be attributed to a transition state such as **C** which does not involve a rate-determining proton transfer. This solvent isotope effect is more consistent with a transition state such as **D** in which a proton transfer occurs to a water molecule acting as a general-base. This postulate further suggests that the $k_1[H^+]$ term in pseudobase decomposition must

Can. J. Chem. Downloaded from www.nrcresearchpress.com by 210.87.254.105 on 09/05/12
For personal use only.

Can. J. Chem. Downloaded from www.nrcresearchpress.com by 210.87.254.105 on 09/05/12
For personal use only.

represent general-acid catalysis by H_3O^+ of the elimination of a hydroxide ion. Although the measured solvent isotope effect $k_1^H/k_1^D = 0.61$ is in the range usually associated with specific-acid catalysis (*i.e.* transition state **C**), there are a number of recent examples in the literature of genuine general-acid catalysis for which similar solvent isotope effects have been found. Thus, in the hydrolysis of ortho esters and of some acetals and ketals isotope effects in the range $k^H/k^D = 0.37$–0.75 have been observed for general-acid catalysis (4, 5). These reactions are somewhat related to pseudobase decomposition, and similar isotope effects might be expected.

The entropies of activation for the k_4 term (Table 4) do not distinguish between the postulated transition states **C** and **D**. The entropies of activation for the reverse step (k_1) vary between -10 and 0 e.u. A value of $\Delta S^{\ddagger} \approx 0$ for this step, as is found for the pseudobases from the 2-methyl-4-nitroisoquinolinium and 10-methylacridinium ions, might be interpreted in terms of transition state **D** if proton transfers occur along pre-formed hydrogen bonds between the pseudobase hydroxyl group and solvating water molecules. The ratios k_1/k_2 and k_3/k_4 for reactions of **1** and **2** are similar for the 9-unsubstituted and 9-phenyl acridine systems (Table 3). We feel that this observation is also most readily accounted for if transition states analogous to **B** and **D** are involved. Since **A** and **C** require formally charged species attacking or being formed at C-9, the enhanced solvation requirements of such species might be expected to be reflected in different k_1/k_2 and k_3/k_4 ratios for the 9-unsubstituted and 9-phenyl derivatives.

The entropies of activation observed for k_3 terms also seem to be too negative to be merely reflecting direct hydroxide attack on the heterocyclic cations. One might predict that such a direct attack would have an entropy of activation similar to the entropy of formation of the pseudobase from heterocyclic cation and hydroxide ion. The greatest discrepancy is between $\Delta S^{\ddagger} = -17$ e.u. for hydroxide ion attack on the cation (k_3) and $\Delta S = +8.7$ e.u. for the equilibrium association of the cation and anion in the 10-methylacridinium system. Interpretation of this reaction as hydroxide ion acting as a general-base for attack by a water molecule would therefore seem to be more consistent with the observed entropies of activation. Such general-base catalysis would be expected to exhibit a considerable solvent isotope effect; however, a small inverse isotope effect ($k_3^H/k_3^D = 0.9$) is actually observed. Although unusual, small isotope effects for general-base catalyzed reactions have been previously observed. Thus, $k^H/k^D = 1.1$ for the general-base catalyzed attack of glycine on phenyl acetate (6). The k_2 step, which is the microscopic reverse of the k_3 term, would then be interpreted as general-acid catalyzed (by a water molecule) decomposition of the neutral pseudobase to the heterocyclic cation. The observed isotope effect $k_2^H/k_2^D = 2.0$ and entropies of activation (-14 to -24 e.u.) are consistent with such an interpretation.

This suggestion that transition state **B** more accurately reflects the hydroxide ion catalyzed reaction than does transition state **A**, is similar to the recent observation that hydroxide attack on the malachite green cation (**5**) to give the carbinol occurs via a general-base mechanism (7). This description of the transition state is also consistent with Ritchie's postulate (8) that the transition states for some related cation–anion nucleophilic addition reactions involve considerable separation of the cation and anion, and are probably somewhat similar to an ion-pair separated by one solvent water molecule. The interpretation of the mechanisms of these reactions in terms of transition states such as **B** and **D** is also supported by our observation of the importance of buffer catalysis in these reactions.

Pseudobase formation from the 10-methylacridinium cations is formally closely related to carbinol formation from triphenylmethyl carbonium ions. These latter reactions have been

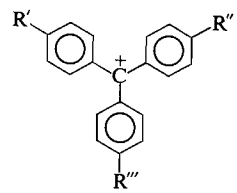

5 R′ = H; R″ = R‴ = $N(CH_3)_2$
6 R′ = R″ = R‴ = $N(CH_3)_2$

extensively studied (9–14). In particular, a comparison between the 10-methylacridinium cation (**1**; R = H) ($pK_{ROH} = 9.86$ (1)) and the crystal violet cation (tris(4-dimethylaminophenyl)-methyl carbonium ion **6**) ($pK_{ROH} = 9.36$ (14)) is of interest since the equilibrium constants for hydroxide addition to these two ions are quite

Can. J. Chem. Downloaded from www.nrcresearchpress.com by 210.87.254.105 on 09/05/12
For personal use only.

similar. At 25°, the pseudo first-order rate constant for attack of water on **6** is 3.5×10^{-5} s^{-1} (9) compared with 2.43×10^{-3} s^{-1} for **1** (R = H). For attack by hydroxide ion, the second-order rate constants are 0.205 M^{-1} s^{-1} for **6** (9) and 552 M^{-1} s^{-1} for **1** (R = H). Thus, although the equilibrium constant for hydroxide addition to **6** is about threefold larger than for **1** (R = H), water attack is 150 times faster and hydroxide attack is over 2500 times faster on **1** (R = H) than on **6**. These rate differences probably arise from steric effects resulting from the presence of an additional aromatic ring on the electrophilic carbon in **6**. In fact, the rates of hydroxide and water attack (k_3 and k_4 in Table 3) on the 10-methyl-9-phenylacridinium ion (**1**; R = Ph) which should involve similar steric effects to the analogous reactions of **6** are within a factor of 10 of the same rate constants for **6**. The result of the above comparison of **1** (R = H) and **6** is not surprising in view of the general observation that in such anion–cation combination reactions there appears to be little correlation between kinetic and equilibrium structural effects (8, 15). Comparison of the relative rates of hydroxide and water attack on these heterocyclic cations gives $\log k_3 - \log k_4 = 5.4$ for both **1** (R = H) and **1** (R = Ph) and $\log k_3 - \log k_4 = 6.9$ for **3** (at 25°). Both of these values are somewhat greater than might be expected (4.5) if Ritchie's N_+ values (15) are assumed to be applicable in these systems.

Experimental

Materials

10-Methylacridinium iodide and 2-methyl-4-nitroisoquinolinium iodide were synthesized as previously described (1). 9-Phenylacridine was prepared from benzoic acid and diphenylamine (16). Methylation with methyl iodide gave 10-methyl-9-phenylacridinium iodide, m.p. 250° (after recrystallization from methanol), lit. m.p. 148–150° (?) (17).

Anal. Calcd. for $C_{20}H_{16}IN$: C, 60.5; H, 4.03; I, 32.0; N, 3.53. Found: C, 60.1; H, 4.51; I, 31.8; N, 3.52.

Buffer solutions were made up from the best available commercial grades of reagents. Buffers used were: chloroacetate (pH < 3); formate (pH = 3–4.5); succinate (pH = 4.5–6); phosphate (pH = 6–8); borate (pH = 8–9.5); carbonate (pH = 9.5–11); phosphate (11–12); standard potassium hydroxide solutions (pH > 12). All kinetic runs were carried out in buffers of ionic strength 0.1, unless indicated otherwise. When necessary, potassium chloride was used as a neutral electrolyte.

Methods

The pK_{ROH} values were measured as previously described (1); by potentiometric titration for the 2-methyl-4-nitroisoquinolinium ion and spectrophotometrically for the 10-methyl- and 10-methyl-9-phenylacridinium ions. All pH measurements were made with a Corning Model 12 Research pH Meter standardized at the reaction temperature with standard buffers (18). All pD values were obtained by the addition of 0.40 to the pH meter reading (19).

Reaction kinetics were measured either with a Durrum–Gibson stopped-flow spectrophotometer or a Cary 16K spectrophotometer (for reactions of the 10-methyl-9-phenylacridinium ion having half times greater than 1 min) by mixing aqueous solutions of the heterocyclic cation (for pseudobase formation) or of the pseudobase (for pseudobase decomposition) with double strength buffer solutions. All solutions were pre-equilibrated at the reaction temperatures (±0.1 °C). All pH values were independently checked after a similar dilution of the stock buffer solutions. Reactions were followed at 410 nm for the 2-methyl-4-nitroisoquinolinium cation, 342 nm for the 10-methylacridinium ion, and 286 nm for the 10-methyl-9-phenylacridinium ion. First-order kinetic plots of $\log (D - D_\infty)$ *vs.* time were prepared, where D is the optical density at time t and D_∞ is the equilibrium optical density. In all cases, such plots were linear for at least 90% of the reaction, and pseudo first-order rate constants (k_{obs}) were determined from the slopes of these lines. The individual rate constants for pseudobase formation (k_f) and decomposition (k_d) were determined as described above.

This research was supported by a grant from the National Research Council of Canada, and a Province of Ontario Graduate Fellowship awarded to W.G.M. We thank Mr. E. P.-C. Wong for the synthesis of 9-phenylacridine and its methiodide salt.

1. J. W. Bunting and W. G. Meathrel. Can. J. Chem. **50**, 917 (1972).
2. A. Albert. The acridines. 2nd Ed. Edward Arnold Ltd., London. 1966. p. xi.
3. H. S. Harned and R. A. Robinson. Trans. Faraday Soc. **36**, 973 (1940).
4. E. H. Cordes. Progr. Phys. Org. Chem. **4**, 1 (1967).
5. T. H. Fife. Acc. Chem. Res. **5**, 264 (1972).
6. W. P. Jencks and J. Carriuolo. J. Am. Chem. Soc. **82**, 675 (1960).
7. C. D. Ritchie. J. Am. Chem. Soc. **94**, 3275 (1972).
8. C. D. Ritchie. Acc. Chem. Res. **5**, 348 (1972).
9. C. D. Ritchie, G. A. Skinner, and V. G. Badding. J. Am. Chem. Soc. **89**, 2063 (1967).
10. E. A. Hill and W. J. Mueller. Tetrahedron Lett. 2565 (1968).
11. C. D. Ritchie and P. O. I. Virtanen. J. Am. Chem. Soc. **94**, 1589 (1972).
12. M. J. Postle and P. A. H. Wyatt. J. Chem. Soc. Perkin II, 474 (1972).
13. C. A. Bunton and S. K. Huang. J. Am. Chem. Soc. **94**, 3536 (1972).
14. O. F. Ginsberg and N. S. Melnkova. J. Gen. Chem. U.S.S.R. **25**, 1109 (1955).
15. C. D. Ritchie and P. O. I. Virtanen. J. Am. Chem. Soc. **94**, 4966 (1972).
16. Reference 2, p. 100.
17. Reference 2, p. 341.
18. R. G. Bates. J. Res. Nat. Bureau Standards, **66A**, 179 (1962).
19. P. K. Glascoe and F. A. Long. J. Phys. Chem. **64**, 188 (1960).

Bufadienolides. 17. Synthesis of 14α- and 14β-Artebufogenin[1]

YOSHIAKI KAMANO AND GEORGE R. PETTIT[2]

Department of Chemistry, Arizona State University, Tempe, Arizona 85281

Received November 24, 1972

Treatment of resibufogenin (**1***a*) or its acetate (**1***b*) with perchloric acid or hydrochloric acid gave 14α- and 14β-artebufogenin (**5***a* and **6***a*, or **5***b* and **6***b*), in addition to 15α-hydroxy-bufalin (**4***a* or *b*). Reaction of epoxide **1***b* with chloranil or boron trifluoride etherate easily afforded 14α- and 14β-artebufogenin acetate (**5***b* and **6***b*) in good yields. Analogous reaction of the isomeric 3β-hydroxy-14α,15α-epoxide **3***a* with perchloric acid, hydrochloric acid, or sulfuric acid again led to 14α- and 14β-artebufogenin (**5***a* and **6***a*) and the 14β,15α-dihydroxy-derivative **4***a*. Similar reaction with periodic acid gave **6***a* and **4***a*.

Lors du traitement de la résibufogénine (**1***a*) ou de son acétate (**1***b*) avec de l'acide perchlorique ou avec de l'acide chlorhydrique, on a obtenu l'artébyfagénine-14α et 14β (**5***a* et **6***a* ou **5***b* et **6***b*), en plus de l'hydroxy-15α bufaline (**4***a* ou **4***b*). La réaction de l'époxyde **1***b* avec du chloranil ou avec de l'éthérate de trifluorure de bore a produit aisément [l'acétate-14α et 14β d'arté bufogénine (**5***b* et **6***B*) avec d'excellents rendements. La réaction similaire de l'époxyde-14α,15α hydroxy-3β isomérique avec de l'acide perchlorique, de l'acide chlorhydrique ou de l'acide sulfurique a conduit de nouveau à l'artébufogénine-14α et 14β (**5***a* et **6***a*) et le dérivé dihydroxy-14β,15α (**4***a*). La réaction identique avec l'acide periodique a conduit aux produits **6***a* et **4***a*. [Traduit par le journal]

Can. J. Chem., 51, 1973 (1973)

In one of the early studies (1) which preceded the bufadienolide structural assignment, 14α-artebufogenin (**5***a*) was prepared from the 14β,-15β-epoxide, resibufogenin (**1***a*), by reaction with concentrated hydrochloric acid and later (2) using perchloric acid. Recently (3), we noted that a small amount of 14α-artebufogenin (**5***a*) could be isolated by column chromatography of 3β,14β-dihydroxy-15α-bromo-5β-bufa-20,22-dienolide (**2**) on alumina. Treatment of the 14α-isomer (**5***a*) with alumina (2) or hydrochloric acid (4) has afforded the epimeric 14β-artebufogenin (**6***a*). Also epimerization of the 14β-isomer (**6***a*) with acid (5) has afforded 14α-artebufogenin (**5***a*). A more direct route to 14β-artebufogenin (**6***a*) has not heretofore been reported.

In the present report we wish to describe new syntheses of 14α- and 14β-artebufogenin (**5***a* and **6***a*) from resibufogenin (**1**) and the isomeric (2) 14α,15α-epoxide **3**. The latter epoxide (**3**) was prepared from 14-dehydrobufalin by oxidation with meta-chloroperbenzoic acid (3)[3]. When 3β-hydroxy-14β,15β-epoxide **1***a* was treated with 70% perchloric acid in acetone (2) and the product carefully chromatographed, 14α-artebufogenin (**5***a*), 14β-artebufogenin (**6***a*), and 3β,-14β,15α-triol **4***a* were obtained in respectively 69 and ~9% yields. Analogous treatment of 3β-acetoxy-14β,15β-epoxide **1***b* gave 14α-artebufogenin acetate (**5***b*), 14β-artebufogenin acetate (**6***b*), 3-acetoxy-14β,15α-diol (**4***b*), and 14α-artebufogenin (**5***a*) (5) in respectively 73, 8, 12, and 8% yields.

Reaction of resibufogenin (**1***a*) with 2 *N* hydrochloric acid in acetone gave 14α-artebufogenin (**5***a*), 14β-artebufogenin (**6***a*), and 15α-hydroxybufalin (**4***a*) in 62, 23.5, and 6% yields. Extension of the reaction to 3β-acetate **1***b* gave the corresponding 3β-acetates, **5***b*, **6***b*, and **4***b* in 60, 22, and 10% yields. The higher yield of 14β-epimer (**6***a* or *b*) resulting from reaction with hydrochloric acid may have been due to the longer contact time. It should also be mentioned that certain etianic acid (7) and pregnane (8) 14β,15β-epoxides have been converted to 14β,15α-dihydroxy derivatives by treatment with perchloric acid.

Reaction of 3β-acetoxy-14β,15β-epoxide **1***b* with chloranil in refluxing xylene or at room temperature with boron trifluoride etherate afforded only the 14α*H*-15-oxo- and 14β*H*-15-oxo-isomers (**5***b* and **6***b*). Best conversion was found using boron trifluoride etherate. Here 14β-artebufogenin was obtained in 60% yield and the 14α-epimer in 20% yield.

[1]For Parts 15 and 16 of this series (Steroids and Related Natural Products 71 and 72) see refs. 13 and 14, respectively.

[2]To whom inquiries should be sent.

[3]A related study employing *p*-nitroperbenzoic acid has been described by Bingham *et al.* (6).

Can. J. Chem. Downloaded from www.nrcresearchpress.com by 210.87.254.42 on 09/05/12
For personal use only.

Can. J. Chem. Downloaded from www.nrcresearchpress.com by 210.87.254.42 on 09/05/12
For personal use only.

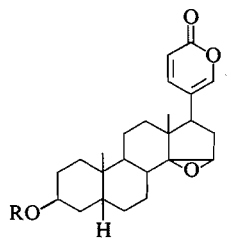

1
a R = H
b R = Ac

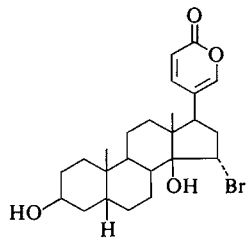

2

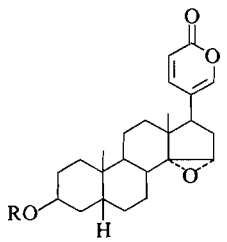

3
a R = H
b R = Ac

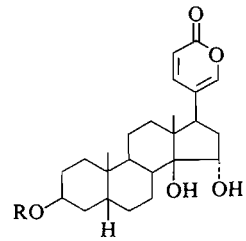

4
a R = H
b R = Ac

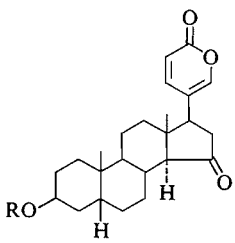

5
a R = H
b R = Ac

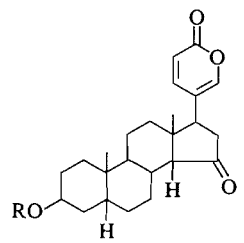

6
a R = H
b R = Ac

Application of the preceding reaction with 4 *N* hydrochloric acid to 3β-hydroxy- or 3β-acetoxy-14α,15α-epoxide **3***a* or *b* gave the 14α*H*-15-oxo- (**5***a* or *b*), 14β*H*-15-oxo- (**6***a* or *b*), and 14β,15α-dihydroxy derivatives (**4***a* or *b*) in respectively 26 or 21, 18 or 14, and 49 or 48% yields. With dilute sulfuric acid in acetone–water as acid catalyst detailed column chromatography of the product led to the 14α*H*- (**5***a* or *b*) and 14β*H*-isomers (**6***a* or *b*) as well as the 14β,15α-dihydroxy derivative (**4***a* or *b*) (3). Similar results were obtained by subjecting 3β-hydroxy-14α,15α-epoxide **3***a* to treatment with dilute perchloric acid in chloroform–acetone. However, reaction of α-epoxide **3***a* with periodic acid in chloroform–acetone gave 14β-artebufogenin (**6***a*) and 15α-hydroxy-bufalin (**4***a*) in 14 and 53% yields. Only a trace of 14α-artebufogenin was detected.

Mayo (9) has suggested that conversion of 14β,15β-epoxides to 14α*H*-15-oxo-derivatives using perchloric acid may be attributed to a 1,2-shift of the C-15 proton. An analogous mechanistic pathway may be operative in the acid-catalyzed reactions we have observed with resibufogenin (**1**) and the corresponding 14α,15α-epoxide **3** (see Scheme 1). In the latter

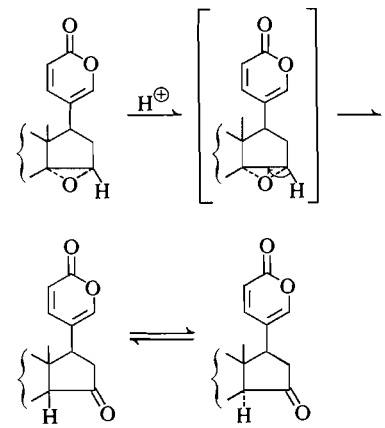

SCHEME 1

case, formation of 14α-artebufogenin is probably the result of epimerizing 14β-artebufogenin. The formation of 14β,15α-diols from 14α,15α-epoxides is analogous to observations made in several earlier studies (10) and we wish to thank a referee for providing this information.

We have previously obtained both 14-dehydrobufalin and resibufogenin (**1***a*) by total synthetic routes (3). Thus, the reactions described above leading to 14α- and 14β-artebufogenin complete total syntheses of these substances.

Experimental

The general experimental techniques have been summarized in the experimental introduction of ref. 3. Authentic specimens of alcohols **4***a* and *b* and the artebufogenins were prepared as previously described (3, 11). The identity of each product was confirmed by results of chromatographic and spectral comparisons with the respective authentic sample. All melting points were observed using a micro hot-stage apparatus (Reichert, Austria) and are uncorrected. Column chromatography refers to the dry method using silica gel (12). All solvent extracts of aqueous solutions were dried over anhydrous sodium sulfate. The identity of each product was established by mixture melting determination and i.r. spectral comparison with an authentic sample.

Can. J. Chem. Downloaded from www.nrcresearchpress.com by 210.87.254.42 on 09/05/12
For personal use only.

Epoxide Ring Opening with 3β-Hydroxy-14β,15β-epoxy-5β-bufa-20,22-dienolide (Resibufogenin, 1a)

Method A. With Perchloric Acid

To a solution of epoxide **1***a* (115 mg) dissolved in acetone (6 ml), 0.05 ml of 72% perchloric acid was added and the mixture was allowed to stand for 30 min at room temperature. The mixture was poured into ice–water and extracted with chloroform. The extract was washed with water, and concentrated *in vacuo* to dryness. The residue (99 mg) was chromatographed on a column of silica gel. Elution with ligroin–acetone 5:1 and 3:1 gave 14α-isomer **5***a* (79 mg), m.p. 265–267° as colorless prisms from acetone, 14β-isomer **6***a* (11 mg), m.p. 128–130° as colorless prisms from methanol, and diol **4***a* (11 mg), m.p. 272–273° as colorless needles from acetone.

Method B. With Hydrochloric Acid

Hydrochloric acid (4 ml of 2 *N*) was added to a solution of **1***a* (100 mg) in acetone (12 ml) and the mixture was allowed to stand for 24 h at room temperature. The mixture was poured into ice–water and extracted with chloroform. The extract was washed with water and solvent evaporated. The residue (97 mg) was chromatographed on a column of silica gel. Elution with ligroin–acetone (5:1) gave **5***a* (62 mg, m.p. 266–267°), **6***a* (24 mg, m.p. 127–129°), and **4***a* (6 mg, m.p. 271–273°).

Epoxide Ring Opening with 3β-Acetoxy-14β,15β-epoxy-5β-bufa-20,22-dienolide (Resibufogenin Acetate, 1b)

Method A. With Perchloric Acid

To a solution of **1***b* (75 mg) in acetone (5 ml), 0.05 ml of 70% perchloric acid was added and the mixture was allowed to stand for 30 min at room temperature. The residue (71 mg) was chromatographed on a column of silica gel. Elution with ligroin–acetone, 19:1, 9:1, and 5:1, provided **5***b* (55 mg), m.p. 221–223°, **6***b* (6 mg), m.p. 233–235°, **4***b* (9 mg), m.p. 271–273°, and **5***a* (6) (6 mg), m.p. 263–265° all as colorless prisms from acetone.

Method B. With Hydrochloric Acid

In the manner described above (**1***a*, method B) β-epoxide **1***b* (50 mg) in acetone (5 ml) was treated with 2 ml of 2 *N* hydrochloric acid. The product (48 mg) was chromatographed on a column of silica gel. Elution with ligroin–acetone 19:1, 9:1, and 5:1 afforded **5***b* (30 mg, m.p. 222–223°), **6***b* (11 mg, m.p. 232–234°), and **4***b* (5 mg, m.p. 269–272°).

Method C. With Chloranil

Chloranil (40 mg) was added to a solution of **1***b* (22 mg) in xylene (5 ml), and the mixture was heated at reflux for 45 min. After dilution with benzene, the mixture was poured into water. The benzene layer was washed with water, dilute sodium bicarbonate, and water, and evaporated to dryness. The residue (30 mg) was chromatographed on a column of silica gel. Elution with ligroin–acetone (9:1) afforded **5***b* (11 mg, m.p. 223–225°) and **6***b* (8 mg, m.p. 223 ~ 234°).

Method D. With Boron Trifluoride Etherate

Freshly distilled boron trifluoride etherate (0.2 ml) was added to a solution of **1***b* (20 mg) in benzene (2 ml)–ether (1 ml), and the mixture was allowed to stand for 10 min at room temperature. After dilution with benzene, the mixture was poured into ice–water. The benzene–ether layer was washed with water, dilute sodium bicarbonate solution, and water, and evaporated *in vacuo* to dryness. The residue (23 mg) was chromatographed on a column of silica gel. Elution with ligroin–acetone (9:1) gave **5***b* (11 mg, m.p. 222–224°) and **6***b* (4 mg, m.p. 232–235°).

Epoxide Ring Opening with 3β-Hydroxy-14α,15α-epoxy-5β-bufa-20,22-dienolide (3a)

Method A. With Perchloric Acid

To a solution of α-epoxide **3***a* (0.20 g) in chloroform (3 ml) – acetone (12 ml), 0.1 ml of 72% perchloric acid solution was added and the mixture was allowed to stand for 48 h at room temperature. After isolation in the manner described above, the product (0.22 g) obtained was chromatographed on a column of silica gel. Elution with ligroin–ether, 5:1 and 3:1, gave **6***a* (57 mg, m.p. 128–130°, prisms from methanol), **5***a* (6 mg, m.p. 266–267°, prisms from acetone), and **4***a* (110 mg, m.p. 271–273°, needles from acetone).

Method B. With Hydrochloric Acid

A solution of α-epoxide **3***a* (70 mg) in chloroform (3 ml) – acetone (12 ml) was treated with 1.5 ml of 4 *N* hydrochloric acid with stirring for 24 h at room temperature. Extraction with chloroform and separation as described above gave the product (68 mg), which was chromatographed on a column of silica gel. Elution with ligroin–ether, 5:1 and 3:1, provided **6***a* (15 mg, m.p. 127–130°), **5***a* (13 mg, m.p. 266–268°), and **4***a* (34 mg, m.p. 272–273°).

Method C. With Sulfuric Acid

To a solution of **3***a* (100 mg) in chloroform (15 ml) – acetone (6 ml) – water (1 ml) was added 1.5 ml of 2 *N* sulfuric acid and the mixture was allowed to stand for 48 h at room temperature. The mixture was poured into water and extracted with chloroform. The extract was washed with water and evaporated (*in vacuo*) to dryness. The product (98 mg) was chromatographed on a column of silica gel. Elution with ligroin–acetone, 5:1 and 3:1, provided **6***a* (18 mg, m.p. 127–130°), **5***a* (4 mg, m.p. 265–268°), and **4***a* (7 mg, m.p. 215–218°).

Method D. With Periodic Acid

To a solution of **3***a* (80 mg) in chloroform (3 ml) – acetone (12 ml) – water (0.2 ml), 60 mg of periodic acid dihydrate was added and the mixture was allowed to stand for 18 h at room temperature. The mixture was poured into water, extracted with chloroform, and the extract was washed with water, and evaporated (*in vacuo*) to dryness. The product (56 mg) was chromatographed on a column of silica gel. Elution with ligroin–acetone (3:1) gave **6***a* (11 mg, m.p. 125–129°) and **4***a* (42 mg, m.p. 271–273°). On t.l.c. (solvent: acetone–chloroform–cyclohexane (3:3:4), silica gel plate developed with concentrated sulfuric acid), the mother liquor of recrystallized **6***a* showed a spot corresponding to **5***a*.

Epoxide Ring Opening with 3β-Acetoxy-14α,15α-epoxy-5β-bufa-20,22-dienolide (3b)

Method A. With Hydrochloric Acid

A solution of α-epoxide **3***b* (0.10 g) in acetone (10 ml) – water (0.1 ml) was stirred with 2 ml of 4 *N* hydrochloric acid for 24 h at room temperature. Following initial separation as described above, the product (99 mg) was chromatographed on a column of silica gel. Elution with ligroin–acetone (9:1 and 5:1) provided **6***b* (26 mg, m.p. 234–235°), **5***b* (14 mg, m.p. 221–222°), and **4***b* (43 mg, m.p. 280–282°).

Method B. With Sulfuric Acid

To a solution of **3***b* (100 mg) in acetone (20 ml) – water (0.5 ml), 2.5 ml of 1 *N* sulfuric acid solution was added and the mixture was allowed to stand for 48 h at room temperature. The solution was poured into water and extracted with chloroform. After isolation (see above) the product (98 mg) was chromatographed on a column of silica gel. Elution with ligroin–acetone mixture (9:1 and 3:1) provided **5***b* (6 mg, m.p. 221–223°), **6***b* (14 mg, m.p. 234–236°), and **4***b* (62 mg, m.p. 280–283°).

Method C. With Boron Trifluoride Etherate

A solution of **3***b* (20 mg) in 4 ml of benzene–ether (1:1) was treated with freshly distilled boron trifluoride etherate for 10 min at room temperature. Isolation of product was performed as described above and provided 21 mg, which was chromatographed on a column of silica gel. Elution with ligroin–acetone (9:1) gave **6***b* (12 mg, m.p. 232–234°) and **5***b* (4 mg, m.p. 222–225°).

The present investigation was supported by Public Health Service Research Grants CA-10612-04, CA-11451-03, and CA-10115-04 from the National Cancer Institute.

1. M. KOTAKE. Sci. Pap. Inst. Phys. Chem. Res. (Tokyo), **24**, 39 (1934).
2. H. LINDE and K. MEYER. Helv. Chim. Acta, **42**, 807 (1959).
3. G. R. PETTIT, Y. KAMANO, F. BRUSCHWEILER, and P. BROWN. J. Org. Chem. **36**, 3736 (1971).
4. M. S. RAGAB, H. LINDE, and K. MEYER. Helv. Chim. Acta, **45**, 1794 (1962).
5. Y. KAMANO, T. ARAI, S. KUMON, and M. KOMATSU. Chem. Pharm. Bull. (Tokyo). In press.
6. K. D. BINGHAM, T. M. BLAIKLOCK, R. C. B. COLEMAN, and G. D. MEAKINS. J. Chem. Soc. C, 2330 (1970).
7. P. HOFER, H. LINDE, and K. MEYER. Helv. Chim. Acta, **43**, 1955 (1960).
8. H. HASEGAWA, Y. SATO, and K. TSUDA. Chem. Pharm. Bull. (Tokyo), **9**, 409 (1961).
9. Molecular rearrangements. Vol. 2. *Edited by* P. De Mayo. John Wiley and Sons, Inc., New York. 1964. p. 1635–1637.
10. A. LARDON and T. REICHSTEIN. Helv. Chim. Acta, **45**, 943 (1962); H. ISHII, T. TOZYO, and D. SATOH. Chem. Pharm. Bull. (Tokyo), **10**, 645 (1962).
11. Y. KAMANO. Chem. Pharm. Bull. (Tokyo), **17**, 1711 (1969).
12. M. KOMATSU and T. OKANO. Yakugaku Zasshi, **87**, 712 (1962).
13. P. BROWN, Y. KAMANO, and G. R. PETTIT. Org. Mass Spect. **6**, 47 (1972).
14. G. R. PETTIT and Y. KAMANO. Chem. Commun. 45 (1972).

Can. J. Chem. Downloaded from www.nrcresearchpress.com by 210.87.254.42 on 09/05/12
For personal use only.

Dissymmetric Oxidation With Methyl 4-Tolyl (*R*)-Sulfoxide

M. H. BENN, PATRICIA CHRISTENSEN, DAN KJERSGAARD, AND CHURAI WATANATADA

Department of Chemistry, The University of Calgary, Calgary, Alberta T2N 1N4

Received August 2, 1972

Methyl 4-tolyl (*R*)-sulfoxide can be used to oxidize (±)-borneol by the carbodiimide–sulfoxide procedure: (−)-camphor is formed in low optical yield; and the residual borneol is correspondingly enriched with its (+)-(1*R*,2*S*,4*R*)-enantiomer.

Le sulfoxyde de méthyle et de tolyle-4 peut être utilisé pour oxyder le bornéol-(±) selon le procédé carboimide-sulfoxyde: le camphre-(−) est obtenu dans des proportions optiquement faibles. Le bornéol résiduaire se trouve enrichi de façon correspondante dans son énantiomère (+)-(1*R*,2*S*,4*R*).

[Traduit par le journal]

Can. J. Chem., 51, 1977 (1973)

Can. J. Chem. Downloaded from www.nrcresearchpress.com by 210.87.254.105 on 09/05/12
For personal use only.

Although dimethyl sulfoxide (**1***a*) appears to be a reagent of choice in the oxidation of primary and secondary alcohols by the sulfoxide–carbodiimide procedure there have been reports that it can be replaced by other sulfoxides; albeit tetramethylene sulfoxide seems to be the only specifically identified substitute (1, 2). If the mechanism of the oxidation is as shown in Scheme 1 (2, 3), it therefore seemed possible that dissymmetric oxidations (the selective oxidation of one enantiomeric alcohol in the presence of the other) might be achieved with a suitable optically-active sulfoxide. We describe here the results of an investigation designed to explore this possibility.

As a conveniently accessible (4) dissymmetric sulfoxide, of known absolute configuration (5), we chose methyl 4-tolyl(+)-(*R*)-sulfoxide (**1***b*). Preliminary experiments with racemic **1***b* established that, in combination with dicyclohexyl carbodiimide (**2**) and phosphoric acid, or pyridinium trifluoroacetate, this sulfoxide could be used to oxidize 1-phenylethanol to acetophenone. However, elevated temperatures were required and, as when dimethyl sulfoxide was employed, the overall conversion of alcohol to ketone was low, with much of the alcohol being lost in side reactions. In addition this system was unattractive for we anticipated that, at the relatively high temperatures which seemed to be needed for the oxidation, acid-catalyzed racemization of the sulfoxide might become troublesome (6). We, therefore, decided to concentrate upon a study of the oxidations of borneol and isoborneol: oxidations which proceed in high yield with dimethyl sulfoxide and in which the product ketone, camphor (**8**), as well as recovered alcohol, could be examined for optical activity.

A summary of the results of these experiments is given in Table 1.

Under the conditions which we employed, isoborneol either resisted oxidation or was predominately converted into camphene. However, racemic borneol (**4**) was oxidized to laevorotatory camphor. The residual borneol was dextrorotatory, thus confirming the selective dissymmetric oxidation of (−)-(2*R*)-borneol by (+)-(*R*)-**1***b*.[1]

The optical purity of **8** and the recovered **4** was very low, 7 and 4% respectively; a result which does not seem attributable to racemization of the sulfoxide since recovered **1***b* was still 62% optically pure. We conclude that either there was poor stereoselection in the formation of the tetracovalent-sulfur intermediate **5** (little preference for the formation of **9***a* rather than *b*); or that if, as Moffat has recently considered (3), **5** is by-passed by the concerted process shown in Scheme 2 this, too, shows little stereoselectivity.

Experimental

Rotations were measured using a Durrum-JASCO O.R.D./C.D. Model 5 spectrometer. A Bendix 2500 gas chromatograph was used for the g.l.c. analyses. The p.m.r. spectra were recorded on Varian A-60 and HA-100 spectrometers. Melting points are uncorrected.

Methyl 4-Tolyl Sulfoxide

Optically active **1***b* was prepared by the literature procedure (5), and had m.p. 76–78°, $[\alpha]_D^{25}$ +145 ± 1° (*c* 3, acetone); lit. (5) m.p. 73.0–74.5°, $[\alpha]_D^{27}$ +145.5° (acetone).

[1]Absolute stereochemistry of camphor and borneol: see ref. 10.

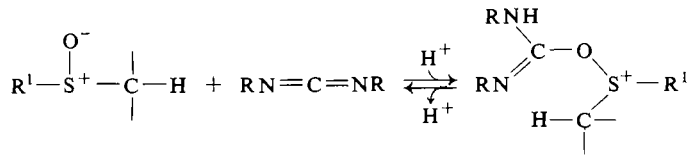

1 2 3

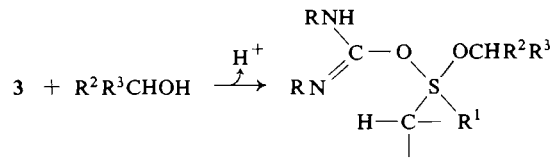

4 5

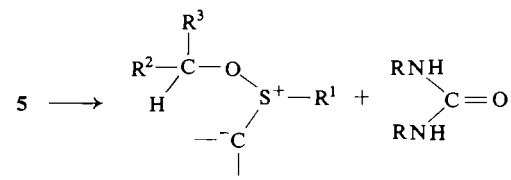

6 7

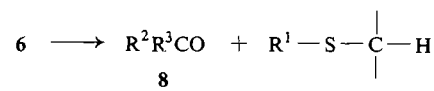

8

SCHEME 1

TABLE 1. Oxidations of borneol and isoborneol

1*b* (mmol)	2 (mmol)	4[b] (mmol)	Catalyst[a] (mmol)	*T* (°C)[c]	*t* (h)	%[d] 8
10	15	5(B)	0	85	24	0
10	15	5(B)	2.2(P)			
			+			
			2.1(P)	85	0.5	30
10	15	5(I)	1.8(P)	85	0.7	0
			+			
			1.5(P)	85	0.7	0[e]
10	15	5(B)	1.8(P)	30	16	—
			1.4(P)	30	72	6
			+			
			1.1(P)	50	19	27
10	10(S)[f]	5(B)	29 (E)	85	1	0
1*a* (mmol)						
4	15	10(B)	2.5(T)	27	2	80

[a]P = Crystalline phosphoric acid; T = pyridinium trifluoroacetate – pyridine; E = triethylamine.
[b]B = Borneol:isoborneol (73:27); I = isoborneol.
[c]±2°.
[d]±1% estimated by g.l.c. and calculated on sulfoxide.
[e]Main product is camphene.
[f]S = Pyridine–SO_3 complex (9).

Can. J. Chem. Downloaded from www.nrcresearchpress.com by 210.87.254.105 on 09/05/12
For personal use only.

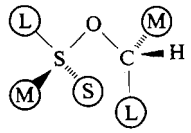

9a

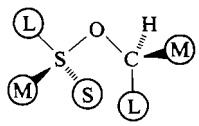

9b

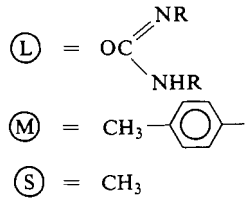

Racemic **1***b* was prepared by the periodate oxidation of methyl 4-tolyl sulfide (7) b.p. 109–112°/0.2 mm, m.p. 55–60°; lit. (7) b.p. 141°/4 mm, m.p. 52–53°.

Catalysts

The crystalline phosphoric acid used was a commercial product (Matheson, Coleman & Bell); the pyridinium trifluoracetate catalyst was prepared *in situ* from trifluoroacetic acid and pyridine (1).

Alcohols

(±)-1-Phenylethanol was prepared by the sodium borohydride reduction of acetophenone. It had b.p. 100–120°/12–15 mm and was ketone-free by g.l.c. analysis (125°/PEGA).

(±)-Isoborneol (Matheson, Coleman, and Bell, practical grade) was recrystallized from acetone – petroleum ether, and then had $[\alpha]_D^{25}$ +0.02° + 0.02° (*c* 5, ethanol), and was >98% pure by g.l.c. analysis (trace of borneol present).

(±)-Borneol; as "racemic borneol" (Nutritional Biochemicals Corp.) had $[\alpha]_D^{25}$ −22.7 ± 0.5° (*c* 5, ethanol), the genuinely racemic isoborneol was epimerized (8) to a mixture of borneol and isoborneol (73:27 by g.l.c. analysis), $[\alpha]_D^{30}$ −0.3 ± 0.1° (*c* 2.5, ethanol) and this product was used in the oxidations.

Oxidation of (±)-1-Phenylethanol

Dicyclohexyl carbodiimide (5.20 g, 25 mmol), (±)-1-phenylethanol (5.50 g, 45 mmol), and methyl 4-tolyl sulfoxide (3.4 g, 22 mmol) were dissolved in sodium – dry benzene (20 ml). To this was added a solution of trifluoroacetic acid (1.26 g, 11 mmol) and pyridine (1.75 g, 22 mmol) in dry benzene (5 ml).

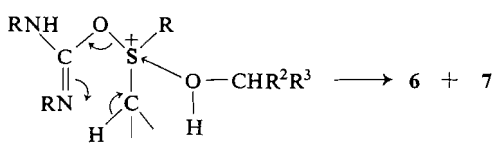

3

SCHEME 2

The reaction mixture was stirred, at room temperature, for 24 h, with rigorous exclusion of moisture. No reaction had taken place so the mixture was stirred and refluxed for 72 h (bath 85°), during which time some solid separated. The reaction mixture was cooled and water (5 ml) added followed by 2 *N* hydrochloric acid (5 ml). After stirring this mixture for 30 min, it was filtered. The filtrate was diluted with ether (50 ml) and the ether phase was washed successively with aqueous sodium bicarbonate, and water, and then dried ($MgSO_4$). Evaporation yielded a pale-brown oil which was distilled to yield a fraction b.p. 90–94°/12 mm. (804 mg) which gave a positive reaction with 2,4-dinitrophenylhydrazine reagent, and was shown by g.l.c. analysis (125°/PEGA) to contain 1-phenylethanol and acetophenone (*ca.* 14:1).

Oxidation of Borneol

Methyl 4-tolyl (+)-(*R*)-sulfoxide (1.54 g, 10 mmol), (±)-borneol-isoborneol (0.77 g, 5 mmol) and dicyclohexyl carbodiimide (3.1 g, 15 mmol) were dissolved in anhydrous benzene (10 ml). To the stirred solution, warmed to 30°, was added crystalline phosphoric acid (180 mg, 1.8 mmol). The reaction mixture was kept at 30°, with rigorous exclusion of moisture, and stirred for 16 h. A white precipitate separated. Additional crystalline phosphoric acid was added (134 mg, 1.4 mmol) and stirring continued for a further 72 h. An n.m.r. analysis revealed only 6% of camphor in the reaction mixture so the temperature was raised to 50° and more phosphoric acid (105 mg, 1.1 mmol) was added. After a further 19 h, p.m.r. analysis revealed that the yield of camphor had risen to *ca.* 25–30%, with 10% camphene, 20% isoborneol, and 35% borneol (as well as dicyclohexyl carbodiimide, methyl 4-tolyl sulfoxide, and methyl tolyl sulfide).

A solution of oxalic acid dihydrate (1.9 g, 15 mmol) in water (50 ml) was then added to the cold reaction mixture, followed by ether (50 ml). After this mixture had been stirred for 1 h it was filtered. The ether phase was separated and washed with aqueous sodium hydrogen carbonate, and water (×3), then dried ($MgSO_4$) and evaporated.

The residue was separated by p.l.c. on Merck silica gel PF 254 + 366 (1m × 20 cm × 1 mm; $CHCl_3$). Extraction of the appropriate bands with chloroform followed by careful evaporation of these extracts (the evaporation of solvent under water-pump pressure was stopped 30 s after the last chloroform disappeared, and the flasks allowed to stand for 5–10 min at room temperature, after which they were of essentially constant weight) yielded the following materials:

(*1*) R_F 0.60 ± 0.06, (−)-camphor (68 mg) (>99.5% by g.l.c. analysis, DEGS, 140°), $[\alpha]_D^{30}$ −2.9 ± 0.2 (*c* 2.4, $CHCl_3$). A second fraction R_F 0.48 ± 0.06, also proved to be camphor (20 mg) (>97% by g.l.c.) $[\alpha]_D^{30}$ −1.7 ± 0.2° (*c* 0.7, $CHCl_3$); lit. (11) $[\alpha]_D$ −41.2°.

(*2*) R_F 0.39 ± 0.03, isoborneol (88 mg) (99% isoborneol:borneol, 93:7 by g.l.c. DEGS 140°), $[\alpha]_D^{30}$ +0.2° ± 0.2 (*c* 2, ethanol).

(*3*) R_F 0.30 ± 0.06, borneol (105 mg) (100% borneol:isoborneol, 97:3 by g.l.c. DEGS, 140°) $[\alpha]_D^{30}$ +0.8 ± 0.2° (*c* 1.8 ethanol); lit. (12) $[\alpha]_D$ +37°.

Can. J. Chem. Downloaded from www.nrcresearchpress.com by 210.87.254.105 on 09/05/12
For personal use only.

(*4*) R_F 0.12 ± 0.06, methyl 4-tolyl sulfoxide (170 mg) (*ca.* 95% pure by p.m.r. analysis), $[\alpha]_D^{30}$ +90 ± 1° (*c* 0.7, acetone).

We thank the National Research Council of Canada for an operating grant which supported this work.

1. K. E. PFITZNER and J. G. MOFFATT. J. Am. Chem. Soc. **87**, 5661 (1965).
2. J. G. MOFFATT. *In* Oxidation: techniques and applications in organic synthesis. Vol. 2. *Edited by* R. L. Augustine and D. J. Trecker. Marcel Dekker Inc., N.Y. 1971. p. 1.
3. J. G. MOFFATT. J. Org. Chem. **36**, 1909 (1971).
4. K. K. ANDERSEN. Tetrahedron Lett. **93** (1962).
5. K. MISLOW, M. M. GREEN, P. LAUR, M. T. MELILLO, T. SIMMONS, and A. L. TERNAY, JR. J. Am. Chem. Soc. **87**, 1958 (1965).
6. K. MISLOW, T. SIMMONS, J. T. MELILLO, and A. L. TERNAY, JR. J. Am. Chem. Soc. **86**, 1452 (1964); J. DAY and D. J. CRAM. J. Am. Chem. Soc. **87**, 4398 (1965).
7. N. J. LEONARD, JR. and C. R. JOHNSON. J. Org. Chem. **27**, 282 (1962); G. KRESZE, E. ROPTE, and B. SCHRADER. Spectrochim. Acta, **21**, 1633 (1965).
8. C. F. WILCOX, JR., M. SEXTON, and M. F. WILCOX. J. Org. Chem. **28**, 1079 (1963).
9. J. R. PARIKH and W. VON E. DOERING. J. Am. Chem. Soc. **89**, 5507 (1967).
10. D. ROGERS and F. H. ALLEN. J. Chem. Soc. B, 632 (1971) and refs. therein.
11. C. WINTHER. Z. Physik. Chem. **60**, 563 (1907).
12. R. H. PICKARD and W. D. LITTLEBURY. J. Chem. Soc. **91**, 1973 (1907).

Can. J. Chem. Downloaded from www.nrcresearchpress.com by 210.87.254.105 on 09/05/12
For personal use only.

Formation of New Tetradentate Schiff Base Metal Chelates

ABDUL MALEK AND JAMES M. FRESCO
Department of Chemistry, McGill University, Montreal, Quebec
Received November 3, 1972

Condensation products of *o*-aminophenol, *N*-substituted-*o*-aminophenols, and 8-amino-1-naphthol with α-diketones have been compared. The basis for the lack of reactivity of these products to yield Schiff base chelates for the cases where the parent diketone is different from glyoxal was examined. Steric factors alone did not appear to influence the reaction.

On a comparé les produits de condensation du *o*-aminophénol, des *o*-aminophénols *N*-substitués, et du amino-8 naphtol-1 avec des α-dicétones. On a examiné la raison du manque de réactivité de ces composés à former des chélates bases de Schiff lorsque la dicétone n'est pas le glyoxal. Les facteurs stériques par eux seuls n'ont pas paru influencer la réaction.

Can. J. Chem., **51**, 1981 (1973)

Introduction

Evidence (1–9) has accumulated in recent years to show that metal ions change the nature of the condensation product of α-diketones with either *o*-hydroxy, or *o*-mercaptoamines and β-mercaptoethylamine. In the absence of metal ions, the condensation product is usually heterocyclic **1** where L is oxygen or sulfur. But the presence of metal ions results in stabilization of the quadridentate Schiff base **2** through complex formation.

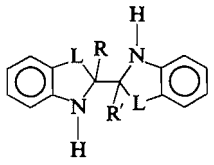

1

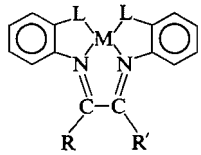

2

Paths that the heterocycle or the corresponding Schiff base tautomer may follow to form the metal chelate have been investigated (1).

It has been shown (10) that the sulfur analogs of structural type **1** undergo metal ion-induced rearrangement more readily than the oxygen analogs. Metal chelates of the thio analog of **1** in which R and R′ are different substituted groups were isolated. However, the oxygen analog reacts with metal ions only when R = R′ = H. This unreactivity was unexpected since the condensation product of *o*-aminothiophenol with salicylaldehyde is the heterocyclic benzthiazoline whereas that of *o*-aminophenol is a Schiff base (7, 11). No chelates of the oxygen analog of structural type **2** with R and R′ groups other than hydrogen atoms have been reported and no satisfactory explanation exists as to why those compounds do not form chelates. Bayer and coworkers (3, 4) explained this lack of chelate formation by assuming that there is steric hindrance between the substituted groups which destabilizes the chelate.

From an examination of models it seems highly unlikely that steric hindrance between the substituted groups is a major factor which can account for such a striking difference in reactivity of these compounds.

The metal chelates of structural type **2**, in which L = NR″(R″ = H, CH_3, C_6H_5, etc.), have not yet been reported. Since a comparison of the spectroscopic and chemical properties of the chelates of structural type **2** where L is varied could provide an understanding of the differences in the reactivities of the parent ligand molecules, a number of these compounds were prepared for study. In addition, since naphthoxazinines **3** provide a case analogous to that of structural

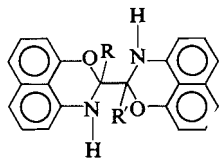

3

type **1** but with the difference that in the former case a six-membered heterocyclic ring is involved, it was of further interest to study the reactivity of these compounds with metal ions and compare them with those of structural type **2**.

Can. J. Chem. Downloaded from www.nrcresearchpress.com by 210.87.254.42 on 09/05/12
For personal use only.

Can. J. Chem. Downloaded from www.nrcresearchpress.com by 210.87.254.42 on 09/05/12
For personal use only.

Experimental

Materials

o-Aminophenol obtained from Eastman Organic Chemicals was recrystallized from ethanol before use. *N*-Methyl-*o*-phenylenediamine monohydrochloride (Eastman), *N*-phenyl-*o*-phenylenediamine (Eastman), glyoxal, 40% aqueous solution (Fisher Scientific Company), pyruvaldehyde, 40% aqueous solution (J. T. Baker Chemical Co.), diacetyl (Fisher), benzil (Eastman), and 2,2′-pyridil (Aldrich Chemical Co. Inc.) were used without further purification. Eastman 8-amino-1-naphthalenesulfonic acid was used for the preparation of 8-amino-1-naphthol hydrochloride without prior purification. Reagent grade nickel chloride hexahydrate and nickel acetate tetrahydrate were obtained from Fisher. Deuterated solvents were obtained from Stohler Isotope Chemicals.

General Methods of Preparation

(i) Benzoxazolines and their Chelates

Benzoxazoline and the 2,2′-mono or disubstituted analogs prepared by the method described by Murase (12) were recrystallized from ethanol.

The nickel chelates were obtained by the following procedure. After dissolution of 0.01 mol of the ligand in 50 ml dry acetone, the solution was shaken in a stoppered flask in the presence of solid sodium hydroxide pellets for 24 h. Upon addition of the pellets, a red–yellow color gradually appeared. Fine particles of the disodium salt of the Schiff base were easily separated from the sodium hydroxide pellets by decantation and subsequent filtration. The yellow disodium salt was unstable in contact with water and alcohols. The nickel chelate was formed by direct addition of the crude sodium salt to an ethanolic solution of nickel chloride (0.01 mol) with vigorous stirring. On addition of water to the ethanol solution the blood-red colored chelate was precipitated. This was filtered, washed first with water and then acetone. Recrystallization from ethanol yielded the pure compound which was dried under vacuum over P_2O_5.

The nickel chelate of 2,2′-bibenzoxazoline was also prepared by direct reaction of nickel acetate with the ligand in ethanol solution as described by Bayer (3). Both methods of preparation yielded identical compounds.

(ii) Naphthoxazinines and their Chelates

The 2,2′-naphthoxazinines were obtained by reaction of 8-amino-1-naphthol with the appropriate α-diketone in a 1:2 molar ratio. The hydrochloride of 8-amino-1-naphthol was obtained from 8-amino-1-naphthalenesulfonic acid by alkali fusion (13). The following procedure was used for the preparation of naphthoxazinines. A 0.02 mol sample of 8-amino-1-naphthol hydrochloride was dissolved in 100 ml water which was previously boiled and cooled to 70°. To this solution a slight excess of the calculated amount of sodium acetate was added to neutralize the acid. A 0.01 mol sample of α-diketone dissolved in a minimum volume of water was added to the 8-amino-1-naphthol solution and the mixture held at this temperature with occasional shaking for about 1 h. Precipitates usually formed gradually. After cooling, the crystals were filtered and washed with water. Recrystallization from ethanol yielded pure compounds.

The nickel chelates of 2,2′-binaphthoxazinine were obtained by the reaction of the ligand with nickel acetate. After 0.01 mol nickel acetate dissolved in 50 ml of ethanol was added to 0.01 mol of the ligand dissolved in 30 ml ethanol, the mixture was refluxed for 1 h. The dark green product formed was separated by filtration and recrystallized from dichloromethane using a Soxhlet extraction system.

(iii) Condensation Products of α-Diketones with N-Methyl- or N-Phenyl-o-phenylenediamine and their Chelates

A solution of 0.02 mol *N*-methyl- or *N*-phenyl-*o*-phenylenediamine in water or ethanol was cooled in an ice bath. A 0.01 mol sample of the appropriate diketone dissolved in water or ethanol was then added slowly with stirring to the amine solution over a period of 1 h. The product appeared gradually and the reaction mixture was stirred overnight. The Schiff base was collected by filtration and was recrystallized from ethanol.

The nickel chelates were prepared by using either one of the following two methods:

Method A: A mixture of 0.02 mol of *N*-methyl- or *N*-phenyl-*o*-phenylenediamine and 0.01 mol of α-diketone dissolved in 50 ml acetone was placed in a stoppered flask. A 0.01 mol sample of nickel chloride dissolved in 20 ml 1:1 ammoniacal solution was added and the contents were allowed to stand at room temperature with occasional stirring for about 1 week. Red or green-colored crystals formed slowly. At the end of the reaction the volume of the solution was reduced by evaporation to increase the yield. After collection by vacuum filtration, the chelate was purified by repeated recrystallization from ethanol–water mixtures.

Method B: This method is essentially the same as the previous one, except the metal ion was reacted directly with the Schiff base obtained by a separate preparation. Both methods provided the same chelate.

Analyses

Microanalyses for carbon, hydrogen, and nitrogen were performed by the Scandinavian Microanalytical Laboratory, Box 25, 2730 Herlev- DK, Denmark.

Nickel was determined by an EDTA titrimetric method (14, 15) after the sample had been ashed at 600° for 1 h and then dissolved in dilute hydrochloric acid. Analytical results are shown in Table 1.

Spectroscopic Measurements

Low resolution mass spectra were obtained with an A.E.I.-MS-902 double focusing mass spectrometer using 70 eV electrons and 8 kV accelerating voltage. The samples were introduced by direct evaporation. A low temperature range (120–130°) was sufficient to obtain the spectra of the free ligands.

Visible and u.v. spectra were recorded with an UNICAM SP 800 u.v. spectrophotometer and with a Beckman DB spectrophotometer connected to a Sargent–Welch SRLG recorder. Absorbance measurements were made in ethanol using 1 cm matched quartz cells.

I.r. spectra in the range 4000–250 cm^{-1} were recorded with a Perkin–Elmer Model 521 grating spectrophotometer. The samples were measured either as KBr pellets, CsBr pellets or as Nujol mulls supported between CsBr plates. Calibration of frequency readings was performed with polystyrene films.

N.m.r. spectra were obtained by using a Varian model

TABLE 1. Analytical data for Schiff bases and their chelates

Compound	% Carbon		% Hydrogen		% Nitrogen		% Nickel	
	Found	Calcd.	Found	Calcd.	Found	Calcd.	Found	Calcd.
$C_{14}H_{12}N_2O_2$	69.9	70.0	5.1	5.0	11.6	11.6		
$C_{14}H_{10}N_2O_2Ni\cdot 2H_2O$	49.8	50.5	4.0	4.2	8.3	8.4	18.0	17.6
$C_{15}H_{14}N_2O_2$	70.3	70.9	5.5	5.6	11.0	11.0		
$C_{16}H_{16}N_2O_2$	70.9	71.6	6.1	6.0	9.9	10.4		
$C_{16}H_{14}N_2O_2Ni\cdot 2H_2O$	54.1	53.2	4.9	5.0	7.6	7.8	15.8	16.3
$C_{16}H_{14}N_2O_2Cd\cdot 2H_2O$	45.5	46.3	4.4	3.9	6.4	6.7		
$C_{16}H_{16}N_4Ni\cdot 2H_2O$	67.0	66.0	6.0	5.5	—	10.6		
$C_{22}H_{16}N_2O_2$	76.2	77.6	5.6	4.7	8.5	8.2		
$C_{22}H_{14}N_2O_2Ni\cdot 2H_2O$	60.7	61.0	4.0	4.2	5.8	6.5		
$C_{26}H_{20}N_4Ni\cdot 2H_2O$	64.2	64.9	6.0	5.0	17.1	11.2		
$C_{26}H_{22}N_6Ni\cdot 2H_2O$	60.9	60.8	4.5	5.1	14.3	16.4	11.4	11.5
$C_{28}H_{26}N_4$	79.3	80.7	6.1	6.3	13.3	13.0		

T-60 spectrometer. The specifications given by the manufacturer are as follows: H_0 field strength 14 092 G; H rotating field frequency 60 MHz (for proton resonance at 14 092 G); resolution: the full line width at half amplitude is ≥ 0.5 Hz; sensitivity: average signal to noise ratio 12:1.

Tetramethylsilane was used as internal or external standard. Measurements were made in chloroform-*d*, dimethylsulfoxide-*d* and pyridine-*d*.

Results and Discussion

Structures of the Schiff Bases

It has been reported (12) previously that the dicondensation of *o*-aminophenols with α-diketones results in the formation of heterocyclic compounds **1**, L = O.

Although in some restricted cases (1) it was possible to isolate the intermediate Schiff bases, in most cases the heterocyclic compound is the only product. A structurally similar compound, 8-amino-1-naphthol was found in the present study to condense with α-diketones forming exclusively the heterocycle, naphthoxazinine **3**.

In contrast to the previous two cases, 2 mol of *N*-methyl- and *N*-phenyl-*o*-phenylenediamines were found to condense with α-diketones to give yellow-colored Schiff bases, **4**. Spectroscopic and chemical evidence in favor of **3** and **4** and additional evidence supporting **1** are discussed in the following sections. The results are summarized in Tables 2 and 3.

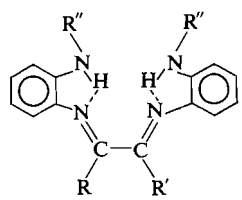

4

(i) I.r. Spectra

All the above three types of compounds have a characteristic sharp band near 3300 cm^{-1} (Table 2). This band is absent in the corresponding metal chelates (Fig. 1). In his investigations with 2,2′-bibenzoxazoline compounds, **1**, Murase (12) assigned this band to the N—H stretching frequency. The presence of this sharp band in the condensation products of 8-amino-1-naphthol with α-diketones indicates that the resultant compounds have the heterocyclic structure **3**. No broad O—H stretching band in the high frequency region was observed in the spectra of these compounds. This indicates the absence of possible Schiff base forms **5** and **6**.

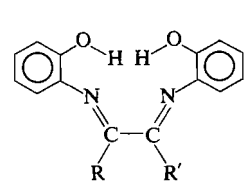

5

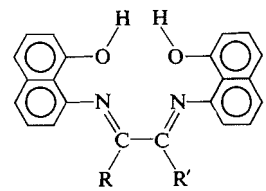

6

The N—H band in the condensation products of *N*-(substituted)-*o*-phenylenediamine with α-diketones is relatively broader and split; this indicates intramolecular hydrogen bonding of the N—H hydrogen with the azomethine nitrogen **4**.

(ii) U.v. Spectra

The spectra of the dicondensation products of *o*-aminophenol and 8-amino-1-naphthol with α-diketones are closely related to those of the primary amines themselves, Table 4. All of these compounds are colorless. The presence of the chromophore such as conjugated azomethine

Can. J. Chem. Downloaded from www.nrcresearchpress.com by 210.87.254.42 on 09/05/12
For personal use only.

TABLE 2. Certain significant i.r., u.v., and n.m.r. spectral bands in the compounds of structural types **1**, **3**, and **4***

Compound	R	R′	R″	N.m.r. peaks (δ p.p.m.) N—H or N—CH_3	N.m.r. peaks (δ p.p.m.) C—H or CH_3	I.r. bands N—H str. (cm^{-1})	U.v. bands (nm)
3*a*	H	H		7.18b	5.24b	3340s	323s, 336s
3*b*	CH_3	CH_3			1.48b	3375s	325s, 336s
1*a*	H	H		7.20″	5.25″	3380s	237s, 293s
1*b*	H	CH_3		7.09′	1.25′	3340s	235s, 294s, 378w
				7.18″	5.00″	3425m	
1*c*	CH_3	CH_3		7.17′	1.29′	3335s	236s, 293s
4*c*	C_6H_5	C_6H_5	CH_3	2.34′		3350m, 3325s	315s, 253s
				3.95′			
4*d*	Py	Py	CH_3	2.64′		3350m, 3270s	314s, 252s
				4.35′			

*′ = singlet, ″ = doublet, b = broad, s = strong, m = medium, w = weak, Py = Pyridyl group.

TABLE 3. Principal peaks in the mass spectra of compounds of structural types **1**, **3**, and **4**

Compound	R	R′	R″	M.p. (°C)	*m/e* (%) formula
3*a*	H	H		215	340(30)$C_{22}H_{16}N_2O_2$, 208(5), 171(90)$C_{11}H_9NO$, 170(100)$C_{11}H_9NO$
3*b*	CH_3	CH_3		259–261	368(5)$C_{24}H_{20}N_2O_2$, 367(8)$C_{24}H_{21}N_2O_2$, 185(21)$C_{12}H_{11}NO$, 184(100)$C_{12}H_{10}NO$, 183(100)$C_{12}H_9NO$
1*a*	H	H		210–212	240(5)$C_{14}H_{12}N_2O_2$, 239(22)$C_{14}H_{11}N_2O_2$, 238(100)$C_{14}H_{10}N_2O_2$, 133(70)C_8H_7NO, 120(97)C_7H_6NO
1*b*	H	CH_3		191	254(100)$C_{15}H_{14}N_2O_2$, 147(88)C_9H_9NO, 146(88)C_9H_8NO, 134(90)C_8H_8NO, 120(73)C_7H_6NO
1*c*	CH_3	CH_3		241	268(40)$C_{16}H_{16}N_2O_2$, 161(100)$C_{10}H_{11}NO$, 146(31)C_9H_8NO, 134(63)C_8H_8NO
1*d*	CH_3	C_6H_5		220–221	330(6)$C_{21}H_{18}N_2O_2$, 223(23)$C_{15}H_{13}NO$, 195(100)$C_{13}H_9NO$, 167(18), 145(19)C_9H_7NO, 133(100)C_8H_7NO
4*c*	C_6H_5	C_6H_5	CH_3	175–178	418(54)$C_{28}H_{26}N_4$, 312(8)$C_{21}H_{18}N_2$, 298(100)$C_{21}H_{18}N$, 282(100)$C_{20}H_{14}N_2$, 221(44)$C_{15}H_{13}N_2$, 209(100)$C_{14}H_{13}N_2$
4*d*	Py	Py	CH_3	143 (dec.)	420(28)$C_{26}H_{24}N_6$, 299(100)$C_{19}H_{15}N_4$, 285(28)$C_{19}H_{15}N_3$, 256(8)$C_{18}H_{13}N_2$, 220(18), 210(18)$C_{13}H_{12}N_3$

(>C=N—) linkage in these compounds should therefore be discounted. This implies that these compounds are heterocyclic.

The spectra of the dicondensation products of *N*-(methyl or phenyl)-*o*-phenylenediamine with α-diketones on the other hand are different than those of the primary amines, Table 4. These compounds are yellow in color, which indicates the presence of chromophoric (>C=N—) linkage, structure **4**.

Base-induced rearrangement. Murase (16) reported earlier that although **1** (R = R′ = H) was insoluble in aqueous alkali, a reddish-yellow color was produced when an excess of potassium hydroxide was added to its ethanol solution and another absorption maximum was observed at 467 nm. This was explained by assuming that 2,2′-bibenzoxazoline tautomerizes to the corresponding Schiff base under the influence of base to yield the anion of **5**.

Can. J. Chem. Downloaded from www.nrcresearchpress.com by 210.87.254.42 on 09/05/12
For personal use only.

Can. J. Chem. Downloaded from www.nrcresearchpress.com by 210.87.254.42 on 09/05/12
For personal use only.

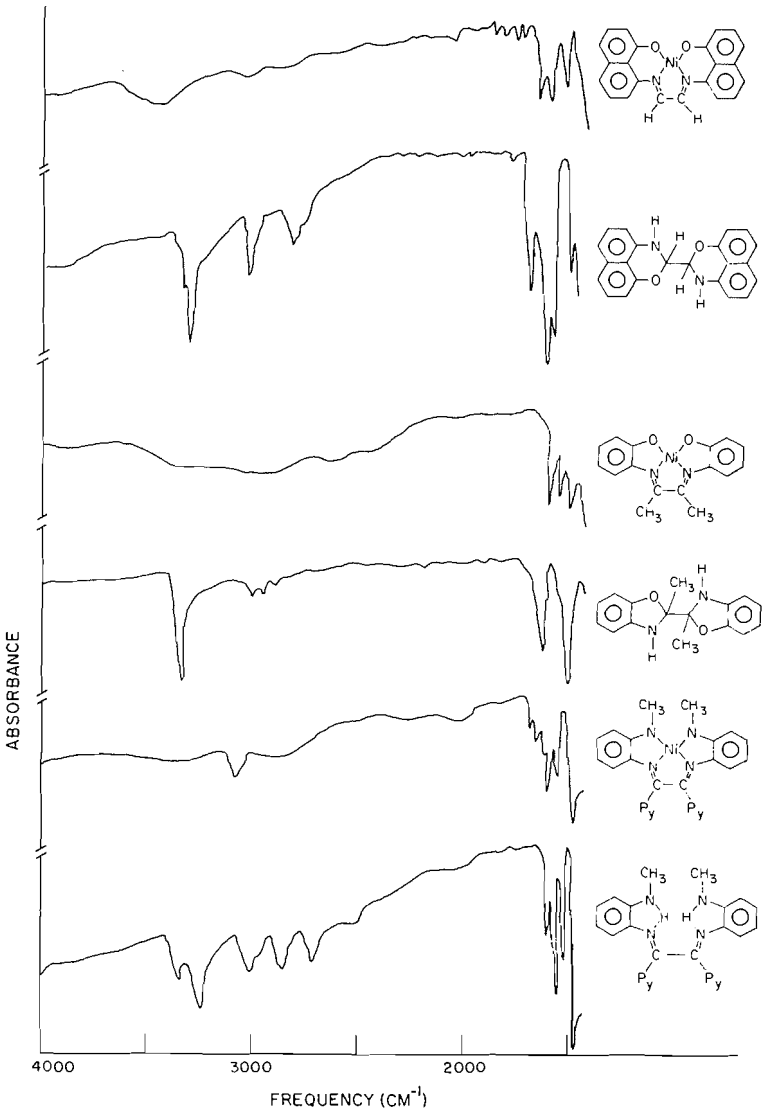

FIG. 1. Comparison of high frequency (4000–1500 cm^{-1}) i.r. spectra of nickel tetradentate chelates and the corresponding free ligands.

The present authors also showed that 2,2′-di- or monosubstituted bibenzoxazolines did not undergo such a rearrangement under identical conditions.

In the present study it was found that substituted bibenzoxazolines and substituted naphthoxazinines developed a reddish-yellow color when a small piece of solid NaOH was added to their dimethylsulfoxide or acetone solutions. The observation was supported by the appearance of new absorption bands in their spectra, Table 4. In all cases the absorption band of the ligands near 300 nm shifted to a higher wavelength after the addition of NaOH. Typical examples are shown in Figs. 2 and 3, and the results are shown in Table 4. This change in the u.v. spectra may be related to the tautomerization of the heterocyclic compound to the corresponding Schiff base. The reason why only unsubstituted 2,2′-bibenzoxazoline and 2,2′-binaphthoxazinine and not their substituted analogs undergo such a change in ethanol and methanol has not been established. It is possible that the Schiff base anion of the substituted analog is such a strong base that it

TABLE 4. Near u.v. and visible absorption bands in the cyclic forms, sodium salts, and the nickel chelates of compounds **1**, **3**, and **4**

Compound	R	R′	R″	Free ligand in ethanol (nm)	Sodium salt in DMSO (nm)	Ni-chelate in ethanol (nm)
8-Amino-1-naphthol·HCl				320s, 331s		
3*a*	H	H		323s, 336s	370s, 510w	322s, 373m, 648m
3*b*	CH_3	CH_3		325s, 336s	368s, 454w	
o-Aminophenol				232s, 286s		
1*a*	H	H		237s, 293s	293s, 325m 480m, 506m	293s, 325m, 530m
1*b*	H	CH_3		235s, 294s, 378w	285s, 333s, 436s	284s, 334m, 500m
1*c*	CH_3	CH_3		236s, 293s,	296s, 322s, 422m	281m, 335m, 490m
N-Methyl-*o*-phenylenediamine·HCl				242s, 292m		
N-Phenyl-*o*-phenylenediamine				238s, 278m, 297m		
4*a*	H	H	CH_3			230s, 314s, 346m
4*b*	H	H	C_6H_5			222vs, 286s 436m, 462m
4*c*	C_6H_5	C_6H_5	CH_3	253s, 315s	No change	
4*d*	Py	Py	CH_3	252s, 314s	No change	252s, 268s, 307s, 420s

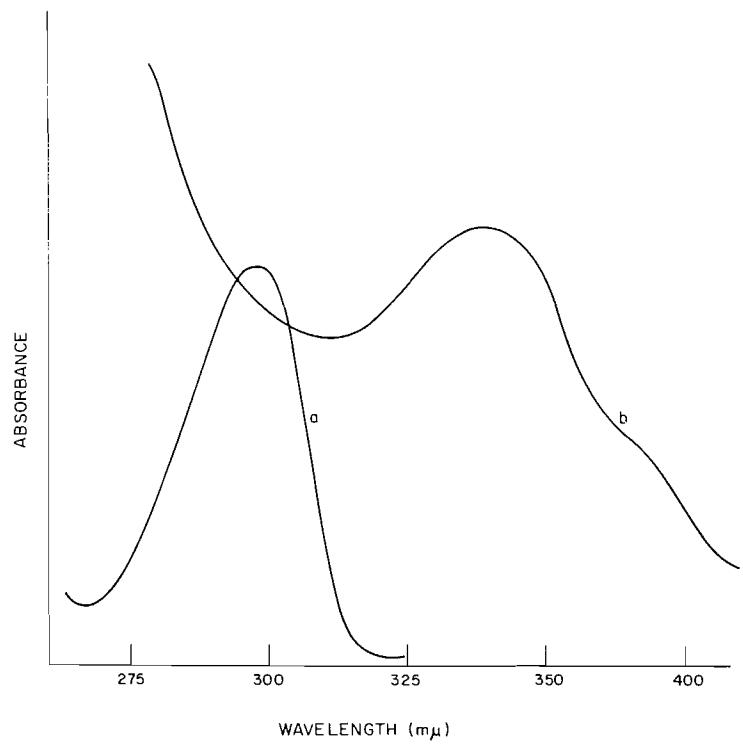

FIG. 2. U.v. spectra of 2,2′-dimethyl-bibenzoxazonine in DMSO; (*a*) normal spectrum; (*b*) spectrum after addition of NaOH.

Can. J. Chem. Downloaded from www.nrcresearchpress.com by 210.87.254.42 on 09/05/12
For personal use only.

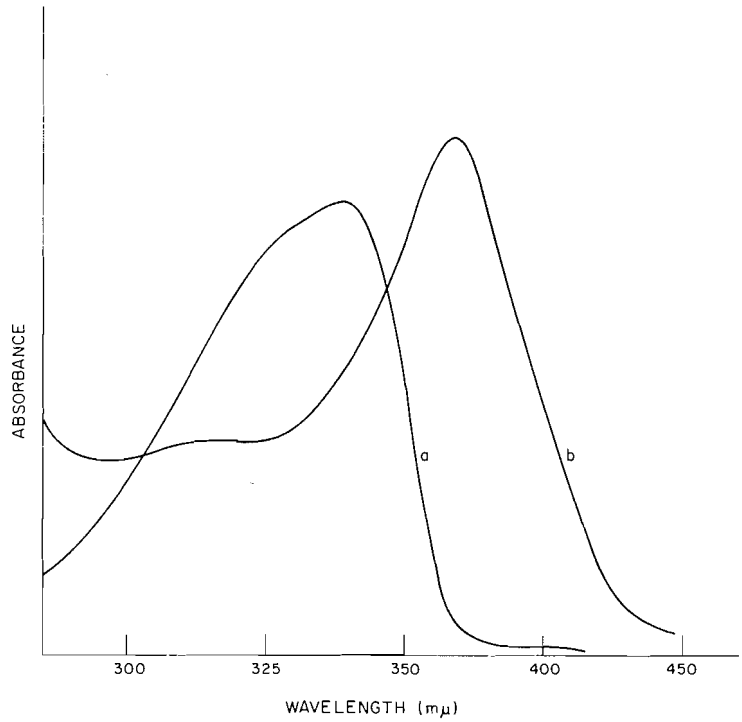

FIG. 3. U.v. spectra of 2,2′-dimethyl-binaphthoxazinine in DMSO; (*a*) normal spectrum; (*b*) spectrum after addition of NaOH.

will immediately rearrange to the heterocyclic form in a protic solvent such as alcohol or water.

The u.v. spectra of the compounds of structural type **4** do not undergo any change on the addition of alkali. This indicates that these compounds have the open Schiff base structure.

(iii) Mass Spectra

The fragmentation pattern in the mass spectra of the compounds of structural types **1**, **3**, and **4** are readily reconcilable with their molecular structures.

In Table 3 the melting points of the compounds and *m/e* values are listed. The relative peak intensities are indicated within brackets. Each peak indicated by its *m/e* value in Table 3 is usually accompanied by a few other peaks of relatively lower intensities; these are not listed.

The mass spectra of compounds of structural types **1** and **3** are uncluttered in the mass region between the molecular peak M and M/2 and have very few peaks of low intensity. This indicates the presence of stable closed structures and that the central carbon–carbon bond between the heterocyclic rings is easily cleaved, breaking the molecule into two halves.

The spectra of the compounds of structural type **4** have complicated patterns between M and M/2. This high mass region has various intense peaks which are assignable to different fragments of the parent molecule. An open-type structure of these compounds is therefore indicated.

It is interesting to note that the mass spectra of **1** have a characteristic peak at *m/e* M − 107. The mass number 107 can be assigned to the fragment

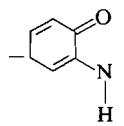

This indicates that the heterocycle is broken at the aliphatic end (breaking the C—O and C—N bonds) before the whole molecule is broken into two halves. The spectra of **3** do not have such characteristic intense bands at M − 156. The difference in the mass spectra of these compounds may be due to the relatively greater stability of six-membered heterocyclic rings of **3** compared to five-membered rings of **1**.

Can. J. Chem. Downloaded from www.nrcresearchpress.com by 210.87.254.42 on 09/05/12
For personal use only.

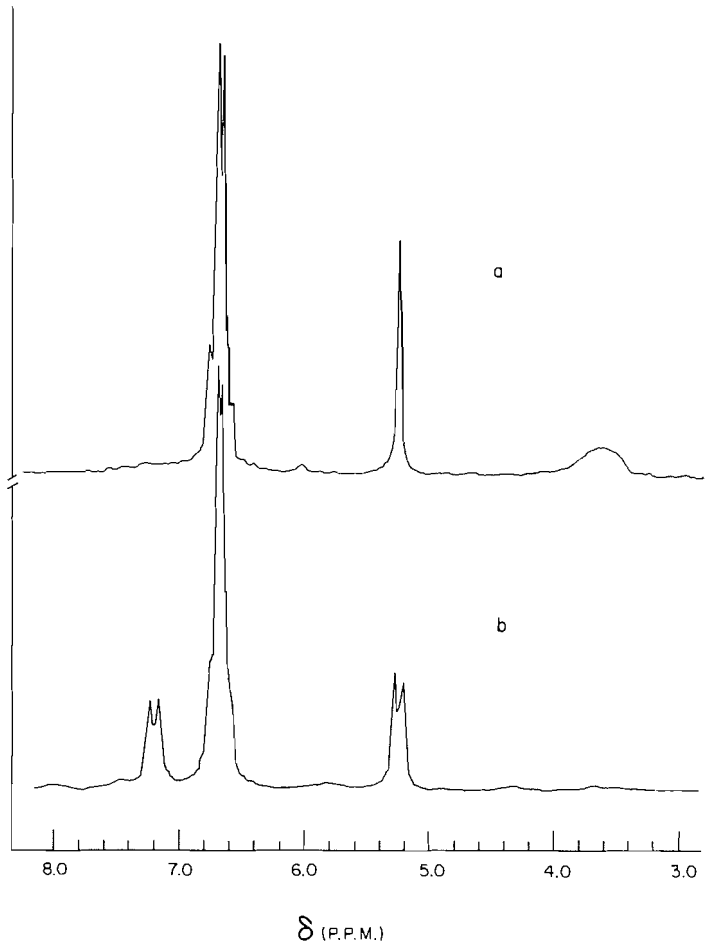

FIG. 4. N.m.r. spectra of 2,2′-bibenzoxazoline in deuterated DMSO; (*a*) spectrum after addition of D_2O; (*b*) normal spectrum.

(iv) N.m.r. Spectra

The results of the n.m.r. spectra are shown in Table 2. These results are compatible with the heterocyclic structures of compounds **1** and **3** and open Schiff base structures of **4**. The N—H signal in the **4** compounds appears upfield compared to those of **3** and **1**. The N—H signal was identified by the fact that it exchanges readily with water; the N—H signal vanishes when D_2O is added to the solution of these compounds.

In the bibenzoxazoline compounds **1***a* and *b*, the C—H and N—H protons mutually split each other. This is exemplified by the spectra of **1***a*, Fig. 4. On deuteration the N—H signal vanishes and the C—H doublet collapses into a singlet.

Quadridentate Schiff Base Metal Chelates

In spite of previous claims (3, 4, 7) that the compounds of structural type **1** (R = R′ = substituted groups) do not form metal chelates, successful methods have been developed in the present study for the preparation of these metal chelates. Additionally, the preparation of the metal chelates of **3** and **4** are reported for the first time. The u.v. spectra of the nickel chelates of these compounds are shown in Table 4 and compared with the spectra of the corresponding sodium salts.

Bayer and his co-workers (3, 4) were the first to show that **1** and its thio analog rearrange in the presence of metal ions to form the metal chelates

Can. J. Chem. Downloaded from www.nrcresearchpress.com by 210.87.254.42 on 09/05/12
For personal use only.

Can. J. Chem. Downloaded from www.nrcresearchpress.com by 210.87.254.42 on 09/05/12
For personal use only.

2. They showed in the case of **1** that such a rearrangement and subsequent chelate formation took place only when R and R′ are hydrogen atoms. No chelates were formed when one or both of the hydrogen atoms were replaced by substituted groups.

Bayer explained this lack of chelate formation in terms of steric hindrance from larger R groups. But the fact that the thio analogs of these compounds (1–3) and **4** readily form metal chelates, dispels the validity of such an explanation.

As noted earlier, Murase (16) showed that 2,2′-bibenzoxazoline **1** (R = R′ = H) developed a color when an excess of KOH was added to its solution in ethanol and another absorption maximum was observed at 467 nm. He ascribed this color and the new band to the Schiff base **5**. He also showed that no such phenomenon was observed in the case of 2-substituted or 2,2′-disubstituted compounds. He concluded that the substituted bibenzoxazolines **1** did not form metal chelates because of their inability to rearrange to the corresponding Schiff base chelates. In the case of 2,2′-binaphthoxazinine **3**, a similar trend was also observed. Through direct reaction with metal acetates, chelate formation took place only when R and R′ were H atoms.

It was found in the present study that all the compounds of structural types **3** and **1** developed a red or yellow color in a molten NaOH–KOH mixture. These colored compounds could be extracted into DMSO. It was later found that the same color also developed when these compounds were shaken in acetone or DMSO in the presence of solid NaOH pellets for several hours. This change in color was associated with shifting of the u.v. bands to higher wave length, Table 4, indicating the tautomerization of the heterocyclic compounds to the open Schiff base form. In acetone, the sodium salt of the Schiff base precipitated out and could easily be separated. The metal chelates were then easily prepared by simply adding the sodium salt to the metal salt in ethanol solution.

The sodium salts of these compounds are very unstable in water, methanol, and ethanol. In ethanol the sodium salts were shown to be converted back to the original cyclic compounds. The rate of this rearrangement to the cyclic form, **1**, is very fast in the case of the 2,2′-substituted compounds and is much slower in the case of the unsubstituted one.

It is now evident from the present study that the reason why **1** and **3** (where R or R′ are substituted groups) do not form metal chelates under mild conditions is not because of steric hindrance between the substituted groups, as was assumed before (3, 4), but rather due to other factors such as electronic, kinetic, or other steric effects.

The authors thank the National Research Council of Canada for financial support of this work.

1. H. JADAMUS, Q. FERNANDO, and H. FREISER. J. Am. Chem. Soc. **86**, 3056 (1964).
2. H. JADAMUS, Q. FERNANDO, and H. FREISER. Inorg. Chem. **3**, 928 (1964).
3. E. BAYER and G. SCHENK. Chem. Ber. **93**, 1184 (1960), **90**, 2325 (1957).
4. E. BAYER. Angew. Chem. **76**, 76 (1964).
5. L. L. UZMAN. Metal binding in medicine. *Edited by* M. J. Seven. Lippincott, Philadelphia, Pennsylvania. 1960. p. 269.
6. F. F. DWYER and D. P. MELLOR. Chelating agents and metal chelates. Academic Press, New York and London. 1964. p. 335.
7. R. G. CHARLES and H. FREISER. J. Org. Chem. **18**, 422 (1953).
8. Y. MUTO. Bull. Chem. Soc. Jap. **33**, 1242 (1960).
9. G. A. BARCLAY, C. M. HARRIS, B. F. HOSKINS, and E. KOKOT. Proc. Chem. Soc. 264 (1961).
10. E. BAYER. Angew. Chem. **73**, 659 (1961).
11. A. MALEK. Ph.D. Thesis. McGill University, Montreal, Quebec. 1972.
12. I. MURASE. Bull. Chem. Soc. Jap. **33**, 59 (1960).
13. F. FICHTER and R. GAGEUR. Chem. Ber. **39**, 3331 (1906).
14. G. SCHWARZENBACH and H. FLASCHKA. Die komplexometrische titration. Ferdinand Enke Verlag, Stuttgart. 1965.
15. J. S. FRITZ and G. H. SCHENK. Quantitative analytical chemistry. Allyn and Bacon Inc., Boston, U.S.A. 1966. p. 468.
16. I. MURASE. Bull. Chem. Soc. Jap. **32**, 827 (1959).

A Wide Line Nuclear Magnetic Resonance Study of Molecular Motion in *n*-Alkyl Ammonium Chlorides

J. TSAU AND D. F. R. GILSON

Chemistry Department, McGill University, P.O. Box 6070, Montreal 110, Quebec

Received December 22, 1972

Wide line n.m.r. studies of *n*-alkyl ammonium chlorides, C_3–C_{10}, show two transitions. The first transition is due to reorientation about the chain axis, the second to a transition to a mesomorphic phase. This phase is probably similar to that observed for the alkali metal salts of fatty acids.

Les études par r.m.n. des chlorure de *n*-alkyl ammonium C_3–C_{10} montrent deux transitions. La première transition est due à la réorientation autour de l'axe de la chaîne, la seconde à une transition en une phase mésomorphe. Cette phase est probablement similaire à celle observée pour les sels alcalins d'acides gras.
[Traduit par le journal]

Can. J. Chem., **51**, 1990 (1973)

Can. J. Chem. Downloaded from www.nrcresearchpress.com by 210.87.254.6 on 09/05/12
For personal use only.

Introduction

The occurrence of solid–solid phase transitions in various homologous series of *n*-alkyl derivatives is well known. Wide line nuclear magnetic resonance methods have been used to study molecular motions in such series, particularly the alkanes themselves (1–3), and the fatty acids and their soaps (4–7). In their extensive studies of the alkali metal salts of fatty acids Dunell and co-workers have observed two line width and second moment transitions, the first due to a change from one crystal form to another, the second due to the appearance of a mesomorphic phase characterized by a low value for the second moment resulting from extensive molecular motion. In general the temperatures of the crystal–crystal transitions for each compound agree well with values obtained by calorimetric or hot stage microscope methods but there is much poorer correlation for the transitions to the "waxy" phase (5).

We have reported (8) the results of a differential scanning calorimetric (d.s.c.) study of the series of *n*-alkyl ammonium chlorides and bromides (C_1 to C_{16}). Transition temperatures and enthalpies were obtained, in some cases these depended on the thermal history of the sample, and entropies of fusion were also measured. The entropy values were less than 5 cal deg^{-1} mol^{-1} indicating the possible existence of a mesomorphic phase analogous to the alkali metal fatty acid salts.

X-Ray structural information on the *n*-alkyl ammonium chloride series is limited, and, with few exceptions, restricted to room temperature studies. The early members of the series, up to C_{10}, have a tetragonal structure at room temperature with the exception of ethyl ammonium chloride which is monoclinic (9–13). The higher members are monoclinic or orthorhombic (14–16). The structures of *n*-propyl and *n*-pentyl ammonium chlorides have been studied at low temperatures and both undergo transitions to a monoclinic structure (12, 13). The d.s.c. studies showed that transitions occurred at or below room temperature for chain lengths less than eight carbon atoms. It appears reasonable therefore to assume that the high temperature phases of the members of the series are tetragonal and a transition to a monoclinic or orthorhombic phase occurs at lower temperatures. The presence of either molecular rotation or statistical disorder in the tetragonal phase has been proposed (16) to explain the conflict between molecular symmetry and site symmetry. The present paper describes the results of a wide line n.m.r. investigation of the *n*-alkyl ammonium chloride salts from C_3 to C_{10}. A study of the methyl ammonium halides has been reported earlier (17).

Experimental

The *n*-alkyl ammonium chlorides were prepared by passing hydrogen chloride gas into a solution of the amine in chloroform or ether, followed by recrystallization (3×) from mixed solvents, ethanol–ether (C_3–C_5), or chloroform–ether (C_6–C_{10}).

Wide line n.m.r. spectra were obtained at 60 MHz using a spectrometer consisting essentially of Varian components with a V3400 high field 9 in. magnet and Fieldial Mark II regulator. Sample temperatures were controlled by a cooled, or heated, flow of dry nitrogen gas through a Dewar system, and measured with copper–

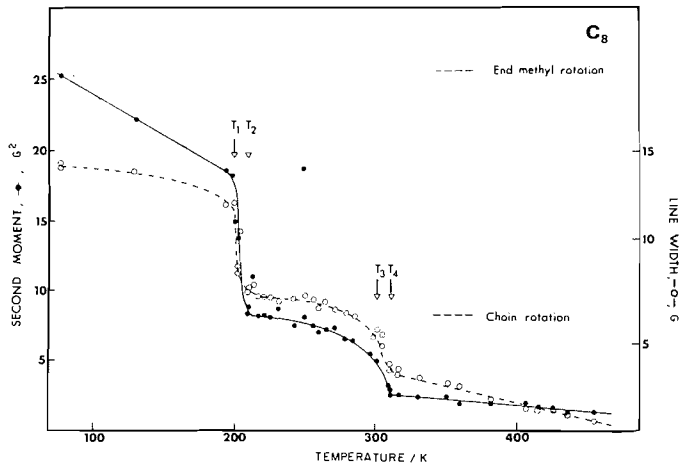

FIG. 1. Temperature dependence of the second moment (filled circles) and line width (open circles) for *n*-octyl ammonium chloride.

constantan thermocouples placed upstream and downstream from the sample. Second moments were computer calculated from the experimental derivative curves, using a program written in this laboratory, and corrected for finite modulation width.

Results

In general the line widths and second moments show similar behavior for all compounds; a gradual decrease from a value greater than 22 G^2 at 77 °K to a value in range of 15 to 18 G^2 at the first transition point, T_1. The second moment then shows an abrupt decrease to a value between 5 and 8 G^2, at temperature T_2, followed by a second transition at a higher temperature, T_3, to a value of 2 to 3 G^2. A steady decrease in second moment then continues to values of about 0.5 G^2 at the melting points. The temperature dependences of the line width and second moment are shown in Fig. 1 for *n*-octyl ammonium chloride. For *n*-butyl and *n*-pentyl ammonium chlorides the two transition temperature ranges are almost coincident. Table 1 lists the transition temperatures and experimental second moment values and also includes the transition temperature of the closest transitions observed in the d.s.c. studies (8).

Discussion

If the crystal structure of a compound is known in sufficient detail the theoretical second moment can be calculated from the van Vleck formula (18). In cases where the structure is not known it is the usual practice to divide the second moment into two contributions, the intramolecular contribution, S_1, and the intermolecular contribution, S_2, The intramolecular second moment can be calculated using accepted values for bond lengths and angles, but the intermolecular contribution must be estimated either by approximate calculations or by comparison with values obtained or calculated for similar compounds. Thus for the *n*-alkyl ammonium chlorides the intramolecular second moments were calculated using bond lengths; C—C = 1.540, C—N = 1.470, C—H = 1.096, and N—H = 1.045 Å and all bond angles were assumed to be tetrahedral. The intermolecular contribution was estimated from values found for other long chain compounds. For the hydrocarbon *n*-$C_{29}H_{60}$ a rigid lattice value of 7.8 G^2 was obtained by Andrew using the known crystal structure (1). In their studies of carboxylic acids and their salts Dunell and co-workers (4–6) have obtained contributions ranging from 6.4 G^2 for potassium caprate and caproate to 9.4 G^2 estimated for sodium stearate. The intermolecular second moment for methyl ammonium chloride in the high temperature form was estimated to be 8.8 G^2 (17). A value of 8.0 G^2 is adopted for the present purposes. In Table 2 the calculated total rigid lattice second moments are listed. In all cases the theoretical values are considerably higher than the experimental. This is not an unexpected result since it is generally observed for long chain compounds and is usually explained as due to the rotation of the end-methyl groups. The calculated second moments for the end-methyl group reorientation case are listed

Can. J. Chem. Downloaded from www.nrcresearchpress.com by 210.87.254.6 on 09/05/12
For personal use only.

Can. J. Chem. Downloaded from www.nrcresearchpress.com by 210.87.254.6 on 09/05/12
For personal use only.

TABLE 1. Experimental second moments and transition temperatures

Chain length (C atoms)	Second moment at 77 °K (G^2)	T_1 (°K)	Second moment at T_1 (G^2)	T_2 (°K)	Second moment at T_2 (G^2)	D.s.c. * transition temperature (°K)	T_3 (°K)	Second moment at T_3 (G^2)	T_4 (°K)	Second moment at T_4 (G^2)	D.s.c. * transition temperature (°K)
3	23.3	148	16.6	200	6.3	188	409	5.0	415	2.0	408
4	27.4	190	19.0	—	—	237	—	—	225	3.0	253
5	26.6	230	17.0	—	—	217	—	—	240	3.0	239
6	22.7	190	15.0	205	7.0	208	255	7.0	266	3.4	264
7	24.1	230	16.0	260	5.0	260	280	5.0	310	3.5	303
8	25.2	195	18.0	210	8.0	276	290	5.0	310	2.4	308
9	24.5	175	16.0	190	8.0	259	318	5.0	324	2.3	325
10	26.4	278	16.0	305	9.0	305	305	7.0	320	2.0	323

*Reference 8.

TABLE 2. Theoretical second moments (G^2)

Chain length (C atoms)	Rigid lattice	End-methyl rotation	Chain rotation
3	33.7	24.9	7.4
4	32.5	25.3	7.6
5	31.7	25.4	7.8
6	31.0	25.7	8.0
7	30.5	25.8	8.0
8	30.2	25.8	8.1
9	29.8	25.9	8.2
10	29.6	26.0	8.2

in Table 2. Agreement with the experimental values at 77 °K is adequate if the uncertainty in the intermolecular second moment is considered. It is possible that the $-\overset{+}{N}H_3$ group reorients as well as, or instead of, the methyl group. Both these possibilities are discarded; the first would reduce the second moment such that unreasonably large intermolecular contributions would be required to explain the magnitudes of the experimental values. Reorientation of the ammonium rather than the methyl group seems unlikely since the polar end of the chain is involved in hydrogen bonding and electrostatic interactions with the neighboring chloride ions.

The observed large reductions in the second moments of long chain compounds generally arise from reorientation about the long chain axis. In calculating the theoretical second moment for this case the same difficulties are encountered as for the rigid lattice calculation; the intramolecular second moment can be obtained fairly easily but the intermolecular contribution cannot. Smith (19) has reviewed the various reduction factors used by different authors. These range from 0.25 to 0.8 and have been applied to "spherical" as well as long chain compounds. In the present case a one-third reduction factor, appropriate to the long chain compounds (1), has been used and the calculated second moments are given in Table 2. The experimental second moments in the region between the two transitions *i.e.* between T_2 and T_3, Fig. 1, are slightly lower than the calculated values but the agreement is again satisfactory in view of the approximations. Between 77 °K and T_1 the second moment decreases steadily. This behavior is commonly observed for long chain compounds and is attributed to increasing amplitudes of torsional motion of the chain. The amplitude necessary to account for the observed reduction in second moment is, however, rather large and some additional motion, such as wagging of the chain, must also occur.

Except for the *n*-octyl and *n*-nonyl compounds the T_1–T_2 n.m.r. transitions correlate approximately with the thermal transitions observed in the d.s.c. study (8) but occur some 10 to 20° lower in temperature. It seems probable that the onset of chain rotation facilitates a crystal–crystal transition.

The second moment transitions which occur over the temperature range T_3 to T_4 reduce the second moments to values of about 2 G^2. These transitions correlate approximately with the d.s.c. transitions which have the largest enthalpy. The low values of the second moment show that molecular motion of a translational nature must occur. This behavior is similar to that observed for the alkali metal salts of fatty acids except that there is no narrow line of modulation width present in the spectra of the *n*-alkyl ammonium chlorides. It appears that the ammonium salts are less susceptible to the presence of impurities and "liquid-like" motion does not occur. The translational motion must involve large groups of molecules and is probably the same as that described by Skoulios and Luzatti (20) for the "waxy" phase of the sodium soaps. This model consists of a double layered ribbon of molecules arranged so that the hydrocarbon chain resembles the bristles on a bottle brush. The member of molecules involved is not known although the ordered domains in mesophases of the liquid crystal type are estimated to be 10^{-5} to 10^{-6} cm in diameter. That a large number of molecules must be involved is evident from the fact that X-ray powder diffraction data can be obtained at temperatures above T_4 (21), but the intensities of the long spacing reflections decrease fairly rapidly with increasing order. A similar behavior

Can. J. Chem. Downloaded from www.nrcresearchpress.com by 210.87.254.6 on 09/05/12
For personal use only.

has been reported for *n*-alcohols (22). The presence of translational motion is consistent with the observed low entropies of fusion (8), although this parameter may also be lowered by the presence of molecular order in the liquid phase.

Financial support from the National Research Council of Canada is gratefully acknowledged.

1. E. R. ANDREW. J. Chem. Phys. **18**, 607 (1950).
2. D. F. R. GILSON and C. A. MCDOWELL. Mol. Phys. **4**, 125 (1961).
3. A. ODAJIMA, J. A. SAUER, and A. E. WOODWARD. J. Phys. Chem. **66**, 718 (1962).
4. B. A. DUNELL and W. R. JANZEN. Wiss. Z. Friedrich–Schiller Univ. Jena, **14**, 191 (1965).
5. T. J. CYR, W. R. JANZEN, and B. A. DUNELL. Adv. Chem. Ser. **63**, 13 (1967). J. A. RIPMEESTER and B. A. DUNELL. Can. J. Chem. **49**, 2906 (1971).
6. J. A. RIPMEESTER and B. A. DUNELL. Can. J. Chem. **49**, 731 (1971).
7. T. J. FLAUTT and K. D. LAWSON. Adv. Chem. Sec. **63**, 26 (1967).
8. J. TSAU and D. F. R. GILSON. J. Phys. Chem. **72**, 4082 (1968).
9. E. W. HUGHES and W. N. LIPSCOMB. J. Am. Chem. Soc. **68**, 1970 (1946).
10. S. B. HENDRICKS. Z. Krist. **67**, 189 (1928).
11. R. W. G. WYCKOFF. Z. Krist. **74**, 25 (1930).
12. M. V. KING and W. N. LIPSCOMB. Acta Cryst. **3**, 222 (1950); Acta Cryst **3**, 227 (1950).
13. J. C. SOUTHARD, R. T. MILNER, and S. B. HENDRICKS. J. Phys. Chem. **1**, 95 (1933).
14. M. GORDON, E. STENHAGEN, and V. VAND. Acta Cryst. **6**, 739 (1953).
15. G. L. CLARK and C. R. HUDGENS. Science, **112**, 309 (1950).
16. J. D. BERNAL. Nature, **129**, 870 (1932).
17. J. TSAU and D. F. R. GILSON. Can. J. Chem. **48**, 717 (1970).
18. J. H. VAN VLECK. Phys. Rev. **74**, 1168 (1948).
19. G. W. SMITH. J. Chem. Phys. **42**, 4229 (1965).
20. A. E. SKOULIOS and V. LUZZATI. Acta. Cryst. **14**, 278 (1961).
21. J. TSAU. Ph.D. Thesis, McGill University, Montreal, Quebec. 1970.
22. K. TANAKA, T. SETO, A. WATANABE, and T. HAYASHIDA. Bull. Inst. Chem. Res. Kyoto Univ. **37**, 281 (1959).

Can. J. Chem. Downloaded from www.nrcresearchpress.com by 210.87.254.6 on 09/05/12
For personal use only.

Allene Oxide Intermediates: Vinylidene Carbene Addition to Carbonyl Compounds

YU-NENG KUO[1] AND MARTIN J. NYE[2]

Department of Chemistry, University of Guelph, Guelph, Ontario

Received August 10, 1972

Solutions of fluorenylidene carbene (**10**) have been generated by treatment of 9-(aminomethylene)-fluorene (**9**) with *n*-butyl nitrite. This vinylidene carbene forms a 1:1 adduct with azobenzene, and with acetone pivaldehyde and tolualdehyde it forms 1:2 adducts containing the 5-fluorenylidene-1,3-dioxolane ring system. Evidence for the intermediacy of an allene oxide (**3**) is presented.

Les solutions de carbène fluorinylidène (**10**) ont été obtenues en traitant l'aminométhylène-9 fluorène (**9**) par le nitrite de *n*-butyle. Ce vinylidène carbène forme un adduit 1:1 avec l'azobenzène et avec l'acétone, le pivaldéhyde et le tolualdéhyde des adduits 1:2 contenant le système cyclique fluorenylidene-5 dioxolane-1,3. L'intermédiaire alleneoxyde (**3**) a été mis en évidence. [Traduit par le journal]

Can. J. Chem., **51**, 1995 (1973)

Introduction

The three isomeric systems: cyclopropanone (**1**), oxyallyl (**2**), and allene oxide (**3**) have attracted attention for a long time as reactive intermediates, and in recent years substituted cyclopropanones (1) and allene oxides (2) have been synthesized. However, there is only one report of an isolation of an oxyallyl system by Fisch and Richards (3), who suggest the structure **4** for the unstable blue non-paramagnetic species obtained in a frozen glass by radiation of lumisantonin; and for this one case, evidence is weak.

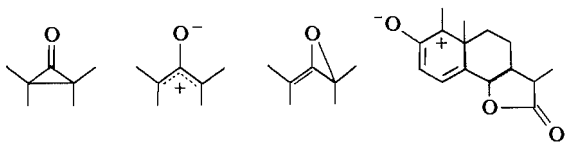

1 **2** **3** **4**

Concerning the experimental thermodynamic stabilities of the three systems, all that is known so far is that 1,1-di-*tert*-butylallene-1,2-oxide[3] (4*a*) and 1,3-di-*tert*-butylallene oxide (2) are less stable than the corresponding cyclopropanones, since both can be thermally isomerized to the cyclopropanone; whereas 1,1,3-tri-*tert*-butylallene-1,2-oxide (4*b*) is very stable thermally and has not been isomerized. Theoretical calculations were first carried out by Burr and Dewar (5) in 1954 using the LCAO method, and oxyallyl was predicted to be less stable than cyclopropanone. Next came a contradictory result by Hoffmann (6) in 1968 using an extended Hückel method, which indicated that oxyallyl should be 60 kcal more stable than allene oxide which should be 7 kcal more stable than cyclopropanone. Then in 1970, Dewar and coworkers (7) confirmed the 1954 result using the newer MINDO/2 method giving cyclopropanone 78 kcal more stable than oxyallyl.

Obviously much more experimental data relevant to the relative stabilities of the isomers (**1–3**) are called for, and high in priority is the synthesis of more examples. One approach is to attempt to synthesize substituted examples of each of the three isomers by carefully selecting stabilizing substituents.

The work reported in this paper was initiated in order to synthesize system **5** and its isomers **6**, **7**, and **8**, and then to investigate their relative stabilities and the possibility of interconversion. This particular system was chosen because the allene oxide **5** might prove to be more stable than the cyclopropanone **7** in contrast to the *tert*-butyl substituted systems. The reasons for this suggestion are firstly that molecular models of **5** show less steric crowding than those of **7** for most R substituents, and secondly that the extra conjugation in **5** might stabilize it relative to **7**. This latter idea is backed up by the fact that the enol **13***a* in acetonitrile solvent contains none of its *aldo* tautomer detectable by n.m.r. (8). The oxyallyl system **6** might also be appreciably stabilized if R'' is a carbonium ion stabilizer such as *p*-tolyl.

[1]Present address: Department of Chemistry, California State University, San Francisco, California.

[2]To whom correspondence should be addressed.

[3]In this case it is not proven whether the *tert*-butyl groups are attached to the 1- or 3-carbon atom.

Can. J. Chem. Downloaded from www.nrcresearchpress.com by 210.87.254.5 on 09/05/12
For personal use only.

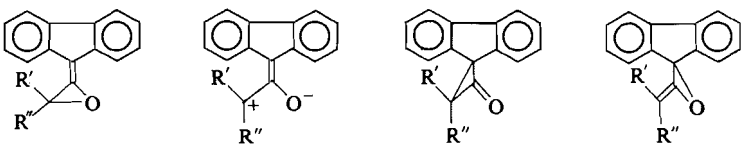

5 6 7 8

	a	*b*	*c*	*d*	*e*	*f*
R′ =	CH_3	H	H	*t*-Bu	CH_3	H
R″ =	CH_3	*t*-Bu	*p*-Tolyl	*t*-Bu	Ph	CCl_3

The synthetic approach to **5** was based on Curtin *et al*'s (9) synthesis of the methylenecyclopropane **11** by treating the enamine **9** with isoamyl nitrite in the presence of 2,3-dimethyl-2-butene. The presumed (9) reaction sequence is initial formation of a diazonium salt followed by loss of nitrogen and a proton to give the carbene **10** which then adds to the alkene to give **11** (see Scheme 1). If one simply replaces the alkene in this synthesis by any other doubly-bonded molecule represented by the general formula X=Y, then on paper one has a general synthesis of compounds of general formula **14**. If X=Y is a carbonyl compound, the product should be an allene oxide, **5**.

This paper reports attempts at this method of synthesis of allene oxides.

Results and Discussion

Numerous different sets of conditions were tried for the reaction between 9-(aminomethylene)-fluorene, *n*-butyl nitrite, and various doubly-bonded molecules. The first part of the reaction, the generation of the carbene **10** with loss of nitrogen was followed by measurement of the volume of gas evolved. The rate was found to be very sensitive to the composition of the medium. For example, while more than 50% of the expected volume of nitrogen is evolved within an hour when the solvent is benzene at 35 °C, no appreciable reaction is observed when the solvent is ether under the same conditions. It was found in general most satisfactory to dispense with the solvent except for solids and reactants in short supply. The temperature generally was raised slowly until at least 50% of the quantitative volume of gas had evolved. The products were then separated by column chromatography.

The following ketones and aldehydes were used as the doubly-bonded reactant: di-*tert*-butyl ketone, acetone, acetophenone, pivaldehyde, tolualdehyde, and chloral. In no case was a stable 1:1-adduct with the carbene **10** obtained. However, in three cases 1:2-adducts having structures **12***a*, *b*, and *c* were isolated as stable crystalline compounds.

The structures were assigned from the spectra of three compounds which are given in tabular form in Table 1. In the p.m.r. spectra, the aliphatic protons of compounds **12***a*, *b*, and *c* occurred at the expected chemical shifts with expected intensity and multiplicity. There was

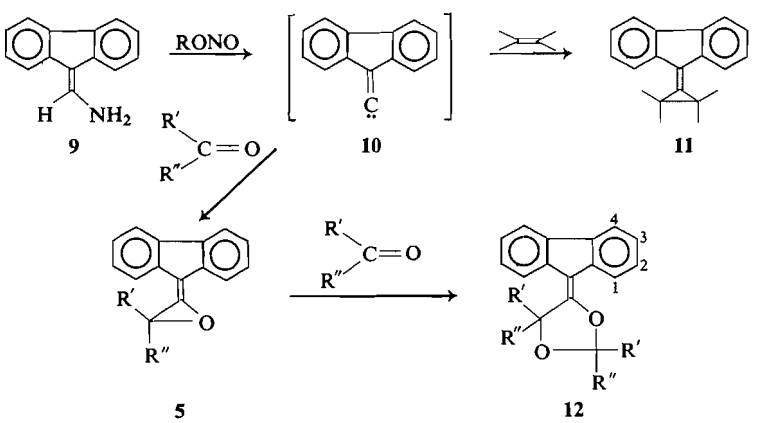

9 10 11 5 12

SCHEME 1

Can. J. Chem. Downloaded from www.nrcresearchpress.com by 210.87.254.5 on 09/05/12
For personal use only.

Can. J. Chem. Downloaded from www.nrcresearchpress.com by 210.87.254.5 on 09/05/12
For personal use only.

TABLE 1. P.m.r. and u.v. data

Compound	P.m.r. δ(p.p.m.)*	U.v. λ_{max}(nm)(ε)†
12*a*	‡8.0–8.2 (qt) 1H (Ar)	283 (18 600)
	7.6–7.9 (m) 3H (Ar)	294 (20 400)
	7.2–7.4 (m) 4H (Ar)	317 (14 300)
	1.91 (s) 6H (Me)	331 (14 800)
	1.66 (s) 6H (Me)	
12*b*	‡8.0–8.2 (qt) 1H (Ar)	290 (15 500)
	7.5–7.8 (m) 3H (Ar)	293 (infl) (15 400)
	7.1–7.4 (m) 4H (Ar)	318 (infl) (14 100)
	5.23 (s) 1H (*tert* H)	315 (15 400)
	4.74 (s) 1H (*tert* H)	
	1.18 (s) 9H (*t*-Bu)	
	1.07 (s) 9H (*t*-Bu)	
12*c*	§8.2–8.4 (qt) 1H (Ar)	287 (infl) (20 400)
	6.9–7.9 (m) 15H (Ar)	299 (21 300)
	6.55 (s) 1H (*tert* H)	318 (17 400)
	6.44 (s) 1H (*tert* H)	331 (20 400)
	2.37 (s) 1H (Me)	
	2.44 (s) 1H (Me)	
13*a*	‖8.1–8.3 (qt) 1H (Ar)	282 (16 900)
	7.1–8.0 (m) 9H	293 (18 600)
	(Ar + OH + vinyl H)	316 (9700)
		325 (infl) (9000)

*Relative to internal TMS; s, singlet; d, doublet; qt, quartet; m, multiplet.
†Solvent: 95% EtOH.
‡Solvent: CCl_4.
§Solvent: $CHCl_3$.
‖Solvent: CH_3CN.

no indication of geometric isomers in **12***b* and *c*, so it is assumed that the isolated compounds are the least hindered *trans* isomers. The aromatic multiplet has a revealing feature for each of **12***a*, *b*, and *c*: a one-proton quartet,[4] is isolated at unusually low field around δ 8.0–8.4 p.p.m. This is interpreted as originating from the proton on C-1 of **12**, which is deshielded by the neighboring oxygen atom of the enol ether. The postulate is corroborated by the observation of a similar quartet for 9-(hydroxymethylene)-fluorene (**13***a*) at δ 8.1–8.3 p.p.m. In the u.v. spectra, four bands characteristic of the fluorenylidene chromophore appear around 285, 295, 315, and 330 nm for all three compounds and the enol **13***a*, whereas compounds containing the fluorene chromophore normally do not absorb above 310 nm. The mass spectra of **12***a*, *b*, and *c* show the expected molecular ions, and the i.r. spectra have no contradictory features.

[4]This quartet has four main peaks spaced approximately equidistantly and of similar intensities, and each shows a further poorly-resolved fine structure.

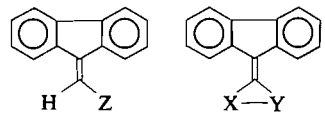

13 **14**

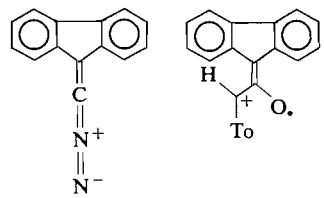

15 **16**

a, Z = OH; *b*, Z = N=CHTo;

c, X—Y = PhN—NPh;

d, Z =

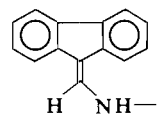

The structures of the products are compatible with intermediate formation of the desired allene oxide followed by its cycloaddition to a further molecule of carbonyl compound. Evidence for the intermediacy of a 1:1 adduct is the analogy to Curtin's work in which a 1:1 adduct (**11**) was isolated, and the following experimental evidence. During column chromatography over silica gel of the product mixture from the reaction between 9-(aminomethylene)-fluorene, acetophenone, and *n*-butyl nitrite, after all the acetophenone had been eluted, a later fraction had a p.m.r. spectrum showing the ratio of aliphatic to aromatic protons exactly right for the allene oxide **5***e* and yet the peaks corresponded to a 50/50 mixture of acetophenone and an unidentified aromatic hydrocarbon product (which must contain a multiple of eight hydrogen atoms). The hydrocarbon product was dark and polymeric in form and resisted attempts to purify it. It is only possible to explain the above observations in terms of decomposition of the chromatographic fraction in question; and it is possible that this fraction contained the allene oxide, which decomposed on work-up to acetophenone and the carbene **10**, which subsequently decomposed to the unidentified product. An alternative mechanism involving a carbonyl

Can. J. Chem. Downloaded from www.nrcresearchpress.com by 210.87.254.5 on 09/05/12
For personal use only.

ylid intermediate instead of **5** cannot however be ruled out, and Martin *et al.* (10) believe such a mechanism to occur during 1:2 adduct formation between dichlorocarbene and benzaldehyde. Evidence on this point could be obtained if the fluorenylidene-1,3-dioxolane products (**12**) would undergo reverse cycloaddition to give back the 1:1 adduct transiently, which could then add to an alkene to give a product, the structure of which would distinguish between the two mechanisms. Along this line **12***b* was heated at 200° for 1 h with dimethylfumarate, but starting material was recovered quantitatively. It is of interest, however, that in the mass spectrometer, **12***c* shows a 50% peak of mass 296 corresponding to the radical ion **16** of the 1:1 adduct, which must arise by loss of a tolualdehyde fragment from the molecule. Likewise **12***a* has a prominent peak *m/e* 234 (4%) corresponding to loss of an acetone fragment, but for **12***b* the peak due to loss of pivaldehyde (*m/e* 274 (4%)) is not prominent; instead a strong peak at 291 (15%) is observed by preferential loss of a *tert*-butyl group. A further uncertainty about the mechanism of the formation of **12** is the fact that it is not experimentally established whether or not the carbene **10** is an intermediate. One can equally well arrive at the products via the diazo intermediate **15** (11) which might then add to the carbonyl reactant before it loses a molecule of nitrogen. However if the carbene **10** is generated, its addition to two molecules of carbonyl compound is reasonable by analogy to other work (10, 12).

After having looked at cycloadditions to the C=O double bond, it was of interest to find out whether a C=N double bond would behave in the same way. Experimentally, neither *N*-phenyl- or *N*-methyl-*p*-tolualdimine yielded products of the desired type. Instead of the new compound *N*-(fluorenylidenemethyl)-*p*-tolualdimine (**13***b*) was obtained in both cases. This product was still obtained if the butyl nitrite was omitted in the reaction conditions. Its formation can be rationalized in terms of addition of 9-(aminomethylene)-fluorene across the double bond of the imine, followed by elimination of aniline or methylamine. The structure of **13***b* is supported by its ready hydrolysis with acid to **9** and tolualdehyde; in fact it was very difficult to isolate in good yield because of its instability to acids and bases. In the absence of catalysts, solutions of **13***b* remain unchanged when heated at 250° for half an hour.

Next to be looked at was the cycloaddition of carbene **10** to N=N double bonds. Azobenzene was treated with 9-(aminomethylene)-fluorene and *n*-butyl nitrite to yield a white crystalline substance m.p. 238–239° having correct elemental analysis and molecular weight (from mass spectroscopy) for the desired product **14***c*. The p.m.r. spectrum showed a complex multiplet between δ 5.7 and 8.2 p.p.m. Since absorption up-field of δ 6.5 p.p.m. is difficult to explain in terms of structure **14***c*, it is thought that **14***c* may have been formed initially, but rearranged intramolecularly to give a product containing a pyrrole ring. The u.v. spectrum is compatible with this idea since it shows a shoulder at 317 nm (ε 9600) indicating more conjugation than in fluorene.

Although adducts were successfully isolated in the cases reported above, yields were low and these positive results were only obtained after numerous variations in the conditions. The inherent difficulty of the reaction is that there exist numerous alternative side-reactions which the reactants can undergo. Most of the products isolated by column chromatography were non-crystalline, but three crystalline side-products were often isolated: the secondary amine **13***d*, 9,9′-biformyl-9,9′-bifluorenyl (**17**) and fluorenone. **13***d* has been suggested by Curtin *et al.* (9) to arise from insertion of the carbene **10** in the NH bond of **9**. He also proposed that **17** could be formed by initial nitrosation of the 9- carbon atom of 9-(aminomethylene)-fluorene followed by loss of nitric oxide to give a radical which dimerizes to give the imine of **17** and thence **17** itself by hydrolysis during work-up. Fluorenone might arise by autoxidation of **9** during work-up for which there are analogies in the literature (13).

Conclusion

Evidence is presented for the intermediacy of allene oxides **5** or their isomers **6**, **7**, and **8**, when 9-(aminomethylene)-fluorene (**9**) is treated with *n*-butyl nitrite in the presence of aldehydes and ketones. The intermediate would then add a further molecule of aldehyde or ketone to give the 1:2 adducts (**12**). It is suggested that further attempts to isolate a stable allene oxide of type **5** should be tried by using different aldehydes and ketones, since the concentration of **5** in the reaction vessel should depend directly on the relative rates of conversion of **10** to **5** and **5** to **12**, and both these rates should depend on the steric

Can. J. Chem. Downloaded from www.nrcresearchpress.com by 210.87.254.5 on 09/05/12
For personal use only.

and electronic effects of R′ and R″, the substituents on the aldehyde or ketone.

Experimental

Melting points were determined on a Meltemp apparatus and are uncorrected. I.r. spectra were obtained on a Beckman model IR5A spectrophotometer in Nujol mulls unless otherwise stated. U.v. spectra were run on a Unicam SP800 spectrophotometer at 25 °C in 1 cm cells. P.m.r. spectra were recorded on a Varian A60A spectrometer using an internal TMS standard. Mass spectra were run on a Varian-Mat CH-7 spectrometer. Microanalyses were performed by A. B. Gygli, Microanalysis Laboratories Limited, Toronto. The following experimental results are selected as examples from the many varied conditions used.

*9-(Hydroxymethylene)-fluorene (**13a**)*

The method used was similar to that of Wislicenus and Waldmuller (14). A mixture of 6.3 g potassium methoxide, 15 g fluorene, 6.7 g ethyl formate, and 75 ml dry ether was refluxed for 4 h over a steam bath. The mixture was cooled and then extracted with 75 ml of water. The water layer was washed with several small portions of ether and then acidified with dilute sulfuric acid. The oil which separated was extracted with ether, and the ether solution washed with dilute sodium bicarbonate solution and then water. The resulting solution was dried over anhydrous magnesium sulfate. Removal of drying agent and evaporation of the ether left a residue of 16.5 g crude product which was distilled under reduced pressure to give 9 g (51%) 9-(hydroxymethylene)-fluorene. I.r.: 3300, 1710, 1681, 1449, 781 cm^{-1}. U.v. and p.m.r.: see Table 1. This compound is a skin irritant, and contact with the hands should be carefully avoided.

*9-(Aminomethylene)-fluorene (**9**)*

The method used was similar to that of Von and Wagner (15). A solution of 12.5 g freshly distilled 9-(hydroxymethylene)-fluorene in 35 ml of dry benzene was placed in an ice bath and dry ammonia gas was passed in for 4 h. Evaporation of the solvent yielded a pale yellow solid, which was extracted with boiling 25% benzene in petroleum ether (b.p. 90–100 °C) mixture. One gram of the secondary amine **13***d* was left undissolved: m.p. 315–317 °C; i.r. 1645, 1274, 769, 719 cm^{-1}. The solution was evaporated to yield 9-(aminomethylene)-fluorene: m.p. 145–147°; i.r. 3472, 3356, 1661, 1285, 775, 734 cm^{-1}; p.m.r. δ 8.1–7.1 p.p.m. (multiplet) 9H (aromatic and vinyl) 5.5 p.p.m. (broad) 2H (NH_2).

*2,2,4,4-Tetramethyl-5-fluorenylidene-1,3-dioxolane (**12a**)*

Butyl nitrite, 8.24 g, was added to a refluxing solution of 9-(aminomethylene)-fluorene, 10.80 g in acetone, 200 ml under an atmosphere of nitrogen. After refluxing for 24 h the solvent was removed *in vacuo* to give 12.2 g of red oil. This was separated by quantitative t.l.c. using 2 mm thickness of Merck Kieselgel G and 15% *n*-hexane in benzene as the solvent. A u.v. lamp was used to visualize the bands. A band having $R_f = 0.3$ yielded 1.2 g of gum which on crystallization from acetone twice gave crystals (0.4 g) of 9,9′-biformyl-9,9′-bifluorenyl (**17**), m.p. 214–215° (lit. (9) m.p. 215–217°); p.m.r. ($CHCl_3$-*d*) δ 9.83 (singlet) 2H (CHO), 7.6–7.0 p.p.m. (multiplet) 16H (aromatic). Evaporation of the mother liquor followed by recrystallization of the gum from hexane yielded 5.0 mg of fluorenone, m.p. 81–82°; i.r. 1718, 1597, 1299, 919, 736; p.m.r. ($CHCl_3$-*d*) 7.8–7.2 p.p.m. (multiplet) (aromatic) identical with authentic sample. A chromatographic band having $R_f = 0.5$ yielded 0.34 g of gum which was crystallized from petroleum ether (b.p. 40–60 °C) to yield 0.17 g (1%) colorless crystals of 2,2,4,4-tetramethyl-5-fluorenylidene-1,3-dioxolane. This was further purified by vacuum sublimation at 90 °C: m.p. 145–146°; i.r. (KBr disk) 1613, 1370, 1263, 1163, 971, 917, 736 cm^{-1}; p.m.r. and u.v. see Table 1; m.s. base peak *m/e*: 206, parent peak (10%) *m/e*: 292.

Anal. Calcd. for $C_{20}H_{20}O_2$: C, 82.16; H, 6.89. Found: C, 82.21; H, 6.91.

Reaction between 9-(Aminomethylene)-fluorene, n-Butyl Nitrite, and Acetophenone

n-Butyl nitrite (1.33 g) was added to a solution of 1.99 g 9-(aminomethylene)-fluorene and 1.56 g acetophenone in 200 ml benzene. After being kept at room temperature for 2 h, the solution was warmed to 60 ± 5° for 12 h. The solvent was then removed by a current of nitrogen to yield a red oil, which was poured onto a silica gel (Woelm activity 1) chromatographic column. Elution with benzene – *n*-hexane mixtures of increasing polarity yielded first acetophenone, then a very small amount of gum showing only aromatic protons in its p.m.r. spectrum, and next 150 mg of a gum which appeared to be a 50/50 mixture of acetophenone and an eight-proton aromatic compound.

*2,4-Di-tert-butyl-5-fluorenylidene-1,3-dioxolane (**12b**)*

To a solution of 3.2 g 9-(aminomethylene)-fluorene in 20 ml pivaldehyde was added 2.4 g of *n*-butyl nitrite. The reaction was carried out under nitrogen in a closed system connected to a gas burette. Eighty percent of the calculated volume of nitrogen expected based on 9-(aminomethylene)-fluorene was evolved after 12 h at room temperature. The excess pivaldehyde was evaporated *in vacuo* and the resulting oil chromatographed through a column of neutral alumina (Woelm activity 1). Elution with benzene – petroleum ether (b.p. 60–80°) of increasing polarity yielded 310 mg (5%) of 2,4-di-*tert*-butyl-5-fluorenylidene-1,3-dioxolane. It was recrystallized twice from petroleum ether (b.p. 60–80°): m.p. 150–151°; i.r. 1650, 1183, 1093, 980, 767, 732 cm^{-1}; p.m.r. and u.v. (see Table 1); mass spectra base peak *m/e*: 191, parent peak (15%) *m/e*: 348.

Anal. Calcd. for $C_{24}H_{28}O_2$: C, 82.73; H, 8.08. Found: C, 82.82; H, 8.00.

*2,4-Di-p-tolyl-5-fluorenylidene-1,3-dioxolane (**12c**)*

n-Butyl nitrite (390 mg) was added to a solution of 490 mg 9-(aminomethylene)-fluorene and 4.33 g *p*-tolualdehyde in 200 ml benzene. The reaction mixture was kept at room temperature for 2 h, at 60 ± 5° for 12 h, and then the solvent was evaporated in a current of dry air to give a red oil which was separated by column chromatography over silica-gel (Woelm activity 1). Elution with *n*-hexane – benzene mixtures yielded 87 mg (8.3%) of 2,4-di-*p*-tolyl-5-fluorenylidene-1,3-dioxolane. It was recrystallized twice from petroleum ether (b.p. 60–80°), m.p. 213–214°; i.r. (KBr disc) 1653, 1198, 1176, 813, 769, 731 cm^{-1}; p.m.r. and u.v. see Table 1; mass spectra base peak *m/e*: 268, parent peak (7%) *m/e*: 416.

Anal. Calcd. for $C_{30}H_{24}O_2$: C, 86.51; H, 5.81. Found: C, 86.44; H, 5.86.

N-(Fluorenylidenemethyl)-p-tolualdimine (13b)

n-Butyl nitrite (580 mg) was added to a solution of 3.05 g *N*-phenyl-*p*-tolualdimine and 500 mg 9-(aminomethylene)-fluorene in 200 ml of benzene. After keeping the reaction mixture at room temperature for 2 h and then warming it to 60 ± 5° for 12 h, the solvent was removed by passing a current of dry air to give a red oil which was separated by column chromatography over silica-gel (Woelm activity 1). The fraction eluting with benzene (60%) – *n*-hexane (40%) solvent yielded 30 mg of yellow crystalline *N*-(fluorenylidenemethyl)-*p*-tolualdimine. It was purified by vacuum sublimation at 100° and recrystallization from ether: m.p. 146–147°; i.r. 1538, 1166, 966, 813, 778, 730 cm^{-1}; p.m.r. (CCl_4) δ 8.8–8.5 (quartet) 1H (C-1 aromatic proton), 8.14 (singlet) 1H (aldiminic CH), 7.8–6.9 (multiplet) 12H (aromatic and vinyl), 2.33 p.p.m. (singlet) 3H (methyl); u.v. λ_{max} (95% ethanol) 236 (ε 44 000), 261 (ε 36 000), 271 (ε 36 000), 375 (ε 36 000) nm; mass spectra parent peak *m/e*: 295.

Anal. Calcd. for $C_{20}H_{17}N$: C, 89.57; H, 5.84; N, 4.59. Found: C, 89.62; H, 6.07; N, 4.52.

Reaction between 9-(Aminomethylene)-fluorene, n-Butyl Nitrite, and Azobenzene

A solution of 2.14 g 9-(aminomethylene)-fluorene, 2.06 g azobenzene, and 1.16 g *n*-butyl nitrite in 250 ml dry ether was refluxed for 40 h. Since the i.r. spectrum showed that much 9-(aminomethylene)-fluorene remained, the solvent ether was distilled from the reaction mixture and 200 ml of the solvent benzene added. Azobenzene (210 mg) and 280 mg butyl nitrite were also added. After refluxing for a further 58 h, the i.r. spectrum of the mixture showed only a small NH band. The solvent was removed *in vacuo* to give a red oil. Column chromatography over silica-gel (Woelm activity 1) yielded 230 mg (5.8%) of a white crystalline compound eluted with 40% benzene in *n*-hexane. It was recrystallized from chloroform twice: m.p. 238–239°; i.r. (KBr disc) 1491, 1449, 773, 735, 699 cm^{-1}; p.m.r. ($CHCl_3$-*d*) δ 8.2–5.7 p.p.m. (multiplet); u.v. λ_{max}(CCl_4) 294 (ε 17 200), 305 (ε 17 600), 316 (inflection) (9600) nm; mass spectra base peak *m/e*: 77, parent peak (83%) *m/e*: 358.

Anal. Calcd. for $C_{26}H_{18}N_2$: C, 87.12; H, 5.06; N, 7.82. Found: C, 87.29; H, 5.20; N, 7.73.

Financial support of the National Research Council of Canada is gratefully acknowledged.

1. N. J. Turro, W. B. Hammond, and P. A. Leermakers. J. Am. Chem. Soc. **87**, 2774 (1965).
2. R. L. Camp and F. D. Greene. J. Am. Chem. Soc. **90**, 7349 (1968).
3. M. H. Fisch and J. H. Richards. J. Am. Chem. Soc. **90**, 1547 (1968).
4. (*a*) J. K. Crandall, W. H. Machleder, and M. J. Thomas. J. Am. Chem. Soc. **90**, 7347 (1968); (*b*) J. K. Crandall and W. H. Machleder. J. Heterocycl. Chem. **6**, 777 (1969).
5. J. G. Burr, Jr. and M. J. S. Dewar. J. Chem. Soc. 1201 (1954).
6. R. Hoffmann. J. Am. Chem. Soc. **90**, 1475 (1968).
7. N. Bodor, M. J. S. Dewar, A. Harget, and E. Haselbach. J. Am. Chem. Soc. **92**, 3854 (1970).
8. Yu-neng Kuo. M.Sc. Thesis. University of Guelph, Guelph, Ontario, 1969.
9. D. Y. Curtin, J. A. Kampmeier, and B. R. O'Connor. J. Am. Chem. Soc. **87**, 836 (1965).
10. C. W. Martin, J. A. Landgrebe, and E. Rapp. Chem. Commun. 1438 (1971).
11. G. W. Cowell and A. Ledwith. Quart. Rev. 139 (1970).
12. W. J. Middleton, D. C. England, and C. G. Krespan. J. Org. Chem. **32**, 948 (1967).
13. J. W. Huffmann and R. P. Elliott. Chem. Ind. (London), 650 (1963).
14. W. Wislicenus and R. M. Waldmuller. Chem. Ber. 785 (1909).
15. I. Von and E. C. Wagner. J. Org. Chem. **9**, 155 (1944).

Can. J. Chem. Downloaded from www.nrcresearchpress.com by 210.87.254.5 on 09/05/12
For personal use only.

The Synthesis of *gem*-Halonitro Sugars and Their Conversion into Epoxynitro Sugars[1]

HANS H. BAER AND WERNER RANK

Department of Chemistry, University of Ottawa, Ottawa, Canada K1N 6N5

Received December 12, 1972

Halogenation of methyl 4,6-*O*-benzylidene-3-deoxy-3-nitrohexopyranosides having the α-D-*talo*, β-D-*galacto*, and α-D-*galacto* configurations, and of the 2,3-dideoxy-3-nitro β-D-*lyxo* and α-D-*lyxo* analogs, smoothly furnished 3-halo-3-deoxy-3-nitro derivatives. The glycosides were chlorinated in methanolic solution with aqueous sodium hypochlorite, and similarly brominated with either bromine in the presence of alkali or *N*-bromoacetamide in the presence of sodium acetate. The analogous nitro glycosides having the β-D-*arabino*, β-D-*manno*, α-D-*manno*, and β-D-*gluco* configurations and also the 2-acetates of the last three compounds were brominated likewise whereas the α-D-*gluco* isomer and its 2-acetate were resistant under the conditions examined. The preferred C-3 configuration in the halonitro products appeared to be that which has an equatorial nitro group and an axial halogen atom in the normal pyranose chair conformation ($^4C_1$). In most instances the halogenation was found to be highly stereoselective in that sense although in some cases the inverse C-3 epimer was formed in a minor proportion. Base treatment of some of the halohydrins led to 2,3-anhydro-3-nitro glycosides. Such epoxide formation may be associated with epimerization at C-2 and -3, for which a mechanism involving a retrograde Henry reaction is postulated.

L'halogénation des méthyl benzylidène-4,6-*O* déoxy-3 nitro-3 hexopyranosides ayant les configurations α-D-*talo*, β-D-*galacto*, et α-D-*galacto*; et des analogues dideoxy-2,3 nitro-3 β-D-*lyxo* et α-D-*lyxo*; conduit aux dérivés halo-3 deoxy-3 nitro-3 selon des réactions douces. Les glycosides ont été chlorés en solution méthanolique par l'hypochlorite de sodium aqueux et bromés de la même façon soit par le brome en présence d'alcalis soit par le *N*-bromo acétamide en présence d'acétate de sodium. Les glycosides analogues nitro ayant les configurations β-D-*arabino*, β-D-*manno*, α-D-*manno* et β-D-*gluco* de même que les acétates en 2 des trois derniers composés ont été bromés de la même façon tandis que l'isomère α-D-*gluco* et son acétate en 2 sont résistants dans les conditions étudiées. La configuration préférée sur le C-3 des produits halonitro apparait être celle qui possède un groupe nitro équatorial et un atome d'halogène axial, dans la conformation chaise normale du pyranose ($^4C_1$). Dans la plupart des exemples, l'halogénation est hautement stéréosélective bien que dans certains cas il se forme en proportion mineure, de l'épimère inverse sur le C-3. Le traitement basique de certains de ces halohydrines conduit aux anhydro-2,3 nitro-3 glycosides. Une telle formation d'époxyde peut être associée à l'épimérisation sur le C-2 et -3 pour laquelle un mécanisme faisant intervenir une réaction de "retro-Henry" a été postulé.

[Traduit par le journal]

Can. J. Chem., **51**, 2001 (1973)

Primary and secondary aliphatic nitro compounds are readily halogenated in the presence of base to afford geminal halonitro derivatives (2, 3). Even though this has long been known, such halogenations apparently have never been tried in nitro carbohydrates, and the few halogen derivatives so far prepared in this field were not of the geminally substituted type. Thus, 2,4,6-tri-*O*-acetyl-3-deoxy-3-nitro-α-D-glucopyranosyl bromide has been made (4) by one of the customary methods for acetobromo sugars from the corresponding α-tetraacetate, and vicinal iodonitro derivatives have been shown (5) to arise by the addition of nitryl iodide to unsaturated sugars. We now report the preparation of several 3-chloro- and 3-bromo-3-deoxy-3-nitrohexopyranosides and describe reactions which some of the products undergo, in particular, epimerization and epoxide formation controlled by stereochemical factors.

Chlorinations were performed by treating the 4,6-*O*-benzylidenated nitro glycosides in methanolic solution with aqueous, 5% sodium hypochlorite solution (or with "Javex" household bleach), normally at room temperature. Crystalline chloro derivatives were smoothly obtained in yields ranging from 75 to over 90%. For bromination, two methods were employed, usually with equal success. The first was similar to the chlorination just mentioned and consisted of generating the sugar nitronate by the provision of alkali at low temperature, which was then followed by bromine addition (Br_2 method).

[1]Part XXVIII in a series on reactions of nitro sugars. For Part XXVII see ref. 1.

Can. J. Chem. Downloaded from www.nrcresearchpress.com by 210.87.254.40 on 09/05/12
For personal use only.

Can. J. Chem. Downloaded from www.nrcresearchpress.com by 210.87.254.40 on 09/05/12
For personal use only.

In the second method *N*-bromoacetamide in the presence of sodium acetate was employed as the brominating agent (NBA method). The latter procedure was especially useful for compounds containing ester groups liable to cleavage under the alkaline conditions of the former procedure.

In many of the halogenations investigated, only one of the two possible C-3 epimeric products was encountered, and on account of the excellent yields it can be stated that the reactions were highly stereoselective. In some cases the second epimer was formed, too, but normally in a minor proportion. We assume that the favored epimer in all events is that which in the stable chair conformation bears the nitro group in equatorial and the halogen atom in axial orientation.

This assumption is based on the analogy to protonation of pyranoside 3-nitronates which invariably produces an equatorial nitro group (6, 7). N.m.r. data of the new products as well as certain chemical reactions were consistent therewith, and hence we have assigned formulas and configurational notations[2] on this premise. It must be admitted, however, that rigorous proof for the configuration of the halonitro carbon atom has not been advanced. In the account that follows, the chemistry of compounds having a *cis*-fused 4,6-benzylidene acetal ring will be treated first, and that of *trans*-fused acetals will be dealt with thereafter. A recent study (9) had revealed considerable differences in the ease of nitronate formation (*i.e.*, proton abstraction from C-3) in dependence of the over-all configuration of the molecule. Since the process of nitronate formation has to precede introduction of a halogen atom it could be expected that there would also be a strong influence of configuration upon the course of halogenation.

Reactions with cis-Fused Acetals

Consonant with the observed, facile formation of their nitronates (9), the methyl 4,6-*O*-benzylidene-3-deoxy-3-nitrohexopyranosides with the α-D-*talo* (**1**), β-D-*galacto* (**2**), and α-D-*galacto* (**3**) configurations, and the methyl 4,6-*O*-benzylidene-2,3-dideoxy-3-nitro-β- and α-D-*lyxo*-hexopyranosides (**4** and **5**) all furnished 3-halo derivatives smoothly in high yields.

Chlorination of **1** gave methyl 4,6-*O*-benzylidene-3-chloro-3-deoxy-3-nitro-α-D-idopyranoside (**6**) which could be isolated in 85% yield when the reaction was performed at 0°. When it was performed at room temperature, **6** could not be isolated but was converted into methyl 2,3-anhydro-4,6-*O*-benzylidene-3-nitro-α-D-talopyranoside (**8**) which crystallized in over 80% yield. This epoxide had previously been obtained in a different way (10). Bromination of **1** by either the Br_2 or the NBA method readily furnished the bromonitro analog **7**. Sodium borohydride reduction of **7** according to Iffland and Criner (11) regenerated **1**, demonstrating that bromination was not attended by any unexpected structural or configurational change. A short treatment of **7** with sodium hydroxide at 25° led to the epoxide **8** in 90% yield. The facile formation of **8** from **6** and **7** strongly supports the *trans*-diaxial halohydrin grouping in these compounds (12*a*).

Chlorination as well as bromination by either method, of the β-D-*galacto* isomer **2** similarly afforded halogen derivatives as single products in good yields. They were methyl 4,6-*O*-benzylidene-3-chloro-3-deoxy-3-nitro-β-D-gulopyranoside (**9**) and its bromo analog **11**. Both products were characterized further by acid-catalyzed debenzylidenation followed by acetylation, to give methyl 2,4,6-tri-*O*-acetyl-3-chloro-3-deoxy-3-nitro-β-D-gulopyranoside (**10**) and its bromo analog **12**, respectively. As in the aforementioned case of **7**, borohydride reduction of **11** regenerated the starting sugar **2** (90% yield). Unlike **7**, however, the bromohydrin **11** did not give an epoxide upon treatment with aqueous alkali. Instead, debromination producing **2** occurred in reversal of the bromination, with the abstraction of Br^+ ion being evidenced by a positive potassium iodide – starch test. When **11** was refluxed in 0.03 *N* methanolic sodium methoxide solution for 20 min it partly survived but largely decomposed with liberation of benzaldehyde.[3] The fact that no epoxynitro sugar was formed in any

[2]Following a suggestion by Professor D. Horton, Columbus, Ohio, and pending the adoption of an official international nomenclature rule for the configuration of sugars that bear unequal geminal substituents on the ring we use the established configurational designations combined with the sequence rule of Cahn *et al.* (8). The substituent which according to this rule has the *higher* priority is thought of as replacing the *hydroxyl group* at the carbon concerned. Thus, for example, if H-3 in the formula of 3-deoxy-3-nitro-D-glucose is replaced by bromine or chlorine (both of which have priority over nitro), the resultant halonitro sugar is regarded as a derivative of D-allose with the halogen atom occupying the place of OH, and the NO_2 group, that of H.

[3]The benzylidene acetal ring in **2** is known to be quite labile towards base (7).

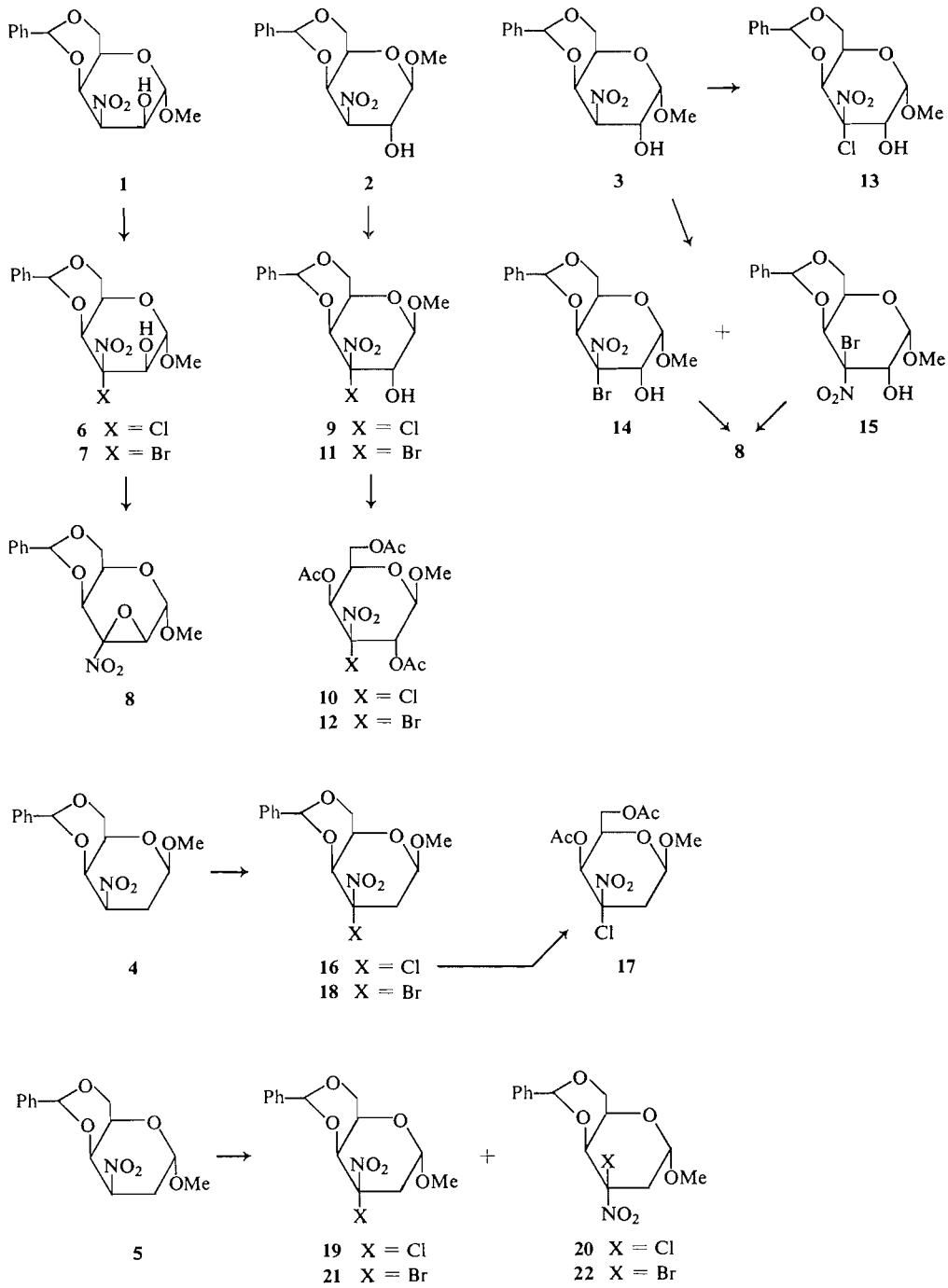

of these base treatments supported the *cis*-bromohydrin configuration.

Chlorination of the α-D-*galacto* isomer **3** afforded methyl 4,6-*O*-benzylidene-3-chloro-3-deoxy-3-nitro-α-D-gulopyranoside (**13**) in over 90% yield. Contrasting with the stereoselectivity of this reaction and all the halogenations of **1** and **2**, bromination of **3** resulted in mixtures of epimers. The Br_2 method gave a crude product (yield, 91%) which exhibited two spots on t.l.c. and showed two benzylidene methine proton resonances (τ 4.48 and 4.30) in an intensity ratio

Can. J. Chem. Downloaded from www.nrcresearchpress.com by 210.87.254.40 on 09/05/12
For personal use only.

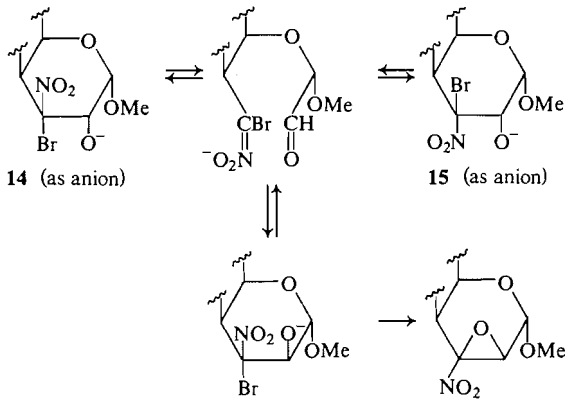

SCHEME I

55:45. Upon chromatographic separation the pure crystalline epimers were isolated in yields of 49 and 33%. The preponderant product was considered to be that which has an equatorial nitro group, *i.e.*, methyl 4,6-*O*-benzylidene-3-bromo-3-deoxy-3-nitro-α-D-gulopyranoside (**14**), and the lesser product was assigned the α-D-*galacto* configuration (**15**). Bromination of **3** by the NBA method gave **14** and **15** in the ratio of 85:15. Reductive removal of the bromine reconverted both **14** and **15** into **3**, thus confirming the epimerism. Interesting observations were made when the products were treated with alkali. It might have been expected that at least one of them (**14**) would incur debromination, like its β-anomer **11**, to give the starting glycoside **3**. However, **14** remained unchanged for 20 h in a methanolic, 0.03 *N* sodium hydroxide solution at room temperature. In refluxing sodium methoxide solution it appeared to suffer far-reaching decomposition (like **11**) but a crystalline product could nevertheless be isolated in 25% yield. The same product arose slowly (10 h) in high yield (72%) from the epimer **15** by action of methanolic hydroxide even at room temperature. Surprisingly it proved identical with the epoxide **8** previously engendered from **1** (via **6** or **7**). These results clearly imply epimerization at C-2, a phenomenon not observed in the alkali treatments of the halonitro compounds having the α-D-*ido* or β-D-*gulo* configuration. The following explanation is offered.

The three bromonitro α-D-glycosides (**7**, **14**, and **15**) have in common substantial strain due to non-bonded interaction of the axial, glycosidic methoxyl group and the axial substituent at C-3. Whereas the structure of **7** with a *trans*-diaxial halohydrin arrangement is conducive to rapid epoxide formation upon proton abstraction from OH-2, this is not the case for **14** and **15**. However, these two compounds may undergo (reversible) ring opening by way of a retrograde Henry reaction, are thus able to epimerize, and therefore they, too, eventually furnish the epoxide **8** (Scheme 1). It appears plausible that ring cleavage occurs more readily in **15** than **14** since an axial nitro group is associated with a higher conformational free energy than an axial bromine atom.[4] In the β-glycoside **11**, which lacks 1,3-diaxial strain, the driving force for a retrograde Henry reaction is diminished, and abstraction of Br^+ by base was observed instead.

The 2-deoxy glycosides **4** and **5** also reacted readily, giving high yields of halonitro derivatives. The β-anomer **4** gave single products, namely methyl 4,6-*O*-benzylidene-3-chloro-2,3-dideoxy-3-nitro-β-D-*xylo*-hexopyranoside (**16**) and its bromo analog **18**. Debenzylidenation of **16** followed by acetylation furnished the corresponding 4,6-diacetate **17**. By contrast, the α-anomer **5** gave mixtures of 3-epimeric halonitro compounds, both in chlorination (the α-D-*xylo* (**19**) and α-D-*lyxo* (**20**) epimers in the ratio 86:14) and in bromination by either method (the α-D-*xylo* (**21**) and α-D-*lyxo* (**22**) epimers in ratios of about 75:25). The epimers could be distinguished by the chemical shifts of their benzylidene methine protons and they were separated by column chromatography. The minor components (**20** and **22**) were characterized by physical data and not by elemental analysis, but spectroscopic evidence including mass spectra supported the structural assignments (see Experimental).

Reactions with trans-Fused Acetals

In nitro glycosides possessing a *trans*-fused 4,6-*O*-benzylidene ring we have so far investigated brominations only. Methyl 4,6-*O*-benzylidene-2,3-dideoxy-3-nitro-β-D-*arabino*-hexopyranoside (**23**) gave with NBA an amorphous bromo derivative (yield, 87%) which appeared uniform according to its n.m.r. spectrum and

[4]For substituted cyclohexanes, values of approximately 0.5 and 1.05 kcal/mol are given for the bromo (12*b*) and nitro (13) substituents, respectively. In 3-deoxy-3-nitro pyranosides an even higher value for the nitro group must be postulated from the results of recent studies in this laboratory (6).

Can. J. Chem. Downloaded from www.nrcresearchpress.com by 210.87.254.40 on 09/05/12
For personal use only.

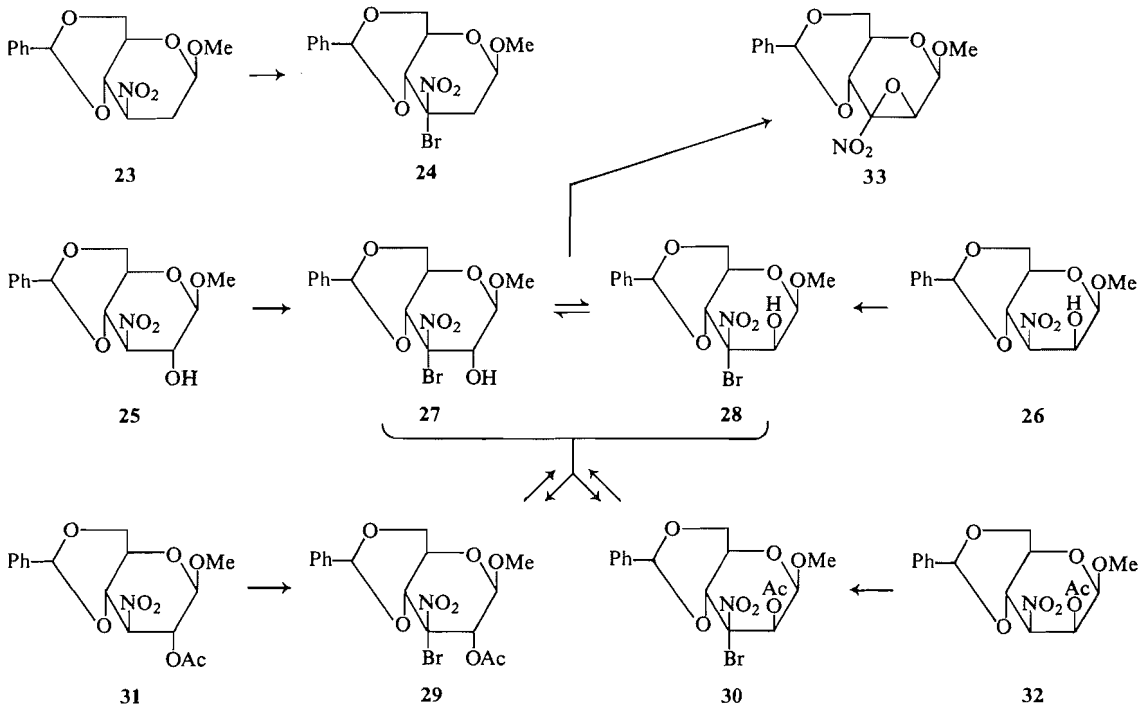

t.l.c. It was assigned the β-D-*ribo* configuration (**24**).

Considerably more complicated were the reactions performed with D-*gluco* and D-*manno* derivatives. It must be recalled in this connection that in the presence of alkali these nitro glycosides form nitronate much less readily than their D-*galacto* and D-*talo* isomers, and moreover that the D-*manno* derivatives are liable to incur rapid epimerization at C-2 (9).

Bromination of the β-D-mannoside **26** at 0° by the Br_2 method did not go to completion. It afforded a mixture which according to integration of signals (τ 4.23, 4.32, 4.42, and 4.48) contained four products in the ratio 5:10:35:50. The compounds present to the extent of 10 and 50% were shown by chromatographic isolation to be unreacted **26** (τ 4.32) and the β-D-glucoside **25** (τ 4.48), respectively. The latter obviously arose by epimerization and failed to be brominated. The two remaining products, together 40% of the mixture, were bromonitro compounds as was first suggested by a shift of the asymmetric nitro vibration from 1550 to 1565 cm^{-1} (14). Although they could be separated chromatographically from the non-brominated material, they could not be separated from each other and were never isolated individually; nevertheless, they were assigned, on the basis of subsequently described experiments, the structures of methyl 4,6-*O*-benzylidene-3-bromo-3-deoxy-3-nitro-β-D-allopyranoside (**27**) (major product, τ 4.42) and -altropyranoside (**28**) (minor product, τ 4.23). The NBA method proved more effective, **26** yielding almost quantitatively a mixture of **27** and **28** in a ratio of 4:1. The near identity of the mixtures of bromo derivatives obtained by the two methods was established by comparison of their i.r. and n.m.r. spectra and optical rotations.[5] It is most noteworthy that either bromination caused extensive epimerization at C-2; whereas for the Br_2 method this could be expected in the light of previous results concerning the action of alkali upon **26** (9), it is remarkable that the sodium acetate present in the NBA method apparently suffices to give the same result.

Bromination of the β-D-glucoside **25** by NBA also produced **27** and **28**, again in a similar ratio (75:15), with some **25** (10%) remaining unre-

[5]A similar mixture of **27** and **28** was produced, also in high yield, by substituting *N*-bromo-succinimide for NBA. Cleavage of the benzylidene ring with concomitant introduction of bromine at C-6 was not observed under our reaction conditions which differ from those of Hanessian's NBS reaction (15).

Can. J. Chem. Downloaded from www.nrcresearchpress.com by 210.87.254.40 on 09/05/12
For personal use only.

Can. J. Chem. Downloaded from www.nrcresearchpress.com by 210.87.254.40 on 09/05/12
For personal use only.

acted. The *manno* isomer **26** was not detected in the product whose n.m.r. spectrum was practically identical with those of the previously obtained mixtures of **27** and **28**, except for weak signals due to remnant **25**. This result was also borne out by close similarities in i.r. spectra and optical rotations. The Br_2 method proved ineffective for bromination of **25**.

Acetylation of a mixture of **27** and **28** by the mild procedure using acetyl chloride in the presence of triethylamine (4, 16) furnished separable 2-acetates **29** and **30** which were isolated in pure form in yields of 70 and 15%. The same acetates were obtained, each in 95% yield and evidently as single products, upon NBA bromination of the 2-*O*-acetyl derivatives **31** and **32** (of **25** and **26**, respectively). Clearly, with the 2-OH group being blocked by acetylation, no epimerization took place on C-2 and the configurations of **27** and **28** at this site have thus been established. In accord therewith were the $J_{1,2}$ coupling constants of **29** (8 Hz) and **30** (0 Hz).

Treatment of the β-D-*altro* bromonitro acetate **30** with 0.04 *N* sodium methoxide in methanol at 0° or at room temperature led to deacetylation followed by 2-epimerization, to give mixtures of **27** and **28**, with the β-D-*allo* derivative (**27**) preponderating four- to five-fold. That is to say, base treatment of **30** at low temperatures produced the same bromonitro compounds, and in virtually the same proportions, as did bromination of **25** or **26**. Reacetylation of a mixture originating from **30** led to isolation of the epimeric, β-D-*allo* acetate **29** in a yield of 65%. The conclusion to be drawn from all these results is that the bromonitro glycosides **27** and **28** (but not their acetates) are readily interconvertible by base, and that a thermodynamic equilibrium tends to be established between them. The epimerization observed in the course of bromination of the β-D-glucoside **25** must exclusively take place on this stage (*i.e.* in **27**) since **25** itself does not epimerize to **26**. The epimerization occurring in the bromination of the β-D-mannoside **26**, shown above to be possible at the stage of **28**, may also take place in **26** itself as can be inferred from previous work,[6] so that perhaps both pathways are utilized in this instance.

Compound **28**, which possesses a *trans*-diaxial bromohydrin structure, was expected to give quite readily an epoxide when treated with base. As previously mentioned, the liberation of **28** from its acetate by methoxide at low temperature was succeeded by partial 2-epimerization; there was no evidence for epoxide formation. However, when mixtures of **27** and **28** were *refluxed* in methoxide-containing methanol for 30 min, epoxide formation did occur. Thus methyl 2,3-anhydro-4,6-*O*-benzylidene-3-nitro-β-D-mannopyranoside (**33**) was isolated in yields of 78 and 84% upon such treatment of the closely similar isomer mixtures originating from brominations of **25** and **26**, respectively. Yields were smaller (41 and 37%) when the acetates **29** and **30** were treated *directly* with boiling methoxide solution, instead of being first saponified (and allowed to epimerize) in the cold; a certain degree of degradation was noticed in these cases.[7] At any rate, the amount of epoxide **33** formed in each instance far exceeded the supply of **28**. This was true even for the alkali treatment of **30** since epimerization following its deacetylation was faster than epoxide formation. The bulk of **33** must therefore be provided by **27** through a mobile, epimeric equilibrium. The epimerization is thought to proceed by reversible ring opening as discussed for **14** and **15**, above.

In the α-anomers of this configurational series, brominations proceeded more sluggishly if at all. Thus, methyl 4,6-*O*-benzylidene-3-deoxy-3-nitro-α-D-glucopyranoside (**34**) failed to react in the Br_2 procedure, and it did not react with NBA in methanol and sodium acetate even when heated under reflux for as long as 10 h. Its 2-acetate **35**, too, was completely inert towards NBA under conditions which had led to nearly quantitative bromination of the β-anomer **31** (3 h at 25°). The α-D-*manno* isomer **36** was only partially brominated by the NBA method although the β-anomer (**26**) had been brominated completely. The mixture obtained was judged on the basis of t.l.c. and n.m.r. evidence (see

[6]Compound **26** was completely (that is, within the limits of detectability by t.l.c.) converted into **25** under conditions of alkalinity comparable to those prevailing in the Br_2 method of bromination (9).

[7]Liberation of benzaldehyde was observed, which is indicative of base-catalyzed β-elimination of the C-4 acetal linkage and implies carbanion formation at C-3. One can only surmise that, at elevated temperature, abstraction of bromine from C-3 becomes markedly competitive with deacetylation. Nitronate so generated would no longer be able to produce epoxide but would undergo other transformations. Compare the behavior of **11** in alkaline media.

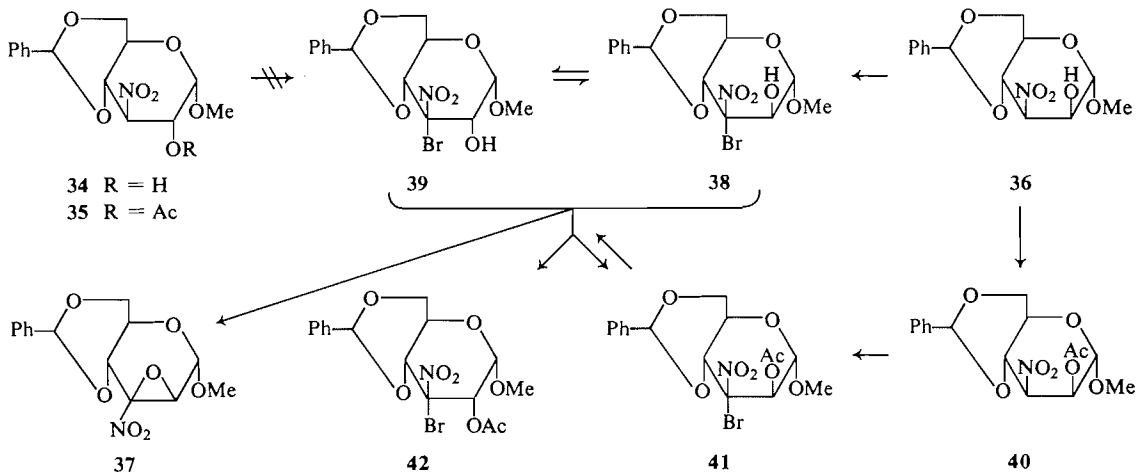

Experimental) to contain some starting material **36**, about 25% of the 2-epimer **34**, and approximately 30% of each of two new products. No attempt was made to separate the products but the presence of two bromonitro derivatives was confirmed by base treatment which afforded the known (10) epoxide, methyl 2,3-anhydro-4,6-*O*-benzylidene-3-nitro-α-D-mannopyranoside (**37**). The latter was isolated in a yield of 51%, which implies that both bromonitro sugars present must have contributed to its formation. Undoubtedly, one of them was methyl 4,6-*O*-benzylidene-3-bromo-3-deoxy-3-nitro-α-D-altropyranoside (**38**) and the other, most likely its α-D-*allo* isomer **39**, in analogy to the β-series. Bromination of the 2-acetate **40** of the α-D-mannoside **36** gave in high yield the 2-acetate **41** of **38** as a crystalline but rather sensitive compound. Deacetylation of **41** at room temperature produced what according to the n.m.r. spectrum was a 2:3 mixture of the same bromonitro sugars that arose in the bromination of **36** (*i.e.* presumably **38** and **39**), and treatment of the deacetylated mixture (or of **41** directly) with refluxing methanolic methoxide again gave the epoxide **37** (yields, 76–82%). Reacetylation of the mixture gave acetates in an approximate ratio of 2:3, and although these could not be separated either, the n.m.r. spectrum suggested that the lesser component was **41**. The major component, then, must have been the acetate of **39**, *i.e.*, presumably the α-D-*allo* derivative **42**. In summary, then, the experiments in this anomeric series have shown that α-D-*manno*, but not α-D-*gluco*, derivatives are effectively brominated by NBA, that epimerizations occur if 2-OH is unprotected, and that the bromonitro derivatives are readily converted into an epoxide.

Stereochemical Considerations

In all the halogenations studied, the preferred configuration arising at C-3 was that which places the nitro group equatorially when the pyranoside ring occupies the normal chair conformation. In a majority of instances a single halonitro derivative was obtained in a high yield, and in certain cases where two products arose these were epimeric at C-2 but stereochemically identical at C-3. However, in some instances C-3 epimers having an axial nitro group were formed as minor products. An explanation for these observations is now to be attempted.

One possibility to be considered is steric control of the approaching, halogen-transferring agent. In principle, the carbanionic site (C-3) in all the nitronates should be freely accessible for attack from the lower side of the glycoside ring while attack from the upper side should be sterically hindered by the axial hydrogen atoms and (or) oxygen functions situated at C-2 and -4. This factor would generally favor axial placement of the incoming halogen and consequently, equatorial placement of the nitro group, and would requi re no qualification for the β-glycosides all of which were indeed halogenated in a stereochemically uniform way. In α-glycosides the axial but more remote methoxyl group presumably reduces somewhat the accessibility of the lower pyranoside face, thereby tending to diminish the degree of stereoselectivity. This was seen in the halogenations of the α-D-*galacto*

Can. J. Chem. Downloaded from www.nrcresearchpress.com by 210.87.254.40 on 09/05/12
For personal use only.

Can. J. Chem. Downloaded from www.nrcresearchpress.com by 210.87.254.40 on 09/05/12
For personal use only.

and α-D-*lyxo* glycosides (**3** and **5**), and bromination seemed to be affected more so than chlorination. In the α-D-*talo* compound (**1**) this effect was not evident, probably because it is small relative to the especially severe hindrance afforded by the two axial oxygen functions on the upper side of the ring. If this line of reasoning is valid one should have expected the α-D-*manno* acetate **40** to give, in addition to the bromo derivative **41** that was produced, at least a small proportion of the corresponding 3-epimer. However, no evidence for formation of the latter has so far been obtained. A similar expectation does not necessarily apply to bromination of the non-acetylated α-D-*manno* compound **36**, since an epimer with axial nitro group, if it is formed as a primary product, may well be too unstable for observation and may suffer rapid epimerization to **38** and (or) **39**.

A further point of interest is the complete inertness of α-D-*gluco* derivatives (**34** and **35**) towards bromination even by the NBA method. It would be hard to visualize that they constitute a category apart as far as the facility of approach of the halogenating agent is concerned. Rather, we are inclined to believe that they failed to form the requisite nitronate salt in the weakly basic reaction medium. The particularly low nitromethylene acidity in 3-deoxy-3-nitro pyranosides having a 2,3,4-triequatorial substituent arrangement has been observed and explained previously (6, 9, 17, 18), but the present finding of an apparent difference in degree between α- and β-anomers is remarkable. Possibly it is a manifestation of a polar effect by which the methoxyl group, through the direction of its dipole in α-glycosides, opposes the development of carbanionic character at C-3.

Spectroscopic Evidence in Support of Configurational Assignments

In earlier work (18) the chemical shift of the benzylidene methine proton signal in n.m.r. spectra of 4,6-*O*-benzylidene-3-deoxy-3-nitrohexopyranosides has proved of diagnostic value for differentiating stereoisomers. Regularities in such shifts observed in the present work tend to support the C-3 configurations of the halonitro derivatives as assigned on the basis of chemical considerations. Table 1 shows that introduction of a halogen atom at C-3 has in some cases little or no effect upon the τ-value of the methine signal whereas in other cases a small but distinct downfield shift (0.1–0.2 p.p.m.) is observed. Virtually unaffected are the signals in those halogen derivatives which possess a *cis*-fused acetal structure and arise either as single (**6**, **7**, **9**, **11**, **13**, **16**, **18**) or as predominant epimers (**14**, **19**, **21**). The group characterized by the downfield shift comprises the minor epimers (**15**, **20**, **22**) in the *cis*-acetal series and all of the products having a *trans*-fused acetal ring. These observations are best explained by assuming that the methine proton experiences a change in shielding when the C_3-halogen bond is *gauche* to the C_4-oxygen bond (*i.e.*, parallel to one of the nonbonding orbitals of O-4) while no such effect is associated with an *anti* orientation of these bonds. When the pyranoside rings are depicted in the $^4C_1$ conformation in agreement with coupling constants found for H-1 and -4, the chemical shift data are thus consistent with the C-3 configurations as allocated. (See the partial formulas **a**–**c**).

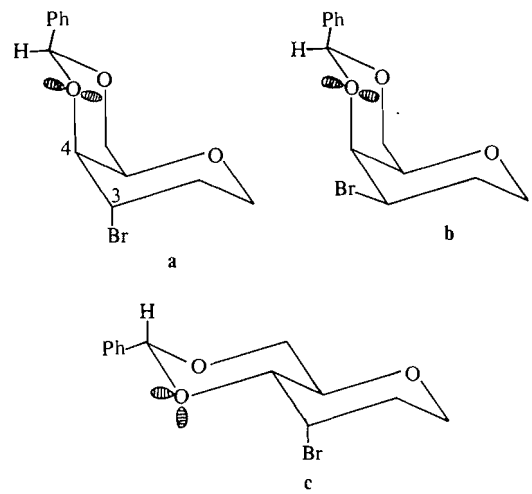

Also in accord with configurations assigned to C-3 are the chemical shifts of the anomeric proton signals insofar as these signals are discernible. In halonitro derivatives presumed to have the "normal" C-3 configuration (impyling axial halogen), the signal of an equatorial H-1 (in α-glycosides) is either virtually unaffected or shifted slightly downfield, and the signal of an axial H-1 (in β-glycosides) is markedly shifted downfield. By contrast, the "abnormal" compounds **15**, **20**, and **22** exhibit a moderate upfield shift of their H-1 signal. At the same time the anomeric methoxyl signals of these three compounds occur about 0.1 p.p.m. upfield from

TABLE 1. Chemical shifts (τ) of n.m.r. signals of halonitro sugars and precursors (100 MHz, in $CDCl_3$)

Compound	$PhCHO_2$	OCH_3	$OCOCH_3$	H-1	H-2	H-4
cis-Acetals						
1	4.41	6.59		5.02	5.37	
6	4.39	6.57		4.95	5.61	5.22
7	4.39	6.57		4.95	5.52	5.12
2	4.48	6.40				
9	4.50	6.43		5.48	5.26	5.45
11	4.51	6.44		~5.45	~5.50	5.30
3	4.51	6.56		5.03	5.28	5.28
13	4.48	6.56		5.01	5.01	5.38
14	4.48	6.55		4.99	~5.20	~5.20
15	4.30	6.64		5.09	~5.7	5.17
4	4.46	6.51				
16	4.44	6.48		5.31	7.20, 7.50	5.53
18	4.44	6.48		5.28	7.22, 7.43	5.43
5	4.43	6.66		4.99	7.40, 7.80	5.27
19	4.42	6.64		4.92	7.00, 7.44	5.47
20	4.28	6.76		5.14	6.96, 7.39	5.32
21	4.41	6.63		4.89	6.94, 7.37	5.33
22	4.28	6.78		5.21	~6.85, 7.30	5.30
trans-Acetals						
23	4.43	6.53		5.48	7.45, 7.77	
24	4.33	6.50		5.21	~7.25	
25	4.49	6.46				
26	4.32	6.44				
27	4.42	6.44				
28	4.23	6.44				
31	4.47	6.52	7.95	5.52	4.61	
29	4.39	6.51	7.93	5.37	4.47	
32*	4.33	6.50	7.89	5.48	4.13	6.05
30	4.21	6.48	7.95	4.96	4.12	
34	4.49	6.55		5.17		
35	4.48	6.61	7.95	4.95	4.73	
36	4.34	6.61		5.28		
40	4.32	6.62	7.94	5.26	4.47	
38	4.24	6.61				
39	4.43	6.55				
41	4.20	6.61	7.99	5.28	4.34	

*See ref. 16.

those of their precursors whereas in all other cases the influence of halogenation upon these signals appears insignificant.

Table 1 shows, furthermore, that the chemical shift of the benzylidene methine proton in non-halogenated glycosides incurs no significant change upon acetylation of the compound in position 2; compare **25**, **26**, **34**, and **36** with their respective 2-acetates **31**, **32**, **35**, and **40**. Assuming that the same holds true for the corresponding bromonitro glycosides one can correlate the 2-acetates **29** and **30** (which were isolated) with the non-acetylated bromination products that show τ 4.42 and 4.23, respectively, and that could not be separated but were designated on this basis as **27** and **28**. By a similar argument one can attribute formulas **38** and **39** to the components showing τ 4.24 and 4.43, of the mixtures resulting from bromination of **36** or deacetylation of **41**.

Experimental

For general preparative instrumental techniques see preceding articles of this series (*e.g.*, refs. 1, 10, 18). Optical rotations were measured at room temperature in chloroform solutions (*c*, 0.5–1) unless otherwise indicated. I.r. spectra were obtained from Nujol mulls on a Beckman IR-20 instrument. The n.m.r. data given for the characterization of compounds (Table 1 and elsewhere)

Can. J. Chem. Downloaded from www.nrcresearchpress.com by 210.87.254.40 on 09/05/12
For personal use only.

Can. J. Chem. Downloaded from www.nrcresearchpress.com by 210.87.254.40 on 09/05/12
For personal use only.

were obtained with a Varian HA-100 spectrometer; a T-60 spectrometer was used for monitoring reactions. The data refer to $CDCl_3$ solutions with TMS as internal standard. The following solvent systems (v/v) were employed for t.l.c. and column chromatography on silica gel: A, carbon tetrachloride – ethyl acetate (7:3); B, the same (4:3); C, petroleum ether (b.p. 30–60°) – ethyl acetate (2:3); D, the same (3:2).

Materials

The nitro glycosides to be halogenated were obtained according to the references given in parentheses: **1** (18), **2** (18, 19), **3** (18), **4** (1), **5** (1), **23** (1, 21*a*), **25** (18, 20, 21*b*), **26** (18, 19), **31** (20, 21*b*, 22), **32** (16), **34** (18, 19), **35** (23), **36** (18). The hitherto unknown *methyl 2-O-acetyl-4,6-O-benzylidene-3-deoxy-3-nitro-α-D-mannopyranoside* (**40**) was prepared by acetylation of **36** with acetyl chloride and triethylamine in methylene chloride as described (16) for the acetylation of **32** (see also the preparation of **29** from **27** + **28**). It was obtained as an amorphous powder in 86% yield; $[\alpha]_D$ +4.5°; ν_{max} 1745 and 1560 cm^{-1} ($OCOCH_3$ and NO_2). N.m.r. (in $CDCl_3$): τ 2.66 (m, 5H, phenyl), 5.03 (q, 1H, H-3), and Table 1; $J_{1,2}$ = 1.5, $J_{2,3}$ = 3.5, $J_{3,4}$ = 11 Hz.

Anal. Calcd. for $C_{16}H_{19}NO_8$ (353.3): C, 54.40; H, 5.42; N, 3.97. Found: C, 54.56; H, 5.29; N, 3.97.

Preparation of Halonitro Glycosides: General

Chlorinations were performed using a reagent grade, 5% aqueous sodium hypochlorite solution, or with equal success, commercial household bleach *Javex*, a product of Bristol-Myers Canada Limited, containing 6% sodium hypochlorite. Brominations were carried out with bromine in alkaline medium (Br_2 method) or with *N*-bromoacetamide in the presence of sodium acetate (NBA method). The procedures are detailed for compounds **6** and **7**. The remaining halonitro derivatives were obtained in the same general way, with occasional modifications as specified. Reactions were routinely monitored by t.l.c.

Upon completion of the halogenations, the products were isolated in one of two ways depending upon their solubility. In each case, the methanolic reaction solution was diluted with water, and part of the methanol was removed by evaporation under reduced pressure (bath temperature, 35°). Frequently the halogenated product separated thereby in crystalline and nearly pure form in large quantity. It was collected by filtration, washed with cold water, and dried in a desiccator before being recrystallized as necessary and specified. This *precipitative procedure* is referred to as work-up (P). When precipitation was unsatisfactory, the solution was concentrated further until most of the methanol was removed, and the remaining aqueous solution was then extracted three times with chloroform. The combined extract was washed twice with water, dried over anhydrous sodium sulfate, and evaporated to afford the product usually in nearly pure form. This *extractive procedure* is referred to as work-up (E).

Methyl 4,6-O-Benzylidene-3-chloro-3-deoxy-3-nitro-α-D-idopyranoside (6)

To an *ice cold* solution of **1** (124 mg) in methanol (30 ml) was added hypochlorite solution (1.2 ml). Inspection by t.l.c. (solvent B) after 5 and 15 min showed absence of **1** and presence of a single, faster moving spot. The solution was neutralized at 0° with 2 *N* acetic acid and worked-up (P). The crude product was recrystallized from ethanol–water to furnish **6** (117 mg, 85%); m.p. 104–105°, $[\alpha]_D$ +48.3°, ν_{max} 3480 and 1570 cm^{-1} (OH and NO_2).

Anal. Calcd. for $C_{14}H_{16}ClNO_7$ (345.7): C, 48.70; H, 4.65; Cl, 10.27. Found: C, 48.80; H, 4.86; Cl, 10.40.

Methyl 4,6-O-Benzylidene-3-bromo-3-deoxy-3-nitro-α-D-idopyranoside (7)

(a) Br_2 Method

To an ice-cold solution of **1** (103 mg) in methanol (15 ml) was added aqueous, 0.1 *N* sodium hydroxide (3.7 ml). The mixture was stirred for 5 min after which bromine was added in small drops until the color of the solution remained slightly yellow. Stirring was then continued for another 5 min and followed by work-up (E). The white product (104 mg) was recrystallized from chloroform–pentane to give **7** (96 mg, 74%); m.p. 126–128°, raised to 129–130° by a second recrystallization. The product had $[\alpha]_D$ +45.5° and ν_{max} 3550, 3490 (OH) and 1565 cm^{-1} (NO_2).

Anal. Calcd. for $C_{14}H_{16}BrNO_7$ (390.3): C, 43.14; H, 4.13; Br, 20.46. Found: C, 43.26; H, 4.17; Br, 20.83.

(b) NBA Method

To a solution of **1** (200 mg) in methanol (20 ml) was added NBA (100 mg) and a saturated, aqueous solution of sodium acetate (2 ml). The reaction mixture was agitated for 30 min at room temperature. Work-up (E) afforded **7** (235 mg, 94%), m.p. 127–129° and undepressed upon admixture of **7** from the Br_2 method. The i.r. spectra of the two products were identical.

Methyl 4,6-O-Benzylidene-3-chloro-3-deoxy-nitro-β-D-gulopyranoside (9)

Chlorination of **2** (62 mg) was carried out at room temperature. According to t.l.c. (solvent C) no **2** was left after 10 min, and a single, faster moving spot was seen. The reaction mixture was allowed to stand for another 15 min, and work-up (E) then gave crude **9** (72 mg) which was recrystallized from ethyl acetate – petroleum ether to give pure **9** (58 mg, 76%); m.p. 166–167°; $[\alpha]_D$ +35.1°, ν_{max} 3480 and 1570 cm^{-1} (OH and NO_2).

Anal. Calcd. for $C_{14}H_{16}ClNO_7$ (345.7): C, 48.70; H, 4.65; Cl, 10.27. Found: C, 48.62; H, 4.78; Cl, 10.26.

Methyl 2,4,6-Tri-O-acetyl-3-chloro-3-deoxy-3-nitro-β-D-gulopyranoside (10)

Compound **9** (200 mg) was debenzylidenated by treatment (24) with 90% trifluoroacetic acid (5 ml) for 20 min at room temperature. The syrupy product obtained upon evaporation failed to crystallize and was therefore acetylated by the boron trifluoride method (22), a reaction time of 20 min being allowed. The acetylation mixture was poured into and stirred with ice water, and the oily product which separated was extracted into chloroform (3 × 30 ml). The extract was washed twice with 5 ml of cold, saturated sodium bicarbonate solution and twice with 5 ml of water. Drying (Na_2SO_4) and evaporation of the solvent gave **10** as a syrup which could be crystallized from chloroform–pentane. The product showed m.p. 91–92°, $[\alpha]_D$ −6.3°, ν_{max} 1765, 1745 ($OCOCH_3$), and 1575 cm^{-1} (NO_2).

Anal. Calcd. for $C_{13}H_{18}ClNO_{10}$ (383.8): C, 40.72; H, 4.73; Cl, 9.25. Found: C, 40.77; H, 4.71; Cl, 9.48.

Can. J. Chem. Downloaded from www.nrcresearchpress.com by 210.87.254.40 on 09/05/12
For personal use only.

Methyl 4,6-O-Benzylidene-3-bromo-3-deoxy-3-nitro-β-D-gulopyranoside (11)

(a) Br_2 Method

To an ice-cooled suspension of **2** (311 mg) in methanol (40 ml) was added aqueous 0.1 *N* sodium hydroxide (11 ml). After stirring for 4 min a clear solution resulted to which bromine was added dropwise until a light yellow color persisted. Stirring at 0° was continued for 15 min and then followed by work-up (P). The product **11** (281 mg, 72%) showed m.p. 75–78°, $[\alpha]_D$ +31.6°, ν_{max} 3450 (OH) and 1565 cm^{-1} (NO_2).

Anal. Calcd. for $C_{14}H_{16}BrNO_7$ (390.2): C, 43.14; H, 4.13; Br, 20.46; N, 3.59. Found: C, 43.03; H, 4.24; Br, 20.38; N, 3.80.

(b) NBA Method

The reaction mixture was heated at reflux temperature for 1 h and then worked-up (P) to furnish **11**, m.p. 77–79°, in a yield of 69%. The i.r. spectrum was identical with that of **11** from (*a*).

Methyl 2,4,6-Tri-O-acetyl-3-bromo-3-deoxy-3-nitro-β-D-gulopyranoside (12)

Compound **11** (140 mg) was debenzylidenated, and the syrupy product acetylated, as described for the preparation of **10** from **9**. Prolonged trituration of the acetylation mixture with ice water gave the triacetate **12** as a solid (103 mg after drying; m.p. 107–108°) which was recrystallized from ethyl acetate – petroleum ether; m.p. 112–113°, $[\alpha]_D$ +25°, ν_{max} 1765, 1740 ($OCOCH_3$) and 1570 cm^{-1} (NO_2).

Anal. Calcd. for $C_{13}H_{18}BrNO_{10}$ (428.2): C, 36.48; H, 4.24; Br, 18.67; N, 3.27. Found: C, 36.60; H, 4.31; Br, 18.69; N, 3.32.

Methyl 4,6-O-Benzylidene-3-chloro-3-deoxy-3-nitro-α-D-gulopyranoside (13)

The glycoside **3** (120 mg) in methanol (15 ml) was treated with hypochlorite solution (1 ml) for 1 h at room temperature. Formation of a uniform product moving faster than **3** was indicated by t.l.c. (solvent D). Work-up (E) furnished crystalline **13** (123 mg, 92%) which upon recrystallization from ethanol–water melted at 121–122°; $[\alpha]_D$ +144°, ν_{max} 3540 and 1570 cm^{-1} (OH and NO_2).

Anal. Calcd. for $C_{14}H_{16}ClNO_7$ (345.7): C, 48.70; H, 4.65; Cl, 10.27. Found: C, 48.53; H, 4.77; Cl, 10.13.

Methyl 4,6-O-Benzylidene-3-bromo-3-deoxy-3-nitro-α-D-gulopyranoside (14) and -α-D-galactopyranoside (15)

(a) Br_2 Method

The glycoside **3** (311 mg) in methanol (40 ml) was treated with 0.1 *N* sodium hydroxide solution (11 ml) for 5 min at 0° and then brominated during 15 min. Work-up (P) afforded a white solid material (355 mg) which according to the t.l.c. (solvent B) was free from starting material but contained two products in similar proportions. An n.m.r. spectrum of the material exhibited two sharp singlets at τ 4.30 and 4.48 with an intensity ratio of 45:55 (benzylidene methine protons). The mixture was chromatographed on a column of silica gel (20 g) which was eluted with solvent C. A clean separation was achieved. The faster moving fraction gave the α-D-*galacto* isomer **15** (130 mg, 33%), m.p. 66°, $[\alpha]_D$ +160.3°, ν_{max} 3540 and 1560 cm^{-1}. The slower fraction gave the α-D-*gulo* isomer **14** (190 mg, 49%), m.p. 118–120°, $[\alpha]_D$ +108°, ν_{max} 3510 and 1560 cm^{-1}.

Anal. Calcd. for $C_{14}H_{16}BrNO_7$ (390.2): C, 43.14; H, 4.13; Br, 20.46. Found for **14**: C, 42.85; H, 4.22; Br, 20.45. Found for **15**: C, 43.27; H, 4.15; Br, 20.72.

(b) NBA Method

The glycoside **3** (93 mg) was completely brominated after 30 min at room temperature. The solid product obtained upon work-up (P) exhibited n.m.r. signals at τ 4.30 and 4.48 in an intensity ratio of 15:85. Column chromatography as described under (*a*) furnished **15** (12.6 mg, 11%) melting at 65–67° and **14** (82 mg, 71%) melting at 119–120°. Identity of the products with those obtained under (*a*) was confirmed by their i.r. spectra.

Methyl 4,6-O-Benzylidene-3-chloro-2,3-dideoxy-3-nitro-β-D-xylo-hexopyranoside (16)

The nitro glycoside **4** (177 mg) was chlorinated in methanol (45 ml) with hypochlorite solution (1.8 ml) at room temperature for 20 min. According to t.l.c. (solvent D) the reaction appeared complete after 10 min. Work-up (E) gave a syrup which was converted into a solid (182 mg, 92%) by dissolution in ethanol and careful addition of water; m.p. 48–49°, $[\alpha]_D$ +18.2°, ν_{max} 1565 cm^{-1} (NO_2).

Anal. Calcd. for $C_{14}H_{16}ClNO_6$ (329.7): C, 51.10; H, 4.89; Cl, 10.77. Found: C, 51.06; H, 4.80; Cl, 10.82.

Methyl 4,6-Di-O-acetyl-3-chloro-2,3-dideoxy-3-nitro-β-D-xylo-hexopyranoside (17)

Debenzylidenation (reaction time 1 h) and subsequent acetylation of **16** (330 mg) was performed as described for the conversion **9** → **10**. The syrupy product was crystallized from cyclohexane to give **17** (192 mg, 65%), m.p. 90–91°, $[\alpha]_D$ +27.5°, ν_{max} 1745 (shoulder at 1760) and 1570 cm^{-1} ($OCOCH_3$ and NO_2).

Anal. Calcd. for $C_{11}H_{16}ClNO_8$ (325.7): C, 40.60; H, 4.95; Cl, 10.86. Found: C, 40.76; H, 5.05; Cl, 10.81.

Methyl 4,6-O-Benzylidene-3-bromo-2,3-dideoxy-3-nitro-β-D-xylo-hexopyranoside (18)

The glycoside **4** (60 mg) was brominated by the NBA method at room temperature. The reaction was complete (t.l.c.) after 15 min and work-up (P) gave **18** (65 mg, 96%) as a white, amorphous powder; $[\alpha]_D$ +22°, ν_{max} 1565 cm^{-1}.

Anal. Calcd. for $C_{14}H_{16}BrNO_6$ (374.2): C, 45.05; H, 4.31; Br, 21.35. Found: C, 45.03; H, 4.12; Br, 21.35.

Methyl 4,6-O-Benzylidene-3-chloro-2,3-dideoxy-3-nitro-α-D-xylo-hexopyranoside (19) and -α-D-lyxo-hexopyranoside (20)

A solution of the glycoside **5** (250 mg) in methanol (30 ml) was treated with hypochlorite solution (2 ml) at room temperature for 2 h. The t.l.c. (solvent D) indicated formation of a major product and a faster moving, minor product. Work-up (E) furnished a syrup (240 mg, 85.5%) whose n.m.r. spectrum displayed two methine proton signals, τ 4.28 and 4.42, with an intensity ratio 14:86. The two products were separated by passage through a column of silica gel (20 g) using solvent D as eluant.

The faster moving fraction gave the α-D-*lyxo* isomer **20** (35 mg, 12.5%) which crystallized from ethanol–water; m.p. 122–123°, $[\alpha]_D$ +126°, ν_{max} 1570 cm^{-1}. The mass spectrum of **20** (mol. wt. 329.74) exhibited an intense molecular ion peak at *m/e* 329. An isotopic distribution pattern conforming to a chloro derivative was observed, A strong peak at *m/e* 298 likely resulted from loss of

Can. J. Chem. Downloaded from www.nrcresearchpress.com by 210.87.254.40 on 09/05/12
For personal use only.

OCH_3, and less prominent peaks at *m/e* 223 and 192 were attributed to loss of C_6H_5CHO from the molecular ion and the aforementioned fragment. Another strong peak was at *m/e* 180.

The slower chromatographic fraction furnished the α-D-*xylo* isomer **19** (188 mg, 67%) which was also crystallized from ethanol–water; m.p. 101–102°, $[\alpha]_D$ +128°, ν_{max} 1565 cm^{-1}. Its mass spectrum also showed a molecular ion peak at *m/e* 329, and the fragmentation pattern was quite similar to that of **20** except for a medium intense peak at *m/e* 177 which was practically absent in the latter.

Anal. Calcd. for $C_{14}H_{16}ClNO_6$ (329.7): C, 51.10; H, 4.89; Cl, 10.77. Found: C, 51.04; H, 4.83; Cl, 10.79.

*Methyl 4,6-O-Benzylidene-3-bromo-2,3-dideoxy-3-nitro-α-D-xylo-hexopyranoside (**21**) and -α-D-lyxo-hexopyranoside (**22**)*

(a) Br_2 Method

The glycoside **5** (200 mg) in methanol (30 ml) was treated for 5 min with aqueous 0.1 *N* sodium hydroxide (6.8 ml). Bromine was then added dropwise in slight excess, and the reaction was allowed to proceed for another 10 min. Work-up (P) gave a crude solid (220 mg, 98%) which showed two spots, both faster than **5**, on t.l.c. with solvent A. The n.m.r. spectrum exhibited methine proton signals at τ 4.28 and 4.41 with an intensity ratio 25:75. The products were separated on a silica gel column (20 g) by elution with solvent A.

The faster moving product obtained from the column was the α-D-*lyxo* isomer **22** (41 mg, 21%), m.p. 105–106°, $[\alpha]_D$ +140.5° (*c*, 0.3), ν_{max} 1565 cm^{-1}. The mass spectrum showed intense molecular ion peaks at *m/e* 373 and 375 in accord with the composition $C_{14}H_{16}BrNO_6$. Less intense peaks were present at *m/e* M − 31, probably due to loss of OCH_3. A single peak of medium intensity was observed at *m/e* 262 and may have resulted from loss of HBr and OCH_3.

The second product eluted from the column was the α-D-*xylo* isomer **21** (156 mg, 69%); m.p. 103–104°, $[\alpha]_D$ +112.5°, ν_{max} 1565 cm^{-1}. Its mass spectrum was very similar to that of isomer **22** but showed an intense peak at *m/e* 221 which was not given by the latter.

Anal. Calcd. for $C_{14}H_{16}BrNO_6$ (374.2); C, 45.05; H, 4.31; Br, 21.35. Found: C, 45.02; H, 4.14; Br, 21.63.

(b) NBA Method

A 60-mg sample of **5** was brominated by NBA. The crude material obtained upon work-up (P) was identical to that obtained under (*a*) according to t.l.c. (solvent A) and n.m.r. spectroscopy, the spectrum showing an intensity ratio 22:78 for the τ 4.28 and 4.41 signals and being otherwise identical with that of the previous product mixture.

*Methyl 4,6-O-Benzylidene-3-bromo-2,3-dideoxy-3-nitro-β-D-ribo-hexopyranoside (**24**)*

The glycoside **23** (200 mg) was brominated by the NBA method at reflux temperature for 1 h. Work-up (P) afforded **24** (222 mg, 87%) as a white amorphous powder; $[\alpha]_D$ −26.2°, ν_{max} 1560 cm^{-1}.

Anal. Calcd. for $C_{14}H_{16}BrNO_6$ (374.2): C, 45.05; H, 4.31; Br, 21.35. Found: C, 45.19; H, 4.23; Br, 21.31.

*Bromination of Methyl 4,6-O-Benzylidene-3-deoxy-3-nitro-β-D-mannopyranoside (**26**)*

(a) Br_2 Method

A mixture of the glycoside **26** (311 mg) in methanol (25 ml) and aqueous 0.1 *N* sodium hydroxide (12.5 ml) was stirred in an ice water bath for 10 min. Bromine was added as in previous examples, and stirring at 0° was continued for 10 min. Work-up (P) gave a white solid material (319 mg) which exhibited four n.m.r. signals in the methine proton region (τ 4.23, 4.32, 4.42, and 4.49; intensity ratios 5:10:35:50). The t.l.c. (solvent A) showed one major spot having the same mobility as the nitro glucoside **25**, one slightly faster moving spot representing new product(s), and a weak, slow-moving spot having the mobility of starting material **26**. The mixture was chromatographed on silica gel (20 g) with the solvent A. All fractions were examined by t.l.c. and pooled appropriately. The fast-moving material (120 mg, $[\alpha]_D$ −39.8°, ν_{max} 1565 cm^{-1}) that was eluted first appeared homogeneous on t.l.c. but was revealed to be a mixture by its n.m.r. spectrum (methine proton signals at τ 4.42 and 4.23 in the ratio 85:15). The major component was assumed to be *methyl 4,6-O-benzylidene-3-bromo-3-deoxy-3-nitro-β-D-allopyranoside* (**27**), and the minor component, its β-D-*altro* isomer **28**.

Continued elution gave some mixed fractions which were discarded, and then a fraction containing pure **25** (93 mg) which was identified with an authentic sample by comparison of n.m.r. and i.r. spectra, t.l.c. and an undepressed mixture m.p. of 180–181°. A subsequent chromatographically uniform fraction gave starting material (**26**) which was identified similarly (mixed m.p. 194–196°, undepressed).

(b) NBA Method

The glycoside **26** (415 mg) was brominated for 1 h in refluxing methanol (40 ml) with NBA (200 mg) in the presence of sodium acetate (4 ml of a saturated aqueous solution). Work-up (P) gave a white solid (507 mg, $[\alpha]_D$ −35.5°) that appeared uniform on t.l.c. (various solvents) but showed two methine proton signals, at τ 4.42 and 4.23 in the intensity ratio 80:20. The i.r. spectrum was identical with that of the chromatographically purified mixture of **27** and **28** described under (*a*). A similar mixture was obtained by reaction with NBA for 5 h at room temperature.

(c) With N-Bromosuccinimide

Substitution of this reagent (71 mg) for NBA in the above reaction gave a product (106 mg, from 103 mg of **26**) whose n.m.r. spectrum was superimposable on that of the aforementioned mixture of **27** and **28**.

*Bromination of Methyl 4,6-O-Benzylidene-3-deoxy-3-nitro-β-D-glucopyranoside (**25**)*

Compound **25** (415 mg) was brominated with NBA as just described for **26**. After 1 h a small amount of **25** remained and a strong, faster moving product spot was observed on t.l.c. (solvent A). This picture did not change upon continued refluxing of the mixture for another 5 h. Work-up (P) gave a crude material (457 mg, $[\alpha]_D$ −41.2°) whose n.m.r. spectrum exhibited three methine proton signals, τ 4.22, 4.41, and 4.48, in the ratio 15:75:10. Except for some minor signals the spectrum was closely similar to that of the mixture of **27** and **28** obtained from

Can. J. Chem. Downloaded from www.nrcresearchpress.com by 210.87.254.40 on 09/05/12
For personal use only.

26, and the same was true for the i.r. spectrum. In view of these similarities and of the similar $[\alpha]_D$-value and t.l.c. pattern it was concluded that the product consisted of **27** and **28** (contaminated by some starting material).

Application of the Br_2 method as described for **26** gave no product after a reaction time of 15 min at 0°; a minute trace of product seemed to appear after 30 min at 25° (t.l.c. with solvent A). Unchanged **25**, m.p. 180°, was isolated in high yield.

Methyl 2-O-Acetyl-4,6-O-benzylidene-3-bromo-3-deoxy-3-nitro-β-D-allopyranoside (29)

(a) From the 2-Acetate 31

Compound **31** (200 mg) was brominated by the NBA method with a reaction time of 3 h at room temperature. Work-up (P) afforded 234 mg (95.5%) of a solid that was uniform in t.l.c. (solvent G) and upon recrystallization from ethyl acetate – petroleum ether afforded pure **29** (197 mg); m.p. 223–225°, $[\alpha]_D$ −69°, ν_{max} 1755 and 1570 cm^{-1} ($OCOCH_3$ and NO_2).

Anal. Calcd. for $C_{16}H_{18}BrNO_8$ (432.3): C, 44.50; H, 4.20; N, 3.24; Br, 18.45. Found: C, 44.58; H, 4.28; N, 3.09; Br, 18.70.

(b) From the Mixture of 27 and 28

A mixture (150 mg) of **27** and **28** originating from bromination of **26** (see earlier) was dissolved in methylene chloride (6 ml) and chilled (0°). To a cold solution of triethylamine (1.93 ml) in dry ether (30 ml) was added acetyl chloride (1.04 ml). The reagent, from which triethylammonium chloride precipitated copiously, was magnetically stirred at 0° for 5 min before the glycoside solution was added. The mixture was stirred for 30 min at 0° and then agitated briefly with cold water. Upon phase separation the aqueous layer was extracted twice with ether. The combined organic layer and extract was washed with three portions of water, dried over Na_2SO_4, and evaporated. The residue gave two spots on t.l.c. (solvent A), the faster spot being much stronger than the slower one. The n.m.r. spectrum showed signals in the region of τ 4.30–4.50 (methine proton and H-2 of **29**) and in the region of 4.10–4.20 (methine proton and H-2 of **30**) in an intensity ratio 80:20. Column chromatography of the mixture on 20 g of silica gel with solvent A led to isolation of the fast-moving component (117 mg, 70.5%) which according to its i.r. spectrum and m.p. 222–224° was identical with **29** described under (*a*). The slower component eluted from the column proved to be the isomer **30** (see the subsequent section).

Methyl 2-O-Acetyl-4,6-O-benzylidene-3-bromo-3-deoxy-3-nitro-β-D-altropyranoside (30)

(a) From the 2-Acetate 32

Compound **32** (150 mg) was brominated with NBA for 1 h at room temperature. Work-up (P) gave crude **30** (174 mg, 95%), m.p. 140–142°, $[\alpha]_D$ −76.2°. Upon recrystallization from ethanol–water the data were m.p 152–153°, $[\alpha]_D$ −80.8°, ν_{max} 1775 and 1565 cm^{-1}.

Anal. Calcd. for $C_{16}H_{18}BrNO_8$ (432.3): C, 44.50; H, 4.20; Br, 18.45. Found: C, 44.43; H, 4.30; Br, 18.64.

(b) From the Mixture of 27 and 28

The slow-moving product obtained from the column (see the preceding section) weighed 24.5 mg (15%), melted at 149–151°, and gave an i.r. spectrum identical with that of **30** from (*a*).

Attempted Bromination of α-D-Glucosides 34 and 35

Compound **34** (311 mg) and NBA (150 mg) were refluxed for 10 h in a mixture of methanol (30 ml) and saturated sodium acetate solution (3 ml). The t.l.c. gave no evidence for product formation, and work-up (P) led to recovery of **34** (242 mg, 78%), m.p. 166–167°, which was identified by its n.m.r. spectrum.

The 2-acetate **35** (100 mg) was similarly treated, with proportionate amounts of reagents, for a period of 3.5 h at room temperature. Upon work-up, 96 mg of unchanged **35**, m.p. 196–197°, was recovered.

Application of the Br_2 method to **34** (as described for **26**) gave no evidence for product formation (t.l.c. with solvent A) after 15 min at 0°, nor after 30 min at 25°. Unchanged **34**, m.p. 166–167°, was recovered.

Bromination of Methyl 4,6-O-benzylidene-3-deoxy-3-nitro-α-D-mannopyranoside (36)

The glycoside **36** (200 mg) was treated with an excess of NBA (400 mg) in refluxing methanol. Inspection by t.l.c. (solvent C) indicated that reaction had taken place but remained incomplete after 3 h; the pattern was essentially unchanged after 4 h. Work-up (P) then gave a white solid (213 mg) which t.l.c. showed to be not uniform but to contain at least one spot that moved faster than the starting material. Some of the latter appeared to be present also. The i.r. band attributable to the asymmetric stretching vibration of the nitro group was split, with one peak being at 1565 and the other at 1550 cm^{-1}. This suggested the presence of bromonitro and nitro sugars in the mixture. The n.m.r. spectrum of the material exhibited four methine proton signals at τ 4.24, 4.34, 4.43, and 4.48. By integration the first signal was seen to constitute 33%, and the last signal, 25% of the total intensity. The two intermediate signals integrated together (42%); however, the one at τ 4.43 could visually be judged to make the greater contribution by far. The signals at τ 4.34 and 4.48 were assigned to residual starting compound **36** and its α-D-*gluco* isomer **34**, respectively. The signals at τ 4.24 and 4.43 were tentatively attributed to *methyl 4,6-O-benzylidene-3-bromo-3-deoxy-3-nitro-α-D-altropyranoside* (**38**) and its α-D-*allo* isomer (**39**). No attempt was made to separate the products, but the presence of bromonitro sugars to an extent of over 50% was shown by the generation of an epoxide as will be described later on.

Methyl 2-O-Acetyl-4,6-O-benzylidene-3-bromo-3-deoxy-3-nitro-α-D-altropyranoside (41)

The 2-acetate **40** (100 mg) was brominated with NBA at room temperature for 2 h. Work-up (P) produced a crystalline material (103 mg, 85%); m.p. 152–153°, $[\alpha]_D$ +12.3°, ν_{max} 1760 and 1570 cm^{-1}. The n.m.r. data in Table 1 together with further observations ($J_{1,2} \sim 0$ Hz; disappearance of the H-3 quartet of **40**) were in accord with structure **41**. The microanalysis was not wholly satisfactory although it did indicate the presence of 93% of the expected amount of bromine in the sample. Instability of the compound resulting in loss of bromine during preparation and storage of the analytical sample might be an explanation.

Can. J. Chem. Downloaded from www.nrcresearchpress.com by 210.87.254.40 on 09/05/12
For personal use only.

Anal. Calcd. for $C_{16}H_{18}BrNO_8$ (432.3): C, 44.50; H, 4.20; Br, 18.45. Found: C, 45.97; H, 4.57; Br, 17.12.

Reactions of Halonitro Glycosides

Borohydride Reductions

For reductive debromination (11), sodium borohydride was added to the ethanolic solution of the bromonitro sugar at room temperature unless specified otherwise. Amounts of reagents and reaction times are given below. For work-up the reaction mixture was slightly acidified with *N* acetic acid, diluted with water, and partially evaporated under reduced pressure to remove most of the ethanol. The product began to separate in crystalline form during this operation; it was collected, washed with water, and dried, and it normally proved pure after one recrystallization from ethanol–water or as specified.

*(a) **1** from **7**.* Compound **7** (200 mg) and $NaBH_4$ (80 mg) in ethanol (40 ml) were allowed to react for 5 min in an ice-water bath. The product (128 mg, 80%), m.p. 174–175°, proved identical with an authentic sample of **1** (lit. m.p. 175° (23), 177–178° (18)) by its i.r. spectrum and on t.l.c. (solvent B). The t.l.c. also suggested the presence of a trace of epoxide **8**.

*(b) **2** from **11**.* Compound **11** (100 mg) and $NaBH_4$ (50 mg) in ethanol (20 ml) were allowed to react for 30 min at 25°. Identity of the product **2** (71 mg, 90%) with an authentic sample was established by comparison of i.r. spectra and an undepressed mixture melting point of 232° (lit. m.p. 230–231° dec. (19), 232° (21)).

*(c) **3** from **14**.* Compound **14** (170 mg) and $NaBH_4$ (80 mg) in ethanol (35 ml) were allowed to react for 10 min at 25°. Upon recrystallization from ethyl acetate – petroleum ether the product **3** (131 mg, 97%) was identical with an authentic sample according to i.r. and n.m.r. spectra; m.p. 165–167° (lit. m.p. 166–167° (18)).

*(d) **3** from **15**.* Compound **15** (20 mg) upon similar debromination gave **3** (12 mg, 75%) that was identified by its i.r. spectrum; m.p. 165–167°.

Alkaline Debromination and Epoxide Formation

*Methyl 2,3-anhydro-4,6-O-benzylidene-3-nitro-α-D-talopyranoside (**8**)*

*(a) From **1** via **6**.* The epoxide **8** was produced when the chlorination of **1** (see the preparation of **6**, above) was carried out at room temperature rather than at 0°. Thus, when **1** (62 mg) in methanol (15 ml) was treated with hypochlorite solution (0.6 ml), t.l.c. (solvent B) showed a single, faster moving spot (presumably **6**) after a reaction time of 15 min, and this spot was replaced by a slower spot corresponding to **8** after 35 min. Work-up (P) including recrystallization from ethanol–water gave **8** (50 mg, 81%), m.p. 215–216°. Its identity with known **8** was established by comparison of i.r. and n.m.r. spectra; lit. (10), m.p. 215–216°.

*(b) From **7**.* To a solution of **7** (35 mg) in methanol (2 ml) were added a few drops of aqueous *N* sodium hydroxide, and the mixture was stirred at 25° for 15 min during which time a white solid separated. Dilution with water and partial evaporation of the mixture afforded 25 mg (90%) of crystalline **8**, m.p. 214–215°.

*(c) From **15**.* Compound **15** (95 mg) was dissolved in methanol (30 ml) to which 1 ml of alcoholic, *N* sodium hydroxide was added. The slow generation of a product having the mobility of **8** was noticed on t.l.c. (solvent D) after a few hours, and the reaction appeared nearly complete after 10 h. The reaction mixture was diluted with water, and methanol was removed by evaporation whereby crystalline if slightly impure **8** (54 mg, 72%) was produced; m.p. 208–210°, $[\alpha]_D$ +89.0°; lit. $[\alpha]_D$ +91.8° (10).

*(d) From **14**.* When **14** was treated with base as under (*c*) it was recovered unchanged even after a prolonged time of exposure (20 h). However, when a sample (30 mg) in methanol (5 ml) together with 0.1 *N* sodium methoxide (1 ml) was heated to reflux for 20 min, reaction did take place to give a major, unidentified product of very low mobility (t.l.c. with solvent C) along with a minor product moving like **8**. Work-up as under (*c*) furnished crystalline **8** (6 mg, 25%), m.p. 213–215°, that was identified also by its i.r. spectrum. The unidentified material remained in the aqueous mother liquor.

*Debromination of **11***

A solution of **11** (50 mg) in ethanol (2 ml) was treated with 0.3 ml of aqueous *N* potassium hydroxide at room temperature. After 30 min all **11** had disappeared and a product having the mobility of **2** was formed (t.l.c. with solvent D). The reaction mixture was diluted with ethanol (10 ml), rapidly deionized by cation exchange, and immediately tested with potassium iodide – starch which produced a blue color. Evaporation of the solution and recrystallization of the residue from ethanol–water gave **2** (24 mg, 62%), m.p. and mixed m.p. 230–232°.

To a solution of **11** (80 mg) in methanol (5 ml) was added 0.1 *N* sodium methoxide in methanol (2 ml). After being refluxed for 20 min the reaction mixture was revealed by t.l.c. (solvent D) to contain a major, very slow-moving product beside some starting material. Dilution of the mixture with water caused **11** (16 mg) to separate; it was identified by its i.r. spectrum. The major reaction product could not be identified, but since a smell of benzaldehyde was noticed it likely was a degradation product. There was no chromatographic evidence for epoxide formation. (2,3-Anhydro glycosides of this type generally move faster than the corresponding 2-hydroxy derivatives.)

*Methyl 2,3-anhydro-4,6-O-benzylidene-3-nitro-β-D-mannopyranoside (**33**)*

*(a) From **30**.* Compound **30** (64.8 mg) was refluxed for 30 min in 0.035 *N* methanolic sodium methoxide solution (8 ml). The cooled solution was deionized with a cation exchange resin, diluted with water, and partially evaporated to remove methanol. A smell of benzaldehyde was noted. White crystals of **33** separated and were washed with water and dried (17 mg, 37%). The melting point, 179–180°, was raised to 182–183° by recrystallization from ethyl acetate – petroleum ether; $[\alpha]_D$ −68.4°. Microanalytical and spectral characterization of the product has been recorded (10).

*(b) From **29**.* Compound **29** (52 mg) gave **33** (15 mg, 40%) in the manner described under (*a*); m.p. 178–180°. The products were identical according to t.l.c., i.r., and n.m.r. spectra.

*(c) From mixtures of **27** and **28***

A mixture of **27** and **28** (60 mg; obtained from bromination of **26**) in methanol (5 ml) was refluxed for 30 min after addition of 0.1 *N* sodium methoxide solution (1.5 ml). Work-up as under (*a*) gave **33** (40 mg, 84%), m.p. 181–182°, identified also by its i.r. spectrum. A similar experiment using a mixture of **27** + **28** originating from

Can. J. Chem. Downloaded from www.nrcresearchpress.com by 210.87.254.40 on 09/05/12
For personal use only.

bromination of **25** gave **33**, m.p. 181–182°, in a yield of 78%.

Methyl 2,3-anhydro-4,6-O-benzylidene-3-nitro-α-D-mannopyranoside (37)

*(a) From **41**.* Compound **41** (65 mg) was refluxed for 30 min in 0.035 *N* methanolic sodium methoxide solution (8 ml). Upon cooling and dilution with water the reaction mixture deposited a voluminous precipitate of **37** which was collected, washed with water, and dried (38 mg, 82%). It melted at 173–174° and its i.r. spectrum was identical with that of **37** prepared by an independent method; lit. m.p. 173–174° (10).

*(b) From mixtures of **38** and **39**.* Eighty milligrams of the mixture of products obtained in the bromination of **36** and presumed to contain **38** and **39** was boiled for 20 min in 7 ml of 0.03 *N* sodium methoxide solution. The product obtained upon work-up and two recrystallizations from ethanol weighed 32.5 mg and proved identical with authentic **37** by an undepressed mixture m.p. 171–173°, and by its i.r. spectrum.

Similarly, a sample (60 mg) of the product of low-temperature deacetylation of **41** (see below) was heated in refluxing methanol (5 ml) and 0.1 *N* sodium methoxide solution (1.5 ml) for 30 min. Cooling and dilution with water gave a precipitate of **37** (36 mg, 76%), m.p. 172–173° (undepressed upon admixture of an authentic sample).

Deacetylation Accompanied by Epimerization

*(a) Reaction of **30**.*

To a solution of the β-D-*altro* acetate **30** (65 mg, 0.15 mmol) in methanol (5 ml) was added 0.30 mmol of sodium methoxide (3 ml of a 0.1 *N* solution). The mixture was allowed to stand at room temperature for 30 min after which time t.l.c. (solvent C) revealed absence of **30** and showed a single, slower spot. Deionization by cation exchange resin, dilution with water, and partial evaporation furnished a white solid (48 mg, 82%) showing $[\alpha]_D$ −38.2°. An n.m.r. spectrum exhibited two methine proton signals at τ 4.41 and 4.22, intensity ratio 80:20. The spectrum was virtually superimposable on those of the mixtures of **27** and **28** obtained in various brominations of **26** (see earlier). Since separation of the products was not possible, the mixture was acetylated by the acetyl chloride – triethylamine method (see the preparation of **29** from **27** + **28**). The solid mixture of acetates obtained was recrystallized twice from ethyl acetate – petroleum ether to give pure β-D-*allo* isomer **29** (34.5 mg, 65%), m.p. 223–225°. The identity of the product with **29** was confirmed by comparison of n.m.r. and i.r. spectra and by t.l.c. (solvent A).

When the above experiment was repeated with the use of only 0.15 mmol of $NaOCH_3$ and a reaction time of 1 h at 0°, the isolated product (52 mg) contained a small amount of unreacted **30** which could be removed by chromatography on silica gel (solvent C) and identified (m.p. 149–151°; i.r. spectrum). The main material eluted from the column (37 mg) was practically identical with previously obtained mixtures of **27** and **28** (product ratio, 85:15).

*(b) Reaction of **41***

To a solution of acetate **41** (86.4 mg, 0.2 mmol) in methanol (10 ml) was added 0.4 mmol of $NaOCH_3$ (4 ml of a 0.1 *N* solution). After 1 h at room temperature a seemingly uniform, more slowly moving product was formed (t.l.c., solvent A). Work-up (P) after 3 h gave a white solid (71 mg, 91%) which according to its i.r. spectrum (ν_{max} 3380 and 1560 cm^{-1}, OH and NO_2) was free from acetyl. The n.m.r. spectrum showed methine proton signals at τ 4.24 and 4.43, and corresponding OCH_3 signals at τ 6.61 and 6.55, tentatively assigned to **38** and **39**, respectively (ratio 4:6). Attempts to separate the products failed. The mixture (150 mg, from repeat experiments) was then acetylated with acetyl chloride and triethylamine in methylene chloride. (See the preparation of **29** from **27** + **28**.) Work-up afforded a solid material (153 mg) which appeared homogeneous on t.l.c. (various systems), having the same mobility as **41**. However, the n.m.r. spectrum revealed the product to be a mixture. The benzylidene methine signals overlapped with H-2 signals and therefore could not be analyzed, but there were two distinct singlets for *O*-acetyl protons, at τ 7.97 and 7.88 (intensity ratio 35:65; total intensity, 3H) which were tentatively attributed to **41** and its α-D-*allo* isomer **42**. Attempts to separate the mixture were unsuccessful.

Support of this work by the National Research Council of Canada is gratefully acknowledged.

1. H. H. Baer and W. Rank. Can. J. Chem. **50**, 1292 (1972).
2. R. Scholl. Ber. **29**, 1823 (1896).
3. R. Junell. Z. Physik. Chem. A, **141**, 71 (1929); Svensk. Kem. Tidskr. **46**, 125 (1934); Arkiv Kemi, Mineral. Geol. **11**B, No. 30, 1 (1934).
4. H. H. Baer, W. Rank, and F. Kienzle. Can. J. Chem. **48**, 1302 (1970).
5. W. A. Szarek, D. G. Lance, and R. L. Beach. Carbohydr. Res. **13**, 75 (1970).
6. H. H. Baer and J. Kovář. Can. J. Chem. **49**, 1940 (1971).
7. H. H. Baer. Adv. Carbohydr. Chem. Biochem. **24**, 69 (1969).
8. R. S. Cahn, C. K. Ingold, and V. Prelog. Experientia, **12**, 81 (1956).
9. H. H. Baer and W. Rank. Can. J. Chem. **49**, 3197 (1971).
10. H. H. Baer and W. Rank. Can. J. Chem. **49**, 3192 (1971).
11. D. C. Iffland and G. X. Criner. J. Am. Chem. Soc. **75**, 4047 (1953).
12. E. L. Eliel, N. L. Allinger, S. J. Angyal, and G. A. Morrison. Conformational analysis. Interscience Publishers, New York, N.Y. 1967. (*a*) p. 101; (*b*) p. 44.
13. H. Feltkamp and N. C. Franklin. J. Am. Chem. Soc. **87**, 1616 (1965). F. R. Jensen, C. H. Bushweller, and B. H. Beck. J. Am. Chem. Soc. **91**, 344 (1969).
14. S. S. Novikov, V. I. Slovetskii, A. A. Fainzil'berg, S. A. Shevelev, V. A. Shlyapochnikov, A. I. Ivanov, and V. A. Tartakovskii. *In* Nitro compounds. *Edited by* T. Urbanski. The Macmillan Company. New York, N.Y. 1964. p. 131.
15. S. Hanessian. Carbohydr. Res. **2**, 86 (1966).
16. W. Rank and H. H. Baer. Can. J. Chem. **49**, 3236 (1971).
17. J. Kovář, K. Čapek, and H. H. Baer. Can. J. Chem. **49**, 3960 (1971).

18. H. H. BAER and W. RANK. Can. J. Chem. **50**, 1216 (1972).
19. H. H. BAER, F. KIENZLE, and T. NEILSON. Can. J. Chem. **43**, 1829 (1965).
20. H. H. BAER and T. NEILSON. Can. J. Chem. **43**, 840 (1965).
21. H. H. BAER. *In* Methods in carbohydrate chemistry. Vol. VI. Academic Press Inc., New York, N.Y. 1972. (*a*) p. 241; (*b*) p. 302.
22. H. H. BAER, F. KIENZLE, and F. RAJABALEE. Can. J. Chem. **46**, 80 (1968).
23. H. H. BAER and F. KIENZLE. Can. J. Chem. **45**, 983 (1967).
24. J. E. CHRISTENSEN and L. GOODMAN. Carbohydr. Res. **7**, 510 (1968).

Can. J. Chem. Downloaded from www.nrcresearchpress.com by 210.87.254.40 on 09/05/12
For personal use only.

Reactions of Phosphorus Pentachloride with Ethyl-, Vinyl-, and Ethynyl(trichloromethyl)carbinol and with 1,1,1-Trichloro-3-nonyn-2-ol[1]

E. Wilkins Reeve and Thomas F. Steckel

Chemistry Department, University of Maryland, College Park, Maryland 20742

Received July 20, 1972[2]

Reactions of phosphorus pentachloride with ethyl(trichloromethyl)carbinol (**2**), (trichloromethyl)-vinylcarbinol (**7**), ethynyl(trichloromethyl)carbinol (**11***a*), and 1,1,1-trichloro-3-nonyn-2-ol (**11***b*) have been studied. Whereas the reaction of phenyl(trichloromethyl)carbinol with phosphorus pentachloride leads to a nearly quantitative replacement of the hydroxyl group by chlorine, the reactions of the aliphatic (trichloromethyl)carbinols are more complicated. Thus the reaction of **2** with phosphorus pentachloride gave 18% of the normal product, 1,1,1,2-tetrachlorobutane (**3**), 13% of 1,1,2-trichloro-1-butene (**4**) from a dehydrohalogenation, and a higher boiling phosphate ester – acid chloride mixture. The alkynylcarbinols (**11**) gave tetrachlorobutynes (**12**) as well as tetrachloroallenes (**13**) by allylic rearrangement. A crystalline phosphate ester of **11***a* was also isolated. Several examples are given of catalytic rearrangements in the vapor phase of 1,1,1-trichloro-2-alkenes to 1,1,3-trichloro-1-alkenes.

On a étudié les réactions du pentachlorure de phosphore avec l'éthyl (trichlorométhyl) carbinol (**2**), le (trichlorométhyl) vinylcarbinol (**7**), l'éthènyl (trichlorométhyl) carbinol (**11***a*) et le trichloro-1,1,1 nonyn-3 ol-2 (**11***b*). Alors que la réaction du phényl (trichlorométhyl) carbinol avec le pentachlorure de phosphore conduit pratiquement quantitativement à la substitution du groupe hydroxyle par un chlore, la réaction avec les (trichlorométhyl) carbinols aliphatiques semble être beaucoup plus compliquée. Ainsi, la réaction de **2** avec le pentachlorure de phosphore conduit à la formation du produit normal (18%), tétrachloro-1,1,1,2 butane, (**3**) ainsi qu'à la formation du trichloro-1,1,2 butène-1 (**4**) (13%), provenant d'une déhydrohalogénation, et d'un mélange phosphate d'ester – chlorure d'acide ayant un point d'ébullition plus élevé. Les carbinols possèdant des groupes alcynes (**11**) produisent des tétrachlorobutynes (**12**) de même que des tétrachloroallènes (**13**) selon un mécanisme impliquant un réarrangement allylique. Un phosphate d'ester cristallin de **11***a* a aussi été isolé. Plusieurs exemples de réarrangements catalytiques en phase vapeur sont rapportés pour les trichloro-1,1,1 alcènes-2 entraînant la formation de trichloro-1,1,3 alcènes-1.

[Traduit par le journal]

Can. J. Chem., **51**, 2017 (1973)

The reaction of phosphorus pentachloride with phenyl(trichloromethyl)carbinol is known to give the corresponding chloride in 87% yield (1). When phenyl is replaced by an aliphatic group, a more complicated set of reactions occurs. The purpose of this work was to study the reactions of the compounds R—CHOH—CCl_3, where R is ethyl, vinyl, ethynyl, and nonynyl, with phosphorus pentachloride to determine the products formed in these reactions. These reactions are of importance because the hydroxyl group in trichloromethylcarbinols cannot be replaced by chlorine by treatment of the carbinol with concentrated hydrochloric acid; the presence of the trichloromethyl group prevents the usual displacement reaction from occurring, even when the alcohol is of the benzylic or allylic type.

The reaction of phosphorus pentachloride with alcohols has been used for over a century to replace the hydroxyl group with chlorine, but the mechanism by which this occurs is even now only imperfectly understood. Several facts are known. First, phosphorus pentachloride is $(PCl_4)^+(PCl_6)^-$ in the crystalline state (2) and in solvents such as phosphorus oxychloride, nitrobenzene, acetonitrile, and benzoyl chloride (3). The reaction occurs with initial stepwise replacement by alkoxy of the chlorines bound to phosphorus but no one has been able to isolate the pentacoordinate chloro ester, $ROPCl_4$ (4). This agrees with the observation that, while many pentacoordinate compounds of phosphorus are known, (5) they appear to be uncommon intermediates in nucleophilic displacements at tetracoordinate phosphorus (6). The reaction products include the alkyl chloride, always with inversion of configuration in the case of saturated alcohols (7); mono-, di-, and triphosphate esters, particularly from primary alcohols (4); and olefins from secondary alcohols, often accompanied by *trans*

[1]Taken in part from the doctoral thesis of Thomas F. Steckel, University of Maryland, 1970.

[2]Revision received March 6, 1973.

Can. J. Chem. Downloaded from www.nrcresearchpress.com by 210.87.254.5 on 09/05/12
For personal use only.

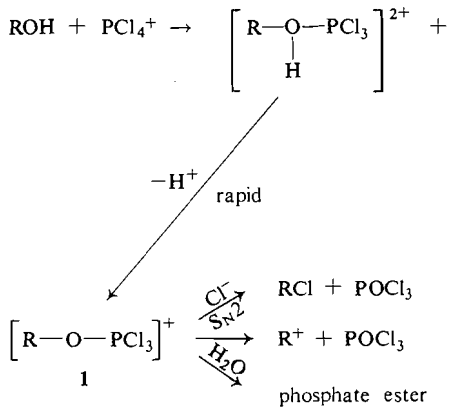

SCHEME 1

addition of chlorine to the double bond (8). Scheme 1 is consistent with the above experimental facts.

The above scheme incorporates the ideas of Gerrard (4) but assumes tetracoordinate intermediates. Independent evidence for the existence of **1** has been obtained from studies of the variation of electrical conductivity during the reaction of alcohols with phosphorus pentachloride in benzene (9).

In our work with vinyl and acetylenic carbinols (Schemes 3 and 4) the reaction intermediates must have a high degree of carbonium ion character to account for the allylic rearrangements observed, and the incipient carbonium ion could be formed by the heterolysis of the alkyl–oxygen bond of **1**. **1** can also react with excess carbinol with the replacement of two more of the phosphorus chlorines.

The reaction of ethyl(trichloromethyl)carbinol (**2**) with phosphorus pentachloride, which has not been studied previously, was found to yield four chlorinated hydrocarbons and ethyl α-chlorobutyrate (Scheme 2). The structures of the products were deduced from their spectra. Compound **5** rearranged completely to **6** during g.l.p.c. analysis.

With benzene instead of ether as the solvent, compounds **3**, **4**, and **5** + **6** were obtained in yields of 4, 2, and 8% respectively, ethyl α-chlorobutyrate was absent, and the major product consisted of another mixture distilling about 100° higher. This contained phosphorus, exhibited strong i.r. absorption at 1295 cm^{-1} characteristic of P=O, and showed splitting of the carbinyl proton attributable to phosphorus. It was concluded to be a mixture of mono- and dichlorophosphate esters of the starting carbinol. The residue appeared to be mostly the triphosphate ester.

As is the case with many unsubstituted alcohols (4), it is clear there is competition between phosphate ester formation and replacement of the hydroxyl group by chlorine. During the latter reaction, dehydrohalogenation occurs to **4** and **5**. Compound **4** is stable, but **5** is thermally unstable; on heating a mixture of **3**, **4**, and **5** at 135° for 2 h, about 50% of **5** is converted to **6**.

The tertiary alcohol, dimethyl(trichloromethyl)carbinol, does not react with phosphorus pentachloride under the above conditions. Others have found that the conversion of this carbinol to the chloride requires several hours heating at 80° with phosphorus pentachloride (10).

Colonge and Lartigau report that (trichloromethyl)vinylcarbinol and phosphorus pentachloride give *trans*-1,1,1,4-tetrachloro-2-butene (**9**) in 48% yield using ether as a solvent (11) (see Scheme 3). We duplicated their results and in addition found that, using benzene as the solvent, **9** was obtained in 34% yield and, based on i.r. and n.m.r. spectra, was contaminated with substituted vinylbenzenes. Unlike most allyl alcohols, (trichloromethyl)vinylcarbinol does not react with concentrated hydrochloric acid containing zinc chloride even after standing for 24 h at room temperature.

Compound **8** could not be isolated; only its allylic isomer **9** was obtained. Colonge and Ducarre (12) reported, on the basis of spectral evidence only, that **9** was stable to heat but was partially converted to **10** by light. We have found that this isomerization occurs quantitatively at 125° during g.l.p.c., and can be carried out catalytically on a preparative scale in 81% conversion by a single pass of the vapors of **9** over copper metal beads at 220°. The driving force for this reaction is probably the resonance stabilization afforded by the vinylidene chloride structure as compared to the unconjugated trichloromethyl group. Over alumina, **9** underwent decomposition.

The reaction of ethynyl(trichloromethyl)carbinol with phosphorus pentachloride has not been studied previously. As with the (trichloromethyl)vinylcarbinol, the reaction is unusual in that the expected chloride (**12***a*) is a minor product; the major component of the volatile

Can. J. Chem. Downloaded from www.nrcresearchpress.com by 210.87.254.5 on 09/05/12
For personal use only.

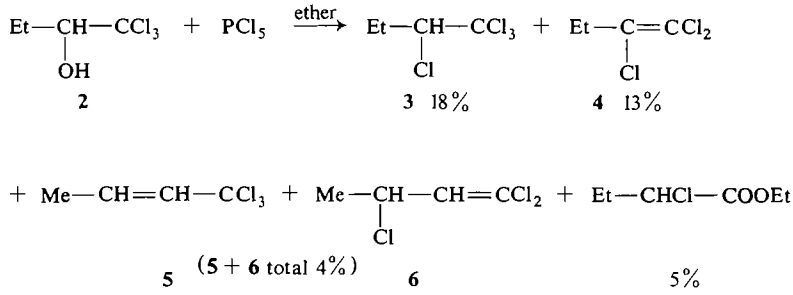

SCHEME 2

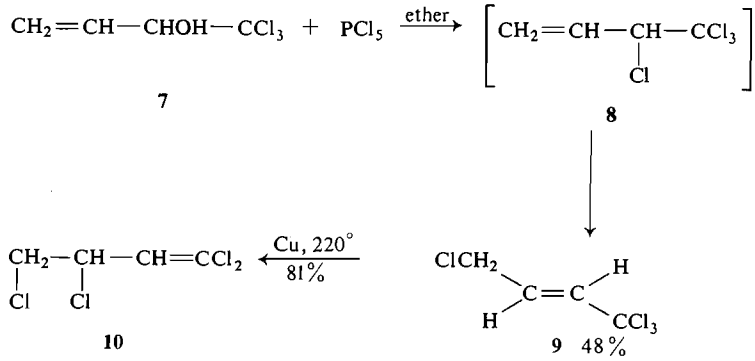

SCHEME 3

fraction of the reaction products is the allene **13***a* formed by an allylic rearrangement accompanying the displacement of the hydroxyl group (see Scheme 4). This presumably occurs by an S_Ni' mechanism.

The phosphate ester **14** could be isolated only when the reaction was carried out by adding phosphorus pentachloride, suspended in benzene, to a benzene solution of the starting carbinol **11***a*. The phosphate ester crystallized from the residue after the volatile fraction had been distilled. Products **12***a* and **13***a* are best obtained by adding the carbinol to the phosphorus pentachloride; thus a 7% yield of the alkyne **12***a* was obtained versus 1% by the reverse addition, but no phosphate ester could be isolated from the non-volatile portion. It seems likely that the triester was not formed with this mode of addition because the phosphorus pentachloride was in excess at all times during the reaction. This might give the monoalkyl chlorophosphate time to react to form the chlorinated hydrocarbons.

The alkyne **12***a* was a stable compound, not isomerized by distillation, by passage through a g.l.p.c. apparatus, or by passage over various catalysts in the vapor phase at 218°. In contrast, the allene **13***a* isomerized quantitatively to the butadiene **15***a* during g.l.p.c. regardless of the chromatographic column employed. The allene did not isomerize during distillation. Since chemical methods of separating the alkyne and allene isomers were unsuccessful, our best sample of **13***a* was an 85% pure (by n.m.r.) fraction, obtained by distillation, with the balance being the alkyne **12***a* together with minor impurities.

The rearrangement of the allene **13***a* to the butadiene **15***a* was found to occur quantitatively during a single pass of the allene in the vapor state over alumina at 218°. Copper beads were also effective in catalyzing the isomerization at this temperature, but two passes were necessary to obtain a 90% conversion. Glass wool, sand, and stainless steel wire loops had no catalytic effect. All attempts to carry out the isomerization

Can. J. Chem. Downloaded from www.nrcresearchpress.com by 210.87.254.5 on 09/05/12
For personal use only.

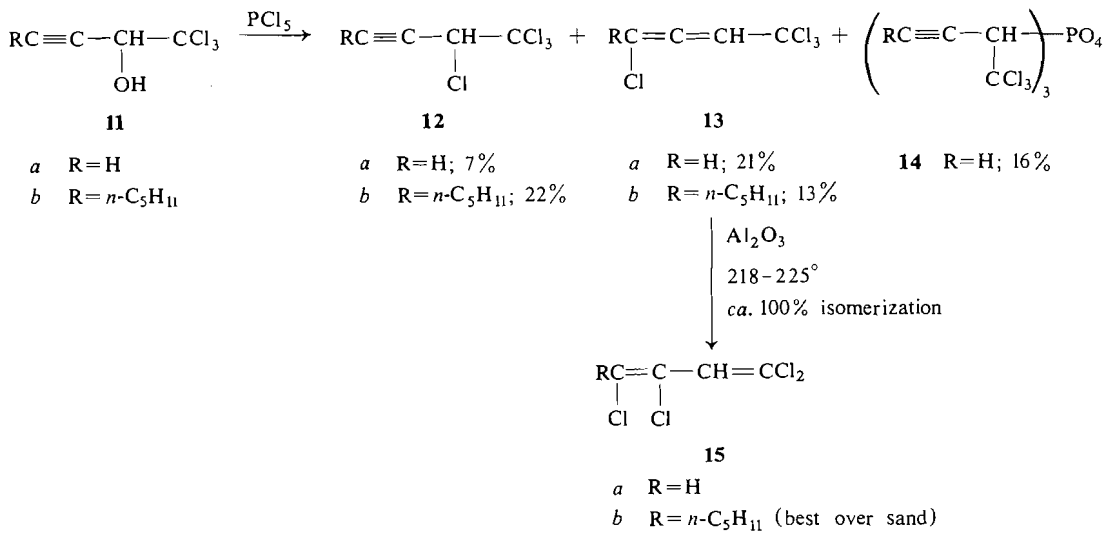

SCHEME 4

in the liquid phase over catalysts such as metallic copper, cupric chloride, copper chromite hydrogenation catalyst, and silica gel were unsuccessful.

To eliminate whatever effect the acetylenic proton might have on the above reactions, *n*-amylacetylene was prepared and converted to 1,1,1-trichloro-3-nonyn-2-ol (**11***b*) by reaction with chloral. The reaction of **11***b* with phosphorus pentachloride was studied by adding the phosphorus pentachloride to the carbinol using benzene as solvent. The crude product containing **12***b* (major component) and its allylic rearrangement product (**13***b*) was obtained in 84% yield (before distillation; 35% after distillation). The undistilled and the distilled materials gave identical n.m.r. spectra. Compound **12***b* was the major fraction formed; this involved a normal replacement of the hydroxyl group. The product **13***b* from the allylic rearrangement was the minor product.

The allene **13***b* rearranged to the diene **15***b* on g.l.p.c., and thus **13***b* could not be obtained pure. This rearrangement could also be carried out as before in the vapor phase at 225° over a variety of substances including alumina, sand mixed with copper powder, and sand alone. Since sand, which is considered to have no catalytic activity, seemed to be best, it appears that the conversion is thermal rather than catalytic. *cis* and *trans* isomers of **15***b* are possible and evidence for their existence was seen in the n.m.r. spectrum where two signals in the ratio of 3.5:1 were observed for the vinyl proton. The isomers were not separated by the g.l.p.c. columns used.

The allene **13***b* was unstable in the liquid phase. After 2 months at room temperature or 30 min at 150°, it was changed to a polymeric material. On heating **13***b* at 150° with finely divided copper metal for 10 min, a dark brown mixture was formed which contained some diene **15***b*. Thus in this case, copper has a limited catalytic effect in the liquid phase.

The alkyne **12***b*, in contrast to the allene **13***b*, was stable in the liquid phase, even when heated either alone or in the presence of copper metal or alumina. It was unaffected by passage of the vapor at 225° over sand or a 1:1 sand and copper powder mixture. However, over alumina at 225°, **12***b* lost two chlorine atoms to give 1,1-dichloro-1-nonen-3-yne (**16**) in about 10% yield, and no starting material could be recovered. During g.l.p.c. analysis at 195°, **12***b* also gave **16** in 5 to 10% yield, but most of the **12***b* could be recovered.

Experimental

Melting points and boiling points are corrected. The i.r. spectra were recorded on a Perkin–Elmer instrument Model 337, using thin films for liquid samples and potassium bromide pellets for solid samples. The mass spectra were recorded on a Varian M-66 mass spectrometer, and the n.m.r. spectra with a Varian A60A instrument. Chemical-shift values are expressed as δ values (p.p.m.) downfield from tetramethylsilane internal standard. Vapor phase chromatographic analyses were carried out on an F & M Model 300 with a helium flow

Can. J. Chem. Downloaded from www.nrcresearchpress.com by 210.87.254.5 on 09/05/12
For personal use only.

Can. J. Chem. Downloaded from www.nrcresearchpress.com by 210.87.254.5 on 09/05/12
For personal use only.

rate of 50 ml/min. The percentage composition figures given for the various fractions are g.l.p.c. percentages. The following chromatographic columns were used: Apiezon (10% Apiezon-L on 60/80 mesh silanized diatomaceous earth (Diatoport-S) packed in a 2 m × 6.35 mm copper tube), silicon fluid (20% Dow-Corning Silicon Fluid #710 on 30/60 mesh Chromosorb P packed in a 2 m × 6.35 mm copper tube), silicon gum rubber (F & M silicon gum rubber on Chromosorb P packed in a 0.7 m × 6.35 mm stainless steel tube).

Elemental microanalyses were performed by Dr. Franz J. Kasler.

*Ethynyl(trichloromethyl)carbinol (**11a**)*

This was prepared by a modification of Shapiro's method (13) in 51% yield from the reaction of sodium acetylide (14) and commercial anhydrous chloral at 0° for 2 h; b.p. 74–82° (14 mm) (lit. (13) 77–81° (16 mm)); n.m.r. ($CDCl_3$) δ 4.90 (1 H, d, J = 2.1 Hz, —C*H*OH—), 3.96 (1 H, broad s, —O*H*), 2.78 (1 H, d, J = 2.1 Hz, *H*C≡).

*1,1,1-Trichloro-3-nonyn-2-ol (**11b**)*

1-Heptyne (15) (32 g, 0.33 mol) in an equal volume of anhydrous ether was added over a 45-min period to 0.3 mol of ethylmagnesium bromide in refluxing ether. After refluxing 2 h, the reaction mixture was cooled in an ice bath under a nitrogen atmosphere and 49 g (0.33 mol) of chloral in an equal volume of ether was added over 1 h; the mixture was then stirred for an additional hour at room temperature. There was obtained 62 g (76%) of the carbinol **11***b*; b.p. 144–149° (16 mm) (lit. (16) 106–110° (4 mm) and 141–142° (12 mm)); n.m.r. (CCl_4) δ 4.69 (1 H, m, —C*H*OH—), 3.44 (1 H, s, O*H*), 2.26 (2 H, m, —CH_2C≡), 1.41 (6 H, m, (—CH_2—)$_3$), 0.91 (t, 3, CH_3—).

*(Trichloromethyl)vinylcarbinol (**7**)*

Twenty-six grams (0.15 mol) of ethynyl(trichloromethyl)carbinol (**11***a*) dissolved in 150 ml ethanol was hydrogenated at room temperature over 1.2 g of 10% palladium-on-carbon catalyst (17) until 0.15 mol of hydrogen had been absorbed. Distillation of the product combined from three such runs gave 61 g (78%) of the carbinol **7**; b.p. 84–87° (30 mm) (lit. 68–69° (12 mm) (13) and 75° (17 mm) (18)); n.m.r. ($CDCl_3$) δ 6.35–5.35 (3 H, m, H_2C=C*H*—), 4.54 (1 H, doublet with some long range splitting, J = 4.8 Hz, J' = 2.4 Hz, —C*H*OH—), 3.6 (1 H, s, —O*H*). The n.m.r. spectra showed the product to be 90–92% pure. Also present were peaks corresponding to the presence of approximately 5% each of **2** and **11***a*.

*Ethyl(trichloromethyl)carbinol (**2**)*

The ethynyl carbinol **11***a* was hydrogenated as above, but the reaction was allowed to go to completion. This took about 20 min, and shaking was continued for another 10 min. From 104 g of **11***a*, there was obtained on distillation 78 g (74%) of the carbinol 2; b.p. 79–84° (28 mm) (lit. (13) 67° (13 mm)); n.m.r. (CCl_4) δ 3.98 (1 H, d of d, J = 9.1, J' = 2.1 Hz, —C*H*OH—), 3.3 (1 H, s, —O*H*), 2.54–1.33 (2 H, m, —CH_2—), 1.12 (3 H, t, J = 7.2 Hz, CH_3—).

*Reaction of Ethyl(trichloromethyl)carbinol (**2**) with Phosphorus Pentachloride*

To 4.4 g (0.025 mol) of **2** dissolved in 16 ml of ether, stirred with a magnetic stirrer and cooled with an ice bath, was added a slurry of 10.4 g (0.05 mol) of phosphorus pentachloride in ether over a period of 10 min. The reaction mixture was stirred for 2 h at room temperature and then decomposed by pouring into ice and water. To this was added 20% potassium hydroxide solution in small portions until the water layer was just basic to litmus; the organic layer was separated, washed twice with 5% sodium carbonate solution, twice with water, dried ($MgSO_4$), concentrated, and distilled giving 1.7 g of a mixture (b.p. 61–76° (34 mm); lit. for **4**: (19) 58° (46 mm), for **6**: (20) 64° (50 mm)). G.l.p.c. analysis (silicon fluid column at 100°) showed the mixture to consist of 49% *1,1,1,2-tetrachlorobutane* (**3**) (18%), 30% *1,1,2-trichloro-1-butene* (**4**) (13%), 10% *1,1,3-trichloro-1-butene* (**6**) (4%), and 11% ethyl α-chlorobutyrate (12%). These compounds had retention times of 42, 15, 17, and 28 min respectively. The presence of 1,1,1-trichloro-2-butene (**5**) was shown by the n.m.r. spectrum of the distilled mixture of chlorinated hydrocarbons prior to g.l.p.c. analysis; it rearranged to **6** during g.l.p.c. analysis.

Spectral data on **3** purified by g.l.p.c.: i.r. of stronger bands (neat) 2970, 2935, 2875, 1450, 1090, 1015, 830, 790–770 (s), 680, and 610 cm^{-1}; n.m.r. (CCl_4) δ 4.25 (1 H, d of d, J = 10.3, J' = 2.3 Hz, —C*H*Cl—), 2.7–1.5 (2 H, m, CH_3CH_2—), 1.2 (3 H, t, J = 7.3 Hz, CH_3—).

Data on **4** purified by g.l.p.c.: i.r. of stronger bands (neat) 2975, 2930, 2875, 1600, 1455, 1425, 1130, 1045, 955, 900 (s), 810 (s), and 735 cm^{-1}; n.m.r. (CCl_4) δ 2.64 (2 H, quartet, J = 7.4 Hz, CH_3CH_2—), 1.18 (3 H, t, J = 7.4 Hz, CH_3—).

Data on **6** purified by g.l.p.c.: i.r. of stronger bands (neat) 2980, 2920, 1620 (s), 1445, 1375, 1260, 1215 (s), 1140 (s), 1010 (s), 925, 885 (s), 835, 670, and 620 (s) cm^{-1}; n.m.r. (CCl_4) δ 6.02 (1 H, d, J = 9.8 Hz, —C*H*=), 4.77 (1 H, m, —C*H*Cl—), 1.62 (3 H, d, J = 6.7 Hz, CH_3).

Identification of ethyl α-chlorobutyrate was based on spectral data obtained on the sample purified by g.l.p.c.: i.r. (neat) 1750 cm^{-1} (ester C=O) (lit. (21) 1750 cm^{-1}; n.m.r. (CCl_4) δ 4.18 (3 H, m, —C*H*Cl— and —CH_2O—), 1.99 (2 H, m, —CH_2CHCl—), 1.32 (3 H, t, J = 7.1 Hz, CH_3—), 1.03 (3 H, t, J = 7.4, CH_3).

Spectral data on **5** was obtained on a sample prepared from **2** and phosphorus pentachloride using benzene as solvent. The reaction mixture was distilled and the major component comprising 47% of the volatile fraction was identified as *1,1,1-trichloro-2-butene* (**5**) from the n.m.r. spectrum of the mixture. It rearranged to **6** on g.l.p.c. analysis and so its spectral data were measured using the 47% mixture: i.r. (neat) 1655 cm^{-1} (C=C); n.m.r. (CCl_4) δ 6.03 (2 H, m, —C*H*=C*H*—), 1.87 (3 H, d, J = 4.9 Hz, CH_3—).

In a separate experiment, the reaction mixture, after pouring into ice and water, was separated and washed with water ten times, stirred with water for 45 min, and washed twice more. Even though no alkali was used in the work-up, the composition of the undistilled product was nearly the same as above; by g.l.p.c.: 53% **3**, 11% **4**, 14% **5** plus **6**, and 18% ethyl α-chlorobutyrate; by n.m.r.: 60% **3** + ethyl α-chlorobutyrate, 21% **4**, 9% **5**, and 6% **6**.

*Reaction of (Trichloromethyl)vinylcarbinol (**7**) with Phosphorus Pentachloride*

To 3.5 g (0.02 mol) of **7** in 13 ml of dry ether at 0° was added a slurry of 8.3 g (0.04 mol) of phosphorus pentachloride suspended in 12 ml of dry ether over a 30 min period under the same conditions as in the reaction of **2**

Can. J. Chem. Downloaded from www.nrcresearchpress.com by 210.87.254.5 on 09/05/12
For personal use only.

above. There was obtained 2.4 g (60% yield) of material prior to distillation, and its n.m.r. spectrum showed it to be 97% *trans-1,1,1,4-tetrachloro-2-butene* (**9**). Distillation gave 1.8 g (48%) of **9**: b.p. 85–88° (21 mm) (lit. (11) b.p. 76–78° (15 mm)). The i.r. was identical with that in the literature (11). The n.m.r. (CCl_4) spectrum showed two narrow complex multiplets at δ 6.42 and 4.15 in the ratio of 1:1 (lit. (12) δ 6.4 (s), 4.1 (m)). The material gave proper elemental analyses for carbon, hydrogen, and chlorine.

*Catalytic Rearrangement of **9** to **10***

A small amount of **9** was injected through a septum into an 8 mm glass U tube packed with copper beads (2 mm diameter) and immersed in a Wood's metal bath (220°). Using nitrogen as a carrier gas, 81% of **10** was collected. No isomerization occurred with sand (Fisher Scientific sea sand) replacing copper. An analytical sample of **10**, *1,1,3,4-tetrachloro-1-butene*, was obtained by collection from the Apiezon g.l.p.c. column. The retention time was 8 min at 125°. Spectral data: i.r. of stronger bands (neat) 3040–2940 (w), 1615 (s), 1440, 1425, 1285, 1205, 1165, 1040, 930, 905 (s), 885 (s), 835 (s), 750, 710, and 625 cm^{-1}; n.m.r. (CCl_4) δ 6.02 (1 H, d, J = 9.7 Hz, —C*H*═), 5.05–4.65 (1 H, m, —C*H*Cl—), multiplet of four peaks at 3.79, 3.77, 3.71, and 3.64 (2 H, m, ClCH_2—). The n.m.r. spectrum is essentially the same as that reported by Colonge and Ducarre (12) for their 60% pure sample of **10**.

Anal. Calcd. for $C_4H_4Cl_4$: C, 24.77; H, 2.08; Cl, 73.15. Found: C, 24.91; H, 1.97; Cl, 73.04.

*Reaction of Ethynyl(trichloromethyl)carbinol (**11a**) with Phosphorus Pentachloride*

To 19.2 g (0.11 mol) of **11***a* dissolved in 60 ml of benzene (stirred and cooled in ice) was added (1 h) a slurry of 47 g (0.225 mol) of phosphorus pentachloride in 40 ml of benzene. After 1 h stirring at 25°, the mixture was poured into ice and the benzene layer was washed (10% sodium carbonate solution, then water), dried ($MgSO_4$), concentrated, and distilled (b.p. 76–81° (26 mm)) giving 4.5 g of a mixture consisting of 5% *3,4,4,4-tetrachloro-1-butyne* (**12***a*) (1% yield), 85% *1,4,4,4-tetrachloro-1,2-butadiene* (**13***a*) (17% yield), and 10% of other compounds (by g.l.p.c. analysis (silicon fluid column at 140°) and n.m.r.). Compounds **12***a* and **13***a* had apparent retention times of 10.7 and 12.3 min respectively; the latter retention time was that of **15***a*, isomerization having occurred. The residue from the distillation of the crude material solidified on cooling, and after recrystallization from cyclohexane, 3.4 g (16%) of *tris(1,1,1-trichloro-3-butyne-2-ol) phosphate* (**14**) was obtained, m.p. 79–80°.

Adding 13 g (0.075 mol) of the carbinol **11***a*, dissolved in 10 ml of benzene, to 31.2 g (0.15 mol) of phosphorus pentachloride suspended in 30 ml of benzene under the above conditions gave 4.6 g of volatile material, b.p. 85–90° (28 mm). G.l.p.c. and n.m.r. analyses showed it to be a mixture of **12***a* (7% yield) and **13***a* (21% yield) with about 10% of impurities. The sample of **12***a* for analysis was prepared by this procedure. No phosphate ester (**14**) could be obtained from the residue.

Spectral and analytical data on *3,4,4,4-tetrachloro-1-butyne* (**12***a*) purified by g.l.p.c.: i.r. of stronger bands (neat) 3300, 2940, 2130, 1210, 965, 815, 735, 665, and 610 cm^{-1}; n.m.r. ($CDCl_3$) δ 5.17 (1 H, d, J = 2.3 Hz, —C*H*Cl—), 2.84 (1 H, d, J = 2.3 Hz, *H*C≡); mass spectrum (70 eV), *M/e* very weak molecular ion peaks at 190 and 192.

Anal. Calcd. for $C_4H_2Cl_4$: C, 25.03; H, 1.05; Cl, 73.92. Found: C, 25.06; H, 1.11; Cl, 73.65.

Spectral and analytical data on *1,4,4,4-tetrachloro-1,2-butadiene* (**13***a*) of 85% purity obtained by distillation: i.r. of stronger bands (neat) 3290, 3145, 1955, 1345, 1225, 1130, 1110, 850, 805, 775, 755, 695, and 600 cm^{-1}; n.m.r. (CCl_4) δ 6.59 (1 H, d, J = 5.5 Hz, ClC*H*═), 6.21 (1 H, d, J = 5.5 Hz, ═C*H*—CCl_3); the mass spectrum (70 eV) showed the molecular ion isotopes as a cluster at *M/e* (relative intensity) 190 (100), 192 (125), 194 (52), 196 (13), and 198 (1). Molecular ion peaks for this compound are much stronger than for **12***a*, but not as strong as for **15***a*.

Anal. Calcd. for $C_4H_2Cl_4$: C, 25.03; H, 1.05; Cl, 73.92. Found: C, 25.30; H, 1.22; Cl, 73.64.

Spectral and analytical data on *tris(1,1,1-trichloro-3-butyne-2-ol)phosphate* (**14**): i.r. of stronger bands (KBr) 3290, 2935, 2135, 1280, 1070, 1030, 970, 910, 825, 800, and 670 cm^{-1}; n.m.r. (CCl_4) δ 5.50 (1 H, d of d, J = 8.2 Hz, J' = 2.1 Hz, >C*H*—CCl_3), 2.83 (1 H, d of d, J = 1 Hz, J' = 2.1 Hz, *H*C≡).

Anal. Calcd. for $C_{12}H_6Cl_9O_4P$: C, 25.54; H, 1.07; Cl, 56.55. Found: C, 25.30; H, 1.10; Cl, 56.35.

*Rearrangement of **13a** to **15a***

This occurred quantitatively during g.l.p.c. analyses regardless of the column employed. It was accomplished on a preparative scale over an alumina catalyst (Fisher activated alumina, 8–14 mesh) at 218° using the glass U tube apparatus described above for the isomerization of **9** to **10**. The isomerization was nearly 100%. The analytical sample of *1,1,3,4-tetrachloro-1,3-butadiene* (**15***a*) was purified by g.l.p.c. (silicon fluid column at 140°); i.r. of stronger bands (neat) 3080, 3035, 1615, 1585, 1255, 1115, 935, 905, 825, and 660 cm^{-1}; n.m.r. ($CDCl_3$) δ 6.60 (1 H, s), 6.36 (1 H, s); the mass spectrum (70 eV) showed the molecular ion isotopes as a cluster at *M/e* (relative intensity) 190 (100), 192 (126), 194 (62), 196 (12), 198 (1).

Anal. Calcd. for $C_4H_2Cl_4$: C, 25.03; H, 1.05; Cl, 73.92. Found: C, 25.30; H, 1.15, Cl, 74.10.

*Reaction of 1,1,1-Trichloro-3-nonyn-2-ol (**11b**) with Phosphorus Pentachloride*

To 7.3 g (0.03 mol) of **11***b* dissolved in 25 ml of benzene (stirred and cooled in ice) was added (30 min) a slurry of 12.5 g (0.06 mol) of phosphorus pentachloride in 15 ml of benzene. After 1 h stirring at 25°, the mixture was poured into ice and neutralized with 20% potassium hydroxide solution. The benzene layer was washed, dried and concentrated as before to yield 6.6 g of a crude product. Distillation was difficult because the material foamed, but was accomplished using Dow defoamers A and Q. There was obtained 2.9 g of a mixture distilling between 147–149° (22 mm). G.l.p.c. analysis (silicon fluid column at 195°) and its n.m.r. spectrum showed the mixture to consist of 60% *1,1,1,2-tetrachloro-3-nonyne* (**12***b*) (22% yield) and 35% *1,1,1,4-tetrachloro-2,3-nonadiene* (**13***b*) (13% yield). **12***b* and **13***b* had apparent retention times of 27 and 21 min respectively; the latter retention time was that of **15***b*, isomerization having occurred.

Spectral and analytical data on *1,1,1,2-tetrachloro-3-nonyne* (**12***b*) purified by g.l.p.c., first on the silicon fluid column at 195° (some decomposition), then on silicon gum rubber at 155°; i.r. of stronger bands (neat) 2960,

Can. J. Chem. Downloaded from www.nrcresearchpress.com by 210.87.254.5 on 09/05/12
For personal use only.

2935, 2860, 2240, 1460, 1285, 1210, 845, 815, 780, 750, 730, and 612 cm^{-1}; n.m.r. (CCl_4) δ 5.05 (1 H, t, J = 2 Hz, —C*H*Cl—), 2.30 (2 H, m, —CH_2C≡), 1.43 (6 H, m, CH_3—CH_2—CH_2—CH_2—), 0.92 (3 H, poorly resolved triplet, CH_3—); the mass spectrum (70 eV) showed the molecular ion isotopes as a cluster at *M/e* (relative intensity) 260 (100), 262 (136), 264 (68), 266 (14), and 268 (1).

Anal. Calcd. for $C_9H_{12}Cl_4$: C, 41.26; H, 4.62; Cl, 54.12. Found: C, 41.50; H, 4.47; Cl, 53.85.

Spectral data on *1,1,1,4-tetrachloro-2,3-nonadiene* (**13***b*) obtained on a distilled sample consisting of 35% **13***b* and 60% **12***b*: i.r. (neat) 1970 cm^{-1} (allene); n.m.r. (CCl_4) δ 6.16 (1 H, t, J = 2.6 Hz, =C=C*H*—).

Rearrangement of **13***b* *to* **15***b*

This could be carried out at 220–225° over sand (preferred), a sand-copper powder mixture, or alumina using the glass U tube apparatus described above for the isomerization of **9** to **10**. The analytical sample of *1,1,3,4-tetrachloro-1,3-nonadiene* (**15***b*) was prepared and purified by g.l.p.c., first on the silicon fluid column at 195° (retention time = 21 min), and then reinjected on the Apiezon column at 170° (retention time = 19 min); i.r. of stronger bands (neat) 3030, 2960, 2930, 2860, 1590, 1460, 1370, 1265, 1110, 930–910, 850, 820, 750, and 675–655 cm^{-1}; n.m.r. (CCl_4) δ 6.50 and 6.34 (1 H, singlets in ratio of 3.5:1, *cis* and *trans* —C*H*=?), 2.53 (2 H, m, —CH_2—CCl=), 1.43 (6 H, m, —CH_2—CH_2—CH_2—), 0.92 (3 H, poorly resolved triplet, CH_3); the mass spectrum (70 eV) showed the molecular ion isotopes as a cluster at *M/e* (relative intensity) 260 (100), 262 (129), 264 (57), 266 (12), and 268 (1).

Anal. Calcd. for $C_9H_{12}Cl_4$: C, 41.26; H, 4.62; Cl, 54.12. Found: C, 41.48; H, 4.40; Cl, 53.93.

1,1-Dichloro-1-nonen-3-yne (**16**)

This was formed in 5% yield during g.l.p.c. of **12***b* on the silicon fluid column at 195°. The column effluent was collected and reinjected on the Apiezon column at 170°; the retention times of **12***b* and **16** on this latter column were 18 and 6 min respectively. Spectral and analytical data on **16**: i.r. (neat) 3030, 2960, 2930, 2850, 2210, 1580, 1460, 1275, 1170, 940–925, 825, 725, and 655 cm^{-1}; n.m.r. (CCl_4) δ 5.85 (1 H, t, J = 2 Hz, ≡C—C*H*=), 2.33 (2 H, m, —CH_2—C≡), 1.43 (6 H, m, —CH_2—CH_2—CH_2—), 0.93 (3 H, poorly resolved triplet, CH_3—); the mass spectrum (70 eV) showed the molecular ion isotopes as a cluster at *M/e* (relative intensity) 190 (100), 192 (58), 194 (8).

Anal. Calcd. for $C_9H_{12}Cl_2$: C, 56.57; H, 6.33; Cl, 37.10. Found: C, 56.30; H, 6.06; Cl, 36.80.

Compound **16** was also obtained in about 10% yield by passage of the vapors of **12***b* over alumina at 225°.

1. SH. MAMEDOV, G. YA. LERNER, and D. N. KHYDYROV. *Zh. Obshch. Khim.* **34**, 53 (1964); Chem. Abstr. **60**, 13172 (1964).
2. D. CLARK, H. M. POWELL, and A. F. WELLS. J. Chem. Soc. 642 (1942).
3. D. S. PAYNE. J. Chem. Soc. 1052 (1953).
4. W. GERRARD and R. J. PHILLIPS. Chem. Ind. (London), 540 (1952).
5. E. L. MUETTERTIES and R. A. SCHUNN. Quart. Rev. Chem. Soc. **20**, 245 (1966).
6. R. D. COOK, P. C. TURLEY, C. E. DIEBERT, A. H. FIERMAN, and P. HAAKE. J. Am. Chem. Soc. **94**, 9260 (1972).
7. C. K. INGOLD. Structure and mechanism in organic chemistry. Cornell University Press, Ithaca, N.Y. 1953. p. 392.
8. H. L. GOERING and F. H. MCCARRON. J. Am. Chem. Soc. **78**, 2270 (1956).
9. M. MURAKAMI and Y. SASAKI. Mem. Inst. Sci. Ind. Research, Osaka Univ. **10**, 181 (1953); Chem. Abstr. **49**, 6864 (1955).
10. S. M. MCELVAIN and C. L. STEVENS. J. Am. Chem. Soc. **69**, 2667 (1947); W. GERRARD and P. L. WYVILL. Res. Appl. Ind. **2**, 536 (1949); Chem. Abstr. **44**, 2440 (1950).
11. J. COLONGE and G. LARTIGAU. Justus Liebigs Ann. Chem. **684**, 10 (1965).
12. J. COLONGE and M. DUCARRE. C.R. Acad. Sci. **261**, 5141 (1965).
13. S. L. SHAPIRO, H. SOLOWAY, and L. FREEDMAN. J. Am. Chem. Soc. **77**, 4874 (1955); D. C. BISHOP, S. C. R. MEACOCK, and W. R. N. WILLIAMSON. J. Chem. Soc. C, 670 (1966).
14. J. H. SAUNDERS. Organic syntheses. Coll. Vol. III. Wiley, New York, N.Y. 1955. p. 416; also ref. 15.
15. K. N. CAMPBELL and B. K. CAMPBELL. Organic syntheses. Coll. Vol. IV. Wiley, New York, N.Y. 1963. p. 119, note 7.
16. N. E. KOLOGRIVONA and V. N. BELOV. Zh. Obshch. Khim. **28**, 3105 (1958), from Chem. Abstr. **53**, 10027 (1959); C. MOUREU and H. DESMOTS. Bull. Soc. Chim. Fr. [3], **27**, 369 (1902).
17. R. MOZINGO. Organic syntheses. Coll. Vol. III. Wiley, New York, N.Y. 1955. p. 687, preparation D.
18. H. NORMANT and J. FICINI. Bull. Soc. Chim. Fr. 1441 (1956).
19. A. T. MORSE and L. C. LEITCH. Can. J. Chem. **33**, 6 (1955).
20. E. C. KOOYMAN and W. M. WAGNER. Rec. Trav. Chim. Pays-Bas, **77**, 923 (1958).
21. A. KIRRMANN and F. DRUESNE. Bull. Soc. Chim. Fr. 1098 (1964).

Silyl-substituted α,β-Unsaturated Ketones from the Reaction of Silylvinylmetallic Reagents with Acid Anhydrides

A. G. Brook and J. M. Duff

Department of Chemistry, University of Toronto, Toronto 181, Ontario

Received November 27, 1972

The reactions of a series of silyl-substituted vinylmetallic reagents with acetic and benzoic anhydride have been investigated as a general route to α,β-unsaturated ketones having a silyl group attached to the carbon–carbon double bond. The reaction has been found to be generally applicable for acetyl derivatives provided low temperatures are used but the reaction with benzoic anhydride gives poorer results. The i.r. and u.v. spectra of the ketones are discussed. The characterization of novel 1,4-dienes obtained as by-products in the syntheses is also described.

Les réactions d'une série de réactifs vinylmétalliques substitués par le silyle sur l'anhydride acétique et benzoique ont été étudiées comme voie générale d'accès aux cétones α,β insaturées avec un groupe silyle attaché à la double liaison carbone–carbone. La réaction est d'application générale pour les dérivés acétyles pourvu qu'on se place aux basses températures mais avec l'anhydride benzoique, cette réaction conduit à des résultats plus pauvres. Les spectres i.r. et u.v. des cétones ont été discutés. La caractérisation des dienes-1,4 nouveaux produits secondaires des synthèses, a été également donnée.

[Traduit par le journal]

Can. J. Chem., **51**, 2024 (1973)

Some years ago several α,β-unsaturated ketones having a silyl group directly attached to the carbon–carbon double bond were synthesized by the hydrosilylation of an acetylenic ketone (1, 2). However, the reaction led to a mixture of α- and β-silylvinyl ketones which proved to be difficult to separate (eq. 1).

[1] $R_3SiH + HC{\equiv}CCOMe \longrightarrow$

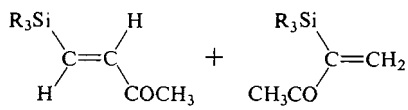

More recently Felix and Weber (3) described a different synthetic approach to β-silylvinyl ketones involving dehydrogenation of the saturated γ-ketosilanes (eq. 2). Another route recently

[2] $R_3SiCH_2CH_2COCH_3 \rightarrow R_3SiCH{=}CHCOCH_3$

used to prepare β-silylvinyl ketones and aldehydes involved the hydrolysis of silylallyl ethers (4) (eq. 3). It appeared to us that a more gen-

[3] $R{-}O{-}CR'{=}C{=}CR''(SiMe_3) \xrightarrow[H_2O]{H^+}$

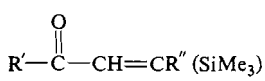

erally applicable route to both α- and β-silyl isomers of this interesting class of compound would be through the coupling of silylvinylmetallic reagents with anhydrides, and the following deals with such couplings using acetic and benzoic anhydride.

Four previously described organometallic reagents were utilized: α-lithiovinyltriphenylsilane (**1**), (5), 1-lithio-1-triphenylsilyl-2-phenylethylene-*E* (**2**) (5), α-trimethylsilylvinylmagnesium bromide (**3**) (6), and β-trimethylsilylvinylmagnesium bromide (**4**) (6). All four reagents coupled with acetic anhydride to give the acetyl derivatives **1***a*, **2***a*, **3***a*, and **4***a* and the triphenylsilyl reagents, **1** and **2**, coupled with benzoic anhydride to give the benzoyl derivatives **1***b* and **2***b*. Using the optimum conditions for these preparations as described in Table 1, the yields varied from 30–80%. In general the couplings with acetic anhydride afforded reasonable yields, but the trimethylsilyl Grignard reagents, **3** and **4**, gave none of the expected benzoyl derivatives under any conditions attempted. All the α,β-unsaturated ketones obtained were stable to mild acidic or basic conditions and the volatile ketones **3***a* and **4***a* could be converted into 2,4-dinitrophenylhydrazones in good yield.

The reactions and the products formed are shown in Scheme 1.

The ketones were found to be very sensitive towards 1,4-addition reactions and in order to minimize further reactions during their preparation it was necessary to use low temperatures.

Can. J. Chem. Downloaded from www.nrcresearchpress.com by 210.87.254.5 on 09/05/12
For personal use only.

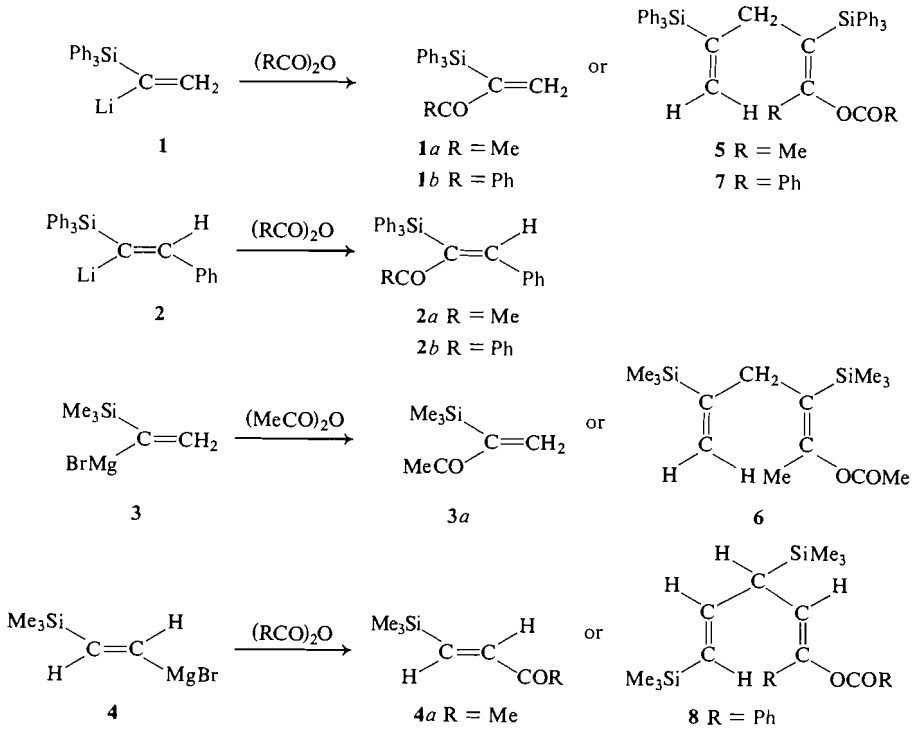

SCHEME 1. Reactions of silylvinylmetallic reagents with acid anhydrides.

The net result of these side reactions was the formation of 1,4-dienes. For example, treatment of α-lithiovinyltriphenylsilane with an excess of acetic anhydride at room temperature afforded a crystalline product (59% yield) along with a small amount of the α,β-unsaturated ketone. This product was assigned the structure **5**. The i.r. spectrum showed strong bands at 5.70 and 6.12 μ which are generally diagnostic of a vinyl acetate. The n.m.r. spectrum showed an aromatic multiplet (30H), two multiplets (each 1H) at δ 6.26 and 5.50 (vinyl protons), a similar multiplet (2H) at 2.95 attributable to the methylene group between two double bonds, and two singlets (each 3H) at 1.88 and 1.83 p.p.m. attributed to the two different methyl groups. The mass spectrum showed the expected parent ion at *m/e* 656. The geometry shown for the vinyl acetate double bond of **5** is assumed. Based on similar evidence, products from the reaction of **3** with acetic anhydride and **1** and **4** with benzoic anhydride were assigned structures **6**, **7**, and **8**, respectively (geometries assumed). The reaction thus appears to be general. As additional structural evidence **6** was subjected to the reactions shown in eq. 4.

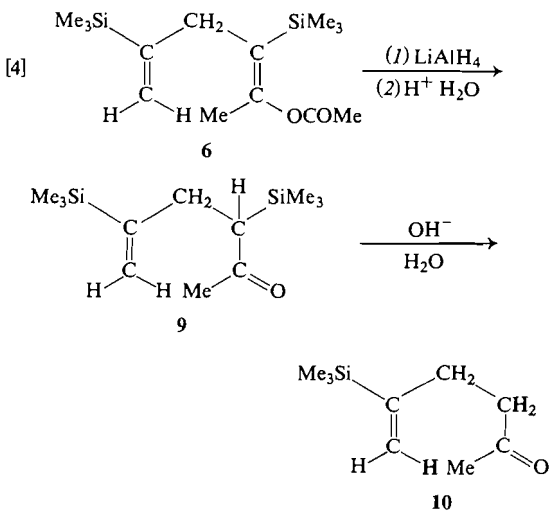

Lithium aluminum hydride reduction followed by acid hydrolysis afforded the β-ketosilane **9** in high yield. This base-sensitive compound in aqueous alkaline dioxane gave the ketone **10** in 72% yield.

An obvious mechanism for the formation of these dienes is the 1,4-addition of the vinyl-

Can. J. Chem. Downloaded from www.nrcresearchpress.com by 210.87.254.5 on 09/05/12
For personal use only.

Can. J. Chem. Downloaded from www.nrcresearchpress.com by 210.87.254.5 on 09/05/12
For personal use only.

TABLE 1. Preparation of α,β-unsaturated ketones

RM	Anhydride (mol)	Temperature (°C)	Product(s)	Yield (%)	M.p. or B.p./mm Hg (°C)	Analytical data: Calcd. C	Calcd. H	Found C	Found H
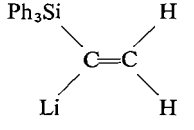	Acetic (2.5)	−78	**1***a*	82	115–116	80.44	6.14	80.69	6.25
		25	**5**	59	189–190	80.44	6.14	80.11	6.12
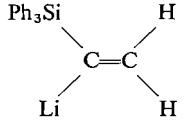	Benzoic (1.2)	−78	**1***b*	42	120–121	83.03	5.68	82.75	5.61
		−78	**7**	38	175–177	83.03	5.68	83.06	5.75
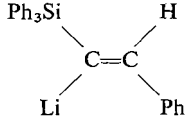	Acetic (2.0)	−78	**2***a*	67	127–128	83.12	5.98	82.89	5.83
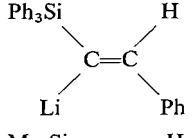	Benzoic (1.1)	−78	**2***b*	29	120–121	84.94	5.62	84.88	5.48
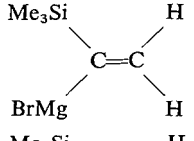	Acetic (3.0)	−120	**3***a*[a]	29[b]	140/760	59.09	9.92	—	—
			6	—	120/0.3	59.09	9.92	58.82	9.94
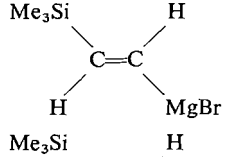	Acetic (3.0)	−120	**4***a*[c]	66[b]	—	59.09	9.92	58.72	9.89
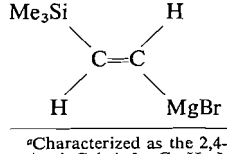	Benzoic (1.0)	−78	**8**	59	190/0.2				

[a]Characterized as the 2,4-dinitrophenylhydrazone, m.p. 163–164°.
Anal. Calcd. for $C_{13}H_{18}N_4O_4Si$: C, 48.43; H, 5.63; N, 17.38. Found: C, 48.41; H, 5.61; N, 17.31.
[b]Yield determined by g.l.p.c. analysis of crude product.
[c]Also characterized as the 2,4-DNPH, m.p. 171–172°.
Anal. Calcd. for $C_{13}H_{18}N_4O_4Si$: C, 48.43; H, 5.63; N, 17.38. Found: C, 48.20; H, 5.99; N, 17.13.

Can. J. Chem. Downloaded from www.nrcresearchpress.com by 210.87.254.5 on 09/05/12
For personal use only.

metallic reagent to the α,β-unsaturated ketone, in the normal manner, to give an enolate ion which is then acetylated or benzoylated by the remaining anhydride. To confirm this pathway 3-triphenylsilylbut-3-en-2-one (**1***a*) was treated with an equimolar amount of α-lithiovinyltriphenylsilane (**1**) at −78°. Hydrolysis gave the expected β-ketosilane **11** in high yield (see eq. 5).

[5] 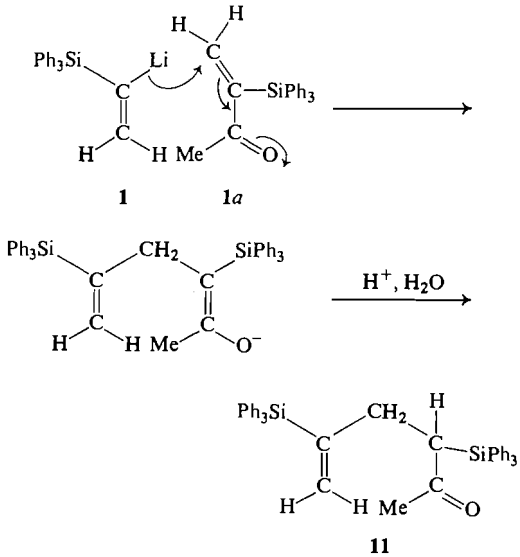

1 **1***a*

The important features of the i.r. and u.v. spectra of the α,β-unsaturated ketones are given in Tables 2 and 3. The carbonyl stretching wavelengths (5.93–6.05 μ) are normal for α,β-unsaturated ketones (typically 5.94–6.02 μ (7)), as previously noted by Felix and Weber (3) for a series of β-silylvinyl ketones. The shift to longer wavelength in the more polar solvent, acetonitrile, is also as expected (8).

The i.r. carbonyl band of β-ketosilanes is generally shifted to about 0.1 μ longer wavelength than that of their carbon analogs (9) (*e.g.* Me_3SiCH_2COMe, 5.89; Me_3CCH_2COMe, 5.82 μ). This effect, probably attributable to inductive release from silicon toward the carbonyl group, may not be as strongly pronounced in the α-silylvinyl ketones since the acetyl derivatives **1***a*–**4***a* absorb at very similar wavelengths.

Unfortunately only one of the six compounds prepared, **4***a*, showed a band (*ca.* 6.29 μ) which could be clearly assigned to a carbon–carbon double bond stretch. No similar band was observed in the α-isomer, **3***a*. Triphenylsilyl compounds in general have i.r. absorption at 6.28 μ and above, associated with the phenyl groups, which probably obscure the carbon–carbon double bond stretch in the four triphenylsilyl ketones.

Five of the six ketones prepared show a u.v. n → π* absorption band which shifts to shorter wavelength with increasing solvent polarity (Table 3). The two trimethylsilyl ketones **3***a* and **4***a* also show a π–π* band which shifts to longer wavelength with increasing solvent polarity. This shift, about 10 nm on changing from cyclohexane to water, is similar to that found in analogous carbon compounds (8).

Although the silyl-substituted α,β-unsaturated ketones undergo n–π* transitions at slightly lower energy than analogous carbon or unsubstituted compounds (typically 305–340 nm, ε 25–100) (7) the small effect is in marked contrast to the effect of direct silicon substitution at the carbonyl chromophore. For example, replacement of a methyl group of acetone by a triphenylsilyl group results in a lowering of the n → π* transition energy by about 26 kcal/mol. Effects of this magnitude (which would have resulted in a shift in λ_{max} from 320 to about 450 nm with silyl substitution) can definitely be ruled out for both α- and β-silylvinyl ketones.

It has been suggested (3) that the main effect of the β-silyl substituent on the n → π* transition of α,β-unsaturated ketones is in stabilizing the π* excited state. The similarity in the n → π* absorption of the α- and β-silyl isomers **3***a* and **4***a* tends to support this and confirms that direct conjugative interaction between the β-silicon atom and the carbonyl group is unimportant (eq. 6).

[6] $Si{-}C{=}C{-}C{=}O \nleftrightarrow \bar{S}i{=}C{-}C{=}C{-}\overset{+}{O}$

However, if lowering the π* level is the only significant effect of silyl substitution then one would predict similar π–π* absorption bands for **3***a* and **4***a*. This is clearly not the case. The π → π* band of the β-silylvinyl isomer, **4***a*, occurs at 13 nm longer wavelength (*ca.* 8 kcal/mol lower energy) and with a somewhat higher extinction coefficient, a result which is not inconsistent with conjugative interaction. It is also of interest to compare the π → π* bands of **3***a* and **4***a* in methanol (Table 3) with those of methyl vinyl ketone (λ_{max} (ethanol) 210), 3-methylbut-3-en-2-one (218), and pent-3-en-

TABLE 2. Spectral data for α,β-unsaturated ketones

Compound	I.r. C=O stretch[a]	U.v. λ_{max} (ε)[b] n → π*	U.v. λ_{max} (ε)[b] Other bands
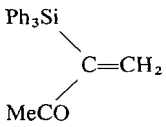	5.98 μ	329 nm (76)[c]	—
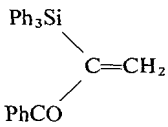	6.03s, 6.09w	322(77), 333(99), 344(110), 357(89), 370(48)	248 nm (12 300)[d]
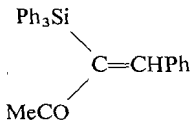	5.93	[e]	257 (15 700)[f]
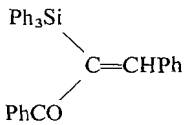	6.05	330(344), 345(348)[g], 359(273), 377(112)	267 (16 200)[f] 248 (24 200)[d]
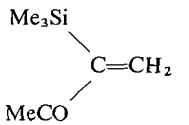	5.98	332(48), 341(45), 355(29), 374(9)	207.5 (7630)[h]
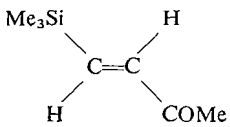	5.88w, 5.95s	327(52), 337(54), 351(49), 365(30), 382(10)	219.5 (10 900)[h]

[a]Carbon tetrachloride solution, s = strong, w = weak.
[b]Cyclohexane solvent. Maxima underlined for n → π* bands.
[c]Fine structure not resolved.
[d]Expected π → π* transition of benzoyl group.
[e]The n → π* band is buried.
[f]Band associated with the triphenylsilylstyryl system (*e.g. trans*-$Ph_3SiCH{=}CHPh$ 261 nm (ε 15 000)).
[g]The n → π* band is a shoulder of the more intense bands.
[h]Measured in 1 mm silica cells with nitrogen purging.

TABLE 3. Effect of solvent polarity on spectra

Compound	I.r.(μ) CCl_4	I.r.(μ) MeCN	U.v. (λ_{max} nm) Band	C_6H_{12}	MeCN	MeOH	H_2O
1*a*	5.98	5.99	n → π*	329	322	317	—
1*b*	6.03, 6.05	6.05 (broad)	n → π*	344	338	330	—
3*a*	5.98	6.01	n → π*	332	323	319	—
			π → π*	207.5	208	210	216
4*a*	5.88, 5.95	5.90, 5.97	n → π*	338	331	325	—
			π → π*	219.5	221.5	223	229

Can. J. Chem. Downloaded from www.nrcresearchpress.com by 210.87.254.5 on 09/05/12
For personal use only.

Can. J. Chem. Downloaded from www.nrcresearchpress.com by 210.87.254.5 on 09/05/12
For personal use only.

2-one (220 nm)[1] (10). Whereas methyl substitution at the double bond causes moderate shifts to longer wavelength (8 nm for α and 10 nm for β) silyl substitution either causes a slightly greater increase (13 nm for β), or no increase at all in the transition wavelength.

To gain some insight into possible causes of these unexpected shifts we have carried out preliminary molecular orbital calculations of the CNDO/2 type (11) on the five model compounds, methyl vinyl ketone, 3-methylbut-3-en-2-one, *trans*-pent-3-en-2-one, and the silyl (*i.e.* SiH_3) analogs of the latter two compounds. Bond lengths were obtained from standard tables (12) and *S-trans* geometries were used. The important results are summarized, in a qualitative manner, in Fig. 1. As expected, each

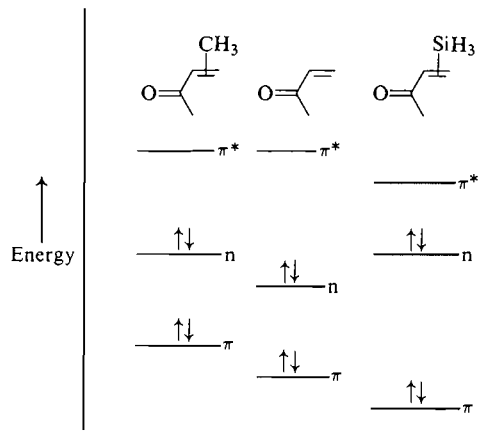

FIG. 1. Qualitative illustration of the results of CNDO calculations for silyl- and methyl-substituted α,β-unsaturated ketones.

compound showed an n-type orbital as the highest filled molecular orbital and a π-type orbital at somewhat lower energy. The lowest energy unfilled molecular orbital was also of the π-type and is designated as π*. The calculations showed a slight raising of the n level on substitution at the double bond with the effect being greatest, though still small, for the α-silyl compound. The π* level remained relatively unchanged with either α- or β-methyl substituents but with silyl substituents the π* energy was substantially lowered. These results are in accord with the observed longer n → π* transition wavelength in the silyl isomers. The effect of substitution on the π molecular orbital was somewhat unexpected. While methyl substitution caused a raising of the level silyl substitution resulted in an equally pronounced lowering of the energy. The predicted result on the π → π* transition are thus a bathochromic shift for the carbon-substituted ketones, as observed, while with the silyl ketones the net effect on the transition energy would depend on the relative amounts by which the π and π* levels were affected. Our calculations predicted a net bathochromic shift on silyl substitution (*i.e.* π* lowered more than π). However, it is reasonable to expect that these effects would depend to some extent on the position of the silyl substituent and the anomalous π → π* spectra of the silyl ketones could thus be explained by different degrees of interaction of an α- or β-silyl group with the π and π* orbitals.

The study of silyl-substituted α,β-unsaturated ketones is in an early stage at present and, in our opinion, more compounds, particularly suitable carbon and other Group IV analogs will be required before final conclusions may be drawn regarding their spectral properties. The present work has introduced a synthetic method which should serve to remedy the deficiency of compounds. Additionally, the demonstrated ease with which these compounds undergo 1,4-addition reactions has shown that they will be versatile intermediates in synthetic organosilicon chemistry.

Experimental

Experiments involving reactive organometallic reagents were carried out under nitrogen using dried, purified solvents. I.r. spectra were recorded on a Perkin–Elmer 237B instrument using 0.1 mm sodium chloride cavity cells. U.v. spectra were determined on Bausch and Lomb or Perkin–Elmer instruments in 10 mm silica cells for n → π* bands and 1 mm cells in the short wavelength region. N.m.r. spectra were determined on Varian A-60 or HR 100 instruments. Melting points were determined on a Fisher–Johns apparatus and are uncorrected.

Conditions of most runs, together with details of yields and analyses are summarized in Table 1.

*3-Triphenylsilylbut-3-en-2-one (**1a**)*

A solution of α-bromovinyltriphenylsilane (1.83 g, 5.0 mmol) in dry diethyl ether (75 ml) at room temperature was treated with 3.75 ml (6 mmol) of *n*-butyllithium in hexane (1.6 *M*). The resulting light yellow solution was stirred for 5 min then was cooled to *ca.* −78° using a Dry-Ice – acetone bath. Addition of acetic anhydride (0.944 ml, 10 mmol) to the resultant light-yellow suspension gave a fine white suspension. After 30 min at

[1]There is no significant difference between methanol and ethanol solvent as regards the π → π* transitions in α,β-unsaturated ketones (8).

Can. J. Chem. Downloaded from www.nrcresearchpress.com by 210.87.254.5 on 09/05/12
For personal use only.

−78° work-up with saturated aqueous ammonium chloride gave a thick oil which crystallized from 30 ml of pentane to give the desired product (1.35 g, 82%) as white solid, m.p. 112–115°. Recrystallization from hexane gave the analytical sample, m.p. 115–116°; n.m.r. (CCl_4) δ 6.27, 6.10 (2d, each 1H, J = 2 Hz) and 2.05 p.p.m. (s, 3H).

*2-Acetoxy-3,5-bis(triphenylsilyl)hexa-2,5-diene (**5**)*

When the above preparation was carried out at −20° a mixture (*ca.* 3:2, respectively) of the ketone **1***a* and compound **5** was obtained.

Addition of acetic anhydride to a solution of α-lithiovinyltriphenylsilane at room temperature gave a 59% yield of **5** on crystallization of the crude reaction product from pentane. Recrystallization from methylene chloride – methanol gave analytically pure material, m.p. 189–190°.

*α-Triphenylsilylvinyl Phenyl Ketone (**1***b*)*

To a solution of the organolithium reagent, prepared as above, from 0.92 g (2.5 mmol) of α-bromovinyltriphenylsilane in ether at −78° was added 0.68 g (3.0 mmol) of benzoic anhydride. After 30 min the resultant suspension was worked-up with saturated aqueous ammonium chloride solution to give an oil. The spectra of this oil indicated that a mixture of products was present. Chromatography on silica gel gave vinyltriphenylsilane (0.26 g, 36%) on elution with carbon tetrachloride. Elution with 1:1 benzene – carbon tetrachloride gave an oil (0.63 g) which was crystallized from hexane to give 0.41 g (42%) of the desired ketone, m.p. 116–120°. Recrystallization from hexane gave pure material, m.p. 120–121°; n.m.r. (CCl_4) δ 6.35, 6.21 p.p.m. (2d, J = 2 Hz).

*1-Benzoyloxy-1-phenyl-2,4-bis(triphenylsilyl)penta-1,4-diene (**7**)*

In a similar experiment to the above, the organolithium reagent from 0.45 g (1.23 mmol) of α-bromovinyltriphenylsilane was treated at −78° with benzoic anhydride (0.31 g, 1.35 mmol). The crude product obtained after work-up was crystallized from methylene chloride – methanol to give 0.18 g (38%) of compound **7**, m.p. 175–180°. Recrystallization from hexane gave the analytical sample, m.p. 175–177°; i.r. (CCl_4) 5.77, 6.26 μ (vinyl benzoate); n.m.r. (CCl_4) δ 6.33, 5.50 (2m, each 1H, C=CH_2), 3.25 p.p.m. (m, 2H, C=C—CH_2—C=C); mass spectrum 780 (2%, M), 303 (70%, $Ph_2SiOCOPh$), 259 (100%, Ph_3Si).

*3-Triphenylsilyl-4-phenylbut-3-en-2-one (**2***a*)*

1-Bromo-1-triphenylsilyl-2-phenylethylene-*Z* (13) (1.50 g, 3.4 mmol; prepared by dehydrobromination of 1,2-dibromo-1-triphenylsilyl-2-phenylethane with pyridine) in 50 ml of dry ether at room temperature was treated with *n*-butyllithium (4 mmol). The resultant deep yellow solution was cooled to −78° and then was treated with acetic anhydride (0.82 ml, 8.0 mmol) to give a fine gelatinous suspension. Work-up after 30 min with ammonium chloride solution gave a thick clear oil which was crystallized from hexane to give 0.91 g (67%) of the desired ketone, m.p. 127–128°; n.m.r. (CCl_4) δ 6.90 (s, 1H, C=CH—) and 1.80 p.p.m. (s, 3H, CH_3CO—).

*α-Triphenylsilylbenzalacetophenone (**2***b*)*

Using the same molar quantities as above, and identical conditions, treatment of the organolithium reagent from **2** with benzoic anhydride gave a complex mixture of products. Crystallization of the crude product from ethanol gave 0.71 g (58%) of *trans*-β-triphenylsilylstyrene. The residual product was chromatographed on silica gel. Elution with 1:1 benzene – carbon tetrachloride gave an oil (0.61 g) which was crystallized from hexane to give 0.46 g (29%) of the required ketone, m.p. 117–119°. Recrystallization from hexane gave m.p. 120–121°, n.m.r. δ 7.0–7.9 p.p.m. (aromatic multiplet).

*4-Trimethylsilylbut-3-en-2-one (**4***a*)*

The Grignard reagent prepared from 16.1 g (0.09 mol) of β-bromovinyltrimethylsilane and magnesium (2.43 g, 0.1 g atom) in 300 ml of tetrahydrofuran was cooled to *ca.* −120° in a liquid nitrogen – methylcyclohexane slush bath. The solution was treated (all at once) with 30.6 g (28.4 ml; 0.3 mol) of acetic anhydride. After 5 min the resultant suspension was allowed to warm up, and then was diluted with ether and worked-up. The organic layer was thoroughly washed with sodium bicarbonate solution to remove acetic acid and excess anhydride, was dried ($MgSO_4$) and then was distilled to a head temperature of 105°. The residue, 10.55 g of light yellow liquid, contained some THF and unidentified material along with the desired α,β-unsaturated ketone. G.l.p.c. analysis of the solution indicated a yield of *ca.* 66%. Pure samples of the ketone were obtained by preparative g.l.p.c. using a 5 ft. × ¼ in. column of 20% SE 30 on Chromosorb W (oven temperature 95°). The pure ketone was a colorless mobile liquid with a pleasant camphoraceous odor, n_D^{21} 1.4480; i.r. (CCl_4) 10.08 μ; n.m.r. (CCl_4) δ 6.89 and 6.40 (J = 19.5 Hz, CH=CH, AB pattern), 2.20 (s, 3H, CH_3CO—), 0.14 p.p.m. (s, 9H, Me_3Si). The large coupling constant between the vinylic protons and the presence of a band at 10.08 μ in the i.r. spectrum indicate that the ketone has *trans*-stereochemistry.

A sample of the purified ketone (0.10 g) was dissolved in dimethyl sulfoxide (10 ml) containing 0.16 g of 2,4-dinitrophenylhydrazine and one drop of concentrated hydrochloric acid. A precipitate formed, and after 5 min methanol was added to give 0.16 g of an orange solid. Recrystallization from methylene chloride – methanol gave the pure dinitrophenylhydrazone (0.14 g, 66%), m.p. 171–172°; n.m.r. ($CDCl_3$) δ 6.81, 6.51 (AB, J = 19.5 Hz, 2H) 2.18 (s, 3H, CH_3C=N—), and 0.22 p.p.m. (s, 9H, Me_3Si).

*1-Benzoyloxy-1-phenyl-3,5-bis(trimethylsilyl)penta-1,4-diene (**8**)*

A solution of the Grignard reagent, prepared from 5.37 g (0.03 mol) of β-bromovinyltrimethylsilane and 0.80 g (0.033 g atom) of magnesium in THF (100 ml), at *ca.* −78°, was treated with benzoic anhydride (6.80 g, 0.03 mol). After 30 min the resultant white suspension was warmed to room temperature and was worked-up as above by adding ether, and then washing in succession with ammonium chloride and sodium bicarbonate solutions. Removal of solvent at reduced pressure gave an oil which was chromatographed on silica gel, eluting with 1:1 benzene – carbon tetrachloride, to give the compound **8**, as a clear thick oil (2.51 g, 59%). This product

Can. J. Chem. Downloaded from www.nrcresearchpress.com by 210.87.254.5 on 09/05/12
For personal use only.

was air sensitive, turning yellow on standing. A sample was distilled (190°/0.2 mm Hg, Kugelrohr); mass spectrum 408 (1%, M), 303 (6.5%, M − PhCO), 105 (70%, PhCO), 73 (100%, Me_3Si); i.r. (CCl_4) 5.75, 6.25 μ (C=O and C=C of a vinyl benzoate); n.m.r. (CCl_4, 100 MHz, see structure below) δ 6.06 (H_A), 5.93 (H_B), 5.54 (H_C),

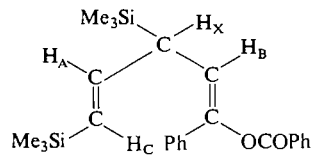

2.92 (H_X) (J_{AX} = 7.4, J_{BX} = 11.4, J_{CX} = 1.2, J_{AC} = 19.6, J_{AB} = J_{BC} = 0 Hz), 0.06 p.p.m. (s, 18H, $2Me_3Si$).

3-Trimethylsilylbut-3-en-2-one (3a)

The Grignard reagent prepared from α-bromovinyltrimethylsilane (27.9 g, 0.15 mol) and magnesium (4.03 g, 0.16 g atom) in THF (275 ml) was diluted with ether (175 ml) and the solution was cooled to *ca.* −120° in a liquid nitrogen – methylcyclohexane slush bath. To the rapidly stirred suspension was added 71.2 g (67 ml; 0.60 mol) of acetic anhydride. After 5 min the mixture was warmed to room temperature and was worked-up as above using ammoniun chloride and sodium bicarbonate solutions. Distillation of the organic layer to a head temperature of 100° gave 33.6 g of light yellow residue. An n.m.r. spectrum indicated that this liquid contained a 1:1 mixture of the desired ketone and the diene, **6**. A similar experiment carried out at −78° gave a 1:4 mixture of ketone and diene respectively.

The volatile product was pumped (25°/0.1 mm) into a Dry-Ice – acetone trap to give 7.7 g of light yellow liquid. This liquid was estimated (by g.l.p.c.) to contain 82% of the desired ketone along with three minor unidentified contaminants. The approximate yield of ketone is thus 29%.

The ketone was purified by preparative g.l.p.c. using the conditions described above for its isomer. The pure compound, a faintly yellow, pleasant-smelling liquid, n_D^{21} 1.4396, boiled at 140° (760 mm) with decomposition. It also decomposed slowly at room temperature but was stable at −20° in the dark. N.m.r. (CCl_4) δ 6.54 and 6.22 (2d, each 1H, J = 2 Hz, C=CH_2), 2.31 (s, 3H, CH_3CO), 0.19 p.p.m. (s, 9H, Me_3Si).

A sample of the impure ketone (0.71 g; 82%) was dissolved in DMSO (10 ml) containing 2,4-dinitrophenylhydrazine (1.0 g) and one drop of concentrated hydrochloric acid. The 0.68 g of product was purified by chromatography on silica gel, m.p. 163–164°; n.m.r. (CCl_4) δ 6.24, 5.95 (2d, each 1H, J = 1.5 Hz), 2.20 (s, 3H, CH_3CO), 0.26 p.p.m. (s, 9H, Me_3Si).

2-Acetoxy-3,5-bis(trimethylsilyl)hexa-2,5-diene (6)

The less volatile product in the above preparation was distilled (120°/0.3 mm; Kugelrohr) to give the pure diene as an oil, n_D^{22} 1.4616; i.r. (liquid film) 5.70, 6.09 μ (C=C—O—$COCH_3$); n.m.r. (CCl_4) δ 5.42, 5.25 (2m, each 1H, C=CH_2), 2.75 (m, 2H, C=C—CH_2—C=C), 2.01 and 1.95 (2s, each 3H, MeC=C and MeC=O), 0.11 and 0.06 p.p.m. (2 s, each 9H, 2 Me_3Si); mass spectrum 284 (1%, M), 169 (13%, M − Me_3Si), 73 (100%, Me_3Si), 43 (19%, MeCO).

Degradation of 2-Acetoxy-3,5-bis(trimethylsilyl)hexa-2,5-diene (6)

(A) To 3,5-Bis(trimethylsilyl)hex-5-en-2-one (9)

A solution of **6** (14.2 g, 0.05 mol) in diethyl ether (100 ml) containing lithium aluminum hydride (1.14 g, 0.03 mol) was heated to reflux for 30 min. The resultant suspension was cautiously worked-up with a slurry of ice and ammonium chloride. Hydrochloric acid (10%) was added to dissolve the aluminum salt and the organic layer was separated, dried, and distilled to give 11.1 g (92%) of pure β-ketosilane **9**, n_D^{22} 1.4600; i.r. (film) 5.89 μ (C=O, β to Si); u.v. (cyclohexane) λ_{max} 285 nm (ε 92); n.m.r. (CCl_4) δ 5.42 and 5.23 (2m, each 1H, C=CH_2), 1.9 (s, 3H, CH_3CO), 0.04 (s, 18H, 2 Me_3Si), 2–3 p.p.m. (complex, 3H, CH_2—CH); mass spectrum 242 (12%, M), 73 (100%, Me_3Si) 43 (10%, CH_3CO).

Anal. Calcd. for $C_{12}H_{26}OSi_2$: C, 59.43; H, 10.81. Found: C, 59.64; H, 10.91.

(B) 5-Trimethylsilylhex-5-en-2-one (10)

A solution of 9.2 g of 3,5-bis(trimethylsilyl)hex-5-en-2-one (**9**, above) in dioxane (50 ml) – water (10 ml) was treated with 0.5 g of potassium hydroxide. The resultant solution was stirred at room temperature for 20 min and then was diluted with ether (3 vol) and was worked-up with dilute hydrochloric acid. The organic layer was dried and distilled to give pure 5-trimethylsilylhex-5-en-2-one (**10**), (5.02 g, 78%), b.p. 80.5°/10 mm; n_D^{20} 1.4460; i.r. (CCl_4) 5.81 μ (C=O); u.v. (cyclohexane) λ_{max} 281 nm (ε 27); n.m.r. (CCl_4) δ 5.53 and 5.34 (2m, each 1H, C=CH_2), 2.45 (m, 4H,—CH_2—CH_2—), 2.10 (s, 3H, CH_3CO), 0.10 p.p.m. (s, 9H, Me_3Si).

Anal. Calcd. for $C_9H_{18}OSi$: C, 63.47; H, 10.65. Found: C, 63.30; H, 10.68.

3,5-Bis(triphenylsilyl)hex-5-en-2-one (11)

A solution of α-bromovinyltriphenylsilane (1.83 g, 5 mmol) in diethyl ether (50 ml) at room temperature was treated with 3.44 ml (5.5 mmol; 1.6 *M*) of *n*-butyllithium. After 20 min the solution was cooled to *ca.* −78° and 1.64 g (5 mmol) of 3-triphenylsilylbut-3-en-2-one (**1a**) was added. The resultant suspension was worked-up with saturated ammonium chloride solution after 5 min to give a glass. Crystallization from hexane gave the required product as white needles, m.p. 131–133° (2.06 g, 67%). Several recrystallizations from hexane and methylene chloride – methanol raised the m.p. to 138–140°; i.r. (CCl_4) 5.90 μ (C=O β to Si); n.m.r. (CCl_4); 100 MHz) δ 5.97 and 5.60 (2m, each 1H, C=CH_2), 3.6–2.5 (m, 3H, CH_2—CH), 1.60 p.p.m. (s, 3H, CH_3CO).

Anal. Calcd. for $C_{42}H_{38}OSi_2$: C, 82.03; H, 6.23. Found: C, 81.92; H, 6.15.

This research was supported by the National Research Council of Canada.

1. L. N. Mashlyakovskii and L. F. Chelpanova. Zh. Obsch. Khim. (Eng. Transl.) **35**, 2009 (1965).
2. N. V. Komarov, V. B. Puchnarevich, S. P. Suschinskaya, G. A. Kalabin, and V. G.

SAKHAROVSKII. Izvest. Akad. Nauk SSSR, Soc. Khim. (Eng. Transl.) 803 (1968).
3. R. A. FELIX and W. P. WEBER. J. Org. Chem. **37**, 2323 (1972).
4. R. MANTIONE and Y. LEROUX. J. Organometal. Chem. **31**, 5 (1971); G. MERAULT, J.-P. PICARD, P. BOURGEOIS, J. DUNOGUES, and N. DUFFAUT. J. Organometal. Chem. **42**, C80 (1972).
5. A. G. BROOK, D. G. ANDERSON, and J. M. DUFF. Can. J. Chem. **48**, 561 (1970).
6. B. F. MIRONOV, A. D. PETROV, and H. G. MAKSIMOVA. Izvest. Akad. Nauk SSSR, Otdel Khim. Nauk, 1954 (1959).
7. L. J. BELLAMY. The infrared spectra of complex molecules. John Wiley & Sons, Inc., New York. 1954.
8. H. H. JAFFE and M. ORCHIN. Theory and applications of ultraviolet spectroscopy. John Wiley & Sons, Inc., New York. 1962. p. 187.
9. A. G. BROOK. Adv. Organometal. Chem. **7**, 95 (1968).
10. Organic electronic spectral data. Wiley-Interscience, New York. Vol. IV, 1958–59, *edited by* J. P. Phillips and F. C. Nacrod; Vol. V, 1960–61, *edited by* J. P. Phillips, R. E. Lyle, and P. R. Jones.
11. P. A. DOBUSH. Program Number 141. Quantum chemistry program exchange. University of Indiana, Bloomington, Indiana.
12. Tables of interatomic distances. Chem. Soc. (London). Spec. Publ. No. 11 (1958).
13. A. G. BROOK and J. M. DUFF. Unpublished studies.

Can. J. Chem. Downloaded from www.nrcresearchpress.com by 210.87.254.5 on 09/05/12
For personal use only.

Effect of Pressure on the Rates of Reaction of Hydrogen Atoms in the Radiolysis of Liquid Ethanol[1]

KAMAL N. JHA AND GORDON R. FREEMAN
Chemistry Department, University of Alberta, Edmonton, Alberta T6G 2G2

Received December 28, 1972

Competition between the reactions

[3] $$H + C_2H_5OH \rightarrow H_2 + CH_3CHOH$$

and

[5] $$H + S \rightarrow HS$$

was measured at 296 *K* at 1 bar and 5.4 kbar. Values of k_5/k_3 at 1 bar and $(\Delta V_5^* - \Delta V_3^*)$ averaged between 1 bar and 5.4 kbar for several solutes S are: cyclohexene, 56, +2.7 cm³/mol; hexene-1, 71, +2.6 cm³/mol; phenol, 25, −3.8 cm³/mol; benzene, 12, −6.5 cm³/mol. The volume of activation of hydrogen atom addition to the aromatic ring is about 8 cm³/mol more negative than that of addition to a mono-olefin. Rate constants of reaction of solvated electrons with these solutes at 295 K, measured by the pulse-radiolysisspectroscopy technique, are (M^{-1} s^{-1}): cyclohexene, $<1 \times 10^4$; hexene-1, 1×10^5; benzene, 4×10^6; phenol, 5×10^7. The phenol reaction with e^-_{solv} does not reduce the hydrogen yield by a proportionate amount, so phenol "catalyses" the decomposition of e^-_{solv} to form hydrogen, perhaps via $C_6H_5OH^-_{solv} \rightarrow C_6H_5O^-_{solv} + H$. The scavenging of hydrogen precursors by hexene-1, benzene, and aniline in *n*-hexane, reported in ref. 6, had $(\Delta V^*_{scavenging} - \Delta V^*_{H_2formation}) = 0, -6$, and -4 cm³/mol, respectively, all three of which may be attributed to hydrogen atom reactions. The yields of hydrogen from solutions of neohexane in cyclopentane at 1 bar and 5.4 kbar indicate that charge transfer occurs from cyclopentane to neohexane, and that the probability of charge transfer is independent of pressure. The methane yields from these solutions indicate that the decomposition of the neohexane ion formed by charge transfer from cyclopentane, to form methane, is inhibited by pressure.

La compétition entre les réactions

[3] $$H + C_2H_5OH \rightarrow H_2 + CH_3CHOH$$

et

[5] $$H + S \rightarrow HS$$

a été mesurée à deux pressions, 1 bar et 5.4 kbar, à 296 K. Le rapport k_5/k_3 a 1 bar, et la difference moyenne des volumes d'activation $(\Delta V_5^* - \Delta V_3^*)$ entre 1 bar et 5.4 kbar, pour plusieurs solutés S ont des valeurs respectivement: cyclohexane, 56, +2.7 cm³/mol; hexène-1, 71, +2.6 cm³/ml; phénol, 25, −3.8 cm³/mol; benzène, 12, −6.5 cm³/mol. La difference entre les volumes d'activation pour l'addition d'un atome H à un noyau aromatique et à un oléfine simple est: $(\Delta V^*_{arom} - \Delta V^*_{olef}) \approx -8$ cm³/mol. Les constantes de vitesse en M^{-1} s^{-1} des réactions e^-_{solv} + S, à 295 K, mesurées par la méthode radiolyse-spectroscopie-pulsée, sont: cyclohexène, $<1 \times 10^4$; hexène-1, 1×10^5; benzène, 4×10^6; phénol, 5×10^7. La réaction e^-_{solv} + phénol ne reduit que peu le rendement d'hydrogène; peut être s'agit-il de la réaction $C_6H_5OH^-_{solv} \rightarrow C_6H_5O^-_{solv} + H$. Les réactions des précurseurs d'hydrogène avec l'hexène-1, le benzène et l'aniline dans le *n*-hexane pour solvant, qui ont été signalées au rèf. 6, ont pour $(\Delta V^*_{scavenging} - \Delta V^*_{H_2formation})$ des valeurs de 0, −6, et −4 cm³/mol, respectivement; ces trois valeurs sont attribuées aux réactions de l'hydrogène atomique. Les variations des rendements d'hydrogène et de méthane obtenus pour des solutions de néohexane dans le cyclopentane, aux pressions de 1 bar et 5.4 kbar sont expliquées par le transfert de charge du cyclopentane au néohexane. La probabilité de transfert de charge ne change pas avec la pression, mais la probabilité de décomposition de l'ion néohexane produit par ce transfert diminue quand la pression augmente.

Can. J. Chem., **51**, 2033 (1973)

Introduction

The study of the effect of pressure upon the behavior of radiolysis intermediates in liquids is being pursued in several laboratories (1–10). The results obtained from such work in hydrocarbons indicate that the ease of scavenging electrons (6, 7) and hydrogen atoms (6) is independent of pressure, while the ease of scavenging positive ions appears to increase with increasing pressure (6, 7). Benzene and aniline were thought to be positive ion scavengers in *n*-hexane (6). These

[1]We are grateful to the National Research Council of Canada for financial assistance.

Can. J. Chem. Downloaded from www.nrcresearchpress.com by 210.87.254.105 on 09/05/12
For personal use only.

Can. J. Chem. Downloaded from www.nrcresearchpress.com by 210.87.254.105 on 09/05/12
For personal use only.

solutes also scavenge hydrogen atoms (11–14) so it is necessary to obtain more information about their reactions with radiolytic species.

Ethanol was chosen as solvent because much is known about the behavior of electrons in it (10) and also because studies can be carried out in both neutral and acidic media. The advantage of strongly acidic solutions is that solvated electrons are rapidly converted into hydrogen atoms, resulting in a convenient medium to study hydrogen atom reactions.

It has been shown that the efficiencies of a variety of hydrogen atom reactions in water increase with increasing pressure (15).

Experimental

Absolute Ethanol from U. S. Industrial Chemical Co. was used. A u.v. spectroanalysis of the alcohol in a 10 cm cell indicated that the concentrations of probable impurities such as carbonyl compound and benzene were $< 1 \times 10^{-5}$ *M*.

Phillips Research Grade hexene-1, cyclohexene, and benzene were stirred with sodium–potassium alloy under vacuum for about 40 h to remove electron-scavenging impurities, then distilled into evacuated ampoules, sealed off, and stored in the dark. These ampoules were opened just prior to use to avoid peroxide formation. Analytical Reagent Grade phenol from B.D.H. Chemicals was mainly used as received because the purification by directional freezing and zone melting did not change the results of either the conventional scavenging or the pulse radiolysis experiments. Phillips Research Grade cyclopentane and neohexane (2,2-dimethylbutane) were purified by the sulfuric acid method described earlier (4). Baker and Adamson Analytical Reagent Grade perchloric acid (mole ratio $HClO_4/H_2O = 1/2$) was used as received.

The techniques used for steady state radiolysis and product analysis have been described elsewhere (1, 6, 10). Irradiation was performed at 296 K with a ^{60}Co γ source at a dose rate of 1×10^{17} eV/g min in ethanol. The dose was 2×10^{18} eV/g.

Rate constants for several reactions of solvated electrons were measured by pulse radiolysis. Solutions were deoxygenated by bubbling with ultrapure argon and irradiated with 0.1 μs pulses of 1.7 MeV electrons. The pulse dose was 3×10^{16} eV/g. The decay half life $t_{1/2}$ of the optical absorption signal at 680 nm was measured for several concentrations of each solute. A plot of $(0.693/t_{1/2})$ was made against solute concentration and the rate constant taken from the slope (16).

Results

Ethanol Solvent

The yield of hydrogen from neutral ethanol was $G(H_2) = 5.2$ at 1 bar and 5.7 at 5.4 kbar, in satisfactory agreement with previously reported values, 5.0 and 5.5, respectively (10).

Ethanol containing 0.10 *M* perchloric acid gave $G(H_2) = 6.1$ at 1 bar and 6.0 at 5.4 kbar.

Yields from the scavenging studies were based on the energy initially absorbed in the solvent only: $g(H_2) = G(H_2)/\varepsilon_s$, where ε_s is the electron fraction of solvent, including the acid when present. A correction was made for hydrogen produced by the direct radiolysis of hexene-1 and cyclohexene in the solutions, using $G(H_2) = 0.8$ (6) and 1.2 (17), respectively. The hydrogen yields from the direct radiolysis of benzene and phenol are so low that no correction was necessary (18).

The decreases in the hydrogen yield, $\Delta g(H_2)$, plotted against the molar concentrations of hexene-1 and cyclohexene in neutral ethanol at 1 bar and 5.4 kbar are shown in Fig. 1. The efficiency of scavenging hydrogen precursors by the olefins decreases with increasing pressure. The efficiency of hexene-1 is slightly higher than that of cyclohexene at both 1 bar and 5.4 kbar.

Figure 2 displays $\Delta g(H_2)$ as functions of benzene and phenol concentrations in neutral ethanol. At high solute concentrations the scavenging efficiencies of the aromatics increase slightly with increasing pressure, although there appears to be a cross-over at low concentrations.

The cross-over of the scavenging curves in Fig. 2 might be due to the participation of two intermediates, such as solvated electrons and hydrogen atoms. Solvated electrons were removed from the competition by rapidly converting them to hydrogen atoms with 0.1 *M* perchloric acid. The effects of benzene and phenol on the hydrogen yields from the acidic solutions are shown in Fig. 3. The scavenging efficiencies of the aromatics increase with pressure at all concentrations. The cross-over was therefore removed

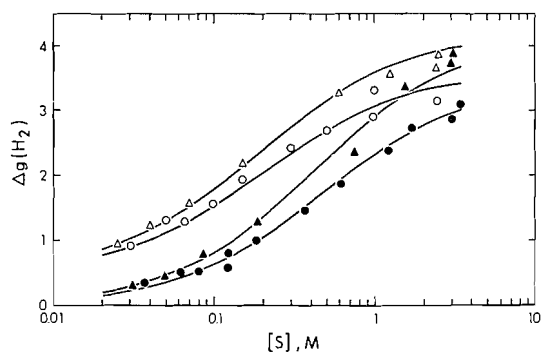

FIG. 1. Decrease in hydrogen yield $\Delta g(H_2)$ from neutral ethanol caused by hexene-1 (△) and cyclohexene (○). Open points, 1 bar; closed points, 5.4 kbar. [S] represents the solute concentration. The curves were calculated from eq. 7.

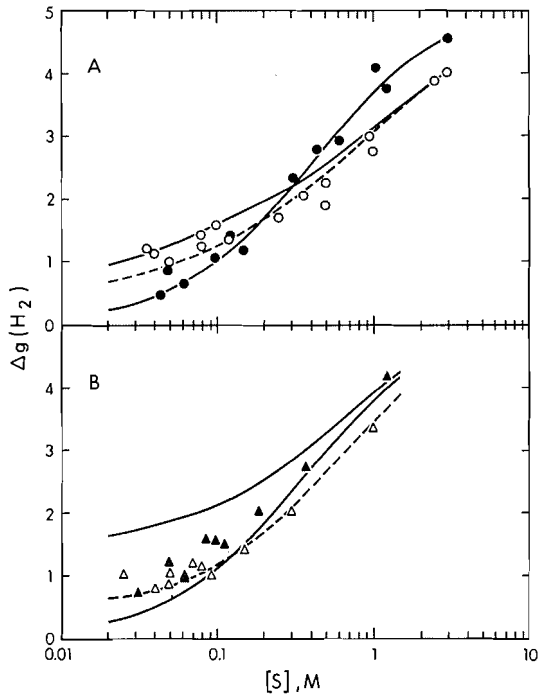

FIG. 2. Decrease in hydrogen yield $\Delta g(H_2)$ from neutral ethanol caused by benzene (○) and phenol (△). Open points, 1 bar; closed points, 5.3 kbar. [S] represents the solute concentration. The full curves were calculated using the rate constants and ratios in Tables 1 and 3. The dashed curves refer to 1 bar and the ratios in Table 3, but use $k_4' = 1 \times 10^6\ M^{-1}\ s^{-1}$ for benzene and $1 \times 10^5\ M^{-1}\ s^{-1}$ for phenol.

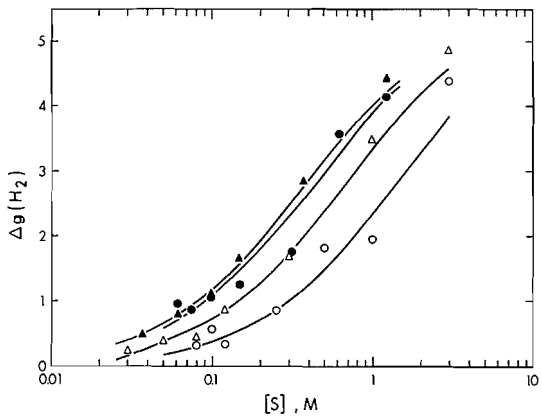

FIG. 3. Decrease in hydrogen yield from acidic ethanol (0.10 M perchloric acid) caused by benzene (○) and phenol (△). Open points, 1 bar; closed points, 5.4 kbar. The curves were calculated from eq. 7.

TABLE 1. Solvated electron reaction rate constants in ethanol at 295 K and 1 bar

Solute	$k_4'(M^{-1}\ s^{-1})$
Cyclohexene	$< 1 \times 10^4$
Hexene-1	1×10^5
Benzene	4×10^6
Phenol	5×10^7
Perchloric acid	3.6×10^{10}*
None	$k_2 = 1.2 \times 10^5 s^{-1}$†

*Reference 16.
†Reference 29.

by the addition of acid, and the remaining $\Delta g(H_2)$ may be attributed to hydrogen atom scavenging.

Olefins could not be used in acidic solutions due to their reactivity with acid.

The values of the rate constants of reaction of solvated electrons with the solutes used in this work were measured by the pulse radiolysis technique, and are listed in Table 1.

Cyclopentane Solvent

The scavenging efficiency of benzene in acidic ethanol increased with increasing pressure (Fig. 3). The same effect in *n*-hexane solvent was attributed to positive charge scavenging (6). An attempt was therefore made to obtain more information about the effect of pressure on the efficiency of charge transfer in liquids.

The yields of hydrogen and methane from the radiolysis of certain saturated hydrocarbon binary solutions deviate from the values "expected" on the basis of the electron fractions of the components (19–22). The deviation has been attributed to charge transfer occurring from the component with the higher ionization potential (I.P.) to the one with the lower I.P. To study the effect of pressure on such systems the yields of hydrogen and methane from solutions of neohexane (2,2-dimethylbutane, I.P. = 10.04 eV (23)) in cyclopentane (I.P. = 10.52 eV (23)) were measured at 1 bar and 5.4 kbar. The yields of hydrogen and methane from pure cyclopentane were not affected by pressure, but those from pure neohexane decreased by 18% and 27%, respectively, when the pressure was increased from 1 bar to 5.4 kbar (Table 2).

Charge transfer from cyclopentane to neohexane would decrease the hydrogen yield and increase that of methane relative to those expected on the basis of the electron fractions of the components of the solution (19, 22). Thus, if charge transfer occurs, $\Delta G = (G_{expected} - G_{observed})$ should be positive for hydrogen and negative for methane. The numbers in parentheses in Table 2

Can. J. Chem. Downloaded from www.nrcresearchpress.com by 210.87.254.105 on 09/05/12
For personal use only.

TABLE 2. H_2 and CH_4 yields obtained from cyclopentane/neohexane solutions at 296 K

	$G(H_2)$		$G(CH_4)$	
ϵ_{NH}*	1 bar	5.4 kbar	1 bar	5.4 kbar
0.00	5.1	5.1	0.03	0.03
0.20	3.88(+0.76†)	3.74(+0.80†)	0.51(−0.16†)	0.28(−0.02†)
0.41	3.44(+0.72†)	3.28(+0.68†)	1.12(−0.43†)	0.53(−0.02†)
1.00	2.81	2.31	1.64	1.20

*ϵ_{NH} = electron fraction of neohexane.
†$\Delta G = (G_{expected} - G_{observed})$, where $G_{expected} = (G_{CP}\epsilon_{CP} + G_{NH}\epsilon_{NH})$, and G_{CP} and G_{NH} represent the product yields from pure cyclopentane and neohexane, respectively.

are ΔG values. The hydrogen yields indicate that charge transfer occurs from cyclopentane to neohexane and that the probability of the reaction is independent of pressure. The methane yields also indicate that charge transfer occurs at 1 bar but $\Delta G(CH_4)$ is very small at 5.4 kbar. High pressure therefore inhibits either the formation of the methane precursor ion by charge transfer, or the decomposition of that ion ($\Delta V^{\ddagger}_{decomposition} - \Delta V^{\ddagger}_{deactivation} \approx 14 \pm 3$ cm^3/mol).

The effects of benzene and aniline on the hydrogen yields from *n*-hexane at high and low pressures (6) were similar to those of benzene and phenol on the yields from acidic ethanol (Fig. 3). It therefore seems probable that the aromatics scavenged hydrogen atoms, rather than positive charge, in *n*-hexane.

Discussion

Neutral Ethanol

The mechanism of hydrogen formation in the γ radiolysis of liquid ethanol can be represented as follows (10, 24).

[1] $C_2H_5OH \rightsquigarrow e^-_{solv}, H^+_{solv}, H$, radicals

[2] $e^-_{solv} \rightarrow C_2H_5O^-_{solv} + H$

[3] $H + C_2H_5OH \rightarrow H_2 + CH_3CHOH$

Reaction 1 represents the situation after geminate neutralization is complete, so e^-_{solv} and H^+_{solv} here represent only the free ions.

In the presence of a trace of electron scavenger, such as the acetaldehyde produced during radiolysis (24, 25), some of the free ion solvated electrons are scavenged and do not produce hydrogen.

[4] $e^-_{solv} + S \rightarrow S^-_{solv} \rightarrow$ no H or H_2

A trace of scavenger has much less effect at high than at low pressures because the value of the ratio k_4/k_2 decreases rapidly with increasing pressure. The value of k_4/k_2 is nearly two orders of magnitude smaller at 5.4 kbar than that at 1 bar (10), which explains why $G(H_2)$ is larger at the high than at the low pressure.

Hexene-1 and Cyclohexene in Neutral Ethanol

Mono-olefins scavenge hydrogen atoms (13, 26, 27). They do not react to an appreciable extent with solvated electrons in the ethanol system (Table 1). Thus, in the hexene-1 and cyclohexene solutions reactions 5 and 6 compete with reaction 3.

[5] $H + S \rightarrow SH$

[6] $H + S \rightarrow H_2 + R'$

where S represents a solute, in this case an olefin.

The curves in Fig. 1 were calculated from eq. 7.

$$[7] \quad \Delta g(H_2) = \Delta g(H_2)_{max}\left\{1 + \frac{k_3[C_2H_5OH]}{(k_5 + k_6)[S]}\right\}^{-1}$$

The values of $\Delta g(H_2)_{max}$ and $(k_5 + k_6)/k_3$ were obtained from plots of $\{\Delta g(H_2)\}^{-1}$ against $\{[C_2H_5OH]/[S]\}$, such as those in Fig. 4, and are listed in Table 3. Probable errors in values of $\Delta g(H_2)_{max}$ are ± 0.1, and in the rate constant ratios are $\pm 10\%$.

The values of $\Delta g(H_2)_{max}$ are larger at 5.4 kbar than at 1 bar because the acetaldehyde impurity prevents some of the hydrogen atoms from forming at 1 bar, due to competition between [2] and [4]. The impurity has a negligible effect on the hydrogen yield at 5.4 kbar, where the loss of electrons through [4] is small (10).

Estimates of k_6/k_5 were obtained by assuming that $k_6/k_5 = 0$ for benzene and putting the total scavengable hydrogen atom yield equal to the value of $\Delta g(H_2)_{max}$ obtained with benzene (see later). Hence,

Can. J. Chem. Downloaded from www.nrcresearchpress.com by 210.87.254.105 on 09/05/12
For personal use only.

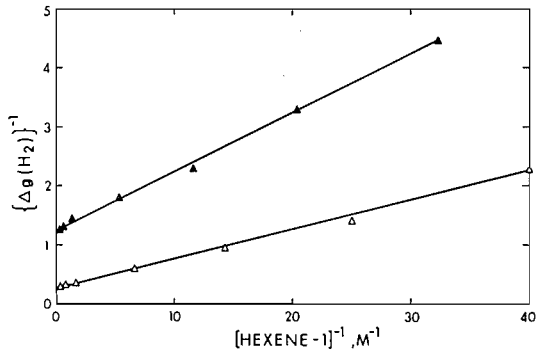

FIG. 4. Plots of $\Delta g(H_2)^{-1}$ against [hexene-1]$^{-1}$ for neutral ethanol (eq. 7). △, 1 bar; ▲, 5.4 kbar (▲ displaced vertically by 1.0 unit for clarity).

$$[8] \quad k_6/k_5 = \frac{\Delta g(H_2)_{max}^{\text{benzene}} - \Delta g(H_2)_{max}^{\text{olefin}}}{\Delta g(H_2)_{max}^{\text{olefin}}}$$

where $g(H_2)_{max}^{\text{benzene}} = 4.7$ at 1 bar and 5.2 at 5.3 kbar. The value $k_6/k_5 = 0.27$ obtained for hexene-1 in ethanol (Table 3) agrees with the value 0.31 reported by Hardwick for hexene-1 in *n*-hexane (27), but the value 0.52 for cyclohexene in ethanol is double the 0.23 reported for cyclohexene in *n*-hexane (27). There are not sufficient data to speculate about the reason for the difference.

The values of rate constant ratios at two pressures were substituted into eq. 9 to obtain the differences in the volumes of activation $\Delta V^{\ddagger}$ of competing reactions.

$$[9] \quad \log\frac{(k_a/k_b)_{P_1}}{(k_a/k_b)_{P_2}} = \frac{(P_2 - P_1)}{2.3RT}(\Delta V_a^{\ddagger} - \Delta V_b^{\ddagger})$$

where $(P_2 - P_1)/2.3RT = 0.095$ mol/cm^3 in the present work. One observes that $(\Delta V_5^{\ddagger} - \Delta V_3^{\ddagger}) \approx +2.7$ cm^3/mol and $(\Delta V_6^{\ddagger} - \Delta V_5^{\ddagger}) = 0$ for both olefins. The latter value is the same as that, $(\Delta V_{10}^{\ddagger} - \Delta V_5^{\ddagger}) = 0$, obtained for hexene-1 in *n*-hexane solvent (6).

$$[10] \quad H + n\text{-}C_6H_{14} \rightarrow H_2 + C_6H_{13}$$

Benzene and Phenol in Acidic Ethanol

In acidic ethanol reactions 2 and 4 are replaced by [11].

$$[11] \quad e^-_{solv} + H^+_{solv} \rightarrow H$$

The results in Fig. 3 were plotted according to eq. 7. The value of $\Delta g(H_2)_{max}$ was taken as $[g(H_2)_0 - 0.5]$, where the unscavengable yield of 0.5 units was estimated from a reworking of earlier results for neutral ethanol (32), and is assumed to be the same in the acidic alcohol, independent of pressure. The values of $(k_5 + k_6)/k_3$ obtained from the plots are listed in Table 3.

Contrary to the behavior of the olefins, the scavenging efficiencies of the aromatic compounds increased with increasing pressure (Table 3). The volume of activation for hydrogen atom addition to benzene is 9 cm^3/mol more negative than that for addition to cyclohexene. The reason for such a difference is not obvious, but the more negative value is associated with the lower rate constant, and more negative volumes of activation are usually associated with more negative entropies of activation (28).

Earlier results (6) may be analysed to obtain $(\Delta V^{\ddagger}_{\text{scavenging}} - \Delta V^{\ddagger}_{H_2\text{formation}})$ in *n*-hexane solvent. The values obtained for several scavengers are listed in Table 4. The difference between hexene-1 and benzene in *n*-hexane is similar to that in ethanol. The present results might indicate that the negative volumes of activation of the benzene and aniline reactions in *n*-hexane were at least partly due to hydrogen atom scavenging, rather than to positive charge reactions as suggested earlier (6).

Benzene and Phenol in Neutral Ethanol

Benzene and phenol have been reported to react with electrons (11, 13) as well as with hydrogen atoms (12–14). An attempt was made to fit the results in Fig. 2, using the hydrogen atom rate constant ratios given in Table 3 and the solvated electron rate constants in Table 1. The total reduction in hydrogen yield was the sum of the yields of scavenged electrons and hydrogen atoms.

$$[12] \quad \Delta g(H_2) = g(e^-_{solv})_{scav} + g(H)_{scav}$$

When $g(e^-_{solv})_{scav}$ was smaller than the free ion yield g_{fi}, the former was calculated from eq. 13.

$$[13] \quad g(e^-_{solv})_{scav} = \left\{\frac{k_4[\text{impurity}] + k_4'[\text{solute}]}{k_2 + k_4[\text{impurity}] + k_4'[\text{solute}]}\right\} g_{fi}$$

At 1 bar, $k_2 = 1.2 \times 10^5$ s^{-1} (29), $k_4[\text{impurity}] = 5 \times 10^4$ s^{-1} and $g_{fi} = 1.7$ (10). The value of $k_4[\text{impurity}]$ was estimated from the observed $g(H_2) = 5.2$ from otherwise pure ethanol and $g(H_2)_0 = 5.7$.

When $g(e^-_{solv})_{scav}$ was greater than g_{fi}, the contribution from spur reactions was read from a

Can. J. Chem. Downloaded from www.nrcresearchpress.com by 210.87.254.105 on 09/05/12
For personal use only.

Can. J. Chem. Downloaded from www.nrcresearchpress.com by 210.87.254.105 on 09/05/12
For personal use only.

TABLE 3. Kinetic parameters of hydrogen atom reactions in ethanol at 296 K

		1 bar			5.4 kbar				
$[HClO_4]$ (M)	Solute	$(k_5 + k_6)/k_3$	$\Delta g(H_2)_{max}$	k_6/k_5	$(k_5 + k_6)/k_3$	$\Delta g(H_2)_{max}$	k_6/k_5	$\Delta V_5^{\ddagger} - \Delta V_3^{\ddagger *}$ (cm^3/mol)	$\Delta V_6^{\ddagger} - \Delta V_5^{\ddagger}$ (cm^3/mol)
0.0	Cyclohexene	85	3.1	0.52	47	3.4	0.53	+2.7	0.0
0.0	Hexene-1	90	3.7	0.27	51	4.1	0.27	+2.6	0.0
0.1	Benzene	12	5.6	0.0	50	5.5	0.0	−6.5	
0.1	Phenol	25	5.6	0.0	57	5.5	0.0	−3.8	

*Average value between 1 bar and 5.4 kbar.

TABLE 4. Differences between the volumes of activation of reactions of hydrogen precursors in *n*-hexane at 296 K*

Scavenger	$\Delta V^{\ddagger}_{scav} - \Delta V^{\ddagger}_{H_2 formation}$ (cm^3/mol)
Carbon tetrachloride	0
Hexadiene-1,3	0
Hexene-1	0
Aniline	−4
Benzene	−6
Benzene in hexane containing 10 mol % ethanol	−9

*Calculated from data in ref. 6.

$g(N_2)$ *vs.* $[N_2O]$ curve (30), using $k(e^-_{solv} + N_2O) = 5 \times 10^9\ M^{-1}\ s^{-1}$ at 1 bar (31) and converting k_4'[solute] into appropriate values of $k(e^-_{solv} + N_2O)[N_2O]$.

Values of $g(H)_{scav}$ were calculated fror [14].

$$[14] \quad g(H)_{scav} = \left\{\frac{k_5[\text{solute}]}{k_3[C_2H_5OH] + k_5[\text{solute}] + k_6[\text{solute}]}\right\} \times g(H)_{max}$$

where $g(H)_{max} = [g(H_2)_0 - 0.5 - g(e^-_{solv})_{scav}]$.

The $\Delta g(H_2)$ curve calculated in the above manner for the phenol solutions at 1 bar was much too high (Fig. 2). To obtain reasonable agreement with the experimental results the value of k_4' had to be reduced by one to two orders of magnitude below that given in Table 1. The dashed curve in Fig. 2*B* was calculated using k_4' 50-fold smaller than the value in Table 1. Benzene showed similar behavior at 1 bar (Fig. 2*A*), but k_4' had to be reduced by a factor of only 2 to 4 to obtain reasonable agreement with experiment. This discrepancy between pulse radiolysis and competition kinetics behavior of phenol, and to a much lesser extent benzene, is not understood. Perhaps [15] occurs. Benzene remains anomalous.

$$[15] \quad C_6H_5OH^-_{solv} \rightarrow C_6H_5O^-_{solv} + H$$

It should be stated that postulation of reaction of quasifree (dry) electrons with phenol and benzene would make the above discrepancies worse.

At 5.3 kbar, hydrogen atom scavenging accounted for essentially all of $\Delta g(H_2)$. The high pressure curves in Fig. 2 were calculated by assuming electron scavenging to be negligible; it might have made some contribution in the phenol solutions (Fig. 2*B*).

Conclusions

$\Delta V^{\ddagger}$ for hydrogen atom addition to an aromatic ring is significantly more negative than that for hydrogen atom addition to a monoolefin.

The apparent rate of reaction of solvated electrons with phenol is much greater when measured by pulse radiolysis than when measured by kinetic analysis of hydrogen yields.

1. D. L. DUGLE and G. R. FREEMAN. J. Phys. Chem. **70**, 1256 (1966).
2. R. R. HENTZ, FARHATAZIZ, D. J. MILNER, and M. BURTON. J. Chem. Phys. **46**, 2995 (1967).
3. U. SCHINDEWOLF, H. KOHRMANN, and G. LANG. Angew Chem. Int. Ed. **8**, 512 (1969).
4. D. W. BRAZIER and G. R. FREEMAN. Can. J. Chem. **47**, 885 (1969).
5. R. R. HENTZ and R. J. KNIGHT. J. Chem. Phys. **52**, 2456 (1970).
6. K. N. JHA and G. R. FREEMAN. Can. J. Chem. **49**, 2651 (1971).
7. R. R. HENTZ and D. W. BRAZIER. J. Chem. Phys. **54**, 554 (1971).
8. M. G. ROBINSON, K. N. JHA, and G. R. FREEMAN. J. Chem. Phys. **55**, 4933 (1971).
9. R. R. HENTZ, FARHATAZIZ, and E. M. HANSEN. J. Chem. Phys. **55**, 4974 (1971).
10. K. N. JHA and G. R. FREEMAN. J. Chem. Phys. **57**, 1408 (1972).
11. M. ANBAR and P. NETA. Int. J. Appl. Rad. Isot. **18**, 493 (1967).
12. M. C. SAUER, JR. and I. MANI. J. Phys. Chem. **72**, 3856 (1968).
13. B. D. MICHAEL and E. J. HART. J. Phys. Chem. **74**, 2878 (1970).
14. P. NETA and R. H. SCHULER. J. Am. Chem. Soc. **95**, 1056 (1972).
15. R. R. HENTZ, FARHATAZIZ, and D. J. MILNER. J. Chem. Phys. **49**, 2153 (1968).
16. K. N. JHA, G. L. BOLTON, and G. R. FREEMAN. Can. J. Chem. **50**, 3073 (1972).
17. G. R. FREEMAN. Can. J. Chem. **38**, 1043 (1960).
18. A. J. SWALLOW. Radiation chemistry of organic compounds. Pergamon Press, Oxford. 1960.
19. T. J. HARDWICK. J. Phys. Chem. **66**, 2132 (1962).
20. P. J. DYNE and J. DENHARTOG. Can. J. Chem. **40**, 1616 (1962).
21. T. KUDO and S. SHIDA. J. Phys. Chem. **71**, 1971 (1967).
22. J. A. STONE and G. MATSUSHITA. Can. J. Chem. **49**, 3287 (1971).
23. R. W. KISER. Introduction to mass spectrometry and its applications. Prentice–Hall, Inc., Englewood Cliffs, N.J. 1965. Appendix IV.
24. S. M. S. AKHTAR and G. R. FREEMAN. J. Phys. Chem. **75**, 2756 (1971).

Can. J. Chem. Downloaded from www.nrcresearchpress.com by 210.87.254.105 on 09/05/12
For personal use only.

25. G. E. ADAMS and R. D. SEDGEWICK. Trans. Faraday Soc. **60**, 865 (1964).
26. F. BUSI and G. R. FREEMAN. J. Phys. Chem. **75**, 2560 (1971).
27. T. J. HARDWICK. J. Phys. Chem. **66**, 291 (1962).
28. K. J. LAIDLER. Chemical kinetics. McGraw–Hill Book Co., New York. 1965. p. 234.
29. J. W. FLETCHER, P. J. RICHARDS, and W. A. SEDDON. Can. J. Chem. **48**, 1645 (1970).
30. J. C. RUSSELL and G. R. FREEMAN. J. Phys. Chem. **72**, 816 (1968). Fig. 5.
31. G. R. FREEMAN. Critical data review on the radiation chemistry of ethanol. NSRDS-NBS. In press.
32. J. J. J. MYRON and G. R. FREEMAN. Can. J. Chem. **43**, 381 (1965).

Can. J. Chem. Downloaded from www.nrcresearchpress.com by 210.87.254.105 on 09/05/12
For personal use only.

Gas Phase Reactions of Fluorine Atoms[1]

THOMAS LONG POLLOCK AND WILLIAM ERNEST JONES
Chemistry Department, Dalhousie University, Halifax, Nova Scotia

Received December 27, 1972

The rate of reaction of F atoms with a series of compounds, CH_4, CH_3F, CH_2F_2, CHF_3, $CHClF_2$, HCl, $CBrF_3$, NH_3, and PH_3 has been determined relative to the chemiluminescent reaction

$$F + NO + Ar \rightarrow FNO^* + Ar \rightarrow FNO + Ar + h\nu$$

by photometry. The fluorine atoms were produced in a flow system from the fluid mixing of molecular fluorine and nitric oxide diluted with argon.

La vitesse de réaction des atomes de fluor avec une série de composés, CH_4, CH_3F, CH_2F_2, CHF_3, $CHClF_2$, HCl, $CBrF_3$, NH_3, et PH_3, a été déterminée en ce qui a trait à la réaction de chemiluminescence suivante

$$F + NO + Ar \rightarrow FNO^* + Ar \rightarrow FNO + Ar + h\nu$$

par photométrie. Les atomes de fluor été produits dans un système à écoulement à partir d'un mélange fluide de fluor moléculaire et d'oxyde azotique dilué à l'aide d'argon.

[Traduit par le journal]

Can. J. Chem., **51**, 2041 (1973)

Introduction

There are few kinetic results available for the reactions of fluorine atoms. Absolute values have been measured for the H_2 (1–4), CH_4 (4, 5), CH_3I (6), CF_3I (6), CCl_4 (7–9), Cl_2 (10), HCl (4), and NO (11) reactions with fluorine atoms. Relative rate determinations by measurement of the total chemiluminescence of HF (12) and product analysis (13–17) have extended the range of compounds to C_1–C_5 alkanes (13, 14, 16) as well as the chlorinated C_1 and C_2 hydrocarbons and fluorocarbons (15–17). Complementing these determinations of the overall rate constants have been the studies designed to elucidate the relative populations of the various vibrational levels of the product HF (12, 18–21).

The reactivity of molecular fluorine and the absence of a simple method for determination of the concentration of fluorine atoms has led to the development of some exotic sources of fluorine atoms in an attempt to circumvent the production of molecular fluorine. These include the photolysis of heavy metal fluorides (4, 18) the electrodeless discharge of CF_4 or SF_6 (9, 12, 21) and the thermal dissociation of N_2F_4 followed by titration of NF_2 with active nitrogen to generate F atoms (2, 5, 10). In a similar vein, Cool and Stephens (22) utilized the fast reaction between molecular fluorine and nitric oxide at room temperature as a fluorine atom source

$$[1] \qquad F_2 + NO \rightarrow FNO + F$$

to initiate the first true chemical laser by fluid mixing. We have chosen to develop this method as a source of fluorine atoms since a subsequent reaction is the combination of F atoms with NO into an electronically excited manifold of FNO which may then decay by emission.

$$[2] \qquad F + NO \xrightarrow{M} FNO^*$$

$$[3] \qquad FNO^* \rightarrow FNO + h\nu$$

This means that the reaction is self-monitoring and photometry of the emission provides a measure of the fluorine atom concentration when the NO is in large excess. Addition of a compound RX capable of reacting with F will cause a decrease in the intensity of the emission proportional to the decrease in the concentration of F atoms thus providing a measure of the relative rates of reactions 2 and 7.

$$[7] \qquad F + RX \rightarrow XF + R$$

Experimental

The fast-flow apparatus consisted of a 40 mm Pyrex cylinder which the F_2 + Ar entered axially from a 10 mm tube while the NO or NO + reactant flowed into the F_2 atmosphere from twenty 0.5 mm jets situated normally to the axial flow (Fig. 1). Gas flows were controlled by needle valves and monitored by capillary flow meters.

[1]The research for this paper was supported by the Defence Research Board of Canada, Grant number 9530-115.

Can. J. Chem. Downloaded from www.nrcresearchpress.com by 210.87.254.5 on 09/05/12
For personal use only.

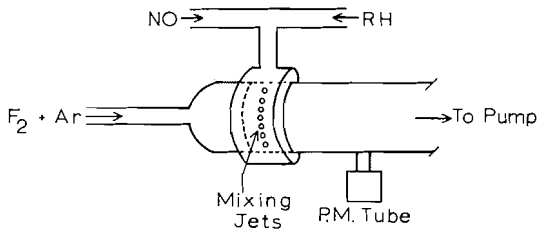

FIG. 1. Schematic of reaction vessel.

Calibrations were either by bleed-out rate from a known volume (NO and reactant) or a bubble flow meter (Ar and F_2). Nitrogen was used as the calibrating gas for the F_2 capillary and the ratio of their viscosities was used to determine the F_2 flow. The pressure in the reaction vessel was measured with a Kel-F 10 oil manometer at the outlet. The 250 l/min pump was protected from fluorine by a charcoal trap. Typical flow conditions were 300 μmol s^{-1} at 3.7 Torr argon which gave a linear velocity of 50 cm s^{-1}.

The photomultiplier tube (EMI 9592B) operating at e.h.t. 1050 V monitored the emission through a tube 8 mm i.d. × 6 cm long situated 5 cm from the mixing jets. The results reported were obtained with the photomultiplier tube positioned at the point of maximum luminosity, determined experimentally. The same results were obtained when the tube was 13 cm from the mixing jets.

Fluorine (Matheson) was supplied from a barricaded tank through thoroughly passivated copper tubing and an activated NaF trap to remove any HF via a Whitey 34RS metering valve to the flow capillary of the Pyrex vacuum system. Ar and H_2 (Canadian Liquid Air) were passed through a molecular sieves column. NO was introduced through supported NaOH at −78 °C. The reactant gases CH_4, CH_3F, CHF_3, $CHClF_2$, HCl, NH_3, PH_3, and $CBrF_3$ (Matheson) were thoroughly degassed and used without further purification as was CH_2F_2 (DuPont).

Purity checks were made on a gas chromatograph equipped with a Gow–Mac thermal conductivity cell and columns of 1/4 in. o.d. copper tubing packed with either 3% squalane on 60–80 mesh silica gel or 20% TCP on 60–80 mesh Gas–Chrom P.

Some samples were also analyzed by mass spectrometry and i.r. spectroscopy.

Results

The intensity of the pale yellow emission as followed by the p.m. tube rose to a plateau value in the presence of excess NO (Fig. 2). The falloff in intensity observed in a hundred-fold excess of NO is due to the geometry of the system. Since the photomultiplier tube is a finite distance from the mixing jets and the distance for $t_{1/2}$ for step 1 varies from ~15 to ~0.15 cm for a 1–100 fold excess, the photon flux in the solid angle viewed by the p.m. tube will vary some with the flow rate of NO. The more rigorous criterion of linearity of I_{em} with F_2 flow at a constant [NO] is fulfilled, however, as can be seen in

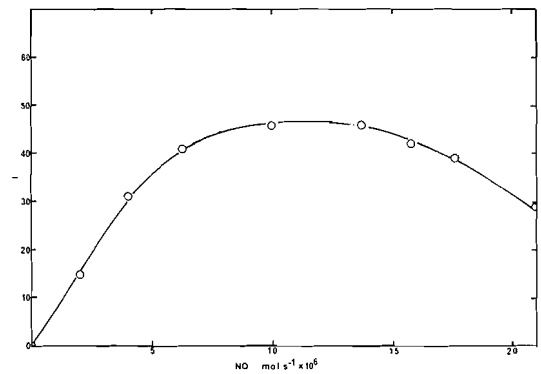

FIG. 2. Emission intensity in arbitrary units *vs.* the nitric oxide flow rate. F_2 flow 0.14 × 10^{-6} mol s^{-1}. Argon flow 300 × 10^{-6} mol s^{-1}. Total pressure = 3.7 Torr.

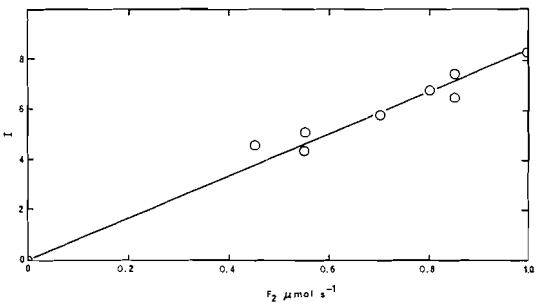

FIG. 3. Emission intensity in arbitrary units *vs.* the fluorine flow rate. NO flow rate 12 × 10^{-6} mol s^{-1}. Total pressure, 3.7 Torr.

Fig. 3. This is predicted by the reaction scheme of Johnston and co-workers (23, 24), modified to include heterogeneous removal of F atoms on the Pyrex surface.

[1] $F_2 + NO \rightarrow FNO + F$

[2] $F + NO + M \rightarrow FNO^* + M$

[3] $FNO^* \rightarrow FNO + h\nu$

[4] $FNO^* + M \rightarrow FNO + M$

[5] $F \xrightarrow{\text{wall}} \text{Product } (SiF_4)$

The assumption of steady-state conditions in the flow tube gives the following expression for the emission intensity I_0.

$$[6]\quad I_0 = \{k_1k_2[F_2][NO]^2[M]\}/\{k_2k_3[NO][M] + k_2k_4[NO][M]^2 + k_4k_5[M] + k_3k_5\}$$

The emission intensity is linearly dependent on

Can. J. Chem. Downloaded from www.nrcresearchpress.com by 210.87.254.5 on 09/05/12
For personal use only.

Can. J. Chem. Downloaded from www.nrcresearchpress.com by 210.87.254.5 on 09/05/12
For personal use only.

the F_2 concentration for a given third body M and constant NO concentration.

When a reactant R—X was mixed with the NO, the photomultiplier output was observed to decrease. This could be ascribed to any of three different causes: (*i*) F_2 + R—X competing successfully with step 1, (*ii*) the polyatomic molecule R—X being a much more efficient quencher in step 4 than the monatomic carrier gas Ar, (*iii*) F + R—X competing successfully with step 2. The first possibility was eliminated for each reactant since a blank run with F_2 and reactant produced no condensable products as determined by the gas chromatograph. It is also pertinent that no emission was observed from any of these blank runs.

The second possible cause was tested by using CF_4 as the reactant. Flow rates of CF_4 up to 10% of the argon carrier gas flow caused no decrease in the photomultiplier current, in fact it increased slightly ($I_0/I = 0.96 - 0.98$). An additional test was supplied by the reactant $CBrF_3$ where $I_0/I = 1.0$ when [RX] $\simeq$ [NO] = [Ar]/15.

The third possibility is then incorporated into the general reaction scheme.

[7] $$F + R—X \rightarrow XF + R$$

together with steps for removal of the radical R,

[8] $$R + NO \rightarrow RNO$$

[9] $$R + F_2 \rightarrow RF + F$$

[10] $$R + FNO \rightarrow RF + NO$$

[11] $$R + F \rightarrow RF$$

[12] $$R + R \rightarrow R_2$$

The mode of removal of R will affect the observed emission only if it produces or removes F atoms. Therefore, we must consider the relative importance of steps 9 and 11. Product analysis could not differentiate between [9], [10], and [11]. Furthermore, the reactivity of FNO in the Pyrex traps does not allow analysis of the products formed in the primary reaction. One can, however, arrive at an order of magnitude rate estimation by considering the relevant rate constants and concentrations. The available bimolecular rate constants for the reactions of CH_3, C_2H_5, and CF_3 and NO are $\sim 10^{11}$ cm^3 mol^{-1} s^{-1} (25–27). The only published values for reaction 9 are for R = H, and the room temperature value is $\sim 2 \times 10^{12}$ cm^3 mol^{-1} s^{-1} (3). When these values are substituted in the rate expressions, the result is

$$\frac{\text{Rate [8]}}{\text{Rate [9]}} > \frac{5}{1}.$$

It is reasonable to assume that k_{10} will not be greater than k_8. Thus, the contribution of step 10 will also be negligible. It is also possible to neglect [11] and [12] relative to [8] under the present experimental conditions. Bearing these facts in mind, the new expression for I is

[13] $$I = k_1k_2[F_2][NO]^2[M]/(k_3 + k_4[M])(k_2[NO][M] + k_5 + k_7[RX])$$

Dividing [6] by [13]

[14] $$\frac{I_0}{I} = 1 + \frac{k_7[RX]}{k_2[NO][M] + k_5}$$

which can be rearranged to give

[15] $$\left(\frac{I_0}{I} - 1\right)^{-1} = \frac{k_5}{k_7[RX]} + \frac{k_2'[NO]}{k_7[RX]}$$

where k_2' is the second order rate constant for step 2.

The data from CHF_3 is plotted in Fig. 4 according to [15]. We conclude from the linearity of the plot that reactions which are second order in radical concentrations, [11] and [12], do not contribute to the removal of R and F, and that steps [1]–[5], [7], and [8] adequately describe the system. The slope is (2.91 $\pm$ 0.08) $\times 10^{-2}$ and the non-zero intercept is (1.99 $\pm$ 0.88) $\times 10^{-2}$. All of the slopes and intercepts,

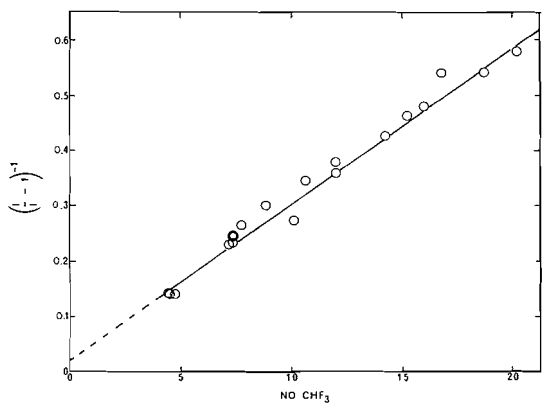

FIG. 4. Dependence of $((I_0/I) - 1)^{-1}$ on the [NO]/[CHF_3] ratio. Total pressure 3.7 Torr. Fluorine flow rate 0.7×10^{-6} mol s^{-1}, nitric oxide flow rate 12×10^{-6} mol s^{-1}.

TABLE 1. Experimental values of k_5/k_7 and k_2'/k_7 and derived values of k_5 for P_{total} = 3.7 Torr

R—X	k_2'/k_7	k_5/k_7 (mol $s^{-1} \times 10^{-6}$)	k_5 (s^{-1})
CH_4	$\leqslant 0.9 \times 10^{-4}$	—	—
CH_3F	$(1.06 \pm 0.18) \times 10^{-4}$	$(3.35 \pm 2.47) \times 10^{-4}$	11.9
CH_2F_2	$(3.96 \pm 0.52) \times 10^{-4}$	$(2.03 \pm 0.79) \times 10^{-3}$	15
CHF_3	$(291 \pm 8) \times 10^{-4}$	$(199 \pm 88) \times 10^{-4}$*	2.5
$CHClF_2$	$(38.9 \pm 0.8) \times 10^{-4}$	$(319 \pm 12) \times 10^{-4}$	29.9
HCl	$(7.8 \pm 0.7) \times 10^{-4}$	$(-7.8 \pm 12.4) \times 10^{-4}$	4.9
$CBrF_3$	1.4 ± 0.5	8.6 ± 2.5	23.1
NH_3	$(1.01 \pm 0.004) \times 10^{-2}$	$(14.6 \pm 0.00) \times 10^{-2}$	53.8
PH_3	$(4.2 \pm 0.4) \times 10^{-3}$	—	—

*Unitless, see Fig. 3.

Figs. 4–7 are listed in Table 1 together with the derived values for k_5. The error limits associated with the experimental data represent the standard deviation as determined from a least squares fit to the data.

The results can be conveniently subdivided into three parts: (*i*) hydrohalocarbons + HCl, (*ii*) perhalocarbon, and (*iii*) group V molecules. Those compounds in division (*i*) were characterized by the property of requiring only a low concentration of reactant to effectively reduce the photomultiplier current almost to the background level ($I_0/I \sim 100$ when [NO]/[RX] ~ 10). On the other hand, those compounds in division (*ii*) required much larger concentrations of reactant ($I_0/I \sim 2$ when [NO]/[RX] ~ 1) to reduce the photomultiplier current at all. The two compounds in division (*iii*) exhibited behavior between the two extremes. In addition,

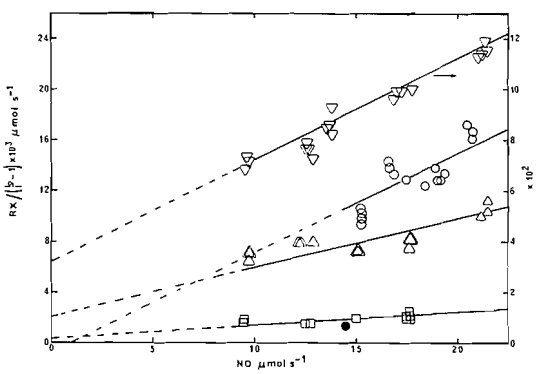

FIG. 5. Dependence of $[RX]/((I_0/I) - 1)$ on the [NO]. Total pressure = 3.7 Torr. ○, HCl, fluorine flow rate 0.18×10^{-6} mol s^{-1}; △, CH_2F_2, fluorine flow rate 0.195×10^{-6} mol s^{-1}; □, CH_3F, fluorine flow 0.18×10^{-6} mol s^{-1}; ▽, $CHClF_2$, fluorine flow 0.12×10^{-6} mol s^{-1}; ●, CH_4, fluorine flow 0.20×10^{-6} mol s^{-1}.

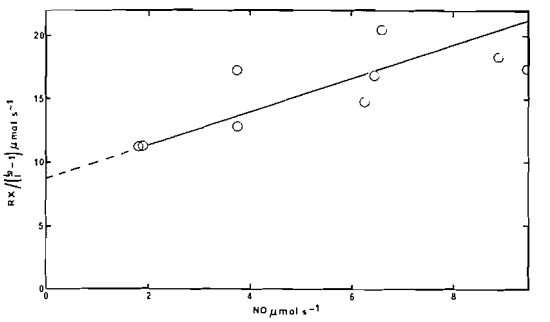

FIG. 6. Dependence of $[RX]/((I_0/I) - 1)$ on the [NO]. Total pressure = 3.7 Torr. ○, $CBrF_3$, fluorine flow, 0.12×10^{-6} mol s^{-1}.

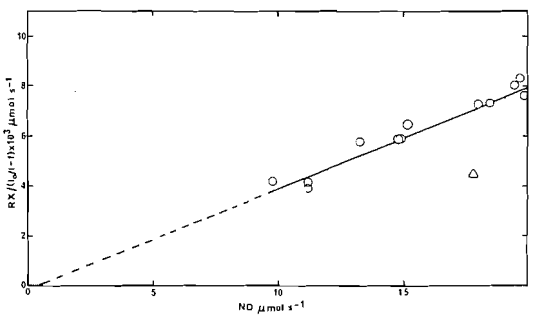

FIG. 7. Dependence of $[RX]/((I_0/I) - 1)$ on the [NO]. Total pressure = 3.7 Torr. ○, NH_3, fluorine flow 0.10×10^{-6} mol s^{-1}; △, PH_3, fluorine flow 0.18×10^{-6} mol s^{-1}.

the PH_3 behavior was anomalous. The intensity of emission decreased when PH_3 was added to the NO flow but, after the PH_3 and NO were turned off and while the F_2 and Ar were still flowing, the intensity first increased then fell off "exponentially" with time to the zero level after a lapse of approximately 5 min. After this

Can. J. Chem. Downloaded from www.nrcresearchpress.com by 210.87.254.5 on 09/05/12
For personal use only.

TABLE 2. Some absolute rate constants and Arrhenius parameters for $F + R—X \rightarrow XF + R$

RX	$k_{298} \times 10^{-13}$ ($cm^3\ mol^{-1}\ s^{-1}$)	$A \times 10^{-13}$ ($cm^3\ mol^{-1}\ s^{-1}$)	E_a ($kcal\ mol^{-1}$)	Reference
CH_4	4.9	33	1.15	5
	4.3			4
	1.0	13*	1.53*	12
	0.68	15*	1.81	16
	≥6			This work
H_2	1.0	15	1.6	2
	3.8			4
	0.4			3
	2			1
	0.75	13*	1.71*	12
	0.15	10.2*	2.50	16
Cl_2	5.3	55	1.4	10
HCl	1.5			4
	0.19	13*	2.54*	12
	0.73			This work
CH_3I	12			6
CF_3I	10			6
CCl_4	0.2			7
	4×10^{-3}			8
	2.4×10^{-5}			9
	6.9×10^{-8}	4*	10.2	17
$CHClF_2$	0.14			This work
	0.05	0.47*	1.35	15
NO	2.8×10^{16}†			11

*Assumed values.
†$cm^6\ mol^{-2}\ s^{-1}$ for Ar as third body in the reaction $F + NO + M \rightarrow FNO + M$.

was observed, the I_0 value would not return to its original level without extended (overnight) pumping on the reaction vessel or prolonged flow of F_2 + excess NO in Argon.

Discussion

The derived values of k_5 listed in Table 1 represent the only available values for the non-homogeneous removal of F atoms in a Pyrex tube. The order of magnitude value from this study is $\sim 10\ s^{-1}$. This suggests that every collision with the wall does not effectively remove the fluorine atom. The scatter, which is random, in the determined values further suggests that the nature of the surface plays a significant role in the ultimate fate of the F atoms which collide with the wall. However, this will not affect the relative rates of reaction as long as self heating effects are eliminated. This condition applies in the present work.

Absolute rate constant values for the reaction between F and R—X derived from the reported rate constant for $F + NO + Ar \rightarrow FNO + Ar$ (11) are compared with available velocity constants in Table 2. The agreement is very good for the hydrogen containing reactants.

A common feature of the abstraction reactions (Table 2) is the low energy barriers to reaction. This is not unexpected in view of the exothermicity of these reactions. This would seem to suggest that the trends in the magnitude of the derived rate constants in Table 3 would have their basis in the A-factor of the Arrhenius expression for k. If such is the case, we can postulate that, in the thermodynamic formulation of the rate constant, the activated complex must become more rigid as one goes from $[F\cdots H\cdots CH_3]^+$ to $[F\cdots H\cdots CF_3]^+$. It is certain that the geometry of the intermediate will change as fluorine atoms replace the protium atoms on methane since the resultant radical changes from D_{3h} symmetry (CH_3) to C_{3v} symmetry (CF_3). This property could be monitored in the HF product. For CHF_3, a greater fraction

Can. J. Chem. Downloaded from www.nrcresearchpress.com by 210.87.254.5 on 09/05/12
For personal use only.

TABLE 3. Rate constants and enthalpy changes for the abstraction reaction of fluorine atoms

R—X	$k_7 \times 10^{-12}$ (cm^3 mol^{-1} s^{-1})	ΔH^* (kcal mol^{-1})
CH_4	≥60	−31.3
CH_3F	53	−33†
CH_2F_2	11	−33†
CHF_3	0.19	−29.8
$CHClF_2$	1.5	−36.4†
HCl	7.3	−33.0
$CBrF_3$	0.004	9.8
NH_3	0.55	−32.9
PH_3	≥22	−59.4

*Reference 28.
†Estimated from D(F—X) − D(R—X).

of the total available energy should appear in the vibrational and rotational levels of the HF but the distribution within the vibrational levels would be more nearly statistical. The period during which the F atom approaches and before the "heavy" non-rearranged CF_3 radical moves away would allow "equilibration" of the available energy. This is in contrast to the CH_4 case where during formation of the HF bond the forming radical (CH_3) changes geometry (an exothermic process) and allows less redistribution of available energy because of a shorter interaction time. The HF bond should thus possess population inversion in its vibrational–rotational levels.

The two group V molecules are also interesting. The measured rate constant for NH_3 is less than that for methane even though the exothermicities are very similar. Qualitatively, the thermodynamic ΔS^* must be positive since, in the activated complex, the NH_3 moiety will lose the property of inversion. This effect will not be as serious in the physically larger PH_3 molecule and this is reflected in the greater room temperature rate constant.

The reaction of F atoms with $CBrF_3$ is endothermic. From the values given in Table 3 for the enthalpy charge and the room temperature velocity constant reported here the A-factor must be of the same order of magnitude as for the other molecules studied.

The inclusion of this molecule illustrates the versatility of this experimentally simple method of following the rates of fluorine atom reactions. A simple, yet powerful method because of its self-monitoring feature.

1. A. F. DODONOV, G. K. LAVROVSKAYA, I. I. MOROSOV, and V. L. TAL'ROZE. Dokl. Akad. Nauk. SSSR, Engl. Transl. **198**, 440 (1971).
2. K. H. HOMANN, W. G. SOLOMON, J. WARNATZ, H. GG. WAGNER, and C. ZETZSCH. Ber. Bunsenges. Phys. Chem. **74**, 585 (1970).
3. S. W. RABIDEAU, H. G. HECHT, and W. B. LEWIS. J. Magn. Reson. **6**, 384 (1972).
4. K. L. KOMPA and J. WANNER. Chem. Phys. Lett. **12**, 560 (1972).
5. H. GG. WAGNER, J. WARNATZ, and C. ZETZSCH. An. Asoc. Quim. Argent. **59**, 169 (1971).
6. I. O. LEIPUNSKII, I. I. MOROSOV, and V. L. TAL'ROZE. Dokl. Akad. Nauk. SSSR. Engl. Transl. **198**, 547 (1971).
7. D. T. CLARK and J. M. TEDDER. J. Phys. Chem. **68**, 2018 (1964).
8. C. ZETZSCH. *In* K. H. Homann and D. I. MacLean. J. Phys. Chem. **75**, 3645 (1971).
9. C. E. KOLB and M. KAUFMAN. J. Phys. Chem. **76**, 947 (1972).
10. J. WARNATZ, H. GG. WAGNER, and C. ZETZSCH. Ber. Bunsenges. Phys. Chem. **75**, 119 (1971).
11. P. KIM, D. I. MACLEAN, and W. G. VALANCE. Abstr. 164th National Meeting Am. Chem. Soc. New York, 1972.
12. N. JONATHAN, C. M. MELLIAR-SMITH, S. OKUDA, D. H. SLATER, and D. TIMLIN. Mol. Phys. **22**, 561 (1971).
13. P. C. ANSON, P. S. FREDRICKS, and J. M. TEDDER. J. Chem. Soc. 918 (1959).
14. G. C. FETTIS, J. H. KNOX, and A. F. TROTMAN-DICKENSON. J. Chem. Soc. 1064 (1960).
15. R. FOON and N. A. MCASKILL. Trans. Faraday Soc. **65**, 3005 (1969).
16. R. FOON and G. P. REID. Trans. Faraday Soc. **67**, 3513 (1971).
17. R. FOON and K. B. TAIT. J. Chem. Soc. Faraday Trans. I **68**, 1121 (1972).
18. J. H. PARKER and G. C. PIMENTEL. J. Chem. Phys. **51**, 91 (1969).
19. J. C. POLANYI and D. C. TARDY. J. Chem. Phys. **51**, 5717 (1969).
20. T. P. SCHAFER, P. E. SISKA, J. M. PARSON, F. P. TULLY, Y. C. WONG, and Y. T. LEE. J. Chem. Phys. **53**, 3385 (1970).
21. N. JONATHAN, C. M. MELLIAR-SMITH, and D. H. SLATER. Mol. Phys. **20**, 93 (1971).
22. T. A. COOL and R. R. STEPHENS. J. Chem. Phys. **51**, 5175 (1969).
23. H. S. JOHNSTON and H. J. BERTIN. J. Mol. Spectrosc. **3**, 683 (1959).
24. D. RAPP and H. S. JOHNSTON. J. Chem. Phys. **33**, 695 (1960).
25. N. BASCO, D. G. L. JAMES, and R. D. SUART. Int. J. Chem. Kinet. **2**, 215 (1970).
26. M. I. CHRISTIE and J. S. FROST. Trans. Faraday Soc. **61**, 468 (1965).
27. B. G. TUCKER and E. WHITTLE. Trans. Faraday Soc. **61**, 484 (1965).
28. D. R. STULL and H. PROPHET (*Project Directors*). JANAF Thermochemical tables. 2nd ed. 1971.

Can. J. Chem. Downloaded from www.nrcresearchpress.com by 210.87.254.5 on 09/05/12
For personal use only.

The Molecular Structures of the Polysulfuryl Fluorides by Vapor Phase Electron Diffraction: $S_2O_5F_2$ and $S_3O_8F_2$

J. LAWRENCE HENCHER

Department of Chemistry, University of Windsor, Windsor, Ontario

AND

S. H. BAUER

Baker Chemical Laboratories, Cornell University, Ithaca, New York 14850

Received November 20, 1972

The molecular structures of the polysulfuryl fluorides, $S_2O_5F_2$ and $S_3O_8F_2$, were determined by vapor phase electron diffraction. In each case it was assumed that a single rotomer was more stable than all others, by at least 2.5 kcal mol^{-1}. The possibility that the sample consisted of a mixture of conformations of comparable stabilities was not explored.

The thermally averaged r_g parameters for $S_2O_5F_2$ are as follows: S=O = 1.398 ± .002 Å; S—F = 1.525 ± 0.005 Å; S—O = 1.611 ± 0.005 Å; ∠SOS = 123.6 ± 0.5°; ∠OS=O = 106.1 ± 0.9°; ∠FS=O = 106.6 ± 0.6°; ∠O=S=O = 126.8 ± 1.2°; ∠OSF = 102.4 ± 1.8°; $\tau_{FS/OS'}$ = 53.8 ± 2.7°; $\tau_{F'S'/OS}$ = 73.7 ± 2.4°. The r_g parameters for $S_3O_8F_2$ are: S=O = 1.402 ± 0.003 Å; S—F = 1.525 ± 0.012 Å; S—O = 1.613 ± 0.006 Å; ∠OSO = 97.8 ± 1.0°; ∠SOS = 123.6 ± 1.2°; ∠OS=O = 106.5 ± 0.8°; ∠FS=O = 105.5 ± 1.2°; ∠O=S=O (bridge) = 128.8 ± 1.4°; ∠O=S=O = 128.5 ± 1.4°; ∠OSF = 101.3 ± 1.5°; $\tau_{SO/SO}$ = 295.3 ± 0.9°; $\tau_{FS/OS}$ = 319.4 ± 2.2°. The standard errors listed are three times the calculated values and are believed to encompass the non-random errors in the analysis.

Les structures moléculaires des fluorures de polysulphuryle, $S_2O_5F_2$ et $S_3O_8F_2$, ont été élucidées par la diffraction des électrons en phase vapeur. Dans chacun des cas, il fut estimé qu'un seul rotamère était plus stable que tous les autres par au moins 2.5 kcal/mol^{-1}. Par suite la possibilité que l'échantillon comporte un mélange de conformations ayant des stabilités comparables n'a pas été explorée. Les paramètres moyennés thermiquement pour le $S_2O_5F_2$ sont les suivants: S=O = 1.398 ± 0.002 Å; S—F = 1.525 ± 0.005 Å; S—O = 1.611 ± 0.005 Å; ∠SOS = 123.6 ± 0.5°; ∠OS=O = 106.1 ± 0.9°; ∠FS=O = 106.6 ± 0.6°; ∠O=S=O = 126.8 ± 0.5°; ∠OSF = 102.4 ± 1.8°; $\tau_{FS/OS'}$ = 53.8 ± 2.7°; $\tau_{F'S'/OS}$ = 73.7 ± 2.4°. Les paramètres pour le $S_3O_8F_2$ sont: S=O = 1.402 ± 0.003 Å; S—F = 1.525 ± 0.012 Å; S—O = 1.613 ± 0.006 Å; ∠OSO = 97.8 ± 1.0°; ∠SOS = 123.6 ± 1.2°; ∠OS=O = 106.5 ± 0.8°; ∠FS=O = 105.5 ± 1.2°; ∠O=S=O (pont) = 128.8 ± 1.4°; ∠O=S=O = 128.5 ± 1.4°; ∠OSF = 101.3 ± 1.5°; $\tau_{SO/SO}$ = 295.3 ± 0.9°; $\tau_{FS/OS}$ = 319.4 ± 2.2°. Les erreurs standards mentionnées représentent trois fois les valeurs calculées et tiennent compte, semble-t-il, des erreurs qui ne sont pas imputables au hasard lors de l'analyse. [Traduit par le journal]

Can. J. Chem., **51**, 2047 (1973)

Introduction

Although it appears that no detailed structures have been reported for $S_2O_5F_2$ and $S_3O_8F_2$, polysulfuryl structures have been proposed on the basis of their infrared and Raman spectra (1, 2). Gillespie and Robinson (3, 4) predicted values for the S—O bond lengths (1.40 Å, terminal and 1.66 Å ,bridge) and ∠O=S=O (120–122°) from correlations of these parameters with force constants and vibrational frequencies.

The structures of the ions $S_2O_7^{2-}$ (5) and $S_3O_{10}^{2-}$ (6, 7) (isoelectronic with $S_2O_5F_2$ and $S_3O_2F_2$, respectively) are notable for the shortness of the terminal S=O separation compared to that in SO_4^{2-} (8) and the larger than tetrahedral bridge angles, ∠SOS. The bridge S–O distance is apparently shorter than a single bond length. Cruickshank (7) attributed these structural effects to an increase in dπ–pπ bond orders, due to delocalization of the lone pair electrons associated with the bridge oxygen. A recent molecular orbital study of the S—O bond by Bartell, Su, and Yow (9) supports involvement of the lone pair electrons but favors a different involvement of the sulfur d orbitals.

The sulfuryl halides exhibit short S—O bonds compared with $SO_2(CH_3)_2$ (10). Either of the above theoretical viewpoints favors increased d orbital utilization, in this case because of the polarizing effect on sulfur by the attached halogen atoms (9, 11).

Because the above interesting factors are presumed to be present in the polysulfuryl fluorides, a structural study was undertaken.

Can. J. Chem. Downloaded from www.nrcresearchpress.com by 210.87.254.105 on 09/05/12
For personal use only.

Can. J. Chem. Downloaded from www.nrcresearchpress.com by 210.87.254.105 on 09/05/12
For personal use only.

Experimental

The samples were obtained in break-seal bottles from R. J. Gillespie of McMaster University. Both samples were produced by fluorination of liquid SO_3 (1). The sample of $S_2O_5F_2$ distilled at 51–52 °C (1 atm) and the sample of $S_3O_8F_2$ distilled at 29–31 °C under a reduced pressure of 3 Torr.

Convergent mode, sectored electron diffraction patterns were recorded on the Cornell Apparatus (12). The nozzle was maintained at about 20 °C. Diffraction patterns were recorded on 4 × 5 in. Kodak Process Plates at 25 and 75 kV for nozzle to plate distances of 12.94 and 26.24 cm. Useful diffraction patterns thus covered the range $5 < q < 140$ Å^{-1} where $q = (40/\lambda) \sin(\theta/2)$. Scale factors were obtained from MgO diffraction patterns recorded concurrently with the gas patterns (13).

Tracings of the diffraction patterns were recorded on a Jarrell Ash microphotometer equipped with a rotating sample stage. The center of each plate was located by an exposed spot from the undeflected beam. Procedures for reducing the above data to relative intensities have been described elsewhere (13–15). The relative intensities are presented for $S_2O_5F_2$ and $S_3O_8F_2$ in Figs. 1 and 2, respectively. Tables of these values, interpolated at integral q, are available from the Depository of Unpublished Data.[1]

Analysis

The experimental molecular intensity was calculated for each set of data depicted in Figs. 1 and 2 according to

$$M_{exp}(q) = [(I(q)/B(q)) - 1]$$

where $I(q)$ is the experimental sectored intensity and $B(q)$ is the background. The resultant curves were then spliced into two composite $(\pi/10)qM_{exp}(q)$ curves for each molecule, as follows:

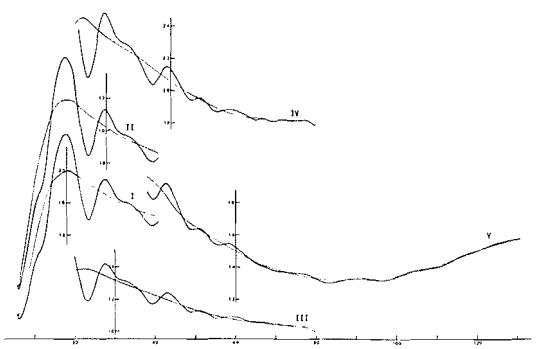

FIG. 1. The sectored diffraction patterns for $S_2O_5F_2$ with deduced backgrounds.

[1]Tables of relative intensities are available, at a nominal charge, from the Depository of Unpublished Data, National Science Library, National Research Council of Canada, Ottawa, Canada K1A 0S2.

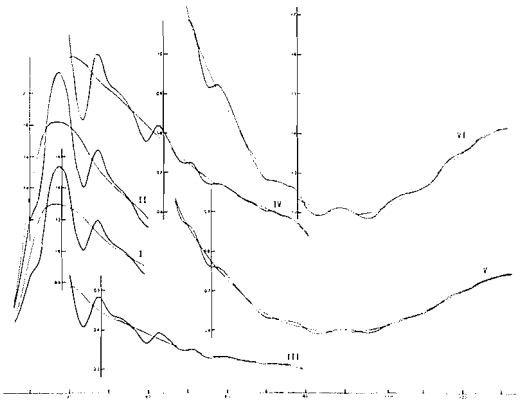

FIG. 2. The sectored diffraction patterns for $S_3O_8F_2$ with deduced backgrounds.

$S_2O_5F_2$ (Set 1 from curves I, IV, and V. Set II from curves II, III, and V of Fig. 1); $S_3O_8F_2$ (Set I from curves I, III, and V. Set II from curves II, IV, and VI of Fig. 2). Each composite was analyzed independently by a least squares procedure (13) which incorporated the Hartley modification (16). Correlation of errors between data points was allowed for by means of a non-diagonal weight matrix (17).

The elastic and inelastic scattering factors inserted in the computer program were those of Tavard *et al.* (18). Phase shifts were calculated from the Bonham and Ukaji expressions (19). Anharmonicity corrections were included in the theoretical $(\pi/10)qM(q)$ curves (20, 21). The structures were parametrized in terms of Hilderbrandt's (22) standard coordinate types; the calculated parameter values are based on the $r_g(0)$ distances.

Results for $S_2O_5F_2$

Two models were tested for $S_2O_5F_2$. One model was assigned C_2 symmetry about the bridge oxygen atom. (A single parameter specified the $-SO_2F$ group rotation about the S—O bridge bonds.) The other model was unsymmetrical and required an independent rotational parameter for each $-SO_2F$ group.

Since it proved impossible to determine all mean square amplitudes independently, they were grouped as follows: $l_1 \equiv l_{S=O} = 0.04$ Å; $l_2 \equiv l_{S-O} = l_{S-F} = 0.05$ Å; $l_3 \equiv l_{OS=O} = l_{FS=O} = l_{O=S=O} = 0.06$ Å; $l_4 \equiv l_{OSF} = 0.065$ Å; l_5 (distances separated by four atoms) $\equiv 0.0884$ Å; l_6 (all other distances) $\equiv 0.123$ Å. Values for l_1–l_4 were based on the known values for SO_2F_2

Can. J. Chem. Downloaded from www.nrcresearchpress.com by 210.87.254.105 on 09/05/12
For personal use only.

(23) and modified by trial and error variation over a $\pm 10\%$ range. The others were determined by least squares while the remaining parameters were constrained. A least squares analysis was carried out for the geometrical parameters and resolution factor while the mean square amplitudes were constrained as outlined above. A systematic variation of the initial values of the rotational parameter(s) over all the staggered and eclipsed conformations resulted in several solutions for each of the above models. The refined values of the rotational parameters and the R factors for these solutions, labelled A–E, are presented in Table 1 for Data Set I. The values of the other parameters did not differ appreciably for the better fitting solutions. Substantially the same results were obtained from the data in Set II. The solutions B–E were tested against the "overall best fit", solution A, according to the R factor significance tests proposed by Hamilton (24, 25). On this basis the alternative solutions for the unsymmetrical model, B–D were rejected as less than 0.5% probable. The comparison test (25) favored solution A over solution E at the 99.5% confidence level.

The "overall best fit" solutions for Sets I and II are listed in Table 2. The arithmetic average parameters given in the third column were inscribed on the structure presented in Fig. 3. The $(\pi/10)qM_{exp}(q)$ and radial distribution curves are shown for Set I in Figs. 4 and 5, respectively. The interatomic distances are given in Table 3 and the correlation matrix is presented in Table 4.

The correlation matrix contains no large elements and therefore the selected parameters were essentially independently determinable. Although all the final calculations were based on optimum fitting of the $(\pi/10)qM_{exp}(q)$ curve, the radial distribution function (Fig. 5) illustrates

TABLE 1. Alternative solutions for the structure of $S_2O_5F_2$ (results for Data Set I)

Solution	$\tau_{F4...S3}$ (deg)	$\tau_{F5...S2}$ (deg)	R*
A	52.4±2.7	71.6±2.4	0.0549
B	316.7±3.5	59.7±3.5	0.0644
C	173.0±3.5	306.1±4.5	0.0681
D	154.0±6	166.4±6	0.1164
E	64.3±2.4		0.0768

$$*R = \frac{\sum_q (\pi/10qM_{exp}(q) - \pi/10qM_{theor}(q))^2 W(q)^{1/2}}{\sum_q (\pi/10qM_{exp}(q))^2 W(q)}$$

where $W(q)$ is the weight.

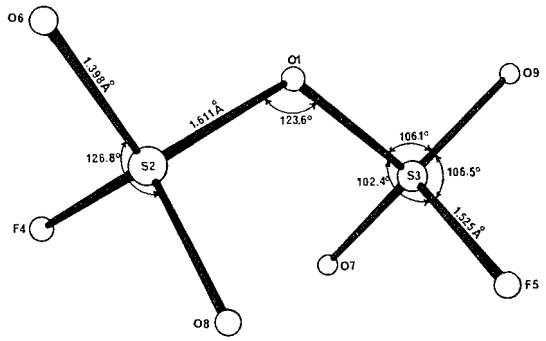

FIG. 3. The molecular structure of $S_2O_5F_2$ with final estimated parameters.

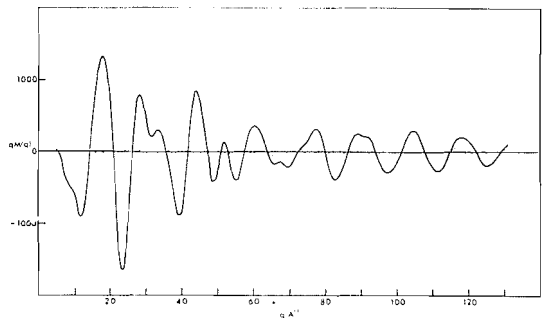

FIG. 4. The experimental molecular intensity, $\pi/10$-$qM(q)$, Set I, for $S_2O_5F_2$, with difference curve for "best fit" solution.

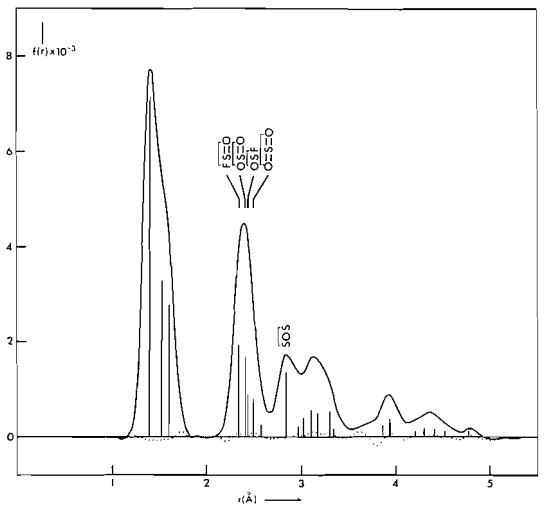

FIG. 5. The radial distribution curve calculated from Set I, $S_2O_5F_2$ with difference curve for "best fit" solution.

TABLE 2. Structural parameters for $S_2O_5F_2$

Parameter	Value		
	Data Set I*	Data Set II*	Average†
S═O	1.398 ±0.002 Å	1.397 ±0.002 Å	1.398±0.002 Å
S—F	1.523 ±0.005 Å	1.527 ±0.005 Å	1.525±0.005 Å
S—O	1.608 ±0.005 Å	1.614 ±0.004 Å	1.611±0.005 Å
∠SOS	123.8 ±0.5°	123.2 ±0.4°	123.6 ±0.5°
∠OS═O	106.2 ±0.9°	106.0 ±0.6°	106.1 ±0.9°
∠FS═O	106.5 ±0.6°	106.6 ±0.5°	106.6 ±0.6°
∠O═S═O‡	126.7 ±1.2°	126.8 ±1.1°	126.8 ±1.2°
∠OSF	102.3 ±1.8°	102.4 ±1.2°	102.4 ±1.8°
$\tau_{F4...S3}$	52.4 ±2.7°	55.1 ±2.4°	53.8 ±2.7°
$\tau_{F5...S2}$	71.6 ±2.4°	75.8 ±2.4°	73.7 ±2.4°
R factor	0.0549	0.0514	

*Quoted uncertainties are three times the calculated values. The factor of 3 has been shown to encompass the non-random errors in the analysis (35) or approximately the 95% confidence level.
†Average values calculated from Sets I and II.
‡Redundant parameter calculated from the others.

TABLE 3. Interatomic distances and root mean square amplitudes (in parentheses) for $S_2O_5F_2$*

	O1	S2	S3	F4	F5	O6	O7	O8	O9
O1	0								
S2	1.611 (0.050)	0							
S3	1.611 (0.050)	2.840 (0.065)	0						
F4	2.445 (0.065)	1.525 (0.050)	3.105 (0.088)	0					
F5	2.445 (0.065)	3.302 (0.088)	1.525 (0.050)	3.859 (0.123)	0				
O6	2.408 (0.060)	1.398 (0.040)	3.929 (0.088)	2.343 (0.060)	4.524 (0.123)	0			
O7	2.408 (0.060)	3.018 (0.088)	1.398 (0.040)	2.581 (0.123)	2.343 (0.060)	4.212 (0.123)	0		
O8	2.408 (0.060)	1.398 (0.040)	3.171 (0.088)	2.343 (0.060)	2.965 (0.123)	2.500 (0.060)	3.342 (0.123)	0	
O9	2.408 (0.060)	3.943 (0.088)	1.398 (0.040)	4.295 (0.123)	2.343 (0.060)	4.773 (0.123)	2.500 (0.060)	4.409 (0.123)	0

*Distances are r_g values quoted in Å and based upon the average parameter values of Table 2.

TABLE 4. Correlation matrix for $S_2O_5F_2$*

	r_{S-O}	∠SOS/2	r_{S-F}	∠OSF	$\tau_{F4...S3}$	$r_{S=O}$	∠OS═O	∠FS═O	$\tau_{F5...S2}$
σ	0.0016	0.1506	0.0017	0.5564	0.9270	0.0006	0.2833	0.1987	0.8131
	1	−0.57	0.25	−0.07	−0.13	−0.04	−0.27	0.04	0.00
		1	−0.08	−0.15	0.04	0.06	0.29	−0.12	0.07
			1	−0.28	−0.10	0.45	0.05	−0.40	−0.07
				1	0.62	−0.23	−0.77	0.67	0.52
					1	−0.09	−0.47	0.32	0.32
						1	0.13	−0.29	−0.09
							1	−0.72	−0.44
								1	0.38
									1

*Computed for Model A, Data Set I.

Can. J. Chem. Downloaded from www.nrcresearchpress.com by 210.87.254.105 on 09/05/12
For personal use only.

Can. J. Chem. Downloaded from www.nrcresearchpress.com by 210.87.254.105 on 09/05/12
For personal use only.

the process of structure determination. What initially appeared as a difficult resolution problem, exhibited by the second peak of the radial distribution curve was apparently offset by the facts that the S . . . S distance (third peak) was substantially resolved, and that the parameters determining the second peak had to be consistent with the remainder of the curve. The large estimated errors, particularly for OSF and O=S=O are nevertheless a reflection of this problem.

Results for $S_3O_8F_2$

The same approach used for $S_2O_5F_2$ was used for $S_3O_8F_2$. A symmetric model (C_{2v} symmetry) was assumed and a converged least squares solution could not be obtained without making the following constraints: the skeletal S—O (bridge) bonds were assumed equal; the terminal S=O bonds were assumed equal; and, the O—S=O angles were assumed equal. The "best fit" model is illustrated in Fig. 6. A systematic variation of the initial values of the conformation determining parameters led to several distinct least squares converged solutions which are given in Table 5. Alternatives to the "best fit" solution were rejected by the R test (22) as less than 0.5% probable. In all runs, the mean square amplitudes were constrained as follows: $l_1 = l_{S=O} = 0.039$ Å; $l_2 = l_{S-F} = l_{S-O} = 0.053$ Å; $l_3 = l_{OS=O} = l_{FS=O}\ l_{O=S=O} = l_{OSF} = l_{SOS} = l_{OSO} = 0.065$ Å; l_4 (2.844 − 3.267 Å) = 0.075 Å, l_5 (3.472 − 3.955 Å) = 0.097 Å; l_6 (4.117 − 4.462 Å) = 0.110 Å; l_7 (4.665 − 6.262 Å) = 0.154 Å.

The "best fit" parameter values are presented in Table 6. The interatomic distances and the correlation matrix are given in Tables 7 and 8, respectively. The experimental molecular scat-

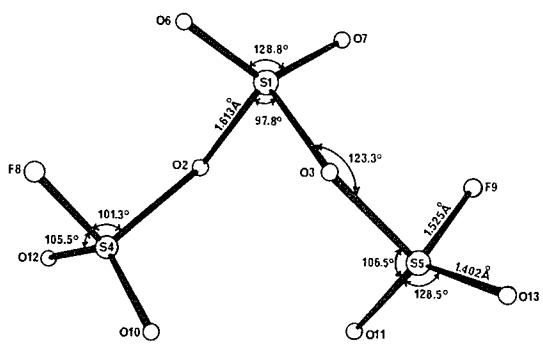

FIG. 6. The molecular structure of $S_3O_8F_2$ with final estimated parameters.

TABLE 5. Alternative solutions for the structure of $S_3O_8F_2$ (results for Data Set I)

Solution	$\tau_{O2...S5}$ (deg)	$\tau_{S1...F9}$ (deg)	R*
A	295.4±1.5	318.9±2.1	0.0755
B	298.8±2.0	54.0±2.8	0.0997
C	183.4±3.6	71.7±4.8	0.1182
D	297.0	176	0.1357
E	167	170.9	0.1565

*See footnote, Table 1.

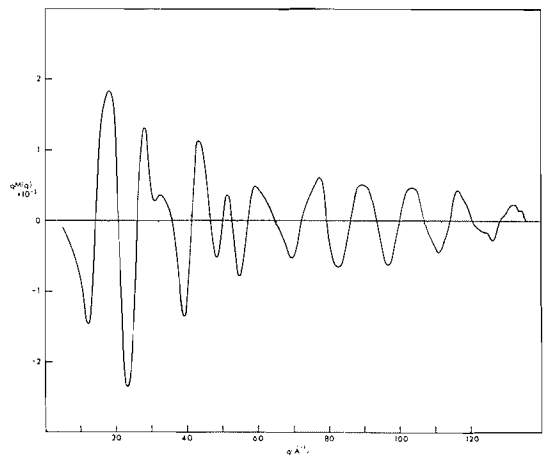

FIG. 7. The experimental molecular intensity, $\pi/10\text{-}qM(q)$, Set I, for "best fit" solution.

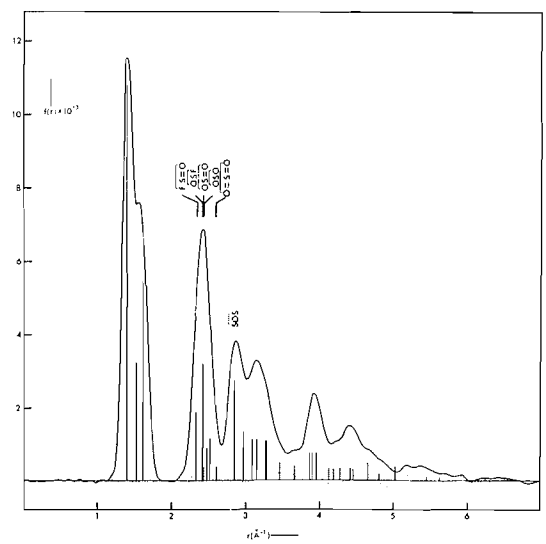

FIG. 8. The radial distribution curve calculated for Set I for $S_3O_8F_2$ with difference curve for "best fit" solution.

TABLE 6. Structural parameters for $S_3O_8F_2$

Parameter	Value		
	Data Set I*	Data Set II*	Average†
S=O	1.402 ±0.002 Å	1.402 ±0.003 Å	1.402±0.003 Å
S—F	1.527 ±0.012 Å	1.524 ±0.012 Å	1.525±0.012 Å
S—O	1.613 ±0.006 Å	1.612 ±0.006 Å	1.613±0.006 Å
∠OSO	97.5 ±0.9°	98.0 ±1.0°	97.8 ±1°
∠SOS	123.9 ±0.9°	123.3 ±1.2°	123.6 ±1.2°
∠OS=O	106.7 ±0.6°	106.3 ±0.8°	106.5 ±0.8°
∠FS=O	105.5 ±1.2°	105.6 ±1.2°	105.5 ±1.2°
∠O=S=O‡ (bridge)	—	—	128.8 ±1.4°
∠O=S=O‡ (terminal)	—	—	128.5 ±1.4°
∠OSF	100.8 ±1.2°	102.0 ±1.5°	101.3 ±1.5°
$\tau_{O2...S5}$	295.4 ±0.8°	295.1 ±0.9°	295.3 ±0.9°
$\tau_{S1...F9}$	319.0 ±2.1°	319.8 ±2.2°	319.4 ±2.2°
R	0.0755	0.0947	

*Uncertainties are three times the calculated values.
†Average values computed from the results of Sets I and II.
‡Redundant parameter.

TABLE 7. Interatomic distances and root mean square amplitudes (in parentheses) for $S_3O_8F_2$

	S1	O2	O3	S4	S5	O6	O7	F8	F9	O10	O11	O12	O13
S1	0												
O2	1.613	0											
	(0.053)												
O3	1.613	2.431	0										
	(0.053)	(0.065)											
S4	2.843	1.613	3.154	0									
	(0.065)	(0.053)	(0.075)										
S5	2.843	3.154	1.613	3.877	0								
	(0.065)	(0.075)	(0.053)	(0.097)									
O6	1.402	2.419	2.419	3.082	3.955	0							
	(0.040)	(0.065)	(0.065)	(0.075)	(0.097)								
O7	1.402	2.419	2.419	3.955	3.082	2.529	0						
	(0.040)	(0.065)	(0.065)	(0.097)	(0.075)	(0.065)							
F8	2.980	2.427	3.472	1.525	4.665	2.480	4.290	0					
	(0.075)	(0.065)	(0.097)	(0.053)	(0.154)	(0.065)	(0.110)						
F9	2.980	3.472	2.427	4.665	1.525	4.290	2.480	5.470	0				
	(0.075)	(0.097)	(0.065)	(0.154)	(0.053)	(0.110)	(0.065)	(0.154)					
O10	3.279	2.419	2.844	1.402	3.267	3.644	4.409	2.331	4.426	0			
	(0.075)	(0.065)	(0.075)	(0.040)	(0.075)	(0.097)	(0.110)	(0.065)	(0.110)				
O11	3.279	2.844	2.419	3.267	1.402	4.409	3.644	4.426	2.331	2.607	0		
	(0.075)	(0.075)	(0.065)	(0.075)	(0.039)	(0.110)	(0.097)	(0.110)	(0.065)	(0.065)			
O12	3.900	2.419	4.462	1.402	5.028	4.117	4.799	2.331	5.634	2.525	4.191	0	
	(0.097)	(0.065)	(0.110)	(0.040)	(0.154)	(1.110)	(0.154)	(0.065)	(0.154)	(0.065)	(0.110)		
O13	3.900	4.462	2.419	5.028	1.402	4.799	4.117	5.634	2.331	4.191	2.525	6.262	0
	(0.097)	(0.110)	(0.065)	(0.154)	(0.040)	(0.154)	(0.110)	(0.154)	(0.065)	(0.110)	(0.065)	(0.154)	

*Distances are r_g values quoted in Angstroms and are based upon the *average* parameter values of Table 6.

tering, $(\pi/10)qM_{exp}(q)$ and the radial distribution curves are shown in Figs. 7 and 8, respectively. As was the case with $S_2O_5F_2$, the valence angles could be determined because the S . . . S distance was resolved and because the accepted valence angles had to be consistent with the well structured outer region of the radial distribution curve.

Discussion

The structures of $S_2O_5F_2$ and $S_3O_8F_2$, given in Tables 2 and 6, show that the bond lengths fall within the expected limits, and the valence bond angles at sulfur follow the valence shell electron pair repulsion theory predictions (26). The bridge angles, ∠SOS, are not significantly different from

Can. J. Chem. Downloaded from www.nrcresearchpress.com by 210.87.254.105 on 09/05/12
For personal use only.

TABLE 8. Correlation matrix for $S_3O_8F_2$*

r_{S-O}	∠OSO/2	∠SOS	τ_{O2S5}	$r_{S=O}$	∠OS=O	r_{S-F}	∠OSF	$\tau_{S1...F9}$	∠FS=O
0.0019	0.3088	0.03341	0.2645	0.0008	0.2156	0.0039	0.3850	0.7237	0.4086
1	−0.19	−0.50	−0.06	0.10	−0.33	0.35	0.03	0.22	−0.36
	1	−0.46	0.76	−0.08	−0.41	−0.19	0.38	0.01	0.25
		1	−0.35	−0.05	0.39	−0.13	−0.39	−0.38	0.24
			1	−0.09	−0.25	−0.14	0.10	−0.03	0.26
				1	−0.12	0.50	−0.03	0.19	−0.29
					1	−0.13	−0.62	−0.45	0.03
						1	−0.08	0.26	−0.57
							1	0.51	−0.02
								1	−0.42
									1

*Computed for Model A, Data Set I.

TABLE 9. Comparison of structural parameters in related molecules

Molecule	S=O (Å)	S—O (Å)	S—F (Å)	∠O=S=O (deg)	∠SOS (deg)	Reference
$S_2O_5F_2$	1.398±0.002	1.611±0.005	1.525±0.005	126.8±1.2	123.6±0.5	This work
$S_3O_8F_2$	1.402±0.003	1.613±0.006	1.525±0.012	128.7±1.4	123.6±1.2	This work
SO_2F_2	1.405±0.003		1.530±0.003	124.0±0.2		27
SO_2FCl	1.408±0.006		1.55 ±0.02	123.7±1.0		28
SO_2Cl_2	1.403±0.003			123 ±2		29
$SO_2(CH_3)_2$	1.425±0.003			127.1±2.4		10
$S_2O_7^{2-}$(K)	1.437±0.004	1.645±0.005			124	5
$S_3O_{10}^{2-}$	1.38 ±0.05	1.54 1.72		122	122	6
$(SO_3)_\infty$	1.41 ±0.03	1.61 ±0.03		128	121	30
S_3O_9	1.371 (axial) 1.430 (equatorial)	1.626		126.1	121.5	36
SOF_4	1.403±0.003		1.552±0.004 (eq) 1.575±0.004 (ax)			32
SO_3F^-(K)	1.43 ±0.01		1.58 ±0.02	112.9		31
HSO_4^-	1.450±0.009	1.613±0.013				33
$C_2H_5SO_4^-$	1.464±0.004	1.603±0.007				34

those in the ions $S_2O_7^{2-}$ and $S_3O_{10}^{2-}$, and $S_5O_{16}^{2-}$ (37). A comparison of the principal geometric parameters with those in the several related species is presented in Table 9, which does, however, reveal several interesting variations.

Due to the necessary constraints that were made to the structure at the central sulfur atom, the alternation in S—O bond length along the chain, exhibited by these ions, could not be observed for $S_3O_8F_2$; however, the closeness of the value obtained (1.613 Å) to that in $S_2O_5F_2$ (1.611 Å) suggests that the difference in lengths is comparable to the estimated uncertainty (±0.006 Å) in this bond length.

The largest difference between the structures of the polysulfuryl fluorides and the sulfuryl halides is in the values of ∠O=S=O. Possibly, this increase in O=S=O angle reflects an increase in the S=O (terminal) bond orders. Bond orders for $S_2O_5F_2$ calculated on the basis of Cruickshank's scheme (7) are $1.6 < n_{S=O} < 2.375$, and $1.2 < n_{S-O}$ (bridge) < 1.25, compared with $1.5 < n_{S=O} < 2$ in SO_2F_2. The lower and upper limits are given for fluorine included or not included, respectively, in the dπ–pπ scheme; the lower limits coincide with the values calculated for $S_2O_7^{2-}$ by the above author (7). A larger bond order is indicated for $S_2O_5F_2$ at both limits. The trend to a larger S=O (terminal) bond order in the polysulfuryls than in SO_2F_2 is indicated by the corresponding shorter S=O bond lengths in the former compounds. While the difference in interatomic distances is marginal it is consistent with the larger O=S=O. That the S—F bond is short in both $S_2O_5F_2$ and $S_3O_8F_2$ compared with SO_2F_2 is consistent with its inclusion in the delocalization scheme. The S—O (bridge) bond length in both compounds is significantly smaller

Can. J. Chem. Downloaded from www.nrcresearchpress.com by 210.87.254.105 on 09/05/12
For personal use only.

Can. J. Chem. Downloaded from www.nrcresearchpress.com by 210.87.254.105 on 09/05/12
For personal use only.

than that in either $S_2O_7^{2-}$ or $S_3O_{10}^{2-}$ (average 1.63 Å) but agrees well with those in $(SO_3)_\infty$, $C_2H_5SO_4^-$, and HSO_3^- in which the bond orders are similar.

The apparent disagreement of the values of S—O and ∠O=S=O with the predictions of Gillespie and Robinson (3, 4) does not disprove the correlation between bond length and force constants but does illustrate the uncertainties involved in their method. The results for the valence parameters are consistent with delocalization of the bridge oxygen electrons throughout the molecule. Although the Cruickshank dπ–pπ bonding scheme may lack quantitative validity, it correctly predicts the structural trends in the present case.

The rotational conformations determined for $S_2O_5F_2$ and $S_3O_8F_2$ represent the best accommodation of the structural parameters to the data. It is assumed that all the other conformations are at least 2.5 kcal mol^{-1} less stable and therefore do not affect the electron diffraction patterns.

We extend our thanks to Professor R. J. Gillespie for helpful discussion. The financial support of the National Research Council of Canada and the Materials Science Center at Cornell University (ARPA-SD-68) is gratefully acknowledged.

1. R. J. Gillespie and E. A. Robinson. Can. J. Chem. **39**, 2179 (1961).
2. H. C. Clark and H. J. Emeleus. J. Chem. Soc. 190 (1958).
3. R. J. Gillespie and E. A. Robinson. Can. J. Chem. **41**, 2074 (1963).
4. R. J. Gillespie and E. A. Robinson. Can. J. Chem. **42**, 2496 (1964).
5. H. R. Lynton and M. R. Truter. J. Chem. Soc. 5112 (1960).
6. D. W. J. Cruickshank. Acta Cryst. **17**, 684 (1964); K. Eriks and C. H. MacGillavry. Acta Cryst. **7**, 430 (1954).
7. D. W. J. Cruickshank. J. Chem. Soc. 5486 (1961).
8. M. Atozi and R. E. Rundle. J. Chem. Phys. **29**, 1306 (1958).
9. L. S. Bartell, L. S. Su, and Hsiukang Yow. Inorg. Chem. **9**, 1903 (1970).
10. H. Oberhammer and W. Zeil. J. Mol. Struct. **6**, 399 (1970).
11. H. H. Jaffe and M. Orchin. Theory and applications of ultraviolet spectroscopy. John Wiley and Sons, Inc. New York, N.Y. 1962. Chapt. 17.
12. S. H. Bauer and K. Kimura. J. Phys. Soc. Jap. **17**, 300 (1962).
13. W. Harshbarger, G. Lee, R. J. Porter, and S. H. Bauer. Inorg. Chem. **8**, 1683 (1969).
14. J. L. Hencher and S. H. Bauer. J. Am. Chem. Soc. **89**, 5527 (1967).
15. S. H. Bauer and A. L. Andreassen. J. Mol. Struct. **12**, 381 (1972).
16. T. G. Strand, D. A. Kohl, and R. A. Bonham. J. Chem. Phys. **39**, 13Ç (1963).
17. Y. Murata and Y. Morino. Acta Cryst. **20**, 605 (1966).
18. C. Tavard, D. Nicholas, and M. Raoult. J. Chim. Phys. **64**, 540 (1967).
19. R. A. Bonham and T. Ukaji. J. Chem. Phys. **36**, 72 (1962).
20. L. S. Bartell. J. Chem. Phys. **23**, 1219 (1955).
21. Kozo Kuchitsu and L. S. Bartell. J. Chem. Phys. **35**, 1945 (1961).
22. R. L. Hilderbrandt. J. Chem. Phys. **51**, 1654 (1969).
23. Sven J. Cyvin. Molecular vibrations and mean square amplitudes. Elsevier Publishing Company, Amsterdam, The Netherlands. 1968.
24. W. C. Hamilton. Statistics in physical science. The Ronald Press Company, New York. 1964.
25. W. C. Hamilton. Acta Cryst. **18**, 502 (1965).
26. R. J. Gillespie and R. S. Nyholm. Q. Rev. Chem. Soc. **11**, 339 (1957); R. J. Gillespie. J. Chem. Educ. **40**, 295 (1963).
27. D. R. Lide, DeE. Mann, and R. M. Fristrom. J. Chem. Phys. **26**, 734 (1957).
28. C. W. Holt and M. C. L. Gerry. Chem. Phys. Lett. **9**, 621 (1971).
29. I. Hargittai. Acta Chim. Acad. Sci. Hung. **57**, 403 (1968).
30. R. Westrik and C. H. MacGillavry. Acta Cryst. **7**, 764 (1954).
31. K. O'Sullivan, R. C. Thompson, and James Trotter. J. Chem. Soc. (A), 2024 (1967).
32. Grete Gunderson and K. Hedberg. J. Chem. Phys. **51**, 2500 (1969); K. Kimura and S. H. Bauer. J. Chem. Phys. **39**, 3172 (1963); J. L. Hencher, D. W. J. Cruickshank, and S. H. Bauer. J. Chem. Phys. **48**, 518 (1968).
33. G. E. Pringle and T. A. Broadbent. Acta Cryst. **19**, 426 (1965).
34. M. R. Truter. Acta Cryst. **11**, 680 (1958).
35. A. L. Andreassen and S. H. Bauer. J. Chem. Phys. **56**, 3802 (1972).
36. W. S. McDonald and D. W. J. Cruickshank. Acta Cryst. **22**, 48 (1967).
37. R. De Vries and F. C. Mijlkoff. Acta Cryst. **B25**, 1696 (1969).

Complete Variational Treatment of the Hydrogen Molecule. I. The Full Electronic Hamiltonian

R. E. KARI,[1] A. C. H. CHAN,[2] G. HUNTER, AND H. O. PRITCHARD[3]

Centre for Research in Experimental Space Science, York University, Downsview, Ontario

Received November 7, 1972

The hydrogen molecule is treated with the $\nabla_1 \cdot \nabla_2$-term regarded as part of the Hamiltonian, rather than as a perturbation as was done by Kolos and Wolniewicz. Specimen results are presented for H_2 and D_2.

La molécule d'hydrogène a été étudiée en considérant que le terme $\nabla_1 \cdot \nabla_2$ fait partie de l'Hamiltonien, plutôt qu'en considérant que celui-ci est une perturbation comme il a été envisagé par Kolos et Wolniewicz. On présente des exemples de résultats obtenus pour H_2 et D_2.

[Traduit par le journal]

Can. J. Chem., **51**, 2055 (1973)

Can. J. Chem. Downloaded from www.nrcresearchpress.com by 210.87.254.42 on 09/05/12
For personal use only.

A detailed review of the discrepancies which existed between the theoretical calculations and the experimental observations for the hydrogen molecule was made a few years ago by Wilkinson and Pritchard (1). At that time it appeared that for the ground state ($X^1\Sigma_g^+$), (*a*) the calculated dissociation energy was too large by about $4\ cm^{-1}$, and (*b*) the calculated vibrational spacings of the low vibrational states were too large, the discrepancy being correlated with the nuclear reduced masses for H_2, HD, and D_2; there was also a slight suspicion that the calculated rotational spacings could be marginally high. Since then, it has been shown by Herzberg (2) that the experimental value for the dissociation energy was in error by between 4 and $5\ cm^{-1}$, and the position now is that the agreement between theory and experiment is as satisfactory as one could expect. The discrepancy in the vibrational spacings still remains, and is certainly not experimental in origin (1). Further, it represents all the more of a theoretical challenge because it is now known that the Born–Oppenheimer method predicted the first three vibrational spacings of the H_2^+ molecule (3, 4) correctly, to within the experimental accuracy (5), and that agreement for some of the lower rotational spacings is equally satisfactory. There is also excellent agreement between experimental (6) and theoretical (3) vibrational spacings for HD^+. If the Born–Oppenheimer method works for H_2^+, there seems no *a priori* reason why it should not also work for H_2, and therefore we have undertaken a thorough re-examination of the theoretical treatment of the ground state of the hydrogen molecule.

We accept at the outset that Kolos and Wolniewicz's 100-term infinite-mass calculation is correct and has converged to an acceptable limit (7) and we suppose that there is a defect in the subsequent evaluation of the vibrational spacings from the infinite-mass internuclear potential. Assuming that the Born–Oppenheimer method is valid (1) we can envisage two reasons why the correct result may not have been obtained: (*i*) that the calculation of the dc_i/dR required for the calculation of the expectation value of ∇_R^2 is an ill-conditioned problem (ref. 8, eq. 27); (*ii*) that it is logically incorrect to treat the $\nabla_1 \cdot \nabla_2$-term in the Hamiltonian in parallel with the ∇_R^2-term (8). We will address a future publication to (*i*) the rigorous calculation of the dc_i/dR, and in this paper we address ourselves to (*ii*) the rigorous treatment of the $\nabla_1 \cdot \nabla_2$-term.

We have noted previously that the $\nabla_1 \cdot \nabla_2$-term should properly be considered as part of the electronic Hamiltonian (9), and to treat it as do Kolos and Wolniewicz (8) means that the operator ∇_R^2 is operating on an incorrect electronic wave function. The effect is obviously small, but could be significant, especially if the correction to the effective internuclear potential were to be skewed about a point near the equilibrium internuclear separation. The expectation value of the operator $\nabla_1 \cdot \nabla_2$ is about $6\ cm^{-1}$ compared with a total energy of about $250\,000\ cm^{-1}$ (8), say one part in 40 000 which would imply that there

[1]Present address: Chemistry Department, Laurentian University, Sudbury, Ontario.

[2]Deceased, February 17th, 1971.

[3]Nuffield Foundation Fellow, Physical Chemistry Laboratory, University of Oxford, 1972–1973.

Can. J. Chem. Downloaded from www.nrcresearchpress.com by 210.87.254.42 on 09/05/12
For personal use only.

should be a correction to the electronic wave function of order 1 in 200 from this term. The subsequent effect of this error on the calculated expectation value for ∇_R^2 is hard to predict with confidence since it is a complicated function of derivatives of the electronic wave function. One has two choices: either one can follow the method of Kolos and Wolniewicz, but treat the $\nabla_1\cdot\nabla_2$- and ∇_R^2-perturbations in tandem, or one can include the $\nabla_1\cdot\nabla_2$-term in the electronic Hamiltonian, thereby losing the simplification that the same electronic wave functions can be used to describe H_2, HD, and D_2. The former choice is logically unacceptable. The first order perturbation correction to the energy would be the Kolos and Wolniewicz result, but to calculate the first order perturbation correction to the wave function, one has to know the (unperturbed) wave functions for excited states of the molecule. In this sense, one would be including part of the non-adiabatic coupling correction in a supposed attempt to calculate the adiabatic energy, and it would be impossible to identify how much non-adiabatic correction had been assimilated into the mass polarization term! Therefore, in this paper, we follow the approach of Gray, Hunter, and Pritchard (10), with the $\nabla_1\cdot\nabla_2$-term included in the original Hamiltonian: this method has the advantage that it is variational throughout, *i.e.* at the Born–Oppenheimer stage, at the adiabatic stage, and at the non-adiabatic stage, the calculated energies are always upper bounds. We do not propose at this time to go beyond the adiabatic approximation, however. We begin with the system of coordinates[4] as defined in Fig. 1 and by standard procedures factorize out the motion of the center of mass of the system, arriving at a kinetic-energy operator T (in atomic units), relative to the center of mass of the system, of the form

$$[1]\quad T = -\tfrac{1}{2}\left\{\frac{1}{\mu_{A1}}[\nabla_\alpha^2 + \nabla_\beta^2] + \frac{2}{M_A}[\nabla_\alpha\cdot\nabla_{AB} + \nabla_\beta\cdot\nabla_{AB} + \nabla_\alpha\cdot\nabla_\beta] + \frac{1}{\mu_{AB}}\nabla_{AB}^2\right\}$$

where

$$[2]\quad \frac{1}{\mu_{A1}} = \frac{M_A + M_1}{M_A M_1} = \frac{M_A + M_2}{M_A M_2} = \frac{1 + M_A}{M_A}$$

and

$$\frac{1}{\mu_{AB}} = \frac{M_A + M_B}{M_A M_B}$$

Now, transforming from center-of-mass coordinates to mid-point-of-the-bond coordinates (7, 10), the kinetic energy operator becomes

$$[3]\quad T = -\tfrac{1}{2}\left\{\nabla_1^2 + \nabla_2^2 + \frac{1}{4\mu_{AB}}(\nabla_1 + \nabla_2)^2 + \frac{1}{\mu_{AB}}\nabla_R^2 + \frac{1}{\mu_A}(\nabla_1\cdot\nabla_R + \nabla_2\cdot\nabla_R)\right\}$$

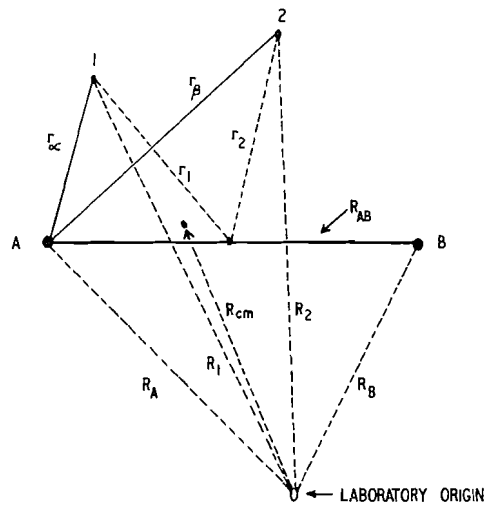

FIG. 1. Illustration of relationship between the two sets of coordinate systems used in the Born–Oppenheimer separation for H_2 and D_2. Center of mass coordinates: $\boldsymbol{r}_\alpha = \boldsymbol{R}_1 - \boldsymbol{R}_A$, $\boldsymbol{r}_\beta = \boldsymbol{R}_2 - \boldsymbol{R}_A$, $\boldsymbol{R}_{AB} = \boldsymbol{R}_B - \boldsymbol{R}_A$. Mid-point of bond coordinates: $\boldsymbol{r}_1 = \boldsymbol{r}_\alpha - \frac{1}{2}\boldsymbol{R}_{AB}$, $\boldsymbol{r}_2 = \boldsymbol{r}_\beta - \frac{1}{2}\boldsymbol{R}_{AB}$, $\boldsymbol{R} = -\boldsymbol{R}_{AB}$.

[4]The choice of systems of coordinates is arbitrary, and largely a matter of convenience, as was noted by Kolos (7). We would at this time add that the three different coordinate systems for effecting the diatomic Born–Oppenheimer separation discussed by Hirschfelder *et al.* (11, 12) are related by a scale parameter (or synonymously by a reduced mass factor in the electronic kinetic energy operator). Whatever coordinate system is used initially, the subsequently determined electronic wave function must be scaled so that the adiabatic electronic energy tends to the correct separated atom limit (9, 10). After this scaling, the electronic wave function is unique: *i.e.* coordinate system independent, so that the calculated adiabatic correction to the electronic energy is also unique. Hirschfelder *et al.*'s discussion of the relative merits of their three different coordinate systems based upon the relative magnitudes of their apparent adiabatic corrections (which included different implicit scaling corrections for each case) is therefore an artefact from the point of view of the essential nature of the Born–Oppenheimer separation.

TABLE 1. Eigenvalues and expectation values calculated via eqs. 5*a* and 5*c* for H_2 and D_2 with $\alpha = 1.0$ and $R = 1.4$ a.u., using the same 20th order wave function as was used by Kolos and Wolniewicz (8): energies in a.u.; $M_A^H = 1836.11686$ a.u., $M_A^D = 3670.4119$ a.u.

	Equation 5*a*		Equation 5*c*	
Quantity	H_2	D_2	H_2	D_2
V(electronic) (V_1)	−3.0633399896		−3.0628572615	−3.0630984744
V(nuclear) (V_2)	0.7142857143		0.7142857143	
$V = V_1 + V_2$	−2.3490542753		−2.3485715472	−2.3488127601
T(electronic)	1.1747118377		1.1745764911†	1.1746441213†
$E = T + V$ (E_5)	−1.1743424376*		−1.1739950561*	−1.1741686388*
∇_i^2-term (ε_6)	0.0003198903	0.0001600245	—	—
$\nabla_1 \cdot \nabla_2$-term (ε_7)	0.0000275787	0.0000137962	—	—
$E = E_5 + \varepsilon_6 + \varepsilon_7$	−1.1739949686	−1.1741686169	−1.1739950561*	−1.1741686388*

*An asterisk marks the solution of an eigenvalue equation, and represents the stage in the calculation at which the total energy E is strictly variational.
†Now includes ε_6 and ε_7: the expectation values for the infinite-mass ∇_i^2-terms are 1.1742291971 a.u. and 1.1744703444 a.u., respectively.

where

$$[4] \qquad \frac{1}{\mu_A} = \frac{M_A - M_B}{M_A M_B}$$

a well-known result (7, 13). For the present, we will confine our attention to the homonuclear molecules H_2 and D_2, with the simplification that the last term in eq. 3 drops out because μ_A^{-1} becomes zero: the complete treatment of the heteronuclear HD would require the retention of this term; eq. 3 then becomes

$$[5] \quad T = -\tfrac{1}{2}\left\{\left(1 + \frac{1}{2M_A}\right)(\nabla_1^2 + \nabla_2^2) + \frac{1}{M_A}\nabla_1 \cdot \nabla_2 + \frac{2}{M_A}\nabla_R^2\right\}$$

where M_A is now either the mass of the proton or the deuteron in atomic units.

Our treatment differs from that of Kolos and Wolniewicz in two respects.[5] They solved the Schrödinger equation with an infinite-mass kinetic energy operator

$$[5a] \qquad T = -\tfrac{1}{2}(\nabla_1^2 + \nabla_2^2)$$

and treated the terms $(2M_A)^{-1}\nabla_1^2$, $(2M_A)^{-1}\nabla_2^2$, $M_A^{-1}\nabla_1 \cdot \nabla_2$, and $2M_A^{-1}\nabla_R^2$ as perturbations. A superior procedure, as we have shown previously (9, 10), would have been to include the first two of these terms in the Hamiltonian, *viz.*

$$[5b] \quad T = -\tfrac{1}{2}\left(1 + \frac{1}{2M_A}\right)(\nabla_1^2 + \nabla_2^2)$$

treating only $M_A^{-1}\nabla_1 \cdot \nabla_2$ and $2M_A^{-1}\nabla_R^2$ as perturbations. The advantage of this slight modification is that the energy (also the wavefunction) is variational at this stage, thereby reducing the uncertainty in the final computed energy. We re-emphasize here that it is quite unnecessary to perform the Born–Oppenheimer separation in the traditional way using infinite-mass nuclei with the natural electronic mass. The version we have described before for H_2^+ etc. (3, 9, 10) which uses a different reduced electronic mass for each molecule is equally valid, and in fact superior as we have just mentioned because one has a variational solution at a later stage in the development of the calculation. Better still is to attempt to solve the Schrödinger equation for H_2 and D_2 with the $\nabla_1 \cdot \nabla_2$-term included in the Hamiltonian, *i.e.*

$$[5c] \quad T = -\tfrac{1}{2}\left\{\left(1 + \frac{1}{2M_A}\right)(\nabla_1^2 + \nabla_2^2) + \frac{1}{M_A}\nabla_1 \cdot \nabla_2\right\}$$

In this way the electronic wave function which will be used to determine the ∇_R^2-correction will be both complete and strictly variational; likewise, the effective Born–Oppenheimer potential, to which this correction is to be added to determine the final rotation–vibration energy levels, is also strictly variational. The required manipulations are lengthy, and will be made available

[5] We note that there is a misprint in the original expression for the Hamiltonian matrix element given by Kolos and Roothaan (14): in their eq. 15 there is a superfluous coefficient 2 associated with the $K_{\bar{p}+1,\,\bar{q}\bar{s}}^{\bar{\mu}}$ term.

Can. J. Chem. Downloaded from www.nrcresearchpress.com by 210.87.254.42 on 09/05/12
For personal use only.

TABLE 2. Expectation values, in cm^{-1}, for the finite-mass and mass-polarization kinetic energy correction terms; 1 a.u. = 219474.72 cm^{-1}

	Equation 5*a*		Equation 5*c*	
Quantity	H_2	D_2	H_2	D_2
∇_i^2-term	70.2078	35.1213	70.1790	35.1141
$\nabla_1 \cdot \nabla_2$-term	6.0528	3.0279	6.0433	3.0255
Total = $\varepsilon_6 + \varepsilon_7$	76.2607	38.1493	76.2222	38.1396

in thesis form shortly (15). Suffice to say at this stage that one requires the same integrals in either the Kolos and Wolniewicz procedure and in ours. However, since the computation of the integrals consumes about 90–95% of the computing time required to perform the calculation for a single pair of values of α and R, the fact that eq. 5*c* is different for each isotopic species is of minimal consequence; the same integrals are required for either H_2 or D_2 with only slightly different scaling factors.

In Table 1 we reproduce specimen results for the same 20th order wave function as is listed in Table 5 of ref. 8, for the exponent $\alpha = 1.0$ and internuclear separation $R = 1.4$ a.u. It can be seen that at this stage in the calculation, there is excellent agreement between the two methods, as one would expect. We conclude therefore that the source of the discrepancy between theory and experiment in respect of the vibrational spacings must, for reasons such as we have outlined at the beginning of this paper, be located in the calculation of the ∇_R^2-term. Table 2 lists, for comparison purposes the expectation values for the finite mass correction and the mass polarization terms corresponding to the wave functions obtained from eqs. 5*a* and 5*c*: they agree very closely of course, with the *percentage* error in the total correction being less for D_2 than for H_2 by a factor of about two.

1. P. G. WILKINSON and H. O. PRITCHARD. Can. J. Phys. **47**, 2493 (1969).
2. G. HERZBERG. J. Mol. Spectrosc. **33**, 147 (1970).
3. G. HUNTER and H. O. PRITCHARD. J. Chem. Phys. **46**, 2153 (1967).
4. C. L. BECKEL, B. D. HANSEN, and J. M. PEEK. J. Chem. Phys. **53**, 3681 (1970).
5. G. HERZBERG and C. JUNGEN. J. Mol. Spectrosc. **41**, 425 (1972).
6. S. TAKEZAWA and Y. TANAKA. J. Chem. Phys. **56**, 6125 (1972).
7. W. KOLOS. Adv. in Quantum Chem. **5**, 99 (1970).
8. W. KOLOS and L. WOLNIEWICZ. J. Chem. Phys. **41**, 3663 (1964).
9. G. HUNTER. J. Chem. Phys. **45**, 3022 (1966).
10. B. F. GRAY, G. HUNTER, and H. O. PRITCHARD. J. Chem. Phys. **45**, 3806 (1966).
11. D. W. JEPSEN and J. O. HIRSCHFELDER. J. Chem. Phys. **32**, 1323 (1960).
12. R. T. PACK and J. O. HIRSCHFELDER. J. Chem. Phys. **49**, 4009 (1968).
13. W. KOLOS and L. WOLNIEWICZ. Rev. Mod. Phys. **35**, 473 (1963).
14. W. KOLOS and C. C. J. ROOTHAAN. Rev. Mod. Phys. **32**, 219 (1960).
15. L. WAGSCHAL. Thesis. York University, Toronto. To be submitted.

Can. J. Chem. Downloaded from www.nrcresearchpress.com by 210.87.254.42 on 09/05/12
For personal use only.

"Transitions vibrationnelles simultanées" d'un donneur et d'un accepteur de proton[1]

ANDRÉ BURNEAU ET JACQUES CORSET

Laboratoire de Spectrochimie Moléculaire, Université de Paris VI, 75230 Paris Cedex O5 et Laboratoire de Chimie Physique, C.N.R.S., 2 rue Henri Dunant, 94320 Thiais

Reçu le 14 novembre 1972

Des absorptions dans le proche infrarouge mettant en jeu simultanément des vibrations de plusieurs molécules, sont mises en évidence pour des mélanges renfermant un donneur de protons RXH et un accepteur R′AB. Les donneurs étudiés sont: le chloroforme, l'eau, le pentachlorophénol, et le méthanol, et les accepteurs: l'acétonitrile, l'acétone, le diméthylsulfoxyde, et la pyridine; pour comparaison, le sulfure de carbone et l'hexachloroacétone sont aussi utilisés comme solvants. On observe non seulement des combinaisons νXH + νAB et νXH + $\nu_3(CS_2)$ mais aussi νXH + νR′, vers 6500 cm^{-1}, si R′ renferme des liaisons CH; ces absorptions à 6500 cm^{-1} n'existent pas si l'on utilise une base R′AB complètement deutériée. Les résultats suggèrent une corrélation entre l'augmentation d'intensité, par formation de liaisons hydrogène, des bandes νXH et de celle des transitions simultanées. Ces transitions, dont l'intensité est quelquefois plus grande que celle des harmoniques 2νXH, contribuent notablement au spectre des donneurs de protons dans le proche infrarouge. Il est probable que ces conclusions, fondées sur l'étude de liaisons hydrogène relativement faibles, peuvent être étendues à des interactions plus fortes; mais l'élargissement des bandes d'absorption rend difficile l'observation des transitions simultanées dans le cas de liaisons hydrogène fortes.

Absorptions simultaneously involving the vibrations of two molecules are brought out of the near infrared spectra of mixtures containing a proton donor RXH and an acceptor R′AB. The donors under study are: chloroform, water, pentachlorophenol, and methanol, and the acceptors: acétonitrile, acetone, dimethylsulfoxide, and pyridine; for comparison, carbon disulfide and hexachloracetone are also used as solvents. Not only the combinations νXH + νAB and νXH + $\nu_3(CS_2)$ are observed, but also νXH + νR′, at about 6500 cm^{-1}, if R′ contains CH bonds; these absorptions at 6500 cm^{-1} do not exist when fully deuterated bases R′AB are used. A correlation between the intensity increase, through hydrogen bonding, of the νXH bands and that of the simultaneous transitions is suggested by the results. In the assignment of the near infrared spectra of proton donors, it is important to take into account the simultaneous transitions because their intensity is sometimes greater than that of the overtones 2νXH. It is likely that these conclusions, founded on the study of relatively weak hydrogen bonds, may be extended to stronger interactions; but the width of the absorption bands in the case of strong hydrogen bond makes the observation of the simultaneous transitions difficult.

Can. J. Chem., 51, 2059 (1973)

Introduction

Au cours de l'étude, dans le proche infrarouge, du spectre de l'eau en interaction avec des solvants organiques accepteurs de protons (1–5), nous avons observé des absorptions mettant en jeu simultanément des vibrations de la molécule d'eau et des molécules de bases. Nous avons pu mettre en évidence de telles transitions vibrationnelles dans d'autres systèmes donneur–accepteur de protons: nous avons déjà publié des résultats préliminaires (6, 7). D'autres auteurs avaient montré l'existence de ce phénomène soit dans des mélanges de gaz comprimés (8, 9), soit dans des phases condensées, à l'état liquide (10–14) ou solide (par ex. 15, 16).[2]

Jusqu'à ces dernières années, il y avait peu d'observations sûres de transitions simultanées dans des mélanges susceptibles de former des liaisons hydrogène. Nous avons donc essayé de savoir si ce phénomène constitue une propriété générale de la liaison hydrogène et de préciser le rôle qu'elle peut y jouer. Pour cela nous avons examiné à la fois des mélanges RXH–BAR′ et RXH–CS_2, le sulfure de carbone étant un solvant quasi inerte.[3] Dans les premiers mélanges, nous avons observé non seulement des transitions νXH + νAB mais aussi νXH + νR′. Dans certains cas, la comparaison du spectre du soluté RXH dans le solvant BAR′ hydrogéné et deutérié nous a permis de prouver l'existence de telles transitions. Dans d'autres cas l'interprétation

[1]Avec la collaboration technique de Jean Limouzi.

[2]Dans la suite nous utiliserons, à propos de ce phénomène, l'expression "transitions vibrationnelles simultanées", suivant en cela les premiers auteurs, plutôt que celle de "double excitation" (13, 15).

[3]RXH désigne le donneur de protons et R′AB un solvant organique ayant un groupement diatomique basique AB et un ou plusieurs radicaux R′.

Can. J. Chem. Downloaded from www.nrcresearchpress.com by 210.87.254.6 on 09/05/12
For personal use only.

du spectre en terme de transition simultanée est probable, sans pour cela être univoque.

Conditions expérimentales

Les spectres ont été enregistrés à l'aide de spectromètres Perkin Elmer 225, Beckman IR 12, et Cary 14, celui-ci étant équipé d'un potentiomètre d'échelle 0–2 ou 0–0.2 unités d'absorbance. La température de stabilisation des solutions dans les faisceaux du Cary 14 est d'environ 30 °C. La largeur de fente spectrale a été maintenue à une valeur égale, au plus, au dixième de la largeur à mi-hauteur de la bande observée. Dans les figs. 1 à 5, les abscisses sont linéaires en longueur d'ondes mais les maximums d'absorption sont repérés en cm^{-1}. La précision de la mesure du nombre d'ondes au maximum d'absorption est estimée, sauf indication contraire, de 1 à 5 cm^{-1}, suivant la forme de la bande. Mais, quand il y a recouvrement de bandes, ou quand ces dernières sont larges, il est possible que le maximum d'absorption ne corresponde que de façon approchée à la position de la transition étudiée. De plus, la fréquence du maximum de certaines bandes, faisant intervenir un vibrateur associé, varie avec la concentration du mélange.

Le "spectre de mesure" est celui d'une solution renfermant des concentrations données de soluté et de solvant, sous une épaisseur e. Le "spectre de référence" est défini théoriquement comme celui qui ne correspond

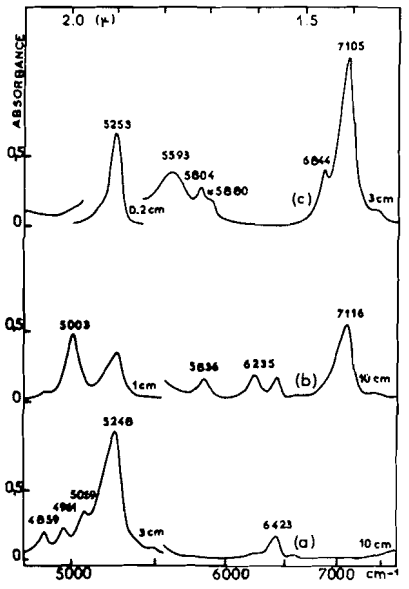

FIG. 2. Spectres d'absorption de H_2O, DHO, et D_2O en solution dans l'acétonitrile-d_3. Concentrations (M): (*a*) D_2O:1 (*b*) D_2O:0.72; DHO:0.25; H_2O:0.03 (*c*) H_2O:1. Les épaisseurs sont indiquées près des spectres.

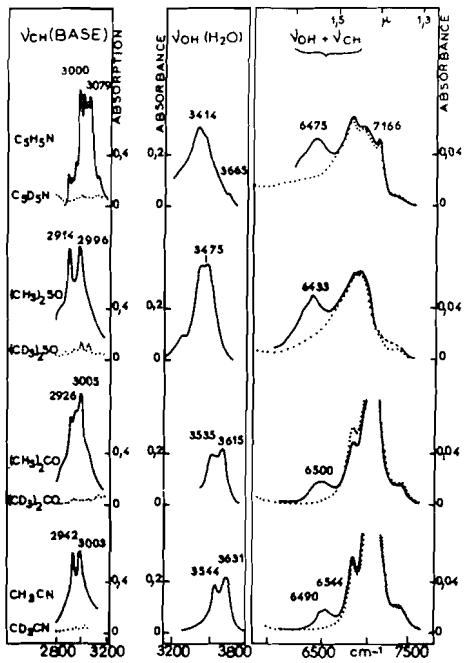

FIG. 1. Spectres d'absorption de H_2O en solutions dans des solvants organiques hydrogénés (courbes en traits pleins) et deutériés (courbes en pointillés) de 3200 à 3800 et de 6000 à 7500 cm^{-1}, et des solvants purs de 2800 à 3200 cm^{-1}. Concentration en eau = 0.5 M. En dessous de 3800 cm^{-1}: l = 0.005 cm; de 6000 à 7500 cm^{-1}: l = 1 cm.

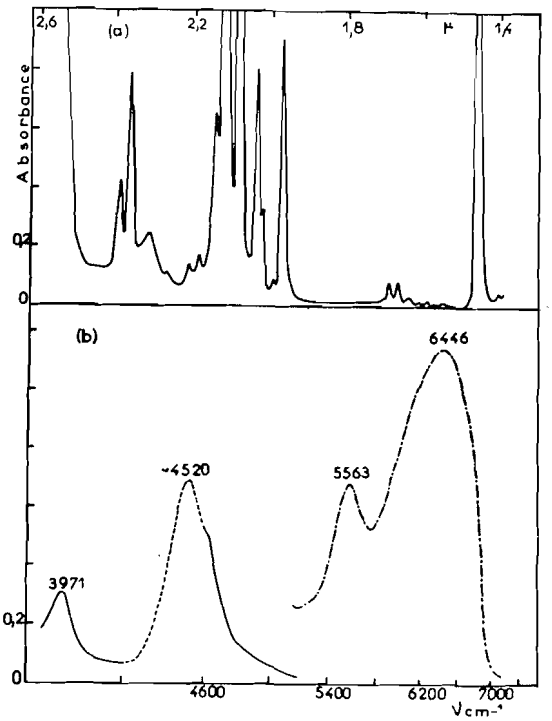

FIG. 3 Spectres d'absorption du pentachlorophénol en solution (*a*) dans le tétrachlorure de carbone (*b*) dans l'acétonitrile-d_3. Concentrations (M): (*a*) 0.1 (*b*) 0.5. Epaisseurs (cm): (*a*) 10(*b*)---1; ---1 × 10.

Can. J. Chem. Downloaded from www.nrcresearchpress.com by 210.87.254.6 on 09/05/12
For personal use only.

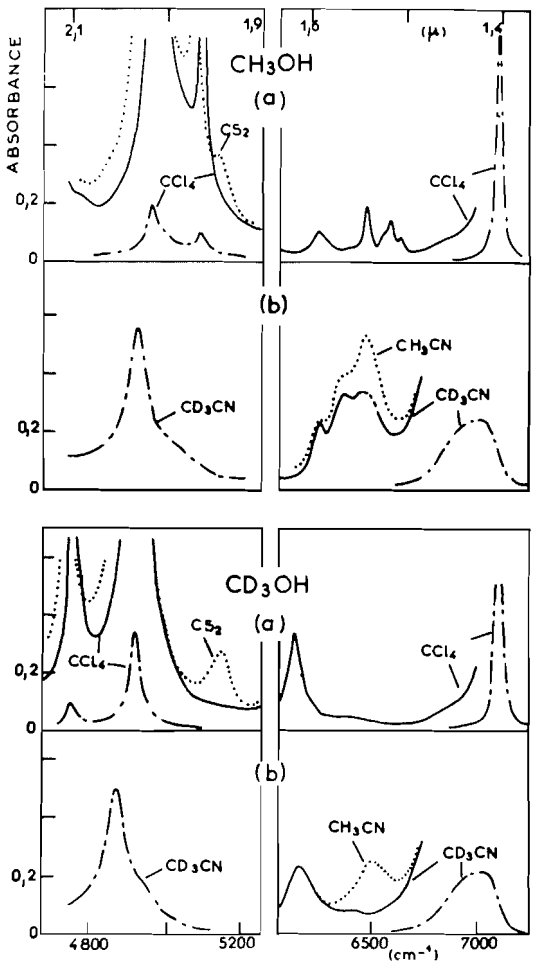

FIG. 4. Spectres d'absorption des molécules CH_3OH et CD_3OH en solution (*a*) dans le tétrachlorure ou le sulfure de carbone, (*b*) dans l'acétonitrile-d_3 ou -h_3. Concentrations (*M*): (*a*) 0.02 (*b*) 0.8. Epaisseurs (cm): (*a*) --- 20, — et ··· 20 × 10; (*b*) --- 1; — et ··· 1 × 10.

qu'aux molécules de solvant dans cet échantillon. Les figs. 1 à 5 ont été obtenues en soustrayant le spectre de référence du spectre de mesure, dans les régions où le solvant n'absorbe que modérément: elles représentent à la fois le spectre du soluté et le spectre éventuel des transitions simultanées. La soustraction a été faite soit par le calcul, soit directement par compensation dans les deux faisceaux du spectromètre Cary 14, en utilisant des cuves convenablement appariées.

Le spectre de référence ne peut pas être obtenu exactement, car il dépend des interactions moléculaires avec le soluté. Pour en obtenir la meilleure approximation, nous avons souvent préparé une solution de référence renfermant un volume de tétrachlorure de carbone égal au volume de soluté dans la solution de mesure, le tétrachlorure de carbone étant inerte et n'absorbant pas dans les régions spectrales étudiées. Sous l'épaisseur *e*, le nombre de molécules de solvant contenues dans les échantillons de référence et de mesure est un peu différent si les volumes de mélange soluté–solvant et CCl_4–solvant ne sont pas identiques; l'état de certaines molécules de solvant dans les deux solutions peut aussi être un peu différent. Cependant, nous pensons que les résultats présentés dans les figs. 1 à 5 sont fiables, surtout pour les solutions diluées, parce que nous avons sélectionné les régions spectrales où le solvant est suffisamment transparent et où les absorptions sont peu sensibles aux interactions. Des défauts de compensation dus à des bandes fines de solvant ont parfois été observés sur des absorptions larges du soluté; ils ne faussent pas l'allure générale du spectre du soluté mais interdisent d'en connaître le profil rigoureux; les régions spectrales correspondantes sont repérées par des courbes en tirets (---) dans les figs. 1 à 5.

Pour préparer les solutions, nous avons utilisé les solvants hydrogénés pour spectrophotométrie, de chez Prolabo, desséchés sur tamis moléculaire 4A; dans le cas du chloroforme, du tamis 5A a été ajouté pour éliminer l'alcool. Le pentachlorophénol provenait de chez Eastman Kodak. Les solvants deutériés ont été

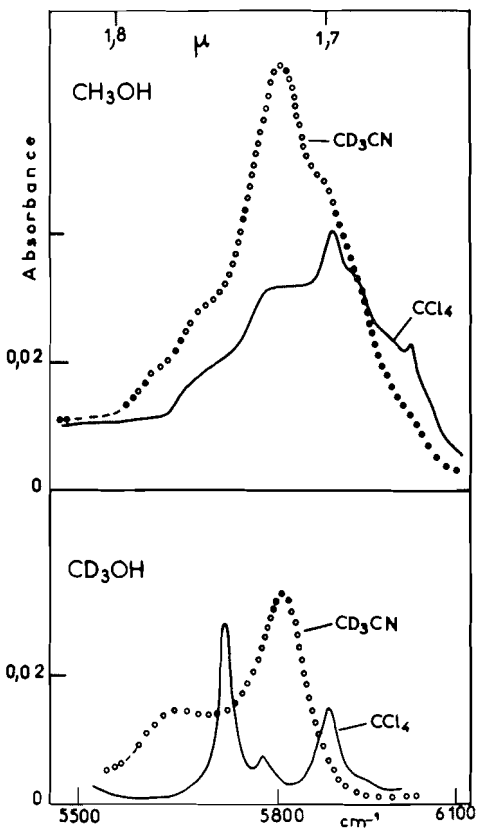

FIG. 5. Spectres d'absorption des molécules CH_3OH et CD_3OH en solution dans le tétrachlorure de carbone (c = 0.02 *M*), et dans l'acétonitrile-d_3 (c = 0.8 *M*). Le produit concentration × épaisseur de cuve est le même pour tous les spectres: $c.l$ = 0.4 cm mol l^{-1}.

Can. J. Chem. Downloaded from www.nrcresearchpress.com by 210.87.254.6 on 09/05/12
For personal use only.

Can. J. Chem. Downloaded from www.nrcresearchpress.com by 210.87.254.6 on 09/05/12
For personal use only.

fournis par C.E.A. France (taux isotopique 99.3 à 99.8%); l'alcool CD_3OH a été préparé à partir de CD_3OD par hydrolyse de l'alcoolate CD_3ONa. Les solvants deutériés ont été utilisés soit pour prouver l'existence de transitions simultanées, soit uniquement à cause de leur transparence. Nous avons vérifié qu'il n'y avait pas d'échange isotopique entre le soluté et le solvant dans les mélanges étudiés ici. Nous nous sommes assurés en particulier que les bandes entre 5800 et 5900 cm^{-1}, dans le spectre du mélange H_2O–CD_3CN ne sont pas dues à l'apparition d'acétonitrile hydrogéné dont les harmoniques 2νCH pourraient absorber dans cette région. Pour cela nous avons examiné le spectre du solvant ayant servi à préparer la solution, après séchage sur tamis moléculaire 4A. Au contraire, nous avons observé un échange isotopique entre les donneurs de protons et l'acétone-d_6. Nous n'avons pas retenu les résultats obtenus avec les mélanges CH_3OH–$(CD_3)_2CO$ parce que la bande observée vers 5200 cm^{-1} peut être non seulement la transition simultanée νOH(CH_3OH) + νCO($(CD_3)_2CO$), mais aussi l'harmonique 2νOD du méthanol CH_3OD qui apparaîtrait au cours du spectre: l'existence de la transition simultanée, très probable, nécessiterait une étude soignée de la cinétique d'échange pour être prouvée. Cependant, l'échange isotopique est suffisamment lent dans le mélange H_2O–$(CD_3)_2CO$ pour que le spectre puisse être étudié, en particulier vers 6500 cm^{-1}.[4]

Résultats

Nous avons étudié des solutions renfermant comme donneurs de protons RXH(D): le chloroforme (6) (figs. 6 et 7), l'eau (figs. 1 et 2, tableau 1), le pentachlorophénol (fig. 3) et le méthanol (figs. 4 et 5, tableaux 2 à 4), et comme accepteurs R′AB divers solvants: l'acétonitrile, l'acétone, le diméthylsulfoxyde (DMSO), et la pyridine. Afin de comparer les propriétés des mélanges avec ou sans liaison hydrogène, nous avons aussi examiné les solutions de méthanol et de chloroforme dans le sulfure de carbone (figs. 4 et 6, tableau 4), et l'hexachloroacétone.

L'attribution préalable du spectre des molécules RXH en solution dans le tétrachlorure de carbone (figs. 4 et 5, tableau 2) (2, 6), dans les régions où sont attendues les transitions simultanées, permet de discuter l'existence de ces dernières.

Mise en évidence des transitions simultanées

Chloroforme

Une transition simultanée νCH($CHCl_3$) + $\nu_3(CS_2)$ mettant en jeu l'absorption la plus intense du sulfure de carbone vers 1520 cm^{-1} avait déjà été mise en évidence (11, 12). Nous avons également démontré l'existence, dans des mélanges chloroforme–accepteurs de protons, des transitions simultanées apparaissant dans des régions spectrales très différentes: νCH($CHCl_3$) + νCN(CD_3CN), νCH($CHCl_3$) + νCO($(CD_3)_2CO$), et νCH($CHCl_3$) + νSO($(CD_3)_2SO$). Ces résultats ayant déjà fait l'objet d'une communication (6), nous n'en reprendrons pas l'analyse ici.

TABLEAU 1. Transitions simultanées dans les mélanges eau–acétonitrile-d_3 (cm^{-1})

Eau		νOH (D)*	νOH (D) + νCN Calcd†	νOH (D) + νCN Obs*
H_2O	ν_1	3544	5811	5804
	ν_3	3629	5896	≈5880
DHO	νOH	3577	5844	5836
D_2O	ν_1	2593	4860	4859
	ν_3	2698	4965	4961

*Fréquences observées pour le mélange eau (concentration totale ≈ 1 *M*) – acétonitrile-d_3.
†Nous avons utilisé νCN = 2267 cm^{-1}, fréquence correspondant à la solution de CD_3CN (fraction molaire 0.25) dans l'eau.

Eau

Nous avons attribué antérieurement le spectre des molécules H_2O, D_2O, et HOD libres, en solution dans le tétrachlorure de carbone (2). Dans les solutions diluées d'eau dans les solvants accepteurs de protons, l'eau est peu autoassociée et l'examen des transitions fondamentales et harmoniques a permis de montrer que la plupart des molécules d'eau sont engagées dans des complexes 1–2 (R′AB...HOH...BAR′); il ne reste une quantité notable de complexes 1–1 (HOH...BAR′) que si la molécule de base est assez encombrante (2, 5, 18).

Transitions νOH(H_2O) + νCH (base) vers 6500 cm^{-1} (fig. 1)

Dans la région de l'harmonique 2νOH, le spectre de la molécule H_2O en solution dans un solvant basique hydrogéné comporte toujours deux massifs d'absorption vers 7000 et 6500 cm^{-1} (fig. 1) (2, 19–22). En opposition, il n'existe pas d'absorption distincte vers 6500 cm^{-1} si l'on utilise un solvant complètement deutérié, toutes les autres conditions d'enregistrement étant identiques (courbes en pointillé).

Le fait que les spectres de l'eau dépendent de la substitution isotopique du solvant prouve que la bande vers 6500 cm^{-1} ne correspond pas

[4]Cet échange devient rapide dans les mélanges H_2O–$(CD_3)_2CO$–CCl_4. Une étude récente (17) est consacrée à la catalyse de la dédeutération de l'acétone-d_6 en milieu acide ou basique.

TABLEAU 2. Attribution proposée pour quelques absorptions des méthanols en solution (cm^{-1})*

Attribution	CH_3OH dans				CD_3OH dans			
	CCl_4	CS_2	CH_3CN	CD_3CN	CCl_4	CS_2	CH_3CN	CD_3CN
ν_1	3644	3629	3541	3546	3645	3631	3541	3546
$\nu_1 + \nu_6$	4962	4946	4925	4925	4923	4904	4872	4874
$\nu_1 + \nu_5$	5091	5072			4766	4748		
$\nu_1 + 2\nu_6$	6272	6252	~6290	6285	6185	6161	6193	6194
$\nu_1 + \nu_3$	6476	6458	6380	6383	5717	5694		~5650
$\nu_1 + \nu CH_3(D_3)$	6582	6561		~6470	5776	5749		
$\nu_1 + 2\delta CH_3(D_3)$	6629	6607			5880	5860		
$2\nu_1$	7119	7092	(7030)	(7030)	7119	7093	(7032)	(7031)
$2\nu_1 + \nu_6$	8426	8388			8388	8345		
$3\nu_1$	10420	10376			10425	10374		

*Vibrations de symétrie A': $\nu_1 = \nu OH(OD)$; $\nu_2 = \nu_a\ CH_3(CD_3)$; $\nu_3 = \nu_s\ CH_3(CD_3)$; $\nu_4 = \delta_a\ CH_3(CD_3)$; $\nu_5 = \delta_s\ CH_3(CD_3)$; $\nu_6 = \delta\ OH(OD)$; $\nu_7 = r\ CH_3(CD_3)$; $\nu_8 = \nu\ CO$. Vibrations de symétrie A'': $\nu_9 = \nu_a\ CH_3(CD_3)$; $\nu_{10} = \delta_a\ CH_3(CD_3)$; $\nu_{11} = r\ CH_3(CD_3)$; $\nu_{12} = \tau\ OH(OD)$. Les fréquences observées pour les vibrations des molécules de méthanol à l'état gazeux et liquide sont indiquées dans la référence 29.

TABLEAU 3. Coefficients d'anharmonicité apparents $x_{ss'}$ pour les méthanols en solution (cm^{-1})

$x_{ss'}$		CH_3OH dans		CD_3OH dans	
		CCl_4	CD_3CN	CCl_4	CS_2
x_{11}	[1]*	84.5	(32)	85.5	84.5
	[2]	85		85	86.5
	[4]	85			86.5
x_{66}	[4]	4	9.5	8	8
x_{13}	[6]	2	−3	−4	
x_{15}	[6]				1
x_{16}	[6]	10	−1		17
	[8]	10.5			19

*Les chiffres entre parenthèses carrées indiquent celles des relations 1 à 9 de la réf. 4 dont ils sont tirés.

uniquement à des vibrations internes de la molécule d'eau: cette bande doit être attribuée à des transitions de combinaisons mettant en jeu simultanément des vibrations de H_2O et de la base. Les seules vibrations qui soient communes à toutes les bases hydrogénées sont celles des groupements CH_3 (ou CH de la pyridine). En effet, les squelettes des molécules utilisées sont très différents: CCN, CCO, CSO, C_5N. De plus, la somme des fréquences vOH + vCH (fig. 1) est de l'ordre de 6500 cm^{-1}. Nous attribuons donc la bande vers 6500 cm^{-1} à la transition simultanée $\nu OH(H_2O) + \nu CH$ (base) (6). Des observations et une attribution analogues ont été faites par Rossarie *et coll.* pour des mélanges d'alcools et d'acétonitrile (14).

Pour les mélanges eau–base hydrogénée, les interprétations antérieures de la bande vers 6500 cm^{-1} doivent être révisées (2, 19–21). En particu-

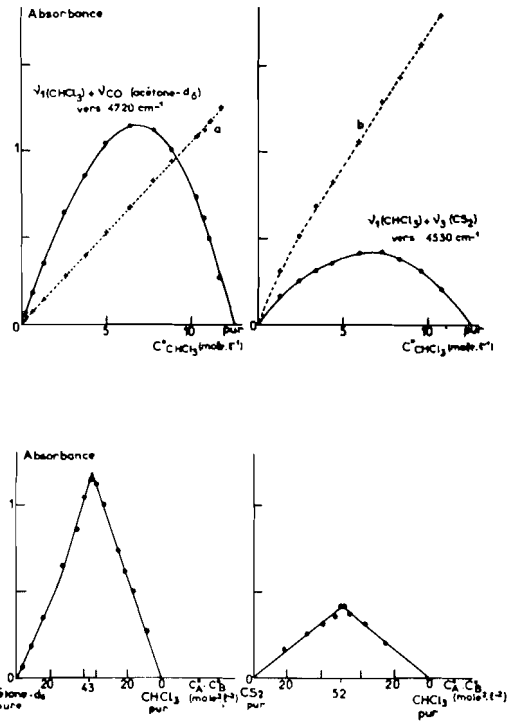

FIG. 6. Evolution de l'absorbance des transitions simultanées pour les mélanges chloroforme–acétone-d_6 (à gauche) et chloroforme – sulfure de carbone (à droite) en fonction de la concentration en chloroforme (en haut) et du produit des concentrations des deux constituants du mélange (en bas). Epaisseur de cuve = 2 cm.

Pour comparaison, courbes en pointillés: (*a*) bande ($\nu_1 + 2\nu_4$) du chloroforme en solution dans le tétrachlorure de carbone, composante vers 5413 cm^{-1}; (*b*) bande ($2\nu_1 + \nu_4$) du chloroforme en solution dans le sulfure de carbone, vers 7075 cm^{-1}.

Can. J. Chem. Downloaded from www.nrcresearchpress.com by 210.87.254.6 on 09/05/12
For personal use only.

TABLEAU 4. Transitions simultanées mettant en jeu le méthanol en solution (cm^{-1})

	CH_3OH				CD_3OH			CD_3OD		
			$(\nu_1 + \nu_x)$			$(\nu_1 + \nu_x)$			$(\nu_1 + \nu_x)$	
ν_x (Solvant)*		ν_1	Calcd	Obs	ν_1	Calcd	Obs	ν_1	Calcd	Obs
ν_3 (CS_2)	1524	3629	5153	≈5140	3631	5155	5149			
νCN (CD_3CN)	2268	3546	5814	≈5808	3546	5814	5808	2622	4890	4885
νCN (CH_3CN)	2259							2627	4886	4877
νCH_3(CH_3CN)	2942	3541	6483	≈6485	3541	6483	6503	2627	5569	≈5555
	3003		6542			6542			5628	

*Valeurs obtenues à partir de solutions diluées dans le méthanol, sauf pour νCH_3 de l'acétonitrile liquide pur.

lier, il n'est pas évident que l'harmonique $2\nu_1(H_2O)$ se situe dans cette région, comme nous l'avions d'abord admis à la suite de Greinacher *et coll.* (2, 19).

Transitions $\nu OH(D)$ (eau) + $\nu CN(CD_3CN)$ (fig. 2)

Pour les mélanges H_2O–CD_3CN (courbe *c*) on ne peut trouver aucune transition intramoléculaire entre 5300 et 6400 cm^{-1}, en combinant les fréquences des vibrations fondamentales de la molécule d'eau soit 1633, 3544, et 3629 cm^{-1}. Les bandes à 5593, 5804, et vers 5880 cm^{-1} doivent donc impliquer d'autres degrés de libertés que ceux correspondant aux seules vibrations internes de H_2O. Nous attribuons les absorptions vers 5804 et 5880 cm^{-1} aux transitions $\nu_1(H_2O)$ + $\nu CN(CD_3CN)$ et $\nu_3(H_2O)$ + $\nu CN(CD_3CN)$ (tableau 1). Il faut remarquer qu'il y a dégénérescence accidentelle entre les vibrations $\nu_a CD_3$ et νCN dans la molécule CD_3CN à l'état liquide (23); il y a donc ambiguïté entre les attributions ν_1 + νCN, ν_3 + νCN, et ν_1 + $\nu_a CD_3$, ν_3 + $\nu_a CD_3$. La bande à 5593 cm^{-1} est observée à la fois dans les mélanges H_2O–CH_3CN et H_2O–CD_3CN, elle ne peut donc être attribuée à une transition simultanée $\nu(H_2O)$ + $\nu_s CD_3$; par ailleurs, la somme des fréquences correspondrait mal. Nous avons en outre observé une absorption analogue pour toutes les solutions de H_2O dans un solvant basique suffisamment transparent; nous l'attribuons à la combinaison $\delta(H_2O)$ + $\nu(H_2O)$ + ν_L entre les vibrations de valence et de déformation de l'eau et les mouvements librationnels du complexe.[5]

Pour les solutions D_2O–CD_3CN (courbe *a*) on observe quatre bandes dans la région 2νOD vers 4700–5500 cm^{-1}. Les bandes à 5069 et 5248 cm^{-1} sont tout à fait analogues aux deux absorptions à 6844 et 7105 cm^{-1} observées pour H_2O dans la région 2νOH (courbe *c*) et sont donc attribuables à des transitions intramoléculaires de même que l'absorption à 6423 cm^{-1}.[6] Mais celles à 4859 et 4961 cm^{-1} n'ont pas leur équivalent dans le spectre de H_2O.[6] Bien qu'un certain nombre de transitions impliquant les seules vibrations de D_2O puissent apparaître dans cette région, il est probable que leur contribution est faible, comme pour H_2O. Nous attribuons les bandes à 4859 et 4961 cm^{-1} aux transitions ν_1 (D_2O) + ν CN(CD_3CN), et ν_3 (D_2O) + ν CN(CD_3CN): les fréquences observées sont extrêmement voisines des fréquences calculées en faisant la somme des fréquences des vibrations fondamentales (tableau 1).

Le spectre (*b*) correspond essentiellement à une solution de HOD et de D_2O dans CD_3CN. En faisant la corrélation avec le spectre de D_2O seul (courbe *a*), on constate que les bandes à 5003, 6235, 7116, et 5836 cm^{-1} mettent en jeu la molécule HOD mais pas D_2O. Les trois premières sont attribuables à des combinaisons des vibrations internes de cette molécule;[6] mais on n'observe aucune absorption notable de HOD entre 5500 et 6000 cm^{-1}, que ce soit à l'état gazeux (24), en solution dans le CCl_4 (2) ou dans l'acétone-d_6. Par contre, la valeur 5836 cm^{-1} correspond assez bien à la somme νOH(HOD) + νCN(CD_3CN). Il est logique que cette absorption n'apparaisse que dans l'acétonitrile et à une fréquence intermédiaire entre celle des transitions ν_1 + νCN et ν_3 + νCN du complexe CD_3-CN...HOH...NCCD_3.

[5]L'écart de fréquence entre la transition (ν_2 + ν_3) à 5253 cm^{-1} et la bande à 5593 cm^{-1} est en effet du même ordre de grandeur que la fréquence de la bande observée vers 400 cm^{-1} pour les solutions de H_2O dans l'acétonitrile (43) et attribuée à des mouvements librationnels (résultats à paraître).

[6]Résultats à paraître.

Can. J. Chem. Downloaded from www.nrcresearchpress.com by 210.87.254.6 on 09/05/12
For personal use only.

Can. J. Chem. Downloaded from www.nrcresearchpress.com by 210.87.254.6 on 09/05/12
For personal use only.

Pentachlorophénol

Parmi les donneurs de protons RXH étudiés, nous avons choisi le pentachlorophénol parce que le groupement R ne renferme aucun atome d'hydrogène, comme dans le cas du chloroforme (6): ceci facilite l'examen du spectre dans le proche infrarouge. Le groupement OH du pentachlorophénol est plus acide que ceux des autres chlorophénols (25, 26): il est susceptible de former une liaison hydrogène relativement forte même avec l'acétonitrile.

Pour le pentachlorophénol en solution dans le tétrachlorure de carbone, la vibration de valence ν OH est à une fréquence relativement faible, 3525 cm^{-1} parce qu'il y a chélation sur les atomes de chlore en ortho (27, 28). Au-dessus de 3950 cm^{-1}, on observe en plus de l'harmonique 2νOH à 6869 cm^{-1}, trois groupes de combinaisons (A, B, et C) impliquant la vibration νOH et centrés respectivement vers 4200, 4750, et 5950 cm^{-1}.

Pour le pentachlorophénol en solution dans l'acétonitrile-d_3, la bande correspondant à la vibration νOH subit une diminution de fréquence de 225 cm^{-1} et est fortement élargie par rapport à la solution dans le tétrachlorure de carbone; en dessous de 1600 cm^{-1}, les autres vibrations mises en jeu dans les combinaisons A, B, et C sont peu perturbées. On comprend donc que les absorptions vers 3971 et 4520 cm^{-1} ne soient plus résolues et aient subi une diminution de fréquence de 200–250 cm^{-1}, tandis que la diminution est double pour la bande 2νOH à 6446 cm^{-1}.[7] Deux attributions peuvent être proposées pour la bande à 5563 cm^{-1}: elle peut correspondre soit au massif C, soit à la transition simultanée νOH (pentachlorophénol) + νCN(CD_3CN). Si l'on admet que la bande à 5563 cm^{-1} correspond au massif C, il convient d'expliquer que l'abaissement de fréquence soit de près de 400 cm^{-1} par rapport à la solution dans le tétrachlorure de carbone, soit environ 150 cm^{-1} trop grand. Pour cela on peut invoquer une résonance de premier ordre entre les niveaux 2νOH et les transitions du groupe C. Mais il nous paraît étonnant qu'une résonance puisse avoir un tel effet sur les fréquences, surtout lorsque les maximums des deux bandes sont séparés de près de 900 cm^{-1}. Par contre, la fréquence 5563 cm^{-1} correspond à la somme νOH (pentachlorophénol) + νCN-(CD_3CN) dans le mélange pentachlorophénol–acétonitrile-d_3. Il est donc probable que cette transition simultanée intervienne dans le spectre de ce mélange.

Méthanol

Le tableau 2 contient l'attribution, au-dessus de 4700 cm^{-1}, des principales absorptions des molécules CH_3OH et CD_3OH en solution dans le tétrachlorure de carbone. La valeur des coefficients d'anharmonicité rassemblés dans le tableau 3 indique que cette attribution est raisonnable.[8] Les bandes les plus intenses sont les combinaisons intramoléculaires νOH + δOH, νOH + δCH_3 (CD_3), et 2νOH (fig. 4). Pour CH_3OH, le massif compris entre 5670 et 6020 cm^{-1} (fig. 5) peut correspondre à de nombreuses transitions: $2\nu CH_3$, $\nu CH_3 + 2\delta CH_3$, $\nu CH_3 + 2\delta$OH. Dans les régions des combinaisons νOH + νCH_3 (fig. 4*a*) et νOH + νCD_3 (fig. 5), $\nu_1 + \nu_3$ est la plus intense (14). Signalons que les fréquences que nous avons mesurées pour ces absorptions diffèrent notablement de celles reportées par Rossarie *et coll.* (14), probablement à cause d'une erreur d'étalonnage de ces derniers.

Solutions dans le sulfure de carbone (fig. 4a)

Les spectres des méthanols en solution dans le sulfure de carbone sont tout à fait semblables à ceux observés pour les solutions dans le tétrachlorure de carbone: la plupart des absorptions ne subissent qu'un faible déplacement de fréquence (tableau 2). Cependant, le spectre de CD_3OH comporte une absorption supplémentaire à 5149 cm^{-1} qui correspond exactement à la transition simultanée ν_1 (CD_3OH) + ν_3 (CS_2) (tableau 4). Le spectre de la solution de CH_3OH dans le sulfure de carbone comporte une épaule nette vers 5140 cm^{-1} qui s'interprète aussi comme la transition simultanée ν_1 (CH_3OH) + ν_3 (CS_2).

Solutions dans l'acétonitrile (figs. 4b et 5)

Dans une solution méthanol–acétonitrile de concentration 0.8 *M* en méthanol, celui-ci est peu autoassocié puisque l'on n'observe qu'une faible épaule vers 3450 cm^{-1} (31). Les vibrations intramoléculaires les plus perturbées sont ν_1, qui diminue d'environ 100 cm^{-1}, et ν_6 qui augmente de 50 cm^{-1} par rapport aux solutions dans

[7]L'allure de la bande côté haute fréquence semble indiquer que certains groupements OH, en faible proportion, restent chélatés en solution dans l'acétonitrile.

[8]La transition $2\nu_1 + \nu_6$ permet d'obtenir des valeurs de x_{11}, à l'aide de la relation [4] de la référence 4, en excellent accord avec celles déjà connues (30) qui sont fournies par les éqs. 1 à 3 (4).

Can. J. Chem. Downloaded from www.nrcresearchpress.com by 210.87.254.6 on 09/05/12
For personal use only.

le tétrachlorure de carbone.[9] D'autres modifications du spectre peuvent correspondre à l'apparition de transitions simultanées.

Le spectre de CD_3OH dans l'acétonitrile-h_3 comporte une bande à 6503 cm^{-1} qui n'existe pas pour les solutions du même alcool dans l'acétonitrile-d_3 (fig. 4*b*). Ce phénomène a aussi été observé pour l'éthanol et le cyclohexanol par d'autres auteurs (14) et nous l'avons discuté ci-dessus dans le cas de l'eau: la bande à 6503 cm^{-1} correspond à la transition simultanée $\nu_1(CD_3OH) + \nu CH_3(CH_3CN)$ (tableau 4). Cette bande est aussi observée vers 6485 cm^{-1} pour CH_3OH; mais dans ce cas, elle se superpose aux combinaisons intramoléculaires ($\nu_1 + \nu CH_3$) de CH_3OH dont l'absorption propre peut être repérée vers 6470 et 6383 cm^{-1} à partir de la solution dans l'acétonitrile-d_3. Pour la solution de CD_3OD dans l'acétonitrile-h_3, nous avons observé la transition simultanée équivalente, soit $\nu_1(CD_3OD) + \nu CH_3(CH_3CN)$, vers 5555 cm^{-1}. Rossarie *et coll.* ont admis que seule la vibration ν_s CH_3 de l'acétonitrile contribue à ces absorptions (14); les résultats portés dans le tableau 4 suggèrent en effet que la contribution de ν_s CH_3 à 2942 cm^{-1} est la plus grande, mais nous ne pouvons pas affirmer, à la précision de nos mesures, que celle de $\nu_a CH_3$ soit négligeable.

La mise en évidence des transitions simultanées $\nu OH + \nu CN$ vers 5800 cm^{-1} est plus délicate parce que les alcools absorbent dans cette région. Pour CD_3OH en solution dans l'acétonitrile-d_3, l'absorption entre 5600 et 5900 cm^{-1} (fig. 5) n'est pas attribuable uniquement au massif ($\nu_1 + \nu CD_3$) de CD_3OH, parce que ce massif a subi, comme ν_1, une diminution de fréquence d'environ 100 cm^{-1} par rapport à la solution dans le tétrachlorure de carbone, et que l'absorption la plus intense est probablement du côté des basses fréquences comme dans le tétrachlorure de carbone. Nous pensons donc que la transition $\nu_1(CD_3OH) + \nu CN(CD_3CN)$ contribue à la bande à 5808 cm^{-1}. Pour CH_3OH, on attend que le massif entre 5600 et 6100 cm^{-1} (fig. 5) soit peu modifié, quand on passe du tétrachlorure de carbone à l'acétonitrile comme solvant, dans la mesure où il ne fait pas intervenir la vibration νOH. L'augmentation d'intensité très nette vers 5808 cm^{-1} correspond donc à la transition $\nu_1(CH_3OH) + \nu CN(CD_3CN)$, à la même fréquence que $\nu_1(CD_3OH) + \nu CN$.

Nous avons aussi observé, pour CD_3OD en solution dans l'acétonitrile-h_3 et -d_3, deux bandes à 4877 et 4885 cm^{-1} que nous attribuons à $\nu_1(CD_3OD) + \nu CN(CH_3CN)$ et $\nu_1(CD_3OD) + \nu CN(CD_3CN)$ (tableau 4), plutôt qu'aux combinaisons ($\nu_1 + \nu CD_3$) de CD_3OD parce que celles-ci sont attendues à une fréquence plus petite. Nous avons aussi vérifié que ces bandes n'étaient pas attribuables à la combinaison ($\nu_1 + \nu_6$) de CD_3OH provenant de l'échange partiel de CD_3OD: aucune absorption appréciable n'apparaissait dans la région $2\nu OH$, vers 7030 cm^{-1}. L'intensité des deux bandes à 4885 et 4877 cm^{-1} est très voisine: la contribution des vibrations $\nu_a CD_3$ de CD_3CN est donc beaucoup plus faible que celle de la vibration νCN.

Discussion

Il n'est pas facile de prouver l'existence de transitions simultanées. D'une part les deux constituants du mélange sont rarement assez transparents. Nous n'avons observé avec certitude que des transitions simultanées impliquant des vibrations de valence (tableau 5) parce qu'elles apparaissent dans les régions spectrales les plus favorables et sont peut-être les plus intenses. D'autre part, il est d'autant plus difficile de mettre en évidence une transition simultanée que la liaison hydrogène est forte, à cause de l'élargissement des bandes. Par exemple, pour le mélange HCl–acétonitrile, nous n'avons pas pu délimiter une région spectrale où l'absorption ne correspondrait qu'à une transition simultanée, alors que la transition $\nu HCl + \nu_3(CS_2)$ serait vraisemblablement observable. Nous avons néanmoins démontré l'existence de transitions $\nu OH + \nu R'$ dans des mélanges H_2O – bases R'AB, $\nu CH + \nu AB$ dans des mélanges $CHCl_3$–R'AB (6), et $\nu OH + \nu CN$ dans H_2O–acétonitrile. Nous avons aussi montré que l'interprétation du spectre dans le proche infrarouge peut être erronée si l'on ne tient compte que des vibrations intramoléculaires.

Nature des molécules impliquées dans les transitions simultanées

Les transitions simultanées observées en solution entre deux molécules A et B, éventuellement susceptibles d'interactions par liaison hydrogène,

[9]L'harmonique $2\nu OH$ devient très large ($\Delta\nu_{1/2} \approx$ 300 cm^{-1}) et si dissymétrique qu'on ne peut donner une signification précise aux fréquences et aux coefficients d'anharmonicité obtenus à partir des maximums d'absorption et portés entre parenthèses dans les tableaux 2 et 3.

TABLEAU 5. Coefficients d'extinction apparents approchés des bandes de transitions simultanées observées $\nu_s + \nu_{s'}$*

ν_s	ν_3 CS_2	νCO $(CCl_3)_2CO$	νCN CD_3CN	νCO $(CD_3)_2CO$	νSO $(CD_3)_2SO$	νCH CH_3CN	νCH $(CH_3)_2CO$	νCH $(CH_3)_2SO$	νCH C_5H_5N
νCH ($CHCl_3$)	6	<1	3	13	21				
νCD ($CDCl_3$)	3								
ν_1 } (H_2O)			7			3	4	6	6
ν_3 }			4						
ν_1 } (D_2O)			5						
ν_3 }			4						
νOH (HOD)			6						
νOH (CH_3OH)	4					2			
νOH(CD_3OH)	5		~7			2			
νOD (CD_3OD)			~6			~2			
νOH (C_6Cl_5OH)			8						

*Unités: $100 \times \varepsilon$(l mol^{-1} cm^{-1}), avec $\varepsilon = (1/cl) \log_{10} (I_0/I)$. Ces coefficients d'extinction sont apparents parce qu'ils ne tiennent pas compte des molécules non complexées: on a en effet utilisé pour concentration celle du soluté introduit dans la solution. D'autre part ces valeurs sont approchées et ne peuvent donner qu'une idée approximative des rapports d'intensité, d'autant plus que la largeur des bandes de transitions simultanées peut être très différente suivant les cas: par exemple $\Delta\nu_{1/2}$ est environ trois fois plus grand pour la bande νOH(C_6Cl_5OH) + νCN(CD_3CN) que pour νOH(HOD) + νCN(CD_3CN).

TABLEAU 6. Intensités approximatives de quelques transitions infrarouges* et Raman†

	CS_2	R′AB $(CCl_3)_2CO$	CD_3CN	CH_3CN	$(CD_3)_2CO$	$(CD_3)_2SO$	$(CH_3)_2SO$
νAB(R′AB)	418‡ (0)	42		2§ (75)	115		122
νCH($CHCl_3$)	4 (31)	5	21		39	75	

*Les intensités infrarouges sont exprimées en 10^8 A (cm^2 molécule^{-1} s^{-1}) avec $A = 1/cl \int \log_n (I_0/I)\, d\nu$ (32). Sauf indication contraire, les intensités des bandes νAB de R′AB et νCH de $CHCl_3$ ont été obtenues respectivement à partir de solutions de R′AB dans le chloroforme et de $CHCl_3$ dans R′AB. Pour νAB, ces valeurs sont approximatives car nous avons tenu compte de l'ensemble des absorptions auxquelles peuvent contribuer ces vibrations.

†On a porté entre parenthèses quelques valeurs de $g_j(45\alpha_j'^2 + 7\gamma_j'^2)$ en (cm^4 g^{-1}) obtenues à l'état gazeux, d'après la référence 33.

‡Il s'agit de l'intensité de la bande ν_3 (CS_2) d'après la référence 34.

§D'après la référence 32.

peuvent se faire soit entre deux molécules voisines A et B libres (hypothèse I), soit à l'intérieur d'un complexe (hypothèse II), soit entre la molécule A dans un complexe et une molécule B de la couche de solvatation de ce complexe (hypothèse III).

Les tableaux 1 et 4 montrent que les vibrations νXH impliquées dans les transitions simultanées observées sont celles des vibrateurs associés. Mais il est difficile de préciser, par l'examen des fréquences, si les groupements AB ou R′ appartiennent à une molécule R′AB complexée (II) ou non (III): ces groupements peuvent en effet contribuer à plusieurs vibrations (fig. 1) (6, 35) et sont peu sensibles à la formation de liaisons hydrogène faibles.

Pour le mélange chloroforme–acétone, la formation de liaisons hydrogène ne peut pas être détectée par l'examen des fréquences mais seulement par l'augmentation d'intensité de la bande νXH (tableau 6) (36). Nous avons néanmoins essayé d'établir une corrélation entre l'intensité des transitions simultanées et la quantité de complexes dans le mélange. On peut en effet faire varier la concentration en complexes, suivant les lois des équilibres, soit en fonction des proportions du mélange binaire, soit en diluant ce mélange par un solvant inerte.

Influence de la proportion du mélange

Nous avons repris une étude analogue à celle que Ketelaar et Hooge ont faite pour le mélange CS_2–Br_2 (11). Nous espérions obtenir des conclusions plus nettes avec le mélange chloroforme–acétone parce que les interactions y sont probablement plus fortes que pour CS_2–Br_2. Pour comparaison, nous avons examiné le mélange chloroforme – sulfure de carbone.

Pour les mélanges sans interaction importante (I), nous admettons, par analogie avec la théorie cinétique des gaz, que l'absorbance de la transition simultanée est proportionnelle au

Can. J. Chem. Downloaded from www.nrcresearchpress.com by 210.87.254.6 on 09/05/12
For personal use only.

Can. J. Chem. Downloaded from www.nrcresearchpress.com by 210.87.254.6 on 09/05/12
For personal use only.

nombre de chocs moléculaires par unité de volume, donc au produit des concentrations $C_A{}^0 C_B{}^0$ des constituants A et B introduits dans le mélange (37). Au contraire, si les transitions simultanées se font à l'intérieur d'un complexe (II), leur absorbance dépend de la constante d'équilibre comme la concentration en complexes C_{AB}. Avec l'hypothèse III, on attendrait un résultat intermédiaire, l'absorbance étant proportionnelle au produit $C_{AB}C_B$ dans le mélange.

Nos résultats (fig. 6) ne permettent pas de mesurer la concentration correspondant au maximum d'absorbance de la transition simultanée avec suffisamment de précision pour choisir entre les hypothèses I et II, suivant les critères définis dans la référence (11). La variation d'absorbance est plus près d'une droite si l'on utilise comme variable le produit des concentrations des constituants A et B, plutôt que la concentration d'un seul constituant; mais l'interprétation détaillée des courbes est compliquée par la présence éventuelle de complexes 2–1 (38). Toutefois la fig. 6 a l'intérêt de prouver l'existence des transitions simultanées d'une façon indépendante de celle utilisée plus haut, puisque leur absorbance passe par un maximum contrairement à celle des transitions intramoléculaires.

Effet de dilution

Dans l'hypothèse I, l'absorbance par unité de longueur est inversement proportionnelle au carré du volume

$$[1] \qquad \frac{A}{l} = aC_A{}^0 C_B{}^0 = a\frac{n_A{}^0 n_B{}^0}{V^2}$$

Dans l'hypothèse II, on a, pour un complexe 1–1:

$$[2] \quad \frac{A}{l} = a'C_{AB} = \frac{a'}{2V}\left\{\left(n_A{}^0 + n_B{}^0 + \frac{V}{K_c}\right) \pm \left[\left(n_A{}^0 + n_B{}^0 + \frac{V}{K_c}\right)^2 - 4n_A{}^0 n_B{}^0\right]^{1/2}\right\}$$

en utilisant la constante K_c exprimée en fonction des concentrations.

La fig. 7 représente l'effet de dilution par le tétrachlorure de carbone sur les transitions $\nu_1(CHCl_3) + \nu CO((CD_3)_2CO)$ et $(\nu_1 + 2\nu_4)$ du chloroforme. L'absorbance de cette dernière transition est inversement proportionnelle au volume, suivant la loi de Beer-Lambert (courbe en trait plein). Au contraire pour la transition simultanée, la variation d'absorbance n'est linéaire ni en $1/V$, ni en $1/V^2$. Ces résultats

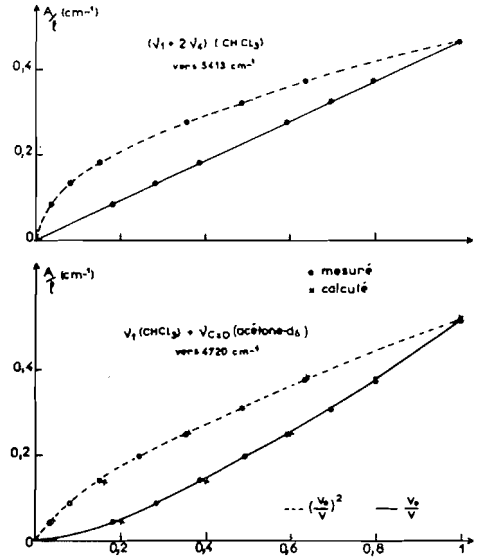

FIG. 7. Effet de la dilution par le tétrachlorure de carbone sur l'intensité de la transition νCH + νCO, dans le mélange chloroforme–acétone-d_6 (en bas) et sur la combinaison $(\nu_1 + 2\nu_4)$ du chloroforme en solution dans le tétrachlorure de carbone (en haut). Fraction molaire en $CHCl_3$ = 0.68, dans le mélange binaire initial de volume V_0.

indiquent que les transitions simultanées mettent bien en jeu au moins une molécule complexée. Les résultats expérimentaux sont en assez bon accord avec les points obtenus par le calcul, en utilisant dans la formule 2 la valeur $K_c = 0.21$ mol^{-1} applicable au complexe 1–1 (36, 39, 40); mais on n'en tirera pas argument pour l'hypothèse II à cause de l'existence possible d'une certaine proportion de complexe 2–1 dans le mélange.

Influence de la force de la liaison hydrogène sur l'intensité des transitions simultanées

Un modèle électrostatique simple a permis de formuler des règles de sélection pour les transitions simultanées dans les phases denses (8, 9, 41). Selon ce modèle, l'interaction électrique a lieu entre deux molécules voisines A et B. En première approximation, on peut se limiter au moment dipolaire induit directement par A dans B et par B dans A: l'existence de transitions $\nu_s + \nu_{s'}$ est due à la non nullité des produits:

$$\left(\frac{\partial\alpha}{\partial q_s}\right)_A\left(\frac{\partial\mu}{\partial q_{s'}}\right)_B \quad \text{et} \quad \left(\frac{\partial\alpha}{\partial q_{s'}}\right)_B\left(\frac{\partial\mu}{\partial q_s}\right)_A, \; q_s \text{ et } q_{s'}$$

Can. J. Chem. Downloaded from www.nrcresearchpress.com by 210.87.254.6 on 09/05/12
For personal use only.

étant des coordonnées normales des molécules A et B, α et μ étant la polarisabilité et le moment dipolaire de ces molécules. Dans cette approximation, on peut observer des transitions simultanées même si les deux molécules ne sont pas polaires; mais il est nécessaire que l'une au moins des deux vibrations considérées ν_s et $\nu_{s'}$ soit active en infrarouge et l'autre en Raman (41). Cependant, en deuxième approximation, il faudrait tenir compte du moment créé "en retour" (8): on pourrait alors observer des transitions simultanées même si, pour les molécules isolées, les deux vibrations considérées ne sont actives qu'en Raman et pas en infrarouge, à condition que l'une au moins des molécules ait un moment dipolaire permanent. En résumé les principaux paramètres qui déterminent l'intensité des transitions simultanées dans deux molécules A et B sont la distance entre ces molécules, leur orientation relative, la variation de leur moment dipolaire et de leur polarisabilité au cours des vibrations considérées.

On peut se demander si la liaison hydrogène renforce l'intensité des transitions simultanées. Les résultats du tableau 5 ne permettent pas de déductions précises. On constate toutefois que l'intensité des transitions simultanées pour les solutions de chloroforme augmente dans l'ordre de basicité du solvant, soit hexachloroacétone,[10] acétonitrile, acétone, et DMSO (tableau 5 et réf. 6). Cependant la force de la liaison hydrogène n'est pas le seul paramètre qui change entre ces solutions. Le fait que l'intensité infrarouge de $\nu_3(CS_2)$ est environ 200 fois plus grande que celle de $\nu CN(CH_3CN)$ (tableau 6) peut expliquer que la transition $\nu CH(CHCl_3) + \nu_3(CS_2)$ soit plus intense que $\nu CH(CHCl_3) + \nu CN(CD_3CN)$, contrairement à ce que laisserait prévoir la force de la liaison hydrogène. D'un autre côté, la transition $\nu CH(CHCl_3) + \nu SO((CD_3)_2SO)$ est beaucoup plus intense que $\nu CH(CHCl_3) + \nu_3(CS_2)$, bien que $\nu_3(CS_2)$ soit nettement plus intense en infrarouge que νSO; mais il faut remarquer que le terme

$$\left(\frac{\partial\alpha}{\partial q_{AB}}\right)_{R'AB}\left(\frac{\partial\mu}{\partial q_{CH}}\right)_{CHCl_3}$$

intervient pour les transitions $\nu CH + \nu AB$ mais pas pour $\nu CH + \nu_3(CS_2)$ puisque $(\partial\alpha/\partial q_3)_{CS_2}$ est nul. Ainsi la liaison hydrogène favorise probablement les transitions simultanées, non seulement en contribuant au rapprochement des molécules mais aussi par l'augmentation de $\partial\mu/\partial q$ qu'elle entraîne toujours pour les vibrations νXH et qui est illustrée pour le chloroforme dans le tableau 6.

En utilisant l'acétone-d_6 et l'hexachloroacétone, nous avons choisi des solvants de basicités très différentes, mais les plus voisins possible du point de vue des propriétés infrarouge et Raman. L'observation de la transition $\nu CH(CHCl_3) + \nu CO((CCl_3)_2CO)$ est incertaine; mais, si elle existe, elle est au moins 10 à 20 fois moins intense que $\nu CH(CHCl_3) + \nu CO((CD_3)_2CO)$. Malheureusement ce résultat ne permet pas de prouver définitivement le rôle particulier de la liaison hydrogène dans les transitions simultanées; en effet, la bande νCO de l'hexachloroacétone est deux à trois fois moins intense en infrarouge, et environ cinq fois moins intense en Raman, que celle de l'acétone-d_6.

En conclusion, remarquons que la contribution des transitions simultanées au spectre d'absorption dans le proche infrarouge peut être importante: ainsi, la fig. 1 montre que, pour le mélange eau–DMSO, la bande $\nu OH + \nu CH_3$ n'est pas beaucoup plus faible que celle correspondant à toutes les transitions intramoléculaires $2\nu_1$, $\nu_1 + \nu_3$, $2\nu_2 + \nu_3$,... de H_2O qui absorbent dans cette région. Nous avons aussi constaté que la transition $\nu CH(CHCl_3) + \nu SO((CD_3)_2SO)$ est plus intense que l'harmonique $2\nu CH$ du chloroforme dilué dans le DMSO-d_6 (6).

Nous exprimons notre gratitude à Mademoiselle Josien, Professeur à l'Université de Paris VI, pour l'intérêt avec lequel elle a suivi l'ensemble de ce travail.

[10]Il a déjà été remarqué que les halogénocétones sont peu basiques (42). Nous-mêmes avons observé que la fréquence νOH du pentachlorophénol en solution dans l'hexachloroacétone, vers 3522 cm^{-1}, est pratiquement la même que pour la solution dans le tétrachlorure de carbone: ceci indique que le pentachlorophénol y reste essentiellement chelaté. L'hexachloroacétone est donc beaucoup moins basique que l'acétonitrile dans lequel la fréquence νOH du pentachlorophénol est de 3300 cm^{-1} environ.

1. A. BURNEAU et J. CORSET. Chem. Phys. Lett. **9**, 99 (1971).
2. A. BURNEAU et J. CORSET. J. Chim. Phys. Physico-chim. Biol. **69**, 142 (1972).
3. A. BURNEAU et J. CORSET. J. Chim. Phys. Physico-chim. Biol. **69**, 153 (1972).
4. A. BURNEAU et J. CORSET. J. Chim. Phys. Physico-chim. Biol. **69**, 171 (1972).
5. A. BURNEAU et J. CORSET. J. Phys. Chem. **76**, 449 (1972).
6. A. BURNEAU et J. CORSET. J. Chem. Phys. **56**, 662 (1972).

7. M. L. JOSIEN et J. LASCOMBE. Conférence Internationale sur la Liaison Hydrogène, Ottawa (1972).
8. L. GALATRY et B. VODAR, C.R. Acad. Sci. Paris **240**, 1072 (1955).
9. J. A. A. KETELAAR. Spectrochim. Acta, **14**, 237 (1959).
10. J. A. A. KETELAAR et F. N. HOOGE. J. Chem. Phys. **23**, 749, 1549 (1955).
11. J. A. A. KETELAAR et F. N. HOOGE. Rec. Trav. Chim. **76**, 529 (1957).
12. S. BĂDILESCU. Rev. Roum. Chim. **15**, 1931 (1970).
13. M. ASSELIN et C. SANDORFY. J. Chem. Phys. **52**, 6130 (1970).
14. J. ROSSARIE, J. C. LAVALLEY, et R. ROMANET. C.R. Acad. Sci. Paris, Ser. B, **273**, 185 (1971).
15. A. RON et D. F. HORNIG. J. Chem. Phys. **39**, 1129 (1963).
16. J. BLANCHARD, L. C. BRUNEL, et M. PEYRON. C.R. Acad. Sci. Paris, Ser. B, **272**, 366 (1971).
17. J. HINE, J. C. KAUFMANN, et M. S. CHOLOD. J. Am. Chem. Soc. **94**, 4590 (1972).
18. P. SAUMAGNE et M. L. JOSIEN. Bull. Soc. Chim. Fr. 813 (1958).
19. E. GREINACHER, W. LÜTTKE, et R. MECKE. Ber. Bunsenges. Phys. Chem. **59**, 23 (1955).
20. A. V. KARYAKIN, A. V. PETROV, et YU. B. GERLIT. Vodorodnaya Svyaz, 181 (1964); Chem. Abstr. **62**, 4783*e* (1965). A. V. KARYAKIN et A. V. PETROV. Sovrem. Metody Anal. 185 (1965); Chem. Abstr. **64**, 7367*d* (1966).
21. G. R. CHOPPIN et M. R. VIOLANTE. J. Chem. Phys. **56**, 5890 (1972).
22. W. C. MCCABE, S. SUBRAMANIAN, et H. F. FISHER. J. Phys. Chem. **74**, 4360 (1970).
23. E. L. PACE et L. J. NOE. J. Chem. Phys. **49**, 5317 (1968).
24. W. S. BENEDICT, N. GAILAR, et E. K. PLYLER. J. Chem. Phys. **24**, 1139 (1956).
25. I. S. PERELYGIN et T. F. AKHUNOV. Opt. Spectrosc. **30**, 367 (1971).
26. S. M. PETROV et V. S. PILYUGIN. Zh. Fiz. Khim. **46**, 163 (1972).
27. P. PINEAU. Thèse Bordeaux, 1961. p. 59.
28. I. S. PERELYGIN et T. F. AKHUNOV. Opt. Spectrosc. **29**, 276 (1970).
29. H. WOLFF, E. WOLFF, et H. E. HÖPPEL. Ber. Bunsenges. Phys. Chem. **72**, 644 (1968).
30. G. DUROCHER et C. SANDORFY. J. Mol. Spectrosc. **15**, 22 (1965).
31. M. KIRSZENBAUM. Thèse de troisième cycle, Paris, 1971.
32. L. A. GRIBOV. Intensity theory for infrared spectra of polyatomic molecules. Original Russian text Academy of Sciences Press, Moscow (1963); *Translation by* P. P. Sutton, Consultants Bureau, New York. 1964.
33. W. F. MURPHY, W. HOLZER, et H. J. BERNSTEIN. Appl. Spectrosc. **23**, 211 (1969).
34. M. CAMEO. Thèse Paris, 1964.
35. M. TRANQUILLE, P. LABARBE, M. FOUASSIER, et M. T. FOREL. J. Mol. Struct. **8**, 273 (1971).
36. J. LASCOMBE, J. DEVAURE, et M. L. JOSIEN. J. Chim. Phys. Physicochim. Biol. **61**, 1271 (1964).
37. G. PANNETIER et P. SOUCHAY. Cinétique chimique. Masson et Cie, Paris. 1964. p. 68.
38. P. COMBELAS, C. GARRIGOU-LAGRANGE, et J. LASCOMBE. Ann. Chim. (Paris), **5**, 315 (1970).
39. E. CONSTANT et L. RACZY. C.R. Acad. Sci. Paris, **253**, 2493 (1961).
40. B. B. HOWARD, C. F. JUMPER, et M. T. EMERSON. J. Mol. Spectrosc. **10**, 117 (1963).
41. F. N. HOOGE et J. A. A. KETELAAR. Physica, **23**, 423 (1957).
42. G. C. LEVY, J. D. CARGIOLI, et W. RACELA. J. Am. Chem. Soc. **92**, 6238 (1970).
43. E. GENTRIC. Thèse de troisième cycle, Brest, 1972. M. H. BARON et C. DE LOZE. J. Chim. Phys. Physicochim. Biol. **68**, 1293 (1971).

Can. J. Chem. Downloaded from www.nrcresearchpress.com by 210.87.254.6 on 09/05/12
For personal use only.

Erratum: Cobalt(II) Mercury Tetrathiocyanate Complexes with Lewis Bases

R. MAKHIJA, L. PAZDERNIK, AND R. RIVEST
Département de chimie, Université de Montréal, Montréal, Québec

Received April 16, 1973
(Ref.: Can. J. Chem. **51**, 438 (1973))

On page 439 in Table 1 the heading for column 5 should read $CoHg(SCN)_4.2P\Phi_3$ instead of $CoHg(SCN)_4$.2trien.

The figure 2137 s at the top of column 4 should appear at the top of column 5.

The figure 2140 s should appear at the top of column 3.

Can. J. Chem. Downloaded from www.nrcresearchpress.com by 210.87.254.6 on 09/05/12
For personal use only.

Can. J. Chem. Downloaded from www.nrcresearchpress.com by 210.87.254.42 on 09/05/12
For personal use only.

Canadian Journal of Chemistry

Published by
THE NATIONAL RESEARCH COUNCIL OF CANADA

Journal canadien de chimie

Publié par
LE CONSEIL NATIONAL DE RECHERCHES DU CANADA

Volume 51 Number 13 July 1, 1973

Volume 51 numéro 13 1 juillet 1973

Studies of β-Diketone Complexes of Rhenium(V). The Molecular and Crystal Structure of *trans*-Dichlorobis(pentane-2,4-dionato)rhenium(IV)[1]

I. D. BROWN, C. J. L. LOCK,[2] AND CHE'NG WAN

Institute for Materials Research, McMaster University, Hamilton, Ontario

Received January 10, 1973

One of the compounds obtained by reacting acetylacetone with oxoethoxodichlorobis(triphenylphosphine)rhenium(V) has been shown by single crystal X-ray diffraction to be *trans*-dichlorobis(pentane-2,4-dionato)rhenium(IV). The crystals are triclinic, $a = 8.032(4)$, $b = 8.344(6)$, $c = 7.429(6)$ Å, $\alpha = 118.1(2)$, $\beta = 92.3(2)$, $\gamma = 55.5(2)°$, $P\bar{1}(C_i^1$, No. 2), $Z = 1$. Intensities were measured with a microdensitometer from photographs recorded on an integrating precession camera. Of the 991 measured reflections all were observed and 984 were used in the refinement. The structure was refined by full matrix least squares to an R_2 value of 0.0685. The compound was found to be a *trans*-monomer, in contrast to the dimeric structure claimed to exist in solution. The ligand atoms bonded to rhenium lie almost exactly at the apices of an octahedron and the bond lengths (Re—Cl, 2.326(8); Re—O1, 1.97(1); Re—O2, 2.01(1) Å) are in the range expected.

La diffraction de rayons X sur monocristal a montré que l'un des composés obtenu dans la réaction de l'acétylacétone sur l'oxoethoxodichlorobis(triphénylphosphine)rhénium(V) est le *trans*-dichlorobis(pentanedionato-2,4)rhénium(IV). Les cristaux sont tricliniques avec $a = 8.032(4)$, $b = 8.344(6)$, $c = 7.429(6)$ Å, $\alpha = 118.1(2)$, $\beta = 92.3(2)$, $\gamma = 55.5(2)°$, $P\bar{1}(C_i^1$, No. 2), $Z = 1$. Les intensités ont été mesurées avec un microdensimètre à partir des photos enregistrées sur une caméra intégratrice en précession. Les 991 réflexions mesurées ont toutes été observées et 984 d'entre elles ont été utilisées dans le raffinement. La structure a été raffinée par la matrice des moindres carrés jusqu'à une valeur de R_2 de 0.0685. Le composé est un monomère *trans*, contrairement à la structure dimère qu'on pensait exister en solution. Les atomes de ligands liés au rhénium sont presque exactement sur les sommets de l'octaèdre et les longueurs de liaison (Re—Cl, 2.326(8); Re—O1, 1.97(1); Re—O2, 2.01(1) Å) sont dans l'intervalle attendu.
[Traduit par le journal]

Can. J. Chem., 51, 2073 (1973)

Introduction

Several types of β-ketoenolate complexes of rhenium have been synthesized (2, 3). Many of these complexes synthesized by Grove *et al.* (3) can exist in different isomeric forms. In order to understand the mechanism of the unusual reaction which gives rise to so many different products it is necessary to know, at least, the detailed molecular structure of the products. To this end we have examined the crystal structures of the reaction products by single crystal X-ray methods.

The product obtained by the reaction of oxodichloroethoxobis(triphenylphosphine)rhenium(V) with refluxing acetylacetone was claimed to be $[ReCl_2(C_5H_7O_2)_2]_2$ (3). Analysis indicated the stoichiometry was $ReCl_2(C_5H_7O_2)_2$ and molecular weight determinations in solution indicated that the material was dimeric. On the basis of infrared spectra and simple arguments about probable coordination numbers of the rhenium atoms the following structure was proposed.

[1]A preliminary report of the structure of the compound appeared in ref. 1.

[2]To whom correspondence should be addressed.

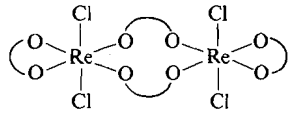

The structure contains two bridging acetylacetonate groups bonded to the rhenium atoms through the oxygen atoms (3). However, no X-ray structure work was reported. Preliminary X-ray work has shown that the compound is a monomer in the solid state and should be named *trans*-dichlorobis-(2,4-pentanedionato)rhenium (IV) (1) and more recently it has been shown the monomeric *trans* structure exists in solution and in the gas phase (4). We describe here the refinement of the crystal structure of this compound.

Experiments

Analyses were performed by Galbraith Laboratories, Inc., Knoxville, Tennessee.

Rhenium metal was obtained from the Rhenium Divison, Chase Brass and Copper Co. Inc., Solon, Ohio. Perrhenic acid was obtained as a solution from S. W. Shattuck Chemical Co., Denver, Colorado. Both materials were used to prepare samples of the grey-green isomer of oxoethoxodichlorobis(triphenylphosphine)rhenium(V) starting material (5). The products of the two reactions were identical. *trans*-Dichlorobis(pentane-2,4-dionato)rhenium(IV) was prepared by the method used by Grove *et al.* (3) to prepare "tetrachlorobis(pentane-2,4-dionato)-μ_2-(pentane-2,4-dionato)dirhenium(IV)."

Anal. calcd. for $C_{10}H_{14}Cl_2O_4Re$: C, 26.4; H, 3.1; Cl, 15.6. Found: C, 26.6; H, 3.1; Cl, 16.1.

Orange plate-like single crystals, suitable for X-ray studies were obtained by slow evaporation of a solution in a 75:25 v/v benzene – carbon tetrachloride solvent mixture at 26–27 °C.

X-Ray Studies

A crystal ($0.15 \times 0.4 \times 0.6$ mm^3) showing uniform extinction under a polarizing microscope was chosen for structural studies. It was mounted along the direction of the longest dimension. Precession photographs of the crystal showed it was triclinic. Precession photographs of the zero layers along [100] and [1$\bar{2}\bar{1}$] were calibrated with a crystal of TiO_2 (rutile) ($a = 4.5929(5)$, $c = 2.9591(3)$ Å (6)) and accurate parameters were calculated. The density of a few crystals were determined by flotation in a tetrabromoethane – carbon tetrachloride mixture. Crystal data are

$C_{10}H_{14}Cl_2O_4Re$ f.w. = 455.3

Triclinic, $a = 8.032(4)$, $b = 8.344(6)$, $c = 7.429(6)$ Å, $\alpha = 118.1(2)$, $\beta = 92.3(2)$, $\gamma = 55.5(2)°$, $V = 334.0$ Å^3, $P\bar{1}(C_i^1$, No. 2), $\rho_o = 2.18$, $Z = 1$, $\rho_c = 2.18(2)$ (23 °C, MoKα, $\lambda = 0.71069$ Å) $\mu = 97.1$ cm^{-1}.

Reflection intensities for the first four layers perpendicular to [100] and the first five layers perpendicular to [1$\bar{2}\bar{1}$] were obtained from films recorded on an integrating precession camera using zirconium filtered MoKα radiation. All intensities were measured using a Joyce–Loebl microdensitometer and then corrected for Lorentz and polarization effects. No absorption corrections were made, and this could introduce a maximum error in F of 10%: the average error would be considerably less than 10%. Standard errors were assigned to each reflection according to the methods of Ibers (7) and Hughes (8) and weights $w = 1/\sigma^2$ were used through the refinement.

Solution of the Structure

The unit cell is triclinic with space group $P1$ or $P\bar{1}$. The centrosymmetric space group was assumed at the beginning of this work and this was confirmed from the Patterson maps as well as subsequent refinement of the structure. Thus the rhenium atom is at a center of symmetry and this was chosen as the origin of the cell. The chlorine and oxygen atoms were located from the Patterson projections on (01$\bar{2}$) and (210). The remaining non-hydrogen atoms were found from successive Fourier synthesis and least squares refinements. At this stage, temperature factors, which were treated as isotropic in the initial refinement, were made anisotropic. The structure was further refined using a full matrix least squares programme CUDLS written by J. S. Stephens for the CDC 6400 computer. Refinement was terminated when no shift of atom parameters greater than $1/10\sigma$ was observed and $R_1 = 0.072$ and $R_2 = 0.0685$.[3] Of the 991 reflections measured, 984 were used in the final refinement. Seven reflections of doubtful accuracy, because they were near the backstop shadow, were given zero weight. The data set recorded represents about 55% of the approximately 1800 reflections which are accessible using a precession angle of 30°. Scattering curves used in the refinement process were obtained from the International tables (9) for Cl, O, and C and from Cromer and Waber (10) for Re. Anomalous dispersion corrections for rhenium and chlorine were taken from Cromer (11).

A difference Fourier map calculated using the structure factors listed in Table 2 had no residual peaks outside plus or minus 1% of the rhenium atom peak. The final atom parameters are shown in Table 1 and the values of F_o and F_c are given in Table 2.[4]

Results and Discussion

Figure 1, which, with Fig. 2, was produced by the ORTEP program written by Johnson (17), shows one complete molecule and the bond lengths and angles are listed in Table 3. The rhenium atom is at the origin of the unit cell, and the shortest Re—Re distance, about 7.4 Å, corresponds to the two rhenium atoms related by the c translation, and thus the compound is monomeric. For the monomer, *cis* and *trans*

[3] $R_1 = \dfrac{\Sigma|\,|F_o| - |F_c|\,|}{\Sigma|F_o|}$; $R_2 = \left(\dfrac{\Sigma\omega(|F_o| - |F_c|)^2}{\Sigma\omega F_o^2}\right)^{1/2}$

[4] Table 2 is available, at a nominal charge, from the Depository of Unpublished Data, National Science Library, National Research Council of Canada, Ottawa, Canada, K1A 0S2.

Can. J. Chem. Downloaded from www.nrcresearchpress.com by 210.87.254.42 on 09/05/12
For personal use only.

TABLE 1. Atom parameters for $Re(acac)_2Cl_2 \times 10^3$*

Atom	x	y	z	U_{11}	U_{22}	U_{33}	U_{12}	U_{13}	U_{23}
Re	0(0)	0(0)	0(0)	35.4(7)	32.4(6)	31.0(4)	−12.0(6)	−8.4(4)	16.0(4)
Cl	260.2(7)	33.7(10)	−50.2(8)	47(3)	59(3)	70(3)	−28(3)	−15(2)	35(3)
O1	225(2)	−321(2)	−82(1)	26(8)	32(5)	28(4)	13(7)	0(5)	13(4)
O2	11(2)	−118(2)	−309(1)	72(10)	53(6)	31(4)	−38(9)	−24(6)	25(5)
C1	308(3)	−508(3)	−269(2)	62(15)	58(10)	48(7)	−45(14)	−25(9)	36(8)
C2	262(3)	−516(2)	−459(2)	55(14)	41(9)	41(7)	−7(12)	−10(8)	25(7)
C3	121(3)	−327(3)	−468(2)	77(13)	42(8)	28(6)	−46(12)	−10(7)	13(6)
C4	481(4)	−734(4)	−283(3)	79(17)	43(9)	76(11)	−32(15)	−44(11)	37(9)
C5	83(3)	−360(4)	−681(3)	146(20)	82(13)	43(7)	−105(17)	−58(11)	39(9)

*Estimated standard deviations in parentheses. U_{ij} is obtained from $\beta_{ij} = 2\pi^2 b_i b_j U_{ij}$ where β_{ij}'s appear as a temperature effect exp $[-(\beta_{11}h^2 + \ldots 2\beta_{12}hk + \ldots)]$ in the structure factor expression and b_i are the reciprocal lattice vectors.

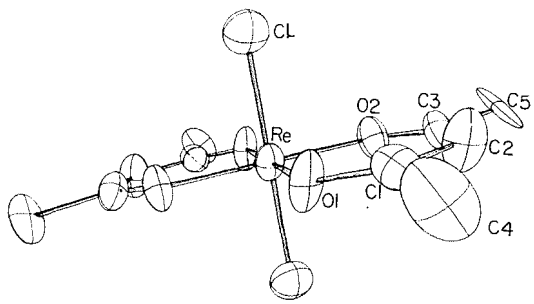

FIG. 1. The molecular structure of $Re(acac)_2Cl_2$. Thermal ellipsoids 50% probability.

TABLE 3. (*a*) Selected distances in $Re(acac)_2Cl_2$*

Atom pair	Distance (Å)	Atom pair	Distance (Å)
Bonded			
Re—Cl	2.326(8)	C1—C2	1.42(3)
Re—O1	1.97(1)	C2—C3	1.36(3)
Re—O2	2.01(1)	C1—C4	1.53(3)
O1—C2	1.30(2)	C3—C5	1.52(3)
O2—C3	1.27(2)		
Non-bonded			
Cl—O1	3.03(2)	Cl—O2(i)	3.05(2)
Cl—O1(i)	3.07(1)	O1—O2	2.80(2)
Cl—O2	3.10(2)	O1—O2(i)	2.83(1)

(*b*) Selected angles in $Re(acac)_2Cl_2$*

Bonds	Angle (deg)	Bonds	Angle (deg)
Cl—Re—O1	89.3(5)	O2—C3—C2	125(2)
Cl—Re—O2	90.9(6)	O1—C1—C4	115(2)
O1—Re—O2	89.4(5)	O2—C3—C5	115(2)
Re—O1—C1	127(1)	C1—C2—C3	125(1)
Re—O2—C3	128(1)	C2—C1—C4	120(1)
O1—C1—C2	125(2)	C2—C3—C5	119(1)

*Estimated standard deviations in parentheses.

configurations are possible; the *trans* configuration was the one found. The pseudo-octahedral coordination around rhenium is elongated along the Re—Cl direction, but the Re—Cl distance (2.326(8) Å) is quite short when compared to values for Re(V) complexes (typically 2.40–2.43(1) Å (12 and references therein)), although the distance is insignificantly different from the 2.353(4) Å found for K_2ReCl_6 (13). The Re—O bond lengths (average 1.99(1) Å) are possibly slightly shorter than Cotton's calculated value for the Re(V)—O single bond (2.04 Å) (14) suggesting that, although the bond order is close to one, some multiple bonding occurs between the oxygen atom and the rhenium atom. The O—Re—O and Cl—Re—O angles are very close to 90° (±1°) required for ideal octahedral coordination at the metal, and thus the inter- and intrachelate ring O—O distances are nearly equal (2.84(1) and 2.80(1) Å, respectively). Bond distances between equivalent sets of atoms within the acetylacetone group differ by about 2σ in the extreme cases and the average values of 1.28 (O—C), 1.39 (C—C ring), and 1.53 Å (C—methyl) agree with values found previously (15).

The ReO1O2 plane and the best weighted least squares plane through O1C1C2C3O2 are almost coplanar (dihedral angle 3.4°) and only one of the methyl carbon atoms, C4, and the rhenium atom are displaced from the latter plane (both 0.08 Å) on the same side. In view of the large positional error of C4 (0.03 Å) this is hardly significant. Both methyl groups show very large thermal motion, and as can be seen in Fig. 1 the motion is probably caused by twisting of the β-ketoenolate ring about an Re—C2 axis. It will be noted that the thermal motion is not symmetric; the motion of C5 is

Can. J. Chem. Downloaded from www.nrcresearchpress.com by 210.87.254.42 on 09/05/12
For personal use only.

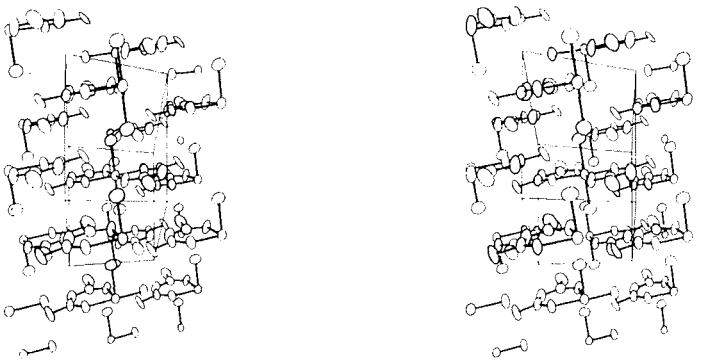

FIG. 2. Stereogram (stereoscopic pair of perspective projections) of $Re(acac)_2Cl_2$ viewed down the b^* axis. The c and a axes run roughly parallel to the horizontal and vertical edges of the paper respectively. The unit cell outlined is shifted by 1/2,1/2,1/2 from the cell used in all calculations in this work.

larger than C4. Both these effects have been observed previously in β-ketoenolate complexes (see references in ref. 15).

The molecules are situated in the unit cell such that the Cl—Re—Cl unit lies almost along the a axis and the molecules form a line. Intermolecular contact along the line is between chlorine atoms. Adjacent lines are arranged such that β-ketoenolate rings on molecules within two adjacent lines are interleaved. Thus, a β-ketoenolate group on a molecule at 0,0,0 in the unit cell is interleaved with β-ketoenolate groups on molecules at $0,1,\bar{1}$ and $1,1,\bar{1}$. In the c direction the chlorine atoms contact the β-ketoenolate groups of adjacent molecules, which are arranged such that the chlorine contact is with one methyl group and the central CH group of a particular β-ketoenolate group. In the b^* direction intermolecular contact is primarily between the chlorine atom on one molecule and a methyl group and its nearest oxygen atom in the β-ketoenolate ring of the next molecule (up or down).

We confirm that previous claims that $Re(C_5H_7O_2)_2Cl_2$ is dimeric (3, 16) are incorrect for the solid state.

We thank the National Research Council of Canada for financial support of this work.

1. C. J. L. LOCK and CHE'NG WAN. Chem. Commun. 1109 (1967).
2. R. COLTON, R. LEVITUS, and G. WILKINSON. J. Chem. Soc. 4121 (1960).
3. D. E. GROVE, N. P. JOHNSON, C. J. L. LOCK, and G. WILKINSON. J. Chem. Soc. 490 (1965).
4. W. D. COURRIER, C. J. L. LOCK, and G. TURNER. Can. J. Chem. **50**, 1797 (1972).
5. N. P. JOHNSON, C. J. L. LOCK, and G. WILKINSON. Inorg. Synth. **9**, 147 (1967). McGraw–Hill, Inc. N.Y.
6. D. T. CROMER and K. HERRINGTON. J. Am. Chem. Soc. **77**, 4708 (1955).
7. J. A. IBERS. Acta Cryst. **9**, 652 (1956).
8. E. W. HUGHES. J. Am. Chem. Soc. **63**, 1737 (1941).
9. J. A. IBERS. International tables for X-ray crystallography. Vol. III. Kynoch Press, Birmingham. 1962. p. 216 *et seq.*
10. D. T. CROMER and J. T. WABER. Acta Cryst. **18**, 104 (1965).
11. D. T. CROMER. Acta Cryst. **18**, 17 (1965).
12. D. BRIGHT and J. A. IBERS. Inorg. Chem. **8**, 709 (1969).
13. H. D. GRUNDY and I. D. BROWN. Can. J. Chem. **48**, 1151 (1970).
14. F. A. COTTON and S. J. LIPPARD. Inorg. Chem. **5**, 416 (1966).
15. E. C. LINGAFELTER and R. L. BRAUN. J. Am. Chem. Soc. **88**, 2951 (1966).
16. G. ROUSCHIAS and G. WILKINSON. J. Chem. Soc. (A), 465 (1966).
17. C. K. JOHNSON. United States Atomic Energy Commission Report—ORNL—3794. Revised, June, 1965.

Can. J. Chem. Downloaded from www.nrcresearchpress.com by 210.87.254.42 on 09/05/12
For personal use only.

An Investigation of the $Sn_{1-x}Sb_xO_2$ System by Mössbauer Spectroscopy

T. BIRCHALL

Department of Chemistry, McMaster University, Hamilton 16, Ontario

AND

R. J. BOUCHARD AND R. D. SHANNON

Central Research Department, E. I. du Pont de Nemours and Company, Wilmington, Delaware 19898

Received January 5, 1973

The $Sn_{1-x}Sb_xO_2$ system has been studied by means of ^{119}Sn and ^{121}Sb Mössbauer spectroscopy. The presence of an unresolved quadrupole splitting in SnO_2 is confirmed. The data show that the oxidation states of the tin and antimony are IV and V, respectively. The conduction electrons resulting from Sb substitution are distributed over the entire lattice. As the Sb content increases, the ^{119}Sn isomer shift and s electron density at the Sn nucleus also increase, as expected for a conduction band composed largely of Sn 5s orbitals.

Le système $Sn_{1-x}Sb_xO_2$ a été étudié à l'aide de la spectroscopie Mössbauer du ^{119}Sn et du ^{121}Sb. La présence d'une scission des raies qui n'a pas été expliquée et qui est causée par la présence d'un quadrupole a été confirmée. Les données démontrent que les états d'oxydation de l'étain et de l'antimoine sont respectivement IV et V. Les électrons responsables de la conduction résultant d'une substitution du Sb sont distribués sur le réseau entier. En même temps que la teneur en Sb augmente, le déplacement isomérique du ^{119}Sn et la densité des électrons s au noyau Sn augmentent tous deux tel que prévu pour une bande de conduction composée surtout d'orbitales 5s du Sn.

[Traduit par le journal]

Can. J. Chem., **51**, 2077 (1973)

Introduction

Stannic oxide, SnO_2, is a semiconducting oxide with the rutile crystal structure and an energy gap of 3.4 eV (1, 2). Because of its high conductivity, transparency, chemical and thermal stability, films of this oxide have been produced commercially for many years. It is well known that the electrical conductivity can be controlled by the use of Sb as a donor impurity. Minimum resistivity is obtained with 1–5% Sb. Larger Sb concentrations lead to increased resistance, probably because of increased lattice disorder. Electrical properties have also been measured on SnO_2:Sb single crystals (3), which can be produced by high-temperature, gas-phase reactions.

Because $Sn_{1-x}Sb_xO_2$ exhibits n-type electrical properties, it is generally assumed that the Sb is present as Sb(V), since to preserve electroneutrality, x atoms of Sb(V) would cause reduction of $x/2$ atoms of Sn(IV) to $x/2$ Sn(II) and provide x electrons to the conduction band. Alternatively, half of the entering Sb(V) could be reduced to Sb(III) with the same effect. However, since the electrical properties of SnO_2:Sb are essentially identical to oxygen-deficient SnO_{2-x} where no Sb^{3+} states are present, Sn(II) is more likely. Electrical properties are not always unambiguous indicators of oxidation states, however, and it would be helpful for our understanding of SnO_2 to verify the oxidation state of the Sb dopant by another technique.

Mössbauer spectroscopy often provides a convenient means for the identification of oxidation states (4) and, in addition, gives information about local site symmetries. We have, therefore, carried out an investigation of the $Sn_{1-x}Sb_xO_2$ system, for x up to 0.1, by this technique.

Experimental

Preparation of Compounds

Solutions of the mixed cations were prepared by dissolving appropriate amounts of reagent grade $SnCl_4 \cdot 5H_2O$ in H_2O to give a final concentration of ~ 0.2 *M*. The Sb was dissolved in aqua regia and added to the Sn solution, to which a small amount of HCl (5 cc/l) was added to prevent premature precipitation of the Sb. The solution was rapidly stirred and ammonia solution was slowly added to p$H = 7$. The resultant gelatinous precipitate was then heated in the mother liquor for ~ 2 h at ~ 100 °C, and washed several times with distilled water, accompanied by several settling and decantation steps. The final product was filtered and dried under vacuum at 100 °C. Portions of these products were heated to 600 °C in air for 16 h; those containing

Can. J. Chem. Downloaded from www.nrcresearchpress.com by 210.87.254.105 on 09/05/12
For personal use only.

TABLE 1. Composition and firing conditions for $Sn_{1-x}Sb_xO_2$

Formula	Code	Firing conditions
SnO_2	40A	25 °C (air)
$Sn_{0.97}Sb_{0.03}O_2$	31B	80–100 °C (vac)
$Sn_{0.95}Sb_{0.05}O_2$	31C	85–100 °C (vac)
$Sn_{0.90}Sb_{0.10}O_2$	31D	85–100 °C (vac)
SnO_2	40C	600 °C 40 h
$Sn_{0.97}Sb_{0.03}O_2$	34B	600 °C 16 h
$Sn_{0.95}Sb_{0.05}O_2$	34C	600 °C 16 h
$Sn_{0.90}Sb_{0.10}O_2$	34D	600 °C 16 h

Sb developed a blue coloration indicative of solid solution formation. X-Ray diffractometer tracings were taken before and after heating with a Norelco diffractometer. Compositions with pure Sn and 3, 5, and 10 mol% Sb were prepared and are listed in Table 1. Samples with 33 and 67 mol% Sb, which are well above the solubility limits of Sb in SnO_2, were also prepared to provide a spectrum containing both combined and unreacted Sb.

Mössbauer Spectra

The Mössbauer system used in this study has been previously described (5). The sources used were $Ba^{119m}SnO_3$, and $Ba^{121m}SnO_3$ obtained from New England Nuclear, and maintained at room temperature (295 °K) throughout. Calibration of the drive velocity was carried out with a ^{57}Co/Pd source and a standard iron foil. The samples for ^{119}Sn spectra all contained 10 mg Sn/cm^2 while those for ^{121}Sb spectra contained $\sim$20 mg Sb/cm^2. ^{119}Sn Spectra of samples of spectroscopically pure SnO_2 were interspersed with the spectra of the other samples and have been used as the reference to which all chemical isomer shifts have been referred. These Sn spectra were computer fitted using the program written by Stone (6). The tin data have been analyzed by fitting the absorption envelope to one Lorentzian line, with no constraints, and to two overlapping Lorentzian lines having equal widths and intensities. In every case, the two line fit was statistically better, as evidenced by the significantly lower χ_A^2 (Table 2), and visually, as shown in Fig. 1. Antimony-121 spectra were fitted as has been described (7) and are referred to InSb at 77 °K as zero velocity.

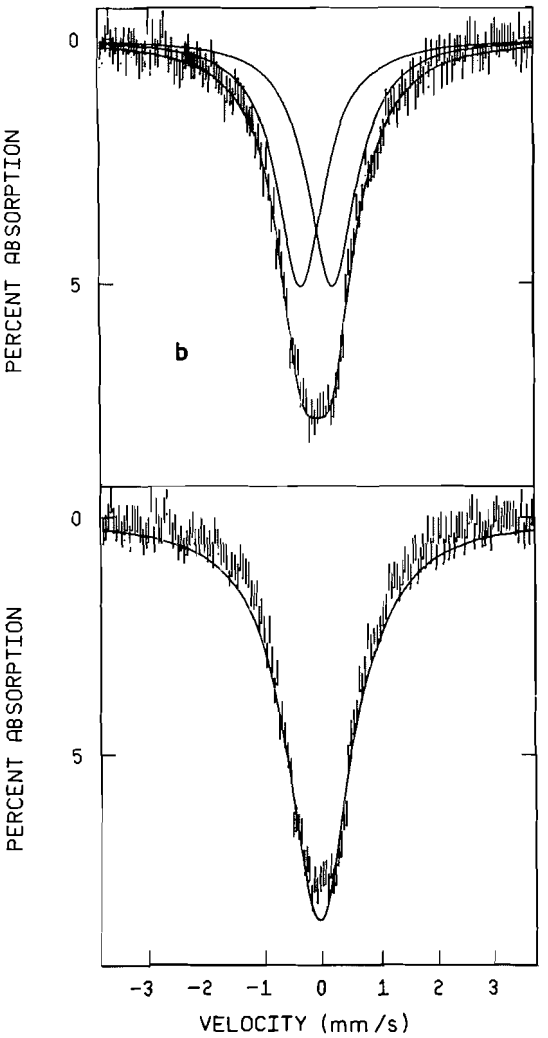

FIG. 1. Mössbauer spectrum of SnO_2 at 295 °K. (*a*) fitted to a single Lorentzian; (*b*) fitted to two Lorentzians with equal width and intensities.

Results and Discussion

X-Ray

The products dried at 100 °C showed a very broad rutile pattern corresponding to a particle size of about 25 Å. The products heated to 600 °C showed sharper peaks and X-ray line broadening calculations give a particle size of 60 to 90 Å, depending on the Sb content. Although no nonrutile peaks were observed in the sample with the highest Sb content (10 mol%), the presence of a second phase cannot be ruled out, since even 5% excess Sb oxide might be present and not observed assuming its X-ray pattern also consisted of weak, broad peaks. The regular increase in line broadening suggests that the Sb is in solid solution, however, with the increased broadening being due to increased asymmetry of the lattice, not to particle size effects.

Mössbauer

In the early tin Mössbauer work, one of the principle source matrices used was SnO_2, since it gave a high recoilless fraction at room temperature. However, some workers have claimed variations in line width depending upon the method of preparation (8) suggesting that the exact composition of the SnO_2 may be in doubt.

Can. J. Chem. Downloaded from www.nrcresearchpress.com by 210.87.254.105 on 09/05/12
For personal use only.

TABLE 2. Mössbauer parameters* for SnO_2 and $Sn_{1-x}Sb_xO_2$

Sample	Temperature (°C)	^{119}Sn One Line δ	Γ	χ^2	^{119}Sn Two Lines δ	Δ	Γ	χ^2	^{121}Sb δ	Γ
SnO_2 spectroscopic pure	295	0	1.46	574	0	0.53	1.12	393		
	295	0	1.40	471	0	0.53	1.06	365		
	295	0	1.39	459	0	0.53	1.07	357		
SnO_2 (40A)	295	0	1.37	480	+0.01	0.55	1.02	366		
SnO_2 (40C)	295	+0.01	1.47	678	+0.01	0.57	1.07	375		
$Sn_{0.9}Sb_{0.1}O_2$ (31D)	295	+0.01	1.47	558	+0.01	0.59	1.02	365	+8.58	2.77
$Sn_{0.95}Sb_{0.05}O_2$ (31C)	295	0	1.35	475	0	0.55	0.99	400		
$Sn_{0.97}Sb_{0.03}O_2$ (31B)	295	0	1.37	549	0	0.56	1.01	429		
$Sn_{0.9}Sb_{0.1}O_2$ (34D)	295	+0.06	1.60	945	+0.06	0.65	1.13	473	+8.21	2.95
$Sn_{0.95}Sb_{0.05}O_2$ (34C)	295	+0.03	1.53	629	+0.04	0.62	1.07	342	+8.35	2.91
$Sn_{0.97}Sb_{0.03}O_2$ (34B)	295	+0.02	1.53	817	+0.03	0.65	1.11	446	+8.38	2.71

*Errors in the isomer shifts are ±0.01 mm/s for ^{119}Sn and ±0.075 mm/s for ^{121}Sb.

In addition, there have been claims for the detection of a unique quadrupole splitting in SnO_2 (9, 10) but little information was provided as to the computational methods used to judge the quality of the spectra; indeed, in one case (10) the quality of the spectra was rather poor. Other groups have attempted to resolve the quadrupole splitting problem in SnO_2 by the application of a magnetic field (11, 12) but this has proved inconclusive.

The crystallographic data for SnO_2 have been re-refined by Baur and Khan (13) and it is clear that the tin atom has six near oxygen neighbors at 2.05 Å: small differences in the Sn—O distances are not statistically significant. However, the O—Sn—O angles are not all equal, and the arrangement of the six oxygens about the Sn is distorted as shown in Fig. 2. This would, of course, give rise to an appreciable asymmetry at the Sn nucleus and a quadrupole splitting would be expected. Whether or not this splitting would be detectable in the Mössbauer spectrum would depend upon its magnitude in relation to the line width parameter, and this is the root of the controversy. Clearly, from an examination of the SnO_2 spectra, (Fig. 1*a*, *b*) there is no *well resolved* quadrupole splitting. However, Fig. 1*a* and the x^2 values indicate that this absorption envelope cannot be fitted to a single Lorentzian line shape. When the absorption is fitted to two lines, a much more significant fit is obtained as Table 2 (x^2 357–393 for 392 degrees of freedom) and Fig. 1*b* show. Analysis of the data in this way clearly shows the presence of a quadrupole splitting of 0.53 mm/s which agrees well with the values reported by Stockler *et al.* (10). This splitting is half the observed line width and therefore just on the limits of resolution. Of the other SnO_2 samples examined, the air dried sample has the same isomer shift and a slightly larger quadrupole splitting, while the one fired at 600 °C has both a higher isomer shift and quadrupole splitting. Compared to the air-dried sample, these differences are small and within experimental error. For reasons discussed below, we believe the isomer shift for SnO_2 (600 °C) to be significantly different from spec. pure SnO_2.

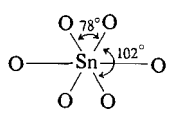

FIG. 2. Arrangement of O atoms about Sn.

The $Sn_{1-x}Sb_xO_2$ samples fired at 85–100° are not single phase systems, since the Sb has not yet entered the SnO_2 rutile lattice. As expected, the ^{119}Sn spectra are not significantly different from samples of undoped SnO_2 prepared under similar conditions. The ^{121}Sb chemical isomer shift indicates that the antimony exists as Sb(V) (14). On firing at 600° the Sb enters the rutile structure to give a single phase system.

Electrical neutrality is preserved by reduction of $x/2$ Sn or Sb atoms to Sn(II) or Sb(III), but the electrons released from these reductions are not localized at the ionic sites where they were created, but are delocalized throughout the entire lattice. The rate at which these electrons

Can. J. Chem. Downloaded from www.nrcresearchpress.com by 210.87.254.105 on 09/05/12
For personal use only.

Can. J. Chem. Downloaded from www.nrcresearchpress.com by 210.87.254.105 on 09/05/12
For personal use only.

are being transferred must be greater than the time for the Mössbauer transition to occur (3.5×10^{-9} s) since no resonance spectra corresponding to either reduced species is observed: concentrations of Sn(II) or Sb(III) as low as 0.4 mol % can be detected under normal conditions. In cases where $x \gg 0.1$, and which X-ray analysis shows to be not a single phase, the ^{121}Sb spectra show the presence of some Sb(III) as well as Sb(V). It is well known that prolonged heating of any antimony oxide results in the formation of Sb_2O_4 which has been demonstrated to contain Sb(III) and Sb(V) (14). The Sb(III) resonance observed is probably the result of such a reaction on the uncombined, excess Sb oxide fraction.

The quadrupole splitting results from the interaction of the nuclear quadrupole moment of the excited state of ^{119}Sn with an electric field gradient. This electric field gradient arises as a result of an asymmetry of valence electrons and/or an asymmetry of neighboring ions. Replacement of a Sn by an Sb atom in the structure will change the lattice contribution to the electric field gradient at the Sn nuclei remaining and this should result in a change in quadrupole splitting from SnO_2 to $Sn_{1-x}Sb_xO_2$. Such a change is indeed observed and, although small, is outside experimental error. The fact that the magnitude of the quadrupole splitting increases indicates that the valence and lattice contributions to the electric field gradient tensor are of the same sign. Whether this sign is positive or negative cannot be ascertained from the data presented here, though this could probably be obtained from a lattice sum calculation. We were unable to satisfactorily analyze the ^{121}Sb spectra in terms of a significant quadrupole interaction, which is not too surprising in view of the large natural line width of the ^{121}Sb resonance and the small quadrupole interaction noted in the ^{119}Sn spectra. This was somewhat disappointing since the sign of the interaction would have been obtained had the splitting been resolvable.

A good correlation is observed between the ^{119}Sn chemical shift and the amount of Sb dopant in the lattice, Fig. 3. Since this plot extrapolates to the chemical shift value for the SnO_2 samples fired at 600°, we believe that the shift reported for this sample is significant. Because the $\delta r/r$ term in the isomer shift expression has a positive sign for ^{119}Sn (15, 16) the

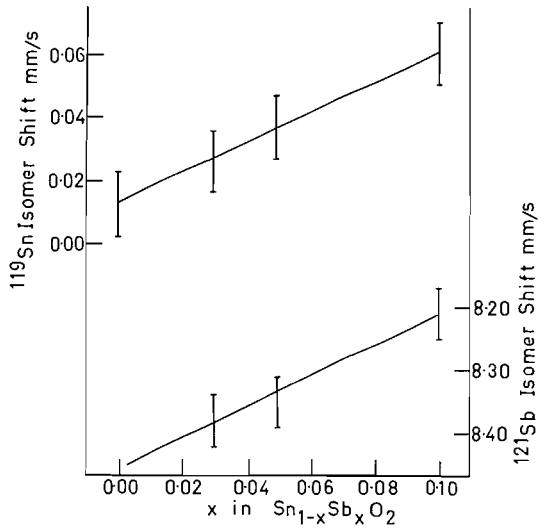

FIG. 3. Plots of ^{119}Sn and ^{121}Sb isomer shifts *vs.* x in the $Sn_{1-x}Sb_xO_2$ system.

increase in isomer shift indicates an increase in s electron density at the nucleus. A similar increase in s electron density at the Sb is also noted but because $\delta r/r$ for Sb is negative (17, 18) this is observed as a decrease in isomer shift. Also, since $\delta r/r$ for ^{121}Sb is greater than that for ^{119}Sn, larger shifts are recorded. Because of the good correlation of both Sn and Sb chemical shifts with the amount of Sb dopant, we conclude that the systems up to and including $Sn_{0.9}Sb_{0.1}O_2$ are indeed single phase, and the X-ray broadening is due to increased asymmetry.

Since the conduction electrons are in band states, not localized levels, every Sn and Sb atom in the lattice will be affected; therefore, the increase in s electron density with increasing conduction electron density is quite reasonable, because the conduction band is composed largely of 5s orbitals (19).

We thank the National Research Council of Canada for financial support.

1. T. ARAI. J. Phys. Soc. Jap. **15**, 916 (1960).
2. E. E. KOHNKE. J. Phys. Chem. Solids, **23**, 557 (1962).
3. D. F. MORGAN and D. A. WRIGHT. Brit. J. Appl. Phys. **17**, 337 (1966).
4. N. N. GREENWOOD and T. C. GIBB. Mössbauer spectroscopy. Chapman and Hall, London. 1971.
5. T. BIRCHALL. Can. J. Chem. **47**, 1351 (1969).
6. A. J. STONE. *Appendix to* G. M. BANCROFT, W. K. ONG, A. F. MADDOCK, and R. K. PRINCE. J. Chem. Soc. (A), 1966 (1967).

7. T. BIRCHALL and B. P. DELLA VALLE. Can. J. Chem. **49**, 2808 (1971).
8. V. S. ZYKOV, E. V. PETROVICH, and YU. P. SMIRNOV. Sov. Phys. J.E.T.P. **22**, 708 (1966).
9. R. H. HERBER and J. SPIJKERMAN. J. Chem. Phys. **42**, 4312 (1965).
10. H. A. STOCKLER, H. SANO, and R. H. HERBER. J. Chem. Phys. **45**, 1182 (1966).
11. B. A. GOODMAN and N. N. GREENWOOD. Chem. Commun. 1105 (1969).
12. N. E. ERICKSON. Chem. Commun. 1349 (1970).
13. W. H. BAUR and A. A. KAHN. Acta Cryst. **B27**, 2133 (1971).
14. J. G. STEVENS and L. H. BOWEN. Mössbauer methodology **5**, 27 (1969).
15. J. P. BOCQUET, Y. Y. CHU, O. C. KISTNER, M. L. PERLMAN, and G. T. EMERY. Phys. Rev. Lett. **17**, 809 (1966).
16. N. N. GREENWOOD, P. G. PERKINS, and D. H. WALL. Phys. Lett. **28A**, 339 (1968).
17. V. A. BRYUKHANOV, B. Z. IOFA, V. KOTHEKAR, S. I. SEMENOV, and V. S. SHPINEL. Zhur. eksp. teor. Fiz. **55**, 160 (1968).
18. S. L. RUBY and G. K. SHENOY. Phys. Rev. **186**, 326 (1969).
19. D. A. WRIGHT. Proc. Brit. Ceram. Soc. **10**, 103 (1968).

Can. J. Chem. Downloaded from www.nrcresearchpress.com by 210.87.254.105 on 09/05/12
For personal use only.

Crystal Structure and Phase Transformations of Sodium Diarsenate, $Na_4As_2O_7$

KIANG Y. LEUNG AND CRISPIN CALVO

Department of Physics and Institute for Materials Research, McMaster University, Hamilton, Ontario

Received November 16, 1972

Sodium diarsenate at room temperature is monoclinic with lattice parameters $a = 5.969(1)$, $b = 10.126(1)$, $c = 12.272(3)$ Å and $\beta = 92.87(2)°$. There are four formula units per cell with space group $C2/c$. The structure was refined by full-matrix least-squares to a final R value of 0.027 utilizing 1157 reflections measured on a Syntex PĪ automatic diffractometer. The anion, consisting of two AsO_4 tetrahedra sharing a common oxygen atom, with a bridging angle of 123.5° at that oxygen atom, lies on a two-fold axis. The bridging As—O bond lengths are 1.783 Å and the average terminal As—O bond length is 1.658 Å uncorrected for thermal motion. Both Na ions show fivefold coordination to oxygen atoms. One of these sodium ions has a long interaction (2.852 Å) with the bridging oxygen atom of the anion. $Na_4As_2O_7$ undergoes a series of phase transformations between room temperature and 220 °C, and a further major transformation near 680 °C.

Le sodium diarsénate est monoclinique à la température ambiante avec comme paramètres du réseau $a = 5.969(1)$, $b = 10.126(1)$, $c = 12.272(3)$ Å et $\beta = 92.87(2)°$. La maille contient quatre unités et le groupe spatial est $C2/c$. La structure a été raffinée par la matrice des moindres carrés jusqu'à une valeur finale R de 0.027, après utilisation de 1157 réflexions mesurées sur un diffractomètre Syntex PĪ automatique. L'anion sur un axe d'ordre deux, est constitué de deux tétraèdres AsO_4 avec un atome d'oxygène en commun, l'angle de portage étant de 123.5° sur cet atome d'oxygène. Les longueurs de liaison As—O du pont sont de 1.783 Å et la longueur moyenne finale pour la liaison AsO est de 1.658 Å, sans apporter de correction pour le mouvement thermique. Les deux ions Na exhibent une coordination de 5 avec les atomes d'oxygène, l'un de ces ions ayant une interaction lointaine (2.852 Å) avec l'atome d'oxygène du pont de l'anion. $Na_4As_2O_7$ subit une série de transformations de phase entre la température ambiante et 220 °C, et une autre transformation majeure près de 680 °C.

[Traduit par le journal]

Can. J. Chem., **51**, 2082 (1973)

Can. J. Chem. Downloaded from www.nrcresearchpress.com by 210.87.254.5 on 09/05/12
For personal use only.

Introduction

To date, little accurate data exists on the structure of systems containing condensed tetrahedral AsO_4 groups. A number of diarsenates have been found to crystallize as analogues of the mineral thortveitite (1), but in these cases, as in all other structures isotypic with thortvietite, ambiguity exists as to the detailed bonding because of disorder at the bridging oxygen atom (2, 3). An additional interest in this system arises because its chemical analog, $Na_4P_2O_7$, manifests a rich variety of phase transformations between room temperature and 600 °C (4–7).

The crystallography of systems containing diortho anions with an overall stoichiometry of $M_2X_2O_7$ and tetrahedrally coordinated X ions have been extensively explored (8, 9). Polymorphic behavior has been noted for a large number of the compounds having this formulation (10–13). The crystallography of systems with the stoichiometry of MX_2O_7 is less well explored but again a number of polymorphs have been reported (14, 15). On the other hand, the crystallographic nature of compounds with composition $M_4X_2O_7$ has been rather ignored, although phase transformations have been reported for $Na_4P_2O_7$, (4–6) $Li_4P_2O_7$ (16, 17) and $Li_4As_2O_7$ (17).

The bonding in those diortho systems with divalent metal cations has been correlated on the basis of local electroneutrality (18). These correlations contain very little of the chemistry of the atoms and ions explicitly in the model since they are related to only the formal charge on the ion and not on the higher moments of this charge density. However, in order to investigate this question further, additional accurate structure resolutions, where the cation to oxygen atom radius and the electronegativities are varied, seem desirable. Further, an understanding of the nature of the transformations in these systems require structural studies of these phases.

Experiments

Crystals of $Na_4As_2O_7$ were grown directly from the melt at 850 °C. The initial charge was formed by heating $Na_2HAsO_4 \cdot 7H_2O$ to about 900 °C. Preliminary photographic work utilizing precession cameras established the space group to be either Cc of $C2/c$ on the basis of the

Can. J. Chem. Downloaded from www.nrcresearchpress.com by 210.87.254.5 on 09/05/12
For personal use only.

extinction conditions. Reflections were absent when $h + k$ = odd or when l = odd and $k = 0$.

The differential thermal analysis traces, taken with the Dupont 900 system, are shown in Figs. 1 and 2. They indicate a transformation near 690 °C and a series of endothermic transformations between room temperature and 220 °C. Melting occurs at 848 °C.

The solid state transformation at 692 °C upon heating is immediately reversible but a single crystal heated to above this transformation decomposed into a powder. However, the transformations between room temperature and 300 °C do not reappear immediately. Figure 2 indicates how these peaks reappear when the sample is allowed to stand at room temperature for a period extending through a number of days.

A ground sphere, 0.01 cm in radius, was used to collect data for the phase stable at room temperature, both for accurate parameters and for the resolution of the crystal structure. The 2θ values of 15 reflections were accurately centered using a Syntex automatic diffractometer and the lattice parameters fitted to these values by least-squares. These results were obtained at 22 °C using MoKα̅ radiation monochromatized with graphite ($\lambda = 0.71069$ Å) and are:

Crystal Data

$Na_4As_2O_7$ f.w. = 353.79
$a = 5.969(1)$, $b = 10.126(1)$, $c = 12.272(3)$ Å, $\beta = 92.87(2)°$, $V = 740.85$ Å^3, $\rho_{exp} = 3.12$g/cm^3, $\rho_{calcd} = 3.16$ g/cm^3, $Z = 4$, space group $C2/c$.

Peaks were scanned at a rate varying between 2 and 24° per min, depending upon the peak count rate. Backgrounds were counted on either side of the peak for the same time period as used in scanning the peak. Reflections whose intensities, after correction for background, were less than 3σ, where σ was determined from counting statistics, were regarded as unobserved. A total of 1157 unique reflections were collected ($2\theta_{max} = 65°$) of which 1011 were regarded as observed. These were corrected for Lorentz, polarization, absorption ($\mu R = 0.59$), using programs in the X-ray 71 package, and extinction as proposed by Larson (19).

The positions of the arsenic atoms were determined form Patterson functions and those of the remaining

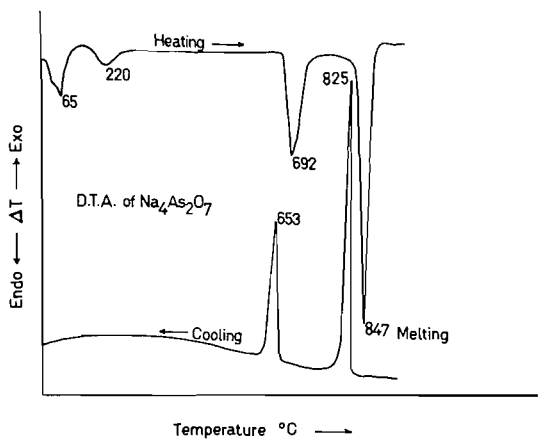

FIG. 1. Differential thermal analysis trace of $Na_4As_2O_7$. Temperatures in degree C are superimposed.

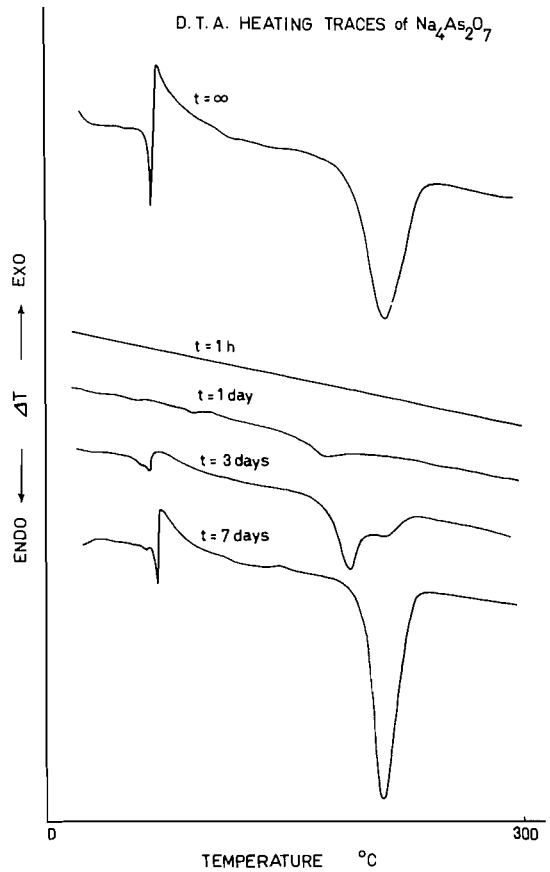

FIG. 2. Differential thermal analysis trace upon heating of $Na_4As_2O_7$ as a function time spent at room temperature between heatings.

atoms determined from difference syntheses. These maps were all consistent with space group $C2/c$. The structure was refined with full matrix least-squares written for the CDC 6400 by J. S. Stephens. Atomic scattering factors for Na^+, As, and O^- obtained from the International Tables for X-ray Crystallography (20) were corrected for dispersion. Convergence was obtained with unit weights and isotropic thermal parameters and then independent anisotropic thermal parameters were varied. For the final refinement weights were set = $\{7.4 - 0.26\ F_o + 0.0031\ F_o^2\}^{-1}$ with coefficients chosen so that $\omega|F_{obs} - F_{calcd}|^2$ would be independent of F_o. No variation of $\Delta F = F_{obs} - F_{calcd}$ with $\sin\theta/\lambda$ was noted. The final R value is 0.027 while $R_\omega = (\Sigma\omega|F_o - F_c|^2/\Sigma\omega F_o^2)^{1/2}$ is 0.037. No residual peaks could be discerned in the final electron density map. The final atomic positional parameters are found in Table 1. Table 2 contains a comparison of the observed and calculated structure factors. The mean deviation of a reflection of unit weight is 0.98.[1]

[1]Table 2 is available, at a nominal charge, from the Depository of Unpublished Data, National Science Library, National Research Council of Canada, Ottawa, Canada K1A 0S2.

Can. J. Chem. Downloaded from www.nrcresearchpress.com by 210.87.254.5 on 09/05/12
For personal use only.

TABLE 1. Atomic and thermal parameters of $Na_4As_2O_7$ with estimated standard deviations in parentheses

	x	y	z	U_{11}*	U_{22}	U_{33}	U_{12}	U_{23}	U_{23}
Na(1)	0.3438(2)	0.3216(2)	0.1273(1)	0.0157(8)	0.0194(7)	0.0146(7)	−0.0024(5)	0.0010(5)	0.0021(5)
Na(2)	0.3118(2)	−0.0155(2)	0.0958(1)	0.0137(8)	0.0209(7)	0.0224(7)	−0.0011(5)	0.0017(6)	0.0023(5)
As	0.14474(5)	0.15226(3)	0.36050(2)	0.0067(2)	0.0084(2)	0.0079(2)	0.0006(1)	0.0004(1)	0.0012(1)
O(1)	0	0.0689(3)	1/4	0.025(2)	0.009(1)	0.017(1)	—	−0.013(1)	—
O(2)	−0.0605(5)	0.1787(3)	0.4442(2)	0.019(2)	0.030(1)	0.016(1)	0.007(1)	0.012(1)	0.005(1)
O(3)	0.3219(4)	0.0360(3)	0.4046(3)	0.012(1)	0.016(1)	0.019(1)	0.005(1)	−0.004(1)	0.0016(8)
O(4)	0.2649(4)	0.2870(2)	0.3133(2)	0.015(1)	0.014(1)	0.015(1)	−0.005(1)	0.000(1)	0.0029(8)

*U_{ij}'s in Å² are computed from $\beta_{ij} = 2\pi^2 b_i b_i U_{ij}$ where $T = \exp -(\beta_{11}h^2 + \ldots + 2\beta_{12}hk + \ldots)$ appear in the structure factor expression and b_j's are reciprocal lattice vectors.

Can. J. Chem. Downloaded from www.nrcresearchpress.com by 210.87.254.5 on 09/05/12
For personal use only.

Description of the Structure

The structure of $Na_4As_2O_7$ consists of anions, formed from AsO_4 groups sharing one corner, arranged in layers, $\frac{1}{2}$ c axis length thick, parelleling the *ab* plane. In each layer the anions are arranged in a hexagonal pattern as seen in Fig. 3 with the As—As vector of any anion at 32.6° to the c axis. The anion contains a crystallographic two-fold axis through the bridging oxygen atom and the As—O—As bond angle is 123.5°. Thus O(3)*a*, O(4)*a*, O(3)*c*, and O(4)*c*, defined in Table 4, lie within 1/4 Å of a plane parallel to the *ab* plane, but O(2)*a* and O(2)*c* do not, as is shown in Fig. 4. Adjacent layers are generated by a center of symmetry, with the anions, regarded as spheres, in this context, showing a pseudo-hexagonal packing.

Na(1) lies between the terminal oxygen atoms of three anions in one layer and nearly directly below an anion in an adjacent layer, as seen as in Fig. 4. It is coordinated to five oxygen atoms contributed by these four anions and bridges across one of these As_2O_7 groups. Na(2) and As nearly have the same z values. Na(2) shares a bridging oxygen atom, O(1)*a*, and a terminal oxygen atom, O(2)*c*, with one anion while the remaining oxygen atoms arise from three additional anions.

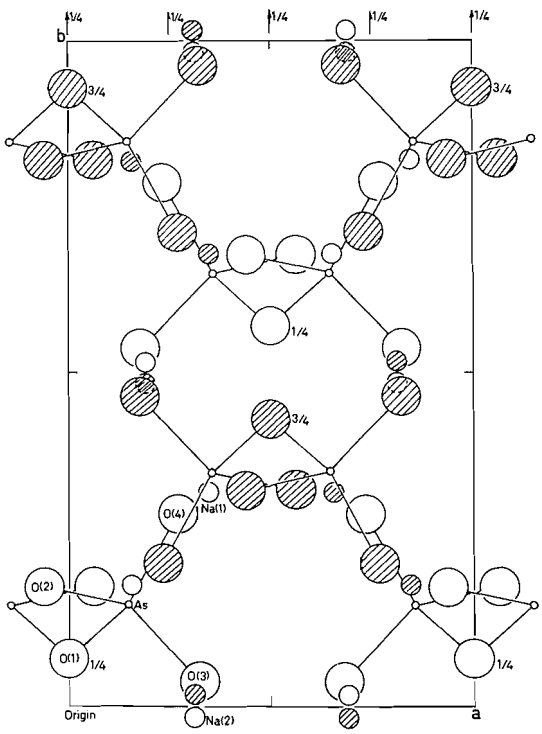

FIG. 3. The structure of $Na_4As_2O_7$ shown in projection onto the *ab* plane. The open circles represent those Na and oxygen atoms within the layer defined by $0 \leq z < 1/2$ and the cross hatched ones those Na and oxygen atoms within the layer defined by $1/2 \leq z < 1$. The largest circles represent oxygen atoms while the smallest ones are arsenic atoms. The intermediate ones represent sodium ions.

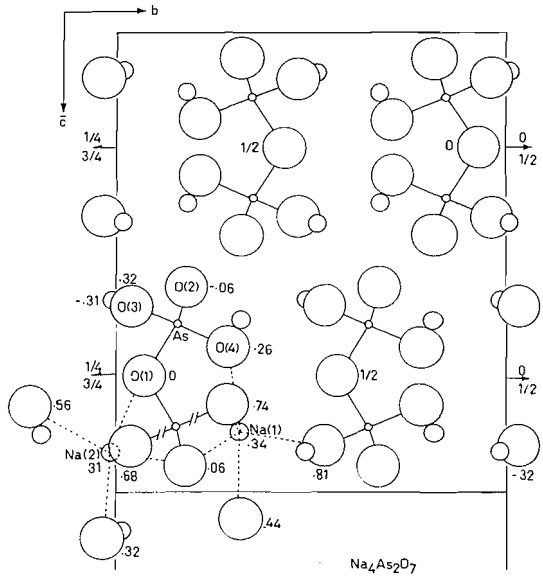

FIG. 4. The structure of $Na_4As_2O_7$ viewed in projection onto the *bc* plane. The small circles are As atoms while the large open ones represent oxygen atoms. The intermediate sized circles are sodium ions.

The bridging oxygen atom of the anion lies on a two-fold axis separated by 1.783(2) Å from the As, noted in Table 3. The terminal As—O bond lengths are substantially and significantly shorter, ranging from 1.655 to 1.659 Å. The minimum thermal corrections to these bonds is 0.003 Å, for the bridging, and 0.002 Å or less for the terminal bonds, based upon the method of Busing and Levy (21). Individual terminal As—O bond lengths are not significantly different. All the O—As—O angles in a tetrahedron that involve the bridging oxygen atom are less than the ideal value, while the remaining angles are all larger than ideal. The As—O—As angle is rather small at 123.5° and results, in part, from the interaction of the bridging with two Na(2) ions.

Each Na ion has only five oxygen atoms within 3.0 Å. The Na(1)—O bond lengths are fairly uniformly distributed between 2.347(3) and

TABLE 3. Bond distances and angles in $Na_4As_2O_7$*

Bond	Distance (Å)	Bonds	Angle (deg)	Bonds	Angle (deg)
As—O(1)*a,c*	1.783(2)†	O(1)—As—O(2)	101.7(1)	O(2)—As—O(3)	113.1(1)
—O(2)*a,c*	1.659(3)	—O(3)	100.9(1)	—O(4)	115.4(1)
—O(3)*a,c*	1.655(3)	—O(4)	109.0(1)	O(3)—As—O(4)	114.7(1)
—O(4)*a,c*	1.659(3)				
As—As(*c*)	3.142(3)	As—O(1)—As	123.5(2)		
Na(1)—O(2)*c*	2.362(3)	O(2)*c*—Na(1)—O(2)*h*	81.2(1)	O(2)*h*—Na(1)—O(3)*g*	87.9(1)
—O(2)*h*	2.347(3)	—O(3)*g*	102.2(1)	—O(4)*a*	171.1(1)
—O(3)*g*	2.409(3)	—O(4)*a*	95.4(1)	—O(4)*c*	90.6(1)
—O(4)*a*	2.379(3)	—O(4)*c*	132.9(1)	O(3)*g*—Na(1)—O(4)*a*	100.9(1)
—O(4)*c*	2.437(3)	O(4)*a*—Na(1)—O(4)*c*	85.7(1)	—O(4)*c*	123.9(1)
Na(2)—O(1)*a*	2.852(2)	O(1)*a*—Na(2)—O(2)*c*	59.4(1)	O(2)*c*—Na(2)—O(3)*d*	85.4(1)
—O(2)*c*	2.506(3)	—O(3)*d*	137.4(1)	—O(3)*e*	113.0(1)
—O(3)*d*	2.359(3)	—O(3)*e*	126.8(1)	—O(4)*g*	129.2(1)
—O(3)*c*	2.248(3)	—O(4)*g*	77.9(1)	O(3)*d*—Na(2)—O(3)*e*	86.9(1)
—O(4)*g*	2.346(1)	O(3)*e*—Na(2)—O(4)*g*	114.4(1)	—O(4)*g*	114.3(1)

*Transformations: $a = x,y,z$; $b = -x,-y,-z$; $c = -x,y,1/2 - z$; $d = x,-y,1/2 + z$; $e = 1/2 + x,1/2 + y,z$; $f = 1/2 - x,1/2 - y,-z$ $g = 1/2 - x,1/2 + y,1/2 - z$; $h = 1/2 + x,1/2 - y,1/2 + z$.
Errors include those arising from the lattice constants in addition to the individual parameter errors.
†Thermal corrections based upon a riding model lead to bond lengths of 1.792, 1.664, 1.667 Å for the As—O(*i*). $i = 1, \ldots, 4$ respectively.

TABLE 4.
(*a*) Bond strengths in $Na_4As_2O_7$*

	As	Na(1)	Na(2)	ΣS_{anion}
O(1)	0.982, 0.982		0.071, 0.071	2.11
O(2)	1.319	0.203	0.146	1.88
		0.211		
O(3)	1.332	0.182	0.205	1.99
			0.268	
O(4)	1.319	0.195	0.211	1.90
		0.171		
ΣS_{cation}	4.95	0.96	0.90	

(*b*) Bond strengths in $Na_4P_2O_7$*

	P(1)	P(2)	Na(1)	Na(2)	Na(3)	Na(4)	ΣS_{anion}
OCE	1.023	1.007	0.176				2.21
O1A	1.312		0.227	0.208		0.175	1.92
O1B	1.309		1.221	1.142	0.168	0.124	1.96
O1C	1.306		0.082	0.146	0.066	0.214	1.98
						0.168	
O2A		1.304	0.192	0.092	0.253		1.85
O2B		1.306		0.192	0.228	0.219	1.95
O2C		1.304	0.194	0.211	0.221		1.91
ΣS_{cation}	4.95	4.92	1.07	1.00	0.94		

*Calculated from $S_i = C_i(r_{0i}/r)^{n_i}$ with

atom(*i*)	C_i	r_{0i}(Å)	n_i
Na^+	1/6	2.449	5.6
As^{5+}	5/4	1.681	4.1
P^{5+}	5/4	1.534	3.2

2.437(3) Å and the $Na(1)O_5$ configuration is a distorted trigonal bipyramid with O(2)*h* and O(4)*a* as the axial oxygen atoms. The four nearest oxygen atoms to Na(2) form a distorted tetrahedron with the O(2)*c*—O(4)*g* edge enlarged to accommodate the fifth oxygen atom, O(1)*a*. The O(1)*a*—O(2)*c* edge is shared with one of the anions. The Na(2)—O distances about the Na(2)—O_4 tetrahedron range from 2.248 to 2.506 Å and the angles lie between 85.4 and

Can. J. Chem. Downloaded from www.nrcresearchpress.com by 210.87.254.5 on 09/05/12
For personal use only.

129.2°. The Na(2)—O(1)*a* interaction is 2.852 Å long and compares with an interaction of 2.426 Å between the bridging oxygen atom and Na(1) in sodium pyrophosphate (6).

Discussion

The structure of $Na_4As_2O_7$ bears considerable resemblance to that of the room temperature polymorph of $Na_4P_2O_7$ (6). The latter structure is orthorhombic with space group $P2_12_12_1$ and unit cell dimensions of $a = 9.367$, $b = 5.390$ and $c = 13.480$ Å. The anion is formed from two PO_4 groups sharing a common oxygen atom with a bridging P—O—P angle of 127.5°. The angle that the P—P vector of the anion subtends with the *c* axis is 9°. This structure also contains layers of pseudo-hexagonally arranged anions and as a result of small displacements assumes a *C* centered cell, with a doubled *c* axis, above 400 °C. Three anions in one layer and three in an adjacent layer are approximately related by a 6_3 axis which becomes a crystallographic symmetry element above 550 °C. Half of the cations lie near this pseudo-axis as shown in Fig. 5. The remaining cations lie between the anion layers and are coordinated to five oxygen atoms. Each anion is stabilized with a non-linear X—O—X group by one strong interaction with one Na^+ in contrast to two weak ones in $Na_4As_2O_7$. In $Na_4P_2O_7$ the anion deviates by about 25° from an eclipsed configuration when viewed parallel to the P—P vector while the comparable average dihedral angle in $Na_4As_2O_7$ is 11°.

As Fig. 5 shows, the bridging oxygen atoms in adjacent layers in $Na_4As_2O_7$ nearly superimposed in projection and a relative shift of 1.8 Å together with the loss of the two-fold axis are needed to establish a pseudo 6_3 axis relationship between the oxygen atoms. In addition, considerable rearrangement of cations is needed to transform from one structure to the other. The phase transformations in $Na_4P_2O_7$ are related to disorder in the direction of the bridging oxygen atom – sodium ion interaction. The fact that O(1) is bonded to two sodium ions precludes similar transformation in $Na_4As_2O_7$.

Typical behavior in X_2O_7 systems has O(1) with the largest amplitude, but in $Na_4As_2O_7$ O(2), one of the terminal oxygen atoms has the largest amplitude. This may be a result of the fact that O(1) is bonded to two cations, whereas in the previous cases the bridging oxygen atom

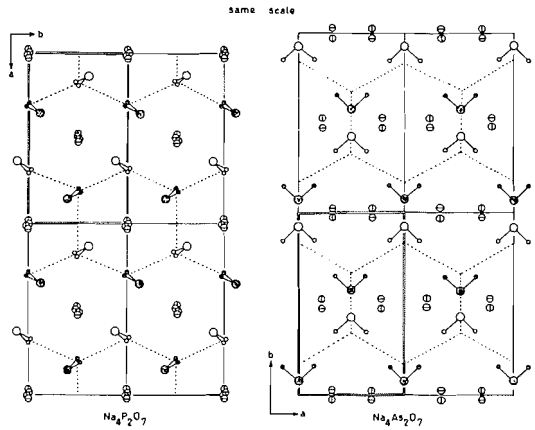

FIG. 5. A comparison of the X—O—X groups and the Na ions bonded to the bridging oxygen atom in $Na_4As_2O_7$ and $Na_4P_2O_7$. The sodium ions are shown as circles with either a horizontal or vertical line. The bridging oxygen atoms are shown with either an open or spotted circle. The smaller circles are X ions with X = As or P.

of the X_2O_7 group bonds strongly to at most one cation. These thermal amplitudes provide no strong evidence for the impending phase transformation however.

The Pauling electrostatic valency (22) is 2.90 at O(1) and 1.85 at the terminal oxygen atoms. From Baur's (18) linear relationship between bond length and electrostatic valency and coefficients derived by Krishnamachari (23) the predicted bond length would be 1.78 Å and 1.675 Å for the As—O(—As) as As—O bond lengths respectively. On the other hand, if the Na(2)—O(1) bonds were ignored they would lead to a greater discrepancy. A more systematic treatment for bonds of varying length has been proposed by Brown and Shannon (24) who show that the bond strength, *s*, can be fitted with a curve of the form $s = C_o(r_o/r)^n$, where r_o and *n* are found by least squares and C_o is given as the formal charge divided by the "normal" coordination number. Table 4 shows the individual bond strengths and the sum about each element. In Table 5 the individual X—O bond lengths are compared with those predicted on the assumption that the calculated valency contribution from the Na^+ is errorless and the difference between the formal charge on the oxygen atom and its formal charge is used to calculate the X—O bond length. Errors in these predicted bond lengths arises from two sources: the

Can. J. Chem. Downloaded from www.nrcresearchpress.com by 210.87.254.5 on 09/05/12
For personal use only.

TABLE 5. Predicted and observed As—O and P—O bond lengths in $Na_4As_2O_7$ and $Na_4P_2O_7$

Bond	Length (Å)	
	Observed	Predicted*
As—O(1)	1.783(2)	1.807(5)
As—O(2)	1.659(3)	1.624(10)
As—O(3)	1.655(3)	1.651(10)
As—O(4)	1.659(3)	1.629(10)
P(1)—OCE	1.633(2)	1.742(4)
P(1)—O1A	1.511(2)	1.475(6)
P(1)—O1B	1.512(2)	1.490(6)
P(1)—O1C	1.513(2)	1.498(6)
P(2)—OCE	1.641(2)	1.753(4)
P(2)—O2A	1.514(2)	1.452(6)
P(2)—O2B	1.513(2)	1.485(6)
P(2)—O2C	1.514(2)	1.474(6)

*Calculated by adjusting the X—O bond length so as to yield $\Sigma S_{O^{2-}} = 2.00$.

individual errors in the Na—O bond lengths and the errors in the estimated values of n and r_o. Only the former contributions are included in Table 5. The agreement in $Na_4As_2O_7$ has to be regarded as reasonably good despite the fact that the effects of thermal motion on the apparent bond lengths have not been applied to either any of the data used. Systematic deviations leading to predicted values of bridging P—O(—P) bonds and smaller terminal ones seem to appear in both these compounds.

This research has been supported by grant number A-940 from the National Research Council of Canada.

1. D. W. J. CRUICKSHANK, H. LYNTON, and G. A. BARCLAY. Acta Cryst. **15**, 491 (1962).
2. J. OZOG, N. KRISHNAMACHARI, and C. CALVO. Can. J. Chem. **48**, 388 (1970).
3. C. CALVO and K. NEELAKANTAN. Can. J. Chem. **48**, 890 (1970).
4. R. VON SAHNEN and G. TAMMAN. Ann. Phys. **10**, 879 (1903).
5. E. P. PARTRIDGE, V. HICKS, and G. V. SMITH. J. Am. Chem. Soc. **63**, 454 (1941).
6. K. Y. LEUNG and C. CALVO. Can. J. Chem. **50**, 2519 (1972).
7. E. M. KURIAN and R. V. TAMHANKAR. Proc. Chem. Symp. Madras, **2**, 143 (1970).
8. B. E. ROBERTSON and C. CALVO. J. Solid State Chem. **1**, 120 (1970).
9. B. E. ROBERTSON and C. CALVO. Acta Cryst. **22**, 665 (1967).
10. K. ŁUKASEWICZ. Bull. Acad. Polon. Sci., Ser. Sci. Chim. **15**, 53 (1967).
11. Z. MELKVI, C. V. STAGER, and C. CALVO. Can. J. Phys. **45**, 83 (1967).
12. P. W. RANBY, D. H. MASH, and S. T. HENDERSON. Brit. J. Appl. Phys. Supp. **4**, 518 (1955).
13. A. N. LAZAREV, T. F. TENISHEVA, and M. A. PETROVA. Izv. Akad. Nauk. SSR Neorg. Mater. **1**, 1379 (1965).
14. L-O. HAGMAN and P. KIERKEGAARD. Acta Chem. Scand. **23**, 327 (1969).
15. G. BISSERT and F. LIEBAU. Acta Crystallogr. **B26**, 233 (1970).
16. T. Y. TIEN and F. A. HUMMEL. J. Am. Ceram. Soc. **44**, 206 (1961).
17. F. REMY. Bull. Soc. Chim. **10**, 3380 (1969).
18. W. H. BAUR. Trans. Am. Crys. Assoc. **6**, 129 (1970).
19. A. C. LARSON. Acta Cryst. **23**, 664 (1967).
20. International tables for X-ray crystallography. Vol. III. Kynoch Press, Birmingham. 1963.
21. W. R. BUSING and H. A. LEVY. Acta Cryst. **17**, 142 (1964).
22. L. PAULING. The nature of the chemical bond. 3rd ed. Cornell University Press, Ithaca. 1960.
23. N. KRISHNAMACHARI. Ph.D. Thesis. McMaster University, 1971.
24. I. D. BROWN and R. D. SHANNON. To be published.

Can. J. Chem. Downloaded from www.nrcresearchpress.com by 210.87.254.5 on 09/05/12
For personal use only.

The Bonding of a Silicon Atom with a Phenyl Ring: the Photoelectron Spectrum of Phenylsilane

RONALD ALLAN NEILL MCLEAN[1]

Department of Chemistry, University of British Columbia, Vancouver 8, British Columbia

Received December 11, 1972

The first band in the photoelectron spectrum of phenylsilane, which is caused by two ionization processes, is shifted to higher energy compared with the corresponding band in the carbon analog, toluene. In particular the highest energy orbital of phenylsilane appears to be stabilized compared to that in toluene probably due to (p → d) π bonding.

La première bande dans le spectre photoélectronique du phénylsilane qui est produit par deux processus d'ionisation, est déplacée vers les plus hautes énergies lorsqu'on compare celle-ci avec la bande correspondante de son analogue dans la série carbonée, le toluène. En particulier, l'orbitale de plus haute énergie du phénylsilane semble être stabilisée si on la compare avec celle du toluène probablement par des liaisons π (du type p → d). [Traduit par le journal]

Can. J. Chem., 51, 2089 (1973)

In our studies (1) of the use of photoelectron spectroscopy for measuring the π bonding interaction between silicon and neighboring atoms, we have obtained the photoelectron spectrum (p.e.s.) of phenylsilane. The spectra of most monosubstituted benzenes indicate that substituent groups can have a considerable effect on the highest energy π orbitals of the phenyl ring, (2, ref. 3, chapt. 11). Groups which have a strong π interaction with the phenyl ring remove the degeneracy present in the highest energy π orbitals of benzene. It was hoped that the lowest energy band in the p.e.s. of phenylsilane, as in the halosilanes (1), would provide some information on π interactions involving the silicon atom.

The photoelectron spectrum of phenylsilane in the region of interest shows that the first band extending from 9.0–9.8 eV has two unresolved components. The first has an adiabatic ionization potential (i.p.) of 9.09 eV and a vertical i.p. of 9.18 eV. The second component, which is much broader, probably has a vertical i.p. of *ca.* 9.43 eV. The carbon analog, toluene, has a somewhat different first band which extends from 8.80–9.60 eV. In this case, the adiabatic i.p. of the first component at 8.80 eV is the vertical and the other component is more clearly resolved than in phenylsilane, with vertical i.p. of 9.35 eV. Although it is obvious that there is vibrational structure on these bands in both compounds, it is too complex to be resolved completely. The first component in each has a progression with spacing *ca.* 800 cm^{-1} partially resolved. This is likely to be the symmetric ring breathing mode as in benzene itself (ref. 3, chapt. 10). Except for a band with maximum at 11.0 eV in phenylsilane (assigned to ionization from a σ bonding orbital involving silicon), the spectra of phenylsilane and toluene are similar at higher energy.

Even without assigning each component of the first band, it is obvious that at least one of the orbitals is considerably more stable in phenylsilane than in toluene. This would be the expected result if the greater π attracting ability of the SiH_3 group more than overcame its expected greater σ donating ability. The latter would have raised the energy of the benzene ring π levels. Additional evidence for this assignment appears in the comparison with benzene itself. The first band in the p.e.s. of benzene (ref. 3, chapt. 10) has a vertical and adiabatic i.p. of 9.24 eV and the band extends to *ca.* 9.7 eV. Therefore the π levels in benzene are at about the same energy as those in phenylsilane, *i.e.* the SiH_3 group is a similar electron attracting group to —H. However, before proceeding with the discussion of these molecules we should compare the results with those of another system which had previously been studied.

The first band in the p.e.s. of phenyltrimethylsilane was compared with that of its carbon analog, *t*-butylbenzene, by Vignollet *et al.* (4). In contrast to the present result, in trimethylsilyl-

[1]Present address: Department of Chemistry, University of Ife, Ile-Ife, Nigeria.

benzene the first band was shifted to lower energy compared to benzene with a splitting of only 0.2 eV. The spectra produced in ref. 4 also indicated that as a whole, the band was shifted to lower energy compared to *t*-butylbenzene. It was concluded from these results that any π attracting ability of the Si atom was overcome by the electron releasing effect caused by the three methyl groups. In addition it could be inferred from the relative positions of the bands in trimethylsilylbenzene and its carbon analog that the net electron releasing effect of the silicon atom was less than that of the carbon atom. This is in disagreement with our present results.

However, an examination of the full spectra of trimethylsilylbenzene and *t*-butylbenzene (ref. 3, p. 296), reveals a slight error in the earlier presentation of the first bands, Firstly, the band in the silicon compound is quite definitely at higher energy than that in the carbon compound, thus bringing the results into agreement with our observations. Secondly, the splitting in the first band of trimethylsilylbenzene is rather greater than 0.2 eV and is about the same as, though more distinct than, that which we observe in silylbenzene. Therefore any conclusions we make from the spectrum of silylbenzene also hold for trimethylsilylbenzene.

The assignment of the components of the bands to ionization from symmetry orbitals is not straightforward, because of the several variable interactions between the ring and the substituent. However, as the a'' orbital (a_2 in C_{2v}) has no electron density at the 1 position of the benzene ring we expect it to be about the same energy in benzene and toluene. Therefore assuming Koopman's theorem to hold, the a'' orbital in toluene has energy -9.35 eV and the a' orbital, -8.80 eV. This assignment is also consistent with the donating effect of the CH_3 group as the a' orbital would be raised in energy by this interaction.

In phenylsilane the a'' level (-9.43 eV) is at slightly lower energy than in toluene. However, there is a considerable stabilization of the a' level (at -9.18 eV) compared to toluene and, although this must be partly due to the reduced M—H donating effect, we believe in line with our earlier results, (1), that there must be some stabilization due to interaction with the Si d orbitals and σ^* (Si—H) orbitals. The same arguments hold for the trimethyl derivatives. Because of the very similar energy levels in the methylated and non-methylated species, it seems that in contrast to the earlier conclusions the inductive effect of the methyl groups have very little influence in these systems. This should be compared with the high energy level in the following halides: CH_3Cl, -11.30 eV (5); $(CH_3)_3CCl$, -10.61 eV (6); SiH_3Cl, -11.65 eV (1), and $(CH_3)_3SiCl$, *ca.* -10.8 eV (7). In these examples the methyl group obviously has a considerable effect on the highest energy level, but the levels in the substituted benzenes discussed here are high enough in energy to be little affected by methyl groups on the substituent atom.

In the light of these results, some recent CNDO/2 calculations on silyl and methyl substituted unsaturated hydrocarbons (8) deserve comment. These calculations, despite not including d orbitals in the silicon basis set, indicated that the $-CH_3$ group acted as a donor and the $-SiH_3$ group as a π acceptor, in agreement with our conclusion. However, although the calculated order of the first ionization potentials is correct for benzene (13.85 eV) > silylbenzene (12.97 eV) > toluene (12.87 eV) it is obvious that the inclusion of d orbitals in the silicon basis set will improve silylbenzene's value relative to benzene and toluene. Our results indicate that the first i.p. of silylbenzene is very close to that of benzene and much higher than that of toluene. Therefore although it is unnecessary to include d orbitals on silicon to predict most of the groundstate properties, it has been shown (9) that to predict the correct relative energies for silicon and carbon compounds, d orbitals must be included in the silicon basis set.

Some earlier Pariser–Parr–Pople calculations carried out by Perkins (10) on *p*-disilylbenzene, indicated, correctly in the light of our present results, that a silicon atom has little net effect on the π *bonding* orbitals of benzene, but a significant stabilizing effect on the antibonding orbitals.

In conclusion, it can be stated that when a silyl group is substituted on a benzene ring it has little net effect on the bonding π electron energies but a net π attracting effect compared to substitution by a methyl group. Further, substitution of the hydrogens of this silyl group with methyl groups also has little effect on π electron levels.

I thank Professors C. A. McDowell and D. C. Frost of the University of British Columbia for the use of their photoelectron spectrometer and their interest in this work, and Dr. A. B. Cornford for some experimental assistance.

1. (*a*) D. C. FROST, F. G. HERRING, A. KATRIB, R. A. N. McLEAN, J. E. DRAKE, and N. P. C. WESTWOOD. Chem. Lhys. Lett. **10**, 347 (1971). (*b*) D. C. FROST, F. G. HERRING, A. KATRIB, R. A. N. McLEAN, J. E. DRAKE, and N. P. C. WESTWOOD. Can. J. Chem. **49**, 4033 (1971). (*c*) R. A. N. McLEAN. In press.
2. A. D. BAKER, D. P. MAY, and D. W. TURNER. J. Chem. Soc. (B), 22 (1968).
3. D. W. TURNER, C. BAKER, A. D. BAKER, and C. D. BRUNDLE. Molecular photoelectron spectroscopy. Wiley–Interscience, London. 1970.
4. Y. VIGNOLLET, J. C. MAIRE, A. D. BAKER, and D. W. TURNER. J. Organomet. Chem. **18**, 349 (1969).
5. J. L. RAGLE, I. A. STENHOUSE, D. C. FROST, and C. A. McDOWELL. J. Chem. Phys. **53**, 178 (1970).
6. K. WATANABE, T. NAKAYAMA, and J. MOTTL. J. Quant. Spectrosc. Radiat. Transfer. **2**, 369 (1962).
7. M. C. GREEN, M. F. LAPPERT, J. B. PEDLEY, W. SCHMIDT, and B. T. WILKINS. J. Organomet. Chem. **31**, C55 (1971).
8. C. G. PITT. Chem. Commun. 816 (1971).
9. F. G. HERRING and R. A. N. McLEAN. Unpublished work.
10. P. G. PERKINS. Theor. Chem. Acta, **12**, 427 (1969).

^{13}C Nuclear Magnetic Resonance Studies. 29. ^{13}C Spectra of Some Alicyclic Methyl Esters[1]

M. GORDON, S. H. GROVER,[2] AND J. B. STOTHERS
Department of Chemistry, University of Western Ontario, London, Ontario

Received January 29, 1973

The shielding effects of the carbomethoxyl group on neighboring carbons in the cyclohexane and *trans*-decalin ring systems have been characterized by ^{13}C n.m.r. examination of ten model compounds. The data show that sufficient differences are exhibited by axial and equatorial groups to permit stereochemical assignments in related systems. The observed trends are compared with those produced by other functional groups. The three-, four-, and five-membered ring cycloalkae carboxylic acid esters were also examined.

Les effets de blindage du groupe carbométhoxyle sur les carbones voisins dans les systèmes cyclohexane et *trans*-décaline ont été étudiés par la r.m.n. du ^{13}C sur dix composés modèles. Les données obtenus montrent que des différences suffisantes existent pour les groupes axial et équatorial pour permettre des attributions stéréochimiques dans ces systèmes. Les tendances observées ont été comparées avec celles causées par d'autres groupes fonctionnels. Les esters d'acide carboxylique cyclique de trois, quatre et cinq unités ont également été examinés. [Traduit par le journal]

Can. J. Chem., **51**, 2092 (1973)

Introduction

In general, the effects of various substituents on the ^{13}C shieldings of neighboring carbons are found to be additive within families of compounds. Consequently, the positions of ^{13}C absorptions for related materials may often be predicted with good precision in a wide variety of systems (1). These trends are of special interest in "fixed" systems, as opposed to freely rotating cases, since the shielding effects of specific groups tend to exhibit marked geometrical dependencies (2). This feature can be valuable for signal assignments in complex spectra and in many cases permits the assignment of stereochemistry. A good example of the utility of these trends for signal assignments has been provided by the complete analysis of the ^{13}C spectra of a series of steroids (3), while the stereochemistry of the A/B ring fusion in steroids is readily determined from the C-19 shielding (4).

The relatively common occurrence of the carbomethoxyl group in natural products prompts one to determine whether the sensitivity of its substituent effects is sufficient to provide another means of characterizing its configuration in alicyclic systems. To this end, we have examined the ^{13}C spectra of some methyl cyclohexane- and *trans*-decalylcarboxylates having both axial and equatorial carbomethoxyl groups. In addition, two conformationally mobile cyclohexane derivatives were included to investigate the possibility of utilizing the ^{13}C data, obtained at ambient temperature, for conformational analysis. Since the dangers associated with the use of proton data obtained at a single temperature for this purpose have been demonstrated by Jensen and coworkers (5), similar difficulties may be anticipated for the ^{13}C approach although reasonable results have been found for some substituents (2*b*, 6). To compare the effects of the carbomethoxyl group on alicyclic carbons in smaller rings, the three-, four-, and five-membered cycloalkanecarboxylates were also examined.

Experimental

The ^{13}C spectra were obtained for 15–20% (w/v) solutions in benzene and/or in deuteriochloroform. The benzene solutions were examined in 12 mm sample cells at 15.1 MHz using a computer-controlled (Varian 620i) HA-type spectrometer equipped with a "homebuilt" proton decoupler (7) and a Varian V4336 probe.[3] The decoupled solvent signal served as an internal ^{13}C lock. With the proton decoupler frequency centered on the benzene protons, the presence or absence of noise modulation furnished noise-decoupled or off-resonance decoupled spectra, respectively. The $CDCl_3$ solutions were examined using a Varian XL-100-15 spectrometer operating in the Fourier transform mode. The solutions were contained in 10 mm tubes which were placed in a

[1]Part 27, ref. 21. Part 28, ref. 22.
[2]Holder of NRCC Scholarships, 1968–1971.

[3]We thank Varian Associates, Palo Alto, Calif. for kindly loaning us this probe for these studies.

Can. J. Chem. Downloaded from www.nrcresearchpress.com by 210.87.254.105 on 09/05/12
For personal use only.

12 mm sample tube containing D_2O, the signal of which was used as the lock.

All peak positions are reported relative to internal tetramethylsilane, a few drops of which were added to the $CDCl_3$ solutions; in benzene the positions were measured relative to the solvent and converted to the TMS scale with the factor 128.7 p.p.m. The precision of the measurements is ± 0.05 p.p.m.

All of the materials employed in this work are known compounds and were available to us from earlier studies (8, 9). In general, the carboxylic acids were prepared and converted to the methyl esters by treatment with diazomethane in the usual manner.

Results and Discussion

The shielding results for the monocyclic esters in $CDCl_3$ solutions are listed in Table 1, together with the solvent shifts found for benzene solutions. The data for the *trans*-decalin derivatives are given in Table 2 in which the values for *trans*-decalin itself are included for comparison; the results for the bicyclic systems were obtained only in $CDCl_3$ solutions. With the exception of the C-2 and -3 signals in the cyclopentane and cyclohexane derivatives, the assignment of individual signals in the spectra of the monocyclic materials is straightforward. Since the general pattern of shielding effects of a variety of substituents leads to a downfield shift of the β-carbon signals and an upfield shift for the γ-carbons, relative to their positions for the parent compound (1), the lower field signal of the C-2/C-3 pair has been assigned to the former nuclei. Although relatively few ^{13}C results for aliphatic methyl esters have been reported (1*b*, 10), the carbomethoxyl effects along an alkyl chain are unexceptional; the substituent shifts are: α, 20; β, 3; γ, −2.5; δ, 0.8, and ε, 0.6 p.p.m. Similar trends are expected for the common alicyclic rings on the basis of results for other substituents.

With the assignments listed in Table 1, one can compare the shieldings of indvidual carbons with the values for the parent hydrocarbons to extract the substituent effects. These results are collected in Table 3. The cycloalkane shieldings reported by Burke and Lauterbur (11) were converted to the TMS scale with the factor 193.7 p.p.m. while the *t*-butylcyclohexane data of Roberts *et al.* (12) were converted using 192.8 p.p.m. (1*b*, 13).

With the exception of the cyclopropyl ester, the trends are similar for each compound. The carbomethoxyl group strongly deshields the directly-bonded carbon while the β-carbons are much less affected in all but the cyclopropyl case. A wide variety of substituents cause a similarly large downfield shift at these carbons ranging from 8–15 p.p.m. (14). If the highfield position of cyclopropane itself is primarily caused by a ring-current effect as originally suggested (11), the marked β effect of these substituents could be ascribed to a diminution of the ring current by the electronegative substituents. It should be noted that the β effects of the carbonyl-containing functional groups tend to be *ca.* 2–3 p.p.m. in aliphatic derivatives; a number of such examples has been collected and discussed in relation to the substituted cyclopropanes (1*b*).

The observed tendency for γ-carbons to absorb upfield from their positions in the corresponding hydrocarbons is quite general for a wide variety of substituents and has been attributed to steric perturbations arising from *gauche* interactions of the substituent and the hydrogen on the γ-carbon (1). While this interpretation is perfectly valid for the alicyclic systems having axial substituents (*syn*-axial interactions with the three- and five-hydrogens) it is apparent that the γ-carbons are significantly shifted upfield in compounds in which the carbomethoxyl group is either held in an equatorial orientation or preferentially exists therein because of destabilizing influences in the axial form. For example, the γ-carbon (C-3) in the cyclobutyl ester exhibits one of the largest upfield shifts although one expects that the quasi-equatorial conformation for the carbomethoxyl group on a four-membered ring is much more stable than the quasi-axial. It may be noted that C-3 in cyclobutanol also exhibits a large upfield shift (11.3 p.p.m.) relative to cyclobutane; this γ effect is appreciably larger than the corresponding shift caused by an axial hydroxyl group in various "fixed" alkylcyclohexanols, *e.g.* 6.6–7.2 p.p.m. (12). Clearly steric perturbations cannot account for these effects if the primary assumption regarding the preferred conformation of monosubstituted cyclobutanes is correct. Analogous trends, however, have been found for the norbornyl series (15–17) for which C-6 is shielded in both *exo*- and *endo*-2-substituted norbornanes relative to its position in norbornane. For each case, *endo*-substituents cause a larger shift but the effects of *exo*-groups are appreciable, usually >1 p.p.m. For example, the γ effects of the hydroxyl at C-6 in the nor-

Can. J. Chem. Downloaded from www.nrcresearchpress.com by 210.87.254.105 on 09/05/12
For personal use only.

Can. J. Chem. Downloaded from www.nrcresearchpress.com by 210.87.254.105 on 09/05/12
For personal use only.

TABLE 1. ^{13}C shieldings* of some methyl cycloalkanecarboxylates, RCOOMe (δ_C, p.p.m. from TMS)

R	C=O	OMe	C-1	C-2	C-3	C-4	Me	Other
Cyclopropyl	175.2	51.5	12.7	8.3				
Cyclobutyl	175.7	51.4	37.9	25.2	18.4			
Cyclopentyl	177.0	51.4	43.7	30.0	25.8			
Cyclohexyl	176.3 (−0.8)	51.2 (−0.3)	43.1 (+0.2)	29.0 (+0.5)	25.4 (+0.5)	25.8 (+0.4)		
1-Methylcyclohexyl	178.0 (−0.7)	51.4 (−0.2)	43.1 (+0.2)	35.5 (+0.6)	23.2 (+0.5)	25.7 (+0.5)	26.3 (+0.3)	
cis-4-*t*-Butylcyclohexyl	175.4 (−0.6)	51.2 (−0.2)	38.9 (+0.4)	28.0 (+0.4)	23.8 (+0.4)	47.9 (+0.5)	27.4 (+0.3)	32.4 (+0.1)
trans-4-*t*-Butylcyclohexyl	176.4 (−0.6)	51.2 (−0.2)	43.4 (+0.3)	29.5 (+0.5)	26.6 (+0.3)	47.3 (+0.5)	27.4 (+0.3)	32.3 (+0.1)
1-Methyl-*cis*-4-*t*-butylcyclohexyl	177.6 (−0.6)	51.3 (−0.1)	43.3 (+0.3)	36.4 (+0.5)	24.8 (+0.3)	47.5 (+0.5)	28.3 (+0.2) 27.4 (+0.3)	 32.2 (+0.3)
1-Methyl-*trans*-4-*t*-butylcyclohexyl	179.2 (−0.6)	51.4 (−0.1)	41.4 (+0.4)	34.3 (+0.6)	22.1 (+0.5)	47.6 (+0.5)	19.6 (+0.3) 27.4 (+0.3)	 32.3 (+0.2)

*In $CDCl_3$ solutions. Values in parentheses are the solvent shifts for benzene solutions, *i.e.* $\delta_C^{C_6H_6} - \delta_C^{CDCl_3}$.

TABLE 2. ^{13}C shieldings of the methyl *trans*-decalylcarboxylates and *trans*-decalin (δ_C, p.p.m. from TMS for $CDCl_3$ solutions)

Orientation* of COOMe	C=O	OMe	C-1	C-2	C-3	C-4	C-5	C-6	C-7	C-8	C-9	C-10
trans-1	175.0	50.5	44.5	29.4	21.8	34.8	34.1	27.0	26.3	31.1	44.7	36.3
cis-1	176.2	50.9	50.2	30.3	25.4	33.5	34.1	26.5	26.4	31.4	44.6	42.1
Nil	—	—	34.3	26.9	26.9	34.3	34.3	26.9	26.9	34.3	43.7	43.7
cis-2	175.4	51.1	34.6	39.1	27.3	30.2	33.8	26.5	26.4	33.6	39.5	43.1
trans-2	175.9	51.1	36.3	42.6	29.1	33.1	33.8	26.6	26.6	33.7	42.4	43.4

*With respect to the C-9 proton.

TABLE 3. Substituent effects of the COOMe group in alicyclic systems (in p.p.m.)

Ring system	Effects at neighboring carbons*			
	α	β	γ	δ
Cyclopropyl	15.3	10.9	—	—
Cyclobutyl	14.6	1.9	−4.9	—
Cyclopentyl	17.2	3.5	−0.7	—
Cyclohexyl	15.4	1.3	−2.3	−1.9
cis-4-*t*-Butylcyclohexyl	11.7	0.2	−4.4	−1.0
trans-4-*t*-Butylcyclohexyl	16.2	1.7	−1.6	−1.6
trans-1-Decalyl†	10.2	2.5(C-2) 1.0(C-9)	−5.1(C-3) −3.2(C-8) −7.4(C-10)	0.5(C-4) −0.2(C-5) −0.6(C-7)
cis-1-Decalyl†	15.9	3.4(C-2) 0.9(C-9)	−1.5(C-3) −2.9(C-8) −1.6(C-10)	−0.8(C-4) −0.2(C-5) −0.5(C-7)
cis-2-Decalyl†	12.2	0.3(C-1) 0.4(C-3)	−4.1(C-4) −4.2(C-9)	−0.7(C-8) −0.6(C-10)
trans-2-Decalyl†	15.7	2.0(C-1) 2.2(C-3)	−1.2(C-4) −1.3(C-9)	−0.6(C-8) −0.3(C-10)

*The α, β, γ, and δ factors are the effects through one, two, three, and four bonds, respectively, given by the difference, $\delta_C^{RCOOMe} - \delta_C^{RH}$; positive values denote downfield shifts.
†*trans*-Decalyl skeletons only; the orientation of COOMe is indicated.

bornanols are −9.7 and −5.2 p.p.m. respectively, while in the corresponding carbomethoxyl derivatives the shifts are −5.0 and −1.4 p.p.m. (15) in the *endo*- and *exo*-esters, respectively. Grutzner *et al.* (15) suggested that the trends for the effects of the *exo*-groups are reminiscent of the well-known W pattern for long-range couplings and that the shielding effects may arise from a similar interaction, namely, overlap of the back lobes of the *exo*-bonding orbitals on C-2 and -6. If this is a contributing factor it follows that such interactions will be even more likely in cyclobutanes because of the closer approach of the carbons involved (C-1 and -3); *viz.* 1.9 *vs.* 2.5 Å.

The data for benzene solutions, listed as incremental shifts in Table 1, show that the carboxyl and methoxyl carbons are shielded in benzene while the remaining carbons are deshielded relative to their values in chloroform. Presumably hydrogen bonding of the carbonyl oxygen with chloroform is responsible for the decreased shielding of the carboxyl carbon which is relayed to the methoxyl carbon. With the exception of the quaternary carbons of the *t*-butyl group, the remaining carbons exhibit a consistent shift of 0.4 ± 0.1 p.p.m. in benzene. Apparently the decreased shift for the quaternary carbons results from the fact that these nuclei are more or less shielded from direct interaction with the solvent by the neighboring methyl groups.

Can. J. Chem. Downloaded from www.nrcresearchpress.com by 210.87.254.105 on 09/05/12
For personal use only.

Can. J. Chem. Downloaded from www.nrcresearchpress.com by 210.87.254.105 on 09/05/12
For personal use only.

Turning to the *trans*-decalin derivatives (Table 2) it becomes apparent that the trends are similar to those found for the cyclohexyl examples. The axial carboxyl carbons absorb at slightly higher fields than their equatorial counterparts while the methoxyl carbon shielding is essentially independent of the orientation of the COOMe group. To compare the shielding effects of the substituent, the differences between *trans*-decalin and the decalyl esters are included in Table 3; the values for *trans*-decalin (Table 2) agree well with the earlier rapid-passage data (18). (In both Tables the axial ester is the first of each pair listed.) The remarkably good agreement between the shielding effects for the 2-carbomethoxy *trans*-decalins and the 4-*t*-butylcyclohexyl derivatives strongly supports the assignments given in Table 2. In contrast, some of the effects listed for the 1-carbomethoxyl cases differ significantly but the apparent discrepancies for methine carbons are not unexpected since this behavior has been noted for a number of norbornyl derivatives (15). Grutzner *et al.* found that deshielding effects of various substituents are attenuated at methine carbons relative to the shifts exhibited by methylene carbons and possible reasons for the trend were discussed (15). This may also account for the somewhat reduced α effect of the axial 1-carbomethoxyl group relative to those found for the 2-decalyl and 4-*t*-butylcyclohexyl cases. It is interesting that carbons separated by four or more bonds from the carbomethoxyl group tend to absorb at slightly higher fields than the analogous centers in the parent hydrocarbon. The largest γ factor for the equatorial esters is found for C-8 in the *cis*-1-decalyl isomer; this is completely consistent because C-8 and the carbomethoxyl group are *gauche* and the γ effect is essentially the same as that for C-8 in the *trans*-1-decalyl derivative. On the other hand, the enhanced γ factors for C-3 and -10 in the latter case are somewhat surprising although there seems little doubt that the assignments are correct. In any event the overall trends are qualitatively consistent with other results.

The consistency of the substituent effects in the 2-decalyl and 4-*t*-butylcyclohexyl systems indicates that either may be employed as models for "pure" axial and equatorial methyl esters with which conformational analysis of the carbomethoxyl group could be done by application of the Eliel equation (19), $K_e = (\delta^{obsd} - \delta^{ax})/(\delta^{eq} - \delta^{obsd})$. As has been noted (1*b*), ^{13}C spectra may, *in principle*, offer advantages for conformational analysis in this simple fashion since more than one center shows a shielding dependence on substituent geometry. Qualitatively the data in Table 3 for the α-, β-, and γ-carbons in the cyclohexyl and 4-*t*-butylcyclohexyl esters appear to support this notion. For each, the effects in the conformationally mobile compound lie between those for the model axial and equatorial compounds and are closer to the latter as expected. Quantitatively, however, it is apparent that different K_e values are obtained depending on which of the positions is chosen. To allow for the small perturbations caused by the anchoring group in the fixed systems the substituent effects listed in Table 3 should be employed rather than the observed shieldings. Since the difference between axial and equatorial substituents is largest at the α-carbon it would appear to be the best choice for estimations of K_e. Since both the 4-*t*-butyl and 2-decalyl systems should be good models, it follows that the α-carbon data for each are equally appropriate; but K_e values, estimated using each of the two, differ by more than a factor of two; *viz.* 4.9 and 10.7. These results clearly show the weakness of the simple approach and emphasize the need for low-temperature studies of the unsubstituted cyclohexyl ester to determine the conformational equilibrium constant, K_e. At best, the present room temperature data indicate the conformational free energy of the carbomethoxyl group to be *ca.* 1.2 ± 0.2 kcal/mol, in agreement with the accepted value (20).

On the positive side, however, it is clearly apparent that the differences in the shielding effects of axial and equatorial carbomethoxyl groups are sufficiently large that stereochemical assignments of configuration for the COOMe group can be made from the ^{13}C data for related systems such as terpenes. Since structures having geminal methyl and carbomethoxyl groups are commonly encountered in nature, the relative orientations of these substituents are of interest and the results for the 1-methylcyclohexanecarboxylates show that the assignment of stereochemistry would be straightforward from the ^{13}C shieldings, especially that of the methyl group.

We wish to thank the National Research Council of Canada for generous support of this work.

1. For general discussions see (*a*) G. C. LEVY and G. L. NELSON. ^{13}C nuclear magnetic resonance for organic chemists. Wiley-Interscience, New York. 1972; (*b*) J. B. STOTHERS. Carbon-13 NMR spectroscopy. Academic Press, New York. 1972; (*c*) J. B. STOTHERS. Appl. Spectros. **26**, 1 (1972).
2. (*a*) D. K. DALLING and D. M. GRANT. J. Am. Chem. Soc. **89**, 6612 (1967); **94**, 5318 (1972). (*b*) G. W. BUCHANAN, D. A. ROSS, and J. B. STOTHERS. J. Am. Chem. Soc. **88**, 4301 (1966); G. W. BUCHANAN and J. B. STOTHERS. Can. J. Chem. **47**, 3605 (1969).
3. H. J. REICH, M. JAUTELAT, M. T. MESSE, F. J. WEIGERT, and J. D. ROBERTS. J. Am. Chem. Soc. **91**, 7445 (1969).
4. B. BALOGH, D. M. WILSON, and A. L. BURLINGAME. Nature, **233**, 261 (1971); J. L. GOUGH, J. P. GUTHRIE, and J. B. STOTHERS. J.C.S. Chem. Commun. 979 (1972).
5. F. R. JENSEN and B. H. BECK. J. Am. Chem. Soc. **90**, 3251 (1968); F. R. JENSEN, C. H. BUSHWELLER, and B. H. BECK. J. Am. Chem. Soc. **91**, 344 (1969).
6. G. W. BUCHANAN and J. B. STOTHERS. Chem. Commun. 1250 (1967).
7. H. BROUWER and J. B. STOTHERS. Can. J. Chem. **50**, 1361 (1972).
8. D. H. MARR and J. B. STOTHERS. Can. J. Chem. **45**, 225 (1967).
9. G. W. BUCHANAN, J. B. STOTHERS, and S.-T. WU. Can. J. Chem. **47**, 3113 (1969).
10. E. LIPPMAA and T. PEHK. Eesti NSV Tead. Akad. Toim, Keem.-Geol. **17**, 210 (1968).
11. J. J. BURKE and P. C. LAUTERBUR. J. Am. Chem. Soc. **86**, 1870 (1964).
12. J. D. ROBERTS, F. J. WEIGERT, J. I. KROSCHWITZ, and H. J. REICH. J. Am. Chem. Soc. **92**, 1338 (1970).
13. G. C. LEVY and J. D. CARGIOLI. J. Mag. Res. **6**, 143 (1972).
14. G. E. MACIEL and G. B. SAVITSKY. J. Phys. Chem. **69**, 3925 (1965); P. H. WEINER and E. R. MALINOWSKI. J. Phys. Chem. **71**, 2791 (1967); K. M. CRECELY, R. W. CRECELY, and J. H. GOLDSTEIN. J. Phys. Chem. **74**, 2680 (1970).
15. J. B. GRUTZNER, M. JAUTELAT, J. B. DENCE, R. A. SMITH, and J. D. ROBERTS. J. Am. Chem. Soc. **92**, 7107 (1970).
16. E. LIPPMAA, T. PEHK, J. PAASIVIRTA, N. BELIKOVA, and E. PLATE. Org. Mag. Res. **2**, 581 (1970).
17. H. BROUWER, M. GORDON, S. H. GROVER, C. T. TAN, K. C. TEO, and J. B. STOTHERS. Unpublished results.
18. E. LIPPMAA and T. PEHK. Eesti NSV Tead. Akad. Toim., Keem.-Geol. **17**, 287 (1968).
19. E. L. ELIEL and R. J. L. MARTIN. J. Am. Chem. Soc. **90**, 682, 689 (1968).
20. J. A. HIRSCH. *In* Topics in stereochemistry. Vol. 1. N. L. Allinger and E. L. Eliel, editors. Wiley-Interscience. N.Y. 1967. p. 208.
21. C. W. DAVID, B. W. EVERLING, R. J. KILIAN, J. B. STOTHERS, and W. R. VAUGHAN. J. Am. Chem. Soc. **95**, 1265 (1973).
22. R. R. FRASER, J. B. STOTHERS, and C. T. TAN. J. Mag. Res. **10**, 95 (1973).

Can. J. Chem. Downloaded from www.nrcresearchpress.com by 210.87.254.105 on 09/05/12
For personal use only.

Stereospecific Conjugate Alkenyl Group Transfer to α,β-Enones Using Vinylalane Reagents

JOHN HOOZ AND ROBERT B. LAYTON[1]

Department of Chemistry, University of Alberta, Edmonton, Alberta

Received January 29, 1973

trans-Alkenyl alanes (easily prepared by hydroalumination of an acetylene) promote the stereospecific 1,4- delivery of the olefinic unit to conjugated ketones. This new conjugate addition reaction provides easy access to *trans*-γ,δ-unsaturated ketones which would otherwise be available with difficulty.

Les alcènylalcanes *trans* (facilement obtenus par hydroalumination d'un acétylenique) introduisent de façon stéréospécifique-1,4 l'unité-oléfine aux cétones conjuguées. Cette nouvelle réaction d'addition conjugée rend les cétones γ,δ insaturées *trans* facilement accessibles, alors que ces dernières sont difficiles à préparer par d'autres voies. [Traduit par le journal]

Can. J. Chem., 51, 2098 (1973)

The β-vinylation of conjugated enones via organocopper "ate" complexes has previously been shown to provide a highly useful, general procedure for appending unsaturated residues to cyclic and acyclic substrates (1) (eq. 1)[2] irrespective of substitution pattern.

[1] $(-C=C-)_2CuLi\cdot L + -C=C-C=O$ (acyclic or cyclic) $\rightarrow -C=C-C-C-C=O$ (acyclic or cyclic)

Several subsequent reports corroborating these results and providing additional interesting applications and extensions of this methodology have appeared, including examples illustrating that the stereochemistry of unsaturation in the organocopper reactant is retained in the product (2–5). This outcome is also contingent on other prior important observations that retention of double bond geometry is preserved, both in: (*i*) converting precursor alkenyl halide to the corresponding lithio species (6, 7), and (*ii*) transforming the resultant organolithium derivative to the appropriate organocopper reagent (8) (eqs 2 and 3).

[2] $C=C(X) \longrightarrow C=C(Li)$

[3] $C=C(Li) \longrightarrow C=C(Cu)$

An effective and unique alternative approach to transferring unsaturated ligands (of the sp type)[3] to conjugated enones makes use of readily available mixed dialkylalkynylalane reagents (eq. 4). This finding (12), in conjunction with a

[4] $R_2AlC\equiv CR' + -C=C-C=O \rightarrow R'C\equiv C-C(-CH-C=O)$

preceding body of evidence,[4] prompted the

[1]Holder of a 1967 Science Scholarship. This work was abstracted in part from a thesis submitted by R. B. Layton to the Faculty of Graduate Studies and Research of the University of Alberta in partial fulfillment of the requirements of the Ph.D. degree, December 13, 1971, and has been discussed in part at the Synthetic Methods and Design Symposium, Carleton University, Ottawa, Canada April 25, 1972.

[2]L = an appropriate complexing reagent (incorporating phosphorus, sulfur; *cf.* (1) and refs. therein).

[3]Although vinylic units can be transferred 1,4- to conjugated enones, albeit in varying degrees of efficiency, from either organocopper (1) or aluminum intermediates (*vide infra*), the situation is considerably different for the conjugate transfer of alkynyl groups. Alkynylcopper reagents are completely ineffective at promoting 1,4-delivery of an acetylenic unit (9, 10) as are acetylenic Grignard reagents (using copper (salt) catalysis (11)), whereas organoalane reagents are uniquely successful (12).

[4]Mixed organoalanes (dialkylalkynyl and di- and trialkylalkenyl) react with a variety of electrophilic functionality in a remarkably specific manner to deliver, almost invariably, only the unsaturated ligand (12–14) in new C—C bond formation.

Can. J. Chem. Downloaded from www.nrcresearchpress.com by 210.87.254.6 on 09/05/12
For personal use only.

Can. J. Chem. Downloaded from www.nrcresearchpress.com by 210.87.254.6 on 09/05/12
For personal use only.

present brief study to explore the possible synthetic potential of conjugate alkenyl transfer from mixed olefinic alanes. In addition to the stereochemical implications inherent in such a study, our prior experience led us to anticipate that some useful synthetic generalizations could emerge regarding the respective efficiencies of Al (and Cu) reagents for conjugate transfer of unsaturated groups. Moreover, since vinylalanes with varying substitution patterns (mono-, di-, and tri-) are available from the appropriate acetylene,[5] the possibility existed of obviating the synthetically tedious, intermediate steps (synthesis of respective *cis*- or *trans*-vinyl halide, followed by eqs. 2 and 3) generally employed when alkenylcuprates are used for conjugate addition.[6]

Diisobutyl *trans*-1-hexenylalane (**1**) was generated by the hydroalumination (diisobutylaluminum hydride) of 1-hexyne (eq. 5). Subsequent

[5] $n\text{-}C_4H_9C{\equiv}CH + (i\text{-}C_4H_9)_2AlH \longrightarrow$

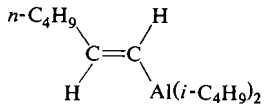

1

reaction with benzalacetone (1.25 h, room temperature, ligroin–benzene solvent) produced, after a hydrolytic work-up, a 67% yield of the product of conjugate transfer of the *trans*-hexenyl unit (eq. 6) (i.r. (film) 1710 (C=O), 970 (*trans*-

[6] $C_6H_5CH{=}CH{-}\overset{O}{\overset{\|}{C}}{-}CH_3 \longrightarrow$

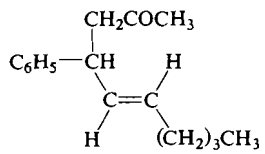

CH=CH) cm^{-1}; n.m.r. ($CDCl_3$) δ 5.45 (m, 2H, $J_{H,H}$ = 15 Hz); mass spectrum, *m/e* M^+ 230).

[5]The hydroalumination of alkynes (with $i\text{-}Bu_2AlH$) involves a *cis*- addition of the Al—H bond to the triple bond to provide (monosubstituted) *trans*-vinylalanes from terminal alkynes and (disubstituted) *cis*-vinylalanes from disubstituted acetylenes. The carbalumination of disubstituted alkynes (using R_3Al) involves a *cis*-addition of the C—Al bond to produce the tri-substituted vinylalane. (15–17).

[6]Isomerically pure vinyl halides may also be synthesized by halogenolysis of vinylalanes (18).

The reaction of **1** with several other α,β-enones gave the results summarized in eqs. 7–9.

[7] $C_6H_5CH{=}CHCOC_6H_5 \xrightarrow{60\%}$

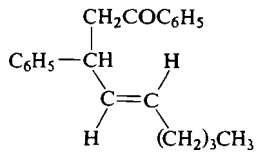

[8]

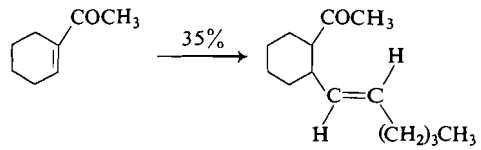

[9] $CH_2{=}CH{-}COCH_3 \xrightarrow{30\%}$

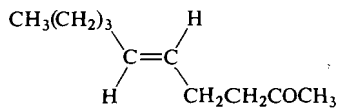

In all instances only the unsaturated ligand of **1** is delivered in 1,4-fashion, and the *trans*-stereochemistry is retained. The selectivity of mixed unsaturated alane **1** thus parallels that encountered previously for acetylenic alane reagents (12), although with somewhat diminished efficiency.

Yields are highest for enone systems carrying a β-aryl substituent (eqs. 6 and 7), a result also analogous to alkynyl conjugate transfer reactions using mixed acetylenic alanes.

Recently, the reduction potentials of a wide variety of α,β-unsaturated carbonyl compounds have been measured in an effort to determine the suitability of substrates toward conjugate addition of organocuprates and possibly other organometallic reagents (19). It was found that a β-phenyl group has a stabilizing effect of +0.4 V (energy difference between intermediate anion radical and parent unsaturated carbonyl system). At present we have no firm experimental evidence to either support or reject the possible intermediacy of anion radicals in conjugate transfer reactions employing organoaluminum reagents. Although undoubtedly a number of complex factors (structural type, geometry, temperature, solvent, etc. (12)) are responsible for promoting successful conjugate addition, we merely note at this time that, among the numerous param-

Can. J. Chem. Downloaded from www.nrcresearchpress.com by 210.87.254.6 on 09/05/12
For personal use only.

eters, the yields of conjugate addition products also appear to correlate well with the reduction potentials.

The lower yield observed for methyl vinyl ketone (eq. 9) is not entirely unexpected in view of its notorious tendency toward base-catalyzed condensation/polymerization reactions.[7]

Although no rigorous attempts have been made to maximize yields, we briefly explored the effect of more polar coordinating solvents such as ether and tetrahydrofuran on the course of the reaction.

In hydrocarbon media, the yield of conjugate addition product for methyl vinyl ketone was *ca.* 15%; addition of an equal volume of ether as cosolvent increased the yield to 30% (eq. 9).

Use of the more strongly coordinating base tetrahydrofuran, however, resulted in the complete suppression[8] of 1,4-addition when acetylcyclohexene was employed as substrate (eq. 8).

Corresponding observations have been made elsewhere which also illustrate the dramatic and influential effect that (apparently) subtle variation of reaction conditions exert on the course of conjugate additions (12). Each substrate doubtless possesses its own unique characteristics, and experimentation is required to define optimal reaction parameters.[9]

Treatment of transoid enones, such as 2-cyclohexenone or isophorone with reagent **1** gave rise to complex mixtures from which no conjugate transfer products could be isolated.[8,10]

[7]Indeed, as a consequence of this tendency, this simple substrate represents a fairly stringent methodological challenge. In connection with a discussion of conjugate additions to enones, it has been noted (20) for example, that "the only examples of organocopper conjugate addition to methyl vinyl ketone involve a lithium divinylcuprate (1) and cuprous chloride catalysis of *m*-methoxybenzylmagnesium chloride (21)." In addition to the present example acetylenic alane reagents (12) and organoboranes (22) may be included.

[8]These reactions are conveniently monitored by i.r. spectroscopy. I.r. analysis of a hydrolyzed aliquot showed complete disappearance of conjugated enone (CO) absorption due to starting material, and considerable hydroxyl absorption. In this, as in the cases of 2-cyclohexenone and isophorone, attempts at isolating or assessing the (presumed) 1,2-addition products from the crude mixture were fruitless, owing to the sensitivity of the tertiary diallylic alcohols.

[9]See footnote 11 of ref. 12 for several additional examples of the effect of reaction variables on conjugate addition and related reactions.

[10]Dialkyl acetylenic alane reagents also fail to effect conjugate addition of the alkyne unit to transoid enones (12).

Despite these intrinsic limitations, it is clear that the directness of this approach, the ease and availability of reagents, and the clean stereochemical outcome, recommend this method as a potentially useful new synthetic device for effecting the stereospecific conjugate transfer of alkenyl groups to enones.

Two recent reports have appeared in connection with synthetic approaches towards prostoglandins which offer promise of widening the range of conjugate addition reactions promoted by Al reagents. Originally, it was noted that the 1,4-alkyne transfer process was restricted to enones capable of adopting a cisoid geometry (12). This has recently been extended by Searle workers, who, employing triacetylenic alanes, have found that a (cyclic) transoid enone structural type can also be accommodated (23). Although inherently wasteful of two organic residues, this extension nonetheless permits direct access to acetylenic ketones which would otherwise be available rather circuitously.

It has also been observed that *trans*-vinyl Al "ate" complexes react with conjugated ketones to transfer only the vinyl ligand in a 1,4-manner and the *trans*-stereochemistry is retained (24). Since this reaction is applicable to transoid enones, it complements the results described here for vinylalanes.

The new alkylation procedure described herein, taken as a body with other recent developments, demonstrates the extraordinary effectiveness and selectivity of conjugate transfer of unsaturated groups promoted by alane (or alanate) reagents. Also, the ready availability of both *cis*- and *trans*-substituted vinylaluminum reagents (25) by hydroalumination of alkynes, combined with the present results, clearly contribute to the expectation that this methodological approach should make possible by further extension the conjugate delivery of either *cis*- or *trans*-substituted vinylic groups to a broad range of enone structures with retention of olefinic geometry.

Experimental

General Considerations

I.r. spectra were recorded using a Unicam SP 1000 i.r. spectrophotometer. N.m.r. spectra were obtained on a Varian A-60 spectrometer using deuteriochloroform as solvent and tetramethylsilane as internal reference. Mass spectra were measured by Dr. A. M. Hogg and his associates using an A.E.I. Model MS-2 spectrometer at an ionization potential of 70 eV. Ligroin, b.p. 63–75°, supplied by Eastman Kodak Co., was successively treated with $KMnO_4$, concentrated H_2SO_4, $KMnO_4$, H_2O, then

refluxed over CaH_2 and distilled from CaH_2 prior to use. Diisobutylaluminum hydride was obtained from Ventron Corp. A representative experimental procedure is described for the conjugate addition to benzalacetone.

4-Phenyl-trans-5-decen-2-one

1-Hexyne (90 mmol) was hydroaluminated with diisobutylaluminum hydride (14.3 ml) in 55 ml of ligroin for 2 h at 50° (18). A solution of benzalacetone (40 mmol) in 20 ml of a mixture of ligroin–benzene (1:1 by volume) was added (0.5 h) at 25°. After stirring the mixture for an additional 0.75 h, i.r. analysis of a dried (Na_2SO_4) ether extract of a hydrolyzed (ice – concentrated HCl) aliquot indicated the complete consumption of starting material; analysis by g.l.p.c. indicated a 67% yield of 4-phenyl-*trans*-5-decen-2-one; i.r. (film) 1710, 1600, 1490, 1450, 970, 700 cm^{-1}; n.m.r. ($CDCl_3$) δ 7.15 (s, 5, C_6H_5), 5.45 (m, 2, CH=CH), 3.79 (q, 1, —C*H*—C_6H_5), 2.75 (d, 2, $COCH_2$), 1.98 (s, 3, CH_3CO), 1.95 (m, 2, —C*H*$_2$—CH=), 1.25 (m, 4, $(CH_2)_2$), 0.8 (t, 3, C*H*$_3$CH$_2$); mass spectrum *m/e* 230 (25), 172 (38), 159 (31), 131 (34), 129 (35), 117 (71), 105 (16), 91 (71), 43 (100).

Anal. Calcd. for $C_{16}H_{22}O$: C, 83.43; H, 9.63. Found: C, 83.79; H, 9.50.

We wish to thank the National Research Council of Canada for financial support of this research.

1. J. Hooz and R. B. Layton. Can. J. Chem. **48**, 1626 (1970).
2. F. Näf and P. Degen. Helv. Chim. Acta, **54**, 1939 (1971); F. Näf, P. Degen, and G. Ohloff. Helv. Chim. Acta, **55**, 82 (1972).
3. C. P. Casey and R. A. Boggs. Tetrahedron Lett. **27**, 2455 (1971).
4. E. J. Corey and R. L. Carney. J. Am. Chem. Soc. **93**, 7318 (1971).
5. C. J. Sih, R. G. Salomon, P. Price, G. Peruzzoti, and R. Sood. Chem. Commun. 240 (1972); C. J. Sih, P. Price, R. Sood, R. G. Salomon, G. Peruzzoti, and M. Casey. J. Am. Chem. Soc. **94**, 3643 (1972).
6. N. L. Allinger and R. B. Hermann. J. Org. Chem. **26**, 1040 (1961).
7. D. Seyferth and L. G. Vaughan. J. Organomet. Chem. **1**, 201 (1963); D. Seyferth and L. G. Vaughan. J. Am. Chem. Soc. **86**, 883 (1964); D. Seyferth. Record Chem. Progr. (Kresge-Hooker Sci. Lib.) **26**, 86 (1965).
8. G. M. Whitesides and C. P. Casey. J. Am. Chem. Soc. **88**, 4541 (1966); G. M. Whitesides' J. S. Filippo, Jr., C. P. Casey, and E. J. Panek. J. Am. Chem. Soc. **89**, 5302 (1967); G. M. Whitesides, C. P. Casey, and J. K. Drieger. J. Am. Chem. Soc. **93**, 1379 (1971).
9. H. O. House and W. F. Fischer. J. Org. Chem. **34**, 3615 (1969).
10. R. B. Layton. Unpublished results.
11. J. H. Rea. Ph.D. Thesis. University of Missouri, Missouri, 1965; Diss. Abstr. **26**, 5043 (1966).
12. J. Hooz and R. B. Layton. J. Am. Chem. Soc. **93**, 7320 (1971).
13. J. Fried, C.-H. Lin, and S. H. Ford. Tetrahedron Lett. 1379 (1969).
14. G. Zweifel, J. T. Snow, and C. C. Whitney. J. Am. Chem. Soc. **90**, 7139 (1968).
15. G. Wilke and H. Muller. Ber. **89**, 447 (1956); G. Wilke and H. Muller. Ann. **618**, 267 (1968); G. Wilke and H. Muller. Ann. **629**, 222 (1960).
16. J. J. Eisch. Organomet. Chem. Rev. B. **4**, 308 (1968).
17. J. J. Eisch and R. Amtmann. J. Org. Chem. **37**, 3410 (1972).
18. G. Zweifel and C. C. Whitney. J. Am. Chem. Soc. **89**, 2753 (1967).
19. H. O. House, L. E. Huber, and M. J. Umen. J. Am. Chem. Soc. **94**, 8471 (1972).
20. G. H. Posner. Org. React. **19**, 1 (1972).
21. S. Danishefsky and B. H. Migdalof. Chem. Commun. 1107 (1969).
22. A. Suzuki, A. Arase, H. Matsumoto, M. Itah, H. C. Brown, M. M. Rogíc, and M. W. Rathke. J. Am. Chem. Soc. **89**, 5708 (1967).
23. R. Pappo and P. W. Collins. Tetrahedron Lett. 2627 (1972).
24. K. F. Bernady and M. J. Weiss. Tetrahedron Lett. 4083 (1972).
25. G. Zweifel and R. B. Steele. J. Am. Chem. Soc. **89**, 5085 (1967).

Can. J. Chem. Downloaded from www.nrcresearchpress.com by 210.87.254.6 on 09/05/12
For personal use only.

The Preparation of Specifically Deuterated *trans*-Cinnamyl Alcohol and *trans*-Cinnamic Acid

DONALD G. LEE AND JAMES R. BROWNRIDGE[1]

Department of Chemistry, University of Saskatchewan, Regina, Saskatchewan S4S 0A2

Received January 16, 1973

The reduction of ethyl phenylpropiolate by lithium aluminum hydride results in partial reduction of the triple bond to give *trans*-cinnamyl alcohol. If ethyl phenylpropiolate is reduced by $LiAlD_4$ followed by work-up with acetone and H_2O the product is the specifically labeled compound, *trans*-3-phenyl-2-propen-1-ol-1,1,2-d_3. If the ester is reduced with $LiAlH_4$ followed by work-up with acetone-d_6 and D_2O the product is *trans*-3-phenyl-2-propen-1-ol-*O*,3-d_2. Oxidation of these two products by sodium ruthenate leads to formation of *trans*-cinnamic acid-α-*d* and *trans*-cinnamic acid-β-*d*, respectively.

La réduction de phénylpropiolate d'éthyle par l'hydrure de lithium et aluminium a pour résultat une réduction partielle de la triple liaison pour conduire à l'alcool cinnamique *trans*. Si ce même ester est réduit par $LiAlD_4$ puis traité par l'acétone et l'eau, le produit obtenu est le phényl-3 propène-2 ol-1 d_3-1,1,2 *trans*, spécifiquement marqué. L'ester est réduit par $LiAlH_4$ puis traité par l'acétone *d*-6 et D_2O, le produit est le phényl-3 propène-2 ol-1 d_2-*O*,3 *trans*. L'oxydation de ces deux composés par le ruthénate de sodium conduit à l'acide cinnamique *trans*, α-*d* et β-*d* respectivement.

[Traduit par le journal]

Can. J. Chem., **51**, 2102 (1973)

The use of specifically labeled organic compounds has become an important procedure in the study of organic reaction mechanisms. In particular, the ability to specifically incorporate deuterium is important for two reasons: (*i*) for the study of isotope effects (1) and (*ii*) because deuterium substitution greatly simplifies proton n.m.r. spectra (2).

We have developed a method which has permitted us to prepare two deuterated cinnamyl alcohols (**1** and **2**) and the corresponding cinnamic acids (**3** and **4**). Although the method as we have used it is specific for these four compounds it is quite likely that it may have general application to many other compounds of this type.

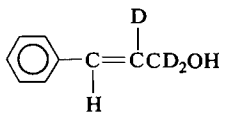

1

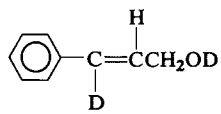

2

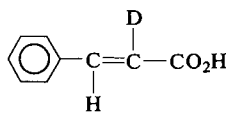

3

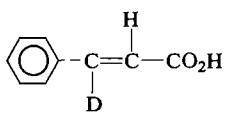

4

Compound **1** was prepared by the partial reduction of ethyl phenylpropiolate (3) with $LiAlD_4$ as indicated in Scheme 1, whereas compound **2** was prepared by reduction with $LiAlH_4$ followed by work-up with acetone-d_6 and dilute D_2SO_4 in D_2O as shown in Scheme 2. The cinnamic acids were obtained by oxidation of the corresponding cinnamyl alcohols with sodium ruthenate (4).

The compounds were identified by use of i.r. and n.m.r. spectroscopy. The proton n.m.r. spectra for compounds **1–4** which provide unambiguous proof of their structures, have been placed in the Depository of Unpublished Data.[2]

The acetone was added in each case to react with any excess reductant before the hydrolysis step was attempted (5). It was observed that if unlabeled acetone was used in Scheme 2 no labeled product was obtained. Presumably an intermediate carbanion capable of abstracting a proton from acetone is formed in the reaction. A probable mechanism for the reaction is outlined in Scheme 3.

Experimental

trans-3-Phenyl-2-propen-1-ol-1,1,2-d_3

Ethyl phenylpropiolate (6.0 g) in 30 ml of anhydrous ether was added from a dropping funnel to 2.18 g of $LiAlD_4$ in 150 ml of absolute ether at room temperature

[1]NRCC Scholarship Holder, 1971–1973.

[2]These spectra are available, at a nominal charge, from the Depository of Unpublished Data, National Science Library, National Research Council of Canada, Ottawa, Canada K1A 0S2.

Can. J. Chem. Downloaded from www.nrcresearchpress.com by 210.87.254.105 on 09/05/12
For personal use only.

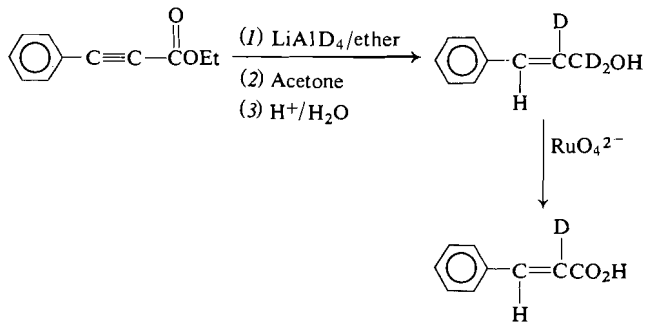

SCHEME 1

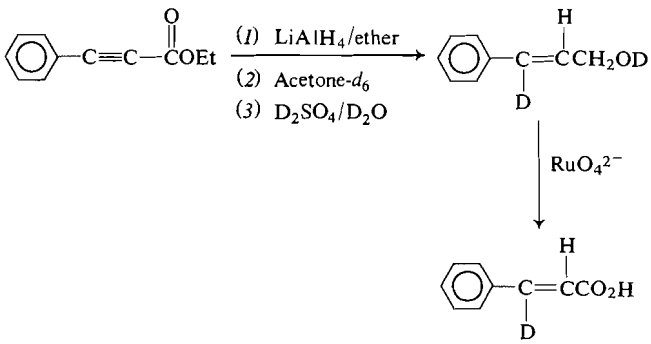

SCHEME 2

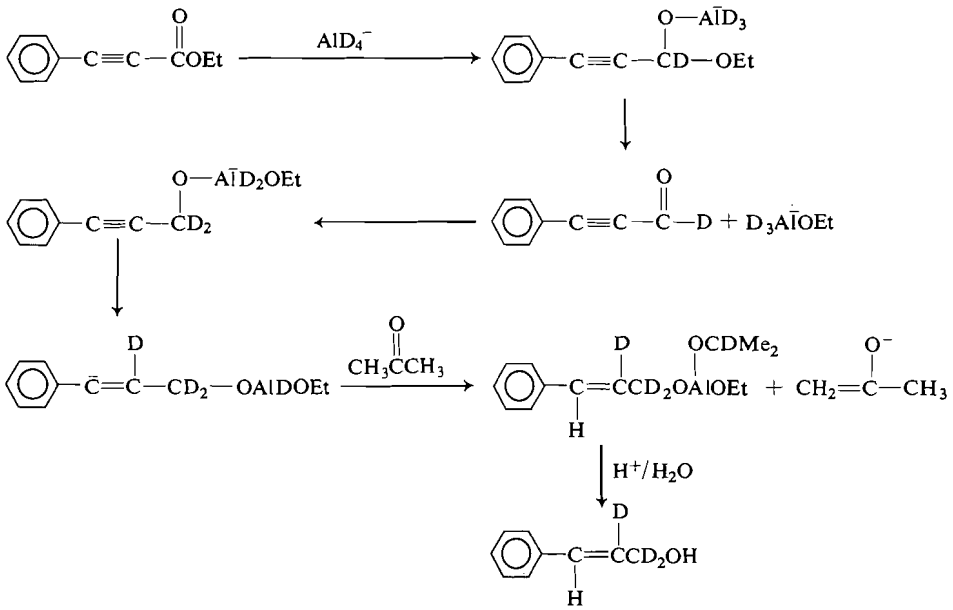

SCHEME 3

Can. J. Chem. Downloaded from www.nrcresearchpress.com by 210.87.254.105 on 09/05/12
For personal use only.

Can. J. Chem. Downloaded from www.nrcresearchpress.com by 210.87.254.105 on 09/05/12
For personal use only.

(3). The solution was then refluxed for 3 h, after which the excess reductant was decomposed with 20 ml of anhydrous acetone followed by 60 ml of cold dilute (0.1 *M*) H_2SO_4. The aluminum hydroxide which precipitated was dissolved by adding 60 ml of 20% H_2SO_4 and the resulting two layers separated. The aqueous layer was extracted with 3 × 50 ml of ether which was combined with the original ether layer and dried over anhydrous calcium chloride. The ether was evaporated and the residue distilled (80°/0.15 mm) to give 3.34 g (71%) of *trans*-3-phenyl-2-propen-1-ol-1,1,2-d_3 which was identified from its i.r. and n.m.r. spectra.

trans-3-Phenyl-2-propen-1-ol-O,3-d_2

As described above, ethyl phenylpropiolate (6.0 g) was reduced with 1.97 g of $LiAlH_4$. After refluxing for 3 h the excess reductant was cautiously decomposed with 3 ml of acetone-d_6 in 20 ml of absolute ether followed by 50 ml of cold dilute (0.1 *M*) D_2SO_4 in D_2O and then by 50 ml of 20% D_2SO_4 in D_2O. The two layers which formed were separated and the aqueous layer extracted as before. The combined ether extracts were dried and evaporated, and the residue distilled to give 3.43 g (73%) of *trans*-3-phenyl-2-propen-1-ol-*O*,3-d_3 which was identified from its i.r. and n.m.r. spectra.

trans-Cinnamic Acid-α-d

This compound was prepared by the oxidation of *trans*-3-phenyl-2-propen-1-ol-1,1,2-d_3 with sodium ruthenate (4). The deuterated cinnamyl alcohol (1.98 g) was suspended in 150 ml of 1.0 *M* aqueous NaOH cooled in an ice–water bath and 604 ml of 0.048 *M* Na_2RuO_4 were added from a dropping funnel. The reaction mixture was stirred continuously and allowed to warm to room temperature overnight. The mixture was filtered through a fine frit to remove the black ruthenium dioxide (RuO_2) which formed, and the filtrate extracted with 3 × 75 ml of ether. The ether layer was dried with anhydrous calcium chloride and evaporated using a water aspirator to leave a liquid (0.3 g, 22% by weight of the total reaction products) which was subsequently identified as benzaldehyde by i.r. and n.m.r. spectra. The aqueous layer was acidified and reextracted with 3 × 75 ml of ether. The ether in turn was dried, filtered, and evaporated leaving a yellow residue. Recrystallization of the residue from ethanol–water gave *trans*-cinnamic acid-α-*d* (1.08 g, 50% yield) identified by i.r. and n.m.r. spectra, m.p; 135–136°, lit. (6) 135°.

trans-Cinnamic Acid-β-d

The oxidation of the *trans*-3-phenyl-2-propen-1-ol-*O*,3-d_2 was carried out in the same manner as described above. The alcohol (0.686 g) was oxidized by 650 ml of 0.0155 *M* Na_2RuO_4 to yield 0.40 g (53% yield) of *trans*-cinnamic acid-β-*d* identified from its i.r. and n.m.r. spectra; m.p. 135–136°.

As was the case for *trans*-cinnamic acid-α-*d*, another reaction product (0.15 g, 27% by weight of the total reaction products) was isolated from the ether layer in the extraction step. The impure sample again appeared to be benzaldehyde. More specifically, one would expect the product to be benzaldehyde-α-*d* as was shown by n.m.r.

The isolation of benzaldehyde from both oxidation procedures indicates that cleavage of the carbon–carbon double bond in the alcohols is a substantial side reaction.

The authors are grateful to the National Research Council of Canada for financial support which sustained this work.

1. L. MELENDER. Isotope effects on reaction rates. Ronald Press, New York. 1960.
2. F. A. BOVEY. Nuclear magnetic resonance spectroscopy. Academic Press, New York. 1969.
3. E. B. BATES, E. R. H. JONES, and M. C. WHITING. J. Chem. Soc. 1854 (1954).
4. D. G. LEE, D. T. HALL, and J. H. CLELAND. Can. J. Chem. **50**, 3741 (1972).
5. R. S. MONSON. Advanced organic synthesis. Academic Press, 1971. Chapt. 2.
6. J. R. A. POLLACK and R. STEVENS (editors). Dictionary of organic compounds. Eyre and Spottiswoode, London. 1965. p. 710.

The Position of Phosphate Groups in the Phosphonomannan of *Hansenula capsulata*, as Determined by Carbon-13 Magnetic Resonance Spectroscopy[1]

PHILIP A. J. GORIN

Prairie Regional Laboratory, National Research Council of Canada, Saskatoon, Saskatchewan S7N 0W9

Received December 18, 1972

The carbon-13 magnetic resonance spectrum of a phosphate of 2-*O*-β-D-mannopyranosyl-α,β-D-mannose was compared with that of the unphosphorylated disaccharide. The positions and number of the signals of C-5's which are coupled to phosphorus-31, together with other spectral data show that the phosphate group is on C-6 of the reducing end-unit (**2**, Fig. 1). This differs from a previous assignment (**1**), thus necessitating a revision (**4**) to the structure **3** proposed for the parent *Hansenula capsulata* phosphonomannan.

Le spectre de résonance magnétique du carbone-13 pour le phosphate, de β-D-mannopyranosyl-2-*O* D-mannose-α,β est comparé à celui d'un disaccharide non-phosphorylé. Les positions et le nombre de signaux correspondant aux positions C-5 qui sont couplés au phosphore-31, ont montré ainsi que d'autres données spectrales que le groupe phosphate se trouve sur la position C-6 de l'unité réductrice terminale (**2**, fig. 1). Ce résultat diffère de l'attribution antérieure (**1**) ce qui, par conséquent entraîne un changement (**4**) en faveur de la structure **3** proposée pour le phosphonomannane *Hansenula capsulata* parent.

[Traduit par le journal]

Can. J. Chem., **51**, 2105 (1973)

The carbon-13 magnetic resonance (c.m.r.) spectra of polyhydroxy compounds have been compared with those of their *O*-methyl ethers, both in the inositol (*1*), pentopyranose and hexopyranose series (2, 3). It was found that the carbon resonance of the $^{13}CHOCH_3$ group in the *O*-methyl ether is approximately 8 p.p.m. downfield from that of the corresponding $^{13}CHOH$ group in the unsubstituted compound. The resonances of the signals of the other carbon atoms were either identical or differed to only a relatively small extent, on going from one compound to the other. By using this observation it has been possible to assign signals to certain carbons in polyhydroxy compounds (1, 2, 4) and conversely it should be possible to identify *O*-methyl ethers by comparison of their c.m.r. spectra with already rationalized spectra of the parent polyhydroxy compound.

An analogous approach is applicable to phosphates since Mantsch and Smith (5) obtained the c.m.r. spectra of the 2′-, 3′- and 5′-phosphates of uridine and found that the resonances of carbons were displaced downfield on phosphorylation of their adjacent hydroxyl groups. In addition it was found by these and earlier workers (6) that both $^{13}C–O–^{31}P$ and $^{13}C–C–O–^{31}P$ coupling takes place in the ribofuranose portion of various nucleotides.

These spectral properties have now made it possible to locate certain of the phosphate groups in the phosphonomannan of *Hansenula capsulata* NRRL Y-1842 (for references to this and other phosphonomannans see ref. 7). Although the polysaccharide gives solutions that are too viscous for spectral studies, a phosphate of 2-*O*-β-D-mannopyranosyl-α,β-D-mannose can be obtained on partial acid hydrolysis which is amenable to examination. Periodate oxidation data suggested that the phosphate group was on one of the C-6's, the non-reducing end-unit being favored (8); (**1**, Fig. 1). In the present study the c.m.r. spectrum of the disaccharide phosphate has been rationalized and the location of the phosphate group determined using the c.m.r. spectra of α- and β-D-mannose, 2,6-di-*O*-methyl-α,β-D-mannose, α,β-D-mannose-2-*d*, α,β-D-mannose-6-phosphate, 2-*O*-β-D-mannopyranosyl-α,β-D-mannose, and methyl β-D-mannopyranoside, on which spectral assignments are available or can be determined.

In general c.m.r. spectra were obtained using solutions of carbohydrate in deuterium oxide maintained at 27 °C. Phosphates were examined as free acids since the acidic form of α,β-D-mannose-6-phosphate gave a well defined spec-

[1]NRCC No. 13142.

Can. J. Chem. Downloaded from www.nrcresearchpress.com by 210.87.254.6 on 09/05/12
For personal use only.

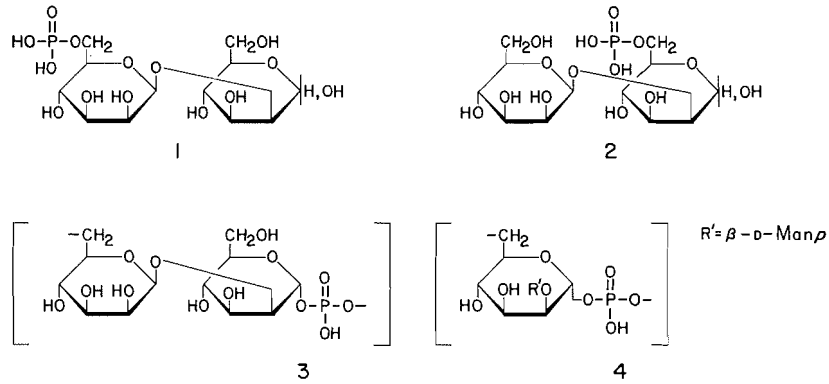

FIG. 1. Old and revised structures for the phosphonomannan of *Hansenula capsulata* and the derived mannobiose-6-phosphate.

trum, whereas the potassium salt gave a C-5 signal that was partially obscured by the C_β-3 signal. C-6 signals of unsubstituted hexoses are generally located at higher field than those of other carbons, and are assignable by the known shielding effect of the substituents on CH_2OH groups (9). However, C-6 signals of CH_2OP groups are more difficult to assign since they are closer to other signals because of the deshielding effect of the phosphate group. They were characterizable, however, by reference to spectra obtained with only partial proton decoupling. The CH_2 groups gave triplets arising from ^{13}C–H coupling, each of the signals being finely split by virtue of ^{13}C–O–^{31}P coupling.

The c.m.r. signals of α- and β-D-mannose have been assigned to carbon atoms by Dorman and Roberts (2) and by Perlin and coworkers (3). Their separate assignments agree except for the relative locations of the C-3 and -2 signals of β-D-mannose, which are at δ_C 73.6 and 71.8 (Table 1). The conclusions of Dorman and Roberts are shown to be correct by comparing the displacements of the ^{13}C signals on going from α,β-D-mannose to 2,6-di-*O*-methyl-α,β-D-mannose (Table 1). The C_β-6 signals are displaced from δ_C 61.6 to 71.3 (or δ_C 70.5) and the C_β-2 signals from δ_C 71.8 to 81.9. The C_β-3 signal at δ_C 73.6, which is not affected by substitution of the adjacent hydroxyl, is displaced only 0.3 p.p.m. to δ_C 73.9. A further confirmation of the assignments could be made by examination of the c.m.r. spectrum of α,β-D-mannose-2-*d*, prepared by an analogous method to that of Isbell *et al.* (10). The C_α-2 and C_β-2 signals should be very small because of the presence of an adjacent deuterium nucleus (11) and it was found that the signals at δ_C 71.2 and 71.8, corresponding respectively to C_α-2 and C_β-2, could not be detected (Table 1).

In agreement with the results of Mantsch and Smith (5) the c.m.r. spectra of α,β-D-mannose and α,β-D-mannose-6-phosphate contain many signals with common resonances (Table 1; Fig. 2 spectra A and C). The resonances of C-1, -2, -3, and -5 signals had undergone little change on phosphorylation whereas the C-6 resonances in the phosphate were displaced 2.2 p.p.m. downfield. The C-6 resonances of the α- and β-phosphate are at δ_C 63.7 with $^2J_{^{13}C-^{31}P}$ = 7 Hz. C_α-5 and C_β-5 signals of α,β-D-mannose (2) at δ_C 72.9 and 76.7 correspond to those in the phosphate at δ_C 72.6 ($^3J_{^{13}C-^{31}P}$ = 7 Hz) and 76.1 ($^3J_{^{13}C-^{31}P}$ = 7 Hz), respectively.

2-*O*-β-D-Mannopyranosyl-α,β-D-mannose was obtained from the mannobiose phosphate (8) by the action of alkaline phosphatase. The structure proposed by Slodki for the disaccharide (8) was confirmed as follows. In a methylation-fragmentation study the 3,4,6-tri-*O*- and 2,3,4,6-tetra-*O*-methyl derivatives of methyl α,β-D-mannopyranoside were obtained and characterized by g.l.c. (12, 13), thus indicating 2-*O*-substitution. The configuration of the linkage is β since the specific rotation of 2-*O*-D-mannopyranosyl-D-mannitol, derived by sodium borohydride reduction, is −43°, lower than +45° reported for 2-*O*-α-D-mannopyranosyl-D-mannitol (14).

The c.m.r. spectrum of 2-*O*-β-D-mannopyranosyl-α,β-D-mannose is complex (Table 1; Fig. 2; spectrum B) but assignments for the C-6

Can. J. Chem. Downloaded from www.nrcresearchpress.com by 210.87.254.6 on 09/05/12
For personal use only.

TABLE 1. Chemical shifts and assignments of c.m.r. signals of mannose and derivatives

Compound	Downfield difference of chemical shifts of assigned signals from that of external TMS, contained in a coaxial capillary in p.p.m. (δ_C)
1. α,β-D-Mannose (2)	94.5 (C_α-1) 94.1 (C_β-1) 76.7 (C_β-5)† 73.6 (C_β-3) 72.9 (C_α-5) 71.8 (C_β-2) 71.2 (C_α-2) 70.8 (C_α-3) 67.5 (C_α-4) 67.1 (C_β-4) 61.6 (C_α-6, C_β-6)
2. α,β-D-Mannose-6-phosphate	94.8 (C_α-1) 94.4 (C_β-1) 76.1 (C_β-5; J 7 Hz) 73.3 (C_β-3) 72.6 (C_α-5; J 7 Hz) 71.9 (C_β-2) 71.3 (C_α-2) 70.6 (C_α-3) 67.1 and 66.7 (αβC4) 63.7 ($C_{\alpha\beta}$-6; J 5 Hz)
3. 2-*O*-β-D-Mannopyranosyl-α,β-D-mannose*	101.4 (C_β-1′) 99.2 (C_α-1′) 94.1 (C_β-1) 92.4 (C_α-1) 80.0 (C_β-2) 78.6 (C_α-2) 76.9 (C_β-5, $C_{\alpha\beta}$-5′) 73.3 ($C_{\alpha\beta}$-3′, C_β-3) 73.1 (C_α-5) 72.4 71.9 71.4 71.0 70.8 70.2 67.7 and 67.3 ($C_{\alpha\beta}$-4, $C_{\alpha\beta}$-4′) 61.6 and 61.3 (C-6′, $C_{\alpha\beta}$-6)
4. Phosphate of 2-*O*-β-D-mannopyranosyl-α,β-D-mannose*	101.4 (C_β-1′) 99.1 (C_α-1′) 94.3 (C_β-1) 92.5 (C_α-1) 79.8 (C_β-2) 78.3 (C_α-2) 76.9 ($C_{\alpha\beta}$-5′) 75.7 (C_β-5, J 7 Hz) 73.3 ($C_{\alpha\beta}$-3′, C_β-3) 72.7 72.1 (C_α-5, J 8 Hz) 71.3 70.8 70.0 67.7 and 67.3 ($C_{\alpha\beta}$-4′, $C_{\alpha\beta}$-4, C_β-4) 64.6 ($C_{\alpha\beta}$-6, J 5 Hz) 61.6 (C-6′)
5. 2,6-Di-*O*-methyl-α,β-D-mannose	94.5 (C_β-1) 91.3 (C_α-1) 81.9 (C_β-2) 81.6 (C_α-2) 75.3 (C_β-5) 73.9 (C_β-3) 72.1 (C_α-5) 71.3 and 70.5 (C_α-3, C_β-6, C_α-6) 67.9 (C_α-4) 67.7 (C_β-4) 59.2 and 59.0 ($OCH_3$2, $OCH_3$6)
6. α,β-D-Mannose-2-*d*	94.5 (C_β-1) 94.2 (C_β-1) 76.8 (C_β-5) 73.6 (C_β-3) 72.9 (C_α-5) 70.7 (C_α-3) 67.5 (C_α-4) 67.3 (C_β-4) 61.6 (C_α-6, C_β-6)

*The carbons with prime numbers are those of the non-reducing end, carbons with nonprime numbers are those of the reducing end, α and β refer to the anomeric configuration of the reducing end.
†Underlined shifts are those used directly in assignment of position of the phosphate group in the mannobiose phosphate.

(from a ^1H coupled c.m.r. spectrum) and C-5 signals can be made. The latter assignment can be made since it has been found in this laboratory (15) that the c.m.r. spectrum of a D-mannopyranosyl unit in an oligosaccharide undergoes little change on substitution with another D-mannopyranosyl unit, except that the resonance of the carbon attached to the glycosyl unit is displaced downfield. Based on this finding the positions of the signals of C-5′ of the non-reducing end-units and C-5 of the reducing end-units of the α- and β-anomers can be predicted by reference to the chemical shifts of C-5 signals of methyl β-D-mannopyranoside (3) and α- and β-D-mannose (2).

Inspection of the c.m.r. spectrum of the unknown phosphate of 2-*O*-β-D-mannopyranosyl-α,β-D-mannose (Table 1; Fig. 2; spectrum D) shows that it resembles that of the unphosphorylated disaccharide except for the C-5 and -6 regions. One C-6 signal of the phosphate has a resonance of δ_C 61.6 corresponding to those at δ_C 61.6 and 61.3 for the C-6's of the disaccharide. The other C-6 signal is coupled (J = 5 Hz) and is displaced 3.2 p.p.m. downfield due to substitution by a phosphate group. The C-5 portions of the phosphate spectrum contain two signals with three-bond ^{13}C–^{31}P coupling. These signals correspond respectively in their resonances and coupling constants (δ_C 72.1, J = 8 Hz; δ_C 75.7, J = 7 Hz) to the C_α-5 and C_β-5 signals of α,β-D-mannose-6-phosphate (δ_C 72.6, J = 7 Hz; δ_C 76.1, J = 7 Hz), respectively, thus indicating a phosphate substituent on O-6 of the reducing end (Fig. 1; **2**). The other possibility, suggested by Slodki (8) namely that the CH_2OP group is located as the non-reducing end-unit (Fig. 1; **1**) is ruled out since its spectrum would contain only one coupled C-5 signal in the vicinity of the corresponding resonance from methyl β-D-mannopyranoside (ref. 3; corrected to δ_C 76.3, for an external TMS standard).

The phosphate was not amenable to a confirmatory methylation-fragmentation experiment, incorporating the Kuhn reaction. The products, following conversion to methyl glycosides, were examined by g.l.c., but only methyl glycosides

Can. J. Chem. Downloaded from www.nrcresearchpress.com by 210.87.254.6 on 09/05/12
For personal use only.

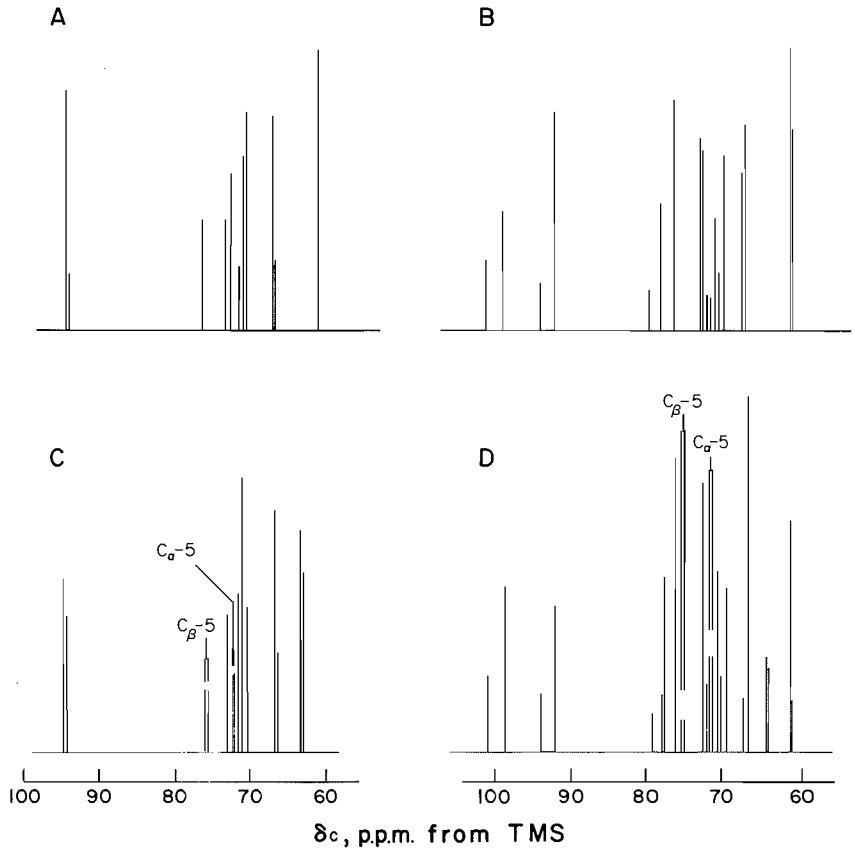

FIG. 2. C.m.r. spectra of α,β-D-mannose (A), α,β-D-mannose-6-phosphate (C), 2-*O*-β-D-Mannopyranosyl-α,β-D-mannose (B), and 2-*O*-β-D-Mannopyranosyl-α,β-D-mannose-6-phosphate (D).

of 2,3,4,6-tetra-*O*-methyl-D-mannose, from the non-reducing end, could be detected. The fate of the phosphorylated unit was not determined.

The structure of the phosphonomannan of *H. capsulata* which was assigned a high proportion of repeating unit **3** (Fig. 1) is therefore incorrect (8). Instead a more highly branched structure must be proposed with a high proportion of a repeating unit containing α-D-mannopyranose units connected by (1 → 6)-phosphorodiester linkages, with each unit substituted in the 2-position by a β-D-mannopyranose unit (Fig. 1; **4**).

Experimental

C.m.r. spectra were obtained using a Varian XL-100-15 n.m.r. spectrometer with Fourier transform and D_2O solutions (4 ml) of 0.3–1.0 g of compound contained in 12 mm diameter × 8 in. tubes at a temperature of 27°. The sweep width was 5000 Hz, the acquisition time 0.4 s and the pulse width 50 μs. 1000–5000 Transients were used, the exact number depending on the sample size and the type of compound examined. Chemical shifts are expressed in p.p.m. and are based on the downfield difference of the resonance signal and that of external TMS contained in a coaxial capillary. Coupling constants *J* are in Hz.

The barium salt of D-mannose-6-phosphate was obtained from Sigma Chemical Co., St. Louis, Mo. It was converted to the free acid by shaking in an aqueous solution with Amberlite 1R120 (H^+ form), followed by filtration and evaporation. 2,6-Di-*O*-methyl-D-mannose was prepared by acid hydrolysis (0.5 *M* H_2SO_4, 100°, 18 h) of methyl 2,6-di-*O*-methyl-α-D-mannopyranoside (16).

Isolation and Characterization of 2-O-β-D-Mannopyranosyl-α,β-D-mannose

The mannobiose phosphate (1.0 g) in water (50 ml) containing sodium bicarbonate (250 mg) was treated with alkaline phosphatase (0.3 ml; from *E. coli*, No. P-4253 supplied by Sigma Chemical Co.) and the solution was deionized with Amberlite 1R120 (H^+ form) and Dowex 1-X8 (bicarbonate form), filtered, and evaporated. The product (0.70 g) had $[\alpha]_D^{25}$ −36° (*c*, 0.3 H_2O). P.m.r. data (D_2O at 70°; shifts are based on the downfield difference δ of the signal from that of a tetramethylsilane

Can. J. Chem. Downloaded from www.nrcresearchpress.com by 210.87.254.6 on 09/05/12
For personal use only.

external standard): δ 5.86 (J = 2 Hz), 5.35 (H-1's of α-anomer); δ 5.57, 5.50 (H-1's of β-anomer). The two sets of signals were in a 2.4:1 ratio. The 2-*O*-β-D-mannopyranosyl-D-mannitol, derived by reduction with aqueous sodium borohydride, had $[\alpha]_D^{25}$ −43° (*c*, 0.3 H_2O), corresponding to a β-linkage (2-*O*-α-D-mannopyranosyl-D-mannitol has $[\alpha]_D^{25}$ +45° (14) and gave a single anomeric signal at δ 5.41).

The linkage position in the reducing disaccharide was confirmed by successive Kuhn methylation, hydrolysis, and treatment with methanolic hydrogen chloride. The products were characterized by g.l.c. of the free glycosides and the mixture obtained on trimethylsilylation as methyl 2,3,4,6-tetra-*O*-methyl-α,β-D-mannoside and methyl 3,4,6-tri-*O*-methyl-α,β-D-mannoside (12, 13), thus indicating a 2-*O*-substituted mannobiose.

An analogous experiment was carried out with the mannobiose phosphate (**2**; Fig. 1), but the only identifiable product was methyl 2,3,4,6-tetra-*O*-methyl-α,β-D-mannopyranoside arising from its non-reducing end unit.

The author would like to thank Mr. M. Mazurek for carrying out c.m.r. spectral determinations.

1. D. E. DORMAN, S. J. ANGYAL, and J. D. ROBERTS. J. Am. Chem. Soc. **92**, 1351 (1970).
2. D. E. DORMAN and J. D. ROBERTS. J. Am. Chem. Soc. **92**, 1355 (1970).
3. A. S. PERLIN, B. CASU, and H. J. KOCH. Can. J. Chem. **48**, 2596 (1970).
4. P. A. J. GORIN and M. MAZUREK. Carbohydr. Res. In press.
5. H. H. MANTSCH and I. C. P. SMITH. Biochem. Biophys. Res. Commun. **46**, 808 (1972).
6. D. E. DORMAN and J. D. ROBERTS. Proc. Natl. Acad. Sci. U.S. **65**, 19 (1970).
7. P. A. J. GORIN and J. F. T. SPENCER. Adv. Carbohydr. Chem. **23**, 367 (1968).
8. M. E. SLODKI. Biochim. et Biophys. Acta, **69**, 96 (1963).
9. L. D. HALL and L. F. JOHNSON. Chem. Commun. No. 10, 509 (1969).
10. H. S. ISBELL, H. L. FRUSH, C. W. R. WADE, and A. J. FATIADI. J. Res. Natl. Bur. Stand., Sect. A 73 (1), 75 (1969).
11. H. SPIESECKE and W. G. SCHNEIDER. J. Chem. Phys. **35**, 731 (1961).
12. P. A. J. GORIN, J. F. T. SPENCER, and S. S. BHATTACHARJEE. Can. J. Chem. **47**, 1499 (1969).
13. S. S. BHATTACHARJEE and P. A. J. GORIN. Can. J. Chem. **47**, 1207 (1969).
14. P. A. J. GORIN and A. S. PERLIN. Can. J. Chem. **34**, 1796 (1956).
15. P. A. J. GORIN. Can. J. Chem. In press.
16. S. S. BHATTACHARJEE and P. A. J. GORIN. Can. J. Chem. **47**, 1195 (1969).

Can. J. Chem. Downloaded from www.nrcresearchpress.com by 210.87.254.6 on 09/05/12
For personal use only.

Proton Magnetic Resonance Studies of Rotational Isomerism in Halotoluene Derivatives. IX. Rotational Barriers and Conformational Energy Differences in $\alpha,\alpha,\alpha',\alpha',\alpha'',\alpha''$, 2,4,6-Nonachloromesitylene

J. PEELING,[1] B. W. GOODWIN,[1] T. SCHAEFER, AND J. B. ROWBOTHAM[2]

Department of Chemistry, University of Manitoba, Winnipeg, Manitoba R3T 2N2

Received January 2, 1973

The activation parameters for the rotation of the dichloromethyl groups in the two conformations of α,α,α′,α′,α″,α″,2,4,6-nonachloromesitylene are reported for solutions in toluene-d_8 and in methylene chloride. In addition, free energies of activation are given for solutions in bromochloromethane, trichloroethylene, and in carbon disulfide. The free energies of activation are lower in the toluene solution than in the other solutions. The entropies of activation are near zero, perhaps slightly negative. The symmetrical conformation is more stable than the unsymmetrical one in all the solvents.

Les paramètres d'activation pour la rotation des groupes dichlorométhyles dans les deux conformations de l'α,α,α′,α′,α″,α″,2,4,6-nonachloromésitylène ont été rapportés pour des solutions dans le toluène-d_8 et le dichlorométhane. De plus, les énergies libres d'activation ont été présentées pour les solutions dans le bromo chlorométhane, trichloroéthylène, et disulfure de carbone. Les énergies libres d'activation sont plus basses dans le toluène que pour les autres solvants; les entropies d'activation sont proches de zéro, voire même légèrement négatives. La conformation symétrique est plus stable que celle qui est non symétrique dans tous les solvants. [Traduit par le journal]

Can. J. Chem., 51, 2110 (1973)

Can. J. Chem. Downloaded from www.nrcresearchpress.com by 210.87.254.42 on 09/05/12
For personal use only.

Introduction

The preferred conformation of the dihalomethyl group in halotoluene derivatives is one in which its C—H bond lies in the plane of the aromatic ring (1–3). The conformation of highest energy, the transition state, is evidently that in which the C—H bond lies in a plane perpendicular to the aromatic ring (4). The energy difference between these conformations in a number of compounds can be measured by monitoring the temperature dependence of their p.m.r. spectra. For example, in α,α,2,4,6-pentachlorotoluene (PCT) rotation by π radians about the sp^2–sp^3 carbon–carbon bond converts **1** to **3** via **2**, thereby interchanging the chemical

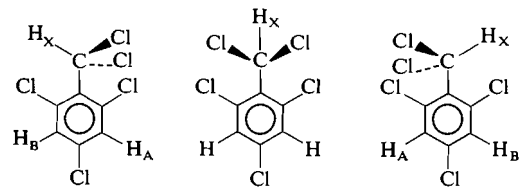

1 **2** **3**

shifts of the ring protons (1). The shape of the ring proton spectrum therefore depends on the rate of rotation, allowing the extraction of the parameters of activation from **1** to **2**. The chemical shift of the side-chain proton, H_x, is invariant to the rotation. On the other hand, in α,α,α′,α′,2,4,5,6-octachloro-*m*-xylene (MOCX)

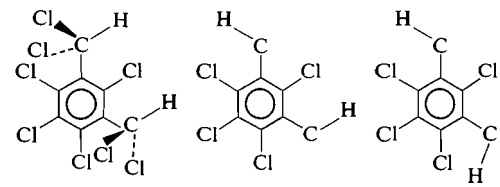

6 **5** **4**

rotation of one of the dichloromethyl groups in any one of **4**, **5**, and **6** converts one conformation into another and the shape of the side-chain proton spectrum now depends on the rotation rate (2). The activation parameters obtained from the side-chain proton spectra in MOCX agree rather well with those from the ring proton spectra in PCT, although it is not possible to distinguish between activation energies for, say, conversion from **4** to **5** and from **5** to **6**.

In α,α,α′,α′,α″,α″,2,4,6-nonachloromesitylene (NCM) the effect of the exchange process on the chemical shifts is somewhat more involved than in PCT or MOCX. Thus, rotation of one of the dichloromethyl groups in **7** converts **7** to

[1]NRCC Scholarship, 1971–1972.
[2]Postdoctorate fellow, 1971–1972.

Can. J. Chem. Downloaded from www.nrcresearchpress.com by 210.87.254.42 on 09/05/12
For personal use only.

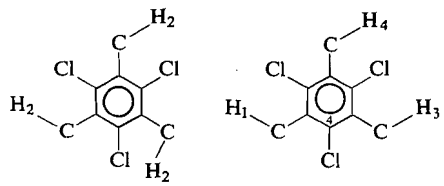

7 8

8 but only rotation of H_3—CCl_2 in **8** will convert **8** back to **7**. Rotation of either of the other two groups in **8** produces an equivalent conformation **8**. But note that any one of these rotations, whether intra- or interconformational, interchanges the chemical shifts of some or of all of the protons and it proves possible to determine the activation parameters for the conversion from **7** to **8** as well as from **8** to **8**.

This paper describes the synthesis of NCM and the determination of its intramolecular activation parameters in toluene-d_8 and methylene chloride solutions. The solubility of NCM in common solvents is restricted but it has been possible to measure the free energy differences between **7** and **8** in a few additional solvents. The free energies of activation for the above conversions are also measured in these solvents.

Experimental

(1) Preparation of NCM

Chlorine gas was bubbled through a solution of mesitylene in CCl_4 in the presence of iron powder until the proton resonance spectrum indicated complete chlorination of the ring positions. After recrystallization, the 2,4,6-trichloromesitylene was further chlorinated in the presence of u.v. light as described for PCT (5). The chlorination was terminated when the proton resonance peaks arising from monochloromethyl groups disappeared. The product was recrystallized twice from CCl_4, m.p. 187–189 °C.

(2) Spectral Measurements

Solutions of NCM, 3.0 mol % in toluene-d_8 and 1.5 mol % in CH_2Cl_2, CH_2ClBr, CCl_2=CHCl, and CS_2, were carefully degassed. Each contained a small amount of tetramethylsilane (TMS) as an internal reference and locking material. The low concentrations of NCM prevented precipitation at low temperatures. Great care was taken in avoiding line shape distortions from saturation or filtering while recording the proton resonance spectra at a sweep rate of 0.02 Hz/s on an HA100-D spectrometer. Calibration of peaks has been described previously (6) as has the measurement of sample temperatures (6).

Results and Discussion

(1) The Exchange Processes

The protons are isochronous in **7** but anisochronous in **8**, so that the proton resonance spectrum displays four peaks at temperatures where rotation about the sp^2–sp^3 carbon–carbon bonds is slow. When one of the dichloromethyl groups in **7** undergoes a rotation by π radians, H_2 exchanges with H_1, H_3, and H_4 of **8**. The latter is converted back to **7** only by rotation of the group H_3—CCl_2 but, because **8** can be produced from **7** in three equivalent ways, the *a priori* probability of the process **7** → **8** is the same as that of the process **8** → **7**. Of course the rate constants for the rotations of the different dichloromethyl groups are determined by their barriers and these need not be the same in **7** and **8**.

Rotation by π radians of the group H_1—CCl_2 in **8** exchanges H_3 and H_4 to form an equivalent **8**. Similarly, rotation of H_4—CCl_2 exchanges H_1 and H_3 to yield another **8**. In both processes the rotating group leaves the shift of its own proton unchanged. Finally, there is no internal rotational process which causes exchange between H_1 and H_4 in **8**.

(2) Assignment of Peaks in Region of Slow Exchange

Figure 1 displays the proton resonance spectrum of NCM in CH_2Cl_2 at temperatures where the exchange is slow. Table 1 gives the chemical shifts for each of the four peaks in toluene-d_8 and CH_2Cl_2 solutions. The three peaks of equal intensity arise from the three anisochronous protons of conformation **7**.

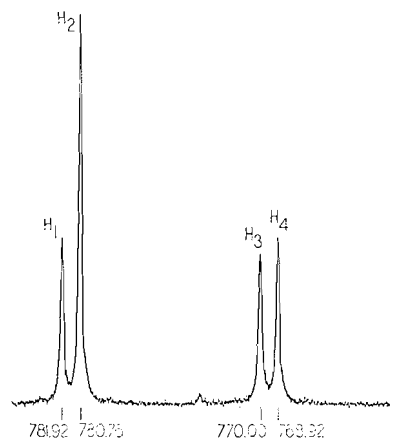

FIG. 1. The p.m.r. spectrum at 100 MHz of a 1.5 mol % solution of NCM in CH_2Cl_2 at 236.6 °K. The assignment of the peaks to conformations **7** and **8** is discussed in the text.

TABLE 1. Proton chemical shifts* of α,α,α′,α′,α″,α″,2,4,6-nonachloromesitylene in toluene-d_8 and methylene chloride

Solvent	T(°C)	H_1	H_2	H_3	H_4
C_7D_8 (3.0 mol %)	−36.3	7.3773	7.3172	7.0902	7.0154
CH_2Cl_2 (1.5 mol %)	−36.6	7.8192	7.8076	7.700	7.6892
$\Delta(CH_2Cl_2 - C_7D_8)$†	—	0.4419	0.4904	0.6098	0.6738

*In p.p.m. downfield from internal TMS.
†Shift in CH_2Cl_2 − shift in C_7D_8, a positive value representing an upfield shift in the aromatic solvent.

(a) Steric Crowding

The peak at 7.808 p.p.m. in CH_2Cl_2 solution clearly arises from the symmetrical conformation **7**. The other peaks can then be assigned to the individual protons in **8** on the basis of their degree of steric interaction with neighboring chlorine atoms, as was done for MOCX (2).[3] For a regular geometry (tetrahedral angles at the side-chain carbon atoms, etc.) the ring Cl–H distance in conformation **1** is 0.5 Å shorter than the sum of the Cl–H van der Waals radii, indicating a high degree of steric crowding even for the actual geometry in **7** and **8**. The time-dependent electric fields from the ring chlorine atom interfere with the diamagnetic charge circulation about the proton (7). The ensuing deshielding is proportional to r^{-6}, where r is the Cl–H distance. Consequently only very slight changes in r (less than 0.1 Å) in the region of the van der Waals contact distance can cause marked changes in the chemical shift of the proton (8).

Consider now the nearest neighbors [L,M] in the [L] Cl_2C—H...Cl [M] moieties of **7** and **8**. For H_1 and H_2 one has [L,M] = [Cl,Cl_2] while for H_3 and H_4 one has [L,M] = [Cl,H]. In terms of relative steric crowding it is therefore reasonable to assign H_1 and H_2 to the peaks at 7.808 and 7.819 p.p.m., respectively (H_2 being known anyway), while H_3 and H_4 are assigned to the high field (greater shielding) peaks at 7.700 and 7.689 p.p.m. from internal TMS. To differentiate (at second order) between H_3 and H_4 one may consider next-nearest neighbors [K,N] in [K,L] Cl_2C—H...Cl [M,N]. One finds [K,N] = [Cl_2,Cl] for H_3 and [H,Cl] for H_4 and assigns H_3 to the peak at lower field, *i.e.*, at 7.700 p.p.m. A similar argument rationalizes the relative shifts of H_1 and H_2.

[3]Calculations based on static electric fields arising from the C—Cl bond dipoles did not reproduce the relative chemical shifts of the protons in MOCX (2).

(b) Aromatic Solvent Induced Shifts (9)

The disc-shaped toluene solvent molecules pack about the solute NCM molecule in such a way that, on average, the solute protons are more often situated above or below than in the plane of solvent molecules (10). The magnetic field from the relatively large induced magnetic moment in the benzene ring will therefore cause a net shielding of the solute protons. This field decreases as the cube of the distance from the solvent molecule and thus the largest aromatic solvent induced shift occurs for those protons which most closely approach the toluene molecule.

The steric model attributes the lowest field peak of NCM in CH_2Cl_2 solution to the proton experiencing the largest degree of steric crowding. Presumably the solvent molecule in the toluene solution can approach this proton least closely. Hence one expects and finds (Table 1) a rough correlation between the aromatic solvent induced shifts and the shielding of the protons of NCM in CH_2Cl_2 solution.

(c) Exchange Broadening

As discussed above, H_3 can exchange its chemical shift with those of all other protons in **7** and **8**, while H_1 and H_4 cannot undergo mutual exchange. In the region where the rotation rate of the $CHCl_2$ group is fast enough to cause noticeable broadening of the individual peaks of Fig. 1, the degree of broadening of the peak of H_3 should therefore be greater than for the other three peaks. In fact, the peak at 7.700 p.p.m. in CH_2Cl_2 solution undergoes exactly this behavior. In toluene solution the peak at 7.090 p.p.m. also displays greater broadening in the region of slow exchange, in agreement with the assignment in Fig. 1 and Table 1 and consistent with the assumed order of the aromatic solvent induced shifts in Table 1.

The internal consistency of the three spectral effects suggests that the assignment of the peaks to the protons in **7** and **8** is a reliable one.

Can. J. Chem. Downloaded from www.nrcresearchpress.com by 210.87.254.42 on 09/05/12
For personal use only.

Can. J. Chem. Downloaded from www.nrcresearchpress.com by 210.87.254.42 on 09/05/12
For personal use only.

(3) Relative Populations of the Conformational Isomers

The calculation of spectral line-shapes as a function of exchange rate requires the relative populations of **7** and **8** as a function of temperature. For the toluene-d_8 solution these were obtained from the relative areas of the two low-field peaks at five temperatures between 202.7 and 240.2 °K. For the solution in CH_2Cl_2 the relative populations were found from eight spectra between 236.6 and 275.6 °K, using the relative areas of the four peaks.

As discussed for MOCX (2) the translational, vibrational, and rotational entropy differences of **7** and **8** are either 0 or about 0.02 e.u. and are neglected. There exists an entropy contribution of R ln 3 for **8** and hence one may write the equilibrium constant as

$$[1] \qquad K = x_8/x_7 = 3 \exp(-\Delta H/RT)$$

where x_8 and x_7 are the mole fractions of **8** and **7** and $\Delta H = H_8 - H_7$ is the enthalpy difference.

The measurements gave $\Delta H = 335 \pm 15$ cal/mol in toluene-d_8 and populations calculated from these values gave theoretical spectra in excellent agreement with experiment between 202.7 and 308.0 °K. At higher temperatures the peaks had coalesced to a single broad band. Similarly, one found $\Delta H = 380 \pm 20$ cal/mol for the CH_2Cl_2 solution and good agreement with experiment up to 304.6 °K.

Relative populations of **7** and **8** were also determined at 232.2 °K for solutions in CS_2, $CHCl{=}CCl_2$, and CH_2ClBr. The results are given in Table 2 and are discussed further below.

(4) The Line-shape Theory and Computer Program

As there is no observable spin–spin interaction between the non-equivalent protons in **8**, the McConnell formulation (11) of the Bloch equations under conditions of exchange was appropriate. The expression for the complex magnetization contained six independent pre-exchange lifetimes τ, four population terms, and four effective T_2 terms. The computer program in Fortran IV took as input data the four populations and T_2 values, the six pre-exchange lifetimes and the frequencies of the exchanging sites. The six independent pre-exchange lifetimes gave separately the rate constants for the inter-conformational conversions between **7** and **8** and the intraconformational conversions from **8** to **8**. A scaling factor allowed the computed spectra to be plotted on a Calcomp plotter. The computations were done on an IBM 360/65 system and the line-shape fitting procedure followed that described for ABX FIT (5).

TABLE 2. Enthalpy differences* between ground state conformations of α,α,α′,α′,α″,α″,2,4,6-nonachloromesitylene in several solvents

Solvent	Dielectric constant (25 °C)	$\Delta H = H_8 - H_7$ (cal/mol)
CH_2BrCl	8.4	296 ± 30
Toluene-d_8	2.4	335 ± 15
CH_2Cl_2	8.9	380 ± 20
$CHCl{=}CCl_2$	3.4	435 ± 30
CS_2	2.6	503 ± 30

*To within experimental error these are also the free energy differences.

(5) Fitted Spectra and Activation Parameters

(a) Temperature Dependence of Peak Positions

Accurate rate constants are contingent upon accurate internal chemical shifts of the exchanging sites at each temperature (12). For the CH_2Cl_2 solution the peak positions vary as $1/T$ between 236.6 and 270.9 °K. The shifts obtained from the regression line agreed extremely well with the experimental spectra and were also used to calculate the site frequencies in the presence of exchange.

In toluene-d_8 solution, where the peak positions were more strongly dependent on temperature, no single function of internal shift versus either T or $1/T$ gave completely satisfactory agreement with experiment. A combination of these functions was used in such a way that the simulated spectra agreed with experiment between 208.9 and 287.1 °K. Extrapolated shift values were then used to fit a further fourteen spectra up to 356.8 °K.

The internal shifts in the other solvents varied only very slightly between 232.2 and 255.2 °K and the exchange rates were determined only at 305.6 °K, very near the coalescence temperature. The free energies of activation were insensitive to immoderately large variations in the internal shift.

(b) Linewidths in the Absence of Exchange

These were assumed to depend on the magnetic field inhomogeneity, which was controlled by monitoring the linewidth of an impurity peak some p.p.m. to high field of the NCM proton peaks. Effective T_2 values for the four sites were

TABLE 3. Activation parameters for the internal rotation processes in α,α,α′,α′,α″,α″,2,4,6-nonachloromesitylene

Parameter	C_7D_8 (3.0 mol %)	CH_2Cl_2 (1.0 mol %)
8 → 7		
E_a (kcal/mol)	15.24 ± 0.25 (0.70)*	16.30 ± 0.40 (0.49)
log A	12.42 ± 0.18 (0.53)	13.00 ± 0.29 (0.35)
$\Delta H‡$ (kcal/mol)	14.69 ± 0.24 (0.72)	15.69 ± 0.40 (0.49)
$\Delta S‡$ (cal/mol °K)	−3.55 ± 0.80 (2.48)	−1.10 ± 1.32 (1.59)
8 → 8		
E_a (kcal/mol)	15.58 ± 0.25 (0.73)	16.70 ± 0.40 (0.49)
log A	12.43 ± 0.18 (0.54)	13.01 ± 0.29 (0.35)
$\Delta H‡$ (kcal/mol)	14.98 ± 0.25 (0.73)	16.09 ± 0.41 (0.49)
$\Delta S‡$ (cal/mol °K)	−3.68 ± 0.81 (2.48)	−1.04 ± 1.33 (1.60)

*The errors not in parentheses are the standard deviations from the linear regression line. Errors in parentheses are *maximum* errors arising from uncertainties in site frequencies and linewidth corrections as discussed in the text.

calculated from the linewidths obtained from a number of spectra at low temperatures and could be checked against the linewidth of the impurity peak.

(c) Fitted Spectra

Only spectra showing considerable exchange broadening were fitted, those between 275.6 and 336.9 °K in CH_2Cl_2 solution and between 258.7 and 356.8 °K in toluene-d_8. Pre-exchange lifetimes for all the exchange processes were extracted at 22 temperatures for the toluene solution and at 16 temperatures for the CH_2Cl_2 solution. In Fig. 2 computed and observed spectra are portrayed at a few representative temperatures for the latter solution.

Plots of ln k *vs.* $1/T$ and of ln (k/T) *vs.* $1/T$, based on the Arrhenius and transition state formulations (12), were prepared for each exchange process in the toluene and CH_2Cl_2 solutions. The linear regression lines had a correlation coefficient of 0.997 for the former and of 0.995 for the latter solution. The activation parameters and their least squares errors are given in Table 3.

(d) Maximum Error Estimates

The r.m.s. errors in Table 3 measure the precision of fit of the rate constant data to straight lines of the type presented in Fig. 3. However, they do not measure systematic errors arising from inaccuracies in the site frequencies, in effective T_2 values and in the temperature measurements. Such errors were estimated as follows:

(i) Site frequency errors

For the CH_2Cl_2 solution the standard deviations from the least squares analysis of the chemical shifts as a function of $1/T$ gave a new

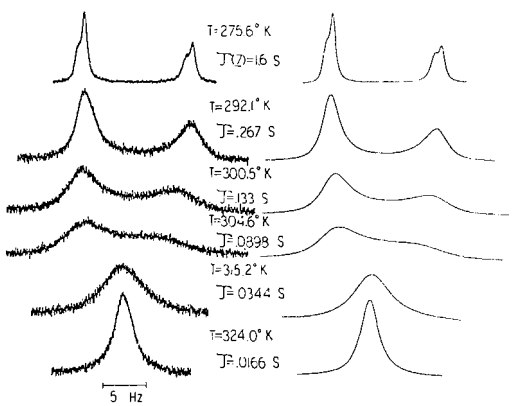

FIG. 2. Calculated and experimental p.m.r. lineshapes at a few representative temperatures are given for a 1.5 mol % solution of NCM in CH_2Cl_2. The pre-exchange lifetimes are indicated for conformation **7**; see text.

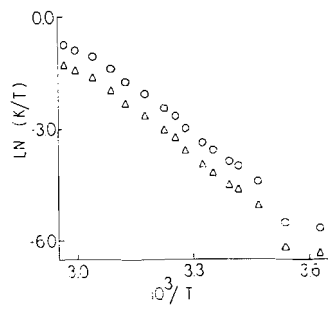

FIG. 3. Plots of ln k/T *vs.* $1/T$ for the activated rotation of the dichloromethyl groups in NCM in CH_2Cl_2 solution. The triangles refer to the process **8** → **8** and the circles to **8** → **7**. The correlation coefficients of the regression lines are both 0.995.

Can. J. Chem. Downloaded from www.nrcresearchpress.com by 210.87.254.42 on 09/05/12
For personal use only.

TABLE 4. Free energies of activation* for the internal rotation in α,α,α′,α′,α″,α″,2,4,6-nonachloromesitylene

Solvent (mol %)	T(°K)†	$\Delta G‡$ (**8** → **7**)	$\Delta G‡$ (**8** → **8**)
C_7D_8 (3.0)	304.6	15.76 ± 0.06	16.10 ± 0.06
CH_2Cl_2 (1.5)	304.6	16.09 ± 0.10	16.47 ± 0.11
CS_2 (1.5)	305.6	16.12 ± 0.12	16.62 ± 0.11
CH_2ClBr (1.5)	305.6	16.22 ± 0.13	16.52 ± 0.10
$CHCl{=}CCl_2$ (1.5)	305.6	16.12 ± 0.12	16.55 ± 0.12

*kcal/mol.
†Ambient probe temperature, being 1 °K lower for the first two solutions because the magnet housing was altered in the interval between the two sets of measurements.

set of site frequencies. These were incorporated into a second line-shape analysis of all spectra above the coalescence temperature. The new set of pre-exchange lifetimes yielded a new set of activation parameters. Their deviation from the original set of parameters was taken as the maximum error arising from inaccuracies in site frequencies. A similar procedure was followed for the toluene solution.

(ii) Effective T_2 errors

T_2 values for the four peaks were calculated from the linewidths measured at a number of low temperatures. The standard deviations gave maximum and minimum T_2 values for each site and these values were used in fitting the computed to the observed spectra in the region of exchange, again allowing an estimate of maximum error in the activation parameters arising from inaccuracies in linewidth corrections.

(iii) Errors in temperature

These are important when there exists only a small temperature range in which rate constants can be extracted from the exchange-broadened spectra. For example, the error in E_a due to an error in T is given (13) by eq. 2. Here σ^2 is a mean square error and ΔT is the temperature

$$[2] \qquad (\sigma_{E_a}/E_a)^2 = (2T^2/\Delta T^2)\,(\sigma_T/T)^2$$

range. In the present work the standard deviation of the temperature was not larger than 0.3 °K. Thus, even for the CH_2Cl_2 solution, where ΔT was only 61.3 °K, the error in E_a introduced by errors in temperature is small relative to the errors introduced by errors in the rate constants. For the toluene solution ΔT was 99.1 °K.

In Table 3 the errors in parentheses are estimates of the maximum errors arising from the three systematic error sources described here. The larger maximum errors in the activation parameters for the toluene solution reflect the larger uncertainties in the site frequencies.

(e) Free Energies of Activation, $\Delta G‡$

These were determined for all five solutions at the normal operating temperature of the magnet and are given in Table 4. The quoted errors include all sources described above but are considerably smaller than those given in Table 3 for a number of reasons. The uncertainty in the ambient temperature is minimal and the latter also happens to be very near the coalescence temperature of the spectra where the lineshape is most sensitive to changes in the rate constant but least sensitive to changes in the site frequencies and in effective T_2 values.

(6) Discussion of Activation Parameters

(a) Free Energy Profile for Rotation

The free energy profile is depicted in Fig. 4, conformation **7** being more stable than **8**. The transition states are indicated by **7′**, **8′**, and **8″**, in which one of the C—H bonds of a side-chain is rotated by π/2 radians out of the plane of the ring,[4] analogous to **2**. It proved impossible to obtain good line-shape fits unless **8′** and **8″**, the transition states for the two processes **8** → **8**, were isoenergetic to within 200 cal/mol and unless **7′**, the transition state for the process **7** → **8**, had a lower free energy than either **8′** or **8″**.

It is interesting to compare the conformations of the transition states of NCM (**8′**, **7′**, and **8″**) with the ground-state conformations **4**, **5**, **6** of MOCX and **9**, **10**, **11** of α,α,α′,α′,2,4,6-hepta-

[4]Previous calculations (14) based on rigid geometries gave the transition state as one in which the C—Cl bond of the side-chain eclipsed the ring C—Cl bond. The calculations of Mannschreck and Ernst (4) allow for bond bending and stretching and clearly give **2** as the transition state of **1**.

Can. J. Chem. Downloaded from www.nrcresearchpress.com by 210.87.254.42 on 09/05/12
For personal use only.

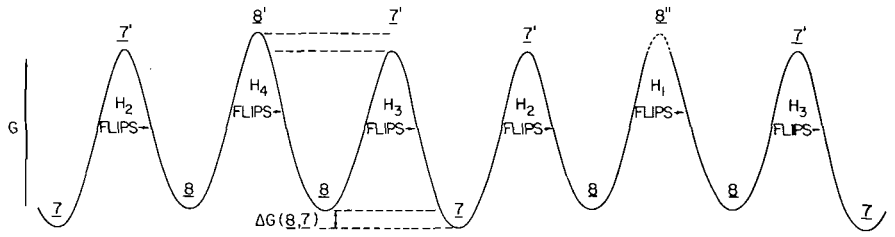

FIG. 4. A free energy profile for the rotation of the dichloromethyl groups in conformations **7** and **8** of NCM. The protons in these groups are numbered in accordance with structures **7** and **8** of the text. Note that the ground state **7** is more stable than the ground state **8** but that **8′** and **8″** are not necessarily of equal free energy; see text.

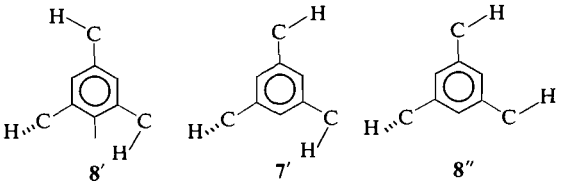

8′ **7′** **8″**

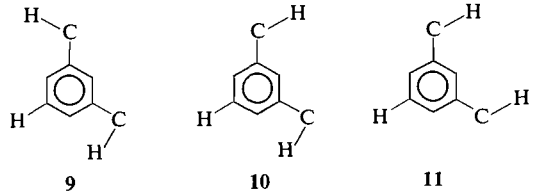

9 **10** **11**

chloro-*m*-xylene (MHCX). The similarities within the groups of structures **4**, **8′**, **9**; **5**, **7′**, **10**; and **6**, **8″**, **11** are clear. Now, it has been shown (2) that **4** and **6** are isoenergetic and of higher energy than **5** and also that **9** and **11** are less stable than **10**. By analogy it is then expected that **8′** and **8″** have approximately the same free energy, higher than that of **7′**. Such comparisons suggest that, in crowded molecules like NCM, steric interactions throughout the conformation and not only in the region of the rotating group are important in determining the energy of the transition state. It is probably coincidental that $\Delta G‡$ (**8** → **8**) − $\Delta G‡$ (**8** → **7**) equals $G_8 - G_7$ to within experimental error (Tables 2 and 4).

(b) Solvent Dependence of the Activation Parameters

$\Delta G‡$ is about 350 cal/mol lower in toluene than in the other solvents (Table 4). A speculative interpretation holds that in the ground state the rather polar C—H bond of the side-chain cannot effectively approach the π electron cloud of the toluene solvent molecules. In the transition state a C—H bond is rotated by π/2 radians out of the plane of the ring, this conformation being somewhat stablilized by a Cl_2C^-—H^+ ... π(acceptor ... donor) interaction with the solvent in a fashion analogous to the hydrogen bond occuring between chloroform and benzene (15, 16).

E_a values in the CH_2Cl_2 solution are about 1 kcal/mol higher than in the toluene solution, as are the respective $\Delta H‡$ values (Table 3). For the latter about half the difference is caused by the more negative $\Delta S‡$ values in the toluene solution, which might be anticipated on the basis of the interaction model above. However, it is a moot point whether in fact the $\Delta S‡$ are significantly different from 0 in either solution.

(c) Comparison With Other Molecules

The $\Delta G‡$ values for NCM are up to 1 kcal/mol higher than in PCT (5) or MOCX (2) for the toluene solutions. In the latter the $\Delta S‡$ values are also near zero, indicating that the higher $\Delta G‡$ values in NCM do indeed reflect the greater steric crowding expected in this molecule.

(7) Solvent Effect on Ground State Stabilities

Conformation **7** has no net dipole moment for symmetry reasons. Conformation **8** will have a net dipole moment and its stability should increase relative to that of **7** as the dielectric constant of the solvent increases (17–21). As can be seen in Table 2 this surmise is not borne out, **8** being least stable relative to **7** in CS_2. If the dipole moment of **8** is small, higher terms in the multipole interaction with the electric fields from the solvent may predominate over the dipolar term, perhaps accounting for the data in Table 2.

The greater stability of the symmetrical form **7** is probably caused by the steric crowding in the vicinity of ring carbon atom 4 in **8**, an interaction which is absent in **7**.

We are grateful to the National Research Council of Canada for financial support.

Can. J. Chem. Downloaded from www.nrcresearchpress.com by 210.87.254.42 on 09/05/12
For personal use only.

1. H. G. GYULAI, B. J. FUHR, H. M. HUTTON, and T. SCHAEFER. Can. J. Chem. **48**, 3877 (1970).
2. J. PEELING, B. W. GOODWIN, T. SCHAEFER, and C. WONG. Can. J. Chem. **49**, 1489 (1971).
3. H. M. HUTTON, J. B. ROWBOTHAM, B. H. BARBER, and T. SCHAEFER. Can. J. Chem. **49**, 2033 (1971).
4. A. MANNSCHRECK and L. ERNST. Chem. Ber. **104**, 228 (1971).
5. B. J. FUHR, B. W. GOODWIN, H. M. HUTTON, and T. SCHAEFER. Can. J. Chem. **48**, 1558 (1970).
6. J. PEELING, T. SCHAEFER, and C. M. WONG. Can. J. Chem. **48**, 2839 (1970).
7. A. A. BOTHNER-BY. J. Mol. Spectrosc. **5**, 52 (1960).
8. T. YONEMOTO. Can. J. Chem. **44**, 223 (1966).
9. P. LASZLO. Prog. Nuc. Mag. Res. Spectrosc. **3**, 231 (1967).
10. A. D. BUCKINGHAM, T. SCHAEFER, and W. G. SCHNEIDER. J. Chem. Phys. **32**, 1227 (1960).
11. H. M. MCCONNELL. J. Chem. Phys. **28**, 430 (1958).
12. G. BINSCH. Topics in Stereochem. **3**, 97 (1968).
13. A. STEIGEL, J. SAUER, D. A. KLEIN, and G. BINSCH. J. Am. Chem. Soc. **94**, 2770 (1972).
14. B. H. BARBER and T. SCHAEFER. Can. J. Chem. **49**, 789 (1971).
15. L. W. REEVES and W. G. SCHNEIDER. Can. J. Chem. **35**, 251 (1957).
16. R. L. LICHTER and J. D. ROBERTS. J. Phys. Chem. **74**, 912 (1970).
17. R. J. ABRAHAM and M. A. COOPER. J. Chem. Soc. B, 202 (1967).
18. R. J. ABRAHAM. J. Phys. Chem. **73**, 1192 (1969).
19. R. J. ABRAHAM and T. M. SIVERNS. Tetrahedron, **28**, 3015 (1972).
20. G. GOVIL and H. J. BERNSTEIN. J. Chem. Phys. **48**, 285 (1968).
21. D. A. DAWSON and W. F. REYNOLDS. Can. J. Ctem. **49**, 3438 (1971).

Can. J. Chem. Downloaded from www.nrcresearchpress.com by 210.87.254.42 on 09/05/12
For personal use only.

^{13}C Nuclear Magnetic Resonance Studies on Molecular Association. I. Self-association of Dipolar Molecules

HAZIME SAITÔ,[1] YUJI TANAKA, SACHIKO NAGATA, AND KENKICHI NUKADA[2]

Basic Research Laboratories, Toray Industries, Inc., Kamakura, Japan

Received June 26, 1972[3]

Self-association of dipolar substances is studied by ^{13}C magnetic resonance. The dilution shifts in carbon tetrachloride are analyzed in terms of the monomer–dimer equilibrium. Downfield ^{13}C shifts of the nitrile and carbonyl groups are observed for the formation of the dimer of acetone, acetonitrile, and ethyl acetate. Upfield ^{13}C shifts, on the other hand, are observed in the methyl and methylene groups of acetone, methylethyl ketone, ethyl acetate, acetonitrile, propionitrile, nitromethane, nitroethane, *N,N*-dimethylformamide, and *N,N*-dimethylacetamide. The equilibrium constants are 0.1–0.5 in units of mole fraction. The downfield ^{13}C shifts of the nitrile and carbonyl groups are interpreted in terms of electric (reaction) field effects imposed by another molecule through dimer formation. The alternation of polarity by polarization of the X–Y group explains the upfield ^{13}C shifts of methyl and methylene groups as shown in the following scheme: $H_3^+—C^-—X^+—Y^-$, where X—Y stands for C=O, C≡N, and NO_2 groups which have been classified as $-I^-$ groups by Pople and Gordon.

La libre association de substances dipolaires a été étudiée à l'aide de la résonance magnétique du ^{13}C. Les déplacements induits par les dilutions dans le tétrachlorure de carbone sont interprétés en terme d'équilibre du monomères–dimère. Les déplacements à champ faible du ^{13}C des groupes nitriles et carbonyle sont observés lors de la formation du dimère de l'acétone, de l'acétonitrile et de l'acétate d'éthyle. Les déplacements à champ fort du ^{13}C, d'autre part, sont observés pour des groupes méthyles et méthylènes de l'acétone de la cétone de méthyle et d'éthyle, de l'acétole dé'éthyle, de l'acétonitrile, du propionitrile du nitrométhane, du nitroéthane, de la *N,N*-diméthyl formamide, et de la *N,N*-diméthyl acétamide. Les constantes d'équilibre sont évaluées à 0.1–0.5 en unités de fraction molaire. Les déplacements à champ faible du ^{13}C des groupes nitriles et carbonyles sont interpretés en termes d'effets de champ électrique (réaction) imposé par un autre molécule lors de la formation du dimère. L'alternance de la polarité causée par la polarisation du groupe X—Y explique les déplacements à champ fort du ^{13}C des groupes méthyles et méthylènes. Tel qu'indiqués dans le schéma: $H_3^+—C^-—X^+—Y^-$, où X—Y représentent les liens C=O, C≡N, et des groupes NO_2 qui ont tous été classifiés comme des groupements $-I^-$ par Pople et Gordon.

[Traduit par le journal]

Can. J. Chem., **51**, 2118 (1973)

Introduction

Recently much attention has been devoted to studies of molecular association by heteronuclear magnetic resonance spectroscopy. Especially in the hydrogen bond system, X—H···Y, studies of X or Y chemical shifts by heteronuclear magnetic resonance are superior to conventional proton spectra with regard to the detection of the charge transfer and/or polarizing effects of the X—H bond. The sensitivity of the chemical-shift displacement due to a slight variation of electron distribution is significantly enhanced by a contribution of the paramagnetic current around the heteroatom under consideration. Therefore, if adequate accuracy of the chemical-shift measurement is attained, a slight variation of the electron distribution, which is unable to be observed by proton spectra, should result in appreciable movement of the chemical shift of the heteroatom. For this reason several sets of data using this method have been accumulated (1–14).

Few studies, on the other hand, have been aimed, using magnetic resonance, at the electrostatic interaction such as the dipolar association which may not be associated with electron transfer as in hydrogen bonding and the charge transfer complex. The equilibrium constant of this sort of association may be generally small owing to the smaller electrostatic energy in comparison with the former. The energy of the dipolar association should be sufficiently larger than kT to stabilize the dipolar pair. It has been suggested that this condition should be easily attained in the case of larger dipoles such as 5 D in the interdipole length ~5 Å (15).

[1]To whom inquiries should be addressed. Address until Sept. 1, 1973: Division of Biological Sciences, National Research Council of Canada, Ottawa, Canada K1A 0R6.

[2]Present address: Pioneering Research and Development Laboratories, Toray Industries, Inc., Otsu, Japan.

[3]Revision received February 27, 1973.

Can. J. Chem. Downloaded from www.nrcresearchpress.com by 210.87.254.40 on 09/05/12
For personal use only.

Can. J. Chem. Downloaded from www.nrcresearchpress.com by 210.87.254.40 on 09/05/12
For personal use only.

Dipolar association has been postulated in the studies of dimerization of nitrobenzene by ^{19}F n.m.r. (16), of dioxane, nitroaniline, and pyridinium dicyanomethylide by dipole moment (15), association between DMSO and nitriles by i.r. (17), and metalorganic compounds by p.m.r. (18). Self-association of acetone (19) and cyclopentanone (20) was also demonstrated by a study of the partition of ketones between water and carbon tetrachloride. A spectroscopic investigation is expected to offer further evidence of such a dipolar association. In this paper, we report a study of ^{13}C shifts on self-association of ketones, nitriles, nitrocompounds, amides, and related dipolar molecules by the dipole–dipole interaction.

Experimental

Measurements of ^{13}C chemical shifts were performed mainly by the ^{13}C INDOR method (21–23). A Varian HA-100 spectrometer was used with a probe doubly tuned to accept 25.15 MHz ^{13}C irradiation frequency as well as 100 MHz proton frequency used for a monitor of the ^{13}C satellite peak. An NMR Specialties HD-60B heteronuclear spin decoupler equipped with a Hewlett-Packard 200 ABR audio frequency oscillator was used to drive 25.15 MHz modulated frequency. All measurements were carried out in the frequency sweep mode with a small amount of TMS dissolved into samples to serve for the field-frequency stabilization. The irradiation power of ^{13}C nucleus was maintained as low as possible. The ^{13}C INDOR spectra, manually swept, were traced on a Varian G-14 external recorder. The accurate irradiation frequency was monitored for each of the inner two peaks of the methyl carbon quartet with a Takeda-Riken TR-3977 radio frequency counter. For this purpose, slightly increased irradiation power was provided to the frequency counter at the exact ^{13}C resonance condition. The measurements were repeated at least five times, and the means of the two inner-peak-frequencies were averaged. By this procedure absolute resonance frequencies of the carbon signal at the unchanged magnetic field which was attained by the field frequency control with TMS signal were obtained. The analyses of dilution curves of ^{13}C signals in carbon tetrachloride were performed with this frequency scale. For convenience ^{13}C chemical shifts were expressed relative to that of neat dioxane, which was determined by replacing with the sample under consideration. The accuracy of the ^{13}C chemical shifts is below $\pm$ 2Hz ($= \pm 0.08$ p.p.m.).

The INDOR method described above renders the observation of ^{13}C shifts of the carbonyl and nitrile groups impossible when they are not directly bonded to protons. In these cases ^{13}C spectra were obtained by the direct method using a frequency sweep at 25.15 MHz on a Varian XL-100-12 spectrometer. This spectrometer has three simultaneously available radio frequency channels, including ^{13}C observing channel, a lock channel (deuteron or proton frequency), and an irradiation channel. The field stabilization was performed by methyl proton or deuteron signals from solute molecules via the lock channel. The samples were contained in 8 mm o.d. tubes. A Varian C-1024 time averaging computer was used to accumulate the spectrum. Accumulation of 500 scans was necessary to observe the broader nitrile carbon which resulted from coupling to the ^{14}N in 0.3 mol fraction carbon tetrachloride solution. Correction of the magnetic field due to the displacement of the lock proton or deuteron shifts is found unnecessary: the displacement is at most 0.02 p.p.m. which is within the experimental error (± 0.08 p.p.m.).

The solvent used in these dilution studies was CCl_4 in all cases. With a view to clarifying a contribution of the reaction field effect, ^{13}C shifts of acetonitrile were examined in various solvents (10 mol %): carbon tetrachloride, dioxane, ethyl acetate, pentachloroethane, diethyl ether, tetrachloroethane, dichloroethane, acetone, nitromethane, acetonitrile, and dimethylsulfoxide. For this purpose a deuteron signal of benzene-d_6 sealed in a capillary inserted into 8 mm o.d. tube was employed for the lock signal. A small amount of cyclohexane (less than 5%) dissolved in the samples was used as a reference of ^{13}C shift.

All materials, which contained ^{13}C in natural abundance, were prepared by distillation after standing over molecular sieve.

Results

To begin with, we investigated the variation of ^{13}C shifts of acetone in carbon tetrachloride solution both by the direct and the INDOR method, as shown in Fig. 1. The upfield and downfield shifts upon increasing concentration of the solute are denoted for the methyl and carbonyl carbons, respectively. A plot of the methyl ^{13}C shift against the carbonyl shifts in Fig. 1 exhibits a linear relationship as illustrated in Fig. 2. Similar results are found for acetonitrile and ethyl acetate. On the basis of these results we postulated that it is possible to ascribe the variation of ^{13}C shifts to a certain molecular interaction. To clarify and support this postulate we analyzed the dilution curves of acetone (Fig. 1), acetonitrile, and ethyl acetate with a model of monomer-dimer equilibrium.[4] With the procedure developed by Happe (24) the equilibrium constant and association shifts Δu are obtained (Tables 1 and 2), which is defined

[4]Although some questions would be raised upon the accuracy of the equilibrium constant deduced from mole fraction units (ref. 25) used in this study and the possibility of higher aggregates, it is our objective of this paper to examine the existence of molecular association in polar molecules and to inquire about the nature of the liquid through the variation of ^{13}C shift. The assumption was made that trimers and higher polymers are not significant because of the fit realized using only monomers and dimers.

Can. J. Chem. Downloaded from www.nrcresearchpress.com by 210.87.254.40 on 09/05/12
For personal use only.

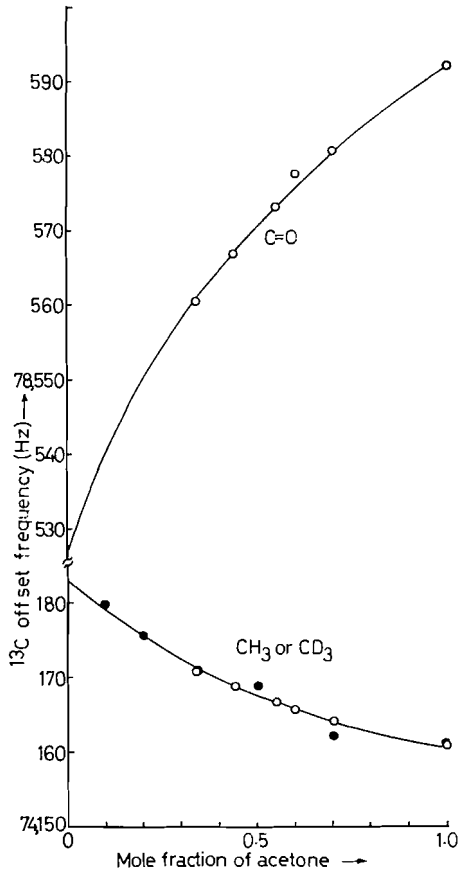

FIG. 1. Plots of the methyl and carbonyl ^{13}C shifts of acetone *vs.* the concentration in carbon tetrachloride. (○: obtained by the direct method with acetone-d_6, ●: obtained by the INDOR method.) ^{13}C shifts are expressed as the sweep-offset frequency in the deuteron lock mode by acetone-d_6. Higher frequency in the frequency sweep mode corresponds with downfield in the field sweep method. Solid lines were obtained by the equilibrium constant, which was calculated by the dilution curve of methyl ^{13}C signal, $K = 0.51$.

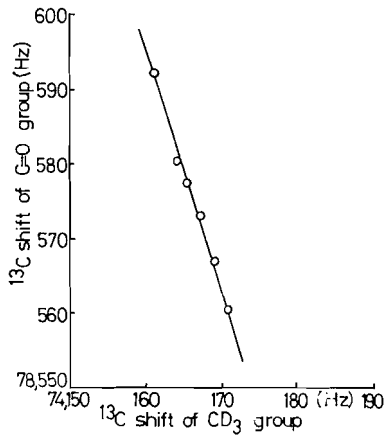

FIG. 2. Plot of ^{13}C shifts of methyl group *vs.* those of the carbonyl group.

TABLE 1. ^{13}C association shifts of dipolar compounds ($CH_3X—Y$)

	^{13}C association shift Δu^a		
	X—Y	Methyl	Proportionality constant^b f
$(CH_3)_2C=O$	−5.9	2.0	−0.34
CH_3CN	−6.9	3.6	−0.52
$CH_3COOCH_2CH_3$	−2.6	3.6	−1.4

$^a\Delta u$ = δ(dimer) − δ(mono), where δ(dimer) and δ(mono) stand for ^{13}C shifts of the dimer and monomer, respectively (in p.p.m.).
$^b\Delta\delta^{13}C(Me) = f\Delta\delta^{13}(X—Y)$, where $\delta^{13}C(Me)$ and $\delta^{13}C(X—Y)$ stand for ^{13}C shifts of methyl and X—Y groups, respectively.

as δ(dimer) − δ(mono), where δ(dimer) is the ^{13}C shift in the dimer and δ(mono) is the ^{13}C shift in the monomer at infinite dilution in carbon tetrachloride. The equilibrium constants thus obtained reproduce the experimental dilution curves.

We also examined methyl and methylene ^{13}C shifts of dipolar substances such as methylethyl ketone, propionitrile, nitromethane, nitroethane, *N*,*N*-dimethylformamide (DMF), and *N*,*N*-dimethylacetamide (DMA) when diluted in CCl_4. The equilibrium constants given in Table 2, $K = 0.1$–0.5 (mol fraction)$^{-1}$, are much smaller than those of the usual hydrogen bond system, $K > 1$. All of the methyl (methylene) ^{13}C shifts except for α methylene group of nitroethane listed in Table 2 show upfield shifts, whereas the corresponding proton signals, methyl or methylene, are displaced downfield. Plots of ^{13}C shifts of acetonitrile *vs.* $(\varepsilon - 1)/(2\varepsilon + 2.5)$ are shown in Fig. 3.

Discussion

Concerning the downfield ^{13}C shifts of the carbonyl[5] and nitrile groups, and the upfield methyl and methylene groups of dipolar molecules by molecular association, three possible explanations come to mind: (*1*) intermolecular magnetic anisotropy, (*2*) the electric (reaction) field effect, (*3*) the inductive effect owing to the

[5]The possibility of hydrogen bonding through the enol form of acetone was discounted by the fact that the enol concentration in pure acetone was reported to be about 2×10^{-4} % (ref. 26). Such a small concentration is incapable of forming intermolecular hydrogen bonds to yield such larger downfield and upfield ^{13}C shifts of the carbonyl and methyl groups, respectively.

TABLE 2. Variations of ^{13}C chemical shifts[a] (in p.p.m.) due to the dipolar associations and their equilibrium constants

		^{13}C shifts[e]				^{1}H shifts (p.p.m.)[e]	
		δ(mono)	δ_1–δ(mono)	K^f	Δu	δ_1–δ(mono)	Δu^g
Acetone		36.40	0.88	0.51	2.0	−0.02	∼−0.02
Methylethyl-ketone	CH_2[b]	20.14	0.80	0.15	3.9	−0.09	−0.39
	CH_3	37.57	0.76	0.13	4.1	−0.01	∼0
Acetonitrile		65.25	0.80	0.13	3.6	−0.06	−0.28
Propionitrile	CH_2[b]	55.71	0.76	0.24	2.7	−0.04	−0.12
	CH_3[c]	55.94	0.76	0.19	3.3	0.11	0.51
Nitromethane		4.17	0.32	0.53	0.91	−0.08	−0.21
Nitroethane	CH_2[b]	3.06	−0.48	0.51	−1.2	−0.11	−0.19
	CH_3[c]	54.35	1.23	0.50	2.9	0.07	0.16
Ethyl acetate		6.34	1.00	0.23	3.6	0.01	∼0
N,*N*-Dimethylformamide	*cis*[d]	34.47[d]	0.64	0.20	2.9	0.03	∼0.12
	trans[d]	29.50[d]	0.48	0.20	2.0	−0.01	∼0
N,*N*-Dimethylacetamide	*cis*[d]	32.05[d]	0.72	0.23	2.5	0.02	∼0.11
	trans[d]	28.87[d]	0.64	0.27	2.0	0	∼0

[a] ^{13}C shifts of methyl group adjacent to the substituent unless otherwise noted.
[b] Methylene carbon adjacent to the substituent group.
[c] β-Methyl carbon.
[d] *N*-Methyl group.
[e] δ(mono) denotes the ^{13}C or proton shifts extrapolated into infinite dilution in carbon tetrachloride solution with respect to dioxane and TMS, respectively. δ_1 stands for the shifts of neat state. Δu = δ(dimer) − δ(mono), where δ(dimer) and δ(mono) stand for ^{13}C shifts of the dimer and monomer, respectively.
[f] In units of (mol fraction)$^{-1}$, error less than 20%.
[g] Δu of the proton shifts is calculated with use of proportionality of ^{13}C shift to the proton shift.

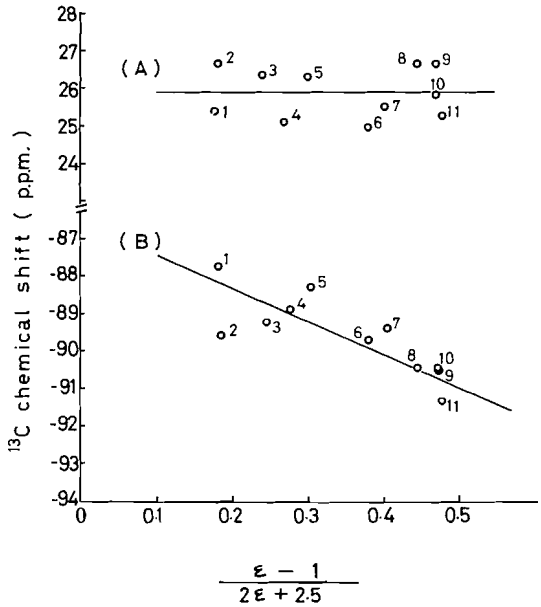

FIG. 3. Plots of ^{13}C solvent shifts of acetonitrile in 10 mol % solution in various solvents (in p.p.m. relative to cyclohexane) against $(\varepsilon - 1)/(2\varepsilon + 2.5)$. (A): Methyl group, (B): nitrile group. Solvents: (1) carbon tetrachloride, (2) dioxane, (3) ethylacetate, (4) pentachloroethane, (5) diethylether, (6) tetrachloroethane, (7) dichloroethane, (8) acetone, (9) nitromethane, (10) acetonitrile, (11) dimethylsulfoxide.

polarization of the substituent dipole, X—Y. Explanations (*1*) and (*2*) are through-space effects, while (*3*) is a through-bond effect.

The intermolecular magnetic anisotropy effect is expected to have the same magnitude of contribution both on proton and ^{13}C nuclei, because it depends primarily upon the molecular geometry. In many cases displacements of the ^{13}C shifts due to molecular association are at least ten times larger than those of proton shifts, although this ratio is only five times in the case of nitro compounds (Table 2). Therefore this is not the major contribution to the displacements of shifts, especially for ^{13}C chemical shift. ^{13}C chemical shifts have been so far explained in terms of the paramagnetic shielding effect which is related to electron density and mean excitation energy.[6] Some authors (23, 32–34) have pointed out the contribution of the electric field effect on ^{13}C chemical shifts. Becconsall *et al.* (23)

[6] It has been reported that there appears a correlation between the electron density and the ^{13}C chemical shift. This is primarily caused by a contribution of the term of the inverse cube of mean 2p electron radius in the paramagnetic current (27). It is generally said that the upfield shift of ^{13}C chemical shift arises from the increased electron density (28–31), if the mean excitation energy remains constant.

Can. J. Chem. Downloaded from www.nrcresearchpress.com by 210.87.254.40 on 09/05/12
For personal use only.

studied the variation of methyl ^{13}C shifts of methyl iodide and acetonitrile in various solvents and concluded that the use of effective dielectric constant was necessary for the application of the reaction field theory to the displacement of ^{13}C chemical shifts. Figure 3 shows ^{13}C shifts of the nitrile group of acetonitrile is approximately linearly dependent on $(\varepsilon - 1)/(2\varepsilon + 2.5)$, while that of methyl group is not. This result shows that the polarization of the nitrile group is related to the electric field effect. Because of the short-lived character of the dipolar pair, as expected from the smaller equilibrium constants, this model is not discriminated from the continuum model such as the reaction field theory. It seems likely that the dipolar field of one dipole is responsible for the polarization of another, the simplest antiparallel model being illustrated in Fig. 4. This sort of orientation was proposed by Dannhauser and Flueckinger (35) with their dielectric study of some nitriles. This explains the downfield ^{13}C shift of the carbonyl and nitrile[7] groups in terms of the electric field effect.[8]

The polarization of the substituent dipole would induce the migration of electrons into the neighbor alkyl group. Pople and Gordon (38) proposed the presence of an alternate polarization in compounds with dipolar substituents such as carbonyl, nitrile, and nitro groups ($-I^-$ group). A schematic of the alternate polarization due to the $-I^-$ group, X—Y, is shown as:

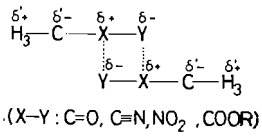

FIG. 4. Antiparallel orientation of CH_3X—Y molecule by the dipole–dipole interaction.

$$H_3{}^+—C^-—X^+—Y^- \quad (X—Y = C{=}O,\ C{\equiv}N,\ NO_2)$$

The additional polarization of the α methyl group, $H_3{}^+—C^-$, by the polarization of $X^+—Y^-$ group, which is induced by the electric field effect described above, makes the ^{13}C and proton signals of this group shift upfield and downfield, respectively.[9] This explanation is in good agreement with experimental data. Similarly the upfield ^{13}C shifts of α methylene groups except for nitroethane are interpreted in terms of the above scheme. It is not clear at present why the α methylene carbon signal of nitroethane does not obey the scheme described above. The β methyl ^{13}C shifts of the ethyl group are shown to undergo the upfield shift due to association (Table 2). This result indicates that the polarization for the ethyl group should be $H_3{}^+C^-—H_2{}^+C^-—X^+—Y^-$ instead of $H_3{}^-C^+—H_2{}^+C^-—X^+—Y^-$ proposed by Pople and Gordon (38.)

It is expected from the above scheme that the amount of the upfield methyl (methylene) ^{13}C shift is proportional to that of the X—Y ^{13}C shift: $\Delta\delta^{13}C(Me) = f\Delta\delta^{13}C(X - Y)$. This relation is shown in Fig. 2. The proportionality constant, f, is given in Table 1. The variation of ^{13}C shifts in DMA and DMF is similarly interpreted in terms of the alternation of polarity: the group of $O^- = C—N^+$ is regarded as the substituent of the $-I^-$ effect.[10,11]

[7]Recently Alei, Jr. and coworkers reported that the ^{15}N liquid association shift of $CH_3C^{15}N$ is +11.3 p.p.m. with respect to the shift in the vapor phase (36). The upfield shift of ^{15}N shift is in accordance with the expectation, $C^+{\equiv}{}^{15}N^-$.

[8]However, no correlation was found between ^{13}C shifts and the reaction field. This result indicates that contribution other than the reaction field might account for the upfield ^{13}C shift of the methyl group. An estimate of the reaction field effect on methyl ^{13}C shifts will be made as follows. According to Horsley and Sternlicht (32), the electric field effect on the ^{13}C resonance of the C—X group is expressed as: $\Delta\sigma_{C-X} = A_{C-X}E_{11}$, where E_{11} is the field component along the bond direction. A_{C-X} is related to the bond polarization, b_{11}, (37) and the bond length, R_{C-X} by the following formula: $A_{CX} = 200b_{11}/(eR_{C-X}) \times 10^{-6}$. The electric field constant $A_{C\equiv N}$ for the nitrile group is calculated to be 11.1×10^{-11}, which is four times larger than A_{CH} of C—H bond (3.0×10^{-11}) (32). If a uniform reaction field (E_{11}) is held along the direction of the C≡N bond, the component along the C—H bond will be $E_{11} \times \cos 70° = 0.34E_{11}$. Accordingly, it is easily recognized that the movement of the methyl ^{13}C shift ($\Delta\sigma_{C-H}$) by the reaction field effect is much smaller than that of nitrile group ($\Delta\sigma_{C\equiv N}$), since $\Delta\sigma_{C\equiv N}/\Delta\sigma_{C-H} \sim 11$.

[9]Similar increased polarization is expected in the case of hydrogen bond formation with protic solvents. Upfield ^{13}C shifts of the methyl group in acetone and acetonitrile are observed (39).

[10]Head-to-tail dipolar association has been proposed for *N,N*-disubstituted amides such as DMF and DMA (40–43).

[11]Momany *et al.* (44) showed by the CNDO/2 calculation of the parallel-plane dimer of *N*-methyl formamide that the more stable complex is the one with the higher degree of charge separation in the molecules of the complex. Then we might consider the electron redistribution mechanism such that a portion of the nitrogen lone pair electrons are donated to the neighboring methyl group through the pseudo π orbital in order to attain the charge separation of stabilization.

Can. J. Chem. Downloaded from www.nrcresearchpress.com by 210.87.254.40 on 09/05/12
For personal use only.

1. H. SAITÔ, K. NUKADA, H. KATO, T. YONEZAWA, and K. FUKUI. Tetrahedron Lett. 111 (1965).
2. H. SAITÔ and K. NUKADA. J. Am. Chem. Soc. **93**, 1072 (1971).
3. H. SAITÔ, Y. TANAKA, and K. NUKADA. J. Am. Chem. Soc. **93**, 1077 (1971).
4. A. LOEWENSTEIN and T. MARGALIT. J. Phys. Chem. **69**, 4152 (1965).
5. J. REUBEN and D. SAMUEL. Israel J. Chem. **1**, 229 (1963).
6. A. E. FLORIN and M. ALEI, JR. J. Chem. Phys. **47**, 4268 (1967).
7. M. ALEI, JR. and A. E. FLORIN. J. Phys. Chem. **73**, 863 (1969).
8. J. REUBEN. J. Am. Chem. Soc. **91**, 5725 (1969).
9. W. M. LITCHMAN, M. ALEI, JR., and A. E. FLORIN. J. Am. Chem. Soc. **91**, 6574 (1969).
10. L. PAOLILLO and E. D. BECKER. J. Mag. Res. **2**, 168 (1970).
11. G. E. MACIEL and R. V. JAMES. J. Phys. Chem. **68**, 437 (1964).
12. G. E. MACIEL and J. J. NATTERSTAD. J. Chem. Phys. **42**, 2752 (1965).
13. G. E. MACIEL and D. D. TRAFICANTE. J. Am. Chem. Soc. **88**, 220 (1966).
14. R. L. LICHTER and J. D. ROBERTS. J. Phys. Chem. **74**, 912 (1970).
15. C. TREINER, J. F. SKINNER, and R. M. FUOSS. J. Phys. Chem. **68**, 3406 (1964).
16. R. W. TAFT, G. B. KLIGENSMITH, and S. EHRENSON. J. Am. Chem. Soc. **87**, 3620 (1965).
17. C. D. RITCHI and A. L. PRATT. J. Am. Chem. Soc. **86**, 1571 (1964).
18. M. D. JOHNSTON, JR., F. P. GASPARRO, and I. D. KUNTZ, JR. J. Am. Chem. Soc. **91**, 5715 (1969).
19. T. F. LIN, S. D. CHRISTIAN, and H. E. AFFSPRUNG. J. Phys. Chem. **71**, 968 (1967).
20. R. L. LYNCH, S. D. CHRISTIAN, and H. E. AFFSPRUNG. J. Phys. Chem. **73**, 3273 (1969).
21. W. A. ANDERSON and R. FREEMAN. J. Chem. Phys. **37**, 85 (1962).
22. E. BAKER. J. Chem. Phys. **37**, 911 (1967).
23. J. K. BECCONSALL and P. H. HAMPSON. Mol. Phys. **10**, 21 (1965).
24. J. A. HAPPE. J. Phys. Chem. **65**, 72 (1961).
25. I. D. KUNTZ, JR., F. P. GASPARRO, M. D. JOHNSTON, JR., and R. P. TAYLOR. J. Am. Chem. Soc. **90**, 4778 (1968).
26. A. GERO. J. Org. Chem. **19**, 1960 (1954).
27. M. KARPLUS and J. A. POPLE. J. Chem. Phys. **38**, 2803 (1963).
28. P. C. LAUTERBUR. J. Am. Chem. Soc. **83**, 1838 (1961).
29. H. SPIESECKE and W. G. SCHNEIDER. Tetrahedron Lett. 468 (1961).
30. W. ADAMS, A. GRIMSON, and G. RODRIGUES. Tetrahedron, **23**, 2513 (1967).
31. F. J. WEIGERT and J. D. ROBERTS. J. Am. Chem. Soc. **90**, 3543 (1968).
32. W. H. HORSLEY and H. STERNLICHT. J. Am. Chem. Soc. **90**, 3738 (1968).
33. J. C. HAMMEL and J. A. S. SMITH. J. Chem. Soc. A, 2883 (1969).
34. A. D. BUCKINGHAM. Can. J. Chem. **38**, 300 (1960).
35. W. DANNHAUSER and A. F. FLUECKINGER. J. Phys. Chem. **68**, 1814 (1964).
36. M. ALEI, JR., A. E. FLORIN, W. M. LITCHMAN, and J. F. O'BRIEN. J. Phys. Chem. **75**, 932 (1971).
37. K. G. DENBIGH. Trans. Faraday Soc. **36**, 936 (1940).
38. J. A. POPLE and M. GORDON. J. Am. Chem. Soc. **89**, 4253 (1967).
39. H. SAITÔ, Y. TANAKA, and S. NAGATA. J. Mag. Res. To be published.
40. J. C. WOODBREY and M. T. ROGERS. J. Am. Chem. Soc. **84**, 13 (1962).
41. A. G. WHITTAKER and S. SIEGAL. J. Chem. Phys. **42**, 3320 (1965).
42. T. YONEZAWA and I. MORISHIMA. Bull. Chem. Soc. Jap. **39**, 2346 (1966).
43. M. RABINOVITZ and A. PINES. J. Am. Chem. Soc. **91**, 1585 (1969).
44. F. A. MOMANY, R. F. MCGUIRE, J. F. YAN, and H. A. SCHERAGA. J. Phys. Chem. **74**, 2424 (1970).

Can. J. Chem. Downloaded from www.nrcresearchpress.com by 210.87.254.40 on 09/05/12
For personal use only.

CNDO–MO Study of the Ozonide Ion and Related Species

JOHN M. SICHEL[1]

Centre de Recherches sur les Atomes et les Molécules, Université Laval, Québec 10, Québec

Received January 8, 1973

The unpaired electron in the ozonide ion (O_3^-) is expected to occupy an antibonding molecular orbital; yet published experimental results indicate a shorter bond length and larger force constants than in neutral ozone. Molecular orbital calculations in the CNDO approximation are reported for this ion and related species (O_3, SO_2, SO_2^-, OF_2^+, OF_2), using both the CNDO/2 and CNDO/BW parametrizations. Both methods predict that the bond lengths in O_3^- are 0.04 Å longer than in O_3, in agreement with qualitative molecular orbital theory, and that the bond angle is 1° less than in O_3. The CNDO/BW method predicts that the electron affinity of O_3 is higher than that of the O atom, in agreement with experiment, since a stabilizing exchange effect outweighs the antibonding nature of the orbital occupied by the extra electron.

Dans l'ion ozonide l'électron célibataire doit se trouver sur une orbitale moléculaire antiliante. Au contraire les résultats expérimentaux actuels indiquent des liaisons plus courtes et des constantes de force de rappel plus grandes que pour la molécule d'ozone. J'ai calculé les orbitales moléculaires pour cet ion et d'autres espèces semblables (O_3, SO_2, SO_2^-, OF_2^+, OF_2) dans l'approximation "CNDO" et avec des paramètres établis selon les méthodes "CNDO/2" et "CNDO/BW". Les deux méthodes s'accordent pour prédire que les liaisons en O_3^- sont plus longues de 0.04 Å que dans la molécule neutre en accord avec la théorie qualitative des orbitales moléculaires, et que l'angle au sommet est de 1° plus petit que dans O_3. La méthode "CNDO/BW" prédit que l'affinité électronique de O_3 est supérieure à celle de l'atome O, en accord avec l'expérience, puisqu'un effet stabilisateur d'échange a plus d'influence que l'effet antiliant de l'orbitale occupée par l'électron additionnel.

Can. J. Chem., **51**, 2124 (1973)

The ozonide ion (O_3^-) is of interest to quantum chemistry since experimental data for this species are in conflict with predictions of simple molecular orbital (MO) theory. According to the usual orbital theory for AB_2 molecules (1), an extra electron added to the ozone molecule should occupy an orbital which is A–B antibonding and B–B′ bonding. The ozonide ion should therefore have "looser bonds" than the neutral ozone molecule; one expects an increase in bond length and a decrease in stretching force constant. Also the bond dissociation energy should be lowered, or equivalently the electron affinity of O_3 should be less than that of the O atom. A detailed analysis of the relationship between orbital bonding character and the effect of orbital occupation on molecular properties has been given by Peyerimhoff *et al.* (2). This type of prediction is in fact correct in most cases, and other simple theoretical methods lead to similar predictions for the ozonide ion (3).

Published experimental evidence, however, indicates that O_3^- may be more tightly bound than expected:

(*i*) Azaroff and Corvin (4) found an O—O bond length of 1.19 Å in KO_3 by X-ray diffraction on a powder sample. This may be compared with 1.278 Å in O_3(5).

(*ii*) The i.r. spectrum of metastable NH_4O_3 recorded at low temperature by Herman and Giguère (3) showed a strong band at 800 cm^{-1}, and two much weaker ones at higher frequencies. In the light of the X-ray diffraction data these authors assigned the band at 800 cm^{-1} to the bending mode ν_2 of the O_3^- ion. (*cf.* 704 cm^{-1} for the O_3 molecule). However, this assignment must now be changed to ν_3, the antisymmetric stretching mode (*cf.* 1050 cm^{-1} in O_3), according to a recent isotope shift study of the O_3^- ion in an Ar matrix by Jacox and Milligan (6).

(*iii*) Finally, Byerly and Beaty (7) have determined an electron affinity of 2.1 ($\pm$0.1) eV for ozone by photodetachment from O_3^-, whereas the electron affinities of O and O_2 (for comparison) are 1.478 and 0.44 eV respectively (8). This corresponds to a bond dissociation energy for O_3^- of 1.7 eV (to O_2 and O^-), compared with 1.04 eV for O_3(9).

MO Calculations

In view of the conflict between the above

[1]Present address: Département de Chimie, Université de Moncton, Moncton, Nouveau Brunswick.

Can. J. Chem. Downloaded from www.nrcresearchpress.com by 210.87.254.40 on 09/05/12
For personal use only.

TABLE 1. Equilibrium bond lengths (in Å)

Molecule	No. valence electrons	CNDO/BW	CNDO/2	Experimental
O_3	18	1.258*	1.167	1.278†
O_3^-	19	1.304	1.201	1.19‡
SO_2	18	1.517*	—	1.432†
SO_2^-	19	1.579	—	—
OF_2^+	19	—	1.151	—
OF_2	20	—	1.176	1.410†

*Reference 20.
†Reference 5.
‡Reference 4.

results and simple MO theory, a quantitative MO calculation of the equilibrium geometry and electronic structure of O_3^- and several related species (O_3, SO_2, SO_2^-, OF_2^+, OF_2) was undertaken using the CNDO approximation (10).

Within the framework of the CNDO approximation, there are a number of parameters to be chosen, for which several sets of recipes have been proposed (11–17), each set defining an MO "method". In this paper I have used two methods parametrized to predict the geometries of molecules containing arbitrary first-row atoms: (*i*) the well-known "CNDO/2" method of Pople and Segal (12), and (*ii*) the "CNDO/BW" method of Boyd and Whitehead (17). The latter method combines atomic parameters from the work of Sichel and Whitehead (13), interatomic electron-repulsion integrals calculated by the formula of Ohno (18), and core-repulsion integrals and core resonance parameters calibrated (17) to fit bond energies and bond lengths of selected molecules. In fact Boyd and Whitehead published several parameter sets (17) which lead to similar values of molecular properties (19, 20). I have used their set I except where otherwise indicated.

The CNDO/BW calculations were performed using the FORTRAN program of Boyd and Whitehead, except that the Jacobi-method matrix diagonalization subroutine was replaced by a faster Householder-method subroutine (21). For open-shell molecules the SCF equations for an unrestricted single determinant were solved as in the work of Pople and Segal (12). The CNDO/2 computations were performed using a modified version of this program. All calculations were optimized with respect to both bond length and bond angle, using an iterative cubic interpolation procedure.

Results

Electronic Configurations

In all calculations the set of occupied orbitals was found to be in accord with the Walsh diagram (1), although the exact order of orbital energies varied somewhat between the two methods and (for open-shell species) between the two spins. Thus, both O_3^- and SO_2^- had the expected $^2B_1$ configurations, which are consistent with the electron spin resonance spectra (22–24).

Bond Lengths

Calculated and experimental bond lengths for the species of interest are shown in Table 1. Both MO methods agree in the prediction that $r_e(O_3^-) > r_e(O_3)$. Molecular orbital calculations should reliably predict trends in bond lengths between species differing by one electron (2). The CNDO/BW method yields an accurate value for $r_e(O_3)$ so that the value of $r_e(O_3^-)$ should be of similar accuracy. For CNDO/2, $r_e(O_3)$ is too low by 0.1 Å so that it is expected that $r_e(O_3^-)$ is similarly low, despite the fortuitous closeness to the reported X-ray value. The low value of $r_e(OF_2)$ further supports this argument. As both MO methods predict an increase of about 0.04 Å, it is suggested that the true bond length in O_3^- is about 1.32 Å, in disagreement with the value of Azaroff and Corvin (4).

Furthermore, the wavefunction for O_3^- shows no reason to expect tighter bonding than in O_3. The extra electron occupies a $2b_1$ (or π^*) antibonding orbital as expected from the Walsh rules (1), and reduces the π-bond order (between bonded O atoms) from 0.702 in O_3 to 0.353 in O_3^-. (By coincidence, these values are valid for both CNDO/BW and CNDO/2 at the appropriate equilibrium geometries.) This trend is in agreement with the matrix i.r. results of Jacox and

Can. J. Chem. Downloaded from www.nrcresearchpress.com by 210.87.254.40 on 09/05/12
For personal use only.

TABLE 2. Equilibrium bond angles (in degrees)

Molecule	No. valence electrons	CNDO/BW	CNDO/2	Experimental
O_3	18	128.4*	119.5†	116.67‡
O_3^-	19	127.3	118.6	100 §
				110 ± 5‖
SO_2	18	115.6*	—	119.5‡
SO_2^-	19	117.9	—	110 ± 5¶
OF_2^+	19	—	110.4	—
OF_2	20	—	106.8†	103.8‡

*Reference 20.
†Not equal to values in ref. 12 where the experimental bond length was assumed.
‡Reference 5.
§Reference 4. This value was supported in ref. 3 on the basis of a force constant analysis, but the analysis is vitiated by an algebraic error. If the error is corrected, a complex value of the bond angle is found for a force field of the form assumed (K. Herman, private communication).
‖Reference 6.
¶Reference 25.

Milligan (6). For SO_2^-, where the only i.r. data indicate a lower stretching force constant than in SO_2(25), there is a similar reduction of π-bond order from 0.707 in SO_2 to 0.353 in SO_2^- (CNDO/BW). Also for OF_2^+, the coefficients of the highest occupied orbital are similar to those of O_3^- and SO_2^-, and the CNDO/2 method predicts that $r_e(OF_2^+) < r_e(OF_2)$ as expected. It seems likely, therefore, that the extra electron in O_3^- does occupy an antibonding orbital in accord with the Walsh rules, and that $r_e(O_3^-) > r_e(O_3)$.

Bond Angles

Table 2 lists the calculated and experimental bond angles. Both MO methods predict only a very slight change in bond angle upon the addition of an electron to ozone. As CNDO/BW predicts (20) a more accurate bond angle for O_3 (116.7°) when parameter set III of ref. 17 is used, a calculation for O_3^- was performed using this parameter set. An equilibrium bond angle of 116.9° was found (for r_e = 1.307 Å), showing again that *differences* in predicted properties between species differing by a single electron are relatively invariant to changes in the MO method. On this basis the true bond angle for O_3^- should be close to 116°.

The small predicted decrease in angle from O_3 to O_3^- is surprising, as the Walsh diagram for AB_2 molecules (1) would suggest a larger decrease upon occupation of the $2b_1$ orbital, whose energy is supposed to decrease with decreasing bond angle due to bonding between the pπ orbitals on the terminal O atoms. However calculations for various values of the bond angle show that the decrease of the $2b_1$ orbital energy with decreasing angle is actually very small in O_3^-, since the bonding effect is almost exactly offset by the increased electrostatic repulsion between the electronic charge distributions on the terminal O atoms, when an extra electron is added to O_3.

Possible Asymmetric Geometry

The above results were obtained assuming a C_{2v} symmetry (two equal bond lengths). It is possible, however, that some excited states of SO_2 and ClO_2 may have (26–29) unequal bond lengths (C_s symmetry). After finding the C_{2v} equilibrium geometry for each molecule, therefore, the possibility of such an asymmetric geometry was examined by calculating the energy for geometries ($r_1 = r_e + \delta r$, $r_2 = r_e - \delta r$, $\theta = \theta_e$). The result is that all species are predicted to have C_{2v} symmetry except for SO_2^-, for which a double minimum was found with δr = 0.03 Å and a small potential barrier of 0.03 eV. This barrier is too small to be significant in view of the approximate nature of the calculation; and *ab initio* calculation including d orbitals (at least) should be necessary to settle the question. In any case, the matrix i.r. spectrum of SO_2^- shows that such a molecular asymmetry, if it exists, must be small (25).

Electron Affinities

Calculated electron affinities and detachment energies are shown in Table 3. The values given were obtained by subtraction of total energies for O_3 and O_3^- at the appropriate geometries, and do not correspond to orbital energies. The large

Can. J. Chem. Downloaded from www.nrcresearchpress.com by 210.87.254.40 on 09/05/12
For personal use only.

TABLE 3. Electron affinities and detachment energies (in eV)

	O_3 (CNDO/BW)	O_3 (CNDO/PS)	SO_2 (CNDO/BW)
Vertical electron affinity	3.728	0.057	2.956
Adiabatic electron affinity	3.940	0.379	3.193
Vertical detachment energy	4.167	0.700	3.404
Photo-detachment threshold (experimental)	2.1*		1.0†

*Reference 7.
†Reference 30.

difference between the two MO methods arises because the CNDO/BW method employs atomic parameters (13) calibrated to reproduce atomic valence-state ionization potentials and electron affinities separately, and the CNDO/2 method does not.

A question of some interest is why the electron affinity of O_3 is larger than that of the O atom (experimental value 1.478 eV (8)), although the additional electron occupies an (A–B) antibonding orbital. This trend is reproduced in the calculated values (for the CNDO/BW method the valence-state electron affinity of O is 2.534 eV), so that it is worthwhile examining the results for the source of the extra stabilization energy, at least in the CNDO model considered. The CNDO/BW energy of the unoccupied $2b_1$ orbital in ozone is -3.592 eV, so that most of the extra stability is correlated with this virtual orbital energy, which may be analyzed as:

$$\varepsilon_{2b_1} = -A_0 + \varepsilon_{chg} + \varepsilon_{exch} + \varepsilon_{AB} + \varepsilon_{BB'}$$
$$= (-2.534 - 0.733 - 8.854 + 7.687 + 0.841)\ \text{eV}$$

In this equation A_0 is the valence-state electron affinity of the oxygen atom, ε_{chg} is the energy associated with the term in the diagonal CNDO Hamiltonian matrix elements due to interaction with net charges, and ε_{exch} is the energy associated with the exchange terms in the same diagonal matrix elements. ε_{AB} is the term due to the off-diagonal matrix elements between π orbitals on a central and an end atom, and $\varepsilon_{BB'}$ similarly for two end atoms.

It can be seen that the positive term ε_{AB} due to antibonding between adjacent atoms is outweighed by the stabilizing "exchange" interaction which diminishes the net repulsion between electronic charge distributions of the same spin. In the CNDO approximation only the intraorbital exchange energy is considered; it remains to be seen whether a similar picture will emerge from a more refined calculation which includes the electron-interaction integrals neglected here.

Force Constants

Molecular orbital calculations can be used to predict potential energy surfaces and therefore force constants, although accurate values should not be expected from semiempirical methods which have not been explicitly calibrated to predict force constants. Calculated and experimental force constants are shown in Tables 4 and 5. A valence force field with no interaction force constants has been assumed. For an AB_2 molecule this takes the form

$$\Delta E = f_r(r - r_e)^2 + \tfrac{1}{2}f_\alpha(\alpha - \alpha_e)^2$$

For O_3 and O_3^-, both methods grossly overestimate the stretching force constant f_r. For

TABLE 4. Stretching force constants (f_r in mdyn/Å)

Molecule	CNDO/BW	CNDO/2	Experimental
O_3	19.1*	49.7	5.7†
O_3^-	15.2	42.4	2.6‡
SO_2	10.9*	—	10.0§
SO_2^-	8.7	—	6.4‖

*Reference 20.
†Reference 31.
‡Reference 6. *Cf.* also footnote § to Table 2.
§Reference 32.
‖Reference 25.

TABLE 5. Bending force constants (f_α/r_e^2 in mdyn/Å)

Molecule	CNDO/BW	CNDO/2	Experimental
O_3	0.61*	0.76	1.28†
O_3^-	0.58	1.02	— ‡
SO_2	0.46*	—	0.79§
SO_2^-	0.37	—	1.78‖

*The calculated bending force constants for AB_2 molecules in ref. 20 are too high by a factor of 2 (R. J. Boyd, private communication).
†Reference 31.
‡No reported value. *Cf.* footnote § to Table 2.
§Reference 32.
‖Reference 25.

Can. J. Chem. Downloaded from www.nrcresearchpress.com by 210.87.254.40 on 09/05/12
For personal use only.

CNDO/2 this is not surprising in view of the values calculated (33) for other molecules, especially those containing oxygen. For CNDO/BW, the computed values for other molecules (19, 20) are on the whole better, but significantly the prediction for O_3 (19) is poor.

O_3^- is predicted to have a lower f_r than O_3 as indicated by the matrix i.r. spectrum (6), but the significance of this prediction must be regarded as doubtful given the size of the error in the actual values. For SO_2 and SO_2^-, the CNDO/BW values are better and SO_2^- is correctly predicted to have the lower stretching force constant.

For the bending force constants (Table 5), both absolute values and trends are poorly predicted.

Conclusion

Molecular orbital calculations in the CNDO approximation indicate that the bond lengths in O_3^- are longer than in O_3, in agreement with simple theory and with recent i.r. data but in disagreement with the result of Azaroff and Corvin (4). The calculations succeed in predicting that the electron affinity of O_3 is higher than that of O, if parameters are used which have been calibrated to predict ionization potentials and electron affinities separately.

I wish to thank Professor Paul A. Giguère for suggesting this problem and for his continued interest and advice. I also thank his colleague, Dr. Kazimiera Herman, for many helpful discussions.

I am grateful to Prof. M. A. Whitehead and his research group for the CNDO/BW computer program, and to the National Research Council of Canada for a research grant.

1. A. D. Walsh. J. Chem. Soc. 2266 (1953).
2. S. D. Peyerimhoff, R. J. Buenker, and J. L. Whitten. J. Chem. Phys. **46**, 1707 (1967).
3. K. Herman and P. A. Giguère. Can. J. Chem. **43**, 1746 (1965).
4. L. V. Azaroff and I. Corvin. Proc. Natl. Acad. Sci. U.S. **49**, 1 (1963).
5. Tables of interatomic distances and configurations in molecules and ions. The Chemical Society, London. 1965.
6. M. E. Jacox and D. E. Milligan. Chem. Phys. Lett. **14**, 518 (1972); J. Mol. Spectrosc. **43**, 148 (1972).
7. R. Byerly and E. C. Beaty. J. Geophys. Res. **76**, 4596 (1971).
8. R. S. Berry. Chem. Rev. **69**, 533 (1969). See also J. Berkowitz, W. A. Chupka, and D. Gutman. J. Chem. Phys. **55**, 2733 (1971).
9. G. Herzberg. Electronic spectra of polyatomic molecules. Van Nostrand, Princeton, N.J. 1966.
10. J. A. Pople, D. P. Santry, and G. A. Segal. J. Chem. Phys. **43**, S129 (1965).
11. J. A. Pople and G. A. Segal. J. Chem. Phys. **43**, S136 (1965).
12. J. A. Pople and G. A. Segal. J. Chem. Phys. **44**, 3289 (1966).
13. J. M. Sichel and M. A. Whitehead. Theoret. Chim. Acta, **7**, 32 (1967); **11**, 220 (1968).
14. K. B. Wiberg. J. Am. Chem. Soc. **90**, 59 (1968).
15. J. Del Bene and H. H. Jaffe. J. Chem. Phys. **48**, 1807 (1968).
16. H. Fischer and H. Kollmar. Theoret. Chim. Acta, **13**, 213 (1969).
17. R. J. Boyd and M. A. Whitehead. J. Chem. Soc. Dalton, 73 (1972).
18. K. Ohno. Theoret. Chim. Acta, **2**, 219 (1964).
19. R. J. Boyd and M. A. Whitehead. J. Chem. Soc. Dalton, 78 (1972).
20. R. J. Boyd and M. A. Whitehead. J. Chem. Soc. Dalton, 81 (1972).
21. G. W. Stewart. Commun. Assoc. Comp. Mach. **13**, 369, 750 (1970).
22. P. W. Atkins and M. C. R. Symons. The structure of inorganic radicals. Elsevier, Amsterdam. 1967. Chapt. 7.
23. S. Schlick. J. Chem. Phys. **56**, 654 (1972).
24. A. Reuveni, Z. Luz, and B. L. Silver. J. Chem. Phys. **53**, 4619 (1970).
25. D. E. Milligan and M. E. Jacox. J. Chem. Phys. **55**, 1003 (1971).
26. R. S. Mulliken. Can. J. Chem. **36**, 19 (1958).
27. J. B. Coon and E. Ortiz. J. Mol. Spectrosc. **1**, 81 (1957).
28. I. Dubois. J. Mol. Struc. **3**, 269 (1969).
29. J. C. Brand, R. W. Redding, and A. W. Richardson. J. Mol. Spectrosc. **34**, 399 (1970).
30. D. Feldmann. Z. Naturforsch. **25***a*, 621 (1970).
31. L. Pierce. J. Chem. Phys. **24**, 139 (1956).
32. S. R. Polo and M. K. Wilson. J. Chem. Phys. **22**, 900 (1954).
33. G. A. Segal. J. Chem. Phys. **47**, 1876 (1967).

Can. J. Chem. Downloaded from www.nrcresearchpress.com by 210.87.254.40 on 09/05/12
For personal use only.

Thermodynamic and Transport Properties of Sodium Benzoate and Hydroxy Benzoates in Water at 25 °C

JACQUES E. DESNOYERS, ROBERT PAGÉ, GÉRALD PERRON, JEAN-LUC FORTIER, PAUL-ANDRÉ LEDUC AND ROBERT F. PLATFORD

Département de chimie, Université de Sherbrooke, Sherbrooke, P.Q. and Canada Centre for Inland Waters, Burlington, Ontario

Received December 27, 1972

The densities, heat capacities, heats of dilution, osmotic coefficients, viscosities, and conductivities of sodium benzoate and the ortho, meta, and para isomers of sodium hydroxybenzoate have been measured in water at 25 °C. The densities and heat capacities of phenol solutions and the osmotic coefficients of aqueous potassium benzoate have also been determined. The addition of an —OH or a —COONa group on a benzene ring has little effect on the properties related to the effective size of the solute (apparent molal volume, B_η viscosity coefficient, and ionic conductivity) but decreases significantly the apparent molal heat capacity. The addition of an —OH group in the meta or para position of sodium benzoate has a similar effect. The large negative contribution to the heat capacity probably reflects the solute–solvent hydrogen bonding. The ortho isomer, which can form an internal hydrogen bond, has a significantly different behavior from that of the other isomers.

The excess properties show no evidence of association at low concentrations although some specific interaction is apparent for the ortho isomer at high concentration. There seems to be some cation–anion structural attraction with the meta and para isomers which again may be related to the hydrogen-bonding ability of these solutes. Sodium and potassium benzoates show signs of association above 1 *m*.

Les densités, capacités calorifiques, chaleurs de dilution, coefficients osmotiques, viscosités, et conductivités du benzoate de sodium et des isomères ortho, méta, et para des hydroxybenzoates de sodium ont été mesurés dans l'eau à 25 °C. Les densités et capacités calorifiques des solutions de phénol et les coefficients osmotiques des solutions de benzoate de sodium ont aussi été déterminées. L'addition de groupements —OH ou —COONa sur un noyau de benzène a peu d'effet sur les propriétés reliées à la dimension effective du soluté (volume apparent molaire, coefficient B_η de viscosité, conductivité ionique) mais décroît de façon appréciable les capacités calorifiques apparentes molaires. L'addition d'un groupement —OH en position méta ou para sur le benzoate de sodium a un effet semblable. La grande contribution négative de ces groupements à la capacité calorifique reflète probablement les effets de liaison hydrogène entre le soluté et le solvant. L'isomère ortho, qui peut former une liaison hydrogène interne, se comporte différemment des autres isomères.

Les propriétés d'excès ne démontrent aucune évidence d'association aux faibles concentrations, même s'il semble y avoir des interactions spécifiques pour l'isomère ortho aux plus fortes concentrations. Il semble y avoir des attractions structurales cation–anion avec les isomères méta et para, interactions qui sont probablement reliées aux possibilités de liaisons hydrogène avec le solvant. Les benzoates de sodium et de potassium semblent s'associer aux concentrations supérieures à 1 *m*.

Can. J. Chem., **51**, 2129 (1973)

Introduction

Systematic studies of aqueous solutions have usually been limited to model electrolyte systems such as alkali halides (1), tetraalkylammonium halides (2), *n*-alkylamine hydrobromides (3–6), or nonelectrolyte systems such as aliphatic alcohols (7), and cyclic ethers (8). Compared to aliphatic solutes the properties of aromatic solutes seem much harder to understand; ions such as tetraphenyl phosphonium, arsonium, and boride appear as either overall structure breakers or makers depending on the property examined (9, 10) and, despite their large size, bolaform dipyridinium salts are often strong structure breakers (11). In addition to the presence of π electrons, the rigidity of the aromatic rings may also influence the behavior of aqueous aromatic solutes. Despite these anticipated difficulties, the importance of their biochemical properties justifies further investigation of their aqueous solutions.

In a continuing study of the hydration of aromatic ions, it was felt useful to examine the three geometrical isomers of monosodium hydroxybenzoates and compare them with sodium benzoate. The addition of a terminal hydroxy group on an aliphatic chain has in general little effect on the solute partial molal volume (12).

Can. J. Chem. Downloaded from www.nrcresearchpress.com by 210.87.254.105 on 09/05/12
For personal use only.

Can. J. Chem. Downloaded from www.nrcresearchpress.com by 210.87.254.105 on 09/05/12
For personal use only.

This series could therefore be a good starting point to study substituent effects and internal hydrogen bonding on solute–solvent and solute–solute interactions. For example, Stein and Tomkiewicz (13) suggested from an n.m.r. study that sodium orthohydroxybenzoate associates in water through π electron interaction while the other two isomers are unassociated.

Relatively few properties of these solutes have been examined in water. Besides a few spectral (14, 15) and solubility (16) measurements most of the studies have been concerned with the ionization and reactivity of the acids. In view of the complexity of the possible solute–solvent and solute–solute interactions it was felt that most of the thermodynamic and transport properties should be determined in water, *i.e.*, densities, heat capacities, ionic conductivities, viscosities, and excess free energies, enthalpies, and entropies. The densities and heat capacities of phenol and the osmotic coefficients of potassium benzoate solutions were also determined to help in the interpretation.

This family of compounds has important biochemical interests; sodium benzoate is a food preservative and salicylic acid has well-known analgesic properties. It is our hope that systematic studies with such solutes will eventually help in understanding their biochemical activity and specificity.

Experimental

The salts used in this study will be abbreviated by: BzNa (sodium benzoate), *o*-HyBzNa, *m*-HyBzNa, and *p*-HyBzNa for the three isomers of sodium hydroxy benzoates. The *o*-HyBzNa (Fisher Scientific) was purified by dissolution in cold absolute ethanol and precipitation with diethyl ether. The other salts were prepared by neutralizing the corresponding acids (Eastman Kodak) with NaOH in methanol. From the p*H* of the aqueous solutions it was ascertained that only the —COOH proton was neutralized.

The acids were purified prior to neutralization by treating the methanol solutions with alumina until all coloration disappeared. The neutralized salts were purified in the same way as *o*-HyBzNa. All these salts showed signs of decomposition when heated or exposed to light when wet. Heating of the solutions was therefore avoided and the salts were dried under vacuum.

All solutions were prepared by weight with water redistilled from an alkaline permanganate solution. The molalities were converted to molarities whenever necessary using the measured densities. All measurements were made on fresh solutions to avoid any decomposition upon standing. In the concentration ranges studied hydrolysis of the weak acid salts caused negligible errors. The temperature was kept at 25 °C and regulated to ±0.002 °C throughout.

The techniques used for density (3), viscosity (4), conductivity (4), heat capacity (17), heat of dilution (18), and isopiestic (19) measurements have all been described elsewhere. The precision of the derived data has also been discussed therein.

Results

The equivalent conductivities Λ were analyzed with the Fuoss–Onsager equation (20),

$$[1]\quad \Lambda = \Lambda_0 - A_\Lambda c^{1/2} + E_\Lambda c \log c + J_\Lambda c$$

where A_Λ and E_Λ are known parameters which can be calculated from the standard conductivities Λ_0 and the properties of the solvent and J_Λ is an adjustable parameter related to solute–solute interaction and to the distance of closest approach a_Λ. The relative viscosities η_r were treated with an extended form (4) of the Jones and Dole equation,

$$[2]\quad \eta_r = \eta/\eta_0 = 1 + A_\eta c^{1/2} + B_\eta c + C_\eta c^2$$

where A_η can be calculated from Λ_0 using Falkenhagen's equation (21), the B_η viscosity parameter depends on the size and hydration of the solute and C_η is an empirical parameter. The apparent molal volumes, heat capacities, and relative enthalpies are given as a function of molarities or molalities by

$$[3]\quad \phi_v = \phi_v^0 + A_v c^{1/2} + B_v c$$

$$[4]\quad \phi_c = \phi_c^0 + A_c c^{1/2} + B_c c$$

$$[5]\quad \phi_L = A_L m^{1/2} + B_L m + C_L m^{3/2} + D_L m^2 + E_L m^{5/2}$$

where the parameters of the limiting Debye–Hückel theory are respectively $A_v = 1.868$, $A_c = 28.99$, and $A_L = 1975$ for 1:1 electrolytes in water at 25 °C (the units of ϕ_v, ϕ_c, and ϕ_L are respectively $cm^3\ mol^{-1}$, $J\ K^{-1}\ mol^{-1}$, and $J\ mol^{-1}$). All higher coefficients measure the deviation from the Debye–Hückel theory for solute–solute interactions.

The osmotic and activity coefficients, φ and γ are obtained in the usual way from isopiestic data (22),

$$[6]\quad \phi = 1 - \frac{2.303A\gamma}{A^3 I} \times \left\{1 + AI^{1/2} - 2\ln(1 + AI^{1/2}) - \frac{1}{1 + AI^{1/2}}\right\} + BI + CI^2 + DI^3 + EI^4$$

Can. J. Chem. Downloaded from www.nrcresearchpress.com by 210.87.254.105 on 09/05/12
For personal use only.

and

$$[7] \quad \ln \gamma = \frac{-2.303A\gamma I^{1/2}}{1 + AI^{1/2}} + 2BI + \frac{3}{2}CI^2 + \frac{4}{3}DI^3 + \frac{5}{4}EI^4$$

where $A\gamma$ is the limiting Debye–Hückel slope, 0.5085 and I is the ionic strength given by $\frac{1}{2}\sum Z_i^2 m_i$. Again all other parameters are adjustable and reflect ion–ion interactions.

Equations 1 to 7 were used to fit all the data, at least at low concentrations. With phenol, the same equations were used for ϕ_v and ϕ_c except for the $c^{1/2}$ term which was removed since phenol behaves like a nonelectrolyte. The viscosities and conductivities are plotted in Fig. 1, the apparent molal volumes and heat capacities in Fig. 2 and the activity coefficients in Fig. 3. The parameters of eq. 1 to 5 are summarized in Table 1 and those of eq. 6 and 7 in Table 2. The actual experimental data are available elsewhere.[1]

Discussion

Solute–solvent interactions should be discussed in terms of the functions ϕ_v^0, ϕ_c^0, B_η, and

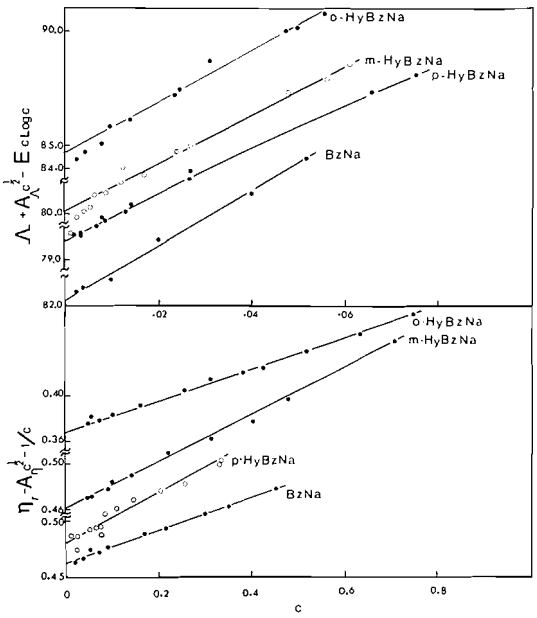

FIG. 1. Viscosities and conductivities of sodium benzoate and hydroxybenzoates in water at 25 °C.

[1]Complete set of the actual experimental data is available, at a nominal charge, from the Depository of Unpublished Data, National Science Library, National Research Council of Canada, Ottawa, Canada K1A OS2.

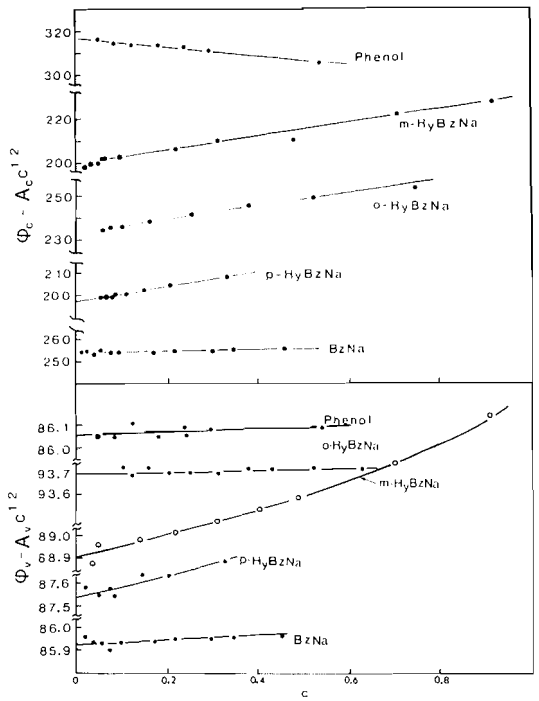

FIG. 2. Apparent molal volumes and heat capacities of phenol, sodium benzoate, and sodium hydroxybenzoates in water at 25 °C.

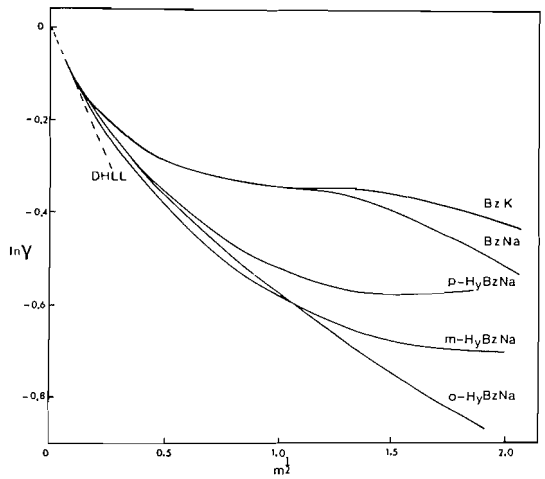

FIG. 3. Activity coefficients of potassium and sodium benzoate and sodium hydroxybenzoates in water at 25 °C.

Λ_0 since they are independent of solute–solute interactions. With the present solutes the interactions are not simple, and we can at best predict their signs. Adding an —OH or —COONa group will increase the degrees of freedom and size of the solute; as such the intrinsic contribution should increase ϕ_v^0, B_η, and ϕ_c^0 and de-

TABLE 1. Transport and thermodynamic properties in water at 25 °C: parameters of eqs. 1 to 5

Parameter	Value				
	BzNa	*o*-HyBzNa	*m*-HyBzNa	*p*-HyBzNa	Phenol
ϕ_v^0 (cm^3 mol^{-1})	85.92	93.70	88.90	87.54	86.06
B_v	0.13	0.02	0.55	0.48	0.06
ϕ_c^0 (JK^{-1} mol^{-1})	253.0	234.5	200.4	197.2	315.8
B_c	5	26	30	34	−13
A_η	0.00919	0.00912	0.00968	0.00958	
B_η (l mol^{-1})	0.463	0.368	0.461	0.480	
C_η	0.144	0.138	0.205	0.222	
Λ_0 (Mho cm^2 eq^{-1})	82.26	84.69	80.10	79.77	
a^* (Å)	2.92	2.61	2.42	2.58	
J_Λ	123	112	100	107	
B_L	−944.0	−4696.5	−3093.3	−1651.8	
C_L	513.4	1905.8	850.9	−6278.5	
D_L				11,654	
E_L				−6509	

*a is the distance of closest approach.

TABLE 2. Osmotic and activity coefficients in water at 25 °C: parameters of eq. 6 and 7

Compound	A	B	C	D	E	m	Data points
BzNa	1.76769	0.05885	−0.022136	−0.0016123	0.0006140	0.1–5.0	20
BzK	1.98009	0.02974	0.003927	−0.0072644	0.0010505	0.1–4.6	20
o-HyBzNa	1.51459	−0.05869	0.006476			0.1–7.6	18
m-HyBzNa	0.99384	−0.00041	0.003398			0.1–6.4	17
p-HyBzNa	1.45797	−0.03964	0.024434	−0.0025659		0.1–3.2	11

crease Λ_0. Any strong coulombic hydration (charge–dipole type) should influence the —COONa group but not —OH; this should be reflected mostly in a decrease in ϕ_v^0 and Λ_0 and increase in B_η. Coulombic hydration probably decreases ϕ_c^0 to some extent, but this effect seems to be small compared with other types of interactions such as the structural ones.

Changes in structural interactions (1) can have a significant influence on the properties of these solutes. The structure-breaking effect will decrease ϕ_c^0, ϕ_v^0, and B_η and increase Λ_0. The structure-making (hydrophobic) interactions will have the opposite effect on ϕ_c^0, B_η, and Λ_0 but have little influence on ϕ_v^0 (there is a compensation between the cavity effect and increase in ice-likeness near hydrophobic solutes (2, 3)).

With the present solutes extra interactions may also arise from inter and intra molecular hydrogen bonding, from the π electrons, from the rigidity of the molecules and from mesomeric and inductive effects. The complexity of all these interactions is such that we cannot hope to find a unique interpretation for all the properties. Still, through a careful examination of the data, we do hope to be able to show the relative importance of the different interactions.

Hydration of —OH and —COONa Groups

The effect of adding an —OH and a —COONa group on the benzene ring is illustrated in Fig. 4 where the changes in ϕ_v^0 and ϕ_c^0 are compared for benzene, phenol, BzNa, and *p*-HyBzNa in water at 25 °C. The volume and heat capacity data for benzene are taken from the literature (9).

The effective sizes of the —OH and —COONa group are small in water as evidenced from the small value of $\Delta\phi_v^0$ corresponding to the addition of one of these groups. The addition of a second group has an even smaller effect on ϕ_v^0. The same is also true for the changes in B_η and Λ_0 when *p*-HyBzNa is compared with BzNa; these differences are $\Delta B_\eta = 0.02$ l mol^{-1} and $\Delta\Lambda_0 = -2.5$ conductance units. The effect on

Can. J. Chem. Downloaded from www.nrcresearchpress.com by 210.87.254.105 on 09/05/12
For personal use only.

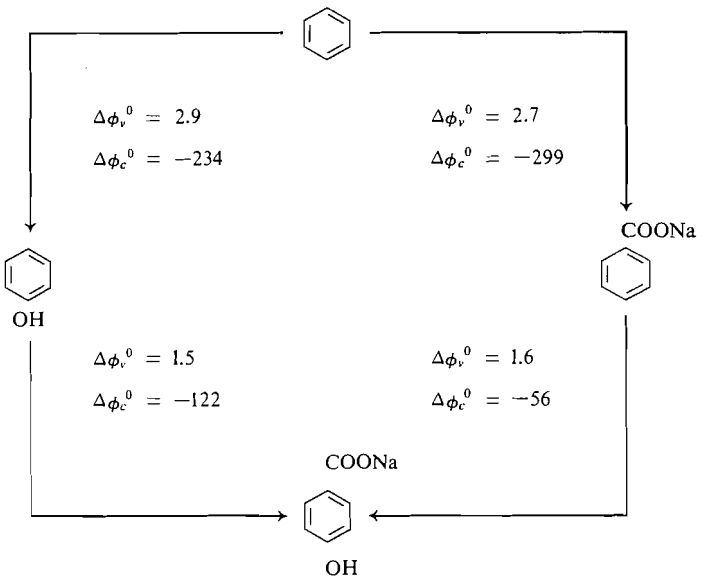

FIG. 4. Effect of the addition of an —OH and a —COONa group on ϕ_c^0 and ϕ_v^0 of benzene.

ϕ_v^0 of adding an ionic $-COO^-$ group would be larger (if ϕ_v^0 of Na^+ is taken as -7 cm^3 mol^{-1} (1), $\Delta\phi_v^0 = 10$ cm^3 mol^{-1}) but still less than the intrinsic contribution expected from the group molecular weight. The small overall contribution of the —OH group is not limited to aromatic compounds; for example ϕ_v^0 of $(C_2H_4OH)_4NBr$ (177 cm^3 mol^{-1}) (12) is about the same as that of Et_4NBr (174 cm^3 mol^{-1}) at 25 °C.

It is tempting to attribute the small effective size of these groups to hydrogen bonding with water, but a comparison of ϕ_v^0 of most aliphatic alcohols in *n*-heptane (23) shows that they are within 1 cm^3 mol^{-1} of the molar volume of the corresponding alkane. Therefore even in nonpolar solvents the effective size of the —OH group is negligible. The exact reason for this is not clear at the moment but it has something to do with the solute molecule itself rather than with structural interactions with the solvent.

The changes in ϕ_c^0 when the groups —OH and —COONa are added to the benzene ring are large and negative while the intrinsic contribution would be expected to be positive. Again this observation is general since ϕ_c^0 of ethanol is 70 J K^{-1} mol^{-1} smaller than that of ethane in water (24).

The interpretation of the heat capacity contribution of the —OH group is easier if it is compared with the corresponding enthalpy. Krishnan and Friedman (25) have shown that the difference between the enthalpy of hydration of the —OH group and that of the terminal —H of the corresponding alkane is constant for most normal alcohols and alkanes and is given at 25 °C by

$$[8]\quad \Delta H^{g\rightarrow w}(OH) = \Delta H_h^0(ROH) - \Delta H_h^0(RH) \simeq -35 \text{ kJ mol}^{-1}$$

Corresponding to this function we may define the heat capacity of hydration related to the replacement of an —H atom by an —OH group,

$$[9]\quad \Delta C_p^{g\rightarrow w}(OH) = \phi_c^0(ROH) - \phi_c^0(RH) - C_p^g(ROH) + C_p^g(RH) \simeq -90 \text{ J K}^{-1} \text{ mol}^{-1}$$

at 25 °C. The data for the heat capacity of the solutes in water (24) and in the gas phase (26) are taken from the literature.

It is surprising that the enthalpy and heat capacity of hydration of the —OH group have the same sign. Since the strength of an interaction usually decreases with temperature, the signs of the corresponding ΔH and ΔC_p are normally opposite. It is therefore probable that $\Delta H^{g\rightarrow w}(OH)$ and $\Delta C_p^{g\rightarrow w}(OH)$ are reflecting different interactions.

The possible components of enthalpies of hydration are given, following Krishnan and Friedman (25), by

Can. J. Chem. Downloaded from www.nrcresearchpress.com by 210.87.254.105 on 09/05/12
For personal use only.

Can. J. Chem. Downloaded from www.nrcresearchpress.com by 210.87.254.105 on 09/05/12
For personal use only.

$$[10]\quad \Delta H^{g\rightarrow w}(OH) = \Delta H(CAV) + \Delta H(VDW) + \Delta H(HB) + \Delta H(STR)$$

where ΔH(CAV) is the enthalpy associated with the process of making a cavity in the solvent to accommodate the solute, ΔH(VDW) with van der Waals and polarization interactions, ΔH(HB) with solute–solvent hydrogen bonding and ΔH(STR) with structural interactions. A corresponding equation may again be written for the heat capacities,

$$[11]\quad \Delta C_p^{g\rightarrow w}(OH) = \Delta C_p(CAV) + \Delta C_p(VDW) + \Delta C_p(HB) + \Delta C_p(STR)$$

The separation of $\Delta H^{g\rightarrow w}$(OH) and $\Delta C_p^{g\rightarrow w}$(OH) into different contributions is somewhat artificial. For example, a good part of hydrophobic hydration can be considered as the work of forming a cavity in water (27). By analogy with the air–water interface there is an increase in the structure of water around the cavity since the —OH group of a water molecule prefers to be hydrogen bonded to another water molecule rather than dangle freely in the cavity. In eqs. 10 and 11 the terms ΔH(CAV) and ΔC_p(CAV) refer to the formation of a cavity in an ideal non-hydrogen-bonded liquid and any accompanying change in hydrogen bonding is considered part of ΔH(STR) and ΔC_p(STR).

These contributions cannot really be determined separately. Still some idea of their relative importance may be obtained indirectly from the properties of non-aqueous solvents and pure liquids. The difference in the enthalpy of transfer, corresponding to the replacement of an —H by an —OH group, from the gas phase to propylene carbonate is $\Delta H^{g\rightarrow PC}(OH) = -21$ kJ mol^{-1} and to dimethylsulfoxide $\Delta H^{g\rightarrow DMS}(OH) = -37$ kJ mol^{-1} (25). With these aprotic solvents, ΔH(HB) and ΔH(STR) are absent. Since these enthalpies of transfer are of the same order of magnitude as those in water, it seems that a good part of $\Delta H^{g\rightarrow w}$(OH) is probably due to the terms H(CAV) + H(VDW) and, as in the case of volumes, have little to do with the particular nature of water. Therefore most of this enthalpy comes from the change in standard state and polarization effects and not from the interactions involving hydrogen-bonding of the solvent.

With $\Delta C_p^{g\rightarrow w}$(OH), the sign of the contributions ΔC_p(CAV) + ΔC_p(VDW) can also be estimated from the properties of pure liquids. Most heat capacities of liquids are larger than those of the corresponding gases. The overall contribution of the two terms ΔC_p(CAV) + ΔC_p(VDW) should therefore be positive. The negative $\Delta C_p^{g\rightarrow w}$(OH) must consequently come from the terms ΔC_p(HB) and ΔC_p(STR).

The interaction between an —OH group and water must be weak since it has little effect on ϕ_v^0, B_η, Λ_0, and enthalpies. On the other hand it must be very temperature dependent to explain the large change in ϕ_c^0. This weak interaction most probably has something to do with the intermolecular hydrogen bond ROH---H_2O. All systems involving hydrogen bonds have abnormally negative ϕ_c^0 (ϕ_c^0 of H_{aq}^+ is much more negative than Li_{aq}^+ (28)) or positive excess heat capacities (this is the case for example of the tetrabutylammonium carboxylates (29)). The ROH---H_2O interaction probably has a negative enthalpy contribution, and it is not unreasonable to assume that this weak interaction strengthens with respect to the H_2O---H_2O interaction as the temperature increases, thus accounting for the negative ϕ_c^0 contribution. In other words temperature weakens the H_2O---H_2O hydrogen bond more than the ROH---H_2O bond, which is not unreasonable considering the difference in the spatial arrangement of these hydrogen-bonded systems.

Comparison of the Ortho, Meta, and Para Isomers

The parameters ϕ_v^0, ϕ_c^0, B_η, and Λ_0 are compared in Fig. 5 for the three geometrical isomers and BzNa. The behavior of Λ_0 is, at least qualitatively, the mirror image of B_η. Since B_η is proportional, and Λ_0 inversely proportional, to the effective size of the moving particle, it seems that both parameters are measuring the same effect; *o*-HyBzNa moves more readily in the solution than either NaBz or the other isomers. On the other hand, ϕ_v^0 of *o*-HyBzNa is significantly larger than that of the other solutes. The presence of an internal hydrogen bond with *o*-HyBzNa will have two main consequences; the free rotation of the —COO^- group will be hindered and the hydrogen bonding with the solvent will be decreased. The decrease in interactions may well explain the higher mobility. Also the increase rigidity will hinder the adaptation to the structure of the liquid and the solute may well occupy more space. Further studies on substituted aromatic solutes in water involving no intramolecular hydrogen bonds and studies

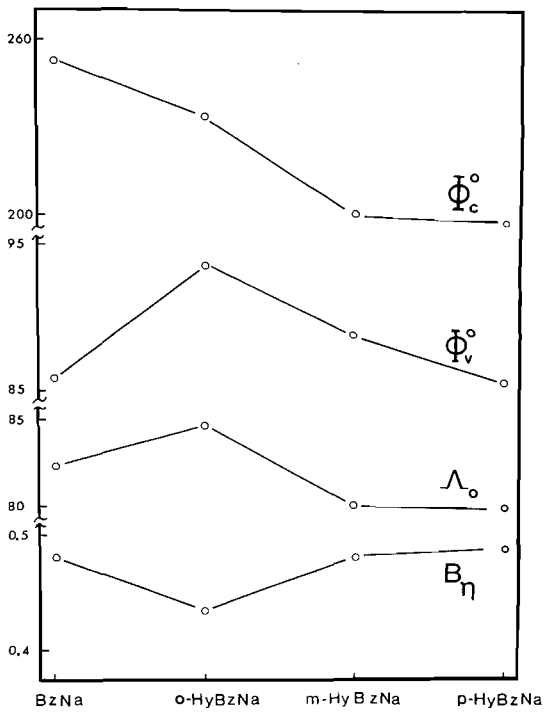

FIG. 5. Standard thermodynamic and transport properties of sodium benzoate and hydroxybenzoate in water at 25 °C.

in non-aqueous solvents would be necessary to confirm these explanations.

The ϕ_c^0 of *o*-HyBzNa is on the other hand more difficult to account for. With many systems ϕ_c^0 and ϕ_v^0 behave similarly. In this respect the higher value of ϕ_c^0 of *o*-HyBzNa is consistent with ϕ_v^0. The internal hydrogen-bonding and reduction in inter-molecular hydrogen bonding would support an increase in ϕ_c^0 when compared with *p*-HyBzNa. On the other hand we would expect it to be even larger than BzNa which is contrary to the experimental observation. It therefore seems that whatever the origin of the interactions with the solvent which causes a decrease in ϕ_c^0 when an —OH group is added to a molecule, it is not fully cancelled by the internal hydrogen bonding.

Except possibly for ϕ_v^0, the difference between the behavior of *m*-HyBzNa and *p*-HyBzNa is small. The observed differences could be related to geometrical factors (the para —OH group may fit slightly better in the structure of water) or inductive effects (larger for para). On the other hand resonance structures cannot readily be written for these solutes in the ionized form, which excludes probably any significant contribution from the mesomeric effect.

Solute–Solute Interactions

The molar excess thermodynamic functions (30) are defined by

$$[12] \qquad G^{EX} = \nu RT(1 - \phi + \ln\gamma)$$

$$[13] \qquad H^{EX} = \phi_L$$

$$[14] \qquad S^{EX} = (H^{EX} - G^{EX})/T$$

where ν, the number of ions formed during the dissociation, is 2 for 1:1 electrolytes.

These functions are plotted in Fig. 6 and compared with the corresponding Debye–Hückel limiting law (DHLL) for BzNa, *o*-HyBzNa, *m*-HyBzNa, and *p*-HyBzNa.

There is more solute–solute attraction with the hydroxybenzoates than with NaBz as evidenced from the more negative G^{EX}. On the other hand, there is no evidence for ion association at low concentrations; the ionic conductance and G^{EX} are all regular. On the other hand, at high concentrations, there are signs of specific ion–ion interactions with *o*-HyBzNa as seen from the cross-over of $\ln\gamma$ when compared with the other hydroxybenzoates (Fig. 3). It is doubtful however if these interactions are as large as

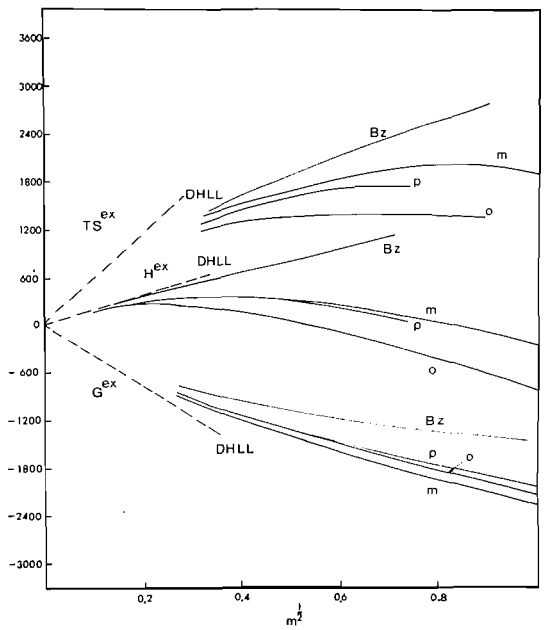

FIG. 6. Excess thermodynamic functions of sodium benzoate and hydroxybenzoates in water at 25 °C.

Can. J. Chem. Downloaded from www.nrcresearchpress.com by 210.87.254.105 on 09/05/12
For personal use only.

Can. J. Chem. Downloaded from www.nrcresearchpress.com by 210.87.254.105 on 09/05/12
For personal use only.

was suggested by Stein and Tomkiewicz (13). As with the properties related to solute–solvent interactions, *m*-HyBzNa and *p*-HyBzNa behave similarly with all the excess properties. At low concentrations ($m < 0.5$), BzNa follows very closely the DHLL with H^{EX} and S^{EX}; but the hydroxybenzoates show negative deviations from the DHLL suggesting some cation–anion structural interactions (31).

The activity data of BzNa (Fig. 3) show a peculiar behavior at high concentrations; the activity coefficient goes through a plateau near 1 *m* above which the activity coefficient shows a steady decrease. The activity of BzK was also measured in order to verify the generality of this effect and the plateau is again present, suggesting some association above these concentrations. Even though there was no evidence of strong hydrophobic character at low concentrations there may be some association similar to micelle formation at these high concentrations.

Information on solute–solute interactions can also be obtained from the parameters, B_v, B_c, J_Λ, and a_Λ of Table 1 which represent the deviations from the DHLL on the corresponding excess functions. These parameters are compared in Fig. 7 for the four sodium salts and phenol. Again BzNa shows no sign of important structural interactions at low concentrations, *m*-HyBzNa and *p*-HyBzNa show some attraction probably of structural origin; hydrophilic–hydrophilic structural attraction (cation-anion) would be reflected in a positive B_c and B_v, a smaller J_Λ and larger a_Λ (31, 32). It should be noted however that the B_v and B_c of *m*-HyBzNa and *p*-HyBzNa are abnormally large and are comparable to those for NaF: $B_v = 0.64$ (31), $B_c = 26$ (28). This again could be related to the particular behavior of hydrogen-bonding solutes (29). The excess properties of *o*-HyBzNa are anomalous since with heat capacities *o*-HyBzNa behaves like the other HyBzNa, with volumes like BzNa and with conductance between BzNa and the other HyBzNa. No simple explanation can at present be offered for these trends.

Finally we could note that the concentration dependence parameters B_v and B_c of phenol in water are comparable with those of BzNa. It therefore seems that, once corrected for the DHLL, the excess properties of BzNa are similar to those of phenol suggesting that the solute–solute interactions involving the —OH group are similar to those of —COONa.

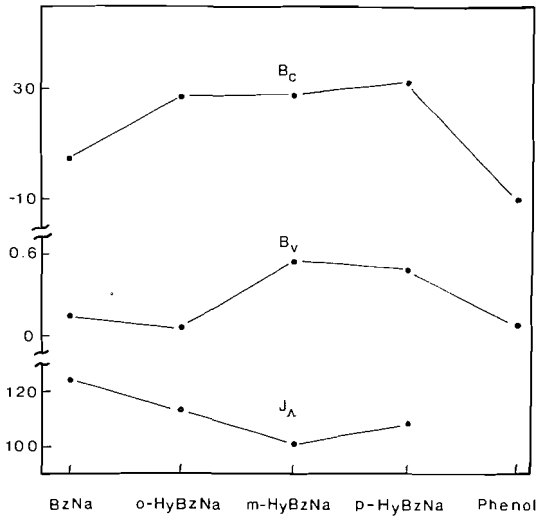

FIG. 7. Comparison of the parameters B_c, B_V, and J_Λ for phenol, sodium benzoate, and hydroxybenzoates in water at 25 °C.

Conclusion

A comparison of the thermodynamic and transport properties of BzNa, HyBzNa, and phenol show that (1) The addition of an —OH or —COONa group on a benzene ring has little effect on properties related to the effective size of the solute in water but decreases significantly the heat capacity. (2) The properties of *m*-HyBzNa and *p*-HyBzNa are similar with all standard and excess properties but those of *o*-HyBzNa are significantly different. (3) All excess properties are normal at low concentrations but do indicate some specific interactions at higher concentrations.

The interpretation of the thermodynamic and transport properties of the substituted benzoates is not simple and most of the explanations offered in terms of solute–solvent and solute–solute interactions are at present speculative. The present study emphasizes the importance of examining many complimentary properties when information on the solvation of complex molecules is sought; otherwise quite erroneous conclusions could easily be drawn. We do hope that the trends observed and the deductions made will be useful in guiding further studies towards a final elucidation of the important interactions between hydrogen-bonding solutes and water.

The authors acknowledge Environment Canada and The National Research Council of Canada for financial

support. One of us (J.-L.F.) is also grateful to N.R.C.C. for the award of a scholarship.

1. J. E. DESNOYERS and C. JOLICOEUR. Modern aspects of electrochemistry. Vol. 5. *Edited by* J. O'M. Bockris and B. E. Conway. Plenum Press, New York. 1969. p. 1; J. E. DESNOYERS. *In* Electrostatic interactions and the structure of water. XVè Conseil International de Chimie Solvay, Brussels. In press.
2. W.-Y. WEN. Water and aqueous solutions. *Edited by* R. A. Horne. Wiley, New York. 1972. Chapt. 15.
3. J. E. DESNOYERS and M. AREL. Can. J. Chem. **45**, 359 (1967).
4. J. E. DESNOYERS, M. AREL, and P.-A. LEDUC. Can. J. Chem. **47**, 547 (1969).
5. J. E. DESNOYERS, R. FRANCESCON, P. PICKER, and C. JOLICOEUR. Can. J. Chem. **49**, 3460 (1971).
6. P.-A. LEDUC, J.-L. FORTIER, and J. E. DESNOYERS. In preparation.
7. F. FRANKS and D. J. G. IVES. Q. Rev. London, **20**, 1 (1966).
8. F. FRANKS, M. A. QUICKENDEN, D. S. REID, and B. WATSON. Trans. Faraday Soc. **65**, 582 (1969).
9. C. JOLICOEUR, P.-R. PHILIP, G. PERRON, P.-A. LEDUC, and J. E. DESNOYERS. Can. J. Chem. **50**, 3167 (1972).
10. C. JOLICOEUR, N. D. THÉ, and A. CABANA. Can. J. Chem. **49**, 2008 (1971).
11. J. E. DESNOYERS and G. PERRON. J. Solution Chem. **1**, 199 (1972).
12. W.-Y. WEN and S. SAITO. J. Phys. Chem. **69**, 3569 (1965).
13. G. STEIN and M. TOMKIEWICZ. Trans. Faraday Soc. **65**, 517 (1969).
14. P. J. PEARCE and R. J. J. SIMKINS. Can. J. Chem. **46**, 241 (1968).
15. S. G. SCHULMAN and H. GERSHON. J. Phys. Chem. **72**, 3297 (1968).
16. A. OSAL and M. KILPATRICK. J. Am. Chem. Soc. **55**, 4440, 4480 (1933).
17. P. PICKER, P.-A. LEDUC, P.-R. PHILIP, and J. E. DESNOYERS. J. Chem. Thermodyn. **3**, 631 (1971).
18. J.-L. FORTIER, P.-A. LEDUC, P. PICKER, and J. E. DESNOYERS. J. Solution Chem. In press.
19. R. F. PLATFORD. J. Phys. Chem. **72**, 4053 (1968).
20. R. FUOSS and F. ACCASCINA. Electrolytic conductance. Interscience Publ., New York. 1959.
21. H. FALKENHAGEN and E. L. VERNON. Phys. Z. **33**, 140 (1932).
22. M. H. LIETZKE and R. W. STOUGHTON. J. Phys. Chem. **66**, 508 (1962).
23. L. A. K. STAVELEY and B. SPICE. J. Chem. Soc. 406 (1952); R. BATTINO. Chem. Rev. **71**, 5 (1971).
24. R. ARNAUD, L. AVEDIKIAN, and J.-P. MOREL. J. Chim. Phys. **76**, 45 (1972).
25. C. V. KRISHNAN and H. L. FRIEDMAN. J. Phys. Chem. **73**, 1572 (1969).
26. Selected values of properties of hydrocarbons and related compounds. American Petroleum Institute. Research project 44 (1967).
27. R. A. PIEROTTI. J. Phys. Chem. **67**, 1840 (1963); M. LUCAS and A. TROBRIAND. C. R., Ser. Chim. C, **274**, 1361 (1972).
28. J.-L. FORTIER, P.-A. LEDUC, and J. E. DESNOYERS. J. Solution Chem. Submitted.
29. P.-A. LEDUC and J. E. DESNOYERS. Can. J. Chem. Submitted.
30. H. L. FRIEDMAN. Ionic solution theory. Interscience, New York. 1962.
31. J. E. DESNOYERS, M. AREL, G. PERRON, and C. JOLICOEUR. J. Phys. Chem. **73**, 3346 (1969).
32. P. R. PHILIP and J. E. DESNOYERS. J. Solution Chem. **1**, 353 (1972).

Can. J. Chem. Downloaded from www.nrcresearchpress.com by 210.87.254.105 on 09/05/12
For personal use only.

On the Unimolecular Decomposition of the tert-Butoxy Radical

C. K. YIP AND H. O. PRITCHARD[1]

Center for Research in Experimental Space Science, York University, Downsview, Ontario

Received November 16, 1972

It is argued that a large apparent pressure dependence in the rate of decomposition of the tert-butoxy radical should not be interpreted in terms of unimolecular reaction theory; the effect is probably heterogeneous in origin.

La dépendance très grande du taux de décomposition des radicaux tert-butoxy sur la pression ne devrait pas être interprété en termes d'une réaction unimoléculaire; un effet de nature hétérogène en est probablement l'origine. [Traduit par le journal]

Can. J. Chem., 51, 2138 (1973)

Can. J. Chem. Downloaded from www.nrcresearchpress.com by 84.22.46.98 on 09/08/12
For personal use only.

It is becoming accepted practice to treat the pressure dependence of the formation of products in complex radical systems in terms of unimolecular reaction theories: this has been done recently, for example, for the tert-butoxy radical produced both thermally (1) and photochemically (2) from di-tert-butyl peroxide; it is the purpose of this note to caution that there can be large pressure effects which do not have their origins in unimolecular fall-off behavior. The thermal decomposition of di-tert-butyl peroxide (DTBP) proceeds, in the presence of high pressures of hydrocarbon (RH), according to (3)

[1] $$\text{DTBP} \rightarrow 2t\text{-BuO}$$

[2] $$t\text{-BuO} \rightarrow \text{acetone} + CH_3$$

[3] $$t\text{-BuO} + \text{RH} \rightarrow t\text{-BuOH} + \text{R, etc.}$$

The results presented below are taken from our previous studies of this reaction with RH = propane or cyclopropane (3–5), and the experimental techniques used have been adequately described elsewhere (3–6).

Figure 1 shows an attempt to deduce the ratio of k_3/k_2 from the rates of formation of *t*-BuOH and acetone at three temperatures, using RH = propane: the diagram is remarkably like those already published for the thermal decompositions of the acetyl (7) and tert-butoxy (1) radicals. Note: (*i*) the large scatter of the points at the lowest temperature where both k_2 and k_3 are low. Figure 2 shows similar results found with RH = cyclopropane at one temperature (115 °C), but in two separate reaction vessels. Note that (*ii*) the results probably separate into two distinct sets, both of which would appear to extrapolate to k_3/k_2 of between 0.05 and 0.1 l mol^{-1} at infinite hydrocarbon concentration; (*iii*) the scatter is largest at low cyclopropane concentrations where $R_3 \propto k_3[\text{RH}]$ is low, especially so because k_3 is extremely small for cyclopropane (4); (*iv*) in two experiments where the vessel had been packed, the effect was probably marginally significant at low hydrocarbon concentration, but inconclusive

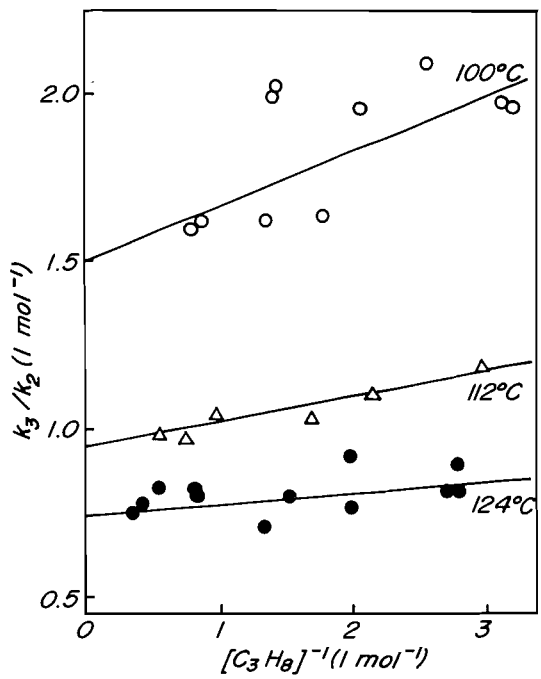

FIG. 1. Apparent variation of k_3/k_2 with hydrocarbon concentration for RH = propane, at three temperatures; data taken from refs. 3 and 5.

[1]Nuffield Foundation Visiting Fellow, Physical Chemistry Laboratory, Oxford University, 1972–1973.

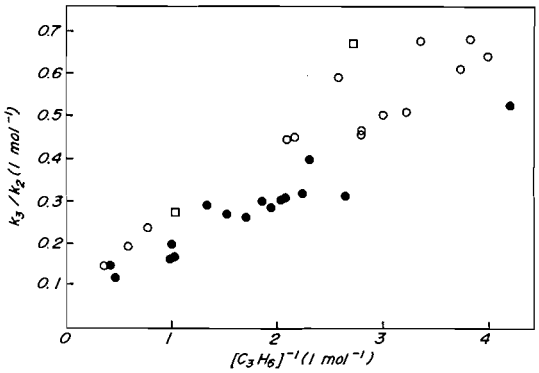

FIG. 2. Apparent variation of k_3/k_2 with hydrocarbon concentration for RH = cyclopropane at 115 °C: open and closed points represent measurements made in two different reaction vessels; square points represent measurements made in a reaction vessel packed with steel balls; data taken from refs. 4 and 5.

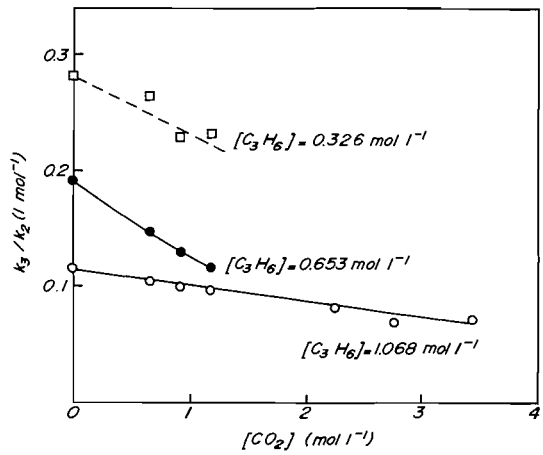

FIG. 3. Apparent variation of k_3/k_2 with carbon dioxide concentration for RH = cyclopropane at 115 °C.

at high hydrocarbon concentration; (*v*) the variation of k_3/k_2 with pressure over the range $0 < [RH]^{-1} \leqslant 3$ l mol^{-1} is at least a factor of four for cyclopropane at 115 °C in Fig. 2, but, at most, only a factor of about 1.3 for propane at the same temperature (*c.f.* Fig. 1).

Points *i* to *iv* can easily be understood if either k_2 or (more probably) k_3 were heterogeneous. Point *v* shows that the pressure dependence cannot be due to fall-off in k_2, since the effect for the *same* radical in different substrates is quite different; furthermore, it seems very likely that for this radical, $p_{1/2}$ is of the order of 100 mm total pressure (say 4×10^{-3} mol l^{-1}) at these temperatures (8), so that at our much greater concentrations (roughly 0.25 to 2.5 mol l^{-1}) a factor of four or more variation in k_2 does not make any sense.

Figure 3 shows the results of a third series of experiments (also at 115 °C) with RH = cyclopropane, in which, using three fixed initial concentrations of cyclopropane, successively larger amounts of carbon dioxide were added. Note that: (*vi*) these experiments were carried out in sequence in one reaction vessel, and are apparently much more reproducible than those shown in Fig. 2: however, those with the lowest cyclopropane concentration show the highest scatter; (*vii*) at the highest pressures, the results seem to be tending towards a value of k_3/k_2 around 0.07 l mol^{-1}, consistent with the results in Fig. 2: however, they do not extrapolate in any simple way using inverse concentrations (*e.g.* $[CO_2]^{-1}$, [total substrate]$^{-1}$, etc.) as the horizontal coordinate; (*viii*) the effect of adding cyclopropane seems to be somewhat greater than the effect of adding carbon dioxide: for example, considering the point at [RH] = 0.653 and $[CO_2]$ = 0.648 mol l^{-1}, increasing [RH] to 1.068 mol l^{-1} reduces k_3/k_2 from 0.147 to 0.104 l mol^{-1}, but keeping [RH] constant and changing $[CO_2]$ to about 1.06 mol l^{-1} would only reduce k_3/k_2 to about 0.120 l mol^{-1}.

Points *vi* and *vii* would be consistent with a heterogeneous component, as, in fact, is point *viii*. Since CO_2 and C_3H_6 have almost identical molecular masses, the diffusion coefficients for CO_2 and C_3H_6 only differ in the molecular-size factor: the cyclopropane molecule is larger than the carbon dioxide molecule, and one would therefore expect cyclopropane to be rather more effective than carbon dioxide in preventing the diffusion of tert-butoxy radicals to the walls in search of labile hydrogen atoms; the effect would not, however, amount to as much as a factor of two in the diffusion coefficients, and in consequence, the slightly greater efficiency for cyclopropane which we observe seems to be reasonable.

One could contrive an explanation of these results in terms of differing reactivities of $(RH)_n$ and $(RH)_n(CO_2)_m$ clusters at these pressures, but it would be hard to account for the increasing scatter at low pressures and temperatures: thus, we conclude that there can be marked pressure dependence in free radical reactions, possibly caused by heterogeneous effects, and the practice of ascribing all the

Can. J. Chem. Downloaded from www.nrcresearchpress.com by 84.22.46.98 on 09/08/12
For personal use only.

pressure dependence to unimolecular fall-off demands positive proof that such effects are absent.

1. P. CADMAN, A. F. TROTMAN-DICKENSON, and A. J. WHITE. J. Chem. Soc. (A), 2296 (1971).
2. F. H. DORER and S. N. JOHNSON. J. Phys. Chem. **75**, 3651 (1971).
3. C. K. YIP and H. O. PRITCHARD. Can. J. Chem. **47**, 4708 (1969).
4. C. K. YIP and H. O. PRITCHARD. Can. J. Chem. **49**, 2290 (1971).
5. C. K. YIP. Ph.D. Thesis. York University, Downsview, Ontario. 1972.
6. C. K. YIP and H. O. PRITCHARD. Can. J. Chem. **50**, 1531 (1972).
7. H. E. O'NEAL and S. W. BENSON. J. Chem. Phys. **36**, 2196 (1962).
8. M. F. R. MULCAHY and D. J. WILLIAMS. Aust. J. Chem. **17**, 1291 (1964).

Can. J. Chem. Downloaded from www.nrcresearchpress.com by 84.22.46.98 on 09/08/12
For personal use only.

Dielectric Constant, Density, and Enthalpy of Transition of Cyclohexane and Neopentane at 500 Atmospheres

HEMMING ART-MING CHEW AND RAYMOND KAI-CHOW CHAN[1]

Department of Chemistry, University of Western Ontario, London, Ontario

Received February 7, 1973

A cell has been described for the simultaneous measurement of the dielectric constant and volume changes at the phase transition of solids at low temperatures and pressures up to 500 atm. The dielectric constants of the high temperature phase of cyclohexane and neopentane at 10 kHz increase with decreasing temperature according to the Clausius–Mossotti equation. The low temperature solid phase of both nonpolar substances has considerably high shear strength and it is suggested that the dielectric data of these substances in the literature may have considerable errors. The enthalpies of fusion and solid–solid transition at 500 atm have been calculated from the experimental results.

Une cellule a été décrite pour mesurer simultanément la constante diélectrique et les changements de volume lors de la transition de phases des solides aux basses températures et sous des pressions atteignant 500 atm. Les constantes diélectriques de la haute température de phase pour le cyclohexane et le néopentane à 10 kHz augmentent lorsque la température décroît selon l'équation de Clausius Mossotti. La phase solide à basse température de ces deux substances non polaires a un pouvoir considérable de cisaillement et on pense que les données de la littérature concernant la constante diélectrique de ces substances comportent des erreurs appréciables. Les enthalpies de fusion et de transition solide–solide sous 500 atm ont été calculées à partir des résultats expérimentaux. [Traduit par le journal]

Can. J. Chem., 51, 2141 (1973)

Introduction

Crystalline solids are generally known to have a negative temperature coefficient of high frequency dielectric constant. This behavior is adequately described by the Clausius–Mossotti equation which suggests that the polarizability of a molecule is independent of temperature. Ice (1) and crystalline methanol (2), in which the contribution due to the infrared polarization decreases with temperature causing their high frequency dielectric constants to decrease with temperature, show departure from this general rule. Crowe and Smyth (3) have reported that several nonpolar solids also show this unusual behavior. While they offered no explanation, their results implied that the density of these solids decreased with temperature. The main objective of our studies is to resolve this anomaly.

A serious problem in the study of the dielectric behavior of solids is caused by the presence of voids of undeterminable dimensions resulting from the cracks in the sample or from the shrinking of the sample away from the electrodes. A dielectric cell in which both could be avoided is an essential prerequisite. We describe an apparatus for the simultaneous, but independent, measurement of the density and dielectric constant of solids. As far as we are aware this is the first apparatus of this type reported for the measurements on solids.

[1]To whom correspondence should be addressed.

Experimental

The dielectric cell designed for the measurement of dielectric constant and volume changes is shown in Fig. 1. All parts are made from stainless steel except the tension spring. L is an 8 cm diameter, 6 cm long block to accommodate the low electrode J and high electrode K. G is a mushroom-shaped piston with O-ring seals H, sliding into M where the solid is contained. G is fastened to the movable plate F which has a container N attached to it. The parallel plate air capacitor D, E is contained in N. The high electrode D of the air capacitor can be moved vertically through the plate P by means of a 40 threads per in. micrometer A with the tube B acting as a guide. The tension spring C is held in place by P and 4 binding posts O. The electrodes D, E, J, and K are electrically insulated by mica, Teflon, and epoxy cement. The force constant of spring C was calibrated by means of a Carver model K laboratory press. The spring is capable of exerting a maximum pressure of 550 atmospheres to a 6.2 mm diameter piston. The friction of the O-ring seals is negligible as shown by the reproducibility of the dielectric results in the heating and cooling part of the cycle (Fig. 4). The pressure exerted on the sample M, which is applied by the tension spring C through G, can be controlled by adjusting the positions of the nuts Q on the binding posts.

Can. J. Chem. Downloaded from www.nrcresearchpress.com by 210.87.254.6 on 09/05/12
For personal use only.

Can. J. Chem. Downloaded from www.nrcresearchpress.com by 210.87.254.6 on 09/05/12
For personal use only.

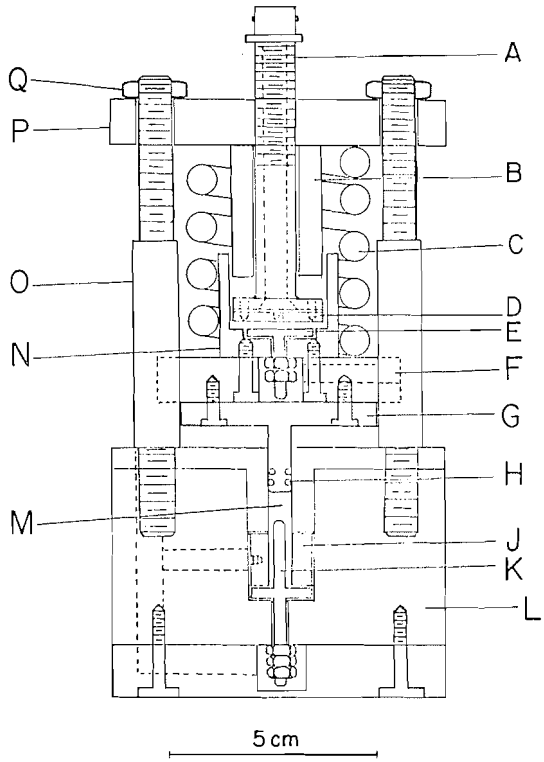

FIG. 1. The cell for dielectric constant and volume measurements.

The capacitance in air of the dielectric cell J K M was 1.048 pF. A calibration with CCl_4 at room temperature showed no stray capacitance in the assembly or in the electrical leads. The complete assembly was kept inside a large metal block with heating wires wound around it and was insulated with polyurethane foam. The insulated metal block was kept in liquid nitrogen contained in a metal dewar. The temperature was controlled and measured with copper–constantan thermocouples. The large thermal capacity of the dielectric cell provided excellent stability of temperature. The variation of temperature inside the solid sample was within ± 0.1 °C. The capacitance bridge and the associated assembly have been described earlier (4).

Measurements were done at constant pressure at different temperatures. Any change in the volume of the solid sample M, caused by thermal expansion or phase transition, produced a change in the distance between D and E. Since the air capacitance between D and E is inversely related to the separation between them, the vertical displacement of G can be easily calculated. Errors caused by the thermal expansion of the metal components of the assembly were too low to make any significant difference in our results.

In order to determine the coefficient of thermal expansion of the solid, it is necessary to know its volume at that temperature. For relatively less volatile substances a known volume of the liquid at room temperature can be introduced into the cell and from the values of the coefficient of thermal expansion, the volume can be calculated at each temperature. For volatile substances *e.g.* neopentane (b.p. 9.5 °C) this method is not convenient and, therefore, the following method was used.

According to the Clausius–Mossotti equation

$$[1] \qquad \frac{\varepsilon - 1}{\varepsilon + 2} = \frac{w[P]}{M(V_0 - \Delta V)} = \frac{d[P]}{M}$$

where w is the weight of the substance occupying V_0 cm^3 at a reference temperature, ΔV is the change in volume at any temperature from the reference temperature, $[P]$ is the molar polarization, and d is the density. Equation 1 can be approximated, after rearrangement, by

$$[2] \qquad \frac{\varepsilon - 1}{\varepsilon + 2} = \frac{w[P]}{MV_0} + \frac{w[P]}{MV_0^2}\Delta V$$

Since the molar polarization of a nonpolar substance is largely due to the electronic polarization, it would be independent of temperature, pressure, or phase transition. The initial volume V_0 can thus be obtained from the ratio of the intercept to the slope of a plot of $(\varepsilon - 1)/(\varepsilon + 2)$ against ΔV. Figure 2 shows such a plot for the high temperature solid phase of neopentane at 500 atm. Note that no knowledge of the density or the weight of the substance is required for this determination.

The enthalpies of fusion and solid–solid transition

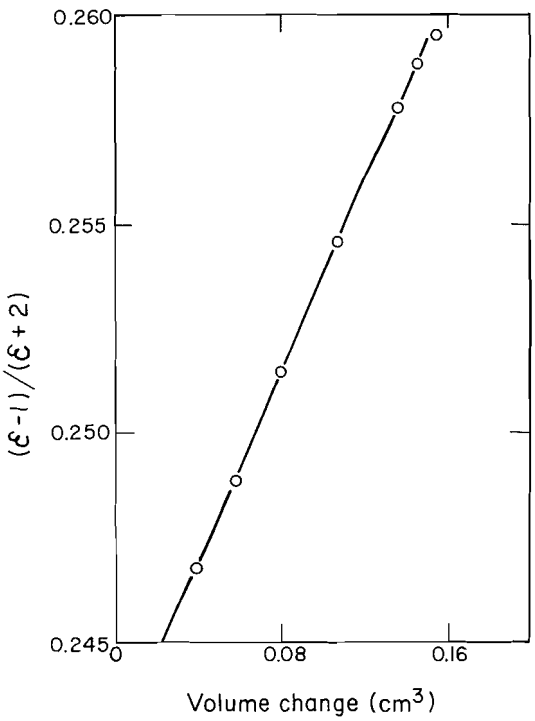

FIG. 2. $(\varepsilon - 1)/(\varepsilon + 2)$ against volume change for neopentane at 500 atm.

TABLE 1. Dielectric constant, density, and molar polarization of cyclohexane at 500 atm

Temperature (°C)	ε	Density (g cm^{-3})	[P] (cm^3 mol^{-1})	Density* (Green and Scheie) (g cm^{-3})
−80.1	2.318	0.977	26.3	
−73.4	2.312	0.970	26.4	
−70.4	2.226	0.905	27.0	
−69.4	2.216	0.901	26.9	
−64.4	2.202	0.893	27.0	0.883
−55.0	2.193	0.888	27.0	0.877
−45.5	2.186	0.883	27.0	0.871
−24.1	2.168	0.873	27.0	0.860
− 7.3	2.153	0.864	27.0	0.850
27.0	2.122	0.855	26.8	
30.0	2.116	0.852	26.8	
31.9	2.111	0.849	26.8	

*At atmospheric pressure.

were measured by a Perkin–Elmer DSC-1B differential scanning calorimeter.

Fischer certified spectranalyzed grade cyclohexane was distilled fractionally with calcium hydride before use. Metheson chemically pure grade neopentane with specified purity of 99.0% minimum was fractionally distilled in a vacuum apparatus and was collected at Dry Ice temperature. The sample was transferred into the dielectric cell inside a pre-cooled dry box at −20 °C.

Results

The measured values of the dielectric constant and density of cyclohexane and neopentane are given at 500 atm and different temperatures in Tables 1 and 2, respectively. Also included are the molar polarization, [P], calculated from eq. 1, and the density data of Green and Scheie (5) for solid cyclohexane at 1 atm. Figures 3 and 4 show the plots of the dielectric constant against temperature at 500 atm along with the atmospheric pressure data from Crowe and Smyth for cyclohexane (3), and Philippe and Piette for neopentane (6).

TABLE 2. Dielectric constant, density, and molar polarization of neopentane at 500 atm

Temperature (°C)	ε	Density (g cm^{-3})	[P] (cm^3 mol^{-1})
−137.4	2.047	0.736	25.4
−130.4	2.053	0.736	25.5
−113.5	2.050	0.724	25.8
− 87.6	2.032	0.714	25.9
− 56.1	2.006	0.703	25.8
− 36.6	1.992	0.697	25.7
− 18.2	1.978	0.691	25.7
− 9.2	1.972	0.688	25.7
0.3	1.964	0.685	25.6
13.1	1.931	0.659	25.9
18.4	1.871	0.637	25.5
21.4	1.867	0.631	25.6
25.0	1.862	0.627	25.7

Our values of the dielectric constant for the solid phases are not only higher than those in the literature, but they also have a qualitatively different temperature dependence. This qualitative difference is seen immediately for cyclohexane after application of only 10 atm pressure and remains unchanged when the pressure is removed. It is evident that the dielectric data for cyclohexane and neopentane in the literature were obtained on solid samples which had voids in them. Under pressure these voids disappear and the sample remains compact even after removal of the pressure. The apparent dielectric constant of a solid containing air gaps (4) is given by

$$[3] \qquad \varepsilon_{app} = \frac{\varepsilon_s}{1 + \delta(\varepsilon_s - 1)}$$

where ε_s is the correct value of the dielectric constant of the solid, and δ is the fractional width of air gaps in the solid sample. The value of δ estimated for Crowe and Smyth's sample at −80 °C would be 5%.

Discussion

Cyclohexane freezes at 6.7 °C at atmospheric pressure to a crystalline solid, I, which transforms to another solid phase, II, at −87.1 °C (7). Neopentane also has two solid phases, the crystalline solid, I, is formed at −16.6 °C and then transforms to phase II at −133.2 °C (8). In both cases the phase I is plastic, in that it readily deforms under pressure, and

Can. J. Chem. Downloaded from www.nrcresearchpress.com by 210.87.254.6 on 09/05/12
For personal use only.

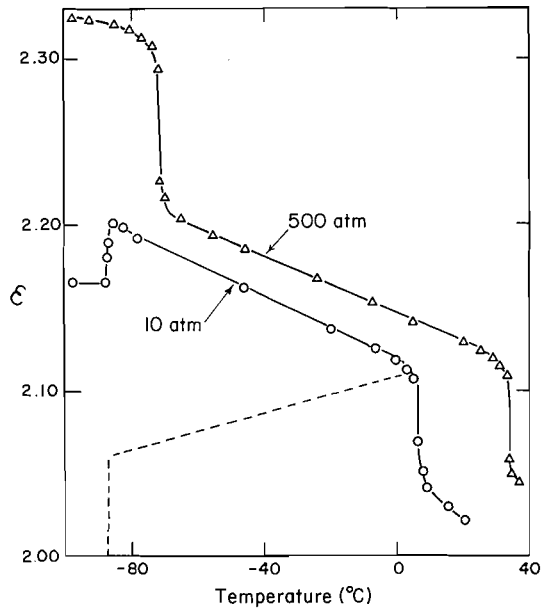

FIG. 3. Dielectric constant against temperature for cyclohexane at 10 and 500 atm and at 10 kHz. The dashed line represents the data of Crowe and Smyth at atmospheric pressure.

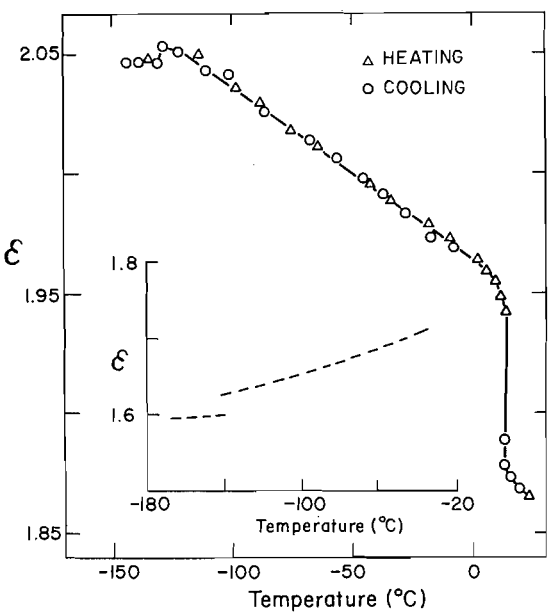

FIG. 4. Dielectric constant against temperature for neopentane at 500 atm and 10 kHz. The insert is the data of Philippe and Piette at atmospheric pressure.

the phase II is relatively hard and brittle (9). Considerably higher pressure is required to deform the phase II. This was evident in the result of our measurement of the effect of pressure on the change in the dielectric constant at I → II transition. It was found that at least 250 atm pressure is required to cause the dielectric constant of cyclohexane to increase at the phase transition. Typical results for cyclohexane are shown in Fig. 3 where the I → II transition at 10 atm produces a decrease in dielectric constant but the same transition at 500 atm produces an increase in dielectric constant. Clearly, the voids produced by the change in density during the I → II transition, which cause an apparent decrease in the dielectric constant, disappear on the application of a minimum pressure of 250 atm. The pressure required to compact the phase II of neopentane is higher than 500 atm as seen in Fig. 4. Thus the values of the dielectric constant and density for the phase II of neopentane are not reliable because of the much lower transition temperature and high shear strength of the solid.

It is worth noting that the comparative measurement of the plasticity of solids by Michels (10) also showed that in the vicinity of the transition temperature, the pressure required to force the low temperature solid phase through a bore is many times higher than that required for the high temperature solid phase.

The calculated values of the molar polarization at 500 atm from the experimental values of dielectric constant and density given in Tables 1 and 2 are 26.9 ± 0.1 and 25.7 ± 0.1 cm^3 mol^{-1} for cyclohexane and neopentane, respectively. This constancy also suggests the essential correctness of our density measurements.

It is worth pointing out that at 20 °C and 1 atm the average literature value of ε for liquid cyclohexane, 2.023 (12, 13) is 0.54% lower than that of n_D^2, 2.034 (14). It is unlikely that this rather unusual situation is due to experimental errors. It is conceivable that the strong ultraviolet absorption of liquid cyclohexane starting at 1800 Å (11) has a tail extending down to the visible region. This additional contribution to n_D^2 may make it larger than ε. Liquid hydrogen at −253 °C shows similar unusual behavior with ε = 1.228 and n_D^2 = 1.232 (15).

Can. J. Chem. Downloaded from www.nrcresearchpress.com by 210.87.254.6 on 09/05/12
For personal use only.

TABLE 3. Parameters used to calculate ΔH at 500 atm

	Fusion		Solid–solid transition	
	Cyclohexane	Neopentane	Cyclohexane	Neopentane
V_1 ($cm^3 mol^{-1}$)	103.8	113	93.5	99
V_2 ($cm^3 mol^{-1}$)	99.5	106	86.2	
ΔV ($cm^3 mol^{-1}$)	4.3	7	7.3	
α_1 ($10^{-4}\,°C^{-1}$)	10.6	8.0	5.2	
α_2 ($10^{-4}\,°C^{-1}$)	5.6	5.3	0.9	
$d\Delta H$ (cal mol^{-1})	−149	−34	−10	
ΔH (cal mol^{-1})				
1 atm	628*	778	1600*	616
500 atm	479	744	1590	
T at 1 atm (°C)	6.7*	− 16.6†	−87.1*	−133.2†
ΔT (°C)				
Calculated	27	30	11	
Experimental	25‡	31	13	11

*Reference 7.
†Reference 8.
‡Reference 17.

The coefficient of thermal expansion at 0 °C and 500 atm for solid cyclohexane derived from dielectric constant is $5.4 \times 10^{-4}\,°C^{-1}$ in reasonable agreement with $5.8 \times 10^{-4}\,°C^{-1}$ obtained from density. The corresponding values for solid neopentane are 5.6×10^{-4} and $5.4 \times 10^{-4}\,°C^{-1}$. The atmospheric density values of Green and Scheie (5) for solid cyclohexane are 1.4% lower than those at 500 atm (Table 1). They found a slightly higher value of $6.8 \times 10^{-4}\,°C^{-1}$ for the coefficient of thermal expansion, which is in fair agreement with the value of $6.3 \times 10^{-4}\,°C^{-1}$ obtained from the dielectric measurements at 0 °C and 10 atm (4). The decrease in the coefficient of thermal expansion with pressure seen here was expected.

The pressure coefficient of dielectric constant $(\partial\varepsilon/\partial p)_T$ at −40 °C for solid cyclohexane calculated from measurements at 10 and 500 atm is $5.1 \times 10^{-5}\,atm^{-1}$, corresponding to a compressibility of $3.2 \times 10^{-5}\,atm^{-1}$ based on the Clausius–Mossotti equation. The extrapolated compressibility at 25 °C is $4.6 \times 10^{-5}\,atm^{-1}$ compared with Bridgman's value of $5.1 \times 10^{-5}\,atm^{-1}$ (16).

Another quantity that is of interest in this work is the effect of pressure on the enthalpy of transition. It can be shown that the difference between the enthalpies of transition at atmospheric and higher pressure is not negligible. The change of enthalpy of transition with respect to pressure for a substance transforming from phase 2 to phase 1 is

$$[4] \quad \left(\frac{\partial \Delta H}{\partial p}\right)_T = (V_1 - V_2) - T(V_1\alpha_1 - V_2\alpha_2)$$

where V_1 and V_2 are the molar volumes; α_1 and α_2 are the coefficients of thermal expansion of phases 1 and 2, respectively. This equation enables one to determine the enthalpy of transition at 500 atm. The calculated values of the change in enthalpy of fusion and of solid–solid transition together with other experimental data are summarized in Table 3. An inspection of eq. 4 shows that a substantial decrease of ΔH with respect to pressure is expected for small ΔV, and large T and $\Delta\alpha$, These conditions are optimal for fusion of cyclohexane. At 500 atm the enthalpy of fusion for cyclohexane decreases by 24% compared to 4.4% for neopentane. On the contrary, the enthalpy of solid–solid transition for cyclohexane hardly changes at all with pressure. It is because the low transition temperature renders the terms with opposite signs in eq. 4 almost identical. The enthalpy of transition decreases by only 0.6% for a pressure change of 500 atm. ΔT is the elevation of fusion or transition temperature at 500 atm, which can also be calculated with the aid of the Clapeyron equation. The calculated values of ΔT using the average values of ΔH and temperature are in fair agreement with the experimental values of ΔT obtained from dielectric measurements.

The authors wish to thank the National Research Council of Canada for financial support.

Can. J. Chem. Downloaded from www.nrcresearchpress.com by 210.87.254.6 on 09/05/12
For personal use only.

1. S. R. GOUGH. Can. J. Chem. **50**, 3046 (1972).
2. P. T. T. WONG and E. WHALLEY. J. Chem. Phys. **55**, 1830 (1971).
3. R. W. CROWE and C. P. SMYTH. J. Am. Chem. Soc. **73**, 5406 (1951).
4. R. K. CHAN and H. A. CHEW. Can. J. Chem. **47**, 2249 (1969).
5. J. R. GREEN and C. E. SCHEIE. J. Phys. Chem. Solids, **28**, 283 (1967).
6. R. PHILIPPE and A. M. PIETTE. Bull. soc. chim. Belg. **64**, 600 (1955).
7. J. G. ASTON, J. SZASZ, and H. L. FINKE. J. Am. Chem. Soc. **65**, 1135 (1943).
8. J. G. ASTON and G. H. MESSERLY. J. Am. Chem. Soc. **58**, 2357 (1936).
9. J. TIMMERMANS. J. Phys. Chem. Solids, **18**, 1 (1961).
10. A. MICHELS. Bull. soc. chim. Belg. **57**, 575 (1948).
11. H. B. KLEVENS and J. R. PLATT. J. Am. Chem. Soc. **69**, 3055 (1947).
12. R. MECKE and R. JOECKLE. Z. Elektrochem. **66**, 255 (1962).
13. A. A. MARYOTT and E. R. SMITH. Table of dielectric constants of pure liquids. Natl. Bur. Stds. Circ. 514 (1951).
14. J. TIMMERMANS. Physico-chemical constants of pure organic compounds. Elsevier. I, 196 (1950) and II, 158 (1965).
15. L. HARTSHORN and J. A. SAXTON. *In* Handbuch der physik. Vol. 16. *Edited by* S. Flügge. Springer-Verlag. 1958. p. 711.
16. P. W. BRIDGMAN. Proc. Am. Acad. Arts. Sci. **77**, 129 (1949).
17. L. DEFFET. Bull. soc. chim. Belg. **44**, 41 (1935).

Can. J. Chem. Downloaded from www.nrcresearchpress.com by 210.87.254.6 on 09/05/12
For personal use only.

Examination of Possible Non-Arrhenius Behavior in the reactions

$$H + C_2H_6 \rightarrow H_2 + C_2H_5$$
$$H + CH_4 \rightarrow H_2 + CH_3$$
$$CH_3 + C_2H_6 \rightarrow CH_4 + C_2H_5$$

THOMAS C. CLARK AND JOHN E. DOVE

Department of Chemistry, University of Toronto, Toronto, Ontario M5S 1A1

Received August 29, 1972

We present a simplified form of the bond-energy–bond-order method of calculating rate coefficients which can be applied to reactions involving multi-atom reactants. Rate coefficients for the reactions

[1] $H + C_2H_6 \rightarrow H_2 + C_2H_5$

[2] $H + CH_4 \rightarrow H_2 + CH_3$

[3] $CH_3 + C_2H_6 \rightarrow CH_4 + C_2H_5$

are calculated for $300 < T < 1800$ °K. The Arrhenius plots of the calculated coefficients are curved, but in the temperature range 400–850 °K where most kinetic measurements have been made the curvature is not large enough to be readily detected. However deviations from a linear Arrhenius plot should be observable if rate measurements are extended to higher temperatures by, *e.g.*, shock tube experiments. The calculated rate coefficients at 300–1800 °K are fitted by the expressions

$$k_1 = 10^{-0.27\pm0.03}T^{3.5} \exp -(5200 \pm 70)/RT$$
$$k_2 = 10^{1.35\pm0.02}T^{3.0} \exp -(8750 \pm 40)/RT$$
$$k_3 = 10^{-3.26\pm0.01}T^{4.0} \exp -(8280 \pm 30)/RT$$

in liter mole second units. These expressions contain powers of T which in each case are greater than predicted by the classical limit of transition state theory. For all three reactions there is now some experimental evidence that the predicted curvature does occur. Some consequences of this behavior are examined.

Nous présentons une forme simplifiée de la méthode énergie de liaison – ordre de liaison pour le calcul des coefficients de vitesse, qui peut être applicable aux réactions engageant des réactants multi-atomiques. Les coefficients de vitesse pour les réactions

[1] $H + C_2H_6 \rightarrow H_2 + C_2H_5$

[2] $H + CH_4 \rightarrow H_2 + CH_3$

[3] $CH_3 + C_2H_6 \rightarrow CH_4 + C_2H_5$

ont été calculés entre $300 < T < 1800$ °K. Les courbes d'Arrhénius des coefficients calculés sont recourbées, mais dans l'intervalle de température 400–850 °K où la plupart des mesures cinétiques ont été faites, la courbure n'est pas suffisamment forte pour être détectée facilement. Cependant, les déviations par rapport à la droite d'Arrhénius peuvent être observées si les mesures de vitesse ont été effectuées à des températures plus élevées, par exemple par des expériences de "shock-tube". Les coefficients de vitesse calculés entre 300–1800 °K satisfont aux expressions

$$k_1 = 10^{-0.27\pm0.03}T^{3.5} \exp -(5200 \pm 70)/RT$$
$$k_2 = 10^{1.35\pm0.02}T^{3.0} \exp -(8750 \pm 40)/RT$$
$$k_3 = 10^{-3.26\pm0.01}T^{4.00} \exp -(8280 \pm 30)/RT$$

en unités litre mole seconde. Ces expressions contiennent des puissances de T qui sont dans chaque cas plus élevées que celles prévues par la limite classique de la théorie de l'état de transition. Pour ces trois réactions il existe maintenant une preuve expérimentale confirmant la courbure prédite. Quelques conséquences de ce fait ont été examinées. [Traduit par le journal]

Can. J. Chem., 51, 2147 (1973)

Introduction

It is customary to use the Arrhenius law to represent the temperature dependence of experimentally measured rate coefficients for bimolecular elementary gas reactions. However, in the case of several important elementary bimolecular reactions in gaseous hydrocarbon chemistry, experimental data indicate a discrepancy in that the rate coefficients at high temperatures lie above the Arrhenius line de-

Can. J. Chem. Downloaded from www.nrcresearchpress.com by 210.87.254.42 on 09/05/12
For personal use only.

Can. J. Chem. Downloaded from www.nrcresearchpress.com by 210.87.254.42 on 09/05/12
For personal use only.

rived from low temperature data. Since there are good theoretical reasons (1*a*) to expect deviations from the Arrhenius law, we decided to investigate the possibility that this discrepancy may be a real effect rather than being due to experimental error. Accordingly, we have used activated complex theory to calculate, over a large temperature range, the rate coefficients of three elementary reactions important in hydrocarbon pyrolysis, namely

[1] $H + C_2H_6 \rightarrow H_2 + C_2H_5$

[2] $H + CH_4 \rightarrow H_2 + CH_3$

[3] $CH_3 + C_2H_6 \rightarrow CH_4 + C_2H_5$

In each case, our calculated absolute values of the rate coefficients correlate the experimental data well. The predicted deviations from the Arrhenius law, particularly above 1000 °K, are large enough to be experimentally significant; the deviations are particularly large in the case of reaction 3.

In our calculations, we have used basically the modified three-center reaction models of Johnston (2), but have applied to them a later formulation of the B.E.B.O. transition state method given by Johnston and Parr (1, 3). We have introduced some approximations of our own which greatly simplify the calculations. The method, with these additional approximations, provides a convenient way of estimating absolute rate coefficients for reactions involving polyatomic species. It also enables an estimate to be made of the error introduced by using the Arrhenius law to extrapolate rate coefficients from one temperature range to another.

By using the B.E.B.O. formulation, we can break down an overall temperature dependence into four components. The first is the usual exponential term containing the potential energy of activation. The second is the temperature raised to some power determined by the classical limit of the partition functions. The third term allows for the temperature variation of quantum effects on the vibrations of the reactants and activated complex. The last is the temperature dependence of the quantum mechanical tunnelling correction for motion along the reaction coordinate. The effect of each contribution can be examined.

Several workers (4–8) have studied reaction 1 over the range 500–900 °K; their rate coefficients are scattered, but in fair agreement. Clark *et al.* (9) suggest that k_1 at 1350 °K is about 50% larger than the value expected from the Arrhenius rate parameters of Baldwin and Melvin (4).

Kurylo and Timmons (10) used a discharge flow system with e.s.r. detection of H atoms to obtain reliable coefficients for reaction 2 over the range 426–727 °K. Other data on reaction 2 (11–14) include two points above 1500 °K which lie above an Arrhenius line through the lower temperature data (11). Dove and Wagner (15) studied the reaction of H atoms with CH_4 at temperatures up to 1100 °K in a discharge–flow system and found agreement with Kurylo and Timmons at lower temperatures; however they observed an apparently anomalously high rate of consumption of H atoms above 850 °K which might indicate departures of k_2 from an Arrhenius form.

In previous kinetic studies (16–19) of reaction 3, its rate has generally been measured relative to that of some reference reaction. We have combined the relative rates with recent data (22–24) on the reference reactions to obtain absolute rate coefficients for reaction 3. The rate coefficients thus obtained from the various studies are found to be in good agreement with one another and to indicate an Arrhenius activation energy of 11.5 to 12.5 kcal mol^{-1} at about 500 °K. McNesby (16) studied the reaction

[3*a*] $CD_3 + C_2H_6 \rightarrow CD_3H + C_2H_5$

whose rate coefficient is expected (16) to be very close to that of reaction 3. At 1350 °K, Clark, Izod, and Kistiakowsky (9) deduced a value for k_3 from studies of high temperature reactions of methyl radicals which was more than 10 times that expected by extrapolation of McNesby's rate parameters. In addition, Clark and Izod (20) deduced that the Arrhenius activation energy for [3] is at least 14 kcal/mol over the range 1200–1500 °K. Recent flow system experiments by Pacey and Purnell (21) have yielded rate coefficients near 1000 °K which are significantly greater than predicted from McNesby's data, and their activation energy of about 16 kcal mol^{-1} is even larger than the value suggested by Clark and Izod for higher temperatures. It is therefore of considerable interest to know the full form of the theoretical temperature dependence of reaction 3, in order to determine whether these apparent discrepancies in the values of k_3 can be genuinely due to the failure of a simple Arrhenius form.

Can. J. Chem. Downloaded from www.nrcresearchpress.com by 210.87.254.42 on 09/05/12
For personal use only.

Method of Calculation

Basic Formulation

In the basic three-center reaction (1*b*), an atom A plus diatom BC, with properties R_{BC}, l_{BC}, ω_{BC}, Γ_{BC} give a linear complex A..B..C, with properties R_{BC}', l_{BC}', l_{BEND}, R_{AB}, l_{AB}, ω_1, ω_{BEND}, Γ_1, Γ_{BEND}, Γ_{RC}. The R's are internuclear separations, and ω's are vibration frequencies. $l = (2\pi kT/F)^{1/2}$ is a classical vibration amplitude, and F is a force constant. The imaginary frequency ω_{RC} is associated with motion along the reaction coordinate over a potential energy barrier of height V. A factor w_i, which is an imaginary number, corrects for interaction terms in the force constant matrix (1*c*). The factors Γ are vibrational quantum corrections (1*b*). Γ_{RC} is the real quantum correction for the imaginary frequency ω_{RC} and is a tunnelling correction factor. The factor β allows for a geometric factor, and any reaction path degeneracy or electronic partition function contributions. For R and l in Å, and ω in cm^{-1}, the rate coefficient for the basic three-center reaction is given in 1 mol^{-1} s^{-1} by

$$k = 1.81 \times 10^7 \beta \Gamma_{RC} \omega_{RC} \frac{R_{BC}'^2 R_{AB}^2}{w_i R_{BC}^2} \times \frac{l_{BC}' l_{AB} l_{BEND}^2}{l_{BC}} \frac{\Gamma_1 \Gamma_{BEND}^2}{\Gamma_{BC}} \exp\left(\frac{-V}{RT}\right)$$

Modifications for Complex Reagents

To allow for the case that there is a multiatom group, such as ethyl, at the center "C", the model of Johnston (2) was adopted. It is:

$$\begin{aligned} &A + B—C—D \rightarrow A...B...C—D \\ \textit{e.g.}\ &H + H—CH_2—CH_3 \rightarrow H...H...CH_2—CH_3 \\ &H + H—C—H_3 \rightarrow H...H...C—H_3 \end{aligned}$$

The force constants associated with each of two perpendicular bending frequencies about ⟨BCD in the complex were calculated as the corresponding reactant force constants multiplied by the bond order of B—C in the complex. The vibrational amplitude term to be introduced into the formula as a result of the presence of the multiatom group at C is simply the reciprocal of the bond order of B—C in the complex. The quantum corrections Γ were calculated from the vibration frequencies of the reactant molecule and complex. In the present work, the bending frequency introduced into the complex was estimated by multiplying the corresponding frequency of the reactant molecule by the square root of the bond order of B—C in the complex. The term introduced into the three-center formula by the molecule at site C with two degenerate bending frequencies ω and a bond order n for B—C in the complex is thus:

$$\frac{1}{n}\left(\frac{\Gamma(\sqrt{n}\omega)}{\Gamma(\omega)}\right)^2$$

We took ω to be the average of the bending frequencies of ethane for reactions 1 and 3, and of methane for reaction 2.

For the case that there was a multi-atom reagent such as methyl at A, the three-center model was modified by introducing (2) a pseudo-diatom E—A as follows:

$$\begin{aligned} &H_3—C + H—CH_2—CH_3 \rightarrow H_3—C...H...CH_2—CH_3 \\ &E—A + B—C—D \rightarrow E—A...B...C—D \end{aligned}$$

First, a geometrical factor $1/4\pi$ should be introduced (1*d*, 2). Two perpendicular bending modes ⟨EAB occur in the complex which were absent in the reactants. Thus two additional vibrational amplitude factors l and two quantum correction factors Γ must be introduced into the simple three-center formula. To allow for CH_3 at the center A, we thus introduce a factor $l^2\Gamma^2/4\pi$.

The bending force constants introduced into the complex by reagent methyl were calculated as follows. An average bending frequency for methane was calculated. A "*G*-factor" (1*e*) for the linear triatomic model H_3—C—H was then used to deduce a bending force constant for the molecule. To find this force constant in the complex, the molecular force constant was multiplied by the C—H bond order in the complex (1*e*, 2). We then used a *G*-factor for the H_3—C...H bend in the complex, to deduce the vibration frequency.

Use of these approximations avoids the lengthy **FG** matrix procedure for finding the bending frequencies of the complex (1*e*). Any resulting uncertainty in the frequencies will be reflected only in the quantum corrections Γ deduced from these frequencies, and thus will vanish at high enough temperatures. For the case of $CH_3 + C_2H_6$ at 400 °K, we have compared our calculated combined quantum correction for the bending frequencies with the correction calculated using frequencies from a complete vibrational analysis by Johnston (2). The excellence of the agreement, within 3%, is

TABLE 1. Input parameters and calculated complex properties

Input parameters		Value		
		Reaction 1 $H + C_2H_6$	Reaction 2 $H + CH_4$	Reaction 3 $CH_3 + C_2H_6$
Masses (a.m.u.)	A	1	1	15
	B	1	1	1
	C	29	15	29
Bond lengths (Å)	R_{AB}	0.74	0.74	1.09
	R_{BC}	1.09	1.09	1.09
	R_{CA}	1.09	1.09	1.54
Frequencies (cm^{-1})	ω_{AB}	4395	4395	2914
	ω_{BC}	2960	2915	2960
	ω_{CA}	2960	2915	940
	$\omega_{\angle BCD}$	1480	1395	1480
Bond energies for models (kcal/mol)	D_{AB}^e	109.3	109.3	111.2
	D_{BC}^e	106.5	111.2	106.5
	D_{CA}^e	120.0	111.2	116.0
Reaction degeneracy		6	4	6
Geometric factor	β	1	1	$1/4\pi$
Complex Properties				
Bond lengths (Å)	R_{AB}'	0.94	0.89	1.30
	R_{BC}'	1.26	1.30	1.24
Potential energy (kcal/mol)	V	12.2	14.3	14.2
Reaction frequency	ω_{RC}	1721i	1488i	1503i
Force constants (10^{+5} dyn/cm)	F_1	1.37	0.71	1.46
	F_2	0.91	1.63	0.53
	F_{12}	1.89	1.89	1.90
	F_B	0.058	0.052	0.076
(for CH_3 reagent)	F	—	—	0.38
Frequencies (cm^{-1})	ω_1	1500	1734	514
	ω_B	673	656	573
	$\omega_{\angle BCD}$	1078	925	1108
(for CH_3 reagent)	ω	—	—	900
Imaginary factor	w_i	1.34i	1.45i	1.93i

almost certainly fortuitous, but the comparison indicates that these approximations are unlikely to introduce any serious error even at low temperatures.

Potential Energy of Activation

We have used the formulation of Johnston and Parr (3), in which the changes in potential energy due to the breaking of one bond and the formation of another are calculated as the sum of three terms. Two of these terms use an empirical relationship between bond order and bond dissociation energy to calculate the interactions A...B and B...C; we consider these terms to remain valid when complicated reagent molecules are involved. The third term is the triplet repulsion between center A and center C. (In each case, when calculating D_e from D_0^0, we included the zero point energies of those molecular vibrations which change when the model molecule is transformed to the complex. The relevant parameters of the model molecules are given in Table 1.) In the simple three-atom case, the triplet repulsion term is calculated from the dissociation energy D_{CA} of the diatomic molecule CA. When complicated reagents are used, it becomes uncertain what is the appropriate dissociation energy to use. Therefore we have explored the use of D_{CA} as a variable parameter, choosing it to give a good fit to the experimental rate coefficient at about 550 °K. Below 500 °K there is an increasing uncertainty

Can. J. Chem. Downloaded from www.nrcresearchpress.com by 210.87.254.42 on 09/05/12
For personal use only.

Can. J. Chem. Downloaded from www.nrcresearchpress.com by 210.87.254.42 on 09/05/12
For personal use only.

in the tunnelling factor and other quantum corrections.

Starting with D_{CA} equal to the model bond dissociation energy CH_3—CH_3 for reactions 1 and 3, and CH_3—H for reaction 2, we found that satisfactory results were obtained for reaction 2. However for reactions 1 and 3 D_{CA} needed to be increased by about 10%. The upper short lines in Figs. 1 and 3 show the rate coefficients calculated when D_{CA} was set equal to the bond dissociation energy as defined above. The lower long solid curves show the rate coefficients obtained when D_{CA} was increased. Note, incidentally, that the general shapes and curvatures of these lines are independent of moderate variations in D_{CA}.

Tunnelling Corrections

Tunnelling corrections Γ_{RC} were evaluated for Eckart potentials with the calculated potential energy of activation V and reaction frequency ω_{RC} of the effective mass of the model (1*b*, 1*e*, 1*f*). We found it convenient to read Γ_{RC} from smooth curves drawn through a plot of $\log_{10}\Gamma_{RC}$ against u_{RC} $(=h\nu_{RC}/kT)$ for various values of α_1 and α_2. Here $\alpha = V/h\nu$; α_1 uses V measured relative to the potential energy minimum of the reactants, and α_2 uses V measured relative to the potential minimum of the products. The data were taken from Table 2.2 of ref. 1.

The shape and height of the calculated activation barrier can be significantly influenced by the value assumed for D_{CA}. We have therefore investigated the possibility that our calculated values of Γ_{RC} might be sensitive to the exact choice of D_{CA}. However we find that for these reactions the 10% increase in D_{CA} alters Γ_{RC} by less than 50% at 300 °K and by smaller amounts at higher temperatures. We believe therefore that our procedure for evaluating the Eckart tunnelling correction is not very seriously in error over most of the temperature range. We are however concerned both about the possibilities of appreciable errors in the calculation of Γ_{RC} near 300 °K and about possible defects in the one-dimensional Eckart tunnelling correction itself at low temperatures. Calculated values of Γ_{RC} for reactions 1, 2, and 3 are 5.6, 3.7, and 3.9 at 400 °K, and as large as 28, 11, and 12.2 at 300 °K.

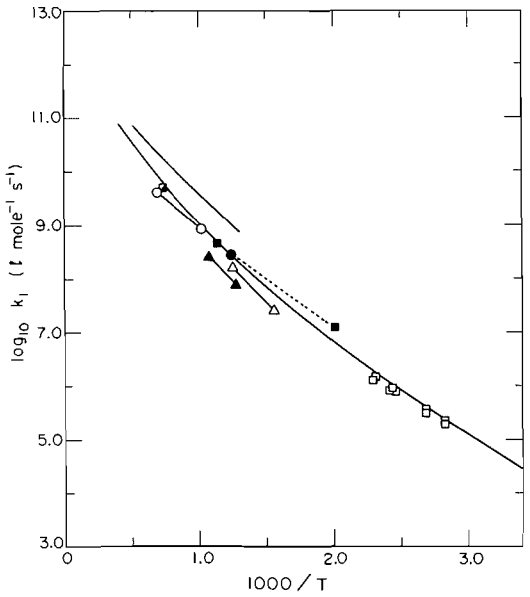

FIG. 1. Temperature dependence of reaction 1, H + $C_2H_6 \rightarrow H_2 + C_2H_5$. Upper solid curve: calculation with D_{CA} equal to bond dissociation energy. Lower solid curve: calculation with D_{CA} increased by 10%. Other lines connect the symbols which represent upper and lower temperature points from the experimental data of; △ ref. 5, ▲ ref. 6, ○ ref. 7, ■ ref. 15. Experimental data points; ● ref. 4, □ ref. 8, ◩ ref. 9,20.

Results and Discussion

Figures 1 to 3 are plots of $\log_{10}k$ against $1000/T$. To obtain the solid calculated curves on

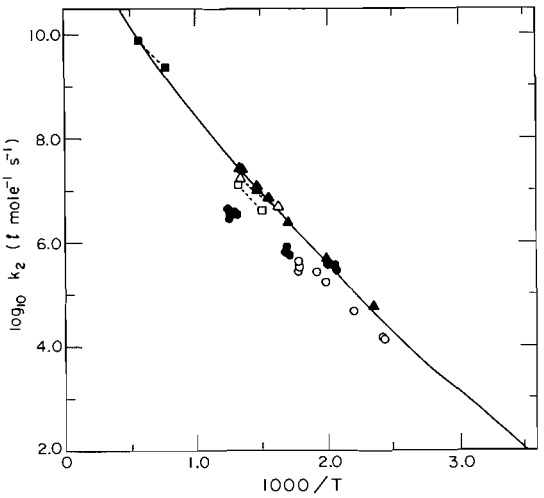

FIG. 2. Temperature dependence of reaction 2, H + $CH_4 \rightarrow H_2 + CH_3$. Solid curve: calculation with D_{CA} equal to bond dissociation energy. Other lines connect the symbols which represent upper and lower temperature points from the data of; □ ref. 5, ■ ref. 11, △ ref. 14. Experimental data points; ▲ ref. 10, ○ ref. 12, ● ref. 13.

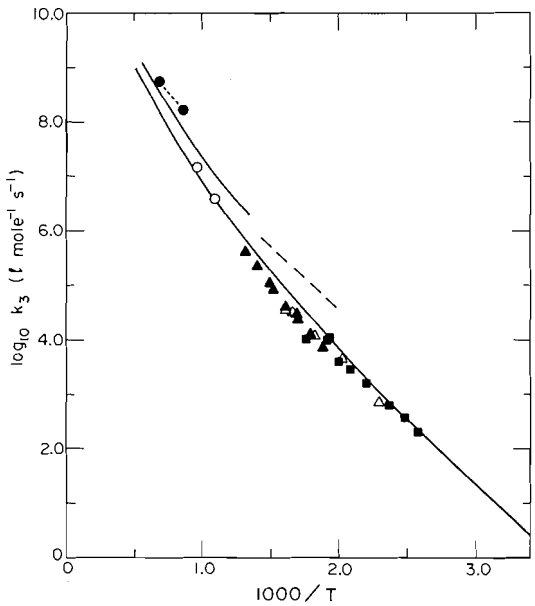

FIG. 3. Temperature dependence of reaction 3, $CH_3 + C_2H_6 \rightarrow CH_4 + C_2H_5$. Upper solid curve: calculation with D_{CA} equal to bond dissociation energy. Lower solid curve: calculation with D_{CA} increased by ~10%. Dashed line: calculated data of ref. 2. Experimental data points; ● ref. 9,20, ▲ref. 16, △ ref. 18, ■ ref. 19, ○ ref. 21.

them, rate coefficients were calculated at 300, 400, 650, 750, 900, 1100, 1350, 1500, 1800 °K, and curves drawn through the points. Experimental data from the literature are also shown. Where possible, data points derived from individual experiments are plotted. However, in some cases (noted in the captions) only two points are shown for an experimental study; these data points were calculated at the lower and upper temperature limits of the study, using the published rate parameters.

H + C_2H_6

Figure 1 is an Arrhenius plot showing a set of calculated coefficients and sets of experimental values. The calculated curve falls within the experimental values in absolute magnitude and gives a reasonable activation energy. The Russian workers (5,6) report values from explosion limits lower than those obtained by more direct methods. Although the set of calculated coefficients is a curve, it should be noted that it approximates well to a straight line between 400 and 850 °K. Serious deviations from this line occur only when data from outside this temperature region are added. Similar curved Arrhenius plots can be seen in the paper by Johnston and Parr (3) for related reactions. It is interesting to note that the curve agrees well with the data of Berlie and Le Roy (8), and with the recent data of Dove and Wagner (15) obtained using e.s.r. detection of H-atoms in a flow system. Agreement is satisfactory with the higher temperature data of Fenimore and Jones (7), and Clark and Izod (20).

To find an analytic form to describe the temperature dependence, the set of coefficients was fitted by the method of least squares to the function:

$$k = AT^n \exp(-E_a/RT)$$

where n was varied in steps of 0.5 between 0.0 and 5.0. The standard deviations in A and E_a were found to be smallest when $n = 3.5$. This empirical power of n is larger by +2.0 than the power expected from simple classical transition state theory.

If a least squares Arrhenius line were fitted to experimental data, or to the theoretical rate coefficients, in the region 400–850 °K, extrapolation to higher temperatures would underestimate the rate coefficients by a factor of about 2 at 1500 °K, and of 3 at 1800 °K. In this case, the size of these errors is close to the scatter in the available experimental rate data, but the difference is nevertheless of the same order at 1350 °K as the increase in k_1 suggested by Clark *et al.* (9) for this temperature.

From the least squares fit, we conclude that our calculated values for k_1 are best described by the expression:

$$k_1 = 10^{-0.27\pm0.03} T^{3.5} \exp(-5200 \pm 70/RT) \quad l\ mol^{-1}\ s^{-1}$$

H + CH_4

Figure 2 shows the calculated rate coefficients and the experimental data (5, 10–14, 20) on an Arrhenius plot. The calculated coefficients are in very good agreement with the experimental data of Kurylo and Timmons (10) which were obtained using a discharge flow system with e.s.r. detection. Note that the data of Majury and Steacie (12) were actually obtained for the reaction −2 and have been converted to values for reaction 2 using the thermodynamic equilibrium constant. Any uncertainties in the equilibrium constant will therefore be reflected in the derived values of k_2. Also, the data of Klein and co-workers (14) are for the reactions of D

Can. J. Chem. Downloaded from www.nrcresearchpress.com by 210.87.254.42 on 09/05/12
For personal use only.

Can. J. Chem. Downloaded from www.nrcresearchpress.com by 210.87.254.42 on 09/05/12
For personal use only.

with CH_4. Again a straight line well describes the temperature dependence between 350 and 800 °K despite tunnelling and quantum effects at these lower temperatures. Deviations from such a line occur above 1000 °K where the rate coefficients are approaching a classical description.

On fitting the theoretical data to the form

$$k_2 = AT^n \exp(-E_a/RT)$$

in the same way as for reaction 1, the best fit was found when $n = 3.0$:

$$k_2 = 10^{1.35\pm0.02}T^{3.0} \exp(-8750 \pm 40/RT) \quad \text{l mol}^{-1}\ \text{s}^{-1}$$

The predicted rate coefficient at 1500 °K is about 2.0 times the value obtained by Arrhenius extrapolation of data below 800 °K.

$CH_3 + C_2H_6$

Figure 3 shows rate coefficients from McNesby (16), Wijnen (18), Trotman-Dickenson *et al.* (19), Pacey and Purnell (21), and the high temperature data of Clark and Izod (20). Relative rate data from refs. 16, 18, and 19 yielded values of k_3 by combination with other rate expressions (22–24). The solid curve calculated by the B.E.B.O. method with slightly increased D_{CA} provides a partial reconciliation of high and low temperature data. The calculated coefficients are in excellent agreement with experimental values near 500 °K and near 1000 °K. Our calculations indicate that the simple Arrhenius extrapolation of rate data for the range 400 to 900 °K will predict a rate coefficient too low by a factor of 4 at 1500 °K. Thus for free radical abstraction reactions of this kind, quite substantial errors can be introduced if a linear Arrhenius extrapolation of low temperature data is made. In fact, the values of k_3 calculated using our model are still about a factor of 3 smaller than the high temperature data of Clark and Izod, so that the experimental Arrhenius plot appears to have even more curvature than we have calculated.

Using the same least squares procedure as used for reactions 1 and 2, the best form for describing the calculated coefficients was found to be

$$k_3 = 10^{-3.26\pm0.01}T^{4.0} \exp(-8280 \pm 30/RT) \quad \text{l mol}^{-1}\ \text{s}^{-1}$$

The exponent n was 4.0, which is greater by 1.5 than the classical value for a linear reaction complex.

Contributions to the Temperature Dependence

The B.E.B.O. formulation of transition state theory does not give a simple analytic functional description of the temperature dependence but it does allow various contributions to be examined. The rate coefficient can be written as

$$k = \gamma T^x \Gamma_{RC} \prod^i \Gamma_i \exp(-V/RT)$$

where $T^{1/2}$ comes from each classical vibrational amplitude so that $x = 5/2$ for reaction 3, $x = 3/2$ for reactions 1 and 2; Γ_{RC} is the tunnelling correction; $\prod^i \Gamma_i$ is the appropriate product of quantum corrections, one for each vibrational frequency involved in reactants and complex, γ is a temperature-independent parameter. Using the standard definition of an Arrhenius activation energy, $E_a = -R\mathrm{d}(\ln k)/\mathrm{d}(1/T)$ the variation of E_a about V can be expressed as:

$$E_a - V = xRT - R\mathrm{d}(\ln \Gamma_{RC})/\mathrm{d}(1/T) - R\,\mathrm{d}(\ln \prod^i \Gamma_i)/\mathrm{d}(1/T)$$

Figure 4 shows the calculated values of $(E_a - V)$, and the individual contributions to $(E_a - V)$, plotted against $1/T$ for reaction 1. Curve I includes all contributions, curve II omits the contribution from the Eckart tunnelling correction. Incidentally, if the Wigner tunnelling correction formula (1*b*) is used, $(E_a - V)$ is found to be between the solid and heavy dashed curves in Fig. 4. Below about 900 °K, the variation of E_a with $1/T$ is relatively slow, and in our calculations this variation is dominated by the Eckart tunnelling factor. The contributions to $(E_a - V)$ from T^x and Γ_i nearly cancel below 900 °K, so that in this temperature range the vibrations make only a small negative contribution to the temperature dependence.

Below 1000 °K, the calculated values of E_a do not vary rapidly with $1/T$, but the variation is still sufficiently large that it should be experimentally detectable. The available experimental data give some support for this prediction of the calculations. For reaction 1, the data of Berlie and Le Roy (8) at 300–600 °K indicate a lower activation energy than data over the range 500–1100 °K, as can be seen from Fig. 1. For reaction 3 there is stronger evidence of low temperature curvature, as shown by the data (16, 18, 19) in Fig. 3.

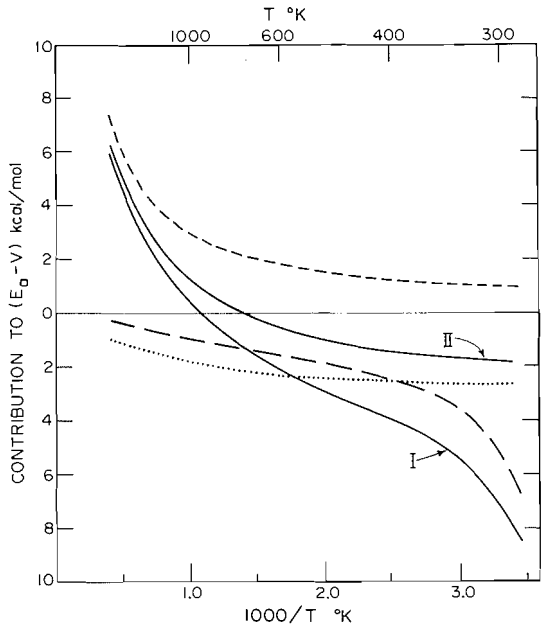

FIG. 4. Temperature dependence of the calculated activation energy for reaction 1: Solid curve I variation of $(E_a - V)$, Solid curve II variation of $(E_a - V)$ without the Eckart tunnelling contribution, – – – Eckart tunnelling contribution, · · · contribution from quantum corrections on stable vibrations, --- contribution from classical $T^{3/2}$ temperature dependence of pre-exponential factor.

The most notable feature of Fig. 4 is the continuing increase in $(E_a - V)$ above 1000 °K. It is this increase which is reflected in the high temperature curvature of the calculated lines in Figs. 1–3. This curvature is due mainly to the T^x term in the expression for k, and is little affected by the tunnelling factor. The other reactions show the same general behavior as depicted in Fig. 4, and the high temperature curvature is even greater in the case of reaction 3 for which $x = 5/2$.

Conclusions

We have shown that the simplified B.E.B.O. method can be used to describe the temperature dependence of rate coefficients for several H-transfer reactions involving complicated reagents over a wide temperature range. The Arrhenius plot of the calculated rate coefficients is continuously curved, but for the temperature range 400–900 °K the predicted curvature is not particularly obvious. However the calculated Arrhenius activation energy increases rapidly with temperature above 1000 °K, especially where the reaction involves abstraction by a radical.

This work was supported by grants from the National Research Council of Canada and from Imperial Oil Limited. T.C.C. wishes to acknowledge that this work was carried out in part during the tenure of an SRC research fellowship at Queen Mary College, University of London, England, 1970–1971.

1. H. S. JOHNSTON. Gas phase reaction rate theory. Ronald, 1966: (*a*) Chapt. 11, (*b*) Chapt. 8, (*c*) Chapt. 4, (*d*) Chapt. 12, (*e*) Chapt. 3, (*f*) Appendix E.
2. H. S. JOHNSTON. Adv. Chem. Phys. **3**, 131 (1960).
3. H. S. JOHNSTON and C. PARR. J. Am. Chem. Soc. **85**, 2544 (1963).
4. R. R. BALDWIN and A. MELVIN. J. Chem. Soc. 1785 (1964).
5. N. I. GORBAN and A. B. NALBANDYAN. Russ. J. Phys. Chem. **36**, 946 (1962).
6. N. N. TIKHOMIROVA, V. V. VOEVODSKII, and V. N. KONDRATIEV. Prog. React. Kinet. **1**, 41 (1961).
7. C. P. FENIMORE and G. W. JONES. 9th International Symposium on Combustion. Academic Press. 1963. p. 604.
8. M. R. BERLIE and D. J. LE ROY. Discuss. Faraday Soc. **14**, 50 (1953).
9. T. C. CLARK, T. P. J. IZOD, and G. B. KISTIAKOWSKY. J. Chem. Phys. **54**, 1295 (1971).
10. M. J. KURYLO and R. B. TIMMONS. J. Chem. Phys. **50**, 5076 (1969).
11. C. P. FENIMORE and G. W. JONES. J. Phys. Chem. **65**, 2200 (1961).
12. T. G. MAJURY and E. W. R. STEACIE. Discuss. Faraday Soc. **14**, 45 (1953).
13. J. W. S. JAMESON and G. R. BROWN. Can. J. Chem. **42**, 1638 (1964).
14. R. KLEIN, J. R. MCNESBY, M. D. SCHEER, and L. J. SCHOEN. J. Chem. Phys. **30**, 58 (1959).
15. J. E. DOVE and H. GG. WAGNER. Unpublished results.
16. J. R. MCNESBY. J. Am. Chem. Soc. **64**, 1671 (1960).
17. J. R. MCNESBY and A. S. GORDON. J. Am. Chem. Soc. **77**, 4719 (1955).
18. M. H. J. WIJNEN. J. Chem. Phys. **23**, 1357 (1955).
19. A. F. TROTMAN-DICKENSON, J. R. BIRCHARD, and E. W. R. STEACIE. J. Chem. Phys. **19**, 163 (1951); A. F. TROTMAN-DICKENSON and E. W. R. STEACIE. J. Chem. Phys. **19**, 324 (1951).
20. T. C. CLARK and T. P. J. IZOD. Dynamic mass spectrometry. Vol. 3. Heyden. 1972. p. 201.
21. P. D. PACEY and J. H. PURNELL. J. Chem. Soc. Faraday I, **68**, 1462 (1972).
22. H. E. VAN DEN BERG, A. B. CALLEAR, and R. J. NORSTROM. Chem. Phys. Lett. **4**, 101 (1969).
23. N. BASCO, D. G. L. JAMES, and R. D. STUART. Int. J. Chem. Kin. **2**, 215 (1970).
24. P. GRAY and A. A. HEROD. Trans. Faraday Soc. **64**, 1568 (1968).

Can. J. Chem. Downloaded from www.nrcresearchpress.com by 210.87.254.42 on 09/05/12
For personal use only.

The Rate Coefficient for $CH_3 + H_2 \rightarrow CH_4 + H$ Measured in Reflected Shock Waves; A Non-Arrhenius Reaction

THOMAS C. CLARK AND JOHN E. DOVE

Department of Chemistry, University of Toronto, Toronto, Ontario M5S 1A1

Received August 29, 1972

Dynamic sampling of reacting gas mixtures behind reflected shock waves has been used to determine the concentration *vs.* time profiles of the products of the recombination chain reactions of methyl radicals in the presence of molecular H_2. The radicals were produced by the rapid pyrolysis of azomethane. By analysis of profiles from experiments in the temperature range 1272–1370 °K we have deduced a value of the rate coefficient of reaction 5: $CH_3 + H_2 \rightarrow CH_4 + H$.

$$k_5 = 4.6 \pm 1.4 \times 10^7 \text{ l mol}^{-1} \text{ s}^{-1} \text{ at } 1340 \text{ °K}$$

It is shown that although this value of k_5 does not lie on the Arrhenius line drawn through lower temperature data, it does lie close to the upward curved Arrhenius plot of values of k_5 calculated by the B.E.B.O. transition state method. Taking a mean activation energy calculated by the B.E.B.O. method, our results suggest the following description for k_5 over the temperature range 1200 to 2000 °K:

$$k_5 = 10^{10.19 \pm 0.30} \exp(-15\,500/RT) \text{ l mol}^{-1} \text{ s}^{-1}$$

Un échantillon dynamique de mélanges gazeux en réaction derrière des chocs d'onde en réflexion a été utilisé pour déterminer les profils de concentration par rapport au temps, des produits de réaction de recombinaison de chaînes des radicaux méthyles en présence de H_2 moléculaire. Les radicaux ont été produits par la pyrolyse rapide de l'azométhane. Par analyse des profils issus des expériences dans l'intervalle de température 1272–1370 °K, nous avons déduit une valeur du coefficient de vitesse pour la réaction 5: $CH_3 + H_2 \rightarrow CH_4 + H$.

$$k_5 = 4.6 \pm 1.4 \times 10^7 \text{ l mol}^{-1} \text{ s}^{-1} \text{ à } 1340 \text{ °K}$$

Bien que cette valeur de k_5 ne se situe pas sur la droite d'Arrhenius obtenue à partir des données correspondants aux plus basses températures, nous avons montré que celle ci est proche du graphique d'Arrhenius courbé en montant et tirée des valeurs de k_5 calculées par la méthode B.E.B.O. sur l'état de transition. En prenant une énergie d'activation moyenne calculée par la méthode B.E.B.O., nos résultats suggèrent la description suivante pour k_5 dans l'intervalle de température de 1200 à 2000 °K:

$$k_5 = 10^{10.19 \pm 0.30} \exp(-15\,500/RT) \text{ l mol}^{-1} \text{ s}^{-1}$$

[Traduit par le journal]

Can. J. Chem., **51**, 2155 (1973)

Introduction

The methyl radical has been shown (1–4) to play an important part in the high temperature chain decomposition of several gaseous hydrocarbons such as methane, ethane, and butane. A knowledge of the reactions of CH_3 is therefore essential to an understanding of these decomposition processes. In recent studies (4, 5), a shock tube coupled to a time-of-flight mass spectrometer has been used to study the high temperature reactions of methyl radicals generated by the rapid pyrolysis of azomethane or dimethyl mercury. The rate of combination of methyl radicals, and the rate of their reaction with ethane, $CH_3 + C_2H_6 \rightarrow CH_4 + C_2H_5$. have been studied in this way. In the present work we have used the same experimental techniques to, determine the rate of reaction of methyl radicals with hydrogen,

[5] $$CH_3 + H_2 \rightarrow CH_4 + H$$

at high temperatures (1272–1370 °K) by pyrolyzing azomethane in the presence of added molecular hydrogen.

The rate coefficient for reaction 5 has been measured at low temperatures by various workers (6–11) whose results are not in very satisfactory agreement. The data of Majury and Steacie for $400 \leqslant T \leqslant 570$ °K are generally accepted as reliable (10–12), although there seems to be no clear reason to reject the data of Davison and Burton (7) or Anderson and Taylor (8). However all of the determinations of the rate coefficient for reaction 5 have been made at temperatures below 600 °K, and there is only one estimate (9) of k_5 above 600 °K. The coefficient for the reverse reaction −5, although more extensively studied (13–16), has been determined reliably only below 800 °K. Since recent calcula-

Can. J. Chem. Downloaded from www.nrcresearchpress.com by 210.87.254.5 on 09/05/12
For personal use only.

Can. J. Chem. Downloaded from www.nrcresearchpress.com by 210.87.254.5 on 09/05/12
For personal use only.

tions (17) have shown that the extrapolation of low temperature data by means of an Arrhenius plot can give a low estimate of a rate coefficient at higher temperatures, we considered it important to determine k_5 at temperatures nearer to those encountered in the pyrolyses of hydrocarbons.

Experimental

The apparatus has been described in detail previously (18). Reacting gas was directly sampled from behind reflected shock waves through a 0.1 mm orifice into the rapidly pumped ion source of a time-of-flight mass spectrometer. Mass spectra were photographically recorded at 20 μs intervals over the 300 to 400 μs duration of an experiment. Shock waves were produced using He or He/N_2 driver gas and 5 Torr initial pressure of reactant mixture containing 0.2 to 2% reagent diluted by neon. The heights of the mass peaks of each species were measured relative to the *m/e* 40 peak of a small known amount of argon included in the mixture as a reference gas. By utilizing the known mass spectrometric sensitivities relative to Ar, as determined in experiments with mixtures of known composition, absolute concentrations could be calculated. This procedure has been described elsewhere (4, 19). An electron energy of 25.0 eV was used in the ion source. Most of the other experimental details including the origin and purification of reagents were exactly as described previously (4). The hydrogen used in this work was Matheson "ultra high purity" grade (99.999%) and was used without further purification.

We performed two sets of experiments. The first repeated as closely as possible previous experiments (4) on azomethane pyrolysis, which were carried out in very similar apparatus, and acted as a standard. A mixture containing 0.16% azomethane, 0.26% argon, and 99.58% neon was used. The second mixture contained 1.87% added molecular hydrogen, 0.16% azomethane, 0.21% argon, and 97.76% neon. The amount of hydrogen added was the minimum which would give measurable changes in the reaction product concentrations. In order to obtain more reliable concentration–time profiles for the reaction products from the somewhat scattered data, the technique of grouping experiments (4, 19) was used. The results of two or three experiments at closely similar temperatures were combined, and the data were averaged. The temperature range of the experiments was restricted to approximately 1250 to 1400 °K. Below 1250° K the dissociation of azomethane was inconveniently slow, whereas above 1400 °K interpretation of the results was made more difficult by redissociation of the product ethane and by the further reaction of ethylene product to form acetylene.

Results

Figure 1 shows the time dependence of the concentrations of ethane, methane, and ethylene determined at 1325, 1340, and 1370 °K, as described above. The contours represent estimated uncertainty limits on the concentrations. We show the results of standard experiments and experiments performed with added hydrogen at the same mean temperatures. As can be seen, the principal effect of adding molecular hydrogen is to cause a significant increase in the amount of methane formed. Methane shows a principal mass peak at *m/e* 16 which is larger, for equal concentrations, than the ethane peak at *m/e* 30 or the fragment peak at *m/e* 26 used to determine ethylene. Thus relatively low concentrations of methane can be determined. Ethylene is difficult to determine since the most useful peak at *m/e* 26 requires correction for the contribution from ethane fragmentation. The correction introduces some further scatter and uncertainty into the data. Thus, in interpreting our data, we have concentrated on explaining the changes in the methane product profiles.

At lower temperatures, the amount of CH_4 formed in the standard experiments was expected to be very small, so that experiments were made using the mixture with added H_2 only. Figure 2 shows the results of these experiments at 1270 and 1311 °K.

Interpretation

The chain mechanism used previously (4) to explain the combination of methyl radicals and the effect of added ethane is:

$$[1] \qquad CH_3 + CH_3 \xrightarrow{(M)} C_2H_6$$

$$[2] \qquad CH_3 + C_2H_6 \rightarrow C_2H_5 + CH_4$$

$$[3] \qquad C_2H_5 \xrightarrow{(M)} C_2H_4 + H$$

$$[4] \qquad H + C_2H_6 \rightarrow C_2H_5 + H_2$$

In the previous work (4) the effect of added ethane was to produce larger, much more easily measured, concentrations of methane and ethylene, and k_1, k_2, and k_4 were determined. In the presence of added molecular hydrogen, the reaction

$$[5] \qquad CH_3 + H_2 \rightarrow CH_4 + H$$

is expected to become important. We have interpreted our present data in terms of reactions 1 to 5. The reaction rate equations for this mechanism were numerically integrated, using values of k_1, k_2, and k_4 taken from refs. 4 and 19, and choosing k_5 to fit the methane profiles in the later part of the reaction time. Several of the reverse reactions also had to be taken into account; in each case the rate coefficient of the reverse reaction was

Can. J. Chem. Downloaded from www.nrcresearchpress.com by 210.87.254.5 on 09/05/12
For personal use only.

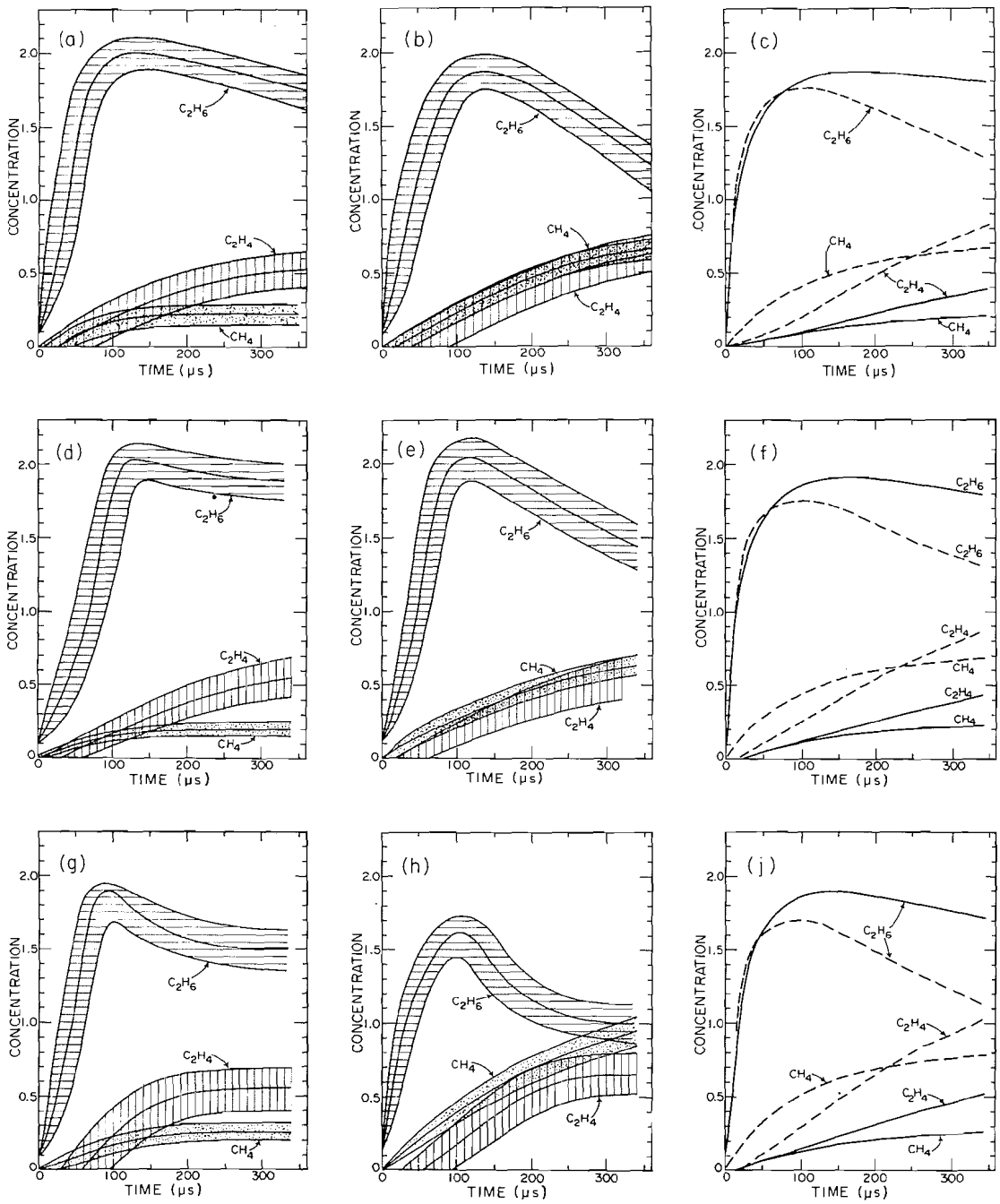

FIG. 1. Product concentration profiles: (*a*), (*b*), (*c*) at 1325 °K; (*d*), (*e*), (*f*) at 1340 °K; (*g*), (*h*), (*j*) at 1370 °K. (*a*), (*d*), (*g*): experimental profiles for the standard mixtures. (*b*), (*e*), (*h*): experimental profiles for the mixture with added hydrogen. (*c*), (*f*), (*j*): calculated profiles. Solid curve: standard mixture. Dashed curve: mixture with added hydrogen.

Can. J. Chem. Downloaded from www.nrcresearchpress.com by 210.87.254.5 on 09/05/12
For personal use only.

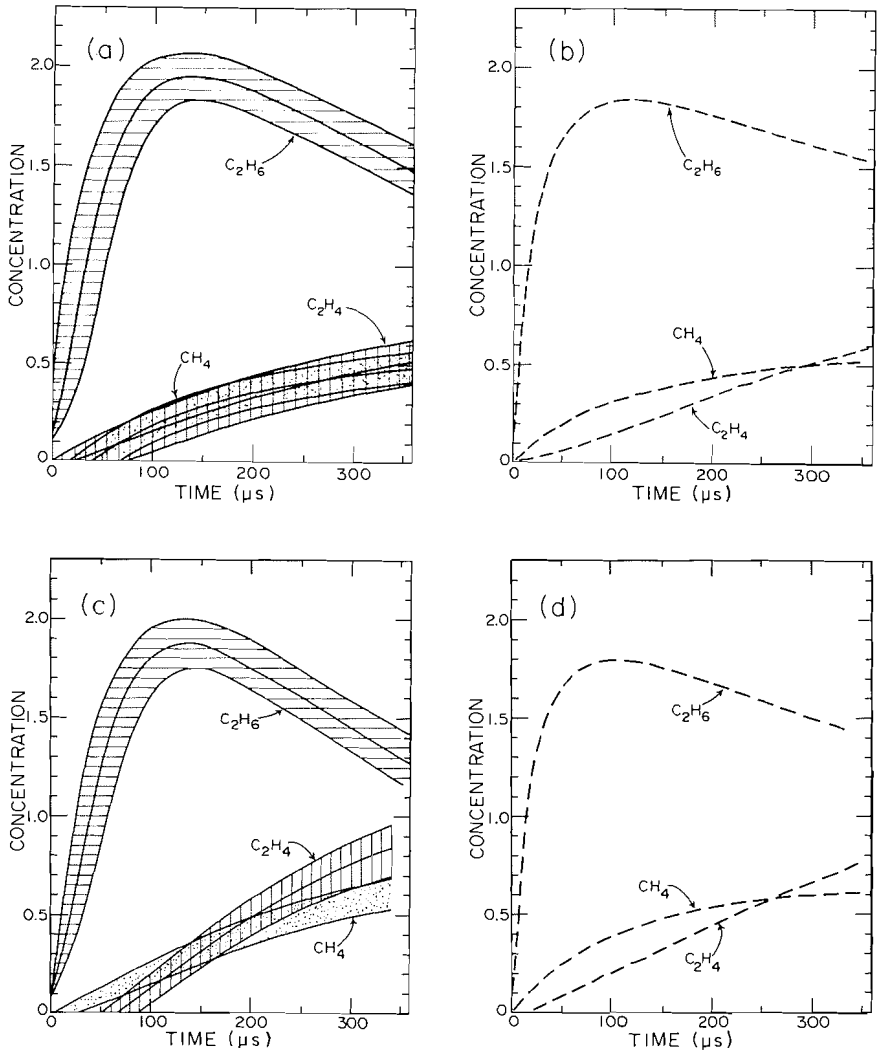

FIG. 2. Product concentration profiles for the mixture with added hydrogen. (*a*), (*b*) at 1270 °K; (*c*), (*d*) at 1311 °K. (*a*), (*c*): experimental profiles. (*b*), (*d*): calculated profiles.

calculated from the forward rate coefficient and the equilibrium constant from ref. 20.

Calculated and experimental profiles are compared in Figs. 1 and 2. The observed methane behavior was well described when $k_5 = 4.6 \times 10^7$ l mol^{-1} s^{-1} at 1340 °K. The small changes in the ethane profiles that occur when H_2 is added were also described. The temperature range of our studies was too small to allow a determination of the energy of activation. However the activation energy could be estimated as 15.5 kcal mol^{-1} from the known endothermicity of the reaction and a calculated activation energy for the reverse reaction (17). With the assumption of this activation energy, the rate coefficient can be expressed as $k_5 = 10^{10.19} \exp(-15\,500/RT)$ l mol^{-1} s^{-1}.

The effects of possible small errors in the value of the equilibrium constant K_5 were investigated, and it was found that changing k_{-5} by a factor of 2 did not affect our conclusions about k_5. In view of the difficulty of measuring ethylene accurately, we have not placed great emphasis on fitting the ethylene profiles. In the absence of added H_2, the calculations tend to underestimate the observed ethylene concentrations, and this has been commented on previously (4). With added

Can. J. Chem. Downloaded from www.nrcresearchpress.com by 210.87.254.5 on 09/05/12
For personal use only.

hydrogen, the ethylene profiles are fitted satisfactorily at 1272, 1312, and 1325 °K. However at 1340 and 1370 °K, the calculations overestimate the ethylene concentration. Although we do not consider this discrepancy serious, we have considered several other elementary reactions which might affect the observed profiles.

The reverse reaction −4 might be expected to reduce the formation of ethylene. However, we have calculated k_{-4} by the B.E.B.O. method (17); even when k_{-4} is increased to 10 times the calculated value, the effects of reaction −4 are negligible. The reaction −4 could become important if the concentration of C_2H_5 were large. Reduction of k_3 would tend to increase $[C_2H_5]$. However k_3 would need to be reduced by a factor of at least 50. The value of k_3 used in our calculations was calculated for the appropriate conditions of temperature and pressure using R.R.K.M. theory and models based on the work of Lin and Laidler (21) and Setser and Rabinovitch (22). Both models gave $k_3 \sim 3 \times 10^6$ s^{-1} at 150 Torr and 1350 °K. We feel that it is improbable that this value is in error by as much as a factor of 10.

We also considered reaction

$$[6] \qquad CH_3 + H \xrightarrow{(M)} CH_4$$

which might affect the yield of methane. We estimated the rate coefficient for this reaction from the thermodynamic equilibrium constant and a calculated value of the rate coefficient k_{-6} for the reverse reaction. We calculated k_{-6} for our experimental temperature and pressure by the R.R.K.M. theory using the model of Setser and Rabinovitch (22). The value of k_6 required to affect the methane formation significantly is 5×10^{10} l mol^{-1} s^{-1}, whereas our calculated value was 2.5×10^9 l mol^{-1} s^{-1}.

These various calculations show that the concentration changes observed when molecular hydrogen is added to the combining methyl radicals are best described by including reaction 5 with a rate coefficient $k_5 = 4.6 \times 10^7$ l mol^{-1} s^{-1} at 1340 °K. Our experimental results are also adequately described by values of k_5 within the range ±30% of this value. However additional uncertainties are introduced by possible errors in the values of the other rate coefficients used in our calculations. Taking these into account, we feel that k_5 is determined within a factor of 2.

Discussion

The lower limit for our value of k_5 determined at 1340 °K is 2.3×10^7 l mol^{-1} s^{-1}. As can readily be seen from Fig. 3, even this lowest value for k_5 is significantly higher than would be given by a straight-line Arrhenius extrapolation of the low temperature direct measurements (11, 15) of k_5. It should be noted that the rate coefficient of reaction 2 reported (4, 19) at 1350 °K was also significantly larger than predicted from low temperature data. In a recent paper (17) we have pointed out that there are theoretical reasons to expect appreciable non-linearity of Arrhenius plots for free radical abstraction reactions; this non-linearity becomes most noticeable when measurements are extended into the temperature range of shock tube studies. The long solid curve in Fig. 3 shows the temperature dependence of k_5 calculated by the B.E.B.O. method as described previously (17); the parameters used in the calculation were those employed for our earlier calculation (17) of k_{-5}, the rate coefficient for the back reaction. Our calculated curve has the same

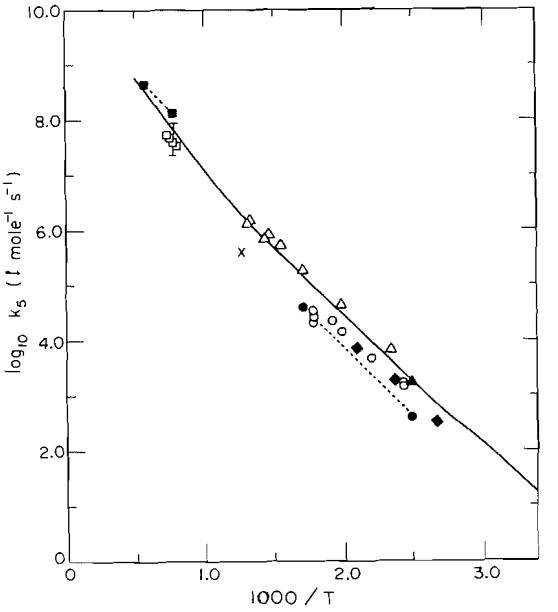

FIG. 3. Arrhenius plot for k_5. Solid curve: B.E.B.O. calculation, this work; ▲, calculated point (24); ○, experimental data (15); ●, upper and lower temperature points of rate parameters (7); ×, experimental data point (9); △, calculated from experimental k_{-5} (13) and thermodynamic equilibrium constant (20); ■, calculated from experimental k_{-5} (14) and thermodynamic equilibrium constant; □, experimental data, this work; ◆, experimental data (11).

form as an earlier calculation by Johnston (23), and agrees well with a point calculated by Polanyi (24) who used a method based on a L.E.P.S. surface. It can be added that our calculated k_5 and k_{-5} closely reproduce the thermodynamic equilibrium constant (20). As shown in Fig. 3, and as expected from our previous paper (17), our calculated values of k_5 also agree well with those deduced by multiplying the equilibrium constant K_5 by Kurylo and Timmons' (13) experimental values of k_{-5}.

Though the agreement among the various experimental data in Fig. 3 is fairly good, the values of k_5 obtained from data (13, 14) on the reverse reaction are systematically 2 to 3 times as large as the directly measured values of k_5. This discrepancy could very well arise from small errors in the experimental measurements. However another possibility which should be mentioned is that the thermodynamic equilibrium constant K_5 is somewhat too high. In this connection, we note that the current value (20) of K_5 (which we have used) is about 10 times larger at 600 °K than that obtained from data in the 1st edition of the JANAF tables, and that this increase is largely due to a change in the recommended ΔH_{f0}^{0} of CH_3 from +32.8 to +35.62 kcal mol^{-1}. If the heat of formation of CH_3 were taken as +34.4 kcal mol^{-1} (this change of 1.2 kcal mol^{-1} should, however, be compared with the currently quoted (20) JANAF uncertainty of ± 0.2 kcal mol^{-1}), the kinetic measurements of forward and reverse rates would agree with one another quite well. Such a change in the thermochemistry would, of course, also affect the calculated potential energy of activation and necessitate a slight revision of the B.E.B.O. calculations, but we find that none of our basic conclusions would be changed.

The above considerations about K_5 do not, in any case, appreciably influence the evaluation of our experimental k_5 at temperatures close to 1340 °K. Our experimental findings do thus support the Arrhenius curvature predicted by transition state calculations and underscore the need for determining rate coefficients at temperatures close to those at which they are to be applied. If we accept the activation energy calculated by the B.E.B.O. method (using current JANAF data) at 1500 °K, and our rate coefficient k_5 at 1340 °K, then the following expression would be expected to hold to within a factor of 2 for k_5 between 1200 and 2000 °K:

$$k_5 = 10^{10.19} \exp(-15\,500/RT)\ \text{l mol}^{-1}\ \text{s}^{-1}$$

This work was supported by grants from the National Research Council of Canada and Imperial Oil Limited.

1. S. W. BENSON and H. E. O'NEAL. Kinetic data on gas phase unimolecular reactions. National Bureau of Standards NSRDS-NBS 21, 1970.
2. P. GRAY, A. A. HEROD, and A. JONES. Chem. Rev. **71**, 247 (1971).
3. T. P. J. IZOD, G. B. KISTIAKOWSKY, and S. MATSUDA. J. Chem. Phys. **56**, 1337 (1972).
4. T. C. CLARK, T. P. J. IZOD, and G. B. KISTIAKOWSKY. J. Chem. Phys. **54**, 1295 (1971).
5. T. C. CLARK, M. A. DI VALENTIN, T. P. J. IZOD, and J. E. DOVE. J. Chem. Phys. **53**, 2982 (1970).
6. T. G. MAJURY and E. W. R. STEACIE. Can. J. Chem. **30**, 800 (1953).
7. S. DAVISON and M. BURTON. J. Am. Chem. Soc. **74**, 2307 (1952).
8. R. D. ANDERSON and H. A. TAYLOR. J. Phys. Chem. **56**, 498 (1952).
9. S. W. BENSON and D. V. S. JAIN. J. Chem. Phys. **31**, 1008 (1959).
10. K. O. KUTSCHKE and E. W. R. STEACIE. J. Phys. Chem. **62**, 866 (1958).
11. H. GESSER and E. W. R. STEACIE. Can. J. Chem. **34**, 113 (1956).
12. H. O. PRITCHARD and G. O. PRITCHARD. Can. J. Chem. **41**, 3042 (1963).
13. M. J. KURYLO and R. B. TIMMONS. J. Chem. Phys. **50**, 5076 (1969).
14. C. P. FENIMORE and G. W. JONES. J. Phys. Chem. **65**, 2200 (1961).
15. T. G. MAJURY and E. W. R. STEACIE. Discuss. Faraday Soc. **14**, 45 (1953).
16. J. W. S. JAMESON and G. R. BROWN. Can. J. Chem. **42**, 1638 (1964).
17. T. C. CLARK and J. E. DOVE. To be published.
18. S. C. BARTON and J. E. DOVE. Can. J. Chem. **47**, 521 (1969).
19. T. C. CLARK and T. P. J. IZOD. Dynamic mass spectrometry. Vol. 3. Heyden. 1972. p. 209.
20. D. R. STULL, H. PROPHET *et al.* JANAF Thermochemical tables. 2nd ed. NSRDS-NBS 37, 1970.
21. M. C. LIN and K. J. LAIDLER. Trans. Faraday Soc. **64**, 79 (1968).
22. B. S. RABINOVITCH and D. W. SETSER. Adv. Photochem. **3**, 1 (1964).
23. H. S. JOHNSTON. Gas phase reaction rate theory. Ronald, 1966. p. 215.
24. J. C. POLANYI. J. Chem. Phys. **24**, 493 (1956).

Can. J. Chem. Downloaded from www.nrcresearchpress.com by 210.87.254.5 on 09/05/12
For personal use only.

Crystalline Adduct Formation Between Quaternary Alkyl Ammonium Salts and Simple Aromatic Compounds[1]

JOSEPH W. HARDY, ELRICK M. WILLIAMS, EDWARD LIPKIN, JEFFREY M. ROSEN, MICHAEL F. ROIZEN, PETER J. BUCHIN, AND EDWARD GODFREY TAYLOR
Department of Chemistry, Williams College, Williamstown, Massachusetts

AND

CHARLES LEONARD TAYLOR AND RAYMOND EVANS MARCH[2]
Department of Chemistry, Trent University, Peterborough, Ontario

Received April 24, 1972[3]

Several crystalline 1:1 adducts of quaternary alkyl ammonium salts with simple aromatic compounds have been prepared. Adduct formation appears to be restricted to certain salt–solvent pairs when the alkyl substituent is *n*-butyl or *i*-amyl, the anion is iodide, perchlorate, nitrate, or picrate and the aromatic compound is benzene, fluorobenzene, or toluene. The standard enthalpy and entropy changes of adduct formation at 25 °C have been obtained from vapor pressure measurements. A linear relationship between these thermodynamic parameters is expressed in the form of an isokinetic temperature. An absorption band at 14.4 μ appears to be characteristic of this series.

Plusieurs produits d'addition (1:1) cristallins ont été proposés à partir de sels d'ammonium quaternaire d'alcoyles et de composés aromatiques simples. La formation de ces produits semble être limitée à certaines paires, solvant-sel, lorsque le groupe alcoyle est le *n*-butyle ou l'*i*-amyle, lorsque l'anion est l'iodure, le perchlorate, le nitrate ou le picrate et aussi lorsque le groupe aromatique est le benzène, le fluorobenzène ou le toluène. Lors de la formation de ces produits à 25 °C, les variations d'enthalpie et d'entropie ont été obtenues à partir de mesures de la tension de vapeur. On exprime la relation linéaire présente entre ces paramètres thermodynamiques sous forme d'une température isocinétique. Une bande d'absorption à 14.4 μ semble être caractéristique de cette série de composés.

[Traduit par le journal]

Can. J. Chem., **51**, 2161 (1973)

Can. J. Chem. Downloaded from www.nrcresearchpress.com by 210.87.254.6 on 09/05/12
For personal use only.

The formation of solid adducts in 1:1 mole ratio between benzene and tetra-*n*-butyl ammonium perchlorate (1), nitrate (2), and picrate (3) has been reported previously. The work reported here seeks to show that the phenomenon is quite general among a number of quaternary alkyl ammonium salts and simple aromatic compounds. Evidence for the extent of adduct formation has been sought through a systematic variation of cation alkyl substituents, anions, and organic compounds. Adduct formation has been found to occur between certain salt–solvent pairs where (*i*) the cation is $(n\text{-butyl})_4N^+$, $(i\text{-amyl})_4N^+$, or $(i\text{-amyl})_3(n\text{-butyl})N^+$; (*ii*) the anion is iodide, perchlorate, nitrate or picrate; and (*iii*) the organic compound is benzene, fluorobenzene, or toluene.

Experimental

Materials

The quaternary alkyl ammonium iodides were prepared in the usual manner from purified tertiary amines and alkyl iodides; nitrates were obtained by metathesis of the quaternary ammonium iodides with silver nitrate. The bromide and the perchlorate salts were prepared from the corresponding hydroxides by neutralization with hydrobromic and perchloric acids, respectively. All salts were purified by multiple recrystallizations and melting points served as an indication of purity: tetra-*n*-propylammonium nitrate (hereafter abbreviated Pr_4NNO_3), m.p. 268–269° (d), tetra-*n*-butyl ammonium iodide (Bu_4NI), m.p. 146°, tetra-*n*-butyl ammonium nitrate (Bu_4NNO_3), m.p. 120°, tetra-*n*-butyl ammonium perchlorate (Bu_4NClO_4), m.p. 210°, tetra-*n*-butyl ammonium bromide (Bu_4NBr), m.p. 117–118°, triisoamyl-*n*-butyl ammonium iodide ($i\text{-Am}_3BuNI$), m.p. 122°, triisoamyl-*n*-butyl ammonium perchlorate ($i\text{-Am}_3BuNClO_4$), m.p. 101–103°, tetraisoamyl ammonium iodide ($i\text{-Am}_4NI$), m.p. 148°, tetraisoamyl ammonium nitrate ($i\text{-Am}_4NNO_3$), m.p. 142°, tetraisoamyl ammonium perchlorate ($i\text{-Am}_4NClO_4$), m.p. 116–117°, and tetra-*n*-amyl ammonium nitrate ($n\text{-Am}_4NNO_3$), m.p. 98–100°.

Benzene, fluorobenzene, and toluene were either of spectrophotometric or reagent quality and were normally used without further purification. Cyclopentadiene was distilled at 50 °C from a mixture of cyclopentadiene and its dimer and stored at −25 °C.

[1]Abstracted in part from the Honors theses of J.W.H. (1966), J.M.R. (1966), M.F.R. (1967), and P.J.B. (1970), the Project Reports of E.L. (1968) and E.M.W. (1968), all of Williams College, Williamstown, Massachusetts.

[2]To whom inquries should be addressed.

[3]Revision received February 8, 1973.

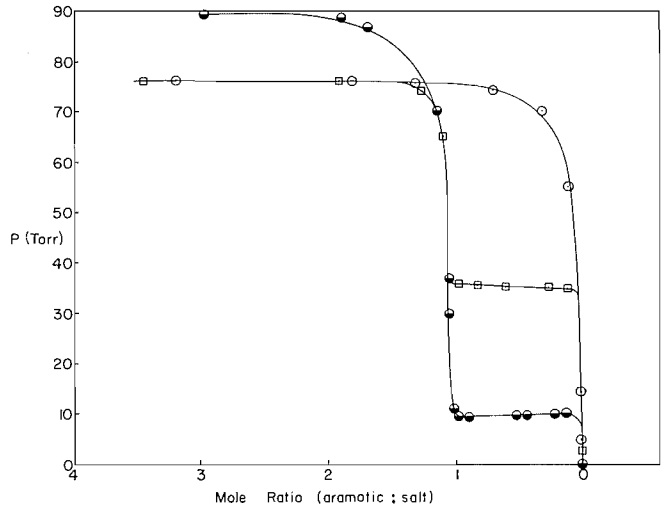

FIG. 1. Vapor pressure–composition curves indicating adduct formation for the systems in *i*-$Am_3BuNClO_4$–benzene ◒ and Bu_4NClO_4–fluorobenzene □. No adduct formation is observed for the system *i*-Am_4NNO_3–fluorobenzene ○.

Vapor pressure – composition curves were determined at 25 °C by means of relatively simple mercury manometer systems having removable sample flasks. Each flask contained initially approximately 1 g of salt per ml of solvent, such as would produce a molar excess of solvent. The flask was warmed in a water bath, evacuated, and the vapor pressure of the solvent was allowed to come to equilibrium over a period of up to several hours, and recorded. All mercury manometer readings were corrected to 0 °C. The flask was then removed from the apparatus, dried, capped, and weighed. Vapor pressure – composition curves were then constructed as shown in Fig. 1; a step-curve displaying a break at 1:1 mole salt–solvent ratio and similar to that previously illustrated (2), was taken as evidence of adduct formation. Vapor pressure – temperature measurements of the molecular adducts were obtained in the range 0–50 °C by submersion of the sample flasks in thermostatted water baths. The maximum expected error in pressure measurements is estimated at ± 0.5 mm. Phase diagrams were constructed in the usual manner from experiments in which appropriate known amounts of salt and solvent were sealed in heavy-walled glass tubing. The tubes were then attached to a shaker and immersed in an oil bath, the temperature of which was raised slowly until the last trace of solid had disappeared.

When adduct-forming salts were added to dry benzene and warmed, two liquid layers were observed. The salt content of the upper layer has been shown (1, 3) to be extremely low, being of the order of 10^{-2} *M*, while that of the lower layer was approximately 10–20 mol %. The two-layer system is often quite stable over a period of weeks.

U.v. absorption spectra of Bu_4NNO_3 and Bu_4NClO_4 with benzene in cyclohexane, with benzene in ethanol, and in pure benzene were determined using Unicam SP800 and Beckmann DB-G spectrophotometers. U.v. spectra of solid samples of Bu_4NNO_3 and the Bu_4NNO_3–C_6H_6 adduct were recorded on the SP800.

I.r. absorption spectra of mulls of Bu_4NNO_3, Bu_4NClO_4, *i*-Am_4NClO_4, *i*-$Am_3BuNClO_4$, *n*-Am_4NNO_3 in benzene, and Bu_4NNO_3 and *n*-Am_4NNO_3 in fluorobenzene were obtained using a Perkin–Elmer 621 grating spectrophotometer.

Results

In Table 1 are summarized the experimental results obtained from vapor pressure – composition studies of all quaternary ammonium salt – solvent pairs studied. For those systems in which adducts were found, the vapor pressure of the adduct is given in Torr at 25 °C.

Data from vapor pressure – temperature measurements of the adduct were treated by the least-mean-square method to obtain the slope *a*, and intercept *b*, from the data expressed in the form $\log P(\text{Torr}) = a/_T + b$. The values obtained for the parameters *a* and *b* for the adducts studied are shown in Table 2; they constitute a concise form of the experimental results obtained for the nine systems examined in detail. Calculated probable errors for the values of *a* are as given and for the values of *b* are ± 0.2.

Adduct formation from solid salt and liquid aromatic solvent may be represented as

[1] $$R_4NX_{(s)} + Ar_{(l)} \rightleftharpoons (R_4NX{-}Ar)_{(s)}$$

which may be regarded as the sum of

[2] $$Ar_{(l)} \rightleftharpoons Ar_{(v)}$$

and

[3] $$R_4NX_{(s)} + Ar_{(v)} \rightleftharpoons (R_4NX{-}Ar)_{(s)}$$

Can. J. Chem. Downloaded from www.nrcresearchpress.com by 210.87.254.6 on 09/05/12
For personal use only.

TABLE 1. Experimental vapor pressure – composition results for salt–solvent pairs studied at 25 °C

Salt	Solvent	Adduct-formation*	Adduct vapor pressure (Torr)
i-$Am_3BuNClO_4$	$-C_6H_6$	Yes	10.0
Bu_4NNO_3	$-C_6H_6$	Yes	15.2†
Bu_4NClO_4	$-C_6H_6$	Yes	24.3‡
i-Am_4NClO_4	$-C_6H_6$	Yes	26.4
i-Am_4NI	$-C_6H_6$	Yes	41.2
i-Am_3BuNI	$-C_6H_6$	Yes	45.8
i-Am_4NNO_3	$-C_6H_6$	Yes	56.4
Bu_4NI	$-C_6H_6$	Inconclusive	—
n-Am_4NNO_3	$-C_6H_6$	No	—
Pr_4NNO_3	$-C_6H_6$	No	—
Bu_4NBr	$-C_6H_6$	No	—
i-$Am_3BuNClO_4$	$-C_6H_5F$	Yes	11.6
Bu_4NNO_3	$-C_6H_5F$	Yes	12.5
i-Am_4NClO_4	$-C_6H_5F$	Yes	33.4
Bu_4-$NClO_4$	$-C_6H_5F$	Yes	35.4
i-Am_4NI	$-C_6H_5F$	Yes	52.0
i-Am_4NNO_3	$-C_6H_5F$	No	—
i-$Am_3BuNClO_4$	$-C_6H_5CH_3$	Yes	12.2
Bu_4NNO_3	$-C_6H_5CH_3$	No	—
i-Am_4NNO_3	$-C_6H_5CH_3$	No	—
Bu_4NNO_3	$-C_5H_6$	No	—

*Observation of plateau in vapor pressure *vs.* composition curve.
†Reference 2.
‡Reference 1.

TABLE 2. Vapor pressure – temperature equation parameters a and b and ΔG_1^0, ΔH_1^0, ΔS_1^0 values (25°) for all adducts studied

Complex	a	b	ΔG_1^0 (cal mol^{-1})	ΔH_1^0 (cal mol^{-1})*	ΔS_1^0 (e.u. mol^{-1})
i-$Am_3BuNClO_4$–C_6H_6	−3080 ± 100	+11.4	−1300 ± 30	−5900 ± 500	−15 ± 2
Bu_4NNO_3–C_6H_6	−3410 ± 50	+12.6	−1100 ± 30	−7400 ± 250	−21† ± 1
i-$Am_3BuNClO_4$–C_6H_5F	−2740 ± 100	+10.2	−1100 ± 30	−4400 ± 500	−11 ± 2
Bu_4NClO_4–C_6H_6	(No values given)		−810	−6100	−18‡
i-$Am_3BuNClO_4$–$C_6H_5CH_3$	−2560 ± 100	+9.68	−500 ± 20	−2900 ± 500	−8 ± 2
i-Am_4NI–C_6H_6	−1830 ± 50	+7.75	−490 ± 20	−160 ± 250	+1.1 +0.9, −0.6
i-Am_4NClO_4–C_6H_5F	−1960 ± 75	+8.11	−490 ± 20	−800 ± 400	−1.1 +0.7, −1.4
Bu_4NClO_4–C_6H_5F	−2860 ± 100	+11.1	−450 ± 20	−4900 ± 500	−15 ± 2
i-Am_3BuNI–C_6H_6	−1790 ± 50	+7.66	−430 ± 20	0 ± 250	+1.4 ± 1
i-Am_4NNO_3–C_6H_6	−1740 ± 25	+7.59	−300 ± 20	+200 ± 130	+1.7 ± 0.5

*Note: $\Delta H_1^0 = \Delta H_2^0 + \Delta H_3^0$; the uncertainty in ΔH_2^0 is ±20 cal. while ΔH_3^0 varies directly with a.
†Reference 2.
‡Reference 1.

ΔG_1^0 values, at 25 °C, for reactions of type [1] were calculated directly from $\Delta G^0 = 2.303\ RT \log P_0/P$, where P_0 is the vapor pressure of the pure solvent, and P is that of the adduct. The values obtained are given in Table 2 and are summarized in Table 3. Literature values (4) for the temperature variation of vapor pressure of benzene, fluorobenzene, and toluene were used to calculate ΔH^0 for reactions of type [2], *i.e.* ΔH_2^0: the values obtained were 8170, 8160, and 8840 cal mol^{-1}, respectively. The experimental results for the temperature variation of adduct vapor pressure were used for the calculation of ΔH_3^0. The enthalpy of solid complex formation from solid salt and liquid solvent, ΔH_1^0 was then calculated as the sum of ΔH_2^0 and ΔH_3^0. The entropy of adduct formation, ΔS_1^0 was calculated from

Can. J. Chem. Downloaded from www.nrcresearchpress.com by 210.87.254.6 on 09/05/12
For personal use only.

TABLE 3. Summary of adduct formation results. ΔG_1^0 (25 °C) in cal mol^{-1}

Salt	Solvent		
	C_6H_6	C_6H_5F	$C_6H_5CH_3$
i-$Am_3BuNClO_4$	−1300	−1100	−500
Bu_4NNO_3	−1100†	−1100	*
Bu_4NClO_4	−810‡	−450	—
i-Am_4NClO_4	−760	−490	—
i-Am_4NI	−490	−230	—
i-Am_3BuNI	−430	—	—
i-Am_4NNO_3	−300	*	*
Bu_4NI	Inconclusive ($\Delta G_1^0 < 100$)	—	—
n-Am_4NNO_3	*	—	—
Pr_4NNO_3	*	—	—
Bu_4NBr	*	—	—
Bu_4N Picrate§	Complex formed		

*Complex sought, but not found.
†Reference 1.
‡Reference 2.
§Reference 3.

[4] $$\Delta S_1^0 = (\Delta H_1^0 - \Delta G_1^0)/T$$

The values are shown in Table 2.

Phase diagrams were obtained for two salt–solvent adduct-forming pairs, *i*-Am_4NNO_3–C_6H_6 and *i*-Am_4NI–C_6H_6 and were very similar in general form to that noted previously for Bu_4NNO_3–C_6H_6 (2). Congruent melting points at approximately 1:1 mole ratio were measured as 76 °C for the *i*-Am_4NNO_3–C_6H_6 system and as 110 °C for the *i*-Am_4NI–C_6H_6 system. Both complexes showed evidence of being largely dissociated in the fused state.

Both solution and solid u.v. spectra of Bu_4NClO_4–C_6H_6 and Bu_4NNO_3–C_6H_6 displayed no significant changes in the character of component absorptions nor any new peaks in the range 195–700 mμ.

It had been reported earlier (2) that the "complex" Bu_4NNO_3–C_6H_6 displayed a new absorption peak at 14.4 μ; we have confirmed the existence of this peak in this "complex" and have found that it occurs in the "complex" forming systems Bu_4NClO_4–C_6H_6, *i*-Am_4NClO_4–C_6H_6, and *i*-$Am_3BuNClO_4$–C_6H_6, but is absent for a mixture of *n*-Am_4NNO_3 and C_6H_6 which has been found not to form an adduct. Preliminary work has indicated that fluorobenzene–salt system spectra follow the same pattern; no peak at 14.4 μ was observed in the case of non-adduct forming *n*-Am_4NNO_3–C_6H_5F mixture while one was observed in the case of an adduct forming Bu_4NNO_3–C_6H_5F mixture.

Discussion

There are three general classes of molecular complexes, *viz.* hydrogen-bonded, clathrate, and charge transfer. While no definite conclusions are drawn as to the nature of the interaction which leads to adduct formation, meaningful comparison with other work can be made and the trends of the data obtained are significant. The band at 14.4 μ which appeared in the i.r. spectra at each of the adducts is probably assignable to C—H out-of-plane bending of the aromatic species held in a crystal lattice, as previously suggested (2). No absorption band was observed in the spectra of solutions of adducts.

In a series of related reactions involving moderate changes in structure the enthalpies and entropies vary, but usually not independently. The relationship between ΔH and ΔS is shown in Fig. 2. The isokinetic temperature obtained from the slope of least squares is 325 °K. This linear change of ΔH with ΔS for a series of related equilibrium involving moderate changes in structure has been reported by several authors (7). The data of Keefer and Andrews (5) with substituted benzene–iodine complexes and those of Yada *et al.* (6) with aliphatic amine – iodine complexes yield isokinetic temperatures of 585 and 542 °K, respectively. The data for the benzene–iodine complex is shown in line with our data for benzene–alkyl quaternary ammonium complexes.

Some of the adducts of this series are quite strongly bonded as is seen from the magnitudes of the enthalpy changes. This tends to eliminate hydrogen bonding as the principal mode of interaction.

All of the adducts are formed in a strict 1:1 stoichiometric ratio and with a steady and reproducible vapor pressure. Such observations are not consistent with clathrate formation.

It is significant that no indication of charge transfer was observed in the u.v. absorption spectra, and the apparent lack of absorption is not readily attributable to the low resolving power or low sensitivity of the instruments used. However, absorption due to the adduct may be masked by the strong bands of benzene. There are many cases of complexes so described

Can. J. Chem. Downloaded from www.nrcresearchpress.com by 210.87.254.6 on 09/05/12
For personal use only.

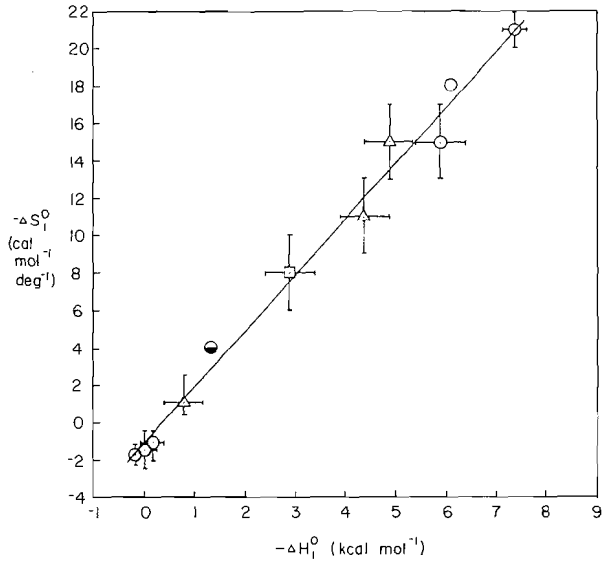

FIG. 2. Variations in ΔS_1^0 with ΔH_1^0 for adduct formation. ○ Benzene – quaternary alkyl ammonium salts (q.a.a.s.) adducts; △ fluorobenzene – q.a.a.s. adducts; □ toluene–q.a.a.s. adduct; ◒ benzene–iodine adduct (ref. 5).

(7) in which absorption due to supposed charge transfer has not been demonstrated. It should be noted that a weak band ($\varepsilon < 10$) near 300 mμ, due to absorption by NO_3^-, was observed for both solid salt and solid complex spectra. Benzene and substituted benzenes have been observed to form charge transfer complexes with I_2 (5), as have aliphatic primary, secondary, and tertiary amines (6), and it may not be unreasonable to suggest that substitution of I_2 by quaternary ammonium salts may lead to similar complex formation.

1. R. P. SEWARD. Inorg. Chem. **3**, 1056 (1964).
2. T. J. PLATI and E. G. TAYLOR. J. Phys. Chem. **68**, 3426 (1964).
3. G. M. POLTORATSKI and K. P. MISCHENKO. Zhur. Fiz. Khim. **39**, 264 (1965).
4. International critical tables of numerical data, physics, chemistry and technology. 1st Ed. Vol. III. McGraw-Hill Book Co. Inc., New York. 1926. p. 221, 223.
5. R. M. KEEFER and L. J. ANDREWS. J. Am. Chem. Soc. **77**, 2164 (1955).
6. H. YADA, J. TANAKA, and S. NAGAKURA. Bull. Chem. Soc. Jap. **33**, 1660 (1960).
7. J. E. LEFFLER. J. Org. Chem. **20**, 1202 (1955).

Can. J. Chem. Downloaded from www.nrcresearchpress.com by 210.87.254.6 on 09/05/12
For personal use only.

Total Synthesis of Eremophilane-type Sesquiterpenoids: (±)-Eremophilenolide, (±)-Tetrahydroligularenolide, and (±)-Aristolochene

EDWARD PIERS[1] AND MICHAEL BERT GERAGHTY

Department of Chemistry, University of British Columbia, Vancouver 8, British Columbia

Received January 8, 1973

The total synthesis of the racemic forms of the eremophilane-type sesquiterpenoids eremophilenolide (**2**), tetrahydroligularenolide (**3**), and aristolochene (**4**) is described. The octalone **7** was converted via an efficient, regioselective route into the keto ester **12**, which served as a common synthetic intermediate for the preparation of the three sesquiterpenoids. Successive subjection of **12** to alkylation, hydrolysis, and decarboxylation afforded the keto acid **14**. Hydrogenation of the latter provided both the *cis*-fused keto acid **20**, which was readily converted into (±)-eremophilenolide (**2**), and the *trans*-fused keto acid **15**, which was similarly transformed into (±)-tetrahydroligularenolide (**3**). Conversion of **12** into the dithioketal **23**, followed by desulfurization and treatment of the resultant olefinic ester **25** with excess methyllithium, provided the olefinic alcohol **27**. Dehydration of the latter yielded (±)-aristolochene (**4**).

La synthèse totale des formes racémiques des sesquiterpénoïdes érémophilènolide (**2**) du type érémophilane, tétrahydroligularénolide (**3**) et l'aristolochène (**4**) est décrite. L'octalone **7** a été converti en passant par un chemin régiosélectif efficace en céto-ester **12**, qui sert d'intermédiaire synthétique commun pour la préparation de trois sesquiterpénoïdes. Lorsque l'on soumet **12** successivement à une alcoylation, à une hydrolyse et à une décarboxylation, l'on obtient alors un céto-acide **14**. L'hydrogénation de ce dernier produit conduit à la fois au céto-acide réuni de manière *cis* **20** qui a été transformé immédiatement en érémophilènolide-(±) (**2**) et au céto-acide réuni de manière *trans* **15** qui a été transformé, de la même façon, en tétrahydroligularenolide-(±) (**3**). La transformation de **12** en dithiocétal **23**, suivi par une désulfurisation et par le traitement de l'ester oléfinique résultant **25** avec du méthyllithium en excès, conduit à l'alcool oléfinique **27**. La déshydratation de ce dernier composé conduit à l'aristolochène-(±) (**4**).

[Traduit par le journal]

Can. J. Chem., 51, 2166 (1973)

Can. J. Chem. Downloaded from www.nrcresearchpress.com by 210.87.254.6 on 09/05/12
For personal use only.

The number of known, naturally occurring eremophilane-type[2] sesquiterpenoids has increased markedly over the past few years (1, 2). To date, approximately 70 different eremophilane-type natural products have been isolated and subjected to structural elucidation. On the other hand, in spite of considerable total effort on the part of a number of research groups, only a few of the structurally fairly-simple members of this class have yielded to total synthesis.[3] We report in this paper the total synthesis of (±)-eremophilenolide (**2**),[4] (±)-tetrahydroligularenolide (**3**), and (±)-aristolochene (**4**).

(+)-Eremophilenolide was isolated (20) from *Petasites officinalis* Moench. and was subsequently shown (21) to possess structure and absolute stereochemistry as depicted in **2**. This compound can be considered as the parent of a small number of eremophilane-type sesquiterpenoids possessing the α,β-unsaturated γ-lactone moiety. Although (−)-tetrahydroligularenolide (**3**) has not as yet been isolated from natural sources, it has been obtained in high yield by palladium-catalyzed hydrogenation of the naturally occurring (−)-ligularenolide (**5**) (22) (absolute configuration as shown). The hydrocarbon (−)-aristolochene, isolated from the roots of *Aristolochia indica*, has been shown (23) to possess structure and absolute configuration as depicted in **4**. This compound is a double bond isomer of the well-known sesquiterpene hydrocarbon (+)-valencene (**6**) (24, 25, 7*b*).

The preparation of the three sesquiterpenoids **2**, **3**, and **4** was accomplished via a common

[1]Fellow of the Alfred P. Sloan Foundation, 1970–1972.

[2]The parent carbon skeleton and the normally-employed numbering system for the eremophilane-type sesquiterpenoids are shown in formula **1**.

[3]To date, the following eremophilane-type and structurally closely related aristolane-type sesquiterpenoids have been totally synthesized: (±)-aristolone (3, 4), (±)-calarene (5), (±)-dehydrofukinone (6), (±)-eremoligenol (7), (±)-eremophil-3,11-diene (8), (±)-eremophilene (7), (±)-fukinone (9–11), (+)-hydroxyeremophilone (11*b*), (±)-ishwarane (12), (±)-*iso*-nootkatone (α-vetivone) (13, 14*a*), (−)-*iso*-nootkatone (α-vetivone) (14*b*), (±)-nootkatone (14*a*, 15, 16), (−)-nootkatone (14*b*), (±)-7-*epi*-nootkatone (14*a*, 17), (±)-tetrahydroeremophilone (18), (±)-valencene (7*b*), and (±)-valerianol (7*b*).

[4]For a preliminary communication, see ref. 19.

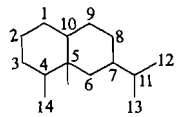

1

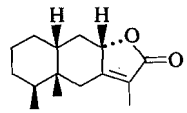

2

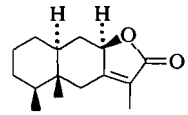

3

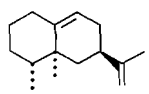

4

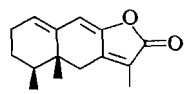

5

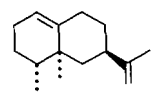

6

synthetic intermediate, the keto ester **12**. The latter was obtained from the octalone **7** (26) by means of the efficient and completely regioselective synthetic route outlined in Scheme 1. Conversion of **7** into the corresponding hydroxymethylene derivative **8** (9), followed by dehydrogenation of the latter with 2,3-dichloro-5,6-dicyanobenzoquinone (27) in dioxan, afforded in 93% overall yield the cross-conjugated keto aldehyde **9**. Oxidation of compound **9** with silver oxide (28) and esterification of the resultant carboxylic acid (**10**) with silver oxide and methyl iodide afforded the keto ester **11** in 85% overall yield. Reduction of **11** with sodium borohydride in pyridine (29) gave, in 86% yield, the crystalline β-keto ester **12**. An alternative, direct conversion of the octalone **7** into the keto ester **12** involving base-promoted condensation of the former with dimethyl carbonate was also considered. However, on the basis of literature precedent (30), it was felt that a reaction of this type would result in carbomethoxylation of **7** at C-1 as well as at the desired position (C-3). Indeed, this direction conversion was later attempted (11*b*) and the product, although claimed to be **12**, was not obtained crystalline and no criterion of purity was given.

Attempted alkylation of **12** with ethyl 2-bromopropionate under a variety of conditions failed. In each case, starting material was recovered in high yield. However, when the sodium enolate of compound **12** was allowed to react with methyl bromoacetate in hot benzene, the desired keto diester **13** was obtained in quantitative yield (see Scheme 1). As shown by the p.m.r. spectrum, this material consisted largely of one diastereomer, and, although the stereochemistry was not rigorously established, literature precedent (30) indicated that the newly alkylated center should possess the configuration shown in **13**. In any event, this point was not crucial, since the next step of the synthesis involved hydrolysis and decarboxylative removal of the tertiary carbomethoxy moiety.

Treatment of the diester **13** with sodium hydroxide in refluxing ethanol–water provided the crystalline keto acid **14** in 82% yield. The stereochemistry of the latter was undoubtedly as indicated, since the epimeric (at C-7) compound would contain a 1,3-diaxial interaction between the angular methyl group and the acetic acid side chain.

In order to obtain (from **14**) a synthetic intermediate suitable for elaboration into (±)-tetrahydroligularenolide (**3**), it was necessary to reduce the carbon–carbon double bond of **14** so as to produce the corresponding *trans*-fused decalone system. On the other hand, reduction to a *cis*-fused decalone was necessary for the production of an intermediate suitable for conversion into (±)-eremophilenolide (**2**).

Hydrogenation of **14** in ethanol over palladium-on-charcoal produced a quantitative yield of the *trans*-fused keto acid **15**. That this hydrogenation had, in fact, afforded the *trans*-fused decalone system was shown conclusively by an independent synthesis of **15**. Thus, treatment of the known decalone **16** (26) with isopropenyl acetate-*p*-toluenesulfonic acid (31) afforded a mixture of the corresponding enol acetates **17** and **18**, in a ratio of approximately 3:2. Reaction of this mixture with 2 equiv of methyllithium in dimethoxyethane (31), followed by addition of methyl bromoacetate, gave a mixture of compounds from which the keto ester **19** could be isolated by column chromatography. Alkaline hydrolysis of **19** yielded the keto acid **15**, identical in all respects with the product obtained by hydrogenation of **14**.

Subjection of compound **14** to hydrogenation with palladium-on-charcoal under basic conditions (ethanolic sodium hydroxide) afforded a quantitative yield of a mixture of the *cis*-fused decalone **20** and the previously obtained *trans*-fused compound **15**, in a ratio of approximately 2:3. At this stage, considerable effort was expended in order to find conditions which would increase the proportion of the desired *cis*-fused decalone **20**. Eventually it was found that hydrogenation of **14** in ethanolic sodium hydroxide using rhodium-on-carbon as catalyst gave improved results. However, under these conditions the ketone carbonyl group was also reduced and it was therefore necessary to oxidize

Can. J. Chem. Downloaded from www.nrcresearchpress.com by 210.87.254.6 on 09/05/12
For personal use only.

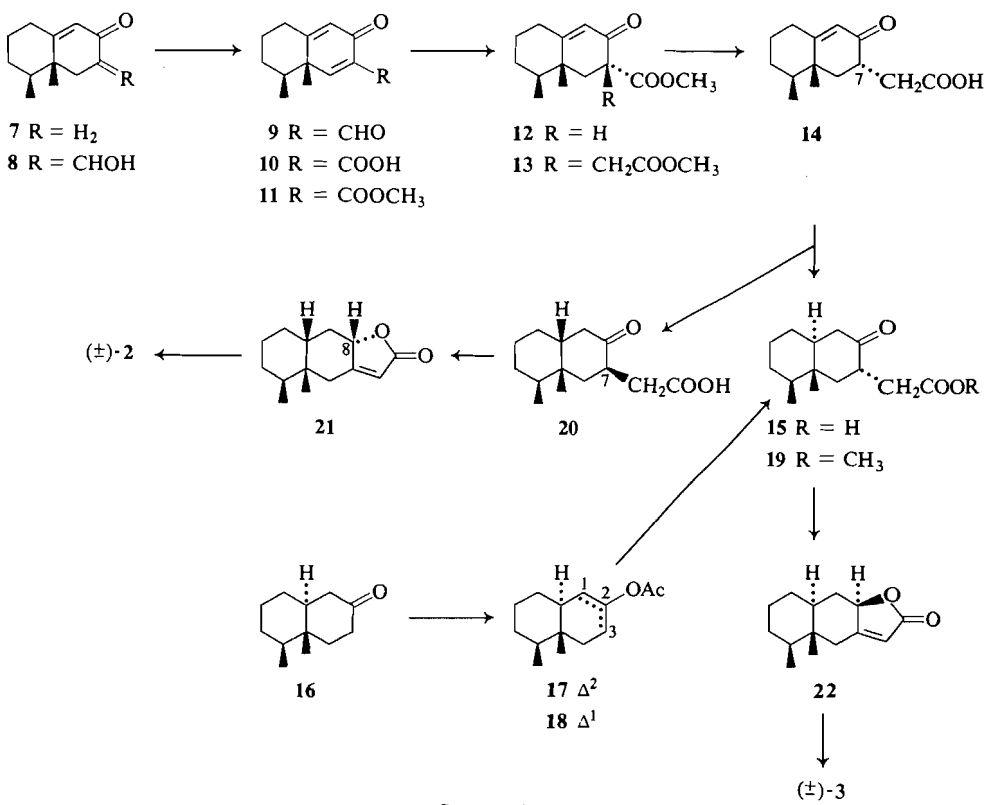

SCHEME 1

the initially formed hydrogenation product. This was readily accomplished by means of ruthenium dioxide – sodium periodate in basic medium (32). There was thus obtained, in high yield, a mixture of **20** and **15** in a ratio of approximately 3:2. The two keto acids were obtained in pure form by careful fractional crystallization of this mixture from hexane–benzene. Since both the hydrogenation and oxidation reactions were carried out under basic, epimerizing conditions, the stereochemistry of the *cis*-fused keto acid should be as indicated in **20**. The latter, on the basis of conformational analysis, would be more stable than the corresponding epimeric (at C-7) compound.

Treatment of the *cis*-fused keto acid **20** with *p*-toluenesulfonic acid in refluxing toluene afforded, in 55% yield, crystalline (±)-11-demethyleremophilenolide (**21**). Since the latter is formed under equilibrating conditions, this compound would be expected to possess the stereochemistry shown in **21** (see ref. 21). This expectation was shown to be correct by the p.m.r. spectrum of the product. The proton at C-8 appeared as a poorly resolved, overlapped pair of doublets, with a width at half-height of 19 Hz, obviously indicating that this proton had an axial orientation. Alkylation (trityl sodium in ether–benzene) of **21** with methyl iodide gave, in 61% yield, racemic eremophilenolide (**2**), which exhibited i.r. and p.m.r. spectra identical with those of an authentic sample of natural (+)-eremophilenolide.[5] This represents the first total synthesis of an eremophilane-type sesquiterpenoid containing the α-methyl-α,β-unsaturated γ-lactone functionality.

Subjection of the *trans*-fused keto acid **15** to a sequence of reactions identical with that described above afforded successively (±)-11-demethyltetrahydroligularenolide (**22**) (94%) and (±)-tetrahydroligularenolide (**3**) (59%). Although an authentic sample of (−)-tetrahydroligularenolide was not obtained, the data

[5]We are very grateful to Professor V. Herout for a sample of (+)-eremophilenolide.

Can. J. Chem. Downloaded from www.nrcresearchpress.com by 210.87.254.6 on 09/05/12
For personal use only.

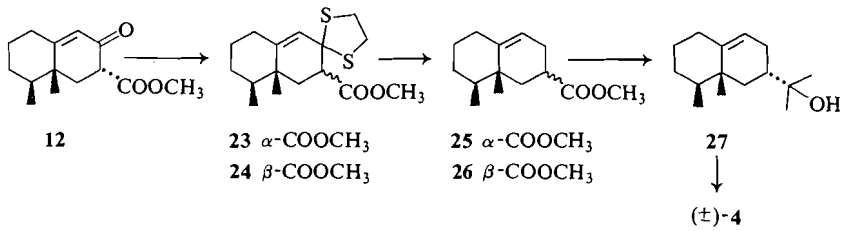

SCHEME 2

obtained from the i.r. and p.m.r. spectra of the synthetic racemate agreed very well with the published data (22).

The keto ester **12** also served as a synthetic intermediate for the preparation of (±)-aristolochene (**4**) (see Scheme 2). Treatment of the former with 1,2-ethanedithiol in acetic acid in the presence of boron trifluoride etherate afforded, in quantitative yield, an epimeric mixture of dithioketal esters **23** and **24**, in a ratio of approximately 4:1. The former could readily be isolated in pure form by fractional crystallization of the mixture from methanol. Desulfurization of **23** with Raney nickel in refluxing ethanol, followed by purification of the crude product by preparative g.l.c. gave the olefinic ester **25**, in 63% yield. Alternatively, desulfurization of a mixture of **23** and **24** (ratio 1:2) yielded a mixture of the olefinic esters **25** and **26** (ratio 1:2). Equilibration of the latter mixture with sodium methoxide in methanol, followed by purification of the resultant material (ratio of **25**:**26** = 9:1) by preparative g.l.c., also provided pure **25**.

When the olefinic ester **25** was allowed to react with an excess of methyllithium in refluxing ether, the olefinic alcohol **27** was obtained in 95% yield. Dehydration of the latter with thionyl chloride in pyridine at 0°, followed by purification of the crude product by column chromatography on silver nitrate-impregnated silica gel, gave (43% yield) pure racemic aristolochene (**4**). This material exhibited spectra (i.r. and p.m.r.) and g.l.c. retention times identical with those of authentic (−)-aristolochene.[6]

Experimental

Melting points and boiling points are uncorrected. The u.v. spectra were measured in methanol solution on a Unicam, model SP 800 spectrophotometer. Routine i.r. spectra were recorded on either a Perkin–Elmer model 137 or 710 spectrophotometer, while all comparison spectra were recorded on a Perkin–Elmer model 457 spectrophotometer. The p.m.r. spectra were taken in deuteriochloroform solution on Varian Associates spectrometers, models T-60, A-60, and/or HA-100. Signal positions are given in the Tiers τ scale, with tetramethylsilane as an internal standard; the multiplicity, integrated peak areas, and proton assignments are indicated in parentheses. The g.l.c. was carried out on Aerograph g.l.c. units, models 700 or 90-P. A column (10 ft × 1/4 in.) packed with 20% Apiezon J on 60/80 mesh Chromosorb W was employed for all analyses. The column temperature and carrier gas (helium) flow-rate (ml/min) are indicated in parentheses. Microanalyses were performed by Mr. P. Borda, Microanalytical Laboratory, University of British Columbia, Vancouver, B.C.

Preparation of Keto Aldehyde **9**

To a solution of 5.0 g (24.2 mmol) of the hydroxymethylene derivative **8** in 250 ml of dry dioxan was added a solution of 5.8 g (29.8 mmol) of 2,3-dichloro-5,6-dicyanobenzoquinone in 250 ml of dry dioxan. The reaction mixture was stirred under an atmosphere of nitrogen at room temperature for 10 min and then diluted with 1150 ml of dichloromethane. The resulting mixture was filtered and the filtrate was passed through a short column of neutral alumina. The alumina was eluted with an additional 500 ml of dichloromethane. Evaporation of the combined dichloromethane solution afforded 4.7 g (95%) of the crystalline keto aldehyde **9**. An analytical sample, obtained by recrystallization of the crude product from hexane, exhibited m.p. 64.5–66°; u.v. λ_{max} 245 mμ (ε 12 600); i.r. ($CHCl_3$) ν_{max} 1700, 1660, 1625, 1600 cm^{-1}; p.m.r. τ −0.33 (s, 1, —CHO), 2.17 (s, 1, β-vinyl H), 3.80 (broad s, 1, α-vinyl H), 8.76 (s, 3, tertiary methyl), 8.87 (unresolved m, 3, secondary methyl).[7]

[6]We are very grateful to Dr. T. R. Govindachari for a sample of (−)-aristolochene.

[7]In the p.m.r. spectrum of each of compounds **4**, **9**–**15** inclusive, **23**, **25**, and **27**, the signal due to the secondary methyl group appeared as a broad band, with very little resolution, while in compounds **3** and **22** this signal appeared as a poorly resolved doublet. Presumably this was, in each case, due to virtual coupling (see reference 33). In contrast, the secondary methyl group of compounds **2**, **20**, and **21** gave rise, in each case, to a clean, well-resolved doublet with the expected coupling constant (6–7 Hz). This observation was eventually used quite consistently to distinguish between those compounds of this series possessing a *trans* (or *trans*-like) ring fusion and those possessing a *cis* ring fusion.

Can. J. Chem. Downloaded from www.nrcresearchpress.com by 210.87.254.6 on 09/05/12
For personal use only.

Can. J. Chem. Downloaded from www.nrcresearchpress.com by 210.87.254.6 on 09/05/12
For personal use only.

Anal. Calcd. for $C_{13}H_{16}O_2$: C, 76.44; H, 7.90. Found: C, 76.64; H, 7.70.

Preparation of Keto Acid ***10***

To a stirred solution of silver nitrate (19.1 g, 0.112 mol) and the keto aldehyde **9** (11.0 g, 0.054 mol) in a mixture of ethanol (200 ml) and water (160 ml) was added dropwise, over a period of 1 h, a solution of sodium hydroxide (8.8 g, 0.22 mol) in water (300 ml). After the reaction mixture had been stirred for an additional 2 h, it was filtered through Celite. The filtrate was evaporated under reduced pressure to a small volume. The residue was diluted with water, washed once with ether, and acidified with 6 *N* hydrochloric acid. The resulting mixture was thoroughly extracted with ether. The combined extracts were washed with brine and then dried over anhydrous magnesium sulfate. Removal of the solvent gave 10.7 g (89%) of the crystalline keto acid **10**. An analytical sample was obtained by recrystallization from hexane–benzene and exhibited m.p. 105°; u.v. λ_{max} 253 mμ (ε 9740); i.r. ($CHCl_3$) ν_{max} 3600–2280 (broad), 1745, 1650, 1600 cm^{-1}; p.m.r. τ −3.55 (broad s, 1, —COOH), 1.57 (s, 1, β-vinyl H), 3.67 (broad s, 1, α-vinyl H), 8.72 (s, 3, tertiary methyl), 8.84 (unresolved m, 3, secondary methyl).

Anal. Calcd. for $C_{13}H_{16}O_3$: C, 70.89; H, 7.32. Found: C, 70.88; H, 7.30.

Preparation of the Keto Ester ***11***

Silver oxide (18.5 g, 0.080 mol) was added to a solution of the keto acid **10** (8.8 g, 0.040 mol) in 240 ml of methanol. To the resultant mixture was added a solution of methyl iodide (11.3 g, 0.078 mol) in 160 ml of methanol. The reaction mixture was stirred at room temperature for 45 min, filtered, and the filtrate was evaporated under reduced pressure. The residue was dissolved in ether and the resulting solution was washed with aqueous sodium bicarbonate, with brine, and then dried over anhydrous magnesium sulfate. Removal of the solvent and distillation of the residue under reduced pressure afforded 9.0 g (96%) of the keto ester **11**, b.p. 147° at 0.1 mm; $n_D^{19.5}$ 1.5388; u.v. λ_{max} 245 mμ (ε 10 550); i.r. (film) ν_{max} 1740, 1720 (shoulder), 1660, 1640 (shoulder) cm^{-1}; p.m.r. τ 2.25 (s, 1, β-vinyl H), 3.85 (broad s, 1, α-vinyl H), 6.12 (s, 3, —$COOCH_3$), 8.79 (s, 3, tertiary methyl), 8.90 (unresolved m, 3, secondary methyl).

Anal. Calcd. for $C_{14}H_{18}O_3$: C, 71.77; H, 7.74. Found: C, 71.53; H, 7.84.

Preparation of Keto Ester ***12***

To a solution of 7.02 g (0.03 mol) of the keto ester **11** in 45 ml of pyridine was added 1.13 g (0.03 mol) of powdered sodium borohydride. External cooling (ice-bath) was required initially to keep the temperature of the reaction mixture below 50°. After the solution had been stirred for 30 min, it was poured into rapidly stirring 2 *N* hydrochloric acid (360 ml). The resulting mixture was extracted thoroughly with ether. The combined extracts were washed with brine, dried over anhydrous magnesium sulfate, and evaporated under reduced pressure. Recrystallization of the residual crude crystalline material from hexane – ethyl acetate gave 5.35 g (76%) of pure keto ester **12**. Column chromatography (silica gel) of the material obtained from the mother liquors afforded an additional 0.7 g (10%) of the desired compound **12**. An analytical sample of keto ester **12** exhibited m.p. 108–108.5°; u.v. λ_{max} 240 mμ (ε 14 920); i.r. ($CHCl_3$) ν_{max} 1740, 1670, 1620 cm^{-1}; p.m.r. τ 4.31 (broad s, 1, vinyl H), 6.30 (s, 3, —$COOCH_3$), 6.57 (pair of doublets, 1, —CH—$COOCH_3$, J = 13.0, 6.0 Hz), 8.88 (s, 3, tertiary methyl), 9.08 (unresolved m, 3, secondary methyl).

Anal. Calcd. for $C_{14}H_{20}O_3$: C, 71.16; H, 8.53. Found: C, 71.02; H, 8.64.

Preparation of the Keto Diester ***13***

To a solution of the keto ester **12** (5.29 g, 22.4 mmol) in dry benzene (180 ml), under an atmosphere of nitrogen, was added 1.04 g (24.6 mmol) of sodium hydride (56% in dispersion oil). When the evolution of hydrogen had ceased (approximately 20 min), 7.5 g (49.0 mmol) of methyl bromoacetate was added all at once. The reaction mixture was gradually heated to 80°, and then refluxed for 2.5 h. The cooled reaction mixture was poured into dilute hydrochloric acid, and the layers were separated. The aqueous layer was extracted further with ether. The combined benzene layer and ether extracts were washed twice with brine and dried over anhydrous magnesium sulfate. Removal of the solvent and distillation of the residual oil under reduced pressure gave a quantitative yield of the keto diester **13** as a viscous oil, b.p. 162–164° at 0.07 mm; u.v. λ_{max} 242 mμ (ε 13 760); i.r. (film) ν_{max} 1740, 1720 (shoulder), 1665, 1640 (shoulder) cm^{-1}; p.m.r. τ 4.22 (broad s, 1, vinyl H), 6.35, 6.41 (s, s, 6, methoxy methyls), 8.98 (s, 3, tertiary methyl), 9.12 (unresolved m, 3, secondary methyl).

Anal. Calcd. for $C_{17}H_{24}O_5$: C, 66.21; H, 7.84. Found: C, 66.29; H, 7.82.

Preparation of Keto Acid ***14***

The keto diester **13** (6.5 g, 21.1 mmol) was dissolved in 210 ml of 5:1 ethanol–water containing 30 g (0.75 mol) of sodium hydroxide and the resulting solution was refluxed under an atmosphere of nitrogen for 30 min. Most of the ethanol was removed under reduced pressure. The residue was diluted with water, washed once with ether, and then acidified with 6 *N* hydrochloric acid. The resulting mixture was extracted with ether, the combined extracts were washed with brine, and then dried over anhydrous magnesium sulfate. Removal of the ether gave 5.0 g of a viscous oil which crystallized on standing. Recrystallization from benzene–hexane gave 3.1 g of pure keto acid **14**. Distillation of the material obtained from the mother liquors (b.p. 190–205° (hot-box) at 0.2 mm), followed by recrystallization of the distillate afforded an additional 1.0 g of keto acid **14** (total yield 82%). An analytical sample exhibited m.p. 127.5–128°; u.v. λ_{max} 238 mμ (ε 14 750); i.r. ($CHCl_3$) ν_{max} 3600–2400 (broad), 1710, 1665, 1620 cm^{-1}; p.m.r. τ −1.30 (broad s, 1, —COOH), 4.28 (broad s, 1, vinyl H), 8.85 (s, 3, tertiary methyl), 9.10 (unresolved m, 3, secondary methyl).

Anal. Calcd. for $C_{14}H_{20}O_3$: C, 71.16; H, 8.53. Found: C, 71.15; H, 8.47.

Preparation of the cis-Fused Keto Acid ***20*** *and the trans-Fused Keto Acid* ***15***

Hydrogenation of the keto acid **14** was carried out at atmospheric pressure and room temperature. A solution of **14** (118 mg, 0.5 mmol) in 3 ml of freshly prepared 0.2 *N* ethanolic sodium hydroxide containing 30 mg of 5% rhodium-on-carbon was hydrogenated until 2 equiv

Can. J. Chem. Downloaded from www.nrcresearchpress.com by 210.87.254.6 on 09/05/12
For personal use only.

of hydrogen were taken up (approximately 5 h). The reaction mixture was filtered and the filtrate was evaporated to dryness. The residue was dissolved in distilled water (4 ml) and 6 mg of ruthenium dioxide was added. To the resulting stirred mixture was added, dropwise, a freshly prepared 5% solution of sodium periodate in distilled water, until the yellowish color of ruthenium tetroxide persisted. The reaction mixture was treated with a few drops of 2-propanol, and then filtered. The filtrate was acidified with dilute hydrochloric acid and then thoroughly extracted with ether. The combined ether extracts were washed with brine and dried over anhydrous magnesium sulfate. Removal of the solvent gave 120 mg of crystalline material, which consisted of a mixture of the *cis*-fused keto acid **20** and the *trans*-fused keto acid **15**, in a ratio of approximately 3:2 (based on the p.m.r. spectrum). Both of the compounds could be obtained in pure form by repeated fractional crystallization of the mixture from varying proportions of hexane–benzene. Although the actual amount of each isomer isolated from the mixture varied somewhat from experiment to experiment, the less soluble compound (*trans*-fused keto acid **15**) was secured in approximately 30% yield, while the more soluble isomer (*cis*-fused keto acid **20**) was obtained in approximately 30–35% yield.

The *trans*-fused keto acid **15** exhibited m.p. 139–140°; i.r. ($CHCl_3$) ν_{max} 3600–2400 (broad), 1705 cm^{-1}; p.m.r. τ 0.04 (broad s, 1, —COOH), 9.00 (s, 3, tertiary methyl), 9.12 (unresolved m, 3, secondary methyl).

Anal. Calcd. for $C_{14}H_{22}O_3$: C, 70.56; H, 9.30. Found: C, 70.80; H, 9.15.

The *cis*-fused keto acid **20** exhibited m.p. 114.5–115°; i.r. ($CHCl_3$) ν_{max} 3600–2400 (broad), 1708 cm^{-1}; p.m.r. τ −1.27 (broad s, 1, —COOH), 9.09 (s, 3, tertiary methyl), 9.12 (d, 3, secondary methyl, J = 7.0 Hz).

Anal. Calcd. for $C_{14}H_{22}O_3$: C, 70.56; H, 9.30. Found: C, 70.42; H, 9.10.

(±)-11-Demethyleremophilenolide (21)

A solution of the keto acid **20** (50 mg, 0.21 mmol) in 12 ml of dry toluene containing 15 mg of *p*-toluenesulfonic acid was refluxed gently under a Dean–Stark water separator in a nitrogen atmosphere for 3 h. The cooled solution was washed with dilute aqueous sodium bicarbonate, with brine and then dried over anhydrous magnesium sulfate. Removal of the solvent, followed by distillation of the residue gave 45 mg of material which crystallized on standing. Recrystallization from hexane yielded 25.5 mg (55%) of the pure lactone **21**, m.p. 112–112.5°; u.v. λ_{max} 216 mμ (ε 14 830); i.r. ($CHCl_3$) ν_{max} 1780, 1745, 1650 cm^{-1}; p.m.r. τ 4.31 (unresolved m, 1, vinyl H, $w_{1/2}$ = 4.0 Hz), 5.26 (broad, unresolved m, 1, C_8H, $w_{1/2}$ = 19.0 Hz), 7.10 (d, 1, C_6H-equatorial, J = 14.0 Hz), 8.99 (s, 3, tertiary methyl), 9.23 (d, 3, secondary methyl, J = 6.0 Hz).

Anal. Calcd. for $C_{14}H_{20}O_2$: C, 76.33; H, 9.15. Found: C, 76.30; H, 9.30.

(±)-Eremophilenolide (2)

To a stirred solution of (±)-11-demethyleremophilenolide (**21**) (68 mg, 0.31 mmol) in 3 ml of dry benzene under an atmosphere of nitrogen was added, dropwise, an ethereal solution of trityl sodium until the red color of the base persisted. After the resulting solution had been stirred at room temperature for 30 min, methyl iodide (142 μl, 2.28 mmol) was added all at once. The solution was stirred for 6 h, diluted with ether, washed with cold water, then brine, and dried over anhydrous magnesium sulfate. Removal of the solvents gave a crude product which was chromatographed over silica gel. Elution with hexane afforded triphenylmethane. Further elution with ether gave 73 mg of material which crystallized on standing. Recrystallization from ether gave 31 mg of pure (±)-eremophilenolide (**2**). Subjection of the material from the mother liquors to column chromatography on silica gel yielded an additional 13 mg of **2** (total yield 61%). An analytical sample of (±)-eremophilenolide (**2**) exhibited m.p. 110.5–111.5°; u.v. λ_{max} 220 mμ (ε 14 600); i.r. ($CHCl_3$) ν_{max} 1740, 1690 cm^{-1}; p.m.r. τ 5.37 (broad unresolved m, 1, C_8H, $w_{1/2}$ = 20.5 Hz), 7.11 (d, 1, C_6H-equatorial, J = 14.5 Hz), 8.21 (unresolved m, 3, vinyl methyl), 8.97 (s, 3, tertiary methyl), 9.20 (d, 3, secondary methyl, J = 6.0 Hz). The i.r. and p.m.r. spectra of this material were identical with those of an authentic sample of natural (+)-eremophilenolide.

Anal. Calcd. for $C_{15}H_{22}O_2$: C, 76.88; H, 9.46. Found: C, 76.58; H, 9.60.

Preparation of the trans-Fused Keto Acid 15

(a) By Hydrogenation of 14 Under Neutral Conditions

A solution of the keto acid **14** (21 mg, 0.089 mmol) in 2 ml of ethanol was hydrogenated at atmospheric pressure and room temperature over palladium-on-charcoal (11 mg) until uptake of hydrogen ceased. Filtration of the reaction mixture, followed by evaporation of the filtrate under reduced pressure afforded a quantitative yield of the *trans*-fused keto acid **15**, shown to be identical (m.p., i.r., and p.m.r. spectra) with the minor product obtained by hydrogenation of the keto acid **14** under basic conditions (*vide supra*).

(b) By Alkylation of the Decalone 16

A solution of the decalone **16** (180 mg, 1 mmol) in 25 ml of isopropenyl acetate containing 100 mg of *p*-toluenesulfonic acid was slowly heated under a Dean–Stark water separator. The acetone – isopropenyl acetate mixture was slowly distilled until the residual volume was about 4 ml. The cooled reaction mixture was poured into aqueous sodium bicarbonate and the resulting mixture was extracted thoroughly with ether. The combined ether extracts were washed with brine and dried over anhydrous magnesium sulfate. Removal of the ether, followed by distillation of the residual oil, afforded 220 mg of the mixture of enol acetates **17** and **18**, b.p. 80–90° (hot-box) at 0.1 mm, in a ratio of approximately 3:2. On the basis of the p.m.r. spectrum, the major compound was the Δ^2-isomer.

A solution of the mixture of enol acetates **17** and **18** in dry dimethoxyethane was added dropwise via a syringe to a stirred solution of methyllithium (2 mmol) in 1.5 ml of dimethoxyethane. To the resulting solution was added, all at once, 0.5 ml of methyl bromoacetate, stirring was continued for 1 min, and the reaction mixture was then poured into cold dilute hydrochloric acid. The resulting mixture was extracted with ether, and the combined ether extracts were washed with water and dried over anhydrous magnesium sulfate. Removal of the solvents gave 237 mg of crude material. Subjection of the latter to column chromatography on silica gel afforded the keto ester **19**, which, upon hydrolysis at room temperature

Can. J. Chem. Downloaded from www.nrcresearchpress.com by 210.87.254.6 on 09/05/12
For personal use only.

with potassium hydroxide in methanol, provided the crystalline keto acid **15**. The latter was shown to be identical (m.p., i.r., and p.m.r. spectra) with the keto acid **15** prepared as described above.

(±)-11-Demethyltetrahydroligularenolide (22)

A solution of the *trans*-fused keto acid **15** (44 mg, 0.19 mmol) in 12 ml of dry toluene containing 15 mg of *p*-toluenesulfonic acid was refluxed gently for 3 h in an atmosphere of nitrogen under a Dean–Stark water separator. The cooled solution was washed with cold, dilute aqueous sodium bicarbonate, with brine, and then dried over anhydrous magnesium sulfate. Removal of the solvent and distillation of the residual material afforded 38 mg (94%) of (±)-11-demethyltetrahydroligularenolide (**22**), m.p. 94–95°. An analytical sample, obtained by recrystallization of this material from hexane, exhibited m.p. 98–99°; u.v. λ_{max} 216 mμ (ε 14 870); i.r. ($CHCl_3$) ν_{max} 1780, 1745, 1645 cm^{-1}; p.m.r. τ 4.34 (unresolved m, 1, vinyl H, $w_{1/2}$ = 4 Hz), 5.33 (unresolved m, 1, C_8H, $w_{1/2}$ = 19 Hz), 7.25 (d, 1, C_6H-equatorial, J = 13.0 Hz), 9.15 (poorly resolved d, 3, secondary methyl, J = 5.5 Hz), 9.36 (s, 3, tertiary methyl).

Anal. Calcd. for $C_{14}H_{20}O_2$: C, 76.33; H, 9.15. Found: C, 76.15; H, 9.03.

(±)-Tetrahydroligularenolide (3)

To a stirred solution of the lactone **22** (85 mg, 0.39 mmol) in 4 ml of dry benzene under an atmosphere of nitrogen was added, dropwise, an ethereal solution of trityl sodium until the red color of the base persisted. After the resulting solution had been stirred at room temperature for 35 min, methyl iodide (160 μl, 2.5 mmol) was added in one portion. The reaction mixture was stirred at room temperature for 6 h, then diluted with ether and poured into ice–water. The organic layer was separated, washed with brine, and dried over anhydrous magnesium sulfate. Removal of the solvents gave 234 mg of residual material which was subjected to column chromatography on silica gel. Elution of the column with hexane yielded triphenylmethane, while elution with ether afforded 82 mg of crude crystalline product. Recrystallization from hexane–ether, followed by further purification (column chromatography) of the material obtained from the mother liquors, provided 53 mg (59%) of pure (±)-tetrahydroligularenolide (**3**), m.p. 91.5–92°; u.v. λ_{max} 220 mμ (ε 14 990); i.r. ($CHCl_3$) ν_{max} 1740, 1685 cm^{-1}; p.m.r. τ 5.38 (unresolved m, 1, C_8H, $w_{1/2}$ = 21 Hz), 7.24 (d, 1, C_6H-equatorial, J = 14.0 Hz), 8.21 (unresolved m, 3, vinyl methyl), 9.09 (poorly resolved d, 3, secondary methyl, J = 5.5 Hz), 9.42 (s, 3, tertiary methyl). Although an authentic sample of (−)-tetrahydroligularenolide was not obtained, the i.r. and p.m.r. data given above agree very well with the published data (22).

Anal. Calcd. for $C_{15}H_{22}O_2$: C, 76.88; H, 9.46. Found: C, 76.65; H, 9.31.

Preparation of the Thioketal Derivative 23

To a solution of the keto ester **12** (1.22 g, 5.2 mmol) in 30 ml of acetic acid was added 2.5 ml of 1,2-ethanedithiol and 1.5 ml of boron trifluoride etherate. The mixture was stirred under nitrogen for 26 h and then diluted with ether. Excess solid sodium bicarbonate was added and the resulting mixture was carefully diluted with cold water. The organic layer was separated, washed successively with aqueous sodium bicarbonate, water, and brine, and then dried over anhydrous magnesium sulfate. Removal of solvent afforded 1.67 g (100%) of crude crystalline material. The p.m.r. spectrum of this material indicated that it was an epimeric mixture of **23** and **24**, in a ratio of approximately 4:1. One recrystallization of this material from methanol yielded 1.16 g (72.5%) of the pure dithioketal **23**, m.p. 110.5–111°; i.r. ($CHCl_3$) ν_{max} 1728 cm^{-1}; p.m.r. τ 4.52 (broad s, 1, vinyl H), 6.32 (s, 3, $-COOCH_3$), 6.52–6.99 (m, 5, $-SCH_2CH_2S-$ and C_7H), 9.07 (s, 3, tertiary methyl), 9.15 (unresolved m, 3, secondary methyl).

Anal. Calcd. for $C_{16}H_{24}O_2S_2$: C, 61.50; H, 7.74; S, 20.52. Found: C, 61.64; H, 7.84; S, 20.35.

The material obtained from the mother liquors of the above recrystallization consisted of compounds **23** and **24** in a ratio of approximately 1:2. Attempts to isolate a pure sample of **24** by column chromatography of this material were not successful.

Preparation of the Olefinic Ester 25

(a) From the Dithioketal 23

To a solution of the dithioketal **23** (594 mg, 1.9 mmol) in 80 ml of ethanol was added about 20 g of W-2 Raney nickel and the resulting mixture was refluxed with stirring under nitrogen for 15 min. The reaction mixture was filtered and the filtrate was evaporated under reduced pressure. Distillation of the residual material gave 373 mg of an oil, b.p. 120° at 0.15 mm, which was shown by g.l.c. analysis (205°, 105) to consist mainly of one compound, accompanied by two minor components. The desired, major component was isolated by preparative g.l.c. (200°, 90), yielding 264 mg (63%) of pure olefinic ester **25**, n_D^{20} 1.4979; i.r. (film) ν_{max} 1735, 808 cm^{-1}; p.m.r. τ 4.72 (unresolved m, 1, vinyl H), 6.36 (s, 3, $-COOCH_3$), 9.06 (s, 3, tertiary methyl), 9.14 (unresolved m, 3, secondary methyl).

Anal. Calcd. for $C_{14}H_{22}O_2$: C, 75.63; H, 9.97. Found: C, 75.46; H, 10.04.

(b) From a Mixture of Dithioketals 23 and 24

A mixture of compounds **23** and **24** (180 mg, 1:2), obtained from the mother liquors of recrystallization of impure **23** (*vide supra*), was subjected to desulfurization with Raney nickel under conditions identical with those described above. Distillation of the crude product gave 102 mg of material which was shown by g.l.c. analysis (205°, 105) to consist mainly (85%) of the epimeric olefinic esters **25** and **26** (approximately 1:2). A solution of this material in 10 ml of 0.82 *M* sodium methoxide in methanol was refluxed under nitrogen for 20 h. The cooled solution was poured into dilute aqueous acetic acid and the resulting mixture was extracted with ether. The combined extracts were washed with water, with brine, and then dried over anhydrous magnesium sulfate. Removal of the solvents, followed by distillation of the residual material, afforded 65 mg of an oil. G.l.c. analysis (205°, 105) of the latter revealed that the ratio of **25** to **26** was now approximately 9:1. The major component, isolated from the mixture by preparative g.l.c. (205°, 105), was shown (i.r. and p.m.r. spectra) to be identical with **25**, prepared as described above.

Preparation of the Olefinic Alcohol 27

An ethereal solution of methyllithium (6 mmol) was added to a cold (0°) solution of the olefinic ester **25**

Can. J. Chem. Downloaded from www.nrcresearchpress.com by 210.87.254.6 on 09/05/12
For personal use only.

(222 mg, 1 mmol) in 8 ml of anhydrous ether. The resulting solution was refluxed under nitrogen for 2.5 h, cooled, and poured into a mixture of Dry Ice in water. The ether layer was separated, successively washed with water and brine, and dried over anhydrous magnesium sulfate. Removal of the solvent gave an oil which, upon distillation under reduced pressure, afforded 212 mg (95%) of the olefinic alcohol **27**, b.p. 125–130° (hot-box) at 0.25 mm; n_D^{20} 1.5075; i.r. (film) ν_{max} 3380, 810 cm^{-1}; p.m.r. τ 4.71 (unresolved m, 1, vinyl H), 8.84, 8.85 (s, s, 6, $-C(OH)(CH_3)_2$), 9.08 (s, 3, tertiary methyl), 9.14 (unresolved m, 3, secondary methyl).

Anal. Calcd. for $C_{15}H_{26}O$: C, 81.02; H, 11.79. Found: C, 80.93; H, 11.67.

(±)-Aristolochene (4)

To a solution of the olefinic alcohol **27** (160 mg, 0.72 mmol) in 5.2 ml of pyridine at 0° was added, dropwise, 520 µl of thionyl chloride. The resulting solution was stirred under a nitrogen atmosphere at 0° for 1 h and then poured into cold, aqueous sodium bicarbonate. The resulting mixture was extracted with ether and the combined extracts were evaporated under reduced pressure. The residue was taken up in ether and the resulting solution was washed successively with water and brine and then dried over anhydrous magnesium sulfate. Removal of the solvent gave 134 mg of crude material. Subjection of the latter to column chromatography on silver nitrate-impregnated silica gel (15%) gave, upon elution with hexane–ether, 57 mg (43%) of pure (±)-aristolochene (**4**), i.r. (film) ν_{max} 3075, 3030, 1645, 887, 810 cm^{-1}; p.m.r. τ 4.70 (unresolved m, 1, vinyl H, $w_{1/2}$ = 9.0 Hz), 5.31 (unresolved m, 2, $=CH_2$, $w_{1/2}$ = 3.0 Hz), 8.29 (unresolved m, 3, vinyl methyl), 9.06 (s, 3, tertiary methyl), 9.17 (unresolved m, 3, secondary methyl). This material exhibited i.r. and p.m.r. spectra identical with authentic (−)-aristolochene.

Anal. Calcd. for $C_{15}H_{24}$: C, 88.16; H, 11.84. Found: C, 88.40; H, 11.90.

Financial support from the National Research Council of Canada and from the University of British Columbia Committee on Research is gratefully acknowledged.

1. T. K. Devon and A. I. Scott. Handbook of naturally occurring compounds. Volume II. Terpenes. Academic Press, New York, N.Y. 1972. pp. 129–134, 136.
2. G. Ourisson, S. Munavalli, and C. Ehret. International tables of selected constants. Vol. 15. Data relative to sesquiterpenoids. Pergamon Press, Inc., New York, N.Y. 1966.
3. C. Berger, M. Franck-Neumann, and G. Ourisson. Tetrahedron Lett. 3451 (1968).
4. E. Piers, R. W. Britton, and W. de Waal. Can. J. Chem. **47**, 831 (1969).
5. R. M. Coates and J. E. Shaw. Chem. Commun. 515 (1968); J. Am. Chem. Soc. **92**, 5657 (1970).
6. M. Ohashi. Chem. Commun. 893 (1969).
7. R. M. Coates and J. E. Shaw. (*a*) Tetrahedron Lett. 5405 (1968). (*b*) J. Org. Chem. **35**, 2597 (1970).
8. E. Piers and R. J. Keziere. Tetrahedron Lett. 538 (1968); Can. J. Chem. **47**, 137 (1969).
9. E. Piers and R. D. Smillie. J. Org. Chem. **35**, 3997 (1970).
10. J. A. Marshall and G. M. Cohen. Tetrahedron Lett. 3865 (1970); J. Org. Chem. **36**, 877 (1971).
11. (*a*) A. K. Torrence and A. R. Pinder. Tetrahedron Lett. 745 (1971); (*b*) A. R. Pinder and A. K. Torrence. J. Chem. Soc. C, 3410 (1971).
12. R. B. Kelly, J. Zamecnik, and B. A. Beckett. Chem. Commun. 479 (1971); Can. J. Chem. **50**, 3455 (1972).
13. J. A. Marshall, H. Faubl, and T. M. Warne, Jr. Chem. Commun. 753 (1967); J. A. Marshall and T. M. Warne, Jr. J. Org. Chem. **36**, 178 (1971).
14. A. van der Gen, L. M. van der Linde, J. G. Witteveen, and H. Boelens. (*a*) Rec. Trav. chim. **90**, 1034 (1971); (*b*) Rec. Trav. chim. **90**, 1045 (1971).
15. M. Pesaro, G. Bozatto, and P. Schudel. Chem. Commun. 1152 (1968).
16. J. A. Marshall and R. A. Ruden. Tetrahedron Lett. 1239 (1970); J. Org. Chem. **36**, 594 (1971).
17. H. C. Odom, Jr. and A. R. Pinder. J. Chem. Soc. Perkin I, 2193 (1972).
18. S. Murayama, D. Chan, and M. Brown. Tetrahedron Lett. 3715 (1968).
19. E. Piers, M. B. Geraghty, and R. D. Smillie. Chem. Commun. 614 (1971).
20. L. Novotný, V. Herout, and F. Šorm. Tetrahedron Lett. 697 (1961).
21. L. Novotný, J. Jizba, V. Herout, F. Šorm, L. H. Zalkow, S. Hu, and C. Djerassi. Tetrahedron, **19**, 1101 (1963).
22. Y. Tanahashi, Y. Ishizaki, T. Takahashi, and K. Tori. Tetrahedron Lett. 3739 (1968); Y. Ishizaki, Y. Tanahashi, T. Takahashi, and K. Tori. Tetrahedron, **26**, 5387 (1970).
23. T. R. Govindachari, P. A. Mohamed, and P. C. Parthasarathy. Tetrahedron, **26**, 615 (1970).
24. G. L. K. Hunter and W. B. Brogden, Jr. J. Food Sci. **30**, 876 (1965).
25. W. D. MacLeod, Jr. Tetrahedron Lett. 4779 (1965).
26. E. Piers, R. W. Britton, and W. de Waal. Can. J. Chem. **47**, 4307 (1969).
27. D. Walker and J. D. Hiebert. Chem. Rev. **67**, 153 (1967).
28. K. J. Clark, G. I. Gray, R. H. Jaeger, and R. Robinson. Tetrahedron, **6**, 217 (1959).
29. S. B. Kadin. J. Org. Chem. **31**, 620 (1966).
30. E. Wenkert, A. Afonso, J. B-son Bredenberg, C. Kaneko, and A. Tahara. J. Am. Chem. Soc. **86**, 2038 (1964).
31. H. O. House and B. M. Trost. J. Org. Chem. **30**, 2502 (1965).
32. R. M. Moriarty, H. Gopal, and T. Adams. Tetrahedron Lett. 4003 (1970).
33. N. S. Bhacca and D. H. Williams. Applications of nuclear magnetic resonance spectroscopy in organic chemistry. Holden-Day, Inc., San Francisco. 1964. p. 36.

Comment: Concerning the Paper of R. P. Mariella and K. H. Brown "A Novel S_N1 Displacement: The Reaction of Tertiary Amines with Acetic Anhydride"

YA. L. GOL'DFARB AND L. I. BELEN'KII

N.D. Zelinsky Institute of Organic Chemistry of the Academy of Sciences of the U.S.S.R., Moscow, B-334, Leninskii Prospekt, 47, U.S.S.R.

Received October 12, 1972

The remarks on the paper of Mariella and Brown (1) concern three points: (*1*) some similar data from the literature were not mentioned; (*2*) the mechanism proposed does not take into account the possibility of catalysis of the reaction; and (*3*) the interpretation of the process as S_N1 displacement is not compatible with known data.

Les remarques concernant la publication de Mariella et Brown englobent trois points: (*1*) des résultats semblables ne sont pas mentionnés dans la littérature; (*2*) le mécanisme proposé ne tient pas compte de la possibilité d'une catalyse de la réaction; (*3*) l'interprétation du processus envisagé comme étant une réaction de déplacement S_N1 n'est pas en accord avec les résultats connus jusqu'à présent.

[Traduit par le journal]

Can. J. Chem., 51, 2174 (1973)

Recently a paper appeared in this Journal describing the cleavage of some tertiary amines by acetic anhydride in which a mechanism for the process was postulated (1). Unfortunately the authors of this paper did not mention that similar reactions had been studied previously. Tiffeneau and Fuhrer (2) had shown at the beginning of the century that tertiary amines bearing benzyl or substituted benzyl groups at the nitrogen atom are cleaved on heating with acetic anhydride while the amines of another structure (*e.g.*, *N*,*N*-dialkyl anilines) are not. They had shown further that the same conditions were suitable for cleavage of some alkaloids having benzyl-like fragments at the nitrogen atom (such as nicotine) (3). Drefahl *et al.* (4) (ref. 2 in ref. 1) had studied the effect of various para-substituents in *N*,*N*-dimethyl benzyl amine on the ability of the latter to undergo cleavage. They had also demonstrated the possibility of splitting *N*,*N*-dimethyl cinnamylmethyl amine as well as the stability of *N*,*N*-dimethyl allyl amine under the conditions used. We have studied the acetic anhydride cleavage of the ArCHR—N bond in *N*-benzyl pyrrolidine, *N*-benzyl piperidine, nicotine, *N*-methylanabasine, *N*-methyl α-phenyl pyrrolidine, -piperidine, -hexamethylene imine as well as some *N*-alkyl polyalkylene imines with no substituent in the α-position (such as *N*-alkyl pyrrolidines and *N*-methyl hexamethylene imine). In our opinion, only the cleavage of dimethyl tert-butyl amine seems to be of fundamental interest among the transformations described by Mariella and Brown (1).

We believe that there is a similarity in mechanism among the cleavage of tertiary amines (5, 6), ethers (7), and thioethers (8) by acid anhydrides or halides and nucleophilic reactions of carboxylic acid derivatives (in particular, anhydrides and halides) *i.e.* esterification, aminolysis, etc. It is known that such reactions are catalyzed by acids and bases. In particular, we have found that acetic acid effectively catalyzes the cleavage of tertiary amines by acetic anhydride. If acetic acid is specially removed from acetic anhydride by distillation over magnesium, the cleavage of amines proceeds very slowly or does not take place at all (5). The ionization of both components is known (9, 10) to increase in the system, acetic acid – acetic anhydride. This fact can explain the high acceleration of aromatic amines acylation by acetic anhydride in the presence of acetic acid (10, 11). Also suggested (12) was another explanation of the same phenomenon in terms of a concerted mechanism dealing with the catalytic effect of unionized CH_3COOH molecules. Both of these schemes are valid for the case of catalytic activity of acetic acid in the cleavage reaction of tertiary amines with acetic anhydride (5).

Purification of acetic anhydride was not mentioned in the paper of Mariella and Brown and therefore, under the conditions used by the authors (1), catalysis by traces of acetic acid was

Can. J. Chem. Downloaded from www.nrcresearchpress.com by 210.87.254.6 on 09/05/12
For personal use only.

[1] 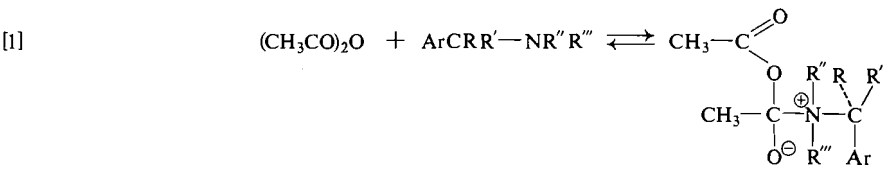

[2] 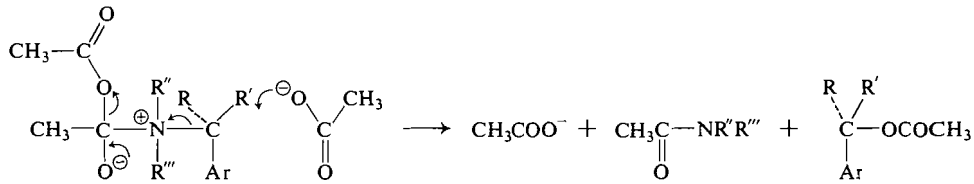

possible. Sodium acetate, in the presence of which the reaction was carried out (1), may also act as a catalyst. Nevertheless, the participation of any catalyst was not considered in the reaction mechanism proposed by Mariella and Brown (1). Another weakness in their mechanism appears to be the purely speculative statement about S_N1 degradation of the intermediate complex, although the authors (1) do discuss the ratio of rates of the reaction single steps (no kinetic data are presented in their paper). As we have shown (5) (*cf.* (3)) no racemization takes place in the course of cleavage of the pyrrolidine ring in nicotine by acetic anhydride. This fact is not compatible with the S_N1 mechanism in its conventional sense. In principle, the retention of optical activity may arise in monomolecular reactions (*i.e.* S_N1 with inversion or S_Ni with retention of configuration). However, additional (kinetic, in particular) information is needed to reach such a conclusion.

Taking into account the retention of optical activity and acetic acid catalysis of nicotine cleavage, it is more logical to propose an S_N2-type mechanism for the reactions described (1). For instance, the mechanism of the reaction catalyzed by acetate ion may be described by eqs. 1 and 2.

The influence of acetic acid as a catalyst on the cleavage of tertiary amines under the action of acetic anhydride was clearly demonstrated by us not only for heterocyclic amines but for aromatic amines as well (*e.g.* *N,N*-dimethyl *p*-methoxybenzyl amine (5)). The reported phenomenon appears to be of general importance since the same catalytic effect of acetic acid was observed by us for the case of ether cleavage (*e.g.* ethyl benzyl ether (7)). In their reply to this comment (15) Mariella and Brown referred to certain papers where no mention of this catalytic effect is to be found. Therefore these references have no bearing on the question under discussion. At the same time it may be noted that Denney and Greenbaum (13) (ref. 8*a* in the reply (15)) have considered the participation of a base in the reaction of anhydrides with amines. We use a similar consideration while discussing the mechanism of acetate anion participation (see above). It is regrettable that in both their paper (1) and reply (15) Mariella and Brown did not discuss the possible role of potassium acetate in the reactions of acetic anhydride with tertiary amines.

Mariella and Brown rejected the S_N2-type mechanism, relying on the fact that benzyl acetate (but not methyl acetate) formation results from interaction of acetic anhydride with benzylic tertiary amines. However it is well known that S_N2 reactions of ammonium salts whose structures are closely related to that of the supposed intermediate considered in ref. 1 proceed predominantly with displacement of the benzyl (but not the methyl) group (*e.g.* ref. 14).

The S_N1 type of mechanism suggested by Mariella and Brown rests mainly on the published data (4) about the effect of the substituent in the benzene ring on the yields of the products: the electron-releasing substituents facilitate the reaction while electron-withdrawing ones slow it down. This fact was related to the differences in stability of respective benzyl cations. However one may find in the paper of Mariella and Brown (1) (see Experimental) data showing the following order for the ease of cleavage: *N,N*-dimethyl benzyl amine > *N,N*-dimethyl benzhydryl amine > *N,N*-dimethyl trityl amine (the yields of acetates are 40, 25 and $<10\%$ respectively). It is difficult to account for this order based on the S_N1 mechanism since the stability of respective cations changes in the opposite direction in this series.

The formation of a quantity of the α-phenyl-

Can. J. Chem. Downloaded from www.nrcresearchpress.com by 210.87.254.6 on 09/05/12
For personal use only.

allyl acetate observed by Mariella and Brown in the cleavage of *N,N*-dimethyl cinnamyl amine (1) may be considered to be a result of an S_N2' mechanism which may be favored due to the steric hindrances for the attack at the CH_2-group adjacent to nitrogen atom. The presence of such steric hindrances is evident from the inspection of space-filling molecular models of the respective intermediate.

In conclusion we would like to note that the mechanism of the cleavage of tertiary amines with acetic anhydride given by Mariella and Brown is clearly an oversimplification and several other mechanisms should also be considered in addition to the one suggested in our comment.

1. R. P. MARIELLA and K. H. BROWN. Can. J. Chem. **49**, 3348 (1971).
2. M. TIFFENEAU and K. FUHRER. Bull. Soc. Chim. Fr. **15**, 162 (1914).
3. M. TIFFENEAU and K. FUHRER. Bull. Soc. Chim. Fr. **9**, 410 (1911).
4. G. DREFAHL, H. LÜCKERT, and W. KÜHLER. J. Prakt. Chem. **11**, 341 (1960).
5. YA. L. GOL'DFARB, R. M. ISPIRYAN, and L. I. BELEN'KII. Zhurn. Obsch. Khim. **39**, 1100 (1969).
6. YA. L. GOL'DFARB, R. M. ISPIRYAN, and L. I. BELEN'KII. Izv. Akad. Nauk SSSR Ser. Khim. 923 (1969).
7. R. M. ISPIRYAN, L. I. BELEN'KII, and YA. L. GOL'DFARB. Izv. Akad. Nauk SSSR Ser. Khim. 2513 (1967).
8. YA. L. GOL'DFARB, R. M. ISPIRYAN, and L. I. BELEN'KII. Doklady Akad. Nauk SSSR, **173**, 101 (1967).
9. M. A. E. MACKENZIE and E. R. S. WINTER. Trans. Faraday Soc. **44**, 159 (1948).
10. V. E. BEL'SKII and M. I. VINNIK. Izv. Akad. Nauk, Ser. Khim. 2132 (1963).
11. V. E. BEL'SKII and M. I. VINNIK. Izv. Akad. Nauk, Ser. Khim. 40 (1964).
12. L. M. LITVINENKO and L. M. ALEKSANDROVA. Ukr. Khim. Zhurn. **27**, 212 (1961).
13. D. B. DENNEY and M. A. GREENBAUM. J. Am. Chem. Soc. **79**, 3701 (1957).
14. C. K. INGOLD. Structure and mechanism in organic chemistry. Cornell University Press, Ithaca, N.Y. 1953. p. 324.
15. R. P. MARIELLA and K. H. BROWN. Can. J. Chem. This issue, following paper.

Can. J. Chem. Downloaded from www.nrcresearchpress.com by 210.87.254.6 on 09/05/12
For personal use only.

Comment: Concerning the Cleavage of Tertiary Amines With Acetic Anhydride

R. P. MARIELLA[1] AND K. H. BROWN

Department of Chemistry, Loyola University, Chicago, Illinois and Continental Can Company, Chicago, Illinois

Received December 29, 1972

The failure of methyl-substituted tertiary amines to yield methyl acetate on cleavage by acetic anhydride indicates that the mechanism proposed by Gol'dfarb and Belen'kii cannot be correct. The results of cleavage of cinnamyldimethylamine are offered as support for the mechanism proposed by Mariella and Brown. Catalysis by acetic acid is not considered to be important.

La tentative pour synthétiser l'acétate de méthyle par clivage d'amines tertiaires substituées par des méthyles à l'aide de l'anhydride acétique s'étant révélée un échec, il en ressort alors que le mécanisme proposé par Gol'dfarb et Belen'kii ne saurait être juste. Les résultats du clivage de la cinnamyldiméthylamine sont rapportés afin de justifier le mécanisme proposé par Mariella et Brown. On considère que la catalyse par l'acide acétique n'est pas un facteur déterminant. [Traduit par le journal]

Can. J. Chem., 51, 2177 (1973)

Can. J. Chem. Downloaded from www.nrcresearchpress.com by 210.87.254.42 on 09/05/12
For personal use only.

It is appropriate now to extend and make further comment on the article "A Novel S_N1 Displacement: The Reaction of Tertiary Amines with Acetic Anhydride" which appeared recently in this Journal (1). Several points concerning the original paper of Mariella and Brown are currently being disputed (2).

The concern of Gol'dfarb and Belen'kii (2) that adequate citation of literature was not made in the paper by Mariella and Brown, while perhaps well intentioned, is certainly not completely researched itself. Three previous papers concerned with the reaction of tertiary amines and acetic anhydride have been published (3–5). Mariella and Brown, in their article (1), gave reference only to the paper by Drefahl *et al.* (4), which was concerned with the structural factors affecting the cleavage of tertiary amines of the benzyldimethyl type. The para-substitution results of the experiments were important in developing a basis for the S_N1 mechanism that was proposed by Mariella and Brown. Drefahl's article itself gave reference to the work of Tiffeneau and Fuhrer (3) so it was deemed unnecessary to re-cite the paper by Tiffeneau in the article of Mariella and Brown. Tiffeneau's work (3) consisted of the acetylation of various tertiary amines. However, the structural implications of the reaction as regards the type of tertiary amines were only cursorily examined. A detailed examination of the work done by Tiffeneau and Fuhrer and of that by Drefahl *et al.* was published in the Ph.D. Dissertation of K. H. Brown (6).[2] Gol'dfarb and Belen'kii certainly could have examined the original source of the Mariella and Brown work had they so desired. Gol'dfarb and Belen'kii's paper "The Effect of Structural and Other Factors on the Cleavage of Tertiary Amines with Acetic Anhydride" (5), as reported by Chemical Abstracts (7), gave only information on the cleavage of heterocyclic tertiary amines by acetic anhydride. In most cases the amines considered were of the benzyl type, and very little structural information concerning non-benzyl type tertiary amines was available from their work. Mariella and Brown are certainly obliged to cite the paper of Gol'dfarb and Belen'kii (5) since it does relate to the more complete study in question.

Indeed, much more is of interest in the paper of Mariella and Brown than merely the cleavage of dimethyl *tert*-butyl amine as suggested by Gol'dfarb and Belen'kii in their "comment" (2). Nowhere in the published literature is any complete structural information available on the reaction of tertiary amines with acetic anhydride. Drefahl *et al.*'s work (4) deals only with the cleavage of benzyl–nitrogen bonds. Tiffeneau's work mentions allyl, phenethyl, and phenyl as groups attached to the tertiary nitrogen. Gol'dfarb and Belen'kii dealt with the benzyl situation or a few others with alkyl substitution on nitrogen. As shown in Table 1 of the paper by Mariella and Brown, a complete structural list of

[1]Author to whom correspondence should be addressed.

[2]The Ph.D. Dissertation may be obtained from University Microfilms, Ann Arbor, Michigan, order no. 71–22, 732.

Can. J. Chem. Downloaded from www.nrcresearchpress.com by 210.87.254.42 on 09/05/12
For personal use only.

tertiary amines was examined under identical conditions as concerned their reactivity with acetic anhydride. Information and data concerning mechanistic conclusions were obtained by Mariella and Brown which were not available from other sources.

We do not believe that acid catalysis occurs in the reaction of tertiary amines with acetic anhydride. Certainly if there was any acetic acid present, it would be un-ionized in the reaction medium, acetic anhydride. Denney and Greenbaum show a mechanism of the reaction of anhydrides with amines to proceed without invoking acid catalysis (8). Similarly, Eliel and Anderson have cleaved benzyldimethyl amine with various esters without the use of catalysts (9). Thus, the contention that acetic acid catalysis is required to explain the results of Mariella and Brown is not a valid criticism of the work.

Among the evidence used to choose a mechanistic pathway was the reaction of cinnamyldimethyl amine. The cinnamyl group, C_6H_5-$CH{=}CHCH_2$, can be considered as an extended allyl group or as a vinylogous benzyl group since structurally it is, in fact, both of these. If one considers the cinnamyl group as a vinylogous benzyl group, the cleavage of the C—N bond in cinnamyldimethylamine is not surprising since by the rule of vinylogy the introduction of a vinyl group between the reaction site and another unsaturated portion of the molecule should give the new compound similar reactivity. Hence $C_6H_5CH_2$—$N(CH_3)_2$ and $C_6H_5(CH{=}CH)$-CH_2—$N(CH_3)_2$ should be of similar reactivity, and, in fact, they are found to be similarly reactive with acetic anhydride.

Interestingly, the reaction of the cinnamyldimethylamine with acetic anhydride gave two products; 60% cinnamyl acetate $CH_3C(=O)OCH_2$-$CH{=}CHC_6H_5$ and 30% α-phenylallyl acetate, $CH_3C(=O)OCH(C_6H_5)CH{=}CH_2$. This is a "typical" product spread for an allylic rearrangement. What seems to have happened is that attack of acetate occurs at two sites of an extended allylic cation *i.e.*, $C_6H_5CH{=}CH{-}CH_2^{\oplus} \leftrightarrow C_6H_5$-$CH(\oplus){-}CH{=}CH_2$. Attack at the primary cationic site would give the cinnamyl acetate while attack at the secondary cationic site would give the α-phenylallyl acetate. The resubmission of the pure cinnamyl acetate to reaction conditions gave only pure cinnamyl acetate and none of the rearranged α-phenylallyl acetate, indicating that equilibration of the product acetates does not occur. An S_N2 attack of acetate on the intermediate below would then give only cinnamyl acetate since there would be no free carbonium ion to resonate. An S_N2' mechanism, with attack at the γ-carbon involves an allylic shift which is

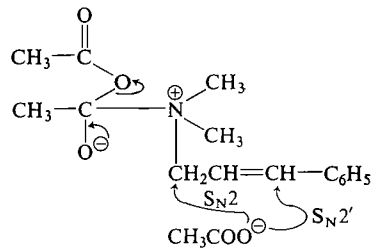

second order and occurs where S_N2 conditions hold, but only where α-substitution sterically retards normal S_N2. It is quite unlikely that an S_N2' mechanism would be operative in the case at hand (10). An S_N1 type mechanism, however, would permit the rearranged product to be formed since the S_N1 proceeds through several stages of ion formation: an "intimate" ion pair, a solvent separated ion pair, and the dissociated ions. Reaction products may result from attack of the nucleophile at any stage. The allylic shift observed in the cinnamyl case could occur during the dissociated ion stage or at the solvent separated ion stage. Also, partial inversion could occur in the "intimate" ion-pair stage since the carbonium ion might still retain its original configuration (10). More evidence for the establishment of an S_N1 type mechanism for the cleavage of tertiary amines by acetic anhydride comes from the work of Drefahl *et al.* (4). Splitting of the C—N bond in *t*-amines with acetic anhydride was observed to be most readily accomplished in those systems which favor ionization to a carbonium ion.

The mechanistic scheme presented by Gol'dfarb and Belen'kii cannot be correct. If R″ or R‴ in their scheme were CH_3, methyl acetate would form. No methyl acetate was found in any of the reactions studied by Mariella and Brown. One of the reasons that two methyl groups on the nitrogen was chosen as a basic structural feature was that the methyl groups were sterically noninterfering and chemically inert. Special attention

was given to try and detect *any* methyl acetate formed during the reaction, but none was detected. Gol'dfarb and Belen'kii merely submit their mechanistic scheme, but offer no further testimony to its validity. Mariella and Brown, however, go much further in that the results of many experiments are used to explain their proposed mechanism, and the results are themselves explained by the mechanism. Furthermore, the reaction of benzyldimethylamine with specially purified acetic anhydride alone gave a 29% yield of benzyl acetate.[3] Thus, the reaction proceeds in the same manner without the necessity of catalysis by acetic acid or sodium acetate.

[3]In order to remove any acetic acid from acetic anhydride, the 98.5% purity acetic anhydride was treated with coarse magnesium filings at reflux for 5 days according to the method of Calcott, English, and Wilbur (11). The acetic anhydride was then fractionally distilled directly into the pre-dried flask which was used for the ensuing reaction. Freshly distilled benzyldimethylamine was added to the acetic anhydride, and the mixture was stirred at reflux for 24 h, using a calcium chloride drying tube to protect against atmospheric moisture contamination. The reaction product, benzyl acetate, was isolated by the same procedure as previously reported (1).

1. R. P. MARIELLA and K. H. BROWN. Can. J. Chem. **49**, 3348 (1971).
2. YA. L. GOL'DFARB and L. I. BELEN'KII. Can. J. Chem. This issue, preceding paper.
3. M. TIFFENEAU and K. FUHRER. Bull. Soc. Chim. Fr. [4], **15**, 162 (1914).
4. V. G. DREFAHL, H. LUCKERT, and W. KOHLER. J. Prakt. Chem. **11**, 341 (1960).
5. YA. L. GOL'DFARB, R. M. ISPERYAN, and L. I. BELEN'KII. Zh. Obshch. Khim. 39 (5) 1100-5 (Russian). (1969).
6. K. H. BROWN. Ph.D. Dissertation. Diss. Abstr. Int. B, 1971, **32** (3), 1440–1.
7. Chem. Abstr. **71**, 704655 (1969).
8. (*a*) D. B. DENNEY and M. A. GREENBAUM. J. Am. Chem. Soc. **79**, 3701 (1957); (*b*) **78**, 877 (1956).
9. E. L. ELIEL and R. P. ANDERSON. J. Am. Chem. Soc. **74**, 547 (1952).
10. J. MARCH. Advanced organic chemistry: reaction, mechanism and structures. McGraw-Hill Book Co., New York, N.Y. 1968. pp. 251–375.
11. W. S. CALCOTT, F. L. ENGLISH, and O. C. WILBUR. Ind. Eng. Chem. **17**, 942 (1925).

Can. J. Chem. Downloaded from www.nrcresearchpress.com by 210.87.254.42 on 09/05/12
For personal use only.

The Crystal and Molecular Structure of Acetamidopentaamminecobalt(III) Perchlorate. A Conjugate Base of Nitrogen Bonded Acetamide

MICHAEL LOUIS SCHNEIDER, GEORGE FERGUSON,[1] AND ROBERT JAMES BALAHURA

Chemistry Department, The University, Guelph, Ontario, N1G 2W1

Received January 3, 1973

The crystal and molecular structure of acetamidopentaamminecobalt(III) perchlorate, $[CH_3CONHCo(NH_3)_5]^{2+}.2ClO_4^-$, has been determined from three-dimensional X-ray data obtained by diffractometer methods. The crystals are monoclinic, space group $P2_1/n(C_{2h}^5$, No. 14) with four formula units in a unit cell of dimensions $a = 13.250(6)$, $b = 10.318(6)$, $c = 10.676(5)$ Å, $\beta = 98.34(3)°$. The structure has been refined by block-diagonal least-squares methods with anisotropic thermal parameters to a final residual R of 0.055 for 1340 observed reflexions. The crystal structure consists of discrete octahedral cations and tetrahedral perchlorate anions. The Co—N (amide) distance is short (1.911(8) Å) while the *trans* Co—N (ammine) bond is long (1.994(8) Å) compared to the equatorial Co—N distances which average 1.963(13) Å. The bond distances in the amide group, C—O 1.267(12) Å and C—N 1.339(12) Å, indicate that a delocalized system plays an important role in the ground state structure of the cation.

La structure moléculaire et cristalline du cobalt(III) acétamidopentaammine perchlorate $[CH_3CONHCo(NH_3)_5]^{2+}.2ClO_4^-$ a été déterminée à l'aide des données tridimensionnelles obtenus des rayons X par des méthodes de diffractométrie. Les cristaux sont monocliniques, de groupe spatial $P2_1/n(C_{2h}^5$, No. 14) comportant quatre unités fondamentales par maille unitaire de dimension $a = 13.250(6)$, $b = 10.318(6)$, $c = 10.676(5)$ Å, $\beta = 98.34(3)°$. La structure a été raffinée par la méthode des moindres carrés (bloc-diagonale) avec des paramètres thermiques anisotropiques jusqu'a un factor d'accord $R = 0.055$ et ce pour tenir compte des 1340 réflexions observées. La structure cristalline consiste en des cations distincts octaédriques et en des anions perchlorates tétraédriques. La longueur de la liaison Co—N (amide) est courte (1.911(8) Å) alors que le lien *trans* Co—N (amine) est long (1.994(8) Å) comparativement aux distances équatoriales Co—N qui mesurent en moyenne 1.963(13) Å. Les longueurs du lien du groupe amide, C—O 1.267(12) Å et C—N 1.339(12) Å indiquent qu'un système délocalisé joue un rôle important dans la structure de l'état stationnaire du cation. [Traduit par le journal]

Can. J. Chem., 51, 2180 (1973)

Introduction

In the reaction of pentaamminecobalt(III) complexes, steric requirements may exert large effects on reaction rates, implying that the orientation of the ligand containing the reaction site may be crucial. As an example, the two extreme orientations of *N*-bonded formamide (R = H) and acetamide (R = CH_3) complexes with pentaamminecobalt(III) are shown in **1** and **2**.

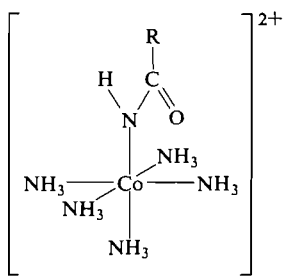

1

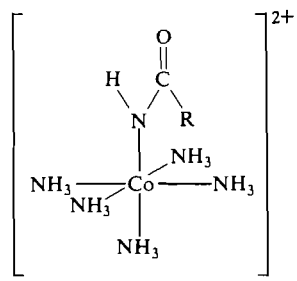

2

[1]To whom correspondence should be addressed.

The chromium(II) reduction of these complexes (1, 2) proceeds according to the equation

$$(NH_3)_5CoNHCOR^{2+} + Cr^{2+} \xrightarrow{H^+} (OH_2)_5CrOCRNH_2 + Co^{2+} + 5NH_4^+$$

the acetamide complex being reduced thirty times slower than the formamide one. As the reductant attacks at the carbonyl oxygen it is tempting to ascribe this rate difference to a change in orientation of the ligand and to attribute orientation (**2**, R = H) to the formamide and (**1**, R = CH_3) to the acetamide derivative. Nuclear Overhauser studies on the formatopentaamminecobalt(III) ion have shown that in d_6-DMSO an orientation analogous to (**2**) is adopted (3). As crystals of the acetamide derivative (**1**, R = CH_3) were readily available, we undertook an X-ray analysis to establish the orientation of the ligand in the solid state. Crystals of the formamide derivative could not be obtained in a suitable crystalline form at this time.

Can. J. Chem. Downloaded from www.nrcresearchpress.com by 210.87.254.42 on 09/05/12
For personal use only.

Can. J. Chem. Downloaded from www.nrcresearchpress.com by 210.87.254.42 on 09/05/12
For personal use only.

TABLE 1. Atomic coordinates*

	x/a	y/b	z/c
Co	2215(1)	2212(1)	−323(1)
Cl(1)	396(2)	273(2)	2940(2)
Cl(2)	4560(2)	−87(3)	2587(3)
N(1)	2046(6)	403(7)	−29(7)
N(2)	755(6)	2454(8)	−178(8)
N(3)	1841(6)	1987(7)	−2140(7)
N(4)	3645(6)	1905(8)	−491(8)
N(5)	2580(6)	2446(7)	1521(7)
N(6)	2383(7)	4111(8)	−571(8)
C(1)	2300(7)	−639(9)	−662(9)
C(2)	2069(9)	−1959(10)	166(10)
O(1)	2744(5)	−554(6)	−1633(6)
O(2)	1300(10)	813(13)	3468(15)
O(3)	−500(8)	824(12)	3186(12)
O(4)	361(10)	180(22)	1642(11)
O(5)	383(9)	−1022(11)	3330(15)
O(6)	3645(8)	−141(12)	3093(12)
O(7)	4414(9)	−711(12)	1392(12)
O(8)	4767(7)	1222(8)	2353(9)
O(9)	5395(7)	−635(10)	3362(11)

*Fractional coordinates $\times 10^4$.

Experimental

Crystal Data for Acetamidopentaamminecobalt(III) perchlorate $C_2H_{19}Cl_2CoN_6O_9$ f.w. = 401.1 Monoclinic a = 13.250(6), b = 10.318(6), c = 10.676(5) Å, β = 98.34(3)°. V = 1444.1 Å^3, Z = 4, ρ_c = 1.84 (21 °C; MoKα, λ = 0.71069 Å). Space group $P2_1/n$ (C_{2h}^5, No. 14). Linear absorption coefficient for X-rays (λ = 0.71069 Å) μ = 16.56 cm^{-1}, $F(000)$ = 821.

The space group was determined uniquely from the systematic absences in the $h0l$ and $0k0$ reflexions as $P2_1/n$. This non-standard space group with equivalent positions $\pm(x,y,z; 1/2 + x, 1/2 - y, 1/2 + z)$ was chosen for convenience. The cell dimensions were obtained from a least-squares treatment of the setting angles of 12 reflexions. The crystal chosen for the data collection was a small thin plate {101} with approximate dimensions 0.02 × 0.2 × 0.3 mm^3. Intensity data were collected to a maximum Bragg angle θ of 25° with our Hilger and Watts Y290 diffractometer. The θ–2θ scan technique was used with a symmetric scan of 0.7° and a scan rate of 0.6 deg/min. Stationary crystal/stationary counter measurements were made of the background counts (17.5 s duration) at each end of the integrated scan. The maximum variation in intensity of standard reflexions was less than 1.2%. The intensities were corrected for Lorentz and polarization factors but not for absorption. Of the 2240 independent reflexions measured, 1340 were considered "observed" ($I > 3\sigma(I)$ where $\sigma(I)$ = [scan + 4 (background)]$^{1/2}$.

Structure Solution and Refinement

The coordinates of the cobalt atom were found from inspection of the three-dimensional Patterson function and the remaining Cl, O, N, and C atoms located by application of the heavy atom method (4). In all calculations of F_c, atomic scattering factors of Cromer and Mann (5) were used for the non-hydrogen atoms and those of Stewart, Davidson, and Simpson (6) for the hydrogen atoms. Corrections were applied for anomalous dispersion of Co and Cl (7). Five cycles of block diagonal least-squares refinement of the non-hydrogen atomic coordinates and isotropic thermal parameters reduced $R_1 = \sum||F_o| - |F_c||/\sum|F_o|$ to 0.092. The non-hydrogen atoms were then allowed to vibrate anisotropically. After the third anisotropic refinement cycle, when R_1 was 0.062, a difference synthesis was calculated but yielded no chemically significant information; in particular we could detect none of the 19 hydrogen atoms in the structure although diffuse electron density was observed around some NH_3 and CH_3 positions. Accordingly a disordered model for the NH_3 and CH_3 hydrogen atoms, with the hydrogen of the acetamido ligand in its calculated position, was allowed for in the structure factor calculations; no hydrogen parameters were refined. Refinement was complete in three more cycles when R_1 = 0.055 and $R_2 = [\sum w(F_o - F_c)^2/\sum wF_o^2]^{1/2}$ = 0.068. The weighting scheme used in the final cycles of refinement was w = 1 if $F_o \leqslant 65.0$, $w = 65/F_o$ if $F_o > 65.0$; unobserved reflexions were given zero weight. On the last cycle of refinement the average shift for all parameters was 0.16 e.s.d., the maximum shift

Can. J. Chem. Downloaded from www.nrcresearchpress.com by 210.87.254.42 on 09/05/12
For personal use only.

TABLE 2. Anisotropic thermal parameters*

	U_{11}	U_{22}	U_{33}	U_{12}	U_{13}	U_{23}
Co	279(6)	240(5)	282(6)	10(6)	37(4)	12(6)
Cl(1)	340(14)	362(13)	465(14)	16(11)	67(11)	48(12)
Cl(2)	393(14)	372(14)	596(16)	−43(12)	−2(12)	100(14)
N(1)	40(5)	25(4)	34(5)	−2(4)	5(4)	−2(4)
N(2)	33(4)	40(5)	59(6)	6(4)	6(4)	11(4)
N(3)	45(5)	23(4)	37(4)	−3(4)	1(4)	0(4)
N(4)	38(5)	38(5)	44(5)	−8(4)	8(4)	−3(4)
N(5)	46(5)	29(5)	32(4)	0(4)	1(4)	0(3)
N(6)	46(5)	33(4)	36(5)	−4(4)	8(4)	3(4)
C(1)	36(6)	22(5)	39(6)	2(4)	2(5)	7(4)
C(2)	59(7)	33(6)	47(6)	−2(5)	10(5)	9(5)
O(1)	55(5)	28(4)	38(4)	3(3)	10(3)	−2(3)
O(2)	90(9)	123(11)	217(15)	−39(8)	−80(9)	11(11)
O(3)	74(7)	122(9)	149(11)	31(7)	22(7)	−57(8)
O(4)	101(11)	376(23)	75(8)	−2(12)	30(7)	22(12)
O(5)	96(9)	66(7)	238(16)	5(6)	4(10)	41(9)
O(6)	73(7)	115(9)	136(10)	2(7)	42(7)	53(8)
O(7)	111(10)	119(10)	131(10)	30(8)	−17(8)	−51(8)
O(8)	69(6)	50(5)	99(7)	−13(4)	−4(5)	28(5)
O(9)	64(6)	101(8)	127(9)	−4(6)	−37(6)	70(7)

*Expressed as $\exp[-2\pi^2(U_{11}h^2a^{*2} + U_{22}k^2b^{*2} + U_{33}l^2c^{*2} + 2U_{12}hka^*b^* + 2U_{13}hla^*c^* + 2U_{23}klb^*c^*)]$, U_{ij} in $Å^2 \times 10^4$ for Co and Cl, $\times 10^3$ for other atoms.

TABLE 3. Interatomic distances (Å) and angles (deg)

(*a*) Bonded distances

Bond	Distance (Å)	Average*	Bond	Distance (Å)	Average*
Co—N(1)	1.910(8)		Cl(1)—O(2)	1.366(13)	
			Cl(1)—O(3)	1.375(12)	
Co—N(6)	1.994(8)		Cl(1)—O(4)	1.383(13)	
			Cl(1)—O(5)	1.401(12)	
Co—N(2)	1.978(9)		Cl(2)—O(6)	1.399(12)	
Co—N(3)	1.945(7)		Cl(2)—O(7)	1.417(13)	
Co—N(4)	1.955(9)		Cl(2)—O(8)	1.408(9)	
Co—N(5)	1.973(8)		Cl(2)—O(9)	1.401(10)	
		1.963(13)			1.394(15)
N(1)—C(1)	1.339(12)				
C(1)—O(1)	1.267(12)				
C(1)—C(2)	1.508(14)				

*Value in parentheses is the r.m.s. deviation from the mean.

(*b*) Valence angles

Bonds	Angle (deg)	Bonds	Angle (deg)
N(1)—Co—N(2)	88.4(3)	O(2)—Cl(1)—O(3)	118.8(8)
N(1)—Co—N(3)	91.6(3)	O(2)—Cl(1)—O(4)	110.0(9)
N(1)—Co—N(4)	89.7(4)	O(2)—Cl(1)—O(5)	108.3(8)
N(1)—Co—N(5)	88.5(3)	O(3)—Cl(1)—O(4)	108.4(8)
N(1)—Co—N(6)	178.1(4)	O(3)—Cl(1)—O(5)	106.8(8)
N(2)—Co—N(3)	89.0(4)	O(4)—Cl(1)—O(5)	103.4(11)
N(2)—Co—N(4)	177.8(3)	O(6)—Cl(2)—O(7)	108.5(7)
N(2)—Co—N(5)	90.4(4)	O(6)—Cl(2)—O(8)	108.0(6)
N(2)—Co—N(6)	90.9(4)	O(6)—Cl(2)—O(9)	114.2(7)

TABLE 3 *(Concluded).*

(*b*) Valence angles

Bonds	Angle (deg)	Bonds	Angle (deg)
N(3)—Co—N(4)	89.9(3)	O(7)—Cl(2)—O(8)	106.3(7)
N(3)—Co—N(5)	179.4(4)	O(7)—Cl(2)—O(9)	110.0(7)
N(3)—Co—N(6)	90.3(3)	O(8)—Cl(2)—O(9)	109.6(6)
N(4)—Co—N(5)	90.6(3)		
N(4)—Co—N(6)	91.0(4)		
N(5)—Co—N(6)	89.8(3)		
Co—N(1)—C(1)	131.0(7)		
N(1)—C(1)—O(1)	122.6(8)		
N(1)—C(1)—C(2)	118.0(9)		
O(1)—C(1)—C(2)	119.4(8)		

(*c*) Non bonding contacts $\leqslant 3.4$ Å

Atom pairs	Distance (Å)	Atom pairs	Distance (Å)
N(1)...O(4)	3.06(2)	N(5)...O(6)	3.35(1)
N(2)...O(4)	3.13(2)	N(5)...O(8)	3.17(1)
N(2)...O(4)^{I}*	3.36(2)	N(5)...O(5)^{II}	3.11(1)
N(2)...O(6)^{II}	3.35(1)	N(5)...O(6)^{II}	3.03(1)
N(2)...O(9)^{II}	3.28(1)	N(6)...O(2)^{II}	3.17(2)
N(2)...O(8)^{III}	3.08(1)	N(6)...O(6)^{II}	3.24(2)
N(3)...O(5)^{I}	3.19(1)	N(6)...O(1)^{IV}	2.98(1)
N(3)...O(1)^{IV}	2.94(1)	N(6)...O(3)^{VI}	3.27(2)
N(3)...O(8)^{III}	3.29(1)	N(6)...O(9)^{III}	3.14(1)
N(4)...O(8)	3.23(1)	C(1)...O(3)^{I}	3.33(1)
N(4)...O(7)^{V}	3.12(2)	O(1)...O(3)^{I}	3.20(1)
N(4)...O(5)^{II}	3.27(2)	O(1)...N(3)	2.90(1)
N(4)...O(3)^{VI}	3.04(2)	O(1)...N(4)	2.99(1)
N(5)...O(2)	3.32(2)		

*The superscripts refer to the following equivalent positions: I, $-x,-y,-z$; II, $1/2-x,1/2+y,1/2-z$; III, $-1/2+x,1/2-y,-1/2+z$; IV, $1/2-x,1/2+y,-1/2-z$; V, $1-x,-y,-z$; VI, $1/2+x,1/2-y,-1/2+z$.

in positional parameter was 0.58 e.s.d., and that for the thermal parameters was 1.06 e.s.d. The X-ray system (8) versions of 1970 and 1972 was used for all major crystallographic calculations; the University of Canterbury data reduction program (9) was used to process our diffractometer tapes and the program to calculate the disordered hydrogen atom position was obtained from Ammon (10). The final positional parameters are listed in Table 1, thermal parameters in Table 2, and interatomic distances and angles in Table 3. A table of observed structure amplitudes and calculated structure factors has been placed with the Depository of Unpublished Data.[2]

[2]Photocopies of the table of observed and calculated structure factors may be obtained at a nominal charge from the Depository of Unpublished Data, National Science Library, National Research Council of Canada, Ottawa, Canada K1A 0S2.

Description of Structure and Discussion

The structure consists of discrete $[Co(NH_3)_5NHCOCH_3]^{2+}$ cations and perchlorate anions. A view of the cation geometry is in Fig. 1. The environment of the cobalt atom is octahedral with a mean *cis* N—Co—N angle of 90.0°.

That the acetamide is nitrogen-bonded to the cobalt atom is clearly established by the physical evidence (1) and confirmed by the successful refinement of this structure. The oxygen atom of the acetamide ligand is pointing between two equatorial *cis* ammines with the methyl group directed away from the Co atom; an exactly similar orientation has been found for the acetatopentaamminecobalt(III) ion (11). The O...N(ammine) intramolecular contact distances, 2.988(10), 2.900(10), do not preclude N—H...O hydrogen bonding but as hydrogen atoms could not be located unequivocally, no real evidence can be produced for it. Even in the absence of

Can. J. Chem. Downloaded from www.nrcresearchpress.com by 210.87.254.42 on 09/05/12
For personal use only.

Can. J. Chem. Downloaded from www.nrcresearchpress.com by 210.87.254.42 on 09/05/12
For personal use only.

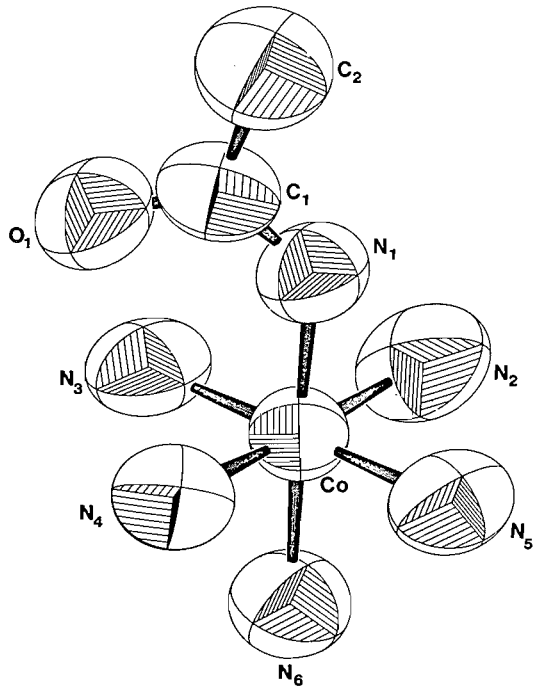

FIG. 1. View of the $[CH_3CONHCo(NH_3)_5]^{2+}$ cation showing our numbering scheme. The thermal ellipsoids are drawn at the 90% probability level.

proven intramolecular hydrogen bonding consideration of relative sizes of the carbonyl oxygen *viz-a-viz* the methyl group would favor the conformation found here.

The N—Co bond *trans* to the amide is slightly longer (1.994(8) Å) than the mean of the four equatorial bonds (1.963(13) Å) and the Co—N(amide) distance (1.911(8) Å) is significantly shorter. These distances may be compared with the average N—Co value found in $Co(NH_3)_6^{3+}$ (1.968 Å) (12) and the shorter value (1.903 Å) reported for the N—Co bonds in $(NH_3)_4$

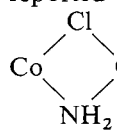

(13). The bond lengths in the amide group are very interesting; the C—O bond length 1.267(12) Å is longer than would be expected for a C=O double bond, 1.23 Å (14), while the C—N distance, 1.339(12) Å, is identical to that found in pyridine 1.340(1) Å (15). Clearly a delocalized system (**3**) is important in the ground state structure of the cation. Lending support to this are the infrared spectra of the acetamide and related complexes. The carbonyl

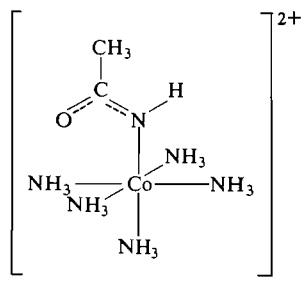

3

stretching frequency for $(NH_3)_5CoNH_2COCH_3^{3+}$ is at 1700 cm^{-1} and for its conjugate base (**3**) at 1560 cm^{-1}, whereas in the free acetamide ν(C=O) appears at 1714 cm^{-1}. These large differences between the carbonyl stretching frequencies of the acidic and basic forms may be rationalized in terms of delocalization in the N—C—O system of the conjugate base, which is not possible in the acidic form. Similar spectral features are found in the acidic and basic forms of the formamide complex ($(NH_3)_5$-

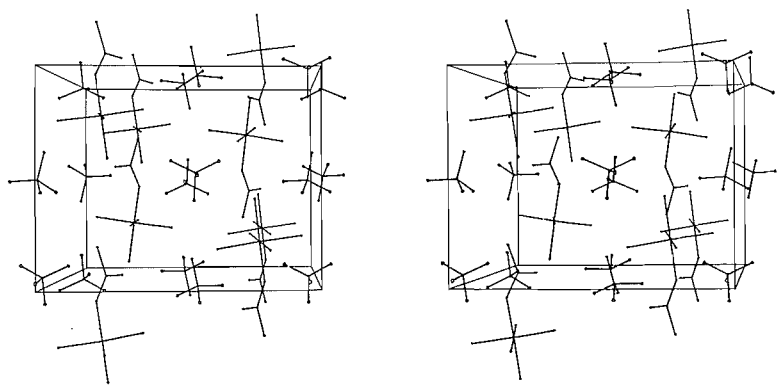

FIG. 2. Stereo-diagram of the contents of the unit cell viewed along the *c*-axis.

$CoNH_2CHO^{3+}$, $\nu C{=}O = 1675\ cm^{-1}$; and $(NH_3)_5CoNHCHO^{2+}$, $\nu C{=}O = 1600\ cm^{-1}$) indicating a similar delocalization.

The other bonded distances in the structure are normal. The Csp^2—Csp^3 distance 1.51(1) Å lies in the range of values usually found for such bonds. The perchlorate anions have their expected tetrahedral geometry with mean O—Cl—O angle 109.3° and mean Cl—O 1.39 Å.

The molecular packing is shown in Fig. 2. The cations and perchlorate ions pack in layers parallel to [011]. Planes of perchlorate ions are found at $x = 0$ and 0.5 with the cations at $x = 0.25$ and 0.75. The shorter intermolecular contacts are listed in Table 3, and for the most part involve ammine or amide N...O(perchlorate) contacts. An analysis of these distances in terms of possible hydrogen bonding would be at best speculative as no hydrogen atoms were located. However, the amide nitrogen N(1) is 3.06(2) Å from a neighboring perchlorate oxygen (O(4)) and the geometrical arrangement (Cl—$\hat{O}$...N 113.9(7), C—$\hat{N}$(H)...O 119.4(7)°) is consistent with this being a weak hydrogen bond.

We are grateful to the National Research Council of Canada for operating grants (A5975 to GF and A6642 to RJB) and for a computing grant (CO357 to GF). All the calculations were performed on the University of Guelph IBM 370/155 computer.

1. R. J. Balahura. Ph.D. Thesis. University of Alberta, Edmonton, Alberta. 1971.
2. R. J. Balahura and R. B. Jordan. J. Am. Chem. Soc. **92**, 1533 (1970).
3. R. J. Balahura and R. B. Jordan. J. Am. Chem. Soc. In press.
4. J. M. Robertson and I. Woodward. J. Chem. Soc. 219 (1937); 36 (1940); G. A. Sim. *In* Computing methods and the phase problem in X-ray crystal analysis. *Edited by* R. Pepinsky, J. M. Robertson, and J. C. Speakman. Pergamon Press, Oxford. 1961.
5. D. T. Cromer and J. B. Mann. Acta. Cryst. **A24**, 321 (1968).
6. R. F. Stewart, E. R. Davidson, and W. T. Simpson. J. Chem. Phys. **42**, 3178 (1965).
7. International tables for X-ray crystallography. Vol. III. The Kynoch Press. 1968. p. 215.
8. J. M. Stewart, G. J. Kruger, H. L. Ammon, C. Dickinson, and S. R. Hall. University of Maryland Computer Science Center Technical Report TR-192 (1972).
9. Program supplied by University of Canterbury Crystallography group and modified at Guelph by Dr. F. C. March.
10. H. Ammon. Personal communication.
11. E. B. Fleischer and R. Frost. J. Am. Chem. Soc. **87**, 3998 (1965).
12. D. W. Meek and J. A. Ibers. Inorg. Chem. **9**, 465 (1970).
13. R. Barro, R. E. Marsh, and W. P. Schaeffer. Inorg. Chem. **9**, 2131 (1970).
14. Tables of interatomic distances in molecules and ions. Supplement. Chemical Society Special Publication No. 18. London, The Chemical Society. 1965.
15. B. Bak, L. Hansen-Nygaard, and J. Rastrup-Andersen. J. Mol. Spectrosc. **2**, 361 (1958).

Can. J. Chem. Downloaded from www.nrcresearchpress.com by 210.87.254.42 on 09/05/12
For personal use only.

Application de la Trichromie Complémentaire à l'étude des complexes métalliques en solution

M. MORIN, M. M. PETIT-RAMEL, ET J. P. SCHARFF

Laboratoire de Chimie Minérale, Université Claude-Bernard Lyon I, 43, Boulevard du 11 Novembre 1918, 69 – Villeurbanne, France

ET

M. R. PÂRIS

Laboratoire de Chimie de Coordination, Université de Dijon, 6, Boulevard Gabriel, 21 – Dijon, France

Reçu le 31 octobre 1972

L'intérêt de la spectrophotométrie trichrome comme méthode d'investigation des équilibres complexes en solution a été démontré à l'aide d'une dizaine d'exemples originaux faisant intervenir divers cations métalliques bivalents (cuivre, vanadyle) ou trivalents (fer, aluminium, yttrium, lanthane) complexés par différents coordinats organiques.

La détermination des coordonnées trichromatiques complémentaires permet la mise en évidence rapide de la formation de complexes colorés simples ou mixtes (en particulier bimétalliques); de leurs domaines d'existence et du nombre d'espèces en solution.

Les limites inhérentes à la méthode sont discutées mais néanmoins celle ci se révèle d'une utilité incontestable pour une première approche des phénomènes de complexation, que l'on doit ensuite compléter par une étude plus quantitative en utilisant les méthodes classiques.

Complementary tri-stimulus spectrophotometry appears as an interesting method for investigation of metal complex equilibria in solution. This has been demonstrated on various examples including bivalent (copper, vanadyl) or trivalent (iron, aluminum, yttrium, lanthanum) metal ions coordinated by several organic ligands.

The formation, p*H* range of existence, and the number of absorbing species in colored solutions of binary or ternary (particularly bimetallic) systems are easily determined by calculation of the complementary tri-stimulus co-ordinates.

The advantages (and disadvantages) of the technique are discussed. This qualitative method appears to be very useful for a first approach of coordination phenomena but needs to be completed by quantitative studies using classical methods.

Can. J. Chem., **51**, 2186 (1973)

Introduction

Le principe de l'emploi de la trichromie complémentaire pour l'étude rationnelle des indicateurs colorés a été mis au point en 1960 par Reilley et ses collaborateurs (1, 2). Ce domaine d'application a donné lieu à de nombreuses publications parmi lesquelles nous pouvons retenir la revue exhaustive de Kotrly (3) ainsi que l'article récent de Kotrly et Vytras (4).

Quelques travaux (5–10) ont montré la valeur de cette méthode d'investigation des équilibres en solution notamment en ce qui concerne les complexes mixtes bimétalliques.

Pour notre part nous avons montré que la méthode pouvait permettre de déceler la formation de complexes métalliques colorés ainsi que le nombre d'espèces en solution et leurs domaines d'existence et ceci beaucoup plus rapidement qu'au moyen des procédés classiques.

Nous illustrerons les possibilités et les limites de la méthode par quelques exemples caractéristiques relatifs à des complexes simples et à des complexes mixtes, soit bimétalliques (du type $M_mM'_{m'}L_n$), soit constitués par un ion métallique et deux coordinats différents (du type $ML_nL'_{n'}$).

Principe des methodes utilisées

Méthode spectrophotométrique trichrome

Nous ne reviendrons pas sur les calculs fondamentaux développés dans l'article original de Reilley (1), nous contentant de poser l'équation générale des coordonnées chromatiques (limitée au terme du premier ordre).

$$[1] \qquad P_r = G_r - J(Q_r - G_r)$$

où les symboles P_r, G_r, et Q_r désignent respectivement les coordonnées chromatiques de la

Can. J. Chem. Downloaded from www.nrcresearchpress.com by 210.87.254.42 on 09/05/12
For personal use only.

Can. J. Chem. Downloaded from www.nrcresearchpress.com by 210.87.254.42 on 09/05/12
For personal use only.

couleur observée, de la couleur incidente et de la couleur absorbée (couleur complémentaire). P_r est alors représenté par les coordonnées trichromatiques x, y, z, se déduisant des flux X, Y, Z (transmittances) par les relations:

$$x = \frac{X}{X + Y + Z}$$

[2] $$y = \frac{Y}{X + Y + Z}$$

$$z = \frac{Z}{X + Y + Z}$$

Dans le cas de la trichromie complémentaire, (seule méthode utilisée dans ce travail), Q_r est représenté par les coordonnées trichromatiques complémentaires u, v, w définies par les relations:

$$u = \frac{U}{U + V + W}$$

[3] $$v = \frac{V}{U + V + W}$$

$$w = \frac{W}{U + V + W}$$

pour lesquelles nous allons expliciter d'une manière concrète et directement utilisable les trois fonctions U, V, et W.

En effet, le principe des déterminations expérimentales consiste à mesurer simultanément avec le pH, au cours d'une neutralisation progressive par la soude, l'absorption lumineuse de solutions de complexes. Après avoir tracé les spectres d'absorption à différents pH, trois domaines du spectre sont sélectionnés et plusieurs longueurs d'onde, en général dix, sont pointées dans chacun d'eux.

La valeur de l'absorbance A est lue pour chaque longueur d'onde et on en fait la somme R dans chaque domaine r

[4] $$R_{(r)} = \sum_{1}^{10} A_r$$

r peut varier de 1 à 3 (3 domaines) et la somme de toutes les absorptions à chaque longueur d'onde sera caractérisée par une fonction U, dans le premier domaine; V, dans le second et W dans le troisième.

U, V, W étant proportionnelles à la concentration de la substance colorée, il en résulte que les "coordonnées de la couleur" u, v, w seront indépendantes de cette même concentration.

La somme $J = U + V + W$ est la "concentration optique" de la solution de complexe. Elle est reliée à la concentration analytique c par la relation

[5] $$J = A \times c \times l$$

où A est l'absorbance totale et l la longueur de la cuve spectrophotométrique.

Dans le cas d'un équilibre simple du type

[6] $$M + L \rightleftarrows ML$$

où M représente l'ion métallique, L l'agent chélatant, et ML le complexe formé par les deux espèces; on peut écrire

[7] $$c_M = [M] + [ML]$$

[8] $$c_L = [L] + [ML]$$

c_M et c_L étant les concentrations totales des réactifs.

Si l'ion métallique est coloré et le coordinat incolore, on peut évaluer successivement les fonctions u, v, w dans le spectre visible. Or nous avons vu que ces fonctions étaient indépendantes de la concentration de l'espèce considérée. D'autre part, si à partir d'un certain pH, le complexe est entièrement formé, un seul colorant ML absorbera, à la dissociation près de celui-ci et la fonction $u = f(c)$, par exemple, présentera un palier correspondant à l'existence de la seule espèce absorbante. Comme la concentration d'une espèce complexe en équilibre est liée directement au pH de la solution, du fait de la forme protonée du coordinat, le graphe $u = f(\text{p}H)$ présentera une ligne droite parallèle à l'axe des pH. Les portions non parallèles à l'axe des abscisses indiquent les zones de transition d'une forme en l'autre.

L'existence d'une seule espèce étant mise en évidence, la colorimétrie trichrome peut encore nous renseigner utilement sur la formation d'un équilibre simple entre deux espèces. Dans ce cas, on constate que les fonctions $u = f(v)$ ou $u = f(w)$ ou encore $v = f(w)$ sont des fonctions linéaires; lorsqu'elles perdent leur linéarité, on peut supposer que l'on se trouve en présence de plus de deux espèces. Il est également possible de prévoir que lorsque l'une de ces fonctions devient ponctuelle, l'équilibre est détruit au profit d'une seule espèce et nous sommes

Can. J. Chem. Downloaded from www.nrcresearchpress.com by 210.87.254.42 on 09/05/12
For personal use only.

ramenés dans les conditions où $u = f(pH)$ reste constante.

Ainsi lorsque nous sommes en présence d'un système inconnu, on peut par le simple tracé d'une série de spectres d'absorption révéler l'existence, soit d'une espèce colorée unique, soit d'un équilibre entre deux espèces, soit encore la présence de plus de deux espèces absorbantes.

Nous illustrons ces trois étapes de la trichromie complémentaire en étudiant des équilibres de complexes connus du point de vue de leur stabilité ionique, ce qui nous permettra d'apprécier la validité de la méthode en même temps que ses limites.

Méthode de calcul de la répartition des différentes espèces

Dans le but de tester les résultats de la méthode précédente nous pouvons calculer les courbes de répartition des espèces en fonction du pH. Le calcul est aisé lorsque l'on connait, ce qui est le cas ici, les constantes de stabilité ionique des divers complexes mis en jeu (8, 12–14).

Dans tous les cas nous avons utilisé une méthode de calcul par approximations successives, dérivée de la méthode d'itération dite "de Newton" et facilement adaptable sur ordinateur.

En effet dans les cas les plus complexes envisagés (espèces mixtes $ML_nL'_{n'}$ et $M_mM'_{m'}L_n$) on dispose des 3 équations exprimant les concentrations totales des trois constituants. On est donc ramené à la résolution de 3 équations F_1, F_2, F_3 non linéaires à trois inconnues X_1, X_2, X_3 (pouvant être [M], [L], [L'] ou [M], [M'], [L]).

On cherche donc les solutions X_1^0, X_2^0, X_3^0 des équations

$$F_i(X_1,X_2,X_3) = 0$$

Il faut pour cela résoudre le système linéaire

$$[9] \qquad \sum_{j=1}^{3} \frac{\partial F_i}{\partial X_j} \cdot dX_j + F_i(X_1,X_2,X_3) = 0$$

avec $dX_j = X_j^0 - X_j$

Le processus d'itération est le suivant: en se donnant des valeurs de départ X_1^1, X_2^1, X_3^1, l'ordinateur calcule les $\partial F_i(X_1^1,X_2^1,X_3^1)/\partial X_j$ et $F_i(X_1^1,X_2^1,X_3^1)$ puis résout le système [9] qui a pour inconnues les dX_j. Les nouvelles valeurs $X_j + dX_j$ sont alors calculées et l'itération est poursuivie jusqu'à ce que $|dX_j/X_j| \leqslant \varepsilon$; ε définissant la précision recherchée.

Resultats expérimentaux

Cas des complexes simples ML_n

(a) Une seule espèce colorée ML existe dans un large domaine de pH

Un exemple particulièrement significatif nous est fourni par le complexe que forment les ions ferriques avec l'acide éthylénediamine-*N*-*N*'-di(*o*-hydroxyphénylacétique). D'après l'étude de Anderegg et L'Eplattenier (11), un seul complexe rouge de stabilité ionique remarquable ($\log \beta_1 = 33.91$) se forme dans une zone de pH allant de 3 à 10. Nous avons pu confirmer ces conclusions en traçant un faisceau de spectres dans le domaine 385–560 nm (où les ions ferriques n'absorbent pas) et en déterminant les courbes $u,v,w = f(pH)$. Les trois fonctions présentent un palier parallèle à l'axe des pH dans le domaine considéré (fig. 1) montrant ainsi l'existence de la seule espèce colorée ML.

(b) Formation successives de plusieurs espèces colorées en fonction du pH

Notre premier exemple concerne les complexes des ions ferriques avec l'acide sulfo-5-salicylique (H_3L). Nous avons montré antérieurement l'existence dans ce système de trois complexes successifs ML, ML_2, et ML_3 dont les constantes de stabilité ont été déterminées potentiométriquement (12): $\log \beta_1 = 12.08$; $\log \beta_2 = 23.22$, et $\log \beta_3 = 30.24$.

Nous avons tracé les spectres d'absorption dans la région 385–535 nm pour différents rapports $R = c_L/c_M$ de réactifs engagés et nous donnons à titre d'exemple les courbes $u,v,w = f(pH)$ obtenues dans le cas où $R = 30$ (fig. 2). Nous avons fait figurer également les courbes de répartition représentant les concentrations des espèces ML_n, en fonction du pH, calculées à

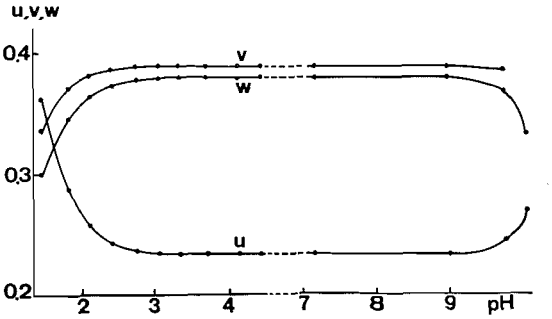

FIG. 1. Courbes $u,v,w = f(pH)$ pour le système Fe(III) – acide éthylènediamine-*N*-*N*'-di-(*o*-hydroxyphénylacétique). $[Fe]_T = [L]_T = 3.10^{-4}$ *M*.

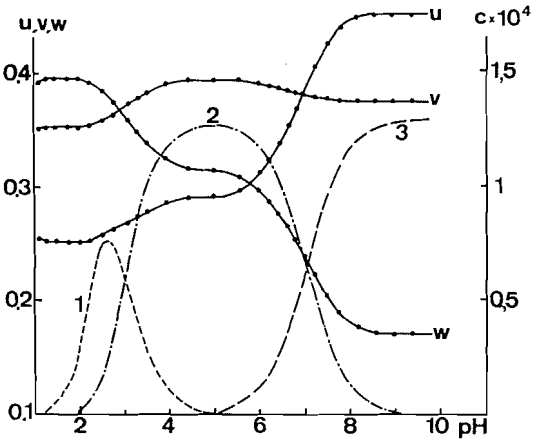

FIG. 2. Méthode trichrome (traits pleins) et courbes de répartition (traits discontinus) pour le système Fe(III) – acide sulfo-5-salicylique. (1) FeL; (2) FeL_2; (3) FeL_3. $[Fe]_T = 1.290 \times 10^{-4}$ *M*; $[L]_T = 3.750 \times 10^{-3}$ *M*.

l'aide des valeurs des constantes indiquées ci-dessus.

On observe de façon très nette le palier correspondant à la formation du premier complexe FeL (coloration violette intense) pour des p*H* compris environ entre 1.50 et 2.50. Les courbes de répartition montrent qu'au delà de p*H* = 2.50 l'espèce ML_2 existe de façon notable, on a donc équilibre entre deux espèces colorées distinctes, ce qui explique que le premier palier des courbes *u,v,w* soit limité à cette valeur.

De même le palier correspondant à la formation du deuxième complexe ML_2 (coloration rouge orangé) est peu marqué. Les courbes de répartition montrent en effet que cette espèce n'existe pratiquement jamais seule en solution mais qu'elle est en équilibre soit avec le premier complexe (p*H* < 5) soit avec le troisième (p*H* > 5). Enfin on observe le palier correspondant à la formation du troisième complexe ML_3 (coloration jaune) pour des p*H* supérieurs à 8.50 en accord avec la courbe de répartition qui montre qu'à partir de cette valeur la concentration en ML_2 devient négligeable et qu'une seule espèce colorée subsiste au sein de la solution.

Cependant il faut souligner que l'existence d'un palier sur les courbes $u,v,w = f(pH)$ ne permet pas de conclure de façon indubitable à l'existence d'une seule espèce colorée. Nous pouvons illustrer ce fait dans le cas des complexes ferriques de l'acide pyrocatécholdisulfonique-3,5: nous avons démontré en effet (13) l'existence de quatre complexes MHL, ML, ML_2, et ML_3 dont deux (MHL et ML) possèdent le même coefficient d'extinction moléculaire.

Les spectres d'absorption exploités dans la région 410–710 nm permettent de tracer les coordonnées trichromatiques complémentaires comme nous l'avons fait sur la fig. 3 pour $R = c_L/c_M = 10$.

L'interprétation des résultats peut se faire d'une façon analogue au cas précédent sauf en ce qui concerne le premier palier observé pour des p*H* < 3. En effet dans ce cas les courbes de répartition montrent que dans cette zone de p*H* acide, deux complexes colorés (bleu–vert) MHL et ML coexistent et ces deux espèces se trouvent avoir le même coefficient d'extinction moléculaire. Cet exemple nous permet d'illustrer de manière tangible les limites de la méthode trichrome.

La méthode trichrome nous a permis, jusque là, d'observer les différents paliers correspondant aux formations successives des complexes simples, au sein d'un même système.

Dans l'exemple suivant, nous allons en atteindre la limite d'utilisation, du fait de l'apparition, non plus successive, mais simultanée, d'au moins deux espèces; c'est le cas du système cuivre–valine, dont la formation a été largement étudiée par diverses techniques: potentiométrique, spectrophotométrique, polarimétrique etc... (14).

Après en avoir calculé la constante de stabilité, nous avions pu tracer les courbes de répartition des espèces en présence: Cu(val), $Cu(val)_2$ et l'ion Cu^{2+} libre en fonction du p*H* (fig. 4), qui mettent en évidence, dès p*H* 6, l'existence d'une

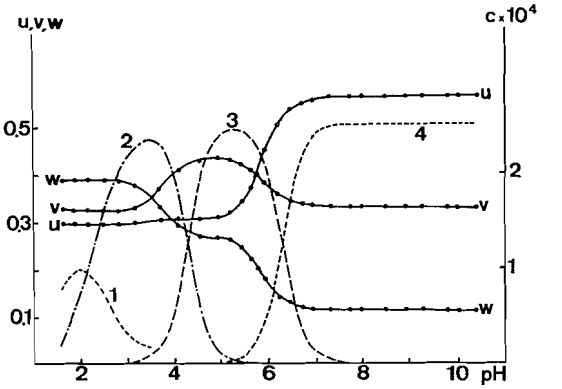

FIG. 3. Méthode trichrome (traits pleins) et courbes de répartition (traits discontinus) pour le système Fe(III) – acide pyrocatécholdisulfonique-3,5. (1) FeHL; (2) FeL; (3) FeL_2; (4) FeL_3. $[Fe]_T = 2.517 \times 10^{-4}$ *M* $[L]_T = 2.500 \times 10^{-3}$ *M*.

Can. J. Chem. Downloaded from www.nrcresearchpress.com by 210.87.254.42 on 09/05/12
For personal use only.

Can. J. Chem. Downloaded from www.nrcresearchpress.com by 210.87.254.42 on 09/05/12
For personal use only.

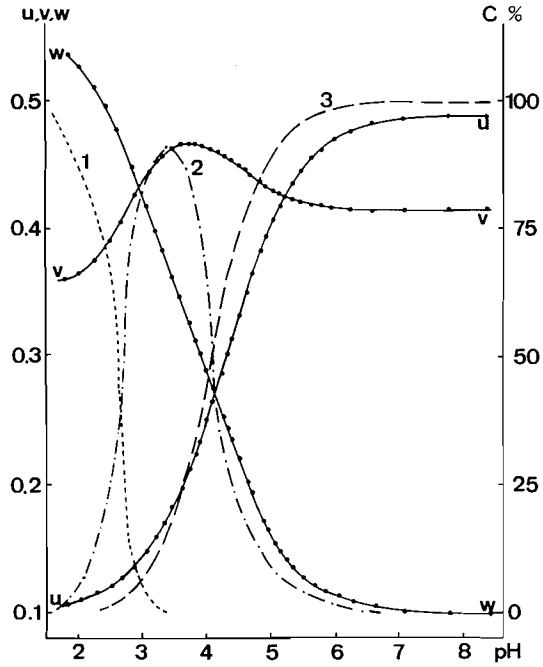

FIG. 4. Méthode trichrome (traits pleins) et courbes de répartition (traits discontinus) pour le système Cu(II)-valine. (1) Cu(II); (2) Cu(val); (3) $Cu(val)_2$. $[Cu]_T = 3.336 \times 10^{-3}$ *M*; $[val]_T = 1.600 \times 10^{-2}$ *M*.

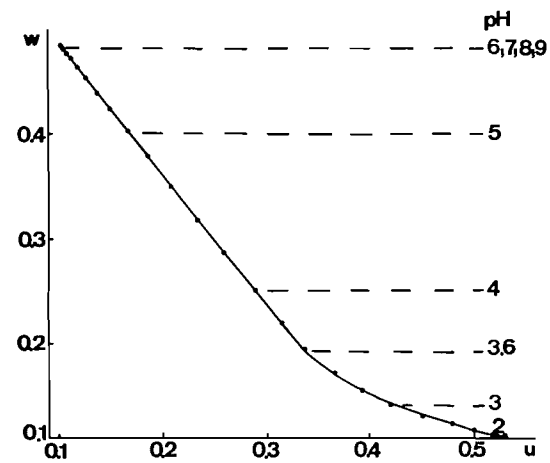

FIG. 5. Courbe $w = f(u)$ pour le système Cu(II)-valine.

espèce absorbante unique, $Cu(val)_2$, ce qui apparait nettement sur le tracé des courbes $u,v,w = f(pH)$ (fig. 4).

D'autre part, l'analyse d'une fonction $w = f(u)$ (fig. 5) montre d'abord:

(*i*) de p*H* 2 à p*H* 3, une variation linéaire caractéristique de la présence de deux espèces qui sont en effet, le cuivre non complexé et le premier complexe Cu(val).

(*ii*) de p*H* 3 à p*H* 3.6, une zone incurvée, restreinte, supposant la présence de plus de deux espèces. En effet, les courbes de répartition font apparaitre la formation simultanée de trois espèces: le cuivre non complexé et les deux espèces chélatées Cu(val) et $Cu(val)_2$.

(*iii*) de p*H* 3.6 à p*H* 6, la fonction redevient parfaitement linéaire et représentative de l'équilibre:

$$Cu(val) + val \rightleftarrows Cu(val)_2$$

(*iv*) enfin à partir de p*H* 6, la fonction devient ponctuelle puisque nous sommes en présence d'une seule espèce $Cu(val)_2$.

Cas des complexes mixtes bicoordinats $ML_nL'_n$

Nous examinerons tout d'abord les données relatives au système Fe(III) – acide sulfo-5-salicylique (H_3L) – acide nitrilotriacétique (H_3L') pour lequel nous avons montré l'existence d'un complexe mixte de formule MLL′ dans un vaste domaine de p*H* allant de 2 à 10. La constante de stabilité ionique $\beta_{11} = [MLL']/[M][L][L']$ a été déterminée potentiométriquement et affinée par nos méthodes habituelles: $\log \beta_{11} = 26.59$.[1]

L'exploitation des spectres d'absorption dans la région 383–560 nm conduit aux courbes $u,v,w = f(pH)$ que nous avons représentées sur la Fig. 6 pour le rapport 1:10:10.

On constate que les trois courbes présentent un palier remarquable dans la zone de p*H* considérée. Le calcul de la répartition des espèces montre que ces paliers sont limités d'une part

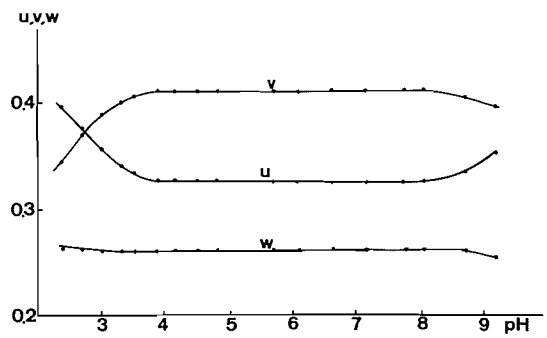

FIG. 6. Courbes $u,v,w = f(pH)$ pour le système Fe(III) – acide sulfo-5-salicylique – acide nitrilotriacétique. $[Fe]_T = 3.600 \times 10^{-4}$ *M*; $[L]_T = [L']_T = 3.600 \times 10^{-3}$ *M*.

[1]Anal. Chim. Acta: à paraitre.

Can. J. Chem. Downloaded from www.nrcresearchpress.com by 210.87.254.42 on 09/05/12
For personal use only.

vers les pH acides par l'existence de l'espèce [FeNTA] et d'autre part vers les pH alcalins par la formation de [$Fe(ASS)_3$]. Nous avons également détecté la présence d'une espèce hydroxydée [FeNTA(OH)] qui coexiste avec l'espèce mixte dans la même région de pH. Cependant ce complexe étant incolore, il n'altère pas les coordonnées trichromatiques et l'on a bien dans ce cas une seule espèce mixte colorée en solution.

Il faut noter que nous avons obtenu des résultats analogues dans le cas du système Fe(III) – acide dihydroxy-2,4 benzoique – acide nitrilotriacétique.

Par contre, si nous examinons maintenant le système mixte cuivre–glycine–valine, le tracé des courbes de répartition (fig. 7) pour lesquelles nous n'avons retenu que le rapport $[M]_T:[L]_T:[L']_T = 1:1:1$ (le plus favorable à la formation de l'espèce mixte) indique en premier lieu, que trois espèces absorbantes sont simultanément présentes à partir de pH 7: le complexe mixte Cu(gly)(val) (environ 50%) et les deux complexes simples $Cu(val)_2$ et $Cu(gly)_2$ dans la proportion de 25% environ. En nous reportant au principe

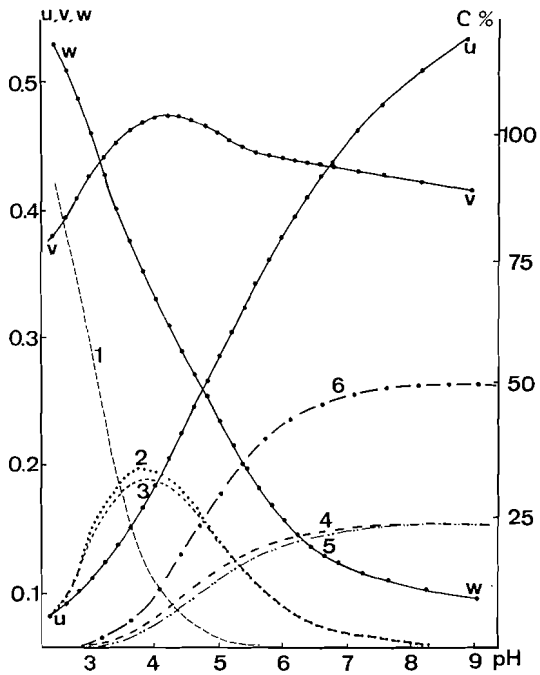

FIG. 7. Méthode trichrome (traits pleins) et courbes de répartition (traits discontinus) pour le système Cu(II)–glycine–valine. (1) Cu(II); (2) Cu(gly); (3) Cu(val); (4) $Cu(gly)_2$; (5) $Cu(val)_2$; (6) Cu(gly)(val) $[Cu]_T = 4.170 \times 10^{-3}$ M; $[gly]_T = [val]_T = 4.200 \times 10^{-3}$ M.

de la méthode trichromatique, les différentes fonctions $u,v,w = f(pH)$ ne doivent pas présenter de palier caractéristique d'une seule espèce absorbante. Ceci est parfaitement vérifié sur la fig. 7 où les trois courbes u, v, w ne présentent aucune partie horizontale.

La substitution des courbes $w = f(u)$ aux courbes $u = f(pH)$, par exemple, n'apporte aucune précision supplémentaire et nous arrivons ici en limite d'utilisation de la méthode, dont les possibilités peuvent être résumées ainsi:

(*i*) la présence d'une seule espèce absorbante se traduit par un palier sur les courbes $u = f(pH)$ et par un point sur les courbes $u = f(v)$.

(*ii*) la présence simultanée de deux espèces absorbantes ne se détectant pas sur les courbes $u = f(pH)$ conduit par contre à une fonction linéaire pour $u = f(v)$.

(*iii*) enfin lorsque ces dernières fonctions ne sont plus rectilignes, nous pouvons en conclure qu'il y a plus de deux espèces absorbantes en présence.

Cas des complexes mixtes bimétalliques $M_mM'_mL_n$

Ces complexes bimétalliques ne semblent pas avoir beaucoup retenu l'attention jusqu'ici; cependant, si leur formation parait relativement rare, à priori, elle peut se révéler extrêmement gênante au cours de la mise au point de dosages complexométriques simultanés de plusieurs métaux. C'est ainsi qu'en 1961, Flaschka, Butcher, et Speights (7), vérifièrent par la trichromie, l'existence d'un tel complexe mixte entre l'acide tartrique, le cuivre et l'aluminium.

Dans un précédent mémoire (8), nous avons pu mettre en évidence, grâce à la méthode trichrome, l'existence du complexe bimétallique formé entre l'acide tartrique, le cuivre et l'yttrium. Comme l'ion tartrate et l'ion citrate ont sensiblement les mêmes propriétés en ce qui concerne la chélation mixte (au nombre de fonctions acides et alcooliques près), il nous a paru intéressant d'étudier le comportement de l'ion citrate, d'une part en présence de cuivre et d'yttrium et d'autre part en présence de cuivre et de lanthane. La méthode trichrome était évidemment tout indiquée dans cette première approche.

Les mesures se font dans un premier temps sur les solutions contenant les citrates de cuivre seuls, considérés comme espèces simples, puis dans un deuxième temps sur les espèces mixtes de

citrate de cuivre–yttrium dont nous ne connaissons pas le nombre à priori.

A partir des deux faisceaux de spectres obtenus dans le domaine de 500 à 850 nm, nous pouvons tracer les coordonnées de la couleur complémentaire u, v, et w pour les complexes simples et u', v', et w' pour les complexes mixtes (fig. 8). Nous observons pour chacune des fonctions, deux paliers caractérisant, dans une zone de pH déterminée, la présence d'une seule espèce colorée et d'une seule espèce mixte, bien différenciées l'une de l'autre. On peut donc en déduire, de prime abord, qu'il se forme entre pH 7 et pH 9 une espèce mixte unique dont la formule $[YCuCit_2(OH)_2]$ a été déterminée par des mesures conjointes d'absorbance et de pH.[2]

Des courbes analogues ont été obtenues pour les systèmes citrates et tartrates de cuivre–lanthane.

Un dernier exemple concerne la recherche d'éventuels complexes entre l'acide citrique et les ions aluminium et vanadyle c'est-à-dire $Al_n(VO)_{n'}$ Cit_m. Or l'examen des coordonnées trichromes en fonction du pH montre que les

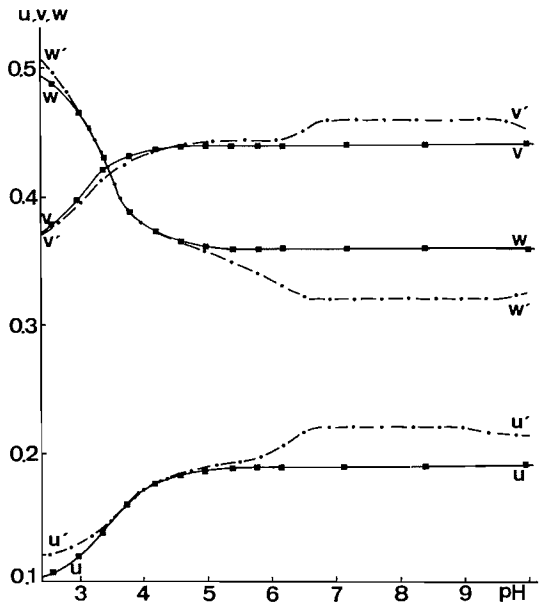

FIG. 8. —, Courbes $u,v,w = f(pH)$ pour le système Cu(II) – acide citrique. $[Cu]_T = 3.060 \times 10^{-3}$ M, $[Cit]_T = 1.500 \times 10^{-2}$ M; - · · · -, Courbes $u',v',w' = f(pH)$ pour le système Cu(II) – Y(III) – acide citrique. $[Cu]_T = 3.060 \times 10^{-3}$ M; $[Y]_T = 3.000 \times 10^{-3}$ M; $[Cit]_T = 1.500 \times 10^{-2}$ M.

[2]J. Inorg. Nucl. Chem: à paraitre.

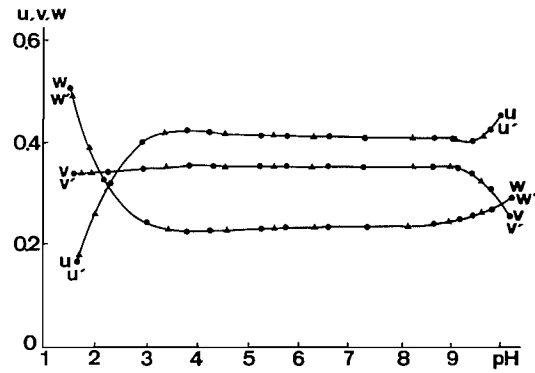

FIG. 9. ●, Courbes $u,v,w = f(pH)$ pour le système VO(II) – acide citrique; ▲, Courbes $u',v',w' = f(pH)$ pour le système Al(III) – VO(II) – acide citrique. $[VO^{2+}]_T = 5.952 \times 10^{-3}$ M; $[Al]_T = 5.952 \times 10^{-3}$ M; $[Cit]_T = 3.000 \times 10^{-2}$ M.

courbes $u = f(pH)$; courbes u, v, w (pour le système vanadyle – acide citrique) et u', v' w' (pour le système aluminium – vanadyle – acide citrique) sont parfaitement confondues (fig. 9).

La présence d'un palier important entre les pH 5 et 9 permet de prévoir un seul citrate simple de vanadyle 1:1 signalé par divers auteurs (15, 16) et après addition d'un sel d'aluminium, il n'y aura que la juxtaposition des citrates simples d'aluminium avec ce même citrate de vanadyle. La formation du complexe mixte bimétallique est donc irréalisable du fait de la grande stabilité du citrate simple de vanadyle (ou de son dimère) (17), interdisant toute compétition avec l'aluminium.

Partie expérimentale

Toutes les mesures de cette étude ont été réalisées à la température standard de 25 °C ± 0.1, en milieu de force ionique 0.5 M maintenue constante par du nitrate de sodium excepté dans le cas des systèmes cuivre–valine et cuivre–glycine–valine où l'électrolyte support était du perchlorate de sodium.

Protométrie

Les mesures de pH ont été effectuées à l'aide d'un compensateur Metrohm E 388 (électrodes Metrohm: type EA 109 UX pour l'électrode en verre et EA 404 pour l'électrode de référence). Les solutions étaient placées dans des cellules thermostatées Tacussel type RMO6 et maintenues sous atmosphère d'azote.

L'étalonnage de la chaine de mesure était vérifié quotidiennement à l'aide des solutions tampons étalons de Bates: biphtalate de potassium 0.05 M (pH = 4.005) et borax 0.05 M (pH = 9.196). La correspondance entre le pH lu et la concentration analytique des protons a été également établie pour chaque cas.

Can. J. Chem. Downloaded from www.nrcresearchpress.com by 210.87.254.42 on 09/05/12
For personal use only.

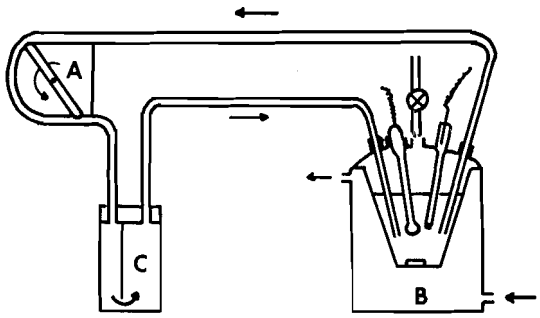

FIG. 10. Schéma de l'appareillage: (*A*) pompe péristaltique; (*B*) cellule potentiométrique; (*C*) cellule spectrophotométrique.

Spectrophotométrie

Le principe de nos déterminations spectrophotométriques consiste à mesurer simultanément avec le p*H*, au cours d'une neutralisation progressive par une base, l'absorption lumineuse de solutions contenant les différents constituants du système. Grâce à une pompe péristaltique (A) la solution circule en permanence de la cellule "potentiométrique" RMO6 Tacussel thermostatée (B) à la cellule "spectrophotométrique" (C) qui est une cuve à circulation (Fig. 10). Nous enregistrons ainsi grâce à un spectrophotomètre Beckman DK 2 A les spectres d'absorption de la solution pour différentes valeurs du p*H*, à différentes longueurs d'onde.

Conclusions

La confrontation de la technique exposée, avec d'autres méthodes spectrophotométriques classiques, et nous pensons particulièrement à la méthode des variations continues et ses extensions (méthodes de Vosburgh et Cooper, de Bent et French, du rapport moléculaire de Yoe et Jones etc...) nous incite à reconnaitre la trichromie complémentaire comme une investigation préliminaire à une étude spectrophotométrique, puisqu'aucune indication sur la stoechiométrie des espèces formées ne peut-être recherchée. Il n'en demeure pas moins, que nous avons démontré, au cours de ce travail, l'intérêt de la spectrophotométrie trichrome, pour la mise en évidence rapide de la formation de complexes colorés simples et mixtes, de leurs domaines d'existence et du nombre d'espèces en solution en fonction du p*H*.

Nous avons volontairement limité cette étude à un aspect purement qualitatif, l'expérience ayant montré qu'une étude quantitative précise des phénomènes de complexation doit être effectuée par des méthodes plus fines, telles que la potentiométrie (ou la polarimétrie dans le cas de coordinats optiquement actifs), méthodes que nous avons employées largement pour l'étude des systèmes envisagés ici (8, 12–14).

C'est d'ailleurs dans le but de tester la valeur des résultats de la méthode trichrome que nous avons étudié des systèmes dont nous avions déterminé antérieurement les constantes de stabilité ionique ce qui nous permettait de calculer les courbes de répartition des différentes espèces en fonction du p*H*. Cette distribution a pu être confirmée dans tous les cas par les résultats de la méthode trichrome qui apparait donc comme une méthode graphique extrêmement simple à mettre en œuvre et donnant des résultats concordant parfaitement avec ceux obtenus par des méthodes expérimentales et mathématiques beaucoup plus fastidieuses (détermination des constantes de stabilité et calcul des courbes de répartition des espèces).

Les limites de la méthode apparaissent dans quelques cas particuliers (existence de deux espèces ayant le même coefficient d'extinction moléculaire ou existence simultanée d'espèces colorées et incolores).

D'autre part la précision obtenue peut être améliorée, notamment par l'emploi de la méthode d'ordonnée pondérée (4) qui s'est montrée supérieure à la méthode des ordonnées selectionnées que nous avons employée pour le calcul des paramètres *u,v,w*. De plus un traitement des données sur ordinateur peut permettre l'automatisation de l'acquisition des coordonnées trichromes (18).

Cependant le processus que nous avons utilisé, présente un tel caractère de simplicité, que la méthode est extrêmement avantageuse pour une première approche d'un système inconnu et beaucoup plus rapide que les méthodes graphiques de Coleman, Varga, et Mastin (19) ou du rang de la matrice de Hugus et El-Awady (20) impliquant l'étude de nombreuses solutions et un traitement mathématique relativement long.

Néanmoins, nous insistons tout particulièrement sur le fait que toutes ces méthodes fournissent essentiellement des renseignements qualitatifs: l'existence et la formule des complexes dans certaines conditions seulement. La résolution précise et complète d'un système nécessite, en outre, qu'une telle étude soit complétée par des mesures quantitatives au moyen des méthodes classiques de la chimie de coordination.

Can. J. Chem. Downloaded from www.nrcresearchpress.com by 210.87.254.42 on 09/05/12
For personal use only.

Nous remercions vivement le Professeur R. A. Pâris pour les conseils et l'aide précieuse qu'il nous a apportés dans la réalisation de ce travail.

1. C. N. Reilley, H. Flaschka, S. Laurent, et B. Laurent. Anal. Chem. **32**, 1218 (1960).
2. C. N. Reilley et A. Smith. Anal. Chem. **32**, 1233 (1960).
3. S. Kotrly. Sb. ved. praci, Vysoka skola chem. technol., Pardubice, **14**, 165 (1966).
4. S. Kotrly et K. Vytras. Talanta, **18**, 253 (1971).
5. H. Flaschka. Talanta, **7**, 90 (1960).
6. H. Flaschka. Talanta, **8**, 8, 342 (1961).
7. H. Flaschka, J. Butcher, et R. Speights. Talanta, **8**, 400 (1961).
8. M. M. Petit-Ramel, M. R. Pâris, et C. M. Blanc. J. Inorg. Nucl. Chem. **34**, 1253 (1972).
9. S. Hirose, I. Ikeuchi, et K. Sakakibara. Bunseki Kagaku, **21**, 183 (1972).
10. S. Hirose et I. Ikeuchi. Bunseki Kagaku, **21**, 759 (1972).
11. G. Anderegg et F. L'Eplattenier. Helv. Chim. Acta, **47**, 1067 (1964).
12. M. Morin, M. R. Pâris, et J. P. Scharff. Anal. Chim. Acta, **57**, 123 (1971).
13. M. Morin et J. P. Scharff. Anal. Chim. Acta, **60**, 101 (1972).
14. M. M. Petit-Ramel et M. R. Pâris. Bull. Soc. Chim. Fr. **7**, 2791 (1968); Bull. Soc. Chim. Fr. **9**, 3070 (1969).
15. R. E. Tapscott et R. L. Belford. Inorg. Chem. **6**, 735 (1967).
16. K. Lal et R. P. Agarwal. J. Ind. Chem. Soc. **46**, 49 (1969).
17. R. H. Dunhill et Mc R. Symons. Mol. Phys. **15**, 105 (1968).
18. K. Vytras et S. Kotrly. Sb. ved. praci, Vysoka skola chem. technol., Pardubice, **26**, 3 (1971).
19. J. S. Coleman, L. P. Varga, et S. H. Mastin. Inorg. Chem. **9**, 1015 (1970).
20. Z. Z. Hugus, Jr. et A. A. El-Awady. J. Phys. Chem. **75**, 2954 (1971).

Can. J. Chem. Downloaded from www.nrcresearchpress.com by 210.87.254.42 on 09/05/12
For personal use only.

The Pulse Radiolysis of Dimethylsulfoxide and Binary Mixtures with Water[1]

T. K. COOPER AND D. C. WALKER

Chemistry Department, University of British Columbia, Vancouver, British Columbia

AND

H. A. GILLIS AND N. V. KLASSEN

Physics Division, National Research Council of Canada, Ottawa, Canada K1A 0S1

Received December 7, 1972

The simultaneous interaction of solvated electrons with strongly solvating water molecules and weakly solvating dimethylsulfoxide (DMSO) molecules has been studied by pulse radiolysis. In all DMSO/H_2O mixtures investigated the solvated electrons have a single absorption band with a maximum intermediate between that of pure DMSO ($\lambda_{max} > 1500$ nm) and that of water ($\lambda_{max} = 720$ nm). There is a nearly linear relationship between the photon energy of λ_{max} and the bulk dielectric constant, indicating that the optical properties of solvated electrons in the mixtures are not dominated by the water. A minimum is observed in the variation of $G\varepsilon_{max}$ with DMSO/H_2O composition which may be associated with intermolecular structure. In mixtures containing >0.2 mole fraction DMSO the solvated electrons have half-lives of 11–18 ns.

The radiation produced oxidizing species in DMSO has a half-life of 1–4 μs and an absorption band centered at 600 nm. This species seems to be present in all DMSO/H_2O mixtures.

Pure DMSO gives a free-ion yield in the range 1.2 to 1.8, as determined separately for the oxidizing and reducing species by bromide and anthracene scavenging experiments respectively. This free-ion yield is in keeping with the dielectric constant of DMSO of 46. The yields in fully deuterated DMSO are ~30% higher than in the protonated material.

L'interaction simultanée des électrons solvatés sur des molécules d'eau fortement solvatantes et des molécules de diméthylsulfoxyde (DMSO) faiblement solvatantes a été étudiée par radiolyse pulsée. Dans tous les mélanges DMSO/H_2O étudiés, les électrons solvatés ont une bande d'absorption simple dont le maximum se situe entre celui du DMSO pur ($\lambda_{max} > 1500$ nm) et celui de l'eau ($\lambda_{max} = 720$ nm). Une relation presque linéaire existe entre l'énergie du photon du λ_{max} et la constante diélectrique du mélange, montrant ainsi que les propriétés optiques des électrons solvatés dans ces mélanges ne sont pas masquées par l'eau. On a observé un minimum dans la variation de $G\varepsilon_{max}$ avec la composition DMSO/H_2O, ce fait peut être associé à une structure intermoléculaire. Dans les mélanges > 0.2 en fractions molaire de DMSO, les électrons solvatés ont des demi-vies de 11–18 ns. L'espèce oxydante produite par la radiation dans le DMSO a une demi-vie de 1–4 μs et une bande d'absorption centrée à 600 nm. Cette espèce semble être présente dans tous les mélanges DMSO/H_2O. Le DMSO pur donne un rendement en ion libre de 1.2 à 1.8, déterminé séparément sur l'espèce oxydante et réductrice par les expériences de piégeage par le bromure et l'anthracène respectivement. Ce rendement en ion libre est en accord avec la constante diélectrique du DMSO de 46. Les rendements dans le DMSO totalement deutérié sont de ~30% plus élevés que pour le DMSO protoné. [Traduit par le journal]

Can. J. Chem., **51**, 2195 (1973)

Introduction

We have previously shown that the solvated electron (e_s^-) in dimethylsulfoxide (DMSO) is very weakly trapped, as evidenced by an absorption band in the near i.r. similar to that found in hydrocarbons (1). This was attributed to the strictly aprotic nature of DMSO which permits solvation of negative ions only through weak ion–dipole interactions. On the other hand, DMSO has a high dielectric constant ($D_s = 46$ at 25 °C), a large dipole moment (4.3 D), and readily solvates positive ions. The free-ion yield of reducing species was measured by the use of N_2O at 0.08 M to be 1.8 ± 0.2 (2). Anthracene (A) has been used as an electron scavenger in pulse radiolysis studies by Koulkes-Pujo *et al.* (3) and Hayon (4) to give yields of $G(A^-)$ of 0.64 and 1.62 respectively. These results will be discussed later in relation to our data using A as an electron scavenger and Br^- as a scavenger for the oxidizing species.

The nature of solvated electrons in many media is being actively investigated. The absorption spectra, and yields, of electrons solvated in binary mixtures of solvents are of interest, particularly when the extent and mode of

[1]N.R.C.C. No. 13107.

Can. J. Chem. Downloaded from www.nrcresearchpress.com by 210.87.254.5 on 09/05/12
For personal use only.

Can. J. Chem. Downloaded from www.nrcresearchpress.com by 210.87.254.5 on 09/05/12
For personal use only.

solvation by the individual solvents differ markedly. Hydrocarbon–alcohol mixtures have been studied in this regard (5–8) but these mixtures are inhomogeneous (9) and clusters of the polar solvent can act as trapping centers for electrons which would otherwise have been lost through geminate recombination. A related effect was noted in formamide/water mixtures where only hydrated electrons were observed. Since in formamide itself no solvated electrons could be detected and were presumed to react rapidly, aggregates of water molecules seemed to simply provide trapping sites (10).

DMSO appears to be an interesting hydrocarbon-like solvent for studying binary mixtures with water because it possesses a high dielectric constant, with a concomitant fairly large free-ion yield, and it is completely miscible with water; in fact DMSO/H_2O mixtures show more intermolecular structure than do the pure liquids (11–16).

Our study on DMSO/H_2O mixtures provides information on the solvated electron and on the fate of the oxidizing species in binary mixtures. We also report measurements on the free-ion yield in pure DMSO.

Experimental

Absorption spectra of transient species were measured by pulse radiolysis methods using 6, 10, 40, or 300 ns pulses (typically 0.4, 0.5, 2, and 5 krad, respectively) of 35 MeV electrons from the linac at the National Research Council of Canada. For the wavelength range below 450 nm a photomultiplier (XP1003) was used as the analyzing light detector, for the range 450–1000 nm a Si photodiode (HP-4207 or EG&G YAG-100) and for the range 750–1500 nm a Ge photodiode (Philco Ford L-4521) was used. Small variations in dose from pulse to pulse were monitored by a secondary emission chamber, or the data were normalized by using the split light-beam detection technique.

In pure DMSO the half-life of the solvated electron was 14 ± 1 ns in agreement with our earlier report (1). In most of the DMSO/H_2O mixtures studied the decay was even faster than in pure DMSO and invariably first order. The solvated electron spectra were usually obtained from the maximum absorption observed when using a 40 ns pulse. However, too much decay of the electron occurs during a 40 ns pulse to permit the determination of $G\varepsilon$. The following method was used to determine $G\varepsilon$ at 1000 nm while $G\varepsilon$ at the other wavelengths were calculated from $G\varepsilon_{1000}$ and the spectra determined with 40 ns pulses. Electron pulses of nominally 6 ns width at half-height were used. The whole detection system had a rise-time of ~4 ns and consisted of a Si photodiode (HP-4207), a 110 MHz pulse amplifier (Keithley 105) and 500 MHz oscilloscope (Tektronix 7904 with 7A19 amplifier). A small component of the response of the HP-4207 has a rise time of μs (see next paragraph). This characteristic of photodiodes has been discussed by Seddon *et al.* (17). We established that this small slow component does not lead to significant errors in kinetic measurements over the first few tens of ns by observing the fast response of the detection system to the Cerenkov emission produced by the irradiation pulse from a piece of Suprasil backed by a mirror at the proper angle to send Cerenkov light through our lens system. The displayed Cerenkov signal reached its maximum 7.5 ns after the start of the pulse, fell to 5% of its maximum 14 ns after the start and to 1% of its maximum 19 ns after the start of the pulse. The pulse, measured in this way, was 8 ns wide at half-maximum. The transient absorptions due to e_s^- in DMSO and water mixtures containing 0.93, 0.72, 0.43, 0.28, and 0.20 mole fraction DMSO were measured at 1000 nm using this fast detection system. The wavelength was set by an interference filter centered at 1000 nm and having a 100 nm bandpass. The maximum absorbance due to e_s^- in DMSO and its water mixtures occurred close to 10 ns after the start of the pulse. The half-life of e_s^- in each solution was determined from a plot of the first order decay. Figure 1 shows the transient absorption due to e_s^- in pure DMSO and the first order plot of the decay. A close approximation to the absorbance corresponding to all the e_s^- produced in a pulse was obtained by extrapolating the decay plot back to mid-pulse (7 ns) as shown in Fig. 1. For all solutions the

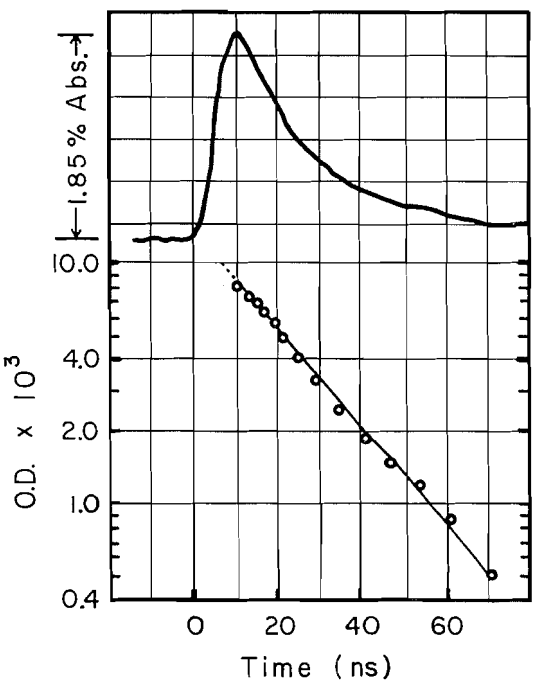

FIG. 1. A copy of the oscilloscope trace of the absorption at 1000 nm due to the e_s^- in DMSO produced by a 6 ns pulse. The sensitivity is 100 mV/div and the sweep speed 10 ns/div. The decay of the absorbance is shown below the trace and the first order line is extrapolated back to mid-pulse.

Can. J. Chem. Downloaded from www.nrcresearchpress.com by 210.87.254.5 on 09/05/12
For personal use only.

extrapolation was small, with O.D.(mid-pulse)/O.D.(max) falling between 1.12 and 1.23. The value of the optical density extrapolated to mid-pulse was used to calculate $G\varepsilon$ at 1000 nm for each solution.

Dosimetry was done with 5×10^{-3} *M* KSCN solutions saturated with N_2O, for which $G\varepsilon_{500}((CNS)_2^-) = 4.2 \times 10^4\ M^{-1}\ cm^{-1}\ (100\ eV)^{-1}$ (18). A potential source of error in measuring $G\varepsilon_{1000}(e_s^-)$ arises from the small component of the HP-4207 response which is slow. We compared the responses of the HP-4207 Si photodiode and the XP 1003 photomultiplier to the absorption due to e_{aq}^- at 715 nm produced by 6 ns pulses under conditions such that the $t_{1/2}$ of e_{aq}^- was 50 μs. Based on the assumption that the photomultiplier response is accurate, the HP-4207 photodiode responded to 86 ± 2% of the absorption at 10 ns, 88 ± 2% at 100 ns and > 99% at 3 μs. To cancel out this potential error, the absorption due to $(CNS)_2^-$ was also measured at short times (100 ns after the pulse) in doing dosimetry for the short-lived e_s^-. This source of error did not exist in measurements made with the EG&G Si photodiode because this detector did not exhibit a slower second component of response, though its initial rise was somewhat slower than that of the HP-4207.

The water was doubly distilled and the vapor, mixed with oxygen, passed through a quartz tube at 750 °C to oxidize organic impurities. Solutions were deaerated by bubbling with pure argon. The solvated electron absorption and decay rates were found to be essentially independent of the method of purification of the DMSO (1). Other chemicals were reagent grade or better.

Results and Discussion

(a) Spectra of Solvated Electrons and an Oxidizing Species in Pure DMSO and Fully Deuterated DMSO

In agreement with previous reports (1, 3) the absorption spectrum of transient species produced in the radiolysis of pure liquid DMSO at room temperature consists of three principal bands. These can be attributed to different species because of their distinct decay characteristics. The bands are: (*i*) a broad absorption stretching into the i.r. with $\lambda_{max} > 1500$ nm with half-life 14 ± 1 ns which we attribute to the solvated electron; (*ii*) a fairly broad band centered at 600 nm attributed to an oxidizing species (either solvent cations or their decomposition products and designated as Ox) whose half-life is 1–4 μs; and (*iii*) absorption bands progressing from 600 nm into the u.v. which arise from at least two species possessing half-lives of ~10 μs and >100 μs.

Figure 2 shows the electron band ($\lambda_{max} > 1500$ nm) and the absorption due primarily to Ox obtained in pure $(CH_3)_2SO$ and pure $(CD_3)_2SO$. The latter absorption, in $(CH_3)_2SO$, consists mainly of a band, due to Ox, with $\lambda_{max} = 600$ nm and $t_{1/2} = 1.6$ μs and a band with $\lambda_{max} < 400$ nm and $t_{1/2} \sim 10$ μs. The initial absorbance was deduced by extrapolation to the end of the pulse from times when the electron band had fully decayed. The spectrum which we attribute to Ox is shown in Fig. 3 as spectrum 2. This was obtained by subtracting from the initial absorption (spectrum 1, Fig. 3) an amount equivalent to a component with $t_{1/2} = 10$ μs. The band centered at 600 nm decays in a first-order manner with half-lives which varied between 1.6 and 4.1 μs on different days. The reason for this variation is not known. However, $G\varepsilon_{max}$ for spectrum 1 of Fig. 3 varied by only ±12% despite the large variation in half-lives.

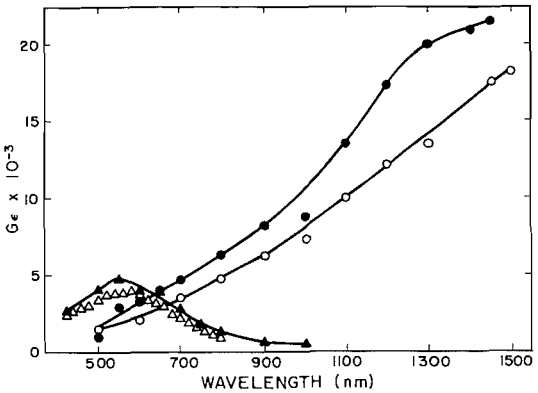

FIG. 2. Transient spectra observed in pure $(CH_3)_2SO$ and pure $(CD_3)_2SO$. Circles represent the initial absorption by solvated electrons only. Triangles refer to the initial absorption which is not due to solvated electrons. ○ and △ are for $(CH_3)_2SO$, ● and ▲ are for $(CD_3)_2SO$.

With short pulses no absorption at all could be detected at $\lambda > 1600$ nm using the Ge detector. This arises from the fact that the Ge detector becomes too slow and inefficient beyond that wavelength (19, 20) to measure the small short-lived absorption due to e_s in this system. However, observations of the steady state absorption during a long radiation pulse (>1 μs) with slower i.r. detectors indicates that the maximum extinction coefficient for the electron band occurs between 1600 and 1800 nm and that $G\varepsilon_{max}$ is <25% larger than $G\varepsilon$ at 1500 nm (1).[2]

Reasons for assigning the broad absorption band with $\lambda_{max} > 1500$ nm to the solvated electron in DMSO include the following: (*i*) its shape, intensity, and position resemble that found in irradiated glassy hydrocarbon com-

[2]Private communication from Dr. E. A. Shaede.

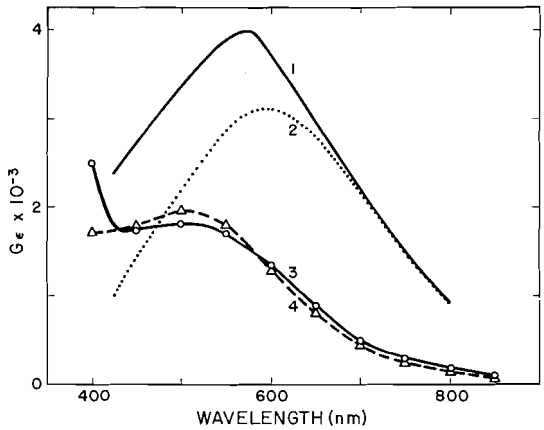

FIG. 3. Curve 1 (same as △ in Fig. 2) is the initial absorption in pure DMSO corrected for absorption by the solvated electron. Curve 2 is the spectrum of the oxidizing species ($t_{1/2}$ = 1.6 μs) in pure DMSO. Curve 2 was obtained by subtracting from Curve 1 an amount equivalent to a component with $t_{1/2}$ = 10 μs. Curve 3 is the initial absorption in 0.2 mole fraction DMSO corrected for absorption due to the solvated electron. Curve 4 is the absorption in 0.2 mole fraction DMSO 0.7 μs after the pulse. In each case a 300 ns, 5 krad pulse was used.

pounds and attributed to trapped electrons; (*ii*) it is eliminated by the presence of known electron scavengers such as Ag^+, N_2O, anthracene, CCl_4, and H^+; (*iii*) it is unaffected by the presence of added Br^-, or small amounts of water; (*iv*) the equivalent increase in both bands shown in Fig. 2 on using deuterated DMSO suggests that the species responsible have a common origin, such as the primary ionization event, and participate in common reactions, such as neutralization.

Substantial evidence for the assignment of the band centered at 600 nm to the primary or secondary oxidizing species formed concurrently with e_s^- includes the following: (*i*) in the presence of Br^- the 600 nm band was eliminated and replaced by the Br_2^- absorption band, (*ii*) high concentrations of efficient electron scavengers which may interrupt geminate ion neutralization increased the 600 nm absorption (*e.g.* 0.5 *M* Ag^+ increased it by ~90%), (*iii*) the absorption is not diminished by the electron scavengers N_2O, anthracene, H^+, and Ag^+, (*iv*) substituting with deuterated DMSO causes the same change as for the electron band indicating a common origin for the two species. Herring and McLean (21) have indicated that the energy separation between the first adiabatic and second vertical ionization potentials in the photoelectron spectrum of a molecule may be equated with the optical absorption band of a cation, in some cases. This energy gap is only 1.4 eV for DMSO (22), which would correspond to a band at ~900 nm for $DMSO^+$ if the ground and first excited states of $DMSO^+$ have similar geometries and comparable solvation energies in liquid DMSO. It is worth noting that in the photoelectron spectrum of $(CH_3)_2S$ the analogous energy level separation is 2.6 eV (22) which corresponds to 480 nm.

Figure 2 shows that $G\varepsilon$ is ~30% larger in the case of the deuterated material for both of these absorption bands. This implies that the 30% difference arises from a change in G rather than ε. Thus, as in water (23, 24), the fraction of ions which become free-ions is substantially larger for the deuterated compound. This is not readily explained in terms of models of geminate recombination based just on bulk dielectric constants, but rather is consistent with a wider *initial* distribution of solvated electrons. This could stem from either (or both) the thermalization and solvation processes. In media of high dielectric constant the material containing the heavier isotope may be less efficient in scattering epithermal electrons, and its longer dielectric relaxation time may result in a more sluggish solvating process.

(*b*) *Free-Ion Yields in Pure DMSO*

(i) Solvated Electrons

Figure 4 shows the values of $G\varepsilon$ at 750 nm for the anthracene negative ion (A^-) resulting from reaction 1 at four concentrations up to

$$[1] \qquad e_s^- + A \rightarrow A^-$$

the solubility limit of anthracene in DMSO. We determined the spectrum of A^- in DMSO and find λ_{max} = 740 nm which can be compared to the λ_{max} ~ 725 nm found in acetonitrile (4). The data points shown in Fig. 4 for A^- at 750 nm have already been corrected for absorption due to the oxidizing species at 750 nm (by measuring the absorption of the latter at 550 nm for each anthracene solution and applying corrections given by the ratio of $\varepsilon_{750}/\varepsilon_{550}$ for the oxidizing species) and likewise for the solvated electron (whose absorbance was monitored at 1275 nm in order to apply the appropriate correction at 750 nm for each concentra-

Can. J. Chem. Downloaded from www.nrcresearchpress.com by 210.87.254.5 on 09/05/12
For personal use only.

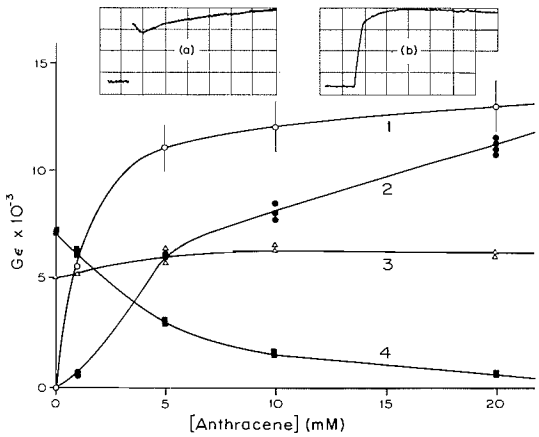

FIG. 4. Graph showing the scavenging of solvated electrons in pure DMSO by anthracene and the formation of anthracene ions. The pulse width was 40 ns. Curve 1: Maximum value of $G\varepsilon$ at 750 nm due to A^-; Curve 2: $G\varepsilon$ at 750 nm due to A^- immediately at the end of the pulse; Curve 3: $G\varepsilon$ at 550 nm due largely to the oxidizing species as observed 100 to 200 nsec after the pulse; Curve 4: $G\varepsilon$ due to solvated electrons at 1250 nm as observed from the maximum absorption during the pulse (not corrected for decay during the pulse nor for detector response time). Insets: (*a*) Oscilloscope trace at 750 nm with 10^{-3} *M* anthracene present. (Vertical scale 1 mV/div, horizontal 200 ns/div.) (*b*) Oscilloscope trace at 750 nm with 10^{-2} *M* anthracene present. (Vertical scale 2 mV/div, horizontal 100 ns/div.)

tion). Typical oscilloscope traces for the absorption at 750 nm in 10^{-3} and 10^{-2} *M* solutions of anthracene in DMSO are shown as insets in Fig. 4. At the lower concentration (inset *a*) the contribution made by the short-lived e_s^- is readily seen. In both traces the contribution from the oxidizing species decreases only slightly over the time period shown since its half-life is about 2 μs.

At all concentrations of anthracene the absorbance due to A^- consists of two components, one of which builds in during the pulse and is larger at the higher concentrations, and another which grows in after the pulse and whose rate of growth increases with [A]. These effects can be recognized by comparison of the traces shown as insets. Figure 4 shows how the immediate $G\varepsilon$ (curve 2) and the maximum $G\varepsilon$ observed after the pulse (curve 1) change with concentration. It should be noted that the latter increases much more rapidly with concentration than the immediate absorption and that the slow component builds in at a much slower rate than the electron decay (as seen by the insets). This suggests that anthracene scavenges the anionic product resulting from reaction of the solvated electron with the solvent, as well as either the solvated electron or its precursor or both.

The effect of anthracene on the yields of oxidizing species and electrons, as measured by the absorptions at 550 and 1250 nm, respectively, are also shown as a function of [A] in Fig. 4. In the work of Hayon (4) and Koulkes-Pujo *et al.* (3) anthracene was used at 5×10^{-3} *M*. It can be seen that at this concentration A reduced the observed yield of e_s^- to $\sim\frac{1}{2}$ its yield in the pure system but that the anthracene then scavenged the decay product of most of these unscavenged electrons. At 2×10^{-2} *M* the observed solvated electron yield was reduced to about 10% but the total yield of A^- was not much higher than at 5×10^{-3} *M*. We suggest that the total yield of A^- at 5×10^{-3} *M* anthracene approximates the free electron yield. It is possible that the small increase in absorbance at 550 nm caused by the addition of anthracene is due to absorption by A^-. By assuming that the extinction coefficient (ε) of A^- at its λ_{max} of 740 nm = $0.99 \times 10^4\ M^{-1}\,cm^{-1}$ (4) we derive from our spectrum of A^- that $\varepsilon = 0.96 \times 10^4\ M^{-1}\,cm^{-1}$ at 750 nm. With this value we calculate $G(A^-)$ at 5×10^{-3} *M* anthracene to be 1.2 ± 0.15. This is very close to $G(N_2)$ from N_2O solutions at $[N_2O] \sim 2 \times 10^{-2}$ *M* but lower than the limiting yield (2). Hayon's value of 1.62 (4) is somewhat larger than this but possibly was not corrected for the significant absorbance by the oxidizing species at the wavelength used to determine $G(A^-)$. The much lower yield of Koulkes-Pujo *et al.* of 0.64 (3) is more difficult to reconcile with ours unless the solvent anions (or whatever is formed from the reaction of e_s^- with DMSO) are consumed by the products from the positive ions prior to their being scavenged by A in their system at 5×10^{-3} *M* in A. It must be noted that in their study the dose per pulse was $\sim 10^2$ times higher and the species responsible for their 625 band decayed according to second order kinetics. Their value of 0.64 may then be equivalent to $G(A^-)$ formed immediately in our system. Bensasson and Land (25) have recently reported a value of ~ 1.4 using biphenyl as an electron scavenger at 10^{-2} *M* and noted that this increases to 1.8 at 10^{-1} *M* biphenyl. Assuming a free-ion yield of 1.2 we calculate ε for e_s^- to be $15\,000\ M^{-1}\,cm^{-1}$

Can. J. Chem. Downloaded from www.nrcresearchpress.com by 210.87.254.5 on 09/05/12
For personal use only.

at 1500 nm in pure DMSO, and the indications are that ε_{max} does not exceed this by more than 25%.[2]

(ii) Oxidizing Species

In the presence of 10^{-2} *M* KBr the electron band was unaffected, but the band at 600 nm was eliminated and a new absorption band centered at 375 nm was produced. The 375 nm band is attributed to Br_2^- by analogy with aqueous systems (26). It presumably arises in a two-step process involving the oxidizing species ($DMSO^+$ or its decay product) by way of an intermediate which could be a simple charge-transfer complex as in reaction sequence [2].

$$[2] \quad Ox + Br^- \rightarrow [Br \leftarrow Ox]^- \xrightarrow{Br^-} Br_2^- + Ox^-$$

The spectrum obtained in the bromide solutions is shown in Fig. 5 and is similar to that reported previously (3). At $[Br^-] > 10^{-2}$ *M* the 600 nm band was totally eliminated, thereby indicating complete scavenging of the oxidizing species responsible for that absorption. The inset of Fig. 5 shows the concentration dependence of the 375 nm absorption on a semi-log plot.

A concentration independent value of $G\varepsilon = (1.5 \pm 0.1) \times 10^4$ was obtained with $[Br^-] > 10^{-2}$ and is identical to that reported by Koulkes-Pujo *et al.* (3). If we assume that ε_{max} for Br_2^- in DMSO is the same as the recently reported value for Br_2^- in H_2O, namely $1.2 \times 10^4\ M^{-1}\ cm^{-1}$ (26), then $G(Br_2^-) = 1.3 \pm 0.15$. This value is approximately equal to the yield of A^- at 5×10^{-3} *M* anthracene and would suggest that the free-ion yield in DMSO is 1.3 ± 0.15, as measured for both oxidizing and reducing species at scavenger concentrations of $\sim 10^{-2}$ *M*. However, the value for $\varepsilon_{max}(Br_2^-)$ in water at 360 nm is also reported to be $\sim 0.83 \times 10^4\ M^{-1}\ cm^{-1}$ (27–29) from which one calculates $G(Br_2^-) = 1.8 \pm 0.2$ in DMSO. This yield is in line with the N_2 yield from N_2O solutions (2) at high $[N_2O]$ and the biphenylide yield (25) at high [biphenyl], and also with the value obtained by Kemp *et al.* (30) for $TMPD^+$ ions in DMSO solutions of tetramethylphenylenediamine (TMPD). Uncertainties in the extinction coefficients of A^- and Br_2^- and in the concentration range where geminate scavenging becomes significant enable us to conclude only that the free-ion yield for pure DMSO lies in the range 1.2 to 1.8. This range fits an empirical correlation between free-ion yield and dielectric constant for a wide range of solvents (4, 31).

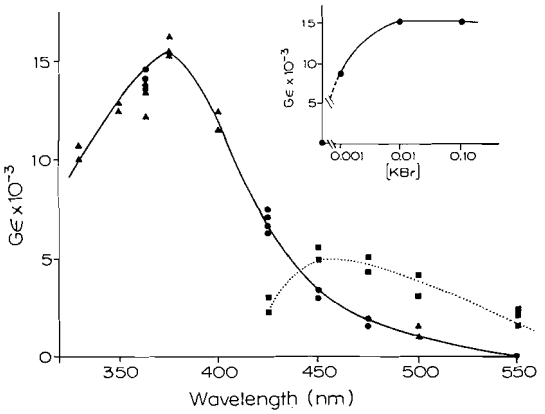

FIG. 5. Absorption spectra for KBr solutions in DMSO. Solid curve refers to Br_2^- spectra; dotted curve refers to transient precursor of Br_2^-. ▲, Br_2^- from 0.1 *M* KBr solution; ●, Br_2^- from 0.01 *M* KBr solution; ■, transient precursor of Br_2^- at 0.01 *M* KBr. Inset: Plot of $G\varepsilon$ at 375 nm for Br_2^- *vs.* [KBr].

The mechanism by which Br_2^- appears to be formed in DMSO can be compared with the analogous reaction in water (26, 29). From the oscilloscope traces for 10^{-2} or 10^{-3} *M* Br^- in DMSO it was evident that the absorption at 375 nm did not build in during the pulse. Furthermore, we seem to have observed an intermediate species formed as a precursor to Br_2^- with an absorption band centered at 450–500 nm. This could readily be distinguished from the 600 nm band because its absorption was almost zero at 650 nm in a 10^{-3} *M* Br^- solution and it decayed with a half-life of ~ 0.8 μs. The latter rate was approximately the same rate with which the Br_2^- absorption at 375 nm built in at this Br^- concentration. At 10^{-2} *M* Br^- both rates were much faster. Thus the transient absorption band, which is shown in Fig. 5, is attributed to an intermediate in reaction 2, perhaps the charge-transfer complex indicated above. An approximate relationship has been found between $h\nu_{max}$ and ionization potential for Br atom charge-transfer complexes with several hydrocarbons and brominated hydrocarbons (32), and the λ_{max} which would be predicted by applying this correlation for the Br atom charge-transfer complex in DMSO (I.P. of DMSO = 8.85 eV (33) is ~590 nm. However, there seems to be no good reason for

Can. J. Chem. Downloaded from www.nrcresearchpress.com by 210.87.254.5 on 09/05/12
For personal use only.

Can. J. Chem. Downloaded from www.nrcresearchpress.com by 210.87.254.5 on 09/05/12
For personal use only.

this relationship to be followed by donor molecules which are as dissimilar as DMSO is to hydrocarbons and brominated hydrocarbons (34). In addition, the complex in reaction 2 may have a negative charge because Ox could be uncharged, so the above-mentioned relationship may be totally irrelevant to this case.

Since 10^{-3} *M* Br^- produces Br_2^- from only about half the free oxidizing species (see inset of Fig. 5), the intermediate of reaction 2 must have an alternative fate besides reaction with Br^-. This other process could be reaction with DMSO.

Absorption due to the 400–500 nm intermediate is fully developed at the end of the 40 ns pulse even in 0.001 *M* KBr, which suggests that $t_{1/2}$ for the oxidizing species is $\leqslant 5 \times 10^{-11}$ s in 0.1 *M* KBr. One might expect species undergoing geminate combination to be scavenged on this time-scale, and therefore the yield of e_s^- should increase; however no increase was observed. This implies that the electron can undergo a spur reaction with the intermediate with the same efficiency with which it reacts with the oxidizing species of DMSO.

(*c*) *Solvated Electrons in DMSO/H_2O Mixtures*

For DMSO/H_2O mixtures two easily resolvable absorption bands are observed for wavelengths >400 nm. One corresponds to the oxidizing species with a maximum at ~600 nm and is comparatively long-lived ($t_{1/2}$ 1 to 4 μs). The other is very short-lived and is attributed to solvated electrons. Figure 6 shows the spectra for the latter species in mixtures consisting of 0, 0.20, 0.28, 0.43, 0.72, 0.93, and 1.0 mole fraction DMSO. Only a single absorption band is obtained for the solvated electron in each mixture. These spectra have been corrected for absorption by the band centered at 600 nm. In the case of pure water the observed solvated electron band corresponds quite closely to the published spectrum of e_{aq}^-, with $G\varepsilon = 4.3 \times 10^4$ molecule $(100\ eV)^{-1}$ M^{-1} cm^{-1} at 720 nm (35).

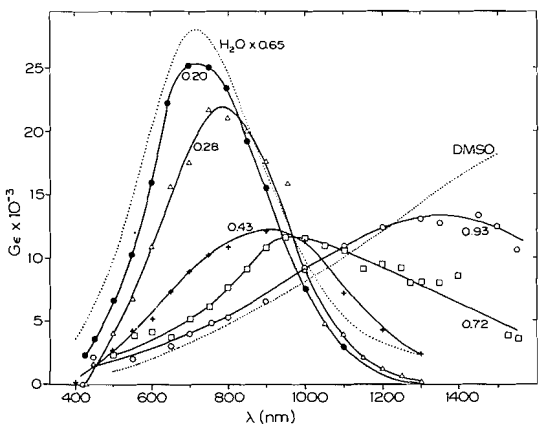

FIG. 6. Absorption spectra of solvated electrons in DMSO/H_2O mixtures; 0, 0.20, 0.28, 0.43, 0.72, 0.93, and 1.0 mole fraction DMSO. The data for pure water have been multiplied by a factor of 0.65 relative to the others. These spectra represent the short-lived solvated electron band only, the longer lived 600 nm band and u.v. bands having been subtracted from the observed absorbances.

(*i*) *Lifetimes of e_s^-*

By following the decay of the absorption at 1000 nm (where the 600 nm band absorption is negligible for all mixtures) after 6 ns pulses it was established that the decay of e_s^- invariably followed first-order kinetics for DMSO/H_2O mixtures (*e.g.* see Fig. 1). Thus the solvated electron appears to decay by reaction with DMSO. The pseudo first-order rate constants obtained are indicated in Table 1 as half-lives (column 6), together with the observed λ_{max}, the width-at-half-height (ΔW), and $G\varepsilon_{max}$ for each mixture. A second-order rate constant was calculated for each mixture from the observed first-order decay rate combined with the bulk concentration of DMSO. These calculated rates are given in column 7 of Table 1 and appear to go through a maximum between 0.43 and 0.20 mole fraction DMSO. At a mole fraction of 0.017 the rate constant is 2.9×10^6 M^{-1} s^{-1} but the rate constant seems to be decreasing as the concentration of DMSO decreases. Meissner *et al.* (36) reported a value of 1.7×10^6 M^{-1} s^{-1} for the reaction of e_s^- with DMSO in alkaline solutions of DMSO slightly more dilute than 0.017 mole fraction.

(*ii*) *Magnitude of $G\varepsilon_{max}$*

Figure 7*a* shows the magnitude of $G\varepsilon_{max}$ for each mixture as a function of composition. As these data have been compensated for decay during the pulse, the minimum in $G\varepsilon_{max}$ between 0.43 and 0.93 mole fraction DMSO apparently does not arise from the faster decay rate of e_s^-, rather both effects may result from the same properties of the solutions. It also seems unlikely that the minimum in $G\varepsilon_{max}$ arises from a minimum in ε_{max} alone and hence we presume that it largely represents the variation in the radiation yield. Our speculation that ε_{max} does

TABLE 1. Properties of solvated electrons in DMSO/H_2O mixtures

Mole fraction DMSO	D_s*	λ_{max} (nm)	ΔW (eV)	$G\varepsilon_{max}$ ($\times 10^{-3}$)	$t_{1/2}$ (ns)	k_2(calcd)† $\times 10^{-6}$ ($M^{-1}s^{-1}$)
0	78	720	0.88	43.0	>1000	—
0.017	78	—	—	—	340	2.9
0.20	75	720	0.83	25.2	18	5.5
0.28	73	790	0.77	21.8	15	5.6
0.43	67	900	0.93	12.1	12	5.6
0.72	57	970	0.83	11.6	11	5.0
0.93	48	~1350	>0.65	13.2	12	4.2
1.00	46	>1500	—	>18.0	14	3.4

*Data taken from ref. 11.
†Calculated from the observed pseudo-first order rate constant and the bulk concentration of DMSO.

not vary in this manner is based simply on the near constancy of ΔW over the full range (Table 1) and the fact that our calculated value of ε_{max} for pure DMSO is quite comparable to ε_{max} for pure water. Therefore, it must be considered whether the minimum in $G\varepsilon_{max}$ between 0.4 and 0.9 mole fraction DMSO can be reasonably attributed to a minimum in $G(e_s^-)$. It is unlikely that a pronounced minimum in $G(e_s^-)$ could result from a marked decrease in the yield of ions escaping geminate recombination (free-ion yield). Firstly, as shown later, the free-ion yield of the concomitant oxidizing species does not show a similar minimum in these same mixtures. Secondly, the bulk dielectric constant for the mixtures changes monotonically with composition (no minimum) and varies only from 80 to 46 over the full range, and so ought not to lead to any pronounced minimum. Perhaps a minimum in $G(e_s^-)$ is the result of a decreased fraction of the free electrons which become solvated. The lifetime of e_s^- is shortest where $G\varepsilon_{max}$ shows the minimum, so that e_s^- reacts faster in the mixture than in pure DMSO. Conceivably, the precursor electron states might also be more reactive in the mixtures. On the other hand, it is possible to interpret a minimum in the fraction of free electrons which become solvated in terms of the structure of DMSO/H_2O mixtures. The yield of solvated electrons should depend on (*a*) the density of pre-existing cavities in the liquid that are suitable as trapping sites, and/or (*b*) the ease with which existing cavities can be modified under the influence of the electric field of the electrons so that they have the dimensions of suitable traps. Many studies of the structure of DMSO–water mixtures have been made (10–14), and the general conclusion

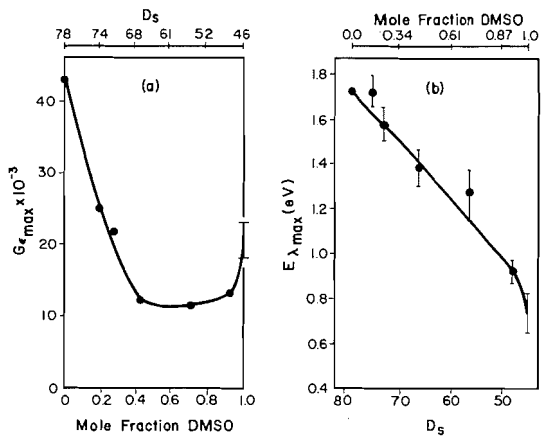

FIG. 7. (*a*) Values of $G\varepsilon_{max}$ for the solvated electron absorption bands (Fig. 6) plotted against the mole fraction DMSO for DMSO/H_2O mixtures. (*b*) Photon energy of the absorption band maxima for the solvated electron in DMSO/H_2O mixtures plotted against the bulk static dielectric constant (25 °C) of the mixture. Non-linear axes showing dielectric constant and mole fraction for (*a*) and (*b*) respectively are given as top abscissae.

drawn from density, viscosity, dielectric, and thermodynamic data is that 2:1, water:DMSO, association occurs to a considerable extent at room temperature. Further, a plot of the energy–volume coefficient, the energy required per unit volume to enlarge a cavity in the solvent, against mole fraction DMSO starts at a low value for pure water, rises quickly to a maximum in the region 25–35 mol% DMSO and then declines slowly as the DMSO is increased to 100% (16). Thus $G\varepsilon$ (and presumably G) and the inverse of the energy–volume coefficient change in a rather similar fashion with composition and this suggests that factor (*b*) above is important in

Can. J. Chem. Downloaded from www.nrcresearchpress.com by 210.87.254.5 on 09/05/12
For personal use only.

Can. J. Chem. Downloaded from www.nrcresearchpress.com by 210.87.254.5 on 09/05/12
For personal use only.

determining the probability of solvation of electrons in these mixtures. However, the concentration of voids might be a minimum around 33 mol% DMSO where the intersolvent bonding is greatest, so factor (*a*) could also be an important, or even the only, factor in determining solvated electron yields.

Bensasson and Land (25) have reported that in the range pure water to ~0.1 mole fraction DMSO the absorbance at 825 nm due to e_{aq}^- decreases in proportion to the energy directly deposited in the water. This led them to suggest that the decrease results because electrons formed in the DMSO do not lead to e_{aq}^-. Our observation that e_s^- in DMSO/H_2O mixtures have single absorption bands intermediate between that in pure water and that in pure DMSO leads us to the different conclusion that the absorption band at low DMSO concentrations, though very similar to that in water, is due to e_s^- and not simply to e_{aq}^-. Koulkes-Pujo *et al.* (37) have reported increasing values of (rate of decay of e_s^-)/$G(e_s^-)$ with increasing DMSO concentration up to 0.08 mole fraction DMSO. Their observation is consistent with an increased decay rate and/or a lower yield of e_s^- with increased concentration of DMSO.

(*iii*) *Variation of* λ_{max}

The λ_{max} of e_s^- in pure DMSO occurs at much longer wavelengths than it does in many other solvents with lower dielectric constants, for example alcohols (38). At the same time, a correlation between the photon energy at the absorption band maxima ($E_{\lambda max}$) and the measured bulk dielectric constants (D_s) of DMSO/H_2O mixtures may exist. The plot of $E_{\lambda max}$ *vs.* D_s in Fig. 7*b* shows that this plot is approximately linear, within experimental error, out to 0.9 mole fraction of DMSO. This suggests a regularly increasing cavity radius and charge delocalization with increasing DMSO content in the mixtures. In addition, the absorption band width-at-half-height (in energy units), ΔW, is fairly constant despite the widely different solvation energies provided by the two solvents separately. If only a small number of molecules were involved in the solvation shell one would expect an enhanced ΔW for mixtures of such dissimilar solvents (39).

In fact the results are somewhat surprising when it is noted that water solvates negative ions by strong hydrogen-bonding whereas DMSO can provide only very feeble solvation of anions through ion–dipole interactions. DMSO is strictly aprotic and should behave like a saturated hydrocarbon, albeit a highly polar one, towards negative ions; and yet, for solvated electrons, the data of Fig. 7*b* indicates that the optical properties of e_s^- in these mixtures are not dominated by the water. This is in sharp contrast to the situation reported for *n*-hexane/ethanol mixtures (6) (perhaps for the reasons mentioned in the Introduction and because of the change in local dielectric constant (40)) and somewhat at variance with the case of tetrahydrofuran/water mixtures (41), where the absorption bands are dominated by the hydroxylic component. It is much more analogous to mixtures of water with alcohols (38) or ammonia (41, 42), or ethylenediamine–tetrahydrofuran mixtures (41).

(*iv*) *Low Temperature Glasses*

Solvated electrons are not stable in pure DMSO and DMSO/H_2O mixtures even in rigid glasses at 77 °K. This was demonstrated using optical absorption spectroscopy during pulse radiolysis, as in the liquid phase experiments, and by e.s.r. studies on γ-irradiated glasses (43). Whereas a DMSO/H_2O glass at 77 °K showed absorption at 600 nm corresponding to a stabilized oxidizing species there was no detectable absorption attributable to a trapped electron lasting longer than ~1 μs. Furthermore, in extensive e.s.r. studies on crystalline DMSO and DMSO-d_6 and on glassy DMSO/H_2O mixtures at 77 °K, no trapped electron signal could be detected. Even when electrons were generated in the e.s.r. cavity by u.v. photolysis of $K_4Fe(CN)_6$ in DMSO/H_2O glasses at 77°K the electrons produced were not stabilized but underwent reaction to produce CH_3 radicals (43). In non-polar hydrocarbon glasses, electrons can readily be trapped and immobilized for long periods at low temperatures, so these effects in DMSO must be attributed to a process with a low activation energy by which the electron can interact with a DMSO molecule of the solvation shell.

(*d*) *The Oxidizing Species in DMSO/H_2O Mixtures*

The 600 nm absorption band which was observed in pure DMSO was also evident in all the DMSO/H_2O mixtures. The position of the

band was almost unaltered by changing the composition from 1.0 to 0.2 mole fraction DMSO. Only the magnitude of the absorbance changed progressively with composition. Furthermore the decay rate of the DMSO oxidizing species was largely unaffected by the composition.

For mixtures containing <0.3 mole fraction DMSO, other absorption bands in the range 400 to 600 nm were very evident. These had different decay characteristics and partly obscured the 600 nm band, thus making it difficult to obtain quantitative measurements of the 600 band in these predominantly aqueous mixtures. For instance, a separate and distinct absorption band with $\lambda_{max} \sim 500$ nm was observed. This 500 nm band grew in after the pulse and decayed more slowly than the 600 nm band. In a 0.2 mole fraction mixture the 500 nm band reached its maximum absorbance ~ 0.7 μs after the end of a 0.3 μs pulse and decayed with a half-life of ~ 12 μs; whereas, in a mixture consisting of 0.066 mole fraction DMSO, the maximum was not reached until ~ 2 μs after the pulse. Thus its formation rate decreased with decreasing DMSO content. The complex behavior in 0.2 mole fraction DMSO can be seen by examination of curves 3 and 4 of Fig. 3. Curve 3 is the spectrum of the initial absorption and curve 4 is the spectrum 0.7 μs later. For wavelengths below 425 nm the situation is also very complicated. For instance, at 400 nm the initial absorbance arises from at least three species with half-lives of approximately 1, 10, and >100 μs. Furthermore, the initial absorbance at 400 nm relative to that at 600 nm is much higher in the 0.2 mole fraction DMSO mixture than it is in pure DMSO. At wavelengths above 600 nm a large fraction of the absorption is due to the Ox band centered at 600 nm with $t_{1/2} = 2$ μs. However, because the 500 nm band overlaps the 600 nm band in dilute solutions the 600 nm band could only be monitored on its long wavelength tail. Thus the absorption was monitored at 715 nm in all mixtures and found to have a half-life for decay of 3 ± 1 μs. The decay rate varied somewhat with dose per pulse and with the total dose accumulated by the sample but not in a consistent or readily identifiable manner. Despite this variation in decay rate the relative values of $G\varepsilon$ of the different mixtures were reproducible.

This procedure, of having to use 715 nm to monitor the oxidizing species which has λ_{max} at 600 nm, was rather unsatisfactory because the band appears to get slightly narrower, or λ_{max} shifts to shorter wavelengths, with progressively increasing water content. Thus the ratio of absorbance at 715 nm to that at 600 nm gets smaller with decreasing DMSO fraction. Nevertheless, this was the only way to explore the yield of oxidizing species over the full composition range. Despite its shortcomings and these uncertainties in the quantitativeness of the data for low DMSO content there is quite interesting information to be gleaned from this study of the oxidizing species in a binary mixture.

The $G\varepsilon$ measured at 715 nm for 300 ns pulses in each DMSO/H_2O mixture is plotted against both mole fraction and electron fraction in Fig. 8. Since the electron fraction is approximately proportional to the dose absorbed by DMSO this latter plot would be a straight line if the yield were proportional to the dose absorbed by the DMSO molecules. For DMSO/H_2O mixtures one might predict an enhanced yield of free-cations of DMSO above the product of (G for the oxidizing species in pure DMSO) × (electron fraction DMSO) for two reasons. Firstly, because of its higher dielectric constant

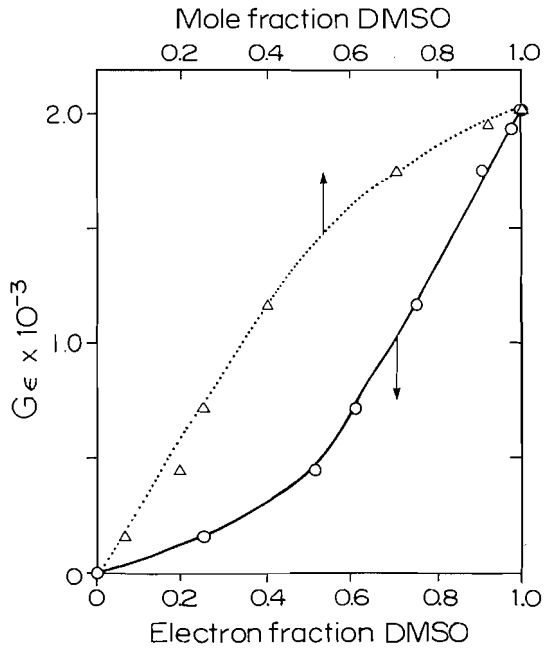

FIG. 8. Variation of $G\varepsilon$ at 715 nm due to the oxidizing species for DMSO/H_2O mixtures as a function of electron fraction DMSO and mole fraction DMSO.

Can. J. Chem. Downloaded from www.nrcresearchpress.com by 210.87.254.5 on 09/05/12
For personal use only.

Can. J. Chem. Downloaded from www.nrcresearchpress.com by 210.87.254.5 on 09/05/12
For personal use only.

the presence of water should decrease geminate recombination and hence increase the free-ion yield of electrons and solvent cations. In this regard, it was found that for a mixture consisting of 0.72 mole fraction DMSO the absorption at 600 nm was almost doubled when $\sim 0.5\ M$ Ag^+ was added to the mixture. Similar increases were found in pure DMSO and are believed to result from an enhanced free-ion yield arising from the capturing of electrons which were otherwise fated to geminate recombination. This enhancement arises both from the high concentration of Ag^+ and the fact that the product, Ag^0, is uncharged, thus interrupting geminate neutralization. On both these counts, the failure of anthracene to increase $G(Ox)$, as shown in Fig. 4, is understandable. Secondly, the ionization potential of DMSO is 8.85 eV (33) which is lower than that of H_2O (12.6 eV). Consequently, in the initial disbursement of energy deposition, if there were collective excitation processes leading to preferential ionization of the component of lower ionization potential, then the presence of water should have enhanced the effective yield of DMSO cations. Both these factors would cause the electron fraction plot in Fig. 8 to be convex upwards, whereas it is convex downwards. However, the data could acquire its observed form from a narrowing, or a shift to slightly shorter wavelengths, of the 600 nm band as the water content increased. This factor could dominate the variation of absorbance at 715 nm with composition. The curvature of the electron fraction plot (Fig. 8) corresponds in direction to the minimum in the $G\varepsilon$ of e_s^- (Fig. 7*a*) and could mean that the free-ion yield is less in mixtures where there is strong intermolecular bonding. However, this correspondence does not hold in detail because in solutions of $\geqslant 0.72$ mole fraction DMSO the yield of oxidizing species of DMSO is almost proportional to the dose deposited in DMSO molecules. In contrast the value of $G\varepsilon_{max}$ for e_s^- is close to its minimum at 0.72 mole fraction DMSO.

The most striking conclusion suggested by Fig. 8 is that there is no important charge-transfer, proton-exchange, or radical interactions between water and the DMSO oxidizing species or its precursor cation. The species responsible for the 600 nm band seems to be largely unaffected by any exchange of H_2O molecules for DMSO molecules in its immediate environment; because its formation, reaction half-life, and optical absorption properties are only altered slightly. (It should be noted that in the 0.5 electron fraction mixture there are 6.5 water molecules for every DMSO molecule.) In hydrocarbon media, various proton acceptors such as ammonia and ethanol (44, 45) have been used as efficient scavengers of the hydrocarbon positive ions. However, we must conclude that the oxidizing species of DMSO does not appear to undergo proton transfer to water. Thus, the proton-transfer or charge-exchange behavior of DMSO is quite different from that of the non-polar aprotic solvents. This is probably a reflection of the strongly dipolar character of DMSO and its facility to afford strong solvation to cations, comparable in fact to that provided by water.

We are most grateful to Dr. K. Lokan and Mr. G. Teather for assistance with the experimental procedures. This work was supported in part by a research grant to D.C.W. from the National Research Council of Canada. T.K.C. also gratefully acknowledges the award of Postgraduate Scholarships from the F. J. Nicholson Family and the National Research Council of Canada.

1. D. C. WALKER, N. V. KLASSEN, and H. A. GILLIS. Chem. Phys. Lett. **10**, 636 (1971).
2. T. K. COOPER and D. C. WALKER. Can. J. Chem. **49**, 2248 (1971).
3. A. M. KOULKES-PUJO, L. GILLES, B. LESIGNE, and J. SUTTON. Chem. Commun. 749 (1971).
4. E. HAYON. J. Chem. Phys. **53**, 2353 (1970).
5. T. J. KEMP, G. A. SALMON, and P. WARDMAN. *In* Pulse radiolysis. *Edited by* M. Ebert *et al.*, Academic Press. 1965. p. 256.
6. B. J. BROWN, N. T. BARKER, and D. F. SANGSTER. J. Phys. Chem. **75**, 3639 (1971).
7. L. B. MAGNUSSON, J. T. RICHARDS, and J. K. THOMAS. Int. J. Radiat. Phys. Chem. **3**, 295 (1971).
8. R. R. HENTZ and G. KENNEY-WALLACE. J. Phys. Chem. **76**, 2931 (1972).
9. A. N. FLETCHER and C. A. HELLER. J. Phys. Chem. **71**, 3742 (1967).
10. D. C. WALKER and S. C. WALLACE. Can. J. Chem. **49**, 3398 (1971).
11. S. A. SCHICHMAN and R. L. AMEY. J. Phys. Chem. **75**, 98 (1971).
12. E. TOMMILA and A. PAJUNEN. Suom. Kemistil. B, **41**, 172 (1968).
13. J. M. G. COWIE and P. M. TOPOROWSKI. Can. J. Chem. **39**, 2240 (1961).
14. G. J. SAFFORD, P. C. SCHAFFER, P. S. LEUNG, G. F. DOEBBLER, G. W. BRADY, and E. F. X. LYDEN. J. Chem. Phys. **50**, 2140 (1969).
15. K. J. PACKER and D. J. TOMLINSON. Trans. Faraday Soc. **67**, 1302 (1971).

16. (*a*) E. A. SYMONS. Can. J. Chem. **49**, 3940 (1971); (*b*) D. D. MACDONALD and J. B. HYNE. Can. J. Chem. **49**, 611 (1971).
17. W. A. SEDDON, E. B. SELKIRK, and J. W. FLETCHER. Int. J. Radiat. Phys. Chem. In press.
18. G. E. ADAMS, J. W. BOAG, J. CURRANT and B. D. MICHAEL. *In* Pulse radiolysis. *Edited by* M. Ebert *et al*. Academic Press, London. 1965. p. 117.
19. N. V. KLASSEN, H. A. GILLIS, and D. C. WALKER. J. Chem. Phys. **55**, 1979 (1971).
20. N. V. KLASSEN, H. A. GILLIS, and D. C. WALKER. J. Chem. Phys. **57**, 3026 (1972).
21. F. G. HERRING and R. A. N. MCLEAN. Inorg. Chem. **11**, 1667 (1972).
22. H. BOCK and B. SOLOUKI. Angew. Chem. Int. Ed. **11**, 436 (1972).
23. D. M. BROWN, F. S. DAINTON, J. P. KEENE, and D. C. WALKER. Proc. Chem. Soc. 266 (1964).
24. E. M. FIELDEN and E. J. HART. Radiat. Res. **33**, 426 (1968).
25. R. BENSASSON and E. J. LAND. Chem. Phys. Lett. **15**, 195 (1972).
26. D. ZEHAVI and J. RABANI. J. Phys. Chem. **76**, 312 (1972).
27. H. C. SUTTON, G. E. ADAMS, J. W. BOAG, and B. D. MICHAEL. *In* Pulse radiolysis. *Edited by* M. Ebert *et al*. Academic Press, New York. 1965. p. 61.
28. M. S. MATHESON, W. A. MULAC, J. L. WEEKS, and J. RABANI. J. Phys. Chem. **70**, 2092 (1966).
29. B. CERCEK. Int. J. Radiat. Phys. Chem. **4**, 25 (1972).
30. T. J. KEMP, J. P. ROBERTS, G. A. SALMON, and G. F. THOMPSON. J. Phys. Chem. **72**, 1464 (1968).
31. G. R. FREEMAN and J. M. FAYADH. J. Chem. Phys. **43**, 86 (1965).
32. J. M. BOSSY, R. E. BÜHLER and M. EBERT. J. Am. Chem. Soc. **92**, 1099 (1970).
33. F. I. VILESOV and B. L. KURBATOV. Dokl. Akad. Nauk. SSSR, **140**, 1364 (1961).
34. (*a*) R. S. MULLIKEN and W. B. PERSON. Ann. Rev. Phys. Chem. **13**, 107 (1962); (*b*) R. E. BÜHLER. J. Phys. Chem. **76**, 3220 (1972).
35. J. P. KEENE. Radiat. Res. **22**, 1 (1964).
36. G. MEISSNER, A. HENGLEIN, and G. BECK. Z. Naturforsch. **B22**, 13 (1967).
37. A. M. KOULKES-PUJO, B. D. MICHAEL, and E. J. HART. Int. J. Radiat. Phys. Chem. **3**, 333 (1971).
38. S. ARAI and M. C. SAUER. J. Chem. Phys. **44**, 2297 (1966).
39. J. L. DYE, M. G. DEBACKER, and L. M. DORFMAN. J. Chem. Phys. **52**, 6251 (1970).
40. G. R. FREEMAN. J. Phys. Chem. **76**, 944 (1972).
41. L. M. DORFMAN, F. Y. JOU, and R. WAGEMAN. Ber. Bunsenges. Phys. Chem. **75**, 681 (1971).
42. R. OLINGER and U. SCHINDEWOLF. Ber. Bunsenges. Phys. Chem. **75**, 693 (1971).
43. T. K. COOPER. Ph.D. thesis. University of British Columbia, Vancouver, British Columbia. 1972.
44. F. WILLIAMS. J. Am. Chem. Soc. **86**, 3954 (1964).
45. J. W. BUCHANAN and F. WILLIAMS. J. Chem. Phys. **44**, 4377 (1966).

Can. J. Chem. Downloaded from www.nrcresearchpress.com by 210.87.254.5 on 09/05/12
For personal use only.

Photochemistry of 2,4-Cyclooctadienone I.[1] In Benzene and Toluene[2]

GORDON L. LANGE AND ELI NEIDERT
Chemistry Department, University of Guelph, Guelph, Ontario
Received September 13, 1972

Irradiation of 2,4-cyclooctadienone (**1**) in benzene or toluene is shown to give in >80% yield two head-to-head dimers. The ring fusions are shown to occur at the α,β-positions of the dienone with *trans–cis* and *trans–anti-trans* stereochemistry. Both dimers may be epimerized to the same product with *cis–anti-cis* ring fusions. Evidence is presented to show that the singlet state is responsible for the *cis–trans* isomerization of **1** to the highly reactive intermediate *trans,cis*-2,4-cyclooctadienone. This intermediate can dimerize in a thermal 2 + 2 cycloaddition or can be generated at −78° and then trapped by 1,3-dienes in a Diels–Alder reaction. A mechanism for the dimerization reaction is discussed.

L'irradiation de la cyclooctadiène-2,4 one (**1**) dans le benzène ou le toluène conduit à deux dimères tête-tête avec un rendement >80%. Les fusions de cycle se produisent sur les positions α,β de la diénone avec la stéréochimie *trans–cis* et *trans–anti-trans*. Les deux dimères peuvent être épimérisés en un même produit avec des fusions de cycle *cis–anti-cis*. L'état singulet responsable de l'isomérisation *cis–trans* de **1** en un intermédiaire hautement réactif *trans–cis* cyclooctadiène-2,4 one, a été prouvé. Cet intermédiaire peut se dimériser selon une cycloaddition [2 + 2] thermique ou bien engendré à −78° puis piégé par des dienes-1,3 selon une réaction de Diels Alder. Un mécanisme pour la réaction de dimérisation a été discuté.
[Traduit par le journal]

Can. J. Chem., **51**, 2207 (1973)

Introduction

The photochemistry of unsaturated cyclooctanones has been the subject of a number of recent publications. Eaton and Lin reported (1) that upon u.v. irradiation, *cis*-2-cyclooctenone was isomerized to *trans*-2-cyclooctenone which either dimerized in a thermal cycloaddition or was trapped by a 1,3-diene in a Diels–Alder reaction. Paquette and Eizember (2) and Crandall *et al.* (2) irradiated 3-cyclooctenone and concluded that an initial Norrish type 1 cleavage was the primary photochemical process involved. Büchi and Burgess (3), and later Chapman and co-workers (3), examined the photochemistry of 2,4,6-cyclooctatrienone and reported that it cleaved to give a ketene intermediate and isomerized to the *trans,cis,cis*-trienone, which underwent a number of thermal reactions. The photochemistry of 2,6- (4, 5) and 2,7-cyclooctadienone (6) has also been reported.

Cantrell and Solomon discussed (4) the photochemistry of 2,4-cyclooctadienone (**1**) with ether, pentane, and methanol as solvents. They reported the isolation in 6–10% yield of a head-to-head, *cis–anti-cis* dimer (m.p. 174°) formed by a 2 + 2 cycloaddition at the α,β positions of two dienone molecules. In the present paper we report our results on the photochemistry of **1** in benzene and toluene. The conclusions differ in a number of important structural and mechanistic aspects from those reported previously (4). In the following paper the photochemistry of **1** in the solvent methanol is discussed.

Results and Discussion

Structure of Dimers

Irradiation of a 1% solution of 2,4-cyclooctadienone (**1**) in benzene using a 350 mμ u.v. source resulted in the rapid disappearance of starting material and the formation in high yield (85%) of a mixture of two dimers, which were readily separated by fractional crystallization from ethyl acetate. Dimer **2** (33%), m.p. 174.5–175.0°, was found to be identical (spectral properties, mixed m.p.) to that prepared and isolated as described previously (4). Dimer **3** (52%), m.p. 89–90°, had not been reported previously. The i.r. spectra indicate that the cycloadditions took place across the α,β-positions and although the n.m.r. spectra will not be discussed in detail they are entirely consistent with the structures to be proposed.

Treatment of either **2** or **3** with methanolic potassium hydroxide at room temperature for 50 h resulted in epimerization to the same dimer, **4**, m.p. 126–127°. Epimerization to this dimer (**4**) indicates that **2** and **3** differ only in their con-

[1]See following paper for Part II.
[2]For preliminary accounts of this work see ref. 23.

Can. J. Chem. Downloaded from www.nrcresearchpress.com by 210.87.254.5 on 09/05/12
For personal use only.

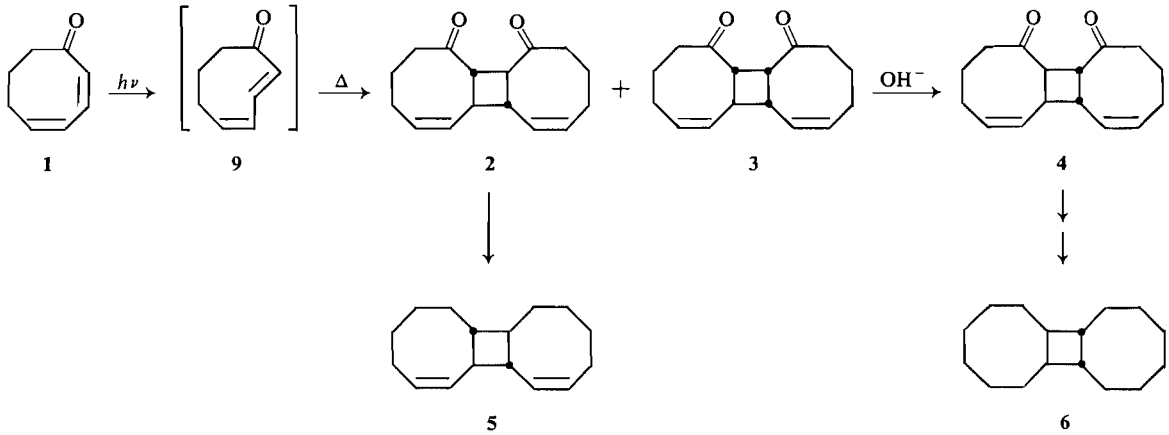

1 9 2 3 4 5 6

figurations at the cyclobutyl positions *alpha* to the carbonyl groups and that either one or both ring fusions in each dimer are *trans*.[3] This result invalidates the *cis–anti-cis* structure proposed previously (4) for the dimer with m.p. 174°. It was reported (4) that the diol diester obtained from this dimer by hydrogenation, Baeyer–Villager oxidation, hydrolysis, and esterification was cleaved relatively slowly by lead tetraacetate, suggesting the presence of a *trans*-1,2-cyclobutanediol moiety. It should be noted that dimer **2**, our proposed structure for the compound with m.p. 174°, would be expected to undergo the same series of reactions in the manner described.

To establish the stereochemistry of the ring fusions in **2**, **3**, and **4**, the conversion of the dimers to known hydrocarbons was attempted. A modified Wolff–Kishner reduction (8) of **2** gave diene **5**, which was identical to the *trans–anti-trans* dimer of *cis,trans*-1,3-cyclooctadiene (9).[4] All attempts to convert **3** or tetrahydro **3**, m.p. 105–106°, to hydrocarbons were unsuccessful presumably because of the close proximity of the carbonyl groups. Hydrogenation of **4** gave tetrahydro **4**[5,6], m.p. 67.0–68.5°, which was converted to a saturated hydrocarbon by preparation of the ethanedithiol diketal followed by Raney nickel desulfurization. This product, **6**, m.p. 57–58°, was identical to the hydrogenation product of the *cis–anti-cis* dimer of *cis,trans*-1,3-cyclooctadiene (9). These conversions conclusively establish the ring fusions in dimers **2** and **4** and as a consequence of the epimerization experiment the structure of **3** can only be as depicted.

Mechanistic Considerations

Having established the structures of the products formed upon irradiation of **1**, next it was appropriate to examine the mechanism of formation of the two dimers, **2** and **3**. In particular, it was desired to examine (*a*) the nature of the excited state involved in the photochemical step, (*b*) the structure of the dimer precursor, if indeed such an intermediate existed, and finally (*c*) the mechanism of the dimerization step itself.

When oxygen, a well-known triplet quencher, was bubbled through a benzene solution of **1** during irradiation, the rate of disappearance of dienone was the same as in a control experiment in which nitrogen was used. Similarly, 0.01–1.0 *M* concentrations of the triplet quencher 1,3-cyclohexadiene (E_T 53 kcal/mol) (10) had no effect on the rate of disappearance of **1**. The quantum yield of intersystem crossing of **1** as determined by the sensitized dimerization of 1,3-cyclohexadiene was found to be <0.01 relative to a value of unity for benzophenone (11). These results suggest that the excited state in the photochemical step is either a singlet or a short-lived triplet. Triplet sensitization experiments were used to differentiate between these two possibilities.

[3]*Trans*-fused bicyclo[6.2.0]alkanones epimerize to the *cis*-fused ketones under alkaline conditions: see refs. 1 and 7.

[4]We thank Dr. Osborn for experimental details prior to publication of their full paper (9).

[5]Tetrahydro **2** has m.p. 70–71° although it was previously reported (4) as a syrup.

[6]Eaton and Lin (1) reported the isolation of two dimers, m.p. 88–90° and 133–134°, upon irradiation of 2-cyclooctenone in cyclohexane. Neither of these dimers is the same as the tetrahydro derivatives of **2**, **3**, or **4**. We thank Prof. Eaton for experimental details in the preparation of the 2-cyclooctenone dimers.

Can. J. Chem. Downloaded from www.nrcresearchpress.com by 210.87.254.5 on 09/05/12
For personal use only.

Can. J. Chem. Downloaded from www.nrcresearchpress.com by 210.87.254.5 on 09/05/12
For personal use only.

Benzene solutions of **1** were irradiated in the presence of the following triplet sensitizers such that the sensitizer absorbed the indicated percentage of incident irradiation: xanthone (99%)[7] (E_T 74.2 kcal/mol) (13), benzophenone (82%) (E_T 68.5 kcal/mol) (13) and Michler's ketone (99%) (E_T 61 kcal/mol) (13). In all three sensitized irradiations there was a very significant decrease in the rate of disappearance of **1**. Although the triplet energy of **1** has not been determined it would be expected to be below that of at least the first two sensitizers. Thus there is no evidence of triplet sensitization and the photochemically reactive state of **1** must be an excited *singlet*.

Next, it was necessary to determine the nature of the photochemical reaction and the structure of the dimer precursor. Benzene (m.p. 5.5°) solutions obviously could not be used for the proposed low temperature experiments but it was found that toluene (m.p. −95°) was a very suitable alternative solvent. Irradiation of a 1% solution of **1** in toluene at room temperature gave a combined yield of 82% dimers **2** and **3**. A similar irradiation was conducted at −78° using a specially constructed low temperature apparatus and the solution was divided into two portions. To one was added a 15-fold excess of the trapping reagent 2,3-dimethyl-1,3-butadiene (DMBD)[8] and both samples were allowed to warm slowly to room temperature. The portion without added diene gave a 40% yield of dimers **2** and **3** and 60% unreacted **1** while the other portion gave a decreased yield of dimers (32%), unreacted **1** (62%) and a crystalline Diels–Alder adduct, **7** (6%); m.p. 45–47°. The spectral data, particularly the presence of two similar methyl groups at τ 8.4 in the n.m.r. spectrum is convincing evidence for the proposed structure of **7**. Irradiation of **1** at room temperature in the presence of 15-fold excess of DMBD gave dimers **2** and **3** (46%) and two adducts: **7**, (15%) and **8** (35%). The strong band in the i.r. spectrum of **8** at 889 cm^{-1} for the terminal methylene

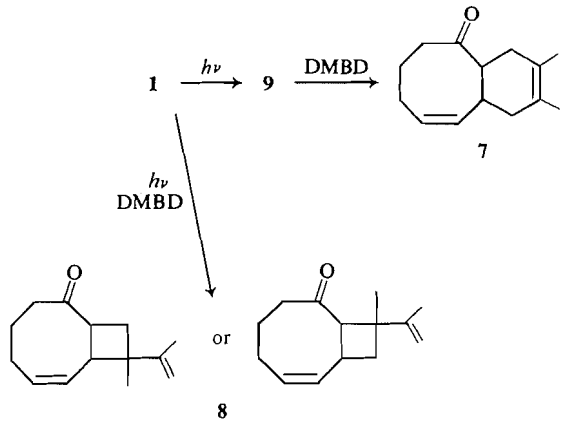

group and the two different methyl singlets in the n.m.r. spectrum (τ 8.4 and 8.7) were particularly useful in assigning a structure to this adduct.

Adduct **8** must have been formed in a photochemical 2 + 2 addition as it was not formed in the trapping experiment. Similar cycloadditions of 1,3-dienes and cycloalkenones have been reported (14). The trapping experiment also showed that the Diels–Alder adduct, **7**, was a thermal 2 + 4 product. This adduct was not formed when a toluene solution of **1** and DMBD was allowed to stand in the absence of light. Thus adduct **7** must have been formed by reaction of DMBD with a highly reactive ground-state species, namely *trans,cis*-2,4-cyclooctadienone (**9**). Cantrell and Solomon (4) reported the formation of *trans*-fused Diels–Alder adducts upon irradiation of **1** in furan and suggested **9** was the reactive species but no low temperature trapping experiments were conducted.

Finally, the dimerization itself must be discussed and an explanation provided for the formation of two dimers. Irradiation of **1** in benzene at concentrations of 0.08 *M* (1%) and 0.38 *M* resulted in the same 44:56 ratio of dimers **2** and **3**,[9] respectively. Similarly, irradiation of **1** in toluene (at room temperature or −78°), in methanol or in the presence of 1,3-dienes caused no change in the dimer ratio. Addition of trapping reagents such as dienes after irradiation of **1** at −78° also caused no change in this ratio but did result in a decreased yield of dimers, indicating competition for the intermediate **9**. Therefore, the dimers must be

[7]To ensure that self-quenching by the sensitizer (12) was not involved, the concentration of xanthone was varied such that it absorbed 90 and 62% of the irradiation and it was found that the rate of disappearance of **1** increased as expected.

[8]This diene was particularly useful as n.m.r. spectroscopy could readily distinguish between the 2 + 2 and the 2 + 4 adducts of **1** and DMBD. When other dienes such as piperylene were used as trapping agents the yield of adducts was higher but the structural assignments were not as straightforward.

[9]Dimer ratios were determined by g.l.c. and as the two peaks overlapped slightly the determinations were accurate to ±3%.

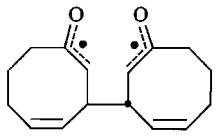

10

formed from two molecules of **9** in a two-step thermal process in which the initially formed diradical, **10**, closes in either a conrotatory or a disrotatory manner to give **2** or **3**, respectively. A similar mechanism has been proposed for the thermal dimerization of *cis,trans*-1,3-cyclooctadiene (9). It was previously suggested (4) that dimerization of **1** proceeded via addition of an excited triplet of **1** to ground-state **1**.

Conclusions

Irradiation of 2,4-cyclooctadienone (**1**) in benzene or toluene resulted in the formation of two dimers, **2**, m.p. 174.5–175.0° and **3**, m.p. 89–90°, in a combined yield of >80%. The structure previously proposed (4) for the former was shown to be in error while the second dimer had not previously been reported. The reason for the high yield of dimers in benzene and toluene as compared with the low yields (8–10% of **2**) in pentane and ether (4) may simply be a reflection of the number of readily abstractable hydrogens available on the solvents (Cantrell reported considerable quantities of polymer formed in pentane and ether) although it is surprising that toluene with three benzylic hydrogens would be such an effective solvent.

From the ultraviolet spectral data (see Experimental) it can be concluded that **1** possesses an intense ($\varepsilon \sim 5800$) π-π^* maximum at ~270 mμ and a weak ($\varepsilon \sim 50$) n-π^* maximum at ~345 mμ. The irradiations could be accomplished using a 350 mμ source and a uranium glass filter ($\lambda > 330$ mμ) (15) and under these conditions it would be expected that almost all the irradiation would be absorbed by the n-π^* band although the tail of the π-π^* band does extend beyond 330 mμ. As the photochemical reaction of **1** is not affected by triplet quenchers, as there is no evidence of intersystem crossing from the singlet to the triplet state and as the reaction is not assisted by triplet sensitizers, we conclude that the singlet state is involved in the photochemical step. Noyori and co-workers (16) reported irradiation of 2-cyclooctenone in methanol to give a methanol adduct via *trans*-2-cyclooctenone is not affected by diene quenchers and a recent review suggested (17) the reactive state in this isomerization may also be a singlet. We believe that the photochemical reaction itself is the *cis–trans* isomerization of the α,β-double bond of **1**. Another possibility that should at least be mentioned is the photochemical formation, possibly via the n-π^* singlet, of an intermediate such as **11**, which could then open to give **9** and other products. Similar intermediates have been suggested by others (7, 18), but in no case, including the present investigation, is there any evidence for their existence.

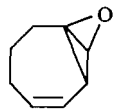

11

The singlet state *cis–trans* isomerization of **1** results in the formation of the highly strained and highly reactive intermediate, *trans,cis*-2,4-cyclooctadienone (**9**). We have presented no spectroscopic evidence for such a species but the low temperature trapping experiments with DMBD leave no doubt that such an intermediate exists and is stable at −78°. Additional evidence for the existence of **9** will be presented in the following paper. This dienone (**9**) has the capability of undergoing ground-state reactions such as dimerization, isomerization to **1** and 2 + 4 addition to suitable trapping reagents such as 1,3-dienes. An attempt to react **9** with cyclopentene gave none of the expected product indicating that a more reactive alkene was required. Corey and co-workers (7) found that *trans*-2-cyclooctenone reacted with 1,1-dimethoxyethylene to give a cycloaddition product but did not react with cyclopentene.

Comparison of the dimerization of **9** with that of *cis,trans*-1,3-cyclooctadiene (9) revealed (*a*) only head-to-head dimers were formed and (*b*) the two most abundant dimers in each investigation had *cis–trans* and *trans–anti-trans* ring fusions. These similarities suggest that a common mechanism may be involved. In the case of the diene dimerization it was proposed that the 1,4-diradical was stabilized because both radicals were allylic while in the present case the diradical **10** is stabilized by the adjacent carbonyl groups. Closure in either a conrotatory or a disrotatory manner then gives the two major dimers.

The formation of dimers has been reported in

Can. J. Chem. Downloaded from www.nrcresearchpress.com by 210.87.254.5 on 09/05/12
For personal use only.

Can. J. Chem. Downloaded from www.nrcresearchpress.com by 210.87.254.5 on 09/05/12
For personal use only.

the irradiation of 2-cycloheptenone (18*a*),[10] 2-cyclooctenone (1), and 2,4,6-cyclooctatrienone (3*b*) but the structures have not been elucidated. Comparison of the stereochemistry of the dimers with those reported here would be of interest particularly as the two dimers of 2-cyclooctenone reported by Eaton and Lin (1) are not the same as any of the tetrahydro derivatives of **2**, **3**, and **4** (see footnote 6).

Experimental

Infrared (i.r.) spectra were recorded on a Beckman Model IR5A spectrophotometer and nuclear magnetic resonance (n.m.r.) spectra were recorded on a Varian A-60A spectrometer using tetramethylsilane as internal standard (TMS, $\tau = 10.0$). Resonance splittings are indicated as singlet (s), doublet (d), triplet (t), doublet of doublets (dd), and multiplet (m). Ultraviolet absorption (u.v.) spectra were recorded on a Unicam SP-800 spectrophotometer and mass spectral (m.s.) analyses were determined on a Varian Mat CH7 low resolution spectrometer.

Analytical thin layer chromatography (t.l.c.) was carried out on 0.25 mm silica gel GF-254 plates while preparative t.l.c. was accomplished on 1.0 mm silica gel PF-254 plates. The solvent system used in each instance will be specified. Column chromatography separations were done on silica gel, 50–200 mesh. Gas liquid phase chromatography (g.l.c.) analyses and separations were run on an Aerograph "Autoprep" Model A-700 with a thermal conductivity detector and the peak areas were determined by triangulation and were not corrected for differences in thermal response. The columns used were: column A, 6 ft × 0.25 in., 20% Carbowax 20M on 60/80 mesh Chromosorb W; column B, 20 ft × 0.375 in., 30% SE 30 on 45/60 mesh Chromosorb W; column C, 6 ft × 0.25 in., 20% SE 30 on 60/80 mesh Chromosorb W. The carrier gas used was helium with a flow rate of 60 ml/min in the 0.25 in. columns and 180 ml/min in the 0.375 in. column. The temperature for the column will be specified. Spinning band distillations were done on a Nester/Faust 117 apparatus with an 18 in. column length.

Microanalyses were performed by H. S. McKinnon, Department of Chemistry, University of Guelph and A. G. Gygli, Toronto, Ontario. All melting points were determined on a Gallenkamp apparatus and are uncorrected. Solvents used in the irradiations were refluxed over calcium hydride and distilled.

Normal irradiations were accomplished in Pyrex or uranium glass (Corning no. 3320) (15) tubes using a Rayonet Photochemical Reactor Model RPR-100 with 16 low-pressure 350 mμ lamps. All samples were deoxygenated by bubbling dry, high purity nitrogen through the solution for 15–30 min depending on the volume of solution. The specially constructed apparatus used in the low temperature experiments consisted of an inner cold finger (60 mm diameter), for the Dry Ice – acetone mixture, surrounded by a cylindrical liner for the irradiation solution which was in turn surrounded by a larger cylindrical liner (100 mm diameter) which could be evacuated to prevent condensation forming on the outside of the apparatus. The solution cavity had a capacity of ~150 ml and a tube run to the bottom of the cavity could be used for degassing the solution or introducing additional reagents as required. The apparatus could be placed conveniently inside the Rayonet Reactor.[11]

Preparation of 2,4-Cyclooctadienone (1)

The procedure of Heap and co-workers (20) was followed and the product after distillation on a spinning band column showed one peak on column A, 140° and column C, 140°. The i.r. and n.m.r. spectral bands for **1** have been recorded in detail but we include here the u.v. maxima in several solvents; λ_{max} (EtOH) 278 mμ (ε 5850); λ_{max} (cyclohexane) 268 mμ (ε 5800), 346 mμ (ε 51); λ_{max} (benzene) 343 mμ (ε ~ 50). The longer wavelength band in ethanol could not be resolved from the 278 mμ band and the shorter wavelength band in benzene was masked by the solvent.

Irradiation of 1 in Benzene

Irradiation of 1.2 g (0.01 mol) of **1** in 120 ml anhydrous benzene at 10–12° in a Pyrex or a uranium glass tube resulted in the rapid disappearance of starting material. G.l.c. analysis (column C, 140°) showed complete consumption of **1** in 4 h. A g.l.c. tracing (column C, 242°) of the crude product showed only two peaks at retention times of 18.7 and 20.8 min in a ratio of 43:57, respectively.

The solvent was removed under vacuum and the residue was triturated with 30 ml ethyl acetate (4) leaving crude dimer **2** as a gray residue. Filtration followed by recrystallization from 1:1 ethyl acetate:benzene yielded 398 mg (33%) pure **2** as colorless crystals, m.p. 174.5–175.0°. G.l.c. analysis (column C, 242°) showed a single peak with retention time 18.7 min. Spectral properties of **2** were as follows; i.r. (KBr) 3000, 1698, 1445, 1345, 1310, 1115, 914, 722, 685 cm^{-1}; n.m.r. ($CDCl_3$) τ 4.24 (4H, m, vinyl), 6.60 (2H, m, —CHCO—), 7.25 (2H, m, —CHC=), 7.43–8.60 (12H, m).

Anal. Calcd. for $C_{16}H_{20}O_2$: C, 78.65; H, 8.25. Found: C, 78.85; H, 8.37.

The solvent was removed from the ethyl acetate filtrate above and the viscous syrup was left in the refrigerator (6°) overnight at which time crystallization had occurred (this dimer would not crystallize if the irradiation was not carried to complete consumption of **1**). Recrystallization from absolute ethanol yielded 625 mg (52%) pure **3** as long, clear crystals, m.p. 89–90°. G.l.c. analysis (column C, 242°) showed one peak with retention time 20.8 min. Spectral properties of **3** were as follows; i.r. (KBr) 3000, 1695, 1355, 1182, 720 cm^{-1}; n.m.r. ($CDCl_3$) τ 4.18 (2H, m, vinyl), 4.53 (2H, m, vinyl), 5.83 (1H, t, $J = 10$ Hz, —CHCO—), 6.47 (1H, d with fine splitting, $J = 10$ Hz, —CHCO—), 6.72–8.90 (14H, m).

Anal. Calcd. for $C_{16}H_{20}O_2$: C, 78.65; H, 8.25. Found: C, 78.83; H, 8.21.

[10]A head-to-head *cis–anti-cis* structure has recently been reported for one of the secondary products from the thermal dimerization of *trans*-2-cycloheptenone (19).

[11]We thank Miss A. Hostetter of the Department of Chemistry, University of Guelph, for the construction of this apparatus.

Can. J. Chem. Downloaded from www.nrcresearchpress.com by 210.87.254.5 on 09/05/12
For personal use only.

An analytical t.l.c. separation of the two dimers could be effected with three passes of chloroform to give the following R_f's: **2**, 0.60: **3**, 0.41. A similar irradiation to that described above using toluene as solvent gave the dimers in a combined yield of 82% (**2**:**3** in a ratio of 42:58).

*Formation of Epimer **4** from Dimers **2** and **3***

A solution of 420 mg (1.72 mmol) **3** and 8.4 g potassium hydroxide in 84 ml methanol was stirred at room temperature under nitrogen for 50 h. To the slightly colored solution was added 400 ml water and the aqueous phase was extracted with chloroform (5 × 50 ml). The combined chloroform extracts were washed with water (2 × 50 ml), saturated brine (2 × 50 ml) and dried ($MgSO_4$). Removal of the solvent under reduced pressure gave 420 mg crude epimer. Recrystallization from 40:60 ethyl acetate:ethanol yielded 320 mg (76%) pure **4** as long crystals, m.p. 126–127°. G.l.c. analysis (column C, 242°) showed only one peak with retention time 20.3 min; i.r. (KBr) 3000, 1692, 1430, 1298, 1043, 732, 718 cm^{-1}; n.m.r. ($CDCl_3$) τ 4.30 (4H, m, vinyl), 5.95 (2H, dd, J = 7 and 2 Hz, —$\overset{|}{C}$HCO), 6.64 (2H, d with fine splitting, J = 7 Hz, —$\overset{|}{C}$HC═), 7.10–8.60 (12H, m).

Anal. Calcd. for $C_{16}H_{20}O_2$: C, 78.65; H, 8.25. Found C, 78.46; H, 8.36.

Similar treatment of 80 mg of **2** yielded 45 mg (58%) of **4**, m.p. 126–127°. The epimers from **2** and **3** had identical g.l.c. retention times as well as i.r. and n.m.r. spectra. A 50:50 mixture of the two epimers had a melting point of 126–127°.

*Wolff–Kishner Reduction of **2***

This modified Wolff–Kishner reduction is similar to a reported procedure (8) for ketones in which there is a possibility of an epimerization side reaction. To a solution of 0.50 g (2.1 mmol) of **2** in 35 ml refluxing absolute ethanol was added 2.5 ml (42.5 mmol) 85% hydrazine hydrate. The solution was heated to reflux for 3.5 h and then poured into a stirred solution of 1.6 g (40 mmol) sodium hydroxide in 35 ml diethylene glycol at 70°. The reaction mixture was continuously distilled while the temperature was raised from 70 to 200°. The temperature was maintained at 200–210° for 5.5 h. The pot residue and distillate were combined, poured into 250 ml water and this aqueous phase extracted with chloroform (5 × 50 ml). The combined extracts were washed with saturated brine (1 × 50 ml) and dried ($MgSO_4$). Removal of the solvent gave a brown syrup, which exhibited no carbonyl absorption in its i.r. spectrum. The crude product was filtered through 10 g silica gel using 150 ml pentane as the eluting solvent. Removal of the solvent gave 0.38 g (87%) of a viscous, colorless syrup which on g.l.c. analysis (column B, 240°) showed a major peak (80%) at 53 min with a slight shoulder at shorter retention time. The major peak was collected from g.l.c. (column B) as a colorless solid; m.p. 30–31°; i.r. (neat) 3010, 2920, 2850, 1456, 1445, 890, 797, 760, 730, 700 cm^{-1}; n.m.r. ($CDCl_3$) τ 4.15–4.80 (4H, m, vinyl), 7.50–9.00 (20H, m). These properties were identical to an authentic sample of **5** which was prepared as reported (9) for comparison. The mixed melting point of the Wolff–Kishner product with an authentic sample of **5** was 30–31°.

Similar treatment of **3** and **4** resulted in the formation of an insoluble precipitate upon reaction with hydrazine hydrate.

*Preparation of Tetrahydro **2**, **3**, and **4***

A solution of 0.10 g (0.41 mmol) of **2** in 50 ml absolute ethanol was vigorously stirred with a catalytic amount of 10% palladium on charcoal under 1 atm of hydrogen until two equivalents of hydrogen were consumed. The reaction mixture was filtered through a mat of filter-aid and the solvent removed. In order for crystallization to occur it was necessary to remove the last traces of alcohol. The compound had previously been reported (4) as a syrup. Recrystallization of the crude saturated dimer from hexane yielded 82 mg (82%) of pure tetrahydro **2** as white crystals; m.p. 70–71°; i.r. (KBr) 1690, 1445, 1332, 1261, 1160 cm^{-1}; n.m.r. ($CDCl_3$) τ 6.71 (2H, m, —$\overset{|}{C}$HCO—), 7.55 (4H, m, —CH_2CO—), 7.90–8.80 (18H, m).

Anal. Calcd. for $C_{16}H_{24}O_2$: C, 77.38; H, 9.74. Found C, 77.45; H, 9.94.

Similar treatment of 0.10 g (0.41 mmol) of **3** followed by recrystallization from hexane yielded 79 mg (79%) of tetrahydro **3**; m.p. 105–106°; i.r. (KBr) 1685, 1450, 1235, 1148, 893, 870 cm^{-1}; n.m.r. ($CDCl_3$) τ 5.95 (1H, t, J = 8 Hz, —$\overset{|}{C}$HCO—), 4.68 (1H, doublet with fine splitting, J = 8 Hz, —$\overset{|}{C}$HCO—), 7.40–9.00 (22H, m).

Anal. Calcd. for $C_{16}H_{24}O_2$: C, 77.38; H, 9.74. Found C, 77.06; H, 9.92.

Similarly, 0.10 g (0.41 mmol) of **4** yielded 85 mg (85%) of tetrahydro **4**; m.p. 67–68°; i.r. (KBr) 1685, 1450, 1222, 1170, 896, 866, 740 cm^{-1}; n.m.r. ($CDCl_3$) τ 6.14 (2H, d, J = 9 Hz, —$\overset{|}{C}$HCO—), 7.30–8.00 (6H, m), 8.00–9.00 (16H, m).

Anal. Calcd. for $C_{16}H_{24}O_2$: C, 77.38; H, 9.74. Found: C, 77.68; H, 9.96.

*Conversion of Tetrahydro **4** to Hydrocarbon **6***

To a solution of 0.16 g (0.65 mmol) of tetrahydro **4** in 3 ml ethanedithiol at room temperature was added 2 ml 98% boron trifluoride etherate and the reaction mixture was stirred 5 h. The homogeneous reaction was then poured into an excess of a chilled sodium hydroxide solution and this aqueous phase was extracted with chilled chloroform (8 × 25 ml) and the combined extracts were washed with chilled water (3 × 30 ml), with saturated brine (3 × 50 ml) and dried ($MgSO_4$). Removal of the solvent gave the crude ethanedithiol diketal which was not purified.

To a solution of this crude diketal in 150 ml absolute ethanol was added 6 g of Raney nickel (W-2) (21) and the suspension was stirred and heated to reflux for 15 h (22). The Raney nickel was filtered and the solvent removed to give 120 mg (85%) crude hydrocarbon which g.l.c. analysis (column B, 250°) showed to consist of 70% of a component with a retention time of 47 min. This compound was collected by g.l.c. as a white solid; m.p. 57–58°; i.r. (KBr) 2900, 1452, 1445, 1358, 953, 875, 848, 744 cm^{-1}. An authentic sample of **6** was prepared as described (9) and was found to be identical to this hydrocarbon prepared by reduction of **4**. The m.p. of a mixture was not depressed.

Can. J. Chem. Downloaded from www.nrcresearchpress.com by 210.87.254.5 on 09/05/12
For personal use only.

Irradiation in Presence of Oxygen

Two identical 1% solutions of **1** in benzene were placed in Pyrex tubes. Through one was bubbled high purity nitrogen for 20 min prior to and during the irradiation while through the other was bubbled oxygen for 20 min prior to and during the irradiation. After 30 min of irradiation the amount of **1** consumed in both cases was determined by g.l.c. (column C). Values of 23.5 and 23.0% consumption of **1** were observed for the nitrogen and oxygen experiments, respectively.

Quenching Experiments with 1,3-Cyclohexadiene

Five solutions of 1% of **1** in benzene were made 0.01, 0.05, 0.10, 0.50, and 1.0 *M* in 1,3-cyclohexadiene and placed in matched Pyrex tubes along with a sixth which contained no diene. Each of the solutions was degassed with purified nitrogen and then uniformly irradiated in a "merry-go-round" apparatus for 20 min. The consumption of **1** in each solution was determined by g.l.c. (column C) relative to an internal standard (*n*-dodecane). The solution without added diene showed 63% consumption of **1** while the values for the other solutions in order of increasing concentration of added diene were 62, 64, 62, 66, and 64% respectively.

Intersystem Crossing Measurements (11)

One benzene solution was made 0.05 *M* in benzophenone and 0.15 *M* in 1,3-cyclohexadiene while a second was made 0.177 *M* in **1** and 0.15 *M* in 1,3-cyclohexadiene. At these concentrations the amount of light absorbed by the two solutions was the same. Both solutions were irradiated uniformly using a "merry-go-round" apparatus and after 5 min the yield of cyclohexadiene dimers was determined in each solution by g.l.c. (column C, 160°). Two dimer peaks (retention times 10.5 and 13.2 min) were observed in the benzophenone solution but these were absent in the other solution. After a total of 15 min irradiation the dimer peaks were considerably larger in the former solution but still absent in the latter and the same was true after 25 min irradiation but by this time the concentration of **1** had decreased significantly in the second solution. Thus no indication of intersystem crossing could be detected within the limits of our measurements.

Sensitization Experiments

The proportion of light absorbed by the components was calculated by determining their relative absorbances at 346 mμ. Four 10 ml benzene solutions each 0.082 *M* (1%) in **1** were placed in matched Pyrex tubes. The first contained no additional compounds, the second contained 340 mg (1.73 mmol) xanthone (E_T 74.2 kcal/mol) (absorbed 99% of irradiation), the third contained 430 mg (2.36 mmol) benzophenone (E_T 68.5 kcal/mol) (82% of irradiation) and the fourth contained 45.2 mg (0.168 mmol) 4,4′-bis(dimethylamino) benzophenone (E_T 61.0 kcal/mol) (99% of irradiation). The four tubes were degassed and then irradiated simultaneously in a "merry-go-round" apparatus for 30 min and the consumption of **1** was determined by g.l.c. (column C) relative to the internal standard *n*-dodecane. The consumption in the first tube was 38% while in the three tubes containing the triplet sensitizers there was no measureable consumption of **1**.

To ensure that self-quenching (12) was not a complication in the xanthone sensitization experiment, the following experiment was conducted. Three 5 ml benzene solutions each 0.082 *M* in **1** were placed in matched Pyrex tubes. To the first was added nothing, to the second was added 5.4 mg (0.028 mmol) xanthone (to absorb 62% of the irradiation) and to the third was added 27.8 mg (0.142 mmol) xanthone (90% of irradiation). The solutions were degassed and uniformly irradiated for 50 min. G.l.c. analysis showed **1** had been consumed to the extent of 58, 18, and 6%, respectively. These values are proportional to the amount of irradiation absorbed by **1** and show that self-quenching was not the reason for the lack of sensitization by xanthone.

Irradiation of 1 with DMBD

A solution of 100 mg (0.82 mmol) **1** and 1.0 g (12 mmol) 2,3-dimethyl-1,3-butadiene (DMBD) in 10 ml benzene was degassed and irradiated for 4 h. The solvent and excess diene were removed under reduced pressure and the residue, upon analysis by programmed g.l.c. (column C, 200–240°), showed five peaks. The first peak (35%, retention time 10.8 min) was collected as a colorless syrup and assigned structure **8**; i.r. (neat) 3050, 3010, 2880, 1700, 1645, 1450, 1370, 1200, 1128, 889, 755 cm^{-1}; n.m.r. ($CDCl_3$) τ 4.00–4.50 (2H, m, —CH=CH—), 5.30–5.50 (2H, m, $\diagdown\!\!\diagup C{=}CH_2$), 6.9–9.3 (10H, m), 8.38 (apparent 3H, s, $CH_3{-}\overset{|}{C}{=}$), 8.73 (apparent 3H, s, $CH_3{-}\overset{|}{C}{-}$); m.s. molecular ion at *m/e* 204. The second peak (4%, retention time 12.5 min) was not isolated. The third peak (15%, retention time 15.8 min) was collected as a white solid and assigned structure **7**; m.p. 45–47°; i.r. (CCl_4) 3010, 2890, 1700, 1420, 1288, 1250, 868, 693 cm^{-1}; n.m.r. ($CDCl_3$) 4.40–4.75 (2H, m, —CH=CH—), 7.2–8.5 (12H, m), 8.38 (apparent 6H, s, $-C(CH_3){=}C(CH_3)-$); m.s. molecular ion at *m/e* 204. The remaining two peaks (46%) had retention times of 32 and 38 min and were assigned to the dimers **2** and **3**.

Low Temperature Irradiation of 1 in Toluene

A solution of 1.22 g (10 mmol) of **1** in 125 ml toluene was placed in the specially constructed low temperature apparatus described previously and irradiated for 2.5 h at −78°. The solution was divided into two equal portions. The first portion was allowed to slowly warm to room temperature, the solvent was removed and the residue upon analysis by programmed g.l.c. (column C, 150–240°) showed 60% **1** and 40% dimers **2** and **3** (42:58). To the second portion was added 12 g DMBD and the solution was allowed to warm to room temperature. G.l.c. analysis of the residue indicated 62% **1**, 6% **7**, and 32% dimers **2**, and **3** (43:57).

When 12 g of piperylene was substituted for DMBD in the trapping experiment above, two adducts (*m/e* 190) were obtained in a combined yield of 12%.

The authors acknowledge financial support from the National Research Council of Canada.

1. P. E. EATON and K. LIN. J. Am. Chem. Soc. **86**, 2087 (1964).
2. (*a*) L. A. PAQUETTE and R. F. EIZEMBER. J. Am. Chem. Soc. **89**, 6205 (1967). (*b*) J. K. CRANDALL, J. P. ARRINGTON, and J. HEN. J. Am. Chem. Soc. **89**, 6208 (1967).
3. (*a*) G. BÜCHI and E. M. BURGESS. J. Am. Chem. Soc. **84**, 3104 (1962). (*b*) L. L. BARBER, O. L. CHAPMAN, and J. D. LASSILA. J. Am. Chem. Soc. **91**, 531 (1969).
4. T. S. CANTRELL and J. S. SOLOMON. J. Am. Chem. Soc. **92**, 4656 (1970).
5. R. NOYORI, H. INOUE, and M. KATÔ. Chem. Commun. 1695 (1970).
6. J. K. CRANDALL and R. P. HASELTINE. J. Am. Chem. Soc. **90**, 6251 (1968).
7. E. J. COREY, J. D. BASS, R. LAMAHIEU, and R. B. MITRA. J. Am. Chem. Soc. **86**, 5570 (1964).
8. R. L. AUGUSTINE. Reduction. M. Dekker, New York. 1968. p. 175.
9. A. PADWA, W. KOEHN, J. MASARACCHIA, C. L. OSBORN, and D. J. TRECKER. J. Am. Chem. Soc. **93**, 3633 (1971).
10. R. E. KELLOGG and W. T. SIMPSON. J. Am. Chem. Soc. **87**, 4230 (1965).
11. (*a*) D. VALENTINE, N. J. TURRO, and G. S. HAMMOND. J. Am. Chem. Soc. **86**, 5202 (1964). (*b*) D. I. SCHUSTER and D. J. PATEL. J. Am. Chem. Soc. **90**, 5145 (1968).
12. (*a*) O. L. CHAPMAN and G. WAMPFLER. J. Am. Chem. Soc. **91**, 5390 (1969). (*b*) P. S. ENGEL and B. M. MONROE. Adv. Photochem. **8**, 253, 303 (1971).
13. J. G. CALVERT and J. N. PITTS, JR. Photochemistry. Wiley, New York. 1966. p. 298.
14. (*a*) T. S. CANTRELL. Chem. Commun. 1656 (1970). (*b*) D. I. SCHUSTER and D. H. SUSSMAN. Tetrahedron Lett. 1657 (1970).
15. (*a*) G. S. HAMMOND, J. SALTIEL, A. A. LAMOLA, N. J. TURRO, J. S. BRADSHAW, D. O. COWAN, R. C. COUNSELL, V. VOGT, and C. DALTON. J. Am. Chem. Soc. **86**, 3197 (1964). (*b*) W. C. AGOSTA and A. B. SMITH, III. J. Am. Chem. Soc. **93**, 5513 (1971).
16. R. NOYORI, A. WATANABE, and M. KATÔ. Tetrahedron Lett. 5443 (1968).
17. D. BRYCE-SMITH. Senior Reporter. Photochemistry. Vol. 1. The Chemical Society, London. 1970. p. 186.
18. (*a*) E. J. COREY, M. TADA, R. LAMAHIEU, and L. LIBIT. J. Am. Chem. Soc. **87**, 2051 (1965). (*b*) R. G. CARLSON and J. H. BATEMAN. Tetrahedron Lett. 4151 (1967).
19. K. G. TAYLOR, W. E. HOBBS, M. S. CLARK, and J. CHANEY. J. Org. Chem. **37**, 2436 (1972).
20. N. HEAP, G. E. GREEN, and G. H. WHITHAN. J. Chem. Soc. C, 164 (1969).
21. R. MOZINGO. Organic syntheses. Coll. Vol. 3. Wiley, New York. 1967. p. 181.
22. F. SONDHEIMER and D. ROSENTHAL. J. Am. Chem. Soc. **80**, 3995 (1958).
23. G. L. LANGE and E. NEIDERT. Tetrahedron Lett. 4215 (1971); 1349 (1972).

Can. J. Chem. Downloaded from www.nrcresearchpress.com by 210.87.254.5 on 09/05/12
For personal use only.

Photochemistry of 2,4-Cyclooctadienone. II[1] In Neutral and Acidic Methanol

GORDON L. LANGE AND ELI NEIDERT

Department of Chemistry, University of Guelph, Guelph, Ontario

Received September 13, 1972

Irradiation of 2,4-cyclooctadienone (**1**) in neutral dry methanol resulted in the formation of 3-methoxy-4-cyclooctenone (18%) and two head-to-head 2 + 2 dimers (combined yield 64%). A similar irradiation in acidic methanol (0.001 *N* HCl) caused a dramatic change in the products formed. A new compound, the dimethyl ketal of *trans,cis*-2,4-cyclooctadienone was formed in 67% yield along with the two dimers (<10%). A mechanism is proposed whereby the photochemically derived *trans,cis*-2,4-cyclooctadienone reacts in thermal processes to give the products described. Low temperature trapping experiments which support this hypothesis are discussed.

L'irradiation du cyclooctadiène-2,4 one (**1**) dans du méthanol neutre anhydre a conduit à la formation du méthoxy-3 cyclooctène-4 one (18%) ainsi qu'à celle de deux dimères 2 + 2 (tête-tête avec un rendement combiné de 64%). Une irradiation similaire dans du méthanol acidifié (0.001 *N* HCl) a provoqué un changement important dans les produits obtenus. Un nouveau composé, la diméthyl cétal du *trans,cis*-cyclooctadiène-2,4 one, a été obtenu avec un rendement de 67% en même temps que les deux dimères (10%). On propose un mécanisme selon lequel la *trans,cis* cyclooctadiène-2,4 one obtenue photochimiquement réagit selon un processus thermique pour donner les produits observés. On discute des résultats obtenus lors d'expérience de captage à basse température qui sont en accord avec cette hypothèse.

[Traduit par le journal]

Can. J. Chem., **51**, 2215 (1973)

Introduction

Irradiation of medium-ring unsaturated ketones in methanol results in the formation of a variety of products involving the solvent. Both 2-cycloheptenone (1) and 2-cyclooctenone (2) upon irradiation in methanol gave the 3-methoxy ketone by addition of solvent across the double bond. In the case of the second ketone, it was shown (2) that the methoxy derivative was formed as a result of thermal nucleophilic attack of methanol on *trans*-2-cyclooctenone, which was formed by photoisomerization of the *cis*-enone. Similarly, irradiation of 2,6-cyclooctadienone in methanol gave 7-methoxy-3-cyclooctenone via the *trans,cis*-dienone (3, 4). Of course, ketenes are often formed upon irradiation of ketones and in methanol solvent the product isolated is the methyl ester (5).

The photochemistry of a number of medium-ring cross-conjugated dienones in methanol has also been investigated. Irradiation of 2,6-cycloheptadienone gave initially the 3-methoxyenone and upon prolonged irradiation dimethoxy adducts were formed (6). Irradiation of both 2,7-cyclooctadienone (7) and 2,8-cyclononadienone (8) gave bicyclic methoxy ketones as the major products and in the latter case the *trans,cis*-dienone was shown to be the precursor of the products. In contrast, irradiation of 2-cyclododecenone in protic or aprotic solvents resulted in photochemical deconjugation of the enone (9).

Irradiation of 2,4-cyclooctadienone (**1**) in methanol has been reported (3) to give 3-methoxy-4-cyclooctenone (30%) and a head-to-head dimer, m.p. 174° (6.5%). The structure of this dimer was discussed in the preceding paper (10). Here we wish to report our findings on the products formed upon irradiation of **1** in neutral and acidic methanol and to discuss some experiments designed to elucidate the mechanism of formation of these compounds.

Results and Discussion

Irradiation of a 1% solution of 2,4-cyclooctadienone (**1**) in dry, neutral methanol with a 350 mμ u.v. source gave dimers **2** (28%) and **3** (36%) and 3-methoxy-4-cyclooctenone (**4**) (18%) as determined by gas liquid chromatography (g.l.c.) using hexadecane as internal standard. Dimer **2**, m.p. 174.5–175.0, was crystallized from an ethyl acetate solution of the irradiation mixture and was shown to be the same as the *trans-anti-trans* dimer isolated from the irradiation of **1** in benzene (10). The other dimer (**3**) could not be crystallized from the mother liquor after removal

[1]For Part I, see preceding paper.

Can. J. Chem. Downloaded from www.nrcresearchpress.com by 210.87.254.6 on 09/05/12
For personal use only.

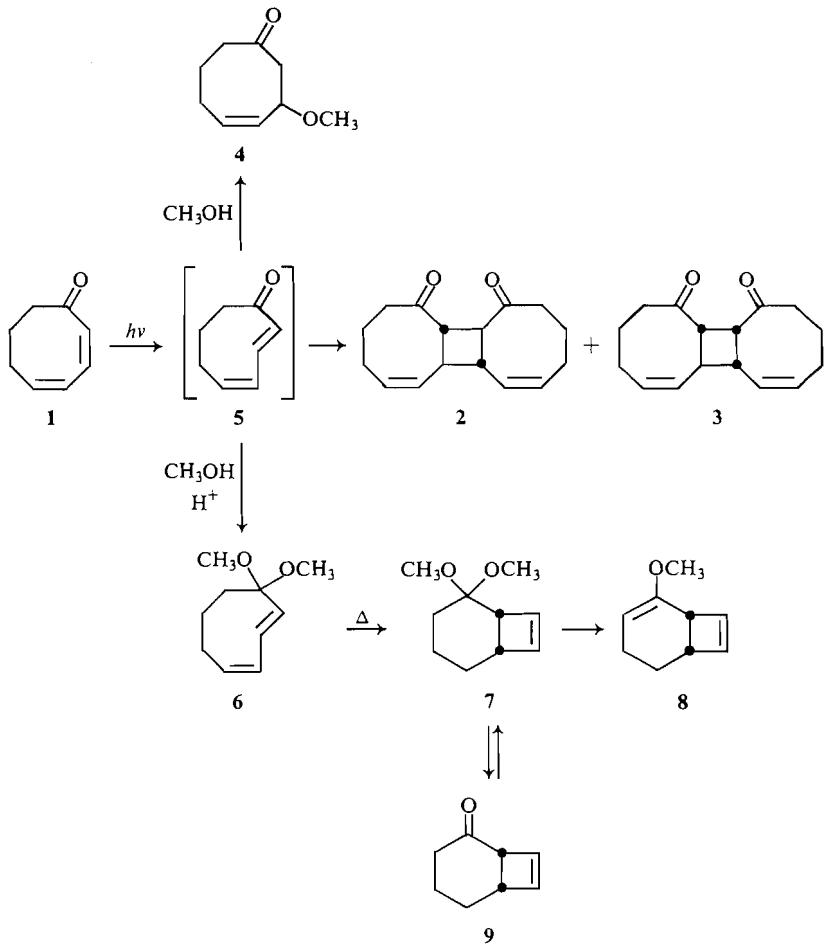

of **2** but its g.l.c. retention time and physical properties (after separation by g.l.c.) left no doubt that it was the *trans–cis* dimer, m.p. 89–90°, which was also obtained in the benzene irradiation (10). The irradiation was repeated using the conditions described by Cantrell and Solomon (3) (0.6% solution, Hanovia 450-W lamp, Pyrex filter) and essentially the same product distribution as outlined above was obtained. The earlier investigators had not reported (3) finding dimer **3** in their irradiation mixture. It should be noted that the ratio of dimers **2**:**3** was 44:56, the same as that found in the benzene and toluene irradiations (10).

When the irradiation was conducted in very dilute acidic methanol there was a dramatic change in the products formed. Irradiation of a 1% solution of **1** in acidic methanol (0.001 *N* HCl) with a 350 mμ source gave only a trace of the methoxyenone (**4**) and less than 10% combined yield of dimers **2** and **3**. But, g.l.c. analysis showed a new peak (~60%) with a retention time of 3 min relative to 10 min for **1** and 18 min for **4**. This volatile product was collected by g.l.c. and found to have the following spectral properties; i.r. no carbonyl absorption; n.m.r. (CCl_4) τ 3.94 (1H, d, $J = 3$ Hz, vinyl), 4.12 (1H, d, $J = 3$ Hz, vinyl), 5.38 (1H, q), 6.54 (3H, s, CH_3—O—), 6.78 (2H, broad s, —C(—)—H at ring fusion), 7.80–8.50 (4H, m, methylene); m.s. molecular ion at *m/e* 136. The n.m.r. spectrum of this compound exhibited some striking similarities to the cyclobutene protons in the spectra of bicyclo[4.2.0]oct-7-en-2-one (**9**) (11) and its ethylene ketal (12). Also, the τ 5.38 resonance is appropriate for the vinyl proton of an enol ether moiety in a 6-membered ring (13). On the basis of this spectral informa-

Can. J. Chem. Downloaded from www.nrcresearchpress.com by 210.87.254.6 on 09/05/12
For personal use only.

Can. J. Chem. Downloaded from www.nrcresearchpress.com by 210.87.254.6 on 09/05/12
For personal use only.

tion and further considerations to be discussed later, the enol ether structure **8** was assigned to this product.

Next it was necessary to explain the formation of **8** from the starting dienone **1**. Heating of dimethyl or diethyl ketals in the presence of a trace of acid is a known procedure for the preparation of enol ethers (13). Also, g.l.c. analysis of dimethyl ketals has been reported (14) to give enol ethers by elimination of methanol. Thus, the bicyclic ketal **7** is a logical precursor to **8**. A sample of **7** was prepared by ketalization of the known bicyclic ketone **9** (11) using trimethylorthoformate in acidic methanol. Injection of **7** onto the g.l.c. column gave only one peak which was collected and found to be identical to **8** thus proving that under our g.l.c. conditions elimination of methanol from **7** was occurring.

The origin of the bicyclic ketal must now be considered. Examination by t.l.c. (silica gel, 15% ether/petroleum ether) of the crude product from irradiation of **1** in acidic methanol revealed a major u.v. positive spot (R_f 0.5) different from **1** (R_f 0.3). Separation of this major band by preparative t.l.c. gave in 67% yield a product (**6**) which possessed the following spectral features: i.r. strong absorption in the region 1150–1050 and at 965 cm^{-1} and no carbonyl band; λ_{max} (CH_3OH) 233 mμ (ε 3150); n.m.r. (CCl_4) τ 3.48–3.96 (2H, m, vinyl), 4.23–4.65 (2H, m, vinyl), 6.83 (6H, s, $>C(OCH_3)_2$), 7.4–9.1 (6H, m, methylenes); m.s. molecular ion at *m/e* 168. The data suggests the compound is a conjugated diene containing a dimethyl ketal moiety. For purposes of comparison, the dimethyl ketal of **1** was prepared by reaction of the dienone with trimethylorthoformate in acidic methanol. This product was also purified by t.l.c. and was found to have quite different spectral properties than those presented above. The i.r. spectrum had no strong absorption in the 900–1000 cm^{-1} region, the u.v. spectrum (λ_{max} (CH_3OH) 239 mμ (ε 7380)) exhibited a much more intense absorption and the n.m.r. spectrum showed two methoxy singlets for the ketal moiety. The mass spectra of the two compounds also had some obvious differences. The u.v. spectra of *cis,cis*-1,3-cyclooctadiene (λ_{max} (cyclohexane) 228 mμ (ε 5620)) (15) and *trans,cis*-1,3-cyclooctadiene (λ_{max} 230.5 mμ (ε 2630)) (15) provided useful comparisons with the ketals. The i.r. spectrum of the *trans,cis*-diene showed strong absorptions at 952 and 970 cm^{-1} which were absent in the *cis,cis*-isomer (15). In addition, photoproduct **6** upon injection onto a g.l.c. column showed only one peak at 3 min which was shown to be identical to **8**, while the dimethyl ketal of **1** gave a peak at 10.5 min which analyzed for the expected composition. From all this evidence it was concluded that **6** must be the dimethyl ketal of *trans,cis*-2,4-cyclooctadienone. The strong band in its i.r. spectrum at 965 cm^{-1} is indicative of a *trans* double bond and the low extinction coefficient in the u.v. spectrum is indicative of a conjugated diene system in which the double bonds are forced into a non-planar conformation by strain (16).

Fonken and co-workers reported (17) that upon heating *trans,cis*-1,3-cyclooctadiene at 80° it isomerized quantitatively to bicyclo[4.2.0]oct-7-ene. If ketal **6** underwent a similar conversion it would be further evidence for the assigned structure. When **6** was heated in refluxing toluene (110°) for 1 h it was converted in >95% yield to the bicyclic ketal **7** as judged by i.r., n.m.r., and analytical t.l.c. Thus injection of **6** onto the g.l.c. column must have resulted in electrocyclic ring closure to **7** followed by elimination of methanol to give **8**.

We propose that **6** was formed from *trans,cis*-2,4-cyclooctadienone (**5**) by ketalization in the acidic methanol solution thus providing even more direct evidence for the existence of the reactive intermediate **5**. Presumably the driving force behind this reaction was the relief of strain in **5** by conversion of the sp^2 hybridized carbonyl carbon to the sp^3 ketal carbon. Another possible route to **6** could be photochemical *cis-trans* isomerization of the ketal of **1**, the latter being formed under the acidic reaction conditions. This possibility was eliminated when it was found that no ketal could be detected when **1** was allowed to sit in acidic methanol (0.001 *N* HCl) for several hours in the dark.

A further insight into the mechanism of the methanol irradiations was provided by some low temperature trapping experiments. A toluene solution[2] of **1** was irradiated at −78°, the u.v. source was turned off and dry neutral methanol

[2]In the preceding paper (10) it was shown that toluene was a suitable solvent for both low and room temperature irradiations.

Can. J. Chem. Downloaded from www.nrcresearchpress.com by 210.87.254.6 on 09/05/12
For personal use only.

was added to the irradiated solution, which was then allowed to warm to room temperature. Examination of the products by g.l.c. using an internal standard showed 7% of methoxyenone **4**, 16% dimer **2**, 22% dimer **3**, and the remainder was starting material. The experiment showed that **4** was indeed formed in a thermal reaction by the addition of methanol to the reactive intermediate **5**.

In a parallel experiment, acidic methanol (7×10^{-4} *N* HCl) was added to a toluene solution of **1** which had been irradiated at −78°. G.l.c. analysis of the products showed 20% of **8** (indicating 20% of **6** actually present in the reaction mixture), 12% combined yield of dimers **2** and **3** and the remainder was **1**. The experiment shows that the *trans,cis*-ketal **6** was formed by an acid catalyzed, ground state reaction of methanol with some reactive intermediate, namely **5**.

The rate of disappearance of **1** in dry methanol was about the same as that in benzene but was about twice that in acidic methanol (0.001 *N* HCl) using the standard irradiation conditions. Some of the inefficiency in these photoreactions is probably the result of thermal isomerization of **5** to starting dienone **1**. In the acidic methanol irradiation, acid catalyzed isomerization of **5** to **1** would result in the decreased rate of disappearance of **1** which was observed. Eaton similarly reported (18) the sensitivity of *trans*-2-cyclooctenone to traces of acid. In our acidic methanol irradiation the concentration of acid is very critical. At a concentration of 0.01 *N* HCl, the rate of disappearance of **1** is very markedly decreased while at 10^{-4} *N* HCl very little **6** is formed and the reaction resembles the normal neutral methanol irradiation.

Conclusions

Irradiation of 2,4-cyclooctadienone (**1**) in dry methanol resulted in the formation of methanol addition product **4** and dimers **2** and **3**. The latter dimer (**3**) had not been reported by previous investigators (3). Irradiation of **1** in acidic methanol (0.001 *N* HCl) gave a good yield of the strained ketal **6** plus a reduced yield of the two dimers. Low temperature trapping experiments showed that the precursor to all these products was the highly reactive *trans,cis*-2,4-cyclooctadienone (**5**), formed in a photochemical *cis–trans* isomerization from **1**. The acid catalyzed formation of ketal **6** illustrates a new and novel method for trapping reactive photochemical intermediates.

Experimental

Spectroscopic instruments and analytical and photochemical equipment were as described in the preceding paper (10). G.l.c. analyses and separations were performed on an Aerograph "Autoprep" Model A-700 using the following columns: column A, 6 ft × 0.25 in., 20% Carbowax 20M on 60/80 mesh Chromosorb W; column B, 6 ft × 0.25 in., 20% SE 30 on 60/80 mesh Chromosorb W. Spectro grade methanol was refluxed with magnesium for 4 h and distilled.

Irradiation of 1 in Neutral Methanol

Irradiation with a 350 mμ source of a solution of 1.2 g (0.01 mol) of **1** in 120 ml dry methanol in a Pyrex tube resulted in the disappearance of starting dienone within 4 h. The solvent was removed and the residue, upon trituration with ethyl acetate, gave a crystalline solid, m.p. 174.5–175.0°, which was shown to be dimer **2** by comparison with a sample from the benzene irradiation of **1** (10). Dimer **3** could not be crystallized from the mother liquor. The complete irradiation mixture was dissolved in chloroform and subjected to g.l.c. analysis (column B, 275°) with hexadecane as internal standard. Product distribution was as follows: 3-methoxy-4-cyclooctenone (**4**) (18%), whose spectral properties were the same as those previously described (3), and dimers **2** (28%) and **3** (36%), whose physical properties after g.l.c. separation were the same as reported in our preceding paper (10).

When 1.2 g (0.01 mol) of **1** in 200 ml dry methanol was irradiated in a Pyrex tube with a 450-W Hanovia type L lamp for 4 h as described by Cantrell and Solomon (3), essentially the same product distribution as detailed above was obtained.

Irradiation of 1 in Acidic Methanol

(*a*) A solution of 1.2 g (0.01 mol) of **1**, 9 μl (0.11 mmol) conc. hydrochloric acid and 120 ml dry methanol in a Pyrex tube was irradiated with a 350 mμ source for 8 h at which time less than 5% of **1** remained. The solvent was removed and the residue, upon g.l.c. analysis (column B, 275°) with internal standard hexadecane, showed less than 10% combined yield of dimers **2** and **3**. An additional g.l.c. analysis (column A, 136°) showed a new peak (~60%) with a retention time of 3 min, starting dienone **1** (< 5%) at 10 min and only a trace of methoxyenone **4** at 18 min. The product at 3 min, which was shown to be **8**, was collected by preparative g.l.c. (column A) and found to have the following spectral properties; i.r. (neat) 3030, 2900, 1650, 1370, 1212, 1158, 798, 780, 725 cm^{-1}; n.m.r. (CCl_4) τ 3.94 (1H, d, J = 3 Hz, vinyl), 4.12 (1H, d, J = 3, vinyl), 5.38 (1H, q, H—C=C—O—), 6.54 (3H, s, CH_3O—), 6.78 (2H, broad s, —C—H at ring fusion), 7.80–8.50 (4H, m, methylene); m.s. molecular ion at *m/e* 136.

Anal. Calcd. for $C_9H_{12}O$: C, 79.38; H, 8.89. Found: C, 79.46; H, 8.98.

(*b*) A solution of 194 mg (1.59 mmol) of **1**, 1.5 μl (0.018 mmol) conc. hydrochloric acid and 19 ml dry methanol in a uranium glass tube (10) was irradiated with a 350 mμ source for 8 h. The solvent was immediately removed at room temperature and the mixture was separated by preparative t.l.c. (15% dry ether/petroleum ether). The major u.v. positive band at R_f 0.5 was re-

moved and yielded 179 mg (67%) of ketal **6**; i.r. (CCl_4) 3010, 2925, 1635, 1138, 1107, 1075, 1057, 965, 680 cm^{-1}; λ_{max} (CH_3OH) 233 mμ (ε 3150); n.m.r. (CCl_4) τ 3.48–3.96 (2H, m, vinyl), 4.23–4.65 (2H, m, vinyl), 6.83 (6H, s, $>C(OCH_3)_2$), 7.4–9.1 (6H, m, methylene); m.s. molecular ion at *m/e* 168. G.l.c. analysis (column A, 136°) of this compound showed only one peak at 3 min which was identical to **8**. Although the ketal **6** is thermally and hydrolytically unstable the following analysis was obtained for the material separated by t.l.c.

Anal. Calcd. for $C_{10}H_{16}O_2$: C, 71.41; H, 9.92. Found: C, 71.84; H, 9.97.

Preparation of Bicyclic Ketal 7

A solution of 100 mg (0.82 mmol) bicyclic ketone **9** (11) and 110 mg (1.04 mmol) trimethylorthoformate in 0.25 ml of a 0.5% solution of *p*-toluenesulfonic acid in dry methanol was left at room temperature for 3 h. The solvent was removed at room temperature and the crude product was separated by preparative t.l.c. (15% dry ether/petroleum ether) to give 12 mg ketone **9** (R_f 0.30) and 66 mg (55% based on reacted ketone) bicyclic ketal **7** (R_f 0.45); i.r. (CCl_4) 3090, 3030, 2920, 1110, 1055, 713 cm^{-1}; n.m.r. (CCl_4) τ 3.81 (1H, d, J = 3 Hz, vinyl), 3.98 (1H, d, J = 3 Hz, vinyl), 6.88 (6H, s, $>C(OCH_3)_2$), 6.80–7.00 (2H, m, $-\overset{|}{\underset{|}{C}}-H$ at ring fusion), 8.00–8.60 (6H, m, methylene); m.s. molecular ion at *m/e* 168. G.l.c. analysis (column A, 136°) of this compound showed only one peak at retention time 3 min which was shown to be enol ether **8**.

Preparation of Dimethyl Ketal of 1

A solution of 300 mg (2.5 mmol) of **1** and 300 mg (2.8 mmol) trimethylorthoformate in 0.5 ml of a 1% solution of *p*-toluenesulfonic acid in dry methanol was left for 1.8 h at room temperature. The solvent was removed and the reaction mixture was separated by preparative t.l.c. (30% dry ether/petroleum ether) to give 73 mg (18%) of the dimethyl ketal of **1** (R_f 0.65); i.r. (CCl_4) 3010, 2930, 1630, 1218, 1152, 1108, 1090, 716 cm^{-1}; λ_{max} (CH_3OH) 239 mμ (ε 7380); n.m.r. (CCl_4) τ 3.8–5.1 (4H, m, vinyl), 6.48 (3H, s, $-OCH_3$), 6.81 (3H, s, $-OCH_3$), 7.5–9.1 (6H, m, methylene); m.s. molecular ion at *m/e* 168. G.l.c. analysis (column A, 136°) showed only one peak at retention time of 10.5 min.

Anal. Calcd. for $C_{10}H_{16}O_2$: C, 71.41; H, 9.92. Found: C, 71.82; H, 9.97.

Thermal Isomerization of Ketal 6

A solution of 50 mg ketal **6** in 5 ml dry toluene was heated to reflux for 1 h. The solvent was removed and examination of the residue by i.r., n.m.r., and analytical t.l.c. revealed that it consisted of >95% bicyclic ketal **7**.

Low Temperature Trapping Experiments

(*a*) A solution of 250 mg (2.04 mmol) of **1** and 125 mg hexadecane (internal standard) in 125 ml dry toluene was placed in a specially constructed low temperature apparatus (10) and irradiated at −78° with a 350 mμ source for 1.5 h. The u.v. source was turned off and 50 ml dry methanol was added with mixing. The solution was allowed to slowly warm to room temperature and the solvents were removed under reduced pressure. Examination of the products by g.l.c. (column A, 136°; column B, 160–275°) showed 7% methoxyenone **4**, 18% dimer **2**, 25% dimer **3** and the remainder was **1**.

(*b*) A solution of 250 mg of **1** and 125 mg hexadecane in 125 ml dry toluene was irradiated at −78° as described above and after turning off the u.v. source a solution of 4 μl conc. hydrochloric acid in 60 ml dry methanol was added with mixing. The solution was allowed to warm to room temperature and the solvents were removed. Examination of the residue by g.l.c. using the conditions as above showed 20% enol ether **8**, 12% combined yield of dimers **2** and **3** and the remainder was **1**. Analytical t.l.c. (15% dry ether/petroleum ether) indicated that **1** was the major component and that ketal **6** was present in about one-third the concentration of **1**.

The authors acknowledge financial support from the National Research Council of Canada.

1. H. Nozaki, M. Kurita, and R. Noyori. Tetrahedron Lett. 2025 (1968).
2. R. Noyori, A. Watanabe, and M. Katô. Tetrahedron Lett. 5443 (1968).
3. T. S. Cantrell and J. S. Solomon. J. Am. Chem. Soc. **92**, 4656 (1970).
4. R. Noyori, H. Inoue, and M. Katô. Chem. Commun. 1695 (1970).
5. L. L. Barber, O. L. Chapman, and J. D. Lassila. J. Am. Chem. Soc. **91**, 531 (1969).
6. H. Nozaki, M. Kurita and R. Noyori. Tetrahedron Lett. 3635 (1968).
7. J. K. Crandall and R. P. Haseltine. J. Am. Chem. Soc. **90**, 6251 (1968).
8. R. Noyori, Y. Ohnishi, and M. Katô. Tetrahedron Lett. 1515 (1971).
9. H. Nozaki, T. Mori, and R. Noyori. Tetrahedron, **22**, 1207 (1966).
10. G. L. Lange and E. Neidert. Can. J. Chem. This issue.
11. R. L. Cargill and J. W. Crawford. J. Org. Chem. **35**, 356 (1970).
12. H. O. House and T. H. Cronin. J. Org. Chem. **30**, 1061 (1965).
13. H. O. House and V. Kramar. J. Org. Chem. **28**, 3362 (1963).
14. K. P. Dimick (*Editor*). G.c. preparative separations. Varian, Palo Alto, California. 1966. pp. 10–16.
15. A. C. Cope and C. L. Bumgardner. J. Am. Chem. Soc. **78**, 2812 (1956).
16. E. A. Braude. Chem. Ind. (London) 1557 (1954).
17. K. M. Shumate, P. N. Neuman, and G. J. Fonken. J. Am. Chem. Soc. **87**, 3996 (1965).
18. P. E. Eaton and K. Lin. J. Am. Chem. Soc. **86**, 2087 (1964).

Can. J. Chem. Downloaded from www.nrcresearchpress.com by 210.87.254.6 on 09/05/12
For personal use only.

The Geometry of the Methyloxocarbonium Ion Trimer: A CNDO/BW Study

JAMES DOUGLAS PULFER[1] AND MICHAEL ANTHONY WHITEHEAD[2]

The Chemistry Department, McGill University, P.O. Box 6070, Montreal 101, Quebec

Received November 15, 1972

Within the Boyd–Whitehead CNDO theory three consistent methods were developed to calculate the carbon–oxygen infrared frequency of several oxocarbonium ions. The first method, type I, showed that the parameters of the CNDO/BW theory are not useful for predicting bond angles. Type II established a correlation between the C(α)—C bond length and the carbon–oxygen frequency. Type III predicted the correct trend for the homologous series of alkyloxocarbonium ions; however, the calculated frequency was consistently higher than experiment by 20–50 cm^{-1}. Conjugation effects were estimated by applying the above methods to the phenyloxocarbonium ion.

Variations on two possible configurations of the methyloxocarbonium ion trimer were studied. The protonated, planar diacetylmethenyloxocarbonium ion, Ac_2HCCO^+, was shown to be the most stable. A type II calculation estimated the C(α)—C bond to be about 1.37 Å. A type III calculation showed the possibility of the existence of the methyloxocarbonium ion dimer.

A l'intérieur de la théorie CNDO de Boyd–Whitehead, trois méthodes cohérentes furent développées pour calculer la fréquence d'absorption en infra-rouge du groupe carbone-oxygène pour plusieurs ions oxocarboniums. La première méthode, type I, a montré que les paramètres de la théorie CNDO/BW ne sont pas utiles lors de la prédiction des angles de liaison. Le type II a permis d'établir une corrélation entre la longueur du lien C(α)—C et la fréquence du lien carbone–oxygène. Le type III a permis de prédire la tendance correcte pour une série homologue d'ions alcoyloxocarboniums; cependant, la fréquence calculée a été constamment plus élevée que les valeurs expérimentales par 20 à 50 cm^{-1}. Les effets de conjugaison ont pu être estimés en appliquant les méthodes ci-haut mentionnées à l'ion phényl oxocarbonium.

Les changements dans les deux conformations possibles du trimère de l'ion méthyloxo carbonium ont été étudiés. La forme protonée et planaire de l'ion diacétylméthènyloxocarbonium, Ac_2HCCO^+, est la plus stable, comme il est démontré. Un calcul selon le type II a permis d'estimer que la longueur de la liaison C(α)—C est d'environ 1.37 Å. Un calcul du type III nous a permis de montrer la possibilité d'existence du dimère de l'ion méthyloxocarbonium. [Traduit par le journal]

Can. J. Chem., 51, 2220 (1973)

Can. J. Chem. Downloaded from www.nrcresearchpress.com by 210.87.254.42 on 09/05/12
For personal use only.

Introduction

There continues to be considerable scientific interest in the geometries and charge distributions of the alkyl-, acyl-, and aryloxocarbonium ions. These ions have been shown to be the active electrophillic reagents in Friedel–Crafts reactions. When Seel (1) first reported the presence of the stable, crystalline methyloxocarbonium tetrafluoroborate $(CH_3CO^+)(BF_4^-)$ salt it was thought (2, 3) that the principle acylating agent in Friedel–Crafts reactions was the linear methyloxocarbonium ion; however, no clear statement could be made on this problem for a number of reasons: Wuhrmann and Susz (4) were the first to report the presence of a weakly absorbing infrared frequency in the $CH_3COCl{\cdot}AlCl_3$ complex at 2200 cm^{-1}, in addition to the strongly absorbing frequency at 2300 cm^{-1}. Cook (5) showed that the 2200 cm^{-1} band was almost nonexistent in the freshly prepared complex, yet in a solution of nitrobenzene the 2300 cm^{-1} band was almost completely replaced by the one at 2200 cm^{-1}. Cassimatis *et al.* (6) have also reported that during attempts to recrystallize the methyloxocarbonium tetrachloroaluminate salt from liquid sulfur dioxide, the crystalline complex converted partly to an amorphous, less structured mass, and the presence of both frequencies was detectable from this material.

For the above reasons, further investigation into the chemistry of the methyloxocarbonium ion has been necessary. Germain *et al.* (7) have isolated two chemically distinct salts from a mixture of acetyl chloride and aluminium trichloride: the familiar methyloxocarbonium tetrachloroaluminate (**1**) and the trimer salt. They postulated that the trimer is the protonated, planar diacetylmethenyloxocarbonium ion, Ac_2HCCO^+; how-

[1]Holder of an NRCC Bursary, 1971–1972.

[2]Author to whom all correspondence should be addressed. Holder of an NRCC Travel Fellowship, 1971–1973.

Can. J. Chem. Downloaded from www.nrcresearchpress.com by 210.87.254.42 on 09/05/12
For personal use only.

ever, they did not discount the possibility that it might be the diacetylmethyloxocarbonium ion, Ac_2CHCO^+.

The skeleton structure and electron charge distribution of the cation in **1** is thought to be known (8, 9); the same cannot be said of the trimer. LeCarpentier and Weiss (9) are in the process of elucidating the crystal structure of the recrystallized tetrachloroaluminate salt of the trimer by X-ray techniques. One of the purposes of the present paper is to theoretically investigate the relative stability of the two most likely conformations of the trimer by means of the Boyd–Whitehead (10, 11) bond length dependent CNDO theory. The two principle structures of the trimer considered have been shown in Figs. 1, 2, and 3.

To discuss the possible conformations of the trimer, it was necessary to study the stereochemistry and charge structures of some related oxocarbonium ions and to try to correlate the geometry of these structures to the observed infrared frequency in a theoretical manner. The phenyloxocarbonium ion and the homologous series of alkyloxocarbonium ions, starting with the methyloxocarbonium ion, were particularly useful. Two major attempts have been put forward to elucidate the structure and electron configuration of the methyloxocarbonium ion. Boer (12) did an X-ray study of the crystal structure of the methyloxocarbonium hexafluoroantimonate salt. Based on the results of that work, the NEMO method (13) was used to try to obtain the electron configuration of the ion. In this calculation it was assumed that the hydrogen atoms were in the tetrahedral positions. An interesting result was obtained. Carbon atom C_2, in Fig. 4, had a formal positive charge of

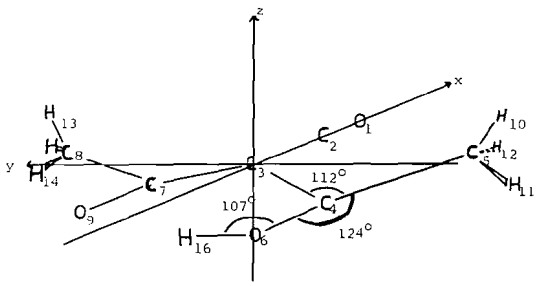

FIG. 1. Coordinates for the protonated planar acetyl- and diacetylmethenyloxocarbonium ions. In the former case, the C_7 atom is replaced by a hydrogen atom. All atoms except the hydrogens, are in the x–y plane.

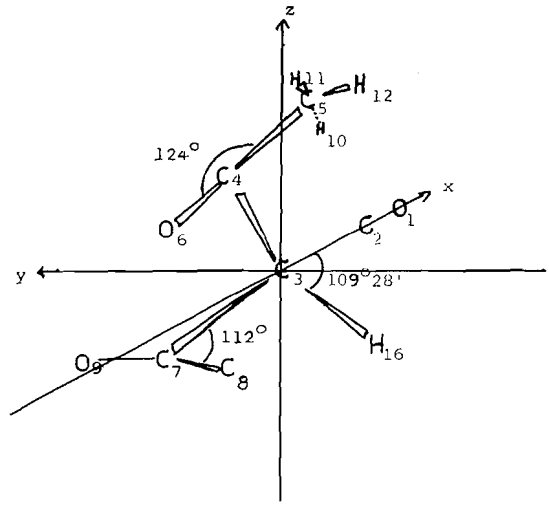

FIG. 2. Coordinates for the diacetylmethyloxocarbonium ion. The $O_6C_4C_5$ plane is rotated 60° to the x–z plane; hydrogen atoms 11 and 12 are staggered with respect to the C_4—O_6 bond. The atoms C_1, C_2, C_3, and C_4 are in the x–z plane. The C_7—C_8 bond bisects angle C_7—C_3—H_{16}.

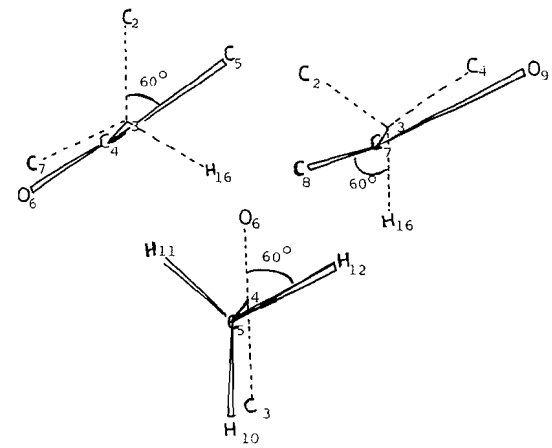

FIG. 3. The sterographic choice of angles used to generate the coordinate system of the diacetylmethyloxocarbonium ion.

1.18 electrons on it. Boer's X-ray work showed that the C_2—C_3 bond length was 1.385 Å.

Veillard and co-workers (8) performed a series of *ab initio* calculations on the methyloxocarbonium ion where the geometry of the C_2—C_3 bond was optimized. After a reasonable value was obtained for this bond, the positions of the three methyl hydrogens were optimized. Both optimizations were carried out with respect to the total energy of the ion. These calculations showed

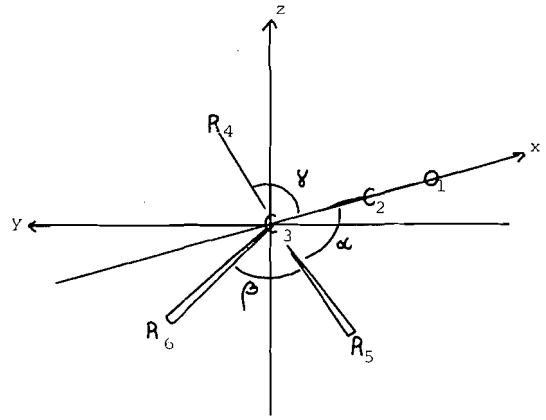

FIG. 4. The coordinates of the alkyloxocarbonium ions: $R_4 = R_5 = R_6$ = Hydrogen, CH_3CO^+; $R_4 = CH_3$, $R_5 = R_6 = H$, $C_2H_5CO^+$; $R_4 = R_5 = CH_3$, $R_6 = H$, $i\text{-}C_3H_7CO^+$; $R_4 = R_5 = R_6 = CH_3$, $t\text{-}C_4H_9CO^+$.

that the C_2—C_3 bond was longer than that reported by Boer, around 1.452 Å. Le Carpentier and Weiss (9) have recently verified this value by X-ray analysis. The *ab initio* charge distribution showed that carbon atom C_2 had a net positive charge of 0.605 electrons. This appears to be a much better estimate, the rest of the formal positive charge being delocalized onto the three equivalent hydrogen atoms in the molecule–ion. The optimum position of the hydrogen atom was found to be the tetrahedral position.

The structures and electron configurations of the other cations in the homologous series are generally less well known. Le Carpentier and Weiss (14) have published some refined results of X-ray studies done on the structure of the ethyl- and isopropyloxocarbonium ions. The structure of the latter ion does not differ significantly from their earlier results (15). The *ab initio* charge distribution of the isopropyloxocarbonium ion has been calculated using a contracted set of gaussian s and p type orbitals (8). The charge on the carbon atom, C_2, was found to be +0.733, and the C_2—C_3 bond was 1.46 Å. There is no X-ray analysis of the tert-butyloxocarbonium hexafluoroantimonate salt.

Veillard and co-workers (8) have pointed out that the molecular structure of methyl cyanide is very similar to the corresponding isoelectronic methyloxocarbonium ion. Corresponding structural data is not available for isobutyronitrile; however, the average length of the C_2—C_3 bond in nitriles of the type $-\overset{|}{\underset{|}{C_3}}-C_2\equiv N$ is around 1.464 Å (16) which is 0.014 Å longer than the length of the corresponding bond in the isopropyloxocarbonium ion (14). The difference is not large and can be partly explained by the higher positive charge located on carbon atom C_2 of the oxocarbonium ion. As a result, the C_2—C_3 bond of the tertbutyloxocarbonium ion was assigned a length of 1.46 Å, which is the same as the comparable bond in tert-butyl cyanide (17).

In addition to these ions, the phenyloxocarbonium ion was studied, in order to estimate how well the various types of calculations might predict the geometry and infrared stretching frequency of a highly conjugated system. The X-ray structure of the phenyloxocarbonium hexafluoroantimonate salt has not been done although the X-ray structure of the covalent complex $Cl_5Sb—O=\overset{|}{\underset{Cl}{C}}—C_6H_5$ has (18). In this complex, the corresponding C_2—C_3 bond was found to be 1.51 Å, an elongated π bond. A much shorter bond would be expected for the ionic salt; consequently, this bond had to be estimated from available data for the isoelectronic phenyl cyanide molecule. Two independent microwave studies of this molecule (19, 20) have shown C_2—C_3 values of 1.4509 Å and 1.419 Å. The shorter length was chosen for these calculations because of the shortening effect of the positive charge at C_2 (Fig. 5).

The infrared spectra are known for all the oxocarbonium ions, including the trimer. The possible existence of the methyloxocarbonium ion dimer was also investigated. No infrared data are available to prove the existence of this ion in solution; however, there is the possibility that the stretching frequency of it might be masked by the stretching frequency of the trimer.

The Calculation

The molecular orbitals and the total energy of each of the organic oxocarbonium ion conformations was evaluated within the LCAO-MO-CNDO-BW approximation (10, 11). The core resonance integral was evaluated as an "overlap ionization potential" between two atomic orbitals k and l on atoms A and B, *i.e.*

Can. J. Chem. Downloaded from www.nrcresearchpress.com by 210.87.254.42 on 09/05/12
For personal use only.

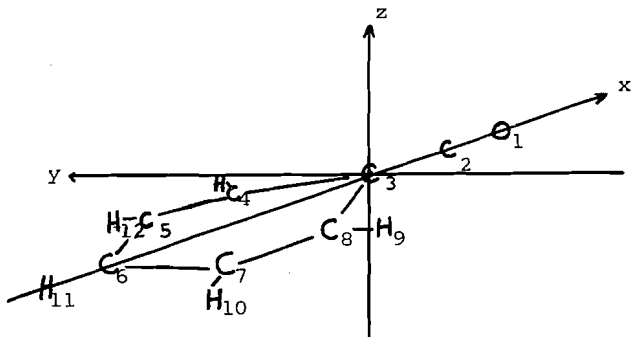

FIG. 5. Coordinates for the aryloxocarbonium ion $C_6H_5CO^+$. $\angle C_4C_3C_8 = 120°$, $\angle C_3C_8H_9 = 120°$, $\angle C_3C_2O_1 = 180°$.

$$[1] \qquad H_{kl} = \beta_{AB}\{I_k + I_l\}S_{kl}$$

Here I_k is the Hinze–Jaffé valence state ionization potential of the kth atomic orbital and S_{kl} is the overlap between the two Slatar type atomic orbitals k and l.

In these calculations, the nuclear–nuclear core repulsion terms between two atoms A and B, N_{AB}, was evaluated as a weighed average between the point charge nuclear repulsion term and the appropriate electron charge interaction between atoms A and B

$$[2] \quad N_{AB} = \lambda_{AB}(Z_AZ_B/R_{AB}) + (1 - \lambda_{AB})Z_AZ_B\gamma_{AB}$$

Here λ_{AB} was defined as

$$[3] \qquad \lambda_{AB} = \exp(-\alpha_{AB}R_{AB})$$

The electron–electron repulsion integral γ_{AB}, in eq. 2, is an average electron repulsion integral between two atoms A and B. It was evaluated by Ohno's method (21), and modified by Sichel and Whitehead (22) to take into account the relative proportions of γ_{ss}, γ_{sp}, γ_{pp}, and $\gamma_{pp'}$, required to yield a homopolar bond within the CNDO approximation.

In Boyd's thesis (23) it is shown that if eqs. 1 and 2 are used to calculate the core resonance integrals and the nuclear–nuclear core repulsion integrals then slightly better and more consistent force constants were obtained than by other methods of calculating H_{kl} and N_{AB}. The parameters, α_{AB} and β_{AB} were determined from diatomic molecules where the internuclear distance was accurately known. The α_{AB} and β_{AB} used in the present calculations were evaluated in the manner outlined above. This set of characteristic constants have been designated parameter set I by Boyd and Whitehead.

In the current calculations the CNDO/BW computer program was fitted with a subprogram for efficiently calculating the optimum geometry of the molecule. This subprogram makes use of a method first developed by Fletcher and Powell (24). A gradient vector for any initially selected geometry was computed for several molecular geometry parameters. From this gradient vector, the subprogram determines the direction of the steepest descent and steps in that direction. The stepsize of each parameter is determined by the size of the partial derivatives of each of the variables. At the new position, another gradient vector and a second total energy were calculated. If the program has stepped too far then a quadratic fit of the points available is made and a new position of the minimum energy found. The process is repeated until the total minimum energy agreed to a specified tolerance, 1×10^{-5}. The method has quadratic convergence and has proven to be superior to other existing methods (24).

Once the optimum geometry was calculated by this method, the several variables employed in the calculation were frozen and the bond length of the carbon oxygen bond was set at two positions bracketing the lowest energy position. A useful stepsize was 0.02 Å. At this stepsize, the anharmonic nature of the potential well of the carbon–oxygen bond was minimized. This made it possible to calculate the force constant using only three points. If the shape of the potential energy curve was badly skewed, *i.e.* one of the terminal points on the interval of interest had a much higher energy than the other, then more points were calculated and a higher order polynomial was used to approximate the total energy function.

Can. J. Chem. Downloaded from www.nrcresearchpress.com by 210.87.254.42 on 09/05/12
For personal use only.

Can. J. Chem. Downloaded from www.nrcresearchpress.com by 210.87.254.42 on 09/05/12
For personal use only.

The interpolating polynomial was the Newton forward difference polynomial (25). The total energy of the molecule was expressed as a function of the carbon–oxygen bond length.

$$[4]\quad E(s) = E_1 + \frac{s}{1!}\Delta E_1 + \frac{s(s-1)}{2!}\Delta^2 E_1 + \frac{s(s-1)(s-2)}{3!}\Delta^3 E_1 + \ldots$$

Δ is the forward difference operator defined as

$$[5]\quad \Delta^n E_1 = \Delta^{n-1} E_2 - \Delta^{n-1} E_1$$

In general, E_m is the total energy of the ion corresponding to a carbon–oxygen bond length x_m where

$$[6]\quad x_m = x_e + \{(n + 1 - 2m)/2\}h, \qquad n \text{ odd}$$

The equilibrium bond length, x_e, was usually the value calculated by the Fletcher–Powell minimization procedure, n is the total number of points in the interpolating polynomial and h is the stepsize between various consecutive points. The variable s, in eq. 4, is a simple function of the bond length x where

$$[7]\quad x = x_e + sh$$

Equation 4 yields a simple relationship for the second derivative of the energy with respect to the carbon–oxygen bond length if three interpolating points were used.

$$[8]\quad \frac{\partial^2 E}{\partial x^2} = \frac{\Delta^2 E_1}{h^2}$$

If the bond has a large degree of anharmonic character to it, then further points must be included in the interpolating polynomial and an equilibrium bond length must be calculated in order to evaluate the second derivative. For most cases, eq. 8 was sufficient to numerically evaluate the second derivative.

Let k_{CO} be the force constant of the carbon–oxygen bond. The second derivative was identified with the force constant.

$$[9]\quad k_{CO} = \{\Delta^2 E_1/h^2\} \cdot K$$

Here K is a conversion factor, from eV/Å^2 to ergs/cm^2. This force constant was used to calculate the infrared stretching frequency.

$$[10]\quad \bar{\nu}_{CO} = \frac{1}{2\pi ch}\sqrt{\frac{\Delta^2 E_1 \cdot K}{\mu_{CO}}}$$

The constant c is the speed of light and μ_{CO} the reduced mass of the carbon–oxygen bond; h is the stepsize mentioned previously.

Results

In order to calculate a consistent carbon–oxygen infrared stretching frequency for a wide range of organic oxocarbonium ions a systematic approach had to be developed. The methyl-, ethyl-, isopropyl-, tert-butyl-, and phenyloxocarbonium ions were used as a basis for testing the three different methods of calculating this particular frequency. In the first method, designated type I, all nearest neighbor geometries that might have an influence on the electron charge structure of the linear chain O_1—C_2—C_3, seen in Fig. 4, were simultaneously varied so as to achieve the most stable geometry. Consequently, all bond lengths shown in Fig. 4 were varied, with the exception of the carbon–hydrogen bonds in the methyl radicals (R_4, R_5, and R_6). These were fixed at 1.09 Å. The bond angles α, β, and γ were also varied at the same time. The resulting geometries for the first three ions mentioned in this series have been presented in Table 1 along with the total energy minimum.

The carbon–oxygen bonds for the methyl- and ethyloxocarbonium ions have been found to be slightly longer (~0.018 Å) than those in the literature; and for the isopropyloxocarbonium ion the calculated carbon–oxygen bond has been shown to be insignificantly longer (~0.008 Å). In general, the slightly longer carbon–oxygen bond lengths are mainly the result of an overestimation of the core nuclear–nuclear repulsion energy terms in the Boyd–Whitehead CNDO theory. In Boyd's thesis (23) there was a discussion of this problem for the carbon monoxide molecule, and the singly ionized carbon monoxide ion. The core nuclear–nuclear repulsion energy terms for carbon monoxide were calculated using eq. 2, and were compared to the Morse potential curve. The calculated values were shown to be consistently too large for all but the equilibrium internuclear distance (1.128 Å). As a consequence, *cataris parebus*, any overestimation of the core repulsion terms will result in an overestimation of the subsequently calculated bond length. Boyd's thesis also shows that parameter set I overestimates the correct bond length for the ionized carbon monoxide molecule by 0.012 Å. These results imply that, within the limitations

TABLE 1. A summary of the bond lengths and angles of the alkyloxocarbonium ions yielding a minimum total energy

RCO$^+$	Molecular geometries Å	Type of calculation I*	II†	III‡	Experimental	Reference
CH_3CO^+	$R(C_2—O_1)$	1.124	1.125	1.124	1.108	9
	$R(C_3—C_2)$	1.471	1.452	1.471	1.452	9
	$R(C_3—H)$	1.101	1.098	1.101	1.09	8
	$\alpha = \beta = \gamma$	109°30′	109°30′	109°28′		
	E_T/eV	−640.3052	−640.3121	−640.3052		
$C_2H_5CO^+$	$R(C_2—O_1)$	1.118	1.130	1.123	1.099	14
	$R(C_3—C_2)$	1.500	1.420	1.488	1.435	14
	$R(C_3—H_5)$	1.110	1.110	1.096	1.09	8
	$R(C_3—CH_3)$	1.572	1.572	1.572	1.550	14
	α	100°36′	100°36′	109°28′		
	β	109°59′	109°59′	109°28′	109.3°§	26
	γ	111°14′	111°14′	109°28′	110.5°	26
	E_T/eV	−803.4625	−803.3632	−803.4126		
i-$C_3H_7CO^+$	$R(C_2—O_1)$	1.124	1.131	1.125	1.116	14
	$R(C_3—C_2)$	1.515	1.440	1.506	1.450	14
	$R(C_3—H_6)$	1.121	1.121	1.113	1.107‖	29
	$R(C_3—CH_3)$	1.570	1.570	1.580	1.551	14
	α	87°12′	87°12′	109°28′	108.3°	14
	β	105°38′	105°38′	109°28′		
	γ	112°12′	112°12′	109°28′	108.3°	14
	E_T/eV	−966.3353	−966.2589	−966.1159		
t-$C_4H_9CO^+$	$R(C_2—O_1)$			1.129	1.160§	17
	$R(C_3—C_2)$			1.460	1.460	17
	$R(C_3—CH_3)$			1.570	1.540	17
	$\alpha = \beta = \gamma$			109°28′	109.5°	17
	E_T/eV			−1112.7322		

*All important geometries were varied, both bond lengths and angles.
†The bond angles found in the type I calculation were frozen; the $C_2—C_3$ bond length taken from experiment; and all other important geometries were varied.
‡The bond angles were fixed at ideal angles: $O_1—C_2—C_3 = 180°$; $C_2—C_3—R_4 = 109°28'$ where R_4 is H— or CH_3—; and the important bond lengths were varied to find a global energy minimum.
§These results are for the isoelectronic nitrile.
‖Cyclopropyl cyanide.

of the theory, the carbon–oxygen bond lengths calculated for the alkyloxocarbonium ions are in reasonably good agreement with experiment.

The carbon–carbon bond lengths presented in Table 1 are also consistently overestimated when compared to experiment. This is primarily due to an overestimation of the core repulsion terms as well. For the two oxocarbonium ions with methyl groups substituted for hydrogens at the C_3 position, the average overestimation for the carbon–carbon $C_2—C_3$ bond is 0.08 Å. The observation implies that in chemically similar systems, it may be possible to apply this overestimation as a correction to any carbon–carbon bond length computed by the Boyd–Whitehead CNDO theory.

The computed angles of the three ions studied by type I calculations were interesting. The angles of the methyloxocarbonium ion were found to be very close to the ideal. This is the same result as was found by Veillard and co-workers (8). In the case of the ethyloxocarbonium ion the angles are close to those found for the isoelectronic ethyl cyanide molecule (26). There is a slight widening of the H—C—H angle, probably due to the increase in the angle γ, which is the result of the increase in the non-neighbors electron–electron repulsion terms between the methyl group and the linear carbon–carbon–oxygen skeleton chain $C_3—C_2—O_1$. The angles found for the isopropyloxocarbonium ion show that the single hydrogen attached to the C_3 carbon atom has floated to a position that allows it to bond with maximum overlap to the carbon p_y atomic orbital. This calculated result arises because the Boyd–Whitehead theory was not parameterized to take non-neighbor interactions explicitly into account (10, 11, 23). As a result,

Can. J. Chem. Downloaded from www.nrcresearchpress.com by 210.87.254.42 on 09/05/12
For personal use only.

Can. J. Chem. Downloaded from www.nrcresearchpress.com by 210.87.254.42 on 09/05/12
For personal use only.

there is a general tendency to overestimate non-neighbor repulsive forces. In the case of the hydrogen atom this has lead to the anomalous result where the angle α is 87°.

The two methyl groups experience roughly the same electron–electron repulsions from the linear carbon–carbon–oxygen C_3—C_2—O_1 systems as did the methyl group in the ethyloxocarbonium ion, as a result the movement of the hydrogen atom to the energetically more stable position has allowed the angle γ to widen further than in the case of the ethyloxocarbonium ion. The angle β has decreased, when compared to the ethyloxocarbonium ion. This was possible because of the significant lengthening of the carbon–hydrogen bond.

Type I calculations do not reproduce a consistent trend in the observed carbon–oxygen infrared frequency of the methyl-, ethyl-, and isopropyloxocarbonium ions. Figure 6 shows that the curve plotted from the calculated infrared frequencies does not consistently reproduce the shape of the experimental curve. Both the ethyl- and the isopropyloxocarbonium ions gave frequencies larger than necessary to reproduce a smooth, consistent approximation to the experimental curve. Consequently, as a method of calculating the frequency of the carbon–oxygen bond, the type I calculation proved to be generally unacceptable. The shape of the total energy surface of the carbon–oxygen bond is not well reproduced by type I calculations, even though this type of calculation generally gives the lowest possible energy. As was previously pointed out, the inconsistency of this type of calculation may be partly the result of parameterization. The CNDO/BW theory has been parameterized for bond length dependence and not for non-neighbor dependence. A new, greatly expanded set of parameters would have to be developed, to take into account the non-neighbor effects.

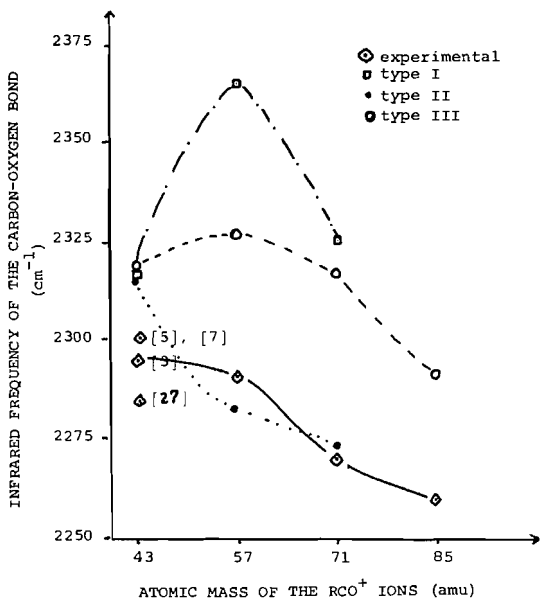

FIG. 6. The frequency of the carbon–oxygen bond as a function of the atomic mass of the alkyloxocarbonium ions where R = CH_3, C_2H_5, i-C_3H_7, t-C_4H_9.

A second method, type II, was developed. The length of the carbon–carbon bond adjacent to the carbon–oxygen bond has a critical effect on the shape of the total energy surface of the ions in the region of the carbon–oxygen bond. This has been described by many authors (6, 7). The extent of the conjugation along the carbon–carbon–oxygen (C_3—C_2—O_1) chain directly affects the frequency of the carbon–oxygen bond. The smaller the conjugation effects, the higher the frequency. For example, the frequency of the methyloxocarbonium ion bond is around 2300 cm^{-1} (3, 7, 27) whereas the phenyloxocarbonium ion carbon–oxygen frequency has been measured to be 2212 cm^{-1}.

Those observations can be rationalized by looking at the gross charge structure of the carbon–carbon–oxygen system. The bulk of the positive charge resides on the carbon atom bonding with oxygen. Typical results have been presented in Table 2. The calculated value for the methyloxocarbonium ion, +0.73 compares favorably with the *ab initio* result obtained by Veillard and co-workers (8) which was +0.605. This high positive charge is thought to be responsible for the high carbon–oxygen frequency observed for the methyloxocarbonium ion. The observed frequency is about 160 cm^{-1} higher than that of the carbon monoxide molecule. The major difference between these two stretching frequencies is the difference in the positive charge on the carbon atom. Any change in this high positive charge causes a corresponding change in the net negative charge on the oxygen atom. In Table 2 it can be seen that the total differential charge density on the oxygen atom increases regularly as the positive charge on the carbon atom C_2 decreases. In the limiting case, carbon monoxide

TABLE 2. Charge distributions from type III CNDO/BW calculations on a homologous series of alkyloxocarbonium ions (RCO^+) where R is CH_3-, C_2H_5-, *i*-C_3H_7-, and *t*-C_4H_9-

Atomic basis	Symmetry	CH_3CO^+	$C_2H_5CO^+$	*i*-$C_3H_7CO^+$	*t*-$C_4H_9CO^+$
O_1	σ	3.1600	3.1747	3.1858	3.1800
	π	3.0134	3.0179	3.0268	3.0585
	σ + π	6.1734	6.1926	6.2126	6.2384
C_2	σ	2.1322	2.1714	2.2057	2.1936
	π	1.1336	1.1255	1.1196	1.1438
	σ + π	3.2658	3.2969	3.3253	3.3374
C_3		4.1655	4.1001	4.0779	3.9874
CH_3(methyl)*			4.0881	4.0776	4.1464
H_6		0.7984	0.8342	0.8657	
(C)H_3†			0.8968	0.9031	0.9002
(C)H_3‡			0.8602	0.8755	0.8654
C_2—O_1§	σ	−0.3821	−0.3699	−0.3638	−0.3757
	π_y	0.8392	0.8421	0.8290	0.8075
	π_z	0.8392	0.8348	0.8420	0.8288
	σ + π	1.2963	1.3069	1.3072	1.2606
C_3—C_2	σ	0.1097	0.1112	0.1095	0.1203
	π_y	0.2672	0.2535	0.2880	0.2925
	π_z	0.2672	0.2632	0.2258	0.2687
	σ + π	0.6441	0.6279	0.6234	0.6815

*Charge on methyl carbon.
†Hydrogen towards carbon–oxygen bond (staggered).
‡Hydrogen away from carbon–oxygen bond.
§Bond order.

would be expected to have the largest total differential charge on the oxygen atom. In preliminary calculations this was the case. The presence of the positive charge has the effect of equalizing the electronegativities of the oxygen and carbon atoms. The result is a higher carbon–oxygen bond order in the oxocarbonium ions than in carbon monoxide. This implies a larger force constant and a higher frequency; all observed frequencies of the oxocarbonium ions are higher than carbon monoxide.

Conjugation of the skeleton chain delocalizes the positive charge on the carbon atom and, as a consequence, lowers the stretch frequency towards that of the free carbon monoxide frequency. A comparison of the results for the planar protonated diacetylmethenyloxocarbonium ion, Ac_2HCCO^+, with those for the tetrahedral case, shown in Table 3, supports the above arguments. The conjugated species has a larger negative charge on the oxygen atom and a smaller total bond order for the carbon–oxygen bond. The calculated infrared stretching frequencies, in Table 4, show that the conjugated ion has a much lower stretching frequency than the tetrahedral case.

For the above reasons, type II calculations were devised as an improvement on the type I calculations and as a method for correlating the C_2—C_3 bond length to the observed frequency. The extent of the conjugation of the carbon–carbon–oxygen (C_3—C_2—O_1) skeleton chain is governed, in large part, by the length of the carbon–carbon bond, and as was previously pointed out, the bond length dependent theory overestimates the carbon–carbon bond lengths. Consequently, in type II calculations, the experimental bond length, when available, or a reasonable estimate of it, based on microwave studies of the isoelectronic alkyl- or phenyl cyanides was substituted. The experimental bond lengths ought to increase the degree of conjugation of the chain; and lower the calculated frequency of the carbon–oxygen bond provided all other aspects of the calculation remain the same. In the type II calculations, no attempt was made to vary the bond angles, those found in type I calculation were used without change. The carbon–oxygen and carbon–radical bonds, *i.e.* C_3—R_4, C_3—R_5, and C_3—R_6, were simultaneously varied to find a new energy minimum. The calculated infrared frequencies were placed in Table 4. In general, the frequencies have been lowered to values very close to experimental; however, Fig. 6 shows that

Can. J. Chem. Downloaded from www.nrcresearchpress.com by 210.87.254.42 on 09/05/12
For personal use only.

TABLE 3. The results of CNDO/BW calculations on a number of conjugated acyl and phenyloxocarbonium ions (RCO^+) where R is acetylmethenyl-, diacetylmethenyl-, diacetylmethyl-, and the phenyl- radicals

Atomic basis	Symmetry	$AcHCHCO^+$ Type III	Ac_2HCCO^+ Type II_2	Ac_2HCCO^+ Type III	Ac_2CHCO^+ Type III	$C_6H_5CO^+$ Type II_2
O_1	σ	3.1578	3.1464	3.1600	3.1684	3.1629
	π	3.1076	3.1736	3.1175	3.0715	3.1136
	σ + π	6.2655	6.3199	6.2776	6.2399	6.2755
C_2	σ	2.1299	2.0855	2.1484	2.1604	2.1084
	π	1.1473	1.2019	1.1483	1.1476	1.1694
	σ + π	3.2773	3.2874	3.2967	3.3080	3.2778
C_3	σ	1.9171	1.9923	1.9427	2.0073	1.9042
	π	2.5190	2.4469	2.5048	2.2948	2.2208
	σ + π	4.4361	4.4392	4.4475	4.3022	4.1251
C_4		3.4100	3.3467	3.3971	3.4599	3.9212
C_5		4.1760	4.3405	4.1824	4.1754	4.0460
O_6 (or C_6)		6.4381	6.4730	6.5212	6.3614	3.9117
H (planar)		0.8135			0.8376*	*o* −0.9102
						m −0.8815
						p −0.8919
H_{16}^+		0.5746	0.5101	0.5125		
C_2—O_1†	σ	−0.3917	−0.4161	−0.2598	−0.2788	−0.5072
	π_y	+0.8494	+0.8308	+0.8390	+0.8049	+0.8193
	π_z	+0.7374	+0.6775	+0.7393	+0.8181	+0.7548
	σ + π	+1.1951	+1.0922	+1.3184	+1.3442	+1.0669
C_3—C_2	σ	−0.1083	−0.1347	−0.4071	−0.5627	−0.1632
	π_y	+0.2084	+0.2548	+0.2104	+0.3337	+0.2828
	π_z	+0.5142	+0.6039	+0.5083	+0.3034	+0.4532
	σ + π	+0.6143	+0.7240	+0.3116	+0.0744	+0.5728

*The tetrahedral hydrogen atom.
†Bond order.

TABLE 4. Three different methods of calculating the carbon–oxygen infrared vibrational frequency of several oxocarbonium ions are compared with experiment

RCO^+	Experimental $\bar{\nu}(cm^{-1})$	Reference	I	II		III	
				Type II_1*	Type II_2†	C_3Tetrahedral	C_3Planar
CH_3CO^+	2300	7	2319	2314		2319	
$C_2H_5CO^+$	2290	3	2364	2283		2326	
i-$C_3H_7CO^+$	2270	3	2325	2273		2317	
t-$C_4H_9CO^+$	2260	3				2292	
$C_6H_5CO^+$	2212	3		2277	2216		2305
$AcHCHCO^+$							2265
Ac_2HCCO^+	2200	7			2212		2234
Ac_2CHCO^+						2278	

*The C_2—C_3 bond length from experimental data, except the phenyloxocarbonium ion.
†The C_2—C_3 bond length estimated.

the correct trends are not predicted by this method. It does show that if the correct carbon–carbon bond length is substituted then reasonable values, close to the observed infrared frequency, could be calculated.

A third method, type III, was devised. The CNDO/BW theory was parameterized for bond length dependence. This parameterization took no account of angular correlation between non-neighbor groups. This implied that angular variation in CNDO/BW calculations might have little meaning. As a consequence, idealized chemical bond angles might be just as reasonable as those obtained by an explicit calculation. The concept of an ideal chemical bond is a simple one. If a chemically related system has nearly tetra-

Can. J. Chem. Downloaded from www.nrcresearchpress.com by 210.87.254.42 on 09/05/12
For personal use only.

Can. J. Chem. Downloaded from www.nrcresearchpress.com by 210.87.254.42 on 09/05/12
For personal use only.

hedral bond angles, then type III calculations would be set up to fix the bond angles in an ideal tetrahedral position. For example, the nearly tetrahedral bond angles of the isoelectronic ethyl cyanide molecule would be a good indication of the ideal angles for the ethyloxocarbonium ion. They would be tetrahedral. In type III calculations, the bond lengths of the carbon–oxygen C_2—O_1, carbon–carbon C_2—C_3, and carbon–radical C_3—R_4, C_3—R_5, and C_3—R_6 bonds were simultaneously varied to find a global energy minimum. The resulting frequencies are uniformly higher than the experimental ones, as can be seen in Fig. 6; however, the trend in the experimental frequencies was reproduced. Of the three methods considered, type III calculations have shown the most consistent results for reproducing the experimental trend of the observed infrared frequencies. The results of the type III CNDO/BW calculations are presented in Tables 1, 2, and 4. If the methyloxocarbonium ion is omitted as a special case, then type III calculations consistently yield frequencies that are about 35 cm^{-1} higher than experiment.

A further calculation could be devised whereby the carbon–carbon C_2—C_3 bond length could be fixed at a chemically reasonable value and the other bond lengths varied along the same idealized angles as were used in type III calculations. This method was used on the phenyloxocarbonium ion and the trimer. It is, in fact, a modification of the type II method. The drawback with this calculation is a lack of generality; however, for specific ions, it can aid in pinpointing the correct C_2—C_3 bond lengths.

Type III calculations have been outlined, in the preceding paragraphs, for the consistent calculation of the infrared stretching frequency of the carbon–oxygen bond in the homologous series of alkyloxocarbonium ions; however, this general scheme was not comprehensive enough. In addition to the aliphatic oxocarbonium ions, it was necessary to ascertain the reliability of the type III calculations for a highly conjugated ion like the phenyloxocarbonium ion. This calculation predicted a rather long carbon–carbon C_2—C_3 bond length, 1.51 Å. The isoelectronic phenyl cyanide molecule has a carbon–carbon length between 1.4509 Å (19) and 1.419 Å (20), the average of these two values being 0.075 Å smaller than the result given by the Boyd–Whitehead calculation. Consequently, the bond length is probably overestimated by at least that length. This analysis has important implications for applying the modified type II calculations to the phenyloxocarbonium ion.

The type III calculation showed a frequency 93 cm^{-1} higher than the experimental value of 2212 cm^{-1} for the phenyloxocarbonium ion. This implied that in cases of high conjugation, the infrared frequency calculated by this method may be overestimated by as much as 90–100 cm^{-1}. In absolute terms this is not very satisfactory. A comparison of the results in Table 4 shows that the calculated infrared frequencies of the phenyloxocarbonium ion are of the same order of magnitude as those for the aliphatic series; however, as has been pointed out previously, type III calculations are only valuable for being able to consistently predict a trend within a series of chemically similar molecule–ions. It is this property that makes them useful. As a consequence of this, caution must be exercised when analyzing the absolute values that result from a type III calculation. This type can point out certain possibilities and trends, but more detailed calculations must follow.

Two modified type II calculations have been carried out on this system in order to try to isolate the major factor that contributes to this rather large error in the frequency. In the first case, type II_1, the carbon–carbon bond was estimated to be the same as the isoelectronic phenyl cyanide molecule (20). The bond angles at O_1, C_2, and C_3 were fixed at ideal values: 120° at C_3 and 180° at C_2. The benzene ring was slightly distorted. The C_3—C_4 type bonds were made a bit longer, 1.402 Å; the others were fixed at 1.394 Å. This was in keeping with the findings of Casado *et al.* (19). The carbon–oxygen bond was the only variable. This calculation gave a frequency of 2277 cm^{-1}, 65 cm^{-1} too high. The frequency and bond lengths are presented in Tables 4 and 5. The C_2—C_3 bond used was about 0.09 Å smaller than the type III value. By shortening this bond there has been a 30 cm^{-1} improvement in the frequency. As in the case of the aliphatic ions, there appears to be a direct correlation between the C_2—C_3 bond length and the calculated frequency.

In the second, modified type II_2, calculation the carbon–carbon bond was estimated as approximately the same as the bond length between two carbon atoms in the sp hybridized valence state. The result was a calculated frequency 4 cm^{-1} above the experimental value. In this calculation the benzene ring was not

TABLE 5. A summary of the calculated results for the phenyloxocarbonium ion

Geometry parameters (Å)	The phenyloxocarbonium ion			Experimental values	
	Type II_1*	Type II_2†	Type III	C_6H_5CN (19)	C_6H_5CN (20)
$R(C_2—O_1)$	1.131	1.140	1.127	1.1581	1.080
$R(C_3—C_2)$	1.419	1.339	1.510	1.4509	1.419
$R(C_4—C_3)$	1.402	1.394	1.394	1.3876	1.402
$R(C_4—H_{13})$	1.080	1.084	1.084	1.0803	1.080
E_T/eV	−1318.2583	−1317.6450	−1318.1761		

*The $C_2—C_3$ bond is taken from microwave studies of the isoelectronic phenyl cyanide.
†The $C_2—C_3$ bond is estimated as a carbon–carbon sp–sp bond length.

distorted. The $C_2—C_3$ bond was shortened 0.171 Å when compared with the type III value. This may seem a large change, however, there is some justification for this type II_2 calculation. Casado *et al.* (19) have shown that electrophillic substituents, like the cyanide radical, distort the shape of the benzene ring. Figure 5 shows the $C_4—C_3—C_8$ bond angle as 120°; however, if an electron withdrawing substituent is situated at the C_3 position, this angle opens up to around 122°, and the carbon–carbon $C_3—C_4$ bonds of the benzene ring lengthen from the normal length of 1.394 Å to 1.402 Å. If this bond angle widened still further, as it might for the $C^{\delta+}—O^{\delta-}$ substituent, then the sp^2 hybridization of the carbon atom C_3 would undergo further reorganization towards an sp hybridized state. Carbon atom C_2 is already in an sp hybridized valence state. In addition, the mean average radii of the electrons in the sp valence state localized on carbon atom C_2 are probably shortened as a result of the large positive charge carried by that carbon atom (+0.73). The net effect of these three factors will be to considerably shorten the $C_2—C_3$ bond, possibly to 1.339 Å which is the carbon–carbon bond length in acetylene.

It would appear that the type III calculation has overestimated the $C_2—C_3$ bond in the phenyloxocarbonium ion more than when the same calculation was applied to the aliphatic series. In the homologous series of ions, the overestimation varied, but was generally around 0.08 Å. It would appear that the same bond in the phenyloxocarbonium ion has been overestimated by between 0.09 Å and 0.17 Å. This leads to the interesting observation that the type III bond length calculation may act as a reflection of the degree of conjugation. The higher the degree of conjugation between the $C_3—C_2—O_1$ chain and the rest of the molecule, the longer the overestimation. For example, the results of type III calculations on the homologous series of alkyloxocarbonium ions have shown that in the cases where the overestimation of the bond length was small, the corresponding overestimation of the frequency was also small. In conclusion, the difference between the calculated and observed frequencies can be directly correlated to the overestimation of the bond length: both within the homologous series and for a highly conjugated system. It is with this conclusion in mind that one must interpret any type III results. Thus in the case where there is almost no possibility of conjugation, as with the methyloxocarbonium ion, the overestimation of the infrared frequency is about 20 cm^{-1}. A reasonably accurate bond length would be expected and this is what is observed. On the other end of the scale, in a highly conjugated system the frequency is in error by 90 cm^{-1} and it is reasonable to suppose that the bond length is also quite a bit larger than the actual figure.

These observations have interesting implications for the applicability of this work to the shapes and structures of the methyloxocarbonium ion dimer and trimer. Modified type II calculations could point the way to an accurate estimation of the bond lengths of the $C_3—C_2—O_1$ skeleton shown in Fig. 1, whereas type III calculations could indicate which, of several possible configurations, is the most stable and, because of its consistency within a given series, point the way to the possible existence of the dimer.

The geometry of the methyloxocarbonium ion trimer is not known although it is thought to be a protonated planar diacetylmethenyloxocarbonium ion (7) as shown in Fig. 1. To apply type III calculations, it is necessary to know the

Can. J. Chem. Downloaded from www.nrcresearchpress.com by 210.87.254.42 on 09/05/12
For personal use only.

TABLE 6. A summary of the geometries calculated for the acetyl-, methenyl-, diacetylmethenyl-, and diacetylmethyloxocarbonium ions

Geometry parameters	$AcHCHCO^+$ Type III	Ac_2HCO^+ Type II_2	Ac_2HCO^+ Type III	Ac_2CHCO^+ Type III
$R(C_2—O_1)$	1.132 Å	1.139 Å	1.136 Å	1.130 Å
$R(C_3—C_2)$	1.481 Å	1.375 Å	1.481 Å	1.471 Å
$R(C_3—C_4)$	1.533 Å	1.533 Å	1.533 Å	1.664 Å
$R(C_4—O_6)$	1.228 Å	1.228 Å	1.228 Å	1.173 Å
$R(O_6—H_{16})$	1.081 Å	1.081 Å	1.081 Å	
$R(C_7—O_9)$		1.228 Å	1.205 Å	1.173 Å
$R(C_3—H_{16})$	1.084 Å			1.093 Å
Ac rotation	0°	0°	2°	60°
E_T	−1273.7994 eV	−1905.7812 eV	−1907.6460 eV	−1906.8102 eV

idealized valence state of carbon atom C_3; consequently two cases were studied. The first considered C_3 in the sp^3 state. The geometry employed for this calculation has been shown in Figs. 2 and 3. The bond lengths were varied and the bond angles were fixed. In this case, five bond lengths were simultaneously varied, the $C_2—O_1$, $C_2—C_3$, $C_3—C_4$, $C_4—O_6$ and the $C_3—H_{16}$ bond lengths. The results of this work have been shown in the last column of Table 6. Two features of note in this calculation are the lengths of the $C_3—C_4$ and $C_4—O_6$ bonds. In the former, the bond length is a long sigma bond and, in the latter case, a shortened pi bond. Normally a carbon–carbon sigma bond would be about 1.54 Å; the calculated length was 1.664 Å. This is probably overestimated by at least 0.08 Å and, if that correction is applied, the result is a bond length of about 1.58 Å, which is an elongated carbon–carbon sigma bond. On the other hand, the normal carbon–oxygen pi bond for the acetyl chloride molecule is 1.25 Å. The corresponding bond in this ion is 1.173 Å which is probably overestimated by about 0.02 Å. The considerable shortening of this bond can be described, in part, by the charge on the carbon atom C_4. As is shown in Table 3 this carbon atom is almost carrying as much formal positive charge as carbon C_2. One other significant feature of this calculation is the energy of the ion. The total energy of this ion is −1906.81 eV.

A second study was carried out where carbon atom C_3 was assigned an sp^2 hybridized valence state. The idealized geometry of this ion is shown in Fig. 1. This is the protonated planar ion favored by Germain *et al.* (7). The hydrogen is situated in a double well potential between the two acetyl radical oxygen atoms. A preliminary calculation showed that the ion was most stable when the oxygen–carbon bonds of the acetyl radicals were nearly parallel and the $O_9—C_7—C_8$ axis was rotated 2° counterclockwise with respect to the x–y plane, *i.e.* counterclockwise in the sense of looking along the $C_3—C_7$ bond from C_3. Starting with this preliminary geometry, six bond lengths were simultaneously varied in this calculation; these six variables were the $C_2—O_1$, $C_2—C_3$, $C_3—C_4$, $C_4—O_6$, $C_7—O_9$, and $O_6—H_{16}$ bonds. The results have been shown in Table 6 as a type III calculation. The total minimum energy of this configuration is −1907.64 eV. This result shows that the planar case is more stable by 19.3 kcal/mol. Tentatively one could conclude that the methyloxocarbonium ion trimer is the protonated planar diacetylmethenyloxocarbonium ion.

A comparison of the stretch frequencies, calculated for the two geometries, provides inconclusive evidence. The tetrahedral case gave a frequency of 2278 cm^{-1}, the planar case, a frequency of 2234 cm^{-1}. This would appear to favor the planar case, as the observed frequency is 2200 cm^{-1}; however, this is not the case. Recall that when type III calculations were applied to the aliphatic ions, the overestimation was around 35 cm^{-1}. In addition, for a moderately conjugated system such as this one, the overestimation is probably around 70 cm^{-1}. If these corrections are applied to the two calculations then in the former case it would become around 2240 cm^{-1} and in the latter about 2160 cm^{-1}.

The gross structure of the ion is probably the planar protonated species. This conclusion is

Can. J. Chem. Downloaded from www.nrcresearchpress.com by 210.87.254.42 on 09/05/12
For personal use only.

based upon the calculated relative stabilities of the two ions. To obtain a more accurate geometry, a modified type II_2 calculation was initiated. With this calculation it is possible to refine the calculated estimates of some of the more important bond lengths such as the C_2—C_3 bond. The results are presented in Table 6. In this calculation, the angles were fixed in idealized positions, and the carbon–carbon C_2—C_3 bond was estimated at 1.375 Å. This estimation was based upon comments made by Veillard and co-workers (8) about the unpublished results of the *o*-methylphenyloxocarbonium ion structure (28). The carbon–carbon C(α)—C bond of this ion has been found by X-ray analysis, to be 1.387 Å, considerably shorter than had been expected; consequently a similar bond length was substituted for that bond in the planar trimer ion. All other bond lengths were frozen at the equilibrium distance established by the type III calculation, except the carbon–oxygen bond. It was varied to find the equilibrium position of this bond for this new geometry. The result was a much less stable ion; however, the infrared frequency, given in Table 4, was only 12 cm^{-1} above the experimentally found value. The stability of the ion could have been greatly improved by relaxing all other bond lengths of significance; however, this is an extremely costly calculation and, besides which, the relative stabilities of the two major cases has already been established. Also, it has already been shown that the major factor influencing the carbon–oxygen stretch frequency is the conjugation of the carbon–carbon bond with the contiguous carbon–oxygen bond. This result, taken together with the results found for the length of the carbon–carbon bond in the phenyloxocarbonium ion tend to suggest that the C_2—C_3 bond length for the planar trimer is between 1.374 Å and 1.387 Å and that the general shape of the ion is that found in Fig.1. The lengths of the other bonds are not as accurately known as this one. In general, those bonds reported for the type II_2 calculation, in Table 3, approximate the geometry of this ion, within the limitations of the theory.

As well as the trimer, there is the interesting possibility that the dimer of the methyloxocarbonium ion might exist. Preliminary calculations have shown that the planar acetylmethenyloxocarbonium ion is more stable than the tetrahedral case. A modified type III calculation was performed on the planar configuration of the dimer.

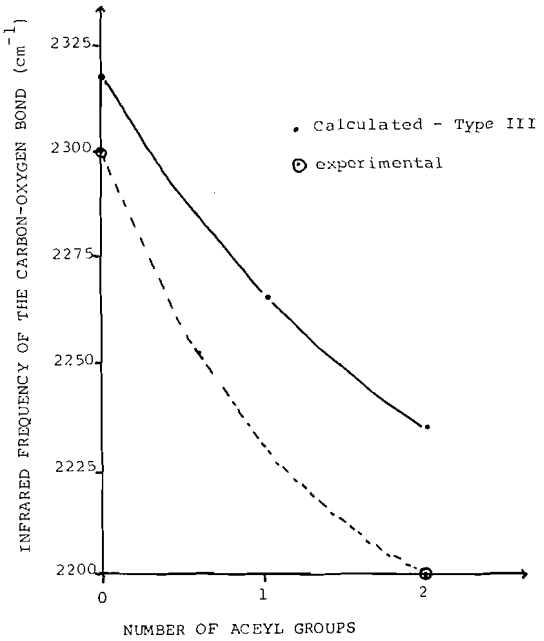

FIG. 7. The frequency of the carbon–oxygen bond as a function of the number of planar acetyl groups substituted in the methyloxocarbonium ion.

In this calculation, the bond lengths found for the planar trimer ion are substituted in all equivalent positions in the dimer except the carbon–carbon, C_2—C_3, and the carbon–oxygen bond C_2—O_1. These two were freely varied to find a global energy minimum. The results have been presented in Table 6. The calculated frequency has been reported in Table 4 at 2265 cm^{-1}. If the experimental values of the methyloxocarbonium ion and the protonated planar diacetylmethenyloxocarbonium ions are plotted along with the type III calculated values of the methyl-, protonated acetylmethenyl-, and diacetylmethenyloxocarbonium ions, shown in Fig. 7, then it is possible to observe a trend similar to the trend found for the type III calculations of the alkyloxocarbonium ions. If this trend is regular, then the experimental value of the protonated acetylmethenyloxocarbonium ion ought to lie at about 2225 cm^{-1}. This value has not been recorded; however, this may be due to the masking effect of the trimer peak. The possibility of its existence shows promise for interesting future work.

The authors would like to thank Mr. Geoff Zeiss and Dr. R. J. Boyd for many thoughtful discussions. This research was supported by the National Research Council

Can. J. Chem. Downloaded from www.nrcresearchpress.com by 210.87.254.42 on 09/05/12
For personal use only.

of Canada, to whom J.D.P. is grateful for the award of a Bursary 1971–72, and M.A.W. is grateful for the award of a Travel Fellowship 1971–73. M.A.W. also thanks Professor A. D. Buckingham of Cambridge University for hospitality 1971–72 and Professor C. A. Coulson of Oxford University for hospitality 1972–73. The McGill Computing Center provided computing facilities on their IBM 360/75.

1. F. SEEL. Z. anorg. allgem. Chem. **250**, 331 (1943).
2. B. SUSZ. C.R. Acad. Sc. Paris, **248**, 2569 (1959).
3. G. A. OLAH. Rev. Roum. Chim. Acad. Rep. Populaire Roumaine, **7**, 1139 (1962).
4. J.-J. WUHRMANN and B. SUSZ. Helv. Chim. Acta, **40**, 722 (1957).
5. D. COOK. Can. J. Chem. **40**, 480 (1962).
6. D. CASSIMATIS, J. P. BONNIN, and T. THEOPHANIDES. Can. J. Chem. **48**, 3860 (1970).
7. A. GERMAIN, A. COMMEYRAS, and A. CASADEVALL. J. Chem. Soc. (D), **12**, 633 (1971).
8. B. REES, A. VEILLARD, and R. WEISS. Theor. Chim. Acta, **23**, 266 (1971).
9. J. M. LE CARPENTIER and R. WEISS. Acta Crystallogr. Sect. B, **28**, 1421 (1972).
10. R. J. BOYD and M. A. WHITEHEAD. J. Chem. Soc. (A), **22**, 3579 (1971).
11. R. J. BOYD and M. A. WHITEHEAD. J. Chem. Soc. Dalton **1**, 73 (1972); 78 (1972); 81 (1972).
12. F. P. BOER. J. Am. Chem. Soc. **90**, 6706 (1968).
13. D. NEWTON, F. P. BOER, and W. N. LIPSCOMBE. Proc. Nat. Acad. Sci. U.S. **53**, 1089 (1965).
14. J. M. LE CARPENTIER and R. WEISS. Acta Crystallogr. Sect. B, **28**, 1430 (1972).
15. J. M. LE CARPENTIER and R. WEISS. J. Chem. Soc. (D), **11**, 596 (1968).
16. M. BARFIELD. J. Am. Chem. Soc. **93**, 1066 (1971).
17. R. L. LIVINGSTON and C. N. R. RAO. J. Am. Chem. Soc. **81**, 285 (1959).
18. J. M. LE CARPENTIER, B. CHEVRIER, and R. WEISS. Bull. Soc. Fr. Mineral. Cristallogr. **91**, 544 (1968).
19. J. CASADO, L. NYGAARD, G. OLE SOERENSEN. J. Mol. Struct. **8**, 211 (1971).
20. D. R. LIDE. J. Chem. Phys. **22**, 1577 (1954).
21. K. OHNO. Theor. Chim. Acta, **2**, 219 (1964).
22. J. M. SICHEL and M. A. WHITEHEAD. Theor. Chim. Acta, **11**, 239 (1968).
23. R. J. BOYD. Ph.D. Thesis. McGill University, Montreal, Quebec. 1970.
24. R. FLETCHER and M. J. D. POWELL. Compt. J. **6**, 163 (1963).
25. A. RALSTON. A first course in numerical analysis. McGraw–Hill Book Co., Inc. 1965. p. 50.
26. R. G. LERNER and B. P. DAILY. J. Chem. Phys. **26**, 678 (1957).
27. G. A. OLAH, S. J. KUHN, W. S. TOLGYESI, E. B. BAKER. J. Am. Chem. Soc. **84**, 2733 (1962).
28. B. CHEVRIER, J. M. LE CARPENTIER, and R. WEISS. Acta Crystallog. Sect. B, **28**, 2673 (1972).
29. J. P. FRIEND and B. P. DAILY. J. Chem. Phys. **29**, 577 (1958).

Can. J. Chem. Downloaded from www.nrcresearchpress.com by 210.87.254.42 on 09/05/12
For personal use only.

The Electrical Polarization of 1,4-Dicyanobenzene

HELMUT HUBER AND GEORGE F WRIGHT

Department of Chemistry, University of Toronto, Toronto, Ontario M5S 1A1

Received November 6, 1972

The anomalous total electric polarization of 1,4-dicyanobenzene has been shown not to be due to high atom polarization by dielectric constant measurement of the solid substance and by its spectral absorption in the far i.r. However the evaluation of atom polarization from the spectral absorption is questioned because these absorptions have a large temperature coefficient in the 50–150 cm^{-1} region. The apparent dipole moment of 1,4-dicyanobenzene in solution has been measured and found to be temperature-dependent.

On a montré que l'anomalie dans la polarisation électrique totale du dicyano-1,4 benzène n'était pas causé par la polarisation des atomes appartenant à des niveaux élevés. Ce fait fut démontré par la mesure de la constante diélectrique de la substance solide et par son spectre d'absorption dans le lointain i.r. Cependant, l'évaluation de la polarisation des atomes à partir du spectre d'absorption est remise en question à cause de la présence d'un coefficient élevé de température pour ces absorptions dans la région de 50 à 150 cm^{-1}. Le moment dipolaire apparent du dicyano-1,4 benzène en solution a été mesuré et est relié à la température.
[Traduit par le journal]

Can. J. Chem., **51**, 2234 (1973)

Can. J. Chem. Downloaded from www.nrcresearchpress.com by 210.87.254.6 on 09/05/12
For personal use only.

Introduction

The polarizations of certain substances in weak 1–5 MHz fields have long been anomalous (1). Such substances are typified by diametrically-opposed substituents. In view of their formally-apparent centrosymmetry such substances might be expected to be devoid of the charge separation called dipole moment. No doubt it was for this reason that when a total polarization (P_T) much more than that which could be attributed to electron polarization (P_E) was found by experiment it was considered to be due to a large atom polarization (P_A). Thus on the basis that

$$P_T = P_E + P_A + P_O$$

then if orientation polarization (P_O) were non-existent, *i.e.* if the nominally centrosymmetric-molecule did not have a dipole moment, the large difference between P_R and P_E would necessarily be a large P_A.

Therefore symmetrically-substituted substances like 1,4-benzoquinone, diarylmercuries, 1,4-dinitrobenzene, *sym*-tetramethylcyclobutanediones and others were said to have abnormally-high atom polarizations (1) although no measurements were made. Instead a theory was proposed (2) to explain abnormally-high atom polarization because of energy imparted to the diametrically-opposed dipoles in such substances by the electric fields imposed upon them.

This postulation of abnormally-high atom polarization in these substances showing anomalous total polarization has been vitiated for several reasons. First a direct method (3) for measurement of combined electron and atom polarization ($P_D = P_E + P_A$ where P_D is called distortion polarization) has been devised which shows that P_A is not abnormally-high in 1,4-benzoquinone (4), 1,4-dinitrobenzene (5), *sym*-tetramethylcyclobutanedione (6), and diphenylmercury (7). Secondly it has been shown in the same publications that the dipole moments that may be calculated from the total polarizations of these substances are temperature-dependent over the range 10–60 °C. According to the prevalent assumption that electron and atom polarization are largely temperature-independent, the temperature-dependent dipole moment must be real, *i.e.* attributable to orientation polarization.

Among the nominally centrosymmetric substances showing unexpected polarization according to the Debye construct is 1,4-dicyanobenzene (1). Since this seeming anomaly was originally attributed to abnormal atom polarization we have now measured it (3). We find that in compressed wafers, the dielectric constant (extrapolated to zero thickness, Fig. 1) is 2.813. Since the density by the air-displacement method (8) is 1.284 at 20° the distortion polarization (P_D) may

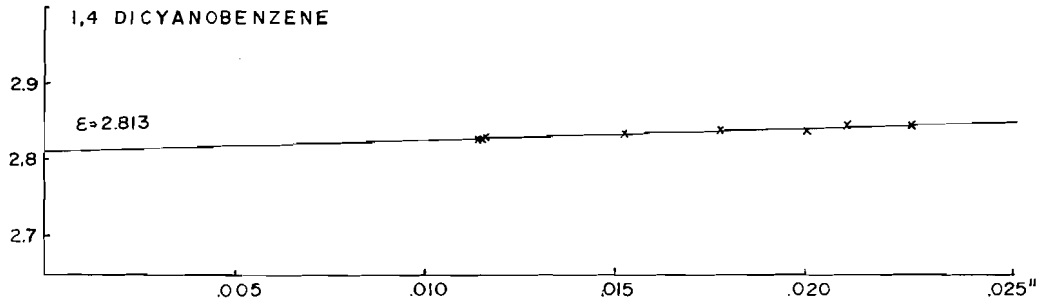

FIG. 1. Dielectric constants *vs.* solid wafer thickness.

TABLE 1. Calculated atom polarizations (P_{A_j}) from spectral absorptions for 1,4-dicyanobenzene in polyethylene wax *vs.* the wax in the reference beam

Spectrometer	ν (cm^{-1})	dν (cm^{-1})	Base line 1	Base line 2	I_0	I	Γ_j	P_{A_j}
IR-11	103	63	74–65		0.6315	0.4041	6124	2.01
PE 301	103	55		74–53	0.4909	0.3296	5029	1.65
PE 301	103	63	74–65		0.6315	0.4203	5881	1.93
IR-11	159	80	62–54		0.3302	0.1845	6223	1.32
IR-11	362	20	33		0.0273	0.0222	256	0.07
IR-11	530	52	19		0.0435	0.0366	381	0.02
IR-11	558	67	18–16		0.0498	0.0263	1720	0.10
IR-11	643	36	14–13		0.0253	0.0187	380	0.02

be calculated as 37.4 cc or only 2.4 cc more than the value of 35.1 cc for electronic polarization calculated from bond polarizabilities (9). This difference of 2.4 cc for P_A (less than 10%) cannot be called an abnormally-high atom polarization. Certainly it cannot account for the unexpected total polarization observed in solutions of 1,4-dicyanobenzene.

There is another way of evaluating atom polarization. Whiffen (10) has used the Kramers–Kronig relationship between molecular refraction and spectral absorption to evaluate P_A for certain substances in the gaseous phase. This relationship takes into account the observation that the electrical reactance of a system becomes greater at the low-frequency side of each resonant absorption band because the masses involved in the intramolecular vibration can "follow" the alternating field at frequencies lower but not higher than the resonant frequency. For each jth absorbance the difference in reactance is designated as a partial atom polarization, P_{A_j}, evaluated by Whiffen's equation

$$P_{A_j} = \frac{NC}{3\pi^2} \int \frac{I_0/I \, d\nu}{\nu_j^2 c}$$

where N is the Avogadro number, C is the vacuum velocity of light, I_0/I is the reciprocal absorption, ν is the specific frequency, c is the concentration, and dν is the width of absorption band. Leaving aside the question whether the vacuum velocity of light is applicable in the condensed phase the summation of these partial atom polarizations in the 50–1000 cm^{-1} range where the contributions are significant is

$$P_A = \Sigma P_{A_j}$$

and where the greatest contributions will come from the absorptions at the lowest frequencies.

The spectra of 1,4-dicyanobenzene in polyethylene wax (3) have been scanned over the 900–50 cm^{-1} range in two spectrometers, the Beckman IR-11 (concentration 15%, path length 0.371 mm) and the Perkin–Elmer 301 (concentration 10%, path length 0.352 mm) and are shown in Table 1 where Γ is the modulus

$$\Gamma = \frac{\log (I_0/I) \, d\nu}{L \cdot c \cdot \nu}$$

L being the path length in mm, c being the concentration and ν the frequency. The band

Can. J. Chem. Downloaded from www.nrcresearchpress.com by 210.87.254.6 on 09/05/12
For personal use only.

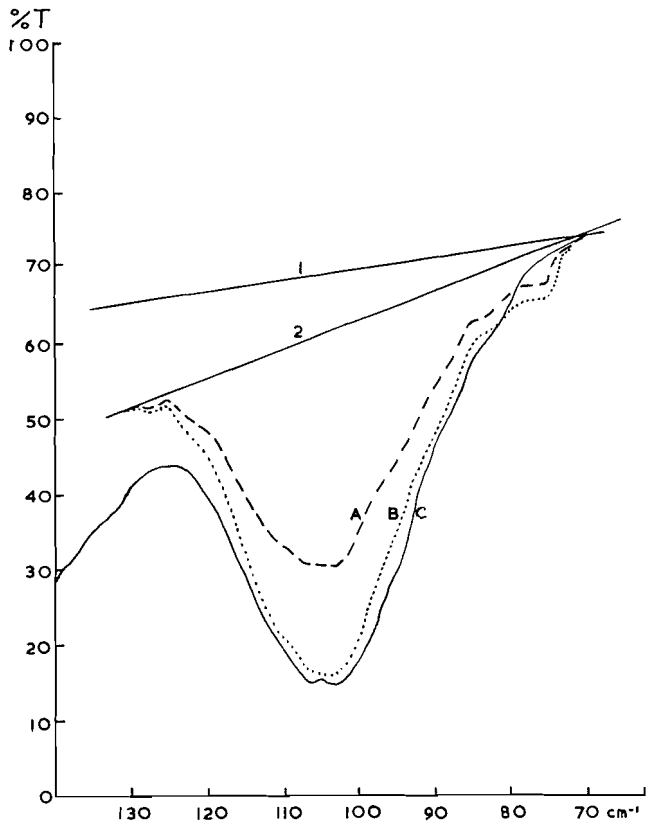

FIG. 2. Spectral absorptions of 1,4-dicyanobenzene in polyethylene wax. (A) PE 301, 10% concentration; (B) PE 301, corrected for 15% concentration; (C) IR-11, 15% concentration; with baselines 1 and 2.

(approximately 103 cm^{-1}) which makes the largest contribution to P_A is shown in Fig. 2.

Because of considerable overlap between this band and one at 159 cm^{-1} of lesser contribution it has been difficult to evaluate the band areas. However, we have chosen two arbitrary baselines, 1 and 2, for calculation of I_0. The calculated values, together with those of lesser contribution are shown in Table 1 using Charney's calculation (11) of each P_{A_j} in terms of $cm^2\ mol^{-1}$ which are comparable with the electrical polarization values

$$P_{A_j} = \Gamma_j(3\pi^2\nu_j)^{-1}$$

It may be seen that the total, $\sum P_{A_j}$, lies between 3.54 and 3.18 $cm^2\ mol^{-1}$. These values are less than 11% of MR_D (35.1 cc) calculated from bond polarization (9) and less than 10% of the distortion polarization determined from compressed wafers. They cannot account for the total polarization found for 1,4-dicyanobenzene.

However, the meaning of the $\sum P_{A_j}$ value ascertained in the condensed phase according to the use of the Kramers–Kronig relationship by Charney *et al.* (11) and others may be questioned. If similar samples on which the data of Table 1 are based are studied at temperature from +40 to −194 °C, profound changes are observed.

First, the "peak" of the absorption at 103 cm^{-1} (+40) is shifted to 108.6 cm^{-1} at −194 °C. Likewise the absorption peak at 155 cm^{-1} (+40°) is shifted to 164 cm^{-1} at −194°. Incidentally the bands at higher frequencies do not shift measurably.

This shift in peak frequency might be attributed to contraction of the crystal lattice although data subsequently to be presented contra-indicate this explanation. However, the other change with decreasing temperature is more profound. It is found that Γ_j increases 337% at j = 164 cm^{-1} at −194° over the value at +40°. Again the intensities at higher frequencies do not change appreciably.

Can. J. Chem. Downloaded from www.nrcresearchpress.com by 210.87.254.6 on 09/05/12
For personal use only.

TABLE 2. Spectra of 2,5-dimethoxy-2,5-dimethyl-3,4-diphenylhexane

Sample state	Concentration (%)	Absorption (cm^{-1})	ΣP_{A_J}	$\Sigma P_{A_J/\varepsilon}$
Glass at +40 °C	31	ν_J 99--111--122--163--207		
		P_{A_J} 0.6--0.2--0.2--0.1--0.3	1.4	0.9
Glass at −190 °C	31	ν_J 101--111--121--164--211		
		P_{A_J} 1.0--0.5--1.1--0.24--0.8	3.6	2.3
Pure, in wafer at +40°	100	ν_J --109------156--187--206		
		P_{A_J} --1.2------0.7--0.1--0.2	2.2	1.4
In polypropylene wax at −190 °C	20	ν_J ---109---147---180---211		
		P_{A_J} --3.6---0.1--0.6--0.6	4.9	3.2

The consequence of these changes is an apparent $\sum P_{A_J}$ at −194° for 1,4-dicyanobenzene of 13.6 cc. The gradual change in $\sum P_A$ over temperatures intermediate between +40 and −194° indicates that higher summations would have been found if we had been able to determine the spectrum at temperatures lower than −194°. It may be noted that the value of 13.6 cc when added to MR_D exceeds the total polarization found for 1,4-dicyanobenzene in benzene (Table 3).

Of course the spectral behavior in the crystalline state might not be comparable with the polarization behavior in solution. We have not been able to make a direct comparison for dicyanobenzene, but the data obtained for *dd,ll*-2,5-dimethoxy-2,5-dimethyl-3,4-diphenylhexane is informative. The earlier studies of this substance (12) showed that it exhibited a temperature-variant dipole moment. The Newman stereochemical diagram for one conformation of this substance

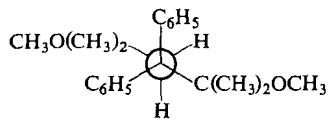

indicates that the observed moment may be attributed to the pivotal bond (13).

This is one of the few substances which we have been able to study spectroscopically in the far i.r. in a state which apparently is not crystalline. Either low solubility or very high background absorption in media such as benzene, carbon tetrachloride, tetrachlorethylene etc. have, so far for us, precluded meaningful solution spectra in this region. However, we have been able to prepare a glass of 31% concentration in polystyrene in which *no* (at least visible) crystallization has occurred. Therefore, we have been able to compare spectra in this glass with those in the pure crystalline state and in a dispersion in polypropylene wax at several temperatures. The data are shown in Table 2.

The magnitude of $\sum P_{A_J}$ may seem to be discrepant from the wafer-measured P_A of −5.7 cc found by capacitance measurement. However, if this anomalously-negative value is adjusted in terms of the phenyl effect (2.0–2.5 cc per phenyl group) (14), it may be seen that at room temperature the spectral and electric values are comparable in magnitude. They are even closer if the spectral $\sum P_{A_J}$ is divided by the dielectric constant, ε, in order to take into account the lower velocity of radiation through the non-gaseous substrate. This agreement probably is fortuitous. Despite the imprecision in the glassy state (due to background absorption from the polystyrene) it is apparent that in the glassy as well as in the crystalline state dimethoxy-dimethyldiphenylhexane shows a strong and temperature-dependent absorption at frequencies between 99 and 211 cm^{-1}. That is to say it behaves like the substances, including 1,4-dicyanobenzene, which show anomalously-high total electric polarizations. If one can assume that our glassy state is non-crystalline then the increased absorption at low temperatures cannot be attributed to the crystal lattice or even to the crystalline state.

In view of all these observations it is questionable whether absorption spectra are useful for evaluation of P_A when they are applied to evaluation of P_A at frequencies below 200 cm^{-1}. Alternatively one may consider whether the unexpected total polarization of 1,4-dicyanobenzene may be due to orientation polarization.

A careful study of the change in total orientation in respect of temperatures between 20 and 40° has now been made in the apparatus described earlier (15) with results shown in Table 3.

Can. J. Chem. Downloaded from www.nrcresearchpress.com by 210.87.254.6 on 09/05/12
For personal use only.

Can. J. Chem. Downloaded from www.nrcresearchpress.com by 210.87.254.6 on 09/05/12
For personal use only.

TABLE 3. Total polarization (P_T) of 1,4-dicyanobenzene as a solute

Solvent	dE/dw	$d\bar{V}/dw$	E solvent	E extrapolated	V solvent	P_T	μ (D) $(MR_D)^{23°}$	μ (D) $(P_D)^{23°}$	Temperature (°C)
Benzene	0.490	−0.260	2.2832	2.2832	1.1378	45.3	0.70	0.61	20
Benzene	0.502	−0.262	2.2724	2.2725	1.1447	45.8	0.72	0.64	25
Benzene	0.520	−0.265	2.2612	2.2615	1.1517	46.3	0.75	0.66	30
Benzene	0.570	−0.267	2.2397	2.2398	1.1670	47.9	0.81	0.69	40
Dioxane	0.736	−0.076	2.2217	2.2218	0.9676	48.4	0.80	0.72	20
Dioxane	0.742	−0.085	2.2005	2.2004	0.9780	48.5	0.82	0.74	30
Dioxane	0.759	−0.098	2.1843	2.1845	0.9897	48.8	0.84	0.76	40

Can. J. Chem. Downloaded from www.nrcresearchpress.com by 210.87.254.6 on 09/05/12
For personal use only.

The apparent dipole moments have been calculated both from the Vogel values for MR_D and from the measured distortion polarization at 23 °C. The results show small but consistent increase in apparent moment in respect of increasing temperature.

It may be seen from Table 3 that the magnitude of the dipole moment (μ) differs in benzene from the larger values found in dioxane. In consideration of the space swept out of the solvent by the candidate substance (16) this difference is not unexpected in view of the small ($\mu = 0.4$ D) but real dipole moment of the dioxane (17) which surrounds this space by contrast to benzene. It is not clear how this difference could be attributed to atom polarization.

In order to relate the apparent moment of 1,4-dicyanobenzene with its thermal behavior one may consider the absorptions in the far i.r. in a different way. The idea that thermal agitation might give rise to orientable dipoles was once considered (2) and then refuted because of the mismatch between the calculated resonance frequency of off-axis bending (*ca.* 10^{13} Hz) and the frequency (*ca.* 10^6 Hz) of electrical polarization measurement. The argument is reasonable, but it leads to the alternative that anomalous total polarization of nominally centrosymmetric molecules must be due to abnormally high atom polarization. The argument has not been reopened since actual measurements (3) showed that in fact such high atom polarizations were not found. The temperature dependence of the apparent moment of 1,4-dicyanobenzene suggests that thermal agitation should again be considered as a cause of orientation polarization in ostensibly centrosymmetric substances.

Perhaps the assignment of specific modes of intramolecular motion to bonds at frequencies below 200 cm^{-1} is not realistic. Inspection of the absorption at *ca.* 103 cm^{-1} for 1,4-dicyanobenzene (Fig. 2) shows that it is by no means simple. Contributions from difference bands in the near i.r., from combinations, and from harmonics in the low frequency region must make large contributions. Indeed the continuous background absorption by benzene and carbon tetrachloride below 150 cm^{-1} (and below their normal vibration modes) must be due to these contributions. It may be significant that none of the spectrometers available to us irradiate the sample monochromatically.

Experimental

Equipment

Dielectric measurements were made in the equipment described previously (15, 3, 12).

Spectral measurements were for the most part made in a Beckman IR-11 spectrometer kindly loaned to us by the U.S. Army. The few attempts to examine solutions in benzene, diozane, and other solvents were made in polyethylene cells (1 mm spacing) supplied by Beckman Instruments Ltd. Dispersions of crystalline sample were prepared as described earlier (3) but in most cases polypropylene (Eastman Epolene) rather than polyethylene wax was used as the dispersing medium because of its relative transparency in the spectral region (80–150 cm^{-1}) of interest.

Temperature-variant spectral studies were made in the regulable low-temperature cell holder sold by Beckman Instruments Inc. (Part No. 195793) which is conveniently adaptable to the IR-11 spectrometer. By means of a perforated rubber sheet 0.25 in. thick under the flange of this cell holder the sample compartment can be maintained water-free. The outer part of the cell holder is equipped with vacuum-tight polypropylene windows (0.625 in. thick) which are retained by aluminium rings (Fig. 3). The inner part (including the liquid nitrogen reservoir, heaters, and thermocouple) encloses a special cell shown in Fig. 4 which has been designed for the Epolene wax wafers or the glassy films which have been examined in this apparatus. The space between the inner and outer part of the complete cell holder is maintained during use at a pressure of 0.001–0.003 Torr to which, of course, the sample must be subjected. In order to compensate for the general opacity of the two polypropylene windows an attenuator (Fig. 5) is used in the reference beam in the same manner as it is used with the pure samples described below.

Pure samples of 0.075 mm thickness are prepared in the die used for fabrication of 0.25 in. diameter wafers with which the dielectric constant of solid substances is determined (3). The sample is similarly ground to ensure random orientation of the crystalline particles. The thin wafers are installed in a sample holder equipped with

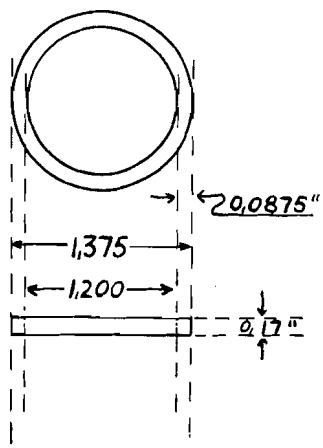

FIG. 3. Retainer ring.

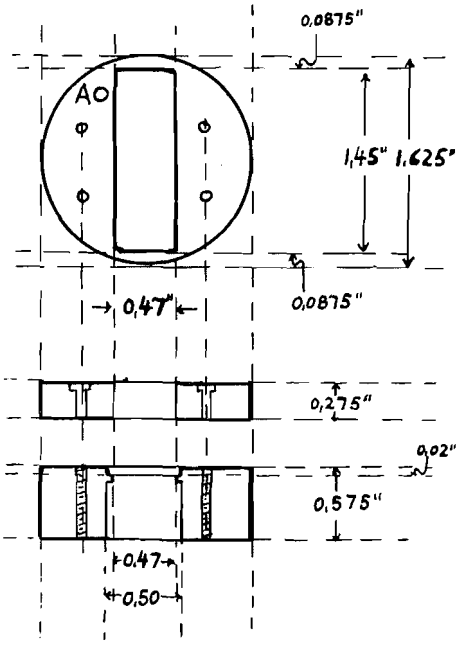

FIG. 4. Sample holder, low temperature cell.

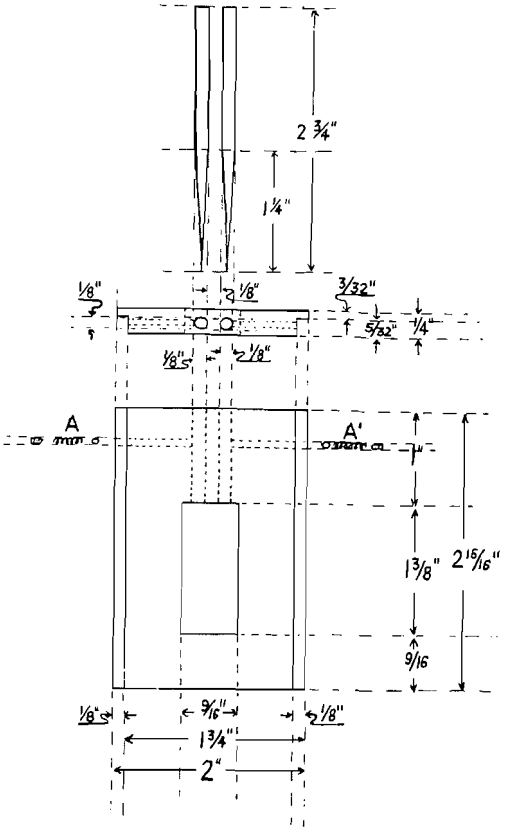

FIG. 5. Attenuator.

tripod screws for position adjustment. This holder may be installed in the reflecting beam condenser (Beckman Part No. 135517) adaptable to the IR-11 at low frequencies. Compensation for reflection losses is accomplished in the reference beam by the attenuator (Fig. 5).

Glassy films are prepared with either polymethylmethacrylate or polystyrene as the glassing matrix. Either of these polymers is dissolved in boiling acetone, butanone-2, or benzene, depending on the solubility of the candidate substance. Then the latter is dissolved at the desired or possible concentration (30–80%) and the solution is evaporated to a viscous melt at about 100°. This molten mass is poured evenly over a hot polished metal plate and evaporation of the volatile solvent is continued (very slowly so as to avoid formation of bubbles) until it is complete. When the plate is cooled to room temperature the glassy film may be peeled off, its thickness measured (about 0.2 mm) and then installed in a cardboard sample holder or in the variable temperature cell holder described above. The technique is not always successful. In any case the film is allowed to stand overnight to ascertain whether spontaneous crystallization occurs. If it does not, then the glass seems to be stable over a long period of time.

The 1,4-dicyanobenzene used in this study has been purified by crystallization from hot acetic acid and hot benzene but the crystals must be ground finely before vacuum drying in order to release solvent, m.p. 227–225°. The 2,5-dimethoxy-2,5-dimethyl-3,4-diphenylhexane has been purified according to procedures previously described (12). Benzene (previously freed from toluene by partial freezing) and dioxane were purified by techniques already described (8).

The authors are grateful to the National Research Council of Canada and the Defence Research Board of Canada for grant funds which made these studies possible.

1. J. W. SMITH. Electric dipole moments. Butterworths, London. 1955.
2. E. I. COOP and L. E. SUTTON. J. Chem. Soc. 1269 (1938).
3. M. BEDARD, H. HUBER, J. L. MYERS, and G. F WRIGHT. Can. J. Chem. **40**, 2278 (1962).
4. H. HUBER and G. F WRIGHT. Can. J. Chem. **42**, 1446 (1964).
5. P. PODLESCHKA, L. WESTLAND, and G. F WRIGHT. Can. J. Chem. **36**, 574 (1958).
6. F. LAUTENSCHLAGER and G. F WRIGHT. Can. J. Chem. **41**, 863 (1963).
7. W. C. HORNING, F. LAUTENSCHLAGER, and G. F WRIGHT. Can. J. Chem. **41**, 1441 (1963).
8. M. V. GEORGE and G. F WRIGHT. Can. J. Chem. **36**, 189 (1958).
9. A. I. VOGEL. J. Chem. Soc. 134 (1946); 607 (1948).
10. D. H. WHIFFEN. Trans. Faraday Soc. **54**, 327 (1958).

Can. J. Chem. Downloaded from www.nrcresearchpress.com by 210.87.254.6 on 09/05/12
For personal use only.

11. E. CHARNEY and E. D. BECKER. J. Am. Chem. Soc. **83**, 4468 (1961).
12. H. SAWATZKY, G. K. WHITE, and G. F WRIGHT. Can. J. Chem. **37**, 1132 (1959).
13. Reference 1, p. 281.
14. H. HUBER and G. F WRIGHT. Can. J. Chem. **42**, 2065 (1964).
15. C. C. MEREDITH and G. F WRIGHT. Can. J. Techn. **33**, 182 (1955).
16. Reference 1, Chapt. 6.
17. A. L. MCCLELLAN. Tables of exp. dipole moments. W. H. Freeman, San Francisco and London. 1963. p. 115.

Can. J. Chem. Downloaded from www.nrcresearchpress.com by 210.87.254.6 on 09/05/12
For personal use only.

Can. J. Chem. Downloaded from www.nrcresearchpress.com by 210.87.254.5 on 09/05/12
For personal use only.

Canadian Journal of Chemistry

Published by
THE NATIONAL RESEARCH COUNCIL OF CANADA

Journal canadien de chimie

Publié par
LE CONSEIL NATIONAL DE RECHERCHES DU CANADA

Volume 51 Number 14 July 15, 1973

Volume 51 numéro 14 15 juillet 1973

Spectroscopic Properties of a Series of Vinyl–Platinum Complexes

T. G. APPLETON,[1] M. H. CHISHOLM,[2] H. C. CLARK,[3] AND L. E. MANZER

Department of Chemistry, University of Western Ontario, London 72, Ontario

Received November 27, 1972

Nuclear magnetic resonance, infrared, and Raman data are given for the series *trans*-$PtRXQ_2$ and *trans*-$[PtRQ_2L]^+$, where R = 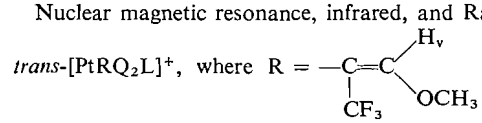 , Q = $(PCH_3)_2C_6H_5$, L = neutral ligand, and Z = anionic ligand. The coupling constants between ^{195}Pt and the trifluoromethyl ^{19}F nuclei and between ^{195}Pt and the vinyl proton H_v both correlate linearly with $^2J_{Pt-CH_3}$ for the corresponding methylplatinum complexes. The results are explained in terms of platinum hybridization in the Pt—C bond dominating the coupling constant.

Les résultats obtenus à l'aide des spectroscopies de résonance magnétique nucléaire, infrarouge et Raman, sont rapportés pour plusieurs composés du type *trans*-$PtRXQ_2$ et *trans*-$[PtRQ_2L]^+$ où R = 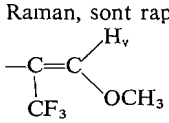 , Q = $(PCH_3)_2C_6H_5$, L = coordinat neutre et Z = coordinat anionique. Les constantes de couplage entre ^{195}Pt et le noyau ^{19}F du groupe trifluorométhyle et entre le ^{195}Pt et le proton H_v du groupe vinyle sont toutes deux reliées linéairement à $^2J_{Pt-CH_3}$ des complexes méthyl platine correspondants. Les résultats sont interprétés en fonction de l'hybridation le long du lien Pt—C qui est le facteur principal en ce qui a trait à la constante de couplage. [Traduit par le journal]

Can. J. Chem., 51, 2243 (1973)

Introduction

A considerable body of evidence has now been collected which supports the contention that the coupling constants $^2J_{Pt-CH_3}$ in methylplatinum(II) complexes, *trans*-$Pt(CH_3)XQ_2$ and *trans*-$[Pt(CH_3)Q_2L]^+$ are determined mainly by properties of the Pt—C bond, in particular the nature of the bonding hybrid orbital used by platinum. For example, $^2J_{Pt-CH_3}$ correlates linearly with $^1J_{Pt-C}$ (1) within a series of methylplatinum complexes and with $^1J_{Pt-H}$ (2) and $^1J_{Pt-P}$ (3) in corresponding hydrido and phosphonato complexes respectively. $^2J_{Pt-CH_3}$ can thus be used as a measure of the *trans*-influence (4) of the ligand *trans* to the methyl group. $^2J_{Pt-CF_3}$ in trifluoromethyl platinum complexes *trans*-$Pt(CF_3)Q_2X$ and *trans*-$[Pt(CF_3)Q_2L]^+$ (2) can also be used as a measure of the *trans*-influence of X^- or L, since $^2J_{Pt-CF_3}$ in these complexes correlates linearly with $^2J_{Pt-CH_3}$ in the corresponding methylplatinum complexes (except for points representing $Sb(C_6H_5)_3$ and to a lesser extent CO). Since the line passed through the origin it was argued that π-bonding did not make an appreciable contribution to the Pt—CF_3 bond and that the Pt—CF_3 coupling

[1]Present Address: Research School of Chemistry, Australian National University, Canberra, Australia.

[2]Present Address: Department of Chemistry, Princeton University, Princeton, New Jersey 08540.

[3]To whom correspondence should be addressed.

Can. J. Chem. Downloaded from www.nrcresearchpress.com by 210.87.254.5 on 09/05/12
For personal use only.

TABLE 1. Characterization data for *trans*-$PtXRQ_2$ and *trans*-$[PtRQ_2L]PF_6$ where

Q = PMe_2Ph and R = 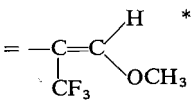

X or L	Analyses: Carbon Calcd.	Carbon Found	Hydrogen Calcd.	Hydrogen Found	Fluorine Calcd.	Fluorine Found	Melting point† (°C)	ν(C≡C) cm^{-1}	Other i.r. and Raman bands	Recrystallization solvents‡
—NCS	38.53	38.48	4.01	4.00	8.71	8.88	151–152	1611	ν_{NC}2085(i.r.)	A
$—NO_2$	37.40	37.45	4.08	4.14	8.87	8.93	§	1610		B§
—CN	40.52	40.10	4.21	4.19	9.16	9.55	102–106	1601	ν_{CN}2110(i.r.)	C
$C_2H_5—NC$	34.67	34.70	3.92	3.81			174–175			A
—:$\overline{CCH_2CH_2CH_2O}$	36.04	35.84	4.04	4.02	21.40	21.06	140	1615	ν_{CO}1255(i.r.)	D
CO	32.77	32.92	3.41	3.56	22.24	22.12	129	1621	ν_{CO}2122(i.r.)	D
$As(C_6H_5)_3$	43.55	42.00	3.95	3.95	16.33	16.66	206	1626		D
$Sb(C_6H_5)_3$	41.68	41.59	3.78	3.87	15.63	15.88	165	1622		D
$P(CH_3)_2(C_6H_5)$‖	59.26	58.95	5.45	5.34			§			D

*All complexes are colorless.
†Melting points are uncorrected.
‡A = $CH_2Cl_2—C_6H_{12}$; B = $(C_2H_5)_2O—C_6H_{12}$; C = $CHCl_3—C_6H_{12}$; D = $CH_2Cl_2—(C_2H_5)_2O$.
§Complex was obtained as an oil.
‖Isolated as $B(C_6H_5)_4^-$ salt.

constant was dominated by a Fermi contact term, and in particular by α^2_{Pt} (*i.e.* the amount of Pt(6s) orbital contribution in the Pt—CF_3 bond)

Within the series of complexes, **1**

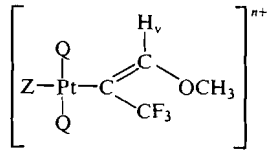

1

1 (*a*) Z = X^-, *n* = 0
(*b*) Z = L, *n* = 1

both the trifluoromethyl ^{19}F nuclei and the vinyl proton H_v show appreciable coupling to ^{195}Pt. However, these two couplings have substantially different paths, although both are over three bonds and are thus somewhat more complex than one bond (*e.g.* $^1J_{Pt-C}$) or two bond (*e.g.* $^2J_{Pt-CH_3}$) coupling constants. It was of interest to determine whether the effect of varying the ligand *trans* to the vinyl group on $^3J_{Pt-C-CF_3}$ and $^3J_{Pt-C=C-H_v}$ was similar to that of varying L or X on $^2J_{Pt-CH_3}$ in corresponding methylplatinum complexes.

Experimental

The complex $Pt\{C(CF_3)=C(OCH_3)H\}\{P(CH_3)_2C_6H_5\}_2Cl$ was prepared as previously described (5).

Analyses were obtained from Schwarzkopf Microanalytical Laboratory Inc., Woodside, N.Y., and Chemalytics Inc., Tempe, Arizona.

In most cases the complexes were extremely difficult to crystallize. Since they were all prepared by similar methods, only a few examples will be outlined.

^1H and ^{19}F spectra were run on a Varian HA-100 spectrometer, the former at 100 MHz with tetramethylsilane as internal reference-lock signal and the latter at 94.1 MHz with "Freon-11" ($CFCl_3$) as the internal reference. Infrared spectra were run as Nujol mulls between CsI disks. Raman spectra were recorded on a Cary 82 spectrometer using a (5145 Å) laser.

Preparation of $[Pt\{C(CF_3)C(OCH_3)H\}Q_2\{As(C_6H_5)_3\}]PF_6$

To an acetone solution of $PtClQ_2\{C(CF_3)C(OCH_3)H\}$ (0.166 g) was added $AgPF_6$ (0.067) in 2 mls of acetone. The solution was magnetically stirred for 1 min and the AgCl removed by centrifugation to give a clear colorless solution. Triphenylarsine (0.082 gm) in acetone was added and the solvent removed on a rotary evaporator to give a clear oil. The oil was taken up in dichloromethane and ether was slowly added until the solution became cloudy. The solution was cooled at −15 °C for 10 h to give white crystals of the desired salt in 65% yield.

Preparation of $[PtQ_2\{C(CF_3)C(OCH_3)H\}(:\overline{CCH_2CH_2CH_2—O})]PF_6$

$AgPF_6$ (0.066 g) in 2 ml of acetone was added to an acetone solution of $PtClQ_2\{C(CF_3)C(OCH_3)H\}$ (0.164 g). The AgCl was removed by centrifugation and $HC{\equiv}CCH_2CH_2OH$ (0.030 g) was added. The solution was stirred for 10 min and the acetone was removed on a rotary evaporator to give a clear oil. The oil was dissolved in dichloromethane, and the addition of diethylether yielded white crystals of the carbene salt in 72% yield.

Preparation of $Pt\{C(CF_3)C(OCH_3)H\}Q_2(NO_2)$

To an acetone solution of $PtClQ_2\{C(CF_3)C(OCH_3)H\}$ (0.160 g) was added $AgClO_4$ (0.052 g). The AgCl was removed by centrifugation and $NaNO_2$ (0.018 g) was added. The solution was stirred for 15 min and the solvent removed on the rotary evaporator. The complex was extracted with dichloromethane and the addition of *n*-hexane gave only an oil. Attempts at recrystallization with a variety of solvents were unsuccessful.

Preparation of $[Pt(C_6H_5)\{P(CH_3)_2(C_6H_5)\}_3](PF_6)$

$AgPF_6$ (0.100 g) was added to $PtCl(C_6H_5)Q_2$ in 5 ml of acetone. The silver chloride was removed by centrifugation and 0.05 ml of $P(CH_3)_2C_6H_5$ was added. The solution was evaporated to dryness, extracted with dichloromethane and passed through a 1 in. Florisil column, eluting with dichloromethane. The volume of the solution was reduced and hexane added. Cooling to 0 °C yielded white crystals which were filtered and washed with diethyl ether. Yield 0.208 g; m.p. 178–180 °C.

Anal. Calcd. C, 43.3; H, 4.6; Found, C, 43.2; H, 4.3.

Results

Characterization, infrared and Raman data for new complexes are given in Table 1 and nuclear magnetic resonance data are given in Table 2.

In the ^1H n.m.r. spectra, the phosphine methyl resonances give overlapping triplets (with satellites from coupling to ^{195}Pt) due to restricted rotation of the vinyl group about the Pt—C bond. This does not necessarily imply extensive π-bonding since there would be considerable steric hindrance to such rotations. The original complex (5) **1** (*a*), X = Cl is exceptional in not showing this P—CH_3 group inequivalence. The inequivalence is most marked when Z is a ligand which would be expected to produce anisotropic chemical shifts, *e.g.* CN^- and I^-. The vinyl proton resonance also appears as a triplet due to coupling with the two equivalent ^{31}P nuclei and is accompanied by ^{195}Pt satellites. The trifluoromethyl resonance appears as a singlet in the ^{19}F n.m.r. spectra and although coupled to ^{195}Pt, no ^{31}P coupling is observed.

Can. J. Chem. Downloaded from www.nrcresearchpress.com by 210.87.254.5 on 09/05/12
For personal use only.

Can. J. Chem. Downloaded from www.nrcresearchpress.com by 210.87.254.5 on 09/05/12
For personal use only.

TABLE 2. N.m.r. data* for complexes *trans*-$PtXRQ_2$ and *trans*-$[PtRQ_2L](PF_6)$ where R = $C(H)(C(=O)OCH_3)(CF_3)$ and Q = $P(CH_3)_2(C_6H_5)$

No. X or L	$\delta_{(P-CH_3)}$	$^2J + {}^4J_{(P-H)}$	$^3J_{(Pt-P-CH_3)}$	$\delta_{(OCH_3)}$	$\delta_{(C=C-H_v)}$	$^4J_{(P-Pt-C=C-H)}$	$^3J_{(Pt-C=C-H)}$	δ_{CF_3}	$^3J_{(Pt-C-CF_3)}$	Other resonances
1 Cl†	1.77	7.3	29.3	3.22	4.97	1.7	55.7	49.8	128	
2 I†	1.88 1.95	7.2 7.2	29.6 29.6	3.27	5.05	1.7	56.4	51.3	126	
3 —NCS	1.79 1.80	7.2 7.2	32.2 29.4	3.16	4.71	1.8	50.2	49.6	122	
4 $—NO_2$	1.68 1.74	6.5 6.5	31.5 29	3.10	4.49	2.0	44	49.3	107	
5 —CN	1.88 1.96	7.5 7.5	32.8 30.8	3.14	4.58	1.8	37.2	48.9	95	
6 C_2H_5NC	1.84 1.88	7.0 7.0	31.5 31.5	3.27	4.94	2.0	40	48.5	98	δ_{CH_2}0.95 δ_{CH_3}3.37
7 $As(C_6H_5)_3$	1.38 1.65	7.5 7.8	29.0 30.0	3.41	5.51	2.0	46	47.7	108	
8 $Sb(C_6H_5)_3$	1.61 1.75	7.3 7.8	24.0 29.0	3.58	6.01	3.0	51	46.9	116	
9 CO	2.02 2.06	8.2 8.2	33.4 33.4	3.26	5.08	2.0	39.6	48.2	97	
10 $:\overset{\frown}{C—CH_2—CH_2—CH_2O}$	1.81 1.86	8.4 8.4	34.3 34.0	3.56	5.45	2.4	30	48.7	78	δ_{OCH_2}4.46 J_{Pt-H}8.0 $\delta_{(:C-C-CH_2)}$1.12 $\delta_{(:C-CH_2)}$2.29 J_{Pt-H} = 7 J_{H-H} = 8
11 $CH_3\overset{O}{\overset{\|}{C}}—CH_3$								48.5	143	
12 $CH_3—C\equiv C—CH_3$								49.0	123	
13 $P(CH_3)_2(C_6H_5)$	1.77 1.60 1.25 d	7.6 6.8 9.4	30.0 29.2 20.6	3.48	4.78	2.2 4.6‡	38	48.1	89	$^4J_{(P-Pt-C-CF_3)}$6.8

*Spectra were recorded in $CHCl_3$ or $CDCl_3$. ^1H chemical shifts in p.p.m. from TMS and ^{19}F chemical shifts in p.p.m. upfield from $CFCl_3$. Coupling constants are given in Hz. d = doublet, t = triplet.
†From ref. 5.
‡Coupling to *trans*-phosphine.

Can. J. Chem. Downloaded from www.nrcresearchpress.com by 210.87.254.5 on 09/05/12
For personal use only.

In Fig. 1, $^3J_{Pt-C-CF_3}$ and $^3J_{Pt-C=C-H_v}$ for the complexes, **1**, are plotted against $^2J_{Pt-CH_3}$ for the corresponding methylplatinum complexes. Except for the point representing L = $Sb(C_6H_5)_3$ both coupling constants in the vinyl complexes **1**(*b*) correlate linearly with $^2J_{Pt-CH_3}$ in corresponding methylplatinum complexes. Since several points lie off the line (for reasons to be discussed later) least squares approximation equations to the lines would be meaningless. However, one point to be noted is that the lines do not appear to pass through the origin. Although the line representing the neutral compounds, **1**(*a*), in Fig. 1, is nearly coincident with that of the cations, previous work (2) has suggested that a distinction should be drawn between the neutral compounds and the cations. We have therefore preserved this distinction although the data of Fig. 1 suggests that it may not be a real one.

In Fig. 2, $^3J_{Pt-C-CF_3}$ is plotted against $^3J_{Pt-C=C-H_v}$. A straight line is obtained which again does not pass through the origin.

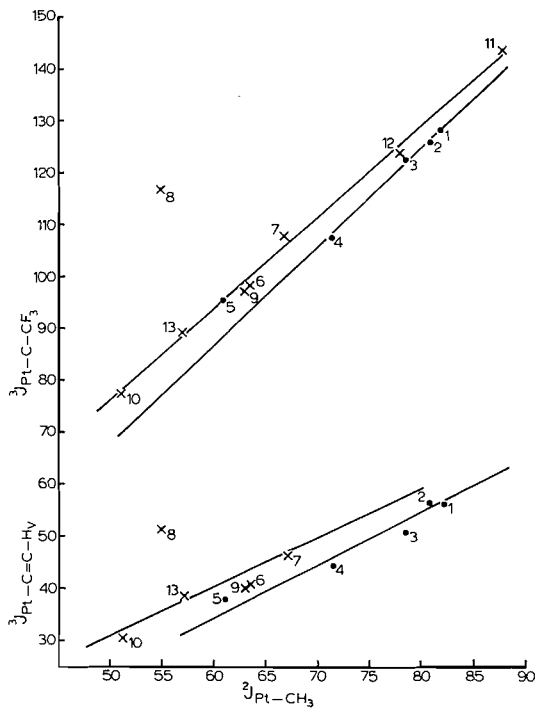

FIG. 1. A plot of $^3J_{Pt-F}$ and $^3J_{Pt-H_v}$ against $^2J_{Pt-H}$ for a series of platinum complexes. The numbering scheme is given in Table 2.

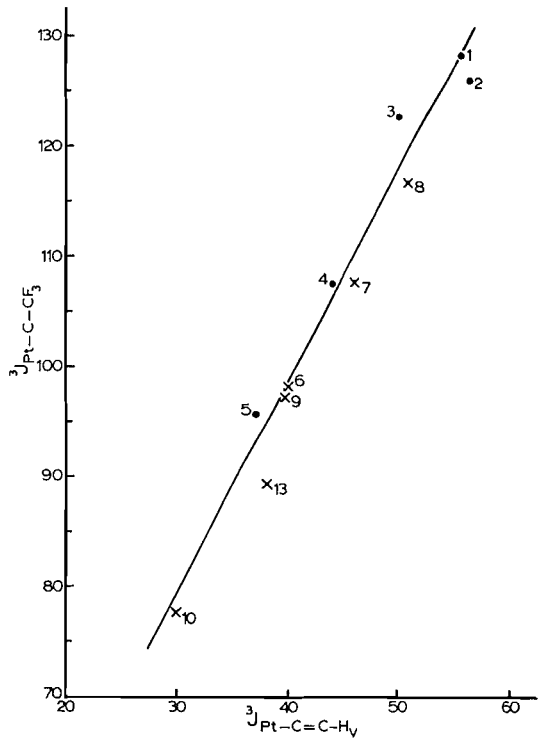

FIG. 2. A plot of $^3J_{Pt-F}$ against $^3J_{Pt-H_v}$ for a series of vinylplatinum complexes. *trans*-Pt{C=C(H$_v$)(CF$_3$)(OCH$_3$)}Q_2Z. The numbers are from Table 2.

Discussion

Properties of the [—C(CF$_3$)=C(OCH$_3$)H] *Group*

Spectroscopic results for some complexes *trans*-$PtRLQ_2^+$ are given in Table 3 to allow a comparison between the properties of the 1-trifluoromethyl-2-methoxyvinyl group and the other organo(R) groups. When Z = C_2H_5NC, CO, or CN^- the C≡X stretching frequency is sensitive to the effective charge on platinum(2) (as pointed out by Hall and Fenske (6) this could include the effect on Pt orbitals of an adjacent positive C atom). The C≡X stretching frequencies clearly show that the effective positive charge on platinum in these vinyl complexes is intermediate between that for R = CH_3 and CF_3.

$^3J_{Pt-P-CH_3}$ for the phosphine *trans* to R in $[RPtQ_3]^+$ has been used to indicate the n.m.r. *trans*-influence (2) of R^-. All the organo (R) groups listed in Table 3 have a high *trans*-

Can. J. Chem. Downloaded from www.nrcresearchpress.com by 210.87.254.5 on 09/05/12
For personal use only.

TABLE 3. Spectroscopic data for the complexes *trans*-PtRZ$\{P(CH_3)_2C_6H_5\}_2^+$

R	Z = $P(CH_3)_2C_6H_5$ $J_{Pt-P-CH_3}$ *cis* to R	*trans* to R	Z = CO ν_{CO}	Z = C_2H_5NC ν_{NC}	Z = CN^- ν_{CN}	Reference
$-CH_3$	30.0	18.5	2095	2234	2111 2118	2, 18
$-C(CF_3)=C(H)(OCH_3)$	30.0 29.2	20.6	2122	2247	2120	
CF_3	28.0	19.0	2140	2256	2134 2143	2
C_6H_5	32.6	17.6				

influence, however the *trans*-influence of the vinyl group is lower than that of the other R groups. For comparison the compound with R = C_6H_5 was studied since the phenyl group also has an sp^2-hybridized carbon atom. The coupling constant $^3J_{Pt-P-CH_3}$ *trans* to C_6H_5 suggests that this group has a significantly higher n.m.r. *trans*-influence than the other R groups studied. (This conclusion has been supported by coupling constants in some organoplatinum(IV) complexes(7)).

Factors Affecting $^3J_{Pt-C-CF_3}$ *and* $^3J_{Pt-C=C-H_v}$

The linear relationships between these coupling constants in the series **1** (Fig. 2) and between these couplings and $^2J_{Pt-CH_3}$ in the corresponding complexes *trans*-$PtCH_3Q_2Z$ suggests that the variations in the coupling constants in the series over the observable range is dominated by variations in Pt hybridization in the Pt—C bond, caused by variations in the *trans*-influence of Z. The appropriate form of the Fermi contact expression for the coupling $^3J_{Pt-C-CF_3}$ is shown in eq. 1 (see ref. 2),

$$[1] \quad {}^3J_{Pt-C-CF_3} \propto \alpha^2_{Pt}\alpha^2_F\gamma_{Pt}\gamma_F f\left(-C\begin{matrix}\diagup\!\!\diagup C\\ \diagdown C\end{matrix}\right)[\psi_{Pt(6S)}(0)]^2[\psi_{F(2S)}(0)]^2(\Delta E)^{-1}$$

where γ_X is the gyromagnetic ratio of nucleus X, α_X^2 is the s-character of the bonding hybrid orbital used by X. $[\psi_{X(NS)}(0)]^2$ is the NS electron density at the nucleus X, $f\left(-C\begin{matrix}\diagup\!\!\diagup C\\ \diagdown C\end{matrix}\right)$ is a function of the geometric and electronic factors controlling transmission of coupling through the vinyl group to the CF_3 group, ΔE is a mean singlet-triplet excitation energy. An analogous expression may be written for coupling to the vinyl proton $^3J_{Pt-C=C-H_v}$. Thus within a *closely related series* coupling constants to the nuclei in the vinyl group can be used as an indication of the *trans*-influence of the ligand *trans*- to the vinyl group *provided* that the electronic and geometrical structure of the vinyl group remains nearly constant. The equation applies only to a purely covalent bond, and any decrease in covalency will cause the coupling constant to decrease. The expression can presumably be generalized for a coupling over *n*-bonds according to eq. 2.

$$[2] \quad {}^nJ_{Pt-A-B---M-X} \propto \gamma_{Pt}\gamma_X\alpha^2_{Pt}\alpha^2_X F(-A-B---M-)[\psi_{Pt(6S)}(0)]^2[\psi_{X(NS)}(0)]^2(\Delta E)^{-1}$$

If this "Fermi Contact" term is dominant, and if $F(-A-B---M-)$ remains nearly constant over the series of compounds concerned, such a coupling constant can be used in a similar way to $^2J_{Pt-CH_3}$, $^1J_{Pt-P}$, etc. The provision that $F(-A-B---M-)$ remain constant is clearly important. An example is provided by the coupling $^3J_{Pt-N-C-H}$. This coupling is dependent on the nature of the ligand *trans* to nitrogen (8) (*i.e.* depends on α^2_{Pt}) but can be affected to a similar extent by changing the geometry of the Pt—N—C—H fragment (8–10).

The tris-phosphine cation, **2**, is interesting from an n.m.r. point of view since $^4J_{(P_2-F)} = 0$,

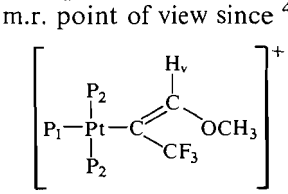

2

$^4J_{(P_1-F)} = 9.4$, $^4J_{(P_2-H_v)} = 2.2$, and $^4J_{(P_1-H_v)} = 4.6$ Hz. These couplings are in line with the well-known tendency of indirect couplings to be larger between *trans* related ligands than between *cis*-ligands.

That the plots in Figs. 1 and 2 do not appear to pass through the origin may have several possible explanations. For example: (*i*) π-bonding between the filled Pt dπ orbitals and empty vinyl π* orbitals could cause a curvature for ligands Z of hypothetically high *trans*-influence (*i.e.* for hypothetical ligands with greater *trans*-influence than alkoxy-carbenes). If this were the reason for the lines not passing through the origin, π-bonding would have to remain nearly constant for the complexes under consideration here. This may be reflected in the small variations in $\nu_{C=C}$ for the vinyl complexes. (*ii*) As well as the appropriate form of eq. 2, the couplings may contain a constant "through space component", as suggested for the complexes, **3** (11).

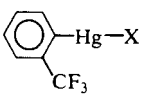

3

If this were the case both $^3J_{Pt-C-CF_3}$ and $^3J_{Pt-C=C-H_v}$ would have to have a through-space component. (*iii*) With ligands of "hypothetically" high *trans*-influence a rehybridization of the vinyl group may occur and the geometrical and electronic factor f(—AB---M) may not remain constant. This is very likely to be the case. However, because of the observed good correlations it appears that f(—AB---M—) does remain constant over the range of complexes studied and $^3J_{Pt-F}$ and $^3J_{Pt-H_v}$ may be used in a similar way to *e.g.* $^2J_{Pt-CH_3}$.

In a previous paper (2) we noted that the ligands CO and $Sb(C_6H_5)_3$ gave points which deviated from the linear plot of $^2J_{Pt-F}$ against $^2J_{Pt-H}$ for the series *trans*-$[PtRL\{P(CH_3)_2(C_6H_5)\}_2]^+$, where R = CH_3 and CF_3 and L = a neutral donor ligand. We suggested that a possible rationale for this observation lay in the synergic bonding properties of CO and $Sb(C_6H_5)_3$ *i.e.* the *trans*-influence of these ligands was dependent on Pt-d to ligand π or π* bonding which in turn was sensitive to the electron density on the metal. In Fig. 1 the point representing the complex $Sb(C_6H_5)_3$ still deviates from the line whilst for L = CO and $CH_3C{\equiv}CCH_3$ (which are generally accepted to utilize a synergic bonding mechanism) there is no such discrepancy. Thus it now seems unlikely that the deviation is entirely attributable to synergism but rather that, for some unknown reason, the value of $^2J_{Pt-CH_3}$ is anomalous for the triphenylstibine complex.

Reactivity

Since the vinyl group is intermediate between CF_3 and CH_3 in electronegativity it was of interest to react the parent compound with $AgPF_6$ in the presence of dimethylacetylene since the course of the reaction is dependent on the organo(R) group and the solvent. For R = CH_3 a stable acetylenic cation is obtained (12) while for R = CF_3 dimerization in acetone occurs to give a cyclobutadiene complex (13) (eq. 3).

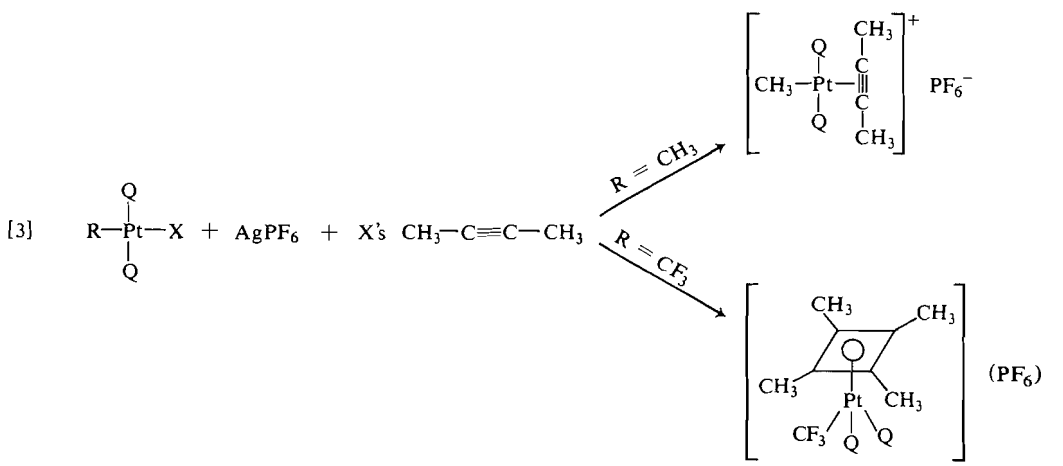

Can. J. Chem. Downloaded from www.nrcresearchpress.com by 210.87.254.5 on 09/05/12
For personal use only.

[4] $\mathbf{1}(a) + AgPF_6 + H{-}C{\equiv}C{-}CH_2CH_2{-}OH \xrightarrow[\text{Acetone}]{}$ 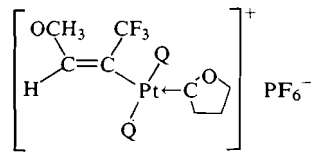 PF_6^-

For R = $C(CF_3){=}C(OCH_3)H$ we were unable to isolate a crystalline complex, however the n.m.r. spectra showed only the presence of the acetylene complex and no evidence of cyclobutadiene formation.

The alkoxycarbene complex was prepared by removal of the chloride from **1**(*a*) with $AgPF_6$ in the presence of the acetylene 1-butyn-4-ol (eq. 4). The reaction appears to be quite general for platinum (13–16) and has been extended to iridium(III) (17).

We are grateful for financial support from the National Research Council of Canada and for the award of an N.R.C.C. Scholarship to L.E.M.

1. M. H. CHISHOLM, H. C. CLARK, L. E. MANZER, and J. B. STOTHERS. Chem. Commun. 1627 (1971).
2. T. G. APPLETON, M. H. CHISHOLM, H. C. CLARK, and L. E. MANZER. Inorg. Chem. **11**, 1786 (1972).
3. F. H. ALLEN, A. PIDCOCK, and C. R. WATERHOUSE. J. Chem. Soc. A, 2087 (1970).
4. T. G. APPLETON, H. C. CLARK, and L. E. MANZER. Coord. Chem. Rev. In press.
5. T. G. APPLETON, H. C. CLARK, and R. J. PUDDEPHATT. Inorg. Chem. **11**, 2074 (1972).
6. M. B. HALL and R. F. FENSKE. Inorg. Chem. **11**, 768 (1972).
7. T. G. APPLETON, H. C. CLARK, and L. E. MANZER. J. Organometal. Chem. To be published.
8. T. G. APPLETON and J. R. HALL. Inorg. Chem. **10**, 1717 (1971).
9. T. G. APPLETON and J. R. HALL. Inorg. Chem. **11**, 117 (1972).
10. T. G. APPLETON and J. R. HALL. Inorg. Chem. **11**, 124 (1972).
11. W. MCFARLANE. Chem. Commun. 609 (1971).
12. M. H. CHISHOLM and H. C. CLARK. Inorg. Chem. **10**, 2557 (1971).
13. M. H. CHISHOLM and H. C. CLARK. J. Am. Chem. Soc. **94**, 1532 (1972).
14. M. H. CHISHOLM and H. C. CLARK. Inorg. Chem. **10**, 1711 (1971).
15. H. C. CLARK and L. E. MANZER. Inorg. Chem. **11**, 2749 (1972).
16. H. C. CLARK and L. E. MANZER. Inorg. Chem. **12**, 362 (1973).
17. H. C. CLARK and L. E. MANZER. J. Organometal. Chem. In press.
18. H. C. CLARK and L. E. MANZER. Inorg. Chem. **11**, 503 (1972).

Can. J. Chem. Downloaded from www.nrcresearchpress.com by 210.87.254.5 on 09/05/12
For personal use only.

Photooxidation of Azomethane[1]

ROBERT SHORTRIDGE AND JULIAN HEICKLEN

Department of Chemistry and Center for Air Environment Studies, The Pennsylvania State University, University Park, Pa., 16802

Received December 15, 1972

The photooxidation of azomethane has been studied at 25 °C and O_2 pressures up to 100 Torr in order to ascertain quantitatively the fate of CH_3O_2 and CH_3O radicals by measuring the quantum yields of CH_3OOH and CH_3OOCH_3 production. The generally accepted reactions include

[3] $2CH_3O_2 \rightarrow 2CH_3O + O_2$

[4*a*] $2CH_3O \rightarrow CH_3OH + CH_2O$

[4*b*] $\rightarrow CH_3OOCH_3$

[5] $CH_3O_2 + CH_3O \rightarrow CH_3OOH + CH_2O$

[6] $CH_3O + O_2 \rightarrow CH_2O + HO_2$

The appropriate rate constant ratios were found to be: $k_5/k_3^{1/2}k_4^{1/2} = 0.31$, $k_{4a}/k_{4b} = 8.9$, and $k_6/k_4^{1/2} = 0.021\ M^{-1/2}\ s^{-1/2}$. The estimated accuracy of these values is ±30%.

La photoxydation de l'azométhane a été étudiée à 25 °C et sous des pressions d'O_2 supérieures à 100 Torr en vue d'étudier quantitativement le sort des radicaux CH_3O_2 et CH_3O par la mesure des rendements quantiques de formation de CH_3OOH et CH_3OOCH_3. Les réactions généralement acceptée comprennent:

[3] $2CH_3O_2 \rightarrow 2CH_3O + O_2$

[4*a*] $2CH_3O \rightarrow CH_3OH + CH_2O$

[4*b*] $\rightarrow CH_3OOCH_3$

[5] $CH_3O_2 + CH_3O \rightarrow CH_3OOH + CH_2O$

[6] $CH_3O + O_2 \rightarrow CH_2O + HO_2$

Les rapports des constantes de vitesse sont: $k_5/k_3^{1/2}k_4^{1/2} = 0.31$, $k_{4a}/k_{4b} = 8.9$, et $k_6/k_4^{1/2} = 0.021\ M^{-1/2}\ s^{-1/2}$. La précision de ces valeurs est évaluée à ±30%. [Traduit par le journal]

Can. J. Chem., **51**, 2251 (1973)

Introduction

We have reexamined the photooxidation of azomethane to determine quantitatively the formation of CH_3OOH and CH_3OOCH_3 from CH_3O_2 and CH_3O radicals. There have been numerous previous investigations of the fates of CH_3O_2 and CH_3O radicals (1), but some conflicts still exist. A convenient source of these radicals is from the photooxidation of azomethane. The mechanism which has generally been accepted is

[1] $CH_3N_2CH_3 + h\nu \rightarrow 2CH_3 + N_2$

[2] $CH_3 + O_2(+M) \rightarrow CH_3O_2(+M)$

[3] $2CH_3O_2 \rightarrow 2CH_3O + O_2$

[4*a*] $2CH_3O \rightarrow CH_3OH + CH_2O$

[4*b*] $\rightarrow CH_3OOCH_3$

[5] $CH_3O_2 + CH_3O \rightarrow CH_2O + CH_3OOH$

[6] $CH_3O + O_2 \rightarrow CH_2O + HO_2$

[7] $CH_3O_2 + HO_2 \rightarrow CH_3OOH + O_2$

The primary photochemical act produces N_2, which can be used as an actinometer, since its quantum yield is unity over a wide range of conditions both in the absence and presence of O_2 (2).

The rate constant ratios which govern CH_3OOH production, $k_5/k_3^{1/2}k_{4a}^{1/2}$ and $k_6/k_{4a}^{1/2}$, were reported by Heicklen and Johnston (3), to be 0.15 and 0.020 $M^{-1/2}\ s^{-1/2}$, respectively at 25 °C. However in the Heicklen and Johnston work, which examined the photooxidation of CH_3I by mass spectral techniques, no direct calibration was made for CH_3OOH; its parent mass spectral sensitivity was assumed to be the same as that for C_2H_5OOH. Also no

[1]C.A.E.S. Report No. 238-72.

Can. J. Chem. Downloaded from www.nrcresearchpress.com by 210.87.254.40 on 09/05/12
For personal use only.

Can. J. Chem. Downloaded from www.nrcresearchpress.com by 210.87.254.40 on 09/05/12
For personal use only.

other accurate determinations of these ratios have been reported.

The rate constant ratio governing CH_3OOCH_3 production, k_{4a}/k_{4b}, has been reported to be between 9 and 12 by Heicklen and Johnston in the same study. Again no direct calibration was made for CH_3OOCH_3; its parent mass spectral peak sensitivity was assumed to be the same as that for $C_2H_5OOC_2H_5$. Furthermore Dever and Calvert (4), using $CH_3N_2CH_3$ photooxidation, did not find CH_3OOCH_3 as a product and concluded that $k_{4a}/k_{4b} > 60$. This finding is more in line with the large rate constant for reaction 4*a* reported by Yee Quee and Thynne (5) (see ref. 1 for a complete discussion).

The present experiments were conducted to extend the earlier study of Heicklen and Johnston (3), which had used CH_3I as the methyl radical source and had been limited to O_2 pressures less than 10 Torr. In the present study, the O_2 pressure has been extended to 100 Torr, and $CH_3N_2CH_3$ was employed instead of CH_3I as a source of CH_3 radicals to avoid the complications associated with iodine atom production.

Experimental

The experimental apparatus and procedure were identical to those reported elsewhere (6). Reaction mixtures were photolyzed in a 500 cc spherical glass vessel at 25 ± 2 °C. The reaction gases exited continuously through a capillary tube connected to 8 mm Pyrex tubing which led through a pinhole to a modified E.A.I. Quadrupole Model 160 mass spectrometer. Only the rates of growth of the CH_3OOH (*m/e* 47 and 48) and the CH_3OOCH_3 (*m/e* 62) product peaks were monitored, inasmuch as the very large background peaks due to N_2 and O_2 effectively prevented observation of the CH_2O (*m/e* 30) and the CH_3OH (*m/e* 31 and 32) product peaks.

The mass spectral sensitivities relative to the *m/e* 58 parent peak of azomethane were determined for the *m/e* 48 peak of CH_3OOH and the *m/e* 62 peak of CH_3OOCH_3. It was necessary to synthesize authentic samples of these two products for this calibration, and the method described by Rieche (7) was followed, except that the CH_3OOH was separated from its ether solution by pumping at about −80 °C in vacuo rather than by the distillation procedure described in the article. Strong surface absorption of both compounds complicated these calibrations, as did a metal surface catalyzed decomposition reaction of CH_3OOH to yield H_2O plus CH_2O. A value of 0.60 ± 0.10 was determined to be the sensitivity of the (*m/e* 62) peak of CH_3OOCH_3 relative to the (*m/e* 58) parent peak of azomethane, and a value of 0.35 ± 0.10 was obtained for the relative sensitivity of the *m/e* 48 peak of CH_3OOH.

In order to generate quantum yields, the *m/e* peak height ratios (48/58) and (62/58) were plotted *vs.* time. The slopes of these plots yielded the rates of production of the CH_3OOH and CH_3OOCH_3 products, when corrected for the relative sensitivity calibration factors and multiplied by the pressure of azomethane present. These product rates were converted to quantum yields by dividing by the N_2 production rate in separate actinometer experiments in the absence of O_2, but at the same $CH_3N_2CH_3$ pressure.

Results

Quantum yields were obtained in a series of runs in which the O_2 pressure was varied from 3 to 104 Torr and the $CH_3N_2CH_3$ pressure maintained at 9–10 Torr. All of the experiments were done at a total pressure of approximately 100 Torr, with N_2 being used as the pressurizing gas when necessary.

A complication in monitoring the CH_3OOH production was encountered with the *m/e* 48 peak, though not with the adjacent *m/e* 47 cracking peak, growing irreproducibly in the dark at higher O_2 pressures. This phenomenon increased in severity with increasing O_2 pressure, and did not seem to involve azomethane, inasmuch as samples containing *only* O_2 at comparable pressures also exhibited (*m/e* 48) peak growth in the dark. It is conceivable that this result can be explained at least in part by the formation of O_3^+ in the mass spectrometer itself. Unfortunately, this problem was responsible for the upper limit of approximately 100 Torr of O_2 in this investigation.

The growth of the mass spectral product peaks was small. Thus, the average uncertainty in most of these quantum yield figures is probably at least as great as in the previous study (3), *i.e.* about 30–40%.

In Table 1 the quantum yield of CH_3OOCH_3, $\Phi\{CH_3OOCH_3\}$, is observed to decrease somewhat with an increase in $[O_2]/I_a^{1/2}$, the fundamental parameter in this system, where I_a is the absorbed intensity. The quantum yield of CH_3OOH production, $\Phi\{CH_3OOH\}$, is about 0.3 at low values of $[O_2]/I_a^{1/2}$, but increases as $[O_2]/I_a^{1/2}$ increases.

Discussion

The mechanism consisting of reactions 1–7 leads to the following rate laws

TABLE 1. Product quantum yields in the photooxidation of azomethane at 25 ± 2 °C and $[CH_3N_2CH_3]$ = 9–10 Torr*

$[O_2]/I_a^{1/2}$ (Torr s)$^{1/2}$	$[O_2]$ (Torr)	$10^3 I_a$ (Torr/s)	$\Phi\{CH_3OOH\}$	$\Phi\{CH_3OOCH_3\}$	F†
218	3.05	0.196	0.36	—	—
390	7.0	0.318	0.29	0.071	9.0
436	6.10	0.194	0.40	—	—
600	13.35	0.492	0.32	0.059	10.5
810	14.4	0.318	0.33	0.066	9.2
1380	19.22	0.194	0.34	—	—
1420	25.2	0.318	0.39	0.063	8.7
1560	31.6	0.195	0.34	—	—
2150	38.3	0.318	0.38	0.042	13.7
2360	58	0.605	0.47	0.041	12.0
2390	42.5	0.318	0.39	0.062	8.9
3040	68	0.500	0.49	0.053	8.7
3060	54.5	0.318	0.50	—	—
3200	71	0.492	0.52	0.059	7.1
3560	84	0.555	0.65	0.057	5.1
3660	90	0.605	0.59	0.045	8.1
3940	100	0.605	0.60	—	—
4150	74	0.318	—	0.045	—
4220	99.5	0.555	—	0.036	—
4650	104	0.500	0.61	0.053	6.4
4690	104	0.492	—	0.040	—
5400	96	0.318	—	0.042	—
					ave. = 8.9 ± 1.5

*Total pressure in all runs was approximately 100 Torr, which was obtained by adding N_2 where necessary.
†$F \equiv (1 - \Phi\{CH_3OOH\} - \Phi\{CH_3OOCH_3\})/\Phi\{CH_3OOCH_3\}$.

$$F \equiv \frac{1 - \Phi\{CH_3OOH\} - \Phi\{CH_3OOCH_3\}}{\Phi\{CH_3OOCH_3\}} = \frac{k_{4a}}{k_{4b}}$$

$$F' = \frac{k_5}{(2k_3k_4)^{1/2}} + \frac{k_6[O_2]/I_a^{1/2}}{k_4^{1/2}(2 - \Phi\{CH_3OOH\})^{1/2}}$$

where

$$F' \equiv \frac{\Phi\{CH_3OOH\}}{(2 - \Phi\{CH_3OOH\})^{1/2}(1 - \Phi\{CH_3OOH\})^{1/2}}$$

Values of F are computed from the data and listed in Table 1. Their average value of 8.9 ± 1.5 gives k_{4a}/k_{4b} good agreement with the value of 9–12 reported by Heicklen and Johnston (3).

The quantity F' is computed and plotted *vs.* $[O_2]/I_a^{1/2}(2 - \Phi\{CH_3OOH\})^{1/2}$ in Fig. 1. The plot is reasonably linear. A least square treatment of the data yields a slope of 1.55×10^{-4} (Torr s)$^{-1/2}$ and an intercept of 0.22. These values give $k_6/k_4^{1/2} = 0.021\ M^{-1/2}\ s^{-1/2}$ and $k_5/(k_3k_4)^{1/2} = 0.31$. The former value

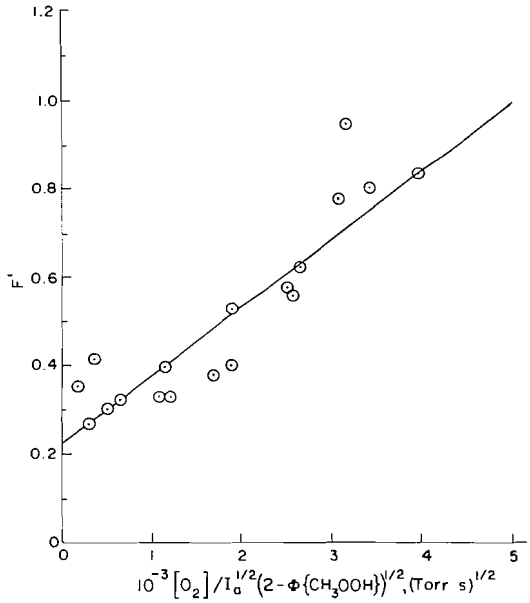

FIG. 1. Plot of $F' \equiv \Phi\{CH_3OOH\}/(2 - \Phi\{CH_3OOH\})^{1/2}(1 - \Phi\{CH_3OOH\})^{1/2}$ *vs.* $[O_2]/I_a^{1/2}(2 - \Phi\{CH_3OOH\})^{1/2}$ in the photooxidation of $CH_3N_2CH_3$ at 25 °C.

Can. J. Chem. Downloaded from www.nrcresearchpress.com by 210.87.254.40 on 09/05/12
For personal use only.

is in good agreement with the value of $0.019\ M^{-1/2}\ s^{-1/2}$ reported by Heicklen and Johnston (3), but the latter value is about a factor of two higher than reported by them.

Finally it should be pointed out that our results provide further evidence against the Russell mechanism (8) in the gas phase. The Russell mechanism is

$$2CH_3O_2 \rightarrow CH_3OH + CH_2O + O_2$$
$$\rightarrow CH_3OOCH_3 + O_2$$

This mechanism predicts that CH_3OOH should not be produced and that $\Phi\{CH_3OOCH_3\}$ should be invariant to $[O_2]/I_a^{1/2}$, both contrary to our findings.

The authors wish to thank Drs. H. A. Wiebe and C. W. Spicer for their help. Comments from Dr. K. O. Kutschke and one referee were of great benefit. This work was supported by the Environmental Protection Agency through the Office of Air Programs under Grant No. AP 01044, for which we are grateful.

1. J. HEICKLEN. Adv. Chem. Series, No. 76, Vol. II, 23 (1968).
2. J. G. CALVERT and J. N. PITTS, JR. Photochemistry. John Wiley and Sons, Inc. New York. 1966. p. 463.
3. J. HEICKLEN and H. S. JOHNSTON. J. Am. Chem. Soc. **84**, 4030 (1962).
4. D. F. DEVER and J. G. CALVERT. J. Am. Chem. Soc. **84**, 1362 (1962).
5. M. J. YEE QUEE and J. C. J. THYNNE. Trans. Faraday Soc. **62**, 3154 (1966).
6. C. W. SPICER, A. VILLA, H. A. WIEBE, and J. HEICKLEN. J. Am. Chem. Soc. **95**, 13 (1973).
7. (*a*) A. RIECHE. Ber. **61**, 951 (1928); (*b*) A. RIECHE and F. HITZ. Ber. **62**, 2458 (1929).
8. G. A. RUSSELL. J. Am. Chem. Soc. **79**, 3871 (1957).

Can. J. Chem. Downloaded from www.nrcresearchpress.com by 210.87.254.40 on 09/05/12
For personal use only.

Commentaire: Observation par spectrometrie infrarouge d'une reaction parasite lors de la reduction de l'acide hexachloroplatinique

MICHEL PRIMET ET MICHEL-VITAL MATHIEU

Institut de Recherches sur la Catalyse, C.N.R.S., 39, boulevard du 11 Novembre 1918, 69100, Villeurbanne, France

Reçu le 6 octobre 1972

Au cours de la préparation de platine supporté par réduction de l'acide chloroplatinique au moyen d'hydrogène, l'acide chlorhydrique formé réagit avec la fluorine constituant les fenêtres de la cellule infrarouge. La chimisorption ultérieure d'eau conduit à l'observation de bandes ν(OH) attribuées à des hydrates du chlorure de calcium.

During the preparation of supported platinum by hydrogen reduction of hexachloroplatinic acid, the hydrochloric acid formed reacts with the fluorine windows of the infrared cell. The subsequent chemisorption of water gives bands due to $CaCl_2$ hydrates.

Can. J. Chem., **51**, 2255 (1973)

Can. J. Chem. Downloaded from www.nrcresearchpress.com by 210.87.254.40 on 09/05/12
For personal use only.

La plupart des catalyseurs platine supporté sont préparés par imprègnation du support au moyen d'acide hexachloroplatinique. L'obtention du métal s'effectue par une réduction au moyen d'hydrogène et s'accompagne de la formation d'acide chlorhydrique. La mesure de l'aire métallique du platine est effectuée par des cycles de titration de l'oxygène adsorbé par l'hydrogène gazeux ou de l'hydrogène adsorbé par l'oxygène gazeux. Quelle que soit la stoechiométrie proposée pour les équations de titration (1–4), l'eau formée serait fixée par le support hydrophile.

Dans les catalyseurs préparés à partir de H_2PtCl_6, une quantité non négligeable de chlore est fixée par le support (5); les propriétés de la phase métallique peuvent donc être perturbées par la présence de l'halogène de même que les schémas proposés pour les cycles de titration H_2–O_2. A la suite de nombreux auteurs (6–8), nous avons donc repris l'étude par spectrométrie infrarouge des interactions du platine déposé avec l'hydrogène, l'oxygène et l'eau.

La méthode de préparation des échantillons est semblable à celle utilisée par d'autres auteurs (6). Le support (Cab-O-Sil H 5 ou Aerosil Degussa) est imprègné par une solution aqueuse de H_2PtCl_6 jusqu'à une teneur en platine de 16%. La cellule utilisée (9) est équipée de fenêtres en fluorine ou en bromure de potassium.

Le solide résultant de l'imprègnation par H_2PtCl_6 est traité à 400 °C sous 200 Torr d'hydrogène pendant une dizaine d'heures, puis mis sous vide à la même température. L'adsorption d'eau sous sa tension de vapeur saturante à température ambiante fournit une large bande centrée vers 3400 cm^{-1} qui disparaît par désorption à 200 °C. Elle est attribuée à de l'eau adsorbée sur la silice. Par contre, l'introduction d'une faible quantité d'eau (2×10^{-2} mmol) fournit un spectre (Fig. 1*a*) présentant deux bandes à 3500 et 3450 cm^{-1}. Celles-ci sont également observées sur le spectre des fenêtres en fluorine de la cellule (Fig. 1*b*), de même que deux autres à 1615 et 1630 cm^{-1} plus difficilement détectables avec le catalyseur à cause de l'absorption de l'échantillon dans ce domaine spectral. Ces quatre bandes sont effacées par une mise sous vide à 25 °C pendant une dizaine d'heures et reformées dans les mêmes conditions.

Au cours de la réduction à 400 °C, un dépôt huileux se forme sur les fenêtres de la cellule; par mise sous vide, la fenêtre apparaît comme dépolie et sa transparence diminue. Lorsque le solide réduit à 400 °C est placé en présence d'hydrogène à température ambiante, puis évacué à 25 °C, l'introduction d'oxygène provoque une sensible augmentation des bandes ν(OH) et des bandes des groupes hydroxyles liés par liaison hydrogène. Aucune bande nouvelle dans le domaine 3550–3300 cm^{-1} n'a pu être détectée.

L'action à 25 °C de faibles incréments de vapeur d'eau sur une silice traitée par HCl à 400 °C fournit les mêmes bandes qu'avec l'échantillon précédent. On pouvait alors penser à une attaque de la silice par HCl avec formation d'un composé volatil qui, condensé sur les fenêtres de la cellule, subirait une hydrolyse en présence de vapeur d'eau. La faible transparence

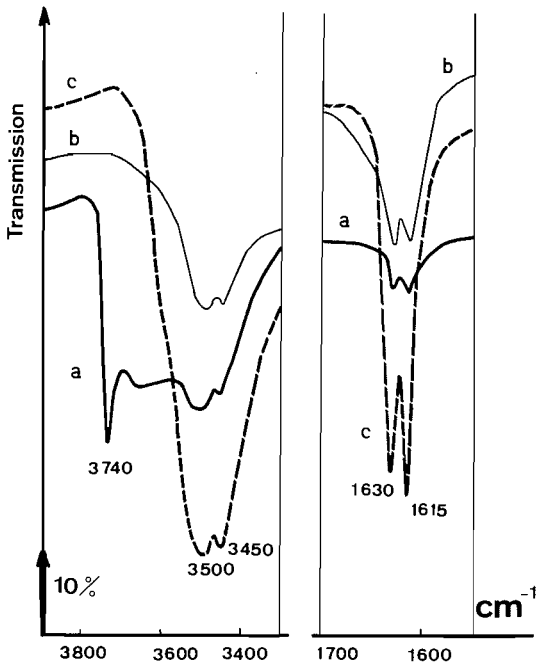

FIG. 1. (*a*), Spectre infrarouge d'un échantillon Pt/SiO_2 à 16% Pt réduit à 400 °C sous H_2, puis sous vide à 400 °C, soumis à l'action de 20 µmol H_2O à température ambiante; (*b*), spectres des fenêtres en CaF_2 de la cellule contenant l'échantillon précédent; (*c*), spectre infrarouge de $CaCl_2$ déshydraté sous vide à 150 °C et soumis à l'action de la vapeur d'eau à 25 °C.

de CaF_2 dans le domaine des vibrations Si—O nous a conduit à reprendre les mesures avec des fenêtres en KBr. Nous n'avons pas retrouvé les bandes vers 3500 et 1600 cm^{-1} mentionnées plus haut; aucune vibration dans le domaine spectral 2000–400 cm^{-1} n'a pu être attribuée à une liaison Si—O. L'hypothèse d'une attaque de la silice par HCl est donc à rejeter.

La nature des fenêtres semble seule responsable des résultats obtenus. Nous avons donc soumis un disque de CaF_2 à l'action de 400 Torr HCl à 25 °C pendant une vingtaine d'heures (un dépôt blanchâtre se forme); après action de la vapeur d'eau, nous retrouvans les bandes à 3500, 3450, 1630, et 1615 cm^{-1} alors qu'une fenêtre de KBr ne fournit pas ces maximums d'absorption dans les mêmes conditions. Seule l'attaque par HCl des fenêtres avec formation de $CaCl_2$ ou de KCl peut expliquer nos résultats expérimentaux. L'action de l'eau sur les produits de réaction conduit à la formation d'hydrates responsables des bandes observées tant que la quantité d'eau introduite reste faible; or $CaCl_2$ fournit de nombreux hydrates (10) alors que KCl ne possède pas d'hydrates connus (11).

Nous avons vérifié cette conclusion en enregistrant le spectre de $CaCl_2$ déshydraté sous vide à 150 °C, puis soumis à l'action de quantités croissantes d'eau à 25 °C (Fig. 1*c*), nous retrouvons les bandes ν(OH) et δ (H_2O) mentionnées plus haut. Ces dernières sont éliminées lors d'un traitement prolongé sous vide de l'échantillon.

L'adsorption d'éthylène sur un disque de fluorine présentant les bandes précédentes ou sur un échantillon de $CaCl_2$ partiellement hydraté entraîne la disparition des maximums d'absorption précédemment détectés et leur remplacement par des bandes relativement larges à 3400 et 1620 cm^{-1}. Une évacuation de l'éthylène entraîne la réapparition des quatre bandes avec diminution d'intensité. Cette perturbation de l'eau liée au chlorure de calcium doit être à rapprocher de celle observée par Kiselev et coll. (12) lors de l'interaction des groupes OH de la silice avec des composés éthylèniques.

En conclusion, le platine supporté ne semble pas présenter de groupes OH superficiels lors des séquences de titration H_2–O_2 ou lors d'une chimisorption d'eau. En conséquence, l'eau formée au cours des opérations de titration ne se dissocie pas sur le métal, ce qui n'invalide pas les équations proposées (1–4). Par contre, au cours de la réduction de H_2PtCl_6 par H_2, l'acide chlorhydrique formé attaque la fluorine en produisant du chlorure de calcium qui peut fournir des hydrates responsables de bandes ν(OH) dans le domaine spectral où des espèces Pt–OH semblent avoir été détectées (6). Une réaction parasite analogue a conduit French et coll. (13) à conférer une acidité protonique à de la silice dispersée dans KBr. Cette réaction parasite est selon Eischens et coll. (14) l'échange des ions K^+ du support KBr par les ions NH_4^+ issus de l'ammoniac gazeux en présence d'eau.

1. J. E. BENSON et M. BOUDART. J. Catal. **4**, 705 (1965).
2. D. E. MEARS et R. C. HANSFORD. J. Catal. **9**, 125 (1967).
3. Y. BARBAUX, B. ROGER, J. P. BEAUFILS, et J. E. GERMAIN. J. Chim. Phys. **67**, 1035 (1970).
4. J. M. BASSET, A. THEOLIER, M. PRIMET, et M. PRETTRE. Vth Int. Congr. on Catalysis, Palm Beach, 1972, papier n° 65.
5. R. MUTIN, J. M. BASSET, et M. PRETTRE. C. R. Acad. Sci. Paris, **273C**, 1704 (1972).

Can. J. Chem. Downloaded from www.nrcresearchpress.com by 210.87.254.40 on 09/05/12
For personal use only.

6. B. A. MORROW et P. RAMAMURTHY. Can. J. Chem. **49**, 3409 (1971).
7. D. D. ELEY, D. M. MORAN, and C. H. ROCHESTER. Trans. Faraday Soc. **64**, 2168 (1968).
8. R. P. EISCHENS et W. A. PLISKINS. Adv. Catal. **10**, 1 (1958).
9. P. PICHAT et M.-V. MATHIEU. La Catalyse au laboratoire et dans l'industrie. Masson et Cie Ed., Paris. 1967. p. 318.
10. P. PASCAL. Nouveau traité de chimie minérale. tome IV. Masson et Cie Ed. Paris. 1958. p. 325.
11. P. PASCAL. Nouveau traité de chimie minérale. tome II. Masson et Cie Ed. Paris. (1963). p. 97.
12. A. V. KISELEV et V. I. LYGIN. Surface Sci. **2**, 236 (1964).
13. R. O. FRENCH, M. E. WADSWORTH, M. A. COOK, et I. B. CUTLER. J. Phys. Chem. **58**, 805 (1954).
14. W. A. PLISKINS et R. P. EISCHENS. J. Phys. Chem. **59**, 1156 (1955).

Can. J. Chem. Downloaded from www.nrcresearchpress.com by 210.87.254.40 on 09/05/12
For personal use only.

Comment: Reply to Primet and Mathieu Concerning the Infrared Observation of PtOH Species

B. A. Morrow and P. Ramamurthy

Department of Chemistry, University of Ottawa, Ottawa, Canada, K1N 6N5

Received January 18, 1973

The i.r. absorption bands due to $CaCl_2$ hydrates, formed on CaF_2 windows during the preparation of silica supported platinum from H_2PtCl_6, should not be confused with those of surface Pt—OH species which are formed by other methods.

Les hydrates de chlorure de calcium formés, sur les fenêtres de fluorites des cellules infrarouges, durant la préparation de platine supporté par de la silice par réduction de l'acide chloroplatinique donnent, dans l'I.R. des bandes d'absorption qu'il ne faut pas confondre avec celles des espèces provenant de Pt—OH qui si trouvent à la surface et qui sont formées par d'autres méthodes.

[Traduit par le journal]

Can. J. Chem., 51, 2258 (1973)

In the preceding paper (1) Primet and Mathieu have implied that our previously reported infrared bands at 3497 and 3544 cm^{-1}, which we attributed to surface PtOH species (2), might also be due to hydrates of $CaCl_2$. This cannot be true for the following reasons:

(*1*) In our spectra, two distinct infrared bands were reported (not a doublet) and these were about 50 cm^{-1} to higher wavenumber than theirs. The 3497 cm^{-1} band is produced only when O_2 is added to a hydrogen covered platinum surface, and the 3544 cm^{-1} band can be produced when water is added to a "reduced" oxygen treated sample. The reader is referred to our original paper for details (2), but better quality spectra showing these features are shown in Fig. 1. The 3497 cm^{-1} band is broader than the sharp 3544 cm^{-1} band and in some instances appears to show some poorly resolved doublet structure. The spectrum in Fig. 1*a* shows this feature as evidenced by a shoulder near 3515 cm^{-1}.

(*2*) Our spectral features are extremely reproducible and can be observed in clean cells equipped with either NaCl or CaF_2 windows. Further, the spectra can be reproduced on silica-supported platinum samples which had been "regenerated" hundreds of times and which were over a year old. Primet and Mathieu's bands presumably can only be seen after the initial reduction of a new SiO_2/H_2PtCl_6 disc, or if they are subsequently observed, the hydrate bands are of diminished intensity.

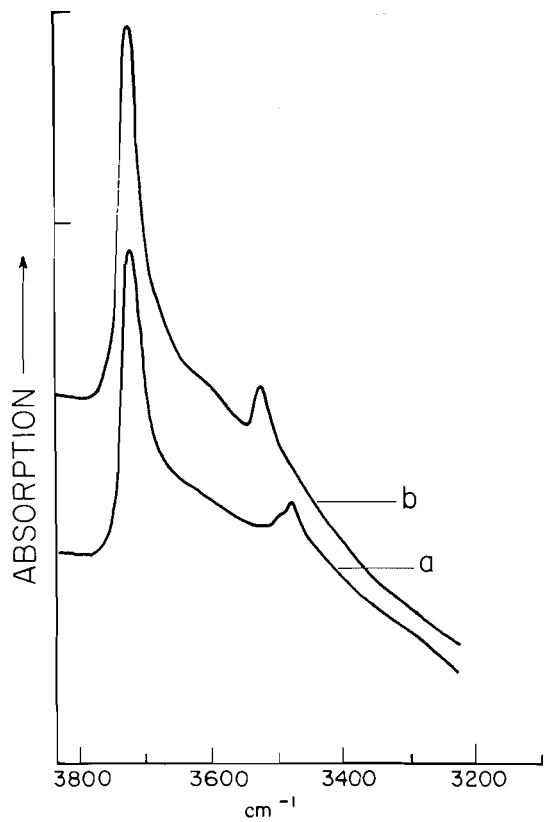

FIG. 1. Infrared spectra of hydroxyl groups on silica-supported platinum. (*a*) 3497 cm^{-1} band. (*b*) 3544 cm^{-1} band. The strong band at 3750 cm^{-1} is due to silica. Ordinate scale refers to the (*b*) spectrum.

Can. J. Chem. Downloaded from www.nrcresearchpress.com by 210.87.254.5 on 09/05/12
For personal use only.

(*3*) Our bands are not removed following prolonged evacuation at room temperature, whereas theirs are removed by this operation.

(*4*) Our observations concerning the addition of ethylene are quite different from those reported by Primet and Mathieu. Indeed, we find that our PtOH bands disappear after adding *any* hydrocarbon and the very intense and well known PtCO band near 2050 cm^{-1} is observed, or it is near 2000 cm^{-1} when a C^{13} hydrocarbon is used (3).

(*5*) Finally, no bands attributable to materials on the cell windows (in the absence of the SiO_2/Pt sample which can be moved at will away from the infrared beam) have ever been detected. This has been checked continuously over a two year period. Further, no bands near 1600 cm^{-1} have ever been detected, a point which has also been checked carefully.

We must stress that the absorptions which we attribute to PtOH surface species are relatively weak in comparison with the SiOH bands of the support and are best observed when the silica itself has been preheated to about 800 °C prior to impregnation with H_2PtCl_6 from anhydrous acetone. The heat treatment makes the support relatively hydrophobic (4) and drives off all of the adsorbed water and removes most of the interacting surface hydroxyl groups which are responsible for the broad tail in the 3700–3300 cm^{-1} region of the spectrum of silica, and the anhydrous acetone prevents extensive rehydration during impregnation. In our experience, unless these precautions are taken, the 3497 and 3544 cm^{-1} bands can almost be obscured by the strong background spectrum near 3500 cm^{-1} due to physically adsorbed water and hydrogen bonded silanol groups.

We can speculate that the failure to detect these bands by earlier workers might be due to these effects, or it is possibly due to the fact that in much of the earlier work (5, 6) alumina has been used as a support and we have already stated why we cannot observe the PtOH bands in this case (2). We should also stress, that only when O_2 is added to "hydrogen covered" platinum do we observe these infrared bands, and in agreement with Darensbourg and Eischens (7) we find no evidence to suggest that H_2O dissociates on pure platinum, or that when H_2 is added to a platinum surface which has been pretreated with O_2, that anything other than water is formed.

1. M. Primet and M-V. Mathieu. Preceding paper.
2. B. A. Morrow and P. Ramamurthy. Can. J. Chem. **49**, 3409 (1971).
3. R. M. Hammaker, S. A. Francis, and R. P. Eischens. Spectrochim. Acta, **21**, 1295 (1965).
4. C. G. Armistead and J. A. Hockey. Trans. Faraday Soc. **63**, 2549 (1967).
5. D. D. Eley, D. M. Moran, and C. H. Rochester. Trans. Faraday Soc. **64**, 2168 (1968).
6. R. P. Eischens and W. A. Pliskin. Adv. Catal. **10**, 1 (1958).
7. D. J. Darensbourg and R. P. Eischens. Paper 21, 5th International Congress on Catalysis, Palm Beach, Florida, Aug. 21–25, 1972.

Can. J. Chem. Downloaded from www.nrcresearchpress.com by 210.87.254.5 on 09/05/12
For personal use only.

Charge Density Distribution in Vanadium Complexes

D. R. EATON AND K. L. CHUA
Department of Chemistry, McMaster University, Hamilton, Ontario
Received November 2, 1972

An empirical method for investigating the effect of substituents on the charge distribution of transition metal complexes is presented. This method is based on the measurement of n.m.r. chemical shifts of paramagnetic compounds and is applied to a series of V(III) complexes. Measurements are reported on the sixteen isomers which result from the systematic replacement of CH_3 groups by CF_3 groups in V(III) trisacetylacetonate. Ninety-nine of the possible 100 ^1H and ^{19}F chemical shifts have been measured. Substituent shifts of several thousand Hz are observed and have been interpreted using a model invoking charge redistribution in both σ and π orbitals. Similar experiments involving phenyl substituents are also reported. The model adopted enables the data to be fitted with a precision of around 2%. The substituent parameters derived from this model are discussed in terms of changes in electron density and the results compared with substituent effects in aromatic compounds. The important differences arise from the three dimensional nature of metal complexes which leads to interactions between the σ and π electrons of a type not found in simple aromatic compounds. The significance of these results to the rationalization of ligand effects on ligand exchange and catalytic reactions is discussed.

Afin d'étudier l'effet des substituants sur la distribution des charges dans des complexes de métaux de transition, on a élaboré une méthode empirique. Cette méthode est basée sur la mesure des déplacements chimiques en r.m.n. de composés paramagnétiques et est appliquée à une série de complexes du V(III). Des mesures furent effectuées sur les seize isomères obtenus lors de la substitution systématique des groupes CH_3 par des groupes CF_3 dans le tris V(III)acétylacétonate. On a mesuré 99 des 100 déplacements chimiques possibles du ^1H et du ^{19}F. Des déplacements induits par les substituants de plusieurs milliers de Hz ont été observés et ont été interprétés en utilisant un modèle impliquant des redistributions des charges dans les orbitales σ et π. On a rapporté aussi des expériences similaires impliquant des substituants phényles. Le modèle adopté a permis d'obtenir des données avec une précision d'environ 2%. Les paramètres des substituants obtenus de ce modèle sont discutés en fonction des changements dans la densité électronique et les résultats sont comparés avec les effets de substituants dans les composés aromatiques. Les différences importantes proviennent de la nature tridimensionelle des complexes métalliques qui implique des interactions entre les électrons σ et π qui ne se retrouvent pas chez les composés aromatiques simples. On discute de l'importance de ces résultats en ce qui a trait à la rationalisation des effets des coordinats sur l'échange des coordinats ainsi que sur les réactions catalytiques.

[Traduit par le journal]

Can. J. Chem., 51, 2260 (1973)

Introduction

We have previously reported (1) n.m.r. studies of complexes of V(III) with mixed ligands and have suggested that experiments of this kind provide a convenient approach to the study of the transmission of substituent effects in transition metal complexes. This topic has significance with respect to the understanding of variations in ligand exchange rates and mechanism with changes in ligand structure. In this earlier paper a qualitative interpretation of the mode of action of substituent effects in these transition metal complexes was proposed and it was concluded that the important parameter was the charge density on the ligand atoms attached to the metal. It was also indicated that it was intended to extend these studies to develop at least an empirical quantitative scale of substituent effects. The present paper represents our efforts in this direction.

β-Diketonate complexes of V(III) have been utilized in this study. These are six coordinated compounds with basically octahedral geometry. The trisacetylacetonate may be regarded as the parent compound of the series. The ligand protons of this compound show large isotropic n.m.r. shifts relative to the free ligand or a diamagnetic complex which have been attributed (2–4) to contact interactions resulting from partial delocalization of the unpaired electrons from the metal d orbitals to the lowest unoccupied ligand π^* orbitals. The basic experiment consists of measuring the change in isotropic shift of a given proton which occurs when there is a change of substituent on one of the other ligands. The substituent changes observed are

Can. J. Chem. Downloaded from www.nrcresearchpress.com by 210.87.254.6 on 09/05/12
For personal use only.

TABLE 1. No. of isomers and resonances of V(III)/acac/tfac/hfac system

Compound	Isomers	Resonances		
		CH_3	CF_3	CH
$V(acac)_3$	1	1	—	1
$V(hfac)_3$	1	—	1	1
$V(acac)_2(hfac)$	1	2	1	2
$V(acac)(hfac)_2$	1	1	2	2
$V(tfac)_3$	2	4	4	4
$V(acac)_2(tfac)$	1	5	1	3
$V(acac)(tfac)_2$	3	8	4	7
$V(hfac)_2(tfac)$	1	1	5	3
$V(hfac)(tfac)_2$	3	4	8	7
V(acac)(tfac)(hfac)	2	6	6	6
Total	16	32	32	36

quite large (the total spread is often several thousand Hz at 100 MHz for a given resonance in a series of substituted compounds) so that experimentally the method is quite sensitive. The *ab initio* calculation of isotropic shifts for transition metal complexes is however fraught with a number of hazards. We have therefore preferred to adopt a more empirical approach to the analysis of the results. This type of approach is exemplified by the use of the various Hammett and Taft σ parameters (5) to describe substituent effects in aromatic compounds. The present case is however substantially more complex than that of aromatic substitution. We have to consider three interconnected π systems in different planes, d orbitals rather than p orbitals are involved, and the octahedral geometry in the lower symmetry of these chelated complexes offers five different substituent positions rather than the three of aromatic systems (ortho, meta, and para). The net result is that rather a large number of parameters are required. A convincing empirical analysis therefore demands a large amount of data. In the present paper we attempt to justify our method of analysis by presenting an essentially complete data set for one system and have then applied the method to other substituents for which we have rather less data.

Results for CH_3 and CF_3 Substitution

N.m.r. spectra of mixed V(III) complexes were obtained by the method described previously (1). Consider first the compounds which can result from the systematic substitution of CF_3 groups for CH_3 groups in the compound $V(acac)_3$. We use the abbreviations acac = acetylacetone (structure **1**), tfac = trifluoroacetylacetone (structure **2**), hfac = hexafluoroacetylacetone (structure **3**). The resulting compounds are tabulated in Table 1. There are a total of 16 different molecules which give rise to 32 chemically distinct CH_3 resonances, 32 CF_3 resonances, and 36 CH resonances. Figure 1 shows the sixteen structures for the general case with two different substituents X and Y and provides the key to the numbering system adopted to present the data.

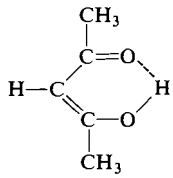

1 acac

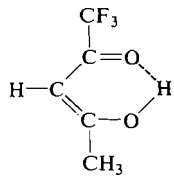

2 tfac

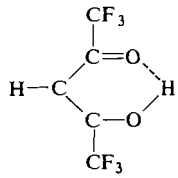

3 hfac

Table 2 presents the observed CH_3 isotropic shifts for the system in which X = CH_3, Y = CF_3. All 32 resonances have been identified and assigned. The isotropic shifts vary from −4054 to −6660 Hz at 100 MHz and 37 °C. We have previously reported (1) the four shifts arising from the three compounds involving acac and hfac. Assignments to compounds with different stoichiometries are unambiguous. Thus in a typical experiment in which hfac is added incrementally to $V(acac)_3$ the two new CH_3 resonances which appear initially are assigned to $V(acac)_2(hfac)$ and the third which appears later to $V(acac)(hfac)_2$. The assignments are then checked by adding acac to $V(hfac)_3$. CH_3 and CH assignments for compounds involving tfac were obtained by using deuterated acac.

Can. J. Chem. Downloaded from www.nrcresearchpress.com by 210.87.254.6 on 09/05/12
For personal use only.

TABLE 2. CH_3 isotropic shifts of V(III)/acac/tfac/hfac system

Compound	Number*	Shifts (Hz) Calculated				Experimental			
$V(acac)_3$	I		−4208				−4208		
$V(acac)_2(tfac)$	II	A,	−4779	B,	−4261	A,	−4808	B,	−4300
		C,	−4006	D,	−5022	C,	−4054	D,	−5031
		E,	−4967			E,	−4981		
$V(acac)_2(hfac)$	III	A=B,	−4826	C=F,	−4983	A=B,	−4836	C=F,	−4982
trans-$V(acac)(tfac)_2$	IV	A=B,	−5136	D=E,	−5625	A=B,	−5120	D=E,	−5598
cis-$V(acac)(tfac)_2$	V	C=F,	−5829	D=E,	−4296	C=F,	−5856	D=E,	−4330
cis'-$V(acac)(tfac)_2$	VI	A,	−5702	C,	−4735	A,	−5740	C,	−4756
		D,	−5106	E,	−4608	D,	−5110	E,	−4610
cis-$V(tfac)_3$	VII		−5449				−5420		
trans-$V(tfac)_3$	VIII	A,	−5029	B,	−5921	A,	−5056	B,	−5870
		E,	−6601			E,	−6654		
trans-V(acac)(tfac)(hfac)	IX	A,	−5892	D,	−6007	A,	−5829	D,	−6004
		E,	−5121			E,	−5126		
cis-V(acac)(tfac)(hfac)	X	C,	−5519	D,	−4970	C,	−5520	D,	−4988
		E,	−4932			E,	−4976		
cis'-$V(hfac)(tfac)_2$	XI	A,	−6039	C,	−5856	A,	−5988	C,	−5790
cis-$V(hfac)(tfac)_2$	XII	A=B,	−5901			A=B,	−5945		
trans-$V(hfac)(tfac)_2$	XIII	C=F,	−6519			C=F,	−6510		
$V(hfac)_2(acac)$	XIV	B=C,	−5727			B=C,	−5734		
$V(hfac)_2(tfac)$	XV	F,	−6597			F,	−6640		

*See Fig. 1.

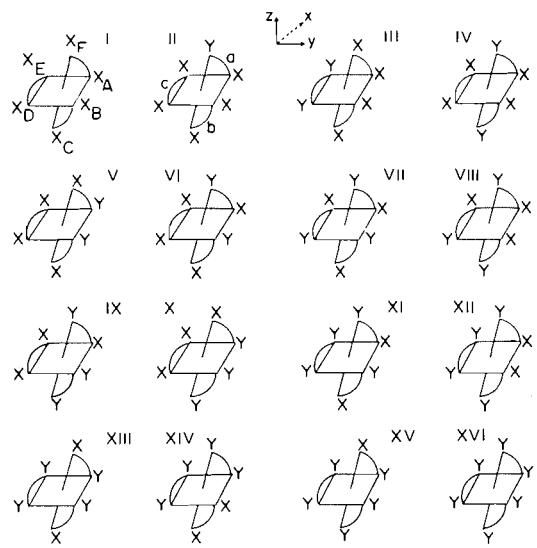

FIG. 1. The sixteen isomers obtained by systematic substitution of a tris chelate $V(XX)_3$.

These experiments enabled the resonances of the tfac ligands to be distinguished from those of the acac ligands. All the compounds except V(acac)(tfac)(hfac) can be identified by experiments involving appropriate pairs of binary mixtures. Lines from V(acac)(tfac)(hfac) were identified by obtaining a variety of spectra from ternary mixtures and eliminating lines previously assigned to other mixed chelates. When two or more isomers of a given compound exist the relative intensities of lines usually sufficed to make assignments to individual isomers. For example in the simple case of $V(tfac)_3$ four CH_3 peaks are observed, three of which are of equal intensity (4). The three of equal intensity must be assigned to the *trans* isomer and the remaining peak to the *cis* isomer. Assignments of lines within a given isomer are based on agreement between observed frequencies and those calculated by the procedure described below. Table 3 gives similar data for the ^{19}F CF_3 shifts. Again all 32 possible resonances have been observed. The range in this case is from −3410 to −5724 Hz at 100 MHz (37 °C) and the assignments are based on experiments similar to those described for the CH_3 spectra. Three of these frequencies were reported previously (1). Thirty-five of the possible 36 CH frequencies are reported in Table 4. The missing resonance belongs to one of the isomers of V(acac)(tfac)(hfac) and is in all probability overlapped by stronger CH_3 resonances present in the complex mixtures used. The spread of the shifts is in this case larger, ranging from −1330 to −5980 Hz at 100 MHz (37 °C). Six of these shifts were reported in the earlier

Can. J. Chem. Downloaded from www.nrcresearchpress.com by 210.87.254.6 on 09/05/12
For personal use only.

TABLE 3. CF_3 isotropic shifts of V(III)/acac/tfac/hfac system

Compound	Number*	Shifts (Hz) Calculated	Experimental
$V(hfac)_3$	XVI	−4510	−4510
$V(acac)_2(tfac)$	II	F, −4159	F, −4152
$V(acac)_2(hfac)$	III	C=D, −4455	C=D, −4152
trans-$V(acac)(tfac)_2$	IV	C=F, −3743	C=F, −3714
cis-$V(acac)(tfac)_2$	V	A=B, −4781	A=B, −4710
cis'-$V(acac)(tfac)_2$	VI	B, −4540 F, −3802	B, −4524 F, −3760
cis-$V(tfac)_3$	VII	−4158	−4150
trans-$V(tfac)_3$	VIII	C, −4162 D, −5021	C, −4080 D, −4998
		F, −3390	F, −3394
trans-V(acac)(tfac)(hfac)	IX	B, −4236 C, −4218	B, −4240 C, −4228
		F, −3790	F, −3394
cis-V(acac)(tfac)(hfac)	X	A, −4464 B, −5220	A, −4536 B, −5156
		C, −4979	C, −4978
cis'-$V(hfac)(tfac)_2$	XI	B, −3574 D, −4344	B, −3566 D, −4377
		E, −4788 F, −4845	E, −4725 F, −4920
cis-$V(hfac)(tfac)_2$	XII	C=F, −4082 D=E, −5792	C=F, −4147 D=E, −5730
trans-$V(hfac)(tfac)_2$	XIII	A=B, −4486 D=E, −3732	A=B, −4526 D=E, −3756
$V(hfac)_2(acac)$	XIV	A=D, −4460 E=F, −4505	A=D, −4480 E=F, −4578
$V(hfac)_2(tfac)$	XV	A, −4057 B, −4850	A, −3984 B, −4999
		C, −5158 D, −4336	C, −5158 D, −4316
		E, −3944	E, −3922

*See Fig. 1.

TABLE 4. CH isotropic shifts of V(III)/acac/tfac/hfac system

Compound	Number*	Shifts (Hz) Calculated	Experimental
$V(acac)_3$	I	−3292	−3292
$V(acac)_2(tfac)$	II	A, −2768 B, −3226	A, −2668 B, −3116
		C, −4040	C, −3964
$V(acac)_2(hfac)$	III	A=B, −4467 C, −1672	A=B, −4486 C, −1700
trans-$V(acac)(tfac)_2$	IV	A=B, −2387 C, −5865	A=B, −2522 C, −5974
cis-$V(acac)(tfac)_2$	V	A=B, −3738 C, −2732	A=B, −3728 C, −2710
cis'-$V(acac)(tfac)_2$	VI	A, −3789 B, −2175	A, −3866 B, −2190
		C, −4390	C, −4470
cis-$V(tfac)_3$	VII	−3445	−3310
trans-$V(tfac)_3$	VIII	A, −1893 B, −3910	A, −1970 B, −3988
		C, −4858	C, −4984
trans-V(acac)(tfac)(hfac)	IX	A, −4134 B, −1338	A, −4221 B, −1330
		C, −5596	C, ?
cis-V(acac)(tfac)(hfac)	X	A, −3548 B, −2957	A, −3579 B, −2906
		C, −3954	C, −3748
cis'-$V(hfac)(tfac)_2$	XI	A, −5081 B, −3032	A, −5104 B, −3028
		C, −2669	C, −2667
cis-$V(hfac)(tfac)_2$	XII	A=B, −3428 C, −3771	A=B, −3551 C, −3610
trans-$V(hfac)(tfac)_2$	XIII	A=B, −4288 C, −2126	A=B, −4220 C, −1980
$V(hfac)_2(acac)$	XIV	A=C, −2541 B, −5999	A=C, −2475 B, −5920
$V(hfac)_2(tfac)$	XV	A, −5040 B, −4257	A, −5014 B, −4229
		C, −1898	C, −1910
$V(hfac)_3$	XVI	−3734	−3734

*See Fig. 1.

Can. J. Chem. Downloaded from www.nrcresearchpress.com by 210.87.254.6 on 09/05/12
For personal use only.

Can. J. Chem. Downloaded from www.nrcresearchpress.com by 210.87.254.6 on 09/05/12
For personal use only.

paper. Thus overall 99 of the possible 100 pieces of data have been obtained.

Analysis of the Data

Examination of the experimental results contained in Tables 2–4 shows that there are clearly large substituent effects of the type defined in the introduction but there is no simple pattern to the data. The most obvious qualitative feature is that increasing CF_3 substitution increases the CH_3 shifts whereas increasing CH_3 substitution decreases the CF_3 shifts. The CH shifts generally follow the trend of the CH_3 or CF_3 groups on the same ligand but the changes are proportionately greater. There are however several exceptions and numerous irregularities in this trend. We have previously suggested a qualitative interpretation of these observations. Our present analysis is based on a modified version of this earlier interpretation.

The model we have adopted is based on the following assumptions.

(*a*) The isotropic shifts arise from contact rather than dipolar interactions. Evidence in favor of this assumption has been presented previously (1, 3) and we do not consider that dipolar interactions represent a significant source of error.

(*b*) The ground states of all these V(III) chelates are orbitally nondegenerate and arise from the e^2 configuration in D_3 symmetry. This point seems to be well established (1) and it is not necessary to consider the type of effects La Mar and Van Hecke (6) have demonstrated for orbitally degenerate ground states.

(*c*) The dominant contact interaction arises from spin transfer from the metal d orbitals to the lowest anti-bonding ligand π^* orbital.[1] A corollary of this assumption is that the observed shifts are proportional to the spin transferred according to the well known McConnell (7) model. In making this assumption we are following the conclusions of several groups (2–4) who have studied isotropic shifts of vanadium complexes. It should be realized though, that even if metal-to-ligand π^* spin transfer is the dominant effect there may be smaller contributions from other mechanisms which could disrupt quantitative analysis.

[1]Only a small amount of mixing with the π^* orbitals is necessary so interactions involving orbitals well separated is energy suffice to cause the shifts. See, for example, ref. 15 for a recent theoretical calculation.

(*d*) The substituent effects are additive, *i.e.*, the effect on the charge distribution of substituting two CF_3 groups on $V(acac)_3$ at specified positions is the sum of the effects of single substitution at the two individual positions. Additivity appears to hold approximately for aromatic systems. The test of this assumption can only lie in the agreement between observed and calculated shifts. It must be expected though that the lack of additivity will be one of the factors leading to incomplete agreement between calculated and experimental values.

Consider first the CH_3 shifts. Figure 2*a* illustrates the overlap between the $p\pi^*$ orbital of the oxygen of a ligand in the *xy* plane and the d_{xz} orbital of vanadium. Based on the above assumptions the neighboring CH_3 shift will be proportional to the amount of spin transferred from the d orbital to the p_π orbital. This in turn depends on two factors, namely the population of the d_{xz} orbital and the ability of the p_π orbital to accept an electron. The first factor was considered in the earlier paper. If all three ligands are identical the occupied d orbitals have the form $(1/\sqrt{2})(d_{xz} - d_{yz})$ and $(1/\sqrt{6})(2d_{xy} - d_{xz} - d_{yz})$. The charge density in the d_{xz} orbital equals that in the d_{xy} and d_{yz} orbitals and has a value of 2/3. This is true for any compound in which the threefold symmetry

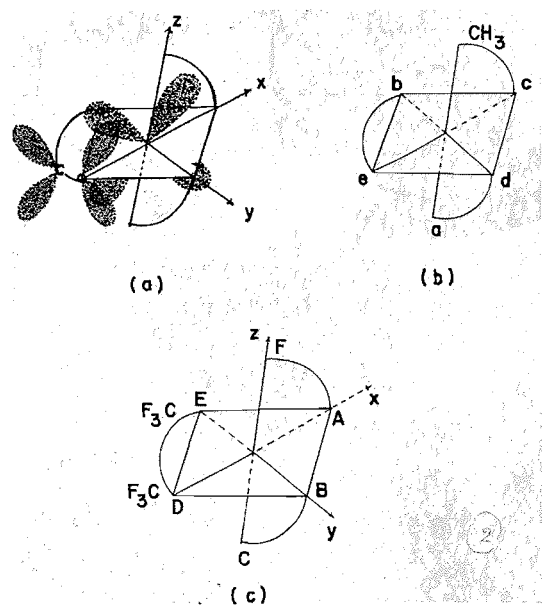

FIG. 2. (*a*) Overlap of d_{xz} and ligand p_π^* orbitals. (*b*) Labelling of substituent parameters. (*c*) Axis system for $V(acac)_2(hfac)$.

Can. J. Chem. Downloaded from www.nrcresearchpress.com by 210.87.254.6 on 09/05/12
For personal use only.

axis is retained, *e.g. cis*-V(tfac)$_3$. For less symmetric cases the form of the occupied orbitals is changed and the occupation values of d_{xy}, d_{xz}, and d_{yz} correspondingly modified. Thus in the extreme case in which the *xy* plane is occupied by a symmetric electron withdrawing ligand which exerts a tetragonal crystal field distortion very much greater than the trigonal distortion present in all these tris chelates the occupied orbitals are d_{xy} and $(1/\sqrt{2})(d_{xz} - d_{yz})$ reducing the population of d_{xz} to 1/2 and increasing that of d_{xy} to 1. The form of the orbitals for intermediate cases was given in ref. 1. In general the population of a d orbital in a plane occupied by oxygens bearing more electron attracting substituents will be increased at the expense of d orbitals in planes containing less electron attracting substituents. The application of this generalization will be considered below.

The second factor mentioned above, namely the ability of the oxygen to accept π electrons, will depend on the charge on the oxygen atom. The more positive charge the greater is the electron accepting ability. Alternatively the more positive the charge the lower the π^* orbital and the better the interaction with the half filled d_π orbital. We might therefore anticipate an inductive effect whereby an electron withdrawing substituent, operating through the σ bonds will induce positive charge to some extent on the more distant oxygens. In principle the effect will be different for each of the five non-neighboring oxygens since none are equivalent by symmetry.

Based on these considerations we have used the empirical eq. 1 to correlate the CH_3 shifts.

$$[1]\quad \Delta\nu = \Delta\nu_0(1 + x)(1 + a + b + c + d + e)$$

The term $(1 + x)$ takes account of the change in d orbital population and $(1 + a + b + c + d + e)$ of the change in the oxygen charge resulting from the inductive effect of substituents in the five possible positions. Both of these factors reduce to unity for the unsubstituted V(acac)$_3$ so that $\Delta\nu_0$ is simply the CH_3 shift for this compound.

This equation was utilized in the following manner in the analysis of the CH_3/CF_3 system. Figure 2*b* shows the labelling of the substituent positions relative to the CH_3 group under consideration. The parameter *a* refers to the *trans* substituent and *b*, *c*, *d*, and *e* to the four nonequivalent *cis* positions. In calculating the CH_3 shifts the relevant parameter is included for each position bearing a CF_3 group and omitted for each position bearing a CH_3 group. Thus for example for the two nonequivalent CH_3 groups of V(acac)$_2$(hfac) the inductive factors are $(1 + a + d)$ and $(1 + b + e)$. Reference to Figs. 1 and 2*b* enables the factors for other CH_3 resonances to be obtained by inspection. The evaluation of the d orbital population factor is perhaps best illustrated by the example shown in Fig. 2*c*. With the axis system as shown d_{xz} and d_{yz} are equivalent but d_{xy} is unique. Further the *xy* plane contains two CF_3 substituents (assumed to be electron withdrawing) and the *xz* and *yz* planes one each. d_{xy} will therefore gain population at the expense of d_{xz} and d_{yz}. We therefore write the population factor as $(1 + x)$ for d_{xy} and $(1 - x/2)$ for d_{xz} and d_{yz}. Inspection of Fig. 2*a* and 2*c* shows that the CH_3 groups A and B obtain spin density by interaction with d_{xy} and the CH_3 groups C and F by interaction with d_{yz} or d_{xz}. The contact shift expressions for these resonances are therefore

$$\Delta\nu_A = \Delta\nu_0(1 + x)(1 + a + d)$$

$$\Delta\nu_C = \Delta\nu_0(1 - x/2)(1 + b + e)$$

Similarly for the CH_3 of V(acac)(hfac)$_2$ we obtain

$$\Delta\nu = \Delta\nu_0(1 + x/2)(1 + a + b + d + e)$$

For the complexes with no two fold symmetry axis d_{xy}, d_{xz}, and d_{yz} all have different populations and two parameters *x* and *y* are required. Appropriate expressions for all 32 CH_3 groups can be readily obtained. The parameters were obtained as follows. Initially it was assumed that *x* has a constant value for all d orbitals the planes of which differ by one CF_3 group as is the case in the above example. No *y* values are then required. If the planes defining the d orbital differed by two CF_3 groups a value equal to twice that assumed above was used. The CH_3 frequencies of V(acac)$_2$(hfac), V(acac)(hfac)$_2$, *cis*-V(tfac)$_3$, and V(acac)$_2$(tfac) were then used to obtain values of the six unknowns *x*, *a*, *b*, *c*, *d*, and *e*. It turned out that the *cis* substituent constants *b*, *d*, and *e* had virtually identical values so the number of adjustable parameters was reduced to four. These four parameters were then further adjusted to give the best fit to all 32 frequencies. The agreement is rather satisfactory. (Standard deviation 5.6%, see

Can. J. Chem. Downloaded from www.nrcresearchpress.com by 210.87.254.6 on 09/05/12
For personal use only.

below.) The agreement can of course be improved by treating x as an adjustable parameter for each compound. The possible variations are not very large since changes in x which improve the agreement for one frequency tend to make it worse for other frequencies. The final calculated frequencies were obtained by optimizing the x and y values and then making a further small adjustment to the substituent parameters. Final calculated frequencies are shown in Table 2. A plot of calculated *vs.* experimental values using this final parameter set is shown in Fig. 3. The standard deviation of the calculated from the experimental values is 1.28% of the total spread of the shifts. (It seems more reasonable to express the standard deviation as a percentage of total spread than of the absolute values. It is actually 0.62% of the average shift.) Of the 1.28% about 0.5% error is attributable to inaccuracies in the measurements and the remainder reflects the inadequacies of the model.

The CF_3 data were treated in exactly the same manner except that the substituent parameter was included for each position bearing a CH_3 group and omitted for each position bearing a CF_3 group rather than *vice versa*. Final calculated frequencies are included in Table 3. The standard deviation of the calculated frequencies is in this case 2.19% of the total spread of the shifts.

The CH frequencies require a slightly modified

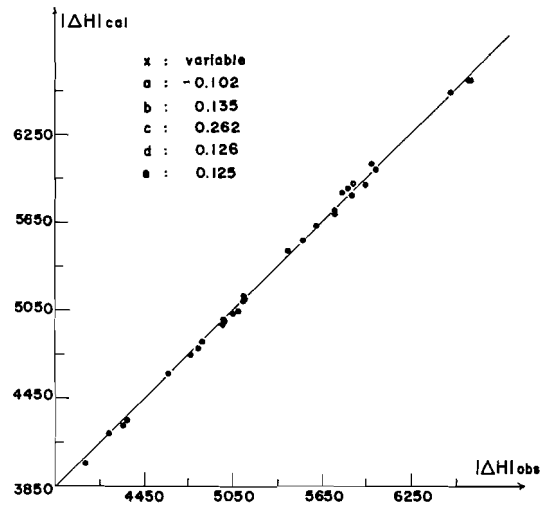

FIG. 3. Comparison of calculated and observed CH_3 chemical shifts. Model with variable x. Shifts in Hz at 100 MHz. CH_3/CF_3 system.

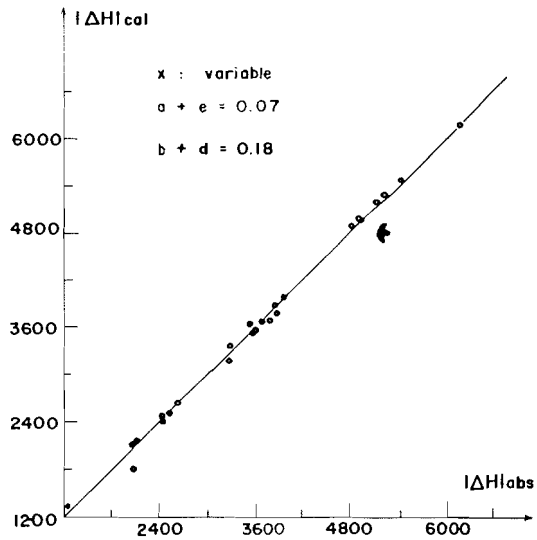

FIG. 4. Comparison of calculated and observed CH shifts. Shifts in Hz at 100 MHz. CH_3/CF_3 system.

procedure. Spin density can reach the γ carbon equally well through either of the two β-diketone oxygens. It is appropriate therefore to include in the population and substituent factors the parameters relating to both oxygens. Thus for example for the acetylacetone CH in $V(acac)_2$-(hfac) the expression becomes

$$\Delta\nu_a = \Delta\nu_0(1 + x_{xy} + x_{yz})[1 + (a + d) + (b + e)]$$
$$= \Delta\nu_0(1 + x/2)(1 + a + b + d + e)$$

Similarly for the CH of the hexafluoroacetylacetone we obtain

$$\Delta\nu_c = \Delta\nu_0(1 - x)(1 - 2a - 2b - 2d - 2c)$$

$\Delta\nu_0$ is obtained in the first case from $V(acac)_3$ and in the second case from $V(hfac)_3$. An average value was used for tfac resonances. It should be noted that a positive substituent parameter is used to express the substituent effect of a CF_3 group on an oxygen bearing a CH_3 and an equal but negative value to allow for the effect of a CH_3 on an oxygen bearing a CF_3. Examination of the above equations and those for the remaining 34 CH shifts shows that the only substituent parameters encountered are the combinations $(a + e)$ and $(b + d)$. In addition to x we have therefore only two variables. Analysis then proceeded in the same manner as for the CH_3 and CF_3 shifts. A plot of calculated *vs.* experimental values using the final parameters is shown in Fig. 4. In this case the standard

TABLE 5. Substituent parameters

System	CH_3	CF_3	CH
V(III)/acac/tfac/hfac	a = −0.102 b = +0.135 c = +0.262 d = +0.126 e = +0.125	a = +0.160 b = −0.113 c = −0.125 d = −0.025 e = +0.046	a+e=0.00 b+d=0.18
V(III)/acac/ϕ—ac/ϕ—ϕ	a = +0.132 b = −0.026 c = −0.038 d = −0.012 e = −0.034		
V(III)/ϕ—ϕ/tf—ϕ/hfac		a = +0.127 b = −0.065 c = −0.126 d = −0.020 e = +0.016	a+e=0.07 b+d=0.18

TABLE 6. d-Orbital population factors* for V(III)/acac/tfac/hfac system

Compound	CH_3 shifts			CF_3 shifts			CH shifts		
	d_{xy}	d_{xz}	d_{yz}	d_{xy}	d_{xz}	d_{yz}	d_{xy}	d_{xz}	d_{yz}
$V(acac)_3$	0.00	0.00	0.00	0.00	0.00	0.00	0.00	0.00	0.00
$V(acac)_2(tfac)$	−0.10	+0.05	+0.05	—	—	−0.02	−0.04	+0.02	+0.02
$V(acac)_2(hfac)$	+0.12	−0.06	−0.06	+0.15	−0.075	−0.075	+0.30	−0.15	−0.15
trans-$V(acac)(tfac)_2$	−0.12	+0.06	+0.06	−0.12	+0.06	+0.06	−0.31	+0.155	+0.155
cis-$V(acac)(tfac)_2$	+0.004	−0.002	−0.002	+0.004	−0.002	−0.002	+0.17	−0.085	−0.085
cis'-$V(acac)(tfac)_2$	−0.03	−0.03	+0.06	−0.02	−0.02	+0.04	−0.13	−0.10	+0.23
cis-$V(tfac)_3$	0.00	0.00	0.00	0.00	0.00	0.00	0.00	0.00	0.00
trans-$V(tfac)_3$	−0.07	+0.04	+0.03	−0.05	+0.03	+0.02	−0.195	+0.33	−0.135
trans-V(acac)(tfac)(hfac)	−0.08	+0.03	+0.05	−0.07	+0.03	+0.04	−0.25	−0.19	+0.44
cis-V(acac)(tfac)(hfac)	−0.04	+0.02	+0.02	−0.02	+0.01	+0.01	−0.018	−0.016	+0.034
cis'-V(hfac)$(tfac)_2$	+0.01	−0.02	+0.01	+0.04	−0.08	+0.04	+0.13	−0.25	+0.12
cis-V(hfac)$(tfac)_2$	−0.006	+0.003	+0.003	−0.13	+0.065	+0.065	−0.01	+0.005	+0.005
trans-V(hfac)$(tfac)_2$	+0.12	−0.06	−0.06	+0.08	−0.04	−0.04	+0.11	−0.055	−0.055
$V(hfac)_2(acac)$	+0.06	+0.06	−0.12	+0.06	+0.06	−0.12	+0.17	+0.17	−0.34
$V(hfac)_2(tfac)$	—	—	+0.014	+0.028	−0.014	−0.014	+0.38	−0.24	−0.14
$V(hfac)_3$	0.00	0.00	0.00	0.00	0.00	0.00	0.00	0.00	0.00

*Value of x in eq. 1.

deviation is 1.97% of the total spread. The calculated frequencies are shown in Table 4. The various parameters derived from the above analyses are collected together in Tables 5 and 6.

Discussion

The validity of an empirical analysis such as that described above is subject to several criteria. First of all it is obvious that the parameters used must reproduce the experimental data with reasonable accuracy. We regard the agreement obtained above as satisfactory. The 1 or 2% discrepancies can very reasonably be ascribed to inadequacies in the model. The most important of these are probably the assumption of a single delocalization mechanism and of additivity of the substituent effects. Secondly the parameters should be internally consistent. Thus if from the CH_3 results we deduce a drift of electrons from *cis* positions towards an oxygen ligand bearing a CF_3 substituent the CF_3 results must indicate enhanced electron density at the CF_3 oxygen obtained from neighboring *cis* CH_3 bearing oxygens. Such consistency should be reflected in opposite signs for corresponding parameters derived from the CH_3 and CF_3 analyses. This result is indeed obtained apart from a small inconsistency in the *e* parameter

Can. J. Chem. Downloaded from www.nrcresearchpress.com by 210.87.254.6 on 09/05/12
For personal use only.

for the CF_3 results. In this case we obtain a small positive value rather than a small negative value. This discrepancy could possibly be rationalized in terms of a direct *cis* interaction with the relatively bulky CF_3 group but we do not believe that it detracts seriously from the overall trend of the results. Similarly the CH parameters should bear some relationship to the CH_3 parameters. Again the zero value of $a + e$ agrees with the opposite signs found for the individual CH_3 parameters and the positive value of $b + d$ is qualitatively as expected. The d orbital population values obtained from the three sets of data are displayed in Table 6. If the model were rigorously correct the three values for a given orbital should be identical. Not surprisingly this equality does not hold particularly well. However there is good agreement in the signs of the changes in orbital populations with substitution and in the overall magnitude of the effect (0–15%). This is probably as much as can be expected. It should be noted that the main discrepancy is that the CH shifts indicate larger population changes than do the CH_3 and CF_3 shifts. This implies that the CH shifts are more sensitive to changes in π spin density than the CH_3 or CF_3 shifts. This is reasonable since other mechanisms such as σ delocalization are certainly expected to be more pronounced at the CH_3 or CF_3 positions.

A final criterion for accepting the analysis is that the results should be physically plausible. This aspect is illustrated by the charge distributions shown diagrammatically in Fig. 5 for two typical complexes. $V(acac)_2(tfac)$ has a single electron withdrawing CF_3 group. This exerts an inductive effect through the σ bonds of the system increasing the positive charge at each of the four *cis* oxygens (Fig. 5*a*). The effect at the oxygen belonging to the same chelating ligand is roughly twice as great as at the other positions. This seems reasonable in view of the availability of an alternative pathway through the σ bonds of the ligand. A little of the negative charge thus withdrawn leaks across to the oxygen *trans* to the substituent. Although not anticipated prior to the analysis of the data, in retrospect this result can be correlated with the many reports of unique *trans* effects in transition metal complexes. In addition to this direct inductive effect on the charge distribution in the σ system of the molecule there is also a polarization of the charge in the metal d orbitals not involved in σ bonding.

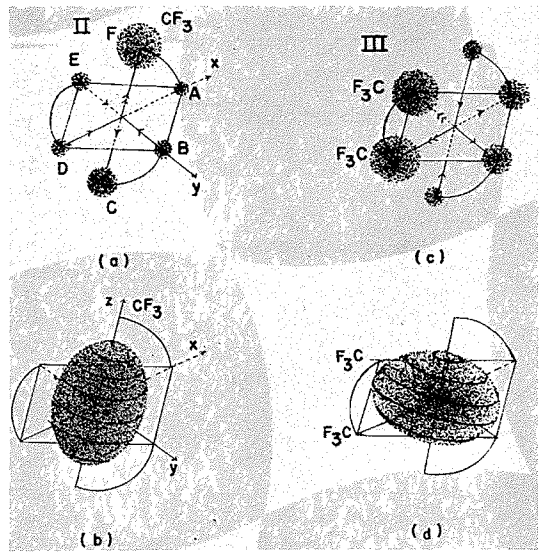

FIG. 5. σ and π charge distribution in two complexes (see text for description).

Instead of there being a spherical distribution of such charge it tends to accumulate in planes containing the electron withdrawing CF_3 group (Fig. 5*b*). In this case the two d orbitals in the planes containing the CF_3 bearing oxygen have gained approximately 5% in population and the orbital in the plane not containing the CF_3 group has lost 10%. Since these are the orbitals involved in π bonding to the ligands there are corresponding changes in the π interactions with the different ligands. These result in enhanced delocalization to the π^* orbitals of ligands not bearing the electron attracting substituent and diminished delocalization to the CF_3 bearing ligand. $V(acac)_2(hfac)$ has two CF_3 substituents and the charge distribution arises from the superposition of the inductive and polarization effects of the two taken individually. The net result is that the two CH_3 bearing oxygens in the same plane as the hfac ligand lose very little negative charge but the two out of this plane lose substantially (Fig. 5*c*). At the same time the d orbitals containing the unpaired electrons are polarized leading to a 12% gain of charge density in the plane of the hfac and a 6% loss in each of the perpendicular planes (Fig. 5*d*). Thus the parameters obtained from the analysis lead to a plausible rationalization of the effect of substituents on the charge distribution of the complexes.

Can. J. Chem. Downloaded from www.nrcresearchpress.com by 210.87.254.6 on 09/05/12
For personal use only.

Can. J. Chem. Downloaded from www.nrcresearchpress.com by 210.87.254.6 on 09/05/12
For personal use only.

Results with Other Ligands

The analysis described above has been extended to several other mixed chelate systems. Initially we sought one further check on the validity of the model. This involves the use of the γ methyl substituted ligand **4**.

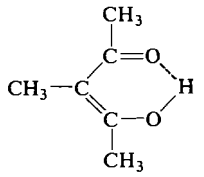

4

The proton n.m.r. spectrum of the tris V(III) complex of this ligand was originally reported by Forman, Murrell, and Orgel in 1959 (2). They observed that the shift of the γCH_3 resonance was opposite in sign to that of the CH in $V(acac)_3$ and this was interpreted as evidence for π spin delocalization. Subsequent investigators have supported this conclusion with other evidence. We argued previously, mainly on the basis of the temperature dependence of the isotropic shifts of the mixed complexes, that the mechanism involved does not change on passing from symmetric to unsymmetric complexes and hence that the evidence in favor of π delocalization in the symmetric complexes implied π delocalization in the unsymmetric complexes. Since our analysis rests on this assumption more direct evidence seemed desirable. Mixed complexes with ligand **4** provide this evidence. For π delocalization in an aromatic system McConnell (7) showed that:

$$a_H = Q\rho_C$$

where a_H is the proton hyperfine coupling and ρ_C the carbon p_π spin density. Theory predicts that Q will be negative for a hydrogen attached to the aromatic carbon and positive for a methyl group so attached (8), hence the change in sign of the CH and C—CH_3 contact shifts. If Q were a true constant in both cases we would expect the C—CH_3 and C—H shifts to be opposite in sign and proportional to each other in magnitude for all mixed complexes in which the C—H is replaced by C—CH_3. Unfortunately it has been shown (9) that Q_{CH_3}, although always positive in sign, can vary in magnitude from compound to compound. If there is π delocalization it is therefore to be expected that the signs of the C—H and C—CH_3 shifts will always be opposite

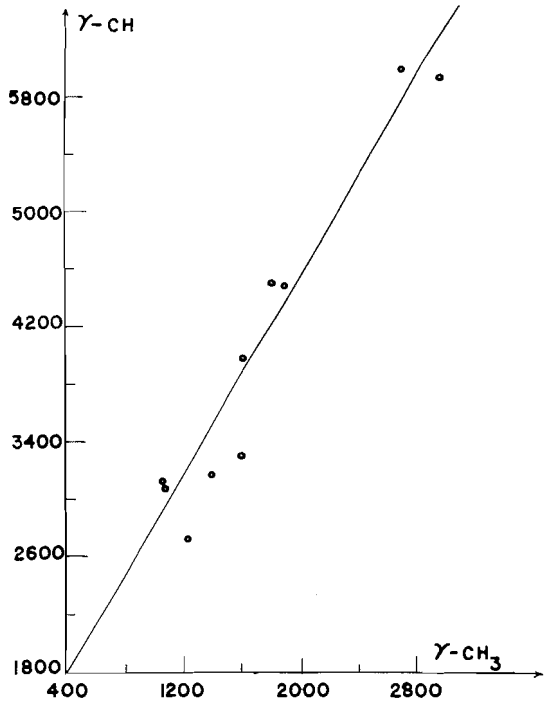

FIG. 6. Variation of γ-CH_3 and γ-CH shifts.

and that the magnitudes will be roughly proportional. The plot in Fig. 6 shows that this expectation is fulfilled. The deviation from strict linearity could result either from variations in Q_{CH_3} or from contributions to the shifts from sources other than π delocalization or from a combination of both effects. In any event it appears that π delocalization is predominant. The isotropic shifts for these mixed complexes are given in Table 7.

We next report results involving mixed complexes with the ligands **5**, **6**, and **7**.

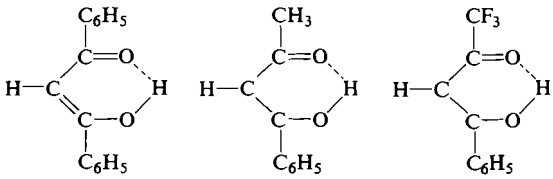

5 **6** **7**

Several investigators (10–13) have provided evidence that a phenyl substituent appears to be rather more electron donating than a methyl substituent in these β-diketonate ligands and our earlier results on the isotropic shifts of V(III) complexes were consistent with this conclusion.

TABLE 7. γ-CH_3 isotopic shifts

Number*	V(III)/γ-CH_3—acac/ϕ—ϕ Compound	Observed shifts	V(III)/γ-CH_3—acac/tfac/hfac Compound	Observed shifts
I	V(γ-CH_3—acac)$_3$	+1588	V(γ-CH_3—acac)$_3$	+1588
II			V(γ-CH_3—acac)$_2$(tfac)	B, +732
				C, +1607
III	V(γ-CH_3—acac)$_2$(ϕ—ϕ)	A=B, +889	V(γ-CH_3—acac)$_2$(hfac)	A=B, +1788
IV			*trans*-V(γ-CH_3—acac)(tfac)$_2$	C, +2698
V			*cis*-V(γ-CH_3—acac)(tfac)$_2$	C, +808
VI			*cis'*-V(γ-CH_3—acac)(tfac)$_2$	C, +1878
XIV	V(γ-CH_3—acac)(ϕ—ϕ)$_2$	B, +761	V(γ-CH_3—acac)(hfac)$_2$	B, +2960

*See Fig. 1.

TABLE 8. CF_3 isotropic shifts of V(III)/ϕ—ϕ/tf—ϕ/hfac system

Compound	Number*	Shifts (Hz) Calculated				Experimental			
V(ϕ—ϕ)$_3$		—				—			
V(ϕ—ϕ)$_2$(tf—ϕ)	II	F, −3909				F, −3900			
V(ϕ—ϕ)$_2$(hfac)	III	D=E, −3674				D=E, −3660			
trans-V(ϕ—ϕ)(tf—ϕ)$_2$	IV	C=F, −3957				C=F, −3962			
cis-V(ϕ—ϕ)(tf—ϕ)$_2$	V	A=B, −4514				A=B, −4454			
cis'-V(ϕ—ϕ)(tf—ϕ)$_2$	VI	B, −4465	F,	−4007		B, −4440	F,	−4014	
cis-V(tf—ϕ)$_3$	VII	−4221				−4252			
trans-V(tf—ϕ)$_3$	VIII	C, −4198	D,	−4908		C, −4274	D,	−4859	
		F, −3701				F, −3720			
cis'-V(hfac)(tfac)$_2$	XI	B, −3794	D,	−4406		B, −3680	D,	−4376	
		E, −4672	F,	−4695		E, −4666	F,	−4736	
cis-V(hfac)(tfac)$_2$	XII	C=F, −3890	D=E,	−5206		C=F, −3990	D=E,	−5076	
trans-V(hfac)(tfac)$_2$	XIII	A=B, −4215	D=E,	−4023		A=B, −4230	D=E,	−4048	
V(hfac)$_2$(ϕ—ϕ)	XIV	A=D, −4461	E=F,	−4593		A=D, −4524	E=F,	−4612	
V(hfac)$_2$(tf—ϕ)	XV	A, −4060	B,	−4720		A, −4020	B,	−4974	
		C, −4981	D,	−4331		C, −5100	D,	−4320	
		E, −4174				E, −4046			
V(hfac)$_3$	XVI	−4510				−4510			

*See Fig. 1.

The spectra of mixed complexes containing CF_3 and C_6H_5 substituents and CH_3 and C_6H_5 substituents have therefore been examined. Table 8 contains the experimentally observed contact shifts for 26 of the possible 32 CF_3 resonances in the CF_3/C_6H_5 system and Table 9 the CH shifts of this system. Thirty of the possible 36 resonances are reported. Analysis proceeded along the lines described for the CH_3/CF_3 system and calculated frequencies are included in Table 9. Figure 7 shows a plot of observed *vs.* calculated frequencies for the CH shifts. A detailed analysis of the shifts of protons on the phenyl ring has not been attempted since the multiplicity of lines creates a considerable assignment problem. Shifts in the CH_3/C_6H_5 system are relatively small and analysis has been confined to the CH_3 resonances. Fourteen of the possible 32 frequencies are reported in Table 10. Derived substituent parameters and d orbital population factors for these two systems are collected together in Tables 5 and 11.

Discussion

The substituent parameters for the phenyl compounds follow the pattern previously discussed. Those derived from the CH_3 shifts are all opposite in sign to the corresponding parameters obtained with CF_3 substituents confirming that a phenyl group does indeed have an opposite effect to a CF_3 group in these transition metal complexes. It is interesting to note that

Can. J. Chem. Downloaded from www.nrcresearchpress.com by 210.87.254.6 on 09/05/12
For personal use only.

TABLE 9. CH isotropic shifts of V(III)/ϕ—ϕ/tf—ϕ/hfac system

Compound	Number*	Shifts (Hz) Calculated	Experimental
$V(\phi—\phi)_3$	I	−3694	−3694
$V(\phi—\phi)_2(tf—\phi)$	II	A, −2462 B, −3873 C, −4881	A, −2420 B, −3853 C, −4828
$V(\phi—\phi)_2(hfac)$	III	A=B, −5218 C, −1381	A=B, −5140 C, −1240
trans-$V(\phi—\phi)(tf—\phi)_2$	IV	A=B, −2647 C, −6179	A=B, −2653 C, −6190
cis-$V(\phi—\phi)(tf—\phi)_2$	V	A=B, −3800 C, −3200	A=B, −3860 C, −3260
cis'-$V(\phi—\phi)(tf—\phi)_2$	VI	A, −3596 B, −2542 C, −4970	A, −3580 B, −2550 C, −4970
cis-$V(tf—\phi)_3$	VII	−3648	−3513
trans-$V(tf—\phi)_3$	VIII	A, −2142 B, −4049 C, −4980	A, −2115 B, −4015 C, −4925
cis'-$V(hfac)(tf—\phi)_2$	XI	A, −5466 B, −3396 C, −2408	A, −5426 B, −3306 C, −2448
cis-$V(hfac)(tf—\phi)_2$	XII	A=B, −3708 C, −3532	A=B, −3766 C, −3557
trans-$V(hfac)(tf—\phi)_2$	XIII	A=B, −4821 C, −1817	A=B, −5266 C, −2074
$V(hfac)_2(\phi—\phi)$	XIV	A=C, −2646 B, −6150	A=C, −2636 B, −6165
$V(hfac)_2(tf—\phi)$	XV	A, −5289 B, −3993 C, −2112	A, −5244 B, −3974 C, −2062
$V(hfac)_3$	XVI	−3734	−3734

*See Fig. 1.

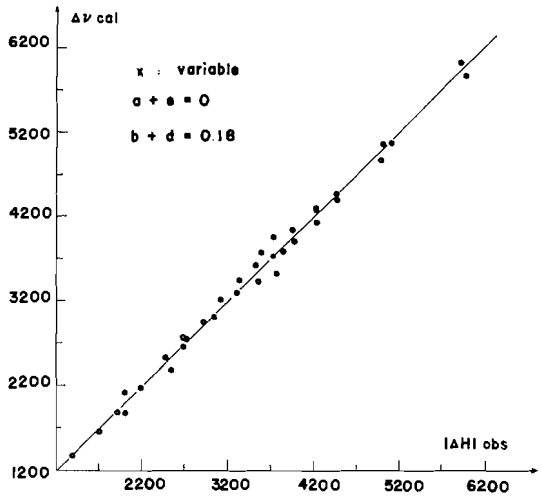

FIG. 7. Comparison of calculated and observed CH shifts. Shifts in Hz at 100 MHz. CF_3/C_6H_5 system.

the *trans* parameter for phenyl *vs.* methyl is quite large but the *cis* parameters are all considerably smaller than those obtained for CF_3. Thus the phenyl group donates electrons to the *cis* positions but withdraws from the *trans* position to such an extent that the net effect is electron withdrawing. This is to be contrasted with CF_3 which withdraws from *cis* positions and donates to the *trans* position but also has a large net withdrawing effect. The parameters obtained from the CF_3 and CH data reflecting the competition of a phenyl group with a CF_3 group are quite similar to those obtained from the CH_3/CF_3 system. It is interesting that the anomaly of a small positive value for *e* is again observed. The orbital population factors in Table 11 also show no new features. They are quite scattered with one or two anomalously high values but the trends relating to the direction of polarization of charge in the metal d_π orbitals are quite clear.

Finally we add some general remarks on the significance of these results. The substituent parameters should be regarded as qualitative indicators of the charge distribution in the σ system. In this respect they are similar to the various Hammett and Taft σ parameters for substituted aromatic compounds. The latter parameters are also often derived from n.m.r. chemical shifts and there are parallel hazards in deriving charge density information from measurements of a variable which is only indirectly related to charge. Confidence in the significance of aromatic substituent parameters rests on their ability to correlate a large variety of diverse physical measurements. If obtained by n.m.r. a given substituent parameter is usually derived from the measurement of a single chemical shift. For transition metal complexes data on substituent effects are much less accessible

Can. J. Chem. Downloaded from www.nrcresearchpress.com by 210.87.254.6 on 09/05/12
For personal use only.

TABLE 10. CH_3 isotropic shifts of V(III)/acac/ϕ—ac/ϕ—ϕ system

Compound	Number*	Shifts (Hz) Calculated				Experimental			
$V(acac)_3$	I		−4208				−4208		
$V(acac)_2(\phi—ac)$	II	A,	−4170	B,	−4187	A,	−4180	B,	−4200
		C,	−4716	D,	−4115	C,	−4780	D,	−4010
		E,	−4017			E,	−4017		
$V(acac)_2(\phi—\phi)$	III	A=B,	−3960	C=F,	−4272	A=B,	−3914	C=F,	−4230
cis-$V(\phi—ac)_3$	VII		−4494				−4480		
trans-$V(\phi—ac)_3$	VIII	A,	−4995	B,	−4314	A,	−4908	B,	−4476
		E,	−4316			E,	−4380		
$V(\phi—\phi)_2(acac)$	XIV	D=E,	−3724			D=E,	−3706		
$V(\phi—\phi)_2(\phi—ac)$	XV	F,	−4322			F,	−4280		

*See Fig. 1.

TABLE 11. (*a*) d-Orbital population factors for V(III)/ϕ—ϕ/tf—ϕ/hfac system

Compound	CF_3 shifts			CH shifts		
	d_{xy}	d_{xz}	d_{yz}	d_{xy}	d_{xz}	d_{yz}
$V(\phi—\phi)_2(tf—\phi)$	—	—	−0.07	−0.12	+0.10	+0.02
$V(\phi—\phi)_2(hfac)$	+0.46	−0.23	−0.23	+0.26	−0.13	−0.13
trans-$V(\phi—\phi)(tf—\phi)_2$	−0.18	+0.09	+0.09	−0.23	+0.115	+0.115
cis-$V(\phi—\phi)(tf—\phi)_2$	+0.005	−0.0025	−0.0025	+0.24	−0.12	−0.12
cis'-$V(\phi—\phi)(tf—\phi)_2$	−0.03	−0.01	+0.04	−0.09	−0.06	+0.15
cis-$V(tf—\phi)_3$	0.00	0.00	0.00	0.00	0.00	0.00
trans-$V(tf—\phi)_3$	−0.11	+0.07	+0.04	−0.23	+0.34	−0.11
cis'-$V(hfac)(tf—\phi)_2$	+0.04	−0.08	+0.04	+0.14	−0.27	+0.13
cis-$V(hfac)(tf—\phi)_2$	−0.02	+0.01	+0.01	−0.10	+0.05	+0.05
trans-$V(hfac)(tf—\phi)_2$	+0.05	−0.025	−0.025	+0.24	−0.12	−0.12
$V(hfac)_2(\phi—\phi)$	+0.04	+0.04	−0.08	+0.055	+0.055	−0.11
$V(hfac)_2(tf—\phi)$	+0.03	−0.02	−0.01	+0.31	−0.16	−0.15
$V(hfac)_3$	0.00	0.00	0.00	0.00	0.00	0.00

(*b*) d-Orbital population factors for V(III)/acac/ϕ—ac/ϕ—ϕ system

Compound	CH_3 shifts		
	d_{xy}	d_{xz}	d_{yz}
$V(acac)_3$	0.00	0.00	0.00
$V(acac)_2(\phi—ac)$	+0.03	−0.01	−0.02
$V(acac)_2(\phi—\phi)$	−0.16	+0.08	+0.08
cis-$V(\phi—ac)_3$	0.00	0.00	0.00
trans-$V(\phi—ac)_3$	+0.12	−0.23	+0.11
$V(\phi—\phi)_2(acac)$	+0.33	−0.165	−0.165
$V(\phi—\phi)_2(\phi—ac)$	−0.01	+0.005	+0.005
$V(\phi—\phi)_3$	0.00	0.00	0.00

and confidence in the significance of the parameters presented here rests on their ability to correlate a large body of n.m.r. data. Direct proportionality between a substituent parameter and the charge on a ligand atom is not implied and is not required if only qualitative discussion of the charge distribution is intended. Similarly we would not place any reliance on the numerical values for orbital populations but merely regard them as a qualitative indication of the movement of charge around the metal atom. Examination of the results keeping in mind these reservations reveals a number of interesting aspects of substituent effects which are unique to transition

Can. J. Chem. Downloaded from www.nrcresearchpress.com by 210.87.254.6 on 09/05/12
For personal use only.

Can. J. Chem. Downloaded from www.nrcresearchpress.com by 210.87.254.6 on 09/05/12
For personal use only.

metal complexes. First of all the movement of charge resulting from unsymmetric substitution is very much greater than that resulting from symmetric substitution. This can be seen most directly by comparing the CH shifts of the symmetric complexes $V(acac)_3$ (−3292 Hz), *cis*-$V(tfac)_3$ (−3328 Hz), and $V(hfac)_3$ (−3734 Hz) with those of an unsymmetric compound, *e.g.* $V(hfac)_2(tfac)$ (−5010, −4220, and −1916 Hz). In the series of symmetric complexes there is an increasing shift representing more charge transfer to the electron withdrawing ligands. In the unsymmetric compound the spread of the shifts is nearly an order of magnitude larger than the difference between $V(acac)_3$ and $V(hfac)_3$. Thus the majority of the charge redistribution represents movement from one ligand to another rather than from the metal to the ligands. We believe that this point has major significance with respect to the activation of substrate molecules in homogeneous catalysis. Thus it is a common observation that catalytic efficiency can depend crucially on the nature of ancillary ligands not directly involved in the reaction. The above observation suggests an obvious rationale for such dependence.

The pattern of charge migration from one ligand to another is revealed in the analysis presented. As with aromatic substitution both σ and π effects are involved. For these three dimensional complexes there are inter-relationships between the σ and π systems not found in planar compounds. A result of this is that there is an inherent tendency for charge movement in the σ and π systems to be opposed. Thus in the present case negative charge moves from acac to hfac ligands in the σ system but from hfac to acac in the π system. Basically this arises because there is charge in d orbitals orthogonal to the σ bonding system which has a spherical distribution in a symmetric complex. In the presence of an unsymmetric ligand field this spherical distribution is distorted to a prolate or oblate spheroid and the distortion is such that the more electron donating ligand has π interactions with the high electron density region. It seems that this effect may also have important mechanistic significance. For example in a complex of suitable geometry an electron withdrawing substituent at a remote point could not only diminish the charge density in the σ bond of a coordinated olefin but could concurrently enhance the density in the olefin π* orbital resulting from back donation. Such a synergistic effect provides an attractive rationale for olefin activation.

A further comparison with aromatic substituent effects is of some interest. Generally an inductively electron withdrawing substituent will qualitatively, if not quantitatively, exert the same influence at the ortho, meta, or para positions of an aromatic molecule. In these transition metal complexes the sign of the effect differs for *cis* and *trans* positions. This difference can again be related to the complexities inherent in a three dimensional system compared to a two dimensional system. Ligands *trans* to each other utilize common metal orbitals to form σ bonds. Ligands *cis* to each other interact with orthogonal metal orbitals. In the latter case the charge distributions in the two metal ligand bonds are polarized leading to a net inductive movement of charge from one ligand to the other. In the former case the involvement of a common metal orbital results in charge gained by the electron withdrawing ligand being shared with the *trans* ligand. This feature could also have considerable significance to substrate activation in catalysis. The implication is that the relative positions of two ligands in a catalytic intermediate may be crucial to the activation process.

In conclusion it seems that the type of qualitative arguments used to rationalize substituent effects on reaction rates and mechanisms in organic chemistry may find application in transition metal chemistry. They must however be used with some sophistication and with due regard to the complications which result from the three dimensional nature of metal complexes.

Experimental

Sources of Chemicals

VCl_3 and V(III) trisacetylacetonate were obtained from the Research Organic/Inorganic Chemical Co. Acetylacetone, hexafluoroacetylacetone, 1,3-diphenyl-1,3-propanedione, 1,1,1-trifluoroacetylacetone, 1-benzoylacetone, and 4,4,4-trifluoro-1-phenyl-1,3-butanedione were purchased from Eastman Kodak Co., and 3-methyl-2,4-pentanedione from Koch Light Lab.

Preparation of Compounds

Deuterated acetylacetone was prepared by adding to acetylacetone in an excess of D_2O, a small amount of sodium carbonate. The mixture was refluxed for 24 h, cooled, and extracted with anhydrous ether. This process was repeated four times, and the mixture then distilled. The fraction boiling at 129 °C was collected. Purity was established by the absence of a proton n.m.r. spectra. It

was further characterized by the isotropic shifts of mixed chelates with $V(hfac)_3$ or $V(\phi\text{—}\phi)_3$.

The complexes $V(hfac)_3$, $V(tfac)_3$, $V(tf\phi)_3$, $V(\phi\text{—}\phi)_3$-$V(\phi\text{—}ac)_3$, and $V(\gamma\text{-Me—}acac)_3$ were prepared by a method analogous to that described by Morris *et al.* (14).

CCl_4 was heated with the passage of N_2 through a side-tube for about 5 min. The respective ligand and VCl_3 were then added and the mixture refluxed for 2 h with stirring. Continuous passage of N_2 gas prevented air-oxidation of the compound. The resulting solution was filtered in a nitrogen atmosphere while hot and the filtrate allowed to cool after which the solvent was removed by vacuum distillation. The resulting brown solid was purified by either recrystallization from CCl_4 or by vacuum sublimation. The former method was employed if the ligand in its pure form is a liquid whereas the alternative was used if it is a solid.

Proton spectra were obtained on a Varian HA-100 instrument using TMS internal reference. ^{19}F spectra were obtained similarly with $CFCl_3$ internal reference, at 94.1 Mc/s and the shifts converted to 100 Mc/s. All spectra were recorded at 37 °C.

We are indebted to the National Research Council of Canada for financial support of this research.

1. D. R. Eaton and K. L. Chua. Can. J. Chem. **49**, 56 (1971).
2. A. Forman, G. N. Murrell, and L. E. Orgel. J. Chem. Phys. **31**, 1129 (1959).
3. D. R. Eaton. J. Am. Chem. Soc. **87**, 3097 (1965).
4. F. Röhrscheid, R. E. Ernst, and R. H. Holm. Inorg. Chem. **6**, 1315 (1967).
5. R. W. Taft. J. Am. Chem. Soc. **79**, 1045 (1957).
6. G. N. La Mar and G. R. Van Hecke. Inorg. Chem. **9**, 1546 (1970); J. Am. Chem. Soc. **91**, 3442 (1969); J. Am. Chem. Soc. **92**, 3021 (1970); J. Magn. Res. **4**, 384 (1971).
7. H. M. McConnell. J. Chem. Phys. **24**, 764 (1956).
8. H. M. McConnell and D. B. Chesnut. J. Chem. Phys. **28**, 107 (1958); D. B. Chesnut. J. Chem. Phys. **29**, 43 (1958).
9. D. R. Eaton, A. D. Josey, R. E. Benson, W. D. Phillips, and T. L. Cairns. J. Am. Chem. Soc. **84**, 4100 (1962).
10. L. G. Van Uitert, W. C. Fernelius, and B. E. Douglas. J. Am. Chem. Soc. **75**, 457 (1953).
11. L. G. Van Uitert, W. C. Fernelius, and B. E. Douglas. J. Am. Chem. Soc. **75**, 2736 (1953).
12. R. L. Lintvedt and H. F. Holtzclaw. Inorg. Chem. **5**, 239 (1966).
13. R. L. Lintvedt and L. K. Kernitsky. Inorg. Chem. **9**, 491 (1970).
14. M. L. Morris, R. W. Mosher, and R. E. Sievers. Inorg. Synth. **9**, 28 (1967).
15. M. J. Scarlett, A. T. Casey, and R. A. Craig. Aust. J. Chem. **24**, 31 (1971).

Can. J. Chem. Downloaded from www.nrcresearchpress.com by 210.87.254.6 on 09/05/12
For personal use only.

The Infrared and Raman Spectra of Powdered and Single-Crystal Barium Chlorate Monohydrate and -deuterate

JOHN E. BERTIE, ANTON M. HEYNS,[1] AND OSCAR OEHLER[2]

Department of Chemistry, University of Alberta, Edmonton, Alberta T6G 2G2

Received January 10, 1973

The infrared and Raman spectra of polycrystalline and single-crystal $Ba(ClO_3)_2 \cdot H_2O$ and $Ba(ClO_3)_2 \cdot D_2O$ have been obtained. The observed bands have been assigned to the various Davydov components of the intramolecular modes and colattice modes. For the water molecule, all of the fundamentals of H_2O, HDO, and D_2O have been located, the anharmonicities of the bending modes have been determined, and those of the stretching modes are essentially the same as for water vapor. The intermolecular coupling is very weak. The effective harmonic force field for the water molecules has been calculated. The stretch–stretch interaction constant is much smaller than for water vapor, reflecting a smaller separation of the asymmetric and symmetric stretching modes. The intermolecular vibrations of the water molecules have been located. For the chlorate ions, in spite of the disorder due to the ^{37}Cl, the spectra can be interpreted in terms of unit cell modes, albeit as a first approximation. The isotope shift of the symmetric Cl—O stretching mode appears to be unusually large. The far-infrared spectra have been tentatively assigned to translational and rotational vibrations involving the Ba^{2+} and ClO_3^- ions.

Les spectres en infrarouge et en Raman ont été obtenus pour les espèces polycristallines et monocristallines de $Ba(ClO_3)_2 \cdot H_2O$ et de $Ba(ClO_3)_2 \cdot D_2O$. Les bandes observées ont été attribuées aux diverses composantes Davydov des modes intramoléculaires. Toutes les bandes fondamentales appartenant à l'H_2O au HDO et au D_2O ayant été localisées, on a pu déterminer pour la molécule d'eau les anharmonicités des modes de torsion; pour celles des modes d'élongation, on a pu déterminer qu'elles étaient identiques à celles obtenues de la vapeur d'eau. Le couplage intermoléculaire est très faible. On a calculé, toujours pour les molécules d'eau, le champ effectif de la force harmonique.

La constante d'interaction élongation-élongation est beaucoup plus petite que dans le cas de la vapeur d'eau, ce qui traduit une séparation plus faible des modes d'élongation asymétrique et symétrique. On a localisé les vibrations intermoléculaires des molécules d'eau. Pour les ions chlorates, malgré la perturbation causée par la présence du ^{37}Cl, les spectres peuvent être interprétés en fonction des modes d'une maille élémentaire, bien que ce ne soit possible qu'en première approximation. Le déplacement isotopique du mode d'élongation symétrique du lien Cl—O semble être anormalement élevé. Les spectres en lointain infrarouge ont été attribués hypothétiquement aux mouvements de translation et de rotation des ions Ba^{2+} et ClO_3^-. [Traduit par le journal]

Can. J. Chem., **51**, 2275 (1973)

Introduction

The crystal structure of $Ba(ClO_3)_2 \cdot H_2O$ is well-known from X-ray (1) and neutron-diffraction (2) studies. The two water molecules in the primitive unit cell are equivalent and are situated on the two-fold axis. Their motion has been studied extensively by deuteron and proton magnetic resonance (3–10) and neutron scattering (11, 12) methods. Infrared (13–16) and Raman (17) spectral studies of polycrystalline $Ba(ClO_3)_2 \cdot H_2O$ have been reported, but the vibrational spectra of single crystals have not been previously obtained using polarized light

[1]Permanent address: Department of Chemistry, University of South Africa, Pretoria, South Africa.

[2]Present address: Laboratorium für Physikalische Chemie, Eidg. Technische Hochschule, Zurich, Switzerland.

Experimental

Single crystals of $Ba(ClO_3)_2 \cdot H_2O$ and $Ba(ClO_3)_2 \cdot D_2O$ were grown by two methods.

(i) Evaporation Method (2)

90 g of $Ba(ClO_3)_2 \cdot H_2O$ (General Chemicals Division, Morristown, N.J., U.S.A.) were dissolved in 300 g of distilled water. After passing the solution through a sintered glass filter, the water was evaporated at a rate of 20 g daily. The resulting single crystals had dimensions up to 1 cm.

(ii) Cooling Method

86 g of $Ba(ClO_3)_2 \cdot H_2O$ were dissolved in 114 g of water at 80 °C. This solution was cooled to room temperature in a closed vessel at a rate of 4 °C per day. A seed crystal was put into the saturated solution at 70 °C, and clear crystals were obtained with dimensions up to 1 cm.

The cooling method was also used for growing $Ba(ClO_3)_2 \cdot D_2O$ single crystals. $Ba(ClO_3)_2 \cdot H_2O$ was recrystallized twice from heavy water, the second time using the cooling method. The product so obtained was

Can. J. Chem. Downloaded from www.nrcresearchpress.com by 210.87.254.42 on 09/05/12
For personal use only.

Can. J. Chem. Downloaded from www.nrcresearchpress.com by 210.87.254.42 on 09/05/12
For personal use only.

judged to be about 95% deuterated from the relative intensities of the OH and OD stretching bands.

The orientation of the crystal axes was determined by X-ray precession and Weissenberg methods. To prepare single-crystal infrared samples plates were cut, using a diamond saw, with the desired orientation and a thickness of about 500 μ. They were then glued to a glass plate with Glyptal cement, and were ground to the required thickness, using bauxite 600 and kerosene. A polyethylene or cesium iodide window was then stuck to the exposed face of the sample using paraffin wax. The glass plate was removed by immersing the glass – sample – window sandwich in acetone for 24 h, and the sample was ready for study. If the sample was found to be too thick it could be affixed to the glass plate again, the window removed by warming the wax, and the sample reground. However, it was found to be impossible to prepare single crystal films thinner than about 20 μ, and this placed severe limitations on the utility of the results obtained. The polycrystalline infrared samples were mulls in Nujol or Fluorolube.

The infrared spectra were recorded using Beckman I.R. 12 and I.R. 11 spectrophotometers, and a Beckman-R.I.I.C. FS 720 interferometer. The resolution was 1 to 2 cm^{-1} for the polycrystalline samples and 2 to 4 cm^{-1} for the single-crystal samples. The spectrometers were calibrated using the standard gases (18). The details of the interferometric methods have been published elsewhere (19). For the polarization studies, Perkin–Elmer wire-grid polarizers were used. The low-temperature samples were held in a Beckman-R.I.I.C. VLT2 variable temperature unit, or in an improved version of this cell constructed in this laboratory.

The Raman spectrometer consisted of a SPEX model 1401 monochromator, SPEX sample-illuminating and detector optics, a cooled FW-130 photomultiplier and photon counting electronics. The 4880 Å line from a Carsons Laboratories model 10SP Ar^+/Kr^+ laser was used to excite the spectra, at a power of about 50 mW after filtering to remove unwanted emission lines. The collecting optics were stopped at $f/1.2$ or 0.9, and the spectral slit width was less than 1 cm^{-1} for all spectra. Single crystals of dimensions 5 × 2 × 2 mm were used and, after determining the orientation of the crystal axes by X-ray methods, the crystal was studied under a polarizing microscope to determine the principal indicatrix axes. The crystal was then aligned in the Raman instrument as described in the next section. The single crystals were mounted on a goniometer head for the room temperature studies. For the low-temperature Raman spectra, the powder and single crystal samples were held in a capillary tube mounted in a SPEX, Harney–Miller cell. To change the polarization of the incident beam and sample the scattered light, a 90° polarization rotator and an analyzer were used. A polarization scrambler was always used immediately in front of the entrance slit. The instrument was calibrated to ±1 cm^{-1} using liquid carbon tetrachloride (20), indene (21), and the manufacturer's statement of linearity to within 1 cm^{-1}, no evidence against this statement having been found. The reproducibility of the frequencies was much better than 1 cm^{-1}, however, and differences of 1 cm^{-1} between lines seen under different polarizations could be determined with certainty.

Crystal Structure and Optical Properties

$Ba(ClO_3)_2 \cdot H_2O$ crystallizes in the monoclinic space group $I2/c(C_{2h}^6)$, with four molecules per unit cell and the unit cell parameters $a = 8.916$ Å, $b = 7.832$ Å, $c = 9.425$ Å, and $\beta = 93°39'$ (2). The Ba^{2+} ions and H_2O molecules are situated on the 2-fold axes (parallel to the b crystal axis) and the ClO_3^- ions are on general positions. It has been shown (2) that the average bond distances and angles of the ClO_3^- ion in $Ba(ClO_3)_2 \cdot H_2O$ agree with those found in $KClO_3$ and $NaClO_3$, the Cl—O bond distances varying from 1.480–1.489 Å and the O—Cl—O bond angles ranging from 105.1–107.1°. The primitive unit cell, from which the selection rules for the vibrational spectra are derived, contains two formula units.

The refractive indices of $Ba(ClO_3)_2 \cdot H_2O$ were determined (1) to be: $\alpha = 1.5622$, $\beta = 1.5777$, and $\delta = 1.635$; the optic axial piane is (010) and the acute bisectrix for the sodium D-line lies at 23.75° to the c-axis with $2V = 55.5°$.

The best alignment of these crystals for Raman spectroscopy is with the incident and scattered light propagating perpendicular to the unique b-axis (22). Because of the shape and size of our crystals, it was more convenient to obtain the spectra at 90 °K with the incident light propagating perpendicular to the b and c axes, along what will be called the x-axis in this paper and which is very close to the a-axis of the crystal, and the scattered light propagating along the b-axis. The crystals were carefully aligned in this configuration by rotating them about the c-axis until the lines at 611 and 621 cm^{-1} in $Ba(ClO_3)_2 \cdot H_2O$ showed complete extinction under $x(bc)b$ and $x(cc)b$ scattering geometries, respectively. (The geometry designation follows ref. 23.) These bands are weak in Fig. 7 but this alignment procedure was, of course, done at gain settings sufficient to yield full-scale deflection under the appropriate polarization. The room temperature crystals were aligned in the same way, and the results were checked by recording spectra with the incident and scattered beams propagating perpendicular to the b-axis, along the indicatrix directions for the sodium-D line. The spectra obtained with this alignment were almost identical to those obtained while collecting the light along the b-axis, indicating that the symmetry conclusions drawn from the spectra collected along b are correct.

Results and Discussion

The infrared and Raman spectra of polycrystalline $Ba(ClO_3)_2 \cdot H_2O$ and $Ba(ClO_3)_2 \cdot D_2O$ are shown in Figs. 1 to 4 and the frequencies and assignments of the bands observed are in Tables 1 and 2. No bands were observed in the frequency regions omitted from Fig. 3. The general features of the assignment are clear. The H_2O stretching vibrations occur at 3500 to 3600 cm^{-1}, the corresponding D_2O vibrations are at 2570 to 2670 cm^{-1}, the H_2O deformation is at 1609 cm^{-1}, the D_2O deformation at 1183 cm^{-1},

Can. J. Chem. Downloaded from www.nrcresearchpress.com by 210.87.254.42 on 09/05/12
For personal use only.

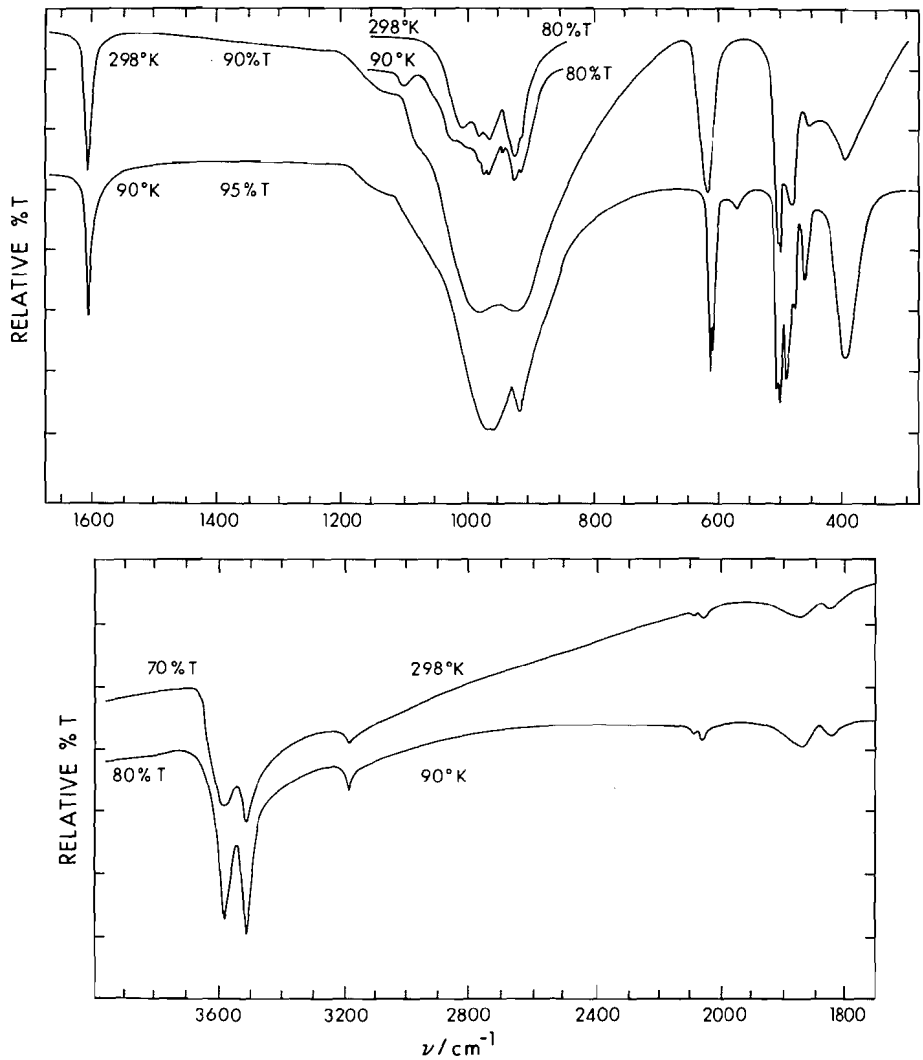

FIG. 1. The infrared spectra of powdered $Ba(ClO_3)_2 \cdot H_2O$ at 300 and 90 °K. Composed from spectra of mulls in Nujol and Fluorolube. The divisions on the intensity scale are 20% T apart.

the Cl—O stretching modes are at 900 to 1000 cm^{-1} and the ClO_3^- deformation modes lie between 470 and 620 cm^{-1}. The vibrations derived from the rotational and translational displacements of the water molecules and chlorate ions and from the translational displacements of the Ba^{2+} ions all lie below about 470 cm^{-1}. Symmetry permits all of these displacements to contribute to each vibration and the assignments are not obvious. However, the frequency shifts upon deuteration indicate that the vibrations at 454 and 395 cm^{-1} in the hydrate and 348 and 290 cm^{-1} in the deuterate primarily involve rotational displacements of the water molecules, and those at 234 and 207 cm^{-1} in the hydrate and 225 and 200 cm^{-1} in the deuterate primarily involve water translational displacements (16).

Upon lowering the temperature some of the bands sharpen and become more intense, and additional fine structure is seen. This is shown for the infrared spectra in Figs. 1 and 2, and similar effects were seen in the Raman spectra. In this respect it should be noted that even at

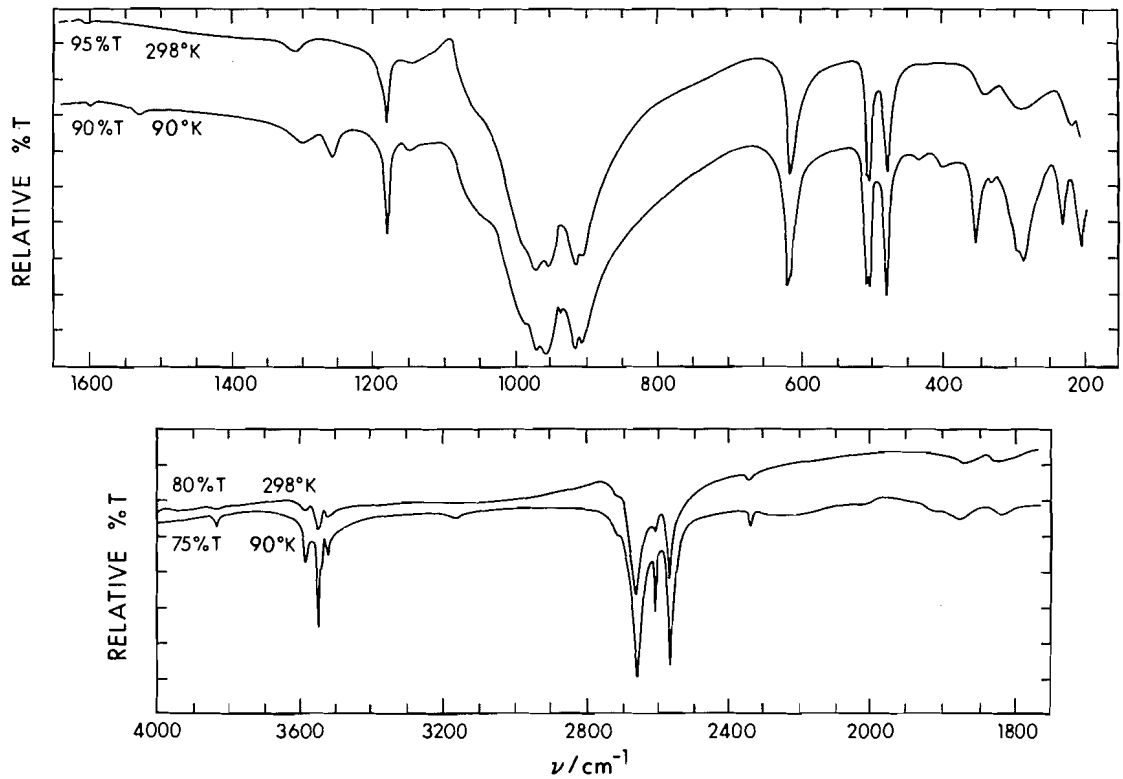

FIG. 2. The infrared spectra of powdered $Ba(ClO_3)_2 \cdot D_2O$ at 300 and 90 °K. Composed from spectra of mulls in Nujol and Fluorolube. The divisions on the intensity scale are 10% T apart.

liquid nitrogen temperatures the bands due to the Cl—O stretching modes are not well resolved in the infrared. These bands are much more complicated than the corresponding Raman bands and may be influenced by reflection effects, longitudinal optic modes, and combination and overtone bands.

The detailed assignment of the spectra will now be discussed using the single crystal polarization data. This is shown in Figs. 5–7 and the frequencies and assignments of the peaks under the various polarizations are given in Tables 1 and 2. The single crystal Raman spectra of $Ba(ClO_3)_2 \cdot D_2O$ are not reproduced, because they were very similar to those of $Ba(ClO_3)_2 \cdot H_2O$ with only the differences that are clear from Table 2. The single crystal infrared spectra were obtained only for samples at 300 °K. These infrared spectra were not of high quality due to the small area of the samples and, therefore, we only report those polarizations which were completely clear. The infrared polarizations became increasingly confused below 400 cm^{-1}, particularly for the hydrate, and no usable infrared polarization data could be obtained below 300 cm^{-1}.

Vibrations of Water Molecules

The water molecules lie on the 2-fold axes of the crystal and the symmetric OH stretching modes form the representation $A_g + A_u$ and the asymmetric OH stretching modes form $B_g + B_u$ under the unit cell group, which is isomorphous with the point group C_{2h}. The single crystal infrared data clearly show the A_u mode (*b*-polarized) at 3516 cm^{-1} in H_2O and 2574 cm^{-1} in D_2O, and the B_u modes (*ac*-polarized) at 3584 and 2668 cm^{-1} in H_2O and D_2O, respectively (Figs. 5 and 6). In the Raman spectra the A_g modes appear at 3514 and 2572 cm^{-1} with the B_g modes at 3582 and 2666 cm^{-1} for H_2O and D_2O, respectively (Table 2 and Fig. 7). The latter two bands could only be detected at low temperature. The intermolecular coupling of the water stretching modes causes the frequency separation between the u- and

Can. J. Chem. Downloaded from www.nrcresearchpress.com by 210.87.254.42 on 09/05/12
For personal use only.

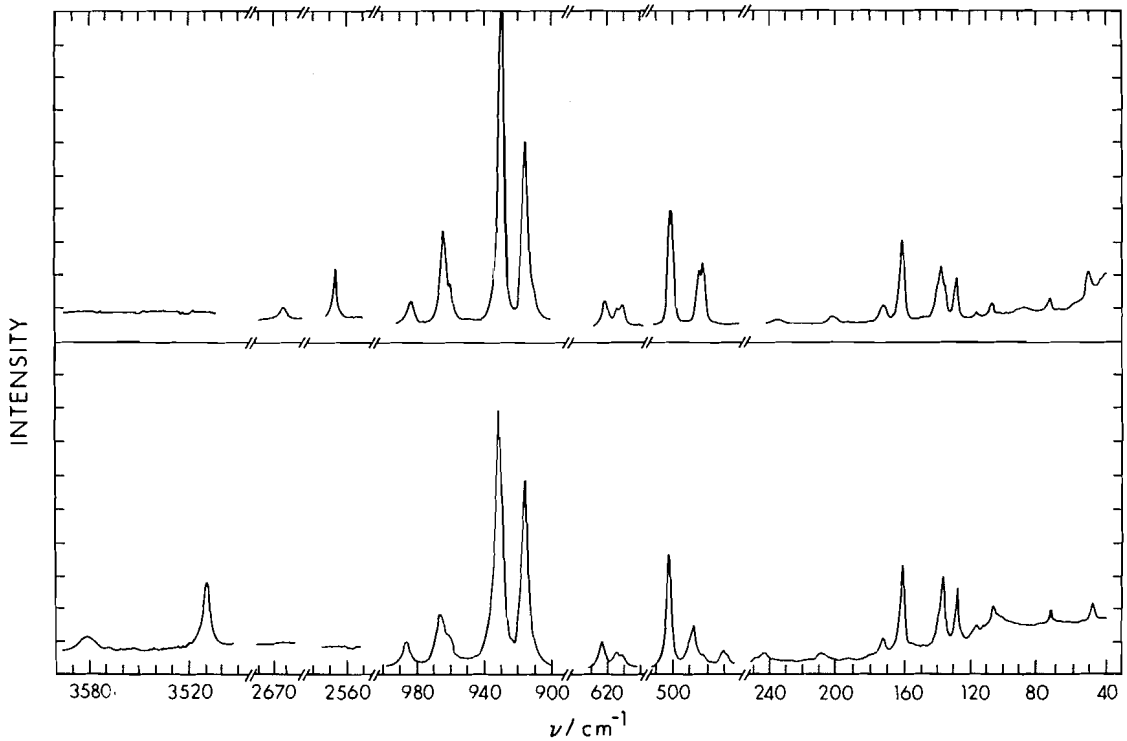

FIG. 3. The Raman spectra of polycrystalline $Ba(ClO_3)_2 \cdot H_2O$ (lower) and $Ba(ClO_3)_2 \cdot D_2O$ (upper) at 90 °K. The divisions on the frequency scale are all 10 cm^{-1} apart.

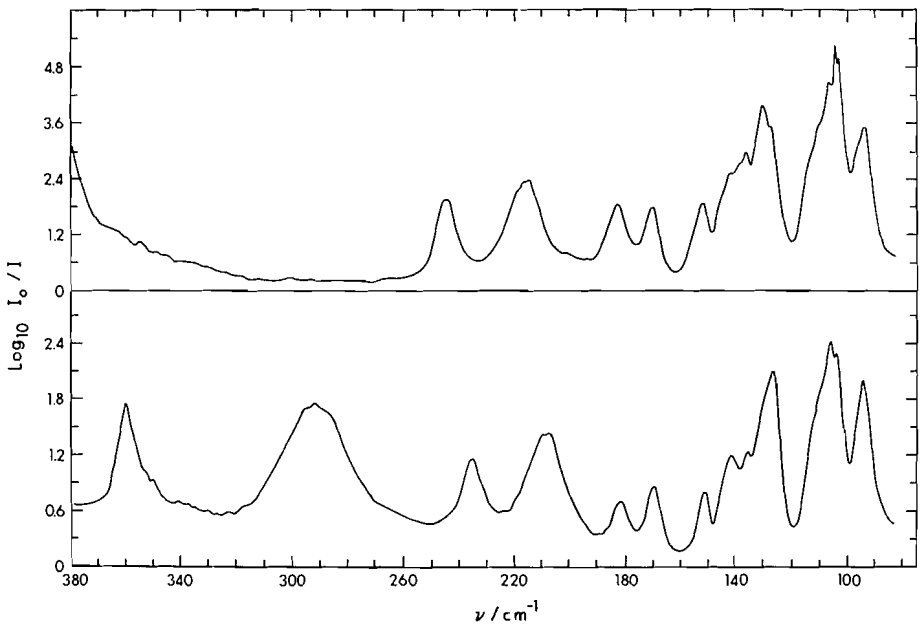

FIG. 4. The far-infrared spectra of $Ba(ClO_3)_2 \cdot H_2O$ (upper) and $Ba(ClO_3)_2 \cdot D_2O$ (lower) at 90 °K.

Can. J. Chem. Downloaded from www.nrcresearchpress.com by 210.87.254.42 on 09/05/12
For personal use only.

TABLE 1. The frequencies in cm^{-1} and assignment of the infrared absorption bands of $Ba(ClO_3)_2 \cdot H_2O$ and $Ba(ClO_3)_2 \cdot D_2O$

$Ba(ClO_3)_2 \cdot H_2O$				$Ba(ClO_3)_2 \cdot D_2O$				
300 °K	90 °K	Intensity	Symmetry*	300 °K	90 °K	Intensity	Symmetry*	Assignment†
3828		w	B_u	3837	3836	w	B_u	
3785		w	A_u	3605		w	A_u	
3584	3584	s	B_u	3584	3584	w	—‡	ν_3'
				3550	3550	s	—‡	ν'(HDO)
3516	3516	s	A_u	3516	3516	w	—‡	ν_1'
3320		w	B_u					
3185	3178	w	A_u					$2\nu_2'$
				3031		vw	A_u	
				3000		vw	B_u	
				2897		vw	B_u	
				2856		vw	A_u	
				2806		vw	—‡	$2\nu_2'$(HDO)
				2718	2718	vw	A_u	
				2668	2663	s	B_u	ν_3'
				2619	2619	m	—‡	ν'(HDO)
				2574	2570	s	A_u	ν_1'
				2493		sh	A_u	
2425		vw	A_u					
				2388		w	B_u	
				2350	2345	w	A_u	$2\nu_2'$
2256		vw	A_u					
2224		vw	B_u	2225		sh	B_u	
2090	2090	sh	B_u	2100		sh	A_u, B_u	
2061	2061	w	B_u					
2000		w	A_u	1988		w	A_u	
1960		sh	B_u	~1950		sh	B_u	
1920		sh	A_u	~1925		sh	A_u	
1908		sh	B_u		1911			
1886		w	A_u					
1879	1870	w	B_u	1880	1878	w	A_u, B_u	
1831	1831	w	A_u	1825	1831	w	A_u	
				1810		sh	B_u	
1741		vw	A_u, B_u	1749		w	A_u, B_u	
1670		vw	B_u					
1609	1609	s	A_u	1609	1609	w	—‡	ν_2'
				1572		vw	A_u, B_u	
1547		w	B_u	1532		w	B_u	
1465		sh	A_u					
1460		sh	B_u	1468		vw	B_u	
1441		vw	B_u					
				1416		w	—‡	ν_2'(HDO)
1415		w	A_u, B_u					
~1380		sh	A_u					
~1345		sh	A_u					
1321		vw	B_u	1313		vw	B_u	
				~1280	~1300	sh	B_u	
					1261	w		
1200		w	B_u	1238		vw	B_u	
				1183	1182	s	A_u	ν_2'
~1150	~1150	sh			1150	w		
	1097	w		1065	1060	sh		
	1020	sh						

Can. J. Chem. Downloaded from www.nrcresearchpress.com by 210.87.254.42 on 09/05/12
For personal use only.

TABLE 1 (*Concluded*)

$Ba(ClO_3)_2 \cdot H_2O$				$Ba(ClO_3)_2 \cdot D_2O$				
300 °K	90 °K	Intensity	Symmetry*	300 °K	90 °K	Intensity	Symmetry*	Assignment†
1005	995	sh		995	990	sh		
	~983	sh						
980	975	s		973	972	s		
960	965	s		953	958	s		ν_1 and ν_3
	946	sh			937	sh		
920	923	s		916	916	s		
912	918	sh		908	908	sh		
620	618	s	B_u	620	621	s	B_u	ν_2
615	615	s	A_u	614	618	s	A_u	ν_2
570	570	sh	A_u					
508	508	m	A_u	508	508	s	A_u	ν_4
504	504	m	B_u	504	504	s	B_u	ν_4
485	493	m	A_u, B_u	481	482	s	A_u, B_u	ν_4
	476	w						
454	460	s	B_u					ν'_R
~445		sh	A_u					
					436	w		
				~400	403	w		
395	395	s	A_u, B_u					ν'_R
				348	360	m	B_u	ν'_R
				290	291	m		ν'_R
234	245	m		225	236	m		ν'_T
207	216	m		200	208	m		ν'_T
175	184	mw		176	182	mw		
165	171	mw		164	170	mw		
148	152	mw		148	156	mw		
138	141	sh		138	142	m		
134	136	m		133	136	m		
126	130	s		125	128	s		
106	110	s		107	~110	s		
102	108	s		103	107	s		
100	105	s		100	105	s		
96	95	s		93	95	s		

*The bands due to B_u modes were polarized in the *ac* plane and those due to A_u modes were polarized parallel to the *b*-axis.
†ν_i' refers to modes of the water molecule; ν_i refers to modes of the ClO_3^- ion numbered according to C_{3v} symmetry. R = rotational and T = translational.
‡The bands assigned to HDO were observed under *b* and *ac* polarizations. The ν_3', ν_2', and ν_1' bands of H_2O in the deuterate were *ac*, *b*, and *b* polarized, respectively.

g-components and is, therefore, extremely weak in this crystal. This can be understood because the water molecules are not hydrogen-bonded to each other and are well separated in the lattice.

The infrared spectra of $Ba(ClO_3)_2 \cdot D_2O$ (Figs. 2 and 6) also show the bands due to the HDO impurity. The 3550 cm^{-1} band is present with similar strengths in the *b* and *ac* polarizations (hereafter termed *abc*-pol.), and arises from the OH stretch of the HDO molecules in the predominantly deuterated lattice. It is accompanied by polarized bands due to the symmetric (3516 cm^{-1}, *b*-pol.) and asymmetric (3584 cm^{-1}, *ac*-pol.) stretching modes of the H_2O molecules in the lattice. The clear appearance of all three of these features can only occur when intermolecular coupling is weak; if it is not weak, bands due to intermolecular OH neighbors confuse the identification of those due to intramolecular OH neighbors. The OD stretching vibration of the HDO molecules occurs at 2619 cm^{-1} (*abc*-pol., Fig. 6).

The strong, *b*-polarized, infrared band at 1609 cm^{-1} in $Ba(ClO_3)_2 \cdot H_2O$ (Fig. 5) clearly arises from the A_u HOH angle deformation mode, ν_2', and the corresponding DOD-mode is at 1183 cm^{-1} (Fig. 6). The DOH bending mode occurs at 1416 cm^{-1} (*abc*-pol., Fig. 6). The Raman-active, A_g deformation mode was not observed, even at low temperatures. The predominantly *b*-polarized band at 3185 cm^{-1}

Can. J. Chem. Downloaded from www.nrcresearchpress.com by 210.87.254.42 on 09/05/12
For personal use only.

TABLE 2. The frequencies in cm^{-1} and assignments of the Raman bands of $Ba(ClO_3)_2 \cdot H_2O$ and $Ba(ClO_3)_2 \cdot D_2O$

$Ba(ClO_3)_2 \cdot H_2O$			$Ba(ClO_3)_2 \cdot D_2O$			
300 °K	90 °K	Symmetry*	300 °K	90 °K	Symmetry*	Assignment†
	3582	B_g		2666	B_g	ν_3'
3514	3512	A_g	2572	2570	A_g	ν_1'
986	987	A_g, B_g	985	986	A_g, B_g	ν_3
965	967	A_g	964	966	A_g	ν_3
959	961	B_g	959	962	B_g	ν_3
934	933	A_g	933	932	A_g	ν_1
931	932	B_g	931	931	B_g	ν_1
918	918	A_g	916	916	A_g	$\nu_1(^{37}Cl)$
915	917	B_g	916	916	B_g	$\nu_1(^{37}Cl)$
621	624	B_g	620	622	B_g	ν_2
			612	614	A_g	$\nu_2(^{37}Cl)$
611	614	A_g	610	611	A_g	ν_2
500	503	A_g, B_g	502	503	B_g	ν_4
			500	502	A_g	ν_4
486	489	A_g	485	486	A_g	ν_4
484	489	B_g	482	483	B_g	ν_4
478	472	B_g				ν'_R
232	245	A_g		234	A_g	ν'_T
224	222					
201	209	A_g, B_g		203	A_g, B_g	ν'_T
			~196			
	175	A_g		176	A_g	
~165sh	173	A_g, B_g	~165sh	174	A_g, B_g	
158	163	A_g, B_g	158	163	A_g, B_g	
	151	A_g, B_g		151	A_g, B_g	
	141sh					
133	137, 136	A_g, B_g	134	140	A_g, B_g	
124	128	A_g, B_g	125	129	A_g, B_g	
	117	A_g	110sh	118	A_g	
	115	B_g				
106	107	A_g, B_g	105	108	A_g, B_g	
	82	A_g, B_g	78	82	A_g, B_g	
70	72	A_g, B_g	71	73	A_g, B_g	
52	50	A_g, B_g	50	50	A_g, B_g	

*The A_g modes were seen under $x(cc)b$ and/or $x(cx)b$ geometry and the B_g modes were seen under $x(bx)b$ and/or $x(bc)b$.
†ν_i' refers to modes of the water molecule; ν_i refers to modes of the ClO_3^- ion numbered according to C_{3v} symmetry. R = rotational and T = translational.

in $Ba(ClO_3)_2 \cdot H_2O$ is assigned to the overtone, $2\nu_2'$. Because the intermolecular coupling is so weak for the OH stretching modes it is undoubtedly a very good approximation to assume that all of the HOH deformation modes lie within 2 or 3 cm^{-1} of the zero-wave-vector, A_u mode. Therefore, 3185 cm^{-1} can be regarded as the overtone of the zero-wave-vector, A_u and A_g deformations at 1609 cm^{-1}.

The energy levels for the bending modes can be represented by

$$G(v) = (v + 1/2)\,\omega_e + (v + 1/2)^2\,\omega_e x_e$$

if the coupling to other modes is ignored (20). Substituting $G(2) - G(0) = 3185$ cm^{-1} and $G(1) - G(0) = 1609$ cm^{-1}, it follows that for the H_2O molecules in $Ba(ClO_3)_2 \cdot H_2O$, $\omega_e = 1642$ cm^{-1} and $\omega_e x_e = -16.5$ cm^{-1}. $\omega_e x_e$ for HDO and D_2O can be calculated from that for H_2O by multiplying by ρ^2, where ρ^2 is the ratio of the appropriate **G**-matrix elements (20, 24). $\omega_e x_e$ is, thus, found to be -12.56 cm^{-1} for HDO and -8.62 cm^{-1} for D_2O. Using these values, $G(2) - G(0)$ can be calculated to be 2807 and 2348 cm^{-1} for HDO and D_2O, respectively. The bands occurring at 2806 cm^{-1} (*abc*-pol.) and 2350 cm^{-1} (*b*-pol.) in the infrared spectra of partially hydrated $Ba(ClO_3)_2 \cdot D_2O$ (Fig. 6) are therefore assigned to $2\nu_2'$ (HDO) and $2\nu_2'(D_2O)$, respectively.

Can. J. Chem. Downloaded from www.nrcresearchpress.com by 210.87.254.42 on 09/05/12
For personal use only.

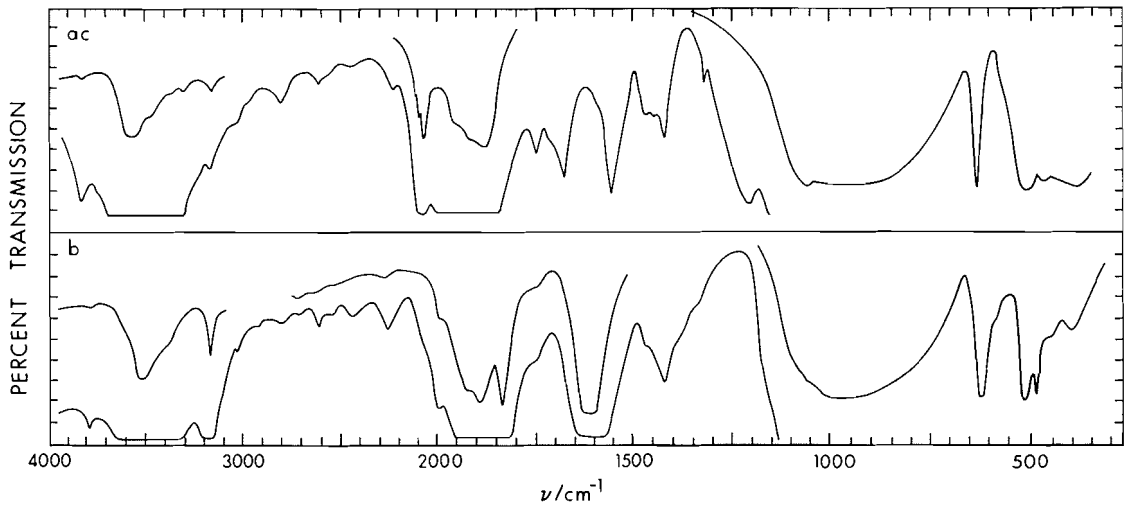

FIG. 5. The infrared spectra of single-crystal $Ba(ClO_3)_2 \cdot H_2O$ at 300 °K, polarized in the *ac* plane (upper) and parallel to the *b*-axis (lower).

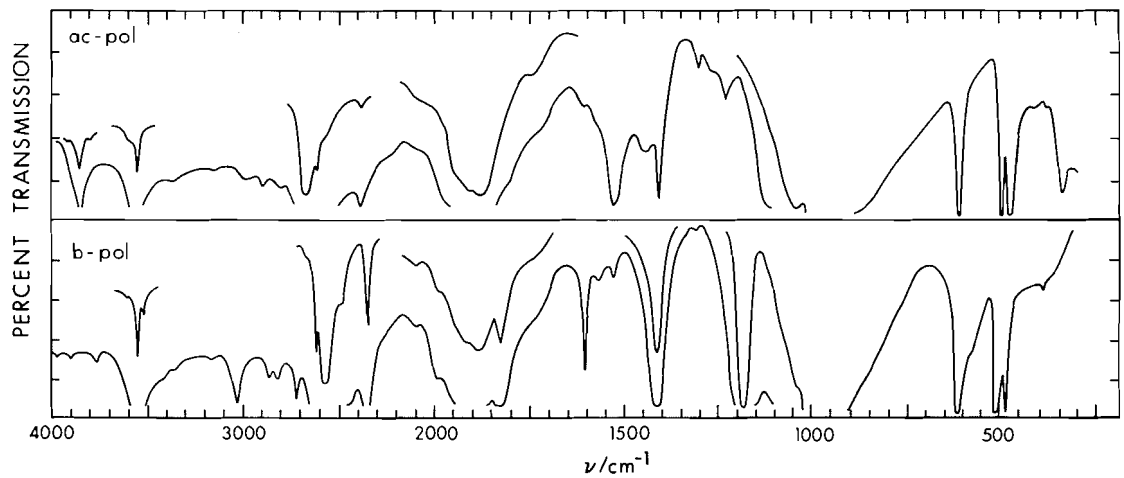

FIG. 6. The infrared spectra of single-crystal $Ba(ClO_3)_2 \cdot D_2O$ at 300 °K, polarized in the *ac* plane (upper) and parallel to the *b*-axis (lower).

This study has yielded complete data on the fundamental vibration frequencies of water in $Ba(ClO_3)_2 \cdot H_2O$. The data were used to calculate the effective intramolecular force field in two ways. First the nine observed frequencies were fitted using the four intramolecular force constants and the program FPERT (25) to yield the calculated frequencies and force constants shown in the left hand side of Table 3. The average error for the H_2O, HDO, and D_2O molecules was 9.2 cm^{-1} or 0.44%, the standard deviation was 12.2 cm^{-1} and the largest individual deviation was 23.8 cm^{-1}. In the second method the observed frequencies were converted to harmonic frequencies in the following way. The deformation modes were corrected using the anharmonicity constants derived above. The stretching modes were corrected using the gas phase values of the anharmonicity constants x_{11}, x_{33}, and x_{13} (26). The harmonic frequencies so obtained are shown in Table 3. The nine frequencies were fitted using the four force constants to yield the calculated frequencies and force constants shown on the right hand side of Table 3. The average error for the three molecules was 0.9 cm^{-1} or 0.046%, the standard

Can. J. Chem. Downloaded from www.nrcresearchpress.com by 210.87.254.42 on 09/05/12
For personal use only.

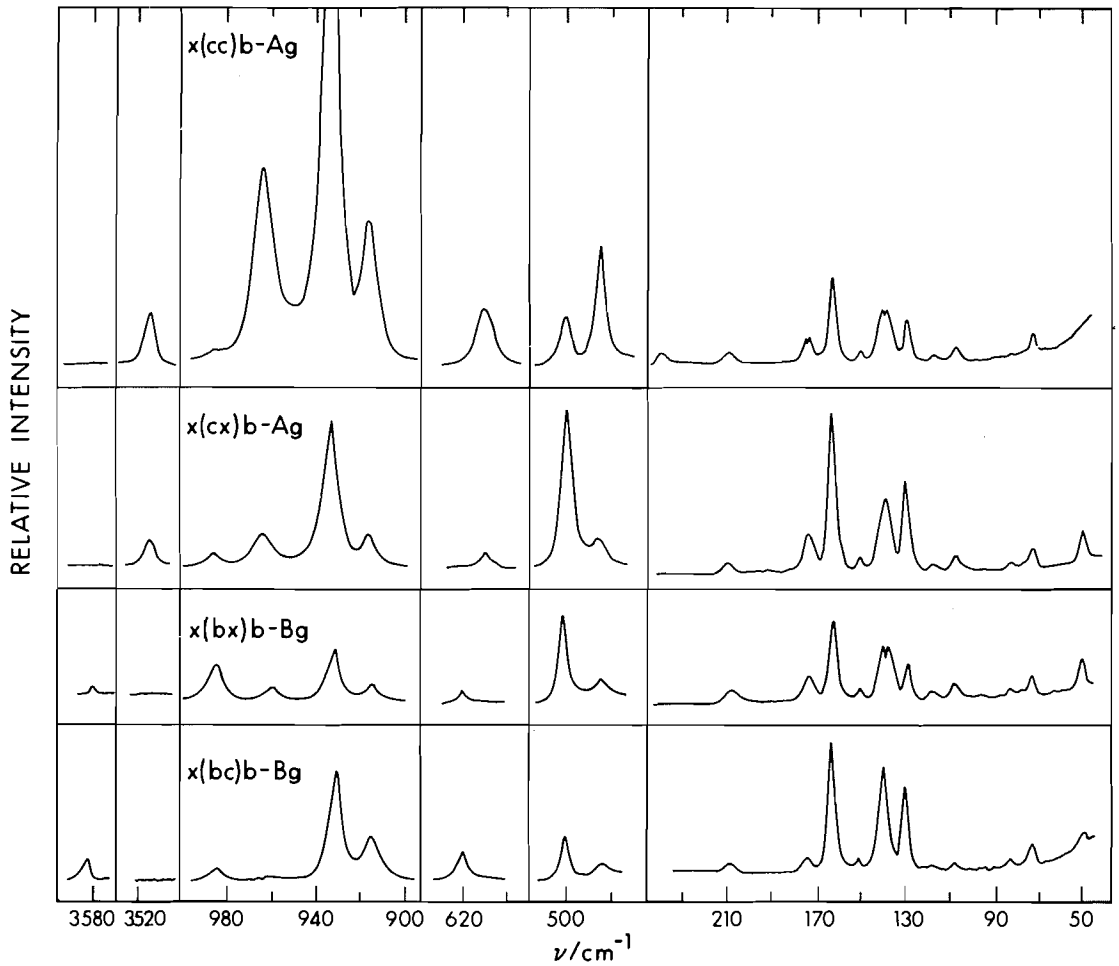

FIG. 7. The Raman spectra of single-crystal $Ba(ClO_3)_2 \cdot H_2O$. The bands above 3500 cm^{-1} and below 250 cm^{-1} are from a sample at 90 °K, and the remaining bands are from a sample at 300 °K. The divisions on the frequency scale are all 20 cm^{-1} apart.

deviation was 1.3 cm^{-1}, and the largest individual deviation was 2.4 cm^{-1}. The close agreement obtained indicates that the gas phase anharmonicities are a good approximation to the true ones for this system.

It is relevant to compare these results with those obtained by Fifer and Schiffer (27) for four hydrates and water vapor. The hydrogen bonding in $Ba(ClO_3)_2 \cdot H_2O$ is weaker than in their hydrates (27). The separation $\nu_3' - \nu_1'$ for H_2O and D_2O is found in this work to be 68 and 94 cm^{-1}, respectively, much smaller than the values 99 and 117 cm^{-1} found for water vapor (26), but larger than the values 29 to 48 cm^{-1} for H_2O and 79 to 83 cm^{-1} for D_2O found for the hydrates of reference 27. The value of F_{rr} found by fitting harmonic frequencies is -0.014 (Table 3), much smaller than the gas-phase value of about -0.1 (27), and this clearly reflects the smaller $\nu_3' - \nu_1'$ separation. The value of F_{rr} cannot be compared with those given by Fifer and Schiffer for other hydrates, because of their different treatment of the anharmonicity and the very low weight assigned to ν_2' in their fitting procedure. However, the differences between $Ba(ClO_3)_2 \cdot H_2O$ and water vapor are in qualitative agreement with the trend pointed out in ref. 27.

There are three rotational vibrations for each water molecule. They can be called the twisting mode, in which the molecules rotate about the two-fold axis, and the wagging and rocking

Can. J. Chem. Downloaded from www.nrcresearchpress.com by 210.87.254.42 on 09/05/12
For personal use only.

TABLE 3. Observed and calculated frequencies and force constants for anharmonic and harmonic H_2O, D_2O, and HDO vibrations in $Ba(ClO_3)_2 \cdot H_2O$*

Compound	Frequencies		Frequencies	
	Observed	Calculated	Harmonic	Calculated
H_2O	3516.0	3519.3	3684.1	3683.6
	1609.0	1622.1	1642.0	1644.0
	3584.0	3599.2	3762.0	3761.5
D_2O	2574.0	2567.0	2662.7	2662.4
	1183.0	1173.5	1200.2	1200.3
	2668.0	2644.2	2763.9	2763.5
HDO	3550.0	3552.5	3722.3	3724.1
	2619.0	2619.3	2712.3	2711.9
	1416.0	1408.4	1441.1	1438.7
	Force constants†			
	$F_r = 6.893$		$F_r = 7.724$	
	$F_{rr} = -0.192$		$F_{rr} = -0.014$	
	$F_{r\delta} = -0.488$		$F_{r\delta} = -0.0678$	
	$F_\delta = 0.769$		$F_\delta = 0.684$	

*The bond length was taken as 0.958 Å and the interbond angle as 110.7°, after ref. 2.
†The units are mdyn/Å for F_r and F_{rr}, mdyn for $F_{r\delta}$, and mdyn Å for F_δ.

modes, representing rotation about the axis in and out of the HOH plane, respectively. The twisting modes of the two water molecules form the representation $A_g + A_u$ under the unit cell group. These do not directly change the orientation of the dipole moment of the water molecule, so the A_u mode can only absorb radiation by changing the induced dipole moments. It is, therefore, expected to absorb more weakly than the wagging and rocking modes in which the direction of the molecular dipole oscillates. These latter modes each form the representation $B_g + B_u$ under the unit cell group. The water rotational modes absorb at 460 and 395 cm^{-1} in the hydrate and at 360 and 291 cm^{-1} in the deuterate. These frequencies are for a sample at 90 °K and at this temperature the absorption is quite strong and sharp (Figs. 1, 2, 4). For a sample at 300 °K the absorptions are much broader and have maxima at 454 and 395 cm^{-1} for the hydrate and at 348 and 290 cm^{-1} for the deuterate (Figs. 1, 2, Table 1). The infrared spectra of single crystals at 300 °K (Figs. 5, 6) show that the bands at 454, 395, and 348 cm^{-1} are predominantly *ac*-polarized and therefore arise from the B_u wagging and rocking modes. There appears to be a significant *b*-polarized component at 395 cm^{-1} in the hydrate which could be assigned to the A_u twisting mode. However a weak feature at 570 cm^{-1} in the hydrate is also *b*-polarized and shifts on deuteration (15), possibly to 400 cm^{-1}, and this may be due to the A_u twist. The only Raman line that can be assigned to water rotational vibrations is at 478 cm^{-1}, in the hydrate at 300 °K, and its polarization shows that it arises from a B_g mode.

Chiba (5) has calculated from deuteron magnetic resonance data that the water rocking mode should lie to high frequency of the wag and the twist, which should be nearly degenerate. His actual frequencies cannot be expected to be too accurate but are 330 and about 245 cm^{-1} for D_2O which correspond to about 450 and 335 cm^{-1} for H_2O. Inelastic neutron scattering studies of single crystals (12) have placed the rock at 477 cm^{-1} and the twist and the wag at 395 ± 5 or 457 ± 6 cm^{-1} in the hydrate. Thus, all of the available data, except the neutron peak at 457 cm^{-1} (12), is consistent with the assignment of the A_u twisting mode at 395 cm^{-1} in the hydrate and 290 cm^{-1} in the deuterate, and the rock and the wag at 454 and 395 cm^{-1} in the hydrate and 360 and 291 cm^{-1} in the deuterate. It is probable that the higher frequency mode is predominantly the rocking vibration, but symmetry permits the wagging and rocking

Can. J. Chem. Downloaded from www.nrcresearchpress.com by 210.87.254.42 on 09/05/12
For personal use only.

Can. J. Chem. Downloaded from www.nrcresearchpress.com by 210.87.254.42 on 09/05/12
For personal use only.

motions to contribute to the same vibrations, which probably explains the polarization of the neutron scattering peak at 457 cm^{-1} (12).

The difference of 24 cm^{-1} between the frequency of the infrared band at 454 cm^{-1} and that of the Raman band at 478 cm^{-1} suggests that the intermolecular coupling may be much larger for the rotational vibrations of the water molecules than for the OH stretching modes. This conclusion must be regarded with caution, however, because the chlorate deformation modes near 480 cm^{-1} have significantly different frequencies in the hydrate and deuterate which probably arises from interaction with the water rotational modes in the hydrate.

The translational vibrations of the water molecules form the representation $A_g + A_u$ for translation along the 2-fold axis and $2B_g + 2B_u$ for translation perpendicular to the 2-fold axis. The bands at 245 and 216 cm^{-1} in the infrared spectra of powdered $Ba(ClO_3)_2 \cdot H_2O$ at 90 °K shift to low frequency by about 4% on deuteration, and can be assigned to ungerade translational vibrations of the water molecules. Similarly the Raman bands at 245 and 209 cm^{-1} at 90 °K, shift to 234 and 203 cm^{-1} in the deuterate and can be assigned to the gerade translational modes of the water molecules. The interpretation of the Raman polarization data is unclear, because both peaks appear to arise from A_g modes, with a B_g mode contributing to the lower frequency one, yet only one A_g mode and two B_g modes are expected.

Vibrations of Chlorate Ions

Normal crystals of $Ba(ClO_3)_2 \cdot H_2O$ are disordered because every fourth chlorine atom is ^{37}Cl. This disorder should only significantly affect the selection rules for the ClO_3^- intramolecular and intermolecular modes and, of course, any other modes that couple with them. In practice, the spectra can be interpreted as though the disorder were not present, because the Raman spectra show reasonably sharp bands with well-defined polarization, as do the infrared spectra of the ClO_3^- deformation modes. The infrared spectra of the Cl—O stretching modes are clearly complicated by factors such as reflection effects and the possible appearance of longitudinal modes, and it does not seem useful to try to assign them. In the following we assign the Raman spectra of the Cl—O stretching and ClO_3^- deformation modes and the infrared spectrum of the deformation vibrations to the various factor group or Davydov components of the vibrations of $^{35}ClO_3^-$ and $^{37}ClO_3^-$. It is apparent that this is a gross simplification because each unit cell contains one $^{37}ClO_3^-$ ion on the average, and it is probable that the bands observed correspond to intensity-weighted density of states curves. However, in the absence of a more rigorous treatment of the spectra of such crystals, the following is presented as a first approximation to the correct assignment, on the understanding that A_g, B_g, etc. are used to concisely describe the polarization behavior of the peaks, rather than to imply that the crystal modes have this symmetry.

The free ClO_3^- ion belongs to the point group C_{3v}, and its vibrations can be classified as the $\nu_1(A_1)$ and $\nu_3(E)$ stretching vibrations, occurring in the range 900–1000 cm^{-1}, the totally symmetric bending vibration, $\nu_2(A_1)$, occurring at about 620 cm^{-1} and the asymmetric bending vibrations, $\nu_4(E)$, at 480–510 cm^{-1} (22, 28, 29). The ClO_3^- ions lie on general positions in the crystal and each A_1 mode of the free ClO_3^- ion yields the representation $A_g + A_u + B_g + B_u$ under the unit cell group. The strongest band in the Raman spectrum of the hydrate, at 934 cm^{-1}, is assigned to the A_g component of the Cl—O stretching mode, ν_1. The B_g component of this mode appears at 931 cm^{-1}. The bands at 918 cm^{-1} (A_g) and 915 cm^{-1} (B_g) are about one-quarter as intense as the ν_1 band and are therefore assigned to the ν_1 mode of $^{37}ClO_3^-$. However, it is clear that the one $^{37}ClO_3^-$ ion per unit cell cannot vibrate in this mode at two distinct frequencies and, in fact, in $Ba(ClO_3)_2 \cdot D_2O$ the A_g and B_g components coincide at 916 cm^{-1}. Different frequencies for the infrared and Raman peaks due to ν_1 of $^{37}ClO_3^-$ have been reported for $KClO_3$ (22). This was interpreted (22) as due to dynamic coupling between the vibrations of $^{35}ClO_3^-$ and $^{37}ClO_3^-$ ions which, if the lack of selection rules because of the disorder is recognized, is equivalent to saying that different parts of the density of states curve have different activities in the two types of spectra. In the case of $Ba(ClO_3)_2 \cdot H_2O$ there is evidence that the first overtone of the water rocking mode at 454 cm^{-1} influences this region and may be responsible for the different frequencies of the A_g and B_g components at 918 and 915 cm^{-1}. Apart from the different fre-

Can. J. Chem. Downloaded from www.nrcresearchpress.com by 210.87.254.42 on 09/05/12
For personal use only.

quencies for the hydrate and deuterate mentioned above, this evidence lies in the relative intensity of these peaks to those, at about 933 cm^{-1}, due to ν_1 of $^{35}ClO_3^-$. In the single crystal spectra at 300 °K these peaks are about one-quarter as intense as those due to ν_1 of $^{35}ClO_3^-$. In the spectrum of the deuterate at 90 °K the intensity ratio is still one-quarter but in that of the hydrate at 90 °K it is one-third. Further, in the Raman spectrum of the powdered deuterate at 300 °K the intensity ratio is one-quarter, as for the single crystal, but the ratio for the powdered hydrate at 300 °K is nearer to two-thirds. These differences are not understood, but they do support the postulate that a phenomenon occurs in the hydrate that does not occur in the deuterate, and this is most obviously attributable to the influence of the overtone of the water rotational mode at 454 cm^{-1}. Even without these complications, the assignment of the bands near to 916 cm^{-1} to the ν_1 mode of $^{37}ClO_3^-$ implies a much greater isotope shift for this mode than is calculated or usually found (22, 28, 29). No explanation can be offered for this, nor is any reasonable alternative assignment apparent.

The appearance of the A_u (615 cm^{-1}), B_u (620 cm^{-1}), A_g (611 cm^{-1}), and B_g (621 cm^{-1}) modes near 620 cm^{-1} in the infrared and Raman spectra of single crystals of $Ba(ClO_3)_2 \cdot H_2O$, indicates that the assignment of these bands to the different components of the symmetric ClO_3^- deformation mode, ν_2, is correct. In the Raman spectra of the deuterate, particularly at lower temperatures, a weak shoulder was seen to occur at 614 cm^{-1}. This lies about 4 cm^{-1} below the average of the frequencies of the four components assigned to $^{35}ClO_3^-$, and its assignment to ν_2 of $^{37}ClO_3^-$ is consistent with the isotope shift usually observed for this mode (28, 29).

The degeneracy of the E-vibrations is lifted under the C_1 site symmetry and the $\nu_3(E)$ and $\nu_4(E)$ modes each yield the representation $2A_g + 2A_u + 2B_g + 2B_u$ under the unit cell group. The single crystal Raman spectra of $Ba(ClO_3)_2 \cdot H_2O$ clearly show two bands at 986 and 965 cm^{-1}, representing the A_g components of the asymmetric stretching modes. The corresponding B_g components were observed at 986 and 959 cm^{-1}.

In the infrared spectra of single crystals of $Ba(ClO_3)_2 \cdot H_2O$, the two b-polarized bands (A_u) at 508 and 485 cm^{-1} and the corresponding ac-polarized bands (B_u) at 504 and 485 cm^{-1} are assigned to the asymmetric, ClO_3^- bending vibrations, ν_4. In the Raman spectra the A_g components of these modes are observed at 500 and 486 cm^{-1} while the B_g components appear at 500 and 484 cm^{-1}.

From this data the site frequency for ν_2 can be determined as 617 and 616 cm^{-1} in the hydrate and deuterate, respectively, by averaging the frequencies of the factor group components. Without the frequencies of the A_u and B_u components, the site frequency for ν_1 can only be estimated as about 932 cm^{-1} in both compounds. The frequencies of the site-group components of the degenerate modes can only be estimated as 985 and 963 cm^{-1} for ν_3 in both compounds, 503 and 485 cm^{-1} for ν_4 in the hydrate, and 504 and 482 cm^{-1} for ν_4 in the deuterate, under the assumption that the site splitting is much greater than the factor group splitting. The results for $KClO_3$ (22) suggest that this assumption may not be valid.

In both the polycrystalline and single crystal infrared spectra, several overtone and combination bands of the Cl—O stretching vibrations were observed in the range 1830–2000 cm^{-1}. These bands are listed in Table 1 along with their polarizations, and are shown in Figs. 5 and 6. The samples studied at 90 °K were too thin to show many of these bands.

Lattice Vibrations Involving the Ba^{2+} and ClO_3^- Ions

The $\boldsymbol{k} = 0$ lattice vibrations of the Ba^{2+} and ClO_3^- ions in $Ba(ClO_3)_2 \cdot H_2O$ form the representation $7A_g + 7A_u + 8B_g + 8B_u$, including the acoustic modes which are identified as $A_u + 2B_u$. As expected from the number of lattice vibrations, the far-infrared and Raman spectra of polycrystalline $Ba(ClO_3)_2 \cdot H_2O$ and $Ba(ClO_3)_2 \cdot D_2O$ are complex. The single crystal Raman spectra show that the majority of these bands are due to both A_g and B_g modes. The single crystal far-infrared spectra also failed to show useful differences in different polarizations.

The translational vibrations of the Ba^{2+} and ClO_3^- ions and the rotational vibrations of the ClO_3^- ions all appear in all four irreducible representations of the unit cell group, and therefore can be expected to interact to yield mixed translational and rotational vibrations. About the only basis for any assignments is the argument that, because the motion of ions is involved, the predominantly translational vibra-

TABLE 4. Lattice vibration frequencies in $KClO_3$, $NaClO_3$, and $Ba(ClO_3)_2 \cdot H_2O$*

		$Ba(ClO_3)_2 \cdot H_2O$ at 90 °K		
$KClO_3$†	$NaClO_3$†	Far-infrared	Raman	
	183	184mw	—	ν_T
	180	—	—	
	176 ν_T	171mw	175w	ν_R
			173w	
161	—		163s	ν_R
		152mw	151w	ν_T
144	142 ν_R	141sh	141sh	
	134	136m	137ms	ν_R
132	ν_R			
	131	130s	128ms	
	124	—		
			117w	ν_R
			115w	
109		110s	—	
		108s	107w	ν_T
		105s	—	
	95	95s	—	
87	86 ν_R	—	—	
83		—	82vw	ν_R
	72	—	72w	
	65 ν_T	—	—	
57		—	50mw	

*Frequencies in cm^{-1}. ν_T or ν_R indicate that the band is tentatively assigned to translational vibrations of Ba^{2+} and ClO_3^- or to rotational vibrations of ClO_3^-, respectively.
†Reference 22.

tions should be strong in the infrared and weak in the Raman. The rotational vibrations of the ClO_3^- ions are likely to be strong in both, although if any vibrations correspond mainly to rotation about the axis of the ClO_3^- group they may be weak in both types of spectra because the intra-ion contributions to the dipole moment and polarizability changes during this motion are only non-zero through the distortion of the ion from C_{3v} symmetry. Because of the simple basis for these ideas the predictions are not expected to hold entirely, but they do enable some tentative assignments to be made.

On this basis, the bands at 184, 152, 110, 108, 105, and 95 cm^{-1} (at 100 °K) (Tables 1, 2, Figs. 3 and 4) are assigned to predominantly translational vibrations. The bands near to 171, 136, and 130 cm^{-1} in both types of spectra, and possibly the band at 163 cm^{-1} in the Raman, are assigned to rotational vibrations about the axes perpendicular to the bisector of the ClO_3^- group, while the Raman bands near 116 and 82 cm^{-1} are assigned to rotational vibrations about the bisector. No assignment of the remaining bands appears to be worthwhile. There is a remarkable similarity between some of the frequencies in $Ba(ClO_3)_2 \cdot H_2O$ and those in $KClO_3$ and $NaClO_3$ (Table 4). The reason for this similarity is unclear, considering the different crystal structures and, presumably, quite different force fields in the different crystals, but the agreement between the frequencies appears to be too extensive to be coincidence. Therefore these frequencies presumably correspond to predominantly ClO_3^- vibrations.

The uncertainty in the above assignments should be abundantly clear, but there appears to be no way of improving on this with the present data.

The National Research Council of Canada is thanked for financial support of this work. We are grateful to Professor R. D. Morton of the Geology Department, University of Alberta, for his advice on cutting and grinding crystal plates.

1. G. KARTHA. Proc. Indian Acad. Sci. Sec. A36, 501 (1952).
2. S. K. SIKKA, S. N. MOMIN, H. RAJAGOPAL, and R. CHIDAMBARAM. J. Chem. Phys. **48**, 1883 (1968).
3. R. D. SPENCE. J. Chem. Phys. **23**, 1166 (1955).
4. A. A. SILVIDI and J. W. MCGRATH. J. Chem. Phys. **33**, 1789 (1960).

Can. J. Chem. Downloaded from www.nrcresearchpress.com by 210.87.254.42 on 09/05/12
For personal use only.

5. T. CHIBA. J. Chem. Phys. **39**, 947 (1963).
6. J. W. MCGRATH and A. A. SILVIDI. J. Chem. Phys. **39**, 3017 (1963).
7. B. PEDERSEN. J. Chem. Phys. **41**, 122 (1964).
8. Z. M. EL SAFFAR. Acta Cryst. **24B**, 1131 (1968).
9. T. CHIBA and K. YOSHINOBU. Bull. Chem. Soc. Jap. **41**, 828 (1968).
10. J. PIETRZAK and A. A. KHANAGOV. Zh. Strukt. Khim. **11**, 544 (1970).
11. H. J. PRASK and H. BOUTIN. J. Chem. Phys. **45**, 699 (1966).
12. C. L. THAPER, B. A. DASANNACHARYA, A. SEQUEIRA, and P. K. IYENGAR. Solid State Commun. **8**, 497 (1970).
13. F. A. MILLER and C. H. WILKINS. Anal. Chem. **24**, 1253 (1952).
14. F. A. MILLER, G. L. CARLSON, F. F. BENTLEY, and W. H. JONES. Spectrochim. Acta **16**, 135 (1960).
15. V. S. TOMAR, H. D. BIST, and D. P. KHANDELWAL. Proc. Nucl. Phys. Solid State Phys. Symp. 15th, **3**, 491 (1970).
16. K. FUKUSHIMA and T. YANAGIDA. Bull. Chem. Soc. Jap. **45**, 2285 (1972).
17. C. SHANTA KUMARI. Curr. Sci. (India) **14**, 204 (1950).
18. Tables of wavenumbers for the calibration of infrared spectrometers. I.U.P.A.C. Butterworths Scientific Publications, London, 1961.
19. J. E. BERTIE and D. A. OTHEN. Can. J. Chem. **50**, 3443 (1972).
20. G. HERZBERG. Infrared and Raman spectra. D. Van Nostrand Co., New York, 1945.
21. J. LOADER. Basic-laser Raman spectroscopy. Heyden and Son Ltd. London, 1970. p. 27.
22. J. B. BATES. J. Chem. Phys. **55**, 494 (1971).
23. T. C. DAMEN, S. P. S. PORTO, and B. TELL. Phys. Rev. **142**, 570 (1966).
24. E. B. WILSON, J. C. DECIUS, and P. C. CROSS. Molecular vibrations. McGraw–Hill, New York, 1955.
25. J. H. SCHACHTSCHNEIDER. Technical report No. 57–65, project number 31450, Shell Development Company, Emeryville, California.
26. W. S. BENEDICT, N. GAILAR, and E. K. PLYLER. J. Chem. Phys. **24**, 1139 (1956).
27. R. A. FIFER and J. SCHIFFER. J. Chem. Phys. **52**, 2664 (1970).
28. G. N. KRYNAUW and C. J. H. SCHUTTE. Z. Phys. Chem. (N.F.) **55**, 113 (1967).
29. C. M. HARTWIG, D. L. ROUSSEAU, and S. P. S. PORTO. Phys. Rev. **188**, 1328 (1969).

Can. J. Chem. Downloaded from www.nrcresearchpress.com by 210.87.254.42 on 09/05/12
For personal use only.

Temperature and Pressure Dependence of ^{35}Cl Nuclear Quadrupole Resonance in $BiCl_3$

G. C. GILLIES AND R. J. C. BROWN

Department of Chemistry, Queen's University, Kingston, Ontario

Received January 18, 1973

The temperature and pressure dependences of the two ^{35}Cl nuclear quadrupole resonances in $BiCl_3$ have been measured. At constant pressure, the temperature coefficients are markedly different and this difference is shown to be due to volume effects associated with different intermolecular bonding.

L'influence de la température et de la pression sur les deux résonances nucléaires quadrupolaires du ^{35}Cl dans $BiCl_3$ a été mesurée. A pression constante, les coefficients de température marquent une certaine différence qui est due aux effets de volume associés aux diverses liaisons intermoléculaires.

[Traduit par le journal]

Can. J. Chem., **51**, 2290 (1973)

Can. J. Chem. Downloaded from www.nrcresearchpress.com by 210.87.254.5 on 09/05/12
For personal use only.

Introduction

The ^{35}Cl nuclear quadrupole resonance (n.q.r.) spectrum of bismuth trichloride consists of two lines, near 19.1 and 16.0 MHz (1). The crystal structure (2) indicates that one chlorine atom in the molecule is close to one extra-molecular bismuth atom, and two "face-bridging" chlorine atoms are each close to two extra-molecular bismuth atoms; the two face-bridging chlorine atoms are reported to be not quite equivalent. Intermolecular bonding has been suggested as a cause of the low values for the n.q.r. frequencies (1), and of the difference between the Raman spectra of gaseous and solid $BiCl_3$ (3); since there are at least two different chlorine atom sites in the solid, the n.q.r. spectrum provides an opportunity for studying two cases of intermolecular bonding in the same sample. The original n.q.r. results (1) indicate that the two resonance frequencies have markedly different temperature dependences, the lower frequency line having a positive temperature coefficient. The present study was undertaken to determine the temperature and pressure coefficients of the two resonance frequencies near room temperature.

Experimental

Details of the spectrometer, and of the equipment used for controlling the temperature and pressure, have been reported previously (4). The resonance frequencies were measured between 238 and 338 K at atmospheric pressure, and at pressures up to 275 MN m^{-2} at temperatures near 298 K.

Results and Discussion

Both resonance frequencies varied essentially linearly with changes in temperature and pressure over the ranges investigated, with the following coefficients. For the 16.0 MHz resonance

$$(\partial\nu/\partial T)_P = +0.38 \pm 0.03 \text{ kHz K}^{-1}$$

$$(\partial\nu/\partial P)_T = -1.22 \pm 0.01 \text{ kHz (MN m}^{-2})^{-1}$$

and for the 19.1 MHz resonance

$$(\partial\nu/\partial T)_P = -1.94 \pm 0.04 \text{ kHz K}^{-1}$$

$$(\partial\nu/\partial P)_T = -0.38 \pm 0.01 \text{ kHz (MN m}^{-2})^{-1}$$

The values of the resonance frequencies at 25 °C were 15 959 ± 1 and 19 159 ± 1 kHz, respectively. The positive temperature coefficient of the lower resonance frequency is confirmed, and it is seen to be associated with a strongly negative pressure coefficient, as in other cases of positive temperature coefficients. The temperature coefficients of the resonance frequencies under constant volume conditions can be obtained from the following equation (5):

$$[1] \qquad \left(\frac{\partial\nu}{\partial T}\right)_V = \left(\frac{\partial\nu}{\partial T}\right)_P + \frac{\alpha}{\beta}\left(\frac{\partial\nu}{\partial P}\right)_T$$

The ratio of thermal expansion coefficient to isothermal compressibility (α/β) has been estimated as $\alpha/\beta \lesssim 3.3$ MN m^{-2} K^{-1} (4), and so for the 16.0 MHz resonance,

$$(\partial\nu/\partial T)_V \cong -3.6 \text{ kHz K}^{-1}$$

while for the 19.1 MHz resonance

$$(\partial\nu/\partial T)_V \cong -3.2 \text{ kHz K}^{-1}$$

The marked difference in the temperature coefficients of the two resonances disappears when the simple corrections for volume changes are made. There are no data available on the asymmetry parameter of either resonance, and so it will be assumed that both asymmetry parameters are small enough that their variations with temperature and pressure produce negligible effects on the observed resonance frequencies; the observed coefficients of the resonance frequencies are then ascribed entirely to variations in the nuclear quadrupole coupling constants. The temperature dependence of the coupling constant at constant volume reflects the effects of lattice vibrations on the time-averaged electric field gradient tensor, and the above result indicates that the two chlorine atom sites are affected by lattice vibrations in approximately the same way. The difference between the two sites lies instead in the different volume dependences of the coupling constants, a result which is consistent with the different intermolecular bonding at the two sites.

It has been shown previously (4) that the temperature coefficient of the ^{209}Bi coupling constant in $BiCl_3$ at constant volume is too large to be accounted for on the basis of vibrational averaging. In the theory of vibrational averaging due to Bayer (6), the temperature dependence of the electric field gradient tensor is calculated assuming that the size and shape of the unit cell, and the average positions of the atoms within the unit cell, remain constant, while the amplitudes of the torsional oscillations increase as the temperature is raised. By combining $(\partial\nu/\partial T)_P$ with $(\partial\nu/\partial P)_T$ using eq. 1, the temperature dependence at constant volume is obtained, but this result contains possible contributions from changes of shape of the unit cell (at constant volume), and changes of the average atomic positions within the unit cell. Hence no numerical comparison of $(\partial\nu/\partial T)_V$ with Bayer theory is justified, beyond observing that the correct order of magnitude is obtained for both ^{35}Cl resonances.

Equipment for this work was purchased using grants from the National Research Council of Canada and the Advisory Research Committee of Queen's University. One of us (G.C.G.) thanks the National Research Council of Canada for the award of a scholarship.

1. H. G. Robinson. Phys. Rev. **100**, 1731 (1955).
2. S. C. Nyberg, G. A. Ozin, and J. T. Szymanski. Acta Cryst. B**27**, 2298 (1971).
3. E. Denchik, S. C. Nyberg, G. A. Ozin, and J. T. Szymanski. J. Chem. Soc. A, 3157 (1971).
4. G. C. Gillies and R. J. C. Brown. Can. J. Chem. **50**, 2586 (1972).
5. T. Kushida, G. B. Benedek, and N. Bloembergen. Phys. Rev. **104**, 1364 (1956).
6. H. Bayer. Z. Phys. **130**, 227 (1951).

Can. J. Chem. Downloaded from www.nrcresearchpress.com by 210.87.254.5 on 09/05/12
For personal use only.

Pyrolysis of Trifluoroacetaldehyde

MICHAEL T. H. LIU, LEON F. LOUCKS, AND ROBERT C. MICHAELSON

Department of Chemistry, University of Prince Edward Island, Charlottetown, Prince Edward Island

Received October 30, 1972

The thermal decomposition of trifluoroacetaldehyde has been studied over the 460–520 °C temperature range, and at pressures from 4 to 400 mm Hg. The experimental rate equation in the high-pressure region is of the form: Rate = $k[CF_3CHO]^{3/2}$ where

$$k = 10^{13.8\pm0.1} \exp(-50\,500 \pm 300/RT)\ cc^{1/2}\ mol^{-1/2}\ s^{-1}$$

The results are consistent with a mechanism initiated by a first order process and terminated by a second order recombination of two CF_3 free radicals. At lower pressures (40 mm Hg), the ratio of k_{init}/k_{term} is pressure dependent and the overall order increases. The effects of added inert gas confirm this pressure dependence.

La décomposition thermique du trifluoracétaldéhyde a été étudiée dans l'intervalle de température 460–520 °C et sous des pressions de 4 à 400 mm Hg. L'équation de vitesse expérimentale dans la région de haute pression est de la forme vitesse = $k[CF_3CHO]^{3/2}$ où

$$k = 10^{13.8\pm0.1} \exp(-50\,500 \pm 300/RT)\ cc^{1/2}\ mol^{-1/2}\ s^{-1}$$

Les résultats sont compatibles avec un mécanisme initié selon un processus de premier ordre puis terminé par une recombinaison de second ordre de deux radicaux libres CF_3. Aux basses pressions (40 mm Hg), le rapport $k_{initial}/k_{final}$ dépend de la pression et l'ordre global augmente. Les effets de gaz inerte ajouté confirment l'influence de la pression. [Traduit par le journal]

Can. J. Chem., 51, 2292 (1973)

Introduction

Arthur and Bell (1) studied the kinetics of the thermal decomposition of trifluoroacetaldehyde at temperatures between 471 and 519 °C, and at pressures up to 180 mm Hg. The main products were trifluoromethane and carbon monoxide in equal amounts together with small amounts of hexafluoroethane and hydrogen. The order of the reaction was 3/2 and the mechanism postulated involved a second-order initiation and third-order termination process.

More recently, Liu and Laidler (2, 3) have reinvestigated the pyrolysis of acetaldehyde over the 480–540 °C temperature range. The mechanism proposed was essentially that of the Rice–Herzfeld scheme, together with a number of other elementary processes. Côme and coworkers (4, 5) published findings similar to those reported by Liu and Laidler. There is general agreement that the experimental results are compatible with a radical chain mechanism which is initiated by a first-order process, and terminated by a second-order combination of methyl radicals. According to the results of Liu and Laidler, the overall order of the thermal decomposition of acetaldehyde is 1.5 at high pressures (> 100 mm Hg) and increases to 1.7 at pressures below 20 mm Hg. These results suggest that both the initiation and termination steps become pressure dependent at low pressures. In view of the apparent differences between the thermal decompositions of acetaldehyde and trifluoroacetaldehyde, the present work was undertaken to see if the pyrolysis of trifluoroacetaldehyde was indeed substantially different from that of acetaldehyde.

Experimental

Trifluoroacetaldehyde (K and K Laboratories Inc.) was prepared from the hydrate by passing the hydrate under vacuum through a column of P_2O_5 packed in glass wool. Bath temperatures up to 90 °C were required to force the hydrate through the column. The trifluoroacetaldehyde was further dried by passing it several times through U-tubes packed with P_2O_5 and then trapped over Na_2CO_3 to remove any residual trifluoroacetic acid. This product was distilled under vacuum from a trap at −95 °C (toluene slush) to a trap at −127 °C (*n*-propanol), with a volatile fraction being trapped with liquid N_2. Gas chromatographic analysis of the purified sample indicated no impurities in excess of 0.1%. The infrared spectrum of the aldehyde at 25 mm Hg agreed with those of Husted and Ahlbrecht (6) and of Dodd, Roberts, and Woodward (7). The infrared spectrum of the high volatility fraction discarded in the distillation revealed the presence of C_2F_4 as an impurity of the original aldehyde; care was taken to remove this impurity.

The decomposition was carried out in a conventional static system. The reaction vessel was a quartz cylinder 418 ml in volume, with a s/v ratio of 0.7 cm^{-1}, enclosed

Can. J. Chem. Downloaded from www.nrcresearchpress.com by 210.87.254.40 on 09/05/12
For personal use only.

Can. J. Chem. Downloaded from www.nrcresearchpress.com by 210.87.254.40 on 09/05/12
For personal use only.

in a furnace consisting of an electrically heated steel cylinder. The temperature of the vessel was controlled to within 0.3 °C by means of a Thermoelectric Model 400 temperature controller.

To initiate a run the trifluoroacetaldehyde was admitted to the vacuum line manifold and a 2 l bulb, and was expanded from this volume to the reaction vessel with the opening of a stopcock. At the end of the run the stopcock was opened and all condensable materials were trapped immediately in spiral traps at −196 °C. The non-condensable fraction was collected in a gas burette. For chromatographic analysis, the gaseous products were swept through a 2-meter Porapak Q column at room temperature and were detected with a hot filament unit.

Pressure measurements in the low-pressure region below about 40 mm Hg, were made with a silicone oil manometer and at higher pressures with a mercury manometer with the mercury surfaces covered with silicone oil.

Prior to every pyrolysis run, some trifluoroacetaldehyde was pyrolyzed in the reaction vessel (usually about 20 mm of reactant). All materials were evacuated from the vessel just before a run and more reactant was admitted to the vessel soon after the run. This procedure was followed to eliminate or reduce surface effects which were mentioned by Arthur and Bell (1), and which in our early runs appeared to cause inconsistent rates of reaction. Examination of the reaction vessel after prolonged use revealed no visible deposits on the surface.

Results and Discussion

Products of the reaction were equimolar amounts of carbon monoxide and trifluoromethane along with small amounts (~0.2% of the total CO for runs at 480 °C and 100 mm Hg reactant) of hexafluoroethane. These were fractionated in a conventional apparatus and identified by gas chromatography.

Reaction rates cited in the discussion are rates of production of CO extrapolated to zero time from a series of runs of varying duration. The overall order of the reaction was examined in detail at 480 °C. Figure 1 reveals that the overall order of the reaction is 3/2 at pressures greater than about 40 mm Hg in agreement with the conclusion of Arthur and Bell (1). However, at lower pressures, a region not investigated extensively by Arthur and Bell, the order of the overall reaction increases as the pressure is lowered (Fig. 2). The overall order is about 1.85 at a pressure of 4 mm Hg. Also shown in Fig. 2 are the results of Liu (3) for the decomposition of acetaldehyde. The rates of decomposition of trifluoroacetaldehyde are less than those of acetaldehyde but the behavior of an increase in the order to a value greater than 3/2 at low pressures is evident in both cases.

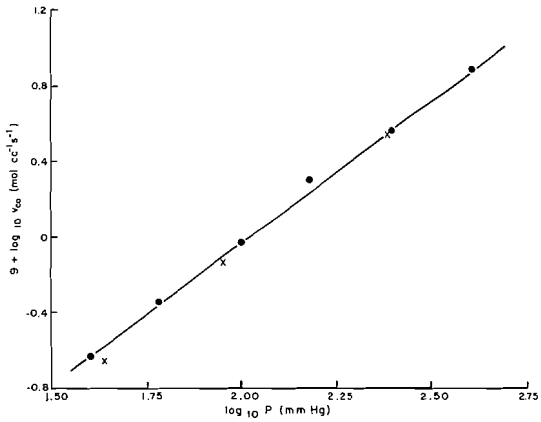

FIG. 1. A plot of the $\log_{10}$ of the overall rate of reaction as a function of the $\log_{10}$ of the pressure of trifluoroacetaldehyde (the high-pressure region). The data indicated by × were obtained early in the study while the data indicated by ○ were obtained in a later series of runs. The solid line was drawn with a slope of 3/2.

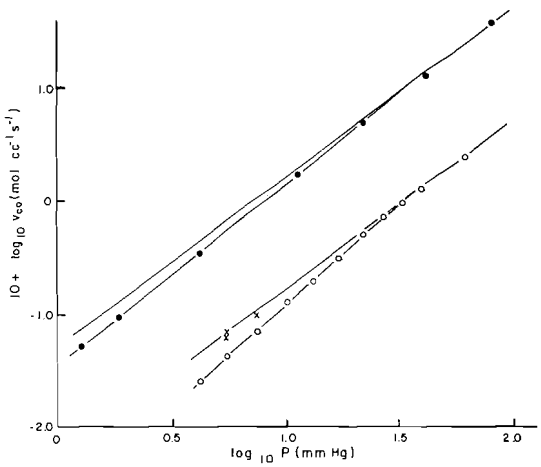

FIG. 2. A plot of the $\log_{10}$ of the overall rate of reaction as a function of the $\log_{10}$ of the pressure of trifluoroacetaldehyde (the low-pressure region): ○, trifluoroacetaldehyde at 480 °C; ×, trifluoroacetaldehyde at 480 °C with CO_2 added; ●, acetaldehyde at 540 °C (data from ref. 3). The solid lines indicate a slope of 3/2 as an extension of high-pressure data.

The fall-off in the rate at lower pressures to produce the higher order was tested by the addition of inert gas. In Fig. 2 the solid straight lines were drawn with the slope of 3/2 for the cases of acetaldehyde and trifluoroacetaldehyde. The addition of 200 mm Hg CO_2 to runs at 5.6 and 7.5 mm Hg trifluoroacetaldehyde increased the rate appreciably and the addition of 250 mm Hg CO_2 to 5.6 mm Hg trifluoroacetaldehyde in-

Can. J. Chem. Downloaded from www.nrcresearchpress.com by 210.87.254.40 on 09/05/12
For personal use only.

creased the rate to the value expected for an overall order of 3/2 (Fig. 2). These experiments confirm the change in order at low pressure and show that 250 mm Hg CO_2 is effective in restoring the reaction to high-pressure conditions.

The temperature dependence of the overall rate was studied in the high-pressure region at a pressure of 100 mm Hg of trifluoroacetaldehyde. The Arrhenius plot provided in Fig. 3 yields the overall rate constant $k = 10^{13.8\pm0.1} \exp(-50\,500 \pm 300/RT)\ cc^{1/2}\ mol^{-1/2}\ s^{-1}$. The activation energy is in good agreement with the value of 49 kcal mol^{-1} obtained by Arthur and Bell. Also the value of $10^{12.2}\ l^{1/2}\ mol^{-1/2}\ s^{-1}$ obtained by Arthur and Bell for the A factor is in good agreement with our experimental frequency factor of $10^{13.8}\ cc^{1/2}\ mol^{-1/2}\ s^{-1}$. The absolute value of the rate constants obtained in this study and in the study of Arthur and Bell agree within a factor of 2, with Arthur and Bell's value being the greater. The reason for the discrepancy in the absolute values is not known.

To explain the experimental observations the following kinetic scheme is suggested for the high-pressure decomposition of trifluoroacetaldehyde.

[1] $CF_3CHO \rightarrow CF_3 + CHO$

[2] $CHO \rightarrow CO + H$

[3] $H + CF_3CHO \rightarrow H_2 + CF_3CO$

[4] $CF_3 + CF_3CHO \rightarrow CF_3H + CF_3CO$

[5] $CF_3CO \rightarrow CF_3 + CO$

[6] $CF_3 + CF_3 \rightarrow C_2F_6$

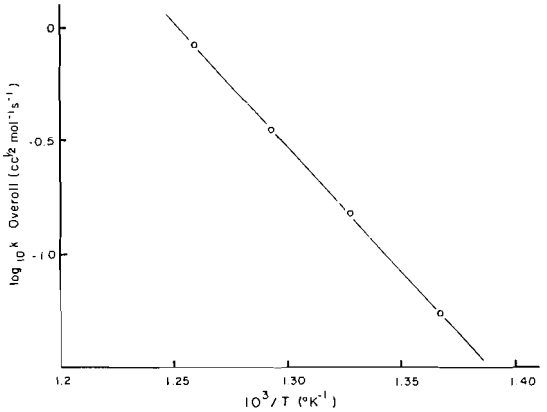

FIG. 3. Arrhenius plot of the overall rate constant for trifluoroacetaldehyde.

A steady-state treatment of the reaction scheme leads to the following expression:

$$v_{CO} = k_4\left(\frac{k_1}{k_6}\right)^{1/2}[CF_3CHO]^{3/2}$$

The low yield of C_2F_6 relative to that of CO and CF_3H satisfies the condition of long chains and thus the above expression can satisfy the rate of production of CO. Furthermore, under these conditions, the rate of formation of CO is equal to the rate of decomposition of trifluoroacetaldehyde and hence is equal to the overall rate of reaction. The relative concentrations of CF_3CO and CF_3 in the reaction system determines which termination process will be important. The steady state condition leads to

$$\frac{[CF_3CO]}{[CF_3]} = \frac{k_4}{k_5}[CF_3CHO]$$

With the use of literature values of $k_4 = 10^{12} \exp -8\,800/RT$ cc $mol^{-1}\ s^{-1}$ (8) and $k_5 = 2.6 \times 10^{10} \exp -10\,000/RT\ s^{-1}$ (9), values of $[CF_3CO]/[CF_3]$ were estimated to be in the range of 10^{-3} to 10^{-4}. It is therefore reasonable to conclude that the termination must involve the recombination of two CF_3 radicals.

Overall Order

The value of 3/2 for the experimental order of reaction in the high pressure region is satisfied by the mechanism given by reactions 1–6. From the Goldfinger rules it follows that a mechanism involving second-order initiation and ββM termination would also satisfy the overall order of 3/2; this was the mechanism suggested by Arthur and Bell. However, such a mechanism could not explain a fall-off in the overall rate constant in the low-pressure region, as both initiation and termination reactions are already pressure dependent. The experimental results for trifluoroacetaldehyde at low pressures show a change in the overall order to values greater than 3/2 and approaching 2. This change is satisfied by the change in the order of reaction 1 to second-order conditions at low pressures, with the termination reaction remaining as the second-order combination of trifluoromethyl radicals, *i.e.* k_{init} shows a pressure dependence while k_{term} is constant and still pressure independent. At even lower pressures, one would anticipate that the combination of the trifluoromethyl radicals would become third order and

Can. J. Chem. Downloaded from www.nrcresearchpress.com by 210.87.254.40 on 09/05/12
For personal use only.

then, with the second-order initiation reaction, the Goldfinger rules would predict a return to 3/2 order overall kinetics.

A comparison of the changes in the overall order of the reactions of acetaldehyde and trifluoroacetaldehyde can be made from Fig. 2, in which it is seen that the shape of the curves is much the same in the two cases. However, it is apparent that the fall-off in CF_3CHO is more pronounced than that of CH_3CHO. This suggests that in the CH_3CHO pyrolysis, the fall-off for CH_3 combination overlaps the pressure dependence of the initiation reaction, while such an overlap is much less readily observed for the CF_3 combination in the case of CF_3CHO pyrolysis.

Ratio of Rate Constants for Initiation and Termination

The pressure dependence of the initiation and termination reactions has been examined in a more detailed form as given in Fig. 4. For the proposed reaction scheme it follows that $k_{overall} = (k_1/k_6)^{1/2} k_4$. The value of k_4 at 480 °C was calculated from the data of Morris and Thynne (8). From the experimental $k_{overall}$ and this value of k_4, k_1/k_6 values were calculated and plotted as a function of pressure in Fig. 4 in a log–log plot. The fall-off of the rate constant ratio is more clearly evident in this figure. The form of the pressure dependence requires a pressure dependence of k_1. This pressure dependence is again seen to commence at about 40 mm Hg and at the lowest pressures studied, for which the slope of the curve in Fig. 4 is about 0.8, the order of the initiation reaction would be 1.8. The effect of added carbon dioxide on the k_1/k_6 ratio is shown again in Fig. 4.

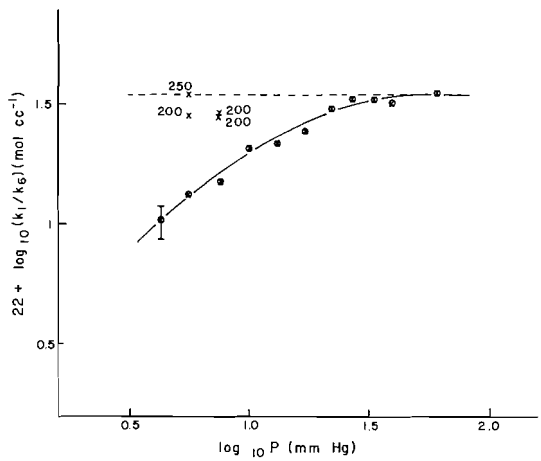

FIG. 4. Plot of $\log k_1/k_6$ against $\log P$ at 480 °C, showing the effects of CO_2. The dashed line is the extension of the high-pressure limit. ⊗, no CO_2 added; ×, CO_2 added at pressures indicated, mm Hg.

The experimental observations described in this paper are satisfied by the reaction scheme given by reactions 1–6. However, the rate enhancement observed by Arthur and Bell for the addition of CO_2 to runs at 75 and 100 mm Hg of CF_3CHO would not be expected. Although the magnitude of the rate enhancement in Arthur and Bell's work (about 25–30% increase for 150–200 mm Hg CO_2) was less than that which we have observed in the low-pressure region (about 40–50% increase for 200 mm Hg CO_2), it was none-the-less a pronounced effect. We regret that in the present study the effect of CO_2 on the rate was not examined in the high-pressure region and we recognize that the rate enhancement in the high-pressure region remains as an unsolved problem in defining the mechanism unequivocally.

Arrhenius Parameters and Bond Dissociation Energies

As already discussed, the A factor and the activation energy determined in this study for the overall reaction in the high-pressure region were in close agreement with the values of Arthur and Bell. A prediction for the value of A_1 can be made with the use of the expression:

$$\log A_{overall} = \tfrac{1}{2} \log A_1 - \tfrac{1}{2} \log A_6 + \log A_4$$

Thus from our experimental value of $\log A_{overall} = 13.8$ and from Morris and Thynne's value of 5.3 for $\log A_4 - \tfrac{1}{2} \log A_6$ it follows that $A_1 \simeq 10^{17.0}$ s^{-1}. Although this value is somewhat high it is in reasonably good agreement with values previously obtained for the unimolecular initiation steps in the pyrolyses of acetaldehyde (2) and ethane (10).

In a similar manner an estimate of the activation energy of reaction (1) can be obtained from the value of $E_4 - \tfrac{1}{2}E_6 = 8.8 \pm 0.2$ kcal/mol reported by Morris and Thynne, combined with our overall activation energy of 50.5 ± 0.3 kcal/mol; it follows that $E_1 \simeq 83$ kcal/mol.

The activation energy E_1 is related to the bond dissociation energy $D(CF_3—CHO)$ which, to a close approximation, may be taken to have the same value. Thus $D(CF_3—CHO) \simeq 83$ kcal/mol. This value may be compared with the

corresponding value of $D(CH_3—CHO) = 79.0 \pm 2.0$ obtained by Liu and Laidler (2) in the pyrolysis of acetaldehyde. It is interesting to note the increase in the bond dissociation energy of the fluorinated compound over that of the hydrogen analog, an increase which in this case amounts to 4.4 kcal/mol. There has been an accumulation of evidence that such an increase is the general case. Studies of $D(CF_3—H)$ by Amphlett, Coomber, and Whittle (11) and Goy, Lord, and Pritchard (12) have provided values in the range of 106.0 to 106.3 kcal/mol, such values being about 2–2.5 kcal/mol greater than $D(CH_3—H)$. The results of Tschuikow-Roux (13), Farmer *et al.* (14), Coomber and Whittle (15), and Goy, Lord, and Pritchard (12) indicate that $D(CF_3—CF_3)$ is about 93–97 kcal/mol, a value about 5–9 kcal/mol greater than $D(CH_3—CH_3)$. Furthermore, Amphlett and Whittle (16) have shown that $D(CF_3CO—H) = 91.1 \pm 2$ kcal/mol and that $D(CF_3CO—H) - D(CH_3CO—H) = 4.1$ kcal/mol. In view of the trend which indicates the increase in bond dissociation energy of various bonds in fluorinated compounds over that of the corresponding hydrogen compounds, it appears that $D(CF_3—CHO) \simeq 83$ kcal/mol is very much of the magnitude expected.

The authors acknowledge the work of Mr. David Hooper and Mr. Wayne Thompson and thank them for their contributions to the experimental procedures. The authors thank the National Research Council of Canada and the Senate Research Committee of the University of Prince Edward Island for financial assistance that made this research possible.

1. N. L. ARTHUR and T. N. BELL. Aust. J. Chem. **18**, 1561 (1965).
2. M. T. H. LIU and K. J. LAIDLER. Can. J. Chem. **46**, 479 (1968).
3. M. T. H. LIU. Ph.D. Thesis. University of Ottawa, Ottawa, Canada. 1967.
4. G. M. CÔME, M. DZIERZYNSKI, R. MARTIN, and M. NICLAUSE. C. R. Ser. C, **264**, 548 (1967).
5. G. M. CÔME, M. DZIERZYNSKI, R. MARTIN, and M. NICLAUSE. Rev. Inst. Fr. Pet. **23**, 1365 (1968).
6. D. R. HUSTED and A. H. AHLBRECHT. J. Am. Chem. Soc. **74**, 5422 (1952).
7. R. E. DODD, H. L. ROBERTS, and L. A. WOODWARD. J. Chem. Soc. 2783 (1957).
8. E. R. MORRIS and J. C. J. THYNNE. Trans. Faraday Soc. **64**, 3027 (1968).
9. J. C. AMPHLETT and E. WHITTLE. Trans. Faraday Soc. **63**, 80 (1967).
10. M. C. LIN and M. H. BACK. Can. J. Chem. **44**, 505 (1966).
11. J. C. AMPHLETT, J. W. COOMBER, and E. WHITTLE. J. Phys. Chem. **70**, 593 (1966).
12. C. A. GOY, A. LORD, and H. O. PRITCHARD. J. Phys. Chem. **71**, 1086 (1967).
13. E. TSCHUIKOW-ROUX. J. Chem. Phys. **43**, 2251 (1965).
14. J. B. FARMER, I. H. S. HENDERSON, F. P. LOSSING, and D. G. H. MARSDEN. J. Chem. Phys. **24**, 348 (1956).
15. J. W. COOMBER and E. WHITTLE. Trans. Faraday Soc. **63**, 1394 (1967).
16. J. C. AMPHLETT and E. WHITTLE. Trans. Faraday Soc. **66**, 2016 (1970).

Can. J. Chem. Downloaded from www.nrcresearchpress.com by 210.87.254.40 on 09/05/12
For personal use only.

Proton Transfer Kinetics in Medium-strong Inorganic Acids[1]

DAVID CHARLES HODGKIN AND PEETER KRUUS

Department of Chemistry, Carleton University, Ottawa, Canada K1S 5B6

Received August 14, 1972[2]

A method of obtaining relative and absolute rate constants for proton transfer equilibria is described. It is suitable for equilibria of the type

$$H_2O + HA \underset{k_r}{\overset{k_d}{\rightleftarrows}} H_3O^+ + A^-$$

in dilute ($< 0.1\ M$) solutions of medium strong inorganic acids. To obtain absolute values of k_d, k_r it is necessary to know the value of ΔV^0 for the equilibrium. Ultrasonic absorption data for aqueous solutions of H_3PO_4, H_3AsO_4, and H_2SO_4 at 20, 10, and 0 °C are presented together with data at 20 °C for H_3PO_3, H_2SeO_3, HIO_4, $NaHSO_4$, $KHSO_4$, and NH_4HSO_4. From analysis of the concentration dependence of the excess absorption, values of K_a are calculated for these acids, and values of k_d, k_r for those where ΔV^0 is available. The K_a obtained are in reasonable agreement with literature values except for HIO_4 and H_2SeO_4. The absolute values of k_r for H_3PO_4, H_3AsO_4, and HSO_4^- indicate that the diffusion controlled recombination process postulated is complete when the ions are about 15 Å from each other.

Une méthode d'obtention des constantes de vitesse relative et absolue pour l'équilibre de transfert du proton a été décrite. Cette méthode convient pour l'équilibre du type

$$H_2O + HA \underset{k_r}{\overset{k_d}{\rightleftarrows}} H_3O^+ + A^-$$

en solutions diluées ($< 0.1\ M$) d'acides inorganiques de force moyenne. Pour obtenir les valeurs absolues de k_d et k_r, il a été nécessaire de connaître la valeur ΔV^0 de l'équilibre. Les données de l'absorption ultrasonique pour les solutions aqueuses de H_3PO_4, H_3AsO_4, et H_2SO_4 à 20, 10, et 0 °C ont été présentées de même que celles de H_3PO_3, H_2SeO_3, KIO_4, $NaHSO_4$, $KHSO_4$, et NH_4HSO_4 à 20 °C. L'analyse de l'excès d'absorption en fonction de la concentration a permis de calculer les valeurs K_a de ces acides et les valeurs k_d, k_r pour ceux dont le ΔV^0 est connu. Les K_a obtenus sont d'un bon accord avec les valeurs de la littérature sauf pour KIO_4 et H_2SeO_4. Les valeurs absolues de k_r pour H_3PO_4, $H_3AsO_4^-$ montrent que le processus postulé pour la recombinaison contrôlée par diffusion, est total lorsque les ions sont séparés de 15 Å environ les uns des autres. [Traduit par le journal]

Can. J. Chem., **51**, 2297 (1973)

Introduction

Estimates for the rate constants for proton transfer reactions in sulfuric acid solutions were made in 1954 by Eigen (1). His calculations were based on the ultrasonic absorption data of Kurtze and Tamm (2).

Since that time, rapid proton transfer in aqueous acid equilibria of the type

$$[1] \qquad HA + H_2O \underset{k_r}{\overset{k_d}{\rightleftarrows}} A^- + H_3O^+$$

has been studied by various means: nuclear magnetic resonance (3), Raman spectroscopy (4), temperature (5) and electric field (6–8) jump techniques, as well as by ultrasonic absorption (9, 10). Such studies have been conducted in various types of solutions: inorganic compounds (3, 4, 6), organic acids (5, 7), proteins (9, 10), as well as for water itself (8). Summaries of proton transfer rates can be found in refs. 11 and 12.

It has generally not been possible to observe the relaxation of such proton-transfer equilibria directly through ultrasonic absorption. The small excess absorption and the difficulty in working with acid solutions make it unlikely that precise enough data can be obtained at the necessary high frequencies, even though apparatus for measurements at such frequencies has become available, *e.g.* ref. 13.

The relaxation time τ can however also be calculated from the measured excess absorption α'/f^2 at low frequencies. For such an analysis,

[1]Taken in part from the thesis submitted by D. C. Hodgkin in partial fulfillment of the requirements for the B.Sc. (Honours) degree.

[2]Revision received March 5, 1973.

Can. J. Chem. Downloaded from www.nrcresearchpress.com by 210.87.254.42 on 09/05/12
For personal use only.

TABLE 1. Rate constants obtained from analysis of ultrasonic absorption data

Row	Acid	T (°C)	k_r ($10^{10}\ M^{-1}\ s^{-1}$)	k_d ($10^8\ s^{-1}$)	K_a (k_d/k_r) ($10^{-3}\ M$)	K_a (lit) ($10^{-3}\ M$)	σ	n	Figure
1	H_3PO_4	20	8.47	8.89	10.5	7.90‡	0.50	11	2
2	H_3PO_4	10	6.53	6.20	9.50	8.52	0.42	5	2
3	H_3PO_4	0	4.45	4.63	10.4	8.97	1.48	5	2
4	H_3AsO_4	20	9.06	5.44	6.0	5.6¶	0.37	6	3
5	H_3AsO_4	10	7.38	2.73	3.7	—	0.43	16	3
6	H_3AsO_4	0	4.10	2.09	5.1	—	1.35	11	3
7	HIO_4	20	26.8	1.13	4.9	23.**	0.24	11	4
8	H_2SeO_3	20	29.7	6.53	2.2	3.5**	0.21	7	4
9	H_3PO_3	20	19.7	28.0	14.2	16.2§	0.24	5	4
10	HSO_4^-*	20	7.57	15.7	20.7	11.8‖	0.33	10	5
11	HSO_4^-	20	5.76	14.2	24.7	11.8	0.21	13	—
12	HSO_4^-†	20	9.0	14.0	15.	11.8	0.2	18	6
13	HSO_4^-	10	4.52	10.8	23.9	15.8	0.56	8	—
14	HSO_4^-†	10	10.0	11.0	11.	15.8	0.2	12	6
15	HSO_4^-	0	2.94	8.35	28.4	21.4	1.30	12	6

*From $NaHSO_4$ data.
†Activity coefficients considered.
‡Reference 20.
§Reference 21.
‖Reference 15.
¶18 °C.
**25 °C.

it is necessary to assume which equilibrium is responsible for the absorption, and to have some thermodynamic data for this equilibrium.

Due to the greater complexity of organic acids, numerous equilibria are present in their solutions which could give rise to ultrasonic absorption. A measurable amount of excess absorption at low frequencies and low concentrations due to equilibria such as that shown in [1] is present also only in medium-strong acids.

An investigation of the concentration dependence of the ultrasonic absorption of 6 medium-strong inorganic acids was carried out. The results are interpreted as due to equilibria of the type shown in [1]. Experimental values of the equilibrium constants can be obtained from the resulting analysis. Absolute values of the rate constants k_d and k_r can be obtained if ΔV^0 for the equilibrium is available.

Experimental

The apparatus and procedure used for the ultrasonic absorption measurements have been described previously (14). Most measurements were carried out at 31.8 MHz with apparatus A (14). Only for a few systems was an extended frequency range (3.5 to 52 MHz) used.

The precision of individual absorption measurements was better than 1%, as judged on the basis of the standard error for obtaining the slope of attenuation *vs.* distance plots. The inaccuracy in the excess absorption, α'/f^2, is of course greater than this. Estimated error limits are given in the large scale plots in Fig. 4. The excess absorption is the relatively small difference between two readings, $\alpha'/f^2 = (\alpha/f^2)_{solution} - (\alpha/f^2)_{water}$.

There are also inaccuracies present due to errors in temperature, especially close to 0 °C, where difficulties were encountered in maintaining constant temperature. This can be seen from the values of the standard deviation:

$$[2]\quad \sigma = \sqrt{\frac{1}{(n-3)}\sum_{i=1}^{n}[(\alpha'/f^2)_{calcd} - (\alpha'/f^2)_{exp}]^2}$$

Column 8 of Table 1 shows σ to be considerably larger for systems at 0 °C.

All solutions were prepared using distilled water redistilled from potassium permanganate solution. Reagent grade acids and salts from Fisher, Anachemia, CIL, or Baker were used without further purification. Stock solutions were made up and their concentrations determined by titration using a pH meter. It is estimated that the concentrations of the subsequently prepared solutions were accurate to better than 2%.

Theoretical Background

The excess absorption, α'/f^2, caused by a relaxation is given by (11):

$$[3]\quad (\alpha'/f^2) = \frac{2\pi^2\kappa_r}{v\kappa_0}\cdot\frac{\tau}{1+\omega^2\tau^2}$$

Here κ_0 is the static compressibility, which can be related to density ρ and the speed of ultrasound v as $\kappa_0 = 1/v^2\rho$. The contribution to the

Can. J. Chem. Downloaded from www.nrcresearchpress.com by 210.87.254.42 on 09/05/12
For personal use only.

Can. J. Chem. Downloaded from www.nrcresearchpress.com by 210.87.254.42 on 09/05/12
For personal use only.

adiabatic compressibility from the relaxing equilibrium is given by κ_r. It can be expanded to be of the form

$$[4] \quad \kappa_r = -\frac{1}{V}\left[\left(\frac{\partial V}{\partial P}\right)_T + \left(\frac{\partial V}{\partial T}\right)_P \cdot \left(\frac{\partial T}{\partial P}\right)_S\right]$$

As $(\partial T/\partial P)_S$ is small for aqueous solutions, the second term in eq. 4 can be neglected when ΔH^0 for the equilibrium is not extremely large. The derivative $(\partial V/\partial P)_T$ can be expanded in terms of θ, the degree of advancement of the equilibrium. Thus

$$[5] \quad \kappa_r = -\frac{1}{V}\left(\frac{\partial V}{\partial \theta}\right)_T\left(\frac{\partial \theta}{\partial P}\right)_T = -\Delta V\left(\frac{\partial \theta}{\partial \ln K}\right)_T\left(\frac{\partial \ln K}{\partial P}\right)_T$$

When the approximation $\Delta V = \Delta V^0$ is made, then κ_r becomes:

$$[6] \quad \kappa_r = \frac{(\Delta V^0)^2}{RT}\cdot\left(\frac{\partial \theta}{\partial \ln K}\right)_T$$

When activity coefficients can be assumed to be unity, then the relationships for τ and $(\partial\theta/\partial \ln K)$ are relatively simple. The relaxation time τ for a reaction as shown in eq. 1 is

$$[7] \quad 1/\tau = k_d + k_r([A^-] + [H_3O^+])$$

The derivative

$$[8] \quad \frac{\partial \theta}{\partial \ln K} = \frac{c\xi(1-\xi)}{(2-\xi)}$$

where c is the stoichiometric concentration and ξ the degree of dissociation.

The value of ξ is related to c and the equilibrium constant K_a by

$$[9] \quad \xi = \frac{-K_a + \sqrt{K_a^2 + 4K_a c}}{2c}$$

The excess absorption (α'/f^2) can then be obtained by appropriate substitution

$$[10] \quad (\alpha'/f^2) = \frac{2\pi^2(\Delta V^0)^2\rho v}{RT}\cdot\frac{c\xi(1-\xi)}{(2-\xi)}\cdot\frac{1}{k_r}\frac{1}{(K_a + 2\xi c)}$$

The expression has been written in a form where k_r and K_a $(= k_d/k_r)$ can be considered as adjustable parameters.

Equations 9 and 10 neglect the effect of activity coefficients. The complete relationships including activity coefficients can be obtained in (11). The derivatives with respect to the degree of dissociation of activity coefficients of the species involved must be known, including the activated state complex.

The acids H_3PO_4, H_3AsO_4, HIO_4, H_2SeO_3, and H_3PO_3 are sufficiently weak so that [9] and [10] can be used for analysis with reasonable accuracy. An 0.05 M solution of H_3PO_4 has approximately $\xi \approx 0.33$, ionic strength ≈ 0.016, $\gamma_\pm^2 \approx 0.93$. This introduces some error ($\sim 3\%$) in the value of ξ calculated through [9]. The error due to neglect of terms of the form $d \ln \gamma_\pm^2 / d \ln \xi$ can in this case be estimated to be of the order of 2% (11). As only a few of the experimental points considered were at concentrations > 0.05 M, the neglect of activity coefficients seems justified in the light of the accuracy of the experimental data.

Equation 10 and a modified form of [9] were also used to analyze the data for $NaHSO_4$ solutions. In this case the ionic strength is higher, so that the errors introduced are greater. In addition, the neglect of absorption due to ion pairing equilibria involving Na^+ and SO_4^{-2} may not be justified. The results for $NaHSO_4$ are thus of a rather approximative nature.

The experimental data was fitted with eq. 10 by choosing a value of ΔV^0 and then using k_r and K_a as adjustable parameters. In adjusting k_r and K_a to give the smallest standard deviations (eq. 2), the following routine was used. A range of values of K_a was chosen. For each value of K_a, the value of k_r giving the smallest standard deviation was then calculated from the relation

$$[11] \quad k_r = \frac{\sum_{i=1}^{n} ((\text{Eq. } 10)_i \times k_r)^2}{\sum_{i=1}^{n} ((\text{Eq. } 10)_i \times k_r)(\alpha^1/f^2)_{\text{expti}}}$$

The symbol $(\text{Eq. } 10)_i \times k_r$ indicates the expression in the r.h.s. of [10] times k_r with the values of c_i and ξ_i (from eq. 9) for the ith data point included. The set K_a, k_r giving the smallest σ was then chosen.

Even if activity coefficients are neglected, the analysis of sulfuric acid solution data is more complex. Equation 8 now becomes

$$[12] \quad \left(\frac{\partial \theta}{\partial \ln K}\right) = \frac{\xi(1+\xi)(1-\xi)}{2-(1-\xi)^2}$$

Can. J. Chem. Downloaded from www.nrcresearchpress.com by 210.87.254.42 on 09/05/12
For personal use only.

and eq. 9 becomes:

$$[13] \quad \xi = \frac{-c - K_a + \sqrt{(c + K_a)^2 + 4K_a c}}{2c}$$

Although eq. 7 is still valid, its form is different when expressed in terms of k_r, K_a, and c. The H_2SO_4 data were analyzed with neglect of activity coefficients taking account of the changes expressed in eqs. 12 and 13.

The H_2SO_4 data was also analyzed using the more accurate forms (11) of eqs. 12 and 7, but leaving [13] unchanged. The activity coefficients were calculated from the Debye–Hückel equation (15). The use of experimental activity data leads to difficulties, as single ion activities are needed, including that of the activated complex. Incorporating changes in eq. 13 would lead to computational difficulties, which seem unjustified in the light of the accuracy of the data.

Results

Figure 1 shows the ultrasonic absorption in aqueous H_3PO_4 solutions up to saturation (14.3 *M*). A smooth curve has been drawn through the points. There may, however, be maxima and minima in the curve as in the case of sulfuric acid (16). α_c refers to the value of the classical absorption arising from viscosity, $\alpha_c/f^2 = 8\pi^2\eta/3v^3$. The absorption was measured as a function of frequency for solutions 0.1, 1.0, 7.0, 14.3 *M* in H_3PO_4. No sign of a relaxation was observed within the frequency range 3.5 to 52 MHz, *i.e.* α/f^2 was constant with frequency within experimental error. As can be seen in Fig. 1, there is an increase in the absorption at small concentrations. Figure 2 shows the absorption at small concentrations (0 to 0.15 *M*) at three temperatures. The data shown in this figure was fitted with eq. 10 using k_r and K_a as adjustable parameters. The results are shown in Table 1, rows 1 to 3 inclusive.

In fitting the H_3PO_4 data, the value of ΔV^0 chosen was -16.2 cm^3 mol^{-1} (15). A value of -15.5 cm^3 mol^{-1} has also been reported (17). As (α'/f^2) varies as $(\Delta V^0)^2$, then k_r would be diminished by nearly 10% if the latter value would be used. The same value of ΔV^0 was used

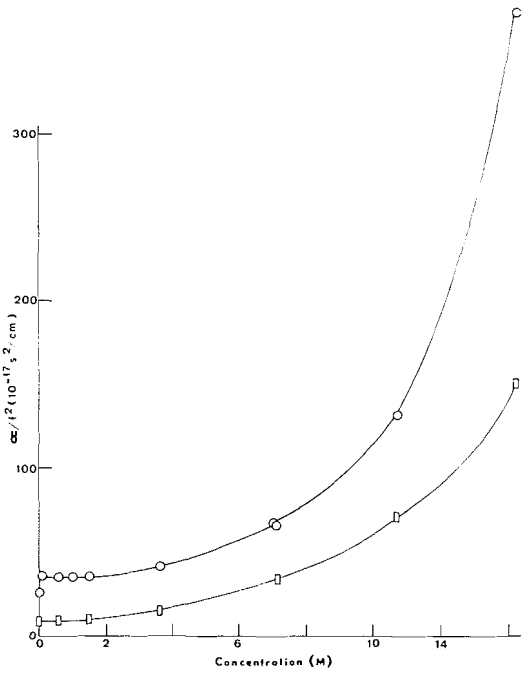

FIG. 1. Ultrasonic absorption in aqueous phosphoric acid solutions: ○, experimental absorption; □, calculated classical absorption.

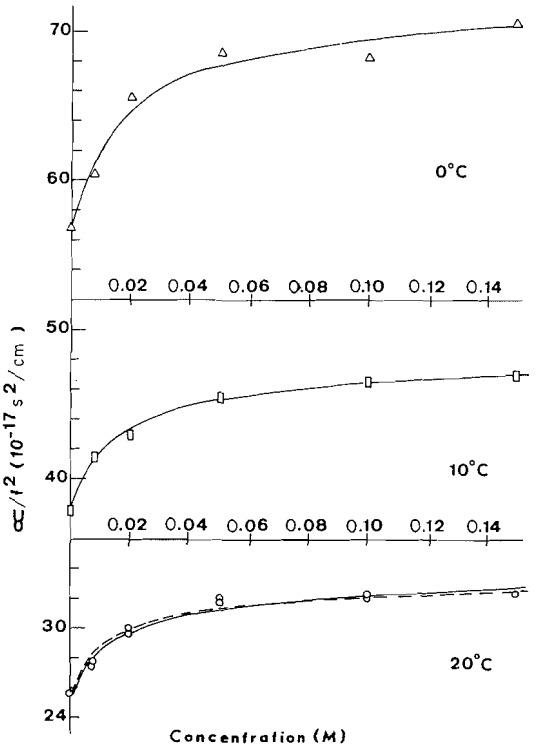

FIG. 2. Ultrasonic absorption in aqueous phosphoric acid solutions at low concentrations: ○, 20 °C; □, 10 °C; △, 0 °C; —, least squares fit (Table 1 rows 1–3,); --- fit assuming literature value of K_a.

Can. J. Chem. Downloaded from www.nrcresearchpress.com by 210.87.254.42 on 09/05/12
For personal use only.

for the three temperatures examined. This can make the calculated value of k_r of the order of 20% smaller than the actual value at 0 °C (10% at 10 °C) if ΔV^0 for H_3PO_4 has the same temperature dependence as for H_2O. For the H_3O^+–OH^- equilibrium, ΔV^0 changes from -26.1 to -23.4 cm^3 mol^{-1} in the 20 degree interval 5 to 25 °C (15). The values of v used throughout were for 20 °C, 1.48×10^5 cm s^{-1}; for 10 °C, 1.43×10^5 cm s^{-1}; for 0 °C, 1.40×10^5 cm s^{-1}. The variation of v and ρ with concentration up to 0.1 M is negligibly small.

In the case of the H_3PO_4 at 20 °C, two curves are shown in order to indicate the sensitivity of eq. 10 to variation in K_a. This sensitivity is also shown in Fig. 7, where k_r and σ are plotted as a function of K_a for H_3AsO_4 at 10 °C. The value of k_r is not very sensitive to changes in K_a. It should be noted that the value of k_r is predominantly determined by data in the higher concentration range, while K_a (and thus k_d) is more sensitive to data in the low concentration range.

Figure 3 shows the curves for H_3AsO_4 corresponding to Fig. 2. Again the fit at 0 °C has a considerably greater standard deviation due to greater imprecision in the experimental data. Data for 3 other medium-strong acids (HIO_4, H_2SeO_3, H_3PO_3) are shown in Fig. 4. In this case (α'/f^2) is plotted *vs.* c to show the amount of imprecision in the data.

In fitting the data in Figs. 3 and 4, a value of -16.0 cm^3 mol^{-1} was used for ΔV^0 in the absence of any literature values. Values of this order of magnitude seem common for equilibria of the type considered (15).

Absorption measurements were taken at 20 °C also for three strong acids, $HClO_4$, HNO_3, and HCl. In this case, no increase in absorption over that of pure water was noted in solutions up to 0.12 M. The value of ξ is in this case so great that $(1 - \xi) \approx 0$, *i.e.* $\alpha'/f^2 \approx 0$.

Figure 5 shows data for H_2SO_4. The 0 °C data are shown with the curve obtained when activity coefficients are neglected. The shape of the experimental and calculated curves are qualitatively different at higher concentrations. The experimental α'/f^2 continues to rise while the calculated α'/f^2 decreases. It was not possible to obtain a meaningful fit for the 0 °C data with consideration of activity coefficients.

The 10 and 20 °C data for H_2SO_4 are shown fitted with the equation taking partial account

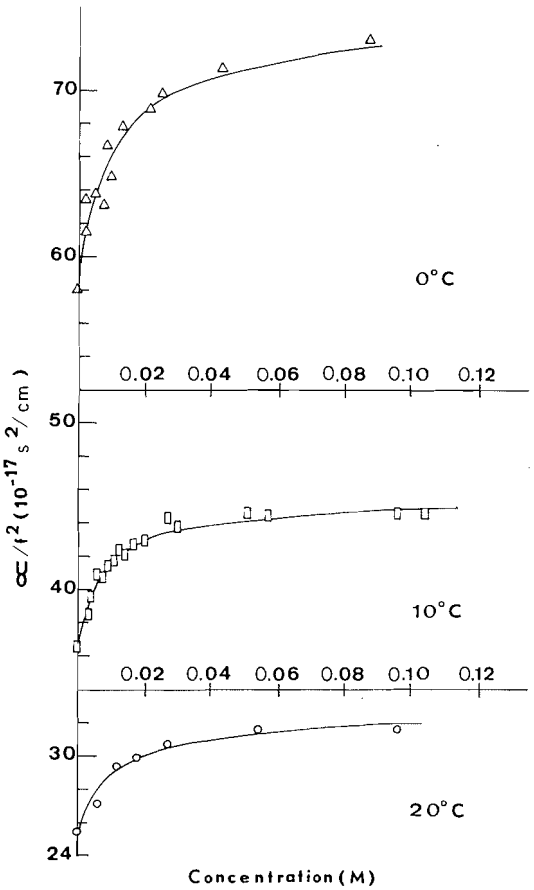

FIG. 3. Ultrasonic absorption in aqueous arsenic acid solutions: ○, 20 °C; □, 10 °C; △, 0 °C; —, Least squares fit (Table 1 rows 4–6).

of activities. The resulting values of ΔV^0 found were -14.3 cm^3 mol^{-1} at 20 °C and -15.5 cm^3 mol^{-1} at 10 °C. This is in good agreement with the literature value -15.5 cm^3 mol^{-1} (18) used for the other H_2SO_4 calculations. Higher values, -20.2 cm^3 mol^{-1} (19) have been reported.

Data for $NaHSO_4$, $KHSO_4$, and NH_4HSO_4 solutions are shown in Fig. 6. The curve shown is for the $NaHSO_4$ data, Table 1 row 10. In this case, as well as in the case of rows 11, 13, and 15, only points below 0.10 M were used to get the best values of K_a and k_r. This makes the neglect of activity coefficients less critical. The data for the 3 salts are completely overlapping within experimental error as seen in Fig. 6. This indicates that ion pairing of the cations with SO_4^{2-} ions may not be of much importance at this temperature, and that the discrepancy between the calculated K_a and that found from other experi-

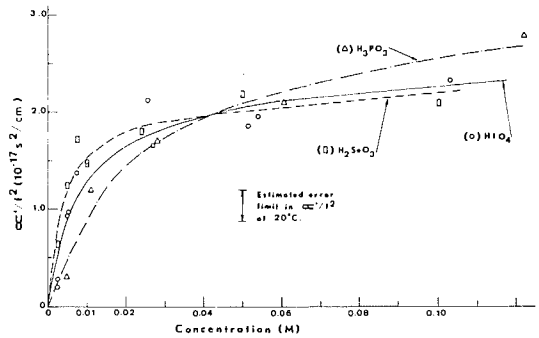

FIG. 4. Excess ultrasonic absorption in aqueous solutions of HIO_4, —○— (Table 1, row 7); H_2SeO_3, ---□--- (Table 1, row 8); H_3PO_3, -·-Δ-·- (Table 1, row 9).

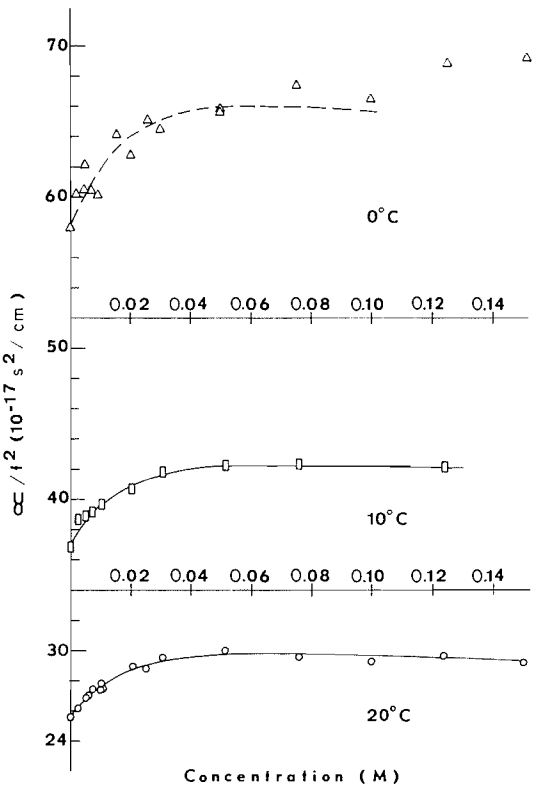

FIG. 5. Ultrasonic absorption in aqueous solutions of sulfuric acid: ○, 20 °C; □, 10 °C; Δ, 0 °C; — least squares fit taking activity coefficients into account (Table 1, rows 12, 14); --- neglecting activity coefficients (Table 1, row 15).

mental methods may be due solely to activity coefficient effects. Figure 7 is included to indicate the sensitivity of the curve-fitting procedure used in obtaining K_a and k_r.

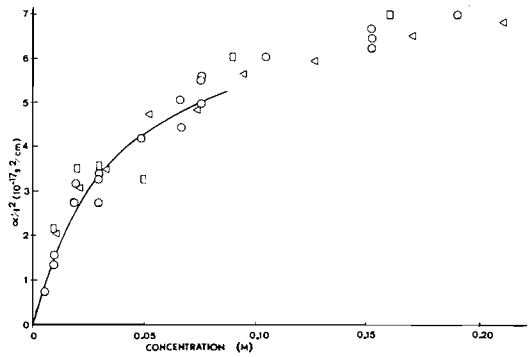

FIG. 6. Excess ultrasonic absorption in aqueous solutions of bisulfate salts: ○, $NaHSO_4$; □, $KHSO_4$; Δ NH_4HSO_4; —, least squares fit to $NaHSO_4$ data (Table 1, row 10).

Discussion

(a) Values of K_a

The equilibrium constants obtained by fitting the experimental curves with eq. 10 are in reasonable agreement with literature values in some cases (Table 1, rows 1, 2, 3, 4, 9, 15). In other cases, they differ considerably from values in the literature. Three literature values can be found for the K_a of H_3PO_3: 1.0×10^{-2} (20), 1.62×10^{-2} (21), and 5.0×10^{-2} (22). The experimental value 1.42×10^{-2} is closest to the second value. It is thus possible that the differences in the values of K_a for HIO_4 and H_2SeO_3 may also be due to unreliable literature values rather than to large errors in the experimental data and its interpretation. Precise values for K_a for medium-strong acids seem difficult to obtain (23).

In the case of HSO_4^-, the differences are however most likely due to an oversimplified model used to interpret the data. The calculated value of γ at 0.10 m^{-1} was in good agreement with experimental values (0.22 as compared to 0.29), but the neglect of activity coefficients in calculating ξ most likely introduces substantial errors. Nevertheless, the values of k_d obtained by neglecting and including activity coefficient effects are not very different (Table 1, rows 11, 12 and 13, 14). The k_r values differ more, as expected, because they are primarily determined by experimental points at higher concentrations (eq. 10), where activity coefficient effects are greater.

(b) Values of k_r, k_d

The excess absorption in the systems studied has been assumed to be due to the single step

Can. J. Chem. Downloaded from www.nrcresearchpress.com by 210.87.254.42 on 09/05/12
For personal use only.

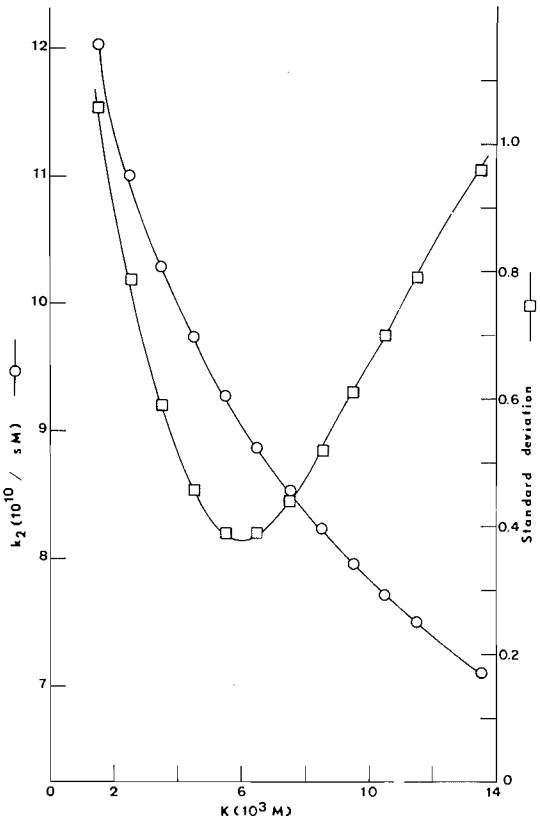

FIG. 7. Variation of k_2 and σ with K in arsenic acid solutions at 10 °C (Table 1, row 5) —○—, k_2 (eq. 16); —□— σ (eq. 2).

equilibrium shown in eq. 1. A more sophisticated model (1) describes the process in two steps:

$$[14]\quad H_3O^+ + A^- \underset{k_2}{\overset{k_1}{\rightleftarrows}} H_3O^+ \,.\, A^- \underset{k_4}{\overset{k_3}{\rightleftarrows}} H_2O + HA$$

Step one is the equilibrium between the free ions and an ion-pair (equilibrium constant $K_{1,2}$). Step two is the equilibrium between the ion-pair and the chemically bonded acid ($K_{3,4}$). Covington *et al.* (23) have discussed this mechanism in some detail.

If it is assumed that step one is rate-determining, then the rate constant k_r in Table 1 can properly be considered to be that for a diffusion-controlled process of the formation of the ion-pair, k_2. Debye (24) has constructed a theory to describe such a process. In the limit of infinite dilution, k_2 can be written as

$$[15]\quad k_2 = \frac{4\pi(D_+ + D_-)}{1000\varepsilon k T} N z_+ z_- e_0^2 \times \left[\exp\left(\frac{z_+ z_- e_0^2}{a\varepsilon k T}\right) - 1\right]^{-1}$$

Here D_+ and D_- are the diffusion coefficients and z_+e_0, z_-e_0 the charges on the cation and the anion, ε is the dielectric constant, N Avogadro's number, k Boltzmann's constant, and a the ion-size parameter describing the distance between ions when the reaction is "complete".

For 1–1 electrolytes, [15] reduces simply to

$$[16]\quad k_2 = 5.32 \times 10^{14}\,(D_+ + D_-) \times [\exp(7.1 \times 10^{-8}/a) - 1]^{-1}$$

The increase in ε cancels approximately the decrease in T in the range 20 to 0 °C. There are several simplifications involved in obtaining eq. 16. However, the use of more sophisticated theories (25, 26) seems unjustified in the light of the limited precision of the experimental results.

The rate constant k_d in the framework of a two-step model must be considered as the ion-pair dissociation rate k_1 of step one, multiplied by the equilibrium constant $K_{3,4}$. The relationship for k_1 derived by Eigen (1) cannot be used directly to analyze the experimental values for k_d.

Values of the activation energy of the recombination reaction can be estimated from the data assuming an Arrhenius form. These estimates are independent of the value of ΔV^0 chosen, if the temperature-independence of ΔV^0 is assumed. The values obtained for H_3PO_4 and H_3AsO_4 are of the order of 4 kcal mol^{-1}, *i.e.* of a magnitude characteristic of diffusion controlled reactions. From [16] it can be seen that this is essentially the activation energy for diffusion.

Values of the distance parameter a can be calculated from the values of k_r. Values of the diffusion coefficients can be calculated from values of the conductivity through the Nernst–Einstein relation (15). Values for D_- were in cases estimated due to the lack of conductivity data. Such estimates are not crucial as $D_+ \gg D_-$ in all cases.

The values of a obtained at the three temperatures for both H_3PO_4 and H_3AsO_4 were in the range 11 to 15 Å. When $a = 15$ Å, the reaction is "complete" when two water molecules are between the ions. The radius of a water molecule

Can. J. Chem. Downloaded from www.nrcresearchpress.com by 210.87.254.42 on 09/05/12
For personal use only.

Can. J. Chem. Downloaded from www.nrcresearchpress.com by 210.87.254.42 on 09/05/12
For personal use only.

is assumed 2.8 Å, while the radius of H_3O^+ and A^- are assumed 1.7 and 2.5 Å, respectively (15).

The same type of analysis was not carried out for the HSO_4^- k_r values listed in Table 1 as their uncertainty is quite large. A more realistic value of k_r for HSO_4^- can be obtained from the more reliable k_d value combined with values of K_a obtained by other methods. When such values of k_r are used, then the a value for HSO_4^- is in the range 11 Å (at 0 °C) to 17 Å (at 20 °C).

The k_r values for H_3PO_3, HIO_4, and H_2SeO_3 are unrealistically large, even in comparison to the H_3O^+–OH^- recombination rate ($k_r = 13 \times 10^{11}$ M^{-1} s^{-1}) (8). These high values may be due to the estimated ΔV^0 being substantially too high. A value of ΔV^0 of approximately -10 instead of -16 cm^3 mol^{-1} would bring the k_2 values down to normal size. The model used to interpret the data may also be at fault. For example, HIO_4 could be present in part in other forms, such as H_5IO_6, $H_4IO_6^-$, $H_3IO_6^{2-}$ (22).

Only for the system HSO_4^- is it possible to compare the above results with those of other workers. Eigen (1) estimated the value of k_r to be 10^{11} M^{-1} s^{-1} and k_d to be 1.5×10^9 s^{-1}. These values are directly comparable to the values 8.4×10^{10} M^{-1} s^{-1} and 1.4×10^9 s^{-1} obtained in this study taking the experimental value of k_d and the literature value of K_a. Irish and Chen (4) obtained a value of 6.4×10^{11} M^{-1} s^{-1} for k_r, but considerably higher concentrations were used in this Raman study. The value of k_r for acetic acid as obtained from a field jump technique (7) is of a similar size as the values reported here for inorganic acids, 7.2×10^{10} M^{-1} s^{-1}.

Conclusions

Experimental data of excess ultrasonic absorption *vs.* concentration in dilute (<0.1 M) solutions of medium-strong inorganic acids can be interpreted with success in terms of the proton-transfer equilibrium present. The experimental curves can be fitted satisfactorily by a two parameter equation. If the ΔV^0 for the equilibrium is known, the absolute values for the rate constants k_r, k_d can be calculated. Without knowledge of ΔV^0, only relative values, *i.e.* K_a, can be obtained.

Experimental data for 6 such acids has been obtained and interpreted to obtain K_a values, and rate constants where ΔV^0 values are available. The K_a values obtained are in reasonable agreement with the literature values for H_3PO_4 and H_3AsO_4 at 3 temperatures and for H_3PO_3 with one of the 3 literature values available at 20 °C. Agreement of the K_a values of HSO_4^-, HIO_4, and H_2SeO_3 with literature values is poorer. In the first case it is most probably due to incomplete consideration of activity coefficient effects, while in the latter cases it may well be due to inaccurate literature values.

The temperature dependence of the k_r values yields reasonable values for the activation energy of the proposed diffusion-controlled reaction. Absolute values of k_r indicate a reaction distance parameter of approximately 15 Å for H_3PO_4, H_3AsO_4, and HSO_4^- indicating that the recombination reaction is essentially complete when the ions are within 2 water molecules of each other. Values of k_r for H_3PO_3, HIO_4, and H_2SeO_3 are unrealistically high when the ΔV^0 value for H_3PO_4 is assumed for them. This may be due to a ΔV^0 for these acids considerably different from those measured for other acids or due to an inadequate model for the equilibrium.

A reanalysis of the ultrasonic data on availability of more accurate thermodynamic data can result in more accurate absolute values of k_r and k_d for such systems. Such an approach seems as promising as the extension of ultrasonic studies to higher frequencies, where sufficiently precise measurements in such acidic systems have not been made as yet.

The authors wish to thank Miss K. Johnstone for technical assistance. The project was supported financially by the National Research Council of Canada and the Inland Waters Branch, Environment Canada. One of the authors (P.K.) gratefully acknowledges the hospitality of the Physics Institute, University of Odense, Denmark, during the time when the manuscript was prepared.

1. M. Eigen. Z. Phys. Chem. **1**, 176 (1954).
2. G. Kurtze and K. Tamm. Acust. **3**, 33 (1953).
3. D. W. Fong and E. Grunwald. J. Am. Chem. Soc. **91**, 2413 (1969).
4. H. Chen and D. E. Irish. J. Phys. Chem. **75**, 2681 (1971); **75**, 2672 (1971).
5. M. C. Rose and J. Stuehr. J. Am. Chem. Soc. **93**, 4350 (1971).
6. P. Hemmes, L. D. Rich, D. L. Cole, and E. M. Eyring. J. Phys. Chem. **75**, 929 (1971).
7. J. J. Auborn, P. Warrick, and E. M. Eyring. J. Phys. Chem. **75**, 2488 (1971).
8. M. Eigen and L. DeMaeyer. Z. f. Elektrochem. **59**, 986 (1955).
9. J. Lang, C. Tondre, and R. Zana. J. Phys. Chem. **75**, 374 (1971).

10. M. HUSSEY and P. D. EDMONDS. J. Phys. Chem. **75**, 4012 (1971).
11. J. STUEHR and E. YEAGER. *In* Physical acoustics. Vol. II-A. *Edited by* W. P. Mason. Academic Press, New York, 1965.
12. M. EIGEN and L. DEMAEYER. *In* Technique of organic chemistry, Vol. VIII, Part II. *Edited by* S. L. Friess, E. S. Lewis, and A. Weissberger. Interscience, New York, 1963.
13. K. G. PLASS. Acust. **19**, 236 (1967–1968).
14. R. J. FANNING and P. KRUUS. Can. J. Chem. **48**, 2052 (1970).
15. H. S. HARNED and B. B. OWEN. The physical chemistry of electrolytic solutions. Reinhold, New York, 1958.
16. J. P. VALLEAU. J. Acoust. Soc. Am. **38**, 669 (1965).
17. A. J. ELLIS and D. W. ANDERSON. J. Chem. Soc. 1765 (1961).
18. P. MUKERJEE. J. Phys. Chem. **65**, 740 (1961).
19. I. M. KLOTZ and C. F. ECKERT. J. Am. Chem. Soc. **64**, 1878 (1942).
20. Handbook of Physics and Chemistry. Chemical Rubber Co.
21. C. J. S. PHILLIPS and R. J. P. WILLIAMS. Inorganic chemistry. Vol. 1. Oxford, 1965.
22. F. A. COTTON and G. WILKINSON. Advanced inorganic chemistry. Interscience, 1962.
23. A. K. COVINGTON, J. G. FREEMAN, and T. H. LILLEY. J. Phys. Chem. **74**, 3773 (1970).
24. P. DEBYE. Trans. Electrochem. Soc. **82**, 265 (1942).
25. H. L. FRIEDMAN. J. Phys. Chem. **70**, 3931 (1966).
26. K. SOLC and W. H. STOCKMAYER. J. Chem. Phys. **54**, 2981 (1971).

Can. J. Chem. Downloaded from www.nrcresearchpress.com by 210.87.254.42 on 09/05/12
For personal use only.

Laser-induced Transient Bleaching of Trapped Electrons in Alkali Halide Single Crystals

ROGER MAY AND DAVID C. WALKER

Chemistry Department, University of British Columbia, Vancouver 8, British Columbia

Received January 12, 1973

F-center electrons in KBr and KI crystals at room temperature are almost totally bleached during the intense light pulse from a Q-switched ruby laser. Recovery of the absorbance is largely complete within microseconds of the end of the pulse such that net loss of trapped electrons, which would result in permanent bleaching, is negligible ($\phi < 10^{-2}$). Transient bleaching seems to result from both a loss of F-centers to form F′-centers and saturation of optical transitions for both the F and F′ bands. Comparisons of transient bleaching effects at 633, 1152, and 694 nm for KBr and KI strongly imply that the trapped electron absorption bands in crystals arise from single optical transitions which are homogeneously broadened. The rate at which the ground state of the F-center is repopulated following laser photolysis is of the order of 10^{-9} s and is very much slower than the analogous process in hydrated electrons. Results are also presented for additively colored and γ-induced F-centers and for F- and F′-centers bleached by ruby laser pulses at low temperatures.

Les électrons du centre F des cristaux de KBr et KI sont presque totalement décolorés à la température ambiante par la lumière intense pulsée d'un laser au rubis Q. L'absorbance retrouvée est quasiment complète à quelques microsecondes de la fin de la pulsation de sorte que la perte nette en électrons piégés, résultant d'une décoloration permanente, est négligeable ($\phi < 10^{-2}$). La décoloration transitoire semble résulter à la fois des pertes en centre F pour former F′ et de la saturation des transitions optiques pour les deux bandes F, F′. Les comparaisons des effets de décoloration transitoire à 633, 1152, et 694 nm pour KBr et KI impliquent fortement que les bandes d'absorption des électrons piégés dans les cristaux proviennent de transitions optiques simples, élargies de façon homogène. La vitesse à laquelle l'état fondamental du centre F est repeuplé dans la photolyse laser, est de l'ordre de 10^{-9} s, c'est à dire beaucoup plus lente que le processus analogue pour les électrons hydratés. Les résultats ont été également présentés pour d'autres couleurs, pour les centres F et F′ décolorés par laser au rubis pulsé aux basses températures.

[Traduit par le journal]

Can. J. Chem., **51**, 2306 (1973)

Introduction

The nature of optical absorption bands of electrons trapped in crystals (*viz.* F-centers) or low temperature amorphous solid (*viz.* e_t^-) has been the subject of much experimental and theoretical investigation. Several photobleaching studies using low intensity illumination have been reported on F-centers (1, 2) and trapped electrons in glasses (3). In those experiments, measurements were made of the net bleaching effects (spectral shifts and quantum yields for electron loss) for the permanent changes resulting from photobleaching.

The application of short, high intensity light pulses from Q-switched ruby lasers has afforded a new perspective to such investigations since it permits very short-lived transient effects to be studied. Mahr (ref. 1, p. 243) has reviewed a series of experiments which employed a Q-switched ruby laser to photolyse F-centers in alkali halide crystals at liquid N_2 temperatures and to follow the relaxation processes occurring *after* the light flash, but with a time resolution which did not permit submicrosecond events to be studied. It has been shown, in this laboratory, that electrons solvated in liquid water at room temperature do not show non-linear absorption during 20 ns ruby laser pulses; thereby indicating a very short lifetime ($< 6 \times 10^{-12}$ s) for the photoexcited state of the hydrated electron when photolyzed at its absorption band maximum (4).

It has been our aim to employ ruby laser photolysis to reveal the nature and origin of optical absorption bands of trapped and solvated electrons, to decide whether the excited state is bound or free, and if the band is homogeneously or heterogeneously broadened. A preliminary account of some of our observations has recently been published (5).

In this paper we describe experiments on the laser photolysis of F-centers (electrons trapped at anion vacancies) in single crystals of potassium bromide and iodide *at room temperature* and

Can. J. Chem. Downloaded from www.nrcresearchpress.com by 210.87.254.6 on 09/05/12
For personal use only.

Can. J. Chem. Downloaded from www.nrcresearchpress.com by 210.87.254.6 on 09/05/12
For personal use only.

F′-centers (electron pairs trapped at anion vacancies) in crystals of potassium bromide and chloride at low temperatures. Several studies of transient bleaching effects of F-centers at low temperatures (typically 80 °K and lower) have been reported previously (ref. 1, p. 243, 6, 7, 8). For instance, Swank and Brown (6) showed that a comparatively long-lived (μs) relaxed excited state of the F-center existed at 80 °K and that the lifetime decreased sharply with increasing temperature so that it could not be measured by them at temperatures >110 °K. In addition Hirai *et al.* (7) studied the formation and decay of F-centers following nanosecond pulse radiolysis and concluded that some electrons were trapped via the relaxed excited state at 80 °K in crystals containing anion vacancies.

In order to answer fully the questions itemized above, it would be preferable to conduct nanosecond flash photolysis at various wavelengths appearing in different regions of the absorption band of one type of trapped electron. However, suitable lasers are not available at high enough powers and, in order to utilize a high power ruby laser to maximum advantage, we selected various media in which the 694 nm ruby laser line appeared in different regions of F and F′ absorption bands. It can be seen in Fig. 1 that for the F-center in KBr at room temperature 694 nm is on the low energy side of λ_{max} and in KI 694 nm is at the F-band maximum. At 77 °K the F-center in KI can be selectively bleached and has been the subject of previous study (ref. 1, p. 243). Similarly F′-centers in KBr and KCl can be selectively bleached at reduced temperatures (where they are stable).

In this study we have used low power c.w. helium/neon lasers, affording lines at 632.8 and 1152 nm, as sources of analyzing light for kinetic photometry. Study of Fig. 1 will show that these laser lines are conveniently positioned to interrogate the behavior of F- and F′-centers both during and immediately after ruby laser photolysis.

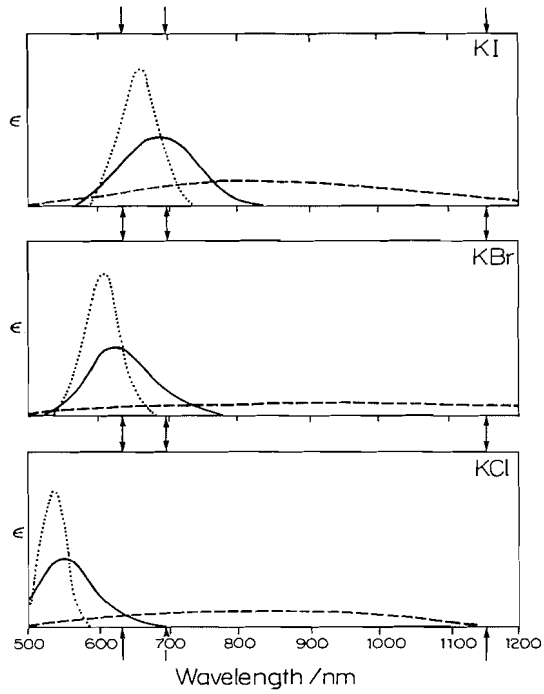

FIG. 1. Representative absorption spectra of F- and F′-centers for KCl, KBr, and KI crystals at various temperatures. ε is the relative extinction coefficient. Solid lines are F-centers at ~298 °K, dotted lines are F-centers at 77 °K and dashed lines are F′-centers at 77 °K. The arrows indicate the wavelengths of the lasers employed, 694, 633, and 1152 nm.

Experimental

Production of F-centers

Single crystals of KBr and KI (Harshaw) of thicknesses varying from 0.25 to 2 cm were polished on opposite faces. For the majority of the experiments described below, F-center coloration to selected absorbances was achieved in these crystals by γ-irradiation in a ^{60}Co source at room temperature. F-center concentrations $\leq 6 \times 10^{16}$ centers cm^{-3} were used throughout. For other experiments (*vide infra*) the crystals were additively colored with potassium vapor in a dual temperature furnace (ref. 2, p. 34). Prior to laser photolysis experiments F-center concentrations in both types of colored crystals were estimated from spectrophotomeric measurements using Smakula's equation and tabulated values of refractive index and oscillator strength (1, 2).

Laser Photolysis

Laser photolysis was performed on the apparatus shown schematically in Fig. 2. The ruby laser (TRG 104A, nominally 1 J of λ = 694.3 nm light) was triggered by shorting contacts on a leaf-type light shutter, E (Ilex). A bleachable dye cell was employed as a Q-switch to produce a 20 ns pulse (FWHM) with maximum intensities of 2×10^{26} photon cm^{-2} s^{-1}. A small fraction of the ruby laser pulse was reflected by a quartz plate M onto a silicon pin photodiode, T (Hewlett Packard, Type 5082-4203, operated at a reverse bias of 20 V) to yield a trigger signal, synchronous with the ruby pulse, for the two oscilloscopes O_1, O_2 (Hewlett Packard, Type 183; Tektronix 7904 with 7A16 and 7B92 plug-in units).

The intensity of 694.3 nm light incident on the sample S was varied by positioning, at *a*, a combination of four spectrophotometric cells C containing aqueous copper sulfate solutions. These solutions could not be bleached significantly at the intensities employed and hence acted

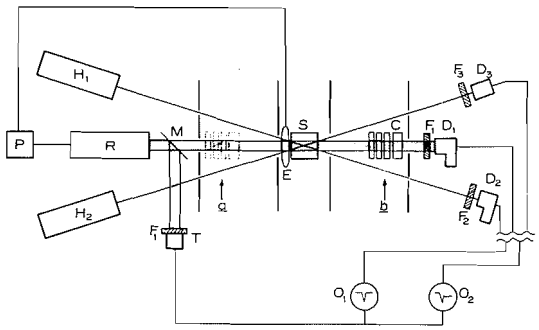

FIG. 2. Schematic diagram of apparatus. S, sample (for low temperature experiments, contained in a Dewar vessel); R, ruby laser head; P, ruby laser power supply, triggered by E; E, leaf-type light shutter; H_1, He/Ne laser, 633 nm; H_2, He/Ne laser, 1152 nm; M, quartz plate; T, Si photodiode (HP 5082–4203) acting as trigger for oscilloscopes; D_1, detector (694 nm), Hamamatsu R213 photomultiplier; D_2, detector (633 nm), R.C.A. 1P28 photomultiplier; D_3, detector (1152 nm), Philco Ford L 4521 Ge photodiode; O_1, O_2, oscilloscopes, Tektronix 7904, Hewlett–Packard 183; F_1, F_2, F_3, narrow band-pass interference filters, as per text; C, Four spectrophotometric cells containing concentrated aqueous solutions of $CuSO_4$ as per text, which could be positioned at either *a*, ahead of S, or *b* behind S.

as linear attenuators. The remaining $CuSO_4$ cells were positioned at *b* such that, in the absence of non-linear absorption by the sample at S, the incident light intensity on the photomultiplier D_1 (Hamamatsu R213) would be the same for identical pulses. The four cells employed had absorbances at 694 nm of 0.5, 1.0, 1.5, and 3.5. Filter F_1 consisted of a 694.3 nm narrow band pass interference filter and neutral density filters of total absorbance, $A = 2.5$.

Ruby laser light which was scattered by the sample and light attenuators was many times more intense than conventional analyzing light sources could cope with, despite the use of four light baffles shown in Fig. 2. To overcome this difficulty, two low power c.w. helium/neon lasers, H_1 (Spectra Physics, Type 132, 2 mW at 632.8 nm) and H_2 (Optics Technology, Type 233, ~2 mW at 1152 nm) placed at angles of about 15° to the ruby laser axis, were employed to provide monochromatic probe beams for kinetic photometry. The use of these c.w. lasers imposed an obvious limitation on spectral investigations but possessed the advantages that kinetic observations could be readily made *during* as well as after the ruby laser pulse and that their pencil beams could be easily directed through only the photolyzed volume element of sample. Even so both detectors D_2 (R.C.A. 1P28 photomultiplier) and D_3 (Philco Ford germanium photodiode, type L 4521) had to be shielded from scattered light by filters F_2 (*four* narrow band pass interference filters, 632.8 nm) and F_3 (1152 nm narrow band pass interference filter and two thicknesses of Kodak Wratten Filter No. 87A). The light shutter, E, was kept open for only 1/100*th* of a second to make the total exposure of the sample to He/Ne laser light trivial compared to that delivered by a ruby laser pulse.

In any particular run, two of the three signals (from D_1, D_2, and D_3) were selected and monitored separately on the oscilloscopes O_1 and O_2. Oscilloscope traces were photographed using Polaroid cameras.

For experiments conducted at reduced temperatures, the sample S was contained in a Dewar vessel with transparent windows. This was either filled with filtered liquid nitrogen for experiments at 77 °K, or alternatively, cold dry nitrogen, boiled from a reservoir of liquid nitrogen, was flowed into the Dewar at various rates such that photolysis could be carried out at selected temperatures between 77 and 300 °K. Crystal temperatures were measured by a copper/constantan thermocouple using a standard potentiometer.

A sample of F-centers at 77 °K was obtained by simply immersing a room temperature irradiated KI crystal in liquid nitrogen. F′-centers were produced *in situ* in KBr and KCl crystals by photolysis of the F-band at reduced temperature with a suitably filtered 30 W projector lamp (9). Crystal temperatures of 123 and 183 °K were used for the experiments on F′-centers in KBr and KCl, respectively, the F′-centers being stable at these temperatures.

Control Experiments

Control experiments were performed on stable solutions of organic dyes which have been shown to exhibit non-linear absorption of 694.3 nm light (10, 11). In this way synchronization of the firing sequence was established and the fast time response of the photoelectric detection systems demonstrated.

Figure 3 shows oscilloscope traces obtained when an aerated $\sim 10^{-5}$ *M* solution of vanadyl phthalocyanine in 1-chloronaphthalene was photolyzed. This solution had respective absorbances at 633 and 694 nm of 0.47 and 1.98 (in a 1 cm path length cell) as determined in a spectrophotometer. Trace (*a*) shows the ruby pulse pro-

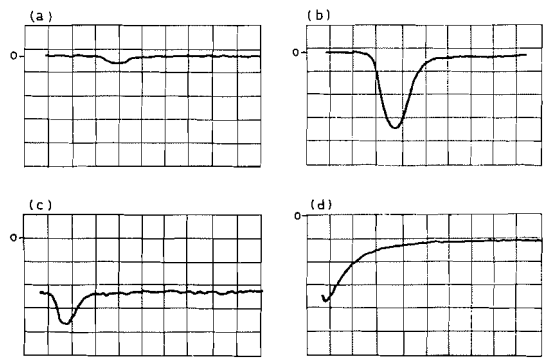

FIG. 3. Tracings of oscilloscope photographs for control experiments: (*a*), (*b*), and (*c*), 10^{-5} *M* solutions of vanadyl phthalocyanine in 1-chloronaphthalene; (*a*) and (*b*) are the transmitted ruby pulses at 694 nm at sweep speeds of 20 ns per division, (*a*) with all cells C at *a*, vertical: 10 mV per division, (*b*) with all cells C at *b*, vertical: 50 mV per division; (*c*) transient signal at 633 nm monitored simultaneously with (*b*), vertical: 20 mV per division, horizontal: 50 ns per division; (*d*) 10^{-5} *M* methylene blue in water monitored at 633 nm with all cells C at *b*, vertical: 20 mV per division, horizontal: 1 μs per division.

Can. J. Chem. Downloaded from www.nrcresearchpress.com by 210.87.254.6 on 09/05/12
For personal use only.

Can. J. Chem. Downloaded from www.nrcresearchpress.com by 210.87.254.6 on 09/05/12
For personal use only.

file under non-bleaching conditions (*i.e.* all the copper sulfate cells C at position *a*, peak incident 694 nm light intensity at S of 6×10^{19} photon cm^{-2} s^{-1}) and (*b*) the profile observed when the ruby beam was unattenuated at the sample S (all cells C in position *b*, maximum incident 694 nm light intensity of 2×10^{26} photon cm^{-2} s^{-1}). The increased signal observed in (*b*) represents a change in transmission from 0.011 to 0.34 which can be expressed as the "fraction bleached", $(A^0 - A)/A^0 = 0.77$ (where A is the absorbance at high incident intensity and A^0 the absorbance under "normal" spectrophotometric conditions, equivalent to all $CuSO_4$ attenuators being at *a*). Trace (*c*) was taken simultaneously with (*b*) and shows the transient effect monitored at 633 nm. The fraction bleached at 633 nm at the pulse maximum was 0.30 and this loss of absorption was observed to repair on a timescale slightly longer than the ruby pulse.

An aerated 10^{-5} *M* solution of methylene blue in water was similarly photolyzed. This solution had $A^0_{694\ nm} = 0.35$ and $A^0_{633\ nm} = 0.97$. Under similar conditions as Fig. 3*a*, *b*, and *c* the fractional bleaching was found to be 0.78 at 694 nm (at the pulse maximum) and 0.57 at 633 nm (at the end of the pulse). As Fig. 3*d* shows, the recovery of 633 nm absorption after the pulse took place on a much longer timescale than for vanadyl phthalocyanine.

Results

The data given in Fig. 4 show the transmitted pulse intensity at the pulse maximum (monitored by D_1) as a function of incident ruby pulse intensity for two irradiated KI crystals having initial absorbances at 694 nm of 0.45 and 1.0. It can be seen that at high pulse intensities the samples are extensively bleached. Similar observations were made with KBr crystals. The inset to Fig. 4 displays observed ruby pulse profiles for the case, (*1*), of low incident ruby intensity, where there is no bleaching, and the case, (*2*), of high incident intensity. The extent of bleaching, narrowing of the pulse and delay of the maximum transmission are evident from comparison of these traces.

Simultaneous monitoring at 633 nm yielded traces such as those presented in Fig. 5. Both frames of Fig. 5 show superpositions of several traces taken with different ruby pulse intensities (see legend). At low light intensities, $\lesssim 10^{23}$ photon cm^{-2} s^{-1}, *only* permanent bleaching of the F-band occurs, the quantum yield of which is very small, $< 10^{-2}$. At intermediate intensities *all* the photobleaching during the pulse lasts for tens of nanoseconds thereafter. At the highest intensities available there is essentially *complete* bleaching during the pulse, of which only ~70% persists after the pulse. The fraction persisting is independent of light intensity once >70%

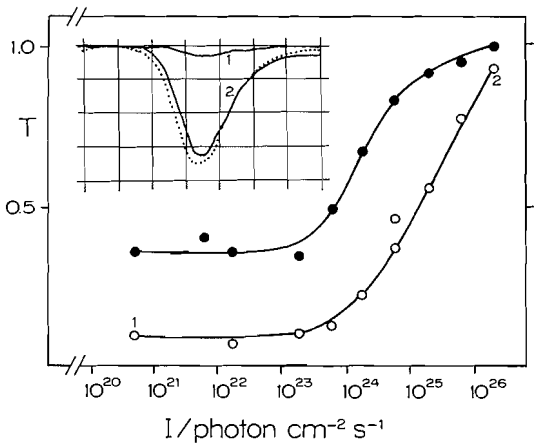

FIG. 4. Transmittance of ruby laser pulse measured at pulse peak at various intensities incident on sample of F-centers in KI crystal at ~295 °K for $A_{694}{}^0 = 0.45$ (solid circles) and $A_{694}{}^0 = 1.0$ (open circles). Inset shows oscilloscope tracings for points 1 and 2 on Fig. 4. The dotted line indicates the profile of incident ruby pulse. Vertical: 10 mV per division, horizontal: 10 ns per division.

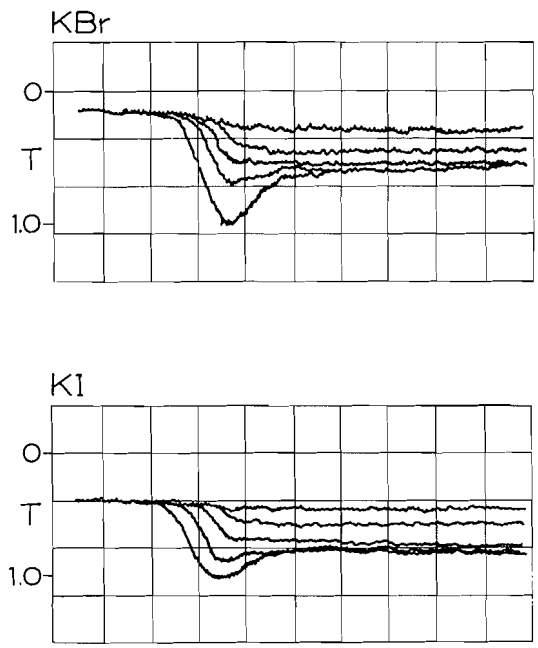

FIG. 5. Oscilloscope tracings showing the transmittance of KI and KBr at 633 nm for five different intensities of ruby light incident upon the crystals (2×10^{23}, 6×10^{23}, 6×10^{24}, 6×10^{25}, and 2×10^{26} photon cm^{-2} s^{-1} for KI and 2×10^{24}, 6×10^{24}, 2×10^{25}, 6×10^{25}, and 2×10^{26} photon cm^{-2} s^{-1} for KBr; in both cases progressing downwards.) Initial absorbance at 694 nm of KI was 1.0 and KBr was 0.5. Vertical: 50 mV per division, horizontal: 10 ns per division.

Can. J. Chem. Downloaded from www.nrcresearchpress.com by 210.87.254.6 on 09/05/12
For personal use only.

bleaching during the pulse has been achieved. This persistent portion recovers with an initial first-order half-life of 0.4 and 7.5 μs for KBr and KI, respectively. However, this repair of absorption does not obey first or second order rate equations for the whole period of recovery.

Similar data to that described above have been obtained for samples with various initial absorbances (at 694 nm) from 0.25 to 1.0 and arising from thick (20 mm) or thin (5 mm) crystals of KBr and KI at low and high F-center concentrations. The extent of transient bleaching processes was evidently not strongly dependent on either absorbance of the sample (at 694 nm) or on F-center concentration.

In order to compare bleaching phenomena at different wavelengths it is convenient to express bleaching by the function $(A^0 - A)/A^0$, termed fraction bleached, which is independent of the extinction coefficient at the different wavelengths. Figures 6 and 7 collate pertinent data for KI and KBr, respectively. For both crystals it can be seen that during the pulse peak the fraction bleached at 633 and 694 nm are essentially coincident. In KBr, F-centers are 50% bleached by a light flux of ~20 photons per F-center, whereas bleaching sets in at lower intensities for KI where the corresponding 50% bleaching value was ~10 at a comparable F-center concentration.

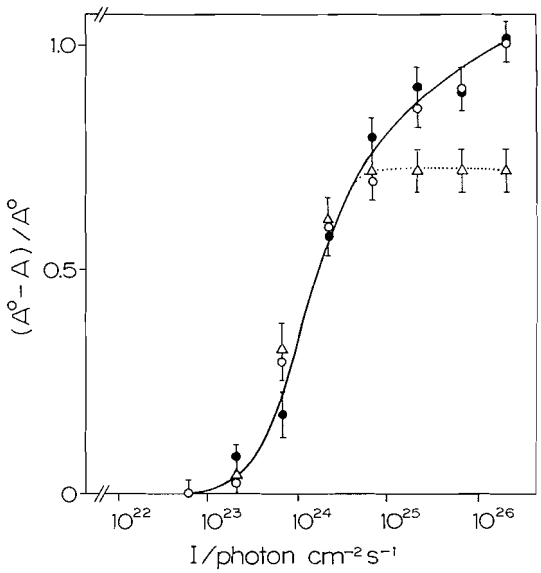

FIG. 6. Fraction bleached, $(A^0 - A)/A^0$, as a function of incident ruby laser intensity, for KI $A_{694}{}^0 = 1.0$. (A^0 is the absorbance at low intensity and A the absorbance at intensity I.) ○, 694 nm at pulse peak; ●, 633 nm during ruby laser pulse peak; △, 633 nm at the end of the ruby laser pulse.

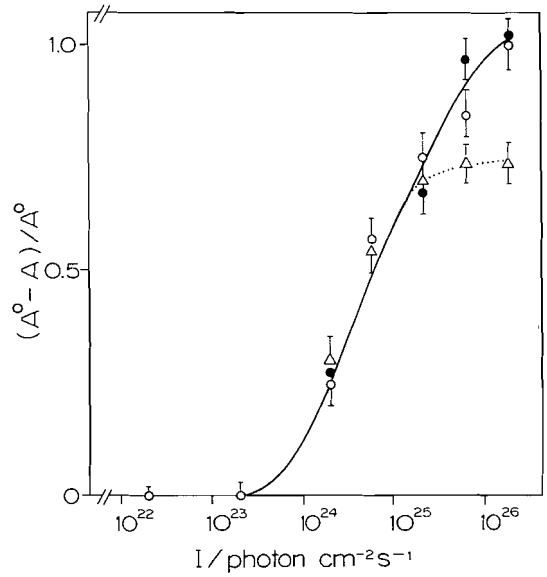

FIG. 7. Fraction bleached, $(A^0 - A)/A^0$, as a function of incident ruby laser intensity, for KBr $A_{694}{}^0 = 0.5$. ○, 694 nm at pulse peak; ●, 633 nm during ruby laser pulse peak; △, 633 nm at the end of the ruby laser pulse.

Transient effects were also monitored at 1152 nm. As Fig. 8 demonstrates, it was found that the ruby pulse induced transient absorption in crystals of KI at 1152 nm. (Analogous results were obtained with KBr.) Some of this absorption appeared during the ruby pulse and some "grew in" over a period of about 1 μs after the pulse.[1] As suggested by a comparison of Fig. 8*c* with Fig. 8*b* the decay of this transient absorption is kinetically coupled to the rate of recovery of F-center absorption at 633 nm. Although at ruby intensities less than $\sim 10^{24}$ photon cm^{-2} s^{-1} the small signals observed at 1152 nm defied actual quantitative comparison with transient

[1]This growing-in of absorption after the pulse cannot be attributed to a significant slow component in the detector's response (as noted in general for Ge detectors (17), because, in several cases, only instantaneous or stepwise changes are observed, see Fig. 9*d* for instance. Furthermore, it cannot arise from concurrent F-band fluorescence at 1152 nm (8) because, in a repeat experiment with the 1152 nm laser switched off, no signal was detected by the photodiode, D_3. Our experimental arrangement was designed to minimize scattered ruby light and consequently had a very low efficiency for observing any fluorescence.

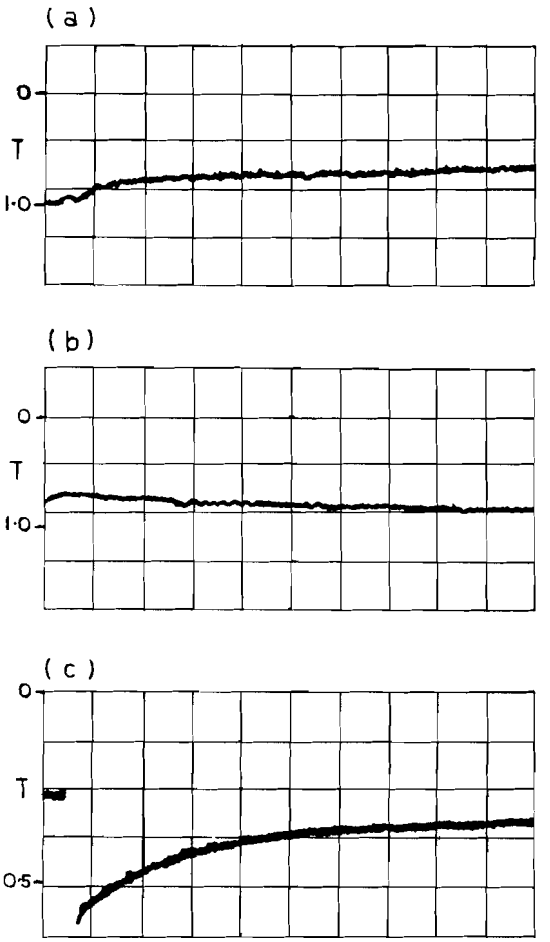

FIG. 8. Oscilloscope traces showing transient changes in transmission in KI at 1152 and 633 nm with cells C in position *b*. (*a*) Absorption created at 1152 nm by ruby pulse, vertical: 5 mV per division, horizontal: 50 ns per division; (*b*) same as (*a*) except horizontal scale is 2 μs per division; (*c*) transient effects at 633 nm monitored simultaneously with (*b*), vertical: 10 mV per division, horizontal: 2 μs per division.

signals at 633 nm, it appeared that the production of end-of-pulse absorption at 1152 nm was a similar function of intensity as the end-of-pulse bleaching at 633 nm.

Laser photolysis of potassium doped crystals of potassium iodide (5 mm thick, initial absorbance at 694 nm, $A_{694}{}^{0} = 0.48$) and potassium bromide (5 mm thick, $A_{694}{}^{0} = 0.10$) produced transient bleaching phenomena which were indistinguishable from the effects reported above for γ-irradiated crystals.

Several low temperature experiments were also performed. A KI crystal containing F-centers ($A_{694}{}^{0} = 0.33$) was exposed to ruby pulses at 77 °K. This caused bleaching at 633 nm only *during* the pulse and this bleaching repaired (see Fig. 9*a*) in a first order manner with a lifetime of 1.4 μs. This recovery rate is in agreement with an earlier observation (ref. 1, p. 243, 12).

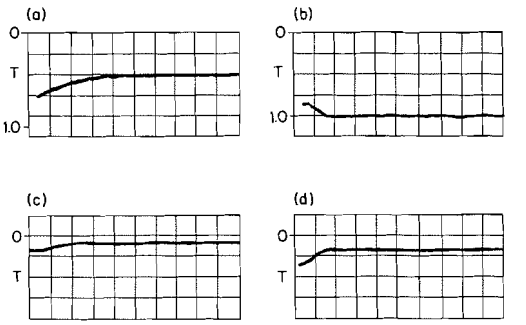

FIG. 9. Oscilloscope traces showing transient effects at low temperatures in KI, KCl, and KBr: (*a*) photolysis of F-centers in KI crystal at 77 °K monitored at 633 nm, vertical: 20 mV per division, horizontal: 1 μs per division; (*b*) photolysis of F′-centers in KCl crystal at 183 °K, monitored at 633 nm; (*c*) photolysis of F′-centers in KBr crystal at 123 °K, monitored at 633 nm; (*d*) photolysis of F′-centers in KBr crystal at 123 °K, monitored at 1152 nm. For (*b*), (*c*), and (*d*) vertical: 5 mV per division, horizontal: 50 ns per division.

A KCl crystal containing F′-centers at 183 °K was also subjected to laser photolysis. Figure 9*b* shows the transient effect observed at 633 nm. It can be seen that essentially all the absorbance which was initially present at this wavelength was bleached during the ruby pulse and this was permanent bleaching. Similar observations were made between 120 and 220 °K, the temperature range studied. No transient effects were observed at 1152 nm. Also the low initial absorbance at 694 nm would have imparted large errors to estimates of bleaching at 694 nm and thus transmitted ruby pulse profiles were not monitored in these experiments.

A sample of F′-centers in KBr was also subjected to ruby laser photolysis at 123 °K. As Fig. 9*c* and *d* show there was a production of absorbance at both 633 and 1152 nm during the ruby pulse. This production occurred only during the pulse and these changes of absorbance were permanent.

Discussion

A primary observation from the above results is that very similar bleaching phenomena during

Can. J. Chem. Downloaded from www.nrcresearchpress.com by 210.87.254.6 on 09/05/12
For personal use only.

Can. J. Chem. Downloaded from www.nrcresearchpress.com by 210.87.254.6 on 09/05/12
For personal use only.

the pulse peak were observed at 633 and 694 nm for F-centers in both KI and KBr crystals at room temperature. Since 633 nm is on the peak of the KBr F-band but on the high energy tail for KI, whereas 694 nm is on the low energy tail for KBr but on the peak for KI, it follows that the coincidence of the bleaching during the pulse strongly suggests that these bands consist entirely of one optical transition which is homogeneously broadened. This is in agreement with theoretical studies (ref. 1, p. 54) in which the ground and excited states are described by 1s and 2p wave functions, respectively. The fact that bleaching sets in at lower intensities for KI than for KBr is qualitatively consistent with the higher extinction coefficient at 694 nm of the F-band in KI.

A second striking effect observed is that, although transient bleaching occurs at comparatively low light fluxes, only a very small fraction of this results in permanent bleaching. In fact, permanent bleaching was so small it was barely detectable after one ruby pulse. However, an estimate of the quantum yield for permanent bleaching of $\phi \lesssim 10^{-2}$ was made for KBr and KI crystals by measuring the net change in transmission at 633 nm caused by several ruby pulses and by calculating the photons absorbed by subtracting the total transmitted light from the total incident light.

Whereas permanent bleaching of F-centers by ruby pulses was insignificant, transient bleaching was prominent. This means that the deexcitation processes leading to the repopulation of the ground state are comparatively slow. It is clear that the transient effects observed cannot be accounted for simply in terms of a 2-level energy scheme involving absorption, stimulated emission and deexcitation processes, because: (*i*), the data shown in Figs. 6 and 7 do *not* fit eq. 1 which may be derived for such a scheme (4),

$$[1] \qquad A^0 - A = 2\varepsilon I_i(1 - 10^{-A})10^3/k_{21}$$

where I_i is the incident intensity (in einstein cm^{-2} s^{-1}) and k_{21} the first order rate constant describing all processes other than stimulated emission by which the excited state is deexcited to the ground state; and (*ii*), the induced absorbance at 1152 nm and the post-pulse effects at 633 nm indicate the involvement of at least one additional transient state. However, some indication of the timescale of the deexcitation processes may be inferred in the following way, and is worthwhile doing for comparison with other types of stabilized electron states.

Considering only ruby laser intensities at which the fraction bleached is very small, say ~ 0.05, then the depletion of the ground state is trivial and the photo-excited state may be regarded as having a low photo-stationary concentration during the pulse peak. This situation approximates to the 2-level scheme to which eq. 1 applies. Taking data for KI from Fig. 6, $(A^0 - A)/A^0 = 0.05$ at $I = 2 \times 10^{23}$ photons cm^{-2} s^{-1} for which $A^0 = 1.0$ and $\varepsilon_{694} = 1.2 \times 10^5$ M^{-1} cm^{-1}, one evaluates k_{21} to be 1.4×10^9 s^{-1}. Furthermore, under these conditions the sample had absorbed $\sim 1.8 \times 10^{15}$ photon cm^{-2} up to the mid-pulse, whereas there were 5×10^{15} F-centers cm^{-2} in the light beam. Thus, 5% bleaching set in when there were ~ 0.36 photons absorbed per F-center per cm^2; which means that the quantum yield for transient bleaching of the ground state was *ca.* 0.14. This then implies that processes which lead to other transient states, and which compete with the direct deexcitation of the excited state, have smaller rate constants than $\sim 0.14k_{21}$, *i.e.* $< 2 \times 10^8$ s^{-1}.

Evidently the rate at which the ground state of the F-center electron in KI at room temperature is repopulated, following photolysis by 694 nm light, is more than two-orders of magnitude slower than the analogous processes in the case of the hydrated electron in liquid water at room temperature (4). Also, this mean lifetime of $\sim 0.7 \times 10^{-9}$ s is long enough to represent spontaneous radiative decay in the case of the crystals, as judged by their absorption band. Comparable data can be derived for KBr, where the higher light intensity required to reach 0.05 bleaching arises simply from its smaller ε_{694}.

The additional transient species involved, which is responsible for the transient absorption at 1152 nm and for some of the absorption at 633 nm immediately at the pulse end, is probably the F′-center. The spectra of F′-centers have been established at reduced temperatures (9) and included in Fig. 1. It can be seen that F′-centers also absorb 694 and 633 nm light. These centers are unstable at room temperature and spontaneously degrade into F-centers. Consequently, we propose that F′-centers are involved as transient species in these experiments. The photolyses at low temperatures show that F′-centers may also be bleached by ruby laser pulses, so that both their formation and bleaching must be considered in the mechanism of the overall photo-bleaching processes.

Can. J. Chem. Downloaded from www.nrcresearchpress.com by 210.87.254.6 on 09/05/12
For personal use only.

A plausible energy level scheme, which qualitatively explains the three photobleaching processes monitored at 633 nm, is shown in Fig. 10. (The F-band manifold of this scheme has been postulated previously (1, 2).) Levels 1 and 2 are respectively the 1s and 2p levels of the F-center. The conduction band (level 3) may be populated thermally from the 2p state of the F-center and from the relaxed 2p state (not shown). The ground state of the F′-center (level 4) may be formed by capture of a conduction band electron by an F-center. The F′-center probably has no bound excited state (9). The various k's are the kinetic rate constants of conversion between the levels noted as subscripts. σ and ρ are the respective absorption cross sections of the F- and F′-centers at 694 nm. (We have included the possibility of stimulated emission for the (2p → 1s) transition of the F-center but a similar process between the conduction band and the F′-center is unlikely because of the density of states in the conduction band.)

At high ruby pulse intensities the near 100% bleaching corresponds to a total saturation of optical transitions of F and F′ electrons. Within a very short time after the end of the pulse electrons populate only the 1s levels of the F- and F′-centers, and the microsecond recovery processes are attributable to thermal decomposition of F′-centers to reform F-centers. At intermediate intensities the predominant process is the conversion of F- to F′-centers; *i.e.* k_{34} is significantly greater than k_{31} in accordance with Pick's observation that at temperatures above 150 °K an F-center has a significantly greater cross-section for capture of another electron than has a vacancy (13, ref. 2, p. 110).

It is of interest to note that the induced bleaching effects are indistinguishable between γ-irradiated crystals (which contain positive hole centers) and potassium doped crystals (which contain no hole bands). Consequently, electrons liberated from F-centers by the ruby light were not recombining with positive holes in the γ-irradiated crystals and the permanent bleaching (observed to have a low quantum yield) must arise from electrons being "lost" by other processes, such as the formation of stable electron aggregate centers.

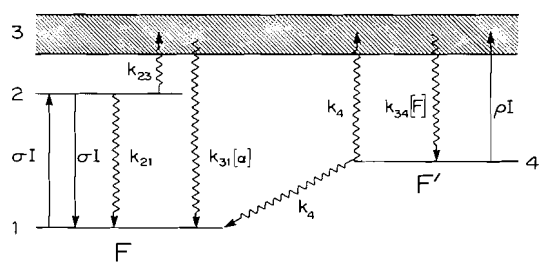

FIG. 10. Proposed energy-level scheme showing absorption and stimulated emission at 694 nm and first order rate constants for interconversion between states. (See text for details.)

Quantitative interpretation of the bleaching data in terms of the energy level scheme (Fig. 10) is complex. Since the transmitted ruby pulse is observed to be asymmetrically shaped with respect to the incident pulse, the system does not reach a photo-stationary state during the pulse so the peak transmitted intensities cannot be readily analyzed at high intensities (14).

A correlation of the loss of absorbance at 633 nm with the production of absorbance at 1152 nm can lead to an estimate of extinction coefficients of the F′-center at 1152 nm. For a particular irradiated KI crystal having an initial absorbance of 0.59 at 633 nm photolyzed with an unattenuated ruby pulse, the absorbance at the end of the pulse was 0.165 compared to a production of absorbance of 0.10 at 1152 nm. Let us assume that the extinction coefficients of the F′-center at 633 and 1152 nm are equal. (This is certainly approximately true at 77 °K (9) and hence, by analogy with the behavior of the F-center (Fig. 1), it is likely to be so at room temperature where, if anything, the spectrum will be broader and the extinction coefficient less wavelength dependent.) Then at the end of the pulse only ~0.065 units of absorbance are due to the F-center and hence ~89% of the F-center electrons were converted to F′-centers by the ruby pulse. If we take the F-center extinction coefficient at 633 nm to be $8.3 \times 10^4\ M^{-1}\ cm^{-1}$ at room temperature (obtained from the F-band spectrum using Smakula's equation, ref. 2), then we calculate the F′-center extinction coefficient at 633 nm to be $3.8 \times 10^4\ M^{-1}\ cm^{-1}$ at room temperature. This may be compared to the 77 °K value of 2.6×10^4 (obtained from ref. 9).

We have noted above that the optical transitions of the F′-center are saturated at high light intensities and indeed near 100% transmission of samples is seen at 633 nm. However, as Fig. 8*a* demonstrates, at comparable light intensities there is transient absorption at 1152 nm produced *during* the ruby pulse peak. This observation could have one of the following implications. Firstly, that the F′ band is heterogeneously

broadened (*i.e.* the overall band is a composite of several overlapping bands, only some of which are bleached by the pulse). This is contrary to theoretical predictions (9). Secondly, that other *unstable* centers, as well as F′, are absorbing at 1152 nm. This latter implication can also explain the high apparent F′ extinction coefficient which was obtained above. It is most likely that these centers are aggregates of the F-center. M and N bands must be ruled out because of their stability at room temperature, as must the unstable R-bands which one would predict not to absorb 1152 nm light (15). In fact, the most likely candidate is an ionized R_2 center, R_2^+, which has been observed by a phase sensitive detection technique in the c.w. laser photolysis of F-centers in KBr (16). The R_2^+ center is an ionized form of the R_2 center which in turn may be considered as an aggregate of two adjacent F-centers (2). The transient effects seen at 1152 nm at room temperature may thus be explained by the following reaction sequence;

$$[2] \qquad F + \alpha \rightleftarrows R_1, R_2^+$$

$$[3] \qquad F' + \alpha \rightleftarrows R_2$$

$$[4] \qquad \alpha + e \rightarrow F \qquad (k_{31})$$

$$[5] \qquad F + e \rightleftarrows F' \qquad (k_{34}/k_{43})$$

where α represents an anion vacancy. It is evident that processes 2 and 3 cannot be easily included in Fig. 10. During the ruby pulse electrons are lost from F-centers and the resulting anion vacancy may interact with F′- or remaining F-centers to form R and R^+ centers. These centers may decay by undergoing further aggregation steps which result in net bleaching of F-centers. Alternatively, these centers may decay by the reverse of processes 2 and 3 above. Indeed the low quantum yield for net bleaching strongly suggests that these latter reactions are predominant. The growth in absorption at 1152 nm immediately after the pulse is accounted for by the decay of R and R^+ centers. The non-first order decay of transient absorption (Fig. 8*b*) at 1152 nm is probably due to overlapping absorption of R_2^+ and F′-centers and the fact that the individual decay rates of R and F′-centers may each dominate at different times during the overall decay to reform F-centers.

The observations at low temperature may also be qualitatively described in terms of the energy level scheme in Fig. 10. At liquid nitrogen temperatures, thermal escape of electrons from the 2p level of the F-center, and from its relaxed state, to the conduction band is likely to be rather slow. Instead, the electrons may ultimately largely populate the relaxed excited state where they have a much longer lifetime (1.4 μs in KI) than at higher temperatures (ref. 1, p. 243, ref. 12).

Finally, the results of Fig. 9*b*, *c*, and *d* show that the F′-center in KCl and KBr at reduced temperature is permanently bleached by the ruby pulse. This is observed as loss of F′ absorption at 633 nm in KCl, and formation of F from F′ resulting in an increase of 633 nm absorption in KBr where $\varepsilon_F > \varepsilon_{F'}$. The increase in absorption at 1152 nm in KBr (Fig. 9*d*) would suggest that one or more F-aggregate centers, which are stable at this temperature, are also formed as a result of F′-photolysis.

We gladly acknowledge Dr. K. E. Rieckhoff for supplying a sample of vanadyl phthalocyanine; Dr. B. A. Saunders for experimental advice concerning additive coloration of crystals; and the Defence Research Board and National Research Council of Canada for financial support.

1. W. B. Fowler (*Editor*). Physics of color centres. Academic Press, New York. 1968.
2. J. H. Schulman and W. D. Compton. Color centres in solids. Pergamon Press, New York. 1963.
3. W. H. Hamill. Radical ions. *Edited by* E. T. Kaiser and L. Kevan. Interscience Publishers, New York. 1968. p. 321.
4. G. A. Kenney-Wallace and D. C. Walker. J. Chem. Phys. **55**, 447 (1971).
5. R. May and D. C. Walker. J.C.S. Chem. Commun. 1972, 1064.
6. R. K. Swank and F. C. Brown. Phys. Rev. **130**, 34 (1963).
7. (*a*) M. Ueta, Y. Kondo, M. Hirai, and T. Yoshinari. J. Phys. Soc. Jap. **26**, 1000 (1969). (*b*) Y. Kondo, M. Hirai, T. Yoshinari, and M. Ueta. J. Phys. Soc. **26**, 1553 (1969). (*c*) M. Hirai, Y. Kondo, T. Yoshinari, and M. Ueta. J. Phys. Soc. **30**, 440 (1971).
8. L. Bosi, P. Podini, and G. Spinolo. Phys. Rev. **175**, 1133 (1968).
9. D. W. Lynch and D. A. Robinson. Phys. Rev. **174**, 1050 (1968).
10. R. M. Danziger, K. H. Bar-Eli, and K. Weiss. J. Phys. Chem. **71**, 2633 (1967).
11. M. L. Spaeth and W. R. Sooy. J. Chem. Phys. **48**, 2315 (1968).
12. D. Frohlich and H. Mahr. Phys. Rev. **141**, 692 (1966).
13. H. Pick. Nuovo Cimento, **VII** (ser X), 498 (1958).
14. L. Huff and L. G. DeShazer. J. Opt. Soc. Am. **60**, 157 (1970).
15. H. Ivey. Phys. Rev. **72**, 341 (1947).
16. M. J. Redman and M. R. Tubbs. Philos. Mag. **24**, 1049 (1971).
17. W. A. Seddon, E. B. Selkirk, and J. W. Fletcher. Private communication.

Can. J. Chem. Downloaded from www.nrcresearchpress.com by 210.87.254.6 on 09/05/12
For personal use only.

A Study of the Proton Nuclear Magnetic Resonance Spectra of Aryl and Mono- and Disubstituted *N*-Methylazoles

RICHARD NOEL BUTLER
Department of Chemistry, University College, Galway, Ireland

Received December 27, 1972

Proton n.m.r. spectra of 111 substituted azoles are compared. The influence of the azole ring on the chemical shifts of substituent phenyl protons is discussed. A correlation between *N*-methyl chemical shifts and the structural characteristics of the *N*-methyl group in mono- and disubstituted azoles is noted.

On compare les spectres r.m.n. du proton de 111 azoles substitués. On discute de l'influence de l'anneau du groupe azole sur les déplacements chimiques des protons appartenant à un substituant phényle. De même on note une corrélation entre les déplacements chimiques du groupe *N*-méthyle et les caractéristiques structurales du *N*-méthyle dans les azoles mono et disubstitués. [Traduit par le journal]

Can. J. Chem., 51, 2315 (1973)

Can. J. Chem. Downloaded from www.nrcresearchpress.com by 210.87.254.6 on 09/05/12
For personal use only.

In recent years a collection of n.m.r. spectra of a wide range of azoles has been built up in separate studies of synthetic and other aspects of azole chemistry. These, when combined, provide useful structural information on the azoles. In this work the p.m.r. spectra of 111 substituted azoles are compared and discussed.

Arylazoles

The effects of the different azole systems on the proton resonances of a substituent phenyl group are summarized in Table 1. Fraser and Haque (1) have reported the upfield shift in the meta- and para-protons ($H_{m,p}$) of the phenyl ring and the accompanying downfield shift in the ortho protons (H_o) on changing a methyl group from the 1- to the 2-position of a methyl substituted-5-phenyltetrazole (compare compounds **5** and **10**, Table 1). The overall effect relative to benzene is considered to arise from a combination of ring anisotropy, nitrogen anisotropy, and an electron donating resonance interaction between the rings in compound **10** which is absent or very small in compound **5** (1–9). A comparison (Table 1) of the relative changes in the chemical shifts of the $H_{m,p}$ and H_o phenyl protons of the following pairs of compounds, **4** *vs.* **9**; **4** *vs.* **8**; **1** *vs.* **6**; **2** and **3** *vs.* **7** shows that this is a general effect in the azoles. In each case changing the *N*-methyl group from the β- to the γ-atom (relative to the atom to which the phenyl group is bonded) results in an upfield shift in the $H_{m,p}$ signal (column 5, Table 1, Part II) and a downfield shift in the H_o signal (column 4, Table 1, Part II). When the *N*-methyl group occupies the β-position, the interaction is lost or greatly diminished and the phenyl protons give a single signal only (compare compounds **1–5**).

The ortho deshielding phenomenon and its disappearance in β-methyl derivatives has been noted previously in substituted phenylpyrazoles (6–9) and also in 3-phenylpyridazines (10), 2,2′-bipyridyl (4, 5), and in aryl-triazines and tetrazines (3). The loss of the interaction has been ascribed to a loss of coplanarity between the rings (6–12) which causes a diminution of the anisotropic effects and a disruption of the resonance interaction. If, as expected, the extent of coplanarity loss is similar for the compounds **1–5** (Table 1, Part I), it is of interest to note the increased deshielding of the phenyl protons with successive replacement of —CH= by —N= in the heterocyclic ring. This probably reflects an increased electron-withdrawing inductive effect in the higher azoles with a possible contribution from nitrogen anisotropy in the case of the tetrazole **5**. Column 5 of Table 1, Part II, shows that the upfield shift of $H_{m,p}$ on going from a β- to a γ-substituted phenylazole also appears to undergo an increase with the number of nitrogen atoms in the ring, suggesting that the factors causing this shielding shift are stronger in the higher azoles. The downfield shift in H_o, which arises simultaneously, is, on the other hand, relatively insensitive to the number of nitrogen atoms in the ring, *e.g.* compounds **6–9**, suggesting that the ortho-deshielding arises from anisotropic effects with little, if any, contribution from the resonance interaction.

Can. J. Chem. Downloaded from www.nrcresearchpress.com by 210.87.254.6 on 09/05/12
For personal use only.

Since all of the compounds **6–10** contain an sp^2 nitrogen atom β- to the phenyl ring a special nitrogen anisotropic effect (including paramagnetic effects of the lone pair and a possible weak hydrogen bonding contribution (2–4)) must be included in the deshielding for these compounds. That such an effect contributes to the ortho-deshielding is suggested from a comparison of compounds **11–13** (Table 1), none of which contains an sp^2 nitrogen atom β to the phenyl ring but all of which contain a ring current. The special ortho-deshielding of compound **12** resulting from removal of the β-Me substituent in compounds **11** and **13** is considerably less than that of the compounds **6–10** while the $H_{m,p}$ shielding is comparable to that of the other diazoles. A comparison of the changes in the ortho-deshielding (column 4, Table 1, Part II) for the compounds **12** → **6–9** → **10** is of interest since it represents the following structural changes about the *C*-phenyl group, =CH—C(Ph)=CH— → —CH=C(Ph)—N= → =N—C(Ph)=N—. Each step involves replacing a β-CH= group by an sp^2 nitrogen atom and the relatively large deshielding for the first step probably reflects a gain in coplanarity as well as —N= anisotropy, whereas the second step, **6–9** → **10** may be an indication of the special contribution of —N= anisotropy. Hence the data in Table 1 suggest that the overall ortho-deshielding relative to benzene is made up of contributions from (*i*) an inductive effect varying with the number of nitrogen atoms in the ring (Table 1, Part I); (*ii*) a ring current effect, *ca.* 0.15 p.p.m. (the average value of the H_o deshielding of the compounds **6–9** less the deshielding due to one =N— atom (0.16 p.p.m.); (this is somewhat greater than the shift for compound **12** since the two β-CH= groups probably cause some loss of coplanarity between the rings), and (*iii*) a nitrogen anisotropic effect, *ca.* 0.16 p.p.m. for each =N— atom β to the phenyl ring (the difference between the average H_o deshielding for compounds **6–9** and compound **10**).

The correlations noted in Table 1 are for arylazoles where the phenyl group is attached to the azole ring at a carbon atom. It is possible that a different transmission of effects could obtain when the phenyl group is attached to the azole ring at a nitrogen atom. A complete set of data on directly comparable β-substituted and β-unsubstituted compounds for the full azole series where the phenyl group is bonded to a nitrogen atom is not readily available. A β-unsubstituted series of 1-*p*-nitrophenylazoles has,

TABLE 1. Chemical shifts (τ) of phenyl protons of arylazoles[a]

PART I:

No.	Compound	τ phenyl	τ phenyl − τ benzene
1	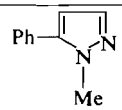	2.61[b]	−0.12
2	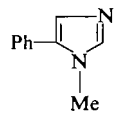	2.61[b]	−0.12
3	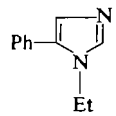	2.60[c]	−0.13
4	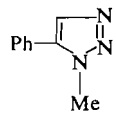	2.53[b]	−0.20
5	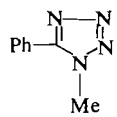	2.36[d]	−0.37

TABLE 1 *(Concluded).*

PART II:

No.	Compound	H_o	$H_{m,p}$	$H_{m,p} - H_o$	ΔH_o[g]	$\Delta H_{m,p}$[h]
6	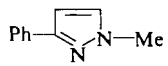	2.20[b]	2.65	0.45	−0.41	+0.04
7	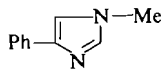	2.28[b]	2.68	0.40	−0.33	+0.07
8	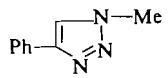	2.22[b]	2.65	0.43	−0.31	+0.12
9	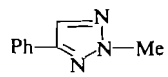	2.26[b]	2.67	0.41	−0.27	+0.14
10	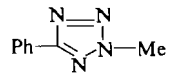	1.87[d]	2.59	0.72	−0.49	+0.23
11	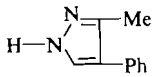	2.66[e]	2.66	—	—	—
12	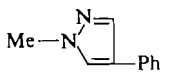	2.60[f]	2.73	0.13	0.06–0.14[i]	0–0.07[i]
13	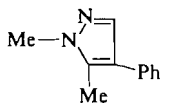	2.74[e]	2.74	—	—	—

[a]Chemical shifts, from internal TMS, are for solutions in $CDCl_3$ at normal probe temperature (*ca.* 35°) unless otherwise stated.
[b]Data from ref. 13.
[c]Data from ref. 12.
[d]Data from ref. 1, see also ref. 40.
[e]Data from refs. 43 and 46.
[f]Data from ref. 7.
[g]$H_o(\tau)$ — $H_o(\tau)$ of corresponding β-*N*-methyl isomer.
[h]$H_{m,p}(\tau) - H_{m,p}(\tau)$ of corresponding β-*N*-methyl isomer.
[i]Differences from compounds **11** and **13**, the β-methyl isomers.

however, been studied (9). Shifts, which were compared directly with nitrobenzene and not with the non-coplanar β-substituted derivatives, gave a value of 0.1 p.p.m. for the ring current effect and 0.7 p.p.m. for the ortho-deshielding in molecules containing two sp^2 nitrogen atoms β to the *N*-phenyl group. This latter value was recognized as a "global" value containing all the effects of the $=\dot{N}-$ atoms and as such included the effects represented by the shifts in Table 1, Part I. Hence there is reasonable agreement between the data herein for *C*-phenylazoles and those reported for *N*-phenylazoles (9). This is best illustrated by using the conclusions from the present approach to predict the shifts for the *N*-phenylazoles and *vice versa*. Taking a ring current effect of 0.15 p.p.m. a deshielding of 0.16 p.p.m. for the effect of each β-sp^2 nitrogen atom and azole inductive effects from Table 1, Part I, (for diazoles 0.1 p.p.m., the average of compounds **1**, **2**, and **11**) gives the following calculated deshielding shifts for the ortho-protons of 1-*p*-nitrophenylazoles: pyrazole, 0.41 p.p.m. (observed (9), 0.40 p.p.m.); imidazole, 0.25 (0.09); 1,2,3-triazole, 0.51 (0.49); 1,2,5-triazole, 0.67 (0.80); 1,2,3,4-tetrazole, 0.68 (0.48). The agreement is reasonable since errors are expected in the values taken from Table 1, Part I, where the azole ring has a methyl substituent. Using the approach of Elguero *et al.* (9) to predict the ortho-deshielding, relative to benzene, of the compounds in Table 1 gives the following: compound **6**, calculated 0.45 p.p.m. (observed, 0.53); **7**, 0.45 (0.43); **8**, 0.45 (0.51);

Can. J. Chem. Downloaded from www.nrcresearchpress.com by 210.87.254.6 on 09/05/12
For personal use only.

9, 0.45 (0.47); **10**, 0.80 (0.86); **12**, 0.10 (0.13), a somewhat better agreement because the complexities of breaking down the "global" sp^2 nitrogen effect do not arise.

Comparison of the magnitudes of the shift differences in Table 1 suggests that anisotropic effects dominate the shifts in the lower azoles and that other effects, such as resonance and inductive effects, may make an appreciable contribution to shifts in the higher azoles, particularly the tetrazoles.

N-Methylazoles

The n.m.r. chemical shifts of *N*-alkyl groups are widely used for structural assignments of isomeric substituted azoles (13–27, 38–43). The *N*-methyl chemical shifts for 105 *N*-methylazoles, measured under similar conditions, are compared in Table 2. In general the τ value for *N*-methyl groups decreases with increasing number of nitrogen atoms in the heterocyclic ring. Within a particular class, the chemical shift (τ) of the *N*-methyl group decreases in the following order for the structure units

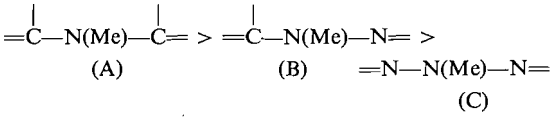

This relationship also applies in an approximate manner across the azole series for comparable compounds. A comparison of the *N*-methyl parent compounds **14** (A unit), diazoles **15** (A unit) and **22** (B unit), triazoles **43** and **48** (B units), **49** (A unit), **44** (C unit), tetrazoles **66** (B unit), **67** (C unit) exemplifies the trend. For *N*-methylpyrrole, **14**, and the diazole series, **15**–**42**, the *N*-methyl signal is above 6.0 τ except for compounds **19** and **26** which contain a NO_2 group interacting with the ring. For triazoles and tetrazoles containing the unit B, the *N*-methyl signal is generally between 5.8–6.0, and is less than 5.8 τ when the unit C is present. Exceptions occur, not unexpectedly, when a strongly activating group, *e.g.* NH_2, is near the *N*-methyl group. The relationship between the chemical shift and the structural units A, B, and C within a particular series is apparent from comparisons of the data in Table 2. For example, with tetrazoles the signal of the 1-alkyl isomer (B unit) is generally 0.15–0.35 p.p.m. upfield from that of the corresponding 2-alkyl isomer (C unit) and with 1,2,4-triazoles the signal of the 4-alkyl isomer (A unit) is 0.1–0.25 p.p.m. upfield from that of the corresponding 1- or 2-alkyl isomers (B units). (Since solvent effects are appreciable, *cf.* refs. 50 and 51, *e.g.* compound **53**, Table 2, comparisons should be confined to data measured in the same solvent.)

The decreased shielding of the *N*-methyl group for the structural series C < B < A probably reflects the greater electron-withdrawing characteristics of the —N= moiety over the —CH= moiety. Lynch[1] has observed a direct correlation between the electron density on the nitrogen atom and the chemical shift of the bonded methyl group (Table 3) which explains the trends noted herein. Electron densities were calculated by the simple HMO method (with α *N*-methyl = α + β, and α_N = α + 0.5β) or by the Wheland–Mann SCF method. Previously correlations have been reported between electron densities and (*i*) proton and ^{13}C chemical shifts of ring C—H groups in azoles (32–34, 50) and (*ii*) amino proton chemical shifts in amino-substituted azoles (23, 35, 36).

Limitations of the Structure — Chemical Shift Relationship

The relationship between the chemical shift of an *N*-methyl group and its appearance in an A, B, or C structural unit began to break down for trisubstituted azoles, the compounds in Table 2 being generally monosubstituted azoles and disubstituted azoles where one of the substituents is the *N*-methyl group. For example the *N*-methyl chemical shifts of 60 trisubstituted pyrazoles ranged between 5.72–7.02 τ and the specific values depended on the nature, type, and combination of substituents (7–9, 51). This is readily explained in terms of Lynch's correlation[1] since it is to be expected that increasing substitution will outweigh structural effects in governing electron densities in the ring. The order of shielding noted for the structural units A, B, and C will also be limited with compounds containing substituents which may interact more strongly with the *N*-alkyl group of one isomer than with that of the other. Thus, for example,

[1]Prior to the submission of this paper B. M. Lynch, Chemistry Department, St. Francis Xavier University, Antigonish, Nova Scotia, had independently arrived at a direct correlation between calculated electron densities and *N*-methyl chemical shifts in azoles (Table 3). Professor Lynch, who was a referee, offered his data for inclusion in this paper.

Can. J. Chem. Downloaded from www.nrcresearchpress.com by 210.87.254.6 on 09/05/12
For personal use only.

TABLE 2. Chemical shifts of *N*-Me protons in substituted azoles[a]

No.	Compound	*N*-Me (τ)	Reference
14	1-methylpyrrole (A unit)	6.45[b]	30
Imidazoles (A unit)	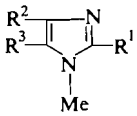		
15	$R^1 = R^2 = R^3 = H$	6.30	28, 29 (*cf.* 39)
16	$R^1 = R^2 = H$, $R^3 = Br$	6.37	28
17	$R^1 = Br$, $R^2 = R^3 = H$	6.36	28
18	$R^1 = R^3 = H$, $R^2 = NO_2$	6.10	28
19	$R^1 = R^2 = H$, $R^3 = NO_2$	5.95	28
20	$R^1 = H$, $R^2 = NO_2$, $R^3 = Br$	6.21	28
21	$R^1 = Br$, $R^2 = NO_2$, $R^3 = H$	6.20	28
3 (Table 1)	$R^1 = R^2 = H$, $R^3 = Ph$	6.04 (CH_2)	12
Pyrazoles (B unit)	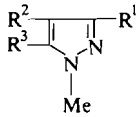		
22	$R^1 = R^2 = R^3 = H$	6.12, 6.19[c]	7, 41 (*cf.* 37 and 39)
23	$R^1 = R^2 = H$, $R^3 = Me$	6.20, 6.27	7, 37
24	$R^1 = Me$, $R^2 = R^3 = H$	6.37, 6.20	7, 37
25	$R^1 = R^3 = H$, $R^2 = Me$	6.30	47
26	$R^1 = R^3 = H$, $R^2 = NO_2$	6.00[d], 5.97	7, 47
27	$R^1 = Me$, $R^2 = Br$, $R^3 = H$	6.23	37
28	$R^1 = Me$, $R^2 = H$, $R^3 = Br$	6.20	37
29	$R^1 = H$, $R^2 = Br$, $R^3 = Me$	6.21	37
30	$R^1 = Br$, $R^2 = H$, $R^3 = Me$	6.28	37
31	$R^1 = R^2 = H$, $R^3 =$ cycloalkyl	6.17	42
32	$R^1 =$ cycloalkyl, $R^2 = R^3 = H$	6.13	42
33	$R^2, R^3 = (CH_2)_4$, $R^1 = H$	6.3	42
34	$R^1, R^2 = (CH_2)_4$, $R^3 = H$	6.2	42
35	$R^2 = R^3 = H$, $R^1 = NH_2$	6.39	45
36	$R^1 = R^2 = H$, $R^3 = NH_2$	6.43	45
37	$R^1 = R^3 = H$, $R^2 = Ph$	6.08	7, 46
38	$R^1 = R^3 = H$, $R^2 = Cl$	6.28	47
39	$R^1 = R^3 = H$, $R^2 = CHO$	6.09	47
1 (Table 1)	$R^1 = R^2 = H$, $R^3 = Ph$	6.18	48
40	$R^2 = R^3 = H$, $R^1 = Ph$	6.15	48
41	$R^1 = Me$, $R^2 = H$, $R^3 = Ph$	6.19	48
42	$R^1 = Ph$, $R^2 = H$, $R^3 = Me$	6.20	48
1,2,3-Triazoles	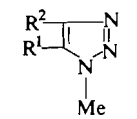		
43	$R^1 = R^2 = H$ (B unit)	5.87, 5.90	28, 50
44	1-Methyl-1,2,5-triazole (C unit)	5.82	50
4 (Table 1)	$R^1 = Ph$, $R^2 = H$ (B unit)	5.92	13
8 (Table 1)	$R^1 = H$, $R^2 = Ph$ (B unit)	5.87	13
9 (Table 1)	(C unit)	5.78	13
45	$R^1 = Br$, $R^2 = H$ (B unit)	6.00	28
46	$R^1 = H$, $R^2 = Br$ (B unit)	5.90[e]	50
47	1-Methyl-4-bromo-1,2,5-triazole (C unit)	5.84	28
1,2,4-Triazoles			
48	1-Methyl-1,2,4-triazole (B unit)	6.00, 6.07	28, 49
49	4-Methyl-1,2,4-triazole (A unit)	6.17, 6.37	12, 49

Can. J. Chem. Downloaded from www.nrcresearchpress.com by 210.87.254.6 on 09/05/12
For personal use only.

TABLE 2. (*Concluded*)

No.	Compound	N-Me (τ)	Reference
50	1-Methyl-5-bromo-derivative (B unit)	6.05	28
51	4-Methyl-5-bromo-derivative (A unit)	6.28	28
52	1-Methyl-5-amino-derivative (B unit)	6.33	28
53	1-Methyl-5-thione-derivative (B unit)	6.25, 6.45[f]	44
54	2-Methyl-5-thione-derivative (B unit)	6.25[f]	44
55	4-Methyl-5-thione-derivative (A unit)	6.55[f]	44
56	1-Ethyl-5-thione-derivative (B unit)	6.00[f] (CH_2)	44
57	2-Ethyl-5-thione-derivative (B unit)	5.9[f] (CH_2)	44
58	4-Ethyl-5-thione-derivative (A unit)	6.10[f] (CH_2)	44
59	1-Benzyl-5-thione-derivative (B unit)	4.6[f]	44
60	4-Benzyl-5-thione-derivative (A unit)	4.8[f]	44
61	1,3-Dimethyl-derivative (B unit)	6.16	49
62	1,5-Dimethyl-derivative (B unit)	6.18	49
63	3,4-Dimethyl-derivative (A unit)	6.36	49
64	1,3,5-Trimethyl-derivative (B unit)	6.32	49
65	3,4,5-Trimethyl-derivative (A unit)	6.53	49

Tetrazoles

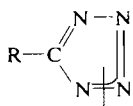

No.	R	R^1(1-isomer) τ (B unit)	R^1(2-isomer) τ (C unit)	Reference
66, 67 (R^1 = Me)[g]	H	5.73	5.54	28
68, 69 (R^1 = Me)	Br	5.87	5.60	28
70, 71 (R^1 = Me)	Me	5.90	5.70	31
72, 73 (R^1 = Me)	NH_2	6.18[j]	5.84	24
74, 75 (R^1 = Ph − CH_2)	NH_2	4.66	4.46	22
76, 77 (R^1 = $PhCH_2$)	NH_2	4.62	4.46	22
78, 79 (R^1 = $PhCH_2$)	$PhCH_2$	4.64	4.35	15
5, 10 (R = Me) (Table 1)	Ph	5.84	5.75	1
80, 81 (R^1 = CH_2COOEt)[h]	2-Thienyl	4.22[f]	4.15[f]	38
82, 83 (R^1 = CH_2COOEt)[h]	2-Furyl	4.25[f]	4.09[f]	38
84, 85 (R^1 = CH_2COOEt)[h]	CH_3OCH_2	4.50[f]	4.25[f]	38
86, 87 (R^1 = CH_2COOEt)[h]	Ph	4.30[f]	4.07[f]	38
88, 89 (R^1 = CH_2COOEt)[h]	NH_2	4.90[f]	4.57[f]	20
90, 91 (R^1 = CH_2COOEt)[h]	CH_3S	4.95[c]	4.67[c]	20
92[i] 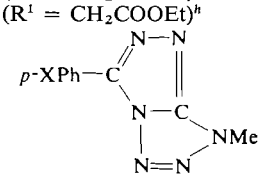		5.80 (*N*-Me)	—	25
93[i] 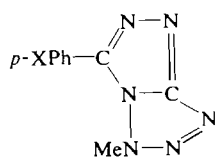		—	5.40 (NMe)	25

[a]Chemical shifts, from internal TMS, are for solutions in $CDCl_3$ at normal probe temperatures (*ca.* 35°) unless otherwise stated.
[b]Measured in cyclohexane at 38° (concentration < 0.1 *M*).
[c]Solvent CCl_4.
[d]Solvent acetone.
[e]A value of 5.78, which conflicts with the present correlation, has also been reported (28).
[f]Solvent DMSO.
[g]The lower number of each pair refers to the 1-substituted isomer.
[h]A similar difference between the 1- and 2-alkyl signal was observed with the corresponding acids.
[i]X = CH_3, H, Br, Cl.
[j]Solvent D_2O. Shift from internal sodium 3-(trimethylsilyl)-propane-1-sulfonate.

Can. J. Chem. Downloaded from www.nrcresearchpress.com by 210.87.254.6 on 09/05/12
For personal use only.

TABLE 3. Correlation of methyl proton shifts in *N*-methylazoles with HMO and Wheland–Mann electron densities[a]

Species	NMe shift τ[b] Observed	Calcd. from HMO	Calcd. from W–M	q_{HMO}	q_{W-M}
1-Methylpyrrole	6.45	6.44	6.46	1.518	1.405
1-Methylimidazole	6.30	6.28_5	6.31_5	1.498	1.393
1-Methylpyrazole	6.19	6.16	6.18	1.482	1.382
4-Methyl-1,2,4-triazole	6.17	6.17	6.11	1.483	1.376
1-Methyl-1,2,4-triazole	6.00	6.03	5.98	1.466	1.365
1-Methyl-1,2,3-triazole	5.87	5.87	5.92	1.445	1.360
1-Methyltetrazole	5.73	5.80	5.73	1.437	1.344
2-Methyltetrazole	5.54	5.49	5.54	1.397	1.328

[a]Data and calculations of B. M. Lynch. See footnote 1.
[b]Slopes of linear regression lines:
Shift = $(-5.519 \mp 0.60) + (7.881 \pm 0.411)q_{HMO}$; standard deviation = 0.042 p.p.m.; correlation coefficient $r = 0.992$.
Shift = $(-10.367 \mp 0.67) + (11.976 \pm 0.49)q_{HMO}$; standard deviation = 0.033 p.p.m.; correlation coefficient $r = 0.995$.

we have noted (24) that with some 5-substituted 1- and 2-methyltetrazoles where the 5-substituent interacts strongly with the ring the chemical shifts of the 1- and 2-methyl groups are similar. In terms of the electron density correlation (Table 3), this implies that the electron density of the 1-N atom was decreased relative to that of the 2-N atom by the 5-substituent although local anisotropic effects could also contribute to such a phenomenon. Some of the compounds in Table 2 display similar effects which arise when substituents such as NO_2, NH_2 are present. For example the compounds **3**, **18**, **19**, **26**, **35**, **36**, **52**, and **72**, fit the general trends rather poorly although the A, B, C structural relationship still holds for directly comparable pairs. However, despite these limitations the trends noted herein will be of value for future structural assignment for isomeric derivatives of the higher azoles.

1. R. R. FRASER and K. E. HAQUE. Can. J. Chem. **46**, 2855 (1968).
2. S. CASTELLANO, H. GUNTHER, and S. EBERSOLE. J. Phys. Chem. **69**, 1446 (1965).
3. H. GUNTHER and S. CASTELLANO. Ber. Bunsenges Physik. Chem. **70**, 913 (1966).
4. T. M. SPOTSWOOD and C. I. TANZER. Aust. J. Chem. **20**, 1227 (1967).
5. J. N. MURRELL, V. M. S. GIL, and F. B. VAN DUIJNEVELDT. Rec. Trav. Chim. **84**, 1399 (1965).
6. B. M. LYNCH and Y. Y. HUNG. Can. J. Chem. **42**, 1605 (1964).
7. L. G. TENSMEYER and C. AINSWORTH. J. Org. Chem. **31**, 1878 (1966).
8. I. FINAR and D. M. RACKHAM. J. Chem. Soc. B, 211 (1968).
9. J. ELGUERO, R. JACQUIER, and S. MONDON. Bull. Soc. Chim. Fr. 1346 (1970); J. ELGUERO, R. JACQUIER, and G. TARRAGO. Bull. Soc. Chim. Fr. 1345 (1970).
10. I. CROSSLAND. Acta Chem. Scand. **20**, 258 (1966).
11. A. ALBERT. Heterocyclic chemistry. Athlone Press, London. 1968. p. 428.
12. R. A. OLOFSON and R. V. KENDALL. J. Org. Chem. **35**, 2246 (1970).
13. S. KOZIMA, T. ITANO, N. MIHARA, K. SISIDO, and T. ISIDA. J. Organomet. Chem. **44**, 117 (1972).
14. L. A. LEE, R. EVANS, and J. W. WHEELER. J. Org. Chem. **37**, 343 (1972).
15. L. HUFF and R. A. HENRY. J. Med. Chem. **13**, 777 (1970).
16. R. N. BUTLER and F. L. SCOTT. J. Org. Chem. **32**, 1224 (1967).
17. K. T. POTTS, H. R. BURTON, T. H. CRAWFORD, and W. S. THOMAS. J. Org. Chem. **31**, 3522 (1966).
18. M. JAPELJ, B. STANOVNIK, and M. TISLER. J. Heterocycl. Chem. **6**, 559 (1969).
19. R. RAAP. Can. J. Chem. **47**, 3677 (1969).
20. R. RAAP and J. HOWARD. Can. J. Chem. **47**, 813 (1969).
21. R. RAAP. Can. J. Chem. **47**, 3677 (1969).
22. F. L. SCOTT and J. C. TOBIN. J. Chem. Soc. C, 703 (1971).
23. M. A. KHAN and B. M. LYNCH. Can. J. Chem. **49**, 3566 (1971).
24. F. L. SCOTT, R. N. BUTLER, and J. FEENEY. J. Chem. Soc. B, 919 (1967).
25. R. N. BUTLER. Can. J. Chem. **50**, 1786 (1972).
26. J. B. DAVIS. Chem. and Ind. (London), 1094 (1968).
27. J. C. N. MA and E. W. WARNHOFF. Can. J. Chem. **43**, 1849 (1965).
28. G. B. BARLIN and T. J. BATTERHAM. J. Chem. Soc. B, 516 (1967).
29. G. S. REDDY, R. T. HOBGOOD, and J. H. GOLDSTEIN. J. Am. Chem. Soc. **84**, 336 (1962).
30. H. J. ANDERSON. Can. J. Chem. **43**, 2387 (1965).
31. J. H. MARKGRAF, W. T. BACHMANN, and D. P. HOLLIS. J. Org. Chem. **30**, 3472 (1965).
32. B. M. LYNCH. Chem. Commun. 1337 (1968).
33. F. J. WEIGERT and J. D. ROBERTO. J. Am. Chem. Soc. **90**, 3543 (1968).
34. B. M. LYNCH and H. J. M. DOU. Tetrahedron Lett. 2627 (1968).
35. B. M. LYNCH, B. C. MCDONALD, and J. G. K. WEBB. Tetrahedron, **24**, 3595 (1968).
36. B. M. LYNCH. Tetrahedron Lett. 1537 (1969).

Can. J. Chem. Downloaded from www.nrcresearchpress.com by 210.87.254.6 on 09/05/12
For personal use only.

37. J. ELGUERO, R. JACQUIER, G. TARRAGO, and H. C. N. TIEN DUC. Bull. Soc. Chim. Fr. 293 (1966).
38. A. K. SORENSEN and N. A. KLITGAARD. Acta. Chem. Scand. **26**, 541 (1972).
39. L. FOWDEN, F. F. NOE, J. H. RIDD, and R. F. M. WHITE. Proc. Chem. Soc. 131 (1959).
40. L. A. LEE and J. W. WHEELER. J. Org. Chem. **37**, 348 (1972).
41. I. L. FINAR and E. F. MOONEY. Spectrochim. Acta, **20**, 1269 (1964).
42. J. D. ALBRIGHT and L. GOLDMAN. J. Org. Chem. **31**, 273 (1966).
43. J. A. MOORE and C. L. HABRAKEN. J. Am. Chem. Soc. **86**, 1456 (1964); J. Org. Chem. **30**, 1892 (1965).
44. A. J. BLACKMAN and J. B. POLYA. J. Chem. Soc. C, 1016 (1971).
45. J. ELGUERO, R. JACQUIER, and S. MIGNONAC-MONDON. Bull. Soc. Chim. Fr. 4436 (1970).
46. P. COHEN-FERNANDES and C. L. HABRAKEN. Rec. Trav. Chim. **86**, 1249 (1967).
47. C. L. HABRAKEN, H. J. HUNTER, and J. C. P. WESTGEEST. Rec. Trav. Chim. **86**, 56 (1967).
48. J.-L. AUBAGNAC, J. ELGUERO, and R. JACQUIER. Bull. Soc. Chim. Fr. 3306 (1969).
49. R. JACQUIER, M.-L. ROUMESTANT, and P. VIALLEFONT. Bull. Soc. Chim. Fr. 2630 (1967).
50. J. ELGUERO, E. GONZALEZ, and R. JACQUIER. Bull. Soc. Chim. Fr. 2998 (1967).
51. J. ELGUERO, R. JACQUIER, and H. C. N. TIEN DUC. Bull. Soc. Chim. Fr. 3727 (1966); A. R. KATRIZKY and J. M. LAGOWSKI. Adv. Heterocycl. Chem. **1**, 316 (1963); **2**, 28 (1963).

Can. J. Chem. Downloaded from www.nrcresearchpress.com by 210.87.254.6 on 09/05/12
For personal use only.

Rearrangements in the Diterpenoid Series. Part II. The Diazotization of Methyl 15-β-amino-13-isopropyl-17-noratis-13-en-18-oate

WILLIAM A. AYER AND PANDURANG D. DESHPANDE

Chemistry Department, University of Alberta, Edmonton, Alberta T6G 2E1

Received January 22, 1973

Treatment of methyl 15-β-amino-13-isopropyl-17-noratis-13-en-18-oate (**1***b*) with sodium nitrite – acetic acid gives rise to a variety of products, including nitrated compounds and norketones. The structures of seven of the products have been established. The reaction of methyl 16-isopropylidene-7,17-secoacon-8(15)-en-18-oate (**2**) with nitrous acid and with dinitrogen tetroxide is described. A simple method for transforming isocyanates to primary amines is presented.

La réaction du méthylamino-β-15 isopropyl-13 noratis-17 ène-13 oate-18 (**1***b*) avec de l'acide acétique – nitrite de sodium donne lieu à plusieurs produits parmi lesquels on trouve des composés nitrés et des norcétones. Les structures de sept de ces produits ont été élucidées. La réaction du méthyl isopropylidene-16 secoacon-7,17 ène-8(15) oate-18 (2) avec de l'acide nitreux et du tétroxyde de diazote est décrite. Une méthode simple pour la transformation des isocyanates en amines primaires est décrite.

[Traduit par le journal]

Can. J. Chem., **51**, 2323 (1973)

In Part I of this series (1) we described the rearrangement of the tosylate **1***a*, which has an atisane skeleton, into the diene **2** which has an aconane skeleton. This rearrangement serves as a model for the proposed (2, 3) biosynthetic transformation of atisine-type alkaloids into alkaloids of the aconitine series. At the same time we have investigated the deamination of the amine **1***b* to see if this method of generating a carbonium ion at C-15 would also lead to rearrangement of the atisane skeleton to an aconane skeleton. This paper dsscribes the rather unexpected results of this latter investigation.

The amine **1***b* was prepared via the acid **1***c*, in turn prepared in 65% yield by Diels–Alder addition of acrylic acid to methyl levopimarate (**3**). Esterification of **1***c* with diazomethane gave the diester **1***d* of known (4) structure and stereochemistry. The transformation of acid **1***c* into the amine **1***b* proved more difficult than was anticipated. When the acid **1***c* was subjected to the conditions of the Schmidt reaction (5) only a small amount (*ca.* 10%) of basic material was obtained. The major product, isolated from the non-basic fraction, was a compound $C_{24}H_{35}NO_3$ to which structure **4** is assigned. The i.r. and n.m.r. spectra (see Experimental) are consistent with the structure, and treatment of the isocyanate **5**, prepared as described below, with concentrated sulfuric acid in chloroform gave compound **4**. It thus appears that acid-catalyzed cyclization of the intermediate isocyanate (arrows in **5**) occurs in preference to hydrolysis and decarboxylation under the conditions of the Schmidt reaction. Efforts to open the lactam ring in **4** by either acid- or base-catalyzed hydrolysis were unsuccessful. An attempt was made to open the lactam ring via the imino-ether **6** (6, 7), prepared by treating **4** with triethyloxonium fluoroborate. However, hydrolysis of **6** with either aqueous acetic acid or aqueous sulfuric acid led only to the regeneration of lactam **4**.

Failure of the Schmidt reaction to give good yields of the desired amine **1***b* prompted us to investigate the Curtius rearrangement (8) of the azide **1***e*. The acid **1***c* was transformed to the acid chloride and this was treated with a solution of sodium azide in acetone. The product consisted of a mixture of the acyl azide **1***e* (2140 cm^{-1}) and the isocyanate **5** (2260 cm^{-1}) as shown by the i.r. spectrum. When this mixture was heated briefly in benzene complete transformation to isocyanate **5** was effected. When the isocyanate **5** was chromatographed over silica gel it was transformed, in part, into the lactam **4**. Various attempts at acid-catalyzed hydrolysis also led primarily to the formation of lactam **4**, usually accompanied by small amounts (5–15%) of the desired amine **1***b*. Attempted hydrolysis under basic conditions gave a different neutral product. This compound was not investigated in detail, but is believed to

Can. J. Chem. Downloaded from www.nrcresearchpress.com by 210.87.254.6 on 09/05/12
For personal use only.

Can. J. Chem. Downloaded from www.nrcresearchpress.com by 210.87.254.6 on 09/05/12
For personal use only.

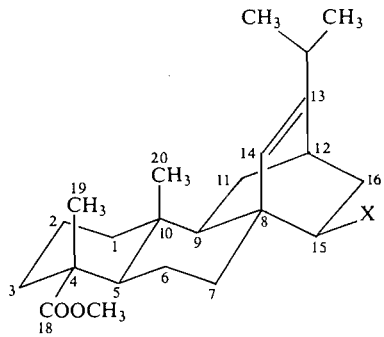

1

a X = OTs
b X = NH_2
c X = COOH
d X = $COOCH_3$
e X = N_3
f X = N—CHO (H)

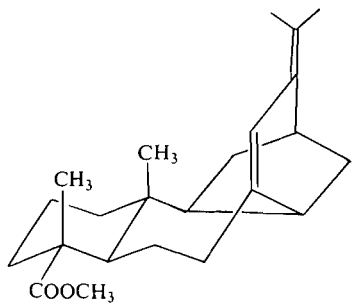

2

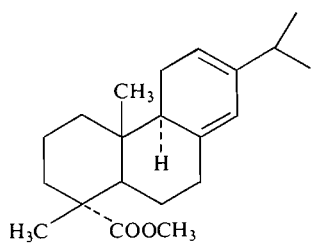

3

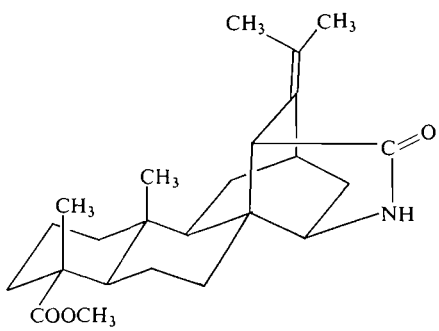

4

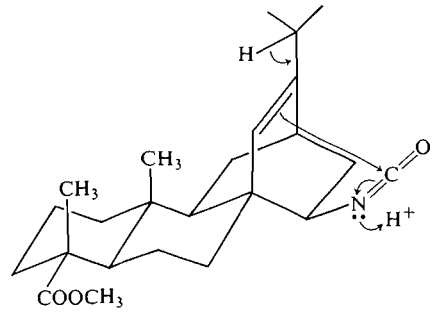

5

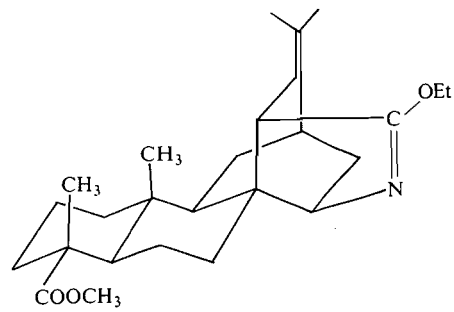

6

be the *sym*-urea **7**, since it showed bands in the i.r. at 3440, 1670, and 1500 cm^{-1}, characteristic (9) of such compounds. *sym*-Ureas are frequently encountered as byproducts in the hydrolysis of isocyanates (8).

In view of the problems encountered in the hydrolysis of the isocyanate we decided to explore a method for the transformation **5** → **1***b* which does not appear to have been exploited previously. Reduction of the isocyanate **5** with sodium borohydride in dimethoxyethane gave the *N*-formyl compound **1***f* in virtually quantitative yield. Acid-catalyzed hydrolysis of **1***f* then gave the amine **1***b* in 75% overall yield from the isocyanate **5**. The amine **1***b* was obtained as a viscous oil which was purified via the crystalline hydrochloride. Since the configuration of the isocyanate group in **5** is assured (retention of configuration expected in the Curtius rearrangement (8); the isocyanate is readily transformed to lactam **4**) and since neither the borohydride reduction nor the hydrolysis of the *N*-formyl compound should lead to inversion, the amino group in **1***b* may be assigned the *endo*-configuration.

With a satisfactory method available for the synthesis of the amine **1***b*, attention was now turned to a study of its deamination. Investiga-

Can. J. Chem. Downloaded from www.nrcresearchpress.com by 210.87.254.6 on 09/05/12
For personal use only.

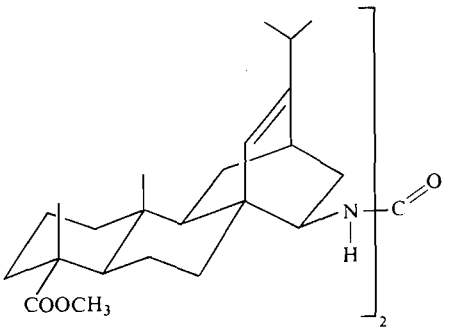

7

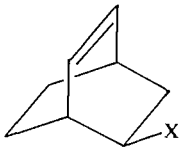

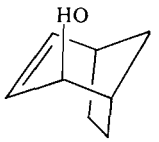

8
a X = NH_2
b X = OTs

9

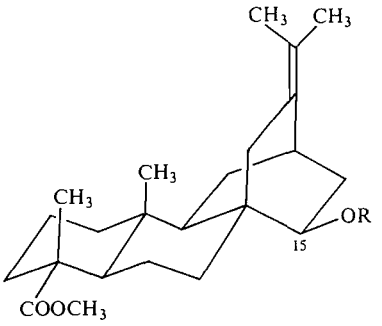

10
a R = $COCH_3$
b R = H

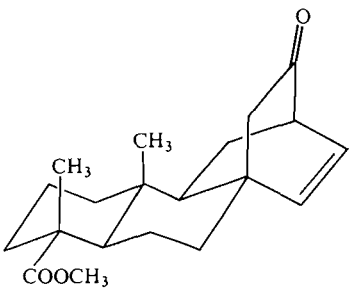

11

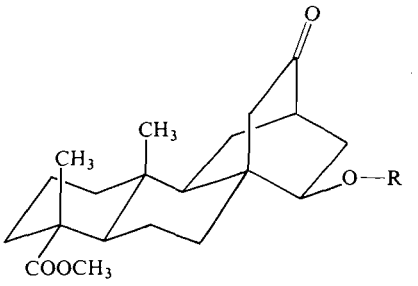

12
a R = $COCH_3$
b R = H
c R = COOEt

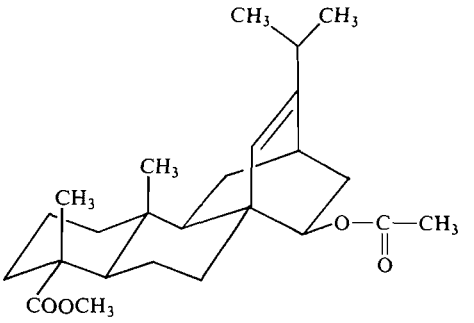

13

tions of the deamination of *endo*-5-aminobicyclo[2.2.2]oct-2-ene (**8***a*) have shown (10, 11) that this compound rearranges in good yield to *exo*-bicyclo[3.2.1]oct-3-en-2-ol (**9**) in aqueous solution, and to a mixture of **9** and the corresponding acetate in glacial acetic acid. The amine **1***b* was diazotized under a variety of conditions (aqueous fluoroboric acid, aqueous hydrochloric acid, aqueous acetic acid, glacial acetic acid). In each case the nonbasic product was a mixture of several components as revealed by its spectroscopic (i.r. and n.m.r.) characteristics and t.l.c. behavior. When a solution of the hydrochloride of **1***b* in glacial acetic acid was treated with an excess of sodium nitrite, nonbasic material was obtained in about 70% yield. A colorless, crystalline product, $C_{23}H_{33}N_3O_8$, separated from an ether solution of the mixture in 12% yield. Early attempts to separate the remaining components of the mixture were unsuccessful. When the diazotization was conducted in aqueous acetic acid a complex mixture of products again resulted. After considerable experimentation a separation procedure was developed (see Experimental) which led to the isolation of seven different crystalline com-

Can. J. Chem. Downloaded from www.nrcresearchpress.com by 210.87.254.6 on 09/05/12
For personal use only.

pounds, including the compound $C_{23}H_{33}N_3O_8$ mentioned above. The molecular formulas of the products, together with their melting points, are listed in Table 1. The assignment of structure to these products is outlined first and then is followed by a discussion of the possible modes of formation.

Compound A, $C_{25}H_{30}O_4$, was assigned structure **10***a* on the following basis: i.r. and n.m.r. spectra indicated the presence of the carbomethoxyl and secondary acetoxyl groups, two methyl groups on saturated carbon (singlets at τ 9.16 (C-10 methyl) and 8.85 (C-4 methyl)), and two methyls on unsaturated carbon (broadened singlets at 8.46 and 8.37). The signal for the proton on C-15 (atisane numbering, see **1**) appeared as an octet with couplings of 9, 3, and 1.5 Hz. The coupling constants of 9 and 3 Hz are consistent with those observed (12) for *vicinal* protons in bicyclo[2.2.2]octane systems. The 1.5 Hz coupling is presumably a W-plan coupling with the *anti* proton on C-14. Methanolysis of **10***a* gave the alcohol **10***b* which on oxidation with Jones' reagent afforded the corresponding ketone, confirming the secondary nature of the hydroxyl function. Structure **10***a* was confirmed by degradation to the known (13) ketoolefin **11**. Ozonolysis of **10***a* gave ketone **12***a* which was hydrolyzed to the alcohol **12***b* and this in turn was transformed to the cathylate **12***c*. Pyrolysis of **12***c* at 240–250° gave the keto olefin **11**. Although we were unable to obtain a sample of **11** for direct comparison, the melting point and spectral properties agree well with those reported (13) for **11**. When compound **10***a* was treated with acetic acid saturated with hydrogen chloride the product showed t.l.c. behavior very similar to that of the known (1) acetate **13**. Although the n.m.r. spectrum indicated that the product was a mixture, the major component gave rise to signals identical with those observed for **13**. This is regarded as confirmatory evidence that the acetoxyl group in **10***a* is *endo* and located at C-15.

TABLE 1. Products isolated after treatment of amine **1***b* with nitrous acid

Product	Formula	M.p. (°C)
A	$C_{25}H_{30}O_4$	145–146
B	$C_{22}H_{32}O_5$	218–222
C	$C_{25}H_{37}NO_6$	130–131
D	$C_{20}H_{28}O_3$	132–133
E	$C_{23}H_{33}N_3O_8$	176–178
F	$C_{23}H_{32}N_2O_6$	136–137
G	$C_{23}H_{33}NO_5$	Amorphous

Compound B, $C_{22}H_{32}O_5$, on first consideration seemed rather anomalous in that the n.m.r. spectrum revealed the presence of only two *C*-methyl groups (singlets at τ 9.14 and 8.84) indicating the loss of two *C*-methyl groups during the deamination process. It was soon recognized however that compound B is identical with the ketoacetate **12***a* obtained on ozonolysis of **10***a*.

Compound C, $C_{25}H_{37}NO_6$, which was isolated in only *ca.* 3% yield, is assigned structure **14** on the basis of the following considerations. Although the highest peak in the mass spectrum appeared at *m/e* 400 and corresponded to an ion $C_{25}H_{36}O_4$, elemental analysis established the presence of nitrogen and is consistent with the molecular formula given. The presence of a nitro group was deduced from the i.r. spectrum which showed absorption bands at 1540 and 1340 cm^{-1}, indicative of a nitro group located on saturated carbon (14). The n.m.r. spectrum of **14** was very informative. The carbomethoxyl and acetoxyl methyls give rise to singlets at τ 6.35 and 8.06, respectively, and the proton *geminal* to the acetoxyl group appears as a doublet of doublets (J = 8 and 2 Hz) at τ 5.36. The C-10 methyl appears at τ 9.34 (shielded by the C_{13}—C_{14} double bond (15)) and the C-4 methyl appears at τ 8.83, while the remaining two methyl groups give rise to singlets at τ 8.24 and 8.28. Since the C—C double bond must be located at 13,14-position (shielding of the C-10 methyl, olefinic proton at τ 4.15) the low chemical shift value for these methyls indicates that the nitro group is located on the same carbon.[1]

As mentioned earlier, the highest mass peak in the mass spectrum appears at *m/e* 400 and corresponds to the loss of HNO_2 from the molecular ion. Elimination of HNO_2 from tertiary nitro compounds upon electron impact is known to be a facile process (17). Attempts to bring about thermal elimination of nitrous acid from **14** were unsuccessful as were attempts to remove the nitro function by hydrogenolysis.

Compound D, $C_{20}H_{28}O_3$, was also isolated in very small amounts and in common with compound B (**12***a*) showed signals for only two

[1]The methyl groups of 2-nitropropane resonate at τ 8.45 (16).

Can. J. Chem. Downloaded from www.nrcresearchpress.com by 210.87.254.6 on 09/05/12
For personal use only.

methyl groups in its n.m.r. spectrum. The presence of a conjugated ketonic function was indicated by absorption in the i.r. at 1670 and 1625 cm^{-1} and in the u.v. at 243 nm. Comparison of compound D with the unsaturated ketone **15** prepared previously (1) revealed their identity.

The determination of the structures of compounds E, F, and G proved to be the most difficult, but was facilitated by the finding that the colorless compound E, which contains

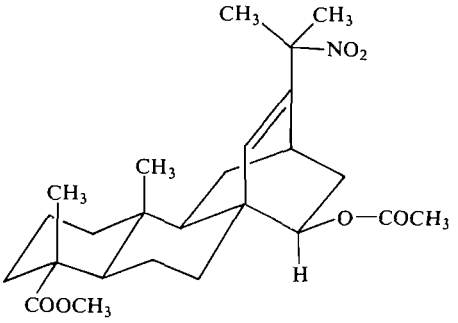

14

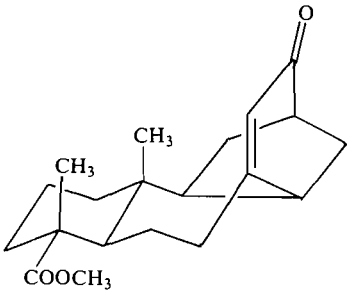

15

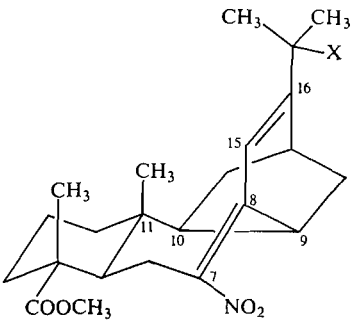

16

a X = NO_2
b X = OH
c X = Cl
d X = ONO

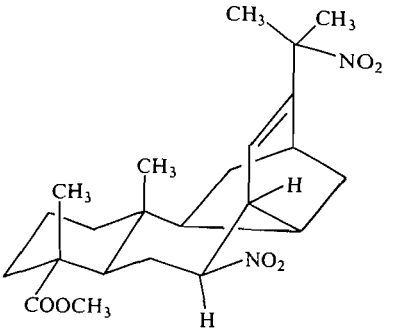

17

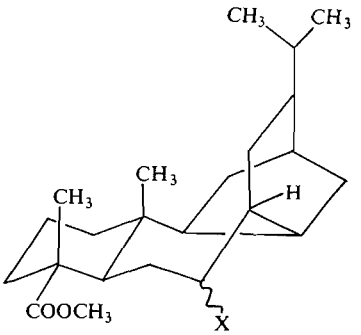

18 X = $NHCOCH_3$
19 X = H

three nitro groups, readily eliminates the elements of nitrous acid when chromatographed over basic alumina to give the yellow compound F, $C_{23}H_{32}N_2O_6$, containing only two nitro groups. Our attention was thus first directed to compound F, to which we assign structure **16***a*. The i.r. spectrum shows absorption bands attributable to nitro groups on both saturated (1545, 1350 cm^{-1}) and unsaturated (1500, 1320 cm^{-1}) carbon (14). The u.v. spectrum, λ_{max} 229 and 348 nm, is consistent with the presence of the nitrodiene chromophore.[2] In the n.m.r. spectrum, the isopropyl methyls resonate at τ 8.24 and 8.20, similar to those in **14**, the C-4 methyl at 8.54, and the C-11 methyl[3] at 9.32. Molecular models indicate that the C-11 methyl lies in the shielding cone of the C_7-C_8 double bond, and that the C-4 methyl is proximate to the nitro group at C-7, perhaps explaining its abnormally low chemical shift. The olefinic proton at C-15

[2]5-Methyl-2-nitro-2,4-hexadiene absorbs at 230 nm (ε 7700) and 335 nm (ε 11 700) (18).

[3]As in the previous paper (1), compounds such as **15** and **16***a*, containing an aconane skeleton, are numbered as derivatives of aconane.

Can. J. Chem. Downloaded from www.nrcresearchpress.com by 210.87.254.6 on 09/05/12
For personal use only.

gives rise to a sharp singlet at τ 2.80, the low chemical shift again perhaps attributable to a deshielding effect of the nitro group at C-7. Catalytic hydrogenation of **16***a* over platinum in ethyl acetate led to a mixture of products from which it was possible to separate a dihydro compound, **17**, in which the C_7-C_8 double bond has been saturated. In this compound the i.r. spectrum shows absorption for nitro groups on saturated carbon only (1540 and 1350 cm^{-1}). In the n.m.r. the signal for the C-11 methyl appears at τ 8.95 and the olefinic proton appears at 4.69. A one-proton multiplet at τ 5.28 is attributable to the proton on C-7. Catalytic hydrogenation of **16***a* over platinum-in-ethanol in the presence of hydrochloric acid gave an 85% yield of basic material, indicating reduction of a nitro group or groups to the amino form. Acetylation of the basic fraction and crystallization from methanol gave a compound $C_{25}H_{41}NO_3$, formulated as the *N*-acetyl compound **18**. Observations pertinent to the structural assignment include the appearance in the n.m.r. spectrum of signals due to an isopropyl group, lack of olefinic absorption, evidence for the presence of a secondary amide, and the similarity of the chemical shifts of the various *C*-methyl groups in **18** to those in the known compound **19** (1).

Compound **18** was the major product (55% yield) isolated from the catalytic hydrogenation (followed by acetylation) in ethanol–HCl. In addition two other crystalline compounds were isolated, each in about 10% yield. One of these had spectroscopic properties very similar to **18** (the mass spectra are virtually identical) and is believed to be the C-7 epimer of **18**. The other minor product has the molecular formula $C_{25}H_{37}N_2O_5Cl$ and is assigned structure **20***a* in which the atisane skeleton has been regenerated from the aconane skeleton. In a parallel series of experiments in which the crude basic product from the catalytic hydrogenation was treated with methanesulfonyl chloride – pyridine rather than acetylated the methanesulfonamide **20***b* (along with the sulfonamides corresponding to **18**) was isolated.[4] The mass spectrum of **20***b* did not show a parent peak. The molecular formula $C_{24}H_{37}N_2O_6SCl$ was inferred from the composition of the ion of highest mass (*m/e* 470, exact mass corresponding to $C_{24}H_{37}NO_4{}^{32}S^{35}Cl$, $M^+ - NO_2$) and supported by combustion analysis. The i.r. spectrum showed absorption bands attributable to sulfonamide (3360, 1140 cm^{-1}), carbomethoxyl (1725 cm^{-1}), and nitro (1545, 1350 cm^{-1}) groups. The n.m.r. spectrum was very similar, except for the signals associated with the sulfonamide group (τ 6.90 (SO_2—CH_3), 5.97 (C-7 proton), 5.07 (N*H*), to that of compound **14**. Pertinent signals include (corresponding signals of **14** in brackets) C-10 methyl τ 9.30 (9.34), C-4 methyl 8.82 (8.83), methyls *geminal* to nitro 8.22 and 8.26 (8.22 and 8.24), carbomethoxyl 6.29 (6.35), C-14 proton 4.15 (4.15), C-15 proton 5.72, J = 8.5 and 3 Hz (5.36, J = 8 and 2 Hz). One possible pathway from **16***a* to **20***c* involved reduction to the hydroxylamine **21** and rearrangement as indicated by the arrows in **21**. Reduction of the resulting imine leads to **20***c*. Alternatively rearrangement

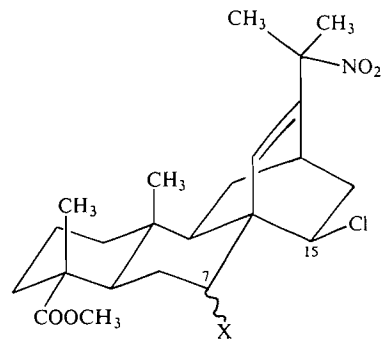

20

a X = $NHCOCH_3$
b X = $NHSO_2CH_3$
c X = NH_2

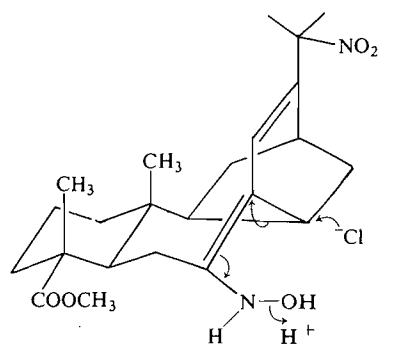

21

[4]Since the sulfonamide **20***b* proved more amenable to isolation and purification than amide **20***a*, the majority of the structural studies on this compound were carried out on the sulfonamide. The results obtained with the amide parallel those with the sulfonamide (see Experimental).

Can. J. Chem. Downloaded from www.nrcresearchpress.com by 210.87.254.6 on 09/05/12
For personal use only.

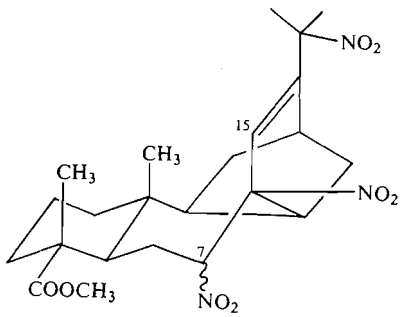

22

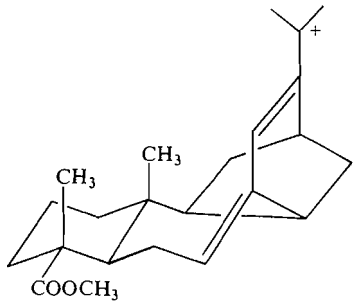

23

could occur at the *C*-nitroso stage leading to the C-7 oximino compounds which could be reduced to **20***c*.

Compound E is assigned structure **22**. When E is chromatographed over basic alumina it loses the elements of nitrous acid and compound **16***a* is formed. The molecular formula was deduced from a consideration of the mass spectrum and from the results of elemental analysis. The highest peak in the mass spectrum appears at *m/e* 433, corresponding to an ion resulting from loss of NO_2 from the molecular ion (mw 479). The base peak in the mass spectrum is at *m/e* 341 ($C_{23}H_{33}O_2$ by h.r.m.s.) and corresponds to an ion such as **23** formed by elimination of three molecules of nitrogen dioxide. The olefinic proton (C-15) appears in the n.m.r. as a broadened singlet at τ 3.92 and is not coupled to the proton geminal to the nitro group at C-7 (τ 5.12). This leads us to favor structure **22** over structure **24** which otherwise accommodates most of the available information. The chemical shift of the C-11 methyl group (τ 8.93) is similar to that in compound **17** (τ 8.95) as is that for the C-4 methyl (τ 8.63 in **22**, 8.69 in **17**) which also supports the location of the double bond at the 15,16-position rather than the 8,15-position. The two remaining methyl groups resonate at τ 8.21, consistent with the presence of a nitro group on the same carbon. Further evidence for the structure of the trinitro compound comes from the alternative mode of formation described below.

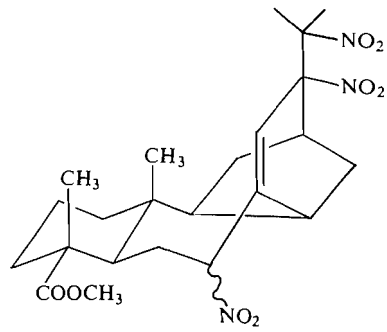

24

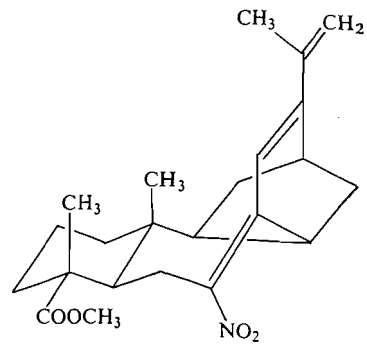

25

Compound G, $C_{23}H_{33}NO_5$, is formulated as **16***b*. Its spectroscopic characteristics are very similar to those of **17** except that **16***b* shows hydroxyl absorption in the i.r. and does not show absorption for a nitro group on saturated carbon. In the n.m.r. the methyl groups geminal to the hydroxyl appear at τ 8.53 and 8.58 (8.20 and 8.24 in **16***a*). When the alcohol **16***b* was subjected to hydrogenation over platinum in the presence of acid and the resulting basic product acetylated compound **18**, previously derived from **16***a*, was obtained.

Attempted dehydration of **16***b* with thionyl chloride in methylene chloride gave the chloro compound **16***c* which on hydrogenation–acetylation also furnished **18**. Alcohol **16***b* was successfully dehydrated to the yellow triene **25** using *p*-toluenesulfonic acid in benzene. The nitrotriene showed absorption maxima in the u.v. at 258 and 382 nm. The presence of the isopropenyl group is indicated by olefinic protons

Can. J. Chem. Downloaded from www.nrcresearchpress.com by 210.87.254.6 on 09/05/12
For personal use only.

at τ 4.80 and 4.59 and vinylic methyl at 8.00 in the n.m.r. as well as by a band in the i.r. spectrum at 900 cm^{-1}. The remaining spectral data are consistent with **16***a*. The formation of the conjugated triene **25** provides important evidence that the substituted isopropyl group in **16***a* and *b* is located on the chromophoric group in those compounds.

With the structures of the many and varied (**10***a*, **12***a*, **14**, **15**, **16***a*, **22**, **16***b*) products of the "deamination" of amine **1***b* reasonably well established we turn now to a consideration of their possible mode of formation.[5]

It has frequently been observed that the products resulting from treatment of a primary amine with nitrous acid differ from those resulting from related solvolytic reactions (19). The amine **8***a*, however, on diazotization undergoes rearrangement to give **9** (10, 11), behavior similar to that observed when the tosylate **8***b* is solvolyzed. In Part 1 of this series it was shown that the tosylate **1***a* undergoes facile rearrangement to the diene **2**. Although the diene **2** could not be detected among the deamination products, three of the nitro compounds, **16***a*, *b*, and **22**, possess the rearranged skeleton of **2**. Since nitration of olefins has been observed under diazotizing conditions (*e.g.*, the formation of ω-nitrocamphene from camphene and sodium nitrite – acetic acid (20)) we decided to investigate the possibility that the rearranged nitro compounds arise via the diene **2**. Indeed when an acetic acid solution of diene **2** was treated with an excess of sodium nitrite the trinitro compound **22** was isolated by direct crystallization in 13% yield. In view of this it was of interest to see whether the use of a limited amount of sodium nitrite in the deamination of **1***b* would lead to the diene **2**. Accordingly amine **1***b* in aqueous acetic acid was treated with 1 equiv of sodium nitrite. Nonbasic material was isolated in *ca.* 16% yield. Crystallization from ether afforded the trinitro compound **16***b*. Chromatography of the residue after crystallization gave the dinitro compound **16***a* plus a noncrystalline material rich in the nitroalcohol **16***b* as indicated by i.r. and t.l.c. The diene **2** could not be detected. It thus appears that the diene **2** may be formed during the nitrous acid treatment but if so its further reaction with the reagent to give nitrated materials competes successfully with deamination of the amine.

Nitrous acid as such is not known to be involved in addition reactions of olefins. It can however give rise to a variety of oxides of nitrogen (NO, NO_2, N_2O_3, N_2O_4) (21) which are reactive towards olefins (22, 23). Dinitrogen tetroxide, for example, adds to olefins to produce *vicinal* dinitro compounds, nitronitrites and, in the presence of oxygen, nitronitrates. The nitronitrites are unstable and readily hydrolyzed to nitroalcohols (22, 23). Similar nitro compounds, along with nitronitroso adducts, are obtained from olefins and nitrous anhydride (23). Although no nitronitroso adducts were isolated, it is possible that they are formed and then oxidized by oxygen to dinitro compounds. Since complete product balance was not obtained, these may also have been formed but have escaped detection. In the following discussion, which is intended to be illustrative rather than definitive, dinitrogen tetroxide is portrayed as the attacking species. The same products may be derived from nitrous anhydride addition, followed by oxidation.

1,4-Addition[6] of N_2O_4 to the diene **2** leads to the dinitro compound **26***a* and nitronitrite **26***b*. Elimination of nitrous acid from **26***a* gives the diene **27***a*. 1,2-Addition of N_2O_4 to **27***a* can give rise to the trinitro compound **22**, which on elimination of nitrous acid gives **16***a*. A similar elimination–addition–elimination sequence on **26***b* leads (via **27***b*) to the nitronitrite **16***d* which after hydrolysis gives nitroalcohol **16***b*. The formation of ketone **15** may be rationalized in terms of 1,2-addition to give nitronitrite **28***a*. Hydrolysis to give **28***b* followed by a reverse Henry reaction (24) (arrows in **28**) either during the alkaline work-up or during the chromatography over alumina would lead to **15**. Homolytic cleavage of nitrite **28***a* could also lead to **15**.

At this stage we decided to see whether any of the postulated intermediates could be detected in the reaction of the diene **2** with dinitrogen tetroxide itself. When an acetic acid solution of the diene was treated with an excess of N_2O_4

[5]Since in many cases the complexity of the product mixtures formed meant that good material balances were not obtained, the following mechanistic speculation is intended only as an aid to the interpretation of the results. For the sake of brevity, usually only one possible pathway is discussed.

[6]An initial 1,2-addition and a subsequent 1,4-addition is also possible.

Can. J. Chem. Downloaded from www.nrcresearchpress.com by 210.87.254.6 on 09/05/12
For personal use only.

the trinitro compound **22** was obtained in 24% yield. Chromatography of the remaining material provided the dinitro compound **16***a* in 13% yield. The only other product which could be isolated in pure form was the nitroacetate **14**, *in which the bicyclo[2.2.2]octane system had been regenerated from the bicyclo[3.2.1]octane system.* Thus the experiment undertaken to gain information regarding the intermediates between the diene and compounds **22**, **16***a*, and **16***b* failed in this respect, but it did suggest that at least some of the products of the original "deamination" which possess the bicyclo[2.2.2]-system may be derived via the diene **2**. As illustrated in Scheme 1, the nitronitrite **28***a* is a possible intermediate in the formation of both **14** and the ketoacetate **12***a*. Loss of the nitrite group as a nitrite ion (the same intermediate carbonium ion may be generated by electrophilic attack of NO_2^+ on the diene **2**) and rearrangement as indicated by the dashed arrows in Scheme 1 leads to **14**. Fragmentation of **28***a* as indicated by the full arrows (Scheme 1) could give rise to the enol nitrite **29** which on hydrolysis would give **12***a*.

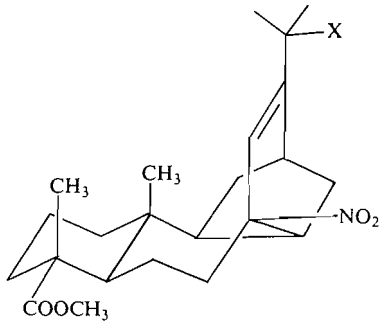

26

a X = —NO_2
b X = —ONO

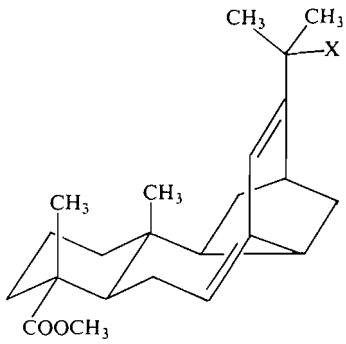

27

a X = —NO_2
b X = —ONO

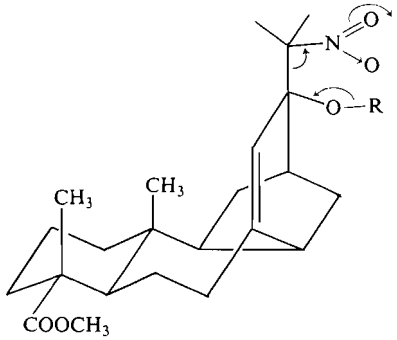

28

a R = NO
b R = H

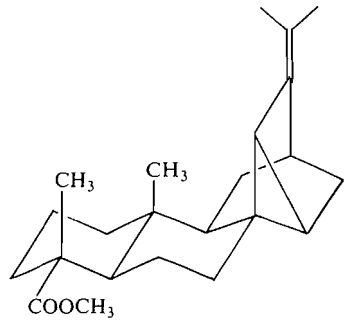

30

The formation of a compound **10***a* is difficult to explain unless it results from acid-catalyzed rearrangement of the diene **2** either by non-terminal protonation at C-15 followed by rearrangement, or by protonation at the isopropylidene group, rearrangement to **13**, and subsequent migration of the double bond in **13**. When the diene **2** was treated with acetic acid – perchloric acid at room temperature, a mixture of the double bond isomers **10***a* and **13***a* was obtained. However, none of **13** could be detected in the product resulting from treatment of amine **1***b* with sodium nitrite – acetic acid. The intermediacy of a vinylcyclopropane (**30**) in the formation of **10***a* from **1***b* cannot be excluded, although this would also involve a (presumably) unfavorable non-terminal protonation in the ring-opening step.

In conclusion we draw attention to the fact that the "deamination" of amine **1***b* takes a much different course than that observed with

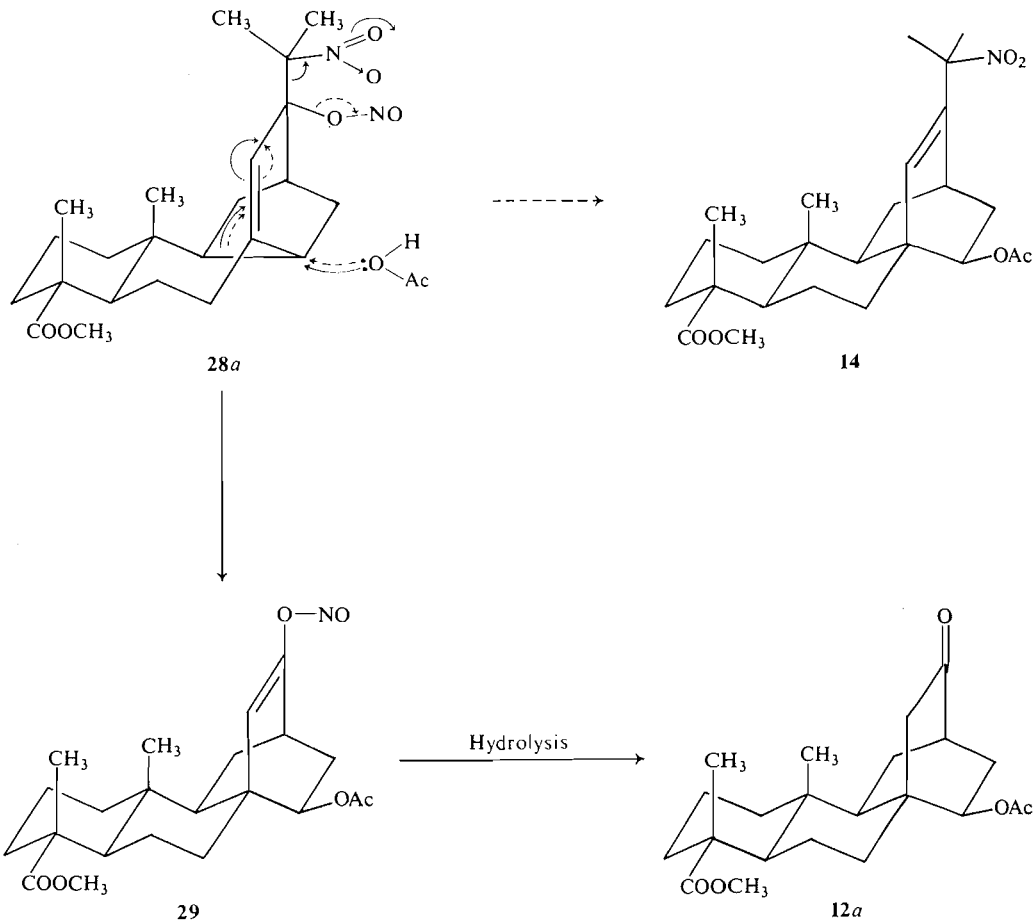

SCHEME 1

the simpler bicyclooctene **8***a*. It does seem probable, however, that the diene **2** is the first-formed product. It is possible that its highly strained nature makes it very susceptible to further reaction, accounting for our failure to isolate **2** directly from the deamination.

Experimental

Melting points were determined on a hot-stage and are uncorrected. Unless otherwise stated i.r. spectra were determined in carbon tetrachloride, u.v. spectra in 95% ethanol, and n.m.r. spectra in deuteriochloroform with tetramethylsilane as internal standard. Mass spectra were determined on an A.E.I. MS-2H or A.E.I. MS-9 mass spectrometer and are reported as *m/e* (relative intensity). High resolution measurements (h.r.m.s.) were performed on the latter instrument. Alumina, unless otherwise specified, means basic alumina of activity II–III (Brockmann scale). Skellysolve B refers to Skelly Oil Company light petroleum, b.p. 62–70°. Microanalyses were performed by G. Gygli, Toronto, and D. Mahlow of this department.

*Methyl 15-β-Carboxy-13-isopropyl-17-noratis-13-en-18-oate (**1c**) (3)*

A solution of methyl levopimarate (10 g, 32 mmol, prepared by esterification of levopimaric acid (25) with ethereal diazomethane) and acrylic acid (20 ml) in benzene (50 ml) was heated under reflux for 9 h. The solution was cooled, concentrated, and the residue was dissolved in ether, dried, and concentrated to give a white solid (12 g). The white solid was dissolved in acetone (60 ml), cyclohexylamine (4.5 ml) added, and the resulting precipitate filtered and washed with cold acetone to give the cyclohexylamine salt of **1***c* (10 g). The salt was suspended in ether (200 ml) and shaken with 10% phosphoric acid (100 ml). The ether layer was washed (H_2O), dried ($MgSO_4$), and concentrated to give acid **1***c* (7.8 g, 20 mmol, 62.5%): m.p. 166–167° (from Skellysolve B); i.r. 3200–2400 (carboxyl OH), 1720, 1700 (C=O of acid, ester) cm^{-1}; n.m.r. τ 9.38 (s, 3, C-10 methyl), 8.95 (d, 6, J = 7 Hz, isopropyl methyls), 8.83 (s, 3, C-4 methyl), 6.28 (s, 3, methoxyl), 4.57 (s, 1, H-14), −0.95 (s, 1, COO*H*).

Anal. Calcd. for $C_{24}H_{36}O_4$: C, 74.23; H, 9.28. Found: C, 74.53, H, 9.10.

Treatment of acid **1***c* with ethereal diazomethane gave

Can. J. Chem. Downloaded from www.nrcresearchpress.com by 210.87.254.6 on 09/05/12
For personal use only.

Can. J. Chem. Downloaded from www.nrcresearchpress.com by 210.87.254.6 on 09/05/12
For personal use only.

the known diester **1***d* (4) identical (m.p., mixed m.p., i.r.) with an authentic sample.

*Schmidt Reaction on Acid **1**c. Isolation of Lactam **4***

A solution of hydrazoic acid (10 ml) in chloroform was added to a solution of acid **1***c* (1.94 g, 5 mmol) in chloroform (25 ml). The mixture was warmed (40°) and concentrated sulfuric acid (3 ml) was added with stirring during a 2.5 h period. The reaction mixture was diluted with water and the layers separated. The aqueous fraction was basified (Na_2CO_3), and extracted with ether. The ether extract was washed (H_2O), dried (Na_2SO_4), and concentrated to give basic product (0.215 g, 11%). The chloroform fraction was washed (H_2O), dried ($MgSO_4$), and concentrated to give nonbasic product (1.41 g, 72%). This was treated with ethereal diazomethane and a portion (0.91 g) of the product chromatographed over silica gel (36 g). Elution with benzene (100 ml) gave 298 mg of an unidentified material. Elution with benzene–ether (1 :1, 200 ml) gave lactam **4** (421 mg) which crystallized from methanol as colorless plates, m.p. 237–238°: i.r. (Nujol) 3360 (NH), 1705 (C=O of ester), 1690 (C=O of lactam) cm^{-1}; n.m.r. τ 9.21 (s, 3, C-10 methyl), 8.85 (s, 3, C-4 methyl), 8.33 (s, 3, isopropylidene methyl), 8.18 (s, 3, isopropylidene methyl), 6.34 (s, 3, methoxyl), 3.86 (s, 1 N*H*).

Anal. Calcd. for $C_{24}H_{35}NO_3$: C, 74.80; H, 9.09; N, 3.63. Found: C, 74.63, 74.32; H, 9.30, 9.20; N, 3.55.

*Attempted Hydrolysis of the Lactam **4** via the Imino-ether **6***

A solution of lactam **4** (102 mg) in methylene chloride (3 ml) was added to a solution of triethyloxonium fluoroborate (165 mg) in methylene chloride (2 ml) and the mixture stirred overnight, then diluted with 10% potassium carbonate solution and the layers separated. The aqueous layer was extracted with methylene chloride, the methylene chloride fractions combined, washed (H_2O), dried ($MgSO_4$), and concentrated to give imino-ether **6** (91 mg); i.r. ($CHCl_3$) 1710 (C=O of ester), 1640 (C=N) cm^{-1}; n.m.r. τ 9.27 (s, 3, C-10 methyl), 8.88 (s, 3, C-4 methyl), 8.80 (t, 3, J = 7 Hz, OCH_2CH_3), 8.42 (s, 3, isopropylidene methyl), 8.37 (s, 3, isopropylidene methyl), 6.48 (s, 3, methoxyl), 6.00 (d, 2, J = 7 Hz, OCH_2CH_3).

A solution of imino-ether **6** (91 mg) in 10% acetic acid – dioxane (1 :1, 20 ml) was heated under reflux for 4 h, then left at room temperature overnight. The solution was concentrated and the residue dissolved in ether. The ether solution was washed (10% Na_2CO_3, H_2O), dried ($MgSO_4$), and concentrated to give lactam **4** (86 mg).

Hydrolysis of imino-ether **6** with 1 *N* sulfuric acid – dioxane (1 :1) also gave lactam **4**.

*Transformation of Isocyanate **5** to Lactam **4***

Concentrated sulfuric acid (1.5 ml) was added dropwise to a warm (40°) stirred solution of isocyanate **5** (540 mg) in chloroform (25 ml). The reaction mixture was then diluted with water and extracted with chloroform. The chloroform extract was washed (H_2O), dried (Na_2SO_4), and concentrated. The product was treated with ethereal diazomethane and chromatographed over silica gel. Elution with benzene–ether (1 :1, 200 ml) gave lactam **4** (72 mg).

*Curtius Reaction on Acid **1**c. Formation of Isocyanate **5***

A solution of acid **1***c* (10 g), thionyl chloride (5 ml), and dry benzene (100 ml) was heated under reflux for 5 h. Excess thionyl chloride was removed by repeated codistillation with benzene, and the solution was concentrated to give the acid chloride (10 g): i.r. 1800 (C=O of acid chloride), 1720 (C=O of ester) cm^{-1}.

To a cooled (5–10°), stirred solution of acid chloride (10 g) in acetone (100 ml) was added during 1 h a solution of sodium azide (2 g) in water (6 ml). The reaction mixture was stirred at 5–10° for one additional hour, then allowed to warm to room temperature and stand for 2 h. The reaction mixture was diluted with water. The oil which separated was taken up in benzene and the benzene removed at reduced pressure. The product thus obtained was a mixture of azide **1***e* and isocyanate **5**: i.r. 2260 (N=C=O), 2140 (N=N=N), 1720 (C=O of ester) cm^{-1}. The mixture was dissolved in dry benzene (60 ml) and the solution was heated under reflux for 3.5 h. Concentration of the solution gave isocyanate **5**: i.r. 2260 (N=C=O), 1720 (C=O of ester) cm^{-1}. Isocyanate **5** (3.6 g) was chromatographed over silica gel (120 g). Elution with benzene (200 ml), benzene–ether (3 :1, 100 ml), ether (100 ml), and ether–chloroform (1 :1, 50 ml) gave isocyanate **5** (2.4 g). Elution with chloroform (200 ml) and chloroform–methanol (9 :1, 200 ml) gave a mixture of isocyanate **5** and lactam **4** (0.33 g). Elution with chloroform–methanol (4 :1, 200 ml) gave lactam **4** (0.8 g).

*Acidic Hydrolysis of Isocyanate **5***

A solution of isocyanate **5** (1.02 g), concentrated hydrochloric acid (25 ml), and dimethoxyethane (40 ml) was heated under reflux for 3 h. The solution was cooled, neutralized (Na_2CO_3), and concentrated. The residue was dissolved in ether, extracted with dilute hydrochloric acid, washed (H_2O), dried, and concentrated to give nonbasic material (0.61 g). Crystallization from methanol gave lactam **4** (0.08 g).

The acidic extract and the washings were combined, basified (Na_2CO_3), and extracted with ether to give amine **1***b* (0.17 g, 17%), identical (i.r., t.l.c.) with that obtained by hydrolysis of the *N*-formyl compound, **1***f*.

*Alkaline Hydrolysis of Isocyanate **5***

A suspension of isocyanate **5** (720 mg), 50% aqueous potassium hydroxide (10 ml), and benzene (10 ml) was heated under reflux for 2 h, then left at room temperature overnight. The suspension was diluted with benzene and the layers separated. The benzene layer was extracted with dilute hydrochloric acid, washed (H_2O), dried ($MgSO_4$), and concentrated to give nonbasic material (656 mg, 91%). A portion of the product (265 mg) was chromatographed over silica gel (14 g). Elution with benzene–ether (1 :1) and crystallization from methanol gave a compound believed to be the *sym*-urea **7** (150 mg): m.p. 158–161°; i.r. 3440 (NH), 1720 (C=O of ester), 1670, 1500 (C=O of *sym*-urea) cm^{-1}.

The acidic extract and washings were combined, basified (Na_2CO_3), and extracted with ether. The ether extract gave 15 mg (2%) of basic product.

*Methyl 15-β-Amino-13-isopropyl-17-noratis-13-en-18-oate (**1**b)*

A solution of isocyanate **5** (10 g) in dimethoxyethane (60 ml) was added to a stirred suspension of sodium borohydride (2.5 g) in dimethoxyethane (400 ml). After

Can. J. Chem. Downloaded from www.nrcresearchpress.com by 210.87.254.6 on 09/05/12
For personal use only.

24 h the reaction mixture was concentrated and the residue treated with dilute hydrochloric acid (1 *N*, 120 ml). The product was extracted with ether, the ether extract washed (H_2O), dried ($MgSO_4$), and concentrated to give the *N*-formyl compound **1***f* (10 g): i.r. 3435, 3400 (NH), 1715 (C=O of ester), 1680 (C=O of amide) cm^{-1}; n.m.r. τ 9.36 (s, 3, C-10 methyl), 8.97 (d, 6, J = 6 Hz, isopropyl methyls), 8.86 (s, 3, C-4 methyl), 6.36 (s, 3, methoxyl), 4.67 (br s, N*H*), 4.67 (s, 1, C=C*H*), 1.96 (s, 1, C*H*O).

A solution of *N*-formyl compound **1***f* (10 g) and ethanolic hydrochloric acid (3:1, 280 ml) was heated under reflux for 5 h. The solution was cooled, neutralized (Na_2CO_3), and concentrated. The residue was diluted with water (200 ml) and ether (300 ml) added. The aqueous layer and the precipitate at the interface of the two layers were separated. The ether layer was extracted with dilute hydrochloric acid, washed (H_2O), dried, and concentrated to give nonbasic material (1.7 g). The acidic extract and washings were combined, basified (Na_2CO_3), and extracted with ether. The ether extract was dried ($MgSO_4$) and concentrated to a viscous oil (7 g). The oil was dissolved in anhydrous ether, cooled (0°), and saturated with hydrogen chloride. Excess solvent was removed and the concentrated solution cooled (0°). The hydrochloride salt of amine **1***b* which precipitated was collected and recrystallized from methyl acetate: yield 6.8 g; m.p. 210–214°; i.r. (Nujol) 3440 (NH_2), 1720 (C=O of ester), 1600, 1580, 1500 cm^{-1}; n.m.r. τ 9.36 (s, 3, C-10 methyl), 8.89 (d, 6, J = 7 Hz, isopropyl methyls), 8.83 (s, 3, C-4 methyl), 6.29 (s, 3, methoxyl), 4.52 (s, 1, C=C*H*), 2.03 (br s, 3, $\overset{+}{N}H_3$).

Anal. Calcd. for $C_{23}H_{38}NO_2Cl$: C, 69.79; H, 9.61; N, 3.54. Found: C, 68.95, 68.56; H, 9.35, 9.37; N, 3.37. (The poor analytical results are attributed to the hygroscopic nature of this salt).

Basification of an aqueous solution of the amine hydrochloride followed by extraction with ether afforded amine **1***b* as a viscous oil. Analytical data were obtained on a sample purified by molecular distillation (120°, 0.05 mm): i.r. 3500–3200 (NH_2), 1720 (C=O of ester), 1660, 1240 cm^{-1}; n.m.r. τ 9.38 (s, 3, C-10 methyl), 8.97 (d, 6, J = 7 Hz, isopropyl methyls), 8.85 (s, 3, C-4 methyl), 6.35 (s, 3, methoxyl), 4.74 (s, 1, C=C*H*).

Anal. Calcd. for $C_{23}H_{37}NO_2$: C, 76.88; H, 10.30; N, 3.90. Found: C, 77.05, 76.74; H, 10.35, 10.37; N, 3.55.

Deamination of Amine 1b. Isolation of Products

Sodium nitrite (700 mg, 10 mmol) was added over a period of 75 min to a stirred solution of amine hydrochloride (2 g, 5 mmol) in glacial acetic acid (16 ml). The mixture was stirred overnight, then sodium nitrite (350 mg, 5 mmol) added and stirring continued for 2 h. The reaction mixture was diluted with ice-cold sodium hydroxide (12 g in 80 ml H_2O) and extracted with ether. The brown, gummy residue was dissolved in ether. The ether fractions were combined, washed (H_2O, dilute HCl, H_2O), dried ($MgSO_4$), and concentrated to give nonbasic product (1.275 g, 71%).

The nonbasic product was dissolved in ether (5 ml) and stored in the cold (0°) overnight. Removal of the supernatant ether solution gave 203 mg (12%) of crystalline trinitro compound **22**: m.p. 175.5–178°; i.r. ($CHCl_3$) 1725 (C=O of ester), 1570, 1550, 1350, 1325 (NO_2) cm^{-1}; n.m.r. τ 8.93 (s, 3, C-11 methyl), 8.63 (s, 3, C-4 methyl), 8.21 (s, 6, isopropyl methyls), 6.25 (s, 3, methoxyl), 5.12 (m, 1, C*H*NO_2), 3.92 (br s, 1, H-15); mass spectrum 433 (M − 46, 2), 386 (10), 357 (27), 341.2481 calcd. for $C_{23}H_{33}O_2$, found 341.2485 (100), 281 (39), 121 (31), 91 (32); mol. wt. (osmometric) 509 (CH_2Br_2).

Anal. Calcd. for $C_{23}H_{33}N_3O_8$: C, 57.61; H, 6.94; N, 8.76; O, 26.69. Found: C, 57.94, 58.25; H, 7.19, 7.03; N, 8.76; O, 26.00.

The noncrystalline material from several experiments was combined (total 2.5 g) and chromatographed over alumina (72 g). Gradient elution with benzene and benzene–ether gave material containing mainly nitro compounds, gradient elution with ether and ether–chloroform gave material containing alcohols.

The chromatographic fractions rich in nitro compounds were combined (206 mg) and chromatographed over neutral alumina (8 g, activity IV). Elution with Skellysolve B gave acetate **10***a* (26 mg) which crystallized from methanol: m.p. 145–146°; i.r. 1740–1730 (C=O of ester), 1380, 1250 cm^{-1}; n.m.r. τ 9.16 (s, 3, C-10 methyl), 8.85 (s, 3, C-4 methyl), 8.46 (s, 3, isopropylidene methyl), 8.37 (s, 3, isopropylidene methyl), 8.02 (s, 3, OCOC*H*$_3$), 7.36 (m, 1, C*H*OAc), 6.37 (s, 3, methoxyl), 5.48 (octet, 1, J = 1.5, 3.5, 9 Hz, H-15); mass spectrum 402 (4), 342 (53), 327 (42), 267 (48), 121 (37), 107 (100).

Anal. Calcd. for $C_{25}H_{38}O_4$ (mol. wt. 402.2770): C, 74.59; H, 9.51. Found (402.2763 (h.r.m.s.)): C, 74.42, 74.94; H, 9.33, 9.41.

Elution with Skellysolve B – benzene (9:1, 225 ml) gave yellow, crystalline dinitro compound **16***a* (23 mg); m.p. 136–137° (from ethanol) λ_{max} 348 (ε 6190), 229 nm (ε 6750); i.r. ($CHCl_3$) 1725 (C=O of ester), 1615 (C=C), 1545, 1350 (NO_2), 1500, 1320 (C=CNO_2) cm^{-1}; n.m.r. τ 9.32 (s, 3, C-11 methyl), 8.54 (s, 3, C-4 methyl), 8.24 (s, 3, isopropyl methyl), 8.20 (s, 3, isopropyl methyl), 6.32 (s, 3, methoxyl), 2.80 (s, 1, H-15); mass spectrum 432 (1), 403.2359 calcd. for $C_{23}H_{33}NO_5$, found 403.2353 (2) 402 (3), 386.2331 calcd. for $C_{23}H_{32}NO_4$, found 386.2334 (100), 135 (19), 121 (25), 107 (49), 91 (38).

Anal. Calcd. for $C_{23}H_{32}N_2O_6$: C, 63.87; H, 7.46; N, 6.48. Found: C, 63.73, 63.87; H, 7.47, 7.60; N, 6.37, 6.39.

Elution with Skellysolve B – benzene (7:3, 135 ml) gave nitroacetate **14** (30 mg); m.p. 130–131° (from Skellysolve B); i.r. ($CHCl_3$) 1730 (C=O of ester), 1540, 1370, 1340 (NO_2) cm^{-1}; n.m.r. τ 9.34 (s, 3, C-10 methyl), 8.83 (s, 3, C-4 methyl), 8.28 (s, 3, isopropyl methyl), 8.24 (s, 3, isopropyl methyl), 8.06 (s, 3, OCOC*H*$_3$), 7.42 (br s, 1, C*H*NO_2), 6.35 (s, 3, methoxyl), 5.36 (d of d, 1, J = 2, 8 Hz, C*H*OAc), 4.15 (s, 1, C=C*H*); mass spectrum 400 (M − 47, 8), 340 (13), 314 (100), 254 (10), 132 (43).

Anal. Calcd. for $C_{25}H_{37}NO_6$: C, 67.09; H, 8.33; N, 3.13. Found: C, 67.10; H, 8.34; N, 3.30.

Elution with benzene (180 ml) gave material (51 mg) which was rechromatographed on silica gel to give unsaturated ketone **15** (14 mg), m.p. 132–133° (from Skellysolve B). This compound was identical (m.p., spectra) with the previously described (1) material.

The chromatographic fractions rich in alcohols were combined and acetylated (total 790 mg). Crystallization from methanol gave acetate **10***a* (80 mg). The noncrystalline material was chromatographed over neutral alumina (26 g, activity IV). Elution with Skellysolve B – benzene (85:15) gave dinitro compound **16***a* (24 mg). Elution with Skellysolve B – benzene (1:1) gave nitroacetate **14** (98 mg). Elution with benzene (100 ml) gave

Can. J. Chem. Downloaded from www.nrcresearchpress.com by 210.87.254.6 on 09/05/12
For personal use only.

ketoacetate **12***a* (39 mg) which was recrystallized from methanol: m.p. 218–222°; i.r. 1720 (C=O of ester, ketone), 1405, 1370 cm^{-1}; n.m.r. τ 9.14 (s, 3, C-10 methyl), 8.84 (s, 3, C-4 methyl), 7.98 (s, 3, $OCOCH_3$), 6.36 (s, 3, methoxyl), 5.34 (br d, 1, C*H*OAc); mass spectrum 376 (5), 316 (22), 290 (100), 257 (63), 121 (90).

Mol. wt. Calcd. for $C_{22}H_{32}O_5$: 376.2249. Found (h.r.m.s.): 376.2247.

Further elution with benzene (250 ml) gave nitroalcohol **16***b* as a wax: λ_{max} 362 (ε 5560), 236 nm (ε 6250); i.r. ($CHCl_3$) 3590 (OH), 1720 (C=O of ester), 1610 (C=C), 1500, 1320 (C=CNO_2) cm^{-1}; n.m.r. τ 9.35 (s, 3, C-11 methyl), 8.53 (s, 3, C-4 methyl), 8.58 (s, 6, isopropyl methyls), 6.28 (s, 3, methoxyl), 2.82 (s, 1, H-15); mass spectrum 403 (20), 386 (29), 385 (26), 368 (33), 356 (18), 338 (27), 137 (50), 135 (74), 121 (27), 109 (46), 81 (48), 69 (19), 67 (26), 55 (49), 43 (100).

Mol. wt. Calcd. for $C_{23}H_{33}NO_5$: 403.2359. Found: 403.2373.

Hydrolysis of Acetate 10a

A solution of acetate **10***a* (24 mg) and sodium methoxide (5 mg) in methanol (2.5 ml) was allowed to stand at room temperature for 80 h. The solution was diluted with water, acidified (HCl), and extracted with chloroform. The chloroform extract was washed (H_2O), dried ($MgSO_4$), and concentrated to give alcohol **10***b* (22 mg); i.r. 3600 (OH), 1720 (C=O of ester), 1240 cm^{-1}; n.m.r. τ 9.14 (s, 3, C-10 methyl), 8.84 (s, 3, C-4 methyl), 8.46 (s, 3, isopropylidene methyl), 8.37 (s, 3, isopropylidene methyl), 6.58 (br d, 1 C*H*OH), 6.36 (s, 3, methoxyl). The mass spectrum showed an apparent molecular ion at *m/e* 360.

Oxidation of Alcohol 10b

Jones' reagent (3 drops) was added to a stirred, cooled (10°) solution of alcohol **10***b* (22 mg) in acetone (4 ml). The reaction mixture was stirred for 5 min, then neutralized (K_2CO_3), diluted with water, and extracted with chloroform. The chloroform extract was washed (H_2O), dried ($MgSO_4$), and concentrated to give a ketone (18 mg) which was purified by molecular distillation: i.r. 1725 (C=O of ester, ketone), 1410, 1245 cm^{-1}; n.m.r. τ 9.06 (s, 3, C-10 methyl), 8.83 (s, 3, C-4 methyl), 8.44 (s, 3, isopropylidene methyl), 8.30 (s, 3, isopropylidene methyl), 6.37 (s, 3, methoxyl). The mass spectrum showed an apparent molecular ion at *m/e* 358.

Conversion of Acetate 10a to Ketoolefin 11

Ozone was bubbled into a cooled (−70°) solution of acetate **10***a* (59 mg) in ethyl acetate (40 ml) at a rate of 0.025 ml/s for 4 min. The blue solution was maintained at −70° for 2 h, allowed to warm to room temperature, then concentrated. The residue was diluted with water (15 ml), 30% hydrogen peroxide (1.5 ml) added, and the mixture heated on a steam bath for 1.5 h. The reaction mixture was cooled and extracted with chloroform. The chloroform extract was dried ($MgSO_4$) and concentrated to give ketoacetate **12***a* (56 mg), identical with that described above.

A solution of ketoacetate **12***a* (25 mg) and potassium hydroxide (2.5 g) in aqueous methanol (1:3, 25 ml) was heated under reflux for 5 h. Methanol was removed, the solution diluted with water, acidified (HCl), and extracted with chloroform. The chloroform extract was washed (H_2O), dried ($MgSO_4$), and concentrated. Treatment with ethereal diazomethane gave ketoalcohol **12***b* (22 mg): m.p. 215–223°.

Freshly distilled ethyl chloroformate (0.6 ml) was added dropwise to a cooled (0°) solution of ketoalcohol **12***b* (22 mg) in pyridine (0.8 ml). A red crystalline solid precipitated. More ethyl chloroformate (0.3 ml) was added and the mixture allowed to stand at room temperature overnight. The reaction mixture was diluted with water, acidified (HCl), and extracted with chloroform. The chloroform extract was washed (H_2O), dried ($MgSO_4$), and concentrated. The residue (30 mg) was dissolved in benzene, filtered through alumina and concentrated to give cathylate **12***c* (21 mg): i.r. 1750–1740 (C=O of ester), 1425, 1370, 1270 cm^{-1}.

Cathylate **12***c* was subjected to pyrolysis in a sealed tube at 240–250° for 1.5 h. The product was sublimed at reduced pressure (95°) to give the known ketoolefin **11** (13 mg): m.p. 166–169° (lit. (13) 166–168°); i.r. (KBr) 1720, 1610 cm^{-1} (lit. (13) 1724, 1616 cm^{-1}).

Attempted Conversion of Acetate 10a to Acetate 13

A solution of acetate **10***a* (67 mg) in glacial acetic acid (3 ml) saturated with hydrogen chloride was allowed to stand at room temperature for 48 h. The solution was concentrated. T.l.c. (silica gel) of the residue showed a single spot, even when mixed with either acetate **13** or acetate **10***a*. The n.m.r. spectrum show signals characteristic of both **13** (τ 9.37 (C-10 methyl), 8.93 (isopropyl doublet), 8.07 (acetoxyl CH_3)) and **10***a* (τ 9.16 (C-10 methyl), 8.02 (acetoxyl CH_3)) in a ratio of approximately 1:2.

Attempted Pyrolysis of Nitroacetate 14

Nitroacetate **14** (25 mg) was impregnated on glass beads in a glass tube and heated to 280–295° at 36 mm for 2 h. The oily material (7 mg) which distilled showed no nitro group absorption in the i.r. spectrum. However, the n.m.r. spectrum showed three signals in the carbomethoxyl region, τ 6.33–6.38, and t.l.c. indicated the presence of several components.

Attempted Hydrogenolysis of Nitroacetate 14

A solution of nitroacetate **14** (18 mg) in methanol (30 ml) was subjected to hydrogenation over Adams' catalyst (30 mg) at room temperature and 50 p.s.i. for 24 h. The solution was filtered and concentrated. The residue was dissolved in benzene, filtered through alumina, and concentrated to give 13 mg of unchanged nitroacetate **14**.

Hydrogenation of Dinitro Compound 16a

(i) Ethyl Acetate

A solution of dinitro compound **16***a* (100 mg) in ethyl acetate (30 ml) was hydrogenated over Adams' catalyst (33 mg) at room temperature and atmospheric pressure for 1 h. The solution was filtered and concentrated to give a mixture of compounds (95 mg). The residue was dissolved in ether and separated into basic (12 mg) and nonbasic (72 mg) fractions. The nonbasic fraction was acetylated and chromatographed over silica gel (6 g). Elution with benzene (125 ml) gave compound **17** (17 mg); m.p. 140–140.5° (from ethanol); i.r. ($CHCl_3$) 1720 (C=O of ester), 1605, 1540, 1350 (NO_2) cm^{-1}; n.m.r. τ 8.95 (s, 3, C-11 methyl), 8.69 (s, 3, C-4 methyl), 8.31 (s, 6, isopropyl methyls), 6.35 (s, 3, methoxyl), 5.28 (m, 1, C*H*NO_2), 4.69 (s, 1, H-15); mass spectrum 388.2488 calcd. for $C_{23}H_{34}NO_4$, found 388.2489 (M − 46, 8),

Can. J. Chem. Downloaded from www.nrcresearchpress.com by 210.87.254.6 on 09/05/12
For personal use only.

358.2508 calcd. for $C_{23}H_{34}O_3$, found 358.2505 (28), 341.2481 calcd. for $C_{23}H_{33}O_2$, found 341.2478 (100), 281.2269 calcd. for $C_{21}H_{29}$, found 281.2269 (54), 121 (44), 107 (69), 105 (52), 91 (57).

Anal. Calcd. for $C_{23}H_{34}N_2O_6$: C, 63.57; H, 7.89; N, 6.45. Found: C, 63.46; H, 7.73; N, 6.36.

(ii) Ethanol

A solution of dinitro compound **16***a* (43 mg) in 95% ethanol (30 ml) was hydrogenated over Adams' catalyst (20 mg) at room temperature and atmospheric pressure for 1 h. The solution was filtered, concentrated, and acetylated. The acetylated material (45 mg) was chromatographed over neutral alumina (3 g, activity II). Elution with benzene (60 ml) gave compound **18** (14 mg): m.p. 80–81° (from methanol); i.r. ($CHCl_3$) 3370 (NH), 1715 (C=O of ester), 1660 (C=O of amide), 1540, 1375 cm^{-1}; n.m.r. τ 9.15 (d, 3, J = 6 Hz, isopropyl methyl), 9.14 (d, 3, J = 6 Hz, isopropyl methyl), 8.87 (s, 3, C-11 methyl), 8.75 (s, 3, C-4 methyl), 8.00 (s, 3, $NCOCH_3$), 6.34 (br s, 1, H-7), 6.33 (s, 3, methoxyl), 3.0 (br s, 1, N*H*); mass spectrum 403.3086 calcd. for $C_{25}H_{41}NO_3$, found 403.3081 (22), 344.2712 calcd. for $C_{23}H_{36}O_2$, found 344.2715 (100), 329 (67), 301 (58), 285 (95), 284 (78), 273 (48), 269 (50), 241 (30), 213 (21), 133 (32), 109 (42), 107 (32), 105 (43).

Anal. Calcd. for $C_{25}H_{41}NO_3$: C, 74.40; H, 10.24; N, 3.47. Found: C, 74.57; H, 10.24; N, 3.49.

(iii) Ethanol – Hydrochloric Acid

A solution of dinitro compound **16***a* (170 mg) in concentrated hydrochloric acid (few drops) and ethanol (40 ml) was hydrogenated over Adams' catalyst for 7 h. The solution was filtered and concentrated. The residue was dissolved in ether and separated into nonbasic material (24 mg) and basic material (118 mg). The basic material was acetylated. Crystallization from methanol gave compound **18** (70 mg). The noncrystalline material was chromatographed over alumina (4 g). Elution with benzene–ether gave compound **18** (13 mg). Further elution with benzene–ether gave the compound epimeric at C-7 with compound **18** (17 mg); i.r. ($CHCl_3$) 3360 (NH), 1725 (C=O of ester), 1540, 1350 cm^{-1}; n.m.r. τ 9.13 (d, 3, J = 6 Hz, isopropyl methyl), 9.11 (d, 3, J = 6 Hz, isopropyl methyl), 8.88 (s, 3, C-11 methyl), 8.72 (s, 3, C-4 methyl), 7.97 (s, 3, $NCOCH_3$), 6.26 (s, 3, methoxyl), 6.10 (br s, 1, H-7), 4.66 (br s, 1, N*H*); mass spectrum 403 (fragmentation pattern as for compound **18**).

Elution with chloroform gave compound **20***a*: m.p. 235–236° (dec.); i.r. ($CHCl_3$) 3435 (NH), 1725 (C=O of ester), 1675 (C=O of amide), 1540, 1500, 1350 cm^{-1}; n.m.r. τ 9.27 (s, 3, C-10 methyl), 8.83 (s, 3, C-4 methyl), 8.25 (s, 3, isopropyl methyl), 8.21 (s, 3, isopropyl methyl), 7.91 (s, 3, $NCOCH_3$), 6.35 (s, 3, methoxyl), 5.95 (br d, 1, H-15), 5.37 (m, 1, H-7); mass spectrum 482 (2), 480 (5), 398 (100), 374.2013 calcd. for $C_{23}H_{31}O_2{}^{35}Cl$, found 374.2017 (52), 38 (3), 36 (11).

Mol. wt. Calcd. for $C_{25}H_{37}N_2O_5{}^{35}Cl$: 480.2392. Found (h.r.m.s.): 480.2395.

In another experiment, the basic product from hydrogenation was treated with methanesulfonyl chloride in pyridine. Crystallization from methanol gave the sulfonamide corresponding to **18**: m.p. 177° (from methanol); i.r. ($CHCl_3$) 3325 (NH), 1705 (C=O of ester), 1330, 1150 cm^{-1}; n.m.r. τ 9.16 (d, 3, J = 6 Hz, isopropyl methyl), 9.13 (d, 3, J = 6 Hz, isopropyl methyl), 8.88 (s, 3, C-11 methyl), 8.75 (s, 3, C-4 methyl), 7.12 (s, 3, NSO_2CH_3), 6.70 (br s, 1, H-7), 6.32 (s, 3, methoxyl), 3.87 (br d, 1, J = 6 Hz, N*H*); mass spectrum 439.2757 calcd. for $C_{24}H_{41}NO_4{}^{32}S$, found 439.2752 (55), 360 (66), 344 (100), 329 (39), 301 (24), 285 (68), 284 (56), 217 (93), 105 (50), 81 (58), 79 (54).

The noncrystalline material (147 mg) was chromatographed over alumina (9 g). Elution with benzene–ether gave the sulfonamide described above (14 mg). Elution with benzene–ether (1 :1, 60 ml) and ether (180 ml) gave the C-7 epimeric sulfonamide (14 mg): m.p. 206–209° (from methanol); i.r. ($CHCl_3$) 3380 (NH), 1720 (C=O of ester), 1330, 1150 cm^{-1}; n.m.r. τ 9.11 (d, 3, J = 6 Hz, isopropyl methyl), 9.10 (d, 3, J = 6 Hz, isopropyl methyl), 8.89 (s, 3, C-11 methyl), 8.78 (s. 3, C-4 methyl), 7.09 (s, 3, NSO_2CH_3), 6.54 (br s, 1, H-7), 6.34 (s, 3, methoxyl), 5.66 (s, 1, J = 7.5 Hz, N*H*); mass spectrum 439.2757 calcd. for $C_{24}H_{41}NO_4{}^{32}S$, found 439.2752.

Elution with chloroform (60 ml) gave compound **20***b* (50 mg): m.p. 188–191° (from Skellysolve B – ether); i.r. ($CHCl_3$) 3360 (NH), 1725 (C=O of ester), 1545, 1340 (NO_2) cm^{-1}; n.m.r. τ 9.30 (s, 3, C-10 methyl), 8.82 (s, 3, C-4 methyl) 8.26 (s, 3, isopropyl methyl), 8.22 (s, 3, isopropyl methyl), 6.90 (s, 3, NSO_2CH_3), 6.29 (s, 3, methoxyl), 5.97 (d, 1, J = 10 Hz, H-7), 5.72 (d of d, 1, J = 8.5, 3 Hz, H-15), 5.07 (d, 1, J = 10 Hz, N*H*), 4.15 (br s, 1, H-14); mass spectrum 470.2129 calcd. for $C_{24}H_{37}NO_4{}^{32}S^{35}Cl$, found 470.2129 (M − 46, 54), 377 (32), 375 (96), 315 (58), 313 (43), 312 (56), 144 (100), 107 (72), 38 (2), 36 (7)

Anal. Calcd. for $C_{24}H_{37}N_2O_6SCl$: C, 55.75; H, 7.21; N, 5.41. Found: C, 55.40; H, 7.10; N, 5.74

*Conversion of Nitroalcohol **16b** to Compound **18***

A solution of nitroalcohol **16***b* (40 mg) and hydrochloric acid (few drops) in ethanol was hydrogenated over Adams' catalyst. The hydrogenated material on work-up gave basic (9 mg) and nonbasic (21 mg) fractions. The basic fraction was acetylated. Crystallization from methanol gave compound **18** (3 mg), identical (t.l.c., i.r.) with that described above.

*Attempted Dehydration of Nitroalcohol **16b***

A solution of nitroalcohol **16***b* (80 mg) and thionyl chloride (1 ml) in methylene chloride (10 ml) was allowed to stand at room temperature for 18 h. The solution was concentrated by codistillation with benzene to give compound **16***c*: λ_{max} 357, 237 nm; i.r. ($CHCl_3$), 1720 (C=O of ester), 1610, 1500, 1320 cm^{-1}; n.m.r. τ 9.33 (s, 3, C-11 methyl), 8.51 (s, 3, C-4 methyl), 8.23 (s, 3, isopropyl methyl), 8.17 (s, 3, isopropyl methyl), 6.29 (s, 3, methoxyl), 2.87 (s, 1, H-15).

Anal. Calcd. for $C_{23}H_{32}NO_4Cl$: Cl, 8.42. Found: Cl, 7.90, 8.47.

Compound **16***c* was hydrogenated in ethanol (30 ml) over Adams' catalyst at room temperature and atmospheric pressure for 2 h. The solution was filtered, concentrated, acetylated, and the product chromatographed over alumina (5 g). Elution with benzene–ether gave compound **18**.

*Acid-catalyzed Dehydration of Nitroalcohol **16b***

A solution of nitroalcohol **16***b* (25 mg), and *p*-toluenesulfonic acid (2.5 mg) in dry benzene (25 ml) was heated under reflux for 1 h. The solution was cooled, then diluted with ether (40 ml). The benzene–ether solution

Can. J. Chem. Downloaded from www.nrcresearchpress.com by 210.87.254.6 on 09/05/12
For personal use only.

was washed (5% Na_2CO_3, H_2O), dried ($MgSO_4$), and concentrated to give compound **27** (24 mg): u.v. λ_{max} 382 (ε 5450), 258 nm (ε 6270); i.r. ($CHCl_3$) 1730 (C=O of ester), 1620 (C=C), 1600, (C=C), 1500, 1320, 900 cm^{-1}; n.m.r. τ 9.34 (s, 3, C-11 methyl), 8.50 (s, 3, C-4 methyl), 8.00 (s, 3, C=C—CH_3), 6.29 (s, 3, methoxyl), 4.80 (s, 1, C=CH_2), 4.59 (s, 1, C=CH_2), 2.77 (s, 1, C=CH); mass spectrum 385 (2), 368 (2), 223 (36), 57 (100).

Reaction of Diene 2 with "Nitrous Acid"

Sodium nitrite (50 mg) was added over a 15 min period to a stirred solution of diene **2** (47 mg) in glacial acetic acid (1 ml). The reaction mixture was allowed to stand overnight, then 50 mg of sodium nitrite was added and the mixture was stirred for 1 h. The reaction mixture was diluted with water, basified (10% NaOH), and extracted with ether. The ether extract was washed (H_2O), dried ($MgSO_4$), and concentrated. Crystallization from ether gave trinitro compound **22** (7 mg, 13%).

Deamination of Amine 1b With Limited Sodium Nitrite

Sodium nitrite (190 mg, 2.7 mmol) was added in portions over a 1 h period to a stirred solution of amine **1***b* (970 mg, 2.7 mmol) in aqueous acetic acid (11 ml). The solution was stirred for 3 h, then separated into basic and nonbasic (165 mg, 16%) material. Crystallization from ether gave trinitro compound **22** (6 mg, 4%). The noncrystalline material (145 mg) was chromatographed over alumina (6 g). Gradient elution with benzene and benzene–ether (32:1) gave dinitro compound **16***a* (12 mg, 7%). Elution with benzene–ether (9:1) gave a mixture (10 mg) of dinitro compound **16***a* and ketone **15**. Elution with ether–chloroform gave nitroalcohol **16***b* (14 mg, 9%).

Reaction of Diene 2 with N_2O_4 in Acetic Acid

A solution of dinitrogen tetroxide (125 mg) in acetic acid (4 ml) was added over a period of 20 min to a stirred solution of diene **2** (185 mg) in glacial acetic acid (10 ml). The solution was stirred for 1 h, then diluted with water and extracted with ether. The ether extract was washed (H_2O), dried ($MgSO_4$), and concentrated. Crystallization from ether gave trinitro compound **22** (57 mg, 24%). The noncrystalline material (178 mg) was chromatographed over alumina (8.5 g). Elution with benzene gave dinitro compound **16***a* (22 mg, 13%). The residue from this crystallization was chromatographed over silica gel. Elution with benzene–ether gave material (7 mg) which crystallized from ethanol when seeded with nitroacetate **14**. Identity with **14** was established by i.r. and t.l.c.

Treatment of Diene 2 with Acetic Acid – Perchloric Acid

A solution of diene **2** (58 mg) and 70% perchloric acid (3 drops) in glacial acetic acid (3.5 ml) was allowed to stand at room temperature for 20 h. The reaction mixture was diluted with water and extracted with chloroform. The chloroform extract was washed (H_2O), dried ($MgSO_4$), and concentrated. The oil (65 mg) obtained was chromatographed over alumina (4 g). Gradient elution with Skellysolve B and Skellysolve B – benzene gave unchanged diene **2** (23 mg). Elution with benzene gave a mixture of acetate **10***a* and acetate **13** (24 mg) as established by n.m.r. Hydrolysis of the mixture of acetates ($KOH-CH_3OH$), followed by esterification (CH_2N_2) and chromatography over alumina yielded, after crystallization from Skellysolve B, the alcohol derived by hydrolysis of **13**, m.p. 92–93°, identical (i.r. and t.l.c.) with a known (1) sample.

We wish to thank Dr. R. V. Lawrence for a very generous sample of the levopimaric acid – acrylic acid Diels–Alder adduct, the National Research Council of Canada for financial support, and the University of Alberta for a dissertation fellowship (to P.D.D.). The authors gratefully acknowledge the help of A. M. Hogg, R. N. Swindlehurst, and G. Bigam in the determination of the n.m.r., i.r., and mass spectra, and L. M. Browne for assistance in various phases of this work.

1. W. A. Ayer and P. D. Deshpande. Can. J. Chem. **51**, 77 (1973).
2. Z. Valenta and K. Wiesner. Chem. and Ind. (London) 354 (1956).
3. R. C. Cookson and M. E. Trevett. J. Chem. Soc. 3121 (1956).
4. N. J. Halbrook, R. V. Lawrence, R. L. Dressler, R. C. Blackstone, and W. Herz. J. Org. Chem. **29**, 1017 (1964).
5. H. Wolff. Org. React. **3**, 307 (1946).
6. E. Bertele, H. Boos, J. D. Dunitz, F. Elsinger, A. Eschenmoser, I. Felner, H. Gribi, H. Gschwend, E. F. Meyer, M. Pesaro, and R. Scheffold. Angew. Chem. Int. Ed. **3**, 490 (1964).
7. H. Muxfeldt and W. Rogalski. J. Am. Chem. Soc. **87**, 933 (1965).
8. P. A. S. Smith. Org. React. **3**, 337 (1946).
9. C. N. R. Rao. Chemical applications of infrared spectroscopy. Academic Press, New York. 1963. p. 264.
10. W. C. Wildman and D. R. Saunders. J. Am. Chem. Soc. **76**, 946 (1954).
11. H. L. Goering, R. W. Greiner, and M. F. Sloan. J. Am. Chem. Soc. **83**, 1391 (1961).
12. K. Tori, Y. Takano, and H. Kitahonoki. Chem. Ber. **97**, 2798 (1964).
13. L. H. Zalkow and N. N. Girotra. J. Org. Chem. **28**, 2037 (1963).
14. Reference 9, pp. 271–272.
15. W. A. Ayer, C. E. McDonald, and J. B. Stothers. Can. J. Chem. **41**, 1113 (1963).
16. Varian Spectra Catalog. Varian Associates, Palo Alto, Calif. Spectrum no. 41.
17. T. R. Aplin, M. Fischer, D. Becher, H. Budzikiewicz, and C. Djerassi. J. Am. Chem. Soc. **87**, 4888 (1965).
18. H. Shechter and F. Conrad. J. Am. Chem. Soc. **76**, 2716 (1954).
19. C. J. Collins. Acc. Chem. Res. **4**, 315 (1971) and references therein.
20. M. Hanack and H. Eggensperger. Ann. **648**, 3 (1961).
21. P. A. S. Smith. Open-chain nitrogen compounds. Vol. 1. W. A. Benjamin, Inc., New York. 1965. p. 7.
22. N. Levy and J. D. Rose. Quart. Rev. **1**, 358 (1947).
23. H. Shechter. Record Chem. Progr. **25**, 55 (1964).
24. P. A. S. Smith. Open-chain nitrogen compounds. Vol. 2. W. A. Benjamin, Inc., New York. 1966. pp. 412–417.
25. V. M. Loeblich, D. E. Baldwin, R. T. O'Connor, and R. V. Lawrence. J. Am. Chem. Soc. **77**, 6311 (1955).

Resolution, Racemization, and Ring Opening of an *o,m'*-Bridged Biphenyl

E. W. WARNHOFF AND P. REYNOLDS-WARNHOFF
Department of Chemistry, University of Western Ontario, London, Ontario

Received January 24, 1973

The ease of racemization and ring cleavage of the dissymmetric *o,m'*-bridged biphenyl **1** has been examined. Although **1** is structurally stable at least to 100°, it racemizes rapidly in the vicinity of 60°. However, if the nitrogen is converted into a better leaving group by quaternization or protonation, the bridge is quickly broken below 80° by nucleophilic displacement at the benzylic carbon atom. U.v. evidence for strain in **1** is presented.

La facilité de racémisation et de rupture de cycle dans le biphényle dissymétrique ponté en *o,m'*-**1** a été examinée. Bien que **1** possède une structure stable au moins jusqu'à 100°, il se racemise rapidement au voisinage de 60°. Cependant, si l'azote est transformé en un meilleur groupe partant par quaternization ou protonation, la rupture du pont est rapide au dessous de 80° par déplacement nucléophile sur l'atome de carbone benzylique. La tension dans **1** a été mise en évidence par u.v.

[Traduit par le journal]

Can. J. Chem., **51**, 2338 (1973)

Can. J. Chem. Downloaded from www.nrcresearchpress.com by 210.87.254.40 on 09/05/12
For personal use only.

The anhydromethine **1** obtained from the Hofmann elimination on the alkaloid caranine **2** (1, 2) has the unusual structure of a biphenyl bridged by a four-atom chain at the *o,m'*-positions. The fact that the bridge of structure **1** could not be completed with Stuart–Briegleb models unless the individual benzene rings were non-planar shows not only that the molecule is strained, but also that the bridge must strongly hinder interconversion of the two atropisomers **3** and **4** (3). The fortunate circumstance that one of the four bridge atoms is a benzylic amino nitrogen allowed demonstration of the hindrance and strain by rendering both optical resolution and bridge cleavage facile. Although there are examples of *m,m'*- and many examples of *o,o'*-bridged biphenyls which have been resolved (4), compound **1** is the only example of an optically active *o,m'*-bridged biphenyl of which we are aware, and as promised earlier (1, footnote 8), we are reporting further chemistry of this interesting molecule.

The strain inherent in **1** ,because of the bridge, first became apparent when the methiodide of the anhydromethine was prepared at room temperature (1). The initial methiodide **5***a* underwent ring scission by nucleophilic attack of iodide on the benzylic carbon to displace the tertiary amine (**5***a* → **6**) which was then quaternized by excess methyl iodide to yield the isolated product **7**. In agreement with this interpretation we now find that quaternization with methyl *p*-toluenesulfonate at room temperature does allow isolation of **5***b*, presumably because of the greatly reduced nucleophilicity of *p*-toluenesulfonate ion compared to iodide ion.

The anhydromethine appears to be stable so long as the nitrogen atom is not positively charged by quaternization or protonation. Even the salts of the anhydromethine with acids whose anions are relatively weak nucleophiles ($HClO_4$, HCl, picric acid) are stable at room temperature, but on warming solutions of these salts in water or ethanol the bridge is readily broken. Thus when **1** was refluxed in 1% aqueous hydrochloric acid, the bridge was broken by displacement of the protonated nitrogen to form the secondary amino alcohol **8***a*. The structure **8***a* was confirmed by acetylation to an *N*-monoacetate **8***d* and an O,*N*-diacetate **8***e*. When the perchlorate or picrate salts were refluxed briefly in ethanol, the bridge was broken by nucleophilic attack of ethanol on the benzylic carbon atom and formation of the ethyl ether **8***b*. Although the above salts were stable at room temperature, the anhydromethine was not stable on dissolution in trifluoroacetic acid at 38°. The n.m.r. spectrum of **1** in trifluoroacetic acid at this temperature gave a triplet for the protonated *N*-methyl absorption (instead of a doublet) and a two-proton singlet at δ 5.29 from the benzylic methylene group, both absorptions requiring the presence of **8***c* with the N protonated (5).

The anhydromethine **1**, m.p. 92–92.5°, as originally prepared from its dissymmetric precursor **2** (1) at 120° was optically inactive, and proof that the molecule could maintain dissymmetry at room temperature was first secured by

Can. J. Chem. Downloaded from www.nrcresearchpress.com by 210.87.254.40 on 09/05/12
For personal use only.

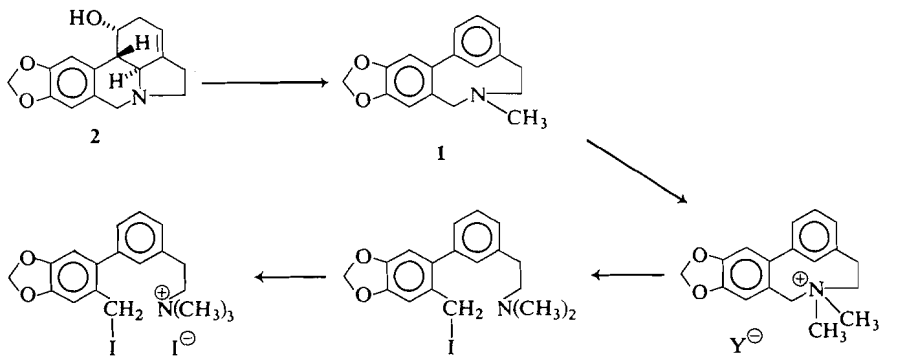

2 1 7 6 5

a Y = $I^{\ominus}$

b Y = $^{\ominus}O_3S$-C$_6$H$_4$-CH_3

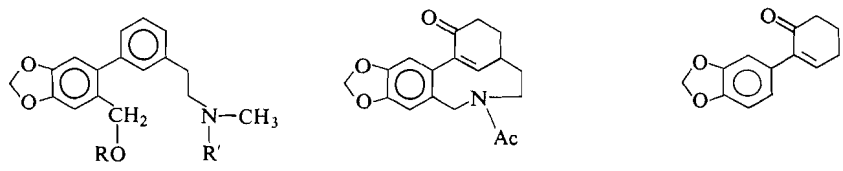

8 9 10

a R = H; R′ = H
b R = C_2H_5; R′ = H
c R = CF_3C=O; R′ = H
d R = H; R′ = Ac
e R = R′ = Ac

resolving the racemic compound at room temperature via its di-*p*-toluyl-L-tartaric acid salt (see Experimental). The (+) enantiomer **4** (3) so obtained had m.p. 75–78° and was of unknown optical purity. At room temperature in solution the anhydromethine is optically stable for at least several days. It was this optical stability at room temperature which prompted the Hofmann degradation of caranine methiodide at room temperature with potassium *t*-butoxide–dimethylsulfoxide which yielded the (−) atropisomer **3** as reported previously (3). When atropisomer **4** was heated to its melting point, it was interconverted with **3** with resolidification to the higher melting racemate **3** + **4**. Enantiomer **4** could also be racemized by boiling (65°) in methanol solution. The loss of optical activity in these two experiments was due to atropisomer interconversion (**4** ⇌ **3**) and not to bridge cleavage because the product in both cases was the racemic anhydromethine **1**.

Further evidence of the strain in this *o,m′*-bridged biphenyl is the characteristic change in the u.v. chromophore (Fig. 1) brought about by bridge cleavage. The benzene rings of **1** are not coplanar and may not even be individually planar whereas the benzene rings of the cleavage product are certainly planar and they may assume a more nearly coplanar arrangement.[1] Yet another example of this distortion of the u.v. chromophore by the short four-atom *o,m′*-bridge in a closely related molecule is the spectrum of the acetylation product of α-

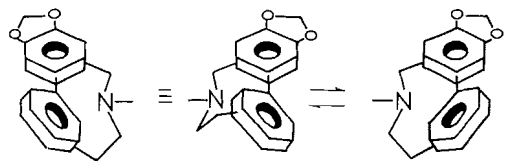

4 **3**

[1]But probably still far from true coplanarity (6).

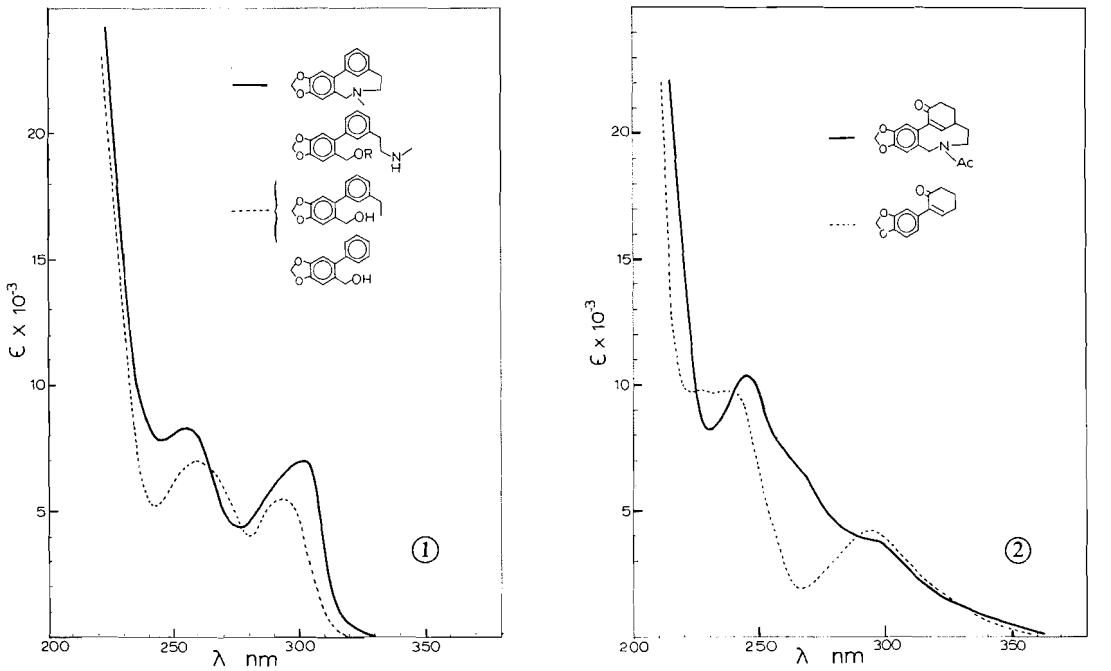

FIG. 1. The u.v. spectra of caranine anhydromethine and three unbridged biphenyls in ethanol.

FIG. 2. The u.v. spectra of bridged and unbridged 2-(3′,4′-methylenedioxyphenyl)-cyclohex-2-enone chromophores in ethanol.

dihydrocaranone **9** (1) compared to the spectrum of 2-(3′,4′ methylenedioxyphenyl)-cyclohexen-2-one (**10**) (Fig. 2).

Experimental

Many of the general procedures are in footnote 19 of ref. 1. Some i.r. spectra were recorded on a Beckman IR-10 instrument. The n.m.r. spectra were recorded on a Varian HA-100 instrument with $CDCl_3$ solutions. Some analyses were by Chemalytics, Inc., Tempe, Arizona.

Caranine Anhydromethine Methotosylate (5b)

A solution of 50 mg of pure **1** and 100 mg of methyl tosylate in 16 drops of CH_3CN was allowed to stand at room temperature for 8 days. Two crops of crystals were obtained totalling 84 mg (99%) of the quaternary tosylate salt **5***b*, m.p. 135–140°; δ 2.24 (s, 3H, $ArCH_3$), 2.5–~3.5 (m, $ArCH_2$), 3.24 (bs, 6H, $+N(CH_3)_2$), 3.5–4.5 (2m, 4H, CH_2NCH_2), 6.0 (AB, 2H, OCH_2O), and 6.5–8.0 (m, 10H, ArH).

Caranine Anhydromethine Perchlorate

To a solution of 50 mg of (±)anhydromethine **1** in 2 ml of HOAc was added 0.2 g of $NaClO_4$. After solution of the $NaClO_4$, the amine perchlorate precipitated. Centrifugation, decantation, and washing with HOAc gave after drying 50 mg (73%) of colorless crystals, m.p. 128–130°. The salt was recrystallized at room temperature by solution in methanol followed by addition of ether. Two such recrystallizations gave 13 mg of long needles, m.p. 132–133°. The u.v. spectrum was identical with that of (±) and (+) **1**.

Anal. Calcd. for $C_{17}H_{17}NO_2 \cdot HClO_4$ (mol. wt. 367.8): C, 55.51; H, 4.93; N, 3.81. Found: C, 55.50; H, 4.93; N, 3.90.

Regeneration of the free base from the perchlorate at room temperature gave recovered (±)anhydromethine **1** whose i.r. and u.v. spectra were identical with those of authentic (±) **1**.

Hydrolysis of Caranine Anhydromethine 1

A solution of 350 mg (1.31 mmol) of (±) **1** in 20 ml of 1% aqueous HCl was refluxed for 1 h. Basification and ether extraction gave 315 mg (84%) of colorless oil which was chromatographed on 10 g of alumina. No trace of **1** remained. EtOAc and EtOAc–EtOH eluted 294 mg of liquid secondary aminoalcohol **8***a*, ν_{max} ($CHCl_3$) 3700–2400 cm^{-1} (broad H-bonded OH and NH) (the two characteristic sharp peaks of **1** at 1307 and 1325 cm^{-1} were absent); λ_{max} (EtOH) 259 (7100) and 294 nm (5500).

The 294 mg of liquid was dissolved in 4 ml of acetic anhydride and allowed to stand at room temperature for 10 min. The solution was diluted with aqueous HCl and extracted with ether. The ether solution was washed with aqueous KOH and water and was then dried and evaporated to leave 295 mg (87%) of colorless liquid N-acetyl derivative **8***d*, ν_{max} ($CHCl_3$) 3435 (OH) and 1635 (amide C=O), λ_{max} (EtOH) 259 (7050) and 294 nm (5600).

A portion (40 mg) of the product **8***a* from another hydrolysis was allowed to react with 1 ml of acetic anhydride in 1 ml of pyridine at room temperature for 6 h. The reaction mixture was partitioned between water and ether. The ethereal layer was washed with dilute aqueous H_2SO_4, 10% aqueous $NaHCO_3$, and saturated

Can. J. Chem. Downloaded from www.nrcresearchpress.com by 210.87.254.40 on 09/05/12
For personal use only.

Can. J. Chem. Downloaded from www.nrcresearchpress.com by 210.87.254.40 on 09/05/12
For personal use only.

aqueous NaCl before being dried over $MgSO_4$. Evaporation of the ether left 45 mg (87%) of colorless oily diacetate **8***e*; ν_{max} (CS_2) 1742 (ester C=O) and 1650 cm^{-1} (amide C=O); δ ($CDCl_3$) 2.08 (s, 6H, CH_3COO and $CH_3C(=O)N$), 2.8–3.0 (m, 5H, Ar—CH_2CH_2—N—CH_3),[2] 3.60 (m, 2H, —CH_2N—C=O), 4.89 (s, 2H, $ArCH_2OAc$), 5.99 (s, 2H, O—CH_2—O), 6.75 (s, 1H, Ar—H), 6.94 (s, 1H, ArH), 7.05–7.45 (m, 4H, ArH).

Anal. Calcd. for $C_{21}H_{23}NO_5$ (mol. wt. 369.4): C, 68.28; H, 6.28; N, 3.79. Found: C, 68.32; H, 6.41; N, 3.30.

Alcoholysis of Caranine Anhydromethine (1)

(*a*) The (±)anhydromethine was stable in neutral ethanol. When 10 mg of (±) **1** was refluxed in 0.5 ml of 99% ethanol for 5 min and allowed to crystallize, there was obtained 6.5 mg of recovered (±) **1**, m.p. 92–92.5° undepressed on admixture with starting material.

(*b*) A 57-mg sample of the perchlorate of (±) **1** was dissolved in 5 ml of 95% ethanol and refluxed for 10 min. Regeneration of free base by basification and extraction with ether gave 40 mg of colorless liquid ring-opened ethyl ether **8***b*. The product was evaporatively distilled at 150° (0.05 Torr), ν_{max} ($CHCl_3$) ~3300 cm^{-1} (broad NH); λ_{max} (EtOH) 258 (6400) and 293 nm (4840).

Anal. Calcd. for $C_{19}H_{23}NO_3$ (mol. wt. 313.4): 1 OC_2H_5, 14.37. Found: OC_2H_5, 13.61.

(*c*) A solution of 42 mg of the picrate of (±) **1** (1) in 5 ml of a mixture of chloroform and 99% ethanol was refluxed for 10 min. Regeneration of the base by passage through 1 g of basic alumina with chloroform eluate gave 20 mg (75%) of colorless liquid ring-opened ethyl ether whose i.r. and u.v. spectra were identical with the sample prepared from the perchlorate salt in section *b*.

Resolution of Caranine Anhydromethine (1)

To a solution of 405 mg (1.52 mmol) of anhydromethine **1** in 10 ml of 95% ethanol was added a solution of 613 mg (1.52 mmol) of di-*p*-toluyl-L-tartaric acid in 9 ml of 95% ethanol. Crystals precipitated almost immediately and the reaction mixture was allowed to stand for 2 days at room temperature. Filtration and washing with 95% ethanol left 638 mg (62%) of white crystals, m.p. 150–154°.

A 549-mg portion of the salt was basified with aqueous NaOH, and the precipitate was centrifuged, washed with water and dried at room temperature to yield 211 mg (94%) of white crystals, m.p. 73–76°. One recrystallization from methanol with minimum heating to effect solution gave 196 mg of long prisms of (+) **1**, m.p. 75–78°, $[\alpha]_D$ +21° (*c*, 0.95 in chloroform); λ_{max} (EtOH) 256 (8270) and 303 nm (7000).

Anal. Calcd. for $C_{17}H_{17}NO_2$ (mol. wt. 267.3): C, 76.38; H, 6.41; N, 5.24. Found: C, 76.25; H, 6.34; N, 5.49.

The mixed m.p. with racemic **1**, m.p. 92–92.5°, was 73–92°.

A 30-mg sample of (+) **1** was heated at 78° for 10 min during which time it melted and then slowly recrystallized completely. The resolidified material had m.p. 92–92.5°, $[\alpha]_D$ 0° (*c*, 1.72 in chloroform). The i.r. spectrum of the racemized material was identical with that of the (+) **1**.

During recrystallization of (+) **1**, if the methanol solution was boiled for ~10 min, the anhydromethine that crystallized had m.p. 92–92.5° and was racemic.

2-(3′,4′-Methylenedioxyphenyl)-cyclohex-2-en-1-one (10)

A solution of 370 mg (1.70 mmol) of 2-(3′,4′-methylenedioxyphenyl)-cyclohexanone (7), m.p. 93–94°, in 5 ml of CCl_4 was stirred (magnetic bar) and treated dropwise with a solution of 297 mg (1.85 mmol) of Br_2 in 4 ml of CCl_4. The reaction mixture was then diluted with more CCl_4, washed with water, dried, and concentrated. The residual oil was dissolved in 5 ml of 2,6-lutidine and refluxed in a N_2 atmosphere for 10 min. The dehydrobromination mixture was diluted with ether, and the lutidine was extracted with aqueous HCl. Evaporation of the dried ether solution left 341 mg (93%) of oil that crystallized. One recrystallization from ethyl acetate–cyclohexane gave 150 mg, m.p. 85–98°. Several more recrystallizations from ethyl acetate followed by sublimation at 90° (0.05 Torr) gave colorless blades of pure **10**, m.p. 99–100°, ν_{max} ($CHCl_3$) 1670 cm^{-1} (C=C—C=O); λ_{max} (EtOH) 238 (9750) and 294 nm (4200).

Anal. Calcd. for $C_{13}H_{12}O_3$ (mol. wt. 216.2): C, 72.21; H, 5.59. Found: C, 72.21; H, 5.62.

Sublimation was necessary to remove ethyl acetate of crystallization which was not removed by drying at elevated temperature.

[2]The N—CH_3 absorption consisted of two peaks, Δδ 5 Hz, which coalesced on raising the temperature to 50°. The two peaks are attributed to slowly interconverting conformers of **8***e*.

1. E. W. WARNHOFF and W. C. WILDMAN. J. Am. Chem. Soc. **79**, 2192 (1957).
2. E. W. WARNHOFF, P. REYNOLDS-WARNHOFF, and S. VALVERDE-LOPEZ. An. Real Soc. Espan. Fis. Quim. Ser. A, **68**, 797 (1972).
3. E. W. WARNHOFF and S. VALVERDE-LOPEZ. Tetrahedron Lett. 2723 (1967).
4. (*a*) B. SMITH. Bridged aromatic compounds. Academic Press, New York. 1964. p. 333; (*b*) D. M. HALL. Progress in stereochemistry. Vol. 4. Butterworths, London, 1969. p. 1.
5. J. C. N. MA and E. W. WARNHOFF. Can. J. Chem. **43**, 1863 (1965).
6. R. J. HIGHET and P. F. HIGHET. J. Org. Chem. **33**, 3096 (1968).
7. W. C. WILDMAN. J. Am. Chem. Soc. **80**, 2567 (1958).

The Fragmentation Mechanism of Cyclobutanol

JOHN L. HOLMES[1]

Department of Chemistry, University of Ottawa, Ottawa, Canada K1N 6N5

AND

ROBIN T. B. RYE

Department of Chemistry, Sir George Williams University, Montreal 107, Quebec

Received January 5, 1973

The mass spectra of cyclobutanol and three ^2H labelled analogs have been studied. The losses of C_2H_4 and $C_2H_5^{\cdot}$ from the molecular ion involve specific fragmentations. Only $CH_3^{\cdot}$ loss from the α-cleaved molecular ion[2] clearly involves hydrogen atom scrambling; this fragmentation also proceeds by a specific mechanism involving C-2 and hydroxyl hydrogen atoms. Loss of water from the molecular ion involves all the hydrogen atoms but in a complex, non-random manner.

Les spectres de masse du cyclobutanol et de trois analogues marqués au deutérium ont été étudiés. Les pertes de C_2H_4 et $C_2H_5^{\cdot}$ à partir de l'ion moléculaire se font par des fragmentations spécifiques. Seule la perte de $CH_3^{\cdot}$ à partir de l'ion moléculaire α clivé implique de façon nette un déplacement au hasard d'un atome d'hydrogène; cette fragmentation se fait également selon un mécanisme spécifique engageant les atomes de C-2 et d'hydrogène hydroxyle. La perte d'eau à partir de l'ion moléculaire engage tous les atomes d'hydrogène selon un mécanisme complexe et non au hasard. [Traduit par le journal]

Can. J. Chem., **51**, 2342 (1973)

The mass spectrum of cyclobutanol has been briefly discussed by Natalis (1) and by Budzikiewicz, *et al.* (2). We have examined the mass spectra of some deuterium labelled cyclobutanols in order to determine whether any of the mechanisms recently proposed for the primary fragmentations of cyclohexanol (3) apply to the C_4 alcohol.

Results and Discussion

Relative peak intensities for the 70 eV mass spectrum of cyclobutanol are shown in Table 1; they agree with published data. Also given in Table 1 are peak intensities for cyclobutanol-OD, 1-d_1-cyclobutanol and 2,2,4,4-d_4-cyclobutanol.

There are only two peaks with relative intensity greater than 10% in the mass spectrum of cyclobutanol. The base peak (*m/e* 44) is accompanied by a weak first field-free region metastable consistent with fast elimination of C_2H_4 from the molecular ion. Under such conditions little hydrogen atom scrambling would be expected. For 2,2,4,4-d_4-cyclobutanol the base peak appears at *m/e* 46 ($M - C_2H_2D_2$): comparison of the peak intensity ratio (*m/e* 46)/(*m/e* 45) in this compound with the equivalent ratio in the unlabelled alcohol shows (after correction for incomplete labelling) that no significant hydrogen scrambling occurs prior to ethylene loss. Similar results are obtained for the d_1-alcohols. Thus ethylene elimination involves the loss of two adjacent methylene groups. The same fragmentation processes have been shown to take place in 1-methyl (4) and 1-ethyl cyclobutanols (5).

The second most intense peak in the mass spectrum (*m/e* 43; relative intensity, 30%) arises mainly through loss of $C_2H_5^{\cdot}$ from the molecular ion. The appropriate metastable is observed, and it is approximately 30 times more intense than that for ethylene loss. If it is assumed that the ratio of total ethylene loss to total ethyl radical loss is the same in the deuterated cyclobutanols as in the unlabelled material a simple calculation shows that there is negligible contribution from loss of $C_2H_4D^{\cdot}$ to the peak at *m/e* 43 in the mass spectrum of 1-d_1-cyclobutanol. For cyclobutanol-OD, however, approximately 50% of the observed peak intensity at *m/e* 43 is due to loss of $C_2H_4D^{\cdot}$ from the molecular ion; in the metastables the loss of $C_2H_4D^{\cdot}$ accounts for 60% of the total ethyl radical loss. Although this latter value is close to that expected for random selection from seven hydrogens and one deuterium in the elimination of the ethyl radical ($C_2H_4D^{\cdot}$:

[1]Author to whom correspondence should be addressed.

Can. J. Chem. Downloaded from www.nrcresearchpress.com by 210.87.254.6 on 09/05/12
For personal use only.

TABLE 1. Relative peak intensities for cyclobutanols at 70 eV

			Relative intensities*	
m/e	Cyclobutanol	Cyclobutanol-OD	1-d_1-Cyclobutanol	2,2,4,4-d_4-Cyclobutanol
76	—	—	—	1.7
75	—	—	—	0.8
74	—	—	—	0.8
73	—	1.4	1.4	0.6
72	1.5	0.6	0.5	0.5
71	0.5	0.3	0.5	—
70	1.0	2.5	0.9	—
61	—	—	—	0.3
60	—	—	—	1.2
59	—	—	—	2.0
58	—	2.8	2.6	1.0
57	3.5	2.1	0.7	1.0
56	—	0.3	2.1	1.0
55	2.3	3.0	0.9	0.9
54	1.1	0.8	0.9	—
53	1.2	1.6	0.5	—
52	—	1.6	0.5	—
47	—	—	—	7.8
46	0.5	4.4	7.0	100.0
45	4.0	100.0	100.0	43.0
44	100.0	20.7	24.0	11.0
43	30.0	9.6	3.0	1.7
42	2.0	6.0	2.0	1.7
41	3.0	2.5	2.0	3.0
40	0.7	1.5	2.0	2.0
39	5.0	4.9	3.0	1.2

*Relative intensities are not corrected for incomplete labelling or for contribution from ^{13}C.

$C_2H_5^{\bullet}$ = 5:3), only a specific elimination mechanism can account for the results obtained for the 1-d_1-alcohol. A specific, rather than a random selection of hydrogen is also required by the results obtained from the 2,2,4,4-d_4-cyclobutanol; the observed ratio of $C_2H_3D_2^{\bullet}$ loss to $C_2H_2D_3^{\bullet}$ in the metastable ion peaks is 35:23, with negligibly small metastables observed for loss of $C_2H_4D^{\bullet}$ and $C_2H_5^{\bullet}$. We conclude that loss of ethyl radical involves the abstraction of a hydrogen atom from specific sites in the α-cleaved molecular ion, *i.e.* from the hydroxyl group and from C-2. The results for the d_4-alcohol also show that *either* there is an isotope effect leading to a preference for hydrogen over deuterium *or* geometrical factors favor abstraction from the hydroxyl group rather than from C-2.

A satisfactory mechanism for ethyl radical loss from cyclohexanol could not be proposed (3) mainly because of uncertainty as to the site of hydrogen abstraction. As the evidence now points to a mechanism involving the α-cleaved molecular ion[2] for ethyl radical loss in both cyclohexanol and cyclobutanol, identification of the abstraction sites in the latter compound may provide the key to the interpretation of the earlier results. This possibility is being given careful study. Ethylene loss from the two compounds occurs apparently by quite different mechanisms; in cyclohexanol involvement of the α-cleaved molecular ion is indicated, whereas C_2H_4 elimination from cyclobutanol is so rapid a process that no metastable ion peak is observed.

A number of other fragmentation processes are worthy of mention even though they give rise to only minor peaks in the mass spectrum.

(i) M — Water, m/e 54

Water loss from the molecular ion is not a favored process, with the peak at *m/e* 54 having

[2]In each case, "α-cleaved ion" will be taken as referring to fission of the 1,4 carbon–carbon bond.

Can. J. Chem. Downloaded from www.nrcresearchpress.com by 210.87.254.6 on 09/05/12
For personal use only.

Can. J. Chem. Downloaded from www.nrcresearchpress.com by 210.87.254.6 on 09/05/12
For personal use only.

TABLE 2. Relative metastable abundances for water and methyl loss from cyclobutanol

(a) Water

	Relative abundance					
	Observed			Random		
Compound	M − HOH	M − HOD	M − DOD	M − HOH	M − HOD	M − DOD
1-d_1-Cyclobutanol	8.6	1.0	—	3	1	—
Cyclobutanol-OD	3.8	1.0	—	3	1	—
2,2,4,4-d_4-Cyclobutanol	3.3	4.0	1.0	3	8	3

(b) Methyl

	M − CH_3	M − CH_2D	M − CHD_2	M − CD_3	M − CH_3	M − CH_2D	M − CHD_2	M − CD_3
1-d_1-Cyclobutanol	2.1	1.1	—	—	1.7	1.0	—	—
Cyclobutanol-OD	2.0	1.1	—	—	1.7	1.0	—	—
2,2,4,4-d_4-Cyclobutanol	1.0	6.0	8.0	2.5	1	6	6	1

Can. J. Chem. Downloaded from www.nrcresearchpress.com by 210.87.254.6 on 09/05/12
For personal use only.

a relative intensity of *ca.* 1%. The metastable abundance data for water loss from the labelled compounds (Table 2) shows that the elimination involves all ring positions. However, as can be seen from Table 2, the relative abundances are not those for complete hydrogen atom scrambling. The preponderance of HOH loss in every case indicates an isotope effect, and the results cannot be fitted to a single mechanism. Molecular geometry renders water loss from the ring-intact form of the molecular ion improbable; we conclude that it takes place primarily from the (rearranged) α-cleaved ion.

(ii) M − OH, m/e 55

In the peaks the intensity ratio $(M - {}^{\prime}OH)^+/(M - HOH)^+$ is close to 2:1; in the metastables, however, the ratio is approximately 1:12. The results for the labelled compounds also show that the hydroxyl group is lost rapidly, before the molecular ion can undergo any appreciable hydrogen atom scrambling (compare unlabelled and -OD alcohols, Table 1). We infer that the hydroxyl group is lost from the ring-intact form of the molecular ion. In cyclohexanol, hydroxyl is not lost from the molecular ion but the comparable fast process is the stereo-specific water loss (3).

(iii) M − Methyl, m/e 57

Methyl loss from the molecular ion gives a significant peak (relative intensity, 3.5%) in the spectrum. In the deuterated alcohols metastable ion peaks are observed for the loss of all possible labelled methyl radicals; relative abundance data are given in Table 2. For the d_1-alcohols the deviations from the random value of the $(M - CH_3)^+/(M - CH_2D)^+$ ratio are small, but significant. For the 2,2,4,4-d_4-cyclobutanol the departure from the random distribution is considerable. The observed values can be well explained by the summation of a random and a specific mechanism. In the mono-deuterated compounds the specific mechanism must yield the "excess" $CH_3^{\bullet}$ and/or $CH_2D^{\bullet}$ loss, while in the d_4-alcohol it must account for the observed "excess" of $CHD_2^{\bullet}$ and $CD_3^{\bullet}$. In the compounds studied, the specific mechanism accounts for approximately 15% of the total methyl loss from the molecular ion.

The suggested specific mechanism involves loss of the terminal carbon from the α-cleaved molecular ion, the third hydrogen atom coming from either C-2 or hydroxyl. The evidence for this proposal is as follows: the ratio of $CH_3^{\bullet}$ to $CH_2D^{\bullet}$ loss for 1-d_1-cyclobutanol indicates excess $CH_3^{\bullet}$ over that required for a random process. The observed ratio of 2.1:1.0 may be divided into a random $CH_3^{\bullet}$ loss (1.7), a specific $CH_3^{\bullet}$ loss (0.4), and a random loss of $CH_2D^{\bullet}$ (1.0). Similarly for cyclobutanol-OD the observed ratio of $CH_3^{\bullet}$ to $CH_2D^{\bullet}$ (2.0:1.1) may be divided into a random $CH_3^{\bullet}$ loss (1.7), a specific $CH_3^{\bullet}$ loss (0.3), a random $CH_2D^{\bullet}$ loss (1.0), and loss of $CH_2D^{\bullet}$ by the specific process (0.1), the latter indicating that the hydroxyl hydrogen atom is involved in the specific methyl loss. (It was not possible, however, quantitatively to determine the relative involvement of C-2 and hydroxyl hydrogens.) For 2,2,4,4-d_4-cyclobutanol, the observed loss of $CH_3^{\bullet}$ and $CH_2D^{\bullet}$ can be wholly assigned to the random process, with the specific elimination accounting for the "excess" $CHD_2^{\bullet}$ and $CD_3^{\bullet}$. The loss of $CD_3^{\bullet}$ in excess of the random value identifies C-2 as an abstraction site.

A recent study has been made by McAdoo *et al.* (5) of the isomeric $C_4H_8O^{+\bullet}$ ions generated from 1-ethyl cyclobutanol and a variety of ketone precursors. All these ions display specific fragmentations for the loss of ethyl and methyl radicals which are at variance with our observations. Moreover, the proposed structures for their $C_4H_8O^{+\bullet}$ ions were $[CH_3CH_2COCH_3]^{+\bullet}$, $CH_3CH^{\bullet}(CO^+H)CH_3$, and $CH_3CH_2(CO^+H)$-$CH_2^{\bullet}$ and therefore we conclude that β-cleavage in cyclobutanol is not a significant process.

In cyclohexanol $CH_3^{\bullet}$ is lost from $(M - HOH)^{+\bullet}$ rather than from the molecular ion (3). The analogous process occurs in the fragmentation of cyclobutanol; a very weak metastable was observed for the loss of $CH_3^{\bullet}$ from $(M - OH)^+$. No attempt was made to determine whether this methyl loss was random or specific because earlier work has shown (6) that $C_4H_7^+$ ions from various precursors undergo complete hydrogen and carbon atom randomization prior to methyl radical elimination. Loss of $CH_3^{\bullet}$ from $(M - HOH)^{+\bullet}$ in the cyclobutanol fragmentation is inferred from the appearance of the peak at *m/e* 39, although no metastable was observed for this process; it has been shown that $C_4H_6^{+\bullet}$ ions lose $CH_3^{\bullet}$ readily (7).

(iv) M − H, m/e 71; (M − H) − H, m/e 70

Loss of the C-1 hydrogen atom has been identified as the origin of the $(M - 1)^+$ peak in

the mass spectrum of cyclohexanol. In the mass spectrum of cyclobutanol, peaks at *m/e* 71 $(M - 1)^+$ and *m/e* 70 show that two hydrogen atoms can be lost from the molecular ion. No metastable was observed for the process $(M - H)^+$, but a weak metastable corresponding to $(M - H) - H$ was found. Analysis of the ion peaks at *m/e* 73 (M), 72, and 71 in the mass spectrum of cyclobutanol-OD shows that the hydroxyl hydrogen atom and one other are lost from the molecular ion with approximately equal ease; the contributions of $(M - H)^+$ and $(M - D)^+$ to the appropriate peak intensities being in the ratio of 3:2.3, respectively. The mass spectrum of 1-d_1-cyclobutanol yielded similar results, confirming the loss of the C-1 hydrogen atom.

Experimental

All spectra were obtained using an A.E.I. MS-902S double focusing mass spectrometer which had been modified to permit defocused operation. Metastable abundance ratios were determined at constant accelerator potential (8) except in the case of 2,2,4,4-d_4-cyclobutanol. For this compound the metastable ion peaks corresponding to loss of $CD_3^{\cdot}$ and HOH overlap. The normal ion peak at *m/e* 58 in the d_4-alcohol is a doublet, with the high mass component arising from the loss of HOH. At moderate resolution ($M/\Delta M \sim 3000$) it was possible to separate the metastable transitions leading to each component of the doublet using the accelerating voltage scan technique (9). All spectra and metastables were measured with an ionizing energy of 70 eV and a source temperature of approximately 100 °C.

Cyclobutanol was prepared from cyclobutanone (Aldrich) by reduction with lithium aluminum hydride. Cyclobutanol-OD was prepared from the alcohol by exchange with D_2O, and was run with excess D_2O in the mass spectrometer. Reduction of the ketone with lithium aluminum deuteride, followed by reduction of the complex with water gave 1-d_1-cyclobutanol. Base-catalyzed exchange of cyclobutanone with D_2O (10) gave 2,2,4,4-d_4-cyclobutanone, which upon reduction with lithium aluminum hydride gave the corresponding alcohol. All the alcohols were purified by g.l.c.

We wish to thank Mr. P. Coulombe for experimental assistance. One of us (J.L.H.) thanks the National Research Council of Canada for financial support.

1. P. NATALIS. Bull. Soc. Roy. Sci. Liege, **31**, 790 (1962).
2. H. BUDZIKIEWICZ, C. DJERASSI, and D. H. WILLIAMS. Mass spectrometry of organic compounds. Holden-Day, Inc., San Francisco. 1967. p. 110.
3. J. L. HOLMES, D. MCGILLIVRAY, and R. T. B. RYE. Org. Mass Spectrom. **7**, 347 (1973).
4. F. W. MCLAFFERTY, D. J. MCADOO, J. S. SMITH, and R. KORNFELD. J. Am. Chem. Soc. **93**, 3720 (1971).
5. D. J. MCADOO, F. W. MCLAFFERTY, and T. E. PARKS. J. Am. Chem. Soc. **94**, 1601 (1972).
6. J. L. HOLMES, D. C. M. TONG, and R. T. B. RYE. Org. Mass. Spectrom. **6**, 897 (1972).
7. P. GOLDBERG, J. A. HOPKINSON, A. MATHIAS, and A. E. WILLIAMS. Org. Mass Spectrom. **3**, 1009 (1970).
8. (*a*) R. W. KISER, R. E. SULLIVAN, and M. S. LUPIN. Anal. Chem. **41**, 1958 (1969); (*b*) J. L. HOLMES and F. M. BENOIT. Mass Spectrometry, M.T.P. International Review of Science. Vol. 5. Butterworths, London. 1972. pp. 276–277.
9. M. BARBER and R. M. ELLIOT. Proceedings of the 12th annual conference on mass spectrometry and allied topics, A.S.T.M. E-14 Committee, Montreal. 1964.
10. M. C. CASERIO, W. H. GRAHAM, and J. D. ROBERTS. Tetrahedron, **11**, 171 (1960).

Can. J. Chem. Downloaded from www.nrcresearchpress.com by 210.87.254.6 on 09/05/12
For personal use only.

Synthesis of Phenols from Diazonium Tetrafluoroborates; a Useful Modification

D. E. HORNING, D. A. ROSS, AND J. M. MUCHOWSKI[1]

Bristol Laboratories of Canada, Candiac, Quebec

Received January 3, 1973

It is shown that phenols are obtained in good yield by the decomposition of aromatic diazonium tetrafluoroborates in refluxing trifluoroacetic acid containing potassium trifluoroacetate.

On démontre que des phénols peuvent être obtenus avec de bons rendements par décomposition des tétrafluoroborates de sel de diazonium aromatique par reflux dans l'acide trifluoroacétique contenant du trifluoroacétate de potassium. [Traduit par le journal]

Can. J. Chem., 51, 2347 (1973)

On several occasions, we have encountered aromatic amines (*e.g.* **1***a* and **2***a*) the diazonium salts of which could not be converted to phenols (**1***d* and **2***b*) under any of the usual (1–4) conditions. This publication describes simple modifications of known procedures (2, 3) which enable one to effect the above transformation with considerable ease. For example, when a solution of the diazonium tetrafluoroborate **1***b* was boiled under reflux in trifluoroacetic acid, containing an equivalent of potassium trifluoroacetate,[2] the salt (**1***b*) could no longer be detected after 20 h. Dilution of this solution with water resulted in the spontaneous hydrolysis of the trifluoroacetate **1***c* to give the phenol **1***d* in high yield. The phenol **2***b* was obtained in a similar way from **2***a*, but in this case the intermediate trifluoroacetate was cleaved by treatment with alkali.

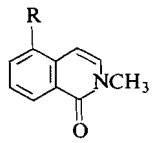

1

a R = NH_2
b R = $N_2^+BF_4^-$
c R = $OCOCF_3$
d R = OH

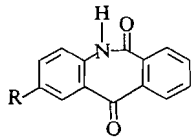

2

a R = NH_2
b R = OH

The synthesis of phenolate esters by the decomposition of diazonium salts in pure carboxylic acid solvents,[3] in particular in glacial acetic acid, has long been known (1), but yields of these esters generally have not exceeded 60% (see, however, ref. 5). In addition, it must be pointed out that Gottstein *et al.* (3) recently have diazotized certain 4-aminoquinolines in trifluoroacetic acid. The salts were then decomposed to phenols (at 5°) by the addition of water. The method described above therefore represents a relatively minor modification of the work of these investigators. It is, however, a modification which is vital, since neither **1***d* nor **2***b* were preparable under the conditions described by these workers. It is because of the exceptional utility[4] of this modified procedure that the work described herein has been submitted for publication.

Experimental

The melting points were determined in a Gallenkamp melting point apparatus and are not corrected. The i.r. spectra were measured with a Perkin–Elmer 237B grating spectrophotometer or a Unicam SP-200G i.r. spectrophotometer. The n.m.r. spectra were recorded with a Varian A-60A spectrometer and are expressed in p.p.m. (δ) from internal tetramethylsilane.

2-Methyl-5-aminoisocarbostyril (1)

This amine was prepared from the nitro compound by

[1]To whom enquiries should be addressed at: Syntex, S. A., Division de Investigacion, Calle Carretera Mexico-Toluca No. 2822, Apartado Postal 10-820, Mexico 10, D.F.

[2]The yields of phenols were considerably diminished in the absence of the salt.

[3]The use of formic acid containing sodium formate was also investigated, but the phenols **1***d* and **2***b* thus obtained were always contaminated with substantial amounts of the products of reductive deamination.

[4]Phenol was produced in > 75% yield by this procedure, and it has recently (6) been shown that simple acylamino phenols are also readily prepared by this method.

Can. J. Chem. Downloaded from www.nrcresearchpress.com by 210.87.254.42 on 09/05/12
For personal use only.

Can. J. Chem. Downloaded from www.nrcresearchpress.com by 210.87.254.42 on 09/05/12
For personal use only.

a modification of the method of Balcom and Furst (7) as described below.

A solution of 2-methyl-5-nitroisocarbostyril (6.18 g, 30.3 mmol; prepared in 85–95% yield by the alkaline ferricyanide oxidation of 2-methyl-5-nitroisoquinolinium iodide (8)) in absolute ethanol (300 ml) containing 100% hydrazine hydrate (6.5 g) and Raney nickel catalyst (1 teaspoon), was heated under gentle reflux for 1 h. The catalyst was removed by filtration through Celite, and the filtrate was evaporated to dryness *in vacuo*. The residue was crystallized from benzene (charcoal) to give the product in two crops; 3.91 g (m.p. 147–149°) and 0.50 g (m.p. 145–146°). Recrystallization of the first crop did not improve its melting point; λ_{max} ($CHCl_3$) 3450, 3375, 1650, 1635, 1598, 1570 cm^{-1}.

Anal. Calcd. for $C_{10}H_{10}N_2O$: C, 68.95; H, 5.79. Found: C, 68.96; H, 6.00.

2-Methyl-5-hydroxyisocarbostyril (2)

Concentrated hydrochloric acid (35 ml) was added to a stirred suspension of the amine (12.2 g, 70 mmol) in water (70 ml) and the mixture thus obtained was cooled to 0° and treated in the usual manner with a solution of sodium nitrite (5.30 g) in water (10 ml). After ½ h at 0°, a solution of sodium tetrafluoroborate (10.98 g) in water (35 ml) was added, and after a further ½ h the product was collected by filtration, washed with a small amount of ice-water and then with a large amount of ether. After drying in a stream of air the solid (15.2 g, 80%) had m.p. 135° dec.

Solid potassium carbonate (3.9 g, 28 mmol) was added cautiously at 0° to trifluoroacetic acid (120 ml), and then the diazonium tetrafluoroborate (15.2 g, 56 mmol) was added all at once. The resultant was stirred at reflux temperature (with protection from moisture) until the solution no longer (20 h) gave a positive test for the diazonium salt (alkaline β-naphthol). The solution was added to water (300 ml), and after 1 h at room temperature the resultant was stored at 0° for 20 h. The tan-colored solid which crystallized was collected by filtration and recrystallized (charcoal) from hot water. The white solid thus obtained (9.0 g, 91%) had m.p. 225–227.5° dec.; λ_{max} (Nujol) 3260–2400 (broad hump), 2733, 1640, 1619, 1585, 1550 cm^{-1}; δ(DMSO-d_6) 3.59 (s, 3H), 6.88 (d, 1H, $J_{3,4}$ = 7.7), 7.34 (q, 1H, J_o = 7.8, J_m = 2.0), 7.44 (t, 1H, J_o = 7.8), 7.50 (d, 1H, $J_{3,4}$ = 7.8), 7.85 (q, 1H, J_o = 7.8, J_m = 2.0). After dissolution of the phenol, the integrated intensity of the DOH peak (this absorption shifted from δ 3.37 to 3.89 on addition of the phenol) increased by precisely the amount required for one proton.

2-Hydroxy-5,6-dihydro-11H-dibenzo[b,e]azepine-6,11-dione (4)

Fluoroboric acid (48%, 300 ml) was added to a suspension (23.8 g, 100 mmol) of the amine (9) in water (400 ml). A solution of sodium nitrite (7.1 g) in water (25 ml) was added in the usual manner at 10–15° and then the solution was cooled to 0°. The solid was collected by filtration, washed successively with ice-cold 10% fluoroboric acid, ice-cold 2-propanol, and ether. After drying in a stream of air the salt weighed 29.9 g (89%).

A solution of the diazonium salt (46.3 g, 137 mmol) in trifluoroacetic acid (500 ml) containing potassium carbonate (9.7 g, 70 mmol) was heated under reflux until a negative diazonium salt test was obtained (72 h). The solvent was removed *in vacuo*, water was added to the residue, and the mixture was extracted with ethyl acetate. The organic phase was extracted with dilute sodium hydroxide, the alkaline phase was made acidic with hydrochloric acid and the product was collected by filtration (after the mixture had first been cooled in ice). The crude product thus obtained was digested with hot ethyl acetate, filtered, and the filtrate after cooling was passed over silica gel (Brinkman, Act II, 40 g per gram of crude phenol). The yellow-colored product (23.02 g) was contained in the first few hundred milliliters of the eluate. Reextraction of the insoluble material from above with hot ethyl acetate and subsequent purification by chromatography gave an additional 1.52 g of the product (total of 24.54 g, 75%). This material was homogeneous by t.l.c. (silica gel, 2% methanol in chloroform) and after sublimation at 200°/0.005 mm it had m.p. 267–269°; λ_{max} (Nujol) 3410, 3150, 1675, 1653 cm^{-1}; δ (DMSO-d_6) 6.76–7.62 (m, 5H), 7.82–8.08 (m, 2H), 9.50 (s, 1H, w_H = 30), 10.60 (d, 1H, $J \sim 1$).

Anal. Calcd. for $C_{14}H_9NO_3$: C, 70.29; H, 3.79; N, 5.86. Found: C, 70.10; H, 3.80; N, 5.95.

The *O*-methyl ether was prepared in 68–72% yield by heating an acetonitrile solution of the potassium salt (generated by treatment of the phenol with potassium carbonate in hot acetonitrile) with a slight excess of dimethyl sulfate. After recrystallization from acetonitrile this material had m.p. 244–245°; λ_{max} (Nujol) 3190, 1670, 1660 cm^{-1}; δ (DMSO-d_6) 3.80 (s, 3H), 7.12–7.83 (m, 6H), 8.05–8.31 (m, 1H), 10.80 (s, 1H, w_H = 6).

Anal. Calcd. for $C_{15}H_{11}NO_3$: C, 71.14; H, 4.37; N, 5.53. Found: C, 71.04; H, 4.24; N, 5.51.

1. Z. E. Jolles. Chemistry of carbon compounds. Vol. IIIA. *Edited by* E. H. Rodd. Elsevier Publishing Company, Amsterdam. 1954. pp. 293–294.
2. J. P. Lambooy. J. Am. Chem. Soc. 72, 5327 (1950).
3. W. J. Gottstein, H. Roberts, I. C. Wells, and L. C. Cheney. J. Org. Chem. **29**, 3065 (1964).
4. A. H. Lewin and T. Cohen. J. Org. Chem. **32**, 3844 (1967).
5. H. H. Hodgson and C. K. Foster. J. Chem. Soc. 435 (1942).
6. O. Ortega and J. M. Muchowski. Unpublished observations.
7. D. Balcom and A. Furst. J. Am. Chem. Soc. **75**, 4334 (1953).
8. D. E. Horning, G. Lacasse, and J. M. Muchowski. Can. J. Chem. **49**, 2787, 2797 (1971).
9. Belgian Patent No. 637 802 (1964); Chem. Abstr. **62**, 10 422 (1965).

Five-membered Heterocyclic Thiones. Part III.[1] 1,2,5-Thiadiazole-3-thiones

D. E. HORNING AND J. M. MUCHOWSKI[2]
Bristol Laboratories of Canada, Candiac, Quebec
Received November 22, 1972

Stable salts of 3-mercapto-1,2,5-thiadiazoles were prepared by the alkaline hydrolysis of the corresponding *N,N*-dimethylthionocarbamates.

Les sels stables de mercapto-3 thiadiazoles-1,2,5 ont été préparés par l'hydrolyse alcaline des *N,N*-diméthylthionocarbamates correspondants. [Traduit par le journal]

Can. J. Chem., **51**, 2349 (1973)

Can. J. Chem. Downloaded from www.nrcresearchpress.com by 210.87.254.40 on 09/05/12
For personal use only.

During the past decade, the chemistry of 1,2,5-thiadiazoles has been investigated in considerable detail (2). These studies have encompassed, among other compounds, the remarkably stable, completely enolic, 3-hydroxy derivatives. The corresponding 3-mercapto compounds have not heretofore been described, although at least one unsuccessful attempt to prepare such substances has been reported (3). This publication describes the synthesis of stable salts of two 3-mercapto-1,2,5-thiadiazoles, one of which is the parent member of the series.

The preparation of the title compounds (see Scheme 1) was based on the rearrangement of thionocarbamates to thiolcarbamates which has been successfully utilized by Newman and Karnes for the conversion of phenols to thiophenols (4). The method was first applied to 4-cyano-3-hydroxy-1,2,5-thiadiazole because it was considered that an electron-withdrawing group at C-4 would impart added stability to the product **5**, irrespective of whether it existed in the thione or the thiol form. Oxygen acylation of **1** (R = CN) was easily accomplished with dimethylthiocarbamyl chloride, and the thionocarbamate thus produced (**2**, R = CN; $\nu_{C=S}$ = 1562 cm^{-1}; see Table 1) rearranged to the thiolcarbamate (**3**, R = CN; $\nu_{C=O}$ = 1693 cm^{-1}) at 130°. Hydrolysis of the thiolcarbamate occurred in refluxing ethanolic potassium hydroxide solution and was accompanied by the expected hydration of the nitrile function. The crude, stable, potassium salt (**4**, M = K) was characterized as the 4-methoxycarbonylmethyl derivative (**6**, R = $CONH_2$, R′ = CH_3)[3] and as the readily purifiable dicyclohexylammonium salt (**4**, M = $(C_6H_{11})_2NH_2$).

In a manner similar to that described above, the parent hydroxy thiadiazole (**1**, R = H) gave a thionocarbamate (**2**, R = H), the rearrangement of which required more vigorous conditions (170°, 3 h) than did the aforementioned cyano analog (**2**, R = CN). Hydrolysis of the thiolcarbamate (**3**, R = H) was effected in the usual manner to give a mixture of salts from which a crystalline mercuric salt (M = Hg/2) could be obtained with ease. The presence of the thiolate in the salt mixture was further substantiated by the preparation of the 4-carboxymethyl derivative (**6**, R = R′ = H; obtained by saponification of the crude, oily, methyl ester).[3]

The thiols derived from the above salts were much less stable than the corresponding hydroxy compounds. Indeed, extraction of the acidified aqueous solution of the crude potassium salt of the parent thiol failed to yield any alkali soluble

[1]For Part II, see ref. 1.

[2]To whom enquiries should be addressed at: Syntex, S.A., Division de Investigacion, Calle Carretera Mexico-Toluca No. 2822, Apartado Postal 10-820, Mexico 10, D.F.

[3]A referee has expressed some reservations concerning the assigned site of alkylation of the ambident anionic system in the salts **4** (R = H, $CONH_2$). In our opinion there can be little doubt that *S*- and not *N*-alkylation occurred in view of the well-known fact that a wide variety of compounds containing the —N—C=S system alkylate, either as the neutral or the anionic species, essentially exclusively on sulfur (6). Indeed, we are unaware of deviations from this pattern irrespective of whether the —N—C=S group is incorporated in an heterocyclic or an acyclic system.

Finally, the n.m.r. spectra (see Table 1) of compounds **6** (R = H, R′ = CH_3 and R = $CONH_2$, R′ = CH_3) are consistent with the assigned structure (*e.g.* the —SCH_2— group in 2-allylthiobenzothiazole appears at δ 3.95 (7)).

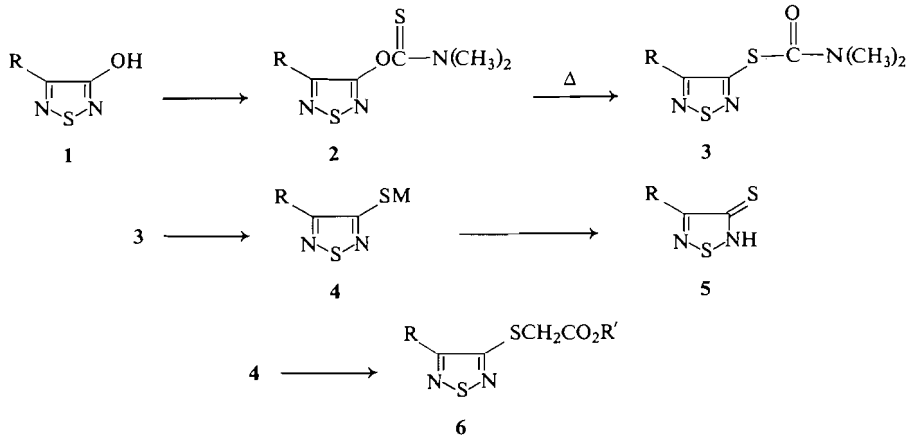

SCHEME 1

TABLE 1. Spectral properties of some 1,2,5-thiadiazoles

Compound	I.r. (cm^{-1})[a]	U.v. spectra[b] λ_{max}(mμ)(log ε)	N.m.r. δ (p.p.m.)[c]
2 (R = H)	3090, 1561[d]	206(3.68), 253(4.24)	3.40(3H), 3.45(3H), 8.50(1H)
2 (R = CN)	2240, 1562[e]	206(3.71), 256(4.30)	
3 (R = H)	3095, 1681[d]	210(3.87), 278(3.94)	3.12(6H), 8.92(1H)
3 (R = CN)	2243, 1693[e]	209(4.00), 274(3.81)	
4 (R = H)[f]	3070[g]		
4 (R = $CONH_2$)[h]	3460, 3290, 3175[g] 2820–2470 (br) 1662, 1597, 1586	209(sh.)(3.76), 233(4.11), 268(4.15), 359(3.53)	
6 (R = R′ = H)	3078, 2705–2390 (br)[g] 1716	208(3.71), 297(3.93)	3.75(3H), 4.05(2H), 8.38(1H)[i]
6 (R = $CONH_2$ R′ = CH_3	3515, 3400, 1747[e] 1698, 1584	208(sh)(3.48), 231(4.05), 242(sh)(3.97), 315(3.75)	3.75(3H), 4.05(2H), 7.58(2H, w_H = 9 Hz)[j]

[a]Recorded with a Unicam SP-200G i.r. spectrophotometer.
[b]Measured in 95% ethanol on a Unicam SP 800 u.v. spectrophotometer.
[c]Recorded in $CDCl_3$ (unless otherwise indicated) with a Varian A-60A spectrometer; all resonances were of singlet multiplicity.
[d]Liquid film.
[e]Measured in chloroform.
[f]Mercuric salt.
[g]Nujol mull.
[h]Dicyclohexylammonium salt.
[i]Spectrum of methyl ester; recorded in CCl_4.
[j]Recorded in DMSO-d_6 – $CDCl_3$ (1:2).

material. The 4-carboxamido derivative was, however, sufficiently stable to be isolable, but a specimen left at room temperature for 1 day was only 50% soluble in dilute sodium hydroxide solution.

The solution i.r. spectrum ($CHCl_3$) of 3-mercapto-4-carboxamido-1,2,5-thiadiazole (**5**, R = $CONH_2$) was devoid of absorptions in the 2600–2500 cm^{-1} region[4] showing that the thione tautomer was the major if not exclusive species present under these conditions.

[4]The SH stretching absorption of thiophene 2- and 3-thiols is reported (5) to occur in the 2540–2510 cm^{-1} region, and 2-methyl-1,2,3-triazole-4-thiol has a strong band at 2540 cm^{-1} (8).

Experimental

The melting points were determined in a Gallenkamp m.p. apparatus and are not corrected.

*3-Cyano-4-hydroxy-1,2,5-thiadiazole (**1**, R = CN)*

This compound was prepared from isonitrosocyanoacetamide and sulfur dichloride according to Ross and Smith (3) but with the following modification: The solid residue obtained after evaporation of the reaction mixture was dissolved in sodium carbonate solution (100 g/l) and the solution was washed with ether. The aqueous phase was made acidic with 10% hydrochloric acid, the product was extracted into ether, the extract was dried over sodium sulfate, treated with activated charcoal and then evaporated *in vacuo*. The residual solid (61–63% yield) had m.p. 157–160° (lit. (3) m.p. 157–160°).

*3-Hydroxy-1,2,5-thiadiazole (**1**, R = H)*

This compound was prepared from glycinamide (9) and

Can. J. Chem. Downloaded from www.nrcresearchpress.com by 210.87.254.40 on 09/05/12
For personal use only.

Can. J. Chem. Downloaded from www.nrcresearchpress.com by 210.87.254.40 on 09/05/12
For personal use only.

sulfur monochloride as described by Weinstock *et al.* (10) except that the crude product was first freed of impurities by solution in sodium carbonate, etc., as described above for the 4-cyano derivative.

4-Cyano-1,2,5-thiadiazol-3-yl-N,N-dimethylthionocarbamate (2, R = CN)

The general procedure of Newman and Karnes (4) was modified as follows: A 55% dispersion of sodium hydride in mineral oil (6.25 g) was washed with hexane, layered with dry DMF (125 ml), and cooled with stirring, in an atmosphere of dry nitrogen, to 0°. The hydroxy nitrile (16.5 g, 130 mmol) was added portionwise, and when gas evolution was complete, dimethylthiocarbamyl chloride (17.6 g, 143 mmol) was added all at once. The cooling bath was removed, and after 20 h at room temperature the solution was poured into ice-water. The mixture was extracted with benzene, the extract was washed with water, dried over sodium sulfate, and evaporated *in vacuo*. The residue was crystallized from benzene – petroleum ether (b.p. 30–60°) to give a yellow solid (21.22 g, 76%), m.p. 84–87°. Recrystallization of this material (charcoal) gave an analytical specimen, m.p. 85–87°.

Anal. Calcd. for $C_6H_6N_4OS_2$: C, 33.63; H, 2.82; N, 26.15. Found: C, 33.68; H, 2.80; N, 26.20.

1,2,5-Thiadiazol-3-yl-N,N-dimethylthionocarbamate (2, R = H)

This compound was prepared in the same way as the above cyano derivative except that the crude oily thionocarbamate was purified by dry column chromatography (11) on silica gel (Brinkman, Activity II–III, 10 g/g substrate) using 2% methanol in chloroform (v/v) as the eluant. The first 200 ml of the eluate (reaction scale, 200 mmol) was discarded, and the next 600 ml contained the pure thionocarbamate (26.83 g). An additional small amount of the product (1.39 g), which was slightly contaminated with more polar substances, was contained in the next 100 ml of the eluate. The main fraction was sufficiently pure to be used in the next step. A portion of this fraction was analyzed.

Anal. Calcd. for $C_5H_7N_3OS_2$: C, 31.73; H, 3.73; N, 22.20. Found: C, 31.79; H, 3.78; N, 22.22.

4-Cyano-1,2,5-thiadiazol-3-yl-N,N-dimethylthiolcarbamate (3, R = CN)

The thionocarbamate (20.5 g, 96 mmol) was heated in an oil bath at 130° under an atmosphere of nitrogen for 40 min. The deeply-colored material was slurried with ether (800 ml), the mixture was filtered, the filtrate was treated with activated charcoal, and finally evaporated *in vacuo*. The residual yellow solid (16.03 g, 78.5%) had m.p. 74–78° and was sufficiently pure to be used in the next step. Recrystallization of this material from benzene–cyclohexane gave a white solid m.p. 79–81°.

Anal. Calcd. for $C_6H_6N_4OS_2$: C, 33.63; H, 2.82; N, 26.15. Found: C, 33.75.; H, 2.80; N, 26.20.

1,2,5-Thiadiazol-3-yl-N,N-dimethylthiolcarbamate (3, R = H)

The chromatographically pure thionocarbamate (18.6 g) was stirred in a nitrogen atmosphere at 170° for 3 h. The deeply-colored oil was dissolved in a small amount of 2% methanol in chloroform, absorbed onto silica gel (20 g, Brinkman, Act II–III) and dried *in vacuo*. This material was placed on top of a dry packed column of silica gel (200 g) and the column was developed with 2% methanol-in-chloroform (100 ml fractions). Fractions 2–3 contained the starting material (5.76 g), and fractions 4–6 contained the product (12.46 g). The recovered starting material was subjected to the above rearrangement conditions (170°, 2.5 h) and after chromatography there was obtained 1.47 g of starting material, and 4.10 g of the thiolcarbamate. The combined product was distilled to give the pure thiolcarbamate (14.12 g, 76%), b.p. 107–108°/0.05 mm. A portion of this material was redistilled for analysis.

Anal. Calcd. for $C_5H_7N_3OS_2$: C, 31.73; H, 3.73; N, 22.20. Found: C, 31.73; H, 3.76; N, 22.46.

4-Carboxamido-1,2,5-thiadiazole-3-thiol dicyclohexylammonium salt (4, R = $CONH_2$)

A solution of 4-cyano-1,2,5-thiadiazol-3-yl-*N,N*-dimethylthiolcarbamate (14.0 g, 65.5 mol) in absolute ethanol (400 ml) containing potassium hydroxide (20.4 g of a 45 wt. % solution, 164 mmol) was heated under reflux for 1 h. The yellow solid (10.0 g, 76.5%; m.p. 265–267° dec.) which separated on cooling was collected by filtration and dried *in vacuo*. This salt was not readily recrystallized, and could not be obtained analytically pure. It was, however, sufficiently pure to be used for alkylation purposes. The thiol was characterized as its dicyclohexylammonium salt which was prepared in the following manner: The crude potassium salt (1.0 g) was dissolved in water, the solution was acidified with 10% hydrochloric acid, and the product was immediately extracted into ethyl acetate. The extract was dried over sodium sulfate and evaporated *in vacuo*. The white solid which remained (594 mg, m.p. 117–121°) was immediately dissolved in ethanol and added to an equimolar amount of ethanolic dicyclohexylamine. Dilution of the solution to turbidity with ether caused the crystallization of the salt (1.01 g), m.p. 166–169°. Recrystallization gave material with m.p. 168–170°.

Anal. Calcd. for $C_3H_3N_3OS_2$:$C_{12}H_{23}N$: C, 52.60; H, 7.65; N, 16.36. Found: C, 52.38; H, 7.67; N, 16.61.

1,2,5-Thiadiazole-3-thiol mercuric salt (4, R = H)

1,2,5-Thiadiazol-3-yl-*N,N*-dimethylthiolcarbamate was hydrolyzed in the manner described for the 4-cyano derivative. The ethanolic solution of the product was evaporated *in vacuo* to give a yellow solid (17.0 g from a 74.6 mmol reaction) which was not easily freed from inorganic materials. It could be shown by alkylation with methyl bromoacetate or by conversion to the mercuric salt, that the above mixture contained *ca.* 62% by weight of the potassium salt. This therefore corresponded to a 90% yield of the thiolate. The mercuric salt was prepared as follows: A solution of the crude salt (1.26 g, 5 mmol) was dissolved in water and the p*H* of the solution (p*H* meter) was adjusted to p*H* 7 by the addition of a few drops of glacial acetic acid. A solution of mercuric acetate (0.8 g, 2.5 mmol) in water (10 ml) was added and the precipitated solid (1.0 g), m.p. 177–180°, was collected by filtration and dried *in vacuo*. Crystallization of this solid from acetone gave material with m.p. 177–179°.

Anal. Calcd. for $C_2HN_2S_2$:0.5 Hg: C, 11.05; H, 0.46; N, 12.88. Found: C, 11.10; H, 0.58; N, 12.98.

4-Carboxamido-3-methoxycarbonylmethylthio-1,2,5-thiadiazole (6, R = H, R′ = CH_3)

The crude potassium salt described above (1.99 g, 10 mmol) and methylbromoacetate (1.8 g, 11.8 mmol) in

methanol (10 ml) was heated under reflux for 1 h. The solution was evaporated *in vacuo*, the residue was treated with hot benzene and filtered. The filtrate on cooling deposited a crystalline solid (1.12 g, 48%) m.p. 144.5–146°. Recrystallization gave material with m.p. 145–146°.

Anal. Calcd. for $C_6H_7N_3O_3S_2$: C, 30.89, H, 3.03; N, 18.01. Found: C, 30.84; H, 3.05; N, 17.88.

3-Carboxymethylthio-1,2,5-thiadiazole (6, R = R′ = H)

(a) From Crude Potassium-1,2,5-thiadiazole-3-thiolate

A solution of the crude salt (1.06 g) in methanol (50 ml) containing an excess of ethyl bromoacetate (1.9 g, 12.4 mmol) was heated at reflux temperature for 1 h. The cooled mixture was filtered and the filtrate was evaporated *in vacuo*. The residue was diluted with water, and the product was extracted into dichloromethane. The extract was dried over sodium sulfate, the solvent was removed *in vacuo*, and the residue was evaporatively distilled at 95–105°/0.05 mm to give the ester (803 mg, 4.23 mmol). On the basis of the yield of the ester obtained, the crude salt described above contained a minimum of 62% by weight of the potassium thiolate. Redistillation of the ester (b.p. 72–74°/0.005 mm) did not remove a small amount of an impurity (< 10%). The ester was therefore saponified as follows. A solution of the ester (380 mg, 2 mmol) in 50% aqueous methanol (20 ml) containing 45 wt. % aqueous potassium hydroxide (250 mg, 2 mmol) was boiled under reflux for 1.25 h. Most of the methanol was removed *in vacuo*, the residue was extracted with benzene, and the aqueous phase was then made acidic with 10% hydrochloric acid. The product crystallized (326 mg, 92%) and had m.p. 127–129°. Two recrystallizations of this material from water gave a solid with m.p. 128–129°.

Anal. Calcd. for $C_4H_4N_2O_2S_2$: C, 27.26; H, 2.29; N, 15.90. Found: C, 27.05; H, 2.31; N, 15.97.

(b) From the Mercuric Salt

Following the method of Soderback (12) for the conversion of mercuric thiolates to sodium thiolates, the mercuric salt (784 mg, 1.8 mmol) was added portionwise to a stirred solution of sodium sulfide nonahydrate (385 mg, 1.6 mmol) in water at 0°. After 30 min at 0°, the test for soluble sulfide ion (sodium plumbite solution) was negative. The mixture was filtered through Celite, the filtrate was diluted with methanol (50 ml), and methyl bromoacetate (400 mg, 2.63 mmol) was added. The solution was heated at reflux temperature for 1 h and then processed in the manner described above to give the crude ester which was saponified without purification. There was obtained a solid (145 mg, 31% based on methyl bromoacetate), m.p. 126–127° identical to the carboxylic acid prepared by method *a*.

1. G. Lacasse and J. M. Muchowski. Can. J. Chem. **50**, 3082 (1972).
2. L. M. Weinstock and P. I. Pollak. Advances in heterocyclic chemistry. Vol. 9. *Edited by* A. R. Katritzky and A. J. Boulton. Academic Press, New York. 1968. pp. 107–163.
3. J. M. Ross and W. C. Smith. J. Am. Chem. Soc. **86**, 2861 (1964).
4. M. S. Newman and H. A. Karnes. J. Org. Chem. **31**, 3980 (1966).
5. S. Gronowitz, P. Moses, and A. B. Hornfeldt. Arkiv. Kemi. **17**, 237 (1961).
6. (*a*)P. A. S. Smith. The chemistry of open-chain organic nitrogen compounds. Vol. I. W. A. Benjamin, Inc., New York. 1965. pp. 163, 261–262, 271. (*b*) P. A. S. Smith. The chemistry of open-chain organic nitrogen compounds. Vol. II. W. A. Benjamin, Inc., New York. 1966. pp. 88, 180.
7. N. S. Bhacca, L. F. Johnson, and J. N. Shoolery. Varian high resolution n.m.r. spectra catalogue. Varian Associates. 1962. p. 136.
8. J. P. Daris and J. M. Muchowski. Unpublished observation.
9. P. S. Yang and M. M. Rising. J. Am. Chem. Soc. **53**, 3183 (1931).
10. L. M. Weinstock, P. Davis, B. Handelsman, and R. Tull. J. Org. Chem. **32**, 2823 (1967).
11. B. Loev and M. M. Goodman. Chem. and Ind. 2026 (1967).
12. E. Soderback. Ann. **465**, 184 (1928).

Can. J. Chem. Downloaded from www.nrcresearchpress.com by 210.87.254.40 on 09/05/12
For personal use only.

Five-membered Heterocyclic Thiones. Part IV.[1] 1,2,4-Thiadiazole-3-thiolates and 1,2,4-Thiadiazole-5-thione

G. LACASSE AND J. M. MUCHOWSKI[2]
Bristol Laboratories of Canada, Candiac, Quebec
Received November 28, 1972

1,2,4-Thiadiazole-5-thione (**2***a*) was synthesized from the corresponding 5-bromo compound. An alternative synthesis of the known 3-methyl-1,2,4-thiadiazole-5-thione is described. It was shown by i.r. spectroscopy that the parent compound and its 3-methyl derivative existed in the thione form in the solid state.

Mercuric-1,2,4-thiadiazole-3-thiolate (**5**) was prepared by cleavage of the corresponding disulfide with mercury. The mercuric salt was converted to a stable (in solution) sodium salt, but the free thio compound was not isolable.

Le thiadiazole-1,2,4 thione-5 (**2***a*) a été synthétisé à partir du composé correspondant bromo-5. On décrit une nouvelle synthèse du composé connu suivant, le méthyl-3 thiadiazole-1,2,4 thione-5. Il a été montré à l'aide de la spectroscopie i.r. que le composé parent et son dérivé méthyl-3 existe à l'état solide sous la forme thione.

Le thiolate-3 mercurique de thiadiazole-1,2,4 (**5**) a été préparé par clivage à l'aide du mercure du disulfure correspondant. Le sel mercurique a été converti en un sel de sodium stable (en solution) mais le composé thio libre n'a pu être isolé. [Traduit par le journal]

Can. J. Chem., **51**, 2353 (1973)

There are two possible 1,2,4-thiadiazole thiols, and ring-substituted representatives of each isomer are known (2,3), but the parent members have not, to our knowledge, been previously described.

3-Substituted-1,2,4-thiadiazole-5-thiones (**2**, Scheme 1) are easily prepared (4) by the base-promoted fragmentation of the corresponding isothiouronium salts (*e.g.*, **1***b*, **1***e*) which in turn are obtained from the readily available (4–7) 5-chloro compounds (1, X = Cl) and thiourea. When the conditions are suitably modified, this method is also applicable to the synthesis of the parent thione (**2***a*).

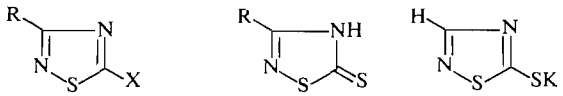

1 **2** **3**

a R = H; X = Br

b R = H; X = S—C(=NH_2^+)—NH_2 Br^-

c R = H; X = SCH_3

d R = CH_3; X = Cl

e R = CH_3; X = S—C(=NH_2^+)—NH_2 Cl^-

f R = CH_3; X = S—P(=O)$(ONa)_2$

a R = H
b R = CH_3

SCHEME 1

The isothiouronium bromide **1***b* (prepared in the usual way from the bromo compound **1***a*), when treated with slightly less than 2 equiv of alkali at room temperature, followed by careful acidification to p*H* 3, gave the crystalline thione **2***a* in 52% overall yield. The structure of this compound was fully substantiated by its elemental analysis and spectral properties (see Table 1), and by conversion to a very stable potassium salt **3** and an oily *S*-methyl ether **1***c*.

The known 3-methyl analog **2***b* of **2***a* was prepared (for comparative purposes) from **1***d* via the isothiouronium salt **1***e* according to the published procedure (4). This thione could also be obtained by the acid-catalyzed decomposition of the salt **1***f* which was prepared from the chloro compound **1***d* and trisodium thiophosphate. This latter substance has often been used to prepare aliphatic thiols from the corresponding halo alkanes (see ref. 8 for example),[3] but to our knowledge it has not heretofore been utilized for the synthesis of heterocyclic thiones.

[1]For Part III, see ref. 1.

[2]To whom enquiries should be addressed at: Syntex, S.A., Division de Investigacion, Calle Carretera Mexico-Toluca No. 2822, Apartado Postal 10-820, Mexico 10, D.F.

[3]We thank Dr. T. Conway of these laboratories for suggesting the use of this reagent.

Can. J. Chem. Downloaded from www.nrcresearchpress.com by 210.87.254.42 on 09/05/12
For personal use only.

TABLE 1. Spectral properties of some 1,2,4-thiadiazole-5-thiones and related compounds

Compound	N.m.r. δ (p.p.m.)[a]	Solvent	I.r. (cm^{-1})[b]
3	8.28 (1H)	DMSO-d_6	1380, 1260, 1180, 1036, 862[c]
2*a*	8.82(1H), 11.98(1H, w_H = 44 Hz)	D_2O	3460, 2660, 1535, 1440, 1298, 1222, 1070, 900, 838, 790[d]
1*c*	2.80(3H), 8.58(1H)	$CDCl_3$	3075, 1463, 1434, 1345, 1321, 1275, 1174, 1063, 1048, 971, 911, 866, 755[e]
2*b*	2.27(3H), 12.85(1H, w_H = 58 Hz)	DMSO-d_6	3450, 3050, 2665, 1592, 1562, 1476, 1421, 1320, 1233, 1095, 1083, 980, 749[d]

[a]Measured with a Varian A-60A spectrometer; all resonances were of singlet multiplicity.
[b]Recorded with a Unicam SP-200G i.r. spectrophotometer.
[c]Nujol mull.
[d]Recorded in KBr.
[e]Liquid film.

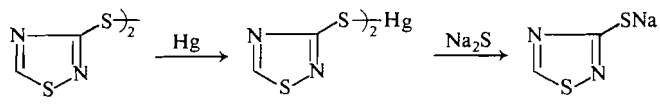

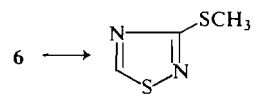

SCHEME 2

3-Mercapto-5-substituted-1,2,4,-thiadiazoles are prepared in several ways (ref. 2, pp. 567–573 and ref. 3, pp. 147–150) none of which is general. The parent member of this series was obtained from the known (9) disulfide **4** (Scheme 2) in a manner identical to that described by Soderback (10) for the preparation of the 5-chloro analog. Thus, cleavage of the above disulfide with mercury gave the stable mercuric salt **5** of 1,2,4-thiadiazole-3-thiol, which was transformed to the corresponding sodium salt **6** with sodium sulfide. The stability of the free thio compound was minimal since extraction of an acidified aqueous solution of the sodium salt did not result in the isolation of any alkali soluble material. Furthermore, it was not possible to isolate the sodium salt **6**, but its presence in solution was confirmed by transformation to the known (11) crystalline *S*-methyl ether **7**.

The solid state i.r. spectrum of 1,2,4-thiadiazole-5-thione (**2***a*) and its 3-methyl analog **2***b* were devoid of absorptions in the 2600–2500 cm^{-1} region,[4] showing that the thione tautomer predominated under these conditions. This contention is supported by the presence of a strong band, tentatively assigned to the C=S stretching

[4]A referee has suggested that the absorption at 2660 cm^{-1} for **2***a* cannot be ignored. In fact, it is exceedingly unlikely that this band is due to the mercapto form of **2***a*, since it is well-known that the SH stretching absorption of a wide variety of mercaptans occurs within the specified region (12). For example, for thiophene-2- and 3-thiols this absorption occurred at 2540–2510 cm^{-1} (13), while isoxazole-5-thiols absorbed at 2550 cm^{-1} (14), and 2-methyl-1,2,3-triazole-4-thiol had a strong band at 2540 cm^{-1} (15). The absence of an absorption in this region for compounds in which thione–thiol tautomerism is possible is now generally considered to be diagnostic of the thione form (16).

U.v. spectroscopy is also often utilized for the study of thione–thiol tautomerism. To be useful, however, the u.v. of an *N*-alkyl and an *S*-alkyl derivative must be compared to that of the thione (thiol), and even then a definite conclusion is often not possible (16).

Can. J. Chem. Downloaded from www.nrcresearchpress.com by 210.87.254.42 on 09/05/12
For personal use only.

Can. J. Chem. Downloaded from www.nrcresearchpress.com by 210.87.254.42 on 09/05/12
For personal use only.

vibration, at 1222 cm^{-1} in **2***a* and 1233 cm^{-1} in **2***b*.[5]

Experimental

The melting points were determined in a Gallenkamp m.p. apparatus and are not corrected.

*1,2,4-Thiadiazole-5-thione (**2***a*) *and potassium-1,2,4-thiadiazole-5-thiolate (**3**)*

A solution of 5-bromo-1,2,4-thiadiazole (9.10 g, 59.5 mmol (19)), in absolute ethanol (250 ml) containing thiourea (4.50 g, 59.1 mmol) was boiled under reflux in a nitrogen atmosphere for 2 h. The solution was evaporated to 50 ml *in vacuo*, 1 *N* sodium hydroxide (118 ml) was added, and the resultant was stirred at room temperature in an atmosphere of nitrogen for 20 min. The solution was extracted with ether (discarded) and the aqueous phase was made acidic to p*H* 3 (p*H* meter) with 4 *N* sulfuric acid. The product was extracted into ether, the extract was dried over sodium sulfate, and evaporated *in vacuo* ($T \leq 20°$) to give the crude crystalline thiol. This material could not be recrystallized; for analysis a small portion of this substance was sublimed at 65°/0.005 mm to give a solid m.p. 93°.

Anal. Calcd. for $C_2H_2N_2S_2$: C, 20.33; H, 1.71; N, 23.71. Found: C, 20.06; H, 1.62; N, 23.90.

The crude thiol from above was dissolved in absolute ethanol (25 ml), an equimolar amount of 1 *N* alcoholic potassium hydroxide was added, and the solution was diluted with dry ether (400 ml). The solid (4.27–5.11 g, 46–55% based on the bromo compound), m.p. 220° dec. was collected by filtration. Crystallization of this material from ethanol–ether (2:3) did not raise the melting point.

Anal. Calcd. for $C_2HN_2S_2K$: C, 15.37; H, 0.65; N, 17.93. Found: C, 15.53; H, 0.74; N, 17.92.

*5-Methylthio-1,2,4-thiadiazole (**1***c*)

A mixture of methyl iodide (3.42 g, 24 mmol) and water (45 ml) containing potassium-1,2,4-thiadiazole-5-thiolate (2.50 g, 16 mmol) was stirred at room temperature for 18 h. The product was extracted into dichloromethane, the extract was dried over sodium sulfate, and evaporated *in vacuo*. The residual oil was distilled at reduced pressure, and a fraction (1.62 g, 77%), b.p. 30–32°/0.1 mm was collected.

Anal. Calcd. for $C_3H_4N_2S_2$: C, 27.25; H, 3.05; N, 21.19. Found: C, 27.36; H, 3.05; N, 21.28.

*1,2,4-Thiadiazol-3-yl Disulfide (**4**)*

The 3-*t*-butylthio-1,2,4-thiadiazole which was required, was prepared by the method of Goerdeler and Budnowski (11) from *t*-butylisothiouronium chloride (20) and dichloromethanesulfenyl chloride (11). It contained an impurity which lacked an aromatic proton absorption in the n.m.r. spectrum. Although this material could be removed at this stage by column chromatography on silica gel, in general it was more conveniently separated at the disulfide stage. The disulfide, was prepared by the partial chlorination (9) of the above sulfide, but the quantity of chlorine was adjusted to the true sulfide content as determined from the n.m.r. spectrum. The crude product was purified by dry column chromatography (21) on silica gel (Brinkman, *ca.* Act. II, 20 g/g of substrate) using chloroform as the eluant. A portion (13 g) of the disulfide when purified in this way (100 ml fractions) gave a crystalline solid (8.4 g, from fractions 16–25), m.p. 116–119° (reported (9) m.p. 119°). The n.m.r. spectrum (1:1 DMSO-d_6 – $CDCl_3$) consisted of a singlet at δ 10.38.

*Mercuric-1,2,4-thiadiazole-3-thiolate (**5**)*

The cleavage of the disulfide was effected by the method of Soderback (10). A mixture of the disulfide (3.4 g, 14.5 mmol), mercury (10 ml), and dry ether (100 ml) was shaken mechanically for 18 h. The ether was decanted and the residual mixture was suspended in ether and decanted from the mercury. The product was collected by filtration, and dried *in vacuo*. It had m.p. 195° dec. (6.2 g, 98%) and could be recrystallized from a large amount of benzene, but the melting point was not improved.

Anal. Calcd. for $C_4H_2N_4S_4Hg$: C, 11.05; H, 0.46; N, 12.88. Found: C, 11.15; H, 0.53; N, 12.97.

*Generation of Sodium-1,2,4-thiadiazole-3-thiolate in situ and Preparation of 3-Methylthio-1,2,4-thiadiazole (**7**)*

The method described by Soderback (10) was used. The above mercuric salt (1.01 g, 2.32 mmol) was added at 0° to a stirred solution of sodium sulfide nonahydrate (504 mg, 2.1 mmol) in water (50 ml). The mixture was stirred in a nitrogen atmosphere at 0° for ½ h, methyl iodide (640 mg, 4.5 mmol) was added, and stirring at room temperature was then maintained for 18 h. Ether was added to the mixture, and after thorough agitation the mixture was filtered through Celite. The ether phase was separated, dried over sodium sulfate, and evaporated *in vacuo*. The residual oil was distilled to give a fraction b.p. 38–40°/0.05 mm (500 mg, 90%). On crystallization from petroleum ether (b.p. 30–60°) at −70°, a solid, m.p. 32° (reported (11), m.p. 32.5°), with physical properties different from 5-methylthio-1,2,4-thiadiazole, was obtained. The n.m.r. spectrum (CCl_4) showed two singlets at δ 2.73 (3H) and 9.88 (1H).

*3-Methyl-1,2,4-thiadiazole-5-thione **2**b*

A mixture of the chloro thiadiazole (**1***d*; 1.34 g, 10 mmol) and an aqueous solution of trisodium thiophosphate (3.40 g, 20 mmol) was stirred at room temperature until solution of the chloro compound had occurred (66 h). The solution was extracted with benzene, and the aqueous phase was made acidic with concentrated hydrochloric acid at 0°. The solid which precipitated (1.27 g, 96%) had m.p. 147–149° (reported (4), m.p. 151°) and was spectroscopically (i.r., n.m.r.) indistinguishable from the thiol prepared by the isothiouronium salt method (4).

[5]The position of this absorption varies considerably (17, 18) and its diagnostic value is thus limited.

1. D. E. Horning and J. M. Muchowski. Can. J. Chem. Preceding paper.
2. W. R. Sherman. Heterocyclic compounds. Vol. 7. *Edited by* R. C. Elderfield. John Wiley and Sons Inc., New York. 1961. pp. 558–578.
3. F. Kurzer. Advances in heterocyclic chemistry. Vol. 5. *Edited by* A. R. Katritzky, A. J. Boulton, and J. M. Lagowski. Academic Press, New York. 1965. pp. 119–204.
4. J. Goerdeler, H. Groschopp, and U. Sommerlad. Ber. **90**, 182 (1957).

5. J. GOERDELER and G. SPERLING. Ber. **90**, 892 (1957).
6. H. SCHROEDER, R. RATZ, W. SCHNABEL, H. ULRICH, E. KOBER, and C. GRUNDEMANN. J. Org. Chem. **27**, 2589 (1962).
7. U. WORFFEL and R. BEHNISCH. Arch. Pharm. **295**, 811 (1962).
8. T. T. CONWAY, A. SHOEB, and L. BAUER. J. Pharm. Sci. **57**, 455 (1968).
9. J. GOERDELER and I. E. TOM. Ber. **98**, 1544 (1965).
10. E. SODERBACK. Ann. **465**, 184 (1928).
11. J. GOERDELER and M. BUDNOWSKI. Ber. **94**, 1682 (1961).
12. L. J. BELLAMY. The infra-red spectra of complex molecules. 2nd ed. Methuen and Co. Ltd. London. 1958. pp. 350–352.
13. S. GRONOWITZ, P. MOSES, and A-B. HORNFELDT. Arkiv. Kemi. **17**, 237 (1961).
14. G. ADEMBRI and R. NESI. J. Heterocycl. Chem. **4**, 54 (1967).
15. J. P. DARIS and J. M. MUCHOWSKI. Unpublished observation.
16. A. R. KATRITZKY and J. M. LAGOWSKI. Advances in heterocyclic chemistry. Vol. 2. *Edited by* A. R Katritzky, A. J. Boulton, and J. M. Lagowski. Academic Press, New York. 1963. pp. 60–66.
17. C. AINSWORTH. J. Am. Chem. Soc. **78**, 4475 (1956).
18. A. J. BLACKMAN and J. B. POLYA. J. Chem. Soc. (C), 1016 (1971).
19. J. GOERDELER, J. OHM, and O. TEGTMEYER. Ber. **89**, 1534 (1956).
20. J. M. SPRAGUE and T. B. JOHNSON. J. Am. Chem. Soc. **59**, 1837 (1937).
21. B. LOEV and M. M. GOODMAN. Chem. and Ind. 2026 (1967).

Can. J. Chem. Downloaded from www.nrcresearchpress.com by 210.87.254.42 on 09/05/12
For personal use only.

Tricyclic Hydrocarbons. II. Carbon-13 Nuclear Magnetic Resonance Spectroscopy as a Method for Unambiguous Structure Determination

GERALD WALLACE BUCHANAN[1] AND ROBERT HARLAN WIGHTMAN

Department of Chemistry, Carleton University, Ottawa, Canada K1S 5B6

Received February 14, 1973

Carbon-13 n.m.r. spectroscopy is demonstrated to be unique as an unambiguous and general method for determining structure in a series of isomeric tricyclic benzenoid hydrocarbons. Observed carbon shieldings for the tricyclic materials are discussed and compared with those for related bicyclic and monocyclic compounds.

On a démontré que la spectroscopie r.m.n. du carbone-13 représente la seule méthode générale et précise pour attribuer les structures d'une série d'hydrocarbures benzènoides tricycliques isomériques. Les blindages des carbones observés pour les produits tricycliques sont discutés et comparés avec ceux reliés aux composés bicycliques et monobicycliques et monocycliques.

[Traduit par le journal]

Can. J. Chem., 51, 2357 (1973)

Can. J. Chem. Downloaded from www.nrcresearchpress.com by 210.87.254.6 on 09/05/12
For personal use only.

Introduction

The lack of facile and unambiguous structure proofs for tetra-substituted benzenoid hydrocarbons has hindered a variety of investigations. Early workers relied on oxidative degradation reactions, which were both time and material consuming, to produce tetracarboxylic acids of a given substitution pattern (1). For some time disagreement regarding structural assignments for these compounds existed (2).

Specifically, the problem involves identification of the linear (*i.e.* 1,2,4,5-substituted) *vs.* the angular (1,2,3,4-substituted) molecules. The six isomeric pairs denoted below will be discussed

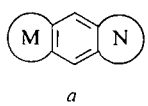

a

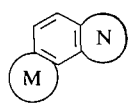

b

1 M = N = 5 **4** M = N = 8 **7** M = 0; N = 5
2 M = N = 6 **5** M = 5; N = 6 **8** M = 0; N = 6
3 M = N = 7 **6** M = 5; N = 7 **9** M = 0; N = 7
10 M = 0; N = 8

in relation to the corresponding bicyclic materials **7, 8, 9,** and **10** (M and N refer to the size of the saturated carbocyclic ring).

The necessity for a generally applicable method of isomer differentiation in these compounds is clear from the recent work of Markl and Fuchs (3) in which structures for **4***a* and *b* have been erroneously assigned. Historically a combination of i.r., u.v., and ^{1}H n.m.r. spectra combined with identification of all precursors in the synthetic sequence have been used in an attempt to solve this problem. In principle the linear and angular isomers should be distinguishable on the basis of the i.r. bands ascribed to the out-of-plane C—H deformation vibrations of the aromatic protons (4). The presence of border-line and combination bands, however, complicates the application of this procedure. In the u.v. spectra the linear arrangement in **1** and **2** produces small bathochromic shifts relative to the angular, but this trend does not persist for the 7–7 and 8–8 isomers **3** and **4** (5). Early investigators in this area assumed that a given isomeric structure followed directly from the synthetic sequence (6). Although identification of precursors is possible (7), it has been demonstrated recently (8, 9) that some of the previously accepted synthetic routes give anomalous products. Furthermore, the mass spectral fragmentation patterns of each pair of isomers are essentially identical (10).

Due to the symmetry of the molecules, the ^{1}H n.m.r. spectra for the aromatic protons do not provide a useful method of isomer identification and the highly coupled methylene regions are difficult to analyze. It is known that carbon-13 n.m.r. (c.m.r.) chemical shifts are an order of magnitude more sensitive to structural change than ^{1}H shieldings (11) and in addition, proton decoupled c.m.r. spectra can be readily analyzed. We herein report the

[1]Author to whom correspondence should be addressed.

TABLE 1. C.m.r. shifts of methylene carbons (δ_C p.p.m. downfield from TMS) ± 0.1*

Compound	Ring size	α	β	γ	α′	β′	γ′
1*a*	M = N = 5	32.4	25.1				
1*b*	M = N = 5	32.7	25.7		31.3		
2*a*	M = N = 6	29.8	22.9				
2*b*	M = N = 6	29.8	22.9		25.3	22.3	
3*a*	M = N = 7	36.4	28.7	32.9			
3*b*	M = N = 7	36.4	28.5	31.9	30.8	27.7	
4*a*	M = N = 8	32.7	32.1	26.3			
4*b*	M = N = 8	33.4	32.7	(26.9)	28.2	31.1	(26.1)
5*a*	M = 5	32.5	25.9				
	N = 6	29.6	23.4				
5*b*	M = 5	32.7	24.9		30.9		
	N = 6	29.4	23.2		26.8	23.2	
6*a*	M = 5	32.7	25.5				
	N = 7	36.3	28.6	32.5			
6*b*	M = 5	33.0	24.9		31.4		
	N = 7	36.1	28.5	31.5	32.7	27.5	
7	N = 5	32.6	25.5				
8	N = 6	29.5	23.3				
9	N = 7	36.8	28.4	32.9			
10	N = 8	32.5	32.5	26.3			

*0.5 *M* solutions in $CDCl_3$.

TABLE 2. C.m.r. shieldings of aromatic carbons (δ_C p.p.m. from TMS) ± 0.1*

Compound	C-1	C-2	C-3	C-4	C-5	C-6
1*a*	141.0	141.0	119.1	141.0	141.0	119.1
1*b*	(141.6)	(139.4)	(139.4)	(141.6)	121.8	121.8
2*a*	133.6	133.6	128.9	133.6	133.6	128.9
2*b*	(133.8)	(133.0)	(133.0)	(133.8)	125.3	125.3
3*a*	140.2	140.2	129.9	140.2	140.2	129.9
3*b*	(140.4)	(139.0)	(139.0)	(140.4)	126.1	126.1
4*a*	138.6	138.6	129.5	138.6	138.6	129.5
4*b*	(139.4)	(137.4)	(137.4)	(139.4)	126.9	126.9
5*a*	134.3	134.3	124.4	141.0	141.0	124.4
5*b*	(134.5)	(132.9)	(140.9)	(142.7)	121.2	127.1
6*a*	(139.8)	(139.8)	123.7	(140.2)	(140.2)	123.7
6*b*	(142.1)	(139.0)	(141.3)	(141.5)	127.1	121.3
7	143.4	143.4	(124.0)	(125.5)	(125.5)	(124.0)
8	136.4	136.4	124.9	128.5	128.5	124.9
9	142.6	142.6	125.5	128.5	128.5	125.5
10	140.8	140.8	125.9	128.7	128.7	125.9

*0.5 *M* solutions in $CDCl_3$.

successful application of c.m.r. to structure determination in tricyclic hydrocarbons and include a discussion of shielding trends for related systems.

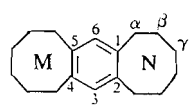

4*a*

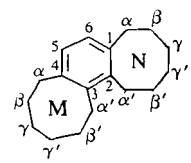

4*b*

Results and Discussion

An example of the numbering scheme used for the linear and angular isomers is presented below for compounds **4***a* and *b*. To facilitate discussion, the methylene carbon shieldings are collected in Table 1 and those for aromatic carbons are in Table 2.

(*a*) *Methylene carbons*

In **1***a*, **2***a*, **3***a*, **4***a*, **7**, **8**, **9**, and **10**, the α-carbon resonances were assigned from specific ^1H decoupling experiments since it is well known that benzylic protons resonate at lower field

Can. J. Chem. Downloaded from www.nrcresearchpress.com by 210.87.254.6 on 09/05/12
For personal use only.

Can. J. Chem. Downloaded from www.nrcresearchpress.com by 210.87.254.6 on 09/05/12
For personal use only.

than those further removed from the aromatic ring. These assignments for **1***a*, **3***a*, **7**, and **9** were supported by the observed integrated intensity ratios. Differences in nuclear Overhauser enhancements for methylene carbons of this type will be minimal. With the exception of **2***a*, **2***b*, **7**, and **8**, no carbon shifts have been reported for the present compounds. Observed methylene shieldings for these four molecules are in reasonable agreement with earlier findings (12, 13).

Examination of the data in Table 1 indicates that methylene carbons in **1***a*, **2***a*, **3***a*, and **4***a* have nearly identical chemical shifts to their bicyclic counterparts **7**, **8**, **9**, and **10** respectively. Apparently no measurable effects are transmitted between the remote alicyclic rings in the linear series. Extension of these observations to the 5–6 linear (**5***a*) and 5–7 linear (**6***a*) tricyclic molecules permits unambiguous assignment of resonances.

The low field shift (32.9 p.p.m.) observed for the γ-carbon in the seven-membered rings of **3***a* and **9** compared with the γ-carbon shift of *ca.* 28.5 p.p.m. in **4***a* and **10** merits comment. From the early work of Grant and Paul (14) the effects of alkyl substitution on the c.m.r. shieldings of saturated alicyclic hydrocarbons were established. Replacement of an α-hydrogen by carbon causes a deshielding of *ca.* 9 p.p.m., and replacement of a β-hydrogen by carbon causes a further deshielding of comparable magnitude. The γ-carbon of **3***a* and **9** has two α-CH_2's and two β-CH_2's whereas *each* γ-carbon of **4***a* and **10** has only one α-CH_2 and two β-CH_2 groupings. Accordingly a considerable downfield shift of the γ-carbon in **3***a* and **9** relative to **4***a* and **10** would be expected.

A similar approach can be used to explain the relatively high field β-carbon shift in **3***a* and **9** (28.4 p.p.m.) compared to that of 32.5 p.p.m. for the β-carbon of **4***a* and **10**. Each β-carbon in **3***a* and **9** possesses two α-CH_2's and *no* β-CH_2 substituents, whereas in **4***a* and **10** each β-carbon has two α-CH_2's and one β-CH_2 group.

Assignments for the angular isomers **1***b*, **2***b*, **3***b*, and **4***b* are based on the assumption that the α-, β-, and γ-carbon resonances will be similar to those in the linear series since remote alicyclic interactions for these carbons have been shown to be minimal. Inter-ring interactions are expected however for the α′-, β′-, and γ′-carbons due to steric factors. No doubt

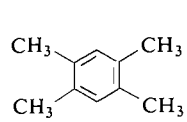

11

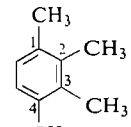

12

the most pronounced effects will occur at the α′-position.

In this context it is important to recall the results of Woolfenden and Grant (15) for durene **11** and prehnitene **12**. The methyls of durene resonate at δ 19.1 whereas those for prehnitene appear at 20.4 and 15.3 p.p.m., respectively. The 2,3-methyl groups of **12** are shielded by *ca.* 5 p.p.m., relative to the 1,4-substituents, a result explained by Grant and Cheney (16) on the basis of sterically induced charge polarization in the C—H bonds. The upfield shifts in the α′-carbon resonances of **2***b*, **3***b*, and **4***b* relative to the α-positions are reminiscent of the methyl shift differences in **12** (*ca.* 5 p.p.m.) and can be reasonably interpreted on similar steric grounds.

It is interesting to note that the α′-carbon of **1***b* is shifted upfield by only 1.4 p.p.m. relative to its α counterpart. Examination of molecular models shows that due to the smaller internal angles in the five-membered rings, the angle θ will increase in **1***b* relative to the

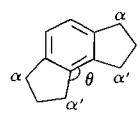

1*b*

corresponding angle in **2***b*, **3***b*, and **4***b*. As a consequence the α′-carbons will be pulled farther apart and the non-bonded repulsions between the methylene protons attenuated, causing the α′-carbons to be correspondingly less shielded.

Employing **1***b* and **2***b* as models, methylene resonances for the 5–6 angular isomer **5***b* can now be assigned with confidence. Here the upfield shift in the α′-resonance (relative to α) of the six-membered ring is less (2.6 *vs.* 4.5 p.p.m.) than in **2***b*, due to the angle distorting effect of the five-membered ring. Conversely the upfield α′-shift in the five-membered ring is greater (1.8 *vs.* 1.4 p.p.m.) than in **1***b*, as expected from substitution of a six-membered ring in the angular position. Additional support for the α- and α′-values for all angular isomers

Can. J. Chem. Downloaded from www.nrcresearchpress.com by 210.87.254.6 on 09/05/12
For personal use only.

was gained from specific proton decoupling experiments on the benzylic hydrogens.

Analogously **1***b* and **3***b* serve as models for the 5–7 angular isomer **6***b*. Again, fusion of the five-membered ring relieves some of the Van der Waals repulsion at the α′-hydrogens of the seven-membered ring, resulting in a smaller upfield shift for this α′-carbon relative to α (3.4 p.p.m.) than is observed in **3***b* (5.6 p.p.m.).

(*b*) *Aromatic Carbons*

Assignments for the linear isomers **1***a*, **2***a*, **3***a*, and **4***a* are straightforward since absorptions for carbons bearing no directly bonded protons retain their singlet structure in the off-resonance decoupling experiment. From the shieldings in **1***a* and **2***a*, assignments in the 5–6 linear isomer **5***a* follow directly. Quaternary carbons in **6***a* have nearly identical shieldings as expected, in view of results for **1***a* and **3***a*.

For **9** and **10**, shifts for C-3,6 *vs.* C-4,5 were assigned by analogy with **8** (12). It is interesting to note the similarity in the C-4,5 shieldings with that of benzene (128.7 p.p.m.). In the case of **7**, the bracketed values in Table 2 indicate a possibility of reversed assignments. Nevertheless it is clear from data for **1***a* and **7** that fusion of a five-membered ring induces appreciable upfield shifts in resonances of C-3 and -6 relative to larger ring materials.

Resonances for C-5 and -6 of the angular isomers **1***b*, **2***b*, **3***b* and **4***b* can be clearly assigned from the off-resonance decoupling experiment due to the inherent symmetry of these molecules. It is not possible, however, to unambiguously assign the quaternary carbons C-1,4 *vs.* C-2,3 in these angular isomers. In any event only small differences (1–2 p.p.m.) separate the resonances.

Using **1***b* and **2***b* as models, assignments for **5***b* follow directly, with the possible interchange of C-1 with -2 and C-3 with -4 resonances. Similarly, employing **1***b* and **3***b*, data for **6***b* can be rationalized.

Conclusions

It is abundantly clear that ^{13}C n.m.r. constitutes a superior method for structure determination in tricyclic hydrocarbons. Nearly all methylene carbon resonances can be unambiguously assigned and isomeric trends explained on steric grounds. Difficulties in assignment of quaternary aromatic carbon resonances on the basis of chemical shifts are obvious and no doubt T_1 measurements will be invaluable in this area in the future.

Experimental

Materials

The tricyclic hydrocarbons were synthesized as previously described (8): Compounds **7, 8, 11,** and **12,** were commercially available samples and were used without further purification. Benzsuberane (**9**) is readily available from 1-benzsuberone which can be obtained commercially (17). Benzocyclooctene (**10**) was prepared according to the procedure of Wittig *et al.* (18).

Spectra

The c.m.r. spectra were obtained at 25.2 MHz using a Varian XL-100-12 NMR spectrometer, most commonly under conditions of complete proton noise decoupling. Spectral accumulations were accomplished with a Varian C-1024 time-averaging computer. Samples were contained in 8 mm tubes and were examined as 0.5 *M* solutions in $CDCl_3$ containing 2% TMS as an internal standard. Off-resonance decoupling experiments were carried out with the proton frequency offset approximately 500 Hz from the center of the proton spectral region.

We thank Mr. A. E. Gustafson for preparation of a sample of benzocyclooctene. Generous financial support from the National Research Council of Canada is gratefully acknowledged.

1. (*a*) R. T. Arnold and R. A. Barnes. J. Am. Chem. Soc. **66**, 960 (1944). (*b*) W. P. Campbell, M. D. Soffer, and T. R. Steadman. J. Am. Chem. Soc. **64**, 425 (1942).
2. L. I. Smith and G. D. Byrkit. J. Am. Chem. Soc. **56**, 1185 (1934).
3. G. Markl and R. Fuchs. Tetrahedron Lett. 4695 (1972).
4. (*a*) L. J. Bellamy. The Infra-red spectra of complex molecules. 1st ed. John Wiley and Sons, Inc., New York, N.Y., 1958. Chapt. 5. (*b*) K. Nakanishi. Infra-red absorption spectroscopy. 1st ed. Nankodo Company Ltd., Tokyo, 1962. pp. 26–27.
5. W. J. Rosenfelder and D. Ginsburg. J. Chem. Soc. 1301 (1957).
6. (*a*) A. D. Campbell and S. N. Slater. J. Chem. Soc. 4353 (1952). (*b*) S. C. Sen Gupta. J. Ind. Chem. Soc. **16**, 89 (1939). (*c*) V. R. Skvarchenko, R. Y. Levina, and O. Y. Okhlobystin. Doklady Akad. Nauk. S.S.S.R. **99**, 789 (1954); Chem. Abstr. **49**, 5414*e* (1955).
7. J. A. Elix, M. V. Sargent, and F. Sondheimer. J. Am. Chem. Soc. **92**, 962 (1970).
8. (*a*) R. H. Wightman, R. J. Wain and D. H. Lake. Can. J. Chem. **49**, 1360 (1971). (*b*) R. T. Arnold and P. N. Craig. J. Am. Chem. Soc. **70**, 2791 (1948).
9. S. A. Patwardhan. Ind. J. Chem. **7**, 105 (1969).
10. C. P. Bahl, D. H. Lake, R. J. Wain, and R. H. Wightman. In preparation.
11. J. B. Stothers. Carbon-13 NMR spectroscopy. Academic Press, New York, N.Y. 1972.

12. L. F. JOHNSON and W. C. JANKOWSKI. Carbon-13 NMR Spectra. John Wiley and Sons, New York, N.Y., 1972.
13. H. L. RETCOFSKY and R. A. FRIEDEL. *In* Spectrometry of fuels. R. A. Friedel, editor. Plenum Press, New York, 1970. p. 90.
14. D. M. GRANT and E. G. PAUL. J. Am. Chem. Soc. **86**, 2984 (1964).
15. W. R. WOOLFENDEN and D. M. GRANT. J. Am. Chem. Soc. **88**, 1496 (1966).
16. D. M. GRANT and B. V. CHENEY. J. Am. Chem. Soc. **89**, 5315 (1967).
17. PL. A. PLATTNER. Helv. Chim. Acta, **27**, 801 (1944).
18. G. WITTIG, H. EGGERS and P. DUFFNER. Justus Liebigs Ann. **619**, 10 (1958).

Can. J. Chem. Downloaded from www.nrcresearchpress.com by 210.87.254.6 on 09/05/12
For personal use only.

Activity Determination of Cobalt in Cobalt–Gold Alloys

S. S. WANG and J. M. TOGURI

Department of Metallurgy and Materials Science, University of Toronto, Toronto, Ontario M5S 1A4

Received January 15, 1973

Activities of cobalt in cobalt–gold liquid alloys from 1250 to 1335 °C were determined by equilibrating the alloy with pure solid CoO under a CO/CO_2 gas mixture of known oxygen partial pressure. The cobalt activities were calculated from the cobalt content of the alloys after equilibration. The activities of gold were calculated by Gibbs–Duhem integration. In the present study, both activities showed positive deviations from ideality. In the terminal region, the cobalt–gold system was found to behave as a regular solution. The temperature effect on the activities was found to be negligible.

Les activités du cobalt dans des alliages liquides cobalt–Au pour des températures allant de 1250 à 1335 °C ont été déterminées par équilibration de l'alliage avec du CoO pur solide sous une atmosphère gazeuse CO/CO_2 possèdant une pression partielle connue d'oxygène. Les activités inhérentes au cobalt ont été évaluées à partir du contenu en cobalt des alliages après équilibration. Les activités de l'or ont été calculées en utilisant une intégration du type Gibbs–Duhem. Dans la présente étude, les deux activités ont montré des déviations positives comparativement au cas idéal. Dans la région terminale, le système Au–cobalt possède un comportement que l'on peut assimiler à celui d'une solution régulière. L'effet de la température sur les activités est négligeable. [Traduit par le journal]

Can. J. Chem., **51**, 2362 (1973)

Can. J. Chem. Downloaded from www.nrcresearchpress.com by 210.87.254.5 on 09/05/12
For personal use only.

Introduction

Data on the thermochemical properties of liquid cobalt–gold alloys are not available. Since these data were required in a study of the cobalt losses to slags, the present study was undertaken. Over the temperature range of interest, the phase diagram of the cobalt–gold system indicates that the composition range of the liquid alloy is limited to a cobalt concentration of approximately 75 at. % (1). Consequently, the activity determinations have been limited to this range.

The method adopted to determine the activities of cobalt in liquid cobalt–gold alloys was to equilibrate the alloys with pure solid CoO and a CO/CO_2 gas mixture of known oxygen partial pressure. The standard state of the cobalt chosen was that of pure supercooled liquid cobalt. The equilibrium involved is

$$[1] \qquad 2CoO_{(s)} = 2Co_{(l)} + O_{2(g)}$$

The equilibrium constant for this reaction is

$$[2] \qquad K_1 = \frac{a_{Co}{}^2 P_{O_2}}{a_{CoO}{}^2}$$

where a's are the respective activities and P_{O_2}, the partial pressure of oxygen.

Although CoO displays deviations from stoichiometry, this deviation is very small particularly in the temperature and oxygen pressure range of this study, as indicated by Smith and Masson (2). Since gold does not enter into solution with the oxide phase, the activity of CoO is assumed to be unity. The cobalt activity can then be expressed as

$$[3] \qquad a_{Co} = \left(\frac{K_1}{P_{O_2}}\right)^{1/2}$$

For the case of pure cobalt, $a_{Co} = 1$ and

$$[4] \qquad P_{O_2}{}^{\text{pure Co}} = K_1$$

Consequently,

$$[5] \qquad a_{Co} = \left(\frac{P_{O_2}{}^{\text{pure Co}}}{P_{O_2}}\right)^{1/2}$$

where P_{O_2} and $P_{O_2}{}^{\text{pure Co}}$ are the oxygen partial pressures at which CoO is in equilibrium with a Co–Au alloy and pure Co respectively. The value of $P_{O_2}{}^{\text{pure Co}}$ can be calculated from a knowledge of the standard free energy change ($\Delta G_1{}^0$) for reaction 1. Using the thermodynamic values recommended by Kubaschewski, Evans, and Alcock (3), the $\Delta G_1{}^0$ can be expressed as

$$[6] \quad \Delta G_1{}^0 = 119\,423 - 0.1T \ln T - 37.26T$$

Experimental

The experimental apparatus used for this study has been described in detail previously (4). It consisted of an alumina reaction tube heated by a temperature controlled molybdenum furnace. The reaction tube contained an alumina tray cemented to an alumina thermocouple protection tube. This assembly, including alumina baffles,

TABLE 1. Experimental results for cobalt–gold alloys

Temperature (°C)	X_{Co}	X_{Au}	Flow rate of CO_2 (cc/min)	Flow rate of CO (cc/min)	P_{O_2} (atm)	a_{Co}	γ_{Co}
1249	0.055	0.945	497	8.9	1.48×10^{-7}	0.101	1.840
1249	0.111	0.889	477	17.1	3.70×10^{-8}	0.202	1.814
1254	0.196	0.804	471	25.3	1.91×10^{-8}	0.299	1.526
1246	0.275	0.725	477	34.2	8.47×10^{-9}	0.405	1.471
1248	0.417	0.583	507	45.0	5.86×10^{-9}	0.500	1.199
1248	0.574	0.426	492	52.8	4.01×10^{-9}	0.604	1.053
1246	0.622	0.378	453	52.8	3.20×10^{-9}	0.659	1.058
1333	0.091	0.909	491	9.9	1.21×10^{-6}	0.099	1.092
1333	0.114	0.886	505	20.4	3.01×10^{-7}	0.199	1.740
1342	0.179	0.821	471	28.5	1.70×10^{-7}	0.294	1.644
1337	0.295	0.705	453	36.6	8.36×10^{-8}	0.395	1.340
1340	0.449	0.551	444	44.7	5.83×10^{-8}	0.490	1.090
1340	0.526	0.474	435	52.8	4.01×10^{-8}	0.591	1.123
1337	0.665	0.335	440	62.1	2.74×10^{-8}	0.690	1.038

rested on an alumina gutter to avoid cracking the main reaction tube during the quenching operation. The temperature variation was ±3 °C over a 2 in. zone.

The required oxygen pressure in the furnace was obtained by using C. P. Matheson grade CO and CO_2. These gases were passed through a Drierite column to remove moisture. The CO_2 was also passed through a copper getter furnace (≃500 °C) to remove residual traces of oxygen. The gas flows were controlled by use of calibrated flow meters. The total flow rate of the CO and CO_2 was 500 ml min^{-1}.

For the oxygen potentials required in this study, the P_{CO_2}/P_{CO} ratio was in the range where the carbon deposition reaction is thermodynamically unfavorable (5).

The purity of the cobalt used in this study was 99.99% while the purity of gold was 99.95%. The alloys were prepared by induction heating under a hydrogen atmosphere.

The experimental procedure was as follows. Approximately 1 g of the prepared alloy was set inside a zirconia crucible and covered with approximately 1 g of solid oxide powder. The crucible was placed into one of the holes of the alumina tray. The system was closed and flushed with argon gas. The tray was slowly pushed into the reaction tube until the hot zone was reached. The gas was then switched to a CO_2/CO gas mixture and the system was left to equilibrate for at least 48 h. After the required time elapsed, the CO_2/CO gas mixture was switched again to purified argon and the samples were quenched by pulling the tray assembly out into the cold regions of the furnace.

Preliminary experiments were carried out to determine the time required for equilibrium. Three alloy samples of the same initial composition were used under the same conditions except over three different equilibrating times; 12 h, 24 h, and 48 h. It was found that 24 h was sufficient. However, to insure the attainment of equilibrium 48 h was adopted as the equilibrating time.

Cobalt was analyzed by an atomic absorption technique as well as spectrophotometrically. Gold was determined by a gravimetric technique using a 5% aqueous hydroquinone solution.

The stoichiometry of the cobalt oxide, after the cobalt activity measurements, was examined by X-ray techniques using the Debye–Scherrer camera. The diffraction patterns showed that the form of the cobalt oxide corresponded to CoO.

Visual examination as well as X-ray diffraction analysis indicated that there was no interaction between CoO and the zirconia crucible.

Results and Discussion

The experimental results for the cobalt activities are presented in Table 1. The accuracy of the activity measurements are estimated to be ±5%. The activities of gold were calculated by use of the Gibbs–Duhem integration. Figure 1 shows the obtained activity–composition curves.

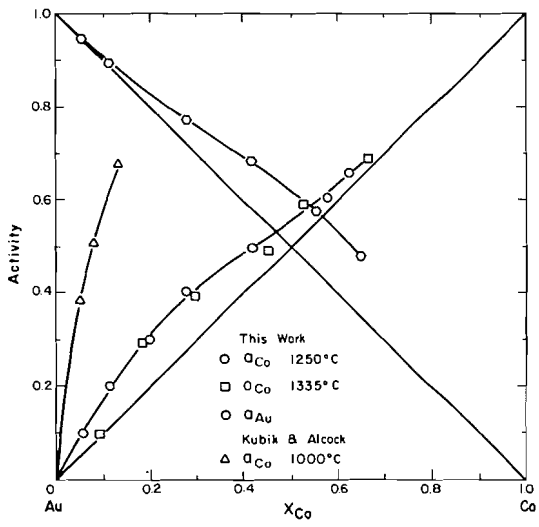

FIG. 1. Relationship between activity and atomic fraction of cobalt.

Can. J. Chem. Downloaded from www.nrcresearchpress.com by 210.87.254.5 on 09/05/12
For personal use only.

Can. J. Chem. Downloaded from www.nrcresearchpress.com by 210.87.254.5 on 09/05/12
For personal use only.

Both cobalt and gold activities exhibit positive deviations from ideality.

From Fig. 1, the effect of an 85 °C temperature change on the cobalt activity appears to be negligible.

Kubik and Alcock (6) determined the activities of cobalt in solid cobalt–gold alloys between 750 and 1000 °C by an EMF method using ThO_2–$YO_{1.5}$ as the solid electrolyte. The determined activities showed large positive deviation from ideality. Their data at 1000 °C is shown for comparison in Fig. 1.

In Fig. 2 $\ln \gamma_{Co}$ values obtained in the present study are plotted against X_{Au}^2 while in Fig. 3 the corresponding $\ln \gamma_{Au}$ values are plotted against X_{Co}^2. The experimental points for $X_{Co} < 0.5$ can be fitted onto a straight line. In the case of $\ln \gamma_{Au}$, the straight line passes through the origin. However, in the case of $\ln \gamma_{Co}$, the straight line does not pass through the origin. The equations for both lines were found by a least square fitting technique as

$$[7] \qquad \ln \gamma_{Au} = -0.0006 + 0.863 X_{Co}^2$$

and

$$[8] \qquad \ln \gamma_{Co} = -0.107 + 0.848 X_{Au}^2$$

Darken (7) has suggested that for most liquid binary metallic systems there appears to exist two terminal compositional regions and a central region. In the two terminal regions, the thermodynamic behavior of the solution is relatively simple, while in the central region the thermodynamics of the solution appear to be much more complicated. In the two terminal regions, if the activity coefficient of the solvent can be represented as

$$[9] \qquad \ln \gamma_{solvent} = \alpha X_{solute}^2$$

from the Gibbs–Duhem equation,

$$[10] \qquad X_{solvent}\, d \ln \gamma_{solvent} + X_{solute}\, d \ln \gamma_{solute} = 0$$

the activity coefficient of the solute can be calculated as

$$[11] \qquad \ln \gamma_{solute} = \alpha X_{solvent}^2 + I$$

where I is the integration constant. If eqs. 9 and 11 are to hold over the entire composition, then I must be zero. However, these relations generally do not apply beyond the terminal region. Thus, in the terminal region there is no requirement that I must be zero.

The present experimental results, as shown in eqs. 7 and 8, follow the forms eqs. 9 and 11. The corresponding α value from eq. 7 is 0.863 while that from eq. 8 is 0.848.

For regular solutions, it is well known that the partial molar heat of mixing of component i can be expressed as,

$$[12] \qquad \Delta \bar{H}_i = RT \ln \gamma_i$$

and the integral heat of mixing of a binary alloy as,

$$[13] \qquad \Delta H^M = X_1\, RT \ln \gamma_1 + X_2\, RT \ln \gamma_2$$

The $\Delta \bar{H}_{Co}$, $\Delta \bar{H}_{Au}$, and ΔH^M at 1250 °C were calculated by use of eqs. 12 and 13, and are

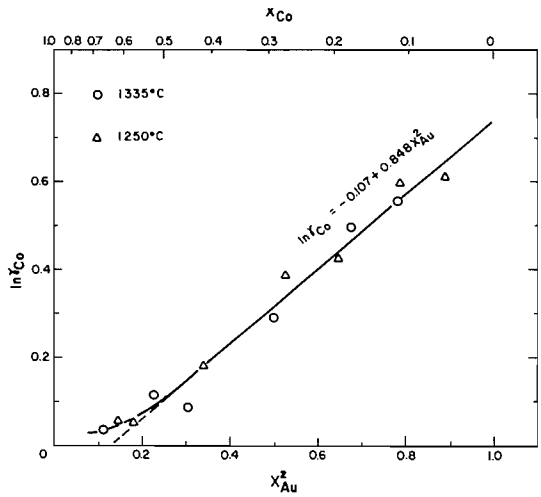

FIG. 2. Relationship between $\ln \gamma_{Co}$ and X_{Au}^2.

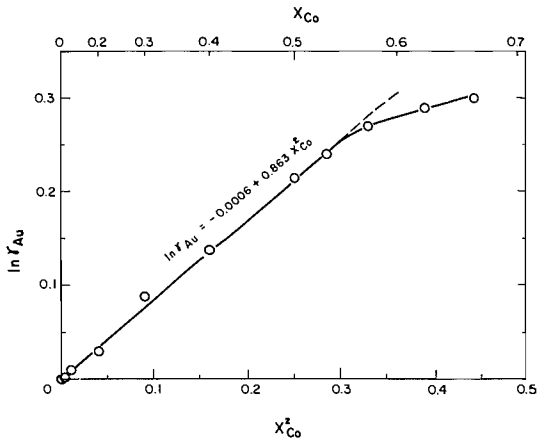

FIG. 3. Relationship between $\ln \gamma_{Au}$ and X_{Co}^2.

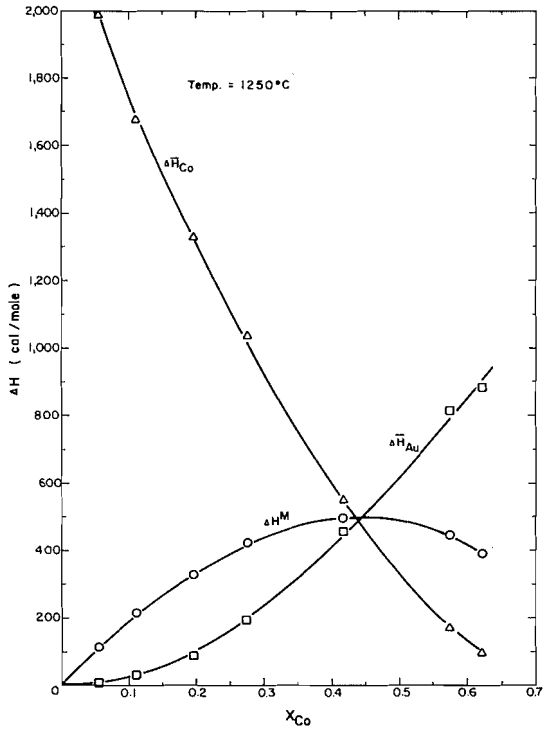

FIG. 4. Calculated enthalpy *vs.* composition at 1250 °C.

plotted in Fig. 4. The maximum integral heat of mixing is 500 cal/mol. Since the heat values for this system are very small, the effect of temperature change on the activity is expected to be negligible. This can be predicted from the van't Hoff expression

$$\left(\frac{\partial \ln a_i}{\partial T}\right)_P = -\frac{\Delta \bar{H}_i}{RT^2}$$

Figure 1, which illustrates the activity–composition relation, shows the insensitive effect of temperature on the activity measurements.

The effect of dissolved oxygen in the cobalt–gold alloys on the activities of cobalt and gold was assumed to be negligible. This was based on the investigation of Averin, Polyakov, and Samarin (8) who determined the solubility of oxygen in liquid cobalt as 0.19, 0.24, and 0.28 wt. % at 1550, 1600, and 1650 °C respectively. These values were confirmed recently by Tankins *et al.* (9) who obtained 0.20 wt. % at 1550 °C.

Conclusions

The activities of cobalt in the cobalt–gold liquid alloys over the temperature range of 1250–1350 °C have been determined. The activities of gold have been calculated by the Gibbs–Duhem integration. Both activities show positive deviation from ideality. The temperature effect on the activities is negligible. The binary alloys behave as a regular solution in the terminal region.

The authors thank the National Research Council of Canada for financial support. The cobalt analysis of the alloys were carried out by Falconbridge Research Laboratories for which the authors are grateful.

1. M. HANSEN. Constitution of binary alloys. McGraw-Hill, York Pa. 1958. p. 195.
2. I. B. SMITH and C. R. MASSON. Can. Met. Q. **9**, 415 (1970).
3. O. KUBASCHEWSKI, E. EVANS, and C. B. ALCOCK. Metallurgical thermochemistry. Pergamon Press, Oxford. 1967.
4. J. M. TOGURI and N. H. SANTANDER. Can. Met. Q. **8**, 167 (1969).
5. A. MUAN and E. F. OSBORN. Phase equilibria among oxides in steelmaking. Addison-Wesley, Mass. 1965.
6. A. KUBIK and C. B. ALCOCK. J. Metal Sci. **1**, 19 (1967).
7. L. S. DARKEN. Trans. Met. Soc. AIME, **239**, 80 (1967).
8. V. V. AVERIN, A. YU. POLYAKOV, and A. M. SAMARIN. Izu. Akad. Nauk. SSSR, Otd. Tekhn. Nauk. **8, 120** (1957).
9. E. S. TANKINS, N. A. GOKCEN, and G. R. BELTON. Trans. Met. Soc. AIME, **230**, 820 (1964).

Can. J. Chem. Downloaded from www.nrcresearchpress.com by 210.87.254.5 on 09/05/12
For personal use only.

On the Mechanism and Substituent Effects of the Tl(III) Oxidation of Phenylethylenes in Methanol

L. NADON, M. TARDAT, M. ZADOR, AND S. FLISZAR

Department of Chemistry, University of Montreal, Montreal, Quebec

Received June 12, 1972[1]

The oxidation of phenylethylenes by $Tl(NO_3)_3$ in methanol proceeds rapidly and selectively to give the products resulting from the migration of aryl groups, *i.e.*, (*i*) the 1,1-dimethoxy-2-phenylethanes from the corresponding styrenes, (*ii*) the phenylacetones from the α-methylstyrenes, and (*iii*) the two possible deoxybenzoines from the 1,1,-diphenylethylenes. The kinetic results, which indicate the formation of the thallic–organic intermediate to be the rate determining step, are discussed in terms of the mechanism of reaction and show the role of the coordination of Tl(III). Hammett's relationship, with $\rho = -4.2$, describes the substituent effects for the competitive oxidation of ring-substituted styrenes and α-methylstyrenes. The relative migratory aptitudes of aryl groups, as determined from the oxidation products of ring-substituted 1,1-diphenylethylenes, is correlated to Brown's σ^+ constants, with $\rho^+ = -2.27$.

L'oxydation des phényléthylènes par le nitrate thallique dans le méthanol conduit rapidement et de manière sélective aux produits résultant de la migration des groupes aryles, c.à.d. (*i*) les diméthoxy-1,1 phényl-2 éthanes à partir des styrènes correspondants, (*ii*) les phénylacétones à partir des α-méthylstyrènes, et (*iii*) les deux désoxybenzoïnes possibles à partir de diphenyl-1,1 éthylènes. Les résultats cinétiques, qui indiquent que la formation de l'intermédiaire organo–thallique constitue l'étape déterminante, sont discutés en termes mécanistiques et, de plus, illustrent le rôle de l'état de coordination du Tl(III). La relation de Hammett, avec $\rho = -4.2$, décrit l'effet de substituants dans l'oxydation compétitive de styrènes et d'α-méthylstyrènes substitués sur le noyau. L'aptitude migratoire relative des groupes aryl, déterminée dans l'étude des produits d'oxydation de diphényl-1,1 éthylènes substitués sur le noyau, est en corrélation avec les constantes σ^+ de Brown, avec $\rho^+ = -2.27$.

Can. J. Chem., **51**, 2366 (1973)

The oxidation of a great number of olefins by thallic salts has been the object of intensive recent studies (1–13), from the point of view of both preparative organic chemistry and of the interesting mechanistic implications. From Henry's fundamental studies, including product distributions and kinetic considerations, a basic mechanistic proposal has developed for the oxidation of a variety of simple olefins by Tl(III) in aqueous acid solutions (1, 2). The oxidation of cyclic olefins, *e.g.* the cyclohexenes, in aqueous (5) and in methanol (4) solutions, the oxidation of chalcones in methanol (8), as well as the oxidation of numerous aromatic olefins, *e.g.* styrene and derivatives thereof, by $Tl(NO_3)_3$ in methanol solution (6) have been investigated.

It appeared that the product distributions depend strongly on the specific experimental conditions. This prompted the present study on $Tl(NO_3)_3$ oxidation in methanol, which considers (*i*) kinetic aspects, (*ii*) the relative reactivity of substituted styrenes, and (*iii*) the migration of substituted phenyl groups in the oxidation of ring substituted 1,1-diphenylethylenes.

[1]Revision received February 27, 1973.

Results and Discussion

Kinetic Studies

The product analysis reported in detail in the Experimental Section indicates that the oxidation of styrene and selected derivatives thereof in methanol solution yields *quantitatively* the dimethylacetals of the corresponding arylethanals.[2]

$$ArCH{=}CH_2 + Tl(NO_3)_3 + 2\,CH_3OH \rightarrow ArCH_2{-}CH(OCH_3)_2 + TlNO_3 + 2HNO_3$$

Styrene and α-methylstyrene were selected for the kinetic studies. At 25 °C, the reaction with thallic salt occurs rapidly, even at low concentrations of both reactants ($\sim 10^{-3}$ *M*). The rate of olefin consumption follows second order kinetics [1],

$$[1] \qquad -d[\text{Olefin}]/dt = k[\text{Olefin}][Tl(III)]$$

as indicated by Fig. 1, expressed in terms of the integrated rate law.

[2]The oxidation of styrene and *p*-bromostyrene by $Tl(NO_3)_3$ in methanol has been reported (6) to give appreciable amounts of glycol ethers, *i.e.* the 1-aryl-1,2-dimethoxyethanes (50–60%). Our investigation fails to confirm this, as explained in the Experimental section.

Can. J. Chem. Downloaded from www.nrcresearchpress.com by 210.87.254.105 on 09/05/12
For personal use only.

TABLE 1. Rate constants for the $Tl(NO_3)_3$ oxidation of styrene and α-methylstyrene*

Olefin	T (°C)	$[HNO_3]$ (M)	$[LiNO_3]$ (M)	$[H_2O]$ (M)	k (M^{-1} s^{-1})
Styrene	5	3.5×10^{-3}	5×10^{-3}	0	3.2
	15			0	6.2
	25			0	12
	35			0	19
	25	5×10^{-3}	15×10^{-3}	0	13.5
	25	15×10^{-3}	5×10^{-3}	0	12.6
	25	20×10^{-3}	0	0	15.6
α-Methylstyrene	5	3.5×10^{-3}	5×10^{-3}	0	27
	15			0	48
	25			0	73
	35			0	110
Styrene	25	3.5×10^{-3}	5×10^{-3}	0	12
				0.28	10.7
				0.56	8.5
				1.11	8.7

*$[Tl(NO_3)_3] = 1.0 \times 10^{-3}$ M, [olefin] $= 1.0 \times 10^{-3}$ M, solvent = methanol.

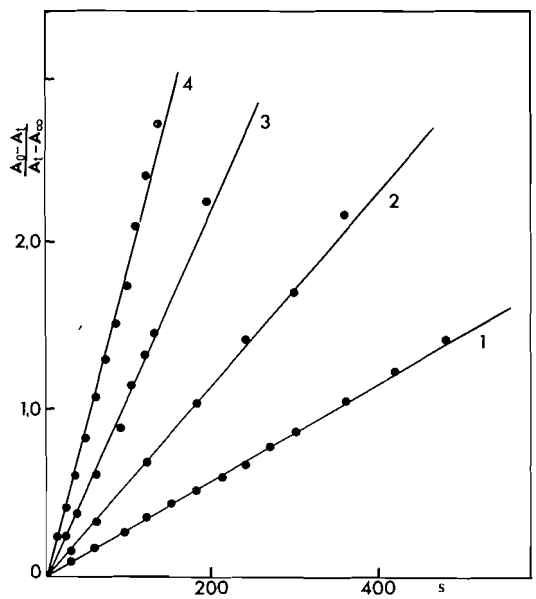

FIG. 1. Integrated second-order rate law for the $Tl(NO_3)_3$ oxidation of styrene. (1) $T = 5$ °C; (2) $T = 15$ °C; (3) $T = 25$ °C; (4) $T = 35$ °C. Solvent = methanol; $[Tl(NO_3)_3] = 1.0 \times 10^{-3}$ M; [styrene] $= 1.0 \times 10^{-3}$ M; $[LiNO_3] = 5 \times 10^{-3}$ M; $[HNO_3] = 3.5 \times 10^{-3}$ M.

The rate constants which were measured under various experimental conditions are indicated in Table 1.

The present kinetic results are thus in accord with those reported by Henry (1) for thallic oxidations in water and by Ouellette *et al.* (9) for the oxidation of styrenes by thallic acetate in acetic acid which both indicate the reactions to be first order in each reactant. It is noted, however, that our rate constants are about 50 times greater than those determined from the thallium acetate oxidation (9) in acetic acid. This can be due to the low stability of the Tl(III)–NO_3 complexes (14), resulting in a highly ionic character of the dominant species Tl^{3+} and $TlNO_3^{2+}$. Indeed, such complexes as TlX_2^+ and TlX_3 which should prevail in acetic acid for $Tl(OAc)_3$ are known to be less reactive (3, 10).

The results given in Table 1 also indicate that the rates are *not inhibited* by the presence of excess nitric acid. This supports the oxidation mechanism suggested by Henry (1) in which the slow step is the formation of the organo-thallic intermediate **1**, eq. 2. In fact, if the decomposition [3] into final products were the slow process, the over-all rate would decrease as the nitric acid concentration is increased.

$$[2]\quad TlX_3 + ArCH{=}CH_2 + CH_3OH \overset{\text{slow}}{\rightleftharpoons} Ar{-}CH(OCH_3){-}CH_2{-}TlX_2 + HX$$

$$[3]\quad \mathbf{1} + CH_3OH \xrightarrow{\text{fast}} \text{Products} + TlX + HX$$

A consideration of all the results reported in the literature indicates that step [3] consists in a competition between two possible reaction paths. These are indicated in Scheme 1, which unifies the proposals which have been considered (2, 5, 6, 9) for various specific experimental conditions and is capable of explaining the depen-

Can. J. Chem. Downloaded from www.nrcresearchpress.com by 210.87.254.105 on 09/05/12
For personal use only.

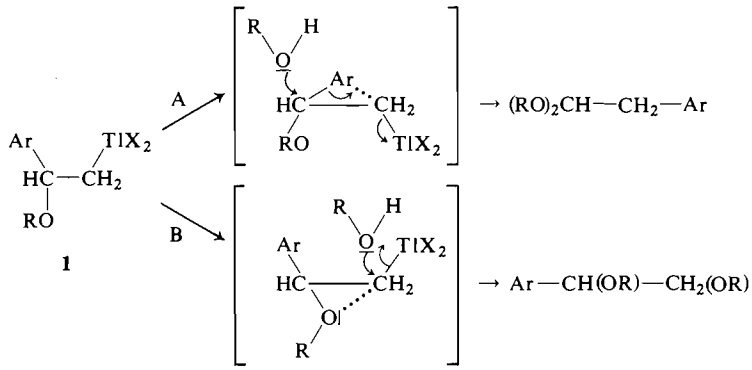

SCHEME 1

dence of the product distribution on the nature of the participating solvent.

As indicated in Scheme 1 for the phenylethylenes, two major modes (A and B) of reaction can take place, *i.e.*, (*i*) path A implying the participation and migration of the phenyl group, already demonstrated by labelling techniques (8, 9), and (*ii*) path B, implying the participation (or even migration) of the OR group of **1**. Such a participation of OR should be favored over an S_N2 substitution of Tl by a solvent molecule, as demonstrated in the case of rigid cyclohexenes (5).

The discrimination between paths A and B depends on the solvent which is used and, hence, on the nature of the OR group in **1**, and on the nature of the migrating group.[3] The formation of dimethylacetals from the corresponding styrenes, which has turned out to be practically quantitative (see Experimental section), is a clear illustration of path A: the phenyl migration is at any rate considerably more important than any participation of the methoxy group. Such a behavior can be attributed to the fact that usually the methoxy group is a poor participating agent. The results which were observed for the 4′-methoxychalcone (8) also support the preferential migratory aptitude of the phenyl group over the participation of the methoxy group.

When the nature of the OR group is changed for a good participating group, it is conceivable that path B may be preferred. This would namely be the case in acetic acid solution (9), where OR = OAc, because the acetoxy is known to be an excellent participating group (11, 15). Alternatively, in cases where the phenyl group is replaced by a group whose migratory aptitude is poor, the relative importance of path B over A is increased to the extent that it may be significant even in methanol solution. This appears to occur in the oxidation of cyclohexene in methanol (6), where path B (formation of diether) represents 15%, as compared to 85% for path A.[4]

It may now be regarded that the product formation (step [3]) is satisfactorily rationalized. From the kinetic point of view, it is, however, step [2] on which attention shall be focused.

The results in Table 1 indicate that α-methylstyrene reacts about 5–10 times faster than styrene, in the range of temperatures investigated. The effect of methyl substitution is thus similar but less pronounced to that observed for the relative reactivities of propylene *vs.* ethylene (2).

The activation parameters calculated from the results of Table 1 are $\Delta H^{\neq} = 9.9 \pm 0.5$ kcal, $\Delta S^{\neq} = -25 \pm 1.5$ e.u. (styrene) and $\Delta H^{\neq} = 7.1 \pm 0.5$ kcal, $\Delta S^{\neq} = -26 \pm 1.5$ e.u. (α-methylstyrene). These activation enthalpies are, hence, similar to the value (7.9 kcal) determined for the $Tl(OAc)_3$ oxidation of *p*-methylstyrene in acetic acid (9).

A more striking observation concerns the influence of water, even in small amounts, on the reaction rates: the presence of 1–2% of water causes a significant decrease of k (Table 1). This

[3]No difference between thallium acetate and nitrate is observed in the product distribution under otherwise identical conditions.

[4]The values have been obtained by measuring the reaction products from the oxidation of cyclohexene, where they are, for path A, cyclopentanecarboxaldehyde and, for path B, the stereoisomeric 1,2-dimethoxycyclohexanes. These results are in full agreement with those reported in the literature (6).

Can. J. Chem. Downloaded from www.nrcresearchpress.com by 210.87.254.105 on 09/05/12
For personal use only.

Can. J. Chem. Downloaded from www.nrcresearchpress.com by 210.87.254.105 on 09/05/12
For personal use only.

TABLE 2. Influence of chloride ions on the rate of oxidation of styrene*

$[Cl^-]$ (M)	R_i ($M\ s^{-1}$) Observed	Calculated
0	10.1×10^{-6}	10.1×10^{-6}
2.5×10^{-4}	8.9×10^{-6}	8.0×10^{-6}
5.0×10^{-4}	5.8×10^{-6}	5.9×10^{-6}
7.5×10^{-4}	3.8×10^{-6}	4.0×10^{-6}
1.0×10^{-3}	2.3×10^{-6}	1.8×10^{-6}
1.5×10^{-3}	0.6×10^{-6}	0.9×10^{-6}
2.0×10^{-3}	$\leq0.3\times10^{-6}$	0
5.0×10^{-3}	$<3\times10^{-10}$	0

*$[Tl(ClO_4)_3] = 1.0\times10^{-3}M$, [styrene] $= 1.0\times10^{-3}M$, $T = 25$°C, $[HClO_4] = 0.2\ M$, solvent = 80% (v/v) methanol – 20% (v/v) water.

can be explained either in terms of a preferential coordination of Tl(III) by water or else in terms of a partial hydrolysis of Tl(III), both of which processes would result in a less reactive thallium species.

The role of the coordination of the thallic ion is further illustrated by the influence of chloride ions, which are known to give stable complexes with Tl(III) (16), on the reaction rates. As indicated by the results in Table 2, chloride ions cause a marked retarding effect on the reaction rates. In order to avoid any interference by nitrate ions, these experiments were carried out in perchloric medium, using (for safety) a 80% (v/v) methanol – 20% water mixture as solvent.

From these results, it may be concluded that $TlCl^{2+}$ is the only Cl-containing reactive species. This, because the rate drops considerably (to less than 3% of its initial value) when $[Cl^-]/[Tl(III)] = 2$, in which case the predominant species is $TlCl_2^+$, instead of $TlCl^{2+}$. Higher chloride concentrations prevent, for all practical purposes, the reaction to occur: this is observed with a ratio $[Cl^-]/[Tl(III)] = 5$, where the predominant species are $TlCl_3$ and $TlCl_4^-$.

These qualitative arguments, deduced from Table 2, lead to the following quantitative interpretation of these results. On the assumption that the stability constants of the various thallium complexes are in the present conditions at least as large as in water,[5] the concentrations $[Tl^{3+}]$ and $[TlCl^{2+}]$ can be evaluated as in ref. 10. Hence, the overall initial rate R_i is

$$[4]\quad R_i = [\text{styrene}]\,(k_{Tl}[Tl^{3+}] + k_{TlCl}[TlCl^{2+}])$$

As indicated in Table 2, the calculated initial rates (eq. 4) are in satisfactory agreement with the corresponding experimental rates, thus supporting the interpretation given above.

The observation that the reactivity of $TlCl^{2+}$ ($k_{TlCl} = 1.8\ M^{-1}\ s^{-1}$) is lower than that of Tl^{3+} ($k_{Tl} = 10.1\ M^{-1}\ s^{-1}$) indicates that the electrostatic effect due to the lowering of the ionic charge is the dominating factor. This is contrary to what had been observed previously in the case of the oxidation of 1,2-cyclohexanedione under similar circumstances, where the present effect was overruled by an opposed "catalytic" effect (10).

Relative Reactivity of Substituted Styrenes

A further insight into the reaction mechanism is given by the study of substituent effects on the rate constants. The relative rates of oxidation of ring-substituted styrenes and α-methylstyrenes have been determined by a competitive method, using excess amounts of olefins with respect to Tl(III). Because the ratio of the products formed is equal to the ratio of the reaction rates, the ratio of the rate constants can be deduced from eq. 5, which is based on the assumption of first order reactions with respect to each olefin (eq. 1).[6]

$$[5]\quad [\text{Product-1}]/[\text{Product-2}] = k_1(\text{Ol-1})/k_2[\text{Ol-2}]$$

It has been verified that k_1/k_2 is independent of the Tl(III) concentration and of the temperature (Table 3).

The reproducibility of the measurements is satisfactory (Table 4), despite the great differences of reactivity which are observed between the invidivual olefins. Each determination of k_1/k_2 has been repeated a minimum of 6 times, and the final results are indicated in Table 5 with a confidence limit of 95%.

It is noted that the results in Table 5 are expressed with respect to the unsubstituted phenylethylene in terms of k_X/k_H, where X stands for the substituent in the phenyl ring. These results

[5]This assumption is verified by analogy with cases where the stability constants are known. There is an increase of stability for complexes of this type due to greater electrostatic interactions in the less polar solvent.

[6]This assumption is further confirmed by the fact that the ratios k_1/k_2 calculated by means of eq. 5 are independent of the ratios of the olefin concentrations.

TABLE 3. Effect of the experimental conditions on the relative rates of Tl(III) oxidation of ring-substituted styrenes in methanol

Olefin-1 (*M*)	Olefin-2 (*M*)	*T*(°C)	$[Tl(NO_3)_3]$	k_1/k_2
p-Chlorostyrene, 1 *M*	Styrene, 1 *M*	−10	0.1	0.158
		0	0.1	0.161
		25	0.1	0.162
		25	0.02	0.155
m-Chlorostyrene, 1 *M*	Styrene, 0.1 *M*	25	0.02	0.027
0.5 *M*	0.1 *M*	25	0.02	0.030
p-Methylstyrene, 1 *M*	Styrene, 0.1 *M*	0	0.1	6.1
		25	0.1	5.9
p-Methoxystyrene, 1 *M*	*p*-Methylstyrene, 1 *M*	25	0.1	10.7*
	Styrene, 10*M*	25	0.1	60

*Corresponding to a value of 63 for *k*(*p*-methoxystyrene)/*k*(styrene).

TABLE 4. Competitive oxidation of *p*-methylstyrene (olefin 1) and styrene (2) in methanol at 25°

p-Methylstyrene (*M*)	Styrene (*M*)	k_1/k_2
1.012	0.995	5.88
0.999	1.004	6.83
0.986	0.989	5.68
1.005	1.015	5.33
0.998	1.013	5.50
0.998	1.013	5.28
0.999	1.004	6.65

TABLE 5. Substituent effects on the rate of Tl(III) oxidation of ring-substituted styrenes and α-methylstyrenes in methanol at 25°

Parent olefins	Substituents (X)	k_X/k_H
Styrenes	*m*-Cl	0.028±0.004
	p-Cl	0.162±0.015
	H	1.000
	p-CH_3	5.9±0.6
	p-CH_3O	63±7
α-Methylstyrenes	*p*-Cl	0.150±0.005
	H	1.000
	p-CH_3	6.4±0.2

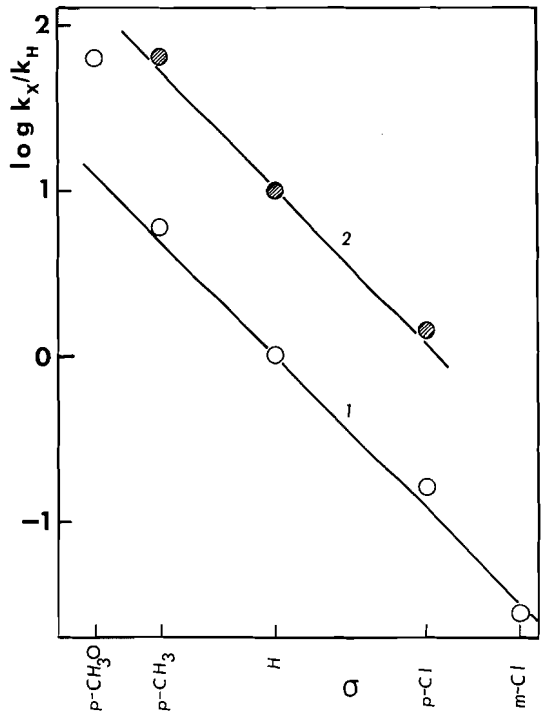

FIG. 2. A verification of Hammett's relationship for the rates of Tl(III) oxidation of ring-substituted styrenes (1) and α-methylstyrenes (2) in methanol. The scale for (2) is shifted by 1 log unit (σ(*p*-CH_3O) = −0.268; σ(*p*-CH_3) = −0.170; σ(H) = 0; σ(*p*-Cl) = +0.227; σ(*m*-Cl) = +0.373).

can be interpreted in terms of Hammett's relationship (Fig. 2).[7]

The negative slope ρ = −4.2 clearly indicates that the overall reaction is favored by electron-releasing substituents; the large ρ value reflects the extreme sensitivity of thallic oxidations to electronic effects. Such a behavior has been noted previously for alkyl substituted ethylenes (2) and for styrenes in acetic acid solution (9). In the latter case, a similar dependence of the reaction rates on substituent effects has been noted, although in acetic acid the product distribution

[7]This correlation is far superior to that which can be obtained using Brown's σ^+ values.

Can. J. Chem. Downloaded from www.nrcresearchpress.com by 210.87.254.105 on 09/05/12
For personal use only.

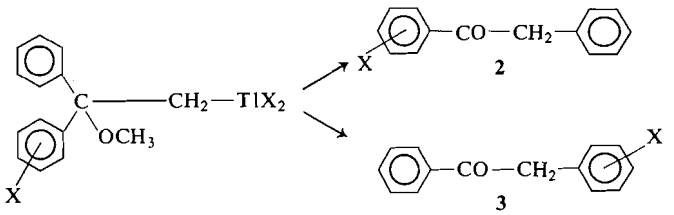

SCHEME 2

is quite different from that observed in methanol. This is in line with the earlier suggestion that the formation of intermediate **1** is rate determining in both methanol and acetic acid.

The ring-substituted α-methylstyrenes react approximately 10 times faster than their styrene analogs. The only oxidation products are the corresponding phenylacetones (Table 1, Experimental section), and *no methylacetophenone could be detected.* This not only indicates that pathway A is followed, but also that any methyl migration is negligible. From the results in Table 5, it also follows that $\rho = -4.2$. Hence, from the observation that the same ρ values are observed for the styrenes and for the α-methylstyrenes, it can be deduced that the methyl group does not exhibit any steric effect which would perturb the transmission of the electronic effects due to the aromatic ring.

Relative Migratory Aptitude of Aryl Groups

Ouellette's studies (9) on the oxidation of styrenes in acetic acid have provided interesting information on the migratory aptitudes of aryl groups. These results, which fit nicely into the proposed mechanism (Scheme 1), represent from this point of view a comparison between the migratory aptitude of the aryl group (path A) *vs.* the participation of OR (path B). The results indicate that electron-releasing substituents on the phenyl group favor its migration.

In methanol solution, however, only path A implying phenyl migration is followed. The relative migratory aptitude of aryl groups can be studied from the competition between two aryl groups under like environment. Derivatives of 1,1-diphenylethylene were chosen for this purpose. Thus, two different carbonyl compounds are formed, depending upon which aryl group has undergone migration (Scheme 2). The deoxybenzoine **2** arises from the migration of the unsubstituted phenyl group, whereas **3** is due to the migration of the substituted one.

TABLE 6. Relative migratory aptitude of aryl groups in the Tl(III) oxidation of 1,1-diphenylethylenes in methanol at 25°

Substituent X	Proportion of **2**	Proportion of **3**	k_X/k_H
m-Cl	0.115	0.885	0.130±0.008
p-Cl	0.341	0.659	0.520±0.005
H			1.000
p-CH_3	0.838	0.162	5.17±0.07
p-CH_3O	≥0.98	≤0.02	≥50

The results reported in Table 6 indicate that electron-releasing substituents attached to a phenyl group favor its migration. In this, the present results agree with those reported by Ouellette *et al.* (9) for the oxidations in acetic acid.

The relative migratory aptitudes are expressed in terms of k_X/k_H, which can be correlated by means of a Hammett equation (Fig. 3). The best fit is obtained by using Brown's σ^+ parameters. The $\rho^+ = -2.27$ value thus calculated for the aryl migration following only path A compares favorably with the ρ^+ value (−1.7) which was determined (9) from the competition between aryl migration and 1,2-diacetate formation.

The present results are, hence, in line with the previous suggestions (6, 8, 9) that the aryl groups migrate toward a carbon atom possessing a more or less developed positive character. The present mechanistic suggestion (Scheme 1) would require a $C^{\delta+}$ character, and the C—Tl bond cleavage is assumed to be concerted with the aryl migration. This is supported by the recent stereochemical study of the oxidation of rigid cyclohexenes (5) which indicated that the decomposition of the organo-thallic intermediate is *not* initiated by the cleavage of the C—Tl bond. The partial positive charge on the C atom under consideration would, of course, result from the important electron-affinity of the Tl to which it is attached.

Can. J. Chem. Downloaded from www.nrcresearchpress.com by 210.87.254.105 on 09/05/12
For personal use only.

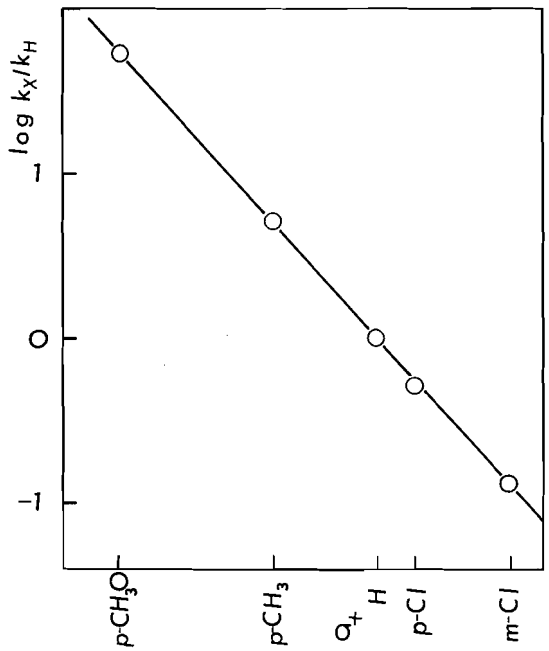

FIG. 3. Hammett plot for the relative migratory aptitudes of aryl groups in the Tl(III) oxidation of ring-monosubstituted 1,1-diphenylethylenes in methanol ($\sigma^+(p\text{-}CH_3O) = -0.778$; $\sigma^+(p\text{-}CH_3) = -0.311$; $\sigma^+(H) = 0$; $\sigma^+(p\text{-}Cl) = +0.114$; $\sigma^+(m\text{-}Cl) = +0.399$).

Conclusions

The oxidation of phenylethylenes by $Tl(NO_3)_3$ in methanol proceeds rapidly and selectively to give the products resulting from the migration of aryl groups, *i.e.* (*i*) the 1,1-dimethoxy-2-phenylethanes from the corresponding styrenes, (*ii*) the phenylacetones from the α-methylstyrenes and (*iii*) the two possible deoxybenzoines from the 1,1-diphenylethylenes.

Kinetic results indicate the reaction to be first order in each reactant. The rate determining step appears to be the formation of the organo–thallic intermediate. The retarding effect of water and Cl^- ions on the reaction rates illustrates the importance of the state of coordination of Tl(III).

Electron-releasing substituents enhance strongly the overall rate of oxidation of ring-substituted styrenes and α-methylstyrenes. The oxidation of ring-substituted 1,1-diphenylethylenes in methanol indicates that electron-releasing substituents strongly favor the migration of the corresponding aryl group, which is in line with the view that the aryl groups migrate toward a $C^{\delta+}$ atom.

Experimental

The thallic nitrate was prepared by dissolving 15 g of thallic oxide in 20 ml concentrated nitric acid, at 60 °C. After cooling, the crystallized $Tl(NO_3)_3 \cdot 3H_2O$ was filtrated and dried in vacuum. The thallic perchlorate solution was prepared by dissolving thallic oxide in aqueous $HClO_4$. The olefins were purchased or prepared and purified by standard methods. The methanol was dehydrated following a standard procedure (17).

The identification of the reaction products was, in general, made by g.l.c. retention times, comparison with authentic samples, and n.m.r. analysis. The g.l.c. analyses were carried out by means of an F and M 5750 gas chromatograph using two different 6 ft columns. For the analysis of the reaction products from the ring-substituted styrenes, 10% Carbowax 20M on Chromosorb PAW-DMCS and Polyphenyl 6 ring columns were used at 142°. The same columns were used at 125° for the oxidation products of the various α-methylstyrenes. For the 1,1-diphenylethylenes, Silicone Rubber UC-W98 (150°) and Polyphenyl 6 ring (195°) columns were used.

The nature of the products, and their yields, obtained from the oxidation of all the olefins investigated, are given in Table 7.

The observation that the oxidation of styrene yields only the dimethylacetal of phenylacetaldehyde, was verified by a comparison with a commercial (Aldrich) sample of acetal. It was also verified that, after acid hydrolysis, only phenylacetaldehyde is obtained. However, to insure a complete hydrolysis, the methanol had to be evaporated and the acetal treated during 1 h with 2 *N* H_2SO_4. Otherwise, the g.l.c. analysis indicates the presence of unreacted acetal. These results were confirmed by test experiments carried out with authentic samples of acetal. The absence of 1-phenyl-1,2-dimethoxyethane in the reaction products was confirmed by means of authentic samples of this product. The acetal and the diether can be separated in g.l.c. on Carbowax 20 M columns and also possess n.m.r. spectra which facilitate their analysis. In the acetal, in CCl_4 solution, the two methoxy groups give a single signal at 3.20 p.p.m. The CH_2 group is revealed by a doublet at 2.8 p.p.m., and the tertiary H by a triplet at 4.4 p.p.m. In the diether, the methoxy groups give two signals at 3.20 and 3.25 p.p.m., the tertiary proton consists of a quartet centered at 4.2 p.p.m., and the CH_2 group a complex signal at 3.4 p.p.m.

The acetals obtained from the oxidation of substituted styrenes have been isolated, after filtration of the thallous nitrate, by washing the methanol solution with a carbonate solution, followed by an extraction by means of ether. The n.m.r. results in CCl_4 solution, with reference to TMS, are indicated in Table 8.

In all cases, the hydrolysis of the acetals has been made in order to confirm the production of the corresponding aldehyde.

The oxidation product from α-methylstyrene has been identified by a comparison with a sample of pure phenylacetone, by g.l.c. (on 2 different columns) and by n.m.r. analysis. The g.l.c. analysis, using acetophenone as internal standard, indicated a yield of 99% of phenylacetone. The n.m.r. spectra of the phenylacetones obtained from their corresponding α-methylstyrenes are indicated in Table 9.

The oxidation product from 1,1-diphenylethylene was identified in g.l.c. by a comparison with a sample of

Can. J. Chem. Downloaded from www.nrcresearchpress.com by 210.87.254.105 on 09/05/12
For personal use only.

TABLE 7. Mass balance for the Tl(III) oxidation of selected phenylethylenes in methanol

Olefin	Olefin used (mmol)	Acetal (mmol)	Carbonyl compound (mmol)
Styrene	0.548	0.546*	
	20.0		16.4†
p-Methylstyrene	7.83	7.16‡	
p-Methoxystyrene	7.23	6.79‡	
p-Chlorostyrene	6.86	6.38‡	
α-Methylstyrene	0.740		0.735*
p-Methyl-α-methylstyrene	7.86		7.30‡
p-Chloro-α-methylstyrene	8.04		7.64‡
1,1-Diphenylethylene	0.536		0.520*
1-*p*-Anisyl-1-phenylethylene	7.20		6.78‡§
1-*p*-Tolyl-1-phenylethylene	7.63		7.02‡§
1-*p*-Chlorophenyl-1-phenylethylene	7.90		7.50‡§
1-*m*-Chlorophenyl-1-phenylethylene	7.82		7.12‡§

*Obtained by g.l.c. of the reaction mixture after completion of the oxidation.
†After hydrolysis of the acetal product. From 20.3 mmol of pure acetal, 17.5 mmol of phenylethanal was obtained.
‡After extraction and isolation of the reaction products.
§Total amount of carbonyl compound, consisting of a mixture of the two isomeric deoxybenzoines.

TABLE 8. N.m.r. spectra of the 1,1-dimethoxy-2-arylethanes produced in the Tl(III) oxidation of ring-substituted styrenes in methanol

Substituent X	δ_{aryl} (p.p.m.)	δ_{CH_2} (d) (p.p.m.)	δ_{CH} (t) (p.p.m.)	δ_{OCH_3} (s)* (p.p.m.)
m-Cl	7.18	2.80	4.40	3.25
p-Cl	7.15	2.80	4.40	3.25
H	7.10	2.80	4.40	3.20
p-CH_3	6.90	2.75	4.40	3.20
p-CH_3O	6.50	2.60	4.35	3.05

*Acetal-methoxy group. For the *p*-methoxy and the *p*-methyl ring substituents, the corresponding protons appear at 3.50 p.p.m. (s) and at 2.25 p.p.m. (s).

TABLE 9. N.m.r. spectra of arylacetones produced in the Tl(III) oxidation of ring-substituted α-methylstyrenes in methanol

Substituent X	δ_{aryl} (p.p.m.)	δ_{CH_2} (s) (p.p.m.)	δ_{CH_3} (s)* (p.p.m.)
p-Cl	6.80	3.40	1.95
H	6.80	3.35	1.90
p-CH_3	6.60	3.30	1.85

*Acetone methyl group. The *p*-methyl ring-substituent appears at 2.15 p.p.m. (s).

deoxybenzoine is observed in g.l.c., using *p*-methoxybenzophenone as internal standard. The identification of all the reaction products was made by comparison with pure samples of 4′-methoxy-, 4′-methyl-, and 4′-chloro-deoxybenzoines, and 4-methoxy-, 4-methyl-, and 4-chlorodeoxybenzoines, all of which were prepared and purified according to literature methods (18).

Kinetic Method

The course of each reaction was followed by ultraviolet spectrophotometry at 270–290 mμ, thus measuring the decrease in olefin concentration. The interpretation of the results was made by means of the integrated second order rate law $x/(a - x) = (A_0 - A_t)/A_t - A_\infty) = kat$, where a = [olefin] = [Tl(III)] and x = concentration of reaction product at time t. The quantities A_0, A_t, and A_∞ are, respectively, the absorbances at time $t = 0$, $t = t$, and $t = \infty$. The rate constant k was calculated from the regression line, as illustrated in Fig. 1. It has been verified that no variation in k occurs when the concentration of the reactants was changed by a factor of 4. Reproducible k values can only be obtained when due care is taken to avoid any polymerization of the olefin while setting up the experiments. The statistical analysis of the results indicates a reproducibility of the k values within 5%.

The competitive kinetic measurements were made by adding 5 ml of a 0.1 *M* solution of thallic nitrate to 5 ml of a solution 1 *M* in each olefin. In most cases, styrene was used as reference compound. Because of the great difference in reactivity between styrene and *m*-chlorostyrene, 0.1 *M* styrene solutions and concentrations of 0.5–1.0 *M* of *m*-chlorostyrene were used, with a 0.02 *M* concentration in thallic nitrate. For the experiments with *p*-methoxystyrene, *p*-methylstyrene was used as reference.

The possible influence of nitrate ions was examined. The kinetic study has revealed a slight increase of the reaction rate by added nitrate ions. However, in the present experimental conditions, a 3-fold excess of nitrate ions in form of $LiNO_3$ does not alter significantly the *ratios* k_X/k_H. For example, in the presence of excess NO_3^-, $k_X/k_H = 6.7$ for the *p*-methylstyrene/styrene system, which compares favorably with the results reported in Table 3.

The financial support given by the National Research Council of Canada is gratefully acknowledged.

Can. J. Chem. Downloaded from www.nrcresearchpress.com by 210.87.254.105 on 09/05/12
For personal use only.

1. P. M. HENRY. J. Am. Chem. Soc. **87**, 990 (1965).
2. P. M. HENRY. J. Am. Chem. Soc. **87**, 4423 (1965).
3. P. M. HENRY. J. Am. Chem. Soc. **88**, 1597 (1966).
4. E. TAYLOR and A. MCKILLOP. Acc. Chem. Res. **3**, 338 (1970).
5. C. FREPPEL, R. FAVIER, J. C. RICHER, and M. ZADOR. Can. J. Chem. **49**, 2586 (1971).
6. A. MCKILLOP, J. D. HUNT, E. C. TAYLOR, and F. KIENZLE. Tetrahedron Lett. **60**, 5275 (1970).
7. H. J. KABBE. Justus Liebigs Ann. Chem. **656**, 204 (1962).
8. W. D. OLLIS, K. L. ORMAND, and I. O. SUTHERLAND. J. Chem. Soc. C, 119 (1970); A. MCKILLOP, B. P. SWANN, and E. C. TAYLOR. Tetrahedron Lett. **60**, 5281 (1970).
9. R. J. OUELLETTE, G. KORDOSKY, C. LEVIN, and S. WILLIAMS. J. Org. Chem. **34**, 4104 (1969).
10. R. FAVIER and M. ZADOR. Can. J. Chem. **47**, 3539 (1969); **48**, 2407 (1970).
11. R. M. MORIARTY and H. GOPAL. Tetrahedron Lett. 345 (1972).
12. C. LION, and J.-E. DUBOIS. C.R. Acad. Sci. Paris, **274**-C, 1073 (1972).
13. J. R. COLLIER and A. S. PORTER. J. Chem. Soc. Chem. Commun. 618 (1972).
14. F. YA. KUL'BA, YU. B. YAKOVLEV, and V. E. MIRONOV. Russ. J. Inorg. Chem. (Engl. Ed.), **10**, 886 (1965).
15. A. STREITWIESER, JR. Solvolytic displacement reactions. McGraw–Hill Book Co., Inc., New York, N.Y. 1962. M. J. STRAUSS, L. J. ANDREWS, and R. M. KEEFER. J. Am. Chem. Soc. **90**, 3473 (1968).
16. D. PESCHANSKI, and S. VALLADAS-DUBOIS. Bull. Soc. Chim. Fr. 1170 (1956); S. AHRLAND, L. GRENTHE, L. JOHANSSON, and B. NOREN. Acta Chem. Scand. **17**, 1567 (1963).
17. A. VOGEL. A textbook of practical organic chemistry. Longman. 1956. p. 169.
18. S. S. JENKINS. J. Am. Chem. Soc. **56**, 682 (1934).

Can. J. Chem. Downloaded from www.nrcresearchpress.com by 210.87.254.105 on 09/05/12
For personal use only.

Rationalization of Carbon-13 Magnetic Resonance Spectra of Yeast Mannans and Structurally Related Oligosaccharides[1]

P. A. J. GORIN

Prairie Regional Laboratory, National Research Council, Saskatoon, Saskatchewan

Received January 2, 1973

The carbon-13 magnetic resonance (c.m.r.) spectra of oligosaccharides, derived from yeast mannans by partial acetolysis, contain signals at δ_c 93.1–105.4 (C-1's) and 79.2–81.2 (C-2's and/or C-3's substituted by mannopyranosyl units). They were assigned on the basis of (*a*) carbons deshielded by attached mannopyranosyl units have resonances at lower field than those of unsubstituted carbons and (*b*) comparison under carefully controlled conditions of the relative sizes of signals of comparable carbons, which have the same resonances, in members of two different homologous series of oligosaccharides. The c.m.r. spectra of certain mannans containing (1 → 6)-linked α-D-mannopyranose main-chains could then be rationalized since they have many signals with resonances in common with those of oligosaccharides, which are derived by partial acetolysis and contain the structures of the side chains.

Les spectres de résonance du carbone-13 (r.m.c.) de certains oligosaccharides, obtenus des mannanes de la levure par acétolyse partielle, contiennent des signaux à δ 93.1–105.4 (C-1) et δ_c 79.2–81.2 (C-2 et/ou C-3 substitué par des unités du type mannopyranosyle). Ceux-ci furent attribués en se basant sur (*a*) l'énoncé suivant lequel les carbones déblindés par les unités mannopyranosyles qui lui sont rattachées résonnent à champ plus faible que les carbones non-substitués et (*b*) la comparaison, dans des conditions strictements contrôlées, des importances relatives des signaux appartenant à des carbones semblables, lesquels résonnent au même endroit, dans les membres de deux séries homologues différentes d'oligosaccharides. Les spectres r.m.c. de certains mannanes contenant des chaînes principales d'α-D-mannopyranoses liés de manière 1 → 6, peuvent alors être rationalisés puisqu'ils possèdent plusieurs signaux que l'on peut assimiler à ceux d'oligosaccharides, qui sont obtenus par acétolyse partielle et qui possèdent les ramifications des chaînes latérales. [Traduit par le journal]

Can. J. Chem., 51, 2375 (1973)

The p.m.r. spectra (1) of yeast mannans can be used as fingerprints for identification and classification of the parent organism. In certain cases the chemical shifts of certain signals are indicative of the presence of certain structures, for example H-1 signals at higher field than δ 5.45 indicate β-D-mannopyranose units (2) and those with δ 5.80 indicate successive (1 → 2)-linked α-D-mannopyranose units (3). The fingerprint and the assignment approaches can be readily extended to carbon-13 magnetic resonance (c.m.r.) spectra of oligosaccharides (4, 5) and polysaccharides (6), since when proton decoupling is used the signals are well-defined with resonances that are reproducible to an accuracy of 1 Hz (0.04 p.p.m.). The present study concerns the assignment of signals of certain resonances to chemical structures in oligosaccharides derived from yeast mannans by partial acetolysis. The presence of signals with the same resonance in the c.m.r. spectrum of a mannan can then serve as an indication of chemical structure. In certain cases when the c.m.r. spectra of the oligosaccharides could not be rationalized it was still possible to use the C-1 portions of the spectrum as fingerprints in identification of related structures in yeast mannans.

The majority of ascomycetous yeasts form cell-wall mannans or galactomannans with main chains of (1 → 6)-linked α-D-mannopyranose units substituted in their 2-positions by α-linked sugar units.[2] The linkages in the side chain vary widely and can be 2-*O*-linked α- or β-D-mannopyranose units or 3-*O*-linked α-D-mannopyranose units, which can be arranged in many combinations (7). The variations of chemical structure are reflected mainly in the c.m.r. signals at low field δ_c 77.2–105.4, which arise from C-1 and from C-2 and/or C-3 that are mannosylated (see ref. 4 for similar effects on the c.m.r. spectrum of laminaribiose). In order to rationalize the c.m.r. spectra of mannans the signals of derived oligosaccharides were first assigned. Two groups of oligosaccharides were examined,

[1]NRCC No. 13152.

[2]In *Citeromyces matritensis* mannan the side chains are α- and β-linked to the main chain (2).

Can. J. Chem. Downloaded from www.nrcresearchpress.com by 210.87.254.42 on 09/05/12
For personal use only.

TABLE 1. Chemical shifts and relative peak heights of c.m.r. signals of certain carbons of (1 → 2)-linked α-D-mannopyranose oligosaccharides

No.		Chemical shift of signals, δ_c in p.p.m. based on downfield difference of signal resonance from that of internal TMS in a coaxial capillary (relative peak heights in parentheses)				
		C-1			C-2	
		Non-reducing end-unit	Internal unit	Reducing end-unit	Reducing end-unit	Internal unit
1	$M\overset{12\alpha}{—}M$ (13)*	103.8 (10)	—	94.4 (17)	80.6 (12)	—
2	$M\overset{12\alpha}{—}M\overset{12\alpha}{—}M$ (20)	103.8 (10)	102.2 (10)	94.3 (8)	80.8 (9)	80.0 (11)
3	$M\overset{12\alpha}{—}M\overset{12\alpha}{—}M\overset{12\alpha}{—}M$ (10)	103.8 (10)	102.3 (14)	94.4 (6)	80.8 (6)	80.0 (14)
4	$M\overset{12\alpha}{—}M\overset{12\alpha}{—}M\overset{12\alpha}{—}M\overset{12\alpha}{—}M$ (10)	103.8 (10)	102.3 (35)	94.4 (8)	80.8 (8)	80.0 (29)

*M = D-Mannopyranose.

those containing only α-linkages and those with α- and β-linkages or β-linkages alone.

(1) Oligosaccharides Containing α-D-mannopyranose Units

In the following discussion the δ_c 93.1–105.4 region which contains C-1 signals is referred to as region A. Region B is used to denote the region between δ_c 79.2 and 81.2 which contains C-2 and/or C-3 signals. These signals are at much lower field than the others (8), because of the deshielding effect of the adjacent *O*-mannosyl group on the carbon atom.

The c.m.r. spectra of a homologous series of (1 → 2)-linked α-D-mannopyranoside oligosaccharides having from two to five units in length contain regions A and B that lend themselves readily to interpretation (see Table 1). The signals at δ_c 94.3–94.4 in region A belong to C-1 of the reducing ends. They are at higher field than other C-1 signals because they are not deshielded by attached mannosyl units. The signals at δ_c 102.1–102.2 arise from C-1's of internal mannopyranosyl units since they are absent from the mannobiose spectrum. By elimination the signals at δ_c 103.4 arise from C-1 of the non-reducing end unit.

It is perhaps significant that these assignments agree with those that can be made on considering the relative sizes of the C-1 signals on one hand and the C-2 signals on the other in a homologous series of (1 → 2)-linked oligosaccharides, despite the potential for the signal response of each carbon to be different (Table 1). The variation in signal size can be due to three factors, namely, difference in the speed of spin-lattice relaxation, different magnitude of nuclear Overhauser effect (n.O.e.), and an insufficiency of data points defining the c.m.r. spectrum. By a process of elimination the former is likely of greatest importance. Allerhand *et al.* (9) have shown that carbon atoms in sucrose have almost identical n.O.e.'s and in recording a c.m.r. spectrum of an oligosaccharide one data point is used every 0.6 Hz to define a signal with a half-height linewidth of 3–7 Hz. The c.m.r. spectra of the homologous series of oligosaccharides, obtained consecutively with as little variation of conditions as possible, showed an increase of the relative sizes of certain C-1 and -2 signals as the series is ascended in a stepwise fashion. Increases in size were observed for the signals at δ_c 102.1–102.2 corresponding to C-1 of internal units and in those at δ_c 80.0 which arise from C-2 of internal units.

Signal assignments can be made in a similar fashion for signals in the c.m.r. spectra of a related homologous series of oligosaccharides (Table 2). These differ from the above series (Table 1) in that the (1 → 2)-linkage attaching the non-reducing end-unit to the adjacent unit is replaced by a (1 → 3)-linkage. As can be seen from Table 1 (nos. 1–4) and Table 2 (nos. 1–3) oligosaccharides in each series have the same resonances for C-1 of the internal units, non-reducing and reducing end-units, and for C-2 of 2-*O*-substituted reducing end-units and internal units. A new signal at δ_c 79.8 corresponding with

Can. J. Chem. Downloaded from www.nrcresearchpress.com by 210.87.254.42 on 09/05/12
For personal use only.

Can. J. Chem. Downloaded from www.nrcresearchpress.com by 210.87.254.42 on 09/05/12
For personal use only.

TABLE 2. α-D-Mannopyranose oligosaccharides containing (1 → 2)- and (1 → 3)-linkages and certain mannans: chemical shifts and relative peak heights of c.m.r. signals

		Chemical shift of signals, δ_c in p.p.m., based on downfield difference of signal resonance from that of internal TMS in a coaxial capillary (relative peak heights in parentheses)						
		C-1			C-2			C-3
No.		3-*O*-Substituted internal and non-reducing end-unit	2-*O*-Substituted internal unit	Reducing end-unit	2,6 Di-*O*-substituted unit	2-*O*-Substituted reducing end-unit	2-*O*-Substituted internal unit	3-*O*-Substituted internal unit
1	$M\overset{13\alpha}{—}M\overset{12\alpha}{—}M$ (10)	103.7 (15)	—	94.4 (10)	—	80.6 (6)	—	79.8 (7)
2	$M\overset{13\alpha}{—}M\overset{12\alpha}{—}M\overset{12\alpha}{—}M$ (12)	103.7 (22)	102.2 (8)	94.4 (10)	—	80.8 (10)	80.0 (13)	79.8 (12)
3	$M\overset{13\alpha}{—}M\overset{12\alpha}{—}M\overset{12\alpha}{—}M\overset{12\alpha}{—}M$ (9)	103.7 (29)	102.2 (22)	94.4 (10)	—	80.8 (11)	80.0 (21)	79.8 (15)
4	$M\overset{13\alpha}{—}M\overset{13\alpha}{—}M\overset{12\alpha}{—}M\overset{12\alpha}{—}M$ (18)	103.7 (16)	102.2 (12)	94.4 (10)	—	80.8 (8)	80.0 (17)	80.0
5	$[M\overset{13\alpha}{—}M]$ (19)	103.8	—	—	—	—	—	—
6	$M\overset{12\alpha}{—}M\overset{13\alpha}{—}M\overset{12\alpha}{—}M\overset{12\alpha}{—}M$ (18)	103.7 (12) (103.9 (15)—non-reducing end unit)	102.2 (24)	94.4 (10)	—	80.8 (6)	80.0 (27)	80.0
						2,6-Di-*O*-substituted unit		
7	*Saccharomyces cerevisiae* mannan (12)	103.7 (10)	102.2 (4)	—	100.2 (6)	80.2 (5)	79.8 (6)	79.8
8	*Saccharomyces rouxii* mannan (13)	103.8 (10)	102.2 (3)	—	100.3 (4)	80.2 (4)	80.0 (5)	—
9	*Saccharomyces fragilis* mannan (1)	103.9 (10)	102.2 (1)	—	100.3 (7)	80.4 (6)	—	—
10	*Endomycopsis fibuliger* mannan (10)	103.9 (10)	—	—	100.3 (8)	80.4 (5)	—	—

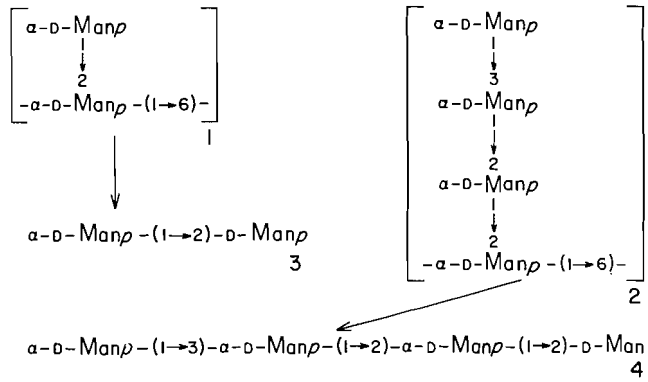

FIG. 1. Structural relationship of portions of mannans of *Saccharomyces fragilis* and *Endomycopsis fibuliger* (**1**) and *Saccharomyces cerevisiae* (**2**) with oligosaccharides (**3** and **4** respectively) formed on partial acetolysis.

C-3 of a 3-*O*-substituted internal unit was also detected in the new series. Unfortunately in region A the signals arising from C-1 of non-reducing end-units and 3-*O*-substituted internal units are superimposed.

The values for resonances of comparable signals in the c.m.r. spectra of D-Man*p*$\overset{13\alpha}{\text{——}}$D-Man*p*$\overset{13\alpha}{\text{——}}$D-Man*p*$\overset{12\alpha}{\text{——}}$D-Man*p*$\overset{12\alpha}{\text{——}}$D-Man*p*,D-Man*p*$\overset{12\alpha}{\text{——}}$D-Man*p*$\overset{13\alpha}{\text{——}}$D-Man*p*$\overset{12\alpha}{\text{——}}$D-Man*p*$\overset{12\alpha}{\text{——}}$D-Man*p* and a linear mannan containing α-(1 → 3)-linkages are also recorded in Table 2. As can be seen, they deviate very little from the values obtained from comparably linked structures in each homologous series of oligosaccharides (Tables 1 and 2).

(2) Oligosaccharides Containing β-D-*Mannopyranose Units Only or Mixed* α- *and* β-D-*Mannopyranose Units*

The c.m.r. spectra of (1 → 2)-linked β-D-mannopyranose oligosaccharides of two to four units in length and a pentasaccharide containing mixed α- and β-linkages were prepared.

In the spectra of the three β-(1 → 2)-linked oligosaccharides some of the chemical shifts in regions A and B of comparable carbons do not correspond on going from one compound to another. Furthermore, the c.m.r. spectra were much more complex than those summarized in Tables 1 and 2: instead of the α-anomer alone appreciable proportions of both α- and β-anomers were present. However, since certain of the signals have resonances within a limited range (see Experimental) some assignments for the tri- and tetrasaccharide spectra can be made. These are as follows: C-1 of α-anomeric reducing end-unit, δ_c 93.8–94.0, β-anomeric reducing end-unit δ_c 95.3; C-1 of non-reducing end-unit, δ_c 100.7–101.2; internal unit, δ_c 102.8. In the mannobiose spectrum the C_β-2 (δ_c 83.2) and C_α-2 resonances (δ_c 80.0) can be assigned with certainty.

Regions A and B of the spectrum of D-Man*p*$\overset{12\alpha}{\text{——}}$D-Man*p*$\overset{12\beta}{\text{——}}$D-Man*p*$\overset{1,2\beta}{\text{——}}$D-Man*p*$\overset{1,2\alpha}{\text{——}}$D-Man (Experimental) could not be rationalized. Only the C-1 signal of the reducing end at δ_c 94.4 corresponded in chemical shift with any previously assigned signal.

(3) Mannans Having a (1 → 6)-Linked α-D-*Mannopyranose Main Chain*

(i) Mannans of Saccharomyces fragilis and Endomycopsis fibuliger

Each mannan has a relatively simple structure consisting mainly of (1 → 6)-linked α-D-mannopyranose main-chain with each unit substituted in the 2-position with a single-unit α-D-mannopyranose side chain (Fig. 1, **1**). The structures differ slightly in that the *Endomycopsis fibuliger* mannan has a small proportion of *O*-α-D-mannopyranosyl-(1 → 3)-α-D-mannopyranose side chains (10, 11) whereas the minor side chain of *Saccharomyces fragilis* mannan is *O*-α-D-mannopyranosyl-(1 → 2)-α-D-mannopyranose (1). The virtually identical c.m.r. spectra (Fig. 2: A and B) lend themselves readily to interpretation. By analogy with the oligosaccharides of the (1 → 2)-linked α-D-mannopyranose series (Table 1) the signals at δ_c 103.9 corresponds to C-1 of the reducing end-units, which shows that the other C-1 signal at δ_c 100.3 belongs to the 2,6-di-*O*-substituted units. Also readily assignable are the C-2 signals at δ_c 80.4 which arise from 2,6-di-

Can. J. Chem. Downloaded from www.nrcresearchpress.com by 210.87.254.42 on 09/05/12
For personal use only.

Can. J. Chem. Downloaded from www.nrcresearchpress.com by 210.87.254.42 on 09/05/12
For personal use only.

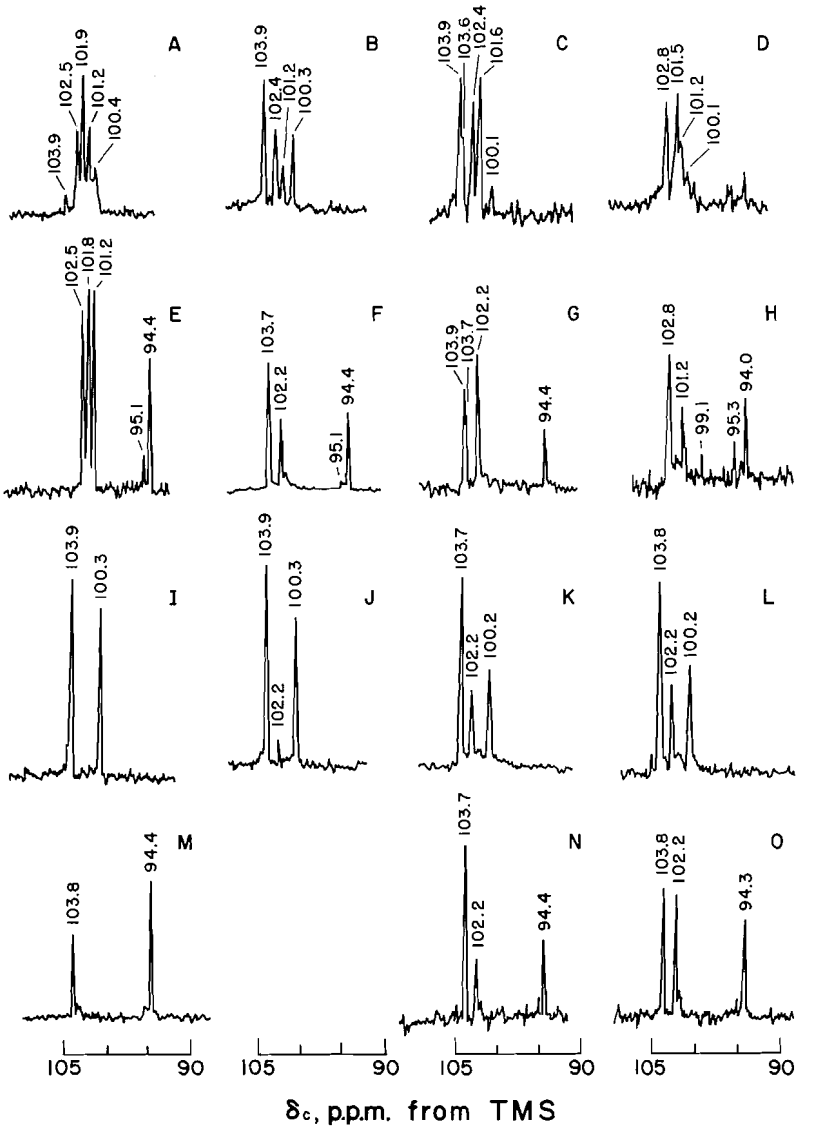

FIG. 2. Region A of c.m.r. Spectra of (*a*) Mannans of *P. pastoris* (A), *M. reukaufii* (B), *D. hansenii* (C), *C. matritensis* (D), *E. fibuliger* (I), *S. fragilis* (J), *S. cerevisiae* (K), and *S. rouxii* (L); (*b*) $M\overset{1,2\alpha}{\text{—}}M\overset{1,2\beta}{\text{—}}M\overset{1,2\beta}{\text{—}}M\overset{1,2\alpha}{\text{—}}M$ (E), $M\overset{1,3\alpha}{\text{—}}M\overset{1,3\alpha}{\text{—}}M\overset{1,2\alpha}{\text{—}}M\overset{1,2\alpha}{\text{—}}M$ (F), $M\overset{1,2\alpha}{\text{—}}M\overset{1,3\alpha}{\text{—}}M\overset{1,2\alpha}{\text{—}}M\overset{1,2\alpha}{\text{—}}M$ (G), $M\overset{1,2\beta}{\text{—}}M\overset{1,2\beta}{\text{—}}M\overset{1,2\beta}{\text{—}}M$ (H), $M\overset{1,2\alpha}{\text{—}}M$ (M), $M\overset{1,3\alpha}{\text{—}}M\overset{1,2\alpha}{\text{—}}M\overset{1,2\alpha}{\text{—}}M$ (N) and $M\overset{1,2\alpha}{\text{—}}M\overset{1,2\alpha}{\text{—}}M$ (O).

O-substituted units. In the *S. fragilis* spectrum the small signal at δ_c 102.3 corresponds to C-1 to the 2-*O*-linked side-chain units.

(ii) Mannans of Saccharomyces cerevisiae and Saccharomyces rouxii

The mannan from bakers yeast (*Saccharomyces cerevisiae*) has a main chain consisting of (1 → 6)-linked α-D-mannopyranose units α-substituted in the 2-positions by side chains, the longest of which is D-Man*p*$\overset{1,3\alpha}{\text{—}}$D-Man*p*$\overset{1,2\alpha}{\text{—}}$D-Man*p*$\overset{1,2\alpha}{\text{—}}$ (Fig. 1, **2**; (12)). Regions A and B of the c.m.r. spectrum of the mannan contains five well-defined signals. These can be assigned by reference to the already assigned signals of D-Man*p*$\overset{1,3\alpha}{\text{—}}$D-Man*p*$\overset{1,2\alpha}{\text{—}}$D-Man*p*$\overset{1,2\alpha}{\text{—}}$D-Man

Can. J. Chem. Downloaded from www.nrcresearchpress.com by 210.87.254.42 on 09/05/12
For personal use only.

(Table 2). It follows (Fig. 2, N and K) that the signal at δ_c 103.7 arises from C-1 of the non-reducing end-units and 3-*O*-substituted units and the signal at δ_c 102.3 from the 2-*O*-substituted units. By analogy with the c.m.r. spectra of the mannans of *E. fibuliger* and *S. fragilis* the signal at δ_c 100.2 should arise from 2,6-di-*O*-substituted units. Region B contains only signals, at δ_c 80.0 and 80.2, although there are carbons from three structurally different units that would be expected to give signals in this region, namely C-2's of 2-*O*- and 2,6-di-*O*-substituted units and C-3 of 3-*O*-substituted units.

The mannan of *Saccharomyces rouxii* has a main chain with (1 → 6)-linked α-D-mannopyranose units substituted in the 2-positions mainly with *O*-α-D-mannopyranosyl-(1 → 2)-α-D-mannopyranose side chains ((11, 13); Fig. 1). It resembles the mannan of *S. cerevisiae* except that it lacks terminal D-Man*p*$\underline{\underline{\ }}^{13\alpha}$ units. The only distinguishing feature of regions A and B of the c.m.r. spectra is that the low field signal of *S. cerevisiae* mannan is at δ_c 103.7 (Fig. 2, K; Table 2) whereas that of the *S. rouxii* mannan is at 103.8 p.p.m. (Fig. 2, L; Table 2). It can be observed that exactly the same chemical shifts of δ_c 103.7 and 103.8 were found for C-1's of oligosaccharides of related structure (Table 2, no. 2 and Table 1, no. 2, respectively; Fig. 2, N and O).

In order to check whether any substituted main-chain units can be detected in the mannans of *S. rouxii* and *S. cerevisiae* the c.m.r. spectrum of a (1 → 6)-linked α-D-mannopyranan (11, 14) was prepared. Its C-1 signal was at δ_c 101.2 and the absence of the resonance in the c.m.r. spectra of the mannans reaffirms (1) that the unsubstituted structural unit is absent.

(iii) Mannans of Metschnikowia reukaufii, Debaryomyces hansenii, Pichia pastoris, and Citeromyces matritensis

It was evident that most of the mannans give C-1 signals (region A) with many resonances in common with those of the longest oligosaccharide formed following partial acetolysis, a technique that preferentially splits (1 → 6)-linkages (13) as depicted in Fig. 1. The only marked difference in the c.m.r. spectra is that the mannan often gives a signal at δ_c 100.3 corresponding to 2,6-di-*O*-substituted units, whereas in the oligosaccharide the same unit has been converted to a reducing end which has a C-1 resonance at much higher field δ_c 94.4.

Taking this into account it should be possible to postulate a possible chemical structure of an unknown mannan using region A of the spectrum as a fingerprint.

Selected examples of spectral resemblance are presented in Fig. 2. The parent yeast and longest oligosaccharide obtained from the mannan are as follows: (M = D-mannopyranose): *E. fibuliger* (M$\underline{\underline{\ }}^{1,2\alpha}$M; spectrum M), *S. fragilis* (M$\underline{\underline{\ }}^{1,2\alpha}$M; spectrum M), *S. rouxii* (M$\underline{\underline{\ }}^{1,2\alpha}M\underline{\underline{\ }}^{1,2\alpha}$M; spectrum O), *S. cerevisiae* M$\underline{\underline{\ }}^{1,3\alpha}M\underline{\underline{\ }}^{1,2\alpha}M\underline{\underline{\ }}^{1,2\alpha}$M; spectrum N), *Metschnikowia reukaufii* (M$\underline{\underline{\ }}^{1,3\alpha}M\underline{\underline{\ }}^{1,3\alpha}M\underline{\underline{\ }}^{1,2\alpha}M\underline{\underline{\ }}^{1,2\alpha}$M; spectrum F), *Debaryomyces hansenii* (M$\underline{\underline{\ }}^{1,2\alpha}M\underline{\underline{\ }}^{1,3\alpha}M\underline{\underline{\ }}^{1,2\alpha}M\underline{\underline{\ }}^{1,2\alpha}$M; spectrum C), *Pichia pastoris* (M$\underline{\underline{\ }}^{1,2\alpha}M\underline{\underline{\ }}^{1,2\beta}M\underline{\underline{\ }}^{1,2\beta}M\underline{\underline{\ }}^{1,2\alpha}$M; spectrum E) and *Citeromyces matritensis* (M$\underline{\underline{\ }}^{1,2\beta}M\underline{\underline{\ }}^{1,2\beta}M\underline{\underline{\ }}^{1,2\beta}$M; spectrum H). As can be seen from Fig. 2 there is a considerable resemblance between the spectra of the oligosaccharides and their parent mannans. In the case of the *D. hansenii* an additional signal at δ_c 101.2 is present in the spectrum of the mannan which is likely from C-1 of an unsubstituted main-chain unit. Similarly, the c.m.r. spectrum of *C. matritensis* mannan differs from that of the (1 → 2)-linked β-D-mannopyranose oligosaccharide in that the former contains only a small signal at δ_c 101.2 corresponding to non-reducing end-units. Instead it contains a strong signal at δ_c 101.5 which likely arises from C-1's of 2,6-di-*O*-substituted units.

(iv) The Mannan from Rhodotorula glutinis

The mannan from *Rhodotorula glutinis* contains alternate (1 → 3)- and (1 → 4)-linked β-D-mannopyranose units (15) and as a solution in D_2O at 70° it gives a simple c.m.r. spectrum consisting of 12 signals, each arising from the 12 structurally distinguishable carbon atoms of the repeating unit. A partial assignment was made following preparation of the c.m.r. spectrum of the (1 → 4)-linked β-D-mannopyranan from ivory nuts (16) dissolved in 5% NaOD in D_2O. Since the mannan is insoluble in D_2O it is necessary to use the same alkaline solvent for the spectral determination on the mannan from

Can. J. Chem. Downloaded from www.nrcresearchpress.com by 210.87.254.42 on 09/05/12
For personal use only.

Rhodotorula glutinis. The spectrum of the (1 → 4)-linked β-D-mannopyranan could be rationalized by referring to the assignments of Dorman and Roberts (8) for β-D-mannose. The resonances of C-2 to -6 of the mannan corresponded closely with those of β-D-mannose with the exception of C-4, which was at 9.6 p.p.m. lower in the mannan with its resulting superimposition on the C-5 signal. A number of the resonances appeared in the c.m.r. spectrum of the mannan from *Rhodotorula glutinis*, but only the two widely-spaced C-1 signals could be assigned with certainty. The other assignments, also presented in the Experimental, are somewhat more tentative with the exception of the C-3 signal of the 3-*O*-substituted units which is downfield from the other C-2 to -6 signals.

In some of the mannobioses the signals of carbons substituted by mannosyl group can be assigned. The deshielding effect of the *O*-mannosyl unit can then be calculated by comparison of the chemical shift of the *O*-substituted carbon with that of the corresponding carbon in α- and β-D-mannose (8), whichever is appropriate (Table 3). For example the downfield displacement of the C-2 signal of 2-*O*-α-D-mannopyranosyl-α-D-mannose is 8.0 p.p.m., compared with that of the C-2 of α-D-mannose. Downfield displacements of the same order were found for C-3 of 3-*O*-α-D-mannopyranosyl-α-D-mannose (7.3 p.p.m.) and 2-*O*-β-D-mannopyranosyl-α-D-mannose (7.6 p.p.m.). Likewise the C-2 signal of 2-*O*-β-D-mannopyranosyl-β-D-mannose is at 8.4 p.p.m. lower field and C-3 signal of 3-*O*-α-D-mannopyranosyl-β-D-mannose is at 7.3 p.p.m. lower field than the corresponding carbons in β-D-mannose.

A greater variation of the downfield displacement values was found on comparing the chemical shifts of C-1′ of α- and β-linked mannobioses, respectively, with those of C-1 of α- and β-D-mannose. Of the values recorded in Table 3, perhaps the most intriguing are those of 2-*O*-β-D-mannopyranosyl-α-D-mannose (5.3 p.p.m.) and its β-anomer (7.4 p.p.m.). The factor or factors responsible for the large difference in values of these relatively more sterically hindered mannobioses will be further investigated.

Experimental

Nuclear Magnetic Resonance Spectroscopy

C.m.r. spectra were obtained using a Varian XL-100-15 n.m.r. spectrometer with Fourier transform on 5% solutions of sugar in D_2O (4 ml) at 70°. Under these conditions approximately 24 000 transients are required. The spectra incorporated 4096 data points with a sweep width of 5000 Hz (198.4 p.p.m.). When comparison of signal size was carried out, the spectra were obtained consecutively, a sweep width of 2500 Hz being used with a correspondingly greater number of transients. In each run the acquisition time was 0.4 s, the pulse width 50 μs, and the maximum decoupling power (10 W) was used, which was centered on 500 Hz downfield from the ^1H resonance of TMS corresponding to the approximate center of the p.m.r. spectra. The hetero-noise bandwidth was 2000 Hz.

Chemical shifts are in p.p.m., the term δ_c describing the downfield difference of the signal resonance and that of external TMS contained in a coaxial capillary. Under such conditions the methyl signal of an internal standard, acetone, was δ_c 31.2 p.p.m.

Some of the c.m.r. spectra of oligosaccharides and mannans are recorded in Tables 1 and 2 and Fig. 2 together with assignments. The other spectra referred to in the above discussion are as follows.

(1) Ivory nut mannan in 5% NaOD in D_2O at 30°

101.7 (C-1), 78.8 (C-4, -5), 73.5 (C-3), 72.2 (C-2), 62.1 (C-6).

(2) Rhodotorula glutinis mannan in 5% NaOD in D_2O at 30°

In the following assignments M^3 and M^4 refer to the 3-*O*- and 4-*O*-substituted β-D-mannopyranose units, respectively, to which the following carbon atoms belong: 101.7 (M^4, C-1), 98.0 (M^3, C-1), 81.2 (M^3, C-3), 78.8 (M^4, C-5), 77.1 (M^4, C-4), 75.4 (M^3, C-5), 73.4 (M^4, C-3), 72.3 (M^4, C-2), 68.9 (M^3, C-2), 66.9 (M^3, C-4), 62.9 (M^3, C-6), 62.0 (M^4, C-6).

(3) 2-O-β-D-Mannopyranosyl-αβ-D-mannose (17)

102.8 (C-1′ of β-anomer), 100.7 (C-1′ of α-anomer), 95.3 (C-1 of β-anomer), 93.7 (C-1 of α-anomer), 81.4 (C-2 of β-anomer), 80.0 (C-2 of α-anomer).

(4) O-β-D-Mannopyranosyl-(1 → 2)-O-β-D-mannopyranosyl-(1 → 2)-αβ-D-mannose (2)

102.8 (C-1 of internal unit), 100.9 (C-1 of non-reducing end-unit), 94.4 (C-1 of β-anomeric reducing end-unit), 93.8 (C-1 of α-anomeric reducing end-unit), 80.6, 80.4 (C-2 of internal unit and α-anomeric reducing end-unit).

(5) O-β-D-Mannopyranosyl-(1 → 2)-O-β-D-mannopyranosyl-(1 → 2)-O-β-D-mannopyranosyl-(1 → 2)-αβ-D-mannose (2)

102.8 (C-1 of internal units), 101.2 (C-1 of non-reducing end-unit), 95.3 (C-1 of β-anomeric reducing end-unit), 94.0 (C-1 of α-anomeric reducing end-unit), 81.2, 81.0, 80.2 (C-2 of 2-*O*-substituted units).

(6) O-α-D-Mannopyranosyl-(1 → 2)-O-β-D-mannopyranosyl-(1 → 2)-O-β-D-mannopyranosyl-(1 → 2)-O-α-D-mannopyranosyl-(1 → 2)-αβ-D-mannose (2)

102.5, 101.7, 101.6, 101.2 (C-1 of non-reducing end-unit and internal units), 95.1 (C-1 of β-anomeric reducing end-unit, small signal) 94.4 (C-1 of α-anomeric reducing end-unit), 80.8 (β-anomer), 80.2, 80.0, 78.7, 78.5 (C-2 of substituted units).

(7) 3-O-α-D-Mannopyranosyl-αβ-D-mannose (21)

103.8 (C-1′ of α and β-anomer), 95.8 (C-1 of α-anomer)

Can. J. Chem. Downloaded from www.nrcresearchpress.com by 210.87.254.42 on 09/05/12
For personal use only.

TABLE 3. Downfield displacement, in p.p.m., of ^{13}C signals of α- and β-D-mannose on replacement of the attached hydroxyl group with an *O*-mannopyranosyl unit

No.		Chemical shift of *O*-substituted carbon signal of mannobiose	Chemical shift of corresponding carbon in α- or β-D-mannose	Downfield displacement of signal	Chemical shift of C-1′ of mannobiose,	Chemical shift of C-1 of α- or β-D-mannose	Downfield displacement of signal
1	2-*O*-α-D-Mannopyranosyl-α-D-mannose	80.0	72.6 (C_α-2)	7.4	103.8	95.8 (α)	8.0
2	3-*O*-α-D-Mannopyranosyl-α-D-mannose	79.8	72.2 (C_α-3)	7.6	103.8	95.8 (α)	8.0
3	3-*O*-α-D-Mannopyranosyl-β-D-mannose	82.7	75.0 (C_β-3)	7.3	103.8	95.8 (α)	8.0
4	2-*O*-β-D-Mannopyranosyl-α-D-mannose*	80.0	72.6 (C_α-2)	7.4	100.7	95.4 (β)	5.3
5	2-*O*-β-D-Mannopyranosyl-β-D-mannose*	81.4	73.0 (C_β-2)	8.4	102.8	95.4 (β)	7.4
6	4-*O*-β-D-Mannopyranosyl-α-D-mannose	—	—	—	101.9	95.4 (β)	6.5
7	6-*O*-α-D-Mannopyranosyl-α-D-mannose	—	—	—	101.5	95.8 (α)	5.7

*The values for Nos. 4 and 5 can be regarded sceptically because of difficulties in definitely assigning signals.

95.3 (C-1 of β-anomer) 82.3 (C-3 of β-anomer), 79.8 (C-3 of α-anomer), 77.8 (C-5 of β-anomer), 75.1, 74.5, 72.7, 72.4, 72.0, 68.9, 67.9, 63.0 (C-6's).

The author would like to thank Mr. M. Mazurek for preparation of c.m.r. spectra.

1. P. A. J. GORIN and J. F. T. SPENCER. Adv. Appl. Microbiol. **13**, 25 (1970).
2. P. A. J. GORIN, J. F. T. SPENCER, and S. S. BHATTACHARJEE. Can. J. Chem. **47**, 1499 (1969).
3. P. A. J. GORIN, M. MAZUREK, and J. F. T. SPENCER. Can. J. Chem. **46**, 2305 (1968).
4. N. YAMAOKA, T. USUI, Z. MATSUDA, K. TUZIMURA, H. SUGIYAMA, and S. SETO. Tetrahedron Lett. 2047 (1971).
5. A. ALLERHAND and D. DODDRELL. J. Am. Chem. Soc. **93**, 2777 (1971).
6. P. A. J. GORIN and J. F. T. SPENCER. Can. J. Microbiol. **18**, 1709 (1972).
7. P. A. J. GORIN and J. F. T. SPENCER. Adv. Carbohydr. Chem. **23**, 367 (1968).
8. D. E. DORMAN and J. D. ROBERTS. J. Am. Chem. Soc. **92**, 1355 (1970).
9. A. ALLERHAND, D. DODDRELL, and R. KOMORSKI. J. Chem. Phys. **55**, 189 (1971).
10. P. A. J. GORIN, J. F. T. SPENCER, and R. J. MAGUS. Can. J. Chem. **47**, 3569 (1969).
11. P. A. J. GORIN, J. F. T. SPENCER, and D. E. EVELEIGH. Carbohydr. Res. **11**, 387 (1969).
12. Y.-C. LEE and C. E. BALLOU. Biochemistry, **4**, 257 (1965).
13. P. A. J. GORIN and A. S. PERLIN. Can. J. Chem. **34**,h1796 (1956).
14. G. H. JONES and C. E. BALLOU. J. Biol. Chem. **244**, 1052 (1969).
15. P. A. J. GORIN, K. HORITSU, and J. F. T. SPENCER. Can. J. Chem. **43**, 950 (1965).
16. K. H. MEYER and H. MARK. Der Aufbau der hochpolymeren organischen Naturstoffe, 168 (1930).
17. P. A. J. GORIN. Can. J. Chem. **51**, 2105 (1973).
18. J. F. T. SPENCER and P. A. J. GORIN. Antonie van Leewenhoek, J. Microbiol. and Serol. **37**, 75 (1971).
19. P. A. J. GORIN and J. F. T. SPENCER. Can. J. Chem. **46**, 3407 (1968).
20. P. A. J. GORIN and A. S. PERLIN. Can. J. Chem. **35**, 262 (1957).
21. P. A. J. GORIN and J. F. T. SPENCER. Can. J. Chem. **48**, 198 (1970).

Can. J. Chem. Downloaded from www.nrcresearchpress.com by 210.87.254.42 on 09/05/12
For personal use only.

Dakin Oxidation of *o*-Hydroxyacetophenone and some Benzophenones: Rate Enhancement and Mechanistic Aspects

M. B. HOCKING

Research Department, Dow Chemical of Canada, Ltd., Sarnia, Ontario and Department of Chemistry, University of Victoria, Victoria, British Columbia

Received July 6, 1972[1]

A synthetic aqueous alkaline hydrogen peroxide solution, made up to approximate the concentrations of caustic and hydrogen peroxide expected from water washing of aerated sodium amalgam, readily oxidized *o*-hydroxyacetophenone to catechol. The relevance of a proposed ester intermediate of this reaction is discussed, and also the possibility of using *o*-hydroxybenzophenone (originating from phenylbenzoate) as a substrate is briefly considered.

Une solution synthétique d'eau oxygénée alcaline a été réalisée pour avoir des concentrations approximatives en caustique et eau oxygénée semblables à celles attendues des eaux de lavage d'amalgame de sodium aéré. Cette solution oxyde facilement l'*o*-hydroxyacétophénone en catéchol. L'intermédiaire ester proposé pour cette réaction a été discuté, la possibilité d'utiliser l'*o*-hydroxyacétophénone (issu du benzoate de phényle) comme substrat a été considérée brièvement. [Traduit par le journal]

Can. J. Chem., **51**, 2384 (1973)

Introduction

Dakin reported (1) in 1909 that alkaline hydrogen peroxide will oxidize *o*- or *p*-hydroxy aromatic aldehydes, **1**, to the corresponding dihydroxyaromatic, **2** (see Scheme 1). While he carried out preliminary investigations with some hydroxyacetophenones, the scope with acetophenones was widened (2, 3) and benzylic ketones included (4) by the later work of Baker and co-workers. Dakin oxidation has been cursorily reviewed (5–7). Mechanistic interpretations have been drawn (5) from the related Baeyer–Villiger oxidation of carbonyl-labelled *p*-methoxyacetophenone, in which it was found that all the label was retained in the carbonyl (8). This finding has since been supported, again by analogy, with retention of the label in the catechol formed when salicylaldehyde is oxidized with oxygen-labelled hydrogen peroxide (9).

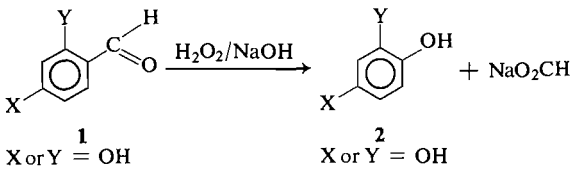

1
X or Y = OH

2
X or Y = OH

SCHEME 1

Dakin oxidation appears capable of satisfying several useful ends not previously considered. It could provide an outlet of greater value than caustic soda for the sodium amalgam produced in mercury cell chlor–alkali production. Aeration of the amalgam, followed by washing with water, gives a dilute aqueous solution of sodium hydroperoxide and sodium hydroxide in water (10) (eqs. 1 and 2). We wished to demonstrate

[1] $$4Na/Hg + O_2 \rightarrow 2Na_2O/Hg$$

[2] $$Na_2O/Hg + 2H_2O \rightarrow NaOH + NaOOH + Hg + H_2\uparrow$$

that this relatively cheap oxidizing solution could be used directly, avoiding the expensive steps of neutralization and distillation required to isolate hydrogen peroxide. *o*-Hydroxyacetophenone appeared to be a useful test substrate, yielding catechol on oxidation. However, as normally run, Dakin oxidation uses only one equivalent of base for each equivalent of hydrogen peroxide (11), and is too slow (16–24 h (11)) to be commercially attractive. The aim of our experiments was to determine a set of conditions where high yields may be achieved in a short reaction time, and, complementary to this, to briefly study mechanistic aspects and alternative substrates for this oxidation.

Experimental

ortho-Hydroxyacetophenone was purchased from Aldrich Chemical Company, checked for purity by n.m.r., and used as received. Caustic was "Dowflake", Dow Chemical of Canada production material, 99.6% purity. Sodium carbonate (anhydrous) and hydrogen peroxide (30%) were Fisher reagent grade chemicals. A Fisher

[1]Revision received March 20, 1973.

Can. J. Chem. Downloaded from www.nrcresearchpress.com by 210.87.254.105 on 09/05/12
For personal use only.

TABLE 1. Summary of Dakin oxidations of *o*-hydroxyacetophenone

Experiment number[a]	Moles of Reactants: Aceto-phenone ketone[b]	Base(s)[c]	H_2O_2	Maximum temperature (°C)[d]	Reaction time (h)[e]	Conversion (%)	Yield (%)[f]: Crude	Yield (%)[f]: Pure
1	0.5	0.5	0.6	51	(24)	94	71	68
2	0.5	1.0	0.6	52	2.0	76	36	33
3	0.1	0.1 + 0.06 Na_2CO_3	0.113	53	0.33	96	80	77
4	0.1	0.1 + 0.06 Na_2CO_3	0.12	49	0.5	95	96	48[g]
5	0.1	0.22	0.12	53.5	1.5	54	96	21[g]
6	0.1	0.10	0.12	48.5	(20)	95	88	78
7	0.1	0.12 Na_2CO_3	0.12	46	1.0	89	87	53
8	0.1	0.10 + 0.06 Na_2CO_3	0.12	50	1.0	97	92	58
9	0.1	0.10 + 0.06 Na_2CO_3	0.12	49–70[h]	0.5	96	81	69
10	0.1	0.08 Na_3PO_4	0.12	41.5	(1.3)	56	85	—
11	0.1	0.10 + 0.04 Na_3PO_4	0.12	48.5	(1.0)	80	86	—
12	0.1	0.20	0.12	53	(1.0)	98	93	72
13	0.1	0.10 + 0.12[g] Alkanox[i]	0.12	49.5	(1.5)	94	90	—
14	0.1	0.10 + 0.127[g] Amway[i]	0.12	47	(1.0)	88	94	66
15	0.1	0.10 + 0.06 Na_2SiO_3	0.12	53	(1.0)	99	94	—
16	0.1	0.10 + 0.10 NH_4OH	0.12	49	(1.5)	97	92	68
17	0.1	0.20 NH_4OH	0.12	44	(1.2)	91	93	51
18	0.1	0.10 + 0.06 Na_2MoO_4	0.12	46.5	1.0	22	≈ 30	0
19	0.1	0.05	0.12	38	(1.0)	46	80	89

[a]Experiments 1–7 in glass, remainder in polyethylene (see Fig. 1).
[b]Experiments 1 and 2 in 710 ml of water, 3 in 200 ml, all others in 275 ml.
[c]Sodium hydroxide unless otherwise stated.
[d]From a starting temperature of 28°, non-thermostatted.
[e]Peroxide remained in those reactions where the time is parenthesized.
[f]Yields based on hydroxyacetophenone consumed. Crude yields by isolation for experiments 1–3, all others by u.v. determination.
[g]Repetition of experiments 4 and 5 in polyethylene, and work-up by salting and ether extraction (see experimental) followed by purification by sublimation gave pure yields of 84 and 52% respectively.
[h]Experiment was thermostatted prior to, and during the reaction, at 49°.
[i]Alkanox and Amway, trade name detergents.

"Accumet" p*H* meter (model 310) was used for p*H* determination and standardized immediately prior to measurement on a buffer near the p*H* to be measured. U.v. spectra were obtained on a Beckman DK-2 ratio recording spectrophotometer.

Hydrogen Peroxide Standardization

Ten-milliliter aliquots of a 1:50 dilution of 30% H_2O_2 were titrated, in acetic acid (25 ml) and aqueous KI (10 ml of 50%) containing 5 drops of 3.7% $(NH_4)_2MoO_4$ catalyst (9), with 0.100 *N* $Na_2S_2O_3$. Titrant (53.1 ml) was required establishing a stock solution H_2O_2 strength of 32 vol % (39.8 wt. %). The density of the stock 30% H_2O_2 at 25° was 1.1325, indicating (9) 36 wt. % H_2O_2. All experiments, except no. 19, were run using portions of the same lot of hydrogen peroxide, the strength of which was periodically checked.

Reaction Vessel Pretreatment

New 500-ml glass vessels were thoroughly washed with methylene chloride, detergent, and hot water and rinsed with distilled water. Ten milliliters of 30% H_2O_2 was added and the vessel filled with 0.1 *N* NaOH and left at room temperature for 24 h. Immediately prior to use, it was thoroughly rinsed with distilled water. Polyethylene vessels were made up from new 500-ml wash bottles pretreated in the same way as the glass vessels.

Peroxide Titrations

Frequent blanks were carried out to improve reproducibility. The reaction aliquot was swirled into a freshly mixed solution of 10% KI (5 ml) and 3.7% $(NH_4)_2MoO_4$ (5 drops) in acetic acid (10 ml) and allowed to stand 20 min before titrating. Standardized (0.100 *N*) sodium thiosulfate was the titrant and starch solution was added near the end point to facilitate determination.

Dakin Oxidation of ortho-Hydroxyacetophenone

The base (usually 0.1 mol, see Table 1) was dissolved, with magnetic stirring, in distilled water (usually 275 ml) in a pretreated polyethylene wash bottle. The ortho-hydroxyacetophenone (usually 13.6 g; 0.1 mol) was then

Can. J. Chem. Downloaded from www.nrcresearchpress.com by 210.87.254.105 on 09/05/12
For personal use only.

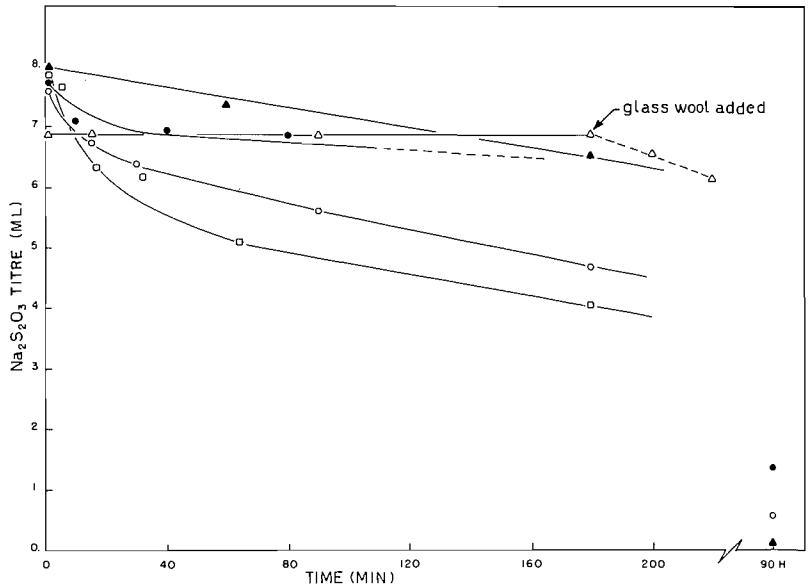

FIG. 1. Stability of aqueous hydrogen peroxide in various alkaline media at 28°. Blanks: NaOH in glass, ●; NaOH + Na_2CO_3 in polyethylene, △; NaOH + Na_2CO_3 in glass, ○; NaOH in polyethylene, ▲; NaOH + Na_2CO_3 at 50° in polyethylene, □.

added, the temperature of the solution adjusted to 28 °C and the 30% hydrogen peroxide (9.4 ml; 0.12 mol) added all at once, with continued stirring throughout. During each reaction the temperature was noted at frequent intervals. Six to eight aliquots of 1 or 2 ml each, depending on the stage of the reaction, were removed at timed intervals during the reaction and titrated iodometrically for peroxide content.

Unreacted starting material was recovered, after slightly acidifying the reaction mixture with glacial acetic acid, by azeotroping with about 100 ml of the water on a boiling water bath under slightly reduced pressure. The insoluble ketone was separated, the rest of the aqueous distillate was saturated with salt and extracted with 2 or 3 small portions of methylene chloride and the combined organic phases dried ($MgSO_4$). Careful distillation of the methylene chloride yielded the unreacted *o*-hydroxyacetophenone. In one or two reactions, when the aqueous distillate after extraction was examined by u.v. absorption, there was evidence of traces (2–10 mg of each) of muconaldehyde and muconic acid, which had been previously observed in peracetic acid oxidations of catechol (12). Approximately 35 mg of catechol had also come over. At no time could any of the intermediate *o*-hydroxyphenylacetate be detected by i.r. or n.m.r. analysis.

The catechol was determined initially by acidifying (acetic acid) the distilland to avoid p*H*-induced shift of the catechol u.v. absorption maximum, making it up to a measured volume with distilled water and then obtaining a catechol concentration figure by comparing the u.v. absorption with that shown by a series of standards. For actual isolation of the catechol three methods were used. The most efficient method was saturation of the aqueous solution with salt and extraction with 5 or 6 small portions of ether (experiment 19). The catechol (4.6 g; 89%) was obtained upon drying and distillation of the ether from the combined extracts. Both of the other work-up methods required initial removal of the water under reduced pressure on a steam bath. One used exhaustive Soxhlet extraction with toluene, the thimble contents being re-ground several times during the extraction. This was used in experiments 1–7, 12, 14, 16, and 17. The other involved trituration of the solid residue with several portions of hot acetone followed by distillation of the combined extracts to remove the acetone (experiments 8 and 9). The catechol was then separated from the traces of salts also extracted by the acetone by vacuum distillation.

Peroxide Stability Experiments

These were conducted in various solutions in the same way as the oxidation experiments above, but as blanks without substrate present (Fig. 1).

Dakin Oxidation of p-Hydroxyacetophenone

To a solution of *p*-hydroxyacetophenone (13.6 g; 0.1 mol) and sodium hydroxide (4 g; 0.1 mol) in distilled water (275 ml) in a polyethylene vessel was added 30% hydrogen peroxide (9.4 ml; 0.12 mol) with stirring. The solution remained homogeneous on the addition of peroxide, in contrast to the *o*-ketone experiments. A small portion of the above solution was placed in an n.m.r. tube, and was scanned in the region of the acetyl methyl at 2 min intervals. As determined by titration for peroxide and by the decrease in the acetyl methyl, and formation and increase of the acetate methyl n.m.r. signals, the rate of this reaction was about the same as the rates of reaction with *o*-hydroxyacetophenone.

Can. J. Chem. Downloaded from www.nrcresearchpress.com by 210.87.254.105 on 09/05/12
For personal use only.

Can. J. Chem. Downloaded from www.nrcresearchpress.com by 210.87.254.105 on 09/05/12
For personal use only.

Hydroquinone Monoacetate

A low yield of hydroquinone monoacetate was obtained by the method of Olcott (13). From a 1 g mole-scale reaction, 4 g of cream colored crystals of the monoester was obtained (m.p. from benzene–hexane 56–60°, lit. (13) 62–63°; proton n.m.r. H_2O from external tetramethylsilane gave: acetate methyl, δ 2.72 p.p.m.; aromatic, 7.38 p.p.m.; integrals 3:4).

Competitive Oxidation–Hydrolysis of p-Hydroxyacetophenone – Hydroquinone Monacetate

p-Hydroxyacetophenone (136.3 mg) and solid sodium hydroxide (40 mg) were dissolved in water (2.7 ml) in a test tube. Hydroquinone monoacetate (152.4 mg) and 30% hydrogen peroxide (113.2 mg) were added simultaneously and the mixture vigorously agitated. A sample, removed and examined by n.m.r., showed a small proton resonance peak for ketone methyl and large peaks for ester and sodium acetate methyls (shifts, from external tetramethylsilane, δ 2.97, 2.72, and 2.35 p.p.m. respectively). Identification was confirmed by seeding with authentic materials. An iodine–thiosulfate titer on a 1-ml aliquot showed that no peroxide remained.

The experiment described above was repeated, but with a preliminary n.m.r. examination of the mixture of all components before peroxide addition. At this point the sharp ketone methyl and ester methyl peak heights were 125 and 112 mm respectively. After peroxide had been added (diluting the solution somewhat), methyl peak heights were: acetate ion 102 mm, ester 50 mm, ketone 15 mm.

Repetition of the experiment two further times, but with 2 equiv of sodium hydroxide (80 mg) and twice the original amount of water (5.4 ml) present initially showed methyl peak heights for acetate ion, 133 and 110 mm, ester, 46 and 29 mm, and ketone, 13 and 10 mm at the end of the reactions.

When the monoester was omitted from the reaction mixtures, no ester methyl was observed during n.m.r. scans at 1 min intervals for the duration of the reaction, and the *p*-hydroxyacetophenone oxidation proceeded more slowly than in the presence of ester. When ketone was omitted from reaction mixtures, ester hydrolysis proceeded more rapidly than in its presence.

Attempted Oxidation of Benzophenone

Using 4 equiv of base and peroxide on a 0.1 g molar scale under the standard Dakin oxidation conditions, only unchanged starting material was obtained.

Oxidation of o-Hydroxybenzophenone

To a stirred solution of the ketone (9.6 g) and sodium hydroxide (4.8 g) in water (200 ml) was added 1 equiv of 30% hydrogen peroxide (5 ml). After 1.5 h virtually no peroxide was left. The components were separated by acidifying (HCl), saturating with salt, and extracting with ether, followed by extractive separations of the acid, phenolic water-soluble, and phenolic water-insoluble fractions. Benzoic acid (1.35 g, m.p. and mixed m.p. 121–123°, and by g.c. retention time), catechol (0.25 g, identified as above, plus n.m.r.), and unchanged starting material (8 g, by g.c. retention time and n.m.r.) were obtained. No salicylic acid could be detected.

When repeated on twice the scale using 5 equiv of peroxide, 10 g of benzoic acid, 4.1 g of catechol, and 1 g of unchanged starting material were obtained.

Oxidation of p-Hydroxybenzophenone

To a stirred solution of the ketone (19.8 g) and sodium hydroxide (18 g) in water (400 ml) was added 30% hydrogen peroxide (45 ml). Peroxide loss was slow, so the reaction was warmed for 1 h in a water bath at 70°. Work-up by the method used for the ortho isomer yielded 2.5 g of benzoic acid and 14.55 g of unchanged starting material. No phenolic product was isolated or detectable.

Oxidation of 4-Hydroxy-4′-methylbenzophenone

This reaction was carried out in exactly the same way as the above using 21.2 g of ketone. *p*-Toluic acid (1.1 g) (m.p. and mixed m.p. 177–180°) and 19 g of unchanged starting material were obtained. No phenolic product was detected.

Oxidation of 2-Furfural

2-Furfural (19 g; freshly redistilled, cut boiling at 156–157°) was added all at once, with stirring to a solution of caustic (8 g) and 30% hydrogen peroxide (18.4 ml) in distilled water (400 ml). After 30 min, when no peroxide was left by titration of an aliquot, the solution was acidified, saturated with salt, and extracted with ether. Separation of the combined extracts into a neutral and an acidic fraction yielded 9.9 g of unchanged 2-furfural (pure, by g.c.) from the former, and 2.4 g crude (0.5 g pure) of 2-furoic acid (m.p. and mixed m.p. 133–134°, and by n.m.r.) from the latter.

A blank reaction (Cannizzaro) carried out as above but omitting the peroxide gave 10 g of unchanged starting material, and 4 g crude (1.2 g pure) 2-furoic acid. No 2-furfuryl alcohol could be detected by n.m.r. in the recovered starting material.

Results and Discussion

The already-optimized procedure of Dakin (11) for the oxidation of salicylaldehyde was taken as a starting point for the study of Dakin oxidation of *o*-hydroxyacetophenone. The effect of a number of variables on conversions and yields is summarized in Table 1.

It was found that doubling the ratio of caustic to hydrogen peroxide in the reaction significantly increased the rate. Twenty to thirty minutes at temperatures of the order of 30° was sufficient to give nearly complete reaction without any loss in conversion or yield from that attainable under normal Dakin conditions. Either 2 equiv of caustic, or a mixture of 1 equiv of sodium carbonate plus 1 equiv of caustic for each equivalent of peroxide gave this result. Thus, experiments 3, 4, 8, 9, and 12 gave faster reactions (See Fig. 2) and similar or better conversions and yields than experiments 1 and 6, which were carried out under normal Dakin conditions. An exception to this generalization was experiment 5, which gave a 96% yield but only 54% conversion. While this should have given as good results as experiment 12 (93 and 98% respec-

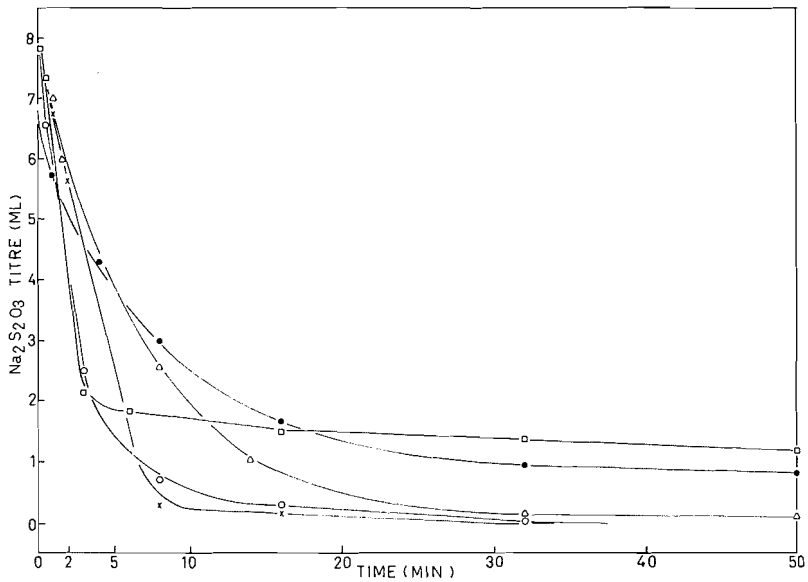

FIG. 2. Peroxide titre *vs.* time for Dakin oxidations at room temperature. Equivalents of base used per equivalent of substrate: 1 NaOH + 1 Na_2CO_3 = ○ (4); 1 NaOH = □ (6), 2 Na_2CO_3 = △ (7); 2 NaOH = X (12), 2 NH_4OH = ● (17). Experiment numbers are given parenthetically.

tively), spontaneous peroxide decomposition in the glass vessel perhaps was responsible for the lower conversion. That this is a likely explanation is shown in Figure 1.

Use of 2 equiv of sodium carbonate, the effect of full carbonation of the alkaline peroxide, results in a significant lengthening of the reaction time, and slightly reduces the conversion and yield (experiment 7).

From the inhomogeneity of reactions using 1 mol of caustic per mol of substrate, and from the homogeneous solutions obtained in the reactions using 2 equiv of base, it appeared that homogeneity may largely be the determining factor for the rate and yield improvements. To test this theory, two experiments (13 and 14) were carried out using 1 equiv of base plus just sufficient synthetic detergent to maintain homogeneity. These reactions gave initial rates as fast as and yields comparable to those obtained by the use of 2 mol of base. However, they still showed the same very slow disappearance of the last 15% of peroxide (Figure 2 and Table 2), found in reactions containing only 1 mol of base, without detergent.

The faster rates throughout the reaction in the presence of 2 equiv of base are probably the result of a p*H* effect combined with a homogeneity difference. In order to determine the effect of a change in p*H* and at the same time to determine whether or not another base could be used in place of caustic or sodium carbonate, reactions were tried using trisodium phosphate, sodium silicate, ammonium hydroxide, and sodium molybdate as alternatives. Other possible bases were too expensive, too insoluble, or could not be obtained by neutralizing aerated sodium amalgam washings to be worth considering for a process. Sodium phosphate, on a sodium ion equivalence basis (*i.e.* as would be obtained on neutralization of NaOOH + NaOH with phosphoric acid), gave only 56% conversion but still a reasonably high yield (experiment 10). When used in conjunction with 1 equiv of caustic the conversion rose significantly but the yield remained at about 86%. This was lower than the yields obtained in reactions using 2 equiv of caustic or caustic–carbonate as the base. Sodium silicate, with which the expected (14) significant spontaneous decomposition of hydrogen peroxide did not materialize, gave a very high conversion and yield (experiment 15). Ammonium hydroxide in conjunction with caustic gave a very high conversion and yield, but alone was not quite so effective and gave a more tarry crude product than any other reaction. Sodium molybdate, as anticipated (14), caused rapid spontaneous decomposition of the

Can. J. Chem. Downloaded from www.nrcresearchpress.com by 210.87.254.105 on 09/05/12
For personal use only.

TABLE 2. *o*-Hydroxyacetophenone reaction performance correlated with p*H*

Experiment number	Bases present[a] (mol)	p*H* of reaction Start[b]	p*H* of reaction End	Residual peroxide (%)[c]	Conversion (%)	Yield[d] (%)
12	0.2 NaOH	13.1	10.6	3	98	93
15	0.1 NaOH, 0.06 Na_2SiO_3	12.7	10.8	3	99	94
8	0.1 NaOH, 0.06 Na_2CO_3	12.8	10.2	< 1	97	92
6	0.1 NaOH	12.3	8.1	18	95	88
13	0.1 NaOH, 0.12 g Alkanox	12.3	8.1	13	94	90
16	0.1 NaOH, 0.1 NH_4OH	12.1	10.0	9	97	92
18	0.1 NaOH, 0.06 Na_2MoO_4	11.9	11.2	< 1	22	≈ 30
14	0.1 NaOH, 0.13 g Amway	11.8	—	16	88	94
11	0.1 NaOH, 0.04 Na_3PO_4	11.8	9.9	2	80	86
19	0.05 NaOH	11.8	7.8	36	46	89
10	0.08 Na_3PO_4	11.9	9.1	17	56	85
7	0.12 Na_2CO_3	10.9	8.6	2	89	87
17	0.2 NH_4OH	10.6	9.5	12	91	93[e]

[a]Per 0.1 mol of *o*-hydroxyacetophenone.
[b]All reactants except ketone present when measured.
[c]Thirty-two minutes after peroxide added.
[d]Yields based on hydroxyacetophenone consumed. Crude yield, usually by u.v. (see Table 1).
[e]Most tarry reaction.

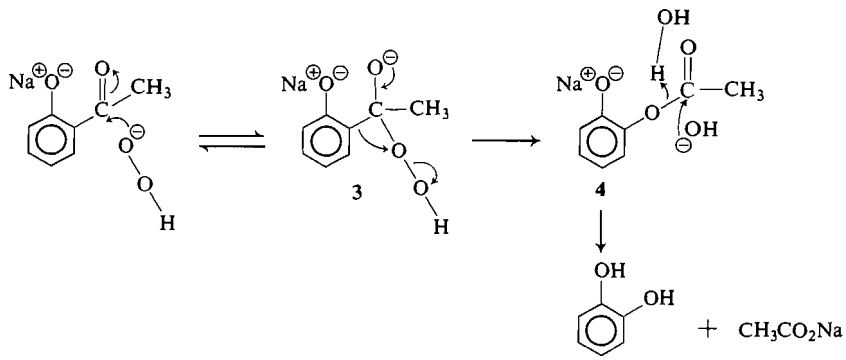

SCHEME 2

peroxide, and gave the lowest conversion (22%) and yield (about 30%) of any reaction in this series.

When the variations in the base are correlated with the p*H* measured before and after the reaction (Table 2), a number of observations can be made. Those reactions where conditions were such that the p*H* remained high (above about 10.5) throughout the reaction are those which were fast with high yields. The one exception is that of the reaction containing molybdate anion. This incurred visible spontaneous peroxide decomposition and, because of the resultant low conversion, the p*H* remained high. The p*H* dropped to 10 or below in the reactions involving sodium phosphate alone, ammonium hydroxide, and those using 1 equiv of caustic or less, with or without detergent, giving lower yields.

The p*H* effect can be explained by considering the hydroperoxide anion concentration. Probably the initial step of a Dakin oxidation involves attack of a hydroperoxide anion on the carbonyl carbon (5), see Scheme 2. Hence, the higher the concentration of hydroperoxide anion, the more rapidly the oxidation should proceed. Since the pK_a of hydrogen peroxide is 11.75 (14), at a p*H* of 11.75 half of the hydrogen peroxide will be dissociated to the hydroperoxide anion while at a p*H* of 9.75 the relative hydroperoxide anion concentration is only 1% of this.[2] Thus, as the p*H* of the oxidizing media falls to 9.5–10 it can

[2]The p*H* range for maximum capricious decomposition of hydrogen peroxide lies in the region of 9.5–12, presumably because it is the region where a significant concentration of hydroperoxide anion, the least stable species of this equilibrium, is present.

Can. J. Chem. Downloaded from www.nrcresearchpress.com by 210.87.254.105 on 09/05/12
For personal use only.

Can. J. Chem. Downloaded from www.nrcresearchpress.com by 210.87.254.105 on 09/05/12
For personal use only.

be expected that a significant decrease in oxidation rate will result. This effect may be the explanation for the very slow final rates observed in experiments 6, 10, 13–17, and 19, where the final p*H* dropped to 10 or below.

Another factor which may contribute to the higher rates at high p*H* is the greater proportion of dissociated phenol in the substrate being oxidized. Phenyl migration is more facile in an intermediate with an ionized hydroxyl, **3**, than in an intermediate in which the hydroxyl is protonated, **5**, which will predominate below a

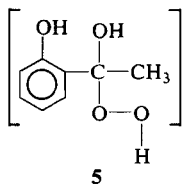

5

p*H* of about 10. The latter is not only likely to retard the reaction by shifting the first equilibrium to the left, but may permit competition of methyl with phenyl migration (no salicylic acid was observed in our reactions). Also, ring oxidation is more likely to compete with acyl oxidation in **5** than in **3**, with its far less electrophilic ring. This may account for the somewhat lower yields observed in a number of the low p*H* experiments.

In an attempt to observe the ester intermediate **4**, only 0.5 equiv of caustic was used in experiment 19. Even with this low caustic ratio the p*H* was sufficiently high for the oxidation to proceed rapidly, and should the ester hydrolysis be significantly slower than oxidation, nearly all the substrate should be oxidized while only half of the ester formed would hydrolyze. Only half the peroxide was consumed in the reaction. Thus, either ester hydrolysis was very fast or the reaction proceeds via a different path. The former explanation is supported by a kinetic study of Hansen (15) on the hydrolysis of catechol monoacetate, in which he found that the second order rate constant is 1175 mol^{-1} s^{-1} at 25°, more than 700 times the rate of hydrolysis of phenyl acetate.

Without anchimeric assistance from the ortho-hydroxyl, the rate of hydrolysis of hydroqinone monoacetate is closer to that of phenyl acetate (15). Accordingly, after an initial preparative scale oxidation of *p*-hydroxyacetophenone to verify the adequacy of the reaction conditions, several competitive oxidation–hydrolysis experiments were undertaken between this ketone and hydroquinone monoacetate. These demonstrated, under a variety of conditions, that *p*-hydroxyacetophenone is more rapidly oxidized than is hydroquinone monoacetate hydrolyzed to the same product, hydroquinone. The somewhat more rapid ester hydrolysis noted in the absence of ketone than in its presence was probably a consequence of more prolonged promotion by the greater availability of hydrogen peroxide (16). This supports the contention that, at least in the oxidation of *p*-hydroxyacetophenone, true ester intermediacy is unlikely.

Transitory intermediacy of species such as **6**, **7**, or **8** could lead to the observed products without ever going through the formation of an ester (Schemes 3–5 do not require ester intermediacy). Of the decomposition pathways (*a*) and (*b*) open to intermediate **6**, alternative (*b*) is more acceptable because phenolate anion is a much better leaving group than hydroxyl ion, and because no ester formation was observed. The formation of intermediate **7** is supported by our finding that, over the p*H* range studied, the higher the p*H* the faster the reaction (Tables 1 and 2), a result easier to explain by the formation step of **7** (*i.e.* direct involvement of phenolate anion), than by the formation step of **6**. Kratzl and co-workers (17) have proposed intermediacy of perester, **8**, to support their agreement with our contention that ester intermediacy is unlikely. They suggest that the perester arises via hydroperoxide radical ring attack followed by aromatization of the quinonoid intermediate. Since perester lifetime is short, our results are also compatible with this suggested pathway.

It is possible that phenyl benzoate, prepared from the cheap industrial raw materials phenol and benzoic acid, might be thermally rearranged to a mixture of hydroxybenzophenones. With this in mind, a few Dakin oxidations were tried with this type of substrate. With 1 equiv of oxidizing agent, about 10% oxidation was achieved with *o*-hydroxybenzophenone. With 5 equiv of oxidant there was about 80% reaction with the ortho isomer, but only about 5% with *p*-hydroxybenzophenone or 4-hydroxy-4′-methylbenzophenone. Benzophenone itself was recovered unchanged.

Clean autoxidation of 2-furfural to 2-furoic

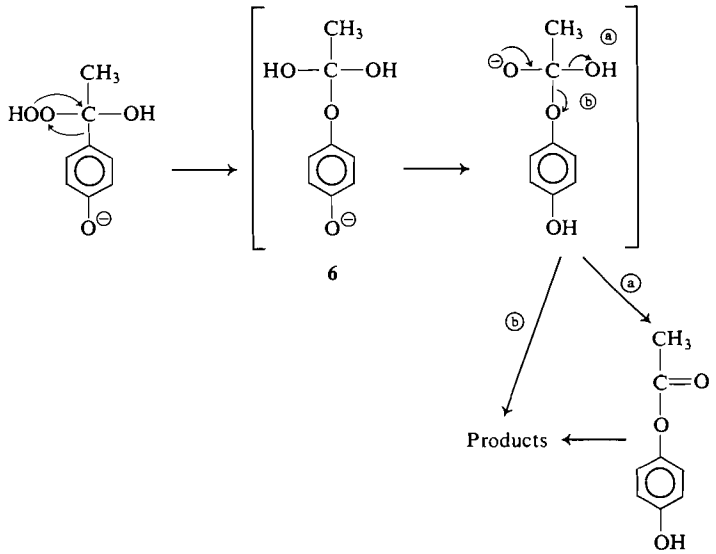

SCHEME 3

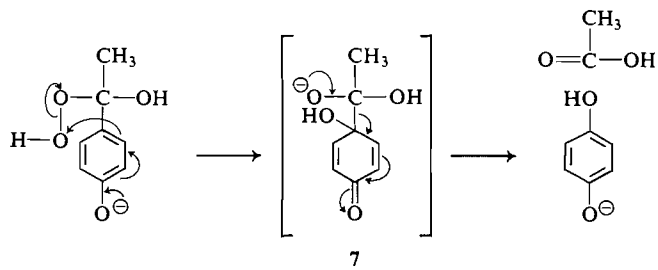

SCHEME 4

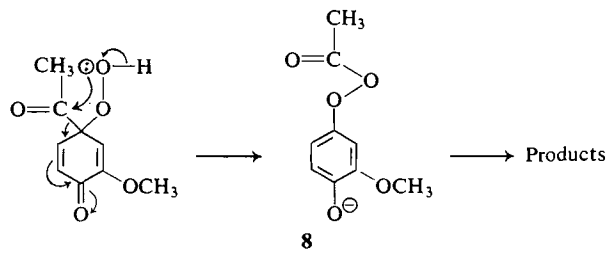

SCHEME 5

acid cannot be achieved. Hence, it was hoped Dakin conditions might be appropriate. It was found, however, that straight Cannizzaro conditions (*i.e.* only caustic present), with no peroxide, gave better results than Dakin conditions. During the course of these experiments Kulnevich *et al.* (18) reported obtaining 2-hydroxyfuran by acidic hydrogen peroxide oxidation of 2-furfural.

The author is grateful to D. J. Peterson for u.v. spectra, H. D. Mak for the n.m.r. spectra, D. G. Lowery for valued technical assistance, and to S. W. Tobey for helpful criticism of the manuscript. He thanks the National Research Council of Canada for partial financial support of this work.

1. H. D. DAKIN. Am. Chem. J. **42**, 477 (1909).
2. W. BAKER, H. G. BONDY, J. GUMB, and D. MILES. J. Chem. Soc. 1615 (1953).

Can. J. Chem. Downloaded from www.nrcresearchpress.com by 210.87.254.105 on 09/05/12
For personal use only.

3. W. BAKER and H. RAISTRICK. J. Chem. Soc. 670 (1941).
4. W. BAKER, E. H. T. JUKES, and C. A. SUBRAHMANYAM. J. Chem. Soc. 1681 (1934).
5. J. B. LEE and B. C. UFF. Quart. Rev. (London) **21**, 429 (1967).
6. M. HUDLICKY. Chem. Listy, **46**, 567 (1952).
7. J. PLIML. Chemie (Prague), **10**, 647 (1958).
8. W. E. DOERING and E. DORFMANN. J. Am. Chem. Soc. **75**, 5595 (1953).
9. M. M. ALEKSANKIN, N. A. VYSOTSKAYA, and A. E. BRODSKII. Kernenergie **5**, 362 (1962). Chem. Abstr. **61**, 16005*d* (1964).
10. Dutch Pat. 58 703. Dec. 16, 1946. To N.V. Koninklijke Nederlandsche Zoutindustrie. Chem. Abstr. **41**, 4899*b* (1947); D. L. SCHECHTER, U.S. Pat. 3 153 576. Oct. 20, 1964. To Dow Chemical Co. Chem. Abstr. **61**, 15698*h* (1964).
11. H. D. DAKIN. Org. Synth. Coll. Vol. I, 143 (1932).
12. A. WACEK and R. FIEDLER. Monatsh. Chem. **80**, 170 (1949).
13. H. S. OLCOTT. J. Am. Chem. Soc. **59**, 392 (1937).
14. W. C. SCHUMB, C. N. SATTERFIELD, and R. L. WENTWORTH. HHydrogen peroxide. Reinhold Publishing Corp., New York. 1955. Pp. 479, 496, 393.
15. B. HANSEN. Acta Chem. Scand. **17**, 1375 (1963).
16. W. P. JENCKS and J. CARIUOLO. J. Am. Chem. Soc. **82**, 1778 (1960).
17. K. KRATZL, W. SCHÄFER, P. CLAUS, J. GRATZL, P. SCHILLING. Monatsh. Chem. **98**A, 891 (1967).
18. V. G. KULNEVICH, L. A. BADOVSKAYA, and G. F. MUZYCHENKO. Khim. Geterotsiklich Soedin. Akad. Nauk Latv. SSR. 582, (1970). Current Abstr. of Chem. and Index Chemicus **38**, 154272, July 1, 1970.

Can. J. Chem. Downloaded from www.nrcresearchpress.com by 210.87.254.105 on 09/05/12
For personal use only.

Thermal Unimolecular Isomerization of 3-Methyl-3-vinyldiazirine

MICHAEL T. H. LIU AND K. TORIYAMA

Department of Chemistry, University of Prince Edward Island, Charlottetown, P.E.I.

Received November 20, 1972

The thermal isomerization of 3-methyl-3-vinyldiazirine in various solvents has been investigated over the temperature range 40–75 °C. The reaction was kinetically first order and unimolecular. The experimental results indicate that this isomerization, as well as the other diazirine decomposition so far investigated, is consistent with a two-step mechanism.

L'isomérisation thermique de la méthyl-3 vinyl-3 diazirine a été étudiée dans divers solvants entre 40 et 75 °C. La réaction est cinétiquement du premier ordre et unimoléculaire. Les résultats expérimentaux indiquent que cette isomérisation, de même que la décomposition de l'autre diazirine étudiée jusqu'à maintenant est en accord avec un mécanisme en deux étapes.

[Traduit par le journal]

Can. J. Chem., 51, 2393 (1973)

Can. J. Chem. Downloaded from www.nrcresearchpress.com by 210.87.254.105 on 09/05/12
For personal use only.

Introduction

Many investigations on carbene chemistry with the use of diazirines have been reported (1), but the nature of the initial mechanistic step involved in their pyrolysis is not well understood. In the gas phase pyrolysis of 3-chloro-3-alkyldiazirines, Frey and Liu (2) have provided some evidence for the intermediate production of carbenes and proposed a transition state for the decomposition of diazirine in which the two carbon–nitrogen bonds are broken simultaneously. Schmitz (3), on the other hand, has argued that an ionic mechanism is more likely to occur, while Mitsch and co-workers (4, 5) favor a mechanism involving the transient existence of diazomethane prior to its loss of nitrogen. Recently, we have studied the thermal decomposition of 3-chloro-3-aryldiazirines (6) and suggested a mechanism involving the breaking of one of the C—N bonds. This process would lead to a diradical and a diazomethane intermediate. We had concluded that the contribution of the latter is probably small due to the lack of solvent effects. The isomerization of 3-methyl-3-vinyldiazirine has been investigated before (7), but the kinetic studies of this process were not measured. The present work was undertaken primarily to obtain the Arrhenius parameters for this isomerization in the hope that the mechanism for diazirines decomposition could be understood.

Experimental

3-Methyl-3-vinyldiazirine was prepared by reacting methyl iodide in the presence of silver nitrate with 3-methyl-3-[β-diethylamino-ethyl]-diazirine according to the method of Schmitz *et al.* (7). The n.m.r. spectrum showed a singlet (CH_3) at τ 8.8 p.p.m. and a multiplet (vinyl grouping) centered at τ 4.95 p.p.m. The solvents used in kinetics studies were carefully dried and distilled before use. Pyrolyses were carried out in sealed tubes immersed in an oil bath which was maintained to ±0.1 °C in the temperature range from 40 to 80 °C. Gas chromatography analysis was conducted with the use of a Perkin–Elmer Flame instrument fitted with a hydrogen flame detector. The rates of reaction were measured by following the disappearance of diazirine (isooctane as an internal standard). The 6 ft column was packed with chromosorb coated with 20% Carbowax 400. The injection and column temperatures were 25 °C. Reproducibility of duplicate analyses was better than 2%. Reaction rates followed by u.v. spectra were measured with Unicam SP 800 at the characteristic absorption of diazirine (λ 378 nm). The detailed experimental procedure was described in our earlier work (6).

Results and Discussion

The thermal isomerization of 3-methyl-3-vinyldiazirine was first order in various solvents, giving primarily 3-methyl-pyrazole according to eq. 1.

[1] 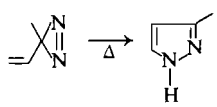

In the cases of carbon tetrachloride and of ethanol solution, the yield of 3-methyl-pyrazole was estimated to be at least 95% by comparison with the u.v. and i.r. spectra of the authentic sample. A small percentage of volatile material was obtained, with the retention time of the chromatographic peak being consistent with butadiene. When *N,N*-dimethylformamide

TABLE 1. Rate constants ($10^4 k$ s^{-1}) for the thermal decomposition of 3-methyl-3-vinyldiazirine

Solvent	Temperature (°C)								Method
	40.0	45.0	50.0	55.0	60.0	65.0	70.0	75.0	
CCl_4	0.616	1.14	2.19	4.00	7.25	12.1	21.9	39.3	V.p.c.
DMFA	0.832	1.57	2.93	5.36	9.78	16.8	—	49.6	V.p.c.
DEGME	0.750	1.43	2.68	5.00	9.07	15.6	—	46.0	U.v.
EtOH (+ H_2O)	0.625	—	2.23	4.09	—	13.1	22.9	39.2	V.p.c.
Aqueous AcOH (90% v/v)	—	—	—	4.02	—	—	—	—	U.v.

(DMFA) and diethylene glycol monoethyl ether (DEGME) were the solvents, the only product was 3-methyl-pyrazole. Table 1 shows the rate constants obtained at each temperature. The energies of activation and the pre-exponential factors, calculated by the least squares method, yielded the following eqs. 2–5. The error limits

$$[2] \quad k_{CCl_4} = 10^{13.70\pm0.10} \times \exp(-25\,600 \pm 200/RT)\ s^{-1}$$

$$[3] \quad k_{DMFA} = 10^{13.60\pm0.06} \times \exp(-25\,400 \pm 100/RT)\ s^{-1}$$

$$[4] \quad k_{DEGME} = 10^{13.70\pm0.10} \times \exp(-25\,500 \pm 120/RT)\ s^{-1}$$

$$[5] \quad k_{EtOH} = 10^{13.70\pm0.05} \times \exp(-25\,600 \pm 200/RT)\ s^{-1}$$

(standard deviations) are those calculated by normal statistical methods.

In considering the mechanism of diazirine decomposition, the initial problem to be dealt with is a choice between a concerted and a two-step mechanism. With this problem in mind, the Arrhenius parameters for various diazirines in Table 5 of ref. 6 were examined. The present study indicates that there is a decrease in activation energy of 3-methyl-3-vinyldiazirine of about 1–2 kcal mol^{-1} from that of 3-chloro-3-phenyldiazirines. The minor solvent effects suggest that the solute–solvent interaction must be nearly the same for both the reactant and transition state. In the thermal decomposition of diazirine, two C—N bonds are broken in the course of the reaction, while only one C—N bond is broken in the isomerization process. If the decomposition occurs by the simultaneous rupture of both bonds, then we may expect a different transition state for the decomposition and the isomerization. However, it is noted that the A factors ($\Delta S^{\ddagger} \sim 2$ e.u.) for the isomerization are similar to those of other diazirine decompositions. This feature indicates that the thermal reaction of all diazirines takes on a similar transition state in gas phase as well as in solution and suggests that, for the decomposition reaction, the breaking of the two C—N bonds occurs in a step-wise manner.

A proposed two-step mechanism (Scheme 1) could involve either a diradical intermediate as in path A or a polar intermediate as in path B. First, we shall look at the evidence for path A by comparing the energy of activation for 3-methyl-3-vinyldiazirine with that for 3,3-dimethyldiazirine (8). For the latter compound a value of 33.16 kcal mol^{-1} was reported for the decompositions carried out at 4 Torr which is in the "fall-off" region. Bridge *et al.* (9) have studied the thermal decomposition of 3-chloro-3-methyldiazirine both at 4 Torr and in the high pressure region. At 4 Torr, the rate constant has fallen to about 75% of its high pressure value. The energies of activation were 27.18 kcal mol^{-1} ($P = 4$ Torr) and 31.07 kcal mol^{-1} ($P = \infty$). It is therefore reasonable to assume that the value of the energy of activation corresponding to k_∞ for 3,3-dimethyldiazirine would be at least 35 kcal mol^{-1}. Although it might be argued that a comparison of this kind is not strictly permissible because this was a reaction in solution, there is reason to believe that such comparison may be meaningful since the parameters for diazirine decomposition are not solvent dependent (6, 7). This statement is substantiated by the results of preliminary investigations of the thermal decomposition of 3-chloro-3-ethyldiazirine in cyclohexene (10) where the ratio $k_{gas}/k_{cyclohexene} = 10^{0.17} \exp(-0.85/RT)$. The lowering of the activation energy by ~ 10 kcal for the vinyl compound is reasonable for the formation of a diradical intermediate such as the one

Can. J. Chem. Downloaded from www.nrcresearchpress.com by 210.87.254.105 on 09/05/12
For personal use only.

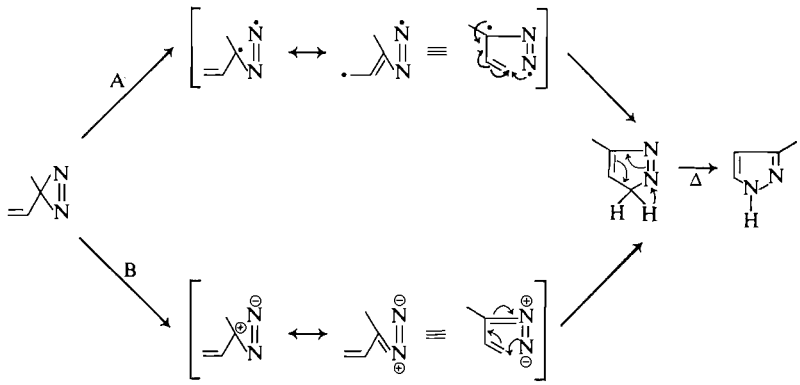

SCHEME 1

TABLE 2. A comparison of solvent effects for some diazirines. The relative rate constants $k_{solvent}/k_{CCl_4}$ at 75 °C are listed

	EtOH	Aqueous AcOH	DMSO	DMFA	DEGME
3-Chloro-3-phenyldiazirine	1	1	1.7	—	1.2
3-Methyl-3-vinyldiazirine	1	1*	—	1.4	1.3

*The comparison was made at 55 °C.

given in path A. More detailed arguments for this statement can be found in ref. 11.

Furthermore, the solvent effects for the isomerization as well as the decomposition of diazirine are shown in Table 2. It is observed that the rate acceleration effect given by $k_{solvent}/k_{CCl_4}$ for 3-chloro-3-phenyldiazirine and 3-methyl-3-vinyldiazirine showed an increase when polar solvents were employed. The effect is rather small and a larger effect would be expected if the rate determining step involved the re-arrangement of diazirine to an ionic intermediate. However, the experimental results of this work do not conclusively rule out the possibility of an ionic mechanism. Path B is equally probable if one considers that the resonance forms of methylvinyldiazomethane consist of linear structures with opposing dipoles:

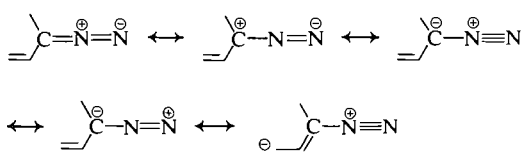

It is seen that the participation of these resonance structures will lead to a compensation in net polarity. Although the dipole moments of methylvinyldiazirine and methylvinyldiazomethane are not known, the dipole moments for these compounds are probably not very different. It is, therefore, not surprising that the observed solvent effect is small. It is also known that the rearrangement of vinyldiazomethane (diazopropene) to pyrazole (12) can occur at room temperature. The rate constants are comparable to those of the isomerization. While there is sufficient evidence that a step-wise mechanism occurs in diazirine decomposition, it is not certain whether the intermediate is of a diradical or an ionic nature.

Grateful acknowledgement is made by one of us, M.T.H.L., for a grants-in-aid of research from National Research Council of Canada and from the Senate Research Committee of U.P.E.I. The authors wish to thank the referees for their valuable comments.

1. W. KIRMSE. Carbene chemistry. 2nd Ed. Academic Press, New York. 1971.
2. H. M. FREY and M. T. H. LIU. J. Chem. Soc. A, 1916, (1970).
3. E. SCHMITZ. Angew. Chem. Int. Ed. **3**, 333 (1964).
4. E. W. NEUVAR and R. A. MITSCH. J. Phy. Chem. **71**, 1229 (1967).
5. P. H. OGDEN and R. A. MITSCH. J. Heterocycl. Chem. **5**, 41 (1968).

Can. J. Chem. Downloaded from www.nrcresearchpress.com by 210.87.254.105 on 09/05/12
For personal use only.

6. M. T. H. LIU and K. TORIYAMA. Can. J. Chem. **50**, 3009 (1972).
7. E. SCHMITZ, C. HÖRIG, and C. GRUNDEMANN. Chem. Ber. **100**, 2093 (1967).
8. H. M. FREY and I. D. R. STEVENS. J. Chem. Soc. 3865 (1962).
9. M. R. BRIDGE, H. M. FREY, and M. T. H. LIU. J. Chem. Soc. A, 91 (1969).
10. M. T. H. LIU and D. CHIEN. To be published.
11. S. W. BENSON. Thermochemical kinetics. John Wiley & Sons, Inc., New York. 1968. p. 86.
12. A. LEDWITH and D. PARRY. J. Chem. Soc. B, 41 (1967).

Can. J. Chem. Downloaded from www.nrcresearchpress.com by 210.87.254.105 on 09/05/12
For personal use only.

Synthesis of Nucleotides from 8,2′-Thioanhydropurine Nucleosides[1]

KELVIN K. OGILVIE AND LEWIS A. SLOTIN[2]
Department of Chemistry, University of Manitoba, Winnipeg, Manitoba
Received January 8, 1973

The 5′-mono and diphosphates of the common 8,2′-thioanhydropurine nucleosides have been prepared and studied with 5′-nucleotidase. alkaline phosphatase, and adenylate kinase. Procedures for the preparation of protected anhydronucleosides and their incorporation into dianhydronucleoside monophosphates have been developed. These nucleotides have been found to be completely resistant to spleen and snake venom phosphodiesterases but are readily converted with Raney nickel into the natural 2′-deoxynucleotides.

Les mono-5′ et diphosphates des nucléosides communs thio-8 anhydro-2′ purine ont été préparés et étudiés avec la nucléotidase-5′, la phosphatase alcaline et la kinase adénylate. Des méthodes pour la préparation d'anhydronucléosides protégés et pour l'incorporation de ceux-ci dans des monophosphates de dianhydronucléoside ont été élaborées. Ces nucléotides se sont montrés complètement résistants aux phosphodiestérases de la rate et du venin de serpent mais se sont facilement transformés avec du nickel de Raney en déoxy-2′ nucléotides naturels. [Traduit par le journal]

Can. J. Chem., **51**, 2397 (1973)

Introduction

Cyclonucleosides (anhydronucleosides) are important analogs of natural nucleosides. They are characterized by having, in addition to the *N*-glycoside linkage, a covalent linkage either directly or via bridging atoms between the 2′, 3′, or 5′ carbons of the sugar and a carbon or nitrogen atom (other than the nitrogen of the glycoside bond) of the purine or pyrimidine base. Previous reports from our laboratory have described convenient methods for obtaining 8,2′-thioanhydropurinenucleosides (1), and the use of anhydropyrimidine nucleosides in the synthesis of anhydro- and arabinonucleotides (2). We wish now to describe the synthesis of anhydropurine nucleoside mono- and diphosphates and dianhydropurine nucleoside monophosphates, their behavior toward certain enzymes, and their conversion to naturally occurring nucleotides. While this work was in progress the synthesis of oligomers of 8,2′-thioanhydroadenosine 5′-phosphate (3*a*) and the synthesis of a dinucleoside monophosphate of 8,2′-anhydro-8-oxy-9-B-D-arabinofuranosyladenine (3*b*) were reported.

Results and Discussion

8,2′-Thioanhydropurine Nucleoside 5′-Mono- and 5′-Diphosphates

An efficient method for the synthesis of monophosphates of natural nucleosides was developed by Yoshikawa *et al.* (4). This method allows the selective 5′-phosphorylation of unprotected nucleosides using partially hydrolyzed phosphoryl chloride in a trialkylphosphate solvent. This method eliminates both the need for protection of either amino or hydroxyl groups and the necessity of absolute dryness generally required in phosphorylations (5).

8,2′-Thioanhydroadenosine (**1***a*), 8,2′-thioanhydroguanosine (**1***b*), and 8,2′-thioanhydroinosine (**1***c*) were successfully converted to their corresponding phosphates **2***a–c* using a large excess of phosphoryl chloride in wet triethyl phosphate (see Scheme 1). **2***a* was obtained in 92% yield and was identical to an authentic sample prepared by cyclization of 2′-O-tosyl-8-bromoadenosine 5′-phosphate (6). The structure of **2***a* was further confirmed by Raney nickel reduction to 2′-deoxyadenosine 5′-phosphate which was dephosphorylated with 5′-nucleotidase to give 2′-deoxyadenosine. Yields of **2***b* and *c* were 43 and 74% respectively and these compounds were identified by Raney nickel reduction to the corresponding 2′-deoxynucleoside 5′-phosphates and subsequent dephosphorylation with 5′-nucleotidase to the natural nucleosides 2′-deoxyguanosine and 2′-deoxyinosine.

The monophosphates **2***a–c* were converted to the diphosphates **3***a–c* via the morpholidate procedure (7). Compounds **2** were treated with morpholine and *N,N*-dicyclohexylcarbodiimide

[1]Part XI in a series on anhydronucleosides.
[2]NRCC Scholarship Holder, 1970–1972.

Can. J. Chem. Downloaded from www.nrcresearchpress.com by 210.87.254.6 on 09/05/12
For personal use only.

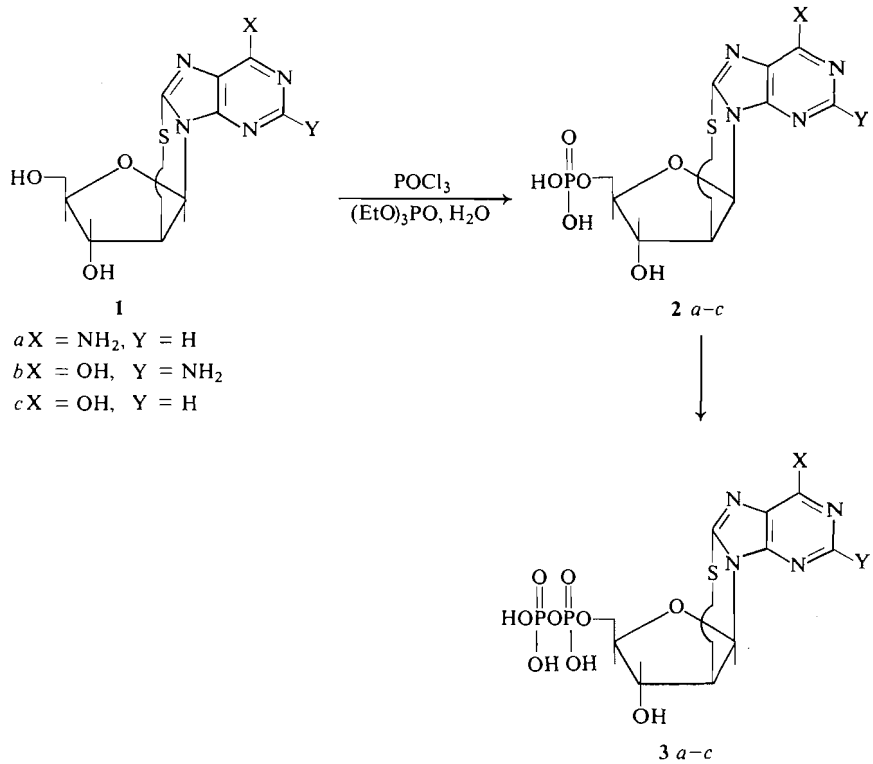

1

a X = NH_2, Y = H
b X = OH, Y = NH_2
c X = OH, Y = H

2 *a–c*

3 *a–c*

SCHEME 1

(DCC) in refluxing aqueous *t*-butanol and the reactions were monitored by electrophoresis at p*H* 7.5. The morpholidates of **2***b* and *c* were obtained in quantitative yields while the morpholidate of **2***a* was produced in 78% and was purified by paper chromatography prior to phosphorylation to **3***a*.

The morpholidates were treated with phosphoric acid and tri-*n*-butylamine in pyridine (8) yielding the diphosphates **3***a–c* in yields of 46, 38, and 43% respectively. The structures were confirmed by electrophoresis, paper chromatography, and phosphate analysis (9).

Enzyme Reactions on the Mono- and Diphosphates

(A) 5′-Nucleotidase

This enzyme selectively removes phosphate from the 5′-position of natural nucleotides. The exact requirements of the enzyme with respect to the nature of the base ring are not known. However it does appear that both the structure (10) and conformation (11–13) of the base ring may be important. In the case of the 5′-monophosphates **2***a–c*, none were substrates of 5′-nucleotidase (6).

(B) Alkaline Phosphatase

This enzyme catalyzes the dephosphorylation of mononucleotides and its action seems to be completely independent of the nature of the base ring (12). As expected all of the compounds **2***a–c* were completely dephosphorylated with alkaline phosphatase.

(C) Adenylate Kinase

This enzyme can convert adenosine 5′-monophosphate (AMP) into adenosine 5′-diphosphate (ADP) and under other conditions will cause the conversion of ADP to AMP and ATP. However neither **2***a* nor **3***a* acted as substrates of adenylate kinase.

Synthesis of Dinucleoside Monophosphates

To test the possibility of incorporating an anhydropurine nucleoside into a nucleotide chain (3), N^6,$O^{3'}$-dibenzoyl-8,2′-thioanhydroadenosine (**4***d*) was condensed with a slight excess of 5′-*O*-monomethoxytritylthymidine 3′-phosphate (14) in pyridine using mesitylenesulfonyl chloride (MSCl). The product (7) was treated with acetic acid to remove the trityl group and chromatographed on paper in solvent

Can. J. Chem. Downloaded from www.nrcresearchpress.com by 210.87.254.6 on 09/05/12
For personal use only.

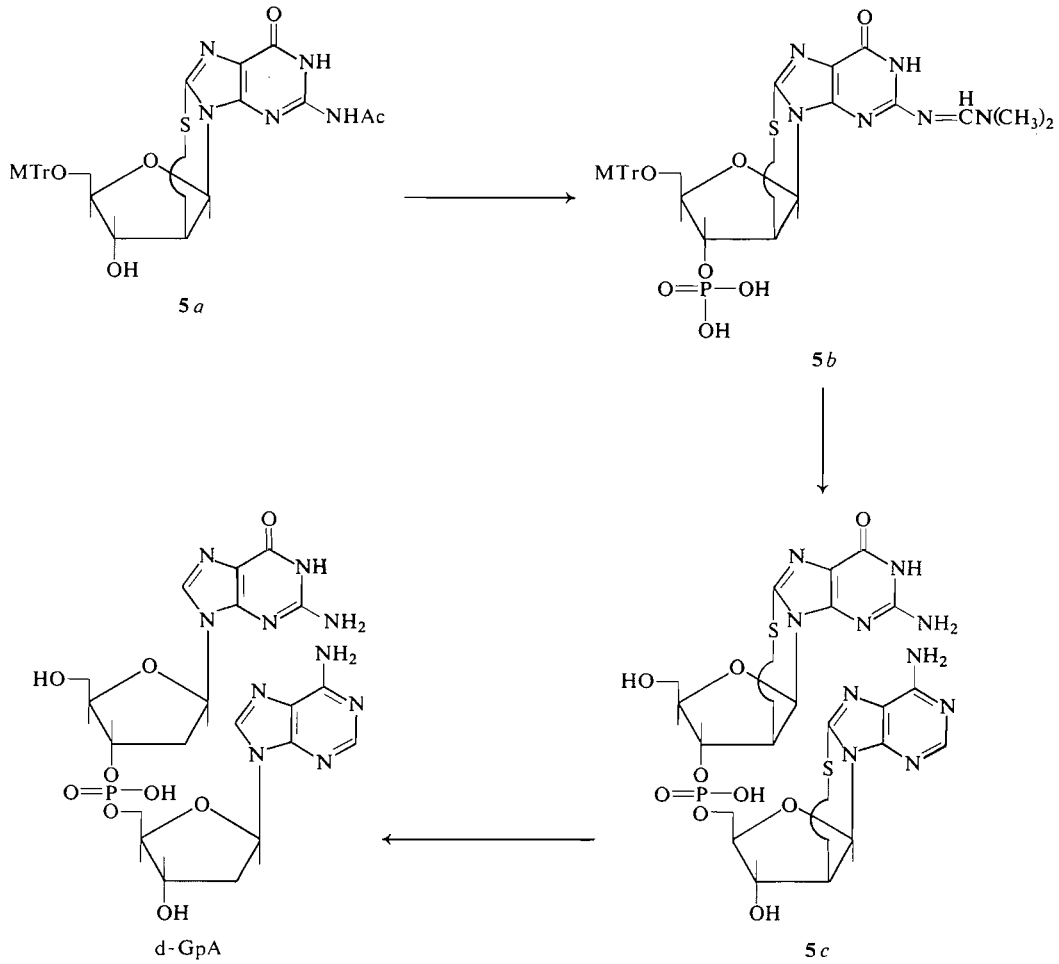

SCHEME 2

A (which also removes the 3′-benzoyl group). The desired product (R_f^A 0.42) was characterized by chromatography and electrophoresis and was treated with spleen phosphodiesterase, producing thymidine 3′-phosphate and N^6-benzoyl-8,2′-thioanhydroadenosine (nucleotide/nucleoside = 1.12). The yield of the nucleotide in this reaction was 20%, and 15% when DCC replaced MSCl as condensing agent.

For the preparation of dianhydronucleoside monophosphates, derivatives with both ring-amino groups and 5′-hydroxyl positions protected were necessary. The compounds 5′-*O*-monomethoxytrityl-N^6-benzoyl-8,2′-thioanhydroadenosine (**4***a*), 5′-*O*-monomethoxytrityl-N^2-acetyl-8,2′-thioanhydroguanosine (**5***a*), and 5′-*O*-monomethoxytrityl-8,2′-thioanhydroinosine (**6***a*) were prepared by the general procedures developed by Khorana and co-workers for natural nucleosides (15).

The synthesis of 8,2′-thioanhydroguanylyl-(3′–5′)-8,2′-thioanhydroadenosine (**5***c*) illustrates (Scheme 2) the general synthesis of the dinucleoside monophosphates. Compound **5***a* was phosphorylated using β-cyanoethylphosphate (3 equiv) and DCC in pyridine. The cyanoethyl group was removed using methanol – concentrated ammonium hydroxide (1 : 1) at 45° for 10 h. These conditions also remove *N*-acyl groups making it necessary to reblock ring amino groups. This is easily accomplished using dimethylformamide dimethyl acetal which introduces the dimethylaminomethylene group at amino positions (16). The resulting intermediate **5***b* was dissolved in 50% aqueous pyridine and passed through a Dowex 50W-X8 (pyridinium form) column. The

Can. J. Chem. Downloaded from www.nrcresearchpress.com by 210.87.254.6 on 09/05/12
For personal use only.

Can. J. Chem. Downloaded from www.nrcresearchpress.com by 210.87.254.6 on 09/05/12
For personal use only.

resulting compound was dried and stirred with **4***d* in pyridine in the presence of more Dowex resin and DCC for 11 days. Protecting groups were removed by first using methanolic ammonia followed by 80% acetic acid and the nucleotide **5***c* was obtained in 22% yield. This nucleotide was completely resistant to both spleen and snake venom phosphodiesterases and was fully characterized including Raney nickel reduction to the known compound deoxyguanylyl-(3′–5′)-deoxyadenosine (17).

8,2′-Thioanhydroinosinyl-(3′–5′)-8,2′-thioanhydroadenosine (**6***c*) and 8,2′-thioanhydroadenylyl-(3′–5′)-8,2′-thioanhydroadenosine (**4***c*), were similarly obtained in 8 and 30% yields starting from **6***a* and **4***a* respectively. Both of these nucleotides were completely resistant to snake and spleen phosphodiesterases. **6***c* was reduced to deoxyinosinyl-(3′–5′)-deoxyadenosine which was fully characterized by enzymes. **4***c* had been prepared previously (18) and was reduced to the known deoxyadenylyl-(3′–5′)-deoxyadenosine (17)

These results clearly indicate that all of the 8,2′-thioanhydropurine nucleosides can be incorporated into anhydronucleotide chains. These anhydronucleotides are of considerable interest in their own right (18) and can be converted with Raney nickel into the naturally occurring 2′-deoxynucleotides.

Experimental

General Methods

Descending paper chromatography was carried out using Whatman 3MM paper. The solvent systems employed were: solvent A, isopropyl alcohol – concentrated ammonium hydroxide – water (7:1:2); solvent B, ethanol–water (7:3); solvent C, *n*-butanol–ethanol–water (4:1:5, organic phase); solvent D, 1 *M* ammonium acetate – ethanol (3:7); solvent E, 0.5 *M* ammonium acetate – ethanol (3:7, adjusted to p*H* 3.5 with acetic acid); solvent F, *n*-propanol – concentrated ammonium hydroxide – water (55:10:35). The solvents were prepared on a volume basis. Thin-layer chromatography was carried out employing the ascending technique in closed jars which were not coated with absorbent paper. All thin-layer chromatography was run on Eastman Chromagram Sheets 6060, silica gel with fluorescent indicator, on strips 10 cm × 2 cm. Thick-layer chromatography was carried out on glass plates (20 cm × 20 cm) coated with a 2 mm thick layer of silica gel DSF-5 (Mondray Chemicals Ltd.). Paper electrophoresis was performed using Whatman 3MM paper in a Savant Flat Plate electrophoretic chamber with a Savant Model HV power supply operated at 2000 V for 1 h; the solution was a triethylammonium bicarbonate buffer (0.05 *M*, p*H* 7.5), prepared by making 15.15 g triethylamine up to 31 volume with water and then bubbling 20 g carbon dioxide through the solution. Nucleosides and their derivatives were detected on paper chromatograms, thin and thick-layer sheets using a u.v. light source (Mineralite, output ~254 nm). Compounds containing trityl or *p*-monomethoxytrityl groups were detected on chromatography by spraying with 10% perchloric acid solution and drying them in a stream of warm air.

I.r. spectra were obtained on a Perkin–Elmer 337 recording instrument using KBr disks for sample preparation. U.v. spectra were obtained on a Cary Model 14 recording spectrophotometer.

Melting points were determined on a Fisher–Johns melting point apparatus and are reported uncorrected. Elemental analyses were performed by Galbraith Laboratories Inc., Knoxville, Tennessee. Samples submitted to them were prepared by crystallization, lyophilization, or precipitation from tetrahydrofuran with hexane followed by heating in a drying apparatus over P_2O_5. In some cases the molecular formula includes fractional moles of solvent as a correction for the analysis. These corrections are added only when a corresponding weight loss was detected on extensive drying of the sample. Phosphate analyses were performed by the method of Lowry and Lopez (9) using ammonium molybdate and ascorbic acid. After release of the phosphate from the nucleotide following alkaline phosphatase action, the phosphate concentration was measured on a Zeiss PMQ 9 absorption spectrometer at 700 nm as the phosphomolybdate. This value is reported relative to the same reaction on an equal concentration of adenosine 5′-monophosphate.

Reagents and Chemicals

Reagent grade pyridine was distilled from *p*-toluene – sulfonyl chloride, redistilled from calcium hydride, and stored over Linde molecular sieves. Reagent grade *N*,*N*-dimethyl-formamide was dried by distillation from calcium hydride and stored over Linde molecular sieves. Reagent grade acetic anhydride was distilled from phthalic anhydride and stored in the dark. *n*-Butanol and phosphoryl chloride were freshly distilled before use. Reagent grade mesitylenesulfonyl chloride purchased from Aldrich was recrystallized from pentane and stored under pentane in the dark. Pyridinium Dowex was prepared by forming a column of Dowex 50W-X8(H^+ form) and washing first with 0.1 *N* HCl(11), then water (11), then 10% aqueous pyridine (11), and finally water (11). Pyridinium mono-β-cyanoethyl phosphate was prepared from the barium salt by passage over a column of Dowex 50W-X8 resin (pyridinium form). The clear solution containing the pyridinium salt was first concentrated to a small volume and then lyophilized to a gum. The gum was dissolved in pyridine and diluted to a known volume and stored in a sealed flask under refrigeration. Sodium hydrogen sulfide solution (40%) was prepared by dissolving 18 g sodium sulfide in 50 ml of water and adding 6.0 g of sodium bicarbonate in small amounts until complete dissolution occurs. Methanol (50 ml) was added with stirring and cooling below 20 °C. Following filtration and washing with methanol the filtrate is concentrated to one-tenth the volume and stored under refrigeration.

Natural nucleosides were purchased from Sigma Chemical Company.

TABLE 1. Properties of anhydronucleoside mono- and diphosphates and isolated 2′-deoxynucleoside 5′-monophosphates

Compound	R_f^F	Rm^{Tp}(p*H* 7.5)	λ_{max} (H_2O) (nm)
2*a*	0.27	0.92	276, 219
2*b*	0.19	0.79	263, 280sh
2*c*	0.33	0.83	265
2′-Deoxyadenosine 5′-phosphate	0.45	0.99	260
2′-Deoxyguanosine 5′-phosphate	0.26	0.88	255, 270sh
2′-Deoxyinosine 5′-phosphate	0.41	0.92	249
3*a*	0.35	1.13	275
3*b*	0.23	0.97	267, 280sh, 263sh
3*c*	0.15	1.01	265

Enzyme Assays

(a) Spleen Phosphodiesterase

Lyophilized spleen phosphodiesterase (10–15 units) obtained from Nutritional Biochemicals Corp. was dissolved in 1 ml of 0.01 *M* sodium pyrophosphate buffer adjusted to p*H* 6.5 with phosphoric acid. An aliquot (0.1 ml) of this solution, 0.2 ml of 0.05 *M* ammonium acetate (adjusted to p*H* 6.5 with acetic acid), and 0.1–1 mg of the nucleotide substrate were incubated at 37 °C. The solution was then applied to Whatman 3MM paper as a band and developed with solvent A. Nucleoside and nucleotide bands were cut out, eluted with water and diluted to a volume of 10 ml. Absorbances were adjusted by using blanks cut from papers treated in the same way as the sample material. The term O.D. unit refers to the extinction of the absorbing material in 1 ml of neutral solution in a quartz cell with a 1-cm path length.

(b) Snake Venom Phosphodiesterase

Two hundred units of snake venom phosphodiesterase obtained from Calbiochem were dissolved in 1 ml of tris-(hydroxymethyl)aminomethane buffer (adjusted to p*H* 9.2 with 0.1 *N* HCl). An aliquot (0.2 ml) of the enzyme solution was added to the nucleotide material (~1 mg) and incubated at 37 °C. The same procedure as in section *a* was then followed.

(c) 5′-Nucleotidase

5′-Nucleotidase (0.5 mg) from Sigma Chemical Co. was dissolved in a p*H* 9.0 buffer (50 ml 0.025 *M* borax and 4.6 ml 0.1 *M* HCl) along with 1 mg nucleotidic material and the solution incubated at 37 °C for 1 h.

(e) Alkaline Phosphatase

Nucleotidic material (1 mg) was treated with 0.1 ml of a suspension of alkaline phosphatase in ammonium sulfate (Sigma Chemical Co.) along with 1 ml p*H* 10.4 buffer (50 ml 0.05 *M* sodium bicarbonate and 16.5 ml of 0.1 *M* sodium hydroxide) and incubated at 37 °C for 5 min.

(e) Adenylate Kinase

(i) Two units of adenylate kinase (Sigma Chemical Co.), nucleotidic material (1 mg), and 0.1 ml p*H* 7.6 buffer (50 ml of tris(hydroxymethyl)aminomethane and 40.3 ml 0.1 *M* HCl) were mixed and the solution incubated at 37 °C for 4 h.

(ii) The conditions were the same as part *i* except 2 mg ATP and 3.4 mg magnesium sulfate were also added.

General Procedures

All reactions of more than 0.2 mmol of the limiting reagent were carried out in tightly stoppered ground glass joint flasks. Reactions of less than 0.2 mmol of the limiting reagent were carried out in Pyrex test tubes (10 ml, screw cap type). Reactions requiring drying by solvent evaporation were performed by evaporation under reduced pressure and air was readmitted through a column (30 cm × 2 cm) of anhydrous magnesium perchlorate.

Synthesis of 8,2′-Thioanhydropurine Nucleoside 5′-Monophosphates (2a-c)

In a typical experiment 200 mg of thioanhydro nucleoside was added to a cold (0 °C) solution of phosphoryl chloride (10 equiv) and water (0.4 equiv) in triethyl phosphate (5 ml). Complete dissolution occurred after 0.5 h and the reaction was continued at 0 °C for an additional 5.5 h. Excess ether was added, the mixture centrifuged, decanted, and the precipitate washed with ether. The resulting solid was dissolved in cold water (2 ml) and stirred at 0 °C for 2 h. Both 8,2′-thioanhydroadenosine 5′-monophosphate (**2***a*) and 8,2′-thioanhydroinosine 5′-monophosphate (**2***c*) precipitated upon addition of excess ethanol. The yield of **2***a* was 236 mg (92%) and the product was identical to that prepared as in the literature (6). The yield of **2***c* was 188 mg (74%). For the guanosine derivative, the aqueous solution was applied to paper chromatograms and developed in solvent F. The band at R_f 0.19 was eluted with water and lyophilized to give 106 mg of 8,2′-thioanhydroguanosine 5′-monophosphate (**2***b*, 43%). General properties of the monophosphates are listed in Table 1 and **2***a–c* were further characterized below.

The monophosphates were dissolved in water and refluxed with Raney nickel for 3 h. Following filtration through Celite powder the products were isolated on paper chromatography in solvent F. Compounds **2***a–c* led respectively to 2′-deoxyadenosine 5′-monophosphate, 2′-deoxyguanosine 5′-monophosphate, and 2′-deoxyinosine 5′-monophosphate. The properties of these are listed in Table 1. Each of the deoxynucleotides was then dissolved in a borate buffer (p*H* 9) and incubated at 37 °C with 5′-nucleotidase. Analysis of the reaction mixtures on paper chromatography showed complete conversion to the corresponding 2′-deoxynucleosides which were identical with authentic samples.

Can. J. Chem. Downloaded from www.nrcresearchpress.com by 210.87.254.6 on 09/05/12
For personal use only.

Can. J. Chem. Downloaded from www.nrcresearchpress.com by 210.87.254.6 on 09/05/12
For personal use only.

8,2′-Thioanhydroadenosine 5′-Diphosphate (3a)

8,2′-Thioanhydroadenosine 5′-monophosphate (50 mg, 0.14 mmol) was refluxed in a *t*-butanol – water mixture (1:1, 2 ml) to which 0.05 ml morpholine had been added. To this refluxing solution, a solution of DCC (115 mg, 0.56 mmol) in *t*-butanol was added dropwise over a period of 3 h. After this time an electrophoresis showed 70% conversion to a new compound (Rm^{T_P} 0.36). Further addition of 4 equiv of morpholine and DCC did not increase the yield after an additional 3 h. The reaction was then filtered and applied directly to paper chromatograms which were developed in solvent F. The band at R_f 0.62 was eluted with water and lyophilized to yield 47 mg (79%) of the morpholidate (R_f^c 0.16, R_f^F 0.62, Rm^{T_P} 0.36 (p*H* 7.5), λ_{max} (H_2O) 275 nm). The morpholidate was not further characterized but was dried by repeated evaporation of pyridine (5 × 0.5 ml). To the residue was added tri-*n*-butylamine (0.95 ml) as well as inorganic phosphoric acid (0.014 ml) which had been previously dried by repeated evaporation of pyridine (5 × 0.5 ml). The mixture was further dried by pyridine evaporation, pyridine added (1.5 ml), and the reaction stirred at room temperature for 48 h. The reaction mixture was then applied to paper chromatograms which were then developed in solvent F. The band at R_f 0.35 was eluted with water and lyophilized giving **3***a* (12.9 mg) in a yield of 46%. The band at R_f 0.62 was eluted with water and lyophilized yielding 10.2 mg of unreacted morpholidate. Properties are listed in Table 1. Phosphate analysis of **3***a* relative to an equal concentration of adenosine 5′-monophosphate was 2.11.

8,2′-Thioanhydroguanosine 5′-Diphosphate (3b)

8,2′-Thioanhydroguanosine 5′-monophosphate (**2***b*, 50 mg, 0.13 mmol) was dissolved in *t*-butanol – water (1:1, 1 ml) to which was added 0.13 ml morpholine. The solution was refluxed for 2 h during which time 90 mg DCC in *t*-butanol (1 ml) was added dropwise. Electrophoretic analysis revealed complete conversion to the morpholidate (R_f 0.54, Rm^{T_P} 0.46 (p*H* 7.5), λ_{max} (H_2O) 265, 280 sh). The solution was filtered and concentrated to dryness *in vacuo*. The residue was extracted twice with ether and then dried by repeated evaporation of pyridine (5 × 0.5 ml). To this was added tri-*n*-butylamine (0.095 ml) as well as inorganic phosphoric acid (0.014 ml) which had been previously dried by repeated evaporation of pyridine. The reaction was further dried by pyridine evaporation, then dissolved in 1.0 ml of pyridine and stirred at room temperature for 2 days. Applying the reaction mixture to paper chromatograms and development in solvent F gave two nucleotide bands R_f 0.54 and 0.23. The band at R_f 0.54 was eluted with water and lyophilized giving 17.3 mg unreacted morpholidate. The band at R_f 0.23 was eluted with water and yielded 22.8 mg **3***b* (37.9%) upon lyophilization (properties are recorded in Table 1). Phosphate analysis of **3***b* relative to an equal concentration of adenosine 5′-monophosphate was 1.93.

8,2′-Thioanhydroinosine 5′-Diphosphate (3c)

8,2′-Thioanhydroinosine 5′-monophosphate (**2***c*) was quantitatively converted to the morpholidate by the same method used above. Electrophoresis showed Rm^{T_P} 0.45 (p*H* 7.5). The 5′-diphosphate **3***c* was synthesized by the procedure outlined above. The paper chromatograms in solvent F gave two bands R_f 0.15 and 0.62. The band at R_f 0.62 was eluted with water and lyophilized to recover 12.8 mg of unreacted morpholidate. The band at R_f 0.15 was also eluted with water and lyophilized to yield **3***c* (26 mg, 43%). (Properties of **3***c* are listed in Table 1). Phosphate analysis of **3***c* relative to an equal concentration of adenosine 5′-monophosphate was 2.19.

Enzyme Studies on 2a–c and 3a 5′-Nucleotidase

One milligram each of **2***a–c* were separately dissolved in 1 ml of buffer solution (p*H* 9.0, 0.025 *M* borax), 0.5 mg of 5′-nucleotidase added, and the solution incubated at 37 °C for 1 h. Examination of the reaction mixtures by paper chromatography and electrophoresis showed no dephosphorylation. However, using the same concentration, adenosine 5′-monophosphate was completely converted to adenosine in 2 min.

Alkaline Phosphatase

Treatment of **2***a–c* with an alkaline phosphatase suspension in ammonium sulfate in the presence of 1 ml of buffer solution (p*H* 10.5, 0.05 *M* ammonium bicarbonate) and incubation at 37 °C gave rapid quantitative hydrolysis to the corresponding thioanhydro nucleosides (**1***a–c*).

Adenylate Kinase (Myokianase)

8,2′-Thioanhydroadenosine 5′-diphosphate (**3***a*, 1 mg, 0.002 mmol), adenylate kinase (1 μl, 2 units) and 0.1 ml tris-buffer (p*H* 7.6) were incubated at 37 °C. Continuous monitoring of the reaction mixture by paper chromatography and electrophoresis for 4 h showed no detectable change in the starting material.

8,2′-Thioanhydroadenosine 5′-monophosphate (**2***a*, 1 mg, 0.003 mmol), adenylate kinase (1 μl, 2 units), ATP (2 mg, 0.003 mmol), magnesium sulfate (3.4 mg, 0.03 mmol), and 0.1 ml tris-buffer (p*H* 7.6) were incubated at 37 °C. Continuous monitoring of the reaction mixture by paper chromatography and electrophoresis showed no detectable change in the starting material.

5′-O-Monomethoxytrityl-N⁶-benzoyl-8,2′-thioanhydroadenosine (4a)

8,2′-Thioanhydroadenosine (**1***a*, 5 g, 17.8 mmol) was dissolved in pyridine and benzoyl chloride (9 ml, 75 mmol) added. The reaction was stirred at room temperature for 2 h, poured into ice water and the aqueous solution extracted with chloroform. After drying over sodium sulfate the chloroform solution was concentrated to a small volume and 11.8 g of white precipitate m.p. 118–119 °C formed upon addition of excess hexane.

Without further purification 5.15 g of this material was dissolved in ethanol–pyridine (3:2, 100 ml), 60 ml 2 *N* sodium hydroxide – ethanol (1:1) added and the solution allowed to stand at room temperature for 5 min. An excess of Dowex 50W-X8 resin (H^+) was added, the solution filtered and the resin washed with warm DMF. The filtrate and washings were combined, concentrated to dryness and the residue washed with ether. Dissolution of the residue in DMF and addition of excess ether gave 1.87 g of a white powder. 1.03 g of this material, monomethoxytrityl chloride (0.99 g, 3.2 mmol) and pyridine (40 ml) were stirred at room temperature overnight. The solution was poured into ice water, extracted with chloroform and the chloroform solution dried over sodium sulfate. Following filtration of the chloroform and concentration to a small volume, **4***a* precipitated (1.55 g, 87%, m.p. 134–136 °C) upon addition of hexane. Chroma-

TABLE 2. Paper and thin-layer chromatographic R_f values of 8,2′-thioanhydropurine nucleoside derivatives

Compound	Paper chromatography* Solvent			Thin layer† Solvent	
	A	B	C	EtOAc	THF
4*a*	0.95	0.95	0.94	0.23	0.63
4*d*	0.88	0.82	0.84	0.25	0.74
5*a*	0.84		0.90	0.06	0.28
5*d*	0.49	0.79	0.55	0.00	0.08
6*a*	0.78	0.86	0.77	0.06	0.22

*Whatman 3MM paper; solvents described in Experimental.
†Eastman chromagram sheets 6060, silica gel with fluorescent indicator.

TABLE 3. Spectral properties of 8,2′-thioanhydropurine derivatives

Compound	U.v. spectra in 95% EtOH λ_{max}, nm (ε)	I.r. spectra*
4*a*	298(18 500), 235(29 300), 285(14 200)sh	5.85, 6.20, 8.05, 14.20
4*d*	297.5(12 300), 232(27 800), 285.5(10 600)sh	5.85, 6.80, 12.75, 14.20
5*a*	270(21 200), 292.5(12 800)sh, 229(19 500)sh	5.75, 5.95, 9.60, 14.15
5*d*	295(14 500), 269(23 600)	5.75, 5.95, 9.60, 12.85
6*a*	265(13 100), 230(17 500)	5.90, 7.15, 14.20

*Principal bands in KBr disk.

tographic and spectral properties are recorded in Tables 2 and 3 respectively.

Anal. Calcd. for $C_{37}H_{31}N_5O_5S$: C, 67.56; H, 4.75; N, 10.65. Found: C, 66.66; H, 4.80; N, 10.41.

*N^6,$O^{3'}$-Dibenzoyl-8,2′-thioanhydroadenosine (**4***d*)*

Compound **4***a* (0.9 g, 1.35 mmol) and benzoic anhydride (3.66 g, 16.2 mmol) were added to pyridine (8 ml) and the resulting solution stirred in the dark at room temperature for 24 h. The reaction was washed with hexane and the resulting oil was concentrated to a gum using ethanol to aid in the removal of the solvent. The residue was dissolved in tetrahydrofuran and 931 mg of material, m.p. 128–130 °C, precipitated as a white solid upon addition of hexane.

Without further purification 0.8 g of this material was dissolved in 80% acetic acid and heated on a steam bath for 15 min. The solution was poured into ice–water with vigorous stirring and the precipitate removed by filtration. The solid was washed with ether and dried to yield **4***d* (18), as a white powder (0.5 g, 96.5%, m.p. 173–174 °C). Chromatographic and spectral properties are recorded in Tables 2 and 3.

Anal. Calcd. for $C_{24}H_{19}N_5O_5S \cdot \frac{1}{2}H_2O$: C, 57.82; H, 4.04; N, 14.05. Found: C, 58.17; H, 4.13; N, 13.38.

*N^2-Acetyl-8,2′-thioanhydroguanosine (**5***d*)*

8,2′-Thioanhydroguanosine (**1***b*, 1.0 g, 3.37 mmol) and tetraethylammonium hydroxide (3.5 ml) were rendered anhydrous by repeated evaporation of pyridine (5 × 20 ml). Pyridine (20 ml) and acetic anhydride (10 ml) were added and the reaction was stirred at room temperature for 24 h after which time a white precipitate formed. The mixture was heated on a steam bath for 3 min to dissolve the precipitate, cooled to room temperature, acetic anhydride added (5 ml), and the solution stirred overnight at room temperature. The reaction was then concentrated to dryness using ethanol–pyridine (3:2, 25 ml) and 2 *N* sodium hydroxide – ethanol (1:1, 15 ml) was added. Following stirring of this solution for 10 min at room temperature an excess of Dowex 50W-X8 resin (H^+) was added. The solution was filtered and the resin washed with hot DMF. The filtrate and washings were combined, concentrated to a small volume and applied to thick-layer plates. One development in chloroform–ethanol (7:3) gave a band at R_f 0.25. This band was eluted with THF concentrated to a small volume and the product precipitated (700 mg, 61%) as a white powder (m.p. 237 °C dec.) upon addition of ethanol. Chromatographic and spectral properties are listed in Tables 2 and 3.

Anal. Calcd. for $C_{12}H_{13}N_5O_5S \cdot \frac{1}{2}H_2O$: C, 41.38; H, 4.05. Found: C, 41.24; H, 4.17.

*5′-O-Monomethoxytrityl-N^2-acetyl-8,2′-thioanhydroguanosine (**5***a*)*

Compound **5***d* (680 mg, 2.0 mmol) and monomethoxytrityl chloride (1.92 g, 6.21 mmol) were dissolved in pyridine (10 ml) and stirred at room temperature for 48 h. The reaction was then added slowly to ice water

Can. J. Chem. Downloaded from www.nrcresearchpress.com by 210.87.254.6 on 09/05/12
For personal use only.

Can. J. Chem. Downloaded from www.nrcresearchpress.com by 210.87.254.6 on 09/05/12
For personal use only.

with vigorous stirring. The resulting precipitate was removed by filtration, dissolved in chloroform, and dried over sodium sulfate. The chloroform solution was filtered, concentrated to a small volume and **5***a* precipitated (598 mg, 50%, m.p. 188 °C dec.) upon addition of excess ether. Chromatographic and spectral properties are listed in Tables 2 and 3.

Anal. Calcd. for $C_{32}H_{29}N_5O_6S$: C, 62.83; H, 4.78; N, 11.45. Found: C, 62.72; H, 4.81; N, 10.85.

5′-O-Monomethoxytrityl-8,2′-thioanhydroinosine (6a)

8,2′-Thioanhydroinosine (**1***c*, 0.5 g, 1.78 mmol) was dried by repeated evaporation of pyridine. DMF (2 ml) and pyridine (25 ml) were added along with monomethoxytrityl chloride (1.64 g, 5.33 mmol) and the solution stirred at room temperature for 4 days. The solution was then poured into ice water. The aqueous mixture was extracted with chloroform (3 × 100 ml) and the chloroform dried over sodium sulfate. Following filtration the chloroform was concentrated to a small volume and **6***a* (330 mg, 33.6%) precipitated as a white powder (m.p. 164–166 °C) upon addition of hexane. Chromatographic and spectral properties are listed in Tables 2 and 3. This compound was identical in all respects to an authentic sample (19).

Thymidylyl-(3′-5′)-N^6-benzoyl-8,2′-thioanhydroadenosine (7)

Compound **4***d* (17 mg, 0.034 mmol) and 5′-*O*-monomethoxytritylthymidine 3′-phosphate (30 mg, 0.05 mmol) were dried by repeated evaporation of pyridine (5 × 1 ml). Mesitylenesulfonyl chloride (10.6 mg, 0.068 mmol) and pyridine (1 ml) were added and the reaction stirred at room temperature for 24 h. Cold water (2 ml) was added and the solution continued stirring for an additional 24 h. Following concentration to dryness, the residue was dissolved in 80% acetic acid (1 ml) and heated on a steam bath for 15 min. After cooling the solution was applied to paper chromatograms and developed in solvent A. The band at R_f 0.42 was eluted with water and lyophilized to give 7 (4.8 mg, 19%). The product had Rm^{T_p} 0.25 and the u.v. spectrum in water showed a maximum at 267.5 nm and a shoulder at 300 nm. Compound 7 could also be obtained using DCC as condensing agent (nucleotide–nucleoside–DCC 1:2:4, 96 h) in 14.6% yield.

Approximately 8.5 $O.D._{260}$ units of 7 were treated with spleen phosphodiesterase for 24 h at 37 °C using standard procedures. The work-up yielded 4.7 $O.D._{267}$ units of T_p(R_f^A 0.10) and 10.8 $O.D._{300}$ units of benzoyl-8,2′-thioanhydroadenosine (R_f^A 0.88). The ratio nucleotide/nucleoside was 0.92. Treatment of 8.5 O.D. units of 7 with snake venom phosphodiesterase under standard conditions led to no detectable degradation.

8,2′-Thioanhydroadenylyl-(3′–5′)-8,2′-thioanhydroadenosine (4c)

Compound **4***a* (167 mg, 0.25 mmol) and β-cyanoethyl phosphate (pyridinium form) (1.5 ml, 0.75 mmol) were dried by repeated evaporation of pyridine (5 × 2 ml). This anhydrous mixture was then dissolved in pyridine (10 ml) and DCC (1.2 g, 5.9 mmol) was added. After standing at 45 °C for 18 h, pyridine–water (3:1, 30 ml) was added and the solution filtered to remove dicyclohexylurea. The filtrate was extracted with three 40 ml portions of hexane. The aqueous pyridine solution was kept at room temperature for 24 h and then evaporated to dryness *in vacuo*. Methanol – concentrated ammonia (1:1, 24 ml) was added to the residue and the resulting solution heated for 10 h at 45° and then concentrated to dryness. DMF (2 ml) and dimethylformamide dimethylacetal (0.2 ml) were added, the solution stirred at room temperature overnight, and then evaporated to dryness. The residue was dissolved in 50% aqueous pyridine and the solution passed through a column of Dowex 50W-X8 (pyridinium form) resin. The column was washed with 50% aqueous pyridine and the eluant concentrated and dried by repeated evaporation of pyridine. The resulting 5′-*O*-monomethoxytrityl-N^6-dimethylaminomethylene-8,2′-thioanhydroadenosine 3′-phosphate (**4***b*) was not purified further but used directly in the condensation reaction.

Compound **4***b* (~0.09 mmol), N^6,$O^{3'}$-dibenzoyl-8,2′-thioanhydroadenosine (**4***d*, 60 mg, 0.1 mmol) and Dowex 50W-X8 (pyridinium form, 0.5 ml) resin were rendered anhydrous by pyridine evaporation. To the anhydrous residue was added pyridine (2 ml) and DCC (246 mg, 1.2 mmol) and the mixture was stirred at room temperature for 11 days. Fifty percent aqueous pyridine (2 ml) was added, the solution filtered and the filtrate extracted with three 20 ml-portions of hexane. The aqueous pyridine layer was kept at room temperature for 24 h and then evaporated. The residue was dissolved in methanol saturated with ammonia at 0 °C (30 ml), kept at 35 °C for 24 h, and then evaporated. The residue was dissolved in 80% acetic acid (10 ml) and heated on a steam bath for 12 min. The solution was cooled and applied to eight paper chromatograms which were then developed in solvent A. The band at R_f 0.20 was eluted with water and gave 16.5 mg (**4***c*, 29.5%) upon lyophilization. The properties of product **4***c* were identical in all respects to those reported in the literature (18); R_f^A 0.20, R_f^B 0.42, R_f^C 0.08, R_f^F 0.43, Rnl^{pA} 0.28 (p*H* 7.5), λ_{max} (H_2O) 271 nm. The product was converted with Raney nickel to deoxyahenylyl-(3′–5′)-deoxyadenosine (15).

Compound **4***c* itself was completely resistant to snake venom and spleen phosphodiesterases at 37 °C for 24 h.

8,2′-Thioanhydroguanylyl-(3′–5′)-8,2′-Thioanhydroadenosine (5c)

5′-*O*-Monomethoxytrityl-N^2-dimethylaminomethylene-8,2′-thioanhydroguanosine 3′-phosphate (**5***b*) was prepared from **5***a* by the same method outlined above for the synthesis of **4***b*. Following passage of an aqueous pyridine solution of **5***b* through a Dowex 50W-X8 (pyridinium) column and drying, the nucleotide was condensed with N^6,$O^{3'}$-dibenzoyl-8,2′-thioanhydroadenosine (**4***d*) using DCC and the procedure outlined earlier. Following basic and acidic deblocking procedures and work-up on paper chromatograms in solvent A, the band at R_f 0.07 was eluted with water and lyophilized to give **5***c* (11.6 mg, R_f^A 0.07, R_f^B 0.40, R_f^C 0.04, R_f^F 0.40, Rm^{pA} 0.24 (p*H* 7.5), λ_{max} (H_2O) 268, 276sh, 220sh). Incubation of the dinucleotide at 37 °C for 24 h with snake venom and spleen phosphodiesterases showed no degradation.

Approximately 5 mg of the dinucleotide in water (1 ml) was refluxed with 1 spoonful of Raney nickel for 6 h. The solution was cooled, filtered with the aid of Celite powder and the filtrate applied to a paper chromatogram.

After development in solvent A, the band at R_f 0.17 was eluted with water and the u.v. spectrum in water showed a maximum at 258 nm.

8,2′-Thioanhydroinosinyl-(3′–5′)-8,2′-thioanhydroadenosine (6c)

Compound **6a** (50 mg, 0.09 mmol) and β-cyanoethyl phosphate (pyridinium form, 0.36 ml, 0.18 mmol) were dried by repeated pyridine evaporation (5 × 1 ml). Mesitylenesulfonyl chloride (59 mg, 0.27 mmol) and pyridine (1 ml) were added and the reaction stirred at room temperature for 7 h. Cold distilled water (1 ml) was added and the reaction stirred at room temperature for 16 h. An additional 1 ml of water was added followed by a saturated salt solution (5 ml). Extraction of the aqueous solution with chloroform resulted in all the phosphorylated material being dissolved in the chloroform. The chloroform solution was concentrated to dryness, 9 *M* ammonium hydroxide added (3 ml) and the solution heated at 60 °C for 1 h. The reaction mixture was applied to paper chromatograms which were developed in solvent A. The band at R_f 0.23 was eluted with water and lyophilized to yield 49 mg of material (R_f^A 0.23, R_f^B 0.72, R_f^C 0.07, Rm^{Tp} 0.65 (p*H* 7.5), λ_{max} (H_2O) 267, 230sh). Forty-seven milligrams of this material was dissolved in 50% aqueous pyridine (5 ml) and passed through a column of Dowex 50W-X8 (pyridinium form) resin. The column was washed with 50% aqueous pyridine and the eluate concentrated to dryness and then rendered anhydrous by repeated pyridine evaporation (5 × 2 ml). To the anhydrous residue was added **4d** (60 mg, 0.1 mmol), DCC (246 mg, 1.2 mmol), and pyridine (2 ml) and the reaction stirred at room temperature for 11 days. Following the same work-up as described above, 4.5 mg of **6c** (8.1%) was obtained from the band at R_f 0.10 in solvent A. (R_f^A 0.10, R_f^B 0.49, R_f^C 0.04, R_f^F 0.45, Rm^{pA} 0.27 (p*H* 7.5), λ_{max} 267.5 nm). The product was completely resistant to spleen and snake venom phosphodiesterases.

Compound **6c** (~3 mg) was dissolved in 0.5 ml water and refluxed with 0.5 spoonful of Raney nickel for 6 h. The mixture was cooled and applied to a paper chromatogram which was developed in solvent A. The band at R_f 0.19 was eluted with water (u.v. maximum (water) 253 nm) and lyophilized. This product (5.5 O.D. units) was incubated with snake venom phosphodiesterase for 7 h at 37 °C. Paper chromatographic examination of the reaction mixture in solvents A, B, and F showed complete degradation to 2′-deoxyinosine (2.79 O.D. units) and 2′-deoxyadenosine 5′-phosphate (3.2 O.D. units). The ratio of nucleotide/nucleoside was 1.09.

We wish to acknowledge financial support from the National Research Council of Canada.

1. K. K. Ogilvie, L. A. Slotin, J. B. Westmore, and D. C. K. Lin. J. Heterocycl. Chem. **9**, 1179 (1972); K. K. Ogilvie, L. Slotin, J. B. Westmore, and D. Lin. Can. J. Chem. **50**, 2249 (1972).
2. K. K. Ogilvie and D. Iwacha. Can. J. Chem. **48**, 862 (1970).
3. (*a*) M. Ikehara and S. Uesugi. J. Am. Chem. Soc. **94**, 9189 (1972); (*b*) M. Ikehara, S. Uesugi, and J. Yano. Nat. New Biol. **240**, 16 (1972).
4. M. Yoshikawa, T. Kato, and T. Takenishi. Bull. Chem. Soc. **42**, 3505 (1969).
5. H. G. Khorana. Some recent developments in the chemistry of phosphate esters of biological interest. J. Wiley and Sons Inc., New York. 1961.
6. M. Ikehara and Y. Ogiso. Tetrahedron, **28**, 3695 (1972).
7. J. G. Moffatt and H. G. Khorana. J. Am. Chem. Soc. **83**, 649 (1961).
8. M. Ikehara and M. Hattori. Biochim. Biophys. Acta, **269**, 27 (1972).
9. O. H. Lowry and J. A. Lopez. J. Biol. Chem. **162**, 421 (1946).
10. Y. Mizuno, M. Ikehara, T. Ueda, A. Nomura, E. Ohtsuka, F. Ishikawa, and Y. Kanai. Chem. Pharm. Bull. **9**, 338 (1961).
11. A. Holy. Coll. Czech. Chem. Commun. **35**, 81 (1970).
12. A. Holy, R. W. Bald, and F. Soung. Coll. Czech. Chem. Commun. **37**, 592 (1972).
13. M. Honjo, Y. Kanai, Y. Furukawa, Y. Mizuno, and Y. Sanno. Biochim. Biophys. Acta, **84**, 696 (1964).
14. G. Weimann and H. G. Khorana. J. Am. Chem. Soc. **84**, 4329 (1962).
15. H. Schaller, G. Weimann, B. Lerch, and H. G. Khorana. J. Am. Chem. Soc. **85**, 3821 (1963).
16. J. Zemlicka and A. Holy. Coll. Czech. Chem. Commun. **32**, 3159 (1967).
17. S. A. Narang, T. M. Jacob, and H. G. Khorana. J. Am. Chem. Soc. **87**, 2988 (1965).
18. S. Uesugi, M. Yasumoto, M. Ikehara, Kn. N. Fang, and P. O. P. Ts'o. J. Am. Chem. Soc. **94**, 5480 (1972).
19. P. A. Rheault. M.Sc. Thesis. University of Manitoba, Winnipeg, Manitoba. 1972.

Can. J. Chem. Downloaded from www.nrcresearchpress.com by 210.87.254.6 on 09/05/12
For personal use only.

Vinyl Azides as Diazoenamines

A. N. THAKORE, J. BUCHSHRIBER, AND A. C. OEHLSCHLAGER
Department of Chemistry, Simon Fraser University, Burnaby 2, British Columbia
Received December 11, 1972

Reaction of vinyl azides with nitrosyl tetrafluoroborate yields 1,2,5-oxadiazoles and 1,2,4-oxadiazoles depending on the structure of the azide. Reaction of 1,2-dialkyl vinyl azides with nitryl tetrafluoroborate gives 2-oxo-1,2,5-oxadiazoles in high yields whereas 1-aryl-2-alkyl vinyl azides gave moderate yields of 3-aryl-1,2,5-oxadiazoles and 5-aryl-1,2,4-oxadiazoles. Acyl chlorides condense with vinyl azides in the presence of aluminum chloride to yield oxazoles. Dimethyl acetylenedicarboxylate condenses with vinyl azides by cycloaddition of the azido function with the alkyne and by cycloaddition of the vinyl group with the alkyne. The latter process occurs only under the influence of $AlCl_3$. The observed reactions are viewed as involving the participation of vinyl azides as *N*-diazoenamines.

La réaction des azotures de vinyle sur le tétrafluoroborate de nitrosyle conduit aux oxadiazoles-1,2,5 et oxadiazoles-1,2,4 dépendant de la structure de l'azoture. La réaction des azotures de dialkyl-1,2 vinyle sur le tétrafluoroborate de nitryle mène aux oxo-2 oxadiazoles-1,2,5 avec des rendements élevés tandis que les azotures d'aryl-1 alkyl-2 vinyle conduisent aux aryl-3 oxadiazoles-1,2,5 et aryl-5 oxadiazoles-1,2,4. Les chlorures d'acyle se condensent aux azotures de vinyle en présence de chlorure d'aluminium pour donner des oxazoles. L'acétylène dicarboxylate de diméthyle se condense aux azotures de vinyle par cycloaddition de la fonction azoture sur l'alkyne et par cycloaddition du groupe vinyle sur l'alkyle. Cette dernière ne se produit qu'en présence de $AlCl_3$. Les réactions observées ont été examinées sous l'angle d'une participation des azotures de vinyle sous forme de *N*-diazoénamines.

[Traduit par le journal]

Can. J. Chem., **51**, 2406 (1973)

Can. J. Chem. Downloaded from www.nrcresearchpress.com by 210.87.254.5 on 09/05/12
For personal use only.

Introduction

The synthetic utility of enamines lies principally in their ability to react with electrophiles at the β-vinyl carbon and undergo cycloaddition at the carbon–carbon double bond (1). The ease of synthesis of the vinyl azide function (2), coupled with HMO calculations (3) and spectral characteristics (3, 4), which indicate there is appreciable electron density at the β-vinyl carbon, make this functional group a logical choice for reaction with electrophiles. The reactions of vinyl azides with acids produce amides via a route most easily rationalized as occurring via protonation of the β-vinyl carbon (5). Reactions with halogens lead to α-haloketones by similar involvement of the β-vinyl carbon (6). The recently reported (7) reactions of vinyl azides with diphenylketene revealed similar nucleophilic behavior of the β-vinyl carbon (see Scheme 1). This latter process may be considered a member of a general class of reactions in which the azide participates as an *N*-diazoenamine.

We have found that vinyl azides react readily with several electrophilic reagents to yield products expected to result from this and closely related transformations (see Scheme 2).

Results and Discussion

Reaction of nitrosyl tetrafluoroborate ($NOBF_4$) with vinyl azides in cold (−15°) acetonitrile results in smooth evolution of nitrogen and production of 1,2,5-oxadiazoles and 1,2,4-oxadiazoles, depending on the structure of the azide. Thus, reaction with 1,2-dialkyl substituted vinyl azides (**1***a–c*) for short periods (30 min – 1 h) followed by addition of water and separation of the organic products gave moderate yields of 1,2,5-oxadiazoles (**2***a*, *b*) (8) and lesser amounts of amides (**3***a–c*). When the reactions were allowed to proceed for extended periods (18 h) the yields of oxadiazoles increased to near 80% while those of the amides decreased to less than 10%. The decreased yields of amides upon prolonged reaction time suggests these products arise from hydrolysis of the azides promoted by the acid (5) (HBF_4) presumably generated during oxadiazole formation.

Reaction of the *trans*-1-azido-1-phenylpropene

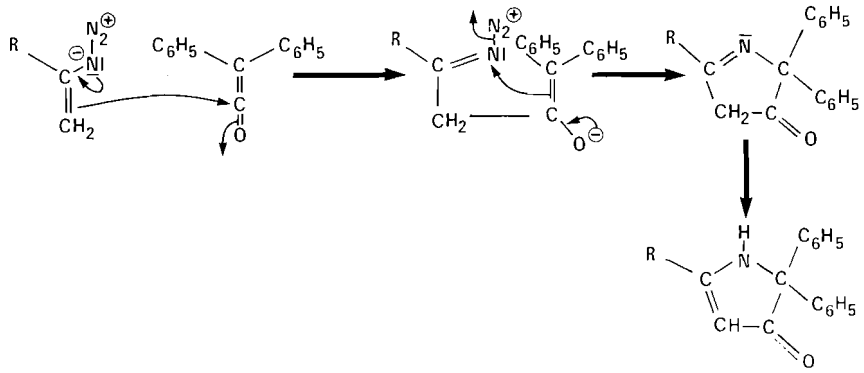

SCHEME 1

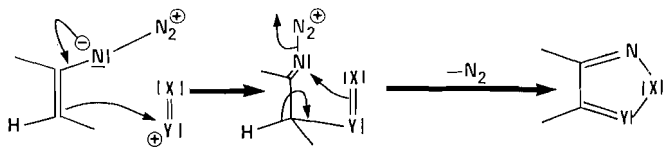

SCHEME 2

(**1***d*) with $NOBF_4$ gave, in addition to the expected 1,2,5-oxadiazole (**2***c*) a comparable amount of 1,2,4-oxadiazole (**4***a*) considered to be formed as shown in Scheme 3. The proposed route to **4** was supported by the detection of benzonitrile in the reaction mixture.

Reactions of 2-alkyl substituted vinyl azides such as **1***e* with $NOBF_4$ gave moderate yields of amides. No evidence for synthetically useful yields of heterocyclic products was obtained.

Reaction of 1,2-dialkyl substituted vinyl azides (**1***a*, *b*) with nitryl tetrafluoroborate (NO_2BF_4) gave high yields of 2-oxo-1,2,5-oxadiazole (**5**, Scheme 4). Extension of this reaction to the 1-aryl-2-alkyl substituted **1***d* gave N_2O, 1,2,5-oxadiazole (**2***c*), 1,2,4-oxadiazole (**4***a*), and benzonitrile. The latter three products were formed in similar proportions to that observed in the reaction of $NOBF_4$ with this azide. In a similar manner reaction of α-azidostyrene (**1***f*) with NO_2BF_4 gave **2***d* and **4***b*. As was the case with reaction with $NOBF_4$, the reaction of 2-alkyl substituted vinyl azides (**1***e*) with NO_2BF_4 did not give synthetically useful yields of heterocyclic products.

We consider the mechanism most consistent with these observations to be that depicted in Scheme 4, where both the $NOBF_4$ and NO_2BF_4 reactions proceed via a common intermediate, **6**. It is noteworthy that **1***d* gives only the product **4***a* of alkyl migration of intermediate **6**. Protonation of **1***d* has been reported (5) to yield amides **3***d* and *e* in a ratio of 0.6:1. Since the latter is considered to be the product of phenyl migration in an intermediate resembling **6**, we expected a product arising from this migration to be present in this reaction. The formal product of phenyl migration in this case would be an α-oximino amide or conceivably an α-keto amido. A v.p.c./mass spectral analysis of the reaction mixture failed to detect a product with a molecular weight corresponding to either of these possibilities.

In an effort to extend the reactions of NO^+ and NO_2^+ with vinyl azides to other electrophiles we studied their reactions with acyl chlorides under a variety of conditions. Reaction of acetyl chloride with **1***a* and *b* at room temperature resulted in evolution of nitrogen and gave, on hydrolytic work, amides **3***a* and *b* as the only identifiable products. In the presence of aluminum chloride the same reaction proceeded with evolution of nitrogen to give a 70% yield of 2,3,5-trimethyl oxazole, **7**.

Although we have not investigated appropriately substituted acyl chlorides which enable one to differentiate the several attractive mechanisms that may be envisioned for the production

Can. J. Chem. Downloaded from www.nrcresearchpress.com by 210.87.254.5 on 09/05/12
For personal use only.

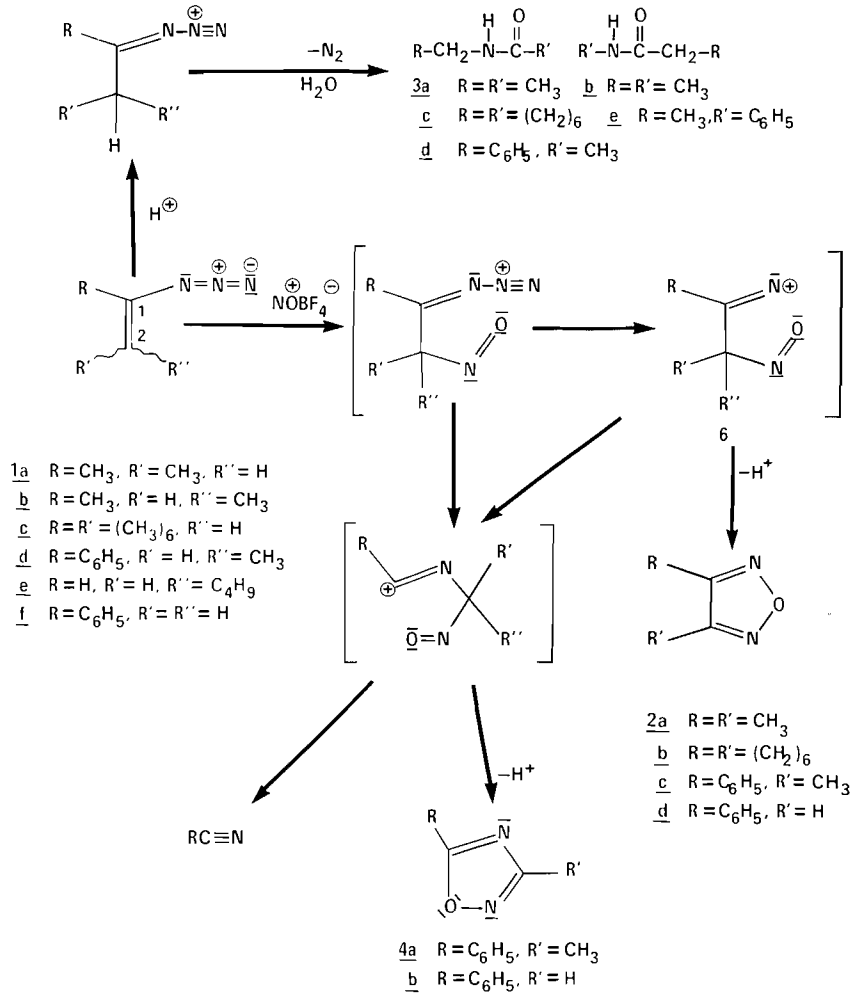

SCHEME 3. Reaction of vinyl azides with $NOBF_4$.

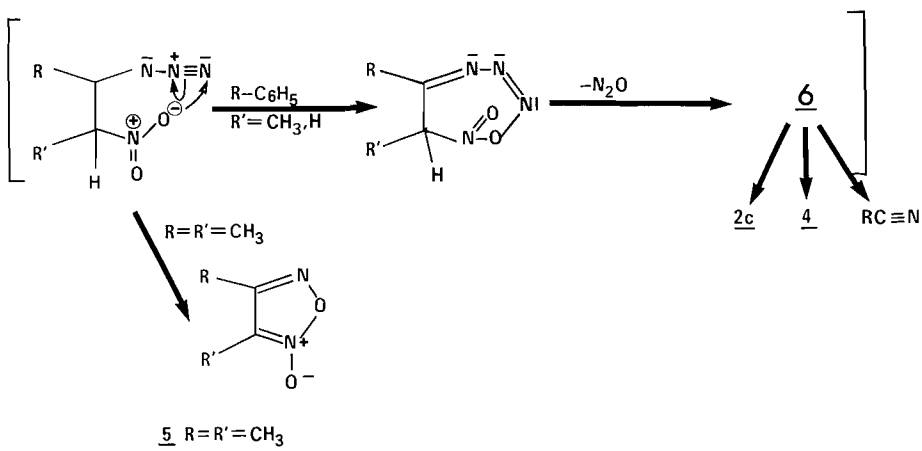

SCHEME 4. Reaction of vinyl azides with NO_2BF_4.

Can. J. Chem. Downloaded from www.nrcresearchpress.com by 210.87.254.5 on 09/05/12
For personal use only.

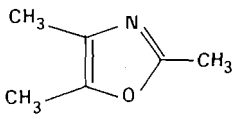

7

of oxazole products from this reaction, we have investigated the reaction of 1-azido-1-phenylpropene (**1***d*) with acetyl chloride. This reaction yielded oxazoles **8**, **9**, and **10** in 17, 7, and 1% yields respectively. These products may be envisioned as being formed by several alternate mechanisms (Scheme 5). Fowler and Hassner (8) have previously demonstrated that reaction of benzoyl chloride with 2-phenyl-3-methyl azirine gives 2,5-diphenyl-4-methyl oxazole (analogous to **8**) via an *N*-benzoyl chloroaziridine.[1]

Thermal (room temperature → 80 °C) reactions of ketene dimer, phenyl isocyanate, benzyl chloride, methyl iodide, cyclohexanone, carbon disulfide, methyl chloroformate, and benzenediazonium tetrafluoroborate with vinyl azides **1***a* and *b* did not produce synthetically useful yields of heterocyclic products. Indeed reactions with these potential electrophiles in several solvents (CH_3CN, $(C_2H_5)_2O$, C_6H_6) with and without added aluminum chloride lead to reactions with solvent (*e.g.* phenylacetamide from benzenediazonium tetrafluoroborate and acetonitrile) and conversion of azides to amides upon hydrolytic work-up.

Since enamines readily undergo cycloaddition reactions with dipolarophilic reagents, we explored the reaction of dimethyl acetylene dicarboxylate (DMAD) with azides **1***a* and *b*. Depending on the reaction conditions either 1:1 or 2:1 DMAD:azide adducts were obtained. Reaction of **1***b* with DMAD at room temperature for 3 days gave triazole **11** (Scheme 6), whose n.m.r. spectrum was unambiguous. In addition to two methoxyl resonances (δ 3.98), two vinyl methyl resonances (one at δ 1.41 appearing as a quartet of quartets (J = 3.5, 0.5 Hz) and a second at 2.19 appearing as a quintet (J = 0.5 Hz)) were evident. A vinyl hydrogen appeared as a quartet of quartets J = 3.5, 0.5 Hz at δ 5.83. This pattern is characteristic of the *trans*-vinyl system of the starting azide **1***b* (4, 5).

This reaction could be catalyzed by addition of aluminum chloride (1 h) but resulted in a significantly lower yield (90 *vs.* 55%) and with formation of a second product (16%). This second product possessed a molecular weight and elemental analysis corresponding to the addition of 2 mol of DMAD to 1 mol of the vinyl azide. It was observed that both azides **1***a* and *b* gave this product in comparable yields. Thus the stereochemistry of the vinyl group is inconsequential or destroyed during this reaction. This 2:1 adduct was the major (55%) product when the reaction was performed by addition of azide to a solution containing a two-fold or greater excess of DMAD and an equivalent of aluminum chloride. It was shown that the 1:1 adduct (11) could not be induced to react further with DMAD in the presence of aluminum chloride, thus it is not a precursor of the 2:1 adduct.

The n.m.r. spectrum of the 2:1 adduct revealed four distinct methoxyl groups, a methyl singlet (δ 2.03), a methyl doublet (δ 0.95, J = 7 Hz), and a methine quartet (δ 3.28). Although both structures **12** and **13** (Scheme 6) are reasonable formulations for the 2:1 adduct based on mechanistic arguments and are consistent with elemental analysis and n.m.r. data, the pyrolytic conversion of the adduct to vinylic products indicates **12** is correct. Thus heating the adduct to 170° produced a mixture of two isomers, the major of which exhibited an n.m.r. spectrum which possessed, in addition to four methoxyl signals, a vinyl methyl singlet (δ 2.84), a vinyl methyl doublet (δ 1.72, J = 7 Hz), and a vinyl hydrogen quartet (δ 6.88, J = 7 Hz). The n.m.r. spectrum of the minor pyrolysis product also contained four methoxyl signals, a vinyl methyl singlet (δ 2.75), a vinyl methyl doublet (δ 1.91, J = 7 Hz), and a vinyl hydrogen quartet (δ 6.20, J = 7 Hz). This observation is compatible with a cyclobutene → butadiene conversion and thus most consistent with **12** as the initial adduct. *A priori* four products (**14**–**17**) could be expected from **12** of undefined stereochemistry. The doublet resonance of the terminal vinyl methyl group (δ 1.72) of the major pyrolysis

[1]A referee has suggested that **8** and **10** could easily be explained by involvement of the antiaromatic *N*-acetyl-2-azirine, **i**.

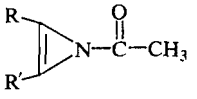

i

Can. J. Chem. Downloaded from www.nrcresearchpress.com by 210.87.254.5 on 09/05/12
For personal use only.

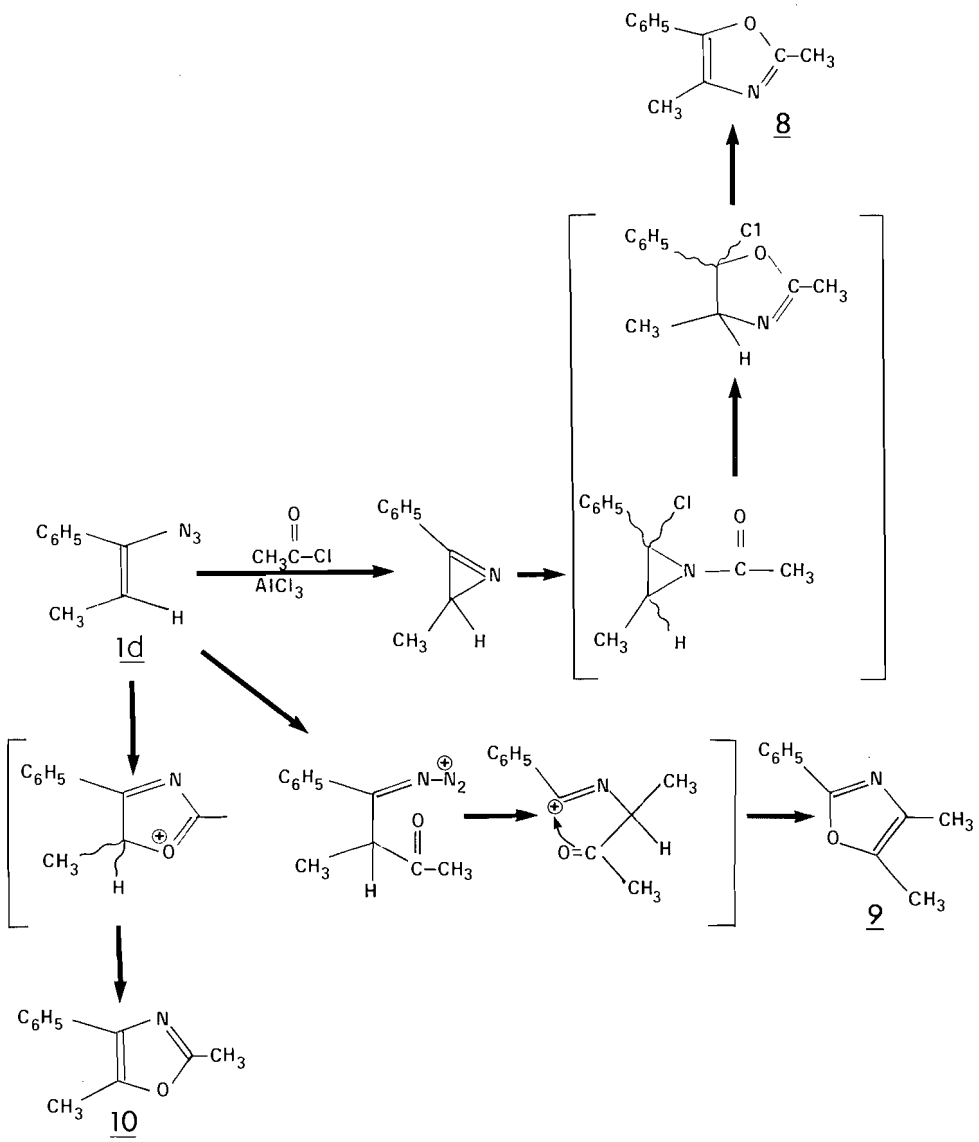

SCHEME 5. Reaction of 1-azido-1-phenylpropene with acetyl chloride.

product is at higher field than the same group of the minor product. This observation allows assignment of a *trans* relationship to this methyl and its vicinal carbomethoxy neighbor in the major isomer and a *cis* relationship in the minor isomer (9).

Comparison of the relative chemical shifts of the vinyl hydrogens associated with the carbons containing these terminal methyls confirms this assignment. The relative stereochemistry of the quaternary methyl and vicinal carbomethoxy about the nitrogen bearing double bonds of the dienic pyrolysis product was deduced by inspection of the chemical shifts of the resonances due to the quaternary methyls. The signal due to this group was at higher field in the major isomer than in the minor isomers. This indicates the quaternary methyl and carbomethoxy function are *cis* to each other in the major isomer and have a *trans* relationship in the minor isomer (9). The major pyrolysis product is thus **14** and the minor product is **15**. Since these two products interconvert thermally under the pyrolysis conditions they would probably inter-

Can. J. Chem. Downloaded from www.nrcresearchpress.com by 210.87.254.5 on 09/05/12
For personal use only.

Can. J. Chem. Downloaded from www.nrcresearchpress.com by 210.87.254.5 on 09/05/12
For personal use only.

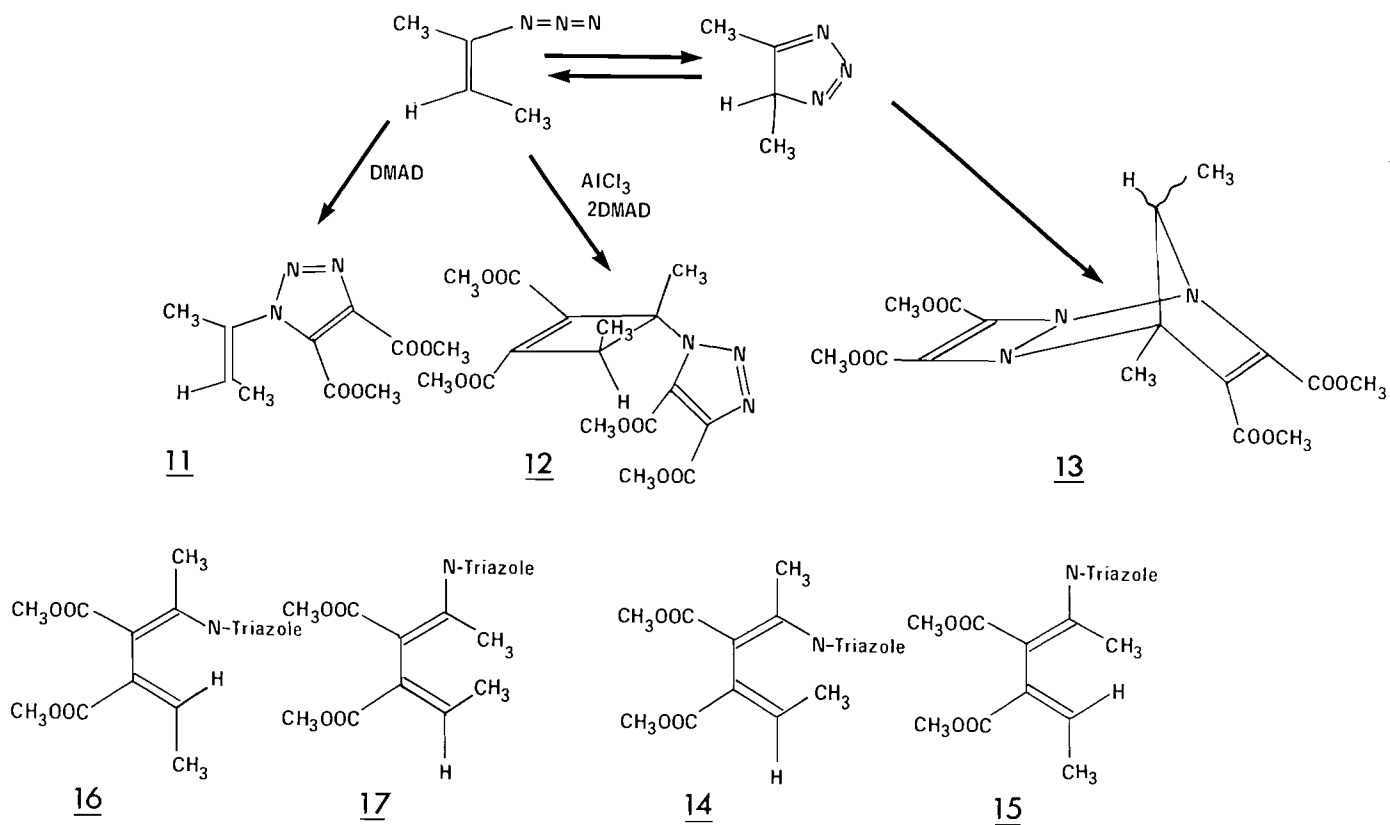

SCHEME 6. Reaction of vinyl azides with dimethylacetylene dicarboxylate (DMAD).

convert with **16** and **17**. Thus, although the stereochemistry of **12** implied by these results is as shown it cannot be assigned with certainty. As noted above both **1***a* and *b* gave **12** in the aluminum chloride catalyzed addition of DMAD to the olefinic linkage of the vinyl azide. In both reactions a triazole was formed. In the case of reaction of **1***b* triazole **11** was formed whereas reaction of **1***a* gave the triazole isomeric with **11** about the olefinic linkage. This suggests the catalyzed addition of DMAD to the olefinic bond of the vinyl azide is stepwise. This addition must be the initial reaction in the formation of the 2:1 adduct since the triazoles (**11**) are not converted to **12** under the reaction conditions.

It can be seen from the above examples that vinyl azides are potentially useful synthetic intermediates when viewed as *N*-diazoenamines.

Experimental

Melting points were obtained on a Fisher–Johns apparatus and are uncorrected. I.r. spectra were recorded with a Perkin–Elmer 457 grating spectrometer. U.v. spectra were recorded on a Unicam SP800 spectrometer. N.m.r. spectra were obtained with Varian A 56/60 and HX100 Spectrometers using tetramethylsilane as an internal standard ($\delta = 0$). Mass spectra were obtained using a Hitachi–Perkin–Elmer RMU6E Spectrometer and an ionization voltage of 80 eV.

Reaction of 1a and b with $NOBF_4$

To a solution of **1***a* or *b* (10) (1 g, 10.3 mmol) in 10 ml acetonitrile at 0° under He was added 1.2 g (20 mmol) $NOBF_4$ over 30 min, nitrogen (mass spectra) evolution was immediate. After 1 h of further stirring the reaction was quenched with water and extracted with three 100-ml portions of ether. The solvent was removed by fractional distillation and the residue fractionated at 20 mm (65°) to yield 0.70 g (~68%) of 3,4-dimethyl-1,2,5-oxadiazole (**2***a*, lit. (11) b.p. (760 mm) 155–156°) which was identified by comparison of its mass and n.m.r. spectra with those published (11) for this compound.

The undistilled residue (0.3 g) was chromatographed on 20 g SiO_2. Initial elution with benzene–methanol (99:1 v/v) gave 0.2 g (19%) of *N*-ethyl acetamide (**3***a*) (5). Continued elution with this solvent system gave 0.1 g (9%) *N*-methyl propionamides (**3***b*) (5). Both amides gave expected i.r., n.m.r., and mass spectra.

This experiment was repeated using 1 g of **1***a* or *b* and allowing the reaction to proceed for 30 min. After this time one-half of the reaction mixture was removed, diluted with water, and extracted (3 × 100 ml) with ether. The ethereal extract was concentrated and analyzed by g.l.p.c. (15% Versamide 900 on Chrom W, 3 ft × 1/8 in. column; temperature programmed 50–150° at 10°/min; using *o*-chlorotoluene as an internal standard) to yield (calcd.) 78–80% of **2***a*, 11% of **3***a*, and 6% of **3***b*. After 18 h the second half of the reaction was similarly analyzed to yield 92–94% of **2***a*, and 1% of a mixture of **3***a* and *b*.

Reaction of 1c with $NOBF_4$

Reaction of **1***c* (1 g, 6.6 mmol) in 10 ml of acetonitrile at 0° under He with 0.89 g (7.6 mmol) of $NOBF_4$ for 1 h followed by the hydrolytic work-up described above gave organic products which were chromatographed on 20 g SiO_2. Elution with benzene gave 0.76 g (75%) of 3,4-hexamethylene-1,2,5-oxadiazole (**2***b*); ν_{max} (film) 2920, 2860, 1450, 1180, 1010, and 930 cm^{-1}; λ_{max} (MeOH) 220 mμ (ε 2420); n.m.r. (CCl_4), δ 2.88 (4H J = 6 Hz, t) and 1.60 (8H, m).

Mol. wt. Calcd. for $C_8H_{12}N_1O$: 152.0949. Found [M^+]: 152.0959.

Continued elution with benzene–methanol (99:1) yielded 9% of lactam **3***c*, m.p. 72.5–73° (lit. (12) m.p. 72–73°); ν_{max} (KBr) 3280 and 1700 cm^{-1}.

Reaction of 1d with $NOBF_4$

To 0.556 g (3.5 mmol) of **1***d* in 15 ml acetonitrile at −10° under He was added a slurry of $NOBF_4$ (0.41 g, 3.1 mmol) in acetonitrile (30 ml). Nitrogen (mass spectra) evolution was immediate. After 18 h at room temperature the solution was quenched with water and extracted continuously with ether. Concentration of the extract gave a solution which was analyzed by g.l.p.c. (2% SE30 on Chrom G, 5 ft × 1/8 in., temperature programmed 50–170° at 6°/min). Reaction products **2***c* (8.8%), **4***a* (12%), and benzonitrile (6%) were identified by mixed injection of authentic samples and comparison of mass spectra obtained on preparatively isolated samples. Yields were calculated *vs.* added internal standard (nitrobenzene).

An authentic sample of 3-phenyl-4-methyl-1,2,5-oxadiazole (**2***c*) was prepared by reaction of 1-oxo-3-methyl-4-phenyl-1,2,5-oxadiazole (13) with PCl_5 (14).

An authentic sample of 3-methyl-5-phenyl-1,2,4-oxadiazole (**4***a*) was prepared by the method of Eloy (15).

Reaction of 1e with $NOBF_4$

The reaction of **1***e* with $NOBF_4$ in acetonitrile was carried out as described above for **1***d*. After the usual hydrolytic work-up the reaction extract was analyzed by a g.l.p.c. (SE 30, temperature programmed 50–290° at 4°/min) mass spectral combination. The only products detectable in more than 5% amounts *vs.* an internal standard were amides (5) (~30%) derived from hydrolysis of the azides (M^+ 115).

Reaction of 1a and b with NO_2BF_4

To 0.5 g (5.2 mmol) **1***a* or *b* in 20 ml of ether at −10 °C under He was added dropwise a solution of 0.68 g (5.5 mmol) NO_2BF_4 in 10 ml of ether. Nitrogen (mass spectra) evolution was immediate. The reaction was allowed to warm to room temperature and was stirred at this temperature for 1 h. After hydrolysis and ether extraction fractional distillation yielded 0.3 g (51%) of **5** (b.p. (16 mm) 100°) which gave a mass spectra identical to that published (11). Analysis of the nonvolatile portion by g.l.p.c. (Versamide 900) *vs.* an internal standard revealed 20% of a mixture of **3***a* and *b*. Repetition of the experiment for 18 h yielded 0.49 g (83%) of **5**.

Reaction of 1d with NO_2BF_4

To the azide (0.5 g) in 10 ml acetonitrile at −10° under He was added a molar equivalent of NO_2BF_4 in the same solvent (20 ml). Upon addition gas evolution (N_2 and

Can. J. Chem. Downloaded from www.nrcresearchpress.com by 210.87.254.5 on 09/05/12
For personal use only.

Can. J. Chem. Downloaded from www.nrcresearchpress.com by 210.87.254.5 on 09/05/12
For personal use only.

N_2O by mass spectral analysis) occurred. After addition (25 min) the solution was stirred at room temperature for 24 h then worked-up by addition of water, extraction with ether, and concentration of the extract. Product identification (**2***c* (17%), **4***a* (24%), benzonitrile (5%)) was made by g.l.p.c./mass spectra analysis (SE 30 column) as described for the $NOBF_4$ **1***d* reaction. Although yields are lower than for reaction of **1***a*, *b* with NO_2BF_4 the alternate products corresponding to **5** and amides were not present. Authentic **5** (R = C_6H_5, R′ = CH_3 and R = CH_3, R′ = C_6H_5) (13) as well as amide hydrolysis products (5) were available for comparisons.

Reaction of ***1****f with* NO_2BF_4

To a 15 ml solution of 1.15 g (8.6 mmol) NO_2BF_4 in acetonitrile at 0° under He was added 1.25 g (8.6 mmol) **1***f* in 12 ml acetonitrile. The solution was stirred at room temperature for 18 h and worked-up in the usual manner. Analysis of the organic products by g.l.p.c./mass spectra (SE 30) indicated two major components both of which possessed $[M]^+$ 146. These were separated by preparative g.l.p.c. (SE 30) and identified as **2***d* (16) (8%) and **4***b* (17) (12.5%) by comparison of n.m.r. and mass spectra with literature values.

Reaction of ***1****a and b with Acetyl Chloride*

To a solution of acetyl chloride (0.81 g, 10 mmol) in 10 ml of dry ether under He was added vinyl azide (**1***a* or *b*), (1.0 g, 10.3 mmol) during 1 h. The evolution of nitrogen was smooth. After stirring for 8 h the reaction was quenched with 10% aqueous $NaHCO_3$. Continuous extraction with ether followed by solvent removal gave only amides **3***a* (5) and *b* (5) (g.l.p.c./mass spectra, Versamide 900).

Repetition of the above using 1.4 g (10.5 mmol) $AlCl_3$ in the initial ether solution gave, after work-up, 1.03 g (70%) of an oil. Distillation (b.p. (15 mm) 65°) of the oil gave 0.8 g (70%) of 2,4,5-trimethyl oxazole (**7**) identified by g.l.p.c., mass spectra and n.m.r. comparison with an authentic sample (18).

Reaction of ***1****d with Acetyl Chloride*

To a solution of acetyl chloride (0.39 g, 5 mmol) in ether (8 ml) under He containing $AlCl_3$ (0.67 g, 5 mmol) was added **1***d* (0.8 g, 5 mmol). The solution was stirred for 2–18 h and worked-up in the usual manner. Analysis by g.l.p.c./mass spectra (5% DEGS on Chrom W, 6 ft × 1/8 in. column, 100° for 30 min, 100–180° at 3°/min) revealed **8** (17%), **9** (7%), **10** (~1%), and amides (3%). Comparison of preparatively g.l.p.c. isolated samples with authentic samples (**8** (19), **9** (20), **10** (19), amides (5)) confirmed the identity of the products.

Reaction of ***1****a and b with DMAD*

Uncatalyzed

An ether solution (20 ml) containing 0.5 g **1***b* (5.2 mmol) and 0.7 g DMAD (4.9 mmol) was stirred for 3 days. Concentration of the solution gave 0.99 g 90% of triazole **11** (b.p. (0.1 mm) 150°) ν_{max} (KCl): 2930, 1735, 1550, 1450, 825, and 810 cm^{-1}.

Mol. wt. Calcd. for $C_{10}H_{13}N_3O_4$: 239. Found (M^+): 239.

$AlCl_3$ Catalyzed

To a solution of 1 g (7 mmol) DMAD and 0.95 g (7.1 mmol) $AlCl_3$ in 20 ml of ether was added 0.7 g (7.1 mmol) of **1***b*. The reaction was stirred for 18 h then quenched with excess 10% aqueous $NaHCO_3$, extracted with ether and chromatographed on 20 g of SiO_2. Elution with petroleum ether gave 0.4 g (23.5%) **11**. Elution with 95:5 petroleum ether : chloroform gave 0.30 g (13%) of **12**, m.p. 98–99°. Repetition of this experiment using an excess of DMAD gave unreacted DMAD, no **11**, and raised the yield of **12** to 15%.

The first experiment was repeated using reverse addition of reactants. Thus *trans*-2-azido-2-butene (**1***b*, 0.5 g, 5.2 mmol) was dissolved in 20 ml of dry ether and the solution cooled to −20 °C. To this was added aluminum chloride (0.8 g) followed by dropwise addition of DMAD (0.7 g, 4.9 mmol). The mixture was warmed to room temperature and after stirring overnight it was diluted with aqueous 10% $NaHCO_3$ until it was weakly basic. Continuous extraction with ether gave 1.00 g of oil. Direct chromatography on 30 g of SiO_2 using 95:5 chloroform – petroleum ether as eluent gave 0.7 g (55%) of **11**.

Similarly reaction of *cis*-2-azido-2-butene (2 g, 20.8 mmol) was added dropwise to a solution of 2.4 g of $AlCl_3$ and DMAD (2.5 g, 17.8 mmol) in 20 ml of ether. After the usual work-up the residual oil was chromatographed on 100 g of SiO_2. Elution with petroleum ether gave 0.9 g of the *cis*-isomer of triazole **11**; ν_{max} (KBr) 2930, 1735, 1550, 1450, 825, and 810 cm^{-1}; n.m.r. ($CDCl_3$): δ 5.85 (1H, quartet, J = 7 of quartet, J = 1 Hz), 3.98 (3H, s), 3.95 (3H, s), 2.21 (3H, sextet, J = 1 Hz), and 1.85 (3H, d, J = 7 of quartet, J = 1 Hz).

Mol. Wt. Calcd. for $C_{10}H_{13}N_3O_4$: 239. Found (M^+): 239.

Elution with 95:5 petroleum ether – chloroform gave 0.2 g (3%) of **12**.

Anal. Calcd. for $C_{16}H_{19}N_3O_8$ ([M^+] 381): C, 50.39; H, 4.99. Found (381): C, 50.52; H, 5.02.

Reaction of ***11*** *with DMAD in the presence of* $AlCl_3$

To a solution of 0.1 g of **11** in 5 ml of ether containing 0.1 g $AlCl_3$ was added 0.2 g DMAD. The reaction was stirred overnight at room temperature then quenched with aqueous 10% $NaHCO_3$. The mixture was continuously extracted with ether which was concentrated. The residue was chromatographed on 20 g SiO_2. Using petroleum ether as the eluent 0.18 g DMAD was recovered. Using 95:5 petroleum ether – chloroform as the eluent 0.08 g of **11** was recovered. T.l.c. analysis of the fractions which would contain **12** revealed its absence.

Pyrolysis of ***12***

A solution of (0.038 g) of **12** in 0.4 ml of nitrobenzene was heated in an n.m.r. tube at 165° for 3 h. The signals due to **12** disappeared and signals attributable of **14** and **15** appeared. Integration of the spectra taken in nitrobenzene after the sample was cooled to room temperature revealed the **14**:**15** ratio to be 87.4:12.6. Because of the interconversion of **14** and **15** at 165° and under conditions necessary for their g.l.p.c. separation analysis was obtained on the mixture obtained from preparative g.l.p.c. (SE 30).

Anal. Calcd. for $C_{18}H_{19}N_3$ ([M^+] 381): C, 50.39; H, 4.99. Found (381): C, 50.47; H, 4.85.

We wish to thank the National Research Council of Canada for financial support of this work through an

operating grant to A.C.O., the Ogilvie Flour Co. Ltd. for a postgraduate fellowship to A.T., and G. Owen of this department for development of g.l.p.c./mass spectrometer interface.

1. A. G. COOK. Enamines: synthesis, structure and reactions. M. Dekker and Co., New York, N.Y. 1969.
2. A. HASSNER. Acc. Chem. Res. **4**, 9 (1971).
3. K. ISOMURA, M. OKADA, and H. TANIGUCHI. Nippon Kagaku Zasshi, **91**, 746 (1970).
4. A. HASSNER and R. W. FOWLER. J. Org. Chem. **33**, 3686 (1968).
5. A. HASSNER, E. S. FERDINANDI, and R. J. ISBISTER. J. Am. Chem. Soc. **92**, 1672 (1970).
6. A. HASSNER and A. B. LEVY. J. Am. Chem. Soc. **93**, 5469 (1971).
7. A. HASSNER, A. S. MILLER, and M. J. HADDADIN. J. Org. Chem. **37**, 2682 (1972).
8. F. W. FOWLER and A. HASSNER. J. Am. Chem. Soc. **90**, 2875 (1968).
9. S. BORY, M. FETIZON, and P. LASZLO. Bull. Soc. Chem. Fr. 2310 (1963).
10. F. W. FOWLER, A. HASSNER, and L. A. LEVY. J. Am. Chem. Soc. **89**, 2077 (1967).
11. H. E. UNGNADE and E. D. LOUGHRAN. J. of Het. Chem. **1**, 61 (1964); G. ENGLERT. Zeit. Fuer. Anal. Chem. **181**, 447 (1961).
12. L. RUZICKA, M. KOBELT, O. FAFLIGER, and V. PRELOG. Helv. Chim. Acta, **32**, 544 (1949).
13. F. B. MALLORY and A. CAMMARATA. J. Am. Chem. Soc. **88**, 61 (1966).
14. G. PONZIO. Chem. Ber. **61**, 1316 (1928).
15. F. ELOY. Bull. Soc. Chim. Belges, **73**, 793 (1964).
16. J. V. BURAKEVICH, A. M. FARE, and G. P. VOLPP. J. Org. Chem. **36**, 5 (1971).
17. C. MOUSSEBOIS and J. F. M. OTH. Helv. Chim. Acta, **47**, 942 (1964).
18. G. THEILIG. Chem. Ber. **86**, 96 (1953).
19. H. BREDERECK, R. GOMPPER, and F. REICH. Chem. Ber. **93**, 1389 (1960).
20. J. H. BOWIE, P. F. DONAGHUE, and H. J. RODDA. J. Chem. Soc. (B) 1123 (1969); J. H. BOWIE, P. F. DONAGHUE, H. J. RODDA, R. G. COOKS, and D. H. WILLIAMS. Org. Mass. Spec. **1**, 13 (1968).

Can. J. Chem. Downloaded from www.nrcresearchpress.com by 210.87.254.5 on 09/05/12
For personal use only.

Can. J. Chem. Downloaded from www.nrcresearchpress.com by 210.87.254.40 on 09/05/12
For personal use only.

Canadian Journal of Chemistry

Published by
THE NATIONAL RESEARCH COUNCIL OF CANADA

Journal canadien de chimie

Publié par
LE CONSEIL NATIONAL DE RECHERCHES DU CANADA

Volume 51 Number 15 August 1, 1973 Volume 51 numéro 15 1 août 1973

The Reaction of Methyl Radicals with Neopentane

PHILIP D. PACEY
Department of Chemistry, Dalhousie University, Halifax, Nova Scotia

Received January 17, 1973

Neopentane was pyrolyzed in a flow reactor system at 793–953 K and 20–400 mm Hg. The rate constant for the initiation reaction,

$$neo\text{-}C_5H_{12} \rightarrow CH_3 + t\text{-}C_4H_9$$

calculated from the observed C_2H_6 yield, was $10^{17.7\pm0.3}$ exp $(-356 \pm 6$ kJ mol$^{-1}/RT)$ s^{-1}, in good agreement with earlier determinations in other temperature ranges. The rate constant of the reaction,

$$CH_3 + neo\text{-}C_5H_{12} \rightarrow CH_4 + neo\text{-}C_5H_{11}$$

calculated from the observed CH_4 and C_2H_6 yields, was $10^{10.5\pm0.1}$ exp $(-67 \pm 2$ kJ mol$^{-1}/RT)$ l mol^{-1} s^{-1}, four to ten times faster than predicted on the basis of earlier work at 404–608 K. From 404–953 K, the Arrhenius plot for this reaction is strongly curved.

Le néopentane a été pyrolysé dans un réacteur en système continu à 793–953 K et 20–400 mm Hg. La constante de vitesse pour la réaction d'initiation,

$$néo\text{-}C_5H_{12} \rightarrow CH_3 + t\text{-}C_4H_9$$

calculée à partir du rendement en C_2H_6 observé, est de $10^{17.7\pm0.3}$ exp $(-356 + 6$ kJ mol$^{-1}/RT)$ s^{-1}, en bon accord avec les déterminations antérieures dans d'autres domaines de température. La constante de vitesse de la réaction,

$$CH_3 + néo\text{-}C_5H_{12} \rightarrow CH_4 + néo\text{-}C_5H_{11}$$

calculée à partir des rendements en CH_4 et C_2H_6, est de $10^{10.5\pm0.1}$ exp $(-67 \pm 2$ kJ mol$^{-1}/RT)$ l mol^{-1} s^{-1}, c'est à dire quatre à dix fois plus rapide que celle prévue à partir des travails précédents effectués à 404–608 K. Dans la zone de température de 404 à 953 K, le tracé d'Arrhénius pour cette réaction est fortement recourbé.

[Traduit par le journal]

Can. J. Chem., 51, 2415 (1973)

The usual method of generation of CH_3 for the study of the metathetical reactions of methyl radicals is the photolysis of acetone or other substrates (1, 2). The rate of formation of CH_4 by the hydrogen abstraction reaction, for example,

[1] $$CH_3 + neo\text{-}C_5H_{12} \rightarrow CH_4 + neo\text{-}C_5H_{11}$$

is compared with the rate of formation of C_2H_6 by the reaction

[2] $$CH_3 + CH_3 \rightarrow C_2H_6$$

The rate constant of reaction 2, k_2, is known from other sources, so k_1 can be calculated. In the temperature range of photolysis, 300–600 K, most reactions like [1] have Arrhenius activation energies of 30–50 kJ mol^{-1} and pre-exponential factors of about 10^8 l mol^{-1} s^{-1}.

These results do not agree with higher temperature studies, in which the CH_3 radicals are generated by thermal decomposition of molecules (3). Specifically, recent studies (4–6) of the reactions of CH_3 with C_2H_6 and n-C_4H_{10} at temperatures above 800 K indicate that (*a*) the rate constants are greater than would be predicted from low temperature data, (*b*)

Can. J. Chem. Downloaded from www.nrcresearchpress.com by 210.87.254.40 on 09/05/12
For personal use only.

activation energies are about 70–90 kJ mol^{-1}, and (*c*) pre-exponential factors are 10^{10}–10^{12} l mol^{-1} s^{-1}. These results suggest that the Arrhenius plots for these reactions are not straight lines but curves. Arrhenius plot curvature is a rarely observed phenomenon, and is of considerable theoretical interest (7). However, the high temperature data are not as extensive as the photolytic data, and combinations of reactions, rather than the single reaction 2, were required at high temperatures to measure the CH_3 concentration.

The object of the present study was to study the reaction of CH_3 with neopentane (2,2-dimethylpropane), reaction 1, using the thermal decomposition of neopentane itself as a source of CH_3. This system is particularly convenient for study, as reaction 1 should be the only source of CH_4 and reaction 2 the only source of C_2H_6.

The Pyrolysis of Neopentane

Neopentane pyrolysis has recently been the subject of three studies in static systems at temperatures from 713 to 873 K (8–10). Data from the three laboratories are in excellent agreement. A mechanism consisting of reactions 1 and 2 and reactions 3–6 explains the rates of formation of the major products. The mechanism

[3] $$neo\text{-}C_5H_{12} \rightarrow CH_3 + t\text{-}C_4H_9$$

[4] $$t\text{-}C_4H_9 \rightarrow i\text{-}C_4H_8 + H$$

[5] $$H + neo\text{-}C_5H_{12} \rightarrow H_2 + neo\text{-}C_5H_{11}$$

[6] $$neo\text{-}C_5H_{11} \rightarrow CH_3 + i\text{-}C_4H_8$$

also explains the reaction order of 3/2 and overall activation energy of 210–243 kJ mol^{-1} observed in the static systems.

Taylor *et al.* (11) have studied the decomposition at higher temperatures (920–1070 K) using very low pressures of neopentane in nitrogen diluent in a flow reactor system. They observed an order of unity and an activation energy of 337 kJ mol^{-1}. However, Baronnet *et al.* (9) have shown that this behavior is predicted by the above mechanism at high temperatures and low pressures, when the chain length of the reaction is very short.

Steady-state analysis of the above mechanism leads to the following relation between the initial rates of formation of CH_4 and C_2H_6:

[7] $$\frac{k_1}{k_2^{1/2}} = \frac{R^0_{CH_4}}{[neo\text{-}C_5H_{12}]} \cdot \left(\frac{1}{R^0_{C_2H_6}}\right)^{1/2}$$

This expression is identical to that used in photolytic work, except that an extra term for reaction of CH_3 with the radical source is not required here.

At the reaction times accessible in static pyrolysis systems (of the order of minutes) observed rates of product formation are significantly less than extrapolated initial rates because of inhibition of the reaction by the isobutene formed. Values of rate constants derived depend greatly on the particular method of extrapolation used (3). For this reason, eq. 7 has not previously been directly applied to the determination of k_1. Côme *et al.* (12) studied the pressure variation of $k_1/k_2^{1/2}$ at one temperature. They assumed

[8] $$R^0_{C_2H_6} = R^0_{H_2} + R^0_{i\text{-}C_4H_{10}} - R^0_{i\text{-}C_5H_{10}}$$

where $i\text{-}C_4H_{10}$ and $i\text{-}C_5H_{10}$ were minor products. Halstead *et al.* (8) calculated k_1, assuming values of k_2 and k_3 to determine $[CH_3]$ by a steady-state calculation.

Reaction 2 is the only reaction resulting in net removal of radicals in the above mechanism, and reaction 3 is the only source of radicals. To maintain a steady radical concentration, the rates of reactions 2 and 3 must be equal. Thus

[9] $$k_3 = \frac{R^0_{C_2H_6}}{[neo\text{-}C_5H_{12}]}$$

Equation 9 was used to determine k_3 by Halstead *et al.* (8). They calculated $R^0_{C_2H_6}$ by assuming it was equal to $R^0_{H_2}$, and extrapolating observed rates of formation of these species to a common point at reaction time $t = 0$. Baronnet *et al.* (9) also determined k_3, assuming eq. 8 was true. Tsang (13) determined k_3 by measuring the CH_4 formed when neopentane was pyrolyzed at about 1200 K in the presence of toluene in a shock tube. In the present work, k_3 has been determined directly from eq. 9, using data from flow reactor studies, from which initial rates can be estimated more readily.

Experimental

The apparatus was similar to that used in a previous study (5).

Neopentane (Phillips Research Grade, 99.88%) was purified by trap-to-trap distillation and, on the day of an experiment, by prolonged and repeated degassing at −196 or −95 °C (toluene slush). The major impurity remaining was *iso*-butane, 0.01 mol %. Impurities of CH_4 and C_2H_6 varied from 1–5 p.p.m.

Three 75 cm-long quartz reactors were used; their internal diameters and surface to volume ratios (S/V)

Can. J. Chem. Downloaded from www.nrcresearchpress.com by 210.87.254.40 on 09/05/12
For personal use only.

were, respectively, (*i*) 1.7 cm, 3.1 cm^{-1}; (*ii*) 0.8 cm, 9.9 cm^{-1}; (*iii*) 0.2 cm, 23 cm^{-1}. Along the axes of reactors (*i*) and (*ii*) was placed a 0.4 cm outside diameter quartz thermocouple well. Reactor (*iii*) was placed along the axis of a 0.8 cm inside diameter quartz tube, which held a moveable thermocouple.

During an experiment, temperatures were measured at 2.5 cm intervals along the reactor using a platinum – platinum – 13% rhodium thermocouple. The computer program described in ref. 5 showed that 93% of the reaction occurred within ±5 °C of the average temperature of reaction during a typical experiment. Reactor diameters, temperatures, and reactant pressures were limited to prevent the endothermicity of the reaction from cooling the gases in the center of the vessel. Using the formula discussed in ref. 5, the maximum temperature drop from reactor wall to axis from this cause was calculated to be 1 °C. To prevent the cooler entering gases from distorting the temperature profile, flow rates were limited to 0.1 mol/h or less. For this flow rate, using method (*i*) of Mulcahy and Pethard (14), the error in the measured reaction rate may be calculated to be 5%.

The reaction products were analyzed by gas chromatography. A 1 m long, 12% NaOH-on-alumina column at 40 °C was used for most analyses, and a 1.5 m, 10% squalane-on-chromosorb P column at 0 °C for products of high molecular weight. Hydrogen was measured with a thermal conductivity detector, and the hydrocarbons with a flame ionization detector.

Results

More than 100 experiments[1] have been performed at reactor temperatures from 793–953 K, reaction pressures from 20–400 mm Hg, and reactor residence times from 0.05–5.1 s, corresponding to conversions varying from 0.1–6.1%. The two major products, methane and isobutene, were formed in equal quantities and together constituted from 90–99.5 mol % of all the products. As reported by earlier workers (8, 9), the yield of hydrogen always exceeded that of ethane, the ratio $[H_2]/[C_2H_6]$ varying from 1.2–2.4. Minor products observed were ethylene, propylene, propane, and 2-methyl-1-butene. Ethylene appeared to be a primary product; the mechanism by which it is formed is not well understood (8). Propylene and propane were secondary products. As reported and interpreted by Baronnet *et al.* (9), the yield of 2-methyl-1-butene was similar in magnitude to the difference $([H_2] - [C_2H_6])$.

Dependence of Rates on Reaction Time

Figures 1*a* and *b* show the dependence of the rates of formation of CH_4 and C_2H_6 on the reactor residence time at 68 mm Hg and 834 K, and 100 mm Hg and 913 K, respectively. In all four cases the rates of product formation decrease as the reaction time increases. A similar effect was observed in the static pyrolysis of neopentane (8, 9), and was shown to be caused by self-inhibition of the reaction by the isobutene formed; in some of these studies the rate observed at the shortest attainable reaction time was less than half of the estimated initial rate. In this flow system much shorter reaction times could be achieved, and the extrapolated initial rates were always within 10% of the nearest observed rate. The solid lines in the figures were calculated by the method of least squares.

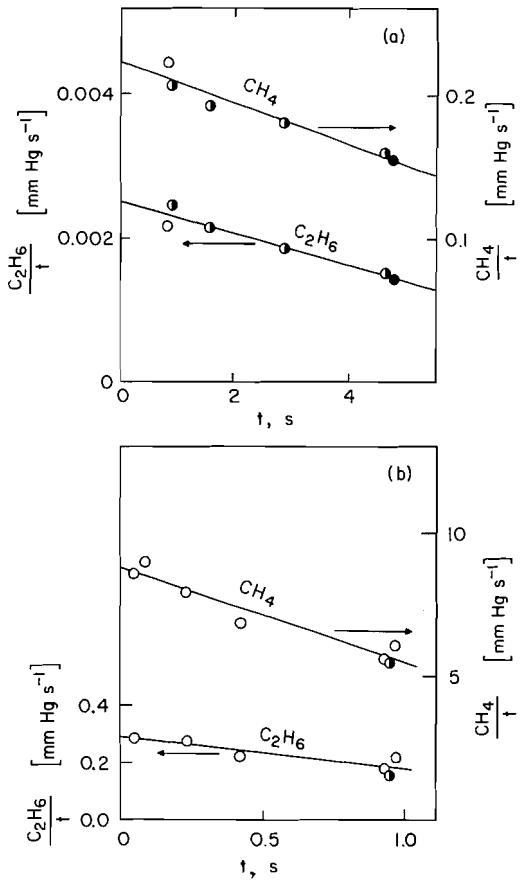

FIG. 1. Rates of formation of CH_4 and C_2H_6 as a function of reactor residence time for pyrolysis of neopentane at (*a*) 68 mm Hg and 834 K and (*b*) 100 mm Hg and 913 K. ●, Reactor (*i*), S/V = 3.1 cm^{-1}; ◑, reactor (*ii*), S/V = 9.9 cm^{-1}; ○, reactor (*iii*), S/V = 23 cm^{-1}.

[1]Tables of data are available, at a nominal charge, from the Depository of Unpublished Data, National Science Library, National Research Council of Canada, Ottawa, Canada, K1A 0R6.

Figures 1*a* and *b* also show that the observed rates were independent of the surface to volume ratio of the reactors.

Dependence of Rates on Pressure

The dependence of the initial rates of formation of CH_4 and C_2H_6 on reaction pressure is shown in Figs. 2 and 3 for reaction at 840 and 914 K, respectively.

In both cases, the data on C_2H_6 formation correlate well with the dashed lines of slope equal to 1.0. This behavior is predicted by the mechanism provided that the initiation reaction 3 is first order and that reaction 2 is the only termination reaction.

The initial rates of CH_4 formation in Fig. 2 correlate well with the dashed line of slope equal to 1.5. As the rate of CH_4 formation is, within 10%, equal to the rate of neopentane removal, the overall reaction is also of order 3/2, in agreement with the results of static pyrolyses (8–10).

In Fig. 3, for a higher reaction temperature, the CH_4 data at high pressures agree with the dashed line of slope 1.5, but the low pressure data lie above this line. This effect was previously observed in static pyrolysis by Baronnet *et al.* (9). They showed that the observation could be explained by the pressure dependence of the recombination rate constant, k_2. At the higher

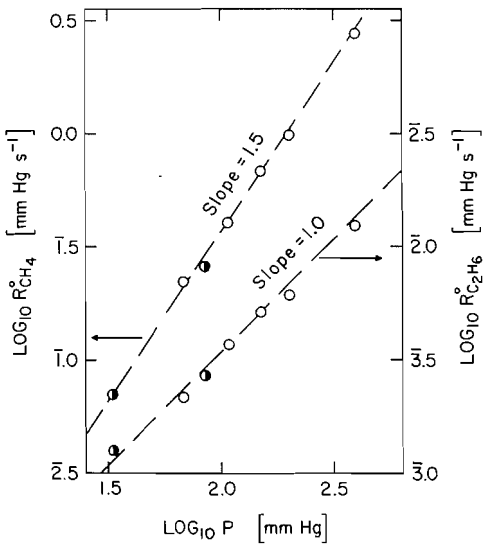

FIG. 2. Order plots for CH_4 and C_2H_6 formation in neopentane pyrolysis at 840 K. ◑, Reactor (*ii*); ○, reactor (*iii*). The dashed lines have slopes of exactly 1.5 and 1.0, respectively, as predicted by the mechanism.

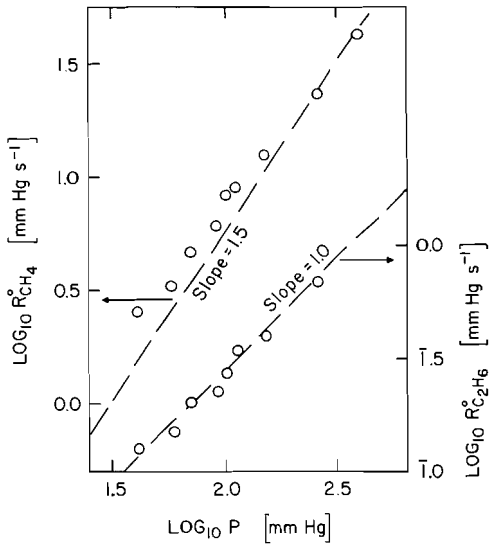

FIG. 3. Order plots for CH_4 and C_2H_6 for pyrolysis of neopentane in reactor (*iii*) at 914 K. The dashed lines have slopes of 1.5 and 1.0, respectively, as suggested by the mechanism.

temperatures of the present experiments (793–953 *vs.* 723–803 K), this pressure dependence should be more pronounced.

The pressure dependence of k_2 causes difficulties in the calculation of k_1 from eq. 7. If the precise value of k_2 were known at every pressure and temperature, it could be substituted in eq. 7 and k_1 determined. However, this pressure dependence is not known with certainty (15). It is necessary, then, either to work at high pressures, where k_2 is pressure independent, or to extrapolate low pressure data to high pressures. Lin and Back (16) have shown that the rate constant of the reverse of reaction 2 can be extrapolated to high pressures using a Lindemann–Hinshelwood plot. It follows that k_2, which must have identical pressure dependence to k_{-2}, can also be extrapolated in this manner.

Two Lindemann–Hinshelwood plots, for reaction temperatures of 953 and 914 K, respectively are shown in Fig. 4. The straight lines were determined by the method of least squares. For the reverse reaction, Lin and Back (16) found that $P_{1/2}$, the pressure at which k_{-2} has dropped to one-half its high pressure value, was 54 mm Hg at 958 K. From Fig. 4, $P_{1/2}$ at 953 K is estimated to be 37 ± 4 mm Hg. In agreement with theory and previous experiments (15), the

Can. J. Chem. Downloaded from www.nrcresearchpress.com by 210.87.254.40 on 09/05/12
For personal use only.

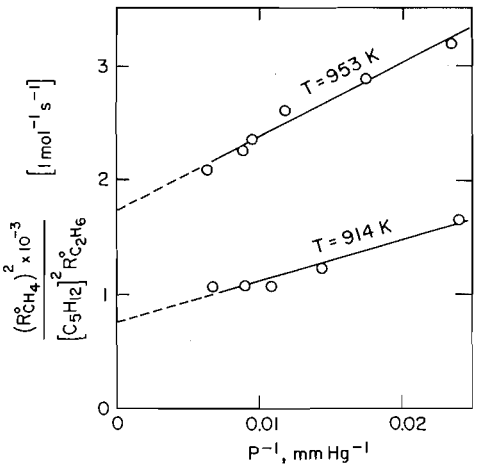

FIG. 4. Lindemann-Hinshelwood style plots for the experimental function, $R^0_{CH_4}{}^2\,[C_5H_{12}]^{-2}\,R^0_{C_2H_6}{}^{-1}$, at varying reaction pressures in reactor (*iii*) at temperatures of 953 and 914 K.

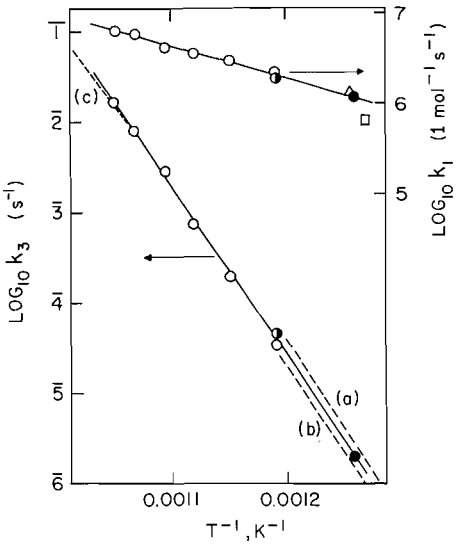

FIG. 5. Arrhenius plots for the rate constants k_1 and k_3. ●, Reactor (*i*); ◑, reactor (*ii*); ○, reactor (*iii*); □, calculated from the data of ref. 12; △, calculated from the data of ref. 8; (*a*) from the data of ref. 8; (*b*) extrapolated from the low temperature data of ref. 9; (*c*) extrapolated from the high temperature data of ref. 13. The solid lines are least squares lines through the data of this work.

values of $P_{1/2}$ estimated became smaller, and farther outside the experimental pressure range, at lower temperatures.

The aim of these experiments was not to study the pressure dependence of k_2, which will not be considered further, but to find the limiting, high pressure value of $R^0_{CH_4}{}^2[C_5H_{12}]^{-2}$-$R^0_{C_2H_6}{}^{-1}$, and then, using eq. 7 to calculate k_1. The extrapolated, high-pressure values of $k_1/k_2{}^{1/2}$ in most cases differed from the nearest observed value by less than 10%, and in all cases differed by less than 20%.

Variation of Reactor Temperature

To calculate k_1 from these high pressure extrapolations, the recently determined value (17) of $k_2 = 2.43 \times 10^{10}$ l mol^{-1} s^{-1} was used. This rate constant was assumed to be temperature independent in the high pressure limit considered here. The resulting values of k_1 (circles) are shown in the form of an Arrhenius plot in the upper part of Fig. 5. For comparison, values of k_1 have been calculated with this value of k_2 from the highest temperature estimates of ref. 8 (triangle) and ref. 12 (square). Both values lie within ±40% of the least squares line through the data of this work. The differences may result from the different methods of extrapolation used.

The Arrhenius activation energy derived from Fig. 5 for k_1 is 67 ± 2 kJ mol^{-1}, where here and subsequently the quoted uncertainty is the standard deviation. This activation energy is much greater than the values 42–50 kJ mol^{-1} found in experiments at lower temperatures and listed in Table 1. The pre-exponential factor from Fig. 5, $10^{10.5\pm0.1}$ l mol^{-1} s^{-1}, is one or two orders of magnitude greater than the low temperature values. Even among the low temperature data in Table 1, there is some indication of a general trend to greater values of $\log_{10} A$ and E_A as the average reaction temperature increases.

The initiation rate constant, k_3, was calculated using eq. 9. Values of k_3 at the same reaction temperature, but different pressures, were averaged and are shown in the lower part of Fig.5. Standard deviations of individual values from the average at a particular temperature were in the range from 4–21%. The solid line was determined by the method of least squares. The dashed line (*a*) represents the highest temperature, static pyrolysis data of Halstead *et al.* (8). Line (*b*) is extrapolated from the static pyrolysis data of Baronnet *et al.* (9). Line (*c*) is extrapolated from data obtained by Tsang (13) by high temperature pyrolysis of neopentane with toluene in a shock tube. In all cases, the

Can. J. Chem. Downloaded from www.nrcresearchpress.com by 210.87.254.40 on 09/05/12
For personal use only.

TABLE 1. Arrhenius Parameters for Reaction 1

Experimental system	Measure of $[CH_3]$	T, (K)	$\log_{10} A$ ($l\ mol^{-1}\ s^{-1}$)	E_A ($kJ\ mol^{-1}$)
$(CH_3)_2$ Hg photolysis ref. 18	Reaction 2	404–524	8.0 ± 0.1	43 ± 1
$(CH_3)_2$ CO photolysis ref. 19	Reaction 2	411–565	8.1 ± 0.1	42 ± 1
$(CD_3)_2$ CO photolysis ref. 20	$CD_3 + (CD_3)_2$ CO	458–582	9.33 ± 0.04	50.2 ± 0.4
Hg photosensitization ref. 21	Reaction 2	503–608	8.7	48
This work	Reaction 2	793–953	10.5 ± 0.1	67 ± 2

agreement between values of k_3 determined by flow pyrolysis and by previous work is excellent.

The solid line leads to the following Arrhenius expression for k_3: $k_3 = 10^{17.7\pm0.3} \cdot \exp(-356 \pm 6\ kJ\ mol^{-1}/RT)\ s^{-1}$. Previous workers have found $k_3 = 10^{18.05\pm0.58} \cdot \exp(-359 \pm 9/RT)$ (8); $k_3 = 10^{16.8} \exp(-343/RT)$ (9); and $k_3 = 10^{16.1} \exp(-327/RT)\ s^{-1}$ (13). The final expression has been reexamined by Tsang (22), who has suggested a revised expression $k_3 = 10^{16.8} \exp(-342/RT)\ s^{-1}$. All the activation energy measurements then would fall in the range 350 ± 9 kJ mol^{-1}, which is exceptional agreement.

Discussion

Comparison with Low Temperature Experiments

Figure 6 allows a more complete comparison of values of k_1 determined by flow pyrolysis (open circles) with those determined by photolysis (squares, ref. 19; triangles, ref. 18; inverted triangles, ref. 20) and the mercury-photosensitized decomposition of neopentane (filled circles, ref. 21). In refs. 18, 19, and 21, k_1 was determined relative to k_2; the results have been recalculated using k_2 from ref. 17. In ref. 20, k_1 was determined relative to the rate constant for the reaction

[10] $CD_3 + (CD_3)_2\ CO \rightarrow CD_4 + CD_3{\cdot}CO{\cdot}CD_2$

The value of k_{10} assumed in ref. 20 was twice as great as that found in four recent investigations (1). This could explain the fact that k_1 from ref. 20 is twice as great as k_1 from ref. 19. The original authors of ref. 18 suggested the lower values calculated for k_1 could have been caused by uneven light illumination.

The straight, dashed line (*a*) in the figure is a least squares line through the data of Trotman-Dickenson *et al.* (19). It can be seen that the pyrolysis data lie well above this line, by 0.7–1.0 log units, or a factor of 5–10. We shall next consider whether it is possible that the pyrolytic data could be in error by such a factor.

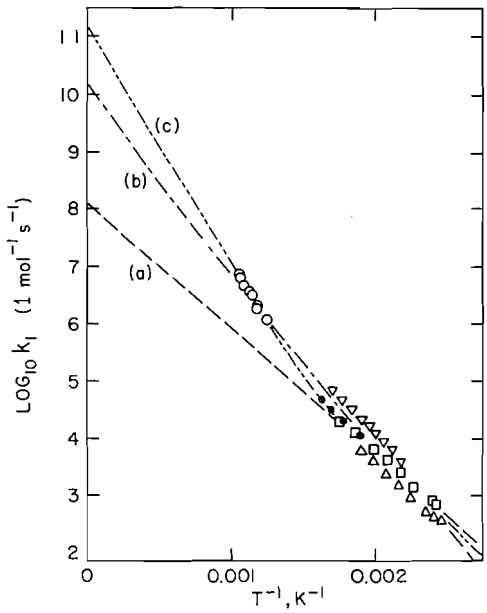

FIG. 6. Arrhenius plot for reaction 1 over a wide temperature range. ○, this work; □, ref. 19; △, ref.18; ▽, ref. 20; ●, ref. 21. Line (*a*), least squares line through the data of ref. 19; (*b*), $k_1 = \Gamma\ 10^{10.2} \exp(-67\ kJ\ mol^{-1}/RT)\ l\ mol^{-1}\ s^{-1}$, where Γ is the tunnelling factor for a truncated parabola from ref. 27; (*c*), $k_1 = 10^{7.8} \exp(-40/RT)\ l\ mol^{-1}\ s^{-1} + 10^{11.2} \exp(-80/RT)\ l\ mol^{-1}\ s^{-1}$.

Possible Systematic Errors

Errors in k_1 could arise from errors in any of the other factors in eq. 7; each will be examined in turn.

The discrepancy in Fig. 6 could be explained

Can. J. Chem. Downloaded from www.nrcresearchpress.com by 210.87.254.40 on 09/05/12
For personal use only.

Can. J. Chem. Downloaded from www.nrcresearchpress.com by 210.87.254.40 on 09/05/12
For personal use only.

if 80–90% of the CH_4 were formed by another reaction, for example, reaction of CH_3 with an impurity, or with H atoms, *t*-butyl radicals or C_5H_{11} radicals, or reaction at a surface.

The major impurity present was isobutane. In all cases CH_4 yields observed were at least ten times as great as the original isobutane concentration. It is impossible that impurities could contribute major quantities of CH_4.

The steady-state concentrations of H, *t*-C_4H_9, and *neo*-C_5H_{11} have been estimated from the mechanism (particularly, reactions 4–6 and the observed rates of formation of H_2, C_2H_6, and C_4H_8, respectively). The rate constant for reaction 5 was assumed equal to the value found by Baldwin and Melvin (23) for the analogous reaction with ethane. The rate constants used for reactions 4 and 6 were those favored by Benson and O'Neal (24). Under all experimental conditions, the calculated concentrations of all three species were lower than the concentration of CH_3. Since reaction 2 is very rapid (about one collision in four is effective), CH_3 must form C_2H_6 via reaction 2 more frequently than it forms CH_4 by any reaction with H, *t*-C_4H_9, or *neo*-C_5H_{11}. C_2H_6 was formed an order of magnitude slower than CH_4, so these reactions, even if their rate constants equalled k_2, could only contribute a maximum of 0.5% of the observed CH_4.

The fact that identical rates were observed in reactors of three different surface to volume ratios indicates that surface reactions could not contribute a major proportion of the CH_4.

The only other ways of removing the discrepancy in Fig. 6 would be to suggest that $R^0_{C_2H_6}$ was underestimated by a factor of 25–100 or that k_2 was overestimated by a factor of 25–100. The first hypothesis can be ruled out by the very short extrapolations required in Figs. 1*a* and *b* and the good agreement between values of k_3 from this work and previous experiments. The second hypothesis would require that k_2 be temperature independent from 300–608 K, and then develop a negative activation energy of 50 kJ mol^{-1} at high temperatures. This is not in accord with the available data (15).

The low temperature data are reasonably consistent among themselves and agree well with experiments on a large number of related reactions (1). It does not seem likely that they can be greatly in error.

It is probable, then, that the values of k_1 in Fig. 6 are correct, and that the Arrhenius plot for this reaction is a curve.

Interpretation

The Arrhenius plot curvature is similar to that observed in studies of the reactions of CH_3 with C_2H_6 and *n*-C_4H_{10} and of C_2H_5 with C_4H_{10} (4–6). The results reported herein are more extensive, however, and the method of calculation simpler.

There are several possible explanations of the observed curvature: the presence of several low frequency vibrations in the transition state, substantial vibrational anharmonicity in the transition state, quantum mechanical tunnelling through the activation energy barrier, and contribution to reaction from more than one reactant state or more than one transition state. Of these, the effect of vibrational anharmonicity is difficult to evaluate quantitatively, but the others will be tested.

According to transition state theory (25), low frequency vibrations in the transition state should each contribute a factor of T to the pre-exponential factor, leading to curvature of the Arrhenius plot in the direction observed. In order to explain the observed magnitude of the curvature, however, it would be necessary to postulate that there are eight or nine more low frequency vibrational modes in the transition state than in the reactants throughout the range 404–953 K. But the low pre-exponential factors observed at low temperatures for reactions of this type suggest that there are very few low frequency vibrations in the transition state (26).

A rough estimation of the effect of tunnelling on this reaction can be seen from curve b in Fig. 6, which shows the function, $k_1 = \Gamma\, 10^{10.2} \exp(-67\ \text{kJ mol}^{-1}/RT)\ \text{l mol}^{-1}\ \text{s}^{-1}$. Here Γ is the tunnelling factor calculated by Sharp and Johnston (27) for the very similar reaction $CF_3 + CH_4 \rightarrow CF_3H + CH_3$, assuming an activation barrier to reaction shaped like a truncated parabola. These tunnelling factors fitted the experimentally observed kinetic isotope effect for that reaction, which is very similar to the kinetic isotope effect for the reaction of CH_3 with C_2H_6 (25). The other factors in the expression for k_1 were chosen to attempt to match curve b to the experimental data.

The figure shows that curve b is close to the

data, but its curvature, or rate of change of slope, is not as great as that of the experimental data. It is quite possible, nevertheless, that a different model for tunnelling could explain both the observed curvature for reaction 1 and the kinetic isotope effect for related reactions.

Curve c in Fig. 6 represents the function, $k_1 = 10^{7.8} \exp(-40 \text{ kJ mol}^{-1}/RT)\ 1 \text{ mol}^{-1} \text{ s}^{-1} + 10^{11.2} \exp(-80 \text{ kJ mol}^{-1}/RT)\ 1 \text{ mol}^{-1} \text{ s}^{-1}$. This function corresponds to a model in which reaction 1 proceeds by two paths, either via two transition states, or from two different reactant vibrational quantum states, or from two types of methyl radicals, as suggested by Hay (28). The model, though crude, can be fitted to the experimental data, as the figure shows.

It is possible that several of these effects may contribute to the observed curvature. At present, the range of the data is not sufficient to distinguish between them.

The low temperature activation energies for the hydrogen abstraction reactions of methyl radicals have been extensively correlated with the bond dissociation energies of the bonds being broken (29, 30). Implicit in these correlations is the assumption that the low temperature activation energies are approximately equal to the height of the activation barrier. If tunnelling occurs, this assumption is not valid. The significance of these correlations is thus reduced.

Whether tunnelling occurs or not, it is clear that the Arrhenius plot for this reaction is a curve. Arrhenius expressions adequately represent the experimental data only within narrow temperature ranges.

The author wishes to thank Prof. J. H. Purnell for his encouragement and the National Research Council of Canada for a grant in support of this research.

1. P. Gray, A. A. Herod, and A. Jones. Chem. Rev. **71**, 247 (1971).
2. A. F. Trotman-Dickenson and G. S. Milne. Tables of bimolecular gas reactions. National Bureau of Standards, Washington. 1967.
3. D. A. Leathard and J. H. Purnell. Ann. Rev. Phys. Chem. **21**, 197 (1970).
4. T. C. Clark, T. P. J. Izod, and G. B. Kistiakowsky. J. Chem. Phys. **54**, 1295 (1971).
5. P. D. Pacey and J. H. Purnell. J. Chem. Soc. Faraday Trans. I, **68**, 1462 (1972).
6. P. D. Pacey and J. H. Purnell. Int. J. Chem. Kinet. **4**, 657 (1972).
7. W. C. Gardiner, Jr., W. G. Mallard, M. McFarland, K. Morinaga, J. H. Owen, W. T. Rawlins, T. Takeyama, and B. F. Walker. 14th Sym. (Int.) Combustion. Combustion Institute. 1972. In press.
8. M. P. Halstead, R. S. Konar, D. A. Leathard, R. M. Marshall, and J. H. Purnell. Proc. Roy. Soc. A**310**, 525 (1969).
9. F. Baronnet, M. Dzierzynski, G. M. Côme, R. Martin, and M. Niclause. Int. J. Chem. Kinet. **3**, 197 (1971).
10. D. J. Frank and W. M. Sackett. Geochim. Cosmochim. Acta, **33**, 811 (1969).
11. J. E. Taylor, D. A. Hutchings, and K. J. Frech. J. Am. Chem. Soc. **91**, 2215 (1969).
12. G. M. Côme, F. Baronnet, G. Scacchi, R. Martin, and M. Niclause. C.R. Acad. Sci. Paris, Ser. C, **267**, 1192 (1968).
13. W. Tsang. J. Chem. Phys. **44**, 4283 (1966).
14. M. F. R. Mulcahy and M. R. Pethard. Aust. J. Chem. **16**, 527 (1963).
15. E. V. Waage and B. S. Rabinovitch. Int. J. Chem. Kinet. **3**, 105 (1971).
16. M. C. Lin and M. H. Back. Can. J. Chem. **44**, 2357 (1966).
17. H. E. Van Den Berg, A. B. Callear, and R. J. Norstrom. Chem. Phys. Lett. **4**, 101 (1968).
18. R. E. Rebbert and E. W. R. Steacie. J. Chem. Phys. **21**, 1723 (1953).
19. A. F. Trotman-Dickenson, J. R. Birchard, and E. W. R. Steacie. J. Chem. Phys. **19**, 163 (1951).
20. J. A. Kerr and D. Timlin. J. Chem. Soc. A, 1241 (1969).
21. E. Furimsky and K. J. Laidler. Can. J. Chem. **50**, 1115 (1972).
22. W. Tsang. Int. J. Chem. Kinet. **1**, 245 (1969).
23. R. R. Baldwin and A. Melvin. J. Chem. Soc. 1785 (1964).
24. S. W. Benson and H. E. O'Neal. Kinetic data on gas phase unimolecular reactions. National Bureau of Standards, Washington. 1970.
25. H. S. Johnston. Gas phase reaction rate theory. Ronald Press, New York. 1966.
26. S. W. Benson. Thermochemical kinetics. Wiley, New York. 1968.
27. T. E. Sharp and H. S. Johnston. J. Chem. Phys. **37**, 1541 (1962).
28. J. M. Hay. J. Chem. Soc. B, 1175 (1967).
29. A. F. Trotman-Dickenson. Chem. Ind. 379 (1965).
30. A. A. Zavitsas. J. Am. Chem. Soc. **94**, 2779 (1972).

Can. J. Chem. Downloaded from www.nrcresearchpress.com by 210.87.254.40 on 09/05/12
For personal use only.

The *gauche* Effect. A Theoretical Study of the Topomerization (Degenerate Racemization) and Tautomerization of Methoxide Ion Tautomer

SAUL WOLFE

Department of Chemistry, Queen's University, Kingston, Ontario

LUIS M. TEL

Departamento de Quimica Fisica, Facultad de Ciencias, Universidad de Valladolid, Spain

AND

I. G. CSIZMADIA

Department of Chemistry, University of Toronto, Toronto, Ontario

Received December 11, 1972

Non-empirical double zeta quality molecular orbital calculations on $^{-}CH_2OH$ as a function of the C—O bond length (r), the rotational angle about the C—O bond (θ), and the pyramidal angle at carbon (ϕ) are described. From the stretching potential curve, $E(r)$, it is shown that dissociation of $^{-}CH_2OH$ proceeds to give CH_2 and OH^{-}. The rotation–inversion surface, $E(\theta,\phi)$, has two types of minima; in both cases the most favorable pyramidal angle at carbon is 105°. The lower minimum corresponds to a structure (the Y conformation) having the hydroxyl proton on the external bisector of the HCH angle. The higher minimum is 6.67 kcal/mol less stable and corresponds to a structure (the W conformation) having the hydroxyl proton on the internal bisector of the HCH angle. The relationship of these results to the *gauche* effect is discussed and it is noted that at certain internuclear distances the nuclear–nuclear repulsion term (E_{nucl}) may overcome the tendency of adjacent electron pairs and polar bonds to exist preferentially in that conformation which has the maximum number of *gauche* interactions between these electron pairs or polar bonds.

The topomerization of $^{-}CH_2OH$, *i.e.*, the conformational transformation from one Y conformation into another, proceeds, via the W conformation as an intermediate, by two separate events, *viz.* rotation about the C—O bond, having a barrier of 10.58 kcal/mol, and pyramidal inversion at carbon, with a barrier of 20.52 kcal/mol. Some factors governing the relative importance of rotation and inversion in degenerate racemization are discussed.

In its ground electronic state CH_3O^{-} is 22.18 kcal/mol more stable than $^{-}CH_2OH$. However, in the low-lying excited states all conformations of $^{-}CH_2OH$ are stabilized relative to CH_3O^{-}. The most stable excited state structure of $^{-}CH_2OH$ corresponds to the energy maximum for rotation–inversion of the ground electronic state.

Les calculs non-empiriques d'orbitales moléculaires (qualité double zeta) sur $^{-}CH_2OH$ sont décrits en fonction de la longueur du lien C—O (r), de l'angle de rotation autour du lien C—O (θ), ainsi que de l'angle pyramidal du carbone (ϕ). A partir de la courbe du potentiel d'élongation, il est démontré que la dissociation de $^{-}CH_2OH$ conduit à la formation de CH_2 et OH^{-}. La surface rotation–inversion $E(\theta,\phi)$, possède deux types de minima; dans les deux cas, l'angle pyramidal le plus favorable au carbone est de 105°. Le minimum le plus bas correspond à une structure (la conformation Y) possédant le proton du groupe hydroxyle sur la bissectrice extérieure de l'angle HCH. Le minimum le plus élevé est de 6.67 kcal/mol moins stable et correspond à la structure (la conformation W) possèdant le proton du groupe hydroxyle sur la bissectrice interne de l'angle HCH. La relation de ces effets avec l'effet *gauche* est discuté; de plus l'on note qu'à certaines distances internucléaires, le terme englobant la répulsion noyau–noyau (E_{nucl}) peut surpasser la tendance des paires adjacentes d'électrons et des liens polaires à exister préférentiellement dans cette conformation qui possède le nombre maximum d'interactions *gauches* entre ces paires d'électrons ou ces liens polaires.

La topomérisation de $^{-}CH_2OH$, *i.e.*, la transformation conformationnelle à partir d'une conformation Y vers une autre, se produit, en passant par la conformation W intermédiaire, selon deux étapes, *viz.* rotation autour du lien C—O ce qui représente une barrière de 10.58 kcal/mol et inversion pyramidale au carbone ce qui représente une barrière de 20.52 kcal/mol. Plusieurs facteurs concernant l'importance relative de la rotation et de l'inversion en ce qui a trait à la racémisation dégénérée sont discutés.

Dans son état électronique fondamental CH_3O^{-} est de 22.18 kcal/mol plus stable que $^{-}CH_2OH$. Cependant dans les plus bas états excités, toutes les conformations de $^{-}CH_2OH$ sont stabilisées comparativement à CH_3O^{-}. La structure du $^{-}CH_2OH$ correspondant à l'état excité le plus stable correspond à l'énergie maximum pour la rotation–inversion de l'état électronique fondamental.

[Traduit par le journal]

Can. J. Chem. Downloaded from www.nrcresearchpress.com by 210.87.254.42 on 09/05/12
For personal use only.

Can. J. Chem. Downloaded from www.nrcresearchpress.com by 210.87.254.42 on 09/05/12
For personal use only.

Introduction

In the course, of *ab initio* theoretical studies related to the *gauche* effect (1–3) we have been interested in the rotation–inversion behavior of carbanions adjacent to a heteroatom (4–7) or second carbanionic center (3). The original work (4–7), which led to the discovery of the *gauche* effect, was performed using minimal basis sets. Calculations of this quality correctly anticipated the tendency of species containing adjacent electron pairs or polar bonds to exist preferentially in that conformation which contains the maximum number of *gauche* interactions between these electron pairs or polar bonds. However, it could not be expected (8) that all of the details of rotation–inversion surfaces associated with such systems, required for an understanding of the physical basis of the *gauche* effect, would be basis set invariant. Therefore, the more recent work, which is being performed with this objective in mind (2, 3, 9–11), employs in all cases basis sets of at least double zeta quality. At the present time this level of calculation represents the practical limit for systems of interest to us.

The work reported here deals with an investigation of hydroxymethylcarbanion, $^{-}CH_2OH$, the tautomeric form of CH_3O^{-}, which can be viewed as the simplest carbanion having an adjacent oxygen atom. This anion is isoelectronic and isoprotic with H_2NOH, whose rotational potential (shown in Fig. 1) has already received some attention (12, 13).

A point of special interest in the geometry optimization of $^{-}CH_2OH$ was the accurate determination of the energetics of the process,

$$H^{+} + {}^{-}CH_2OH \rightarrow CH_3OH$$

required for a comparison of the proton affinities of $^{-}CH_2OH$ and $^{-}CH_2SH$. It is an experimental fact (14) that the kinetic acidity of a proton at a carbon adjacent to sulfur is several orders of magnitude greater than that of a proton at carbon adjacent to oxygen. This has been attributed to d_{π}–p_{π} stabilization of the intermediate in the former case (14, 15). Since it has not been necessary to postulate d-orbital conjugation to account for the *stereochemical* properties of sulfur-stabilized carbanions (1, 4–7), it seemed reasonable to suppose that some, as yet unrecognized, non-conjugative explanation might account for the *chemical* difference between oxygen and sulfur.

Method

An extensive contracted Gaussian basis set was employed which has been optimized for C and O atoms by Huzinaga (16), and by Basch *et al.* for H (17). For $^{-}CH_2OH$ this consisted of a total of 80 GTF contracted to 26 basis functions, corresponding to a double zeta basis set. The same basis set was used for a study of CH_3O^{-}, CH_3OH, and $CH_3OH_2^{+}$ (9). Since the Hartree–Fock limit was approached quite well in the CH_3OH calculation, the results for $^{-}CH_2OH$ were expected to be reliable. All computations were performed on an IBM 360/65 computer using the IBMOL 4 system (18).

Results and Discussion

The Conformational Hypersurface of $^{-}CH_2OH$

To generate a complete conformational hypersurface of $^{-}CH_2OH$ it would have been necessary to determine the variation of the total energy with respect to each of the $3N - 6$ internal coordinates. For practical reasons, however, it is customary in an *ab initio* calculation to investigate the effects of only one, two or, perhaps, three internal coordinates. For $^{-}CH_2OH$ the independent variables selected for study were the C—O bond length (r), rotation about the C—O bond (θ), and pyramidal inversion at carbon (ϕ), because it seemed likely that these would have the greatest effects upon the stereochemistry of the anion.

The resulting four-dimensional hypersurface $E(r,\theta,\phi)$ was then generated in two stages. In the initial stage, variation of r was examined and two cross-sections of the hypersurface were obtained, corresponding to tetrahedral bond angles at carbon ($\phi = 110°$) and, using the energy minima of H_2NOH as a guide (12, 13), the 0° (**1**, termed the Y conformation) and 180° (**2**, termed the W conformation) rotational conformations ($\theta = 0$, 180°). These results, presented in Table 1 and illustrated in Fig. 2, indicate minima at 1.500 (**1**) and 1.508 Å (**2**).

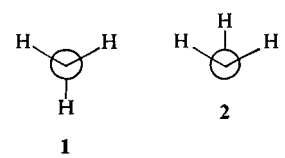

1 **2**

It is possible, using these data, to identify the products of dissociation of $^{-}CH_2OH$. Only heterolytic bond cleavage can be considered, because of the closed shell SCF treatment, and

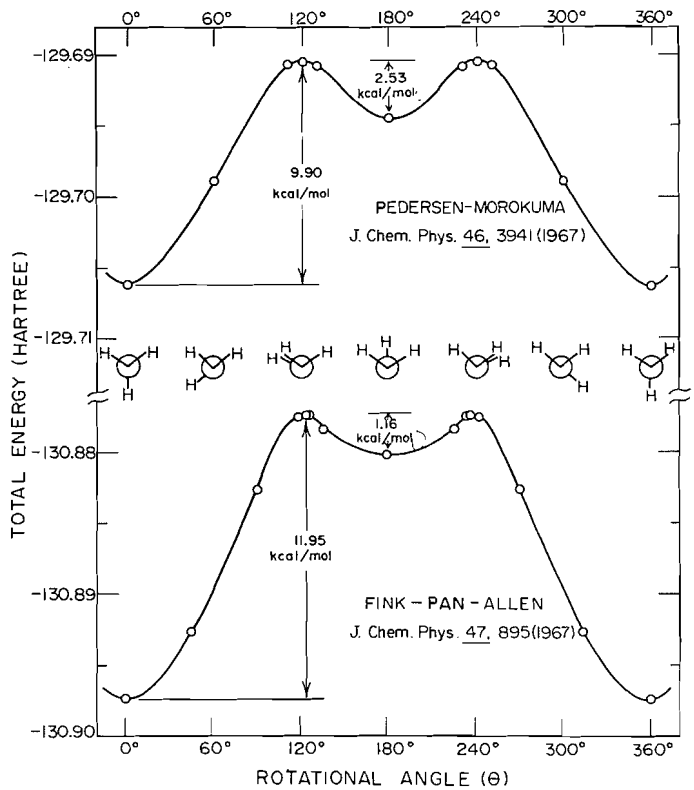

FIG. 1. The computed rotational potential of hydroxylamine.

TABLE 1. Variation of the total energy values and their components with C—O internuclear distance in **1** and **2**

		R (bohr)				
Compound		2.19856	2.69856	3.69856	5.69856	8.69856
1	E_T (Hartree)	−114.19704	−114.30505	−114.26348	−114.18701	−114.17556
	$V_{ne} + T$	−238.64193	−229.71641	−218.06082	−206.27494	−198.12539
	V_{ee}	85.25117	81.00711	75.33349	69.56784	65.41382
	V_{nn}	39.19372	34.40425	28.46385	22.52009	18.53600
2	E_T	−114.18705	−114.29469	−114.25880	−114.18499	−114.17471
	$V_{ne} + T$	−238.63062	−229.70208	−218.02685	−206.23425	−198.11689
	V_{ee}	85.16964	80.94231	75.26757	69.51350	65.40028
	V_{nn}	39.27393	34.46507	28.50048	22.53575	18.54190

two such processes might be proposed as indicated in eqs. 1 and 2.

[1] $^{-}:CH_2—OH \rightarrow :CH_2 + OH^{-}$

[2] $^{-}:CH_2—OH \rightarrow :CH_2^{2-} + OH^{+}$

Equation 1 was expected to represent the favored route, on the basis of simple electronegativity arguments. Moreover, because the ground state of OH^+ has triplet multiplicity, this species does not represent a closed shell problem. The energetics of both routes were computed, with the results shown in Table 2. Clearly route [2] is less favorable, by almost 0.8 hartree. However, it is also evident that our calculations converge to slightly higher values than the energies of the dissociated products. It is possible that these correspond to a local maximum in the Morse potential; such maxima in theoretically computed potential curves have been observed previously (19) and have also

Can. J. Chem. Downloaded from www.nrcresearchpress.com by 210.87.254.42 on 09/05/12
For personal use only.

TABLE 2. The energetics of ionic dissociation* of $^{-}CH_2$—OH

Path [1]		Path [2]	
CH_2 ($^1A_1$)	− 38.860934	CH_2^{2-} ($^1A_1$)	− 38.399181
OH^- ($^1\Sigma^+$)	− 75.320304	OH^+ ($^3\Sigma^-$)	− 74.953197
$CH_2 + OH^-$	−114.181238	$CH_2^{2-} + OH^+$	−113.352378

*Bond lengths and bond angles of the fragments were chosen to be the same as those of the dissociating molecule.

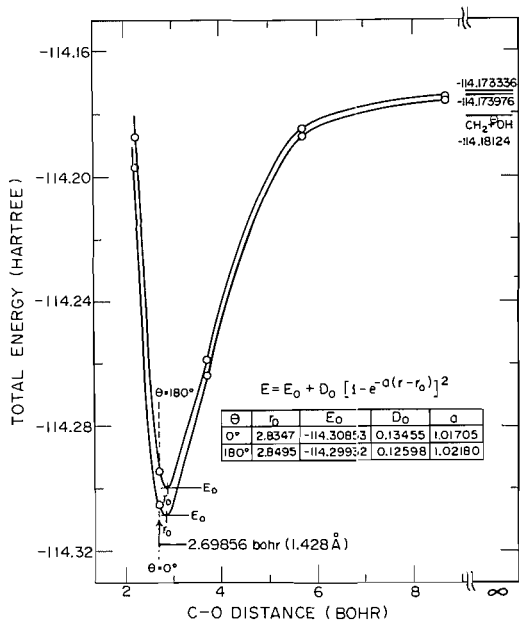

FIG. 2. The Morse potential functions of $^{-}CH_2OH$ in conformations **1** (lower curve) and **2** (upper curve). The energetics of path [1] are also shown.

been detected experimentally, in predissociation (20). Alternatively, the present result may simply be an artefact of the particular geometry employed.

In the second stage of the work, a rotation–inversion surface $E(\theta,\phi)$ was generated using the experimental C—O bond length of methanol (1.428 Å). This was done to facilitate a direct comparison with the previous calculations on the parent compound (CH_3OH) and the tautomeric form (CH_3O^-) of $^{-}CH_2OH$ (9). The computed total energy values and their components are summarized in Table 3, and the rotation–inversion surface for this C—O bond length is shown in Fig. 3. This figure shows the energy maximum, corresponding to structure **3**, and two equivalent saddle points (**4**), as well as the two minima corresponding to **1** and **2**. The Y conformation, as in H_2NOH, represents the lowest minimum on the energy surface. Two cross-sections of this surface associated with inversion at carbon are shown in Fig. 4 and five cross-sections, associated with rotation about the C—O bond, are given in Fig. 5. The energy components of two of these rotational curves, $\phi = 120°$ (planar configuration at carbon) and $\phi = 110°$ (tetrahedral configuration at carbon) are shown in Fig. 6.

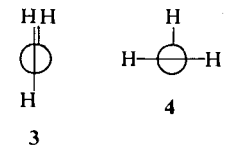

Topomerization of $^{-}CH_2OH$

With Figs. 3–5 in hand it is possible to provide a theoretical discussion of the process, referred to as "degenerate racemization" (21*a*), or "topomerization" (21*b*), whereby a species such as $^{-}CH_2OH$ transforms itself by some combination of rotation and inversion from one structure into an identical or enantiomeric structure. Scheme 1 illustrates the various possible routes for such a process in the present case.

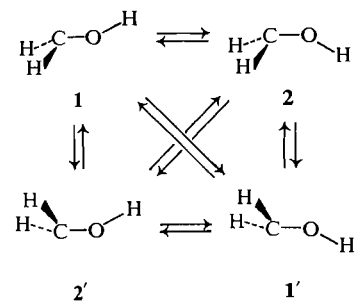

SCHEME 1. Topomerization of $^{-}CH_2OH$. Horizontal arrows: rotation along the C—O bond or in-plane inversion at oxygen. Vertical arrows: pyramidal inversion at carbon. Diagonal arrows: rotation–inversion.

Can. J. Chem. Downloaded from www.nrcresearchpress.com by 210.87.254.42 on 09/05/12
For personal use only.

TABLE 3. Computed energy values and their components associated with the rotation–inversion surface of $^{-}CH_2OH$

		$\phi°$				
$\theta°$		120*	115	110†	105	100
0	E_T	−114.27482	−114.29296	−114.30505	−114.30751	−114.30535
	$V_{ne} + T$	−229.42352	−229.55206	−229.71641	−229.95128	−230.23498
	V_{ee}	80.967865	80.979422	81.007116	81.097140	81.220908
	V_{nn}	34.180838	34.279674	34.404250	34.546632	34.708722
60	E_T			−114.29316	−114.29904	
	$V_{ne} + T$			−229.73416	−229.96025	
	V_{ee}			81.017263	81.091816	
	V_{nn}			34.423731	34.569391	
90	E_T	−114.25401	−114.27359	−114.28667	−114.29256	−114.29160
	$V_{ne} + T$	−229.53496	−229.59305	−229.74417	−229.97578	−230.27191
	V_{ee}	81.090646	81.011031	81.015485	81.091084	81.218619
	V_{nn}	34.190301	34.308420	34.442018	34.592139	34.761686
120	E_T		−114.27514	−114.28616	−114.29065	−114.28822
	$V_{ne} + T$		−229.57123	−229.73864	−229.98413	−230.29315
	V_{ee}		80.978830	80.995681	81.081221	81.217685
	V_{nn}		34.317257	34.456793	34.612257	34.787247
180	E_T	−114.27482	−114.28636	−114.29469	−114.29688	−114.29263
	$V_{ne} + T$	−229.42352	−229.51298	−229.70208	−229.96367	−230.28458
	V_{ee}	80.967865	80.906507	80.942316	81.041197	81.186061
	V_{nn}	34.180838	34.320114	34.465075	34.625587	34.805885

*Planar carbon.
†Tetrahedral bond angles at carbon.

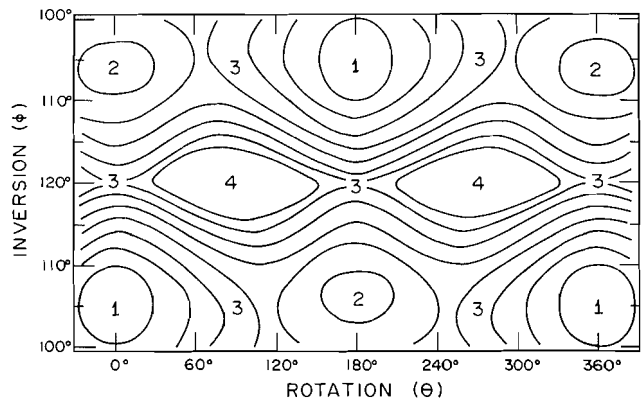

FIG. 3. Rotation–inversion surface ($E(\theta,\phi)$) of $^{-}CH_2OH$ at the methanol C—O bond length (1.428 Å).

The meaning of Scheme 1 is that the interconversion of **1** and **1′** (≡ **1**) must involve one of the following combinations: (*A*) rotation about the C—O bond and pyramidal inversion at the carbanionic center; (*B*) rotation about the C—O bond and in-plane inversion at oxygen; (*C*) in-plane inversion at oxygen and pyramidal inversion at carbon. In each case the process may be characterized by a single barrier (*i.e.*, combined rotation–inversion) or by two discrete barriers (*i.e.*, via an intermediate) which may or may not have equal heights. The problem then is to select the favored route from these twelve possibilities.

Structure **3**, which represents the barrier for combined rotation–pyramidal inversion, is 33.6 kcal/mol less stable than **1**. Although the barrier to in-plane inversion was not computed in the

Can. J. Chem. Downloaded from www.nrcresearchpress.com by 210.87.254.42 on 09/05/12
For personal use only.

Can. J. Chem. Downloaded from www.nrcresearchpress.com by 210.87.254.42 on 09/05/12
For personal use only.

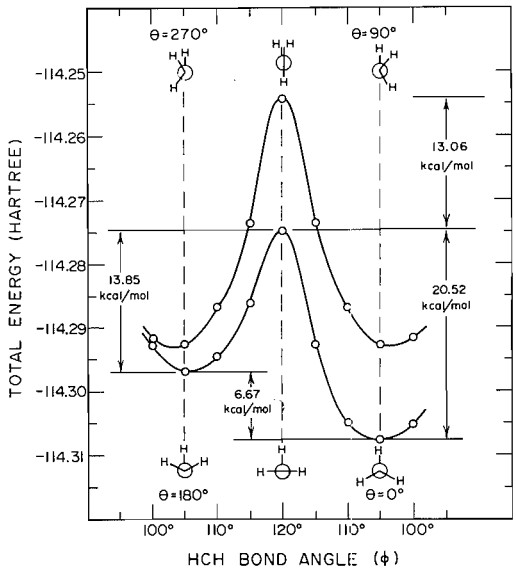

FIG. 4. Two inversion cross-sections of the rotation–inversion surface of $^{-}CH_2OH$. Upper curve: the cross-section through $\theta = 90°$ ($\equiv 270°$). Lower curve: the cross-section through $\theta = 0°$ ($\equiv 180°$).

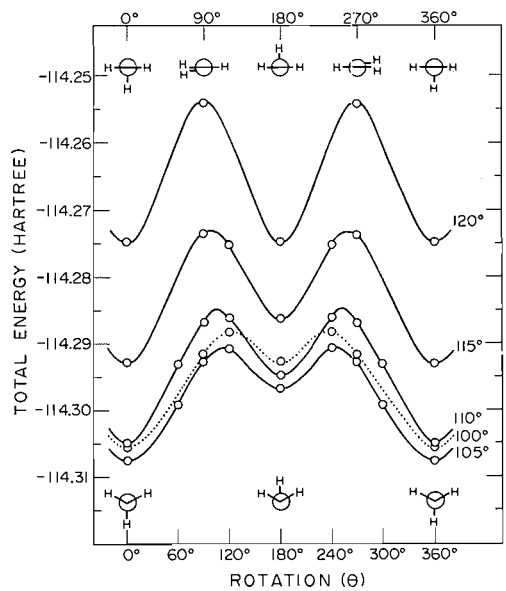

FIG. 5. Five rotational cross-sections of the rotation–inversion surface of $^{-}CH_2OH$.

present work, this barrier must also be greater than 30 kcal/mol since calculations employing the same type of basis set used here (9) give values of 31.5 kcal/mol for in-plane inversion of both H_2O and CH_3OH. The energetics associated with path *A*, via **2** ($\equiv$ **2′**) as an intermediate, are shown in Fig. 7. The barrier height is 20.52 kcal/mol in this case so that path *A*, with stepwise rotation and pyramidal inversion, is clearly the route of topomerization of $^{-}CH_2OH$. Moreover, of the two events depicted in Fig. 7, rotation about the C—O bond requires less energy. The topomerization of $^{-}CH_2OH$ may, therefore, be described as (pyramidal) inversion-dominated. This conclusion would not be affected by the addition of d-type functions to carbon or the simultaneous addition of d-type functions to carbon and p-type functions to hydrogen, because these cause an increase in the inversion barrier (22).

The rotational potential of $^{-}CH_2OH$, shown in the bottom curve of Fig. 5, corresponds closely to that of H_2NOH, shown in Fig. 1. It is very probable, therefore, that the conclusion just reached for $^{-}CH_2OH$ can be extended to H_2NOH. Indeed, it has been demonstrated experimentally that degenerate racemization of alkyl-substituted hydroxylamines is an inversion-dominated process (23).

It is now of interest to inquire into the factors which can be expected to govern the mechanism of degenerate racemization in the general case $R_nX—YR_m$ (n, m = 1, 2; X, Y = C^-, N, O, P, S) (**5**). The following empirical observations facilitate the discussion:

(*i*) For rotation-dominated processes, two-fold barriers are in the range 10 ± 5 kcal/mol (H_2O_2 (24), H_2S_2 (25), N_2H_4 (26), FCH_2OH (2)), three-fold barriers are in the range 5 ± 3 kcal/mol (27) (C_2H_6, C_2H_5F, CH_3NH_2), and six-fold barriers are in the range 0–1 kcal/mol (9, 10).

(*ii*) For pyramidal inversion-dominated processes, barriers associated with central atoms of the First Row are almost an order of magnitude less than those associated with atoms of the Second Row (CH_3^- (5.2 kcal/mol; (22)) < SiH_3^- (39.9 kcal/mol; (28)); NH_3 (5.5 kcal/mol (29)) < PH_3 (37.2 kcal/mol; (30)); OH_3^+ (<1 kcal/mol; (31)) < SH_3^+ (28 kcal/mol; (32)).

(*iii*) Directly attached electron-withdrawing substituents cause an increase, and electron-releasing substituents a decrease in barriers to pyramidal inversion (33–36). Symmetrical systems of the First Row ($C_2H_4^{-2}$ (3), hydrazines (37, 38)) show slightly increased ($\sim$2–3 kcal/mol barriers to pyramidal inversion (relative to the corresponding methyl or hydrogen-substituted analogs (36)) because of electron pair – electron pair repulsive interactions which, in general,

Can. J. Chem. Downloaded from www.nrcresearchpress.com by 210.87.254.42 on 09/05/12
For personal use only.

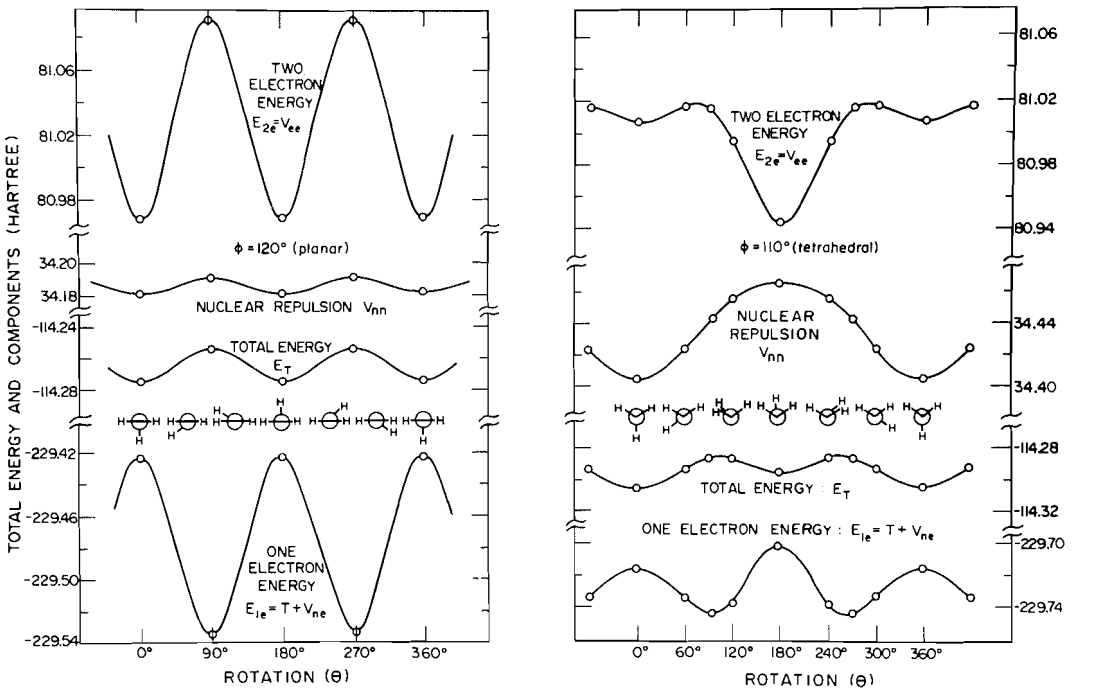

FIG. 6. The total energy of $^{-}CH_2OH$ and its components associated with rotational cross-sections through $\phi = 120°$ (planar geometry at carbon) and $\phi = 110°$ (tetrahedral geometry at carbon).

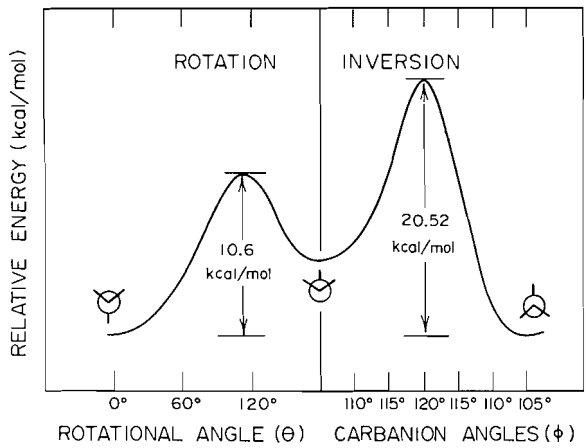

FIG. 7. The energetics of the preferred route of degenerate racemization of $^{-}CH_2OH$.

have less effect than electronegativity differences. Surprisingly, symmetrical systems below the First Row (diphosphines (26.2 kcal/mol; (39)), diarsines (27 kcal/mol; (40)) are reported to have *lower* inversion barriers than the parent phosphines and arsines (42–46 kcal/mol (34)).[1]

[1]For a "modicum of doubt" concerning the diarsine value, see ref. 34*a*; and for evidence that the value quoted for diphosphine actually refers to an association–dissociation process, see ref. 34*b*.

(*iv*) p_π–d_π conjugative effects have relatively little effect on barriers to pyramidal inversion (33, 34), but p_π–p_π conjugation can confer substantial stabilization upon the planar intermediate in the inversion process (41, 42) and, thus, cause a decrease in the barrier.

In view of the relative magnitudes of the barriers, it can be seen that when X or Y is an atom below the First Row, and pyramidal inversion at this center is possible, this will be the

Can. J. Chem. Downloaded from www.nrcresearchpress.com by 210.87.254.42 on 09/05/12
For personal use only.

dominant process associated with degenerate racemization. The situation is more interesting when the inversion center is an atom of the First Row because rotation and inversion have comparable barriers. The electron pair repulsive effects noted above cause inversion to be dominant in $C_2H_4^{-2}$ and in hydrazines. The electron-withdrawing effect of oxygen (χ_C, 2.55; χ_N, 3.04, χ_O, 3.44 (43)) causes a sufficient increase in the barrier at adjacent carbon or nitrogen to make pyramidal inversion at these centers the dominant process in $^-CH_2OH$ and substituted hydroxylamines. However, the electron-releasing effect of sulfur (χ_S, 2.58 (43)) has the opposite effect on adjacent nitrogen and, in sulfenamides, degenerate racemization is rotation dominant (44). Aminophosphines (χ_P, 2.19 (43)) have a trigonal planar structure at nitrogen (11) because of the substantial electron release from P to N.

Relationship of the Present Results to the gauche Effect

The formal definition of the *gauche* effect given in the Introduction predicts the W conformation **2** to be more stable than the Y conformation **1**. This prediction is incorrect. Although **2** is a minimum on the rotation–inversion surface, it is 6.67 kcal/mol less stable than **1**. We believe (2, 3) that the *gauche* effect of adjacent electron pairs is the result of a tendency of these electron pairs to behave as though they have no stereochemical significance, *i.e.*, a quasi-spherical structure. According to this view, termed rule 3 of the *gauche* effect, the tendency towards the *gauche* effect is bond pair – bond pair > bond pair – lone pair > lone pair – lone pair. Although this formulation has predictive utility (1) it should be noted that it is based on the electronic component of the total energy term. This quantity, E_T, contains, besides the electronic component ($E_{elec} = V_{ne} + V_{ee} + T$), the nuclear–nuclear repulsion term ($V_{nn} = V_{nucl}$).

The total energy difference between **1** and **2** is given by

$$\begin{aligned}\Delta E_T &= E_T^1 - E_T^2 \\ &= (E_{elec}^1 + E_{nucl}^1) - (E_{elec}^2 + E_{nucl}^2) \\ &= (E_{elec}^1 - E_{elec}^2) + (E_{nucl}^1 - E_{nucl}^2) \\ &= \Delta E_{elec} + \Delta E_{nucl}\end{aligned}$$

The data of Table 1 indicate that, at each of the C—O bond lengths examined in the present work, ΔE_T and ΔE_{nucl} are negative quantities and ΔE_{elec} is positive. Consequently, the more crowded conformation **2** is stabilized relative to **1** by a more negative electronic term and, at the same time, is destabilized by a more positive nuclear term. The balance between the two effects is such that nuclear–nuclear destabilization outweighs the electronic stabilization. Figure 8 shows these changes in $-\Delta E_T$, $-\Delta E_{nucl}$, and Δ_{elec} as a function of C—O bond length. It is evident that the energy difference between the two upper curves ($-\Delta E_T = -\Delta E_{elec} - \Delta E_{nucl}$) has its maximum numerical value in the region of the optimized C—O bond length (1.500 Å). As the C—O distance increases, both ΔE_{nucl} and ΔE_{elec} decrease numerically, and their sum, ΔE_T, also decreases numerically because ΔE_{nucl} is more greatly affected by the change in the bond length.

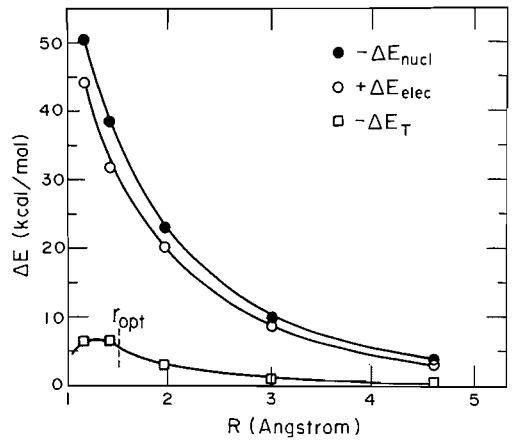

FIG. 8. A plot of ΔE_{elec}, $-\Delta E_{nucl}$, and $-\Delta E_T$ ($\Delta E = E_1 - E_2$) for conformations **1** and **2** as a function of C—O bond length.

These considerations reveal that there may be exceptions to rule 3 of the *gauche* effect (45, 46) depending on the balance between the nuclear and electronic terms which, in turn, will depend upon both the internuclear distance and the sizes and types of ligands attached to the central atoms X and Y (*cf.* **5**).[2] It should also be noted that this analysis of the structure of $^-CH_2OH$ in terms of nuclear and electronic interactions is a conformational analog of the stretching potential of a diatomic system. This type of analysis seems to have general utility (47).

[2]In $^-CH_2SH$ the W conformation is more stable than the Y conformation because $\Delta E_{elec} > \Delta E_{nucl}$ (7, 48).

Can. J. Chem. Downloaded from www.nrcresearchpress.com by 210.87.254.42 on 09/05/12
For personal use only.

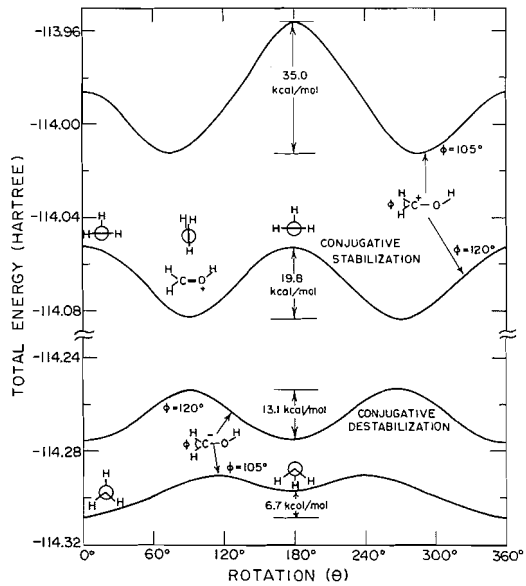

FIG. 9. A comparison of the rotational potentials of $^{-}CH_2OH$ and $^{+}CH_2OH$ at $\phi = 105°$ and $\phi = 120°$.

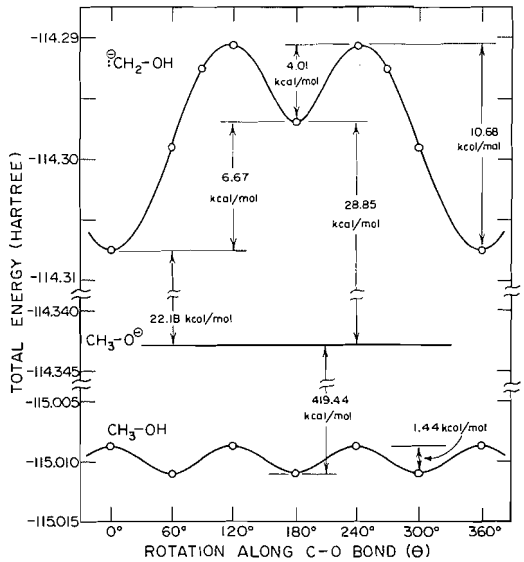

FIG. 10. The energy of CH_3O^- and the rotational potentials of CH_3OH and $^{-}CH_2OH$ (at $\phi = 105°$).

Figure 9 shows the rotational potentials of $^{-}CH_2OH$ and $^{+}CH_2OH$ at $\phi = 105°$ (the optimized pyramidal angles of the anion) and at $\phi = 120°$ (the optimized angles at carbon for the cation). The 120° curves show the contrasting effects of *conjugative stabilization* (19.8 kcal/mol with respect to the reference state $\mathbf{4}^{+}$) and *conjugative destabilization* (49, 50) (13.1 kcal/mol with respect to the reference state $\mathbf{4}^{-}$). As expected, the two curves have opposite phase. The 105° curves also have opposite phase.

Tautomerization of $^{-}CH_2OH$

Figure 10 shows the rotational potentials of methanol (9), $^{-}CH_2OH$ in its most favored pyramidal configuration at carbon ($\phi = 105°$), as well as the energy of methoxide ion (9). The energetics associated with the removal of a methyl proton from CH_3OH are 441.62 kcal/mol and the resulting anion, $^{-}CH_2OH$, is 22.18 kcal/mol less stable than its tautomer CH_3O^-. Although this latter energy difference is in the range expected for a ground state process, we considered that the transition state for tautomerization (*cf.* eq. 3) might not be accessible in a thermal process. It was of interest, therefore,

[3] 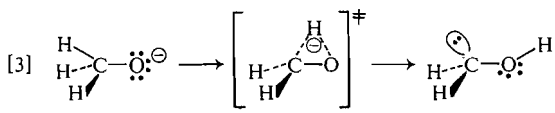

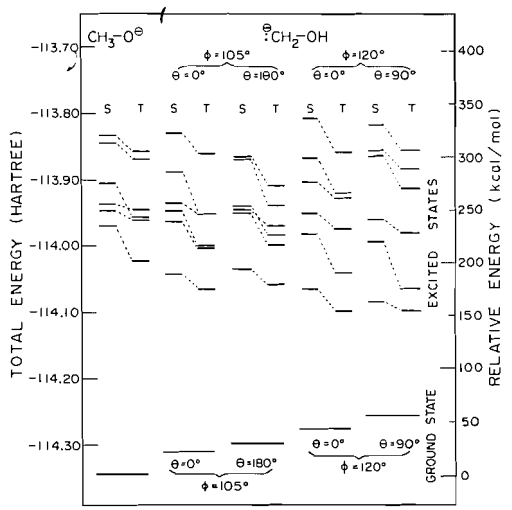

FIG. 11. A comparison of singlet and triplet energy levels of CH_3O^- and $^{-}CH_2OH$.

to examine the possibility of inducing tautomerization photochemically.

Comparison of the energy levels of CH_3O^- (first two columns of Fig. 11) with those of $^{-}CH_2OH$ shows that all conformations of the carbanion are stabilized relative to CH_3O^- in the low-lying excited states. Figure 11 also shows a reversal of ground state conformational properties of the carbanion similar to that noted for FCH_2OH (51). This effect is sufficiently large

to cause the ground state structure (3) corresponding to conjugative destabilization to become the most stable structure in the excited states.

A more detailed analysis of the energetics associated with the photochemical interconversion of CH_3O^- and $^-CH_2OH$, and their relationship to the relative ease of abstraction of the O—H and C—H protons of CH_3OH, is in preparation.

We thank the National Research Council of Canada for financial support of this work and for the award of a Special Grant.

1. S. WOLFE. Acc. Chem. Res. **5**, 102 (1972).
2. S. WOLFE, A. RAUK, L. M. TEL, and I. G. CSIZMADIA. J. Chem. Soc. B, 136 (1971).
3. S. WOLFE, L. M. TEL, J. H. LIANG, and I. G. CSIZMADIA. J. Am. Chem. Soc. **94**, 1361 (1972).
4. S. WOLFE, A. RAUK, and I. G. CSIZMADIA. J. Am. Chem. Soc. **89**, 5710 (1967).
5. A. RAUK, S. WOLFE, and I. G. CSIZMADIA. Can. J. Chem. **47**, 113 (1969).
6. S. WOLFE, A. RAUK, and I. G. CSIZMADIA. J. Am. Chem. Soc. **91**, 1567 (1969).
7. S. WOLFE, A. RAUK, L. M. TEL, and I. G. CSIZMADIA. J. Chem. Soc. D, 96 (1970).
8. J. M. LEHN. Pure Appl. Chem. **25**, 129 (1971).
9. L. M. TEL, S. WOLFE, and I. G. CSIZMADIA. J. Chem. Phys. In press.
10. L. M. TEL, S. WOLFE, and I. G. CSIZMADIA. Int. J. Quant. Chem. In press.
11. I. G. CSIZMADIA, A. H. COWLEY, M. W. TAYLOR, L. M. TEL, and S. WOLFE. J. Chem. Soc. Chem. Commun. 1147 (1972).
12. L. PEDERSON and K. MOROKUMA. J. Chem. Phys. **46**, 3941 (1967).
13. W. H. FINK, D. C. PAN, and L. C. ALLEN. J. Chem. Phys. **47**, 895 (1967).
14. S. OAE, W. TAGAKI, and A. OHNO. Tetrahedron, **20**, 417 (1964).
15. D. L. COFFEN. Rec. Chem. Progr. **30**, 275 (1969).
16. S. HUZINAGA. J. Chem. Phys. **50**, 1371 (1969).
17. H. BASCH, M. B. ROBIN, and N. A. KUEBLER. J. Chem. Phys. **47**, 1201 (1967).
18. A. VEILLARD. IBMOL: Computation of wave functions for molecules of general geometry, Version 4. IBM Research Laboratory, San Jose, California.
19. I. G. CSIZMADIA, B. T. SUTCLIFFE, and M. P. BARNETT. Can. J. Chem. **42**, 1645 (1964).
20. G. HERZBERG and L. G. MUNDIE. J. Chem. Phys. **8**, 263 (1940).
21. (*a*) M. RABAN, F. B. JONES, JR., and G. W. KENNEY, JR. Tetrahedron Lett. 5055 (1968); (*b*) G. BINSCH, E. L. ELIEL, and H. KESSLER. Angew. Chem. Int. Ed. Engl. **10**, 570 (1971).
22. PH. MILLIE and G. BERTHIER. Int. J. Quant. Chem. **2S**, 67 (1968); R. E. KARI and I. G. CSIZMADIA. J. Chem. Phys. **50**, 1443 (1969).
23. M. RABAN and G. W. J. KENNEY, JR. Tetrahedron Lett. 1295 (1969); M. RABAN, and D. KOST. J. Org. Chem. **37**, 499 (1972); M. RABAN. Personal communication.
24. A. VEILLARD. Chem. Phys. Lett. **4**, 51 (1969).
25. A. VEILLARD and J. DEMUYNCK. Chem. Phys. Lett. **4**, 476 (1970).
26. E. L. WAGNER. Theor. Chim. Acta. **23**, 115 (1971).
27. J. P. LOWE. Progr. Phys. Org. Chem. **6**, 1 (1968).
28. A. RAUK. Personal communication.
29. A. RAUK, L. C. ALLEN, and E. CLEMENTI. J. Chem. Phys. **52**, 4133 (1970); R. E. KARI and I. G. CSIZMADIA. J. Chem. Phys. **56**, 4337 (1972).
30. J. M. LEHN and B. MUNSCH. J. Chem. Soc. D, 1327 (1969).
31. J. W. MOSKOWITZ and M. C. HARRISON. J. Chem. Phys. **43**, 3550 (1965).
32. D. DARWISH. Mech. React. Sulfur Compounds, **3**, 33 (1968).
33. R. D. BAECHLER and K. MISLOW. J. Am. Chem. Soc. **93**, 773 (1971).
34. (*a*) R. D. BAECHLER, J. P. CASEY, R. J. COOK, G. H. SENKLER, JR., and K. MISLOW. J. Am. Chem. Soc. **94**, 2859 (1972); (*b*) H. C. E. MCFARLANE and W. MCFARLANE. J. Chem. Soc. D, 1189 (1972).
35. J. M. LEHN. Top. Curr. Chem. **15**, 311 (1970); J. B. LAMBERT. Top. Stereochem. **6**, 19 (1971).
36. A. RAUK, L. C. ALLEN, and K. MISLOW. Angew. Chem. Int. Ed. Engl. **9**, 400 (1970); A. RAUK, J. D. ANDOSE, W. G. FRICK, R. TANG, and K. MISLOW. J. Am. Chem. Soc. **93**, 6507 (1971).
37. J. E. ANDERSON, D. L. GRIFFITH, and J. D. ROBERTS. J. Am. Chem. Soc. **91**, 6371 (1969).
38. M. J. S. DEWAR and B. JENNINGS. J. Am. Chem. Soc. **91**, 3655 (1969); H. KESSLER and D. LEIBFRITZ. Tetrahedron Lett. 4297 (1970).
39. J. B. LAMBERT, G. F. JACKSON, and D. C. MUELLER. J. Am. Chem. Soc. **92**, 3093 (1970).
40. J. B. LAMBERT, G. F. JACKSON, and D. C. MUELLER. J. Am. Chem. Soc. **90**, 6401 (1968).
41. W. EGAN, R. TANG, G. ZON, and K. MISLOW. J. Am. Chem. Soc. **93**, 6205 (1971).
42. R. H. BOWMAN and K. MISLOW. J. Am. Chem. Soc. **94**, 2861 (1972).
42. R. H. BOWMAN and K. MISLOW. J. Am. Chem. Soc. **94**, 2861 (1972).
43. A. L. ALLRED. J. Inorg. Nucl. Chem. **17**, 215 (1961).
44. J. KAY, M. D. GLICK, and M. RABAN. J. Am. Chem. Soc. **93**, 5224 (1971).
45. O. EXNER, D. N. HARPP, and J. G. GLEASON. Can. J. Chem. **50**, 548 (1972).
46. O. EXNER., V. JEHLIČKA, and J. FIRL. Coll. Czech. Chem. Commun. **37**, 466 (1972).
47. S. WOLFE and I. G. CSIZMADIA. To be published.
48. S. WOLFE, M. H. WHANGBO, L. M. TEL, and I. G. CSIZMADIA. To be published.
49. K. MÜLLER and A. ESCHENMOSER. Helv. Chim. Acta, **52**, 1823 (1969).
50. K. MÜLLER. Helv. Chim. Acta, **53**, 1112 (1970).
51. S. WOLFE, L. M. TEL, and I. G. CSIZMADIA. J. Am. Chem. Soc. In press.

Can. J. Chem. Downloaded from www.nrcresearchpress.com by 210.87.254.42 on 09/05/12
For personal use only.

Dihedral Angular Dependence of H—N—C—H Coupling Constants. Protonated Amines in Trifluoroacetic Acid

ROBERT R. FRASER, ROGER N. RENAUD,[1] JOHN K. SAUNDERS,[2] AND YUK Y. WIGFIELD

Department of Chemistry, University of Ottawa, Ottawa, Canada K1N 6N5

Received February 12, 1973

Measurements of vicinal H—N—C—H coupling constants in the conjugate acids of two tertiary amines having known rigid conformations provide support for the validity of the Karplus relation for this type of coupling constant. Seven vicinal coupling constants agree to within 0.5 Hz with those calculated from the expression $J = 9.8 \cos^2 \phi - 1.8 \cos \phi$.

Les mesures des constantes de couplage H—C—N—H dans les acides conjugués de deux amines tertiaires de conformations rigides connues permettent d'établir la validité de la relation de Karplus pour ce type de constante de couplage. Sept constantes de couplage vicinal sont en accord, à 0.5 Hz près, avec celles calculées utilisant l'expression $J = 9.8 \cos^2 \phi - 1.8 \cos \phi$.

[Traduit par le journal]

Can. J. Chem., **51**, 2433 (1973)

Can. J. Chem. Downloaded from www.nrcresearchpress.com by 210.87.254.40 on 09/05/12
For personal use only.

It is well known that, under conditions of slow exchange, vicinal H—N—C—H coupling constants are observed in the n.mr. spectra of the conjugate acids of alkylamines (1). Such conditions obtain when spectra of alkyl or aryl amines are determined using trifluoroacetic acid (TFA) as solvent (2, 3). An extensive survey of the difference in chemical shift between protons α to nitrogen in amines versus their conjugate acids in TFA was carried out by Ma and Warnhoff (3). In addition to providing characteristic shift data, they pointed out that the multiplicity of the signal for the α-protons revealed the primary, secondary or tertiary nature of the amine. Subsequently, little advantage has been taken of TFA as a solvent for n.m.r. studies of amines. Surprisingly also, very little data concerning the angular dependence of H—N—C—H coupling constants in this solvent has appeared (*vide infra*). We wish to describe the measurement of a number of these coupling constants and the assessment of their adherence of the Karplus relation (4).

The Karplus relationship is undoubtedly the most general and useful stereochemical relationship in n.m.r. spectroscopy. In a recent review (4), Anet and Anet document the large number of cases in which H—X—Y—Z systems exhibit a dependence of the magnitude of the H–Z coupling constant on the dihedral angle between the H—X and Y—Z bonds. In addition a number of more recent papers offer further examples of a Karplus type behavior of the vicinal coupling constants in the $^{19}F—C—C—H$ (5), $^{13}C—O—C—H$ (6), $^{13}C—N—C—H$ (6), $^{31}P—S—C—H$ (7), P—O—C—H (8), $^{199}Hg—C—C—H$ (9), and $^{13}C—C—O—^{31}P$ (10) structural units. The exact form of the Karplus equation varies considerably, a number of different geometric expressions to approximate the $[\cos]^2$ dependence of J on the dihedral angle ϕ having been utilized (11–13). We will employ the form $J = A \cos^2\phi + B \cos\phi + C$(14). Refinements of the equation to include the effects of orientation of electronegative substituents (15) need not be considered here.

Both experimental (16–19) and theoretical (19) evidence has been presented that H—C—N—H coupling constants in amides have a dihedral angular dependence. The same is likely true for H—C—N—H couplings when the nitrogen is tetracoordinate and positively charged. The first such indication was described by Lambert and coworkers (20) who ascribed the observed splittings of 10.0 and 2.3 Hz in the $^{+}NH_a—CH_a$ portion of *N*-methylpiperidinium ion to J_{aa} and J_{ae} respectively. Subsequently values for J_{aa} of 7.5–9.6 and for J_{ae} of 1–2 Hz have been reported for a variety of nitrogen heterocycles by several groups of workers (21–

[1]Present address: National Research Council of Canada, Ottawa, Canada.

[2]Present address: Département de chimie, Université de Sherbrooke, Sherbrooke, Québec.

TABLE 1. N.m.r. spectral parameters for 0.2 *M* solutions of **1** and **2** in TFA

	Chemical shifts*						Coupling constants† (Hz)						
Compound	H_A	H_B	H_C	H_D	H_M	H_X	AB	AX	BX	CD	CX	DX	MX
1	3.43	4.26	3.92	4.09		8.0‡	−12.1	10.0	3.9	−13.0	0.0	4.6	
2	4.69	5.17			5.78	8.0	−14.0	7.8	6.0				7.5

*Reported on the δ scale (p.p.m. downfield from TMS).
†Both **1** and **2** in TFA showed a coupling constant of 5.3 Hz for $J_{H-\overset{+}{N}-CH_3}$. No resolvable long-range coupling could be detected for either compound.
‡Not observable, but has been seen at δ 8.0 (23) when the rate of relaxation at nitrogen is sufficiently rapid.

23, 36). Since the existing data is limited to examples of vicinal couplings between protons having $\phi = 60$ or 180° in flexible six-membered rings whose chair–chair equilibria could not be precisely determined, we have examined the H—N—C—H couplings in two protonated amines in which five different dihedral angles are present. The results support the originally proposed (20) Karplus relation for these coupling constants.

Previous studies in this laboratory involved the synthesis of two conformationally fixed tertiary amines: the bridged biaryl amine, **1** (24) and the isoindoline, **2** (25). Dissolution of **1** in TFA produces a single conjugate acid which possesses two asymmetric structural features. Rotation about the bond joining the two aromatic rings is prevented by the ortho-methyl groups (26) thus preserving the biaryl asymmetry. And since deprotonation of the conjugate acid of **1** is slow on the n.m.r. time scale, the nitrogen atom acts as a pseudoasymmetric center. For these reasons the n.m.r. spectrum of **1** in TFA shows separate signals for each of the four protons α to nitrogen.[3] Each of these is coupled with the N—H proton and with its diastereotopic partner. The spectrum was rigorously analyzed as an ABCDX spectrum to yield the parameters listed in Table 1.

Measurements on a Dreiding model of **1** indicate the protons of one methylene group to have φ's of 40 and 160° (±5°), and those of the other methylene group to have φ's of 40 and 80°. Assignment of the n.m.r. signals is made in the following way. The largest vicinal coupling, J_{AX}, is attributed to the proton having $\phi = 160°$ on the basis of the previous results (20–23). H_B, the diastereotopic partner of H_A, is identified by its geminal splitting with H_A. Since H_D has a vicinal splitting of the same magnitude as H_B, it is assigned to the proton having the same φ as H_B (40°). The remaining proton H_C has $\phi = 80°$. These assignments are illustrated in the three-dimensional formulae of Fig. 1.[4]

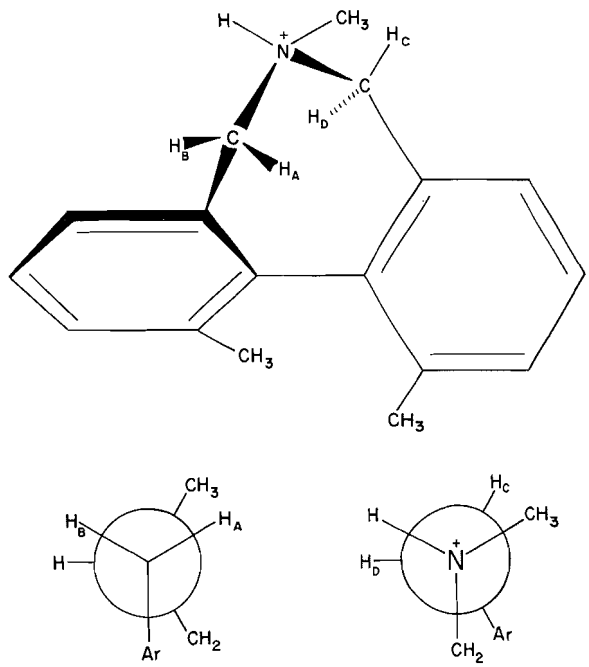

FIG. 1. A three-dimensional representation of **1**-H^+ in TFA showing the proton assignments.

[3]The spectrum was measured during simultaneous spin-decoupling of the ^{14}N nucleus and also the aromatic protons. This reduced the line-widths of the α-protons from 0.6 to 0.2 Hz.

[4]The three alternative assignments all lack any correlation between $J_{H-N-C-H}$ and φ. In view of the widespread adherence of vicinal coupling constants to the Karplus relation these alternatives appear highly unlikely.

Can. J. Chem. Downloaded from www.nrcresearchpress.com by 210.87.254.40 on 09/05/12
For personal use only.

TABLE 2. A comparison of vicinal couplings obtained experimentally and by calculation using $J = 9.8 \cos^2 \phi - 1.8 \cos \phi$

Compound	Proton	ϕ (degree)	J_{exp} (Hz)	J_{calcd}
1	H_A	160	10.0	10.3
	H_B	40	3.9	4.4
	H_C	80	0.0	0.0
	H_D	40	4.6	4.4
2	H_A	0	7.8	8.0 (7.4)*
	H_B	120	6.0	3.3 (6.2)*
1 and **2**	$\overset{+}{N}—CH_3$	$\frac{2(60°) + 180°}{3}$	5.3	4.9

*Calculated for the conformation of 2 in which there is a distortion of 15° from complete planarity.

The spectrum of **2** in TFA reveals the presence of two conjugate acids in a ratio of 4:1. Accurate peak measurements were possible for the absorptions due to the major isomer only. Analysis of the $CH_2—\overset{H}{\overset{|}{\overset{+}{N}}}$ pattern as an ABX system gave the parameters listed in Table 1. The two methylene protons show unequal coupling (6.0 and 7.8 Hz) to the proton on nitrogen in **2**-H^+. It is usually found that in five-membered heterocyclic compounds $J_{cis} > J_{trans}$ (4). Exceptions to this rule[5] are limited to a few saturated heterocycles (27, 28) and in one case an unsaturated heterocycle studied by Anet and Muchowski (30). They observed $J_{trans} = J_{cis}$ in the two isomeric 2,3-dimethylindolines. Nevertheless, sufficient examples of heterocycles with a double bond in the ring and having $J_{cis} > J_{trans}$ are known (31) to cause Anet and Anet to conclude that assignments on this basis are reliable (4). It is therefore reasonable to assign the *cis* configuration to the protons in **2**-H^+ which exhibit the larger vicinal coupling constant.

The methine proton in **2**-H^+ shows only one splitting of 7.5 Hz. This proton *is most likely*[6] *cis* to H_A since both are coupled equally with H_X. The assignments made on this basis are shown in Fig. 2. Finally, as Table 1 shows, in both **1** and **2** in TFA the $H—\overset{+}{N}—CH_3$ coupling is 5.3 Hz.

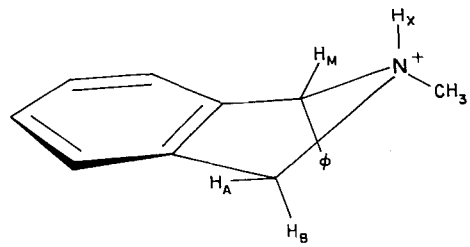

FIG. 2. The most probable configuration and conformation for the major isomer of **2**-H^+ in TFA.

Discussion

It is noteworthy that the vicinal H—C—N—H coupling constants in the conjugate acids of **1** and **2** vary considerably as do their respective dihedral angles. The best agreement obtainable between the observed J's and those calculated from the dihedral angle is provided by eq. 1.

$$[1] \qquad J = 9.8 \cos^2 \phi - 1.8 \cos \phi$$

As indicated in Table 2, agreement is obtained to within 0.5 Hz in all cases except for $J_{120°}$ in **2** which has $J_{exp} > J_{calcd}$ by 2.7 Hz. This particular deviation from eq. 1 is very likely due to a puckering of the five-membered ring as has been previously encountered in substituted indanes (32). If an angular distortion of 15° from planarity in the direction shown in Fig. 2 is assumed, then the calculated values (given in brackets in Table 2) for J in **2**-H^+ agree to within 0.5 Hz with the

[5]An apparent exception has been eliminated by the recent X-ray determination of the configuration of toxol (29).

[6]One might question the fact that this assignment requires the methyl and phenyl groups to be *cis* in the more abundant isomer. It is, however, most probable that the 4:1 ratio of the two conjugate acids reflects the relative rates of protonation of **2** from the two sides since Booth and Little have shown this to be a kinetically controlled process in a study of *cis*-3,5-dimethylpiperidine in TFA (23).

Can. J. Chem. Downloaded from www.nrcresearchpress.com by 210.87.254.40 on 09/05/12
For personal use only.

experimental ones. It can be concluded that the vicinal coupling constants determined herein have magnitudes consistent with the predictions of the Karplus relation, thereby providing support for the proposals of previous workers (20–23). Such dependence of J on geometry should prove to be of considerable value in the conformational analysis of amines.[7]

Without wishing to detract from the usefulness of the Karplus relation in the present instance, it is important to recall its limitations. Jackman and Sternhell (33) have discussed in considerable detail the different factors which can influence the magnitude of vicinal coupling constants. Difficulties in assessing the importance of factors other than dihedral angle led these authors to conclude that angles cannot be determined to better than 10° under the best of conditions using vicinal coupling constant data. Their conservative attitude must also apply to the present case.

Experimental

All n.m.r. measurements were made using a Varian HA-100 spectrometer equipped with an NMR Specialties SD-100 spin-decoupler. Line positions were obtained from an average of five measurements and are accurate to better than 0.15 Hz. Coupling constants obtained from the exact analysis will have similar accuracy. Melting points are uncorrected. Calculation of the ABCDX system was carried out using the NMR CAL program on a Nicolet 1083 computer.

N-Methyl-6,7-dihydro-1,11-dimethyl-5H-dibenz[c,e]-azepine (1)

This compound was prepared by methylation (Clarke–Eschweiler) of the corresponding secondary amine (24) in essentially quantitative yield. The product, after crystallization from methanol–water, had m.p. 93–94°; (lit. (26) m.p. 50.5–52°); n.m.r. (δ scale) 2.15 (6H, s) 2.25 (3H, s) 3.17 (4H, AB_q, J = 12) 7.1–7.3 (6H, m).

In view of the discrepancy between its melting point and that previously reported, **1** was converted to its methiodide which, after crystallization 4 times from ethanol, had m.p. 258–259° (lit (26) m.p. 256°).

Anal. Calcd. for $C_{18}H_{22}NI$: C, 56.98; H, 5.85, N, 3.69. Found: C, 56.65; H, 6.13; N, 3.61.

2-Methyl-1-phenylisoindoline (2)

The synthesis of this compound has been reported previously (35).

[7]With the aid of these vicinal coupling constants, the conformation of *N*-methyl-5,6-dihydro-7*H*,12*H*-dibenz-[*d*, *f*]azocine could be unambiguously determined (34).

We thank the National Research Council of Canada for financial support of this work.

1. E. GRUNWALD, A. LOWENSTEIN, and S. MEIBOOM. J. Chem. Phys. **27**, 630 (1957).
2. W. F. REYNOLDS and T. SCHAEFER. Can. J. Chem. **41**, 540 (1963); W. F. REYNOLDS and T. SCHAEFER. Can. J. Chem. **42**, 2641 (1964).
3. J. C. N. MA and E. W. WARNHOFF. Can. J. Chem. **43**, 1849 (1965).
4. F. A. L. ANET and R. ANET. *In* Determination of organic structures by physical methods. Vol. 3. Nachod and Phillips (editors). Academic Press, New York, 1971. p. 392.
5. K. L. WILLIAMSON, S. MOSSER, and D. E. STEDMAN. J. Am. Chem. Soc. **93**, 7208 (1971).
6. R. U. LEMIEUX, T. L. NAGABHUSHAN, and B. PAUL. Can. J. Chem. **50**, 773 (1972).
7. J. R. CAMPBELL and L. D. HALL. Chem. and Ind. 1138 (1971).
8. L. D. HALL and R. B. MALCOLM. Can. J. Chem. **50**, 2092 (1972).
9. J. E. GALLE and A. HASSNER. J. Am. Chem. Soc. **94**, 3930 (1972).
10. (*a*) H. H. MANTSCH and I. C. P. SMITH. Biochem. Biophys. Res. Commun. **46**, 808 (1972); (*b*) R. D. LAPPER, H. H. MANTSCH, and I. C. P. SMITH. J. Am. Chem. Soc. **94**, 6243 (1972).
11. M. KARPLUS. J. Chem. Phys. **30**, 11 (1959).
12. M. KARPLUS. J. Am. Chem. Soc. **85**, 2870 (1963).
13. E. B. WHIPPLE. J. Mag. Res. **5**, 163 (1971).
14. M. BARFIELD and M. KARPLUS. J. Am. Chem. Soc. **91**, 1 (1969).
15. K. G. R. PACHLER. J. Chem. Soc. Perkin II, 1936 (1972); K. G. R. PACHLER. J. Mag. Res. **8**, 183 (1972).
16. V. F. BYSTROV, S. L. PORTNOVA, V. F. ISETLIN, V. T. IVANOV, and Y. A. OVCHINNIKOV. Tetrahedron, **25**, 493 (1969).
17. M. T. CUNG, D. CANET, P. GRANGER, M. MARRAUD, and J. NÉEL. C.R. Acad. Sci. Ser. C, **269**, 580 (1969).
18. G. N. RAMACHANDRAN, R. CHANDRASEKARAN, and K. D. KOPPLE. Biopolymers. **10**, 2113 (1971).
19. M. BARFIELD and H. L. GEARHART. J. Am. Chem. Soc. **95**, 641 (1973), and refs. therein.
20. J. B. LAMBERT, R. G. KESKE, and D. K. WEARY. J. Am. Chem. Soc. **89**, 5921 (1967).
21. F. G. RIDDELL and J. M. LEHN. J. Chem. Soc. B, 1224 (1968).
22. H. BOOTH and R. U. LEMIEUX. Can. J. Chem. **49**, 777 (1971).
23. H. BOOTH and J. H. LITTLE. J. Chem. Soc. Perkin II, 1846 (1972).
24. R. R. FRASER and Y. Y. WIGFIELD. Tetrahedron Lett. 2515 (1971); see also R. R. FRASER, G. BOUSSARD, I. D. POSTESCU, and J. J. WHITING. Can. J. Chem. **51**, 1109 (1973).
25. R. R. FRASER and R. N. RENAUD. Can. J. Chem. **49**, 755 (1971).
26. K. MISLOW, M. A. W. GLASS, H. B. HOPPS, E. SIMON, and G. H. WAHL, JR. J. Am. Chem. Soc. **86**, 1710 (1964).
27. F. A. L. ANET. J. Am. Chem. Soc. **84**, 747 (1962).

Can. J. Chem. Downloaded from www.nrcresearchpress.com by 210.87.254.40 on 09/05/12
For personal use only.

28. M. GREGSON, W. D. ALLIS, B. T. REDMOND, I. O. SUTHERLAND, and H. H. DIETRICHS. Chem. Commun. 1394 (1968).
29. L. H. ZALKOW, E. KEINAN, S. STEINDEL, A. R. KALYANARAMAN, and J. A. BERTRAND. Tetrahedron Lett. 2873 (1972).
30. F. A. L. ANET and J. M. MUCHOWSKI. Chem. and IND. 81 (1963).
31. S. STERNHELL. Quart. Revs. **23**, 236 (1969).
32. R. A. AUSTIN and C. P. LILLYA. J. Org. Chem. **34**, 1327 (1969).
33. L. M. JACKMAN and S. STERNHELL. Applications of nuclear magnetic resonance spectroscopy in organic chemistry. 2nd ed. Pergamon Press, Oxford, 1969. p. 292.
34. R. N. RENAUD, R. B. LAYTON, and R. R. FRASER. In preparation.
35. R. R. FRASER and R. N. RENAUD. Can. J. Chem. **49**, 746 (1971).
36. B. R. LOWRY and A. C. HUITRIC. J. Org. Chem. **37**, 1316, 2697 (1972).

Can. J. Chem. Downloaded from www.nrcresearchpress.com by 210.87.254.40 on 09/05/12
For personal use only.

The Electrical Polarizations of Mercuric Chloride and Dimethylmercury

HELMUT HUBER AND GEORGE F WRIGHT

Department of Chemistry, University of Toronto, Toronto, Ontario M5S 1A1

Received November 17, 1972

The apparent dipole moments calculated from solutions of mercuric chloride and dimethylmercury have been found to alternate between high and low values over the temperature range extending from 8.5 to 50 °C. The significance of this alternation is discussed.

Les moments dipolaires apparents calculés pour des solutions de chlorure mercurique et de diméthylmercure alternent suivant la température qui varie de 8.5 à 50 °C, entre des valeurs hautes et basses. L'importance de cette alternance est discutée. [Traduit par le journal]

Can. J. Chem., **51**, 2438 (1973)

Can. J. Chem. Downloaded from www.nrcresearchpress.com by 210.87.254.6 on 09/05/12
For personal use only.

Introduction

A quandary arose in 1934 when it was found (1) that diphenylmercury and some 4,4′-disubstituted derivatives which would appear structurally to be centrosymmetric (therefore devoid of moment) did in fact exhibit total electrical polarizations which might be interpreted as evidence for dipole moments. Shortly this apparent anomaly was interpreted as abnormally high atom polarization (P_A) (2) but later a method for measuring P_A was devised (3) and perfected. Insofar as these measurements are meaningful they indicate that the candidate compounds do not display abnormally high atom polarizations. The difference between the total polarizations and the sum of the measured P_A plus the estimated electron polarization (P_E) must then according to the Debye concept (2) be attributed to orientation polarization (P_0). The latter is expressed by the Debye construct as dipole moment.

In any circumstance the combined $P_A + P_E$, *i.e.* the distortion polarization (P_D), by the Debye construct ought to be practically temperature independent. Therefore the total polarizations of solutions in media of low or unmeasurable dipole moment containing diphenylmercury (4), benzoquinone (5), 1,4-dinitro-benzene (6), and other substances (7) were determined over a range of temperatures extending from 8.5 to 50°. As might be expected the total polarizations differed in respect of temperature. However, unexpectedly the dipole moments calculated from these total polarizations also were temperature-dependent. Because the latter phenomena are not in accord with the Debye construct they have been described as apparent dipole moments. Recently 1,4-dicyanobenzene (9) has been included in the same category.

In order to explain this temperature dependence it has been proposed (8) that the ostensibly-symmetric substances are in fact excited to dissymmetric states which react with the electric field to show an orientation polarization. The extent of P_0 can be accounted for only if it be assumed that 20–40% of the molecules are excited. The ambient environment ought amply to supply the necessary energy. Moreover the variation in apparent moment must be related to the temperature of the environment.

We have sought a correlative phenomenon to relate to this temperature-dependence and have found only that the substances which display it all have strong absorption bands in the 50–200 cm^{-1} spectral region. Moreover these absorption bands have been found to change markedly in intensity over the temperature range of 79–313 °K. This intensity variance has been reported in detail for 1,4-dicyanobenzene (9).

It must be pointed out that the absorbances, which are too broad for detailed analysis, have been determined in the absorption spectrometers currently available.

No obvious way of demonstrating the hypothesis for temperature-dependence of dipole moments has heretofore been apparent to us. First our temperature range for measurement has been limited at best to 8.5–50 °C. Second some of the apparent moments increase with increasing temperature while others decrease. It seems obvious that the molecular species which we have examined are too complex for simple interpretation.

Consequently we have sought simpler candi-

TABLE 1. Polarization of mercuric chloride in benzene

Temperature (°C)	α	$-\beta$	ε_0	ε_{extr}	$\overline{V}_0$	$\overline{V}_{extr}$	P_T (cc)	μ (D) MR_D	μ (D) P_D
8.5	0.540	0.920	2.3085	2.3085	1.12204	1.12206	43.2	0.92	0.77
9.3	0.628	0.928	2.3068	2.3068	1.12307	1.12311	47.0	1.01	0.87
10	0.730	0.912	2.3046	2.3046	1.12414	1.12410	53.5	1.15	1.04
15	0.744	0.940	2.2940	2.2941	1.13098	1.13098	54.3	1.18	1.06
20	0.716	0.992	2.2829	2.2830	1.13777	1.13792	48.0	1.05	0.92
22.5	0.664	0.988	2.2799	2.2797	1.14111	1.14118	46.1	1.01	0.88
25	0.662	0.996	2.2738	2.2740	1.14461	1.14442	45.8	1.00	0.87
30	0.674	1.00	2.2621	2.2621	1.15180	1.15180	46.7	1.04	0.90
32.5	0.684	1.01	2.2572	2.2571	1.5541	1.15535	47.5	1.06	0.93
35	0.828	1.01	2.2513	2.2513	1.15917	1.15919	55.0	1.23	1.12
37.5	0.760	1.02	2.2467	2.2467	1.16260	1.16282	51.3	1.16	1.03
40	0.564	1.02	2.2414	2.2416	1.16638	1.16640	41.3	0.92	0.75
50	0.510	1.04	2.2218	2.2216	1.18148	1.18160	38.8	0.86	0.68

dates. The first to be examined is mercuric chloride, with only 4 degrees of freedom. A polarization greater than that expected for this nominally-linear molecule has earlier been reported (10) and has been attributed to non-linearity of Cl—Hg—Cl in benzene solution.

We have first examined the possibility that this "abnormal" polarization might be due to high distortion polarization, $P_E + P_A = P_D$. This determination of P_D in solid wafers (where P_0 is not expected) was at first fraught with difficulty. Although mercuric chloride is largely unionized, even in aqueous solution, we found that a reaction occurs between the mercury in our Au–Hg amalgam (3) and mercuric chloride. This reaction inactivated our electrical circuit. However it has been found that the interposition of a very thin layer of Petrolatum between the amalgam and the wafer prevents this reaction and permits a precise determination. The plot of apparent dielectric constant *vs.* wafer thickness is linear leading to an extrapolated ε at zero thickness of 5.560. The density (5.44 at 20°) has been determined by air displacement in the apparatus earlier described (11), so the distortion polarization is found to be 30.1 cc. Since the molecular refraction calculated according to Eisenlohr is 24.7 cc the difference, P_A, is 5.4 cc. This is appreciable (18% of P_D) but it cannot account for the polarization in solution.

The total polarization of mercuric chloride in benzene solution has been determined from 8.5 to 50 °C at 13 different temperatures. Because of the low solubility at least five complete determinations were made at each temperature. The results are presented in Table 1, and these results are plotted in Fig. 1. The dipole value for 50° is not included because the imprecision is greater than those shown by the vertical limits drawn in the figure. It may be noted in Table 1 that in consideration of the values for dipole moment with respect to temperature for this triatomic molecule there is a difference from those of the more complex substances examined previously. It may be seen that this apparent moment of mercuric

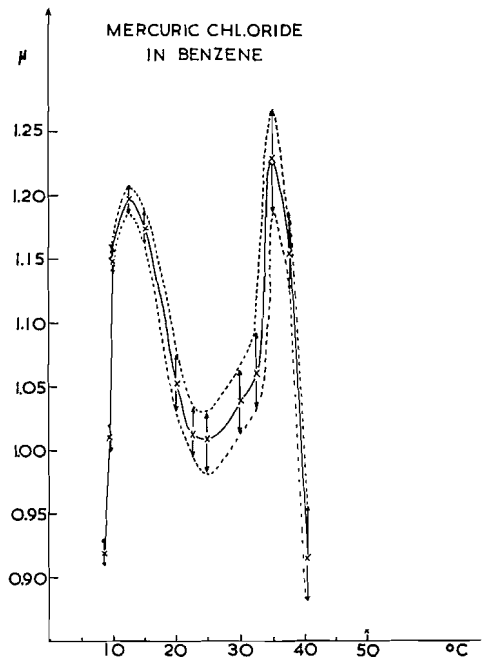

FIG. 1. Dipole moment *vs.* temperature.

Can. J. Chem. Downloaded from www.nrcresearchpress.com by 210.87.254.6 on 09/05/12
For personal use only.

TABLE 2. Polarization of mercuric bromide in benzene

Temperature (°C)	α	β	ε_0	ε_{extr}	$\overline{V}_0$	$\overline{V}_{extr}$	P_T (cc)	μ (D) MR_D	μ (D) P_D
20	0.696	−0.972	2.2829	2.2828	1.13777	1.13776	64.6	1.27	1.14
30	0.512	−1.024	2.2621	2.2622	1.15180	1.15182	48.7	0.95	0.75
40	0.380	−1.046	2.2414	2.2414	1.16638	1.16652	39.4	0.67	0.32

chloride increases, and then decreases twice over the temperature range examined.

For further consideration of this behavior it may be informative to refer to the far-i.r. absorption spectrum shown in Fig. 2. The lowest frequency band shifting from 76 to 77 cm^{-1} during a temperature change from 313 to 79 °K in the solid state has its counterpart (at 70 cm^{-1}) in the vapor-phase spectrum (12) of this substance (attributed to molecular bending) but the very broad band (dv = 38 to 44 cm^{-1} from 313 to 79 °K) is not mentioned by Klemperer and Lindemann and is observed only in the condensed state where its peak shifts from 105 to about 110 cm^{-1} over the same temperature range. If the 76–77 cm^{-1} band represents the Cl—Hg—Cl bending frequency (12) in all states then the broad band of large integrated intensity at 105–110 cm^{-1} would seem to be a complex of excitations characteristic of bending in the condensed state. The greater-than-twofold increase in intensity for this band at 79 °K *vs.* 313 °K would indicate that these excitations are characteristic of the higher temperature; *i.e.* a greater population at −194° is in the ground state and thus available for excitation by the imposed radiation of the spectrometer.

If indeed these excited states were distributed between unsymmetrical ones which can be oriented by the electromagnetic field at 0.5 MHz and symmetrical ones which cannot be so oriented then the relative populations of these states at different temperatures would be expected to affect the apparent moments shown in Fig. 1. Specifically one might conclude that the ambient temperature at 25 °C contributes largely to symmetrical excited states by contrast to those at 14 and 34 °C which contribute largely to unsymmetrical states. It is unfortunate that the limitations of our technique preclude examination outside the +8.5–50° range; the cyclic behavior might continue in either direction.

The case of mercuric chloride is a special one. Polarization studies with mercuric bromide in benzene show only a downward trend of apparent moment with increasing temperature. The results, shown in Table 2 are based on a measured distortion polarization of 37.3 cc. It may be significant that the far-i.r. spectral absorption, shown in Fig. 3, occurs at frequencies of 50 and 72–74.5 cm^{-1}. The band at 50 cm^{-1} probably corresponds with that observed at 41 cm^{-1} by Klemperer and Lindemann at 973 °K. Both bands are approximately of equal width and equal intensity at 313 °K. The increased intensity

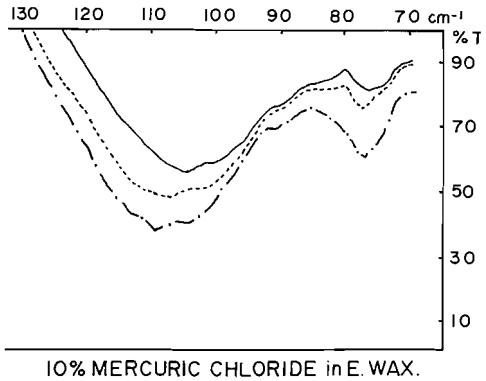

FIG. 2. Absorption spectra *vs.* temperature: (—) +40 °C; (·) −50 °C; (··) −190 °C.

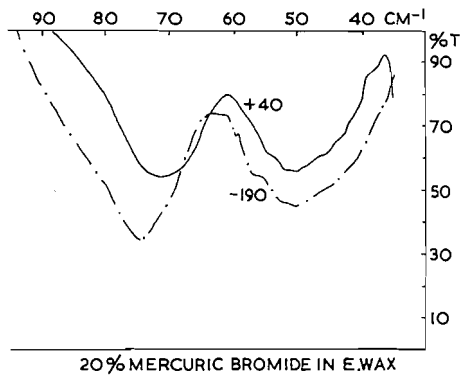

FIG. 3. Absorption spectra *vs.* temperature (°C).

Can. J. Chem. Downloaded from www.nrcresearchpress.com by 210.87.254.6 on 09/05/12
For personal use only.

TABLE 3. Apparent moments of dimethylmercury, calculated from MR_D = 22.60 cc according to Halverstadt–Kumler

Medium	Temperature (°C)	α	β	ε	ε_{extrap}	$\overline{V}_0$	$\overline{V}_{extr}$	P_T (cc)	μ (D)
Benzene	12.5	0.144	0.766	2.30097	2.30097	1.12751	1.12749	30.59	0.61
	20.0	0.150	0.782	2.28314	2.28312	1.13768	1.13766	31.03	0.63
	25.0	0.150	0.784	2.27413	2.27412	1.14465	1.14464	31.30	0.65
	30.0	0.156	0.786	2.26305	2.26304	1.15170	1.15168	31.84	0.67
	35.0	0.085	0.798	2.25116	2.25115	1.15899	1.15890	28.27	0.53
	37.5	0.050	0.796	2.24602	2.24602	1.16258	1.16248	27.04	0.47
	40.0	0.114	0.796	2.24014	2.24004	1.16632	1.16622	30.09	0.62
Dioxane	20.0							33.3	0.71
Cyclohexane	10.0	0.050	0.942	2.02418	2.02416	1.29218	1.29220	23.32	0.18
	15.0	0.056	0.944	2.01601	2.01599	1.29987	1.29994	23.90	0.25
	20.0	0.105	0.982	2.00802	2.00802	1.30767	1.30780	24.81	0.32
	25.0	0.104	0.984	1.99894	1.99887	1.31554	1.31564	25.03	0.34
	30.0	0.089	0.985	1.99110	1.99108	1.32396	1.32395	24.54	0.31
	35.0	0.058	0.988	1.98259	1.98260	1.33223	1.33226	22.97	0.14
	37.5	0.048	0.989	1.97846	1.97839	1.33672	1.33679	22.53	0
	40.0	0.066	1.004	1.97459	1.97466	1.34081	1.34076	22.93	0.13
	42.5	0.096	0.992	1.96953	1.96952	1.34501	1.34508	25.32	0.37
	45.0	0.116	0.996	1.96532	1.96455	1.34934	1.34936	26.72	0.46
	50.0	0.075	0.998	1.95675	1.95678	1.35844	1.35834	24.60	0.32

at 79 °K is less than doubled. So mercuric chloride and bromide behave differently.

On the other hand the polarization behavior of dimethylmercury resembles to some extent that of mercuric chloride. This more complex substance, being a liquid, cannot be examined spectroscopically by our i.r. equipment in condensed states because of general background absorption, either pure or in benzene or carbon tetrachloride. Likewise laser-induced Raman spectra are uninformative, either in the liquid state at 313 °K or when rapidly condensed from vapor to solid at 79 °K. However the measurements of electrical polarization as recorded in Table 3 show the cyclic temperature dependence. The change of moment is idealized in Fig. 4 as interconnected points, each representing the average of at least five complete determinations. As might be expected the magnitude of apparent moment is greatest in dioxane and least in cyclohexane, benzene being intermediate.

Thus two relatively simple candidates show an alternating dependence in moment upon changes of near-ambient temperatures. Other temperature-dependent moments have not shown such alternating behavior. But in retrospect we were originally probably misled by the apparent linearity in moment-diminution for benzoquinone (5) with increasing temperature. Certainly the similar variation for diphenylmercury

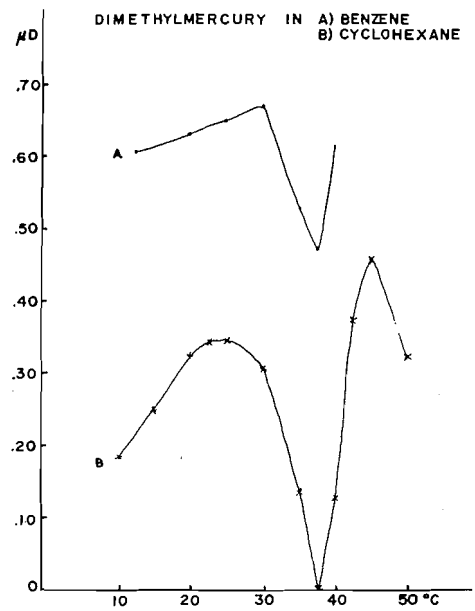

FIG. 4. Dipole moment *vs.* temperature.

(4), for 1,4-dinitrobenzene (6) and other complex substances has not shown a linear relationship. We do not know how the values of these moments change at temperatures outside the range of our instrument (13).

Some may ask why this moment-temperature dependence has not been observed for the large

Can. J. Chem. Downloaded from www.nrcresearchpress.com by 210.87.254.6 on 09/05/12
For personal use only.

number of substances whose moments have been determined (14). We suggest that such variations may be hidden within polarizations due to permanent moments. They may be observable when precision of measurement exceeds by an order of magnitude our present ± 0.001 pF. Extension of the temperature range by pressurization of the test-capacitance may also be helpful.

It may also be asked whether in view of simpler physical methods for determination of molecular structure it is worthwhile to pursue the tedious techniques of electrical polarization measurements at various temperatures. We have tried to assemble an instrument in which the specific volume and the dielectric constant of a single sample could be determined for a range of temperatures at one time, within the present limits of precision during the time period (30 min) needed for a determination We have not been successful. but in principle such an instrument could be built. An air capacitance of about 1000 pF would be desirable.

Finally it may be asked whether, in view of the relatively-simple though less precise determination of electrical polarization in the gaseous phase, there is sufficient information to be gained from the condensed phases to warrant study. From the viewpoint of the chemist the appreciable number of chemical reactions that occur in the liquid phase is a sufficient answer.

Experimental

The techniques used in this study have been outlined previously (13, 6, 3). Mercuric chloride and bromide have been crystallized from ethanol before use. Dimethylmercury was purified by distillation at 96 °C.

1. G. C. HAMPSON. Trans. Faraday. Soc. **30**, 877 (1934).
2. J. W. SMITH. Electric dipole moments. Butterworth's, London. 1955. pp. 256–290.
3. M. BEDARD, H. HUBER, J. L. MYERS, and G. F WRIGHT. Can. J. Chem. **40**, 2778 (1962).
4. H. SAWATZKY and G. F WRIGHT. Can. J. Chem. **36**, 1555 (1958); **41**, 1441 (1962).
5. C. C. MEREDITH, L. WESTLAND, and G. F WRIGHT. J. Am. Chem. Soc. **79**, 2385 (1957).
6. P. PODLESCKA, L. WESTLAND, and G. F WRIGHT. Can. J. Chem. **36**, 574 (1958).
7. C. C. MEREDITH and G. F WRIGHT. Can. J. Chem. **38**, 1177 (1960).
8. H. HUBER and G. F WRIGHT. Can. J. Chem. **42**, 1446 (1964).
9. H. HUBER and G. F WRIGHT. Can. J. Chem. **51**, 2234 (1973).
10. A. R. TOURKY and H. A. RIZK. Can. J. Chem. **35**, 630 (1957); J. Phys. Chem. **64**, 565 (1960).
11. M. V. GEORGE and G. F WRIGHT. Can. J. Chem. **36**, 189 (1958).
12. W. KLEMPERER and L. LINDEMANN. J. Chem. Phys. **25**, 397 (1956).
13. C. C. MEREDITH and G. F WRIGHT. Can. J. Techn. **33**, 182 (1955).
14. A. L. MCCLELLAND. Tables of experimental dipole moments. W. H. Freeman Co., San Francisco. 1963.

Can. J. Chem. Downloaded from www.nrcresearchpress.com by 210.87.254.6 on 09/05/12
For personal use only.

Solute Radical Inactivation of the Sulfhydryl Enzyme Papain – Sensitization and Protection[1]

G. M. GAUCHER, BARBARA L. MAINMAN, AND D. A. ARMSTRONG
Department of Chemistry, University of Calgary, Calgary, Alberta T2N 1N4
Received January 12, 1973

Particularly pure N_2O-purged papain solutions (2×10^{-5} *M*; p*H* 6.8) were irradiated at 0 °C for different times with ^{60}Co γ-rays, in the presence of 10–30 m*M* solutions of acetate, isobutanol, and thiocyanate. In comparison to OH radicals, these solute radicals substantially enhanced papain inactivation. Calculated inactivation probabilities per papain–radical reaction (*i.e.* 0.43 for OH and 1.00 for solute radicals) support this finding.

In situ protection of both N_2-purged and N_2O saturated papain solutions by cysteine was found to occur only at cysteine: papain molar ratios above 15:1, while below this ratio substantial sensitization occurred, reaching a maximum at a 2:1 ratio. This enhanced inactivation of papain at low cysteine concentrations is primarily repairable in nature, and probably due to CysS· attack on papain's active site sulfhydryl. Only at relatively high cysteine:papain ratios (>30) can protection be ascribed simply to radical scavenging.

Des solutions particulièrement pures de papaine, libérées de N_2O, (2×10^{-5} *M*; p*H* 6.8) furent irradiées à 0 °C pendant des temps variables avec des rayons-γ ^{60}Co, en présence de solutions 10–30 m*M* d'acétate, d'isobutanol, et de thiocyanate. En comparaison des radicaux OH, ces radicaux dissous favorisent de manière significative l'inactivation de la papaine. Les probabilités calculées d'inactivation par réaction radical–papaine (*i.e.* 0.43 pour OH et 1.00 pour radicaux dissous) sont en accord avec les résultats trouvés.

La protection *in situ* des solutions de papaine, libérées en N_2 et saturées en N_2O, par la cystéine n'est seulement valable que pour un rapport molaire cystéine:papaine supérieure à 15:1 alors qu'en-dessous de ce rapport une sensibilisation non-négligeable se produit et atteint un maximum pour un rapport 2:1. Cette inactivation favorisée de la papaine à des concentrations faibles en cystéine est principalement reparable dans la nature et semble causée par l'attaque du CysS· sur la fonction sulphydryle composant le site actif de la papaine. On ne peut avoir une protection assimilable au trappage radicalaire par la cystéine qu'à des rapports relativement élevés cystéine:papaine (>30). [Traduit par le journal]

Can. J. Chem., **51**, 2443 (1973)

Introduction

A previous publication (1) from this laboratory reported a study of the radiolysis of the sulfhydryl protease, papain, in dilute aqueous solutions. The overall radiation sensitivity of the enzyme was high compared to that of other enzymes, but, as in earlier work (2), it was found that a substantial fraction of the inactivated papain molecules could be reactivated by post-irradiation chemical repair with 1000-fold excess of cysteine. From a comparison of *G* (inactivation) in N_2O-saturated and N_2-purged solutions it was concluded that e_{aq}^- was more effective in deactivating papain than OH and that it also gave a higher yield of repairable inactivation.

The papain solutions used in this early work were 10^{-2} *M* in sodium acetate (p*H* 6.9) and contained two species of protein, active and inactivatable papain, at a total concentration of 2.1×10^{-5} *M*. In addition to recent chromatographic developments (3) which have made it possible to obtain much purer papain preparations, we have found it possible to omit the sodium acetate and hence irradiate essentially solute-free papain solutions. These changes represent a considerable simplification of the system and we have therefore redetermined the inactivation yields. The experimental procedures and results will be given in greater detail elsewhere. The purpose of this paper is to report the extremely high specificity of $\cdot CH_2CO_2^-$, isobutanol radicals, and certain other radicals for the inactivation of papain. The results are of considerable interest since the high concentration of organic molecules in the cytoplasm of living cells will undoubtedly provide large numbers of aliphatic and other free radicals — not only through direct action, but also by the scavenging of OH, H, and e_{aq}^- formed from water. The present data show that such solute radicals are potentially highly damaging to macromolecular

[1]Issued as Publication No. 73-01 from the Biopolymer Research Group, University of Calgary.

Can. J. Chem. Downloaded from www.nrcresearchpress.com by 210.87.254.105 on 09/05/12
For personal use only.

Can. J. Chem. Downloaded from www.nrcresearchpress.com by 210.87.254.105 on 09/05/12
For personal use only.

targets such as sulfhydryl enzymes, and they shed further light on the phenomenon of protection.

Experimental

The present experiments were carried out with a standardized preparation of high activity papain for which the average k_{cat} of 44 preparations was 11.50 ± 0.91 s^{-1} *vs.* a k_{cat} of 5–6 for commercial crystalline papain (1). Similar high activity papain preparations have recently been reported (4). In our presently utilized procedure, partially purified activated papain is bound to a papain-specific inhibitor linked to an agarose gel, which is supported in a chromatography column (3). After washing with eight column volumes of 2×10^{-2} *M* sodium acetate (p*H* 6), the active enzyme was eluted with N_2-purged double-distilled water and made up to the desired concentration immediately before use. The resulting solution contained less than 10^{-4} *M* sodium acetate.

All papain solutions were bubbled further with N_2 or N_2O and then transferred to radiation cells sealed from the atmosphere. After exposure to ^{60}Co radiation, aliquots were assayed for sulfhydryl content and enzymatic activity as previously described (1). The latter assay was carried out both with and without a post-irradiation preassay incubation with cysteine to effect repair (see above and ref. 1).

For nitrogen-purged solutions the above procedure gave the same *G* inactivation values as: (*a*) preparations in which the sodium acetate (p*H* 6) wash solution was replaced with a 2×10^{-2} *M* $NaClO_4$ solution, resulting in an even further reduction in the final acetate concentration, and (*b*) preparations in which the papain solutions in distilled water were made up to 2×10^{-2} *M* in $NaClO_4$ prior to irradiation. The identical yields observed in distilled water and in the presence of the radiochemically inert (5) $NaClO_4$ in *b* show that increasing the electrolyte concentration up to 2×10^{-2} *M* is without effect on the inactivation yields. However, since excessively high concentrations such as 0.1 *M* may have an effect, the electrolyte concentrations in the present experiments were kept $\leq 20 \times 10^{-2}$ *M*.

Results and Discussion

Figure 1 shows plots of the percentage residual activity *vs.* irradiation time for 2×10^{-5} *M* N_2O-purged solutions of papain containing various added solutes. Since all solvated electrons form OH in reaction 1, the total initial yield of OH

[1] $$e_{aq}^- + N_2O + H^+ \rightarrow N_2 + OH$$

radicals is 5.9 per 100 eV (6). From the known rate constants for the reactions of OH with papain (7), CNS^- and isobutanol (8) and assuming homogeneous kinetics, it can be shown for the conditions in Fig. 1 that ≥90% of OH would have undergone reactions 2–4 in preference to reaction with papain. For the case of acetate the

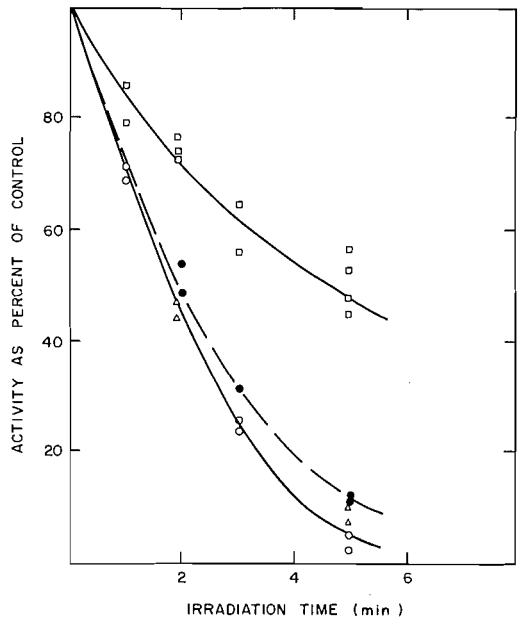

FIG. 1. Dose-inactivation plots for ~2×10^{-5} *M* aqueous papain solutions irradiated at 0 °C with ^{60}Co γ-rays at a dose rate of 5.75 ± 0.09 × 10^{16} eV ml^{-1} min^{-1} under N_2O and in the presence of various solutes. p*H* of acetate solutions = 6.9, all others = 6.2 ± 0.2. All enzyme activities were determined without post irradiation repair. □, no added solute; ○, 20 m*M* isobutanol; △, 10 m*M* NaSCN; ●, 20 m*M* Na Acetate.

[2][2] $$OH + C_4H_9OH \rightarrow H_2O + R\cdot$$

[3] $$OH + CNS^- \rightarrow OH^- + CNS\cdot$$

[4] $$CNS\cdot + CNS^- \rightarrow \cdot(CNS)_2^-$$

proportion undergoing reaction 5 under our conditions is about 65% (5, 8). The radicals

[5] $$OH + CH_3CO_2^- \rightarrow H_2O + \cdot CH_2CO_2^-$$

formed in reactions 2, 3–4, and 5 attack papain and the dose-inactivation plots in Fig. 1 clearly show that there is enhanced inactivation where OH is replaced by either $\cdot CH_2CO_2^-$, R·, or $\cdot(CNS)_2^-$.

The magnitude of *G* (inactivation) calculated from the initial slopes of plots such as those in Fig. 1 represents the combined damage caused by OH or the solute radicals formed from it, the hydrogen atom (G_H = 0.6 (9)) and molecular

[2]R· is assumed to be predominantly

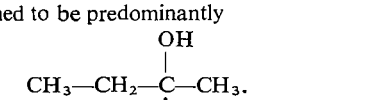

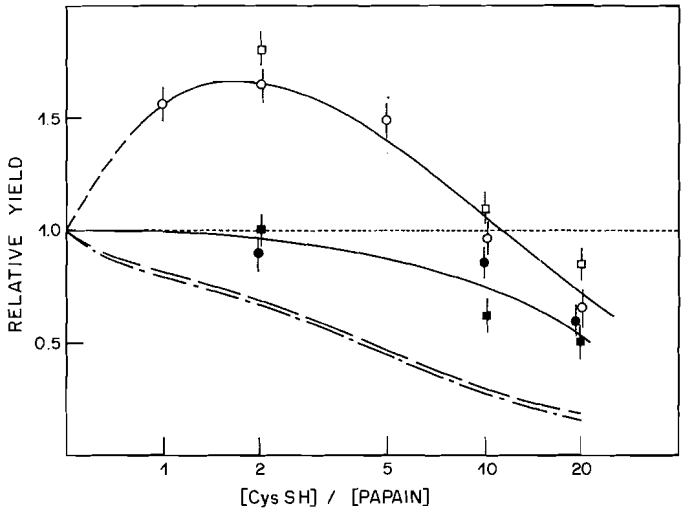

FIG. 2. Relative inactivation yields as a function of [CysSH]/[Papain]. Relative yield = G (inactivation, cysteine present)/ G (inactivation, cysteine absent). Solid and open points indicate relative yields for non-repairable and total inactivation respectively while circles and squares are for N_2- and N_2O-purged solutions respectively. The —·- line is the calculated fraction of OH radicals reacting with papain in N_2O-saturated solutions, and the — — line the corresponding fraction of total radicals (OH and e_{aq}^-) reacting with papain in N_2-purged solutions.

hydrogen peroxide ($G_{H_2O_2}{}^M = 0.75$ (9)). Redpath (10) has cited unpublished results which discount the importance of H as an inactivating agent and we shall also neglect it. Hydrogen peroxide on the other hand produces ~60% repairable and 40% non-repairable damage to papain (11). After allowing for these contributions the inactivation caused by each of the above radicals can be calculated and compared with the total yields of these radicals to give the net probability of papain inactivation per radical. These probabilities are given in Table 1.

The sulfhydryl group of cysteine 25 is essential to the activity of papain and analysis for this group (see ref. 1 for assay method) indicates that a large fraction of the inactivation by $\cdot CH_2CO_2^-$ occurs via the destruction of this cysteine residue, the initial attack being probably:

TABLE 1. Probability of inactivation per reaction of papain with various free radicals

Radical	Total inactivation	Non-repairable inactivation
OH	0.43±0.08	0.11
$\cdot(CNS)_2^-$	1.00±0.08	0.31
R· (isobutanol)	1.00±0.08	0.53
$\cdot CH_2CO_2^-$	1.00±0.08	0.54

[6] Papain—SH + $\cdot CH_2CO_2^- \rightarrow$

Papain—S· + $CH_3CO_2^-$

A similar situation occurs with the isobutanol radical and the enhanced inactivation observed here with $\cdot(CNS)_2^-$ is in agreement with a recent publication of Redpath (10). The high specificity of certain free radicals for the inactivation of papain is thus confirmed and extended by this report. Furthermore the fact that these radicals are either negatively charged or apolar is in agreement with the presence of positive (12) and apolar (13) sub-sites at the active site of papain.

There is considerable interest in the protection of biological molecules by cysteine and related thiols. In our earlier paper the protection of papain against non-repairable radiochemical damage was demonstrated using 6×10^{-5} M nitrogen-purged enzyme solutions and cysteine: papain ratios of 2:1, 5:1, and 10:1. Because of the possible complicating effects of the presence of both acetate and inactive papain in our earlier study, the phenomenon has been reinvestigated. In addition the measurements have been extended to include total and non-repairable damage in both nitrogen-purged and N_2O-saturated solutions. In these experiments cysteine concentrations were sufficiently low (see Fig. 2) compared to those routinely used under our

Can. J. Chem. Downloaded from www.nrcresearchpress.com by 210.87.254.105 on 09/05/12
For personal use only.

Can. J. Chem. Downloaded from www.nrcresearchpress.com by 210.87.254.105 on 09/05/12
For personal use only.

postirradiation repair conditions (*i.e.* a molar ratio cysteine:papain of 1000:1), so that any chemical repair by cysteine as in reaction 7, which is relatively slow (1, 14), would be

[7] PapainSSCys + CysSH → PapainSH + CysSSCys

negligible. Hence any protective effect of cysteine must be ascribed to faster reactions such as: (*a*) radical scavenging as in reactions 8, 8*a*, and 9

[8] $e_{aq}^- + CysSH \rightarrow Cys\cdot + SH^-$

[8*a*] $Cys\cdot + CysSH \rightarrow CysH + CysS\cdot$

[9] $OH + CysSH \rightarrow H_2O + CysS\cdot$

or (*b*) *in situ* repair of unstable papain radicals, as in reactions 10 and 11.[3]

[10] Papain—H + OH → Papain· + H_2O

[11] Papain· + CysSH → Papain—H + CysS·

G values for inactivation in the presence of various concentrations of cysteine were obtained from plots such as those in Fig. 1. The ratio *G* (inactivation, cysteine present):*G* (inactivation, cysteine absent), termed the "relative yield", is plotted against cysteine:papain in Fig. 2. Generally interpreted, relative yields of less than unity indicate protection, while those greater than unity indicate sensitization.

From the known (5, 7, 8) rate constants of reactions 9 and 10, and assuming homogeneous kinetics, one can calculate the fraction of OH which should react with papain at each cysteine:papain ratio. Likewise from the rate constants (5, 7) of reactions 8 and 12, the fraction of elec-

[12] $e_{aq}^- + Papain \rightarrow Papain^-$

trons reacting with papain can be calculated. The average of the two is given by the dashed line in Fig. 2 and should correspond to the fraction of total radicals (e_{aq}^- + OH) which attack papain in N_2-purged solutions. The OH fraction, given by the dot-dashed line, should correspond to the fraction of OH attacking papain in the N_2O-saturated solutions. If the products of reactions 8, 8*a*, 9, and 11 did not react with papain then the relative yields should follow these lines or even lie below them, if reaction 11 yields active papain. As can be seen, whether with or without post-irradiation repair, the relative yields both for N_2-purged and N_2O-saturated solutions all lie substantially above these lines, indicating that protection by straightforward radical scavenging does not occur. Also it should be noted that reaction 11 may yield inactive papain (see below).

Of particular interest is the observation that at low cysteine:papain ratios, where most OH (and e_{aq}^- in N_2-purged solution) react with papain, the relative yield for total inactivation shows a strong sensitization which reaches a maximum at cysteine:papain ≃ 2. There may be a number of factors contributing to this complex behavior. For example, adsorption of cysteine onto charged sites of the enzyme may alter the nature of the free radical reactions with papain, causing a higher inactivation efficiency. Also fixation of damaged papain rather than restoration to the active form is possible in reaction 11 (*cf.* the effects reported in ref. 17). However, almost all of the enhanced damage is repairable and this coupled with present knowledge (16, 18) of the radiation chemistry of SH compounds suggests that the formation of CysS· radicals in reactions 8, 8*a*, 9, and 11, and their subsequent attack on the enzyme is more important. Hence, we propose that the following reactions are involved.

At high cysteine:papain ratios or in the absence of papain, CysS· radicals would be expected (16, 18) to disappear through the reactions:

[13] $CysS\cdot + CysS^- \rightleftharpoons CysSS^-Cys$

[14] $CysS\cdot + CysSS^-Cys \rightarrow CysS^- + CysSSCys$

However, in the presence of papain and with low cysteine:papain ratios reactions 15 and 16

[15] $CysS\cdot + PapainS^- \rightleftharpoons PapainSS^-Cys$

[16] $CysS\cdot + PapainSS^-Cys \rightarrow CysS^- + PapainSSCys$

should be favored, since the pK_a of the SH group of papain will be lower than that of cysteine due to hydrogen-bonding interactions (12) at the active site. Since PapainSSCys is known (14) to be repairable via reaction 7 this could well explain the substantial enhancement of repairable damage. The fact that the relative yields with repair by CysSH are also above the dashed line in Fig. 2 suggests that CysS· radicals are also capable of causing non-repairable damage. These radicals are thermochemically more stable and

[3]This reaction has not actually been observed, but one assumes that it should proceed with a rate constant of about $10^6\ M^{-1}\ s^{-1}$ or larger as with lysozyme free radicals (15) and other large radical species (16).

thus less reactive than OH. In addition to the high selectivity for RS^- anions, CysS· may have an affinity for papain's active site imidazolium ion by virtue of its carboxylate anion (12). This and other reactions with other amino acid residues located in close proximity to this imidazolium ion could lead to the observed non-repairable inactivation.

Further investigations are underway to pinpoint more clearly the reasons for the sensitization of papain inactivation at low cysteine concentrations. However, the present work has clearly demonstrated that the protection of a sulfhydryl enzyme by another thiol can be a highly complex phenomenon. In fact if our interpretation is correct, the efficiency of the protector will depend not only on k_8/k_{12} and k_9/k_{10}, but also on k_{13}/k_{15} and K_{13}/K_{15}. Thus, as in the present instance, a sulfhydryl protector may be a sensitizer under certain conditions. In this connection it is interesting to note that some non-sulfhydryl sensitizers may also exhibit protective effects at higher concentrations (see ref. 19 and references cited therein).

Finally, the high efficiency with which isobutanol, acetate, and thiocyanate radicals inactivate papain, is particularly relevant to radiobiology, given the high probability of forming cytoplasmic solute radicals. At present the efficiency of such radicals appears to be due largely to their selectivity for papain's active site sulfhydryl, and such effects are likely to apply to other biologically important enzymes.

The authors wish to acknowledge financial assistance from the Defence Research Board and National Research Council of Canada

1. G. M. GAUCHER, B. L. MAINMAN, G. P. THOMPSON, and D. A. ARMSTRONG. Radiat. Res. **46**, 457 (1971).
2. A. PIHL and T. SANNER. Radiat. Res. **19**, 27 (1963).
3. S. BLUMBERG, I. SCHECTER, and A. BERGER. Eur. J. Biochem. **15**, 97 (1970).
4. K. R. LYNN and D. LOUIS. In press.
5. M. ANBAR and P. NETA. Int. J. Appl. Radiat. Isotop. **18**, 493 (1967).
6. G. E. ADAMS, J. W. BOAG, J. CURRANT, and B. D. MICHAEL. *In* Pulse radiolysis. *Edited by* M. Ebert, J. P. Keene, A. J. Swallow, and J. H. Baxendale. Academic Press, London. 1965. p. 117.
7. J. R. CLEMENT, D. A. ARMSTRONG, N. V. KLASSEN, and H. A. GILLIS. Can. J. Chem. **50**, 2833 (1972).
8. R. L. WILLSON, C. L. GREENSTOCK, G. E. ADAMS, R. WAGEMAN, and L. M. DORFMAN. Int. J. Radiol. Phys. Chem. **3**, 211 (1971).
9. J. K. THOMAS. Adv. Rad. Chem. **1**, 103 (1969).
10. J. L. REDPATH. Int. J. Radiat. Biol. **22**, 99 (1972).
11. G. M. GAUCHER, B. L. MAINMAN, and D. A. ARMSTRONG. To be published.
12. C. J. JOLLEY and J. A. YANKEELOV. Biochemistry, **11**, 164 (1972).
13. A. BERGER, I. SCHECHTER, H. BENDERLI, and N. KURN. Peptides-1969. North-Holland, Amsterdam. 1971. p. 290.
14. L. A. SLUYTERMAN. Biochim. Biophys. Acta, **139**, 430 (1967).
15. J. V. DAVIES, M. EBERT, and R. J. SHALEK. Int. J. Radiat. Biol. **14**, 19 (1968).
16. G. E. ADAMS, G. S. MCNAUGHTON, and B. D. MICHAEL. Trans. Faraday Soc. **64**, 902 (1968), and prior refs. cited therein.
17. J. HOLIAN and W. M. GARRISON. Nature, **221**, 57 (1969).
18. J. W. PURDIE, H. A. GILLIS, and N. V. KLASSEN. Chem. Commun. **19**, 1163 (1971); and private communication.
19. E. I. POWERS, R. C. RICHMOND, and M. SIMIC. Nature New Biol. **238**, 260 (1972).

Can. J. Chem. Downloaded from www.nrcresearchpress.com by 210.87.254.105 on 09/05/12
For personal use only.

The Preparation of 1,1′-Carbonyl- and 1,1′-Sulfinyl-dipyrazoles and their Reactions with Carbonyl Compounds

K. I. THE, L. K. PETERSON, AND E. KIEHLMANN

Chemistry Department, Simon Fraser University, Burnaby 2, British Columbia

Received January 18, 1973

The compounds 1,1′-carbonylbis(3-methylpyrazole) (**1**), 1,1′-carbonylbis(3,5-dimethylpyrazole) (**2**), and 1,1′-sulfinyldipyrazole (**3**) have been prepared. They react with aldehydes and ketones in the presence of metal ion catalysts to form 1,1′-alkylidenedipyrazoles together with carbon dioxide, from **1** and **2**, or sulfur dioxide, from **3**. Tetrapyrazol-1-ylmethane results from the pyrolysis at 200° of 1,1′-carbonyldipyrazole in the presence of cobalt(II) chloride.

La préparation du carbonyl-1,1′ bis (méthyl-3 pyrazole) (**1**), carbonyl-1,1′ bis (diméthyl-3,5 pyrazole) (**2**) et sulfinyl-1,1′ dipyrazole (**3**) a été rapportée. Ces composés réagissent sur les aldéhydes et cétones en présence de catalyseurs ion métallique pour conduire aux alkylidène-1,1 dipyrazoles et gaz carbonique pour le **1** et **2** et anhydride sulfureux pour **3**. Le tétrapyrozyl-1 méthane résulte de la pyrolyse à 200° du carbonyl-1,1′ dipyrazole en présence de chlorure de cobalt(II). [Traduit par le journal]

Can. J. Chem., **51**, 2448 (1973)

As previously reported (1, 2), 1,1′-carbonyldipyrazole reacts with various carbonyl compounds in the presence of metal salt catalysts, liberating carbon dioxide to form 1,1′-alkylidenedipyrazoles. We have now prepared the related compounds 1,1′-carbonylbis(3-methylpyrazole), 1,1′-carbonylbis(3,5-dimethylpyrazole), and 1,1′-sulfinyldipyrazole in order to study steric and electronic substituent effects.

Experimental

Elemental analyses were performed by the departmental analyst. Melting points are uncorrected. The n.m.r. spectra[1] were recorded on a Varian A 56/60 using $CDCl_3$ as solvent and TMS as internal standard. Mass spectra were determined with a double-focusing RMU-6E Hitachi Perkin–Elmer instrument, and for all compounds reported below (**1–13**), the mass corresponding to the observed parent peak was in agreement with the calculated molecular weight.[2]

Preparation of 1,1′-Carbonylbis(3-methylpyrazole) (1)

3-Methylpyrazole (0.10 mol) in dry ether (50 ml) was added slowly, under a nitrogen atmosphere, to a stirred ethereal (200 ml) suspension of sodium amide (0.10 mol); the mixture was stirred for 16 h at 25° and then heated at reflux temperature for 4 h. With the reaction vessel attached to the vacuum system, phosgene (0.05 mol) was condensed onto the mixture, which was initially held at −78° for 1 h, then heated under reflux for several hours, again under a nitrogen atmosphere. The sodium chloride precipitate (0.10 mol) was filtered off and the solvent was distilled under N_2 to give a yellow solid which was purified by zone fractionation under vacuum to yield pure **1**, m.p. 68–69°, in 80% yield.

Anal. Calcd. for $C_9H_{10}N_4O$: C, 56.8; N, 29.4; H, 5.3. Found: C, 56.5; N, 29.6; H, 5.2.

N.m.r.: τ 7.63 (s, 3H, CH_3), 3.68 (d, 1H, 4-H, J = 3.0 Hz), 1.37 (d, 1H, 5-H, J = 3.0 Hz).

Preparation of 1,1′-Carbonylbis(3,5-dimethylpyrazole) (2)

Compound **2** was prepared from 3,5-dimethylpyrazole according to the method used for compound **1**; m.p. 85–86° (lit. (3) 89–90°); yield, 70%.

Anal. Calcd. for $C_{11}H_{14}N_4O$: C, 60.6; N, 25.7; H, 6.4. Found: C, 60.8; N, 25.8; H, 6.5.

N.m.r.: τ 7.75 (s, 3H, 3-CH_3), 7.52 (d, 3H, 5-CH_3, J = 1.0 Hz), and 3.95 (m, 1H, 4-H).

Preparation of 1,1′-Sulfinyldipyrazole (3)

Compound **3** was prepared in the same way as 1,1′-carbonyldipyrazole (2), using thionyl chloride in place of phosgene; yield, 55%; m.p. 73–74°.

Anal. Calcd. for $C_6H_6N_4OS$: C, 39.5; N, 30.8; H, 3.2. Found: C, 39.6; N, 31.1; H, 3.4.

N.m.r.: τ 2.23 (q, 1H, 3-H, J_{34} = 1.6, J_{35} = 0.5 Hz), 3.53 (q, 1H, 4-H, J_{45} = 2.7, J_{34} = 1.6 Hz), and 2.00 (q, 1H, 5-H, J_{45} = 2.7, J_{35} = 0.5 Hz).

Reactions of 1 with Carbonyl Compounds

(*a*) With acetone: The following procedure is typical of all reactions in this section. A mixture of **1** (0.90 mmol), dry acetone (~5 ml), and cobalt(II) chloride (~4 mg) was heated in a sealed tube at 90–95° for 16 h to liberate CO_2 quantitatively (only traces of CO_2 were detected at 25°). The solid product was purified by zone fractionation under vacuum to yield 2,2-bis(3-methylpyrazol-1-yl)-propane (**4**); yield, 70%; m.p. 101–102°.

[1]N.m.r. spectra and bands showing unresolved fine structure are signified by an asterisk.

[2]The mass spectra of compounds **1–13** exhibited strong parent peaks in all cases. Major fragments corresponding to loss of pyrazolyl or methylpyrazolyl moieties were observed. Compounds **1**, **2**, and 1,1′-carbonyldipyrazole gave rise to di(methylpyrazolyl), and dipyrazolyl recombination species, respectively.

Can. J. Chem. Downloaded from www.nrcresearchpress.com by 210.87.254.40 on 09/05/12
For personal use only.

Can. J. Chem. Downloaded from www.nrcresearchpress.com by 210.87.254.40 on 09/05/12
For personal use only.

Anal. Calcd. for $C_{11}H_{16}N_4$: C, 64.7; N, 27.5; H, 7.8. Found: C, 65.2; N, 27.6; H, 8.0.

N.m.r.: τ 7.80 (s, 6H, $C(CH_3)_2$, 7.72 (m, 6H, 3-CH_3), 3.98 (d*, 2H, 4-H, J = 2.3 Hz) and 2.78 (d*, 2H, 5-H, J = 2.3 Hz).

(*b*) Acetone-d_6 gave 2,2-bis(3-methylpyrazol-1-yl)-hexadeuteropropane (**5**); yield, 85%; m.p. 102–103°.

N.m.r.: τ 7.73 (s*, 3, CH_3), 4.00 (d*, 1H, 4-H, J = 2.4 Hz), 2.83 (d*, 1H, 5-H, J = 2.4 Hz).

(*c*) Acetaldehyde gave 1,1-bis(3-methylpyrazol-1-yl)-ethane (**6**); yield, 65%.

Anal. Calcd. for $C_{10}H_{14}N_4$: C, 63.2; N, 29.5; H, 7.4. Found: C, 63.2; N, 28.6; H, 7.6.

N.m.r.: τ 7.78 (s*, 6H, ring-CH_3), 4.00 (d*, 2H, 4-H, J = 2.3 Hz), 2.55 (m*, 2H, 5-H), 3.60 (9, 1H, >CH—CH_3, J = 6.7 Hz), and 7.83 (m*, 3H, >CH—CH_3).

(*d*) Cyclobutanone gave 1,1-bis(3-methylpyrazol-1-yl)-cyclobutane (7); yield, 75%; m.p. 43.5–45°.

Anal. Calcd. for $C_{12}H_{16}N_4$: C, 66.7; N, 25.9; H, 7.4. Found: C, 66.6; N, 25.6; H, 7.6.

N.m.r.*: 7.73 (s, 6H, CH_3), 3.98 (d, 2H, 4-H, J = 2.4 Hz), 2.77 (d, 2H, 5-H, J = 2.4 Hz), 7.93 and 6.83 (m, 6H, —$(CH_2)_3$—).

(*e*) Cyclopentanone gave 1,1-bis(3-methylpyrazol-1-yl)-cyclopentane (**8**); yield, 30%; m.p. 121–122°.

Anal. Calcd. for $C_{13}H_{18}N_4$: C, 67.8; N, 24.4; H, 7.8. Found: C, 67.7; N, 24.3; H, 7.9.

N.m.r.*: τ 7.75 (s, 6H, CH_3), 4.00 (d, 2H, 4-H, J = 2.4 Hz), 2.68 (d, 2H, 5-H, J = 2.4 Hz), 8.17 and 7.13 (m, 8H, —$(CH_2)_4$—).

(*f*) 4-Methylcyclohexanone gave 1,1-bis(3-methylpyrazol-1-yl)-4-methylcyclohexane (**9**); yield, 60%; m.p. 77.5–78.5°.

Anal. Calcd. for $C_{15}H_{22}N_4$: C, 70.1; N, 21.8; H, 8.2. Found: C, 69.9; N, 21.6; H, 8.5.

N.m.r.: τ 9.13 (m, 3H, —CH_2—CH(—CH_3)—), 7.72 and 7.75 (2s, 6H, —N=C(—CH_3)—), 4.13 and 3.92 (2d*, 2H, 4-H, J = 2.3 Hz), 3.13 and 2.43 (2d*, 2H, 5-H, J = 2.3 Hz), and 7–9 (complex band, 9H, cyclohexane ring).

Reactions of 2 with Ketones

The procedure was essentially the same as that used with compound **1** above, except that temperatures of 150–170° were required to facilitate reaction.

(*a*) Acetone gave 2,2-bis(3,5-dimethylpyrazol-1-yl)propane (**10**); yield, 65%; m.p. 80–81.5°.

Anal. Calcd. for $C_{13}H_{20}N_4$: C, 67.3; N, 24.1; H, 8.6. Found: C, 67.5; N, 24.1; H, 6.6.

N.m.r.: τ 7.77 (s, 6H, 3-CH_3), 4.17 (broad band, 2H, 4-H), 8.32 (d, 6H, 5-CH_3, J = 0.8 Hz), and 7.87 (s, 6H, >$C(CH_3)_2$).

(*b*) Cyclobutanone gave 1,1-bis(3,5-dimethylpyrazol-1-yl)-cyclobutane (**11**); yield, 50%; m.p., 72–73°.

Anal. Calcd. for $C_{14}H_{20}N_4$: C, 68.8; N, 22.9; H, 8.2. Found: C, 68.9; N, 22.6; H, 8.3.

N.m.r.: τ 7.78 (s, 6H, 3-CH_3), 4.22 (m*, 2H, 4-H), 8.13 (d, 6H, 5-CH_3, J = 0.8 Hz), 8.00 and 6.73 (complex bands, 6H, —$(CH_2)_3$—).

(*c*) With methyl ethyl ketone, CO_2 was evolved quantitatively, together with a difficult-to-purify oil and 3,5-dimethylpyrazole. The latter was identified by i.r., n.m.r., and mass spectra. The expected compound 2,2-bis(3,5-dimethylpyrazol-1-yl)-butane was not detected.

(*d*) With cyclohexanone, CO_2 was evolved quantitatively together with an impure oil and 3,5-dimethylpyrazole. The expected compound 1,1-bis(3,5-dimethylpyrazol-1-yl)-cyclohexane was not detected.

Reactions of 3 with Ketones

(*a*) With acetone: A typical procedure was as follows: Dry acetone (~5 ml), 1,1′-sulfinyldipyrazole (2.05 mmol), and a catalytic amount of dry $CoCl_2$ were sealed under vacuum into a reaction vessel and cooled in liquid nitrogen. On warming from −196° to room temperature, a blue solution, gradually turning yellow, was observed. After 16 h, the products were SO_2 (quantitatively), identified by its i.r. spectrum and vapor phase molecular weight (M(calcd.), 64.06; M(obsd.), 63.8), and a residue of solids which was purified by zone fractionation to yield 2,2-dipyrazol-1-ylpropane (75% yield), identified by its m.p. and i.r., mass, and n.m.r. spectra (2, 4).

(*b*) Cyclobutanone gave 1,1-dipyrazol-1-ylcyclobutane (80% yield) by its m.p. and i.r., mass, and n.m.r. spectra (2).

(*c*) Cyclopentanone, a reaction temperature of 120–130° was required; the product was identified as 1,1-dipyrazol-1-ylcyclopentane (35% yield) by its m.p. and i.r., mass, and n.m.r. spectra (2, 4).

(*d*) 4-Methylcyclohexanone gave 1,1-(dipyrazol-1-yl)-4-methylcyclohexane at room temperature, in 60% yield, and identified by its m.p. and i.r., mass, and n.m.r. spectra (2).

The Reaction of 1,1′-Carbonyldipyrazole with Benzophenone

A preliminary experiment indicated that no reaction occurs between 1,1′-carbonyldipyrazole and benzophenone in the presence of a catalytic amount of cobalt(II) chloride in refluxing THF (2). However, when equimolar quantities (1.75 mmol) of these two reagents and a trace of dry $CoCl_2$ were heated in a sealed tube at 190–200° for 16 h, carbon dioxide (1.16 mmol) and a mixture of brown solid and liquid products was formed. The solid was purified by zone fractionation and recrystallization from methanol, yielding white crystals of diphenyldipyrazol-1-ylmethane (**12**); yield, 25%; m.p. 153–154°.

Anal. Calcd. for $C_{19}H_{16}N_4$: C, 76.0; N, 18.7; H, 5.3. Found: C, 75.6; N, 18.8; H, 5.3.

N.m.r.: τ 3.83 (q, 2H, 4-H, J_{45} = 2.5, J_{34} = 1.8 Hz), 2.53 (m, 4H, 3-H and 5-H), 3.07 and 2.72 (m, 10H, C_6H_5).

The Pyrolysis of 1,1′-Carbonyldipyrazole

Pure 1,1′-carbonyldipyrazole was found to be stable up to 180°; however, a sample (2.34 mmol) heated at 190° for 16 h, in the presence of a catalytic amount of dry $COCl_2$, yielded CO_2 (0.97 mmol) and a brown residue. Tetrapyrazol-1-ylmethane (**13**) was separated from the residue by zone fractionation; yield, 50%; m.p., 146–147° (lit. (4), 146–147°).

N.m.r.: τ 2.07 (q, 3-H, J_{34} = 1.8, J_{35} = 0.7 Hz), 3.45 (q, 4-H, J_{45} = 2.9, J_{34} = 1.8 Hz), and 2.23 (q, 5-H, J_{45} = 2.9, J_{35} = 0.7 Hz).

Discussion

1,1′-Carbonylbis(3,5-dimethylpyrazole) (**2**) and the new compounds 1,1′-carbonyl-bis(3-methylpyrazole) (**1**) and 1,1′-sulfinyldipyrazole (**3**) are obtained in high yield by the reaction of

[1] 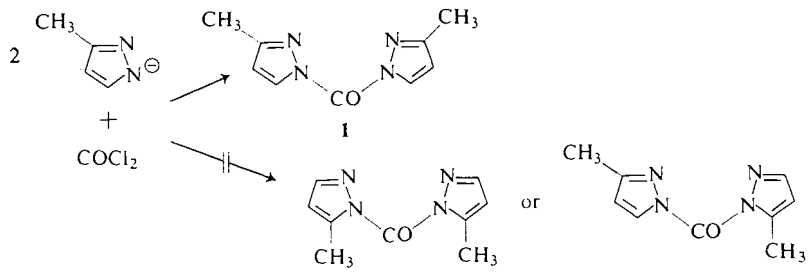

1 14

the appropriate sodium pyrazolide salt with either phosgene or thionyl chloride, in a manner analogous to the procedures reported in the literature for the synthesis of 1,1′-sulfinyldiimidazole (5) and various derivatives of 1,1′-carbonyldipyrazole (1, 3, 6–8) and 1,1′-carbonyldiimidazole (9). Compound **1** is obtained as a single substance, there being no evidence for the formation of the isomeric 1,1′-carbonylbis-(5-methylpyrazole) or the mixed isomer **14** (eq. 1).

Thus N-1, though more remote than N-2 from the electron-releasing methyl group, is clearly the more nucleophilic center in the methylpyrazolide anion. Compounds **1**–**3** are sensitive to moisture, being hydrolyzed to free base and carbon dioxide or sulfur dioxide. They are readily characterized on the basis of m.p., elemental analysis, and i.r., mass, and p.m.r. spectral measurements; the assignment of the lowest-field resonance to H-5 of **1** and **3** is related to the electron-withdrawing effect of the C=O or S=O group attached at N-1. The resonances of the 3- and 5-methyl groups in compound **2** can be distinguished on the basis of similar arguments (10).

Like 1,1′-carbonyldipyrazole, compounds **1**, **2**, and **3** react with aldehydes and ketones, in the presence of catalytic amounts of cobalt(II) chloride, to yield dipyrazol-1-ylmethanes and CO_2 and SO_2 (eq. 2). However, whereas most

[2] $$(py)_2XO + R_2CO \rightarrow R_2C(py)_2 + XO_2$$

X = C or S
py = pyrazol-1-yl, 3-methylpyrazol-1-yl, or 3,5-dimethylpyrazol-1-yl

of the reactions of 1,1′-carbonyldipyrazole occur at room temperature, more vigorous conditions *viz.* 100–110° and 160–180°, are required with compounds **1** and **2**, respectively. Although the sulfinyl compound **3** reacts readily at room temperature, it is less reactive than the corresponding carbonyl compound as shown by the exclusive formation of carbon dioxide when acetone was allowed to compete for both reagents. It is noteworthy that Staab and Wendel (5) have reported the opposite reactivity order for the corresponding imidazole derivatives. The reactivity decrease in the series 1,1′-carbonyldipyrazole > **1** > **2** clearly indicates that both the 3- and the 5-methyl substituent are sterically active during the course of the reaction; unfortunately, one cannot deduce, from this evidence alone, the relative significance of steric effects on individual steps of the detailed reaction mechanism.

Bulky groups also influence the reactivity of the ketones. Thus, the catalytic reaction of 1,1′-carbonyldipyrazole with benzophenone only occurs at 190–200° to give diphenyldipyrazol-1-ylmethane (**12**); and 1,1′-carbonyldipyrazole condenses with itself at 190–200°, in the presence of cobalt(II) chloride, to yield tetrapyrazol-1-ylmethane (**13**) (eqs. 3 and 4). Neither reaction

[3] $$(py)_2CO + (C_6H_5)_2CO \xrightarrow[190\text{–}200^\circ]{CoCl_2} (py)_2C(C_6H_5)_2 + CO_2$$

[4] $$2(py)_2CO \xrightarrow[190\text{–}200^\circ]{CoCl_2} (py)_4C + CO_2$$

is observed in the absence of catalyst. Interestingly, 1,1′-carbonyldipyrazole reacts preferentially with benzophenone (eq. 3) rather than with itself (eq. 4) which is consistent with the general rule that resonance interactions of the type

$$>N-\overset{|}{C}=O \leftrightarrow >\overset{\oplus}{N}=\overset{|}{C}-\overset{\ominus}{O}$$

make the carbonyl carbon of an amide less electropositive, *i.e.*, less susceptible to nucleophilic attack than that of a ketone. In view of this fact, it is surprising indeed that 1,1′-carbonyldipyrazole reacts *at all* according to eq. 4; one may

Can. J. Chem. Downloaded from www.nrcresearchpress.com by 210.87.254.40 on 09/05/12
For personal use only.

attribute the enhanced reactivity of its carbonyl group, relative to simple amide systems, to a preferred delocalization of the nitrogen lone pair of electrons over the aromatic pyrazole ring, rather than over the three atoms forming the amide group. I.r. spectroscopic measurements (2) provide further support for this interpretation.

Our studies with 1,1′-carbonylbis(3,5-dimethylpyrazole) (**2**) indicate a dramatic limitation to the number of stable derivatives which may be obtained with ketones. Thus, acetone and cyclobutanone react at 160° in the established typical fashion, yielding 2,2-bis(3,5-dimethylpyrazol-1-yl)propane (**10**) and 1,1-bis(3,5-dimethylpyrazol-1-yl)cyclobutane (**11**), respectively. The comparable reactions with methyl ethyl ketone and with cyclohexanone, on the other hand, produce carbon dioxide, 3,5-dimethylpyrazole and unidentified oils which are presumably decomposition products of the desired 1,1′-alkylidene(3,5-dimethylpyrazoles). A study of models suggests several favorable conformations for **10** and **11**, respectively. However, models of the unknown 2,2-bis(3,5-dimethylpyrazol-1-yl)butane and 1,1-bis(3,5-dimethylpyrazol-1-yl)cyclohexane are sterically congested, locked structures; considerable interaction between the N-2 lone electron pair and the C-3 proton of the hydrocarbon moiety could lead to facile decomposition.

The authors wish to express their sincere thanks to Maki Belluce for technical assistance and to the National Research Council of Canada for financial support.

1. L. K. PETERSON and K. I. THE. Chem. Commun. 841 (1972).
2. K. I. THE and L. K. PETERSON. Can. J. Chem. **51**, 422 (1973).
3. H. A. STAAB. Justus Liebigs Ann. Chem. **622**, 31 (1959).
4. S. TROFIMENKO. J. Am. Chem. Soc. **92**, 5118 (1970).
5. H. A. STAAB and K. WENDEL. Justus Liebigs Ann. Chem. **694**, 86 (1966).
6. W. RIED and H. J. SCHUBERT. Justus Liebigs Ann. Chem. **653**, 181 (1962).
7. Q. MINGOIA. Gazz. Chim. Ital. **61**, 449 (1931).
8. K. V. AUWERS and H. STUHLMANN. Chem. Ber. **59B**, 1043 (1926).
9. H. A. STAAB. Angew. Chem. **74**, 407 (1962).
10. L. G. TENSMEYER and C. AINSWORTH. J. Org. Chem. **31**, 1878 (1966).

Can. J. Chem. Downloaded from www.nrcresearchpress.com by 210.87.254.40 on 09/05/12
For personal use only.

The Use of Polymer Supports in Organic Synthesis. II.[1] The Syntheses of Monoethers of Symmetrical Diols

JACK Y. WONG AND CLIFFORD C. LEZNOFF
Department of Chemistry, York University, Downsview, Ontario

Received January 25, 1973

An insoluble polymer support system was used as a unique method of blocking one functional group of a completely symmetrical difunctional compound. The monotetrahydropyranyl and monotrityl ethers of the symmetrical diols, HO—$(CH_2)_n$—OH, where n = 2, 4, 6, 8, and 10, were prepared. Reaction conditions for the preparation of the monotetrahydropyranyl ether of 1,10-decanediol were optimized.

Un système impliquant un support polymérique insoluble a été utilisé pour bloquer un groupe fonctionnel d'un composé difonctionnel complètement symétrique. Les éthers monotétrahydropyranylé et monotritylé des diols symétriques HO—$(CH_2)_n$—OH, où n = 2, 4, 6, 8, et 10, ont été préparés. Les conditions expérimentales pour la préparation de l'éther monotétrahydropyranylé du décanédiol-1,10 ont été optiminiséa. [Traduit par le journal]

Can. J. Chem., **51**, 2452 (1973)

Can. J. Chem. Downloaded from www.nrcresearchpress.com by 210.87.254.105 on 09/05/12
For personal use only.

The concept of using an insoluble polymer support as a selective blocking group of one functional group of a completely symmetrical difunctional compound was recently demonstrated (1). In this paper the syntheses of monotetrahydropyranyl and monotrityl ethers of the completely symmetrical diols, HO—$(CH_2)_n$—OH, where n = 2, 4, 6, 8, and 10 are described.

The commercially available Merrifield resin (2) (2% cross-linked polystyrene beads with 1.7 mmol of —CH_2Cl groups/g of resin, obtained from Schwarz/Mann) was modified, according to the procedure of Kusama and Hayatsu (3), to an insoluble polymer containing acid chloride groups, (P)—C_6H_4—CH_2COCl (**1**). The acid chloride **1** contained 0.8 mequiv. Cl/g of polymer as determined by the modified Vollhard procedure (4). Polymer **1** contains only one in six functionalized phenyl groups along the polymer chain and hence the acid chloride polymer **1** acts as a dilute reagent.

In a typical reaction sequence as outlined in Scheme 1, resin **1** and an excess of symmetrical diol, **2***a–e*, reacted in pyridine to give the resin, **3***a–e*, in which one of the alcohol groups was attached to the insoluble polymer through an ester linkage.[2] The unreacted excess diol can be readily recovered by simple filtration of this polymer. This reaction represents a selective blocking of one alcohol group of a completely symmetrical diol. The minimum amount of the diol attached to the polymer was determined by base hydrolysis of **3***a–e* to give back the starting diol. It is recognized that base hydrolysis of **3***a–e* could be incomplete even after long reaction times and hence the amount of diol obtained after base hydrolysis represents a minimum amount of diol attached to the polymer. The polymer **3***a–e* contained approximately 0.05–0.2 mmol of **2***a–e* per gram.

Reaction of resin esters **3***a–e* with trityl chloride in pyridine (5, 6) gave the resin trityl ether, **4***a–e*. Base hydrolysis of **4***a–e* gave the monotrityl ethers **5***a–e* in amounts ranging from 0.048 mmol of **5***e*/g of **4***e* to as much as 0.087 mmol of **5***a*/g of **4***a*. In addition, the acid polymer **6** was recovered.

The monotrityl ethers, **5***a–e*, were hydrolyzed with 80% acetic acid (5) to give trityl alcohol and the parent diols, **2***a–e*, in a 1:1 ratio. Elemental analysis and the mass spectral data of **5***a–e* were entirely consistent with the assigned structures. Ethers, **5***a–e* gave parent ions in their mass spectra. In addition, all spectra of **5***a–e* showed a base peak at m/e 243 resulting from the cleavage of the ethers and the formation of the bulky trityl cation. This mode of cleavage of bulky tertiary ethers is well documented (7). The i.r. spectra of **5***a–e* showed broad O—H absorption at 3450 cm^{-1} and

[1]For Part I, see ref. 1.

[2]The possibility exists that two adjacent phenyl rings are functionalized and hence both ends of the symmetrical diols, **2***a–e*, could attach themselves to the polymer. The use of a large excess of diol greatly diminishes the chance of this occurring.

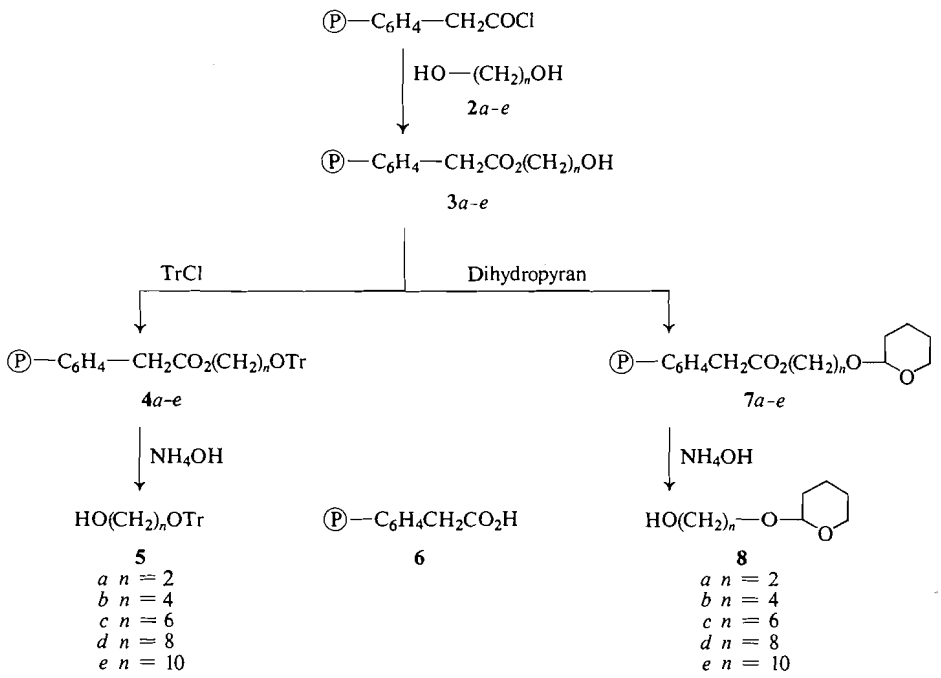

SCHEME 1

aromatic absorption at 1600 cm^{-1}. The i.r. spectra of **3***a–e* and **4***a–e* were uninformative.

The quantity of **5***a–e* from **3***a–e* was not as high as expected and it was suspected that the bulkiness of the trityl group was inhibiting the base hydrolysis of **4***a–e*. In an experiment designed to test this hypothesis resin **4***e* was treated with concentrated HCl in dioxane to give the diol **2***e* and trityl alcohol in 0.12 mmol/g of **4***e*. Thus the yield of the tritylation step is quite high and the moderate quantity of **5***e* obtained is likely due to the inefficiency of the base hydrolysis of **4***e*. The bulkiness of the trityl group may add to the inefficiency of the final base cleavage reaction resulting in decreased quantities of **5***a–e*. Thus some mono trityl ether remains attached to the polymer.

In an attempt to see if polymer **6** was reusable, **6** was converted back to the acid chloride **1**, by treatment with thionyl chloride, and the sequence of reactions repeated using 1,10-decanediol, **2***e*, as a model.

The quantity of **5***e* obtained from once used polymer was less than 50% of that obtained using fresh polymer **1** (see Experimental). The used polymer **6** was again converted to **1** and the sequence repeated a second time using alcohol **2***b*. The yield of **5***b* from twice used polymer was less than 25% of that obtained using fresh polymer **1**. If one considers that base hydrolysis of polymer **4***b* is incomplete because of the inefficiency of the base cleavage and perhaps the bulkiness of the trityl group, then it is reasonable to expect that the used polymer **6** has less carboxy groups liberated and hence available for subsequent reactions. It should also be noted that every subsequent recyclization of polymer **6** resulted in a browner polymer.

Thus, in the formation of monotrityl ethers the base cleavage of the ether from the polymer is incomplete resulting in lower yields and the polymer liberated is not highly suitable for regeneration as subsequent cycles result in even lower yields.

The polymer support synthesis of monotrityl ethers of symmetrical diols gave the monoethers in moderate quantities on a mole basis. In order to demonstrate the formation of monoethers of symmetrical diols in higher quantities on a mole basis, it was decided to synthesize the monotetrahydropyranyl ethers of the symmetrical diols **2***a–e*. The reduced steric requirements of the tetrahydropyranyl group as compared to the trityl group should result in higher yields of monoethers.

Reaction of resin **3***a–e* in anhydrous dioxane

Can. J. Chem. Downloaded from www.nrcresearchpress.com by 210.87.254.105 on 09/05/12
For personal use only.

Can. J. Chem. Downloaded from www.nrcresearchpress.com by 210.87.254.105 on 09/05/12
For personal use only.

with excess dihydropyran, anhydrous sodium sulfate and *m*-benzene-disulfonic acid as a catalyst gave, after 48 h at room temperature,[3] resin **7***a–e*. Subsequent base cleavage of **7***a–e* yielded resin **6** and **8***a–e* in quantities averaging 0.035 mmol/g of **7***a–e*.

The reaction of **3***a–e* with dihydropyran was incomplete as evidenced by the isolation of the parent diols, **2***a–e*, from the base cleavage of **7***a–e*. The monotetrahydropyranyl ethers, **8***a–e*, were separated from the parent diols, **2***a–e*, by preparative t.l.c. on alumina prepared from an aqueous slurry containing 1% sodium bicarbonate. T.l.c. on silica gel, even prepared with sodium bicarbonate always resulted in hydrolysis of **8***a–e* to **2***a–e* and dihydropyran. The pure tetrahydropyrans, **8***a–e* were rechromatographed on alumina containing 1% sodium bicarbonate and pure **8***a–e* showed no evidence of hydrolysis on this adsorbant system, thus showing that the starting diols obtained in the hydrolysis of **7***a–e* were, in fact, due to incomplete reaction of **3***a–e* and not due to hydrolysis of **8***a–e* in the work-up of the reaction.

The monotetrahydropyranyl ethers, **8***a–e*, were hydrolyzed on silica gel to give dihydropyran and the parent diols, **2***a–e*, in a 1:1 ratio. Elemental analysis and the mass spectral data of **8***a–e* were entirely consistent with the assigned structures. Ethers, **8***c–e* exhibited very weak parent ions in their mass spectra, while **8***a–b* showed no parent ions at all. In addition, however, **8***a–e* all exhibited the tetrahydropyranyl cation as the base peaks of the spectra. The weak parent ions and the formation of the tetrahydropyranyl cation is consistent with published data on the mass spectra of tetrahydropyranyl ethers (8).

The i.r. spectra of the monotetrahydropyranylethers **8***a–e* were almost identical to each other; and showed much broader absorptions at 3450 (O—H) and 1080 cm^{-1} (C—O—C) than the diols **2***a–e*. The i.r. spectra of **7***a–e* were uninformative and were not useful for characterization.

[3]The reaction of diols **2***a–e* with **1** to give **3***a–e* for the preparation of the trityl ethers, **5***a–e*, were conducted partially at higher temperatures (see Experimental). Although more diol became attached to the polymer at higher temperatures, it was felt that the more inaccessable functional groups reacted at these higher temperatures resulting in loss of starting material and deterioration of the polymer.

The resin **6** recovered from the hydrolysis of **7***a–e* was converted back to polymer **1**, by treatment with thionyl chloride, and the sequence of reactions leading to **8***e* was repeated. The quantity of **8***e* obtained from once-used polymer was only 50% of that obtained from the fresh polymer and hence polymer **6** generated from the hydrolysis of **7***a–e* is also not a very suitable regenerable polymer and exhibits similar characteristics to polymer **6** regenerated from the hydrolysis of **4***a–e*. Thus the inefficiencies of the base cleavage reaction of **4***a–e* and **7***a–e* and the deterioration of the polymer by $SOCl_2$[4] appear more responsible for the incomplete regeneration of **1** from **6** than the bulkiness of the trityl group of **4***a–e*. One of the drawbacks of organic synthesis on insoluble polymer support systems is the long reaction times involved in the various reactions on the insoluble polymer. It was thus decided to do a time study on the various reactions leading to the formation of **8***e* as a model system.

Polymer **1** was reacted with **2***e* at various times as shown in Table 1. Subsequent base cleavage of the product **3***e* for 48 h gave back the starting diol, **2***e*, in maximum yield for a reaction time of **1** with **2***e* of 48 h showing that for the initial attachment of the diol to the polymer, the standard time of reaction, 48 h, was optimum.

The reaction of **3***e* with dihydropyran for different times was performed. As shown in Table 2, reaction was essentially complete after 24 h instead of the standard reaction time of 48 h. In fact the yield of **8***e*, obtained after base hydrolysis of **7***e* was slightly lower for longer reaction times.

The effect of time on the base hydrolysis of **7***e* was next examined. As indicated in Table 3, base hydrolysis of **7***e* to yield **8***e* was complete after 48 h. Thus the standard conditions were best for the base cleavage step.

Thus a practical general method of synthesizing monotrityl and monotetrahydropyranyl ethers of symmetrical diols has been outlined.

The insoluble polymer support synthesis of monotrityl ethers of symmetrical diols is preferable to the synthesis of the monotetrahydropyranyl ethers of symmetrical diols as they are obtained in higher quantities, while the tetra-

[4]The polymer turns pale brown on treatment with $SOCl_2$.

Can. J. Chem. Downloaded from www.nrcresearchpress.com by 210.87.254.105 on 09/05/12
For personal use only.

TABLE 1. The effect of time on the reaction of **1** with **2***e*

Amount of **1** (g)	Time of reaction (h)	*Yield of **2***e* (g)
4.0230	1	0.0189
4.0631	10	0.0219
4.0781	24	0.0303
4.1162	48	0.0382

*Obtained by based hydrolysis of 3*e* for 48 h.

TABLE 2. The effect of time on the reaction of 3*e* with dihydropyran

Amount of 3*e* (g)	Time of reaction (h)	*Yield of **8***e* (g)
4.0244	2	0.0081
4.0707	10	0.0291
4.0166	24	0.0373
4.0266	48	0.0336

*Obtained by base hydrolysis of 7*e* for 48 h.

TABLE 3. The effect of time on the base cleavage of 7*a–e*

Amount of 7*e* (g)	Time of reaction (h)	Yield of **8***e* (g)
4.0968	1	0.0098
4.0971	24	0.0305
4.1009	48	0.0386
4.1148	72	0.0385

hydropyranyl ethers are always contaminated by starting diol which must be separated by preparative t.l.c.

The use of insoluble polymers as blocking groups of other symmetrical difunctional organic compounds is in progress using means other than the inefficient base hydrolysis of products from the insoluble polymer. The search for a more regenerable polymer is also under investigation.

Experimental

All melting points were determined on a Kofler hot stage and are uncorrected. The i.r. spectra were recorded on a Unicam SP1000 i.r. spectrophotometer using neat compounds or Nujol mulls. Mass spectra were recorded on a Hitachi-Perkin-Elmer RMU-6 mass spectrometer. Silica gel, and alumina, prepared with a 1% $NaHCO_3$ aqueous slurry, were used for thin and thick-layer chromatography. [Microanalyses were performed by Dr. C. Daessle of Montreal and G. Gygli of Toronto.

*Acid Chloride Resin **1***

The Merrifield resin (2) (2% cross-linked polystyrene beads having 1.7 mmol of $-CH_2Cl$ groups/g of resin was obtained from Schwarz/Mann and converted to **1** according to the procedure of Kusama and Hayatsu (3). Resin **1** contained 0.8 mmol Cl/g of polymer as determined by the modified Vollhard procedure (4).

Preparation of the Alcohol Resins, 3a–e

A typical example is given for the preparation of resin 3*e*. A suspension of 4.12 g of Ⓟ—C_6H_4—CH_2—COCl in 30 ml of anhydrous pyridine and 2.71 g of 1,10-decanediol, **2***e*, was stirred under exclusion of moisture ($CaCl_2$-tube) at room temperature for 24 h and at 100 °C for 24 h. The resin was collected by filtration and washed three times with pyridine, three times with pyridine–water (1:1), three times with water, three times with ethanol, and finally three times with ether.

Preparation of the Trityl Resins, 4a–e

A standard procedure is given for the synthesis of **4***e*. A mixture of 3.02 g of resin 3*e* and 2.0 g of chlorotriphenylmethane in 40 ml of anhydrous pyridine were stirred for 48 h at room temperature under exclusion of moisture ($CaCl_2$-tube). The resin was then collected by filtration and washed four times with pyridine, three times with pyridine–water (3:1), three times with pyridine–water (1:1), six times with water, three times with ethanol–water (1:1), once with acetone, three times with ethanol, and at least three times with dry ether.

Release of the Monotritylalcohols, 5a–e, from Resins 4a–e

In a standard procedure, 3.22 g of resin **4***e* was treated with 20 ml of a 1:1 mixture of dioxane and concentrated ammonia in a stoppered flask with magnetic stirring for 48 h. The resin was filtered and washed six times with water, once with acetone, three times with ethanol, and three times with ether. The aqueous filtrate was extracted with three aliquots of ether. The combined ether extracts were washed six times with water, dried over Na_2SO_4 and evaporated to give a slightly impure oil which was purified by preparative t.l.c. on silica gel (eluant 10% $CHCl_3$ – 90% C_6H_6) to give 0.0645 g of analytically pure **5***e* (see Table 4 for physical and mass spectra data on **5***a–e*). No starting diol **2***e* was detected.

Preparation of the Tetrahydropyranyl Ether Resins 7a–e

In a typical procedure, 4.01 g of resin 3*e* (prepared by reaction of **1** with **2***e* for 48 h at room temperature only) was suspended in 30 ml of anhydrous dioxane. Excess dihydropyran (5.00 g) and 0.10 g of *m*-benzenedisulfonic acid was added as a catalyst. To the mixture was added 2.00 g of anhydrous sodium sulfate to absorb liberated water and the reaction was stirred for 24 h under exclusion of moisture ($CaCl_2$-drying tube). The resin was filtered, neutralized with anhydrous pyridine (to prevent hydrolysis of the monopyranyl ether) and filtered twice. Then the resin was washed twice with pyridine–water (1:1), ten times with water (to remove sodium sulfate), three times with ethanol, and at least three times with dry ether.

Release of the Monotetrahydropyranyl Alcohols, 8a–e, from Resins 7a–e

A suspension of 4.01 g of resin 7*e* and 30 ml of a 1:1 mixture of dioxane and concentrated ammonium hydroxide was stirred for 48 h at room temperature. The resin was filtered and washed as before in the preparation of **5***a–e*. An identical work-up as before yielded an impure oil. Preparative t.l.c. on alumina prepared with a 1%

TABLE 4. Physical and mass spectral data of 1-*O*-trityl-1,*n*-alkanediols

Compound	M.p. (°C)	Yield (mmol/g polymer)	Analysis Found C	Analysis Found H	Analysis Calculated C	Analysis Calculated H	Mass spectra *m/e* M^+ (% of base peak)
$TrO(CH_2)_2OH$	95–96*	0.087	82.64	6.72	82.89	6.58	3.80
$TrO(CH_2)_4OH$	65–67	0.074†	83.17	7.51	83.13	7.23	2.31
$TrO(CH_2)_6OH$	68–69	0.085	83.31	7.89	83.33	7.78	0.59
$TrO(CH_2)_8OH$	oil	0.072	83.35	8.13	83.51	8.25	5.63
$TrO(CH_2)_{10}OH$	oil	0.048‡	83.30	8.64	83.65	8.65	6.87

*Literature 98–100° (6).
†From twice and thrice used polymer only 0.012 and 0.006 mmol/g of 4*b* respectively were obtained.
‡From once used polymer only 0.019 mmol/g of 4*e* were obtained.

TABLE 5. Physical and mass spectral data of 1-*O*-tetrahydropyranyl-1,*n*-alkanediols

Compound **8**	Yield (mmol/g polymer)	Analysis Found C	Analysis Found H	Analysis Calculated C	Analysis Calculated H	Mass spectra *m/e* M^+ (% of base peak)
a	0.034	57.27	9.44	57.53	9.59	0.00
b	0.027	62.30	10.65	62.07	10.34	0.00
c	0.036	65.35	10.89	65.54	10.92	0.15
d	0.034	67.83	11.30	67.43	11.61	0.35
e	0.036*	69.80	11.63	69.48	11.80	0.26

*From once used polymer only 0.017 mmol of 8*e*/g polymer 7*e* was obtained.

slurry of $NaHCO_3$, and using 2:3 benzene – petroleum ether gave 0.0373 g of analytically pure **8***e* and 0.0126 g of recovered **2***e*. (See Table 5 for physical and mass spectral data on **8***a–e*.)

Determination of the Amounts of Diols, 2a–e, on Resins 3a–e

A suspension of 4.11 g of resin **3***e* in a 1:1 mixture of dioxane and concentrated ammonium hydroxide was stirred at room temperature for 48 h. The resin was filtered and washed in the same manner as for the release of **8***e* from **7***e*. An identical work-up as before yielded 0.03 g of **2***e*.

Regeneration of Polymer 1 from Polymer 6

The acid resin **6** was treated with thionyl chloride in toluene and refluxed for 24 h with stirring according to Kusama and Hayatsu (3).

The authors wish to acknowledge the support of the National Research Council of Canada for a grant in aid of this research.

1. C. C. LEZNOFF and J. Y. WONG. Can. J. Chem. **50**, 2892 (1972).
2. R. B. MERRIFIELD. J. Am. Chem. Soc. **85**, 2149 (1963); R. B. MERRIFIELD. Sci. **150**, 178 (1965).
3. T. KUSAMA and H. HAYATSU. Chem. Pharm. Bull. **18**, 319 (1970).
4. J. M. STEWART and J. D. YOUNG. Solid phase peptide synthesis. W. H. Freeman, San Francisco. 1969. p. 27; P. B. HAWK, B. L. OSER, and W. H. SUMMERSON. Practical physiological chemistry. 13th ed. Blakiston, 1954. p. 955.
5. A. M. MICHELSON and A. R. TODD. J. Chem. Soc. 951 (1953); G. WEIMANN and H. G. KHORANA. J. Am. Chem. Soc. **84**, 419 (1962).
6. B. HELFERICH, P. E. SPEIDEL, and W. TOELDTE. Chem. Ber. **56**, 769 (1923).
7. H. BUDZIKIEWICZ, C. DJERASSI, and D. H. WILLIAMS. Mass spectrometry of organic compounds. Holden-Day Inc., San Francisco. 1967. p. 261.
8. H. BUDZIKIEWICZ. *In* Biochemical applications of mass spectroscopy. *Edited by* G. R. Walker. Wiley-Interscience, New York. 1972. p. 262.

Can. J. Chem. Downloaded from www.nrcresearchpress.com by 210.87.254.105 on 09/05/12
For personal use only.

Total Synthesis of Spirobenzylisoquinoline Alkaloids. Part III. (±)-Ochrobirine[1]

STEWART MCLEAN AND JOHN WHELAN
Department of Chemistry, University of Toronto, Toronto, Ontario
Received November 8, 1972

The route to spirobenzylisoquinoline alkaloids through a Pictet–Spengler cyclization of a suitable 1,2-indanedione has been modified, by the introduction of a 3-bromo substituent into the indanedione, with a view to providing a general synthesis of spirobenzylisoquinoline alkaloids bearing two oxygen functions on ring C. A highly stereoselective synthesis of (±)-ochrobirine has been achieved.

L'accès aux alcaloïdes du type spirobenzylisoquinoléine par une cyclisation selon Pictet–Spengler d'une indane dione-1,2 adéquate, a été modifié par l'introduction d'un substituant bromo-3 sur l'indanedione en vue d'obtenir une synthèse générale d'alcaloïdes spirobenzylisoquinoléine porteurs de deux fonctions oxygénées sur le cycle C. Une synthèse hautement stéréosélective de l'ochrobirine (±) a été réalisée.
[Traduit par le journal]

Can. J. Chem., **51**, 2457 (1973)

Can. J. Chem. Downloaded from www.nrcresearchpress.com by 210.87.254.5 on 09/05/12
For personal use only.

The term spirobenzylisoquinoline alkaloids has been applied to a group of alkaloids isolated from certain *Corydalis* and *Fumaria* species and having the skeleton shown in **1**. This structural class has been recognized for a relatively short time, and all members of it known at present can be described by structure **1** in which variations of substitution occur only in rings A and C (1). In ochotensimine (**1***a*) and ochotensine (**1***b*), the first members of this class to be recognized (2), ring C carries a single substituent, a methylene group at C-14; alkaloids with oxygen functions (at carbonyl or carbinol oxidation levels) at one or both of positions 9 and 14 have been described more recently. We reported in 1968 (3) the first total synthesis of a member of this class, (±)-ochotensimine, and since then the descriptions of several syntheses of this alkaloid, ochotensine, and some of the alkaloids with oxygen functions in ring C have appeared.

The synthetic plan of the majority of the successful syntheses of these alkaloids has been related to the one we used to synthesize ochotensimine: the condensation of an indanedione (such as **2**) with a phenylethylamine (such as **3**), each suitably substituted, followed by manipulation of the functionality of the intermediate to provide the target molecule. Ochrobirine (**1***c*) (4), for example, has been synthesized from the methylenedioxyindanetrione (**2** with C=O in place of C—X) and subsequent reduction of the dione intermediate (**4** with C=O in place of C—X) (5, 6); **1***c* is also an example of a spirobenzylisoquinoline alkaloid that has been synthesized by a different route proceeding, nevertheless, through the same dione intermediate (7). We recognized that our original synthetic plan could be developed into a general synthesis of those spirobenzylisoquinoline alkaloids with two oxygen functions on ring C if a suitable functional group could be introduced into position 3 of the indanedione precursor (**2**). In principle at least, this group (X), which could subsequently be converted into an oxygen function distinguishable from the aromatic ketone already present, would allow control to be maintained throughout the synthesis of both functionality and stereochemistry at the sites destined to be C-9 and -14 in the final product, and provide controlled routes to any of the target alkaloids.

We have found that the substituent X most suitable for this purpose is bromine and we have converted the methylenedioxyindanedione **2***a*, already available to us from our earlier work (3), to its monobromo derivative **2***b*. A Pictet–Spengler reaction of **2***b* with the dihydroxyphenylethylamine **3**, produced the spiro compound **4***a* which appears to be a single epimer and, although its stereochemistry is not proven at this stage, its subsequent fate can most readily be explained if it is the epimer shown in **5**.

The phenolic hydroxyl groups were protected by conversion to a mixed carbonate and the

[1]Taken from the Ph.D. Thesis of John Whelan, University of Toronto. References 3*a* and *b* constitute Parts I and II, respectively.

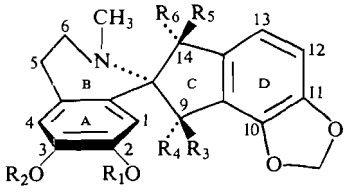

1

	R_1	R_2	R_3	R_4	R_5	R_6
a Ochotensimine	CH_3	CH_3	H	H	$=CH_2$	
b Ochotensine	CH_3	H	H	H	$=CH_2$	
c Ochrobirine	$-CH_2-$		H	OH	OH	H

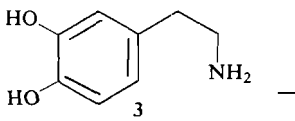

3

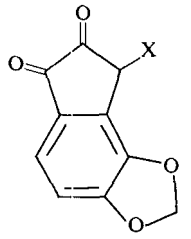

2

a X = H
b X = Br

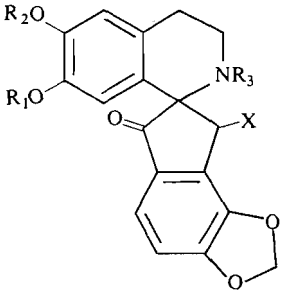

4

a $R_1 = R_2 = H; R_3 = H; X = Br$
b $R_1 = R_2 = CH_3OCO; R_3 = CHO; X = Br$
c $R_1 = R_2 = CH_3OCO; R_3 = CHO; X = OH$
d $R_1 + R_2 = CH_2; R_3 = CHO; X = OH$

nitrogen was then formylated with acetic–formic anhydride. The product **4***b* was treated with aqueous acetic acid containing silver acetate in order to replace the bromine with a hydroxyl group and form **4***c*. This reaction appears to have taken place with net inversion at the reaction site and produced the alcohol **4***c* with the same configuration at C-9 as ochrobirine (as illustrated in **6**). The alcohol **4***c* was protected as its tetrahydropyranyl ether and the protecting groups were removed from the catechol system, which was then methylenated to provide an intermediate possessing the methylenedioxybenzene moiety found in ochrobirine (**1***c*) and several other spirobenzylisoquinoline alkaloids.

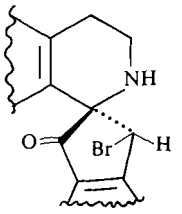

5

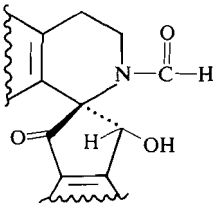

6

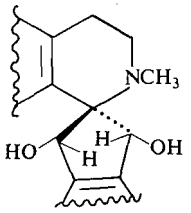

7

The alcohol function was regenerated by hydrolysis of the tetrahydropyranyl ether, the ketonic and amide carbonyl functions were reduced with lithium aluminum hydride, and (±)-ochrobirine (**1***c*) (the stereochemistry is illustrated by **7**) was isolated. This material formed crystals, m.p. 237–241°, identical in spectroscopic and t.l.c. characteristics with the authentic alkaloid; comment has been made previously (6, 7) on the variation in the values reported for the melting point of ochrobirine,

Can. J. Chem. Downloaded from www.nrcresearchpress.com by 210.87.254.5 on 09/05/12
For personal use only.

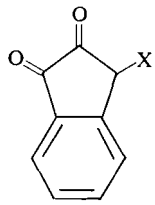

8

a X = H

b X = Br

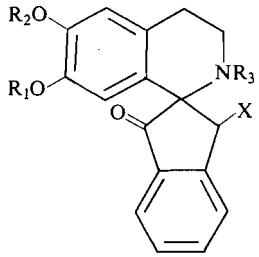

9

a $R_1 = R_2 = H; R_3 = H; X = Br$

b $R_1 = R_2 = CH_3OCO; R_3 = CHO; X = Br$

c $R_1 = R_2 = CH_3OCO; R_3 = CHO; X = OH$

d $R_1 + R_2 = CH_2; R_3 = CHO; X = OH$

and our value is in accord with that reported by Manske and coworkers (6).

This route was explored first starting with the unsubstituted parent 1,2-indanedione (**8***a*) because of its greater accessibility, and the details of the reactions in the exploratory model series and in the main series (leading to alkaloids) can conveniently be discussed together. The reaction sequence produced a series of highly functionalized intermediates, most of which were fairly unstable and resisted isolation and purification by standard procedures; none was obtained crystalline. It was, therefore, generally necessary to carry forward to the next step material in as pure a condition as could be obtained in the circumstances; in each case a reference sample was purified until it appeared to be homogeneous by t.l.c. (or a mixture of epimers in the case of tetrahydropyranyl ethers), and characterized by spectroscopic methods. Our description of the details of the reaction steps, including their stereochemical features, is based on these data, a reasonable expectation for the predictability of recognized processes, and the successful outcome of the synthetic sequence, which has led to an alkaloid of established structure and stereochemistry (4); consequently, this synthesis of **1***c* does not serve in the usual sense to confirm the structure and stereochemistry assigned to the alkaloid, instead the assignments made to the alkaloid show the most probable course, particularly with respect to stereochemistry, followed by the synthesis.

Monobromination of the indanedione **8***a* under controlled conditions provided an excellent yield of **8***b*; care was required to prevent dibromination and other unwanted reactions from occurring, and the methylenedioxy derivative (**2***a*) appeared to be even more sensitive to the reaction conditions, but essentially quantitative conversion could be achieved under the correct conditions. The Pictet–Spengler reaction of **8***b* with the hydrochloride of dihydroxyphenylethylamine **3** provided the spiro compound **9***a* in good yield (50%); in the main series the yield of **4***a* was even better (>70%). In both series the appearance in the n.m.r. spectrum of a single peak in the range characteristic of the proton at the C-Br position pointed to the production of a single epimer at C-9. The bromo ketones were readily degraded by base, but the bromine resisted displacement under a wide range of conditions that used external nucleophiles that were not strong bases. Attempts to introduce an oxygen function directly at an earlier stage by acetoxylation of **8***a* did not lead to the desired isomer. We turned, therefore, to an approach which would introduce a substituent capable of providing intramolecular assistance in the displacement of the bromine. To this end the *N*-formyl derivative **9***b* was prepared by the action of acetic–formic anhydride on the derivative of **9***a* in which the phenolic hydroxyl groups had been protected as mixed carbonates; these conversions were carried out in excellent yields both in the model series and in the main series where **4***b* was obtained. Treatment of **9***b* with silver acetate in hot aqueous acetic acid now led to a clean replacement of the bromine by a hydroxyl group. It seems probable, therefore, that the *N*-formyl group has served, as intended, to provide intramolecular assistance in the displacement of the bromine (8), and this appears to be possible only when these groups have the *trans*-relationship depicted in **5**; furthermore, the solvolysis must then have taken place with net inversion of configuration at C-9 since parallel results were obtained (with a yield of 90% under slightly milder solvolysis conditions) in the main series and the product obtained (**4***c*) can be assigned the *cis*-configuration shown in **6** because it led ultimately, under conditions where no further stereochemical change at C-9 would be expected, to ochrobirine, which has been assigned this configuration at C-9 (4).

Careful basic hydrolysis of the carbonate **9***c* regenerated the catechol in ring A and this was methylenated by treatment with methylene iodide and base in dimethylformamide in the

Can. J. Chem. Downloaded from www.nrcresearchpress.com by 210.87.254.5 on 09/05/12
For personal use only.

Can. J. Chem. Downloaded from www.nrcresearchpress.com by 210.87.254.5 on 09/05/12
For personal use only.

presence of a copper catalyst (3, 9). An acceptable but not good yield of the desired methylenedioxybenzene derivative (**9***d*) was obtained, but several by-products were also isolated; in the main series the situation was even worse and the yield of desired product (15%) from **4***c* was considered to be unacceptably low. Since it appeared probable that the β-hydroxy ketone of ring C was largely responsible for the difficulty encountered in the methylenation reaction, in the main series the hydroxyl function was protected as its tetrahydropyranyl derivative prior to methylenation. The methylenation reaction was now highly successful and an excellent yield of the methylenedioxy compound was obtained. (Spectroscopic evidence indicated that the tetrahydropyranyl derivatives existed as pairs of epimers differing in configuration in the tetrahydropyran ring; this was of no consequence with respect to the development of the stereochemistry of the alkaloidal skeleton.) We have commented previously (3) on the desirability of carrying out the formation of a methylenedioxybenzene moiety early in a synthesis and before sensitive functional groups are present because of the vigorous conditions required to effect methylenation of a catechol; in the present synthesis, however, the activated phenolic character of **3** was required to obtain an acceptable yield of product in the Pictet–Spengler step, and the recent description of a relatively mild methylenation reaction (8) was of critical value to our synthetic plan.

In the model series, after the formyl group had been removed by hydrolysis, it was found that the presence of the hydroxyl group prevented successful completion of the Eschweiler–Clarke *N*-methylation reaction. Consequently, in the main series hydrolysis was carried out under conditions that removed only the tetrahydropyranyl group and formed **4***d* (the sequence from **4***c* was carried out with an over-all yield greater than 85%), and both the ketone and the amide carbonyl groups were reduced by addition of lithium aluminum hydride. (±)-Ochrobirine (**1***c*) uncontaminated by the epimeric diol was obtained (in 53% yield); the stereoselectivity of this reduction is most readily attributed, as has been proposed by others (5, 6), to internal delivery of hydride to the carbonyl group at C-14 from an aluminum hydride complex formed first at the C-9 hydroxyl group. Under the conditions we used some *N*-demethylochrobirine was also isolated, resulting from reductive removal of the *N*-formyl group by the lithium aluminum hydride; however, this yielded further (±)-ochrobirine (19% from **4***d*) on re-formylation and lithium aluminum hydride reduction.

Experimental

Melting points were determined on a Thomas-Kofler micro hot stage. Spectrometers used were a Perkin–Elmer 237B or 257 for i.r. spectra, a Unicam SP800 for u.v. spectra, a Varian T-60 for n.m.r. spectra, a CEC 21-490 for mass spectra, and an AEI MS-902 for accurate mass measurements. Unless otherwise indicated, chloroform solutions were used to obtain i.r. spectra and the wavelengths of significant absorptions are reported in μ, and chloroform-*d* solutions (with tetramethylsilane as internal standard) were used to obtain n.m.r. spectra and chemical shifts are reported on the τ scale followed in parentheses with an indication of the multiplicity of the signal (singlet, doublet, etc. are abbreviated to their initial letters) and the number of protons associated with it. Since the intermediates obtained were non-crystalline and generally unstable, they could not be characterized by microanalysis; some were too unstable to provide satisfactory mass spectra, the parent-molecule ion frequently being absent and ions indicative of thermal degradations being present, but the *m/e* values of the more abundant ions (followed in parentheses by an indication of their relative abundance) and the accurate mass measurements of certain significant ions are reported for key intermediates where these values could be obtained.

*The 3-Bromo-1,2-indanediones (**8***b*, **2***b*)

(a) Model Series

Pyridinium bromide perbromide (800 mg; 2.5 mmol) was added to a solution of 1,2-indanedione (3) (290 mg; 2.0 mmol) in 25 ml of glacial acetic acid and the mixture was heated on a steam bath with vigorous swirling. As soon as the red color faded (5–10 min), the reaction mixture was poured into 400 ml of ice-water and thoroughly extracted with methylene chloride. The extract, after it had been washed with water until neutral, afforded 3-bromo-1,2-indanedione (**8***b*) (390 mg; 1.7 mmol) as an unstable amber oil. Spectroscopic characteristics: i.r. 5.64, 5.77; n.m.r. 1.8–2.4 (complex; 4), 4.34 (s; 1); mass spectrum 226, 224 (equal intensity; mol. ions corresponding to $C_9H_5BrO_2$).

(b) Methylenedioxy Series

4,5-Methylenedioxy-1,2-indanedione (3) (190 mg; 1.0 mmol) was brominated with pyridinium bromide perbromide (400 mg; 1.25 mmol) under the same conditions, and the bromo derivative **2***b* (280 mg; 1.0 mmol) was obtained as an unstable amber oil. Spectroscopic characteristics: i.r. 5.65, 5.81; n.m.r. 2.65 (AB q, J = 8 Hz, int. chem. shift 33 Hz; 2), 3.67 (narrow m; 2), 4.46 (s; 1).

The Spiro Skeletons (Pictet–Spengler Cyclization)

(a) Model Series

A mixture of the bromo dione **8***b* (390 mg; 1.7 mmol) and β-(3,4-dihydroxphenyl)ethylamine hydrochloride (429 mg; 2.25 mmol) in 30 ml of absolute ethanol was heated at 68–70° with vigorous stirring under nitrogen

Can. J. Chem. Downloaded from www.nrcresearchpress.com by 210.87.254.5 on 09/05/12
For personal use only.

for 24.5 h. The reaction mixture was cooled, diluted with 250 ml of 3% hydrochloric acid, and extracted with methylene chloride. The aqueous solution was cooled to 0°, very carefully neutralized (to Fisher short range Alkacid ribbon) by the addition of solid sodium bicarbonate, and thoroughly extracted with methylene chloride. This extract afforded the bromospiroisoquinoline **9***a* (300 mg; 0.83 mmol) as a dark unstable oil. Spectroscopic characteristics: i.r. 2.75, 2.81, 3.05 (broad), 5.80; n.m.r. ($CDCl_3$–CH_3OD): 1.9–2.8 (complex; 4), 3.29 (s; 1), 3.95 (s; 1), 4.24 (s; 1) (remainder of the spectrum obscured by solvent).

Methyl chloroformate (*ca.* 2.4 mmol) was added dropwise to a stirred solution of **9***a* (300 mg; 0.83 mmol) in 25 ml of pyridine cooled to 0°. The reaction mixture was allowed to warm up to room temperature and stirring was continued for 20 h. Solvent was removed by vacuum distillation at room temperature, and the residue was taken up in methylene chloride, washed with water, and recovered in the usual manner as an amber oil (i.r. 5.65, 5.79).

This intermediate was redissolved in 10 ml of methylene chloride cooled to 0°, and 1 ml of acetic–formic anhydride was added dropwise to the stirred solution. The solution was allowed to warm up to room temperature and stirring was continued for 20 h. Solvent was removed at reduced pressure, the residue was dissolved in methylene chloride which, after it had been washed with water, afforded the formylated product **9***b* (382 mg; 0.76 mmol) as an amber oil. Spectroscopic characteristics: i.r. 5.63, 5.77, 5.96; n.m.r. 1.76 (s; 1), 1.9–2.6 (complex; 4), 2.78 (s; 1), 3.49 (s; 1), 4.38 (s; 1), 6.10 (s; 3), 6.20 (s; 3), 5.6–7.2 (complex; 4).

(b) Methylenedioxy Series

3-Bromo-4,5-methylenedioxy-1,2-indanedione (**2***b*) (280 mg; 1.0 mmol) and β-(3,4-dihydroxyphenyl)ethylamine hydrochloride (221 mg; 1.16 mmol) in 15 ml of absolute ethanol formed, under the conditions described above, the spiro compound **4***a* (286 mg; 0.71 mmol) which was isolated as an unstable yellow solid. (N.m.r. ($CDCl_3$–CH_3OD): 2.66 (AB q, J = 8 Hz, int. chem. shift 26 Hz; 2), 3.38 (s; 1), 3.76 (narrow m; 2), 4.00 (s; 1), 4.39 (s; 1) remainder of spectrum obscured by solvent.) This intermediate was immediately treated with methyl chloroformate and then acetic–formic anhydride under the conditions used in the model series, and the intermediate **4***b* (322 mg; 0.58 mmol) was isolated as an amber foam. Spectroscopic characteristics: i.r. 5.64, 5.79, 5.96; n.m.r. 1.78 (s; 1), 2.75 (AB q, J = 8 Hz, int. chem. shift 30 Hz), 2.81 (s; 1), 3.47 (s; 1), 3.85 (narrow m; 2), 4.43 (s; 1), 6.16 (s; 3), 6.22 (s; 3), 5.8–7.2 (complex; 4); mass spectrum 468(3), 364(10), 350(30), 349(100), 348(29), 334(13), 305(13), 293(15), 277(27), 276(28), 248(20), 220(14), 191(19), 190(20), 177(16), 164(17), 163(22), 123(14), 117(17); mass measurements 468.09020 (P-Br, $C_{23}H_{18}O_{10}N$, 468.09307), 349.05639 ($C_{16}H_{13}O_9$, 349.05596; $C_{19}H_{11}O_6N$, 349.05864).

Displacement of Bromine

(a) Model Series

Silver acetate (490 mg; 3.0 mmol) was added to a solution of the protected bromo spiro compound **9***b* (382 mg; 0.75 mmol) in 25 ml of 90% aqueous acetic acid, and the mixture was vigorously stirred at 100–105° under nitrogen with exclusion of light for 10 h. The reaction mixture was cooled, diluted with 400 ml of ice-water, and thoroughly extracted with methylene chloride. The extract, after it had been washed with water, afforded the hydroxy compound **9***c* (200 mg; 0.45 mmol) as an amber oil. Spectroscopic characteristics: i.r. 5.63, 5.77, 6.03; n.m.r. ($CDCl_3$–CH_3OD) 1.76 (s; 1), 2.0–2.6 (complex; 4), 2.80 (s; 1), 3.62 (s; 1), 4.80 (s; 1), 6.10 (s; 3), 6.21 (s; 3) (remainder of spectrum obscured by solvent).

(b) Methylenedioxy Series

The same reaction was carried out with **4***b* (254 mg; 0.59 mmol), carrying the methylenedioxy group in ring D, and the hydroxy compound **4***c* (210 mg; 0.53 mmol) was isolated as a brown solid after a reaction time of 8 h. Spectroscopic characteristics: i.r. 5.64, 5.79, 6.03; n.m.r. 1.78 (s; 1), 2.78 (AB q, J = 8 Hz, int. chem. shift 28 Hz; 2), 2.82 (s; 1), 3.55 (s; 1), 3.86 (narrow m; 2), 4.78 (broadened s, sharpened on addition of D_2O; 1), 6.12 (s; 3), 6.18 (s; 3), 5.8–7.4 (complex; 4); mass spectrum 467(37), 440(40), 439(57), 424(34), 412(36), 380(38), 366(34), 350(75), 349(91), 336(65), 334(74), 322(100), 321(62), 320(35), 293(46), 279(47), 277(72), 262(46), 249(32), 222(34), 221(36), 220(55), 219(40), 192(37), 191(47), 190(38), 178(38), 177(72), 165(47), 163(90), 151(35), 137(42); mass measurements 467.08433 (P-H_2O, $C_{23}H_{17}O_{10}N$, 467.08525), 349.05606 ($C_{16}H_{13}O_9$, 349.05596; $C_{19}H_{11}O_6N$, 349.05864), 322.07087 ($C_{18}H_{12}O_5N$, 322.07154).

Methylenation

The hydroxy compound **4***c* (146 mg; 0.30 mmol) in 5 ml of dry methylene chloride was refluxed with 0.04 ml of dihydropyran and a trace of *p*-toluenesulfonic acid for 1.5 h under nitrogen. The mixture of epimeric tetrahydropyranyl derivatives (182 mg), which showed two spots on t.l.c., was isolated in the usual manner, and then dissolved in 15 ml of methanol. A solution of sodium bicarbonate (100 mg; 1.2 mmol) in 10 ml of water was added over a period of 10 min to the stirred methanol solution, which was kept at room temperature and under nitrogen. After a further 4 h, the solution was diluted with 150 ml of water and extracted with methylene chloride. The phenolic material (128 mg) obtained from the extract was dissolved in 30 ml of dimethylformamide containing methylene iodide (50 mg; 1.8 mmol), potassium carbonate (300 mg; 2.3 mmol), and cupric oxide (200 mg). The reaction mixture was blanketed with nitrogen, stirred vigorously, and heated to 120–125° for 1.5 h. It was then cooled, diluted with 350 ml of ice-water, and thoroughly extracted with methylene chloride. The extract afforded a residue (129 mg), a mixture of epimeric tetrahydropyranyl derivatives, which was dissolved in 12 ml of 0.5 *N* hydrochloric acid; the reaction mixture was stirred at room temperature under nitrogen for 2.5 h, diluted with 200 ml of water and thoroughly extracted with methylene chloride. After it had been washed with water, the extract was evaporated and the methylenedioxy compound **4***d* (100 mg; 0.26 mmol) was obtained as an amber solid. Spectroscopic characteristics: i.r. 5.81, 6.05; n.m.r. 1.70 (s; 1), 2.74 (AB q, J = 8 Hz, int. chem. shift 29 Hz; 2), 3.34 (s; 1), 3.80 (s; 2), 3.95 (s; 1), 4.13 (narrow m; 2), 4.78 (broadened s, sharpened on addition of D_2O; 1), 5.6–7.5 (complex; 4).

(±)-Ochrobirine

Lithium aluminum hydride (0.35 mmol) as an 0.05 *M*

solution in ether was added dropwise to a stirred solution of the keto amide **4***d* (32 mg; 0.084 mmol) in 40 ml of dry tetrahydrofuran at 0° under nitrogen. Stirring was continued for a further 2.5 h while the reaction mixture was allowed to warm up to room temperature; solid lithium aluminum hydride (30 mg; 0.8 mmol) was then added and the solution was refluxed for 30 min. The solution was cooled to 0°, and excess lithium aluminum hydride was carefully decomposed by dropwise addition of cold 5% hydrochloric acid. The solution was diluted with 25 ml of water, made basic with solid sodium bicarbonate, and thoroughly extracted with methylene chloride. After it had been washed with water, the extract afforded a residue which was subjected to preparative layer chromatography on silica gel G with elution by 85:14:1 methylene chloride – methanol – concentrated ammonium hydroxide. This provided (±)-ochrobirine (16 mg; 0.044 mmol) and its *N*-demethyl analog (8 mg; 0.022 mmol). The latter was *N*-formylated under the conditions described above, and then reduced with lithium aluminum hydride (15 mg; 0.40 mmol) in refluxing tetrahydrofuran to provide a further supply of (±)-ochrobirine (6 mg; 0.016 mmol). The (±)-ochrobirine was recrystallized from acetone–hexane and obtained as cream-colored prisms, m.p. 237–241° (lit. 235 (6), 210–212 (7), 185–187° (5)). The t.l.c. behavior (three systems) and n.m.r., i.r., u.v., and mass spectra were identical to those of an authentic sample of the alkaloid and the spectroscopic values corresponded to those reported (5–7) for natural and synthetic materials.

We thank the National Research Council of Canada for financial support of this work; fellowship support to J. Whelan from his source and from Kodak Canada Ltd., is also gratefully acknowledged. Professor D. B. MacLean of McMaster University provided friendly encouragement and the reference samples and spectra.

1. S. McLean and J. Whelan. MTP international review of science. Organic chemistry series I. Vol. IX. *Edited by* K. Wiesner. Butterworths, London, 1972. Chapt. 5. M. Shamma. The alkaloids. *Edited by* R. H. F. Manske. Vol. XIII. Academic Press, New York, 1971. p. 165.
2. S. McLean and M.-S. Lin. Tetrahedron Lett. 3819 (1964). S. McLean, M.-S. Lin, and R. H. F. Manske. Can. J. Chem. **44**, 2449 (1966).
3. (*a*) S. McLean, M.-S. Lin, and J. Whelan. Tetrahedron Lett. 2425 (1968). (*b*) S. McLean, M.-S. Lin, and J. Whelan. Can. J. Chem. **48**, 948 (1970).
4. R. H. F. Manske, R. G. A. Rodrigo, D. B. MacLean, D. E. F. Gracey, and J. K. Saunders. Can. J. Chem. **47**, 3589 (1969).
5. T. Kametani, S. Hibino, and S. Takano. Chem. Commun. 925 (1971); J. Chem. Soc. Perkin I, 391 (1972).
6. B. Nalliah, Q. A. Ahmed, R. H. F. Manske, and R. Rodrigo. Can. J. Chem. **50**, 1819 (1972).
7. N. E. Cundasawmy and D. B. MacLean. Can. J. Chem. **50**, 3028 (1972).
8. C. U. Pittman, S. P. McManus, and J. W. Larsen. Chem. Revs. **72**, 357 (1972).
9. M. Tomita and Y. Aoyagi. Chem. Pharm. Bull. (Japan), **16**, 523 (1968).

Can. J. Chem. Downloaded from www.nrcresearchpress.com by 210.87.254.5 on 09/05/12
For personal use only.

The Cumulative Acceleration by Methyl Substituents on the Rate of Addition of 4-Chlorobenzenesulfenyl Chloride to Olefins[1]

GEORGE H. SCHMID AND DENNIS G. GARRATT

Department of Chemistry, University of Toronto, Toronto, Ontario M5S 1A1

Received February 22, 1973

The rate of addition of 4-chlorobenzenesulfenyl chloride to ethylene and all six of its methylated derivatives has been measured in 1,1,2,2-tetrachloroethane at 25° by means of the stopped flow and a competitive technique. A plot of log k_{rel} *vs.* the number of methyl groups on the carbon–carbon double bond is linear. This establishes that the methyl groups have a cumulative acceleration on the rate contrary to previous reports. The use of the competitive method of obtaining rates of arenesulfenyl chloride additions to olefins suffers from the fact that thermodynamically rather than kinetically controlled product mixtures are often formed.

La vitesse d'addition du chlorure de chloro-4 benzènesulfènyle sur l'éthylène et ses six dérivés méthylés, a été mesurée dans le tétrachloro-1,1,2,2 éthane à 25° par les techniques de compétition et de flux bloqué. Le tracé du log k_{rel} en fonction du nombre de groupes méthyle sur la double liaison carbone–carbone est une droite; ceci montre que les groupes méthyle ont un effet d'accélération cumulatif sur la vitesse contrairement aux publications antérieures. L'utilisation de la méthode compétitive dans l'obtention des vitesses d'addition des chlorures d'arène sulfényle pêche par la fait que les produits thermodynamiques se forment souvent de préférence aux produits cinétiques. [Traduit par le journal]

Can. J. Chem., **51**, 2463 (1973)

Introduction

The fact that methyl substituents on a carbon–carbon double bond have a cumulative acceleration on the rates of electrophilic addition for reactions in which a bridged intermediate is involved in their mechanism was first pointed out by Bartlett and Sargent (2). Such a substituent effect has been observed in the epoxidation of olefins by peracetic acid (3) and the ionic bromination (4) and chlorination (5) of olefins.

A very different effect of methyl substitution is observed in the acid-catalyzed hydration of simple alkenes where the rate-determining step is the addition of a proton to the double bond to form an open carbonium ion, with resultant concentration of charge upon *one* of the carbon atoms of the double bond (6). Thus an olefin such as isobutylene, which can form a tertiary carbonium ion, reacts at least 1000 times faster than propylene which can form only a secondary carbonium ion. Further substitution of methyl groups at the less methylated end of the double bond produces no increase in the hydration rate of the compound. Consequently no cumulative acceleration by methyl substitution is found for a reaction in which an open ion is involved in its reaction mechanism.

[1]Reaction of Sulfenyl Chlorides and their Derivatives. VIII. For Part VII, see ref. 1.

The mechanism of the addition of alkane and arene sulfenyl chlorides to olefins is known to involve a bridged episulfonium ion (7). Consequently the rate of this addition reaction should exhibit such cumulative acceleration by methyl substitution. Thaler (8) found that the relative rates of addition of methanesulfenyl chloride to a series of olefins obtained using a competition technique do not show such a cumulative effect. Beverly and Hogg (9) on the other hand have found that the rate of addition of 2,4-dinitrobenzenesulfenyl chloride to a number of olefins gives a linear Taft plot.

We wish to report experimental results which will reconcile the results of Thaler and Hogg.

Results

We have measured the rate of addition of 4-chlorobenzenesulfenyl chloride to ethylene (**1**) and all its methylated derivatives (**2**–**7**) in 1,1,2,2-tetrachloroethane (TCE) at 25 °C by means of the stopped flow technique using a Durrum–Gibson stopped-flow spectrophotometer. The rate of disappearance of 4-chlorobenzenesulfenyl chloride was followed by measuring the decrease in its absorption at 392.5 nm. The addition was found to exhibit normal second order kinetics, first order in olefin and first order in sulfenyl chloride to 80% completion of the reaction. The rate data are presented in Table 1.

Can. J. Chem. Downloaded from www.nrcresearchpress.com by 210.87.254.6 on 09/05/12
For personal use only.

TABLE 1. The specific rate constants for the addition of 4-chlorobenzenesulfenyl chloride to a series of methyl substituted ethylenes in tetrachloroethane at 25°

Compound	No. of methyl groups	k_2 (M^{-1} s^{-1})	k_{rel}	No. of runs
Ethylene (**1**)	0	65.1 ± 3.0	1.0	8
Propene (**2**)	1	205 ± 18	3.14	6
cis-2-Butene (**3**)	2	1340 ± 100	20.6	16
trans-2-Butene (**4**)	2	434 ± 13	6.66	11
Isobutylene (**5**)	2	551 ± 50	8.46	6
2-Methyl-2-butene (**6**)	3	3030 ± 210	46.5	25
2,3-Dimethyl-2-butene (7)	4	7760 ± 540	119	30

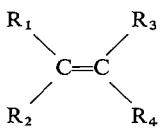

	R_1	R_2	R_3	R_4
1	H	H	H	H
2	CH_3	H	H	H
3	CH_3	H	CH_3	H
4	CH_3	H	H	CH_3
5	CH_3	CH_3	H	H
6	CH_3	CH_3	CH_3	H
7	CH_3	CH_3	CH_3	CH_3

We have also determined the relative rates by means of competition experiments using 4-chlorobenzenesulfenyl chloride rather than methanesulfenyl chloride used by Thaler. Using this method, equimolar excesses of two olefins were allowed to react with an inadequate supply of 4-chlorobenzenesulfenyl chloride. The product composition was determined by g.l.c. as well as n.m.r. and was found to vary with time. When the product composition was determined immediately after mixing, the product ratios so obtained were identical within experimental error to the values obtained by means of the stopped flow technique. If the reaction mixture was allowed to stand at 25° for as long as several days an equilibrium mixture was finally obtained. These data are given in Table 2.

TABLE 2. Product composition under kinetic and thermodynamic control of the addition of 4-chlorobenzenesulfenyl chloride to a series of methyl substituted ethylenes in tetrachloroethane at 25°

Compound	Product composition		k_{rel}*
	Initial	Equilibrium	
Ethylene (**1**)	1.0	1.0	1.0
Propene (**2**)	3.0	0.8	3.14
cis-2-Butene (**3**)	21	7.3	20.6
trans-2-Butene (**4**)	6.7	2.6	6.66
Isobutylene (**5**)	8.5	1.18	8.46
2-Methyl-2-butene (**6**)	46.4	9.11	46.5
2,3-Dimethyl-2-butene (7)	120	7.47	119

*Determined by stopped flow technique.

Discussion

From the data in Table 1, it is clear that there is a corresponding increase in the rate of addition of 4-chlorobenzenesulfenyl chloride with an increase in the number of methyl groups on the olefin. The cumulative nature of this increase is illustrated in Fig. 1 in which the log k_{rel} for addition of bromine, chlorine, and 4-chlorobenzenesulfenyl chloride is plotted against the number of methyl groups on the double bond. These data for the addition of 4-chlorobenzenesulfenyl chloride are clearly consistent with the findings of Hogg as well as our expectations regarding the mechanism of arenesulfenyl chloride addition to olefins but are contrary to the findings of Thaler.

The data in Table 2 explain why the results of Thaler do not appear to be consistent with the data in Table 1. The product composition depends upon whether the experiment is carried out under conditions of kinetic or thermodynamic control. The results of Thaler using the competition technique appear to have been obtained under conditions of thermodynamic

Can. J. Chem. Downloaded from www.nrcresearchpress.com by 210.87.254.6 on 09/05/12
For personal use only.

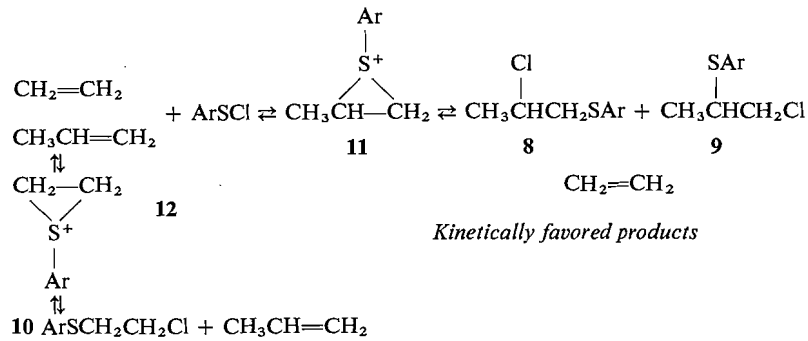

SCHEME 1

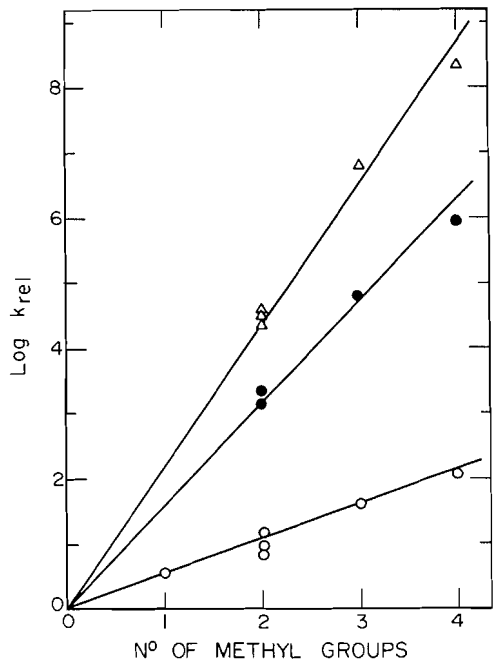

FIG. 1. Cumulative effect of methyl groups on chlorination Δ, bromination ●, and arenesulfenation ○.

rather than kinetic control. Considerable evidence has been presented that the kinetically controlled adducts, formed from the addition of alkane and arenesulfenyl chlorides, can undergo isomerization (10) under conditions of thermodynamic control. Such *anti*-Markownikoff isomerization is occurring in this system and can be detected by n.m.r. The initial and final product compositions for the additions where such

TABLE 3. Product composition of addition of 4-chlorobenzenesulfenyl chloride to unsymmetric alkenes **2**, **5**, and **6** in 1,1,2,2-tetrachloroethane at 25°

	Initial product composition		Final product composition	
Alkene	M*	aM*	M*	aM*
Propene (**2**)	61.8	38.2	31.7	68.3
Isobutylene (**5**)	11.7	88.3	94.5	5.5
2-Methyl-2-butene (**6**)	35.0	65.0	92.0	8.0

*M = Markownikoff; aM = anti-Markownikoff.

isomerization can be detected are given in Table 3. Furthermore it has recently been reported (11) that an exchange of arenesulfenyl chloride can occur between an adduct and an olefin. This too occurs under the conditions of the competition experiment. Thus our results, as well as those of Thaler can be explained in the following way. Addition of 4-chlorobenzenesulfenyl chloride to an equimolar excess of ethylene and propene will give initially a mixture of products containing predominently the propene adducts **8** and **9** since they are the kinetically favored products. With time an exchange will occur to form an equilibrium mixture of adducts **8**, **9**, and **10** containing predominently **10**. As previously noted this exchange most likely occurs by reformation of the episulfonium ions **11** and **12** as illustrated in Scheme 1. The adducts of 4-chlorobenzenesulfenyl chloride undergo exchange slowly enough that we can observe the kinetically controlled product distribution in the competition experiments as well as equilibration to the

Can. J. Chem. Downloaded from www.nrcresearchpress.com by 210.87.254.6 on 09/05/12
For personal use only.

TABLE 4. Physical properties and chemical analysis for adducts of 4-chlorobenzenesulfenyl chloride to olefins **1–7**

Olefin	M.p. or b.p. (°C)	%C		%H		%S	
		Calcd.	Found	Calcd.	Found	Calcd.	Found
Ethylene (**1**)	27–28	46.39	46.32	3.89	4.04	15.48	15.50
Propene (**2**)	97–98/10μ	48.88	49.17	4.56	4.70	14.50	14.56
cis-2-Butene (**3**)	dec.	51.07	51.29	5.14	5.21	13.63	13.79
trans-2-Butene (**4**)	dec.	51.07	51.07	5.14	5.07	13.63	13.75
Isobutylene (**5**)	78.5–79/20μ	51.07	51.39	5.14	5.07	13.63	13.81
2-Methyl-2-butene (**6**)	76/10μ (dec.)	53.02	53.01	5.66	5.54	12.87	12.78
2,3-Dimethyl-2-butene (**7**)	89/10μ (dec.)	54.76	54.47	6.12	6.15	12.18	12.38

thermodynamic product distribution. Use of methanesulfenyl chloride rather than 4-chlorobenzenesulfenyl chloride would be expected to accelerate the exchange reaction and as a result the observed product distribution would not be that of kinetic control. To support this view, we have found that the equilibrium for exchange between 2-chloropropyl methyl sulfide and isobutylene is established within 1 h at room temperature in *n*-heptane. Clearly exchange was occurring in the competitive experiments carried out by Thaler.

Our results are in accord with those of Thaler in one respect. From the plot in Fig. 1 it is clear that the cumulative effect of methyl groups on the rate is least for the addition of 4-chlorobenzenesulfenyl chloride and greatest for the addition of chlorine. Thus the methyl substituents on the episulfonium ion contribute less toward delocalizing the positive charge than do the methyl substituents on the bromonium or chloronium ion. This is consistent with the ability of the three heteratoms to support a positive charge; S > Br > Cl.

Experimental

All melting and boiling points are uncorrected. Microanalyses were carried out by A. B. Gygli Microanalysis Laboratory, Toronto, Ontario.

The *olefins* were obtained commercially and their purity was verified by g.l.c. and n.m.r.

4-Chlorobenzenesulfenyl chloride was prepared as previously described (12).

1,1,2,2-Tetrachloroethane was purified as previously described (12).

Kinetics

Solutions for kinetic runs were prepared in general by direct weighing. If the olefin was a gas at room temperature, the gas was bubbled into a given quantity of solvent and its' concentration was determined by titration with a standard solution of 4-chlorobenzenesulfenyl chloride. After the kinetic runs, the olefin concentrations were redetermined. No loss of olefin by evaporation was ever detected. The kinetics were carried out as previously described (12).

Product Composition

The reactions were carried out in n.m.r. tubes immersed in a constant temperature bath at 25°. The olefin was added dropwise as quickly as possible into a sulfenyl chloride solution in $CDCl_3$. The n.m.r. tubes were placed in pulverized Dry Ice as soon as the reaction was complete as determined by a colorless solution. The n.m.r. measurements were carried out on a Varian T-60 instrument at 30° (probe temperature). The n.m.r. tubes were then replaced in the bath (25°) until equilibrium composition was observed.

Analytical samples were prepared using analytical grade 4-chlorobenzenesulfenyl chloride and the commercially available olefins. The reactions were carried out in ACS grade methylene chloride at room temperature. On removal of the solvent the adducts were often analytically pure as determined by n.m.r. and g.l.c. Otherwise they were purified by g.l.c. or distillation. The physical properties and chemical analysis of the adducts are given in Table 4. Selected n.m.r. data are presented in Table 5.

Exchange Reactions with Methanesulfenyl Chloride Adducts

The existence of exchange between adducts of methanesulfenyl chloride and alkenes in *n*-heptane at 25° was shown by adding 2-chloropropyl methyl sulfide to a solution of isobutylene. Within 10–15 min of addition the characteristic peaks of the adduct of *p*-chlorobenzenesulfenyl chloride and isobutylene apeared in the n.m.r.

Competitive Experiments With 4-Chlorobenzenesulfenyl Chloride

To solutions equimolar in each of two olefins, *e.g.* ethylene and propene, was added enough 4-chlorobenzenesulfenyl chloride to account for 35–45% of the olefin present. Samples were immediately injected into the g.l.c. using a 1/4 in. × 13 ft column of 5% Carbowax on Chromosorb G to separate the products. All adducts were easily separated (except for Markownikoff – *anti*-Markownikoff isomers). Injections were continued over several days until equilibrium was observed to have been reached. The instrument was calibrated to show linearity of peak area versus concentration dependence for the adducts.

Can. J. Chem. Downloaded from www.nrcresearchpress.com by 210.87.254.6 on 09/05/12
For personal use only.

Can. J. Chem. Downloaded from www.nrcresearchpress.com by 210.87.254.6 on 09/05/12
For personal use only.

TABLE 5. N.m.r. parameters of 4-chlorobenzenesulfenyl chloride adducts*

Olefin	Proton				Chemical shift			
	1	2	3	4	1	2	3	4
Ethylene	CH_2Cl	CH_2S	—	—	3.62	3.18	—	—
Propene (M adduct)	CH_3CHCl	CH_3CHCl	CH_2S	—	1.58 ,d		3.34m	—
Propene (aM adduct)	CH_3CHS	CH_3CHS	CH_2Cl	—	1.25, d		3.34m	—
Isobutylene (M adduct)	$(CH_3)_2CCl$	CH_2S	—	—	1.64, s	3.33, s	—	—
Isobutylene (aM adduct)	$(CH_3)_2CS$	CH_2Cl	—	—	1.30, s	3.46, s	—	—
cis-2-Butene	CH_3CHS	CH_3CHS	CH_3CHCl	CH_3CHCl	1.38, dd†	3.56, o	1.53, dd	4.20, o
trans-2-Butene	CH_3CHS	CH_3CHS	CH_3CHCl	CH_3CHCl	1.36, d	3.30, m	1.56, d	4.16, m
2-Methyl-2-butene (M adduct)	$(CH_3)_2CCl$	CH_3CHS	CH_3CHS		1.66, d‡	1.46, d‡	3.31, q	
2-Methyl-2-butene (aM adduct)	$(CH_3)_2CS$	CH_3CHCl	CH_3CHCl		1.30, d‡	1.67, d‡	3.93, q	
2,3-Dimethyl-2-butene	$(CH_3)_2CS$	$(CH_3)_2CCl$			1.35, s	1.76, s		

*d = doublet; o = octet; dd = doublet, doublet; m = multiplet.
†J_2 = 8.0, J_3 = 1.5 Hz, *threo*; J_2 = 6.0 Hz, *erythro*.
‡J_3 = 2.5 (aM), 2.0 Hz (M); J_3 = 7.5 (aM), 7.0 Hz (M).

Continued financial support from the National Research Council of Canada is gratefully acknowledged.

1. G. H. SCHMID and V. J. NOWLAN. J. Org. Chem. **37**, 3086 (1972).
2. P. D. BARTLETT and G. D. SARGENT. J. Am. Chem. Soc. **87**, 1297 (1965).
3. D. SWERN. Chem. Revs. **45**, 1 (1949).
4. J. E. DUBOIS and G. MOUVIER. Tetrahedron Lett. 1629 (1965).
5. M. L. POUTSMA. Science, **157**, 997 (1967).
6. P. RIESZ, R. W. TAFT, JR., and R. H. BOYD. J. Am. Chem. Soc. **79**, 3724 (1957).
7. W. H. MUELLER. Angew. Chem. Internat. Edit. **8**, 482 (1969).
8. W. A. THALER. J. Org. Chem. **34**, 871 (1969).
9. G. M. BEVERLY and D. R. HOGG. J. Chem. Soc. B, 175 (1971).
10. G. M. BEVERLY and D. R. HOGG. Chem. Commun. 138 (1966).
11. G. H. SCHMID and P. H. FITZGERALD. J. Am. Chem. Soc. **93**, 2547 (1971).
12. G. H. SCHMID, V. M. CSIZMADIA, V. J. NOWLAN, and D. G. GARRATT. Can. J. Chem. **50**, 2457 (1972).

Can. J. Chem. Downloaded from www.nrcresearchpress.com by 210.87.254.6 on 09/05/12
For personal use only.

Photoreactions of Nitroso Compounds in Solution.[1] XXIII. A Novel Oxidative Photoreaction of Nitrosamines and Nitrosamides

Y. L. CHOW, J. N. S. TAM, C. J. COLÓN, AND K. S. PILLAY

Department of Chemistry, Simon Fraser University, Burnaby, British Columbia

Received May 31, 1972[2]

Novel oxidations attending the photorearrangement of a nitrosamide and the photoaddition of nitrosamine are described and compared with the corresponding non-oxidative photoreactions.hWith proper filters, disproportionation during photorearrangement of *N*-nitrosohexylacetamide and tautomerization during nitrosopiperidine photoaddition to cyclohexene can be minimized to give improved yields of the *anti*-dimers of *C*-nitroso compounds. These side reactions are shown to be exclusively derived from secondary photoreactions of the *C*-nitroso compounds. In the presence of oxygen, the courses of the photoreactions are diverted cleanly to form nitrate esters. Oxygen reacts with nitric oxide, both in the free state and when paired with the C-radical thus diverting the course of the reaction. The rate constant of radical combination between a C-radical and nitric oxide is estimated to be in the range of 2×10^7 s^{-1}.

De nouvelles oxydations accompagnant le photoréarrangement de la nitrosamide et la photoaddition de la nitrosamine sont décrites et comparées avec les photoréactions non-oxydantes correspondantes. Avec des filtres convenables, la dismutation durant le photoréarrangement de la *N*-nitrosohexylacétamide et la tautomérisation durant la photoaddition de la nitrosopiperidine au cyclohexène peuvent être réduites au minimum pour ainsi donner de meilleurs rendements en dimères-*anti* des composés *C*-nitroso. Ces réactions parasites proviennent, tel qu'il a été démontré, exclusivement de photoréactions secondaires des composés *C*-nitroso. En présence d'oxygène, le cheminement des photoréactions est nettement modifié pour former des esters nitrate. L'oxygène réagit avec l'oxyde nitrique, à la fois à l'état libre et lorsque pairé au C-radical, pour ainsi dévier le chemin de la réaction. La constante de vitesse de la combinaison radicalaire entre le C-radical et l'oxyde nitrique semble se situer dans les alentours de 2×10^7 s^{-1}.

[Traduit par le journal]

Can. J. Chem., 51, 2469 (1973)

Can. J. Chem. Downloaded from www.nrcresearchpress.com by 210.87.254.42 on 09/05/12
For personal use only.

Introduction

It has been established that various nitroso derivatives are photolabile (2–6). Photorearrangements of *N*-nitrosoamides (2–4) and nitrites (5) in neutral solutions are characterized intramolecularly by the exchange reaction between an δ-hydrogen atom and the nitroso group. Photoreaction of a nitrosamine requires the presence of an acid (6); photoaddition to an olefin, however, finds no parallel in the photolysis of *N*-nitrosamides and nitrites. In spite of the wide difference in their reaction pattern, there are certain mechanistic features common to these photoreactions: namely recombination of an alkyl radical and nitric oxide (or a nitric oxide donor) in the product forming step (2, 7). We have reported that, in the course of the photorearrangement of nitrites, oxygen not only fails to quench the photoreaction but diverts the major reaction pathway to form the rearranged nitrates (8) which can be regarded as the oxidation products of the corresponding *C*-nitroso compounds. This new photooxidation process is now found to be a common feature for the photoreactions of *N*-nitrosamides and *N*-nitrosamines. In view of the clean and efficient reaction, this photooxidation is a potentially useful method for nitrate ester synthesis. The purpose of this paper is to describe these photooxidative processes and to compare them with the corresponding non-oxidative photoreactions.

Results

Photoaddition of Nitrosamines

We have established that in the presence of an acid a nitrosamine photolytically adds to cyclohexene to give *trans*-1-nitroso-2-aminocyclohexane (**1**) as the primary product (9, 10). The reactions of a *C*-nitroso alkane such as **1**, has been fairly well studied by us (6, 10) and other groups (11, 12); those reactions which are relevant to the present discussion are summarized in the lower part of Scheme 1. Recently, Mackor and de Boer have suggested that the oximation process **1** → **3** is also promoted by light (13). In general, photoaddition carried out under an inert gas in a Pyrex apparatus gives *anti*-dimer **2**

[1]For paper XXII of this series, see ref. 1.

[2]Revision received April 10, 1973.

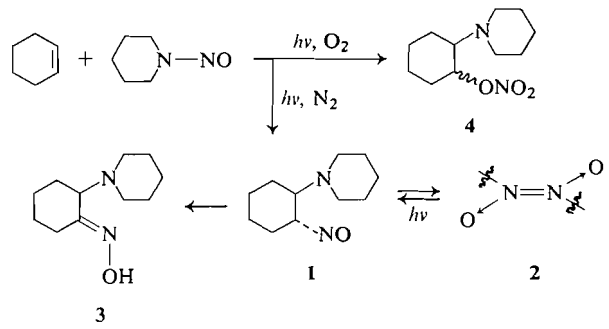

SCHEME 1

and oxime **3** in which the yield of **2** is low owing to light-catalyzed decompositions (6, 9, 10).

When photoaddition of *N*-nitrosopiperidine to cyclohexene was carried out with light >350 nm at $-25 \sim -50°$, the u.v. absorption at 290 nm due to *anti*-dimer **2** increased rapidly to a maximum then decreased slowly on prolonged irradiation. Under the usual work-up (9, 10) 2-piperidinocyclohexanone oxime **3** was obtained in good yield in addition to a small quantity of dimer **2**. After the absorbance at 290 nm reached its maximum value, the photolysis was terminated and the reaction mixture worked-up under the conditions given in the Experimental, a crude dimer fraction could be isolated in 30–35% yield. In view of the slow decomposition to the oxime **3** and incomplete photoaddition, the yield of *anti*-dimer **2** was actually higher than that indicated. The dimer was shown to be the *anti*-dimer of *trans*-1-nitroso-2-piperidinocyclohexane as indicated by the strong i.r. absorption at 1210 cm^{-1} and the n.m.r. signal at τ 4.43.

However, the u.v. profile of *N*-nitrosopiperidine photoaddition to cyclohexene showed a simple zero order decrease of 345 nm band intensity without emergence of the *anti*-dimer peak at 290 nm when a stream of oxygen was substituted for nitrogen. Under a less rich supply of oxygen, the *anti*-dimer absorption appeared during the photoaddition with reduced intensity; this dimer absorption disappeared on prolonged irradiation under oxygen. From these photolysates the hydrochlorides of *cis*- and *trans*-1-nitrato-2-piperidinocyclohexane (**4**) were isolated by fractional crystallization. The i.r. spectrum of the crude basic extract exhibited a weak peak at 1715 cm^{-1} indicating the presence of a minor amount of 2-piperidinocyclohexanone **6** (9). The free bases **4** were unstable on standing and, on attempted chromatography, were decomposed to a dark red resin. The crude product was however reduced with hydrazine hydrate catalyzed by Pd/C (14) to a mixture of *cis*- and *trans*-2-piperidinocyclohexanol (**5**) in a good yield; this reagent specifically reduced the nitrates **4** to the corresponding alcohols **5** leaving cyclohexanone **6** as the stable hydrazone. The n.m.r. spectrum of the crude basic extract showed methine proton signals at τ 6.65 (the axial proton of *trans*-**5**) and 5.92 (the equatorial proton of *cis*-**5**) in the ratio of 67:33. This ratio indicates that the isomeric ratio of nitrates *trans*-**4**:*cis*-**4** was about 2:1. The chromatography of cyclohexanols **5** was, however, only partially successful giving semi-pure *trans*-**5** as a low melting solid. Attempted *p*-nitrobenzoylation of **5** was not successful; cyclohexanols **5** were recovered. Treatment of cyclohexanols **5** with acetic anhydride in pyridine gave the expected acetates which, on chromatography, were decomposed to starting material **5**.

Under similar irradiation conditions, oxidative photoaddition of *N*-nitrosodimethylamine to cyclohexene cleanly gave a mixture of the hydrochlorides of *trans*- and *cis*-1-nitrato-2-dimethylaminocyclohexane (**4**, dimethylamino instead of piperidino group). The isomeric ratio is nearly 1:1 as indicated by the n.m.r. spectrum. The crude residue was reduced by sodium borohydride to give a mixture of *trans*- and *cis*-2-dimethylaminocyclohexanol.

Photorearrangement of Nitrosamides[3]

We have established that irradiation of *N*-nitroso-*N*-hexylacetamide (**7**) in a Pyrex appar-

[3]A part of this result was published as a preliminary account (31).

Can. J. Chem. Downloaded from www.nrcresearchpress.com by 210.87.254.42 on 09/05/12
For personal use only.

TABLE 1. Percentage yields* of products in the photolysis of *N*-nitroso-*N*-hexylacetamide (**7**) in benzene

Entry	Condition	**8**	**11**	**10**	**9**	Remark
1	N_2, >280 nm	37	37	6	20	†
2	He, >280 nm	45	30	1	18	†
3	N_2, >400 nm	58	42	0	0	
4	O_2, >280 nm	0	10	12	43	‡
5	O_2, >280 nm	0	22	11	44	†, §
6	O_2, >400 nm	0	26	12	47	

*The percentages were calculated on the basis of 1 mol of the product being produced from 1 mol of the nitrosamide.
†Nitrobenzene and nitrophenols were detected.
‡Nitrobenzene (5%), *o*-nitrophenol (4%), *p*-nitrophenol (2%), and *N*-formylacetamide were isolated.
§The experiment was run under oxygen pressure (400 mm Hg).

atus (transparent above 280 nm) under an inert atmosphere leads to the rearrangement product, *N*-(4-nitrosohexyl)acetamide which is isolated as *anti*-dimer **8**, and minor quantities of oxidation products, *N*-(4-nitratohexyl)acetamide (**9**) and *N*-nitro-*N*-hexylacetamide (**10**) (2). In addition *N*-hexylacetamide (**11**) and other minor products derived from β-scission of the amido radical and oxidation of the solvent (such as nitrobenzene and nitrophenols from benzene) were also isolated (15*a*). Reasons have been presented to suggest that the oxidation products, nitrate **9** and nitroamide **10**, are derived from a disproportionation of nitric oxide and are not due to oxygen present as an impurity in the inert gas (2, 15*a*). In the accompanying paper (16) these disproportionation processes have been shown to arise from photolysis of *anti*-dimer **8**. It follows that if the absorption peak of *anti*-dimer **8** at 290 ~ 340 nm is not irradiated, the disproportionation can be prevented. As expected when nitrosamide **7** was irradiated with a light source >400 nm, *anti*-dimer **8** was obtained in a good yield in addition to the parent amide **11**; no oxidation products, such as nitrate **9**, nitroamide **10**, and nitrophenols, were detected (Table 1). The ratio of the two products **8** and **11** remained essentially unchanged over a 10-fold increase of the initial concentration of nitrosamide **7**.

Under oxygen atmosphere, irradiation of a benzene solution of nitrosamide **7** through a Pyrex filter or with light >400 nm resulted in the formation of the oxidation products, nitrate **9**, nitroamide **10**, and the parent amide **11** (Table 1). The oxidation products of benzene (nitrobenzene and nitrophenols) were also obtained by no *anti*-dimer **8** was isolated; weak dimer absorption at

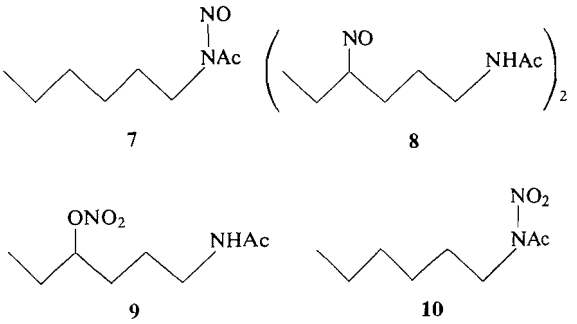

7 **8** **9** **10**

290 nm could be observed if oxygen supply was low. The yields of nitrate **9** remained in the vicinity of 50% with 10-fold increase in the concentration of **7**. Curiously, on irradiation of a benzene solution of nitrosamide **7** saturated with nitric oxide in a Pyrex vessel, neither the rate of photolysis was retarded nor were oxidation products, such as **9** or nitrobenzenes, detected; from the photolysate only *anti*-dimer **8** (36%) and the parent amide **11** (57%) were obtained. A benzene solution saturated with a commercial nitric oxide exhibited an u.v. absorption maximum in the 290–350 nm region which was possibly due to the absorption of nitrogen dioxide[4] (either in NO_2 or N_2O_4 forms).

Discussion

While the primary photoproduct is a *C*-nitroso compound in both photorearrangement of a

[4]This absorption is no longer observable in a solution of nitric oxide purified in a vacuum line. The solubility of NO in water is 7.34 ml/100 ml at 0°, in ethanol 26.3 ml/100 ml at 25° (quoted from Handbook of Chemistry and Physics, 46th ed., The Chemical Rubber Co., Cleveland, Ohio, 1965). In cyclohexane, the NO concentration has been determined to be 2.06×10^{-3} *M* at 800 Torr and 20 °C (ref. 15*b*).

Can. J. Chem. Downloaded from www.nrcresearchpress.com by 210.87.254.42 on 09/05/12
For personal use only.

Can. J. Chem. Downloaded from www.nrcresearchpress.com by 210.87.254.42 on 09/05/12
For personal use only.

nitrosamide and photoaddition of a nitrosamine, the final products of these two photoprocesses are quite different after irradiation in a Pyrex apparatus. In the former case considerable amounts of oxidation products, nitrate **9** and nitroamide **10**, are formed and in the latter case tautomerization product, oxime **3**, is the major one. In the accompanying paper it is shown (16) that the *C*-nitroso intermediates are undergoing a secondary reaction; in the former case it is a light-catalyzed disproportionation reaction and in the latter a tautomerization as in Scheme 1. It is suggested that the discrepancy between the disproportionation pathway on one hand and the tautomerization pathway on the other arises from the difference in media as well as in the structures. The tautomerization of **1** is catalyzed by the protic solvent and an acid (10–12); in the accompanying paper (16), light-catalyzed tautomerization of **1** will be discussed. Obviously if the dimer of the *C*-nitroso compound is preserved in the photolysate by avoiding irradiation at its absorption wavelength (about 290 nm) during the photolysis, the secondary reactions of *anti*-dimers **2** and **8** will not occur. The improved yields of *anti*-dimers **2** and **8** observed in those photolyses equipped with an appropriate filter system support this argument. It is noteworthy that under such selective excitation conditions the photolysis of a nitrosamide is completely free from any oxidation product (2, 15*a*) and the photoaddition of nitrosamine gives no detectable secondary photoproducts (6, 17). Some pertinent examples of the selective excitation of *N*-nitrosamides are described in the thesis written by one of us (18), and others are under further investigation (19).

There are a few questions arising from the wavelength-dependent photorearrangement of nitrosamide **7**, to which unfortunately there are no satisfactory explanations at the moment since the mechanism of the nitrosamide photorearrangement has not been well established (2–4, 15*a*). These questions will be discussed on the basis of the currently accepted mechanism (2–4) which, although undoubtedly only a simplified version of the true mechanism, should, nevertheless, serve to identify some of the inadequacies of our present understanding. First of all, the use of commercial NO gives essentially the same product pattern **8** and **11** as that of the >400 nm nitrosamide photorearrangement. The conclusion that the observed disproportionation in the >280 nm photorearrangement is derived from the secondary photolysis of *C*-nitroso dimer **8** is supported by the observation that impurities in NO gas, absorbing at 290–350 nm, act as an internal filter to block the irradiation of dimer **8**. It further leads us to a surprising conclusion that externally added NO does not participate in the disproportionation and also does not promote the formation of *C*-nitroso compound; it scarcely even scavenges the amido radical to regenerate **7**, in view of the photolysis rate remaining unaffected. Although in this case it is very tempting to ascribe a "cage effect"[5] to photodissociated radical pair **12**, this assumption does not seem to be a compelling one since it will be shown later that the radical pair **12** is reacting with oxygen efficiently. The well documented fact that NO in condensed or solid phase is predominantly N—N bonded in polymeric forms (21) leads us to assume that the external NO is similarly associated in solution. Such polymeric NO present in the bulk may neither interact nor exchange with NO in **12**. A proposal of a "tight radical pair" for **12** appears reasonable and can account for this as well as >400 nm photolysis under nitrogen. The presence of a radical pair in red-light photolysis of a *C*-nitroso monomer has been demonstrated by de Boer's group recently (11*b*).

Disproportionation of nitric oxide in the course of a radical reaction is known (22). In the accompanying report (16) we shall demonstrate that photolysis of *anti*-dimer **8** through Pyrex causes disproportionation through dissociation to the corresponding *C*-radical and NO as the primary step. No doubt this explains the product pattern observed in the >290 nm photorearrangement under nitrogen. It follows that NO generated in the photolysis of *anti*-dimer **8** is different from that generated by >400 nm irradiation of nitrosamide **7**. Since red-light photolysis (>690 nm) of 2-nitroso-2-methylpropane also causes disproportionation (11*b*), it is untenable to assume a difference in vibrationally excited NO being responsible for this discrepancy. It is more probable that a "tight radical pair" **12***b* is formed and collapses immediately to *C*-nitroso monomer of **8** in photo-

[5]In the photolysis of nitrites, Akhtar and Pechat (20) reported that no "cage effect" is involved in the rearrangement.

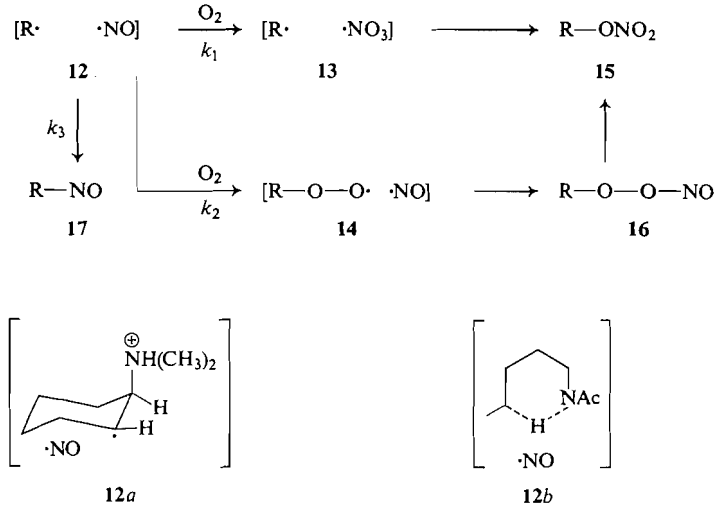

SCHEME 2

rearrangement of **7**. In other words, the difference arises from states of "bound" NO and "free" NO.

We have presumed that the H-atom source in the formation of parent amide **11** comes from benzene as the result of displacement reactions by $\cdot NO_3$ and $\cdot NO_2$ formed during >280 nm photolysis. This clearly does not explain the formation of **11** in the >400 nm photorearrangement of **7** since no nitrobenzenes are isolated. Although benzene might be considered as the source by a direct H-atom transfer to the amido radical, this has not been substantiated by finding a dehydrogenation product (such as biphenyl) in the photolysate. There must be a certain amount of stabilization in an amido radical which makes the H-atom abstraction from benzene rather improbable. At present the H-atom source in the formation of the parent amide **11** remains a challenging question.

Returning now to the photolyses in the presence of oxygen, the reaction pathway is cleanly diverted to the formation of oxidation products such as nitrates **4** and **9**. From the fact that the oxidation occurs exclusively even if irradiation has been carried out with a pertinent filter system (to avoid irradiation of the *anti*-dimer peak), it is concluded that *anti-dimers 2 and 8 are not necessary intermediaries for the oxidation process.* It is envisaged that oxygen intercepts the radical pair, such as **12**, before its collapse to *C*-nitroso compound **17**. In view of the argument presented above for the photorearrangement of *N*-nitrosamides, this stage can be represented by radical pair **12***b*. The mechanism of *N*-nitrosamine photoaddition elucidated by us (7) suggests the corresponding radical pair is **12***a* but not necessarily a "tight" one. The oxidation of the radical pair **12** can follow either one of the two possibilities to give radical pair **13** or **14** (Scheme 2). Peroxy nitrite **16** is expected to be an unstable species which rearranges rapidly to **15**, very likely through the peroxy bond scission.

An overview of the various photoprocesses is provided in Scheme 2. It is now in order to discuss the relative importance and the implications of these processes. First of all, the rate of radical combination[6] (**12** → **17**) is nearly equal to the rate of either oxidation processes (**12** → **13** or **14**) as demonstrated by the partial formation of *C*-nitroso compound **17** (equivalent to dimer **2** and **8**) under a limited supply of oxygen; at a higher supply of oxygen, radical pair **12** is totally intercepted and there is no u.v. absorption of the dimer **2** or **8** at 290 nm. Assuming the oxidation has a diffusion controlled rate constant (k_1 or $k_2 = 10^{10}\ M^{-1}\ s^{-1}$) (24) the upper limit of k_3 can be estimated to be $2.2 \times 10^7\ s^{-1}$ at the oxygen concentration of $4.5 \times 10^{-2}\ M$ at 25°

[6]Studies in gas phase kinetics show that the bimolecular rate constants of combinations of methyl radical with oxygen and with nitric oxide are about the same $10^8\ M^{-1}\ s^{-1}$ (23).

Can. J. Chem. Downloaded from www.nrcresearchpress.com by 210.87.254.42 on 09/05/12
For personal use only.

Can. J. Chem. Downloaded from www.nrcresearchpress.com by 210.87.254.42 on 09/05/12
For personal use only.

(25). We have argued that the recombination rate constant k_3 must be very high in order to explain the stereospecific formation of *trans*-1-nitroso-2-dimethylaminocyclohexane observed previously (17) and the analogue **1** obtained in the present work; in relative sense k_3 must be much faster than that of the cyclohexane ring inversion in **12***a*; the rate of the ring inversion, however, cannot be reliably estimated at present. The success of the present oxidation process derives from the fact that at moderate concentrations of oxygen, radical pair can be intercepted before its collapse; thus the photoreaction is cleanly diverted to nitrate formation.

The relative importance of the two oxidation processes (**12** → **13** or **14**) may be discussed now. Studies in gas phase kinetics show that the reaction of NO with oxygen is complex and no *a priori* prediction of the relative rates is possible (26). The clean nitrate formations suggests that oxygen does not attack the radical pair in a random manner. If the pathway **12** → **14** → **16**→ **4** was the correct mechanism, it would have afforded *trans*-nitrate **4** stereospecifically, assuming pernitrite **16** rearranges to **4** by the peroxy bond scission. This pathway is clearly untenable since experimentally we have observed scrambling of the stereochemistry in nitrate-**4** (*trans*:*cis* = 2:1). The alternative pathway **12** → **13** → **4** can accommodate the stereochemical result and is the more likely mechanism. The combination of nitrogen trioxide with radical R· is probably a slower process than the ring inversion in **12***a*. Isolation of nitrophenols during the oxidative photorearrangement also supports the intermediacy of nitrogen trioxide which has been proposed to attack benzene followed by the nitrate rearrangement leading to these nitrophenols (15*a*). Among other radicals present during the oxidative photorearrangement, neither oxygen nor NO is known to attack the benzene nucleus; a peroxy radical attack requires a circuitous route to yield nitrophenols.

Attention should be called to the fact that the present oxidative photoreaction is a simple and clean preparative method for nitrate esters that requires no strong nitric acid nor expensive silver nitrate. Furthermore, nitrates are stable to photolysis. While the hydrochloride of nitrate **4** is stable to ordinary operations, the free base is unstable due to a base catalysed decomposition of the nitrate moiety. Apparently one of these decompositions is the elimination of nitrous acid to give ketone[7] **6** which is always found as a minor product during the liberation of the free base **4** (2) but is absent in the crude hydrochloride of **4**. The stereochemical consequence of this oxidative photoaddition gives a mixture of *trans*- and *cis*-**4** in 2:1 ratio. Assuming that various possible side reactions during isolation and reduction of nitrate **4** operate nearly identically with both the *cis*- and *trans*-isomeric compounds, this ratio is indicated by the ratio of the isomeric cyclohexanols **5** obtained by the specific reduction. It is interesting that the acetates of cyclohexanols **5** are hydrolyzed back to **5** on adsorbing on an alumina column. The hydrolysis is no doubt facilitated by the displacement of the acetate group assisted by the neighboring amino group participation (27). Since *p*-nitrobenzoate group is a better leaving group than acetate, the hydrolysis may have taken place more rapidly during working-up.

Finally, it is important to mention that oxygen does not quench the excited states of nitrosamines and nitrosamides from which the primary photoprocesses occur. In view of the generally accepted fact that a triplet state is susceptible to an oxygen quenching (28), it may be suggested that the photoreaction is initiated from a singlet state of the nitroso compounds. In the case of photodecompositions of nitrosopiperidine, our kinetic studies by flash excitation (7) have verified the singlet state reaction. A similar study on nitrosamide photodecomposition does not allow us to draw a conclusion since both singlet and triplet sensitization lead to the decomposition (18).

Experimental

For the general conditions of experiments and spectroscopy, see our previous publication (6). For the photolysis a Hanovia medium pressure mercury lamp (654A36, 200 W) was used in conjunction with a suitable filter system. A Pyrex photolysis apparatus cut off the light source below 290 nm. For > 350 nm light source, a filter solution of 2,7-dimethyl-3,6-diazacyclohepta-1,6-diene perchlorate (0.01% aqueous solution) or a Norex filter (29) was used. For > 400 nm light source, a sodium nitrite sodium phthalate solution (30) was used as filter which cut off the light energy below 400 nm.

Photoaddition of N-Nitrosopiperidine

A solution of *N*-nitrosopiperidine (4.5 g), cyclohexene

[7]The ketone could have been formed through a peroxy radical intermediate as has been proposed by de Boer's group in the related oxidative study of nitrosocyclohexane (13). Apparently this process is not important in the present case.

Can. J. Chem. Downloaded from www.nrcresearchpress.com by 210.87.254.42 on 09/05/12
For personal use only.

(4.9 g), concentrated hydrochloric acid (3.5 ml), and methanol (500 ml) was irradiated with a light source > 350 nm at −25° for 2 h. Sodium carbonate (5.5 g) was added to the blueish green photolysate with stirring. The white precipitate (1.73 g) was filtered and washed with water. Partial concentration of solvent gave a second crop of crystals (550 mg). The combined crops were recrystallized from a mixture solvent of methylene chloride – methanol to give white crystals of the *anti*-dimer of *trans*-1-nitroso-2-piperidinocyclohexane (**2**): m.p. 170–172°; i.r. 1210, 1185, 1100, 1055, 1030, and 695 cm^{-1}; n.m.r. τ 4.43 ($w_{1/2}$ = 25 Hz, 1H) and 6.8–7.8 (m, 5H).

Subsequent precipitates obtained by evaporation of solvent contained mostly 2-piperidinocyclohexanone oxime (**3**) (9) contaminated with a minor amount of the *anti*-dimer **2**.

Oxidative Photoaddition of N-Nitrosopiperidine

A solution of *N*-nitrosopiperidine (6.84 g, 0.06 mol), cyclohexene (3.28 g, 0.04 mol) and concentrated hydrochloric acid (6 ml) in methanol (340 ml) was irradiated under oxygen atmosphere at −10° for 3 h. A filter solution of 2,7-dimethyl-3,6-diazacyclohepta-1,6-diene perchlorate, was circulated through the cold finger. The bulk of methanol was removed and the residual solution was washed with ether and was neutralized with potassium carbonate to p*H* 7.5. The basic extract (6.8 g) showed strong absorptions at 1625, 1275, and 865 cm^{-1} for a nitrate group and a medium peak at 1715 cm^{-1} for a carbonyl group.

The crude basic fraction was reduced with hydrazine hydrate in the presence of Pd/C in methanol solution (14) for 18 h. The reduced product was isolated in the usual manner to give an oil which exhibited no i.r. absorptions typical of nitrate and carbonyl groups. The oil was distilled under 0.5 mm Hg to give the major fraction of b.p. 84° (4.2 g): i.r. 3440, 1305, 1105, 1080, and 1060 cm^{-1}; n.m.r. τ 5.92 (m, $w_{1/2}$ = 7 Hz), 6.28 (D_2O exchangeable), and 6.65 (dt, J = 4 and 9 Hz): *m/e*(%) 183(M^+), 140(12), 125(35), 124(100), 111(54), 98(93), and 84(50). This fraction solidified at room temperature. The solid was chromatographed on an alumina column. Elution with methylene chloride gave a fraction which showed single spot on a t.l.c. plate. This fraction was distilled to give *trans*-2-piperidinocyclohexanol (**5**): n.m.r. τ 7.47(m), 6.68 (dt, J = ~4 and 11 Hz).

When the above solid was treated with *p*-nitrobenzoyl chloride in pyridine and was worked-up in the usual manner, the starting material, a mixture of *cis*- and *trans*-2-piperidinocyclohexanol, was recovered.

Acetylation with acetic anhydride – pyridine gave a crude product which shows i.r. absorption at 1735 and 1240 cm^{-1}. Chromatography of the crude acetylation product on an alumina column gave the acetate of the *cis*-cyclohexanol **5** which was sublimed at 55°/0.02 mm: i.r. 2860, 2800, 1735, and 1240 cm^{-1}; n.m.r. τ 4.63 ($w_{1/2}$ = 6 Hz, 1H), 7.46 (m), 7.95 (s, 3H), and 8.35 (m); *m/e*(%) 225(9), 182(19), 166(10), 125(12), 124(100), 111(6), 110(5), 98(8), 84(9) and 43(8). This acetate gradually decomposes on storage. Further elution afforded a mixture of *cis* and *trans*-cyclohexanol **5**.

In a separate experiment, a solution of *N*-nitrosopiperidine (2.3 g, 0.02 mol), cyclohexene (2.56, 0.03 mol), and concentrated hydrochloric acid (2 ml, 0.024 mol) in methanol (140 ml) was irradiated under similar conditions. The methanol was evaporated to a small volume under vacuum at a water bath temperature of 10° (if heated, the solution darkens). The methanol was cooled to 0° and then ether was added gradually to produce slight cloudiness from which crystals (1.1 g) appeared upon standing: m.p. 159–161° (dec.). They were recrystallized three times from 2-propanol to give the hydrochloride of *cis*-1-nitrato-2-piperidinocyclohexane (4); m.p. 169–170°; i.r. 2500, 1640, 1266, and 870 cm^{-1}; n.m.r. (D_2O) τ 4.47 (m, $w_{1/2}$ = 12 Hz, 1H), 6.76 (m, 3H), 7.12 (m, 2H), 8.33 (m, 14H).

Anal. Calcd. for $C_{11}H_{21}N_2O_3Cl.H_2O$: C, 47.05; H, 7.48; N, 9.98; Cl, 12.65. Found: C, 46.82; H, 7.89; N, 10.12; Cl, 12.56.

The mother liquor was cooled for another 3 months at −10° to give a second crop of crystals (300 mg) which showed in the n.m.r. spectra a broad multiplet at τ 4.77. These crystals were recrystallized three times from a mixture of 2-propanol – ether to afford the hydrochloride of *trans*-1-nitrato-2-piperidinocyclohexane (4): m.p. 134–137°; i.r. 3250, 2650, 2530, 1630, 1270, and 880 cm^{-1}; n.m.r. (D_2O) τ 4.77 (m, $w_{1/2}$ = 25 Hz, 1H), 6.65 (b, 5H), 8.15 (m, 14H).

Anal. Calcd. for $C_{11}H_{21}N_2O_3Cl$: C, 49.90; H, 7.95; N, 10.58; Cl, 13.40. Found: C, 50.10; H, 7.76; N, 10.42; Cl, 13.27.

Oxidative Photoaddition of N-Nitrosodimethylamine

A solution of *N*-nitrosodimethylamine (1.48 g, 0.02 mol), cyclohexene (3.28 g, 0.04 mol), and concentrated hydrochloric acid (2 ml) in methanol (130 ml) was photolyzed in the similar manner under oxygen for 1.5 h. The usual work-up afforded the hydrochlorides of *cis*- and *trans*-2-dimethylamino-1-nitratocyclohexane; darkened at 109° and decomposed at 119–122° with evolution of a gas; i.r. 1640, 1280, and 870 cm^{-1}; n.m.r. (D_2O) τ 4.3 (m, $w_{1/2}$ = 10 Hz, 1H), 4.7 (m, $w_{1/2}$ = 25 Hz, 1H), 6.5 (superimposed double triplet, J = 3.5 ~ 4 and 12 Hz, 2H), 7.1 and 7.2 (two singlets, 6H), 7.5–7.9 (m, 8H).

Anal. Calcd. $C_8H_{17}N_2O_2Cl$: C, 42.76; H, 7.57; N, 12.47; Cl, 15.81. Found: C, 42.87; H, 7.47; N, 12.35; Cl, 15.70.

The mother liquor of 4 was evaporated to give a syrup which was dissolved in methanol (50 ml). The solution was treated with $NaBH_4$ (1.54 g, 0.04 mol) added in small portions while stirring. After 12 h the solution was treated with concentrated hydrochloric acid (20 ml) and then with water (40 ml). Basification of the solution and extraction with CH_2Cl_2 afforded, upon evaporation of the CH_2Cl_2, an oil (2.2 g) of the *cis* and *trans* mixture (ratio 1:1) of 2-dimethylaminocyclohexanol: i.r. 3450, 1270, 980, 960, and 880 cm^{-1}; n.m.r. τ 6.0 (m, 1H); 7.0 (m, 1H), 7.8 (s, 6H), 7.8 – 9.2 (m, 8H).

Photolysis of N-Nitroso-N-hexylacetamide (7)

A benzene solution of nitrosamide **7** was photolyzed in the same apparatus as above and the results were summarized in Table 1. The isolation and characterization of the products follows the procedure of the previous publication (2).

Nitrate **9** was reduced with lithium aluminum hydride followed by a treatment with benzoyl chloride – pyridine to give *N*-(4-benzoyloxyhexyl)-*N*-ethylbenzamide: i.r. 1720, 1630, 1275, and 1115 cm^{-1}; n.m.r. τ 9.04 (t, 3H,

J = 7 Hz), 8.88 (t, 3H, J = 7 Hz), 4.97 (m, 1H); m/e(%) 353(M^+), 248(3), 232(4), 162(15), 105(100), and 77(35).

For the photolysis under nitric oxide atmosphere, a manometric pressure device was used to maintain the pressure at 1 atm. Before the introduction of nitric oxide, the whole system was carefully displaced with helium gas.

For the photolyses under oxygen, the supply of oxygen was regulated to 1 ~ 3 bubbles per second. Other procedures follow those described in photorearrangement.

The authors thank the National Research Council of Canada, the Defence Research Board of Ottawa and the President's Research Fund of Simon Fraser University for financial support of this work.

1. Y. L. Chow, C. J. Colón, H. H. Quon, and T. Mojelsky. Can. J. Chem. **50**, 1065 (1972).
2. Y. L. Chow, N. S. Tam, and A. C. H. Lee. Can. J. Chem. **47**, 2441 (1969).
3. L. P. Kuhn, G. G. Kleinspehn, and A. C. Duckworth. J. Am. Chem. Soc. **89**, 3858 (1967).
4. O. E. Edwards and R. S. Rosich. Can. J. Chem. **45**, 1287 (1965).
5. M. Akhtar. Adv. Photochem. **2**, 263 (1964); R. H. Hesse. Adv. Free Radical Chem. **3**, 83 (1969).
6. Y. L. Chow, S. C. Chen, and D. W. L. Chang. Can. J. Chem. **48**, 157 (1970) and previous papers quoted therein.
7. M. P. Lau, A. J. Cessna, Y. L. Chow, and R. W. Yip. J. Am. Chem. Soc. **93**, 3803 (1971).
8. Y. L. Chow, T. Hayasaka, and J. N. S. Tam. Can. J. Chem. **48**, 508 (1970).
9. Y. L. Chow. Can. J. Chem. **43**, 2711 (1965).
10. Y. L. Chow, C. J. Colón, and S. C. Chen. J. Org. Chem. **32**, 2109 (1967).
11. (*a*) A. Mackor, Th. A. J. W. Wajer, and Th. J. de Boer. Tetrahedron Lett. 2115 (1966), 2757 (1967); (*b*) J. A. Maassen. Ph.D. dissertation. University of Amsterdam. 1972.
12. B. G. Gowenlock and W. Lüttke. Quart. Rev. **12**, 321 (1958).
13. A. Mackor and Th. J. de Boer. Rec. Trav. Chim. **89**, 164 (1970).
14. L. P. Kuhn. J. Am. Chem. Soc. **73**, 1510 (1951).
15. (*a*) Y. L. Chow and J. N. S. Tam. J. Chem. Soc. C 1138 (1970). (*b*) D. S. Tsiklis and G. M. Svetlova. Zh. Fyz. Khim., **32**, 1476 (1958).
16. Y. L. Chow, J. N. S. Tam, K. S. Pillay. Can. J. Chem. This issue.
17. Y. L. Chow, D. W. L. Chang, and S. C. Chen. Can. J. Chem. **49**, 3069 (1971).
18. J. N. S. Tam. Ph.D. Thesis. Simon Fraser University, 1970.
19. Y. L. Chow and R. A. Perry. Tetrahedron Lett. 513 (1972) and the unpublished results.
20. M. Akhtar and M. M. Pechet. J. Am. Chem. Soc. **86**, 265 (1964).
21. (*a*) A. L. Smith, W. E. Keller, and H. L. Johnston. J. Chem. Phys. **19**, 189 (1951); (*b*) C. E. Dinerman and G. E. Ewing. J. Chem. Phys. **53**, 626 (1970) and the papers cited in these two refs.
22. (*a*) J. F. Brown, Jr. J. Am. Chem. Soc. **79**, 2480 (1957); (*b*) L. G. Donaruma and D. J. Camody. J. Org. Chem. **22**, 635 (1957).
23. (*a*) F. B. Marcotte and W. A. Noyes, Jr. Discuss. Faraday Soc. **10**, 236 (1951); (*b*) R. W. Durham and E. W. R. Steacie. J. Chem. Phys. **20**, 582 (1952).
24. A. A. Lamola and N. J. Turro. Energy transfer and organic photochemistry. Interscience Publisher, New York, N.Y., 1969. p. 34.
25. J. Horiuti. Sci. Paper, Inst. Phys. Chem. Research, Tokyo, **17**, 341, 125 (1931).
26. J. Heicklin and N. Cohen. Adv. Photochem. **5**, 157 (1968).
27. B. Capon. Quart. Rev. **18**, 45 (1964).
28. V. Kasche and L. Lindquist. J. Phys. Chem. **68**, 817 (1964); M. A. Herbert, J. W. Hunt, and H. E. Johns. Biochem. Biophys. Res. Commun. **33**, 643 (1968).
29. N. J. Turro and R. Engel. J. Am. Chem. Soc. **91**, 7113 (1969).
30. C. M. Orlando, Jr., H. Mark, A. K. Bose, and M. S. Mankas. J. Org. Chem. **33**, 2512 (1968).
31. Y. L. Chow and J. N. S. Tam. Chem. Commun. 747 (1969).

Can. J. Chem. Downloaded from www.nrcresearchpress.com by 210.87.254.42 on 09/05/12
For personal use only.

Photoreactions of Nitroso Compounds in Solution.[1] XXIV. Photooxidation and Photodecomposition of *C*-Nitroso Compounds

Y. L. CHOW, J. N. S. TAM, AND K. S. PILLAY

Department of Chemistry, Simon Fraser University, Burnaby 2, British Columbia

Received May 31, 1972[2]

Irradiation of the *anti*-dimers of *C*-nitroso compounds under nitrogen caused dissociation to the corresponding *C*-nitroso monomer which underwent photodisproportionation, tautomerization, and dimerization. Similar irradiation underhoxygen led principally to nitrate and nitro compound formation. The disproportionation of *N*-(4-nitrosohexyl)acetamide was shown to occur by photodissociation of the *C*-nitroso monomer to the alkyl radical and nitric oxide. Under an oxygen atmosphere, those *C*-nitroso compounds which could undergo facile photodissociation were quickly oxidized to nitrates. As a result, mixtures of the corresponding *cis*- and *trans*-*C*-nitrates were obtained from the *anti*-dimer of *trans*-1-nitroso-2-chlorocyclohexane. The *anti*-dimer of *trans*-1-nitroso-2-piperidinocyclohexane was photolytically tautomerized to the corresponding oxime under nitrogen and was oxidized chiefly to the *C*-nitro compound under oxygen; the two processes obviously share a common intermediate. Mechanisms for these photoprocesses are suggested.

L'irradiation dans une atmosphère d'azote des dimères-*anti* de composés *C*-nitroso a provoqué la dissociation de ceux-ci pour donner le monomère *C*-nitroso correspondant lequel a subi une photodismutation, une tautomérisation et une dimérisation. Une irradiation similaire dans une atmosphère d'oxygène a conduit principalement à la formation des produits nitrate et nitro. La dismutation de la *N*-(nitroso-4 hexyl) acétamide se produit par photodissociation du monomère *C*-nitroso en radical alcoyle et en oxyde nitrique tel qu'il a été démontré. Sous une atmosphère d'oxygène, ces composés *C*-nitroso qui peuvent subir une photodissociation facile ont été très rapidement oxydés en nitrates. Par suite, à partir du dimère-*anti* du *trans* nitroso-1 chloro-2 cyclohexane on a pu obtenir un mélange des *C*-nitrates *cis* et *anti* correspondants. Le dimère *anti* du *trans* nitroso-1 piperidino-2 cyclohexane a été tautomérisé photolytiquement pour donner l'oxyme correspondant sous azote et a été oxydé surtout en composé *C*-nitro sous oxygène; ces deux processus doivent nécessairement posséder un intermédiaire commun. Par suite, on suggère des mécanismes pour ces procédés photochimiques. [Traduit par le journal]

Can. J. Chem., 51, 2477 (1973)

Can. J. Chem. Downloaded from www.nrcresearchpress.com by 210.87.254.105 on 09/05/12
For personal use only.

There are many experimental features of nitrosoalkane chemistry that cannot be satisfactorily explained in terms of conventional electronic and steric theories. A nitrosoalkane solution will spontaneously form an equilibrium mixture of monomer **1** and dimers **2** and **3** (2), although the driving force remains obscure (3). The dimers have been shown to possess an azodioxy linkage **2** and **3** in ambient conditions and are colorless in contrast to a deep blue to green color exhibited by the monomer (2). In solution, *primary* and *secondary* nitrosoalkanes have a great tendency to exist as the dimers, whereas the *tertiary* analogs remain mostly monomeric (4). Both electronic and steric effects have been invoked to explain this difference (2–6).

Having an α-hydrogen, *primary* and *secondary* nitrosoalkanes may also irreversibly tautomerize to the corresponding oximes **4**. Although this tautomerization is generally slower than the dimerization process, it is accelerated by acid and base catalysis (7–9). Recently, de Boer's group (10), expanding upon the earlier work of Gowenlock and Trotman (2), has demonstrated that a colorless *anti*-dimer **2**, when irradiated at 320–360 nm at a low temperature, dissociates into a blue–green nitrosoalkane **1** which spontaneously dimerizes at about −70° to the corresponding less stable *syn*-dimer **3**. The latter compound is thermally transformed to the *anti*-dimer on slight warming (see Scheme 1).

C-Nitroso monomers generally exhibit weak absorptions near 680 (ε ~10) and 270 nm (ε ~80), and a strong one at 220 nm (ε *ca.* 5000). The former two bands have been assigned to $n_N \rightarrow \pi^*$ (11) and $n_O \rightarrow \pi^*$ (12) transitions respectively. The long wavelength absorption for an *anti*-dimer **2** occurs in the 280 ~ 300 nm region and that of a *syn*-dimer **3** around 260 ~ 275 nm. Pertinent to the present discussion, it

[1]For Part XXIII of this series, see ref. 1.
[2]Revision received March 12, 1973.

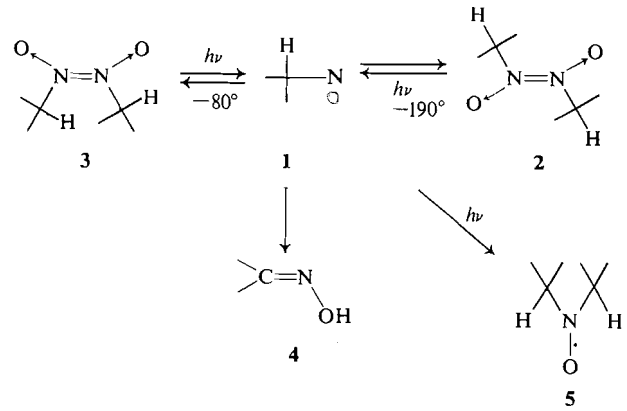

SCHEME 1

should be mentioned that photolysis of a *C*-nitroso monomer gives a stable radical, nitroxide **5**, in which the primary photochemical act has been shown to be dissociation to alkyl and nitric oxide radicals (13, 14). Suggestions of other types of *C*-nitroso compound photoreactions, such as reduction (15), lack convincing proof and may well be the result of secondary reactions. For a *C*-nitroso group, an electronically excited state analogous to that of a carbonyl group (16) is conceivable, but has not been well defined. In connection with our studies of nitrosamine and nitrosamide photolysis, we have been investigating photoreactions of *C*-nitroso compounds. A recent report on the photooxidation of nitrosocyclohexane (17) prompts us to disclose our results on oxidative and non-oxidative photoreactions of some *C*-nitroso compounds.

Results

Photodecomposition

Since our source of *C*-nitroso compounds were dimers, throughout this report irradiation was carried out in a Pyrex apparatus (energy cut-off <290 nm) so that both dimer and monomer absorption bands were excited; the former excitation promoted the dissociation of dimers **2** or **3** to the corresponding monomer (10).

Irradiation of a benzene solution of the *anti*-dimer of *N*-(4-nitrosohexyl)acetamide (**6**) (18) in a Pyrex flask under nitrogen caused a rapid disappearance of the u.v. absorption peak at 290 nm and gave *N*-(4-nitratohexyl)acetamide (**8**) (18) and *N*-hexylacetamide (**7**) in the ratio of *ca.* 1:3. The oxime corresponding to the tautomerization was not detected in the photolysate. This product distribution suggests that a disproportionation of the *C*-nitroso compound has occurred in which nitrate **8** was formed at the expense of two other *C*-nitroso molecules. However, a similar irradiation of *anti*-dimer **6** in a solution saturated with a commercial nitric oxide resulted in the recovery of the starting material **6** nearly quantitatively.

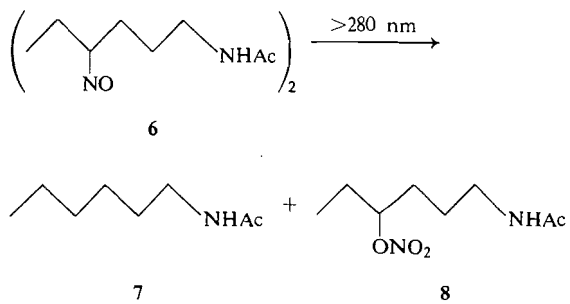

The *anti*-dimer of *trans*-1-nitroso-2-chlorocyclohexane (**9**) was prepared by addition of nitrosyl chloride to cyclohexene (19–21). On irradiation of a benzene solution of the *anti*-dimer **9** under nitrogen, a white crystalline precipitate formed on the surface of the reaction vessel. The white solid melted at 135–140° and exhibited u.v. absorption at 275 nm which is gradually shifted to 298 nm on standing in a dark place. Recrystallization of this precipitate from benzene gave only the *anti*-dimer **9** as white crystals. This precipitate was the corresponding *syn*-dimer of *trans*-1-nitroso-2-chlorocyclohexane. The crude product isolated from benzene solution exhibited i.r. absorption at 1640, 1280, and 880 for a nitrate and for an *anti*-dimer at 1450 and 1210 cm^{-1}, but no i.r. absorption for a nitro group. Chromatography of this crude

Can. J. Chem. Downloaded from www.nrcresearchpress.com by 210.87.254.105 on 09/05/12
For personal use only.

Can. J. Chem. Downloaded from www.nrcresearchpress.com by 210.87.254.105 on 09/05/12
For personal use only.

product afforded *anti*-dimer **9** and a fraction which was shown to contain *trans*-1-nitrato-2-chlorocyclohexane (**10**) and cyclohexyl chloride in nearly equal amounts. An analysis by v.p.c. showed that the peak of the *trans*-nitrate **10** contained a small shoulder which was tentatively assigned to the corresponding *cis*-nitrate. Photodecomposition of the *anti*-dimer **9** in a methanol solution was very slow; from the photolysate, *N,N,O*-tri(2-chlorocyclohexyl)hydroxylamine (**11**) was obtained in addition to nitrates **10** and cyclohexyl chloride.

When a methanol solution of the *anti*-dimer of *trans*-1-nitroso-2-piperidinocyclohexane (**13**) (22) containing hydrochloric acid was irradiated at 5 °C, 65–75% of *anti*-1-piperidinocyclohexanone oxime (**14**) was obtained. The tautomerization was slow at room temperature in the absence of irradiation. The crude product showed no i.r. absorption due to a nitrate or a nitro group. Although there were trace amounts of other products, they could not be isolated in pure states. In this photodecomposition as well as the above two cases, there were always traces of other by-products that could be stable radical compounds of nitroxides as de Boer's group has shown by e.s.r. spectroscopy (23). The diffused n.m.r. signals shown by the crude product indicated the presence of paramagnetic substances, although lack of an e.s.r. facility prevented us from confirming this.

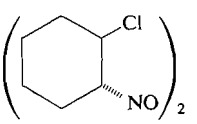

9

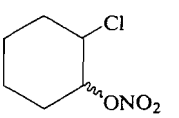

10

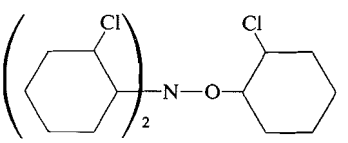

11

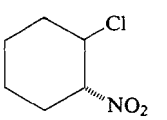

12

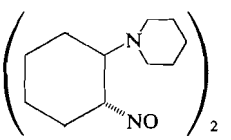

13

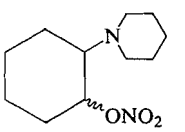

15

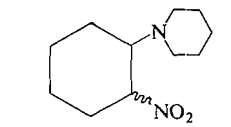

16

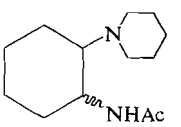

17

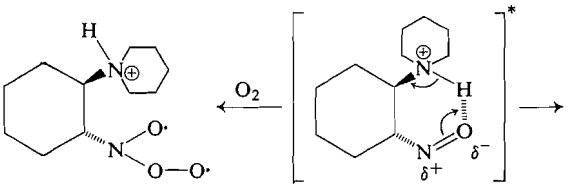

19 18

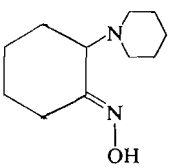

14

Photooxidation

When the photolysis of **6** was carried out under an atmosphere of oxygen instead of nitrogen, nitrate **8** was produced cleanly and in excellent yield. That this was a genuine photooxidation process was established by the fact that a benzene solution of *anti*-dimer **6** saturated with oxygen was stable indefinitely when stored in a dark place. That the oxidation was not initiated by a singlet oxygen (24) (generated, possibly, by a self-photosensitization) was demonstrated by the failure of a methanol solution of **6** to undergo a change when singlet oxygen was generated *in situ* by rose bengal photosensitization.

Oxidative irradiation of *anti*-dimer **9** in a methanolic solution containing perchloric acid or in a benzene solution caused quick disappearance of the *anti*-dimer absorption at 295 nm and precipitation of *syn*-dimer **9**. During the methanol solution photolysis the new absorption at 275 nm due to the corresponding *syn*-dimer was also observed. Owing to precipitation of the *syn*-isomer the photolysis required a prolonged irradiation for completion. From these photolyses *trans*-1-nitrato-2-chlorocyclohexane (**10**) and *trans*-1-nitro-2-chlorocyclohexane (**12**) were isolated by column chromatography. The corresponding *cis*-isomer of **12** was not detected in the photolysate in spite of careful chromatography. The presence of a small amount of the

Can. J. Chem. Downloaded from www.nrcresearchpress.com by 210.87.254.105 on 09/05/12
For personal use only.

cis-isomer of nitrate **10** is suggested by the v.p.c. analysis in which a small shoulder appeared at a slightly longer retention time than that of *trans*-**10**. Some chromatographic fractions of **10** also showed a weak n.m.r. signal at about τ 6.0 that can be assigned to the CHCl proton of the *cis*-isomer. The weak i.r. absorption at 3400 and in the 900–1000 cm^{-1} region, observed in the crude product obtained from the photooxidation in the methanol solution, leads us to suspect the presence of a small amount of the corresponding oxime from tautomerization; this oxime was not isolated. The *trans*-configuration in both cases was assigned on the basis of the large coupling constants of the methine protons in nitrate **10** and nitro compound **12**. Analysis of the product by v.p.c. showed that the photooxidation afforded nitrate **10** and nitro compound **12** in nearly 1:1 ratio. Extensive efforts to reduce the nitrate and nitro groups in **10** and **12** have failed. A mixture of lithium aluminum hydride and aluminum chloride, or catalytic hydrogenation, reduced these functional groups as well as cleaved C—Cl bond to variable extents.

Photooxidation of *anti*-dimer **13** in a benzene solution gave a tarry crude product which showed strong i.r. absorption at 1550, 1320, 1620, and 1270 cm^{-1} and medium absorption at 1710 cm^{-1}. The tarry material was not present in the crude product when the photooxidation was carried out in methanol in the presence of hydrochloric acid: the crude product (hydrochloride salts) exhibited weak i.r. absorptions at 1720, 1635, 1240 and strong absorptions at 1550 and 1450 cm^{-1}. It was shown that this crude product contained *cis*- and *trans*-1-nitro-2-piperidinocyclohexane (**16**) as the major product and minor amounts of *cis*- and *trans*-1-nitrato-2-piperidinocyclohexane (**15**) (1) and 2-piperidinocyclohexanone. The salt was hydrogenated in the presence of platinum catalyst, and then neutralized to give a crude mixture of free bases; the i.r. spectrum showed that the nitrate and nitro groups were completely reduced. Acetylation of the crude base and chromatography gave a small amount of 2-piperidinocyclohexanol (a mixture of *cis*- and *trans*-isomers) (1) and the remainder as various mixtures of *trans*- and *cis*-1-acetamido-2-piperidinocyclohexane (**17**). The ratio of the *cis*- to *trans*-isomer **17** was determined, from an analysis of the n.m.r. spectrum, to be 2:3. From the n.m.r. spectrum of a chromatographic fraction containing *trans*-**17** as the major product, the *trans*-configuration was readily determined from the coupling pattern of the methine proton ($CHNHCOCH_3$). In other fractions, although two methyl signals for the acetyl group were discernible, the chemical shift of the methine proton of the *cis*-**17** was apparently superimposed on that of *trans*-**17**. However, it was fortunate that signals due to the methine as well as methyl protons of *cis*- and *trans*-**17** were well separated when the n.m.r. spectrum of a mixture was determined in the presence of a shift reagent, tris(dipivaloylmethanato)europium (25). In agreement with a *cis*-isomer being a better chelating ligand than a *trans*-isomer, it is pertinent to mention that the signals of methyl and methine protons of the *cis*-**17** were shifted downfield much more than those of *trans*-**17**. In the present case the chemical shift differences of methyl and methine protons were merely <10 Hz in a $CDCl_3$ solution, the corresponding shift differences in the presence of the europium complex were 74 and 48 Hz respectively. This observation may possibly prove useful for differentiating the configurations of isomers.

Discussion

Owing to the facile interconversion of *C*-nitroso compounds under photolytic conditions, it is usually difficult to be certain whether an observed reaction should be attributed to a nitroso monomer or its dimer. For this reason, the reactions of both monomers and dimers are treated together here, except for those steps where a clear distinction can be made. The results described above and those published earlier encompass a wide range of reactions that compete with each other in deciding the fate of a photoexcited *C*-nitroso compound. The favored pathway is decided by the structure of the *C*-nitroso compound as well as by the reaction conditions. Under the experimental irradiation conditions, all the dimers **6**, **9**, and **13** rapidly dissociate to the corresponding monomers, which then undergo further photoreactions. In the case of *anti*-dimer **6**, it is a rapid disproportionation, for **9** a rapid recombination mixed with a slow disproportionation, while for dimer **13** it is overwhelmingly a tautomerization.

Disproportionation during photolysis of dimer **6** has some precedent in nitrite photolysis (26) and in a free radical reaction in the presence of external nitric oxide (27, 28). The primary photoprocess is no doubt the well established step of

Can. J. Chem. Downloaded from www.nrcresearchpress.com by 210.87.254.105 on 09/05/12
For personal use only.

homolytic dissociation to give a C-radical and nitric oxide (13, 14). Owing to an internal filter effect associated with commercial nitric oxide which hinders photoexcitation of the dimer absorption at 295 nm, the identity of the generated nitric oxide with respect to the external one could not be determined.[3] It is clear that the oxidation products obtained in >290 nm photolysis of *N*-nitroso-*N*-hexylacetamide are derived from this disproportionation process of **6** which is the primary photorearrangement product (1, 18); the mechanism of this disproportionation process has been discussed elsewhere (26–29).[4] The lack of disproportionation reactions during >400 nm photolysis of the nitrosamide (1) suggests that the reactive intermediates (either C-radical or nitric oxide) generated in this photolysis are not the same as those generated in the photolysis of *anti*-dimer **6**. We have suggested that a "tight radical pair" generated in >400 nm photolysis prevents liberation of the nitric oxide which ordinarily initiates disproportionation (1). Red-light photolysis (>680 nm) of 2-nitroso-2-methylpropane also yields *t*-butylnitrate and allied disproportionation products[5] (30) in which the presence of a radical pair has been demonstrated. It is believed that only when the members of the radical pair are genuinely "free" from each other, can disproportionation (and nitroxide formation) occur.

The photolysis of *anti*-dimer **9** under nitrogen is more complicated due to the relatively fast formation of the *syn*-dimer of **9** by a kinetically controlled dark reaction. In comparison to the *syn*-dimers of nitrosocyclohexane and other nitrosoalkanes, *syn*-**9** is surprisingly stable; however, the factors responsible for this stability remain unknown. The slow photodissociation of monomer **9** yields disproportionation products as well as hydroxylamine **11**; the latter is apparently formed via the corresponding nitroxide.

Predominant tautomerization during the photolysis of *anti*-dimer **13**, no doubt, has its origin in the proximity of the proton-donating piperidinium group at the 2-position with respect to the *C*-nitroso moiety. In view of the large difference in the rates of irradiated and thermal tautomerizations under comparable conditions, we believe that there is a certain amount of light catalysis in the process. Mackor and de Boer (17, 31) have reported a red-light catalyzed tautomerization of nitrosocyclohexane monomer (generated at 80°) in cyclohexane to yield cyclohexanone oxime in *ca.* 90% yield; in this photolysis e.s.r. signals of the corresponding nitroxide has been detected but no disproportionation product has been reported. One may envisage a vibrationally excited *C*-nitroso monomer, probably derived from a radiationless decay of an electronically excited manifold, to undergo facile tautomerization. Alternatively, photoexcitation may create a dipolar *C*-nitroso species, such as **18**, which triggers a facile proton transfer.

Generally speaking, the results of *anti*-dimer photooxidation in Pyrex apparatus and those of red-light photooxidation of nitrosocyclohexane (17) and 2-nitroso-2-methylpropane (30) can be characterized by the formation of nitrates and nitro compounds, although the ratios can vary considerably. It should be mentioned that nitro compounds were not formed in our photolysis under nitrogen and that the oxidations are genuine photoreactions as shown by control reactions in the dark. Also, the oxidations are not initiated by a singlet oxygen (24). Furthermore, the photooxidation takes place from a *C*-nitroso monomer since no reaction has been observed without irradiation at the dimer absorption near 290 nm.

Inspection of the oxidation products shows that all the nitrates obtained as the result of photooxidation of the *anti*-dimers have lost the stereochemical integrity of the original *trans*-configuration. In contrast, nitro compound **12** maintains the original *trans*-configuration of *anti*-dimer **9**. The conditions used in the photooxidation of *anti*-dimer **13** do not allow us to predict the stereochemical consequences since the scrambling of the configuration in **16** can have arisen from nitro–nitronate tautomeric equilibrium (32) through acid or base catalysis. The dissimilarity in the stereochemical results

[3]For a discussion of the polymeric state of nitric oxide in solution see ref. 1.

[4]For obvious reasons gas kineticists (ref. 28) favor the generation of $\cdot NO_3$ by disproportionation of three molecules of NO. In solution it is more likely NO attacks a *C*-nitroso monomer to form the azonitrate ester intermediate which eliminates nitrogen to give nitrate (27). The absence of the corresponding nitro compound in our photolysis products supports the latter mechanism (however, see ref. 31 for a comparison).

[5]An assumption that only a vibrationally excited ·NO from >290 nm photolysis can undergo disproportionation becomes questionable from this experiment.

Can. J. Chem. Downloaded from www.nrcresearchpress.com by 210.87.254.105 on 09/05/12
For personal use only.

suggest that nitro and nitrate formations occur by separate pathways. Indeed, during red-light photooxidation of nitrosocyclohexane, Mackor and de Boer have observed that while the yields of nitrocyclohexane increase as the reaction temperature is lowered, the yield of cyclohexyl nitrate remains virtually stationary.

In photooxidations, scrambling of the nitrate configurations means that at some point the C—NO bonds of the monomer must be broken and that C—ONO_2 bonds are formed. It follows that the nitrate formation must be derived from photodissociation of *C*-nitroso monomers which is the common pathway to disproportionation. Under the photooxidation conditions, clearly the generated nitric oxide is quickly intercepted by oxygen to become nitric trioxide[6] (28). The combination of the alkyl radical with nitric trioxide completes the oxidation process to give the corresponding nitrate, which is stable to further irradiation. This mechanistic interpretation shares a common principle with the oxidation during nitrosamine photoaddition and nitrosamide photorearrangement described in the preceding paper (1); namely, oxygen captures nitric oxide quickly regardless of the existence of the latter as the radical pair. This mechanism requires that any dimer which can undergo photodissociation should be able to undergo photooxidation to form the corresponding nitrate; the efficiency of this is determined by the lifetime of the *C*-nitroso monomer and its ease of C—N bond scission. In agreement, the *C*-nitroso monomer of dimer-**6** photodisproportionates most efficiently and, therefore, is oxidized exclusively to nitrate whereas the ones derived from dimer **9** and **13** are oxidized only partially to nitrate **10**, owing to its facile dimerization and nitro compound formation (*vide infra*).

Since conservation of the *trans*-configuration in the formation of nitro compound **12** requires that the C—NO bond remain intact during the reaction, it follows that some primary photochemical act other than photodissociation must be responsible for the oxidation to the nitro compound. A perspective view of product patterns in the photolysis of various *C*-nitroso compounds leads us to believe that the nitro compound formation process in photooxidation shares a common reactive intermediate with the process[7] of tautomerization in the corresponding photolysis under nitrogen. Tentatively we ascribe a vibrationally excited state of a *C*-nitroso monomer, such as **18**, to this intermediate. Probably oxygen captures such an excited species instantaneously, before it can undergo other processes, leading to a diradical **19** which is also proposed by de Boer's group (17, 30). In the presence of a suitable substrate, peroxy radical **19** may abstract an H-atom (from ethylbenzene) or add (to styrene) (30); otherwise **19** may shed the extra oxygen atom by oxidizing another *C*-nitroso monomer to give two nitro compounds. Without going into detail, the various photochemical processes of *C*-nitroso compounds can be summarized in Scheme 2. We assume that the same excited state **20** is responsible for all the primary photochemical reactions. Studies are underway to see if there is more than one excited state involved in the photoprocesses and what type(s) of excited state are involved.

The mechanism of the nitro group formation discussed above assumes excited *C*-nitroso monomers as the reactive species, on the basis of (*i*) the facile dissociation of a *C*-nitroso dimer to the corresponding monomer on irradiation at $-190°$ (10), and (*ii*) the formation of the corresponding *C*-nitro compound during photooxidation of a *C*-nitroso monomer (17, 30) with red-light. At present an alternative possibility of the excited dimers **9** and **13** being the reactive species cannot be ruled out completely. Conceivably a photoexcited dimer may react with oxygen to form an intermediate **23** which then decomposes to a nitro compound such as **12** and **16**. If this is the case, it may be inferred that *anti*-dimer **6** photodissociates to the monomer readily and is photooxidized totally to nitrate **8**, whereas photoexcited *anti*-dimers **9** and **13** have a sufficiently long lifetime to react with oxygen directly to give nitro compounds **12** and **16**. The validity of this interpretation awaits clarification in future.

[6]Depending on the structure, oxygen and alkyl radical combination is no doubt also possible. Such a pathway has been found in the photooxidation of nitrosocyclohexane (17).

[7]Perhaps the dimerization process can be included if it is also a light-catalyzed reaction; an unambiguous proof is, however, not available at present.

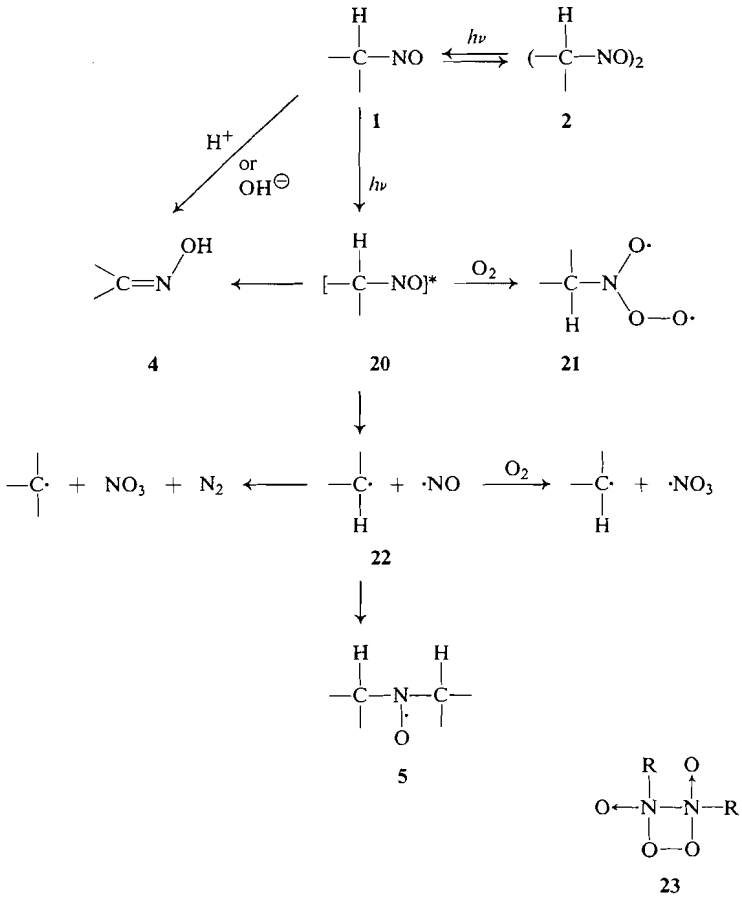

SCHEME 2

Experimental

The apparatus and conditions for spectroscopic analyses were the same as those described in the previous publication (1). The photolysis was carried out in a Pyrex apparatus with a Hanovia mercury lamp 654A36 (200 W).

Photolysis of the anti-dimer of N-(4-Nitrosohexyl)-acetamide (6)

(A) A benzene solution (220 ml) of *anti*-dimer **6** (101 mg) (18) was photolyzed under nitrogen for 2 h. The solvent was evaporated to give an oil (105 mg). This crude oil was chromatographed on a silicic acid column to give *N*-(4-nitratohexyl)acetamide (**8**, 32 mg) (18) the parent amide (**7**, 57 mg) and *anti*-dimer **6** (19 mg).

(B) A solution of *anti*-dimer **6** (10 mg) in benzene (15 ml) was purged with helium and was saturated with nitric oxide. The solution was irradiated for 1 h and was evaporated to give a solid residue which contained *anti*-dimer **6** as shown by t.l.c. and i.r. analysis. The same solution kept at room temperature in the dark for 48 h also gave the unreacted *anti*-dimer **6**.

(C) A solution of *anti*-dimer **6** (20 mg) in benzene (30 ml) was irradiated under oxygen for 4 h. The crude residue showed strong i.r. absorptions at 1625, 1275, and 865 cm^{-1}. Preparative t.l.c. separation gave nitrate **8** (15.3 mg) and a trace amount of the parent amide **7**.

(D) A solution of *anti*-dimer **6** (60 mg), rose bengal (25 mg), and methanol (100 ml) was irradiated in the presence of oxygen with a tungsten lamp (500 W) for 10 h during which the absorption peak at 293 nm decreased less than 5%. The recovered product was shown to be *anti*-dimer **6**.

Photolysis of the anti-Dimer of trans-1-Nitroso-2-chlorocyclohexane (9)

(A) The dimer was prepared according to the method of Ponder *et al.* (19) and was recrystallized from absolute ethanol: m.p. 150–152° (lit. (19) 152–153°); n.m.r. τ 4.28 (m) and 5.5 in the ratio of 1:1; i.r. 1460 and 1210 cm^{-1}.

A solution of *anti*-dimer **9** (1 g) in benzene (100 ml) was photolyzed under nitrogen atmosphere. In 0.5 h, a precipitate covered the photocell. The white crystals were scraped off the surface of the photocell now and then, and irradiation was continued for 7 h. The crystalline precipitate (260 mg) was washed with ether and dried overnight: m.p. 135–140°. An ethanol solution of the crystals exhibited u.v. absorption at 275 nm which shifted gradually to 295 nm after 10 h. Recrystallization from benzene gave white crystals that exhibited the identical

Can. J. Chem. Downloaded from www.nrcresearchpress.com by 210.87.254.105 on 09/05/12
For personal use only.

Can. J. Chem. Downloaded from www.nrcresearchpress.com by 210.87.254.105 on 09/05/12
For personal use only.

i.r., n.m.r., and mass spectra as those of *anti*-dimer **9**. The residue from the photolysate showed i.r. absorption at 1640, 1450, 1285, 1210, and 850 cm^{-1}. Alumina chromatography of this crude product gave **9** (540 mg) and a fraction of oil; i.r. 1635, 1280, 860, and 750 cm^{-1}; n.m.r. τ 5.05 (m), 6.10 (m), and 6.4 (m). V.p.c. analysis of the oil (on a 3% SE 30 column at 90°) showed that cyclohexylchloride and *trans*-1-nitrato-2-chlorocyclohexane (**10**) were present in nearly 1:1 ratio. However, the peak of the latter compound exhibited a weak shoulder which was tentatively assigned to the corresponding *cis*-isomer of **10**.

A solution of *trans*-dimer **9** (1 g) in methanol (100 ml) was photolyzed under nitrogen for 37 h until the 295 nm peak disappeared. After the usual working-up, the crude oil (950 mg) was taken up in methanol from which a white solid (145 mg) deposited. Recrystallization of the solid from methanol gave white crystals of *N,N,O*-tri(2-chlorocyclohexyl)hydroxylamine (**11**); m.p. 110–112°, i.r. 1045 and 730 cm^{-1}, *m/e* 381, 383, 385, 264, 266, 229, and 231. The residue obtained from the removal of **11** exhibited strong absorption at 1640, 1285, 850, and 750 cm^{-1}. V.p.c. analysis of the oil showed that cyclohexyl chloride and **10** were present in 1:1 ratio.

(B) A solution of *trans*-dimer **9** (1 g) in methanol containing aqueous perchloric acid (1.2 g) was photolyzed under oxygen. The original u.v. absorption of the *trans*-dimer at 295 nm shifted to 275 nm in 0.5 h irradiation and *cis*-dimer precipitated out gradually. The precipitate disappeared slowly and finally the peak at 275 nm disappeared after 5 h irradiation. In a benzene solution the same situation was observed.

The benzene photolysate was evaporated to give a resin which showed i.r. absorption at 1725(w), 1630(s), 1550(s), 1375(s), 1280(s). This resin was chromatographed on an alumina column. With petroleum ether *trans*-1-nitrato-2-chlorocyclohexane (**10**) was eluted and was sublimed to give an oil; i.r. 1630, 1280, 860, and 750 cm^{-1}; n.m.r. τ 8.35 (m, 6H), 7.78 (m, 2H), 6.10 (dt, J = 4 and 8 Hz, 1H) and 5.02 (dt, J = 4 and 8 Hz, 1H); *m/e* (% at 15 eV) 136 (10), 134 (30), 121 (40), 119 (100), 85 (80), 84 (90), 70 (55), 69 (65).

Continuing elution with petroleum ether gave mixtures of nitrate **10** and nitro compound **12** and, finally, with 20% benzene in petroleum ether a fraction of oil which showed a single spot on t.l.c. This oil was distilled to a colorless oil of *trans*-1-nitro-2-chlorocyclohexane (**12**); i.r., 1550, 1370, 850, and 745 cm^{-1}; n.m.r. τ 5.495 (dt, J = 10 and 4 Hz, 1 H) and 5.735 (dt, J = 10 and 4 Hz; 1H); *m/e* (%) 127 (4), 118 (1.7), 116 (4.6), 97 (4), 81 (100), 79 (31) and 77 (12).

Analysis of the crude product by v.p.c. (3% SE 30 column at 90°) from either photooxidation in methanol or in benzene showed that the ratio of nitrate **10** (R_t 2.7 min) and nitro compound **12** (R_t 3.2 min) is about 1:1. The shoulder corresponding to *cis*-isomer of **10** is also observed in the former peak.

Photolysis of the anti-Dimer of trans-1-Nitroso-2-piperidinocyclohexane (13)

(A) A solution of *anti*-dimer **13** (250 mg) (22), concentrated hydrochloric acid (0.3 ml), and methanol (300 ml) was photolyzed under nitrogen for 0.5 h. The methanol solution was basified, evaporated, and extracted with methylenechloride. After working-up, the crude resin was chromatographed to give 2-piperidinocyclohexanone oxime (**14**, 145 mg).

(B) The *anti*-dimer (1.0 g) and concentrated hydrochloric acid (2.5 ml) in methanol (500 ml) was irradiated through a Pyrex filter, under oxygen atmosphere for 1 h. The solvent was evaporated to give a semi-solid; the i.r. spectrum of which exhibited weak absorptions at 1720 and 1635 cm^{-1} but strong absorptions at 1550, 1450, and 1370 cm^{-1} for a nitro group. Chromatography on an alumina column gave several fractions of mixtures of *cis*- and *trans*-1-nitro-2-piperidinocyclohexanes (**16**) which exhibited n.m.r. signals at τ 5.33 (dt, J = 11 and 5 Hz) and 5.15 (m, $w_{1/2}$ = 6 Hz) in various ratios.

The crude product was hydrogenated in MeOH in the presence of platinum black and the free base (840 mg) was liberated with potassium carbonate. The free base (420 mg) was acetylated with acetic anhydride and sodium acetate. The crude product (360 mg) was isolated in the usual manner to afford an oil: 3300, 1640, 1540, 1265 cm^{-1}; n.m.r. τ 8.05(s) and 7.93(s) in the ratio of 3:2. Chromatography of this oil in an alumina column gave various mixtures of *trans*- and *cis*-1-acetamido-2-piperidinocyclohexane (**17**, 35%) and a mixture of *cis*- and *trans*-2-piperidinocyclohexanol (13%) (1). One of the acetamido fractions contained *ca.* 85% of the *trans*-isomer and was sublimed to give an oil: i.r. 3300, 1640, 1545, 1305, 1255, and 1100 cm^{-1}; n.m.r. 8.05 (s), 7.57(m) and 6.63(dt, J = 10 and 4 Hz, 1H) and 3.27 (NH); *m/e* (%) 224 (M^+), 179 (15), 165 (15), 124 (67), 110 (18), 98 (23), 84 (50) and 41 (100). The *trans*-isomer **17** was also prepared by reduction of the *anti*-dimer **13** with lithium aluminum hydride in ether.

A mixture of *cis*- and *trans*-acetamide in $CDCl_3$ solution in the presence of tris(dipivaloylmethanato)-europium exhibited signals at τ 4.63 (m, $w_{1/2}$ = 23 Hz) and 6.47 (s) for the *trans*-isomer and 3.83 (m, $w_{1/2}$ = 10 Hz) and 5.24(s) for *cis*-isomer.

The authors are grateful to the National Research Council of Canada, Defence Research Board, Ottawa and the President's Research Fund, Simon Fraser University, for financial supports of this project.

1. Y. L. Chow, J. N. S. Tam, C. J. Colón, and K. S. Pillay. Can. J. Chem. This issue.
2. B. G. Gowenlock and J. Trotman. J. Chem. Soc. 1670 (1956); 419 (1955).
3. R. Hoffman, R. Gleiter, and F. B. Mallory. J. Am. Chem. Soc. **92**, 1460 (1970).
4. B. G. Gowenlock and W. Lüttke. Quart. Rev. **12**, 321 (1954).
5. V. von Keussler and W. Lüttke. Z. Electrochem. **63**, 614 (1959).
6. R. R. Holmes. J. Org. Chem. **29**, 3076 (1964).
7. L. G. Donaruma. J. Org. Chem. **23**, 1338 (1958).
8. A. DiGiacomo. J. Org. Chem. **30**, 2614 (1965).
9. G. Collin, R. Höhn, H. G. Hauthal, H. Hübner, W. Pritzkow, W. Rolle, H. Schaefer, and M. Wahren. Ann. **702**, 55 (1967).
10. A. Mackor, Th. A. J. W. Wajer, and Th. J. de Boer. Tetrahedron Lett. 2757 (1967).
11. L. Orgel. J. Chem. Soc. 1267 (1953); J. Mason. J. Chem. Soc. 3904 (1957).

12. K. NAKAMOTO and R. RUNDLE. J. Am. Chem. Soc. **78**, 1116 (1956).
13. (*a*) A. MACKOR, TH. A. J. W. WAJER, TH. J. DE BOER, and J. D. W. VAN VOORST. Tetrahedron Lett. 2115 (1966). (*b*) J. A. MAASSEN, H. HITTENHAUSSEN, and TH. J. DE BOER. Tetrahedron Lett. 3213 (1971).
14. J. DICKSON and B. G. GOWENLOCK. Liebigs Ann. **745**, 52 (1971).
15. (*a*) E. BAMBERGER. Chem. Ber. **35**, 1606 (1902). (*b*) H. MAUSER and H. HEITZER. Z. Naturforsch. **20**b, 200 (1965).
16. A. COX and T. J. KEMP. Introductory photochemistry. McGraw-Hill Book Co. (U.K.) Ltd., London, 1970. p. 72.
17. A. MACKOR and TH. J. DE BOER. Rec. Trav. Chim. **89**, 164 (1970).
18. Y. L. CHOW, J. N. S. TAM, and A. C. H. LEE. Can. J. Chem. **47**, 2441 (1969).
19. B. W. PONDER, T. E. WALTON, and W. J. POLLOCK. J. Org. Chem. **33**, 3957 (1968).
20. W. PRITZKOW, H. SCHAEFER, P. PABST, A. EBENROTH, and J. BLYER. J. Prakt. Chem. **29**, 123 (1965).
21. M. OHNO, M. OKAMOTO, and N. NUKADA. Tetrahedron Lett. 4047 (1965).
22. Y. L. CHOW, C. J. COLÓN, and S. C. CHEN. J. Org. Chem. **32**, 2109 (1967); Y. L. CHOW, S. C. CHEN, and D. W. L. CHANG. Can. J. Chem. **46**, 157 (1970).
23. TH. A. J. W. WAJER, A. MACKOR, TH. J. DE BOER, and J. D. W. VAN VOORST. Tetrahedron, **23**, 4021 (1967); A. MACKOR, TH. A. J. W. WAJER, and TH. J. DE BOER. Tetrahedron, **24**, 1623 (1968).
24. C. S. FOOTE. Acc. Chem. Rev. **1**, 104 (1968).
25. R. F. BUTTERWORTH, A. G. PERNET, and S. HANESSIAN. Can. J. Chem. **49**, 981 (1971).
26. Y. L. CHOW, T. HAYASAKA, and J. N. S. TAM. Can. J. Chem. **48**, 508 (1970).
27. J. F. BROWN, JR. J. Am. Chem. Soc. **79**, 2480 (1957); L. G. DONARUMA and D. J. CAMODY. J. Org. Chem. **22**, 635 (1957).
28. J. HEICKLEN and N. COHN. Adv. photochem. **5**, 157 (1968).
29. Y. L. CHOW and J. N. S. TAM. J. Chem. Soc. C, 1138 (1970).
30. J. A. MAASSEN. Ph.D. dissertation. University of Amsterdam, 1972.
31. A. MACKOR. Ph.D. dissertation. University of Amsterdam, 1968.
32. F. G. BORDWELL. Acc. Chem. Res. **3**, 281 (1970); F. G. BORDWELL and K. C. YEE. J. Am. Chem. Soc. **92**, 5933, 5939 (1970); F. G. BORDWELL, K. C. YEE, and A. C. KNIPE. J. Am. Chem. Soc. **92**, 5945 (1970).

Can. J. Chem. Downloaded from www.nrcresearchpress.com by 210.87.254.105 on 09/05/12
For personal use only.

The Dehydrogenation and Dehydration of 2-Propanol Vapor on Manganese Ferrite

EUGENE FRANCIS MCCAFFREY AND ROBERT ANDERSON ROSS
Department of Chemistry, Lakehead University, Thunder Bay, "P", Ontario
Received September 8, 1972

The dehydrogenation and dehydration of 2-propanol on manganese ferrite has been studied between 306 and 362 °C. The selectivity for dehydrogenation was constant throughout the temperature range. At 362 °C a trace of condensation of the alcohol to mesityl oxide was detected, <0.1% v/v of the reaction products.

La déhydrogénation et la déhydratation du propanol-2 sur la ferrite de manganèse ont été étudiées entre 306 et 362 °C. La sélectivité en faveur de la déhydrogénation s'est avéré constante à toutes les températures. A 362 °C une trace de condensation de l'alcool en oxyde de mésityle a pu être détectée <0.1% v/v des produits de la réaction. [Traduit par le journal]

Can. J. Chem., **51**, 2486 (1973)

Introduction

This article describes some experiments on the catalytic reactions of 2-propanol over manganese ferrite. The work was carried out to see if any links could be found with previous studies on alcohol decompositions using spinel oxide catalysts (1, 2) and also with recent experiments in which manganese(II) oxide was evaluated as a catalyst in the simultaneous dehydration and dehydrogenation of 2-propanol vapor (3).

Experimental

Apparatus and Procedure

The all-glass flow system and the methods of analysis have been described previously (3). To establish the experimental conditions for which the reaction rate was not influenced by external or internal diffusion, the influence of space velocity, catalyst mass, and particle size were studied in the usual manner (3). As a result the kinetic measurements were performed at atmospheric pressure with a flow rate of 300 ml min^{-1} (normal temperature and pressure) and the catalyst particle size was kept less than 0.1 mm.

All reaction rate measurements were made after the establishment of a steady activity level.

Materials

Manganese ferrite, $MnFe_2O_4$, was prepared by heating manganese(II) oxide (3) and iron(III) oxide (99.99% w/w Alfa Inorganics Inc.) to 1300 °C in flowing nitrogen for 48 h. The final X-ray powder photograph confirmed the $MnFe_2O_4$ structure (4). The surface area was 0.22 m^2 g^{-1} (B.E.T. krypton; −196 °C; σ = 21.5 Å^2).

2-Propanol and acetone were "spectroquality" reagents and their u.v. absorption characteristics were the same as those given on their accompanying certificates. All gaseous reagents and the nitrogen carrier (Canadian Liquid Air Ltd.) were 99.99% pure.

Results and Discussion

The activity of the ferrite was tested at 400 °C with 1 g of the material and an alcohol partial pressure of 9.37 Torr. The catalyst was stable and carbon dioxide was not detected in the reaction products.[1]

The Effect of 2-Propanol Partial Pressure on the Reaction Rates

The partial pressure of 2-propanol was varied between 3.17 and 15.62 Torr at 362 and 306 °C. There was a very slight but measurable trend for the selectivity for dehydrogenation to decrease with increase in the alcohol partial pressure at 306 °C. Approximate values of 0 and 0.2 were determined from logarithmic plots (3) for the reaction orders with respect to 2-propanol partial pressure for both reactions at 306 and 362 °C, respectively. These low values of reaction orders probably indicate that the catalyst surface was highly saturated with adsorbed alcohol.

The Effects of Hydrogen and Propylene

At 362 °C the effect of varying the total hydrogen partial pressure from 1.00 to 51.67 Torr on the rates of reaction of 9.37 Torr partial pressure alcohol was examined. The reaction rates increased slightly and monotonously with increase in the hydrogen partial pressure over the entire

[1]Complete set of tabular data is available, at a nominal charge from the Depository of Unpublished Data, National Science Library. National Research Council of Canada, Ottawa, Canada K1A 0S2.

Can. J. Chem. Downloaded from www.nrcresearchpress.com by 210.87.254.105 on 09/05/12
For personal use only.

Can. J. Chem. Downloaded from www.nrcresearchpress.com by 210.87.254.105 on 09/05/12
For personal use only.

pressure range such that with 51.67 Torr total hydrogen pressure the rates of dehydrogenation and dehydration had increased by about 36 and 28%, respectively. When the added hydrogen was removed on completion of the experiments, the catalyst activity returned to its original level after 2 h. Hydrogen has also been reported to enhance the rate of the dehydrogenation reaction over chromia-alumina catalysts (5) possibly by increasing the donor nature of the catalyst. However, it may be more likely that a fairly insensitive adsorption/desorption equilibrium condition exists between hydrogen and some adsorbed species.

From 306 to 362 °C with propylene partial pressure from 0.10 to 50.77 Torr and 9.37 Torr alcohol partial pressure, propylene had no real influence on the rates of either the dehydrogenation or dehydration reactions. This may be interpreted in terms of a very rapid saturation of adsorption sites or that an extremely fast desorption of propylene occurs.

The Effects of Water Vapor and Acetone

The effect of changing the total water vapor partial pressure from 0.11 to 2.86 Torr was studied at 362 °C with 9.37 Torr partial pressure alcohol. The rates of both reactions were slightly depressed by addition of water vapor. The maximum effect was observed with 2.86 Torr total water vapor pressure when the values of the rates of dehydration and dehydrogenation were lowered by 7 and 18%, respectively. After the removal of the added water vapor, the catalyst activity returned to its original value in 30 min.

The very small dependence of the rate of dehydration on the partial pressure of water vapor differs from the results found with manganese(II) oxide, where the order of the dehydration reaction with respect to water vapor pressure was -0.5 (3). However, the result is similar to that established for reaction of 2-propanol over nickel(II) oxide (6) and the earlier result for dehydration of ethanol over γ-alumina (2). These observations indicate that manganese ferrite is much less susceptible to poisoning by water vapor than was manganese(II) oxide (3) which points to possible differences in the types of dehydration sites on the two catalysts. Adsorption of water vapor on coordination unsaturated species (7) on the surface of manganese(II) oxide might be expected to form a more stable intermediate adsorbed complex than that on the ferrite.

At 362 °C and with 9.37 Torr alcohol partial pressure, the acetone partial pressure was varied from 1.00 to 5.43 Torr. Both reaction rates were depressed monotonously and in step such that the selectivity for dehydrogenation remained constant over the pressure range and an approximate reaction order of -0.1 with respect to acetone partial pressure was determined for each reaction. The activity for the dehydrogenation reaction returned to within 3% of its initial value when the added acetone was removed from the system. However, the activity for dehydration was permanently reduced by 12% at the steady level of catalyst activity.

The Effect of Temperature on the Reaction Rates

Experiments were carried out with 9.37 Torr partial pressure 2-propanol at various temperatures from 306 to 362 °C. The rates of the dehydrogenation and the dehydration reactions as well as the selectivity for dehydrogenation are given in Table 1. At 362 °C, mesityl oxide composed less than 0.1% v/v of the reaction products.

The selectivity observed with manganese ferrite does not differ significantly from that found for manganese(II) oxide (3), several other transition metal oxides (6), and magnesium, calcium, strontium, and barium oxides (8). On the other hand, it has been reported that dehydration of 2-propanol was favored on nickel ferrite catalysts (1). Since both nickel and manganese ferrites are inverse spinels (9), the difference in their selectivities appears not to be related to the cation distribution within the

TABLE 1. Effect of temperature on the rates of dehydrogenation, r_1, and dehydration, r_2, of isopropyl alcohol over manganese ferrite using 9.37 Torr partial pressure alcohol

Catalyst temperature (°C)	Rate of dehydrogenation (mol m^{-2} s^{-1}) $\times 10^8$	Rate of dehydration (mol m^{-2} s^{-1}) $\times 10^8$	Selectivity $\frac{r_1}{r_1 + r_2}$
362	126.0	14.4	0.90
349	92.0	10.5	0.90
336	61.2	6.7	0.90
324	40.0	4.6	0.90
306	17.9	2.2	0.89

lattice. Such a relationship has been proposed to account for selectivity differences shown by a series of alumina-spinel oxides in the decomposition of ethyl alcohol (2).

1. E. LICHTNER and G. SZALEK. Z. Chem. **8**, 314 (1968).
2. D. E. R. BENNETT and R. A. Ross. J. Catal. **17**, 122 (1970).
3. D. G. KLISSURSKI, E. F. MCCAFFREY, and R. A. Ross. Can. J. Chem. **49**, 3778 (1971).
4. American Society for Testing Materials, Card Index, 1967.
5. C. DANIEL and J. C. KURIACOSE. Curr. Sci. **36**, 606 (1967).
6. D. G. KLISSURSKI, E. F. MCCAFFREY, and R. A. Ross. Paper 3, Vth Int. Congr. Catal. Palm Beach. 1972.
7. O. V. KRYLOV. Catalysis by nonmetals. Academic Press, New York and London. 1970.
8. E. F. MCCAFFREY, T. A. MICKA, and R. A. Ross. J. Phys. Chem. **76**, 3372 (1972).
9. T. J. GRAY. *In* High temperature oxides, Part IV. *Edited by* A. M. Alper. Academic Press, New York and London. 1971.

Can. J. Chem. Downloaded from www.nrcresearchpress.com by 210.87.254.105 on 09/05/12
For personal use only.

Determination of Excess Volumes of Cyclohexane + Benzene Mixtures with a Mechanical Oscillator Densimeter[1]

OSAMU KIYOHARA[2] AND G. C. BENSON

Division of Chemistry, National Research Council of Canada, Ottawa, Canada K1A 0R6

Received February 28, 1973

Two methods of calibrating an Anton Parr densimeter were investigated. Values of the excess volume of cyclohexane + benzene mixtures obtained from density measurements at 25 °C with this instrument agree well with results in the literature.

Deux méthodes d'étalonnage, d'un densimètre Anton Parr ont été envisagées. Les volumes d'excès des mélanges cyclohexane + benzène ont été calculés à partir des densités mesurées, à 25 °C, avec cet appareil; l'accord avec les résultats rapportés dans la littérature est excellent.

Can. J. Chem., 51, 2489 (1973)

Can. J. Chem. Downloaded from www.nrcresearchpress.com by 210.87.254.42 on 09/05/12
For personal use only.

This note reports values of excess volumes obtained from measurements of density on the system cyclohexane + benzene with an oscillator type densimeter (Digital Densimeter DMA O2C, manufactured by Anton Parr K.G.). The primary purpose of the work was to examine the suitability of this instrument for studying the excess volumes of mixtures of nonelectrolytes.

The DMA O2C densimeter is based on a design developed by Kratky and co-workers (1–3). In it, the density of a fluid (gas or liquid) is determined by measuring the resonant frequency of a mechanical oscillator, a U-shaped Duran 20 glass tube, filled with the fluid. The method assumes a linear relation

$$[1] \qquad d = AT^2 + B$$

between the density, d, of the fluid and the square of the period, T, of the oscillator. A and B are constants of the instrument and their values are determined by calibration with two fluids of known densities, water and air generally being used for this purpose. Under favorable circumstances, differences in density can be determined within $\pm 1.5 \times 10^{-6}$ g cm^{-3}, thus the instrument is well suited to the study of dilute aqueous solutions and to the determination of partial molar volumes (2, 4–6). However, this accuracy is limited to differences which are less than about 0.05 g cm^{-3}. The operating manual for the DMA O2C points out that the approximation associated with the use of eq. 1 leads to errors which increase in the measurement of larger density differences, and gives an upper bound of $\pm 1 \times 10^{-3}$ g cm^{-3} for differences of 3 g cm^{-3}. Recently, the DMA O2C has been used to determine densities of mixtures of organic liquids and to obtain excess volumes for systems in which the variation in density is much greater than 0.05 g cm^{-3} (7, 8). It is therefore important to study in more detail the suitability of the densimeter for such measurements.

Two different ways of calibrating the densimeter were investigated. Method I followed the manufacturer's instructions, and used water and air as standards. The water was twice distilled in a Pyrex still, and prior to its use it was boiled to remove dissolved air. The temperature of the oscillator chamber was controlled at 25.000 ± 0.002 °C. It was monitored continuously with a quartz thermometer and the observed oscillator periods were corrected to 25.000 °C. François *et al.* (9) reported that their densimeter was sensitive to changes in atmospheric pressure. To investigate this effect further, our densimeter was placed in a metal box with a window, and the pressure was increased above the ambient by about 15 Torr. This experiment failed to reveal any clear-cut pressure dependence and, within the reproducibility of the measurements, the change in the period of the oscillator filled with air agreed with the value estimated from the increase in the density of the air.

The second calibration (method II) was carried out over a more limited range of density, 0.74–1.05 g cm^{-3}, and should therefore give a better description of the behavior of the oscillator for densities of interest in our work.

[1]NRCC No. 13185.

[2]NRCC Postdoctorate Fellow 1971–1973.

TABLE 1. Molar excess volume V^E of mixtures of cyclohexane + benzene containing mole fraction x of cyclohexane at 25 °C

x	V^E(cm^3 mol^{-1})	x	V^E(cm^3 mol^{-1})
0.05443	0.1296	0.53501	0.6501
0.10395	0.2359	0.53965	0.6496
0.14783	0.3236	0.54486	0.6499
0.16064	0.3418	0.60482	0.6301
0.20153	0.4091	0.61647	0.6222
0.27293	0.5066	0.63063	0.6181
0.28480	0.5250	0.69248	0.5662
0.28878	0.5290	0.71962	0.5363
0.32679	0.5695	0.74827	0.5031
0.34887	0.5850	0.75253	0.4967
0.36937	0.6049	0.79043	0.4427
0.43128	0.6359	0.85327	0.3373
0.45339	0.6443	0.86238	0.3202
0.45757	0.6464	0.95263	0.1221
0.48451	0.6489		

Oscillator periods were determined for water and ten organic liquids for which the densities (relative to water) were measured in a magnetic float densimeter (10). The method of least squares was used to fit eq. 1 to the results and the standard error of estimate for the representation was 0.000057 g cm^{-3}. Over the range of density considered in method II, the values of the density at 25 °C derived from the two calibrations are related by the equation

$$[2] \qquad d_I = 1.0002663 d_{II} - 0.0002952$$

Thus a density of 0.7 g cm^{-3} will be low by about 1×10^{-4} g cm^{-3} if the instrument is calibrated by method I. Although eq. 2 is characteristic of our particular densimeter, it should also provide an approximate indication of the error which can occur when this type of instrument is used without a careful calibration for the range of density under investigation.

In deriving excess volumes from density results, there will be some cancellation between systematic errors in the densities of the mixtures and of the pure components. However, the use of a calibration based only on water and air can lead to significant errors in the excess volume when the densities of the components are very different.

Powell and Swinton (11) have suggested that the system cyclohexane + benzene be adopted as a standard for testing dilatometers. Samples of cyclohexane and benzene were purified chromatographically and a series of mixtures of known mole fractions were prepared from these by weight, applying corrections for buoyancy effects. Densities at 25 °C were obtained from the densimeter readings, using the calibration by method II. The results for cyclohexane and benzene were 0.773598 and 0.873524 g cm^{-3}, respectively. The values of the excess volume, V^E, for the mixtures are summarized in Table 1. These are represented by the least squares equation

$$[3] \quad V^E/\text{cm}^3\,\text{mol}^{-1} = x(1-x)[2.61313 - 0.10497(1-2x)]$$

where x is the mole fraction of cyclohexane. The standard error of estimate for this representation is 0.0017 cm^3 mol^{-1}.

Our values of V^E can be compared with values measured recently by dilatometric (12) and magnetic float (10) techniques. A least squares analysis was carried out on the three sets of results, assigning equal statistical weight to each of the 132 points. This led to the equation

$$[4] \quad V^E/\text{cm}^3\,\text{mol}^{-1} = x(1-x)[2.60446 - 0.09188(1-2x) + 0.03492(1-2x)^2]$$

with a standard error of estimate equal to 0.0018 cm^3 mol^{-1}. Figure 1 shows a plot of the deviations of the individual experimental results from eq. 4. Also shown are curves representing the deviations of the smoothed results for each of the investigations. It can be seen that most of the deviations are less than ±0.5%, and that our results are in good agreement with the values obtained by the other methods. For the system

Can. J. Chem. Downloaded from www.nrcresearchpress.com by 210.87.254.42 on 09/05/12
For personal use only.

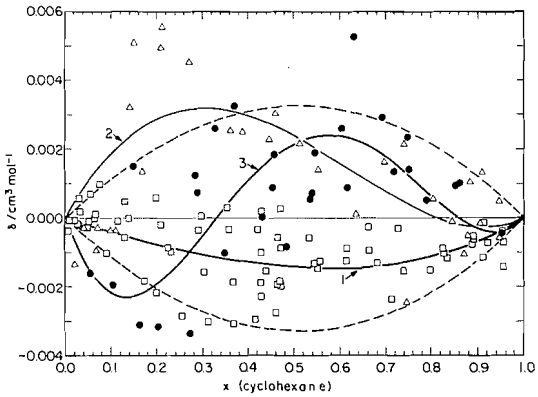

FIG. 1. Comparison of experimental results for molar excess volume of cyclohexane + benzene mixtures at 25 °C: Points and curves represent deviations from eq. 4 (*i.e.* $\delta = V^E - V^E$ (eq. 4)); □, Stokes, Levien, and Marsh (12): curve 1, $V^E/\text{cm}^3\ \text{mol}^{-1} = x(1-x)\cdot[2.5988 - 0.0901(1-2x) + 0.03445(1-2x)^2]$; Δ, Weeks and Benson (10): curve 2, $V^E/\text{cm}^3\ \text{mol}^{-1} = x(1-x)\cdot[2.6141 - 0.0744(1-2x) + 0.0337(1-2x)^2]$; ●, present work: curve 3, smoothed results represented by eq. 3; broken curves correspond to deviations of ±0.5%.

cyclohexane + benzene, the densities of the components differ only by 0.1 g cm^{-3}, and the values of the excess volume are not altered significantly (*i.e.*, less than 0.0002 cm^3 mol^{-1}), if the densimeter is calibrated by method I instead of method II.

We wish to thank Mr. P. J. D'Arcy and Mr. C. J. Halpin for technical assistance during this investigation.

1. H. STABINGER, H. LEOPOLD, and O. KRATKY. Monatsh. Chem. **98**, 436 (1967).
2. O. KRATKY, H. LEOPOLD, and H. STABINGER. Z. Angew. Phys. **27**, 273 (1969).
3. H. LEOPOLD. Elektron. **19**, 297 (1970).
4. L. BØJE and A. HVIDT. J. Chem. Thermodyn. **3**, 663 (1971).
5. C. TONDRE and R. ZANA. J. Phys. Chem. **76**, 3451 (1972).
6. P. R. PHILIP, J. E. DESNOYERS, and A. HADE. Can. J. Chem. **51**, 187 (1973).
7. A. BARLATIER, R. MEYER, H. DESPLANCHES, and J. METZGER. C.R. Acad. Sci. Paris Ser. C, **273**, 1473 (1971).
8. D. BALLET. Thèse de Spécialité. Université de Clermont–Ferrand, Clermont–Ferrand, France, 1972.
9. J. FRANÇOIS, R. CLÉMENT, and E. FRANTA. C.R. Acad. Sci. Paris Ser. C, **273**, 1577 (1971).
10. I. A. WEEKS and G. C. BENSON. J. Chem. Thermodyn. **5**, 107 (1973).
11. R. J. POWELL and F. L. SWINTON. J. Chem. Eng. Data, **13**, 260 (1968).
12. R. H. STOKES, B. J. LEVIEN, and K. N. MARSH. J. Chem. Thermodyn. **2**, 43 (1970).

Can. J. Chem. Downloaded from www.nrcresearchpress.com by 210.87.254.42 on 09/05/12
For personal use only.

Further Studies of γ-Irradiated Propylene Carbonate Glasses

ERIC A. SHAEDE

Saskatchewan Accelerator Laboratory, University of Saskatchewan, Saskatoon, Saskatchewan S7N 0W0

AND

MARTYN C. R. SYMONS[1]

Chemistry Department, The University of Leicester, Leicester LE1 7RH, England

Received January 30, 1973

An earlier postulate, that physically trapped electrons (e_t^-) are responsible for a narrow e.s.r. singlet at $g = 2.0028$ formed by exposure of glassy propylene carbonate to ^{60}Co γ-rays at 77 °K, is re-examined. An alternative, that propylene carbonate radical anions are formed, in which the extra electron is largely confined to an antibonding orbital on the carbonate moiety, is favored. The primary new evidence for this anion is the detection of satellite e.s.r. lines which were lost on bleaching or thermal decay of the central line, and which occurred in the correct field regions to be assigned to ^{13}C hyperfine structure from the carbonate carbon of the anion.

The complicated set of proton hyperfine lines is now assigned largely to the radical **1** and the mechanisms by which this radical may be formed are discussed. The previously observed temperature dependence of the proton hyperfine features can now be understood in terms of thermal restrictions on the motions of the methyl group and the adjacent methylene protons.

On a étudié de nouveau un ancien postulat selon lequel des électrons piégés physiquement (e_t^-) sont responsables de l'étroit singulet en R.S.E. à $g = 2.0028$ consécutivement à l'exposition du carbonate de propylène vitreux à des rayons-γ ^{60}Co à 77 °K. On favorise une autre alternative selon laquelle il se formerait des anions radicalaires du carbonate de propylène où l'électron en surplus serait surtout limité à une orbitale anti-liante de l'entité carbonate. Le nouvel argument principal en faveur de cet anion est la détection de bandes satellites en r.s.e. lesquelles sont perdues lors de la décoloration ou de la dégénérescence thermique de la bande centrale et qui apparaissent dans les bonnes régions du champ pour pouvoir être attribuées à la structure hyperfine du ^{13}C appartenant au carbone du carbonate de l'anion. Le patron compliqué des bandes hyperfines du proton est maintenant attribué surtout au radical **1** et les mécanismes responsables de la formation de ce radical sont discutés. La relation déjà observée entre les bandes hyperfines du proton et la température peut maintenant être expliqué en termes de restrictions thermiques sur les mouvements du groupe méthyl et des protons du groupe méthylène adjacent. [Traduit par le journal]

Can. J. Chem., **51**, 2492 (1973)

Introduction

This paper describes a continuation of a recent study (1) of radiation effects in glassy propylene carbonate (4-methyl-2-dioxolone; hereafter, PC), which reference should be consulted for an introductory survey of the subject. In this (1), a central narrow e.s.r. singlet was tentatively assigned to physically trapped electron centers (e_t^-) such as are commonly encountered in irradiated saturated aliphatic compounds such as alcohols, ethers, amines, and hydrocarbons (2). We now advance evidence which goes against this earlier hypothesis, and suggest instead that the central singlet is a property of propylene carbonate anions.

A detailed interpretation of the complex set of proton hyperfine lines previously detected is also offered, and an attempt is made to explain the effect of changes in temperature on these hyperfine features.

[1]To whom correspondence should be addressed.

Experimental

Details were as described previously (1) except that a more powerful ^{60}Co source was used, giving a nominal dose rate of *ca.* 4 Mrad. h^{-1}. Aqueous solutions covering a range of concentrations all appeared glassy, and gave well resolved e.s.r. sextets when Mn^{2+} salts were added (3).

Results and Discussion

(a) The Central Singlet

Our new experiments have confirmed all the previously reported details pertaining to this singlet, of which Figs. 2 and 3 of ref. 1 are typical. Factors in favor of the trapped electron (e_t^-) theory have been presented in detail (1). Some arguments against the concept are now considered.

Can. J. Chem. Downloaded from www.nrcresearchpress.com by 210.87.254.105 on 09/05/12
For personal use only.

Can. J. Chem. Downloaded from www.nrcresearchpress.com by 210.87.254.105 on 09/05/12
For personal use only.

(*i*) The *g*-value is slightly greater than that of the free-spin (2.0028 as against 2.0023), whilst all those for well established e_t^- centers are slightly less than 2.0023.

(*ii*) The optical absorption thought to be associated with this center comprised a broad band in the 300–500 nm region, having a maximum at *ca.* 370 (1). This is a higher energy band than any previously found for e_t^- centers and since the band energy increases as the trap depth increases, this implies an extremely deep trap. However, it is general experience that the deepest traps are formed by compounds containing hydroxyl groups, and it has been elegantly demonstrated by Smith and Pieroni (4) that the hydroxyl protons are directly responsible for this depth. We would therefore have expected to find that e_t^- centers in propylene carbonate had an absorption band to long wavelengths of the bands for alcohols which are found in the 500–600 nm region (2).

(*iii*) It is known that carbonate ions react with electrons to give CO_3^{3-} ions (5), and that carboxylic acids can give $(RCO_2H)^-$ anions (6). By analogy, it might be expected that carbonate esters would give the corresponding anions by electron capture. Since O-protonation or O-alkylation has only a minor effect upon the magnetic properties of ions such as CO_2^- or PO_3^{2-} (7), we would expect PC^- to have *g*-values close to those for CO_3^{3-}, ($g_\parallel = 2.0016$, $g_\perp = 2.0032$), (5), but with *g* closer to the free-spin value, the ^{13}C hyperfine tensor components close to, but somewhat larger than, those for $^{13}CO_3^{3-}$ ($A_\parallel(^{13}C) = 171.3$ G, $A_\perp(^{13}C) = 111.3$ G) (5). Thus the *g*-value of 2.0028 is quite reasonable for PC^-, the isotropy being either fortuitous, or arising because the anion is rotating rapidly.

The best test of the radical anion theory would therefore be to detect e.s.r. features for radicals containing ^{13}C. Hyperfine structure in the expected regions has indeed been detected (Fig. 1*a*), and these lines were selectively lost on photobleaching or thermal annealing (Fig. 1*b*). Since these lines appear as anisotropic features centered on the main singlet with about the required relative intensities, we assign them to PC^- radical anions, and conclude that the isotropy of the g-tensor is fortuitous.

The derived ^{13}C hyperfine data ($A_{iso} = 153$ G, $2B = 28$ G) are reasonable for the carbonate carbon in PC^-. The increase in A_{iso} relative to CO_3^{3-} (131 G) is as expected in view of the

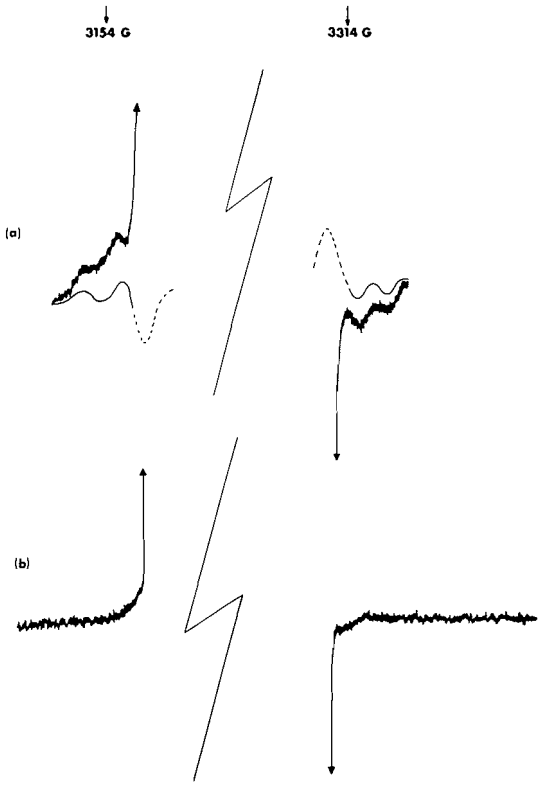

FIG. 1. First derivative e.s.r. spectra for propylene carbonate glasses after exposure to ^{60}Co γ-rays at 77 °K showing the wings of the main features at very high gain: (*a*) before decay of the central line, showing features assigned to PC^- radicals containing ^{13}C, and (*b*) after decay of the central line, at the same gain, showing loss of these features.

effective increase in the electronegativity of two of the ligands (7–9). The relatively small $2B$ value is not expected, but probably results from a slight libration of the anion at 77 °K. Alternatively the features taken as perpendicular (Fig. 1*a*) may be cross-over lines for a non-axial symmetric A-tensor. Indeed, the changes closely parallel those induced by crystal-field changes and librations in the hyperfine parameters for NO_2, CO_2^-, and PO_3^{2-} radicals (10). We conclude that, despite the strong arguments that can be made in favour of e_t^- centers (1), the species is, in all probability, PC^-. An important fact apparently favouring e_t^- was the marked ease of saturation of the singlet species (1). However, RCO_2H^- radicals are also very readily saturated (11), so that this is not diagnostic. We conclude that the center is almost certainly PC^- rather than e_t^-.

One interesting result of this suggestion is that CO_3^- radical anions may, in part, be formed by photochemical breakdown of these anions:

[1] 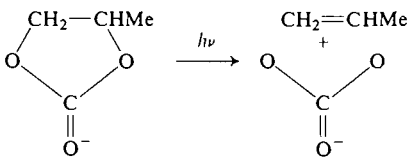

These anions (CO_3^-), previously detected both by their optical and e.s.r. spectra in the irradiated glasses (1), were found to increase markedly in concentration during ultraviolet photolysis.

An important observation in the previous study of the e.s.r. singlet (1) was its rather rapid decay even at 77 °K. This decay seemed to be characterized by non-homogeneous second-order kinetics (1). Since we are now able to conclusively assign the e.s.r. line to PC^-, it is necessary to re-examine the decay process. One would hardly expect such a large species as PC^- to be mobile at 77 °K and similarly, as will be elaborated on later, the expected stable counter species PCH^+ would also be immobile. Therefore it is necessary to postulate that the electrons are only very weakly bound to the propylene carbonate molecules in a low energy antibonding orbital. A rapid exchange reaction 2,

[2] $$PC^- + PC \rightarrow PC + PC^-$$

must exist in the glassy matrix to allow charge transfer through the medium until neutralization occurs via reaction 3,

[3] $$PC^- + PCH^+ \rightarrow PC + \text{"PCH"}$$

The "PCH" species would most likely spontaneously decompose, possibly to give the radical species **1** (which will be shown later to be the major other paramagnetic species present) and molecular hydrogen.

(b) The Proton Hyperfine Components

A typical e.s.r. spectrum of the type under consideration is given in Fig. 2*a*, and also in Figs. 2*b*, 4*a*, and 4*b* of ref. 1. Because of the effect of various physical constraints upon certain of these components, it was suggested that they comprise three sets of doublets, designated B, D, and E, with proton coupling constants of 42, 83, and 124 G respectively (1).

We now find that very similar spectra are obtained when γ-irradiated aqueous glasses are annealed. Initially, the e.s.r. spectra of such glasses were dominated by the characteristic features of hydroxyl radicals, but on controlled thermal annealing these were lost, and replaced by features very similar to those in Fig. 2*a* (see Fig. 2*b*). By far the most probable reaction for hydroxyl radicals is (12):

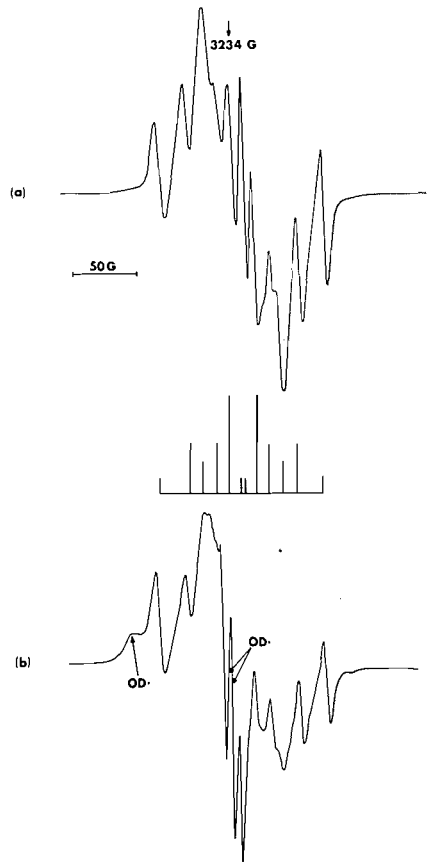

FIG. 2. First derivative e.s.r. spectra for propylene carbonate after exposure to ^{60}Co γ-rays at 77 °K, showing features assigned to

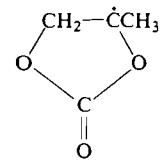

radicals (*a*) for the pure material; the stick spectrum reconstruction underneath represents the predicted lines using $a(CH_3) = 22$ G and $a(CH_2) = 31.5$ G; (*b*) for an aqueous (D_2O) solution, after partial annealing, showing features assigned to ȮD radicals also.

Can. J. Chem. Downloaded from www.nrcresearchpress.com by 210.87.254.105 on 09/05/12
For personal use only.

[4] $\cdot OH + PC \longrightarrow CH_2{-}\dot{C}Me + H_2O$

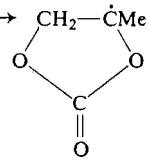

1

and we have therefore endeavored to explain these features, together with the changes noted previously (1) entirely in terms of species **1**. The most reasonable e.s.r. spectrum for **1** would com-

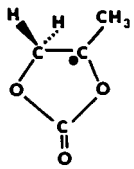

1

prise a 1:3:3:1 quartet of coupling *ca.* 20 G from the methyl group, each line being split further into 1:2:1 triplets by the methylene protons. This would occur provided the conformation is symmetrical, as in **2**, in which case the methylene

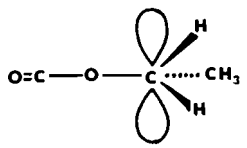

2

proton coupling would be *ca.* 30 G (13). (These values are reduced from those for comparable hydrocarbon radicals because of slight delocalization onto the oxygen atom (13).)

However, libration about the C—C bond, or any static spread over a range of conformations, would render the methylene protons inequivalent, and this would change the 1:2:1 triplet into 1:(1 + 1):1 sets of lines, with the central doublet liable to appear as a single broad line. Thus the spectrum might well comprise sets of triplets having a narrow–broad–narrow appearance, the outer lines remaining narrow because these dynamic or static effects are out-of-phase modulations, which leave the sum of the hyperfine coupling constants of the two protons approximately unchanged.

Similarly, free rotation for the methyl group might well be inhibited at 77 °K. This often results in a narrow–broad–broad–narrow appearance of the four lines, for similar reasons.

Just these sorts of changes are indeed found in the spectra under consideration. A stick spectrum reconstruction, based on radical **1**, with $a(CH_3) = 22$ G and $a(CH_2) = 31.5$ G is given under Fig. 2*a*. The resolved $M_I = \pm 1/2$ lines from the methyl groups are clearly broadened relative to the $M_I = \pm 3/2$ components, but on heating the normal 1:3:3:1 intensities are found (*cf.* Fig. 7*a* of ref. 1). Again, the central lines are often very broad in the spectra in ref. 1, although in several instances they are of nearly the correct intensity (*cf.* Fig. 2*a*). In spectra for the frozen aqueous solutions these lines are clearly detected (Fig. 2*b*) which suggests that the preferred conformation is the symmetric form indicated in **2**, rather than a twisted configuration as in **3**.

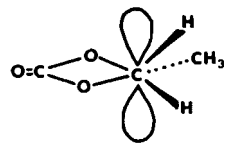

3

We conclude that **1** is the major radical species responsible for these hyperfine components. Nevertheless the various changes outlined in ref. 1 cannot all be accommodated in terms of restricted rotation effects, and it seems probable that at least one other radical is present in low concentration. We have been unable to distinguish separate features however.

Radical **1** is in fact the most likely species to be formed in irradiated propylene carbonate glasses. The primary actions of the radiation may be represented as [5],

[5] $PC \rightsquigarrow PC^*, PC^+, e^-$

We now know that the fate of the electrons is captured by the matrix to form PC^-. The primary positive ion PC^+ very likely immediately transfers a proton to one of the adjacent PC molecules to form radical species **1** and PCH^+ which presumably would be stable. Radical species **1** may also be formed via reaction 3 discussed above or it may be formed from PC* (*i.e.* propylene carbonate electronically excited by the radiation) via reactions 6 and 7,

[6] $PC^* \rightarrow \mathbf{1} + H\cdot$

[7] $PC + H\cdot \rightarrow \mathbf{1} + H_2$

since the tertiary hydrogen bond is the most

Can. J. Chem. Downloaded from www.nrcresearchpress.com by 210.87.254.105 on 09/05/12
For personal use only.

easily broken. Thus the overall yield of radical **1** in irradiated PC could be quite large.

One of us (E.A.S.) wishes to thank the University of Saskatchewan for financial support.

1. E. A. SHAEDE. Can. J. Chem. **50**, 782 (1972).
2. L. KEVAN. Actions Chim. Biol. Radiat. **13**, 57 (1969).
3. I. S. GINNS and M. C. R. SYMONS. J. Chem. Soc. Dalton Trans. 143 (1972).
4. D. R. SMITH and J. J. PIERONI. Can. J. Chem. **45**, 2723 (1967).
5. S. A. MARSHALL and R. A. SERWAY. J. Chem. Phys. **45**, 4098 (1966); R. S. EACHUS and M. C. R. SYMONS. J. Chem. Soc. A, 790 (1968).
6. J. E. BENNETT and L. H. GALE. Trans. Faraday Soc. **64**, 1174 (1968).
7. M. C. R. SYMONS. Unpublished observations.
8. L. PAULING. Proc. Nat. Acad. Sci. U.S.A. **14**, 359 (1928); J. Chem. Phys. **51**, 2767 (1969).
9. A. BEGUM, A. R. LYONS, and M. C. R. SYMONS. J. Chem. Soc. A, 2290 (1971).
10. M. C. R. SYMONS. J. Chem. Soc. A, 1998 (1970); J. H. SHARP and M. C. R. SYMONS. J. Chem. Soc. A, 3075 (1970).
11. S. LUKAC, J. TEPLY, and K. VACEK. J. Chem. Soc. Faraday Trans. I, **68**, 1377 (1972).
12. J. F. GIBSON, M. C. R. SYMONS, and M. G. TOWNSEND. J. Chem. Soc. 269 (1959).
13. M. C. R. SYMONS. J. Chem. Soc. 277 (1959).

Can. J. Chem. Downloaded from www.nrcresearchpress.com by 210.87.254.105 on 09/05/12
For personal use only.

Hydrated Electrons Formed in the Flash Photolysis of Ag° and Tl°

NORMAN BASCO, SUNIL K. VIDYARTHI, AND DAVID C. WALKER
Chemistry Department, University of British Columbia, Vancouver, British Columbia

Received February 14, 1973

The transient species Ag^0, formed in the reduction of Ag^+ by hydrated electrons, may be photodissociated to e_{aq}^- again by light in the absorption band of Ag^0 centered at ~315 nm.

$$Ag^0 \xrightarrow{h\nu} Ag^+ + e_{aq}^-$$

It suggests that this band is a charge-transfer-to-solvent band. The photon energy threshold for photoionization of Ag^0 (3.0 eV) is substantially smaller than the vacuum photoelectric work function of silver metal (4.5 eV). Analogous results were obtained in solutions of Tl^+ indicating that Tl^0 may also yield e_{aq}^- on photolysis at ~300 nm. The experiments utilized a double flash photolysis technique, in which hydrated electrons were produced by u.v. photolysis of SO_4^{2-} in the first flash, reacted with Ag^+ or Tl^+ to give the short-lived intermediates Ag^0 (lifetime ~60 μs) and Tl^0 (lifetime < 20 μs) which were photolyzed by a second flash containing light in a restricted wavelength range.

Les espèces transitoires contenant Ag^0, obtenues de la réduction de Ag^+ par des électrons hydratés, peuvent être photodissociées de nouveau pour donner des e_{aq}^- par la lumière à la bande d'absorption de Ag^0 centrée à ~315 nm.

$$Ag^0 \xrightarrow{h\nu} Ag^+ + e_{aq}^-$$

Ce fait suggère que cette bande en est une typique d'un transfert de charges au solvant. La limite énergétique du photon pour la photoionisation de Ag^0 (3.0 eV) est beaucoup plus petite que la fonction de travail photoélectrique (dans le vide) de l'argent métallique (4.5 eV). Des résultats analogues furent obtenus pour des solutions de Tl^+ ce qui signifient que le Tl^0 peut aussi libérer des e_{aq}^- lors de la photolyse à ~300 nm. Les expériences furent basées sur la technique de photolyse à double éclair dans laquelle les électrons hydratés sont produits par la photolyse en u.v. du SO_4^{2-} lors du premier éclair, puis ont réagi avec du Ag^+ ou Tl^+ pour donner naissance aux intermédiaires (existence éphémère) Ag^0 (temps de vie ~60 μs) et Tl^0 (temps de vie < 20 μs) qui sont photolysés par la suite à l'aide d'un second éclair composé de lumière possédant des longueurs d'onde discrètes. [Traduit par le journal]

Can. J. Chem., 51, 2497 (1973)

Introduction

Pulse radiolysis studies of hydrated electron reactions with several transition metal ions have led to the identification of some "unusual" oxidation states, in which the transient ions, or atoms, created have strong optical absorption bands in the region of 300 nm in liquid solutions (1–4) and glassy matrices (5, 6). An analogous species is Ag^0 formed by reaction 1

[1] $Ag_{aq}^+ + e_{aq}^- \rightarrow Ag^0 \quad k_1 = 3.2 \times 10^{10}\ M^{-1}\ s^{-1}$ (2)

which has a lifetime governed largely by reaction 2.

[2] $Ag^0 + Ag^+ \rightarrow Ag_2^+ \quad k_2 = 5.9 \times 10^9\ M^{-1}\ s^{-1}$ (4)

Ag^0 has also been detected and identified by e.s.r. in γ-irradiated low temperature solids containing Ag^+ ions (7, 8).

Results have recently been reported on the observation of a transient species produced in the double flash photolysis of aqueous $NaOH/H_2$ solutions, in which hydrated electrons created in the first flash by u.v. photolysis of OH^- (and other anions) react to form transient species which may then be photolyzed by the second flash which contains light of restricted wavelengths (9, 10). In this paper we wish to report experiments of a similar nature involving Ag^0 and Tl^0 as the intermediates.

Experimental

The apparatus has been described in detail elsewhere (10). It consists basically of a 42.5 cm suprasil reaction vessel placed between two conventional 50 cm suprasil flash photolysis lamps called "main" and "auxiliary". Spaces are provided so that Corning color glass light filters may be placed between either lamp and the reaction vessel. The lamps can be fired successively at any time delay down to a microsecond. The flashes are typically 20 μs width-at-half-height. The main was used at 625 J and the auxiliary at 825 J energy. Monitoring of absorbing species was conducted in two ways, firstly by a spectro flash and spectrograph combination and secondly by laser photometry. The latter permits absorptions to be

Can. J. Chem. Downloaded from www.nrcresearchpress.com by 210.87.254.40 on 09/05/12
For personal use only.

TABLE 1. Transmission characteristics (relative to maximum) of Corning glass filters used between auxiliary lamp and reaction vessel

Filter #	Wavelength (nm) of transmission*				
	3%	10%	50%	90%	97%
9-54	216	223	240	288	300
7-54†	231(411)	236(401)	253(390)	283(367)	298(353)
0-53	279	290	303	334	344
0-52	339	342	350	380	389
3-74	385	390	415	461	497
3-70	486	493	507	548	573

*Error limit = ±3 nm.
†7-54 has a transmission band in the relevant region of the spectrum. The wavelengths in brackets indicate the long wavelength limits of this band. The maximum transmission at ~320 nm is an absolute transmission of 89%.

observed *during* and after the flashes but of course only at the laser wavelength. A 7 mW He/Ne laser was used as the monitoring light source in the experiments reported here for following transient changes in the absorbance of hydrated electrons at 633 nm. The Corning glass filters used in this work had the transmission characteristics shown in Table 1.

Solutions of Ag_2SO_4 with Na_2SO_4 were made from "Analar" grade Ag_2SO_4 and Na_2SO_4 dissolved in triply distilled water as described (10) and deoxygenated by bubbling with pure He gas. Concentrations of Ag^+ in the range 10^{-5} to 10^{-6} *M* were selected so that e_{aq}^- would react almost exclusively with Ag^+, according to reaction 1, but not too rapidly so that there was adequate absorption due to e_{aq}^- for it to be conveniently monitored during and after the flashes. A typical half-life of ~3–15 μs for e_{aq}^- was convenient. Since e_{aq}^- was produced at ~10^{-6} *M* by the main flash, loss of e_{aq}^- in bimolecular decay reactions was not serious. Na_2SO_4 was generally present at ~10^{-3} *M* so that there was suitable light absorption from the main flash to create ~10^{-6} *M* e_{aq}^-. For experiments with thallous, Tl_2SO_4 was used in place of Ag_2SO_4. For experiments requiring a scavenger for the oxidizing species "Aristar" grade 2-propanol and "Analar" grade sodium formate were utilized.

Results

In Ag_2SO_4/Na_2SO_4 solutions the short wavelength light ($\lambda < \sim 220$ nm) of the main flash (no light filter between it and the reaction vessel) was absorbed by SO_4^{2-} according to reaction 3

$$[3] \qquad SO_4^{2-} + h\nu \rightarrow e_{aq}^- + SO_4^-$$

to generate hydrated electrons (11, 12). Strong absorption of the 633 nm laser light by e_{aq}^- occurs during the main flash as shown in Fig. 1, e_{aq}^- being the only species in these systems absorbing significantly at this wavelength. This reacts rapidly with Ag^+. With a 0-53 filter between the auxiliary lamp and reaction vessel an auxiliary absorption peak such as that shown in

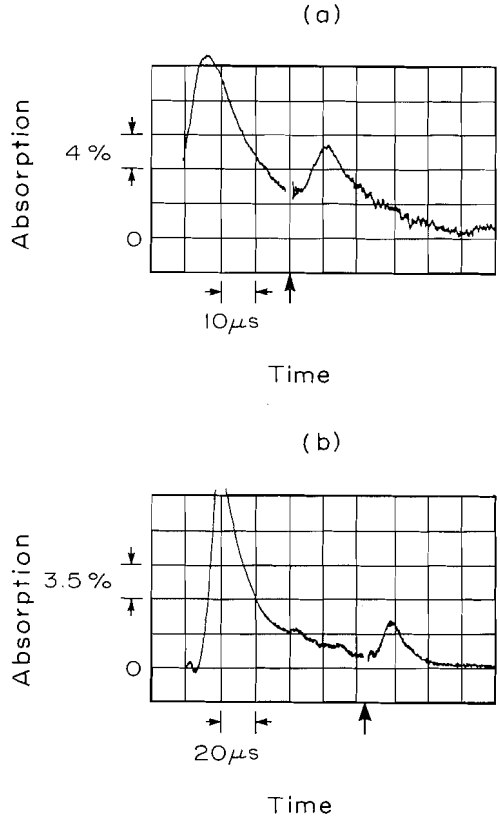

FIG. 1. Oscilloscope traces showing absorption by e_{aq}^- at 633 nm during main and auxiliary flashes in a 10^{-5} *M* solution of Ag^+ in 10^{-3} *M* Na_2SO_4. A 0-53 filter was included between the auxiliary lamp and the reaction vessel. The arrow indicates the triggering pulse for the auxiliary lamp, (*a*) shows a time delay of 35 μs and (*b*) for 95 μs between the main and auxiliary flashes.

Fig. 1 was obtained. This shows traces obtained for 35 and 95 μs delays between main and auxiliary flashes. At very short delay times the second absorption peak was comparable in size to the first peak showing that most of the hydrated electrons originally formed were regenerated by the second flash containing only $\lambda > 270$ nm.

The magnitude of the second absorption peak decreased with increasing delay time between the firing of the main and auxiliary lamps. Figure 2 shows these data for a solution containing Ag^+ at 5×10^{-6} *M*, the ordinate being proportional to the concentration of the intermediate at various times compensated for small variations in the main flash intensity as registered by the hydrated electron concentration in the main absorption peak. The decay of the transient

Can. J. Chem. Downloaded from www.nrcresearchpress.com by 210.87.254.40 on 09/05/12
For personal use only.

TABLE 2. Ratio of peak absorbances (due to e_{aq}^-) in auxiliary/main flashes for Ag^+ (5×10^{-6} *M*) and Tl^+ (2×10^{-5} *M*) solutions with various light filters between the auxiliary lamp and reaction vessel for the same delay time between flashes (60 μs for Ag^+, 30 μs Tl^+)

Filter	9-54	7-54	0-53	0-52	3-74	3-70
Ag^+, *A*(aux)/*A*(main)	0.19	0.15	0.11	0.06	0.03	<0.01
Tl^+, *A*(aux)/*A*(main)	0.35	0.31	0.27	0.20	<0.04	<0.04

species was approximately first order, as indicated by the inset of Fig. 2, with a half-life of ~42 μs.

On adding an additional layer of the 0-53 filter the absorption in the auxiliary peak was reduced significantly for a given delay time. On replacing the 0-53 filter by a 0-52 filter the auxiliary absorption peak was reduced to about half that found for the same delay with 0-53. On further exchanging the filter to 3-74 the absorption was reduced to ~25% that found with 0-53 whereas 3-70 eliminated the auxiliary absorption peak. These data are included in Table 2 for a 5×10^{-6} *M* Ag^+ solution. These filter experiments indicate: (*a*) almost all e_{aq}^- may be regenerated by one auxiliary flash containing $\lambda > 270$ nm at short times, so the absorption is substantial at $\lambda > 270$; (*b*) a considerable fraction of the absorption band leading to photoregeneration of e_{aq}^- lies in the range 270 to 320 nm; (*c*) the band responsible is fairly broad and certainly extends to ~400 nm.

Absorption spectra were taken at various times after either flash using light from an 80 J spectroflash directed down the length of the reaction vessel and focussed onto the slit of a small Hilger and Watts quartz prism spectrograph containing 35 mm HP4 photographic film. Immediately after the main flash the absorption spectrum corresponded quite closely to that of e_{aq}^-, as reported previously (10). Figure 3 shows the spectrum obtained for three conditions: (*i*) 35 μs after the main flash, when ~90% of e_{aq}^- had reacted with Ag^+ present at $\sim 10^{-5}$ *M*; (*ii*) 13 μs after the auxiliary lamp which was fired 38 μs

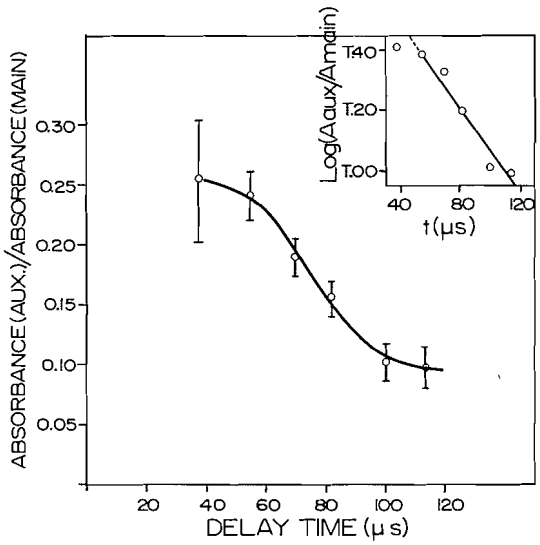

FIG. 2. Plot showing the decay of the transient as a function of time in a 5×10^{-6} *M* Ag^+ solution. The ordinate is the ratio of absorbances due to hydrated electrons during the peak of the auxiliary flash relative to the main flash. The abscissa represents the time delay between the flashes. Inset shows the same information plotted according to first-order rate law. (The particularly large uncertainty in the first data point arises mainly from the existence of significant absorption still by e_{aq}^- from the main flash).

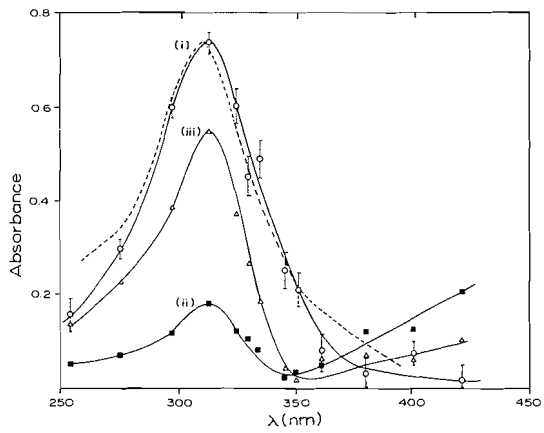

FIG. 3. Absorption spectra in the wavelength range 250 to 425 nm for a 10^{-5} *M* Ag^+ solution taken under the following conditions: (*i*) 35 μs after the main flash (⊙). (*ii*) 13 μs after the firing of the auxiliary flash (*i.e.* during the auxiliary flash) which was fired 38 μs after the main flash (△). (*iii*) 30 μs after the auxiliary flash which was fired 38 μs after the main flash (■). A 0-53 filter was included between the auxiliary lamp and the reaction vessel. The dashed line is a published spectrum assigned to Ag^0(3).

Can. J. Chem. Downloaded from www.nrcresearchpress.com by 210.87.254.40 on 09/05/12
For personal use only.

Can. J. Chem. Downloaded from www.nrcresearchpress.com by 210.87.254.40 on 09/05/12
For personal use only.

after the main. In this experiment a 0-53 filter was present between the auxiliary lamp and the reaction vessel; and (*iii*) 30 μs later, when e_{aq}^- had again reacted with Ag^+.

Further evidence that products of reaction 1 were responsible for the auxiliary absorption peak is derived from experiments using various Ag^+ solutions. For instance, it was shown that SO_4^- radicals, formed in reaction 3, were not involved because comparable traces to those of Fig. 1 were obtained from the following two solutions: (*a*) 3 m*M* Na_2SO_4, 5 μ*M* Ag_2SO_4 and 1 m*M* 2-propanol (2-propanol is reputed to react rapidly with SO_4^- radical ions (13)) and (*b*) 3 m*M* NaOH, 5 μ*M* Ag_2SO_4 and 1 m*M* HCOONa. In this latter solution e_{aq}^- was formed by photolysis of OH^- ($OH^- \xrightarrow{h\nu} OH + e_{aq}^-$) and the OH radical scavenged by formate ions. This latter mixture also shows that Ag^{2+} ions from reaction 4 are not responsible for the auxiliary absorption peak. Ag^{2+} could be formed in reaction 4 (the OH perhaps arising from SO_4^- in the SO_4^{2-} experiments) but is excluded by the presence of the formate.

[4] $$Ag^+ + OH \rightarrow Ag^{2+} + OH^-$$

Solutions of thallous ions were studied in an analogous manner. For a solution containing 10^{-5} *M* Tl_2SO_4 and 10^{-3} *M* 2-propanol traces similar to Fig. 1 were obtained and on changing the filters the data of Table 2 were found for a delay between main and auxiliary of 30 μs. The intermediate was evidently photodissociated mainly by light centered around ~300 nm. In this case the transient decayed more rapidly than in the Ag^+ system. Reactions 5 and 6 are known to occur (2, 14) and are expected to be involved here as with the Ag^+ system, but where $k_6 > k_2$ (14).

[5] $$Tl^+ + e_{aq}^- \rightarrow Tl^0 \quad k_5 \sim 1.1 \times 10^{10}\ M^{-1}\ s^{-1}$$ (2)

[6] $$Tl^0 + Tl^+ \rightarrow Tl_2^+$$

Discussion

The laser photometry data indicate that hydrated electrons, produced during the main flash by far u.v. photolysis of SO_4^{2-} in reaction 3, react rapidly with Ag^+ according to reaction 1, thereby creating a transient species (half-life ~ 42 μs at 5×10^{-6} *M* Ag^+) which can be photodissociated by the auxiliary lamp to yield e_{aq}^- again. Light filter experiments show that the transient is photolyzed by wavelengths centered around 300 nm but extending to 400 nm. This is entirely consistent with the spectra shown in Fig. 3. Curve (*i*) shows the spectrum of the transient 35 μs after the main flash, curve (*ii*) its loss during the auxiliary flash, and (*iii*) its formation again 30 μs after the auxiliary flash. Absorption at long wavelengths in curve (*ii*) also corroborate the formation of e_{aq}^-. The transient evidently has an absorption band centered ~315 ± 5 nm and this is the band which leads to photodissociation to e_{aq}^-.

Also sketched in Fig. 3 is the spectrum reported by Baxendale *et al.* (3) with λ_{max} at 310 nm and assigned by them to Ag^0 which compares very closely to our transient. Consequently we conclude that photolysis during the Auxiliary flash can be represented by photoionization process [7].

[7] $$Ag^0 \xrightarrow{h\nu} Ag^+ + e_{aq}^-$$

This conclusion is corroborated by a comparison of the estimated extinction coefficient, and by the decay kinetics displayed in Fig. 2. We estimated the extinction coefficient of Ag^0 at λ_{max} (315 nm) by the following procedure. The flash intensity absorbed is given by the analytical form, $I_a = ate^{-bt}$ (15) where b is $1/t_{max}$. The value of a was obtained experimentally from a solution which was the same as that of Fig. 3 except that it contained no Ag^+ (*i.e.*, e_{aq}^- very long-lived) because in this solution the maximum absorbance could be related directly to the total number of electrons formed, *i.e.* a/b^2. It is now assumed that all e_{aq}^- react with Ag^+ to give Ag^0 and that the latter decay by reaction 2 with $k_2 = 6 \times 10^9\ M^{-1}\ s^{-1}$. Thus $[Ag^0]$ at 35 μs was calculated by integration of the equations

$$d[e_{aq}^-]/dt = a\,te^{-bt} - k_1[Ag^+][e_{aq}^-]$$

$$d[Ag^0]/dt = k_1[Ag^+][e_{aq}^-] - k_2[Ag^+][Ag^0]$$

This value of $[Ag^0]$ at 35 μs was used to evaluate the extinction coefficient of Ag^0 from the experimental absorbance shown in Fig. 3, curve (*i*). The value obtained was about $2.5 \times 10^4\ M^{-1}\ cm^{-1}$, which compares remarkably well with the published value of $2.3 \times 10^4\ M^{-1}\ cm^{-1}$ at 313 nm (3*b*).

The rate of decay of the transient is consistent with it being Ag^0 but not with Ag_2^+ or Ag^{2+}. Ag_2^+ is formed in reaction 2 and may decay by reaction 8 to yield Ag^{2+} (4, 16).

[8] $Ag_2^+ + Ag^+ \rightarrow Ag^{2+} + Ag_2^0 \quad k_8 = 3.8 \times 10^9\ M^{-1}\ s^{-1}$ (4)

Both Ag_2^+ and Ag^{2+} are believed to absorb at $\lambda < 400$ nm and the 310 nm band has recently been tentatively assigned to Ag_2^+ rather than Ag^0 (16). However when we calculate the time at which Ag^0, Ag_2^+, and Ag^{2+} reach their maximum concentrations, by the procedure indicated above using the published values of k_1, k_2, and k_8 and our $[Ag^+]$, then we find the maxima occur essentially during the main flash for Ag^0, 50–85 μs afterwards for Ag_2^+ and at even later times for Ag^{2+}. Thus our laser photometry data can only be explained if Ag^0 was the photodissociated species. The decay shown in Fig. 2 yields a value of $k_2 = 3.3 \times 10^9\ M^{-1}\ s^{-1}$ for reaction 2, which is somewhat smaller than the published values, averaging $6 \times 10^9\ M^{-1}\ s^{-1}$ (4, 16).

A similar interpretation may be applied to the results on Tl^+ solutions which strongly implies that Tl^0 was the short-lived transient which may be photodissociated by light between 250–350 nm giving e_{aq}^- according to process [9].

[9] $$Tl^0 \xrightarrow{h\nu} Tl^+ + e_{aq}^-$$

The thallous system seems to be quite similar to the silver system except that Tl^0 decays more rapidly.

The occurrence of process [7] implies that the absorption band of Ag^0 centered around 315 nm corresponds to a charge-transfer-to-solvent (CTTS) band. This is supported by the high oscillator strength of 0.63 which we calculate for the transition based on the spectrum of Fig. 3 and the value of ε_{max} evaluated above. It may be a common feature of the unusual valence state species (hyper-reduced states), many of which absorb in this spectral region, for these bands to be CTTS bands. Indeed, when Ni^{2+} solutions were examined in this same way rather similar effects were found, which implies that the transient ion Ni^+ may be photodissociated again into Ni^{2+} and e_{aq}^- by light ~300 nm. Rather similar results were obtained with other transition metal ions but not with Cu^{2+}. (It should be noted that these transients were very short-lived and could not be involved in our experiments on the bimolecular combination of e_{aq}^- (10) even if transition metal ions were present as trace impurities.)

Attempts to produce e_{aq}^- by flash photolysis of metallic silver in this apparatus, either in the form of a semi-transparent silver mirror or as colloidal particles, have been unsuccessful. It should be noted however that the photon energy threshold for process [7] is at about 3.0 eV (~400 nm), which is about 1.5 eV smaller than the vacuum photoelectric work function for silver metal (17).

We are grateful to the National Research Council of Canada and the Defence Research Board of Canada for financial support of this research.

1. G. E. Adams, J. H. Baxendale, and J. W. Boag. Proc. Chem. Soc. 241 (1963).
2. J. H. Baxendale, E. M. Fielden, C. Capellos, J. M. Francis, J. V. Davies, M. Ebert, C. W. Gilbert, J. P. Keene, E. J. Land, A. J. Swallow, and J. M. Nosworthy. Nature, **201**, 468 (1964).
3. (*a*) J. H. Baxendale, E. M. Fielden, and J. P. Keene. Proc. Roy. Soc. **A286**, 320 (1965). (*b*) J. H. Baxendale, E. M. Fielden, and J. P. Keene. Pulse Radiolysis. *Edited by* M. Ebert. Academic Press, London. 1965. p. 207.
4. J. Pukies, W. Roebke, and A. Henglein. Ber. Bunsenges. Phys. Chem. **72**, 842 (1968).
5. D. M. Brown and F. S. Dainton. Trans. Faraday Soc. **62**, 1139 (1966).
6. A. Barakatt, M. Ottolenghi, and J. Rabani. J. Phys. Chem. **76**, 203 (1972).
7. L. Shields. J. Chem. Phys. **45**, 2232 (1966).
8. B. L. Bales and L. Kevan. J. Chem. Phys. **55**, 1327 (1971).
9. N. Basco, G. A. Kenney, and D. C. Walker. Chem. Commun. 917 (1969).
10. N. Basco, G. A. Kenney-Wallace, S. K. Vidyarthi, and D. C. Walker. Can. J. Chem. **50**, 2059 (1972).
11. J. Barrett, M. F. Fox, and A. L. Mansell. J. Phys. Chem. **69**, 2996 (1965).
12. E. Hayon and T. T. McGarvey. J. Phys. Chem. **71**, 1472 (1967).
13. L. Dogliotti and E. Hayon. J. Phys. Chem. **71**, 2511 (1967).
14. B. Cercek, M. Ebert, and A. J. Swallow. J. Chem. Soc. (A), 612 (1966).
15. N. Basco, A. B. Callear, and R. G. W. Norrish. Proc. Roy. Soc., **A260**, 459 (1961).
16. P. L. T. Bevan. Private Communication.
17. Handbook of chemistry and physics. The Chemical Rubber Co., Ohio. 1970.

Can. J. Chem. Downloaded from www.nrcresearchpress.com by 210.87.254.40 on 09/05/12
For personal use only.

Effect of Solute–Solute Interaction on Molecular Luminescence in Rigid Glasses: Anomalous Thioxanthenone Phosphorescence and Anthracene Fluorescence[1]

R. O. Loutfy,[2] D. F. Williams, and R. W. Yip

Division of Chemistry, National Research Council of Canada, Ottawa, Canada K1A 0R6

Received March 14, 1973

The phosphorescence spectra and lifetimes of thioxanthenone in a number of rigid matrices at 77 °K was found to be dependent on the concentration, rate of cooling of the glass, and on the wavelength of excitation. At 77 °K and at concentrations greater than $\sim 5 \times 10^{-5}$ *M*, aggregates of thioxanthenone are believed to be responsible for a new phosphorescence band at 472 nm, and a corresponding absorption band at 390–395 nm.

The formation of aggregates is also believed to be responsible for the variations, with excitation wavelength, of the fluorescence lifetime of anthracene in polymethacrylate at ambient temperatures.

Le spectre de phosphorescence et les durées de vie de la thioxanthénone dans un certain nombre de matrices rigides à 77 °K, dépendent de la concentration, de la vitesse de refroidissement du verre et de la longueur d'onde d'excitation. A 77 °K et pour des concentrations supérieures à $\sim 5 \times 10^{-5}$ *M*, on pense que les agrégats de thioxanthénone formés sont responsables d'une nouvelle bande de phosphorescence à 472 nm et de la bande d'absorption correspondante à 390–395 nm.

De même, cette formation d'agrégats est tenue pour responsable des variations, avec la longueur d'onde d'excitation, de la durée de fluorescence de l'anthracène dans le polyméthacrylate aux températures ambiantes. [Traduit par le journal]

Can. J. Chem., **51**, 2502 (1973)

Recently, several examples of anomalous phosphorescence involving aromatic ketones in low temperature glasses have been reported (1–5). They have variously been attributed (*i*) to the population of two singlet manifolds of the same molecule (Michler's ketone) (1), (*ii*) to differences in local environment (Michler's ketone) (2), (*iii*) to the existence of two different conformations of the solute molecule (butyrophenone) (3), and (*iv*) to photoproducts (1-indanone and 1-tetralone) (4). In the present note, we report two further examples of anomalous luminescence, involving simple aromatic molecules, which are unlikely to be due to the above causes or to impurity. We have observed anomalous phosphorescence from dilute solutions of thioxanthenone in glass matrices (10^{-5}–10^{-4} *M*) at 77 °K and anomalous fluorescence from anthracene in polymethyl methacrylate (10^{-4} *M*). We suggest that anomalous emission originate from aggregates in both cases even though many of the features of the emission were similar to those which could be due to triplet excimer (6) and to the population of two emitting triplet states (a violation of Kasha's rule (7)) by intersystem crossing from two singlet states of the same molecule (1). The results stress the importance of carrying out low temperature absorption and phosphorescence excitation measurements under different conditions when investigating possible instances of triplet excimer emission or emission from two triplet states of the same molecule. In contrast to the usual suggestion of *slow* cooling of dilute solutions in the preparation of glass matrices for emission study, our results clearly show that to minimize aggregation, it is necessary to *rapidly* cool dilute solutions. Even under these very improbable conditions, some aggregation can be observed.

The phosphorescence spectrum of a dilute sample (1×10^{-5} *M*) of thioxanthenone in 4:1 methylcyclohexane–isopentane (MCIP) or methylcyclohexane (MC) matrices at 77 °K was similar to that reported earlier (8). At higher concentrations (5×10^{-5}–10^{-4} *M*), however, the phosphorescence spectrum in MCIP (or EPA) and the lifetime was dependent on the wavelength of excitation. As shown in Fig. 1, a new phosphorescence band at 472 nm became more pronounced (relative to the normal peak at 443 nm) as the excitation wavelength was

[1]NRCC No. 13261.

[2]NRCC Postdoctorate Fellow, 1971 to present.

Can. J. Chem. Downloaded from www.nrcresearchpress.com by 210.87.254.5 on 09/05/12
For personal use only.

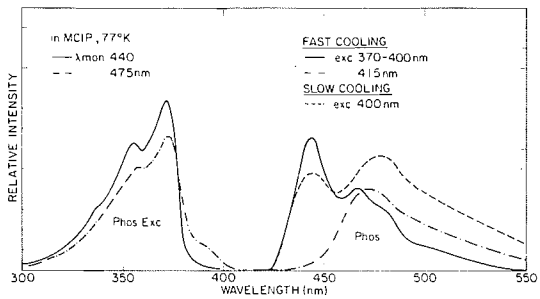

FIG. 1. Phosphorescence and phosphorescence excitation spectra of 10^{-4} *M* thioxanthenone in MCIP at 77 °K (*a*) fast cooling phosphorescence: (—) λ_{ex} 370 or 400 nm; (- - -) λ_{ex} 415 nm, phosphorescence excitation: (—) λ_{mon} 440 nm and (- - -) λ_{mon} 475 nm, (*b*) slow cooling phosphorescence (---) λ_{ex} 400 nm.

increased above the absorption maximum at 380 nm. The new phosphorescence band at 472 nm decayed exponentially with a $\tau = 0.13$ s in MCIP or EPA (λ_{ex} 400 nm, λ_{mon} 475 nm), whereas the normal emission decayed with a $\tau = 0.16$ s in EPA and 0.15 s in MCIP (λ_{ex} 363 nm, λ_{mon} 440 nm). These observations were similar to those reported for Michler's ketone (1) and Michler's thione (6) and could be due to excitation of two different singlet states (of the same molecule) as postulated recently by Klöpffler (1), but which may be due to excimer emission, aggregate emission, or microcrystalline emission.

We therefore searched for (and found) an absorption band which corresponded to the phosphorescence band at 472 nm. Both the absorption and phosphorescence excitation spectra[3] of thioxanthenone in MCIP (or EPA) (1×10^{-4} *M*) at 77 °K revealed a weak shoulder at ~390 nm (395 nm in EPA). At room temperature, the shoulder was absent. These observations, particularly the latter one, appear to rule out impurity as an explanation. Since at 77 °K, there exists a ground state absorption which corresponds to the emission at 472 nm, excimer emission is also ruled out.

The phosphorescence spectrum of thioxanthenone crystal at 77 °K showed a structureless emission (λ_{max} 510 nm) $\tau = 0.098$ s which was independent of the wavelength of excitation. In view of these observations, the most likely explanation for the anomalous phosphorescence is due to aggregate formation and not microcrystals. The degree of aggregation depends upon both solute concentration and the solvent used. The aggregate emission in MCIP was displaced to the red from that in EPA.

Aggregation was confirmed when we studied the effect of rate of cooling of the glass matrix on the phosphorescence spectrum. A sample prepared by cooling over several hours exhibited a definite peak at long wavelength, whereas this sample rapidly-cooled showed only a slight shoulder (see Fig. 1).

Lifetime measurements were used as one sample quality control for a recent experimental investigation concerning the differences between the temperature dependence 300–1.8 °K of the fluorescence lifetime of anthracene in polymethyl methacrylate solutions and anthracene single crystals (9). Naturally for any meaningful comparison, particularly at low temperatures, it was necessary to show that no solute aggregation had taken place. As a test for the absence of aggregates the fluorescence lifetime at 4 °K was measured as a function of emission wavelength. Occasionally the sample fluorescence lifetime was not independent of emission wavelength, indicating aggregation, though the solute concentration was $\sim 10^{-5}$ *M* and aggregation was not expected. Furthermore samples seemingly produced under exactly the same conditions did not always show the same extent of aggregation, and indeed aggregation was sometimes completely absent even for more concentrated solutions. No other experimental probe was found to be as sensitive to aggregation as the fluorescence decay rate in this case, though under extreme conditions absorption studies also showed crystallite formation.

[3]Excitation spectra were obtained using a Farrand Spectrofluorimeter Mark I.

1. W. KLÖPFFLER. Chem. Phys. Lett. **11**, 482 (1971).
2. P. R. CALLIS and R. W. WILSON. Chem. Phys. Lett. **13**, 417 (1972).
3. P. J. WAGNER, M. MAY, and A. HAUG. Chem. Phys. Lett. **13**, 545 (1972).
4. N. Y. C. CHU and D. R. KEARNS. J. Am. Chem. Soc. **94**, 2619 (1972).
5. M. E. LONG, Y. H. LI, and E. C. LIM. Mol. Photochem. **3**, 221 (1971).
6. D. S. L. BLACKWELL, C. C. LIAO, R. O. LOUTFY, P. DE MAYO, and S. PASZYC. Mol. Photochem. **4**, 171 (1972).
7. M. KASHA. Discuss. Faraday Soc. **9**, 14 (1950).
8. G. S. HAMMOND, A. A. LAMOLA, and W. G. HERKSTROETER. J. Am. Chem. Soc. **86**, 4537 (1964).
9. I. H. MUNRO, L. M. LOGAN, F. D. BLAIR, F. R. LIPSETT, and D. F. WILLIAMS. Mol. Cryst. Liq. Cryst. **15**, 297 (1972).

Can. J. Chem. Downloaded from www.nrcresearchpress.com by 210.87.254.5 on 09/05/12
For personal use only.

Crystal Structure of 1,3,5,7-Tetrasulfur-2,4,6,8-tetramethylimide, $S_4(NCH_3)_4$

ALISTAIR L. MACDONALD AND JAMES TROTTER

Department of Chemistry, University of British Columbia, Vancouver 8, British Columbia

Received January 15, 1973

Crystals of $S_4(NCH_3)_4$ are orthorhombic, $a = 25.483(6)$, $b = 15.842(3)$, $c = 5.642(2)$ Å, $Z = 8$, space group *Fdd*2, required molecular symmetry C_2. The structure was determined with CuKα diffractometer data by Patterson and Fourier methods, and refined by full-matrix least-squares methods to $R = 0.067$ for 473 observed reflexions. The eight-membered ring has a crown conformation, with approximate C_{4v} symmetry, and the bonds at each nitrogen atom are slightly but significantly non-planar. Mean bond lengths are S—N = 1.677(4), C—N = 1.479(7) Å.

Les cristaux de $S_4(NCH_3)_4$ sont orthorhombiques, $a = 25.483(6)$, $b = 15.842(3)$, $c = 5.642(2)$ Å, $Z = 8$, groupe d'espace *Fdd*2, la symetrie minimum de la molecule est C_2. La structure a été determinée à partir de methodes de Patterson et Fourier, et a été affinée par les methodes moins carrées (matrice complète) à $R = 0.067$ pour 473 reflexions observées. La cycle de huit membres a une conformation d'un coronne, la symetrie étant à peine de C_{4v}, et les liaisons à chaque atome de nitrogene sont significament non-plans. Les distances moyennes des liaisons sont S—N = 1.677(4), C—N = 1.479(7) Å.

Can. J. Chem., **51**, 2504 (1973)

Introduction

There are eight known compounds of general formula $S_{8-x}(NH)_x$, $x = 0$–4, in which no two nitrogen atoms are adjacent, and the crystal structures have been determined for S_8 (1), S_7NH (2), three isomers of $S_6(NH)_2$ (2–4), $S_5(NH)_3$ (5), and $S_4(NH)_4$ (6, 7). All contain molecules with eight-membered puckered rings, and each molecule lies on a crystallographic two-fold symmetry element, except 1,3-$S_6(NH)_2$ (4). All the corresponding *N*-methyl sulfur imides are known (8), but no structural analyses have been reported. A puckered ring has been predicted for $S_4(NCH_3)_4$ (9), and dipole moment measurements suggest non-planar S_2NC groupings (8 and references therein). We now describe an X-ray crystal study of $S_4(NCH_3)_4$.

Experimental

Crystals of $S_4(NCH_3)_4$ (9) from hexane are colorless needles (usually several cm in length) elongated along *b*; since the crystals shattered when cut normal to the needle axis, it proved difficult to obtain one suitably small for the X-ray analysis, but eventually one of dimensions 0.2 × 0.5 × 0.2 mm was found, and the crystal data were determined from film and diffractometer measurements:

$C_4H_{12}N_4S_4$ f.w. = 244.4

Orthorhombic, $a = 25.483(6)$, $b = 15.842(3)$, $c = 5.642(2)$ Å, $V = 2277.7$ Å^3, $\rho_o = 1.437$ (flotation in aqueous KI), $Z = 8$, $\rho_c = 1.425$ (20 °C, CuKα, $\lambda = 1.5418$ Å, $\mu = 70$ cm^{-1}). Space group Fdd^2 (C_{2v}^{19}), from systematic absences.

Intensities were measured on a Datex-automated G.E. XRD 6 diffractometer, with a scintillation counter, CuKα radiation (Ni filter and pulse-height analyzer), and a θ–2θ scan over a range in 2θ of (1.80 + 0.86 tan θ) degrees at a speed of 2° min^{-1}, with background counts at each end of the scan. All 611 independent reflexions with $2\theta \leqslant 146°$ were measured, and 473 were classified as observed, having $I > 3\sigma(I)$, where $\sigma^2(I) = S + B + (0.03S)^2$, S = scan count, B = normalized background count. The intensity of a check reflexion, measured every 30 reflexions, fell to 50% of its initial value during the data collection; comparison with films indicated a uniform reduction for all reflexions, and because of the difficulty of obtaining suitable crystals the same crystal was used throughout, and the check reflexion data were used to reduce all intensities to the same scale. Structure amplitudes were derived as usual; no absorption correction was made.

Structure Analysis

The molecule is required to have C_2 symmetry. The structure was determined by Patterson and electron-density methods, and refined by full-matrix least-squares methods, finally with anisotropic thermal parameters, scattering factors from ref. 10, and anomalous dispersion corrections for sulfur ($\Delta f' = 0.03$, $\Delta f'' = 1.2$). Hydrogen atoms could not be located. The weighting scheme was $\sqrt{w} = 1$ when $|F_o| \leqslant 57$, $\sqrt{w} = 57/|F_o|$ when $|F_o| > 57$, $\sqrt{w} = 0.3$ for unobserved reflexions, and the final R values were 0.067 for the observed reflexions, and 0.081 for all data. Measured and calculated structure factors are in the Depository of Unpublished Data.[1]

Final positional and thermal parameters are in Table 1.

[1]Complete set of data is available, at a nominal charge, from the Depository of Unpublished Data, National Science Library, National Research Council of Canada, Ottawa, Canada, K1A 0S2.

Can. J. Chem. Downloaded from www.nrcresearchpress.com by 210.87.254.5 on 09/05/12
For personal use only.

TABLE 1. Final parameters (e.s.d.'s) × 10^4, t.f. = exp $-(b_{11}h^2 + ... 2b_{12}hk....)$

Atom	x	y	z	b_{11}	b_{22}	b_{33}	b_{12}	b_{13}	b_{23}
S(1)	681(1)	720(1)	0	18(1)	44(1)	380(9)	−6(1)	16(2)	30(3)
S(2)	−448(1)	1087(1)	6(8)	19(1)	34(1)	358(9)	3(1)	−19(2)	20(3)
N(1)	730(3)	−236(5)	1244(16)	15(1)	42(4)	285(29)	3(2)	3(6)	−4(9)
N(2)	159(3)	1221(4)	1119(18)	21(2)	26(3)	441(36)	−1(2)	10(7)	18(9)
C(1)	204(5)	1663(7)	3431(25)	28(3)	48(5)	500(50)	−1(3)	−22(10)	−69(14)
C(2)	922(5)	−314(7)	3695(24)	19(2)	54(5)	410(42)	1(3)	−17(9)	−13(14)

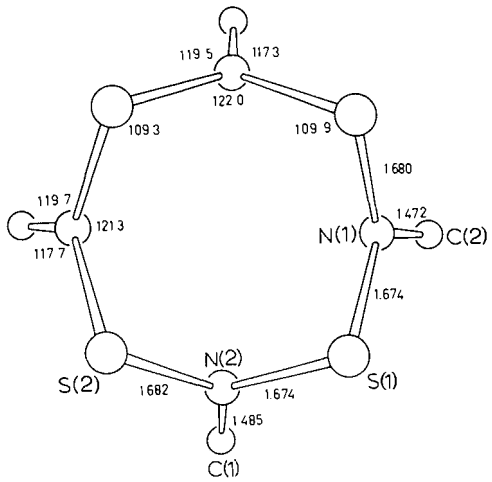

FIG. 1. Bond lengths and angles in $S_4(NCH_3)_4$; standard deviations for S—N, N—C, N—S—N, S—N—S, S—N—C are 0.009, 0.015 Å, 0.4, 0.6, 0.8°, respectively.

Discussion

The molecule (Fig. 1) contains an eight-membered, puckered ring of alternating sulfur and nitrogen atoms, with a crown conformation, and with the methyl groups bonded to nitrogen; the molecular symmetry is approximately C_{4v}. All the atoms of one type (S, N, or C) lie in one plane parallel to (001); the distance between the S and N planes is 0.67 Å, and that between the N and C planes is 1.34 Å. The geometry at each of the two independent nitrogen atoms is slightly but significantly non-planar, with the carbon atoms displaced by 0.28 and 0.29 Å from the SNS planes, the N—C bonds being 11° out of these planes. Similar nonplanarity may be present in $S_4(NH)_4$, where the N—H bonds make angles of 10° with the SNS planes, although the deviations are not statistically significant (11).

The thermal parameters correspond approximately to rigid-body vibration, with some additional motion of the methyl groups. The minimum translational motion (root-mean-square displacement 0.17 Å) is along c, *i.e.* the C_2 (approximate C_4) molecular axis, with displacements of 0.19 and 0.23 Å approximately along the cross-ring N...N directions. Minimum rotational motion (3.7°) is about the C_2 axis, with rotations of 4.3 and 5.4° about axes normal to C_2 and to S—N bonds.

Bond lengths and angles are included in Fig. 1. The mean S—N bond length is 1.677(4) Å (1.686 Å if a thermal motion correction is applied), the value in $S_4(NH)_4$ being 1.674(4) Å. This length is intermediate between the sum of the single-bond radii (1.74 Å) and the double-bond length of 1.54 Å found in $N_4(SF)_4$ (12), suggesting an intermediate bond order (13) and delocalization of nitrogen lone-pair electrons, in agreement with the observation that $S_4(NCH_3)_4$ is an extremely weak base (14). However the S—N—S—N torsion angles, 91.8 and 94.6°, and the N—S—N valency angles, 109.3 and 109.9°, are similar to the values in S_8, 99.3 and 107.8°, and it has been argued (15) that if the bonds in S_8 are single-bonds, then 1.67 Å is the expected single-bond length for S—N bonds involving sp^3 hybridization at sulfur. The mean C—N bond distance, 1.479(7) Å (1.485 Å if corrected for thermal liberation), is normal. The valency angles are close to the values expected for sp^3 hybridization at sulfur and sp^2 at nitrogen.

The crystal structure is shown in Fig. 2. Intermolecular contacts are normal, the shortest being S...C, 3.90; S...S, 3.925; C...C, 3.92 and 4.01 Å.

We thank Professor N. L. Paddock and Mr. R. W. Harrison for crystals and discussion, the University of British Columbia Computing Centre for assistance, and the National Research Council of Canada for financial support.

Can. J. Chem. Downloaded from www.nrcresearchpress.com by 210.87.254.5 on 09/05/12
For personal use only.

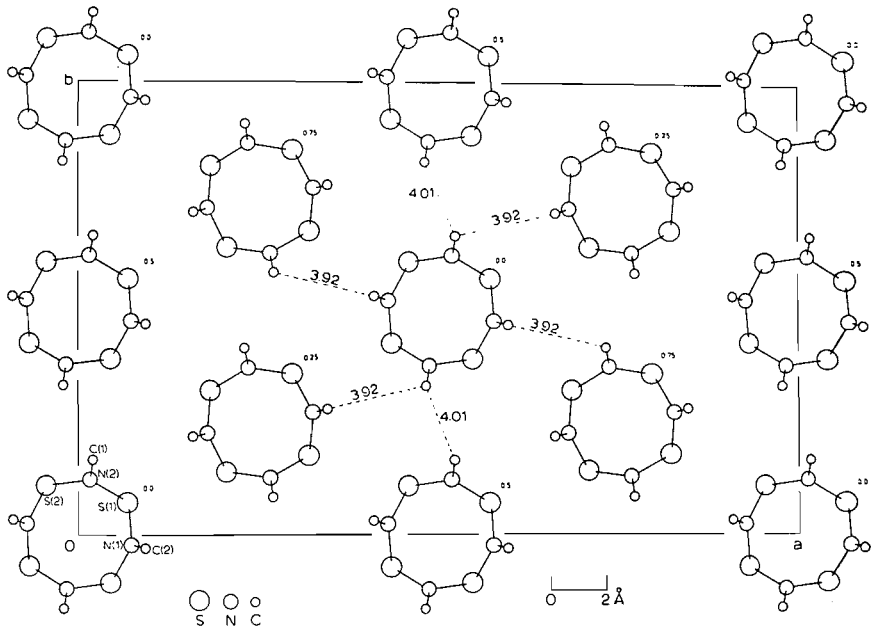

FIG. 2. Structure of $S_4(NCH_3)_4$ viewed along *c*.

1. S. C. ABRAHAMS. Acta Cryst. **8**, 661 (1955).
2. J. WEISS. Z. anorg. Chem. **305**, 190 (1960); J. WEISS and H.-S. NEUBERT. Acta Cryst. **18**, 815 (1965).
3. J. C. VAN DE GRAMPEL and A. VOS. Acta Cryst. **B25**, 611 (1969).
4. H. J. POSTMA, F. VAN BOLHUIS, and A. VOS. Acta Cryst. **B27**, 2480 (1971).
5. H. GARCÍA-FERNÁNDEZ and C. RÉRAT. C.R. Acad. Sci. Paris, C, **262**, 1866 (1966).
6. E. W. LUND and S. R. SVENDSEN. Acta Chem. Scand. **11**, 940 (1957).
7. R. L. SASS and J. DONOHUE. Acta Cryst. **11**, 497 (1958).
8. W. I. GORDON and H. G. HEAL. J. Inorg. Nucl. Chem. **32**, 1863 (1970).
9. B. D. STONE and M. L. NIELSEN. J. Am. Chem. Soc. **81**, 3580 (1959).
10. International tables for X-ray crystallography. Vol. III. Kynoch Press, Birmingham. 1962.
11. T. M. SABINE and G. W. COX. Acta Cryst. **23**, 574 (1967).
12. O. GLEMSER. Angew. Chem. (Int. Ed.), **2**, 530 (1963).
13. D. CHAPMAN and T. C. WADDINGTON. Trans. Faraday Soc. **58**, 1679 (1962).
14. R. W. HARRISON. Private communication.
15. R. GLEITER. J. Chem. Soc. (A), 3174 (1970).

Can. J. Chem. Downloaded from www.nrcresearchpress.com by 210.87.254.5 on 09/05/12
For personal use only.

Solvation of Cl^- and O_2^- with H_2O, CH_3OH, and CH_3CN in the gas phase

R. YAMDAGNI, J. D. PAYZANT, AND P. KEBARLE

Department of Chemistry, University of Alberta, Edmonton, Alberta T6G 2G2

Received February 16, 1973

Determination of the temperature dependence of the equilibrium constants $K_{n,n-1}$ for the reactions $A^-B_n = A^-B_{n-1} + B$ where A^- equals Cl^- and O_2^- and B is HOH, CH_3OH, or CH_3CN leads to the corresponding $\Delta H^0_{n-1,n}$, $\Delta G^0_{n-1,n}$, and $\Delta S^0_{n-1,n}$ values. The experimental technique is based on mass spectrometric detection of ions escaping from a high pressure ion source. At $n = 1$, Cl^- is solvated most strongly by methanol, then CH_3CN and HOH. At higher n a cross over is observed with water becoming the best solvent. These results are in agreement with the positive transfer enthalpies and free energies for Cl^- from the liquid solvents HOH → CH_3OH and HOH → CH_3CN reported in the literature.

O_2^- is solvated more strongly than Cl^- appearing thus as an ion of "size" intermediate between Cl^- and F^-. Again CH_3OH gives the highest interaction for $n = 1$, however for $n > 1$ water gives stronger interactions.

La détermination de l'influence de la température sur les constantes d'équilibre $K_{n,n-1}$ pour les réactions $A^-B_n = A^-B_{n-1} + B$ où $A^- = Cl^-$ et O_2^- et B = HOH, CH_3OH, et CH_3CN, conduit aux valeurs correspondantes pour $\Delta H^0_{n-1,n}$, $\Delta G^0_{n-1,n}$ et $\Delta S^0_{n-1,n}$. La technique expérimentale est basée sur la détection par spectrométrie de masse, des ions sortant d'une source d'ions à haute pression. Pour $n = 1$, Cl^- est le plus solvaté par le méthanol puis CH_3CN et HOH. Pour n plus élevé, une interversion se produit et c'est l'eau qui devient le meilleur solvant. Ces résultats sont en accord avec les enthalpies et énergies libres de transfert pour Cl^- dans les solvants liquides HOH → CH_3OH et HOH → CH_3CN, rapportées dans la littérature.

O_2^- est solvaté plus fortement que Cl^- indiquant ainsi que la taille de cet ion est intermédiaire entre Cl^- et F^-. CH_3OH montre encore la plus forte interaction pour $n = 1$, cependant pour $n > 1$, c'est l'eau qui conduit aux interactions les plus fortes. [Traduit par le journal]

Can. J. Chem., **51**, 2507 (1973)

Can. J. Chem. Downloaded from www.nrcresearchpress.com by 210.87.254.40 on 09/05/12
For personal use only.

Introduction

A comparative study of the gas phase solvation of the halide ions by water and acetonitrile molecules was published earlier (1). The present work extends the study to the O_2^- ion and includes methanol as a new solvent. The O_2^- ion is an important ion in the ionosphere and troposphere (2) where it results from electron capture by O_2. The superoxide ion O_2^- is stable also in condensed phases. Thus paramagnetism and X-ray crystal studies of the solid metal superoxides (NaO_2, KO_2, etc.) have shown (3) that these contain discrete free radical anions O_2^-. The O_2^- ion although unstable in aqueous solution plays an important role in biological systems (4). The superoxide ion is stable in aprotic solvents. Solutions of alkylamine superoxide in aprotic solvents have been used to study the reactivity of the superoxide ion as a nucleophilic reagent (5).

In the gas phase the O_2^- ion forms stable hydrates $O_2^-(H_2O)_n$ (6) and other solvates: $O_2^-(CH_3OH)_n$, $O_2^-(CH_3CN)_n$ etc. Thus the stabilities of these solvates can be studied and some interesting information on this symmetric singly charged diatomic ion can be obtained.

All measurements described in the present work are based on the determination of the temperature dependence of the gas phase equilibria $(n,n-1)$ observed in a high pressure mass spectrometer ion source.

$$(n,n-1) \qquad A^-B_n = AB^-_{n-1} + B$$

Experimental

The apparatus and method of measurement have been described in considerable detail elsewhere (7, 8). Only a brief outline will be given here. The equilibrium constants $K_{n-1,n}$ were determined by mass spectrometric detection of ions escaping from the reaction chamber-ion source. At equilibrium the $K_{n-1,n}$ are given by

$$K_{n-1,n} = \frac{P_{A^-(B)_n}}{P_{A^-(B)_{n-1}} P_B} \approx \frac{I_{A^-(B)_n}}{I_{A^-(B)_{n-1}} P_B}$$

$$K_{n,n-1} = 1/K_{n-1,n}$$

where P_X represents the partial pressures in the ion source and I_X the mass spectrometrically detected ion intensities of the respective species. It is assumed that the measured ion intensity ratios reflect the ratio of the partial pres-

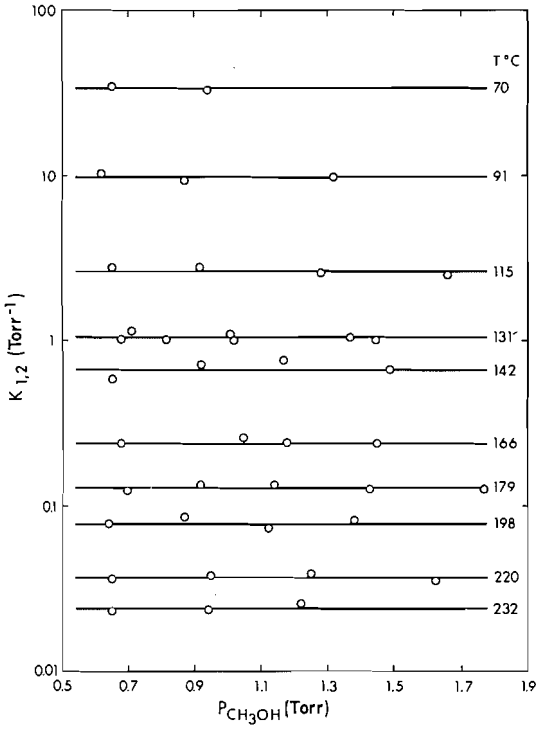

FIG. 1. Equilibrium constants $K_{1,2}$ for the reaction $O_2^-.CH_3OH + CH_3OH = O_2^-(CH_3OH)_2$ as a function of methanol pressure. Total pressure is 4.0 Torr (O_2).

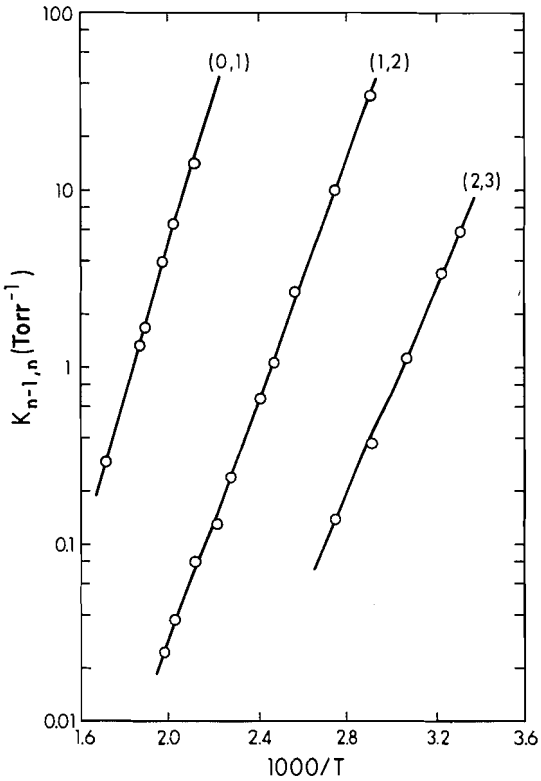

FIG. 2. Van't Hoff plots of equilibrium constants $K_{n-1,n}$ for reactions $(n-1,n)$: $O_2^-(CH_3OH)_{n-1} + CH_3OH = O_2^-(CH_3OH)_n$, $n = (1, 2, 3)$.

sures. In a typical experiment the pressure of carrier gas (O_2) in the ion source is ~5 Torr and the partial pressure of solvent vapor is varied over the 0.5–2.0 Torr range. Under these conditions the half life of the forward clustering reactions $(n-1,n)$ is short ($t_{1/2} < 30$ μs) (2). Since the average ion spends about 1 ms in the ion source (9) and undergoes a large number of collisions the measured ion intensities should give the thermodynamic equilibrium concentrations.

A 2 kV electron beam of $\sim 10^{-8}$ A entering the ion source through a narrow slit (1.5 × 0.01 mm) is used for ionization. The ions are sampled from the ion source through a slit (1.5 × 0.01 mm) which is mounted about 4 mm below the plane of the electron beam. The liquid solvent was kept in a thermostated bulb and its vapor was introduced through a capillary into the flowing (~25 atm cc min^{-1}) carrier gas. The flow rate was monitored with a calibrated flowmeter and the partial pressure of the solvent in the ion source was calculated by "weight loss" measurements (7, 8).

The negative ion O_2^- was observed in O_2 (9), and is presumably produced by third body capture of thermal electrons:

$$e + 2O_2 = O_2^- + O_2$$

The Cl^- ion was generated by the addition of small quantities (~0.01 Torr) of CCl_4 (6) to the carrier gas. The reaction probably involved is dissociative electron capture by CCl_4:

$$e + CCl_4 = Cl^- + CCl_3$$

The Cl^-, CH_3OH, and CH_3CN experiments described in this paper were done before the pulsed electron multiscaling technique was developed (7). Therefore the kinetics of the approach to the equilibria $(n-1,n)$ was not studied for that system. The O_2^- values were obtained with the multiscaling technique.

The absolute accuracy of the quoted ΔH° and ΔG° values is difficult to assess. Most accurate are the ΔG° values corresponding to the experimental temperature range. The ΔH° values and ΔG°_{298} values depend on a correct evaluation of the slope in the Van't Hoff plots. The standard deviation of the slope corresponds generally to less than ±3% of the ΔH° values. However, the error is probably closer to ±5%. The largest actual error is expected in the ΔS° values since the least square treatment used does not take into account systematic deviations of the measured equilibrium constants and temperature.

Results and Discussion

The equilibrium constants for the reaction

$$A^-B_{n-1} + B = A^-B_n$$

were measured at different temperatures with

Can. J. Chem. Downloaded from www.nrcresearchpress.com by 210.87.254.40 on 09/05/12
For personal use only.

TABLE 1. Experimentally determined enthalpy, entropy, and free energy changes for the reaction: $A^-B_n = A^-B_{n-1} + B^*$

A	B		$(n,n-1)$ (1,0)	(2,1)	(3,2)	(4,3)	(5,4)
F^-	H_2O†	ΔH^0	23.3	16.6	13.7	13.5	13.2
		ΔS^0	17.4	18.7	20.4	36.9	30.7
		ΔG^0	18.1	11.0	7.6	5.5	7.1
O_2^-	H_2O‡	ΔH^0	18.4	17.2	15.4	—	—
		ΔS^0	20.1	25.1	28.2	—	—
		ΔG^0	12.5	9.7	7.0	—	—
	CH_3OH	ΔH^0	19.1	15.5	13.5	—	—
		ΔS^0	21.9	24.8	27.9	—	—
		ΔG^0	12.5	8.1	5.2	—	—
	CH_3CN	ΔH^0	16.4	14.2	11.9	9.5	—
		ΔS^0	17.4	22.0	24.7	22.4	—
		ΔG^0	11.2	7.7	4.5	2.8	—
Cl^-	H_2O†	ΔH^0	13.1	12.7	11.7	11.1	—
		ΔS^0	16.5	20.8	23.2	25.8	—
		ΔG^0	8.2	6.5	4.5	3.4	—
	CH_3OH	ΔH^0	14.2	13.0	12.3	11.2	10.5
		ΔS^0	14.8	19.4	23.6	26.4	25.5
		ΔG^0	9.8	7.2	5.2	3.3	2.9
	CH_3CN§	ΔH^0	13.4	12.2	10.6	6.2	—
		ΔS^0	14.3	18.9	20.1	10.8	—
		ΔG^0	9.2	6.6	4.6	3.0	—

*ΔH^0 and ΔG^0 (298 °K) values in kcal/mol. ΔS^0 values in e.u. standard state, 1 atm.
†Reference 9*a*.
‡Reference 9*b*.
§Reference 1.

various solvent (B) pressures. A typical case is shown in Fig. 1 where the equilibrium constants are plotted against the CH_3OH pressure. It can be seen that the equilibrium constants are independent of solvent pressure within experimental error. The Van't Hoff plots ($n = 1, 2, 3$) for the O_2^- methanol system are shown in Fig. 2. The thermodynamic values of ΔH^0, ΔS^0, and ΔG^0 were derived from such plots for all the systems studied and are listed in Table 1. Some previous data from this laboratory are also included in the table for comparison.

For a visual comparison, the variation of $\Delta H^0_{n-1,n}$ with n for the ions F^-, O_2^-, and Cl^- are shown in Fig. 3. We may start the discussion with the behavior of Cl^- which is a typically "medium size" spherical negative ion. The highest $\Delta H^0_{1,0}$ value is observed with CH_3OH followed by CH_3CN and HOH. Methanol and water are both protic solvents while CH_3CN is aprotic. The dependence of the $\Delta H^0_{1,0}$ interactions (of Cl^-) on the nature of the protic solvents RH was examined in an earlier paper (10) which dealt with hydrogen bonding to negative ions. It was concluded that the $\Delta H^0_{1,0}$, which corresponds to the dissociation energy of the hydrogen bond $D(Cl^-—HR)$, increases with the proton donating power, *i.e.*, with the gas phase acidity of HR. The higher $\Delta H^0_{1,0}$ for methanol relative to water was ascribed to a higher gas phase acidity of methanol which was in agreement with gas phase acidity measurements by Brauman (11). The present results extend the comparison to higher n. In Fig. 3 one observes that methanol remains a better "solvent" also for higher n but that the difference between methanol and water decreases. Extrapolation of these $\Delta H^0_{n,n-1}$ values indicates a possible cross over, *i.e.* a larger ΔH^0 for water at the $\Delta H^0_{5,4}$ step. Earlier gas phase solvation work (1, 9) has indicated that the trends in the $\Delta H^0_{n,n-1}$ values observed even for only the first four or five steps reflect differences in the total single ion enthalpies and free energies of solvation. This seems to be the case also for the Cl^-

Can. J. Chem. Downloaded from www.nrcresearchpress.com by 210.87.254.40 on 09/05/12
For personal use only.

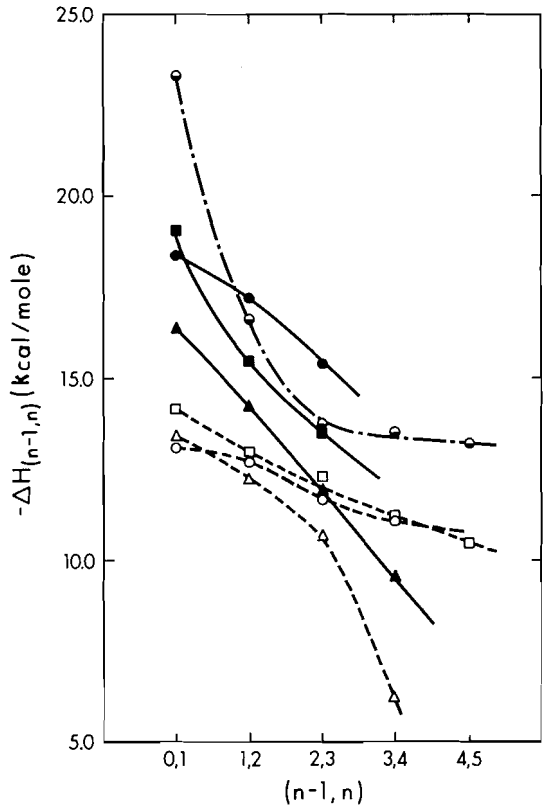

FIG. 3. Plot of $-\Delta H^0_{n-1,n}$ for solvation reaction in the gas phase: ●, $O_2^-(H_2O)_n$; ■, $O_2^-(CH_3OH)_n$; ▲, $O_2^-(CH_3CN)_n$; ○, $Cl^-(H_2O)_n$; □, $Cl^-(CH_3OH)_n$; △, $Cl^-(CH_3CN)_n$; ◑, $F^-(H_2O)_n$.

solvation by water and methanol. Since the measured differences between the $\Delta H^0_{n,n-1}$ for methanol and water are small and followed by a possible cross over, the present results indicate only a small difference between the total enthalpies of solvation of Cl^- by water and methanol. Choux and Benoit (12) have estimated a small positive enthalpy for transfer of Cl^- from H_2O to CH_3OH: $\Delta H_{transfer} = +1.9$ kcal/mol. If this estimate is correct then the indicated cross over in Fig. 3 is probably real. The free energy differences (Table 1) show a trend similar to that of the ΔH^0 differences, however the relative decrease of the $\Delta G^0_{n,n-1}$ for methanol is more rapid, such that a reversal with water becoming more favored is observed already for the $\Delta G^0_{4,3}$ step. This suggests that the free energy of Cl^- transfer from HOH to CH_3OH should be positive and larger than the corresponding ΔH^0 transfer, a result which is in agreement with conclusions of Parker and co-workers (13).

A comparison between the $\Delta H^0_{n,n-1}$ and $\Delta G^0_{n,n-1}$ values for Cl^- and the other halide ions and the protic and aprotic solvents HOH and CH_3CN was reported earlier (1). The most significant finding was that acetonitrile at close range (low n) gives stronger interactions than water but that the interactions become very much less favorable at high n. Furthermore it was found (1) that the small ions (F^-) showed stronger interactions with water while the interaction with acetonitrile became relatively more favorable as the size of the ion increased. This result was found to be in agreement with transfer enthalpies and free energies for the liquid solvents (HOH → aprotic solvent) which had been determined (12, 13) to be positive for small ions (F^-) becoming progressively smaller and turning negative for large ions (I^-).

The solvation of O_2^- (Fig. 3 and Table 1) fits similar general trends. The $\Delta H^0_{n,n-1}$ values of Fig. 3 show that O_2^- falls between F^- and Cl^- and may thus be considered as an ion which has a "radius" falling between those of F^- and Cl^-. Correspondingly the difference between the values for HOH and CH_3CN observed for O_2^- is larger than that observed for the larger Cl^- ion. It is also found that the solvation by methanol becomes unfavorable at much smaller $n,n-1$ values since a crossover occurs already after $\Delta H^0_{1,0}$. We are led to expect that ion transfer from the liquid solvent water to methanol should show transfer enthalpies which decrease as the size of the ion is increased. This is borne out by the determinations of Choux and Benoit (12).

Of course the O_2^- ion is not spherically symmetrical. The simple MO description puts the three outer electrons in the doubly degenerate nonbonding $2_p\pi_g$ orbital. This means that in the unperturbed O_2^- the negative charge should be spread out to the two ends of the ion. One would expect that the presence of a molecule like HOH and CH_3OH with a partially positively charged hydrogen atom will induce a partial shift of electronic charge to the one side of the O_2^- ion with the polar molecule attaching itself effectively to that side. The behavior of O_2^- as an ion "smaller" than Cl^- is thus not unexpected. The addition of a second and further molecules might then engage both oxygen atoms. Unfortunately the data in Fig. 3 do not seem to

Can. J. Chem. Downloaded from www.nrcresearchpress.com by 210.87.254.40 on 09/05/12
For personal use only.

show a consistent behavior. Thus the hydrates show a small fall off between $\Delta H^0_{1,0}$ and $\Delta H^0_{2,1}$ (compared to that of F^-) however the methanol results give a fairly large fall off for the same step.

From the general position of the O_2^- in Fig. 3 one can predict that its total enthalpy of hydration will be close but lower than that for F^-. Since $\Delta H_h(F^-) = -113$ kcal/mol and $\Delta H_h(Cl^-) = -81.3$ kcal/mol (14) one might expect a $\Delta H_h(O_2^-) \approx -100$ kcal/mol. The transfer enthalpy from water to methanol should be small and positive while that to acetonitrile also positive but considerably larger.

1. R. YAMDAGNI and P. KEBARLE. J. Am. Chem. Soc. **94**, 2940 (1972).
2. J. D. PAYZANT and P. KEBARLE. J. Chem. Phys. **56**, 3482 (1972).
3. F. A. COTTON and G. WILKINSON. Advanced inorganic chemistry. 2nd ed. Interscience Publishers, John Wiley. 1966.
4. R. NILSON, F. M. PICK, and R. C. BRAY. Biochim. Biophys. Acta, **1969**, 192 (1969).
5. M. V. MERRITT and D. T. SAWYER. J. Org. Chem. **35**, 2157 (1970).
6. P. KEBARLE, M. ARSHADI, and J. SCARBOROUGH. J. Chem. Phys. **49**, 817 (1968).
7. A. J. CUNNINGHAM, J. D. PAYZANT, and P. KEBARLE. J. Am. Chem. Soc. **94**, 7627 (1972).
8. J. D. PAYZANT, R. YAMDAGNI, and P. KEBARLE. Can. J. Chem. **49**, 3308 (1971).
9. (*a*) M. ARSHADI, R. YAMDAGNI, and P. KEBARLE. J. Phys. Chem. **74**, 1475 (1970); (*b*) M. ARSHADI and P. KEBARLE. J. Phys. Chem. **74**, 1483 (1971).
10. R. YAMDAGNI and P. KEBARLE. J. Am. Chem. Soc. **93**, 7139 (1971).
11. J. I. BRAUMAN and L. K. BLAIR. J. Am. Chem. Soc. **92**, 5586 (1970).
12. G. CHOUX and R. L. BENOIT. J. Am. Chem. Soc. **91**, 6221 (1969).
13. R. ALEXANDER, E. C. F. KO, Y. C. MAC, and A. J. PARKER. J. Am. Chem. Soc. **89**, 3703 (1967).
14. J. E. DESNOYERS and C. JOLICOEUR. Modern aspects of electrochemistry. Vol. 5. *Edited by* H. O'M. Bockris and B. E. Conway. Plenum Press, N.Y. 1969.

Can. J. Chem. Downloaded from www.nrcresearchpress.com by 210.87.254.40 on 09/05/12
For personal use only.

Free-energy Relationships in Coordination Chemistry. III. A Comprehensive Index to Complex Stability

E. NIEBOER[1] AND W. A. E. MCBRYDE

Department of Chemistry, University of Waterloo, Waterloo, Ontario

Received November 7, 1972

Efforts to relate metal-complex stability constants to some property of the metal ions involved have led to the development of a correlating numerical index Q with the following characteristics: (*i*) Q is a two parameter quantity involving ionic charge and electronegativity, which may assume different values for a particular metal according to the type of ligand with which complexes are formed; (*ii*) linear relationships are obtained for plots of log K_{ML} *vs.* Q for various metals and more than thirty ligands. The effect of the thermodynamic and structural properties of ligands and metal complexes on the slope and intercept in this correlation is discussed. Two new indices to class b behavior are introduced, one for metal ions and one for ligands. The index Q is shown to be related to other published indices of ionic or covalent, class a or class b, behavior of metals and ligands; the alternative ways of assigning Q may be regarded as reflecting the varying degrees of ionic or covalent character in the complexes of a given metal.

Dans le but de relier les constantes de stabilité métal-complexe à certaine propriété des ions métalliques, on a développé un indice numérique de corrélation Q possèdant les caractéristiques suivantes: (*i*) Q est un paramètre double engageant la charge ionique et l'électronégativité. Il peut avoir des valeurs différentes pour un métal particulier selon le type de ligand avec lequel les complexes se forment. (*ii*) Des relations linéaires ont été obtenues en portant log K_{ML} en fonction de Q pour divers métaux et pour plus de trente ligands. L'effet des propriétés thermodynamique et structurale des ligands et des complexes métalliques sur la pente et l'ordonnée à l'origine dans cette corrélation, a été discuté. Deux nouveaux indices de classe b ont été introduits, un pour les ions métaux et un pour les ligands. L'indice Q peut être relié à d'autres indices publiés, ionique ou covalent, classe a ou classe b, comportement des métaux et ligands; les autres méthodes d'attribution sur Q peuvent refléter des degrés variables dans le caractère ionique ou covalent des complexes pour un métal donné. [Traduit par le journal]

Can. J. Chem., 51, 2512 (1973)

Introduction

The classification of donors and acceptors in inorganic reactions has provided a useful framework for the rationalization of metal-complex formation in solution. The original division of acceptors (metal ions) by Ahrland, Chatt, and Davies (1) into class a and class b was based on complex stability in solution as measured by equilibrium constants. These ideas were then extended to the ligand donor atoms: class a donors (*e.g.*, N, O, F) are preferred by class a acceptors, and class b donors (*e.g.*, P, S, Cl) by class b acceptors. More recently Ahrland (2–5) has made the generalization that class a reactions in aqueous medium tend to be entropy stabilized, while class b interactions tend to be enthalpy controlled (exothermic). This thermodynamic criterion is useful, but cannot be used in a clear-cut diagnostic test for any individual reaction (see below).

Pearson's concept (6–10) of hard and soft acids and bases (h.s.a.b.) is a more comprehensive analysis of chemical reactivity. Class a donors and acceptors are referred to as "hard" and the corresponding class b entities are designated "soft". Donor atoms were characterized by a consideration of properties such as polarizability, redox potential, and electronegativity, and by a comparison of their relative affinities for the acids H^+ (hard) and CH_3Hg^+ (soft). Acceptors were then characterized by their preference for the "hard" and "soft" bases. The ability of donor and acceptor atoms to participate in π-back bonding was also considered to be an essential feature of "soft" behavior by Arhland and Pearson.

The use of the vague terms "soft" and "hard" has been criticized (11) on the grounds that they cannot be associated with a single known physical parameter such as polarizability, or with bonding phenomena such as π-back bonding. Williams and Hale (11), Klopman (12), and Jørgensen (13) all agree that the gross fea-

[1]Present address: Department of Chemistry, Laurentian University, Sudbury, Ontario.

Can. J. Chem. Downloaded from www.nrcresearchpress.com by 210.87.254.5 on 09/05/12
For personal use only.

Can. J. Chem. Downloaded from www.nrcresearchpress.com by 210.87.254.5 on 09/05/12
For personal use only.

tures of class a and class b behavior are explained satisfactorily by the relative importance of ionic and covalent bonding as modified by solvent effects. London energies and classical polarization may also be important, but are more difficult to assess. Jørgensen (13) expresses the opinion that additional stabilization may also be achieved when one partner of a covalent bond has a low ionization energy and the other has low-energy continuum orbitals. The second atom is then able to take over a small amount of electron density from the first. This charge invasion of continuum orbitals of low energy is thought to take place in systems where the traditional π-back bonding has been implied.

Several indices of class a and b behavior for acceptors and donors have been reported. Craig and Nyholm (14) have proposed $R = \sum I_M(r_M + r_L)/Z^2$ as an index to the character of metal ions; here $\sum I_M$ is the sum of the ionization energies of the metal up to charge Z, and r_M and r_L are ionic radii of the metal and ligand respectively. Class b character is assigned to an ion when $R > 19$, class a when $R < 15$, and intermediate character for $15 < R < 19$. Williams and Hale (11) noted that large values of the similar parameter $\sum I_M r_c$ (in which r_c is the interionic distance in halides) were found for the elements with strongest b character. For a series of bivalent halides the reciprocal of this parameter multiplied by 0.85 closely matched the fraction of ionic character calculated for the partial ionic/covalent bond model (15). The implication here is that a high degree of covalent bond character correlates with class b character in metal ions. Klopman (12) has reproduced in part, and with good agreement, the series of "hard" and "soft" central atoms and ligands established empirically by Ahrland *et al.* and Pearson (1–10). He calculated acceptor and donor electronegativities in solution from ionization energies, electron affinities, ionic sizes, and hydration energies. A related "softness" parameter has been defined by Ahrland (5); and another proposed by Pearson and Mawby (16) also agrees well with Klopman's index.

The present work is concerned with correlation of the magnitude of stability constants with properties of the metal ion. It is surprising that the class a and b indices just mentioned have not been widely tested as indices of complex stability in solution, though other atomic parameters have been employed for a long time (17–19). Thus charge/size ratios for ions have found limited application for class a acceptors. Functions such as Z^2/r_M and Z^2/r_{eff} must be employed when ions of different charge type are considered. The effective radius, r_{eff}, is the sum of the cationic crystal radius r_M and an amount related to the radius of the donor atom of the ligand. For instance, ionic hydration energies vary linearly with $Z^2/(r_M + 0.85)$ (11, 20). The most comprehensive and successful correlation achieved so far is that between log K_{ML} (74.5% by volume of dioxane) of acetylacetone and dibenzoylmethane complexes with the last stepwise ionization potential or with ZX_M, where X_M is the Haissinsky electronegativity, of the metal ion (17, 19, 21–25).

Our attempts to apply these parameters to such systems as EDTA met with very limited success. However, these efforts led to the development of a new index, hereafter described as Q, which is somewhat related to the ZX_M scale, and somewhat related to other parameters by which metals and ligands have been categorized. The value of Q for a given metal, though arrived at empirically, appears in many cases to be dependent on the ligand with which it has been combined. This is taken to reflect the variation in size and especially in bonding character of different donor atoms. In working with the new index we became aware of other derived parameters by which ligands could be characterized and metal–ligand stabilities correlated, and of a new scale for the classification of acceptors.

The Stability Index Q

The index Q may be defined as follows:

$$[1] \qquad Q = (a\delta ZX_M + bX_M^2)/(a + b)$$

In this, X_M is the electronegativity of the metal ion according to Allred (26) and Z is the ionic charge; a and b are integral weighting factors (0, 1, 2....); δ is a parameter calculated with the aid of Slater atomic shielding constants (27) and is intended to compensate in the case of certain elements for an effective increase in electronegativity due to small size or extra covalent bonding character. For some metal ions the choice of integers a and b or of the parameter δ appears to depend on the ligand with which the metal is combined. The particular ways in which

Can. J. Chem. Downloaded from www.nrcresearchpress.com by 210.87.254.5 on 09/05/12
For personal use only.

TABLE 1. Correlations of metal complex stabilities with Q

Ligand number	Ligand[a]		Number of ions	Slope ρ	Intercept on Q axis Q_{int}	Standard deviation of log K_{ML}	Correlation factor r	Index $\frac{\rho Q_{int}}{n}$
1	Dibenzoylmethane (75% by volume of dioxane)		23	2.69	−0.53	0.37	0.995	−0.71
2	Acetylacetone (75% by volume of dioxane)		16	2.69	−0.13	0.32	0.995	−0.17
3	4,5-Dihydroxybenzene-1,3-disulfonic acid		12	4.10	+0.79	0.49	0.995	+1.62
4	Acetylacetone		20	2.32	1.09	0.32	0.986	1.26
5	Ethylenediaminetetraacetic acid		26	8.36	1.46	0.66	0.995	2.03
6	Nitrilotriacetic acid		23	5.34	1.52	0.59	0.986	2.02
7A	8-Hydroxyquinoline-5-sulfonic acid		12	4.55	1.56	0.19	0.998	3.55
8	Hydroxide		27	2.84	1.60	0.33	0.996	4.54
9	8-Hydroxyquinoline		12	4.89	1.66	0.20	0.998	4.06
10	1,2-Dihydroxybenzene		9	5.32	1.73	0.59	0.987	4.60
11A	Acetic acid		8	1.00	1.85	0.06	0.992	1.85
12	5-Sulfosalicylic acid		14	4.17	1.81	0.42	0.990	3.77
13	*N*-Methyliminodiacetic acid		12	4.82	1.87	0.35	0.991	3.00
14	Salicylaldehyde (50% by volume of dioxane)		11	3.28	1.99	0.17	0.997	3.26
15	Salicylic acid		10	4.96	2.03	0.37	0.996	5.03
16A	Iminodiacetic acid		12	5.08	2.06	0.38	0.993	3.49
17A	Pyridine-2,6-dicarboxylic acid		10	4.50	2.07	0.37	0.987	3.11
18A	Ethylenediamine-*N*,*N*′-diacetic acid		6	8.62	2.17	0.62	0.989	4.68
19	Salicylaldehyde		5	3.10	2.24	0.10	0.999	3.47
20A	Pyridine-2-carboxylic acid		11	4.56	2.28	0.28	0.982	5.20
21	Glycine		12	4.87	2.40	0.35	0.993	5.84
22A	Benzoic acid		4	1.00	2.52	—	—	2.52
23	Phenol		3	2.52	2.70	0.01	1.00	6.80
24	1,10-Phenanthroline		8	6.79	2.47	0.16	0.999	8.39
25	2,2′-Bipyridyl		7	6.81	2.69	0.44	0.987	9.16
26	Triethylenetetramine		9	14.35	2.75	0.72	0.996	9.86
27	Ethylenediamine	log K_{ML}	9	8.63	2.82	0.30	0.998	12.17
		log β_2	10	15.00	2.82	1.00	0.994	10.58
28	Ammonia		13	4.66	2.95	0.55	0.987	13.75
29	Cyanide	log β_4	4	40.68	2.97	1.58	0.990	30.2
30	Pyridine		10	2.75	3.05	0.17	0.995	8.39
31	Fluoride	Line I ($\mu = 0.5$)	9[b]	2.15	2.00	0.09	0.999	4.30
		Line II ($\mu = 0.5$)	9[b]	2.41	3.69	0.23	0.993	8.89
		Line I ($\mu = 0$)	11	2.20	1.64	0.21	0.997	3.61
		Line II ($\mu = 0$)	8	2.51	3.51	0.21	0.995	8.81
32	Chloride	Line I	18[c]	2.43	1.09	0.38	0.988	2.65
		Line II	13[d]	2.64	3.30	0.46	0.978	8.71
33	Bromide	Line I	8[e]	3.28	1.15	0.35	0.997	3.77
		Line II	10[f]	3.51	3.46	0.64	0.974	12.14
7B	8-Hydroxyquinoline-5-sulfonic acid		5[g]	3.24	1.52	0.11	0.982	2.46
11B	Acetic acid		10[i]	1.55	1.74	0.11	0.997	2.70
16B	Iminodiacetic acid		15[h]	3.98	1.88	0.25	0.993	2.49
18B	Ethylenediamine-*N*,*N*′-diacetic acid		11[h]	4.17	1.61	0.30	0.976	1.68
20*B*	Pyridine-2-carboxylic acid		15[i]	2.10	1.62	0.17	0.992	1.70
22B	Benzoic acid		2	1.80	2.52	—	—	4.54

[a]Unless indicated otherwise, the reaction medium is water with an ionic strength of 0–0.1 in the majority of cases.
[b]See Fig. 1 for ions correlated.
[c]Tl^{3+}, Hg^{2+}, Ag^{+}, alkaline earths, alkali metals, lanthanides, Y^{3+}, Sc^{3+}, Tl^{+}, Pu^{3+}.
[d]Tl^{3+}, Pd^{2+}, Cd^{2+}, In^{3+}, Bi^{3+}, Pb^{2+}, Sn^{2+}, Ga^{3+}, Fe^{3+}, Cu^{2+}, Ni^{2+}, Mn^{2+}, Zn^{2+}, Be^{2+}.
[e]Hg^{2+}, Tl^{3+}, Ag^{+}, Sc^{3+}, Y^{3+}, Tl^{2+}, Ce^{3+}, Cs^{+}, K^{+}.
[f]Tl^{3+}, Pd^{2+}, Bi^{3+}, Cd^{2+}, In^{3+}, Cu^{2+}, Pb^{2+}, Sn^{2+}, Fe^{3+}, Zn^{2+}.
[g]Lanthanides; and alkaline earths if $Q = \delta Z X_M$.
[h]H^{+}, lanthanides, and alkaline earths.
[i]H^{+}, Pb^{2+}, lanthanides, and alkaline earths.

Can. J. Chem. Downloaded from www.nrcresearchpress.com by 210.87.254.5 on 09/05/12
For personal use only.

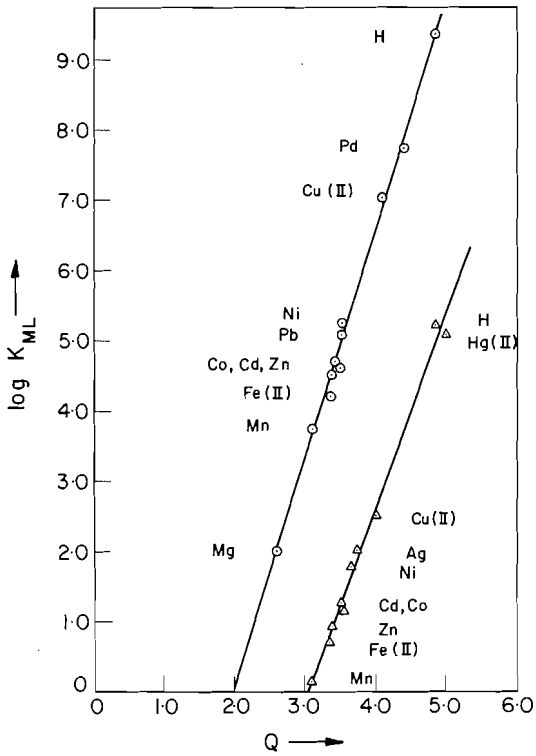

FIG. 1. Metal complex stabilities of hydroxide and fluoride ions as a function of Q: open circles and lower Q-scale, hydroxide ion (μ = 0; 20, 25 °C); open triangles and upper Q-scale, fluoride ion (μ = 0.5 M $NaClO_4$, 25 °C).

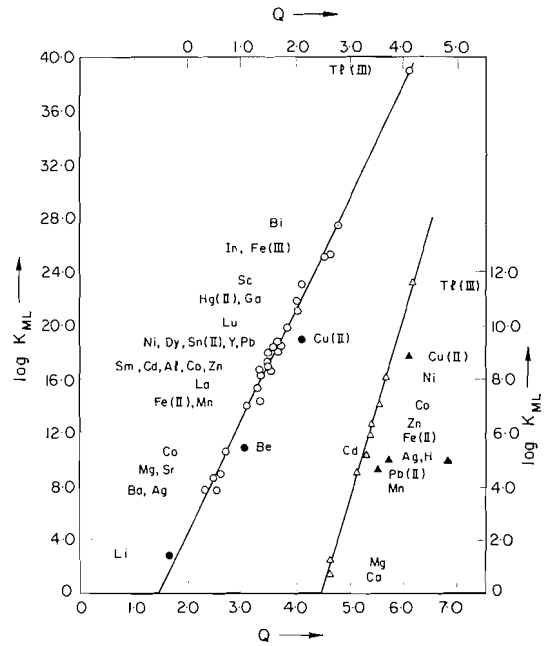

FIG. 2. Metal complex stabilities of ethylenediaminetetraacetic acid and 1,10-phenanthroline as a function of Q: open and closed circles and lower Q-scale, EDTA (μ = 0.1 M, 20 °C); open and closed triangles and upper Q-scale, 1,10-phenanthroline (μ = 0.1 M, 25 °C). The data represented by the closed symbols were omitted from the regression analyses.

Q values are assigned to individual ions are specified in the next section.

It was found that when the first stepwise stability constants for the complexes of a given ligand with a series of metal ions were plotted against the appropriate Q values of the metal ions, a straight-line relationship ensued. The results of a regression analysis of over thirty ligand systems are summarized in Table 1, and are represented for seven ligands in Figs 1–4. The slopes, intercepts, correlation coefficients r (28), and the standard deviations of log K_{ML} were evaluated by a routine least-squares treatment that assigned all "error" to the ordinate. The data employed[2] (29) in the regression analysis were selected with care to include information obtained under the same experimental conditions, preferably by one group of workers. The comparisons were further limited to stability constants for 1:1 metal–ligand complexes mainly because of availability of data, but also to minimize steric and configurational contributions to the free energies examined.

From these linear correlations two parameters emerge which, as will be shown, have considerable capacity for the characterization of metal–ligand stabilities. These are the slope ρ and the intercept on the Q axis, Q_{int}.

Q-Values for Metal Ions

The specific assignment of Q values to metal ions is shown in Table 2. At first glance these assignments seem arbitrary but in fact they were arrived at rather easily. Although comments on the variation of Q for a given metal among different ligands will be reserved for a later section, it is evident from Table 2 that the index is independent of the nature of the ligand for enough metal ions to enable a characteristic plot of log K_{ML} *vs.* Q to be established in each case.

[2]Tabular form of the actual data are available, at a nominal charge, from the Depository of Unpublished Data, National Science Library, National Research Council of Canada, Ottawa, Canada, K1A 0S2.

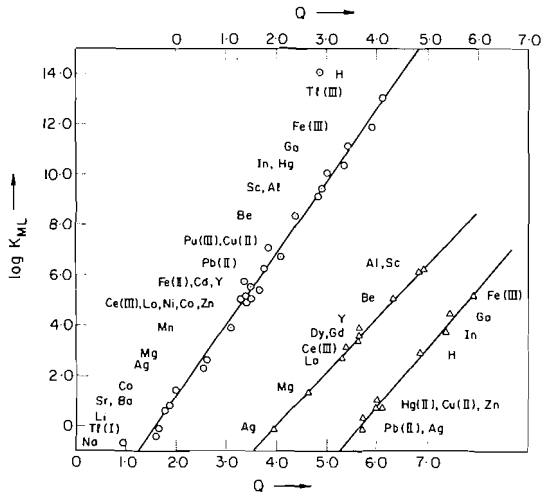

FIG. 3. Metal complex stabilities of salicylaldehyde and pyridine as a function of Q: open circles, salicylaldehyde (50%, by volume of dioxane, 25 °C); open triangles, pyridine (μ = 0.5 M, 25 °C).

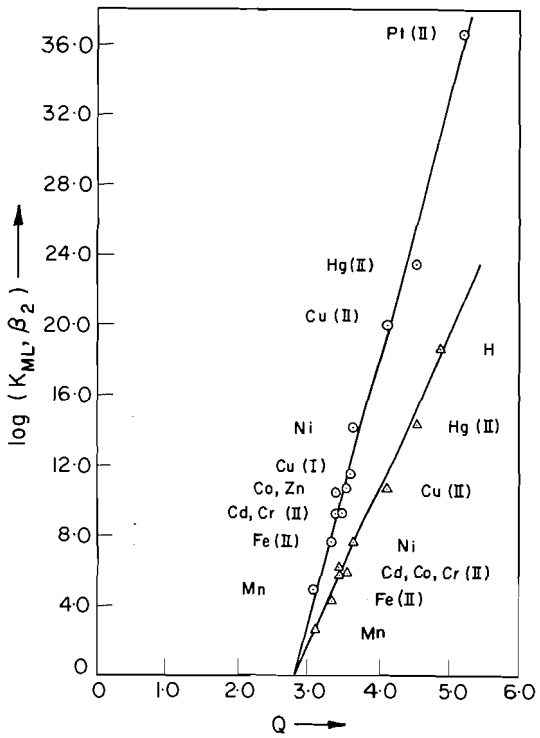

FIG. 4. Metal complex stabilities of ethylenediamine as a function of Q: open circles, log β_2 (μ = 1 M, 25 °C); open triangles, log K_{ML} (μ = 1 M, 25 °C).

Additional metal ions could then be fitted to the regression line by a suitable choice of the weighting coefficients, a and b, or by the use of the coefficient δ mentioned previously, and discussed in more detail in the next section. Average electronegativity values (ref. 26, Table 3) were employed in the computation of Q, although values from Table 2 in the same paper occasionally improved the fit to the linear correlations for Co^{2+}, Ni^{2+}, Cd^{2+}, Zn^{2+}, and Ca^{2+}. Since electronegativity is not a uniquely defined characteristic of an atom or ion, its value for a particular metal may exhibit some variation according to the method by which it was assigned or to the ligand with which it is combined. For instance Allred's values are based on the enthalpies of formation of metal halides, and show a dependence on the nature of the halide. In the case of Co^{2+} and Ni^{2+}, X_M values of 1.88 and 1.91, respectively, were suitable for most ligands, but values of 1.85 and 1.87, respectively, gave better correlation for pure oxygen donors. When $\log K_{ZnL} > \log K_{CdL}$, $X_M = 1.64$ for Cd^{2+} but when $\log K_{CdL} > \log K_{ZnL}$ a value of $X_M = 1.74$ was employed. A value of 1.69 was used for Zn^{2+} except for ligands *1*, *2*, and *4*, where Allred's average value (1.65) gave better results. For Ca^{2+} a value of 1.0 was adequate for all ligands except 5 and 6 where the choice of 1.05 provided a better fit. No value for the electronegativity of Cu^{2+} was reported by Allred. A value of 2.02 was found to be consistent with most of the linear correlations obtained, although the value of 2.00 reported elsewhere (30, 31) gave improved fits for the halide ions, ammonia, and pyridine.

As indicated in Table 2 a characteristic Q value can be associated with each functional group. For polyfunctional ligands the Q value related to the entire ligand molecule is evaluated by taking the arithmetic mean of the Q values appropriate to each functional group. For instance, in the case of EDTA, aluminum has a value

$$Q = 4[(X_M^2 + ZX_M)/2] + 2X_M^2/6$$
$$= (2ZX_M + 4X_M^2)/6.$$

Evaluation of δ

The assignment of δ values by means of Slater screening constants is arbitrary, though supported by some degree of logic. The shielding constant S (27) subtracted from the nuclear

Can. J. Chem. Downloaded from www.nrcresearchpress.com by 210.87.254.5 on 09/05/12
For personal use only.

TABLE 2. Q Values for metal ions*

Ions	Q	δ	Ligand number
Na^+, K^+, Cs^+, Rb^+	ZX_M	1.0	*1, 2, 8*
	X_M^2	—	*32, 33*
Li^+	δZX_M	1.69	*1, 2, 5, 8*
Cu^+	δZX_M	2.12	*28, 30*
	X_M^2	—	*27*
Ag^+	X_M^2	—	*24–26, 28, 30*, N-donor in *21, 20A*; *31*
	ZX_M	1.0	*1, 2, 31*
	δZX_M	1.31	*5, 6, 8, 11A, 32, 33*; O-donor in *21, 20A*
Tl^+	ZX_M	1.0	*1, 8, 11B, 31, 32, 33*
	X_M^2	—	*27, 28*
Ca^{2+}, Sr^{2+}, Ba^{2+}	ZX_M	1.0	*1, 3, 8, 31*; O-donor in *7A* and *9* (but see Table 1, footnote g)
	δZX_M	1.30	other O-, NO-, N-donors
	X_M^2	—	*32*
Mg^{2+}, Mn^{2+}, Zn^{2+}	ZX_M	1.0	All donors except *31* for Zn^{2+} and *32 for* Mg^{2+}
Zn^{2+}	δZX_M	1.25	*31*
Mg^{2+}	X_M^2	—	*32*
H^+, Fe^{2+}, Co^{2+}, Ni^{2+}, Cu^{2+}	X_M^2	—	All donors
Cr^{2+}, V^{2+}, (Sn^{2+})	ZX_M	1.0	*20A, 27* (*5, 32*)
Be^{2+}	δZX_M	1.39	*1, 2, 4, 8, 10, 12, 31*
	ZX_M	1.0	*5, 6, 32*
Cd^{2+}	ZX_M	1.0	Most ligands
	δZX_M	1.25	*32, 33*
	X_M^2	—	*1, 2, 4*
Hg^{2+}	$X_M^2(\equiv ZX_M)$	1.0	*5, 20A, 25, 29, 31, 32, 33*; O-donor in *6, 16A, 21*
	δZX_M	1.25	*8, 28, 30*; N-donor in *6, 16A, 21*
	$(X_M^2 + \delta ZX_M)/2$		*26, 27*
Pb^{2+}	ZX_M	1.0	*8, 20B, 22B, 31, 32, 33*
	X_M^2	—	All others
Y^{3+}, lanthanides, Actinides	ZX_M	1.0	All donors†
Al^{3+}	ZX_M	1.0	*31*, hydroxyl group in pure oxygen donors
	X_M^2	—	N-donors in *5, 6, 17A*
	$(X_M^2 + ZX_M)/2$		Carboxyl donors in *5, 6, 17A*
Fe^{3+}, Ga^{3+}, Bi^{3+}	ZX_M	1.0	*31* and hydroxyl group
	X_M^2	—	*32, 33*, any N-donor groups
	$(X_M^2 + ZX_M)/2$		Carbonyl and carboxyl groups
In^{3+}	ZX_M	1.0	*8, 31*, N-donor and hydroxyl group
	$(X_M^2 + ZX_M)/2$		*32, 33*, carbonyl and carboxyl groups
Tl^{3+}	ZX_M	1.0	*5, 8, 32, 33*
	X_M^2		*24, 25, 32, 33*
Sc^{3+}	ZX_M	1.0	*5, 6, 32, 33*
	δZX_M	1.20	*1, 2, 4, 8, 31–33*
	X_M^2	—	*32, 33*
Pt^{2+}, Pd^{2+}	ZX_M	1.0	*14, 21*
	X_M^2	—	*27, 28, 32, 33*

*When $Q = ZX_M + \delta ZX_M$, a has a value of unity and b of zero; similarly when $Q = X_M^2$, b has a value of unity and a of zero; a and b both have values of unity when $Q = (ZX_M + X_M^2)/2$. This covers all cases in this table.
†$Q = X_M^2$ transfers these ions from line I to line II of Cl^- and Br^-.

charge A provides a rough measure of the effective screened nuclear charge at the periphery of an atom or ion. The factor δ in this work takes the form of the ratio of two $(A - S)$ values. In the case of the three small ions (H^+, Li^+, Be^{2+}) the $(A - S)$ values compared (Table 3) are for a typical alkali or alkaline earth metal ion and the value for the related "atypical" small ion.

As indicated earlier, electronegativities are known to depend on the nature of the chemical bond and the bonding orbitals for which they are evaluated (32–35). It appears (Table 2) that when the Allred X_M values are used, ZX_M adequately describes the reactivity of Ba^{2+}, Ca^{2+}, and Sr^{2+} with the halide ions and oxygen donors of relatively low Q_{int} values (Table 1). However,

Can. J. Chem. Downloaded from www.nrcresearchpress.com by 210.87.254.5 on 09/05/12
For personal use only.

TABLE 3. Evaluation of δ[a]

Ion	$(A - S)$	$(A - S)^*$	$(A - S)_{ave}$	Electron for which $(A - S)$ calculated	δ
Na^+, K^+, Rb^+	2.20	—	—	*n*s or *n*p	1.0
H^+	1.00	—	—	1s	2.20/1.0 = 2.20
Li^+	1.30	—	—	2s	2.20/1.3 = 1.69
Mg^{2+}, Ca^{2+}, Sr^{2+}, Ba^{2+}	3.20	—	—	*n*s or *n*p	1.0
Be^{2+}	2.30	—	—	2s	3.20/2.30 = 1.39
Ca^{2+}, Sr^{2+}, Ba^{2+}	3.20	—	—	*n*s or *n*p	
	2.00	—	—	$(n - 1)$d	
	—	—	2.60	average[b]	2.60/2.00 = 1.30
Zn^{2+}, Cd^{2+}, Hg^{2+}	4.70	5.20	—	*n*s or *n*p	
		8.85	—	$(n - 1)$d	
			7.025*	Average*[b]	
			5.86	Average[c]	5.86/4.70 = 1.25
Ag^+, Cu^+, Au^+	3.70	4.20	—	*n*s or *n*p	
		7.85	—	$(n - 1)$d	7.85/3.70 = 2.12
			6.02*	Average*[b]	
			4.86	Average[c]	4.86/3.70 = 1.31

[a]The symbol * identifies the effective nuclear charge of the d^9s excited state.
[b]The average value for *n*s and $(n - 1)$d.
[c]The average of the preceeding average and $(A - S)$.

for most ligands these values are too small. The δ values in Table 3 for these ions are thought to correct their electronegativity values for the increased effective nuclear charge that is expected if the ligand donor electrons are exposed to a field that is intermediate between that acting on a $(n - 1)$d and a *n*s electron. The $(n - 1)$d and *n*s orbitals are known to be comparable for these ions (ref. 20, pp. 48–51). Since electronegativity values have been shown to be a function of the effective nuclear charge (36), the use of Slater rules seems reasonable. Similar arguments are applicable for Sc^{3+}.

Ions with d^{10} configuration are believed to be capable of easy distortion by an anion, and this should increase the effective nuclear charge of the cation (14, 37). In addition, the energy difference between the d^{10} ground state and the lowest d^9s excited state is quite small for Cu^+, Ag^+, Au^+, and Hg^{2+} (38). Thus a higher effective nuclear charge would result from ds mixing. In our evaluation of δ the average effective nuclear charges of the ground and excited states are compared to that of the ground state.

The small standard deviations associated with individual log K_{ML} values in the Q correlation for these atypical ions indicate that δ has empirical validity.

Factors Influencing the Slope ρ

It is evident from Table 1 and Figs. 1–5 that ρ varies widely. In addition, it is evident that the steeper slopes correspond to greater complex stabilities for ligands with comparable values of Q_{int}. The most obvious dependence of ρ is on the number of donor groups:[3] $\rho_{27}(K_{ML})/2\rho_{28} = 0.93$; $\rho_{26}/2\rho_{27}(K_{ML}) = 0.83$; $\rho_{27}(\beta_2)/2\rho_{27}(K_{ML}) = 0.87$; $\rho_9/(\rho_{23} + \rho_{30}) = 0.93$; $\rho_{21}/(\rho_{28} + \rho_{11A}) = 0.86$. These ratios of slopes reflect Bjerrum's statistical effect (17). The effect of Brønsted–Lowry basicity difference is illustrated by pyridine, *30*, and ammonia, *28*: $\rho_{28}/\rho_{30} = 1.69$. Since ions of both traditionally accepted class a and b behavior are correlated for these ligands (Fig. 3), Pearson's classification of pyridine as "softer" than ammonia is questionable. In fact, group electronegativity evaluation for these ligands (39) rank ammonia as the less electronegative of the two. In the Lewis sense, pyridine is the poorer electron donor.

In the sequence F^- (ρ = 2.2, 2.5), Cl^- (ρ = 2.4, 2.6), OH^- (ρ = 2.8), Br^- (ρ = 3.3, 3.5), and CN^- ($\rho/4$ = 10) a good relationship exists between the slopes and Klopman's "softness"

[3]We designate by ρ_j the slope found in the regression analysis for the ligand numbered *j* in Table 1.

Can. J. Chem. Downloaded from www.nrcresearchpress.com by 210.87.254.5 on 09/05/12
For personal use only.

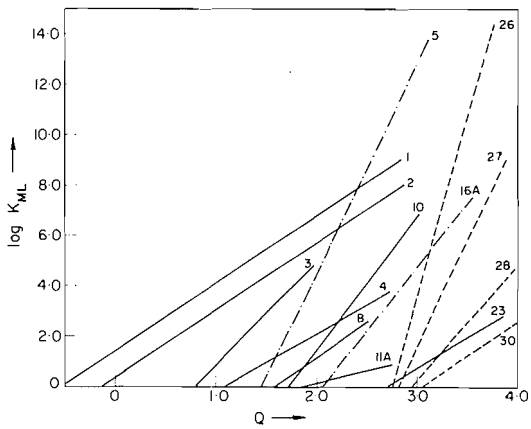

FIG. 5. Metal complex stabilities as a function of Q. The ligand numbers correspond to those in Table 1; numbers *1, 2, 3, 4, 8, 10, 11A* and *23* are oxygen donors; *26–28, 30* are nitrogen donors; while *5* and *16A* are nitrogen–oxygen donors.

parameter (12), where softness increases in the order $F^- < OH^- < Cl^- < Br^- \ll CN^-$ (see also Ahrland (5)). Klopman takes into account the relative energies in solution of the occupied "frontier" (valence) orbitals of the donor and acceptor. When these are comparable, electron transfer is favorable (class b behavior). Consequently, the slopes in the sequence carboxyl ($\rho = 1.0$), enol ($\rho = 2.32$), phenol ($\rho = 2.52$), OH^- ($\rho = 2.84$) probably reflect the increasing class b behavior of these functional groups.

The chelate effect and perhaps ring size (r.s.) are evident in the following ligand series: $\rho_{25}/2\rho_{30} = 1.24$, r.s. = 5; $\rho_{15}/(\rho_{23} + \rho_{11A}) = 1.41$, r.s. = 6; $\rho_{20A}/(\rho_{30} + \rho_{11A}) = 1.22$, r.s. = 5; $\rho_{10}/2\rho_{23} = 1.05$, r.s. = 5.

The normal and structural substituent effects defined in Part I (28) also exhibit diagnostic behavior in the present correlations. The normal substituent effect gives lower values of ρ as electron-withdrawing substituents reduce the availability of donor electrons: $\rho_{12}/\rho_{15} = 0.84$; $\rho_{7A}/\rho_9 = 0.93$; $\rho_3/\rho_{10} = 0.77$. A more vivid illustration of this is provided by the family of salicylaldehyde ligands treated in Part I (28), the data for which are not reported in Table 1: $\rho_{substituted}/\rho_{unsubstituted} = 0.91$ (5-chloro), 0.86 (4-chloro), 0.83 (3-chloro), 0.63 (5-nitro). The Q_{int} values are nearly identical for all these numbers. This we believe is also diagnostic of a normal substituent effect. For the remaining members of this salicylaldehyde family the ratio of slopes continues to decrease, but is accompanied by a change in Q_{int} to lower values: $\rho_{substituted}/\rho_{unsubstituted} = 0.60$ (3-nitro), 0.06 (3,5-dinitro). Excessively charged substituents such as nitro and sulfo groups are known to cause the breakdown of linear free-energy relationships (Parts I (28) and II (40)), and this is reflected in the change in Q_{int}.

In contrast, constancy of slope ρ and changes in Q_{int} are diagnostic of the structural substituent effect: $\rho_1/\rho_2 = 1.0$; $\rho_{24}/\rho_{25} = 1.0$; and perhaps for the ligands *9*, *20A*, and *21*, $\rho_{21}/\rho_9 = 1.0$; $\rho_{20A}/\rho_9 = 0.93$.

Factors Influencing the Q_{int} Value

Changes in Q_{int} (ΔQ_{ij}) will be designated negative when the value for ligand i is algebraically greater than that for ligand j, and *vice versa*. As just indicated, such changes accompanied by constancy of the slope ρ appear to be diagnostic of the structural substituent effect. The following are illustrative examples: $\Delta Q_{25,24} = -0.22$; $\Delta Q_{2,1} = -0.40$; $\Delta Q_{21,20A} = -0.12$; $\Delta Q_{21,9} = -0.74$. Changes in solvent are characterized primarily by changes in Q_{int}, although in this case a small change in ρ occurs also: $\Delta Q_{4,2} = -1.22$; $\Delta Q_{19,14} = -0.25$.

Incorporation of a single functional group into an aromatic system is accompanied by a shift of Q_{int} to higher values: $\Delta Q_{4,19} = 1.15$; $\Delta Q_{11A,22A} = 0.67$; $\Delta Q_{8,23} = 1.10$; $\Delta Q_{28,30} = 0.10$. If these observations are combined with the occurrence of high Q_{int} values for nitrogen donors and relatively low Q_{int} values for oxygen donors, the conclusion is suggested that the higher the Q_{int} value of a ligand the greater is its class b character for complex formation in solution. Supporting evidence for this is found in the case of cyanide ion.

It thus appears that both ρ and Q_{int} increase with class b behavior. This has prompted us to consider the quantity $\rho\Delta Q_{int}/n$ (where n represents the number of monodentate ligand atoms or the total number of donor groups in a multidentate ligand) as a comprehensive index of class b character. Calculated values of this index are given in the last column of Table 1. Notice, for instance, the order of class b character suggested by the values of this parameter in the following series of ligands: OH^- (4.54); pyr. (8.39); Cl^-

Can. J. Chem. Downloaded from www.nrcresearchpress.com by 210.87.254.5 on 09/05/12
For personal use only.

Can. J. Chem. Downloaded from www.nrcresearchpress.com by 210.87.254.5 on 09/05/12
For personal use only.

(8.71, line II); F^- (8.81, line II); Br^- (12.14, line II); NH_3 (13.75); CN^- (30.2).

The behavior of the halides requires some further discussion. As shown in Table 1 these ions give rise to two regression lines; they appear to exhibit ambivalence toward the correlation sought (see Fig. 1 for fluoride). This may be taken to signify that they partake of both class a and b character. The traditionally class a metal ions for the most part fall on line I and those of intermediate and class b character on line II. The only deviations from this pattern are observed for Hg^{2+}, Ag^+, and Tl^+, which fall on line I in the case of Cl^- and Br^-, and Tl^{3+} which fits either line ($Q = ZX_M$, line II; $Q = X_M^2$, line I). These ions still have a large favorable entropy contribution to the free energy in their reaction with these anions (3), and this may account for their association with the class a group. In addition, it is perhaps consistent with our arguments (see below) that for the anions of greater class b character (Cl^-, Br^-) $Q = X_M^2$ for nearly all metal ions whereas for the fluoride ion $Q = ZX_M$. In the case of the former ligands, $Q = X_M^2$ places the lanthanides on line I and $Q = ZX_M$ places them on line II, in a fashion similar to that for Tl^{3+}. Pearson (9, 10) classifies F^- and Cl^- as "hard" and Br^- as borderline. The present study suggests that these three ions have more in common than is currently accepted.

Another interesting pattern may be deduced from the data on Table 1. It concerns the relationship of nitrogen–oxygen donors to the parent nitrogen donor compound. Two interesting series may be discerned: ligands *5*, *18A*, *27*, and *6*, *16A*, *21*, *28*. The former is related to ethylenediamine and the latter to ammonia by progressive N-substitution by acetate arms. The ρ values are nearly constant within each family, while Q_{int} changes in almost regular increments: $\rho_5(8.36)$, $\rho_{18A} = 8.62$, $\rho_{27} = 8.63$; $\Delta Q_{5,18A} = +0.71$ and $\Delta Q_{18A,27} = +0.65$; similarly $\rho_6(5.3)$, $\rho_{16A} = 5.08$, $\rho_{21} = 4.87$, $\rho_{28} = 4.66$; $\Delta Q_{6,16A} = +0.54$, $\Delta Q_{16A,21} = +0.34$, $\Delta Q_{21,28} = +0.55$. The parameter $\rho Q_{int}/n$ also decreases rapidly in each family as more oxygen functional groups are attached. These observations will be interpreted in the following section.

Thermodynamic Considerations

It will be beneficial to introduce some aspects of Prue's treatment of the thermodynamics of metal complex formation (41). The change in free energy ΔG^0 is expressed as

$$[2] \qquad \Delta G^0 = -RT \ln \bar{v} - RTb + w'$$

where $\bar{v}$ represents the partition function quotient which in its simplest approximation may be replaced by the molar volume of the metal complex; $-RTb$ is the molar electrostatic energy, and w' the temperature-independent covalent term. RTb and w' contribute to ΔH^0 but not to ΔS^0. In addition, temperature-dependent functions of $\bar{v}$ and b contribute to ΔH^0 and ΔS^0, and a term $R \ln \bar{v}$ must also be added to ΔS^0. Any changes in the vibrational, rotational, and translational motions that accompany metal complex formation, including those of solvent, can contribute to all three thermodynamic quantities through the partition function terms. Such contributions are expected to be the largest for reactions in a polar medium such as water.

A consideration of volume changes shown (42) to accompany ion associations in solution is also pertinent. Neutralization of carboxylic acids is accompanied by large molar volume changes (*e.g.*, +11 ml/mol for protonation of acetate ion). The presence of a positive charge, as, for instance, in the monoprotonated glycine molecule, reduces the magnitude of this effect somewhat. Protonation of amines is generally characterized by sizeable negative molar volume changes (*e.g.*, −6 ml/mol for ammonia). In this case the presence of a negative charge makes the volume change more positive, while a positive charge makes it considerably more negative. For example, addition of a second proton to the monoprotonated form produces the following volume changes for the indicated species: ethylenediamine, −11 ml/mol; EDTA, −2 ml/mol. A linear correlation has been observed for changes in entropy and volume on ionization of fifty-three aqueous acids (43). Such volume changes have been shown to contribute as much as 0.5 kcal/ml to the free energy change for these reactions (42, 43). A similar relationship would appear to apply for metal-complex formation reactions.

The thermodynamic form of such contributions has not been determined but entry through the partition function term in eq. 2 seems likely, since volume increments should parallel changes in the vibrational, rotational, and translational

Can. J. Chem. Downloaded from www.nrcresearchpress.com by 210.87.254.5 on 09/05/12
For personal use only.

motion of solvent molecules. Schwarzenbach (44) in his evaluation of the effective dielectric constants for proton transfer reactions involving bases of the type just mentioned does not consider contributions to the free energy from volume changes. Sizeable volume changes can be shown to accompany some of the reactions treated by Schwarzenbach, and thus his values of the microscopic dielectric constant are likely underestimated.

An examination of metal-ligand enthalpies and entropies (29, 45) reveals that metal complex formation with neutral ligands such as ammonia or ethylenediamine is accompanied not only by negative enthalpy changes, but also by negative entropy changes. The latter reflect the negative volume changes discussed above for the protonation of these ligands. It is also readily confirmed that the formation of metal complexes with oxygen–nitrogen donors is characterized by both favorable ΔH^0 and ΔS^0 values (29, 45). We envisage, by analogy with the protonation reactions discussed, that N-substitution by acetate arms in nitrogen donor molecules results in a more positive molar volume change for the corresponding metal-complex formation reaction. Consequently, oxygen–nitrogen donors have, so to speak, the best of two worlds: the large positive entropy characteristic of oxygen donors (positive molar volume change) and the large negative enthalpy characteristic of the more class b nitrogen donors. The observed shift to lower Q_{int} values that accompanies the successive incorporation of carboxyl groups and the retention of the relatively high ρ value of the parent N-donor are interpreted to reflect this duality, respectively. Schwarzenbach (45) has also discussed the possibility that highly charged ligands promote a low effective dielectric constant and a more positive temperature dependence of this parameter, which would make ΔH^0 more negative. Further investigation may well reveal some relationship between these dielectric and volume effects.

The available enthalpy–entropy data (3, 4, 29, 45) support another general trend: ligands with high Q_{int} values tend to participate in enthalpy-favored reactions, while reactions of ligands with low Q_{int} values tend to be largely entropy-dominated. The molar volume changes accompanying the protonation of OH^- and the phenoxide ion also substantiate such a comparison: 21.3 ml/mol (Q_{int} = 1.6) and 17–18 ml/mol (Q_{int} = 2.7), respectively.

It is expected that drastic structural changes such as those observed for a family of ligands exhibiting the structural substituent effect make an important contribution to the partition function terms. The factors likely to contribute will necessarily be properties solely (28) of the ligand, of which the following are examples: molecular volume or bulk of ligand, a more favorable conformational change owing to ligand rigidity (44), a vibrational, rotational, or translational change for solvent molecules on complex formation, due to the release of ligand-induced electrostriction. The specific hydrogen bonding to water molecules observed for 2,2′-bipyridyl and 1,10-phenanthroline (46) is an example of the latter. In addition, it should be emphasized that a systematic increase in the hydrophobicity (44, 47–49) of ligands in a related series may produce a reduction in the effective dielectric constant and a concomitant positive increase in the temperature gradient of this parameter. This would render the ΔH^0 values of complex formation more negative (44)[4]. Lowering of the microscopic dielectric constant would of course, also increase the magnitude of the *RTb* term in eq. 2. The analogy of the structural substituent effect (constant ρ and large ΔQ_{ij}) and the medium effect is striking (*e.g.*, Fig. 5, lines 1, 2, 4).

Ligand Architecture

In an earlier section we have emphasized several systematic trends in ρ and Q_{int} values which characterize various aspects of ligand architecture. Some of these special effects are illustrated in Fig. 5: number of donor atoms, lines *26*, *27*, *28*, as well as the pairs *10,23* and *5,16A*; the structural substituent effect, lines *1*, *2*; the medium effect, lines *2*, *4*; and the systematics of N,O-donors by pairs *5,27* and *16A,28*. Two additional features about the relationship of N,O-donors to the parent N- and O-constituents are of interest. The first concerns the Q_{int} changes discussed for N-substitution by acetate. The Q_{int} values of simple N,O-ligand systems are approximated well by the arithmetic mean of the values exhibited by the parent N and

[4]It is for this reason that an exothermic reaction need not necessarily imply class b behavior.

TABLE 4. Classification of metal ions

Class	Ions[a]
Class a	Li(1.39), K^+(1.46), Na^+(1.55), Rb^+(1.56), Cs^+(1.57), Ba^{2+}(1.74), Sr^{2+}(1.78), Ca^{2+}(1.84), La^{3+}(2.42), Ce^{3+}(2.45), Pr^{3+}(2.48), Nd^{3+}(2.51), Mg^{2+}(2.58), Sm^{3+}(2.59), Y^{3+}(2.65), Gd^{3+}(2.69), Dy^{3+}(2.74), Ho^{3+}(2.75), Er^{3+}(2.77), Tm^{3+}(2.81), Be^{2+}(2.85), Lu^{3+}(2.87), Sc^{3+}(3.07), Pu^{3+}(3.15), Al^{3+}(3.50), Np^{3+}(3.59), U^{3+}(3.72), Mn^{2+}(3.96), Ti^{2+}(4.15).
Borderline	Zn^{2+}(4.54), V^{2+}(4.60), Cr^{2+}(4.66), Ga^{3+}(4.82), In^{3+}(5.26), Fe^{2+}(5.39), Cd^{2+}(5.51), H^+(5.52), Co^{2+}(5.61), Fe^{3+}(5.72), Ni^{2+}(5.73), Tl^+(5.90), Sn^{4+}(5.99), Sn^{2+}(6.38), Cu^{2+}(6.41), Cu^+(6.53),
Class b	Pb^{2+}(7.18), Tl^{3+}(7.49), Hg^{2+}(7.80), Ag^+(7.85), Bi^{3+}(7.87), Pd^{2+}(8.28), Pb^{4+}(9.18), Pt^{2+}(9.41), Au^+(14.32).

[a]The value of the quantity $(X_M)^2(r_M + 0.85)$ is given in parentheses following each ion. X_M values are from (26), and r_M values from ref. 20, pp. 151–153 and (51).

O donor ligands: for example,

$$Q_{int}(\text{glycine}) = \tfrac{1}{2}\,(Q_{int}(\text{acetic acid}) + Q_{int}(\text{ammonia}))$$

This additivity principle is consistent with that mentioned earlier in connection with the individual Q values of metal ions in correlations of N,O-donors.

The second point of interest is the observation of two lines for the correlation in some N,O-donor systems (*7A,7B*; *16A,16B*; *18A,18B*; *20A,20B*) and for carboxylic acids (*11,22*). The lanthanide cations, the alkaline-earth ions, and sometimes H^+ and Pb^{2+}, fall on the B lines, while all other metal ions considered fall on the A lines. The latter correlations are accepted as normal. The B lines for N,O-donor ligands have low Q_{int} values (Table 1) which are characteristic of the oxygen function in the ligand, and have slopes that are considerably smaller than that expected for the parent nitrogen functional group. This distinction between A and B lines disappears when the ratio of the number of oxygen donor groups to nitrogen donor groups reaches 2:1 (alkaline earths) or 3:1 (lanthanide cations). The interpretations now rendered to explain these observations are largely speculative, but they are actually susceptible to experimental substantiation (*e.g.*, by n.m.r.). The observed Q_{int} and ρ values suggest that B-line metal ions exhibit a reduced affinity for the nitrogen donor atom compared to the A-line ions. This reduced affinity may imply an "outer" sphere interaction. In contrast, the two lines for the 1:1 acetate complexes would seem to imply that B-line ions form "inner" sphere 1:1 complexes, while the A-line ions form "outer" sphere complexes with the acetate ion. "Outer sphere" complexes are often comparable in stability to "inner sphere" complexes (50).

New Indices to Class b Behavior

The quantity $(X_M)^2(r_M + 0.85)$ has been found to reproduce (Table 4) the various metal-ion classifications reviewed in the Introduction; here r_M is the cationic crystal radius and 0.85 is an appropriate constant assumed to reflect the radius of O and N donor atoms (20). The division of metal ions into class a, borderline, and class b categories in Table 4 is arbitrary. The choice of the above function finds additional justification from the fact that values of $d/(X_M)^2 r_e$, with d a suitable scaling constant and r_e the equilibrium internuclear distance in chloride complexes, closely match the fractional ionic characters calculated for solid chloride complexes (11, 15, 52).

We have already discussed the success of the quantity $\rho Q_{int}/n$ in reproducing established class b character of ligands. It is informative to interpret Q_{int} as the Q value of the hypothetical metal ion for which $K_{ML} = 1$. This common point of reference conveniently arranges the ligands according to the magnitude of the Q values of these hypothetical metal ions. Consequently, ligands of low Q_{int} values (*e.g.*, EDTA) have $K_{ML} > 1$ even for metals with small values (<2) of the index Q, while ligands of high Q_{int} values (*e.g.*, ammonia) have $K_{ML} < 1$ for these same metal ions.

Significance of the Parameter Q

The quantity Z^2/r_e is accepted as a good index to metal-complex formation reactions of as-

Can. J. Chem. Downloaded from www.nrcresearchpress.com by 210.87.254.5 on 09/05/12
For personal use only.

Can. J. Chem. Downloaded from www.nrcresearchpress.com by 210.87.254.5 on 09/05/12
For personal use only.

sumed high ionic character (17, 20). In the previous section we introduced the parameter $(X_M)^2 r_c$ as a suitable index to class b behavior. If we accept the conclusion of Williams and Hale (11) and Klopman (12) that class a character is the ability of acceptors and donors to participate in electrostatic interactions, and class b character in covalent interactions, then the index Q may be visualized as the geometric mean of an ionic and a covalent index: $Q = (Z^2/r_c \cdot (X_M)^2 r_c)^{1/2} = ZX_M$. There is also evidence (52–54) that for complexes of relatively low ionic character $(X_M)^2/r_c$ may be regarded as proportional to the ionic energy. In this case Q would reduce to the value $(X_M)^2$, the value used in all correlations of the borderline metal ions of the first-row transition series (d^6 to d^9 ions) and for correlations of nearly all metal ions with anions of moderate class b character such as chloride and bromide ions.

The parameter Q may also be considered as the geometric mean of the quantities $\sum I_M$ and $(X_M)^2$. Sanderson (55) has illustrated the existence of a linear relationship between $(\sum I_M)^{1/2}$ and Z. In fact, $(\sum I_M)^{1/2} = (2.5 \pm 0.3)Z$ for most of the metal ions considered in the present correlations. Consequently, $Q = \text{constant} \cdot (\sum I_M \cdot (X_M)^2)^{1/2}$. The sum of the ionization potentials measures the electron-attracting power of a gaseous metal ion, and $(X_M)^2$ the electron-attracting power of an ion in a complex molecule (34). Both quantities are important in the partial ionic/covalent model of bonding (11, 15, 52–54).

We conclude from these deliberations linking Q to established ionic and covalent indices and to atomic properties important in the partial ionic/covalent bond model, and from the thermodynamic considerations set out earlier that eq. 2 adequately describes metal complex formation in solution. Thus the gross features of metal complex formation are determined by the thermal contributions to the free energy and the relative magnitudes of the ionic and covalent energies. All these contributions are obviously dependent on the nature of both the ligand and metal ion. The success and versatility of the index Q, we believe, is in part due to the incorporation of the ligand-dependent parameters a, b, and δ in its definition (eq. 1). In addition, the ligand dependence of the Q-correlations is taken into account, and indeed is estimated, by the parameters ρ and Q_{int}. The weakness of previous correlations of this sort has been the omission of any allowance for this dependence of complex stability on the nature of the ligand, and this has led to their limited applicability. In contrast, the dependence of the Q-correlations on the ligand as measured by ρ and Q_{int} allowed a novel and systematic discussion of ligand architecture and of other factors important in complex formation. The large number and diversity of the ligand systems and metal ions treated also attest to a versatility lacking for other indices. The successful correlation of the metal complex stabilities of a ligand with metal ions of both extreme class a and class b character is especially noteworthy. (See, *e.g.*, Figs. 1–4).[5]

Finally, abnormal behavior of metal ions in their reaction with ligands may be detected when unusually large deviations occur in the Q-correlations. For example, the destabilizations characteristic of Cu(II), Pb(II), Ag(I), and H(I) complexes with 1,10-phenanthroline and 2,2′-bipyridyl discussed in Part I (28) show up clearly in Fig. 2. The deviations observed for the Cu(II)–, Be(II)–EDTA complexes in Fig. 2 suggest that the magnitudes of the respective

[5]We agree with a referee that a comment on the relation of the correlations of the present study to the dual parameter scale for the strength of Lewis acids and bases introduced by Misono and co-workers (56, 57) is warranted. Our index Q and their "hardness" parameter X $(=(X_M^2 + \Sigma I_n + 2X_M \Sigma I_n^{1/2})/10)$ have similar contributions, and our parameter $X_M^2(r_M + 0.85)$ and their "softness" index Y $(= 10\,(I_n/I_{n+1})(r_M/n^{1/2}))$ yield similar metal ion classifications (see Table 4). In fact, for many ions the magnitude of the parameter $(X + Y)/2$ most closely resembles our Q values. However, this agreement must be fortuitous because of the arbitrary nature of defining Q, X, and Y. The work of Misono *et al.* differs from ours in that metal complex stabilities are fitted to a two-parameter equation $(\log K_{ML} = \alpha X + \beta Y + \gamma)$ rather than a single-parameter one $(\log K_{ML} = \rho Q + \text{intercept})$. In addition, the systems treated by them are mostly simple monodentate ligands (our ligand numbers *4*, *8*, *11*, *28*, *30–33*, oxalate, and thiosulfate). The large deviations observed from the two parameter equations for metal ions of distinct class b character required (57) a re-evaluation of Y by an iterative procedure using the experimental stability data $(\log K_{ML} = \alpha' X + \beta' Y' + \gamma')$. Very few of these improved values (Y') are available. The trend observed for the ligand parameter β' seems to parallel that described for the ligand index $\rho Q_{int/n}$.

A successful single-parameter equation seems to us more useful than a two-parameter equation, since the former is simpler by one variable. Also their emphasis on the relationship of covalency to "hardness" seems suspect in the light of the evidence reviewed and discussed in the present work.

stability constants (provided the experimental data are reliable) are unusually low.

This work was supported by a grant from the National Research Council of Canada for which grateful acknowledgment is made. One of the authors (E.N.) records his thanks for the award of a National Research Council of Canada Postgraduate Fellowship. We also thank Mrs. J. L. McCourt of this laboratory for assistance with the statistical analyses.

1. S. AHRLAND, J. CHATT, and N. R. DAVIES. Q. Rev. London, **12**, 265 (1958).
2. S. AHRLAND. Struct. Bonding, Berlin, **1**, 207 (1966).
3. S. AHRLAND. Helv. Chim. Acta, **50**, 306 (1967).
4. S. AHRLAND. Struct. Bonding, Berlin, **5**, 118 (1968).
5. S. AHRLAND. Chem. Phys. Lett. **2**, 303 (1968).
6. R. G. PEARSON. J. Am. Chem. Soc. **85**, 3533 (1963).
7. R. G. PEARSON. Chem. Br. **3**, 103 (1967).
8. R. G. PEARSON. Surv. Prog. Chem. **5**, 1 (1969).
9. R. G. PEARSON. J. Chem. Educ. **45**, 581 (1968).
10. R. G. PEARSON. J. Chem. Educ. **45**, 643 (1968).
11. R. J. P. WILLIAMS and J. D. HALE. Struct. Bonding, Berlin, **1**, 249 (1966).
12. G. KLOPMAN. J. Am. Chem. Soc. **90**, 223 (1968).
13. C. K. JØRGENSON. Struct. Bonding, Berlin, **3**, 106 (1967).
14. D. P. CRAIG and R. S. NYHOLM. *In* Chelating agents and metal chelates. *Edited by* F. P. Dwyer and D. P. Mellor. Academic Press, New York. 1964. p. 51.
15. R. G. PEARSON and H. B. GRAY. Inorg. Chem. **2**, 358 (1963).
16. R. G. PEARSON and R. J. MAWBY. Halogen chemistry. Vol. 3. *Edited by* V. Gutmann. Academic Press, New York. 1967. p. 55.
17. F. J. C. ROSSOTTI. *In* Modern coordination chemistry. *Edited by* J. Lewis and R. G. WILKINS. Interscience Publishers, New York. 1960. pp. 1–77.
18. A. E. MARTELL and M. CALVIN. Chemistry of the metal chelate compounds. Prentice–Hall, New York. 1952. pp. 181–206.
19. S. CHABEREK and A. E. MARTELL. Organic sequestering agents. J. Wiley and Sons, New York. 1959. pp. 163–173.
20. C. S. G. PHILLIPS and R. J. P. WILLIAMS. Inorganic chemistry. Vol. 1. Oxford University Press, New York and Oxford. 1965. pp. 159–164.
21. R. M. IZATT, W. C. FERNELIUS, C. G. HAAS, and B. P. BLOCK. J. Phys. Chem. **59**, 80 (1955); **59**, 170 (1955).
22. L. G. VAN UITERT and W. C. FERNELIUS. J. Am. Chem. Soc. **76**, 379 (1954).
23. L. G. VAN UITERT, W. C. FERNELIUS, and B. E. DOUGLAS. Atomic energy commission document NYO-3372. March 5, 1952.
24. L. G. VAN UITERT, W. C. FERNELIUS, and B. E. DOUGLAS. J. Am. Chem. Soc. **75**, 2736 (1953).
25. L. G. VAN UITERT and W. C. FERNELIUS. J. Am. Chem. Soc. **76**, 375 (1954).
26. A. L. ALLRED. J. Inorg. Nucl. Chem. **17**, 215 (1961).
27. J. C. SLATER. Phys. Rev. **36**, 57 (1930).
28. E. NIEBOER and W. A. E. MCBRYDE. Can. J. Chem. **48**, 2549 (1970).
29. L. G. SILLÉN and A. E. MARTELL. Stability constants of metal–ion complexes. Chem. Soc. Spec. Publ. No. 17, London, 1964; Suppl. No. 1. Chem. Soc. Spec. Publ. No. 25, London, 1971.
30. W. GORDY and W. J. O. THOMAS. J. Chem. Phys. **24**, 439 (1956).
31. L. PAULING. The nature of the chemical bond. Cornell University Press, Ithaca, New York. 1939. pp. 58–75; also 3rd ed. 1960. pp. 64–107.
32. R. P. ICZKOWSKI and J. L. MARGRAVE. J. Am. Chem. Soc. **83**, 3547 (1961).
33. J. HINZE, M. A. WHITEHEAD, and H. H. JAFFÉ. J. Am. Chem. Soc. **85**, 148 (1963).
34. J. HINZE and H. H. JAFFÉ. J. Am. Chem. Soc. **84**, 540 (1962).
35. G. KLOPMAN. J. Am. Chem. Soc. **86**, 1463 (1964).
36. A. L. ALLRED and E. G. ROCHOW. J. Inorg. Chem. **5**, 264 (1958).
37. B. E. DOUGLAS and D. H. MCDANIEL. Concepts and models of inorganic chemistry. Blaisdell Publishing Company. Waltham. 1965. pp. 89 and 347.
38. L. E. ORGEL. An introduction to transition metal chemistry. Methuen and Co. Ltd., London. 1960. pp. 66–68.
39. D. H. MCDANIEL and A. YINGST. J. Am. Chem. Soc. **86**, 1334 (1964).
40. E. NIEBOER and W. A. E. MCBRYDE. Can. J. Chem. **48**, 2565 (1970).
41. J. E. PRUE. J. Chem. Educ. **46**, 12 (1969).
42. F. J. MILLERO. Chem. Rev. **71**, 147 (1971); W. KAUZMANN, A. BODANSZKY, and J. RASPER. J. Am. Chem. Soc. **84**, 1777 (1962).
43. L. G. HEPLER. J. Phys. Chem. **69**, 965 (1965); T. G. SPIRO, A. REVESZ, and J. LEE. J. Am. Chem. Soc. **90**, 4000 (1968).
44. G. SCHWARZENBACH. Pure Appl. Chem. **24**, 307 (1970).
45. J. CHRISTENSEN and R. M. IZATT. Handbook of metal ligand heats. Marcel Dekker. New York. 1970.
46. M. J. FAHSEL and C. V. BANKS. J. Am. Chem. Soc. **88**, 878 (1967).
47. J. G. KIRKWOOD and F. H. WESTHEIMER. J. Chem. Phys. **6**, 506 (1938).
48. C. TANFORD and J. G. KIRKWOOD. J. Am. Chem. Soc. **79**, 5333 (1967); C. TANFORD. J. Am. Chem. Soc. **79**, 5348 (1957).
49. C. F. WILCOX and C. LEUNG. J. Am. Chem. Soc. **90**, 336 (1968).
50. M. T. BECK. Coord. Chem. Rev. **3**, 91 (1968).
51. J. KLEINBERG, W. J. ARGERSINGER, JR., and E. GRISWOLD. Inorganic chemistry. D. C. Heath and Company, Boston, 1960. pp. 72–81.
52. R. S. EVANS and J. E. HUHEEY. J. Inorg. Nucl. Chem. **32**, 777 (1970).
53. R. S. EVANS and J. E. HUHEEY. J. Inorg. Nucl. Chem. **32**, 373 (1970).
54. J. E. HUHEEY and R. S. EVANS. J. Inorg. Nucl. Chem. **32**, 383 (1970).
55. R. T. SANDERSON. Chemical periodicity. Reinhold, New York. 1960. Chapt. 3.
56. M. MISONO, E. OCHIAI, Y. SAITO, and Y. YONEDA. J. Inorg. Chem. **29**, 2685 (1967).
57. M. MISONO and Y. SAITO. Bull. Chem. Soc. Jap. **43**, 3680 (1970).

Can. J. Chem. Downloaded from www.nrcresearchpress.com by 210.87.254.5 on 09/05/12
For personal use only.

Oxidation of Some Transition-Metal Cyanide Compounds by Hydroxyl Radical

W. L. WALTZ, S. S. AKHTAR, AND R. L. EAGER

Department of Chemistry and Chemical Engineering and the Saskatchewan Accelerator Laboratory, University of Saskatchewan, Saskatoon, Saskatchewan

Received February 6, 1973

The oxidation of some transition-metal cyanide compounds by hydroxyl radical in aqueous media has been investigated by pulse radiolysis. For compounds of the type, $M(CN)_6^{4-}$ where M is Fe, Ru, and Os, and for $Mo(CN)_8^{4-}$, the mechanism of their reaction with hydroxyl radical involves single electron transfer with the formation of the intensely colored metal complexes of the same stoichiometry as the starting materials. The u.v.–visible absorption spectra for these products for the iron, ruthenium, and osmium systems are reported along with the associated second order rate constants for their formation. The reaction of $Mo(CN)_8^{4-}$ with hydroxyl radical has been studied by a competition technique using sodium bicarbonate. The values of the second order rate constants are near those expected of diffusion-controlled reactions and they range between *ca.* 5×10^9 to 1×10^{10} M^{-1} s^{-1}.

L'oxydation de quelques composés métal de transition-cyanure par le radical hydroxyle en milieu aqueux, a été étudiée par radiolyse pulsée. Pour les composés du type $M(CN)_6^{4-}$ où M = Fe, Ru et Os et pour $Mo(CN)_8^{4-}$, le mécanisme de la réaction avec le radical hydroxyle fait intervenir un transfert simple d'électron avec formation de complexes métalliques intensément colorés de même stoechiométrie que les produits de départ. Les spectres d'absorption u.v.–visible de ces produits dans les systèmes fer, ruthénium et osmium, ont été rapportés de même que les constantes de vitesse de second ordre associées à leur formation. La réaction de $Mo(CN)_8^{4-}$ avec le radical hydroxyle a été étudiée par une technique de compétition utilisant le bicarbonate de sodium. Les valeurs des constantes de vitesse du second ordre sont voisines de celles que l'on attend pour des réactions contrôlées par diffusion et leur domaine s'étend de 5×10^9 à 1×10^{10} M^{-1} s^{-1}. [Traduit par le journal]

Can. J. Chem., **51**, 2525 (1973)

Introduction

In the radiolysis of aqueous media near neutral p*H*, the hydrated electron, e_{aq}^-, and the hydroxyl radical, OH, occur as the primary reducing and oxidizing species, respectively (1). While numerous studies of the reactions of the hydrated electron with transition metal complexes have been carried out (1–3), relatively few reports have been presented on the reactions of OH with metal complexes (2, 4). The reaction mechanisms of hydroxyl radical with metal complexes can potentially involve either electron or atom transfer. Such reactions are not only of fundamental interest in the area of radiation chemistry but also in a broader sense to the study of inorganic reaction mechanisms. A case in point is the reaction of OH with ferrocyanide ion, reaction 1 (2, 4–7),

$$[1] \quad OH + Fe(CN)_6^{4-} \rightarrow OH^- + Fe(CN)_6^{3-}$$

that involves an electron transfer mechanism with the formation of the stable and intensely light-absorbing ferricyanide product. The characteristics of this reaction have also provided a sound basis for the use of this reaction in radiation dosimetry, particularly in conjunction with pulse radiolysis, and as a standard for determining rate constants for hydroxyl radical reactions by competition techniques (5–7). Of further interest to this study is the recent report (8) that the reactions of transition metal pentacyanonitrosyl ions with OH radical exhibit a linear free energy relationship. In this context, we wish to report the results of a pulse radiolysis investigation of the reactions of OH radical with a series of stable transition-metal cyanides involving systems capable of exhibiting well characterized higher oxidation states of the metal center.

Experimental

The technique of pulse radiolysis used in this work, involving spectrophotoelectric recording, is similar to that described elsewhere (1, 9), although in this case the monitoring light source was a 150 W xenon arc lamp and the detector was a RCA 1P28 photomultiplier tube (five stages used). The initial absorbance of the hydrated electron at 578 nm ($\varepsilon = 1.09 \times 10^4$ M^{-1} cm^{-1} (10)) in aqueous 10^{-3} *M* NaOH and 10^{-3} *M* methanol solutions was used to set the dose level. Changes in the dose level from one pulse to another were monitored with a secondary electron emission monitor (s.e.m.). The s.e.m. was used to normalize the data points to a common dose for the evaluation of absorption changes in competition

Can. J. Chem. Downloaded from www.nrcresearchpress.com by 210.87.254.40 on 09/05/12
For personal use only.

Can. J. Chem. Downloaded from www.nrcresearchpress.com by 210.87.254.40 on 09/05/12
For personal use only.

experiments and in the determination of product spectra. The molar extinction coefficients, ε, of the absorbing products were determined relative to that of e_{aq}^- (*vide supra*) assuming that the yield of e_{aq}^- to be essentially equal to that of OH radical (1).

Triply distilled water was used to prepare all solutions. The compounds, $K_4[Ru(CN)_6]\cdot 3H_2O$ and $K_4[Mo(CN)_8]\cdot 2H_2O$, were kindly supplied by Dr. A. W. Adamson, and $K_4[Os(CN)_6]\cdot 3H_2O$ was obtained from City Chemical Corporation (New York). Reagent quality (Shawinigan) $K_4[Fe(CN)_6]\cdot 3H_2O$ and $NaHCO_3$ were used. Isopropanol (Fisher Spectroscopic Grade and BDH Aristar) and methanol (Fisher Spectroscopic Grade) were used without further purification. Nitrous oxide (Matheson, minimum purity 98.0%) was further purified by trap-to-trap distillation where necessary. All other materials were of reagent quality. The syringe and degassing-bulb techniques used for the preparation and handling of solutions were similar to those described elsewhere (3). The solutions were prepared on the day of use, and those containing cyanide materials were protected from light.

Results and Discussion

On irradiation of neutral or slightly alkaline aqueous solutions, the primary radical species formed are the hydrated electron, e_{aq}^-, hydroxyl radical, and to a lesser extent hydrogen atom (1, 3). The reactions of e_{aq}^- with the cyanides of Fe(II), Ru(II), Os(II), and Mo(IV) are relatively slow processes (2, 11) so that the decay of e_{aq}^- in aerated media will involve principally reaction 2

$$[2] \qquad e_{aq}^- + O_2 \rightarrow O_2^- \text{ (or } HO_2)$$

while in saturated nitrous oxide solutions its decay will be via reaction 3 to give OH radical (1, 3).

$$[3] \qquad e_{aq}^- + N_2O \rightarrow N_2O^- \xrightarrow{H^+} N_2 + OH$$

In aerated media, both OH and O_2^- (or HO_2 in acidic media, pK_a 4.5 (1)) will be present after the pulse while in N_2O saturated solutions OH will be the major radical species. Previous studies (*5b*, 6) on the oxidation of ferrocyanide by HO_2 and O_2^- indicate that HO_2 is nearly five orders of magnitude slower in reactivity than OH and that O_2^- is unreactive so that on time scales shorter than a millisecond as used here the reactions of O_2^- and HO_2 with $Fe(CN)_6^{4-}$ are negligible. The other cyano compounds studied are weaker reducing agents than ferrocyanide with the possible exception of $Os(CN)_6^{4-}$ so that the reactions of O_2^- and HO_2 with these materials are expected to be of negligible importance. This expectation seems to be borne out as no changes in the levels of absorption of the products formed initially by the reactions of OH (*vide infra*) were observed for time scales as long as 1 ms after the pulse.

On irradiation of neutral, aerated solutions containing $Fe(CN)_6^{4-}$, $Ru(CN)_6^{4-}$, or $Os(CN)_6^{4-}$, a rapid increase in optical absorption in the blue and near u.v. regions occurs and leads to the attainment of a stable level of absorption. If the solutions are saturated with nitrous oxide, the final absorbance is now about twice that of the aerated solutions. Plots of the optical spectra of the stable products for the osmium and ruthenium systems are shown in Fig. 1. The stable product of irradiated aqueous $Ru(CN)_6^{4-}$ exhibits peaks at 470 ($\varepsilon = 920\ M^{-1}\ cm^{-1}$) and at 330 nm ($\varepsilon = 2140\ M^{-1}\ cm^{-1}$) and a shoulder at 355 nm. These features are in accord with the qualitative spectrum reported (12) for $Ru(CN)_6^{3-}$.[1] The spectrum of tetrabutylammonium hexacyanoosmium(III) measured in ethanol (13) shows peaks at 412 ($\varepsilon = 1450\ M^{-1}\ cm^{-1}$) and at 332 nm ($\varepsilon = 1680\ M^{-1}\ cm^{-1}$) and this corresponds closely to that for irradiated $Os(CN)_6^{4-}$ media with peaks at 410 ($\varepsilon = 1400\ M^{-1}\ cm^{-1}$) and at 325 nm ($\varepsilon = 1520\ M^{-1}\ cm^{-1}$).

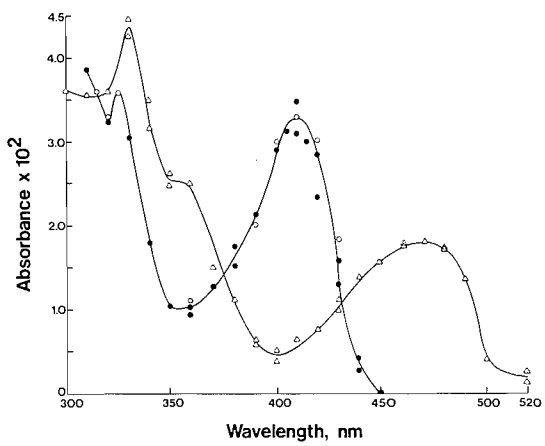

FIG. 1. Absorption spectra of the stable products arising from irradiation of aerated, aqueous solutions of $Os(CN)_6^{4-}$ and $Ru(CN)_6^{4-}$. △, $2 \times 10^{-4}\ M\ K_4[Ru(CN)_6]$, $[OH]_{max} \sim 5.0\ \mu M$. ○ and ●, $1 \times 10^{-4}\ M\ K_4[Os(CN)_6]$. The spectrum is comprised of points from two separate experiments at $[OH]_{max} \sim 5.9\ \mu M$. Half-band width of 4 nm for the monochromator; light path length of 4 cm.

[1]The peak given here as 470 nm is reported (12) at 455 nm, however the spectrum shown in the article suggests that the peak is actually closer to 470 nm.

TABLE 1. Values for the rate constants for the reactions of hydroxyl radical

Compound	Concentration	$k_c \times 10^{9a-d}$ (M^{-1} s^{-1}, ~25 °C)	Method of determination	E^0 (V, $M^{n+} - M^{n+1}$)
$K_4[Fe(CN)_6]$	80–140 μ*M*	11.2 ± 1.7 (21)	Formation of product	−0.36[e]
	2 m*M*	8.0	Isopropanol competition	
$K_4[Ru(CN)_6]$	40–200 μ*M*	5.7 ± 0.8 (31)	Formation of product	−0.86[f]
	1 m*M*	4.4	Isopropanol competition	
$K_4[Os(CN)_6]$	50–200 μ*M*	10.3 ± 1.2 (36)	Formation of product	—
	1 m*M*	8.6	Isopropanol competition	
	0.1 m*M*	10.2	Methanol competition	
$K_4[Mo(CN)_8]$	3–20 m*M*	5.8 ± 0.6	$NaHCO_3$ competition (50 m*M*)	−0.73[e]
$NaHCO_3$	50 m*M*	0.036 ± 0.003 (6)	Formation of product	—
	50 m*M*	0.038	Isopropanol competition	

[a]The values of k_c determined from the rates of formation of products are the average values for both aerated and N_2O saturated solutions. The numbers in parentheses represent the number of determinations. The wavelengths of observation were 420 nm for $Fe(CN)_6^{3-}$; 330, 355, and 470 nm for $Ru(CN)_6^{3-}$; 330 and 410 nm for $Os(CN)_6^{3-}$.
[b]The values of k_c derived from alcohol competition are based upon the rate constants for the reaction of hydroxyl radical with isopropanol of 2.15×10^9 M^{-1} s^{-1} and with methanol of 9.0×10^8 M^{-1} s^{-1}. The wavelengths of observation were 410 nm for $Fe(CN)_6^{3-}$ and $Os(CN)_6^{3-}$ and 350 nm for $Ru(CN)_6^{3-}$.
[c]The experiments involving $NaHCO_3$ were carried out in N_2O saturated solutions (p*H* ~8.2) and the wavelength of observation of CO_3^- was 578 nm.
[d]The value of k_c for $Mo(CN)_8^{4-}$ is based upon an average value for the reaction of HCO_3^- and OH of 3.7×10^7 M^{-1} s^{-1}.
[e]Cited in ref. 21.
[f]Reference 12.

For ferrocyanide solution, the product exhibited a peak at 420 nm ($\varepsilon = 1040$ M^{-1} cm^{-1}) in excellent agreement with the reported values for $Fe(CN)_6^{3-}$ (1, 5, 6, 12, 13).

The kinetics of formation of the foregoing product materials were investigated under conditions where the concentrations of the metal complexes were in great excess of the maximum OH concentrations. Under these conditions, the formation of products obeyed a first order rate law. The apparent first order rate constants for the ruthenium and osmium systems were independent of dose (*ca.* 1 to *ca.* 6 μ*M* $[OH]_{max}$) and of wavelength, and they were the same whether the solutions were aerated or saturated with N_2O. Concentration studies indicated that the observed first order rate constants, k_{obs}, were linearly dependent on the concentrations of the metal complexes: the second order rate constants, k_c, evaluated from the values of k_{obs} are summarized in Table 1. The value of k_c of $(1.12 \pm 0.17) \times 10^{10}$ M^{-1} s^{-1} found in this study for $Fe(CN)_6^{4-}$ corresponds well with previously reported values of $(1.25 \pm 0.1) \times 10^{10}$ (5) and $(9.3 \pm 0.5) \times 10^9$ M^{-1} s^{-1} (7) obtained by pulse radiolysis.

As a confirmation of the participation of OH radical in these reactions, the competition reactions in aerated media between the metal complexes and the alcohols, isopropanol and methanol, whose reactions with OH have been well characterized (1, 2, 7), were carried out. The effect on the absorbance, *A*, of the product, by the presence of alcohol was found to be described by eq. 4

$$[4] \qquad \frac{A_0}{A} = 1 + \frac{k_{alc}[\text{alcohol}]}{k_c[\text{complex}]}$$

where A_0 is the absorbance in the absence of alcohol, and where k_{alc} and k_c are the respective second order rate constants for the particular alcohol and for the complex. The values obtained for k_c taking as the values of k_{alc} for isopropanol and methanol to be 2.15×10^9 and 9.0×10^8 M^{-1} s^{-1}, respectively, (7) are summarized in Table 1. These are in agreement within an experimental error of *ca.* 15% with the directly measured values; however the values obtained using isopropanol are consistently low. The reason for this is not apparent; the presence of impurities seems to be ruled out as two different sources of isopropanol were used.

The foregoing results indicate that $Ru(CN)_6^{4-}$ and $Os(CN)_6^{4-}$ react with hydroxyl radical by a single electron transfer mechanism in analogy to the well established behavior of $Fe(CN)_6^{4-}$, reaction 1. Both the nature of the product spectra and independence of the rate of product formation on wavelength indicate that $Ru(CN)_6^{3-}$ and $Os(CN)_6^{3-}$ are the sole observed products. The lack of dose dependence on the rate of

Can. J. Chem. Downloaded from www.nrcresearchpress.com by 210.87.254.40 on 09/05/12
For personal use only.

Can. J. Chem. Downloaded from www.nrcresearchpress.com by 210.87.254.40 on 09/05/12
For personal use only.

formation of the products confirms that the bimolecular recombination reaction of OH was not significant in the measurements.

Sharma (14) has shown through ^{60}Co irradiation studies that $Mo(CN)_8^{4-}$ also reacts with OH via a single electron transfer to give $Mo(CN)_8^{3-}$. Because $Mo(CN)_8^{3-}$ absorbs in the same region as the intensely absorbing and photosensitive $Mo(CN)_8^{4-}$ (11), it was not feasible to monitor directly the reaction of $Mo(CN)_8^{4-}$ and OH. Instead this reaction was observed indirectly by its competition with the reaction of HCO_3^- with OH. The reactions of OH with HCO_3^- and CO_3^{2-} lead to the formation of CO_3^- that absorbs intensely in the visible region with a peak at 600 nm (15–18). Since rate constants reported for the reactions of OH with HCO_3^- and CO_3^{2-} seem dependent upon conditions, the rate constant for the HCO_3^- used in this work was determined by both direct and competition measurements under the same conditions as used for the measurement of the $Mo(CN)_8^{4-}$ reaction. These values (Table 1) are in accord with the previously reported values for HCO_3^- that range from 1 to $8 \times 10^7\ M^{-1}\ s^{-1}$ (16–18). Included in Table 1 is the value of k_c for the reaction of $Mo(CN)_8^{4-}$ and OH evaluated using an average value of $3.7 \times 10^7\ M^{-1}\ s^{-1}$ for the bicarbonate reaction.

The reactions of hydroxyl radical with $Fe(CN)_6^{4-}$, $Ru(CN)_6^{4-}$, $Os(CN)_6^{4-}$, and $Mo(CN)_8^{4-}$ clearly involve a single electron transfer mechanism to yield complexes of the same stoichiometry with the metal center in the next higher oxidation state, and the second order rate constants are near those expected of diffusion-controlled reactions. In contrast, the reactions of OH with $Fe(CN)_5NO^{2-}$, $Co(CN)_5NO^{3-}$, $Mn(CN)_5NO^{3-}$, and $Cr(CN)_5NO^{3-}$ are somewhat slower (8, 18*b*). The rate constants for these pentacyanonitrosyl complexes range between $1.2 \times 10^7\ M^{-1}\ s^{-1}$ for the iron complex to $4.0 \times 10^9\ M^{-1}\ s^{-1}$ for the chromium system, and a linear free energy relationship (l.f.e.r.) is exhibited between the logarithms of the rate constants and the stretching frequencies of the coordinated NO group. In the case of the cyano complexes, the near diffusion-controlled values of the rate constants indicate that the transition states are close to the levels of the starting materials. As such, the degree of selectivity of any possible l.f.e.r. would be expected to be quite small. In this regard, it should be noted that the Ru(II) and Mo(IV) systems that are much weaker reducing agents than is ferrocyanide as shown by their half-cell potentials (see Table 1), are only slightly less reactive towards hydroxyl radical.

The difference in reactivity between the pentacyanonitrosyl complexes and the cyano complexes may be a manifestation of different mechanisms of reaction with hydroxyl radical. While the identities of the initial reaction products for the nitrosyl systems are uncertain, the results of an investigation of $Fe(CN)_5NO^{2-}$ by Buxton and co-workers (18*b*) suggest that the reaction with OH does not involve either electron transfer or detachment of NO. Thus the reaction mechanism of the pentacyanonitrosyl complexes may involve OH addition possibly to the coordinated NO group in contrast to the electron transfer mechanism encountered for the cyano complexes. Several additional features are suggestive in regard to the possibility of OH addition to the coordinated NO group. The l.f.e.r. exhibited by the nitrosyl systems shows that the lower is the NO stretching frequency the higher is the value of the rate constant for the OH reaction (8). Thus the nitrosyl complexes with the higher rate constants are those with a relatively higher electron density on the NO group (19). If the reactions of the nitrosyl complexes with OH involved electron transfer, it might be expected that $Mn(CN)_5NO^{3-}$ with an E^0 of -0.6 V (20) would be more reactive than either $Ru(CN)_6^{4-}$ or $Mo(CN)_8^{4-}$ (see Table 1) whereas it is found to be less reactive ($k_c = 2.4 \times 10^9\ M^{-1}\ s^{-1}$ (8)).

A final point concerns the use of the cyano compounds for pulse radiolysis dosimetry and competition kinetics. Ferrocyanide has proven particularly advantageous owing in part to its high reactivity towards OH and to the intense absorption of the ferrocyanide product at 420 nm. In this regard, the high reactivity of $Ru(CN)_6^{4-}$ coupled with the intense absorption of the ruthenium(III) product at a somewhat longer wavelength (470 nm) than that for ferrocyanide may prove to be useful. An additional advantage for the ruthenium system is that while both the iron and ruthenium complexes are quite photosensitive to light in the blue – near u.v. region (10), the ruthenium system should be less susceptible to photolytic degradation owing to its lower intrinsic absorption in this region (12). It should be noted however that the long term

stability of $Ru(CN)_6^{3-}$ is less than that of $Fe(CN)_6^{3-}$ (12), although this does not appear to be a complication on the time scales employed in pulse radiolysis.

We wish to acknowledge the financial support for this investigation by the National Research Council of Canada. It is also a pleasure to acknowledge the technical assistance of Messrs. D. Jennings and E. Kozar for help in operation of the accelerator and of Mr. D. Storer for the development of the s.e.m.

1. M. S. MATHESON and L. M. DORFMAN. Pulse radiolysis. The M.I.T. Press, Cambridge, Mass. 1969.
2. M. ANBAR and P. NETA. Int. J. Appl. Radiat. Isot. **18**, 493 (1967).
3. E. J. HART and M. ANBAR. The hydrated electron. Wiley–Interscience, New York, New York. 1970.
4. E. T. DENISOV. Usp. Khim. Engl. Transl. **40**, 24 (1971).
5. (*a*) J. RABANI and M. S. MATHESON. J. Am. Chem. Soc. **86**, 3175 (1964); (*b*) D. ZEHAVI and J. RABANI. J. Phys. Chem. **76**, 3703 (1972).
6. G. E. ADAMS, J. W. BOAG, and B. D. MICHAEL. Trans. Faraday Soc. **61**, 492 (1965).
7. R. L. WILLSON, C. L. GREENSTOCK, G. E. ADAMS, R. WAGEMAN, and L. M. DORFMAN. Int. J. Radiat. Phys. Chem. **3**, 211 (1971).
8. B. JEŻOWSKA-TRZEBIATOWSKA, E. KALECIŃSKA, and J. KALECIŃSKI. Bull. Acad. Pol. Sci. Ser. Sci. Chim. **19**, 265 (1971).
9. R. L. EAGER, V. KABACHIA, W. L. WALTZ, R. J. WOODS, and K. J. MCCALLUM. Can. J. Chem. In press.
10. E. M. FIELDEN and E. J. HART. Radiat. Res. **32**, 564 (1967).
11. W. L. WALTZ and A. W. ADAMSON. J. Phys. Chem. **73**, 4250 (1969).
12. D. D. DEFORD and A. W. DAVIDSON. J. Am. Chem. Soc. **73**, 1469 (1951).
13. J. J. ALEXANDER and H. B. GRAY. J. Am. Chem. Soc. **90**, 4260 (1968).
14. B. K. SHARMA. Can. J. Chem. **46**, 2757 (1968).
15. G. E. ADAMS, J. W. BOAG, and B. D. MICHAEL. Trans. Faraday Soc. **61**, 1417 (1965); **61**, 1674 (1965).
16. J. P. KEENE, Y. RAEF, and A. J. SWALLOW. Pulse radiolysis. *Edited by* M. Ebert, J. P. Keene, A. J. Swallow, and J. H. Baxendale. Academic Press, New York, New York. 1965. pp. 99–106.
17. J. L. WEEKS and J. RABANI. J. Phys. Chem. **70**, 2100 (1966).
18. (*a*) G. V. BUXTON. Trans. Faraday Soc. **65**, 2150 (1969); (*b*) G. V. BUXTON, F. S. DAINTON, and J. KALECIŃSKI. Int. J. Radiat. Phys. Chem. **1**, 87 (1969).
19. P. T. MANOHARAN and H. B. GRAY. Inorg. Chem. **5**, 823 (1966).
20. W. JAKÓB and T. SENKOWSKI. Rocz. Chem. **38**, 1751 (1964).
21. B. M. CHADWICK and A. G. SHARPE. Adv. Inorg. Chem. Radiochem. **8**, 83 (1966).

Can. J. Chem. Downloaded from www.nrcresearchpress.com by 210.87.254.40 on 09/05/12
For personal use only.

Complex Fluoroanions in Solution. IV. Fluorocomplexes involving MoF_6, MoF_6^-, and MoF_5[1]

S. BROWNSTEIN

Division of Chemistry, National Research Council of Canada, Ottawa, Canada K1A 0R9

Received April 4, 1973

Complexes of MoF_5 or MoF_6^- with BF_3, AsF_5, TaF_5, and NbF_5 have been prepared and partially characterized by infrared and fluorine resonance spectroscopy and X-ray powder diffraction. MoF_6 was not found to form complexes with binary fluorides nor fluoroanions.

Les complexes de MoF_5 ou de MoF_6^- avec du BF_3 ,AsF_5, TaF_5 et NbF_5 ont été synthétisés et caractérisés partiellement à l'aide de la spectroscopie infrarouge et de résonance du fluor ainsi qu'à l'aide de la diffraction des rayons-X (poudre). Il a été trouvé que le MoF_6^- ne forment pas de complexes avec des fluorures binaires ainsi qu'avec des fluoro anions. [Traduit par le journal]

Can. J. Chem., **51**, 2530 (1973)

Introduction

There are now many examples of fluorine bridging in solution to yield complex fluoroanions (ref. 1 and references cited therein). It is not yet clear what factors are responsible for the stability of certain complex fluoroanions and the instability of others and more information is required to explain the results reported thus far. Since complex fluoroanions of WF_4 have been obtained an investigation of molybdenum fluoride species appeared promising (1).

Molybdenum hexafluoride forms charge transfer complexes with $(CH_3)_4X$, where X is Si, Ge, or Sn (2). It also reacts with methylmethoxosilanes or dimethyl sulfite to give methoxomolybdenum(VI) fluorides (3). Reactions with organic bases to give hepta- or octaco-ordinate structures, as with WF_6, have also been reported (4). Alkali metal salts of MoF_6^- have been prepared and are isostructural with the corresponding tungsten and rhenium salts (5). The nitrosyl salt has also been synthesized and its infrared spectrum recorded (6). Complexes of MoF_5 with acetonitrile and chloroacetonitrile have been prepared and their infrared spectra described (7).

Experimental

All sample preparation and handling was done with standard vacuum line techniques or using a vacuum dry box. Those portions of the vacuum line which might come in contact with molybdenum hexafluoride were constructed with stainless steel bellows valves employing Teflon seats. Reagent and solvent purification and storage were accomplished as previously described (8, 9).

[1]NRCC No. 13277.

Molybdenum hexafluoride, purchased from Ozark-Mahoning Ltd., was used without further purification. Potassium hexafluoromolybdate (5), nitrosyl hexafluoromolybdate (6), and molybdenum pentafluoride (10) were prepared by established procedures.

Tetra-n-butylammonium Hexafluoromolybdate, (TBA)MoF_6

(TBA)I and MoF_6, in excess, were allowed to react in sulfur dioxide as solvent and all volatile materials were then pumped off under high vacuum. The pale cream powder has an X-ray powder diffraction pattern similar to (TBA)MF_6, where M is Ta, Nb, Sb, or W.

Anal. calcd. for (TBA)MoF_6: Mo, 21.2. Found: Mo, 20.1.

Fluorine resonance spectra were obtained on a Varian Associates HA-100D spectrometer operating at 94.1 MHz. Chemical shifts are reported as p.p.m. from internal $CFCl_3$. X-Ray powder photographs were taken with Cu radiation in 114 mm diameter Debye-Scherer cameras. Infrared spectra of the compounds dispersed in potassium bromide disks were obtained with a Perkin–Elmer 621 spectrophotometer.

Results and Discussion

No change in the fluorine resonance spectra and hence no interaction was observed in methylene chloride and in sulfur dioxide solutions between MoF_6 and BF_3, PF_5, AsF_5, TaF_5, NbF_5, MoF_5, (TBA)BF_4, and (TBA)SbF_6. Therefore molybdenum hexafluoride is not very reactive as a fluorine donor nor as a fluorine acceptor in fluorine bridge bonding. Molybdenum pentafluoride was found to be unreactive with BF_3 and PF_5 in all the solvents investigated and with AsF_5 in fluorotrichloromethane as solvent. However in sulfur dioxide, sulfuryl chlorofluoride, and methylene chloride solutions there is a rapid reaction with the solvent in the

Can. J. Chem. Downloaded from www.nrcresearchpress.com by 210.87.254.40 on 09/05/12
For personal use only.

Can. J. Chem. Downloaded from www.nrcresearchpress.com by 210.87.254.40 on 09/05/12
For personal use only.

presence of AsF_5, SbF_5, TaF_5, or NbF_5 to give a complex mixture. These reactions were not further investigated.

When PF_5 is added to a suspension of $KMoF_6$ in liquid sulfur dioxide the fluoride resonance spectrum of phosphorus pentafluoride is clearly evident, but with BF_3 or AsF_5 as the binary fluoride no fluorine resonance spectrum is observed. With the two latter fluorides a yellow-orange solution was obtained. The solution was decanted from the solid and all volatile materials removed under high vacuum. The solids were found, by X-ray powder diffraction patterns, to be KBF_4 and $KAsF_6$, respectively. With TaF_5 and NbF_5 as the binary fluorides $KTaF_6$ and $KNbF_6$ were obtained in the same manner. These results may be explained in terms of reaction 1 where N is boron and $x = 3$ and where N is arsenic, tantalum, and niobium and $x = 5$.

$$[1] \qquad KMoF_6 + NF_x \rightarrow KNF_{x+1} + MoF_5$$

The yellow compound MoF_5 is soluble in sulfur dioxide to give a yellow-orange solution and does not produce a high resolution fluorine resonance spectrum since it is paramagnetic. Reaction 1 is similar to that observed with KWF_6 except for the fact that WF_5 is not stable and reacts further to give identifiable products (1).

The fluorine resonance spectra of reaction mixtures containing equimolar quantities of PF_5, BF_3, or AsF_5 with nitrosyl hexafluoromolybdate were similar to those obtained with potassium hexafluoromolybdate. However with $NOMoF_6$ as starting material and BF_3, an X-ray diffraction photograph of the solid, remaining after removal of volatile materials under vacuum, indicated the presence of $NOMoF_6$ and a new compound, not $NOBF_4$. With AsF_5 as the binary fluoride, $NOAsF_6$ and a new compound, not $NOMoF_6$, were found in the solid residue. It therefore seems that in these cases a complex fluoroanion is formed and continues to exist to some extent in the solid phase.

The infrared spectrum of nitrosyl hexafluoromolybdate was obtained, with some difficulty, by deposition on the cell windows directly from the vapor phase (6). Extensive hydrolysis was found to occur in Nujol mulls and KBr disks. These results were confirmed in the present studies. It was found that in addition to various peaks from hydrolysis products produced in the KBr disks a strong band attributed to a molybdenum fluorine stretch was observed at 550 cm^{-1} for $KMoF_6$ and at 560 cm^{-1} for $NOMoF_6$. The infrared spectrum of the reaction product of $NOMoF_6$ and BF_3 has, in addition to the lines previously observed from hydrolysis products, a strong line at 570 cm^{-1} from a molybdenum–fluorine stretch and three lines at 1040, 1080, and 1120 cm^{-1} attributed to boron–fluorine stretching frequencies. The latter three lines agree in position and intensity with those found at 1030, 1080, and 1120 cm^{-1} for NH_4BF_4 in a KBr disk (11). The infrared spectrum of the reaction product of $NOMoF_6$ and AsF_5 has a strong molybdenum–fluorine stretching frequency at 570 cm^{-1} and very strong bands at 700 and 390 cm^{-1} attributed to arsenic–fluorine stretching and bending modes. Infrared absorption lines are found at 700 and 398 cm^{-1} in $(TBA)AsF_6$ (8). From the combined results of fluorine resonance and infrared spectra and X-ray powder diffraction data it seems safe to conclude that a complex fluoroanion species is produced by reaction of $NOMoF_6$ with BF_3 and with AsF_5.

With silver as cation there is good evidence from fluorine resonance and infrared spectroscopy and X-ray powder diffraction studies for complex fluoroanion formation between MoF_5 and BF_4^-. In this case the complex is soluble in methylene chloride and a strong line is found at 145.5 from fluorine bonded to boron in the complex anion along with a much weaker line at 151.0 p.p.m. from BF_4^-. There does not appear to be any complex formation between MoF_5 and PF_6^-, AsF_6^-, nor SbF_6^- with silver and tetrabutylammonium as cations.

The clearest evidence for complex fluoroanions involving Mo(V) is found with silver and tetrabutylammonium as cations. The fluorine resonance spectrum of an equimolar solution of $(TBA)NbF_6$ and MoF_5 is shown in Fig. 1. Those peaks marked with an asterisk are attributed to $Nb_2F_{11}^-$ and have been reported previously (9). The major remaining peaks at −199.4, −161.1, and perhaps 142 p.p.m. are assigned to fluorines bonded to niobium in structure **1**, where X is niobium.

They are listed in Table 1 along with other reported complex fluoroanions of niobium for purpose of comparison. Since there is an unpaired electron on molybdenum(V) it is unlikely that fluorine resonance signals would be observed for fluorines directly bonded to molyb-

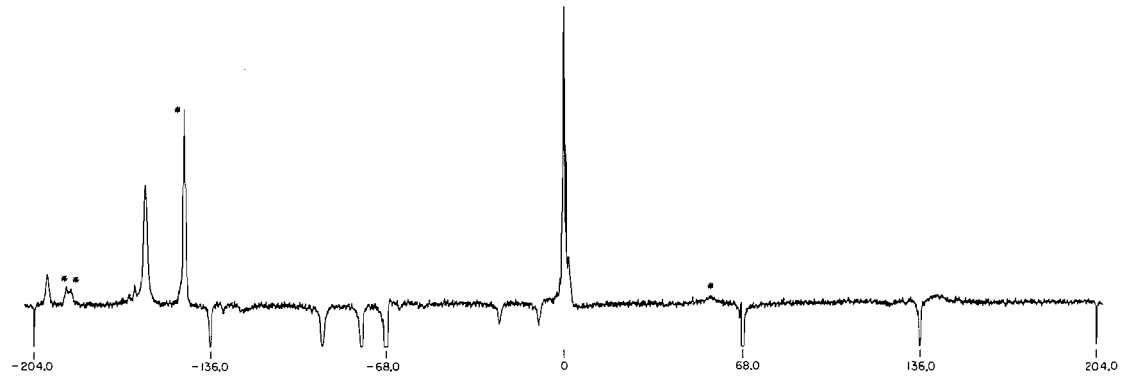

FIG. 1. The fluorine resonance spectrum of an equimolar methylene chloride solution of (TBA)NbF_6 and MoF^5 at $-110°$.

TABLE 1. Fluorine chemical shifts (p.p.m.) and spin coupling contants (Hz) in polyfluoroanions

Ion	δ_1	δ_2	δ_3	δ_4	δ_5	$J_{1,2}$	$J_{1,3}$	$J_{2,3}$	$J_{3,4}$	$J_{3,5}$	$J_{4,5}$
$MoNbF_{11}^-$	—	—	142	−161.1	−199.4	—	—	—	—	—	—
$Nb_2F_{11}^-$*			59	−145.5	−191.3				40	180	40
$SbNbF_{11}^-$*	131.5	118	101.7	−156.5	−205	—	—	—	—	—	—
$TaNbF_{11}^-$*	−108.7	−69.4	−40	−149.4	−197.4	40	180	40			
$WNbF_{10}^-$†		−68.7	—	−138	—			68	—	—	—
$MoTaF_{11}^-$		—	—	−58.6	−89.9	—	—	—	26	240	26
$Ta_2F_{11}^-$*			−80.8	−72.0	−115.1				41.8	165	23.0
$SbTaF_{11}^-$*	134.0	117.0	100.6	−78.6	−125.7	90	—	40	43	172	23
$WTaF_{10}^-$†		−67.4	—	−65.6	−94.6			58	34	230	24

*Reference 9.
†Reference 1. This ion is like 1 except that F_1 is absent.

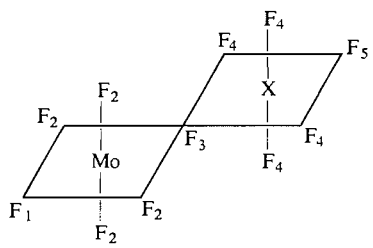

1

denum. The line at −199.4 is assigned to F_5 and that at −161.1 to F_4 from comparison with the chemical shifts found for other niobium containing complex fluoroanions. The observed intensity ratio of 1:4.7 is consistent with this assignment considering the errors introduced by different line widths and probably different relaxation times. The hetero-anion $MoNbF_{11}^-$ is 1.25 times more abundant than the homo-anion $Nb_2F_{11}^-$. A possible route for the formation of $Nb_2F_{11}^-$ is by reaction (2) which is analogous to the reactions

[2] $2MoNbF_{11}^- \leftrightarrows Nb_2F_{11}^- + Mo_2F_{11}^-$ or $MoF_5 + MoF_6^-$

previously discussed for the disproportionation of polyfluoroanions involving tantalum, niobium, and antimony (9).

The fluorine resonance spectrum of an equimolar solution of $AgTaF_6$ and MoF_5 is shown in Fig. 2. Those peaks marked with an asterisk are attributed to $Ta_2F_{11}^-$ and have been reported previously (9). The doublet at −89.9 with a spin–spin splitting of 240 Hz is assigned to F_5 on the basis of its chemical shift and the magnitude of its spin coupling which is assigned as $J_{3,5}$. These values are listed in Table 1 along with those for fluorine bonded to tantalum in other complex fluoroanions to facilitate a comparison. The triplet at −58.6 is assigned to F_4 with equal spin coupling constants $J_{3,4}$ and $J_{4'5}$ of 26 Hz. The F_5 resonance is not sufficiently sharp to resolve this coupling although there is a suggestion of it. The observed intensity ratio of 1:4.1 for F_5 and F_4 is consistent with this assignment. The peak at −43 is from unreacted TaF_6^- and those at −148, −120, and −85 are from fluorine on molybdenum in hydrolyzed species. These lines vary in relative

Can. J. Chem. Downloaded from www.nrcresearchpress.com by 210.87.254.40 on 09/05/12
For personal use only.

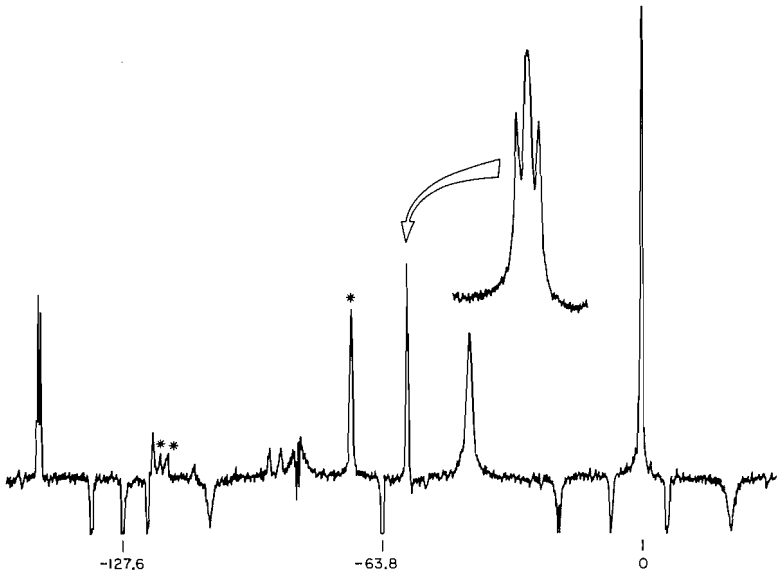

FIG. 2. The fluorine resonance spectrum of an equimolar methylene chloride solution of $AgTaF_6$ and MoF_5 at −105°.

TABLE 2. The effect of a binary fluoride upon the chemical shift of a probe nucleus

Probe nucleus	Chemical shift with binary fluoride (p.p.m.)				
	MoF_5	WF_4	NbF_5	TaF_5	SbF_5
Equatorial F on tantalum	−58.6	−65.6	−69.4	−72.0	−78.6
Terminal F on tantalum	−89.9	−94.6	−108.7	−115.1	−125.7
Equatorial F on niobium	−161.1	−138	−145.5	−149.4	−156.5
Terminal F on niobium	−194.4		−191.3	−197.4	−205

intensity from sample to sample with both silver and tetra-*n*-butylammonium as cations.

It is possible to order the relative electron withdrawing abilities of a binary fluoride as part of a polyfluoroanion from its effect upon the chemical shifts of a particular fluorine species in the other part of the polyfluoroanion (9). From the change in chemical shift for both the equatorial and terminal fluorines bonded to tantalum one obtains the following order of electron withdrawing ability. $MoF_5 < WF_4 < NbF_5 < TaF_5 < SbF_5$. Using the terminal fluorine bonded to niobium as a probe the order is $NbF_5 < MoF_5 < TaF_5 < SbF_5$. From the equatorial fluorines bonded to niobium the order $WF_4 < NbF_5 < TaF_5 < SbF_5 < MoF_5$ is obtained. The data summarizing these results are listed in Table 2. Although there are irregularities in the position of MoF_5 in the niobium complex fluoroanions it appears that this method may have promise in ordering the results obtained from studies of complex fluoroanions.

The author wishes to thank Miss Gayle Benson for preliminary studies with MoF_6 and $NOMoF_6$.

1. S. BROWNSTEIN. J. Inorg. Nucl. Chem. In press.
2. R. R. MCLEAN, D. W. A. SHARP, and J. M. WINFIELD. Chem. Commun. 452 (1970).
3. D. W. WALKER and J. M. WINFIELD. J. Fluorine Chem. **1**, 376 (1971).
4. (*a*) F. N. TEBBE and E. L. MUETTERTIES. Inorg. Chem. **7**, 172 (1968). (*b*) E. L. MUETTERTIES. *In* Advances in the chemistry of the co-ordination compounds. *Edited by* S. Kirschner. MacMillan. New York. 1961. p. 517.
5. G. B. HARGREAVES and R. D. PEACOCK. J. Chem. Soc. 4212 (1957).
6. J. R. GREICHMAN, E. A. SMITH, S. S. TROND, and P. R. OGLE. Inorg. Chem. **1**, 661 (1962).
7. J. C. FUGGLE, D. W. A. SHARP, and J. M. WINFIELD. J. Fluorine Chem. **1**, 427 (1971).
8. S. BROWNSTEIN. Can. J. Chem. **47**, 605 (1969).
9. S. BROWNSTEIN. Inorg. Chem. **12**, 584 (1973).
10. T. J. OUELLETTE, C. T. RATCLIFFE, D. W. A. SHARP, and A. M. STEVEN. Inorg. Synth. **13**, 146 (1972).
11. S. BROWNSTEIN and J. PAASIVIRTA. Can. J. Chem. **43**, 1645 (1965).

Can. J. Chem. Downloaded from www.nrcresearchpress.com by 210.87.254.40 on 09/05/12
For personal use only.

Total Synthesis of (±)-Trachylobane, a Pentacyclic Diterpenoid with a Tricyclooctane System

R. B. KELLY, J. EBER, AND H. K. HUNG

Department of Chemistry, University of New Brunswick, Saint John, New Brunswick

Received March 6, 1973

A total synthesis of (±)-trachylobane, a pentacyclic diterpenoid possessing a tricyclo[3.2.1.$0^{2,7}$]octane system, is described. Completion of the synthesis of trachylobane confirms the validity of the structure assigned to this diterpenoid and provides corroboration of structures assigned to diterpenoids from which it has been obtained as a conversion product.

On décrit une synthèse totale du (±)-trachylobane, un diterpénoide pentacyclique possédant un système tricyclo[3.2.1.$0^{2,7}$]octane. En complétant ainsi la synthèse du trachylobane, on a confirmé la structure assignée à ce diterpénoide et corroboré les structures proposées aux diterpénoides desquels il a été obtenu comme produit de conversion. [Traduit par le journal]

Can. J. Chem., **51**, 2534 (1973)

Trachylobane (**1**) is the naturally occurring (1) parent hydrocarbon of a group of biogenetically important diterpenoidal acids and alcohols which are characterized by a tricyclo[3.2.1.$0^{2,7}$]-octane system incorporated into ring C (1–3). The isolation from *Trachylobium* of diterpenoids possessing the trachylobane skeleton was first reported in 1965 (2) and since then further reports of the isolation of new members of the trachylobane group have appeared (3). It was not until 1971, however, that the parent hydrocarbon, trachylobane (**1**), was isolated from natural sources.

The trachylobane skeleton has, for some time, been associated with interesting speculations regarding the biogenesis of the diterpenes. In fact, ten years before the discovery of the trachylobane group, a non-classical carbonium ion (**2**) related to trachylobane was suggested as an intermediate in the biosynthesis of various diterpenoidal skeleta (4). Consequently, the eventual discovery of the trachylobanes in nature inspired considerable experimentation directed toward interconversions involving trachylobane and the tetracyclic diterpenoids (*e.g.* 2*c*, 5).

The tricyclooctane system present in the

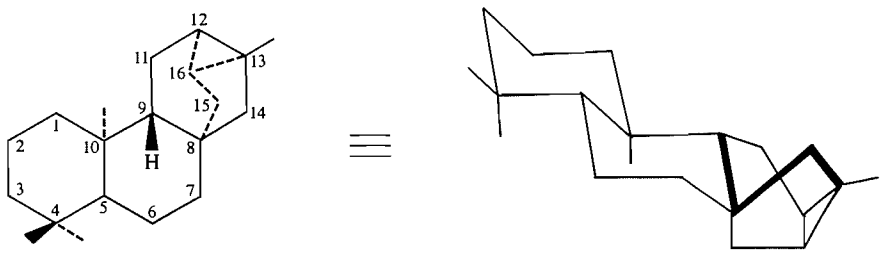

1

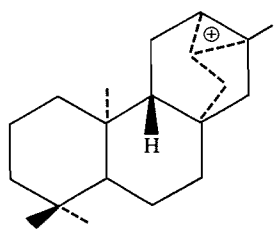

2

Can. J. Chem. Downloaded from www.nrcresearchpress.com by 210.87.254.42 on 09/05/12
For personal use only.

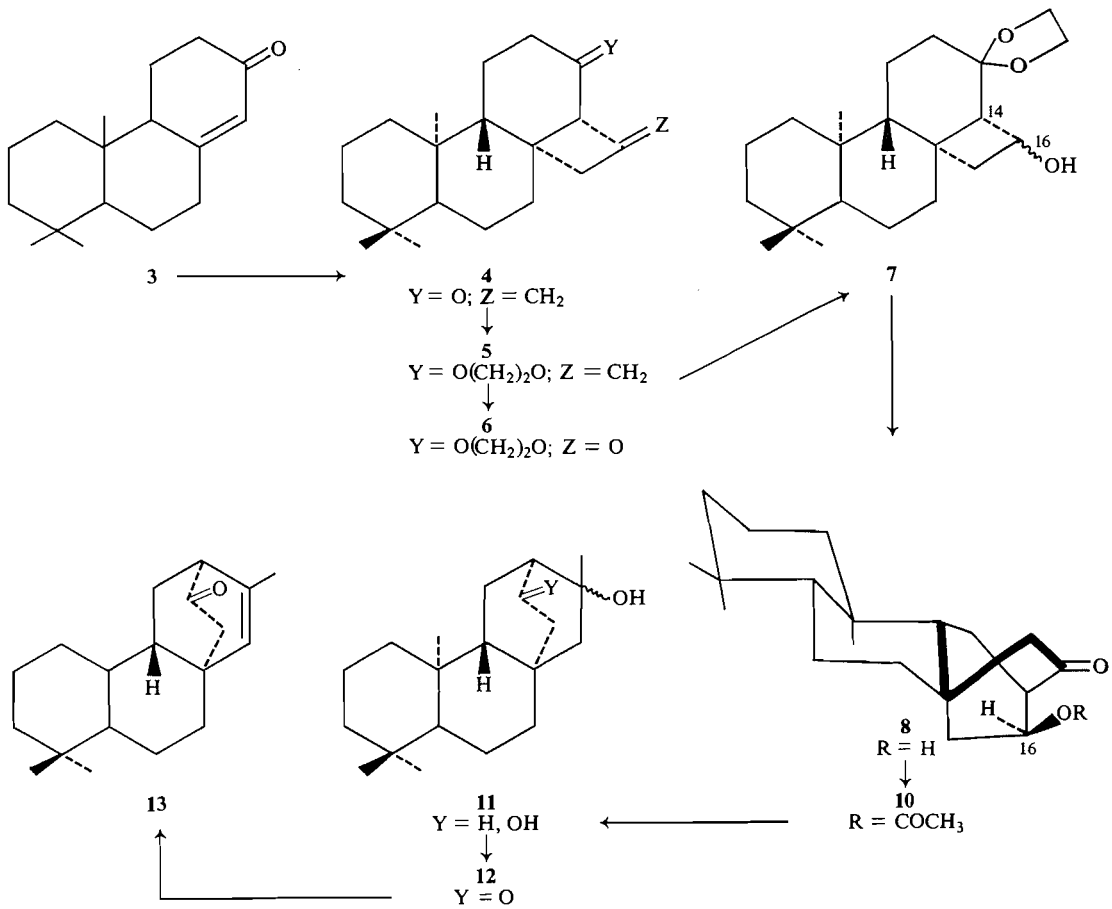

SCHEME 1

trachylobane skeleton is also found in the sesquiterpenoids ishwarone (6) and ishwarane (6) and we have recently described a total synthesis of the latter (7). We now wish to describe a total synthesis of trachylobane (**1**) which confirms the validity of the structure assigned to this diterpenoid and provides corroboration for the structures assigned to diterpenoids from which it has been derived as a conversion product (2, 3). The synthetic route is outlined in Schemes 1 and 2.

Stereo- and regiospecific photo-addition of allene (7 and refs. cited) to the totally synthetic (8) unsaturated ketone **3** afforded, in 70% yield, the crystalline adduct **4**. Consistent with structure **4**, the i.r. spectrum of the adduct showed carbonyl absorption at 1710 cm^{-1} and bands at 1675 and 875 cm^{-1} due to the exocyclic methylene and, in the n.m.r. spectrum, there was a multiplet at δ 4.95 (2H) attributable to the exocyclic methylene.[1]

Oxidation of the crystalline ketal **5** of **4** with osmic acid-periodate gave the crystalline cyclobutanone (**6**) in 93% yield (from **4**). The i.r. spectrum of **6** showed carbonyl absorption 1777 cm^{-1} due to the cyclobutanone and the n.m.r. spectrum was devoid of signals attributable to vinylic protons but showed a multiplet (4H) at δ 3.77 due to the ethylene group of the ketal function.

The cyclobutanone (**6**) was reduced to the crystalline cyclobutanol (**7**) in 97% yield with lithium aluminum hydride. The alcohol (**7**) had spectral properties consistent with the assigned structure. Thus, the i.r. spectrum showed

[1]Only spectral data pertinent to the discussion will be given in this section; for further details see Experimental.

Can. J. Chem. Downloaded from www.nrcresearchpress.com by 210.87.254.42 on 09/05/12
For personal use only.

Can. J. Chem. Downloaded from www.nrcresearchpress.com by 210.87.254.42 on 09/05/12
For personal use only.

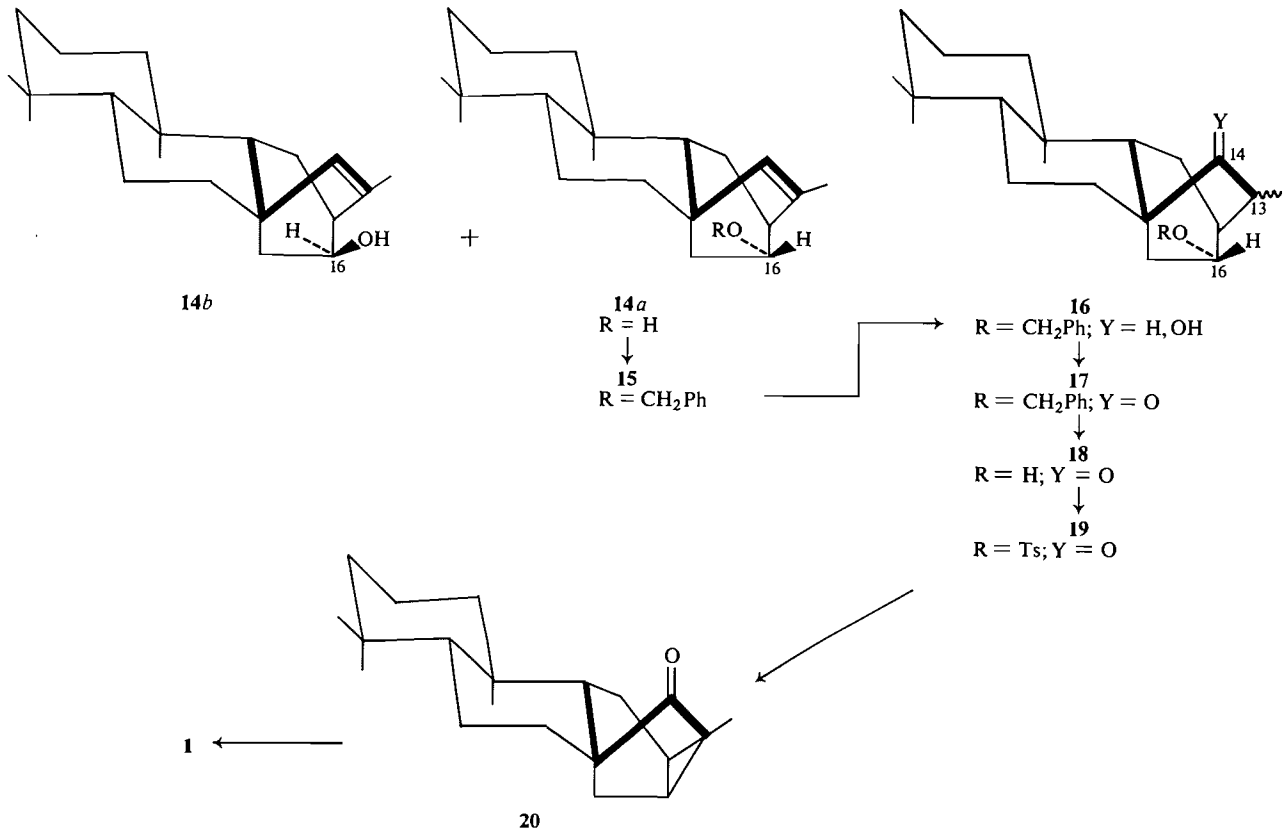

SCHEME 2

Can. J. Chem. Downloaded from www.nrcresearchpress.com by 210.87.254.42 on 09/05/12
For personal use only.

hydroxyl absorption at 3500 cm^{-1} and, in the n.m.r. spectrum, there was a doublet (1H) at δ 2.77 due to the methine at C-14 and a multiplet (1H) at δ 4.30 due to the C-16 proton.[2]

Treatment of **7** with aqueous hydrochloric acid in tetrahydrofuran resulted in deketalization followed by skeletal rearrangement to give, directly, the crystalline keto alcohol **8** in 97% yield. The conversion **7** → **8** involves deketalization followed by retro-aldolization to give the intermediate keto aldehyde **9** then aldol condensation to give **8** (*cf.* 7). The structure assigned

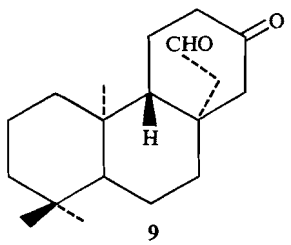

9

to the keto alcohol is supported by its i.r. spectrum which showed bands at 3370 (hydroxyl) and 1720 cm^{-1} (ketone) and by a multiplet (1H) in the n.m.r. spectrum at δ 4.17 due to the proton at C-16. In contrast with previous experience of this type of rearrangement (7), apparently only a single epimer was formed which has been assigned the stereostructure represented by **8** for reasons given in the sequel.

Conversion of **8** to the acetate **10** and treatment of the latter with methyl lithium followed by acid hydrolysis afforded the crystalline diol **11** in 85% yield. The i.r. spectrum of **11** was devoid of carbonyl absorption and the n.m.r. spectrum showed a singlet (3H) at δ 1.27 (CH_3—C—OH).

Jones oxidation (9) of the diol **11** gave, in 86% yield, the keto alcohol **12** (i.r. 3360 and 1710 cm^{-1}) as a crystalline compound. Dehydration of **12** with *p*-toluenesulfonic acid in boiling benzene gave the crystalline enone **13** in 78% yield. The spectral properties of the dehydration product were consistent with structure **13**. Thus, there were bands in the i.r. spectrum at 1725 (ketone) and 1647 cm^{-1} (double bond) and, in the n.m.r. spectrum, there was a doublet at δ 1.75 (vinylic methyl) and a multiplet at 5.77 (vinylic proton).

Reduction of the enone **13** with lithium aluminum hydride and chromatography of the product on silica gel afforded two epimeric enols **14***a* (m.p. 147–148°; yield 55%) and **14***b* (m.p. 135–136°; yield 42%). The i.r. spectra of the epimeric enols were similar, both displaying hydroxyl absorption at 3250–3300 cm^{-1} and a band at *ca.* 1650 due to the double bond. In the n.m.r. spectrum of the higher melting epimer there was a doublet (3H) at δ 1.68 (vinylic methyl), a multiplet (1H) at 3.87 (proton at C-16), and a multiplet (1H) at 5.48 (vinylic proton); in the case of the lower melting epimer the corresponding signals occurred at δ 1.76, 3.83, and 5.72 respectively.

The assigned stereoconfigurations at C-16 of the epimeric enols is based on the observation that, in the case of the higher melting epimer, the n.m.r. spectrum shows that the singlet (δ 1.08) for one of the tertiary methyl groups appears *ca.* 15 Hz downfield relative to the singlets (δ 0.80 and 0.85) for the other two tertiary methyl groups attached to C-4. No such pronounced deshielding effect is observed in the spectrum of the lower melting epimer in which the relevant singlets appear at δ 0.80 and 0.87 (superimposed singlets for two methyl groups). This effect was attributed to deshielding of the angular methyl group by the hydroxyl group. Consequently, the higher melting epimer was assigned structure **14***a*, in which the hydroxyl group is closer to the angular methyl group than in **14***b*. The latter structure must then be assigned to the lower melting epimer.

Unlike **14***b*, the enol **14***a* leads to a keto tosylate (**19**) in which the tosylate function is favorably aligned for an S_N2_i displacement by the carbanion at C-13 to form the cyclopropyl ketone **20**. For this reason, **14***a* rather than **14***b* was chosen for the continuation of the synthesis. However, based on experience gained during the synthesis of ishwarane (7) it seems likely that either epimer could have been chosen.

Reasoning similar to that applied to **14***a* (*vide supra*) can now be used to assign the configuration at C-16 of the keto alcohol **8**. Singlets for the three methyl groups appear at δ 0.83, 0.88, and 0.95. Thus, in contrast with **14***a*, no single methyl group is significantly deshielded relative to the other two by the hydroxyl group. In analogy with **14***b*, this requires that the configuration at C-16 be as shown in **8** in which the hydroxyl group is farther removed from the angular methyl group than it would be in the epimeric orientation. The fact that none of the

[2]The numbering system shown in **1** is adhered to throughout.

pertinent methyl groups in the diol **11**, which has the same configuration at C-16 as **8**, is deshielded relative to the others provides substantiation for this stereochemical assignment.

Conversion of **14***a* to the benzyl ether **15** followed by hydroboration afforded a single crystalline alcohol **16** in 55% yield (from **14***a*) the i.r. spectrum of which showed hydroxyl absorption at 3450 cm^{-1}. In addition to the signals due to the benzyl group, the n.m.r. spectrum exhibited a doublet (1H) at δ 2.75 (proton at C-14) and a multiplet (1H) at 3.68 (proton at C-16). The stereochemistry at C-13 and -14 is unknown but this is of no consequence so far as the synthetic route is concerned.

Oxidation of **16** with the Sarett reagent (10) gave, in 65% yield, the crystalline ketone **17** (i.r. 1710 cm^{-1}) which, on hydrogenolysis of the benzyl group gave the crystalline keto alcohol **18** in 76% yield (i.r., 3460 and 1690 cm^{-1}; n.m.r., devoid of signals for benzyl group).

The keto alcohol **18** was converted to the tosylate **19** and the latter was transformed in 52% yield into the crystalline cyclopropyl ketone **20** by heating at 60° for 2 h in dimethyl sulfoxide containing an excess of methylsulfinyl carbanion (11). The spectral properties of this key condensation product were consistent with structure **20**. Thus, the u.v. spectrum showed a maximum at 209 nm (ε 3800) due to absorption of the cyclopropyl ketone; the i.r. spectrum showed carbonyl absorption at 1720 cm^{-1} but was devoid of bands attributable to hydroxyl or tosylate absorption; the n.m.r. spectrum showed a partially obscured multiplet at *ca.* δ 0.60 due to protons on the cyclopropane ring and singlets for four tertiary methyl groups.

Finally, the cyclopropyl ketone **19** was reduced to the hydrocarbon **1** by the Barton modification (12) of the Wolff–Kishner reduction. After purification by t.l.c., the hydrocarbon was obtained as an oil in 56% yield. The spectral properties of the reduction product were consistent with structure **1**; the i.r. spectrum showed no carbonyl absorption and the n.m.r. spectrum showed a multiplet at δ 0.65 due to the protons on the cyclopropane ring and singlets for four tertiary methyl groups.

The identity of the synthetic hydrocarbon **1** with an authentic sample of trachylobane was established by the following criteria: identity of i.r. and n.m.r. spectra; identical retention times on v.p.c. (single peak on co-injection).

Experimental

Instrumentation, Methods, and Materials

Melting points were determined on a Fisher–Johns apparatus and are uncorrected. The i.r. spectra were recorded on a Perkin–Elmer model 237 B spectrophotometer and u.v. spectra were determined with a Perkin–Elmer Coleman model 124 instrument. The n.m.r. spectra were recorded with a Varian T-60 instrument; chemical shifts were expressed in p.p.m. (δ-values) downfield from the signal for tetramethylsilane which is used as an internal standard.

V.p.c. was performed on a Hewlett-Packard model 5750 instrument fitted with a stainless steel column (6 × 1/8 in) packed with 10% of UC-W98 (silicone gum-rubber) on diatoports (80–100 mesh). The t.l.c. was carried out on silica gel GF-254 procured from Brinkman Instruments (Canada) Ltd.

Reaction products were isolated by the following procedure. The product was extracted into the specified solvent and the extract was washed two or three times with appropriate aqueous solutions as indicated. The original aqueous layer (if any) and the aqueous washings were extracted three times with the solvent and the combined extracts were dried over anhydrous magnesium sulfate, filtered, and evaporated *in vacuo* on a rotary evaporator.

Petroleum ether refers to the fraction with boiling point range 30–60°.

Brine refers to a saturated solution of sodium chloride.

Photo-adduct 4

Photo-addition of allene to the unsaturated ketone **3** was carried out at −70° using a 450 W mercury vapor immersion lamp with a Corex sleeve. A solution of 8.0 g of **3** and 44.0 g of allene in 1500 ml of freshly distilled hexane was irradiated for 1 h then the reaction solution was left at room temperature overnight to allow excess allene to escape. The solvent was evaporated *in vacuo* and the residue was chromatographed on a column of 250 g of silica gel with benzene as solvent. Crystallization of the eluted material from ether afforded 6.56 g (70%) of **4**, m.p. 112°; ν_{max} (Nujol) 1710 (ketone), 1675, and 875 with overtone at 1750 cm^{-1} (exocyclic CH_2); n.m.r. ($CDCl_3$) δ 0.83 (s, 6H, superimposed singlets for two tertiary methyls), 0.90 (s, 3H, tertiary methyl), 4.95 (m, 2H, vinylic protons).

Anal. Calcd. for $C_{20}H_{30}O$: C, 83.86; H, 10.56. Found: C, 84.21; H, 10.82.

Ketal 5

A solution of 5.47 g of **4**, 550 mg of *p*-toluenesulfonic acid monohydrate, and 16.5 ml of ethylene glycol in 550 ml of benzene was refluxed under a nitrogen atmosphere for 30 min. During reflux water was separated in a Dean–Stark adapter. The cooled reaction solution was worked-up in the usual manner with potassium bicarbonate solution and water. Crystallization of the resulting material from ether – petroleum ether gave 6.14 g (98%) of **5**, m.p. 116.5°; ν_{max} (Nujol) 1675 and 880 with overtone at 1760 cm^{-1} (exocyclic CH_2); n.m.r. ($CDCl_3$), δ 0.78, 0.82 and 0.87 (s, 3H each, tertiary methyls), 3.93 (br s, 4H, ethylene of ketal function), 4.94 (m, 2H, vinylic protons).

Anal. Calcd. for $C_{22}H_{34}O_2$: C, 79.95; H, 10.37. Found: C, 80.31; H, 10.38.

Can. J. Chem. Downloaded from www.nrcresearchpress.com by 210.87.254.42 on 09/05/12
For personal use only.

Can. J. Chem. Downloaded from www.nrcresearchpress.com by 210.87.254.42 on 09/05/12
For personal use only.

Cyclobutanone 6

A solution of 600 mg of **5**, 5.1 ml of water, and 60 ml of dioxan was treated with a solution of 60 mg of osmic acid in 2.4 ml of pyridine. After stirring for 15 min in the dark, the reaction solution was treated over a period of 1 h, with 690 mg of sodium metaperiodate dissolved in 6.9 ml of water. The resulting mixture was stirred at room temperature in the dark for 2 days. Solid material was removed by filtration, the filtrate extracted with ether, and the extracts were worked-up in the usual manner with 10% sodium bisulfite solution and water. Crystallization of the product from ether – petroleum ether afforded 570 mg (95%) of **6**, m.p. 142–143°; ν_{max} (Nujol) 1777 cm^{-1} (ketone); n.m.r. (CCl_4), δ 0.78, 0.83, and 0.87 (s, 3H each, tertiary methyls), no signals for vinylic protons.

Anal. Calcd. for $C_{21}H_{32}O_3$: C, 75.86; H, 9.70. Found: C, 76.06; H, 10.02.

Cyclobutanol 7

A solution of 153 mg of **6** in 10 ml of ether was added dropwise to a suspension of 200 mg of lithium aluminum hydride in 10 ml of ether over a period of 20 min. The reaction mixture was stirred at room temperature for 16 h then refluxed for 15 min. The cooled reaction mixture was treated with 0.3 ml of brine, stirred for 5 h, dried with anhydrous sodium sulfate, and filtered. The solid material was washed well with ether and the washings combined with the filtrate and evaporated *in vacuo*. Crystallization of the residue from ether afforded 151 mg (98%) of **7**, m.p. 142°; ν_{max} (Nujol) 3475 cm^{-1} (OH); n.m.r. (CCl_4), δ 0.77, 0.81 and 0.84 (s, 3H each, tertiary methyls). 2.77 (d, J = 3.5 Hz, 1H, methine at C-14), 3.87 (br s, 4H, ethylene of ketal function), 4.30 (m, 1H, H—C—OH).

Anal. Calcd. for $C_{21}H_{34}O_3$: C, 75.41; H, 10.25. Found: C, 75.34; H, 10.48.

Keto Alcohol 8

A solution of 1.20 g of **7** in 90 ml of tetrahydrofuran was treated with 72 ml of 1 *M* aqueous hydrochloric acid and left under nitrogen at room temperature for 21 h. The reaction solution was extracted with chloroform and the extracts were worked-up in the usual manner with saturated sodium bicarbonate solution and water. Crystallization of the product from methylene chloride – petroleum ether afforded 1.04 g (97%) of **8**, m.p. 237°; ν_{max} 3370 (OH) and 1720 cm^{-1} (ketone); n.m.r. ($CDCl_3$), δ 0.83, 0.88 and 0.95 (s, 3H each, tertiary methyls), 4.17 (m, 1H, H—C—OH).

Anal. Calcd. for $C_{19}H_{30}O_2$: C, 78.57; H, 10.41. Found: C, 78.90; H, 10.50.

Keto Acetate 10

Conversion of 1.85 g of **8** in the usual manner with acetic anhydride in pyridine followed by crystallization of the product from methylene chloride – petroleum ether gave 1.94 g (92%) of **9**, m.p. 175°; ν_{max} 1740 cm^{-1} (broad band, acetate and ketone); n.m.r. ($CDCl_3$), δ 0.85, 0.88 and 0.99 (s, 3H each, tertiary methyls), 2.00 (s, 3H, acetate), 5.07 (H—O—Ac).

Anal. Calcd. for $C_{21}H_{32}O_3$: C, 75.86; H, 9.70. Found: C, 76.00; H, 9.71.

Diol 11

A solution of 500 mg of **10** in 20 ml of tetrahydrofuran was added dropwise to 10 ml of a 1 *M* ether–tetrahydrofuran solution of methyl lithium under nitrogen; during the addition the methyl lithium solution was cooled on an ice bath. The reaction solution was stirred at room temperature for 1 h then treated dropwise with 24 ml of 0.5 *M* aqueous hydrochloric acid. The product was extracted with methylene chloride and the extracts were worked-up in the usual manner with sodium bicarbonate solution and brine. Crystallization of the product from methylene chloride – petroleum ether gave 393 mg (85%) of **11**, m.p. 182°; ν_{max} 3260 (OH); n.m.r. ($CDCl_3$), δ 0.82 (s, 3H, tertiary methyl), 0.87 (s, 6H, superimposed signals for two tertiary methyls), 1.27 (s, 3H, CH_3—C—OH), 3.97 (m, 1H, H—C—OH).

Anal. Calcd. for $C_{20}H_{34}O_2$: C, 78.38; H, 11.18. Found: C, 78.34; H, 11.19.

Keto Alcohol 12

A solution of 210 mg of **11** in 25 ml of acetone was treated dropwise at room temperature with an 8 *N* solution of Jones' reagent (9) until a persistent orange color was observed. Excess oxidizing reagent was deactivated by the addition of 1 ml of methanol. The reaction mixture was poured into 100 ml of 5% sodium carbonate and the product was extracted into ether. The ether extracts were washed with brine, dried, and evaporated *in vacuo*. Crystallization of the residue from methylene chloride – petroleum ether gave 179 mg (86%) of **12**, m.p. 207–208°; ν_{max} (Nujol) 3360 (OH) and 1710 cm^{-1} (ketone); n.m.r. ($CDCl_3$), δ 0.77, 0.80 and 0.87 (s, 3H each, tertiary methyls), 1.40 (s, 3H, CH_3—C—OH).

Anal. Calcd. for $C_{20}H_{32}O_2$: C, 78.90; H, 10.60 Found: C, 78.82; H, 10.58.

Enone 13

A solution of 1.09 g of **12** and 1.08 g of *p*-toluenesulfonic acid monohydrate in 1080 ml of benzene was refluxed for 5 h while water was separated in a Dean–Stark adapter. The cooled benzene solution was added to 600 ml of saturated sodium bicarbonate solution, the layers were separated, and the aqueous layer was extracted with ether. The benzene layer and the ether extracts were washed with brine, combined, dried, and evaporated *in vacuo*. Chromatography of the residue on a column of 135 g of silica gel impregnated with 20% silver nitrate with 2.5% of ether in petroleum ether as solvent followed by crystallization from petroleum ether afforded 800 mg (78%) of **13**, m.p. 94°; ν_{max} (Nujol) 1725 (ketone), 1647 and 805 cm^{-1} (olefin); n.m.r. ($CDCl_3$), δ 0.81 (s, 3H, tertiary methyl), 0.87 (s, 6H, superimposed signals for two tertiary methyls), 1.75 (d, J = 2 Hz, 3H, vinylic methyl), δ 5.77 (m, 1H, vinylic proton).

Anal. Calcd. for $C_{20}H_{30}O$: C, 83.86; H, 10.56. Found: C, 84.01; H, 10.67.

Enols 14a and b

A solution of 426 mg of **13** in 10 ml of ether was added dropwise to a stirred mixture of 300 mg of lithium aluminum hydride and 10 ml of ether. The mixture was stirred at room temperature for 5 h then refluxed for 1 h, cooled, and treated with 0.3 ml of brine. After stirring overnight, anhydrous sodium sulfate was added and stirring was continued for 30 min. The solid material was collected by filtration and washed well with ether. The combined filtrate and washings were evaporated *in vacuo*. The residue was combined with similar material, resulting from the reduction of 800 mg of **13** as described above, and chromatographed on a column of 75 g of silica gel with 4–8% of ether in petroleum ether as solvent.

Can. J. Chem. Downloaded from www.nrcresearchpress.com by 210.87.254.42 on 09/05/12
For personal use only.

Enol ***14a***

Crystallization of the first fraction eluted from the column from ether afforded 676 mg (55%) of **14***a*, m.p. 147–148°; ν_{max} (Nujol) 3340 (OH), 1640 and 800 cm^{-1} (olefin); n.m.r. ($CDCl_3$), δ 0.80, 0.85 and 1.08 (s, 3H each, tertiary methyls), 1.68 (d, J = 2 Hz, 3H, vinylic methyl), 3.87 (m, 1H, H—C—OH), δ 5.48 (m, 1H, vinylic H).

Anal. Calcd. for $C_{20}H_{32}O$: C, 83.27; H, 11.18. Found: C, 83.60; H, 11.37.

Enol ***14b***

Crystallization of the second fraction from the column from methylene chloride – petroleum ether afforded 512 mg (42%) of **14***b*, m.p. 135–136°; ν_{max} (Nujol) 3250 (OH), 1652 and 790 cm^{-1} (olefin); n.m.r. ($CDCl_3$), δ 0.80 (s, 3H, tertiary methyl), 0.87 (s, 6H, superimposed signals for two tertiary methyls) 1.76 (d, J = 2 Hz, vinylic methyl), 3.83 (m, 1H, H—C—OH), 5.72 (m, 1H, vinylic proton).

Anal. Calcd. for $C_{20}H_{32}O$: C, 83.27; H, 11.18. Found: C, 83.71; H, 11.26.

Benzyl Ether ***15***

A mixture of 635 mg of **14***a*, 635 mg of sodium hydride, and 53 ml of benzene was refluxed under a nitrogen atmosphere for 5 h. Benzyl chloride (2.65 ml) was then added and reflux was continued under nitrogen for an additional 17 h. After cooling, the reaction mixture was treated dropwise with 5 ml of methanol then added to 100 ml of water. The benzene layer was separated and the aqueous layer extracted with ether. The benzene layer and the ether extracts were combined and evaporated *in vacuo*. The residual oil was chromatographed on a column of 90 g of silica gel with 2% of ether in petroleum ether as solvent. The product obtained from the column was rechromatographed on a column of 30 g of silica gel impregnated with 20% of silver nitrate. Elution of the column with 1% of ether in petroleum ether and crystallization of the product from the column from pentane afforded 675 mg (80%) of **15**, m.p. 66°; ν_{max} 3030–3000, 2000–1600, and 800–680 (multiple bands, aromatic), and 1647 cm^{-1} (olefin); n.m.r. ($CDCl_3$), δ 0.81, 0.86 and 1.12 (s, 3H each, tertiary methyls), 3.57 (m, 1H, H—C—O), 4.47 (s, 2H, benzylic methylene), 5.55 (m, 1H, vinylic proton), 7.30 (m, 5H, aromatic protons).

Anal. Calcd. for $C_{27}H_{38}O$: C, 85.66; H, 10.12. Found: C, 85.56; H, 10.21.

Benzyl Ether Alcohol ***16***

A solution of 145 mg of **15** in 3 ml of tetrahydrofuran under a nitrogen atmosphere was treated, while cooled on an ice bath, with 0.8 ml of a 1 *M* tetrahydrofuran solution of borane. The reaction solution was allowed to warm to room temperature and left under nitrogen for 16 h. After the addition of 0.6 ml of water the reaction solution was treated with 1.5 ml of 3 *M* sodium hydroxide followed by 1.5 ml of 30% hydrogen peroxide solution. The reaction solution was stirred at 40° for 45 min. The product was extracted into ether and the extracts were worked-up with brine in the usual manner. Purification of the product by t.l.c. on silica gel with ether – petroleum ether (1:1) as solvent followed by crystallization from pentane afforded 88 mg (68%) of **16**, m.p. 54–56°; ν_{max} (Nujol) 3450 cm^{-1} (OH); n.m.r. ($CDCl_3$), δ 0.83, 0.85, and 1.10 (s, 3H each, tertiary methyls), 1.11 (d, J = 6.5 Hz, 3H, secondary methyl), 2.75 (d, J = 3 Hz, 1H, H—C—OH), δ 3.68 (m, 1H, H—C—O), 4.48 (s, 2H, benzylic protons), 7.30 (m, 5H, aromatic protons).

Anal. Calcd. for $C_{27}H_{40}O_2$: C, 81.76; H, 10.17. Found: C, 81.82; H, 10.61.

Keto Benzyl Ether ***17***

A solution of 135 mg of **16** in 2.1 ml of pyridine was added to a mixture of 215 mg of chromic anhydride in 2.1 ml of pyridine. The mixture was stirred in the dark at room temperature for 4 h. The pyridine was evaporated *in vacuo*, the residue suspended in water, and the product extracted into ether. The extracts were worked-up in the usual manner with brine. Purification of the oily product by t.l.c. on silica gel with ether – petroleum ether (1:3) as solvent followed by crystallization from petroleum afforded 90 mg (67%) of **17**, m.p. 80–81°; ν_{max} (Nujol) 1710 cm^{-1} (ketone); n.m.r. ($CDCl_3$), δ 0.83 (s, 6H, superimposed signals for two tertiary methyls), 1.17 (s, 3H, tertiary methyl), 1.20 (d, J = 6.5 Hz, 3H, secondary methyl), 3.68 (m, 1H, H—C—O), 4.47 (s, 2H, benzylic protons), 7.28 (m, 5H, aromatic protons).

Anal. Calcd. for $C_{27}H_{38}O_2$: C, 82.18; H, 9.71. Found: C, 82.35; H, 9.80.

Keto Alcohol ***18***

The keto benzyl ether **17** (70 mg) in 25 ml of methanol was hydrogenated at atmospheric pressure over 35 mg of palladium–charcoal catalyst (10% Pd) for 1 h. Removal of the catalyst by filtration, evaporation of the solvent *in vacuo* and crystallization of the residue from petroleum ether afforded 41 mg (76%) of **18**, m.p. 158°; ν_{max} (Nujol) 3460 (OH) and 1690 cm^{-1} (ketone); n.m.r. ($CDCl_3$), δ 0.85 (s, 6H, superimposed signals for two tertiary methyls), 1.17 (s, 3H, tertiary methyl), 1.20 (d, J = 6.5 Hz, 3H, secondary methyl), 4.07 (m, 1H, H—C—OH).

Anal. Calcd. for $C_{20}H_{32}O_2$: C, 78.89; H, 10.60. Found: C, 79.16; H, 10.75.

Cyclopropyl Ketone ***20***

A solution of 116 mg of **18** in 3.5 ml of pyridine was treated with 270 mg of *p*-toluenesulfonyl chloride and left at room temperature for 3 days. After the addition of 25 ml of ice-water, the reaction solution was stirred on an ice bath for 20 min. The product was extracted into ether and worked-up in the usual manner with cold 2 *M* hydrochloric acid and brine. The crystalline tosylate (**19**, 170 mg) was used without further purification for the next step.

The following reaction was carried out in a dry nitrogen atmosphere. The tosylate (170 mg), suspended in 5 ml of dry dimethyl sulfoxide, was treated with 1.1 ml of a 0.5 *M* dimethyl sulfoxide solution of methylsulfinyl carbanion (11). The mixture was heated, with stirring, at 60° whereupon the tosylate dissolved within a few minutes and heating was continued for 2 h. After cooling, the reaction solution was treated with 0.5 ml of water and diluted with ether. The ether solution was worked-up in the usual manner with brine and water. Purification of the product by t.l.c. on silica gel with ether – petroleum ether (1:3) as solvent followed by crystallization from petroleum ether afforded 54 mg (52%) of **20**, m.p. 85°; λ_{max} (EtOH) 209 nm (ε 3800); ν_{max} (Nujol) 1720 cm^{-1} (ketone); n.m.r. (CCl_4), *ca.* δ 0.60 (m, 2H, protons on cyclopropane ring), 0.81, 0.86, 1.03, and 1.06 (s, 3H each, tertiary methyls).

Mol. Wt. Calcd. for $C_{20}H_{30}O$: 286. Found (mass spectrum): 286.

(±)-Trachylobane ***1***

The reduction of **20** to trachylobane (**1**) was carried out in a dry nitrogen atmosphere as follows (*cf.* 12, 7). A solution of 52 mg of **20** in 6 ml of a stock solution prepared by dissolving 690 mg of sodium in 60 ml of diethylene glycol was treated with 0.4 ml of anhydrous hydrazine (12) and immersed in an oil bath at 210°. More anhydrous hydrazine (*ca.* 0.8 ml) was added until the reaction solution was refluxing freely and the temperature of the solution was 180°; the solution was allowed to reflux at this temperature for 14 h then an additional 1 ml of anhydrous hydrazine was added and reflux was continued for 1 h. Hydrazine was distilled from the reaction flask until the temperature of the solution reached 210°. After keeping the reaction solution at 210° for 24 h, it was cooled, diluted with ether and worked-up in the usual manner with cold 1 *M* hydrochloric acid, 1 *M* sodium carbonate, and brine. Purification of the product by t.l.c. on silica gel with pentane as solvent afforded 28 mg (56%) of **1** as an oil which gave rise to a single peak on v.p.c. with a retention time of 17.0 min (column temperature programmed from 94° to 250° at 10°/min), i.r., devoid of carbonyl absorption; n.m.r. ($CDCl_3$) δ 0.65 (m, 2H, protons on cyclopropane ring), 0.80, 0.83, 0.94, 1.13 (s, 3H each, tertiary methyls).

Anal. Calcd. for $C_{20}H_{32}$: C, 88.16; H, 11.84. Found: C, 88.35; H, 11.93.

The synthetic hydrocarbon **1** was identical with an authentic sample of trachylobane obtained from natural sources (i.r. and n.m.r. spectra, a single peak on v.p.c. when coinjected with the authentic sample).

We are grateful to the National Research Council of Canada for a grant in support of this work.

We are also grateful to Professors A. G. González and B. M. Fraga, Universidad de la Laguna, Tenerife, Spain, for a sample of trachylobane, to Professor J. St. Pyrek, Polska Akademia Nauk, Warsaw, for a sample of trachylobane and n.m.r. spectra of trachylobane and to Professor G. Ourisson, Université Louis Pasteur, Strasbourg, France, for an n.m.r. spectrum of trachylobane.

1. A. G. González, J. L. Bretón, B. M. Fraga, and J. G. Luis. Tetrahedron Lett. 3097 (1971).
2. (*a*) G. Hugel, L. Lods, J. M. Mellor, D. W. Theobald, and G. Ourisson. Bull. Soc. Chim. Fr. 2882 (1965); (*b*) G. Hugel, L. Lods, J. M. Mellor, D. W. Theobald, and G. Ourisson. Bull. Soc. Chim. Fr. 2888 (1965); (*c*) G. Hugel, L. Lods, J. M. Mellor, and G. Ourisson. Bull. Soc. Chim. Fr. 2894 (1965).
3. (*a*) J. St. Pyrek. Tetrahedron, **26**, 5029 (1970); (*b*) L. F. Bjeldanes and T. A. Geissman. Phytochemistry, **11**, 327 (1972).
4. E. Wenkert. Chem. and Ind. 282 (1955).
5. (*a*) R. A. Appleton, A. J. McAlees, A. McCormick, R. McCrindle, and R. D. H. Murray. J. Chem. Soc. C, 2319 (1966); (*b*) R. R. Sobti and S. Dev. Tetrahedron Lett. 3939 (1966).
6. References cited in ref. 7.
7. R. B. Kelly, J. Zamecnik, and B. A. Beckett. Can. J. Chem. **50**, 3455 (1972).
8. R. F. Church, R. E. Ireland, and J. A. Marshall. J. Org. Chem. **31**, 2526 (1966).
9. K. Bowden, I. M. Heilbron, E. R. H. Jones, and B. C. L. Weedon. J. Chem. Soc. 39 (1946).
10. G. I. Poos, G. E. Arth, R. E. Beyler, and L. H. Sarett. J. Am. Chem. Soc. **75**, 422 (1953).
11. E. J. Corey and M. Chaykovsky. J. Am. Chem. Soc. **87**, 1345 (1965).
12. D. H. R. Barton, D. A. Ives, and B. R. Thomas. J. Chem. Soc. 2056 (1955).

Can. J. Chem. Downloaded from www.nrcresearchpress.com by 210.87.254.42 on 09/05/12
For personal use only.

Determination of the Basicities of a Series of Substituted Benzyldimethylamines in 50% Aqueous Methanol

DONALD G. LEE AND R. SRINIVASAN

Department of Chemistry, University of Saskatchewan Regina Campus, Regina, Saskatchewan

Received June 28, 1972

The basicities of a series of substituted benzyldimethylamines have been determined potentiometrically in 50% (by weight) aqueous methanol. An excellent Hammett correlation ($\rho = -1.38$) is obtained. The larger value of ρ in aqueous methanol as compared to water (-1.14) is interpreted in terms of a greater capability of water to solvate ammonium ions, thus suppressing the stabilizing or destabilizing effect of ring substituents.

Les basicités d'une série de benzyldiméthylamines substituées ont été déterminées par potentiométrie dans le méthanol aqueux à 50% en poids. Une excellente corrélation de Hammett ($\rho = -1.38$) a été obtenue. La valeur plus élevée de ρ dans le méthanol aqueux comparée à celle déterminée dans l'eau (-1.14) a été interprétée par une capacité plus grande de solvatation des ions ammoniums par l'eau supprimant ainsi l'effet stabilisateur ou déstabilisateur des substituants du cycle. [Traduit par le journal]

Can. J. Chem., **51**, 2542 (1973)

Introduction

A knowledge of the acid–base properties of a substrate is essential to a complete understanding of any reaction which is subject to acid catalysis or inhibition. Hence before undertaking a study of such a reaction it is necessary to first determine the basicity constants of the reactants. Consequently we have determined the pK_{BH^+} values (as defined by eq. 1) of several substituted benzyldimethylamines in connection with a study of the oxidation of tertiary amines by bromine (1).

[1] 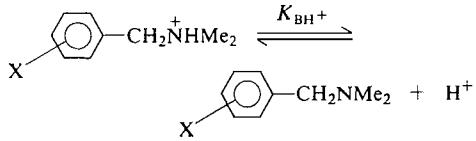

The recent development of standard buffers for aqueous alcohol solvents (2) permitted the use of potentiometric methods in 50% (by weight) aqueous methanol. This solvent was chosen because its *Y*-value (3) corresponds closely to that of the medium in which the oxidation reaction was studied (1).

Experimental

Reagents, Solvents, and Buffers

The solvent (50% aqueous methanol by weight) was prepared by mixing 63.3 ml of spectroquality methanol (MC/B) with 50 ml of water which had been purified by distillation from an all glass Corning AG-3 still.

Benzyldimethylamine, supplied by the Aldrich Chemical Co., was purified by distillation to give a colorless liquid, b.p. 74–75°/15 mm (lit. b.p. 73–74°/15 mm) (4). All other amines were purified by distillation just prior to use and the purity was checked by g.l.c. using a 30 ft column packed with the detergent, Tide.

Standardization of the p*H* meter was accomplished using the procedure of the National Bureau of Standards (5). For this purpose two buffer solutions were prepared as follows: (*i*) 0.2722 g of KH_2PO_4, 0.5359 g Na_2HPO_4-$7H_2O$, and 0.1169 g of NaCl in 1000 g of solvent (p*H* 8.232 at 25°); (*ii*) 0.3003 g of acetic acid, 0.6804 g of NaOAc $3H_2O$ and 0.2922 g of NaCl in 1000 g of solvent (p*H* 5.591 at 25 °C).

The p*H* meter, which utilized a glass and a calomel electrode, was standardized at a p*H* of 8.232 with the phosphate buffer thermostated at 25.0 ± 0.1° in a constant temperature cell. The p*H* of the acetate buffer solution was measured as 5.620, which is in reasonably good agreement with the reported value of 5.591 in this solvent (5).

Determination of pK_{BH^+} Values

The pK_{BH^+} values for the substituted benzyldimethylamines were determined at 25.0 ± 0.1° using a standard experimental procedure (6).

In a typical potentiometric titration, 20 ml of the amine solution in 50% aqueous methanol (*ca.* 0.01 *M*) was placed in a cell thermostated at 25.0 ± 0.1° and covered with aluminum foil to minimize evaporation of methanol. Portions ranging from 0.01 to 0.05 ml of perchloric acid in 50% aqueous methanol (*ca.* 0.20 *M*) were added from a microliter syringe, the solution being stirred well after each addition, and the p*H* was recorded. The titration was carried out over a p*H* range not less than two units on either side of the pK_{BH^+} value of the amine. The entire process of adding the titrant and recording the p*H* reading was repeated with a solution of KOH in 50% aqueous methanol (*ca.* 0.20 *M*) in a similar fashion. Corrections were made for the slight dilution involved in this

Can. J. Chem. Downloaded from www.nrcresearchpress.com by 210.87.254.6 on 09/05/12
For personal use only.

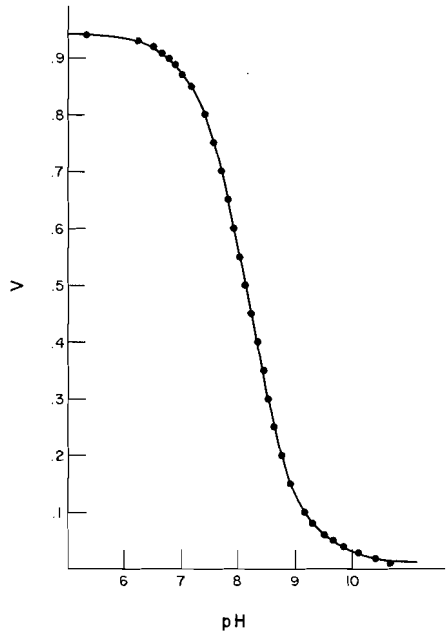

FIG. 1. Curve for the titration of benzyldimethylamine with dilute perchloric acid. The solid line is the theoretical curve; the closed circles are experimental points.

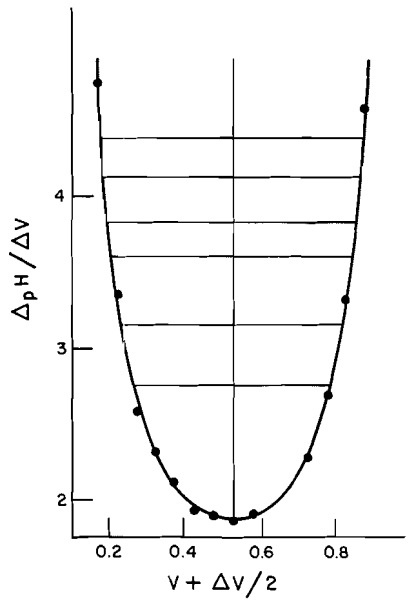

FIG. 2. Parabolic curve used for estimating the pK_{BH^+} of benzyldimethylamine.

process (6) and plots of titer (V) *vs.* pH for both acid and base titrations were found to give sigmoidal curves (Fig. 1). The pH value at the inflection point of each sigmoidal curve refers to the pK_{BH+} value of the amine. A differential method was adopted to estimate the inflection point. A plot of the ratio $\Delta pH/\Delta V$ *vs.* $V + \Delta V/2$ (the mid-point of the titer added) gave, as expected, a symmetric parabola (Fig. 2). The $V + \Delta V/2$ value through which the axis of symmetry of the parabola passes, would give the volume of titrant at which the amine is half protonated and the corresponding pH value, read from the sigmoidal curve, represents the approximate pH_{BH+} value of the amine. This value was then adjusted by use of a curve-fitting technique until the theoretical and experimental curves matched. The required adjustments were not great (usually about ± 0.02 pH units).

It was assumed that the pK_{BH+} values of the amines are insensitive to the small changes in ionic strength accompanying the titration. The activity coefficients of the species involved in the equilibrium were also assumed to be unity since the concentrations of the amines were small (*ca.* 0.01 M).

Syntheses of Substituted Benzyldimethylamines

The substituted benzyldimethylamines were prepared by a modification of the procedure described by Eliel *et al.* (7). As a typical example the synthesis of *p*-chlorobenzyldimethylamine is described in detail below and the results for other substituted benzyldimethylamines are summarized in Table 1.

Benzene (120 ml) was cooled in ice to the freezing point and gaseous dimethylamine was passed through it until 38.7 g (0.86 mol) had been absorbed. Gradual addition of a solution of *p*-chlorobenzyl chloride (33.81 g, 0.21 mol) in benzene (150 ml) to the stirred amine solution resulted in the precipitation of a white solid. This mixture was allowed to stand at room temperature for 4 days in a well stoppered flask. Then about 6 N hydrochloric acid (200 ml) was added gradually with constant stirring, whereupon two layers separated. The aqueous layer was washed with ether to remove traces of benzene and neutralized with a solution of KOH, the reaction flask being immersed in cold water during the addition of base. When the solution was distinctly basic, an oily layer separated. The latter was extracted into ether and the ethereal solution dried over anhydrous $MgSO_4$. Evaporation of the solvent then gave crude *p*-chlorobenzyldimethylamine which was purified by vacuum distillation (b.p. 87.5–88.5°/9 mm; lit. b.p. 90–95°/9–11 mm) (7) to give 26 g (73%) of colorless liquid which was shown to be a single pure compound by use of g.l.c.

For the purposes of analysis the amine was then converted to the solid hydrobromide derivative using the following procedure (8).

The amine (17 g, 0.1 mol) was dissolved in ether (250 ml) and HBr gas was passed through the solution at room temperature. The HBr gas was generated by dropwise addition of bromine to stirred dry tetrahydronaphthalene at 25° (9). The HBr gas was purified from traces of bromine by passing it through tetrahydronaphthalene and dried by passing it over silica gel. The colorless crystalline *p*-chlorobenzyldimethylamine hydrobromide, obtained in quantitative yields, was crystallized several times from ethanol–ether solutions (m.p. 198–199°) and identified from the analytical data reported in Table 2.

m-Methylbenzyl chloride was obtained from K & K Laboratories, Inc., while *p*-cyanobenzyl bromide and

Can. J. Chem. Downloaded from www.nrcresearchpress.com by 210.87.254.6 on 09/05/12
For personal use only.

TABLE 1. Analytical data for identification of the substituted benzyldimethylamines*

Substituent	Yield (%)	Boiling point† (°C/mm)	Melting point of hydrobromide (°C)	Elemental analysis‡ (%)
H	§	74–75/15 (73–74/15 (4))	144–145	C, 50.53(50.01) H, 6.51(6.53)
p-Cl	73	87.5–88.5/9 (90–95/9–11 (7))	198–199	C, 43.29(43.14) H, 5.16(5.23)
p-Br	98	109/11–12	209–210	C, 36.29(36.64) H, 4.41(4.44)
m-CH_3	79	83/14	189–190	C, 52.06(52.17) H, 6.95(7.00)
p-CH_3	82	94–95/23	174–175	C, 52.18(52.17) H, 7.04(7.00)
p-NO_2	76	142–146/12–14 (140–146/13–14 (7))	177–178	C, 41.40(41.40) H, 5.19(5.02)
p-CN	71	102–103/3	255–256	C, 49.65(49.81) H, 5.48(5.43)
m-CN	70	84–85/1.9	208–209	C, 50.77(49.81) H, 5.67(5.43)
m-F	68	66–67/10	187–188	C, 46.13(46.18) H, 5.58(5.60)
p-F	97	58–59/8.7 (61–62/6.5 mm (10))	177–178	C, 46.33(46.18) H, 5.74(5.60)
m-Cl	99		200–202	C, 42.90(43.12) H, 5.15(5.23)

*The n.m.r. spectrum was found to be consistent with the assigned structure in each case.
†Literature values in parentheses.
‡Elemental analysis was done by Chemalytics, Tempe, Arizona. Calculated values in parentheses.
§Obtained from the Aldrich Chemical Company.

p-methylbenzyl bromide were purchased from Pfaltz & Bauer, Inc. The remaining substituted benzyl halides used were supplied by Aldrich Chemical Co., Inc. Dimethylamine gas was obtained from Matheson of Canada Ltd.

Results and Discussion

The pK_{BH^+} values obtained as described above have been summarized in Table 2. For comparison purposes the values previously obtained in aqueous solutions have been included in Table 2. It should be noted, however, that the pK_{BH^+} values reported here refer to a particular standard state (50% aqueous methanol) and while they may be used to indicate relative basicities they cannot be extrapolated directly to any other standard state.

The Hammett plot shown in Fig. 3 gives a ρ value of -1.38 (11). It is of interest to compare this value with that reported by Rosenblatt *et al.* (12) for the same reaction in water, $\rho = -1.14$. The larger value of ρ obtained with the former solvent reflects the greater solvating abilities of water as compared to methanol. Since water is more capable of solvating ammonium ions the stabilizing or destabilizing influence of ring substituents is suppressed in an aqueous medium.

TABLE 2. pK_{BH^+} values of substituted benzyldimethylamines in 50% aqueous methanol at 25.0 ± 0.1 °C

Substituent	Acid titration	Base titration	Average	Value in* aqueous solutions
p-Me	8.31	8.35	8.33	9.22
m-Me	8.22	8.32	8.27	
H	8.17	8.23	8.20	9.03
p-F	7.92	8.00	7.96	8.94
p-Br	7.73	7.78	7.76	
m-F	7.70	7.75	7.73	
m-Cl	7.67	7.62	7.65	8.67
p-Cl	7.79	7.80	7.80	8.83
m-CN	7.25	7.27	7.26	
p-CN	7.16	7.20	7.18	
p-NO_2	7.04	7.09	7.07	8.14

*Taken from ref. 12.

Can. J. Chem. Downloaded from www.nrcresearchpress.com by 210.87.254.6 on 09/05/12
For personal use only.

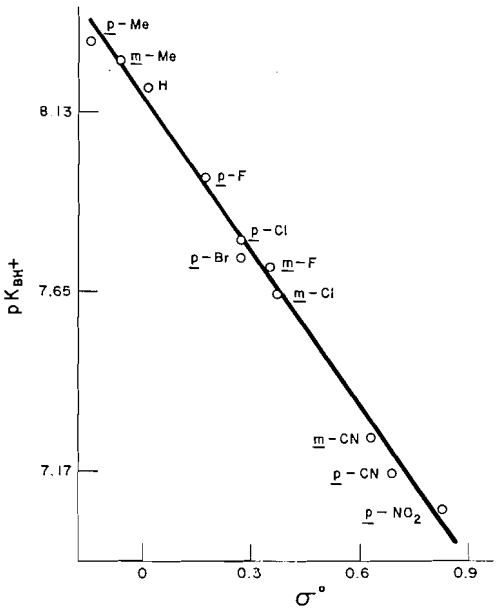

FIG. 3. Hammett plot correlating the pK_{BH^+} values of substituted benzyldimethylamines.

Good Hammett plots were obtained when either σ or σ° substituent constants were used; the correlation coefficients being 0.991 and 0.997 respectively (13). When attempts were made to use other substituent constants (*e.g.* σ^+ and σ^-) much lower correlation coefficients were obtained. Hence it would appear that the methylene group effectively isolates the ring from direct conjugation with the nitrogen.

The authors are grateful to the National Research Council of Canada for support for this work and one of us (R.S.) is pleased to acknowledge the receipt of a scholarship (1968–1971) from the Saskatchewan Research Council.

1. D. G. LEE and R. SRINIVASAN. Can. J. Chem. This issue. Following article.
2. R. G. BATES. The chemistry of nonaqueous solvents. Vol. I. *Edited by* J. J. Lagowsky. Academic Press, New York and London. 1966. Chapt. 3.
3. E. GRUNWALD and S. WINSTEIN. J. Am. Chem. Soc. **70**, 846 (1948); A. H. FAINBERG and S. WINSTEIN. J. Am. Chem. Soc. **79**, 1597, 1602, 1608 (1957); S. WINSTEIN, A. H. FAINBERG, and E. GRUNWALD. J. Am. Chem. Soc. **79**, 4146 (1957).
4. R. C. WEAST. Editor. Handbook of chemistry and physics. 49th Ed. The Chemical Rubber Co., Cleveland, Ohio. 1968. p. C-576.
5. M. PAABO, R. A. ROBINSON, R. G. BATES. J. Am. Chem. Soc. **87**, 415 (1965).
6. A. ALBERT and E. P. SERJEANT. Ionization constants of acids and bases. Methuen and Co. Ltd., London. 1962. Chapt. 2.
7. E. L. ELIEL, T. N. FERDINAND, and M. C. HERMANN. J. Org. Chem. **19**, 1693 (1954).
8. W. J. HICKINBOTTOM. Reactions of organic compounds. 3rd Ed. Longmans, New York. 1957. p. 401.
9. D. R. DUNCAN. *In* Inorganic synthesis. Vol. I. *Edited by* H. C. Booth. McGraw-Hill Book Company, New York. 1939. p. 151.
10. F. N. JONES and C. R. HAUSER. J. Org. Chem. **27**, 4020 (1962).
11. L. P. HAMMETT. Physical organic chemistry. McGraw-Hill, New York. 1970. Chapt. 11.
12. D. H. ROSENBLATT, L. A. HULL, D. C. DELUCA, G. T. DAVIS, R. C. WEGLEIN, and H. K. R. WILLIAMS. J. Am. Chem. Soc. **89**, 1158 (1967).
13. D. V. HUNTSBERGER. Elements of statistical inference. Allyn and Bacon, Inc., Boston. 1965.

Can. J. Chem. Downloaded from www.nrcresearchpress.com by 210.87.254.6 on 09/05/12
For personal use only.

The Oxidation of Benzyldimethylamine by Bromine

DONALD G. LEE AND R. SRINIVASAN

Department of Chemistry, University of Saskatchewan, Regina Campus, Regina, Saskatchewan

Received June 28, 1972

The rates of oxidation of several substituted benzyldimethylamines by bromine in 50% aqueous acetic acid have been determined spectrophotometrically. Electron-withdrawing substituents decrease the rate of reaction with the Hammett ρ value being -0.95. The reaction is subject to general base catalysis and substitution of deuterium in the α-position decreases the rate of reaction by approximately 30%, thus indicating that the α-C—H bond is cleaved in the slow step of the reaction. All results are consistent with a mechanism which involves, in the rate determining step, loss of an α-hydrogen atom as a proton with concomitant transfer of electrons from nitrogen to the oxidant.

Les vitesses d'oxydation de plusieurs benzyldiméthylamines substituées par le brome dans l'acide acétique à 50% aqueux, ont été déterminées par spectrophotométrie. Les substituants électroattracteurs diminuent la vitesse de réactions avec une constante de Hammett de -0.95. La réaction est sujette à une catalyse basique généralisée et la substitution par le deutérium sur la position α diminue la vitesse de la réaction de 30% environ, indiquant ainsi que la liaison α-C—H est rompue dans l'étape lente de la réaction. Tous les résultats sont compatibles avec un mécanisme impliquant dans l'étape déterminante de vitesse la perte d'un atome d'hydrogène-α en tant que proton et le transfert compétitif d'électrons de l'azote à l'oxydant. [Traduit par le journal]

Can. J. Chem., 51, 2546 (1973)

Introduction

The oxidation of amines by halogens has a long history dating from 1900 when Wilstatter and Iglauer (1) treated *N*-methyl alkaloids with aqueous chlorine and found that tropidine, tropane, and *N*-methylpiperidine were demethylated. Later, when trimethylamine was cleaved by aqueous chlorine, *N*-chlorodimethylamine and formaldehyde were found to be the major products (2).

The oxidative cleavage of tertiary amines by aqueous bromine has recently been studied by Deno and Fruit (3) primarily to explore the synthetic potential of this reaction. From a limited study of the reaction mechanism they proposed that the slow step involved loss of an α-hydrogen as a proton and the abstraction of the lone pair of electrons on nitrogen by bromine. The synthetic utility and limitations of the oxidation of tertiary amines by aqueous bromine have also been discussed by these authors. This reaction has the advantage of simplicity of reagents and reaction conditions. In addition yields are generally very good and the reaction was also found to be rapid for those amines studied. Furthermore, the inertness of amides towards aqueous bromine affords a means of protecting and reforming primary and secondary amines. On the other hand the reaction suffers from the disadvantages of poor selectivity with unsymmetrical amines, competing bromination of aromatic rings, particularly the alkoxy-substituted aromatics so prevalent in alkaloids, and bromine addition to unsaturated systems.

In view of the synthetic usefulness of this oxidative process we have undertaken an investigation of the reaction mechanism. An understanding of the mechanism, apart from being interesting in its own right, often provides control and flexibility in its synthetic applications. Furthermore, it was anticipated that a study of the mechanism would complement the work of Deno and Fruit (3) and as a result, the reaction would become more attractive for synthetic and degradative purposes.

Experimental

Solvents and Reagents

Reagent grade acetic acid, supplied by the Fisher Scientific Company, was used without further purification since it was observed to be resistant to oxidation by bromine under the conditions of these experiments. Bromine (Mallinckrodt analytical reagent grade) was also used directly without prior purification. The preparation and purification of the substituted benzyldimethylamines have been described in the preceding paper (4). Benzyldimethylamine-α,α-d_2 was obtained from Merck, Sharp and Dohme of Canada Ltd. Its chemical purity was verified by g.l.c. and its isotopic composition was confirmed by n.m.r.

Can. J. Chem. Downloaded from www.nrcresearchpress.com by 210.87.254.105 on 09/05/12
For personal use only.

Can. J. Chem. Downloaded from www.nrcresearchpress.com by 210.87.254.105 on 09/05/12
For personal use only.

Kinetic Methods

The rates of bromine oxidations can be estimated by following the reduction of Br_2 either iodometrically (3, 5, 6) or spectrophotometrically (7–9). The iodometric method is preferable since it can be used to follow the rate of the reaction in aqueous buffered media similar to those used for synthetic purposes. However, it was found that this method did not give adequate reproducibility when attempts were made to study the rate over a significant portion of the reaction. Previous workers who have used this method have been content to follow the rate during the initial 10% of the reaction (3); however, it is apparent that the results would be more meaningful if the rate of the reaction was followed for at least one half life. Consequently, an attempt was made to use a spectrophotometric method similar to the procedure which has been described for monitoring the rate of bromine substitutions (7).

The primary difficulty with the spectrophotometric method is associated with the fact that Br_3^-, which forms as the reaction proceeds, has a very strong absorption in the same region as Br_2. Consequently, the absorption band of Br_2 becomes obscured by the greater absorption of Br_3^- in buffered aqueous solutions. However, in mixed solvents such as 50% aqueous acetic acid, the absorption bands of Br_2 and Br_3^- intersect at 449 nm and the total amount of unreduced bromine (Br_2 plus Br_3^-) can be monitored at that particular wavelength (10). Hence, although 50% aqueous acetic acid is not the most common solvent for synthetic purposes it was used since more precise kinetic data could be obtained in this medium.

The absorption spectra of solutions of bromine (3.50×10^{-3} *M*) in 50% aqueous acetic acid with and without addition of potassium bromide were recorded and the point of intersection of the absorption curves of Br_2 and Br_3^- was found to remain constant at 449 nm. Furthermore the Br_2–Br_3^- system was found to follow Beer's law closely ($\varepsilon = 125.3$) between 5.07×10^{-3} and 1.78×10^{-3} *M*, the working kinetic range.

In a typical kinetic experiment solutions of the amine and bromine (the amine concentration being at least five times that of the bromine concentration) in 50% aqueous acetic acid were thermostated at 25.0 ± 0.1°. Then 2 ml of the amine solution and 1 ml of the bromine solution were added to a teflon-stoppered glass cuvette and a timer was started. After thoroughly mixing the solution by inverting the cuvette several times it was placed in the thermostated cell compartment of a Unicam SP500 Series 2 spectrophotometer and the absorbance at 449 nm was recorded at intervals using the amine solution in 50% aqueous acetic acid as the reference. A plot of ln (absorbance) against time was then prepared and the pseudo first-order rate constant calculated from the slope of the resulting straight line. For the first 50% of the reaction the deviations of the experimental points from the statistically best fit straight line were generally random; however when data up to 75% completion were analyzed, the pseudo first-order plots showed curvatures toward slower rates. This observation could be accounted for quantitatively by the formation of Br_3^- which is a less vigorous oxidant than Br_2 (11). A typical rate plot has been reproduced in Fig. 1.

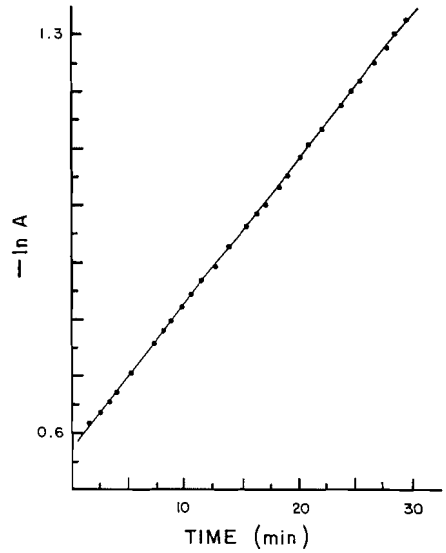

FIG. 1. Pseudo first-order rate plot.

Product Analysis

To a stirred solution of benzyldimethylamine (16.9 g, 0.125 mol) in 50% aqueous acetic acid (50 ml) at room temperature, bromine (4 g, 0.025 mol) in 50% aqueous acetic acid (75 ml) was added gradually. The solution was allowed to stand for about 3 h by which time the bromine had almost disappeared. The reaction mixture was added directly to 300 ml of 3 *M* hydrochloric acid containing 2,4-dinitrophenylhydrazine (9.90 g, 0.05 mol). The precipitated dinitrophenylhydrazone was filtered and dried to give 5.62 g (0.020 mol, 80%) of crude product (m.p. 228–232°). Crystallization from ethanol gave purified material (m.p. 235–236°; lit. m.p. 237° (12)), which was confirmed to be the 2,4-dinitrophenylhydrazone derivative of benzaldehyde from a mixed melting point measurement with an authentic sample.

Acidity Measurements

The acidities of solutions used in these experiments were measured by indicator procedures using *m*-nitroaniline and *p*-nitroaniline as indicators (13).

The pK_{BH^+} value for *m*-nitroaniline in 50% acetic acid was determined by use of eq. 1. The p*H* of the solution

$$[1] \qquad pK_{BH^+} = pH - \log([B]/[BH^+])$$

was changed by addition of variable amounts of 70% $HClO_4$ and the ratio $[B]/[BH^+]$ determined spectrophotometrically. The average pK_{BH^+} value calculated in this way was found to be 2.43 ± 0.03 in reasonable agreement with the value previously reported for this indicator in aqueous solutions of various mineral acids (13). Then by application of the indicator overlap technique (14) the pK_{BH^+} of *p*-nitroaniline was found to be 0.97, in excellent agreement with previous results (13). The H_0 values of 50% aqueous acetic acid solutions containing different concentrations of the amines which were used in kinetic experiments were then calculated from absorption measurements. The data obtained for the benzyldimethylamines are included in Table 1. From the data in this table it is quite apparent that the acidity of the medium is

TABLE 1. Pseudo first-order rate constants for the oxidation of substituted benzyldimethylamines by bromine in 50% acetic acid at 25.0 ± 0.1°

Substituent	Total amine concentration (M)	H_0	k_1(min^{-1})
H	0.243	3.26	2.57×10^{-2}
	0.194	3.24	1.81×10^{-2}
	0.155	3.17	1.18×10^{-2}
	0.116	3.12	7.99×10^{-3}
	0.0776	3.02	3.97×10^{-3}
	0.0605	2.98	2.75×10^{-3}
p-CN	0.190	3.21	4.71×10^{-2}
	0.152	3.14	3.04×10^{-2}
	0.122	3.12	2.17×10^{-2}
	0.0913	3.07	1.39×10^{-2}
	0.0609	2.98	7.36×10^{-3}
p-F	0.227	3.21	2.53×10^{-2}
	0.182	3.18	1.72×10^{-2}
	0.146	3.12	1.26×10^{-2}
	0.0909	3.00	5.78×10^{-3}
	0.0728	2.97	4.03×10^{-3}
	0.0567	2.91	2.88×10^{-3}
m-Me	0.234	3.27	2.79×10^{-2}
	0.188	3.22	1.91×10^{-2}
	0.150	3.14	1.30×10^{-2}
	0.113	3.09	8.10×10^{-3}
	0.0750	3.02	4.01×10^{-3}
	0.0585	2.96	2.65×10^{-3}
p-Cl	0.214	3.24	3.01×10^{-2}
	0.172	3.17	2.12×10^{-2}
	0.137	3.12	1.44×10^{-2}
	0.103	3.08	8.79×10^{-3}
	0.0686	2.98	4.60×10^{-3}
	0.0535	2.95	3.02×10^{-3}
m-Cl	0.213	3.23	3.73×10^{-2}
	0.171	3.19	2.55×10^{-2}
	0.137	3.16	1.76×10^{-2}
	0.102	3.07	1.11×10^{-2}
	0.0682	2.98	5.47×10^{-3}
p-Me	0.282	3.28	3.25×10^{-2}
	0.226	3.25	2.24×10^{-2}
	0.181	3.21	1.52×10^{-2}
	0.136	3.14	9.52×10^{-3}
	0.0903	3.07	4.70×10^{-3}
	0.0705	3.02	3.21×10^{-3}
m-F	0.219	3.21	3.09×10^{-2}
	0.175	3.18	2.18×10^{-2}
	0.140	3.12	1.52×10^{-2}
	0.150	3.08	9.40×10^{-3}
	0.0699	2.99	4.87×10^{-3}
	0.0545	2.94	3.25×10^{-3}
m-CN	0.196	3.16	4.62×10^{-2}
	0.157	3.14	3.17×10^{-2}
	0.125	3.10	2.26×10^{-2}
	0.0940	3.03	1.47×10^{-2}
	0.0620	2.96	7.36×10^{-3}
p-Br	0.212	3.23	3.06×10^{-2}
	0.170	3.18	2.23×10^{-2}
	0.127	3.10	1.40×10^{-2}
	0.106	3.07	9.53×10^{-3}
	0.0849	3.00	6.91×10^{-3}
	0.0637	2.95	4.45×10^{-3}
	0.0425	2.85	2.33×10^{-3}

dependent on the amount of amine present and that this fact must be taken into consideration in any quantitative treatment of the reaction kinetics.

Results

Since the oxidation of benzyldimethylamine was found to give benzaldehyde as the principal organic product (in agreement with the results obtained by Deno and Fruit (3) in an aqueous buffered medium) it is probable that the stoichiometry in both solvents can be represented by eq. 2. Furthermore it is to be expected that

$$[2]\quad RCH_2NR'R'' + Br_2 + H_2O \rightarrow RCHO + R'R''NH + 2HBr$$

the gross features of the reaction mechanism will be similar in the two solvent systems. However, it is not unlikely that some of the details may change significantly; for example, it is quite probable that the same rate law would pertain in both solvents, but it would be surprising if identical Hammett "ρ" and Brønsted "β" constants were obtained.

A logical starting point in the study of any reaction mechanism is to obtain the empirical rate law for the process. This was done by determining the order of the reaction with respect to each of the reactants. The results, obtained by varying the concentration of oxidant and reductant, indicated that the reaction was first order in bromine (Fig. 2) but that the order with respect to amine was slightly greater than unity (Fig. 3).

Consequently the rate law for the reaction can be expressed in the form of eq. 3, and the pseudo

$$[3]\quad -d[Br_2]/dt = k_2[\text{Amine}]^{1.1}[Br_2]$$

first-order rate constants obtained when the reaction was studied in the presence of excess amine would be given by eqs. 4 and 5.

Can. J. Chem. Downloaded from www.nrcresearchpress.com by 210.87.254.105 on 09/05/12
For personal use only.

Can. J. Chem. Downloaded from www.nrcresearchpress.com by 210.87.254.105 on 09/05/12
For personal use only.

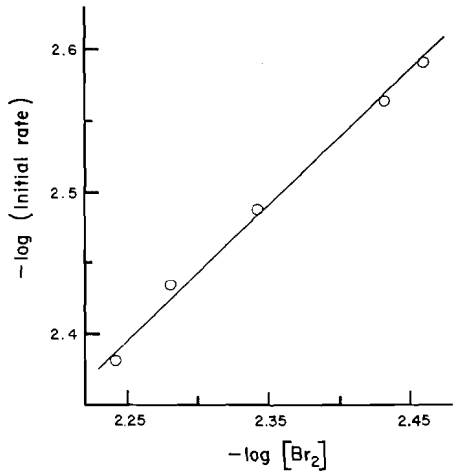

FIG. 2. Plot for determining the order with respect to bromine. Slope = 0.94 ± 0.06.

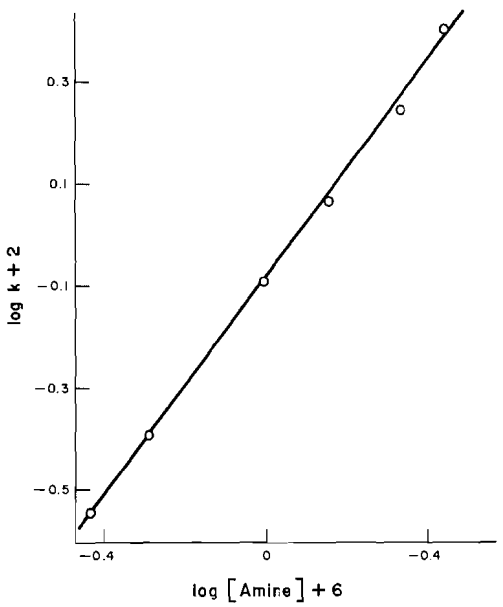

FIG. 3. Plot for determining the order with respect to benzyldimethylamine. Slope = 1.09 ± 0.02.

$$[4] \qquad -d[Br_2]/dt = k_1[Br_2]$$

$$[5] \qquad k_1 = k_2[\text{Amine}]^{1.1}$$

The decrease in rate of reaction associated with increasing acidity (Fig. 4) is undoubtedly due to a deactivating protonation of the amines which can be quantitatively accounted for if the pK_{BH^+} values for the amines are known. However because of the high acidity of 50% acetic

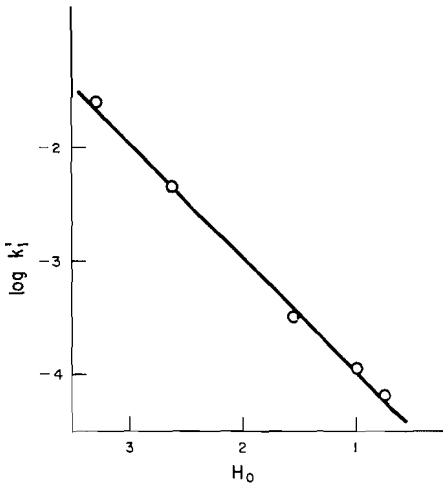

FIG. 4. Variation of rate with H_0.

acid accurate estimates of basicity constants cannot be obtained in this medium. Instead the pK_{BH^+} values were determined, as previously described (4), in 50% aqueous methanol. The necessity of changing to a different solvent system introduces the possibility of error in both the absolute and the relative rate constants for different amines. However an attempt to minimize such errors was made by using two solvents of similar *Y*-values (15), which can be expected to have similar solvating abilities. However, an understanding of the origin of *Y*-values makes it clear that two such solvent systems would have similar solvating properties with respect to carbonium ions, and not necessarily with respect to ammonium ions. Consequently this introduces a possible error into the ρ value that has been calculated by application of the Hammett equation (16) to the data in Table 1. However the error is not likely to be so large as to seriously affect the general conclusions that may be drawn.

The sign and magnitude of the ρ value and the correlation of rates with σ^0 substituent constants (and the lack of correlation with σ^+ constants) suggest that the amine fragment in the transition state is electron deficient compared to the ground state and that the electron deficiency is mostly on the nitrogen rather than on the benzylic carbon.

The reaction rate was found to be unaffected by light. No change in rate was observed when the reaction vessel was irradiated with a 250 W sunlamp. Hence, a free radical mechanism is probably not involved. Similar results were ob-

TABLE 2. Salt effects on the oxidation of benzyldimethylamine in 50% aqueous acetic acid*

Salt	[Salt](M)	H_0	k_1'(min^{-1})	$k_{1\,(adj)}$(min^{-1})†
Sodium chloride	0	3.17	1.14×10^{-2}	1.14×10^{-2}
	0.20	3.09	6.65×10^{-3}	8.00×10^{-3}
	0.40	3.03	4.28×10^{-3}	5.91×10^{-3}
	0.60	2.96	3.29×10^{-3}	5.34×10^{-3}
Sodium perchlorate	0.20	3.09	8.02×10^{-3}	9.64×10^{-3}
	0.40	3.05	6.63×10^{-3}	8.74×10^{-3}
	0.60	3.00	5.45×10^{-3}	8.06×10^{-3}
Sodium acetate	0.10	3.28	1.58×10^{-2}	1.23×10^{-2}
	0.15	3.28	1.72×10^{-2}	1.34×10^{-2}
	0.20	3.28	1.87×10^{-2}	1.55×10^{-2}
	0.40	3.34	2.53×10^{-2}	1.71×10^{-2}
Sodium benzoate	0.10	3.18	1.70×10^{-2}	1.66×10^{-2}
	0.20	3.21	2.13×10^{-2}	1.94×10^{-2}
	0.40	3.21	3.10×10^{-2}	2.85×10^{-2}

*[Total amine] = 0.155 M; [Br_2] = 5.36×10^{-3} M; temperature = 25.0 ± 0.1°.
†Rate constants adjusted to an H_0 of 3.17.

tained by Deno and Fruit (3) for the oxidation reaction in aqueous buffered medium.

That the reaction is subject to base catalysis was shown by studying the rates in the presence of several basic and non-basic salts. The results, which are presented in Table 2 and Fig. 5, clearly indicate that the rate is accelerated in the presence of sodium acetate and sodium benzoate, but slightly decreased in the presence of sodium chloride and sodium perchlorate. The acceleration caused by addition of acetate or benzoate ions is a clear indication of general base catalysis, whereas the decrease caused by the addition of chloride and perchlorate ions can be accounted for if one assumes that the transition state involves a significant participation by water. Addition of salts such as NaCl and $NaClO_4$ cause a decrease in the activity of water with the larger effect observed for chloride ion being in agreement with the known hydration properties of Cl^- and ClO_4^- (17). Similar trends attributed to the decrease in the activity of water accompanying the addition of these salts, have been reported in the literature (13, 18). For example, the effects of added salts on the kinetics of thallic ion oxidation of olefins in strongly acidic medium have also been explained in terms of the activity of water being altered by salts (19).

The addition of these salts to the solution alters its acidity. However, since the response of the rate to changes in acidity is known quantitatively it is possible to adjust all the rates to a common H_0 value. The adjusted rate constants are given in the last column of Table 2.

The observation of base catalysis also explains why the order with respect to amine is slightly greater than unity (Fig. 3). The amine in addition to being a reductant can also act as a base and thus increase the rate of reaction slightly.

The rate of oxidation of benzyldimethylamine-α,α-d_2 was found to be significantly slower than the rate of oxidation of the unlabelled compound under comparable conditions (Table 3). Rate decreases of this magnitude could be a reflection of either a secondary isotope effect (20) or a small primary isotope effect (21). A distinction between these two possibilities can be made by noting that the magnitude of the effect decreases by an amount well beyond the limits of experimental error when sodium acetate or sodium benzoate is added to the solution. Addition of these ions should cause no change in the magnitude of a secondary isotope effect, but could influence the primary effect if the rate determining step involved transfer of an α-proton to a base.

If the decrease in rate is due to a small primary isotope effect it follows from the theory elaborated by Westheimer (21) that the transition state must be extremely unsymmetrical with respect to transfer of the hydrogen to the base; *i.e.* either the carbon–hydrogen bond must be relatively intact *or* extensively cleaved in the transition state. If the former case were true adding more base would tend to make the transi-

Can. J. Chem. Downloaded from www.nrcresearchpress.com by 210.87.254.105 on 09/05/12
For personal use only.

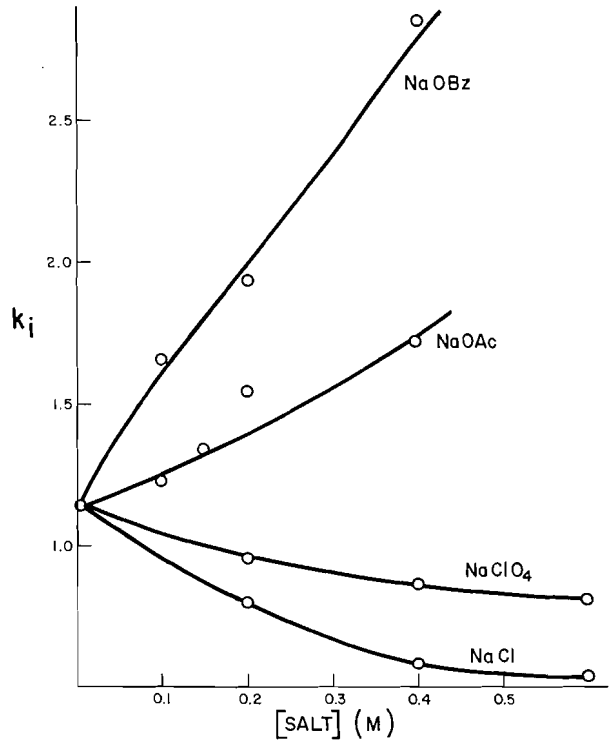

FIG. 5. Effect on rate of adding various salts.

TABLE 3. Isotope effects for the oxidation of benzyldimethylamine in 50% aqueous acetic acid

[Total amine] (M)	k_1(H) (min^{-1})	k_1(D) (min^{-1})	k_1(H)/k_1(D)
0.243	2.56×10^{-2}	1.90×10^{-2}	1.39 ± 0.04
	2.58×10^{-2}	1.86×10^{-2}	
		1.81×10^{-2}	
0.241	2.38×10^{-2}	1.74×10^{-2}	1.36 ± 0.01
	2.37×10^{-2}	1.76×10^{-2}	
0.176	1.43×10^{-2}	1.03×10^{-2}	1.38 ± 0.02
	1.43×10^{-2}	1.05×10^{-2}	
0.176	3.08×10^{-2}	2.54×10^{-2}	1.23 ± 0.02*
	3.11×10^{-2}	2.50×10^{-2}	
0.146	2.86×10^{-2}	2.39×10^{-2}	1.21 ± 0.03†
	2.98×10^{-2}	2.42×10^{-2}	

*[Sodium acetate] = 0.40 M.
†[Sodium benzoate] = 0.40 M.

tion state more symmetrical, and thus predict an increase in the magnitude of the isotope effect (in conflict with the experimental observations). On the other hand, if the proton was almost completely transferred to the base during the rate-limiting step, an increase in base concentration would tend to make the transition state even less symmetrical and thus reduce the magnitude of the isotope effect, in agreement with the data summarized in Table 3.

Hence the experimental results are most consistent with the suggestion that the diminution in rate which is observed on deuterium substitution is a consequence of a small primary isotope effect.

Discussion

The reaction mechanism is at least partially defined by the observations that the slow step involves cleavage of the α-carbon–hydrogen bond and that the transition state is electron deficient.

Carbon–hydrogen bond cleavage could be accomplished by either a homolytic or a heterolytic reaction. The possibility of a homolytic reaction is, however, eliminated by the observation that the rate is not changed on irradiation of the reaction vessel. Other free radical processes are known to be sensitive to light (22). Furthermore since the reaction rate correlates best with σ^0

Can. J. Chem. Downloaded from www.nrcresearchpress.com by 210.87.254.105 on 09/05/12
For personal use only.

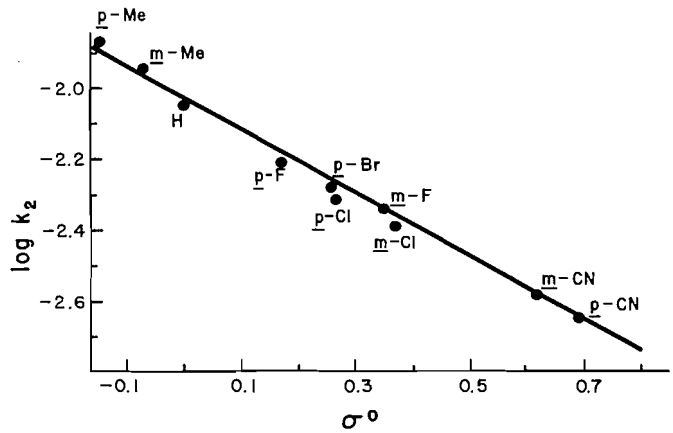

FIG. 6. Hammett plot for the oxidation of substituted benzyldimethylamines by bromine. [Amine] = 1.00×10^{-6}. Slope = -0.95 ± 0.04. Correlation coefficient = 0.99.

substituent constants affording a ρ value of −0.95, it also appears that a benzylic hydrogen is not abstracted as a hydride ion by bromine (Fig. 6). Such an abstraction would be expected to yield a much more negative ρ value. In reactions where considerable evidence for hydride transfer exists as in the oxidation of alcohols by bromine (23, 24) and the oxidation of amines by triphenylmethyl cation (3), ρ values of −2.29 and −2.0 were observed.

The negative ρ value also indicates that the rate determining step does not involve a simple loss of the α-hydrogen as a proton. Such a process would produce a negative charge on the transition state and the reaction would be expected to exhibit a positive ρ value. Loss of the α-hydrogen as a proton concomitant with electron transfer from the nitrogen to the oxidant is however, suggested by the experimental observations. In addition the small isotope effect is consistent with a transition state in which the α-carbon–hydrogen bond is extensively cleaved, and the observed base catalysis suggests that the hydrogen is transferred as a proton.

All of the results described herein are in quantitative agreement with the reaction sequence shown in Scheme 1.

This mechanism is also consistent with the previously reported product studies (3). For example, oxidation of dimethylpropylamine gave propanal as the main product, presumably because of the greater stability of intermediate **1** as compared to **2**. The former is a trisubstituted carbon–

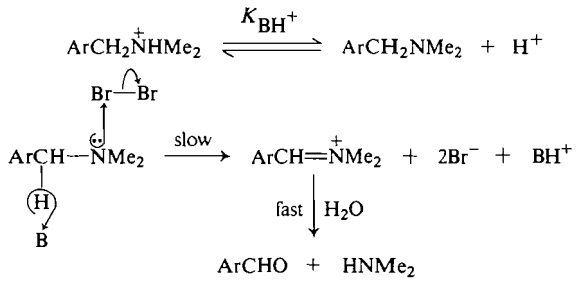

SCHEME 1

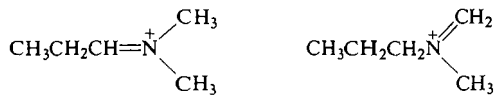

1 2

nitrogen double bond whereas the latter is only disubstituted. Similarly the oxidation of dipropylbenzylamine gives mainly benzaldehyde because **3** allows for direct conjugation of the carbon–nitrogen double bond with the aromatic ring whereas **4** does not.

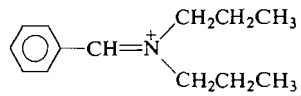

3

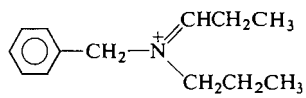

4

Can. J. Chem. Downloaded from www.nrcresearchpress.com by 210.87.254.105 on 09/05/12
For personal use only.

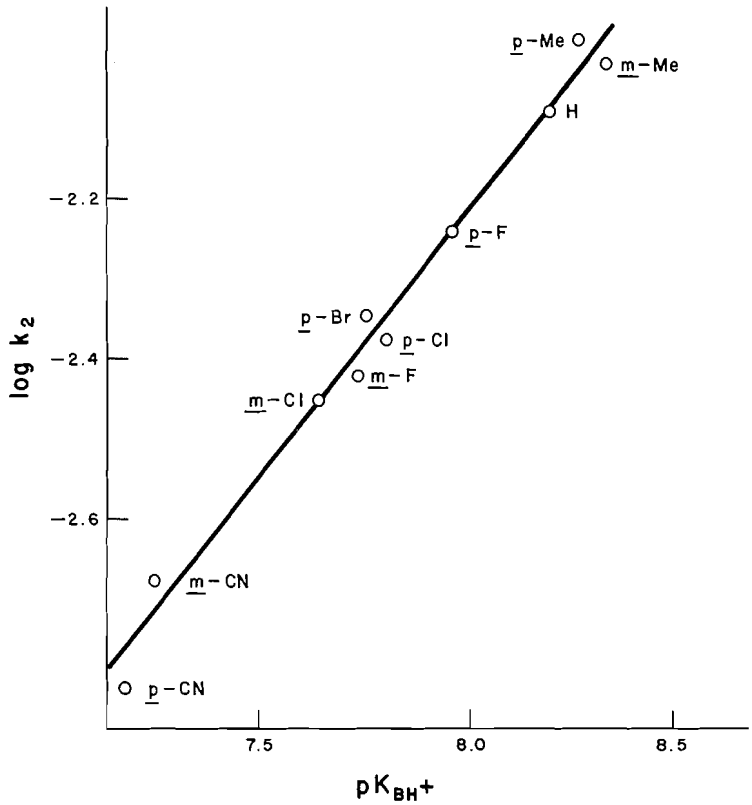

FIG. 7. Brønsted relationship between the rate of oxidation (in 50% aqueous acetic acid) and the basicity of substituted benzyldimethylamines (in 50% aqueous methanol). Slope = 0.67 ± 0.03. Correlation coefficient = 0.99.

The same reasoning also explains why the oxidation of benzyldimethylamine, which is described in this paper, gave benzaldehyde as the primary product, and it is significant to note that the yield of benzaldehyde increased from 52 to 70–80% on going from benzyldipropylamine to benzyldimethylamine.[1]

These observations also point out a difference between this reaction and the oxidation of the corresponding compounds by chlorine dioxide (25). The latter reaction, which is apparently initiated by a free radical abstraction results in preferential methyl cleavage during the oxidation of benzyldimethylamine.

Furthermore the Brønsted plot (Fig. 7) with $\alpha = +0.67$ indicates that there is a similarity between the transition state and the protonated amine (26). Had the substituent interactions on the protonation and oxidation reactions been identical a Brønsted slope of $\alpha = 1.00$ would have been expected. It is possible that the deviation from unity may be a solvent effect; however it should also be noted that an α of the magnitude observed in this work has been reported for other reactions where iminium ions have been proposed as intermediates (25).

The reaction also exhibits a steric effect; for example, oxidation diisopropyl – *n*-propylamine gives 50% propanal and only 21% acetone while benzylbis(1-methylbenzyl)amine gives 75% benzaldehyde and 5% acetophenone (3). It is possible

[1]It should be noted that the small primary isotope effect observed for this reaction may also be partially as a consequence of the fact that benzyldimethylamine can undergo cleavage of either the *N*-benzyl or the *N*-methyl bonds. Deuteration of the α-benzyl hydrogens would promote methyl cleavage and thus reduce the observed isotope effect.

Can. J. Chem. Downloaded from www.nrcresearchpress.com by 210.87.254.105 on 09/05/12
For personal use only.

to understand these results by noting that since the transition state also involves a base, which acts as a proton abstractor, disubstitution of the α-carbon would interfere with approach of base at that position.

The authors are grateful to the National Research Council of Canada for financial support of this work, and one of us (R.S.) is pleased to acknowledge the receipt of a scholarship (1968–1971) from the Saskatchewan Research Council.

1. R. WILSTATTER and F. IGLAUER. Ber. **33**, 1636 (1900).
2. A. HANTZSCH and W. GRAF. Ber. **38**, 2154 (1905).
3. N. C. DENO and R. E. FRUIT. J. Am. Chem. Soc. **90**, 3502 (1968).
4. D. G. LEE and R. SRINIVASAN. Can. J. Chem. This issue. Preceding article.
5. U. P. ZIMMERMAN and E. BERLINER. J. Am. Chem. Soc. **84**, 3953 (1962).
6. E. BERLINER and J. C. POWERS. J. Am. Chem. Soc. **83**, 905 (1961).
7. E. M. ARNETT and G. B. KLINGENSMITH. J. Am. Chem. Soc. **87**, 1023, 1032, 1038 (1965).
8. R. M. KEEFER, J. H. BLAKE, and L. J. ANDREWS. J. Am. Chem. Soc. **76**, 3062 (1954).
9. R. M. KEEFER, A. OTTENBERG, and L. J. ANDREWS. J. Am. Chem. Soc. **78**, 255 (1956).
10. F. H. WESTHEIMER. Organic experiments. 2nd Ed. *Edited by* L. F. Fieser. Raytheon Education Co., Lexington, Mass. 1968. p. 310.
11. R. SRINIVASAN. Ph.D. Thesis, The University of Saskatchewan, Regina Campus, Regina, Saskatchewan, 1971.
12. A. I. VOGEL. A textbook of practical organic chemistry. 3rd Ed. Longmans Green and Co., London. 1956. p. 723.
13. M. A. PAUL and F. A. LONG. Chem. Rev. **57**, 1 (1957).
14. C. H. ROCHESTER. Acidity functions. Academic Press, New York. 1970. p. 16.
15. J. E. LEFFLER and E. GRUNWALD. Rates and equilibrium of organic reactions. Wiley, New York. 1963. pp. 297–300.
16. L. P. HAMMETT. Physical organic chemistry. McGraw-Hill, New York. 1970. Chapt. 11.
17. R. A. ROBINSON and R. H. STOKES. Electrolyte solutions. Butterworths Scientific Publications, London. 1959. p. 59.
18. M. OJEDA and P. A. H. WYATT. J. Phys. Chem. **68**, 1857 (1964).
19. P. M. HENRY. J. Am. Chem. Soc. **87**, 990 (1965).
20. E. A. HALEVI. Progress in physical organic chemistry. **1**, 109 (1963).
21. L. MELANDER. Isotope effects on reaction rates. Ronald Press, New York. 1960; F. H. WESTHEIMER. Chem. Rev. **61**, 265 (1961).
22. W. A. PRYOR. Introduction to free radical chemistry. Prentice-Hall Inc., Englewood Cliffs, N.J. 1966.
23. C. G. SWAIN, R. A. WILES, and R. F. W. BADER. J. Am. Chem. Soc. **83**, 1945 (1961).
24. P. AUKETT and I. R. L. BARKER. Chem. Ind. (London), 193 (1967); J. Chem. Soc. Perkin II, 568 (1972).
25. D. H. ROSENBLATT, L. A. HULL, D. C. DE LUCA, G. T. DAVIS, R. C. WEGLEIN, and H. K. R. WILLIAMS. J. Am. Chem. Soc. **89**, 1158 (1967).
26. R. P. BELL. The proton in chemistry. Cornell University Press, Ithaca, New York. 1959. Chapt. X.

Can. J. Chem. Downloaded from www.nrcresearchpress.com by 210.87.254.105 on 09/05/12
For personal use only.

N-Methylamino Acids in Peptide Synthesis. III. Racemization during Deprotection by Saponification and Acidolysis[1]

JOHN R. MCDERMOTT AND N. LEO BENOITON

Department of Biochemistry, University of Ottawa, Ottawa, Canada K1N 6N5

Received March 5, 1973

The racemization of *N*-methylamino-acid derivatives in aqueous sodium hydroxide and hydrogen bromide in anhydrous acetic acid and other solvents has been investigated by determining the products of the reaction with an amino-acid analyzer after deprotection. Whereas MeIle-OMe, Z-MeIle, and the *N*-unmethylated derivatives were only slightly racemized (<2%), Z-MeIle-OMe (18–24%), Z-Ala-MeLeu-OMe (22%), and Z-Ala-MeLeu-OBu^t (7%) were appreciably racemized by aqueous sodium hydroxide. It is suggested that these derivatives racemize because of the absence of an >*N*—H or carboxyl group whose ionization would suppress ionization of the neighboring α-*C*—H bond. Z-MeIle and Z-Ala-MeLeu were substantially racemized (68% in 4 h and 34% in 1 h, respectively) by 5.6 *N* hydrogen bromide in acetic acid. The extent of racemization by acid varied with acid strength, polarity of solvent, and time. Incorporation of label into both isomers of Ala-MeLeu from a solution of the tritiated reagent established that ionization at the α-*C*—H bond had occurred. No racemization was caused by aqueous acid or by hydrogen chloride.

La racémisation des dérivés d'acide aminé *N*-méthylé dans la soude aqueuse et HBr dans l'acide acétique et autres solvants, a été étudiée par détermination des produits de réaction sur un analyseur d'acide aminé après déprotection. Tandis que le MeIle-OMe, Z-MeIle et les dérivés *N*-non méthylé subissent une racémisation légère (<2%), le Z-MeIle-OMe (18–24%), Z-Ala-MeLeu-OMe (22%) et Z-Ala-MeLeu-OBu^t (7%) se racémisent de façon notable dans la soude aqueuse. On pense que la racémisation de ces dérivés est due à l'absence d'un >N—H ou d'un groupe carboxyle dont l'ionisation empêcherait celle de la liaison voisine α-*C*—H. Z-MeIle et Z-Ala-MeLeu subissent une racémisation substantielle (68% en 4 h et 34% en 1 h respectivement) en présence d'acide bromhydrique 5.6 *N* dans l'acide acétique. L'étendue de la racémisation varie avec la force de l'acide, la polarité du solvant et la durée. Le marquage isotopique dans les deux isomère Ala-MeLeu à partir d'une solution de réactif tritié montre que l'ionisation se fait sur la liaison α-*C*—H. Il n'y a pas de racémisation par l'acide aqueux ou par l'acide chlorhydrique.

[Traduit par le journal]

Can. J. Chem., **51**, 2555 (1973)

Protection of the amino function by the benzyloxycarbonyl group (2) and the carboxyl function as its methyl ester (3) is a widely used strategy in peptide synthesis. Selective deprotection of the *N*-terminus is accomplished by acidolysis, usually with hydrogen bromide in acetic acid (4), or by hydrogenation (2), and saponification is used to selectively remove the methyl ester (3). Racemization has generally been assumed to be negligible during these reactions, although a recent report (5) shows that saponification of a benzyloxycarbonyl-dipeptide methyl ester can cause a small degree of racemization.

Experience with derivatives of *N*-methylamino acids has been limited, and no one has investigated their susceptibility to racemization under conditions of saponification and acidolysis. Saponification has been used for the deprotection of several *N*-benzyloxycarbonyl- (6, 7) and *N*-*t*-butyloxycarbonyl-*N*-methylamino-acid (7) methyl esters, giving products in good yields with satisfactory optical rotations. An apparently stereochemically pure protected dipeptide, Z-Cys(Bzl)-MeTyr,[2] was obtained in excellent yield by saponification of the methyl ester (9). However, saponification of Ac-MePhe-OMe (6) and Z-MeAsp(OMe)-OMe (1) was attended by considerable racemization, and the seemingly curious observation that Ac-MeTyr-NHPh in ethanolic sodium hydroxide racemized more quickly than the corresponding unmethylated derivative is recorded in the literature (10).

[1]Supported by a grant from the Medical Research Council of Canada. N.L.B. is an Associate of the M.R.C.C., J.R.M. was a Fellow of the M.R.C.C. For Part II of this series, see ref. 1.

[2]The abbreviations for the amino-acid and peptide derivatives are those recommended by the IUPAC–IUB Commission on Biochemical Nomenclature (8). When not indicated, the amino-acid symbols represent the L-isomer, except for glycine.

Can. J. Chem. Downloaded from www.nrcresearchpress.com by 210.87.254.40 on 09/05/12
For personal use only.

TABLE 1. Racemization during the saponification of methyl esters*

Compound	Normality of NaOH	NaOH used (mol. equiv.)	Time (h)	Diastereomer formed (%)
Z-Ala-MeLeu-OMe	4	2	1/4	11
Z-MeIle-OMe	2	2	3	12
Z-MeIle-OMe	4	2	2	9
Z-MeIle-OMe	1	1.1	24	12
Z-Ala-Leu-OMe	1	1.1	1	<0.1
Boc-Ala-Pro-OMe	1	1.1	3	<0.1
Z-Ile-OMe	1	1.1	24	1.0
MeIle-OMe†	1	5	3	0.8
Z-MeIle-OH	2	2	3	0.8

*Two-three volumes of methanol added to the aqueous NaOH.
†No methanol added.

Products with high optical rotations were also obtained when *N*-benzyloxycarbonyl,*N*-methyl-amino-acid methyl esters were deprotected with 37% hydrogen bromide in acetic acid (6). However, measurement of optical activity is not a reliable test of stereochemical purity and small degrees of racemization may have been missed. We present here studies on the racemization attending the saponification and acidolysis of some *N*-methylated amino-acid and peptide derivatives by analysis with an amino-acid analyzer of the diastereomeric products of the reactions.[3] This work developed from the observation that two peaks corresponding to the L,L- and L,D-isomers were obtained on analysis with an amino-acid analyzer of Ala-MeLeu prepared by the saponification and hydrogenolysis of Z-Ala-MeLeu-OMe.

MeLeu-OMe.HBr was prepared by the hydrogenation of Z-MeLeu-OMe (6) in the presence of one molecular equivalent of hydrogen bromide, and coupled to Z-Ala by the mixed-anhydride method. The resulting oily protected dipeptide was saponified with 2 mol. equiv. of sodium hydroxide (1.25 *M* in 75% aqueous methanol), using the minimum reaction time required as determined by t.l.c. in a pilot experiment, and the product was converted to the free dipeptide by hydrogenation. Analysis showed it to contain 11% of the L,D-isomer. However, only 0.6% of the L,D-isomer was obtained on hydrogenation of Z-Ala-MeLeu-OBzl prepared by the same coupling technique (12). Thus considerable racemization had occurred during the saponification reaction—a surprising result in view of the general acceptance of this reaction in peptide synthesis.

Racemization was also detected when Z-MeIle-OMe was saponified under various conditions. The results together with data from other saponification experiments are shown in Table 1. Z-MeIle-OH underwent only slight racemization, as did Z-Ile-OMe, but no racemization was detected in the saponification of Z-Ala-Leu-OMe and Boc-Ala-Pro-OMe, thus emphasizing the different properties of the *N*-methyl derivatives.

It is difficult to compare the ease of racemization of esters of *N*-methylamino-acid derivatives with those of the corresponding amino-acid derivatives because the latter are hydrolyzed more readily than the former (15). It could be argued that since the amino-acid ester derivative is in contact with base for a shorter period of time, it would be expected to racemize less. To determine whether or not *N*-methylamino-acid derivatives are intrinsically more prone to racemize, the behavior of the *t*-butyl esters of Z-Ala-MeLeu and Z-Ala-Leu was investigated. As a precaution, only the neutral material was analyzed since unusual cases where *t*-butyl esters were saponified have been reported (16). The results in Table 2 show that both compounds racemized to some extent, and that there was a significant difference between the two compounds in the ease of racemization although it is less marked than the difference between the two methyl ester derivatives.

[3]A preliminary account of this work has appeared (11). The synthesis of the reference compounds and the chromatographic data for the various diastereomers are described in the accompanying paper (12). Analysis of diastereomeric products with an amino-acid analyzer has been used for determining amino-acid enantiomers (13), and as a test for racemization during peptide synthesis (14).

Can. J. Chem. Downloaded from www.nrcresearchpress.com by 210.87.254.40 on 09/05/12
For personal use only.

TABLE 2. Racemization of *t*-butyl esters by base*

Compound	Normality of NaOH	NaOH used (mol. equiv.)	Time (h)	Diastereomer formed† (%)
Z-Ala-MeLeu-OBu^t	1	1.1	1	3.3
Z-Ala-MeLeu-OBu^t	4	2	1/4	3.7
Z-Ala-Leu-OBu^t	1	1.1	1	0.3
Z-Ala-Leu-OBu^t	4	2	1/4	0.5

*Four volumes of methanol added to the aqueous NaOH.
†Corrected for the presence of a small amount of L,D-isomer in the starting material.

It is reasonable to assume that racemization occurred as a result of simple ionization at the α-carbon-hydrogen bond of the *N*-methylamino acid, although isoracemization in which the asymmetry is lost by ionization without dissociation (17, 18) cannot be ruled out. Why do *N*-methylamino-acid derivatives racemize more readily than the corresponding amino-acid derivatives? In an *N*-monosubstituted amino-acid ester, the $>N$—H will generally be more acidic than the α-*C*—H. Thus in base, this group will ionize first and so protect the neighboring *C*—H bond from ionization. In an *N*-substituted *N*-methylamino-acid ester, no such effect obtains, and the α-*C*—H will ionize more readily. Similarly, ionization of the free carboxyl group of an *N*-substituted *N*-methylamino acid will prevent further ionization at the α-carbon atom (19). Alternatively, Neuberger has proposed that the electron-donating methyl group favors the polar immonium form of the amide bond and that this encourages ionization of the neighboring *C*—H bond (19). From both these theories it would be predicted, however, that *N*-substituted proline derivatives should racemize as readily as *N*-methylamino-acid derivatives, but this is not the case. The reason for this is not clear.

Although the above results were obtained with only two systems (Ala-MeLeu and MeIle) there is nothing to suggest that they are not applicable to *N*-methylamino acids in general. It therefore appears that saponification should not be used during the synthesis of peptides containing *N*-methylamino-acid residues.

Racemization also occurred during the deprotection of *N*-methylamino-acid derivatives with hydrogen bromide in acetic acid. Z-Ala-MeLeu, prepared from the *t*-butyl ester, gave 0.4% L,D-isomer on hydrogenation, whereas treatment with 5.6 *N* hydrogen bromide in acetic acid gave 17% of the L,D-isomer. It was further discovered that Ala-MeLeu itself was racemized under these conditions. The effect of acid strength and duration of exposure on racemization was investigated (Table 3). Deprotection of Z-MeIle and Z-D-Me*a*lle was achieved with little racemization using 2.5 *N* hydrogen bromide, but stronger acid (5.6 *N*) over an extended period gave considerable racemization. An extended treatment of Z-Gly-Ala-MeLeu with the same acid also gave a partially racemized product. No racemization was detected for the derivatives of Ala-Leu and Ala-Pro, and only 0.3% for Z-Ile, even under drastic conditions.

During the above studies, it was found that the extent of racemization of Ala-MeLeu varied considerably, and not always in the predicted manner. Freshly prepared solutions of hydrogen bromide in acetic acid gave the highest values, and it was thought that accumulation of moisture in the reagent might be depressing the racemization. Indeed, when water was added deliberately to the reagent, no racemization took place.

Experiments with other solvents revealed that the extent of racemization increases with the polarity of the solvent (ether < dioxane < acetic acid). Various hydrogen chloride solutions did not cause racemization.

Thus concentrated hydrogen bromide in a dry, polar solvent can racemize *N*-methylamino-acid derivatives. Again, the presence of an $>N$—H group next to the α-*C*—H appears to inhibit racemization—contrast the values obtained for Z-MeIle (34%) and MeIle (3%) under the same conditions.[4] The difference between the values for Z-Ala-MeLeu and Z-Ala-Leu cannot be ascribed to different rates of cleavage of the benzyloxycarbonyl group, since the free peptide

[4]The results of Ikutani who showed that some *N*,*N*-dimethylamino acids, which lack the $>N$—H group, are unusually susceptible to racemization by hot dilute aqueous acid (20) are consistent with this view.

Can. J. Chem. Downloaded from www.nrcresearchpress.com by 210.87.254.40 on 09/05/12
For personal use only.

TABLE 3. Racemization under the influence of anhydrous acid

Compound	Reagent	Time (h)	Diastereomer formed (%)
Z-Ala-MeLeu	5.6 *N* HBr–AcOH	1	17
Z-Ala-MeLeu	2.5 *N* HBr–AcOH	4	9.4
Z-Ala-MeLeu	5.6 *N* HBr–AcOH*	4	6.5
Z-Ala-MeLeu	5.6 *N* HBr–AcOH*	17	22
Z-Ala-MeLeu	5.6 *N* HBr–AcOH*	66	49
Ala-MeLeu	2.5 *N* HBr–AcOH	17	35
Ala-MeLeu	2.5 *N* HBr–nitromethane	17	14†
Ala-MeLeu	6.2 *N* HBr–dioxane	17	9.0
Ala-MeLeu	2.5 *N* HBr–dioxane	17	1.0
Z-Ala-MeLeu	HBr–ether, saturated	4	0.2
Ala-MeLeu	1.1 *N* HCl–AcOH	17	0.2
Ala-MeLeu	4.0 *N* HCl–dioxane	17	<0.1
Ala-MeLeu	2.5 *N* HBr–80% aq. AcOH	4	<0.1
Ala-MeLeu	Trifluoroacetic acid	17	<0.1
Z-MeIle	5.6 *N* HBr–AcOH	4	34
Z-D-Me*a*Ile	5.6 *N* HBr–AcOH	4	5
Z-MeIle	2.5 *N* HBr–AcOH	1	1
Z-D-Me*a*Ile	2.5 *N* HBr–AcOH	1	<0.5
MeIle	5.6 *N* HBr–AcOH	4	3
Ile	5.6 *N* HBr–AcOH	4	0.5
Z-Gly-Ala-MeLeu	5.6 *N* HBr–AcOH	17	40‡
Boc-Ala-Pro	5.6 *N* HBr–AcOH	17	<0.1
Z-Ala-Leu	5.6 *N* HBr–AcOH	17	<0.1
Z-Ile	5.6 *N* HBr–AcOH	4	0.3

*Old reagent.
†Several by-products formed.
‡Approximate value, since relative color yields not known.

itself undergoes racemization. This then is an unambiguous demonstration of the relative ease with which *N*-methylamino-acid derivatives racemize.

The acid-catalyzed racemization of amino acids in 6 *N* hydrochloric acid is well known (13, 19). Ionization of the α-*C*—H bond has been proposed as the mechanism (19), as follows:

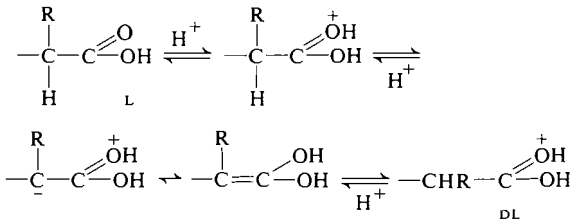

Thus, heating amino acids in tritiated hydrochloric acid resulted in some incorporation of tritium into the α-position. The specific activity found for alanine was 3.5 times less than the value expected from the degree of racemization, however, and this has been attributed to an isotope effect (21).

Our results can be interpreted in these terms, since strong acid and polar solvent are essential requirements for racemization. To determine whether ionization and protonation were taking place, Ala-MeLeu was incubated in a tritiated solution of hydrogen bromide in acetic acid. The extent of racemization was determined on the analyzer as usual, and the amount of tritium incorporated into each diastereomer was determined by passing a second sample of the solution through the analyzer column, collecting the effluent in fractions, and determining their radioactivity with a liquid scintillation counter. The results are shown in Fig. 1. The peptide was found to contain 10% of the L,D-isomer, having a specific activity 6.5% of that of the original solution. The difference between these two values can be attributed to an isotope effect (21). The L,D-isomer also contained 2.6 times as much radioactivity as the L,L-isomer, a difference which can be attributed to asymmetric induction. A similar steric effect, although in an opposite sense, has been observed for isoleucine in tritiated hydrochloric acid, where the isoleucine had 1.4 times the radioactivity present in the *allo*-isoleucine formed by racemization (21). Ionization and protonation, therefore, unquestionably had taken place.

Can. J. Chem. Downloaded from www.nrcresearchpress.com by 210.87.254.40 on 09/05/12
For personal use only.

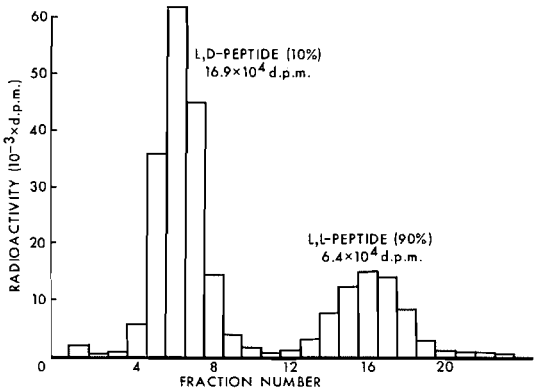

FIG. 1. Radioactivity incorporated into Ala-MeLeu after 4 h in tritiated HBr in acetic acid (saturated) at room temperature. The specific activity of the resulting L-Ala-DL-MeLeu was 1.17×10^6 d.p.m./mmol, corresponding to 9% of that of the original solution.

Again, the result for the proline dipeptide appears to be inconsistent with the theory that racemization is inhibited by the presence of an $>N$—H group next to the α-*C*—H, unless ionization of the derivative were followed by protonation solely at the "L"-position. A preliminary labelling experiment with Ala-Pro in tritiated hydrogen bromide in acetic acid gave an incorporation of less than 10% (the limit of detection with the system used) of that obtained for Ala-MeLeu, making this explanation unlikely.

It is evident that from a practical viewpoint, hydrogenation is to be preferred over acidolysis with hydrogen bromide for cleavage of benzyloxycarbonyl groups from *N*-methylamino-acid derivatives.

Experimental

Materials and Methods

L-Alanine, L-isoleucine, L-leucine, and L-proline were obtained from General Biochemicals, Chagrin Falls, Ohio, D-*allo*-isoleucine from ICN Nutritional Biochemicals, Cleveland, Ohio, and Boc-Ala from Pierce Chemical Company, Rockford, Illinois. Benzyloxycarbonyl-amino acids were prepared by the original procedure (2) as described by Greenstein and Winitz (22). Solvents were purified and dried by standard methods before use. Acetic acid was dried over $CaSO_4$, which was removed by filtration. Hydrogenations were done in the presence of 10% palladium on charcoal catalyst at atmospheric pressure. Solutions of hydrogen bromide were prepared by passing the gas (Matheson of Canada, Whitby, Ontario) into the solvent at 0 °C with the exclusion of moisture. Organic solvent extracts were dried with $MgSO_4$ and evaporated under reduced pressure using a rotary evaporator. Proton nuclear magnetic resonance (n.m.r.) (Varian T-60) and t.l.c. on silica gel GF_{254} in $CHCl_3$–MeOH (9:1) were used routinely to confirm the identity and purity of oils.

Analyses of diastereomeric amino acids and peptides were performed on a Beckman model 120B amino-acid analyzer using the long column (50 cm, AA-15 resin) and an intermediate length column (15 cm, Aminex A-5 resin) eluted with 0.20 *N* sodium citrate buffer, p*H* 4.25, at a flow rate of 68 ml/h (34 ml/h for MeIle (23)).[3] Benzyloxycarbonyl derivatives were deprotected by hydrogenation in 80% acetic acid for 4 h. *t*-Butyl-ester derivatives were treated with trifluoroacetic acid for 30 min before hydrogenation. The *t*-butyloxycarbonyl group was also removed with trifluoroacetic acid.

Z-Ala-MeLeu-OMe

Isobutyl chloroformate (2.6 ml; 20 mmol) was added to a solution of Z-Ala (4.66 g; 20 mmol) and triethylamine (2.8 ml; 20 mmol) in tetrahydrofuran (10 ml) at −10 °C, and the solution was stirred for 90 s. To this was added MeLeu-OMe.HBr (4.8 g; 20 mmol), prepared by the hydrogenation of Z-MeLeu-OMe (6) in the presence of 1 mol. equiv. of HBr, in tetrahydrofuran (15 ml) containing triethylamine (2.8 ml) and the suspension was stirred for 1 h at −10° and overnight at 0°. The reaction mixture was concentrated to an oil which was taken up in ethyl acetate (100 ml). The ethyl acetate was washed with water, *N* HCl, water, 5% aqueous $NaHCO_3$, and water (each 2 × 25 ml), dried, and evaporated. The residual oil was dried *in vacuo*. Yield 5.86 g (80%), homogeneous by t.l.c.; n.m.r. analysis consistent with the structure.

Z-Ala-Leu-OMe

This was obtained as an oil (88% yield) in the same manner from Z-Ala and Leu-OMe.HCl.

Z-Ala-Leu

Z-Ala-Leu-OMe (3 g) was dissolved in a mixture of methanol (9 ml) and 1 *N* NaOH (9 ml). After 1 h water (20 ml) was added, the solution was washed with ether (20 ml) and acidified to p*H* 1 with 4 *N* HCl. The resulting oil was extracted into ethyl acetate (2 × 30 ml), the extract was dried and evaporated to an oil. The oily Z-Ala-Leu was converted to the dicyclohexylammonium salt as described (24), recrystallized, m.p. 162–163°, lit. m.p. 163° (24), and regenerated as described (24). Yield 2.3 g, 80%.

Boc-Ala-Pro

Boc-Ala-Pro-OBzl was obtained as an oil (61%) by coupling Pro-OBzl.HCl (25) with the mixed anhydride of Boc-Ala. This was dissolved in ethyl acetate and hydrogenated for 8 h. Evaporation of the solvent gave an oil which was crystallized twice from ether – light petroleum b.p. 30–60°. Yield 94%, m.p. 154–155°, $(\alpha)_D^{28}$ −89.9° (*c*, 1 in ethanol).

Anal. Calcd. for $C_{13}H_{22}N_2O_5.H_2O$: C, 51.3; H, 8.1; N, 9.2. Found: C, 50.8; H, 8.2; N, 9.1.

Z-MeIle, Z-D-MeAlle

These compounds were prepared from Z-Ile and Z-D-*a*lle by the room-temperature methylation procedure (1) using NaH (3 mol. equiv.) and methyl iodide (8 mol. equiv.) in tetrahydrofuran.

Can. J. Chem. Downloaded from www.nrcresearchpress.com by 210.87.254.40 on 09/05/12
For personal use only.

Can. J. Chem. Downloaded from www.nrcresearchpress.com by 210.87.254.40 on 09/05/12
For personal use only.

Boc-Ala-Pro-OMe, Z-MeIle-OMe, Z-Ile-OMe

The corresponding acid (1 mmol) was dissolved in ether (5 ml) and an ethereal solution of diazomethane was added dropwise until the first yellow color persisted. The excess reagent was destroyed with a drop of acetic acid, and the solution was evaporated to an oil. These oils were used without purification for the saponification experiments.

MeIle-OMe

Z-MeIle-OMe was hydrogenated in 80% aqueous acetic acid for 4 h, the solvent was removed by evaporation, and the resulting oil was dried *in vacuo* over KOH.

MeLeu-OBu^t

Z-MeLeu (8.0 g) (1) was *t*-butylated for 48 h using the method of Roeske (26). Yield 9.0 g (94%). The oil was hydrogenated in ethyl acetate (80 ml) for 4 h giving another oil upon evaporation of the solution (5.1 g, 98%). The n.m.r. analysis was consistent with the structure.

Z-Ala-MeLeu-OBu^t

This compound was prepared as an oil (R_f 0.78 on t.l.c.) in 87% yield by the mixed-anhydride coupling of Z-Ala (6.16 g) and MeLeu-OBu^t (5.10 g). Analysis after deprotection showed that it contained 0.4% of L,D-isomer.

Z-Ala-MeLeu

Z-Ala-MeLeu-OBu^t (6 g) was left in trifluoroacetic acid for 30 min at room temperature. The solution was evaporated and the product was partitioned between 5% aqueous $NaHCO_3$ and ether. The aqueous layer was brought to p*H* 1 with 4 *N* HCl, extracted with ethyl acetate (2 ×), and the extracts were dried and evaporated to give an oil. Yield 4.8 g (94%), R_f 0.7 on t.l.c.; n.m.r. analysis consistent with the structure.

Z-Ala-Leu-OBu^t

This was prepared by the mixed-anhydride coupling of Z-Ala with Leu-OBu^t (26) and recrystallized from ether – light petroleum. Yield 93%, m.p. 89–91°, lit. m.p. 90–92° (27). Analysis of a sample after deprotection showed that it contained 0.15% of the L,D-isomer.

Ala-MeLeu

Z-Ala-MeLeu (from the *t*-butyl ester) was hydrogenated in 80% aqueous acetic acid for 4 h. The solvent was evaporated and the crystalline product was dried *in vacuo* over KOH. Analysis showed that it contained 0.4% of the L,D-isomer. This compound was used for the acid-catalyzed racemization experiments.

Z-Gly-Ala-MeLeu

Z-Gly-Ala-MeLeu-OBu^t (0.1 g), prepared by coupling Z-Gly with Ala-MeLeu-OBu^t using *N*-hydroxysuccinimide–dicyclohexylcarbodiimide (12), was left in trifluoroacetic acid for 1 h at room temperature. The solution was evaporated and the residual oil was used directly.

Saponification

Methyl Esters

The methyl ester (0.5–2 mmol) was dissolved in methanol (2–3 times the volume of the NaOH solution used), and the aqueous NaOH was added. The mixture was shaken for the required time and water (20 ml) was added. Any neutral material was removed by extraction with ether (2 × 10 ml) and the aqueous layer was acidified to p*H* 1 with 4 *N* HCl (p*H* 3 with aqueous citric acid for Boc-Ala-Pro). The product was extracted into ethyl acetate (2 × 20 ml), the extracts were dried and evaporated, and the residue was deprotected and analyzed. The MeLeu-OMe reaction mixture was acidified to p*H* 2 and analyzed directly.

t-Butyl Esters

After the addition of water, the product was extracted into ethyl acetate (2 × 15 ml), the extracts were dried and evaporated.

Acid-catalyzed Racemization

The sample (0.1 mmol) was dissolved in the appropriate reagent (1 ml) in a flask protected from moisture. After the required time the solution was evaporated and the residue was dissolved in 0.2 *N* sodium citrate, p*H* 2.2, for analysis.

Tritium Exchange Experiments

Tritiated acetic acid was prepared by warming a mixture of ^3H_2O (25 mCi, 1 ml) and acetic anhydride (0.925 ml) at 60° for 24 h. Anhydrous $CaSO_4$ was added to remove the slight excess of water, the mixture was filtered, and hydrogen bromide was passed into the solution at 0 °C until saturation had occurred. Ala-MeLeu (43.6 mg; 0.2 mmol) was dissolved in the tritiated reagent (0.5 ml), and after 4 h the mixture was diluted to 10 ml with acetic acid. An aliquot (1.5 ml) was evaporated, the residue was taken up in 0.2 *N* sodium citrate, p*H* 2.2, and this was analyzed (Aminex A-5 resin, 15-cm column, p*H* 4.25 eluting buffer) for the peptide isomers and radioactivity with the amino-acid analyzer by incorporating a flow-cell scintillation counter assembly (Nuclear-Chicago model 4526) between the outlet of the column and the mixing coil. The two radioactive peaks coincided with the two ninhydrin-positive peaks. A second run was carried out, this time collecting the effluent from the column in 1.5 ml fractions, Each fraction was diluted with 15 ml of Aquasol (New England Nuclear, Boston, Massachusetts) and its radioactivity was measured with a Beckman LS-133 liquid scintillation counter. The values were corrected using a standard curve for tritium. The specific activity of the original solution was determined from the diluted solution, and found to be 1.28×10^7 d.p.m./mmol ^3H.[5]

Ala-Pro (36.8 mg; 0.2 mmol) was treated as described above, the radioactivity of the isomers being determined using the flow-cell assembly. Analysis showed 1% of the L,D-peptide, the labelled product having a specific activity 0.8% of that of the original solution.

We thank Dr. J. Rudinger and Dr. M. Goodman for helpful discussions.

[5]Assuming that the reaction mixture (1.54×10^8 d.p.m.) contained 12.2 mmol H^+: 0.6 mmol from the 0.2 mmol of peptide, 2.8 mmol of HBr, and 8.8 mmol (0.5 ml) of acetic acid. The increase in volume obtaining during the saturation of the acetic acid with HBr has not been taken into account. If a 25% increase had taken place, the specific activity of the solution would be 1.47×10^7 d.p.m./mmol.

1. J. R. McDERMOTT and N. L. BENOITON. Can. J. Chem. **51**, 1915 (1973).
2. M. BERGMANN and L. ZERVAS. Ber. **65**, 1192 (1932).
3. M. BODANSZKY and M. A. ONDETTI. Peptide synthesis. Interscience publishers, New York, N.Y. 1966. pm 43.
4. D. BEN-ISHAI and A. BERGER. J. Org. Chem. **17**, 1564 (1952).
5. G. W. KENNER and J. H. SEELY. J. Am. Chem. Soc. **94**, 3259 (1972).
6. J. R. COGGINS and N. L. BENOITON. Can. J. Chem. **49**, 1968 (1971).
7. R. K. OLSEN. J. Org. Chem. **35**, 1912 (1970).
8. IUPAC–IUB commission on biochemical nomenclature. J. Biol. Chem. **247**, 977 (1o72).
9. R. L. HUGUENIN and R. A. BOISSONNAS. Helv. Chim. Acta, **44**, 213 (1961).
10. M. BOVARNICK and H. T. CLARKE. J. Am. Chem. Soc. **60**, 2426 (1938).
11. J. R. McDERMOTT and N. L. BENOITON. *In* Chemistry and biology of peptides: Proc. of the 3rd American Peptide Symposium, Boston, 1972. *Edited by* J. Meienhofer. Ann Arbor Publishers, Ann Arbor, Mich. 1972. p. 369.
12. J. R. McDERMOTT and N. L. BENOITON. Can. J. Chem. This issue.
13. J. M. MANNING and S. MOORE. J. Biol. Chem. **243**, 5591 (1968).
14. (*a*) M. BODANSZKY and L. E. CONKLIN. Chem. Commun. 773 (1967). (*b*) N. IZUMIYA and M. MURAOKA. J. Am. Chem. Soc. **91**, 2391 (1969).
15. J. E. PURDIE and N. L. BENOITON. Can. J. Chem. **49**, 3469 (1971).
16. R. SCHWYZER, B. ISELIN, H. KAPPELER, B. RINIKER, W. RITTEL, and H. ZUBER. Helv. Chim. Acta, **46**, 1975 (1963); S. BAJUSZ, T. LAZAR, and Z. PAULAY. Acta Chim. Acad. Sci. Hung. **41**, 329 (1964).
17. D. J. CRAM and L. GOSSER. J. Am. Chem. Soc. **86**, 5457 (1964).
18. J. KOVACS, H. CORTEGIANO, R. E. COVER, and G. L. MAYERS. J. Am. Chem. Soc. **93**, 1541 (1971).
19. A. NEUBERGER. Adv. Protein Chem. **4**, 297 (1948).
20. Y. IKUTANI. Bull. Chem. Soc. Jap. **43**, 3602 (1970).
21. J. M. MANNING. J. Am. Chem. Soc. **92**, 7449 (1970).
22. J. P. GREENSTEIN and M. WINITZ. Chemistry of the amino acids. John Wiley and Sons, New York. NY. 1962. p. 891.
23. J. R. COGGINS and N. L. BENOITON. J. Chromatogr. **52**, 251 (1970).
24. E. KLIEGER, E. SCHRÖDER, and H. GIBIAN. Ann. **640**, 157 (1961).
25. R. E. NEUMAN and E. L. SMITH. J. Biol. Chem. **193**, 97 (1951).
26. R. W. ROESKE. Chem. Ind. 1121 (1959).
27. A. I. MIROSHNIKOV, A. A. KIRYUSKIN, and YU. A. OVCHINNIKOV. Zh. Obshch. Khim. **40**, 429 (1970).

Can. J. Chem. Downloaded from www.nrcresearchpress.com by 210.87.254.40 on 09/05/12
For personal use only.

N-Methylamino Acids in Peptide Synthesis. IV. Racemization and Yields in Peptide-bond Formation[1]

JOHN R. MCDERMOTT AND N. LEO BENOITON

Department of Biochemistry, University of Ottawa, Ottawa, Canada K1N 6N5

Received March 5, 1973

The racemization of an *N*-methylamino-acid residue during peptide-bond formation and mixed-anhydride activation has been investigated using Ala-MeLeu-Gly and Ala-MeLeu as model peptides. The results were compared with those for Ala-Leu-Gly, Ala-Leu, and Ala-Pro. The extents of racemization were determined by analysis of the diastereomeric products of the reactions after deprotection, using an amino-acid analyzer. Extensive racemization was detected after the hydrolysis of the mixed anhydrides of Bz-MeLeu, Z-Ala-MeLeu, and Z-Ala-Leu, but not of Boc-Ala-Pro and Z-MeIle. Significant racemization (2.8–39%) was observed when Z-Ala-MeLeu was coupled with Gly-OBzl by various methods in the presence of salts such as triethylamine hydrochloride or *p*-toluenesulfonate. Only coupling through the *N*-hydroxysuccinimide (HONSu) ester gave stereochemically pure product. In the absence of salt, less racemization was observed, but only couplings using *N*-ethoxycarbonyl-2-ethoxy-1,2-dihydroquinoline and *N,N'*-dicyclohexylcarbodiimide–HONSu gave essentially pure products. Polar solvents promoted racemization, but excess base did not. Chemical evidence that the racemization intermediate is an oxazolium-5-oxide has been obtained by trapping the intermediate as an addition product (a pyrrole) in 85% yield.

The yields obtained by various coupling methods have been determined for several model peptides. Couplings at the carboxyl group of an *N*-methylamino acid gave high yields only in the absence of salt, except for coupling by the HONSu ester method. Couplings to an *N*-methylamino group gave high yields, except for coupling by the *p*-nitrophenyl ester method. Couplings to Ala-MeLeu-OBu^t gave higher yields than couplings to Ala-MeLeu-OBzl, presumably due to piperazine-dione formation by the latter.

La racémisation d'un reste acide aminé *N*-méthyle lors de la formation de la liaison peptidique et de l'activation par anhydride mixte, a été étudiée en utilisant les peptides modèles Ala-MeLeu-Gly et Ala-MeLeu. Les résultats ont été comparés à ceux obtenus pour Ala-Leu-Gly, Ala-Leu et Ala-Pro. L'étendue de racémisation a été déterminée par analyse des diastéréoisomères après déprotection et emploi d'un analyseur d'acide aminé. Une racémisation importante a été détectée après hydrolyse des anhydrides mixtes de Bz-MeLeu, Z-Ala-MeLeu et Z-Ala-Leu mais pas pour Boc-Ala-Pro et Z-MeIle. Une racémisation notables (2.8–39%) a été observée lors du couplage du Z-Ala-MeLeu sur le Gly-OBzl par les diverses méthodes en présence de sels tels que le chlorohydrate ou para toluène sulfonate de triéthylamine. Seul le couplage par l'ester de la *N*-hydroxy succinimide (HONSu) conduit à un produit de pureté stéréochimique. En l'absence de sel, la racémisation est plus faible mais seuls les couplages par le *N*-éthoxycarbonyl éthoxy-2 dihydro-1,2 quinoléine et le complexe *N,N'*-dicyclohexylcarbodiimide–HONSu donnent des produits essentiellement purs. Les solvants polaires favorisent la racémisation mais pas un excès de base. L'intermédiaire de racémisation oxyde-5 d'oxazolium a été mis en évidence par piegeage sous forme de produits d'addition (un pyrrole) avec un rendement de 85%.

Les rendements obtenus dans les divers couplages ont été déterminés sur différents peptides modèles. Les couplages sur le carboxyle d'un acide aminé *N*-méthylé se font avec des rendements élevés en l'absence de sel sauf pour la méthode de l'ester HONSu. Les couplages sur le groupe *N*-méthylamino se font avec des rendements élevés sauf pour la méthode de l'ester *p*-nitrophényle. Les couplages de l'Ala-MeLeu-OBu^t sont meilleurs que ceux de l'Ala-MeLeu-OBzl probablement à cause de la formation par ce dernier d'une pipérazine dione. [Traduit par le journal]

Can. J. Chem., 51, 2562 (1973)

Peptides containing *N*-methylamino acids form an important group of antibiotics (2) and are also of interest as analogs of peptide hormones (3). Many peptides of *N*-methylamino acids have been synthesized, but systematic studies in this area of peptide synthesis have not been carried out. The synthesis of these peptides is attended with the problems of the lack of crystallinity of intermediates, the tendency of intermediates to cyclize and the lesser reactivity of the methylamino group or steric hindrance (4), though the latter does not always manifest itself. Racemization has generally been assumed to be less of a problem than for ordinary peptides, because of the inability of *N*-acyl *N*-methylamino-acid de-

[1]Supported by a grant from the Medical Research Council of Canada. N.L.B. is an Associate of the M.R.C.C., J.R.M. was a Fellow of the M.R.C.C. For Part III of this series, see ref. 1.

Can. J. Chem. Downloaded from www.nrcresearchpress.com by 210.87.254.105 on 09/05/12
For personal use only.

Can. J. Chem. Downloaded from www.nrcresearchpress.com by 210.87.254.105 on 09/05/12
For personal use only.

rivatives to form oxazolones (5), and because of their structural similarity to derivatives of proline whose resistance to racemization is well known. However, several observations are completely inconsistent with this assumption. Both *N*-methylphenylalanine and proline can be racemized by acetic anhydride in acetic acid (6), but only *N*-methyltryptophane and not proline was racemized by ketene at acid p*H* (7). Z-Gly-MePhe[2] was partially racemized as was Z-Gly-Phe during the formation of the *p*-nitrophenyl ester using tris-(*p*-nitrophenyl) phosphite but Z-Gly-Pro was not (9). And finally, a product with a lower specific rotation than that of the same product prepared by a different method was obtained from the DCCI-mediated coupling of Z-Cys(Bzl)-MeTyr with IleOMe (10). In the previous paper we have demonstrated the tendency of *N*-methylamino-acid derivatives to racemize during saponification and acidolysis (1). In this paper, we present a study on the racemization of *N*-methylamino-acid residues during peptide-bond formation, and a comparison of the yields obtainable by different methods for several model peptides.[3]

Our interest in racemization of *N*-methylamino acids during peptide synthesis arose from the observation that a mixed-anhydride coupling of Bz-MeLeu with *p*-nitroaniline gave a product devoid of optical activity (12). In preliminary experiments, it was then found that no optical activity remained after the mixed anhydride formed from Bz-MeLeu and ethyl chloroformate at 0° had been hydrolyzed. The extents of racemization for some other derivatives subjected to the same admittedly rather drastic activation conditions followed by hydrolysis are given in Table 1. Z-MeLeu racemized very little, but the extents of racemization of Z-Ala-MeLeu and Bz-MeLeu approached those of Z-Ala-Leu and Bz-Leu. Boc-Ala-Pro resisted racemization, as expected, but Bz-Pro racemized sufficiently to indicate that one should not disregard completely the possibility that proline residues might racemize during couplings.[4] The consistently low values observed for the two proline derivatives show that proline is atypical in not behaving like other imino acids, as has already been observed in the previous paper (1).

TABLE 1. Extent of racemization during the hydrolysis of mixed anhydrides*

Compound	Diastereomer or D isomer formed (%)
Bz-Leu	50†
Bz-MeLeu	45†
Bz-Pro	6.5†
Z-MeIle	<0.5‡
Z-Ala-MeLeu	26.5‡
Z-Ala-Leu	38‡
Boc-Ala-Pro	0.1‡

*Mixed anhydride formed by reaction with ROCOCl–Et_3N in THF at 0° for 5 min. Water was then added.
†Determined by measurement of optical rotation. EtOCOCl used.
‡Determined by analysis after deprotection. Bu^tOCOCl used.

Further studies were then carried out on actual peptide synthesis using several standard coupling methods. The extents of racemization and the yields have been obtained throughout this work by determining the deprotected diastereomeric products of the reaction using an amino-acid analyzer. This method was chosen because the sensitivity and speed of this type of analysis have been demonstrated (14, 15) and because of our own experience with the analyzer (16). The elution conditions used and the elution times and ninhydrin color yields for the various diastereomeric pairs are given in Table 2.[5] The elution times and relative color yields for each pair were determined by analysis of the peptides prepared from the racemic amino acid, and the identity of the peaks and the absolute color yields for each isomer were established by analysis of the L,L-peptide. The standard instrument column and buffers,[6] plus the Aminex A-5 column which has been a standard part of our instrument for several years, sufficed for separating all the

[2]The abbreviations for the amino-acid and peptide derivatives are those recommended by the IUPAC–IUB Commission on Biochemical Nomenclature (8). When not indicated, the amino-acid symbols represent the L isomer, except for glycine. Other abbreviations used: DCCI, *N*,*N*′-dicyclohexylcarbodiimide; EEDQ, *N*-ethoxycarbonyl-2-ethoxy-1,2-dihydroquinoline; HONSu, *N*-hydroxysuccinimide; NMM, *N*-methylmorpholine; NEPIS, *N*-ethyl-5-phenylisoxazolium-3′-sulfonate; THF, tetrahydrofuran.

[3]A preliminary account of this work has appeared (11).

[4]Partial racemization of a proline residue during coupling has in fact been reported (for the DCCI-mediated coupling of Bz(NO_2)-Pro with *p*-nitrophenol) (13).

[5]It is interesting to note the decrease in ninhydrin color constants in going from Ala-Leu-Gly (24.3), to Gly-Ala-MeLeu (13.6), Ala-MeLeu-Gly (5.7), Ala-MeLeu (1.1), and MeAla-Leu (<0.05).

[6]The concentrations given for the p*H* 4.25 buffer in refs. 11, 16, and 17 are in error. The correct concentration is 0.20 *N*.

TABLE 2. Chromatographic data for analysis of diastereomers*

Compound	Elution time (min)	Color constant
Ala-MeLeu	43.5	1.1
Ala-D-MeLeu	34.5	1.0
Ala-Leu	40	17.2
Ala-D-Leu	31	14.6
Ala-MeLeu-Gly	35	5.7
Ala-D-MeLeu-Gly	41	5.2
Ala-Leu-Gly	33, 96†	24.3
Ala-D-Leu-Gly	38, 120†	21.9
Ala-Pro‡	158	7
Ala-D-Pro‡	142	9
MeIle§	63	5.2
D-Me*a*Ile§	57	4.5

*Beckman model 120B amino-acid analyzer, Aminex A-5 (15 cm) resin, eluted with 0.20 *N* sodium citrate, p*H* 4.25, at 68 ml/h; 57 °C.
†AA-15 (50 cm) resin.
‡AA-15 (50 cm) resin, eluted with p*H* 3.28 buffer (85 min), followed by p*H* 4.25 buffer.
§Elution at 34 ml/h (16). Other constants at 34 ml/h: Ile, 39.1 (92 min); *a*lle, 39.3 (83 min); MeAla-Leu, 0.3 (82 min).

diastereomeric pairs. Though no experiments designed to test sensitivity were carried out, the peptide peaks were well enough separated to allow detection of about 1 part in 1000 of the other isomer, as has been reported by other workers (14, 15). The *N*-methylisoleucine–*N*-methyl-*allo*-isoleucine pair were less well separated, allowing detection of about 1 part in 200.

The methods used for the synthesis of the *N*-methylleucine peptides are shown in Scheme 1. Points to note are that the syntheses of the L,L-isomers had to be carried out without using saponification or acidolysis with hydrogen bromide, both of which cause racemization (1), and that the tripeptide was obtained by using DCCI–HONSu as the coupling agent for the reason which is apparent from Table 4.

The coupling of Z-Ala-MeLeu to Gly-OBzl was used to determine the extent of racemization during peptide-bond formation by various procedures. The crude product of the reaction was deprotected by hydrogenation, and the resulting tripeptide analyzed. The initial series of couplings were done in the presence of triethylamine *p*-toluenesulfonate or hydrochloride, derived from the salt of the appropriate Gly-OBzl. The results are shown in Table 3, together with those obtained for coupling Z-Ala-Leu to Gly-OBzl for comparison. Racemization occurred in varying degrees for all the coupling methods studied, except the HONSu ester method. Moreover, in

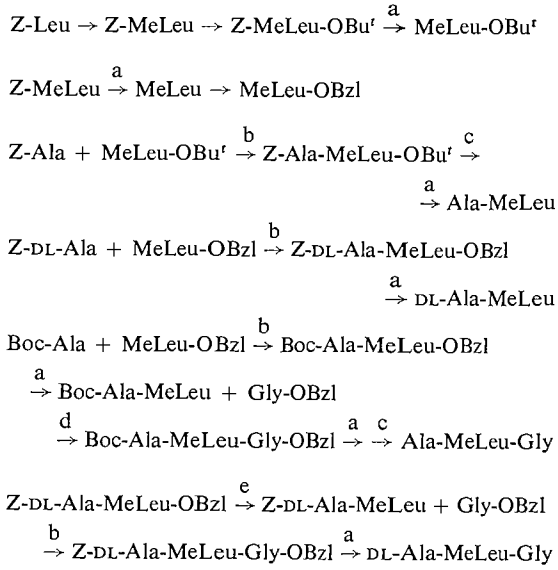

SCHEME 1. a, hydrogenation; b, mixed anhydride; c, trifluoroacetic acid; d, DCCI–HONSu; e, saponification.

all cases but one, the *N*-methylamino acid suffered more racemization than did the corresponding amino acid in the analogous peptide. The low extents of racemization obtained for Z-Ala-Leu-Gly-OBzl using DCCI–HONSu and EEDQ are in accord with the literature (15, 18, 19) except for the report of Kemp *et al.* (20). In the case of the DCCI–HONSu coupling, racemization clearly occurred during the formation of the active ester, since no diastereomer was formed when the HONSu ester was coupled. When *N*-methylmorpholine was used as base for the mixed-anhydride couplings, instead of depressing the degree of racemization as it normally does (21), it had the opposite effect.

In Table 4 are shown the results for couplings carried out using Gly-OBzl in the absence of salt of tertiary base. In this later work, crystalline Boc-Ala-MeLeu was used in preference to the oily benzyloxycarbonyl derivative. In a test case (DCCI), the yield and extent of racemization were, as expected, very similar for the two compounds. DCCI–HONSu and EEDQ caused much less racemization than in experiments with salt present, the former yielding a stereochemically pure product. The enhancement of racemization by salts (22, 23) has been attributed to the basicity of the anion (the chloride ion in particular) (13), the increased ionic strength of the medium (24),

Can. J. Chem. Downloaded from www.nrcresearchpress.com by 210.87.254.105 on 09/05/12
For personal use only.

TABLE 3. Yields and extents of racemization during couplings to Gly-OBzl in the presence of salt*

Coupling method	Z-Ala-Leu	Z-Ala-MeLeu	
	$TosOH.Et_3N$	$TosOH.Et_3N$	$HCl.Et_3N$
DCCI–HONSu	0.4 (93)	2.8 (77)	11 (71)
HONSu ester			<0.1 (91)
EEDQ	0.5 (78)	15 (68)	7.7 (74)
Bu^tOCOCl–Et_3N	2.0 (84)	7.0 (66)†	8.2 (63)
DCCI	16 (89)	15 (64)	27 (58)
NEPIS‡		39 (45)	

*Percent of L,D-peptide formed, determined by analysis after deprotection. The yields (figures in parentheses) were determined by weighing the neutral product of the reaction. Couplings were carried out in THF in the presence of the designated salt.
†13 (74) in AcOEt; 13 (70) using NMM as base; 29 (74) in AcOEt using NMM as base.
‡In CH_3CN.

TABLE 4. Yields and extent of racemization during the coupling of Boc-Ala-MeLeu with Gly-OBzl*

Coupling method	Solvent	L,D-Peptide formed (%)	Yield (%)
DCCI–HONSu	THF	<0.1	93
EEDQ	THF	0.5	86
DCCI	THF	15	78
DCCI	AcOEt	26	82
DCCI + Et_3N†	THF	14	55
Bu^tOCOCl–Et_3N‡	THF	6.4	60
Bu^tOCOCl–Et_3N‡	AcOEt	14	65
Bu^tOCOCl–Et_3N§	THF	3.9	36
Bu^tOCOCl–NMM‡	THF	15	68
NEPIS	CH_3CN	20	52

*Free base. Results determined by analysis after deprotection.
†One molar equivalent.
‡90-s activation, −10°.
§30-s activation, −15°.

and more recently to both of these (25). We have shown that the addition of an equivalent amount of triethylamine to a DCCI coupling did not increase the percentage of L,D-isomer. Thus the racemization is not base-catalyzed, and only the increased ionic strength can be appropriate as an explanation here. The seemingly anomalous results obtained with *N*-methylmorpholine may be due to the higher solubility in THF of *N*-methylmorpholine hydrochloride compared to triethylamine hydrochloride, leading to an increased ionic strength of the solution. The mixed-anhydride coupling at −15° using a 30-s activation time (the conditions for minimum racemization) (21) gave less diastereomer but at the expense of a considerably reduced yield.

Racemization was considerably enhanced for both the mixed-anhydride and DCCI couplings when ethyl acetate was used instead of the less polar THF. This dependence on solvent polarity could explain why high extents of racemization were obtained for the NEPIS coupling where the solvent was acetonitrile. It is interesting to note that with this reagent under similar conditions (absence of chloride), Smart *et al.* were able to couple the racemization-prone Bz-Leu without diastereomer formation (22).

The absence of base catalysis indicates that the mechanism involved is not a simple α-hydrogen abstraction. *N*-Acyl *N*-methylamino acids cannot form oxazolones, and this has led to the oxazolonium salt **1** being proposed as the racemization intermediate (9, 13, 26). The oxazolonium (or more correctly the 5-oxo-Δ^2-oxazolinium) cation can racemize by loss of proton to give the mesoionic oxazolium-5-oxide **3** or by tautomerism to the 5-hydroxy-oxazolium cation **2**. The resonance stabilization of these two derivatives (the oxazolium ring is in fact pseudoaromatic (27)) could contribute to the ease with which *N*-methylamino-acid derivatives racemize.

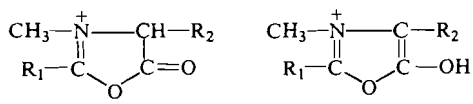

1

2

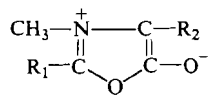

3

Oxazolonium derivatives were thought to be extremely unstable, and evidence for their existence was derived from cryoscopic data obtained with Bz-MeGly in sulfuric acid (28) and from their implication in the mechanism of the Dakin–

Can. J. Chem. Downloaded from www.nrcresearchpress.com by 210.87.254.105 on 09/05/12
For personal use only.

Can. J. Chem. Downloaded from www.nrcresearchpress.com by 210.87.254.105 on 09/05/12
For personal use only.

West reaction (29). Recently, however, several stable oxazolonium perchlorates have been prepared by treating *N*-substituted *N*-acylamino acids in acetic anhydride with perchloric acid (30).

The oxazolonium cation is a powerful acylating agent, giving a transient yellow color, ascribed to structure **3** when it is added to an amine (31, 32). We observed an immediate yellow color when we prepared the mixed anhydride of Bz-MeLeu or added DCCI to Bz-MeLeu. The oxazolium-5-oxides, prepared *in situ*, also undergo a 1,3-dipolar cycloaddition reaction with activated double and triple bonds (31), and we have made use of this reaction to show that oxazolonium-type intermediates can be formed under peptide coupling conditions. Z-Ala-MeLeu and DCCI were left in THF at room temperature for 10 min. Upon addition of methyl propiolate **4**, carbon dioxide was immediately evolved, and *N*,*N*′-dicyclohexylurea and the crystalline pyrrole **5** were obtained in about 85% yield. The plausible "classical" products of the

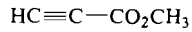

4

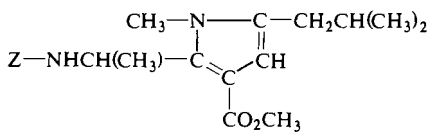

5

reaction would have been the *N*-acylurea derivative, which could not have been formed in large amounts, and the symmetrical anhydride of the protected peptide (33). But neither of these has the structural features required for a 1,3-dipolar cycloaddition reaction, therefore the pyrrole must have come from the oxazolium-5-oxide (**3**: R_1 = Z-NHCH(CH_3)—; R_2 = —$CH_2CH(CH_3)_2$), presumably formed in the reaction by cyclization to the oxazolonium cation followed by loss of a proton. This mechanism is consistent with the observations that the extent of racemization is (i) markedly dependent on solvent polarity and, seemingly, ionic strength which would be expected for a charged intermediate, and (ii) not affected by base, base catalysis being unnecessary for cyclization to an oxazolonium cation, the presumed rate-determining step.

The deprotonated mesoionic ring structure **3** is extremely unstable, and decomposes by dimerization (acylation at C-4) when unsubstituted at C-4(R_2 = H) (32). Treatment of Bz-MeGly with DCCI yielded the dimer resulting from α-*C*-acylation (34). It follows that if the oxazolonium cation is an intermediate in the coupling of *N*-methylamino-acid residues, the possibility that α-*C*-acylation might take place when sarcosyl is the coupling residue should be kept in mind. A practical implication of ignoring this danger might be that in the design of a synthesis, the decision to condense peptide fragments at sarcosyl residues in order to avoid racemization could prove to be more of a nuisance than an expedience.

It thus transpires that *N*-methylamino-acid residues seem to be just as prone to racemize during couplings as amino-acid residues, and even more so in the presence of salts. This is contrary to the generally accepted notions, which stem from their apparent structural similarity to prolyl residues, and could be attributed to the formation of the oxazolonium intermediate by the *N*-methylamino-acid derivative. The striking difference in behavior between the *N*-methylamino acid and proline could be due to the failure of the latter to form the oxazolonium intermediate. This in fact was proposed by Goodman and Stueben to account for the difference in behavior observed in the formation of the *p*-nitrophenyl esters (9). They suggested that the rigidity of the proline ring prevents the formation of a second contiguous ring. This appears to us a plausible explanation, but it must be borne in mind that under appropriate conditions, an oxazolonium intermediate can be formed even from a proline derivative. This had been suggested by Williams and Young (13) and has now been proved by Boyd and Wright who prepared the oxazolonium perchlorate from Bz(NO_2)-Pro (30).

The yields of tripeptide were determined in conjunction with the extents of racemization from the amino-acid analysis chromatogram (except as indicated in Table 3) for all the foregoing coupling reactions, and the results appear in Tables 3 and 4. They varied from 93% (DCCI–HONSu) to 52% (NEPIS) in the absence of triethylammonium salt and from 77% (DCCI–HONSu) to 45% (NEPIS) in the presence of salt. The yield was lowered by the presence of salt in all but the conventional mixed-anhydride case, where salt is always present. It is noticeable that

TABLE 5. Yields for couplings to an *N*-methylamino-acid ester component*

Coupling method	MeLeu-OBzl†	Ala-MeLeu-OBzl‡	Ala-MeLeu-OBu^t‡
DCCI	96	46	96
DCCI–HONSu	96	61	98
Bu^{t}OCOCl–Et_3N	92	68	92
EEDQ	91	93	95
p-Nitrophenyl ester	29	67	94

*Yields (%) determined by analysis after deprotection.
†Z-Ala coupled to the ester *p*-toluenesulfonate.
‡Z-Gly coupled to the ester hydrochloride. Ninhydrin color constant for Gly-Ala-MeLeu, 13.6.

the two racemization-free coupling methods (DCCI–HONSu and EEDQ) gave the best yields. It is known that β-alanyl derivatives can be formed as side-products during DCCI–HONSu couplings when the formation of the intermediate HONSu ester is slow (35). A good correspondence was found between the yield of the tripeptide calculated from the amino acid analysis and the weight of the total neutral product, indicating that the amount of any such impurities in our case could not have been appreciable.

The yields for couplings between three other pairs of reactants were determined and the results are given in Table 5. Excellent yields of the dipeptide were obtained in all but the *p*-nitrophenyl-ester coupling. Allusions to the lesser reactivity of an *N*-methylamino group in couplings have been made (4, 36). From our findings it appears that couplings to an *N*-methylamino group proceed smoothly, with the exception of a classical activated-ester coupling, but that only moderate yields result when a *C*-terminal *N*-methylamino acid is activated for synthesis. More experiments with different peptides are needed to confirm this generalization.

The two tripeptides in Table 5 were used to investigate the importance of cyclization to the piperazine-2,5-dione, which is known to be a problem in synthesis with both proline and *N*-methylamino-acid derivatives (4). The dipeptide *t*-butyl ester gave very high yields indicating that the *t*-butyl ester provided adequate protection against this side reaction, whereas the dipeptide benzyl ester gave considerably lower yields, presumably because of the competing cyclization reaction (the piperazine-dione was not isolated). A high yield was nevertheless obtained with the benzyl ester when EEDQ was the coupling reagent. The explanation for this is not apparent to us.

Experimental

Materials and Methods

Amino acids were obtained from General Biochemicals, Chagrin Falls, Ohio; Boc-Ala and HONSu from Pierce Chemical Company, Rockford, Illinois; DCCI from Schwarz-Mann, Orangeburg, New York; EEDQ and NEPIS from Aldrich Chemical Company, Milwaukee, Wisconsin; methyl propiolate from K & K Laboratories Inc., Plainview, New York; Aminex A-5 resin from Bio-Rad Laboratories, Richmond, California. Benzyloxycarbonylamino acids were prepared by the original procedure as described by Greenstein and Winitz (ref. 37, p. 891). Solvents were purified and dried by standard methods before use. Light petroleum refers to the fraction boiling between 30–60°. Organic solvent extracts were dried with $MgSO_4$ and evaporated under reduced pressure using a rotary evaporator. When not specified, hydrogenations were carried out at atmospheric pressure in 80% aqueous acetic acid in the presence of 10% palladium on charcoal catalyst for 4 h. The catalyst was removed by filtration, the solution was evaporated, the evaporation was repeated several times after the addition of water, and the residue was dried *in vacuo* over KOH pellets. Optical rotations were determined with a Perkin Elmer model 141 polarimeter using a 1 dm tube. Proton nuclear magnetic resonance (n.m.r.) (Varian T-60) and t.l.c. on silica gel GF_{254} in chloroform–methanol (9:1) were used to confirm the identity and purity of oils. Diastereomeric amino acids and peptides were analyzed with a Beckman model 120B amino-acid analyzer according to Spackman *et al.* (38) using the conditions described in Table 2. Both the extent of racemization and the yield of a reaction were calculated from the same chromatogram of an aliquot of deprotected peptide using the data in Table 2.

The following compounds were prepared as indicated: Bz-Leu and Bz-Pro (ref. 37, p. 1266), Bz-MeLeu (40), Z-MeLeu (41), Boc-Ala-Pro (1), Z-Ala-Leu and Z-DL-Ala-Leu (42), Gly-OBzl.TosOH, Gly-OBzl.HCl, and Gly-OBzl (ref. 37, p. 928), Z-Ala-MeLeu (oil, containing 0.4% of the L,D-isomer) from the *t*-butyl ester (1).

MeLeu-OBzl.TosOH

A mixture of *N*-methyl-L-leucine (3.3 g, from the hydrogenation of Z-MeLeu in aqueous acetic acid), *p*-toluenesulfonic acid monohydrate (4.87 g), benzyl alcohol (20 ml), and benzene (60 ml) was heated under reflux for 36 h, the water formed being trapped in a Dean–Stark tube (44). The benzene was evaporated off,

Can. J. Chem. Downloaded from www.nrcresearchpress.com by 210.87.254.105 on 09/05/12
For personal use only.

Can. J. Chem. Downloaded from www.nrcresearchpress.com by 210.87.254.105 on 09/05/12
For personal use only.

ether (100 ml) and light petroleum (200 ml) were added, and the solution was left overnight at 0°. The crystals were collected, and recrystallized from ethyl acetate – methanol – light petroleum. Yield 7.0 g (72%), m.p. 116–117°, $[\alpha]_D^{25}$ −2.2° (*c*, 1 in ethanol).

Anal. Calcd. for $C_{21}H_{23}NO_5S$: 61.9; H, 7.2; N, 3.4 Found: C, 61.5; H, 7.1; N, 3.4.

Boc-Ala-MeLeu

Boc-Ala (1.89 g) and MeLeu-OBzl.TosOH (4.04 g) were coupled by the mixed-anhydride method using Bu^{t}OCOCl (1.3 ml) and triethylamine (1.38 ml) in ethyl acetate (20 ml) at −10° as described below. The neutral product was an oil (3.6 g; 92%), giving a single spot on t.l.c., and whose n.m.r spectrum was consistent with the structure (Boc-Ala-MeLeu-OBzl). The oil was hydrogenated in ethyl acetate for 8 h. Removal of the solvent left an oil which crystallized upon trituration with light petroleum, and which was recrystallized from ether – light petroleum. Yield 2.0 g (75%), m.p. 107–109°, $[\alpha]_D^{28}$ −55.1° (*c*, 1 in ethanol).

Anal. Calcd. for $C_{12}H_{28}N_2O_5$: C, 56.9; H, 9.0; N, 8.9. Found: C, 56.4; H, 9.1; N, 8.4.

A sample (20 mg) was left in trifluoroacetic acid (0.5 ml) for 30 min and then analyzed. The product contained none (<0.1%) of the diastereomer.

Reference Compounds

The elution times and relative ninhydrin color yields for each diastereomeric pair of peptides were obtained by chromatography of the peptides synthesized from a racemic starting material. For convenience, in the case of the two *N*-methylamino acid peptides, one isomer of each diastereomeric pair was actually the enantiomorph of the L,D-isomer which was analyzed for. Moreover, some racemization undoubtedly occurred during the synthesis of these peptides at the mixed-anhydride coupling and saponification stages; however, the products would still be a mixture of diastereomers in equal amounts *i.e.*, L,L + D,D = D,L + L,D. The assignments of the two peaks obtained during chromatography and the absolute color yields of the isomers were then established by chromatography of a known amount of the stereochemically pure L,L-isomer.

N-methyl-L-isoleucine and *N*-methyl-D-*allo*-isoleucine were obtained by hydrogenation of Z-MeIle and Z-D-MeaIle prepared by the room-temperature methylation of Z-Ile and Z-D-*a*Ile (41). Ala-DL-Leu and Ala-DL-Pro were prepared from L-alanine *N*-carboxyanhydride and the free amino acid by the method of Manning and Moore (14), and used for analysis without purification. Ala-Leu was obtained by leaving Boc-Ala-Pro in trifluoroacetic acid for 30 min, evaporating the solution, and drying the residue *in vacuo* over KOH.

DL-Ala-Leu-Gly was obtained by hydrogenation (8 h) of Z-DL-Ala-Leu-Gly-OBzl, prepared by the mixed-anhydride (Bu^{t}OCOCl–Et_3N) coupling of Z-DL-Ala-Leu with Gly-OBzl.TosOH in THF. Ala-Leu-Gly was obtained by hydrogenation (8 h) of Z-Ala-Leu-Gly-OBzl prepared by the DCCI–HONSu-mediated coupling of Z-Ala-Leu with Gly-OBzl.TosOH as described below.

DL-Ala-MeLeu, as the hydrochloride, was obtained by a mixed-anhydride (Bu^{t}OCOCl–Et_3N) coupling of Z-DL-Ala (0.545 g) and MeLeu-OBzl.TosOH (1.06 g) in ethyl acetate (15 ml). The neutral product was isolated as an oil (1.07 g, 97%) which was hydrogenated in 80% aqueous acetic acid containing 2*N* HCl (1 mol. equiv.).[7] Ala-MeLeu was obtained by hydrogenation of Z-Ala-MeLeu.

DL-Ala-MeLeu-Gly was obtained by hydrogenation (8 h) of Z-DL-Ala-MeLeu-Gly-OBzl. The latter was the neutral product (oil, 0.55 g, 80%) obtained by the mixed-anhydride (Bu^{t}OCOCl–Et_3N) coupling of Z-DL-Ala-MeLeu (0.465 g) and Gly OBzl.TosOH (0.453 g) in THF as described below. The Z-DL-Ala-MeLeu (oil) was the acidic product (0.74 g, 77%) obtained by the saponification (2 h) of Z-DL-Ala-MeLeu-OBzl (0.97 g) in a mixture of methanol (8 ml) and 4 *N* NaOH (2.5 ml). Ala-MeLeu-Gly was the product obtained from the DCCI–HONSu-mediated coupling of Boc-Ala-MeLeu and Gly-OBzl described below. This was the first coupling to have given pure L,L-peptide.

Racemization during Hydrolysis of Mixed Anhydrides

The test compound (1–2 mmol) was dissolved in THF (5 ml) containing triethylamine (1 mol. equiv.) at 0°. Isobutyl chloroformate (1 mol. equiv.) was added with stirring, followed by water (2 ml) 5 min later. After 1 h at 0°, the THF was evaporated, and the residue was partitioned between ether (5 ml) and 5% aqueous $NaHCO_3$ (5 ml). The aqueous layer was acidified to p*H* 1 (p*H* 3 for Boc-Ala-Pro) with 3 *N* HCl, extracted with ethyl acetate, and the extract was dried and evaporated. Benzyloxycarbonyl derivatives were deprotected by hydrogenation, Boc-Ala-Pro by treatment with trifluoroacetic acid for 30 min, and the products were analyzed. The optical rotations of the benzoyl derivatives were measured, with the following results: Bz-Leu, $[\alpha]_D^{24}$ 0.0° (*c*, 1.8 in dimethylformamide); Bz-MeLeu, $[\alpha]_D^{24}$ −6.5° (*c*, 1 in dimethylformamide); Bz-Pro, $[\alpha]_D^{25}$ −83.3° (*c*, 4 in ethanol). Original values were, respectively: +7.0°, −54.0°, and −95.4°.

Coupling Methods for Racemization Experiments

The following methods were employed for coupling Z-Ala-Leu, Z-Ala-MeLeu, and Boc-Ala-MeLeu (0.5 mmol) with Gly-OBzl (0.5 mmol) (Tables 3 and 4). When salts of Gly-OBzl were used, triethylamine (0.5 mmol) was added to the ester salt. After the reaction, the solvent was removed by evaporation, the residual oil was taken up in ethyl acetate (10 ml), and the solution was washed with *N* HCl (2 × 5 ml), 5% aqueous $NaHCO_3$ (2 × 5 ml), and water (2 × 5 ml). The extract was dried and concentrated to an oil which was analyzed after deprotection by hydrogenation for 8 h. For couplings with Boc-Ala-MeLeu, aqueous citric acid was used instead of HCl for washing, and the hydrogenation was followed by treatment with trifluoroacetic acid (1 ml) for 30 min.

(i) DCCI (45)

DCCI (110 mg) was added to the reactants in the appropriate solvent (2 ml) and the mixture was stirred at room temperature for 18 h. The mixture was cooled, filtered, and the filtrate was evaporated.

---

[7]In the absence of HCl, only a small amount of ninhydrin-positive material was formed, presumably due to cyclization of the ester to the piperazine-dione after loss of the benzyloxycarbonyl group.

(ii) DCCI–HONSu (18)

As for the DCCI coupling except that HONSu (57 mg) was added to the reaction mixture before the DCCI.

(iii) HONSu Ester (46)

As for the DCCI–HONSu coupling except that the Gly-OBzl.HCl (0.101 g) in THF (1 ml) containing triethylamine (0.069 ml) was added 1 h after the DCCI and HONSu.

(iv) Mixed Anhydride (47)

The carboxy-containing component, base (0.069 ml of triethylamine or 0.056 ml of *N*-methylmorpholine), and isobutyl chloroformate (0.065 ml) were stirred in the solvent (2 ml) at −10° C for 90 s. The ester in THF (2 ml) was added, and the mixture was stirred at −10° for 1 h, and at room temperature for 1 h. One coupling was done under different conditions (Table 4).

(v) EEDQ (19)

A solution of the two reactants and EEDQ (129 mg; 5% excess) in THF (2 ml) was stirred at room temperature for 18 h. The neutral product was isolated as described above except that four washings with *N* HCl were carried out to remove the quinoline.

(vi) NEPIS (48)

The carboxy-containing component was stirred with NEPIS (127 mg) and triethylamine (0.069 ml) in acetonitrile (2.5 ml) at 0 °C for 1 h. The ester in cold acetonitrile (1 ml) was added, the mixture was stirred at 0° for 2 h, and then overnight at room temperature.

Couplings of Z-Ala + MeLeu-OBzl

Z-Ala (112 mg; 0.5 mmol) and MeLeu-OBzl.TosOH (202 mg) were coupled in THF (5 ml) using the methods described above. The neutral product was isolated and deprotected by hydrogenation in 80% aqueous acetic acid containing *N* HCl (0.5 ml) for 8 h. A solution of Z-Ala-ONp (39), MeLeu-OBzl.TosOH (202 mg), and triethylamine (0.069 ml) in dimethylformamide (2 ml) was kept at 37 °C for 36 h (43). The total neutral product was deprotected for analysis.

Couplings of Z-Gly + Ala-MeLeu-OR

Ala-MeLeu-OBzl.HCl (0.63 g; 91%; m.p. 157–160°; hygroscopic) was obtained by leaving Boc-Ala-MeLeu-OBzl (0.81 g) in dioxane containing hydrogen chloride (3.9 *N*, 10 ml) at room temperature for 1 h and evaporating the solution.

Ala-MeLeu-OBu^t.HCl (0.56 g; 70%; m.p. 176–178°) was prepared by hydrogenation of Z-Ala-MeLeu-OBu^t (1.1 g) (1) in *t*-butanol containing HCl (1 mol. equiv.) for 4 h. The product was obtained as a white solid by evaporating the solvent and drying the residual gel *in vacuo* over KOH.

Z-Gly (0.063 g) and Ala-MeLeu-OBzl.HCl (0.104 g) or Ala-MeLeu-OBu^t.HCl (0.092 g) were coupled in THF (2 ml) using the general methods described above, with triethylamine to neutralize the HCl. The nitrophenyl-ester coupling was carried out in dimethylformamide at 37° for 24 h. The neutral products were isolated to give Z-Gly-Ala-MeLeu-OBzl and Z-Gly-Ala-MeLeu-OBu^t as oils which were hydrogenated for 8 h. The *t*-butyl ester was treated with trifluoroacetic acid (1 ml) for 1 h before hydrogenation.

The color constant for Gly-Ala-MeLeu was determined from the deprotected product of the mixed-anhydride coupling of the benzyl ester. The product was washed with ether and dried *in vacuo* over KOH.

Trapping of Racemization Intermediate

Z-Ala-MeLeu (0.85 g) and DCCI (0.502 g) were stirred in THF (20 ml) at room temperature for 10 min. The mixture was cooled in ice, and methyl propiolate (0.50 ml) was added. There was an immediate evolution of carbon dioxide. The mixture was stirred at 0 °C for 2 h and then evaporated. The residue was suspended in acetone (20 ml), the mixture was kept at −10° for 3 h, and the *N,N'*-dicyclohexylurea (0.45 g; 83%) was filtered off. The filtrate was evaporated, the residue was taken up in ethyl acetate, and the solution was washed twice with aqueous $NaHCO_3$ and water, dried, and evaporated. The residual oil was crystallized (0.80 g) from ether – light petroleum and recrystallized from methanol–water. Yield 0.71 g (79%), m.p. 106–108°, n.m.r. δ($CDCl_3$–TMS): 7.31 (s, 5, $-C_6H_5$); 6.49 (s, 1, pyrrole); 5.11 (s, 2, $-CH_2O-$); 4.9 (b, 2, $-NHCH\langle$); 3.73 (s, 3, $-OCH_3$); 3.42 (s, 3, $\rangle NCH_3$); 2.84 (d, 2, $-CH_2-$, J = 7.0 Hz); 1.8 (m, 1, $\rangle CH-$); 1.52 (d, 3, CH_3-, J = 6.0 Hz); 0.92 (d, 6, $(CH_3)_2=$, J = 6.2 Hz).

Anal. Calcd. for $C_{21}H_{28}N_2O_4$: C, 67.7; H, 7.6; N, 7.5. Found: C, 67.4; H, 7.8; N, 7.3.

We thank Dr. J. Rudinger for most helpful discussions.

1. J. R. McDERMOTT and N. L. BENOITON. Can. J. Chem. This issue.
2. E. SCHRÖDER and K. LÜBKE. The peptides. Vol. II. Academic Press, New York, N.Y. 1966. p. 396.
3. J. RUDINGER. *In* Drug design. *Edited by* E. J. Ariens. Vol. II. Academic Press, New York, N.Y. 1971. p. 319.
4. J. RUDINGER. *In* Peptides: Proc. of the 5th European Peptide Symposium, Oxford. 1962. *Edited by* G. T. Young. Oxford University Press, Oxford. 1963. p. 133.
5. M. BODANSZKY and M. A. ONDETTI. Peptide synthesis. Interscience Publishers, New York, N.Y. 1966. p. 137.
6. H. E. CARTER and C. M. STEVENS. J. Biol. Chem. **133**, 117 (1940).
7. R. W. JACKSON and W. M. CAHILL. J. Biol. Chem. **126**, 37 (1938).
8. IUPAC–IUB commission on biochemical nomenclature. J. Biol. Chem. **247**, 977 (1972).
9. M. GOODMAN and K. C. STUEBEN. J. Org. Chem. **27**, 3409 (1962).
10. R. L. HUGUENIN and R. A. BOISSONNAS. Helv. Chim. Acta, **44**, 213 (1961).
11. J. R. McDERMOTT and N. L. BENOITON. *In* Chemistry and biology of peptides: Proc. of the 3rd American Peptide Symposium, Boston, 1972. *Edited by* J. Meienhofer. Ann Arbor Publishers, Ann Arbor, Mich. 1972. p. 369.
12. N. L. BENOITON. Unpublished results.
13. M. W. WILLIAMS and G. T. YOUNG. J. Chem. Soc. 3701 (1964).

Can. J. Chem. Downloaded from www.nrcresearchpress.com by 210.87.254.105 on 09/05/12
For personal use only.

14. J. M. MANNING and S. MOORE. J. Biol. Chem. **243**, 5591 (1968).
15. N. IZUMIYA and M. MURAOKA. J. Am. Chem. Soc. **91**, 2391 (1969); N. IZUMIYA, M. MURAOKA, and H. AOYAGI. Bull. Chem. Soc. Jap. **44**, 3391 (1971).
16. J. R. COGGINS and N. L. BENOITON. J. Chromatogr. **52**, 251 (1970).
17. N. L. BENOITON and J. R. COGGINS. *In* Progress in peptide research, Vol. 2; Proc. of the 2nd American Peptide Symposium, Cleveland, 1970. *Edited by* S. Lande. Gordon and Breach, New York, N.Y. 1972. p. 145.
18. E. WÜNSCH and F. DREES. Chem. Ber. **99**, 110 (1966); F. WEYGAND, D. HOFFMANN, and E. WÜNSCH. Z. Naturforsch. **21b**, 426 (1966).
19. B. BELLEAU and G. MALEK. J. Am. Chem. Soc. **90**, 1651 (1968).
20. D. S. KEMP, Z. BERNSTEIN, and J. REBEK. J. Am. Chem. Soc. **92**, 4756 (1970).
21. G. W. ANDERSON. J. E. Zimmerman, and F. M. CALLAHAN. J. Am. Chem. Soc. **89**, 5012 (1967).
22. N. A. SMART, G. T. YOUNG, and M. W. WILLIAMS. J. Chem. Soc. 3902 (1960).
23. G. W. ANDERSON, J. BLODINGER, and A. D. WELCHER. J. Am. Chem. Soc. **74**, 5309 (1952); F. WEYGAND, A. PROX, L. SCHMIDHAMMER, and W. KÖNIG. Angew. Chem. **75**, 282 (1963).
24. M. GOODMAN and W. J. MCGAHREN. Tetrahedron, **23**, 2031 (1967).
25. A. W. WILLIAMS and G. T. YOUNG. J. Chem. Soc. Perkin I, 1194 (1972).
26. A. NEUBERGER. Adv. Protein Chem. **4**, 297 (1948).
27. R. HUISGEN. *In* Aromaticity. Chem. Soc. Special Publ. No. 21, London. 1967. p. 51.
28. J. L. O'BRIEN and C. NIEMANN. J. Am. Chem. Soc. **79**, 80 (1957).
29. J. W. CORNFORTH and D. F. ELLIOT. Science, **112**, 534 (1950).
30. G. V. BOYD and P. H. WRIGHT. J. Chem. Soc. Perkin I, 909 (1972).
31. R. HUISGEN, H. GOTTHARDT, H. O. BAYER, and F. C. SCHAEFER. Angew. Chem. (Int. ed.), **3**, 136 (1964).
32. G. V. BOYD and P. H. WRIGHT. J. Chem. Soc. Perkin I, 914 (1972).
33. E. SCHRÖDER and K. LÜBKE. The peptides. Vol. I. Academic Press, New York, N.Y. 1965. p. 109.
34. C. V. GRECO, R. P. GRAY, and V. G. GROSSO. J. Org. Chem. **32**, 4101 (1967).
35. F. WEYGAND, W. STEGLICH, and N. CHYTIL. Z. Naturforsch. **23b**, 1391 (1968); H. GROSS and L. BILK. Tetrahedron, **24**, 6935 (1968).
36. P. A. JAQUENOUD. Chimia, **14**, 373 (1960).
37. J. P. GREENSTEIN and M. WINITZ. Chemistry of the amino acids. John Wiley and Sons, New York, N.Y. 1962.
38. D. H. SPACKMAN, W. H. STEIN, and S. MOORE. Anal. Chem. **30**, 1190 (1958).
39. F. MARCHIORI, R. ROCCHI, and E. SCOFFONE. Gazz. Chim. Ital. **93**, 834 (1963).
40. J. R. COGGINS and N. L. BENOITON. Can. J. Chem. **49**, 1968 (1971).
41. J. R. MCDERMOTT and N. L. BENOITON. Can. J. Chem. **51**, 1915 (1973).
42. E. KLIEGER, E. SCHRÖDER, and H. GIBIAN. Ann. **640**, 157 (1961).
43. M. BODANSZKY. Acta Chim. Acad. Sci. Hung. **10**, 335 (1957).
44. J. D. CIPERA and R. V. V. NICHOLLS. Chem. Ind. 16 (1955).
45. J. C. SHEEHAN and G. P. HESS. J. Am. Chem. Soc. **77**, 1067 (1955).
46. G. W. ANDERSON, J. E. ZIMMERMAN, and F. M. CALLAHAN. J. Am. Chem. Soc. **85**, 3039 (1963).
47. R. A. BOISSONNAS. Helv. Chim. Acta, **34**, 874 (1951); J. R. VAUGHAN. J. Am. Chem. Soc. **73**, 3547 (1951); T. WIELAND and H. BERNHARD. Ann. **572**, 190 (1951).
48. R. B. WOODWARD, R. A. OLOFSON, and H. MAYER. J. Am. Chem. Soc. **83**, 1010 (1961).

Can. J. Chem. Downloaded from www.nrcresearchpress.com by 210.87.254.105 on 09/05/12
For personal use only.

A Comparative Proton Magnetic Resonance Study of the Molecular Conformation of Uracil and 6-Aza Uracil Nucleosides and Nucleotides

DONALD J. WOOD[1] AND FRANK E. HRUSKA

Department of Chemistry, University of Manitoba, Winnipeg, Manitoba R3T 2N2

AND

RICHARD J. MYNOTT[1] AND RAMASWAMY H. SARMA

Department of Chemistry, The State University of New York at Albany, Albany, New York 12222

Received January 15, 1973

Proton magnetic resonance data for uridine and uridine-5′-monophosphate, and the corresponding 6-azauracil analogs, are presented and discussed in terms of their overall three dimensional conformations in aqueous solution. The data reveal a destabilizing influence of the 6-aza base upon the gog and g′–g′ conformation of the ribose phosphate moiety.

Les données obtenues de la résonance magnétique du proton pour l'uridine, l'uridine-5′-monophosphate ainsi que les analogues correspondants aza-6 uracil, sont présentées et interprétées en termes de conformation totale tridimensionelle en solution aqueuse. Les données révèlent une influence déstabilisante de la base aza-6 sur la conformation g–g et g′–g′ de l'entité ribose-phosphate.

[Traduit par le journal]

Can. J. Chem., **51**, 2571 (1973)

Introduction

There has been considerable interest in the antimetabolite behavior of 6-azauridine (azaU) which is known to have potent anti-leukemic properties (1). The nucleoside itself is not effective but is converted *in vivo* to 6-azauridine-5′-monophosphate (5′-azaUMP, Fig. 1) which inhibits the transformation of orotidine-5′-monophosphate (5′-OMP) to uridine-5′-monophosphate (5′-UMP) by the decarboxylating enzyme, orotidine-5′-monophosphate decarboxylase. Recently Saenger and Suck (2) have, by X-ray analyses, found that the *gauche–gauche* conformation about the $C_{4'}$—$C_{5'}$ bond which occurs exclusively in all previously-investigated nucleoside-5′-monophosphates is not assumed by 5′-azaUMP.

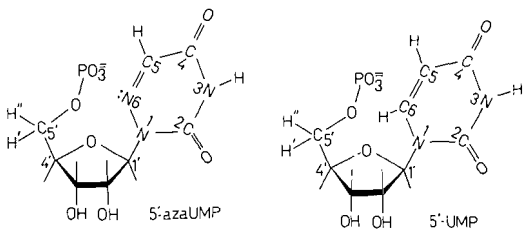

FIG. 1. Structural formula for 6-azauridine-5′-monophosphate (5′-azaUMP) and uridine-5′-monophosphate (5′-UMP).

[1]Postdoctoral Fellow.

The authors suggest that the presence of an unusual conformation (*gauche–trans*) might explain the inhibitory capacity of the aza derivative. In the present study we have obtained and analyzed the p.m.r. spectra of U(uridine), 5′-UMP, azaU, and 5′-azaUMP. Comparison of the p.m.r. data indicates that the presence of the 6-aza base has a marked destabilizing influence upon the *gauche–gauche* conformation of 5′-azaUMP and, therefore, that an unusual conformation of its ribose phosphate moiety is retained in aqueous solution.

Materials and Methods

Top grade azaU, 5′-azaUMP, and 5′-UMP were obtained from Calbio-Chem. The p.m.r. spectra of azaU (D_2O, 0.1 *M*, p*D* = 7.0, 30 °C, internal reference 3-trimethylsilylpropanesulfonic acid, DSS) were recorded at 220 MHz (Varian spectrometer, Canadian 220 Centre). Spectra for 5′-UMP and 5′-azaUMP (D_2O, 0.1 *M*, p*D* = 8.0, 30 °C, internal reference tetramethylammonium chloride, TMA) were obtained in the Fourier transform mode; details for obtaining FT spectra have been presented elsewhere (3). Both ^{31}P-decoupled and ^{31}P-coupled spectra were obtained and analyzed using LAME (4). Computer simulations of both the ^{31}P-decoupled and ^{31}P-coupled ^1H spectra were generated as a final test of the p.m.r. data. The experimental and simulated spectra for the mononucleotides are reproduced in Figs. 2–5. The experimental data are given in Table 1; the chemical shift and coupling constant data for U are taken from ref. 5. We would like to draw attention to, in particular, the 4′-region of 5′-UMP and 5′-azaUMP. In the case of 5′-UMP, a distinct sharpening of the

Can. J. Chem. Downloaded from www.nrcresearchpress.com by 210.87.254.40 on 09/05/12
For personal use only.

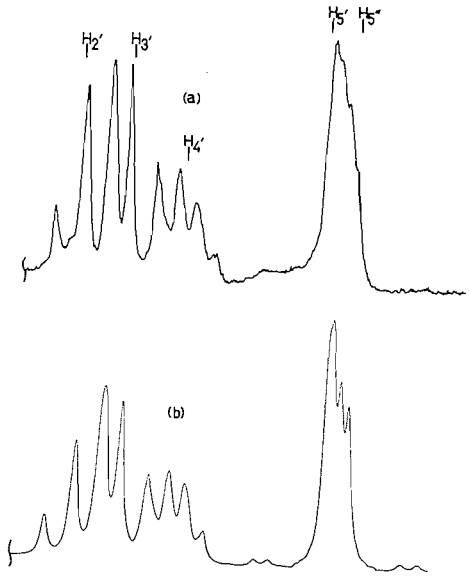

FIG. 2. (*a*) 100 MHz Fourier transformed spectrum of uridine-5′-monophosphate (5′-UMP) in D_2O, pD = 8.0, 0.10 *M*, with the phosphorus atom decoupled (2′ to 5″ region only). (*b*) Computer simulated spectrum.

4′-region is a consequence of P-decoupling (compare Figs. 2*a* and 3*a*). However, in the case of 5′-azaUMP, no difference is noted in the 4′-region of the ^{31}P-coupled and ^{31}P-decoupled spectra (Figs. 4*a* and 5*a*). LAME analysis generates a 1.8 Hz[2] P–$H_{4'}$ coupling for fitting of the experimental 4′-transitions of 5′-UMP, whereas no significant coupling (<0.1 Hz) was generated in the iterative fitting of the 4′-transitions of 5′-azaUMP. Thus, the presence of a long-range four-bond coupling between P and H-4′ is indicated for the uracil derivative but not for the 6-aza derivative.

Results and Discussion

It has been demonstrated that Karplus treatments of the vicinal 4′- to 5′-hydrogen coupling constants can yield information regarding the conformation about the $C_{4'}$—$C_{5'}$ bond of a nucleoside moiety (7–9). The main conclusion of these earlier studies was that the exocyclic CH_2OH group of a nucleoside interconverts, in solution, between the three principle staggered conformations (Fig. 6) with the relative populations of the conformational isomers dependent upon a number of factors including the nature of the base, furanose ring puckering, and solvent properties (9). In recent studies (8, 9), we have evaluated the $C_{4'}$—$C_{5'}$ conformational problem in terms of the experimental *sum* of $J_{4'5'} + J_{4'5''}$.

[2]A 2.2 Hz P–$H_{4'}$ coupling in 5′-UMP was reported by Smith *et al.* (6).

The use of this sum relies solely on the reasonable assumption that any vicinal *trans* H–H coupling (*ca.* 8–10 Hz) is larger than *all gauche* H-H couplings (*ca.* 2–4 Hz) experienced during the course of rotation about the $C_{4'}$—$C_{5'}$ bond. The sum allows for discussion of the relative contributions of the *gauche–gauche* (g–g) rotamer and the *combined* contribution from the *gauche–trans* (g–t) and *trans–gauche* (t–g) rotamers (Fig. 6). Evaluation of the individual contributions from the g–t and the t–g isomers requires, first of all, an absolute spectral assignment of the 5′-hydrogens which can be ultimately carried out only by selective deuteration at the 5′-position (a reasonable assignment for several molecules, based on phosphate field effects, has been presented by Remin and Shugar (10)). In addition corrections for the orientation-dependent effect of the electronegative furanose-ring oxygen (11) need be applied to, in particular, the *gauche* couplings. Until such time that these corrections can be estimated, it is our contention that the use of the sum $J_{4'5'} + J_{4'5''}$ provides a more than adequate guide for monitoring perturbations in time-averaged conformations about the $C_{4'}$—$C_{5'}$ bond in a nucleoside or nucleotide.

Assuming that these sums provide a meaningful basis for monitoring nucleoside (tide) structure, then a number of qualitative predictions

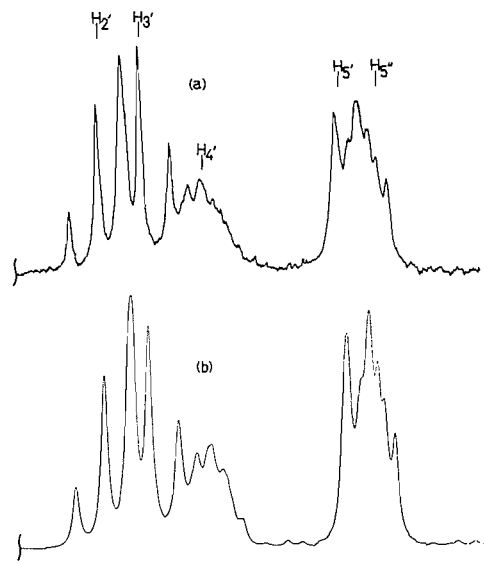

FIG. 3. (*a*) 100 MHz Fourier transformed spectrum of uridine-5′-monophosphate (5′-UMP) in D_2O, pD = 8.0, 0.10 *M*, without phosphorus decoupled (2′ to 5″ region). (*b*) Computer simulated spectrum.

Can. J. Chem. Downloaded from www.nrcresearchpress.com by 210.87.254.40 on 09/05/12
For personal use only.

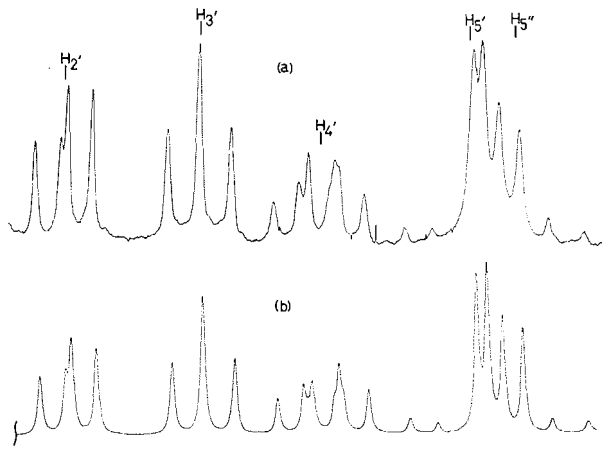

FIG. 4. (*a*) 100 MHz Fourier transformed spectrum of 6-azauridine-5′-monophosphate (5′-azaUMP) in D_2O, pD = 8.0, 0.10 *M*, with phosphorus decoupled (2′ to 5″ region). (*b*) Computer simulated spectrum.

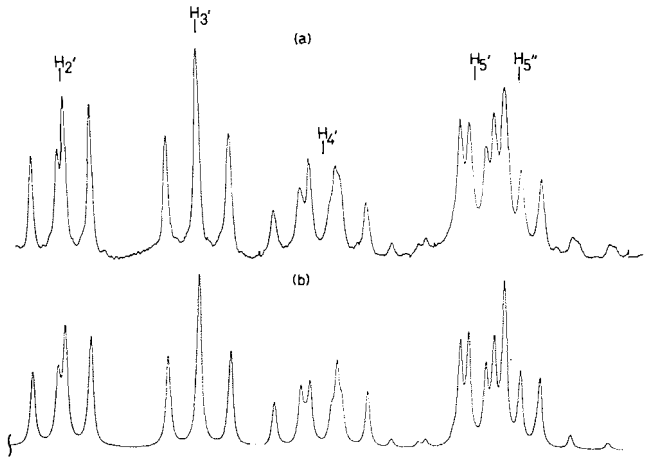

FIG. 5. (*a*) 100 MHz Fourier transformed spectrum of 6-azauridine-5′-monophosphate (5′-azaUMP) in D_2O, pD = 8.0, 0.10 *M*, without phosphorus decoupled (2′ to 5″ region).

can be made using Fig. 6. Clearly for the g–g conformation in which the 5′-O lies above the ring, the magnitudes of both $J_{4'5'}$ and $J_{4'5''}$ are predicted to be small (2–4 Hz) since the coupled nuclei are oriented *gauche*. However, if the 5′-O lies off the ring in either the g–t or t–g rotamer the 4′-hydrogen lies *trans* to one of the 5′-hydrogens and the corresponding vicinal coupling is expected to be large (*ca.* 8–10 Hz). Thus, any perturbation resulting in an *increase* in the g–g rotamer population should be manifest by a *decrease* in the experimental *sum* $J_{4'5'} + J_{4'5''}$ whereas an increase in the g–t and/or t–g populations, at the expense of the g–g conformer, should result in an *increase* in the observed sum (7, 8). Also, perturbations in molecular conformation about the $C_{5'}$—$O_{5'}$ bond can be monitored in an analogous fashion (12) (Fig. 7). In the g′–g′ rotamer, the P atom is *gauche* to each of the methylene hydrogens and therefore the *sum* $J_{P\text{-}H_{5'}} + J_{P\text{-}H_{5''}}$ is expected to be small (*ca.* 6 Hz) (13). In the g′–t′ and t′–g′ rotamers, however, the *sum* is expected to be large (*ca.* 24 Hz) since the P -atom is now *trans* to one of the 5′-hydrogens (13).

The experimental sums, $J_{4'5'} + J_{4'5''}$ (7.4 Hz for U; 8.8 Hz for azaU), indicate that the presence of the 6-azauracil base has a destabilizing influence, relative to uracil, upon the g–g orientation about the $C_{4'}$—$C_{5'}$ bond of a nucleoside.

Can. J. Chem. Downloaded from www.nrcresearchpress.com by 210.87.254.40 on 09/05/12
For personal use only.

Can. J. Chem. Downloaded from www.nrcresearchpress.com by 210.87.254.40 on 09/05/12
For personal use only.

TABLE 1. P.m.r. parameters* for D_2O solutions of U, 6-aza-U, 5′-UMP, and 5′-azaUMP at 30 °C

Parameter	U†	azaU	5′-UMP	5′aza-UMP
$\nu_{1'}$	5.90	6.13	2.81	2.96
$\nu_{2'}$	4.34	4.58	1.24	1.43
$\nu_{3'}$	4.22	4.37	1.17	1.20
$\nu_{4'}$	4.13	4.09	1.07	1.00
$\nu_{5'}$	3.91	3.82	0.84	0.75
$\nu_{5''}$	3.80	3.69	0.78	0.68
ν_5	5.88	7.40	2.80	4.27
ν_6	7.89	—	4.93	—
$J_{1'2'}$	4.4	3.6	5.3	4.2
$J_{2'3'}$	5.3	5.2	5.0	5.4
$J_{3'4'}$	5.5	5.8	3.9	5.4
$J_{4'5'}$	3.0	3.2	2.5	4.6
$J_{4'5''}$	4.4	5.6	3.0	6.1
$J_{5'5''}$	−12.7	−12.4	−13.5	−11.3
$J_{1'5}$	0.35	0.61	<0.2	0.55
$J_{P\text{-}4'}$	—	—	1.8	<0.2
$J_{P\text{-}5'}$	—	—	3.2	5.6
$J_{P\text{-}5''}$	—	—	5.1	6.1
$J_{4'5'} + J_{4'5''}$	7.4	8.8	5.5	10.7
$J_{P\text{-}5'} + J_{P\text{-}5''}$	—	—	8.3	11.7

*Chemical shifts in p.p.m. of U and aza U are relative to internal DSS whereas those for the phosphates are relative to internal TMA (coupling constants in Hz).
†Taken from ref. 5.

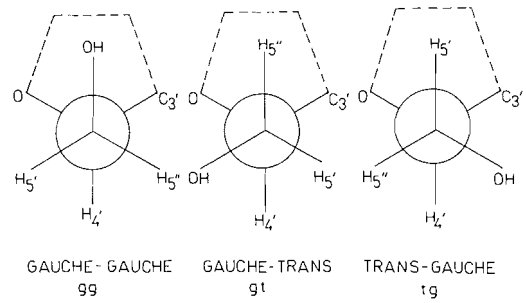

FIG. 6. Staggered conformations about the $C_{4'}$—$C_{5'}$ bond.

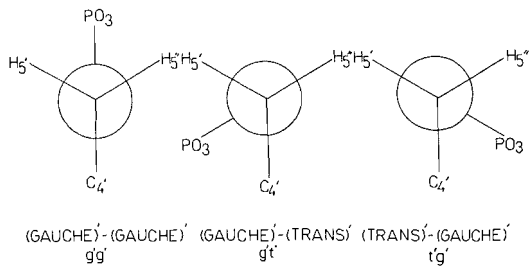

FIG. 7. Staggered conformations about the $C_{5'}$—O_5 bond.

The apparent destabilizing effect is even more pronounced for the monophosphate derivatives for which an *increase* of 5.2 Hz in the sum is evident when uracil is substituted by the 6-aza base (Table 1). Manipulation of eqs. 1–3 in ref. 7 allows for derivation of a simple relationship between P_{gg} (the fractional population of the g–g rotamer) and $\sum$(the observed sum of $J_{4'5'} + J_{4'5''}$):

$$[1] \qquad P_{gg} \simeq (12 - \textstyle\sum)/8$$

which provides rough estimates of g–g population. Substitution of the data into eq. 1 leads to P_{gg} values: U (60%); azaU (40%); 5′-UMP (80%); 5′-azaUMP (15%).

A similar expression may be derived for the $C_{5'}$—$O_{5'}$ bond of the monophosphates. Assuming $J_{P\text{-}H}$ (*gauche*) $\simeq$ 3 Hz and $J_{P\text{-}H}$ (*trans*) $\simeq$ 21 Hz (13), we can derive the relationship

$$[2] \qquad P_{g'g'} \simeq (24 - \textstyle\sum')/18$$

where $P_{g'g'}$ and $\sum'$ are the population of the g′–g′ rotamer and the observed sum $J_{P\text{-}5'} + J_{P\text{-}5''}$. The derived $P_{g'g'}$ values, 5′-UMP (90%), 5′-azaUMP (70%) suggest a but slight destabilizing influence of the 6-aza base upon the g′–g′ rotamer of a 5′-nucleotide.

Support for the above arguments is provided by the long-range four-bond $J_{P\text{-}4'}$ coupling in 5′-UMP (revealed by the decoupling experiments, Figs. 2, 3) but not in 5′-azaUMP (Figs. 4, 5). Four-bond H–H coupling constants are known to be strongly dependent upon the stereochemical arrangement of the intervening bonds

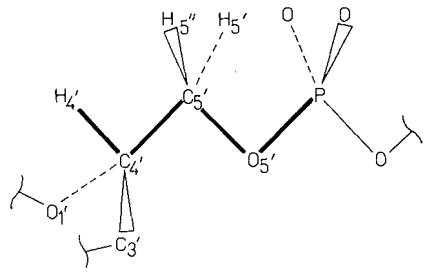

FIG. 8. The all *trans*, "W", spatial arrangement between the phosphorus atom and the 4′-proton.

and largest for the all-*trans* (W) conformation (14). Hall and coworkers (13, 15–17) have presented clear evidence that H–P coupling in H—C—C—O—P fragments follow a similar stereo-relationship. The "W" relationship between the phosphorus and 4′-hydrogen, of a 5′-mononucleotide, is encountered when the molecule is simultaneously oriented g–g and g′–g′ (Fig. 8) but is destroyed by rotation about *either* of the $C_{4'}$—$C_{5'}$ or $C_{5'}$—O bonds into one of the *trans* conformations. Thus, in view of the work by Hall *et al.* concerning the stereospecificity of four-bond H–P couplings in phosphate esters, we are inclined to present the $^4J_{P\text{-}4'}$ values for 5′-UMP (1.8 Hz) and 5′-azaUMP (<0.1 Hz) as further evidence for the suggested destabilizing influence of a 6-azauracil base upon the g–g and g′–g′ conformers.

The apparent destabilization of the g–g and g′–g′ rotamers in 5′-azaUMP is most reasonably interpreted in terms of a repulsive electrostatic interaction between the 6-aza nitrogen and the negatively charged 5′-phosphate.[3] This electrostatic interpretation, mentioned by Saenger and Suck (2) in their discussion of the crystal conformation of 5′-azaUMP, is supported by theoretical calculations (2, 23) which indicate that the C-6 position of the uracil base is a *positive* center whereas the 6-aza nitrogen is *negative*. These theoretical estimates of charge density at the 6-position and the negative charge on the phosphate, at neutral or basic p*H*, form a reasonable basis for discussion of *not only* the calculated *decrease* in the g–g rotamer in going from 5′-UMP to 5′-azaUMP *but also* of our calculated *increase* in g–g population of 5′-UMP relative to U (which suggests the presence of an attractive interaction between a uracil base and a 5′-phosphate) and our calculated *decrease* in g–g population of 5′-azaUMP relative to azaU. Furthermore our estimates of the rotamer populations at the nucleoside level point to a repulsion between the 6-azanitrogen and the 5′-hydroxyl of azaU but the interaction must certainly be attenuated relative to that involving a negatively charge phosphate in the 5′-nucleotide.

A consideration of space-filling molecular models leads us to suggest at this point a probable sequence of rotation of a g–g, g′–g′ oriented 5′-nucleotide into one of the *trans* conformations about the $C_{4'}$—$C_{5'}$ and $C_{5'}$—O bonds. In the g–g conformation steric interactions of the phosphate with the base and 2′,3′-hydrogens tends to restrict rotation about the $C_{5'}$—O bond to the g′–g′ conformation. However, after rotation of the molecule about the $C_{4'}$—$C_{5'}$ bond into the g–t, or t–g, form, rotation about $C_{5'}$—O becomes less sterically hindered. We suggest, therefore, that the appearance of the g′–t′ and t′–g′ rotamers of a 5′-mononucleotide is likely only after rotation of the molecule out of the g–g form, which in the case of 5′-azaUMP is most reasonably traced to the suggested base-phosphate repulsion.

The vicinal ribose H–H coupling constants $J_{1'2'}$, $J_{2'3'}$ and $J_{3'4'}$ can be discussed via the Karplus relation in terms of a favored mode of ring puckering. In a qualitative manner the similarity in corresponding *J* values indicates a similar ribose conformation for U, 5′-UMP, azaU, and 5′-azaUMP, which may be reasonably considered in terms of an equilibrium model involving interconversion between C-2′ *endo* and C-3′ *endo* mode[4] (7). Comparison of the

[3]This interpretation assumes an *anti* conformation for the uracil and 6-azauracil derivatives. In this conformation the 6-position of the base is located over the ribose and in close proximity to the 5′-O when the molecule is oriented g–g. Available spectroscopic evidence suggests that the *anti* range of conformers is favored, for these molecules, in both the crystal state and in aqueous solution (2, 18–22).

[4]The authors realize that furanose conformations have been discussed in terms of the 20 possible puckering modes (26). We also realize that use of p.m.r. data to confirm the presence of *one* particular mode is futile and consider the approach outlined recently (27) which discusses segments of the pseudorotational cycle thought to be significantly populated. By C-2′ *endo* we mean simply that conformation in which $H_{1'}$, $H_{2'}$ assume a quasi axial:axial (a:a) relationship and $H_{3'}$, $H_{4'}$ a quasi equatorial:equatorial (e:e) relationship and by C-3′ *endo* that conformation in $H_{1'}$, $H_{2'}$ are quasi e:e and $H_{3'}$, $H_{4'}$ are quasi a:a. In effect we mean by C-3′ *endo* and C-2′ *endo* terms the N and S conformations in the nomenclature recently presented (28) (see also ref. 3 for a useful discussion of furanose puckering).

Can. J. Chem. Downloaded from www.nrcresearchpress.com by 210.87.254.40 on 09/05/12
For personal use only.

relative magnitudes of $J_{1'2'}$ and $J_{3'4'}$ for the nucleotides suggests a slight preference for a C-2′ *endo* mode in 5′-UMP but a slight preference for a C-3′ *endo* mode in 5′-azaUMP. In the crystal state, the ribose moieties assume similar conformations; U (18) and azaU (19) are C-3′ *endo* while 5′-azaUMP (2) is C-3′ *endo* C-2′ *exo*. The crystal data for 5′-UMP are not available; however, in UpA the uridine fragment is found in the C-3′ *endo* C-2′ *exo* conformation (24, 25).

Conclusion

P.m.r. data for 6-azauridine and 6-azauridine-5′-monophosphate are presented and compared to those of the corresponding uracil derivatives. The data reveal a pronounced destabilizing effect of the 6-azauracil base upon the *gauche–gauche* conformation of the 5′-monophosphate. This effect is also noted at the nucleoside level but to a lesser extent. These observations are interpreted in terms of an electrostatic repulsion between the electronegative 6-azanitrogen of the base and the 5′-phosphate (or hydroxyl) group. Our evidence indicates a predominance of an unusual (*trans*) conformation about the $C_{4'}$—$C_{5'}$ bond of 5-azauridine-5′-monophosphate in aqueous solution in accord with observations of Saenger and Suck for the crystalline nucleotide, and lends support to their rationalization of the antimetabolite behavior of the molecule.

NOTE ADDED IN PROOF: A recent publication (29) has discussed the consequences of substitution by the aza nitrogen at the 6-position of uridine on the ribose chemical shifts and conformation. Also of interest is the X-ray study (30) of formycin, a C-ribosyl nucleoside with an aza nitrogen *ortho* to the glycosyl linkage; the structural features of this molecule also point to an electrostatic repulsion between this aza nitrogen and the sugar $O_{5'}$ atom.

This research was supported in part by grants from the National Research Council of Canada, The Research Corporation of New York, The National Cancer Institute of NIH, and the National Science Foundation. The Faculty of Graduate Studies of the University of Manitoba are gratefully acknowledged for a post-doctoral fellowship to D. J. Wood. The fast Fourier transform system was bought by funds furnished by the National Science Foundation and the State University of New York. The authors acknowledge illuminating discussions with Drs. B. Pullman, A. Saran, W. Saenger, and M. Sundaralingam. We also thank Dr. W. Saenger for forwarding to us a copy of his reprint (ref. 2), and Dr. Arthur A. Grey and Mrs. Valerie Robinson of the Canadian 220 MHz Centre, Sheridan Park, Ontario, Canada, for obtaining 220 MHz spectra.

1. R. E. HANSCHUMACHER, P. CALABRESI, A. D. WELCH, V. BONO, H. FALLOU, and E. FREI. Cancer Chemotherapy Reports **21**, 1 (1962); J. SKODA. Prog. Nuc. Acid Res. **2**, 197 (1963).
2. W. SAENGER and D. SUCK. Private communication; manuscript submitted for publication.
3. R. H. SARMA and R. J. MYNOTT. J. Am. Chem. Soc. **95**, 1641 (1973).
4. C. W. HAIGH and J. M. WILLIAMS. J. Mol. Spectrosc. **32**, 398 (1969).
5. T. SCHLEICH, B. J. BLACKBURN, R. D. LAPPER, and I. C. P. SMITH. Biochemistry, **11**, 137 (1972).
6. I. C. P. SMITH, H. H. MANTSCH, R. D. LAPPER, R. DESLAURIERS, and T. SCHLEICH. Proceedings, international symposium on the conformation of biological molecules and polymers. Symposia on quantum chemistry and biochemistry. B. Pullman and E. D. Bergman (editors). Vol. 4. Academic Press, 1973. In press.
7. F. E. HRUSKA, A. A. GREY, and I. C. P. SMITH. J. Am. Chem. Soc. **92**, 4088 (1970).
8. F. E. HRUSKA, A. A. SMITH, and J. G. DALTON. J. Am. Chem. Soc. **93**, 4334 (1971).
9. F. E. HRUSKA. Proceedings, international symposium on the conformation of biological molecules and polymers. Symposia on quantum and biochemistry. B. Pullman and E. D. Bergman (editors). Vol. V. Academic Press, 1973. In press.
10. M. REMIN and D. SHUGAR. Biochem. Biophys. Res. Commun. **48**, 636 (1972).
11. D. H. WILLIAMS and N. S. BHACCA. J. Am. Chem. Soc. **86**, 2742 (1964).
12. F. E. HRUSKA, D. J. WOOD, and J. G. DALTON. Can. J. Chem. In preparation.
13. L. D. HALL and R. B. MALCOLM. Chem. Ind. 92 (1968).
14. (*a*) A. RASSAT, C. W. JEFFORD, J. M. LEHN, and B. WAEGELL. Tetrahedron Lett. 233 (1964); (*b*) M. BARFIELD and B. CHAKRABARTI. Chem. Rev. **69**, 757 (1969).
15. L. D. HALL and R. B. MALCOLM. Can. J. Chem. **50**, 2092 (1972).
16. L. D. HALL and R. B. MALCOLM. Can. J. Chem. **50**, 2102 (1972).
17. B. DONALDSON and L. D. HALL. Can. J. Chem. **50**, 2111 (1972).
18. E. A. GREEN, R. SHIONO, and R. D. ROSENSTEIN. Chem. Commun. 53, 1973.
19. C. H. SCHWALBE and W. SAENGER. Biochem. Biophys. Res. Commun., **44**, 57 (1971).
20. G. T. ROGERS and T. L. V. ULBRICHT. Eur. J. Biochem. **22**, 457 (1971).
21. F. E. HRUSKA. Can. J. Chem. **49**, 2111 (1971).
22. M. P. SCHWEIZER, A. D. BROOM, P. O. P. TS'O, and D. P. HOLLIS. J. Am. Chem. Soc. **90**, 1042 (1968).

Can. J. Chem. Downloaded from www.nrcresearchpress.com by 210.87.254.40 on 09/05/12
For personal use only.

23. B. PULLMAN and A. PULLMAN. Quantum biochemistry, Interscience, New York, 1963. p. 714, 832.
24. M. C. SEEMAN, J. L. SUSSMAN, and H. M. BERMAN. Nature, **233**, 90 (1971).
25. J. RUBIN, T. BRENNAN, and M. SUNDARALINGAM. Biochemistry, **11**, 3112 (1972).
26. M. SMITH and C. D. JARDETZKY. J. Mol. Spectrosc. **28**, 70 (1968).
27. L. D. HALL, P. R. STEINER, and C. PEDERSEN. Can. J. Chem. **48**, 1155 (1970).
28. C. ALTONA and M. SUNDARALINGAM. J. Am. Chem. Soc. **94**, 8205 (1972).
29. M. P. SCHWEIZER, E. B. BANTA, J. T. WITKOWSKI, and R. K. ROBINS. J. Am. Chem. Soc. **95**, 3770 (1973).
30. P. PRUSINER, T. BRENNAN, and M. SUNDARALINGAM. Biochemistry, **12**, 1196 (1973).

Can. J. Chem. Downloaded from www.nrcresearchpress.com by 210.87.254.40 on 09/05/12
For personal use only.

Photo-additions of Naphthalene Derivatives with Substituted Ethylenes: Influence of Methoxy- and Cyano-substituents on the Products

TERENCE RICHARD CHAMBERLAIN AND JOHN JAMES MCCULLOUGH[1]

Department of Chemistry, McMaster University, Hamilton, Ontario

Received December 18, 1972

Irradiation of 2-methoxynaphthalene and acrylonitrile in ethanol affords *exo*- and *endo*-7-cyano-6-methoxy-2,3-benzobicyclo[4.2.0]octa-2,4-diene, in the ratio 30:70. The structures are assigned from the n.m.r. spectra. The *endo* compound is the more stable, and on base equilibration predominates (90%). These adducts eliminate a methoxy-group on treatment with *tert*-butoxide at 80°, to afford 2,3-naphthocyclobutene carboxamide. Irradiation of 2-cyanonaphthalene and methyl vinyl ether in ethanol gives a complicated mixture of adducts which includes the cyclobutane 7-methoxy-6-cyano-2,3-benzobicyclo-[4.2.0]octa-2,4-diene as a major product (35%). Also formed are 7-methoxy-2,3(8-cyanobenzo)bicyclo-[3.3.0]octa-2,7-diene (8%), 8-methoxy-10-cyano-1,2-benzocycloocta-1,3,5-triene (18%), and a dimer of the latter (7%), and 8-methylene-5-methoxy-2,3(10-cyanobenzo)bicyclo[2.2.1]heptene (35%). The structures of the latter adducts are assigned from spectroscopic data, including nuclear Overhauser effects. Possible mechanisms for formation of the latter adducts, and a rule for prediction of regiospecificity in cyclobutane formation, are proposed.

L'irradiation du méthoxy-2 naphtalène et de l'acrylonitrile dans l'éthanol conduit à l'*exo* et l'*endo* cyano-7 méthoxy-6 benzo-2,3 bicyclo[4.2.0] octadiène-2,4 dans le rapport 30:70. Les structures ont été attribuées à partir des spectres r.m.n. Le composé *endo* est plus stable et prédomine par équilibration basique (90%). Ces adduits éliminent un groupe méthoxy par traitement au *tert*-butoxyde à 80° pour conduire au naphto-2,3 cyclobutène carboxamide. L'irradiation du cyano-2 naphtalène et du méthyl-vinyléther dans l'éthanol conduit à un mélange complexe d'adduits comprenant le cyclobutane méthoxy-7 cyano-6 benzo-2,3 bicyclo[4.2.0] octadiène-2,4 comme produit majoritaire. Comme autres produits, on trouve le méthoxy-7 (cyano-8 benzo)-2,3 bicyclo[3.3.0] octadiène-2,7 (8%), le méthoxy-8 cyano-10 benzo-1,2 cyclooctatriène-1,3,5 (18%), le dimère de ce dernier (7%), et le méthylène-8 méthoxy-5 (cyano-10 benzo)-2,3 bicyclo[2.2.1] heptène (35%). Les structures des derniers adduits ont été attribuées à partir des données spectroscopiques, en particulier par des effets Overhauser nucléaires. Les mécanismes possibles de formation de ces derniers adduits et une règle pour prédire la régiospecificité de la formation du cyclobutane ont été proposés. [Traduit par le journal]

Can. J. Chem., **51**, 2578 (1973)

Previous work in our laboratory has shown that, in photo-additions of naphthalene with various substrates, the donor–acceptor properties of the reactants can determine the structures of products (1–4). For example, in the photoreaction of naphthalene with acrylonitrile (2), a protonation process has been discovered (3*a*), which is certainly dependent on the acceptor role of acrylonitrile. The reaction of naphthalene and pyrrole, however, is best explained by assuming the pyrrole to act as an electron donor (4).

The possible importance of charge-transfer in the photo-addition reactions of benzene and its derivatives with substituted ethylenes (5, 6) has been pointed out by Bryce-Smith (7). The light-induced additions of benzene with cyclobutene (8, 9), tetramethylethylene (10, 11), and 2-butene (11) have been reported. The tetramethylethylene reaction is influenced by an acid catalyst (10), suggesting that charge-transfer processes are important, *cf.* naphthalene–acrylonitrile addition (3).

Recently, photochemical additions of anthracene and 9-cyanoanthracene with dienes in the $4\pi + 4\pi$ and $4\pi + 2\pi$ modes have been described, and the authors have remarked on the effect of the electron-withdrawing, cyano-group on the products formed (12).

One approach we have taken in attempting to evaluate the importance of charge-transfer in photochemical additions was to study the reactions of naphthalene, substituted with an electron-donating or electron-withdrawing group with oppositely substituted ethylenes (1).

[1]Author to whom correspondence should be addressed at McMaster University. Presently (1972–1973) on sabbatical leave at the Laboratory of Chemical Biodynamics, Lawrence Berkeley Laboratory, University of California, Berkeley, California 94720.

Can. J. Chem. Downloaded from www.nrcresearchpress.com by 210.87.254.6 on 09/05/12
For personal use only.

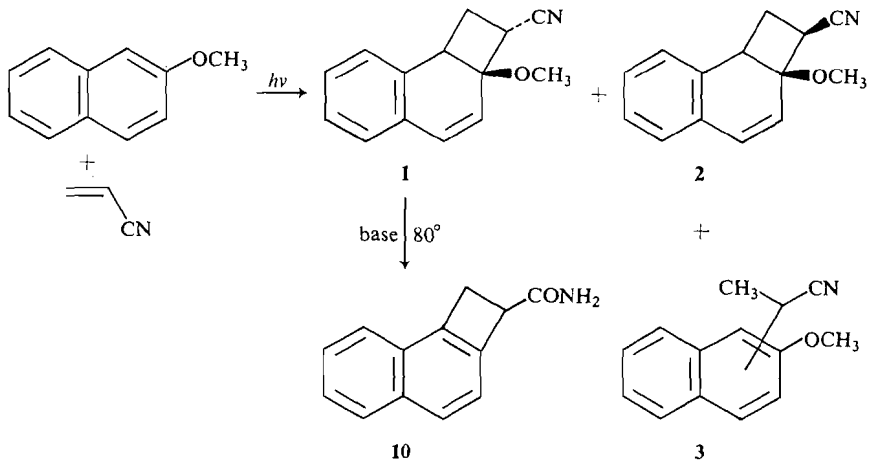

SCHEME 1

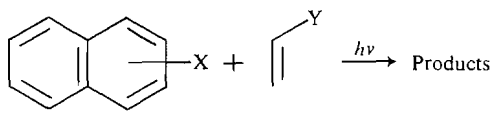

(X is electron-donating, Y is electron-withdrawing or vice versa)

In this paper, we are reporting the structures of the adducts formed on photolysis of methoxynaphthalene and acrylonitrile, and of 2-cyanonapthalene with methoxyethylene. The idea of studying these pairs of reactants followed the reports of Schulte-Frohlinde and co-workers (13), in which they describe the effect of donor–acceptor properties of a quencher and quenchee, on singlet and triplet quenching. The present study is a step in the continuation of our work with napthalene and acrylonitrile (2, 3, 14).

Results

2-Methoxynaphthalene and Acrylonitrile

The dimerization of 2-methoxynaphthalene in a $4\pi + 4\pi$ mode is apparently the only photochemical process known for this compound (15, 16). Irradiation of 2-methoxynaphthalene and acrylonitrile in ethanol using a pyrex filter causes a smooth addition to occur.[2] The reaction is shown in Scheme 1.

The product distribution was measured by v.p.c., which gave **1**, 70%; **2**, 25%, and **3** ~3%. The cycloadducts **1** and **2** were separated by column chromatography and fractional crystallization, and both were crystalline solids. Their structures were assigned as follows. Equilibration with *tert*-butoxide showed that **1** and **2** are epimers, with **1** the more stable (see below). The gross structures followed from this and their mass spectra, the latter showing weak parent ions of *m/e* 211, with the base peaks at *m/e* 158 corresponding to methoxynaphthalene cation, resulting from cyclobutane ring cleavage (14). Adduct **1** also decomposed on sensitized photolysis, giving 2-methoxynaphthalene, a known reaction of this ring system (2, 3). This evidence indicated that **1** and **2** were the epimeric 7-cyano-6-methoxy-2,3-benzobicyclo[4.2.0]octa-2,4-dienes.

The detailed structures were assigned from the n.m.r. spectra, which are shown in Fig. 1, and the data are collected in Table 1.

In adduct **1**, the doublet of doublets at 3.36 was removed by treatment with methoxide and D_2O in pyridine, which identifies the resonance with H-7, α to the nitrile. The doublet of triplets at 3.52 may then be assigned to H-1, and the splitting pattern, together with the result of decoupling experiments which show that coupling between H-1 and -7 is small, demands that H-1 and -7 cannot be vicinal, and the nitrile function must be at C-7.

The stereochemistry of the nitrile substituent is more difficult to assign. Equilibration of **1** with *tert*-butoxide gives a mixture of **1** and **2** in the ratio 9:1 (v.p.c.), showing that the minor photolysis product is also the less stable isomer. The latter is also quite labile, and was observed to revert to the equilibrium mixture on crystallization from hot petroleum. This was in part responsible for the difficulty experienced in isolating **2**.

[2]This contrasts with the reported lack of reaction between 2-methoxynaphthalene and maleic anhydride on irradiation (15*a*), a result which we have confirmed.

Can. J. Chem. Downloaded from www.nrcresearchpress.com by 210.87.254.6 on 09/05/12
For personal use only.

Can. J. Chem. Downloaded from www.nrcresearchpress.com by 210.87.254.6 on 09/05/12
For personal use only.

TABLE 1. N.m.r. data for cyclobutane adducts*

	H-1	H-4	H-5	H-7	H-8,8′	CH_3	Other
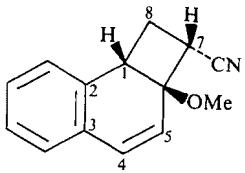 **1**	3.52, dt J = 10.0, 1.5	6.92, d J = 10.0	5.83, dd J = 10.0, 1.5	3.36, dd J = 9.0, 10.0	2.45, 1.72 J_{gem} = 10.5	3.03, s	7.15, m benzenoid
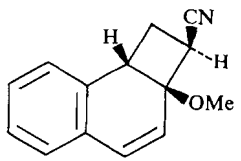 **2**	3.87, ddt $J_{(t)}$ = 9.0	6.82, d J = 10.0	5.65, dd J = 10.0, 1.0	3.15, ddd J = 9.0, 2.5, 1.5	1.80, 2.42 (both m)	3.08, s	7.15, m benzenoid
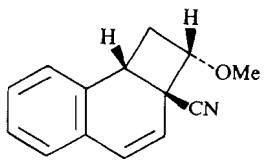 **5**	~3.4	6.65, d J = 10.0	5.65, dd J = 10.0, 1.5	4.35, dd J = 8.5, 7.0	2.45, m	3.48, s	7.10, m benzenoid

*Chemical shifts (p.p.m.), coupling constants (Hz), and multiplet structures of proton resonances in **1**, **2**, and **5**; s = singlet, d = doublet, t = triplet, m = multiplet, dd = doublet of doublets, etc.

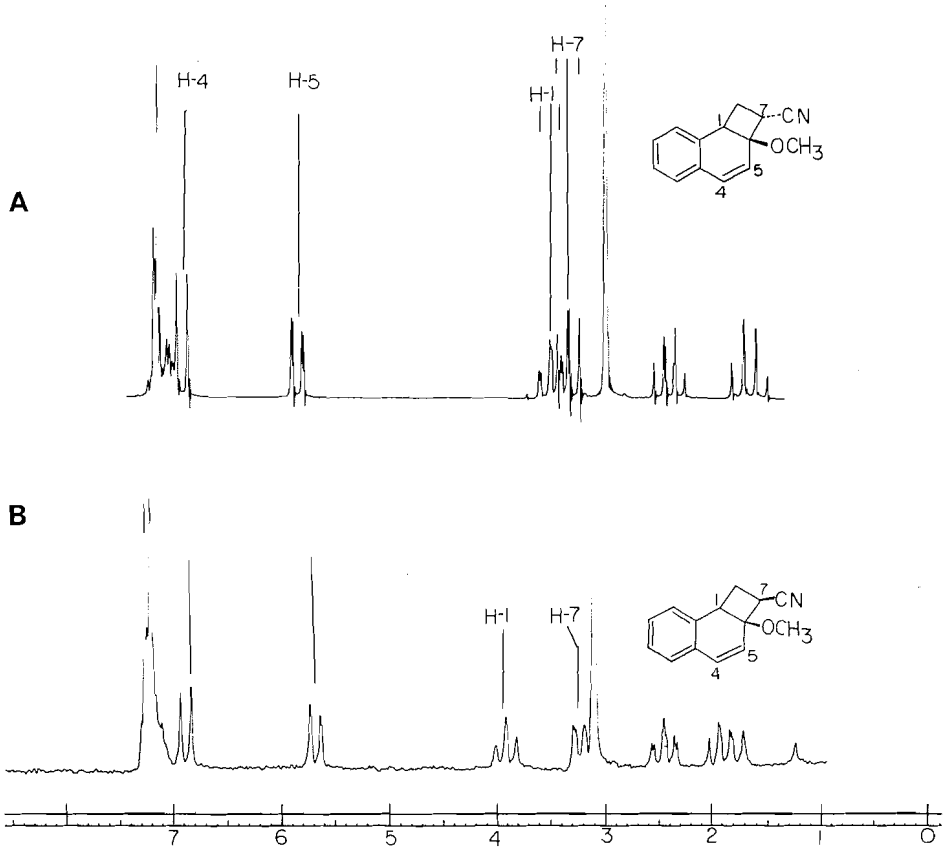

FIG. 1. 100 MHz n.m.r. spectra of **1** and **2**. A, spectrum of **1** (*endo*); B, spectrum of **2** (*exo*). The solvent was $CDCl_3$.

Noting that in the demethoxy series the *endo*-isomer **4** is the more stable (14), the above observation on the equilibration of **1** and **2** suggests **1** is *endo* and **2** is *exo*. This assignment is supported by the n.m.r. spectra at 100 MHz, which are shown in Fig. 1 and Table 1.

The important difference in the n.m.r. spectra appears in the resonances of H-7. In **1**, this resonance is a doublet of doublets, with J = 9.0 and 10.0 Hz. The resonance was positively identified with H-7 since it was removed by treatment with base and deuterium oxide, as already mentioned. The corresponding resonance in **2**, however, is a doublet with J = 9.0 Hz, further split with small coupling constants of 2.5 and 1.5 Hz. The magnitudes of these coupling constants point to the *endo* configuration for **1** and *exo* for **2**, if the four-membered ring has the same geometry in these adducts as in the demethoxy compound **4**, shown in Scheme 2. The shape of the latter is known from an X-ray study (14). In **1**, H-7 will be axial and should therefore be coupled strongly to the methylene group protons, since axial–axial and axial–equatorial vicinal coupling constants in cyclobutanes are large (17). In compound **2**, however, H-7 experiences one equatorial–equatorial coupling to the methylene group, and this is consistent with the coupling constant of 2.5 Hz (17). The large vicinal coupling (9.0 Hz) is, of course, due to the equatorial–axial splitting.

In both of the isomers, the H-1 resonance is basically a triplet with J = 9.0 and 10.0 Hz, which is consistent with the assigned structures shown in Scheme 2.

Spin decoupling experiments demonstrated that there are some small, long-range splittings in these compounds. For example, H-1 is coupled to H-5 in both isomers, with J = 1.0–1.5 Hz. In **2**, H-1 is also coupled to H-7 with J = 1.5 Hz, a splitting which appears to be absent from **1**, and, interestingly, is also absent

Can. J. Chem. Downloaded from www.nrcresearchpress.com by 210.87.254.6 on 09/05/12
For personal use only.

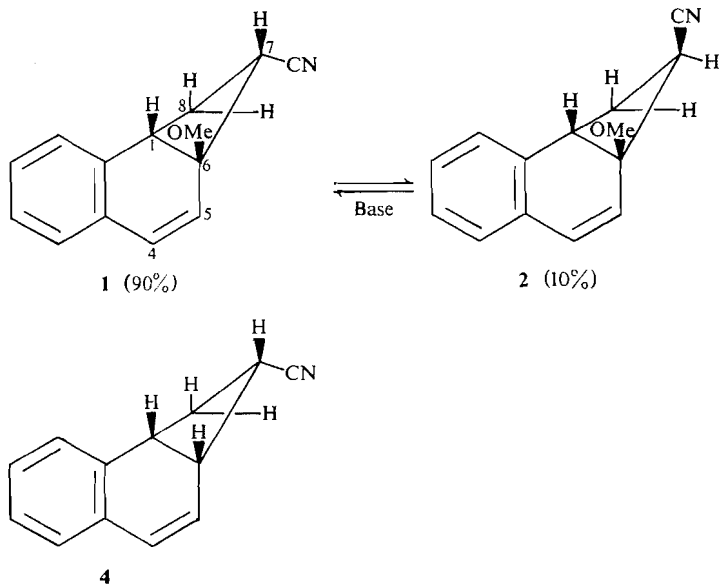

1 (90%) 2 (10%)

4

SCHEME 2

from the spectrum of **4** (14). This further strengthens the argument that **1** and **4** have essentially the same stereochemistry.

Treatment of a mixture of **1** and **2** with *tert*-butoxide in *tert*-butyl alcohol at reflux (80°), followed by aqueous acid work-up, resulted in expulsion of the methoxy group and aromatization to form the naphthalene derivative, 1,2-naphthocyclobutene-3-carboxamide (**10**). The structural evidence is given in the experimental. The above photo-addition is therefore a key to a convenient route to the 2,3-naphthocyclobutene system.

The substituted naphthalenes **3** were not purified on account of their oily nature and low yield. The n.m.r. spectrum of the fraction from chromatography of the photolysis mixture containing these products showed the characteristic methyl resonances (doublets) at high field, methine quartets, and the aromatic multiplet at low field (2). Thus, there is no doubt that substituted naphthalenes are formed, although their precise structures are unknown.

2-Cyanonaphthalene and Methoxyethylene

The photo-dimerization of 2-cyanonaphthalene has recently been reported (18). Irradiation of 2-cyanonaphthalene and methoxyethylene in ethanol, using a Pyrex filter, afforded five 1:1 adducts. These were separated by column chromatography and all were crystalline solids. The assigned structures are shown in Scheme 3.

Since one of the products is particularly photolabile, the relative yields are variable, and the figures in Scheme 3 represent yields in a typical run. The product distribution was measured by v.p.c.

Structure **5** was easily assigned by comparison with cyclobutane structures obtained in other reactions (see above, and ref. 2). The compound decomposed on photolysis, consistent with the cyclobutane structure (2, 3). In the n.m.r. spectrum, which is described in Table 1, the significant features are the resonances (doublets) at 6.65 and 5.65 due to the vinylic protons, and the doublet of doublets at 4.35 with coupling constants of 8.5 and 7.0 Hz. The latter is assigned to H-7 (α to the methoxy-group), and since the resonance is a doublet of doublets, it shows that the methoxy-group is at C-7. We tentatively assign the *endo*-stereochemistry to the methoxy function, by analogy with **1**, **2**, and **4**; **5** is therefore *endo*-7-methoxy-6-cyano-2,3-benzobicyclo[4.2.0]octa-2,4-diene.

The three other monomeric adducts were suspected not to be cyclobutane derivatives, since they were relatively stable to irradiation, and did not cleave in the fashion expected for cyclobutanes on electron impact (14). Their structures are derived mainly from the n.m.r. spectra, which are described below and in Fig. 2. The numbering used agrees with Scheme 3.

The n.m.r. spectrum of **6** (220 MHz, $CDCl_3$ solution) had the following resonances (number-

Can. J. Chem. Downloaded from www.nrcresearchpress.com by 210.87.254.6 on 09/05/12
For personal use only.

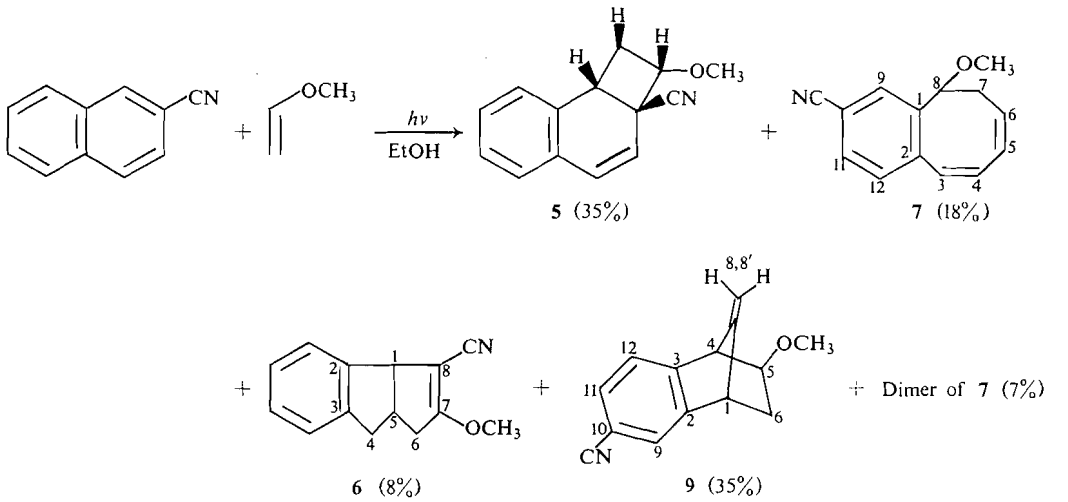

SCHEME 3

ing as in Scheme 3): 7.48 (area 1) and 7.23 (area 3) both multiplets, assigned to the aromatic ring; a complex multiplet at 3.15 (area 1), assigned to H-5; and a doublet at 4.34 (area 1), assigned to H-1. This doublet, which had $J = 7.0$ Hz, collapsed to a singlet when the multiplet at 3.15 (H-5) was irradiated. The remaining resonances, of the two methylene groups, occurred at 2.36 (doublet $J = 18.0$ Hz), 2.82 (multiplet), and 3.20 (multiplet). The resonance of the methoxy group was a singlet (area 3) at 4.02, which is consistent with a methyl vinyl ether (19). The downfield shift of one proton of the aromatic ring indicates that this proton is in the deshielding region of, and close to the cyano-group (20, 2*b*). The mass spectrum showed ions of *m/e* 211 (100) (parent and base peak) and 115 (46) (indenyl cation). In the i.r., the cyano-function absorbed at 2200 cm^{-1}, showing that it is conjugated with the double bond. The evidence all points to the structure 7-methoxy-8-cyano-2,3-benzobicyclo[3.3.0]octa-2,7-diene (**6**).

Compound **7** showed in the n.m.r. (100 MHz, $CDCl_3$ solvent) the protons of the aromatic ring at 7.80 (area 1) doublet, $J = 2$ Hz assigned to H-9; at 7.54 (area 1) doublet of doublets, $J = 2.0$ and 8.0 Hz due to H-11; at 7.24 (area 1) doublet, $J = 8.0$ Hz assigned to H-12. The diene system gave resonances at 6.53 (area 1) doublet, $J = 12.0$ Hz assigned to H-3; at 6.22 (area 1) doublet, $J = 12.0$ Hz assigned to H-4. The latter doublet was broadened by coupling to other protons, probably H-5 and -6. The resonance assigned to H-5 and -6 occurred at 5.66 (area 2) as overlapping singlets, and the protons of the methylene group (H-7) resonated at 2.54 and 3.02 (both areas 1). The methine proton H-8 resonated at 5.12 (area 1) doublet of doublets, $J = 11.0$ and 4.0 Hz. The methoxy group gave a singlet at 3.24 (area 3).

The above data show that the aromatic ring carried the cyano-group, that there are two ethylenic bonds, and that there is a methoxy-group and three aliphatic protons. These data allow the ring-expanded structure of **7** to be assigned. It does not, however, permit the location of the methoxy- or cyano-groups to be determined.

The latter structural details were determined by nuclear Overhauser effect (n.O.e.) measurements. These measurements were performed as described by Bell and Saunders (21). The increases in intensity in the observed signals, when various resonances were irradiated, are summarized in Fig. 2.

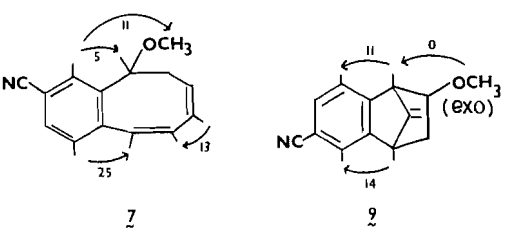

7 8

FIG. 2. Nuclear Overhauser effects in adducts **7** and **8**. Arrow tail indicates proton irradiated; arrow head indicates proton observed. Values give % increase in the observed signal intensity.

Can. J. Chem. Downloaded from www.nrcresearchpress.com by 210.87.254.6 on 09/05/12
For personal use only.

Can. J. Chem. Downloaded from www.nrcresearchpress.com by 210.87.254.6 on 09/05/12
For personal use only.

The 20–25% enhancement of the H-12 signal intensity when H-3 resonance was irradiated, and the observed effects between H-9 and -8 and the methoxy-group, provide good evidence that the latter is at C-8, and the cyano-group at C-10. The enhancement of 13% in the H-4 resonance when that of H-5 is irradiated shows the double bonds are conjugated.

The u.v. spectrum had λ_{max} (EtOH) 280 mμ, log ε 3.87. The spectrum of 1-phenylbuta-1,3-diene has λ_{max} (EtOH) 280 mμ, log ε 4.50 (22).

Thus, the evidence points to the structure 8-methoxy-10-cyano-1,2-benzocycloocta-1,3,5-triene **7**.

A relatively insoluble, dimeric compound was also formed. Structure **8** is tentatively assigned to this compound, on the basis of n.m.r. (see experimental) data and on the assumption that the cyclization occurs via the most stable biradical intermediate.

The adduct which is assigned structure **9** is difficult to isolate in a pure form, and slowly crystallizes as waxy plates (from ethanol), which were sublimed, m.p. 50–52°.

The n.m.r. spectrum revealed the *exo*-methylene group resonances as a doublet, at 6.21 ($J_{8,8'}$ = 2.0 Hz) and a doublet of doublets at 5.91 ($J_{8,8'}$ = 2.0, $J_{1,8'}$ = 0.7 Hz); both had areas 1. The aromatic ring carried the cyano-group, and the resonances were at 7.89, doublet ($J_{9,11}$ = 2.0 Hz) assigned to H-9; at 7.70, doublet of doublets ($J_{9,11}$ = 2.0 and $J_{11,12}$ = 8.0 Hz) assigned to H-11; and at 7.26, doublet ($J_{11,12}$ = 8.0 Hz) assigned to H-12.

The resonances assigned to the bridgehead methine protons occurred at 4.03 as a broadened doublet with $J_{1,4}$ = 4.0 Hz attributed to H-4, and the H-1 resonance was at 3.48, but was partly obscured by the singlet of the methoxy-group which occurred at 3.56. The resonance of H-5 occurred at 4.27 and was coupled to the protons of the methylene group with J_{exo} = 3.5 and J_{endo} = 11.0 Hz. H-5 was not coupled to H-4, indicating that the methoxy group had the *exo*-stereochemistry (23*b*). The methylene group protons resonated at 1.46 (*endo*) and 2.44 (*exo*), and J_{gem} was 13.5 Hz.

The n.m.r. spectrum of **9**, particularly the coupling pattern, is consistent with the benzobicyclo[2.2.1]heptene system (23). To establish the relative positions of the methoxy and cyano-group, n.O.e. were measured. The results are shown in Fig. 2. Thus when the signal assigned to H-4 was irradiated, a 12% enhancement of the H-12 resonance was noted. Similarly, irradiation of H-1 caused a 11% enhancement of the H-9 signal. These results point to structure **9**, *exo*-5-methoxy-7-methylene-2,3-(2′-cyano) benzobicyclo[2.2.1]hept-2-ene.

NOTE ADDED IN PROOF: Recently, results of an independent study of 2-naphthonitrile and methyl vinyl ether photo-addition were described (41). Unfortunately, this paper did not include spectroscopic data or melting points, so that we are unable at present to compare the products described with those reported here. Some of our structural assignments differ from those of Mizuno *et al.* In particular, the benzonorbornene adduct **9** could in fact correspond to the cyclobutene adduct II in Mizuno's paper. The n.m.r. data which we obtained for **9** could well fit Mizuno's structure II. It is likely that the cyclobutene is the correct structure, and is probably formed by irradiation of the benzocycloctatriene, **7**.

Discussion

Regiospecificity in Cyclobutane Formation

Mixed photo-additions of naphthalene with ethylenic substrates are known to afford cyclobutanes (2, 3). The present study has shown that this type of addition can also occur with 2-methoxy- and 2-cyanonaphthalene, if appropriate ethylenic substrates are used. It has also recently been reported that 2-cyanonaphthalene and tetramethylethylene add to form a cyclobutane on irradiation (24). Inspection of structures **1**, **2**, **4**, and **5** reveals that the following directive effects appear to be operating. First, addition occurs at the 1,2-bond of the naphthalene nucleus; if there is a substituent in the nucleus, addition occurs at the 1,2-bond carrying the substituent. Second, when mono-substituted naphthalenes and ethylenes react, the substituents are *vicinal* in the cyclobutane product, *e.g.*, **1**, **2**, and **5**.

While more than one specific interaction may be responsible for the observed directive effect, the following simple rule seems adequate for predictive purposes. That is, ring closure occurs from the most stable open-chain intermediate, which we represent as an ionic species. For example, closure of **11** would lead to **1** and **2**, as shown in Scheme 4.

The cation part of **11** consists of an allylic

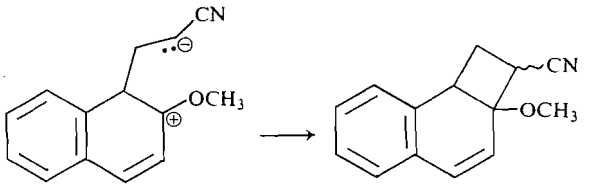

11 1 and 2

SCHEME 4

Can. J. Chem. Downloaded from www.nrcresearchpress.com by 210.87.254.6 on 09/05/12
For personal use only.

carbonium ion, stabilized by linear conjugation with a phenyl group, and with a methoxy group, all of which should contribute to stabilization.

This species **11** should be preferred over isomeric structures, in which bonding to the acrylonitrile moiety is at other positions of the substituted naphthalene ring, or at the unsubstituted ring. We also note that formation of the predominant cyclobutane **4** from naphthalene and acrylonitrile should involve the most stable intermediate, *i.e.* **11** without the methoxy group, since the cation center in that case is the relatively stable cinnamyl carbonium ion. The same rule accounts for formation of **5** from 2-cyanonaphthalene and methyl vinyl ether, and for the direction of addition of ethylenes to benzonitrile (6).

The intermediates such as **11** are represented as polar species, rather than biradicals because the excited states from which they are formed are singlets, and are best represented as spin-paired structures. Naphthalene and acrylonitrile add via S_1 (3*b*), and it is very likely that the additions of 2-methoxy- and 2-cyanonaphthalene are also singlet reactions (25).

The above rule for singlet additions of simple arene derivatives may be regarded as a counterpart of the "most stable biradical rule" which holds for many triplet additions (26, 27). In mentioning triplets, we note that the triplet states (T_1) of naphthalene and its non-carbonyl derivatives[3] appear to be photochemically quite inert, and this observation will be discussed elsewhere.

Isolation of substituted type products **3** from the 2-methoxynaphthalene-acrylonitrile reaction, albeit in low yield, is consistent with a donor–acceptor situation in which the acrylonitrile is the acceptor. The acrylonitrile should become electron-rich while bonded in an exciplex, and accept a proton from the solvent (3).

The formation of **10** on treatment of **1** and **2** with *tert*-butoxide at 80° is of synthetic interest. The photo-addition is thus the basis of a simple route to the naphthocyclobutene ring system of **10**, giving a compound with useful functionality in the four-membered ring. We are presently studying photo-additions of other substituted arenes, where the substituents is a potential leaving group, to attempt to extend this synthesis to other derivatives.

Possible Routes to Structures 6, 7, and 9

In contrast to the well-established $2\pi + 2\pi$ addition (28*a*) which can lead to adducts **1**, **2**, **4**, and **5**, the structures **6**, **7**, and **9** must be formed in a more complicated manner. However, although the latter adducts apparently have no precedent in arene photochemistry, it is possible to account for their formation without invoking any bizarre processes.

For example, it is known that on irradiation of benzene, fulvene is formed (29). Hence, the process shown in the first part of Scheme 5 is a suggested route for the formation of **9**.

In **7**, since the methoxy group is at C-8 (not C-7), as shown by the n.O.e., this compound cannot arise from **5**. It was also shown that **5** decomposes to 2-cyanonaphthalene on irradiation, and does not yield **7**. To account for the ring-expanded structure **7**, we propose that addition of methyl vinyl ether occurs not at the position of high bond order (the 1–2 bond of the naphthalene (30)) but on the bond from C-8 to the angular carbon, as shown in Scheme 5. Such an addition is formally a $2\pi + 6\pi$ addition, which is excited state symmetry allowed (28*b*), but is a rare process (31). This addition results in a temporary loss of aromaticity in the intermediate, which can be regained in one ring by the electrocyclic reaction in which the cyclo-

[3]2-Acetylnaphthalene adds to methyl cinnamate on irradiation (39), and this may be a triplet process.

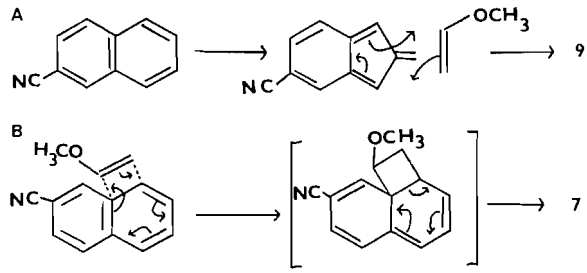

SCHEME 5. Proposed mechanisms for formation of **7** and **9**

butane ring is ruptured and the eight-membered ring of **7** is formed.

Compound **6** is the minor product, but has an intriguing structure, which is supported by all the spectral data.[4] A mechanism leading to structure **6** can be envisioned, which comprises (*a*) $2\pi + 6\pi$ cycloaddition of methyl vinyl ether to the 2–3 bond of the 2-cyanonaphthalene, (*b*) ring opening of the intermediate to give a benzocyclooctatriene,[5] (*c*) 1,5-bonding followed by a 1,4-hydrogen shift to give the fused five-membered rings of **6**. These proposed steps all have precedent, either in ground or excited state chemistry (32–34).

In conclusion, photo-additions of simple naphthalenes with ethylene derivatives can afford substituted benzobicyclo[4.2.0]octa-2,4-dienes (2, 3, 14), which have been obtained in low yield by less direct routes (35). Also, the question of which reactant has which substituent in these mixed additions can be of the utmost importance, since the nature and complexity of the products may depend on the configuration of substituents. This dependence may result from an increased preference for $2\pi + 6\pi$ addition *vs.* $2\pi + 2\pi$, but a more precise explanation must await the results of further investigations.

Experimental

Materials and equipment used, unless stated otherwise, were as described elsewhere (2, 3, 14). 2-Cyanonaphthalene was from Eastman Kodak Co., and was recrystallized from light petroleum, b.p. 30–60°, and had m.p. 66–67°. 2-Methoxynaphthalene was from Aldrich and had m.p. 73–74°, from 95% ethanol. Methyl vinyl ether was from Matheson of Canada, Ltd. N.m.r. spectra were taken in $CDCl_3$ solution. Chemical shifts are given as p.p.m. (δ) downfield from tetramethylsilane, and coupling constants are in Hz.

Microanalyses were by the Spang Microanalytical Laboratory, Ann Arbor, Michigan.

Photo-reaction of 2-Methoxynaphthalene and Acrylonitrile

2-Methoxynaphthalene (6.0 g, 0.0379 mol) and acrylonitrile (30.0 g, 0.565 mol) in ethanol (1 l) were irradiated through Pyrex, in the usual apparatus for 12 h. A considerable amount of insoluble material was formed. The solution was evaporated and the residue was extracted with ether. The ether extracts were filtered and on evaporation gave 7.0 g of product mixture. Analysis of the latter by v.p.c. (5 ft × 1/8 in. SE-30 on Chromosorb Wat 190°) showed 2-methoxynaphthalene at 2 min, and product peaks at 6 and 6.5 min (ratio 80:20). Minor products (~2%) were noticed, retention times 7–9 min. The crude mixture was chromatographed on 500 g of silica gel in a 60 × 4.0 cm column, slurry-packed in benzene–hexane (4:1). This solvent was used for elution and 250 ml fractions were collected. Fractions 1–5 contained 2-methoxynaphthalene (2.066 g). Fractions 6–12 contained the minor components (total 0.1413 g) which were combined and chromatographed again (see below). Fractions 13–20 were mixtures of **1** and **2** (measured using the relative areas in the n.m.r. spectrum of the vinylic proton peaks), in a ratio of approximately 2:1. These fractions were crystalline, total 3.67 g. The yield of adducts was 71%, based on reacted 2-methoxynaphthalene. Fractional crystallization (3 times) of this mixture

[4]A referee has pointed out that the benzocyclobutene structure **I** is also consistent with our data. However, we favor structure **6** because **I** has both methine protons

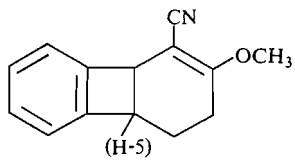

I

benzylic, and in our experience, bridgehead, benzylic protons resonate at 3.5–4.0 δ (2), while the resonance of H-5, of **6** is at 3.15 δ. It is also known that the parent ring system of **I** rearranges under mild conditions to the isomeric benzobicyclo[4.2.0]octa-2,4-diene (35). It is therefore unlikely that **I** would have survived our isolation procedures, although it may be the primary photoproduct.

[5]A similar sequence can account for the formation of benzocyclooctatetraene derivatives, and possibly the dimethyl-3,4-benzotricyclo[3.3.0.$0^{2,8}$]octa-3,6-diene-6,7-dicarboxylate, reported as products from irradiation of naphthalene and dimethyl acetylene dicarboxylate (40).

Can. J. Chem. Downloaded from www.nrcresearchpress.com by 210.87.254.6 on 09/05/12
For personal use only.

Can. J. Chem. Downloaded from www.nrcresearchpress.com by 210.87.254.6 on 09/05/12
For personal use only.

(3.20 g) from ether – light petroleum afforded 2.50 g of *endo*-7-cyano-6-methoxy-2,3-benzobicyclo[4.2.0]octa-2,4-diene (**1**), m.p. 85–86°. The n.m.r. and i.r. spectra are described in the text.

Anal. Calcd. for $C_{14}H_{13}ON$: C, 79.59; H, 6.20; N, 6.63. Found: C, 79.50; H, 6.22; N, 6.69.

The mother-liquors of the crystallization of **1** were enriched in the second component **2** (n.m.r. monitoring). The combined liquors were evaporated, and further quantities of **1** mixed with **2** were separated by crystallization from ether – light petroleum, b.p. 30–60°. This process was repeated several times, and a gum residue was obtained from the final mother-liquors from two experiments, which n.m.r. analysis showed to be a mixture of **1** and **2**, in the ratio 1:3. The latter was chromatographed on a 52 × 3.0 cm column of silica gel for t.l.c., (Merck, A. G., grain size 10–40μ) slurry packed in benzene. Elution was with benzene, under 5 p.s.i. pressure of nitrogen and 20 ml fractions were collected. Fractions 62–80 contained 0.5960 g of a mixture of **1** and **2**, the earlier fractions being almost pure **1**. Fractions 80–90 contained **2**, the *exo*-isomer, (60 mg), m.p. 79–81° from hexane.

Anal. Calcd. for $C_{14}H_{13}ON$: C, 79.59; H, 6.20; N, 6.63. Found: C, 79.74; H, 6.35; N, 6.60.

Base-catalyzed Epimerization of 1

To a solution of potassium (0.2748 g, 0.00703 g atom), purified according to Fieser and Fieser (36) in *tert*-butyl alcohol (50 ml) under nitrogen and at ambient temperature, was added 0.1034 g, 0.519 mmol of the methoxynitrile **1**, dissolved in *tert*-butyl alcohol (10 ml). The solution was stirred magnetically at ambient temperature for 21 h. The colorless solution was neutralized (5 ml in HCl), concentrated under vacuum, and extracted with ether. The ether extracts were washed with saturated NaCl solution, saturated $NaHCO_3$, and finally water. The ether solution was dried ($MgSO_4$) and evaporated. The residue (0.0946 g, 91.5%) was analyzed by n.m.r. on the T-60, and was shown to be a mixture of **1** and **2** in the ratio 9:1.

Base-catalyzed Aromatization of 1

The adducts of 2-methoxynaphthalene and acrylonitrile (**8** and **9**) (0.1049 g, 0.526 mmol) in *tert*-butyl alcohol (10 ml) were added to a solution of potassium *tert*-butoxide in *tert*-butyl alcohol (from 0.1780 g potassium and 50 ml *tert*-butyl alcohol). The mixture was stirred and heated under reflux in a nitrogen atmosphere for 2 h. The cool solution was neutralized with 5 ml of 1 *N* HCl, washed with aqueous NaCl–$NaHCO_3$, and dried ($MgSO_4$). Evaporation afforded a gum residue (0.18 g), which gave 0.09 g of white solid, m.p. 105–115° on trituration with ether. The latter was crystallized from ethyl alcohol giving crystals of **10**, 0.0214 g, 22% m.p. 202–204°.

Anal. Calcd. for $C_{13}H_{11}NO$: C, 79.21; H, 5.58; N, 7.10%. Found: C, 79.24; H, 5.56; N, 7.14%.

The compound is identified as 1,2-naphthocyclobutene-3-carboxamide from the following spectroscopic evidence. The i.r. spectrum (KBr disc) showed no nitrile band, but had absorption at 1665 (amide carbonyl) and 3400–3500 cm^{-1} (—NH_2 group). The u.v. spectrum (95% ethanol) had a band at 226 mμ, log ε = 4.95. Naphthalene has λ_{max} at 220 mμ, log ε 5.12 (37). The n.m.r. spectrum (CF_3COOH) using acetic acid as internal standard had a multiplet (area 6) centered at 7.3 (aromatic ring protons). The methylene and methine protons of the four-membered ring comprised an ABM system. The methine resonance was a doublet of doublets at 4.2 (J = 5.5 and 2.0 Hz), while the AB multiplet of the methylene group was centered at 3.4 and J_{AB} was 14.0 Hz. The spectrum was run on the T-60, and chemical shifts are only approximate.

Photo-reaction of 2-Cyanonaphthalene and Methoxyethylene

For this reaction, the Hanovia lamp immersion apparatus was fitted with a Dry-Ice condenser, and the solution was cooled in an ice–salt mixture. 2-Cyanonaphthalene (1.8857 g, 0.0123 mol) and methoxyethylene (38.6 g, 0.66 mol) in ethyl alcohol, 95% (320 ml), were irradiated in the usual way for 12 h. The solution was evaporated, and the residue triturated with ether. V.p.c. analysis of the ether solution (5 ft × 1/8 in. of 4% QF-1 on Diatoport at 180°) showed five components with retention times between 6 and 10 min. Retention times and fractional composition for each component are given below. The dimer **8**, 0.0924 g, which was insoluble, was filtered and had m.p. 270–280°. The dimeric adduct showed resonances between 7.0 and 8.0 (area 3) indicating that the cyano-group was in the aromatic ring; an AB quartet centered at 6.3, J = 12.0 Hz (area 2) is assigned to the vinylic protons; resonances at 4.5, 2.3, and 1.7 assigned to the methine and methylene protons. A singlet (area 3) at 3.2 is attributed to the methoxy-group. The u.v. spectrum had λ_{max} (EtOH–CH_2Cl_2) 270 mμ, log ε 4.54, and is similar to *p*-cyanostyrene, which has λ_{max} $CHCl_3$ 258 mμ, log ε 4.15 (38), if account is taken of the two chromophores, alkyl substitution, and cyclic structure in **8**. The assigned structure is the head-to-head cyclobutane dimer of **7**, with the 5,6 bonds of **7** forming the four-membered ring.

The ether solution was evaporated and the mixture (2.0907 g) chromatographed on a 59 × 2.0 cm column of silica gel for t.l.c. (240 g) (E. Merck, A. G., grain size 10–40μ), slurry-packed in and eluted with benzene. A pressure of 5 p.s.i. was used to give a flow rate of 2 drops/s, and 20 ml fractions were collected. 2-Cyanonaphthalene, m.p. 66–67° (1.1045 g), was found in fractions 13–17. Adduct **6** (0.0532 g), m.p. 80–96° (94–95° from hexane), was found in fractions 23–27. It was identified as 8-cyano-7-methoxy-2,3-benzobicyclo[3.3.0]-octa-2,7-diene. Fractions 29–31 were mainly compound **7** (0.1148 g), m.p. 70–106° (111–112° from hexane), which is assigned the structure 8-methoxy-1,2-(12-cyanobenzo)-cycloocta-1,3,5-triene. Fractions 32–36 contained the cyclobutane adduct **5** (0.1539 g), m.p. 73–74° from hexane, identified as 6-cyano-7-methoxy-2,3-benzobicyclo[4.2.0]-octa-2,4-diene. Fractions 38–42 were mixtures of compounds **11** and **9** (0.070 g), while the latter alone (0.0458 g) was found in fractions 43–50. This gave crystals, m.p. 50–51°, on slow crystallization from ethanol–water or on slow sublimation at 1 mm. Structure **9** was identified as 6-methoxy-7-methylene-2,3-(10-cyanobenzo)-bicyclo-[2.2.1]heptene. Elution with a further 2 l of benzene afforded intractable material (~0.150 g) which from the n.m.r. spectrum appeared to be a mixture of several compounds. The column was finally stripped with 0.5 l of ether, and 0.3988 g of mixture was obtained, which gave 0.0561 g of the above dimer **8** on trituration with ether. Total yield of **8** was 0.1485 g, m.p. 296–297° from ethanol. Recovery from the column was 2.0588 g, 98%.

Analytical figures for the isomeric photo-adducts **5–9**: Anal. Calcd. for $C_{14}H_{13}ON$: C, 79.59; H, 6.20; N, 6.63. Found for **5**: C, 79.58; H, 6.25; N, 6.52. Found for **7**: C, 79.49; H, 6.16; N, 6.61. Found for **6**: C, 79.60; H, 6.35; N, 6.55. Found for **9**: C, 79.40; H, 6.20; N, 6.49. Found for **8**: C, 79.52; H, 6.18; N, 6.71.

V.p.c. analysis of the photolysis mixture gave the following composition: (**5**), 35.5% at 6.2 min; (**7**), 17.5% at 5.9 min; (**6**), 7.0% at 9.5 min; and (**9**), 35.5% at 6.7 min. There was in addition a minor peak appearing as a shoulder at 7.0 min, about 4%, corresponding to a compound which has not been identified.

Photo-sensitized Decomposition of the Cyclobutane Adducts

The cyclobutane from 2-methoxynaphthalene and acrylonitrile (**1**) (30 mg), 2-methoxynaphthalene (60 mg), and an internal standard (*cis*-7-cyano-2,3-benzobicyclo-[3.2.0]heptane (2*b*) (14 mg) in ethanol (13 ml) were irradiated at 313 mμ with a monochromator. Aliquots were withdrawn at known time intervals and were analyzed by v.p.c. on 5 ft × 1/8 in. of 4% QF-1 on Diatoport at 175°. The disappearance of adduct **1** was linear with time, and about 30% had decomposed in 2 h. The rate of decomposition was the same when 2-cyanonaphthalene was used as sensitizer.

A similar experiment with the adduct of 2-cyanonaphthalene and methyl vinyl ether (**5**), using 2-cyanonaphthalene as sensitizer showed that the adduct decomposed more rapidly, about 70% reacting in 2 h.

The major adduct of naphthalene and acrylonitrile (**4**) was checked for photostability in a similar way. It was found that naphthalene and benzophenone, but not fluorenone, would act as sensitizers for its decomposition.

Deuterium Exchange of Nitrile (1)

Treatment of nitrile (**1**) (50 mg) in dry pyridine (0.3 ml) and D_2O (0.1 ml) with sodium methoxide (15 mg) at 50° for 5 h resulted in exchange of one proton in the adducts for deuterium. The exchange was observed by n.m.r., and the experiment served to identify the methine proton α to the nitrile group.

We thank Dr. K. Saunders and Mr. B. Sawyer for measuring the nuclear Overhauser effects, Dr. R. F. Childs for the procedure for deuterium exchange of **1**, and Mr. B. R. Ramachandran for help with this experiment. We are grateful to the National Research Council of Canada for financial support.

1. This work was presented in part at the 101st Meeting of the American Chemical Society, Los Angeles, California, April 1971. Abstract No. ORGN-123.
2. (*a*) J. J. McCULLOUGH, C. CALVO, and C. W. HUANG. Chem. Comm. 1176 (1968); (*b*) J. J. MJïCCULLOUGH and C. W. HUANG. Can. J. Chem. **47**, 757 (1969).
3. (*a*) R. M. BOWMAN, T. R. CHAMBERLAIN, C. W. HUANG, and J. J. McCULLOUGH. J. Am. Chem. Soc. **92**, 4106 (1970); (*b*) R. M& BOWMAN and J. J. McCULLOUGH. Chem. Commun. 948 (1970).
4. (*a*) J. J. McCULLOUGH, C. W. HUANG, and W. S. WU. Chem. Commun. 1368 (1970); (*b*) J. J. McCULLOUGH and W. S. WU. Tetrahedron Lett. 3951 (1971); (*c*) J. J. McCULLOUGH, W. S. WU, and C. W. HUANG. J. Chem. Soc. Perkin II, 370 (1972).
5. B. EM JOB and J. D. LITTLEHAILES. J. Chem. Soc. C, 886 (1968).
6. J. G. ATKINSON, D. E. AYER, G. BUCHI, and E. W. ROBB. J. Am. Chem. Soc. **85**, 2257 (1963).
7. D. BRYCE-SMITH. Chem. Commun. 806 (1969).
8. R. SRINIVASAN. I.B.M. J. Res. Develop. **15**, 34 (1971).
9. R. SRINIVASAN. J. Am. Chem. Soc. **92**, 3555 (1971).
10. D. BRYCE-SMITH, B. E. FOULGER, A. GILBERT, and P. J. TWITCHETT. Chem. Commun. 794 (1971).
11. K. E. WILZBACH and L. KAPLAN. J. Am. Chem. Soc. **93**, 2073 (1971).
12. N. C. YANG and J. LIBMAN. J. Am. Chem. Soc. **94**, 1406 (1972); N. C. YANG, J. LIBMAN, L. BARRETT, JR., M. H. HUI, and R. L. LOESCHEN. J. Am. Chem. Soc. **94**, 1408 (1972).
13. S. ANDER, H. BLUME, G. HEINRICH, and D. SCHULTE-FROHLINDE. Chem. Commun. 745 (1968); D. SCHULTE-FROHLINDE and R. PFEFFERKORN. Ber. Bunsenges. Phys. Chem. **72**, 330 (1968).
14. R. M. BOWMAN, C. CALVO, J. J. McCULLOUGH, R. C. MILLER, and I. SINGH. Can. J. Chem. **51**, 1060 (1973).
15. (*a*) J. S. BRADSHAW and G. S. HAMMOND. J. Am. Chem. Soc. **85**, 3953 (1963); (*b*) P. WILANAT and B. K. SELINGER. Austral. J. Chem. **21**, 733 (1968); (*c*) J. S. BRADSHAW, N. B. NIELSEN, and D. P. REES. J. Org. Chem. **33**, 259 (1968).
16. B. K. SELINGER and M. STERNS. Chem. Commun. 978 (1969).
17. E. B. WHIPPLE and G. R. EVANEGA. Org. Mag. Res. **2**, 1 (1970).
18. T. W. MATTINGLY, JR., J. E. LANCASTER, and A. ZWEIG. Chem. Commun. 595 (1971).
19. H. A. SZYMANSKI and R. E. YELIN. N.M.R. Band Handbook. Plenum Press, New York, N.Y. 1968. pp. 85–90.
20. G. JONES and W. J. RAE. Tetrahedron Lett. **22**, 3021 (1966); F. BELL and J. SPANSWICK. J. Chem. Soc. C, 1887 (1966).
21. R. A. BELL and J. K. SAUNDERS. Can. J. Chem. **48**, 1114 (1970).
22. H. M. WALBORSKY and J. F. PENDLETON. J. Am. Chem. Soc. **82**, 1405 (1960).
23. (*a*) K. TORI, K. AONO, Y. HATA, R. MUNEYUKI, T. TSUZI, and H. TANIDA. Tetrahedron Lett. **22**, 9 (1966); (*b*) J. MEINWALD and Y. C. MEINWALD. J. Am. Chem. Soc. **85**, 2514 (1963).
24. T. S. CANTRELL. J. Am. Chem. Soc. **94**, 5930 (1972).
25. T. R. CHAMBERLAIN, J. D. GREEN, and J. J. McCULLOUGH. Unpublished observations.
26. N. J. TURRO and P. D. BARTLETT. J. Org. Chem. **30**, 1849 (1965).
27. R. M. BOWMAN, J. J. McCULLOUGH, and J. S. SWENTON. Can. J. Chem. **47**, 4503 (1969).
28. R. B. WOODWARD and R. HOFFMAN. The conservation of orbital symmetry. Verlag Chemie, Gmbk, Weinheim/Bergstr. 1970; (*a*) Chapter 6; (*b*) p. 70.
29. H. F. ANGUS, J. M. BLAIR, and D. BRYCE-SMITH. J. Chem. Soc. 2003 (1960).
30. A. STREITWIESER. Molecular orbital theory for organic chemists. John Wiley and Sons, Inc., New York, N.Y. 1961. p. 170.
31. G. B. GILL. Quart. Rev. Chem. Soc. **22**, 364 (1968).
32. R. O. KAN. Organic photochemistry. McGraw-Hill Book Co. Inc., New York, N.Y. 1966. pp. 51–54.

Can. J. Chem. Downloaded from www.nrcresearchpress.com by 210.87.254.6 on 09/05/12
For personal use only.

33. H. E. ZIMMERMAN and H. IWAMURA. J. Am. Chem. Soc. **92**, 2015 (1970).
34. H. A. S. GORDON and J. R. McNESBY. J. Chem. Phys. **31**, 853 (1959).
35. P. J. COLLIN and W. H. F. SASSE. Tetrahedron Lett. 1689 (1968); A. M. BRAUN. J. Org. Chem. **35**, 1208 (1970); C. A. MATUSZAK and L. DICKSON. J. Org. Chem. **37**, 3345 (1972).
36. L. FIESER and M. FIESER. Reagents for organic synthesis. Vol. I. John Wiley and Sons, Inc., New York, N.Y. 1967. p. 905.
37. H. H. JAFFÉ and M. ORCHIN. Theory and applications of ultraviolet spectroscopy. John Wiley and Sons, Inc., New York, N.Y. 1962. p. 301.
38. H. A. LAITINEN, F. A. MILLER, and T. D. PARKS. J. Am. Chem. Soc. **69**, 2707 (1947).
39. D. R. ARNOLD, L. B. GILLIS, and E. B. WHIPPLE. Chem. Commun. 918 (1969).
40. E. GROVENSTEIN, JR., T. C. CAMPBELL, and T. SHIBATA. J. Org. Chem. **34**, 2418 (1969).
41. K. MIZUNO, C. PAC, and H. SAKURAI. J. Chem. Soc. Chem. Commun. 219 (1973).

Can. J. Chem. Downloaded from www.nrcresearchpress.com by 210.87.254.6 on 09/05/12
For personal use only.

High Temperature Aqueous Electrolyte Concentration Cells and the Ionization of Liquid Water to 200 °C

DIGBY D. MACDONALD,[1] P. BUTLER,[2] AND D. OWEN

Research Chemistry Branch, Whiteshell Nuclear Research Establishment, Atomic Energy of Canada Limited, Pinawa, Manitoba R0E 1L0

Received December 1, 1972

High temperature aqueous electrolyte concentration cells with and without liquid junction are described. These cells were used to measure the ionization constant of water in 0.1, 0.25, 0.5, and 1.0 mol/kg KCl solutions at temperatures to 200 °C. Extrapolation to infinite dilution yielded the following functions for the temperature dependence of log K_w^0 and the thermodynamic parameters for ionization: log $K_w^0 = -4046.16/T + 3.537 - 0.01323T$; $\Delta G^0 = 77458.0 - 67.71T + 0.253187T^2$ J/mol; $\Delta H^0 = 77458.0 - 0.253187T^2$ J/mol; $\Delta S^0 = 67.71 - 0.5063T$ J/K mol; $\Delta C_p^0 = -0.5063T$ J/K mol.

Des cellules de concentration aqueuse d'électrolytes à haute température, avec ou sans jonction liquide, ont été décrites. Ces cellules ont été utilisées pour mesurer la constante d'ionisation de l'eau dans des solutions à 0.1, 0.25, 0.5, et 1.0 mol/kg de KCl, à des températures allant jusqu'à 200 °C. L'extrapolation à la dilution infinie a conduit aux fonctions suivantes pour l'influence de la température sur log K_w^0 et sur les paramètres thermodynamiques d'ionisation: log $K_w^0 = -4046.16/T + 3.537 - 0.01323T$; $\Delta G^0 = 77458.0 - 67.71T + 0.253187T^2$ J/mol; $\Delta H^0 = 77458.0 - 0.253187T^2$ J/mol; $\Delta S^0 = 67.71 - 0.5063T$ J/K mol; $\Delta C_p^0 = 0.5063T$ J/K mol. [Traduit par le journal]

Can. J. Chem., 51, 2590 (1973)

Introduction

An accurate method for determining ionic activities, pH, and equilibrium phenomena in solution is through the use of electrolyte concentration cells. This class of reversible cell may be divided into two types, *viz.* those with and without liquid junction, represented by cells I and II, respectively.

I $\quad Pt(H_2)/HCl(a_1)/HCl(a_2)/(H_2)Pt$

II $\quad Pt(H_2)/HCl(a_1),[AgCl]/Ag/[AgCl],HCl(a_2)/(H_2)Pt$

These cells have been investigated extensively at temperatures less than 100 °C (1, 2). Variations of cells I and II have been used to measure transport numbers, hydrogen ion activity and dissociation constants for weak acids and bases (1, 2). In two recent publications Mesmer *et al.* (3, 4) described an electrolyte concentration cell with liquid junction (*i.e.* cell I) which is capable of precise acidity measurements at elevated temperatures. This cell was used to determine the apparent ionization constant for water ($Q_w = m_{H^+} \cdot m_{OH^-}$) in 1 mol/kg KCl solution to 292 °C (3) and the hydrolysis of Al^{3+} in KCl solution to 150 °C (4).

In this paper we describe simple and reliable high temperature concentration cells with and without liquid junction. These cells were designed to provide accurate potentiometric acidity measurements at elevated temperatures as part of a program in this laboratory to study hydrolytic processes in high temperature water. The accuracy of these cells is demonstrated in the present work by measuring the ionization constant for water in 0.1, 0.25, 0.5, and 1.0 mol/kg KCl solutions at temperatures between 25 and 200 °C. Plots of log K_w *vs.* ionic strength, extrapolated to infinite dilution, yield log K_w^0 values which agree to within $\pm 0.2\%$ with the best data in the literature which have been derived from conductance techniques. This close agreement demonstrates that the apparatus described here is capable of yielding precise acidity measurements in high temperature water. These concentration cell techniques are being applied to the study of hydrothermal precipitation reactions and to the determination of transport numbers for ions in aqueous solution at elevated temperatures.

Experimental

Electrochemical Cells

The electrolyte concentration cells used in this study are shown in Fig. 1. The cell body consisted of a 300 ml titanium autoclave which was gold-plated on the inside surface to minimize contamination of the solution in the outer compartment. The inner compartment was ma-

[1]To whom correspondence should be addressed. Present address: Department of Chemistry, Victoria University of Wellington, Wellington, New Zealand.

[2]Summer student, May – September, 1972.

Can. J. Chem. Downloaded from www.nrcresearchpress.com by 210.87.254.40 on 09/05/12
For personal use only.

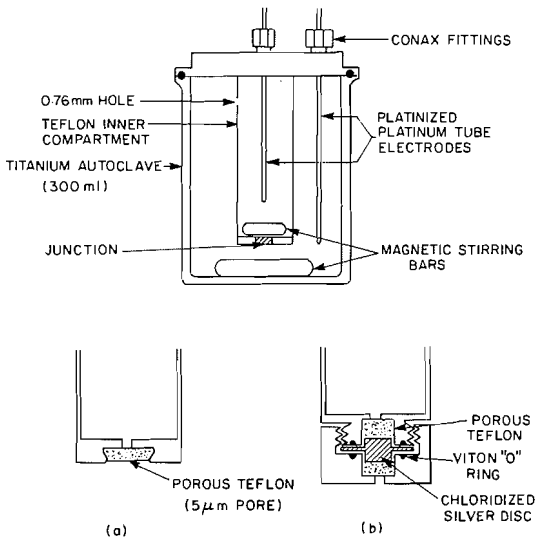

FIG. 1. High temperature aqueous electrolyte concentration cell.

chined from Teflon to a wall thickness of 1.5 mm. This wall thickness allowed rapid thermal equilibration of the two compartments after a sudden temperature change. Both compartments contained Teflon covered magnetic stirring bars to agitate the solutions. These stirring bars were activated by a rotating magnet located beneath the aluminum oil bath used to control temperature.

The reversible hydrogen electrodes consisted of pure platinum tubes (3 mm od., 1.5 mm i.d.) which were sealed at the lower ends. The tubes were insulated from the autoclave body by Conax fittings containing Teflon sheaths and cones. The electrodes were lightly platinized by electrolysis in a dilute solution of chloroplatinic acid immediately before use. Chromel–alumel thermocouples (0.8 mm diameter) were inserted into the platinum tubes to monitor the temperatures of the compartments.

The junctions used in cells I and II are shown in Figs. 1*a* and *b*, respectively. For cell I, the junction consisted of a porous Teflon disc (3 mm thick, 6.4 mm diameter, 10 μm pore size) which was pressed into the tapered cavity shown in Fig. 1*a*. Initial experiments showed that the porous Teflon did not always produce a satisfactory junction and electrolytic contact between the compartments was frequently interrupted. This resulted in erratic behavior of the potential difference between the two hydrogen electrodes. This phenomenon was attributed to the failure of expelling air from the pores because of the non-wettability of Teflon. Two techniques were used to overcome this problem. First, an electric discharge was passed through the Teflon disc in the presence of water vapor. This procedure produced a wettable surface presumably due to hydroxylation of the Teflon surface by hydroxyl radicals produced in the spark discharge. The second technique, and the one most often adopted, was to boil the Teflon disc in a saturated solution of KCl and then cool. During boiling, air was expelled from the pores in the Teflon disc and replaced by KCl solution when cooled. The boiling/cooling procedure was repeated over two or three cycles. Of the two techniques, the second one was found to produce the most reliable junctions.

The junction used in cell II consisted of a chloridized silver disc separated from the solutions by porous Teflon discs which were treated as described above. Direct contact between the two compartments was prevented by using Viton O rings. The silver disc was chloridized by anodizing in a slightly acidified 10% KCl solution for 30 min at a current density of 2 mA/cm². The silver discs were freshly chloridized before each run.

The autoclave was degassed by cyclic compression/decompression with pure hydrogen. This procedure was repeated at least five times to remove all traces of oxygen from the system and the pressure was finally adjusted to 0.6 MPa (6 bar) for cell I and 0.2 MPa (2 bar) for cell II. The lower pressure employed in cell II was required to reduce the rate at which AgCl was reduced by hydrogen at high temperature (5–8). The porous Teflon plugs also reduced the rate of reduction that occurred at the silver chloride surface, presumably by reducing the rate of diffusion of dissolved hydrogen to the surface. Even so, it was found that sufficient reduction occurred at 150 °C over 24 h to cause a change in color of the silver chloride surface from red-brown to silver. This probably reflects the formation of silver metal at the electrode surface. This color change was frequently accompanied by mV or tens of mV deviations in potential and experiments using cell II were restricted to a few hours duration at temperatures greater than 150 °C.

The entire autoclave was immersed in an oil bath which allowed temperatures (25–200 °C) to be controlled to ±0.1 °C. The system was brought to temperature in steps to ensure that the two compartments did not differ by more than 5° C. This procedure minimized distillation from the outer compartment to the inner compartment during heat-up and in the reverse direction during cool-down. Distillation was also minimized by maintaining a pressure of hydrogen in the system, and by having a hole of small diameter (0.76 mm) between the two compartments.

All potential measurements were made using a Beckman Research p*H* meter. This instrument was capable of detecting 0.1 mV changes in the potential difference between the two hydrogen electrodes. Potentials were recorded after they had become constant to within 0.1 mV for at least 15 min.

Solutions

Dilute solutions of HCl and KOH (0.010 mol/kg) in potassium chloride solutions (0.1–1.0 mol/kg) were prepared from reagent grade chemicals. The solutions were stored in tightly stoppered Teflon containers to minimize contamination due to atmospheric carbon dioxide.

Results

Cell I

Since the pressure of hydrogen is the same in both compartments the potential (E) of the inner compartment electrode with respect to the outer compartment electrode is given by eq. 1

$$[1] \qquad E = \frac{2.303RT}{F}\log\frac{(a_{H^+})_2}{(a_{H^+})_1} + E_j$$

where subscripts 1 and 2 designate the outer and inner compartments, respectively, and E_j is the

Can. J. Chem. Downloaded from www.nrcresearchpress.com by 210.87.254.40 on 09/05/12
For personal use only.

Can. J. Chem. Downloaded from www.nrcresearchpress.com by 210.87.254.40 on 09/05/12
For personal use only.

liquid junction potential. Since the inner compartment contained the KOH solution, we write

$$[2] \qquad (a_{H^+})_2 = a_{H_2O} K_w/(a_{OH^-})_2$$

where K_w is the ionization constant of water in the solution of interest, and a_i is the activity of species i in the system. Recognizing that

$$[3] \qquad a_i = \gamma_i m_i$$

where γ_i and m_i represent the activity coefficient and molal concentration, respectively, then substitution of eqs. 2 and 3 into eq. 1 results in the following expression for $-\log K_w$

$$[4] \quad -\log K_w = -\frac{F(E - E_j)}{2.30RT} - \log [(m_{H^+})_1(m_{OH^-})_2] - \log \frac{\gamma_{H^+}\gamma_{OH^-}}{a_{H_2O}}$$

Liquid junction potentials for cell I at high temperatures can be estimated using the Henderson equation (2, 3)

$$[5] \qquad E_j = -\sum D_i[(m_i)_2 - (m_i)_1]$$

where the D_i coefficients are given by

$$[6] \qquad D_i = RT|Z_i|\lambda_i/(Z_i F \sum(|Z_i|)\bar{m}_i\lambda_i)$$

The quantity $\bar{m}_i$ is the average concentration of species i in the two compartments, Z_i is the ionic charge, and λ_i is the equivalent conductance. Equivalent conductances for K^+, Cl^-, H^+, and OH^- at temperatures to 400 °C have been estimated by Quist and Marshall (9) and were used here to evaluate E_j. In the present study, the liquid junction potential rarely exceeded 1 mV which represents a minor correction to the measured potential (typically 500 mV).

The activity coefficient term in eq. 3 is equated to the analytical expression given by Harned and Cook. (10)

$$[7] \quad \log \frac{\gamma_{H^+}\gamma_{OH^-}}{a_{H_2O}} = -\frac{2S\sqrt{I}}{1 + A\sqrt{I}} + BI + CI^{3/2}$$

which has been used by Mesmer, Baes, and Sweeton (3) for cells of type I at elevated temperatures. The various coefficients in eq. 7 have the following values

$$[8] \qquad S = 1.814 \times 10^6/(\varepsilon T)^{3/2}$$

$$[9] \qquad A = 50.30\, a/(\varepsilon T)^{1/2}$$

$$[10] \qquad B = 0.266 + 5.2 \times 10^{-4} t$$

$$[11] \qquad C = -0.0350 - 4.88 \times 10^{-4} t$$

where a is a temperature independent parameter equal to 3.6 for KCl, ε is the dielectric constant for water (11), and I is the ionic strength of the solution. Since the ionic strengths of both compartments were kept nearly equal we equate I in eq. 7 to the average value. Equation 7 reproduces experimental data to better than 1% up to 3 mol/kg KCl and 60 °C, and the work of Mesmer *et al.* (3) indicates that these coefficients are acceptable to much higher temperatures.

Cell II

The potential of cell II for uniform hydrogen pressure is given by eq. 12

$$[12] \qquad E = \frac{2.303RT}{F} \log \frac{(a_{H^+,2})(a_{Cl^-,2})}{(a_{H^+,1})(a_{Cl^-,1})}$$

Expansion of this expression and substitution of eqs. 2 and 3 results in the following expression for $-\log K_w$

$$[13] \quad -\log K_w = -\frac{FE}{2.303RT} - \log (m_{H^+})_1(m_{OH^-})_2 - \log \frac{\gamma_{H^+}\gamma_{OH^-}}{a_{H_2O}} + \log \frac{(m_{Cl^-})_2}{(m_{Cl^-})_1} + \log \frac{(\gamma_{Cl^-})_2}{(\gamma_{Cl^-})_1}$$

where, as before, E is the potential difference between the inner and outer compartment platinum electrodes. We assume that, although the ionic strengths are well outside the Debye–Hückel range, the *ratio* of activity coefficients is given by eq. 14

$$[14] \quad \log \frac{(\gamma_i)_2}{(\gamma_i)_1} = -Z_i^2 S \frac{\sqrt{I_2} - \sqrt{I_1}}{(1 + \sqrt{I_2})(1 + \sqrt{I_1})}$$

It should be noted that, since $I_2 \approx I_1$, the contribution that the above term makes to $-\log K_w$ is small (usually $< 1\%$) and any error inherent in the above assumption is probably within the total experimental error.

Numerical values for $\log K_w$ in 0.1, 0.25, 0.5, and 1.0 mol/kg KCl solutions at temperatures between 25 and 200 °C are plotted in Figs. 2–5. Interpolated values at 25 °C intervals are plotted in Fig. 6 as a function of ionic strength. Extrapolation of $\log K_w$ to infinite dilution yields the numerical values for $\log K_w^0$ which are listed in Table 1.

Discussion

The values for $\log K_w^0$ listed in Table 1 are plotted in Fig. 7 together with similar data ob-

Can. J. Chem. Downloaded from www.nrcresearchpress.com by 210.87.254.40 on 09/05/12
For personal use only.

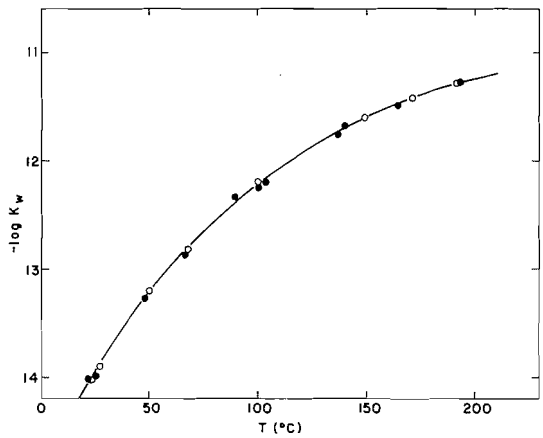

FIG. 2. The dependence of $-\log K_w$ on temperature in 0.1 mol/kg KCl solution; ●, cell I; ○, cell II.

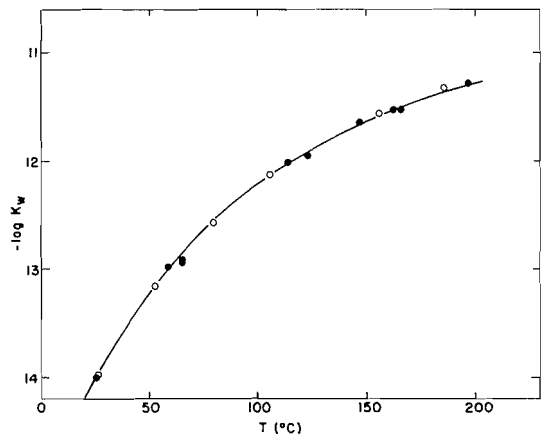

FIG. 3. The dependence of $-\log K_w$ on temperature in 0.25 mol/kg KCl solution; ●, cell I; ○, cell II.

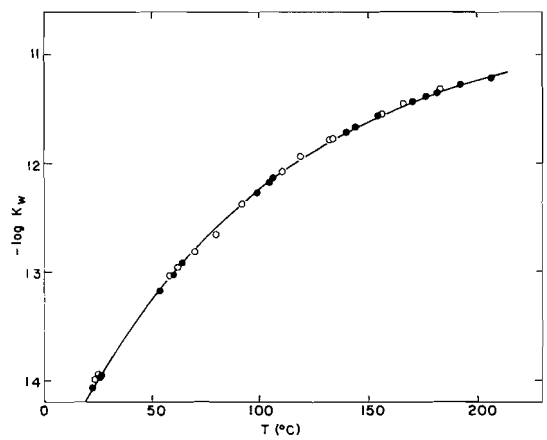

FIG. 4. The dependence of $-\log K_w$ on temperature in 0.5 mol/kg KCl solution; ●, cell I; ○, cell II.

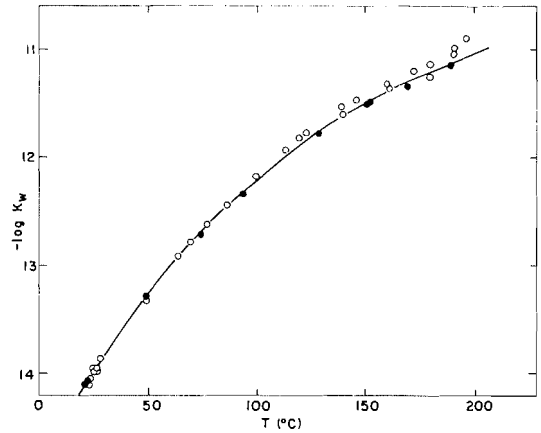

FIG. 5. The dependence of $-\log K_w$ on temperature in 1 mol/kg KCl solution: ●, cell I; ○, cell II.

tained using both galvanic cell (8, 13) and conductance techniques (12). The present data agree to within $\pm 0.2\%$ with the values of Fisher and Barnes (12), which were derived from conductance measurements on the system acetic acid – ammonium acetate – ammonia. Good agreement is also obtained at 175 and 200 °C with the data of Dobson and Thirsk (8), which were derived from e.m.f. measurements on galvanic cells of the type H_2/HCl (or NaOH), NaCl [AgCl]/Ag. At lower temperatures (*i.e.* 100, 125, and 150 °C) the data of Dobson and Thirsk (8) are not in good agreement with either our values or the conductance measurements of Fisher and Barnes (12). However, the close agreement between the present e.m.f. data and the conductance values indicates that the data of Dobson and Thirsk at these lower temperatures are in error by approximately ± 0.1 in $\log K_w^0$ (*i.e.* $\pm 1\%$). At temperatures less than 100 °C, the data reported here are in excellent agreement with the very precise values of Harned and Robinson (13), which were also derived from galvanic cell measurements.

The present data were obtained over a sufficiently wide temperature range that meaningful values for the thermodynamic parameters of ionization at S.V.P. (ΔG^0, ΔH^0, ΔS^0, and ΔC_p^0) could be obtained. It was found that the experimental data are represented within experimental error (see Table 1) by eq. 15.

$$[15] \quad \log K_w^0 = -4046.16/T + 3.537 - 0.01323T$$

(standard deviation = 0.016)

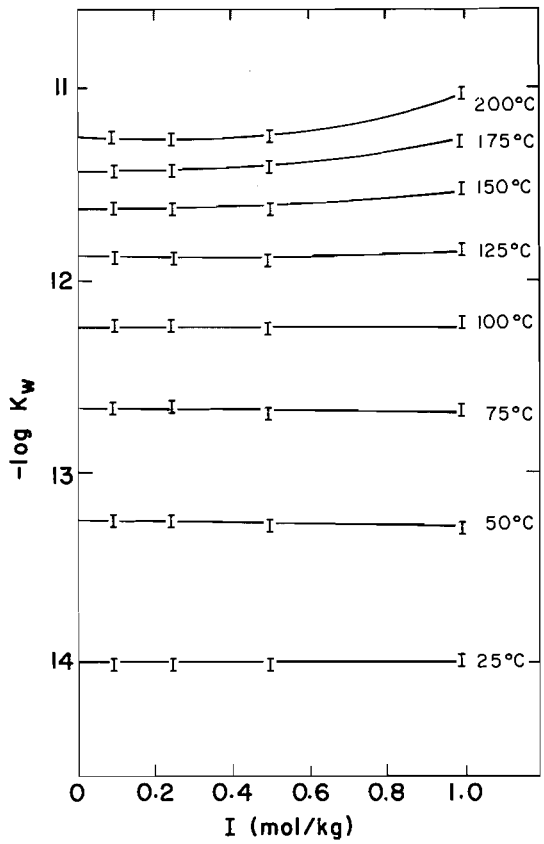

FIG. 6. The variation of $-\log K_w$ with ionic strength at various temperatures.

TABLE 1. Numerical values for the ionization constant of water at elevated temperature

T (°C)	$-\log K_w^0$ Observed	$-\log K_w^0$ Calculated*
25	13.99	13.98
50	13.24	13.26
75	12.68	12.69
100	12.24	12.24
125	11.88	11.89
150	11.64	11.62
175	11.43	11.42
200	11.26	11.27

*Calculated using eq. 15.

and the standard free energy change by

[16] $\Delta G^0 = 77458 - 67.17T + 0.253187T^2$ J/mol

Differentiation of eq. 16 and application of standard relationships between free energy, entropy, enthalpy, and heat capacity resulted in the following expressions for ΔH^0, ΔS^0, and ΔC_p^0 at S.V.P.

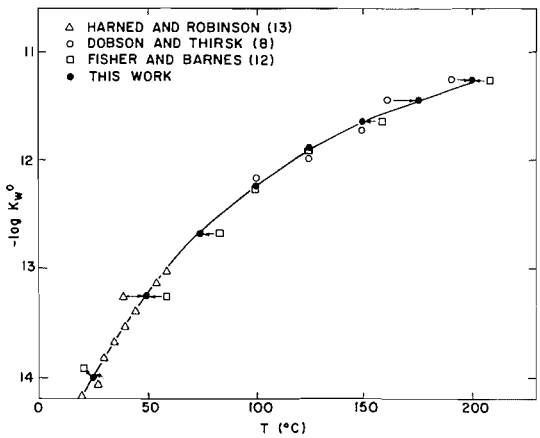

FIG. 7. The dependence of $-\log K_w^0$ on temperature for the ionization of water.

[17] $\Delta H^0 = 77458.0 - 0.253187T^2$ J/mol

[18] $\Delta S^0 = 67.71 - 0.5063T$ J mol

[19] $\Delta C_p^0 = -0.5063T$ J/K mol

Numerical values for ΔG^0, ΔH^0, ΔS^0 and ΔC_p^0 for the ionization of liquid water at 25 °C were calculated from eqs. 16 to 19 and found to be 77 458 J/mol, 54 951 J/mol, −83.2 J/K mol, and −151 J/K mol, respectively. Dobson and Thirsk (8) have analyzed log K_w^0/temperature data from previous studies in detail using a number of analytical functions to represent the temperature dependence of log K_w^0. The value obtained in the present study for ΔG^0 (25 °C) agrees within ±0.2% with the values derived by Dobson and Thirsk (8). The value derived here for ΔH^0 (25°) of 54 951 J/mol is 2–3% lower than calorimetric values of 56 576 J/mol (14) and 55 647 J/mol (15). However, Dobson and Thirsk (8) show that the value obtained for ΔH^0 (25 °C) from ionization data is sensitive to the function chosen to represent the temperature dependence of log K_w^0. Thus, for functions of the type

[20] $$RT \ln K_w^0 = \sum_{i=0}^{n} a_i T^i$$

ΔH^0 (25 °C) is found to vary from 43 036 J/mol for $n = 2$ to 57 739 J/mol for $n = 5$. For $n = 3$ they find ΔH^0 (25 °C) = 54 735 J/mol which is in good agreement with the present work. Similarly, the temperature dependence of ΔH^0 at 25 °C, *i.e.*

Can. J. Chem. Downloaded from www.nrcresearchpress.com by 210.87.254.40 on 09/05/12
For personal use only.

Can. J. Chem. Downloaded from www.nrcresearchpress.com by 210.87.254.40 on 09/05/12
For personal use only.

ΔC_p^0 (25 °C), is highly sensitive to the value of n chosen for eq. 20 and varies from 0 J/K mol ($n = 2$) to −713 J/K mol for $n = 5$. The value obtained in the present study (−151 J/K mol) is in good agreement with the value of −150 J/K mol found by Dobson and Thirsk (8) for $n = 3$.

Differentiation of eq. 15 with respect to temperature, and putting $(d \log K_w^0/dT) = 0$, leads to values of 280 °C and −11.09 for T_{max} and $(\log K_w^0)_{max}$, respectively. These values are in excellent agreement with the experimental values of 275 °C and −11.01 as determined by Fisher and Barnes (12) from conductance measurements. Furthermore, values for $\log K_w^0$ extrapolated to the range 200 to 300 °C using eq. 15 agree to within 1% with the values determined from conductance data (12).

In the present work the dependence of the term $\gamma_{H^+}\gamma_{OH^-}/a_{H_2O}$ on ionic strength is represented by eq. 7. This expression has been found accurate to <1% in 0–3 mol/kg KCl at temperatures to 60 °C (10). The lack of dependence of $\log K_w$ on ionic strength, as shown in Fig. 6, demonstrates that eq. 7 is acceptable to temperatures as high as 125 °C. At higher temperatures, positive deviations occur, particularly in 1 mol/kg KCl. This deviation has also been noted by Mesmer, Baes, and Sweeton (3), and can be attributed to ion pairing to form (H^+Cl^-) and (K^+OH^-). Association of KOH has been suggested to occur at room temperature (16), and is expected to become increasingly important as temperature increases due to the decrease in the dielectric constant of water.

Previous investigations (5–8) of the H_2/H^+Cl^--[AgCl]/Ag system at elevated temperatures have shown that the reduction of AgCl occurs spontaneously,

$$AgCl + \tfrac{1}{2}H_2 = Ag + H^+ + Cl^-$$

This process results in a decrease in potential with time from the theoretical reversible value due to the establishment of local hydrogen cells at the silver/silver chloride electrode and due to the change in acidity of the solution. In the present study, we attribute the scatter in $\log K_w$ data at elevated temperatures, when measured with cell II (see Fig. 5), to the reduction of AgCl. Analysis of the solutions after a run showed that the change in H^+ concentration was sufficient to account for the observed scatter, and suggest that the existence of local hydrogen cells at the Ag/AgCl surface are of minor importance in the present system. It is possible that since the Ag/AgCl electrodes are opposed the interference from hydrogen cells at the surface tend to cancel. However, in view of the uncertainties associated with the behavior of silver/silver chloride electrodes in hydrogen rich systems, we recommend the use of cell I in the determination of acidities at elevated temperatures.

1. R. A. Robinson and R. H. Stokes. Electrolyte solutions. Butterworths, London. 1959.
2. G. Kortüm. Treatise on electrochemistry. 2nd ed. Elsevier, Amsterdam. 1965.
3. R. E. Mesmer, C. F. Baes, and F. H. Sweeton. J. Phys. Chem. **74**, 1937 (1970).
4. R. E. Mesmer and C. F. Baes. Inorg. Chem. **10**, 2290 (1971).
5. M. H. Lietszke, R. S. Greeley, W. T. Smith, and R. W. Stoughton. J. Phys. Chem. **64**, 652 (1960).
6. R. N. Royhoudhury and C. F. Bonilla. J. Electrochem. Soc. 103 (1956); 241 (1956).
7. G. Kortüm and W. Haussermann. Ber. Bunsenges, **69**, 594 (1965).
8. J. V. Dobson and H. R. Thirsk. Electrochim. Acta, **16**, 315 (1971).
9. A. S. Quist and W. L. Marshall. J. Phys. Chem. **69**, 2984 (1965).
10. H. S. Harned and M. A. Cook. J. Am. Chem. Soc. **59**, 2304 (1937).
11. G. C. Akerlof and H. I. Oshry. J. Am. Chem. Soc. **72**, 2846 (1950).
12. J. R. Fisher and H. L. Barnes. J. Phys. Chem. **76**, 90 (1972).
13. H. S. Harned and R. A. Robinson. Trans. Faraday Soc. **36**, 973 (1940).
14. T. Ackermann. Disc. Faraday Soc. **24**, 180 (1957).
15. J. D. Hale, R. M. Isatt, and J. J. Christenson. J. Phys. Chem. **67**, 2605 (1963).
16. R. A. Robinson and H. S. Harned. Chem. Rev. **28**, 419 (1941).

Erratum: Investigations of Substituent Effects by Nuclear Magnetic Resonance Spectroscopy and All-valence Electron Molecular Orbital Calculations. II. 4-Substituted α-Methylstyrenes and α-*t*-Butylstyrenes

G. K. HAMER, I. R. PEAT, AND W. F. REYNOLDS
Department of Chemistry, University of Toronto, Toronto, Ontario M5S 1A1

Received April 16, 1973
(Ref. Can. J. Chem., **51**, 915 (1973))

Can. J. Chem., **51**, 2596 (1973)

Table 2 on page 917 should read as follows:

TABLE 2. Vinyl proton chemical shifts (in p.p.m. relative to $(CH_3)_4Si$) and coupling constants (in Hz) for 4-substituted α-*t*-butylstyrenes at infinite dilution in cyclohexane-d_{12}

Substituent	δ_{H_B}	δ_{H_C}	$\Delta\delta$(B − C)	J_{BC}
H	4.7200	5.1367	−0.4167	1.79
CH_3	4.6958	5.1092	−0.4134	1.87
$C(CH_3)_3$	4.7110	5.1156	−0.4046	1.87
F	4.7256	5.1513	−0.4257	1.68
Cl	4.7247	5.1538	−0.4291	1.60
Br	4.7247	5.1518	−0.4271	1.58
OCH_3	4.7035	5.1088	−0.4053	1.91
$N(CH_3)_2$	4.6896	5.0776	−0.3880	2.07
NO_2	4.7780	5.2399	−0.4619	1.19

Erratum: Structure of Radicals Produced by γ-Radiolysis. Part 2. Radicals Derived from 5-Membered Alicyclic Molecules

RON E. LINDER AND A. CAMPBELL LING
Department of Chemistry, West Virginia University, Morgantown, W.V. 26506

Received May 8, 1973
(Ref.: Can. J. Chem. **50**, 3982 (1972))

Can. J. Chem., **51**, 2596 (1973)

In Table 1 of that article, the data given for the cyclopentenyl radical should read

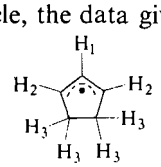

$a_1 = 3.0$ $a_1 = 3.1$
$a_2 = 14.0$ $a_2 = 14.0$
$a_3 = 21.5$ $a_3 = 21.6$

where data for hyperfine splitting constants a_2 and a_3 have become interchanged in this line of the table.

Can. J. Chem. Downloaded from www.nrcresearchpress.com by 210.87.254.40 on 09/05/12
For personal use only.

Can. J. Chem. Downloaded from www.nrcresearchpress.com by 210.87.254.42 on 09/05/12
For personal use only.

The Interaction of Organomercury Pollutants with Biologically Important Sites: An X-ray study of the 2:1 Complex between Methylmercury and Penicillamine

YAU SHING WONG, PETER C. CHIEH, AND ARTHUR J. CARTY[1]

Department of Chemistry, University of Waterloo, Waterloo, Ontario

Received May 24, 1973

The toxic pollutant methylmercurychloride forms 1:1 and 2:1 complexes with the sulfur amino acid DL-penicillamine. The mode of binding of the methylmercury by penicillamine has been established by a three-dimensional X-ray study of $[CH_3Hg]_2(SC(CH_3)_2CHNH_2COO)$.

Le polluant toxique méthylchlorure de mercure forme des complexes 1:1 et 2:1 avec le soufre de l'acide aminé DL-pénicillamine. Le mode de complexation du dérivé méthylmercure avec la pénicillamine a été établi grâce à une étude tridimensionnelle par rayon-X de $[CH_3Hg]_2(SC(CH_3)_2CHNH_2COO)$.

Can. J. Chem., 51, 2597 (1973)

Methylmercuric chloride is the extremely toxic form of the heavy metal which has caused numerous deaths and many cases of brain damage (1). Recent work has re-emphasized the inherent biological dangers in mercury pollution to human, animal, and plant life in view of the apparent ease of conversion of inorganic mercury to CH_3HgCl by biological methylation processes involving, for example, methyl group transfer from methylcorrinoids (2,3), present in microorganisms. In order to understand and combat the inhibitory effects of methylmercury it is essential to have detailed knowledge, currently lacking, of the mode of bonding between CH_3Hg— and the various sites (ligands) present in protein and enzyme molecules. We have carried out structural studies on model complexes of methylmercury with sulfur amino acids and we describe herein the characterization of complexes with DL-penicillamine $HSC(CH_3)_2CH(NH_2)COOH$.

Scheme 1 summarizes products obtained from CH_3HgCl and the zwitterionic form $[HSC(CH_3)_2CH(\overset{+}{N}H_3)COO^-]$ of DL-penicillamine.

Microanalysis indicated that crystals A and B were 2:1 complexes of methylmercury with penicillamine whereas C was a 1:1 complex. The i.r. spectra of complex B showed coordination of the deprotonated sulfhydryl group and the amino group but did not unequivocally establish bonding of the carboxylate group to methylmercury. An X-ray study was undertaken to unambiguously define the nature of the metal — amino acid linkage. Crystal data: $(CH_3Hg)_2[SC(CH_3)_2CH(NH_2)COO]$; orthorhombic crystals, space group *Pbcn*; $a = 19.70$ Å, $b = 10.48$ Å, $c = 11.97$ Å; $Z = 8$, ρ_{meas} (flotation) = 3.06 g cm^{-3}, $U = 2475.9$ Å^3, $\rho_{calcd} = 3.114$ g cm^{-3}. The intensities of 1047 independent reflections were measured on a GE XRD6 automatic diffractometer using MoK_α radiation; 935 reflections were considered observed and used in the analysis. The structure was solved by the heavy atom method and refined by least squares using anisotropic thermal parameters, to the present R value of 0.085.[2] The molecular structure is shown in Fig. 1. The binuclear molecule consists of a deprotonated penicillamine ligand in the form $^-SC(CH_3)_2CH(NH_2)COO^-$ bonded via the sulfur atom to one methylmercury unit and via the amino group to the other mercury atom. The coordination geometry around Hg(1) can best be described as linear, two coordinate with an S—Hg—C angle of 176.4° although a very weak interaction of Hg(1) with O(2) of a neighboring molecule may be indicated by a distance of 2.851

[1]To whom correspondence should be addressed.

[2]A structure factor table is available, at nominal charge, from the Depository of Unpublished Data, National Science Library, National Research Council of Canada, Ottawa, Canada K1A 0S2.

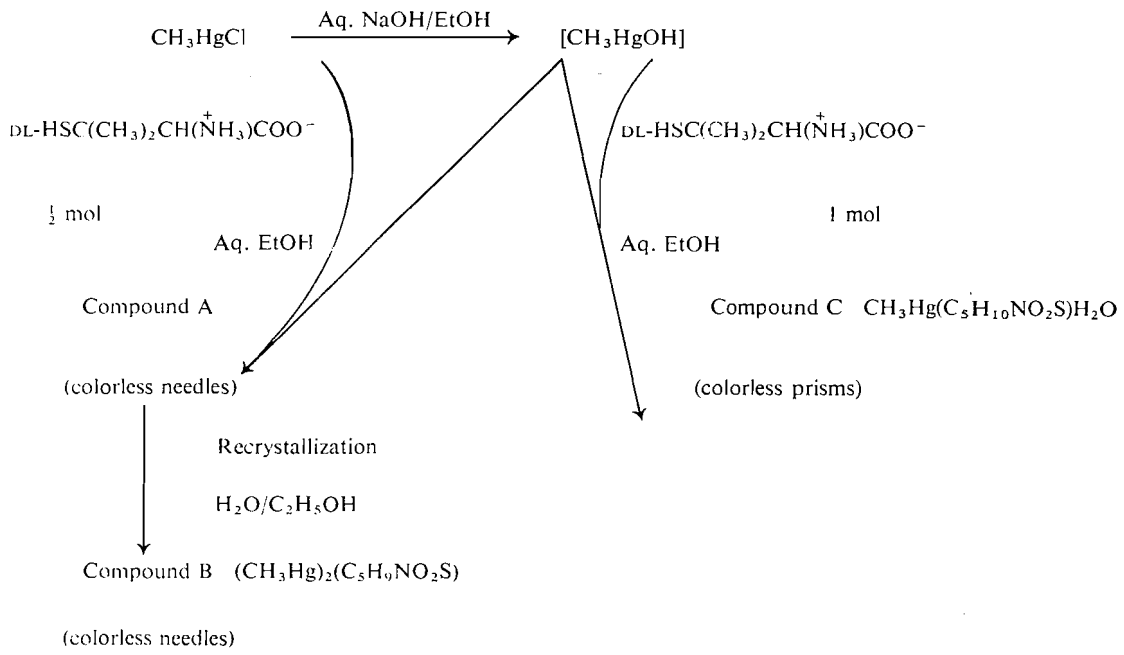

SCHEME 1

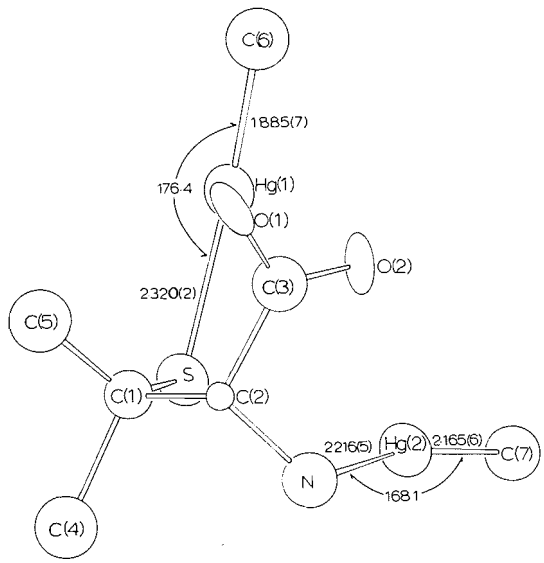

FIG. 1. A view of the molecular structure of the 2:1 complex between methylmercury and penicillamine, $(CH_3Hg)_2[SC(CH_3)_2CH(NH_2)COO]$, illustrating the atomic numbering and pertinent molecular parameters.

Å which is barely within the sum of Van der Waals radii for mercury (1.50 Å) (4) and oxygen (1.40 Å). In agreement with Hg(1) having a *characteristic* coordination number of two, the Hg(1)—S bond length of 2.320(2) Å is very similar to the Hg—S distances (average 2.330(7) Å) in $[C_6H_5N{=}C(OCH_3)S]_2Hg$ (5) where mercury is also two coordinate. By contrast, in $Hg(SCN)_2As(C_6H_5)_3$ where the characteristic coordination number is three the Hg—S distances average 2.54 Å (6) and in tetrahedrally coordinated mercury complexes Hg—S distances greater than 2.50 Å are usually observed (for a summary of X-ray data see ref. 7). Hg(2) is coordinated in approximately linear fashion to a methyl carbon atom and the nitrogen atom of the penicillamine amino group. The apparent deviation of the N—Hg(2)—C(7) angle from 180° may be attributable to the proximity of O(2) of the carboxylate group to Hg(2). The Hg(2)—O(2) distance of 2.708(4) Å is much longer than expected for covalent Hg—O bonds (2.00–2.30 Å) (8) but significantly shorter than the sum of the Van der Waals radii. The Hg(2)–O(2) interaction may be, in part, responsible for the significant difference in Hg(1)—C(6) (1.885(7) Å) and Hg(2)—C(7) (2.165(6) Å) distances although lack of accurate literature data for Hg—Csp^3 bond lengths preclude a detailed discussion. The Hg(2)—N bond length of 2.216(5) Å compares favorably with the Hg—N distance (2.10 Å) in H_2NHgCl (9) but is considerably shorter than in $Cl_3CHgCl{\cdot}C_{12}H_8N_2$ (10) (2.61 Å average) where the *o*-phenanthroline is only weakly

Can. J. Chem. Downloaded from www.nrcresearchpress.com by 210.87.254.42 on 09/05/12
For personal use only.

bound. The bonding of the $—NH_2$ group to Hg(2) implies that the complex is a zwitterion with the positive center localized in the $—NH_2—Hg—CH_3$ moiety and the negative center on the carboxylate group.

This structure determination demonstrates unequivocally that amino acids are capable of binding two methylmercury moieties. Previously it had been assumed that nitrogen containing bases would not form complexes with methylmercury (1*b*) and hence that arginine, lysine, and histidine would not be implicated in methylmercury poisoning. Preliminary work has shown that monoclinic crystals of complex A contain the amino acid bonded to mercury in similar fashion to B whereas in complex C only the sulfur atom of the deprotonated penicillamine molecule is implicated in bonding. A full X-ray study of complex C is in progress.

The results of this work can be compared with studies (11) of Hg^{2+} complexation by L-cysteine, *S*-methyl-L-cysteine, and DL-methionine. Whereas the Hg^{2+} ion has the ability to bind two amino acid sites simultaneously (11), the present work suggests that the CH_3Hg^+ species has little residual Lewis acidity after coordinating a sulfur or amino group. This is in agreement with studies which indicate a low complexing ability for organomercurials in general (12).

We are grateful to the Department of National Health and Welfare for financial support of this work.

1. (*a*) L. DUNLAP. Chem. Eng. News, July 5th (1971), p. 22. (*b*) J. M. WOOD. *In* Advances in environmental science and technology. Vol. 2. *Edited by* J. N. Pitts and R. L. Metcalf. Wiley, New York. 1971. p. 39.
2. J. M. WOOD, F. S. KENNEDY, and C. G. ROSEN. Nature, **223**, 753 (1969).
3. N. IMURA, E. SUKEGAWA, S. K. PAN, K. NAGAO, J. Y. LIM, T. KWAN, and T. UKITA. Science, **172**, 1248 (1971).
4. D. GRDENIĆ. Q. Rev. **19**, 303 (1965).
5. R. S. MCEWEN and G. A. SIM. J. Chem. Soc. A, 1552 (1967).
6. R. C. MAKHIJA, A. L. BEAUCHAMP, and R. RIVEST. Chem. Commun. 1043 (1972).
7. S. E. LAWTON. Inorg. Chem. **10**, 328 (1971).
8. C. MAHON and D. BRITTON. Inorg. Chem. **10**, 2331 (1971).
9. W. N. LIPSCOMB. Acta Crystallogr. **4**, 266 (1961). L. NIJSEN and W. N. LIPSCOMB. Acta Crystallogr. **5**, 604 (1952).
10. A. D. REDHOUSE. Chem. Commun. 1119 (1972).
11. D. F. S. NATUSCH and L. J. PORTER. J. Chem. Soc. A, 2527 (1971).
12. A. J. CANTY and G. B. DEACON. Aust. J. Chem. **21**, 1757 (1968). A. J. CANTY and B. M. GATEHOUSE. Acta Crystallogr. B, **28**, 1872 (1972).

Can. J. Chem. Downloaded from www.nrcresearchpress.com by 210.87.254.42 on 09/05/12
For personal use only.

Can. J. Chem. Downloaded from www.nrcresearchpress.com by 210.87.254.6 on 09/05/12
For personal use only.

Canadian Journal of Chemistry

Published by
THE NATIONAL RESEARCH COUNCIL OF CANADA

Journal canadien de chimie

Publié par
LE CONSEIL NATIONAL DE RECHERCHES DU CANADA

Volume 51 Number 16 August 15, 1973

Volume 51 numéro 16 15 août 1973

The Fluorescence of CS_2 Vapor

C. LAMBERT[1] AND G. H. KIMBELL

Defence Research Establishment, Valcartier and Centre de Recherches sur les Atomes et les Molecules, P.O. Box 880, Courcelette, Quebec

Received December 27, 1972

The fluorescence of carbon disulfide vapor was measured as a function of both wavelength of excitation and wavelength of fluorescence. It was found necessary to invoke a vibrational cascade model in order to account for the observations. Vibrational deactivation occurred on every collision, whereas electronic deactivation was found to require about ten collisions.

The quenching by the foreign gases Ar, N_2, O_2, CO_2, COS, SF_6, and C_3H_8 of CS_2 fluorescence excited by a wavelength of 320.0 nm was measured and the rate constants computed. The degree of efficiency could be correlated with the complexity of the molecule as determined by its polarizability.

La fluorescence des vapeurs de disulfure de carbone a été mesurée en fonction de la longueur d'onde d'excitation et aussi de la longueur d'onde de fluorescence. Il a été nécessaire, d'utiliser un modèle possédant des vibrations en cascade afin d'expliquer les résultats observés. Une désactivation en ce qui a trait aux vibrations, se produit pour chaque collision alors qu'une désactivation électronique semble nécessiter environ dix collisions. L'extinction par divers gaz étrangers Ar, N_2, O_2, CO_2, COS, SF_6, et C_3H_8, de la fluorescence du CS_2 provenant de l'excitation par une longueur d'onde de 320.0 nm a été mesurée et les constantes de vitesse calculées. Les degrés d'efficacité peuvent être reliés à la complexité de la molécule telle que déterminée selon sa polarisabilité. [Traduit par le journal]

Can. J. Chem., 51, 2601 (1973)

Introduction

Fluorescence of CS_2 vapor was first observed by Heicklen (1). He measured the total fluorescent emission between 420.0 and 650.0 nm, excited by different wavelengths varying between 280.0 and 350.0 nm. The quenching constant was calculated for pressures of CS_2 ranging from 10^{-2} to 10^2 Torr. Despite some large fluctuations in the data, a simple mechanism of a single state excitation (both vibrational and electronic) and collisional deactivation appeared to be obeyed. It appeared that electronic quenching occurred on every collision. CS_2 is not dissociated at these wavelengths and no evidence was obtained for any processes other than fluorescence quenching.

Herman, Herman, and Akriche (2) observed that an afterglow followed an electrical discharge through vapor of CS_2 but were unable to observe any structure in the spectra.

Arnold and Kimbell (3) studied the radiation emitted by shock-heated CS_2–Ar mixtures. Using a spectrophotometric technique they ascertained that the emitting state was likely to be the $^3A_2$ state observed by Kleman (4) in absorption. Following this work they attempted (5) to re-analyze the CS_2 afterglow. From their work it was possible to suggest that the state observed using the shock excitation technique was unlikely to be the same as produced in the afterglow (a result of CS + S recombination).

[1]Present address: CEGEP de Trois Rivières, Trois Rivières, Québec.

Can. J. Chem. Downloaded from www.nrcresearchpress.com by 210.87.254.6 on 09/05/12
For personal use only.

Very recently, during the course of the present work, Brus (6) measured the laser-excited fluorescence of CS_2 vapor and measured a double exponential decay suggestive of two emitting states. One of the lifetimes observed was in good agreement with that observed by Douglas (7).

Although a number of observations of emission from CS_2 vapor has been made, only suggestions have been made regarding spectral assignments. Also, in light of the recent work on NO_2 (8, 9) showing a vibrational cascade mechanism for the fluorescence deactivation process, further studies were made in an attempt to look for structure and to measure the quenching constants while varying the wavelengths of both excitation and observed fluorescence. Thus it was hoped that these studies would further clarify the mechanism of the quenching process and perhaps contribute further information towards a positive identification of some of the emitting levels.

The quenching of the fluorescence of triatomic molecules by foreign gases has been studied by many workers. The quenching of NO_2 fluorescence was studied recently by Myers, Silver, and Kaufman (11) in 1966. They obtained the quenching constants for thirteen inert gases. These values ranged from 1/25 to 1/2 of gas kinetic collision number and increased with increasing molecular complexity. These workers also observed that the quenching constant was dependent on the fluorescence wavelength. Mettee (12) in his studies of SO_2 fluorescence found quenching constants of a similar order of magnitude but no wavelength dependence. Brus has obtained some initial rate constants for the quenching of CS_2 fluorescence by several foreign gases. He employed a N_2 laser at 337.1 nm for excitation and observed the fluorescence decay. Prior to this report and the present work we are unaware of any additional work on the quenching of CS_2 fluorescence by foreign gases.

Measurements were made of the quenching constant for eight collision partners. The best empirical relation appears to exist between the probability of fluorescence quenching per gas kinetic collision and the polarizability of the molecule.

Experimental

The apparatus used is shown in Fig. 1. In general it is a standard method for exciting and observing fluorescence in the gas phase using a double monochromator system for excitation and detection. The detection system can use either a monochromator or narrow-band filter for selection of a narrow spectral band of the fluorescence. The fluorescence signal was amplified using phase sensitive techniques and an appropriate photomultiplier.

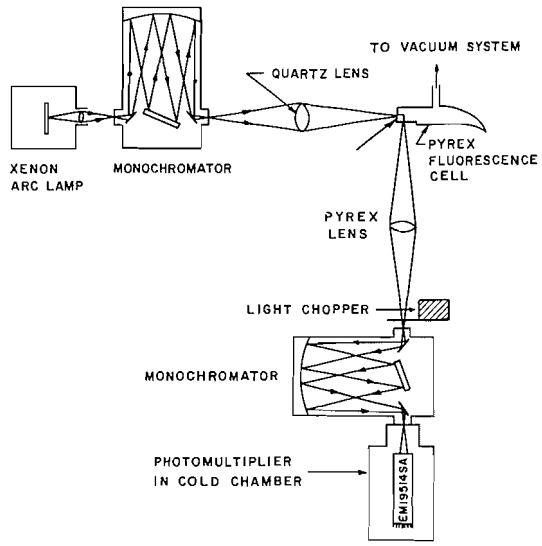

FIG. 1. Schematic of apparatus.

The excitation source was a Hanovia Model 901 C1 150 watt xenon lamp. Wavelength selection for excitation was made by a 0.25 m Jarrell-Ash monochromator equipped with a 2360 lines/mm grating blazed at 300.0 nm. With 2.3 nm slits at the entrance and exit, a nominal bandpass of 5.0 nm was maintained. Exciting radiation was concentrated in the cell using quartz optics. The Pyrex cell was equipped with "suprasil" quartz windows.

Fluorescence, perpendicular to the exciting radiation, was collected by a Pyrex lens and focussed onto the slit of an identical monochromator equipped with a 1180 lines/mm grating blazed at 600.0 nm. For experiments wherein the total radiation was captured, a Corning Sharp Cut, CS 3-72 filter was used to eliminate the scattered radiation below 420.0 nm. The photomultiplier used was an EMI 9514 SA and had an "S" response. Phase sensitive techniques using a PAR Model HR-8 lock-in amplifier were used and the output recorded using an Esterline-Angus recorder. Cooling of the photomultiplier was accomplished using a Products for Research Model TE 102 TS cooling chamber cooled to $-20\,^{\circ}C$.

The carbon disulfide used was Fisher Certified Reagent Grade, Infrared Spectranalyzed. The CS_2 was degassed several times prior to use by repeated freezing in a trap of liquid nitrogen. The pressure of CS_2 was measured using a Wallace and Tiernan gauge for the range 0.1 to 20 Torr (± 0.05 Torr) and an NRC Alphatron gauge for lower pressures.

All quenching experiments were carried out at a CS_2 pressure of 10^{-2} Torr. An average value of the fluorescence over a period of about 10 mins was recorded. The wavelength chosen for excitation was 320.0 nm and the bandpass 5.0 nm. All the gases used, except propane,

Can. J. Chem. Downloaded from www.nrcresearchpress.com by 210.87.254.6 on 09/05/12
For personal use only.

were 99.99% pure as stated by Matheson and used without further purification. Propane was commercial grade. Pressures were measured using the Alphatron, precalibrated for the individual gas.

Results

Simple Stern–Volmer Model

For the simplest case where a molecule is excited to a single electronic energy level the following reaction sequence may be said to apply.

$$[1] \qquad CS_2 + h\nu \xrightarrow{I_x k_a} CS_2^*$$

$$[2] \qquad CS_2^* \xrightarrow{k_f} CS_2 + h\nu \qquad \tau = 1/k_f$$

$$[3] \qquad CS_2^* + CS_2 \xrightarrow{k_q} 2CS_2$$

From the stationary state approximation it is possible to obtain

$$[4] \qquad [CS_2^*] = \frac{I_x k_a [CS_2]}{k_f + k_q [CS_2]}$$

and if

$$[5] \qquad I = \alpha k_f [CS_2^*]$$

then

$$[6] \qquad I = \frac{\alpha I_x k_a k_f [CS_2]}{k_f + k_q [CS_2]}$$

where k_a represents the rate constant for light absorption; k_f, the rate constant for fluorescence; k_q, the rate constant for self-quenching; I, the fluorescence intensity measured in arbitrary units; and I_x, the intensity of the exciting radiation, or

$$[7] \qquad \frac{P}{I} = B[1 + QP]$$

where

$$Q = k_q/k_f,\ P = [CS_2] \text{ and } B = \frac{1}{\alpha I_x k_a}$$

This is the simple Stern–Volmer expression. Thus from measurements of the fluorescent radiation as a function of CS_2 pressure, the validity of this expression can be evaluated.

The spectral distribution of the fluorescent emission for an excitation wavelength (λ_E = 310.0 nm) and two different pressures of CS_2 is shown in Fig. 2. At the lowest pressure used (not shown) a shift in the intensity maximum towards shorter wavelengths was observed. No structure was observed under any of the conditions used. The long wavelength cut-off is not real as shown in view of the decreasing spectral sensitivity of the photomultiplier in this region.

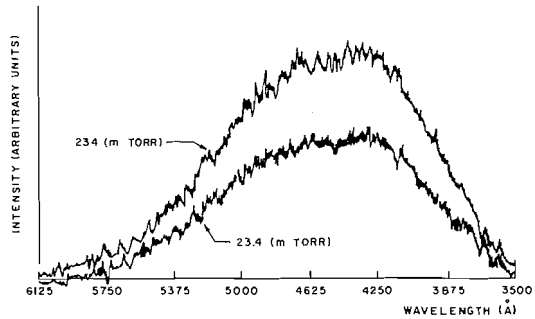

FIG. 2. Photomultiplier recordings of CS_2 fluorescence spectra at two pressures of CS_2.

Measurements of the total fluorescence intensity were made in two ways: (*1*) use of a Corning C.S. 3-72 filter permitted all wavelengths above 420.0 nm to reach the detector; (*2*) the entire fluorescence spectrum was measured using a monochromator and measurements made of the area under the curve.

When these data were plotted using eq. 7, the curves were linear in apparent agreement with the simple Stern–Volmer quenching relationship. Figure 3 shows two curves with λ_E = 310.0 and λ_E = 320.0 nm. Table 1 contains the data for four values of λ_E. These data were obtained using the sharp cut-off filter which gave the most precise measurements of the quenching. The error limits represent the standard deviation of the data points from the line such as shown in Fig. 3. Plots of the sort shown in Fig. 3 were obtained at pressures ranging from 3 to 300 mTorr.

Further studies were made of the fluorescence

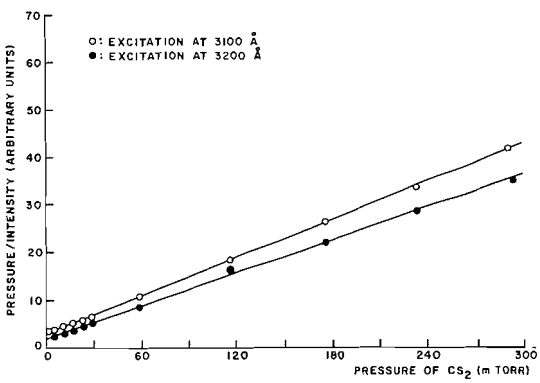

FIG. 3. Stern–Volmer quenching curves: observation of total fluorescence using Corning CS 3-72 filter.

TABLE 1. Variation of the quenching constant as a function of the wavelength of excitation

Wavelength of excitation (nm)	Quenching constant, Q ($Torr^{-1}$)	Radiative lifetime* (μs)	% Error on Q
300.0	45.4	5.67±0.15	2.7
310.0	48.9	6.12±0.14	2.3
320.0	79.4	9.93±0.64	6.5
330.0	101.8	12.73±0.34	2.7

*Assuming $k_q = 8 \times 10^6$ $Torr^{-1}$ s^{-1}.

TABLE 2. The fluorescence as a function of the wavelength of excitation and emission

Wavelength of excitation (nm)	Wavelength of emission (nm)	Quenching constant, Q ($Torr^{-1}$)	Radiative lifetime* (μs)	% Error on Q
290.0	390.0	60.8	7.6±1.0	15
	430.0	48.2	6.0±0.8	14
	480.0	45.5	5.5±1.0	18
	540.0	54.8	6.8±1.5	21
305.0	387.5	92.8	11.6±0.8	7
	425.0	62.4	7.8±0.4	6
	462.5	55.3	6.9±0.6	9
	500.0	69	8.6±1.5	18
310.0	390.0	72.4	9.0±0.4	4
	430.0	62.9	7.9±0.3	3
	480.0	58.9	7.3±0.4	5
	540.0	48.1	6.0±0.4	7
320.0	387.5	135	16.9±3.3	20
	425.0	102	12.8±1.3	10
	462.5	102	12.8±1.6	13
	500.0	97	12.1±1.9	15
340.0	390.0	204	25.5±3.5	14
	430.0	116	14.5±1.5	10
	480.0	119	15 ±2	14
	540.0	105	13.2±1.3	10

*Assuming $k_q = 8 \times 10^6$ $Torr^{-1}$ s^{-1}.

using five wavelengths of excitation and over the same pressure range. In this case, however, the fluorescence signal was recorded using a monochromator with slits set for 12.5nm. These data are shown in Table 2. A definite variation in the quenching constant Q is evident with both wavelength of excitation and fluorescent wavelength.

In addition to the above observations it was noted that at the lowest pressure of CS_2 used, a shift in the intensity maximum towards shorter wavelengths became apparent.

Vibrational Cascade Model

The results discussed above, therefore, suggest that the simple Stern–Volmer mechanism with only one excited level is insufficient as an explanation. A vibrational cascade model such as used to explain NO_2 fluorescence (8) may be described in the following way. This model assumes a vibrational deactivation of the primary excited level prior to re-emission of a photon. Although thoroughly developed by the authors of ref. 8, a brief summary will be included here for completeness.

$$[8] \quad -\frac{d[X_1]}{dt} = (k_{f_1} + k_{e_1}[X] + k_{v_1}[X])[X_1] - k_a I_x[X]$$

Can. J. Chem. Downloaded from www.nrcresearchpress.com by 210.87.254.6 on 09/05/12
For personal use only.

Can. J. Chem. Downloaded from www.nrcresearchpress.com by 210.87.254.6 on 09/05/12
For personal use only.

$$[9] \quad -\frac{d[X_2]}{dt} = (k_{f_2} + k_{e_2}[X] + k_{v_2}[X])[X_2] - k_{v_1}[X][X_1]$$

$$[10] \quad -\frac{d[X_i]}{dt} = (k_{f_i} + k_{e_i}[X] + k_{v_i}[X])[X_i] - k_{v_{i-1}}[X][X_{i-1}]$$

where [X] is the concentration of molecules in the ground electronic state, the $[X_i]$'s are the concentrations of the vibrational levels of the excited electronic state, k_f is the first order rate constant for radiation, k_V is the second order rate constant for vibrational quenching, k_e is the second order rate constant for electronic level quenching, k_a is the absorption coefficient, and I_x is the intensity of the incident radiation.

In order to simplify the analysis it is necessary to make some further assumptions:

(*a*) The rate constants are independent of the particular vibrational level of the upper emitting state. Although not strictly true in some cases, as recently proven (10), there is insufficient information to facilitate the development of such a detailed model.

(*b*) Only the energy transfer rates present in eqs. 8–10, are important. This ignores loss by diffusion, radiation of vibrational energy of the upper state, and collisionally-induced vibrational excitation.

Insertion of a diffusion dependent term $k_d[CS_2^*][CS_2]^{-1}$ in eq. 4 leads to

$$[11] \quad \frac{[CS_2]^2}{I} = \frac{1}{\alpha I_x k_a} \times \left[\frac{k_q}{k_f}[CS_2]^2 + [CS_2] + \frac{k_d}{k_f}\right]$$

A plot of $[CS_2]^2/I$ against $[CS_2]$ shows zero intercept; thus it appears adequate to neglect diffusive losses.

(*c*) All excited levels lying within $\Delta\nu$ of ν_E contribute to the fluorescence intensity in proportion to their concentration. $\Delta\nu = \nu_E - \nu_f$.

For the stationary state the populations of the excited states are given by

$$[12] \quad X_1 = \left(\frac{k_a I_x}{k_f}\right)\left[\frac{[X]}{1 + (Q_E + Q_V)[X]}\right]$$

$$[13] \quad X_i = \left[\frac{Q_V[X]}{1 + (Q_E + Q_V)[X]}\right][X_i - 1]$$

where $Q_E = k_e/k_f$ is the quenching constant for electronic energy; $Q_V = k_v/k_f$ is the quenching constant for vibrational energy. If the intensity is summed over all levels one can obtain

$$[14] \quad \frac{[X]}{I} = \frac{k_f}{k_a I_x}\left[1 - \left[\frac{1 + [X]Q_E}{1 + [X](Q_E + Q_V)}\right]^n\right]$$

where $[X] = P = [CS_2]$. Further, if $k_f/k_a I_x = B$ and $S = Q_E/Q_V = k_e/k_v$, this reduces to

$$[15] \quad \frac{P}{I} = \frac{B(1 + Q_V S P)}{1 - \left[\frac{Q_V P}{1 + Q_V(1 + S)P}\right]^n}$$

In this equation the exponent n represents the total number of excited levels contributing to the intensity of fluorescence; this number depends on the average value of the vibrational quantum transferred ($\Delta\nu_{vib}$) on each deactivating collision and on the difference in energy between the exciting radiation and the fluorescent radiation, *i.e.*

$$[16] \quad n = 1 + (\nu_E - \nu_f)/\Delta\nu_{vib}$$

where ν_E = wavelength of incident radiation; ν_f = wavelength of fluorescent radiation. For high pressures $P \gg 1/Q_V$ and eq. 15 reduces to

$$[17] \quad \frac{P}{I} = \frac{BQ_V PS(1 + S)^n}{[(1 + S)^n - 1]}$$

where from eq. 7

$$[18] \quad Q_{obs} = \frac{Q_V S(1 + S)^n}{[(1 + S)^n - 1]}$$

or $Q_{obs} = Q_V G(n,S)$. In order to check the applicability of this model it is necessary to calculate the function $G(n,S)$ for various values of n and S. Values are given in Table 2. An increase in n for fixed S corresponds to increasing $\Delta\nu$. Figure 4 shows the variation in Q_{obs} with $\Delta\nu$ for three values of S and differing values of $\Delta\nu_{vib}$. The best combination of S and $\Delta\nu_{vib}$ found to fit the data were $S = 0.1$ and $\Delta\nu_{vib} = 1000\ cm^{-1}$. For a value of τ radiative = 15 μs (see next section), $k_q = 7 \times 10^6\ Torr^{-1}\ s^{-1}$. (This assumes the molecular diameter of CS_2 to be 5 Å.) The value of Q_V can be obtained by eq. 18 and Table 3. It is then possible to calculate k_e and k_v. *e.g.* $k_e = 0.76 \times 10^{-10}\ cm^3\ molecule^{-1}\ s^{-1}$ and $k_v = 7.6 \times 10^{-10}\ cm^3 molecule^{-1}\ s^{-1}$.

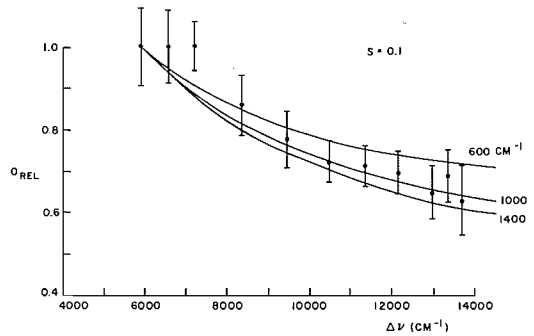

FIG. 4. Comparison of calculated and relative quenching constants as a function of $\Delta\nu = \nu_E - \nu_F$. Reference value is at 6000 cm^{-1}. $\Delta\nu_{vib}$ has been used as the parameter for the theoretical curves.

TABLE 3. Values of function $G(n,S)$

	G for S =		
n	0.2	0.1	0.05
2	0.654	0.576	0.537
4	0.386	0.315	0.282
6	0.300	0.224	0.197
8	0.260	0.187	0.154
10	0.238	0.163	0.129
12	0.225	0.146	0.113
14	0.217	0.135	0.101
16	0.211	0.128	0.092
18	0.208	0.122	0.085
20	0.205	0.117	0.080
22	0.203	0.114	0.076
24	0.202	0.111	0.072
26	0.201	0.109	0.069
28	0.201	0.107	0.067
30	0.201	0.106	0.065

Radiative Lifetime

Heicklen measured the absorption coefficient of CS_2 and from this calculated a radiative lifetime for the fluorescing state of 3.2 μs. Douglas measured a value of 15 μs which in addition to those measured for SO_2 and NO_2 is abnormally long. This latter author proposed a mechanism whereby the lifetime is lengthened by the mixing of the levels of one electronic state with those of another from which there was no allowed transition to the ground state. This type of vibrational–electronic mixing can result in a situation where some molecules excited to the upper state can spend a portion of their lifetime in the state from which fluorescence is forbidden. This then could result in a lengthening of the lifetime.

Recently Brus has remeasured the lifetimes of CS_2 excited by an N_2 pulsed laser at 337.1 nm. He discovered a double exponential decay of the fluorescing radiation and attributed this to the presence of two excited states contributing to the fluorescence signal. The longer-lived of the two states was found to have a lifetime equal to 17 ± 2 μs in excellent agreement with Douglas. The shorter lived state was found to have a lifetime of 2.9 ± 0.3 μs. These emissions were tentatively assigned to the S and U states designated by Kleman. Recent work of Merer *et al.* (13) has aided greatly in the clarification. Merer *et al.* found that, at room temperature, hot bands of the V system extend to 340.0 nm and mask the weaker S and U bands. Thus Brus excited a hot band of the V system ($^1B_2$–$^1\Sigma_g^+$) in addition to an underlying triplet. The V system consists of the Renner–Teller mixed components of the $^1\Delta_u$ state. Thus it appears that Douglas using excitation at 320.0 nm also has measured the lifetime of the V state. It is thus possible and likely that more than one state has contributed to the fluorescence as measured in the present experiments.

It is therefore essential to consider whether or not the interpretation reported above could be in error. Reverting to the simple Stern–Volmer model (eq. 7) consider the contributions of both states. Let the two excited states be designated by 1 and 2. Then $I_{total} = I_1 + I_2$

$$[19]\quad I_{total} = \frac{\alpha_1 I_{x_1} k_{a_1} k_{f_1} P}{k_{f_1} + k_{q_1} P} + \frac{\alpha_2 I_{x_2} k_{a_2} k_{f_2} P}{k_{f_2} + k_{q_2} P}$$

and

$$[20]\quad \frac{I}{P} = \frac{1}{B_1}\left(\frac{1}{1 + k_{q_1}\tau_1 P}\right) + \frac{1}{B_2}\left(\frac{1}{1 + k_{q_2}\tau_2 P}\right)$$

therefore

$$[21]\quad \frac{P}{I} = \frac{B_1 B_2 (1 + k_{q_1}\tau_1 P)(1 + k_{q_2}\tau_2 P)}{B_1(1 + k_{q_1}\tau_1 P) + B_2(1 + k_{q_2}\tau_2 P)}$$

where $\tau_1 = 17$ μs, $k_{q_1} = 1.2 \times 10^{-10}$ cm^3 $molecule^{-1}$ s^{-1}; $\tau_2 = 2.9$ μs, $k_{q_2} = 7.9 \times 10^{-10}$ cm^3 $molecule^{-1}$ s^{-1} from Brus (6).

$$[22]\quad k_{q_1}\tau_1 \cong k_{q_2}\tau_2$$

hence

$$[23]\quad \frac{P}{I} = \frac{B_1 B_2}{B_1 + B_2}(1 + k_{q_1}\tau_1 P)$$

or

Can. J. Chem. Downloaded from www.nrcresearchpress.com by 210.87.254.6 on 09/05/12
For personal use only.

TABLE 4. Quenching of CS_2 fluorescence by foreign gases*

Collision partner	Q_M ($Torr^{-1}$)	% Error	k_M (cm^3 $molecule^{-1}$ s^{-1} $\times 10^{-10}$)	$\pi\sigma_q^2$ (cm^2 $molecule^{-1}$ $\times 10^{-16}$)	D (Å)	$\pi\sigma_c^2$ (cm^2 $molecule^{-1}$ $\times 10^{-16}$)	P
Ar	15.4	8.6	0.22±0.02 (0.17±0.03)	4.3±0.3 (3.5±0.6)	3.418	55.6	0.08
N_2	34.6	10	0.49±0.05 (0.20±0.05)	8.7±0.8 (3.6±0.9)	3.681	59.2	0.15
O_2	34.8	4.6	0.49±0.03 (0.32±0.05)	9.2±0.5 (6.0±1.0)	3.433	55.8	0.16
CO_2	73.0	6.4	1.0 ±0.04	21 ±1.2	3.996	63.5	0.34
COS	88.1	8	1.2 ±0.07	28 ±2.3	4.13	65.4	0.43
SO_2	104.	6.1	1.5 ±0.06	34 ±1.8	4.29	67.8	0.51
SF_6	114.0	5.4	1.6 ±0.06	44 ±2.0	5.01	78	0.57
C_3H_8	150.0	8.5	2.1 ±0.12	44 ±3.2	5.06	79.5	0.56

*Values obtained by Brus (6) are included in parentheses for comparison.

$$\frac{P}{I} = \frac{B_1 B_2}{B_1 + B_2}(1 + k_{q_2}\tau_2 P)$$

Thus it is concluded that in this particular case where coincidentally eq. 22 is valid the experimental results can only be interpreted in terms of a vibrational cascade in the upper state. It is, however, not possible to discriminate between the two states. So it appears that in this work, using broad band excitation, only the V was excited and thus vibrational relaxation within this state was observed. Brus also found that the relative proportions of the two components contributing to the double exponential decay were independent of pressure. This eliminates the possibility that one state is converted into the other.

Quenching of Fluorescence by Foreign Gases

In the presence of foreign gases the simple mechanism discussed earlier must be modified to include the following

$$[3a] \qquad CS_2^* + M \xrightarrow{k_M} CS_2 + M$$

It is possible to derive, following the stationary state approximation the expression

$$[24] \qquad \frac{I_0}{I} = 1 + \frac{k_M[M]}{k_f + k_q[CS_2]}$$

where I_0 is the fluorescence intensity in absence of foreign gas, M, and I is that measured in the presence of M. For constant $[CS_2]$ the slope of the plot of I_0/I *vs.* [M] is equal to

$$\frac{k_M}{k_f}\frac{1}{1 + \frac{k_q}{k_f}[CS_2]}$$

where k_M/k_f shall be called the quenching constant, Q_M. The factor

$$\frac{1}{1 + \frac{k_q}{k_f}[CS_2]}$$

was evaluated to be 0.75 using the value of the fluorescence lifetime equal 15 μs (7) and $k_q = 0.76 \times 10^{-10}$ cm^3 $molecule^{-1}$ s^{-1}. This is in agreement with Heicklen who measured $(k_q/k_f)[CS_2] = 0.36 \pm 0.05$. Figure 5 shows the Stern–Volmer plots for the eight foreign gases used and Table 4 lists the values of k_M calculated from the slopes of these curves. Similarly, included are the values of $\pi\sigma^2$, the quenching cross-section, and the values of the steric factor obtained by dividing this cross-section by that calculated using the values of the gas viscosity collision diameters taken from Hirschfelder, Curtiss, and Bird (14). The % error was obtained from the 95% confidence interval on the slopes of the lines shown in Fig. 5. It can be seen from

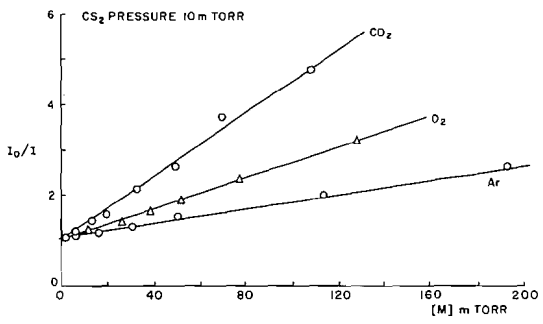

FIG. 5. Typical Stern–Volmer plots for M = Ar, O_2, CO_2.

Can. J. Chem. Downloaded from www.nrcresearchpress.com by 210.87.254.6 on 09/05/12
For personal use only.

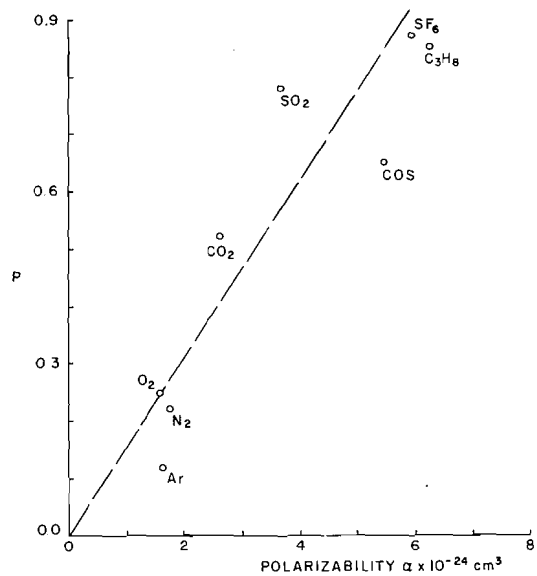

FIG. 6. Correlation of quenching probability per gas kinetic collision, P, with polarizability of the collision partner.

the table that there is excellent agreement with the recent data of Brus.

It has been stated by Mettee (12) that the quenching efficiencies for SO_2 fluorescence correlate well with the polarizability of the quenching partner. This appears also to be so for CS_2 as shown in Fig. 6, although with so few data points it is difficult to conclude a great deal. A similar graph plotting P *vs.* $1/\Delta E$ where ΔE is the energy discrepancy for nearest resonant energy transfer exhibits considerably more scatter. It would be very interesting to use these data to verify the recent theory of Thayer and Yardley (15), however, insufficient information with too few polar quenchers exists at present.

Conclusions

The simple Stern–Volmer model of fluorescence quenching is insufficient to explain the observed variation in quenching coefficient with exciting and fluorescing wavelength in CS_2 vapor. It is necessary to use a more complex model involving vibrational relaxation of an upper state prior to quenching. This relaxation has not been observed previously and, in fact, some authors have suggested that the high collision efficiencies for electronic deactivation suggest that it is not present (1, 6). Vibrational relaxation occurs with a rate constant equal to 7.6×10^{-10} cm^3 molecule^{-1} s^{-1}, approximately the gas kinetic rate of 2.3×10^{-10} cm^3 molecule^{-1} s^{-1}. Electronic quenching requires about 10 collisions or about 1/10 the gas kinetic rate. This is within the error of the observations of previous workers. The size of the vibrational quantum transferred is approximately 1000 cm^{-1}. This frequency is an approximate mean of the three normal vibrations of ground state CS_2 and thus is a reasonable value. The value of the rate of electronic quenching is in good agreement with the measurement of Brus on the longer-lived state (1.2×10^{-10} cm^3 molecule^{-1} s^{-1}) if the lifetime measured by Douglas is used. These results are in good agreement with those recently made on similar molecules, *i.e.* NO_2, SO_2.

The collision cross-sections for the quenching of CS_2 fluorescence by eight collision partners were measured and found to correlate adequately with the polarizability of the quencher.

1. J. HEICKLEN. J. Am. Chem. Soc. **85**, 3562 (1963).
2. L. HERMAN, R. HERMAN, and J. AKRICHE. J. Quant. Spectrosc. Radiat. Transfer, **3**, 77 (1963).
3. S. J. ARNOLD and G. H. KIMBELL. J. Phys. Chem. **73**, 3751 (1969).
4. B. KLEMAN. Can. J. Phys. **41**, 2034 (1963).
5. S. J. ARNOLD and G. H. KIMBELL. Can. J. Chem. **49**, 451 (1971).
6. L. E. BRUS. Chem. Phys. Lett. **12**, 116 (1971).
7. A. E. DOUGLAS. J. Chem. Phys. **45**, 1007 (1966).
8. L. F. KEYSER, S. Z. LEVINE, and F. KAUFMAN. J. Chem. Phys. **54**, 355 (1971).
9. S. E. SCHWARTZ and H. S. JOHNSTON. J. Chem. Phys. **51**, 1286 (1969).
10. G. HANCOCK and I. W. M. SMITH. Chem. Phys. Lett. **8**, 41 (1971); H. W. SIDEBOTTOM, K. OTSUKA, A. HOROWITZ, J. G. CALVERT, B. R. RABE, and E. K. DAMON. Chem. Phys. Lett. **13**, 337 (1972).
11. G. H. MYERS, D. M. SILVER, and F. KAUFMAN. J. Chem. Phys. **44**, 718 (1966).
12. H. D. METTEE. J. Phys. Chem. **73**, 1071 (1969).
13. CH. JUNGEN, D. N. MALM, and A. J. MERER. Chem. Phys. Lett. **16**, 302 (1972).
14. J. O. HIRSCHFELDER, C. F. CURTISS, and R. B. BIRD. Molecular theory of gases and liquids. J. Wiley and Sons, Inc., 1954. Appendix I.
15. C. A. THAYER and J. T. YARDLEY. J. Chem. Phys. **57**, 3992 (1972).

Can. J. Chem. Downloaded from www.nrcresearchpress.com by 210.87.254.6 on 09/05/12
For personal use only.

Proton N.M.R. Spectra of some Cyclopentadienyltitanium Compounds

ALEXANDR GLIVICKY[1] AND JAMES DUNCAN MCCOWAN
Department of Chemistry, Queen's University, Kingston, Ontario

Received March 26, 1973

N.m.r. spectra obtained preliminary to studies of compounds of the form Cp_2TiRCl and Cp_2TiR_2 raise questions about some previous interpretations of related spectra.

Les spectres r.m.n., obtenus antérieurement à l'étude des composés de la forme Cp_2TiRCl et Cp_2TiR_2, ont soulevé certaines questions quant aux interprétations précédantes des spectres se rattachant à ceux-ci.
[Traduit par le journal]

Can. J. Chem., **51**, 2609 (1973)

Introduction

Preliminary to a study of the stability and reactivity of cyclopentadienyl titanium, a catalogue of ^1H n.m.r. spectra was developed for reference. These spectra have been compared with those already reported (1–8) and any significant differences examined.

Procedures

Since many of the subject compounds are air sensitive, all manipulations were either within a nitrogen-filled glove box or within a vacuum line.

The glove box atmosphere was dry nitrogen (99.9% purity supplied by Matheson of Canada Limited and Canox Limited) which entered the box through a column packed with Linde molecular sieves No. 5A and was continually circulated, once within the box, through a Vac Corporation HE-493 Dri-Train. Glassware used within the box had been previously dried within high vacuum vessels that could be placed, sealed, within the interchange. The interchange itself could be evacuated to 6 Nm^{-2} before being flushed with nitrogen.

In the glove box, samples were prepared to known concentrations and component ratios in n.m.r. tubes fitted with tapers. They were degassed three times while frozen to liquid nitrogen temperatures on a vacuum line outside of the glove box and sealed at 10^{-2} Nm^{-2}. Spectra were obtained using frequency sweep on a Bruker HX-60 spectrometer. Tetramethyl silane was employed both as reference and as lock. All the samples were measured at 294 ± 1 °K. All shifts are reported relative to tetramethylsilane ($\tau = 10$). The accuracy of the reported τ values is better than $\pm 0.02\tau$.

$Cp_2Ti(C_6H_5)_2$ was prepared by the method of Summers *et al.* (9); $Cp_2Ti(C_6H_5CH_2)_2$ by the method of Razuvaev *et al.* (10); and $CpTi(C_6H_5CH_2)_3$ by the method of Cannell (11). Except for $Cp_2Ti(C_6H_5CH_2)Cl$, other organometallic materials were obtained from Alfa Inorganics.

The preparation of $Cp_2Ti(C_6H_5CH_2)Cl$ is based on a method by Dubsky and Jacot-Guillarmod (12), and is recommended for preparation of related compounds.

Dioxane (5.1 mmol) was added slowly with constant stirring to a 50 ml flask containing a 1.02 *M* solution of $C_6H_5CH_2MgCl$ (5.1 mmol) in tetrahydrofuran. After stirring for 15 min, the mixture was filtered and the filtrate evaporated to dryness. The white residue of $(C_6H_5CH_2)_2Mg$ was washed three times with pentane, dried for ½ h at reduced pressure, and finally dissolved in 15 ml of benzene.

$(C_6H_5CH_2)_2Mg$ (2.5 mmol) so prepared was added slowly, in benzene solution, to a 50 ml flask containing Cp_2TiCl_2 (1.54 g, 6.2 mmol), benzene (20 ml) and a magnetic stirring bar. After stirring for an additional 10 min, the resulting violet mixture was filtered through a fine frit. Addition of a two fold excess of *n*-pentane to the violet filtrate precipitated crystals. After approximately 20 h, the liquid was decanted and the remaining violet black crystals were dried at reduced pressure. Elemental analysis was by Alfred Bernhardt (Elbach).

Anal calcd. for $C_{17}H_{17}TiCl$: C, 67.02; H, 5.62; Cl, 11.64; Ti, 15.72. Found: C, 66.72; H, 5.61; C, 11.82; and Ti, 15.79.

It should be noted that the sample used in the above analysis was deliberately exposed to air for 6 h before being sealed in an evacuated tube and sent for analysis. The resulting analysis would tend to disprove the recent suggestion (6) that decomposition is rapid in air at room temperature.

The "melting point" was 365 °K with decomposition, as determined in an evacuated capillary. A value of 380 °K has been reported in an argon atmosphere (6).

Results and Discussion

N.m.r. data are presented in Tables 1 to 7. Chemical shifts are nearly independent of concentration. On the other hand, solvent influence is marked. The reported values can be explained in terms of the shielding contributions of the solvent (13, 14), as can most values reported in the literature (2–8), but some anomalies exist among the literature values. These are discussed below.

[1]Present address: Research Department, Imperial Oil Limited, Sarnia, Ontario.

Can. J. Chem. Downloaded from www.nrcresearchpress.com by 210.87.254.5 on 09/05/12
For personal use only.

TABLE 1. N.m.r. shifts of $Cp_2Ti(C_6H_5)_2$ in different solvents

Solvent	Concentration ($M \times 10^3$)	τ values	
		Cp protons*	Ring protons†
CCl_4	1	3.85	3.22 s
C_2Cl_4	2	3.90	3.20 s
CH_2Cl_2	2	3.80	3.07 s
$CDCl_3$	—	3.80	3.08 s
C_6H_{12}	4	3.97	3.22 s
C_6D_6	26	4.27	3.03 mc‡
$C_6D_6 + CH_2Cl_2$	—	4.24	3.07 mc
C_6F_6	30	3.77	3.25 mc
Acetone	—	3.98	—
CH_3OH	—	3.82	3.15 mc

*Sharp singlet.
†s = singlet; mc = center of the multiplet.
‡Peak of 2.98τ was tentatively assigned to *o*-protons and that at 3.08τ to *m*- and *p*-protons.

TABLE 2. N.m.r. shifts of $Cp_2Ti(C_6H_5)Cl$ in different solvents

Solvent	Concentration ($M \times 10^3$)	τ values	
		Cp protons*	Ring protons†
C_2Cl_4	20	3.72	3.28 mc
CH_2Cl_2	—	3.67	3.15 s
C_6H_{12}	10	3.79	3.28 mc

*Sharp singlet.
†s = singlet; mc = center of the multiplet.

TABLE 3. N.m.r. shifts of $Cp_2Ti(C_6H_5CH_2)_2$ in different solvents

Solvent	Concentration ($M \times 10^3$)	τ values			
		Cp protons*	CH_2 protons*	Ring protons†	
				m-, *p*-	*o*-
CCl_4	30	4.12	8.13	3.27 mc	2.92 mc
C_2Cl_4	—	4.12	8.12	—	—
CH_2Cl_2	100	4.05	8.13	—	—
$CDCl_3$	400	4.05	8.09	3.18 mc	2.85 mc
$CDCl_3$(216K)	400	4.02	8.10	3.18 mc	2.85 mc
C_6H_{12}	10	4.22	—	—	—
C_6D_6	145	4.45	8.12	3.12 mc	2.77 mc
C_6F_6	113	4.02	8.20	3.33 mc	3.00 mc
THF	—	4.02	—	2.90 mc	3.25 mc
Acetone	—	3.95	—	3.02 mc	

*Sharp singlet.
†s = singlet; mc = center of the multiplet.

The Results of Waters and Mortimer

Waters and Mortimer (6) comment on the "abnormal" chemical shift observed for the cyclopentadienyl protons of $Cp_2Ti(C_6H_5CH_2)Cl$ in chloroform. However, in the present work, it was found that dissolving $Cp_2Ti(C_6H_5CH_2)Cl$ in $CDCl_3$ led rapidly to the formation of an intensely red solution by the following process:

[1] $2Cp_2Ti(C_6H_5CH_2)Cl + 2CDCl_3 \rightarrow$
$2Cp_2TiCl_2$ + bibenzyl
+ combination products of solvent radicals

Some $CpTiCl_3$ was also identified.

In order to verify that the reported spectra (6) were indeed those of the decomposition products, the chemical shifts of Cp_2TiCl_2 and of bibenzyl

Can. J. Chem. Downloaded from www.nrcresearchpress.com by 210.87.254.5 on 09/05/12
For personal use only.

Can. J. Chem. Downloaded from www.nrcresearchpress.com by 210.87.254.5 on 09/05/12
For personal use only.

TABLE 4. N.m.r. shifts of $Cp_2Ti(C_6H_5CH_2)Cl$ in different solvents

Solvent	Concentration ($M \times 10^3$)	τ values			
		Cp protons*	CH_2 protons*	Ring protons†	
				m-, *p-*	*o-*
C_2Cl_4	10	3.94	7.63	—	—
CH_2Cl_2	200	3.87	7.54	3.58 mc	3.08 mc
C_6H_{12}	5	4.17	—	—	—
C_6D_6	—	4.35	7.60	—	—
C_6F_6	100	3.88	7.70	3.35 mc	3.03 mc
Acetone-d_6	—	(3.73)	(7.55)	—	—

*Sharp singlet.
†s = singlet; mc = center of the multiplet.

TABLE 5. N.m.r. shifts of $CpTi(C_6H_5CH_2)_3$ in different solvents

Solvent	Concentration ($M \times 10^3$)	τ values		
		Cp protons*	CH_2 protons*	Ring protons†
C_2Cl_4	100	4.23	7.03	2.97 mc
$C_2Cl_4+CH_2Cl_2$(3:1)	—	4.17	7.00	2.97 mc
C_6H_{12}	—	4.27	—	3.00 mc
C_6H_6	—	—	7.20	—
THF	20	4.10	6.97	2.92 mc
Pentane	20	4.17	6.93	2.95 mc

*Sharp singlet.
†s = singlet; mc = center of the multiplet.

TABLE 6. N.m.r. shifts of Cp_2TiCl_2 in different solvents

Solvent	Concentration ($M \times 10^3$)	τ value*
CH_2Cl_2	Saturated solution	3.45
THF	Saturated solution	3.45
Acetone	50	3.38
$CDCl_3$	—	3.41
C_6D_6	10	4.08
Toluene	60	4.12
Nitrobenzene	Saturated solution	3.32
CCl_4	Saturated solution	3.52

*Sharp singlet.

in $CDCl_3$ were measured. They correspond exactly to those shifts reported (6) for the monobenzyl compound. Probably the same situation exists for the neopentyl compound. It seems certain that the reported values (6) are for the decomposition products, and that the subsequent discussion of "abnormal" behavior is without meaning.

The Results of Nesmeyanov et al.

The singlet resonance arising from the cyclopentadienyl protons of Cp_2TiCl_2 dissolved in tetrahydrofuran (Table 6) is inconsistent with the report of Nesmeyanov *et al.* (15) but agrees with reports from other investigators (1, 2, 16). Nesmeyanov observed two resonances, one close to that reported here and the other 0.25τ upfield, which coalesced into a singlet when the

TABLE 7. N.m.r. shifts of $CpTiCl_3$ in different solvents

Solvent	Concentration ($M \times 10^3$)	τ value*
C_2Cl_4	20	3.10
CH_2Cl_2	—	2.95
$CDCl_3$	—	2.94
C_6D_6	10	3.77
THF	—	2.82
CCl_4	Saturated solution	3.02

*Sharp singlet.

system was heated to 408 °K. He interpreted the results in terms of nonequivalent protons.

A more plausible explanation is the presence of $(Cp_2TiCl)_2O$ in Nesmeyanov's sample. An n.m.r. spectrum of this material showed its resonance to be 0.25τ upfield from that of Cp_2TiCl_2 in tetrahydrofuran. Moreover, this material disproportionates (17) with polymerization of one of the products

[2] $2n(Cp_2TiCl)_2O \rightarrow nCp_2TiCl_2 + (Cp_2Ti{\cdot}O)_n$

This reaction, which proceeds visibly at room temperature, is very rapid at 408 °K. Since the fine yellow polymeric solid produces no observable proton resonance, all of Nesmeyanov's observations are explained.

The Results of Beachell and Butter

Beachell and Butter (2) have examined the influence of the electronegativity and electronic character of ligands R on the chemical shifts of the cyclopentadienyl protons in the compounds $(C_5H_5)_2TiR'R''$.

In one case, cyclopentadienyl proton chemical shifts of four compounds, $Cp_2Ti(CH_3)_2$, $Cp_2Ti(CH_3)Cl$, Cp_2TiCl_2, and $CpTiCl_3$ are plotted against the summed electronegativities of the "first atom" of the R groups and an excellent linear relationship is obtained. On this basis it is concluded that methyl, chlorine, and cyclopentadienyl ligands contribute an equal electronic effect. While the observation that the data for $Cp_2Ti(CH_3)Cl$ lie intermediate between those of the dimethyl and dichloro compounds is not unexpected, the apparent equivalence of the effects of the π bonded cyclopentadienyl and the methyl and chlorine is more surprising.

It is also fortuitous, since three of the values are in doubt. Both the value for $Cp_2Ti(CH_3)_2$ and that for $CpTiCl_3$ differ from those reported in Table 1 of the same paper, with the further difference that the $CpTiCl_3$ value was obtained in tetrahydrofuran (18). The $CpTiCl_3$ and Cp_2TiCl_2 values both differ from those reported here, the latter substantially.

Taking the tabulated values for $Cp_2Ti(CH_3)_2$ and $Cp_2Ti(CH_3)Cl$ and the value from Table 6 for Cp_2TiCl_2, a constant increment for ring proton chemical shift in the series $Cp_2Ti(CH_3)_nCl_{2-n}$ is still obtained, but with δ/n equal to 0.29. While these data could still be fitted to the correlation with electronegativity attempted by Beachell and Butter, the value for $CpTiCl_3$ could not. This fact, taken with the lack of linearity in some analogous series, suggests that there is little justification for simple correlations of cyclopentadienyl ring proton chemical shift with the electronegativity of the "first atom".

The authors thank the National Research Council of Canada, the Ontario Department of University Affairs, and Queen's University for financial support of this research. The award of fellowships to one of us (A.G.) by the Ontario Government and by Queen's University is gratefully acknowledged.

1. A. F. Reid and P. C. Wailes. J. Organomet. Chem. **2**, 329 (1964).
2. H. C. Beachell and S. A. Butter. Inorg. Chem. **4**, 1133 (1965).
3. M. D. Rausch and D. J. Ciappenelli. J. Organomet. Chem. **10**, 127 (1967).
4. P. C. Wailes, H. Weigold, and A. P. Bell. J. Organomet. Chem. **33**, 181 (1971).
5. G. Fachinetti and C. Floriani. Chem. Commun. 654 (1972).
6. J. A. Waters and G. A. Mortimer. J. Organomet. Chem. **22**, 417 (1970).
7. M. D. Rausch. Inorg. Chem. **3**, 300 (1964).
8. I. S. Kolomnikov, T. S. Lobeeva, V. V. Gorbachevskaya, G. G. Aleksandrov, Yu. T. Struckhov and A. E. Vol'pin. Chem. Commun. 972 (1971).
9. L. Summers, R. H. Uloth, and A. Holmes. J. Am. Chem. Soc. **77**, 3604 (1955).
10. G. A. Razuvaev, V. N. Latyaeva, and L. I. Vyshinskaya. Dokl. Chem. **189**, 884 (1969).
11. L. G. Cannell. Private communication.
12. G. J. Dubsky and A. Jacot-Guillarmod. Helv. Chim. Acta, **52**, 1735 (1969).
13. L. M. Jackman and S. Sternhell. Applications of n.m.r. spectroscopy in organic chemistry. Pergamon Press, Oxford. 1969. p. 104.
14. A. D. Buckingham, T. Schaefer, and W. G. Schneider. J. Chem. Phys. **32**, 1227 (1960).
15. A. N. Nesmeyanov, E. I. Fedin, O. V. Nogina, N. S. Kochetkova, V. A. Dubovitsky, and P. V. Petrovsky. Tetrahedron, Suppl. 8, 389 (1966).
16. P. M. Druce, B. M. Kingston, M. F. Lappert, T. R. Spalding, and R. CM Srivastava. J. Chem. Soc. A, 2106 (1969).
17. S. A. Giddings. Inorg. Chem. **3**, 684 (1964).
18. C. A. Sloan and W. A. Barber. J. Am. Chem. Soc. **81**, 1364 (1959).

Can. J. Chem. Downloaded from www.nrcresearchpress.com by 210.87.254.5 on 09/05/12
For personal use only.

The Crystal Structure of $KAlP_2O_7$

HOK NAM NG AND CRISPIN CALVO

Institute of Materials Research, McMaster University, Hamilton, Ontario

Received December 22, 1972

$KAlP_2O_7$ crystallizes as monoclinic crystals with $a = 7.308(8)$, $b = 9.662(6)$, $c = 8.025(4)$ Å, $\beta = 106.69(7)°$, $z = 4$ and space group $P2_1/c$. The structure was refined from 1394 observed reflections by full-matrix least-squares method to a final R value of 0.032. The $P_2O_7^{4-}$ anion consists of a pair of corner-sharing PO_4 groups in a nearly staggered configuration. The mean bridging and terminal P—O bond lengths are 1.607 and 1.509 Å, respectively, and the P—O—P angle is 123.2°. The anions lie in planes parallel to (001). The Al ions are bonded to six oxygen atoms contributed by anions in three layers of P_2O_7 groups. The average Al—O bond length is 1.889 Å. The potassium ion is coordinated to ten oxygen atoms lying within a spherical shell with inner and outer radii of 2.739 and 3.185 Å.

$KAlP_2O_7$ crystallise sous forme monoclinique avec $a = 7.308(8)$, $b = 9.662(6)$, $c = 8.025(4)$ Å, $\beta = 106.69(7)°$, $z = 4$ et le groupe spatial est $P2_1/c$. La structure a été raffinée à partir des 1394 réflexions observées par la méthode des moindres carrés jusqu'à obtention d'une valeur finale pour R de 0.032. L'anion $P_2O_7^{4-}$ comprend une paire de groupes PO_4 ayant un côté commun, dans une configuration presque éclipsée. Les longueurs moyennes des liaisons P—O du pont et du bout sont respectivement de 1.607 et 1.509 Å et l'angle P—O—P est 123.2°. Les anions sont situés dans des plans parallèles à (001). Les ions Al sont liés à six atomes d'oxygène venant des anions des trois couches de groupes P_2O_7. La longueur moyenne de la liaison Al—O est de 1.889 Å. L'ion potassium est coordiné à dix atomes d'oxygène se trouvant à l'intérieur d'une enveloppe sphérique de rayons interne et externe de 2.739 et 3.185 Å.

[Traduit par le journal]

Can. J. Chem., 51, 2613 (1973)

Can. J. Chem. Downloaded from www.nrcresearchpress.com by 210.87.254.105 on 09/05/12
For personal use only.

Introduction

Although the structures of a number of divalent metal pyrophosphates are presently known, relatively little can be said about the structures of the $M^IM^{III}P_2O_7$ compounds, where M^I is a monovalent metal and M^{III} is a trivalent metal. The compound $KAlP_2O_7$ was first characterized by d'Yvoire (1) and later by Klyucharov and Skoblo (2). Gamondès, d'Yvoire, and Boule prepared two groups of $M^IM^{III}P_2O_7$ compounds (3). The first group consists of $KAlP_2O_7$ and $NaFeP_2O_7$-I and the second group consists of $NaAlP_2O_7$ and $NaFeP_2O_7$-II. An irreversible phase transformation from $NaFeP_2O_7$-I to $NaFeP_2O_7$-II was observed at 750 °C. From their X-ray powder patterns $NaFeP_2O_7$-II and $NaAlP_2O_7$ were considered to be isostructural and their structures to be related to that of α-$Cu_2P_2O_7$. The former two compounds belong to the space group $P2_1/c$ while α-$Cu_2P_2O_7$ belongs to the space group $C2/c$ (4); the lowering of symmetry results from the replacement of the symmetry equivalent Cu atoms in α-$Cu_2P_2O_7$, by Na and Fe or Na and Al atoms in an ordered manner. $KAlP_2O_7$ and $NaFeP_2O_7$-I, both with the space group $P2_1/c$, were also thought to be isostructural, but their structure was not known.

While attempting to grow crystals of $AlPO_4$ with the cristobalite structure by using KH_2PO_4 as a flux, we obtained some large colorless crystals which were identified as $KAlP_2O_7$. The structure investigation of $KAlP_2O_7$, as a representation of the group $M^IM^{III}P_2O_7$-I was deemed worthwhile in order to seek its relationship to that of the group $M^IM^{III}P_2O_7$-II compounds, and determine whether $KAlP_2O_7$ has polymorphic modifications analogous to $NaFeP_2O_7$.

Experiments

Crystals of $KAlP_2O_7$ were prepared by heating a mixture of 20% (mol) $AlPO_4$ and 80% KH_2PO_4 in a platinum crucible. The mixture was melted and the temperature was held at 1100 °C for 6 h. It was then cooled at a rate of 6 °C/h to 600 °C and quenched to room temperature. Clear and colorless parallelopipeds of $KAlP_2O_7$ could be separated from the powdery matrix by washing the product in boiling water.

Precession photographs showed that $0k0$ reflections with k odd and $h0l$ reflections with l odd were absent. The space group was confirmed to be $P2_1/c$. Accurate lattice parameters were determined by a least-squares fit to 15 2θ values measured with the Syntex PĪ automatic diffractometer. The values obtained are listed in Table 1 along with other crystal data. Also included in Table 1 are the lattice parameters determined from powder patterns by Gamondès *et al.*, who also determined the

Can. J. Chem. Downloaded from www.nrcresearchpress.com by 210.87.254.105 on 09/05/12
For personal use only.

TABLE 1. $KAlP_2O_7$* crystal data

Parameter	Value† This work	Reference 3
a (Å)	7.308(8)	7.329
b (Å)	9.662(6)	9.654
c (Å)	8.025(4)	8.045
β (degree)	106.69(8)	106.93
Volume (Å^3)	542.77	
ρ_{expti}(g/cm^3)		2.923
ρ_{calcd}(g/cm^3)	2.927	
z	4	

*Formula weight, 241.11; μ (linear absorption coefficient), 23.6 cm^{-1}; space group $P2_1/c$.
†Estimated standard deviations in parentheses.

density of $KAlP_2O_7$ to be 2.923 g/cm^3, corresponding to four formula units per unit cell.

A good quality single crystal of $KAlP_2O_7$, ground into spherical shape, with a radius of 0.012 cm was selected for intensity measurements. Intensity data were collected on a Syntex $P\bar{1}$ automatic diffractometer using graphite monochromatized MoKα radiation (λ = 0.71069 Å). The mode of scan used was θ/2θ at a variable rate. Reflections whose intensity corrected for background was less than three times the standard deviation were considered unobserved. A total of 2275 symmetry-independent reflections was collected, among which 1394 reflections were considered observable ($I > 3\sigma$). The data were corrected for Lorentz, polarization, and absorption effects ($\mu R = 0.28$).

The structure was determined from Patterson functions and subsequent electron density and difference electron density maps. The structure was refined by minimizing $\Sigma\omega(|F_o| - |F_c|)^2$ using a full-matrix least-squares program written by J. S. Stephens for the CDC 6400. Atomic scattering curves for K^+, Al^{3+}, P^{5+}, and O^{2-} were taken from Cromer and Waber (5) and those for the potassium and phosphorus atoms were corrected for anomalous dispersion (6). The atomic positions were refined together with individual isotropic temperature factors until the R value converged to 0.066. The anisotropic components of the temperature factors of K^+ and then of the other atoms were allowed to vary. A weighting function $\omega = (1.27 - 0.03F_o + 0.001F_o^2)^{-1}$ was chosen so that the square of the difference between the observed and calculated structure factors $\omega(\Delta F)^2$ would be independent of the local average value of $|F_o|$. Unobserved reflections were given zero weight if their calculated structure factor was less than the local minimum observable value; otherwise they were given a value 0.9 times the local minimum observable value. For a small number (seven) of intense reflections, all at low $\sin\theta/\lambda$, the calculated structure factor was substantially larger than the observed value. Correction was then applied for secondary extinction. The refinement terminated when the maximum shift in the parameters was less than one-third of the estimated standard deviation. The final R value is 0.032 and the residual

$$R_2 = \left[\frac{\sum \omega(|F_o|^2 - |F_c|^2)}{\sum \omega|F_o|^2}\right]^{1/2}$$

is 0.043. The final positional and thermal parameters are shown in Table 2. The calculated and observed structure factors are listed in Table 3.[1] The value of the mean deviation of a reflection of unit weight is 0.96.

Discussion

The pyrophosphate group in $KAlP_2O_7$ (Fig. 1) is formed from two slightly distorted PO_4 tetrahedra which share O(1). The plane containing the two phosphorus and the bridging oxygen atoms, or the plane of the anion, is approximately parallel to the *ac*-plane. The $P_2O_7^{4-}$ group nearly has C_s symmetry with the plane of the anion as the pseudo mirror plane. O(4) and O(5) deviate slightly from this plane since the dihedral angle between the O(4)—P(2)—O(1) plane and the O(5)—P(1)—O(1) plane is about 9°. The P—O—P bridge angle is 123°, which is smaller than any of the bridge angles in those pyrophosphates reported to date. The P(1)—O(1) bond (1.610 Å) is slightly longer than the P(2)—O(1) bond (1.604 Å). The terminal P—O bonds are also different. The shortest terminal P—O bonds are the P(1)—O(5) bond (1.502 Å) and the P(2)—O(4) bond (1.485 Å) which are the closest to the plane of the molecule. The average lengths of the terminal P—O bonds are 1.511 and 1.506 Å for the P(1) and P(2) tetrahedra, respectively. For both tetrahedra the O—P—O angles subtended by the terminal oxygen atoms are all larger than the ideal tetrahedral angle except O(2)—P(2)c—O(6), whereas those subtended by the central oxygen atom and the terminal oxygen atoms are all less than 109° 28′. These and other important bond lengths and bond angles are listed in Table 4.

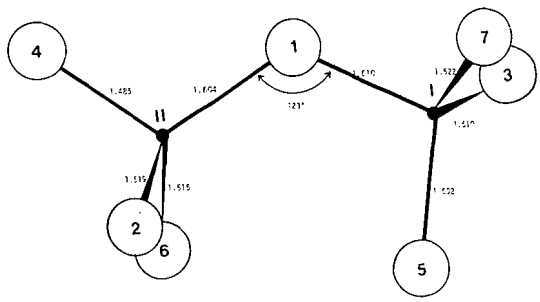

FIG. 1. Geometry of the $P_2O_7^{4-}$ anion in $KAlP_2O_7$. The phosphorus atoms are labelled I and II and the oxygen atoms are labelled 1 to 7. Bond lengths are in Å.

[1]Table 3 is available, at a nominal charge, from the Depository of Unpublished Data, National Science Library, National Research Council of Canada, Ottawa, Canada K1A 0S2.

Can. J. Chem. Downloaded from www.nrcresearchpress.com by 210.87.254.105 on 09/05/12
For personal use only.

TABLE 2. Positional and thermal parameters of $KAlP_2O_7$*

Atom	Position type	x	y	z	U_{11}†	U_{22}	U_{33}	U_{12}	U_{13}	U_{23}
K	4(e)	0.18038(8)	0.31735(7)	0.05451(8)	0.0150(2)	0.0177(3)	0.0141(2)	0.0001(2)	0.0008(2)	0.0013(2)
P(1)	4(e)	0.43728(8)	0.63270(6)	0.18908(7)	0.0057(2)	0.0050(2)	0.0059(2)	0.0005(2)	0.0016(2)	−0.0002(2)
P(2)	4(e)	0.12959(8)	0.90439(6)	0.83234(7)	0.0061(2)	0.0050(2)	0.0052(2)	0.004(2)	0.0017(2)	0.0001(2)
Al	4(e)	0.2369(1)	0.59985(8)	0.76048(8)	0.0063(3)	0.0056(3)	0.0061(3)	0.0000(2)	0.0016(2)	0.0002(2)
O(1)	4(e)	0.3305(2)	0.9514(2)	0.8071(2)	0.0089(7)	0.0088(7)	0.0119(7)	−0.0012(5)	0.0060(5)	−0.0026(6)
O(2)	4(e)	0.0865(2)	0.7397(2)	0.2553(2)	0.0088(7)	0.0053(7)	0.0119(7)	−0.0003(5)	0.0022(5)	0.0013(5)
O(3)	4(e)	0.6363(2)	0.5725(2)	0.2356(2)	0.0069(6)	0.0078(7)	0.0144(7)	0.0013(5)	0.0033(5)	−0.0007(5)
O(4)	4(e)	0.1490(2)	0.5905(2)	0.5215(2)	0.0135(7)	0.0161(8)	0.0064(6)	−0.0038(6)	0.0032(5)	−0.0002(6)
O(5)	4(e)	0.3216(3)	0.6053(2)	0.0046(2)	0.0142(8)	0.0129(8)	0.0066(6)	−0.0003(6)	0.0007(6)	−0.0008(6)
O(6)	4(e)	0.9833(2)	0.4959(2)	0.2238(2)	0.0070(6)	0.0079(7)	0.0089(6)	−0.0026(5)	0.0021(5)	−0.0011(5)
O(7)	4(e)	0.4450(2)	0.7835(2)	0.2451(2)	0.0079(6)	0.0058(7)	0.0133(7)	0.0000(5)	0.0028(5)	−0.0017(5)

*Estimated standard deviation in parentheses.
†Calculated from $\beta_{ij} = 2\pi^2 b_i b_j U_{ij}$ where $T = \exp[-(\beta_{11}h^2 + 2\beta_{12}hk + \ldots)]$ is the thermal factor appearing in the structure factor expression and b_i's are reciprocal lattice vectors.

TABLE 4. Molecular geometry in $KAlP_2O_7$*

(*a*) P_2O_7 group

Bond	Distance (Å)	Bonds	Angle (deg)
P(1)—O(1)c	1.610(2)†	P(1)—O(1)c—P(2)c	123.2(2)
—O(3)	1.510(2)		
—O(5)	1.502(2)	O(1)c—P(1)—O(3)	104.8(2)
—O(7)	1.522(2)	—O(5)	105.1(2)
		—O(7)	107.0(2)
P(2)c—O(1)c	1.604(2)		
—O(2)	1.519(2)	O(3)—P(1)—O(5)	113.9(2)
—O(4)	1.485(2)	—O(7)	110.1(2)
—O(6)	1.515(2)	O(5)—P(1)—O(7)	115.0(2)
P(1) —P(2)c	2.827(3)	O(1)c—P(2)c—O(2)	107.4(2)
		—O(4)	107.3(2)
		—O(6)	105.5(2)
		O(2)—P(2)c—O(4)	113.3(2)
		—O(6)	108.6(2)
		O(4)—P(2)c—O(6)	114.3(2)

(*b*) Al environment

Bond	Distance (Å)	Bonds	Angle (deg)
Al—O(2)c	1.894(2)		
—O(7)c	1.925(2)	O(4)—Al—O(2)c	89.5(2)
—O(3)i	1.902(2)	—O(7)c	90.5(2)
—O(6)i	1.892(2)	—O(3)i	89.8(2)
—O(4)	1.841(2)	—O(6)i	89.8(2)
—O(5)	1.878(2)		
		O(5)—Al—O(2)c	90.9(2)
Al—P(1)c	3.103(2)	—O(7)c	91.2(2)
—P(2)	3.141(2)	—O(3)i	89.7(2)
—P(2)c	3.186(2)	—O(6)i	88.7(2)
		O(4)—Al—O(5)	178.4(2)
		O(2)c—Al—O(3)i	173.8(2)
		O(7)c—Al—O(6)i	173.5(2)
		O(2)c—Al—O(7)c	89.1(2)
		—O(6)i	84.4(1)
		O(3)c—Al—O(7)c	97.1(2)
		—O(6)i	89.5(2)

(*c*) K environment

Bond	Distance (Å)	Bonds	Angle (deg)
K—O(2)s	2.900(3)	O(1)c—K—O(2)i	142.1(2)
—O(2)i	2.739(3)	—O(2)s	90.4(1)
—O(6)	2.832(3)	—O(3)i	95.5(1)
—O(6)i	2.853(2)	—O(3)s	101.0(1)
—0(3)s	2.989(2)	—O(4)s	138.7(1)
—O(3)i	3.184(3)	—O(5)	48.30(5)
—O(7)s	2.767(3)	—O(6)	50.24(5)
—O(1)c	3.004(2)	—O(6)i	92.7(1)
—O(4)s	3.185(3)	—O(7)s	65.6(1)
—O(5)	3.034(3)		

TABLE 4 (*Concluded*).

(*c*) K environment (*Concluded*)

Bond	Distance (Å)	Bonds	Angle (deg)
		O(2)i—K—O(2)s	90.8(1)
		—O(3)i	75.1(1)
		—O(3)s	116.1(2)
		—O(4)s	52.1(1)
		—O(5)	104.2(1)
		—O(6)	103.3(1)
		—O(6)i	52.2(1)
		—O(7)s	146.3(2)
		O(2)s—K—O(3)i	163.6(1)
		—O(3)s	76.1(1)
		—O(4)s	48.4(1)
		—O(5)	127.8(2)
		—O(6)	52.7(1)
		—O(6)i	112.4(1)
		—O(7)s	111.5(2)
		O(3)i—K—O(3)s	117.5(1)
		—O(4)s	123.0(2)
		—O(5)	50.7(1)
		—O(6)	121.7(2)
		—O(6)i	52.1(1)
		—O(7)s	84.9(2)
		O(3)s—K—O(4)s	75.8(1)
		—O(5)	113.3(1)
		—O(6)	115.8(1)
		—O(6)i	163.9(1)
		—O(7)s	51.0(1)
		O(4)s—K—O(5)	150.9(1)
		—O(6)	92.9(1)
		—O(6)i	99.3(1)
		—O(7)s	126.7(2)
		O(5)—K—O(6)	75.2(1)
		—O(6)i	53.1(1)
		—O(7)s	82.4(1)
		O(6)—K—O(6)i	80.4(1)
		—O(7)s	110.3(2)
		O(6)i—K—O(7)s	130.7(2)

*Oxygen atom positions are derived from those listed in Table 2 by operations of the screw axis, *c*-glide plane and center of inversion designated by O(*n*)s, O(*n*)c, and O(*n*)i, respectively.

†Estimated standard deviations in parentheses include uncertainties in the unit cell dimension.

The $P_2O_4^{4-}$ group is propagated in the *ab* plane by the two-fold screw axes to form a sheet. Adjacent sheets are generated by the *c*-glide planes to form the network for the entire structure (Figs. 2 and 3). The distance between adjacent sheets is 3.84 Å as compared to 4.35 Å found in α-$Cu_2P_2O_7$ (4).

The aluminum ion is octahedrally coordinated with six oxygen atoms with an average Al—O bond length of 1.889 Å. Four of these oxygen

Can. J. Chem. Downloaded from www.nrcresearchpress.com by 210.87.254.105 on 09/05/12
For personal use only.

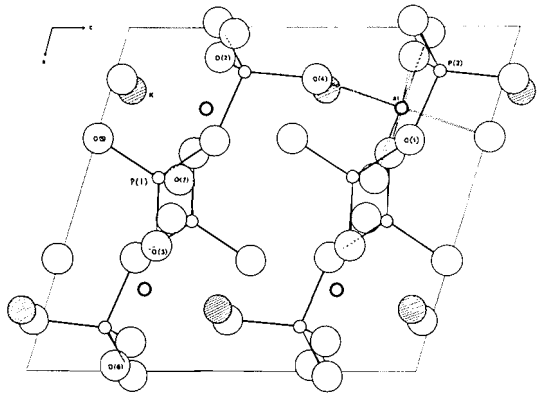

FIG. 2. Structure of $KAlP_2O_7$ projected onto the *ac*-plane. Small open circles are phosphorus atoms, large open circles are oxygen atoms, small double circles are aluminum atoms, and large shaded circles are potassium atoms.

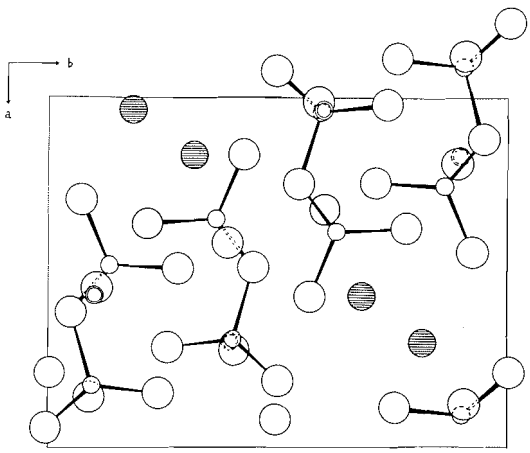

FIG. 3. Structure of $KAlP_2O_7$ projected onto the *ab*-plane. Same legends as in Fig. 2.

atoms (O(2)c, O(3)i, O(6)i, and O(7)c) from three different $P_2O_7^{4-}$ groups in the same sheet nearly lie on a plane while O(4) and O(5) from the adjacent sheets complete the octahedron. Thus the Al ion serves to link three pyrophosphate sheets (Fig. 2) and this may account for the small distance between sheets in $KAlP_2O_7$. The AlO_6 octahedron is distorted with the axial bonds (1.841 and 1.878 Å to O(4) and O(5)) considerably shorter than the equatorial bonds, which average 1.903 Å, and two O—Al—O angles in the equatorial plane significantly different from 90° (Table 4). It should be noted that O(4) is involved in the shortest Al—O and P—O bond, but forms the longest bond, among the nearest ten, with the other cation, K^+ (3.185 Å). Potassium shares oxygen atoms with two pyrophosphate sheets with bond lengths ranging from 2.739 to 3.185 Å.

The distortion of the $P_2O_7^{4-}$ ion from two regular corner-sharing tetrahedra (in $KAlP_2O_7$) is similar to that found in other pyrophosphate compounds. The difference between the terminal and the bridging P—O bond lengths, for a P—O—P bond angle near 109°, has been ascribed to the result of $d\pi$–$p\pi$ bonding by Cruickshank (8), who predicted bond lengths of 1.51 and 1.64 Å for the terminal and bridging bonds, respectively. Table 5 lists the average P—O bond lengths and bridge angles of the non-linear $P_2O_7^{4-}$ groups found in various pyrophosphate compounds. Experimentally this difference in terminal and bridging P—O bonds is always smaller than the predicted value of 0.13 Å. Cruickshank attributed this to the opening of the P—O—P bridge angle and as a result the bridging P—O bonds acquire some π-character from the orbitals in the P—O—P plane as well. It can be seen from Table 5 that a decrease in the P—O—P angle is indeed correlated with an increase in the difference between the bridging and terminal P—O bonds in a general way. In $KAlP_2O_7$ the P—O—P angle of 123° is the smallest among the pyrophosphate compounds listed in Table 5, and yet the difference of 0.10 Å in the P—O bonds is still less than the predicted 0.13 Å. The P_2O_7 group in the present compound has a staggered C_s symmetry while all the remaining staggered P_2O_7 groups have pseudo C_2 symmetry and show P—O—P angles larger than 130°. The anions showing eclipsed configurations all have angles lying in the range between 127 and 138°.

By way of contrast, the variation of individual bond length in a distorted coordination polyhedron AX_n was correlated by Baur with the bond strengths, p_x, received by the individual anions (9). That is, the anion is no longer considered to be isolated. This idea was quantitatively summarized by the equation

$$d(\text{A—X}) = \langle d(\text{A–X})\rangle + b\Delta p_x$$

where Δp_x is the difference between the p_x of one individual anion and the mean p_x of all anions in the coordination polyhedron. The mean cation–anion distance $\langle d(\text{A—X})\rangle$ and b are empirically derived constants, and the appro-

Can. J. Chem. Downloaded from www.nrcresearchpress.com by 210.87.254.105 on 09/05/12
For personal use only.

TABLE 5. Angle at the bridging oxygen atom and average bridging and terminal P—O bond lengths in various pyrophosphate compounds

Compound*	∠P—O—P (deg)	d(P—O_b) (Å)	d(P—O_t) (Å)	Difference (Å)
Staggered P_2O_7-I				
$KAlP_2O_7$	123	1.607	1.509	0.10
Eclipsed P_2O_7				
$Na_4P_2O_7$(7)	127	1.637	1.513	0.12
α-$Ca_2P_2O_7$(11)	130	1.597	1.510	0.09
β-$Ca_2P_2O_7$(12)	130	1.627	1.516	0.11
	138	1.603	1.521	0.08
$Cd_2P_2O_7$(13)	132	1.625	1.515	0.11
α-$Sr_2P_2O_7$(14)	134	1.598	1.497	0.10
Staggered P_2O_7-II				
$Na_4P_2O_7 \cdot 10H_2O$(15)	130	1.612	1.523	0.09
$Na_2H_2P_2O_7 \cdot 6H_2O$(16)	136	1.598	1.519	0.08
α-$Ni_2P_2O_7$(17)	137	1.602	1.537	0.065
α-$Zn_2P_2O_7$(18)	139	1.603	1.536	0.07
	148	1.582	1.505	0.08
α-$Co_2P_2O_7$(19)	143	1.580	1.517	0.07
α-$Mg_2P_2O_7$(20)	144	1.591	1.516	0.075
α-$Cu_2P_2O_7$(4)	157	1.570	1.525	0.05

*Reference numbers in parentheses.

TABLE 6. Observed and calculated P—O distances in $KAlP_2O_7$*

Anion	p_0	Δp_0	d_{obs} (Å)	d_{calcd} (Å)	$d_{obs} - d_{calcd}$
Side 1					
O(1)	2.60	+0.54	1.610	1.596	+0.014
O(3)	1.95	−0.11	1.510	1.525	−0.015
O(5)	1.85	−0.21	1.502	1.514	−0.012
O(7)	1.85	−0.21	1.521	1.514	+0.007
Mean	2.06	0	1.536	1.537	−0.001
Side 2					
O(1)	2.60	+0.51	1.604	1.593	+0.011
O(2)	1.95	−0.14	1.519	1.522	−0.003
O(4)	1.85	−0.24	1.485	1.511	−0.026
O(6)	1.95	−0.14	1.515	1.522	−0.007
Mean	2.09	0	1.531	1.537	−0.006

*$d_{calcd} = 1.537 + 0.109\Delta p_0$.

priate equation for the PO_4 tetrahedron was given by Baur as

$$d(\text{P—O}) = 1.537 + 0.109\Delta p_0$$

The predicted P—O distances for the two PO_4 tetrahedra in $KAlP_2O_7$ are compared with the observed values in Table 6. The results are generally satisfactory except for O(4).

Baur extended the idea of Δp_x correlation to the variation of Si—O—Si bridge angle in the disilicates (10). He showed a correlation between the bridge angle and $\Delta d_{(om)}$ which is the difference between the experimentally observed bridging Si—O bond length and the mean Si—O bond length $\langle d(\text{Si—O})\rangle$. Figure 4 shows the plot of $\Delta d_{(om)}$ versus the P—O—P bridge angle for 16 pyrophosphate compounds. The value for $\langle d(\text{P—O})\rangle$ chosen here is the actual mean P—O distance averaged over all the P—O bonds in the particular structure. The plot shows an inverse relationship between the bridge angle and $\Delta d_{(om)}$, but the correlation is rather poor.

The possibility of a phase transformation for $KAlP_2O_7$ was investigated by differential thermal analysis from 25 to 500 °C in air. A very small endothermic effect was observed at 455 °C.

Can. J. Chem. Downloaded from www.nrcresearchpress.com by 210.87.254.105 on 09/05/12
For personal use only.

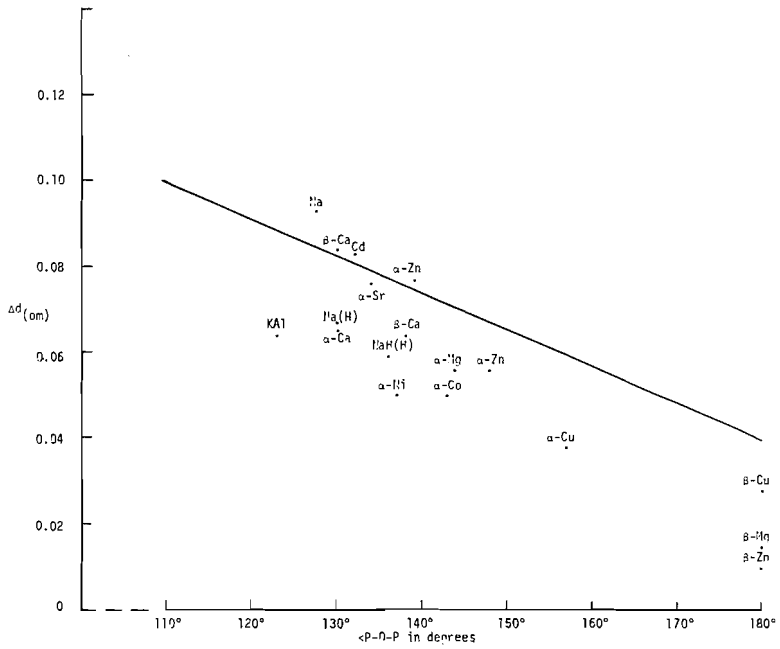

FIG. 4. Plot of $\Delta d_{(om)}$ *vs.* P—O—P bridge angle for 16 pyrophosphate compounds (for α-$Zn_2P_2O_7$ and β-$Ca_2P_2O_7$, the structure has two non-equivalent pyrophosphate groups). Na(H) and NaH(H) denote the compounds $Na_4P_2O_7 \cdot 10H_2O$ and $Na_2H_2P_2O_7 \cdot 6H_2O$, respectively. The solid line corresponds to Cruickshank's prediction.

However, precession photographs taken at 25, 430, and 500 °C on the same crystal showed no change in space group symmetry, and very little change in cell dimensions and intensity of the reflections.

If $NaFeP_2O_7$-I is isostructural with $KAlP_2O_7$ and $NaFeP_2O_7$-II is structurally related to α-$Cu_2P_2O_7$ as suggested by Gamondès *et al.* (3), a comparison between the structures of $KAlP_2O_7$ and α-$Cu_2P_2O_7$ should reveal some structural relationship between the two groups of $M^IM^{III}P_2O_7$ compounds and the nature of the phase transformation of $KAlP_2O_7$.

The space group of $NaFeP_2O_7$-II, $P2_1/n$, differs from the space group $C2/c$, to which α-$Cu_2P_2O_7$ belongs, by the absence of two-fold rotation axes through the bridging oxygen atom in the former in addition to a rotation of the a and c axes. In Fig. 5 the projection of the α-$Cu_2P_2O_7$ structure onto the $a'c'$ plane has been reproduced after applying the transformation $\boldsymbol{a}' = -\boldsymbol{a}$, $\boldsymbol{c}' = \boldsymbol{a} + \boldsymbol{c}$, so as to show space group symmetry $I2/n$. The dimension of this transformed unit cell for α-$Cu_2P_2O_7$ becomes $a' = 6.876$ Å, $b' = 8.113$ Å, $c' = 9.439$ Å, $\beta' = 113.8°$.

In both α-$Cu_2P_2O_7$ (Fig. 5) and $KAlP_2O_7$ (Fig. 2) the pyrophosphate anion, in a nearly staggered configuration, forms sheets parallel to the ab plane. In the former case the P—O—P plane contains the b axis and nearly lies in the ac plane in the present case. This change destroys the nearly hexagonally close-packed array of oxygen atoms which characterize the sheets in

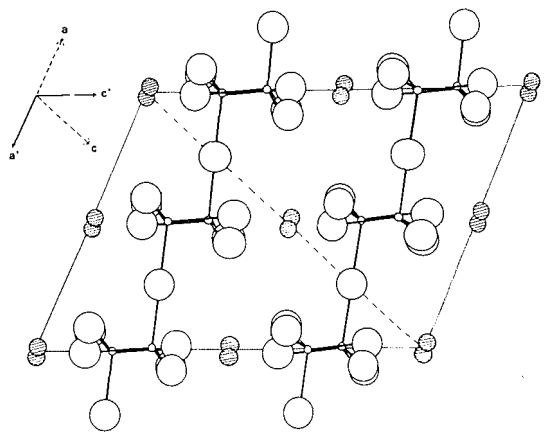

FIG. 5. Projection of the α-$Cu_2P_2O_7$ structure along the b-axis in the transformed space group $I2/n$. Small open circles are phosphorus atoms, large open circles are oxygen atoms, and shaded circles are copper atoms.

Can. J. Chem. Downloaded from www.nrcresearchpress.com by 210.87.254.105 on 09/05/12
For personal use only.

α-$Cu_2P_2O_7$. In addition the pyrophosphate groups are rotated so as to subtend an angle of $-11°$ with the sheet directions, rather than $+17°$, so as to accommodate the aluminum ion. This destroys the octahedral site between sheets creating the pseudo cubical sites occupied by K^+ in $KAlP_2O_7$. These changes suggest that gross rearrangements are involved in the change between $NaFeP_2O_7$-I and $NaFeP_2O_7$-II and that the analogous change is unlikely to account for the DTA anomaly seen in $KAlP_2O_7$.

The authors wish to thank Mrs. S. Leung for growing the crystals and the National Research Council of Canada for financial support in terms of a research grant and a Postdoctorate Fellowship (H.N.N.).

1. F. D'Yvoire. Bull. Soc. Chim. Fr. 1224 (1962).
2. Ya. V. Klyucharov and L. I. Skoblo. Dokl. Akad. Nauk. SSSR, **154**, 634 (1964).
3. J. P. Gamondès, F. D'Yvoire, and A. Boule. C.R. Acad. Sc. Paris, **272C**, 49 (1971).
4. B. E. Robertson and C. Calvo. Acta Cryst. **22**, 665 (1967).
5. D. T. Cromer and J. T. Waber. Acta Cryst. **18**, 104 (1965).
6. D. T. Cromer. Acta Cryst. **18**, 17 (1965).
7. K. Y. Leung and C. Calvo. Can. J. Chem. **50**, 2519 (1972).
8. D. W. J. Cruickshank. J. Chem. Soc. 5486 (1961).
9. W. H. Baur. Trans. Am. Cryst. Assoc. **6**, 129 (1970).
10. W. H. Baur. Am. Miner. **56**, 1573 (1971).
11. C. Calvo. Inorg. Chem. **7**, 1345 (1968).
12. N. C. Webb. Acta Cryst. **21**, 942 (1966).
13. C. Calvo and P. K. L. Au. Can. J. Chem. **47**, 3409 (1969).
14. L. O. Hagman, I. Jansson, and C. Magneli. Acta Chem. Scand. **22**, 419 (1968).
15. W. S. McDonald and D. W. J. Cruickshank. Acta Cryst. **22**, 43 (1967).
16. R. L. Collins and M. Willis. Acta Cryst. **27B**, 291 (1971).
17. K. Łukaszewicz. Bull. Acad. Pol. Sci. Ser. Sci. Chim. **15** (2), 47 (1967).
18. B. E. Robertson and C. Calvo. J. Solid State Chem. **1**, 120 (1970).
19. N. Krishnamachari and C. Calvo. Acta Cryst. **B28**, 2883 (1972).
20. C. Calvo. Acta Cryst. **23**, 289 (1967).

Can. J. Chem. Downloaded from www.nrcresearchpress.com by 210.87.254.105 on 09/05/12
For personal use only.

Crystal Structure of α-VPO_5

BYRON JORDAN AND CRISPIN CALVO

Department of Physics, McMaster University, Hamilton, Ontario

Received March 21, 1973

α-VPO_5 crystallizes in the tetragonal space group $P4/n$ with $a = 6.014(7)$ and $c = 4.434(2)$ Å. The structure, isotypic with that of α-VSO_5, was refined by full-matrix least-squares method to an R value of 0.089 using 239 independent reflections. The vanadium ion lies on a crystallographic four-fold axis, as does one of the oxygen atoms, and the P on a site of $\bar{4}$ symmetry. A second oxygen atom, as a result of disorder, occurs in two positions which are mirror reflected with respect to the *ac* plane. The structure consists of highly distorted VO_6 groups with bond lengths along the *c* axis of 1.580(11) and 2.853(11) Å while the remaining four V—O bond lengths are all 1.858(8) Å. The P—O bond lengths in the PO_4 tetrahedron are 1.541(8) Å with the PO_4 groups bridging across four chains of VO_6 groups.

L'αVPO_5 cristallise dans le groupe d'espace tétragonal $P4/n$ avec $a = 6.014(7)$ et $c = 4.434(2)$ Å. La structure, isotype de celle de l'αVSO_5, a été raffinée par les méthodes matricielles des moindres carrés jusqu'à une valeur R de 0.089 après 239 reflexions indépendantes. L'ion vanadium se trouve sur l'axe cristallographique d'ordre 4 de même que l'un des oxygènes, le P sur le site de symétrie $\bar{4}$. Un second atome d'oxygène résultant du désordre, se trouve dans deux positions qui sont images par rapport à un miroir du plan *ac*. La structure comprend des groupes VO_6 hautement distordus avec les longueur de liaison sur l'axe *c* de 1.580(11) et 2.853(11) Å tandis que les longueurs des quatres autres liaisons V—O sont toutes de 1.858(8) Å. Les longueurs des quatres autres liaisons P—O dans le tétraèdre PO_4 sont de 1.541(8) Å avec des groupes PO_4 traversant en pont quatre chaînes de groupes VO_6.

[Traduit par le journal]

Can. J. Chem., **51**, 2621 (1973)

Introduction

The structures of a series of ABO_5 compounds with A in an octahedrally and B in a tetrahedrally coordinated site have been reported. Cations such as S^{6+}, P^{5+}, and Mo^{6+} occur in the B sites and V^{5+}, V^{4+}, Ta^{5+}, Nb^{5+}, and Mo^{5+} have been reported in the A site. Two crystalline forms are known for these substances; an orthorhombic form reported for β-VSO_5(1) and β-VPO_5(2) and a tetragonal form for $MoPO_5$(3), $VMoO_5$(4), $TaPO_5$(5), $NbPO_5$(6), α-VSO_5(7), and now α-VPO_5. Aside from VPO_5 only VSO_5 occurs in both phases, but unlike the present compound, single crystals of the α form of VSO_5 have not been obtained.

The preparation and unit cell parameters of both phases of VPO_5 have been reported by Bordes and Courtine (8) while the α form was prepared by Ladwig (9) and uncharacterized form by Brown and Hummel (10). Bordes and Courtine (8) found that the β-VPO_5 formed from a mixture of ammonium phosphate and ammonium metavanadate at 595 °C but the α phase appeared upon dehydration of $VPO_5 \cdot 2H_2O$ at 120 °C. Both substances were prepared under one atmosphere of O_2. Further, they found that, whereas the α form appeared to undergo reversible hydrolysis with the *c* axis length depending upon the value of X in $VPO_5 \cdot XH_2O$, the β form remained anhydrous under similar treatment. Since there is a great deal of interest in the optical (11) and electrical properties of V_2O_5–P_2O_5 glasses (12) and concern over the structural nature of these (13, 14), a detailed structure of this polymorph seems warranted.

Experiments

Crystals of α-VPO_5 were prepared from equal molar amounts of P_2O_5 (Fisher Scientific) and V_2O_5 (Fisher Scientific) weighed in stoppered bottles filled in a Dry Box. The components were well mixed and then transferred to a platinum crucible which was directly inserted into a furnace pre-heated to 200 °C. The temperature was then raised and kept at 850 °C over night, and then cooled at a rate of 10–15 °C/h to below 700 °C. At this point the power to the furnace was removed and the furnace plus sample allowed to cool to room temperature. Yellow-green dendritic crystalline plates formed on the surface of a darker green glass-matrix. α-VPO_5 will occur throughout the crucible when cooled more slowly, however. The crystals cleaved easily. All photographs indicated some disorder since the reflections were about 3 times longer parallel to *c* than in the *ab* plane. Prolonged heating in air up to 500 °C caused further disorder as indicated by an extension of the diffraction spot. However, crystals survived storage at room temperature and cooling to 150 °K. A very weak electron paramagnetic resonance signal arising from V^{4+}, whose maximum possible concentration was below 1%, was detected. The crystals are stable at least to 1140 °C without a loss of weight.

A small plate crystal with dimensions 1.5 × 1.5 × 0.1 mm was used to collect all the crystallographic data

Can. J. Chem. Downloaded from www.nrcresearchpress.com by 210.87.254.42 on 09/05/12
For personal use only.

Can. J. Chem. Downloaded from www.nrcresearchpress.com by 210.87.254.42 on 09/05/12
For personal use only.

TABLE 1. Atomic and thermal parameters for α-VPO_5 with standard errors in parentheses

Atom	x	y	z	U_{11} (Å^2)*	U_{22} (Å^2)	U_{33} (Å^2)	U_{12} (Å^2)	U_{13} (Å^2)	U_{23} (Å^2)
V	1/4	1/4	0.2139(5)	0.0019(14)	U_{11}	0.0165(11)	—	—	—
P	1/4	3/4	1/2	0.0030(18)	U_{11}	0.0189(16)	—	—	—
O(1)	1/4	1/4	0.858(2)	0.011(5)	U_{11}	0.018(4)	—	—	—
O(2)	0.1965(13)	0.9522(12)	0.2987(17)	0.012(3)	0.009(3)	0.0227(3)	−0.001(3)	−0.002(3)	0.002(3)
O(3)†	1/2 − x	y	z	U_{11}	U_{11}	U_{33}	$-U_{12}$	$-U_{13}$	U_{22}

*Calculated from $\beta_{ij} = 2\pi^2 b_i b_j U_{ij}$ where $T = \exp[-(\beta_{11}h^2 + 2\beta_{12}hk + \ldots)]$ is the thermal factor in the structure factor expression.
†Derived from parameters of O(2) with a site occupancy of 0.33(2).

Can. J. Chem. Downloaded from www.nrcresearchpress.com by 210.87.254.42 on 09/05/12
For personal use only.

using graphite monochromatized MoKα radiation. Accurate parameters were refined using least-squares from 2θ values obtained with a Syntex $P\bar{1}$ diffractometer. The crystal data are as follows:

α-VPO_5 f.w. = 161.91

Tetragonal, $a = 6.014(7)$, $c = 4.434(2)$ Å, $V = 160.37$ Å^3, (at 21 °C), $Z = 2$, $\rho_x = 3.353$ g/cm^3. Space group: $P4/n$ $F_{000} = 472$, $\lambda_\alpha = 0.71069$ Å. Extinct reflections are $hk0$ with $h + k =$ odd.

All the reflections in a hemisphere up to a 2θ angle of 60° were collected. The intensity was measured at variable scan rates from 2 to 24° per min, depending upon the peak intensity and backgrounds measured at 1° removed from the peak. Reflections whose intensity measure was less than 3σ were regarded as unobserved. The intensities were corrected for absorption using a linear absorption coefficient of $\mu = 36.2$ cm^{-1} and then symmetry equivalent reflections were averaged.

Refinement proceeded from the atomic coordinates reported for $VMoO_5$ (4) with P^{5+} in place of Mo^{5+}. Atomic scattering factors for V^{5+} were obtained from Cromer and Waber (15) and P and O were obtained from the International Table for X-ray crystallography (16). Dispersion corrections were applied. The structure was refined by a full-matrix least-squares program prepared for the CDC 6400 by J. S. Stephens. Weights, $\omega = [2.5 + 0.01F_o^2]^{-1}$, were chosen so that the difference between the observed and calculated structure factors would be independent of the magnitude of the observed structure factor. When convergence had been obtained with isotropic thermal parameters the components of the anisotropic thermal parameters were allowed to vary. As anticipated the U_{33} parameters were large and, in addition, the U_{11} parameter for O(2) indicated two disordered positions with a root-mean-squared displacement of about 0.5 Å. A model allowing for two separate positions for this oxygen atom, one at either end of this principal axis of this apparent thermal ellipsiod with variable occupancy, was tested. The R value changed from 0.12 to 0.10. Further refinement reduced the R value to 0.089 for 248 reflections of which 9, showing large deviations, were not included. The final value for the disorder parameter, the fractional occupancy of the O(2) site, is 0.67(2). The atomic parameters are in Table 1. The observed and calculated structure factors are in Table 2.[1] A final difference synthesis showed some residual peaks of about 0.03 of the vanadium peak at the vanadium site and peaks about half this height at 0, 1/2, 0.653 and 0, 1/2, 0.405.

Description of the Structure

The structure of α-VPO_5 is composed of chains of distorted VO_6 octahedra coincident with the four-fold axes as shown in Fig. 1. The four oxygen atoms in the *ab* plane are shared with four different PO_4 groups and each of the oxygen atoms of the PO_4 group is shared with a separate chain of VO_6 octahedra. The two disordered configuration for O(2) are derived from a structure where the V—O(2) and P—O(2) bonds coincide with either the

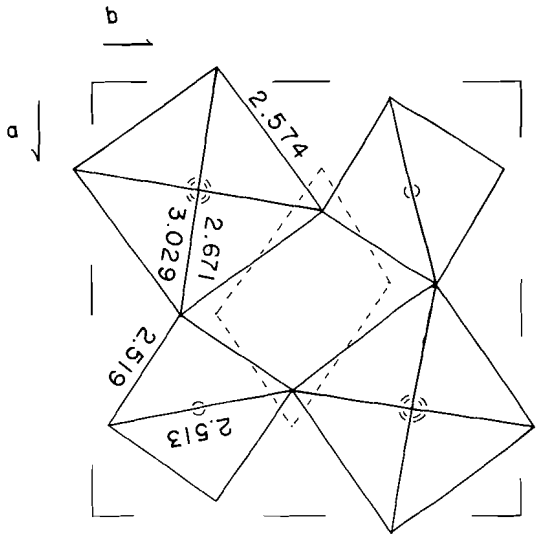

FIG. 1. The structure of α-VPO_5 projected onto the *ab* plane. Oxygen atoms lie at the corners of the polyhedra. The vanadium ions are represented by the double circle and phosphorus ions by the single circles. The corners of the dotted parallelogram represent the position of the oxygen atoms when disordered. The O—O lengths in Å are indicated.

ac or *bc* planes by a coupled rotation of the VO_6 groups in a given layer either all clockwise or all counterclockwise. At the present time it is not known whether this disorder is temperature dependent or results from errors in the stacking of mica-like sheets frozen in at the time of growth although significant intensity changes occur upon cooling.

The bond strength (S_i) – bond length (R) empirical curve (17) given by $S_i = (5/4)(1.714/R)^{5.1}$, suggests a regular VO_6 octahedral should have V—O bond lengths of 1.85 Å. The VO_6 groups are distorted from this regular VO_6 group by a displacement of the vanadium ion by about 0.37 Å along the *c* axis. Both oxygen atoms on the *c* axis move away from the displaced vanadium atom; the nearest by 0.1 Å and the furthest by 0.56 Å.

Discussion

Of all the structures isotypic with α-VPO_5 the present refinement is the only one which reports a disorder. Since the others were refined varying the individual thermal parameters isotropically only, it cannot be ascertained whether a similar phenomena occurs elsewhere in the series. Without a detailed resolution of these other structures it cannot be safely assumed that this disorder is characteristic of the structure rather than the compound. The possibility that these structures deviate slightly from stoichiometry cannot be discounted although the ease with which they form glasses suggests that the devia-

[1]Photocopies of Table 2 are available, at a nominal charge, from the Depository of Unpublished Data, National Science Library, National Research Council, Ottawa, Canada K1A 0S2.

TABLE 3. Bond lengths and angles in α-VPO_5 with standard errors in parentheses*

Bond	Distance	Bonds	Angle (deg)	Bonds	Angle (deg)
V—O(1)	1.580(11)	O(1)—V—O(2)	101.6(2)	O(2)—V—O(2)*b*	87.7(3)
—O(2)	1.858(7)	—O(1)	180.0	—O(2)*c*	156.7(4)
—O(1)*a*	2.853(11)				
P—O(2)	1.541(8) (4X)	O(2)—P—O(2)*c*	109.1(4)		
		—O(2)*d*	109.7(4)		

*Transformations: $a = x, y, 1 - z$; $b = y, 1/2 - x, z$; $c = 1/2 - x, 1/2 - y, z$; $d = 1/2 + x, -y, -z$.

TABLE 4. Comparison of bond lengths and bond strength in V_2O_5, VPO_5, and VSO_5 compounds

	V_2O_5		β-VPO_5		α-VPO_5		β-VSO_5		α-VSO_5	
Bond	Length (Å)	S_i	Length (Å)	S_i	Length (Å)	S_i	Length (Å)	S_i	Length (Å)	S_i
V—O(1)	1.58	1.893	1.566	1.981	1.580	1.893	1.594	1.810	1.63	1.615
—O(2)	1.78	1.031	1.849	0.849	1.856	0.828	2.005	0.562	2.04	0.514
—O(3)	1.88	0.780	1.886	0.768	1.856	0.828	2.016	0.546	2.04	0.514
—O(4)	1.88	0.780	1.886	0.768	1.856	0.828	2.056	0.494	2.04	0.514
—O(5)	2.02	0.541	1.902	0.735	1.856	0.828	2.056	0.494	2.04	0.514
—O(6)	2.78	0.106	2.591	0.158	2.857	0.093	2.284	0.289	2.47	0.194
		ΣS_i 5.13		5.26		5.34		4.19		3.87

*From $S_i = (5/4)(1.714/R)^{5.1}$ with R as bond lengths. The parameters 1.741 and 4.1 were derived from V^{5+} coordinated to oxygen atoms.

tions in the crystal are not likely to be the cause of the residual peaks. Twinning, with the twin plane through the phosphorus atom, does predict peaks near the positions found in the difference synthesis, but the agreement is by no means perfect.

In α-VSO_5(7) the vanadium ions are tetravalent and, as a result, the distortion of the VO_6 octahedron is less pronounced than in α-VPO_5. In particular the V—O(1) bond lengths are 1.63(3) and 2.47(3) Å while the remaining V—O bond lengths are 2.04 Å long in the former compound. As can be seen in Table 4, similar changes occur in this group between the α and β phases of the sulfate and the phosphate. It is common to ignore the long V—O bond and discuss only five orbitals for the vanadium oxygen system. However, if these bond orders, S_i, are taken as guides to the strength of the bonds it is just as serious an error to regard the short bonds as equivalent to the other five as it is to ignore the long one with regards to the V—O bonds of intermediate length. From the view of crystal packing, the distorted octahedron seems to be the basic unit in all these structures.

In this regard the discrepancy between the parameters presented here and those reported by Bordes and Courtine (8) ($a = 6.20$, $c = 4.11$ Å) should be noted. These values suggest that the V—O(1) *a* bond is about 0.22 Å shorter than that reported in Table 3 and the V—O(2) bond is about 0.10 Å longer. The relative direction of these changes is consistent with a redistribution of the bond about the vanadium ion but the magnitudes are not consistent with the predictions of the bond strength – bond length curve. These authors also report an expansion of the *c* axis by 0.16 Å between 130 and 700 °C. An expansion of this order of magnitude is unusual and substantially larger than the lattice expansion we could detect.

Caution should be exercised in deriving structural information concerning the V_2O_5–P_2O_5 glasses from the structures of α-VPO_5, β-VPO_5, and V_2O_5 alone. Structure sensitive data including electron spin resonance of V^{4+}, nuclear magnetic resonance of ^{51}V, and conductivity of the glasses have not provided a satisfactory resolution of this problem. Since the average tetrahedral P—O bond lengths differ by about 10% from that of V—O (1.71 Å) some replacement of P^{5+} by V^{5+} in the tetrahedral site would not be unexpected. Such a replacement has been proposed in $V_{1+x}Mo_{1-x}O_5$ when x deviates positively from zero. However, it is not possible to change continuously from either VPO_5

Can. J. Chem. Downloaded from www.nrcresearchpress.com by 210.87.254.42 on 09/05/12
For personal use only.

structure to that of V_2O_5. Each of these structures however, contain chains of octahedra involving alternately long and short V—O bonds nearly parallel to the axis of the chain. Thus, such chains, but of finite length, might be expected in the glasses on structural grounds. The replacement of a V—O—V interaction equatorial to the axis of the chain by V—O—P interaction will involve small changes in the bonding, and none in bond order, relative to the bond strength in the strong V—O bond and will preserve the approximately axial nature of the field gradient reported by Landsberger and Bray (14).

This research was supported by a grant A-0948 from the National Research Council of Canada.

1. P. KIERKEGAARD and J. M. LONGO. Acta Chem. Scand. **19**, 1906 (1965).
2. R. GOPAL and C. CALVO. J. Solid State Chem. **5**, 432 (1972).
3. P. KIERKEGAARD and M. WESTERLUND. Acta Chem. Scand. **18**, 2217 (1964).
4. H. A. EICK and L. KIHLBORG. Acta Chem. Scand. **20**, 722 (1966).
5. J. M. LONGO, J. W. PIERCE, and J. A. KAFALAS. Mater. Res. **6**, 1157 (1971).
6. J. M. LONGO and P. KIERKEGAARD. Acta Chem. Scand. **20**, 72 (1966).
7. J. M. LONGO and R. J. ARNOTT. J. Solid State Chem. **1**, 394 (1970).
8. E. BORDES and PIERRE COURTINE. C. R. Acad. Sc. Paris, **270**, 1375 (1972).
9. G. LADWIG. Z. Anorg. Allg. Chem. **364**, 225 (1969).
10. J. J. BROWN and F. A. HUMMEL. Trans. Br. Ceram. Soc. **64**, 419 (1965).
11. G. W. ANDERSON and W. D. COMPTON. J. Chem. Phys. **52**, 6166 (1970).
12. M. SAYER, A. MANSINGH, J. M. REYES, and G. ROSENBLATT. J. Appl. Phys. **42**, 2857 (1971).
13. G. F. LYNCH, M. SAYER, S. L. SEGAL, and G. ROSENBLATT. J. Appl. Phys. **42**, 2587 (1971).
14. F. R. LANDSBERGER and P. J. BRAY. J. Chem. Phys. **53**, 2757 (1970).
15. D. T. CROMER and J. T. WABER. Acta Cryst. **18**, 104 (1965).
16. International Tables for X-ray Crystallography. Vol. III. Kynoch Press, Birmingham. 1963.
17. I. D. BROWN and R. D. SHANNON. Acta Cryst. A, **29**, 266 (1973).

Can. J. Chem. Downloaded from www.nrcresearchpress.com by 210.87.254.42 on 09/05/12
For personal use only.

A General Method of Calculating the Water Activity of Supersaturated Aqueous Solutions from Ternary Data

J. SANGSTER, T. T. TENG, AND F. LENZI[1]

Département de Génie chimique, Ecole Polytechnique, Université de Montréal, Montréal, Québec

Received January 25, 1973

Recently developed methods of predicting water activities of multicomponent aqueous solutions use binary data. At high concentrations these methods are limited inasmuch as they require binary data beyond the solubility limit of individual solutes. A method is proposed whereby ternary water activity data may be used to calculate water activities of supersaturated binary solutions. The new method is compared with two extrapolation procedures on a known system and gives the best agreement. Values of the water activities for supersaturated solutions of KNO_3 (3.8 to 7.6 *m*) and K_2SO_4 (0.7 to 2.3 *m*) at 25 °C are obtained.

Des méthodes de prédiction de l'activité de l'eau de systèmes aqueux à composants multiples ont été récemment proposées. Ces méthodes demandent des données binaires, mais sont limitées par le manque de ces données au-delà de la limite de solubilité des solutés individuels. Une méthode de calcul des activités de l'eau des solutions binaires sursaturées est proposée à partir de données ternaires. Cette méthode est appliquée à un système connu et donne de meilleurs résultats que deux méthodes d'extrapolation. Les valeurs de l'activité de l'eau à 25 °C ont été établies pour des solutions sursaturées en K_2SO_4, de 0.7 à 2.3 *m*, et en KNO_3, de 3.8 à 7.6 *m*.

Can. J. Chem., **51**, 2626 (1973)

Introduction

The prediction of the water activity, a_w, of aqueous solutions is of both theoretical and practical interest (1, 8). This is especially true of solutions of moderate to high concentrations.

This paper describes a recently developed method that uses binary data to predict a_w values for multicomponent aqueous solutions, applicable to both electrolytes and non-electrolytes, up to total concentrations as high as 12 *m*. The reverse method is used herein to calculate "virtual" water activities, *i.e.*, a_w's for a solute beyond its solubility limit, from ternary a_w data. These are of definite thermodynamic interest. Robinson and co-workers (1), in calculating excess free energies of mixing for systems involving K_2SO_4, needed values for the osmotic coefficient of this salt $\varphi_{K_2SO_4}$, beyond its solubility limit. They estimated $\varphi_{K_2SO_4}$ from weighted averages of $\varphi_{Na_2SO_4}$ and $\varphi_{Rb_2SO_4}$. The predictive method of the present work is used to find virtual values of $\varphi_{K_2SO_4}$, in answer to Robinson's requirement, and also of KNO_3. It is a general method, applicable to both electrolytes and non-electrolytes.[2]

[1]To whom correspondence should be addressed.

[2]Stokes and Robinson (5) have used a similar method to obtain a_w values for supersaturated mannitol solutions.

The Zdanovskii Relation

A method of predicting a_w's which uses binary solution data has been found (4) to be equally applicable to electrolytes and non-electrolytes. It uses the linear molality relation for isopiestic solutions discovered empirically by Zdanovskii in 1936 (3). It is presented here in sketch form only, since it has been tested in detail elsewhere (4). If a ternary aqueous solution, of electrolytes 1 and 2 at molalities m_1 and m_2, respectively, is in isopiestic equilibrium with two binary solutions of molalities m_{01} and m_{02}, then

$$[1] \quad m_1/m_{01} + m_2/m_{02} = 1 \text{ at constant } a_w$$

Relation 1 was discovered independently in 1966 by Stokes and Robinson (5), where it was applicable to semi-ideal solutions of non-electrolytes at isopiestic equilibrium. In a survey of 117 ternary aqueous systems reported in the literature, it was found (4) that most of these obeyed Zdanovskii's rule (eq. 1) to a good approximation up to moderate concentrations. Equation 1 held well for a majority of electrolyte/electrolyte, electrolyte/non-electrolyte, and non-electrolyte/non-electrolyte ternary aqueous solutions.

To take account of deviations from Zdanovskii linearity, eq. 1 may be written (6) in the form

Can. J. Chem. Downloaded from www.nrcresearchpress.com by 210.87.254.5 on 09/05/12
For personal use only.

Can. J. Chem. Downloaded from www.nrcresearchpress.com by 210.87.254.5 on 09/05/12
For personal use only.

[2] $m_1/m_{01} + m_2/m_{02} + by_1y_2m = 1$

where

$$m = m_1 + m_2$$

$$y_1 = m_1/m$$

and

$$y_2 = m_2/m$$

Equation 2 defines b, an empirical deviation parameter. In the previous publication (4), the ternary systems were divided arbitrarily into groups A, B, and C, according to the magnitude of b, thus: group A, $0 < |b_{ave}| < 0.02$; group B, $0.02 < |b_{ave}| < 0.1$; group C, $|b_{ave}| > 0.1$. Zdanovskii plots of a system from each group are given in Figs. 1–3 of ref. 4.

The use of equation 1

[1] $m_1/m_{01} + m_2/m_{02} = 1$

to find a_w for a ternary aqueous solution of total molality $(m_1 + m_2)$ is essentially a determination of the equivalent isopiestic m_{01} or m_{02} (4). The given data are: m_1, m_2, and a_w *vs.* molality curves for each solute in its own solution. An estimate of the unknown a_w is made, the corresponding values of m_{01}' and m_{02}' are read off, and the sum S

$$m_1/m_{01}' + m_2/m_{02}' = S$$

is calculated. If $S \neq 1$, a second iteration can be performed, using $m_{01}'' = Sm_{01}'$ (or $m_{02}'' = Sm_{02}'$). The process is repeated until S is as close as desired to unity. The value of m_{01} or m_{02} at this point gives the a_w of the ternary solution. The a_w values calculated in this manner are usually within 0.5% of experimental values (4).

The use of eq. 1 in this method of calculation requires that the unknown a_w lie in the common range of a_w binary data available. This imposes a practical criterion for the reliability or feasibility of the calculation. The requirement is $(a_w)_{mixture} > a_w^*$ where a_w^* is the higher of the two limiting a_w's of the binary data. Exceeding the criterion implies extrapolating the a_w *vs.* m curve beyond a_w^*, with attendant uncertainty, since in practice an empirical polynomial is fitted to the a_w *vs.* molality data.

Finding "Virtual" Water Activities

It sometimes happens that ternary isopiestic solution data include solutions whose a_w's are smaller than the binary a_w^* defined above. If a_w^* represents the solubility limit of solute 2 then eq. 1 can be used in reverse to find a_w's of solute 2 beyond a_w^*, that is, "virtual" a_w's, or a_w's of supersaturated solutions.

The given data in this kind of calculation are: a_w of the ternary solution, m_1,m_2, and m_{01}, where m_{01} is the isopiestic molality of the more soluble solute. This a_w is the "virtual" water activity, and the isopiestic m_{02} is found by solving eq. 1 for this quantity. If greater accuracy is desired, eq. 2, which includes the correction factor b, may be used instead. Since b cannot be found at a_w's less than a_w^*, extrapolated values would have to be used.

Virtual water activities have previously been found by a weighted extrapolation procedure of the φ's of closely related electrolytes. Hidalgo and Orr (7) used this method to calculate φ's for supersaturated solutions of NaCl, KCl, RbCl, and CsCl up to 20 m; LiCl was the reference salt. The present paper will show that this procedure, while useful for extrapolation not far beyond the solubility limit, may not be reliable at concentrations much beyond this point.

Results

The corrected Zdanovskii relation 2 is used to calculate virtual a_w's for three salts: (*a*) $NaNO_3$ beyond 6 m (a check of the method on a "known" salt); (*b*) K_2SO_4 beyond its solubility limit, 0.7 m; and (*c*) KNO_3 beyond its solubility limit, 3.8 m.

(a) $NaNO_3$, the "Known" Salt

The Zdanovskii relation 2 may be rearranged to give

[4] $$m_{02} = \frac{m_2}{1 - \frac{m_1}{m_{01}} - \frac{bm_1m_2}{m}}$$

Equation 4 is used to find a_w's of $NaNO_3$ solutions beyond 6 m ($a_w = 0.845$) from data (9–12) of the ternary systems (*i*) $LiNO_3(1)$–$NaNO_3(2)$–H_2O; (*ii*) $NaCl(1)$–$NaNO_3(2)$–H_2O; and (*iii*) $UO_2(NO_3)_2(1)$–$NaNO_3(2)$–H_2O. The values for b used in equation 4 were found from: $LiNO_3/NaNO_3$, $b = -0.080 + 0.111a_w$; $NaCl/NaNO_3$, $b = -0.080 + 0.109a_w$; $UO_2(NO_3)_2/NaNO_3$, $b = 0.063 - 0.06a_w$. These relations are based on ternary isopiestic data at $a_w > 0.845$ (10,11,13). Table 1 presents calculated m_{02} and corresponding a_w values together with experimental m_{02} values interpolated from data in the

TABLE 1. Water activities beyond 6 *m* of $NaNO_3$ at 25 °C by the Zdanovskii method: ternary systems X(1)–$NaNO_3$(2)–H_2O

Electrolyte partner X(1)	a_w	Ternary solutions m_1	Ternary solutions m_2	Isopiestic binary solutions m_{01}	Isopiestic binary solutions m_{02}(exptl)	m_{02}(calcd)	a_w(calcd)
NaCl	0.8409	3.2773	1.3406	4.2410	6.1643	6.2008	0.8401
		2.4376	2.5280			6.1533	0.8412
		0.8255	4.9034			6.1511	0.8413
$LiNO_3$	0.8253	1.3153	4.6067	4.1530	6.8650	6.8611	0.8254
		2.5360	2.5830			6.8970	0.8246
		3.3705	1.2315			6.9203	0.8240
$LiNO_3$	0.8223	2.5860	2.6141	4.1944	6.9950	7.0886	0.8202
$UO_2(NO_3)_2$	0.8135	1.6864	1.9876	2.3460	7.3760	7.4108	0.8127
$LiNO_3$	0.7859	1.6344	5.7246	4.9610	8.6500	8.6520	0.7858
		3.1007	3.1583			8.6759	0.7852
		4.0751	1.4889			8.7101	0.7844
$UO_2(NO_3)_2$	0.7811	1.2193	4.6767	2.6780	8.8400	8.8401	0.7811
$LiNO_3$	0.7627	4.7612	1.1607	5.4400	9.6955	9.6634	0.7633
		3.9546	2.5668			9.6763	0.7631
		2.9590	4.3363			9.6950	0.7627
		1.6953	6.6150			9.7049	0.7625
$UO_2(NO_3)_2$	0.7543	1.3678	5.2462	2.9670	10.088	10.095	0.7541
		2.1646	2.5514			10.222	0.7512

TABLE 2. Experimental water activity of $NaNO_3$ at 25 °C beyond 6 m*

m	a_w
6.033	0.8439
6.1643	0.8409
6.236	0.8393
6.397	0.8354
6.865	0.8253
7.376	0.8135
7.667	0.8070
7.747	0.8055
7.859	0.8028
8.650	0.7859
8.840	0.7811
8.945	0.7792
8.992	0.7783
9.670	0.7632
9.889	0.7589
10.088	0.7543

*Data from refs. 10–12, 14.

literature (10–12, 14); Table 2 presents these literature data.[3] Calculated and experimental values are plotted in Fig. 1. Also included in this figure are virtual a_w's calculated by a weighted

[3]Table 2 is presented here to supplement existing data up to 6 *m* in a standard reference (15).

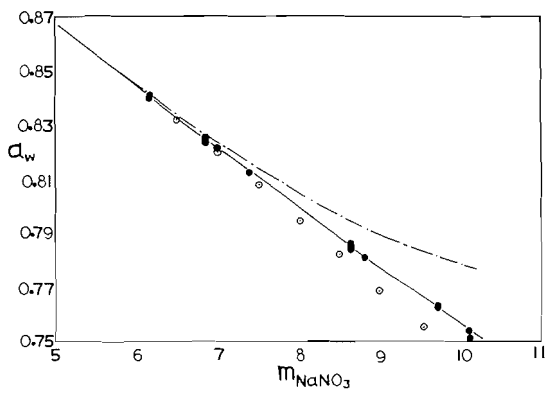

FIG. 1. Water activities of $NaNO_3$ solutions at 25 °C. -·-·- extrapolation of polynomial fitted in the range 0–6 *m*; — experiment; ● Zdanovskii method (average values); ⊙ weighted extrapolation.

extrapolation method using data for $LiNO_3$ and NH_4NO_3. Water activities for $NaNO_3$ solutions to 6 *m*, and for those of $LiNO_3$ and NH_4NO_3 to 13 *m* were taken from a standard reference (15), and the a_w ratios $NaNO_3/LiNO_3$/and $LiNO_3/NH_4NO_3$ were calculated.

(b) K_2SO_4 beyond 0.7 m (a_w = 0.975)

Virtual a_w's were found, using eq. 4, from data (1) of the ternary systems (*i*) Na_2SO_4(1)–K_2SO_4-

Can. J. Chem. Downloaded from www.nrcresearchpress.com by 210.87.254.5 on 09/05/12
For personal use only.

TABLE 3. Virtual a_w's of K_2SO_4 at 25 °C beyond 0.7 m by the Zdanovskii method: ternary systems X(1)–K_2SO_4(2)–H_2O

Electrolyte partner X(1)	a_w	Ternary solutions m_1	Ternary solutions m_2	Isopiestic binary solutions m_{01}	Isopiestic binary solutions m_{02}(calcd)
KCl	0.9739	0.6770	0.1242	0.8184	0.7465
		0.6317	0.1616		0.7336
		0.5406	0.2442		0.7418
		0.4925	0.2862		0.7392
Na_2SO_4	0.9735	0.3816	0.3816	0.7517	0.7526
KCl		0.6036	0.2008	0.8197	0.7892
Na_2SO_4	0.9730	0.5331	0.2379	0.7667	0.7496
		0.4327	0.3446		0.7651
		0.2724	0.5127		0.7787
KCl	0.9700	0.6862	0.2290	0.9422	0.8766
NaCl		0.6761	0.2252	0.9082	0.8657
Na_2SO_4	0.9698	0.4412	0.4415	0.8709	0.8650
KCl		0.6902	0.2301	0.9429	0.8937
NaCl		0.6789	0.2262	0.9122	0.8689
NaCl	0.9696	0.6659	0.2401	0.9197	0.8553
		0.5923	0.3228		0.8926
KCl	0.9654	0.7907	0.2630	1.0886	1.0053
NaCl		0.7786	0.2590	1.0424	1.0026
KCl	0.9647	0.8614	0.2203	1.1100	1.0330
		0.7396	0.3341		1.0452
		0.6740	0.3917		1.0371
Na_2SO_4	0.9608	0.8027	0.3846	1.1705	1.1506
		0.4987	0.6886		1.1550
NaCl	0.9551	1.0211	0.3397	1.3441	1.3742
KCl	0.9544	1.0547	0.3516	1.4375	1.4052
NaCl		1.0340	0.3444	1.3643	1.3827
KCl	0.9505	1.1418	0.3798	1.5593	1.5170
NaCl		1.1195	0.3724	1.4753	1.4973
NaCl	0.9439	1.2687	0.4226	1.6602	1.7293
NaCl	0.9266	1.8084	0.3781	2.1348	2.3435
		1.6389	0.5585		2.2933
		1.5084	0.7000		2.2851

(2)–H_2O; (*ii*) KCl(1)–K_2SO_4(2)–H_2O; and (*iii*) NaCl(1)–K_2SO_4(2)–H_2O for $a_w < 0.975$. An average value for b for each system was used, calculated from the original data for $a_w > 0.975$: (*i*) $b_{ave} = -0.077$; (*ii*) $b_{ave} = +0.061$; and (*iii*) $b_{ave} = -0.027$.

The results are given in Table 3, and plotted in Fig. 2. Also included in this figure are a_w values at 0.8, 1.0, and 1.2 m calculated by Robinson (1) using the weighted comparison method.

(c) KNO_3 beyond 3.8 m ($a_w = 0.926$)

Virtual a_w's were found, using eq. 4, from data (12) of the ternary systems (*i*) $NaNO_3$(1)–KNO_3(2)–H_2O; (*ii*) KCl(1)–KNO_3(2)–H_2O; and (*iii*) NaCl(1)–KNO_3(2)–H_2O for $a_w < 0.926$. For systems (*i*) and (*ii*), the b_{ave} values used were +0.007 and +0.053, respectively (11, 12). In system (*iii*), b was a function of a_w, and an extrapolated value ($b = +0.14$ at $a_w = 0.8947$) was used; this is illustrated in Fig. 3. The results are given in Table 4.

For purposes of comparison, virtual a_w's of KNO_3 were calculated by the weighted extrapolation method described in section (*a*), using data for KNO_3, $NaNO_3$, and $LiNO_3$. The virtual a_w's for KNO_3 appear in Fig. 4.

Can. J. Chem. Downloaded from www.nrcresearchpress.com by 210.87.254.5 on 09/05/12
For personal use only.

TABLE 4. Virtual a_w's of KNO_3 at 25 °C beyond 3.8 m by the Zdanovskii method: ternary systems X(1)–KNO_3(2)–H_2O

Electrolyte partner X(1)	a_w	Ternary solutions m_1	Ternary solutions m_2	Isopiestic binary solutions m_{01}	Isopiestic binary solutions m_{02}(calcd)
KCl	0.9157	1.6042	1.6049	2.6374	4.5955
$NaNO_3$	0.9148	1.8357	1.8817	3.0584	4.7846
KCl	0.9055	1.8260	1.8362	2.9474	5.5317
KCl	0.9039	1.8607	1.8615	2.9957	5.6485
NaCl	0.8947	1.8541	1.8623	2.9621	7.6328

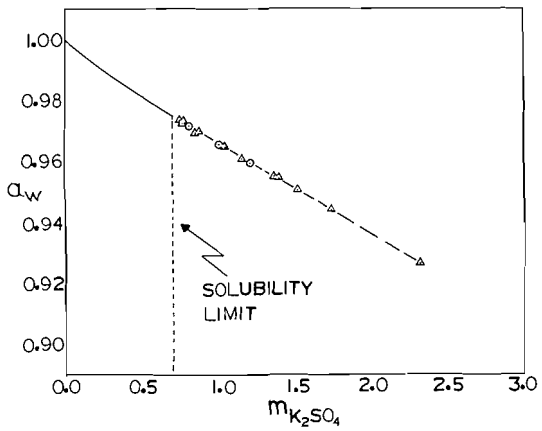

FIG. 2. Water activities of K_2SO_4 solutions at 25 °C. △ Zdanovskii method (average values); ⊙ weighted extrapolation.

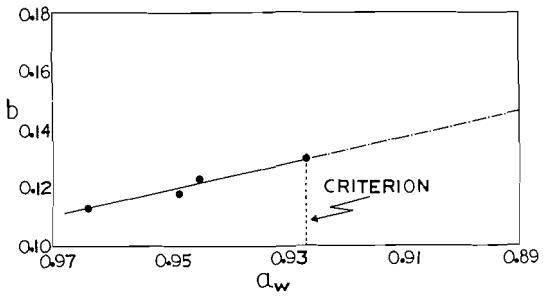

FIG. 3. The Zdanovskii deviation parameter b as a function of water activity for the system NaCl–KNO_3–H_2O.

Discussion

(a) Check of the Method Using the "Known" Salt, $NaNO_3$

Figure 1 shows that the a_w values calculated by our method follow quite closely the experimental line. The maximum value of the deviation $|m_{02}(\text{exptl.}) - m_{02}(\text{calcd.})| = \Delta m(\text{max})$ from Table 1 is 0.13 m, and the average deviation

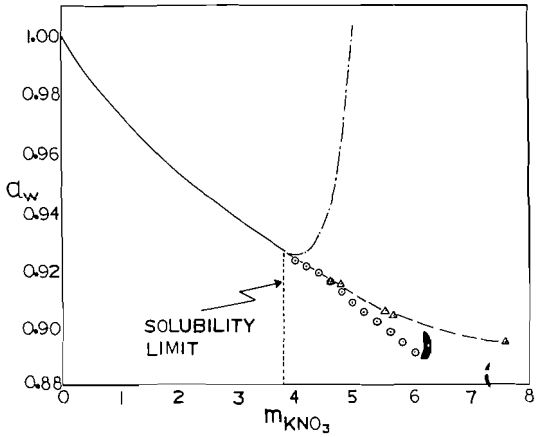

FIG. 4. Water activities of KNO_3 solutions at 25 °C. △ Zdanovskii method (average values); ⊙ weighted extrapolation; ----- extrapolation of polynomial fitted in the range 0–3.8 m.

Δm (ave) is 0.032 m. The corresponding values for Δa_w(max) and Δa_w(ave) are 0.0031 and 0.0007. This suggests that the Zdanovskii method can be used to find virtual a_w's with an expected average uncertainty of approximately 0.0007, or 0.1% at $a_w = 0.8$.

(b) Virtual Water Activities of K_2SO_4 Solutions

Figure 2 shows virtual water activities of this salt up to 2.25 m. The extrapolated values found by Robinson (1) coincide with those found from the Zdanovskii method; these are compared at round molalities as follows (the first of each pair is Robinson's value): 0.8 m: 0.9718, 0.9720; 1.0 m: 0.9656, 0.9655; 1.2 m: 0.9595, 0.9595. Thus weighted extrapolation not far beyond the solubility limit yields results in accord with the Zdanovskii method.

(c) Virtual Water Activities of KNO_3 Solutions

Figure 4 shows that there is a divergence between weighted extrapolation values and those of the Zdanovskii method, at concentrations

Can. J. Chem. Downloaded from www.nrcresearchpress.com by 210.87.254.5 on 09/05/12
For personal use only.

much beyond the solubility limit. We believe the Zdanovskii method may be more reliable, for the following reasons. The weighted extrapolation method assumes a continuous uni-directional differential relation between the physical chemical properties of solutions of like salts. Though this may be justified in many examples, it is not necessarily true for all systems. The Zdanovskii method, when it uses group B and C systems, assumes a constant b_{ave} value (or, if b is strongly a_w-dependent, extrapolates an appropriate value) for a_w's beyond the solubility limit. This procedure, though it contains a residue of arbitrariness, does at least recognize a deviation parameter obtained from experiment. Insofar as it does so, the Zdanovskii method would seem to be inherently safer than simple weighted extrapolation.

The Zdanovskii method is strengthened if group A ternary systems are used, for then $b \simeq 0$, and no assumptions have to be made beyond the unlikelihood of a sudden large change in the value of b beyond the solubility limit. Both the weighted extrapolation and Zdanovskii methods are preferable to simple extrapolation of a_w–molality curves fitted by polynomials or other functions.

(d) The Use of "Virtual" Water Activities

Virtual water activities of single solutes are of great practical interest, since these would be required for prediction of a_w for concentrated multicomponent systems, either by the Zdanovskii method (4), or the more precise method of Reilly, Wood, and Robinson(2). These water activities can then be used to compute solubilities of salts in multicomponent systems, *i.e.*, to predict phase diagrams (16*a*, *b*).

The calculation of virtual a_w's by the present Zdanovskii method requires ternary solution data at water activities beyond the solubility limit of one of the solutes. Although the literature contains isopiestic data of a large number of ternary solutions, few of these data meet this requirement. Since virtual water activities are of definite practical importance, we hope that the necessary ternary data will soon be forthcoming.

We thank the National Research Council of Canada for financial aid.

1. R. A. ROBINSON, R. F. PLATFORD, and C. W. CHILDS. J. Solution Chem. **1**, 167 (1972).
2. P. J. REILLY, R. H. WOOD, and R. A. ROBINSON. J. Phys. Chem. **75**, 1305 (1971).
3. A. B. ZDANOVSKII. Tr. Solyanoi Lab. Akad. Nauk SSSR, No. 6, 1936.
4. H. CHEN, J. SANGSTER, T. T. TENG, and F. LENZI. Can. J. Chem. Eng. **51**, 234 (1973).
5. R. H. STOKES and R. A. ROBINSON. J. Phys. Chem. **70**, 2126 (1966).
6. A. N. KIRGINTSEV and A. V. LUK'YANOV. Russ9 J. Phys. Chem. **40**, 953 (1966).
7. A. F. HIDALGO and C. ORR. J. Chem. Eng. Data, **13**, 49 (1968).
8. R. A. ROBINSON and V. E. BOWER. J. Res. Natl. Bur. Stand. **69A**, 365 (1965).
9. R. A. ROBINSON, R. H. WOOD, and P. J. REILLY. J. Chem. Thermodyn. **3**, 461 (1971).
10. A. N. KIRGINTSEV and A. V. LUK'YANOV. Radiokhimiya, **6**, 449 (1964).
11. A. N. KIRGINTSEV and A. V. LUK'YANOV. Russ. J. Phys. Chem. **39**, 653 (1965).
12. C. P. BEZBORUAH, A. K. COVINGTON, and R. A. ROBINSON. J. Chem. Thermodyn. **2**, 431 (1970).
13. A. N. KIRGINTSEV and A. V. LUK'YANOV. Russ. J. Phys. Chem. **38**, 867 (1964).
14. A. N. KIRGINTSEV and A. V. LUK'YANOV. Russ. J. Phys. Chem. **39**, 389 (1965).
15. R. A. ROBINSON and R. H. STOKES. Electrolyte solutions. 2nd ed. (revised). Butterworths, London. 1970.
16. (*a*) A. B. ZDANOVSKII. Zh. Fiz. Khim. **22**, 1475 (1948); (*b*) A. B. ZDANOVSKII. Tr. Vsesoyuz. Nauchn.-Issled. Inst. Galurgii, 26 (1949).

Can. J. Chem. Downloaded from www.nrcresearchpress.com by 210.87.254.5 on 09/05/12
For personal use only.

Isotropic Nuclear Magnetic Resonance Shifts of Co(II) Complexes with Mixed Ligands

D. R. EATON AND K. L. CHUA

Department of Chemistry, McMaster University, Hamilton, Ontario

Received February 15, 1973

Isotropic n.m.r. shifts of several Co(II) complexes involving β-diketonate ligands are reported. A change of substituent on one β-diketonate ligand significantly affects the shifts of protons or fluorine atoms on the other β-diketonate ligand of the same compound. An argument is presented to suggest that these substituent shifts arise predominantly from contact rather than dipolar effects. The pattern of shifts is compared with that previously observed for β-diketone complexes of V(III) and a similar interpretation is proposed.

Les déplacements chimiques isotropes (en r.m.n.) de plusieurs complexes du Co(II) contenant des coordinats du type β-dicétonate ont été étudiés. Le changement d'un substituant sur un des coordinats β-dicétonate a modifié de manière significative les déplacements chimiques des protons ou des fluors sur l'autre coordinat β-dicétonate du même composé. On présente alors une hypothèse selon laquelle les déplacements chimiques des substituants proviennent principalement des effets de contact plutôt que des effets dipolaires. Le patron des déplacements chimiques est comparé à celui observé antérieurement pour des complexes de V(III) contenant des coordinats β-dicétone; une interprétation similaire est avancée.
[Traduit par le journal]

Can. J. Chem., 51, 2632 (1973)

Introduction

The isotropic shifts observed in the n.m.r. spectra of paramagnetic transition metal complexes provide a sensitive method for the investigation of bonding in transition metal complexes. We have been interested of late in utilizing this method to study the transmission of substituent effects in complexes with mixed ligands. Such studies have been reported involving octahedral complexes of V(III) (1,2) and of Cr(II) (3) and tetrahedral complexes of Ni(II) (4). The detailed interpretation of the results has varied in the different cases but all show the common feature that the effects observed have been attributed to contact rather than dipolar interactions. In principle, the introduction of a substituent in a metal complex can induce a change in the magnetic anisotropy of a molecule and hence cause dipolar shifts. If large, such an effect could invalidate interpretations based on contact mechanisms. It seemed worthwhile to investigate the magnitude of such dipolar shifts by choosing to work with complexes in which they are expected to be present. Such a study would at least provide an indication of the errors which could arise from the neglect of dipolar interactions in other systems. The present paper reports some results obtained in this area.

Distorted octahedral complexes of Co(II) are known to possess large magnetic anisotropies and therefore to exhibit dipolar shifts (5). Complexes of the stoichiometry $Co(acac)_2L_2$ (acac = acetylacetonate, and L = a wide variety of monodentate ligands) have been extensively studied (6–10). Most of these studies have been concerned with the isotropic shifts of protons on the ligand, L. LaMar (11), however, has reported large differences in the acac shifts with changes in the ligand L. He concluded that these changes were dipolar in origin. Comparison of the shifts of the protons on L with those on the acac ligand lead to the conclusion that the species in solution had distorted octahedral geometry with the L ligands occupying *trans* positions. The shifts of the acac protons were interpreted as arising from a combination of dipolar and contact effects and a series of ligands L was presented in which the contact contribution becomes progressively more dominant. More recently Horrocks and Hall (12) have measured the anisotropy of the magnetic susceptibility of a single crystal of the compound in which L = pyridine and used this data to calculate the dipolar contribution to the isotropic n.m.r. shifts. Their conclusions are consistent with the interpretation presented by LaMar.

Results

In the present experiments the intent was to investigate the effect of making a substituent change on one of the β-diketone ligands on the

Can. J. Chem. Downloaded from www.nrcresearchpress.com by 210.87.254.42 on 09/05/12
For personal use only.

TABLE 1. Isotropic n.m.r. shifts* of Co(II) β-diketonate complexes

Compound†	Resonance	Shift for L = Pyridine	CD_3CN	DMSO	Dioxane
X = CH_3	CH_3	−2518	− 878	−1992	—
1	CH	−2151	− 656	− 7	—
X = C_6H_5	ortho	−2629	−2369	−2294	—
2	meta	− 886	− 856	− 812	—
	para	− 564	− 614	− 474	—
	CH	−1390	−1645	+ 80	—
X = $C(CH_3)_3$	$C(CH_3)_3$	−1740	−1190	−1290	—
3	CH	—1316	− 671	+1461	—
X = CF_3	CF_3	−3400	−4065	−3279	−3092
4	CH	+2460	− 274	+2536	+3582

*Shifts in Hz at 100 MHz, 33 °C.
†$Co(XCO.CH.CO.X)_2L_2$; ligand 1–4, see text.

TABLE 2. Isotropic n.m.r. shifts* of mixed Co(II) complexes

Compound†	Resonance	Shift for L = Pyridine	DMSO
X = CH_3(**1**)	CH_3	−2454	‡
Y = C_6H_5(**2**)	CH_x	−2005	
	CH_y	−1674	
	ortho	−2704	
	meta	− 920	
	para	− 594	
X = CH_3(**1**)	CH_3	—	‡
Y = $C(CH_3)_3$(**3**)	CH_x	−1951	
	CH_y	−2418	
	$C(CH_3)_3$	−1949	
X = C_6H_5(**2**)	$C(CH_3)_3$	−1850	−1538
Y = $C(CH_3)_3$(**3**)	CH_x	−1724	+ 948
	CH_y	—	—
	ortho	−2478	−1834
	meta	− 864	− 669
	para	− 492	− 326
X = CH_3(**1**)	CH_3	−2100	−1910
Y = CF_3(**4**)	CH_x	−1891	+ 897
	CH_y	+ 901	+1746
	CF_3	‡	‡

*Shifts in Hz at 100 MHz, 33 °C.
†$Co(XCOCHCOX)(YCOCHCOY)L_2$.
‡Not observed.

isotropic shifts of the other β-diketone ligand. By using different monodentate ligands L we hoped to vary the proportions of the dipolar and contact contributions to the isotropic shifts and hence deduce whether the substituent changes are predominantly dipolar or contact in origin. It was first necessary to measure the shifts for several symmetric chelates with different substituents on the β-diketone. Each chelate was examined with several different axial ligands L. These results are presented in Table 1. We then proceeded to examine the mixed chelates to ascertain the substituent effects. Results for mixed chelates are given in Table 2.

The β-diketone ligands involved have structures **1**–**4**. Co(II) chelates of β-diketone ligands tend to be polymeric in non-coordinating solvents such as chloroform. This is manifested by

Can. J. Chem. Downloaded from www.nrcresearchpress.com by 210.87.254.42 on 09/05/12
For personal use only.

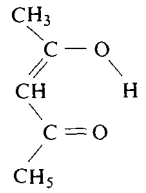

1

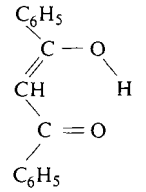

2

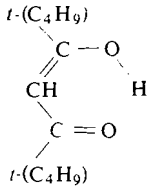

3

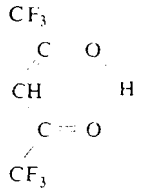

4

the appearance of a complex n.m.r. spectrum. However in coordinating solvents a two line spectrum appears which is assigned to octahedral species such as $Co(acac)_2L_2$. With excess of ligand L this is the only species present. Excess can be assured by using L as the solvent. Since we are interested only in the β-diketone resonances deuterated solvents were used throughout. Addition of a second β-diketone ligand to such a solution leads to the formation of mixed chelates. Thus if ligand **4** is added to a solution of the Co(II) complex of ligand **1** in pyridine additional lines appear attributable to the mixed chelate. On continued addition the resonances attributable to the symmetric chelate with ligand **4** appear. The correctness of the assignments of the mixed ligand complex can then be checked by adding ligand **1** to the Co(II) chelate of ligand **4**. In simple systems such as these there are no assignment problems.

A number of difficulties restricted the systems available for study. For some of the complexes the lines are exceedingly broad. This is particularly true for compounds in which the β-diketone has trifluoromethyl substituents. LaMar (11) noted similar linewidth variations, though not so pronounced, and suggested that they arose from varying electron spin relaxation times due to spin–orbit interaction with low lying excited states. Relatively slow exchange with ligand L is also possible. Measurement of the temperature dependence of the shifts revealed some deviations from Curie law below −25 °C which could be due to slowing down of the fast exchange between free and complexed axial ligand. However we would not disagree with LaMar's explanation of the linewidth effects. Measurements in some solvents were also limited by oxidation of the complexes.

Discussion

Although the data available are limited we are able to arrive at a relatively unambiguous conclusion regarding the importance of dipolar effects. It is apparent from the results in Table 2 that significant substituent effects are observed in some, but not all, cases.

Mixed complexes involving the ligands **1** and **2**, **1** and **3**, **1** and **4**, and **2** and **3** have been examined with L = pyridine and L = dimethylsulfoxide. Significant substituent shifts are observed in all cases with L = pyridine and in the last two cases with L = dimethylsulfoxide. It is not certain whether the inability to observe shifts in the remaining two cases is due to the shifts being too small to observe, to the resonances of the mixed chelates being too broad to observe, or to the failure to form mixed complexes. In cases where the shifts of two or more resonances on the same mixed chelate are observed they are in the same direction relative to the symmetric chelate, *e.g.* both the CH_3 and the CH resonance of ligand **1** move to high field in the mixed complex with ligand **4**. The most significant observation though is that in each case resonances on one ligand are shifted in the opposite direction to those on the other ligand in a mixed complex. Thus in the series of mixed complexes with L = pyridine the CH resonance of ligand **1** is shifted +146, +200, and +360 Hz from its position in the symmetric $Co(acac)_2L_2$ for the cases in which the second ligand is **2**, **3**, and **4**, respectively. The CH resonance of the second ligand is concurrently shifted −284, −1102, and −1559 Hz when this ligand is **2**, **3**, or **4**, respectively. Examination of the data in Tables 1 and 2 reveals that this pattern holds throughout.

The pyridine ligands of $Co(acac)_2py_2$ are exchanging rapidly with free ligand in solution on the n.m.r. time scale. It is therefore permissible (12) to neglect the orientation of the pyridine molecule with respect to the metal–nitrogen bond when considering the geometry of the $Co(acac)_2py_2$ molecule. Given that the complex has a *trans* configuration (11) the symmetry of the molecule is therefore D_{2h}. The magnetic susceptibility tensor has three principal axes uniquely defined by the symmetry axes of

Can. J. Chem. Downloaded from www.nrcresearchpress.com by 210.87.254.42 on 09/05/12
For personal use only.

Can. J. Chem. Downloaded from www.nrcresearchpress.com by 210.87.254.42 on 09/05/12
For personal use only.

the molecule. If one of the acac ligands is replaced by hfac (ligand **4**) C_{2v} symmetry is retained. The elements of symmetry of the C_{2v} point group (a C_2 axis and two planes) suffice to define three principal axes for the magnetic susceptibility which are identical with those of $Co(acac)_2py_2$. The dipolar shift of a proton is given by the expression (12)

$$\frac{\Delta\nu}{\nu}\text{dip} = -\frac{1}{3N}\left[\chi_z - \frac{\chi_x}{2} - \frac{\chi_y}{2}\right]\left(\frac{3\cos 2\theta - 1}{r^3}\right)_{av} - \frac{1}{2N}[\chi_x - \chi_y]\left(\frac{\sin^2\theta\cos 2\Omega}{r^3}\right)_{av}$$

In this expression θ and Ω are angles relating the position of the proton in question to the principal axes of the magnetic susceptibility tensor. The angular functions in this expression have identical values for the two CH protons of $Co(acac)_2L_2$ since they are equivalent by symmetry. Since both the positions of the CH protons and the directions of the principal axes are unchanged on passing to Co(acac) (hfac)py_2 it follows that the angular functions for the two CH protons of this mixed complex are also identical. Any change in the dipolar shift of the two protons resulting from a change in the magnetic anisotropy of the mixed chelate compared with the symmetric chelate must therefore be identical in sign and magnitude for both protons. This is clearly not the case, in fact in every compound examined the two protons in question shift in opposite directions. We deduce therefore that the substituent shifts are predominantly contact in origin and that any dipolar component, if present, is relatively small.

Given this conclusion it becomes valid to compare the present results with those previously reported (1,2) for V(III) complexes which were also interpreted assuming a contact mechanism. Octahedral Co(II) complexes have a T_1 ground state which splits to A and E states on application of a tetragonal distortion.[1] In the present case the A state is lower and is separated from the excited E state by the tetragonal distortion energy ζ. The V(III) complexes also have a nondegenerate ground state. The type of effects predicted (13) for mixed complexes arising from an orbitally degenerate ground state and observed with Cr(II) compounds (3) are therefore not to be anticipated. Consider specifically the CH resonances which are common to all the ligands used. LaMar (11) suggested that the shift of this proton in the Co(II) complexes resulted from the combination of a downfield dipolar shift and an upfield contact shift with the dipolar shift becoming progressively less important as the tetragonal splitting ζ becomes larger. In the A ground state of the molecule the unpaired electrons occupy the d_{xy}, $d_{x^2-y^2}$ and d_{z^2} orbitals. The results in Table 1 show that the CH shifts of the symmetric complexes with ligands **2**, **3**, and **4** are all to high field of those for ligand **1** with the same axial ligand L^2 and hence we deduce that ζ is larger for these ligands and that mixing of the A state with excited states through spin–orbit coupling less important. If we consider only the ground state configuration direct delocalization of spin to the π orbitals of the β-diketonate ligand cannot occur since none of the spin containing orbitals d_{xy}, $d_{x^2-y^2}$ or d_{z^2} has the correct symmetry to mix with the π orbitals of ligands in the xy plane. If the spin is in the π system, as the most recent analyses has concluded (14), an indirect or polarization mechanism must be involved. According to the model originally proposed by Levy and Orgel (15) such a mechanism will lead to a preference for electrons of α spin in the d_{xz}, d_{yz} orbitals and a corresponding preponderance of β spin delocalized to the ligands. The situation in the V(III) complexes is exactly the opposite with the unpaired electrons being contained in d orbitals with the correct symmetry to interact with ligand π orbitals leading to α spin delocalization. In this manner the opposite signs of the contact shift in the two cases may be rationalized.

Consider now the results for the mixed complexes contained in Table 2. In the V(III) case in mixed complexes of acac (ligand **1**) and hfac (ligand **4**) the CH of the acac is shifted to low field and that of the hfac to high field (1). In the Co(II) case the acac resonance moves to high field and the hfac resonance to low field. If α spin delocalization is involved in the first case and β spin delocalization in the second case the results are clearly equivalent. Our analysis of the V(III) system involved two factors the first dependent on the populations of the various spin containing d orbitals and the second on the

[1]The further small splitting of the E state if the symmetry is D_{2h} rather than D_{4h} can be neglected in this discussion.

[2]The CH shift of ligand **1** in acetonitrile appears anomalous in this respect.

ability of a ligand oxygen to accept an electron, *i.e.*, on its charge. These factors usually acted in concert to enhance the shifts. In the Co(II) case the first factor is inapplicable since the interacting d orbitals are in all cases fully populated. The second factor, however, remains operative and reflects the movement of charge in the σ system brought about by substituent changes on other ligands. It may be significant that the substituent shifts are on the whole smaller in the Co(II) compounds than in the V(III) compounds. The implication is that they cannot be amplified by changes in orbital populations.

It would not be advisable to extend this analysis in a quantitative manner. It suffers from all the limitations discussed previously in the V(III) case plus the added complication that dipolar effects, although not predominant, may still be of some importance. The significant point is perhaps the observation of substituent effects of the same type as those previously observed in V(III) complexes in a system involving a different metal and a different delocalization mechanism. We would suggest that such effects may be of quite general importance in transition metal chemistry and that isotropic n.m.r. shifts may provide a very convenient probe. We also conclude that contact effects are more important than dipolar effects in determining changes in the isotropic shifts caused by ligand substitution. This is consistent with an earlier suggestion (16) regarding isotropic shifts in first row transition metal complexes but in no way disagrees with the results of Horrocks and Hall (12) showing that there is a substantial dipolar contribution to the absolute shifts in these Co(II) compounds.

Experimental

Source of Chemicals

Co(II) acetylacetonate and Ni(II) acetylacetonate were obtained from the Research Organic/Inorganic Chemical Co. and $CoCl_2 \cdot 6H_2O$ from D.B.D.H. Laboratory. Hexafluoroacetylacetone, 1,3-diphenyl-1,3-propanedione, and 2,2,6,6-tetramethyl-3,5-heptanedione were purchased from Eastman Kodak Co. and dimethylsulfoxide-d_6, pyridine-d_5, and acetonitrile-d_3 from Merck Sharp and Dohme Co.

Preparation of Compounds

The Co(II) β-diketone complexes were prepared as follows.

The appropriate ligand (0.02 mol) was dissolved in a small amount of methanol and added to about 30 ml of distilled water with stirring. The mixture was heated gently and 6 *N* ammonia solution added until the solution showed slightly basic to litmus paper. A second solution was prepared by dissolving 0.1 *M* $CoCl_2 \cdot 6H_2O$ in about 30 ml of distilled water. The two solutions were mixed with stirring. (If no precipitate appeared, more ammonia was added until a precipitate did appear, then 4 drops excess were added.) The precipitate was collected, washed with H_2O, and dried under vacuum.

Sample Preparation

Solution of di-adduct of Co(II) β-diketonate was prepared by adding the coordinating solvent to the corresponding β-diketonate in the mole-ratio of 320:1 so that the coordinating solvent was present in excess to ensure that all the Co(II) β-diketonate was coordinated and existed in a monomeric form. CCl_4 was then added to give a final concentration of 0.005 *N*.

Proton spectra were obtained using a Varian HA-100 instrument at 37 °C with TMS internal reference. ^{19}F spectra were obtained on a Varian DP 60 instrument using $CFCl_3$ internal reference, at 56.4 Mc/s and the shifts converted to 60 Mc/s.

We are indebted to the National Research Council of Canada for financial support of this research.

1. D. R. EATON and K. L. CHUA. Can. J. Chem. **49**, 56 (1971).
2. D. R. EATON and K. L. CHUA. Can. J. Chem. In press.
3. G. N. LAMAR and G. R. VAN HECKE. J. Magn. Res. **4**, 384 (1971).
4. D. R. EATON and W. D. PHILLIPS. J. Chem. Phys. **43**, 392 (1965).
5. J. P. JESSON. J. Chem. Phys. **47**, 579 (1967).
6. J. A. HAPPE and R. L. WARD. J. Chem. Phys. **39**, 1211 (1963).
7. W. D. HORROCKS, R. C. TAYLO, and G. N. LAMAR. J. Am. Chem. Soc. **86**, 3031 (1964).
8. R. W. KLUIBER and W. D. HORROCKS. Inorg. Chem. **6**, 166 (1967).
9. R. W. KLUIBER and S. KOPYCINSKI. J. Inorg. Nucl. Chem. **30**, 1891 (1968).
10. T. VONEZAWZ, I. MORISHIMA, Y. AKANA, and K. FUKUTA. Bull. Chem. Soc. Jap. **43**, 379 (1970).
11. G. N. LAMAR. J. Magn. Res. **1**, 185 (1969).
12. W. D. HORROCKS and D. W. HALL. Inorg. Chem. **10**, 2368 (1971).
13. W. C. LIN and L. E. ORGEL. Mol. Phys. **7**, 130 (1964).
14. M. J. SCARLETT, A. T. CASEY, and R. A. CRAIG. Aust. J. Chem. **24**, 31 (1971).
15. D. A. LEVY and L. E. ORGEL. Mol. Phys. **3**, 583 (1960).
16. D. R. EATON. J. Am. Chem. Soc. **87**, 3097 (1965).

Can. J. Chem. Downloaded from www.nrcresearchpress.com by 210.87.254.42 on 09/05/12
For personal use only.

Crystal and Molecular Structure of the Synthetic Intermediate, 2-Bromo-3-methoxy-5-hydroxy-5,6,7,8,9,10,13,14-octahydro-8-methyl-10,13-*N*-acetylaminomethano-phenanthrene, $C_{19}H_{24}O_3NBr$

H. LYNTON and P. Y. SIEW

Department of Chemistry, University of New Brunswick, Fredericton, New Brunswick

Received March 5, 1973

Crystals of the synthetic intermediate, 2-bromo-3-methoxy-5-hydroxy-5,6,7,8,9,10,13,14-octahydro-8-methyl-10,13-*N*-acetyl aminomethano-phenanthrene, $C_{19}H_{24}O_3NBr$, are monoclinic, space group $P2_1/n$, unit cell dimensions $a = 10.62(1)$, $b = 14.47(2)$, $c = 23.88(2)$ Å, $\beta = 99.4(2)°$, $z = 8$ with two molecules in the asymmetric unit. The structure was solved by the heavy atom method and refined by full matrix least squares to $R = 0.096$ for 2120 observed reflections. The conformation was found to be *cis* at the junction between rings A and B making further cyclization to obtain an A ring nitrogen bridge not possible.

Les cristaux de l'intermédiaire synthétique, bromo-2 méthoxy-3 hydroxy-5, octahydro-5,6,7,8,9,10,13,14 méthyl-8, *N*-acétylaminoéthano-10,13 phénanthène, $C_{19}H_{24}O_3NBr$, sont du type monoclinique appartenant au groupe $P2_1/n$ dont les dimensions de la maille unitaire sont $a = 10.62(1)$, $b = 14.47(2)$, $c = 23.88(2)$ Å, $\beta = 99.4(2)°$, $z = 8$ avec deux molécules par maille asymétrique. La structure a été élucidée par la méthode des atomes lourds et a été raffinée à l'aide de la méthode des moindres carrés (matrice complète) jusqu'à $R = 0.096$ et ce, pour 2120 réflections observées. On a trouvé que la conformation est du type *cis* à la jonction entre les cycles A et B ce qui entraîne l'impossibilité de former par cyclisation subséquente un anneau du type A contenant un azote qui forme un pont.

[Traduit par le journal]

Can. J. Chem., **51**, 2637 (1973

Introduction

In the light of a possible synthesis of the alkaloid songorine, $C_{21}H_{30}O_3N$ (**1**), a stereospecific synthesis of a prerequisite intermediate pentacyclic keto lactam, $C_{17}H_{19}O_4N$ (**2**), has been reported (1). Prior attempts to look for potential intermediates resulted in the synthesis of 2-bromo-3-methoxy-5-hydroxy-5,6,7,8,9,10,13,14-octahydro-8-methyl-10,13-*N*-acetylaminomethano-phenanthrene, $C_{19}H_{24}O_3NBr$ (**3**). As the stereochemistry of compound (**3**) could not be fully established from spectroscopic data, an X-ray structure analysis was undertaken.

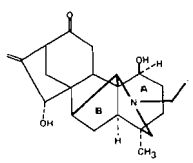

1

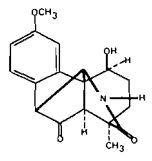

2

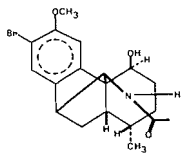

3

Results

Crystal Data

$C_{19}H_{24}O_3NBr$ m.w. = 395.3 Monoclinic, $a = 10.62(1)$, $b = 14.47(2)$, $c = 23.88(2)$ Å, $\beta = 99.4(2)°$, $v = 3620$ Å^3, $\rho_0 = 1.42(1)$ gm cm^{-3}, $z = 8$, $\rho_c = 1.42$ gm cm^{-3} (20 °C, MoKα, $\lambda = 0.71069$ Å). The space group is $P2_1/n$ ($C^5{}_{2h}$) No. 14 in *International Tables for X-ray Crystallography Vol. 1* (2) with two molecules in the asymmetric unit.

X-Ray Data

The intensity data were collected on a Picker computer-controlled four angle diffractometer using a $\theta/2\theta$ scan with β-filtered MoKα radiation and a scintillation detector. A scan speed of 1°/min was used with a scan range of 1.5° corrected for dispersion. The background count was taken for 20 s at each end of the scan range. Data were corrected against a standard reflection taken at intervals of 20 readings. The *hkl* and $\bar{h}kl$ octants were explored to a maximum 2θ of 40°. There were 3380 accessible reflections in this region of which 2120 were considered observed. The threshold count was taken as 0.05 times the background count or 5 counts, whichever was the greater. The crystal was needle

Can. J. Chem. Downloaded from www.nrcresearchpress.com by 210.87.254.5 on 09/05/12
For personal use only.

shaped with dimensions 0.40 × 0.24 × 0.20 mm^3. The needle axis *a*, was mounted parallel to the ϕ axis of the diffractometer. The linear absorption coefficient for MoKα radiation is μ = 17.8 cm^{-1}. No corrections were made for absorption or extinction.

Structure Analysis

A three-dimensional Patterson synthesis, and subsequent Fourier syntheses established all atoms other than hydrogen. All atoms are in general positions.

Refinement was carried out by minimizing the quantity $\sum\omega(|F_o| - |F_c|)^2$ for observed reflections only, using successive cycles of full-matrix least squares and anisotropic thermal parameters for all atoms. The weighting function used was $\omega = 1/1 + [(|F_o| - P_2)/P_1]^4$ with P_1 = 2 and P_2 = 11. Scattering factor curves used were those given in ref. 3, Table 3.3.1.A, with corrections for anomalous dispersion for bromine (ref. 3, Table 3.3.2.C.) The final agreement factor $R = \sum(||F_o| - |F_c||)/\sum|F_o|$ was 0.096. In the last cycle no parameter shift exceeded 0.1 times the established standard deviation. A difference synthesis showed residual peaks of height ranging from 0.3 to 0.9 e Å^{-3}. These were attributed to hydrogen atoms, although no attempt was made to establish their coordinates.

The table of final parameters and a set of structure factors based on these has been placed in the Depository of Unpublished Data.[1]

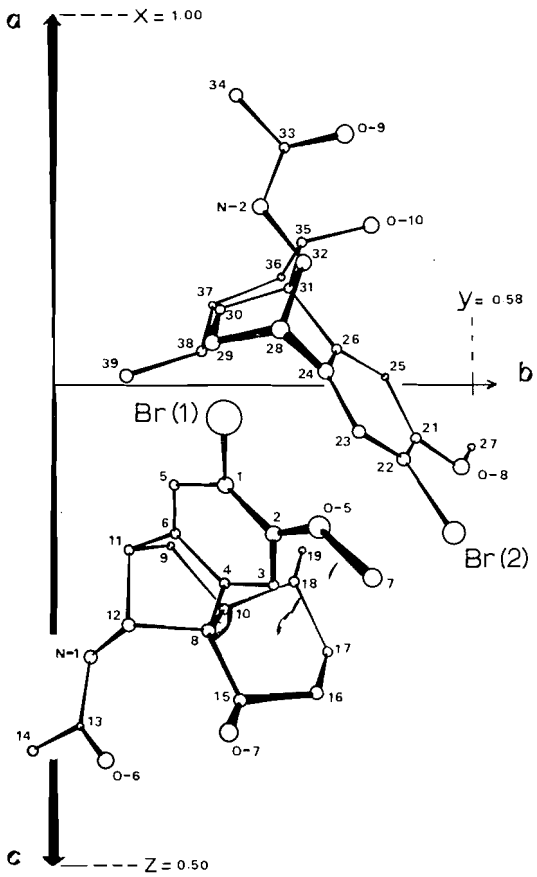

FIG. 1. Projection of the two molecule asymmetric unit (direction cosines of the normal to the plane of projection 0.707:0:0.707, refered to orthogonal axes X_o along *a*, Y_o along *b* and Z_o along *c**).

TABLE 1. Summary of bond distances for $C_{19}H_{24}O_3NBr$

Atoms		Distance (Å)
Ring system		
	C—C (aromatic)	1.38(3)–1.43(3)
	C—C	1.46(3)–1.63(3)
Side groups		
	C(ring)—O	1.37(2)
	C—O (alcohol)	1.42(3)–1.44(3)
	C—O (methoxy)	1.48(3)
	C=O	1.21(3)–1.25(3)
	C—N	1.43(2)–1.47(2)

Discussion

Figure 1 shows the relative orientation of the two molecules in the asymmetric unit. A brief summary of the bond distances is given in Table 1. The *cis* conformation between the A and B rings at C(8)[C(31)] and C(10)[C(30)] makes further cyclization of the A ring not possible between the nitrogen and the C(18)[C(38)] atom. As a consequence, this compound was considered to be of no further use as a possible intermediate in the alkaloid synthesis.

We wish to thank Dr. K. Wiesner for suggesting the problem, Dr. F. R. Ahmed of the National Research Council of Canada for use of his computer programs and the National Research Council of Canada for financial support.

1. K. WIESNER, P-T HO, D. CHANG, and J. F. BLOUNT. Experientia, **28**, 766 (1972).
2. International tables for X-ray crystallography. Vol. I. The Kynoch Press, Birmingham, England. 1965.
3. International tables for X-ray crystallography. Vol. III. The Kynoch Press, Birmingham, England. 1962.

[1]Complete set of tabular data is available, at a nominal charge, from the Depository of Unpublished Data, National Science Library, National Research Council of Canada, Ottawa, Canada, K1A 0S2.

Can. J. Chem. Downloaded from www.nrcresearchpress.com by 210.87.254.5 on 09/05/12
For personal use only.

Reversible Inhibition of the Esterase Activity of Carboxypeptidase A by Carboxylate Anions[1]

JOHN W. BUNTING AND CHESTER D. MYERS
Department of Chemistry, University of Toronto, Toronto, Ontario M5S 1A1

Received January 24, 1973

Reversible inhibition of the hydrolysis of *O*-(hippuryl)-L-3-phenyllactic acid by carboxypeptidase A has been studied for 26 carboxylate ion inhibitors at 25°, p*H* 7.5, and ionic strength 0.2 (NaCl). Competitive inhibition, partially competitive inhibition, and mixed inhibition kinetics were observed. Within homologous series, strictly competitive inhibition by the lower members gave way to partially competitive inhibition with higher members, while homologs having very large hydrocarbon moieties displayed mixed inhibition kinetics. Partially competitive inhibition in this system is not consistent with a scheme involving only 1:1 enzyme–inhibitor complexes; rather, higher order enzyme–inhibitor complexes will be necessary for a complete description of the inhibition mechanism.

Inhibition constants ($\log K_i$) for the aliphatic carboxylate ions which are strictly competitive inhibitors, are closely correlated linearly with Hansch's π-parameter for hydrophobicity. This *quantitatively* confirms the importance of hydrophobic interactions between carboxypeptidase A and inhibiting ions. Carboxylate ions containing aromatic rings are less effective inhibitors than expected on the basis of the π-parameters of their hydrocarbon moieties. The dependence of $\log K_i$ on π in this system is unusually strong for a binding phenomenon, and suggests that an inhibitor-dependent conformational change may also be involved.

L'inhibition réversible de l'hydrolyse de l'acide *O*-(hippuryl) phényl-3 L-lactique par la carboxypeptidase A a été étudiée par rapport à 26 inhibiteurs (ion carboxylate) à 25°; p*H* 7.5 et force ionique 0.2 (NaCl). On a observé des cinétiques d'inhibition compétitive, d'inhibition compétitive partielle et d'inhibition mixte. A l'intérieur d'une même série, l'inhibition seulement compétitive par des membres inférieurs a donné lieu à de l'inhibition compétitive partielle par les membres supérieurs alors que les homologues possédant des entités hydrocarbure très grandes possèdent un cinétique d'inhibition mixte. L'inhibition compétitive partielle dans ce système n'est pas en accord avec un processus impliquant des complexes inhibiteur–enzyme 1:1; au contraire, des complexes inhibiteur–enzyme d'ordre plus élevé seront nécessaires afin d'expliciter complètement le mécanisme d'inhibition.

Les constantes d'inhibition ($\log K_i$) pour les ions carboxylate aliphatique lesquels sont des inhibiteurs seulement de compétition, sont reliées intimement de façon linéaire avec le paramètre-π de Hansch en ce qui a trait à l'hydrophobie. Ce fait confirme *quantitativement* l'importance d'interactions hydrophobes entre la carboxypeptidase A et les ions responsables de l'inhibition beaucoup moins efficaces qu'il était prévisible en se basant sur les paramètres-π de leur entité hydrocarbure. La relation entre le $\log K_i$ et π dans ce système, est forte ce qui est inhabituel pour un phénomène de fixation et suggère ainsi qu'un changement conformationnel relié à l'inhibiteur peut ainsi être impliqué.

[Traduit par le journal]

Can. J. Chem., **51**, 2639 (1973)

Both the peptidase and esterase activities of carboxypeptidase A are well-known to be reversibly inhibited by carboxylate anions (1–9). Systematic studies on the dependence of the nature and extent of this inhibition on the structure of the inhibiting anion are lacking, however. A systematic study is particularly important in the light of the variety of inhibition mechanisms that have been observed for various carboxylate anions. Thus, competitive, non-competitive, and mixed inhibitory modes[2] have all been observed for different anions with a common substrate, carbobenzoxyglycyl-L-phenylalanine (1). On the other hand, both competitive and non-competitive inhibition kinetics have been observed for the same inhibitor against different peptide substrates. Furthermore, inhibition of peptidase activity by 3-phenylpropanoate (hydrocinnamate) ion has been suggested to be a mixture of competitive, non-competitive, and mixed inhibitory modes (11). Other studies of individual carboxylate ion inhibitors and assignment of inhibition modes abound in the literature.

Much of this work is clouded by the fact that inhibition studies have often been carried out at substrate concentrations where substrate activation or inhibition is also important. Consequently, some measured inhibition constants can only be considered to be "apparent" con-

[1]For a preliminary communication, see ref. 45.
[2]Terminology of Dixon and Webb (10).

Can. J. Chem. Downloaded from www.nrcresearchpress.com by 210.87.254.5 on 09/05/12
For personal use only.

Can. J. Chem. Downloaded from www.nrcresearchpress.com by 210.87.254.5 on 09/05/12
For personal use only.

stants rather than true binding constants, since the inhibitor molecules may be competing for either or both of the substrate binding sites (12, 13). The only substantial attempt (2) at correlating inhibitor structure with inhibitory capacity is marred by the fact that the substrate which was used (carbobenzoxyglycyl-L-tryptophan), displays substrate inhibition at the substrate concentration (0.05 *M*) at which the inhibitors were evaluated (14).

Interference from these substrate activation and inhibition phenomena in the assignment of inhibitory modes of peptidase activity has been overcome by the choice of tripeptide substrates which are relatively free of these effects (6). Depending upon the inhibitor chosen, competitive, non-competitive and mixed inhibition kinetics may still be observed, however. In a recent elegant study using a stopped-flow fluorescence technique (15), mixed inhibition kinetics with peptide substrates were shown to arise through a combination of competitive and non-competitive inhibitory modes. A sufficiently comprehensive study to allow the rationalization of the dependence of inhibitory mode on inhibitor structure was not attempted, however.

We feel that a comprehensive systematic study is required of the reversible inhibition of both the esterase and peptidase activities of carboxypeptidase A by carboxylate anions. Such a study should clarify many of the apparently anomalous, and sometimes contradictory, inhibition data that are in the literature, and at the same time may throw some light on the interpretation of the profound differences in the activity of this enzyme towards peptide and ester substrates (16–20). We report herein, the first part of such a study, into the dependence of the inhibition of esterase activity on the structure of aliphatic and aromatic carboxylate anion inhibitors, since many of the present results are of interest in their own right. Comparison will be made at a later time with a similar study, which is currently underway in our laboratory, on the inhibition of peptidase activity.

Experimental

Materials

All carboxylic acids were obtained commercially. Solids were recrystallized to melting points in agreement with literature values. Liquids were distilled, and fractions having boiling points consistent with literature data were selected. The identity of each carboxylic acid was also checked by p.m.r. spectroscopy. Stock solutions of the sodium salts of each carboxylic acid were prepared by careful titration of a known weight of the acid in aqueous solution (or suspension) to p*H* 7.5 with standard sodium hydroxide solution.

O-(Hippuryl)-L-3-phenyllactic acid was purchased from Fox Chemical Co., Los Angeles. Bovine carboxypeptidase A was obtained as a suspension in toluene from Worthington Biochemical Corp. Enzyme stock solutions were prepared by dialysis of this suspension against 1 *M* sodium chloride in 0.05 *M* tris buffer, p*H* 7.5, containing 10^{-4} *M* zinc nitrate at 4°. Enzyme concentrations were estimated spectrophotometrically at 278 nm ($\varepsilon = 6.42 \times 10^4\ M^{-1}\ cm^{-1}$) (21).

Methods

All reactions were studied at 25°, ionic strength 0.2 (NaCl), p*H* 7.5. Hydrolysis of the ester was followed by titration with standard potassium hydroxide solution (0.0025 *M*) on a p*H*-stat which consisted of the following Radiometer Corp. components: Syringe Buret SBUla, Type TTTlc Titrator and Type SBR2c Titrigraph. Substrate concentrations were always less than 4×10^{-4} *M*, so that substrate inhibition which becomes important at higher concentrations of *O*-(hippuryl)-L-3-phenyllactic acid could be neglected (18, 22, 23). Enzyme concentrations were in the range $7.1 \times 10^{-10} - 2.8 \times 10^{-9}$ *M*.

For each inhibitor, inhibition constants were determined by measuring initial velocities of the enzymic hydrolysis at approximately ten different substrate concentrations for each of two or more different inhibitor concentrations. The set of data at each inhibitor concentration was inspected graphically (E/v_0 *vs.* $1/S$) for linearity, and fitted by computer according to the regression technique of Wilkinson (24). For the uninhibited enzyme, the parameters obtained were $K_m = 7.18 \times 10^{-5}$ *M* and $k_{cat} = 2.50 \times 10^4\ min^{-1}$. Literature values for this substrate at p*H* 7.5, 25°, but at different ionic strengths, are in the ranges $K_m = (5.1 - 8.8) \times 10^{-5}$ *M* and $k_{cat} = (2.80 - 3.47) \times 10^4\ min^{-1}$ (23).

For those carboxylate anions that exhibited competitive inhibition kinetics, the apparent Michaelis constant, K_m^{app}, at inhibitor concentration *I*, was used to calculate the inhibition constant K_i, from the relationship (10)

$$K_i = I/(K_m^{app}/K_m - 1)$$

Light-scattering measurements were made on a Brice-Phoenix Universal 1000-D Light Scattering Photometer in solution under the same experimental conditions as were used for the kinetic experiments, except that the enzyme and substrate were absent.

Results

For each of the straight chain alkanoate ions from acetate to octanoate, reciprocal plots (E/v_0 *vs.* $1/S$) typical of competitive inhibition were obtained at a number of inhibitor concentrations (examples in Fig. 1). Calculation of inhibition constants at each inhibitor concentration gave values which were independent of the inhibitor concentration in the series from acetate to hexanoate ions (Table 1). However, for

Can. J. Chem. Downloaded from www.nrcresearchpress.com by 210.87.254.5 on 09/05/12
For personal use only.

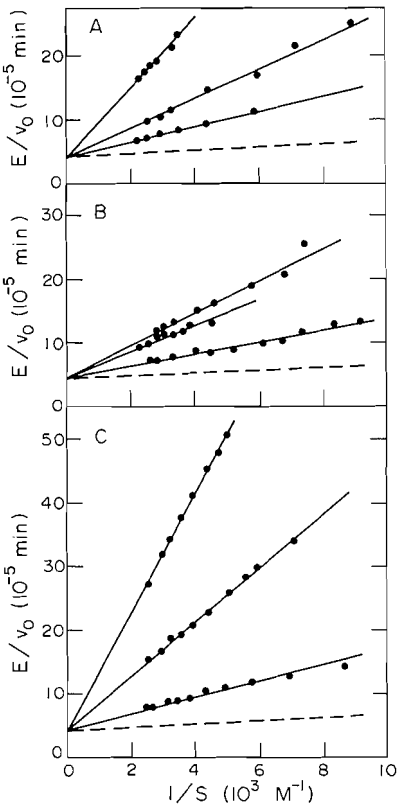

FIG. 1. Reciprocal plots for the inhibition of the hydrolysis of *O*-hippuryl-L-3-phenyllactic acid by carboxypeptidase A. A: propanoate, I = 21.3, 42.6, 63.9 mM; B: butanoate, I = 1.72, 2.58, 5.17 mM; C: octanoate, I = 2.02, 5.05, 8.07 mM. Dotted line indicates velocity in the absence of inhibitor.

the heptanoate and octanoate ions, the inhibition constants obtained were dependent on inhibitor concentration (Table 1), and in each case decreased with increasing inhibitor concentration. Such a phenomenon is typical of what has been termed partially competitive inhibition (10). With the nonanoate ion, the reciprocal plots are typical of mixed inhibition rather than competitive inhibition (Table 2).

Some branched chain alkanoate ions with small hydrocarbon moieties (up to five carbon atoms) also gave competitive inhibition constants that were independent of the inhibitor concentration (Table 1). Likewise, strictly competitive inhibition was also observed for the cyclopropane- and cyclobutanecarboxylate ions. However, cyclopentane- and cyclohexanecarboxylate ions displayed partially competitive inhibition, as was also the case for the cyclohexylacetate and 3-cyclohexylpropanoate ions (Table 1). With the 4-cyclohexylbutanoate ion, mixed inhibition kinetics were again observed (Table 2).

The benzoate and the ω-phenylalkanoate ions up to the 4-phenylbutanoate ion all displayed strictly competitive inhibition kinetics (Fig. 2 and Table 1). The slight trend in K_i apparent in Table 1 for the 5-phenylpentanoate ion may be due to partially competitive inhibition but experimental error cannot be completely ruled out. The 6-phenylhexanoate and also the 2-naphthalenecarboxylate ions gave mixed inhibition kinetics (Table 2).

The anionic inhibitors for carboxypeptidase A that were included in the present study display three characteristic types of reversible inhibition kinetics, *viz.* strictly competitive, partially competitive, and mixed inhibition. None of the carboxylate anions in the present study is a noncompetitive inhibitor for the hydrolysis of *O*-hippuryl-L-3-phenyllactic acid by this enzyme. Furthermore, a pattern to the dependence of the various types of inhibition on the size of the hydrocarbon moiety of the inhibiting ion is

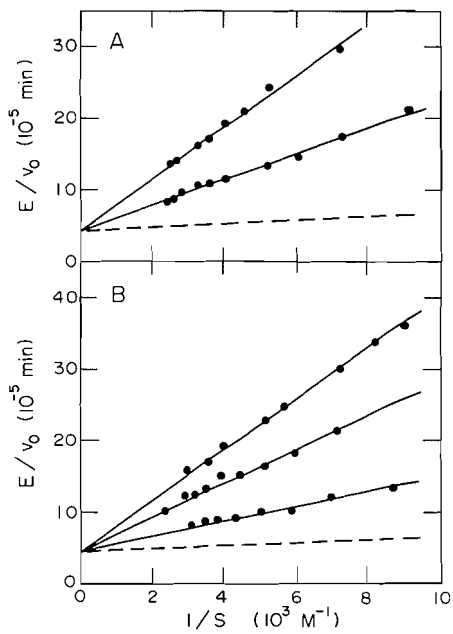

FIG. 2. Reciprocal plots for the inhibition of the hydrolysis of *O*-hippuryl-L-3-phenyllactic acid by carboxypeptidase A. A: phenylacetate, I = 2.81, 4.23 mM; B: 5-phenylpentanoate, I = 0.696, 2.26, 3.38 mM. Dotted line indicates the velocity in the absence of inhibitor.

TABLE 1. Inhibition constants for competitive inhibitors (RCO_2^-) of carboxypeptidase A*

No.	R	Inhibitor concentration (M)	% Inhibition†	K_m^{app} (M)	K_i (M)	Average K_i (M)
1	CH_3	8.34×10^{-2}	32	2.02×10^{-4}	4.60×10^{-2}	
		0.124	36	2.22×10^{-4}	5.93×10^{-2}	5.3×10^{-2}
2	CH_3CH_2	2.13×10^{-2}	56	4.06×10^{-4}	4.58×10^{-3}	
		4.26×10^{-2}	67	6.11×10^{-4}	5.67×10^{-3}	
		6.39×10^{-2}	77	1.00×10^{-3}	4.95×10^{-3}	5.1×10^{-3}
3	$CH_3(CH_2)_2$	1.72×10^{-3}	36	2.20×10^{-4}	8.35×10^{-4}	
		2.58×10^{-3}	49	3.31×10^{-4}	7.14×10^{-4}	
		5.17×10^{-3}	62	5.10×10^{-4}	8.40×10^{-4}	8.0×10^{-4}
4	$CH_3(CH_2)_3$	7.29×10^{-4}	48	3.13×10^{-4}	2.17×10^{-4}	
		1.46×10^{-3}	65	5.83×10^{-4}	2.04×10^{-4}	2.1×10^{-4}
5	$CH_3(CH_2)_4$	6.33×10^{-4}	33	2.06×10^{-4}	3.38×10^{-4}	
		1.26×10^{-3}	60	4.71×10^{-4}	2.27×10^{-4}	
		1.90×10^{-3}	69	6.58×10^{-4}	2.44×10^{-4}	2.7×10^{-4}
6	$CH_3(CH_2)_5$	9.88×10^{-4}	25	1.59×10^{-4}	5.12×10^{-4}	
		1.98×10^{-3}	60	4.86×10^{-4}	3.44×10^{-4}	
		2.97×10^{-3}	78	1.02×10^{-3}	2.26×10^{-4}	‡
7	$CH_3(CH_2)_6$	2.02×10^{-3}	30	1.95×10^{-4}	1.18×10^{-3}	
		4.04×10^{-3}	53	3.83×10^{-4}	9.24×10^{-4}	
		5.05×10^{-3}	70	6.77×10^{-4}	5.98×10^{-4}	
		8.07×10^{-3}	83	1.41×10^{-3}	4.10×10^{-4}	‡
8	$(CH_3)_2CH$	4.94×10^{-3}	42	2.69×10^{-4}	1.80×10^{-3}	
		9.90×10^{-3}	64	5.61×10^{-4}	1.45×10^{-3}	1.6×10^{-3}
9	$(CH_3)_2CHCH_2$	2.89×10^{-4}	40	2.37×10^{-4}	1.26×10^{-4}	
		1.16×10^{-3}	71	7.48×10^{-4}	1.24×10^{-4}	1.2×10^{-4}
10	$(CH_3)_3C$	1.04×10^{-3}	32	2.00×10^{-4}	5.81×10^{-4}	
		2.76×10^{-3}	53	3.80×10^{-4}	6.44×10^{-4}	6.1×10^{-4}
11	$(CH_3)_3CCH_2$	1.15×10^{-4}	40	2.35×10^{-4}	5.07×10^{-5}	
		9.22×10^{-4}	78	1.11×10^{-3}	6.40×10^{-5}	5.7×10^{-5}
12	Cyclopropyl	9.36×10^{-3}	58	4.58×10^{-4}	1.72×10^{-3}	
		1.87×10^{-2}	74	7.91×10^{-4}	1.87×10^{-3}	1.8×10^{-3}
13	Cyclobutyl	4.63×10^{-4}	48	3.29×10^{-4}	1.29×10^{-4}	
		7.14×10^{-4}	54	3.91×10^{-4}	1.60×10^{-4}	
		1.43×10^{-3}	75	8.52×10^{-4}	1.31×10^{-4}	1.4×10^{-4}
14	Cyclopentyl	5.89×10^{-4}	37	2.29×10^{-4}	2.69×10^{-4}	
		8.80×10^{-4}	68	6.30×10^{-4}	1.13×10^{-4}	
		1.17×10^{-3}	76	8.91×10^{-4}	1.02×10^{-4}	‡
15	Cyclohexyl (C_6H_{11})	1.02×10^{-3}	26	1.68×10^{-4}	7.85×10^{-4}	
		2.63×10^{-3}	63	5.54×10^{-4}	3.92×10^{-4}	
		3.93×10^{-3}	80	1.21×10^{-3}	2.49×10^{-4}	‡
16	$C_6H_{11}CH_2$	2.22×10^{-3}	26	1.69×10^{-4}	1.64×10^{-3}	
		3.69×10^{-3}	41	2.63×10^{-4}	1.38×10^{-3}	
		4.56×10^{-3}	51	3.57×10^{-4}	1.15×10^{-3}	
		5.54×10^{-3}	66	6.03×10^{-4}	7.50×10^{-4}	
		7.96×10^{-3}	78	1.04×10^{-3}	5.87×10^{-4}	‡
17	$C_6H_{11}(CH_2)_2$	5.97×10^{-4}	28	1.77×10^{-4}	4.06×10^{-4}	
		9.95×10^{-4}	46	2.90×10^{-4}	3.23×10^{-4}	
		1.59×10^{-3}	66	6.04×10^{-4}	2.15×10^{-4}	‡
18	C_6H_5	1.48×10^{-2}	41	2.40×10^{-4}	6.33×10^{-3}	
		2.95×10^{-2}	58	4.40×10^{-4}	5.75×10^{-3}	6.0×10^{-3}

Can. J. Chem. Downloaded from www.nrcresearchpress.com by 210.87.254.5 on 09/05/12
For personal use only.

TABLE 1 (*Concluded*).

No.	R	Inhibitor concentration (M)	% Inhibition†	K_m^{app} (M)	K_i (M)	Average K_i (M)
19	$C_6H_5CH_2$	2.81×10^{-3}	58	4.37×10^{-4}	5.51×10^{-4}	
		4.23×10^{-3}	70	6.90×10^{-4}	4.91×10^{-4}	5.2×10^{-4}
20	$C_6H_5(CH_2)_2$	2.50×10^{-4}	26	1.64×10^{-4}	1.95×10^{-4}	
		4.95×10^{-4}	47	3.05×10^{-4}	1.52×10^{-4}	1.7×10^{-4}
21	$C_6H_5(CH_2)_3$	8.75×10^{-4}	28	1.87×10^{-4}	5.47×10^{-4}	
		1.02×10^{-3}	29	1.90×10^{-4}	6.18×10^{-4}	
		1.74×10^{-3}	46	2.91×10^{-4}	5.70×10^{-4}	5.8×10^{-4}
22	$C_6H_5(CH_2)_4$	6.96×10^{-4}	26	1.63×10^{-4}	5.48×10^{-4}	
		2.26×10^{-3}	69	4.16×10^{-4}	4.72×10^{-4}	
		3.38×10^{-3}	79	6.58×10^{-4}	4.14×10^{-4}	‡

*At p*H* 7.5, 25°, ionic strength 0.2 (NaCl).
†At 2.0×10^{-4} M substrate.
‡K_i depends on inhibitor concentration, partially competitive inhibition.

TABLE 2. Parameters for inhibition of carboxypeptidase A by some carboxylate anion mixed Inhibitors*

Anion	Inhibitor concentration (M)	% Inhibition†	K_m^{app} (M)	k_{cat}^{app} (min^{-1})
Nonanoate	3.83×10^{-3}	59	1.70×10^{-4}	1.49×10^4
	6.22×10^{-3}	76	1.12×10^{-4}	7.27×10^3
	8.41×10^{-3}	78	9.15×10^{-4}	6.41×10^3
4-Cyclohexylbutanoate	8.59×10^{-4}	49	7.02×10^{-5}	1.38×10^4
	1.28×10^{-3}	62	1.73×10^{-4}	1.41×10^4
	2.11×10^{-3}	78	8.31×10^{-5}	6.15×10^3
6-Phenylhexanoate	9.49×10^{-4}	40	9.09×10^{-5}	1.69×10^4
	2.10×10^{-3}	62	4.82×10^{-5}	8.99×10^3
	2.63×10^{-3}	71	3.31×10^{-5}	6.78×10^3
2-Naphthalenecarboxylate	5.09×10^{-4}	42	3.38×10^{-5}	1.36×10^4
	1.52×10^{-3}	65	3.02×10^{-5}	8.04×10^3
	3.56×10^{-3}	89	9.75×10^{-5}	3.16×10^3

*At p*H* 7.5, 25°, ionic strength 0.2 (NaCl).
†At 2.0×10^{-4} M substrate.

apparent. In all cases, the lower members of the series are strictly competitive inhibitors; the inhibition changes to partially competitive with higher members of a series, and eventually to mixed inhibition with very large hydrocarbon moieties. The large 2-naphthalenecarboxylate ion is also a mixed inhibitor, whereas the analogous smaller benzoate ion is a strictly competitive inhibitor.

Dixon and Webb (10) have shown that partially competitive inhibition kinetics will arise from Scheme 1, in which the catalytic activities

$$E + S \rightleftharpoons E.S \qquad \text{Dissociation constant: } K_s$$
$$E + I \rightleftharpoons E.I \qquad K_i$$
$$E.I + S \rightleftharpoons E.I.S \qquad K_{is}$$
$$E.S + I \rightleftharpoons E.I.S \qquad K_{si}$$
$$E.S \xrightarrow{k} E + P$$
$$E.I.S \xrightarrow{k} E.I + P$$

SCHEME 1

of the two complexes E.S. and E.I.S are the

Can. J. Chem. Downloaded from www.nrcresearchpress.com by 210.87.254.5 on 09/05/12
For personal use only.

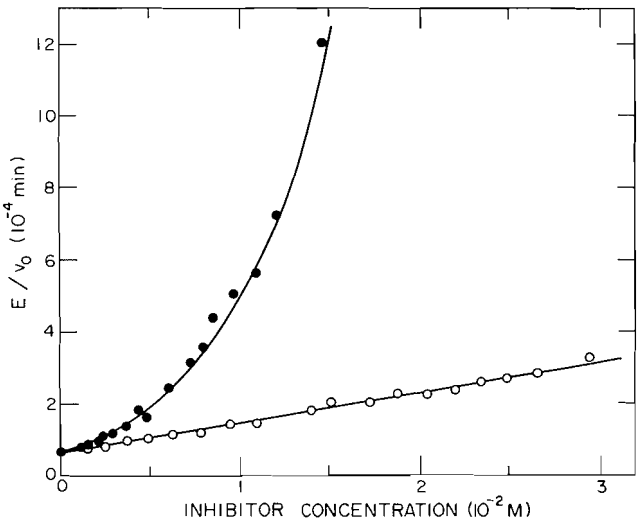

FIG. 3. Dependence of E/v_0 on I at 2.0×10^{-4} M substrate for cyclohexylacetate ion (●) and cyclopropanecarboxylate ion (○).

same. Scheme 1 gives rise to the dependence of initial velocity on inhibitor concentration in eq. 1. Equation 1 predicts that at constant sub-

$$[1] \qquad \frac{v_0}{E} = \frac{k}{1 + \frac{K_s}{S}\frac{(1 + I/K_i)}{(1 + I.K_s/K_i.K_{is})}}$$

strate concentration, a plot of E/v_0 *vs.* I should approach a maximum value at large inhibitor concentrations. However, the experimentally determined dependence of E/v_0 on inhibitor concentration for the cyclohexylacetate ion (a partially competitive inhibitor) in Fig. 3 shows no approach to a maximum over the experimentally accessible range of inhibitor concentration (up to 95% inhibition). Instead, the curve in Fig. 3 suggests a greater than first-power dependence on inhibitor concentration. Similar data for the cyclopropanecarboxylate ion is also included in Fig. 3. As expected for a strictly competitive inhibitor, the dependence of E/v_0 on I for this ion is linear (up to greater than 80% inhibition). From the slope of this plot we have estimated (10) a value of $K_i = 1.7 \times 10^{-3}$ M, which is in close agreement with the value obtained by varying the substrate concentration at constant inhibitor concentration (Table 1).

We therefore feel that the relatively simple scheme outlined above for partially competitive inhibition is not operative in the present cases. Reaction schemes involving complexes in which at least two inhibitor anions are bound to each enzyme molecule seem to be necessary in order to account for the observed dependence of K_i on inhibitor concentration for the anions with which we have observed partially competitive inhibition kinetics.

It is possible that the observation of partially competitive and mixed inhibition kinetics with some inhibitors in this study may perhaps be related to the tendency of the substrate, *O*-(hippuryl)-L-3-phenyllactic acid, to form higher order enzyme–substrate complexes (13, 22). We have attempted to minimize such effects by working only at substrate concentrations where substrate inhibition is minimal. However, the possibility exists that those anions that are not strictly competitive inhibitors, may be able to promote binding at one or both substrate binding sites via an initially formed enzyme–inhibitor complex. Kinetic schemes taking into account this possibility and also the higher order enzyme–inhibitor species noted above, would be relatively complex. At the present time, we do not have sufficient data to allow an analysis of the various kinetic schemes that are possible.

We thought that the occurrence of mixed inhibition kinetics with the largest anions may have been due to complications arising from the aggregation of these species to form micelles. However, a light scattering study of aqueous solutions of sodium 6-phenylhexanoate under

Can. J. Chem. Downloaded from www.nrcresearchpress.com by 210.87.254.5 on 09/05/12
For personal use only.

Can. J. Chem. Downloaded from www.nrcresearchpress.com by 210.87.254.5 on 09/05/12
For personal use only.

the experimental conditions used in the kinetic studies gave no evidence of aggregation at the concentrations used in the inhibition studies. Furthermore, literature data suggest that the critical micelle concentration for the nonanoate ion is greater than 0.1 *M* at 25° (25, 26), which is a much higher concentration than was used for the observation of mixed inhibition kinetics with this ion (Table 2). We therefore feel that micelle formation is not an important factor in the present studies, and should not be implicated in the interpretation of the various forms of inhibition kinetics that are observed.

Carboxypeptidase A catalyzes the hydrolysis of the C-terminal amide bonds of peptides and analogous ester bonds, with a preference for C-terminal amino acids (or α-hydroxycarboxylic acids) that have hydrocarbon side-chains (27). In general, it has been found that carboxylate anions with similar types of hydrocarbon moieties are reversible inhibitors of the enzyme (1–9). X-ray crystallographic studies of this enzyme in the crystalline state have indicated that the active-site region does contain a convenient hydrophobic pocket for the acceptance of such entities (28–31). In an attempt to quantitatively describe the observed inhibitor specificity we investigated the possibility that the inhibition constants of the strictly competitive inhibitor anions were related to the Hansch π-parameters (32–34) for their hydrocarbon groups. This parameter, which is based upon the distribution coefficients of solutes between water and 1-octanol, has often been successfully used to reflect hydrophobic character in linear free energy correlations (33). From Fig. 4, it is clear that the log K_i values for the aliphatic carboxylate ions that are strictly competitive inhibitors of esterase activity (except hexanoate) are closely correlated with π (correlation coefficient = 0.966), with the straight chain, branched chain and cyclic alkyl groups all being accommodated by the same line:

$$[2] \qquad -\log K_i = 1.77\pi + 0.50$$

The inhibitors containing aromatic rings are not accommodated by this same equation. The plot for the strictly competitive inhibitors, $C_6H_5(CH_2)_nCO_2^-$ ($n = 0$–3), is not linear, although the first two members may be considered to lie on a line of similar slope to that of eq. 2 (broken line in Fig. 4). The larger anions

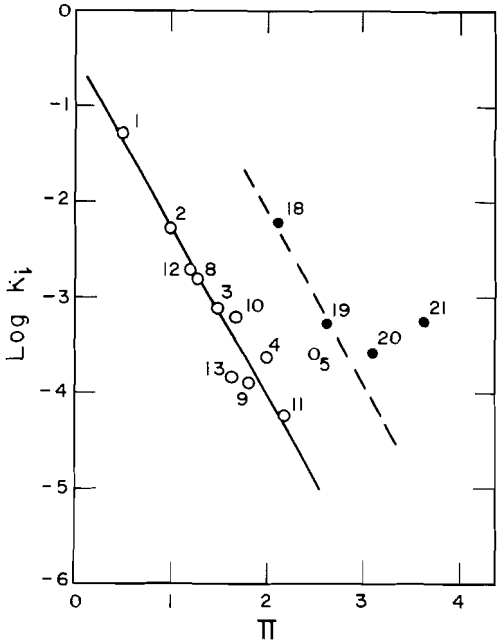

FIG. 4. Dependence of log K_i on π for strictly competitive inhibitor anions. Carboxylate ions are indicated by numbers which correspond to those in Table 1.

in this group ($n = 2$, 3) appear to be less effective inhibitors than the π values of their hydrocarbon groups would suggest, even allowing for an apparent inherent difference in inhibitory effectiveness between aliphatic and aromatic acids. Straight chain alkanoate ions larger than pentanoate, also are much less effective inhibitors than is consistent with their hydrophobic character. We feel that such hydrocarbon moieties are probably too large to fit into the hydrophobic pocket in their energetically most favorable conformations.

The pentanoate ion shows a slightly larger deviation from the correlation line in Fig. 4 than do any of the smaller aliphatic carboxylate ions. This suggests that the *n*-butyl group may be slightly longer than the maximum length that an *n*-alkyl group may be to fit into the hydrophobic pocket in its energetically most favorable conformation. Using Corey–Pauling–Koltun models, we have measured the distance from the carboxylate carbon atom to the end of the hydrocarbon chain in the pentanoate ion in its most extended conformation. This distance, 7.1 Å, should approximately reflect the length of the hydrophobic pocket that is accessible to an alkyl moiety.

Can. J. Chem. Downloaded from www.nrcresearchpress.com by 210.87.254.5 on 09/05/12
For personal use only.

Through eq. 2, one might predict that K_i for competitive inhibition of esterase activity by formate ion ($\pi = 0$) would be approximately 0.3 *M*. Thus, under our experimental conditions (ionic strength 0.2), the maximum concentration of formate ion (0.2 *M*) would lead to only 15% inhibition at substrate concentration 2×10^{-4} *M*.

Attempts to correlate the inhibition constant data with the steric parameter, E_s (35), or the electronic parameter, σ^* (35), rather than π, were unsuccessful. Thus, the 2,2-dimethylpropanoate ion and butanoate ions have similar K_i values (Table 1), although the E_s values of their alkyl groups are quite different (-1.54 for $(CH_3)_3C$; -0.36 for $CH_3CH_2CH_2$ (35)).

Discussion

In the past, the most extensively studied carboxylate ion inhibitors for carboxypeptidase A have been the phenylacetate and 3-phenylpropanoate ions. Literature values of K_i for these ions at p*H* 7.5 and 25° (but at various ionic strengths) lie in the range 0.39–0.73 m*M* for phenylacetate (1, 5, 6) and 0.062–0.19 m*M* for 3-phenylpropanoate (1, 5, 6, 7). Our inhibition constants for these two ions (Table 1) lie within these ranges. Our K_i value for the 4-phenylbutanoate ion (0.58 m*M*) is approximately half of two previously reported values (1.1 and 1.37 m*M* (1, 5)), although our data are consistent with previous reports that this ion is a less effective inhibitor than its next lower homolog, 3-phenylpropanoate (5). We have observed strictly competitive inhibition with each of these ions, which is in accord with studies on their inhibition of this enzyme towards *O*-hippuryl-L-mandelic acid (5) and carbobenzoxyglycyl-L-phenylalanine (1). However, a recent report (6) indicates that phenylacetate and 3-phenylpropanoate ions act as non-competitive inhibitors for the hydrolysis of carbobenzoxyglycylglycyl-L-phenylalanine and hippuryl-L-phenylalanine.

On several occasions (2, 4), acetate ion has been reported not to inhibit this enzyme, even in one case (2), in the presence of 1 *M* sodium acetate. Our data suggest that this ion is a significant inhibitor of esterase activity (K_i = 53 m*M*). Although an early report suggests that propanoate and butanoate ions display mixed inhibition kinetics towards carbobenzoxyglycyl-L-phenylalanine hydrolysis (1), we find that all the simple alkanoate ions are competitive inhibitors for the hydrolysis of *O*-hippuryl-L-3-phenyllactic acid. Similarly, benzoate ion is a strictly competitive inhibitor in our study, which was not the case in an earlier investigation (1).

Some of these apparently anomalous results may be due to the differences that have been observed between the peptidase and esterase activities of carboxypeptidase A (16–20), and also possibly to differences in experimental conditions. Furthermore, it has recently been demonstrated (15) that the phenylacetate, 3-phenylpropanoate, 3-iodopropanoate, and butanoate ions simultaneously display both competitive and non-competitive components in their inhibition of dansyl-glycyl-L-tryptophan hydrolysis by carboxypeptidase A. This requires at least two distinct binding sites for these carboxylate ions, and suggests that the predominant mode of inhibition observed for different substrates may be very dependent on substrate structure. It is possible that mixed inhibition kinetics for ester hydrolysis observed in the present study may arise in a similar manner. However, it should be noted that we have not observed any examples of purely non-competitive inhibition of ester hydrolysis, whereas this form of inhibition is well known for peptide hydrolysis (6).

Overall, our results are in qualitative agreement with an earlier more limited study (2) on the dependence of inhibitor effectiveness on structure, although as noted above, this earlier study was carried out under conditions where substrate inhibition has since been shown to be important.

It is clear from the X-ray crystallographic investigation (28–31) of carboxypeptidase A and carboxypeptidase–ligand complexes that there is a convenient hydrophobic pocket in the active-site region of the enzyme for the acceptance of apolar side chains of substrate and inhibitor molecules. It is also apparent that the negatively charged carboxylate group can be conveniently accommodated by an electrostatic interaction with the positively charged guanidinium group of arginine-145, or alternatively, coordinated to the active site zinc ion. Both types of electrostatic interaction have been observed in crystals of small molecule – carboxypeptidase complexes. The binding of a *p*-iodophenylpropanoate ion has been interpreted as involving a Zn^{2+} –

Can. J. Chem. Downloaded from www.nrcresearchpress.com by 210.87.254.5 on 09/05/12
For personal use only.

carboxylate interaction, whereas the binding of glycyl-L-tyrosine involves an ion pair between the tyrosine carboxylate group and the arginine-145 side-chain. It is possible that either (or both) of these interactions are important for the binding of carboxylate ion inhibitors in solution, and that some of the different inhibition modes that we have observed may result from different accommodations for the carboxylate groups of various inhibiting ions.

A p.m.r. spectroscopic investigation (36) of the binding of 3-phenylpropanoate ions to manganese – carboxypeptidase A in solution has indicated that a water molecule is displaced from the coordination sphere of the manganese ion upon inhibitor binding. This is consistent with the carboxylate group being coordinated to the metal ion in this case. Similarly, line-broadening in the p.m.r. spectrum of methoxyacetate ions in the presence of manganese–carboxypeptidase has been shown to be consistent with the coordination of this species to the active-site metal ion (37). It is clear, however, from the crystallographic investigation of *p*-iodophenylpropanoate–carboxypeptidase complexes, that there are at least four sites in the enzyme molecule at which these ions may be bound (28). Multiple binding of 3-phenylpropanoate ions to cobalt – carboxypeptidase A has also been observed by spectroscopic methods (38, 39). The observation of mixed inhibition kinetics with anions having large hydrocarbon entities may be a reflection of preferential binding at one or more of these other sites when the hydrocarbon group is no longer sufficiently small to be accommodated in the active-site hydrophobic pocket. The close correlation with π for the smaller carboxylate ions is strong evidence in support of these ions all being bound in a similar manner. The data in Fig. 3 for the cyclohexylacetate ion suggest that at least for this ion, and also presumably for the other ions that display partially competitive inhibition kinetics, multiple binding sites also exist in solution.

The slope of the log K_i *vs.* π correlation line (eq. 2) is considerably larger than has previously been observed for the binding of small molecules to macromolecules through "hydrophobic bonding". Typical pre-π factors in correlations of binding constants with π are in the range 0.46–0.84 (33, 40). Thus, the relationship in eq. 2 suggests an unusually strong dependence of binding on the hydrophobic character of the hydrocarbon moiety of the inhibiting anion. Consideration of homologous pairs of anions that fit eq. 2 allows the calculation of the contribution of a methylene unit to the binding of an inhibitor ion to the enzyme. The data in Table 3 suggest that the free energy change for binding per methylene unit in these reactions is 1.46 $\pm$ 0.05 kcal/mol. This value is considerably larger than expected for the free energy of transfer of a methylene unit between an aqueous and hydrocarbon environment. This latter value has been estimated to be approximately 0.8 kcal/mol in various studies (41, 42). Such a change would give rise to a pre-π factor of approximately 1.1 which is somewhat greater than is found in most correlations of hydrophobic character with ligand binding to macromolecules (33, 40), but considerably less than the value of 1.77 in eq. 2. Thus, if our observed $\Delta(\Delta F) = 1.46$ kcal/mol/methylene unit reflects the free energy change for the transfer of a methylene unit from bulk aqueous solution to the hydrophobic cavity at the active-site of the enzyme, one is forced to conclude that this cavity is more hydrophobic than a hydrocarbon solvent, a phenomenon that is of doubtful physical significance.

An alternative interpretation would be to suggest that, in addition to the transfer of a methylene unit from water to a less polar environment, the pre-π factor is also reflecting one or more other factors which are also dependent on the hydrophobic character of the binding ligand. The X-ray crystallographic studies indicate that considerable conformational changes occur in this enzyme in the vicinity of the active-site upon ligand binding (28–31). We suggest that the large pre-π factor of eq. 2 is the sum of the effects of the hydrophobic character of the inhibiting ion on both inhibitor binding (*i.e.*

TABLE 3. Differences in free energy of binding of homologous inhibitors to carboxypeptidase A

R_1	R_2	$\Delta(\Delta F)$* (kcal/mol)
CH_3	CH_3CH_2	1.40
CH_3CH_2	$CH_3(CH_2)_2$	1.11
$(CH_3)_2CH$	$(CH_3)_2CHCH_2$	1.52
$(CH_3)_3C$	$(CH_3)_3CCH_2$	1.41
Cyclopropyl	Cyclobutyl	1.52
C_6H_5	$C_6H_5CH_2$	1.45

*Calculated from $\Delta(\Delta F) = RT \ln (K_i^1/K_i^2)$.

Can. J. Chem. Downloaded from www.nrcresearchpress.com by 210.87.254.5 on 09/05/12
For personal use only.

hydrophobic bonding) and on producing a conformational change in the enzyme. This interpretation assumes that the conformational change upon formation of the enzyme–inhibitor complex is directly related to the hydrophobic character of the ligand. Such an assumption is not without precedent; Helmer *et al.* (43) have observed that the binding of small molecules to bovine serum albumin produces changes in optical rotation that correlate with the hydrophobic character of the ligand. These changes in optical rotation are believed to reflect conformational changes in the protein upon ligand binding. Furthermore, the changes in optical rotation are much more dependent on the hydrophobic character of the ligand (pre-π factor 2.23) than are the binding constants for these same ligands to this protein (pre-π factor 0.75).

The observed differences in the binding of strictly aliphatic carboxylate anions and those containing aromatic rings are puzzling. The differences cannot be due merely to the presence of a ring since both acyclic and cyclic aliphatic carboxylates seem to be reasonably well correlated by eq. 2. The lower ω-phenylalkanoic acid anions seem to lie on a line of similar slope to that for the aliphatic carboxylate ions (Fig. 4). The difference in inhibitory effectiveness for equally hydrophobic (*i.e.* equal π-values) hydrocarbon moieties between the two groups of inhibitors is

$$\log K_i(\text{aliphatic}) - \log K_i(\text{aromatic}) = -1.9$$

This relationship may be interpreted as meaning that carboxylate ions containing aromatic rings are inherently less potent inhibitors than strictly aliphatic carboxylate ions, but the reasons for this difference remain unclear at the present time. It is interesting to note that in a recent study (44) of the reversible inhibition of chymotrypsin by alkyl- and ω-phenylalkyl-boronic acids, a difference between aliphatic acids and phenyl substituted acids was observed. Here, however, based upon their hydrophobic character as expressed by π-values, the acids containing aromatic rings were *more* effective inhibitors than their aliphatic counterparts. For this system we have calculated

$$\log K_i(\text{aliphatic}) - \log K_i(\text{aromatic}) = 1.2$$

As is the case for carboxypeptidase A, the reasons for this inherent difference between aliphatic and aromatic inhibitors of chymotrypsin are not known.

This research was supported by a grant from the National Research Council of Canada, and an NRCC Scholarship awarded to C.D.M.

1. E. Elkins-Kaufman and H. Neurath. J. Biol. Chem. **178**, 645 (1949).
2. E. L. Smith, R. Lumry, and W. J. Polglase. J. Phys. Chem. **55**, 125 (1951).
3. H. Fujioka and K. Imahori. J. Biol. Chem. **237**, 2804 (1962).
4. J. E. Coleman and B. L. Vallee. Biochemistry, **3**, 1874 (1964).
5. E. T. Kaiser and F. W. Carson. Biochem. Biophys. Res. Commun. **18**, 457 (1965).
6. D. S. Auld and B. L. Vallee. Biochemistry, **9**, 602 (1970).
7. L. D. Byers and R. Wolfenden. J. Biol. Chem. **247**, 606 (1972).
8. H. Neurath and G. H. Schwert. Chem. Rev. **46**, 69 (1950).
9. P. H. Petra. Methods Enzymol. **19**, 460 (1970).
10. M. Dixon and E. C. Webb. Enzymes. 2nd ed. Longmans Green and Co. Ltd., London, 1967. p. 315.
11. R. Lumry and E. L. Smith. Discuss. Faraday Soc. **20**, 105 (1955).
12. W. N. Lipscomb. Acc. Chem. Res. **3**, 81 (1970).
13. J. W. Bunting and J. Murphy. Biochem. Biophys. Res. Comm. **48**, 1316 (1972).
14. B. L. Vallee. Federation Proc. **23**, 8 (1964).
15. D. S. Aul, S. A. Latt, and B. L. Vallee. Biochemistry, **11**, 4994 (1972).
16. J. E. Coleman and B. L. Vallee. Biochemistry, **1**, 1083 (1962).
17. J. E. Coleman and B. L. Vallee. J. Biol. Chem. **236**, 2244 (1961).
18. J. R. Whitaker, F. Menger, and M. L. Bender. Biochemistry, **5**, 386 (1966).
19. R. C. Davies, D. S. Auld, and B. L. Vallee. Biochem. Biophys. Res. Commun. **31**, 628 (1968).
20. J. F. Riordan, M. Sokolovsky, and B. L. Vallee. Biochemistry, **6**, 3609 (1967).
21. R. T. Simpson, J. F. Riordan, and B. L. Vallee. Biochemistry, **2**, 616 (1963).
22. W. O. McClure, H. Neurath, and K. A. Walsh. Biochemistry, **3**, 1897 (1964).
23. R. C. Davies, J. F. Riordan, D. S. Auld, and B. L. Vallee. Biochemistry, **7**, 1090 (1968).
24. G. N. Wilkinson. Biochem. J. **80**, 324 (1961).
25. H. B. Klevens. J. Phys. Chem. **52**, 130 (1948).
26. A. N. Cambell and G. R. Lakshminarayanan. Can. J. Chem. **43**, 1729 (1965).
27. R. P. Ambler. Methods Enzymol. **11**, 155 (1967).
28. T. A. Steitz, M. L. Ludwig, F. A. Quiocho, and W. N. Lipscomb. J. Biol. Chem. **242**, 4662 (1967).
29. G. N. Reeke, Jr., J. A. Hartsuck, M. L. Ludwig, F. A. Quiocho, T. A. Steitz, and W. N. Lipscomb. Proc. Nat. Acad. Sci. U.S. **58**, 2220 (1967).
30. W. N. Lipscomb, G. N. Reeke, Jr., J. A. Hartsuck, F. A. Quiocho, P. H. Bethge, M. L. Ludwig, T. A. Steitz, H. Muirhead, and J. C. Coppola. Brookhaven Symp. Biol. **21**, 24 (1968).

31. W. N. LIPSCOMB, G. N. REEKE, JR., J. A. HARTSUCK, F. A. QUIOCHO, and P. H. BETHGE. Phil. Trans. Roy. Soc. London, Ser. B. **257**, 177 (1970).
32. T. FUJITA, J. IWASA, and C. HANSCH. J. Am. Chem. Soc. **86**, 5171 (1964).
33. C. HANSCH. Acc. Chem. Res. **2**, 232 (1969).
34. A. LEO, C. HANSCH, and D. ELKINS. Chem. Rev. **71**, 525 (1971).
35. R. W. TAFT, JR. Steric effects in organic chemistry. M. S. Newman (ed.). John Wiley and Sons, Inc., New York, 1956. p. 556.
36. R. G. SHULMAN, G. NAVON, B. J. WYLUDA, D. C. DOUGLAS, and T. YAMANE. Proc. Nat. Acad. Sci. U.S. **56**, 39 (1966).
37. G. NAVON, R. G. SHULMAN, B. J. WYLUDA, and T. YAMANE. Proc. Nat. Acad. Sci. U.S. **69**, 86 (1968).
38. S. A. LATT and B. L. VALLEE. Biochemistry, **10**, 4263 (1971).
39. S. A. LATT, D. S. AULD, and B. L. VALLEE. Federation Proc. **29**, 666 (1970).
40. C. HANSCH. Drug design. Vol. 1. E. J. Ariens (ed.). Academic Press, New York, 1971. p. 271.
41. C. TANFORD. J. Am. Chem. Soc. **84**, 4240 (1962).
42. P. MUKERJEE. Adv. Colloid Interface Sci. **1**, 241 (1967).
43. F. HELMER, K. KIEHS, and C. HANSCH. Biochemistry, **7**, 2858 (1968).
44. V. K. ANTONOV, T. V. IVANINA, A. G. IVANOVA, I. V. BEREZIN, A. V. LEVASHOV, and K. MARTINEK. FEBS Lett. **20**, 37 (1972).
45. J. W. BUNTING and C. D. MYERS. Chem. Commun. 826 (1972).

Can. J. Chem. Downloaded from www.nrcresearchpress.com by 210.87.254.5 on 09/05/12
For personal use only.

Ring Opening of Dihydro-1,4-oxathiins

MAURICE ARMAND CORBEIL, MICHAEL CURCUMELLI-RODOSTAMO, ROBERT JAMES FANNING, BRUCE ALLAN GRAHAM, MARSHALL KULKA, AND JAMES BENJAMIN PIERCE

Uniroyal Limited, Research Laboratories, Guelph, Ontario

Received December 8, 1972

Acid hydrolysis of 5,6-dihydro-2-methyl-1,4-oxathiin-3-carboxanilide gives 2-(2-hydroxyethylthio)-acetoacetanilide enol. 3-Carbonyl-substituted 5,6-dihydro-1,4-oxathiins were found to undergo ring cleavage by nucleophilic nitrogen attack on C-2. Thus the following reactions were observed: 3-acetyl-5,6-dihydro-2-methyl-1,4-oxathiin on treatment with hydrazine gives 4-(2-hydroxyethylthio)-3,5-dimethylpyrazole, instead of the hydrazone. The 1,4-oxathiins, *N*-(5,6-dihydro-2-methyl-1,4-oxathiin-3-ylcarbonyl)-*N'*-phenylurea and 5,6-dihydro-2-methyl-1,4-oxathiin-3-carboxylic acid hydrazide rearrange to give 5-(2-hydroxyethylthio)-6-methyl-1-phenyluracil and 4-(2-hydroxyethylthio)-3-methyl-2-pyrazolin-5-one, respectively. Finally, treatment of 5,6-dihydro-2-methyl-1,4-oxathiin-3-carbonyl chloride with 2-aminopyridine and with 2-aminopyrimidine affords 4*H*-3-(2-hydroxyethylthio)-2-methylpyrido[1,2-*a*]pyrimidin-4-one and 4*H*-3-(2-hydroxyethylthio)-2-methylpyrimido[1,2-*a*]pyrimidin-4-one, respectively, as the predominant products.

L'hydrolyse acide du dihydro-5,6 méthyl-2 oxathiine-1,4 carboxanilide-3 a produit l'énol (hydroxy-2 éthylthio)-2 acétoacétanilide. Les composés dihydro-5,6 oxathiine-1,4 carboxyl-3 substitués ont subi un clivage du cycle consécutivement à l'attaque de la position C-2 par un azote nucléophile. Par suite, les réactions suivantes furent observées: l'acétyl-3 dihydro-5,6 méthyl-2 oxathiine-1,4 a produit lors d'une réaction avec l'hydrazine l'(hydroxy-2 éthylthio)-4 diméthyl-3,5 pyrazole au lieu de l'hydrazone. Les oxathiines-1,4 *N*-(dihydro-5,6 méthyl-2 oxathiine-1,4 carbonyl-3) *N'*-phénylurée et l'hydrazide de l'acide dihydro-5,6 méthyl-2 oxathiine-1,4 carboxylique-3 ont produit par réarrangement l'(hydroxy-2 éthylthio)-5 méthyl-6 phényl-1 uracile et l'(hydroxy-2 éthylthio)-4 méthyl-3 pyrazoline-2 one-5, respectivement. Finalement, la réaction du chlorure de dihydro-5,6 méthyl-2 oxathiine-1,4 carbonyle-3 avec l'amino-2 pyridine et avec l'amino-2 pyrimidine à conduit, comme produits principaux, à l'(hydroxy-2 éthylthio)-3-4*H* méthyl-2 pyridopyrimidine[1,2-*a*]one-4 et à l'(hydroxy-2 éthylthio-3-4*H* méthyl-2 pyrimido pyrimidine[1,2-*a*]one-4 respectivement. [Traduit par le journal]

Can. J. Chem., 51, 2650 (1973)

The discovery that 5,6-dihydro-1,4-oxathiins and more particularly 5,6-dihydro-2-methyl-1,4-oxathiin-3-carboxanilide (Vitavax®)[1] (**1**) and its sulfone (Plantvax®) possess systemic fungicidal properties (1) has stimulated interest in 1,4-oxathiin chemistry and has given impetus to the search for other systemic fungicides.

The purpose of this paper is to discuss the ring opening of several 3-carbonyl-substituted 5,6-dihydro-1,4-oxathiins by nucleophilic attack on C-2.

Recently Wilson demonstrated that 5,6-dihydro-2-methyl-1,4-oxathiin undergoes acid-catalyzed hydrolytic cleavage to form (2-hydroxyethylthio)-2-propanone (2). It has been found in this laboratory that 5,6-dihydro-2-methyl-1,4-oxathiin-3-carboxanilide (**1**) undergoes similar hydrolytic cleavage with formation of the enol form **2** of 2-(2-hydroxyethylthio)acetoacetanilide (**3**) (eq. 1). This compound was also prepared from 2-mercaptoethanol and 2-chloroacetoacetanilide.

That the hydrolysis product is the enol **2** and not the keto form **3** has been demonstrated by the purple color it gives in alcoholic ferric chloride, by its rapid dissolution in aqueous sodium and ammonium hydroxide, and by its i.r. and n.m.r. spectra. The ketone carbonyl band is absent in the i.r. spectrum and the singlet at 15.5 p.p.m. in the n.m.r. spectrum is indicative of an enolic proton. The enolization appears to be aided by the sulfur atom since unsubstituted β-ketoamides are largely ketonic. Similar enolization has been observed in 2-thio-1,3-diketones (3).

The cleavage product **2** was converted readily to **1** by heating in benzene with azeotropic water

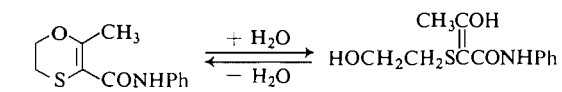

[1] **1** **2**

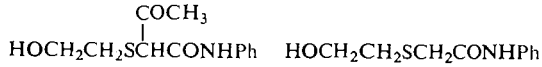

3 **4**

[1]®Uniroyal's registered trademark.

removal in the presence of an acid catalyst. As expected, it is sensitive to base, and in aqueous sodium hydroxide undergoes deacetylation to furnish 2-(2-hydroxyethylthio)acetanilide (**4**). Similar deacetylations have been previously observed (4–6). **2** forms a 2,4-dinitrophenylhydrazone (**5**) which is also obtained by treatment of the oxathiin **1** with 2,4-dinitrophenylhydrazine reagent. The n.m.r. spectrum of the hydrazone shows a singlet at 4.67 p.p.m. which is not affected on treatment of the sample with deuterium oxide. Assignment of this singlet to a proton at C-2 shows the hydrazone to have the imine structure **5**, rather than the alternative enamine structure **6**.

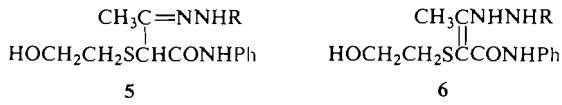

5 **6**

R = 2,4-dinitrophenyl

Mattsson and Bertilsson have shown that 5,6-dihydro-2-methyl-1,4-oxathiin-3-carboxanilide (**1**) can also be cleaved by amines (7). Thus a solution of **1** and pentylamine on standing at room temperature for several days affords 2-(2-hydroxyethylthio)-3-pentylaminocrotonanilide. A number of reactions of 3-carbonyl-substituted 5,6-dihydro-1,4-oxathiins involving nucleophilic attack on C-2 by nitrogen have been encountered in this laboratory.

One such reaction constitutes an example of the known conversion of β-alkoxy-α,β-unsaturated ketones to pyrazoles on treatment with hydrazine (8). Thus from 3-acetyl-5,6-dihydro-2-methyl-1,4-oxathiin (**7**) and hydrazine a product was obtained which was identified as 4-(2-hydroxyethylthio)-3,5-dimethylpyrazole (**8**). The n.m.r. spectrum (DMSO-d_6) of this product (**8**) shows a singlet at 2.23 p.p.m. attributed to two equivalent methyl groups and two triplets at 2.56 and 3.45 p.p.m. characteristic of the two methylenes of a 2-hydroxyethylthio group.

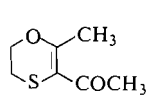

7

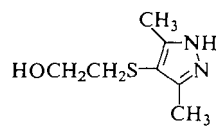

8

The preparation of the oxathiin **7** now warrants brief consideration. Reaction of 3-chloro-2,4-pentanedione with 2-mercaptoethanol in the presence of sodium bicarbonate gave a neutral and an acidic compound (Scheme 1). The acidic compound, presumably **9**, was converted to the desired oxathiin **7** by acid-catalyzed dehydration. The neutral product was identified as **10** by comparison of its i.r. and n.m.r. spectra with those of an authentic sample prepared by acetylation of (2-hydroxyethylthio)-2-propanone (2). It probably formed by rearrangement of **9**. A similar rearrangement, observed in this laboratory, consists in the conversion of ethyl 2-(2-hydroxyethylthio) acetoacetate (**11**) to ethyl (2-acetoxyethylthio)acetate (**12**) in the presence of sodium ethylate (eq. 2).

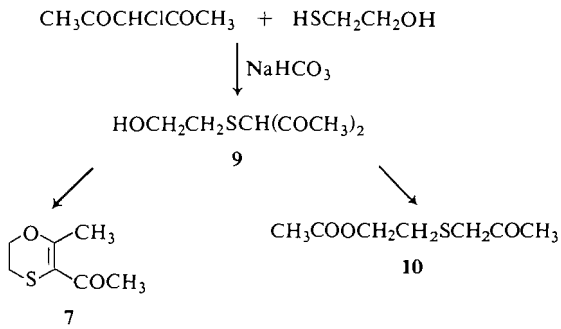

SCHEME 1

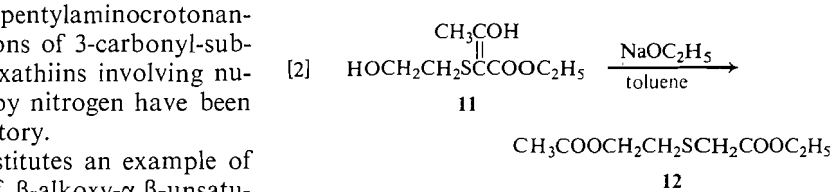

11

$CH_3COOCH_2CH_2SCH_2COOC_2H_5$

12

The identity of compound **12** was established by comparison of its i.r. and n.m.r. spectra with those of the compound obtained by acetylation of ethyl (2-hydroxyethylthio)acetate (9).

Another reaction involving nucleophilic attack by nitrogen on C-2 of a 1,4-oxathiin gave a 2-hydroxyethylthio-substituted uracil. Thus *N*-(5,6-dihydro-2-methyl-1,4-oxathiin-3-ylcarbonyl)-*N'*-phenylurea (**13**), prepared from 5,6-dihydro-2-methyl-1,4-oxathiin-3-carbonyl chloride (**14**) and *N*-phenylurea, when heated in refluxing toluene in the presence of sodium hydride rearranged to 5-(2-hydroxyethylthio)-6-methyl-1-phenyluracil (**15**) in 57% yield (Scheme 2). Compound **15** was also obtained in an attempt to make **13** by the method of Wolfe and Trimitsis (10). Thus treatment of ethyl 5,6-dihydro-2-methyl-1,4-oxathiin-3-carboxylate (**16**) (*1b*) with *N*-phenylurea and sodium hydride in toluene at reflux temperature gave **15** in 55% yield. Since, as shown above, compound **13** rearranges to

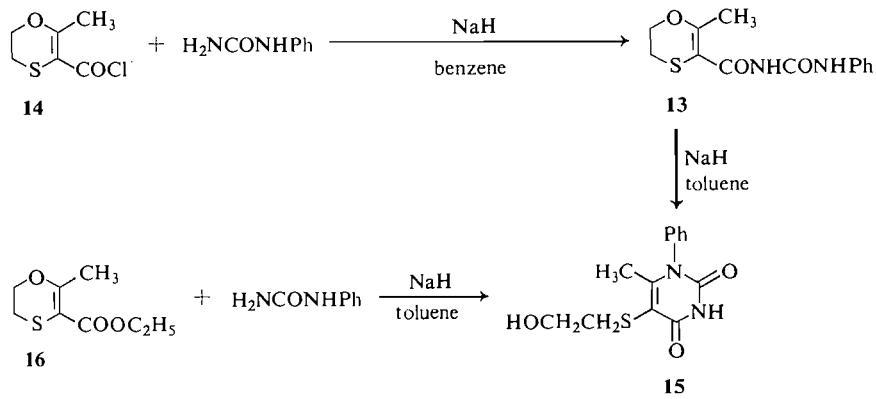

SCHEME 2

15 in a suspension of sodium hydride in refluxing toluene, it is probably an intermediate in the reaction of the ester **16** with *N*-phenylurea to form **15**. The i.r. and n.m.r. spectra of the rearrangement product **15** are in agreement with the proposed structure. The solubility of the product in aqueous sodium hydroxide and the fact that the *N*-methyl derivative can easily be prepared by the method of Senda and Suzui (11) provided further evidence for the uracil structure **15**. Confirmation of the presence of the alcoholic function came from the conversion of **15** to a chloride on treatment with thionyl chloride in chloroform. 1-(5-Chloro-2-methylphenyl)-5-(2-hydroxyethylthio)-6-methyluracil was obtained from ethyl 5,6-dihydro-2-methyl-1,4-oxathiin-3-carboxylate **16** and *N*-(5-chloro-2-methylphenyl)-urea in the same manner as was **15**.

A further example of ring opening of a dihydro-1,4-oxathiin by intramolecular nitrogen attack was encountered when an *n*-butanol solution of 5,6-dihydro-2-methyl-1,4-oxathiin-3-carboxylic acid hydrazide (**17**) was heated at reflux to give the rearranged isomer 4-(2-hydroxyethylthio)-3-methyl-2-pyrazolin-5-one (**18**) (eq. 3). The n.m.r. spectrum of **18** shows the two methylene triplets characteristic of a 2-hydroxyethylthio group. The solubility of **18** in aqueous sodium carbonate and its u.v. absorption at 242 nm are in accord with the assigned 2-pyrazolin-5-one structure. A strong band in the i.r. spectrum (KBr) between 2400 and 2900 cm^{-1}, ascribed by De Stevens and co-workers (12) to the pyrazolinone zwitterion, shows the important contribution of the tautomeric form **19**.

Cleavage of the dihydro-1,4-oxathiin ring was also demonstrated in the reaction of the acid chloride **14** with 2-aminopyridine in benzene in

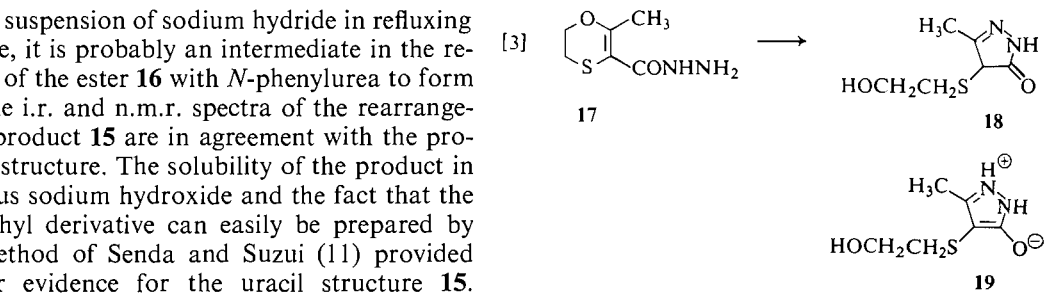

the presence of triethylamine. This reaction gave the amide **20** in only 4% yield. The major reaction product **21**, isolated in 56% yield, was identified as 4*H*-3-(2-hydroxyethylthio)-2-methylpyrido[1,2-*a*]pyrimidin-4-one (**21***a*), an isomer of **20**.

The i.r. spectrum of compound **21** revealed the presence of a hydroxyl group. The n.m.r.

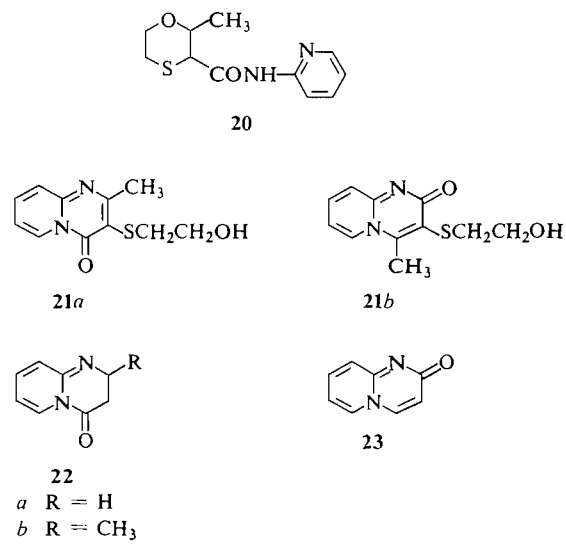

a R = H
b R = CH_3

spectrum shows two triplets (J = 6Hz), centered at 3.67 and 2.98 p.p.m., instead of the methylene multiplets present in the spectra of dihydro-1,4-oxathiins. The foregoing data indicated that cleavage of the dihydro-1,4-oxathiin ring had occurred resulting in the formation of a 2-hydroxyethylthio group. At this stage, structures **21***a* and **21***b* were considered for compound **21**.

The problem of distinguishing between a 2- and a 4-pyrido[1,2-*a*]pyrimidinone is not new and has been the subject of several investigations (13–19). In particular, it has been shown by Adams and Pachter (15) and by Allen *et al.* (19) that the u.v. spectra of 2- and 4-pyrido[1,2-*a*]-pyrimidinones are characteristically different in the relative values of the extinction coefficients of the maxima occurring in the regions of 240–270 nm (region *a*) and 300–400 nm (region *b*). Typically the 4-ones show a ratio of extinction coefficients $\varepsilon_b/\varepsilon_a$ greater than 1 whereas for 2-ones this ratio is less than $\frac{1}{3}$. Table 1 lists the u.v. data for compounds **22***a* and **23** (19) together with those we found for compound **21**. Comparison of the extinction-coefficient ratios ($\varepsilon_b/\varepsilon_a$) clearly indicates that **21** has the 4-one structure **21***a* rather than the alternative 2-one structure **21***b*.

Structure **21***a* received further spectroscopic support. The n.m.r. spectrum of compound **21** shows a single-proton doublet (8.93 p.p.m.) downfield from the bulk of aromatic absorption by 0.9 p.p.m. In structure **21***a* the low-field position of this doublet can be attributed to the deshielding of the 6-proton by the keto group whereas a similar effect is not possible in structure **21***b*. A comparable deshielding was found by Mendel for the 6-proton of compound **22***b* (20).

Confirmation of structure **21***a* rests on chemical evidence. Formation of the alternative structure **21***b* would be expected to involve the intermediacy of the minor reaction product **20**.

TABLE 1. Comparison of u.v. data of 2- and 4-pyrido[1,2-*a*]pyrimidinones*

Compound	λ_a	ε_a	λ_b	ε_b	$\varepsilon_b/\varepsilon_a$
21*a*	248	11.5	352	14.3	1.24
22*a*†	248	10.0	348	10.0	1.00
	258	9.6			
23†	268	10.0	324	3.2	0.31

*The wavelength is given in nm and the extinction coefficient is expressed as $\varepsilon \times 10^{-3}$.
†U.v. data from ref. 19.

The latter, however, was shown not to be a reaction intermediate, since it was recovered quantitatively after being subjected to the reaction conditions.

Reaction of the acid chloride **14** with 2-amino-3-, -4-, and -5-methylpyridine furnished the 4-pyrido[1,2-*a*]pyrimidinones **24***a*, **24***b*, and **24***c*, respectively. The dihydro-1,4-oxathiin carboxamides were shown by n.m.r. spectroscopy to form in low yield.

However, reaction of compound **14** with 2-amino-6-methylpyridine and with 2-amino-4,6-dimethylpyridine led exclusively to the amides **25***a* and **25***b*. Clearly, the 6-methyl group hinders attack of the electrophile on the ring nitrogen. Failure of the ring nitrogen of 2-amino-6-methylpyridine to participate in reactions with bifunctional electrophiles has been well documented (13, 21–23).

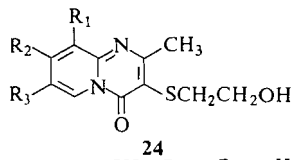

24

a $R_1 = CH_3$, $R_2 = R_3 = H$
b $R_1 = R_3 = H$, $R_2 = CH_3$
c $R_1 = R_2 = H$, $R_3 = CH_3$

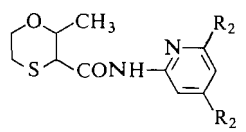

25

a $R_1 = CH_3$, $R_2 = H$
b $R_1 = R_2 = CH_3$

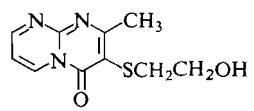

26

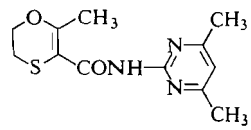

27

Treatment of the acid chloride **14** with 2-aminopyrimidine furnished the 4-pyrimido[1,2-*a*]pyrimidinone **26**. The structural assignment follows from the presence in the n.m.r. spectrum of a low-field absorption (centered at 9.2 p.p.m.) due to the C-6 and -8 protons (see above) and from analogy with the behavior of the 2-aminopyridines. As expected, reaction of compound **14** with 2-amino-4,6-dimethylpyrimidine yielded only the amide **27**.

Experimental

I.r. spectra were obtained on Perkin-Elmer 237B or 521 grating i.r. spectrometers. The n.m.r. spectra were recorded using an R-20 Hitachi Perkin-Elmer spectrometer and are expressed in p.p.m. (δ values) relative to tetramethylsilane as standard. Melting points were determined on a Gallenkamp melting point apparatus and are

uncorrected. Ultraviolet spectra were measured on a Perkin-Elmer 402 spectrometer and the analyses were performed on a Perkin-Elmer 240 elemental analyzer.

2-(2-Hydroxyethylthio)acetoacetanilide Enol (2)

To a solution of 2-chloroacetoacetanilide (53 g, 0.25 mol) in methanol (50 ml) and pyridine (25 g) was added 2-mercaptoethanol (20 g, 0.26 mol) and the solution stirred for 15 min with occasional cooling on a water bath maintaining the temperature at 35 to 40°. The reaction mixture was allowed to stand at room temperature for 2 h and then poured into water (200 ml). The material obtained by solidification of the precipitated oil was collected, washed well with cold water, and dried. Crystallization from toluene gave large white crystals (54.6 g or 87.5%) of m.p. 64–66°. Recrystallization from toluene yielded a pure product melting at 66–67°. N.m.r. ($CDCl_3$): 15.5 (1H, s, OH), 9.33 (1H, s, NH), 7.33 (5H, m, aromatic), 3.67 (2H, m, CH_2O), 2.63 (2H, t, CH_2S), 2.63 (1H, t, OH), 2.33 (3H, s, CH_3); i.r. ($CHCl_3$): 3680, 3620, 3325 cm^{-1}.

Anal. Calcd. for $C_{12}H_{15}NO_3S$: C, 56.89; H, 5.96; N, 5.52. Found: C, 56.80; H, 6.20; N, 5.61.

The enol **2** was converted in 65% yield to 2-(2-chloroethylthio)acetoacetanilide enol by treatment with thionyl chloride in benzene at room temperature, m.p. 83–85°.

Anal. Calcd. for $C_{12}H_{14}ClNO_2S$: C, 53.03; H, 5.19; N, 5.15; Cl, 13.04; S, 11.8. Found: C, 53.05; H, 5.61; N, 5.66; Cl, 12.8; S, 11.8.

Ring Opening of 5,6-Dihydro-2-methyl-1,4-oxathiin-3-carboxanilide with Aqueous Acid

A mixture of 5,6-dihydro-2-methyl-1,4-oxathiin-3-carboxanilide (23.5 g, 0.10 mol), 10% aqueous hydrochloric acid (100 ml), and toluene (200 ml) was heated to 80° while stirred rapidly. The mixture was maintained at this temperature for 1 h, allowed to cool, and the aqueous and organic layers were then separated. The toluene phase was extracted with cold 10% aqueous sodium hydroxide (2 × 100 ml) and the aqueous extract acidified with dilute hydrochloric acid. The product immediately oiled out of the acidic solution. It was extracted with toluene (2 × 100 ml) and the toluene phase was reduced in volume (to about 75 ml) by distillation under reduced pressure. The product was crystallized from the remaining toluene by cooling to −20° and scratching to induce crystallization. Thus was obtained 2-(2-hydroxyethylthio)acetoacetanilide (14.5 g or 57%) of m.p. 63–67°. The i.r. spectrum of this material proved to be identical to that of the material isolated from reaction of 2-chloroacetoacetanilide with mercaptoethanol.

5,6-Dihydro-2-methyl-1,4-oxathiin-3-carboxanilide (1)

To a solution of 2-(2-hydroxyethylthio)acetoacetanilide enol (**2**) (23.5 g, 0.09 mol) in benzene (65 ml) was added *p*-toluenesulfonic acid (0.1 g) and the reaction mixture was heated under reflux for 2 h with azeotropic water removal in a Dean–Stark trap. The solution was diluted with benzene (100 ml) and then washed with cold 5% aqueous sodium hydroxide and with water. The solvent was distilled off *in vacuo* and the residue crystallized from toluene to yield white crystals (19.9 g or 90%) of m.p. 93–95°. N.m.r. ($CDCl_3$): 9.33 (1H, s, NH), 7.5 (5H, m, aromatic), 4.80 (2H, m, CH_2O), 3.52 (2H, m, CH_2S), 2.36 (3H, s, CH_3).

Anal. Calcd. for $C_{12}H_{13}NO_2S$: C, 61.28; H, 5.53; N, 5.96. Found: C, 61.29; H, 5.58; N, 5.87.

Deacetylation of 2-(2-Hydroxyethylthio)acetoacetanilide (2) to 2-(2-Hydroxyethylthio)acetanilide (4)

To a solution of 2-(2-hydroxyethylthio)acetoacetanilide (25 g, 0.1 mol) in benzene (100 ml) was added 10% aqueous sodium hydroxide (100 ml) and the reaction mixture stirred at 35 to 40° for 1.5 h. The reaction mixture was cooled and the precipitate collected, washed with water, and dried. The white solid thus obtained (15.5 g or 70%) melted at 80–81° and did not depress the m.p. of an authentic sample of 2-(2-hydroxyethylthio)acetanilide prepared from 2-mercaptoethanol and chloroacetanilide. The i.r. spectrum was identical with that of the authentic sample.

The treatment of 2-(2-hydroxyethylthio)acetanilide with thionyl chloride in chloroform yielded 2-(2-chloroethylthio)acetanilide in 65% yield, m.p. 91–93°.

Anal. Calcd. for $C_{10}H_{12}ClNOS$: C, 52.27; H, 5.26; N, 6.09. Found: C, 52.10; H, 5.20; N, 5.93.

2,4-Dinitrophenylhydrazone (5) of 2-(2-Hydroxyethylthio)acetoacetanilide (2)

To a solution of 5,6-dihydro-2-methyl-1,4-oxathiin-3-carboxanilide (10.5 g, 0.045 mol) in methanol (250 ml) was added a solution of 2,4-dinitrophenylhydrazine (9 g, 0.045 mol) in concentrated sulfuric acid (100 ml), water (400 ml), and methanol (100 ml). After allowing the reaction mixture to stand at room temperature for 2 days, the orange crystals were filtered, washed with water and with methanol, and dried. The yellow solid (18 g or 90%) melted at 188–190° and at 191–193° after recrystallization from acetonitrile. N.m.r. (DMSO-d_6): 10.86 (1H, s, NH), 10.31 (1H, s, NH), 6.8–8.9 (8H, m, aromatic), 4.9 (1H, t, J = 5.5 Hz, OH), 3.4–3.8 (2H, m, CH_2O), 2.72 (2H, t, J = 6.5 Hz, CH_2S), 2.29 (3H, s, CH_3); i.r. (KBr): 3240, 3310, 3590 cm^{-1}.

Anal. Calcd. for $C_{18}H_{19}N_5O_6S$: C, 49.87; H, 4.41. Found: C, 50.26; H, 4.52.

The same compound was obtained when 2-(2-hydroxyethylthio)acetoacetanilide (**2**) was treated similarly with 2,4-dinitrophenylhydrazine.

3-Acetyl-5,6-dihydro-2-methyl-1,4-oxathiin (7)

Sodium bicarbonate (92.4 g, 1.1 mol) was added to a stirred mixture of 3-chloro-2,4-pentanedione (24)(134.5 g, 1 mol), benzene (400 ml), 2-mercaptoethanol (78.1 g, 1 mol), and water (200 ml). After 0.5 h the organic layer was separated and extracted with 2 *N* sodium hydroxide (500 ml). The organic layer was washed with water (200 ml) and concentrated *in vacuo* to yield *(2-acetoxyethylthio)-2-propanone* (**10**) (5.9 g or 3.4%), a colorless liquid of b.p. 100° at 0.4 mm. N.m.r. ($CDCl_3$): 4.16 (2H, t, J = 6.5 Hz, CH_2O), 3.33 (2H, s, CH_2CO), 2.72 (2H, t, J = 6.5 Hz, CH_2S), 2.26 (3H, s, CH_3CO), 2.04 (3H, s, acetoxy); i.r. (film): 1730 (ester CO), 1700 cm^{-1} (ketone CO).

Anal. Calcd. for $C_7H_{12}O_3S$: C, 47.70; H, 6.86. Found: C, 47.52; H, 6.76.

The aqueous sodium hydroxide extract from above was acidified with hydrochloric acid and extracted with benzene (2 × 250 ml). The organic extracts were combined, added to *p*-toluenesulfonic acid (5 g), and heated to reflux with azeotropic removal of the water formed in the

reaction. When no further water was liberated the reaction mixture was cooled and washed successively with 1 *N* sodium hydroxide (200 ml) and water (200 ml). The organic layer was concentrated *in vacuo* to a syrup which was distilled through a vigreux column to give 3-acetyl-5,6-dihydro-2-methyl-1,4-oxathiin (**7**) (43 g or 27%), a yellow liquid of b.p. 89–90° at 0.5 mm. N.m.r. ($CDCl_3$): 4.31 (2H, m, CH_2O), 2.96 (2H, m, CH_2S), 2.26, 2.23 (each 3H, s, CH_3); i.r. (film): 1670 (CO), 1635 cm^{-1} (C=C).

Anal. Calcd. for $C_7H_{10}O_2S$: C, 53.13; H, 6.37. Found: C, 52.79; H, 6.45.

*Rearrangement of Ethyl 2-(2-hydroxyethylthio)acetoacetate (**11**) to form Ethyl (2-acetoxyethylthio)-acetate (**12**)*

A sample of ethyl 2-(2-hydroxyethylthio)acetoacetate was prepared by the method given in ref. 1*b* and was not isolated. Thus to ethyl 2-chloroacetoacetate (25) (15.0 g, 0.089 mol) and 2-mercaptoethanol (6.8 g, 0.089 mol) in a mixture of toluene (200 ml) and water (50 ml) was added sodium bicarbonate (7.5 g, 0.089 mol). The reaction mixture was stirred for 18 h, the phases were separated, and some toluene (100 ml) distilled from the toluene phase to remove any residual water. To the resulting toluene solution of ethyl 2-(2-hydroxyethylthio)acetoacetate was added 6 drops of a 10% solution of sodium ethoxide in absolute ethanol. The mixture was heated on a steam bath for 2 h and the toluene was then removed under reduced pressure. The residue was distilled to give ethyl (2-acetoxyethylthio)acetate (10.2 g or 56%), b.p. 96–100° at 0.4 mm. This material proved to be identical in every respect to a sample made by acetylation of ethyl (2-hydroxyethylthio)acetate (9). N.m.r. ($CDCl_3$): 4.24 (2H, t, J = 6.5 Hz, OCH_2CH_2), 4.19 (2H, quartet, J = 7.2 Hz, OCH_2CH_3), 3.28 (2H, s, SCH_2CO), 2.86 (2H, t, J = 6.5 Hz, SCH_2CH_2), 2.05 (3H, s, CH_3CO), 1.27 (3H, t, J = 7.2 Hz, CH_3CH_2); i.r. (film): 1635, 1225, 1025 cm^{-1}.

*Reaction of 3-Acetyl-5,6-dihydro-2-methyl-1,4-oxathiin (**7**) with Hydrazine to form 4-(2-Hydroxyethylthio)-3,5-dimethylpyrazole (**8**)*

To a stirred solution of 3-acetyl-5,6-dihydro-2-methyl-1,4-oxathiin (3.16 g, 0.02 mol) in isopropanol (5 ml), cooled in an ice-water bath, was added dropwise a solution of aqueous hydrazine hydrate (85%, 1.3 g, 0.022 mol) in isopropanol (5 ml). After standing 12 h the reaction mixture was filtered to yield 4-(2-hydroxyethylthio)-3,5-dimethylpyrazole (**8**) (2.5 g or 73%) of m.p. 162–163°. Recrystallization from isopropanol gave colorless prisms: m.p. 162–163°. N.m.r. (DMSO-d_6): 3.45 (2H, t, J = 7 Hz, CH_2O), 2.56 (2H, t, J = 7 Hz, CH_2S), 2.23 (6H, s, $2CH_3$); i.r. (KBr): 1565, 1040 cm^{-1}; u.v.: λ_{max} (MeOH) 235 nm (1520).

Anal. Calcd. for $C_7H_{12}N_2OS$: C, 48.80; H, 7.02; N, 16.26. Found: C, 48.64; H, 7.16; N, 15.86.

*N-(5,6-Dihydro-2-methyl-1,4-oxathiin-3-ylcarbonyl)-N'-phenylurea (**13**)*

To a mixture of sodium hydride (7.2 g, 0.3 mol) and *N*-phenylurea (41 g, 0.3 mol) in dry benzene (270 ml) and dimethylformamide (30 ml), which had been warmed and stirred for 1.5 h, was added dropwise over 25 min a solution of 5,6-dihydro-2-methyl-1,4-oxathiin-3-carbonyl chloride (**14**) (1*b*) in benzene prepared from the corresponding acid (50 g, 0.33 mol) and thionyl chloride. The reaction mixture was then stirred and heated under reflux for 1 h and finally let stand at room temperature overnight. It was washed with 5% aqueous sodium hydroxide, dried over sodium sulfate, and the solvent removed. The residual oil solidified and the solid was recrystallized three times from ethanol (charcoal) to give white crystals (10.4 g or 12%) of m.p. 120–123°. N.m.r. ($CDCl_3$): 10.57 (1H, s, NH, D_2O exchangeable), 8.84 (1H, s, NH, D_2O exchangeable), 7.3 (5H, m, aromatic), 4.35 (2H, m, CH_2O), 2.86 (2H, m, CH_2S), 2.25 (3H, s, CH_3).

Anal. Calcd. for $C_{13}H_{14}N_2O_3S$: C, 56.09; H, 5.07; N, 10.06. Found: C, 56.27; H, 5.24; N, 9.81.

*5-(2-Hydroxyethylthio)-6-methyl-1-phenyluracil (**15**)*

*(a) From Ethyl 5,6-Dihydro-2-methyl-1,4-oxathiin-3-carboxylate (**16**) and N-Phenylurea*

To a mixture of sodium hydride (8.4 g, 0.35 mol), *N*-phenylurea (40 g, 0.29 mol), and dry toluene (300 ml), which had been allowed to stand for 1 h, was added ethyl 5,6-dihydro-2-methyl-1,4-oxathiin-3-carboxylate (49.8 g, 0.27 mol) (1*b*). The mixture was heated under reflux. In about 45 min the solids dissolved almost completely and then precipitation began. The reaction mixture was stirred and heated under reflux for 2 h and subsequently let stand overnight; it was then treated with excess 5% aqueous sodium hydroxide and filtered. The aqueous phase was separated and acidified with concentrated hydrochloric acid. The precipitate was filtered, washed with water, dried, and washed with hot acetone and ethanol yielding a white solid (40.7 g or 55%) of m.p. 237–243°. Further purification by reprecipitation from aqueous sodium hydroxide followed by recrystallization from acetic acid yielded a product melting at 247.5–249°. N.m.r. (DMSO-d_6): 11.53 (1H, s, NH, D_2O exchangeable), 7.44 (5H, s, aromatic), 4.68 (1H, t, OH, D_2O exchangeable), 3.43 (2H, t, CH_2O), 2.73 (2H, t, CH_2S), 2.10 (3H, s, CH_3); i.r. (KBr): 3440, 1484, 1050, 760, 700 cm^{-1}.

Anal. Calcd. for $C_{13}H_{14}N_2O_3S$: C, 56.09; H, 5.07; N, 10.06. Found: C, 56.55; H, 5.27; N, 10.40.

*(b) From N-(5,6-Dihydro-2-methyl-1,4-oxathiin-3-ylcarbonyl)-N'-phenylurea (**13**)*

To a solution of *N*-(5,6-dihydro-2-methyl-1,4-oxathiin-3-ylcarbonyl)-*N'* phenylurea (**13**) (6.0 g, 0.022 mol) in dry toluene (40 ml) was added sodium hydride (0.6 g, 0.026 mol). The mixture was heated under reflux for 3 h, cooled to room temperature, and extracted with 5% aqueous sodium hydroxide (40 ml). The aqueous phase was separated after filtration and acidified with concentrated hydrochloric acid. The precipitate was collected, washed with water, and dried to yield a white solid (3.5 g or 57%) of m.p. 241–246°. The identity of this product with that obtained by method (*a*) was established by comparison of i.r. spectra and by m.m.p. determination.

5-(2-Hydroxyethylthio)-3,6-dimethyl-1-phenyluracil

5-(2-Hydroxyethylthio)-6-methyl-1-phenyluracil (**15**) was methylated in aqueous sodium hydroxide with dimethyl sulfate in the usual manner (11). The yield of the product after crystallization from toluene and from acetone – petroleum ether was 76%, m.p. 136–137.5°. N.m.r. ($CDCl_3$): 7.3 (5H, m, aromatic), 3.68 (3H, t, CH_2O + OH), 3.40 (3H, s, CH_3), 2.84 (2H, t, CH_2S), 2.28 (3H, s, CH_3).

Anal. Calcd. for $C_{14}H_{16}N_2O_3S$: C, 57.51; H, 5.51; N, 9.58. Found: C, 57.80; H, 5.76; N, 9.52.

5-(2-Chloroethylthio)-6-methyl-1-phenyluracil

To a stirred solution of 5-(2-hydroxyethylthio)-6-methyl-1-phenyluracil (**15**) (20 g, 0.068 mol) in chloroform (500 ml) was added over 40 min a solution of thionyl chloride (10 ml) in chloroform (50 ml). The reaction mixture was heated under reflux for 2 h, let stand overnight at room temperature, and filtered. The solvent and excess thionyl chloride were removed from the filtrate and the residue recrystallized from acetone and ethanol to yield a white solid (17.0 g or 84%) of m.p. 205–206.5°. N.m.r. (DMSO-d_6): 11.53 (1H, s, NH), 7.39 (5H, s, aromatic), 3.72 (2H, t, CH_2Cl) 2.99 (2H, t, CH_2S), 2.10 (3H, s, CH_3); i.r. (KBr): OH bands absent.

Anal. Calcd. for $C_{13}H_{13}ClN_2O_2S$: C, 52.60; H, 4.41; N, 9.44. Found: C, 52.99; H, 4.47; N, 9.03.

1-(5-Chloro-2-methylphenyl)-5-(2-hydroxyethylthio)-6-methyluracil

This was prepared from ethyl 5,6-dihydro-2-methyl-1,4-oxathiin-3-carboxylate (**16**) and *N*-(5-chloro-2-methylphenyl)urea as above. The product melted at 242–244° and the yield was 31%. N.m.r. (DMSO-d_6): 11.6 (1H, s, NH), 7.40 (3H, m, aromatic), 4.65 (1H, s, OH), 3.52 (3H, t, CH_2O), 2.77 (2H, t, CH_2S), 2.11, 2.07 (each 3H, s, CH_3).

Anal. Calcd. for $C_{14}H_{15}ClN_2O_3S$: C, 51.45; H, 4.62; N, 8.57. Found: C, 51.31; H, 4.58; N, 8.86.

*5,6-Dihydro-2-methyl-1,4-oxathiin-3-carboxylic Acid Hydrazide (**17**)*

A suspension of 5,6-dihydro-2-methyl-1,4-oxathiin-3-carboxylic acid (32 g, 0.2 mol) in thionyl chloride (20 ml, 0.28 mol) and benzene (200 ml) was heated at 70° until the solid dissolved. The reaction mixture was concentrated *in vacuo* to a syrup which was dissolved in chloroform (50 ml) and added dropwise to a stirred solution of hydrazine hydrate (85%, 100 ml) in chloroform (200 ml) cooled in an ice bath. After addition of the acid chloride was completed, the reaction mixture was kept at room temperature for 12 h before the chloroform layer was separated and extracted with cold 2.5 *N* hydrochloric acid (600 ml). The acidic aqueous extract was added to sodium bicarbonate (150 g) to give a weakly basic solution which was extracted with chloroform (2 × 200 ml). The chloroform extracts were combined and concentrated *in vacuo* to a syrup which was crystallized from ethanol to give the hydrazide (15.9 g or 46%) as colorless needles of m.p. 129.5–130.5°. N.m.r. (DMSO-d_6): 5.1 (3H, broad, NH), 4.2 (2H, m, CH_2O), 2.96 (2H, m, CH_2S), 1.97 (3H, s, CH_3); i.r. (KBr): 1650 cm^{-1} (CO).

Anal. Calcd. for $C_6H_{10}N_2O_2S$: C, 41.36; H, 5.79; N, 16.08. Found: C, 41.38; H, 5.80; N, 16.18.

*Rearrangement of 5,6-Dihydro-2-methyl-1,4-oxathiin-3-carboxylic Acid Hydrazide (**17**) to 4-(2-Hydroxyethylthio)-3-methyl-2-pyrazolin-5-one (**18**)*

A solution of 5,6-dihydro-2-methyl-1,4-oxathiin-3-carboxylic acid hydrazide (3.48 g, 0.02 mol) in *n*-butanol (20 ml) was heated under reflux for 24 h. The crystals, which formed on cooling, were filtered and washed with isopropanol to yield 4-(2-hydroxyethylthio)-3-methyl-2-pyrazolin-5-one (**18**) (2.85 g or 82%) of m.p. 187–189°. Recrystallization from ethanol gave colorless needles: m.p. 188–190°. N.m.r. (DMSO-d_6): 8.5 (3H, broad, NH + OH), 3.48 (2H, t, J = 7 Hz, CH_2O), 2.55 (2H, t, J = 7 Hz, CH_2S), 2.18 (3H, s, CH_3); i.r. (KBr): 2900–2600 cm^{-1} (zwitterion), 3420, 1030 cm^{-1} (primary OH); u.v.: λ_{max} (MeOH) 242 nm (2650).

Anal. Calcd. for $C_6H_{10}N_2O_2S$: C, 41.36; H, 5.79; N, 16.08. Found: C, 41.54; H, 5.84; N, 16.12.

*5,6-Dihydro-2-methyl-N-(2-pyridyl)-1,4-oxathiin-3-carboxamide (**20**) and 4H-3-(2-Hydroxyethylthio)-2-methylpyrido[1,2-a]pyrimidin-4-one (**21a**)*

A solution of 5,6-dihydro-2-methyl-1,4-oxathiin-3-carbonyl chloride (**14**) (1*b*) in benzene (prepared from the corresponding acid (16 g, 0.125 mol) in benzene (250 ml) and thionyl chloride (18 g, 0.152 mol)) was added dropwise over 2 h to a stirred mixture of 2-aminopyridine (9.4 g, 0.1 mol), triethylamine (10.2 g), and benzene (300 ml). The reaction mixture was kept at 4–5° during the addition and then left to stand at room temperature overnight. The precipitate (mainly $Et_3N.HCl$) was collected and washed thoroughly with hot benzene. The solvent was removed from the filtrate under reduced pressure and the residue placed in a funnel, pressed, and washed with a little cold acetonitrile. Two crystallizations from acetonitrile afforded compound **21***a* (12.2 g or 56%) of m.p. 109–111.5°. N.m.r. ($CDCl_3$): 8.93 (1H, d, aromatic), 7.95–7.00 (3H, complex, aromatic), 4.15 (1H, s, OH), 3.67 (2H, t, J = 6 Hz, CH_2O), 2.98 (2H, t, J = 6 Hz, CH_2S), 2.72 (3H, s, CH_3); i.r. (KBr): 3270, 1670, 1625 cm^{-1}; u.v.: λ_{max} (EtOH) 248 (11 500), 352 nm (14 300).

Anal. Calcd. for $C_{11}H_{12}N_2O_2S$: C, 55.93; H, 5.12; N, 11.86. Found: C, 55.98; H, 5.12; N, 11.80.

The hydrobromide of **21***a* was prepared by addition of 60% HBr to a solution of the base in acetone. Recrystallization from acetonitrile containing a little water gave crystals of m.p. 235–236° (dec.).

Anal. Calcd. for $C_{11}H_{13}BrN_2O_2S$: C, 41.65; H, 4.13; N, 8.83. Found: C, 41.39; H, 4.22; N, 8.87.

The combined acetonitrile washings and mother liquors from the purification of **21***a* were evaporated under reduced pressure and the residue dissolved in chloroform. The chloroform solution was washed with aqueous sodium bicarbonate and warm water and then dried over sodium sulfate. A small amount of **21***a* (0.4 g, m.p. 110–112°) was obtained from the aqueous washings. The solid material isolated from the chloroform solution was recrystallized from 95% ethanol to give the amide **20** (0.9 g or 4%) of m.p. 108.5–110°. N.m.r. ($CDCl_3$): 8.76 (1H, s, NH), 8.34–6.85 (4H, complex, aromatic), 4.36 (2H, m, CH_2O), 2.93 (2H, m, CH_2S), 2.25 (3H, s, CH_3); i.r. (KBr): 3160, 1670, 1655, 1600 cm^{-1}.

Anal. Calcd. for $C_{11}H_{12}N_2O_2S$: C, 55.93; H, 5.12; N, 11.86. Found: C, 55.73; H, 5.11; N, 11.93.

From the ethanolic mother liquors an additional amount of compound **21***a* was obtained (0.6 g, m.p. 109–111°).

*Stability of Compound **20** under the Reaction Conditions*

A solution of 0.83 g of the amide **20** in benzene (40 ml) containing triethylamine (0.5 g) was kept for 3 h at 5° and an additional 3 h at room temperature. The solvent and triethylamine were removed under reduced pressure. The residue, 0.80 g, melted at 106–109°; it was identified as **20** by i.r., n.m.r., and m.m.p.

Compounds ***24a***, ***24b***, ***25a***, ***25b***, and ***27***

The following procedure was used for the preparation of these compounds. To a stirred slurry or solution of the aminopyridine or 2-amino-4,6-dimethylpyrimidine (0.10 mol) in benzene (300 ml) containing triethylamine (10.2 g) was added dropwise over 1.5 h a solution of the acid chloride **14** (0.12 mol) in benzene (100 ml). The reaction mixture was kept at about 5° during the addition and then left to stand at room temperature overnight. The reaction mixture was filtered and the precipitate washed with benzene. The benzene was removed from the filtrate under reduced pressure and the residue purified by crystallization.

*4H-3-(2-Hydroxyethylthio-2,9-dimethylpyrido[1,2-a]-pyrimidin-4-one (**24a**)*

Yield: 10.2 g or 41%; m.p. 92–92.5° (Me_2CHOH); n.m.r. ($CDCl_3$): 8.88 (1H, d, aromatic), 7.80–6.95 (2H, complex, aromatic), 4.32 (1H, t, J = 7 Hz, OH), 3.88–3.45 (2H, m, CH_2O), 2.97 (2H, t, CH_2S), 2.74, 2.56 (each 3H, s, CH_3); i.r. (KBr): 3410, 1653, 1620 cm^{-1}.

Anal. Calcd. for $C_{12}H_{14}N_2O_2S$: C, 57.59; H, 5.64; N, 11.20. Found: C, 57.63; H, 5.83; N, 11.22.

The *O*-acetyl derivative of compound **24***a* was prepared by heating briefly on a steam bath a solution of **24***a* in pyridine with excess Ac_2O; m.p. 78.5–79° (petroleum ether).

Anal. Calcd. for $C_{14}H_{16}N_2O_3S$: C, 57.53; H, 5.52; N, 9.59. Found: C, 57.41; H, 5.52; N, 9.45.

*4H-3-(2-Hydroxyethylthio)-2,8-dimethylpyrido[1,2-a]-pyrimidin-4-one (**24b**)*

Yield: 12.2 g or 49%; m.p. 133–134° (benzene); n.m.r. ($CDCl_3$): 8.88 (1H, d, aromatic), 7.43–6.90 (2H, complex, aromatic), 4.05 (1H, s, OH), 3.65 (2H, t, CH_2O), 2.94 (2H, t, CH_2S), 2.72, 2.50 (each 3H, s, CH_3); i.r. (KBr): 3410, 1670, 1638 cm^{-1}.

Anal. Calcd. for $C_{12}H_{14}N_2O_2S$: C, 57.59; H, 5.64; N, 11.20. Found: C, 57.43; H, 5.77; N, 11.24.

The hydrobromide of **24***b* (prepared as that of **21***a*) was recrystallized from ethanol to give material of m.p. 222–223° (dec.).

Anal. Calcd. for $C_{12}H_{15}BrN_2O_2S$: C, 43.52; H, 4.56; N, 8.45. Found: C, 43.49; H, 4.69; N, 8.17.

The *O*-acetyl derivative of **24***b* (prepared as that of **24***a*) melts at 90–91° (petroleum ether – acetone).

Anal. Calcd. for $C_{14}H_{16}N_2O_3S$: C, 57.53, H, 5.52; N, 9.59. Found: C, 57.52; H, 5.46; N, 9.47.

*5,6-Dihydro-2-methyl-N-(6-methyl-2-pyridyl)-1,4-oxathiin-3-carboxamide (**25a**)*

Yield: 21.3 g or 85%; m.p. 87–89° (EtOH); n.m.r. ($CDCl_3$): 8.76 (1H, s, NH), 8.20–6.78 (3H, complex, aromatic), 4.36 (2H, m, CH_2O), 2.92 (2H, m, CH_2S), 2.43, 2.27 (each 3H, s, CH_3); i.r. (KBr): 3360, 1666 cm^{-1}.

Anal. Calcd. for $C_{12}H_{14}N_2O_2S$: C, 57.59; H, 5.64; N, 11.20. Found: C, 57.77; H, 5.78; N, 10.93.

The hydrobromide of **25***a* (prepared as that of **21***a*) was crystallized from acetone to give crystals of m.p. 178–179° (dec.).

Anal. Calcd. for $C_{12}H_{15}BrN_2O_2S$: C, 43.52; H, 4.56; N, 8.45. Found: C, 43.61; H, 4.59; N, 8.45.

*5,6-Dihydro-2-methyl-N-(4,6-dimethyl-2-pyridyl)-1,4-oxathiin-3-carboxamide (**25b**)*

Yield: 16.6 g or 63%; m.p. 128–129° (EtOH); n.m.r. ($CDCl_3$): 8.53 (1H, s, NH), 7.81 (1H, s, aromatic), 6.66 (1H, s, aromatic), 4.33 (2H, m, CH_2O), 2.91 (2H, m, CH_2S), 2.37, 2.29, 2.25 (each 3H, s, CH_3); i.r. (KBr): 3350, 1660 cm^{-1}.

Anal. Calcd. for $C_{13}H_{16}N_2O_2S$: C, 59.08; H, 6.10; N, 10.60. Found: C, 58.89; H, 6.23; N, 10.27.

The hydrobromide of **25***b* (prepared as that of **21***a*) melts at 170–170.5° (acetone).

Anal. Calcd. for $C_{13}H_{17}BrN_2O_2S$: C, 45.23; H, 4.96; N, 8.11. Found: C, 45.50; H, 4.92; N, 8.01.

*5,6-Dihydro-2-methyl-N-(4,6-dimethyl-2-pyrimidyl)-1,4-oxathiin-3-carboxamide (**27**)*

Yield: 8 g or 30%; m.p. 143–144° (acetone); n.m.r. ($CDCl_3$): 8.67 (1H, s, NH), 6.77 (1H, s, aromatic), 4.40 (2H, m, CH_2O), 2.98 (2H, m, CH_2S), 2.45 (6H, s, $2CH_3$), 2.29 (3H, s, CH_3); i.r. (KBr): 3220, 1680 cm^{-1}.

Anal. Calcd. for $C_{12}H_{15}N_3O_2S$: C, 54.33; H, 5.70; N, 15.84. Found: C, 54.69; H, 5.67; N, 15.63.

*4H-3-(2-Hydroxyethylthio)-2,7-dimethylpyrido[1,2-a]-pyrimidin-4-one (**24c**)*

To a stirred mixture of 2-amino-5-methylpyridine (10.8 g, 0.1 mol), triethylamine (10.5 g), and benzene (300 ml) was added dropwise over 2 h a solution of the acid chloride **14** (0.125 mol) in benzene (100 ml.). The reaction mixture was kept at 3–7° during the addition and then left to stand at room temperature overnight. The cooled reaction mixture was filtered and the precipitate treated with cold water (100 ml). The insoluble material was collected and dried in an oven under reduced pressure. Crystallization from ethanol–water (10:1) afforded crystals (8.8 g or 35%) of m.p. 122–123°. The benzene filtrate yielded an additional amount of product (1.5 g, m.p. 118–121°). N.m.r. ($CDCl_3$): 8.82 (1H, s, aromatic), 7.80–7.30 (2H, complex, aromatic), 3.65 (2H, t, CH_2O), 2.96 (2H, t, CH_2S), 2.73, 2.45 (each 3H, s, CH_3); i.r. (KBr): 3395, 1653, 1625 cm^{-1}.

Anal. Calcd. for $C_{12}H_{14}N_2O_2S$: C, 57.59; H, 5.64; N, 11.20. Found: C, 57.90; H, 5.40; N, 11.22.

The hydrobromide of **24***c* (prepared as that of **21***a*) was recrystallized from ethanol to give material of m.p. 239° (dec.).

Anal. Calcd. for $C_{12}H_{15}BrN_2O_2S$: C, 43.52; H, 4.56; N, 8.45. Found: C, 43.55; H, 4.54; N, 8.46.

The *O*-acetyl derivative of compound **24***c* (prepared as that of **24***a*) melts at 119–120° (petroleum ether).

Anal. Calcd. for $C_{14}H_{16}N_2O_3S$: C, 57.53; H, 5.52; N, 9.59. Found: C, 57.60; H, 5.61; N, 9.54.

*4H-3-(2-Hydroxyethylthio)-2-methylpyrimido[1,2-a]-pyrimidin-4-one (**26**)*

To a stirred mixture of 2-aminopyrimidine (9.5 g, 0.1 mol), triethylamine (10.2 g), and benzene (300 ml) was added dropwise over 1 h a solution of the acid chloride **14** (0.125 mol) in benzene (100 ml). The reaction mixture was kept at 3–5° during the first 2 h of the reaction and then left to stand at room temperature overnight. The precipitate was collected by filtration and washed with a little cold benzene. Then it was dissolved in water and the resulting solution basified with ammonia and extracted with chloroform. The extract was dried over sodium sulfate and the chloroform and triethylamine removed under reduced pressure. The crystalline residue (7.4 g) melted at 138–145°. Recrystallization from acetonitrile furnished crystals (5 g or 21%) of m.p. 150–152°. The

benzene filtrate and washings yielded an additional small amount of product (0.5 g, m.p. 147–150°). N.m.r. ($CDCl_3$): 9.37–8.99 (2H, complex, aromatic), 7.34–7.10 (1H, m, aromatic), 3.85–3.40 (3H, complex, CH_2O + OH); on addition of D_2O this absorption is replaced by a triplet, 2H, $J = 6$ Hz, CH_2O), 3.01 (2H, t, $J = 6$ Hz, CH_2S), 2.72 (3H, s, CH_3); i.r. (KBr): 3380, 1652, 1613 cm^{-1}.

Anal. Calcd. for $C_{10}H_{11}N_3O_2S$: C, 50.63; H, 4.67; N, 17.72. Found: C, 50.49; H, 4.63; N, 17.70.

The *O*-acetyl derivative of compound **26** (prepared as that of **24***a*) melts at 134–134.5° (petroleum ether – acetone).

Anal. Calcd. for $C_{12}H_{13}N_3O_3S$: C, 51.61; H, 4.69; N, 15.05. Found: C, 51.70; H, 4.72; N, 14.89.

Grateful acknowledgment is made to the National Research Council of Canada for financial assistance, to W. R. Boos, M. J. Ross, and W. P. Klimstra for providing the analyses and the n.m.r. and i.r. spectra, and to Dr. W. A. Harrison who carried out similar reactions with 2-aminothiazoles and participated in discussions.

1. (*a*) B. VON SCHMELING and M. KULKA. Science, **152**, 659 (1966). (*b*) B. VON SCHMELING, M. KULKA, D. S. THIARA, and W. A. HARRISON. U.S. patents 3,249,499 (1966), 3,393,202 (1968), 3,3o9,214 (1968), and 3,402,241 (1968); Can. patents 787,893 (1968), 791,151 (1968), 824,243 (1970), and 825,665 (1969).
2. G. E. WILSON. J. Am. Chem. Soc. **87**, 3785 (1965).
3. Z. YOSHIDA, H. OGOSHI, and T. TOKUMITSU. Tetrahedron, **26**, 2987 (1970).
4. A. J. HODGKINSON and B. STASKUN. J. Org. Chem. **34**, 1709 (1969).
5. J. M. STRALEY and A. C. ADAMS. Org. Synth. Coll. Vol. **4**, 415 (1963).
6. R. J. GROUT, B. M. HYNAM, and M. W. PARTRIDGE. J. Chem. Soc. C, 1590 (1969).
7. O. V. MATTSSON and B. E. BERTILSSON. German Offen. 2,133,450 (1972).
8. R. FUSCO. *In* The chemistry of heterocyclic compounds. Vol. 22. *Edited by* A. Weissberger. Interscience, New York and London. 1967. p. 54.
9. G. SCHRADER. U.S. patents 2,909,557 (1959) and 2,929,834 (1960).
10. J. F. WOLFE and G. B. TRIMITSIS. Can. J. Chem. **47**, 2097 (1969).
11. S. SENDA and A. SUZUI. Chem. and Pharm. Bull. (Tokyo), **6**, 476 (1958). Chem. Abstr. **53**, 10237*d* (1959).
12. G. DE STEVENS, A. HALAMANDARIS, P. WENK, and L. DORFMAN. J. Am. Chem. Soc. **81**, 6292 (1959).
13. H. ANTAKI and V. PETROW. J. Chem. Soc. 551 (1951).
14. R. ADAMS and I. J. PACHTER. J. Am. Chem. Soc. **74**, 4906 (1952).
15. R. ADAMS and I. J. PACHTER. J. Am. Chem. Soc. **74**, 5491 (1952).
16. I. J. PACHTER. J. Org. Chem. **26**, 4157 (1961).
17. G. R. LAPPIN. J. Org. Chem. **26**, 2350 (1961).
18. A. HALLEUX and H. G. VIEHE. J. Chem. Soc. C, 881 (1970).
19. C. F. H. ALLEN, H. R. BEILFUSS, D. M. BURNESS, G. A. REYNOLDS, J. F. TINKER, and J. A. VANALLAN. J. Org. Chem. **24**, 779 (1959).
20. A. MENDEL. J. Heterocycl. Chem. **9**, 935 (1972).
21. G. R. LAPPIN. J. Am. Chem. Soc. **70**, 3348 (1948).
22. G. R. LAPPIN, Q. R. PETERSEN, and C. E. WHEELER. J. Org. Chem. **15**, 377 (1950).
23. G. R. LAPPIN. J. Org. Chem. **23**, 1358 (1958).
24. J. J. D'AMICO. U.S. patent 2,704,791 (1955).
25. W. R. BOEHME. Org. Synth. Coll. Vol. **4**, 592 (1963).

Investigation of Factors Affecting Conformational Preference in Complex Haloethane Derivatives by Classical Energy Calculations[1]

WILLIAM F. REYNOLDS AND DONALD J. WOOD

Department of Chemistry, University of Toronto, Toronto, Ontario M5S 1A1

Received January 15, 1973

Classical energy calculations are used in combination with Abraham's electrostatic theory of solvation energy to estimate rotamer energy differences for haloethane derivatives. The calculations are tested by comparing experimental and calculated ΔE values for several di- and tetrahaloethanes. There is good agreement for chloro and bromo derivatives but poorer agreement for fluoro and iodo derivatives. ΔE values in solution are also estimated for 14 complex chloro- and bromoethanes which we have previously investigated by n.m.r. spectroscopy. The calculations generally parallel the experimental results as reflected by vicinal coupling constants. They are particularly useful for trends in conformational preference for closely related compounds and are used in conjunction with vicinal coupling constants to identify diastereomers produced by halogenation of alkenes. Steric interactions, dipole–dipole interactions and solvation energy are all important in determining conformational preference for complex haloethanes in solution.

Les calculs classiques d'énergie ont été utilisés combinés à la théorie électrostatique d'Abraham pour l'énergie des rotamères dans les dérivés d'haloéthane. Les calculs ont été testés en comparant les valeurs de ΔE expérimentale et théorique pour plusieurs di et tetrahaloéthanes. Pour les dérivés chloro et bromo, l'accord est bon mais faible dans le cas des dérivés fluoro et iodo. Les valeurs de ΔE en solution ont été aussi calculées pour quatorze chloro et bromoéthanes complexes que nous avons étudiés précédemment par spectroscopie r.m.n. Les calculs suivent généralement les résultats expérimentaux qui se reflètent dans les constantes de couplage vicinal. Les calculs ont été particulièrement utiles pour prévoir les tendances dans les conformations préférentielles des composés en étroite relation et ont été employés avec les constantes de couplage vicinal pour identifier les diastéréoisomères issus de l'halogénation des alcènes. Les interactions stériques, les interactions dipole–dipole et l'énergie de solvatation sont toutes importantes pour déterminer la conformation privilégiée des haloéthanes complexes en solution.

[Traduit par le journal]

Can. J. Chem., **51**, 2659 (1973)

Can. J. Chem. Downloaded from www.nrcresearchpress.com by 210.87.254.40 on 09/05/12
For personal use only.

Introduction

While experimental energy differences have been determined for a large number of simple ethane derivatives (1), there is little information available for complex ethane derivatives (*i.e.* ethane derivatives with three non-equivalent rotational isomers (rotamers)). We have been interested in determining conformational preference of complex ethanes in solution by n.m.r. spectroscopy (2–5). By monitoring changes in vicinal coupling constants with solvent, it was possible to deduce orders of rotamer energy levels for a number of complex ethane derivatives (2, 4, 5), but no quantitative energy differences could be obtained.

Classical energy calculations have proved useful for determining conformational energy differences (6), even for macromolecules (7). This approach allows discussion of conformational preference in terms of non-bonded (steric) interactions, dipole–dipole interactions, etc. These calculations often do not include solvation effects. However, Abraham and co-workers have developed an electrostatic model for solvation effects (8) which has provided quantitative estimates of solvation energies for a number of simple polar ethane derivatives (9). Consequently, we decided to combine classical energy calculations with Abraham's electrostatic calculations in an attempt to obtain at least semi-quantitative estimates of energy differences for complex substituted ethanes as well as to determine factors affecting conformational preference in these derivatives. One additional possible application which we hoped to check was the use of these calculations for the identification of diastereomers produced by halogenation of alkenes.

Details of Calculations

Classical energy calculations can be performed with varying degrees of sophistication. We decided to keep our calculations as simple as possible

[1]Taken in part from the Ph.D. Thesis of D. J. Wood, University of Toronto, 1972.

TABLE 1. Non-bonded potential parameters, bond lengths, bond dipole moments, and torsional barriers for CONCAL calculations

(a) Non-bonded potential parameters

Atom	α^a	N^a	VDW (Å)[b]
C	0.93	5.2	1.70
C(phenyl)	1.22	5.2	1.77
H	0.42	0.9	1.20
Br	3.34	21.8	1.95
Cl	2.28	16.0	1.80
I	5.11	30.1	2.15
F	0.38	7.8	1.35

(b) Bond lengths and bond dipole moments

Bond	Bond length (Å)[c]	Bond dipole moments (D)[d]
C—C (aliphatic)	1.54	0.0
C—C (aromatic)	1.40	0.0
C—C_6H_5	1.52	0.40
C—H (aliphatic)	1.11	−0.30
C—H (aromatic)	1.09	—
C—F	1.35	1.51
C—Cl	1.78	1.56
C—Br	1.94	1.48
C—I	2.10	1.29

(c) Torsional barrier terms

Bond	β^e	U_0(kcal mol^{-1})[e]	Reference
C(aliphatic)—C(aliphatic)	3	2.88	1
C(aliphatic)—C(aromatic)	6	0.04	1

[a]Terms are defined in eq. 5. α values are from ref. 17 while *N* is from ref. 16.
[b]Van der Walls' radii taken from ref. 11 (C(phenyl) from ref. 37).
[c]Reference 38.
[d]Reference 15. Effects of aromatic C—H bonds not included.
[e]Terms defined in eq. 2.

in the hope that reasonable energy levels could be estimated for a minimal expenditure of computer time.

While many classical energy calculations involve energy minimization techniques in which bond energies and bond lengths are varied to find the most stable geometry (6), this is a complex and time consuming procedure. Consequently, it was decided to use fixed bond angles and bond lengths to simplify the calculations. During the course of this investigation, Abraham and Parry reported results of similar calculations for simple substituted ethanes using fixed bond angles and bond lengths (10). However, they used different potential functions for non-bonded and dipolar interactions and restricted their calculations to the gas phase.

Bond lengths used in this investigation are given in Table 1. C—C—H and C—C—F angles in the ethyl group were taken as 109.5°. For other groups bonded to ethane (X = Cl, Br, I, CH_3, C_6H_5), X—C—C and X—C—X angles were fixed at 110.5° for di-substituted ethanes, 111.0° for tri-substituted ethanes, and 111.5° for tetra-substituted ethanes. A regular hexagonal geometry was assumed for the phenyl group.

The total energy, E_n, for rotamer **n** of a substituted ethane is assumed to be

$$[1] \quad E_n = E_{TOR} + E_{DIP} + E_{NB} + E_{SOLV}$$

where E_{TOR} represents the torsional barrier for rotation about a C—C bond, E_{DIP} represents the interaction between polar groups, E_{NB} represents steric or non-bonded interaction energies and E_{SOLV} represents the solvation energy. With this formulism, only energy differences between rotamers are significant.

The torsional contribution is given by

$$[2] \quad E_{TOR} = 0.5\ U_0(1 + \cos \beta\phi)$$

where U_0 is the barrier height for rotation about the unsubstituted carbon–carbon bond (the

Can. J. Chem. Downloaded from www.nrcresearchpress.com by 210.87.254.40 on 09/05/12
For personal use only.

Can. J. Chem. Downloaded from www.nrcresearchpress.com by 210.87.254.40 on 09/05/12
For personal use only.

torsional term is assumed to be unaffected by substituents (11, 12), ϕ is the dihedral angle, and β defines the symmetry of the barrier. Values for these parameters are given in Table 1.

The effect of interactions between polar bonds was estimated by treating polar bonds as point dipoles acting at the center of the polar bond. This interaction is given by (13)

$$[3] \quad E_{DIP} = \sum^{i \neq j} \frac{1}{A} \frac{1}{|\boldsymbol{R}|^3} \times \left(\boldsymbol{U}_i \cdot \boldsymbol{U}_j - \frac{3(\boldsymbol{U}_i \cdot \boldsymbol{R})(\boldsymbol{U}_j \cdot \boldsymbol{R})}{|\boldsymbol{R}|^2} \right)$$

where $\boldsymbol{U}_i$ and $\boldsymbol{U}_j$ are the dipole moment vectors of the dipolar bonds i and j, $\boldsymbol{R}$ is the distance vector joining the two point dipoles, and A is the internal dielectric constant. Bishop and Craig estimated that $A = 1.5$ for a carbon framework, based upon the bond refraction of a C—C bond (14). Consequently this value was used. For reasons discussed in part *a* of the Discussion, calculations were normally performed using bond dipole moments (Table 1) although calculations for simple haloethanes were also carried out using group dipole moments (15).

The most commonly used non-bonded interaction potential functions are the exponential ("6-exp") and the Lennard-Jones ("6-12") functions (6). Scott and Scheraga recommended the use of the latter function since it contains only two adjustable parameters as opposed to three for the "6-exp" energies and because the "6-exp" function incorrectly predicts interaction energies at small internuclear separations (16). In addition, a variety of different parameters have been suggested for the "6-exp" functions (10). Consequently, we chose the "6-12" function to minimize parameterization.

With this function, for n non-bonded interactions,

$$[4] \quad E_{NB} = \sum_n^{i<j} [d_{ij}/r_{ij}^{12} - e_{ij}/r_{ij}^{6}]$$

where

$$[5] \quad e_{ij} = \frac{362.45\alpha_i\alpha_j}{(\alpha_i/N_i)^{1/2} + (\alpha_j/N_j)^{1/2}}, \quad d_{ij} = (e_{ij}r_{min}^{6})/2$$

and where r_{ij} is the separation between atoms i and j, α is the atomic polarizability, N is the "effective number of valence electrons" and r_{min} is the sum of the van der Waals' radii for i and j (16). Parameters used in the calculation are given in Table 1. The only parameter worthy of comment is α for phenyl carbons where α was increased by 0.29, corresponding to one-half the contribution from a C=C bond (17).

Solvation energy was calculated according to Abraham's electrostatic theory, using eq. 13 of ref. 8*a*. This divides the solvation energy into dipolar, E_{DISOL}, and quadrupolar, E_{QSOL}, reaction field terms (no corrections were made for solvent–solute dipole–dipole interactions (8*c*)). The quadrupolar term was calculated using the mid-point of the ethyl C—C bond as the origin to simplify the calculation. This may introduce a small error, since the calculation really should be carried using the geometric center of the molecule as the origin (8*b*).

The solute radius (assuming a spherical solute molecule) and the solute refractive index must be known for the solvation calculations. The solute radius, a, can be calculated from the molar volume $\overline{V}$:

$$[6] \quad \overline{V} = \text{M.W.}/d = 4/3(\pi a^3 N)$$

In cases where the density, d, was not known, $\overline{V}$ was estimated by assuming additivity of molar volumes, *e.g.*

$$\overline{V}_{C_6H_5CHClCH_2Cl} - \overline{V}_{C_6H_5CH_2CH_2Cl} = \overline{V}_{CH_2ClCH_2Cl} - \overline{V}_{CH_3CH_2Cl}$$

Unknown refractive indices were estimated from molar refractivities (18). A full listing of these parameters is available elsewhere (19).

A computer program, CONCAL, was written to carry out the calculation of the terms from eq. 1. The program as written can handle up to 30 atoms, 10 dipolar bonds, and one or two bond rotations. Calculation of non-bonded interactions between atoms whose relative positions are unchanged by rotation are suppressed to minimize the number of calculations. The program prints out all energy terms from eq. 1 and total energy for each conformation generated by incremental changes (usually 2°) of bond rotation angles. Thus, for example, in 1-phenyl-1,2-dibromoethane, calculations were performed for rotation about both the C_α—C_β bond and the C_α—C_6H_5 bond. In all compounds, energy minima corresponded (within 10°) to staggered conformations about the C_α—C_β bond. The phenyl groups were invariably calculated to have a conformation which minimized non-bonded

TABLE 2. Solvation energies for several haloethane derivatives

(a) Energy difference (ΔE) between gauche and anti rotamers (ΔE in kcal/mol)

	1-Bromo-2-phenylethane		1,2-Dibromo-1-phenylethane		1,2-Dibromo-3,3-dimethylbutane	
Solvent	ΔE_{CALCD}	ΔE_{EXP}(20)	ΔE_{CALCD}	ΔE_{EXP}[a]	ΔE_{CALCD}	ΔE_{EXP}[a]
CCl_4	0.51	0.51	0.73	0.73	−0.83	−0.83
$CHCl_3$	0.40	0.38	0.64	0.70	−1.06	−1.09
$(CH_3)_3C—Cl$	0.30	—	0.55	0.68	−1.22	−1.06
$(CH_3)_2C=O$	0.26	0.26	0.50	0.60	−1.31	−1.26
$(CH_3)_2S=O$	0.24	0.00	0.46	0.55	−1.37	−1.36

(b) Dipolar (E_{DISOL}) and quadrupolar (E_{QSOL}) solvation energy terms for individual rotamers

		1,2-Dibromo-1-phenylethane				1,2-Dibromo-3,3-dimethylbutane			
Solvent	Isomer	Dipole moment	$-E_{DISOL}$	$-E_{QSOL}$	$-E_{SOLV}$	Dipole moment	$-E_{DISOL}$	$-E_{QSOL}$	$-E_{SOLV}$
CCl_4	*anti*[b]	0.60	0.02	0.24	0.27	0.20	0.00	0.16	0.17
	gauche[b]	2.24	0.33	0.06	0.39	2.55	0.43	0.12	0.55
$(CH_3)_2S=O$	*anti*[b]	0.60	0.06	0.54	0.60	0.20	0.01	0.34	0.35
	gauche[b]	2.24	0.86	0.12	0.98	2.55	1.02	0.26	1.28

[a]Calculated using method from ref. 21. The *gauche* rotamer is 2 while the *anti* rotamer is 1 (see Table 4). Rotamer 3 has a negligible population (2, 5). Data from refs. 2 and 5.
[b]Assuming Br—C—C—Br dihedral angles of 185 and 65° for *anti* and *gauche* forms respectively.

interactions with other groups. A full listing of the program is available elsewhere (19).

Experimental

Most experimental results have been previously reported (2–5). Spectra for 1,2-dichloro-1-phenylethane and *erythro*- and *threo*-1,2-dichloro-1-phenylpropane were obtained and analyzed using previously reported procedures (2). Dielectric constants, ε, used in the calculations corresponded to those measured experimentally for the solutions for which n.m.r. spectra were recorded. They were measured at 30 °C using a WTW DKO3 Dekameter.

Results and Discussion

The discussion is divided into four parts: (*a*) testing of the applicability of Abraham's theory of solvation energy to complex substituted ethanes, (*b*) testing of our particular model for classical energy calculations by comparing calculated and experimental energy differences for simple haloethanes, (*c*) discussion of CONCAL results for complex substituted ethanes, and (*d*) experimental confirmation of the tentative assignments of diastereomers provided by CONCAL plus vicinal coupling constants.

For all compounds, it is assumed that volume differences, ΔV, and entropy differences, ΔS, between rotamers are zero, *i.e.* it is assumed that $\Delta E = \Delta G$.

(a) Applicability of the Electrostatic Model of Solvation Energy to Complex Substituted Ethanes

Abraham's electrostatic theory of solvation energy (8) provides at least qualitative predictions of the change in rotamer energy with solvent for several complex haloethanes (2, 3, 5), although it breaks down for 1-phenyl-1,2,2-trihaloethanes (3). In an attempt to determine whether the theory gave quantitative answers for other complex ethane derivatives, solvation energy calculations were performed for three compounds for which experimental energy differences were either available or could be estimated; 1-bromo-2-phenylethane, 1,2-dibromo-1-phenylethane and 1,2-dibromo-3,3-dimethylbutane. Results are given in Table 2.

No experimental gas phase energy values are available to allow comparison of calculated and experimental changes in ΔE on going from the gas phase to various solvents. Consequently calculated and experimental energy differences in CCl_4 were assumed equal and calculated values in other solvents were expressed relative to this value. Experimental results for 1-bromo-2-phenyl ethane are those of Lin (20) while ΔE values for other compounds were estimated using the approach suggested by Snyder (21).

Can. J. Chem. Downloaded from www.nrcresearchpress.com by 210.87.254.40 on 09/05/12
For personal use only.

TABLE 3. Comparison of experimental and calculated energy differences[a] for symmetrically substituted di- and tetrahaloethanes

X	State	ΔE_{NB}[b]	ΔE_{DIP}	ΔE_{TOR}	ΔE_{DISOL}	ΔE_{QSOL}	ΔE_{CALCD}	$\angle_g$[c]	ΔE_{EXP}	Reference
(a) 1,2-di-X-ethanes										
F	Gas	−0.02	+1.18	+0.07	—	—	+1.23	66	+0.2	10
		(−0.02)	(+1.30)[d]	(+0.07)	—	—	(+1.35)	(66)		
Cl	Gas	+0.10	+0.80	+0.12	—	—	+1.02	68	+1.2	1
		(+0.10)	(+0.92)	(+0.12)	—	—	(+1.14)	(68)		
Cl	Neat	+0.18	+0.87	+0.03	−2.27	+1.19	+0.00	64	+0.30	29
		(+0.14)	(+0.97)	(+0.07)	(−2.69)	(+1.70)	(+0.19)	(66)		
Br	Gas	+0.29	+0.62	+0.19	—	—	+1.10	70	+1.77	1
		(+0.24)	(+0.75)	(+0.28)	—	—	(+1.27)	(72)		
Br	Neat	+0.36	+0.65	+0.12	−1.50	+0.86	+0.49	68	+0.94	29
		(+0.29)	(+0.79)	(+0.19)	(−1.90)	(+1.30)	(+0.67)	(70)		
I	Gas	+0.83	+0.38	+0.48	—	—	+1.69	76	+2.6	10
		(+0.83)	(+0.56)	(+0.48)	—	—	(+1.87)	(76)		
(b) 1,1,2,2-tetra-X-ethanes										
F	Gas	−0.02	+1.19	+0.07	—	—	+1.24	66	+1.16	1
		(−0.02)	(+1.31)	(+0.07)	—	—	(+1.36)	(66)		
Cl	Gas	−0.47	+0.54	−0.02	—	—	+0.05	58	0.0	1
		(−0.47)	(+0.56)	(−0.02)	—	—	(+0.07)			
Cl	Neat	−0.47	+0.58	−0.03	−1.38	+0.77	−0.53	60	−1.1	1
		(−0.47)	(+0.60)	(−0.03)	(−1.63)	(+1.00)	(−0.53)	(60)		
Br	Gas	−0.95	+0.44	−0.02	—	—	−0.53	58	0.0	10
		(−0.95)	(+0.50)	(−0.02)	—	—	(−0.47)	(58)		
Br	Neat	−0.95	+0.44	−0.02	−1.16	+0.62	−1.07	58	0.85	
		(−0.94)	(+0.53)	(−0.03)	(−1.50)	(−0.90)	(−1.04)	(60)	−0.75	1

[a]Symbols are defined in text following eq. 1.
[b]Energy difference between *gauche*- and *anti*-rotamer (the *anti* rotamer for 1,1,2,2-tetrahaloethanes is defined as the rotamer in which each halogen atom is *anti* to another halogen. ΔE in kcal/mol.
[c]Dihedral angle of *gauche*-rotamer.
[d]Values in brackets calculated using group dipole moments.

This allows one to estimate ΔE values from vicinal coupling constants for compounds in which one of the rotamers has a negligible population (both compounds fulfil this requirement (2, 5)).

As can be seen in Table 2, there is very good agreement between experimental and calculated changes in ΔE, indicating that Abraham's theory can be applied to these compounds. The results for the two dibromo compounds are particularly informative. The calculations indicate a smaller change in ΔE for 1-phenyl-1,2-dibromoethane than for 1,2-dibromo-3,3-dimethylbutane, as observed experimentally. This arises from differences in both dipolar and quadrupolar solvation terms (Table 2). These differences are due to the polarity of the C_α—C_6H_5 bond (the C_α–*t*-butyl bond in the dibromoalkane is assumed to have $\mu = 0$). This also accounts for the solvent dependence of ΔE for 1-phenyl-2-bromoethane and points out the necessity of considering all neighboring polar bonds (*i.e.* using bond moments) in solvation energy calculations for complex substituted ethanes.

(b) Symmetrically Substituted Dihalo- and Tetrahaloethanes

Calculations were performed for these compounds, for which energy differences are available, to check the accuracy of the classical energy calculations. Abraham has pointed out that experimental solution energy differences generally have not been corrected for the variation of ΔE with temperature and really correspond to ΔE at 0 °K (8*a*). Consequently, experimental values have been corrected to 30 °C, using eq. 18 of ref. 8*a*. Results are given in Table 3.

There is generally satisfactory agreement between experimental and calculated results for the chloro and bromo derivatives. This is important since all of the complex ethanes which we have investigated are chloro and/or bromo derivatives. The calculations indicate that nonbonded (steric) interactions, dipolar interactions

Can. J. Chem. Downloaded from www.nrcresearchpress.com by 210.87.254.40 on 09/05/12
For personal use only.

TABLE 4. CONCAL calculation of energy difference and populations for 1,2-di-X-1-phenylethanes

X	Solvent	ΔE_{2-1}[a]	ΔE_{3-1}	n_1[a]	n_2	n_3	$\langle J_{AC}\rangle_{EXP}$[b]	$\langle J_{BC}\rangle_{EXP}$
Br	CCl_4	0.70	2.76	0.76	0.24	0.00	11.07	5.00
Br	$CDCl_3$	0.60	2.52	0.72	0.27	0.01	10.90	5.16
Br	$(CH_3)_3C—Cl$	0.51	2.31	0.69	0.29	0.02	10.82	5.15
Cl	CCl_4	0.55	1.51	0.67	0.27	0.06	8.45	6.17
Cl	$CDCl_3$	0.40	1.22	0.61	0.31	0.08	7.94	6.55
Cl	$(CH_3)_3C—Cl$	0.30	1.03	0.56	0.34	0.10	7.82	6.53

[a]Energy differences (in kcal/mol) and populations refer to rotamers shown below (R ≡ C_6H_5).
[b]Coupling constants in Hz. Values from ref. 2 (X = Br) or this work (X = Cl).

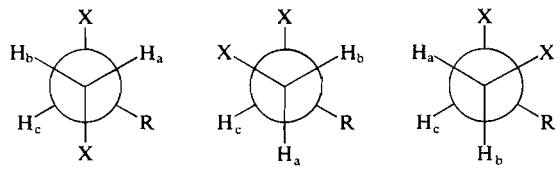

and, in solution, solvation energy are all important in determining conformational stability. Results are similar for calculations using group and bond dipole moments.

The results for 1,1,2,2-tetrachloroethane in the gas phase are particularly interesting. The experimental ΔE value of zero is surprising since one might have expected both dipolar and non-bonded interactions to be greater in the *gauche* forms. However the calculations suggest a larger non-bonded interaction in the *anti* form, leading to the small ΔE value. This probably occurs because the "6-12" potential goes through a minimum at the sum of the van der Waals' radii. With the larger X—C—X and X—C—C angles, the separation of *gauche* chlorine atoms falls close to this distance, making *gauche* chlorines more stable than *anti* chlorines where the separation is larger.

The calculations overestimate the stability of the *anti* rotamer for 1,2-difluoroethane. Abraham and Parry noted even larger discrepancies for this compound (10), suggesting that both the "6-12" and "6-exp" potentials may be too hard. However, since in both this investigation and that of Abraham and Parry (10), better results were obtained for more highly substituted fluoro derivatives, this may not be the whole answer. Csizmadia and co-workers obtained better agreement for 1,2-difluoroethane using quantum mechanical calculations (22). Agreement for 1,2-diiodoethane is better using the "6-exp" potential (10), than the "6-12" potential. The latter potential may be too soft for iodine.

Tri-substituted ethanes and unsymmetrically di- and tetra-substituted ethanes show similar agreement between calculated and experimental results (19).

In summary, agreement between calculated and experimental results is generally satisfactory, with best results for bromo and chloro derivatives. Interestingly, the calculations show the same strengths and weaknesses of those of Abraham and Parry (10), even though entirely different steric and dipolar potentials were used.

(c) Complex Substituted Ethanes

There are no experimental ΔE values for the complex substituted ethanes which we have investigated. Consequently, calculated ΔE values are compared with vicinal coupling constants and, where possible, with the order of energy levels deduced from the variation of these coupling constants with solvent and temperature (2, 3). Results for complex substituted ethanes are given in Tables 4–6.

(i) 1,2-Dihalo-1-phenylethanes

The calculated energy levels for the 1,2-dibromo derivative (Table 4) are identical to those deduced experimentally (2, 21) and the changes in population with solvent parallel to the changes in coupling constants (assuming that an *anti* coupling constant is greater than a *gauche* coupling constant). Furthermore, the calculations suggest that n_3 is negligibly small, as deduced experimentally (2). Snyder's approximate method (21) (see above) gives $\Delta E_{2-1} = +0.73$ kcal/mol in CCl_4 while CONCAL gives $+0.70$ kcal/mol.

The calculations for 1,2-dichloro-1-phenyl-

Can. J. Chem. Downloaded from www.nrcresearchpress.com by 210.87.254.40 on 09/05/12
For personal use only.

TABLE 5. CONCAL calculations of energy differences and populations for 1,2-di-X-2Y-1-phenylethanes

Isomer	X	Y	Solvent	ΔE_{5-4}	ΔE_{6-4}	n_4[a]	n_5	n_6	$\langle J_{AB}\rangle_{CALCD}$[b]	$\langle J_{AB}\rangle_{EXPT}$[c]
(a) 1,2-Dihalo-1-phenylpropanes										
erythro	Br	CH_3	$CDCl_3$	1.19	1.20	0.78	0.11	0.11	—[d]	10.16
threo	Br	CH_3	$CDCl_3$	−0.01	1.32	0.47	0.48	0.05	—[d]	5.68
erythro	Cl	CH_3	$CDCl_3$	0.44	0.67	0.55	0.27	0.18	—[d]	7.82
threo	Cl	CH_3	$CDCl_3$	−0.21	0.48	0.35	0.49	0.16	—[d]	6.00
(b) 1-Phenyl-1,2,2-trihaloethanes										
—	Br	Br	CCl_4	0.83	1.55	0.75	0.19	0.06	7.47	7.35
erythro	Br	Cl	CCl_4	1.06	1.24	0.77	0.13	0.10	7.66	7.86
threo	Br	Cl	CCl_4	0.49	1.50	0.66	0.29	0.05	6.79	6.02
erythro	Cl	Br	CCl_4	0.16	1.06	0.52	0.40	0.08	5.76	5.66
threo	Cl	Br	CCl_4	0.71	0.80	0.63	0.20	0.17	6.66	6.58
—	Cl	Cl	CCl_4	0.27	0.84	0.53	0.34	0.13	5.88	5.98

[a]Energy differences (in kcal/mol) and populations refer to rotamers shown below (R ≡ C_6H_5, E ≡ *erythro* isomer, T ≡ *threo* isomer).
[b]Estimated using eq. 7 (see text).
[c]Experimental values from refs. 2 and 3 or this work (in Hz).
[d]No coupling constants were calculated for this set due to limited number of data points for electronically similar compounds.

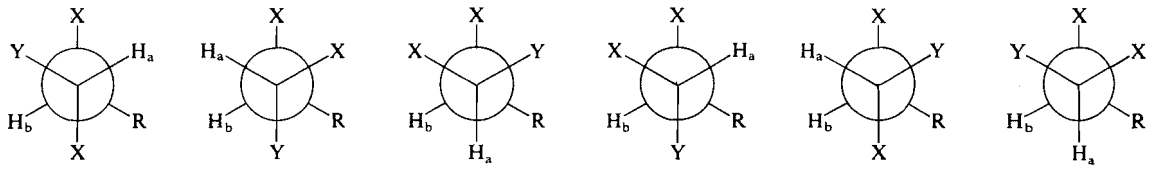

TABLE 6. CONCAL calculations of energy differences, populations and coupling constants for 1,1,2-tri-X-propanes

X	Solvent	ΔE_{5-4}[a]	ΔE_{6-4}	n_4[a]	n_5	n_6	$\langle J\rangle_{CALCD}$[b]	$\langle J\rangle_{EXP}$[c]
Br	CCl_4	−0.79	−0.44	0.15	0.55	0.30	3.17	3.20
Br	$CDCl_3$	−0.78	−0.82	0.12	0.42	0.46	3.07	3.20
Br	$(CH_3)_3C—Cl$	−0.76	−1.08	0.09	0.34	0.57	2.93	3.19
Br	$(CH_3)_2C=O$	−0.76	−1.25	0.08	0.28	0.64	2.91	3.11
Br	$(CH_3)_2S=O$	−0.75	−1.36	0.07	0.25	0.68	2.87	2.94
Cl	CCl_4	−0.47	−0.28	0.21	0.46	0.33	3.64	3.60
Cl	$CDCl_3$	−0.41	−0.69	0.16	0.32	0.51	3.39	3.56
Cl	$(CH_3)_3C—Cl$	−0.38	−0.96	0.13	0.24	0.63	3.28	3.50
Cl	$(CH_3)_2C=O$	−0.36	−1.12	0.11	0.20	0.69	3.18	3.24
Cl	$(CH_3)_2S=O$	−0.35	−1.22	0.10	0.17	0.73	3.13	3.01

[a]Energy differences (in kcal/mol) and populations refer to rotamers shown below (R ≡ CH_3).
[b]Estimated using eq. 7 (see text).
[c]Experimental values from ref. 3 (in Hz).

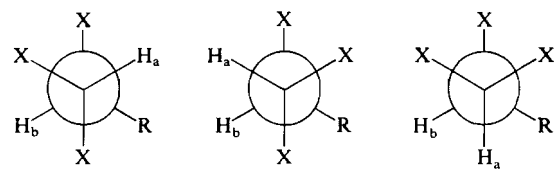

ethane indicate a smaller population of rotamer **1** than for the dibromo derivative and a significant population for **3** which increases with ε. The smaller value of $\langle J_{AB}\rangle$ is consistent with the smaller value of n_1 while the decrease in $\langle J_{AB}\rangle$ + $\langle J_{BC}\rangle$ with increasing ε is consistent with the calculated non-zero value of n_3 (since both coupling constants are *gauche* in **3**). Snyder's method cannot be applied since $n_3 \neq 0$.

As previously suggested (2), the preference

Can. J. Chem. Downloaded from www.nrcresearchpress.com by 210.87.254.40 on 09/05/12
For personal use only.

Can. J. Chem. Downloaded from www.nrcresearchpress.com by 210.87.254.40 on 09/05/12
For personal use only.

for rotamer **1** in the 1,2-dihalo-1-phenylethanes is due to both steric and dipolar interactions. For example, for 1,2-dibromo-1-phenylethane in CCl_4, **1** is calculated to be more stable than **2** by 0.42 kcal/mol due to steric interactions and 0.28 kcal/mol due to dipolar interactions. The importance of dipolar interactions is consistent with our observation that even remote substituents can alter conformational preference due to dipolar interactions (4).

(ii) erythro and threo 1,2-Dihalo-1-phenylpropanes

Calculations for these compounds were carried out for only one solvent ($CDCl_3$) since they involve minimization of energy with respect to three independent rotations and take considerable computer time. $CDCl_3$ was chosen since the energy level for the *threo* derivative had been estimated in this solvent (2).

The calculated populations for these compounds are generally consistent with available evidence concerning conformational preference (2) although there are two minor discrepancies. From the temperature-independence of $\langle J_{AB} \rangle$ for the *threo* dibromo derivative in $CDCl_3$ and from the intermediate value of $\langle J_{AB} \rangle$, the energy order $E_5 < E_4 < E_6$ was deduced (2). However, these observations are also consistent with rotamers **4** and **5** of equal energy and **6** much less stable, as calculated. In the case of the *threo* derivatives, the larger value of $\langle J_{AB} \rangle$ for the dichloro compound is apparently inconsistent with the calculated values for n_4. While this could, in part, reflect electronegativity differences (29), it is probably due to inadequacies in the calculations. In this case, a difference of only 0.2 kcal for ΔE_{5-4} has a profound effect on calculated populations, since ΔE_{5-4} is very small.

The most important observation is that the calculations correctly predict the relative order of n_4 values for each *erythro–threo* pair (assuming that the magnitude of $\langle J_{AB} \rangle$ is approximately proportional to n_4). This suggests the possibility that the calculations could be used in conjunction with vicinal coupling constants to identify *erythro* and *threo* isomers produced by halogenation of alkenes. The identification of diastereomers from these reactions is important in view of the interest in mechanisms of halogen addition to alkenes (23, 24). There appears to be no general method for identifying diastereomers and previous attempts to use n.m.r. spectroscopy for this purpose have led to contradictory conclusions (25–28).

(iii) 1-Phenyl-1,2,2-trihaloethanes

These compounds were produced by halogenation of the appropriate β-halostyrenes (3). Since diastereomers were produced simultaneously and were extremely similar in physical properties (3), this seemed like a particularly rigorous test of the usefulness of classical energy calculations to identify isomer pairs. Results are given in Table 5.

There is a substantial difference in n_4 values for each pair of diastereomers. Fortunately, there is a correspondingly large difference in $\langle J_{AB} \rangle$ values for these compounds, making the assignment of diastereomers straightforward. In fact, for all of the 1-phenyl-1,2,2-trihaloethanes except for the two *threo* derivatives, calculated n_4 values parallel experimental $\langle J_{AB} \rangle$ values.

In view of the electronic similarities for these six compounds as well as for the 1,1,2-trihalopropanes (assuming phenyl and methyl groups both have small electronic effects), it was decided to attempt to estimate a self-consistent set of coupling constants for these derivatives:

$$[7] \qquad \langle J_{AB} \rangle = n_4 J_4 + n_5 J_5 + n_6 J_6$$

Experimental $\langle J_{AB} \rangle$ values and calculated n_4, n_5, and n_6 values for 1-phenyl-1,2,2-trihaloethanes in CCl_4[2] and 1,1,2-trihalopropanes in CCl_4 and $(CH_3)_2S{=}O$ were used to solve for J_4, J_5, and J_6, using the least-squares criterion. Best values were $J_4 = 9.3$, $J_5 = 1.8$, and $J_6 = 2.6$ Hz. The latter two values are reasonable for *gauche* coupling constants. While 9.3 Hz is smaller than many *anti* coupling constants, it is not unreasonably small. Extrapolation of variable temperature results for $\langle J_{AB} \rangle$ for 1-phenyl-1,2,2-tribromoethane to low temperatures gave a value of 9.7 Hz for the *anti* coupling constant (19), in good agreement with the above value.

There is good agreement between all experi-

[2]Results for other solvents were not used since these compounds apparently do not obey Abraham's solvation theory in polar solvents (3). No calculations were performed for the 1,2-dihalo-1-phenylethanes since in this system there are six coupling constants for the three rotamers. Consequently, a very large number of measurements would be necessary for an adequate least squares fit. Similarly, coupling constants were not estimated for 1,2-dihalo-1-phenylpropanes since there were only four data points to estimate three coupling constants.

Can. J. Chem. Downloaded from www.nrcresearchpress.com by 210.87.254.40 on 09/05/12
For personal use only.

mental and calculated coupling constants for 1-phenyl-1,2,2-trihaloethanes except for the *threo* 1-chloro-1,2-dibromo derivative (with respective r.m.s. errors of 0.34 and 0.13 Hz with and without this derivative). The calculations appear to overestimate n_4 for the latter compound in CCl_4. This presumably accounts for the reversal of the *threo* derivatives in the comparison of n_4 and $\langle J_{AB} \rangle$. The agreement between calculated and experimental coupling constants was always significantly worse if J_4, J_5, and J_6 values were estimated with one or both assignments of *erythro–threo* pairs reversed (19). While this does not prove the assignments, it certainly supports them. Experimental evidence in support of the assignments is given in part *d*.

The calculations suggest that the differences in conformational preference for isomer pairs are primarily due to differences in steric interactions. For example, for the 2-bromo-1,2-dichloro derivatives the steric and dipolar energy values for **5** relative to **4** are respectively 0.02 and 0.25 kcal/mol for the *erythro* derivative and 0.53 and 0.23 kcal/mol for the *threo* derivative. This illustrates the sensitivity of the calculations since these differences in steric interactions are not apparent from an inspection of the rotamers (Table 5).

(iv) 1,1,2-Trihalopropanes

If one counts the total number of *gauche* steric interactions (involving Cl, Br, and CH_3 groups) and strong *gauche* dipolar interactions (Cl and Br), the predicted energy level order is: **4** (two steric, one dipolar interaction) $<$**5** (three steric, one dipolar interaction), $<$**6** (three steric, two dipolar interactions). This simplistic approach, which worked for several phenylethane and alkane derivatives (2, 5), obviously breaks down for this system since the small $\langle J_{AB} \rangle$ values (Table 6) strongly suggest small values for n_4.

The CONCAL calculations are clearly superior to first-order predictions of the type outlined above since CONCAL predicts that **4** is the least stable rotamer for both compounds in all solvents (Table 6). Furthermore, there is excellent agreement (r.m.s. error = 0.14 Hz) between experimental and calculated coupling constants, using the same values for J_4, J_5, and J_6 as given in *iii*.

The reason for the relative instability of **4** becomes apparent from a consideration of the individual energy terms. For example, for 1,1,2-trichloropropane, the difference in steric interactions, ΔE_{5-4} and ΔE_{6-4}, are respectively -0.44 and -0.40 kcal/mol. These are almost identical to the previously discussed (see part *b*) difference in steric interactions between *gauche* and *anti* rotamers of 1,1,2,2-tetrachloroethane (-0.47 kcal/mol). In addition, there is a slightly more favorable dipolar interaction for **5** ($\Delta E_{5-4} = -0.12$ kcal/mol). This arises from stabilizing interactions between proximate $\overset{\delta+}{C}—\overset{\delta-}{Cl}$ and $\overset{\delta\delta-}{C}—\overset{\delta\delta+}{H}$ bonds. By contrast, there is an unfavorable dipolar interaction in **6**, ($\Delta E_{6-4} = +0.74$ kcal/mol) due to *gauche* C—Cl bonds. However, this is compensated by the increased solvent stabilization of **6**, which has the greatest dipole moment. This leads to a predicted reversal of stability for **5** and **6** at high dielectric constant. In summary, the calculations suggest that a combination of stabilizing *gauche* interactions between CH_3 and Cl groups in both **5** and **6** and solvent stabilization of **6** lead to **4** being the least stable rotamer. Similar *gauche* interactions have been invoked to account for the stability of the *gauche* rotamers of 1-halopropanes (10, 30).

The close similarity between experimental and calculated coupling constants (even to the extent of predicting correct relative magnitudes of changes in $\langle J_{AB} \rangle$ with solvent for the two compounds), suggests that the electrostatic solvent theory is applicable for 1,1,2-trihalopropanes. By contrast, it did not work for 1-phenyl-1,2,2-trihaloethanes in polar solvents (3). This supports our suggestion that the latter breakdown was due to specific interactions involving the phenyl group (3).

(d) Chemical and Spectroscopic Identification of Erythro and Threo Pairs

It was decided to attempt to identify the *erythro* and *threo* isomers of 1-phenyl-1,2,2-trihaloethanes by carrying out a dehydrohalogenation reaction followed by spectroscopic identification of the halostyrene derivatives produced by this reaction.

Chlorination of *trans*-β-bromostyrene in CH_2Cl_2 at room temperature gave a mixture of two products (mixture A). The major product (81%) had the larger coupling constant in CCl_4 and corresponded to the isomer tentatively identified in part *c* as *threo*-2-bromo-1,2-dichloro-1-phenylethane. The reaction mixture was further

TABLE 7. Product distribution for dehydrohalogenation of 1-phenyl-1,2,2-trihaloethanes and n.m.r. spectral data used for identifying product β-dihalostyrenes

(a) Dehydrohalogenation products for mixtures of erythro- and threo-1-phenyl-1,2,2-trihaloethanes

From mixture A (see text)			From mixture B		
Peak	Peak position (in p.p.m. relative to TMS)	%	Peak	Peak position (p.p.m.)	%
1	7.11	4	1	7.10	20
2	7.03	58	2	7.03	62
3	6.81	9	3	6.78	5
4	6.79	4	4	6.73	3
5	6.62	15	5	6.71	5
6	6.44	8	6	6.61	5

(b) Substituent effects of β-halogens upon α-proton chemical shifts in cis and trans β-halostyrenes

X	Isomer	$\Delta\delta_\alpha$[a]
Br	*trans*	+0.41
Br	*cis*	+0.37
Cl	*trans*	+0.12
Cl	*cis*	−0.09

(c) Predicted and experimental chemical shifts for β-dihalostyrenes (δ scale)

Isomer[b]	Predicted chemical shift[c]	Experimental chemical shift
7	7.11	7.11
10	6.94	7.03

[a]Relative to unsubstituted styrene (δ_α = 6.62 p.p.m.).
[b]See Fig. 1.
[c]Predicted shift equals shift for unsubstituted styrene plus effects of two substituents, *e.g.* Cl *trans* and Br *cis* to the phenyl group for 7.

reacted with 0.5 *M* potassium *t*-butoxide in *t*-butyl alcohol and worked-up according to the method of Fahey and Schubert (31). The n.m.r. spectrum of the reaction product showed six vinyl proton singlets, presumably corresponding to six different dihalostyrenes (see Table 7). This is the expected result (see Fig. 1), assuming only *trans*-dehydrohalogenation (32). The two peaks at lowest field are identified as peaks due to α-protons, both from the chemical shifts and because they were significantly broadened by long-range coupling to the phenyl protons (only α protons should show this coupling (33)).

The styrene with the vinyl peak at 7.03 δ is produced in such large yield that it clearly must be produced from the major isomer.[3] This styrene is either **7** or **10**. There has been considerable success in identifying vinyl derivatives by n.m.r. spectroscopy, assuming additivity of substituent effects (34, 35). Consequently, the chemical shifts of styrene and β-halostyrenes were measured in CCl_4. Chemical shifts of the β-dihalostyrenes were then predicted, assuming additive effects due to the β substituents. The results suggest that the predominant product is **10** (Table 7). Calculations based on three other sets of additive substituent parameters (34–36) gave the same prediction (19). **10** would be produced by *trans*-dehydrohalogenation of *threo*-1-phenyl-2-bromo-1,2-dichloroethane (see rotamer $\mathbf{6}_T$, X = Cl, Y = Br). Consequently, the *threo* product must be the major product and have the larger vicinal coupling constant, as predicted by CONCAL.

Bromination of a 50:50 mixture of *cis*- and *trans*-β-chlorostyrene in CCl_4 at 5 °C again gave two products (mixture B) with the major

[3]A β-dihalostyrene is the expected major product since the β hydrogen should be more acidic than the α hydrogen.

Can. J. Chem. Downloaded from www.nrcresearchpress.com by 210.87.254.40 on 09/05/12
For personal use only.

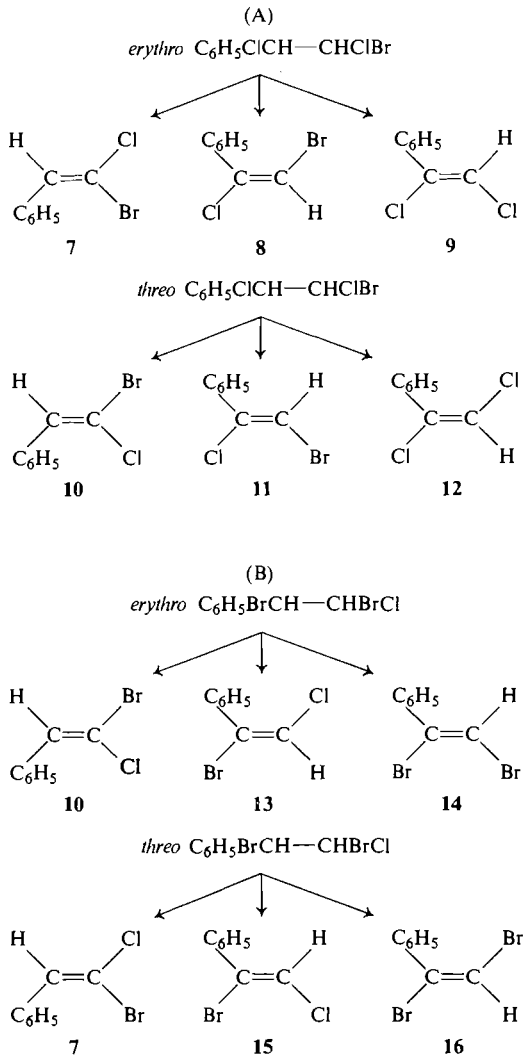

FIG. 1. Possible dihalostyrenes produced by dehydrohalogenation of mixtures of *erythro*- and *threo*-1-phenyl-1,2,2-trihaloethanes.

product (64%) having the larger coupling constant (bromination of the *trans*-styrene in CH_2Cl_2 gave a 50:50 mixture). Dehydrohalogenation of the mixture from CCl_4 again gave **10** as the major product. This indicates that in this case the major halogenation product with the larger coupling constant was *erythro*-1-phenyl-2-chloro-1,2-dibromoethane (assuming *trans*-dehydrohalogenation, see Table 5). This again confirms the prediction by CONCAL.

The first conclusion that can be drawn from the results in this part is that CONCAL can be used in conjunction with vicinal coupling constants to identify diastereomers produced by halogenation of alkenes. The results are also of interest from a mechanistic point of view. Chlorination of *trans*-β-bromostyrene yields 81% of the *threo* product, *i.e.* the *cis* product (see rotamer $\mathbf{6}_T$, Table 5). However, this does not necessarily imply *cis*-addition. As pointed out by Fahey (23, 31), the chlorination of phenylalkenes involves a linear carbonium ion and the product distribution depends upon the relative rates of rotation about the C—C bond and of ion pair collapse, as well as the conformational preference of the carbonium ion.

The results of the bromination of β-chlorostyrene indicate a greater fraction of the *trans*-product, consistent with the results of Fahey for halogenation of 1-phenylpropenes (31).

Summary and Conclusions

We have shown that Abraham's electrostatic theory of solvation energies can be applied to complex substituted ethanes while classical energy calculations reproduce the experimental rotamer energy differences for a number of simple chloro- and bromoethanes.

The two techniques used in conjunction reproduce the energy differences for complex ethanes (as reflected by vicinal coupling constants) with reasonable accuracy. The calculations appear to be most useful for detecting trends in conformational preference for related series of compounds. For example, the experimental coupling constants for 1-phenyl-1,2,2-trihaloethanes and 1,1,2-trihalopropanes are accurately reproduced using a single set of *gauche*- and *anti*-vicinal coupling constants in conjunction with the calculated rotamer populations. One important application of this ability to detect differences in conformational preference is the ability to use the CONCAL calculations to identify diastereomers produced by chlorination or bromination of alkenes.

By breaking down energy differences into differences in steric interactions, dipole–dipole interactions, solvation energies, etc., the calculations allow the rationalization of some unexpected results such as the stability of *gauche*-rotamers in 1,1,2,2-tetrachloroethane and 1,1,2-trichloropropane. The calculations indicate that all three of the above factors are important in determining conformational preference in complex substituted ethanes.

Can. J. Chem. Downloaded from www.nrcresearchpress.com by 210.87.254.40 on 09/05/12
For personal use only.

Financial support from the National Research Council of Canada is gratefully acknowledged.

1. J. P. LOWE. Progress in physical organic chemistry. Vol. VI. *Edited by* A. Streitwieser Jr. and R. W. Taft. Interscience, New York. 1968.
2. W. F. REYNOLDS and D. J. WOOD. Can. J. Chem. **47**, 1295 (1969).
3. W. F. REYNOLDS and D. J. WOOD. Can. J. Chem. **49**, 1209 (1971).
4. G. K. HAMER, W. F. REYNOLDS, and D. J. WOOD. Can. J. Chem. **49**, 1755 (1971).
5. D. A. DAWSON and W. F. REYNOLDS. Can. J. Chem. **49**, 3438 (1971).
6. J. E. WILLIAMS, P. J. STANG, and P. R. SCHLEYER. Annual review of physical chemistry. Vol. XIX. *Edited by* H. Eyring. Annual Reviews Inc., Palo Alto, California. 1968. p. 531.
7. H. A. SCHERAGA. Chem. Rev. **71**, 195 (1971).
8. (*a*) R. J. ABRAHAM and M. A. COOPER. J. Chem. Soc. D, 588 (1966); (*b*) R. J. ABRAHAM and M. A. COOPER. J. Chem. Soc. B, 202 (1967); (*c*) R. J. ABRAHAM. J. Phys. Chem. **73**, 1192 (1969).
9. R. J. ABRAHAM and R. H. KEMP. J. Chem. Soc. B, 1240 (1971) and references therein.
10. R. J. ABRAHAM and K. PARRY. J. Chem. Soc. B, 539 (1970).
11. L. PAULING. The nature of the chemical bond. Cornell University Press, Ithaca, New York. 1960. pp. 187–193.
12. J. LIELMEZS and B. J. HAGAN. Theor. Chim. Acta, **15**, 89 (1969).
13. J. LEHN and G. OURISSON. Bull. Soc. Chim. Fr. 1113 (1965).
14. D. M. BISHOP and D. P. CRAIG. Mol. Phys. **6**, 139 (1963).
15. L. E. SUTTON. Determination of organic structures by physical methods. Vol. 1. Academic Press, New York. 1965. Chapt. 9.
16. R. A. SCOTT and H. A. SCHERAGA. J. Chem. Phys. **45**, 2091 (1966).
17. J. A. A. KETELAAR. Chemical constitution. Elsevier, Amsterdam. 1953. p. 90.
18. Handbook of chemistry and physics. 51st Ed. *Edited by* R. C. Weast. Chemical Rubber Co., Cleveland, Ohio. 1971.
19. D. J. WOOD. Ph.D. Thesis, University of Toronto, Toronto, Ontario. 1972.
20. WEI-CHUWAN LIN. J. Chem. Phys. **52**, 2805 (1970).
21. E. I. SNYDER. J. Am. Chem. Soc. **88**, 1165 (1966).
22. S. WOLFE, A. RAUK, L. M. TEL, and I. G. CSIZMADIA. J. Chem. Soc. (B) 136 (1971).
23. R. C. FAHEY. Topics in stereochemistry. Vol. III. *Edited by* e. L. Eliel and N. L. Allinger. Interscience, New York. 1968.
24. P. B. DE LA MARE and R. BOLTON. Electrophilic additions to unsaturated systems. *Edited by* C. Eaborn. Elsevier, New York. 1965.
25. R. A. AUERBACH and C. A. KINGSBURY. Tetrahedron, **27**, 2069 (1971) and references therein.
26. G. H. SCHMID. Can. J. Chem. **46**, 3415 (1968).
27. J. C. RANDALL, R. L. VAULX, M. E. HOBBS, and C. R. HAUSER. J. Org. Chem. **30**, 2035 (1965).
28. G. P. NEWSOROFF and S. STERNHELL. Aust. J. Chem. **21**, 747 (1968).
29. R. J. ABRAHAM and G. GATTI. J. Chem. Soc. B, 961 (1969).
30. E. L. ELIEL, N. L. ALLINGER, S. J. ANGYAL, and G. A. MORRISON. Conformational analysis. Interscience, New York. 1965. p. 16.
31. R. C. FAHEY and C. SCHUBERT. J. Am. Chem. Soc. **87**, 5172 (1965).
32. G. KÖBRICH and P. BUCK. Chemistry of acetylenes. *Edited by* H. G. Viehe. Marcel Dekker Press, New York. 1069. Chapt. 2.
33. M. J. BARFIELD, C. J. MACDONALD, I. R. PEAT, and W. F. REYNOLDS. J. Am. Chem. Soc. **93**, 4195 (1971).
34. S. W. TOLBY. J. Org. Chem. **34**, 1281 (1969).
35. J. W. EMSLEY, J. FEENEY, and L. SUTCLIFFE. High resolution nuclear magnetic resonance spectroscopy. Pergamon Press, New York. 1965. p. 716.
36. L. J. DOLBY, C. WILKINS, and T. G. FREY. J. Org. Chem. **31**, 1110 (1966).
37. A. BONDII. J. Phys. Chem. **68**, 441 (1964).
38. Tables of interatomic distances and configuration in molecules and ions. Chem. Soc. (London) Spec. Publ. No. 11 (1958) and No. 18 (1965).

Can. J. Chem. Downloaded from www.nrcresearchpress.com by 210.87.254.40 on 09/05/12
For personal use only.

Dielectric Relaxation and Intramolecular Rotation in Aliphatic Ketones

JOHN CROSSLEY

Department of Chemistry, Lakehead University, Thunder Bay, Ontario

Received April 2, 1973

Dielectric constants and losses have been obtained for a number of aliphatic and aromatic ketones in cycloexane, *n*-hexadecane, decalin and paraffin oil – cyclohexane mixtures at up to ten frequencies between 1 and 145 GHz at 25 °C. Static dielectric constants have also been measured at 2 MHz. The results for each system have been analyzed in terms of a Cole–Cole distribution. The relaxation times and their viscosity dependence are discussed in terms of dipole reorientation by intramolecular and whole molecule rotations.

Les constantes et les pertes diélectriques ont été obtenues pour un certain nombre de cétones aliphatiques et aromatiques dans le cyclohexane, *n*-hexadécane, décaline et dans des mélanges d'huile de parafinne – cyclohexane jusqu'à dix fréquences de 1 à 145 GHz à 25 °C. Les constantes diélectriques statiques ont été également mesurées à 2 MHz. Les résultats pour chaque système ont été analysés par rapport à la distribution Cole–Cole. Les temps de relaxation et leurs variations en fonction de la viscosité ont été discutés par rapport à la réorientation dipolaire par des rotations intramoléculaires et celles de la molécule entière.

[Traduit par le journal]

Can. J. Chem., **51**, 2671 (1973)

Can. J. Chem. Downloaded from www.nrcresearchpress.com by 210.87.254.5 on 09/05/12
For personal use only.

Introduction

Dielectric relaxation times have been obtained for some carefully chosen aliphatic amines (1), bromides (2), ketones (3), and alkenes (4) as part of a systematic study of the factors governing the mechanisms of dipole reorientation in aliphatic chain compounds. For the straight chain 1-aminoalkanes and 2-alkanones, the mean relaxation times are virtually independent of the size of the *n*-alkyl group, and dipole reorientation apparently occurs by the intramolecular rotation of the terminal $-NH_2$ and $-COCH_3$ groups, respectively. The relaxation times for the primary amines are independent of the location of the $-NH_2$ group on the alkyl chain. In contrast, if the carbonyl group of a normal alkanone is removed from the chain end, the relaxation time detectably lengthens, probably because the intramolecular process is restricted and whole molecule rotation makes an increased contribution to the dielectric absorption. The intramolecular process is apparently restricted in secondary and tertiary amines, which have much longer relaxation times than the primary amines. Dipole reorientation in 1-alkenes and *n*-alkylbromides appears to involve the rotation of a variety of molecular segments from the polar end group to the whole molecule, and their relaxation times which lengthen with increased chain length are longer than those for analogous primary *n*-alkylamines and 2-alkanones.

In this paper the previous work on ketones is extended to include compounds in which intramolecular rotation may be restricted. Several of the previously examined ketones have been measured in more viscous solvents. The viscosity dependence of the mean dielectric relaxation time may be influenced by the degree to which whole molecule and intramolecular rotations contribute to the absorption, since intramolecular relaxation times have been considered to be relatively insensitive to the macroscopic viscosity (5) which is not the case for molecular relaxation times.

Experimental

The apparatus and procedure employed to determine dielectric constants, ε', and dielectric losses, ε'', at 1–145 GHz have been described previously (6–8). Static dielectric constants, ε_0, were measured at 2 MHz using a WTW Dipolmeter. All the chemicals were dried and distilled prior to use. The polar solute concentrations for all the solutions were generally about 0.03 mol fraction. The paraffin oil – cyclohexane mixtures contained about 30% by volume paraffin oil (Canlab). Viscosities (η) were measured using Ubbelhode type viscometers.

Results

The experimental η, ε' ($\pm 0.5\%$), and ε'' ($\pm 5\%$) values measured at 25 °C are given in Table 1 which has been placed in the Depository

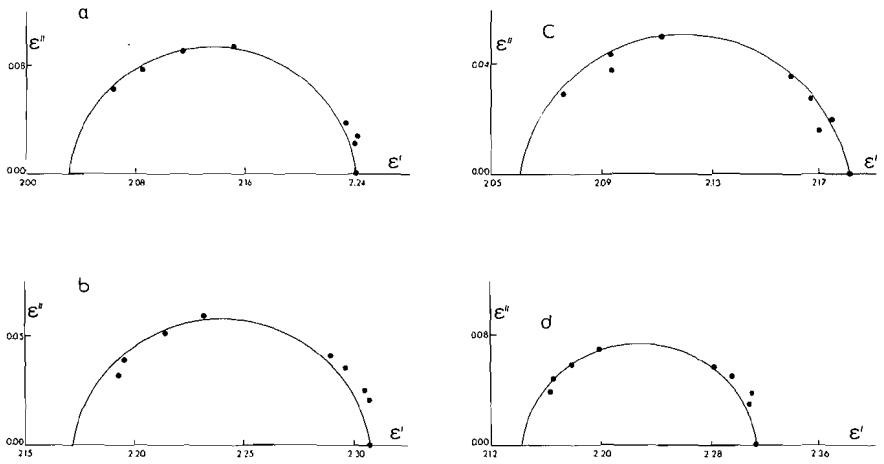

FIG. 1. Cole–Cole plots for 7-tridecanone in (*a*) cyclohexane, (*b*) decalin, (*c*) hexadecane, and (*d*) paraffin oil – cyclohexane at 25 °C. The experimental points were measured at 35.1, 24.0, 16.2, 9.32, 2.48, 1.93, 1.25, 0.97, and 0.002 GHz. The 2.48 GHz point is absent for the cyclohexane solution.

TABLE 2. Dielectric relaxation data at 25 °C (the units for τ_0 and μ are picoseconds and Debyes, respectively)

Compound	Cyclohexane			Decalin			Hexadecane			Paraffin oil – cyclohexane		
	τ_0	α	μ	τ_0	α	μ	τ_0	α	μ	τ_0	α	μ
2-Hexanone*	4.0	0.04	2.62	5.2	0.09	2.63	4.8	0.15	2.70	6.6	0.05	2.36
2-Nonanone*	5.9	0.14	2.73	8.3	0.09	2.56	8.5	0.15	2.65	12.5	0.06	2.57
5-Nonanone*	7.2	0.06	2.63	9.7	0.06	2.58	9.6	0.10	2.60	12.1	0.06	2.40
7-Tridecanone	13.8	0.07	2.53	20.8	0.08	2.53	19.4	0.10	2.58	24.2	0.08	2.47
8-Pentadecanone*	17.1	0.13	2.57	24.8	0.12	2.54	24.0	0.13	2.58	31.8	0.14	2.55
2-Nonadecanone*	8.3	0.18	2.61	11.2	0.17	2.54	12.8	0.16	2.60	15.6	0.13	2.48
10-Nonadecanone*	22.0	0.15	2.58	32.0	0.11	2.52	31.9	0.11	2.58	38.9	0.13	2.53
11-Heneicosane	22.2	0.11	2.43	35.3	0.09	2.44	—	—	—	—	—	—
di-*t*-Butyl ketone	3.4	0.05	2.51	—	—	—	—	—	—	—	—	—
2,2-Dimethyl-3-heptanone	6.9	0.09	2.44	—	—	—	—	—	—	—	—	—
3-*n*-Butyl-2-heptanone	19.7	0.10	2.59	—	—	—	36.9	0.11	2.68	—	—	—
1,3-Diphenyl-2-propanone	12.5	0.10	2.57	—	—	—	—	—	—	—	—	—
Hexanophenone	18.8	0.11	2.75	39.3	0.08	2.68	41.2	0.09	2.65	55.4	0.09	2.67

*From ref. 3.

of Unpublished Data.[1] For all the systems it is possible to draw depressed center semicircular arcs through the experimental points, within the experimental error, when plotted in the complex plane and Fig. 1 shows some typical data. Consequently, the ε', ε'', and ε_0 values for each solute–solvent system were analyzed for a mean relaxation time, τ_0, a Cole–Cole distribution parameter, α, and a high frequency dielectric constant, ε_∞, using a computer fit to the Cole–Cole equations (9). Apparent dipole moments, μ, were calculated as before (3) from the ε_0 and ε_∞ values. The τ_0, α, and μ data are presented in Table 2. The errors involved in the above methods have been discussed (10).

[1]Copies of Table 1 are available at a nominal charge, from the Depository of Unpublished Data, National Science Library, National Research Council of Canada, Ottawa, Canada K1A 0S2.

Discussion

The mean relaxation times for 7-tridecanone and 11-heneicosanone in cyclohexane solution

Can. J. Chem. Downloaded from www.nrcresearchpress.com by 210.87.254.5 on 09/05/12
For personal use only.

Can. J. Chem. Downloaded from www.nrcresearchpress.com by 210.87.254.5 on 09/05/12
For personal use only.

are consistent with those previously obtained for 8-pentadecanone and 10-nonadecanone (3). These symmetrically substituted ketones have much longer relaxation times than any of the 2-alkanones and dipole reorientation, by twisting around the R—C and R′—C bonds, is apparently restricted when both R and R′ in

R—C—R′ have about five or more carbon atoms (the relaxation time for 5-nonanone, R = R′ = 4 carbon atoms, is not significantly longer than that for 2-nonanone). Similar results have been obtained for aliphatic ethers (11). The relaxation time for di-*t*-butyl ketone is quite short and very similar to that for acetone, 3.2 ps, in dilute solution (12). In addition, α is also quite small and it would appear that the *t*-butyl groups do not interfere with one another in the intramolecular twisting mechanism which is the major process of dipole reorientation. The relaxation time for 2,2-dimethyl-3-heptanone is quite similar to those for the nonanones (3), also in cyclohexane solution. Thus the two methyl groups adjacent to the carbonyl group of the former molecule are insufficient in size to hinder intramolecular rotation to any significant extent. In contrast, the *n*-butyl group in 3-*n*-butyl-2-heptanone appears to have a marked steric effect. The relaxation time for this molecule in cyclohexane is considerably longer than those for the 2-alkanones, and in the more viscous hexadecane, it is longer than that for 10-nonadecanone. It would appear that rotation of the whole molecule makes an important contribution to the dielectric absorption of this substituted heptanone. The Cole–Cole distribution parameter α is considerably greater than zero; however, the data could not be analyzed in terms of contribution from two reasonable relaxation times. The mean relaxation time for 1,3-diphenyl-2-propanone is much shorter than that for benzophenone (13), 19 ps in cyclohexane at 25 °C, which has a somewhat similar shape and size. Benzophenone is an essentially rigid molecule and thus intramolecular twisting about the benzyl – carbonyl group bonds must make a significant contribution to the dielectric absorption of 1,3-diphenyl-2-propanone. This is not unreasonable since the resonance effects thought to be responsible for the high barrier to intramolecular rotation in benzophenone are considerably reduced in the propanone. Unlike the aliphatic ketones, segmental rotations are largely unimportant for this aromatic ketone and the possibility of two overlapping Debye dispersions due to whole molecule and intramolecular rotations is more probable. Although the Cole–Cole plot for this compound in cyclohexane does not show any distinct separation, it is possible to obtain a good fit to the experimental ε' and ε'' data using $\tau_1 = 18$ ps, $\tau_2 = 5$ ps, and $C_1 = 0.7$, which are not unreasonable values for the above processes. The mean relaxation times for hexanophenone, benzophenone (13), and acetophenone (14) in cyclohexane at 25 °C are 18.8, 19, and 10.2 ps, respectively, and the respective values in decalin also at 25 °C are 39.3, 34.6 (15), and 17.5 ps. The resonance effects which restrict intramolecular rotation in benzophenone are not as important for acetophenone. The mean relaxation time for the latter is shorter than expected for molecular rotation and its dielectric absorption data may be analyzed in terms of two relaxation times which can be reasonably assigned to whole molecule and intramolecular rotation. Hexanophenone is similar in size to benzophenone and the mean relaxation times of these two ketones in both cyclohexane and decalin are quite close. For hexanophenone it would appear that the steric effect of the alkyl group, together with the resonance effect of the aromatic group, give rise to a high barrier to intramolecular rotation and dipole reorientation is dominated by rotation of the whole molecule.

The relaxation time of a rigid molecule lengthens with increased solvent viscosity, but experiments have shown (16) that the viscosity dependence of the relaxation time does not conform to a simple relationship and is considerably influenced by the shape of the solute molecule and the relative size of the solute and solvent molecules. However, the ketones under investigation are non-spherical in shape and although τ_0 will not be directly proportional to the macroscopic viscosity it should detectably lengthen if the rotation of the whole molecule makes any significant contribution to the dielectric absorption. Intramolecular rotation occurs with relatively little displacement of surrounding molecules and the relaxation times have generally been considered to be independent of viscosity. Thus for a system in which dipole reorientation is achieved by both whole molecule (τ_1) and intramolecular (τ_2) rotation the ratio τ_1/τ_2 would be expected to increase with increased viscosity

TABLE 3. Ratios of relaxation times in cyclohexane (τ_C), decalin (τ_D), hexadecane (τ_H), and paraffin oil – cyclohexane (τ_P), and reduced relaxation times in cyclohexane (τ_{RC}) and paraffin oil – cyclohexane (τ_{RP}) at 25 °C ($\eta_D/\eta_C = 3.5$; $\eta_H/\eta_C = 3.8$)

Solute	τ_D/τ_C	τ_H/τ_C	τ_P/τ_C	η_P/η_C	τ_{RP}/τ_{RC}
2-Hexanone	1.3	1.2	1.7	8.5	0.17
2-Nonanone	1.4	1.4	2.1	13.1	0.16
5-Nonanone	1.4	1.3	1.7	8.4	0.18
7-Tridecanone	1.5	1.4	1.9	10.5	0.17
8-Pentadecanone	1.5	1.4	1.9	11.6	0.16
2-Nonadecanone	1.4	1.5	1.9	11.6	0.16
10-Nonadecanone	1.5	1.5	1.8	11.7	0.15
11-Heneicosanone	1.6	—	—	—	—
3-*n*-Butyl-2-heptanone	—	1.9	—	—	—
Hexanophenone	2.1	2.2	3.0	12.1	0.43

and may give rise to a distortion of the Cole–Cole plot, which should facilitate an analysis in terms of two relaxation times. The Cole–Cole plots for the ketones in decalin, hexadecane, and paraffin oil – cyclohexane are as symmetrical as those obtained in the less viscous cyclohexane (Fig. 1). The relaxation times in Table 2 do lengthen with increased solvent viscosity, however; *i.e.* cyclohexane < decalin ≃ hexadecane < paraffin oil – cyclohexane.

A comparison of the effect of increased viscosity on the relaxation time of each ketone is given in Table 3, and, as expected even for rigid molecules, the viscosity ratios are much greater than the corresponding relaxation time ratios. The τ_P/τ_C value for 2-nonanone appears to be anomalously high when compared with the values for the other 2-alkanones; however, the viscosity of the 2-nonanone in paraffin oil – cyclohexane solution was greater than the others. In order to partially correct for the differences in viscosity of the paraffin oil – cyclohexane solvents, the reduced relaxation time (τ_0/η) ratios are presented in the last column of Table 3. Hexanophenone and 3-*n*-butyl-2-heptanone had previously been considered to be rigid molecules and the ratios for these compounds in Table 3 are greater than those for the other ketones in all the solvents. The values for the first seven ketones in Table 3 are very similar which is somewhat surprising in view of the earlier interpretation of the cyclohexane data (3). In addition, the small differences between the relaxation times of the 2-alkanones in cyclohexane are magnified in the more viscous solvents, and it would appear that whole molecule rotation does contribute to the absorption of the 2-alkanones, but the magnitude of this contribution is less than it is for the symmetrically substituted ketones. However, it was not possible to obtain sensible analyses in terms of two relaxation times, probably because segmental rotations, which are not possible for the analyzable aromatic ketones, also contribute to the absorption. In fact, for a majority of the ketones, the distribution parameters listed in Table 2 show no significant increase with increased solvent viscosity which might indicate that the intramolecular and whole molecule relaxation times are lengthened by the same factor. The effect of viscosity on these processes for aliphatic molecules has not been investigated in any systematic studies and consequently there is little with which to compare the values in Table 3. For *n*-octylbromide dipole reorientation is thought to occur by a variety of segmental rotations and τ_H/τ_C at 25 °C is 1.2 (17). The τ_D/τ_C value for anisole at 25 °C is about 1.2 and in solution the intramolecular relaxation process has a weight factor of about 0.65 (18, 5). The τ_D/τ_C value for both acetophenone and benzophenone is about 1.7 (14, 15).

In conclusion the results presented in Tables 2 and 3 indicate that the dielectric absorption of hexanophenone and 3-*n*-butyl-heptanone contains large contributions from the rotation of the molecule as a whole. Intramolecular and molecular rotation contribute to the absorption of the other alkanones, the relative magnitude of these contributions depends on the degree to which the intramolecular process is sterically restricted. Unfortunately, possibly because the viscosities were insufficient, detectable separation of the Cole–Cole arcs into regions which could be assigned to intramolecular and molecular relaxations were not obtained.

The author wishes to thank the National Research Council of Canada for a grant to support this work.

1. S. P. TAY and J. CROSSLEY. J. Chem. Phys. **56**, 4303 (1972).
2. S. P. TAY and J. CROSSLEY. Can. J. Chem. **50**, 2031 (1972).
3. J. CROSSLEY. J. Chem. Phys. **56**, 2549 (1972).
4. J. CROSSLEY. J. Chem. Phys. To be published.
5. E. L. GRUBB and C. P. SMYTH. J. Am. Chem. Soc. **83**, 4873 (1961).

Can. J. Chem. Downloaded from www.nrcresearchpress.com by 210.87.254.5 on 09/05/12
For personal use only.

6. W. F. HASSELL, M. D. MAGEE, S. W. TUCKER, and S. WALKER. Tetrahedron, **20**, 2137 (1964).
7. S. E. KEEFE and E. H. GRANT. Rev. Sci. Instrum. **39**, 1800 (1968).
8. S. K. GARG, H. KILP, and C. P. SMYTH. J. Chem. Phys. **43**, 2341 (1965).
9. K. S. COLE and R. H. COLE. J. Chem. Phys. **9**, 341 (1941).
10. M. D. MAGEE and S. WALKER. Trans. Faraday Soc. **62**, 3093 (1966).
11. S. DASGUPTA, K. N. ABD. EL NOUR, and C. P. SMYTH. J. Chem. Phys. **50**, 4810 (1969).
12. D. H. WHIFFEN and H. W. THOMPSON. Trans. Faraday Soc. **41A**, 114 (1946).
13. D. B. FARMER and S. WALKER. Trans. Faraday Soc. **63**, 966 (1967).
14. D. B. FARMER. Ph.D. Thesis. University of Aston in Birmingham. 1967.
15. J. T. VIJ and K. K. SRIVASTAVA. Bull. Chem. Soc. Jap. **43**, 2313 (1970).
16. E. L. GRUBB and C. P. SMYTH. J. Am. Chem. Soc. **83**, 4122 (1961).
17. K. HIGASI, K. BERGMANN, and C. P. SMYTH. J. Phys. Chem. **64**, 880 (1960).
18. D. B. FARMER, A. HOLT, and S. WALKER. J. Chem. Phys. **44**, 4116 (1966).

Can. J. Chem. Downloaded from www.nrcresearchpress.com by 210.87.254.5 on 09/05/12
For personal use only.

N.M.R. Studies of Anhydrous Hydrogen Fluoride Solutions[1]

JACOB SHAMIR AND AHARON NETZER[2]

Department of Inorganic and Analytical Chemistry, The Hebrew University of Jerusalem, Israel

Received December 20, 1972

Solutions of anhydrous HF and SO_2 and electrolytes in anhydrous HF have been studied by n.m.r. Both ^1H and ^{19}F chemical shifts were studied as a function of concentration and temperature. The dimerization constant and the enthalpy of the reaction $2HF \rightleftarrows (HF)_2$ were calculated.

The results for electrolyte solutions were interpreted on the basis of two effects, ionization and the H-bond breaking effect. A linear relationship exists between δ_0, the molal chemical shft, and the ionic crystallographic radii. A temperature effect was also observed and interpreted. Solutions of salts of Lewis acids were also studied but results are less conclusive; it was shown, however, that their δ_0 values are smaller than those of alkali fluorides.

Les solutions anhydres de HF et SO_2 et d'électrolytes dans HF anhydre ont été étudiées par RMN. Les déplacements chimiques de ^1H et ^{19}F ont été étudiées en fonction de la concentration et de la température. La constante de dimérisation et l'enthalpie de la réaction $2HF \rightleftarrows (HF)_2$ ont été calculées.

Les résultats pour les solutions d'électrolytes ont été interprétés en fonction de deux effets: l'ionisation et la rupture de la liaison H. Une relation linéaire existe entre δ_0, déplacement chimique molal, et le rayon ionique cristallographique. Un effet de température a été aussi observé et interprété. Les solutions de sels d'acides de Lewis ont été également étudiées mais les résultats sont moins concluants; il a été montré cependant que les valeurs δ_0 correspondantes, sont plus petites que celles de fluorures alcalins.

[Traduit par le journal]

Can. J. Chem., **51**, 2676 (1973)

Introduction

Anhydrous hydrogen fluoride is a highly polymerized liquid. There is no clear evidence for the extent of association or of the configuration of the polymeric molecules in the liquid state. The structure of the gaseous phase has indicated the existence of cyclic polymers. On the other hand, the heat of vaporization of the liquid is rather low for a highly associated liquid. It can therefore be concluded that not much of a change occurs in the average number of polymer units per mole of HF in the transition from liquid to gas.

Depolymerization of an associated compound can be achieved in either of two ways. One is to heat the associated substance, and especially to vaporize the liquid and lower the pressure of the vapor. The second is to dilute the associated liquid with a chemically inert liquid. In this study the second method was used.

On the basis of experimental data such as the Hammet function (H_0) of mixtures of HF and SO_2 and their i.r. and Raman spectra, Hyman (1) concluded that SO_2 behaves as an inert solvent with regard to HF, and it may therefore be assumed that dilution of HF with SO_2 would cause depolymerization of HF by breaking the H-bonds. More recently, Gillespie and Humphreys (2) have provided evidence for non-ionization/reaction of SO_2 in HF using a cryoscopic technique. Both anhydrous HF and SO_2 are liquid at room temperature when kept under their own pressure and are miscible in all proportions.

Many n.m.r. studies (3) have shown that when a polymerized liquid is depolymerized by dilution with an inert liquid, the ^1H resonance of the particular hydrogen involved in the H-bond is shifted to a higher field. A similar effect was therefore expected in the case of anhydrous HF. In every H-bond, another atom is involved, *e.g.*, F, O, or N. Very little is known about how the n.m.r. of these atoms is affected when they are involved in H-bonding.

In the system HF–SO_2 it is assumed that as the concentration of HF decreases, a depolymerization effect takes place:

$$(HF)_n \rightarrow (HF)_{n-k} + (HF)_k$$

It is probably more correct to assume that a

[1]Presented in part at the 1st Winter Fluorine Conference, St. Petersburg, Florida, 1972.

[2]To whom correspondence should be addressed. Present address: Water and Wastewater Treatment Research, Canada Centre for Inland Waters, P.O. Box 5050, Burlington, Ontario.

Can. J. Chem. Downloaded from www.nrcresearchpress.com by 210.87.254.42 on 09/05/12
For personal use only.

Can. J. Chem. Downloaded from www.nrcresearchpress.com by 210.87.254.42 on 09/05/12
For personal use only.

number of polymeric species of varying chain lengths exist simultaneously in solution. Only in very dilute solutions can it be assumed that the monomer and dimer are the dominant species.

The interpretation of the n.m.r. data becomes rather complicated as the various chemical shifts for the different species present in solution are unknown and only one weighted average signal can be measured.

The data obtained at low HF concentrations have been interpreted in terms of an equilibrium between monomeric and dimeric forms of HF. From the values of the dimerization constant, K_D, at different temperatures the enthalpy of dimerization was calculated. In addition, some measurements were made of the temperature dependence of ^1H and ^{19}F chemical shifts, which could also be interpreted as being a characteristic property of the H-bond itself rather than mainly a reflection of changes in the relative amounts of various H-bonded species in equilibrium.

In recent years various ionic solutions have been studied by n.m.r. spectroscopy. Some of these have recently been reviewed by Hinton and Amis (4). In most studies carried out in solution one observes only the weighted average signal. This is the result of fast chemical exchange on the n.m.r. time scale, among the various species present. This causes the interpretation to be rather difficult unless separate chemical shifts for the different species can be determined. The observed weighted-average signal could be formulated as:

$$[1] \qquad \delta_{obs} = \sum(p_i\delta_i)$$

where p_i is the fraction of the total number of nuclei with chemical shift δ_i.

In this paper we present some results obtained by studying electrolyte solutions of alkali fluorides and salts of the Lewis acids, BF_3, AsF_5, and SbF_5 in anhydrous HF. Anhydrous HF is a highly acidic non-aqueous solvent and most solutes in it behave as bases as they become protonated by the solvent. Only a few solutes act as acids in this strongly acidic medium and these are mainly fluoride acceptors such as BF_3, AsF_5, and SbF_5. Alkali fluorides act as bases and dissociate as follows

$$[2] \qquad MF \rightleftarrows M^+ + F^-$$

$$[3] \qquad F^- + (HF)_n \rightleftarrows [(HF)_nF]^-$$

The first step we will term the *ionizing effect*. The solute dissociates into ions and the fluoride ion attaches itself to a neutral molecule to become a larger anion. The second step, the *H-bond breaking step*, involves depolymerization

$$[4] \qquad (HF)_n \rightleftarrows (HF)_{n-k} + (HF)_k$$

Solutions of salts of the Lewis acids studied can be considered as 1 : 1 electrolytes and not as bases. The major process is the ionic dissociation

$$[5] \qquad MAF_x \rightleftarrows M^+ + AF_x^-$$

where M is an alkali metal, and A is boron, arsenic, or antimony; x is 4 or 6.

Experimental

Chemicals

Anhydrous Hydrogen Fluoride

Highly purified HF was obtained by fractional distillation of commercial anhydrous HF (Matheson). Its minimum specific conductivity was 2×10^{-6} ohm^{-1} cm^{-1} at room temperature. The details of the distillation column have been described elsewhere (5).

Sulfur Dioxide

Commercial sulfur dioxide (Matheson), reputed to be 99.99% pure, was condensed into a nickel vessel containing P_2O_5. The SO_2 was cooled to liquid N_2 temperature and all the non-condensable gases pumped off until a vacuum of the order of 10^{-6} Torr was achieved. The SO_2 was then allowed to warm-up to room temperature and stand overnight. The i.r. spectra of gaseous SO_2 samples showed no bands that could be attributed to water or other impurities. In addition, a high gain ^1H n.m.r. spectrum gave no indication of the presence of protons.

Metal Fluorides and Complex Fluorides

Commercial products were used and had the following purities: LiF, 99.6%; NaF, 99.6%; KF, 99%; RbF, 99.8%; CsF, 99%; $KSbF_6$, 95%; $NaBF_4$, 99.9%; KPF_6, 98%; $NaAsF_6$, 97%; $KAsF_6$, 98%.

The alkali fluorides were heated at 120 °C overnight, before being transferred in an inert atmosphere Dry Box to KEL-F vessels (0.75 in. o.d. × 6 in.). The complex fluorides were used without prior heating.

Preparation of Solutions

All the solutions were prepared and handled on the KEL-F section of the metal vacuum line. The concentrations of the HF-SO_2 solutions were determined by weight. The solutions were prepared either directly in KEL-F n.m.r. tubes, or, when a low concentration of one of the constituents was required, in a larger KEL-F vessel (0.75 in. o.d. × 6 in.) and some of it was then poured under vacuum into the n.m.r. tube.

The electrolyte solutions were prepared in (0.75 in. o.d. × 6 in.) KEL-F containers fitted with KEL-F valves. The concentrations were determined by weight. The tubes were charged with the appropriate dried salt in a Dry Box; they were then attached to the KEL-F section of the vacuum line evacuated, and the appropriate amount of

Can. J. Chem. Downloaded from www.nrcresearchpress.com by 210.87.254.42 on 09/05/12
For personal use only.

anhydrous HF distilled in. The prepared solution was then poured, under vacuum, into the KEL-F n.m.r. tube using a Y-connection. The usual procedure was to start out by preparing the highest concentration and then diluting it further.

N.M.R. Measurements

N.M.R. Instrumentation

All measurements were performed on a Varian Analytical n.m.r. spectrometer, Model A-56/60 using KEL-F n.m.r. tubes. A Varian Automatic Voltage Regulator, Type 1581-A, was used to stabilize the voltage. The temperature was regulated by a Varian V-6040 temperature controller with a pressure switch modification for regulating the nitrogen flow.

The original instrument could detect fluorine resonances in the range from 8 000 Hz to low field to 11 000 Hz to high field of CCl_3F. For our purposes an extension of this region was needed, and this was achieved by the addition of extra crystals.

Reference Materials

TMS and CCl_3F were used as external references, respectively. The need for bulk diamagnetic susceptibility corrections was found to be negligible.

^1H Signals

All recordings were made with a 50 Hz sweep time of 250 s. For each sample 5–7 recordings were made, usually on the same chart, with a shift of 5 Hz in the sweep offset setting between one reading and the next. The numerical values of the chemical shifts, which never differed by more than ± 0.5 Hz, were then averaged. The reference calibration was done twice, once before the sample measurement and once after.

^{19}F Signals

In measurements of the fluorine resonance, a considerable broadening was observed as the solutions became dilute in anhydrous HF. This necessitated changing the sweep width, keeping it always as narrow as possible. As a result, the precision of the measurements was lower and the average error was about ± 1.0 Hz. In this case too, the reference calibration was done twice.

Results and Discussion

The HF–SO_2 System

In all the samples measured, only one resonance signal was observed for either ^1H or ^{19}F. This signal is therefore an average over all the HF molecules present in various degrees of polymerization. Apparently, the exchange rate is sufficiently fast for the signals to be completely collapsed.

The value of the chemical shift varies with the HF concentration. The lowest concentration at which signals could be observed and measured was at 0.639 *m* of HF (mole fraction = 0.0393): at this concentration the ^1H resonance has shifted by +2.78 p.p.m. (at 34 °C) and the ^{19}F resonance by −8.34 p.p.m. (at 38.5 °C), both with reference to pure anhydrous HF. The data are presented graphically in Figs. 1–3.

^1H Resonances and Concentration Dependence at Different Temperatures

The ^1H chemical shifts at 34° are presented as a function of the mole fraction of HF in Fig. 1. The data obtained at −31.5° is identical to the data presented in Fig. 1, except in the low concentration region (Fig. 2). The chemical shift, as seen in Figs. 1 and 2, moves towards higher field almost linearly with decreasing concentration. The degree of polymerization is higher at lower temperatures, and it is therefore to be expected that the change in chemical shift with concentration is more pronounced at lower temperatures. This is seen in Fig. 2, where the slope in the dilute region is steeper at lower temperatures. Assuming that in the region of low HF concentration (0.639–2.039 *m*) the dominant species are the monomer and the dimer, the

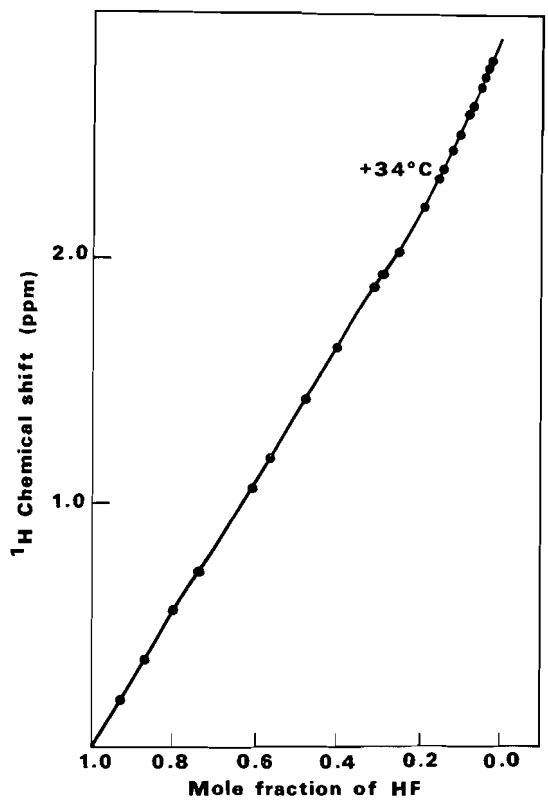

FIG. 1. Variation of proton chemical shift, expressed in p.p.m. with reference to pure anhydrous HF *vs.* concentration expressed in mole fraction in the HF–SO_2 system at 34 °C.

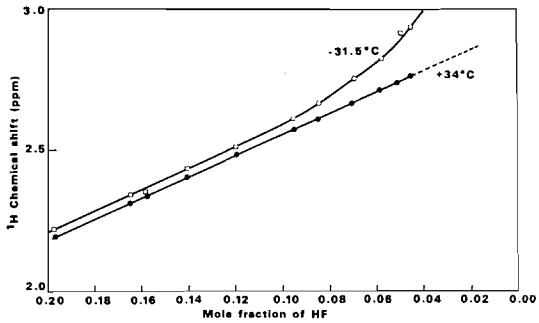

FIG. 2. Enlarged plot of the low HF concentration region: variation of proton chemical shift, expressed in p.p.m. with reference to pure anhydrous HF *vs.* concentration expressed in mole fraction in the HF–SO_2 system at 34 °C and −31.5 °C.

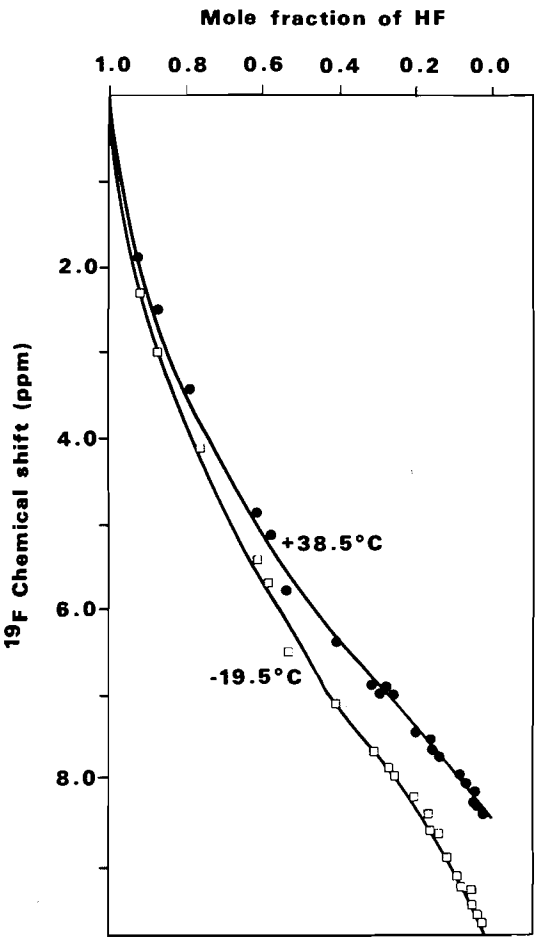

FIG. 3. Variation of fluorine chemical shift expressed in p.p.m. with reference to pure anhydrous HF *vs.* concentration expressed in mole fraction in the HF–SO_2 system at two temperatures.

observed chemical shift will be given by the following equations

$$[6] \qquad \delta_{obs} = (\delta_M P_M) + (\delta_D P_D)$$

$$[7] \qquad \delta_{obs} = \left(\delta_M \frac{X_M}{X_T}\right) + \left(\delta_D \frac{2X_D}{X_T}\right)$$

where $X_T = X_M + 2X_D$; and δ_M, δ_D are the chemical shifts of monomer and dimer, P_M, P_D are the fraction of the total number of nuclei in monomer or dimer form, X_M, X_D are the mole fractions of monomers and dimers, and X_T is the total mole fraction.

The dimerization constant is therefore given by

$$[8] \qquad K_D = \frac{[X_D]}{[X_T - 2X_D]^2}$$

From formula 7 we can derive

$$[9] \qquad \delta_{obs}\frac{X_T}{X_M} = \delta_M + \delta_D\frac{2X_D}{X_M}$$

or

$$[10] \qquad \delta_{obs} Y = \delta_M + \delta_D Z$$

where

$$Y = \frac{X_T}{X_M} \quad \text{and} \quad Z = \frac{2X_D}{X_M}$$

If one plots values for $\delta_{obs} Y$ *vs.* Z for the best value of K_D, a straight line should be obtained. From the slope of the line and its intersection both δ_M and δ_D can be calculated. Such a computation was done according to the method of Groves *et al.* (6) using a CDC 6400 computer. The results are tabulated below for two temperatures, the shifts being relative to pure anhydrous HF.

TABLE 1.

Temperature (°C)	δ_D(Hz)	δ_M(Hz)	K_D
+34	98.7	197.3	7.5
−31.5	106.1	379.3	123.0

In using these values the chemical shift was recalculated taking into account the K_D, δ_M, and δ_D values. The calculated values were compared to the δ_{obs} and were found to be in agreement within ±0.6%. In studying the chemical shifts as a function of pressure in the gas phase, Mackor *et al.* (7) obtained a value of 4.35 p.p.m. (261 Hz) for δ_M at room temperature.

Can. J. Chem. Downloaded from www.nrcresearchpress.com by 210.87.254.42 on 09/05/12
For personal use only.

Can. J. Chem. Downloaded from www.nrcresearchpress.com by 210.87.254.42 on 09/05/12
For personal use only.

From the values of K_D at different temperatures, the enthalpy of the dimerization was calculated

$$\Delta H = \frac{-\mathrm{d} \ln K}{\mathrm{d}(1/T)} R$$

The value found was

$$\Delta H = -6.29 \text{ kcal/mol}$$

In the cyclic hexamer – monomer equilibrium, one obtains $6\,HF \rightleftarrows (HF)_6$. This would mean that six H bonds are formed and accordingly this would result in a value of $-6.29 \times 6 = -37.74$ kcal/mol. This is in good agreement with other data of ΔH in the literature where different methods have been used. These data lie between -38.0 and -40.8 kcal/mol (8).

^{19}F Resonances

The results are presented in Fig. 3, which shows that the ^{19}F resonances shift towards lower field, as the HF concentration decreases. This is in contrast to the results obtained in n.m.r. studies of HF in the gas phase (7, 9). Our studies of the temperature effect in pure liquid anhydrous HF, as discussed later, also indicate that both ^1H and ^{19}F resonances shift towards higher field as the temperature increases. All these parameters, namely decreasing pressure in the gas phase, increasing the temperature of pure liquid anhydrous HF, and diluting HF solutions, result in depolymerization, and therefore, should be reflected by a shift towards higher field in the n.m.r. spectra. High field ^{19}F chemical shifts have been observed in the gas phase and in pure anhydrous HF, but not in $HF–SO_2$ solutions. This exception could be explained as the result of an enormous "solvent effect". This effect has been studied by Evans (10, 11) who compared the chemical shifts of CCl_4 solutions of various compounds containing fluorine with those of similar compounds containing hydrogen. For instance, CF_4 at infinite dilution in CCl_4 has a chemical shift of 9.24 p.p.m., compared to 0.5 p.p.m. in case of CH_4. In both cases, no interaction between solute and solvent is expected. The large "solvent effect" in the case of ^{19}F chemical shifts is a result of changes in the paramagnetic term, σ_{para}^{AA}, for the electrons localized on fluorine; whereas, for hydrogen, the dominant term is the diamagnetic term, σ_{AA}^{dia}, in the Ramsey equation (ref. 3, p. 130). The "solvent effect" observed in the ^{19}F n.m.r. of $HF–SO_2$ solution is large and in the opposite direction when compared to changes resulting from the breaking of H-bonds. Among the various factors responsible for the "solvent effect", Evans lists the extent to which the fluorine atom is protected from the influence of the solvent. In the case of HF, and especially when H-bonds are broken, the fluorine is under a greater influence from the solvent. In addition, this solvent has a large dipole moment, strongly polarizing the H-bonded fluorine. Observing such a large "solvent effect" and not being able to separate it from the H-bond breaking effect, did not enable us to interpret the ^{19}F n.m.r. data quantitatively.

Temperature Effect in Pure Anhydrous HF

The changes in the n.m.r. spectrum of pure liquid anhydrous HF were studied as a function of temperature. Raising the temperature causes a change in the chemical shift towards higher field, which is related to a depolymerization process. This is observed in both the ^1H and ^{19}F resonances and is in agreement with other studies (7). The data are presented graphically in Fig. 4.

The approximate linear dependence is given by

$$\delta_{^1H}(HF) = 7.70 + (t \times 1.20 \times 10^{-2}) \text{ p.p.m.}$$
(with respect to external TMS)

$$\delta_{^{19}F}(HF) = 198.65 + (t \times 4.0 \times 10^{-2}) \text{ p.p.m.}$$
(with respect to external CCl_3F)

where t is the temperature in °C.

It should be mentioned that the chemical shifts

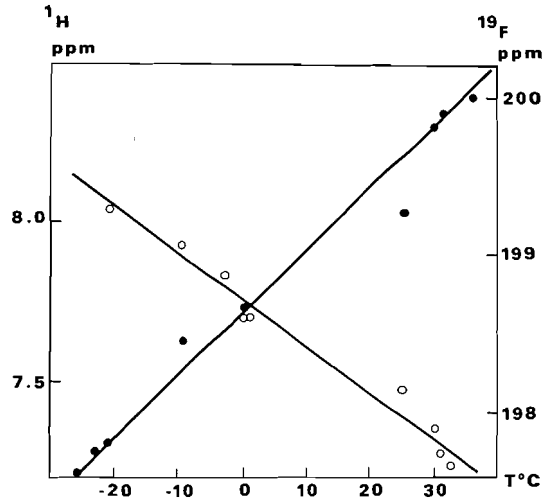

FIG. 4. ^1H and ^{19}F n.m.r. chemical shifts of anhydrous HF as a function of temperature.

TABLE 2. ^1H and ^{19}F molal chemical shifts (δ_0) for salts of Lewis acids in anhydrous HF, expressed in p.p.m./molal concentration

	H				F			
Compound	Room temperature (°C)	δ_0	Low temperature (°C)	δ_0	Room temperature (°C)	δ_0	Low temperature (°C)	δ_0
KBF_4	31	0.045	−23	0.038	30	0.42	−23	0.31
$NaBF_4$	31	0.03			27	0.21		
$KAsF_6$	25	0.097	1	0.093	25	1.03	0	0.55
$NaAsF_6$	35	0.12			35	0.81		
$KSbF_6$	27	0.2	0	0.15	31	2.18		
KF	31	0.24	−9.5	0.23	36	2.03	23	1.86
NaF	32	0.33	−3	0.30	31	2.30	−9	2.04

reported in the literature for both ^1H and ^{19}F in anhydrous HF vary slightly. For ^1H, the values lie between 7.8 and 8.85 p.p.m. (7, 9, 12, 13) and for ^{19}F, they range from 194.0 to 200.0 p.p.m. (7, 9, 14–16). These differences result from differences in the temperature at which the measurements were made and may also be due to the purity of the anhydrous HF.

Electrolyte Solutions

Alkali Fluorides

In all cases only one exchange averaged line was observed in both the ^1H and ^{19}F n.m.r. spectra. The data presented in Figs. 5–8, represent the chemical shifts of the ^1H and ^{19}F resonances with respect to anhydrous HF *vs.* the molality of the solutions at different temperatures. All the observed shifts are towards lower field. They all increase almost linearly as the concentration increases. In addition, the molal chemical shifts, δ_0, were calculated from the region of dilute concentrations.

$$\delta_0 = \left(\frac{d\delta}{dc}\right)_{c=0}$$

These values are summarized in Table 2 and will be discussed later.

An n.m.r. study of the $(HF_2)^-$ anion in various bifluoride salts of some butylamines has shown that ^1H resonances lie between 4.76 and 4.86 p.p.m., and ^{19}F resonances lie between 32.1 and 49.6 p.p.m. to low-field of pure anhydrous HF (17). The highest electrolyte concentration in this study was that of CsF which reached a value of 13.09 *m* (CsF:HF = 1:3.8). In this particular solution the ^1H chemical shift was 3.97 p.p.m. (238.4 Hz) and the ^{19}F chemical shift was 30.68 p.p.m. (1730.5 Hz) to low field of pure anhydrous HF. These values are rather close to those obtained for the $(HF_2)^-$ anion. As no levelling off is indicated in these curves, one is inclined to assume that the ionization process is a total one and therefore linear change is taking place.

If the ionic dissociation was the only process involved then one would expect that the chemical shift would only be dependent on the fluoride ion concentration and would not be influenced by the cation. But this is not the case, and a very pronounced relationship is noticed between the ionic crystal radii and the molal chemical shift (δ_0) as presented in Fig. 9. The second effect therefore to be considered is that of bond-breaking, *i.e.* depolymerization of the solvent molecules. The observed chemical shift is the sum of two contributions

$$\delta_{obs} = \delta_{ion} + \delta_{bb} \quad [11]$$

where δ_{obs} is the observed molal chemical shift, δ_{ion} is the molal ionization chemical shift, and δ_{bb} is the molal bond-breaking chemical shift.

The influence of depolymerization on the n.m.r. signals of HF has been reported earlier in this paper. It was established that the ^1H resonance shifts towards higher field as the degree of depolymerization increases. Since δ_{obs} is negative (towards lower field) and the δ_{bb} is positive, one has to conclude that δ_{ion} is negative and its absolute magnitude is greater than that of δ_{bb}.

$$|\delta_{ion}| > |\delta_{bb}|$$

Assuming that complete ionization occurs, δ_{ion} would be expected to be the same for all salts. Therefore the difference in δ_{obs} for the various salts has to be interpreted in terms of

Can. J. Chem. Downloaded from www.nrcresearchpress.com by 210.87.254.42 on 09/05/12
For personal use only.

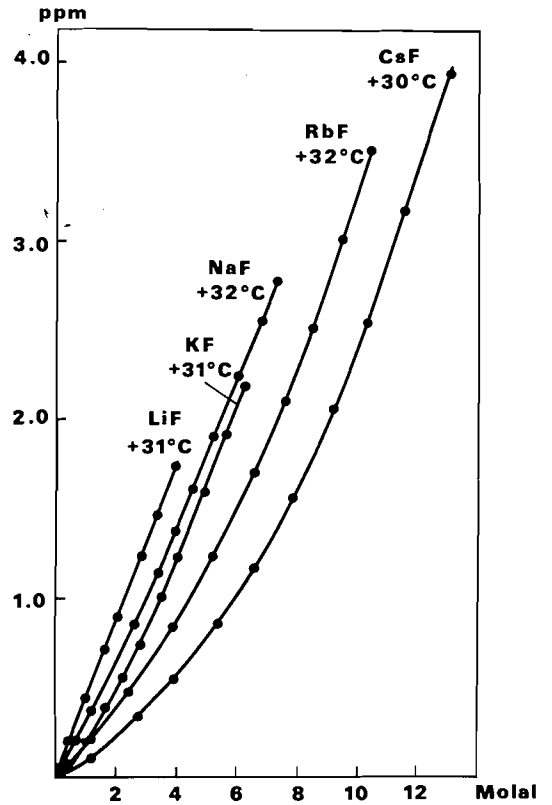

FIG. 5. Variation of proton chemical shifts expressed in p.p.m. with reference to pure anhydrous HF, *vs.* concentration, expressed in molality of various solutes.

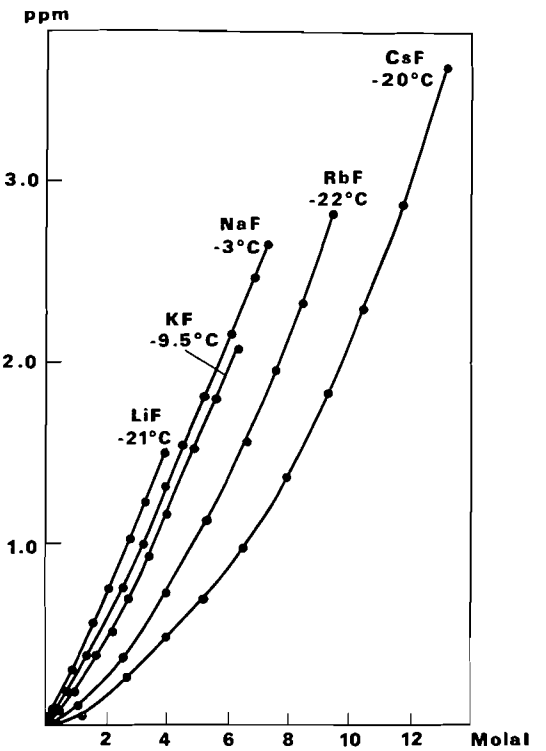

FIG. 6. Same as Fig. 5 for lower temperatures.

the depolymerization process. Since the signs of δ_{obs} and δ_{bb} are opposite, an increase in $|\delta_{obs}|$ reflects a decrease in δ_{bb} and vice versa.

From Fig. 9 it is seen that $|\delta_{obs}|$ is smallest for the Cs cation and largest for Li cation; in other words, δ_{bb} is largest for Cs and smallest for Li. An increase in the ionic crystallographic radius causes an increase in the degree of depolymerization.

Fabricand and Goldberg (18) studied the p.m.r. chemical shifts in alkali halide aqueous solutions. They too noticed that when plotting the crystal radii of cations and anions versus the relative to the molal proton chemical shifts, a straight line was obtained. They inferred that the average number of hydrogen bonds in water near an ion, is proportional to the ionic radius and that the number decreases with increasing radius. In aqueous solutions the two effects are δ_{bb} and δ_E, where δ_E is the polarization shift resulting from distortion of the electronic

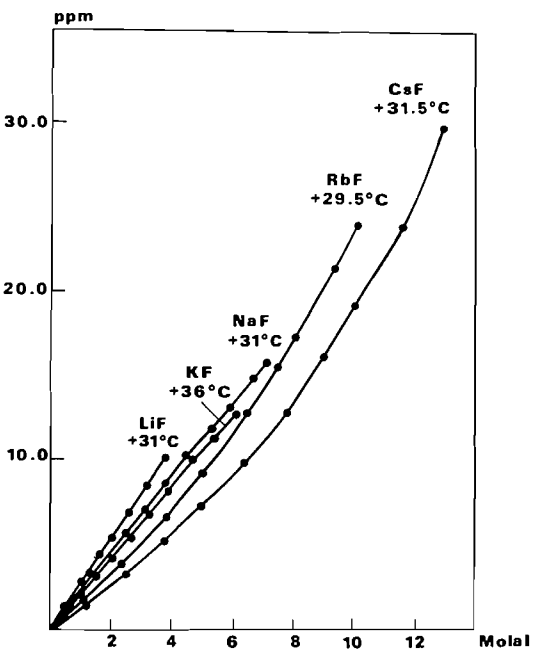

FIG. 7. Variation of fluorine chemical shifts expressed in p.p.m. with reference to pure anhydrous HF, *vs.* concentration, expressed in molality, of various solutes.

Can. J. Chem. Downloaded from www.nrcresearchpress.com by 210.87.254.42 on 09/05/12
For personal use only.

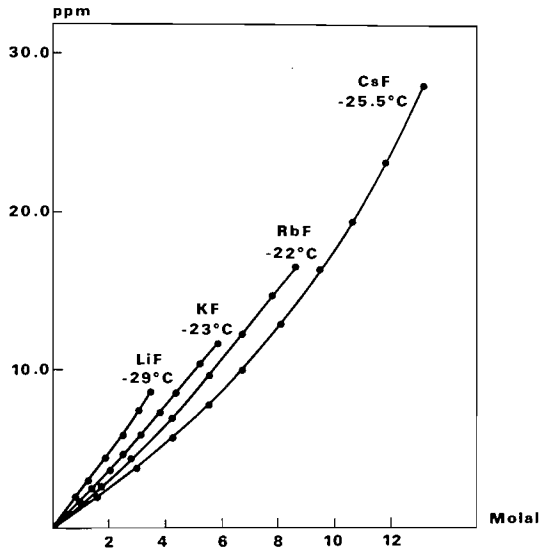

FIG. 8. Same as Fig. 7 for lower temperatures.

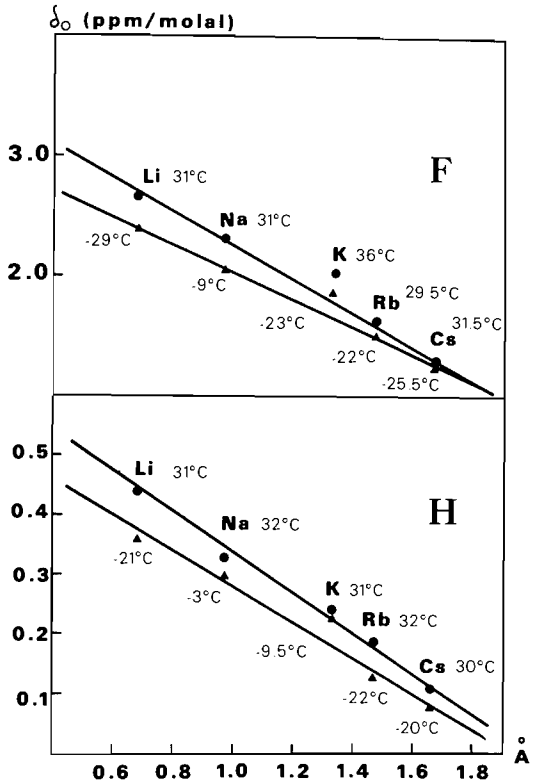

FIG. 9. δ_0 – molal chemical shifts of hydrogen and fluorine expressed in p.p.m./molality *vs.* crystallographic radii expressed in Å.

structure of water by the ionic electric field. In the case of HF, the polarization effect reaches an extreme situation when the solvent itself ionizes. Our observations are, therefore, very similar to previous findings for water, and we conclude that larger ions cause a larger bond-breaking effect, and as a result $|\delta_0|$ decreases as the ionic radius increases.

From Fig. 9 it is seen that a linear relationship exists between the ionic crystallographic radii and the observed molal chemical shifts. This similarity would not necessarily be predictable since water is a three dimensional system while HF is a two dimensional system.

Our results are also in agreement with those of Gillespie and Humphreys (2), who have shown that at low molarities (less than 0.15 *m*) the alkali metal fluorides act as simple 1 : 1 electrolytes. But at higher concentrations, there is substantial deviation from ideal behavior, which in our work we have attributed to ionization and H-bond breaking effects.

Temperature Effect

A comparison of the $|\delta_0|$ values at lower temperatures with values for the same salt at higher temperatures shows that $|\delta_0|$ is usually somewhat smaller at lower temperatures. The degree of polymerization in the pure solvent increases with decreasing temperature. Therefore, the number of H-bonds to be broken in order that a particular degree of depolymerization be attained with the same amount of solute will be greater at lower temperatures, and as a result $|\delta_{bb}|$ will be larger, and $|\delta_0|$ will therefore decrease, which is indeed observed.

Transverse Relaxation Times

From the width of the lines at their half height, the transverse relaxation times, T_2, were calculated. The ^1H resonances are observed to vary slightly, while in the case of the ^{19}F resonances, the width increases with increasing concentration. This change in line width varied from several Hz to several thousand Hz. This effect has already been observed by Solomon and Bloemberger (19), who studied the relaxation times of anhydrous HF and the changes caused by addition of water or potassium fluoride. We do not know of any explanation other than that given by these authors. Their explanation takes into account the effects of ionization, which presumably stabilizes the long ionized chains of $[(HF)_nF]^-$.

Can. J. Chem. Downloaded from www.nrcresearchpress.com by 210.87.254.42 on 09/05/12
For personal use only.

Salts of Lewis Acids

The solubilities of the alkali salts of Lewis acids studied were lower and the chemical shifts were also smaller than those of alkali fluorides, making these results less accurate. However, some general statements can be summarized. Both hydrogen and fluorine resonances shift towards lower field with respect to pure anhydrous HF, and this would indicate that in these cases too, the ionizing or polarizing effect is stronger than the bond-breaking effect. The observed molal chemical shifts, as summarized in Table 2, are smaller than the molal chemical shifts of alkali fluoride solutions. If one considers all the ionizing equilibria it seems that it really is a much more complicated system than the alkali fluoride solutions. The following equilibria can coexist

[12] $MAF_6 \rightleftarrows M^+ + AF_6^-$

[13] $AF_6^- \rightleftarrows AF_5 + F^-$

[14] $F^- + (HF)_n \rightleftarrows [(HF)_nF]^-$

[15] $2HF + AF_5 \rightleftarrows (H_2F)^+ + AF_6^-$

(A = P, As, Sb; M = Na, K). Steps 13 to 15 can be summarized by cancelling the ionization and dissociation of the complex AF_6^-. The net reaction can be written

$$(HF)_{n+2} \rightleftarrows (H_2F)^+ + [(HF)_nF]^-$$

which is really the self-dissociation of HF. It is possible that the dissociation of the salt MAF_6 would thus increase the self-dissociation of the solvent. One notices that the equilibria involved are rather complicated, and since no separate δ values for the various species involved are known, it is impossible to analyze the results quantitatively.

We would like to express our appreciation to the Ford Foundation for their financial support for this research.

1. H. H. HYMAN. HF as a strong acid solvent. Ph.D. Thesis. Illinois Institute of Technology, Chicago, Ill., 1960.
2. R. J. GILLESPIE and D. A. HUMPHREYS. J. Chem. Soc. (A), 2311 (1970).
3. J. W. EMSLEY, J. FEENEY, and L. H. SUTCLIFFE. High resolution n.m.r. spectroscopy. Vol. 1. Pergamon Press. 1965. pp. 534–539.
4. J. F. HINTON and E. S. AMIS. Chem. Rev. **67**, 367 (1967).
5. J. SHAMIR and A. NETZER. J. Sci. Instr. **1**, 770 (1968).
6. P. D. GROVES, P. J. HUCK, and J. HOMER. Chem. Ind. 915 (1967).
7. E. L. MACKOR, C. MACLEAN, and C. W. HILBERS. Rec. Trav. Chim. **87**, 655 (1968).
8. J. H. SIMONS and J. H. HILDEBRAND. J. Am. Chem. Soc. **46**, 2183 (1924).
9. D. K. HINDMAN and C. D. CORNWELL. J. Chem. Phys. **48**, 2017 (1968).
10. D. F. EVANS. Proc. Chem. Soc. 115 (1958).
11. D. F. EVANS. J. Chem. Soc. 877 (1960).
12. W. G. SCHNEIDER, H. J. BERNSTEIN, and J. H. POPLE. J. Chem. Phys. **28**, 601 (1958).
13. C. MACLEAN and E. L. MACKOR. Proc. Colloque Ampere XI, Eindhoven. North Holland. 1963. p. 108.
14. H. S. GUTOWSKY and C. J. HOFFMAN. J. Chem. Phys. **19**, 1259 (1951).
15. G. A. OLAH, S. J. KUHN, and W. J. TOLGYOSI. J. Am. Chem. Soc. **81**, 6350 (1959).
16. E. FLUCK. Die Kernmagnetische Resonanz und ihre anwendung in der Anorganische Chemie. Spring Verlag, Berlin. 1963.
17. J. SORIANO, J. SHAMIR, A. NETZER, and Y. MARCUS. Inorg. Nucl. Chem. Lett. **5**, 209 (1969).
18. B. P. FABRICAND and S. GOLDBERG. J. Chem. Phys. **34**, 1624 (1961).
19. I. SOLOMON and H. BLOEMBERGER. J. Chem. Phys. **25**, 261 (1956).

Can. J. Chem. Downloaded from www.nrcresearchpress.com by 210.87.254.42 on 09/05/12
For personal use only.

1:2 Trimethylphosphine Complexes of the Group IV Tetrahalides, *trans*-$MX_4.2P(CH_3)_3$ and *trans*-$MX_4.2P(CD_3)_3$ (where M = Si, Ge, or Sn; X = Cl or Br); Assignment of Metal–Phosphorus modes

D. K. Frieson and G. A. Ozin[1]

Lash Miller Chemistry Laboratories and Erindale College, University of Toronto, Toronto, Ontario M5S 1A1

Received January 5, 1973

The vibrational spectra of some 1:2 trimethylphosphine adducts of the group IV tetrahalides, which contain ligands in a *trans* configuration, are examined in detail using perdeutero-trimethylphosphine to facilitate the assignment of all metal-halogen and metal–phosphorus stretching modes. Preparation of $SiCl_4.2PMe_3$ with a 1:1 mixture of $P(CH_3)_3$ and $P(CD_3)_3$ enables an almost unambiguous assignment of the spectrum of this adduct. Normal coordinate calculations for all adducts are reported.

Les spectres vibrationnels de certains composés d'addition 1:2 de la triméthylphosphine et de tétrahalogénures du groupe IV qui contiennent des coordinats dans une configuration *trans*, ont été étudiés en détail grâce à l'utilisation de la perdeutéro-triméthylphosphine afin de rendre plus facile l'attribution de tous les modes d'élongation des liaisons métal–halogène et métal–phosphore. La préparation du $SiCl_4.2PMe_3$ à partir d'un mélange 1:1 de $P(CH_3)_3$ et de $P(CD_3)_3$ a permis l'interprétation presque sans ambiguité du spectre de ce composé d'addition. On présente aussi pour tous les composés les calculs en coordonnées normales. [Traduit par le journal]

Can. J. Chem., **51**, 2685 (1973)

Can. J. Chem. Downloaded from www.nrcresearchpress.com by 210.87.254.40 on 09/05/12
For personal use only.

Introduction

The proliferation of adducts of the form $MX_4.nL$ reported in the literature is convincing evidence of the tendency of group IV tetrahalides to seek a maximum covalency of six through the formation of coordinate bonds with sufficiently strong electron donors (1). In the case where 1:2 adducts are formed, the possibility of *cis–trans* isomerism arises. The *trans* stereochemistry in group IV appears to be favored. X-Ray crystallography has established the *trans*-octahedral structures of several pyridine adducts of the type $MX_4.2py$ where MX_4 = SiF_4, $SiCl_4$, $GeCl_4$, $SnCl_4$, $SnBr_4$, $SeCl_4$, and $PbCl_4$ (2). In group IV, tin tetrahalide is unique in the formation of *cis* adducts (3); a *cis* adduct of a silicon or germanium tetrahalide involving monodentate ligands has yet to be demonstrated.

While crystallographic data must often be reverted to for conclusive proof of a given structure, vibrational spectroscopy can, in principle, be used to differentiate between a *cis* and a *trans* stereochemical configuration. Thus, a *trans* (D_{4h}) molecule should show two metal–halogen stretching frequencies in the Raman effect (the totally symmetric a_{1g} mode and the "antiphase" b_{1g} mode) and one in the infrared (the asymmetric e_u mode). In contrast, the *cis* (C_{2v}) molecule should show four such frequencies, two of which will be strong in the Raman spectrum but weak in the infrared (a_1 modes), and two of which will be strong in the infrared spectrum but weak in the Raman (b_1 and b_2 modes). (See Fig. 1.)

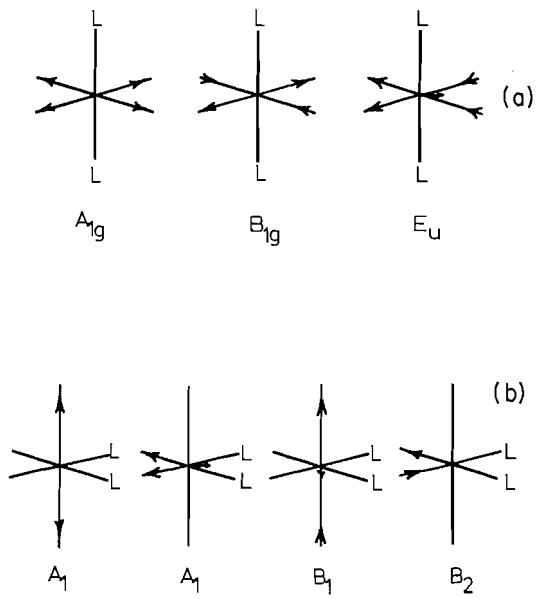

FIG. 1. (*a*) ν(M—X) modes of an $MX_4.2L$ complex having D_{4h} symmetry. (*b*) ν(M—X) modes of an $MX_4.2L$ complex having C_{2v} symmetry.

[1]To whom all correspondence should be addressed.

Can. J. Chem. Downloaded from www.nrcresearchpress.com by 210.87.254.40 on 09/05/12
For personal use only.

Trimethylphosphine has been shown to form 1:2 adducts with some group IV tetrahalides (4–6), and the vibrational spectra of these $MX_4.2PMe_3$(MX_4 = $SiCl_4$, $SiBr_4$, $GeCl_4$, and $SnCl_4$) compounds have been reported (5). The close similarity of the spectra and the observation of the typical D_{4h} spectral pattern of metal–halogen stretching frequencies (two Raman active and one infrared active) in the spectra have led Beattie and Ozin (5) to assign a *trans* stereochemistry to this system. Blayden and Webster (7) have recently confirmed this assignment with an X-ray study of $SiCl_4.2PMe_3$. In spite of the excellent vibrational data, the complexity of the spectra of molecules of this size precludes an unambiguous assignment of many fundamental modes.

The purpose of the present study is to investigate more thoroughly the spectra of these adducts using isotopic substitution as a means of conclusively identifying all skeletal stretching modes, particularly the metal–phosphorus vibrational frequencies.

Experimental

Silicon tetrachloride, silicon tetrabromide, germanium tetrachloride, and tin tetrachloride were purified by multiple distillation *in vacuo* in all-glass systems. Trimethylphosphine was dried over molecular sieve which had been heated to *ca* 300 °C under vacuum for at least 24 h. It was subsequently stored over calcium hydride in a break-seal ampoule. Perdeutero-trimethylphosphine was prepared by the method of Mann and Wells (8) substituting deuterated methyl iodide for methyl iodide (9) and isolating the ligand as the silver iodide derivative $[AgI.PMe_3]_4$ (10). The ligand was regenerated under vacuum by gentle heating, collected in a cold trap, and dried over molecular sieve as previously described.

Solvents (diethyl ether, benzene) were dried by reflux over calcium hydride for at least 24 h, followed by vacuum distillation onto more CaH_2 over which it was stored.

All reagents were thoroughly dried, outgassed, and vacuum distilled into break-seal ampoules prior to use. All glass apparatus was used throughout to avoid grease contamination.

The trimethylphosphine adducts (with the exception of $SnCl_4.2PMe_3$) were prepared at −78 °C under vacuum by distilling an excess of trimethylphosphine into a reaction flask containing an ether solution of the appropriate acceptor. The adduct precipitated immediately. After the reaction mixture had been allowed to come to room temperature and to interact for a period of time (at least 1 h), the ether solvent together with excess volatile reagent was removed by distillation. Bistrimethylphosphine tin tetrachloride was similarly prepared by direct interaction of tin tetrachloride with an excess of trimethylphosphine with subsequent removal of excess free ligand.

Solutions of $SiCl_4.2PMe_3$ and $SiBr_4.2PMe_3$ in benzene were prepared *in vacuo* for spectroscopic examination. Ampoules were then opened in a dry-box where the solutions were immediately transferred to infrared cells just before the spectrum was run. Nujol (Na dried) mulls were also prepared in the dry-box using standard techniques. $GeCl_4.2PMe_3$ and $SnCl_4.PMe_3$ were found to be insoluble in common covalent, noncoordinating solvents.

Raman spectra were recorded with a Spex 1401 double-spectrometer using argon-ion laser (4880 Å) excitation, while infrared spectra were obtained with a Perkin–Elmer 180 spectrometer with the use of high density polythene sample plates.

The computer programs used for the calculations of the vibrational spectra are based on those of Schactschneider's GMAT, FMAT, and EIGV and were run on an IBM 7094 computer system.

Results and Discussion

The total deuteration studies using $P(CD_3)_3$ remove any ambiguity in the assignment of the metal–halogen stretching frequencies of these adducts. Two low frequency Raman bands and one degenerate high frequency infrared band are readily recognized as the typical spectral pattern ($e_u + a_{1g} + b_{1g}$) of a formally D_{4h} *trans*-octahedral molecule (assuming free rotation of the ligands in solution). The frequencies of these bands are comparatively unaltered by isotopic substitution. The totally symmetric stretching mode generally gives the strongest line in the Raman spectrum and in solution it is polarized.

Metal–halogen stretching frequencies

Compound	ν(MX) anti	sym	asym	ν_1 (MX_4)*
$SiCl_4.2PMe_3-h_9$	234	295	416/387	429
$SiBr_4.2PMe_3-h_9$	140	204	323	249
$GeCl_4.2PMe_3-h_9$	225	267	285/251	397
$SnCl_4.2PMe_3-h_9$	235	269	291/272	368

*Reference 11.

For the tetrachloride adducts, this band is found to lie some 100–130 cm^{-1} below the ν_1 band of the parent compound. Qualitatively, this is indicative of a substantial weakening of the metal–halogen bond as a result of the increased electron density on the central metal atom when two donor ligands are coordinated. This is an expected trend which is also reflected in the increase in the length of the M—X bond (2.25 Å in $SiCl_4.2PMe_3$ (7) as compared to 2.02 Å in $SiCl_4$ (12), for instance).

It is interesting to note the relative constancy of position of the symmetric and antiphase

Can. J. Chem. Downloaded from www.nrcresearchpress.com by 210.87.254.40 on 09/05/12
For personal use only.

modes through the tetrachloride series. The position of the asymmetric frequency on the other hand varies considerably since this mode involves movement of the central metal atom. The asymmetric stretching mode is doubly-degenerate (e_u symmetry) in a formal D_{4h} system but the degeneracy is removed in the solid state where the site symmetry (in the crystal) is C_{2h} (7). This explains the observation of a strong doublet for this e_u mode in the solid state spectra of all four adducts. Where spectra can be obtained from solution, this doublet collapses into a broad singlet which is the strongest absorption in the infrared spectrum.

Considerable difficulty arises when assigning the symmetric metal–phosphorus stretching vibration. This band is typically found at low frequencies in the region of the skeletal deformational modes which are subject to extensive coupling with ligand deformations of the same symmetry. (See calculations.) As a result, total deuteration produces a shift of all frequencies in this region. To circumvent this problem, mixed $P(CH_3)_3/P(CD_3)_3$ studies were undertaken in the case of $SiCl_4.2PMe_3$. When the adduct is prepared from a 1:1 mixture of non-deuterated- and per deutero-trimethylphosphine, the metal–phosphorus stretching modes split into 1:2:1 triplets whose components correspond to the three products possible from the reaction. (The Raman spectrum of the $P(CH_3)_3$ and $P(CD_3)_3$ mixture displays no evidence for methyl exchange over a period of time.) Identification of the mode is thus easily accomplished. Its position is relatively constant through the series and compares well with metal–phosphorus stretching frequencies of similar compounds in group III. For example, the ν_{sym}(In—P) band is assigned from single crystal Raman studies to the band at 135 cm^{-1} in $InCl_3.2PMe_3$ (13) and the ν_{sym} (Al—P) mode is probably the 133 cm^{-1} band in $AlCl_3.2PMe_3$ (14). The metal–nitrogen mode is also observed at low frequencies in similar nitrogen-donor adducts (15).

Metal-phosphorus stretching frequencies

Compound	ν(M—P)	
	sym	asym
$SiCl_4.2PMe_3-h_9$	158	478
$SiBr_4.2PMe_3-h_9$	156	462
$GeCl_4.2PMe_3-h_9$	146	380
$SnCl_4.2PMe_3-h_9$	157	354

Other workers have recognized the comparative invariance of the ligand modes in a variety of adducts as a means of separating them from skeletal modes (16). Deuteration of the ligand confirms previous assignments of these modes.

Ligand deformational modes*

Compound	a_{1g}	e_u	e_g
$SiCl_4.2PMe_3$	350 (313)	293 (260)	283/269 (243/223)
$SiBr_4.2PMe_3$	350 (308)	299 (260)	285/266 (243/227)
$GeCl_4.2PMe_3$	347 (306)	—†	279 (238)
$SnCl_4.2PMe_3$	338 (300)	—†	258 (223)

*Figures in parentheses refer to perdeutero-species.
†Hidden under $\nu(MCl)_{asym}$.

With two trimethylphosphine ligands *trans* to each other in a complex having C_{2h} symmetry, the representation of *ligand* stretching and deformational modes is

$$\Gamma^{C_{2h}}(l, \delta) = 2(2a_g + b_g + a_u + 2b_u)$$

where $l \equiv \Delta l \equiv$ P—Me bond stretching; $\delta \equiv \Delta\delta \equiv PMe_3$ deformation. If the ligands are considered to rotate freely about the metal–phosphorus bond, the adduct may be regarded as a formally D_{4h} symmetry type. The above representation then becomes

$$\Gamma^{D_{4h}}(l, \delta) = 2(a_{1g} + a_{2u} + e_g + e_u)$$

where correlation has been along a C_2' axis of the D_{4h} molecule. Thus, there are four fundamental modes of vibration, two Raman active and two infrared active, associated with both stretching and deformational motions of the ligands.

The four stretching modes which are typically found in the region of 670–760 cm^{-1} undergo spectral shifts of *ca.* 60–70 cm^{-1} on deuteration. In the deformation region, three of the four

TABLE 1. Structural parameters*

Compound	r(Å)	
	(M—X)	(M—P)
$SiCl_4.2PMe_3$	2.25	2.26
$SiBr_4.2PMe_3$	2.59	2.26
$GeCl_4.2PMe_3$	2.35	2.32
$SnCl_4.2PMe_3$	2.58	2.50

*r(P—Me), 1.86 Å; ∠(M—P—Me), 117.8°; ∠(Me—P—Me), 100.0°.

TABLE 2. Force constants for $MX_4.2PMe_3$

$MX_4.2PMe_3$	MCl_6^{n-}†	$SiCl_4.2PMe_3$	$SiBr_4.2PMe_3$	$GeCl_4.2PMe_3$	$SnCl_4.2PMe_3$
f_d		1.600	1.500	1.420	1.550
f_r	f_b	1.399	1.103	1.199	1.329
f_{dd}		0.020	0.080	0.062	0.150
f_{rr}^{cis}	f_{bb}^{cis}	0.156	0.123	0.130	0.154
f_{rr}^{trans}	f_{bb}^{trans}	0.078	0.061	0.065	0.077
f_{rd}	f_{bb}^{cis}	0.156	0.123	0.130	0.154
f_α	f_β	0.273	0.183	0.226	0.146
f_β	f_β	0.273	0.183	0.226	0.146
$f_{\alpha\alpha}$	$f_{\beta\beta}^{adj}$	0.015	0.010	0.072	0.008
$f_{\alpha\beta}$	$f_{\beta\beta}^{adj}$	0.015	0.010	0.072	0.008
$f_{\beta\beta}$	$f_{\beta\beta}^{adj}=f_{\beta\beta}^{adj}$	0.015	0.010	0.072	0.008
$f_{r\alpha}$	$f_{b\beta}^{adj}$	0.160	0.125	0.123	0.057
$f_{r\beta}$	$f_{b\beta}^{adj}$	0.160	0.125	0.123	0.057
$f_{d\beta}$	$f_{b\beta}^{adj}$	0.160	0.107	0.123	0.057
f_t		2.870	2.870	2.870	2.870
f_{tt}		−0.010	−0.010	−0.010	−0.010
f_δ		0.233	0.233	0.233	0.233
$f_{\delta\delta}$		0.010	0.010	0.010	0.010
f_γ‡		0.087	0.087	0.087	0.087

*Units of mdyn/Å.
†Reference 22.
‡f_γ was multiplied by l^2 for convenience in the calculations. Similarly $f_{\beta\beta}$ was multiplied by r^2 while all other force constants not in units of mdyn/Å were multiplied by the bond lengths they subtended.

possible modes can be identified. These typically shift 30–40 cm^{-1} with isotopic substitution of hydrogen. The e_g-type deformation appears to be split in both $SiCl_4.2PMe_3$ and $SiBr_4.2PMe_3$ and may conceivably be so in $GeCl_4.2PMe_3$ and $SnCl_4.2PMe_3$ also, with one-half of the doublet hidden in the $\nu(M—X)_{asym}$ band. Raman spectra of the former two in benzene solution indicate that here the degeneracy of the mode remains unperturbed. This supports the assignment of both solid state bands to this mode.

There are, in addition to the afore-cited modes, two ligand "rocking" vibrations. Since these normally occur in the range 220–180 cm^{-1} and are usually highly mixed with skeletal deformations, they will not be discussed at this point.

$SiCl_4.2PMe_3$

The spectra of this adduct, in the solid state and in benzene solution, are to be found in Tables 3 and 4, respectively. Table 5 contains the calculated and observed spectra together with the approximate description of each mode.

Three sets of experiments were performed including spectroscopic examination of $SiCl_4.2PMe_3$ which had been prepared from (*a*) nondeuterated-trimethylphosphine, (*b*) perdeuterotrimethylphosphine, and (*c*) a 1:1 mixture of nondeuterated- and perdeuterotrimethylphosphine. The total deuteration experiment enabled a complete separation of ligand and acceptor modes in the region above 200 cm^{-1}, although little information was obtained for modes below this range due to the high degree of mixing as previously described. The silicon–chlorine stretching frequencies are easily identified as those which are unperturbed by deuteration.

The Raman spectrum of bis(perdeutero-trimethylphosphine) silicon tetrachloride (Fig. 2) illustrates a classic case of Fermi resonance (17) and provides a rare example for a halide complex in which the strongest band in the spectrum is *not* the totally symmetric metal–halogen stretching vibration.

The mixed nondeuterated/perdeutero-trimethylphosphine experiment has been briefly described in the preceding section. Preparation of $SiCl_4.2PMe_3$ from a 1:1 mixture of PMe_3-h_9 and PMe_3-d_9 will yield a mixture of the adducts $SiCl_4.2(PMe_3\text{-}h_9)$, $SiCl_4.(PMe_3\text{-}h_9).(PMe_3\text{-}d_9)$, and $SiCl_4.2(PMe_3\text{-}d_9)$ in a statistical ratio of 1:2:1. The spectrum of this mixture (hereafter denoted as $SiCl_4.2PMe_3$-h_9/d_9) will thus be a summation of the spectra of $SiCl_4.2PMe_3$-h_9 and $SiCl_4.2PMe_3$-d_9 with additional bands which belong uniquely to $SiCl_4.(PMe_3\text{-}h_9).(PMe_3\text{-}d_9)$.

The Si—P stretching modes are very strongly coupled with the result that the symmetric and

Can. J. Chem. Downloaded from www.nrcresearchpress.com by 210.87.254.40 on 09/05/12
For personal use only.

TABLE 3. Vibrational Spectra of $SiCl_4.2PMe_3$

$SiCl_4.2PMe_3(h_9/d_9)$		$SiCl_4.2PMe_3(h_9)$		$SiCl_4.2PMe_3(d_9)$		Approximate description of mode
Raman	I.r.	Raman	I.r.	Raman	I.r.	
	~965s,br		~965s,br			
	868vw		866w			
	855w		855w		850vw	ν(SiP)asym + ν(SiCl)asym
	~835(?)vvw				835vw	
	806s				807s	$\rho_t(CH_3)$
782w	783s			~780vw	784s	
753s	754s	752ms	754s		~746(?) vvw	
691mw	691w			690w	691w	$\nu(PMe_3)$
682, 678 ms		678s				
	677(?)vw				676w	
642, 638 w	~645(?)vw, br			641, 637 w	~642vw, br	
614ms				613ms		$\nu(PMe_3)$
	615w		615vw		618mw	$\nu_3(SiCl_4)$?
	~478msh		478s			
	468s					ν(SiP)asym
	~457msh				458s	
	413, 385 vs,br		416, 387 vs,br		413, 388 vs,br	ν(SiCl)asym
350w, 334mw, 312m	332w	350m		313vs		$\delta(PMe_3)$
295vvs		295vs		290s		ν(SiCl)sym
	293mw		293s			
	268m					$\delta(PMe_3)$
	260w				260s	
283vwsh, 270w, 249w, 222w		283mw, 269m		243mwsh, 223w		$\delta(PMe_3)$
	244(?)vw		244w			$\delta(PMe_3)$
	218mw		222m		218m	δ(SiCl)i.p+ $\nu_4(SiCl_4)$?
235s		234s		234s		ν(SiCl)antiphase
204w,br		207m				δ(SiCl).o.p.+ $\rho_r(PMe_3)$
190w				189m		$+\delta(PMe_3)$
	190vw		~192vw		191w	δ(SiCl)i.p.
180, 174 m		180ms				δ(SiCl)o.p.+ $\delta(PMe_3)$
				170s		$+\nu$(SiP)
154ms		158ms		150ms		ν(SiP)sym
		58mw		54mw		$\rho_r(PMe_3)+$
		41ms		40m		δ(SiCl)o.p.

asymmetric levels of the $SiCl_4.(PMe_3\text{-}h_9).(PMe_3\text{-}d_9)$ adduct lie between the respective levels of the $SiCl_4.2PMe_3\text{-}h_9$ and $SiCl_4.2PMe_3\text{-}d_9$ species. Thus, the asymmetric silicon–phosphorus stretching band is a *triplet* in the spectrum while the symmetric stretching band is most certainly an unresolved *triplet* centered midway between the corresponding bands of the h_9 and d_9 adducts. This is convincing evidence for the assignment of the band at 158 cm^{-1} to the symmetric silicon–phosphorus stretching frequency.

Can. J. Chem. Downloaded from www.nrcresearchpress.com by 210.87.254.40 on 09/05/12
For personal use only.

TABLE 4. Vibrational spectra of $SiCl_4.2PMe_3$ in benzene solution

$SiCl_4.2PMe_3(h_9)$		$SiCl_4.2PMe_3(d_9)$		$SiCl_4.2PMe_3(h_9/d_9)$		Approximate description of mode
Raman	I.r.	Raman	I.r.	Raman	I.r.	
	475 s,br				~475 msh 462 sbr	ν(SiP)asym
			455 s,br		~455 msh	
	413 vs,br		412 vs,br		412 vs,br	ν(SiCl)asym
~345 m,p				~353 vw		
				331 m,p	~330 vw	δ(PMe_3)
		311 vs,p		312 ms,p		
296 s,p		301 ms,p		299 vs,p		ν(SiCl)sym
	290 m				~287 w	
~276 vw	~264 m				267 m	δ(PMe_3)
			258 m		258 mw	
236 w,dp				238 mw,dp		ν(SiCl)antiphase
					244 (?)	
	221 m		221 m		219	δ(SiCl)i.p. + ν_4(SiCl)
					193 (?)	

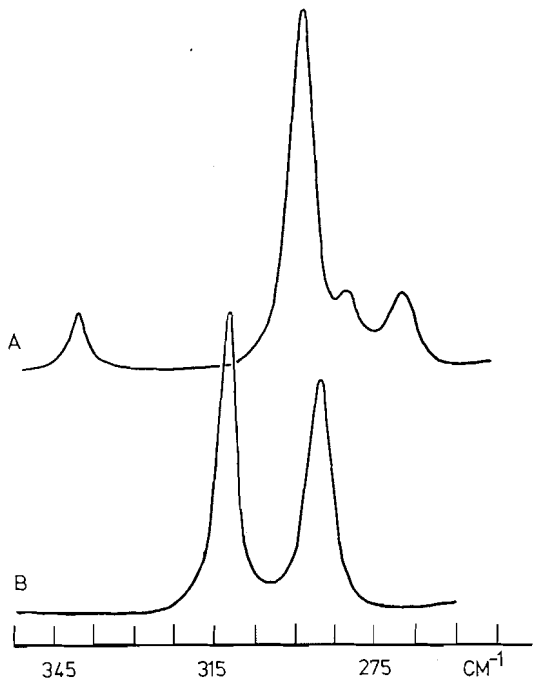

FIG. 2. Fermi resonance between Raman active A_{1g} modes of $SiCl_4.2P(CD_3)_3$. (*a*) Raman spectrum of $SiCl_4.2P(CH_3)_3$; (*b*) Raman spectrum of $SiCl_4.2P(CD_3)_3$.

$SiBr_4.2PMe_3$

The vibrational spectra of nondeuterated- and bis(perdeutero-trimethylphosphine) silicon tetrabromide have been examined and are found in Tables 6 and 7. Calculated and observed spectra appear together in Table 8 with the most probable description of each mode. Considered in conjunction with the assigned spectrum of $SiCl_4.2PMe_3$, the assignment of the fundamental stretching frequencies is quite straightforward. The totally symmetric silicon–bromine stretching frequency is the polarized band at 204 cm^{-1}, the strongest in the Raman spectrum. The asymmetric mode is split in the solid state but coalesces to a singlet at 338 cm^{-1} in benzene solution. Four bands appear in close proximity in the lower region of the Raman spectrum of this adduct and all experience small shifts on deuteration. The strongest of these bands occurs at 156 cm^{-1}. In cognizance of the position of the silicon–phosphorus stretching frequency in $SiCl_4.2PMe_3$-h_9, this band is assigned to that mode in $SiBr_4.2PMe_3$-h_9.

$GeCl_4.2PMe_3$

The striking similarity of the spectrum of this adduct to that of $SiCl_4.2PMe_3$ strongly suggests that a *trans*-octahedral configuration is maintained. (See Tables 9 and 10.) The two strong peaks at 285 and 251 cm^{-1} in the infrared spectrum are assigned to the asymmetric germanium–chlorine stretching mode where the degeneracy has been removed in the solid state.

In the Raman spectrum, the totally symmetric germanium–chlorine stretching mode is the very intense band at 267 cm^{-1} while the antiphase mode is the medium intensity band at 225 cm^{-1}. Neither of these bands shift on deuteration. Conversely, the peak at 145 cm^{-1} shifts to 138 cm^{-1} in the perdeutero analog and is as-

Can. J. Chem. Downloaded from www.nrcresearchpress.com by 210.87.254.40 on 09/05/12
For personal use only.

TABLE 5. Calculated spectrum of $SiCl_4.2PMe_3$

$SiCl_4.2PMe_3(h_9)$		Approximate description of mode†	Symmetry type	$SiCl_4.2PMe_3(d_9)$	
Observed	Calculated			Calculated	Observed
754	733	$\nu(PMe_3)$	e_u	697	691
752	732	$\nu(PMe_3)$	e_g	696	690
	695	$\underline{\nu(PMe_3)} + \nu(SiP)$	a_{2u}	664	
678	690	$\nu(PMe_3)$	a_{1g}	656	613
478	460	$\underline{\nu(SiP)} + \nu(PMe_3)$	a_{2u}	452	458
416, 387	434	$\nu(SiCl)$	e_u	434	413, 388
350	365	$\underline{\delta(PMe_3)} + \nu(SiP)$	a_{1g}	347	311
	332	$\delta(PMe_3) + \delta(SiCl)$o.p.	a_{2u}	317	
295	287	$\nu(SiCl)$	a_{1g}	284	290
293	275	$\delta(PMe_3)$	e_u	264	260
283, 269	269	$\underline{\delta(PMe_3)} + \delta(SiCl)$o.p.	e_g	251	243, 223
244	242	$\underline{\delta(PMe_3)} + \delta(SiCl)$i.p.	e_u	231	218
234	236	$\nu(SiCl)$	b_{1g}	236	234
222	216	$\delta(SiCl)$i.p.	b_{2g}	216	218
207	196	$\underline{\delta(SiCl)}$o.p. $+ \rho_r(PMe_3) + \delta(PMe_3)$	e_g	188	189
180	189	$\underline{\delta(SiCl)}$o.p. $+ \delta(PMe_3) + \nu(SiP)$	a_{2u}	180	170
192	156	$\underline{\delta(SiCl)}$i.p. $+ \rho_r(PMe_3) + \delta(SiCl)$o.p.	e_u	151	191
158	155	$\underline{\nu(SiP)} + \delta(PMe_3)$	a_{1g}	144	150
	153	$\underline{\delta(SiCl)}$o.p.	b_{2u}	153	
58	110	$\underline{\rho_r(PMe_3)} + \delta(SiCl)$o.p.	e_g	104	54
	74	$\underline{\rho_r(PMe_3)} + \delta(SiCl)$o.p.	e_u	69	

signed to the symmetric germanium–phosphorus stretching frequency. An alternative assignment is the band at 172 cm^{-1}, but in light of the position of the corresponding mode in the silicon analogs, this is probably somewhat higher than expected.

$SnCl_4.2PMe_3$

The spectra of this adduct and its perdeutero-analog are found in Tables 11 and 12. The intense band at 269 cm^{-1} is assigned to the totally symmetric "breathing" mode of the assumed square planar $SnCl_4$ residue. As in the previous three adducts, the asymmetric mode appears to be split in the solid state, giving an intense doublet at 291 and 272 cm^{-1}, but the insoluble nature of the compound prevents confirmation of this assignment.

An examination of the Raman spectrum (Table 12) discloses bands at 157 and 123 cm^{-1}, either of which may be assigned to the symmetric tin–phosphorus stretching frequency. Although an unequivocal assignment is impossible, calculations support assignments to the 157 cm^{-1} band. The other band is preferably assigned to a deformational mode.

The asymmetric tin–phosphorus stretching mode is assigned to the infrared band at 354 cm^{-1} which shifts to 323 cm^{-1} on deuteration.

As in the case of the $GeCl_4.2PMe_3$ adduct, a correlation of calculated and observed frequencies has been made in Table 12.

Conclusion

We may summarize the vibrational data for the 1:2 trimethylphosphine complexes of the group IV tetrahalides, by stating that deuteration studies using $P(CD_3)_3$ and mixed ligand studies using $P(CH_3)_3/P(CD_3)_3$ have proven to be of considerable value in helping to distinguish internal ligand modes, halogen stretching modes, and metal–phosphorus stretching modes. In this way we have been able to assign with a reasonable degree of certainty, the symmetric and asymmetric metal–phosphorus stretching modes for most of the complexes studied and from the frequencies, calculate the respective k_{MP} band stretching force constants.

Can. J. Chem. Downloaded from www.nrcresearchpress.com by 210.87.254.40 on 09/05/12
For personal use only.

TABLE 6. Vibrational spectra of $SiBr_4.2PMe_3$

$SiBr_4.2PMe_3(h_9)$		$SiBr_4.2PMe_3(d_9)$		Approximate description of mode
Raman	I.r.	Raman	I.r.	
			840 w	
	962 s		797 s	$\rho_r(CH_3)$
	~785 w,br	778 vw	780 wsh	
753 vwsh	750 m		690 w	$\nu(PMe_3)$
748 mw		688 w	675 w	$\nu(PMe_3)$
		637 w	637 w	
676 m		611 m		$\nu(PMe_3)$
	~673 vw		615 w	$\nu(PMe_3)$
	462 ms		441 s	ν(SiP)asym
350 w		308 w		$\delta(PMe_3)$
	~349 mwsh		~348 mwsh	
	~331 wsh		~329 wsh	
	~323 s,br		~317 s,br	ν(SiBr)asym
	299 mw		260 m	$\delta(PMe_3)$
~285 w,br		~243 w,br	242 vw	
	270 w		231 w	$\delta(PMe_3)$
~266 w		~227 w		
			218 vw	
~233 w	209 mw			$\rho_r(PMe_3) + \delta$(SiBr)o.p.
	225 mw		200 mw	
204 vs		192 vs		ν(SiBr)sym
	176 m		172 m	δ(SiBr)o.p.
156 s		152 ms		ν(SiP)sym
~140 ms	138 s	138 s		ν(SiBr)antiphase
~131 msh		126 mwsh		δ(SiBr)i.p.
120 mw		118 m		δ(SiBr)o.p. + $\rho_r(PMe_3)$
~ 41 (?) vvw				
35 w				

TABLE 7. Vibrational spectra of $SiBr_4.2PMe_3$ in benzene solution

$SiBr_4.2PMe_3(h_9)$		$SiBr_4.2PMe_3(d_9)$		Approximate description of mode
Raman	I.r.	Raman	I.r.	
	489 s		~490 m	$\nu_3(SiBr_4)$
	459 s		~440 s	ν(SiP)asym
~351 w,p		302 w,p		$\delta(PMe_3)$
	~338 vs,br		~337 vs,br	ν(SiBr)asym
	290 m		254 m	$\delta(PMe_3)$
~264 w,p		249 mw,p		$\delta(PMe_3) + \nu_1(SiB_4)$
	~265 vw		~234 w	$\delta(PMe_3)$
	~218 w		192 mw,br	
200 vs,p		193 vs,p		ν(SiBr)sym
	175 m		171 mw	

Can. J. Chem. Downloaded from www.nrcresearchpress.com by 210.87.254.40 on 09/05/12
For personal use only.

TABLE 8. Calculated spectrum of $SiBr_4.2PMe_3$

$SiBr_4.PMe_3(h_9)$		Approximate description of mode†	Symmetry type	$SiBr_4.2PMe_3(d_9)$	
Observed*	Calculated			Observed*	Calculated
750	730	$\nu(PMe_3)$	e_u	694	690
748	729	$\nu(PMe_3)$	e_g	693	688
673	693	$\underline{\underline{\nu(PMe_3)}}$‡ + ν(SiP)	a_{2u}	662	615
676	689	†(PMe_3)	a_{1g}	655	611
462	450	$\underline{\underline{\nu(PMe_3)}}$ + δ(SiBr)o.p. + $\nu(PMe_3)$	a_{2u}	440	441
350	359	$\underline{\underline{\delta(PMe_3)}}$ + ν(SiP) + $\nu(PMe_3)$	a_{1g}	339	308
323	351	ν(SiBr) + δ(SiBr)o.p. + δ(SiBr)i.p.	e_u	350	317
	306	$\underline{\underline{\delta(PMe_3)}}$ + δ(SiBr)o.p. + $\rho_r(PMe_3)$	a_{2u}	291	
299	264	$\delta(PMe_3)$	e_u	245	260
285, 266	264	$\delta(PMe_3)$	e_g	244	243, 227
204	181	$\underline{\underline{\nu(SiBr)}}$ + $\delta(PMe_3)$ + ν(SiP)	a_{1g}	177	192
225	173	$\underline{\underline{\nu(SiBr)}}$ + $\rho_r(PMe_3)$ + δ(SiBr)o.p.	e_u	167	200
233	160	$\rho_r(PMe_3)$ + δ(SiBr)o.p.	e_g	151	209
156	147	$\underline{\underline{\nu(SiP)}}$ + ν(SiBr) + $\delta(PMe_3)$	a_{1g}	139	152
140	140	$\underline{\underline{\nu(SiBr)}}$	b_{1g}	140	138
176	133	$\underline{\underline{\delta(SiBr)}}$o.p. + $\delta(PMe_3)$ + ν(SiP)	a_{2u}	127	172
131	118	$\underline{\underline{\delta(SiBr)}}$i.p.	b_{2g}	118	126
	112	$\underline{\underline{\delta(SiBr)}}$i.p. + $\rho_r(PMe_3)$	e_u	109	
120	83	$\underline{\underline{\delta(SiBr)}}$o.p. + $\rho_r(PMe_3)$	e_g	79	118
	77	δ(SiBr)o.p.	b_{2u}	77	
	63	$\underline{\underline{\delta(SiBr)}}$o.p. + $\rho_r(PMe_3)$ + δ(SiBr)i.p.	e_u	59	

*Solid-state spectra.
†Potential energy contributions of less than 10% have been neglected.
‡Terms which form a major part of the mode are *underscored*; those forming *ca.* > 75% are underscored twice.

Normal Coordinate Analysis

Normal coordinate analysis of the $MX_4.2PMe_3$ adducts and their perdeutero-analogs were performed in C_{2v} symmetry using the Wilson **F–G** matrix method. Bond lengths and angles from the crystal structure were used for $SiCl_4.2PMe_3$ (7). Bond lengths of the square-planar MX_4 residue of the other adducts were obtained by multiplying the bond length in the parent molecule (18–20) by a factor corresponding to the increase in the Si—Cl distance upon complex formation. With the methyl group considered as a point mass, the coordinated PMe_3 structural parameters of $SiCl_4.2PMe_3$ were assumed in all cases. Likewise, the metal–phosphorus bond length was taken to be the sum of the appropriate covalent radii (21). This, in fact, corresponded exactly with the distance found in the crystal structure in the case of $SiCl_4.2PMe_3$ (see Table 1).

Internal coordinates are defined on the following pages. There are 33 normal modes of vibration if the methyl groups are considered as point masses where

$$\Gamma_{vib} = 11A_1 + 5A_2 + 8B_1 + 9B_2$$

Force fields of chemically and structurally related species were used where they existed. A scheme of 13/16 (PCl_6^-) was chosen for $SiCl_4.2PMe_3$ (22). Since a similar force field was not available for $SiBr_4.2PMe_3$, force constants were obtained from a (3/4) (PCl_6^-) scheme by multiplying the stretch and stretch–interaction constants by the factor $f_r(SnBr_6^{2-})/f_r(SnCl_6^{2-})$; and the bend and bending–interaction constants by the factor $f_\alpha(SnBr_6^{2-})/f_\alpha(SnCl_6^{2-})$ (23). The force fields of $GeCl_6^{2-}$ and $SnCl_6^{2-}$ (22) were transferred directly to $GeCl_4.2PMe_3$ and $SnCl_4.2PMe_3$, respectively. Only minor adjustments in some interaction constants of $SiBr_4.2PMe_4$ and

Can. J. Chem. Downloaded from www.nrcresearchpress.com by 210.87.254.40 on 09/05/12
For personal use only.

TABLE 9. Vibrational spectra of $GeCl_4.2PMe_3$

$GeCl_4.2PMe_3(h_9)$		$GeCl_4.2PMe_3(d_9)$		Approximate description of mode
Raman	I.r.	Raman	I.r.	
	758s		693 vw	$\nu(PMe_3)$
759 mw		692 w		$\nu(PMe_3)$
		641, 634 vw	774 vw	
	683 w		599 vw	$\nu(PMe_3)$
674 mw		609 mw		$\nu(PMe_3)$
	380 w		353 w	ν(GeP)asym
347 m		306 m		$\delta(PMe_3)$
	285, 251 s		283, 259 s	ν(GeCl)asym
279 wsh		252 vwsh, 238 vw		$\delta(PMe_3)$
267 vvs		262 vvs		ν(GeCl)sym
225 m		224 m		ν(GeCl)antiphase
	221 m		203 m	
199 w		204 w		
	195 s		191 m	
180 mwsh		178 mw		
172 m		160 m		
	170 w		169 w	
	159 w		154 w	
146 m		138 m		ν(GeP)sym
64 w		60 w		
56 w		54 w		
44 mw		39 mw		

TABLE 10. Calculated spectrum of $GeCl_4.2PMe_3$

$GeCl_4.2PMe_3(h_9)$		Approximate description of mode*	Symmetry type	$GeCl_4.2PMe_3(d_9)$	
Observed	Calculated			Calculated	Observed
758	731	$\nu(PMe_3)$	e_u	695	693
759	726	$\nu(PMe_3)$	e_g	689	692
683	687	$\nu(PMe_3)$	a_{2u}	653	599
674	687	$\nu(PMe_3)$	a_{1g}	653	609
380	373	$\underline{\nu(GeP)} + \delta(PMe_3)$	a_{2u}	358	353
347	358	$\underline{\delta(PMe_3)} + \nu(GeP)$	a_{1g}	340	306
285, 251	329	$\nu(GeCl)$	e_u	437	283, 259
—	305	$\delta(GeCl)o.p. + \delta(PMe_3) + \nu(GeP)$	a_{2u}	299	—
—	271	$\underline{\delta(PMe_3)} + \nu(GeCl)$	e_u	258	—
267	267	$\underline{\nu(GeCl)}$	a_{1g}	265	262
279	261	$\delta(PMe_3)$	e_g	241	238
221	233	$\delta(PMe_3) + \nu(GeCl) + \delta(GeCl)i.p.$	e_u	223	203
225	219	$\nu(GeCl)$	b_{1g}	219	224
195	183	$\nu(GeP) + \delta(PMe_3)$	a_{2u}	174	191
146	150	$\underline{\nu(GeP)} + \delta(PMe_3)$	a_{1g}	140	138
172	145	$\underline{\rho_r(PMe_3)} + \delta(GeCl)o.p.$	e_g	137	160
180	125	$\delta(GeCl)i.p.$	b_{2g}	125	182, 176
170, 159	124	$\underline{\rho_r(PMe_3)} + \delta(GeCl)i.p. + \delta(GeCl)o.p.$	e_u	119	169, 154
64, 65	87	$\underline{\delta(GeCl)}o.p. + \rho_r(PMe_3)$	e_g	84	60, 54
	86	$\delta(GeCl)o.p.$	b_{2u}	84	
	55	$\underline{\delta(GeCl)}o.p. + \delta(GeCl)i.p.$	e_u	52	

*See Table 8 for notation.

Can. J. Chem. Downloaded from www.nrcresearchpress.com by 210.87.254.40 on 09/05/12
For personal use only.

TABLE 11. Vibrational spectra of $SnCl_4.2PMe_3$

$SnCl_4.2PMe_3(h_9)$		$SnCl_4.2PMe_3(d_9)$		Approximate description of mode
Raman	I.r.	Raman	I.r.	
	779 vw			
	759 m		691 w	$\nu(PMe_3)$
759 w		691 vw		$\nu(PMe_3)$
	695 w		675 w	
		644, 638 vvw		
	674 w		629 mw	$\nu(PMe_3)$
668 w	667 vw	608 w		$\nu(PMe_3)$
534 vw	533 m	516 vvw	525 m	(impurity or hydrolysis)
	354 wsh		323 wsh	ν(SnP)asym
338 mw		300 ms		$\delta(PMe_3)$
	291, 272 s		293, 271 s	ν(SnCl)asym
269 s		265 s		ν(SnCl)sym
258 vwsh		223 wsh		$\delta(PMe_3)$
	236 wsh		231 wsh	
235 mw		235 mw		ν(SnCl)antiphase
200, ~177 vw		200, ~180 vw		
	190 w		171 wsh	
		162 mw		
157 mw		139 mw		ν(SnP)sym
	153 m		154 m	
146 vwsh		146 wsh		
123 mw		119 mw		

TABLE 12. Calculated spectrum of $SnCl_4.2PMe_3$

$SnCl_4.2PMe_3(h_9)$		Approximate description of mode*	Symmetry type	$SnCl_4.2PMe_3(d_9)$	
Observed	Calculated			Calculated	Observed
759	728	$\nu(PMe_3)$	e_u	691	691
759	727	$\nu(PMe_3)$	e_g	690	691
668	691	$\nu(PMe_3)$	a_{1g}	658	608
674	687	$\nu(PMe_3)$	a_{2u}	653	629
354	366	$\underline{\nu(SnP)} + \delta(PMe_3)$	a_{2u}	348	323
338	367	$\underline{\delta(PMe_3)} + \nu(SnP)$	a_{1g}	348	300
291, 272	301	$\overline{\nu(SnCl)}$	e_u	301	293, 271
269	282	$\nu(SnCl)$	a_{1g}	279	265
—	263	$\delta(PMe_3)$	e_u	243	—
258	263	$\delta(PMe_3)$	e_g	243	223
235	229	$\nu(SnCl)$	b_{1g}	229	235
236	226	$\nu(SnP) + \delta(PMe_3)$	a_{2u}	218	231
190	175	$\underline{\rho_r(PMe_3)} + \delta(SnCl)o.p. + \delta(SnCl)i.p.$	e_u	170	171
200, 177	159	$\underline{\overline{\delta(SnCl)}}o.p. + \rho_r(PMe_3)$	e_g	152	200, 180
146	158	$\delta(SnCl)i.p.$	b_{2g}	158	146
157	157	$\underline{\nu(SnP)} + \delta(PMe_3)$	a_{1g}	146	139
153	144	$\underline{\overline{\delta(SnCl)}}o.p.$	a_{2u}	140	154
	127	$\underline{\overline{\delta(SnCl)}}i.p. + \rho_r(PMe_3)$	e_u	124	
	110	$\overline{\delta(SnCl)}o.p.$	b_{2u}	110	
123	99	$\underline{\rho_r(PMe_3)} + \delta(SnCl)o.p.$	e_g	94	119
	62	$\underline{\delta(SnCl)}o.p. + \rho_r(PMe_3)$	e_u	58	

*See Table 8 for notation.

Can. J. Chem. Downloaded from www.nrcresearchpress.com by 210.87.254.40 on 09/05/12
For personal use only.

$GeCl_4.2PMe_3$ were necessary. Metal–phosphorus stretching force constants were chosen to reproduce observed frequencies and were found to be in the range 1.1–1.4 mdyn/Å (see Table 2). The excellent fits which these force fields produce exonerate the rather arbitrary nature of such a transference. Nevertheless one should not attach too much significance to the force fields *per se*.

The transference scheme and force constants are shown below.

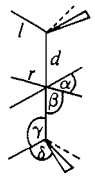

We wish to thank the National Research Council of Canada and Erindale College for financial support of this work and NRCC for a scholarship for D.K.F.

1. I. R. BEATTIE. Q. Rev. **17**, 382 (1963).
2. (*a*) V. BAIN, R. C. G. KILLEAN, and M. WEBSTER. Acta Cryst. B**25**, 156 (1969). (*b*) R. C. G. KILLEAN. Unpublished work. (*c*) R. HULME, G. J. LEIGH, and I. R. BEATTIE. J. Chem. Soc. 366 (1960). (*d*) M. MILNE, I. R. BEATTIE, M. WEBSTER, H. E. BLAYDEN, P. J. JONES, R. C. G. KILLEAN, and J. L. LAWRENCE. J. Chem. Soc. A, 482 (1969). (*e*) M. MILNE. Unpublished work.
3. (*a*) C. I. BRANDEN. Acta Chem. Scand. **17**, 759 (1963). (*b*) I. LINDQVIST. Inorganic adduct molecules of oxo-compounds. Springer, Berlin. 1963. (*c*) Y. HERMODSSON. Acta Cryst. **13**, 656 (1960). (*d*) H. E. BLAYDEN and M. WEBSTER. Unpublished work.
4. I. R. BEATTIE and G. A. OZIN. J. Chem. Soc. A, 2267 (1969).
5. I. R. BEATTIE and G. A. OZIN. J. Chem. Soc. A, 370 (1970).
6. G. A. OZIN. J. Chem. Soc. D, 104 (1969).
7. H. E. BLAYDEN and M. WEBSTER. Inorg. Nucl. Chem. Lett. **6**, 703 (1970).
8. F. G. MANN and A. F. WELLS. J. Chem. Soc. 708 (1938).
9. P. J. D. PARK and P. J. HENDRA. Spectrochim. Acta, **24**A, 2081 (1968).
10. F. G. MANN, A. F. WELLS, and D. PURDIE. J. Chem. Soc. 1831 (1937).
11. K. NAKAMOTO. Infrared spectra of inorganic and coordination compounds. Wiley–Interscience, New York. 1963.
12. R. R. REYNOLDS and K. HEDBURG. J. Chem. Phys. **50**, 4986 (1969).
13. G. A. OZIN. J. Chem. Soc. A, 1307 (1970).
14. I. R. BEATTIE and G. A. OZIN. J. Chem. Soc. A, 2373 (1968).
15. (*a*) I. R. BEATTIE, T. R. GILSON, and G. A. OZIN. J. Chem. Soc. A, 2772 (1968). (*b*) I. R. BEATTIE and G. A. OZIN. J. Chem. Soc. A, 542 (1969).
16. G. A. OZIN. Ph.D. Thesis, Oxford, 1967.
17. G. A. HERZBERG. Infrared and Raman spectra of polyatomic molelcules. D. Van Nostrand Co., Inc., New York. p. 217ff. 1945.
18. M. W. LISTER and L. E. SUTTON. Trans. Faraday Soc. **37**, 393 (1941).
19. Y. MORINO, Y. NAKAMURA, and T. IIJIMA. J. Chem. Phys. **32**, 643 (1960).
20. R. L. LIVINGSTON and C. N. R. RAA. J. Chem. Phys. **30**, 339 (1959).
21. COTTON and WILKINSON. Advanced inorganic chemistry. 2nd ed. Interscience, New York, p. 105. 1962.
22. I. R. BEATTIE, T. GILSON, K. LIVINGSTON, V. FAWCETT, and G. A. OZIN. J. Chem. Soc. A, 718 (1967).
23. S. SUNDARAM. Proc. Phys. Soc. **91**, 764 (1967).

Can. J. Chem. Downloaded from www.nrcresearchpress.com by 210.87.254.40 on 09/05/12
For personal use only.

Preparation, Infrared and Raman Spectra, and Stereochemistries of Pentacoordinate Trimethylphosphine Complexes, $MX_4.P(CH_3)_3$ and $MX_4.P(CD_3)_3$ where M = Ge or Sn and X = Cl or Br

D. K. FRIESON AND G. A. OZIN[1]

Lash Miller Chemistry Laboratories and Erindale College, University of Toronto, Toronto, Ontario

Received January 5, 1973

The 1:1 adducts $MX_4.PMe_3$ (M = Ge or Sn; X = Cl or Br) are prepared by recrystallization of the respective 1:2 complexes from excess MX_4 acceptor. Solid state infrared and Raman Spectra and X-ray powder photographs suggest that these adducts are all trigonal bipyramidal with the ligand in an axial position. Normal coordinate calculations in C_{3v} symmetry (axial ligand) and C_s symmetry (equatorial ligand) support this assignment. The rather high ν(MP) frequencies indicate unusually strong metal–phosphorus donor bonds in these compounds.

Les produits d'addition 1:1 $MX_4.PMe_3$ (M = Ge ou Sn; X = Cl ou Br) ont été préparés par recristallisation des complexes 1:2 correspondants à partir d'un excès de MX_4 accepteur. Les spectres infrarouge et Raman (état solide) et les photographies obtenues par rayons-X (poudre) suggèrent que ces composés d'addition possèdent tous une structure du type bipyramide trigonale avec le coordinat en position axiale. Des calculs en coordonnées normales pour une symétrie C_{3v} (coordinat axial) et une symétrie C_s (coordinat équatorial) sont en accord avec cette attribution. Les fréquences ν(MP) assez élevées sont généralement caractéristiques des liens forts donneurs métal–phosphore de ces composés.
[Traduit par le journal]

Can. J. Chem., 51, 2697 (1973)

Introduction

The vibrational spectra and stereochemistry of 1:2 adducts of trimethylphosphine with certain Group IV tetrahalide acceptor molecules have recently been discussed and their stability noted (1, 2). A number of other 1:2 triorganyl phosphine adducts with $SnCl_4$ have also been reported and their vibrational (2*a*, 2*b*) and Mössbauer (2*b*) spectra discussed. In all cases, *trans*-octahedral $MX_4.2L$ stereochemistries have been assigned to the 1:2 adducts. 1:1 Complexes of $SnCl_4$ with triphenylphosphine and tricyclohexylphosphine have been prepared (2*b*) but their vibrational spectra and structures as yet remain unassigned. Trimethylphosphine also tends to favor the formation of 1:2 complexes with the Group III (3) and the Group V trihalides (4, 5), the notable exception being $GaCl_3.PMe_3$ (3). The 1:2 trimethylphosphine complex of gallium trichloride is not known. These observations are to be compared with the tendency of trimethylamine to form stable 1:2 complexes in Group III (6) but unstable 1:2 and stable 1:1 complexes in Group IV (1, 7). Again gallium trichloride is the exception in Group III, the 1:2 adduct $GaCl_3.2NMe_3$ dissociating easily to $GaCl_3.NMe_3$ when the trimethylamine solvent is removed. $SiCl_4.NMe_3$ is also completely dissociated at room temperature. These trends suggest the possibility of producing the first examples of 1:1 PMe_3 complexes of the Group IV tetrahalides by introducing a small amount of the ligand into a large excess of acceptor solvent. Such experiments have yielded interesting results and are described in this paper.

Experimental

The Group IV tetrahalide reagents MX_4(M = Si, Ge, or Sn and X = Cl or Br) were purified by multiple trap-to-trap distillation *in vacuo*. The trimethylphosphine ligand was prepared and purified as described previously (1). The adducts were prepared *in vacuo* in thick-walled all glass reaction tubes by distilling a small quantity of ligand onto a large excess of the acceptor species at −78 °C. As the reagents warmed and the tetrahalide melted reaction occurred, this reaction tended to be quite sudden and violent and care had to be exercized to control the temperature of the mixture near the melting point of the acceptor.

In the reaction of excess $GeCl_4$ or $SnCl_4$ with PMe_3, the 1:2 product is initially formed. Recrystallization of these products from the excess acceptor at 140 and 100 °C respectively slowly yielded the 1:1 complexes. The Raman spectra of the mixtures was periodically examined and when no further change could be detected, the reaction was taken to be complete. In contrast, the 1:1 adducts of $GeBr_4$ and $SnBr_4$ are formed even in an excess of trimethylphosphine. (There was some evidence for the

[1]To whom correspondence should be addressed.

Can. J. Chem. Downloaded from www.nrcresearchpress.com by 210.87.254.5 on 09/05/12
For personal use only.

Can. J. Chem. Downloaded from www.nrcresearchpress.com by 210.87.254.5 on 09/05/12
For personal use only.

formation of $GeBr_4.2PMe_3$ but the adduct proved very unstable and the results could not be reproduced.) For $SiCl_4$ and $SiBr_4$, only 1:2 adducts are formed despite prolonged recrystallization from excess acceptor (1, 2). The *per deutero*-trimethylphosphine analogs of all 1:1 adducts were also prepared. In addition, the known trimethylamine complexes $GeCl_4.NMe_3$ and $SnCl_4.NMe_3$ were made for the purposes of comparison and were identified by their vibrational spectra (8, 9).

The Raman spectra of the solids were obtained with a Spex 1401 Raman spectrometer and Carson argon or krypton ion laser excitation (4880 or 5682 Å) while far infrared spectra were recorded with a Perkin–Elmer 180 spectrometer. Solution data could not be obtained due to the insoluble nature of the compounds.

X-Ray powder photographs of $GeCl_4.NMe_3$, $GeCl_4.PMe_3$, $SnCl_4.NMe_3$, and $SnCl_4.PMe_3$ were obtained using a collimated beam type camera and the Straumanis method of film mounting. Monochromatic X-rays at $\lambda = 1.542$ Å from a copper source were used. Unfortunately these materials gave only low angle reflections so that it was necessary to calculate the Bragg angles on the assumption of uniform and negligible film shrinkage. These data are listed in Table 15.

The adducts were analyzed for total halide content by quantitatively hydrolyzing a known weight of the compound in 0.1 *M* HNO_3 followed by argentiometric titration. The results are shown in the table below. All manipulations were carried out under vacuum or in a dry box which was continuously purged with dried air.

Total halide analysis

	% X	
Adduct	Calculated	Found
$GeCl_4.PMe_3$	48.8	48.7
$SnCl_4.PMe_3$	42.1	42.0
$GeBr_4.PMe_3$	68.3	69.5
$SnBr_4.PMe_3$	62.1	61.6

Results and Discussion

The reaction of PMe_3 with an excess of $SiCl_4$, $SiBr_4$, $GeCl_4$, or $SnCl_4$ invariably produced the six-coordinate complex while the reaction with $GeBr_4$ or $SnBr_4$ always led to the formation of a 1:1 adduct even when the ligand was held in excess. (There was some indication for the formation of the 1:2 complex, $GeBr_4.2PMe_3$, but the results could not be reproduced.) However, when $GeCl_4.2PMe_3$ and $SnCl_4.2PMe_3$ were recrystallized from $GeCl_4$ and $SnCl_4$ at *ca.* 140 °C and *ca.* 110 °C respectively, compounds which analyzed correctly as 1:1 complexes resulted. In contrast 1:1 adducts of $SiCl_4$ and $SiBr_4$ could not be induced to form, despite prolonged recrystallization at temperatures above 150 °C. These latter results agree with observations by Beattie and Ozin (2).

Donor–acceptor compounds of the main groups now abound in the literature. Molecular weight determinations where possible have led most authors recently to favor a monomeric molecular formulation although the validity of such results is open to question due to the strong propensity of these adducts to dissociate in solution (10). Nevertheless, available crystal structure data generally support this contention. Among the known structures are $SiCl_4.2PMe_3$ (11), $GeCl_4.NMe_3$ (12), $SnCl_4.2POCl_3$ (13), and a host of *bis* pyridine adducts $MX_4.2py$ (14) where MX_4 is SiF_4, $SiCl_4$, $GeCl_4$, $SnBr_4$, $SeCl_4$, or $PbCl_4$. While the insoluble nature of the $MX_4.PMe_3$ adducts of this study in common inert solvents precludes accurate molecular weight determinations, the inherent simplicity of the spectra support the assumption that these species also are covalent monomers.

In five-coordinate complexes of this type, structures may be based on either of two possible geometries: the trigonal bipyramid or the square pyramid, each with various possible geometric isomers. Examples of square pyramidal (10 electron valence shell) configurations are extremely rare. (Indeed, to our knowledge, only two species are known to have this geometry: $InCl_5^{2-}$ (15) and $SbPh_5$ (16)). Most five-coordinate structures are based on the trigonal bipyramid and the structures of the $MX_4.PMe_3$ adducts will be discussed in terms of this configuration. Thus, for a 1:1 adduct, two possible isomers exist: the ligand may be in an axial, staggered conformation (5) in which case the adduct has C_{3v} symmetry (where it should be noted that intermediate rotameric conformations of the ligand would reduce the symmetry of the adduct below C_{3v}); or the ligand may occupy an equatorial site giving the molecule formally C_{2v} symmetry if free rotation about the metal–phosphorus bond is assumed and C_s if not (Table 1, Fig. 1).

As most five-coordinate molecules are found to be trigonal bipyramids, similarly most five-coordinate 1:1 adducts are C_{3v} symmetry types. The recent X-ray crystal structure proves this to be the case for $GeCl_4.NMe_3$ (12) while the vibrational spectra of $TiCl_4.PMe_3$ (9) and other $MX_4.NMe_3$ adducts (where MX_4 = SiF_4, $SiCl_4$, $TiCl_4$, or $SnCl_4$) (8, 9) strongly support an axial ligand. The only known exceptions are the $TiCl_4.PH_nMe_{3-n}$ complexes (where n = 1, 2, or 3) in which the vibrational

TABLE 1. Selection rules of ν(MX) and ν(MP) modes of $MX_4.PMe_3$ species*

Geometry	Ligand position	Point group	Γ_{MX}	Γ_{MP}
Trigonal Bipyramid	Axial	C_{3v}	$2a_1$(R, P; i.r.) + e(i.r.; R)	a_1(R, P; i.r.)
	Equatorial	C_{2v}	$2a_1$(R, P; i.r.) + b_1(i.r., R) + b_2(i.r., R)	a_1(R, P; i.r.)

*Free rotation of the ligand assumed.

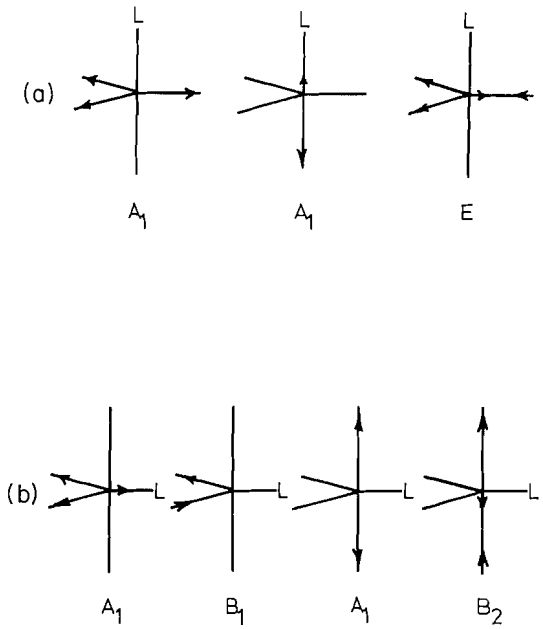

FIG. 1. (*a*) ν(MX) modes of the C_{3v} symmetry model $MX_4.L$; (*b*) ν(MX) modes of the C_{2v} symmetry model $MX_4.L$.

spectra suggest that the ligand is in an equatorial position (9).

As previously demonstrated (1) metal–halogen stretching vibrations can be identified as those bands which do not shift appreciably upon deuteration of the trimethylphosphine ligand, provided there is not severe coupling with ligand modes of the same symmetry. However, the narrow spectral region in which these bands tend to appear in the complexes studied here, and the appearance of ligand deformational modes in the same region can result in a certain amount of confusion as to which bands shift and which do not. There is also the problem of Raman and infrared coincidences (or near-coincidences) and there authenticity. Inspection of the spectra in Tables 7, 9, 11, and 13 reveals *at least three* bands which may be attributed to ν(MX) modes. These results are not unambiguous in their stereochemical implications although data supplied by X-ray powder photographs of $GeCl_4.NMe_3$, $SnCl_4.NMe_3$ and $SnCl_4.PMe_3$ (Table 15) lend strong support to the C_{3v} model. The recent X-ray crystal structure of $GeCl_4.NMe_3$ (12) has confirmed previous vibrational spectroscopic evidence (8) for an axial ligand (C_{3v} symmetry) and X-ray powder photographs (Table 15) prove $SnCl_4.NMe_3$ and $SnCl_4.PMe_3$ to be isomorphous with this adduct. While isomorphous crystals do not necessarily imply isostructural compounds, it is a highly probable event for chemically related species such as these. Numerous examples in the literature attest to this fact (see for example refs. 17, 18), as indeed does the isostructural pair $GeCl_4.NMe_3$ (12) and $SnCl_4.NMe_3$ (19). It is unfortunate and disquieting that $GeCl_4.PMe_3$ should yield the anomalous result in this respect. Nevertheless, the similarity of the spectra strongly suggest that the $MX_4.PMe_3$ compounds are isostructural and the isomorphicity of the $SnCl_4.PMe_3$ complex with the trimethylamine adducts is taken as evidence of an axial PMe_3 ligand in this series pending a more definitive study using single crystal X-ray techniques.

While metal–halogen stretching vibrations are relatively unperturbed by isotopic substitution, ν(MP) modes tend to shift 10–20 cm^{-1} due to the increased mass of the ligand when it is deuterated. For this reason the high frequency peaks at 536, 421, 537, and 423 cm^{-1} in the spectra of $GeCl_4.PMe_3$, $GeBr_4.PMe_3$, $SnCl_4.PMe_3$, and $SnBr_4.PMe_3$ respectively are assigned to metal–phosphorus stretches. The positions of these bands are indicative of unusually strong metal phosphorus bonds, and force constants of the order of 3.8–4.0 mdyn/Å for $MCl_4.PMe_3$ and 2.3–2.4 mdyn/Å for $MBr_4.PMe_3$ adducts were required to reproduce these frequencies in G.V.F.F. calculations (see later). However it would be dangerous to

Can. J. Chem. Downloaded from www.nrcresearchpress.com by 210.87.254.5 on 09/05/12
For personal use only.

Can. J. Chem. Downloaded from www.nrcresearchpress.com by 210.87.254.5 on 09/05/12
For personal use only.

attempt to relate these values quantitatively to bond strengths since the frequencies were found to be highly dependent upon interaction force constants in the force field. On the other hand, the effects of the strong donor bonds are reflected in the spectral position of stretching frequencies in the MX_4-residue since one would expect that the added electron density on the central atom should result in a weakening of the metal–halogen bonds. Thus, comparing the ν(GeCl) frequencies in $GeCl_4.PMe_3$ with those in $GeCl_4.NMe_3$ (8) where the *germanium–nitrogen* stretching frequency of 234 cm^{-1} typifies a much weaker dative bond, one finds the germanium–chlorine stretching modes at substantially higher frequencies in the latter complex (305–405 cm^{-1} as compared to 265–235 cm^{-1}).

Up to this point, the spectral analysis has been in terms of a covalent monomeric species. There are, however, two features in these spectra which deserve special mention. The first is the almost identical frequency of the ν(MP) modes in the respective germanium and tin tetrahalide analogs and the second is the magnitude of change in the ν(MP) frequency on passing from chloride to bromide analog. A plausible alternative explanation for this behavior, which seems to suggest a phosphorus–halogen bond, is formulation of the compounds as the products of the oxidative coupling reaction $[MX_3^-][Me_3PX^+]$ known to occur for certain adducts in Group V (5). However, the spectra rule out this possibility and the most reasonable chemical formulation for the Group IV complexes of this study remains the five-coordinate adduct and detailed interpretation of the spectra to follow will be in terms of this configuration.

$GeCl_4.PMe_3$

The solid state Raman and infrared spectra of $GeCl_4.PMe_3$ and its *per deutero*-analog are shown in Table 7. In order to identify the germanium–chlorine stretching frequencies it is necessary to correlate all spectral absorptions of $GeCl_4.P(CH_3)_3$ with those of $GeCl_4.P(CD_3)_3$. Table 7 shows the favored correlation but alternatives will be discussed below.

The most obvious coincidence is the strong Raman and infrared band at 267 cm^{-1}. Clearly unperturbed by deuteration, it is ascribed to a germanium–chlorine stretching mode. Similarly both the 323 cm^{-1} Raman band and the 319 cm^{-1} infrared band belong to ν(GeCl) vibrations. Although these bands are very close, the question arises as to whether they are indeed true coincidences. The 328 cm^{-1} component of the Raman doublet at 323/328 cm^{-1} does shift on deuteration of the ligand and the strong Raman peak at 278 cm^{-1} which appears to be in resonance with the 267 cm^{-1} band is found at 240 cm^{-1} in the spectrum of the deuterated adduct. However, the fate of the Raman band at 290 cm^{-1} is obscure: it could be unaffected by deuteration and appear in the 287 cm^{-1} band of the d_9-adduct in which case it would be a ν(GeCl) mode, or it could shift to 251 cm^{-1} in which case it is a deformation of the ligand. It is precisely the interpretation of this point which renders the spectra somewhat ambiguous for if it is accepted that this is a germanium–chlorine stretch, the spectra would imply the equatorial ligand site. Clearly more information is required.

Inspection of Table 8 will show that G.V.F.F. calculations in both C_{3v} and C_s (formally C_{2v}) symmetry give acceptable agreement with the observed spectrum. It must be noted, however, that an inordinately (and unacceptably) large axial stretch interaction force constant ($f_{dd} \sim 34\%$ of f_d) was required to fit the axial germanium–chlorine stretching frequencies of the C_s model. The C_{3v} force field seems to be more reasonable in this respect. Comparison of the spectrum of $GeCl_4.PMe_3$ with similar adducts (Table 2) also tends to favor an axial ligand. The spectra of the C_{2v} complexes $TiCl_4.PH_nMe_{3-n}$ $n = 1$ or 2, for example, clearly display *four* distinct and well-separated metal–halogen stretching vibrations while the spectrum of the C_{3v} complex $TiCl_4.PMe_3$ (9) resembles $GeCl_4.PMe_3$ with a set of *three* metal–halogen stretching modes in a narrow spectral range. It also displays a rather high frequency ν(TiP) mode. Owing to the substantial weakening of

TABLE 2. Fundamental stretching frequencies of $GeCl_4.PMe_3$ and $TiCl_4.PMe_3$*

Mode	Frequency (cm^{-1})	
	$TiCl_4.PMe_3$	$GeCl_4.PMe_3$
$\nu_{as}(MX_3)$	413 s (i.r.)	319 m (i.r.)
$\nu_s(MX_3)$	355 s (R, i.r.)	267 s(R, i.r.)
ν(MX)	379 s (i.r.)	323 m(R)
ν(MP)	488 m (i.r.)	536 s (R, i.r.)

*Reference 9.

Can. J. Chem. Downloaded from www.nrcresearchpress.com by 210.87.254.5 on 09/05/12
For personal use only.

the germanium–chlorine bonds as a result of the strong dative bond from phosphorus, comparison of the spectrum with $GeCl_4.NMe_3$ (8) is less enlightening but the foregoing considerations suggest $GeCl_4.PMe_3$ be assigned a C_{3v} stereochemistry.

$GeBr_4.PMe_3$

Unlike its tetrachloride analog, this adduct spontaneously forms in an excess of either reactant. The spectra of the deuterated and nondeuterated compounds are listed in Table 9. Germanium–bromine stretching modes characteristically appear at low frequencies and are unperturbed by isotopic substitution of the ligand. The strong Raman band at 295 cm^{-1} is quite obviously a ν(GeBr) mode. Although peaks at 233 cm^{-1} and 329 cm^{-1} are close to the ν_1 and ν_3 modes of free germanium tetrabromide (21), they are also assigned to germanium–bromine stretches in the adduct. The unchanging intensity of these peaks after extensive pumping on the complex by means of a liquid nitrogen trap and also after brief opening of the cell to the atmosphere justifies this assignment.

The infrared spectra are dominated by a very intense broad band centered at *ca.* 200 cm^{-1} which possibly contains two components. If this is so, four ν(GeBr) modes would imply the C_{2v} structure. Calculations in C_s symmetry however lend little support to this proposition for, in spite of an unacceptably large axial interaction force constant ($f_{dd} \approx 33\%$ of f_d), it was impossible to raise the calculated symmetric axial stretch and lower the asymmetric stretch sufficiently to fit observed values. G.V.F.F. calculations using reasonable values of force constants demonstrate that these spectra are best rationalized in terms of a C_{3v} stereochemistry (see Table 10).

Three bands in this region of the spectrum remain unassigned. The weak absorptions at *ca.* 270 cm^{-1} shift to lower frequencies on deuteration and are quite obviously ligand deformations. The strong Raman peak at 246 cm^{-1} appears to shift to 213 cm^{-1}. It is also attributed to a ligand deformational mode, while the medium shoulder at *ca.* 209 cm^{-1} is assigned to a ligand rocking vibration due to its appearance at *ca.* 182 cm^{-1} in the d_9-spectrum (this mode appears at 190 cm^{-1} in $InI_3.2PMe_3$ (3)). The unperturbed modes at 109 and 85 cm^{-1} are clearly skeletal deformations.

The germanium–phosphorus stretching mode in this adduct appears *ca.* 100 cm^{-1} below the analogous mode in $GeCl_4.PMe_3$. If the acceptor strengths of $GeCl_4$ and $GeBr_4$ were comparable one would of course expect to observe similar ν(GeP) frequencies in the two adducts. But clearly, the inability of $GeBr_4$ to form a 1:2 complex with PMe_3 and the comparative ease of formation of the *bis*trimethylphosphine adduct of $GeCl_4$ suggest much weaker Lewis acid properties toward PMe_3 in the tetrabromide. The effect of the weaker dative bond probably explains the lower germanium–phosphorus stretching frequency. The parallel change in the ν(SnP) frequency can be rationalized in a similar fashion.

$SnCl_4.PMe_3$

The spectrum of this adduct, particularly the nondeuterated complex, bears a close resemblance to the spectrum of $SnCl_4.NMe_3$ (19). X-Ray powder photographs show these two compounds to be isomorphous. This lends much support to the interpretation of the spectra on the basis of a C_{3v} stereochemistry, although G.V.F.F. calculations yield equally acceptable agreement with the observed spectrum for both models (see Table 12). As in the case of the C_s symmetry calculation of $GeCl_4.PMe_3$, this analysis however required a rather large (but in this case not unacceptable) axial interaction force constant ($f_{dd} \approx 14\%$ of f_d) to provide a reasonably close fit.

Inspection of the spectra in Table 11 reveals *three* medium to strong bands which do not shift when the ligand is deuterated. These are unequivocally tin chlorine stretching frequencies. There is, however, a fourth peak at *ca.* 350 cm^{-1} which is also relatively unperturbed by deuteration. *A priori*, the vibrational spectra would suggest that the ligand occupies an equatorial site but the fact that the X-ray powder

TABLE 3. ν(MX) modes of $SnCl_4.PMe_3$ and $SnCl_4.NMe_3$*

Mode	Frequency (cm^{-1})	
	$SnCl_4.PMe_3$	$SnCl_4.NMe_3$
$\nu_{as}(MX_3)$	326 s (i.r.)	367 vs (i.r.)
$\nu_s(MX_3)$	335 vs (R)	345 s (R)
ν(MX)	295 m (R)	318 m (R)

*Reference 19.

Can. J. Chem. Downloaded from www.nrcresearchpress.com by 210.87.254.5 on 09/05/12
For personal use only.

photographs of $SnCl_4.PMe_3$ and $SnCl_4.NMe_3$ are virtually superimposable and that the vibrational spectra are remarkably similar (see Table 3) favor the opposite conclusion. This band may then be due to splitting of the degenerate asymmetric ν(SnCl) mode, but unfortunately solution data could not be obtained to confirm this assignment.

$SnBr_4.PMe_3$

The quality of the spectra of this adduct suffers due to the low frequencies at which the modes of interest appear. Below 200 cm^{-1} the shift of modes associated with motion of the ligand is proportionately less. The spectrum however, is very similar to that of $GeBr_4.PMe_3$.

The 245 cm^{-1} Raman band shifts to 201 cm^{-1} on deuteration and appears to be in resonance with the 180 cm^{-1} band because of the intensity changes observed (see Table 13). The infrared bands at 256 cm^{-1} and *ca.* 192 cm^{-1} are clearly tin–bromine stretching frequencies but the 165 cm^{-1} band is assigned to a skeletal deformation. The Raman band at 180 cm^{-1} is also attributed to a ν(SnBr) mode. Thus, three ν(SnBr) modes can be identified. The unshifted band at 139 cm^{-1} is unreasonably low to be a tin–bromine stretch although calculations in C_s symmetry would place the a'-type axial mode in this region. However, at the same time the a'' mode is calculated over 50 cm^{-1} too high and cannot be lowered without using an unacceptably large interaction force constant. G.V.F.F. calculations (Table 14) in C_{3v} symmetry suggest that this spectrum is best interpreted in terms of this stereochemistry. The band at 139 cm^{-1} is most probably a skeletal deformation mode.

Normal Coordinate Analysis

Normal coordinate analyses were performed on the two possible structures of a monomeric adduct based on a trigonal bipyramidal stereochemistry:

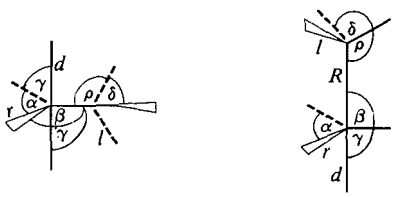

C_s (equatorial ligand) C_{3v} (axial ligand)

the C_{3v} model which contains the ligand in an axial position and the C_s model in which the ligand occupies an equatorial site. Equatorial metal-halogen bond lengths were taken directly from the parent molecules (22–24) while the axial bond lengths were multiplied by the ratio of the axial bond length to the equatorial bond length in molecular PCl_5 (25) to reflect the weaker axial bond known to exist in five coordinate species. The metal-phosphorus interatomic distance was taken as the sum of the covalent radii (26). Bond angles in both models were those of the idealized trigonal bipyramid: the structures were assumed to be undistorted. The structural parameters of the ligand were transferred unaltered from coordinated trimethylphosphine in $SiCl_4.2PMe_3$ whose crystal structure is known (11). These data are listed in Table 4. Internal coordinate definitions are shown below.

Force constants for both the C_s and the C_{3v} models were transferred from the tetrahedral and octahedral species $GaCl_4^-$ and $GeCl_6^{2-}$ for $GeCl_4.PMe_3$, and $InCl_4^-$ and $SnCl_6^{2-}$ for $SnCl_4.PMe_3$ according to the scheme adopted by Beattie and co-workers for the isoelectronic pentachloro-anions (27). For the tetrabromide adducts the tetrahedral force constants of $GaBr_4^-$ and $InBr_4^-$ (28) were initially chosen together with the octahedral force field of $SnBr_6^{2-}$ (29). Since $GeBr_6^{2-}$ is not known, an approximate force field was obtained by multiplying the appropriate $SnBr_6^{2-}$ force constants by the factor $f_{ij}(GeCl_6^{2-})/f_{ij}(SnCl_6^{2-})$. The transference schemes are delineated in Tables 1 and 6. Direct transference in general produced values which were in rather poor agreement with observed frequencies. For $GeCl_4.PMe_3$, a 3/4-scheme was somewhat more successful but, since the equatorial stretching modes were computed too high and the axial modes too low in both models, f_r and f_d were reduced and increased respectively. Interaction force constants were also adjusted to produce an acceptable fit. A satisfactory fit was also obtained for both

TABLE 4. Structural parameters (Å)*

Compound	r(M—X^{ax})	r(M—X^{eq})	r(M—P)
$GeCl_4.PMe_3$	2.16	2.11	2.32
$GeBr_4.PMe_3$	2.36	2.29	2.32
$SnCl_4.PMe_3$	2.38	2.31	2.50
$SnBr_4.PMe_3$	2.52	2.44	2.50

*r(P—C) = 1.86 Å; ∠(C—P—C) = 100°; ∠(M—P—C) = 117.8°.

TABLE 5. C_s force constants* for $MX_4.PMe_3$

$MX_4.PMe_3$	MX_5^{n-}†	$GeCl_4.PMe_3$	$GeBr_4.PMe_3$	$SnCl_4.PMe_3$	$SnBr_4.PMe_3$
f_r	f_a	1.103	1.430	1.776	1.340
f_d	f_b	1.059	0.897	1.580	1.025
f_R		3.500	2.300	4.000	2.400
$f_{rr} = f_{rR}$	f_{aa}	0.110	0.220	0.127	0.130
f_{dd}	f_{bb}^{trans}	0.357	0.296	0.220	0.015
f_{rd}	f_{bb}^{cis}	0.133	0.139	0.154	0.120
$f_\alpha = f_\beta$	f_α	0.136	0.130	0.085	0.080
f_γ	f_β	0.226	0.205	0.146	0.145
$f_{\alpha\beta} = f_{\beta\beta}$	$f_{\alpha\alpha}$	0.023	0.030	0.147	0.020
$f_{\alpha\gamma} = f_{\beta\gamma}$	$\frac{1}{2}(f_{\alpha\alpha} + f_{\beta\beta}^{adj})$	0.052	0.117	0.078	0.066
$f_{\gamma\gamma}$	$f_{\beta\beta}^{adj}$	0.072	0.102	0.008	0.014
f_{Rl}		0.350		0.400	
f_l		2.870	2.870	2.870	2.870
f_{ll}		−0.010	−0.010	−0.010	−0.010
f_δ		0.233	0.233	0.233	0.233
$f_{\delta\delta}$		0.010	0.010	0.010	0.010
f_p		0.087	0.087	0.087	0.087

*In units of mdyn/Å.
†Reference 27. The subscripts "a" and "α" indicate tetrahedral force constants while "b" and "β" refer to octahedral force constants according to the scheme delineated by Beattie for MCl_5 species.

TABLE 6. C_{3v} force constants* for $MX_4.PMe_3$

$MX_4.PMe_3$	MX_5^{n-}†	$GeCl_4.PMe_3$	$GeBr_4.PMe_3$	$SnCl_4.PMe_3$	$SnBr_4.PMe_3$
f_r	f_a	1.304	1.473	1.776	1.340
f_d	f_b	1.299	1.247	1.529	1.200
f_R		3.800	2.300	4.000	2.400
$f_{rr} = f_{rR}$	f_{aa}	0.130	0.263	0.178	0.130
f_{Rd}	f_{bb}^{trans}	0.067	0.196	0.077	0.040
f_{rd}	f_{bb}^{cis}	0.133	0.139	0.154	0.120
f_α	f_α	0.102	0.130	0.085	0.080
$f_\beta = f_\gamma$	f_β	0.170	0.205	0.146	0.145
$f_{\alpha\alpha}$	$f_{\alpha\alpha}$	0.017	0.030	0.147	0.020
$f_{\alpha\beta} = f_{\alpha\gamma}$	$\frac{1}{2}(f_{\alpha\alpha} + f_{\beta\beta}^{adj})$	0.039	0.117	0.078	0.066
$f_{\beta\beta} = f_{\beta\gamma} = f_{\gamma\gamma}$	$f_{\beta\beta}^{adj}$	0.054	0.102	0.008	0.014
$f_{r\alpha} = f_{r\beta} = f_{r\gamma}$	$f_{b\beta}^{adj}$	0.090		0.057	
$f_{d\gamma}$	$f_{b\beta}^{adj}$	0.090		0.057	
$f_{R\beta}$	$f_{b\beta}^{adj}$	0.090		0.057	
f_{Rl}		0.380		0.400	0.240
f_l		2.870	2.870	2.870	2.870
f_{ll}		−0.010	−0.010	−0.010	−0.010
f_δ		0.233	0.233	0.233	0.233
$f_{\delta\delta}$		0.010	0.010	0.010	0.010
f_p		0.087	0.087	0.087	0.087

*In units of mdyn/Å.
†See second footnote of Table 5.

models of $SnCl_4.PMe_3$ by an upward adjustment of f_d to effect an increase in the symmetric axial tin–chlorine stretching frequency.

Particular difficulty was encountered in fitting the axial stretching frequencies of the tetrabromide complexes. In the C_s structure of $GeBr_4.PMe_3$, it was necessary to increase the interaction force constant f_{dd} substantially to accomplish a reduction in the asymmetric mode and an increase in the symmetric mode. Agreement is still rather poor, but further increase would make f_{dd} unreasonably large. Distortion of the axial bonds each 15° off the axis did not appreciably alter the frequencies. Similar adjustments were necessary for $SnBr_4.PMe_3$ and for the C_{3v} symmetry models.

Large f_{MP} force constants were required to approximately reproduce observed metal–phos-

Can. J. Chem. Downloaded from www.nrcresearchpress.com by 210.87.254.5 on 09/05/12
For personal use only.

TABLE 7. Vibrational spectrum of $GeCl_4.PMe_3$

$GeCl_4.PMe_3$-h_9		$GeCl_4.PMe_3$-d_9		Approximate description of mode
Raman	I.r.	Raman	I.r.	
780 w	779 mw	713 w	712 w	$\nu(PMe_3)$
698 mw	696 m	643 vw		
	675 w	633 mw	631 s	$\nu(PMe_3)$
536 s	533 s	517 s	515 s	ν(GeP)
530 msh	526 msh	511 msh	508 msh	
328	mbr			$\delta(PMe_3)$
323				
		324 m		ν(GeCl)
	319 msh		319 msh	ν(GeCl)
290 mwsh		287 mbrsh		$\delta(PMe_3)$
278 s		~251 mw		$\delta(PMe_3)$
		240 m		
267 s	269 sbr	267 ms	269 sbr	ν(GeCl)
231 m		203 m		$\rho_r(PMe_3)$
	~198 vwsh		199 w	δ(GeCl)
170 ms	167 w	170 m	167 mw	δ(GeCl)
142 s	~136 w	140 ms	138 w	δ(GeCl)

TABLE 8. Calculated and observed vibrational frequencies for $GeCl_4.PMe_3$ (cm^{-1}): potential energy contributions > 75% considered pure modes; potential energy contributions < 30% neglected

P.E. contribution	C_s Sym	C_s Calcd	Obsd Raman	Obsd I.r.	C_{3v} Calcd	C_{3v} Sym	P.E. contribution
$\nu(PMe_3)$	a''	728		779 mw	726	e	$\nu(PMe_3)$
$\nu(PMe_3)$	a'	727	780 w				
$\nu(PMe_3)$	a'	677	698 mw	696 m	679	a_1	$\nu(PMe_3)$
ν(GeP)	a'	506	536 s	533 s	514	a_1	ν(GeP)
ν(GeCleq)	a'	334	323 mbr		316	a_1	ν(GeClax)
δ(GeClax), ν(GeCl)o.p.	a''	327		319 msh	333	e	ν(GeCleq)
ν(GeCleq), $\delta(PMe_3)$	a'	310	290 mwsh, 278 s		261	e	$\delta(PMe_3)$
ν(GeClax)	a'	266	267 s	269 sbr	271	a_1	ν(GeCleq)
$\delta(PMe_3)$	a'	261					
$\delta(PMe_3)$	a''	260	231 m		225	a_1	ν(GeClax)
ν(GeCleq), ν(GeClax)	a'	217					
ν(GeCleq), δ(GeCl)o.p.	a'	184		198 vwsh	162	e	$\rho_r(PMe_3)$, δ(GeCl)i.p.
ν(GeClax), δ(GeCl)o.p.	a''	176		167 w			
					175	e	δ(GeCl)o.p
δ(GeCl)o.p., δ(GeCl)i.p.	a'	172	170 ms				
δ(GeCl)o.p., $\rho_r(PMe_3)$	a''	140		136 w			
					126	e	$\rho_r(PMe_3)$
$\rho_r(PMe_3)$, δ(GeCl)o.p.	a'	128	142 s				
δ(GeCl)o.p.	a''	127					
δ(GeCl)i.p., δ(GeCl)o.p.	a'	98					
δ(GeCl)o.p., $\rho_r(PMe_3)$	a''	83					
δ(GeCl)i.p., δ(GeCl)i.p.	a'	76					

Can. J. Chem. Downloaded from www.nrcresearchpress.com by 210.87.254.5 on 09/05/12
For personal use only.

TABLE 9. Vibrational spectra of $GeBr_4.PMe_3$

$GeBr_4.PMe_3$-h_9		$GeBr_4.PMe_3$-d_9		Approximate description of mode
Raman	I.r.	Raman	I.r.	
770 vw	772 m	705 vw		$\nu(PMe_3)$
		635 vvw	637 vw	
679 w	680 m	613 w	614 ms	$\nu(PMe_3)$
	674 m	603 vw	594 m	$\nu(PMe_3)$
	474 mw		450 w	hydrolysis
421 vs	422 ms	400 s	401 s	ν(GeP)
	377 m		356 mw	hydrolysis
	348 mw		317 wsh	$\delta(PMe_3)$
	329 m		327 m	ν(GeBr)
267 w	270 vwsh		256 wsh	$\delta(PMe_3)$
246 s	248 wsh	213 s		$\delta(PMe_3)$
233 s	230 mwsh	232 s	230 msh	ν(GeBr)
~209 msh		~182 wsh		$\rho_r(PMe_3)$
	~208 } sbr		207 } sbr	ν(GeBr)
195 s	~195 }	194 s	192 }	
109 s		108 ms		δ(GeBr)
85		85 ms		δ(GeBr)
~74 wsh				

TABLE 10. Calculated and observed vibrational frequencies for $GeBr_4.PMe_3$ (cm^{-1}): P.E. contributions > 75% considered a pure mode; P.E. contributions < 30% neglected

C_s model			Observed		C_{3v} model		
P.E. contribution	Symmetry type	Calcd. frequency	Raman	I.r.	Calcd. frequency	Symmetry type	P.E. contribution
$\nu(PMe_3)$	a''	727		772 m	726	e	$\nu(PMe_3)$
$\nu(PMe_3)$	a'	727	770 vw				
$\nu(PMe_3)$	a'	706	679 w	680 m	706	a_1	$\nu(PMe_3)$
ν(GeP)	a'	424	421 vs	422 ms	426	a_1	ν(GeP)
ν(GeBreq)	a'	343		329 m	301	e	ν(GeBreq)
$\delta(PMe_3)$	a'	306	267 w	270 vwsh	306	a_1	$\delta(PMe_3)$ + δ(GeBr)o.p.
ν(GeBrax)	a''	300	233 s	230 mwsh	212	a_1	$\nu(GeBreq)_3$
$\delta(PMe_3)$	a'	259	246 s	248 wsh	260	e	$\delta(PMe_3)$
$\delta(PMe_3)$	a''	257					
ν(GeBreq)	a'	198	211 ms	208 s			
ν(GeBrax)	a'	151	195 s	195 s	166	a_1	ν(GeBrax) + ν(GeBreq) + ν(GeP)
ν(GeBreq) + $\rho_r(PMe_3)$	a'	155	205 w		150	e	$\rho_r(PMe_3)$ + ν(GeBreq)
ν(GeBreq) + δ(GeBr)o.p. + ν(GeP) + ν(GeBrax)	a'	145	109 s		135	a_1	δ(GeBr)o.p.
$\rho_r(PMe_3)$ + ν(GeBrax)	a''	134	85 s		104	3	$\rho_r(PMe_3)$ + δ(GeBr)i.p.
$\rho_r(PMe_3)$ + δ(GeBr)o.p.	a'	106					
$\rho_r(PMe_3)$ + ν(GeBrax)	a''	98	78 wsh				

Can. J. Chem. Downloaded from www.nrcresearchpress.com by 210.87.254.5 on 09/05/12
For personal use only.

TABLE 11. Vibrational spectra of $SnCl_4.PMe_3$

$SnCl_4.PMe_3$-h_9		$SnCl_4.PMe_3$-d_9		Approximate description of mode
Raman	I.r.	Raman	I.r.	
772 vw, 757 vvw	772 vw, 760 m	708 ww, 698 vw, 689 vw	691 vw	$\nu(PMe_3)$
694 w	695 ms, 669 w	606 mw, 635 w, 629 w	595 w, 629 m	$\nu(PMe_3)$
537 w, 531 wsh	538 ms	518 mw, 512 wsh	515 m	$\nu(SnP)$
358 w	350 msh	351 wsh	352 m	(see text)
335 ws		336 ms		$\nu(SnCl)$
324 wsh	326 sbr	320 ms	327 msh	$\nu(SnCl)$
295 m	295 mbr	296 s	295 sbr	$\nu(SnCl)$
278 m		264 m	271 msh	$\delta(PMe_3)$
270 w	273 msh	244 wsh, 234 mbr		$\delta(PMe_3)$
259 mv		227 wsh		$\delta(PMe_3)$
229 w		201 vw		$\rho_r(PMe_3)$
186 mwbr				$\rho_r(PMe_3)$
165 wsh		169 sbr		$\delta(SnCl)$
157 mbr		155 msh		$\delta(SnCl)$

TABLE 12. Calculated and observed frequencies for $SnCl_4.PMe_3$: P.E. contributions > 75% considered pure modes; P.E. contributions < 30% neglected

C_s model			Observed		C_{3v} model		
P.E. contributions	Symmetry type	Calcd. frequency	Raman	I.r.	Calcd. frequency	Symmetry type	P.E. contributions
$\nu(PMe_3)$	a''	727	757 vvw	760 m	726	e	$\nu(PMe_3)$
$\nu(PMe_3)$	a'	722	772 vw	772 vw			
$\nu(PMe_3)$	a'	678	694 w	695 ms	678	a_1	$\nu(PMe_3)$
$\nu(SnP)$	a'	494	537 w	538 ms	494	a_1	$\nu(SnP)$
$\nu(SnCleq)$	a'	347	358 w	350 msh			
$\nu(SnCleq)$	a'	337	335 vvs		333	a_1	$\nu(SnCleq)$, $\nu(SnClax)$
$\nu(SnClax)$	a''	333	324 wsh	326 sbr	336	e	$\nu(SnCleq)$
$\nu(SnClax)$	a'	281	295 m	295 mbr	291	a_1	$\nu(SnClax)$, $\nu(SnCleq)$
$\delta(PMe_3)$	a''	262	270 w	273 msh	261	e	$\delta(PMe_3)$
$\delta(PMe_3)$	a'	258	278 m				
$\delta(PMe_3)$	a'	232	259 mw		223	a_1	$\delta(PMe_3)$
$\rho_r(PMe_3)$, $\delta(SnCl)$o.p.	a''	156	229 w		156	e	$\rho_r(PMe_3)$, $\delta(SnCl)$o.p.
$\delta(SnCl)$o.p.	a'	160	165 wsh		146	a_1	$\delta(SnCl)$o.p.
$\delta(SnCl)$o.p.	a''	148	157 mbr		144	e	$\delta(SnCl)$o.p.
$\delta(SnCl)$o.p.	a''	147					
$\delta(SnCl)$o.p.	a'	142					
$\rho_r(PMe_3)$	a'	113	186 mwbr		86	e	$\rho_r(PMe_3)$, $\delta(SnCl)$o.p.
$\delta(SnCl)$o.p., $\rho_t(PMe_3)$	a''	84					

Can. J. Chem. Downloaded from www.nrcresearchpress.com by 210.87.254.5 on 09/05/12
For personal use only.

TABLE 13. Vibrational spectra of $SnBr_4.PMe_3$

$SnBr_4.PMe_3$-h_9		$SnBr_4.PMe_3$-d_9		Approximate description of mode
Raman	I.r.	Raman	I.r.	
774 vw	772 mw	687 vw		$\nu(PMe_3)$
757 vw	755 mw			$\nu(PMe_3)$
		636 vvw	635 w	
684 w	683 m	616 vw	616 mw	$\nu(PMe_3)$
667 vw	663 w	604 w		$\nu(PMe_3)$
423 m	422 s	404 mw	403 s	ν(SnP)
	~352 vw		~315 vw	$\delta(PMe_3)$
331 w	331 w	294 w		$\delta(PMe_3)$
287 vw		264 vw		$\delta(PMe_3)$
269 w		252 vw, 230 vw		$\delta(PMe_3)$
	256 mw		257 ms	ν(SnBr)
245 mw		201 s		$\delta(PMe_3)$
	192 vsbr		198 s, br	ν(SnBr)
180 msh		180 s		ν(SnBr)
170 s		155 msh		$\rho_r(PMe_3)$
160 msh	162 sbr	~167 mwsh	165 m	δ(SnBr)
139 ms		141, ~135, 101 mw		δ(SnBr)

TABLE 14. Calculated and observed frequencies for $SnBr_4.PMe_3$: P.E. contributions > 75% considered pure modes; P.E. contributions < 30% neglected

C_s			Observed		C_{3v}		
P.E. contributions	Symmetry type	Calcd. frequency	Raman	I.r.	Calcd. frequency	Symmetry type	P.E. contributions
$\nu(PMe_3)$	a''	727	774	772 mw	726	e	$\nu(PMe_3)$
$\nu(PMe_3)$	a'	725	757 vw	755 mw			
$\nu(PMe_3)$	a'	706	684 w	683 m	669	a_1	$\nu(PMe_3)$
ν(SnP)	a'	403	423 m	422 s	424	a_1	ν(SnP)
$\delta(PMe_3)$	a''	264	287 w		264	e	$\delta(PMe_3)$
$\delta(PMe_3)$	a'	265	269 w				
ν(SnBreq), $\delta(PMe_3)$	a'	252	245 mw		256	a_1	ν(SnBrax), $\delta(PMe_3)$
δ(SnBreq)	a'	253		256 mw	242	e	ν(SnBreq), $\delta(PMe_3)$
ν(SnBrax)	a''	248		182 vsbr	192	a_1	ν(SnBreq)
ν(SnBreq)	a'	188	180 s		160	a_1	ν(SnBrax), ν(SnBreq)
$\rho_r(PMe_3)$, δ(SnBr)o.p.	a''	145		162 sbr	144	e	$\rho_r(PMe_3)$
$\rho_r(PMe_3)$	a'	143	160 msh				
ν(SnBrax)	a'	141	139 ms		107	a	δ(SnBr)o.p.
δ(SnBr)o.p.	a'	122					
δ(SnBr)o.p.	a''	100			100	e	δ(SnBr)o.p
$\rho_r(PMe_3)$, δ(SnBr)o.p.	a'	98					
δ(SnBr)o.p.	a''	93					
δ(SnBr)o.p., $\rho_r(PMe_3)$	a''	70			78	e	δ(SnBr)o.p., $\rho_r(PMe_3)$

Can. J. Chem. Downloaded from www.nrcresearchpress.com by 210.87.254.5 on 09/05/12
For personal use only.

TABLE 15. X-Ray powder data* for $MCl_4.N(CH_3)_3$ and $MCl_4.P(CH_3)_3$ where M = Ge or Sn

	$\sin^2\theta_i$							
	$GeCl_4.PMe_3$		$GeCl_4.NMe_3$		$SnCl_4.NMe_3$		$SnCl_4.PMe_3$	
1	0.00105	w	0.00129	w				
2	0.00142	vw	0.00209	w	0.00196	s	0.00196	s
3	0.00175	w	0.00259	s				
4	0.00235	m	0.00323	m	0.00304	m	0.00300	m
5	0.00281	mw	0.00395	s	0.00403	w	0.00412	w
6	0.00319	vw	0.00430	w				
7	0.00364	vw	0.00506	vw	0.00526	m	0.00521	vw
8	0.00439	s	0.00654	m	0.00643	mw	0.00637	m
9	0.00481	ms	0.00741	w	0.00747	w	0.00753	w
10	0.00526	w	0.00852	vw				
11	0.00610	vw	0.00999	w	0.01020	ms	0.01013	ms
12	0.00650	vw	0.01056	ms				
13	0.00753	mw	0.01173	mw				
14	0.00859	vw	0.01242	ms	0.01242	s	0.01234	s
15	0.00924	ms	0.01336	vw	(0.01401)	w	0.01401	w
16	0.01042	vvw	0.01476	w				
17	0.01114	ms	0.01613	m				
18	0.01203	w	0.01720	vvw				
19	0.01352	w	0.01869	mw	0.01840	m	0.01840	m
20	0.01509	vvw	0.02244	mw	0.02214	m	0.02214	m
21	0.01784	w	0.02445	vw				
22	0.01964	w	0.02543	s	0.02532	vs	0.02532	vs
23	0.02122	w	0.02665	w	0.02654	mw	0.02643	mw
24	0.02296	mw	0.02756	w				
25	0.02424	w	0.02883	w				
26	0.02587	vw	0.03170	mw	0.03194	m	0.03170	m
27	0.02756	w	0.03368	mw	0.03356	ms	0.03368	ms
28	0.02965	vvw	0.03534	vw				
29	0.03207	m	0.03638	vw				
30	0.03381	vw	0.03783	w				
31	0.03612	w	0.04026	w				
32	0.03850	vvw	0.04192	w				
33	0.04012	vw	0.04534	vw	0.04491	vw	0.04462	vw
34	0.04178	vw	0.04607	vw	0.04607	w	0.04607	w
35			0.04950	w				
36			0.05133	w				
37			0.05398	vvw				
38			0.05897	vvw				
39			0.06349	vw				
40			0.07100	mw	0.07082	m	0.07100	m

*Correlation between the adducts $GeCl_4.NMe_3$, $SnCl_4.NMe_3$, and $SnCl_4.PMe_3$ is indicated.

phorus stretching frequencies. Interaction force constants were also introduced for the chlorides. The final force fields for C_s and C_{3v} symmetries are listed in Tables 5 and 6. No attempt was made to obtain an exact fit since an infinite number of solutions is possible.

We wish to thank the National Research Council of Canada for a N.R.C.C. scholarship for D.F.K. and for financial support of this work.

1. D. K. FRIESEN and G. A. OZIN. Can. J. Chem. (1973). In press.
2. I. R. BEATTIE and G. A. OZIN. J. Chem. Soc. (A), 2267 (1969).
2. (*a*) R. RIVEST, S. SINGH, and C. ABRAHAM. Can. J. Chem. **45**, 3137 (1967). (*b*) A. J. CARTY, T. HINSPERGER, L. MIHICHUK, and H. D. SHARMA. Inorg. Chem. **9**, 2572 (1970).
3. I. R. BEATTIE and G. A. OZIN. J. Chem. Soc. (A), 2373 (1968).
4. R. R. HOLMES and E. F. BERTAUT. J. Am. Chem. Soc. **80**, 2980 (1958).

Can. J. Chem. Downloaded from www.nrcresearchpress.com by 210.87.254.5 on 09/05/12
For personal use only.

5. J. C. SUMMERS and H. H. SISLER. Inorg. Chem. **9**, 862 (1970).
6. I. R. BEATTIE, T. GILSON, and G. A. OZIN. J. Chem. Soc. (A), 1092 (1968).
7. C. J. WILKINS and D. K. GRANT. J. Chem. Soc. 927 (1953).
8. I. R. BEATTIE and G. A. OZIN. J. Chem. Soc. (A), 370 (1970).
9. I. R. BEATTIE and T. GILSON. J. Chem. Soc. (A), 2960 (1969).
10. I. R. BEATTIE. Q. Rev. **17**, 382 (1963).
11. H. E. BLAYDEN and M. WEBSTER. Inorg. Nucl. Chem. Lett. **6**, 703 (1970).
12. M. S. BILTON and M. WEBSTER. J. Chem. Soc. Dalton, 722 (1972).
13. C. I. BRANDEN. Acta Chem. Scand. **17**, 759 (1963).
14. (*a*) V. BAIN, R. C. G. KILLEAN, and M. WEBSTER. Acta Cryst. **B25**, 156 (1969). (*b*) R. C. G. KILLEAN. Unpublished work. (*c*) R. HULME, G. J. LEIGH, and I. R. BEATTIE. J. Chem. Soc. 366 (1960). (*d*) M. MILNE, I. R. BEATTIE, M. WEBSTER, H. E. BLAYDEN, P. J. JONES, R. C. G. KILLEAN, and J. L. LAWRENCE. J. Chem. Soc. (A), 482 (1969).
15. D. S. BROWN, F. W. B. EINSTEIN and D. G. TUCK. Inorg. Chem. **8**, 14 (1969).
16. P. S. WHEATLEY and G. WITTIG. Proc. Chem. Soc. 251 (1962).
17. G. A. OZIN. J. Chem. Soc. (A), 1307 (1970).
18. I. R. BEATTIE and G. A. OZIN. J. Chem. Soc. (A), 542 (1969).
19. I. R. BEATTIE and T. GILSON. J. Chem. Soc. 6595 (1965).
20. R. BAUMGÄRTNER, W. SAWODNY, and J. GOUBEAU. Z. Anorg. Allg. Chem. **333**, 172 (1964).
21. K. NAKAMOTO. Infrared spectra of inorganic and coordination compounds. Wiley–Interscience, New York.
22. M. W. LISTER and L. E. SUTTON. Trans. Faraday Soc. **37**, 393 (1941).
23. Y. MORINO, Y. NAKAMURA, and T. IIJIMA. J. Chem. Phys. **32**, 643 (1960).
24. R. L. LIVINGSTON and C. N. R. RAA. J. Chem. Phys. **30**, 339 (1959).
25. Interatomic distances. Chemical Society, London. 1958.
26. COTTON and WILKINSON. Advanced inorganic chemistry. 2nd ed. Interscience, New York. p. 105.
27. I. R. BEATTIE, T. GILSON, K. LIVINGSTON, V. FAWCETT, and G. A. OZIN. J. Chem. Soc. (A), 718 (1967).
28. A. MÜLLER and B. KREBS. J. Mol. Spectrosc. **24**, 180 (1967).
29. S. SUNDARAM. Proc. Phys. Soc. **91**, 764 (1967).

Can. J. Chem. Downloaded from www.nrcresearchpress.com by 210.87.254.5 on 09/05/12
For personal use only.

Binary Transition Metal Dinitrogen Complexes. Part II. Matrix Infrared and Raman Spectra, Structure, and Bonding of $Pt(N_2)_n$ (where $n = 1$–3)

E. P. KÜNDIG, M. MOSKOVITS, AND G. A. OZIN

Lash Miller Chemical Laboratories, and Erindale College, University of Toronto, Toronto, Ontario

Received January 9, 1973

The products of the cocondensation reactions of Pt atoms with N_2 at 4.2–10 °K are investigated by matrix isolation infrared and Raman spectroscopy and are shown to be binary dinitrogen complexes of the form $Pt(N_2)_n$. Examination of the reaction products in pure $^{14}N_2$, in $^{14}N_2/^{15}N_2$, in dilute $^{14}N_2$/Ar, in $^{14}N_2/^{15}N_2$/Ar as well as $^{14}N_2/^{14}N^{15}N/^{15}N_2$/Ar matrices establishes the stoichiometries of the complexes to be $n = 1$–3. Structural assignments can be made for the complexes $Pt(N_2)$ and $Pt(N_2)_3$ which contain end-on bonded dinitrogen and are found to be similar to the corresponding dinitrogen and carbonyl complexes of nickel and palladium. $Pt(N_2)_2$ appears to be the exception in this series of complexes, for which side-on bonded dinitrogen is proposed.

On the basis of the Cotton–Kraihanzel force field of approximation and the isotope intensity sum rules, isotopic frequencies are computed for the NN stretching modes of the individual complexes and isotopic absorption intensities for $Pt(N_2)_3$ and are found to be in close agreement with the observed values. In the case of $Pt(N_2)$, the scrambled $^{14}N^{15}N$ isotope data establish that the dinitrogen ligand is bonded to the Pt atom in an end-on fashion. On the basis of its unusual spectroscopic behavior $Pt(N_2)_2$ is proposed to have sideways bonded dinitrogen ligands. $Pt(N_2)_3$ in solid α-N_2 is found to be slightly distorted from a regular triangular planar molecule but appears to be regular D_{3h} in solid argon. Calculations show that a substitutional site symmetry of C_2 for $Pt(N_2)_3$ satisfactorily accounts for all the spectral lines observed for the complex in nitrogen. Comparisons are made within the group of binary dinitrogen complexes $M(N_2)_n$ where $n = 1$–3 and with the corresponding binary carbonyl complexes $M(CO)_n$. The relationship between the dinitrogen complexes NiN_2, PdN_2, and PtN_2 and nitrogen chemisorbed on those same metals is discussed.

Les produits de cocondensation d'atomes de Pt avec du N_2 à 4.2–10 °K ont été étudiés à l'aide de la spectroscopie infrarouge et Raman (isolement de la matrice) et se sont révélés être des complexes binaires diazotés du type $Pt(N_2)_n$. L'examen des produits de la réaction dans les milieux $^{14}N_2$ pur, $^{14}N_2/^{15}N_2$, $^{14}N_2$/Ar dilué, $^{14}N_2/^{15}N_2$/Ar ainsi que $^{14}N_2/^{14}N^{15}N/^{15}N_2$/Ar, a fixé la stoechiométrie (n) des complexes égale à 1–3. Des attributions structurales peuvent être effectuées pour les complexes $Pt(N_2)$ et $Pt(N_2)_3$ qui contiennent les groupes diazotés liés aux extrémités et qui, par suite, ressemblent aux complexes correspondant du nickel et du palladium comportant des groupes diazote et carbonyle. Le $Pt(N_2)_2$ semble être l'exception dans cette série de complexes puisque l'on propose pour ceux-ci que les groupes diazotés sont liés de côté.

En se basant sur le champ de force Cotton–Kraihanzel et sur les règles d'additivité des intensités isotopiques, on a pu calculer les fréquences isotopiques pour les modes d'élongation NN des complexes individuellement ainsi que les intensités d'absorption isotopique par le $Pt(N_2)_3$; ces résultats sont en accord avec les valeurs observées. Dans le cas du $Pt(N_2)$, les données se rattachant aux isotopes $^{14}N^{15}N$ mélangés, ont montré que le coordinat diazoté est lié à l'atome de Pt par les extrémités. En se basant sur son comportement spectroscopique inhabituel le $Pt(N_2)_2$ semble posséder des coordinats diazotes liés de côté. Le $Pt(N_2)_3$ dans le N_2 solide semble ne pas correspondre à cause de torsions légères à une molécule planaire triangulaire mais par contre semble être un D_{3h} régulier dans l'argon solide. Des calculs ont montré qu'un site de symétrie C_2 pouvant être substitué, explique assez bien pour le $Pt(N_2)_3$ toutes les bandes spectrales observées pour le complexe dans l'azote. Des comparaisons sont faites à l'intérieur du groupe de complexes binaires diazotés $M(N_2)_n$ où $n = 1$–3 et avec les complexes binaires carbonylés correspondant $M(CO)_n$. On discute de la relation présente entre les complexes diazotés NiN_2, PdN_2, et PtN_2 et l'azote chemisorbé sur ces mêmes métaux. [Traduit par le journal]

Can. J. Chem., 51, 2710 (1973)

Introduction

We have recently shown that the products of the cocondensation reactions of monatomic Ni and Pd vapors with pure N_2 or dilute N_2/Ar mixtures at 4.2–10 °K are binary dinitrogen complexes of the form $Ni(N_2)_n$ and $Pd(N_2)_m$ where $n = 1$–4 and $m = 1$–3 (1). The bonding of the dinitrogen ligand in these complexes was shown to be similar in a number of respects to the coordinated dinitrogen molecule in dinitrogen complexes that are stable at room temperature as well as CO in carbonyls. For example, the

Can. J. Chem. Downloaded from www.nrcresearchpress.com by 210.87.254.6 on 09/05/12
For personal use only.

Can. J. Chem. Downloaded from www.nrcresearchpress.com by 210.87.254.6 on 09/05/12
For personal use only.

molecular structures of $Ni(N_2)_n$ and $Pd(N_2)_m$ were shown to be similar to the corresponding binary carbonyls $Ni(CO)_n$ and $Pd(CO)_m$. Also the Cotton–Kraihanzel force field approximation (2) and isotope intensity sum rules (3, 4) applied usually to CO in carbonyls, were shown to be equally successful for predicting the frequencies and intensities of infrared active NN stretching modes for coordinated N_2 in binary dinitrogen complexes and their mixed isotopic molecules (1).

As a continuation of our work on the Ni/N_2 and Pd/N_2 systems, we have now investigated the matrix cocondensation reactions of monatomic Pt vapors with N_2 and N_2/Ar at 4.2–10 °K and we find that by and large its behavior mirrors that of Pd in many respects. It nevertheless deviates from the behavior of both the Pd/N_2 and Ni/N_2 systems in some striking instances discussed below (5, 6).

A relationship between NiN_2 and that of N_2 chemisorbed on Ni has also been recently discussed (7) and it is of considerable interest therefore to try to obtain the analogous data for PtN_2 and to compare it with the available infrared data for N_2 chemisorbed on Pt metal (8).

Burdett, Graham, and Turner using similar metal atom – dinitrogen matrix cocondensation reactions, have reported that Ni, Cr, Pt, and Cu can *only* form monodinitrogen complexes of the form MN_2 (9). Our own data for the nickel–dinitrogen system differed markedly from theirs in several respects and necessitated a reappraisal of their data and an interpretation of our data in terms of the four complexes, $Ni(N_2)_n$ (where $n = 1$–4) (1).

For the platinum–dinitrogen system reported here, our matrix infrared data again differ with the corresponding data reported by Turner *et al.* Rather than forming a single complex PtN_2 as proposed by Turner *et al.*, we find that *three* dinitrogen complexes of platinum, $Pt(N_2)_m$ (where $m = 1$–3) are formed.

It is noteworthy that very few dinitrogen complexes of platinum, which are stable at room temperature, have been reported in the literature. The only available data refer to three closely related binuclear complexes of platinum containing dinitrogen, which were reported by Volkov and Volkova and were formulated as containing the linear Pt—N≡N—Pt grouping (10).

Briefly, our technique involves the cocondensation of Pt atoms with N_2 or N_2 in Ar at 4.2–10 °K followed by spectroscopic examination. Matrix infrared and matrix Raman were both used. The latter carries with it the possibility of performing matrix depolarization measurements thereby identifying the totally symmetric vibrational modes (11).

Mixed isotopic matrix gases were also used to help establish the coordination number of the reaction products under different degrees of matrix dilution. In the case of monodinitrogen complexes, the mode of attachment of the dinitrogen to the metal atom, that is, whether end-on or side-on, can be determined from the $^{14}N^{15}N$ isotope data. Finally, warmup experiments were performed which aid in the assignment of the spectral lines to the several species present in the matrix.

Experimental

Monatomic Pt vapor was generated by directly heating either a thin (0.008 in.) ribbon filament of Pt with AC or Pt wire (0.010 in.) wound around a tungsten rod (0.025 in.). The platinum (99.99%) was supplied by McKay Inc., New York, or Imperial Smelting, Toronto. Research grade $^{14}N_2$ (99.99%) and Ar (99.99%) were supplied by Matheson. Isotopically enriched $^{15}N_2$ (99.5%) was supplied by Prochem. A mixture of $^{14}N_2$, $^{15}N^{14}N$, and $^{15}N_2$ in the ratio 1:2:1 was prepared by the conventional technique and the relative concentrations of the isotopic molecules checked by gas phase Raman spectroscopy (Fig. 1).

The furnace used for the evaporation of the metals has been described previously (1). The rate of metal atom depositions was continuously monitored using a quartz crystal microbalance (12). The deposition rate was set such that the probability that a metal atom had another metal atom as a nearest neighbor in either the N_2 or Ar f.c.c.

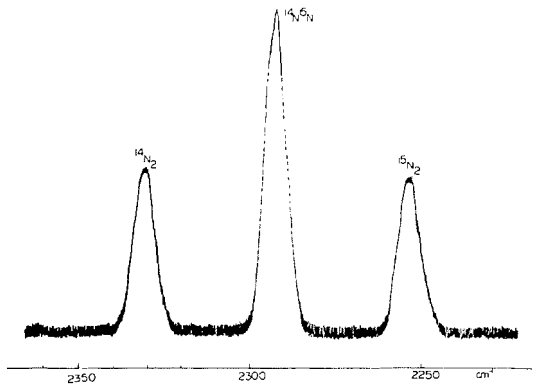

FIG. 1. The gas phase Raman spectrum of a statistical 1:2:1 mixture of $^{14}N_2$:$^{14}N^{15}N$:$^{15}N_2$ at about 100 Torr pressure.

lattice was approximately 1 in 10^3. Matrix gas flows, controlled by a calibrated micrometer needle valve, were usually in the range 2–8 mmol/h. In the infrared experiments matrices were deposited on a cryotip cooled to either 4.2 or 10 °K by means of an Air Products liquid helium transfer system or a Displex closed cycle helium refrigerator. Spectra were recorded on a Perkin Elmer 180 spectrophotometer. In the Raman experiments the matrices were deposited on a liquid helium cooled (4.2 °K) cryotip. Spectra were recorded on a Spex model 1401 Raman spectrophotometer using Carson argon ion 4880 Å and 5145 Å laser excitation.

Results

Tris(dinitrogen)platinum(0),Pt(N_2)$_3$ in Solid N_2

When platinum atoms are cocondensed with pure $^{14}N_2$ at 10 °K the main feature of the matrix infrared spectrum is a doublet at 2217.1, 2206 cm^{-1} (the 2206 cm^{-1} line being the more intense) with two other very weak lines at about 2177 and 2148 cm^{-1} (Fig. 2*a*). The corresponding matrix Raman spectrum besides the lines belonging to $^{14}N_2$ and $^{14}N^{15}N$ (in natural abundance 0.3%) shows only one strong polarized line at 2258 cm^{-1} (Fig. 3).

When the matrix infrared experiment was repeated using a $^{14}N_2$:$^{15}N_2 \cong 1.33:1$ mixture,

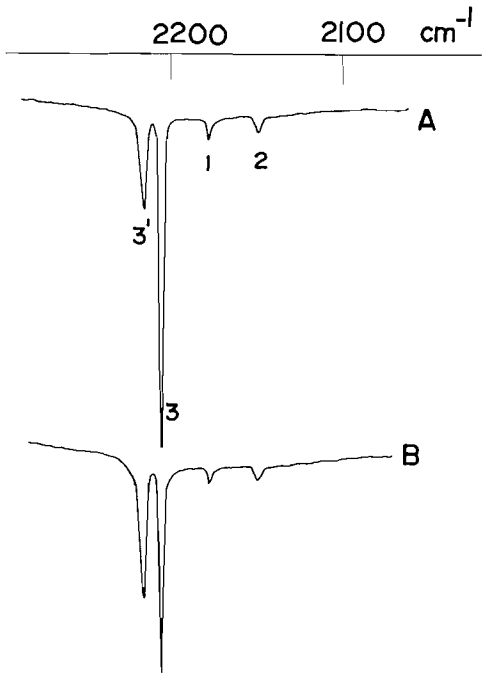

FIG. 2. The matrix infrared spectrum of the products of the cocondensation reaction of Pt atoms with pure $^{14}N_2$: (*A*) at 10 °K and (*B*) after warm-up to 35 °K.

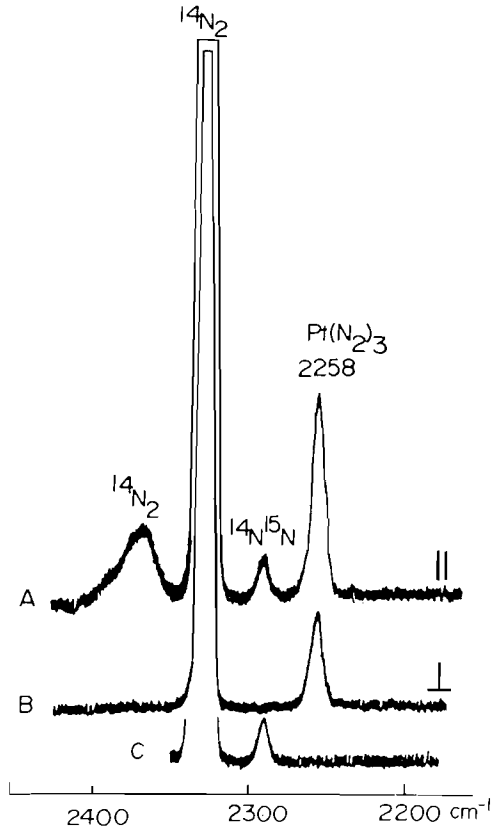

FIG. 3. The matrix Raman spectrum of the products of the cocondensation reaction of Pt atoms with pure $^{14}N_2$ at 4.2 °K: (*A*) parallel polarization, (*B*) crossed polarization and (*C*) after warm-up to 40 °K.

the spectrum shown in Fig. 4 was obtained. The main lines observed at 2217.1 and 2206 cm^{-1} in pure $^{14}N_2$ were replaced by *two* groups of lines at 2239.5, 2234, 2217.1, 2206, and 2151.5, 2145.8, 2141.0, 2132.5 cm^{-1}. In pure $^{15}N_2$ a doublet at 2141.0, 2132.5 cm^{-1} was observed.

The multiplet isotope structure for the Pt/$^{14}N_2$/$^{15}N_2$ reaction is very similar to that previously observed for the analogous Pd/$^{14}N_2$/$^{15}N_2$ reaction and a *prima facie* interpretation suggests the formation of a tris-dinitrogen platinum complex. A detailed analysis of the spectrum, to be described later, proves that the observation of only four new lines when going from $^{14}N_2$ to $^{14}N_2$/$^{15}N_2$ is *only* compatible with a tris-dinitrogen complex, Pt(N_2)$_3$ where the four new lines are associated with the mixed isotopic species Pt($^{14}N_2$)$_2$($^{15}N_2$) and Pt($^{14}N_2$)($^{15}N_2$)$_2$.

Can. J. Chem. Downloaded from www.nrcresearchpress.com by 210.87.254.6 on 09/05/12
For personal use only.

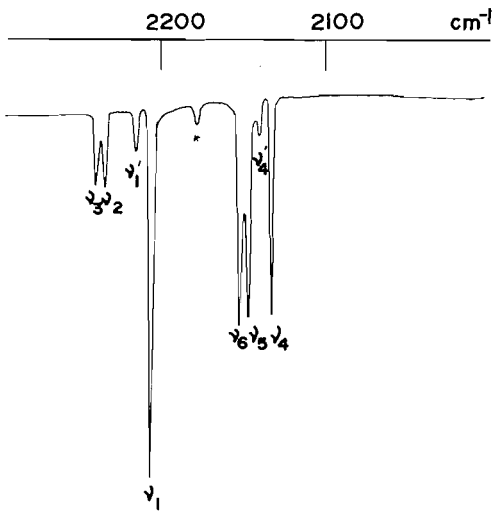

FIG. 4. The matrix infrared spectrum of the products of the cocondensation reaction of Pt atoms with a $^{14}N_2$:$^{15}N_2 \cong 1.33$:1 mixture at 10 °K. The asterisk shows a small amount of $Pt(N_2)$.

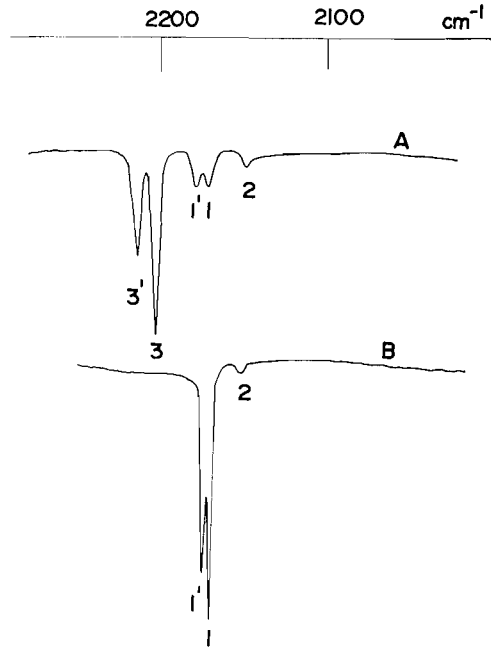

FIG. 5. The matrix infrared spectrum of the products of the cocondensation reaction of Pt atoms with (*A*) $^{14}N_2$:Ar = 1:3 mixture at 10 °K and (*B*) a $^{14}N_2$:Ar = 1:20 mixture at 10 °K.

Bis(dinitrogen)platinum(0),Pt(N_2)$_2$ and Mono(dinitrogen)platinum(0),Pt(N_2) in Solid Argon

When platinum atoms were cocondensed with dilute $^{14}N_2$:Ar = 1:20 mixtures at 10 °K, a strong doublet was observed at 2173, 2169 cm^{-1} in the infrared spectrum; together with a very weak line at about 2150 cm^{-1} (Fig. 5*b*). The corresponding lines observed in the $^{15}N_2$:Ar = 1:10 experiment were at 2104.5, 2095.5, and 2079 cm^{-1}. On warm-up to 35 °K, the absorption at 2150 cm^{-1} (in, for example, $^{14}N_2$:Ar = 1:10) grows in intensity while the doublet at 2173/2169 cm^{-1} gradually decays. Similar results were obtained in more dilute matrices ($^{14}N_2$:Ar = 1:1000) as shown in Fig. 6 which shows the intensity changes of the doublet at 2173/2168 cm^{-1} compared to the absorption at 2150 cm^{-1}, during warm-up to 30 °K. The intensity ratio of the 2173/2168 cm^{-1} components is observed to be approximately equal on deposition at 10 °K but changes during warm-up until at 30 °K, the 2168 cm^{-1} component predominates. The identity of the species giving rise to the new NN stretching modes at 2173/2168 and 2150 cm^{-1} in $^{14}N_2$/Ar matrices will be discussed below.

When the infrared experiment was repeated using a $^{14}N_2$:$^{15}N_2$:Ar = 1:1:100 mixture, the doublet at 2173/2168 cm^{-1} in $^{14}N_2$/Ar becomes a "doublet of doublets" at 2172.8/2168.3 and 2101.0/2096.5 cm^{-1} (Fig. 7*a*). This confirms the assignment of the 2173/2168 cm^{-1} doublet to a mono-dinitrogen complex, $Pt(N_2)$.

When Pt was evaporated into a 1:2:1:200 $^{14}N_2$/$^{14}N^{15}N$/$^{15}N_2$/Ar, aside from the two doublets at 2170/2166 and 2098/2094, a triplet of lines was observed at 2128/2132/2136 with absorbances roughly in the ratio 1:2:1. These are obviously associated with the molecule consisting of a Pt atom bonded to an atom of $^{15}N^{14}N$ and their significance will be discussed below.

Warmup experiments were carefully performed on the $^{14}N_2$:$^{15}N_2$:Ar = 1:1:100 matrix (Figs. 7*b*–7*e*) and show the initial disappearance of the absorptions assigned to $Pt(N_2)$ and the simultaneous growth of lines at 2150.0, 2140.9, and 2078.5, 2069.2 cm^{-1}. The line originally observed at 2150 cm^{-1} in $^{14}N_2$/Ar matrices (after warm-up to 35 °K) thus becomes a *quartet* isotope pattern in $^{14}N_2$/$^{15}N_2$/Ar and confirms its assignment to a bis-dinitrogen platinum complex, $Pt(N_2)_2$.

Prolonged warm-up of $Pt(N_2)_2$ at 35 °K

Can. J. Chem. Downloaded from www.nrcresearchpress.com by 210.87.254.6 on 09/05/12
For personal use only.

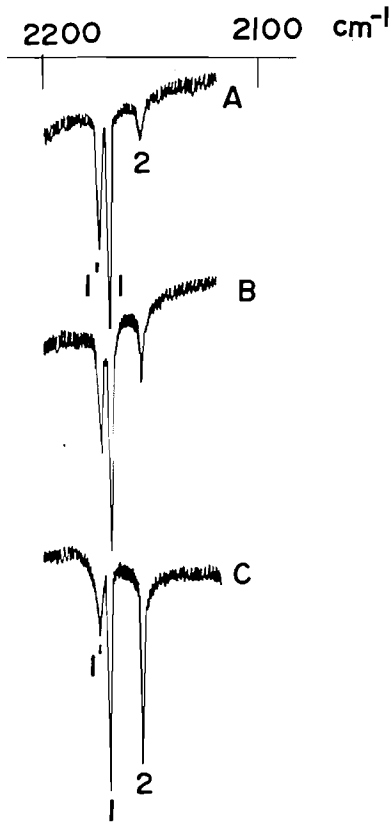

FIG. 6. The matrix infrared spectrum of the products of the cocondensation reaction of Pt atoms with a $^{14}N_2$:Ar = 1:1000 mixture at 10 °K: (*A*) before warm-up, (*B*) warm-up to 25 °K, (*C*) warm-up to 30 °K.

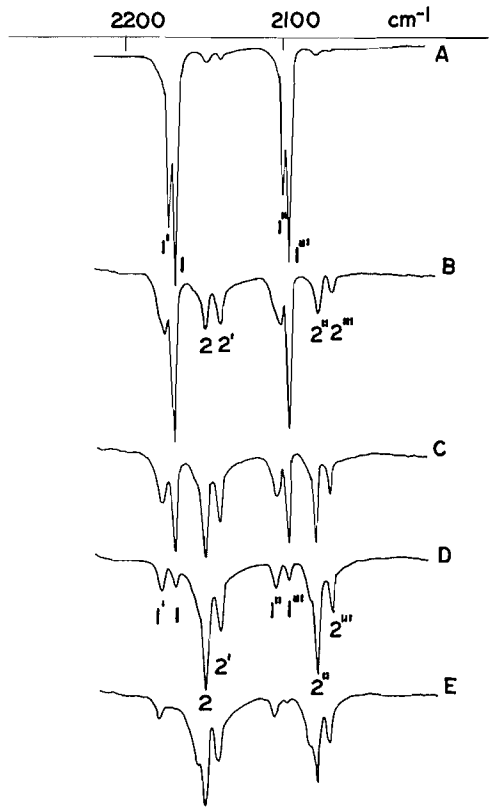

FIG. 7. The matrix infrared spectrum of the products of the cocondensation reaction of Pt atoms with a $^{14}N_2$:$^{15}N_2$:Ar = 1:1:100 at 10 °K: (*A*) before warm-up, (*B*)-(*E*) successive warm-up experiments at 20, 25, 30, and 35 °K.

produced a small splitting of the absorptions at 2150 and 2018.5 (Fig. 7*e*) which is assigned to a matrix splitting.

Discussion

Tris(dinitrogen)platinum(0),Pt(N_2)$_3$

The doublet structure at 2217.1, 2206 cm^{-1} observed for $Pt(N_2)_3$ in solid nitrogen (Fig. 2*a*) resembles in many respects the similar doublet at 2251, 2241 cm^{-1} for $Pd(N_2)_3$ also in solid nitrogen. For example, on allowing the $Pt/^{14}N_2$ cocondensate to warm up to 30–35 °K (Fig. 2*b*) the absorbance of the line at 2217.1 cm^{-1} grows while that of the 2206 cm^{-1} line diminishes, until they are approximately equal in absorbance. In dilute N_2/Ar matrices, which had been deposited at 25 °K and allowed to warm up to 35 °K, the doublet structures at 2217.1/2206 and 2141.1/2132.5 cm^{-1} assigned to $Pt(^{14}N_2)_3$ and $Pt(^{15}N_2)_3$, respectively, appear as single lines at about 2209 and 2138 cm^{-1}, respectively. In the $^{14}N_2/^{15}N_2$ mixed isotope experiment we noted that only *four* new lines appeared in addition to those at 2217.1, 2206 (in $^{14}N_2$) and 2141, 2132.5 (in $^{15}N_2$) cm^{-1}.

If the line at 2217.1 cm^{-1} were an independent species it would have to be a mono-dinitrogen species since it forms a doublet at 2217.1, 2141 cm^{-1} in the $^{14}N_2/^{15}N_2$ experiment. However, the mono-dinitrogen species has been identified at 2173/2168 cm^{-1} in the $^{14}N_2$:Ar = 1:1000 experiment in which *no* line is observed at 2217.1 cm^{-1}.

This behavior parallels very closely that observed for $Pd(N_2)_3$ and on the basis of similar reasoning, we prefer to assign both components

Can. J. Chem. Downloaded from www.nrcresearchpress.com by 210.87.254.6 on 09/05/12
For personal use only.

Can. J. Chem. Downloaded from www.nrcresearchpress.com by 210.87.254.6 on 09/05/12
For personal use only.

of the 2217.1, 2206 cm^{-1} doublet to the single species $Pt(^{14}N_2)_3$ rather than to two dinitrogen species in the matrix.

One must therefore conclude that the line at 2217.1 cm^{-1} (and its $^{15}N_2$ analog at 2141 cm^{-1}) belongs to $Pt(N_2)_3$, being one of the two components of the E' mode with its degeneracy removed and that, as with $Pd(N_2)_3$, the observed growth and decay behavior of the doublet is an annealing effect. In detail, when first deposited the matrix is irregular, hence the distortion of the $Pt(N_2)_3$ species from D_{3h} is at a minimum. When warmed the N_2 matrix anneals, thereby increasing the distortion of the $Pt(N_2)_3$ from D_{3h} to C_2, the substitutional site symmetry in α-N_2. However, it would appear that the distortion problem can be obviated by depositing Pt atoms into N_2/Ar matrices at 25 °K and then annealing at 35 °K. Under these conditions it is probable that $Pt(N_2)_3$ is a regular D_{3h} triangular planar molecule.

Frequency and Intensity Calculations for $Pt(N_2)_3$

We have recently shown that the method of Bor (3) and Haas and Sheline (4), used for calculating the effect of $^{13}C^{16}O/^{12}C^{18}O$ isotopic substitution on the relative intensities of the infrared bands of metal carbonyls, can also be applied successfully to $^{14}N_2/^{15}N_2$ isotopic substituted dinitrogen complexes of Ni and Pd (1) and that the Cotton–Kraihanzel force field approximation (2) usually applied to carbonyls is equally applicable to binary dinitrogen complexes. We therefore use an identical approach to that previously outlined for $Pd(N_2)_m$ where $m = 0$–3 to calculate the intensities and frequencies of the mixed isotopic species $Pt(N_2)_m$.

Using the notation outlined below:

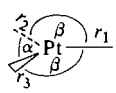

where f_{rr} is associated with α and f_{rr}' with β and the C_2 axis is taken collinear with r_1. The force constants for the $Pt(N_2)_3$ molecules were calculated by applying a least squares analysis to the observed frequencies assuming the Cotton–Kraihanzel force field simplification. The calculated and observed frequencies and force constants are shown in Table 1.

The intensity calculations were performed on the basis of a regular trigonal planar, rather than a C_2 molecule since it was felt that *before* warm-up the former structure represented the molecule more accurately than the latter. The results of the intensity calculations are also shown in Table 1. The agreement is quite good and when taken with the excellent correspondence of the observed and calculated NN stretching frequencies, provides convincing evidence for the structural and vibrational assignments and favors a C_2 substitutional site symmetry for $Pt(N_2)_3$ in solid α-N_2 (13). This rationale is given additional support by the close agreement between the observed and calculated intensity relationship of the split E' NN stretching modes of $Pt(^{14}N_2)_3$ as observed after warm-up when full C_2 symmetry is assumed (see Table 1).

Mono(dinitrogen)platinum(0),$Pt(N_2)$

The Mode of Attachment of the Dinitrogen Ligand to Platinum and the Cause of the Doublet Splitting 2173/2168 cm^{-1}

The mode of attachment of N_2 to a metal atom in MN_2 can be shown to be either end-on or side-on by using metal atom cocondensation reactions with statistical mixtures of nitrogen isotopes $^{14}N_2$:$^{14}N^{15}N$:$^{15}N_2$ = 1:2:1 diluted in Ar (7). The expected patterns of NN absorptions are shown below.

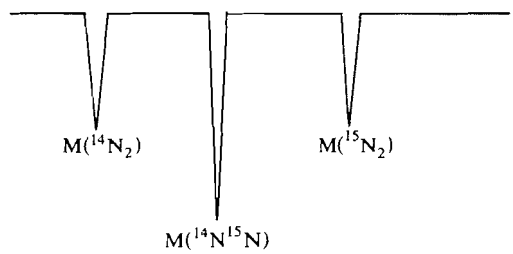

For side-on bonded N_2 three approximately equally spaced lines with absorption intensities in the ratio 1:2:1 are expected. This pattern has been observed for CoN_2 (14).

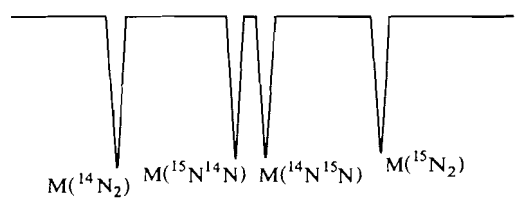

For end-on bonded dinitrogen four lines with a closely spaced central doublet are expected where

TABLE 1. Isotope frequency and integrated infrared absorption intensities* for $Pt(^{14}N_2)_m(^{15}N_2)_{3-m}$ (where $m = 0$–3) in solid nitrogen

Frequency notation		Frequency		Intensity†		
		Calculated	Observed	Calculated	Observed‡	Assignment‡
I.r.	ν_1	2206.2	2206.0	0.441	0.435	A(I)
	ν_1'	2217.1	2217.1			B(I) B(II)
	ν_2	2234.0	2234.0	0.065	0.069	A(V)
	ν_3	2241.9	2239.5	0.030	0.068	A(II)
	ν_4	2131.4	2132.5	0.250	0.216	A(VI)
	ν_4'	2141.9	2141.0			B(VI) B(V)
	ν_5	2144.6	2145.8	0.194	0.194	A(II)
	ν_6	2152.1	2151.5	0.109	0.200	A(V)
R	ν_7	2255.7	2258.0			A(I)

*The integrated infrared absorption intensities for $Pt(^{14}N_2)_3$ in solid N_2 after warm-up are 2206.0 (I_{obs} 1.063; I_{calcd} 1.096), 2217.1 (I_{obs} 1.000; I_{calcd} 1.000). The intensities have been normalised with the 2217.1 cm^{-1} line set to 1.00.
†Intensities quoted in absorbance units, and calculated for an isotopic mixture $^{15}N_2/^{14}N_2 = 0.75$.
‡Same notation used as in ref. 1.

TABLE 2. Calculated and observed isotope frequencies* for $Pt(^nN^mN)_p(^nN^mN)_{2-p}$ where n, $m = 14$, 15 and $p = 0$–2

Frequency† notation	Observed frequency	Calculated frequency	Assignment‡
ν_3 (i.r.)	2150.0	2150.4	$Pt(^{14}N_2)_2$ Σ_u^+ or B_2
ν_5 (i.r.)	2140.9	§ 2143.6	$Pt(^{14}N^{15}N)(^{14}N_2)$ A_1
ν_4 (i.r.)		§ 2142.6	$Pt(^{14}N_2)(^{15}N_2)$ A_1
ν_6 (i.r.)	2116 ‖ 2113	2114.0	$Pt(^{14}N^{15}N)_2$ Σ_u^+ or B_2
ν_7 (i.r.)	(2107)	2107.0	$Pt(^{14}N^{15}N)(^{15}N_2)$ A_1
ν_8 (i.r.)	2103	2103.0	$Pt(^{14}N^{15}N)(^{14}N_2)$ A_1
ν_1 (i.r.)	2078.5	2077.4	$Pt(^{15}N_2)_2$ Σ_u^+ or B_2
ν_2 (i.r.)	2069.2	§ 2067.9	$Pt(^{14}N_2)(^{15}N_2)$ A_1
ν_9 (i.r.)		§ 2067.0	$Pt(^{14}N^{15}N)(^{15}N_2)$ A_1

*$k_{NN} = 18.90$ and $k_{NN,NN} = -0.16$ mdyn/Å.
†See ref. 1 for explanation of notation.
‡The first symmetry type shown refers to a $D_{\infty h}$ molecule and the second to a D_{2d} molecule.
§Overlap.
‖Probably due to the various isotopic arrangements $(^{14}N^{15}N)Pt(^{15}N^{14}N)$, $(^{14}N^{15}N)Pt(^{14}N^{15}N)$ and $(^{15}N^{14}N)Pt(^{14}N^{15}N)$ if end-on dinitrogen is assumed.

the absorption intensities of the four lines are equal. This pattern has been observed for NiN_2 (1, 7) and by Shilov and co-workers (15) for $[Ru(NH_3)_5N_2]^{2+}$.

The central doublet for end-on bonded N_2 arises from the non-equivalence of the mixed isotopic species $M—^{14}N\equiv^{15}N$ and $M—^{15}N\equiv^{14}N$.

In the case of Pt the interpretation of the scrambled isotopic results is complicated slightly by the matrix split of the NN absorption associated with the $Pt(N_2)$ species. Thus the type of bonding of the N_2 to the Pt does not immediately follow from the $^{14}N_2/^{14}N^{15}N/^{15}N_2$/Ar with Pt experiments. This necessitates the following analysis.

The two components of the doublet at 2173/2168 may in turn arise from two end-on bonded $Pt(N_2)$ species, two side-on bonded $Pt(N_2)$ species or one end- and one side-on bonded $Pt(N_2)$ species. The "difference" between the two $Pt(N_2)$ species is likely a multiple trapping site effect. Assuming these four possible causes for the 2173/2168 cm^{-1} doublet labeled below for convenience

(*i*)	2173	(s)	A
	2168	(s′)	B
(*ii*)	2173	(e)	A
	2168	(s′)	B
(*iii*)	2173	(s)	A
	2168	(e′)	B

Can. J. Chem. Downloaded from www.nrcresearchpress.com by 210.87.254.6 on 09/05/12
For personal use only.

Can. J. Chem. Downloaded from www.nrcresearchpress.com by 210.87.254.6 on 09/05/12
For personal use only.

(*iv*)	2173	(e)	A
	2168	(e′)	B

where e, e′ = end-on bonded dinitrogen, s, s′ = side-on bonded dinitrogen, the patterns that one would expect to observe in the $Pt/^{14}N^{15}N$ region (where the splitting of the $Pt^{14}N^{15}N/Pt^{15}N^{14}N$ is of the same order as the matrix splitting, that is, approximately 4 cm^{-1}) are shown in Fig. 8[1] for each of the four possible situations. Only the pattern corresponding to case (*iv*) matches that observed experimentally, hence both components 2173 and 2168 cm^{-1} are associated with end-on bonded dinitrogen in $Pt(N_2)$. If $Pt(N_2)$ may be assumed to be a linear triatomic molecule, one can in principle obtain from each of the two sets of four lines associated with each of the two $Pt(N_2)$ species (A and B) the three stretching force constants f_{NN}, f_{PtN} and $f_{PtN,NN}$. In practice one finds that the near linear dependance of the four equations relating the N—N stretching fundamental to the atomic masses and force constants together with the error in the position of the lines associated with the $Pt/^{14}N^{15}N$ molecules makes it impossible to determine the values of the three force constants unambiguously. The interdependance of f_{PtN} and $f_{PtN,NN}$ is especially marked and reasonable fits could be obtained with $f_{PtN,NN}$ anywhere in the range 0 to 0.5 mdyn/Å. Accordingly we report in Table 3 the force constants calculated on the basis of the simple valence force field approximation ($f_{PtN,NN} = 0$).

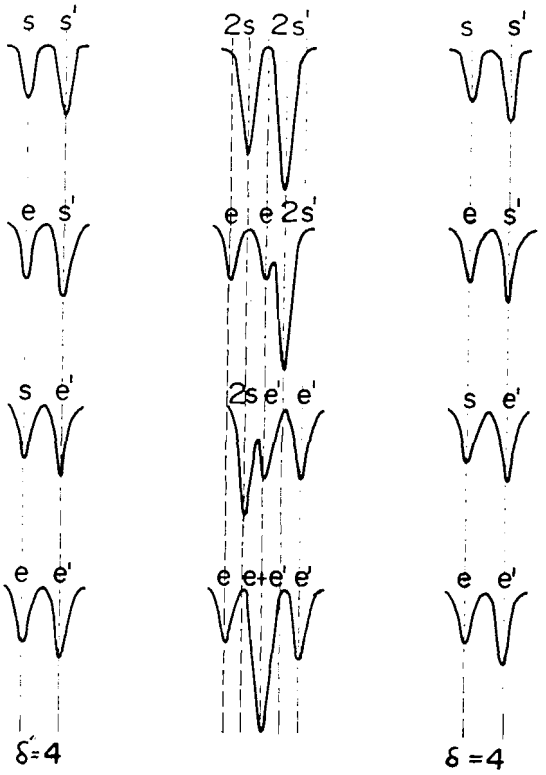

FIG. 8. Schematic representation of the isotope patterns expected for the $Pt(N_2)$ molecule when using statistical mixtures of nitrogen isotopes $^{14}N_2:{}^{14}N^{15}N:{}^{15}N_2 = 1:2:1$ in argon (s, s′ = side-on and e, e′ = end-on bonded dinitrogen; see text).

[1]The 2 in 2s and 2s′ of Fig. 8 is meant to indicate the expected overlap between the isotope lines of side-on (s or s′) bonded $Pt^{14}N^{15}N$ and $Pt^{15}N^{14}N$.

Bis(dinitrogen)platinum(0),Pt(N₂)₂

The characterization of $Pt(N_2)_2$ proved to be difficult in part because appreciable concentrations of the species could only be obtained by careful warmup experiments of $Pt(N_2)$ and in part due to its unusual character vis-à-vis bis-dinitrogen complexes of Pd and Ni. A number of approaches were used to try to maximize the absorptions assigned to $Pt(N_2)_2$. For example, Pt atom depositions with concentrated $^{14}N_2/Ar = 1/3$ mixtures were attempted. These gave mainly $Pt(N_2)_3$ (Fig. 5*a*); however, by changing to $N_2/Ar = 1/20$ the spectra showed

TABLE 3. Calculated and observed frequencies for linear Pt^mN^nN where $m, n = 14, 15$

(*a*) Molecule A*

ν		
Observed	Calculated	Assignment
2172.8	2173.1	$Pt^{14}N_2$
2138.5	2138.6	$Pt^{15}N^{14}N$
2134.5	2134.6	$Pt^{14}N^{15}N$
2100.5	2099.4	$Pt^{15}N_2$

*$k_{PtN} = 2.04$, $k_{NN} = 18.94$ mdyn/Å.

(*b*) Molecule B*

ν		
Observed	Calculated	Assignment
2168.3	2169.1	$Pt^{14}N_2$
2134.5	2134.7	$Pt^{15}N^{14}N$
2130.5	2130.6	$Pt^{14}N^{15}N$
2096.5	2095.5	$Pt^{15}N_2$

*$k_{PtN} = 2.05$, $k_{NN} = 18.86$ mdyn/Å.

predominantly $Pt(N_2)$ (Fig. 5*b*). Depositions at higher temperatures (25 °K) gave predominantly $Pt(N_2)_3$.

It was noted that matrices which initially contained predominantly $Pt(N_2)$ or comparable amounts of $Pt(N_2)$ and $Pt(N_2)_2$, upon warmup, showed the growth of the absorption assigned to $Pt(N_2)_2$ and the gradual disappearance of $Pt(N_2)$. Using this approach, and $^{14}N_2/^{15}N_2/Ar = 1/1/100$ mixtures, a characteristic *quartet* pattern (Fig. 7) was observed which could be assigned to the NN stretching modes of the isotopic molecules $Pt(^{14}N_2)_n$ $(^{15}N_2)_{2-n}$ where $n = 0$–2.

The corresponding $^{14}N_2/^{14}N^{15}N/^{15}N_2/Ar = 1/2/1/100$ matrix was carefully warmed up to 35–40 °K. The infrared spectrum before warmup shows all of the lines assigned to the mono-dinitrogen isotopic molecules $Pt(^{14}N_2)$, $Pt(^{14}N^{15}N)$, $Pt(^{15}N^{14}N)$ and $Pt(^{15}N_2)$ which gradually decrease in intensity, with the appearance of new absorptions which can be associated with mixed isotopic bis-dinitrogen species, containing the $^{14}N^{15}N$ scrambled molecule (Table 2). Although some band overlaps of mixed isotopic $Pt(N_2)$ and $Pt(N_2)_2$ molecules can be anticipated, these new absorptions can be associated with the isotopic molecules $Pt(^{14}N^{15}N)(^{14}N_2)$[I], $Pt(^{14}N^{15}N)(^{15}N_2)$[II] and $Pt(^{14}N^{15}N)_2$[III].

Frequency and Force Constant Calculations for $Pt(N_2)_2$

The force constants and frequencies were calculated by applying a least squares analysis of the observed isotopic frequencies for the molecules $Pt(^{14}N_2)_n(^{15}N_2)_{2-n}$ assuming the Cotton–Kraihanzel approximation. The calculated and observed frequencies ν_1 to ν_4 for the three molecules $n = 0$–2 are compared in Table 2. The agreement is within 1.7 cm^{-1}. These calculations can apply equally well to a bis-dinitrogen complex containing end-on bonded N_2 (linear $D_{\infty h}$) or side-on bonded N_2 (pseudotetrahedral D_{2d} or square planar D_{2h}). Regardless of the geometry the calculations provide convincing evidence for our vibrational assignment of those lines to a Pt/N_2 complex containing two N_2 molecules.

Although in principle one can decide between the end-on and side-on structures on the basis of $^{14}N_2/^{14}N^{15}N/^{15}N_2/Ar$ mixed isotopic experiments, since one would expect 7 new lines to appear in the $^{14}N^{15}N$ stretching region for the linear molecule while only 3 new lines appear for the D_{2d} and square planar D_{2h} cases, the overlap of lines made the interpretation of the spectra difficult. Thus, although only three (2116, 2113, and 2103 cm^{-1}) new $^{14}N^{15}N$ absorptions with perhaps a fourth very weak feature at 2107 cm^{-1} were observed, we do not believe the data to be of sufficiently high quality to merit drawing any definite conclusions from it.

Concentration Behavior and Warm-up Characteristics of the Binary Dinitrogen Complexes of Platinum

From our experience with binary dinitrogen and carbonyl complexes it has proven possible to relate qualitatively the difference between the force constant of the free ligand and the respective C.K. force constant in a series of closely related compounds to their relative thermodynamic stabilities.

A justifiable assumption would appear to be that ΔH_{ML}, the average metal–ligand bond energy, is given by

$$\Delta H_{ML} \propto k^L - k_{C.K.}{}^L$$

where k^L and $k_{C.K.}{}^L$ are the free ligand and C.K. bond stretching force constants, respectively, and that ΔH_C, the enthalpy of decomposition of the compound to the metal atom and free ligand, is given by

$$\Delta H_C \propto n\Delta H_{ML}$$

where n is the coordination number with respect to the ligand.

This proposal receives support by examining the computed values of ΔH_C for the binary dinitrogen complexes of Ni, Pd, and Pt as a function of n (see Fig. 9 and Table 5). (Although decomposition to the metal atom and free nitrogen also involves the entropy of decomposition which in general would increase with increasing n, we make the assumption that its contribution to the free energy of decomposition is smaller than that of ΔH_C.) The results for Ni and Pd as expected parallel their warm-up behavior and confirm that the most stable complexes are those with the highest stoichiometry, $Ni(N_2)_4$ and $Pd(N_2)_3$. In the case of Pt, however, the data indicate that $Pt(N_2)_2$ is the most stable complex rather than $Pt(N_2)_3$ and one might anticipate some peculiar concentration and warm-up characteristics for the series $Pt(N_2)_n$. For example, upon warm-up, one might have expected the absorption assigned to $Pt(N_2)_2$ to grow at the expense of both $Pt(N_2)$ and $Pt(N_2)_3$.

Can. J. Chem. Downloaded from www.nrcresearchpress.com by 210.87.254.6 on 09/05/12
For personal use only.

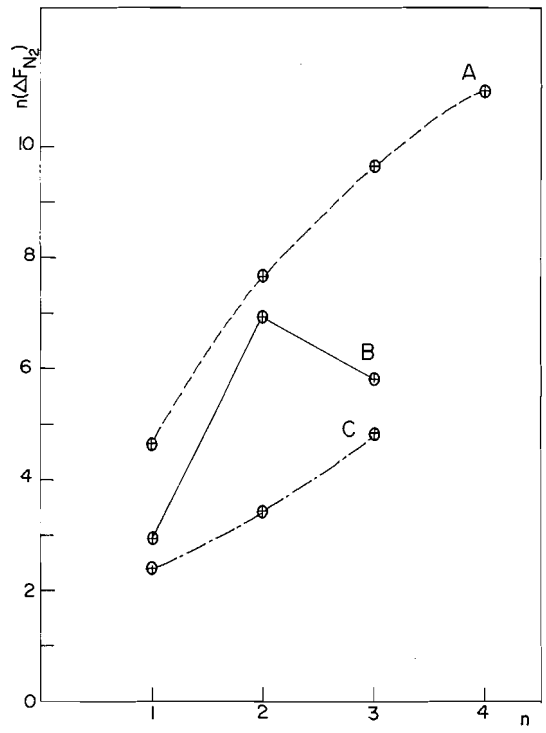

FIG. 9. Graphical representation of ΔH_C (in arbitrary units) as a function of the coordination number n: (*A*), $Ni(N_2)_n$; (*B*), $Pt(N_2)_n$; and (*C*), $Pd(N_2)_n$.

In fact we found that in warm-up experiments performed in $N_2/Ar = 1:10$–$1:100$ mixtures which initially show $Pt(N_2)$ and $Pt(N_2)_2$ but no $Pt(N_2)_3$, the $Pt(N_2)_2$ increased in intensity at the expense of $Pt(N_2)$. Under these conditions $Pt(N_2)_3$, however, was never observed to form by further reaction of $Pt(N_2)_2$ with N_2.

When Pt atoms were deposited into $N_2/Ar = 1:10$ mixtures at higher temperatures (25 °K), appreciable quantities of $Pt(N_2)_3$ and $Pt(N_2)$ were formed and smaller amounts of $Pt(N_2)_2$. Warm-up studies of these matrices at 35 °K show only the growth of $Pt(N_2)_2$ at the expense of $Pt(N_2)$, while the absorption intensity of $Pt(N_2)_3$ did *not* change. Similar results were obtained with more concentrated matrices $N_2/Ar = 1:3$ (Fig. 5*a*) when deposited at 10 °K.

In pure N_2 matrices (Fig. 2*a*) $Pt(N_2)_3$ was always the major product although some $Pt(N_2)$ and $Pt(N_2)_2$ were always formed. Such was not the case in the analogous Pd and Ni experiments.

One possible explanation for this peculiar warm-up behavior is that there is a high activation energy separating the $Pt(N_2)_2$ from the $Pt(N_2)_3$. This implies that in the experiments in which the N_2:Ar ratios are high or in the cases when the ratios were of intermediate values but deposition was carried out at higher temperatures, $Pt(N_2)_3$ forms via a one step tetramolecular reaction and does not decompose upon further warm-up to the $Pt(N_2)_2$. Thus, although $Pt(N_2)_3$ is thermodynamically less stable than $Pt(N_2)_2$, the former is prevented from decomposing to the latter because of the kinetic restraint.

Both of these effects would be in keeping with a $Pt(N_2)_2$ complex which is somehow structurally different from the other two complexes. For instance, by assuming a complex with sideways bonded dinitrogen ligands (either D_{2d} or square planar D_{2h}), both the inordinate thermodynamic stability and the kinetic effect are explained; the former being due to the saturation of the four coordination sites on the Pt while the latter is due to the structural rearrangement that would have to take place when going from a sideways bonded bis-dinitrogen to an end-on bonded tris-dinitrogen platinum complex.

This hypothesis is further strengthened by noting that the stretch–stretch interaction force constant for $Pt(N_2)_2$ is *negative* which makes it unique among the various Ni, Pd, and Pt binary dinitrogen species.

Jones (17) has shown that the CO stretch–stretch interaction force constant in carbonyls is positive. Assuming that his arguments may be carried over to binary dinitrogen complexes, one arrives at the same conclusion for the case of end-on bonded dinitrogen.

Jones' eq. 4 which reads

$$F_{kl} = -F_l(S_l)_k$$

in which F_{kl} is the interaction force constant linking internal coordinate k with l, F_l is the primary force constant associated with internal coordinate l and S_l is the change in internal coordinate l due to a unit positive change in internal coordinate k is almost generally valid and can therefore be used in determining the sign of F_{N_2,N_2} expected for sideways bonded dinitrogen in $Pt(N_2)_2$.

Consider a D_{2d} molecule as shown below (where the diagram is not meant to imply anything about the nature of the NN at PtN bonding).

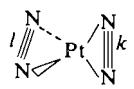

Can. J. Chem. Downloaded from www.nrcresearchpress.com by 210.87.254.6 on 09/05/12
For personal use only.

TABLE 4. The calculated Cotton–Kraihanzel NN bond stretching force constants for $Pt(N_2)_n$ (where n = 1–3)

Molecule	Point symmetry	f_r	f_{rr}	$f_{rr'}$
$Ni(N_2)_4$	T_d	19.85	0.34	
$Ni(N_2)_3$	D_{3h}	19.38	0.59	
$Ni(N_2)_2$	$D_{\infty h}$	18.76	0.48	
$Ni(N_2)$	$C_{\infty v}$	17.97*		
$Pd(N_2)_3$	C_2†	20.97	0.09	0.19
$Pd(N_2)_2$	$D_{\infty h}$	20.87	0.28	
$Pd(N_2)$	$C_{\infty v}$	20.19*		
$Pt(N_2)_3$	C_2†	20.43	0.17	0.31
$Pt(N_2)_2$	$D_{\infty h}$	18.90	−0.16	
$Pt(N_2)$	$C_{\infty v}$	19.44*		

*For the sake of consistency Cotton–Kraihanzel rather than exact force constants are listed for the mono-dinitrogen complexes.
†See text.

Stretching bond k reduces the π bonding within it and also decreases the π overlap with the metal. The π overlap between the metal and the other dinitrogen (l) is thereby increased, decreasing the π bonding within bond l and increasing internal coordinate l. Hence $(S_l)_k$ is positive and F_{kl} is negative.

Thus a negative N—N stretch–stretch interaction force constant is in keeping with a sideways bonded $Pt(N_2)_2$.

Summary of Structure and Bonding in Binary Dinitrogen Complexes of Ni, Pd, and Pt

Molecular dinitrogen complexes of Ni, Pd, and Pt of the form $Ni(N_2)_n$ (where n = 1–4), $Pd(N_2)_m$, and $Pt(N_2)_m$ (where m = 1–3) can be synthesized and stabilized by metal atom–nitrogen matrix cocondensation methods. These binary dinitrogen complexes have, with the exception of $Pt(N_2)_2$, been shown to be similar to the corresponding binary carbonyl complexes in a number of ways, some of which have been discussed previously (1). The behavior of Pt in the group deserves special attention. We note, for instance (Fig. 9), that the order of stability of the dinitrogen complexes as indicated by the quantity $n(\Delta F_{N_2})_n$ is in general Ni > Pt > Pd and, with the exception of $Pt(N_2)_2$, a monatomic increase in stability (Fig. 9) and C.K. force constants (Table 4) is observed with increasing coordination number. The inverse order observed for Pd and Pt is presumably a manifestation of the lanthanide contraction, and is in keeping with the Allred–Rochow electronegativities for the respective metals, X_{Ni} (1.75) > X_{Pt} (1.44) > X_{Pd} (1.35), concomitant with the synergic σ donor – π^* acceptance mechanism generally used to explain the bonding of dinitrogen to transition metals.

Relationship between PtN_2 and N_2 Chemisorbed on Pt

We have recently suggested that a connection exists between our earlier studies of NiN_2 and N_2 chemisorbed on Ni (7). In Table 6, van Hardeveld and van Montfoot's data (8) for N_2 chemisorbed on silica supported Ni, Pd, and Pt particles is compared with our own for the analogous MN_2 complexes. We note that the trend for ν_{NN} is Ni < Pt < Pd just as in the case of MN_2. We also observe that in all three cases ν_{NN} is *higher* for the chemisorbed N_2 than for the corresponding MN_2. This would indicate that, assuming one can extend our previously stated argument relating $n\Delta F_{N_2}$ with ΔH_C to the case of chemisorbed N_2, the metal–nitrogen bond strength is lower in chemisorbed N_2 than in the corresponding MN_2 complex. As discussed in ref. 7, this may arise from the fact that a surface metal atom releases some of its electrons into the conduction band of the metal. This formally raises the oxidation state of the metal, thereby decreasing the extent of backbonding below that which takes place when a single metal atom is bonded to a nitrogen molecule.

It is interesting to note in the last column of Table 6 that the extent of bond weakening is approximately the same for the three metals when going from MN_2 to the chemisorbed ligand. Thus a great deal of insight into the bonding of N_2 to surface metal atoms may be obtained by comparison with the parallel MN_2 molecules, vindicating the view that the forces which bind molecules to surfaces upon chemisorption are in

Can. J. Chem. Downloaded from www.nrcresearchpress.com by 210.87.254.6 on 09/05/12
For personal use only.

TABLE 5. Comparison of frequency and bond stretching force constant depressions for binary dinitrogen complexes of nickel, palladium, and platinum

Coordination number	$(\Delta\nu_{N_2})_{Ni}$	$(\Delta F_{N_2})_{Ni}$	$\Delta H_C^* = n\Delta H_{ML}$
$n = 4$	154	2.75	11.00
3	191	3.22	9.66
2	224	3.84	7.68
1	239	4.63†	4.63
	$(\Delta\nu_{N_2})_{Pd}$	$(\Delta F_{N_2})_{Pd}$	ΔH_C
$n = 3$	87	1.63	4.89
2	94	1.73	3.46
1	115	2.41†	2.41
	$(\Delta\nu_{N_2})_{Pt}$	$(\Delta F_{N_2})_{Pt}$	ΔH_C
$n = 3$	116	2.17	6.51
2	178	3.70	7.40
1	160	3.16†	3.16

*See text for explanation of ΔH_C and $n\Delta H_{ML}$ notation.
†For the sake of consistency, Cotton–Kraihanzel rather than exact force constants are used in calculating ΔF_{N_2} and ΔH_C for the mono-dinitrogen complexes.

TABLE 6. Comparison between stretch frequencies of N_2 chemisorbed on Ni, Pd, and Pt and the analogous MN_2 complexes

M	$\nu_{NN\ chemisorbed\ N_2}$*	$\nu_{NN\ MN_2}$†	$\Delta\nu_{CN_2}$‡	$\Delta\nu_{MN_2}$§	$\Delta\nu_{MN_2}/\Delta\nu_{CN_2}$
Ni	2202	2090	128	240	1.9
Pd	2260	2213	70	117	1.7
Pt	2230	2170	100	162	1.6

*Data of ref. 8.
†Where a matrix split exists the mean frequency is listed.
‡$\nu_{free\ N_2} - \nu_{chemisorbed\ N_2}$.
§$\nu_{free\ N_2} - \nu_{NN\ stretch\ for\ MN_2}$ (where M = Ni, Pd, Pt).

many ways similar to those operating in more conventional metal ligand coordination complexes (16).

NOTE ADDED IN PROOF: Recent data reported by D. Gruen *et al.* (J. Chem. Phys., in press) indicate the existence of an end-on bonded $Pt(N_2)_2$ complex. They report, however, their inability to produce a $Pt(N_2)_3$ complex. The source of this discrepancy has not yet been established.

We wish to thank Mr. Ted Huber and Mr. Bill Hughes for technical assistance and the National Research Council of Canada and the Research Corporation for financial support.

1. H. HUBER, E. P. KÜNDIG, M. MOSKOVITS, and G. A. OZIN. J. Am. Chem. Soc. **95**, 332 (1973); E. P. KÜNDIG, M. MOSKOVITS, and G. A. OZIN. J. Mol. Struct. **14**, 137 (1972).
2. F. A. COTTON and C. S. KRAIHANZEL. J. Am. Chem. Soc. **84**, 4432 (1962).
3. G. BOR. J. Organomet. Chem. **10**, 343 (1967).
4. H. HAAS and R. K. SHELINE. J. Chem. Phys. **47**, 2996 (1967).
5. E. P. KÜNDIG, M. MOSKOVITS, and G. A. OZIN. Can. J. Chem. **50**, 3587 (1972).
6. R. L. DEKOCK. Inorg. Chem. **10**, 1205 (1971).
7. M. MOSKOVITS and G. A. OZIN. J. Chem. Phys. **58**, 1251 (1973).
8. R. VAN HARDEVELD and A. VAN MONTFOOT. Surf. Sci. **4**, 396 (1966).
9. J. K. BURDETT, M. A. GRAHAM, and J. J. TURNER. J. Chem. Soc. Dalton, 1620 (1972).
10. V. M. VOLKOV and L. S. VOLKOVA. Russ. J. Inorg. Chem. **16**, 1382 (1971).
11. H. HUBER, G. A. OZIN, and A. VANDER VOET. Nature Phys. Sci. **232**, 166 (1971).
12. M. MOSKOVITS and G. A. OZIN. J. Appl. Spectrosc. **26**, 481 (1972).
13. R. W. G. WYCKOFF. Crystal structures. Vol. 7. Interscience, New York. p. 29.
14. G. A. OZIN and A. VANDER VOET. Can. J. Chem. (1973). In press.
15. YU G. BOROD'KO, A. K. SHILOVA, and A. E. SHILOV. Russ. J. Phys. Chem. **44**, 349 (1970).
16. R. P. EISCHENS. Acc. Chem. Res. **5**, 74 (1972).
17. L. H. JONES. J. Mol. Spectrosc. **5**, 133 (1960).

Can. J. Chem. Downloaded from www.nrcresearchpress.com by 210.87.254.6 on 09/05/12
For personal use only.

Binary Dioxygen Complexes of Nickel, Palladium, and Platinum, $M(O_2)$ and $(O_2)M(O_2)$, in Low Temperature Matrices

H. HUBER, W. KLOTZBÜCHER, G. A. OZIN,[1] AND A. VANDER VOET

Lash Miller Chemistry Laboratory and Erindale College, University of Toronto, Toronto, Ontario M5S 1A1

Received January 18, 1973

The cocondensation reactions of nickel, palladium, and platinum atoms with gaseous oxygen or dilute oxygen–argon mixtures at 4.2–10 °K give rise to binary transition metal dioxygen complexes. Variable concentration and diffusion controlled warm up studies, $^{16}O/^{18}O$ isotopic substitution studies, normal coordinate and isotope intensity calculations establish the complexes to be of the types $M(O_2)$ and $(O_2)M(O_2)$. Both the mono- and bisdioxygen complexes contain the dioxygen molecules coordinated to the metal atom in a side-on fashion, with a unique D_{2d} "spiro"-type structure favored for the bis-complexes. Frequency and bond stretching force constant trends within the series of complexes are examined and suggest that the O—O and M—O values increase with increasing coordination number, and thus with an increase in partial positive charge on the metal. This trend in O—O stretching frequencies is not in accord with the evaluation of metal–dioxygen bond strengths as based on the degree of reversibility of dioxygen coordination.

Les réactions de cocondensation des atomes de nickel, palladium et platine avec l'oxygène gazeux ou des mélanges dilués d'oxygène-argon à 4.2–10 °K, conduisent à des complexes binaires métal de transition – dioxygène. Les études sur la variation de concentration et sur la diffusion contrôlée par réchauffement, les effets de substitution isotopique $^{16}O/O^{18}$, les calculs de coordinat normal et de l'intensité isotopique, montrent que les complexes sont du type $M(O_2)$ et $(O_2)M(O_2)$. Les deux complexes mono et bis-dioxygène possèdent des molécules de dioxygène coordinées au métal d'une façon latérale conférant ainsi une structure unique de type D_{2d} "spiro" favorable dans le cas de bis complexes. L'évolution de la fréquence et de la constante de force d'élongation à l'intérieur d'une série de complexes a été examinée et laisse penser que l'accroissement des valeurs O—O et M—O va de pair avec le nombre de coordination ainsi que l'accroissement de la charge partielle positive sur le métal. Cette évolution dans les fréquences d'élongation O—O n'est pas en accord avec les valeurs des forces de liaison métal–dioxygène basées sur le degré de réversibilité de la coordination du dioxygène.

[Traduit par le journal]

Can. J. Chem., **51**, 2722 (1973)

Introduction

As a continuation of our studies concerning the reactivity of monoatomic transition metal vapors with small gaseous molecules at cryogenic temperatures (1), it was decided to investigate the cocondensation reactions of nickel atoms with dioxygen. In a preliminary report (2) evidence was presented for the existence of binary dioxygen complexes, namely $Ni(O_2)$ and $(O_2)Ni(O_2)$. These experiments have now been extended to include all members of this group (Ni, Pd, Pt) and have been able to show that mono- and bisdioxygen complexes are capable of existence for all three metals.

Binary dioxygen complexes of this type can be considered to be simple "model sub-units" for more complicated synthetic and naturally occurring dioxygen complexes that are usually stable at normal temperatures and that make use of metal-activated molecular dioxygen. These binary dioxygen complexes can be thought of as having a fundamental relationship to any system in which the interaction between a metal and dioxygen is important, for example, the reactivity of coordinated dioxygen in synthetic and naturally occurring dioxygen carriers (3), oxidation reactions on metal based catalysts (4), etc.

This paper describes a series of cocondensation reactions between Ni, Pd, and Pt atoms and molecular oxygen at 4.2–10 °K in both pure O_2 and O_2/Ar matrices, as studied by matrix isolation infrared spectroscopy. The experiments include variable concentration studies of dioxygen in argon, diffusion controlled warm up studies, ^{18}O isotopic substitution (both $^{16}O^{18}O$ and $^{18}O_2$) and normal coordinate and isotope intensity calculations. The data for $M(O_2)$ and $(O_2)M(O_2)$ provide information regarding (*a*) the mode of dioxygen coordination, (*b*) the relative disposition of the dioxygen molecules in the bisdioxygen complexes and, (*c*) the force constants (and hence approximate strengths) of the metal–oxygen and oxygen–oxygen bonds in the mono- and biscomplexes.

[1]To whom correspondence should be addressed.

Can. J. Chem. Downloaded from www.nrcresearchpress.com by 210.87.254.105 on 09/05/12
For personal use only.

Can. J. Chem. Downloaded from www.nrcresearchpress.com by 210.87.254.105 on 09/05/12
For personal use only.

Experimental

Monoatomic Ni and Pd vapors were generated by directly heating a 0.010 in. ribbon filament of the metal with a.c. in a furnace which has been described previously (1*c*). Platinum vapor was obtained by heating a 0.030 in. tungsten rod around the center of which were wound several turns of 0.010 in. Pt wire. The nickel, palladium, and platinum metal (99.99%) were supplied by McKay Inc., New York. Research grade $^{16}O_2$ (99.99%) and Ar (99.99%) were supplied by Matheson. Isotopically enriched $^{18}O_2$ (93%) was supplied by Miles Research Laboratories. Statistically scrambled mixtures of $^{16}O_2/^{16}O^{18}O/^{18}O_2$ were prepared by subjecting $^{16}O_2/^{18}O_2$ mixtures at about 200 Torr to a continuous tesla discharge. The scrambling process and concentration ratios were monitored by gas phase Raman measurements.

The rate of metal atom deposition was continuously followed and controlled using a quartz crystal microbalance (5). The deposition rate was set such that the probability of a metal atom having another metal atom as nearest neighbor in the argon lattice was approximately 1/1000. Matrix gas flows, controlled by a calibrated micrometer needlevalve, were maintained in the range 2–8 mmol per h. In the infrared experiments the matrices were deposited on a CsI window cooled to either 4.2 °K by an Air Products liquid helium cryotip transfer system or to 10 °K by means of an Air Products Displex closed cycle helium refrigerator. I.r. spectra were recorded using Perkin–Elmer 621 and Beckmann IR-12 spectrophotometers. Matrix Raman experiments were attempted but were generally unsuccessful due to laser diffusion and photodecomposition processes. Raman matrices were deposited on an aluminum tip and cooled to 4.2 °K. Spectra were recorded on a Spex 1401 Raman spectrophotometer using both Carson argon ion (4880 and 5145 Å) and krypton ion (6471 and 5682 Å) laser excitation. Normal coordinate calculations were performed using Schachtschneider's GMAT and EIGV programs for the M.V.F.F. analysis.

Results

As some of the details of the nickel dioxygen cocondensation reactions already have been described briefly (2), the approach to the matrix infrared experiments and the interpretation of the results can best be illustrated in detail by reference to the palladium dioxygen system. The similar procedure and interpretation of the data for Ni and Pt will only be referred to in tabular form.

The Palladium–Dioxygen Cocondensation Reaction

When Pd atoms were cocondensed with dilute $^{16}O_2$:Ar (1:200) mixtures at 4.2–10 °K, *two* sharp infrared absorptions are observed in the O—O stretching region at 1110.8 and 1023.5 cm^{-1} (see Fig. 1*B*), characteristic of coordinated dioxygen (3*a*, 3*b*). The intensities of these lines were shown to be directly proportional to the metal deposition time. The *relative* intensities of these lines were found to be very sensitive to the $^{16}O_2$:Ar ratio; and for example, at ratios less than 1:200 the absorption at 1023.5 cm^{-1} became dominant and at $^{16}O_2$:Ar = 1:1000 is the only band visible. In more concentrated matrices the band at 1110.8 cm^{-1} predominates and is the only line observed in pure $^{16}O_2$ (Fig. 1*A*) matrices (see later). Diffusion controlled warm up experiments on dilute matrices indicated that the higher frequency absorption increases in intensity with increase in temperature at the expense of that at lower frequency (Fig. 2).

When Pd atoms are cocondensed with a dilute argon matrix containing isotopically enriched oxygen ($^{18}O_2$:Ar = 1:200), *two* sharp absorptions are observed at 1048.5 and 966.5 cm^{-1}, which are shifted by 62.3 and 61.0 cm^{-1} from the $^{16}O_2$ counterpart lines (Fig. 1*C*). From this series of data, it is possible to deduce that *two*

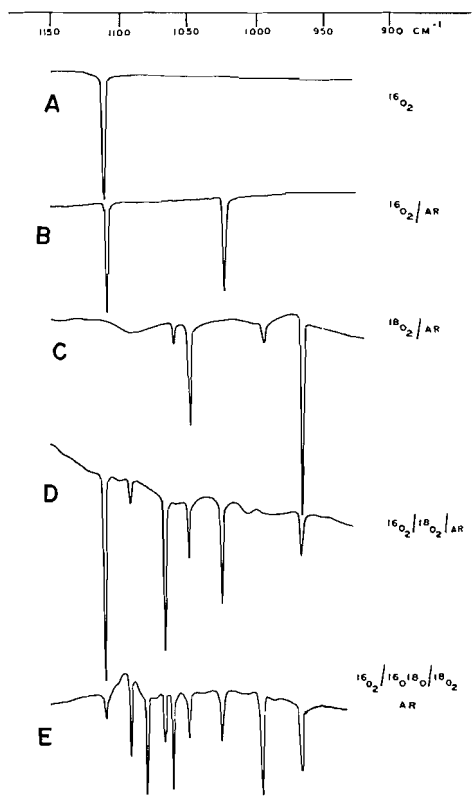

FIG. 1. The matrix infrared spectrum of the products of the cocondensation reaction of Pd atoms with (*A*) pure $^{16}O_2$, (*B*) $^{16}O_2$:Ar ≅ 1:200, (*C*) $^{18}O_2$:Ar ≅ 1:200, (*D*) $^{16}O_2$:$^{18}O_2$:Ar ≅ 2:1:600, and (*E*) $^{16}O_2$:$^{16}O^{18}O$:$^{18}O_2$:Ar ≅ 1:2:1:800, at 4.2 °K showing the characteristic isotope patterns of both $Pd(O_2)$ and $(O_2)Pd(O_2)$.

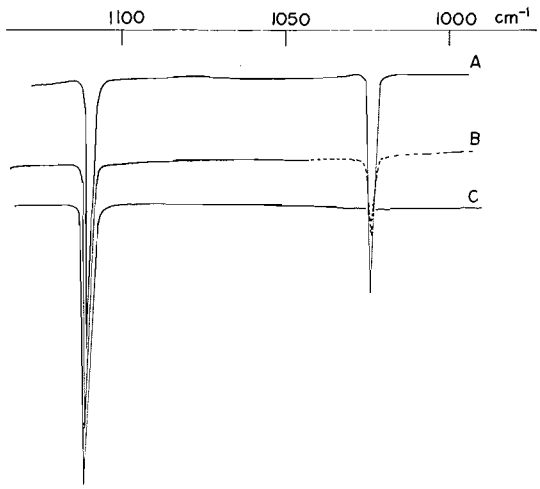

FIG. 2. Similar spectrum to that shown in Fig. 1*B* after successive warm-up experiments at 35 °K each for 10 min.

distinct palladium–oxygen species exist in dilute O_2/Ar matrices and a *single* species in pure $^{16}O_2$ and in O_2/Ar = 1:1000, where the higher frequency absorption (1110.8 ($^{16}O_2$)/1048.5 ($^{18}O_2$)) corresponds to a higher coordination complex than the lower. Fortunately the 1110.8 to 1023.5 cm^{-1} frequency separation is sufficiently large to permit meaningful mixed $^{16}O_2/^{16}O^{18}O/^{18}O_2$ isotope experiments on the two species without the complication of band overlap, which in principle should yield information concerning their stoichiometries, the nature of the metal–dioxygen bonding and the mode of attachment of the dioxygen molecule(s) to the metal atom (that is, whether end or side-on bonding). For the sake of clarity of presentation, each of these species will be discussed separately.

The 1023.5 Absorber, Monodioxygen Palladium, $Pd(O_2)$

When Pd atoms are cocondensed with a dilute $^{16}O_2:^{18}O_2$:Ar = 2:1:600 mixture at 4.2–10 °K (Fig. 1*D*) a doublet is observed at 1023.5 and 966.5 cm^{-1}. This 57 cm^{-1} splitting would indicate that the species responsible for the absorption at 1023.5 cm^{-1} contains a *single* dioxygen molecule. The mode of attachment of the dioxygen to the metal atom can be defined in principle by consideration of the intensity pattern and the number of lines observed when using a statistical mixture of dioxygen isotopes in dilute argon matrices (mixture used in this work: $^{16}O_2/^{16}O^{18}O/^{18}O_2$/Ar = 1:2:1:800). The spectrum obtained with this mixture is expected to be one of the two following patterns illustrated below:

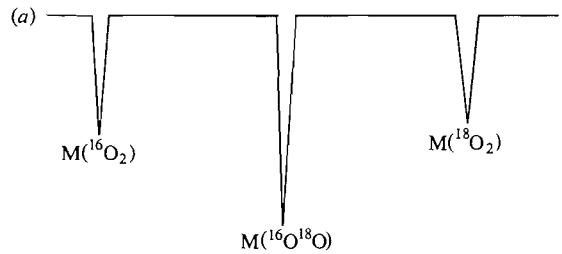

A *three*-line spectrum, consisting of approximately equally spaced lines, with absorption intensities in the ratio 1:2:1. This multiplet pattern characterizes a single dioxygen molecule coordinated to the metal so as to form an isosceles triangle in which the oxygen atoms are equivalent (*i.e.*, side-on bonding). The central component shows the spectral equivalence of the mixed isotopic molecules $M(^{16}O^{18}O)/M(^{18}O^{16}O)$, and as it carries a statistical weighting factor of two as compared to the unscrambled species it is therefore expected to be twice as intense as the outer two components.

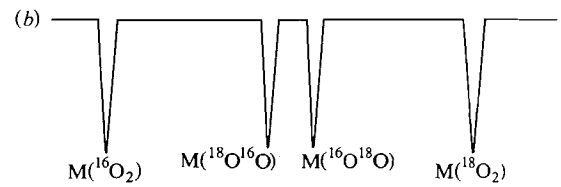

A *four*-line spectrum with a closely spaced central doublet with absorption intensities in the ratio 1:1:1:1, characteristic of a single dioxygen molecule coordinated in an "end-on" linear or non-linear fashion and having spectroscopically non-equivalent oxygen atoms. The inequivalence but equal weighting of $M(^{16}O^{18}O)$ and $M(^{18}O^{16}O)$ results in the small separation and equal intensities of the central doublet. Similar considerations have been able to distinguish between possible modes of attachment in transition metal – dinitrogen complexes (7, 8).

When Pd atoms were cocondensed with a dilute scrambled mixture ($^{16}O_2/^{16}O^{18}O/^{18}O_2$/Ar = 1:2:1:800) the matrix infrared spectrum showed a 1:2:1 *triplet* of approximately equally spaced lines at 1024.0, 995.5, and 967 cm^{-1} (Fig. 1*E*). The three-line spectrum was carefully examined under conditions of high resolution. All three were found to have *identical* band widths of 2 cm^{-1} at half height. The slit width used for the scan was 1 cm^{-1} with a scan speed of 2 cm^{-1}

Can. J. Chem. Downloaded from www.nrcresearchpress.com by 210.87.254.105 on 09/05/12
For personal use only.

Can. J. Chem. Downloaded from www.nrcresearchpress.com by 210.87.254.105 on 09/05/12
For personal use only.

per min. The central component remained unsplit under these conditions with an absorption intensity approximately twice that of the two outer components. It would thus appear that in dilute O_2/Ar matrices, Pd forms a monodioxygen species $Pd(O_2)$ in which the dioxygen molecule is acting as a ligand, bonding to the metal atom in a symmetrical side-on fashion.

Very similar results were obtained for both nickel (see, for example, Fig. 3) and platinum atoms with dilute O_2/Ar matrices. The data for all three monodioxygen complexes are presented in Tables 1–3. A matrix splitting effect of about 5 cm^{-1} was observed for platinum monodioxygen (see later).

The 1110.8 cm^{-1} Absorber, Bisdioxygen Palladium, $(O_2)Pd(O_2)$

When Pd atoms are cocondensed with a dilute $^{16}O_2/^{18}O_2$/Ar = 2:1:600 matrix at 4.2–10 °K, in addition to the doublet previously assigned to the monodioxygen species, four lines are observed at 1110.8, 1091.5, 1066.7, and 1048.0 cm^{-1} (Fig. 1*D*). This band pattern indicates that the absorbing species contains *two* equivalent dioxygen molecules and the lines are easily assigned to the isotopic species $(^{16}O_2)Pd(^{16}O_2)$, $(^{16}O_2)Pd(^{18}O_2)$, and $(^{18}O_2)Pd(^{18}O_2)$, as shown in Tables 2 and 5. A similar situation is observed in pure oxygen matrices as shown in Table 4 (see later).

In principle the mode of attachment of the dioxygen molecules to the metal in the bis-compound can be determined from $^{16}O^{18}O$ experiments, and indeed with a scrambled mixture (identical to that used in the monodioxygen experiments) the original absorption at 1110.8 in $^{16}O_2$/Ar was split into a *six*-line spectrum (Fig. 1*E*) which could be assigned to the possible isotopic combinations of a $(O_2)Pd(O_2)$ molecule as shown below:

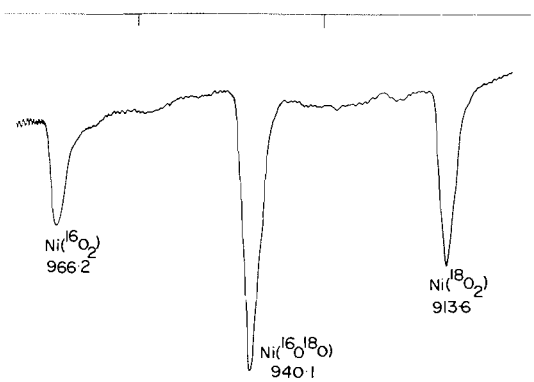

FIG. 3. The matrix infrared spectrum of the products of the cocondensation reaction of Ni atoms with $^{16}O_2$: $^{16}O^{18}O$:$^{18}O_2$:Ar ≅ 1:2:1:800 at 4.2 °K showing the characteristic oxygen isotope pattern for mono-dioxygen nickel containing sideways bonded dioxygen.

TABLE 1. Vibrational assignments of the oxygen stretching modes in binary dioxygen complexes $M(O_2)$ where M = Ni, Pd, or Pt

Molecule	Frequency (cm^{-1}) for M = Ni	Pd	Pt
$M(^{16}O_2)$	966.2	1024.0	926.6
$M(^{16}O^{18}O)$	940.1	995.5	901.4
$M(^{18}O_2)$	913.6	967.0	875.2

Molecule	Frequency (cm^{-1})
$(^{16}O_2)Pd(^{16}O_2)$	1111.5
$(^{16}O_2)Pd(^{16}O^{18}O)$	1092.2*
$(^{16}O^{18}O)Pd(^{16}O^{18}O)$	1080.5
$(^{16}O_2)Pd(^{18}O_2)$	1067.2
$(^{16}O^{18}O)Pd(^{18}O_2)$	1060.5
$(^{18}O_2)Pd(^{18}O_2)$	1048.5

*Note that owing to a 7% impurity of $^{16}O^{18}O$ in the commercially available $^{18}O_2$ gas, a very weak absorption at 1092.2 cm^{-1} belonging to $(^{16}O_2)Pd(^{16}O^{18}O)$ is also observed in the $^{16}O_2$/$^{18}O_2$ mixed isotope experiments.

This "sextet pattern" indicates a non-degenerate vibration of two equivalent dioxygen molecules each containing equivalent oxygen atoms. The second and fifth components of the multiplet indicate the equivalence of the oxygen atoms in each O_2 unit, since if the molecules were attached in an end-on fashion (non-equivalent), further splitting or line broadening of the lines due to the rearrangement of the $(^{16}O^{18}O)$ component would be expected. This broadening is not observed and all six components of the sextet are equally sharp. The absence of the lines assigned to the species $Pd(^{16}O^{18}O)_2$ in pure $^{16}O_2/^{18}O_2$ matrices, and the non-equivalence of the (16–16) (18–18) and (16–18)(16–18) species clearly indicated in the spectrum shows that the original oxygen molecules remain intact upon bonding to the metal atom.

Since a planar (D_{2h}) structure would have *cis*- and *trans*-isomers for the (16–18)(16–18) molecule and since no splitting is observed at the frequency assigned to the species (1080.5 cm^{-1}), the D_{2d} "spiro" structure is proposed (Fig. 4). This symmetry model is also favored from

TABLE 2. Infrared spectra (in the oxygen stretching region) observed following the deposition of palladium atoms with oxygen† molecules in an argon matrix at 10 °K

$^{16}O_2$:Ar (1:200)	$^{18}O_2$:Ar (1:200)	$^{16}O_2$:$^{18}O_2$:Ar (2:1:600)	$^{16}O_2$:$^{16}O^{18}O$:$^{18}O_2$:Ar (1:2:1:800)
1110.8*		1111.0	1111.5
		1091.5†	1092.2
			1080.5
		1066.7	1067.2
			1060.5
	1048.5*	1048.0	1048.5
1023.5		1023.5	1024.0‡
			995.5‡
	966.5	966.5	967.0‡

*Diffusion controlled warm up at 35 °K causes these bands to increase in intensity at the expense of the low frequency bands.
†The $^{18}O_2$ sample contains 7% of $^{16}O^{18}O$ as purchased from Miles laboratories.
‡The integrated absorption intensity of this triplet was approximately 1:2:1 (Fig. 1*E*).

TABLE 3. Infrared spectra (in the oxygen stretching region) observed following the deposition of platinum atoms with oxygen molecules in an argon matrix at 10 °K

$^{16}O_2$:Ar (1:50)	$^{18}O_2$:Ar (1:50)	$^{16}O_2$:$^{18}O_2$:Ar (1:1:100)	$^{16}O_2$:$^{16}O^{18}O$:$^{18}O_2$:Ar (1:2:1:200)	$^{16}O_2$ (Pure)
1050.2		1050.0	1050.0	1052.6
1047.2		1047.2	1048.2	1049.6
			1030.6	
			1027.6	
			1021.6	
			1017.8	
		1004.0	1003.8	
		1001.6		
			1000.6	
			998.4	
	991.4	991.4	991.4	
	989.0	989.4	989.0	
926.4		926.4	926.6	
920.8		920.8	920.8	
			901.4	
	874.8	875.2	875.2	
	868.8		869.0	

Dewar–Chatt maximum π-bond overlap considerations (see later).

Very similar results were obtained for both nickel and platinum atoms (see for example Tables 3 and 5 and Fig. 5) and establish the existence of bisdioxygen complexes $(O_2)M(O_2)$ for all three metals. Only in the case of platinum atoms was a doublet structure with a small splitting (2–5 cm^{-1}) observed for each line (Fig. 5) in both pure dioxygen and dilute dioxygen–argon matrices (see later).

Observation and Assignment of Low Frequency Modes

Only in matrices in which the O—O stretching modes of $Pd(^{16}O_2)$ and $(^{16}O_2)Pd(^{16}O_2)$ were arranged to be *totally* absorbing, was it possible to observe weak lines at 504 and 427 cm^{-1} assignable to Pd—O stretching modes. On the basis of their concentration dependencies and warm-up behavior and similar νMO frequencies to stable synthetic dioxygen complexes (6), these two lines could be associated with the metal–oxygen

Can. J. Chem. Downloaded from www.nrcresearchpress.com by 210.87.254.105 on 09/05/12
For personal use only.

TABLE 4. Infrared spectra (in the oxygen stretching region) observed following the deposition of palladium atoms with a pure oxygen* matrix at 10 °K§

$^{16}O_2$		$^{16}O_2$:$^{18}O_2$	$^{16}O_2$:$^{16}O^{18}O$:$^{18}O_2$
1112.3†	1114.7	1114.6	1114.6
	1110.0	1109.6	1109.6
		1095.5	1095.6
		1091.3	1091.3
			1083.5
			1079.2
		1070.0	1069.8
		1065.5	‡
			1063.1
			1059.5
		1051.5	1051.5
		1047.5	1047.7

*The $^{18}O_2$ sample contains 7% of $^{16}O^{18}O$ as purchased from Miles Laboratories.

†Appears as a single line after deposition, splits into a doublet on warming to 15–35 °K. Initially the strongest component is at 1114.7 cm^{-1}. This intensity order reverses on warming to 35 °K.

‡One-half of the doublet is hidden by the strong doublet at 1063.1, 1059.5.

§All infrared absorptions in these pure oxygen matrices observed as doublets with a splitting in the range 3.8–50. cm^{-1} (see text).

stretching modes of the bis- and monocomplexes, respectively. In the nickel atom – dioxygen reactions, similar weak lines were observed at 535 and 505 cm^{-1} assignable to the Ni—O modes of the bis- and monodioxygen compounds. Analogous low frequency modes in the Pt/O_2 system could not be observed, presumably because of their low intensity.

Bisdioxygen Complexes in Solid Oxygen

Having established that the highest stoichiometry complex formed in the Pd/O_2 reaction is $(O_2)Pd(O_2)$ which in argon matrices appears to have the spiro D_{2d} structure, it is interesting to consider the analogous data in pure oxygen matrices. The spectra obtained in argon and

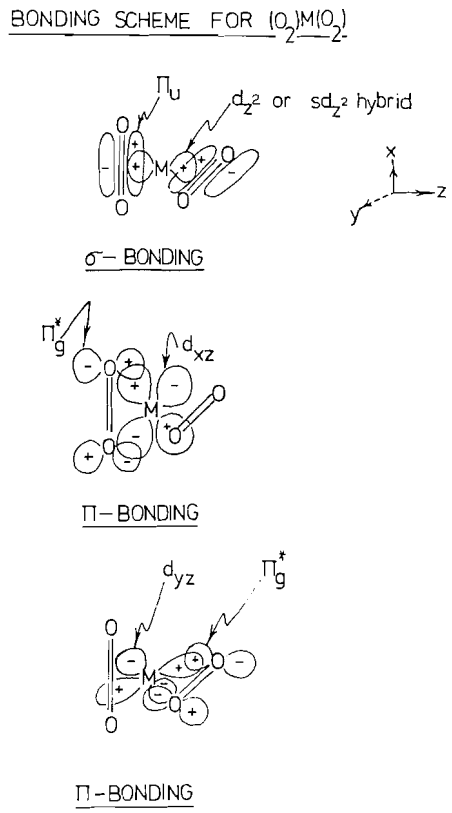

FIG. 4. Schematic molecular orbital π-bonding model for a bis-dioxygen complex $(O_2)M(O_2)$. The complex contains two equivalent dioxygen molecules (where all oxygen atoms are also equivalent) bonding in a sideways fashion in a D_{2d} configuration, to the central metal atom. (The σ-bonding not considered here, is represented by the heavy arrows.)

TABLE 5. Observed and calculated frequencies for isotopic species of the bisdioxygen complexes $(O_2)M(O_2)$ (where M = Ni, Pd, or Pt)

Molecule	Frequency (cm^{-1})*			Assignment
	Ni	Pd	Pt	
$(^{16}O_2)M(^{16}O_2)$	1062.0 (1062.1)	1111.5 (1111.1)	1050.0	νO—O
$(^{16}O_2)M(^{16}O^{18}O)$	1045.2 (1044.3)	1092.2 (1092.4)	1030.6	νO—O
$(^{16}O^{18}O)M(^{16}O^{18}O)$	1035.2 (1032.5)	1080.5 (1080.1)	1021.6	νO—O
$(^{16}O_2)M(^{18}O_2)$	1018.2 (1020.3)	1067.2 (1067.3)	1003.8	νO—O
$(^{16}O^{18}O)M(^{18}O_2)$	1016.2 (1013.7)	1060.5 (1060.5)	1000.6	νO—O
$(^{18}O_2)M(^{18}O_2)$	1001.4 (1001.6)	1048.5 (1047.9)	991.4	νO—O
$(^{16}O_2)M(^{16}O_2)$	535.0 (535.4)	504.0 (503.7)		νM—O

*Calculated frequencies are shown in parentheses and are based on the M.V.F.F. force constants listed in Table 8.

Can. J. Chem. Downloaded from www.nrcresearchpress.com by 210.87.254.105 on 09/05/12
For personal use only.

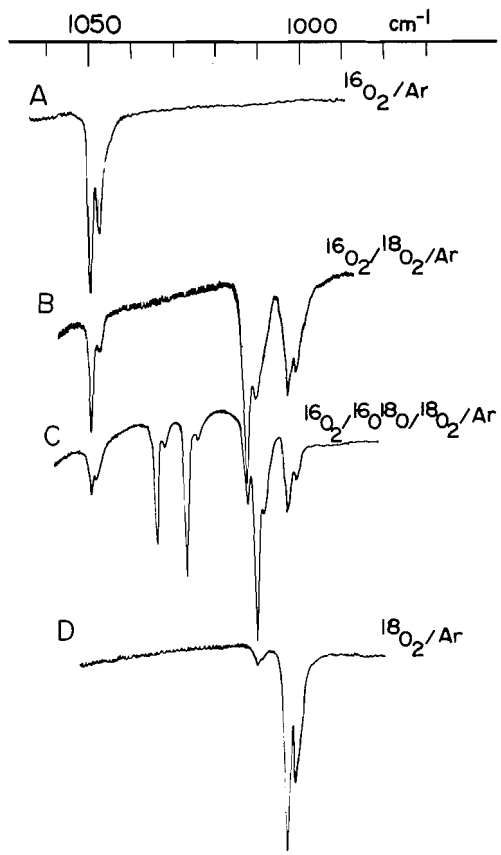

FIG. 5. The matrix infrared spectrum of the products of the cocondensation reaction of Pt atoms with (*A*) $^{16}O_2$:Ar ≅ 1:50, (*B*) $^{16}O_2$:$^{18}O_2$:Ar ≅ 1:1:100, (*C*) $^{16}O_2$:$^{16}O^{18}O$:$^{18}O_2$:Ar ≅ 1:2:1:200 and (*D*) $^{18}O_2$:Ar ≅ 1:50 showing the characteristic isotope pattern of $(O_2)Pt(O_2)$.

oxygen matrices show gross similarities in terms of the frequencies and intensities of the observed lines. However, the spectra in $^{16}O_2$, $^{16}O_2/^{18}O_2$, and $^{16}O_2/^{16}O^{18}O/^{18}O_2$ matrices show a doublet splitting of all the O—O stretching modes (see for example Fig. 6).

An examination of the reported crystal structures of solid oxygen is quite informative in terms of the possible sites of palladium atoms in the lattice. Solid oxygen exists in three crystalline modifications. The low, intermediate, and high temperature phases are referred to as α-, β-, and γ-oxygen respectively with phase transition temperatures α-O_2 (0–23.9 °K), β-O_2 (23.9–43.6 °K), and γ-O_2 (43.6–54.4 °K). The two low temperature phases have been studied extensively by diffraction methods (ref. 9 and references therein). α-O_2 is monoclinic with a $C2/m$ (C_{2h}^3) space group and has two molecules in the unit cell whose axis is perpendicular to the two-fold symmetry axis (see Fig. 7). The molecules are at positions having $2/m$ symmetry, that is, at a center of symmetry (C_{2h}) as suggested by Cairns and Pimentels' (10) tentative interpretation of the infrared spectra of solid α-oxygen. The β-phase has been assigned the space group $R\bar{3}m$ (D_{3d}^5) which can be described in terms of a primitive rhombohedral cell containing one molecule oriented parallel to the trigonal axis and occupying a site of D_{3d} symmetry.

From considerations of the bond length (1.18 Å) and van der Waals radius (1.4 Å) of oxygen and the atomic radius of palladium (1.38 Å), it appears unlikely that the palladium atom would reside in any of the interstitial sites of either the α or β oxygen lattices. The palladium

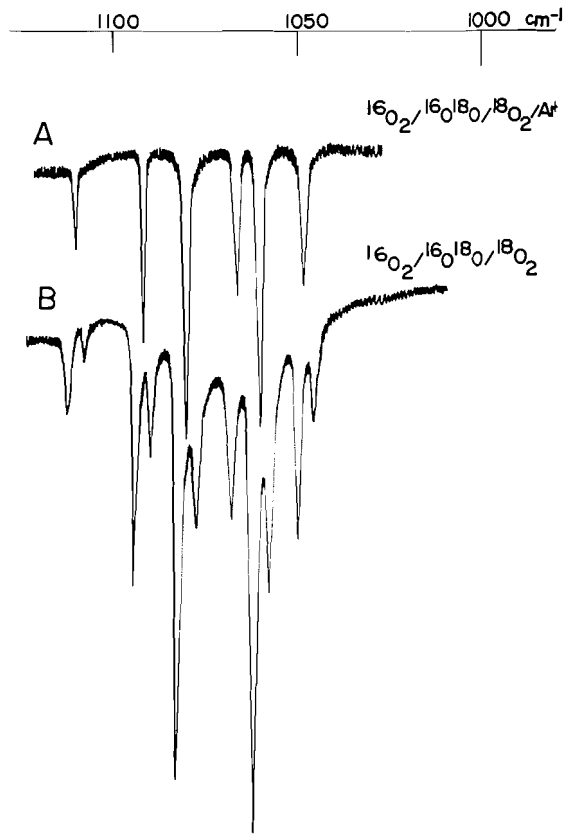

FIG. 6. The matrix infrared spectrum of the products of the cocondensation reaction of Pd atoms with (*A*) $^{16}O_2$:$^{16}O^{18}O$:$^{18}O_2$:Ar ≅ 1:2:1:800 and (*B*) $^{16}O_2$:$^{16}O^{18}O$:$^{18}O_2$ ≅ 1:2:1 (see text).

Can. J. Chem. Downloaded from www.nrcresearchpress.com by 210.87.254.105 on 09/05/12
For personal use only.

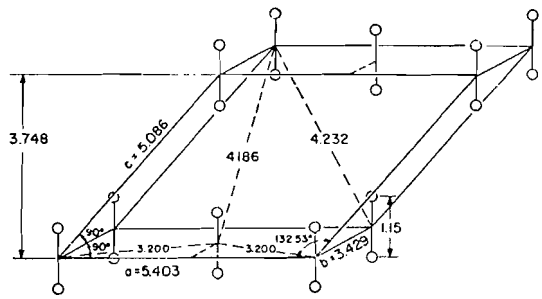

FIG. 7. The crystal structure of α-O_2 showing the monoclinic unit cell ($C2/m$). There are two molecules in the primitive unit cell centred at (000) and $(\frac{1}{2}\frac{1}{2}0)$ with the O—O bonds approximately normal to the *ab* plane.

atom must then reside in the more spacious C_{2h} substitutional site when in the α-O_2 lattice or the D_{3d} substitutional site when in the β-O_2 lattice about which there are four nearest O_2 neighbors. Preferential interaction of the palladium atom in a substitutional site with two nearest neighbor O_2 molecules (it is a matter of conjecture whether a fluxional situation exists) is then the most favored scheme for the formation of $(O_2)Pd(O_2)$ in solid oxygen.

When palladium atoms are deposited into a pure $^{16}O_2$ matrix at 4.2 °K, the infrared spectrum initially shows a *single* νO—O absorption at 1112.3 cm^{-1} (Fig. 8). However, on warming the matrix to 10–30 °K, this singlet absorption splits into a closely spaced doublet at 1114.7 and 1110.0 cm^{-1} (Fig. 8).

The warm up characteristics of the oxygen absorption of $(O_2)Pd(O_2)$ in solid oxygen would appear to indicate that when first deposited, at 4.2 °K the oxygen lattice can be considered to be in a disordered or glassy phase (evidence in favor of this stems from Pimentel's infrared data of O_2 when deposited at 4.2 °K, which shows significant lattice imperfections in the solid so prepared). The $(O_2)Pd(O_2)$ molecule experiences an averaged local field and thereby gives rise to a single oxygen absorption (1112.3 cm^{-1}). When the oxygen matrix is warmed, it is annealed (presumably in a somewhat non-uniform manner) thereby increasing the regularity of its α-O_2 and β-O_2 crystalline lattice portions. The $(O_2)Pd(O_2)$ molecule now feels the perturbing effect of the two different substitutional lattice sites (C_{2h} and D_{3d} in the α- and β-O_2 lattices, respectively) and gives rise to the observed closely spaced doublet structure or matrix splitting (Fig. 8).

In the case of Ni and Pt atoms deposited into

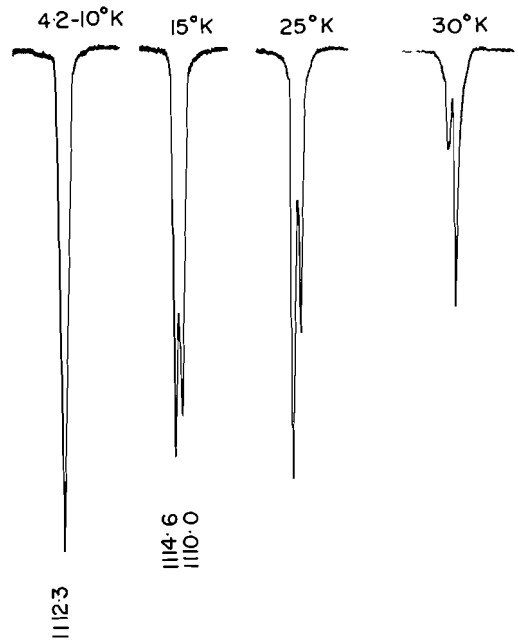

FIG. 8. The matrix infrared spectrum of $(^{16}O_2)Pd(^{16}O_2)$ formed in the cocondensation reaction of Pd atoms with pure $^{16}O_2$ on deposition at 4.2–10 °K, and after successive warm-up experiments at 15, 25, and 30 °K each for 10 min.

pure $^{16}O_2$ matrices, a similar matrix splitting effect is observed for the complexes $(O_2)Ni(O_2)$ and $(O_2)Pt(O_2)$ with components centered at 1064.0 and 1053.2 cm^{-1} and 1052.6 and 1049.6 cm^{-1}, respectively. The cause of these splittings is probably related to site effects similar to those described for $(O_2)Pd(O_2)$.

Normal Coordinate Calculations for Binary Mono- and Bisdioxygen Complexes of Nickel, Palladium, and Platinum

For synthetic dioxygen complexes that are stable at room temperature and which have been shown to contain the dioxygen ligand bonded to the metal in a side-on fashion, two limiting mechanical local models have been considered for the $M(O_2)$ residue of the complex. These two models have been referred to as monodentate and isosceles and are illustrated below:

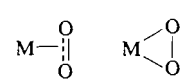

As a significant reduction of the bond order of the oxygen molecule is observed for the binary

Can. J. Chem. Downloaded from www.nrcresearchpress.com by 210.87.254.105 on 09/05/12
For personal use only.

TABLE 6. Representative examples of synthetic dioxygen complexes (frequencies and force constants)

Molecule	ν_1‖	ν_2‖	k_{MO}	k_{OO}	Reference
$Pt(O_2)(PPh_3)_2$†	828	472	2.1.2.2	3.0	6*c*
$Ni(O_2)(t\text{-BuNC})_2$†	898	552	2.4	3.5	6*c*
$Pd(O_2)(t\text{-BuNC})_2$†	893	484	2.1	3.5	6*c*
$Rh(O_2)Cl(PPh_3)_2(t\text{-BuNC})$†	892	576	3.2	3.3	6*c*
$Ir(O_2)(PPh_3)_3Cl$†	852	563	*	*	3*a*
$(M^+)_2(O_2^{2-})$‡			1.2		12
$(M^+)(O_2^-)$‡				5–6	12
$Pd(O_2)$§	1023.5	427	1.35	4.15	This work
$(O_2)Pd(O_2)$§	1110.8	504	1.84	5.50	This work
O_2				11.32	

*Values not reported.
†Stable at room temperature.
‡Alkali metal ionic peroxides and superoxides, stable under conditions of matrix isolation.
§Stable under conditions of matrix isolation.
‖ν_1 and ν_2 are the O—O and M—O A_1 type stretching modes.

dioxygen complexes of the present study, indicating significant back bonding, the present analysis is best considered in terms of delocalized bonding of the isosceles type. (We note that insignificant lowering of the C=C bond order or bond stretching force constant for ethylene in Zeise's salt, points to the relevance of the monodentate model for this type of side-on bonded olefin complex (11).)

Normal Coordinate Analysis of $Pd(O_2)$ and $(O_2)Pd(O_2)$

$Pd(O_2)$

The palladium monodioxygen compound with side-on bonded O_2 is assumed to have the isosceles triangular structure of C_{2v} symmetry as shown below. Representative O—O and Pd—O bond lengths are taken at 1.4 and 2.1 Å, respectively.

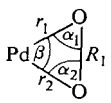

The number and types of vibrational modes expected are $4A_1 + 2B_2$ and on the basis of the internal coordinates indicated in the diagram the symmetry coordinates are:

$$A_1 \quad S_1 = \Delta R_1$$
$$S_2 = 1/\sqrt{2}(\Delta r_1 + \Delta r_2)$$
$$S_3 = 1/\sqrt{2}(\Delta\alpha_1 + \Delta\alpha_2)$$
$$S_4 = \Delta\beta$$
$$B_2 \quad S_5 = 1/\sqrt{2}(\Delta r_1 - \Delta r_2)$$
$$S_6 = 1/\sqrt{2}(\Delta\alpha_1 - \Delta\alpha_2)$$

The approximation of a force field for the monodioxygen complex is fairly difficult since there is not a great deal of force constant data available in the literature for coordinated dioxygen. Some representative examples are listed in Table 6 for anionic, matrix isolated alkali metal peroxides and superoxides (12) as well as a number of synthetic dioxygen complexes (6*c*).

The Cotton–Kraihanzel force field approximation (13), which was applied successfully to binary dinitrogen and carbonyl compounds, is based on the ability to decouple the ligand stretching modes from the metal-ligand modes. Since, in the case of the isosceles model for dioxygen complexes, such coupling is expected to be *significant*, a more complete force field was desired. To obtain a reasonable frequency fit for $Pd(O_2)$, a M.V.F.F. and a least squares analysis of the data were employed. The dependence of the O—O and Pd—O frequencies on the values of k_{OO} and k_{PdO} and suitable interaction and angular force constants was thoroughly investigated and resulted in the force field listed in Table 7. The agreement between the observed and calculated frequencies also shown in Table 7 is excellent.

It should be noted here that the evaluation of this force field was made on the assumption that the observed Pd—O stretching frequency was of the A_1 type and that the B_2 mode was too weak to observe. It could be argued that the interaction force constant f_{PdOPdO} might be negative, as was assumed for the superoxide calculations (12), but reduction of this interaction force constant in the present analysis only increased the

Can. J. Chem. Downloaded from www.nrcresearchpress.com by 210.87.254.105 on 09/05/12
For personal use only.

Can. J. Chem. Downloaded from www.nrcresearchpress.com by 210.87.254.105 on 09/05/12
For personal use only.

calculated value for the B_2 mode. Furthermore, the calculations indicated that to obtain a frequency fit compatible with a reversed assignment unreasonably low values of f_r or unreasonably high values of f_{rr} would be required. Hence the assignment to the symmetric metal–ligand mode was favored.[2] By similar iteration procedures, force fields were calculated for the nickel and platinum monodioxygen complexes and the results are also shown in Table 7.

$(O_2)Pd(O_2)$: The D_{2d} "Spiro" Configuration

On the basis of D_{2d} symmetry concluded from the observation of the six component multiplet pattern in the spectrum of $Pd/^{16}O_2/^{16}O^{18}O/^{18}O_2/Ar$, and using the same bond distances as used in the monodioxygen complex, the **G** matrix of the biscomplex could be evaluated. The internal and symmetry coordinates of the vibrational modes (including redundancies) are shown below:

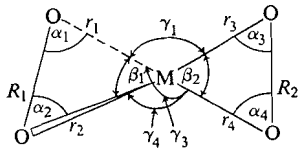

(Eight torsional coordinates (τ) were included in the analysis.)

$$
\begin{aligned}
A_1\ S_1 &= 1/\sqrt{2}(\Delta R_1+\Delta R_2)\\
S_2 &= 1/2(\Delta r_1+\Delta r_2+\Delta r_3+\Delta r_4)\\
S_3 &= 1/2(\Delta\alpha_1+\Delta\alpha_2+\Delta\alpha_3+\Delta\alpha_4)\\
S_4 &= 1/\sqrt{2}(\Delta\beta_1+\Delta\beta_2)\\
S_5 &= 1/2(\Delta\gamma_1+\Delta\gamma_2+\Delta\gamma_3+\Delta\gamma_4)\\
S_6 &= 1/2\sqrt{2}(\Delta\tau_1-\Delta\tau_2-\Delta\tau_3+\Delta\tau_4+\Delta\tau_5\\
&\qquad -\Delta\tau_6-\Delta\tau_7+\Delta\tau_8)\\
A_2\ S_7 &= 1/2\sqrt{2}(\Delta\tau_1+\Delta\tau_2+\Delta\tau_3+\Delta\tau_4-\Delta\tau_5\\
&\qquad -\Delta\tau_6-\Delta\tau_7-\Delta\tau_8)
\end{aligned}
$$

$$
\begin{aligned}
B_1\ S_8 &= 1/2(\Delta\gamma_1-\Delta\gamma_2-\Delta\gamma_3+\Delta\gamma_4)\\
S_9 &= 1/2\sqrt{2}(\Delta\tau_1+\Delta\tau_2+\Delta\tau_3+\Delta\tau_4+\Delta\tau_5\\
&\qquad +\Delta\tau_6+\Delta\tau_7+\Delta\tau_8)\\
B_2\ S_{10} &= 1/\sqrt{2}(\Delta R_1-\Delta R_2)\\
S_{11} &= 1/2(\Delta r_1+\Delta r_2-\Delta r_3-\Delta r_4)\\
S_{12} &= 1/2(\Delta\gamma_1+\Delta\gamma_2-\Delta\gamma_3-\Delta\gamma_4)\\
S_{13} &= 1/\sqrt{2}(\Delta\beta_1-\Delta\beta_2)\\
S_{14} &= 1/2\sqrt{2}(\Delta\tau_1-\Delta\tau_2-\Delta\tau_3+\Delta\tau_4-\Delta\tau_5\\
&\qquad +\Delta\tau_6+\Delta\tau_7-\Delta\tau_8)\\
E_{1a}\ S_{15} &= 1/\sqrt{2}(\Delta r_3-\Delta r_4)\\
S_{16} &= 1/\sqrt{2}(\Delta\alpha_3-\Delta\alpha_4)\\
S_{17} &= 1/2(\Delta\gamma_1+\Delta\gamma_2-\Delta\gamma_3-\Delta\gamma_4)\\
S_{18} &= 1/2\sqrt{2}(\Delta\tau_1+\Delta\tau_2-\Delta\tau_3-\Delta\tau_4+\Delta\tau_5\\
&\qquad +\Delta\tau_6-\Delta\tau_7-\Delta\tau_8)\\
S_{19} &= 1/2\sqrt{2}(\Delta\tau_1+\Delta\tau_2-\Delta\tau_3-\Delta\tau_4-\Delta\tau_5\\
&\qquad -\Delta\tau_6+\Delta\tau_7+\Delta\tau_8)\\
E_{1b}\ S_{20} &= 1/\sqrt{2}(\Delta r_1-\Delta r_2)\\
S_{21} &= 1/\sqrt{2}(\Delta\alpha_1-\Delta\alpha_2)\\
S_{22} &= 1/2(\Delta\gamma_1-\Delta\gamma_2+\Delta\gamma_3-\Delta\gamma_4)\\
S_{23} &= 1/2\sqrt{2}(\Delta\tau_1-\Delta\tau_2+\Delta\tau_3-\Delta\tau_4+\Delta\tau_5\\
&\qquad -\Delta\tau_6+\Delta\tau_7-\Delta\tau_8)\\
S_{24} &= 1/2\sqrt{2}(\Delta\tau_1-\Delta\tau_2+\Delta\tau_3-\Delta\tau_4-\Delta\tau_5\\
&\qquad +\Delta\tau_6-\Delta\tau_7+\Delta\tau_8)
\end{aligned}
$$

These internal and symmetry coordinates are applicable to both pure $^{16}O_2$ and $^{18}O_2$ isotopic species, with appropriate changes in the mixed species where the symmetry is lowered C_{2v} in case of $(^{16}O_2)Pd(^{18}O_2)$, C_2 in case of $(^{16}O^{18}O)$-$Pd(^{16}O^{18}O)$, and C_s in the species $(^{16}O_2)Pd$-$(^{16}O^{18}O)$ and $(^{18}O_2)Pd(^{16}O^{18}O)$.

As in the case of the monodioxygen complexes, a M.V.F.F. was derived and the values of ν_{OO} and ν_{PdO} were calculated for the various $^{16}O/^{18}O$ isotopic combinations. Certain simplifying assumptions were made for these calculations, namely that the angle–stretch and angle–angle interaction force constants as well as the torsional force constants were equal to zero. After several iterations the final force field as shown in Table 8 was obtained. It should be mentioned that the calculations were based on the assignment of the Pd—O stretching frequency to the B_2 mode. The possibility of the assignment of this band to the E mode was tested, but a frequency fit could be made only with unreasonably low values of k_{PdO}. Similar calculations were done for $(O_2)Ni$-(O_2) (with the NiO stretching frequency (B_2) at 535 cm^{-1}) and the resulting force field is also

[2]NOTE ADDED IN PROOF: Assignment of the metal–oxygen stretching frequencies to the A_1 and B_2 modes for the mono and bisdioxygen complexes, respectively, was confirmed by intensity calculations. For $Pd(O_2)$ the ratio of relative intensities is approximately $I_{B_2}/I_{A_1} = \tan^2\theta$ where $\theta = \angle OPdO$. For the given bond lengths, θ is approximately equal to 40° and the ratio $I_{B_2}/I_{A_1} \sim 1/8$, therefore if only one MO stretching mode is observed for the monodioxygen complex it must be the A_1. For $(O_2)Pd(O_2)$ it can be shown that $I_E/I_B \sim \tan^2\theta$ and for $\theta \sim 40°$, $I_E/I_{B_2} \sim 1/8$. The MO mode is therefore assigned to the B_2 mode.

TABLE 7. Observed and calculated frequencies and M.V.F.F. force constants for the monodioxygen complexes $M(O_2)$, where M = Ni, Pd, or Pt

(*a*) Frequencies

		$Ni(O_2)$		$Pd(O_2)$		$Pt(O_2)$	
Mode*	Compound	Obsd.	Calcd.	Obsd.	Calcd.	Obsd.	Calcd.
ν_1	$M(^{16}O_2)$	966.2	966.9	1024.0	1023.8	926.6	927.3
ν_1	$M(^{16}O^{18}O)$	940.1	940.5	995.5	995.2	901.4	901.4
ν_1	$M(^{18}O_2)$	913.6	912.9	967.0	965.6	875.0	874.5
ν_2	$M(^{16}O_2)$	504	503.2	427	427.3	—	375–415

*ν_1 is the O—O stretching mode and ν_2 is the corresponding M—O stretching mode. The calculated frequencies are shown in parenthesis.

(*b*) M.V.F.F. force constant

	Value		
Parameter	$Ni(O_2)$	$Pd(O_2)$	$Pt(O_2)$*
k_{OO}	3.4	4.15	3.28–3.24
k_{MO}	1.55	1.35	1.20–1.50
$k_{MO.OO}$	0.45	0.45	0.44
$k_{MO.MO}$	0.40	0.24	0.20–0.24

*The Pt—O stretching mode was not observed. In the calculations a range of values of k_{MO} was used (1.20–1.50 mdyn/Å) to give a range of possible νPt—O values (375–415 cm^{-1}). The corresponding k_{O-O} values required for the fit of ν_{O-O} ranged between 3.28 and 3.24 mdyn/Å.

TABLE 8. M.V.F.F.* for bisdioxygen nickel and palladium, $(O_2)Ni(O_2)$ and $(O_2)Pd(O_2)$

	Value	
Parameter	$(O_2)Pd(O_2)$	$(O_2)Ni(O_2)$
f_R	5.50	5.00
f_r	1.84	2.19
f_{RR}	0.37	0.25
f_{Rr}	0.32	0.12
f_{rr}	0.20	0.20
f_{rr}'†	0.17	0.50

*Units in mdyn/Å. See text for notation.
†Stretch–stretch interaction between Pd—O bonds of different O_2 ligands.

listed in Table 8. The calculated and observed frequencies for these $M(O_2)_2$ molecules are listed in Table 5 and the close agreement provides convincing evidence for the correctness of our vibrational and structural assignments.

It is significant that the force constants for the oxygen–oxygen stretching mode and for the metal–oxygen stretching mode both *increase* with increased coordination number.

Complete M.V.F.F. calculations were not performed for the platinum bisdioxygen molecule since the low frequency Pt—O mode was *not* observed in any of the experiments. However, it is not unreasonable to expect similar force constant trends upon going from $Pt(O_2)$ to $(O_2)Pt(O_2)$.

Although it was mentioned earlier that the expected coupling of the ligand and metal–ligand modes influenced the choice of a more complete force field, this does not mean that a Cotton–Kraihanzel force field cannot be established for dioxygen complexes. Indeed we performed such C.K. calculations for the high frequency O—O stretching modes (which may be referred to as the "monodentate" model) and obtained quite reasonable agreement between the observed and calculated frequencies of the bisdioxygen complexes of Ni, Pd, and Pt (Table 9). The best fit M.V.F.F. bond stretching force constants (listed in Table 8) are found to be slightly smaller than the corresponding C.K. values (listed in Table 9).

Intensity Calculations for the O—O Stretching Modes of Isotopically Substituted $(^nO^mO)M(^nO^mO)$ (where M = Ni, Pd, or Pt; n, m = 16 or 18)

The absorption intensities of two modes belonging to the same symmetry type which can couple, can be evaluated using the isotope inten-

Can. J. Chem. Downloaded from www.nrcresearchpress.com by 210.87.254.105 on 09/05/12
For personal use only.

TABLE 9. Observed and calculated frequencies* for the isotopic bisdioxygen complexes ($^nO^mO$)M($^nO^mO$) (where M = Ni, Pd, or Pt; n, m = 16 or 18) based on the Cotton–Kraihanzel force field approximation

	Frequency* (cm^{-1})		
Molecule	Ni	Pd	Pt
($^{16}O_2$)M($^{16}O_2$)	1062.0 (1062.0)	1111.5 (1111.5)	1050.0 (1050.0)
($^{16}O_2$)M($^{16}O^{18}O$)	1045.2 (1045.2)	1092.2 (1092.5)	1030.6 (1030.6)
($^{16}O^{18}O$)M($^{16}O^{18}O$)	1035.2 (1032.1)	1080.5 (1080.1)	1021.6 (1020.4)
($^{16}O_2$)M($^{18}O_2$)	1018.2 (1024.2)	1067.2 (1067.3)	1003.8 (1004.3)
($^{16}O^{18}O$)M($^{18}O_2$)	1016.2 (1014.6)	1060.5 (1060.4)	1000.6 (1000.2)
($^{18}O_2$)M($^{18}O_2$)	1001.4 (1001.3)	1048.5 (1047.9)	991.4 (989.9)
	Value		
Force constant	Ni	Pd	Pt
f_R†	6.052	6.236	5.427
f_{RR}	0.736	0.413	0.231

*Calculated frequencies in parentheses.
†Force constant units mdyn/Å.

sity rules (for all coordinates of a given symmetry species) shown below (17):

$$\sum_k I_k = \sum_{k'k''} \frac{\partial \boldsymbol{\mu}}{\partial S_{k'}} \cdot \frac{\partial \boldsymbol{\mu}}{\partial S_{k''}} G_{k'k''}$$

$$\sum_k \frac{I_k}{\lambda_k} = \sum_{k'k''} \frac{\partial \boldsymbol{\mu}}{\partial S_{k'}} \cdot \frac{\partial \boldsymbol{\mu}}{\partial S_{k''}} F_{k'k''}{}^{-1}$$

For example, in a number of binary dinitrogen and carbonyl complexes (18, 19) it was found that these intensity sum rules could be used in conjunction with the Cotton–Kraihanzel force field approximation, to predict relative absorption intensities for NN and CO infrared active stretching modes, respectively. Their application to these systems simply involves the determination of the components of the transition dipole moment vectors with respect to each symmetry coordinate S_k, where in the C.K. approximation $G_{k'k''}$ simply equals the reduced mass of the ligand and $F_{k'k''}{}^{-1}$ is an element of the matrix inverse to the force constant matrix $F_{k'k''}$.

Since homonuclear diatomic molecules do not undergo a net dipole change during bond stretching, the resultant mode is not infrared active. However, when the diatomic molecule is coordinated to a metal atom in an "end-on" fashion, ligand stretching is accompanied by a net dipole change as shown below

$$M{-}N\overrightarrow{\equiv}N \qquad \boldsymbol{\mu}' \neq 0$$

resulting in infrared activity of the mode. If one considers an oxygen molecule coordinated to a metal atom in a "side-on" fashion as postulated for $M(O_2)$ and $(O_2)M(O_2)$, it is apparent that the oxygen–oxygen stretching mode does not involve a dipole change and must gain its infrared activity from a transition dipole moment induced by coupling with the metal–oxygen stretching mode of the same symmetry. Therefore, it should be possible to define a transition dipole moment vector $\boldsymbol{\mu}'$ for the O—O stretching mode which is directionally dependent on the transition dipole moment vectors for the M—O stretching modes as shown below:

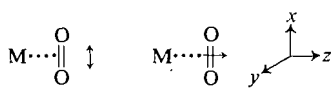

$\mu_x = \mu_y = 0$ $\qquad$ $\mu_z \neq 0$

It was felt that within the limits of the C.K. approximation, the non-zero components of the decoupled transition dipole moment vectors ($\boldsymbol{\mu}_z'$) could be used to predict relative absorption intensities for the O—O stretching modes of the isotopic bisdioxygen molecules. As an example, let us consider the schematic model for ($^{16}O_2$)M($^{16}O_2$) shown below.

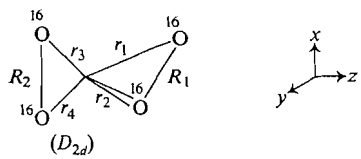

(D_{2d})

Can. J. Chem. Downloaded from www.nrcresearchpress.com by 210.87.254.105 on 09/05/12
For personal use only.

TABLE 10. Calculated and observed* relative absorption intensities for the isotopic molecules ($^nO^mO$)M($^nO^mO$) (where M = Ni, Pd, or Pt; n, m, = 16 or 18)

Molecule	Ni†	Pd	Pt
($^{16}O_2$)M($^{16}O_2$)	1.99	1.80 (1.68)	1.57 (1.86)
($^{16}O_2$)M($^{16}O^{18}O$)	8.51	7.81 (6.34)	6.92 (5.17)
($^{16}O^{18}O$)M($^{16}O^{18}O$)	9.39	9.29 (9.19)	9.21 (7.02)
($^{16}O_2$)M($^{18}O_2$)	4.40	3.97 (3.83)	3.04 (3.46)
($^{16}O^{18}O$)M($^{18}O_2$)	10.00	10.00 (10.00)	10.00 (10.00)
($^{18}O_2$)M($^{18}O_2$)	2.76	2.99 (3.69)	3.35 (3.16)

*The observed intensities were measured by assuming a triangular contour for the infrared band and using the expression $I = \Delta\nu_{1/2}[1 + \gamma \log \gamma/(1 - \gamma)]$ where $\Delta\nu_{1/2}$ = width of band at half height, γ = fractional transmittance, and $I = -\int \log \gamma \, d\nu$. Observed relative intensities presented in parentheses.

†Spectra of poor quality. See text.

It is possible to depict diagrammatically the two possible O—O stretching modes of symmetry type A_1 and B_2 with the corresponding M—O modes:

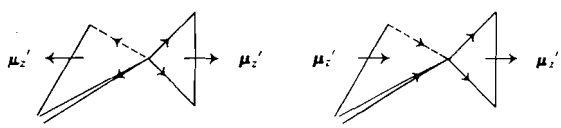

$$A_1$$

$$S_1 = 1/\sqrt{2}(\Delta R_1 + \Delta R_2)$$

$$S_2 = 1/2(\Delta r_1 + \Delta r_2 + \Delta r_3 + \Delta r_4)$$

$$B_2$$

$$S_1 = 1/\sqrt{2}(\Delta R_1 - \Delta R_2)$$

$$S_2 = 1/2(\Delta r_1 + \Delta r_2 - \Delta r_3 - \Delta r_4)$$

The vector sum of the transition dipole moment vectors for the A_1 mode is of course equal to zero, making this mode infrared inactive. However, the B_2 mode is expected to be infrared active and the intensity sum rules may be applied.[3]

Applying this method individually to each of the six isotopic molecules ($^nO^mO$)M($^nO^mO$) (where n, m = 16 or 18) and multiplying the intensity of each by its expected statistical abundance (and correcting for the true concentration ratio of $^{16}O_2$:$^{16}O^{18}O$:$^{18}O_2$) a set of expected relative intensities may be obtained as summarized in Table 10. Comparison of these calculated absorption intensities with those observed for $Pd(O_2)_2$ and $Pt(O_2)_2$ show remarkably close agreement and support the validity of the model and the frequency assignments used in the computations. Even though the $Ni(O_2)_2$ spectra were not of high quality the same general trends in the predicted and observed intensity pattern were quite apparent.

[3]C.K. force constants were used since they correspond more closely to the decoupled or monodentate model.

Discussion of Results

As found for $M(O_2)$ and $(O_2)M(O_2)$ (where M = Ni, Pd, or Pt) and many synthetic dioxygen carriers, the side-on mode of bonding appears to be the more common form (14), which is not unexpected for transition metals in relatively low oxidation states (15). The fact that $(O_2)M(O_2)$ is pseudotetrahedral (D_{2d}) rather than planar (D_{2h}) would tend to favor M(0) rather than M(II) complexes.

The addition of O_2 to Ni, Pd, and Pt atoms in these matrix cocondensation reactions can be discussed in terms of the π-bonding scheme of Chatt and Dewar (16). A delocalized three center molecular orbital scheme involving the symmetry allowed metal orbitals and an in-plane π^* of O_2 describes the situation more satisfactorily than a localized model in terms of O_2^{2-} or O_2^- (3*b*). The degree of back bonding which occurs will depend upon the relative energies and the amount of overlap between the orbitals.

It is interesting to try to relate briefly Ibers' (14*c*) rationale for the factors affecting reversible oxygen uptake in synthetic dioxygen carriers, to our data for binary dioxygen complexes. Ibers proposes that an increase in electron density at the metal accomplished by reducing the electronegativity of halide substituents or upon changing the metal in a complex (for example,

Can. J. Chem. Downloaded from www.nrcresearchpress.com by 210.87.254.105 on 09/05/12
For personal use only.

Ir > Rh > Co in the series indicated below)

Complex	r(O—O)(Å)	r(M—O)(Å)	Oxygen uptake properties	Reference
$[Co(O_2)(2{=}phos)_2]BF_4$	1.420	1.902 1.871	Irreversible	14*a*
$[Rh(O_2)(diphos)_2]PF_6$	1.418	2.026 2.025	Reversible	14*c*
$[Ir(O_2)(diphos)_2]PF_6$	1.625	1.961 1.990	Irreversible	14*c*

will *enhance* O_2 uptake properties. This would appear to be borne out by the above crystallographic data and is in fact also reflected in the order of the O—O stretching frequencies and bond stretching k_{OO} force constants for the binary monodioxygen complexes $Ni(O_2)$, $Pd(O_2)$, and $Pt(O_2)$, which parallel (in an inverse fashion) the order of O—O bond lengths in the Co, Rh, and Ir complexes tabulated above, that is: r(O—O), Å, Rh $\simeq$ Co < Ir;[4] k(O—O), mdyn/Å, Pd > Ni > Pt; ν(O—O), cm^{-1}, Pd > Ni > Pt.

As mentioned earlier, the D_{2d} assignment for $(O_2)M(O_2)$, as well as being favored on spectroscopic grounds, is also preferred on a Dewar–Chatt π-bonding scheme (see Fig. 4). From maximum π-bonding overlap considerations, the use of the mutually orthogonal d_{xz}, d_{yz} orbitals is required and would necessitate that the dioxygen molecules adopt a "spiro" conformation about the metal atom. In this context it is important to note than on increasing the coordination number of the metal from one in $M(O_2)$ to two in $(O_2)M(O_2)$ where M = Ni, Pd, and Pt, the infrared active νOO stretching mode shifts to higher frequencies.

The degree of electron density transferred to π^* antibonding orbitals on the O_2 through the intermediary of the metal will depend on the other ligands on the complex. The νOO frequency order on passing from $M(O_2)$ to $(O_2)M(O_2)$ does follow the trend expected on the Chatt–Dewar concept of O_2 bonding, that is, $(O_2)M(O_2) > (M)O_2$. Thus, on increasing the dioxygen coordination number, the degree of charge transfer per O_2 molecule from the π metal orbitals would decrease as would the amount of π^* back bonding, resulting in a strengthening of the O—O bond upon passing from the mono- to biscomplex, as is observed. However, the order observed for the metal–oxygen stretching modes (and k_{MO} bond stretching force constants) is $(O_2)Pd(O_2)$ > $Pd(O_2)$ and $(O_2)Ni(O_2)$ > $Ni(O_2)$, which is *not* that expected from the rationalization of the reversible dioxygen uptake being related to those compounds containing dioxygen ligands with shorter O—O bond lengths (14*c*) (or high k_{OO} with higher M—O bond lengths and presumably lower k_{MO} force constants). This observation would seem to imply that the earlier descriptions of the bonding of O_2 to metals might be an oversimplification of the factors involved in the dioxygen carrying problem.

In our opinion, although the formal charge transfer to each dioxygen ligand in $(O_2)M(O_2)$ appears to be less than in $M(O_2)$, the "total" charge transfer from the metal, or the formal (fractional) oxidation state of M for the biscomplex, could conceivably be greater than that in the monocomplex. Furthermore, a shorter O—O bond for the dioxygen in $(O_2)M(O_2)$ as compared to $M(O_2)$ (deduced from νOO and k_{OO} values) would have the effect of shorten-

[4]As the difference in r(O—O) for the Co and Rh complexes is not significant when considered with the standard deviations, we have put the oxygen–oxygen bond length in $[Rh(O_2)(diphos)_2]PF_6$ approximately equal to that in $[Co(O_2)(2{=}phos)_2]BF_4$.

Can. J. Chem. Downloaded from www.nrcresearchpress.com by 210.87.254.105 on 09/05/12
For personal use only.

ing the PdO bond in the biscomplex compared to the monocomplex. If either of these effects were operative, one can then rationalize the stronger O—O and M—O bonds in the bisdioxygen complexes.

We wish to thank Dr. Martin Moskovits for many helpful discussions and the National Research Council of Canada and the Research Corporation for financial assistance.

1. (*a*) G. A. Ozin, H. Huber, E. P. Kündig, and M. Moskovits. Can. J. Chem. **50**, 2385 (1972). (*b*) E. P. Kündig, M. Moskovits, and G. A. Ozin. Can. J. Chem. **50**, 3587 (1972). (*c*) E. P. Kündig, M. Moskovits, and G. A. Ozin. J. Mol. Struct. **14**, 137 (1972); Nature, **235**, 98 (1972).
2. H. Huber and G. A. Ozin. Can. J. Chem. **50**, 374) (1972).
3. (*a*) J. Valentine, D. Valentine, and J. P. Collman. Inorg. Chem. **10**, 219 (1971). (*b*) L. Vaska. Acc. Chem. Res. **1**, 335 (1968). (*c*) J. P. Collman. Acc. Chem. Res. **1**, 136 (1968). (*d*) R. O. C. Norman and J. R. L. Smith. Oxidases and related redox systems. Vol. 1. *Edited by* T. E. King, H. S. Mason, and M. Morrison. Wiley, New York, N.Y. 1965. p. 131.
4. (*a*) L. C. Schroeter. Sulphur dioxide. Pergamon Press, Oxford. 1966. p. 34. (*b*) J. P. Collman, M. Kubota, and J. W. Hosking. J. Am. Chem. Soc. **89**, 4809 (1967).
5. M. Moskovits and G. A. Ozin. J. Appl. Spectrosc. **26**, 481 (1972).
6. (*a*) R. Horn, E. Weissberger, and J. P. Collman. Inorg. Chem. **9**, 2367 (1970). (*b*) P. J. Hayward, D. M. Blake, G. Wilkinson, and C. J. Nyman. J. Am. Chem. Soc. **92**, 5873 (1970). (*c*) A. Nakamura, Y. Tatsuno, M. Yamamoto, and S. Otsuka. J. Am. Chem. Soc. **93**, 6052 (1971).
7. G. A. Ozin and A. Vander Voet. Can. J. Chem. **51**, 637 (1973).
8. M. Moskovits and G. A. Ozin. J. Chem. Phys. **58**, 1251 (1973).
9. C. S. Barrett, L. Meyer, and J. Wasserman. J. Chem. Phys. **47**, 592 (1967).
10. B. R. Cairns and G. C. Pimentel. J. Chem. Phys. **43**, 3432 (1965).
11. M. J. Grogan and K. Nakamoto. J. Am. Chem. Soc. **90**, 918 (1968); **88**, 5454 (1966).
12. L. Andrews. J. Am. Chem. Soc. **90**, 7368 (1968); J. Chem. Phys. **50**, 4288 (1969); **53**, 3922 (1969); **54**, 4935 (1971); **57**, 1327 (1972).
13. F. A. Cotton and C. S. Kraihanzel. J. Am. Chem. Soc. **84**, 4432 (1962).
14. (*a*) N. W. Terry, E. L. Amma, and L. Vaska. J. Am. Chem. Soc. **94**, 653 (1972). (*b*) M. S. Weininger, I. F. Taylor, and E. L. Amma. Chem. Commun. 1172 (1971). (*c*) J. A. McGinnety, N. C. Payne, and J. A. Ibers. J. Am. Chem. Soc. **91**, 6301 (1969).
15. R. Mason. Nature, **217**, 543 (1968).
16. (*a*) J. Chatt. J. Chem. Soc. 2939 (1953). (*b*) M. J. S. Dewar. Bull. Soc. Chim. Fr. **18**, C71 (1951).
17. E. B. Wilson, J. C. Decius, and P. F. Cross. Molecular vibrations. McGraw-Hill Publishing Co., London. 1955.
18. H. Huber, E. P. Kündig, M. Moskovits, and G. A. Ozin. J. Am. Chem. Soc. **95**, 332 (1973).
19. J. H. Darling and J. S. Ogden. Inorg. Chem. **11**, 666 (1972).

Can. J. Chem. Downloaded from www.nrcresearchpress.com by 210.87.254.105 on 09/05/12
For personal use only.

Binary Mixed Dinitrogen–Carbonyl Complexes of Nickel(0), $Ni(N_2)_m(CO)_{4-m}$ (where $m = 1$–3)

E. P. KÜNDIG, M. MOSKOVITS, AND G. A. OZIN

Lash Miller Chemistry Laboratory, and Erindale College, University of Toronto, Toronto, Ontario

Received January 25, 1973

Nickel atoms have been cocondensed in various $^{12}C^{16}O/^{14}N_2$, $^{12}C^{16}O/^{14}N_2/Ar$, and $^{12}C^{18}O/^{14}N_2/^{15}N_2/Ar$ matrices and the infrared and Raman spectra of the products recorded at 4.2–10 °K. In addition to the infrared absorptions associated with the known compounds $Ni(N_2)_4$ and $Ni(CO)_4$, other NN and CO stretching modes are observed which can be ascribed to the mixed carbonyl–dinitrogen species $Ni(N_2)_m(CO)_{4-m}$ where $m = 1$–3. Confirmation of the molecular constitutions and vibrational assignments of the isolated species was obtained from (*a*) variable concentration experiments in which either N_2 or CO was arranged to be in excess, (*b*) diffusion controlled warm-up experiments in the range 10–35 °K, and (*c*) isotope substitution experiments using $^{14}N_2/^{15}N_2/^{12}C^{18}O/Ar$ matrices in which the total nitrogen to carbon monoxide ratio was varied. Cotton–Kraihanzel k_{CO} and k_{NN} force constants are computed for the mixed compounds $Ni(CO)_3(N_2)$, $Ni(CO)_2(N_2)_2$, and $Ni(CO)(N_2)_3$ and trends within the series are discussed in terms of the σ-donor and π-acceptor bonding properties of the N_2 and CO ligands. An analysis is presented in which the changes in the CO and N_2 bond stretching force constants in passing from $Ni(CO)_m$ to $Ni(CO)_m(N_2)_{4-m}$ and from $Ni(N_2)_{4-m}$ to $Ni(CO)_m(N_2)_{4-m}$ are related to the change in σ and π orbital populations. The results of that analysis indicate that CO is both a better σ donor and a better π acceptor than N_2. Integrated absorbances of the bands associated with the species $Ni(CO)_m(N_2)_{4-m}$ are measured and are used to compute ratios of the transition dipole moments $(\mu_{CO}')_m$ and $(\mu_{N_2}')_m$ for CO and N_2 respectively. The observed trends for $(\mu_{CO}')_m$ and $(\mu_{N_2}')_m$ as functions of m are found to be in keeping with the changes in the respective CO and N_2 π orbital populations.

On a étudié la cocondensation d'atomes de nickel dans plusieurs milieux $^{12}C^{16}O/^{14}N_2$, $^{12}C^{16}O/^{14}N_2/Ar$, et $^{12}C^{18}O/^{14}N_2/^{15}N_2/Ar$ et on a enregistré les spectres infrarouge et Raman des produits à 4.2–10 °K. En plus des absorptions infrarouges associées avec les composés connus $Ni(N_2)_4$ et $Ni(CO)_4$, d'autres modes d'élongation NN et CO, qui peuvent être associés aux espèces mixtes carbonyle-diazote $Ni(N_2)_m(CO)_{4-m}$ où $m = 1$–3, ont été observés. La confirmation des structures moléculaires ainsi que des attributions des vibrations pour les espèces isolées a été obtenue à partir des (*a*) expériences à concentration variable où soit N_2 soit CO était en excès (*b*) expériences de chauffage de 10–35 °K contrôlées par diffusion et (*c*) expérience de substitution isotopique en utilisant un milieu $^{14}N_2/^{15}N_2/^{12}C\ ^{18}O/Ar$ dans lequel on a changé le rapport entre l'azote total et le monoxyde de carbone. Les constantes de force Cotton–Kraihanzel K_{CO} et K_{NN} ont été calculées pour les composés mélangés $Ni(CO)_3(N_2)$, $Ni(CO)_2(N_2)_2$, et $Ni(CO)_2(N_2)_3$ et les tendances à l'intérieur de cette série sont discutées en termes des propriétés de liaisons, donneur et accepteur, des coordinats N_2 et CO. On présente une analyse dans laquelle les changements dans les constantes de force pour l'élongation des liens CO et N_2 lors du passage de $Ni(CO)_m$ à $Ni(CO)_m(N_2)_{4-m}$ et de $Ni(N_2)_{4-m}$ à $Ni(CO)_m(N_2)_{4-m}$ sont reliés au changement de population dans les orbitales σ et π. Les résultats de l'analyse ont montré que le CO est à la fois un meilleur σ-donneur et un meilleur π-accepteur que le N_2. Les absorbances intégrées des bandes associées aux espèces $Ni(CO)_m(N_2)_{4-m}$ ont été mesurées et ont été utilisées afin d'obtenir les rapports des moments dipolaires de transition $(\mu_{CO}')_m$ et $(\mu_{N_2}')_m$ pour CO et N_2 respectivement. La tendance observée pour $(\mu_{CO}')_m$ et $(\mu_{N_2}')_m$ en fonction de m sont, comme il est prouvé, en accord avec les changements des populations respectives de l'orbitale π du CO et du N_2. [Traduit par le journal]

Can. J. Chem., 51, 2737 (1973)

Introduction

Since the discovery that N_2 can form dinitrogen complexes which are isoelectronic and isostructural with CO in carbonyl complexes, there has been a great deal of literature written concerning the similarities and differences between N_2 and CO as neutral ligands (1–5). For example, despite the obvious greater stability of CO complexes over their N_2 analogs, one finds that the decrease in the former's force constant from that of free CO is always less than that of the latter. This has led some authors (6) to speculate that N_2 may be a better acceptor than CO. A variety of techniques has been used to determine the relative importance of σ and π bonding of coordinated CO and N_2 in analogous carbonyl and dinitrogen complexes.

For example, Chatt *et al.* (5) used ligand fre-

Can. J. Chem. Downloaded from www.nrcresearchpress.com by 210.87.254.6 on 09/05/12
For personal use only.

Can. J. Chem. Downloaded from www.nrcresearchpress.com by 210.87.254.6 on 09/05/12
For personal use only.

quency and bond stretching force constant shifts, Darensbourg (4) used infrared frequencies and absorption intensities, Bancroft *et al.* (2) used Mössbauer partial isomer shifts and partial quadrupole splittings, while Purcell (1) and Fenske and co-workers (3) used approximate molecular orbital calculations. The general consensus reached by most of these authors was that N_2 is weaker in both its σ-donor and its π-acceptor function in bonding to the metal, than is CO. Only in the case of Bancroft's Mössbauer data (for a series of low spin iron(II) complexes) and Fenske's theoretical studies was it possible to separate quantitatively the relative σ-donor and π-acceptor characteristics of N_2 relative to CO.

Obviously, a unique insight into this problem may be gained by studying the properties of complexes, where CO and N_2 are in direct competition with each other for bonding electrons. In this paper we discuss such a situation.

Transition metal atom vapors in their monatomic form are extremely reactive and are proving to be convenient starting materials for a wide variety of inorganic syntheses at cryogenic temperatures. This type of "synthesis with metal atoms" has been reviewed recently (7).

In a matrix infrared study involving the cocondensation of nickel atoms with dilute $^{12}C^{16}O$/Ar matrices DeKock (8) was able to assign the four carbonyl stretching modes associated with the compounds $Ni(CO)_m$ where $m = 1$–4.

Recently, we reported matrix infrared and Raman data for the products of the cocondensation reaction of nickel atoms with dilute $^{14}N_2$/Ar matrices (9) in which we were able to identify the binary nickel dinitrogen compounds $Ni(N_2)_m$ where $m = 1$–4 with end-on bonded dinitrogen (10), which are isostructural and isoelectronic withDeKock's binary nickel carbonyls, $Ni(CO)_m$. More recently still, Rest (11) reported the matrix synthesis of $Ni(CO)_3N_2$, by matrix u.v.-photolysis of $Ni(CO)_4$ in dilute N_2/Ar mixtures.

In this paper we are reporting infrared and Raman spectroscopic data for $Ni(CO)_m(N_2)_{4-m}$ where $m = 1$–3, formed in the cocondensation reaction of nickel atoms with CO/N_2 and CO/N_2/Ar matrices at 4.2–10 °K.

Experimental

Monatomic Ni vapor was generated by directly heating a thin (0.010 in.) ribbon filament of the metal with AC. The nickel (99.99%) was supplied by McKay Inc, New York. Research grade $^{14}N_2$ (99.99%), $^{12}C^{16}O$ (99.99%), and Ar (99.99%) were supplied by Prochem. Gas mixtures were prepared by conventional vacuum line techniques.

The furnace used for the evaporation of the metals has been described previously (12). The rate of metal atom depositions was continuously monitored using a quartz crystal microbalance (13). The deposition rate was set such that the probability that a metal atom had another metal atom as a nearest neighbor in either the N_2 or Ar f.c.c. lattice was approximately 1 in 10^3 assuming equal sticking coefficients for all species. Matrix gas flows, controlled by a calibrated micrometer needle valve, were usually in the range 2–8 mmol/h. In the infrared experiments matrices were deposited on a CsI window cooled to 10 °K by means of an Air Products Displex closed cycle helium refrigerator. Spectra were recorded on a Perkin Elmer 180 spectrophotometer. In the Raman experiments the matrices were deposited on a liquid helium cooled (4.2 °K) aluminum tip. Spectra were recorded on a Spex model 1401 Raman spectrophotometer using Carson argon ion 4800 and 5145 Å laser excitation.

Two different approaches were used to achieve the desired mixed carbonyl–dinitrogen complexes: (*i*) cocondensation of Ni atoms with CO/N_2/Ar mixtures (total CO/N_2:Ar = 1:10) at 4.2–10 °K which yields all of the lower coordination number, mixed species $Ni(CO)_x(N_2)_y$ where $x + y \leqslant 4$ followed by matrix annealing at 30–35 °K to yield the tetracoordinate species $Ni(CO)_m(N_2)_{4-m}$ or (*ii*) cocondensation of Ni atoms with the same CO/N_2/Ar mixtures but at approximately 30 °K. Method (*ii*) apparently yielded a thermodynamically equilibrated mixture since little change could be induced by further annealing while method (*i*) required prolonged annealing to achieve the same results.

As well as runs containing 1:1 mixtures of N_2/CO in argon, experiments were carried out with gas mixtures containing excess N_2, for example, CO/N_2/Ar = 1/9/20 at 4.2–10 °K followed by annealing to 30 °K. Under these conditions the species containing the greatest number of N_2 ligands were favored. (The stability of these complexes apparently increases with increasing number of CO ligands.) Prolonged warming to 30–35 °K caused these species to decline gradually in relative abundance. Experiments of this sort helped in assigning the observed absorptions to the various species in the matrix.

Two main types of runs were performed. The first used mixtures of $^{12}C^{16}O$ with $^{14}N_2$ with various amounts of argon. The second used $^{12}C^{18}O$ with $^{14}N_2/^{15}N_2$/Ar mixtures of various ratios. The data from the latter set of experiments were used to aid in the assignment, determine the stoichiometries and calculate the C.K. force constants of the products formed. In the matrix–Raman experiments, metal atoms were deposited into pure $^{12}C^{16}O/^{14}N_2$ mixtures containing excess $^{14}N_2$ to maximize the formation of the less stable dinitrogen species.

Results and Discussion

When Ni atoms were cocondensed with $^{12}C^{16}O$:$^{14}N_2$:Ar = 1:1:20 mixtures at 10 °K and then annealed at 30 °K, apart from the strong infrared absorption assigned to $^{12}C^{16}O$ (2138 cm^{-1}) and its weak $^{12}C^{18}O/^{13}C^{16}O$ (2090 cm^{-1}) isotopic counterpart and $Ni(^{12}C^{16}O)_4$ at

Can. J. Chem. Downloaded from www.nrcresearchpress.com by 210.87.254.6 on 09/05/12
For personal use only.

2048 cm^{-1}, five new absorptions were observed in the NN stretching region at 2269.6, 2264.4, 2257.6, 2240.0, and 2210.3 cm^{-1}, and five absorptions in the CO stretching region at 2100.6, 2084.3, 2029.4, 2005.0, and 1991.3 cm^{-1} (Figs. 1, 2).

A number of features of this spectrum are worth noting. First, the spectroscopic *absence* of $Ni(N_2)_m$ and $Ni(CO)_m$ where m = 1–3 but the *presence* of the more stable tetracarbonyl $Ni(CO)_4$ at 2049.7 cm^{-1} (T_2). Second, the much larger infrared absorption intensities of the new CO stretching modes compared to their NN counterpart stretching modes. Third, *all* of the new NN stretching modes shift to *higher* frequencies compared to $Ni(N_2)_4$ whereas *four* CO stretching modes shift to *lower* and *two* to *higher* frequencies compared to $Ni(CO)_4$. In addition to the strong carbonyl stretching modes below 2048 cm^{-1}, the much weaker and very sharp absorptions observed at about 2100.6 and 2084.3 cm^{-1} are tentatively assignable to totally symmetric CO stretching modes (of which the stronger carbonyl modes mentioned above are their asymmetric counterparts).

These preliminary data are qualitatively what one would expect for the formation of *three* new molecules $Ni(CO)_3(N_2)$, $Ni(CO)_2(N_2)_2$, and $Ni(CO)(N_2)_3$.

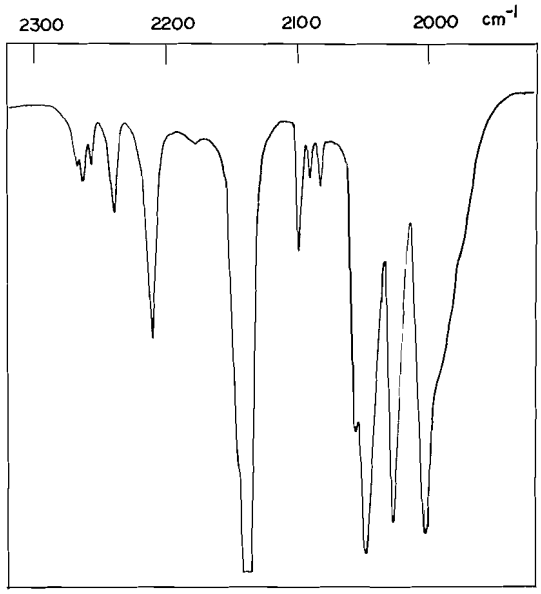

FIG. 1. The matrix infrared spectrum of the products of the cocondensation reaction of Ni atoms with $^{12}C^{16}O$: $^{14}N_2$:Ar = 1:1:20 mixture at 10 °K.

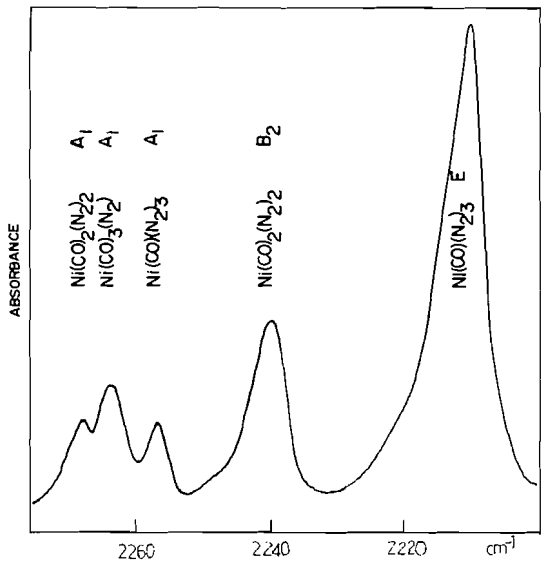

FIG. 2. The same as Fig. 1 but showing the νNN stretching region under conditions of high resolution with scale expansion.

Matrix Infrared Experiments

Monocarbonyl Trisdinitrogen Nickel(0), $Ni(CO)(N_2)_3$

When nickel atoms were cocondensed with $^{12}C^{16}O$:$^{14}N_2$:Ar = 1:9:20 at 10 °K and annealed at 30 °K, and the infrared spectrum compared to the 1:1:20 run described earlier (Fig. 1), it is apparent that higher dinitrogen species $Ni(N_2)_4$, $Ni(N_2)_3(CO)$ are being preferentially formed and one can assign the observed infrared lines shown below:

$Ni(N_2)_3(CO)$, (C_{3v}), ν_{A_1}CO, 2005.0 cm^{-1}; ν_ENN, 2210.3 cm^{-1}; ν_{A_1}NN, 2257.6 cm^{-1}.

$Ni(N_2)_4$, (T_d), ν_{T_2} NN 2173.0 cm^{-1} (9).

The observed $^{12}C^{18}O$ isotopic shift for $Ni(N_2)_3$-(CO) from 2005 to 1959 cm^{-1} is in excellent agreement with the calculated value (Tables 1, 2).

Using an isotopic mixture $^{12}C^{18}O$:$^{14}N_2$:$^{15}N_2$:Ar = 1:1:1:30 and experimental conditions similar to above, the multiplet structure of the NN stretching mode at 2210.3 cm^{-1} was carefully examined under conditions of high resolution (Fig. 3).

Four isotopic molecules for $Ni(N_2)_3(CO)$ are expected using $^{12}C^{18}O/^{14}N_2/^{15}N_2$/Ar isotopic mixtures as shown above. Because the ^{15}N isotopic shift for the E type infrared NN stretching mode of $Ni(N_2)_3(CO)$ is expected to be about

TABLE 1. Observed and calculated frequencies and observed integrated absorbances due to $Ni(CO)_m(N_2)_{4-m}$ (m = 1, 2, 3) obtained by cocondensing Ni atoms with $^{12}C^{16}O$ and $^{14}N_2$ in argon matrices

ν_{obsvd}	ν_{calcd}	A*	Mode	Assignment
2269.6	2268.0	0.393	νNN (A_1)	$Ni(CO)_2(N_2)_2$
2264.4	2264.3	0.622	νNN (A_1)	$Ni(CO)_3N_2$
2257.6	2257.7	0.227	νNN (A_1)	$NiCO(N_2)_3$
2240.0	2240.0	0.672	νNN (B_2)	$Ni(CO)_2(N_2)_2$
2210.3	2210.4	2.240	νNN (E)	$NiCO(N_2)_3$
2100.6	2100.6	0.629	νCO (A_1)	$Ni(CO)_3N_2$
2084.3	2086.2	0.230	νCO (A_1)	$Ni(CO)_2(N_2)_2$
2049.7 }		20.950	νCO (T_2)	$Ni(CO)_4$
2058.6 }				
2029.4	2030.6	8.950	νCO (E)	$Ni(CO)_3N_2$
2005.0	2005.9	11.280	νCO (A_1)	$NiCO(N_2)_3$
1991.3	1992.2	10.820	νCO (B_1)	$Ni(CO)_2(N_2)_2$

*Integrated absorbance (units cm^{-1}) = $\int \log (I_0/I)\, d\nu$. Where lines overlap, as for example those at 2269.6, 2264.4, and 2257.6, A was obtained by fitting Lorentz line shapes to the bands and integrating numerically.

TABLE 2. Observed and calculated frequencies due to $Ni(CO)_m(N_2)_{4-m}$ where m = 1, 2, 3 obtained by cocondensing Ni atoms with $^{12}C^{18}O$ and $^{14}N_2/^{15}N_2$ mixtures in argon matrices

ν_{obsvd}	ν_{calcd}	Assignment
2265br*	2268.0 }	(A_1) $Ni(C^{18}O)_2(^{14}N_2)_2$
	2264.3 }	(A_1) $Ni(C^{18}O)_3{}^{14}N_2$
	2257.7 }	(A_1) $Ni(C^{18}O)(^{14}N_2)_3$
2253	2255.6	(A') $Ni(C^{18}O)_2(^{14}N_2)(^{15}N_2)$
2246	2245.9	(A') $Ni(C^{18}O)(^{14}N_2)_2{}^{15}N_2$
2240	2239.1	(B_2) $Ni(C^{18}O)_2(^{14}N_2)_2$
2232	2232.1	(A') $Ni(C^{18}O)^{14}N_2(^{15}N_2)_2$
2211	2210.4	(E) $Ni(C^{18}O)(^{14}N_2)_3$, (A'') $Ni(C^{18}O)(^{14}N_2)_2{}^{15}N_2$
2191	2191.7	(A_2) $Ni(C^{18}O)_2(^{15}N_2)_2$, ($A_1$) $Ni(C^{18}O)_3{}^{15}N_2$
2174	2175.0	(A') $Ni(C^{18}O)_2{}^{14}N_2{}^{15}N_2$
2161	2163.2	(B_2) $Ni(C^{18}O)_2(^{15}N_2)_2$, ($A'$) $Ni(C^{18}O)(^{14}N_2)(^{15}N_2)_2$
2147	2146.6	(A') $Ni(C^{18}O)(^{14}N_2)_2{}^{15}N_2$
2138	2135.4	(A'') $Ni(C^{18}O)^{14}N_2(^{15}N_2)_2$, ($E$) $Ni(C^{18}O)(^{15}N_2)_3$ and $^{12}C^{16}O$†
2053		(T_2) $Ni(^{12}C^{16}O)_4$†
2046	2046.4	(A_1) $Ni(C^{18}O)_3(^{14}N_2)$, (A_1) $Ni(C^{18}O)_3(^{15}N_2)$
2031	2034.0 }	(A_1) $Ni(C^{18}O)_2(^{14}N_2)_2$, ($A'$) $Ni(C^{18}O)_2(^{14}N_2)(^{15}N_2)$
	}	(A_1) $Ni(C^{18}O)_2(^{15}N_2)_2$
1983	1981.7	(E) $Ni(C^{18}O)_3(^{14}N_2)$, (E) $Ni(C^{18}O)_3(^{15}N_2)$
1959	1958.0 }	(A') $Ni(C^{18}O)(^{14}N_2)_2(^{15}N_2)$
	1957.7 }	(A_1) $Ni(C^{18}O)(^{15}N_2)_3$, (A_1) $Ni(C^{18}O)(^{14}N_2)_3$
	1957.4 }	(A') $Ni(C^{18}O)(^{14}N_2)(^{15}N_2)_2$
1945	1944.2 }	(B_1) $Ni(C^{18}O)_2(^{14}N_2)_2$
	}	(A'') $Ni(C^{18}O)_2(^{14}N_2)(^{15}N_2)$
	}	(B_1) $Ni(C^{18}O)_2(^{15}N_2)_2$

*Broad band.
†7% $^{12}C^{16}O$ impurity in commercially available $^{12}C^{18}O$ (93%).

75 cm^{-1}, it is necessary to use $^{12}C^{18}O$ isotopic substitution to shift the interfering strong $^{12}C^{16}O$ absorption (2138–2148 cm^{-1}) also to lower wave numbers.

The expected $^{14}N_2/^{15}N_2$ multiplets for a tris-dinitrogen molecule (assuming C_{3v} symmetry) is then a *six*-line pattern (see for example the $^{14}N_2/^{15}N_2$ data for $Pd(N_2)_3$ (14)), that is, a triplet in the $^{14}N_2$ region and a triplet in the $^{15}N_2$ region. The $^{14}N_2$ triplet was resolved although the lowest component of the $^{15}N_2$ triplet expected at 2135 cm^{-1} was obscured by the 7% residual

Can. J. Chem. Downloaded from www.nrcresearchpress.com by 210.87.254.6 on 09/05/12
For personal use only.

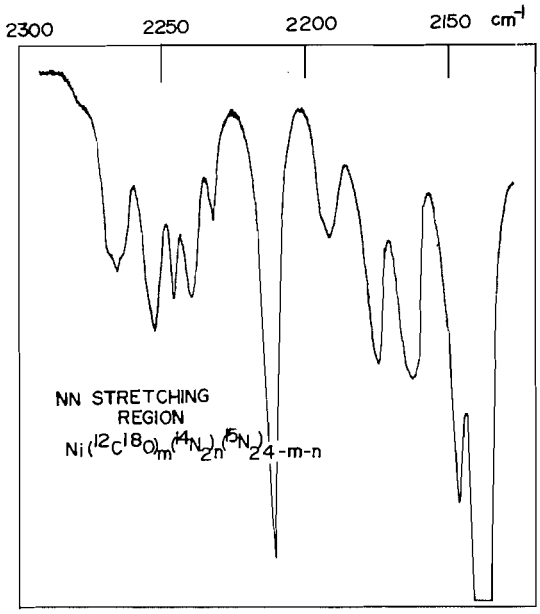

FIG. 3. The matrix infrared spectrum of the products of the cocondensation reaction of Ni atoms with $^{12}C^{18}O$: $^{14}N_2$:$^{15}N_2$:Ar = 1:1:1:30 showing the ^{14}N and ^{15}N isotope multiplet structure for the series of complexes $Ni(^{12}C^{18}O)_m(^{14}N_2)_n(^{15}N_2)_{4-n-m}$ (where m = 1–3 and n = 0–3).

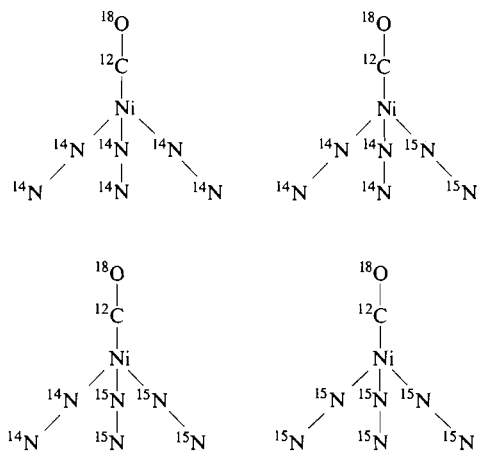

$^{12}C^{16}O$ in the isotopic $^{12}C^{18}O$ (see Table 2). These data serve to characterize $Ni(N_2)_3(CO)$ and place the ligand assignments on a firm basis.

It is interesting to note that prolonged warm-up of the species $Ni(N_2)_4$ and $Ni(N_2)_3CO$ in the presence of CO caused a decrease in intensity of the absorptions associated with these species, whereas the other absorptions presumably belonging to $Ni(CO)_2(N_2)_2$ and $Ni(CO)_3(N_2)$ were affected to only a minor extent. This would again indicate that the higher carbonyl species are more stable than the higher dinitrogen species.

Tricarbonyl Monodinitrogen Nickel(0) and Dicarbonyl Bisdinitrogen Nickel(0), $Ni(CO)_3(N_2)$ and $Ni(CO)_2(N_2)_2$

When Ni atoms were cocondensed with either $^{12}C^{16}O$:$^{14}N_2$:Ar = 1:1:20 or 9:1:20 at 10 °K and annealed at 30 °K, the absorptions associated with higher carbonyl species were always predominant compared to the analogous dinitrogen species. Examination of the infrared spectra shows the absence of $Ni(N_2)_4$ and very little $Ni(CO)(N_2)_3$ but the presence of considerable quantities of $Ni(CO)_4$, $Ni(CO)_3(N_2)$, and $Ni(CO)_2(N_2)_2$.

The distribution of absorption intensities under these conditions supports our initial tentative assignments of $Ni(CO)_3(N_2)$ and $Ni(CO)_2(N_2)_2$ as follows: $^{12}C^{16}O$:$^{14}N_2$:Ar = 1:1:20 or 9:1:20:

$Ni(^{12}C^{16}O)_3(^{14}N_2)$, (C_{3v}), ν_{A_1}NN, 2264.4 cm^{-1}; ν_{A_1}CO, 2100.6 cm^{-1}; ν_ECO, 2029.4 cm^{-1}.

$Ni(^{12}C^{16}O)_2(^{14}N_2)_2$, (C_{2v}), ν_{A_1}NN, 2269.6 cm^{-1}; ν_{B_2}NN, 2240.0 cm^{-1}; ν_{A_1}CO, 2084.3 cm^{-1}; ν_{B_1}CO, 1991.3 cm^{-1}.

The observed $^{12}C^{18}O$ isotopic shifts for $Ni(^{12}C^{18}O)_3(^{14}N_2)$ and $Ni(^{12}C^{18}O)_2(^{14}N_2)_2$ are in excellent agreement with the calculated values (see Tables 1, 2).

Using experimental conditions similar to the above, we cocondensed Ni atoms with $^{12}C^{18}O$: $^{14}N_2$:$^{15}N_2$:Ar = 1:1:1:30 mixtures in order to determine the multiplet structure of the NN stretching modes which we have assigned to $Ni(CO)_3(N_2)$ and $Ni(CO)_2(N_2)_2$. Two C_{3v} isotopic molecules are expected (shown below) for $Ni(CO)_3(N_2)$

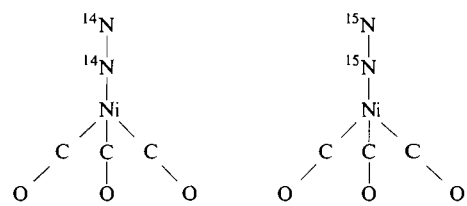

using $^{14}N_2/^{15}N_2$ mixed isotopes which should yield a *single* NN stretching mode in the $^{14}N_2$ region and a *single* $^{15}N_2$ counterpart mode shifted by approximately 73 cm^{-1} to lower frequencies.

Can. J. Chem. Downloaded from www.nrcresearchpress.com by 210.87.254.6 on 09/05/12
For personal use only.

Can. J. Chem. Downloaded from www.nrcresearchpress.com by 210.87.254.6 on 09/05/12
For personal use only.

A doublet is observed at 2265 and 2191 cm^{-1} consistent with this prediction and serves to characterize the monodinitrogen-tricarbonyl molecule, $Ni(CO)_3(N_2)$. These vibrational assignments are in excellent agreement with those recently reported by Rest (11) for $Ni(CO)_3(N_2)$ produced in the matrix u.v. photolysis of $Ni(CO)_4$ isolated in dilute N_2/Ar matrices at 17 °K.

In this context, it seems reasonable to assign some disturbingly intense infrared absorptions in the 2100–2000 cm^{-1} region, which were not accounted for in DeKock's (8) $Ni(CO)_m$ study, to the mixed complex $Ni(CO)_3(N_2)$ presumably formed from "trace nitrogen impurities" in the CO/Ar mixtures or cryopumped onto the central cold plate during the matrix isolation experiment.

Having satisfactorily identified the NN and CO stretching modes belonging to $Ni(CO)_3(N_2)$ and $Ni(CO)(N_2)_3$, it remains to confirm that the observed infrared absorptions at 2269.6, 2240.0, 2084.3, and 1991.3 cm^{-1} belong to the dicarbonyl–bisdinitrogen complex $Ni(CO)_2(N_2)_2$.

Three isotopic molecules are expected for $Ni(CO)_2(N_2)_2$ using $^{12}C^{18}O$ and $^{14}N_2/^{15}N_2$ mixtures:

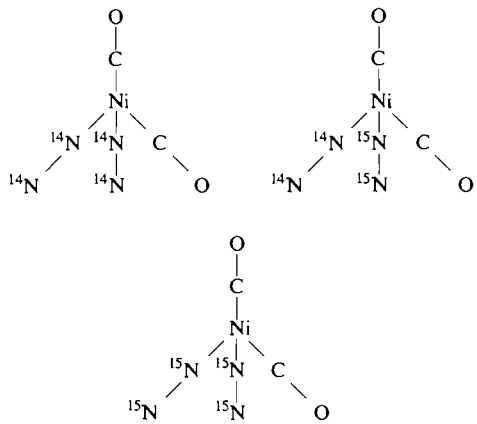

which should yield a *triplet* pattern in the $^{14}N_2$ region and a similar *triplet* pattern, shifted to lower frequencies by about 75 cm^{-1}, in the $^{15}N_2$ region.

This doublet of triplets multiplet structure was observed at 2265, 2253, 2240 and 2191, 2174, 2161 cm^{-1} (Tables 1, 2) and adequately serves to characterize the dicarbonyl-bisdinitrogen molecule, $Ni(CO)_2(N_2)_2$.

Matrix Isolation Laser Raman Experiments

Although we have been able to obtain high quality matrix Raman spectra for $Ni(N_2)_4$ in Ar (9), the analogous measurements for the mixed species $Ni(CO)_m(N_2)_{4-m}$ in Ar proved to be considerably more difficult primarily because of laser absorption throughout the visible range 4880–6471 Å and subsequent local heating of the matrix leading to decomposition.

This local heating effect by the laser beam was minimized by using extremely low power laser excitation. Reasonable quality Raman spectra could be obtained by cocondensing Ni atoms with $^{12}C^{16}O$:$^{14}N_2$ = 1:3 mixtures at 25–30 °K (see Fig. 3). The results showed that all of the molecules $Ni(CO)_m(N_2)_{4-m}$ were present under these conditions in comparable proportions. (In agreement with pure $^{12}C^{16}O$:$^{14}N_2$ = 1:1 matrix infrared experiments, our analogous 1:1 Raman experiments show predominantly $Ni(CO)_4$ and only minute quantities of the mixed carbonyl–dinitrogen species.)

The Raman data for the 1:3 mixture shown in Fig. 4, apart from the intense lines due to $^{12}C^{16}O$ (2138 cm^{-1}) and $^{14}N_2$ (2328 cm^{-1}) and much less intense lines due to natural abundance isotopes $^{12}C^{18}O$, $^{13}C^{16}O$ and $^{14}N^{15}N$, show weak lines at 2266, 2242, 2112, 2173 cm^{-1} assignable to NN stretching modes and 2098, 2076, 2048, 2026, 2002, 1996 cm^{-1} assignable to CO stretching modes of $Ni(CO)_m(N_2)_{4-m}$.

The correlation between the matrix Raman and matrix infrared data is excellent for the lines which are expected to show coincidences (that is, matrix shifts observed on passing from pure

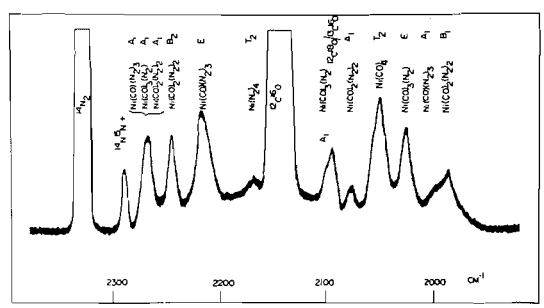

FIG. 4. The matrix Raman spectrum of the products of the cocondensation reaction of Ni atoms with $^{12}C^{16}O$:$^{14}N_2$ = 1:3 at 25–30 °K (spectrum recorded at 4.2 °K) showing all of the species $Ni(^{12}C^{16}O)_m(^{14}N_2)_{4-m}$ (where m = 0–4).

TABLE 3. Calculated Cotton–Kraihanzel force constants for $Ni(CO)_m(N_2)_{4-m}$ ($m = 1, 2, 3$)

	f				
Molecule	CO	NN	CO,CO	NN,NN	CO,NN
$Ni(CO)(N_2)_3$	16.2903	20.4149		0.2758	0.2511
$Ni(CO)_2(N_2)_2$	16.8220	20.8951	0.7968	0.2289	0.2494
$Ni(CO)_3N_2$	17.1851	20.6862	0.5351		0.6040

CO/N_2 matrices to CO/N_2:Ar = 1:10 matrices are within ± 4 cm^{-1}).

Frequency and Cotton–Kraihanzel Force Constant Calculations for Isotopically Substituted $Ni(CO)_m(N_2)_{4-m}$

We have reported previously (9) that the Cotton–Kraihanzel force field approximation (15) applied usually to carbonyls is also successful in predicting NN stretch frequencies of binary dinitrogen complexes. We therefore use this approximation in calculating the force constants for the mixed carbonyl–dinitrogen complexes $Ni(CO)_m(N_2)_{4-m}$ assuming end-on bonded ligands and symmetries as shown below.

Molecule	Symmetry	ν_{NN}	ν_{CO}
$Ni(CO)(N_2)_3$	C_{3v}	A_1+E	A_1
$Ni(CO)_2(N_2)_2$	C_{2v}	A_1+B_2	A_1+B_1
$Ni(CO)_3(N_2)$	C_{3v}	A_1	A_1+E

The best values of the force constants for each of the three molecules $Ni(CO)_m(N_2)_{4-m}$ were obtained by a least squares fit. All reasonable assignments of the various lines among the three molecules were attempted. Those reported give by a substantial margin the best fit. It is gratifying that the assignment which gave the best fit is also that deemed most likely on the basis of matrix experiments containing either excess N_2 or CO. Calculated frequencies based on these force constants are listed in Tables 1 and 2. The values of the calculated force constants are listed in Table 3. These data are also plotted in Fig. 5 together with the corresponding data for $Ni(CO)_m$ and $Ni(N_2)_m$ where $m = 1 \rightarrow 4$.

The trends in the computed force constants illustrated in Fig. 5 are noteworthy. In particular one notes that the NN stretching force constant for $Ni(CO)_2(N_2)_2$ is larger than that of the other two mixed carbonyl dinitrogen species.

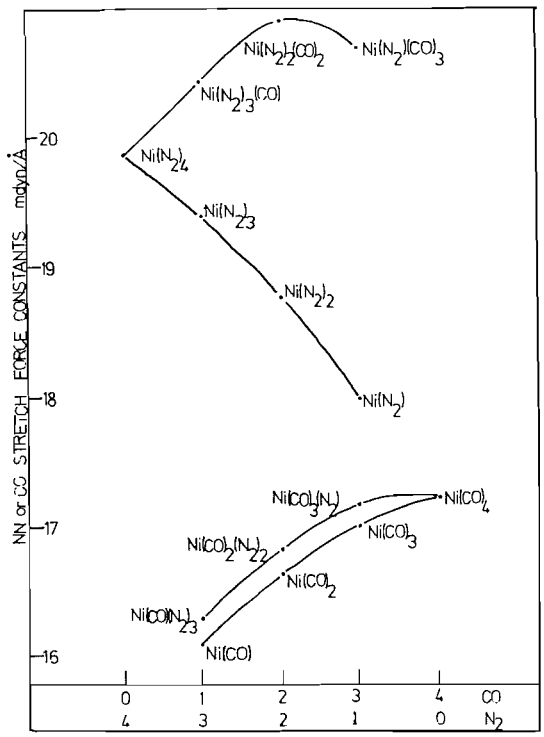

FIG. 5. Graphical plot of the NN and CO Cotton–Kraihanzel bond stretching force constants for the species $Ni(CO)_m(N_2)_{4-m}$, $Ni(CO)_m$ and $Ni(N_2)_m$ (where $m = 1$–4) as a function of m.

These observations are discussed in the next section.

The Relative Donor and Acceptor Properties of CO and N_2

Despite the fact that the relative donor and acceptor properties of ligands have been discussed widely in the current literature, these quantities are seldom rigorously defined. Accordingly for the purpose of the subsequent discussion we define the basicity and acidity of a ligand as follows.

Can. J. Chem. Downloaded from www.nrcresearchpress.com by 210.87.254.6 on 09/05/12
For personal use only.

Can. J. Chem. Downloaded from www.nrcresearchpress.com by 210.87.254.6 on 09/05/12
For personal use only.

We assume that one can define a donor orbital and an acceptor orbital for the free ligand. For example, in CO the 5σ orbital of the free CO is the donor orbital and the 2π is the acceptor orbital; while in free N_2 the correct donor orbital is not $3\sigma_g$ but rather, following Fenske's notation (3), $\theta_5 = (1/\sqrt{2})(2\sigma_u + 3\sigma_g)$ which is centered on the N atom about to bond to the metal. Thus although more than one orbital is involved in the donation, one can form a linear combination of these, thereby defining a single "donor orbital". The proper acceptor orbital of N_2 is $1\pi_g$.

After the ligand bonds one can, in principle, express the ligand's charge distribution in a basis of the *free* ligand *molecular* orbitals; in this manner the σ donor ability of the ligand is defined by $n_\sigma^0 - n_\sigma$ where n_σ^0 is the σ-orbital occupation of the free ligand ($n_\sigma^0 = 2$ in the case of CO and N_2), while n_σ is the σ-orbital occupation of the bonded ligand.

Similarly the acceptor ability of the ligand is defined by $n_\pi - n_\pi^0$ where n_π^0 and n_π have analogous definitions ($n_\pi^0 = 0$ in CO and N_2). For simplicity we write

$$\sigma = n_\sigma^0 - n_\sigma$$

and

$$\pi = n_\pi - n_\pi^0$$

and we say that ligand L_1 is a better σ-donor (base) towards a particular metal atom or ion than ligand L_2 if $\sigma_1 > \sigma_2$ with a similar definition existing for relative π-acceptor ability (acidity).

Turning our attention specifically to the $Ni(CO)_m(N_2)_{4-m}$ case, we assume (in an analogous fashion to Fenske and co-worker (16)) that the CO bond stretching force constant in the above series of compounds may be written

$$f_m^{CO} = an_{\sigma m}^{CO} + bn_{\pi m}^{CO} + c$$

This equation can be rewritten as

$$[1] \qquad f_m^{CO} = d - a\sigma_m^{CO} + b\pi_m^{CO}$$

where $d = 2a + c$. We also assume that an identical equation holds for the CO stretch force constants K_m^{CO} of the series of binary carbonyls $Ni(CO)_m$, namely

$$[2] \qquad K_m^{CO} = d - a\sigma_m^{CO'} + b\pi_m^{CO'}$$

where the prime distinguishes the orbital populations in the $Ni(CO)_m$ case from that of $Ni(CO)_m(N_2)_{4-m}$. So that

$$[3] \quad f_{4-m}^{N_2} = d' - a'\sigma_{4-m}^{N_2} + b'\pi_{4-m}^{N_2}$$

and

$$[4] \quad K_{4-m}^{N_2} = d' - a'\sigma_{4-m}^{N_2'} + b'\pi_{4-m}^{N_2'}$$

Now if eq. 1 is assumed to hold for free CO and free CO^+, the quantity a would be given by

$$a = K_{CO} - K_{CO^+}$$

where K_{CO} and K_{CO^+} are, respectively, the bond stretching force constants of CO and CO^+. Similarly a' would be given by

$$a' = K_{N_2} - K_{N_2^+}$$

with analogous definitions for K_{N_2} and $K_{N_2^+}$. It is unlikely that this should be exactly the case; nevertheless one might at least expect the signs of a and a' to be correctly given by the above equations. Thus a is a negative quantity while a' is a positive quantity.[1] At the same time one expects both b and b' to be negative quantities implying the generally accepted fact that the ligand force constant decreases as the π overlap increases. Accordingly eqs. 1 and 3 will take the forms

$$[5] \qquad f_m^{CO} = d + |a|(\sigma_m^{CO} - \gamma\pi_m^{CO})$$

and

$$[6] \quad f_{4-m}^{N_2} = d' - a'(\sigma_{4-m}^{N_2} + \gamma'\pi_{4-m}^{N_2})$$

respectively, where γ and γ' are, respectively, $|b/a|$ and $|b'/a'|$. Similar equations hold for K_m^{CO} and $K_{4-m}^{N_2}$.

It is evident therefore that the force constants of bonded CO depend on a $(\sigma - \pi)$-like term while those of bonded N_2 on a $(\sigma + \pi)$-like term. This explains to some extent the greater decrease in the NN stretching frequencies (from that of the free ligand) observed in N_2 complexes than the corresponding decrease in the CO stretch force constant in the analogous carbonyls.

The data shown in Fig. 5 indicate that the CO stretch force constants for the species $Ni(CO)_m(N_2)_{4-m}$ are increased only *slightly* from those of the analogous $Ni(CO)_m$ complexes, while the NN stretch force constants are *markedly* in-

[1] $K_{CO} = 18.46$, $K_{CO^+} = 19.26$, $K_{N_2} = 22.37$, $K_{N_2^+} = 19.50$ mdyn/Å. These quantities were calculated from observed vibrational frequencies reported by Herzberg (17).

Can. J. Chem. Downloaded from www.nrcresearchpress.com by 210.87.254.6 on 09/05/12
For personal use only.

creased in the former species from those of the analogous $Ni(N_2)_{4-m}$ complexes. Furthermore, the NN stretch force constants for the $Ni(CO)_m(N_2)_{4-m}$ molecules are in every case *larger* than $K_4^{N_2}$, *i.e.*, that of $Ni(N_2)_4$, while the CO stretching force constant in the $Ni(CO)_m(N_2)_{4-m}$ molecules are in every case *smaller* than K_4^{CO}, *i.e.*, that of $Ni(CO)_4$. This implies (see eqs. 5 and 6) that the addition of $(4-m)$ N_2's to $Ni(CO)_m$ to form $Ni(CO)_m(N_2)_{4-m}$ causes the quantity $(\sigma^{CO} - \gamma\pi^{CO})$ to increase less than it does on adding $(4-m)$ CO's to form $Ni(CO)_4$; while on adding m CO's to $Ni(N_2)_{4-m}$ to form $Ni(CO)_m(N_2)_{4-m}$ the quantity $-(\sigma^{N_2} + \gamma'\pi^{N_2})$ increases more than it does on adding m N_2's to form $Ni(N_2)_4$. An analysis of the nine different possibilities[2] regarding the relative σ-donor, π-acceptor properties of the two ligands indicates that these trends are only consistent with CO's being a better acceptor than N_2. Furthermore, the fact that $f_{4-m}^{N_2} > K_{4-m}^{N_2}$ while $f_m^{CO} \simeq K_m^{CO}$ implies that in the former case there is both a large σ change and a large π change while in the latter case both σ and π changes are small. Hence CO is a better σ donor than N_2 or at least equal to it.

Turning our attention to the apparently anomalous value of $f_1^{N_2}$, we find that this too is a result of the better acceptor ability of CO over that of N_2. As one proceeds from $Ni(CO)_3N_2$ to $Ni(CO)(N_2)_3$ (*i.e.*, as $4-m$ increases), $\pi_{4-m}^{N_2}$ is expected to *increase* due to decrease in the number of CO's. (This is opposite to the trend one expects in $Ni(N_2)_m$ where there are no CO's to compete for the back donated electrons.) At the same time the presence of CO's on the Ni makes the metal more acidic, thereby increasing σ donation by the N_2's. Thus reducing the number of CO's *reduces* $\sigma_{4-m}^{N_2}$. The quantity $\sigma_{4-m}^{N_2} + \gamma'_{4-m}{}^{N_2}$ would therefore have a minimum, and $f_{4-m}^{N_2}$ a maximum, when the slope of $\sigma_{4-m}^{N_2}$ *vs.* $4-m$ is equal but opposite in sign to the slope of $\pi_{4-m}^{N_2}$ *vs.* $4-m$. A maximum is, in fact, observed for $f_2^{N_2}$ $(Ni(CO)_2(N_2)_2)$.

Infrared Intensities

Darensbourg (4) has attempted in several publications to relate the integrated infrared absorption intensities of bonded CO and N_2 to the π electronic charge transfer from the metal to the ligand. He has shown, for instance, that the absorbance due to the NN vibration correlates with its stretching frequency in a series of related dinitrogen complexes. This correlation indicates in fact that the transition dipole depends on both the σ as well as the π overlap.

We have measured the integrated absorbance of the bands associated with the species $Ni(CO)_m(N_2)_{4-m}$ (where bands overlapped, the individual components were obtained by means of a Lorentz line shape fit), but because the concentration of these species in the matrix is not known accurately, only ratios $(\mu_{CO}'/\mu_{N_2}')_m$, where μ_{CO}' and μ_{N_2}' are the transition dipole moments of the CO and N_2 ligand within the molecule $Ni(CO)_m(N_2)_{4-m}$, could be calculated.

The quantity μ_{CO}'/μ_{N_2}' was obtained from the relations

$$[7] \qquad \sum I_m = c_m \sum_{k'k''} \frac{\partial \boldsymbol{\mu}}{\partial S_{k'}} \cdot \frac{\partial \boldsymbol{\mu}}{\partial S_{k''}} G_{k'k''}$$

where c_m is an unknown constant proportional to the concentration of $Ni(CO)_m(N_2)_{4-m}$, and the other quantities are defined in ref. 4.

After obtaining μ_{CO}'/μ_{N_2}' one can substitute back into [7] and obtain $c_m\mu_{CO}'^2$ and $c_m\mu_{N_2}'^2$. All of these quantities are listed in Table 4. It is noteworthy that both $c_m\mu_{CO}'^2$ and $c_m\mu_{N_2}'^2$ *decrease* with *increasing m*.

Although the values c_m are not known one expects c_m to *decrease* as *m decreases*, thus, if anything μ_{CO}' and μ_{N_2}' both *increase* even more rapidly than indicated in Table 4 with decreasing number of CO's. This observation is in fact easily understandable. The decrease in μ_{CO}' with increasing number of CO ligands may be given the conventional explanation that the back-donated electrons must be shared by more CO's as the number of CO's increases, hence the π overlap population to an individual CO decreases, while the increase in μ_{N_2}' with increasing number of N_2's is explained by assuming that the number

TABLE 4. Calculated μ_{CO}'/μ_{N_2}' values for the molecules $Ni(CO)_m(N_2)_{4-m}$

m	Molecule	μ_{CO}'/μ_{N_2}'	$c_m\mu_{CO}'^2$	$c_m\mu_{N_2}'^2$
1	$NiCO(N_2)_3$	3.60	76.9	5.94
2	$Ni(CO)_2(N_2)_2$	3.97	55.7	3.53
3	$Ni(CO)_3N_2$	4.34	22.8	1.21

[2]These are: CO is an equal donor and an equal acceptor, an equal donor and a better acceptor, an equal donor and a worse acceptor, a better donor and an equal acceptor, a better donor and a better acceptor, a better donor and a worse acceptor, etc. than N_2.

of CO's present in the molecule determines the quantity of charge available for backbonding to the dinitrogens; this being a direct result of the fact that CO is a much better acceptor than N_2.

These observations are therefore in keeping with the view (4) that the transition dipole associated with the vibration of a ligand like CO or N_2 increases with increasing π overlap in a series of related compounds, here $Ni(CO)_m(N_2)_{4-m}$.

It should be pointed out that this observation does not preclude a dependence of μ_{CO}' or μ_{N_2}' on the σ-donor population as well as the π but rather it reflects the fact that in the $Ni(CO)_m(N_2)_{4-m}$ series, it is mainly the π overlap which changes as m varies.

Summary

Using the combined techniques of matrix infrared and Raman spectroscopy and isotope substitution we have been able to characterize for the first time the binary mixed dinitrogen–carbonyl complexes of nickel, $Ni(CO)_m(N_2)_{4-m}$ (where m = 1–3), formed in the cocondensation reaction of Ni atoms with $CO/N_2/Ar$ mixtures at 4.2–40 °K. The vibrational data for these complexes, when taken in conjunction with the data for the binary dinitrogen and carbonyl complexes $Ni(N_2)_m$ and $Ni(CO)_m$ (where m = 1–4) have proven to be of considerable value in shedding new light on the bonding properties of N_2 and CO in the unique situation, when bonded to the same metal atom and thereby competing for the same bonding electrons.

An analysis has been presented for the series of complexes $Ni(CO)_m(N_2)_{4-m}$ which attempts to correlate the changes in the C.K. CO and N_2 force constants with the respective changes in the σ and π orbital populations. With this type of approach, it has proven possible to effect a qualitative separation of the relative σ-donor and π-acceptor properties of the two ligands where the conclusions are found to be in agreement with those reported independently by Chatt *et al.* (5), Darensbourg (4), Bancroft *et al.* (2), and Fenske and co-workers (3), that is, CO is both a better σ-donor and a better π-acceptor than N_2.

We wish to thank Mr. Ted Huber for valuable technical assistance and the National Research Council of Canada, the Research Corporation, and Erindale College for financial assistance.

1. K. F. PURCELL. Inorg. Chim. Acta, **3**, 540 (1969).
2. G. M. BANCROFT, R. E. GARROD, A. G. MADDOCK, M. J. MAYS, and B. E. PRATER. J. Am. Chem. Soc. **94**, 647 (1972).
3. K. G. CAULTON, R. L. DEKOCK, and R. F. FENSKE. J. Am. Chem. Soc. **92**, 515 (1970).
4. D. J. DARENSBOURG. Inorg. Chem. **11**, 1436 (1972), **10**, 2399 (1971).
5. J. CHATT, D. P. MELVILLE, and R. L. RICHARDS. J. Chem. Soc. A, 2841 (1969).
6. J. P. COLLMAN, M. KUBOTA, F. D. VASTINE, J. Y. SUN, and J. W. KANG. J. Am. Chem. Soc. **90**, 5430 (1968).
7. G. A. OZIN and A. VANDER VOET. Acc. Chem. Res. In press.
8. R. L. DEKOCK. Inorg. Chem. **10**, 1205 (1971).
9. H. HUBER, E. P. KÜNDIG, M. MOSKOVITS, and G. A. OZIN. J. Am. Chem. Soc. **94**, 332 (1973).
10. M. MOSKOVITS and G. A. OZIN. J. Chem. Phys. In press.
11. A. J. REST. J. Organomet. Chem. **40**, C76 (1972).
12. E. P. KÜNDIG, M. MOSKOVITS, and G. A. OZIN. J. Mol. Struct. **14**, 137 (1972).
13. M. MOSKOVITS and G. A. OZIN. J. Appl. Spectrosc. **26**, 481 (1972).
14. H. HUBER, E. P. KÜNDIG, M. MOSKOVITS, and G. A. OZIN. Can. J. Chem. **50**, 2385 (1972).
15. F. A. COTTON and C. S. KRAIHANZEL. J. Am. Chem. Soc. **84**, 4432 (1962).
16. M. B. HALL and R. F. FENSKE. Inorg. Chem. **11**, 1619 (1972).
17. G. HERZBERG. Spectra of diatomic molecules. Van Nostrand Co. Inc., New York. 1964.

Can. J. Chem. Downloaded from www.nrcresearchpress.com by 210.87.254.6 on 09/05/12
For personal use only.

Transport Numbers for Hydrochloric Acid at Elevated Temperatures

DIGBY D. MACDONALD[1,2] AND D. OWEN

Research Chemistry Branch, Whiteshell Nuclear Research Establishment, Atomic Energy of Canada Limited, Pinawa, Manitoba R0E 1L0

Received December 15, 1972

Transport numbers for H^+ and Cl^- have been measured as a function of concentration and temperature to 200 °C using electrolyte concentratio. ells. The infinite dilution transport number for H^+ decreases with temperature while that for Cl^- increases. This temperature dependence is discussed in terms of thermal destruction of the three dimensional structure of liquid water.

Les nombres de transport pour H^+ et Cl^- ont été déterminés en fonction de la concentration et de la température jusqu'à 200 °C en utilisant des cellules de concentration en électrolytes. Le nombre de transport à la dilution infinie pour H^+ décroît avec la température alors que celui de Cl^- croît. La discussion de cette dépendance vis à vis de la température a porté sur la destruction thermique de la structure tridimensionnelle de l'eau liquide. [Traduit par le journal]

Can. J. Chem., **51**, 2747 (1973)

Can. J. Chem. Downloaded from www.nrcresearchpress.com by 210.87.254.5 on 09/05/12
For personal use only.

A fundamental electrochemical property of an ion in solution is its transport number, *i.e.* the fraction of the total current carried by the ion under electrolysis. The experimental techniques used to derive transport numbers for ions at room temperature have been well reviewed by Robinson and Stokes (1), but little work has been reported on extending these techniques to higher temperatures. In this paper we describe the use of electrolyte concentration cells with and without liquid junction to determine the transport numbers of H^+ and Cl^- ions in hydrochloric acid at temperatures to 200 °C. Smith and Dismukes (2) have previously measured transport numbers in 0.1 mol/l KCl and NaCl solutions at temperatures to 125 °C using the moving boundary technique. Quist and Marshall (3) extrapolated these data to 400 °C to calculate limiting equivalent conductances for the single ions Na^+, H^+, K^+, NH_4^+, Li^+, Cl^-, and OH^- over the same temperature range.

The two compartment high temperature concentration cell with liquid junction [I] has been described elsewhere (4) and is similar in design to that used by Mesmer, Baes, and Sweeton (5) for high temperature acidity measurements in aqueous systems

$$[I] \qquad Pt,H_2 \left| \begin{matrix} H^+Cl^- \\ (m_1) \end{matrix} \right. \vdots \left. \begin{matrix} H^+Cl^- \\ (m_2) \end{matrix} \right| H_2,Pt$$

The concentric compartments contained lightly platinized platinum tube electrodes which also served as thermocouple wells for temperature measurement. The solutions in the two compartments were agitated by Teflon covered magnetic stirring bars which were activated by a rotating magnet located beneath the aluminum oil bath used for temperature control. Electrolytic contact between the two compartments was maintained through a porous (10 μm pore) Teflon disc. All potential measurements were made using a Beckman Research p*H* meter. A typical experiment consisted of loading cell I with the appropriate solutions ($m_1 = 0.10$, $m_2 = 1.00$, 0.50, 0.10, and 0.05 mol/kg), degassing followed by pressurization with hydrogen gas to 0.3 MN/m^2 and then heating the cell in steps of 10–15 °C up to 200 °C. Potentials (E_T) were measured after thermal equilibrium had been achieved and recorded after they had become sensibly constant (change <0.1 mV/h). The measured potentials are listed in Table 1 and were reproducible to about ± 0.2 mV as determined by triplicate experiments.

Potentials (E) for the concentration cell without liquid junction, [II],

$$[II] \qquad Pt,H_2 \left| \begin{matrix} H^+Cl^-, [AgCl] \\ (m_1) \end{matrix} \right| Ag \left| \begin{matrix} [AgCl], H^+Cl^- \\ (m_2) \end{matrix} \right| H_2,Pt$$

were calculated from the data of Greeley *et al.* (6) for the cell $Pt,H_2|H^+Cl^-$, [AgCl]|Ag at elevated temperatures and are listed in Table 1. The polynomial [1] was fitted to the potential data for cells I and II

$$[1] \qquad E_T = C_0 + C_1E + C_2E^2$$

[1]To whom correspondence should be addressed.

[2]Present address: Department of Chemistry, Victoria University of Wellington, Wellington, New Zealand.

TABLE 1. Potentials for cells I and II and transport numbers for H^+ and Cl^- as a function of m_2 and temperature

T (°C)	m_2 (mol kg^{-1})	E_T (V)	E^* (V)	t_{Cl^-}	t_{H^+}
25	1.000	0.0191	0.1189	0.151	0.849
	0.500	0.0133	0.0798	0.157	0.843
	0.100	0.0000	0.0000	0.169	0.831
	0.050	−0.0055	−0.0335	0.174	0.826
60	1.000	0.0256	0.1311	0.196	0.804
	0.500	0.0172	0.0889	0.196	0.804
	0.100	0.0000	0.0000	0.195	0.805
	0.050	−0.0073	−0.0367	0.195	0.805
90	1.000	0.0307	0.1403	0.218	0.782
	0.500	0.0208	0.0953	0.219	0.781
	0.100	0.0000	0.0000	0.220	0.780
	0.050	−0.0088	−0.0395	0.221	0.779
125	1.000	0.0366	0.1498	0.240	0.760
	0.500	0.0251	0.1027	0.243	0.757
	0.100	0.0000	0.0000	0.249	0.751
	0.050	−0.0109	−0.0431	0.251	0.749
150	1.000	0.0407	0.1564	0.254	0.746
	0.500	0.0280	0.1077	0.258	0.742
	0.100	0.0000	0.0000	0.267	0.732
	0.050	−0.0123	−0.0448	0.271	0.729
175	1.000	0.0445	0.1614	0.266	0.734
	0.500	0.0308	0.1109	0.272	0.728
	0.100	0.0000	0.0000	0.286	0.714
	0.050	−0.0138	−0.0473	0.292	0.708
200	1.000	0.0477	0.1661	0.285	0.715
	0.500	0.0339	0.1205	0.287	0.713
	0.100	0.0000	0.0000	0.292	0.708
	0.050	−0.0150	−0.0488	0.294	0.706

*Interpolated from the data of Greeley *et al.* (6).

by a least squares technique at each temperature. The coefficients in eq. 1 and the associated standard deviations obtained by this procedure are listed in Table 2 for various temperatures between 25 and 200 °C.

Transport numbers for chloride ion, t_{Cl^-}, were calculated (1) from data listed in Table 1 using eq. 2

$$[2] \qquad t_{Cl^-} = (dE_T/dE)_{m_2}$$

where subscript m_2 designates the concentration of HCl at which the differential was evaluated. Transport numbers for hydrogen ion, t_{H^+}, were then evaluated using the relationship

$$[3] \qquad t_{H^+} = 1 - t_{Cl^-}$$

The above values were extrapolated by plots of t_{H^+} and t_{Cl^-} *vs.* $\sqrt{m_2}$ to $m_2 = 0$ to obtain the infinite dilution values listed in Table 2.

Plots of $t_{H^+}^\circ$ and $t_{Cl^-}^\circ$ *vs.* temperature to 200 °C are shown in Fig. 1. The values obtained in this work at 25 °C agree within experimental error (±0.005) with the accepted values listed by Robinson and Stokes (1) but differ by up to 5% from the values calculated from the limiting conductance data of Quist and Marshall (3) at higher temperatures. However, the data of Quist and Marshall were obtained by extrapolation of transport numbers for 0.1 mol/l KCl and NaCl solutions from $T < 125$ °C to higher temperatures together with conductance data for these and HCl solutions at elevated temperatures. In view of the errors inherent in extrapolations of this type, the differences found between the two sets of data are surprisingly small.

The data plotted in Fig. 1 shows that the infinite dilution transport numbers for H^+ and Cl^- exhibit "normal" variation with temperature, *i.e.* the cation and anion transport numbers approach equality with increasing temperature. Sodium chloride solutions exhibit similar be-

Can. J. Chem. Downloaded from www.nrcresearchpress.com by 210.87.254.5 on 09/05/12
For personal use only.

TABLE 2. Coefficients for eq. 1 and transport numbers at infinite dilution for H^+ and Cl^- at temperatures to 200 °C

T (°C)	C_0(V)*	C_1	C_2 (V^{-1})	$t_{H^+}{}^0$	$t_{Cl^-}{}^0$
25	0.0001556	0.16895	−0.07571	0.82_0†	0.18_0†
60	−0.00009338	0.19511	0.00415	0.80_5	0.19_5
90	−0.00005736	0.22020	−0.008321	0.77_5	0.22_5
125	−0.00008051	0.24880	−0.02804	0.74_6	0.25_4
150	−0.00015512	0.26731	−0.04203	0.72_6	0.27_4
175	−0.00008058	0.28614	−0.06308	0.70_3	0.29_7
200	−0.00046373	0.29166	−0.02026	0.70_2	0.29_8

*$C_0 = 0$ for a perfect fit. Standard deviations for eq. 1 are 0.000137, 0.000083, 0.000051, 0.000072, 0.000140, 0.000073, and 0.000445 V at 25, 60, 90, 125, 150, 175, and 200 °C, respectively.
†Robinson and Stokes (1) list values for $t_{H^+}{}^0$ and $t_{Cl^-}{}^0$ at 25 °C of 0.8209 and 0.1791, respectively.

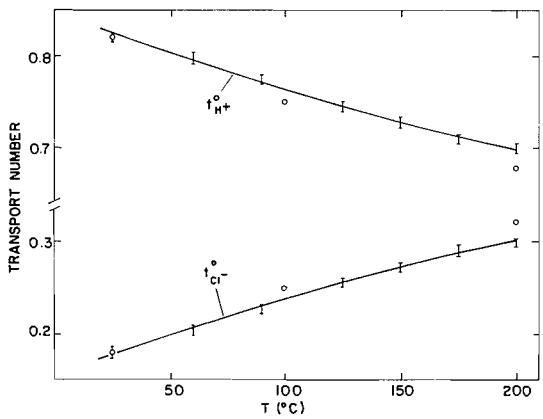

FIG. 1. Transport numbers at infinite dilution for H^+ and Cl^- at temperatures to 200 °C. I, this work; ○, calculated from the data of Quist and Marshall (3).

havior whereas in KCl solutions, the opposite has been observed to occur (1, 2).

It is generally recognized (1) that the abnormally high transport number for H^+ in aqueous solution is due to high mobility via a chain mechanism. In this mechanism the proton jumps from one water molecule to a neighboring one via the formation of a hydrogen bond. The rate at which this occurs is believed to be determined by the rate of rotation of water molecules into the hydration sheath of the H_3O^+ ion as the proton passes along the chain (7). This chain mechanism operates in parallel with the motion-in-a-viscous-fluid mechanism commonly used to describe the transport properties of ions other than H^+ or OH^-, *e.g.* Cl^-. At low temperatures this chain mechanism predominates and accounts for the large mobility observed for the proton in aqueous solution. However, it is likely that this process is highly cooperative in nature in that proton transfer cannot take place until a suitable orientation is attained by the rotating acceptor water molecule. Simple geometric considerations indicate that the required orientation is such that the molecule also satisfies the spatial requirements for tetrahedral bonding within the surrounding network of bonded water molecules. Accordingly, these orientations, on average, will be favored over the average orientation presented by a rotating non-bonded acceptor molecule. Thus, an increase in temperature, which results in destruction of the tetrahedral structure of water, will disfavor transport by the chain mechanism and the motion of hydrated H^+ in the field will be increasingly determined by the viscosity of the medium. In this manner, it is expected that the fractional increase in mobility of the proton for a given increase in temperature will be less than that for other small ions. The data of Quist and Marshall (3) show that this is indeed the case for ions such as Li^+, Na^+, K^+, NH_4^+, Cl^-, HSO_4^-, and SO_4^{2-}. Thus, for a hydrogen chloride solution the fraction of charge carried by H^+, and hence $t_{H^+}{}^0$, will decrease with rising temperature as observed.

1. R. A. ROBINSON and R. H. STOKES. Electrolyte solutions. Butterworths, London. 1959.
2. J. E. SMITH, JR., and E. B. DISMUKES. J. Phys. Chem. **67**, 1160 (1963); **68**, 1603 (1964).
3. A. S. QUIST and W. L. MARSHALL. J. Phys. Chem. **69**, 2984 (1965).
4. D. D. MACDONALD, P. BUTLER, and D. OWEN. To be published.
5. R. E. MESMER, C. F. BAES, JR., and F. H. SWEETON. J. Phys. Chem. **74**, 1837 (1970).
6. R. S. GREELEY, W. T. SMITH, R. W. STOUGHTON, and M. H. LIETZKE. J. Phys. Chem. **64**, 652 (1960).
7. B. E. CONWAY, J. O'M. BOCKRIS, and H. LINTON. J. Phys. Chem. **24**, 834 (1956).

Can. J. Chem. Downloaded from www.nrcresearchpress.com by 210.87.254.5 on 09/05/12
For personal use only.

Evidence for Reactive Intermediates Formed During Pyrolyses of α-Betaines: A Mass Spectrometric Investigation[1]

RUDOLPH A. CHAMPA[2] AND D. L. FISHEL[3]

Department of Chemistry, Kent State University, Kent, Ohio 44242

Received June 18, 1971[4]

Pyrolytic decomposition of glycine betaine, 2-(*N*-pyridyl)acetic acid betaine and 2-(*N*-pyridyl)propionic acid betaine were conducted in inlet systems of two mass spectrometers of differing geometries. Evidence was obtained for primary thermolysis with loss of carbon dioxide to give an ylid from each betaine. The ylids may react further by several alternate pathways involving either hydrogen abstraction, rearrangement and teleomerization, or by divalent carbon transfer by insertion reactions.

La décomposition pyrolytique des bétaines de la glycine, de l'acide (*N*-pyridyl)-2 acétique et de l'acide (*N*-pyridyl)-2 propionique, a été effectuée dans les systèmes d'introduction de deux spectromètres de masse de géométrie différente. La thermolyse primaire a été mise en évidence par perte de gaz carbonique et formation d'un ylure à partir de chaque bétaine. Les ylures peuvent réagir ensuite selon diverses voies: perte d'hydrogène, réarrangement et téléomérisation ou transfert de carbone divalent par réaction d'insertion.
[Traduit par le journal]

Can. J. Chem., 51, 2750 (1973)

Introduction

The structure usually presented for glycine betaine, **1**, suggests that this compound or derivatives might undergo a simple heterolytic thermal dissociation to give singlet methylene, **2**, either directly or via ylid, **3**

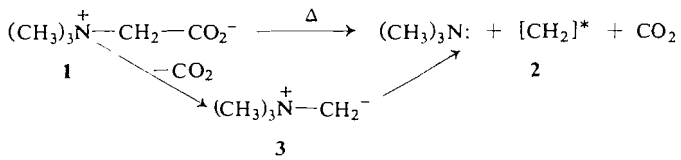

The analogous structure for pyridinium betaines, **4**, should be even more easily decarboxylated to an ylid, **5**, expected to readily undergo further transformation or serve as a methylenating agent

4 **5**

a, R=H
b, R=CH_3

We here report our investigations of these possibilities for genesis of products derived from α-betaine decompositions.

No recent work is reported on thermolytic reactions of glycine betaine, free of base or other reagents. Willstätter (2) reported interconversion with isomeric methyl *N*,*N*-dimethylaminoacetate at temperatures from 135° to 293°. Others have independently reported trimethylamine, dimethylamine, carbon dioxide, and nitrogen as products of pyrolytic distillation of glycine betaine as well as the rearrangement ester (3, 4). Volatile bases which reduced ammoniacal silver oxide or Fehling's solution but which gave no Schiff test nor hydrazone formation, were also obtained. The molecularity and other details of the rearrangement to methyl *N*,*N*-dimethylaminoacetate have not been established. The other reported products may result subsequent to formation of reactive intermediates by simple pyrolytic cleavage reactions such as **1** → **3**, **1** → **2**, or **3** → **2**.

Decarboxylation of α-haloacids on heating with pyridine to give ylids has been presumed to occur via initial formation of pyridinium

[1]Taken, in part, from ref. 1.

[2]Present address: Space and Missile Systems Organization, P.O.B. 92960, Worldway Postal Center, RSSE, Los Angeles, Calif. 90009.

[3]To whom correspondence should be addressed.

[4]Revision received March 16, 1973.

Can. J. Chem. Downloaded from www.nrcresearchpress.com by 210.87.254.40 on 09/05/12
For personal use only.

TABLE 1. Ion intensity variation with ionization energy for glycine betaine pyrolysis at 315°, 0.2 Torr

	Ionization energies (eV)			
m/e	8	10	15	20
41				1.5
42			13.0	19.3
43			5.5	6.4
44			8.8	10.8
45			2.1	2.3
56			3.0	2.9
57			2.6	2.7
58	43.8	100.0	100.0	100.0
59	100.0	84.0	25.8	12.7
60	4.3	11.9	1.4	—
72	13.8	13.9	17.5	14.2
73	55.3	16.4	3.7	2.4
117	40.4	13.4	2.7	1.4
131	2.5	4.0	0.2	0.1

betaines (5). Evidence for ylids was isolation of *N*-alkylpyridinium halides supposed to arise from rapid protonation of the ylids. Attempts to isolate betaines by the reaction between 2,5-dimethylpyrazine and α-haloacids at room temperature are reported to give the analogous *N*-alkyl-2,5-dimethylpyrazinium salts (6).

Methylene (or carbene) and its substituted derivatives as well as a variety of ylids have been firmly established as reactive intermediates with finite lifetimes characterizable both chemically and spectroscopically. Much of the recent chemistry has been summarized in various monographs and reviews (7–10). Direct identification of these intermediates might be accomplished via electronic (11) or mass spectrometry. Carbenes are difficult to measure by the latter technique other than in specially designed apparatus (12) but ylids appear to have sufficient stability to be easily identified by either method.

As an alternative to direct detection of methylene, one might identify products which could be shown to result from either typical insertion and/or addition reactions or via transfer from an ylid. The least complicated array of products would be obtained if those initially produced were swept away or quenched before further attack by reactive species. Our approach to this technique of early product identification is to conduct pyrolysis reactions with small samples directly in the inlet system of a mass spectrometer. Expansion into the low pressure of the inlet system or spectrometer source effectively removes the initial products from the reaction zone and they are ionized and examined at once by mass spectrometry.

Results and Discussion

Mass spectra given as Tables 1–7 are typical of the data obtained. Peak intensities were reproducible to within 5% owing to care in maintaining nearly constant conditions from run to run, including temperatures and pressures, sampling times and sample size as well as instrument operating parameters. All the latter were routinely cycled and optimized for each analysis. We are confident that under these conditions, spectra obtained for betaine pyrolyses products may be directly compared with spectra for suspected pure stable components to unmask evidence for reactive intermediates.

Glycine Betaine

Glycine betaine is not directly ionized as such in a mass spectrometer since it is not volatile[5]. Ionization during introduction of betaine samples was not detectable at temperatures below 260° and then only weak spectra were realized until the sample temperature approached 300°. An *m/e* 117 peak (apparent molecular ion) observed at temperatures >260° must be associated with

[5]Attempts to sublime glycine betaine through a 3 mm distance at $\sim 10^{-5}$ Torr/200–300° produced samples which show no n.m.r. absorption characteristic of betaine. Peaks corresponding to methyl *N,N*-dimethylaminoacetate were easily recognizable, however.

Can. J. Chem. Downloaded from www.nrcresearchpress.com by 210.87.254.40 on 09/05/12
For personal use only.

TABLE 2. Mass spectra of methyl *N,N*-dimethylaminoacetate as a function of ionization energy; source temperature 290° and 170°*, pressure 2 × 10^{-5} Torr

	Relative intensity							
m/e	8 eV	20 μA	12 eV		20 eV	100 μA	70 eV	
30							7.4	(5.1)
42					1.7		13.9	(13.2)
43					0.6		3.1	(2.5)
44					0.9		2.6	(1.9)
45					0.9		3.9	(3.7)
56							1.1	(1.0)
57							4.4	(3.7)
58	50.5	(18.8)	100.0	(100.0)	100.0	(100.0)	100.0	(100.0)
59			4.4	(2.7)	4.0	(3.2)	4.0	(4.0)
116						(0.4)	0.2	(0.5)
117	100.0	(100.0)	48.0	(65.9)	16.7	(24.4)	8.9	(15.6)
118		(11.3)	2.6	(3.2)	0.8	(1.2)	0.4	(0.7)

*Values in parentheses were obtained at 170°.

TABLE 3. Mass spectrum of glycine betaine by direct-insertion pyrolysis; source, 300°, 8 × 10^{-7} Torr; ionization energy, 70 eV, 100 μA; 30 s scan time

*m/e**	Relative intensity	*m/e*	Relative intensity	*m/e*	Relative intensity
14	2.6	32	1.3	57	7.30
15	13.6	36	2.9	58	100.0
17	2.2	38	1.0	59	10.0
18	10.1	40	2.0	72	3.9
26	0.8	41	3.6	73	2.6
27	2.1	42	25.7	84	0.5
28	5.3	43	6.0	85	1.2
28†	4.5	44	25.5	103	3.0
29	1.2	44†	9.1	104	0.2
29†	3.5	51	15.2	116	1.4
30	11.1	52	5.5	117	1.2
31	2.5	56	3.3	131	0.2

*Metastable ions were recorded at 14.5, 15.5, 26.9, 28.8, 31.8, 46.1, 54.2, and 68.2.
†Peak doublets were resolved at these masses, footnoted values were higher in mass.

the rearrangement isomer, methyl *N,N*-dimethylaminoacetate for which good spectra can be easily obtained at lower temperatures. Betaine derivatives incapable of thermal rearrangement gave analogous results (2-(*N*-pyridyl)acetic acid and 2-(*N*-pyridyl)propionic acid betaines do not exhibit molecular ions at any temperature).

Flash pyrolyses of ≃0.1 mg samples of glycine betaine in the all glass inlet system produced the spectra of Table 1. Comparison with spectra obtained in an identical manner for methyl *N,N*-dimethylaminoacetate (Table 2) suggests two concurrent thermolysis reactions for betaine in addition to rearrangement to the ester. These are illustrated in Scheme 1 (processes which do *not* involve loss of radical to give cation). Clearly neither the *m/e* 73 nor the *m/e* 59 species arise by ion-fragmentation of the ester as they are absent in low voltage spectra of the latter but constitute the major ions for the betaine. High resolution mass measurements for the *m/e* 73, 72, 59, and 58 species confirm an atomic composition consistent with Scheme 1 (*m/e* 73 = $(CH_3)_3\overset{+}{N}CH_2^-$; *m/e* 59 = $(CH_3)_3N$:; *m/e* 72 and 58 are the fragment ions resulting from loss of H·). Reduction in relative ion intensity for both *m/e* 73 and 59 with increased ionization energy is also consistent with their identification as molecular species. On the other hand, *m/e* 72 and 58 represent an increased proportion of the total ion current with initial increases in ionization energy, consistent with formation by ion

Can. J. Chem. Downloaded from www.nrcresearchpress.com by 210.87.254.40 on 09/05/12
For personal use only.

TABLE 4. Mass spectra of "stable" 2-(*N*-pyridyl)acetic acid betaine thermolysis products; Source, 295°, 0.03 Torr; ionizing energies are nominal instrument readings, ionizing current 10 μA; (relative intensities indicated)

	Relative intensity			
m/e	15 eV	20 eV	25 eV	70 eV
37				3.3
38				4.8
39		18.1	21.8	11.6
41				3.5
42				2.8
44	68.1	100.0	100.0	100.0
49				2.5
50			16.4	10.6
51		21.5	34.1	13.5
52	26.4	51.4	43.8	19.3
53			10.5	4.2
65			10.5	3.4
66		19.4	11.8	3.9
67			11.0	3.2
78		15.9	13.8	5.3
79	100.0	91.0	56.7	24.5
80				2.7
93			10.5	3.5
94	45.1	41.0	24.4	9.1
95			10.0	3.2

TABLE 5. Mass spectrum of 2-(*N*-pyridyl)acetic acid betaine by direct insertion pyrolysis; source, 210°, 8×10^{-7} Torr; ionization energy, 70 eV, 100 μA; 30 s scan time following sample introduction*

m/e	Relative intensity	*m/e*	Relative intensity	*m/e*	Relative intensity
26	3.1	52	4.8	107	1.5
27	2.4	53	4.0	185§	2.0
28	8.4	63.1†		186§	1.0
34.3†		64.8†		187§	3.4
39	3.7	65	2.0	188§	1.1
41	2.8	66	1.5	279§	0.3
44	100.0	67	2.6	280§	0.4
45	1.3	78	3.5	281§	0.3
45.5‡		79	6.6	372§	0.05
46‡		92	1.8	374§	0.1
46.5‡		92.5‡		376§	0.02
47.8†		93§	5.5		
50	1.6	94§	43.8		
51	2.9	95	14.2		

*Fragment ions of < 1% relative intensity are not listed.
†*m/e* values for metastable ion peaks.
‡Identified as doubly-charged ions.
§Ions which persist in low voltage (8 eV, 20 μA) spectra.

fragmentation. The *m/e* 58 species likely is derived in part from all three molecular species present. It is clearly the principal fragment from the ester ($M^{\cdot +} = 117$) and is also the known principal fragment in trimethylamine spectra (1, 13). We also observed a metastable ion at *m/e* 46.1 in 70 eV spectra of glycine betaine consistent with the process: $73^+ \rightarrow 58^+ + CH_3$.

Carbon dioxide is a major volatile product from betaine pyrolyses at atmospheric pressure. Its absence in low voltage spectra is due to its high appearance potential ($\simeq$13.8 eV). In addi-

Can. J. Chem. Downloaded from www.nrcresearchpress.com by 210.87.254.40 on 09/05/12
For personal use only.

TABLE 6. Time variation of the mass spectrum for 2-(*N*-pyridyl)-acetic acid betaine by repetitive scanning (30 s); direct-insertion pyrolysis at 185°; ionizing energy, 20 eV, 100 μA; source pressure, 2×10^{-6} Torr

	Peak intensity at time (min)			
m/e	Initial*	2	3	5 (maximum ion current)
18	9	8		
44	7	13	12	90
79	5	6	18	57
94	18	30	165	1300
95	10	17	90	540
96			7	33
107			7	24
172			4	19
185				80
186		2	10	65
187			19	385
188				85
278				13
279			6	35
280				82
281			4	26

*The initial spectrum was obtained as soon as the sample probe was introduced to the heated block.

TABLE 7. Mass spectrum of 2-(*N*-pyridyl)propionic acid betaine by direct insertion pyrolysis; source, 210°, 4×10^{-6} Torr; ionizing energy, 70 eV, 100 μA; scan time, 30 s*

m/e	Relative intensity	*m/e*	Relative intensity	*m/e*	Relative intensity
22	2.9	65	1.5	160.5§	
26	2.2	67	2.5	161.5§	
27	5.5	77	1.2	172	1.1
28	14.5	78	3.1	185	1.2
29	3.5	79	9.1	211	1.8
39	3.2	80	31.5	212	0.6
41	2.8	93	3.2	213	5.2
42	1.6	94	2.9	214‡	4.1
44	97.5	106	8.8	215	7.6
45	3.2	107‡	7.6	216	1.9
50	1.5	108	100.0	320	0.6
51	3.2	109	19.5	321‡	1.2
52	5.8	110	1.4	322	0.9
53	6.3	132	1.1	323	0.4
54	1.3	134	5.0		
59.3†		135	1.8		
		136	1.5		

*Fragment ions 1% relative intensity are not recorded.
†Metastable ion peak.
‡These ions persist in low voltage spectra.
§Doubly charged ions.

tion, this lowest molecular weight pyrolysis species is expected to diffuse more rapidly which may account for its low intensity in high voltage spectra.

The highly unstable ylid, *m/e* 73, would be expected to decompose or rearrange very rapidly. Thus it could further cleave to methylene plus trimethylamine as an alternate to formation of the latter directly from the betaine (dotted line, Scheme 1). The ylid might also undergo

Can. J. Chem. Downloaded from www.nrcresearchpress.com by 210.87.254.40 on 09/05/12
For personal use only.

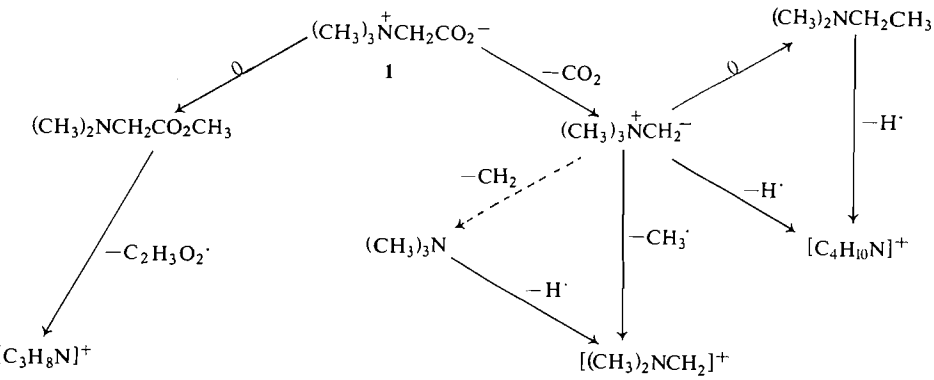

SCHEME 1. Proposed routes for pyrolyses and ion-fragmentation (bracketed ions) of glycine betaine at low ionizing energies.

Stevens rearrangement to ethyldimethylamine

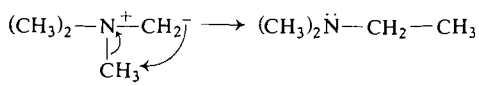

The stable product resulting from such a rearrangement would account for the persistence of the *m/e* 73 contribution in low voltage spectra obtained via the glass inlet system in which products are "stored" for relatively long times, (Table 1).

Trimethylamine radical-ion might also result by ion fragmentation of the ylid radical-ion but this is less likely at low ionization energies. Attempts were made to establish formation of methylene during pyrolysis by observing *m/e* 14 during direct sample introduction. These experiments were conducted by pre-focussing the mass spectrometer on fragment-ion *m/e* 14 at high ionizing energies, then reducing the ionization energy just prior to sample pyrolysis. No signal was obtained under these conditions. This may be due to the difficulty inherent in optimizing tuning parameters, in particular the ion-repeller voltage in the absence of a signal at low voltages, or may indicate that this short life-time species is not present in sufficient concentrations in the gas phase to enable detection during betaine pyrolyses (12).

Evidence for a reactive intermediate that is a source of methylene is provided by the molecular ion species observed at *m/e* 131 which occurs in all low voltage as well as 70 eV spectra. This has a composition of $C_6H_{13}NO_2$ (high resolution mass measurement) and may result from C—H insertion of methylene (either directly or by transfer from the ylid) in either glycine betaine itself or in methyl *N,N*-dimethylaminoacetate. One may argue for insertion in the ester as more likely if attack is by free methylene, since methylene is an electrophile. Such insertion products would also contribute to the fragmentation spectrum observed for glycine betaine (*i.e.*, the stable products from thermolysis of glycine betaine).

Methylene insertion on the ester would be statistically favored at methyl. Extension of the ester alkyl chain to ethyl, for example, yields a product which has a mass spectrum identical to that for the methyl ester excepting the molecular ion region; *m/e* 131 and attendant isotope peaks replace *m/e* 117 and 118 peaks.

Higher molecular weight species would be expected if an appreciable concentration of the reactive intermediate was present in the condensed phase. The absence of peaks above *m/e* 131 in glycine betaine spectra suggests that thermolysis products are either rapidly volatilized or that the intermediate methylide is "quenched", via Stevens rearrangement, for example. Gas phase reactions between the 131 species and either methylene or methylide during direct insertion analysis is expected to be almost nil at the pressures of the mass spectrometer source ($\simeq 10^{-5}$ Torr).

Although the formation of methylene as an entity is not rigidly established here, there are few other realistic explanations for the origin of the *m/e* 131 ion. An alternate suggestion for its structure is that of the betaine (or its rearrangement products) which might result by nucleophilic attack of the ylid on glycine betaine with

Can. J. Chem. Downloaded from www.nrcresearchpress.com by 210.87.254.40 on 09/05/12
For personal use only.

displacement of trimethylamine

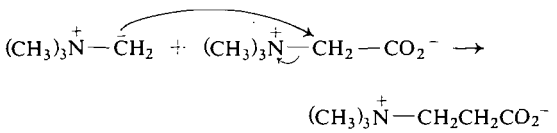

The latter betaine, however, is not stable at temperatures >140° but readily undergoes decomposition via Hoffman elimination to acrylic acid (2).

Thus, we feel the evidence supports the reactions presented in Scheme 1 when small amounts of glycine betaine are pyrolyzed at low pressures. In addition to molecular rearrangement, methylene is produced in a two step sequence via trimethylammonium methylide. The methylide may also abstract protons from any available source yielding a stable quaternary salt if suitable anions were available.

Pyridine Betaines

Coe (14) has observed that the pyridinium chlorides obtained for reactions between ethyl chloroacetate and various alkylpyridines are extremely hygroscopic; we confirm this and also wish to note that some small amount of water appears to be structurally bound to the betaines. Completely satisfactory elemental analyses could not be obtained for this reason. This tenaciously held water was identified by p.m.r. spectra taken in deuterium oxide as solvent, there being a signal for a singlet which intensifies on adding a small amount of water.

Mass spectra typical of those obtained for **4***a* and **4***b* are presented in Tables 4–7. Ionization characteristics similar to those for glycine betaine were observed. Ionization does not occur at temperatures below the thermal decomposition point (<150°); molecular ions are absent.[6]

A small sample of **4***a* decomposed at 295° and "stored" at 0.03 Torr then introduced via the all-glass inlet system led to intense ions at *m/e* 44, 52, 79, and 94 in low voltage spectra (Table 4). These ions provide evidence for decomposition involving initial C—C cleavage yielding the pyridine methylide, **5***a*, which abstracts a proton from any available source to give the *m/e* 94 species (Scheme 2). The most intense ion in low voltage spectra at *m/e* 79 is evidence for C—N cleavage. This could arise by subsequent fragmentation of the methylide, **5***a*, or the *m/e* 94 species. The absence of ions at *m/e* 58 suggests the latter path although the $C_2H_2O_2$ species which might give this ion may be too reactive to be observable as an ion in the mass spectrometer under these conditions. The *m/e* 52 ion is typical for pyridines that do not involve substitution at other than the nitrogen atom (16).

When a direct insertion sampling technique was employed (Table 5) the gross features of the spectrum from *m/e* 12–95 were much the same. Of greater interest was the appearance of new ions over the range from *m/e* 95–377; these higher mass ions were persistent even in low voltage spectra (8 eV, 20 μA) indicating they represent stable products derived from thermal decomposition of the pyridine betaine. In general ion–molecule reactions following electron impact require relatively high pressures and concomitant high ionizing energies (ref. 17, see particularly chapt. 11) and can thus be discarded as a source of these high molecular weight ions. The most intense ions in the high mass range are found at simple multiples of 94 less one, two, or three a.m.u. A logical explanation is that these higher molecular weight species are the result of dimerization, trimerization, etc., in the condensed phase, of pyridine methylide or a rearranged isomer of the ylid. In fact, exact mass measurements give the composition for the ions at *m/e* 93, 186, and 279 as C_6H_7N, $C_{12}H_{14}N_2$, and $C_{18}H_{21}N_3$, respectively. Recent work by Paquette, *et al.* (18) shows that certain 1H-azepine derivatives easily undergo thermochemical dimerization. Rearrangement of pyridine methylide to 2H-azepine is readily formulated and this isomer should no less easily dimerize than does 1H-azepine.[7] Although Paquette does not report evidence for trimers or higher oligomers of his compounds, the expected products of dimerization should be capable of continued cycloaddition reactions.

[6]Since our original submission, analogous behavior has been reported by Grønneberg and Undheim (15) for 3-hydroxypyridinium betaines; these workers report loss of CO_2 to give an apparent molecular ion. Intermolecular reactions involving the 3-hydroxy group are prominent in subsequent interpretation of their results.

[7]Since our work was completed, Grønneberg and Undheim (15) have independently suggested a 2H-azepine structure via rearrangement of ylids they presumed to arise from 3-hydroxypyridinium betaines. They do not report observation of teleomerization products from these systems, however.

Can. J. Chem. Downloaded from www.nrcresearchpress.com by 210.87.254.40 on 09/05/12
For personal use only.

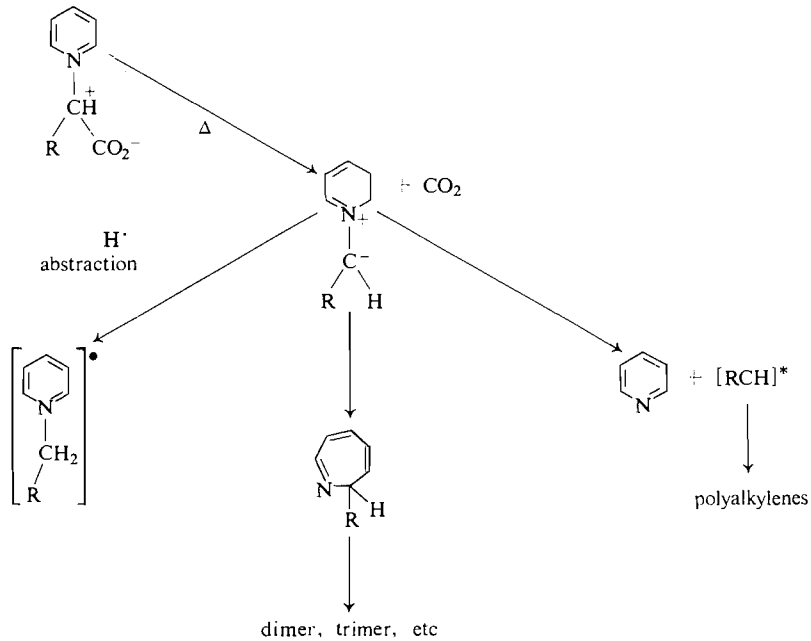

SCHEME 2. Proposed routes for pyrolyses of 2-(*N*-pyridyl)alkanoic acid betaines.

The direct insertion pyrolysis mass spectrum of methyl substituted derivative, **4***b*, shows features similar to the spectrum of **4***a*. This compound would be expected to decompose with loss of CO_2 to give the methyl pyridinium methylide, **5***b*, at *m/e* 107. Dimerization, etc. should give ions at *m/e* 214, 321, etc. Ions are observed at all expected *m/e* values and with relative intensities similar to their analogs in the spectrum of **4***a*.

In some spectra obtained by direct insertion pyrolysis of either the **4***a* or **4***b* derivatives, low intensity ions appeared as a group pattern of peaks 1 a.m.u. apart in approximate Gaussian distribution. This pattern was repeated at intervals of either 14 or 28 a.m.u. (respectively, for **4***a* and **4***b*) to the upper mass limit set for the scan. This pattern is analogous to that shown by a mixture of hydrocarbon homologues for the molecular ion region and it is suggestive of the formation of polyalkylenes by methylene polymerization or by methylene transfer from the ylid. An alternative for **4***b* is that the derived ylid may cleave with rearrangement to ethylene and pyridine, followed by subsequent polymerization of the ethylene. This would not, however, explain the analogous mass spectral results for **4***a*.

Scheme 2 presents a summary of reactions we believe to occur on thermolytic decomposition of *N*-pyridine betaines at low pressures.

Experimental

General

Melting points were determined in a capillary with a Hoover–Thomas melting point apparatus and are uncorrected; infrared spectra were determined with a Perkin–Elmer Model 337 spectrometer and p.m.r. spectra were determined with a Varian Associates A-60 spectrometer; data were consistent with structures assigned.

Materials

Betaine was obtained as the monohydrate (Eastman Kodak Company) which deliquesces if exposed to the atmosphere. It was freed from traces of atmospheric moisture in an oven at 100° for 10–15 min and stored in a desiccator over potassium hydroxide.

2-(N-pyridyl)acetic acid betaine was synthesized as follows:[8] Dry, reagent grade pyridine (7.9 g, 0.1 mol) was added to ethyl chloroacetate (12.3 g, 0.1 mol) and allowed to stand until completely solidified (about 24 h). The intermediate, ethyl 2-(*N*-pyridyl)acetate chloride salt was formed in almost quantitative yield. It was dissolved in absolute ethanol (50 ml) and added to a hot solution of potassium hydroxide (6.5 g, 0.1 mol) in ethanol (150 ml). There was an immediate precipitation of potassium

[8]The procedure for synthesis of pyridine betaine is adapted from a method reported to us by Dr. R. T. Myers of our department, who kindly provided us with the initial samples used in this study. See also ref. 14.

Can. J. Chem. Downloaded from www.nrcresearchpress.com by 210.87.254.40 on 09/05/12
For personal use only.

chloride and the color of the solution turned dark orange. No further precipitation occurred after about 4 h and the potassium chloride was removed by filtration. Potassium chloride again precipitated from the filtrate and after 20 h was removed. This two-step precipitation and filtration always seemed to be necessary to obtain product free of potassium chloride. The second filtrate was stored at −5°; crude 2-(*N*-pyridyl)acetic acid betaine crystallized and was collected after 3 days. Concentration of the mother liquor afforded additional solid product on similar treatment. The combined crude product (12.2 g, 89%) was recrystallized from ethanol three times and gave faintly colored (yellow) product (5.48 g, 40%) m.p. 150–160° d. Further recrystallization merely removed the coloration; the melting behavior was identical. A dried sample gave the following analysis:

Anal. Calcd. for $C_7H_7NO_2$: C, 61.38; H, 5.11; N, 10.21.

Anal. Calcd. for $C_7H_7NO_2 \cdot \frac{1}{8}H_2O$: C, 60.03; H, 5.06; N, 10.00.

Found: C, 60.43; H, 5.23; N, 9.92.

N.m.r. (D_2O) τ = 5.65 (s, 2, —CH_2—), τ = 2–3 (m, 5, Ar—H), τ = 6.13 (s, H_2O).

2-(N-pyridyl)propionic acid betaine was synthesized by a procedure analogous to that above from pyridine and ethyl 2-bromopropionate. Overall yield of purified product was 17.8% m.p. 164–170°d. A dried sample was analyzed:

Anal. Calcd. for $C_8H_9NO_2$: C, 63.57; H, 5.96; N, 9.27.

Anal. Calcd. for $C_8H_9NO_2 \cdot 0.4\ H_2O$: C, 60.68; H, 6.19, N, 8.84.

Found: C, 60.56; H, 5.58; N, 8.62

N.m.r. (D_2O) τ = 1.00–2.15 (m, 5, Ar—H), τ = 4.66 (q, 1, —CH(CH_3)—, J = 7.4 c.p.s.), τ = 8.12 (d, 3, CH_3CH, J = 7.2 c.p.s.), τ = 5.4 (s, H_2O).

Mass Spectrometric Studies

Samples of the betaines were pyrolyzed in 0.1 to 1.0 mg amounts directly in the mass spectrometer inlet systems maintained at a fixed temperature. In the CEC Model 21-103C an all-glass heated inlet (temperature 295 ± 5°) with 3 l reservoir was used; volatiles were leaked into the source. In the AEI MS-12 a similar all-glass inlet system (1 l reservoir) or the source direct-insertion probe were used. Residual gas pressure above the decomposing samples varied from 10^{-2} to 0.2 Torr in the glass inlet systems and was ~4×10^{-7} Torr in the source.

Voltage scanning from *m/e* 25–250 required 15 min in the CEC 21-103C. Magnetic scanning from *m/e* 350–12 was done in ~30 s on the AEI MS-12. Other data are recorded in the tables; electron energies are nominal meter readings and are uncorrected.

We are indebted to the staff and director R. E. Farrell of the Broadway Laboratory of the Standard Oil Company of Ohio for mass spectra obtained early in this investigation with a CEC 21-103C. The A.E.I. MS-12 was purchased in part with funds provided under a National Science Foundation Matching Funds Grant.

1. R. A. CHAMPA. M.Sc. Thesis. Kent State University, Kent, Ohio. 1970.
2. R. WILLSTÄTTER. Berichte, **35**, 584 (1902).
3. V. STANEK. Z. Zuckerind. (Bohm), **27**, 479 (1902).
4. H. T. STRAW and H. T. CRANFIELD. J. Soc. Chem. Ind. 40T (1936).
5. K. W. RATTS, R. K. HOWE, and W. G. PHILLIPS. J. Am. Chem. Soc. **91**, 6115 (1969).
6. E. V. HORT and P. E. SPOERRI. J. Am. Chem. Soc. **77**, 5898, (1955).
7. J. A. BELL. *In* Progress in physical organic chemistry. Vol. 2. Interscience, New York. 1964.
8. W. KIRMSE. Carbene chemistry. Academic Press, New York. 1964.
9. W. KIRMSE. Angew. Chem. Int. Ed. **4**, 1 (1965).
10. A. WILLIAM JOHNSON. Ylid chemistry. Academic Press, New York. 1966.
11. G. HERZBERG and J. SHOOSMITH. Nature, **183**, 1801 (1959).
12. S. N. FONER and R. L. HUDSON. J. Chem. Phys. **45**, 49 (1966).
13. G. HVISTENDAHL and K. UNDHEIM. Org. Mass. Spectrom. **3**, 821 (1970).
14. D. G. COE. J. Org. Chem. **24**, 882 (1959).
15. T. GRØNNEBERG and K. UNDHEIM. Acta Chem. Scand. **25**, 2807 (1971).
16. H. BUDZIKIEWICZ, C. DJERASSI, and D. H. WILLIAMS. Mass spectrometry of organic compounds. Holden–Day, San Francisco. 1967. Chapt. 20.
17. F. H. FIELD, M. S. B. MUNSON, and D. A. BECKER. *In* Ion molecule reactions in the gas phase. Adv. Chem. Ser. No. 58. Am. Chem. Soc., Washington, D.C. 1966.
18. L. A. PAQUETTE, J. H. BARRETT, and D. E. KUHLA. J. Am. Chem. Soc. **91**, 3616 (1969).

Can. J. Chem. Downloaded from www.nrcresearchpress.com by 210.87.254.40 on 09/05/12
For personal use only.

The Reactions of Organometallic Compounds Involving Silicon. Reactions of Methyldiphenyl-, Triphenylsilyl-sodium, -potassium, -rubidium, and -caesium with 9-Methylfluorene in Tetrahydrofuran

MUHAMMAD ABDUL HAMID[1]

Department of Chemistry, The University of Manchester Institute of Science and Technology, Sackville Street, Manchester, M60 1QD, England

Received January 26, 1973

The reactions of triphenylsilyl-sodium (Ph_3SiNa), diphenylmethylsilyl-sodium ($Ph_2MeSiNa$), triphenylsilyl-potassium (Ph_3SiK), triphenylsilyl-rubidium (Ph_3SiRb), and triphenylsilyl-caesium (Ph_3SiCs) with 9-methylfluorene in tetrahydrofuran (THF) were studied using the stop-flow technique at low temperatures. The rate constant k ($l\ mol^{-1}\ s^{-1}$) depends on the nature of the cation; at $-50\,°C$ k is 11.5 for Ph_3SiNa, 29.5 for $Ph_2MeSiNa$, 26.8 for Ph_3SiK, 35.6 for Ph_3SiRb, and 47.9 for Ph_3SiCs. It seems that the organosilylalkali–metal compounds (R_3SiM) exist in the form of contact ion-pair and therefore the reactivity of an ion-pair is determined by the Coulombic binding energy of the pair. The thermodynamic constants of activation for these reactions were calculated for $-50\,°C$ and compared with the corresponding values of triphenylsilyl-lithium Ph_3SiLi reaction with 9-methylfluorene in THF. The plots of log k, ΔS^*, and ΔH^* against $1/(r_c + 2)$ and ΔS^* against ΔH^* were drawn to show that Li^+ due to its existence as solvent separated ion-pair behaves differently to its Na^+, K^+, Rb^+, and Cs^+ counterparts.

The electronic spectra of R_3SiM, 9-methyl-fluoren-9-yl-sodium, -potassium, -rubidium and -caesium were determined at temperatures varying from 20 to $-80\,°C$. A red shift was observed in spectra of R_3SiNa at low temperatures; this was attributed to the increase in dipole moment which occurs during the electronic transition. The spectra of 9-methylfluoren-9-yl-sodium, -potassium, -rubidium, and -caesium were compared with their lithium counterpart to explain the effects of gegenion on the solvation of these species.

On a étudié les réactions dans le tétrahydrofuranne du triphénylsilyl-sodium (Ph_3SiNa), du diphénylméthylsilyl-sodium ($Ph_2MeSiNa$), du triphénylsilyl-potassium (Ph_3SiK), du triphénylsilyl-rubidium (Ph_3SiRb) et du triphénylsilyl-caesium (Ph_3SiCs) avec le méthyl-9 fluorène en utilisant la technique d'interruption de débit pour des basses températures. La constante de vitesse K ($l\ mol^{-1}\ s^{-1}$) varie selon la nature du cation: à $-50\,°C$, K est égal à 11.5 pour Ph_3SiNa, 29.5 pour $Ph_2MeSiNa$, 26.8 pour Ph_3SiK, 35.6 pour Ph_3SiRb et 47.9 pour Ph_3SiCs. Il semble que les composés du type organosilylalcalino-métal (R_3SiM) existent sous la forme de paire d'ions intimes et que par conséquent la réactivité de cette paire d'ions est déterminée par l'énergie d'interactions coulombiennes de la paire. Les constantes thermodynamiques d'activation pour ces réactions ont été calculées à $-50\,°C$ et comparées avec les valeurs correspondantes de la réaction du triphénylsilyl-lithium (Ph_3SiLi) avec le méthyl-9 fluorène dans le THF. Les courbes du log k, ΔS^* et ΔH^* en fonction de $1/(r_c + 2)$ et de ΔS^* en fonction de ΔH^* ont été faites afin de montrer que le Li^+, à cause de son existence sous forme d'une paire d'ions solvatés, possède un comportement différent de celui des autres entités Na^+, K^+, Rb^+, et Cs^+.

Les spectres électroniques des R_3SiM, méthyl-9 fluorènyl-9-sodium, -potassium, -rubidium et -caesium ont été déterminés pour des températures allant de 20 à $-80\,°C$. Un déplacement vers le rouge à été observé dans les spectres du R_3SiNa à basses températures; ce fait a été relié à l'augmentation du moment dipolaire qui se produit lors de la transition électronique. Les spectres des méthyl-9 fluorènyl-9-sodium -potassium, -rubidium et -caesium ont été comparés avec ceux obtenus du dérivé lithié (Li) correspondant afin d'expliquer les effets de l'ion complémentaire sur la solvatation de ces espèces.

[Traduit par le journal]

Can. J. Chem., **51**, 2759 (1973)

The dependence of the reactivity of organometallic compounds on the nature of the gegenion has been of significant interest in the anionic reactions. The reactivity of the ion pair of alkali metal salt of living polystyrene has been found to be increased with increasing the size of gegenion in the anionic polymerization of styrene in dioxane (1–4) while in THF (5–7) the order is reversed. The effect of changing the gegenion for the reactions of triphenylsilyl-alkali-metal compounds with 1,1-diphenylethylene in THF has been reported by Evans *et al.* (8). It has been found that when alkali metal was lithium, exceptional results were obtained both in the kinetics and in the spectroscopic experi-

[1]Present address: Department of Chemistry, Purdue University, Lafayette, Indiana 47907.

Can. J. Chem. Downloaded from www.nrcresearchpress.com by 210.87.254.105 on 09/05/12
For personal use only.

Can. J. Chem. Downloaded from www.nrcresearchpress.com by 210.87.254.105 on 09/05/12
For personal use only.

ments. The reactions of substituted silyl-lithiums with 9-methylfluorene (9) have been reported previously; the results for the reactions of Ph_3SiNa, $Ph_2MeSiNa$, Ph_3SiK, Ph_3SiRb, and Ph_3SiCs with 9-methylfluorene in THF are now presented.

Experimental

Materials

9-Methylfluorene (9), hexaphenyldisilane (10), and THF (11) were purified and dried as described previously. Ph_3SiNa, $Ph_2MeSiNa$, Ph_3SiK, Ph_3SiRb, and Ph_3SiCs were prepared by the cleavage of corresponding symmetrical disilanes by the respective metal in THF using a method similar to that described for the organosilyllithium compounds (10). The rubidium and caesium films were prepared by heating the calcium turning with the respective metal chloride under high vacuum conditions.

Spectral Measurements

In order to determine the spectra and the extinction coefficients of the product for the reaction between R_3SiM and 9-methylfluorene in THF, the reactants were mixed under high vacuum conditions using the procedure similar to that described in the previous paper (12). The spectra of the R_3SiM and 9-methylfluoren-9-yl-alkali metal compounds were determined at temperatures varying from 20 to -80 °C using the same technique as described for 9-phenylfluoren-9-yl-lithium (12).

Kinetic Measurements

The reactions of Ph_3SiNa, $Ph_2MeSiNa$, Ph_3SiK, Ph_3SiRb, and Ph_3SiCs with 9-methylfluorene in THF were studied under high vacuum conditions at low temperatures using the stop-flow technique (13). The rate of formation of product 9-methylfluoren-9-yl-sodium, -potassium, -rubidium, and -caesium was most conveniently followed by observing the change of optical density at 510, 500, 510, and 500 nm, respectively, with time. The order of reaction in R_3SiM and 9-methylfluorene was determined using the procedure similar to that described in the previous paper (12).

Results

Spectra

The spectra of Ph_3SiK, Ph_3SiRb, and Ph_3SiCs in THF showed an absorption maxima at 363, 368, and 376 nm, respectively. The values obtained for extinction coefficients at maximum absorption were in agreement with those reported previously by Evans *et al.* (8) for Ph_3SiM reagents within the experimental error of $\pm 2\%$. The spectra of Ph_3SiM determined at low temperatures (20 to -80 °C) did not show any significant change in their maximum absorption. The slightly low values found for $\varepsilon\lambda_{max}$ at reduced temperatures could be due to the condensation of the water vapors on the surface of the sample cell. The spectra of Ph_3SiNa and $Ph_2MeSiNa$ determined in THF and 1,2-dimethoxyethane (DME) showed that the position of maximum absorption gradually changed at low temperatures in both the solvents, therefore the extinction coefficients were calculated at the respective λ_{max} (see Table 1 and Fig. 1).

TABLE 1. Spectral values for R_3SiNa

Compound	Solvent	Temperature (°C)	λ_{max} (nm)	$10^{-4}\ \varepsilon\lambda_{max}$
Ph_3SiNa	THF	20	340	1.41
	THF	−20	344	1.38
	THF	−80	346	1.31
	DME	20	343	1.42
	DME	−20	348	1.41
	DME	−80	356	1.40
$Ph_2MeSiNa$	THF	20	337	1.15
	THF	−20	348	1.15
	THF	−80	354	1.13
	DME	20	340	1.16
	DME	−20	350	1.16
	DME	−80	356	1.15

The red colored product of reaction between R_3SiNa and 9-methylfluorene in THF, 9-methylfluoren-9-yl-sodium showed one distinct absorption peak at 480 nm ($\varepsilon\lambda_{max} = 1.03 \times 10^3$) and a shoulder at 510 nm at 20 °C, which developed into a distinguishable absorption peak at low temperatures. The 510 nm absorption peak was used to study the chemical kinetics of R_3SiNa reactions with 9-methylfluorene in THF. The extinction coefficients calculated at 510 nm are 8.93, 9.27, and 9.7×10^2 at 20, −30, and −80 °C, respectively. The red colored product for the reaction of Ph_3SiK and Ph_3SiCs with 9-methylfluorene in THF, 9-methylfluoren-9-

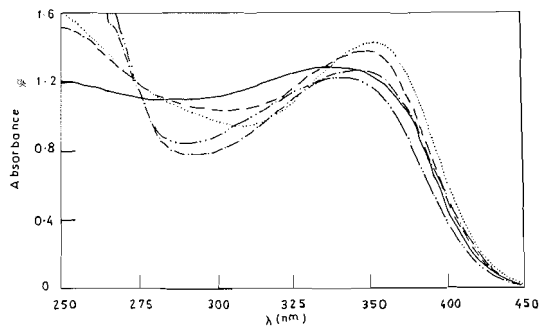

FIG. 1. The effect of temperature on the absorption spectra of R_3SiNa in THF solution; path-length = 1 mm: Ph_3SiNa (8.75×10^{-4} *M* at 20 °C), ····· at −80 °C and ····· at 20 °C; $Ph_2MeSiNa$ (1.12×10^{-3} *M* at 20 °C) ··· at −80 °C, --- at −50 °C and — at 20 °C.

Can. J. Chem. Downloaded from www.nrcresearchpress.com by 210.87.254.105 on 09/05/12
For personal use only.

yl-potassium and -caesium both gave typical broad spectra with maximum absorption at 500 nm (see Fig. 2). The values calculated for the $\varepsilon\lambda_{max}$ are 1.15×10^3 and 1.11×10^3 for 9-methylfluoren-9-yl-potassium and -caesium, respectively. No significant change was observed in the spectra of these compounds determined at reduced temperatures. The red colored product of reaction between Ph_3SiRb and 9-methylfluorene in THF, 9-methylfluoren-9-yl-rubidium showed three distinct absorption peaks at 532 ($\varepsilon\lambda_{max}$ 8.83×10^2), 500 ($\varepsilon\lambda_{max}$ 1.27×10^3), and at 476 nm ($\varepsilon\lambda_{max}$ 1.13×10^3) and a shoulder at 446 nm at 20 °C (see Fig. 2). The spectrum of 9-methylfluoren-9-yl-rubidium was slightly changed at reduced temperatures. For example, two new absorption peaks appeared at 510 and 538 nm overlapping the 500 and 532 nm absorption peaks, respectively. A shoulder at 550 nm was also observed at reduced temperatures.

Kinetics

The rate of reaction of Ph_3SiNa and $Ph_2MeSiNa$ with 9-methylfluorene in THF were measured at −30 °C to investigate the order of reaction whereas the corresponding reactions of Ph_3SiK, Ph_3SiRb, and Ph_3SiCs were most conveniently measured at −50 °C. The concentration of R_3SiM and 9-methylfluorene was varied from 2.25×10^{-3} to 1.611×10^{-2} *M* and from 2.06×10^{-3} to 1.611×10^{-2} *M*, respectively. To establish the order of reaction in the respective reactant, four experiments were carried out varying the concentration of one reactant and keeping the concentration of other one constant in the ratio of 1:2 to 2:1. At least ten repeat reaction curves were obtained to check the reproducibility of the system. It was observed that the reproducibility was very good. The order of reaction found from the dependence of the initial rate of reaction on the initial reagent concentration was 1.03 in Ph_3SiNa, Ph_3SiK and Ph_3SiRb, 1.01 in $Ph_2MeSiNa$, and 0.97 in Ph_3SiCs. For this sequence of R_3SiM the order in 9-methylfluorene was 0.96, 1.02, 1.01, 1.0, and 1.0. The analysis of the optical density *vs.* time curve for these reactions confirmed that the overall order of reaction was 2. These reactions may be considered as irreversible under the conditions of the experiments, since second order kinetics held for at least 90% of the reactions.

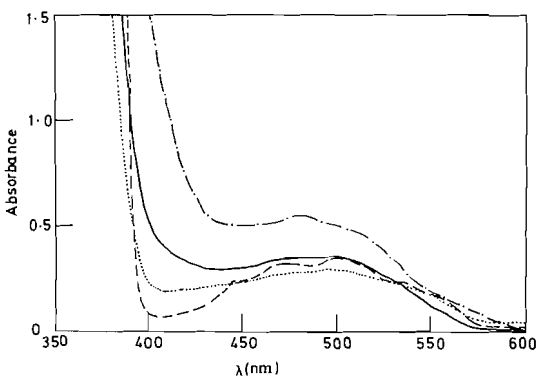

FIG. 2. Absorption spectra of 9-methylfluoren-9-yl-alkalimetal compounds in THF at 20 °C; path-length = 1 mm: ·····, 9-methylfluoren-9-yl-sodium (5.15×10^{-3} *M*);—, 9-methylfluoren-9-yl-potassium (3.28×10^{-3} *M*); ---, 9-methylfluoren-9-yl-rubidium (2.83×10^{-3} *M*); and ···, 9-methylfluoren-9-yl-caesium (3.16×10^{-3} *M*).

The activation energy (E_a) was found from the change in the rate constant of reaction over the temperature range of −10 to −56 °C (see Table 2). The values found for E_a from the Arrhenius

TABLE 2. Temperature dependence of rate constant

Compound	Temperature (°C)	k (l mol^{-1} s^{-1})
$Ph_2MeSiNa$	−12	63.1
	−18	54.7
	−30	46.2
	−38	38.2
	−45	32.0
	−52	28.5
Ph_3SiNa	−10	29.1
	−22	21.9
	−30	18.6
	−38	15.5
	−45	12.9
	−52	11.0
Ph_3SiK	−19	118.7
	−25	85.1
	−30	69.1
	−38	47.9
	−46	31.5
	−50	26.8
	−52	24.1
Ph_3SiRb	−20	182.3
	−30	104.6
	−40	64.9
	−50	35.2
	−56	25.2
Ph_3SiCs	−25	263.8
	−30	190.4
	−35	141.8
	−42	79.6
	−50	48.0
	−56	30.9

TABLE 3. Thermodynamic constants of activation for the reaction between Ph_3SiM and 9-methylfluorene in THF at $-50\,°C$

Parameter	Value				
	Ph_3SiLi	Ph_3SiNa	Ph_3SiK	Ph_3SiRb	Ph_3SiCs
k (l mol^{-1} s^{-1})	0.5	11.5	26.8	35.6	47.9
A (l mol^{-1} s^{-1})	1.5×10^6	5.2×10^3	3.5×10^6	2.8×10^7	1.4×10^9
ΔH^* (kcal mol^{-1})	6.2	2.2	4.7	5.5	7.2
ΔG^* (kcal mol^{-1})	13.2	11.8	11.4	11.3	11.2
ΔS^* (cal mol^{-1} deg^{-1})	−31.5	−43.0	−30.1	−26.0	−18.0

plots were 2.7, 2.3, 5.2, 6.0, and 7.6 kcal mol^{-1} for Ph_3SiNa, $Ph_2MeSiNa$, Ph_3SiK, Ph_3SiRb, and Ph_3SiCs reactions with 9-methylfluorene respectively. The thermodynamic constants of activation calculated for $-50\,°C$ are given in Table 3. The results quoted have the following estimated systematic errors: k and A, $\pm 7\%$, ΔH^* and ΔG^*, $\pm 5\%$, and ΔS^*, $\pm 9\%$.

Products of Reactions

For product analysis the reactions of R_3SiM with 9-methylfluorene in THF were carried out at temperatures consistent to those used in the kinetic experiments under high vacuum conditions. The concentrations of the reactants were used similar to those described in the kinetics experiments. The reaction mixture was quenched with deuterium oxide, after complete reaction. The product formed when the reaction mixture was quenched was isolated by distilling off the THF. The residue material was dissolved in *n*-hexane, washed with water and then dried by storing over anhydrous magnesium sulfate. The solution was filtered and evaporated to dryness. The components of the product were isolated by fractional crystallization and preparative t.l.c. All the components were identified by their melting points, elemental analysis, and n.m.r. spectra.

It was found in all the cases that only 9-hydrogen atom of 9-methylfluorene was replaced by alkali metal atom of R_3SiM regardless of the concentration ratio of the reactants used in these reactions.

Discussion

The yellow-colored solution of R_3SiNa compounds in THF gives typical broad spectra as shown in Fig. 1. The values of λ_{max} and $\varepsilon\lambda_{max}$ of Ph_3SiNa spectrum are slightly different from those quoted by Evans *et al.* (8) (see Table 1). The broad absorption spectrum of a large molecule such as R_3SiNa is not unusual because the molecule has the choice of a variety of initial and final vibrational and rotational states all belonging to the same electronic transition. Furthermore, in solutions the vibrational-rotational fine structure is generally masked by solute–solvent interaction, and continuous absorption bands result in the spectrum. At low temperatures a well resolved spectrum of a molecule would be expected with an unaltered absorption maximum. However, in the spectra of R_3SiNa the absorption maximum is gradually changed to longer wavelength at low temperatures. This gradual red shift in absorption maximum at low temperatures could be explained by considering the fact that the R_3SiNa molecule experiences an increase in dipole moment on excitation which results in a gain in solvation energy for this state. Another factor which could be responsible for the red shift in the spectra of R_3SiNa is the promotion of ionization of these species at low temperatures. However, this latter factor should not be considered very important in this work because it does not explain the *gradual and reversible* red shift at low temperatures.

The spectra of R_3SiNa determined in DME were similar to those in THF. A small red shift caused in the spectra of R_3SiNa in DME could be explained using the arguments suggested by Hogen-Esch and Smid (14) in their studies of ion-pairs of carbanions, that DME because of its bidentate coordination behavior acts as a better solvating agent than that of THF for alkali metal ions.

The spectra of R_3SiM reagents in THF solution shifts toward longer wavelength as the ionic radius of the cation increases, but they do not overlap the spectra of 9-methylfluoren-9-yl-alkalimetal compounds. Hence the spectra of

Can. J. Chem. Downloaded from www.nrcresearchpress.com by 210.87.254.105 on 09/05/12
For personal use only.

Can. J. Chem. Downloaded from www.nrcresearchpress.com by 210.87.254.105 on 09/05/12
For personal use only.

R_3SiM do not interfere with the wavelengths of the products selected to study the kinetics of these reactions. The red shift observed in the spectra of R_3SiM compounds with the increase in the radius of gegenion is consistent with the results reported for various anionic species (8, 14–18).

It has been reported in a previous paper (9) that the shape of 9-methylfluoren-9-yl-lithium spectra was unaltered whereas the values of $\varepsilon\lambda_{max}$ increase as the temperature was reduced from 20 to −88 °C. This increase in the $\varepsilon\lambda_{max}$ was attributed to the formation of solvent separated ion pairs at reduced temperatures from the contact ion pairs that exist at room temperature. The same phenomenon was observed in the case of 9-methylfluoren-9-yl-sodium, where a new absorption peak was developed at 510 nm at the expense of 480 nm peak when the temperature was reduced from 20 to −80 °C. The increase in $\varepsilon\lambda_{max}$ was relatively small in the case of 9-methylfluoren-9-yl-sodium as compared to its lithium counterpart, which could be an indication that the formation of solvent separated ion pairs was more difficult in the case of 9-methylfluoren-9-yl-sodium than -lithium at reduced temperatures. On the other hand no change in $\varepsilon\lambda_{max}$ was observed in the case of 9-methylfluoren-9-yl-potassium, -rubidium, and -caesium at reduced temperatures. Therefore, it could be concluded that these species exist as contact ion pairs in THF even at −80 °C. Similar results have also been reported by Smid and co-worker (14) in their studies of ion pairs of fluorenylalkali-metal compounds in THF.

The red shift of 6 to 10 nm observed in the absorption peaks of 500 and 532 nm at reduced temperatures in the spectrum of 9-methylfluoren-9-yl-rubidium is in marked contrast with its potassium and caesium counterparts. However, this behavior of 9-methylfluoren-9-yl-rubidium could not be explained at this stage.

It was quite easy to prepare Ph_3SiNa and $Ph_2MeSiNa$ in THF by the cleavage of the corresponding symmetrical disilanes using sodium metal, but it was not possible to prepare phenyldimethylsilyl-sodium using the same method. Furthermore, the cleavage of 1,2-diphenyl-1,1,2,2-tetramethyldisilane by sodium, sodium–mercury amalgam in DME at 50 °C also failed. Unsuccessful attempts to prepare $PhMe_2SiNa$ by the cleavage of 1,2-diphenyl-1,1,2,2-tetramethyldisilane have also been reported by Fearon and Gilman (19).

The reaction was first order in both reactants and the overall second order kinetics were retained to at least 90% of the total reaction. These kinetics results were further supported by the results obtained from product analysis that only 9-hydrogen atom of 9-methylfluorene was replaced by alkali metal atom of R_3SiM. In accordance with these results the reactions under investigation could be postulated as follows

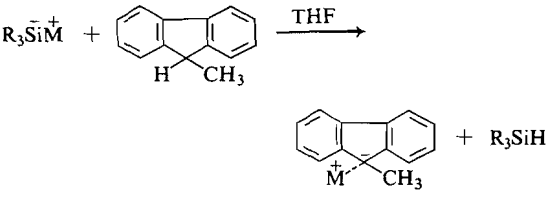

The rate sequence for these reactions is as follows: Ph_3SiLi (9) < Ph_3SiNa < Ph_3SiK < Ph_3SiRb < Ph_3SiCs. This order is consistent with the results reported for various anionic reactions (1, 8) when the organometallic species exist as contact ion-pairs.

The plot of log k against $1/(r_c + 2)$, where r_c is the ionic radius of cation is an excellent straight line for the cation Na^+, K^+, Rb^+, and Cs^+ whereas Li^+ lies well below the line (see Fig. 3). Such a linear relation between log k and $1/(r_c + 2)$ signifies the importance of Coulombic attraction between the ion pair on the reactivity of Ph_3SiM reagents. A similar linear relation has also been reported for log k and $1/(r_c + 2)$ by Evans *et al.* (8) for the reactions of Ph_3SiM with 1,1-diphenylethylene in THF, with the only ex-

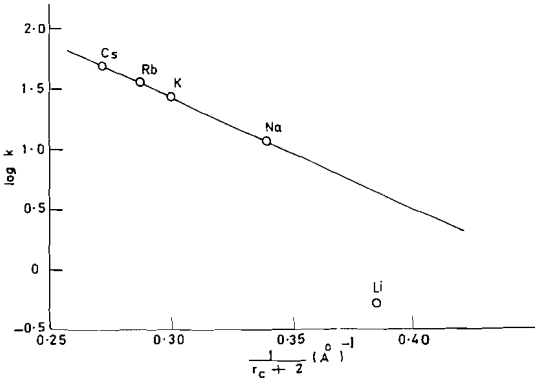

FIG. 3. Plot of log k against $1/(r_c + 2)$.

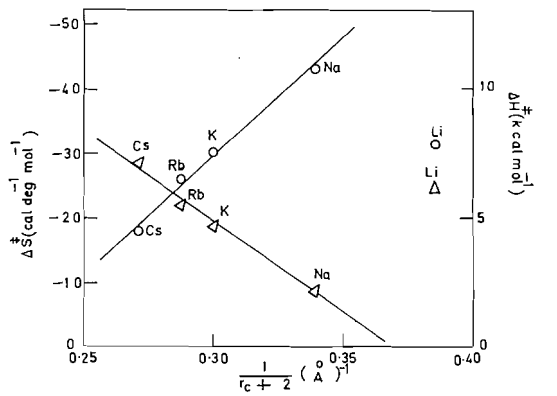

FIG. 4. △, Plot of $\Delta H^{\ddagger}$ against $1/(r_c + 2)$; ○, plot of $\Delta S^{\ddagger}$ against $1/(r_c + 2)$.

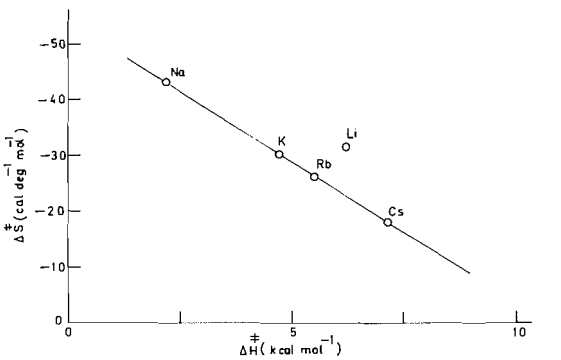

FIG. 5. Plot of $\Delta S^{\ddagger}$ against $\Delta H^{\ddagger}$.

ception that the Li^+ lay well above the line in their plot.

The plots of $\Delta H^{\ddagger}$ and $\Delta S^{\ddagger}$ against $1/(r_c + 2)$ and $\Delta S^{\ddagger}$ against $\Delta H^{\ddagger}$ also show that Li^+ behaves differently to its Na^+, K^+, Rb^+, and Cs^+ counterparts (see Figs. 4 and 5). The analysis of these plots confirms the views already put forward that Ph_3SiNa, -K, -Rb, and -Cs all exist as contact ion pairs and therefore behave in a similar fashion while the exceptional behavior of Ph_3SiLi is due to its existence in the form of solvent separated ion pairs.

In the system involving Na^+, K^+, Rb^+, and Cs^+ the values of $\Delta H^{\ddagger}$ and A factor increase linearly from Na^+ to Cs^+, while the values of $\Delta S^{\ddagger}$ become more positive for the same sequence (see Table 3 and Fig. 5). In accordance with these results it could be suggested that both activation enthalpy and entropy are responsible in determining the rate of these reactions.

In the case of Li^+ the reactant (Ph_3SiLi) and the product (9-methylfluoren-9-yl-lithium) both exist as solvent separated ion pairs. Since the reaction involves equal solvation of the initial and the transition state, this deprives the system of some driving force. Furthermore, this accounts for the slower rate of reaction for Ph_3SiLi as compared to its Na^+, K^+, Rb^+, and Cs^+ counterparts, contrary to the fact that the solvent separated ion pairs should react more rapidly than the contact ion pairs.

Finally, the relative reactivity of Ph_3SiNa and $Ph_2MeSiNa$ is consistent with the fact that the replacement of a phenyl by a methyl group increases the electronegativity of the silyl anion.

1. D. N. BHATTACHARYYA, J. SMID, and M. SZWARC. J. Phys. Chem. **69**, 624 (1965).
2. F. S. DAINTON, G. C. EAST, G. A. HARPELL, N. R. HURWORTH, K. J. IVIN, R. T. LAFLAIR, R. H. PALLEN, and K. M. HUI. Makromol. Chem. **89**, 257 (1965).
3. G. ALLEN, G. GEE, and C. STRETCH. J. Polym. Sci. **48**, 189 (1960).
4. C. STRETCH and G. ALLEN. Polym. **2**, 151 (1961).
5. D. N. BHATTACHARYYA, C. L. LEE, J. SMID, and M. SZWARC. Polym. **5**, 54 (1964).
6. D. N. BHATTACHARYYA, C. L. LEE, J. SMID, and M. SZWARC. J. Phys. Chem. **69**, 612 (1965).
7. H. HOSTALKA, R. V. FIGINI, and G. V. SCHULZ. Makromol. Chem. **71**, 198 (1964).
8. A. G. EVANS, M. LL. JONES, and N. H. REES. J. Chem. Soc. Perkin II, 389 (1972).
9. A. G. EVANS, M. A. HAMID, and N. H. REES. J. Chem. Soc. (B), 2164 (1971).
10. A. G. EVANS, M. LL. JONES, and N. H. REES. J. Chem. Soc. (B), 961 (1967).
11. J. E. BENNETT, A. G. EVANS, J. C. EVANS, E. D. OWEN, and B. J. TABNER. J. Chem. Soc. (B), 3954 (1963).
12. M. A. HAMID. Can. J. Chem. **50**, 3761 (1972).
13. D. DADLEY and A. G. EVANS. J. Chem. Soc. 418 (1967).
14. T. E. HOGEN-ESCH and J. SMID. J. Am. Chem. Soc. **88**, 307 (1966).
15. A. STREITWIESER, JR. and J. I. BRAUMAN. J. Am. Chem. Soc. **85**, 2633 (1963).
16. H. E. ZAUGG and A. D. SCHAEFER. J. Am. Chem. Soc. **87**, 1857 (1965).
17. N. V. VELTHORST and G. J. HOIJLINK. J. Am. Chem. Soc. **87**, 2429 (1965).
18. H. V. CARTER, B. J. MCCLELLAND, and E. WARHURST. Trans. Faraday Soc. **56**, 455 (1960).
19. F. W. G. FEARON and H. GILMAN. J. Organomet. Chem. **9**, 403 (1967).

Can. J. Chem. Downloaded from www.nrcresearchpress.com by 210.87.254.105 on 09/05/12
For personal use only.

The Anharmonicity Correction for Kinetic Isotope Effect Calculations

JAN BRON AND SYLVIA O. HACKER

Department of Chemistry, University of Natal, Durban, South Africa

Received March 12, 1973

The kinetic isotope effect, in the ring opening of a triatomic system, is corrected for anharmonicity in the vibrational ground state. For this system it is found that the correction is small and not larger than uncertainties caused by other assumptions made in kinetic isotope effect calculations.

L'effet isotopique sur la cinétique de l'ouverture de cycle d'un système triatomique a été corrigé en tenant compte de l'anharmonicité de l'état vibrationnel fondamental. Pour ce système, on a trouvé une petite correction de l'ordre des incertitudes issues des suppositions faites dans les calculs de l'effet isotopique sur la cinétique. [Traduit par le journal]

Can. J. Chem., 51, 2765 (1973)

Can. J. Chem. Downloaded from www.nrcresearchpress.com by 210.87.254.42 on 09/05/12
For personal use only.

Introduction

The theoretical evaluation of kinetic isotope effects is usually carried out by application of transition state theory and statistical mechanics. By making many assumptions (1), the expression obtained is usually called the harmonic approximation. It has been discussed in great detail by Bigeleisen and co-worker (2) and Wolfsberg and co-worker (3).

One of the assumptions leading to the harmonic approximation is, as implied in the name, that the molecule vibrates harmonically. It has been shown (1) that for *equilibrium* isotope effects this assumption may lead to considerable error. Although equilibrium constants have been corrected for anharmonicity before (4), to give rather unexpected results, it was Wolfsberg *et al.* (5) who realized the importance of a constant term, G_0, in the expansion of the vibrational–rotational energy in powers of $(n_i + \frac{1}{2})$. This refers to the familiar (6) expression

$$[1] \quad E_v(n) = G_0 + \sum\omega_i(n_i + \tfrac{1}{2}) + \sum x_{ij}(n_i + \tfrac{1}{2})(n_j + \tfrac{1}{2})$$

in which the vibrational energy levels are assumed to be non-degenerate.

One of the first attempts to correct transition state calculations for anharmonicity has been made by Weston (7). However, the constant term, G_0, has been ignored. The anharmonicity correction for kinetic isotope effects has never been determined correctly. Because these calculations are carried out routinely now, it is worthwhile to determine the importance of this correction in kinetic isotope effect calculations.

General Considerations

If only the ground state is considered, the correction due to anharmonicity for the zero-point harmonic energy, $\frac{1}{2}\sum\omega_i$, is

$$[2] \quad \text{AZPE} = G_0 + \tfrac{1}{4}\sum x_{ij} = E_v(0) - \tfrac{1}{2}\sum\omega_i$$

The dimension of energy is wave numbers. Because the ground state is the most important accessible vibrational state at reasonable temperatures, only the correction due to AZPE will be considered. For some equilibria it has been shown that the correction for anharmonicity of the excited states is indeed small (1).

The expression for $E_v(0)$, referred to as ZPE has been given before (1) and shall not be reproduced. It should be noted, however, that it is only valid for a stable molecule. One of the terms in ZPE, $-\frac{1}{4}\sum B_e^{(\alpha\alpha)}$, is a simplification of the much more complicated term (8):

$$[3] \quad -\frac{1}{4}\sum B_e^{(\alpha\alpha)} = \frac{\hbar}{8\pi c}\sum_i \left[\sum_\alpha \frac{A_{ii}'^{(\alpha\alpha)}}{I_{\alpha\alpha}^{(e)}} + \sum_{\alpha<\beta} \frac{a_i^{(\alpha\alpha)}a_i^{(\beta\beta)} - (a_i^{(\alpha\beta)})^2}{I_{\alpha\alpha}^{(e)}I_{\beta\beta}^{(e)}} - \frac{3}{8}\left(\sum_\alpha \frac{a_i^{(\alpha\alpha)}}{I_{\alpha\alpha}^{(e)}}\right)^2\right]$$

All symbols used have been defined by Nielsen (6). Equation 3 should be used for transition states, because the relationships leading to its simplification break down. The running index i for a transition state has a maximum value of $(3N - 7)$ rather than $(3N - 6)$.

For the isotope effect (k_1/k_2) in the reactions

Can. J. Chem. Downloaded from www.nrcresearchpress.com by 210.87.254.42 on 09/05/12
For personal use only.

[4] $$\Delta_1 \overset{k_1}{\rightleftharpoons} \Delta_1^* \rightarrow P_1$$

$$\Delta_2 \overset{k_2}{\rightleftharpoons} \Delta_2^* \rightarrow P_2$$

in which the reactants Δ_1 and Δ_2 only differ in isotopic substitution and Δ^* stands for the transition state and P for the products, the anharmonicity correction is

[5] $$\text{ACOR} = \exp\,[-(\Delta\text{AZPE})hc/kT]$$

The quantity ΔAZPE is defined as

$$\Delta\text{AZPE} = \text{AZPE}(\Delta_2) - \text{AZPE}(\Delta_1) - \text{AZPE}(\Delta_2^*) + \text{AZPE}(\Delta_1^*)$$

From a knowledge of geometry and force field of the species involved, ΔAZPE and hence ACOR can be evaluated.

The Model

The ring opening of an equilateral triangular, triatomic molecule, with each side equal to 1.524 Å (9) and leading to a bent transition state, may serve as the reaction for which the anharmonicity correction will be determined. All three atoms have an atomic weight of 14 in the species that is not isotopically substituted. The effect of isotopic substitution in the various positions can now be investigated. For example, the isotope effect and the corresponding anharmonicity correction can be evaluated if the rate of reaction of a species with isotope substitution at the position where the bond is being broken is compared with the unsubstituted case.

The reaction is supposed to take place in the ideal gas phase. The two reacting systems that will be compared are:

[6]

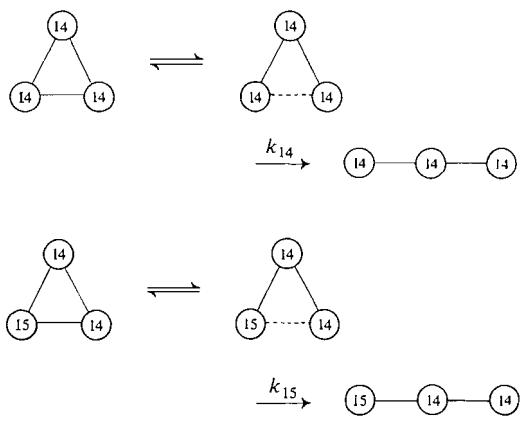

In these two reacting systems isotopic substitution takes place at the bond being broken. This bond will vary in length, while the other two remain unchanged. The kinetic isotope effect for the above reactions is then defined as k_{14}/k_{15}.

The Calculation of the Anharmonicity Correction and Isotope Effect

For the initial and transition states the changes in bond length have been chosen as the three internal coordinates. For symmetry reasons it is convenient to choose for the initial state a linear combination of internal coordinates. These are for all initial states, regardless of the fact that the symmetry may be changed on isotopic substitution, $S_1 = (r_1 + r_2 + r_3)/\sqrt{3}$, $S_2 = (2r_1 - r_2 - r_3)/\sqrt{6}$, and $S_3 = (r_2 - r_3)/\sqrt{2}$, in which, for example, r_1 means the change in bond distance between atoms 1 and 2.

From the choice of internal coordinates it follows that all diagonal force constants are the same for the initial state. This basically also holds for the transition state, except that the diagonal force constant which corresponds to the bond being broken (the reaction coordinate) has been taken as zero. The magnitudes of the non-zero diagonal quadratic, cubic, and quartic force constants for the *basic force field* (see below) are 4.37 mdyn/Å (9), −52.4 mdyn/Å^2, and 209.8 mdyn/Å^3, respectively. All off-diagonal force constants are taken as zero. The force constants strictly refer to the derivatives of the potential energy with respect to internal coordinates and exclude any multiplicative constant. The cubic force constant is −12 times and the quartic force constant 48 times the quadratic force constant, a trend *approximately* followed by most molecules (10, 11). There are other ways of estimating force constants (12), but the key data are lacking and the results obtained are not necessarily better in this case.

The transformation of force constants in internal coordinates to force constants in dimensionless normal coordinates (6) has been accomplished by the method of Pariseau *et al.* (13). Because the change in isotopic mass, the geometry of the transition state, and the force field are rather arbitrary, they have been varied in a systematic way to establish their importance in determining the magnitude of the anharmonicity correction of kinetic isotope effects. All quanti-

TABLE 1. The anharmonicity correction as a function of the geometry of the transition state

Geometry of t.s.*	AZPE (cm^{-1})†		200 °K		700 °K	
	t.s. (14)	t.s. (15)	k.i.e.‡	ACOR	k.i.e.	ACOR
1.0*h*	−38.09	−37.44	1.061	0.996	1.022	0.999
0.8*h*	−38.60	−37.96	1.059	0.996	1.020	0.999
0.6*h*	−37.74	−37.09	1.057	0.996	1.018	0.999
0.4*h*	−36.52	−35.85	1.053	0.996	1.015	0.999
0.2*h*	−35.62	−34.93	1.050	0.996	1.012	0.999

*h is the height of the triangle representing the initial state (i.s.). The number nh, (n = 1.0, . . . , 0.2), is the height of the transition state (t.s.) where only the reacting bond is changed with respect to i.s.

†t.s. (14) refers to the transition state without isotopic substitution, while t.s. (15) refers to the transition state where one of the atoms of weight 14, at the position where the bond is being broken, has been replaced by its isotope of weight 15. The corresponding initial states, i.s. (14) and i.s. (15), have an AZPE value of −56.64 and −55.38 cm^{-1}, respectively.

‡The kinetic isotope effect (k.i.e.) calculated by means of the harmonic approximation (2, 3) in which symmetry numbers have been ignored.

ties connected with the reaction coordinate in, for example, eq. 3 have been set equal to zero.

Results and Discussion

If the rates of reaction of the two systems [6] at 200 °K are compared, the kinetic isotope effect, as can be seen in the first line of Table 1, is about 1.06 (6%). The anharmonicity correction is quite small, only 0.996 (0.4%) at this temperature. At 700 °K the correction becomes 0.999, which is negligible. As is also true for the other results listed in Table 1, the basic force field has been used and the geometry of the initial and transition states is the same.

The remainder of Table 1 shows other interesting results. If only the reacting bond is allowed to stretch while leaving the remaining two unchanged, the small anharmonicity correction does not vary, contrary to the isotope effect which decreases slightly. It appears that AZPE for the transition state, similar to ACOR, is almost insensitive towards geometry of the transition state. Although the frequencies have not been listed, the magnitudes of AZPE for the initial and transition states are only 3–4% of the zero-point energies.

The anharmonicity correction as a function of the force field of the transition state is listed in Table 2. The force field for the initial state is the basic one and, as before, the geometry of both states is the same. Again the conclusion is simple; even for greatly differing cubic and quartic force constants the correction is smaller than 2.5% at temperatures higher than 200 °K. When the cubic and quartic force constants in internal coordinates are zero, the correction is very close to one (but not exactly). It can also be seen that the correction is more sensitive towards changes in the cubic force constants than to changes in the quartics.

TABLE 2. The anharmonicity correction as a function of the cubic and quartic force constants.

Force field of t.s.*	ACOR	
	200 °K	700 °K
coqo	1.000	1.000
cuqo	0.994	0.998
coqu	1.001	1.000
cuqh	0.995	0.999
cuqd	0.997	0.999
chqu	1.000	1.000
cdqu	0.978	0.994
chqh	0.999	1.000
cdqd	0.980	0.994

*Key to the code: c = cubic force constant; q = quartic force constant; o = zero; u = unchanged; h = halved; d = doubled. The letters cuqd, for example, mean the cubic force constants are unchanged and the quartic force constants doubled with respect to the basic force field (see text).

A spectacular increase in ACOR can be achieved decreasing the mass of the isotope to almost zero. Although without physical significance, the correction can be as large as 6537 at 200 °K, if an atom of mass 14 is replaced by one of 0.1. However, for any reasonable mass ratio the correction stays small. The results of the determination of the mass dependence of ACOR can be found in Table 3.

For the basic force field and geometry, isotopic substitution at the position away from the bond being broken reduces the isotope effect to 1.003 and ACOR to 1.000 at 200 °K. Double substitution at the bond being broken shows that

Can. J. Chem. Downloaded from www.nrcresearchpress.com by 210.87.254.42 on 09/05/12
For personal use only.

TABLE 3. The anharmonicity correction as a function of mass

	200 °K		700 °K	
X*	k.i.e.†	ACOR	k.i.e.†	ACOR
0.1	0.000	6537	0.001	12.31
1	0.003	2.267	0.159	1.263
5	0.272	1.123	0.643	1.034
10	0.717	1.027	0.889	1.008
15	1.061	0.996	1.022	0.999
20	1.319	0.980	1.108	0.994
100	2.468	0.941	1.438	0.983

*Mass of the isotope at the bond being broken. Transition and initial states have the same geometry. The basic force field has been used.
†Symmetry numbers are ignored.

the isotope effect and anharmonicity correction are roughly additive (1.117 and 0.991 at 200 °K, respectively).

Some other corrections have also been determined. The corrections for effective rotational constants (6), rotational stretching (14), and replacing the sum by an integral (15) in the rotational partition function are in all calculations less than 0.1% and can be safely ignored under normal conditions for the proposed reactions.

The authors would like to thank the South African Council for Scientific and Industrial Research for financial assistance and Miss S. E. Nieuwoudt for her help in computer programming.

1. J. BRON and M. WOLFSBERG. J. Chem. Phys. **57**, 2862 (1972).
2. J. BIGELEISEN and M. WOLFSBERG. Adv. Chem. Phys. **1**, 15 (1958).
3. M. WOLFSBERG and M. J. STERN. Pure Appl. Chem. **8**, 225 (1964).
4. J. W. PYPER and F. A. LONG. J. Chem. Phys. **41**, 2213 (1964).
5. M. WOLFSBERG, A. A. MASSA, and J. W. PYPER. J. Chem. Phys. **53**, 3138 (1970).
6. H. H. NIELSEN. Rev. Mod. Phys. **23**, 90 (1951).
7. R. E. WESTON, JR. J. Chem. Phys. **31**, 892 (1959).
8. M. WOLFSBERG. J. Chem. Phys. **50**, 1484 (1969).
9. HS. H. GÜNTHARD, R. C. LORD, and T. K. MCCUBBIN, JR. J. Chem. Phys. **25**, 768 (1956).
10. K. KUCHITZU and Y. MORINO. Bull. Chem. oc. Jap. **38**, 814 (1965).
11. K. MACHIDA. J. Chem. Phys. **44**, 4186 (1966).
12. S. REICHMAN, D. F. SMITH, JR., and J. OVEREND. Spectrochim. Acta **26A**, 927 (1970).
13. M. A. PARISEAU, I. SUZUKI, and J. OVEREND. J. Chem. Phys. **42**, 2335 (1965).
14. E. B. WILSON, JR. J. Chem. Phys. **4**, 526 (1936).
15. K. F. STRIPP and J. R. KIRKWOOD. J. Chem. Soc. **19**, 1131 (1951).

Can. J. Chem. Downloaded from www.nrcresearchpress.com by 210.87.254.42 on 09/05/12
For personal use only.

Model Experiments Directed towards the Synthesis of *N*-Aminopeptides

AMADEO FAILLI, VERN NELSON, HANS IMMER, AND MANFRED GÖTZ
Department of Chemistry, Ayerst Research Laboratories, P.O. Box 6115, Montreal 101, Quebec
Received February 15, 1973

Since modified peptides embodying a 1,1-disubstituted hydrazide (II) have not been described previously, model experiments were carried out to determine suitable reaction conditions for their preparation. The synthesis of model compounds of type II is the subject of this paper.

On a effectué des expériences modèles afin de déterminer les conditions de réaction appropriées pour la préparation de peptides modifiés contenant une hydrazide disubstituée en 1,1. La synthèse de composés modèles de type II fait l'objet de la présente publication.

[Traduit par le journal]

Can. J. Chem., 51, 2769 (1973)

Can. J. Chem. Downloaded from www.nrcresearchpress.com by 210.87.254.6 on 09/05/12
For personal use only.

Introduction

Among natural products of pronounced physiological activity are numerous peptides. Typical examples are the kinins (1) and the recently discovered hypothalamic releasing hormones (2). The therapeutic application of peptides is, however, limited due to rapid enzymatic degradation in the alimentary tract after oral administration. Even on parenteral administration most of these compounds lose their potency much faster than desired. The elimination of this shortcoming is, therefore, a classical goal of peptide chemistry. A number of approaches have been explored in the past to improve the stability and to prolong the physiological lifetime of therapeutically interesting peptides, for instance: the use of alkylated aminoacids (3), the replacement of amide by ester groups (4), the substitution of D- for L-aminoacids (5), of the elongation of the peptide linkage by an additional —NH— to form a hydrazide of type I (6). These changes are in general accompanied by either considerable or total loss of activity. Some loss of activity, hopefully combined with increased pharmacological specificity, is frequently acceptable, since many natural products are effective at minimal concentrations (7).

Since modified peptides embodying a 1,1-disubstituted hydrazide (II) have not been described previously, model experiments were carried out to determine suitable reaction conditions for their preparation. The synthesis of model compounds of type II is the subject of this paper.

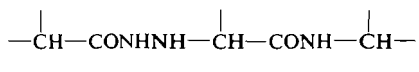

I

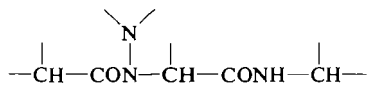

II

Methods

The versatile and elegant four-component condensation of Ugi (8) provided easy access to the desired peptide analogues. This reaction was modified so that the substituted hydrazones were prepared separately and then allowed to react with the isonitrile and the carboxylic acid as shown in Scheme 1. In the simplest case, the product is a dipeptide analogue in which one nitrogen atom carries a dialkylamino substituent.

Results

The addition of isonitriles to hydrazones was expected (8) to proceed with a rather low reaction rate in view of the reduced basicity of the hydrazones compared to the amine derivatives. Nevertheless Ugi products were obtained in acceptable yields, since the addition of the isonitrile and the carboxylic acid was followed by an irreversible rearrangement. Zinner and Bock (9) also succeeded in using hydrazines in the Ugi reaction in connection with the synthesis of substituted tetrazoles.

Tables 1–3 list the compounds prepared. Examples **1–4** (Table 1) represent reaction products of cyclohexanone dimethylhydrazone, ethyl

Can. J. Chem. Downloaded from www.nrcresearchpress.com by 210.87.254.6 on 09/05/12
For personal use only.

TABLE 1. Four component reaction products of general structure:

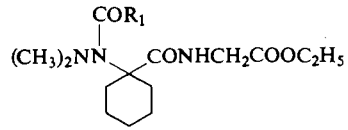

Compound	R_1	Reaction conditions	Yield (%)	M.p. (°C)	Crystallization solvent	Formula	Analysis (%) Calculated C	H	N	Found C	H	N
1	H	4 h, r.t.	69	87–88	Hexane/methylene chloride	$C_{14}H_{25}N_3O_4$	57.17	8.42	14.04	56.33	8.50	14.12
2	C_6H_5	30 h, r.t.	69	90–92	Diisopropylether	$C_{20}H_{29}N_3O_4$	63.97	7.79	11.19	64.11	7.85	11.51
3	$pNO_2C_6H_4$	48 h, r.t.	82	86–88	Hexane/methylene chloride	$C_{20}H_{28}N_4O_6$	57.13	6.71	13.33	57.35	6.74	13.19
4	$CH_2NHCOCH_2NHCOOCH_2C_6H_5$	7 day, reflux	14	138–39	Hexane/methylene chloride	$C_{25}H_{37}N_5O_7$	57.79	7.18	13.48	57.73	7.21	13.56
5	H	4 h, r.t.	63	84–86	Diisopropylether	$C_{20}H_{29}N_3O_4$	63.97	7.79	11.19	63.97	7.85	11.21
6	$pNO_2C_6H_4$	24 h, r.t.	74	116–17	Acetone/diisopropylether	$C_{26}H_{32}N_4O_6$	62.89	6.50	11.28	63.08	6.55	11.29

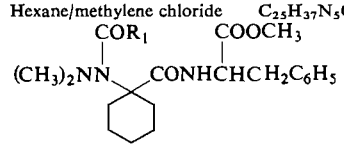

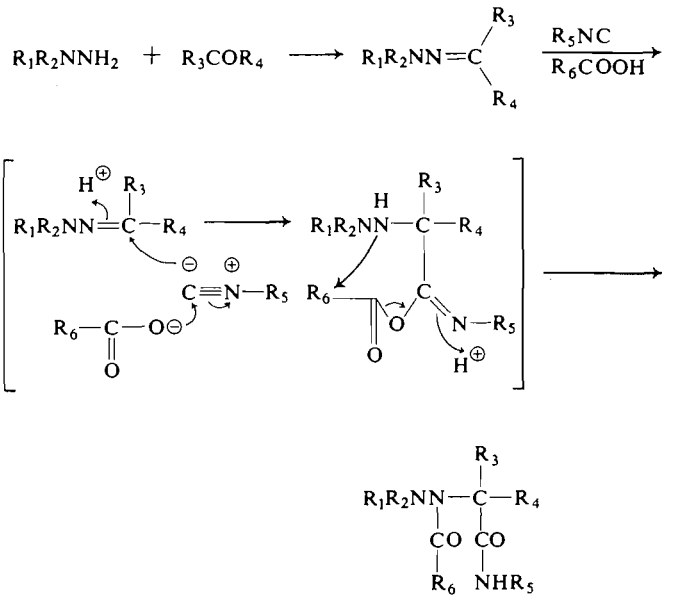

SCHEME 1

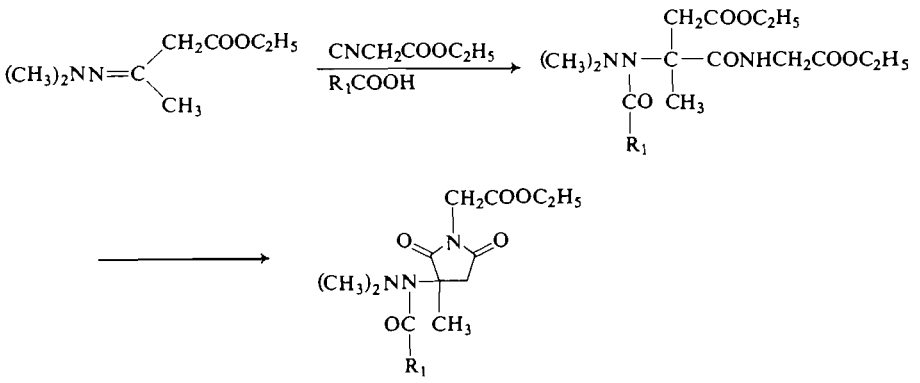

SCHEME 2

isocyanoacetate (10) and a carboxylic acid. It is evident that the reaction rate was considerably reduced with increasing bulk of the substituent R_1. This was also true for substances **5** and **6**, where the isonitrile derived from D,L-phenylalanine methylester was employed. Replacement of cyclohexanone by ethyl acetoacetate as carbonyl component led to Ugi products which underwent ring closure to 2,5-dioxopyrrolidines (Scheme 2), under mildly basic conditions. In some cases ring closure occurred spontaneously without base treatment (**7**, **8**, **12**).

Examples **9**, **10**, and **11** of Table 2 clearly demonstrate the influence of R_1 substituents on reaction rate. The latter depends on the conversion of A to B and is determined by the electrophilic character of the carbonyl group of the acid (Scheme 3).

Finally, the use of cyclohexylisonitrile and the

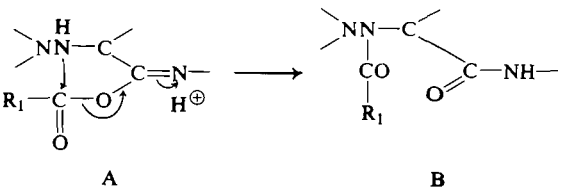

SCHEME 3

Can. J. Chem. Downloaded from www.nrcresearchpress.com by 210.87.254.6 on 09/05/12
For personal use only.

Can. J. Chem. Downloaded from www.nrcresearchpress.com by 210.87.254.6 on 09/05/12
For personal use only.

TABLE 2. Four component reaction products of general structure:

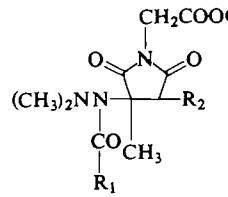

Compound	R_1	R_2	Reaction Conditions	Yield (%)	M.p. (°C)	Crystallization solvent	Formula	Analysis (%) Calculated C	H	N	Found C	H	N
7	H	H	21 h, r.t.	59	89–92	Hexane/methylene chloride	$C_{12}H_{19}N_3O_5$	50.52	6.71	14.73	50.47	6.74	14.72
8	CH_3	H	10 day, r.t.	23	112–15	Hexane/methylene chloride	$C_{13}H_{21}N_3O_5$	52.16	7.07	14.04	52.11	7.02	14.12
9	C_6H_5	H	9 day, r.t.	33	100–02	Hexane/ethylacetate	$C_{18}H_{23}N_3O_5$	59.82	6.42	11.62	60.06	6.49	11.70
10	$pNO_2C_6H_4$	H	8 day, r.t.	64	179–82	Ethylacetate	$C_{18}H_{22}N_4O_7$	53.20	5.46	13.79	53.02	5.56	13.94
11	$pClC_6H_4$	H	7 day, reflux	39	123–25	Hexane/methylene chloride	$C_{18}H_{22}ClN_3O_5$	54.62	5.60	10.62	54.60	5.75	10.42
12	H	C_6H_5	4 day, r.t.	30	123–24	Hexane/methylene chloride	$C_{18}H_{23}N_3O_5$	59.82	6.41	11.63	60.09	6.46	11.63

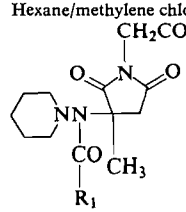

13	H		18 h, r.t.	71	89–92	Diisopropyl ether	$C_{15}H_{35}N_3O_5$	55.37	7.13	12.92	55.51	7.21	13.08
14	C_6H_5		12 day, r.t.	62	140–44	Diisopropyl ether	$C_{21}H_{27}N_3O_5$	62.82	6.78	10.47	62.88	6.85	10.46
15	$pNO_2C_6H_4$		12 day, r.t.	60	232–35	Ethylacetate	$C_{21}H_{26}N_4O_7$	56.49	5.87	12.55	56.65	5.92	12.60
16	$pClC_6H_4$		7 day, reflux	49	153–55	Hexane/methylene chloride	$C_{21}H_{26}ClN_3O_5$	57.80	5.96	9.63	57.84	6.12	9.56

Can. J. Chem. Downloaded from www.nrcresearchpress.com by 210.87.254.6 on 09/05/12
For personal use only.

TABLE 3. Four component reaction products of general structure:

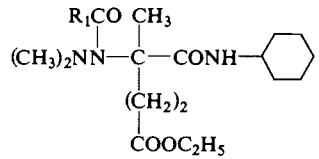

Compound	R_1	Reaction conditions	Yield (%)	M.p. (°C)	Crystallization solvent	Formula	Analysis (%) Calculated C	H	N	Found C	H	N
17	H	3 h, r.t.	62	81–83	Hexane/ether/ methylene chloride	$C_{17}H_{31}N_3O_4$	59.80	9.15	12.31	59.47	9.28	12.42
18	C_6H_5	24 h, r.t.	70	79–80	Hexane/methylene chloride	$C_{23}H_{35}N_3O_4$	66.16	8.45	10.06	66.07	8.47	10.22

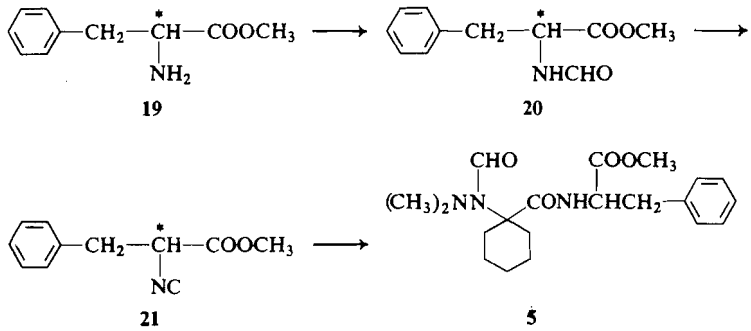

SCHEME 4

dimethylhydrazone of 4-ketopentanoic acid ethyl ester in the Ugi reaction was investigated. The reaction went smoothly and the reaction rate was again dependent on R_1 (structures **17**, **18**).

Whenever an asymmetric center is generated in the Ugi reaction a racemate is obtained (structures **7**–**18**), at least in the absence of inducing agents (11). It was now interesting to ascertain if isonitriles derived from optically active amino acid esters retain optical activity under the conditions employed. L-Phenylalanine methyl ester (**19**) (12) was converted into *N*-formyl-L-phenylalanine methyl ester (**20**) (12, 13) which was transformed into the isonitrile (**21**) with phosgene under mild conditions. The optically active isonitrile (**21**) was condensed with cyclohexanone-dimethylhydrazone in the presence of formic acid to yield **5** (Scheme 4) which showed no optical activity (14). The application of the Ugi reaction utilizing 1,1-dialkylated hydrazines to a peptide problem of pharmacological interest will be described separately (15).

Experimental

General Procedures[1]

(a) Synthesis of 1–8, 12, 17, 18

To a stirred, ice-cold solution of the isonitrile (0.1 mol) and the hydrazone (0.1 mol) in CH_2Cl_2 (50 ml) the solution of the carboxylic acid (0.1 mol) in CH_2Cl_2 (50 ml) was added dropwise. After the appropriate time the solution was diluted with 100 ml CH_2Cl_2 and washed with 4 *N* NH_4OH (100 ml), H_2O (100 ml), and saturated NaCl solution (100 ml). The organic phase was dried over Na_2SO_4, filtered, and evaporated to dryness *in vacuo*. The residue was crystallized.

(b) Synthesis of 9–11, 13–16

The residue obtained under (*a*) was dissolved in $CHCl_3$ (250 ml) and refluxed for 90 min in the presence of 40 g anhydrous K_2CO_3. The solids were filtered off, the solvent evaporated *in vacuo* and the residue crystallized.

L-*Phenylalanine methyl ester hydrochloride (19) (12)*

A solution of L-phenylalanine (25 g, 0.15 mol) in anhydrous methanol (250 ml), saturated with anhydrous hydrogen chloride, was heated to reflux for 5 min. The solvent was removed *in vacuo* and the residue crystallized from methanol – diisopropyl ether (16.0 g): m.p. 159–161° $[\alpha]_D$ + 38.7 (*c* 2.9 in EtOH).

Anal. Calcd. for $C_{10}H_{14}ClNO_2$: C, 55.68; H, 6.50; N, 6.50. Found: C, 55.79; H, 6.62; N, 6.59.

N-Formyl-L-phenylalanine methyl ester (20) (12, 13)

A hot solution of sodium formate (123 g, 0.18 mol) in 98% formic acid (14 ml) was added to a warm solution of L-phenylalanine methyl ester hydrochloride (22.0 g, 0.1 mol) in formic acid (15 ml). After 1 h the mixture was filtered, and acetic anhydride (29 ml, 0.245 mol) was added over a period of 20 min under ice cooling. After 1 h at room temperature the acids were removed *in vacuo*. The residual oil was dissolved in acetone (100 ml), filtered, and fractionally distilled. Yellow oil (19.7 g): b.p. 133–136°/0.88 mm; $[\alpha]_D$ + 32.5° (*c* 2.5 in EtOH).

Anal. Calcd. for $C_{11}H_{13}NO_3$: C, 63.75; H, 6.32; N, 6.75. Found: C, 63.51; H, 6.48; N, 6.74.

Methyl-2-isocyano-3-phenylpropionate (21)

A solution of phosgene (5.2 g, 0.052 mol) in dry CH_2Cl_2 (45 ml) was added dropwise to a stirred solution of *N*-formyl-L-phenylalanine methyl ester (10.0 g, 0.048 mol) and *N*-methylmorpholine (13 g, 0.125 mol) in dry CH_2Cl_2 (25 ml) at −30°. The solution was stirred at −30° for an additional 30 min, filtered, and the filtrate concentrated *in vacuo*. Benzene was added to the residue followed by filtration and concentration. The residue was distilled to afford a yellow oil (6.47 g): b.p. 97°/0.3 mm; γ_{max} ($CHCl_3$) 2150, 1746 cm^{-1}; n.m.r. ($CDCl_3$) 3.20 (d, *J* 7 Hz, 2H, —CH_2—), 3.77 (3H, $COOCH_3$), 4.48 (two doublets, *J* 7.5 and 5 Hz, 1H, —*CH*—), 7.30 p.p.m. (5H, aromatic); $[\alpha]_D$ −10.0° (*c* 1.0 in MeOH).

Anal. Calcd. for $C_{11}H_{11}NO_2$: C, 69.82; H, 5.86; N, 7.40. Found: C, 68.72; H, 5.97; N, 7.42.

N-[1-(N-Dimethylamino)formamido]cyclohexylcarbonyl phenylalanine methyl ester (5)

To a solution of cyclohexanone dimethylhydrazone (3.70 g, 0.026 mol) and L-methyl 2-isocyano-3-phenylpropionate (5.0 g, 0.026 mol) in dry CH_2Cl_2 (15 ml) a

[1]Reaction conditions are given in Tables 1–3.

Can. J. Chem. Downloaded from www.nrcresearchpress.com by 210.87.254.6 on 09/05/12
For personal use only.

solution of formic acid (1.2 g, 0.026 mol) in dry CH_2Cl_2 (15 ml) was added under ice cooling. The solution was stirred at room temperature for 20 h, diluted with CH_2Cl_2 (30 ml), and washed with 0.5 *N* NH_4OH (15 ml), H_2O (15 ml), and saturated NaCl solution (15 ml). The organic phase was dried over Na_2SO_4, concentrated and crystallized from diisopropyl ether as white needles (6.2 g); m.p. 84–86°; γ_{max} ($CHCl_3$) 1735 1660 cm^{-1}; n.m.r. ($CDCl_3$) 1.45 and 2.00 (1OH, —CH_2—), 2.74 (6H, NCH_3), 3.16 (d, *J* 6.5 Hz, 2H, phenyl —CH_2—), 3.75 (3H, $COOCH_3$), 4.88 (multiplet, 1H, —CH—), 6.52 (d, *J* 7 Hz, 1H, *NH*), 7.25 5H, aromatic), 8.33 p.p.m. (1H, CHO); $[\alpha]_D$ nil (*c* 1.0 in MeOH).

Anal. Calcd. for $C_{20}H_{29}N_3O_4$: C, 63.97; H, 7.79; N, 11.19. Found: C, 63.97; H, 7.85; N, 11.21.

We would like to thank Dr. G. Schilling and his staff for providing the microanalyses and spectral data.

1. E. SCHRÖDER and K. LÜBKE. The peptides. Vol. II. Academic Press, New York and London, 1966. p. 4.
2. A. V. SCHALLY, A. ARIMURA, and A. J. KASTIN. Science, **179**, 341 (1973).
3. (*a*) R. L. HUGUENIN and R. A. BOISSONNAS. Helv. Chim. Acta, **44**, 213 (1961); (*b*) K. JOST, J. RUDINGER, and F. SORM. Coll. Czech. Chem. Commun. **26**, 2496 (1961).
4. M. M. SHEMYAKIN, L. A. SHCHUKINA, E. I. VINOGRADOVA, G. A. RAVDEL, and YU. A. OVCHINNIKOV. Experientia, **22**, 535 (1966).
5. (*a*) C. H. SCHNEIDER and V. DUVIGNEAUD. J. Am. Chem. Soc. **84**, 3005 (1962); (*b*) E. D. NICOLAIDES, M. K. CRAFT, and H. A. DEWALD. J. Med. Chem. **6**, 524 (1963).
6. P. OEHME, J. BERGMANN, H. G. MÜLLER, R. GRUPE, H. NIEDRICH, W. E. VOGT, and F. JUNG. Acta biol. med. germ. **28**, 121 (1972) and papers cited therein.
7. E. SCHRÖDER and K. LÜBKE. The peptides. Vol. II. Academic Press, New York and London, 1966. p. 128.
8. I. UGI. Angew. Chem. **74**, 9 (1962).
9. G. ZINNER and W. BOCK. Arch. Pharm. **304**, 933 (1971).
10. I. UGI, U. FETZER, U. EHOLZER, H. KNUPFER, and K. OFFERMANN. Angew. Chem. **77**, 492 (1965).
11. G. W. GOKEL, D. MARQUARDING, and I. K. UGI. J. Org. Chem. **37**, 3052 (1972) and refs. cited therein.
12. F. BERGEL, J. M. JOHNSON, and R. WADE. J. Chem. Soc. 3802 (1962).
13. R. G. JONES. J. Am. Chem. Soc. **71**, 644 (1949).
14. See also: H. L. MAIA, B. RIDGE, and H. N. RYDON. J. Chem. Soc. Perkin I, 98 (1973).
15. H. IMMER, V. NELSON, W. ROBINSON and M. GÖTZ. Liebigs Ann. Chem. Submitted.

Can. J. Chem. Downloaded from www.nrcresearchpress.com by 210.87.254.6 on 09/05/12
For personal use only.

The Direct Observation of a Stereospecific Pentadienyl – Cyclopentenyl Cation Cyclization

N. W. K. CHIU AND T. S. SORENSEN

Department of Chemistry, The University of Calgary, Calgary, Alberta

Received February 20, 1973

Two isomeric 1,2,4,5-tetramethylpentadienyl cations (**4***a* and **4***b*) have been observed in FSO_3H–SO_2ClF at −125°. They undergo stereospecific thermal cyclizations to cyclopentenyl cations in accord with the Woodward–Hoffmann rules.

Les deux cations isomères (**4***a* et **5***a*) du tétraméthyl-1,2,4,5 cyclopentadiényle ont été observés dans un mélange de FSO_3H–SO_2ClF à −125°. Ils subissent des cyclisations thermiques stéréospécifiques qui les transforment en cations cyclopentènyles suivant les règles de Woodward–Hoffmann.

[Traduit par le journal]

Can. J. Chem., **51**, 2776 (1973)

Introduction

There are now many literature examples (1–7) in which a substituted dienylic cation undergoes a thermal cyclization reaction to yield a cyclopentenyl cation.

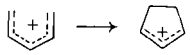

This reaction was one of the first to be treated by Woodward and Hoffmann (8). It can be described as an electrocyclic transformation and is predicted to proceed in a conrotatory manner.[1] In our previous paper relating to the stereochemistry of this transformation (9), we reported the thermal acid cyclization of the isomeric dienols **1***a–c* (via the presumed intermediacy of the dienylic cation **2**) to the cyclopentenyl cation **3***a* or **3***b*. The cyclization is nearly stereospecific and indeed proceeds in a conrotatory manner as predicted by the Woodward–Hoffmann rules (8).

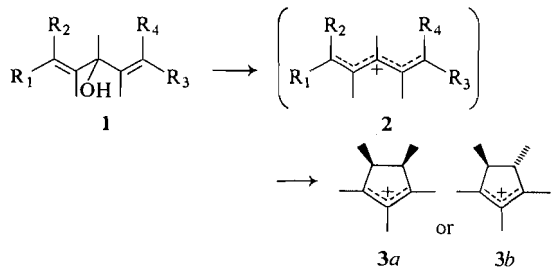

a $R_1=R_3=CH_3$, $R_2=R_4=H$
b $R_1=R_4=CH_3$, $R_2=R_3=H$
c $R_2=R_4=CH_3$, $R_1=R_3=H$

(In all cases — indicates a methyl group.)

However, the failure to directly observe the presumed dienylic cation intermediate **2** must inevitably lead to some doubt about the existence of **2** as an intermediate. Furthermore, the non-observation of **2** curtailed our original intention to examine the cyclization by both the thermal and photochemical processes.

In another attempt, we chose the homologous dienylic cation systems **4** and **5**, whose precursors are the dienols **6** and **7** respectively.

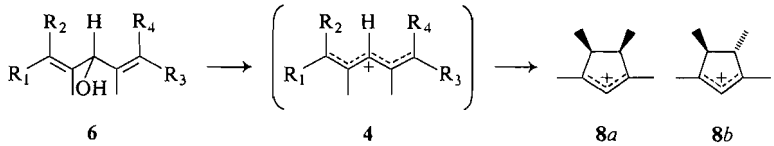

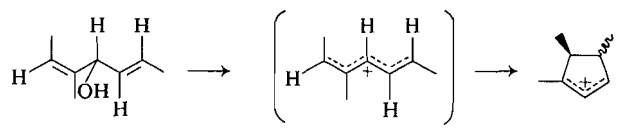

a $R_1=R_3=CH_3$, $R_2=R_4=H$
b $R_1=R_4=CH_3$, $R_2=R_3=H$
c $R_2=R_4=CH_3$, $R_1=R_3=H$

[1]Confirmed also by extensive CNDO/2 calculations.

Can. J. Chem. Downloaded from www.nrcresearchpress.com by 210.87.254.42 on 09/05/12
For personal use only.

Can. J. Chem. Downloaded from www.nrcresearchpress.com by 210.87.254.42 on 09/05/12
For personal use only.

The steric interactions responsible for the instability (nonplanarity) of **2** are shown by molecular model studies to be mainly due to the following interaction.

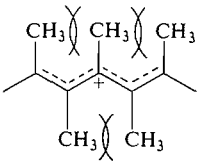

This interaction is reduced in **4** and even more so in **5**, at least in some of the geometric forms of these. An excellent precedent exists for the expectation that the removal of a C-3 methyl group in **2** will result in dienylic ion stability (to cyclization). The ion **10** has a half-life of 2.3×10^3 s at $-57°$ whereas ion **11** has a half-life of 4.6×10^4 s at 25° (6).

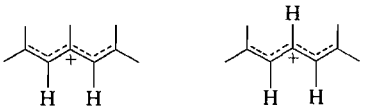

10 **11**

Results

There are three geometric isomers of 3,5-dimethylhepta-2,5-dien-4-ol (**6**), *viz.*, 2E,5E (**6***a*), 2E,5Z (**6***b*) and 2Z,5Z (**6***c*). These isomeric alcohols were prepared as follows:

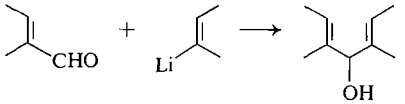

6*a*

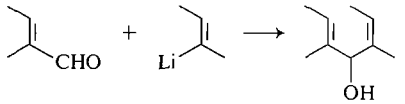

6*b*

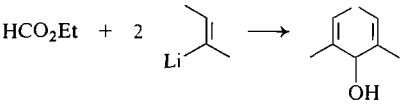

6*c*

In addition to the expected isomers, these preparations invariably yielded one of the other isomers as a minor by-product (geometric impurity). Thus alcohols **6***a*, **6***b*, and **6***c* contained **6***b*, **6***a*, and **6***b*, respectively, as an impurity. Fractional distillation at reduced pressure gave **6***a*, **6***b* and **6***c* in 88, 92, and 88% geometric purity, as determined by n.m.r. spectroscopy. The structure of these alcohols is shown by the method of synthesis and by the chemical shift values obtained for the C-2, -4, and -6 protons. The C-4 proton exhibits a broad singlet absorption at τ 5.80 in **6***a*, 5.20 in **6***b*, and 4.76 in **6***c*. The C-2 and -6 protons of the symmetrical isomers **6***a* and **6***c* show the expected quartet of quartets pattern (2H) centered at τ 4.52 and 4.76 respectively. The unsymmetrical alcohol **6***b* shows the expected double set of a quartet of quartets centered at τ 4.73 and 4.52. The C-4 proton peak was used for the analytical geometric purity determinations. This peak in **6***c* partially overlaps with that of the C-2 proton but fortunately **6***c* cannot be a significant impurity in **6***a* or **6***b* from the method of synthesis.

Similarly, the alcohol **7**, in predominantly (>85%) the geometry (2Z,5E) shown in the formula, was prepared from *trans*-crotonaldehyde and *trans*-2-butenyl-2-lithium.

Carbonium Ion Preparations

The isomeric alcohols **6***a*, **6***b*, and **6***c* were added to some or all of the following acids: H_2SO_4 (86–100%), $ClSO_3H$, CF_3SO_3H, FSO_3H, FSO_3H–SbF_5 (4:1), SbF_5–SO_2ClF (1:2), and FSO_3H–SO_2ClF (1:4). The temperature of addition ranged from -125 to 0°. In FSO_3H–SO_2ClF (1:4) at $-125°$, the dienol **6***a* gave mainly the dienylic ion **4***a*, dienol **6***b* gave **4***b* and a large amount of polymeric material, and dienol **6***c* gave only polymer. Invariably, the two cyclic ions **8***a* and **8***b* were also formed as by-products. At $-83°$, dienylic cations **4***a* and **4***b* both cyclized at about the same rate ($t_{1/2} \simeq 1$ h) to give mainly **8***b* and **8***a* respectively. With all other acid systems (temperature of addition $> -80°$) no dienylic cations were observed, only mixtures of cations **8***a* and **8***b* in varying ratios (Table 1). These results were actually obtained prior to the very low temperature studies and it subsequently became obvious from the cyclization rate of **4***a* and **4***b* why no dienylic cations were observed. In some cases, a third cyclic ion **8***c* was also formed as a component of the mixture.

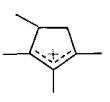

8*c*

The structure of these ions was confirmed by n.m.r. spectroscopy. The n.m.r. spectral data for

TABLE 1. Initial ratios of **8***a* and **8***b* obtained

Acid	Alcohol	Temperature of addition* (°C)	% ions **8***a*	**8***b*	**8***c*	Corrected† **8***a*:**8***b*
85.5% H_2SO_4	**6***a*	0	25	73	2	18:82
88.5% H_2SO_4	**6***a*	−5	22	75	3	15:85
93.5% H_2SO_4	**6***a*	0	18	80	2	9:91
96.3% H_2SO_4	**6***a*	0	18	80	2	9:91
	6*b*	0	70	28	2	76:24
	6*c*	−5	78	22	0	78:22
98.1% H_2SO_4	**6***b*	0	77	23	0	83:17
	6*c*	−5	80	20	0	80:20
100.1% H_2SO_4	**6***a*	0	17	83	0	8:92
	6*b*	0	75	25	0	80:20
$ClSO_3H$	**6***b*	−70	65	35	0	
	6*c*	−80	Polymers only			
FSO_3H	**6***a*	−70	13	87	0	3:97
	6*b*	−40	78	22	0	84:16
	6*b*	−70	78	22	0	84:16
	6*c*	−40	20	40	40	
	6*c*	−65	17	33	50	
CF_3SO_3H	**6***a*	−30	8	57	35	
	6*c*	−30	10	20	70	
	6*c*	−10	6	19	75	
4:1 FSO_3H–SbF_5	**6***c*	−65	17	33	50	

*Cooling bath temperature.
†Since the starting alcohols contained geometric impurity (see text), these values have been corrected as if 100% pure alcohols were used.

TABLE 2. N.m.r. data for **8***a*, **8***b*, **4***a*, and **4***b*

Ion	Chemical shift (τ)*		Assignment
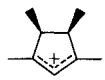 **8***a*	8.620, 8.542	doublet, $J \simeq 7.8$ Hz	CH_3 on C-4 and -5
	7.04	broad	CH_3 on C-1 and -3
	6.47	multiplet	H on C-4 and -5
	2.42	singlet	H on C-2
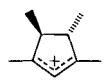 **8***b*	8.542, 8.472	doublet, $J \simeq 7.0$ Hz	CH_3 on C-4 and -5
	7.04	broad	CH_3 on C-1 and -3
	6.91	multiplet	H on C-4 and -5
	2.46	singlet	H on C-2
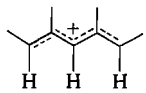 **4***a*	7.64	singlet	CH_3 on C-2 and -4
	7.38	doublet, $J \simeq 6.5$ Hz	CH_3 on C-1 and -5
	1.58	quartet, $J \simeq 6.5$ Hz	H on C-1 and -5
	1.54	singlet	H on C-3
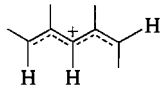 **4***b*	7.67	singlet	CH_3 on C-2 and -4
	7.45	multiplet (not resolved)	CH_3 on C-1 and -5
	1.52	multiplet (not well resolved)	H on C-1, -3, and -5

*Center of peak.

Can. J. Chem. Downloaded from www.nrcresearchpress.com by 210.87.254.42 on 09/05/12
For personal use only.

Can. J. Chem. Downloaded from www.nrcresearchpress.com by 210.87.254.42 on 09/05/12
For personal use only.

4*a*, **4***b*, **8***a*, and **8***b* are listed in Table 2, that for **8***c* has previously been reported (2). The chemical shifts observed for the dienylic cations **4***a* and **4***b* are similar to those observed for related systems (2, 6). The actual ground-state geometry of the ions (see ref. 1) cannot be determined by n.m.r. spectroscopy because of the lack of vicinal protons (and hence of vicinal coupling constants) on the cation framework. From previous results, the ground-state geometry is assumed to be the "W" or 2E,3E configuration (see ref. 3 for a proposed rational nomenclature for dienylic cations).

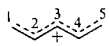

"W" or 2E, 3E

The assigment of the stereochemistry of **8***a* and **8***b* was based on their equilibrium ratio (K = **8***b*/**8***a* = 3.5 ± 0.1), obtained in H_2SO_4, which by analogy to ions **3***a* and **3***b*, should favor the *trans* ion **8***b* and by a comparison of their n.m.r. spectra with that found for **3***a* and **3***b* (9). For example, the C-4 and -5 methyl groups in **3***a* (*cis*) appear at a higher field than in **3***b* (*trans*) and a corresponding observation is consistent with the assignments for **8***a* and **8***b*.

For all acid systems other than SO_2ClF–FSO_3H (4:1) the relative amounts of the cyclized ions **8***a*, **8***b*, and **8***c*, in mixtures, were determined by peak area measurements using the C-2 proton n.m.r. peak at τ 2.42 in **8***a*, and 2.46 in **8***b*, and the C-2 methyl peak of **8***c* at τ 7.86. The details are given in the experimental section. The acid addition of alcohols **6***a* and **6***b* was in most cases quite smooth. In contrast, **6***c* reacted violently with all acids except H_2SO_4 to form large amounts of apparently polymeric material. When the aprotic SbF_5:SO_2ClF (1:2) acid solvent system was used, all three alcohols were at first poorly soluble and then reacted violently, only gummy residues being obtained.

The dienylic alcohol **7** was added to 100% H_2SO_4, FSO_3H, and FSO_3H–SbF_5 (4:1). In FSO_3H and FSO_3H–SbF_5, the dienylic ion **5** was observed at −70°. Ion **5** was found to rearrange slowly to give the cyclic ion **9***b* (FSO_3H, −40°, $t_{1/2} \simeq 1$ h) which in turn rearranges to **9***c* at higher temperature (FSO_3H, 20°, $t_{1/2} \simeq 10$ min). In 100% H_2SO_4 one is limited in the temperature of the preparation to 0° or slightly lower (supercooled solution) and in this solvent only **9***c* was obtained on addition of the alcohol.

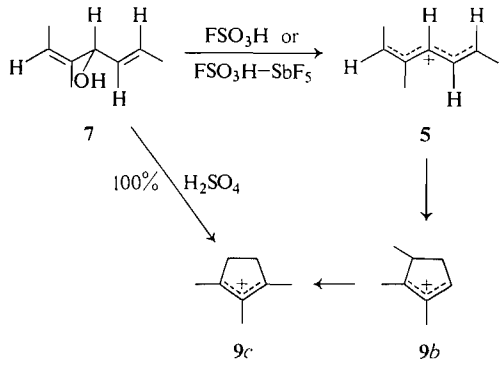

7 5 9*c* 9*b*

The structures of these ions were confirmed by n.m.r. spectroscopy (Table 3.)

Discussion

The observable dienylic cation **4***a* cyclizes to give predominantly the cyclopentyl cation **8***b* (the *trans* dimethyl configuration at C-4 and -5) while **4***b* gives predominantly **8***a*. As discussed in the earlier papers (6, 9), this is consistent with a conrotatory process in which the "U" or 2Z,3Z geometry of the dienylic cation cyclizes to a cyclopentenyl cation. The equilibrium involved

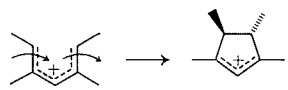

4*a* "U" or 2Z,3Z **8***b*

in getting from the ground-state 2E,3E configuration to the 2Z,3Z configuration has been discussed (6, 9). In the above results, a direct dienylic cation cyclization is involved and we therefore have excellent evidence for the existence of this species in those cases where only the cyclized ions are observed on dienol addition, *i.e.* the pentamethyl results (9) and the higher temperature results in this work (Table 1). The results for dienols **6***a* and **6***b*, *i.e.* showing considerable stereospecificity in the particular cyclopentenyl cation formed, are similar to the results obtained for the pentamethyl case and need be discussed no further.

The behavior of **6***c* presents a dilemma since a cyclization of the initially formed dienylic cation should have produced the *trans* ion **8***b*. However, in sulfuric acid (the only acid solvent not leading to considerable polymer formation or the production of considerable **8***c*), the *cis* ion **8***a* is formed in predominant amount (slightly higher stereospecificity than from even **6***b*). This is not

TABLE 3. N.m.r. data for **5**, **9***b*, and **9***c*

Ion	Chemical shift (τ)*		Assignment
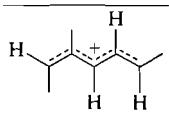 **5**	7.79	singlet	CH_3 on C-3
	7.32	broad (unresolved)	Two terminal CH_3
	2.50	triplet ($J \simeq 13.0$ Hz)	H on C-5
	1.37	multiplet	H on C-2, -4, and -6
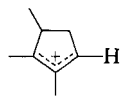 **9***b*	8.45	doublet ($J \simeq 7.5$ Hz)	CH_3 on C-5
	7.69	singlet	CH_3 on C-2
	6.95	singlet	CH_3 on C-1
	6.75, 6.37	multiplets	H on C-4 and -5
	0.29	broad	H on C-3
9*c*	7.82	singlet	CH_3 on C-2
	7.10	singlet	CH_3 on C-1 and -3
	6.50	singlet	H on C-4 and -5

*Center of peak.

a thermodynamic result since we have already stated that the equilibrium **8***b*/**8***a* favors **8***b*. Rather than postulate a disrotatory closure in **4***c*, it seems more reasonable to postulate an isomerization at the dienylic ion stage **4***c* → **4***b*; the ring closure of **4***b* then yielding the observed *cis* cyclic ion **8***a*. There are several good reasons why this might happen:

1. The transition state for the ring closure of **4***c* is particularly bad (large methyl–methyl repulsion).

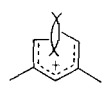

4*c*

The alternative two stage process may then represent a lower energy pathway for reaction.

2. For steric reasons (9), the dienylic ion **4***c* (in any configuration) is not expected to be as stable as **4***b*; however, **4***a* is expected to be the most stable. The rate constants for possible isomerization and ring closure steps are shown schematically below.

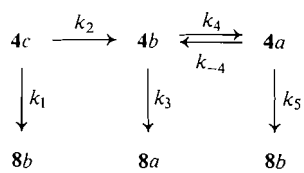

It seems possible that k_2 and k_4 may be competitive with k_1 and k_3 (and even a k_{-4} step and k_5 may be competitive). This would explain the lack of complete stereospecificity in **4***b* → **8***a* and **4***a* → **8***b*. In the case of **4***c*, the rate constant k_2 may actually be larger than k_1 so that cyclization occurs predominantly via **4***b*, leading to the *cis* ion **8***a*.

In the corresponding pentamethyl dienylic cations **2***a–c*, an analogous behavior, *i.e.* **2***c* → **3***a*, was not observed, the expected *trans* ion **3***b* always being the major product. This difference can be satisfactorily rationalized because, as pointed out in the Introduction, there is reason to expect the cyclization rate constants k_1, k_3, and k_5 to be smaller in the tetramethyl series, under investigation in this work. The isomerization rate constants k_2 and k_4 may not, however, be very different in the two cases. We believe therefore that in the pentamethyl series, k_1 is larger than k_2.

The formation of **8***c*, the rearranged cyclic ion, occurs mainly with alcohol **6***c* and only in certain acid solvents, in particular CF_3SO_3H and SbF_5–FSO_3H. This ion must be formed in the initial rather violent reaction sequence which takes place when the alcohol and acid are mixed since it can be shown that the rearrangement of **8***a* and **8***b* to **8***c*, while it does go to completion, is a very slow reaction on the time scale needed for the addition procedure. Also the formation of **8***c* can be correlated with the amount of polymer formed in the addition reaction. The virtual

Can. J. Chem. Downloaded from www.nrcresearchpress.com by 210.87.254.42 on 09/05/12
For personal use only.

absence of **8***c* in some of the solvents studied indicates to us that these particular reactions are virtually free from hydride shifts occurring *after* the initial cyclization process since a hydride shift mechanism is the most obvious way of explaining the formation of **8***c*.

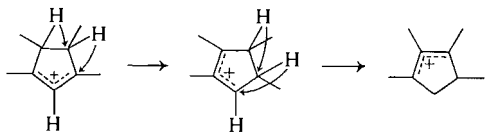

8*a* or **8***b* **8***c*

The trimethylpentadienyl cation system **5** could not be successfully used to study the pentadienyl → cyclopentenyl stereochemistry. Even in one of the strongest acid systems known (FSO_3H–SbF_5), the dienylic ion **5** does not give **9***a* as an observable product on cyclization. One has therefore no way of determing the stereochemistry of the cyclization process since the first observable product **9***b* has lost one asymmetric center.

In this work, we have shown for the first time an observable dienylic cation → cyclopentenyl cation cyclization which is nearly stereospecific. This complements the previous results (9) because in that study, dienylic cations were not actually observed, even though there was abundant presumptive evidence that they were involved as intermediates.

The thermal cyclization rates of **4***a* and **4***b* are extremely rapid and any photochemical studies will of necessity have to be carried out at extremely low temperatures.

Experimental

Boiling points are uncorrected. Distillations were done on either a stainless steel spinning band column or an auto annular Teflon spinning band column (Nester/Faust). The n.m.r. spectra of all neutral compounds were obtained as *ca.* 10% solutions in carbon tetrachloride with tetramethylsilane as internal standard using a Varian Associates A-60 or HA-100 spectrometer. The n.m.r. spectra of all ion solutions were obtained with tetramethylammonium cation as internal standard (τ 6.90) using the HA-100 spectrometer equipped with a variable temperature probe. Microanalyses were performed by the Microanalysis Lab., The University of Calgary.

3,5-Dimethyl-(2E,5Z)-heptadien-4-ol (6b)

A solution of 32.6 g (0.24 mol) of *trans*-2-bromobut-2-ene in 30 ml of ether was added slowly over 0.75 h to 3.5 g (0.5 mol) of lithium ribbon containing 1% sodium in 100 ml of ether at 0° under an argon atmosphere. To the resulting alkenyl lithium solution was added a solution of 21 g (0.25 mol) of tiglaldehyde in 25 ml of ether over 1 h, stirring being continued for a further hour at 20°. The reaction mixture was then filtered through glass wool into an ice cold solution of 30 g ammonium chloride in 150 ml of water with vigorous stirring. The ether layer was separated and the aqueous layer was extracted with three 75 ml portions of ether. The combined ether layers were washed with 10% carbonate solution and dried over potassium carbonate. Distillation of the residue at reduced pressure gave 16.0 g (46%) of colorless liquid, b.p. 85–85.5°/11 mm. During the course of distillation, five fractions were collected at this temperature and n.m.r. analyses showed that they had the same geometric purity (92% **6***b* and 8% **6***a*), n.m.r. peaks centered at τ 8.54 (12H, multiplet, two terminal methyls and C-3 and -5 methyls); 5.20 (1H, singlet, C-4 proton); 4.73 (1H, quartet of quartets, $J \simeq 6.0$ and 0.9 Hz, C-2 proton), and 4.52 (1H, quartet of quartets, $J \simeq 6.6$ and 1.3 Hz, C-6 proton). The OH peak is variable.

Anal. Calcd. for $C_9H_{16}O$: C, 77.09; H, 11.50. Found: C, 77.20; H, 11.58.

3,5-Dimethyl-(2Z,5Z)-heptadien-4-ol (6c)

To a solution of *trans*-2-butenyl-2-lithium prepared as above from 95 g (0.7 mol) of *trans*-2-bromobut-2-ene and 9.7 g (1.4 mol) of lithium in 200 ml of ether was added a solution of 26 g (0.35 mol) of ethyl acetate and worked up as usual to give 15.3 g (31%) of light yellow liquid, b.p. 52–6°/2 mm. Redistillation gave a very lightly yellow fraction, b.p. 81–2°/11 mm and a colorless fraction, b.p. 82°/11 mm. These two fractions had identical geometric purity (86% **6***c* and 14% **6***b*). The colorless fraction was found to dehydrate in about 2 days at 0° whereas the colored fraction was stable indefinitely and hence this was used for the study as reported in this paper. N.m.r. peaks centered at τ 8.31 (12H, multiplet, two terminal methyls and C-3 and -5 methyls); 4.76 (1H, singlet, C-4 protons), and 4.76 (2H, quartet of quartets, C-2 and -6 protons). The OH peak is variable.

Anal. Calcd. for $C_9H_{16}O$: C, 77.09; H, 11.50. Found: C, 76.98; H, 11.29.

3,5-Dimethyl-(2E,5E)-heptadien-4-ol (6a)

From 68 g (0.5 mol) of *cis*-2-bromobut-2-ene, 7 g (1 mol) of lithium, and 42 g (0.5 mol) of tiglaldehyde, there was obtained 35 g (50%) crude alcohol, b.p. 90–5°/14 mm. On redistillation, six fractions were collected, b.p. 83–4°/9 mm. They were shown by n.m.r. analyses to have identical geometric purity (88% **6***a* and 12% **6***b*). N.m.r. peaks centered at τ 8.39 (6H, doublet, $J \simeq 6.7$ Hz, each doublet split into quartets, $J \simeq 1.0$ Hz, two terminal methyls); 8.56 (6H, multiplet, C-3 and -5 methyls); 5.80 (1H, singlet, C-4 proton), and 4.52 (2H, quartet of quartets, $J \simeq 6.7$ Hz and 1.3 Hz, C-2 and -6 protons). The OH peak is variable.

Anal. Calcd. for $C_9H_{16}O$: C, 77.09; H, 11.50. Found: C, 76.57; H, 11.70.

3-Methyl-(2Z,5E)-heptadien-4-ol (7)

The same procedure used for the preparation of **6** was used to prepare **7**. From 27 g (0.2 mol) of *trans*-2-bromobut-2-ene, 2.8 g (0.4 mol) of lithium, and 14 g (0.2 mol) of crotonaldehyde, there was obtained 11 g (44%) of a colorless liquid, b.p. 83–4°/13 mm. N.m.r. peaks centered at τ 8.36 (9H, multiplet, two terminal methyls and C-3 methyl); 5.06 (1H, multiplet, C-4 proton); 4.80 and 4.49 (3H, multiplet, C-2, -5, and -6 protons).

Can. J. Chem. Downloaded from www.nrcresearchpress.com by 210.87.254.42 on 09/05/12
For personal use only.

Anal. Calcd. for $C_8H_{14}O$: C, 76.14; H, 11.18. Found: C, 74.69; H, 11.56.

Preparation of the Ions

All ion solutions were made to *ca.* 8% weight of alcohol/volume of acid solvent by adding 50 mg of the alcohol to 0.6 ml of the acid. The concentrations of sulfuric acid were determined by titration. Chlorosulfonic acid (B.D.H.), fluorosulfonic acid (Diaprep. Inc., N.M.R. grade), and sulfuryl chloride fluoride (Research Organic/Inorganic Chemical Corp.) were used without further purification. Antimony pentafluoride and trifluoromethylsulfonic acid were purified by double distillation. When sulfuric acid was used as solvent, the hexane extraction method was followed. In all other acids, direct additions of the alcohol or a solution of alcohol in deuterochloroform or trichloromonofluoromethane (1:2 ratio) were used.

Equilibration of 8a and 8b

Mixtures of **8***a* and **8***b* in 88–93% H_2SO_4 were equilibrated at 0° until no appreciable changes occurred as indicated by n.m.r. spectroscopy. An equilibrium ratio of 3.53 ± 0.10 was obtained favoring the *trans* ion **8***b*.

The authors wish to thank the National Research Council of Canada for financial support.

1. N. C. DENO and C. U. PITTMAN, JR. J. Am. Chem. Soc. **86**, 1871 (1964).
2. T. S. SORENSEN. Can. J. Chem. **42**, 2768 (1964); **43**, 2744 (1965).
3. N. C. DENO, C. U. PITTMAN, JR., and J. O. TURNER. J. Am. Chem. Soc. **87**, 2153 (1965).
4. T. S. SORENSEN. J. Am. Chem. Soc. **89**, 3782, 3794 (1967).
5. D. M. BROUWER and J. A. VAN DOORN. Rec. Trav. Chim. Pays-Bas, **89**, 333 (1970).
6. T. S. SORENSEN and R. Z. BLADEK. Can. J. Chem. **50**, 2806 (1972).
7. R. KURUPATI. Ph.D. Thesis. The University of Calgary, Calgary, Alberta (1971). p. 174.
8. R. B. WOODWARD and R. HOFFMANN. J. Am. Chem. Soc. **87**, 395 (1965).
9. P. H. CAMBPELL, N. W. K. CHIU, K. DENGAU, I. J. MILLER, and T. S. SORENSEN. J. Am. Chem. Soc. **91**, 6404 (1969).

Can. J. Chem. Downloaded from www.nrcresearchpress.com by 210.87.254.42 on 09/05/12
For personal use only.

The Observation of Two Different Base-catalyzed Processes Occurring in Directly Observable Carbonium Ion Rearrangements

N. W. K. CHIU AND T. S. SORENSEN

Department of Chemistry, The University of Calgary, Calgary, Alberta

Received February 20, 1973

In aqueous sulfuric acid, *cis*-1,3,4,5-tetramethylcyclopentenyl cation (**1***a*) has been found to rearrange not only to the *trans* isomer (**1***b*) but also to 1,2,3,4-tetramethylcyclopentenyl cation (**1***c*). The **1***a* → **1***b* and **1***a*/**1***b* → **1***c* rearrangements follow H_0 with slopes of 0.94 and 0.45 respectively. The **1***a* → **1***b* rearrangement involves a neutral intermediate, 1,2,4,5-tetramethylcyclopentadiene, whereas the **1***a*/**1***b* → **1***c* rearrangement involves a termolecular or intramolecular push–pull process.

Dans l'acide sulfurique, le cation *cis* tétraméthyl-1,3,4,5 cyclopentenyle (**1***a*) se réarrange non seulement en isomère *trans* (**1***b*) mais aussi en cation tétraméthyl-1,2,3,4 cyclopentenyle (**1***c*). Les réarrangements **1***a* → **1***b* et **1***a*/**1***b* →**1***c* se font suivant H_0 avec des pentes de 0.94 et 0.45 respectivement. Le passage **1***a* → **1***b* se fait par un intermédiaire neutre tétraméthyl-1,2,4,5 cyclopentadiène, tandis que les réarrangements **1***a*/**1***b* →**1***c* se font selon un processus push–pull termoléculaire et intramoléculaire.

[Traduit par le journal]

Can. J. Chem., 51, 2783 (1973)

Introduction

A number of directly observable carbonium ion rearrangements in sulfuric acid occur by a base-catalyzed mechanism (1). These appear, however, to fall into two distinct categories:

1. Those in which k_{rearr} appears to approximately follow the acidity function, H_0, of the solvent, with unit slope.

2. Those in which this slope is only about 0.5.

This differentiation has involved a comparison of different ion systems, but in this paper it is shown that it is possible to have the same starting ion rearranging to two different products, where one process belongs to category 1 and the other to category 2. This fortunate occurrence allows one to differentiate the two processes on mechanistic grounds and, therefore, to define them in other than the rather empirical H_0 correlation.

Results and Discussion

The two ion rearrangements studied were:

1. The interconversion of *cis*-1,3,4,5-tetramethylcyclopentenyl cation, **1***a*, and *trans*-1,3,4,5-tetramethylcyclopentenyl cation, **1***b*.

2. The rearrangement of either **1***a* or **1***b* into a third isomeric ion, the 1,2,3,4-tetramethylcyclopentenyl cation, **1***c*.

Ions **1***a* or **1***b* were prepared *in situ* in 84–100% H_2SO_4 and in pure FSO_3H, and could each be obtained in about 90% geometric purity. The n.m.r. spectra of **1***a*, **1***b*, and **1***c* are sufficiently different so that this tool can be used to quantitatively follow the reactions. The actual peaks used were the C-2 protons of **1***a* and **1***b* at τ 2.42 and 2.46 respectively and the C-2 methyl of **1***c* at τ 7.86. The n.m.r. data on these ions are reported in a separate paper (2).

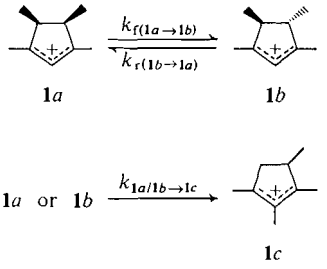

(In all cases — indicates a methyl group.)

1*a* ⇌ **1***b* *Kinetics*

The equilibrium ratio of the two ions was determined to be $K_{1b/1a} = 3.5 \pm 0.2$ (2), favoring, as expected (1), the *trans* isomer. The most accurate kinetic data are obtained therefore by measuring the rate of the forward reaction $\mathbf{1a} \xrightarrow{k_{f(1a\rightarrow 1b)}} \mathbf{1b}$. The reaction was studied in sulfuric acid solvent concentrations ranging from 93.5 to 100.1% (concentrations corrected for dilution during the preparation (1)) at 0 °C and employing carbonium ion concentrations of 10% weight of alcohol per volume of acid. Under these conditions, the second reaction **1***a* or **1***b* → **1***c* is negligible.

The kinetic data gave good reversible first-

Can. J. Chem. Downloaded from www.nrcresearchpress.com by 210.87.254.105 on 09/05/12
For personal use only.

Can. J. Chem. Downloaded from www.nrcresearchpress.com by 210.87.254.105 on 09/05/12
For personal use only.

TABLE 1. Kinetics for **1***a* ⇌ **1***b* at 0°

% H_2SO_4*	$k_{f(1a\rightarrow 1b)}$ (s^{-1})†	k_1 (s^{-1})‡
100.1	8.5×10^{-6}	2.1×10^{-5}
98.1	3.0×10^{-5}	7.5×10^{-5}
96.3	8.2×10^{-5}	2.0×10^{-4}
93.5	1.8×10^{-4}	4.5×10^{-4}

*Corrected, 10% ion concentrations.
†Average of at least four runs at each acid concentration. The error is estimated at ±10%.
‡Calculated values (see text).

order plots and Table 1 lists the values of $k_{f(1a\rightarrow 1b)}$ for the various solvent concentrations. Except for the 100.1% acid data, log $k_{f(1a\rightarrow 1b)}$, when plotted against H_0 (Fig. 1), results in a reasonably linear correlation with a slope of about 0.94.

1*a* or **1***b* → **1***c* *Kinetics*

In this reaction, an equilibrium constant $K_{1c/1a+1b}$ was not observed; however, a minimum value is ⩾250 ($\Delta G \geqslant 3$ kcal/mol), based on the prevailing signal to noise ratio for the C-2 methyl group of **1***c* and correcting for the three proton size of this signal. The reaction was studied in 85.5 to 100.1% H_2SO_4 and in FSO_3H at 0 °C. The data gave good simple first-order plots once the **1***b*/**1***a* equilibrium was established and the resulting rate constants are reported in Table 2. A plot of log $k_{1a/1b\rightarrow 1c}$ *vs.* H_0 (Fig. 1), forcing a linear relationship, gives a slope of about 0.45 for the lower percent acid data. However, the plot appears to follow a curve which

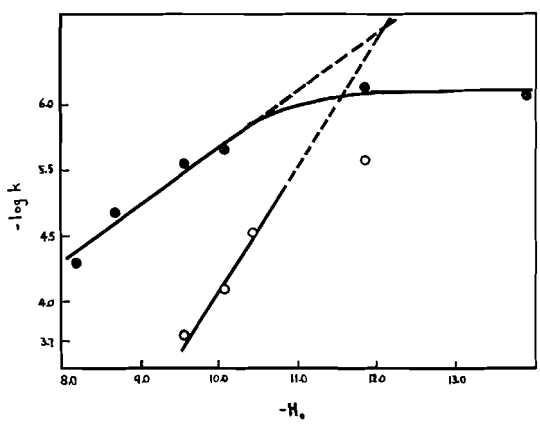

FIG. 1. (○) Plot of $-\log k_{f(1a\rightarrow 1b)}$ against $-H_0$, (●) plot of $-\log k_{1a/1b\rightarrow 1c}$ against $-H_0$, and (--) the extrapolation of both curves to higher H_0 values. The slope is 0.94 for the lower line and 0.45 for the higher, thereby showing the predicted changeover in the observed mechanism at higher H_0 values.

TABLE 2. Kinetics for **1***a*/**1***b* → **1***c* at 0°

Acid	$k_{1a/1b\rightarrow 1c}$ (s^{-1})*
FSO_3H	4.7×10^{-6}†
FSO_3H	2.7×10^{-6}‡
100.1% H_2SO_4	3.2×10^{-6}†
100.1% H_2SO_4	2.3×10^{-6}‡
96.3% H_2SO_4	7.1×10^{-6}
93.5% H_2SO_4	9.0×10^{-6}
88.5% H_2SO_4	2.1×10^{-5}
85.5% H_2SO_4	5.2×10^{-5}

*Average of at least four runs at each acid concentration. The error is estimated at ±10%.
†Starting ion mainly **1***a*, **1***a*/**1***b* equilibrium not initially established.
‡Starting ion mainly **1***b*, **1***a*/**1***b* equilibrium not initially established.

levels off as H_0 gets bigger. One point which needs to be emphasized is that the slope at any point in this curve is much less than that observed for the **1***a* ⇌ **1***b* kinetics and it will be seen later that there is no particular mechanistic reason to expect any linearity of log $k_{1a/1b\rightarrow 1c}$ and H_0 in this reaction.

Comparison of $k_{f(1a\rightarrow 1b)}$ *and* $k_{1a/1b\rightarrow 1c}$

The **1***a* ⇌ **1***b* reaction at the lower sulfuric acid concentrations is much faster than the **1***a*/**1***b* → **1***c* reaction, *e.g.*, a factor of 20 in 93.5% H_2SO_4. However, a very rough extrapolation of both rates (Fig. 1) to very high H_0 solvents leads to the prediction of equal rates about $H_0 = -12$ to -13 and for the **1***a*/**1***b* → **1***c* reaction to be the faster above this. Fluorosulfonic acid is reported to have $H_0 = -13.9$ (3) and the above prediction is experimentally verified since the **1***a*/**1***b* equilibrium is not established in this solvent until the **1***a*/**1***b* → **1***c* reaction is well over 50% complete. The rates for **1***a* → **1***c* and for **1***b* → **1***c* are in fact different (Table 2).

Reaction Mechanisms

Category One

The **1***a* ⇌ **1***b* equilibrium constant and the acid dependence of the interconversion rates are very similar to those of the closely related *cis*- and *trans*-1,2,3,4,5-pentamethylcyclopentenyl cations, **2***a* ⇌ **2***b*, a slope of log k_{rearr} *vs.* H_0 of 0.99 (1) for the latter compared to 0.94 for the former.

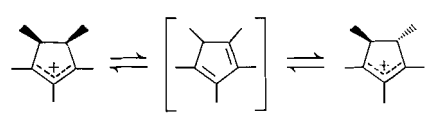

2*a* **3** **2***b*

Can. J. Chem. Downloaded from www.nrcresearchpress.com by 210.87.254.105 on 09/05/12
For personal use only.

The mechanism for the **2***a* ⇌ **2***b* interconversion has been shown previously to involve the intermediacy of the diene **3** and the same mechanism, therefore, appears very reasonable for **1***a* ⇌ **1***b*.

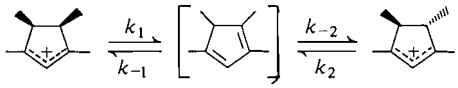

1*a* **4** **1***b*

In order to evaluate k_1 and k_2, the diene **4** was added to the strong acid solvents. Under the experimental conditions, where k_1 and k_2 are negligibly slow, the ratio of **1***a*/**1***b* observed is equal to k_{-1}/k_{-2}. This same procedure has previously been shown to yield reliable estimates of k_{-1}/k_{-2} for the **2***a* ⇌ **2***b* reaction. The ratio obtained from this study was 1.5 ± 0.2 favoring the thermodynamically less stable *cis* ion, **1***a*. Similar nonequilibrium protonation is also observed with **3** although the ratio is closer to unity. This ratio is *independent* of the strength of the acid and protonation occurs at C-4 since, within experimental error, only **1***a* and **1***b* are formed. However, the diene **4** was only *ca.* 94% pure and since the isomeric impurity **5** on protonation yields **1***c*, it is difficult to exclude the possibility

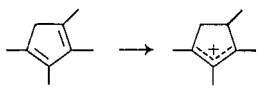

5 **1***c*

that up to 2 or 3% of **1***c* might have been formed in the protonation of diene **4**.

Assuming a steady-state concentration for **4**, then

$$k_{f(1a\rightarrow 1b)} = \frac{k_1 k_{-2}}{k_{-1} + k_{-2}}$$

and since $k_{-1}/k_{-2} = 1.5$, therefore, $k_1 = 2.5\ k_{f(1a\rightarrow 1b)}$. Similarly, $k_2 = 0.5\ k_{f(1a\rightarrow 1b)}$.

It now seems reasonable to suppose that those base-catalyzed reactions belonging to category 1, with slope of about unity for log k_{rearr} *vs.* H_0, are always characterized by the intermediacy of the corresponding diene. This type of reaction is by no means limited to *cis–trans* interconversions but has as a general characteristic, the possibility of returning from the diene back to the starting cation so that in general $k_f \neq k_1$.

Category Two

For the reaction **1***a*/**1***b* → **1***c*, we considered initially, as a working hypothesis, that it would

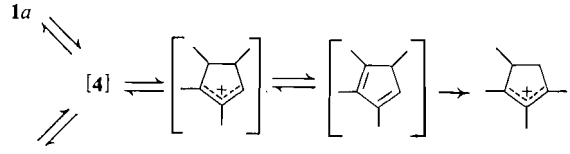

1*b* **6** **7** **1***c*

SCHEME 1

likely involve the sequence shown in Scheme 1. It seemed reasonable to suppose that a complex steady-state reaction of this type might show a different acid dependence from the **1***a* ⇌ **1***b* interconversion. In order to investigate some of the intermediate steps, the cyclopentenyl cation **6** was prepared by the addition of 3,4-dimethylhepta-2,5-dien-4-ol, **8**, to FSO_3H or FSO_3H–SbF_5 at −70°. A dienylic cation intermediate **9** is presumably formed initially which then cyclizes to give a mixture of the *cis* and *trans* isomers of **6** (for the cyclization of dienylic cations to cyclopentenyl cations, see refs. 2, 4–10).

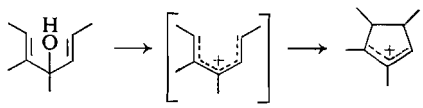

8 **9** **6**

Ion **6** rearranges only to **1***c*; the rate constant $k_{6\rightarrow 1c}$ was determined and is reported in Table 3. Since the conversion of **6** to **1***c* is much faster than the conversion of **1***a*/**1***b* → **1***c*, steps subsequent to the formation of **6** cannot be rate determining. Projected experiments involving diene **7** thus became redundant. One can, therefore, substitute the following expression in place of Scheme 1.

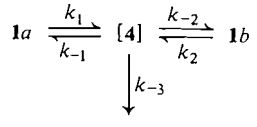

1*c*

TABLE 3. Kinetics for **6** → **1***c* in FSO_3H

Temp. (°C)*	$k_{6\rightarrow 1c}$ (s^{-1})†
−45	5.1×10^{-4}
−55	1.3×10^{-4}
−65	1.8×10^{-5}
0	1.7×10^{-1}‡

*±1°.
†Average of two runs at each temperature. The error is estimated at ±10%.
‡Extrapolated value.

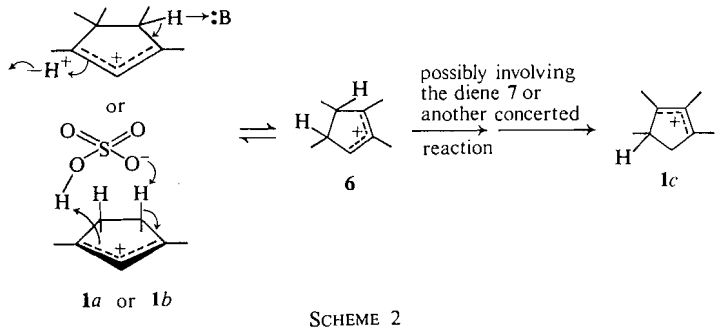

SCHEME 2

Assuming a steady-rate concentration for **4**, the overall rate constant for the formation of **1***c* from an equilibrium **1***a*/**1***b* mixture is

$$k_{1a/1b\rightarrow 1c} = k_{-3}\frac{k_1 + k_2K}{k_{-1} + k_{-2}}$$

and on substituting $k_{-1} = 1.5\ k_{-2}$, $K = 3.5$, and $k_2 = \frac{1}{5}k_1$, one obtains $k_{1a/1b\rightarrow 1c} = 0.7\ k_{-3}k_1/k_{-2}$. For comparison purposes, $k_f(\mathbf{1}a \rightarrow \mathbf{1}b)$ was equal to $k_1/2.5$. The only way $k_{1a/1b\rightarrow 1c}$ might have a different acid dependence from $k_f(\mathbf{1}a \rightarrow \mathbf{1}b)$ would be for the ratio k_{-3}/k_{-2} to vary, itself, as a function of the acid concentration. This certainly seems an acceptable possibility but experimental evidence is totally lacking, since protonation of **4**, even in very strong acids, does not yield **6** and hence **1***c*. We feel, therefore, that Scheme 1 does not represent the mechanism for **1***a*/**1***b* → **1***c* and, in particular, that the diene **4** is not an intermediate in the reaction.

About the only mechanism which has the required prerequisites, *i.e.*, base-catalyzed but no diene **4**, would be a termolecular[1] or intramolecular push–pull process (10) whereby a base species removes a proton and in a concerted process another proton comes on at the opposite end as shown in Scheme 2.

The acid dependence of such a process is unpredictable; however, the observed behavior is not inconsistent with such a mechanism, assuming the proton removal step is the more important. Also, one would not necessarily expect a linear H_0 correlation since no acid–base equilibria are involved.

In FSO_3H and 100.1% H_2SO_4 solvents, it is possible that a hydride shift mechanism operates since these are well-known in related cases (5, 7–11) (Scheme 3).

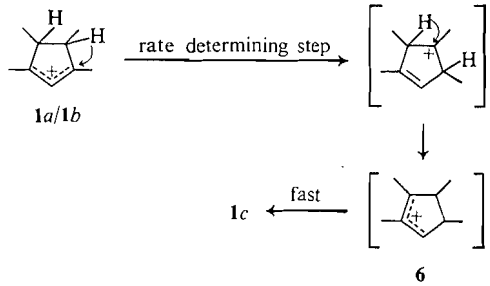

SCHEME 3

However, such a happening does not affect the central features of the **1***a*/**1***b* → **1***c* reaction, namely the solvent dependence and the observed slope of 0.45 in the weaker sulfuric acid solvents.

There are in the literature (10, 12) several other examples of base-catalyzed carbonium ion rearrangements where the k_{rearr} *vs.* H_0 slope is much less than unity. These, and the example described in this paper, have a unifying feature, *viz.* in each case a cation much less stable than either the reactant or the product is proposed as a key reaction intermediate. We suggest that this intermediate will always be formed by a concerted mechanism not involving diene. There are, therefore, two quite distinct classes of base-catalyzed carbonium ion rearrangements.

Experimental

Kinetics

The basic procedures used are similar to those reported for the pentamethyl case (1). Kinetic data are reported in Tables 1, 2, and 3.

Equilibrium of 1a/1b → 1c

Cation samples of **1***a* or **1***b* in 96% H_2SO_4 were kept at 0° for 120 h (minimum) and analyzed by n.m.r. spectroscopy. No peaks attributable to either **1***a* or **1***b* were observed. A minimum value of $K_{1c/1a+1b}$ was estimated to be $\geqslant 250$.

[1]The solvent is undoubtedly highly structured (polymeric) as a result of hydrogen bonding and the term termolecular is misleading in this sense.

Can. J. Chem. Downloaded from www.nrcresearchpress.com by 210.87.254.105 on 09/05/12
For personal use only.

Preparation of 1,2,4,5-Tetramethylcyclopentadiene (4)

A cation mixture of **1***a*/**1***b* (from 3 g of 2,4-dimethyl-2,5-heptadien-4-ol and 30 ml of concentrated H_2SO_4 at 0°) was injected slowly into the vortex of a vigorously stirred solution of 30% aqueous NaOH and ether at −5°. The ether layer was separated and the aqueous layer was extracted with ether (3 × 50 ml). The combined ether solution was washed with saturated brine and dried over anhydrous K_2CO_3. After removal of the ether under reduced pressure, micro distillation of the residue gave 1.7 g of colorless liquid, b.p. 40.5° at 12 Torr. V.p.c. (5 ft × 1/4 in. SE-30 on Chromosorb W at 65°) and n.m.r. analyses indicated 94% **4**, 3% of 1,2,3,4-tetramethylcyclopentadiene (**5**) (identified by co-injection with authentic sample), and 3% of an unidentified component.

Diene **4** shows n.m.r. peaks centered at τ 8.99 (C-5 methyl, doublet, J = 7.8 Hz); 8.24 (C-1 and -4 methyls, singlet); 8.13 (C-2 methyl, singlet); 7.53 (C-5 hydrogen, quartet, J = 7.8 Hz), and 4.30 (C-3 hydrogen, broad singlet).

Protonation of 4

Diene **4** was added to 98% and 100% H_2SO_4 at 0°. N.m.r. analysis of the resulting solution indicated 95% of **1***a* and **1***b* in the ratio of 1.5 ± 0.2 favoring **1***a* and 5% of **1***c*. In FSO_3H and 4:1 FSO_3H–SbF_5, the ratio **1***a*/**1***b* was 1.3 ± 0.2 with 15–25% of **1***c*.

Preparation of 3,4-Dimethylhepta-2,5-dien-4-ol (8)

Using the general preparative method for 3,5-dimethylhepta-2,5-dien-4-ol (2), from 9.8 g (0.1 mol) of 3-methylpent-3-en-2-one, 12.1 g (0.1 *m*) of 1-bromo-1-propene (*cis–trans* mixture), and 1.4 g (0.2 mol) of lithium, 7 g (60%) of **8** was obtained, b.p. 63–6° at 9 Torr.

N.m.r. analysis showed peaks at τ 4.25–4.75 (C-2, -5, and -6 protons); 8.20–8.55 (C-1, -3, and -7 methyls); 8.64 and 8.72 (C-4 methyl, two singlets due to the two isomers, *i.e.* (2E,5E) and (2E,5Z)). The OH peak is concentration dependent.

Preparation of 1,2,4,5-Tetramethylcyclopentenyl cation (6)

Dienol **8** (75 mg) was added to 0.5 ml of FSO_3H or FSO_3H–SbF_5 with stirring at −78°. N.m.r. analysis of the resulting solutions showed the presence of cation **6** (mixture of *cis* and *trans*). N.m.r. peaks were observed at τ 0.39 and 0.45 (C-3 proton); 6.38 and 6.82 (C-4 and -5 protons, broad), 6.99 (C-1 methyl, singlet), 7.74 (C-2 methyl, singlet), and 8.47–8.65 (C-4 and -5 methyl, multiplet). All peaks for the *cis* and *trans* isomers overlap except those for the C-3 proton.

The authors wish to thank the National Research Council of Canada for financial support.

1. T. S. SORENSEN, I. J. MILLER, and C. M. URNESS. Can. J. Chem. **48**, 3374 (1970).
2. N. W. K. CHIU and T. S. SORENSEN. Can. J. Chem. This issue.
3. R. J. GILLESPIE. Acc. Chem. Res. **1**, 202 (1968).
4. P. H. CAMPBELL, N. W. K. CHIU, K. DEUGAU, I. J. MILLER, and T. S. SORENSEN. J. Am. Chem. Soc. **91**, 6404 (1969).
5. R. Z. BLADEK and T. S. SORENSEN. Can. J. Chem. **50**, 2806 (1972).
6. N. C. DENO and C. U. PITTMAN, JR. J. Am. Chem. Soc. **86**, 1871 (1964).
7. T. S. SORENSEN. Can. J. Chem. **42**, 2768 (1964).
8. T. S. SORENSEN. Can. J. Chem. **43**, 2744 (1965).
9. N. C. DENO, C. U. PITTMAN, JR., and J. O. TURNER. J. Am. Chem. Soc. **87**, 2153 (1965).
10. T. S. SORENSEN. J. Am. Chem. Soc. **89**, 3782, 3794 (1967).
11. T. S. SORENSEN. J. Am. Chem. Soc. **87**, 5075 (1965).
12. N. C. DENO and R. R. LASTOMIRSKY. J. Am. Chem. Soc. **90**, 4085 (1968).

Can. J. Chem. Downloaded from www.nrcresearchpress.com by 210.87.254.105 on 09/05/12
For personal use only.

Steric Effects in the Baeyer–Villiger Reaction of Simple Ketones

MITCHELL A. WINNIK AND VALERIE STOUTE

Erindale College and the Lash Miller Laboratories, Department of Chemistry, University of Toronto, Toronto, Ontario M5S 1A1

Received February 12, 1973

The reactions of simple alkyl ketones with peroxytrifluoroacetic acid (PTFA) and peroxymaleic acid (PMA) have been examined. Magnitudes of steric effects in the Baeyer–Villiger reaction have been determined, the largest being a factor of 13 in neopentyl to ethyl migration in 5,5-dimethyl-3-hexanone. PMA is consistently more selective toward electronic differences in migrating groups. PTFA shows the greater sensitivity to steric effects.

On a examiné les réactions de cétones alcoyles simples avec l'acide peroxytrifluoroacétique (PFTA) et l'acide peroxymaléique (PMA). On a déterminé les grandeurs des effets stériques dans la réaction de Baeyer–Villiger, le plus grand effet étant un facteur de 13 lors de la migration du néopentyle par rapport au groupement éthyle pour la diméthyl-5,5 hexanone-3. Le PMA est régulièrement plus sélectif vis-à-vis des différences électroniques dans les groupes migrateurs. PTFA possède une plus grande sensibilité pour ce qui est des effets stériques. [Traduit par le journal]

Can. J. Chem., 51, 2788 (1973)

Introduction

While steric effects in the Baeyer–Villiger reaction (1) have received attention in bicyclic systems (2), ortho-substituted acetophenones (3), and benzaldehydes (4), simple aliphatic ketones have not been studied. Analytical difficulties abound and before the days of n.m.r. such study would have been impossible. While one might expect that migratory aptitudes of aliphatic groups, 3° > 2° ~ benzyl > 1° > Me, would have a steric component (the larger group always migrates in preference), Emmons and co-workers found almost no difference in the migratory aptitudes of ethyl and neopentyl when comparing the reaction of their respective phenyl ketones (5). Several years ago, one of us employed the Baeyer–Villiger reaction as a tool in the analysis of a mixture of long chain aliphatic ketones (6). It was necessary to assume indiscriminate migration of primary alkyl groups in the reaction of the ketones with peroxytrifluoroacetic acid. This seemed, in light of Emmons' results, to be a good approximation; but, as a control, 3-heptanone was subjected to these conditions. It was found that *n*-butyl migrated in preference to ethyl by 2 to 1. This paper presents the results of our study of the effect of steric bulk on the relative migratory aptitude of alkyl groups in the Baeyer–Villiger reaction.

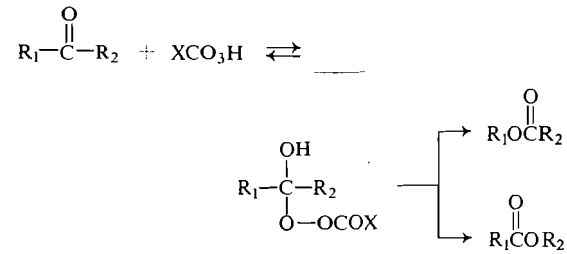

Results

Methyl Ketones

The Baeyer–Villiger reaction was carried out at room temperature (23 ± 1°) on a series of methyl primary alkyl ketones in methylene chloride solution. The reactions were run to completion using twofold excess of peroxytrifluoroacetic acid (PTFA) in the presence of anhydrous disodium hydrogen phosphate or using fourfold excess of peroxymaleic acid (PMA) without added buffer. The reactions employing PTFA ordinarily were over in an hour, although, to ensure completion of the reaction, they were routinely stirred 90 min before working them up. Reactions employing PMA required 48 h stirring at room temperature to achieve complete reaction. No attempt was made to study the kinetics under these conditions. The former peracid requires a solid buffer in the reaction mixture, and, PMA reac-

Can. J. Chem. Downloaded from www.nrcresearchpress.com by 210.87.254.40 on 09/05/12
For personal use only.

Can. J. Chem. Downloaded from www.nrcresearchpress.com by 210.87.254.40 on 09/05/12
For personal use only.

tions deposit solid maleic acid during the course of the reaction. Both situations make it impossible to study the kinetics of the reaction under conditions identical to this product study.

Extent of methyl migration was assayed by n.m.r. The methyl resonance, in all cases, was well resolved and upfield of the methylene resonance of the corresponding isomeric ester. The small amounts of methyl esters produced required calibration of the attenuator. Calibration data, including correlation coefficients, are presented in detail in the experimental section. The methyl resonances were scanned at increased amplitude and the weight of the methyl peak was divided by its amplification factor. The very small values of methyl migration in methyl isobutyl ketone and methyl neopentyl ketone were calibrated by interpolating from known mixtures of the appropriate pure esters. We estimate the error in these measurements to be approximately $\pm 5\%$. The limit of our ability to detect methyl ester under these conditions is about 0.05%.

The extent of methyl migration for the ketones studied is collected in Table 1. The amount of methyl migration in methyl *n*-propyl ketone is half that observed in methyl ethyl ketone. Further homologation of the alkyl chain results in much smaller changes in extent of methyl migration. These differences are probably real, since they are outside of experimental error and are reflected in the amount of methyl migration found with both peracids. They may reflect conformational differences of the chains in methylene chloride solution. 2-Undecanone poses a peculiar problem here in that the product nonyl acetate is unusually sensitive to hydrolysis. Nonyl alcohol interferes with the assay procedure. The methylene protons adjacent to the OH fall on top of the ester O-methyl singlet. The product of the PMA oxidation underwent enough hydrolysis in 24 h reaction (3–10%) to obscure measurement of the extent of methyl migration in this case. Even with PTFA, when worked up in the usual way and allowed to stand at room temperature in CCl_4 in an n.m.r. tube, nonyl acetate underwent extensive hydrolysis.

TABLE 1. Methyl migration for $RCOCH_3$

R	CF_3CO_3H	R/CH_3	PMA	R/CH_3
Ethyl	1.38%[a]	72[b]	0.37%[a]	270[b]
Propyl	0.69	150	0.22	450
Butyl	0.78	130	0.25	400
Pentyl	0.51	200	0.15	670
Nonyl	0.65	150	—[c]	—[c]
Isobutyl	0.32	310	0.13	770
Neopentyl	0.12	830	0.10	1000
Benzyl	<0.05	>2000	<0.05	>2000

[a]Percent methyl migration.
[b]Ratio of migratory aptitude alkyl/methyl.
[c]Could not be measured due to partial ester exchange.

PMA is consistently more selective in the oxidation of methyl ketones. This difference of three- to fourfold increase in the selectivity probably reflects an increase in its sensitivity to electronic effects, when compared to PTFA. As the steric bulk of the alkyl group increases, this selectivity diminishes, suggesting that electronic and steric requirements lead to opposing effects.

Ethyl Ketones

The Baeyer–Villiger reaction of ethyl *n*-alkyl ketones was carried out under conditions identical to those described above. Both n.m.r. and mass spectral assays were employed. In the cases of 1-phenyl-2-butanone and neopentyl ethyl ketone, the CH_2—O protons of the respective esters were clearly resolved at 60 MHz. The esters from the reaction of isobutyl ethyl ketone could be resolved clearly only at 100 MHz. Partial resolution could be obtained at 60 MHz. The normal 3-alkanones did not lend themselves to an n.m.r. assay. Partial resolution was observed at 220 MHz for these reaction products. These partially resolved spectra were very useful since they allowed estimation of migratory aptitudes, which served as a convenient check on the more rigorous analyses.

Attempts to separate the product esters by g.l.c. failed, except in the case of 3-hexanone. Ethyl butanoate and propyl propanoate could be separated on a carefully packed 30 ft Carbowax 4000 column or on a 150 ft Carbowax 4000 coated capillary column. Our assay for 3-alkanones depended upon the propensity of ethyl alkanoates to give an intense ion in the mass spectrum at *m/e* 88, whereas propanate esters give peaks at *m/e* 57 and 75. The mass spectrometer was calibrated, in each instance, with known mixtures of the product esters and the composition of the Baeyer–Villiger product mixture was determined from the *m/e* 88/75 ratio by interpolation.

Table 2 lists the ratio of ethyl migration to

TABLE 2. Product ratios for ethyl ketones

R/Ethyl	CF_3CO_3H	Calcd.[a]	PMA	Calcd.[a]
Propyl	1.75[b]	2.0	1.89[b]	1.7
Butyl	1.56	1.8	2.13	1.5
	1.6[c]		1.7[c]	
Pentyl	1.85	2.8	2.08	2.5
	1.7[c]		2.0[c]	
Nonyl	2.04	2.1	2.38	—
Isobutyl	4.76[d]	4.3	4.54[d]	2.9
Neopentyl	13.3[e]	11.6	11.9[e]	3.7
Benzyl	17.5[e]		25.0[e]	

[a]Calculated from the ratio of alkyl/methyl migration in the pertinent 2-alkanone to ethyl/methyl migration in 2-butanone.
[b]Mass spectrometric assay.
[c]220 MHz n.m.r. assay.
[d]100 MHz n.m.r. assay.
[e]60 MHz n.m.r. assay.

alkyl migration for both peracids. Also included in the table is the ratio of alkyl to ethyl migratory aptitudes, calculated from the methyl ketone data by comparing the ratio of alkyl/methyl migration to ethyl/methyl migration. It is interesting to note that, unlike the methyl ketones, the ethyl ketones show little change in selectivity in changing from PTFA to PMA as the peracid. Increasing the steric bulk of the alkyl group increases its tendency to migrate. *n*-Propyl acts as though it is larger than ethyl. Isobutyl contributes a factor of three over *n*-butyl to the relative migratory aptitude of the alkyl moiety, and neopentyl approximately another factor of three. The large migratory aptitude for benzyl indicates that electronic considerations are also important in the migration of this group.

Discussion

Steric Effects

Substitution of methyl groups on the β-carbon of 2- and 3-alkanones causes fairly small changes in the migratory aptitudes of the alkyl portion relative to methyl and ethyl. Extent of alkyl migration increases fairly regularly with the bulk of the alkyl group. Parallel effects are seen in the methyl and ethyl ketones and with both peracids. The largest difference is a factor of 13.3 seen in the reaction of ethyl neopentyl ketone with PTFA. This represents a difference in the free energy of activation ($\Delta\Delta G^{\ddagger}$) of neopentyl over ethyl migration of 1.5 kcal/mol.

We favor a steric origin for this change in migratory aptitude. One easily can visualize the origin of this steric effect in Newman projections of the Criegee intermediate by assuming that migration takes place *anti*-periplanar to the

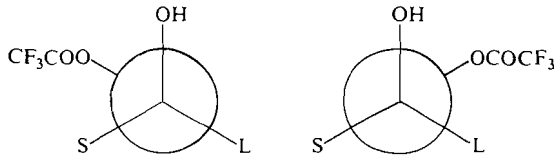

departing carboxylate and that the product-determining transition state has similar steric demands. This argument has been advanced before (5). It is well to remember Curtin's admonition (8) that, if migration is slow with respect to rotation, the product ratio is determined solely by the ratio of the energies of the two transition states and not by the rotamer populations of the intermediate.

Comparison of the Peracids

Two papers by Emmons present examples of the change in relative migratory aptitude as a function of peracid. Emmons noted initially (5) that phenyl cyclohexyl ketone suffered 22% phenyl migration with PTFA and 11% phenyl migration with peroxyacetic acid in the presence of 1 *M* CF_3CO_2H. In later work (7), he observed that, in the reactions of desoxybenzoin, PMA gave a 7:1 ratio of benzyl to phenyl migration, whereas with PTFA, equal amounts were found. In both examples he concluded that migration was concerted with O—O bond cleavage and that the reaction involving the poorer leaving group was more selective.

Our results indicate that the situation is not so simple. PMA here is consistently more selective than PTFA when one is comparing two groups, which differ in the ability to stabilize positive charge by delocalization in the transition state. In the comparison of methyl with primary alkyl, PMA is about four times more selective. Comparing primary alkyl with benzyl, PMA is 1.4 times as selective. Where the comparison is between two primary alkyl groups (and one might expect a similar electronic demand) very small differences are observed between the two peracids.

Robertson and Swelin (9) visualize a homolytic pathway for O—O bond cleavage in the Criegee intermediate, derived from the reaction of peroxyacetic acid and benzophenones containing electron withdrawing groups. The normal Baeyer–Villiger products are produced by a 1,2 radical migration of one of the phenyl groups. A change in reaction mechanism, they assert, is responsible for the change in migratory apti-

Can. J. Chem. Downloaded from www.nrcresearchpress.com by 210.87.254.40 on 09/05/12
For personal use only.

Can. J. Chem. Downloaded from www.nrcresearchpress.com by 210.87.254.40 on 09/05/12
For personal use only.

tudes of phenyl and *p*-nitrophenyl when peroxyacetic acid is used instead of PTFA. To our knowledge, alkyl migrations to radical centers are not known (10), and the absence of methyl migration in the *t*-butoxy radical argues against a radical pathway in our experiments. In addition, maleic acid is a much stronger acid than acetic acid (pK_a = 1.83 *vs.* 4.75, respectively, in water) (11) and a better leaving group from the Criegee intermediate.

We are well aware of the dangers of trying to present mechanistic conclusions based upon small differences in relative rate constants. With this in mind, we would like to comment on some of our more surprising data: in the reaction with methyl ketones, there is a pronounced decrease in the selectivity of PMA as the bulk of the alkyl groups increases. PMA is about fourfold more selective than PTFA in reaction with 2-butanone, three times as selective in the homologous 2-alkanones, and, in neopentyl methyl ketone, the selectivity drops to 20%. This suggests that PTFA, which carries out this Baeyer–Villiger reaction 50 times faster than PMA (as estimated from half-times for reaction), is more sensitive to steric effects.

This trend abates in the ethyl ketones where the two peroxyacids show very similar selectivity toward ethyl/alkyl migration. In one case, however, PTFA, is the more selective peroxyacid. It shows 11% increased selectivity over PMA in the oxidation of neopentyl ethyl ketone.

Likely sources of diminished steric sensitivity of PMA may be visualized in the drawing below. The assumption of *anti*-periplanar migration implies that the leaving group is in the staggered conformation with respect to the non-migrating group and the hydroxyl, which eventually becomes the ester carbonyl. Migration takes place with relief of steric interaction between the non-migrating and leaving groups.

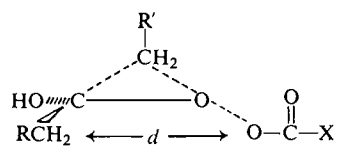

A source of the smaller steric requirement for migration, when maleic acid is the leaving group, might be a later transition state in that reaction and hence a greater distance *d* between these groups. Another source, which is tempting to invoke, particularly in methylene chloride solution, involves specific hydrogen bonding requirements, for the second carboxyl function in PMA, which render the leaving group rigid and sterically remote from the non-migrating group. We have no specific evidence on either point. We have carried out a few experiments with trichloroperoxyacetic acid, which has a bulkier X group, but these reactions are not as clean as those with PMA and PTFA.

PMA asserts its more selective nature in the oxidation of 1-phenyl-2-butanone, suggesting that there is an electronic component to benzyl migration in the Baeyer–Villiger reaction. The electronic contribution to benzyl migration here, however, can be estimated to be less than 1 kcal per mol. If we assume the benzyl function to be approximately isosteric with the isobutyl group,[1] less than a factor of four need be explained by the ability of benzyl to stabilize a positive charge in the transition state for migration.

Experimental

Materials

All ketones, with the exception of 5,5-dimethyl-3-hexanone, were obtained commercially. All esters, excluding ethyl decanoate (K and K laboratories) and ethyl acetate (Fisher Scientific Co.), were prepared by standard methods. In each case, the compound was checked on a Varian T-60 n.m.r. spectrometer and a Perkin-Elmer 337 grating i.r. spectrophotometer. Purification was effected by careful distillation through a 10 in. Vigreux column or through a Nester–Faust spinning band column, depending on the nature of the impurities. Before use, each compound was assayed by gas chromatography using a Varian Aerograph Model 1440-2 gas chromatograph equipped with a flame ionization detector. No compound was used unless shown to be greater than 99% pure on two of the following columns: (1) 11 ft. × 1/8 in. 10% Carbowax 4000 on Chromasorb P 80/100 mesh; (2) 10 ft. × 1/8 in. 10% diethylene glycol succinate on Chromasorb W 100/120 mesh; (3) 150 ft × 0.02 in. capillary with SE-30 coating.

Hydrogen peroxide (98%) (FMC corporation) was standardized by permanganate titration. Trifluoroacetic anhydride (Eastman or Baker) and maleic anhydride (Fisher Scientific Co.) were used without further purification.

5,5-Dimethyl-3-hexanone

Dry, finely powdered cadmium chloride (16.5 g, 0.09 mol) was added to an ice-cold solution of ethyl magnesium bromide (0.18 mol) in 65 ml of dry ether.

[1]Benzyl is more closely isosteric with isoamyl. If benzyl is larger than isobutyl in the region of interest, the electronic enhancement of benzyl migration is even smaller than this value (Keith Yates, private communication).

TABLE 3. N.m.r. assay of methyl ketones[a]

Mixture	% methyl ester	Slope[b] (M)	Intercept[b] (C)	Correlation coefficient
Methyl propanoate – ethyl acetate	0.256–0.840	0.973	0.024	0.997
Methyl hexanoate – pentyl acetate	0.106–0.675	1.02	0.027	0.989
Methyl 3-methyl butanoate – isobutyl acetate	0.072–0.337	1.21	0.030	0.999
Methyl 3,3-dimethyl butanoate – neopentyl acetate	0.095–0.250	1.11	0.026	0.991
Ethyl 3,3-dimethyl butanoate – neopentyl propanoate	8.30–11.78[c]	1.04	−0.025	0.990

[a]Measured by peak weights.
[b]Known composition = M (measured composition) + C.
[c]Percent ethyl ester.

The suspension was stirred at room temperature for 40 min before being cooled again to 5°. To this cold reaction mixture, 10 ml (0.106 mol) of *t*-butyl acetyl chloride in 30 ml of dry ether was added slowly, after which the mixture was refluxed with stirring for 90 min. Cooled to room temperature, the final product mixture was poured onto ice, leading to the formation of a white precipitate. Concentrated sulfuric acid was added dropwise until this precipitate just dissolved. The ethereal layer was separated, washed with successive portions of water, 10% sodium carbonate, and water, and then dried over magnesium sulfate. Distillation through a 10 in. Vigreux column gave the ketone (10.1 g or 79%), b.p. 136°.

Trifluoroperoxyacetic Acid

The peracid solution (*ca.* 1 *M*) was prepared fresh for each oxidation reaction. Trifluoroacetic anhydride (6.1 g, 0.029 mol) in methylene chloride was carefully added to 98% hydrogen peroxide (0.87 g, 0.025 mol) in 15 ml of methylene chloride at 0°. Once the addition was completed, the reactants were periodically agitated until a homogenous solution was observed. The solution was then diluted to 25 ml at room temperature and a 1 ml aliquot titrated iodometrically.

Peroxymaleic Acid

Maleic anhydride (2.45 g, 0.025 mol) was added to a suspension of 98% hydrogen peroxide (0.73 g, 0.021 mol) in 10 ml of methylene chloride at room temperature. Once the anhydride had dissolved, the methylene chloride was brought to reflux and maintained there for 30 min. The peroxymaleic acid solution thus formed was cooled and used directly in the oxidation reaction. This procedure was found to be superior to all other methods for producing this peracid.

Oxidations with Trifluoroperoxyacetic Acid

One procedure was found to give smooth, facile oxidation of all the ketones studied. The peracid solution (10 ml, *ca.* 0.010 mol) was added slowly from a pressure-equalizing dropping funnel to a mechanically stirred suspension of disodium hydrogen phosphate (4.25 g, 0.030 mol, previously dried over phosphorus pentoxide) in a solution of the ketone (*ca.* 0.005 mol) in 10 ml of methylene chloride, maintained at 23° ± 1°. Vigorous stirring was continued for 90 min to insure complete reaction. The reaction was quenched with water and the organic phase washed twice with water. The aqueous layers were combined and back-washed with 30 ml of methylene chloride. The combined organic layers were dried over magnesium sulfate and the solvent removed under reduced pressure. The reaction products were dissolved in carbon disulfide or carbon tetrachloride to be assayed by n.m.r., as described below.

Oxidations with Peroxymaleic Acid

To the entire solution of peroxymaleic acid (*ca.* 0.025 mol), prepared as above and maintained at 23° ± 1°, was added a solution of the ketone (*ca.* 0.005 mol) in 10 ml of methylene chloride. The contents of the reaction flask were stirred vigorously for 48 h after which they were mixed with 30 ml of water. This was enough to dissolve the white precipitate of maleic acid formed during the oxidation. The organic layer was separated, washed three times with 25 ml portions of phosphate buffer (0.5 *M*, p*H* 6.5) and once with a further 30 ml portion of water, dried over magnesium sulfate, and the solvent evaporated under reduced pressure. The reaction products were taken up in carbon disulfide or carbon tetrachloride before being assayed by n.m.r.

N.m.r. Analysis of Ester Mixtures

This assay was used for the product mixtures from oxidation of all the methyl ketones and of 5-methyl-3-hexanone, 5,5-dimethyl-3-hexanone, and phenyl-2-butanone. In every case, the two well-resolved signals, corresponding to the groups *alpha* to the ester oxygen in each of the two products, were scanned on a Varian T-60 n.m.r. spectrometer using a sweep width of 100 Hz and a sweep time of 50 s. The smaller of the two signals was then scanned 5 to 10 times at each of two increased amplitudes. Each scan was retraced several times to insure the reproducibility of the instrument and the phase was always carefully adjusted to make the base line of the peaks as straight as possible. The filter dial was always set at 2 so that, at the sweep width used, the peaks were smooth as well as broad. The areas under the peaks (in Xerox copies of these spectra) were then carefully cut out, weighed, corrected to the same amplitude, and the weight contribution, made by one hydrogen to each ester signal, calculated.

In the case of the products from 5-methyl-3-hexanone and 5,5-dimethyl-3-hexanone, similar spectra were run on a Varian HA 100 as well. Here the relative concentrations of the two esters were such that the signals could be compared at one amplitude.

The procedure was calibrated by subjecting series of known mixtures of esters to the same assay. For each series examined, plots were made of the known com-

Can. J. Chem. Downloaded from www.nrcresearchpress.com by 210.87.254.40 on 09/05/12
For personal use only.

TABLE 4. Mass spectrometric assay of ethyl esters[a]

Mixture	Alkyl/ethyl ester	Slope[b] (M)	Intercept[b] (C)	Correlation coefficient
Ethyl butanoate – propyl propanoate	1.39–1.85	0.631	0.222	0.999
Ethyl pentanoate – butyl propanoate	1.40–2.20	1.84	−0.560	0.989
Ethyl hexanoate – pentyl propanoate	2.49–3.64	1.84	−0.774	0.999
Ethyl decanoate – nonyl propanoate	1.50–3.66	2.34	−0.681	0.999

[a]Measured by peak height.
[b]Alkyl/ethyl ester ratio = M [(intensity at m/e 75)/(intensity at m/e 88)] + C.

positions versus the measured values. Slopes, intercepts, and correlation coefficients are collected in Table 3.

Mass Spectrometric Analysis of Ester Mixtures

This method was used for the product mixtures from the reaction of all ketones of the type $RCH_2CH_2\overset{O}{\overset{\|}{C}}CH_2CH_3$. All spectra were run on neat samples, using a Bell and Howell mass spectrometer model 21-490, at 70 eV and source temperature of 100° ± 10°. Four traces were collected for each sample. The m/e 75/88 values obtained for known mixtures were plotted against the alkyl/ethyl ester ratio as indicated in Table 4. Baeyer–Villiger product ratios were determined from their m/e 75/88 values by interpolation on these plots.

We wish to thank the National Research Council of Canada for financial support. Miss Stoute wishes in addition to thank the P.E.O. Sisterhood for a fellowship.

1. P. A. S. SMITH. *In* Molecular rearrangements. Vol. 1. *Edited by* P. de Mayo. Interscience, New York. 1963. p. 568.
2. J. MEINWALD and E. FRAUENGLASS. J. Am. Chem. Soc. **82**, 5235 (1960); R. R. SAUERS and G. P. AHEARN. J. Am. Chem. Soc. **83**, 2759 (1961); R. R. SAUERS and J. A. BEISLER. J. Org. Chem. **29**, 210 (1964).
3. (*a*) W. H. SAUNDERS, JR. J. Am. Chem. Soc. **77**, 4679 (1955). (*b*) E. E. SMISSMAN, J. PENGMAN LI, and ZAFAR ISRAILI. J. Org. Chem. **33**, 4231 (1968).
4. Y. OGATA and Y. SAWAKI. J. Am. Chem. Soc. **92**, 4189 (1972).
5. M. F. HAWTHORNE, W. D. EMMONS, and K. S. MCCALLUM. J. Am. Chem. Soc. **80**, 6393 (1958).
6. R. BRESLOW and M. A. WINNIK. J. Am. Chem. Soc. **91**, 3083 (1969).
7. R. W. WHITE and W. D. EMMONS. Tetrahedron, **17**, 31 (1962); S. L. FRIESS and N. FARNHAM. J. Am. Chem. Soc. **72**, 5518 (1950).
8. D. Y. CURTIN. Rec. Chem. Prog. **15**, 111 (1954).
9. J. C. ROBERTSON and A. SWELIN. Tet. Lett. 2871 (1967).
10. C. WALLING. *In* Molecular rearrangements. Vol. 1. *Edited by* P. de Mayo. Interscience, New York. 1963. p. 416.
11. Handbook of chemistry and physics. 46th ed. Chemical Rubber Co. Cleveland. p. D-78.

Can. J. Chem. Downloaded from www.nrcresearchpress.com by 210.87.254.40 on 09/05/12
For personal use only.

Can. J. Chem. Downloaded from www.nrcresearchpress.com by 210.87.254.105 on 09/05/12
For personal use only.

The Crystal and Molecular Structure of the Adduct Formed by the Reaction of Tributylphosphine and *p*-Chlorobenzylidenemalononitrile

GEORGE FERGUSON, COLIN ALAN FYFE, AND WAYNE CLIFFORD MARSH
Department of Chemistry, University of Guelph, Guelph, Ontario N1G 2W1

Received February 19, 1973

Crystals of the 1:1 adduct of tributylphosphine with *p*-chlorobenzylidenemalononitrile are monoclinic, a = 13.719(2), b = 12.557(5), c = 14.229(3) Å, β = 110.59(2)°, Z = 4, space group $P2_1/c$. The structure was determined with diffractometer data by direct methods and refined by block-diagonal least-squares calculations to R = 0.10 for 1405 observed reflections. The structure is zwitterionic with the positive charge localized on the phosphorus atom and the negative charge mainly on the terminal —C(CN)$_2$ group.

Les cristaux de l'adduit 1:1 de la tributylphosphine avec le *p*-chlorobenzylidenemalononitrile sont monocliniques avec a = 13.719(2), b = 12.557(5), c = 14.229(3) Å, β = 110.59(2)°, Z = 4, le groupe spatial est $P2_1/c$. La structure a été déterminée à partir des données du diffractomètre par les méthodes directes et les moindres carrés après raffinement juisqu'à un R = 0.10 pour 1405 réflexions observées. La structure est zwittérionique avec la charge positive localisée sur l'atome de phosphore et la charge négative principalement sur le groupe —C(CN)$_2$ terminal. [Traduit par le journal]

Can. J. Chem., 51, 2794 (1973)

All the reactions involving the interaction of nucleophiles with electronegatively substituted alkenes can be rationalized in terms of an initial attack of the nucleophile on the β-carbon atom of the alkene to form the intermediate (**1**), whose further reaction can give rise to a variety of products depending on the conditions (eq. 1;

[1] 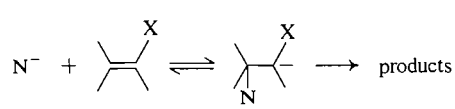

1

X is an electronegative sustituent) (1). The existence of species of type **1** has been verified in the case of substituted stilbenes for charged nucleophiles (2–4).

When the nucleophile is uncharged, a special case of eq. 1 arises and a zwitterion should be formed, eq. 2. One case where an adduct of 1:1

[2] 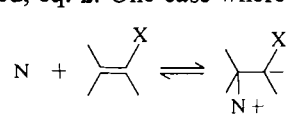

stoichiometry has been experimentally observed in such an attack by a neutral nucleophile is the interaction of tributylphosphines with benzylidenemalononitriles (5). Horner and Klupfel (5) originally formulated the structure as the zwitterion (**2**). Since then, several other possible structures have been considered (6, 7).

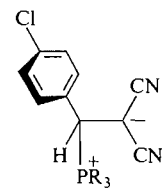

2

A recent n.m.r. investigation (7) has concluded that the zwitterionic structure (**2**) was correct. Because of the direct relevance of these compounds to the theory of nucleophilic alkene substitution reactions, the structure analysis of the 1:1 adduct of tributylphosphine with *p*-chlorobenzylidenemalononitrile was undertaken in an attempt to confirm the results of the n.m.r. investigation.

Experimental

The adduct crystallized from dioxan as yellowish irregular fragments. A small crystal was mounted and sealed in a thin-walled capillary (when left in the open the crystals showed evidence of decomposition and of being hydroscopic). Unit-cell and space group data were obtained from various rotation, Weissenberg, and precession photographs; accurate cell parameters were obtained by a least-squares procedure applied to the setting angles of 12 general reflections measured on a diffractometer.

Crystal Data

$C_{22}H_{32}ClN_2P$ (mol. wt. 390.9): monoclinic, a =

TABLE 1. Atomic positional* and thermal† parameters‡

Atom	x	y	z	U_{11}	U_{22}	U_{33}	U_{12}	U_{13}	U_{23}
Cl	5827(3)	5786(4)	2560(3)	62	140	110	−26	33	1
P	1165(3)	4025(3)	2740(2)	60	59	38	−3	25	1
N(1)	−0134(9)	3467(9)	−0903(8)	97	83	46	7	15	−8
N(2)	1673(9)	1338(9)	1509(8)	103	68	72	11	2	−15
C(1)	4563(11)	5362(13)	2232(10)	74	100	61	2	33	−1
C(2)	4358(11)	4238(13)	2094(10)	77	110	74	−1	37	−13
C(3)	3337(10)	3866(12)	1855(9)	58	103	64	2	33	4
C(4)	2535(10)	4572(11)	1780(8)	62	75	40	−2	27	1
C(5)	2755(10)	5679(10)	1904(9)	79	58	49	−11	26	2
C(6)	3777(11)	6040(12)	2141(10)	71	100	60	−14	20	6
C(7)	1413(9)	4234(10)	1567(8)	62	82	33	−11	29	−6
C(8)	1092(9)	3220(10)	0924(8)	56	67	42	7	15	−4
C(9)	0433(10)	3365(10)	−0087(9)	66	57	62	7	35	−6
C(10)	1412(9)	2193(11)	1240(9)	68	67	43	9	17	−10
C(11)	1299(11)	5327(12)	3348(9)	76	70	36	−2	37	−8
C(12)	0944(12)	5219(13)	4295(10)	97	82	41	−3	41	−12
C(13)	1286(13)	6271(13)	4931(11)	114	86	55	13	49	−13
C(14)	2458(13)	6375(14)	5463(12)	107	122	73	−2	9	−23
C(15)	−0146(11)	3545(12)	2443(10)	66	99	58	−1	28	−7
C(16)	−0976(10)	4264(12)	1720(10)	59	99	64	3	27	8
C(17)	−2074(11)	3871(15)	1609(10)	48	145	76	14	11	−7
C(18)	−2915(13)	4510(18)	0839(15)	76	199	129	16	41	−7
C(19)	2050(11)	3076(11)	3600(9)	87	69	45	9	16	21
C(20)	3140(11)	3525(14)	4216(10)	79	121	52	14	21	11
C(21)	3888(14)	2670(17)	4725(13)	97	152	101	36	8	−11
C(22)	5007(15)	3069(20)	5197(14)	71	226	102	34	−13	−15

*Fractional coordinates $\times 10^4$.
†T.F. = exp $[-2\pi^2(U_{11}h^2a^{*2} + U_{22}k^2b^{*2} + U_{33}l^2c^{*2} + 2U_{12}hka^*b^* + 2U_{13}hla^*c^* + 2U_{23}klb^*c^*)]$; U_{ij} in Å$^2 \times 10^3$.
‡The estimated standard deviations in thermal parameters U lie in the range 0.002–0.014 Å^2.

13.719(2), b = 12.557(5), c = 14.229(3) Å, β = 110.59(2)°,[1] U = 2295 Å^3, Z = 4, D_c = 1.13 g cm^{-3}, $F(000)$ = 840. Cu K_α = 1.5418 Å, μ(Cu K_α) = 21 cm^{-1}. Space group $P2_1/c$ (C_{2h}^5) from systematic absences: $h0l$ when l is odd, $0k0$ when k is odd.

The intensities of all reflections with 2θ(Cu K_α) < 114° (minimum interplanar spacing 0.92 Å) were measured on a PDP 8-I controlled Hilger and Watts Y290 four-circle diffractometer, with a scintillation counter, approximately monochromatic Cu K_α radiation (nickel filter and pulse-height analyzer), and a θ/2θ step scan of 80 steps of 0.01° each. Background counts of 20 s were made at the beginning and end of each scan. No absorption corrections were applied. The crystal decomposed slowly in the X-ray beam as measured by the falloff of counts from standard reflections throughout the course of the data collection. The crystal did not appear to have moved from its original mounting, as going through the crystal alignment process after data collection yielded the same orientation parameters for the standard reflections as had been obtained initially. Allowance for the crystal decomposition was made by scaling the intensity data by means of the counts from the standard reflections. Lorentz and polarization factors were applied, and the structure factors were derived in the usual way. Reflections which had a net count of less than 3σ above background, where σ(I) is defined by $\sigma^2(I) = S + B + (0.05\,S)^2$ and S and B are the scan and background counts respectively, were taken as being unobserved. These reflections were assigned structure factors equal to the measured values but were excluded from the refinement. Of the 2764 possible reflections with 2θ < 114°, 1405 (51%) were classified as observed.

[1]Throughout this paper the estimated standard deviations are given in parentheses and refer to the last significant figure.

Structure Analysis

The data were placed on an absolute scale by Wilson's method (8), and normalized structure amplitudes E were derived. The 411 E's greater than 1.5 were used in the structure determination utilizing the PHASE (9) link of the X-ray 72 system. Initially the 100 largest E's were phased and these were then used to phase the remaining 311 E's greater than 1.5. An E map based on the 411 phased E's revealed the positions of 22 of the 26 non-hydrogen atoms, the missing atoms being in the n-butyl groups. A difference Fourier synthesis at this stage revealed the positions of the four missing atoms.

The structure was refined by block-diagonal least-squares methods, with the scattering curves of ref. 10, the function minimized being $\omega(|F_o| - |F_c|)^2$ with final weights, $\omega = 0$ for the unobserved reflections and $\omega = 1$ for $F_o < F^*$, and F^*/F_o for $F_o \geq F^*$. A value of 12.0 for F^* was found to be suitable from an analysis of $\omega(|F_o| - |F_c|)^2$ over ranges of $|F_o|$. Four cycles of refinement with isotropic temperature factors reduced R to 0.16. Six further cycles with all atoms allowed to vibrate anisotropically gave a final R of 0.10 for the 1405 observed data, and

Can. J. Chem. Downloaded from www.nrcresearchpress.com by 210.87.254.105 on 09/05/12
For personal use only.

TABLE 2. Interatomic distances (Å) and angles (deg)

(*a*) Bond lengths

Cl—C(1)	1.715(15)	C(8)—C(9)	1.41(1)
		C(8)—C(10)	1.39(2)
P—C(7)	1.837(13)		
P—C(11)	1.828(15)	C(9)—N(1)	1.15(1)
P—C(15)	1.801(15)	C(10)—N(2)	1.15(2)
P—C(19)	1.830(13)		
		C(11)—C(12)	1.59(2)
C(1)—C(2)	1.44(2)	C(12)—C(13)	1.58(2)
C(2)—C(3)	1.40(2)	C(13)—C(14)	1.52(2)
C(3)—C(4)	1.39(2)	C(15)—C(16)	1.53(2)
C(4)—C(5)	1.42(2)	C(16)—C(17)	1.54(2)
C(5)—C(6)	1.40(2)	C(17)—C(18)	1.52(2)
C(6)—C(1)	1.34(2)	C(19)—C(20)	1.55(2)
		C(20)—C(21)	1.49(2)
C(4)—C(7)	1.52(2)	C(21)—C(22)	1.53(2)
C(8)—C(7)	1.54(2)		

(*b*) Bond angles

C(7)—P—C(11)	106.4(6)	P—C(15)—C(16)	113.8(10)
C(7)—P—C(15)	108.9(6)	C(15)—C(16)—C(17)	110.4(12)
C(7)—P—C(19)	114.2(6)	C(16)—C(17)—C(18)	111.9(15)
C(11)—P—C(15)	109.7(7)		
C(11)—P—C(19)	109.5(6)	P—C(19)—C(20)	115.0(10)
C(15)—P—C(19)	108.1(7)	C(19)—C(20)—C(21)	112.0(14)
		C(20)—C(21)—C(22)	113.0(17)
P—C(7)—C(4)	110.9(7)	Cl—C(1)—C(2)	118.1(11)
P—C(7)—C(8)	108.4(9)	Cl—C(1)—C(6)	122.0(12)
C(4)—C(7)—C(8)	114.0(11)	C(2)—C(1)—C(6)	119.8(13)
		C(1)—C(2)—C(3)	119.4(14)
C(7)—C(8)—C(9)	116.4(10)	C(2)—C(3)—C(4)	120.3(13)
C(7)—C(8)—C(10)	125.8(9)	C(3)—C(4)—C(5)	119.2(12)
C(9)—C(8)—C(10)	117.8(10)	C(3)—C(4)—C(7)	123.9(12)
		C(5)—C(4)—C(7)	116.9(12)
C(8)—C(9)—N(1)	177.6(17)	C(4)—C(5)—C(6)	119.9(12)
C(8)—C(10)—N(2)	179.3(18)	C(5)—C(6)—C(1)	121.4(14)
P—C(11)—C(12)	108.4(10)		
C(11)—C(12)—C(13)	107.3(13)		
C(12)—C(13)—C(14)	113.9(14)		

$$Rw = [\Sigma\omega(F_o - F_c)^2/\Sigma\omega F_o^2]^{1/2} = 0.11$$

The maximum ratio of shift to e.s.d. on the final cycle was 0.5. Measured and calculated structure factors have been placed in the Depository of Unpublished Data.[2] A final difference synthesis showed maximum fluctuations of 0.7 eÅ^{-3}. Although a large number of peaks were in reasonable positions for hydrogen atoms, no attempt was made to include them in the analysis.

The positional and thermal parameters are listed in Table 1. Bond lengths and angles and their standard deviations are given in Table 2. Figure 1 is a stereoscopic view of the molecule produced by ORTEP (11). The molecular packing is shown in Fig. 2.

[2]A complete set of tabular data is available at a nominal charge from the Depository of Unpublished Data, National Science Library, National Research Council of Canada, Ottawa, Canada, K1A 0S2.

Discussion

The crystal structure (Fig. 2) contains discrete molecules. The two shortest contacts both involve the terminal N atoms of the cyano groups. Atom N(1) is only 3.34(2) Å from a neighboring C(7) atom (related by $-x, 1-y, -z$). Atom N(2) is 3.29(1) Å distant from an adjacent Cl atom (related by $1-x, \frac{1}{2}+y, \frac{1}{2}-z$). These and all other intermolecular distances correspond to, or are greater than, van der Waals contacts.

The molecular structure is shown in Fig. 1 and geometry details are in Table 2. Carbon (7) is clearly in a tetrahedral configuration (the bond angles at C(7) are between 108 and 114°); the C(7)—P bond is the same length as the P—C-

Can. J. Chem. Downloaded from www.nrcresearchpress.com by 210.87.254.105 on 09/05/12
For personal use only.

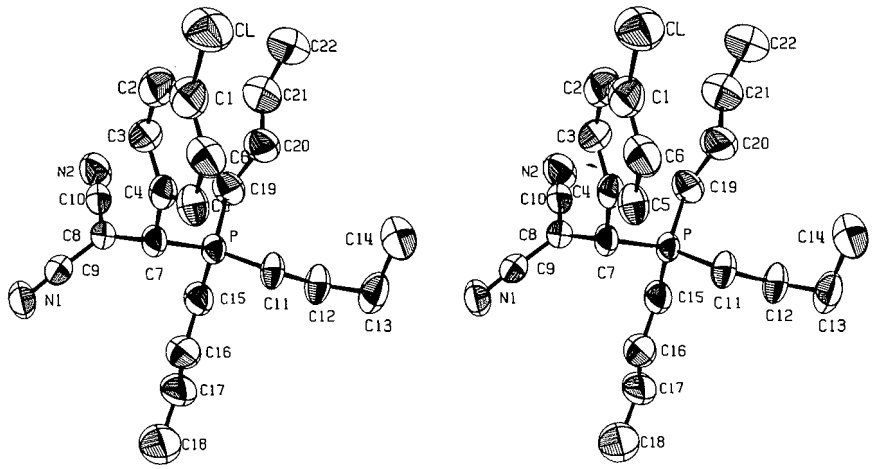

FIG. 1. Stereo view of the structure of the adduct, produced by ORTEP (11).

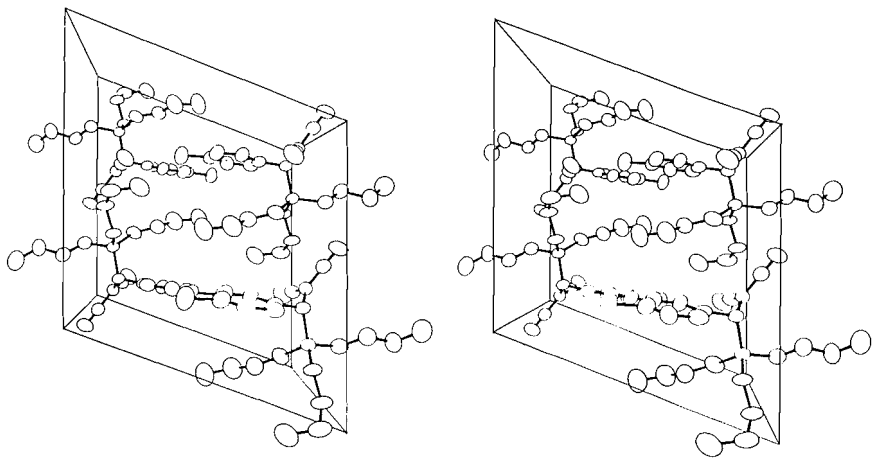

FIG. 2. Stereo view of the four molecules in the unit cell. The origin of the cell is at the lower left corner with $a \rightarrow$, $c \uparrow$, and b vertical.

(butyl) bonds; the coordination around the phosphorus is tetrahedral, and the configuration at C(8), the atom to which the cyano groups are bonded, is planar, implying sp^2 hybridization at C(8).

All the above features establish formulation (**2**) as the correct one with the positive charge localized on the phosphorus and the negative charge on the terminal $C(CN)_2$ group. The bond lengths found for the structure are not significantly different from expected values (12); the relatively high standard deviations obtaining from crystal decomposition preclude any really detailed discussion of fine structure. Mean molecular dimensions include P^+—$C(sp^3)$ 1.824(14), Csp^2—Csp^3 1.53(2), Csp^3—Csp^3 1.54(2), Csp^2—C(N) 1.40(1), and C≡N 1.15(1) Å.

The results presented thus substantiate fully the conclusions of the n.m.r. investigation, and it is considered that the characterization of the intermediate which ensues makes it suitable as a model for substitution reactions of this type. Further investigations using complete n.m.r. line shape analysis and stopped flow kinetics are currently in progress.

We are grateful to the National Research Council of Canada for operating grants A5975 (to G.F.) and A5876 (to C.A.F.) and for a computing grant C0357 (to G.F.).

We thank Dr. David F. Rendle for producing the ORTEP diagrams and assistance with the calculations.

Can. J. Chem. Downloaded from www.nrcresearchpress.com by 210.87.254.105 on 09/05/12
For personal use only.

1. S. PATAI and Z. RAPPOPORT. *In* The chemistry of alkenes. *Edited by* S. Patai. Interscience Publishers, Inc., London. 1964.
2. R. STEWART and D. J. KROEGER. Can. J. Chem. **45**, 2173 (1967).
3. D. J. KROEGER and R. STEWART. Can. J. Chem. **45**, 2163 (1967).
4. C. A. FYFE. Can. J. Chem. **47**, 2331 (1969).
5. L. HORNER and K. KLUPFEL. Ann. Chem. **591**, 69 (1955).
6. Z. RAPPOPORT and S. GERTLER. J. Chem. Soc. 1360 (1964).
7. C. A. FYFE and M. ZBOZNY. Can. J. Chem. **50**, 1713 (1972).
8. A. J. C. WILSON. Nature, **150**, 152 (1942).
9. X-Ray 72 Program System; Tech. Rep. Tr-192 (1972). *Edited by* J. M. Stewart. University of Maryland Computer Science Center, College Park, Maryland.
10. International tables for X-ray crystallography. Vol. III. The Kynoch Press, Birmingham. 1962.
11. C. K. JOHNSON. Rep. No. ORNL-3794. Oak Ridge National Laboratory, Oak Ridge, Tenn. 1965.
12. Chem. Soc. Spec. Publ. The Chemical Society, London. 1965. No. 18.

Can. J. Chem. Downloaded from www.nrcresearchpress.com by 210.87.254.105 on 09/05/12
For personal use only.

Some Cobalt(II) Complexes in Non-aqueous Systems

K. E. JOHNSON AND J. L. MEYER

Department of Chemistry, University of Saskatchewan, Regina, Saskatchewan S4S 0A2

Received November 22, 1972

By following the variation of absorptivity and energy of the principal electronic transitions with addition of ligand it is shown that $CoCl_2$ gives rise to $CoCl_4^{2-}$ in γ-butyrolactone and $Co(NO_3)_2$ gives rise to dodecahedral $Co(NO_3)_4^{2-}$ in γ-butyrolactone, propylene carbonate, and acetone.

En suivant la variation de l'absorption et de l'énergie des transitions électroniques principales par addition de ligand, on a montré que le $CoCl_2$ conduit à $CoCl_4^{2-}$ dans la γ-butyrolactone et $Co(NO_3)_2$ au $Co(NO_3)_4^{2-}$ dodécahedral dans la γ-butyrolactone, le carbonate de propylène et l'acétone.

[Traduit par le journal]

Can. J. Chem., 51, 2799 (1973)

Can. J. Chem. Downloaded from www.nrcresearchpress.com by 210.87.254.105 on 09/05/12
For personal use only.

The interaction of simple salts with excess of ligand to form complexes is confused in several systems by the solvent's ability to complex appreciably with the metal ion. Thus, $[Co(H_2O)_6]^{2+}$ is the species produced by aqueous solution of several Co(II) salts. We have noted in previous work (1) that $Co(NO_3)_2$ dissolved in a molten alkali nitrate to give dodecahedral $[Co(NO_3)_4]^{2-}$ (2) and in dimethyl sulfone to give a dodecahedral species with apparently half the molar absorptivity of $[Co(NO_3)_4]^{2-}$ which reverted to $[Co(NO_3)_4]^{2-}$ on the addition of excess alkali nitrate. $Co(ClO_4)_2$ in dimethyl sulfone gave an octahedral Co(II) species with a spectrum very similar to that of $CoSO_4$ in 98% H_2SO_4 (3); addition of alkali nitrate to this dimethyl sulfone solution converted the Co(II) to $[Co(NO_3)_4]^{2-}$. It is well known that $CoCl_2$ in molten chlorides (4) and even in concentrated HCl exists as the tetrahedral $CoCl_4^{2-}$.

It is the purpose of this article to show that dodecahedral $[Co(NO_3)_4]^{2-}$ is readily produced in γ-butyrolactone, propylene carbonate, and acetone and that tetrahedral $CoCl_4^{2-}$ is obtained in γ-butyrolactone.

Experimental

Reagent-grade (99%) γ-butyrolactone, propylene carbonate, and acetone were used as supplied, lithium nitrate and lithium chloride were oven-dried at 150 °C, cobalt chloride dehydrated (5), cobalt nitrate prepared according to Addison and Logan (6), and cobalt nitrate trihydrate by heating the hexahydrate for 12 h at 90 °C. Spectra were recorded with a Beckman DK-2A spectrophotometer.

Results and Discussion

The spectrum of $CoCl_2$ in γ-butyrolactone with varying molar ratios of lithium chloride (n) showed two main peaks and a shoulder at 15 kK for $n > 2$. The shoulder became more pronounced at $n = 3$ but stayed constant in intensity at $n > 3$. If the molar absorptivity and peak energy are plotted as a function of n (Fig. 1), distinct changes of slope occur at $n = 2$. It appears that by $n = 2$ $CoCl_4^{2-}$ is the dominant cobalt species in solution. Furthermore, the intensity of the strongest peak varies roughly

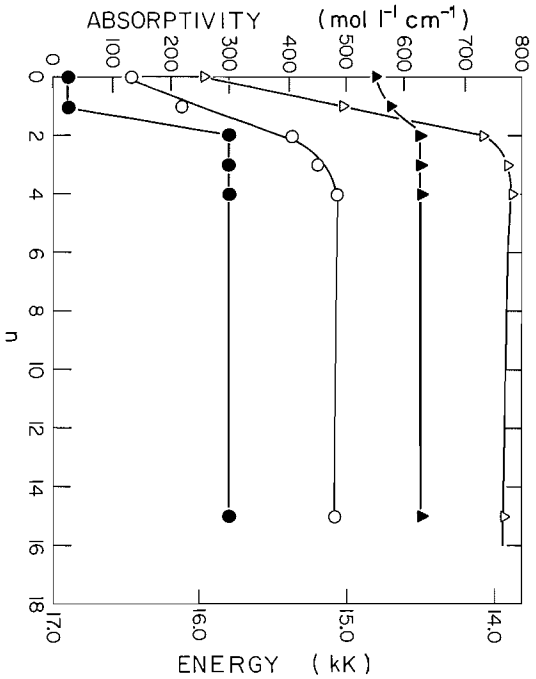

FIG. 1. Spectral maxima of $CoCl_2 + n$LiCl in γ-butyrolactone: △ absorptivity and ▲ energy of lower energy band *vs.* n; ○ absorptivity and ● energy of higher energy band *vs.* n; $CoCl_2$ concentration range 2.4–6.4 × 10^{-3} M.

as 1:2:3 for $n = 0$, 1, 2, suggesting that 1/3, 2/3, and 3/3 of the added $CoCl_2$ is converted to tetrahedral $CoCl_4^{2-}$ at these respective stages, the remainder being octahedrally bound as $CoCl(solvent)_5^+$ and therefore weakly absorbing. The alternative explanation that tetrahedral $CoCl_2(solvent)_2$, $CoCl_3(solvent)^-$, and $CoCl_4^{2-}$ are successively formed and that their absorptivities are in the ratio 1:2:3 is much less likely.

The spectra of $Co(NO_3)_2 + nLiNO_3$ solutions in γ-butyrolactone, propylene carbonate, and acetone were identical to those obtained from $Co(NO_3)_2 \cdot 3H_2O + nLiNO_3$. They all contain a band close to 19 kK with a molar absorptivity, in terms of added Co(II), ranging from 45–60 at $n = 0$ to 80–120 at $n = 9$. The plots (Fig. 2) of absorptivity *vs.* n are somewhat more curved than for the chloride with breaks at $n = 1$–2. The peak energy curves all drop from one energy at $n = 0$ to a virtually constant value for $n > 1$. In addition to the main band a broad absorption was noted for the propylene carbonate and acetone solutions with $\nu_{max} = 8.5$ and 8.8 kK, respectively, the $\varepsilon_{max} = 10$ and 8, respectively. This band shifted to higher energies as n increased and ε_{max} doubled over the range $n = 0$ to $n = 9$.

All the nitrate solution spectra compare closely with those of $Co(NO_3)_4^{2-}$ mentioned above. What is more the ratio of the final to initial absorptivities of approximately 2:1 suggests that we start with half the added cobalt dodecahedrally coordinated by nitrate and half of it coordinated, presumably octahedrally, by solvent molecules. The greater curvature of the nitrate plots is in accord with the lesser stability of the nitrate *vs.* the tetrahedral chloride complex, *i.e.* a large excess of nitrate is required to drive the formation of $Co(NO_3)_4^{2-}$ to completion. The intermediate formation of mixed nitrate–solvent complexes is also consistent with the data.

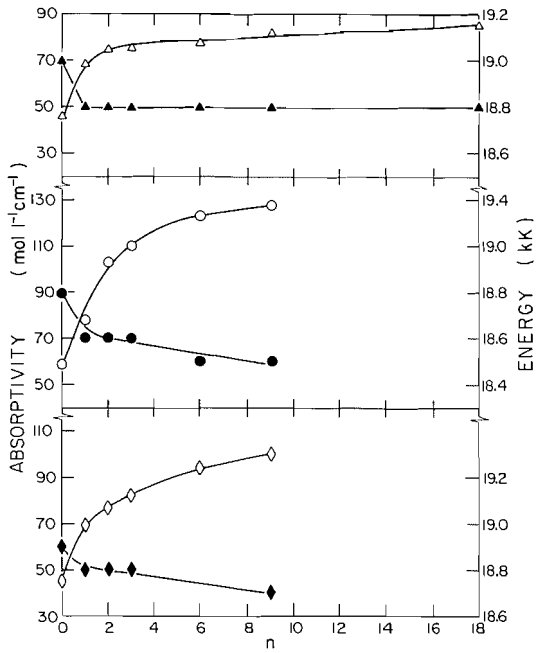

FIG. 2. Absorptivity (open points) and energy (closed points) of principal band of $Co(NO_3)_2 + nLiNO_3$ *vs.* n for butyrolactone (squares), propylene carbonate (circles), and acetone (triangles). $Co(NO_3)_2$ concentration ranges 1.3–17 × 10^{-2} M (butyrolactone), 0.9–1.0 × 10^{-2} M (propylene carbonate), and 1 × 10^{-2} M (acetone).

We thank the National Research Council of Canada for financial support.

1. K. W. FUNG and K. E. JOHNSON. Can. J. Chem. **47**, 4699 (1969).
2. F. A. COTTON and J. G. BERGMAN. J. Am. Chem. Soc. **86**, 2941 (1964).
3. J. R. DICKINSON and K. E. JOHNSON. J. Mol. Spectrosc. **33**, 414 (1970).
4. K. E. JOHNSON and J. R. DICKINSON. *In* Advances in molten salt chemistry. Vol. II. Plenum Press, New York. In press.
5. G. BRAUER (*Editor*). Handbook of preparative inorganic chemistry. 2nd ed. Vols. 1 and 2. Academic Press, New York. 1965.
6. C. C. ADDISON and N. LOGAN. Adv. Inorg. Chem. Radiochem. **6**, 71 (1964).

Can. J. Chem. Downloaded from www.nrcresearchpress.com by 210.87.254.105 on 09/05/12
For personal use only.

Effect of Dose on the Yield of Trapped Electrons in Aliphatic Amine Glasses

TOSHIYASU ITO, SHOJI NODA, KENJI FUEKI, AND ZEN-ICHIRO KURI

Department of Synthetic Chemistry, Faculty of Engineering, Nagoya University, Chikusa-ku, Nagoya, Japan

Received January 29, 1973

An electron spin resonance (e.s.r.) and photoconductivity study has been made of the effect of dose on the yield of trapped electrons in γ-irradiated aliphatic amine glasses at 77 °K. It is shown that the effect of dose on the trapped electron yield can be correlated with matrix polarity.

Une étude par r.p.e. et photoconductivité a été effectuée sur l'effet de la dose sur le rendement en électrons piégés dans des verres d'amine aliphatique γ-irradiés à 77 °K. Une corrélation entre l'effet de la dose sur le rendement en électrons piégés et la polarité de la matrice a été ainsi établie.

[Traduit par le journal]

Can. J. Chem., 51, 2801 (1973)

Can. J. Chem. Downloaded from www.nrcresearchpress.com by 210.87.254.6 on 09/05/12
For personal use only.

Introduction

In a previous paper (1) we have reported the electron spin resonance (e.s.r.) and optical absorption characteristics of trapped electrons produced in γ-irradiated aliphatic amine glasses at 77 °K, demonstrating that there is a correlation between such spectroscopic characteristics and matrix polarity. Recently we have also made an optical bleaching study of trapped electrons in the same amine glasses (2), showing that there are bound excited states for trapped electrons in these matrices.

In this note we report the effect of dose on the yield of trapped electrons in aliphatic amine glasses at 77 °K, as studied by both e.s.r. and photoconductivity measurements. It is shown that the effect of dose on the trapped electron yield can be correlated with matrix polarity for a variety of matrices including the amines.

Experimental

Aliphatic amines (2-methyl-*n*-amylamine, diisopropylamine, and triethylamine) were purified as previously described (2). E.s.r. measurements were carried out on trapped electrons with a conventional X-band spectrometer using 100 kc.p.s. magnetic field modulation. In some experiments at high doses, optical absorption measurements were made on trapped electrons.

The photoconductivity cell was made from quartz and had a cylindrical shape with a diameter of 20 mm. Thin stainless steel mesh was used as electrodes. The spacing between the electrodes was 1 mm and their diameter was 10 mm. The electrodes were 3 mm from the cell window. The sample was distilled into the cell from a storage bulb on a vacuum line and was thoroughly degassed prior to γ-irradiation. In photoconductivity experiments on the γ-irradiated samples the light beam was directed through the semi-transparent electrodes. The light source was a Toshiba 500 W i.r. lamp. A Toshiba VR-68 filter was used to cut off light below about 680 nm. A d.c. electric field was 1.8 kV cm^{-1}. The photocurrent was amplified by a Kawaguchi Electric Works NA-16E electrometer and the output from the electrometer was recorded on a Toa Electronics EPR-2T recorder.

Results and Discussion

The experimental results are given in Figs.1–3, in which both the trapped electron concentration and the initial photocurrent are presented as a function of dose. Figure 1 shows the results for triethylamine. It can be seen from Fig. 1 that with increasing dose the concentration of trapped electrons increases initially, reaches a maximum and then decreases down to nearly zero. The photocurrent intensity behaves exactly in the same manner with dose. The curve of photocurrent *vs.* dose can be superimposed on that of trapped electron concentration *vs.* dose on a normalized scale. The agreement

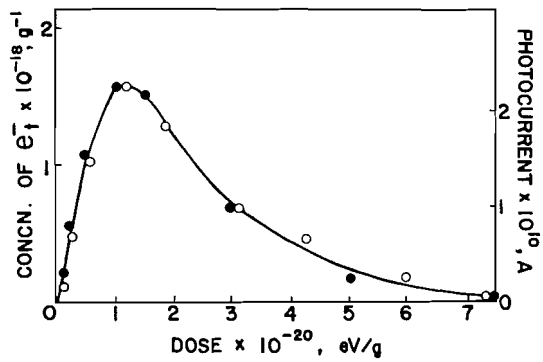

FIG. 1. Dose dependence of trapped electron concentration and of photocurrent for triethylamine at 77 °K: ○, trapped electron concentration; ●, photocurrent.

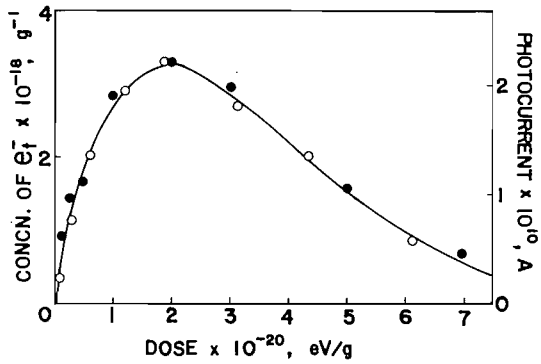

FIG. 2. Dose dependence of trapped electron concentration and of photocurrent for diisopropylamine at 77 °K: ○, trapped electron concentration; ●, photocurrent.

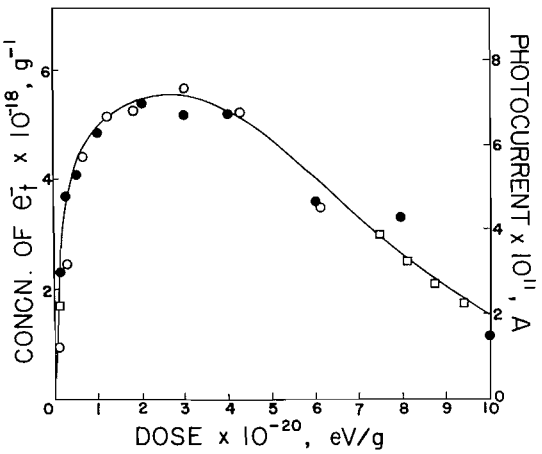

FIG. 3. Dose dependence of trapped electron concentration and of photocurrent for 2-methyl-*n*-amylamine at 77 °K: ○, trapped electron concentration (e.s.r.); □, trapped electron concentration (optical); ●, photocurrent.

between the two types of dose-dependence curves indicates that the photo-induced charge carriers are probably electrons. The maximum concentration of trapped electrons is $1.6 \times 10^{18}\ g^{-1}$ and the maximum photocurrent is 2.3×10^{-10} A. The dose at which the concentration of trapped electrons is maximum is 2.0 Mrad.

Figure 2 shows the results for diisopropylamine. The dose dependence of the trapped electron concentration and of the photocurrent is similar to that observed for the triethylamine. The maximum concentration of trapped electrons is $3.2 \times 10^{18}\ g^{-1}$ and the maximum photocurrent is 2.2×10^{-10} A at a dose of 3.1 Mrad.

Figure 3 shows the results for 2-methyl-*n*-amylamine. Again the dose dependence of the trapped electron concentration and of the photocurrent is similar to those observed for the triethylamine and the diisopropylamine. The maximum concentration of trapped electrons and the maximum photocurrent are $5.7 \times 10^{18}\ g^{-1}$ and 6.8×10^{-11} A, respectively, at a dose of about 4.8 Mrad. Since the e.s.r. spectrum of trapped electrons in 2-methyl-*n*-amylamine glass was broad (1), it was difficult to measure reliably the e.s.r. spectral intensity of trapped electrons at high doses where the trapped electron signal was partially masked by the radical spectrum. In these cases, the relative concentration of trapped electrons was measured by the optical absorption method and it was normalized to fit the dose–yield curve at a low dose.

The maximum concentration of trapped electrons and the dose yielding such a maximum are both in decreasing order for 2-methyl-*n*-amylamine, diisopropylamine, and triethylamine. This is in the order of decreasing matrix polarity, since the magnitude of permanent dipole moment of the matrix molecule is ~1.1 D for 2-methyl-*n*-amylamine, ~0.85 D for diisopropylamine, and 0.66 D for triethylamine. It is expected that the more polar the matrix, the higher is the yield of trapped electrons because stronger electron–solvent dipole interactions in the more polar matrix would make electron localization occur more efficiently in the matrix. It should be noted, however, that the more polar the matrix, the smaller is the maximum photocurrent. If it is assumed that the probability of optical transitions to the conduction band is about the same for trapped electrons in the three amines, the photocurrent should be proportional to the product of the trapped electron concentration, the electron mobility, μ, and the average lifetime, τ, of an electron in the conduction band in these amines. Using the observed values of the photocurrent and the trapped electron concentration, we can inversely estimate the relative magnitudes of $\mu\tau$ in these amines; $\mu\tau$(2-methyl-*n*-amylamine):$\mu\tau$(diisopropylamine):$\mu\tau$(triethylamine) = 1:6:12. We see that $\mu\tau$ decreases with increasing matrix polarity. This trend may be interpreted in terms of the charge transport mechanism in which mobile electrons are temporarily trapped in the matrix (3); and the

Can. J. Chem. Downloaded from www.nrcresearchpress.com by 210.87.254.6 on 09/05/12
For personal use only.

TABLE 1. Dose at which the concentration of trapped electrons is maximum at 77 °K (in units of Mrad)

Matrix	E.s.r.	Optical	Photo-conductivity	μ_d[k] (D)	ε_s[k] (at 298 °K)
Alkaline ice	~6[a]	~10[b]		1.85	
Ethylene glycol	10[c]			2.26	37.7
Methanol	9.6[c]			1.70	32.6
Ethanol	11[c]	9.6[d]		1.69	24.3
i-Propanol	7.7[c]			1.69	18.3
n-Propanol	6.4[c]			1.69	20.1
i-Butanol	4.8[c]			1.64	17.7
n-Butanol	4.7[c]	3.8[d]		1.67	17.1
n-Pentanol	5.0[c]				13.9
Methyltetrahydrofuran	4.0[e]; 5.6[f]			1.75[m]	4.6
2-Methyl-*n*-amylamine	4.8[g]		4.3[g]	1.1[m]	
Diisopropylamine	3.1[g]		3.1[g]	0.85[m]	2.9[m]
Triethylamine	2.0[g]; 2.2[e]		2.0[g]	0.66	2.42
Methylcyclohexane	2.2[h]			0	2.03
3-Methylpentane	1.5[e]	1.5[i]		0	1.88[m]
3-Ethylpentane		1.0[i]		0	1.94
3-Methylhexane			0.8[j]	0	1.93

[a]Reference 8.
[b]Reference 9.
[c]Reference 11.
[d]Reference 12.
[e]Reference 13.
[f]Reference 14.
[g]This work.
[h]Reference 15.
[i]Reference 16.
[j]Reference 17.
[k]Reference 18.
[m]Values estimated from those of similar compounds.

transient trapping time is presumably longer in the more polar matrix, making the electron mobility lower. Also, the permanent electron-trapping efficiency is expected to be higher in the more polar matrix, giving smaller τ.

We now consider the cause of decrease in trapped electron yield with increasing dose. This decrease arises probably from the reaction of mobile and trapped electrons with radiation-produced radicals and/or positive holes (4). The correlation between matrix polarity and the dose yielding the maximum concentration of trapped electrons suggests that the positive holes, which can migrate through the matrix, play a role in decreasing the trapped electron yield, since it is known that positive holes migrate through non-polar matrices such as hydrocarbon glasses while they are immediately trapped in polar matrices such as alcohol glasses (5). Also, it is conceivable that dielectron formation may play a part for the decrease in trapped electron yield at high doses. Experimental evidence has been reported for the existence of dielectrons trapped in polar liquids and solids (6–9). A recent theoretical study also indicates that the trapped dielectron is energetically stable relative to two single trapped electrons, suggesting the possible existence of dielectrons in polar matrices (10).

The correlation between matrix polarity and the dose yielding the maximum concentration of trapped electrons found for the amines can be observed more generally for a variety of matrices. Table 1 summarizes the relevant data available at present with remarks on the method of measurement: e.s.r., optical absorption, and photoconductivity. Table 1 includes various matrices covering a wide range of matrix polarity: alkaline ice (10 *M* NaOH), alcohols, ether, amines, and hydrocarbons. In Table 1 are also given the gas-phase values of permanent dipole moment, μ_d, of the matrix molecules and the static dielectric constants, ε_s, of the matrix compounds at room temperature. Matrix polarity is approximately in decreasing order from the top to the bottom. These data lend further support for the arguments put forward above.

Can. J. Chem. Downloaded from www.nrcresearchpress.com by 210.87.254.6 on 09/05/12
For personal use only.

We thank Mr. N. Kato for his assistance in photoconductivity measurements.

1. S. NODA, K. FUEKI, and Z. KURI. Chem. Phys. Lett. **8**, 407 (1971).
2. S. NODA, K. FUEKI, and Z. KURI. Can. J. Chem. **50**, 2699 (1972).
3. L. KEVAN. J. Phys. Chem. **76**, 3830 (1972).
4. A. EKSTROM, R. SUENRAM, and J. E. WILLARD. J. Phys. Chem. **74**, 1883 (1970).
5. W. H. HAMILL. *In* Radical ions. *Edited by* E. T. Kaiser and L. Kevan. Wiley–Interscience, New York. 1968. Chapt. 9.
6. R. CATTERALL and M.C. R. SYMONS. J. Chem. Soc. A, 13 (1966).
7. N. BASCO, G. A. KENNEY-WALLACE, S. K. VIDYARTHI, and D. C. WALKER. Can. J. Chem. **50**, 2059 (1972).
8. J. ZIMBRICK and L. KEVAN. J. Am. Chem. Soc. **89**, 2483 (1967).
9. L. KEVAN, D. R. RENNEKE, and R. J. FRIAUF. Solid State Commun. **6**, 469 (1968).
10. D.-F. FENG, K. FUEKI, and L. KEVAN. J. Chem. Phys. **58**, 3281 (1973).
11. T. SASAKI, S. OHNO, and K. KAWATSURA. Chem. Lett. 91 (1972).
12. S. FUJII and J. E. WILLARD. J. Phys. Chem. **74**, 4313 (1970).
13. D. P. LIN and L. KEVAN. J. Chem. Phys. **55**, 2629 (1971).
14. J. TEPLÝ, I. JANOVSKY, F. KISS, and K. VACEK. Int. J. Radiat. Chem. **4**, 265 (1972).
15. M. SHIROM and J. E. WILLARD. J. Am. Chem. Soc. **90**, 2184 (1968).
16. A. EKSTROM, R. SUENRAM, and J. E. WILLARD. J. Phys. Chem. **74**, 1888 (1970).
17. T. HUANG and L. KEVAN. J. Am. Chem. Soc. **95** (1973).
18. R. C. WEAST (*Editor*). Handbook of chemistry and physics. 50th Ed. Chemical Rubber Co., Cleveland, Ohio. 1969.

Can. J. Chem. Downloaded from www.nrcresearchpress.com by 210.87.254.6 on 09/05/12
For personal use only.

Can. J. Chem. Downloaded from www.nrcresearchpress.com by 210.87.254.105 on 09/05/12
For personal use only.

Canadian Journal of Chemistry

Published by
THE NATIONAL RESEARCH COUNCIL OF CANADA

Journal canadien de chimie

Publié par
LE CONSEIL NATIONAL DE RECHERCHES DU CANADA

Volume 51 Number 17 September 1, 1973

Volume 51 numéro 17 1 septembre 1973

Proton Transfer Reactions of Carbon Acids. III. Effect of Solvent Change on the Equilibrium and Kinetic Parameters of the Reaction of Di-(4-nitrophenyl)methane with Alkoxide Bases

JAE-HANG KIM[1] AND KENNETH T. LEFFEK

Chemistry Department, Dalhousie University, Halifax, Nova Scotia

Received March 22, 1973

The equilibrium constants, the second-order rate constants, and the activation parameters have been determined for the proton transfer from di-(4-nitrophenyl)methane to ethoxide ion in a series of mixed solvents containing various amounts of acetonitrile in ethanol. The quantities have been interpreted in terms of the general postulates of the Miller–Parker theory of solvation effects.

On a déterminé les constantes d'équilibre, les constantes de vitesse du second ordre ainsi que les paramètres d'activation pour le transfert d'un proton du di-(nitro-4 phényl) méthane à l'ion éthoxyde dans plusieurs mélanges de solvants contenant des quantités variables d'acétonitrile dans l'éthanol. Les données obtenues furent interprétées en fonction des postulats de la théorie de Miller–Parker traitant des effets de solvatation. [Traduit par le journal]

Can. J. Chem., **51**, 2805 (1973)

Introduction

Several proton transfer reactions between substituted methanes and bases in organic solvents have been studied kinetically with respect to the determination of the activation parameters and isotope effects (1–6). In the previous paper in this series (6) the reaction of di-(4-nitrophenyl)methane with alkoxide bases in the corresponding alcohol solvents was investigated. The variation of the activation parameters $\Delta H^{\ddagger}$ and $\Delta S^{\ddagger}$ with alkoxide–alcohol identity was interpreted in terms of solvation effects during the activation process. This paper presents a study of the effect of changing the solvating characteristics of the alcohol solvents by the addition of certain percentages of an aprotic co-solvent, acetonitrile, on the equilibrium constants and kinetic parameters of the same reaction 1 with two alkoxides,

[1] $(NO_2C_6H_4)_2CH_2 + \bar{O}AlK \rightleftharpoons [(NO_2C_6H_4)_2CH]^- + HOAlk$

ethoxide and *t*-butoxide. However, since the largest changes in these parameters take place when the alcohol content of the solvent is low, this work is actually an investigation of the reaction in acetonitrile solvent containing various concentrations of alcohol.

The objective of the study is to ascertain whether the reaction parameters change in a manner consistent with the previous interpretation (6) and with solvent effect theory in general.

Results and Discussion

Equilibrium Measurements

Optical density measurements on equilibrium mixtures of substrate and alkoxide may be used to determine the molar absorptivity (ε) of the colored anion of the substrate and also the equilibrium constant K for the reaction. From

[1]Post-doctoral Fellow 1971–1972.

TABLE 1. Equilibrium constants (25 °C) for the reaction of di-(4-nitrophenyl)methane with alkoxide ions and the molar absorptivity of the methane anion

Alkoxide/%v/v alcohol in acetonitrile solvent	K	ε (l mol^{-1} cm^{-1} at 770 nm)
$C_2H_5O^-$/5% ethanol	810	45 500
$C_2H_5O^-$/10% ethanol	650	23 800
$C_2H_5O^-$/20% ethanol	145	8 700
$C_2H_5O^-$/80% ethanol	20	2 600*
$C_4H_9O^-$/50% *t*-butanol	17 200	22 200

*At 560 nm wavelength.

the equilibrium expression 2

$$[2] \quad \frac{K}{[\mathrm{AlkOH}]} = K' = \frac{[\mathrm{A}^-]}{[\mathrm{AlkO}^-]([\mathrm{AH}] - [\mathrm{A}^-])}$$

which applies to reaction 1 when the alkoxide is in large excess but of only moderate concentration, and in which AH is the substrate carbon acid and A^- its anion, eq. 3 may be derived.

$$[3] \quad [\mathrm{AH}]/(\mathrm{o.d.}) = 1/K'\varepsilon\,[\bar{\mathrm{O}}\mathrm{Alk}] + 1/\varepsilon$$

where o.d. is the optical density.

A plot of [AH]/(o.d.) *vs.* $1/[\bar{\mathrm{O}}\mathrm{Alk}]$ gives a good straight line for all the solvent systems recorded in Table 1. Both ε and K are subject to large random errors since ε is quite large and is the reciprocal of the intercept of the graph. The error in ε also appears in K as this is calculated from the slope of the graph ($1/K'\varepsilon$). Thus, the values for K and ε collated in Table 1 are probably no better than ±20%, but may be interpreted with due regard to these limits.

The position of the absorption peak of the substrate anion changes from 560 nm in 80% v/v ethanol in acetonitrile to 770 nm in 20% v/v (or less) ethanol in acetonitrile, which must correspond to a change in the solvation shell from alcohol to a mixture of alcohol and acetonitrile. Large solvent shifts are quite common for carbanions; we recently reported a 40 nm shift for the sodium salt of diethyl 2,4-dinitrophenylmalonate between DMSO and methanol (7) and Bowden and Stewart (8) found a shift of 120 nm for the anion of tri-(4-nitrophenyl)methane between ethanol and 40 mol % ethanol in DMSO, although the anion of di-(4-nitrophenyl)methane showed a shift of less than 20 nm for the same solvent pair.

The data in Table 1 show that increasing the alcohol content of the solvent decreases both the equilibrium constant and the molar absorptivity of the anion.

Both the alkoxide ion and the carbanion are undoubtedly preferentially solvated by the alcohol molecules, since acetonitrile is a poor anion solvator (9). Moreover, the alkoxide ion, being smaller with a more concentrated charge, is the more strongly solvated of the two anions by alcohol–anion hydrogen bonding. Thus, increase in alcohol content stabilizes the alkoxide ion to a greater extent than it stabilizes the carbanion and causes a reduction in the equilibrium constant. Miller and Parker (10) and Parker (11) have postulated that in dipolar aprotic solvents, the polarizability of the anion causes the solvation to be greater the larger the anion. This effect again predicts the results observed in Table 1 with the large methane anion most stabilized in the acetonitrile-rich solvents.

Kinetic Measurements

First-order rate constants were measured for the reaction of eq. 1, using a large excess of alkoxide base and a rate equation derived for the equilibrium condition (1). A least-squares computation was carried out for a plot of k_1 *vs.* alkoxide concentration for each temperature studied and the slopes, equal to the second-order rate constants for the reactions, were obtained. These first- and second-order rate constants are shown in Table 2. The activation parameters derived from the k_2 values are given in Table 3.

The second-order rate constants decrease as the alcohol content of the solvent is increased, but the enthalpy of activation also decreases, which is more than compensated by an increasingly negative entropy of activation.

The variation of the rate constants with solvent composition are as expected for this type

Can. J. Chem. Downloaded from www.nrcresearchpress.com by 210.87.254.105 on 09/05/12
For personal use only.

Can. J. Chem. Downloaded from www.nrcresearchpress.com by 210.87.254.105 on 09/05/12
For personal use only.

TABLE 2. Rate constants for the reaction of di-(4-nitrophenyl)methane with alkoxide ions

(*a*) Ethoxide in 80% v/v ethanol in acetonitrile; initial concentration $(NO_2C_6H_4)_2CH_2 = 2 \times 10^{-3}$ *M*

	10^2[ethoxide] (*M*)				
	3.87	7.68	9.62	11.56	
Temperature (°C)	k_1 (s^{-1})				k_2 (l mol^{-1} s^{-1})
20.0	1.18	1.31	1.38	1.44	3.5 ± 0.1
25.0	1.64	1.88	1.95	1.97	4.4 ± 0.9
30.0	2.21	2.43	2.50	2.67	5.7 ± 0.5
35.0	3.31	3.64	3.86	3.93	8.4 ± 0.8
40.0	4.07	4.57	4.74	4.91	11.0 ± 0.8
45.0	5.20	5.65	5.94	6.23	13.3 ± 0.7

(*b*) Ethoxide in 20% v/v ethanol in acetonitrile; initial concentration $(NO_2C_6H_4)_2CH_2 = 3.43 \times 10^{-4}$ *M*

	10^2[ethoxide] (*M*)					
	0.35	0.87	1.15	1.91	2.42	
Temperature (°C)	k_1 (s^{-1})					k_2 (l mol^{-1} s^{-1})
20.0	0.249	0.267	0.284	0.298	0.334	3.8 ± 0.4
25.0	0.301	0.335	0.347	0.363	0.418	5.0 ± 0.8
30.0	0.415	0.440	0.466	0.504	0.625	9.4 ± 2
35.0	0.500	0.535	0.564	0.609	0.755	11.3 ± 2
40.0	0.779	0.802	0.853	0.932	1.05	13.1 ± 2
45.0	0.904	0.965	0.999	1.19	1.27	19.0 ± 2

(*c*) Ethoxide in 5% v/v ethanol in acetonitrile; initial concentration $(NO_2C_6H_4)_2CH_2 = 5.4 \times 10^{-5}$ *M*

	10^2[ethoxide] (*M*)							
	0.16	0.29	0.41	0.58	0.76	1.23	1.59	
Temperature (°C)	k_1 (s^{-1})							k_2 (l mol^{-1} s^{-1})
20.0	0.15	0.21	0.25	0.33	0.43	0.56	0.67	36 ± 2
25.0	0.18	0.27	0.33	0.42	0.54	0.75	0.90	51 ± 2
30.0	0.25	0.36	0.45	0.68	0.77	1.06	1.51	84 ± 4
35.0	0.37	0.56	0.75	0.98	1.10	1.69	1.98	113 ± 5
40.0	0.58	0.83	0.98	1.31	1.67	2.32	2.85	159 ± 40
45.0	0.73	1.08	1.51	2.03	2.42	3.73	3.83	230 ± 20

(*d*) *t*-Butoxide in 50% v/v *t*-butanol in acetonitrile, initial concentration $(NO_2C_6H_4)_2CH_2 = 5.43 \times 10^{-5}$ *M*

	10^3[*t*-butoxide] (*M*)						
	0.67	1.68	3.77	5.64	7.86	11.8	
Temperature (°C)	k_1 (s^{-1})						k_2 (l mol^{-1} s^{-1})
25.0	0.11	0.16	0.23	0.37	0.41	0.51	39 ± 4
30.0	0.12	0.19	0.27	0.42	0.44	0.65	47 ± 3
35.0	0.15	0.21	0.39	0.50	0.53	0.79	56 ± 5
40.0	0.19	0.30	0.45	0.67	0.71	0.98	70 ± 6
45.0	0.24	0.35	0.58	0.88	0.97	1.22	90 ± 9

TABLE 2. (*Concluded*)

(*e*) *t*-Butoxide in 20% v/v *t*-butanol in acetonitrile; initial concentration $(NO_2C_6H_4)_2CH_2 = 5.43 \times 10^{-5}$ *M*

	10^3[*t*-butoxide] (*M*)						
	0.84	1.54	2.05	2.87	2.97	4.30	
Temperature (°C)	k_1 (s^{-1})						k_2 (l mol^{-1} s^{-1})
20.0	0.20	0.32	0.47	0.50	0.51	0.64	120 ± 20
25.0	0.21	0.33	0.55	0.63	0.64	0.72	150 ± 30
30.0	0.25	0.42	0.70	0.81	0.83	0.94	210 ± 40
35.0	0.32	0.55	0.86	1.08	1.23	1.33	310 ± 50
40.0	0.40	0.73	1.12	1.36	1.46	1.70	385 ± 50
45.0	0.50	0.94	1.44	1.88	2.04	2.27	540 ± 80

TABLE 3. Activation parameters of proton transfer reactions from di-(4-nitrophenyl)methane to alkoxide base

Base	Solvent (% alcohol in acetonitrile)	$\Delta H^{\ddagger}$ (kcal mol^{-1})	$\Delta S^{\ddagger}$ (cal mol^{-1} deg^{-1})	$\Delta G^{\ddagger}$ (kcal mol^{-1} at 300 °K)
Ethoxide	5	13.1 ± 0.4	−6.7 ± 1.4	15.1
Ethoxide	20	11.1 ± 1.1	−17.8 ± 3.6	16.4
Ethoxide	80	9.8 ± 0.4	−22.6 ± 1.4	16.6
t-Butoxide	20	10.8 ± 0.5	−12.3 ± 1.5	14.5
t-Butoxide	50	7.6 ± 0.3	−25.8 ± 0.9	15.3

of reaction in which the negative change is dispersed over a larger molecular entity on going from the initial state to the transition state. In terms of Miller–Parker theory (11), the alcohol is a much better anion solvator than acetonitrile and solvation by alcohol is stronger the smaller the anion. Thus, the initial state alkoxide is stabilized to a greater extent than the transition state as the alcohol content is increased, and this produces a smaller k_2 the greater the alcohol content. It is seen from Table 2 that most of the change in k_2 takes place between the alcohol contents of 5 and 20%, which indicates that there is a marked preferential solvation by alcohol molecules.

Another way of wording the same explanation is to say that the alkoxide ion is a stronger proton abstractor in acetonitrile-rich solvents since it is less strongly solvated by acetonitrile, than it is by alcohol in alcohol-rich solvents, with which it forms hydrogen bonds.

While the above arguments account readily for the free energy changes (*i.e.* the relative rates), the enthalpies of activation change in the opposite direction, decreasing with increasing alcohol content of the solvent. Since the Parker theory accounts for the rate changes with solvent variation of a large number of reactions, it seems reasonable to accept its general premises and develop a solvation theory for proton transfer reactions within its framework, but which at the same time is consistent with the observed enthalpies and entropies of activation.

In the previous paper in this series (6) it was postulated that in the initial state solvation shell there was a large amount of solvent–solute interaction, alcohol hydrogen-bonded to the alkoxide ion, whereas the transition state solvation shell featured solvent–solvent interaction, resulting from the lack of charge concentration in the much larger transition state. Thus, with increased alcohol content the solvation of the initial state would be stronger in free energy terms but the enthalpy of activation would be decreased because of the effect of having more alcohol molecules surrounding the inner solvation shell. The energy required to break one alcohol–alkoxide hydrogen bond would be offset by the formation of a new alcohol–alcohol hydrogen bond. That is, it requires less

Can. J. Chem. Downloaded from www.nrcresearchpress.com by 210.87.254.105 on 09/05/12
For personal use only.

energy to break out one alcohol molecule from the solvation shell if the solvent molecule intermediately adjacent to it in the next solvent layer is another alcohol molecule, rather than an acetonitrile molecule.

A direct consequence of the formation of more solvent–solvent hydrogen bonds as the transition state is formed is that more alcohol molecules are tied down in the transition state than in the initial state giving rise to larger negative entropies of activation with increasing alcohol content.

Experimental

The preparation of materials and measurement of the equilibrium constants were carried out as previously described (6).

All the kinetic measurements were made with a Durrum-Gibson stopped-flow spectrophotometer with a Kel-F flow system and an optical cell of 2 mm light-pathlength. The technique used was essentially that already given (6), except that stock solutions of alkoxide in solvents containing 20% alcohol or less were prepared by making a suspension of solid alkoxide in acetonitrile in a dry-box and then adding the appropriate quantity of alcohol. Recently, Chattopadhyay and Coetzee (12) have pointed out a potential source of error in the use of the Durrum stopped-flow spectrophotometer. At temperatures other than ambient, the solutions in the valve block section of the flow system are not in thermal equilibrium with the thermostated reservoir which contains the drive syringes. Thus, it is possible that the temperature of the reacting solution in the cuvette is not that of the reservoir if insufficient solution is driven through the system to transfer solution from the drive syringes to the cuvette. We believe our experimental technique avoided this source of error. Fluid from an external constant temperature bath was pumped with a heavy duty pump through the drive syringe reservoir and also through the observation cuvette housing. To measure a rate constant the drive syringes were filled and allowed to equilibrate to the reservoir temperature which remained constant to ± 0.03 °C. Two or three trial runs were made and observed on the oscilloscope in nonstorage mode. If these appeared satisfactory and reproducible, the oscilloscope was switched to the storage mode and between four and six runs were made in rapid succession and superimposed on the oscilloscope screen. These runs nearly always superimposed exactly giving one slightly broadened trace and were carried out within a total time of less than 1 min. Using this technique, the actual temperature of the solution in the cuvette must be very close to that of the reservoir. The first-order rate constants were generally obtained from oscilloscope traces covering the range 50–100% transmittance, using a computer program which converted the transmittance values to absorbance before calculation of the rate constants. Examples of kinetic runs have been given previously (6).

The authors are grateful for financial support by the National Research Council of Canada.

1. E. F. CALDIN and J. C. TRICKETT. Trans. Faraday Soc. 772 (1953).
2. E. F. CALDIN and G. LONG. Proc. R. Soc. A, **228**, 263 (1955).
3. W. D. KOLLMEYER and D. J. CRAM. J. Am. Chem. Soc. **90**, 1784 (1968).
4. E. F. CALDIN, M. KASPARIAN, and G. TOMALIN. Trans. Faraday Soc. **64**, 2802 (1968).
5. E. F. CALDIN, A. JARCZEWSKI, and K. T. LEFFEK. Trans. Faraday Soc. **67**, 110 (1971).
6. A. JARCZEWSKI and K. T. LEFFEK. Can. J. Chem. **50**, 24 (1972).
7. K. T. LEFFEK and P. H. TREMAINE. Can. J. Chem. **49**, 1979 (1971).
8. K. BOWDEN and R. STEWART. Tetrahedron, **21**, 261 (1965).
9. L. P. HAMMETT. Physical organic chemistry. McGraw-Hill, New York. 1970. Chap. 8.
10. J. M. MILLER and A. J. PARKER. J. Am. Chem. Soc. **83**, 117 (1961).
11. A. J. PARKER. Q. Rev. **16**, 163 (1962).
12. P. K. CHATTOPADHYAY and J. F. COETZEE. Anal. Chem. **44**, 2117 (1972).

Can. J. Chem. Downloaded from www.nrcresearchpress.com by 210.87.254.105 on 09/05/12
For personal use only.

The Structure of Thiobinupharidine

J. T. WRÓBEL AND B. BOBESZKO
Department of Chemistry, University of Warsaw, Warsaw, Poland
AND
T. I. MARTIN, D. B. MACLEAN, N. KRISHNAMACHARI, AND C. CALVO
Department of Chemistry, McMaster University, Hamilton, Ontario
Received March 21, 1973

The spectroscopic properties of thiobinupharidine and its isomer, neothiobinupharidine, of established structure, have been examined and compared. From this study it was possible to deduce the structure and relative configuration of the alkaloid. The structure has been firmly established and the absolute configuration determined by the study of the crystal structure of thiobinupharidine dihydrobromide dihydrate, $C_{30}H_{42}O_2N_2S \cdot 2HBr \cdot 2H_2O$. The crystals are orthorhombic with space group $C222_1$, a = 25.128(6), b = 9.869(2), c = 26.380(6) Å, and Z = 8. The structure was refined, using full-matrix least-squares techniques with 1934 reflections, to a final R value of 0.097. The thiobinupharidine moiety hydrogen bonds to one of two types of H_2O–Br–H_2O spiral chains in the structure. The tetrahydrothiophene ring is distorted from planarity, and this together with the nonequivalence of the S and C atoms in the ring causes the molecule to deviate from C_2 symmetry.

Les propriétés spectroscopiques de la thiobinupharidine et de son isomère néothiobinupharidine de structure établie, ont été examinées et comparées. De cette étude, il a été possible de déduire la structure et la configuration relative de l'alcaloide. La structure et la configuration absolue ont été déterminées de façon sûre par l'étude de la structure cristalline du dibromhydrate de la thiobinupharidine dihydratée $C_{30}H_{42}O_2N_2S \cdot 2HBr \cdot 2H_2O$. Les cristaux sont orthorhombiques de groupe spatial $C222_1$, a = 25.128(6), b = 9.869(2), c = 26.380(6) Å et Z = 8. La structure a été raffinée par la technique matricielle des moindres carrés avec 1934 réflexions jusqu'à une valeur finale pour R de 0.097. Le groupe thiobinupharidine est lié par pont hydrogène à l'un des deux types de chaînes spirales H_2O—Br—H_2O dans la structure. Le cycle tétrahydrothiophène est distordu par rapport au plan; ce fait, en plus de la non équivalence des atomes S et C du cycle, cause une déviation a la symétrie C_2 pour la molécule.
[Traduit par le journal]

Can. J. Chem., **51**, 2810 (1973)

Thiobinupharidine ($C_{30}H_{42}N_2O_2S$, (**1**)) was first reported in 1962 by Achmatowicz and Bellen (1) who described the properties of the base and some of its salts. The molecular formula assigned to this alkaloid, over which there was originally some question, was confirmed a few years later by mass spectrometry (2). In the original paper it was noted that this alkaloid had twice the number of carbon, nitrogen, and oxygen atoms present in the *Nuphar* alkaloid, deoxynupharidine ($C_{15}H_{23}NO$, (**2**)) of established structure (3) and the authors anticipated that there would be structural similarities between the new sulfur-containing alkaloid and **2**. A number of structures were considered in which two molecules of **2** were joined, but the exact nature of the union between the two molecules was not established. In later papers (2, 4) it was concluded from spectroscopic and other data that two molecules of **2** were joined through a new sulfur-containing ring.

The second sulfur-containing alkaloid to be isolated from *Nuphar* species was an isomer of **1** designated neothiobinupharidine (**3**) (4). From an examination of the spectroscopic properties of **1** and **3** (2, 4) it was concluded that they were stereoisomers. The i.r. spectra of the two bases were very similar, their p.m.r. spectra were distinctly different (see below), but their mass spectra (m.s.) were virtually identical. The structure of **3** was elucidated through an *X*-ray analysis of neothiobinupharidine dihydrobromide tetrahydrate (5, 6). The X-ray studies established the gross structure and the relative configuration at all chiral centers but not the absolute configuration of the molecule. The original supposition that two deoxynupharidine molecules were incorporated into **3** was substantiated. The two molecules were incorporated without alteration of relative configuration at any center other than C(7).

In the past several years other sulfur-contain-

Can. J. Chem. Downloaded from www.nrcresearchpress.com by 210.87.254.42 on 09/05/12
For personal use only.

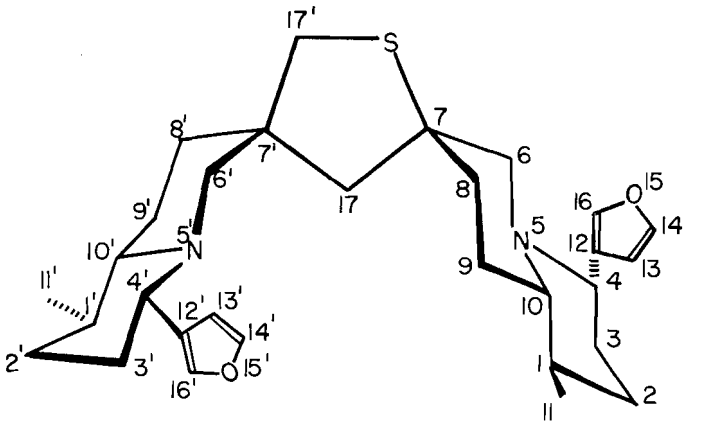

Ia THIOBINUPHARIDINE ($C_{30}H_{42}N_2O_2S$)

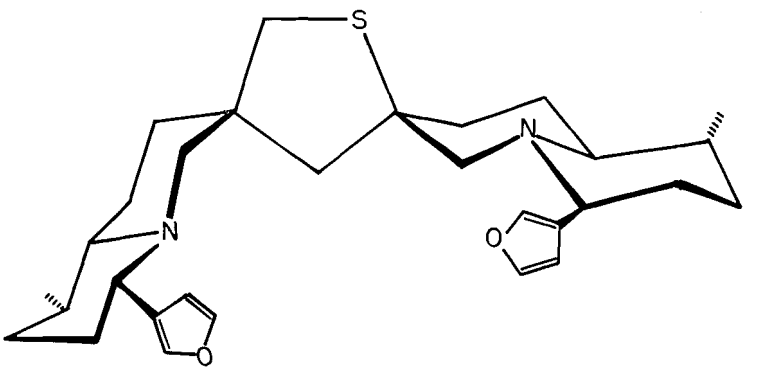

Ib

ing alkaloids of *Nuphar* have been reported. LaLonde *et al.* (7) have isolated two isomeric carbinolamines designated 6,6′-dihydroxythionuphlutine-A and -B and have reduced their immonium perchlorates to the apparently stereoisomeric thionuphlutines-A and -B ($C_{30}H_{42}N_2O_2S$). Thionuphlutine-A has very recently been shown to be identical with thiobinupharidine (8). It has been proposed (8) that nuphleine isolated some years ago (9) and 6,6′-dihydroxythionuphlutine-A are identical although a direct comparison has not been made. The isolation from *N. luteum* of a sulfoxide of neothiobinupharidine has also been reported (10). An alkaloid ($C_{30}H_{42}N_2O_3S$) named thionupharoline (11) has also been described and recent work in the authors' laboratories has shown it to be a hydroxyl derivative of **1**. Thus these sulfur alkaloids are all closely related and it seems that thiobinupharidine and thionuphlutine-B are stereoisomers of one another and of neothiobinupharidine. It was to examine the nature of the stereoisomerism between **1** and **3** that this work was undertaken.

We began our study by re-examining the spectra of **1** and **3** in the hope that we might clarify the stereochemical differences between the two molecules in this way. *trans*-Quinolizidines exhibit Bohlmann bands in their i.r. spectra and these bands are evident as expected in the spectrum of neothiobinupharidine (2, 4). When equimolar solutions of **1** and **3** were examined under the same conditions, it was observed that the Bohlmann bands in each spectrum were of nearly equal intensity although differing slightly in complexity. Thus it seems that **1** like **3** has two *trans*-quinolizidine rings.

The m.s. of **1** and **3** were reported some years

Can. J. Chem. Downloaded from www.nrcresearchpress.com by 210.87.254.42 on 09/05/12
For personal use only.

Can. J. Chem. Downloaded from www.nrcresearchpress.com by 210.87.254.42 on 09/05/12
For personal use only.

TABLE 1. Characteristic ions in the m.s. of thiobinupharidine and neothiobinupharidine

	Relative abundance (%)		
m/e	Thiobinupharidine	Neothiobinupharidine	Composition
94	40	38	C_6H_6O
107	23	20	C_7H_7O
136	11.5	9.5	$C_9H_{12}O$
178	100	100	$C_{11}H_{16}NO$
230	35	43	$C_{15}H_{20}NO$
231	10	12.5	$C_{15}H_{21}NO$
247	1.3	1.2	$M^+/2$
264	1.3	1.6	$C_{15}H_{22}NOS$
359	8.5	10.5	$C_{21}H_{31}N_2OS$
427	1.1	1.3	$C_{26}H_{39}N_2OS$
447	1.6	2.8	$C_{29}H_{39}N_2O_2$
451	0.5	0.6	$C_{27}H_{35}N_2O_2S$
461	2.0	2.7	$C_{30}H_{41}N_2O_2$
465	0.75	0.9	$C_{28}H_{37}N_2O_2S$
479	0.3	0.35	$C_{29}H_{39}N_2O_2S$
494	30	28	$C_{30}H_{42}N_2O_2S$

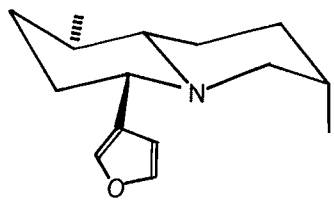

2 DEOXYNUPHARIDINE

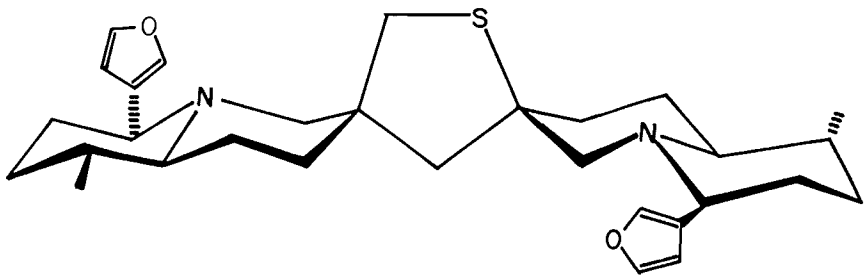

3 NEOTHIOBINUPHARIDINE
($C_{30}H_{42}N_2O_2S$)

ago (2) and that of **3** examined by high resolution very recently (10). We have confirmed the earlier observation that the spectra of **1** and **3** are very similar (Table 1) and have found by high resolution mass measurements that the compositions of the major ions in the two spectra are identical.

The p.m.r. spectra of the two alkaloids (Figs. 1 and 2) have now been examined at 220 MHz and the anomalies of the earlier studies (4) have been clarified. The interpretation of the spectra was aided greatly by referring to the studies of LaLonde and co-workers on the spectrum of deoxynupharidine (12) and on the spectra of model quinolizidines (13). Even so, the spectra

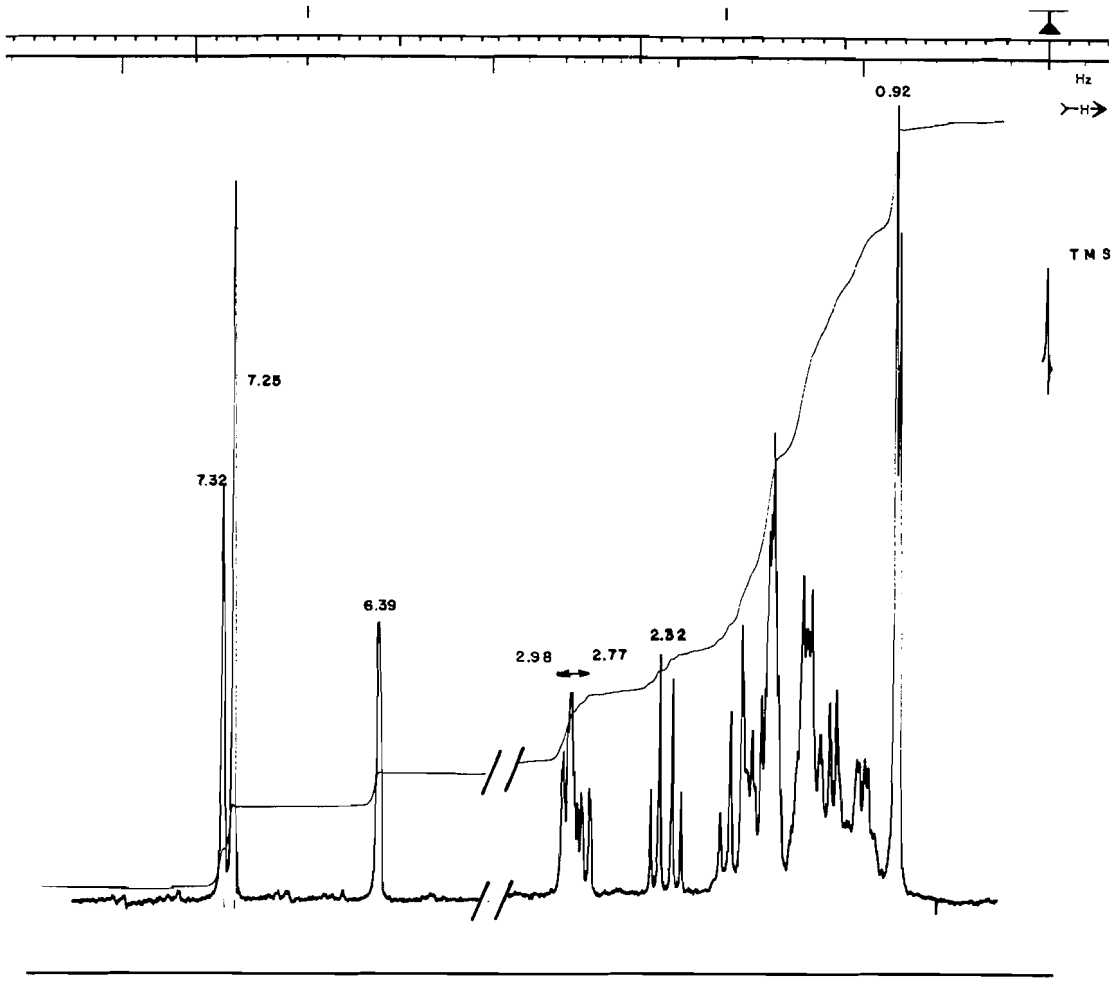

FIG. 1. The 220 MHz n.m.r. spectrum of thiobinupharidine.

are very complex and only a few of the protons of each were assignable.

In the spectrum of thiobinupharidine there is a signal of area 6 centered at δ 0.91 (J = 5 Hz) assignable to two CH—CH_3 groups. Similarly in **3** there is a signal of area 6 centered at δ 0.85 (J = 5.5 Hz). These resonances are very similar to the equatorial methyl resonance at C-1 of deoxynupharidine which is found at δ 0.92 (J = 5.6 Hz). Contrary to the earlier report there are no signals corresponding to methyl groups at quaternary carbon centers in either **1** or 3 nor are there any other signals attributable to CH_3 groups in the spectrum. The signals corresponding to the furan protons appear in **1** at δ 6.39 (2H, broad singlet, $w_{1/2}$ = 7 Hz) assigned to the β-protons of the two furan rings and at δ 7.25 (2H, singlet, $w_{1/2}$ = 4 Hz) and 7.32 (2H, singlet $w_{1/2}$ = 5 Hz) assigned to the α-protons. In the spectrum of **3** the furan signals are more complex appearing at δ 6.34 (1H, broad singlet $w_{1/2}$ = 3 Hz) and 6.52 (1H, broad singlet, $w_{1/2}$ = 3 Hz) attributable to the β-protons, and at 7.23 (1H, broad singlet, $w_{1/2}$ = 3 Hz) and 7.32 (3H, multiplet) assignable to the α-protons. These observations concerning the furan protons are in accord with those made earlier (4) which led originally to the incorrect conclusion that **1** must be a more symmetrical molecule than **3**. In the spectrum of **1** there are complex signals of area 4 in the region δ 2.77–2.98 attributed to the two protons α to the furan rings at C(4) and C(4′) and to the two equatorial protons at C(6) and C(6′). These assignments are made by

Can. J. Chem. Downloaded from www.nrcresearchpress.com by 210.87.254.42 on 09/05/12
For personal use only.

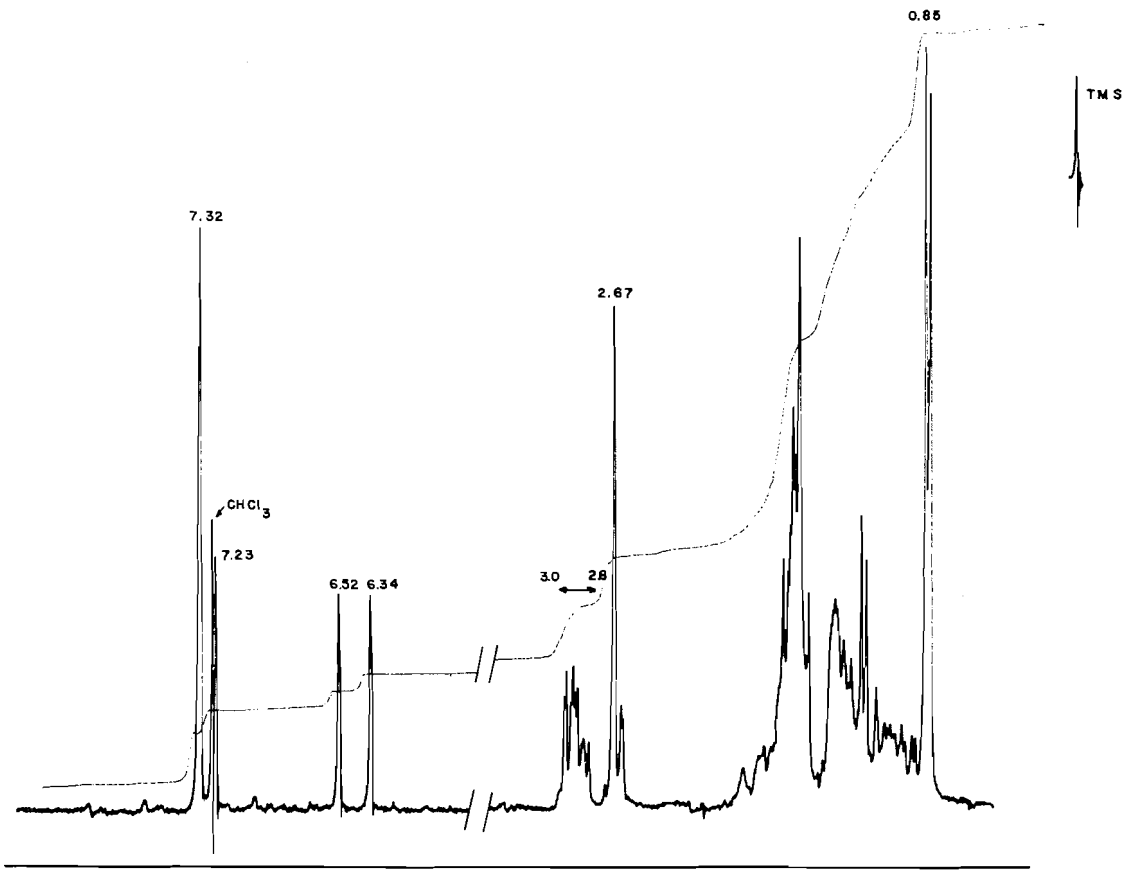

FIG. 2. The 220 MHz n.m.r. spectrum of neothiobinupharidine.

analogy with the chemical shifts of the corresponding protons in **2**. There is also in the spectrum of **1** a well-defined AB quartet centered at δ 2.32 (J = 11.5 Hz) attributed to the methylene adjacent to sulfur. In the spectrum of **3** the C(4) and C(4′) and the C(6) and C(6′) equatorial protons also appear in a complex pattern in the region δ 2.60–3.00. Superimposed on this complex pattern is a singlet at δ 2.67 (2H, $w_{1/2}$ = 3 Hz) attributed to the methylene adjacent to sulfur.

In recent studies on model compounds LaLonde *et al.* (13) have found that axial thiomethylene groups on quinolizidine systems absorb at δ 2.80 while equatorial thiomethylene groups absorb at 2.40. The thiomethylene group of **3** is known to be axial from the *X*-ray study and appears at δ 2.67. The much higher field absorption of the thiomethylene group of **1** at δ 2.32 would suggest by analogy that it is equatorial with respect to the quinolizidine ring. Therefore, this accounts for one of the stereochemical differences between the two molecules. Assuming that stereochemical differences between **1** and **3** reside in the tetrahydrothiophene ring and that the configuration at all other centers is the same, as the p.m.r. data suggest, there are two possible structures **1***a* and **1***b* for **1** in which the sulfur linkage to the second ring is equatorial and axial, respectively.

Until the finding that thiobinupharidine and thionuphlutine-A were identical there did not seem to be a method to differentiate between **1***a* and **1***b*. However, LaLonde (14) has presented evidence for the equatorial character of the C(7)—S linkage in thionuphlutine-A (thiobinupharidine) based on the formation of **1** by reduction of the immonium perchlorate derived from 6,6′-dihydroxythionuphlutine-A. In reduction experiments with borodeuteride and borohydride, he found evidence for sulfur participation, probably through an episulfonium ion, in

Can. J. Chem. Downloaded from www.nrcresearchpress.com by 210.87.254.42 on 09/05/12
For personal use only.

directing the attack of D^- or H^- on the carbon–nitrogen double bond of the immonium salts. In the case where an equatorial sulfur was present deuteride attack was found to occur in a manner that introduced deuterium into an equatorial position, whereas when an axial sulfur was present the entering deuterium was introduced into an axial position. In the reduction cited above the entering deuterium occupied an equatorial position in the reduction product. Thus, the evidence favors structure **1***a* for thiobinupharidine.[1] (This structure has been confirmed through the X-ray crystal structure determination on thiobinupharidine dihydrobromide dihydrate discussed below.)

The structure found in the X-ray study for the hydrobromide is shown in Fig. 3. As concluded from the spectroscopy the structures of thiobinupharidine and neothiobinupharidine (6) are very similar particularly if it is assumed that **3** has the same absolute configuration as that determined for **1**. The major difference between thiobinupharidine and neothiobinupharidine lies in the fact that S and C(17′) (Fig. 3) are equatorial to the two quinolizidine systems in the former, whereas they are axial in the latter. Consequently C(17) is axial in thiobinupharidine and equatorial in neothiobinupharidine.[2] In both isomers the S, C(17′), C(7), and C(17) atoms lie in a plane and C(7′) is displaced from the plane by 0.28 Å in the present structure and 0.49 Å in neothiobinupharidine. Since the mean deviations of the atoms defining the plane is 0.004 Å in the former case and 0.006 Å in the latter these displacements are significant.

Pertinent bond distances and angles are found in Table 2. As in neothiobinupharidine, there are some unusually and significantly long bond lengths in the sulfur-containing ring. The S—C bond lengths lie on either side of the expected value of 1.81 Å (15), unlike those in neothiobinupharidine where both the C—S bond lengths are shorter than 1.81 Å. The thermal parameter for S is unusually large in both isomers (see Table 3) suggestive of disorder, but that of C(17′) is small in the present compound and large in neothiobinupharidine.

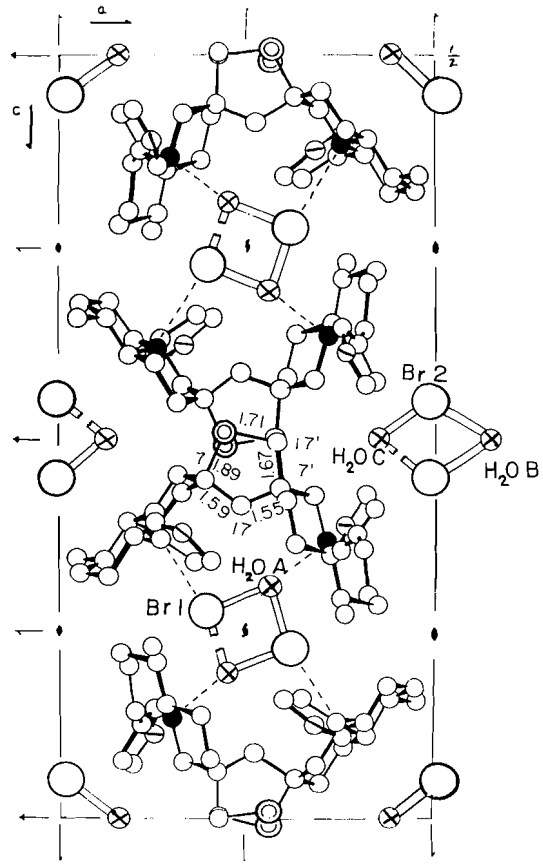

FIG. 3. The structure of thiobinupharidine dihydrobromide dihydrate projected down [010]. Only half the unit cell contents are shown. (○) Br; ◎ S; ⊗ H_2O; ● N; ⊘ O; (o) C.

The average $C(sp^3)$—$C(sp^3)$ bond length in the structure is 1.55 Å, in good agreement with the accepted value of 1.54 Å. The only bond of this type which exceeds the average value by as much as three standard deviations is that between C(17′) and C(7′) in the present structure. A similar anomaly in bond length is found in neothiobinupharidine. The mean C=C and C—O bond distances in the furan rings are both 1.39 Å compared with C=C, 1.361 and 1.351 Å, and C—O, 1.362 Å and 1.361 Å, found in furan (16) and furan-3,4-dicarboxylic acid (17), respectively. The average C—N bond length at

[1]In a recent personal communication Professor R. T. LaLonde has informed us that he has reached the same conclusion regarding the structure of thiobinupharidine and has found that the structure of thionuphlutine-B is that represented in **1***b*. His conclusions were reached as the result of more extensive chemical and spectroscopic studies on the alkaloids and on model systems. We thank Professor LaLonde for sending us a preprint of the paper he has prepared on his studies and which is in press in the Journal of the American Chemical Society.

[2]The same numbering system is used for both isomers and differs from that used by Birnbaum (6).

Can. J. Chem. Downloaded from www.nrcresearchpress.com by 210.87.254.42 on 09/05/12
For personal use only.

Can. J. Chem. Downloaded from www.nrcresearchpress.com by 210.87.254.42 on 09/05/12
For personal use only.

TABLE 2. Bond lengths and angles in thiobinupharidine dihydrobromide dihydrate with standard errors in parentheses

Bond	Distance (Å)	Bond	Distance (Å)	Angle	Degrees	Angle	Degrees
S—C(17′)	1.71(2)			C(7)—S—C(17′)	99(2)		
C(17′)—C(7′)	1.67(3)			S—C(17′)—C(7′)	104(2)		
C(7′)—C(17)	1.56(3)			C(17′)—C(7′)—C(17)	105(2)		
C(17)—C(7)	1.59(3)			C(7′)—C(17)—C(7)	111(3)		
C(7)—S	1.89(3)			C(17)—C(7)—S	103(1)		
N(5)—C(6)	1.53(3)	N(5′)—C(6′)	1.53(3)	C(10)—N(5)—C(6)	109(2)	C(10′)—N(5′)—C(6′)	111(2)
C(6)—C(7)	1.58(3)	C(6′)—C(7′)	1.51(4)	N(5)—C(6)—C(7)	111(2)	N(5′)—C(6′)—C(7′)	114(2)
C(7)—C(8)	1.44(4)	C(7′)—C(8′)	1.44(4)	C(6)—C(7)—C(8)	113(2)	C(6′)—C(7′)—C(8′)	114(2)
C(8)—C(9)	1.55(4)	C(8′)—C(9′)	1.54(4)	C(7)—C(8)—C(9)	113(2)	C(7′)—C(8′)—C(9′)	112(2)
C(9)—C(10)	1.62(4)	C(9′)—C(10′)	1.54(4)	C(8)—C(9)—C(10)	106(2)	C(8′)—C(9′)—C(10′)	115(2)
				C(9)—C(10)—N(5)	109(2)	C(9′)—C(10′)—N(5′)	108(2)
C(10)—N(5)	1.58(3)	C(10′)—N(5′)	1.57(4)				
				N(5)—C(10)—C(1)	109(2)	N(5′)—C(10′)—C(1′)	105(2)
C(10)—C(1)	1.52(4)	C(10′)—C(1′)	1.49(4)	C(10)—C(1)—C(2)	110(2)	C(10′)—C(1′)—C(2′)	110(4)
C(1)—C(2)	1.62(4)	C(1′)—C(2′)	1.55(4)	C(1)—C(2)—C(3)	106(2)	C(1′)—C(2′)—C(3′)	109(3)
C(2)—C(3)	1.47(4)	C(2′)—C(3′)	1.52(5)	C(2)—C(3)—C(4)	116(2)	C(2′)—C(3′)—C(4′)	108(2)
C(3)—C(4)	1.59(4)	C(3′)—C(4′)	1.61(4)	C(3)—C(4)—N(5)	103(2)	C(3′)—C(4′)—N(5′)	103(2)
C(4)—N(5)	1.57(3)	C(4′)—N(5′)	1.57(3)	C(4)—N(5)—C(10)	109(2)	C(4′)—N(5′)—C(10′)	110(2)
C(12)—C(13)	1.46(4)	C(12′)—C(13′)	1.47(4)	C(16)—C(12)—C(13)	103(2)	C(16′)—C(12′)—C(13′)	102(2)
C(13)—C(14)	1.38(4)	C(13′)—C(14′)	1.37(4)	C(12)—C(13)—C(14)	114(3)	C(12′)—C(13′)—C(14′)	113(2)
C(14)—O(15)	1.41(4)	C(14′)—O(15′)	1.37(3)	C(13)—C(14)—O(15)	100(2)	C(13′)—C(14′)—O(15′)	105(2)
O(15)—C(16)	1.35(4)	O(15′)—C(16′)	1.41(4)	C(14)—O(15)—C(16)	116(2)	C(14′)—O(15′)—C(16′)	111(2)
C(16)—C(12)	1.42(4)	C(16′)—C(12′)	1.39(4)	O(15)—C(16)—C(12)	107(2)	O(15′)—C(16′)—C(12′)	110(2)

Can. J. Chem. Downloaded from www.nrcresearchpress.com by 210.87.254.42 on 09/05/12
For personal use only.

TABLE 2.(*Concluded*)

Bond	Distance (Å)	Bond	Distance (Å)	Angle	Degrees	Angle	Degrees
C(1)—C(11)	1.53(5)	C(1′)—C(11′)	1.56(4)				
C(4)—C(12)	1.45(4)	C(4′)—C(12′)	1.43(4)				
				C(8)—C(7)—S	113(2)	C(8′)—C(7′)—C(17′)	114(2)
				C(8)—C(7)—C(17)	113(2)	C(8′)—C(7′)—C(17)	111(2)
				C(6)—C(7)—S	101(2)	C(6′)—C(7′)—C(17′)	105(2)
				C(6)—C(7)—C(17)	113(2)	C(6′)—C(7′)—C(17)	107(2)
				C(3)—C(4)—C(12)	115(2)	C(3′)—C(4′)—C(12′)	111(2)
				N(5)—C(4)—C(12)	108(2)	N(5′)—C(4′)—C(12′)	111(2)
				C(4)—C(12)—C(16)	123(2)	C(4′)—C(12′)—C(16′)	130(2)
				C(4)—C(12)—C(13)	134(2)	C(4′)—C(12′)—C(13′)	127(2)
				C(2)—C(1)—C(11)	108(2)	C(2′)—C(1′)—C(11′)	105(2)
				C(10)—C(1)—C(11)	113(2)	C(10′)—C(1′)—C(11′)	112(3)
Br(1)—OA	3.36(2)	OA—Br(1)—OAa	126.9(4)				
Br(1)—OAa*	3.28(2)	OA—Br(1)—N(5)	119.6(5)				
Br(1)—N(5)	3.43(2)	OAa—Br(1)—N(5)	101.9(5)				
OAa—N(5)	2.80(3)	Br(1)—OA—Br(1)a	120.1(3)				
		Br(1)—OAa—N(5′)	103.5(3)				
		Br(1)a—OAa—N(5′)	124.4(3)				
Br(2)—OB	3.28(2)	Br(2)—OB—Br(2)a	121.7(3)				
Br(2)—OC	3.28(2)	Br(2)—OC—Br(2)a	113.4(3)				
		OB—Br(2)—OC	131.8(3)				

*Br(1)a and OAa are related to Br(1) and OA by the 2_1 axis parallel to [010] direction and passing through ($x = \frac{1}{4}$, $z = \frac{3}{4}$). Br(2) and Br(2)a are related by the twofold axis parallel to [100] direction and passing through ($y = \frac{1}{2}$, $z = \frac{1}{2}$).

TABLE 3. Atomic positions in thiobinupharidine dihydrobromide dihydrate with standard errors in parentheses

Atom	x	y	z	U
S	0.2191(4)	0.7932(12)	0.4900(4)	0.120(3)
C(1)	0.0586(10)	0.712(3)	0.6588(10)	0.076(9)
C(1′)	0.3714(11)	0.826(3)	0.7064(11)	0.079(9)
C(2)	0.0257(12)	0.846(3)	0.6749(12)	0.084(10)
C(2′)	0.4215(13)	0.741(4)	0.7184(13)	0.105(11)
C(3)	0.0648(10)	0.956(3)	0.6784(10)	0.058(8)
C(3′)	0.4120(11)	0.596(3)	0.7018(11)	0.071(9)
C(4)	0.0963(10)	0.991(3)	0.6280(10)	0.056(8)
C(4′)	0.4041(9)	0.596(3)	0.6413(9)	0.049(7)
N(5)	0.1281(8)	0.858(2)	0.6172(8)	0.051(6)
N(5′)	0.3520(7)	0.684(2)	0.6334(8)	0.053(6)
C(6)	0.1607(10)	0.878(3)	0.5690(10)	0.058(8)
C(6′)	0.3373(10)	0.678(3)	0.5774(10)	0.058(8)
C(7)	0.1896(9)	0.743(2)	0.5531(8)	0.051(7)
C(7′)	0.2918(9)	0.771(2)	0.5633(8)	0.046(7)
C(8)	0.1536(11)	0.620(3)	0.5489(11)	0.069(8)
C(8′)	0.2996(13)	0.909(3)	0.5788(11)	0.082(9)
C(9)	0.1222(12)	0.602(3)	0.5985(12)	0.078(10)
C(9′)	0.3155(12)	0.920(3)	0.6349(11)	0.077(10)
C(10)	0.0877(11)	0.737(3)	0.6092(10)	0.071(9)
C(10′)	0.3638(10)	0.834(3)	0.6506(11)	0.063(9)
C(11)	0.0197(13)	0.594(3)	0.6554(13)	0.096(11)
C(11′)	0.3822(12)	0.968(3)	0.7305(13)	0.099(11)
C(12)	0.1338(10)	0.107(3)	0.6319(10)	0.053(8)
C(12′)	0.3969(10)	0.461(3)	0.6226(9)	0.053(8)
C(13)	0.1816(11)	0.126(3)	0.6619(10)	0.068(9)
C(13′)	0.4183(11)	0.403(3)	0.5755(11)	0.065(9)
C(14)	0.2015(12)	0.256(3)	0.6586(11)	0.085(9)
C(14′)	0.4060(10)	0.268(3)	0.5703(10)	0.062(8)
O(15)	0.1651(9)	0.313(2)	0.6237(8)	0.093(7)
O(15′)	0.3803(8)	0.235(2)	0.6136(8)	0.101(7)
C(16)	0.1256(11)	0.229(3)	0.6080(11)	0.079(9)
C(16′)	0.3730(12)	0.349(3)	0.6448(12)	0.074(9)
C(17)	0.2403(9)	0.710(3)	0.5869(9)	0.051(7)
C(17′)	0.2842(6)	0.750(2)	0.5011(8)	0.018(5)
OA	0.2768(7)	0.550(2)	0.6927(7)	0.076(6)
OB	0.5583(12)	1/2	1/2	0.108(11)
OC	0.4229(14)	0	1/2	0.133(13)
Br(1)	0.1960(1)	0.7937(3)	0.7274(1)	*
Br(2)	0.4947(2)	0.2430(5)	0.4494(2)	*

*	U_{11}(Å²)	U_{22}(Å²)	U_{33}(Å²)	U_{12}(Å²)	U_{13}(Å²)	U_{23}(Å²)
Br(1)	0.072(2)	0.048(2)	0.047(2)	0.006(2)	−0.001(2)	0.003(2)
Br(2)	0.125(3)	0.148(4)	0.152(4)	−0.031(3)	0.016(3)	−0.044(4)

These values were obtained from

$$\beta_{ij} = 2\pi^2 b_i b_j U_{ij}$$

where the β_{ij}'s appear in the structure factors as

$$\exp\left[-(\beta_{11}h^2 + 2\beta_{12}hk + \ldots)\right]$$

and the b_i's are reciprocal lattice vectors.

1.56 Å, is larger than expected from values reported in related structures (6).

The alkaloids in both isomers possess a pseudo twofold axis. The nonplanarity of the S-containing ring and the inequivalence of S and C(17′) destroy this element of symmetry. In the present structure S has a large thermal motion parameter while C(17′) has a very small one, suggestive of a disorder resulting in an unequal mixture of two orientations in which S and C(17′) interchange as a result of a rotation of 180° about the pseudo twofold axis. In neothiobinupharidine it is tempting to attribute the residual peak in the difference synthesis to a similar rotation of the molecule but with the axis of rotation substantially displaced from the

Can. J. Chem. Downloaded from www.nrcresearchpress.com by 210.87.254.42 on 09/05/12
For personal use only.

Can. J. Chem. Downloaded from www.nrcresearchpress.com by 210.87.254.42 on 09/05/12
For personal use only.

center of the C(17′)—S bond. In the structure at hand, however, this should cause an apparent shortening of the S—C(7) and S—C(17′) bonds, and a lengthening of the C(17′)—C(7′) bond. The S—C(17′) and C(17′)—C(7′) bond lengths of 1.71 and 1.67 Å are consistent with this, but not the S—C(7) bond, whose length is 1.89 Å and thus deviates by more than 4σ from the comparable distance in neothiobinupharidine. At present it is not possible to account for these features in this structure.

The packing in the structure is defined by the arrangement of the organic moiety between two types of spirals containing hydrogen-bonded water molecules and bromide ions. The first spiral contains Br(1) and H_2OA and is propagated by a 2_1 axis parallel to the *b* axis while the second contains Br(2), H_2OB, and H_2OC and is generated by the twofold axes parallel to *a* through the water molecules. The first spiral interacts with the thiobinupharidine through N(5) and N(5′) with Br(1) and H_2OA, respectively, and the stabilization of this interaction is reflected in the smaller thermal parameters for the atoms in the first spiral compared with the second. The interatomic interactions suggestive of hydrogen bonding are included in Table 2. The Br(1)—OA, Br(1)—OAa, Br(2)—OB, and Br(2)—OC distances at 3.36(2) Å for the first and 3.28(2) Å for the remainder are similar to the distances of 3.26 and 3.39 Å observed for similar interactions in quinuclidinylbenzilate hydrobromide (18) and capaurine hydrobromide (19), respectively. In these latter structures the bromide ion – quaternary nitrogen distances were 3.18 and 3.12 Å respectively. The corresponding distance in the present structure is 3.43 Å between Br(1) and N(5). It appears that given the configuration of the neothiobinupharidine moiety it is not possible to pack two bromide ions into this entity efficiently in the structure and that the water molecules permit the separation of the halide ions while allowing the organic framework to come into contact at the appropriate separations defined by the van der Waals' radii.

Experimental

Apparatus, Methods, and Materials

M.s. were determined on a C.E.C. 21-110B double-focusing mass spectrometer. Samples were introduced through a direct inlet system. Relative intensity data were obtained from low resolution m.s. recorded under identical conditions at 70 eV and at 140 μA and at a source temperature of 200 °C and a source pressure of 2×10^{-6} Torr. The high resolution mass spectra (h.r.m.s.) were recorded on Ilford Q-2 photographic plates which were developed in the usual manner. The spectra were then recorded on magnetic tape, using a Gaertner comparator-densitometer linked to a Datex system. They were processed on a CDC-6400 computer using a modified version of the HIRES program of Tunnicliff and Wadsworth (20). The compositions of all ions formed by electron impact and discussed in this paper were established by high resolution measurements and agreed with calculated values within the limits ±5 mmass units. A comparison of the intensities of the ions in the spectra of **1** and **3** is found in Table 1.

I.r. spectra of **1** and **3** were recorded on a Perkin-Elmer 521 spectrometer. Samples were made up at a concentration of 0.03 *M* (15 mg/ml) in carbon tetrachloride, using a solution cell with NaCl windows and a path length of 0.5 mm. The total area of the three absorption bands with maxima at 2740, 2760, and 2780 cm^{-1}, the Bohlmann bands, was estimated and found to be nearly equal.

P.m.r. spectra were recorded at 220 MHz on a Varian 220 HR spectrometer using a field sweep mode. Samples were dissolved in $CDCl_3$ using added TMS as internal locking signal. Chemical shifts are quoted relative to TMS = 0.0 δ.

In the X-ray experiments a crystal with dimensions 0.17 × 0.12 × 0.07 mm and a Syntex $P\bar{1}$ automatic diffractometer with graphite monochromatized MoKα radiation were used throughout this investigation. Unit cell parameters were obtained by least squares from 15 accurately centered reflections. The crystal data are as follows:

$C_{30}H_{42}O_2N_2S \cdot 2HBr \cdot 2H_2O$ FW = 692.68

$a = 25.128(6)$, $b = 9.869(2)$, $c = 26.380(6)$ Å, volume = 6545.6 Å^3, $D_m = 1.41$ g/cm^3, $Z = 8$, $D_x = 1.407$ g/cm^3, space group $C222_1$

The systematic absences are $h + k$ odd in general and $00l$ for l odd. Data were collected up to 2θ equal to 35°. Reflections were scanned at a rate between 2 and 24° per min depending upon the peak intensity. Backgrounds were measured at 1° removed from the peak. A total of 1934 unique reflections (consisting of hkl, $hk\bar{l}$ pairs) were observed of which 1452 had intensity greater than 3σ. The data were corrected for Lorentz and polarization effects but not for absorption. The linear absorption coefficient, μ, is 27.3 cm^{-1} and the average μR value is 0.19.

The atomic positions were determined from the Patterson function and subsequent electron density and difference electron density. The structure was refined using full-matrix least squares using a program written by J. S. Stephens for the CDC 6400. Atomic scattering factors were obtained from the International Tables for X-ray Crystallography (21) and corrected for anomalous dispersion. Weights, ω, were assigned such that ΔF would be locally independent of F_o by setting

$$\omega = [157\text{–}1.67F_o + 0.0103F_o^2]^{-1}.$$

The anisotropic components of the thermal parameters for Br and isotropic thermal parameters of the remaining atoms were varied resulting in a minimum R value of 0.091 with Friedel equivalent reflections averaged. These

Friedel equivalent pairs were then separated and the absolute configuration sought using about 200 pairs which showed greater than 20% difference in their measured intensities. Structure factor calculations for the two alternate configurations showed that the deviations were in the direction consistent with the proposed configuration in over 70% of the cases. This configuration was then refined using all 1934 reflections yielding a final R value of 0.085 for observed reflections only when all shifts were less than 0.3 of the calculated standard deviation. For all the reflections the final R value was 0.097. A final difference synthesis showed no peaks greater than 1/6 of a carbon peak. No attempt was made to locate hydrogen atoms. Table 3 contains the final atomic parameters. A list of selected bond distances and angles in the molecule appears in Table 2, and the observed and calculated structure factors are compared in Table 4.[3]

Thiobinupharidine Dihydrobromide Dihydrate

Thiobinupharidine (50 mg) was dissolved in hot methanol and a 1:1 mixture of methanol and concentrated hydrobromic acid was added dropwise to a pH of 3–4. The fine colorless needles that separated on cooling were recrystallized from a 1:1 mixture of acetone and water. The crystals melted at 245–247°.

Anal. Calcd. for $C_{30}H_{42}N_2O_2S \cdot 2HBr \cdot 2H_2O$: C, 52.02; H, 6.92; N, 4.04; Br, 23.09. Found: C, 52.06; H, 6.85; N, 4.08; Br, 23.11.

Conversion of the hydrobromide to the free base by treatment of an aqueous solution with ammonia followed by extraction with ether and subsequent workup gave thiobinupharidine identical with an authentic specimen.

We thank the National Research Council of Canada for financial support of this work.

[3]Table 4 is available, at a nominal charge, from the Depository of Unpublished Data, National Science Library, National Research Council of Canada, Ottawa, Canada K1A 0S2.

1. O. ACHMATOWICZ and Z. BELLEN. Tetrahedron Lett. 1162 (1962).
2. O. ACHMATOWICZ, H. BANASZEK, G. SPITELLER, and J. T. WRÓBEL. Tetrahedron Lett. 927 (1964).
3. J. T. WRÓBEL. Alkaloids, **8**, 441 (1967).
4. O. ACHMATOWICZ and J. T. WRÓBEL. Tetrahedron Lett. 129 (1964).
5. G. I. BIRNBAUM. Tetrahedron Lett. 4149 (1965).
6. G. I. BIRNBAUM. Acta Cryst. **23**, 536 (1967).
7. R. T. LALONDE, C. F. WONG, and W. P. CULLEN. Tetrahedron Lett. 4477 (1970).
8. R. T. LALONDE and C. F. WONG. Phytochemistry, **11**, 3305 (1972).
9. T. N. IL'INSKAYA, A. D. KAZOVKOV, and T. G. MONAKHOVA. Khim. Prir. Soedin. **3**, 178 (1967).
10. J. T. WRÓBEL, A. IWANOW, J. SZYCHOWSKI, J. POPLAWSKI, C. K. YU, T. I. MARTIN, and D. B. MACLEAN. Can. J. Chem. **50**, 1968 (1972).
11. J. T. WRÓBEL. Rocz. Chem. **44**, 457 (1970).
12. C. F. WONG, E. AUER, and R. T. LALONDE. J. Org. Chem. **35**, 517 (1970).
13. R. T. LALONDE, C. F. WONG, and H. G. HOWELL. J. Org. Chem. **36**, 3703 (1971).
14. R. T. LALONDE. U.S. Clearinghouse Fed. Sci. Tech. Inform. P.B. Rep. 1970, No. 192810; Chem. Abstr. **74**, 392086.
15. G. VALLE, V. BUSETTI, M. MAMMI, and G. CARAZZOLO. Acta Cryst. B, **25**, 1432 (1969).
16. B. BAK, D. CHRISTENSEN, W. B. DIXON, L. HANSEN-NYGAARD, J. R. ANDERSEN, and M. SCHOTTLÄNDER. J. Mol. Spectrosc. **9**, 124 (1962).
17. D. E. WILLIAMS and R. E. RUNDLE. J. Am. Chem. Soc. **86**, 1660 (1964).
18. A. MEYERHOFFER and D. CARLSTRÖM. Acta Cryst. B, **25**, 1119 (1969).
19. H. SHIMANOUCHI, Y. SASADA, M. IHARA, and T. KAMETANI. Acta Cryst. B, **25**, 1310 (1969).
20. D. D. TUNNICLIFF and P. A. WADSWORTH. Anal. Chem. **40**, 1826 (1968).
21. INTERNATIONAL TABLES FOR X-RAY CRYSTALLOGRAPHY, Vol. III. Kynoch Press, Birmingham, England. 1962.

Can. J. Chem. Downloaded from www.nrcresearchpress.com by 210.87.254.42 on 09/05/12
For personal use only.

Processus photophysiques dans la molécule de colchicine

H. ROIGT ET R. M. LEBLANC

Université du Québec à Trois-Rivières, Groupe de Biophysique, Département de Chimie-Biologie, C.P. 500, Trois-Rivières, Québec

Reçu le 6 mars 1973

Un diagramme de Jablonski est proposé pour la molécule de colchicine. A cette fin des résultats primordiaux ont été tirés de l'étude de l'absorption u.v.-visible, de la luminescence à 77 °K et de la photolyse. Ainsi le rendement de phosphorescence a été trouvé égal à 0.86 et un résultat important concerne la mise en évidence de l'établissement de pont hydrogène entre la colchicine et le solvant.

The photophysics of colchicine has been studied by absorption and luminescence spectroscopy. The quantum yield of phosphorescence has been found to be 0.86. The quantum yield measurements of colchicine photodegradation in different solvents are reported. The polarity and hydrogen bond character of the solvents are observed to play an important role in these measurements. The Jablonski diagram is proposed for the colchicine molecule.

Can. J. Chem., **51**, 2821 (1973)

Can. J. Chem. Downloaded from www.nrcresearchpress.com by 210.87.254.42 on 09/05/12
For personal use only.

Introduction

Une des principales caractéristiques de la colchicine réside dans son pouvoir antimitotique spécifique (1, 2). Un excellent résumé des propriétés apparaît dans l'article de Wallace et Ertel (3). Bien que possédant au point de vue médical des effets secondaires nocifs et imprévisibles, la colchicine est encore étudiée et utilisée fréquemment surtout dans les laboratoires de génétique cellulaire.

Or, un travail récent démontre que l'on peut inverser l'action biologique de la Colcemide (*N*-méthyl *N*-désacétyl colchicine) par irradiation du produit à 366 nm. Ce comportement est expliqué par la photodégradation de la substance (4). Pourtant, d'autres auteurs (5) observent des effets différents selon la région spectrale d'irradiation utilisée.

On s'aperçoit donc qu'une explication définitive ne pourra être formulée que lorsqu'une étude quantitative approfondie sur la photoinactivation de la colchicine aura été entreprise. Si l'on en juge par les travaux antérieurs (6–14) les résultats concernant la photodégradation quantique ne sont pas nombreux. Notre étude tente de combler cette lacune en examinant les processus photochimiques primaires et en établissant un bilan énergétique compte tenu d'un résultat préliminaire lié à la phosphorescence de la colchicine (15).

Partie expérimentale

Les solvants tels le tétrachlorure de carbone (spectranalyzed), le chloroforme (spectranalyzed, 0.75% C_2H_5OH), le dichlorométhane (spectranalyzed), le méthanol (99.9% pur), le *n*-propanol (certified normal), l'isopropanol (certified A.C.S.), le *n*-butanol (reagent A.C.S.), l'isobutanol (certified), le tertiobutanol (certified), le 1,4-dioxane (certified, 99% pur), le benzène (spectranalyzed), le formamide (certified), le *N*,*N*-diméthylformamide (certified A.C.S.), l'acétonitrile (certified A.C.S.) sont tous des produits Fisher et ont été employés sans autre purification. Il en est de même du mélange diéthyl éther, isopentane, éthanol, 5:5:2, (EPA mixed solvent, American Instrument Co. Inc.) et de l'éthanol à 95% (C.I.P., Gatineau, Québec). L'eau est distillée dans un système Barnsted.

Les standards de luminescence appartiennent à un ensemble de photosensibilisateurs (Organic Laboratory Chemicals, J. T. Baker Chemical Co., Phillipsburg, New Jersey, kit 4040).

L'oxalate de potassium et le chlorure ferrique (Fisher, reagent grade) ont servi à la préparation de l'actinomètre $K_3Fe(C_2O_4)_3.3H_2O$, lequel est recristallisé trois fois dans l'eau distillée tiède, à l'abri de la lumière.

Les cristaux verts obtenus sont séchés à l'air et récupérés dans un flacon teinté. Une solution sulfurique 0.006 *M* de ferrioxalate de potassium est ensuite préparée selon la technique élaborée par Hatchard et Parker (16).

L'acétate de sodium (reagent. Anachemia Chemicals Ltd.) et la 1,10-phénanthroline (certified A.C.S., Fisher) sont aussi utilisés tels quels dans la préparation des solutions nécessaires à l'obtention du complexe de couleur rouge avec les ions Fe^{2+}.

Les critères de pureté de la colchicine utilisée, ainsi que la description des caractéristiques du spectrophotomètre Unicam SP 1800 et du spectrofluorimètre Perkin-Elmer MPF 2A, ont déjà été mentionnés dans une publication antérieure (15). Cependant pour la détermination des rendements quantiques de phosphorescence, le photomultiplicateur HTV R106 a été remplacé par le HTV R136. Les spectres d'émission furent corrigés à l'aide de la réponse spectrale relative du photomultiplicateur au moyen d'une calculatrice électronique Hewlett-Packard 9820 A qui intégrait automatiquement les aires sous les courbes dans une unité commune. Les échantillons contenus dans des tubes en quartz ne présentaient aucune trace d'eau qui aurait eu pour effet de fendiller le verre

TABLEAU 1. Coefficients d'absorption de la colchine dans différents solvants

Solvant	λ_{max}(log ε) (±1 nm)			
Eau	354 (4.21)	246 (4.50)	234 (4.43)	199
Méthanol	352 (4.22)	243 (4.46)	234 (4.44)	206
Ethanol 95%	351 (4.22)	243 (4.47)	234 (4.43)	202 (4.40)
n-Propanol	351 (4.19)	244 (4.42)		202
2-Propanol	350 (4.23)	243 (4.60)	234 (4.44)	
n-Butanol	351 (4.21)	244 (4.45)		
t-Butanol	350 (4.20)	242 (4.40)		204
Tetrachlorure de carbone	347 (4.20)	260 (4.21)		
Chloroforme	350 (4.21)	242 (4.42)		
Dichlorométhane	343 (4.22)	248 (4.42)		
Benzène	344 (4.22)			
1,4-Dioxane	342 (4.19)	266 (4.11)		
Formamide	350 (4.22)	255 (4.29)		
N,*N*-Diméthyl formamide	344 (4.14)	262 (4.09)		
Acétonitrile	343 (4.19)	230 (4.45)		

(EPA solide) à 77 °K. Les tubes eux mêmes étaient maintenus en place par une garniture intérieure en Teflon, système qui avait pour effet d'obtenir des résultats reproductibles. Chacun des résultats est la moyenne d'une série de cinq ou six essais effectués dans des conditions expérimentales différentes.

Le système d'irradiation comporte les parties suivantes: une lampe au mercure General Electric AH4, 125 W, "pression moyenne"; un réflecteur cylindrique; une lentille convergente; un filtre de chaleur Chance No. HAI; un filtre optique 366 nm Chance No. 0.X.1; un diaphragme à iris ainsi qu'un bloc d'irradiation.

Le bloc d'irradiation comporte trois cellules de quartz, cylindriques, de 1 cm de trajet optique et de 2.75 cc de volume, calées dans des rainures à cet effet. Au milieu du bloc et placée perpendiculairement, avec un angle de 45° par rapport au faisceau incident, se trouve une lamelle de quartz de 1.5 mm d'épaisseur que répartit la lumière incidente en deux faisceaux perpendiculaires, dans le rapport: 7% réfléchie à angle droit et 93% traversant sans aucune déviation. Ce rapport est indépendant de l'intensité incidente.

La cellule latérale contient toujours de l'actinomètre et la densité optique mesurée à 5100 Å sert au calcul de l'intensité lumineuse émise par la lampe (éliminant ainsi les erreurs dues à une fluctuation possible de l'intensité durant l'irradiation).

La cellule arrière contient également de l'actinomètre et sert au calcul de la quantité de photons qui n'a pas été absorbée par la solution de colchicine: on peut ainsi corriger la valeur du rendement quantique de photodégradation obtenue.

Enfin la cellule frontale contient la solution dont on veut étudier la photolyse.

Les solutions de colchicine ayant servies à l'irradiation n'ont pas été dégazées à l'inverse de celles qui ont été utilisées pour la détermination des rendements de phosphorescence. En effet quelques expériences ont montré que le rendement quantique de dégradation de la colchicine demeurait dans les limites de l'erreur expérimentale quand on passait d'une solution non dégazée à une solution dégazée (pression inférieure à 10^{-5} Torr).

Résultats et discussion

Absorption

Certains résultats concernant l'absorption des molécules appartenant à la même famille que la colchicine ont déjà fait l'objet d'une importante étude de la part de Šantavý et coll. (17).

D'autres travaux portant sur les tropolones en particulier, prouvent la spécificité des bandes d'absorption dont l'une commune à tous ces composés et située vers 350 nm (arrangement du cycle tropolone) (18–20).

Quant à nous, nous nous sommes penchés plutôt sur l'effet de solvant, en restreignant notre champ d'investigation à la molécule de colchicine uniquement. Il va sans dire que les résultats concernant les coefficients d'absorption moléculaire sont absolument nécessaires pour le calcul des rendements quantiques de photoisomérisation de la colchicine.

Le tableau 1 concerne directement l'absorption en fonction du solvant, les coefficients d'absorption étant calculés par la méthode des moindres carrés. L'intervalle de concentrations se situe entre 10^{-3}–10^{-6} M, sauf le tétrachlorure de carbone (10^{-5}–10^{-6} M).

On note en premier lieu que la valeur de ces coefficients ε est relativement élevée ($\varepsilon \geqslant 12000$) ce qui implique des transitions $\pi\pi^*$ pour toutes ces bandes. Ceci est vérifié en outre par le déplacement bathochrome des maxima lorsque la polarité du solvant augmente.

On s'aperçoit aussi que le nombre des bandes d'absorption varie selon le solvant utilisé, mais celle entre 340 et 355 nm demeure toujours.

Can. J. Chem. Downloaded from www.nrcresearchpress.com by 210.87.254.42 on 09/05/12
For personal use only.

Can. J. Chem. Downloaded from www.nrcresearchpress.com by 210.87.254.42 on 09/05/12
For personal use only.

Un résultat important concerne l'absorption de la colchicine dans le formamide d'une part et dans son dérivé *N*,*N*-diméthylé d'autre part. Le maximum se déplace de 350–344 nm quand on passe du premier au second. Ce déplacement relativement important ne peut être expliqué uniquement par la variation du moment dipolaire du solvant. En effet, ici intervient un effet de liaison hydrogène c'est-à-dire que l'augmentation en intensité du ou des ponts hydrogènes entre la colchicine et le solvant conduit au même phénomène qu'une augmentation dans la polarité de ce dernier. Le doublet électronique libre sur l'azote du formamide est beaucoup plus disponible que dans le cas du *N*,*N*-diméthylformamide à cause d'un empêchement stérique provoqué par les groupements méthyle dans ce dernier cas. Il en découle donc une plus grande capacité à établir des liaisons hydrogène dans le cas du formamide et le déplacement de λ_{max} observé est tout à fait normal. Un tel effet a été commenté pour d'autres molécules (21).

Luminescence

Aucune fluorescence n'a été décelée, cependant une importante phosphorescence apparaît entre 380 et 600 nm, caractérisée par un spectre peu structuré avec un maximum d'intensité à 423 nm et une bande 0–0 à 402 nm dans l'*e.p.a.* La nature de cette luminescence a déjà fait l'objet d'un travail publié récemment (15).

Le choix des standards pour la mesure du rendement relatif de phosphorescence de la colchicine a été conditionné par l'énergie de son état triplet, $E_{T_1} = 71.5$ kcal mol^{-1}. A cette fin nous avons choisi la benzophénone (22), l'acétophénone (23) et le biphényle (24). Le rendement de phosphorescence ϕ_P(Colc.) a été déterminé à l'aide de la relation proposée par Parker et Rees (25):

$$[1] \qquad \phi_P(\text{Colc.}) = \phi_S(H/A)_S/(H/A)_{\text{Colc.}}$$

Colc. et S, indices se rapportant respectivement à la colchicine et au standard; H, hauteur maximum du spectre d'émission pour une même longueur d'onde d'excitation; A, aire sous le spectre, corrigée, d'après la réponse du photomultiplicateur.

Dans le cas des deux premiers standards la corrélation est excellente et indique une valeur moyenne ϕ_P(Colc.) = 0.86 (15 essais à différentes longueurs d'onde d'excitation), tandis qu'avec le biphényle on obtient une valeur de 0.18.

Cependant dans ce dernier cas, Parker et Hatchard (24) signalent que la valeur trouvée pour le biphényle n'est qu'approximative. Quant à nous, nous considérons qu'elle doit être erronée compte tenu des résultats obtenus avec les autres standards. Quoiqu'il en soit le calcul des rendements de photodégradation de la colchicine confirmera cette assertion.

Photolyse

En utilisant le dispositif d'irradiation décrit dans la partie expérimentale, on mesure par spectrophotométrie la décroissance de densité optique de la bande d'absorption $\pi\pi^*$ vers 350 nm, absorption due au cycle tropolone qui sera le siège d'un photoréarrangement. Cette bande est idéale pour une telle mesure puisqu'elle disparaît presque complètement dans le spectre des lumicolchicines β et γ dont le coefficient d'absorption à 350 nm, calculé à partir du graphique de Grewe et Wulf (12), est égal à: $\varepsilon = 1650$ l mol^{-1} cm^{-1}, soit une valeur équivalente au dixième de celle de la colchicine.

La figure 1 montre l'aspect spectral que revêt cette photodégradation dans l'eau. Des spectres semblables ont déjà été publiés mais ils concernaient la photoisomérisation de la lumicolchicine α (26) et celle de la *N*-méthyl, *N*-désacétyl colchicine (13).

Après un certain temps d'irradiation, il apparaît deux nouvelles bandes dont les maxima se situent respectivement à 223 et à 266 nm, absorptions caractéristiques des lumicolchicines β et γ. On note également la présence de quatre points isobestiques soit à 211, 228, 257 et 301 nm. La bande située à 350 nm diminue beaucoup d'intensité tout en se déplaçant vers les courtes longueurs d'onde (diminution de la conjugaison dans le cycle), tandis que les maxima à 199 et à 246 nm deviennent des minima.

Toujours sur la fig. 1, il est important de remarquer que la photodégradation de la colchicine n'est pas linéaire en fonction du temps, d'où l'obligation de recourir à une intensité d'irradiation plus faible et aussi à des intervalles d'irradiation plus courts. On a donc utilisé une intensité incidente corrigée, voisine de 10^{14} quanta s^{-1} cm^{-2} et dans ce cas on a noté une décroissance uniforme de la densité optique en fonction du temps, ce, durant 5 min à peu près, et pour deux séries de solvants, soient les chlorométhanes

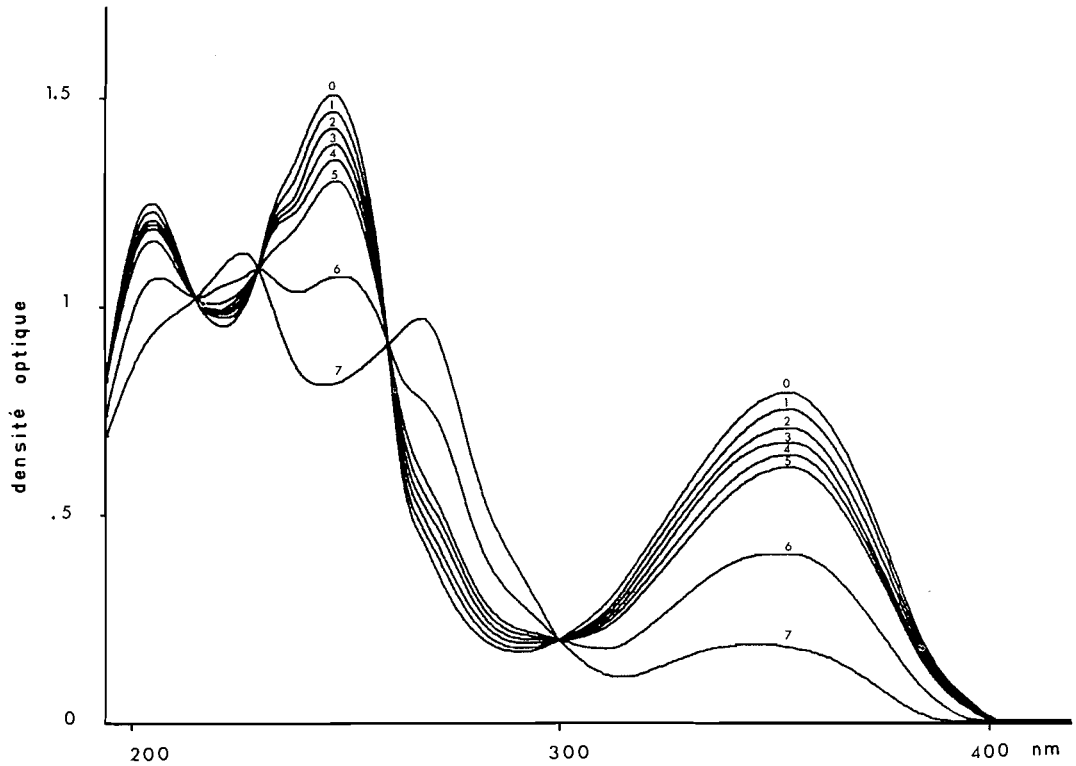

FIG. 1. Photodegradation de la colchicine en solution aqueuse. 4.9×10^{-5} *M*; p*H* = 5.8; $I_{abs} = 2 \times 10^{15}$ quanta s^{-1} cm^{-2}; temps d'irradiation 0: 0 min, 1: 10 min, 2: 20 min, 3: 30 min, 4: 40 min, 5: 50 min, 6: 120 min, 7: 240 min.

d'une part (fig. 2*a*), et les alcools d'autre part (fig. 2*b*). Le temps au bout duquel la linéarité disparaît, dépend du solvant: plus celui-ci est polaire, plus le temps est long. C'est la pente de ces droites qui sert à calculer le rendement quantique de photoisomérisation de la colchicine, selon l'équation:

$$[2] \quad \Phi(\text{Colc.}) = \frac{\Delta(\text{d.o.})_{350\,nm} \times N_0 \times V}{t \times \varepsilon_{max} \times I_{abs}}$$

Φ(Colc.): rendement quantique de photoisomérisation de la colchicine; $\Delta(\text{d.o.})_{350\,nm}$: diminution de densité optique du maximum vers 350 nm; N_0: 6.023×10^{20} molécules cm^{-3}; V: volume de la solution de colchicine irradiée en cm^3; t: temps d'irradiation en s; ε_{max}: coefficient d'absorption moléculaire vers 350 nm en 1 mol^{-1} cm^{-1}; I_{abs}: intensité absorbée par la colchicine en quanta s^{-1} cm^{-2}.

Effet de solvant

En plus des deux séries de solvants cités précédemment, ont été utilisés le benzène (faible probabilité de réaction d'abstraction d'hydrogène), le formamide et son dérivé *N*,*N*-diméthylé pour une comparaison possible quant à l'établissement de liaisons hydrogène. Les résultats apparaissent dans le tableau 2.

Dans l'une ou l'autre des séries de solvants étudiés, on remarque une diminution du rendement quantique de photodégradation en fonction du moment dipolaire du solvant.

Cet effet est expliqué par la formation d'un complexe de solvatation soluté – solvant, d'autant plus stable que le moment dipolaire est élevé.

Le cas du formamide et de son dérivé *N*,*N*-diméthylé, offre un aspect intéressant de l'intervention des ponts hydrogène et de leur importance dans les processus photophysiques. En effet, en passant du formamide à son dérivé, on assiste à une augmentation du simple au double du rendement de photodégradation et l'explication de ce phénomène ne peut résider uniquement dans la différence de moment dipolaire entre les deux molécules de solvant. Cette variation est

Can. J. Chem. Downloaded from www.nrcresearchpress.com by 210.87.254.42 on 09/05/12
For personal use only.

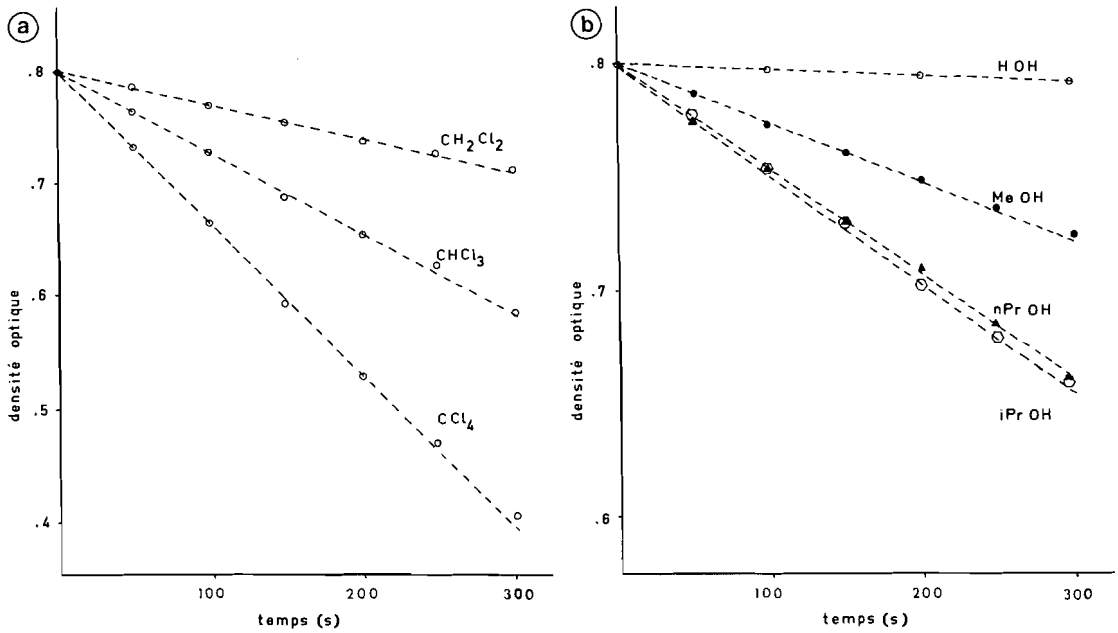

FIG. 2. Décroissance du maximum d'absorption vers 350 nm en fonction du temps d'irradiation: (*a*) cas des chlorométhanes; (*b*) cas des alcools.

TABLEAU 2. Rendements quantiques de photodegredation de la colchine dans différents solvants

Solvant	Concentration (*M*)	$I_{abs} \times 10^{14}$ (quanta s^{-1} cm^{-2})	Φ(Colc.) (±10%)	$\mu \times 10^{19}$ (u.e.s. c.g.s.)
CCl_4	5×10^{-5}	1.01	0.11	0
$CHCl_3$	"	1.12	0.050	10.2
CH_2Cl_2	"	1.07	0.030	15.4
H_2O*	"	1.21	0.003_5	18.5
MeOH	"	1.22	0.020	17.0
PrOH	"	1.23	0.037	16.9
i-PrOH	"	1.14	0.037	16.7
C_6H_6	"	1.02	0.016	0
$HCONH_2$	"	0.32	0.016	
$HCON(Me)_2$	"	0.18	0.030	

*En ce qui a trait à la *N*-méthyl,*N*-désacétyl colchicine, Aronson et Inoué (4) avaient trouvé comme rendement quantique de dégradation: $\Phi = 3 \times 10^{-3}$ dans l'eau; $\Phi \simeq 36 \times 10^{-3}$ dans le *n*-butanol. Ces résultats sont très voisins des nôtres.

essentiellement due au fait que dans le formamide, le doublet électronique libre sur l'atome d'azote est beaucoup plus disponible donc du même coup, beaucoup plus apte à ériger un ou plusieurs ponts hydrogène avec la molécule de colchicine. Le complexe colchicine–formamide serait donc beaucoup plus stable à cause de ces liaisons hydrogène et inhiberait la photoisomérisation de la colchicine.

L'établissement de ponts hydrogène entre la colchicine et le solvant pourrait très bien expliquer l'action antimitotique de la substance.

Par contre, le cas du benzène est marginal: si l'on s'en tient à la valeur du moment dipolaire des molécules de solvant, le benzène devrait donner à peu près le même résultat que le tétrachlorure de carbone. Or il n'en est rien et il se pourrait bien que dans ce cas on assiste à un

Can. J. Chem. Downloaded from www.nrcresearchpress.com by 210.87.254.42 on 09/05/12
For personal use only.

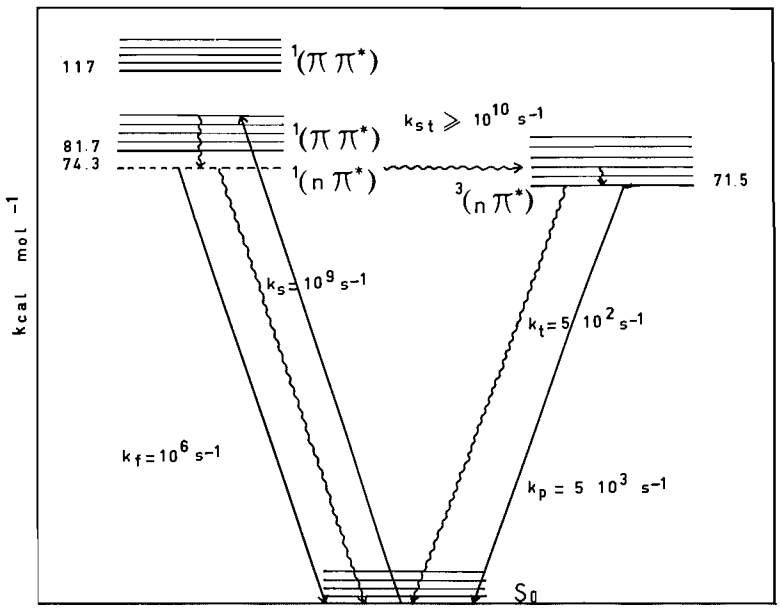

FIG. 3. Diagramme de Jablonski. (→) processus radiatif; (⇝) processus non radiatif.

transfert de charge qui diminuerait du même coup la photodégradation de la colchicine.

Autres effets

Des essais préliminaires sur quelques solutions portent à croire qu'un effet de concentration existe, surtout dans l'isopropanol. En effet le rendement quantique de photodégradation augmente proportionnellement avec la concentration. Or quand on sait que l'isopropanol est le solvant le plus apte à donner lieu à une réaction secondaire d'abstraction d'hydrogène en présence d'une fonction cétone (21), on conçoit donc qu'un tel effet soit tout à fait normal avec la colchicine qui possède aussi un groupement cétone sur le cycle tropolone.

Des études en ce sens sont actuellement en cours avec parallèlement des essais sur l'effet d'intensité, de la longueur d'onde d'irradiation, et aussi de p*H* (27).

Diagramme de Jablonski

Les processus photophysiques les plus importants que subit la colchicine, peuvent se résumer dans les étapes suivantes:

$$(\text{Colc.})_{S_0} + \text{solvant} \rightarrow (\text{complexe})_{S_0}$$

$$(\text{complexe})_{S_0} + h\nu \rightarrow (\text{complexe})^*_{S_n}$$

$$(\text{complexe})^*_{S_n} \rightarrow (\text{Colc.})_{S_0} + \text{solvant}$$

$$(\text{complexe})^*_{S_n} \rightarrow (\text{Colc.})^*_{S_1} + \text{solvant}$$

$$(\text{Colc.})^*_{S_1} \rightarrow (\text{Colc.})^*_{T_1}$$

$$(\text{Colc.})^*_{T_1} \rightarrow (\text{Colc.})_{S_0} + h\nu'$$

$$(\text{Colc.})^*_{S_1, T_1} \rightarrow \text{photoproduits}$$

Le complexe solvant–colchicine absorbe un photon, ce qui le conduit à un état excité S_n. Suite à cette absorption, le processus de conversion interne du complexe libère la molécule de colchicine qui demeure à l'état excité $^1(n\pi^*)$. A partir de S_1, aucune désactivation radiative n'est observée. Par contre la constante de conversion interne k_s, correspondant à une désactivation thermique $S_1 \rightarrow S_0$ est calculée théoriquement (28) $k_s = 10^9\ s^{-1}$.

Toujours à partir de S_1, on assiste à un croisement inter-système $S_1 \rightarrow T_1$ dont la constante de vitesse calculée théoriquement est égale à $k_{st} \geqslant 10^{10}\ s^{-1}$.

A partir de cet état triplet $^3(n\pi^*)$, il y a alors émission de phosphorescence (77 °K) avec $k_p = 5 \times 10^3\ s^{-1}$ (15).

Au sujet du processus photochimique qui conduit à l'isomérisation de la molécule, le mécanisme proposé par Chapman et coll. (29) relatif aux tropolones, ferait intervenir l'état triplet. Ceci reste cependant à vérifier dans le cas de la colchicine.

La transition la plus importante demeure le croisement inter-système $S_1 \rightarrow T_1$, ce qui signifie

Can. J. Chem. Downloaded from www.nrcresearchpress.com by 210.87.254.42 on 09/05/12
For personal use only.

que la plupart des molécules se retrouvent en T_1 après l'absorption d'un photon.

Tous ces processus sont schématisés sur le diagramme de la fig. 3.

En conclusion de cette étude photophysique de la colchicine, on peut affirmer que les résultats concernant le rendement quantique de photoisomérisation viennent corroborer ceux obtenus précédemment sur le rendement de phosphorescence. Ces deux processus primaires sont de loin les plus importants que subit la molécule et on s'aperçoit que la somme des deux rendements approche l'unité.

Nous tenons à exprimer notre gratitude au Conseil national de recherches du Canada ainsi qu'au Conseil de Recherches pour la Défense (# 9530-117) qui ont fourni l'apport financier à notre étude.

1. O. J. EIGSTI et P. DUSTIN. Colchicine in agriculture, medicine, biology and chemistry. Iowa State College Press, Ames, Iowa. 1955.
2. J. W. COOK et J. D. LOUDON. The alkaloids. Vol. II. Academic Press Inc., New York. 1952.
3. S. L. WALLACE et N. H. ERTEL. Bull. Rheum. Diseases, **20**, 582 (1969).
4. J. ARONSON et S. INOUÉ. J. Cell. Biol. **45**, 470 (1970).
5. J. H. MILLER et M. C. STEPHANI. Physiol. Plant. **24**, 264 (1971).
6. M. HÜBLER. Arch. Pharm. **171**, 205 (1865).
7. H. STRUVE. Z. Anal. Chem. **12**, 164 (1873).
8. C. JACOBI. Arch. Exp. Path. Pharmacol. **27**, 129 (1890).
9. D. I. MACHT. Science, **66**, 653 (1927).
10. R. GREWE. Naturwiss. **33**, 187 (1946).
11. F. ŠANTAVÝ. Coll. Czech. Chem. Commun. **16**, 655 (1951).
12. R. GREWE et W. WULF. Chem. Ber. **84**, 621 (1951).
13. O. A. NEUMÜLLER, H. J. KUHN, G. O. SCHENCK, et F. ŠANTAVÝ. Liebigs Ann. Chem. **674**, 122 (1964).
14. N. H. ERTEL et S. L. WALLACE. Biochem. Med. **4**, 181 (1970).
15. H. ROIGT et R. M. LEBLANC. Can. J. Chem. **50**, 1959 (1972).
16. C. G. HATCHARD et C. A. PARKER. Proc. R. Soc. London, A, **235**, 518 (1958).
17. A. D. CROSS, J. HRBEK, JR., J. L. KAUL, et F. ŠANTAVÝ. Festshrift Kurt Mothes zum 65, Geburtstag, Veb. Gustav. Fisher Verlag Jena. 1965.
18. F. ŠANTAVÝ. Publ. Fac. Med. Brno, **19**, 149 (1946).
19. F. ŠANTAVÝ. Collect. Czech. Chem. Commun. **14**, 145 (1949).
20. F. ŠANTAVÝ et T. REICHSTEIN. Helv. Chim. Acta, **33**, 1606 (1950).
21. A. A. LAMOLA et M. J. TURRO. Energy transfer and organic photochemistry. Interscience Publishers, New York. 1969.
22. E. GILMORE, G. GIBSON, et D. MCLURE. J. Chem. Phys. **20**, 829 (1952).
23. E. GILMORE, G. GIBSON, et D. MCLURE. J. Chem. Phys. **23**, 399 (1955).
24. C. A. PARKER and C. G. HATCHARD. Analyst, **87**, 644 (1962).
25. C. A. PARKER et W. T. REES. Analyst, **85**, 587 (1960).
26. G. O. SCHENCK, H. J. KUHN, et O. A. NEUMÜLLER. Tetrahedron Lett. **12** (1961).
27. R. M. LEBLANC et coll. En préparation.
28. N. J. TURRO. Molecular photochemistry. W. A. Benjamin Inc., New York. 1967.
29. W. G. DAUBEN, K. KOCH, O. L. CHAPMAN, et S. L. SMITH. J. Am. Chem. Soc. **83**, 1768 (1961).

Can. J. Chem. Downloaded from www.nrcresearchpress.com by 210.87.254.42 on 09/05/12
For personal use only.

The Synthesis of Miserotoxin and Structural Analogs[1]

HANS H. BAER, SHUET-HING LEE CHIU, AND DOUGLAS C. SHIELDS
Department of Chemistry, University of Ottawa, Ottawa, Canada K1N 6N5

Received February 21, 1973

The condensation of 2,3,4,6-tetra-*O*-acetyl-α-D-glucopyranosyl bromide with a variety of nitro alcohols led to nitroalkyl β-D-glucopyranoside tetraacetates. The following nitro alcohols were employed: 3-nitro-1-propanol, 2-nitro-1-propanol, 1-nitro-2-propanol, 2-nitro-1-butanol, 2-nitro-3-pentanol, and 2-methyl-2-nitro-1-propanol. The free 3-nitropropyl and 2-methyl-2-nitropropyl glycosides were obtained from their tetraacetates by deacetylation with sodium methoxide, whereas methanolysis catalyzed by methyl *p*-toluenesulfonate was employed for deacetylation of the other tetraacetates. Evidence for the presence of epimers in glycosides having a chiral center in the aglycon was obtained. Physical data of synthetic 3-nitropropyl β-D-glucopyranoside agreed with those of miserotoxin, the poisonous principle recently isolated from *Astragalus miser* varieties.

La condensation du bromure de tétra-*O*-acétyl-2,3,4,6 α-D-glucopyranosyl avec plusieurs nitro alcools a conduit aux tétraacétates de nitroalcoyl du β-D-glucopyranosides. On a employé les nitro alcools qui suivent: nitro-3 propanol-1, nitro-2 propanol-1, nitro-1 propanol-2, nitro-2 butanol-1, nitro-2 pentanol-3, et méthyl-2 nitro-2 propanol-1. Les nitropropyl-3 et méthyl-2 nitropropyl-2 glycosides libres ont été obtenus à partir de leur tétraacétates par déacétylation par le méthylate de sodium, alors que la méthanolyse catalysée par le *p*-toluènesulfonate de méthyle a été utilisée pour la déacétylation des autres tétraacétates. On a mis en évidence la présence d'épimères dans les glycosides possédant un centre chiral dans l'aglycon. Des données physiques pour le nitropropyl-3 β-D-glucopyranoside sont en accord avec celles de la miserotoxine, l'entité toxique récemment isolée des variétés d'*Astragalus miser*.

[Traduit par le journal]

Can. J. Chem., 51, 2828 (1973)

Certain varieties of timber milkvetch (*Astragalus miser*), a plant indigenous to the western regions of North America, contain a poison that may cause illness or death in livestock feeding in areas infested with the plant (1–7). The poisonous principle, which has been named miserotoxin, was isolated by Stermitz, Norris, and Williams (8) who adduced spectral and chemical evidence for its structure as 3-nitropropyl β-D-glucopyranoside (**1**). In continuation of our studies (9) on applications of the Koenigs–Knorr reaction to nitro glycoside syntheses, we decided to attempt a synthesis of **1**, which would corroborate the structural assignment of the natural product and, furthermore, we undertook to synthesize a number of β-D-glucopyranosides containing various other nitroalkyl groups as aglycons. It was thought that possession of such structural analogs might be valuable in biochemical and toxicological research bearing on the problem of miserotoxin. It is noteworthy that no simple nitroalkyl glycosides have thus far been reported in the literature, with the exception of 2-nitroethyl β-D-glucopyranoside tetraacetate (10). Attempted deacetylation of this compound led to cleavage of the glycosidic bond.

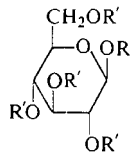

1 –**6** R′ = H
1*a*–**6***a* R′ = Ac

1,**1***a* R = $-CH_2CH_2CH_2NO_2$

2,**2***a* R = $-CH_2\underset{\displaystyle NO_2}{\underset{|}{C}}HCH_3$

3,**3***a* R = $-\underset{\displaystyle CH_3}{\underset{|}{C}}HCH_2NO_2$

5,**5***a* R = $-\underset{\displaystyle CH_2CH_3}{\underset{|}{\overset{\displaystyle NO_2}{\overset{|}{C}}}}HCH_3$

4,**4***a* R = $-CH_2\underset{\displaystyle NO_2}{\underset{|}{C}}HCH_2CH_3$

6,**6***a* R = $-CH_2\underset{\displaystyle CH_3}{\underset{|}{C}}HCH_3$

Condensation of 2,3,4,6-tetra-*O*-acetyl-α-D-glucopyranosyl bromide (α-acetobromoglucose, (**7**)) with 3-nitro-1-propanol in chloroform in the presence of silver oxide afforded crystalline 3-nitropropyl 2,3,4,6-tetra-*O*-acetyl-β-D-glucopyranoside (**1***a*) in 46% yield. It is well known and

[1]Presented at the 8th International Symposium on the Chemistry of Natural Products, New Delhi, February, 1972. Miserotoxin was synthesized by D.C.S. (M.Sc. Thesis, University of Ottawa, 1970) and its analogs by S.H.L.C. (Ph.D. Thesis, University of Ottawa, 1971).

generally accepted that the Koenigs–Knorr reaction of **7**, when carried out in the normal manner, results in inversion of the anomeric configuration to give β-D-glucosides (11). The optical rotation and n.m.r. data of **1***a* were in full accord therewith (see Experimental). Deacetylation of **1***a* with sodium methoxide gave in 90% yield analytically pure but amorphous **1**. Its optical rotation and spectral data agreed with this structure and with data recorded (8) for natural miserotoxin.[2] Toxicity tests on chickens showed that synthetic **1** corresponded in its activity to milkvetch extracts.[3]

Next, we synthesized the nitroalkyl β-D-glucopyranosides **2**–**6**, where the 2-nitropropyl, 1-methyl-2-nitroethyl, 2-nitrobutyl, 1-ethyl-2-nitropropyl, and 2-methyl-2-nitropropyl groups served as aglycons. The selection of nitroalcohols to be condensed with α-acetobromoglucose thus represented primary and secondary alcohols as well as primary, secondary, and tertiary nitro compounds. It had to be considered that, with the exception of the tertiary nitro compound **6**, the glycosides to be synthesized would be sensitive towards base, a fact which had to be taken into account in the conduct of operations. Compounds **2**–**5** all are β-nitroalkyl acetals that are capable of anion formation at the nitro group and consequently are prone to eliminative cleavage of the glycoside bond (12, 13; see also later on). Performance of the Koenigs–Knorr condensation by use of the efficient, but strongly basic, condensing agent silver oxide therefore was deemed inadvisable. Silver carbonate appeared less objectionable in this respect, but due to its lower reactivity the condensations, especially those with secondary alcohols, were expected to require more time so that the advantage of reduced basicity was feared to be offset by a prolonged exposure of the product to the agent. In fact, exploratory experiments using either condensing agent proved unsatisfactory. However, good results were obtained when a combination of silver carbonate and silver perchlorate was used, an improved variant in the customary Koenigs–Knorr conditions first recommended by Wolfrom and co-workers (14) and occasionally employed by others (15). Its efficiency is based on the fact that the rate-determining dissociation of the glycosyl halide becomes a homogeneous-phase reaction in the presence of soluble silver perchlorate. Perchloric acid produced upon alcoholysis of intermediary glycosyl perchlorate is then neutralized by silver carbonate, thus regenerating silver perchlorate of which, for this reason, a catalytic amount only is needed (14). Nevertheless, in some of our cases, we observed smoother reaction when a stoichiometric amount was employed. Yields and physical constants of the nitroalkyl β-D-glucopyranoside tetraacetates **2***a*–**6***a* obtained are indicated in Table 1.

The 2-nitropropyl glycoside **2***a* theoretically is capable of existing in two diastereoisomeric forms due to epimerism at the nitromethine carbon. Since racemic 2-nitro-1-propanol was used in the synthesis, the formation of such epimers was expected and, indeed, the crystalline analytical sample (m.p. 135–137°) consisted of two components in approximately equal proportions as was revealed by its n.m.r. spectrum. Thus, the signal of the aglycon methyl group consisted of two doublets, δ 1.46 and 1.60, each having a spacing of 7 Hz. At low field, the signal attributable to the anomeric proton was also a pair of doublets (δ 4.48 and 4.53); each had a spacing of 7.5 Hz which indicated 1,2-diaxial proton orientation and hence the β-configuration for both components. The components were indistinguishable chromatographically, and no attempts at separation were made. Products having somewhat lower melting points (*e.g.*, 125–127°) were obtained in some runs, and these might have differed in epimer ratio. However, the problem was not investigated further in this case.

Similar observations were made in syntheses with 1-nitro-2-propanol. Preparations of 1-methyl-2-nitroethyl β-D-glucopyranoside tetraacetate (**3***a*) varying in their melting points were obtained, and in this instance, a more detailed study was made. From n.m.r. spectra it became evident that mixtures differing in epimer composition had arisen. One such (crystalline) mixture (**3***a*$_1$) was isolated in 35% yield when the condensation of **7** was performed as usual in chloroform solution in the presence of silver car-

[2]One minor discrepancy was in the asymmetric nitro vibration in the i.r., which we observed at ν_{max} 1545 cm^{-1}, that is, in the usual range for nitroalkane groups, whereas Stermitz and coworkers (8) reported ν_{max} 1520 cm^{-1}. The latter value probably is erroneous as it appears too low for a primary aliphatic nitro moiety.

In an attempt to prepare the tetraacetate **1***a* by acetylation of **1** with acetic anhydride and sodium acetate (reaction conditions not stated), the authors (8) obtained a hexaacetyl derivative whose aglycon they formulated as an *N,O*-diacetyl hydroxamic acid. We were unable to prepare such a product from synthetic **1**.

[3]Details to be published elsewhere.

TABLE 1. Nitroalkyl β-D-glucopyranosides

Tetraacetate	m.p. (°C)	$[\alpha]_D$ (in chloroform)	Yield (%) (based on alcohol)	Free glycoside	M.p. (°C)	$[\alpha]_D$ (in methanol)	Yield (%)
1*a*	116	− 4.8	42	**1**		−24.0 (H_2O)	90
2*a*	135–137	−18.4	43	**2**	115–117	−12.3	65
3*a*$_1$	128–129	−14.6	35	**3**		−18.3	56
3*a*$_2$	139–142	−17.2	18				
4*a*	86–88	−18.8	42	**4**	144–145	−22.0	81
5*a*$_1$	125–126	−19.6	50	**5**		−28.6	61
5*a*$_2$	136–139	−21.6	16				
6*a*	158–159	−20.1	40	**6**	141–142	−23.3	81

bonate and a relatively small amount of silver perchlorate. The epimeric components present showed a chemical shift difference in their aglycon methyl signals such that the two doublets overlapped to give a nearly symmetrical triplet (J = 6 Hz). In the region of δ 4.3–4.6 there occurred two quartets assignable to the nitromethyl group protons of two epimeric components, and two nearly coinciding doublets for the anomeric protons. Both of these doublets had a 7.5 Hz spacing, which precludes the contingency of α,β-anomerism. Condensation in the presence of an increased amount of perchlorate under otherwise unchanged conditions led to isolation of **3***a*$_1$ and, in addition, a higher-melting product **3***a*$_2$. The latter was the sole product isolated when the nitro alcohol was allowed to react with silver perchlorate as condensing agent but in the absence of silver carbonate. The yield was low (18%) under these conditions as might be expected in view of the absence of an acid scavenger.[4] The specific rotation of **3***a*$_2$ was very similar to that of **3***a*$_1$, and its n.m.r. spectrum suggested that aglycon epimers were present in a different ratio.

The n.m.r. spectrum of the 2-nitrobutyl glycoside tetraacetate **4***a* (m.p. 86–88°) showed no evidence for the existence of epimers although aglycon epimerism should be possible in this structure, too. However, samples varying somewhat in their melting points were obtained in different runs, and in one instance (which could not be reproduced) a crop melting at 99–103° was isolated; this might be an indication that epimers were present. Perhaps, in the analytical sample a single epimer had crystallized fortuitously, or else it contained epimers which were not differentiated spectroscopically.

With silver perchlorate and silver carbonate, the condensation of 2-methyl-3-pentanol led to a 1-ethyl-2-nitropropyl glycoside tetraacetate **5***a*$_1$ of m.p. 125–126°. Condensation promoted by mercuric cyanide in 1,2-dichloroethane solution was also tried with this alcohol, and a pure glycoside (**5***a*$_2$) of m.p. 136–139° was isolated. The mercuric cyanide method (17) is widely employed in glycoside synthesis (18) although it may entail complications due to incorporation of cyanide in the sugar (19).[5] As a consequence of the presence of two asymmetric centers in the aglycon of **5***a*, four diastereoisomers of this structure could have arisen. The n.m.r. spectra of the products **5***a*$_1$ and **5***a*$_2$ were difficult to analyze, especially since signals of sugar ring protons at C-1 and -6, and aglycon protons at C-1′ and -2′, were crowded together in the δ 4–5 region. However, in both spectra the signals at highest field (δ 0.9 approximately), which were due to the methyl part of the aglycon ethyl group, appeared as double triplets. Similarly, the anomeric proton signal, which at least in **5***a*$_2$ was clearly recognizable at δ 4.47, had the character of two (nearly coinciding) doublets with J = 7.5 Hz. These features suggested that the products were mixtures of diastereoisomeric β-D-glucosides.

No complications from aglycon epimerism were to be expected in the 2-methyl-2-nitropropyl derivative **6***a*. The n.m.r. spectrum of the product was readily interpretable in terms of the assigned structure.

[4]Silver perchlorate in nitromethane solution was introduced by Bredereck *et al.* (16) as a reagent capable of promoting glycosyl substitution on trityl ethers. In that case, insoluble trityl perchlorate is formed instead of perchloric acid, and acidity is not a problem.

[5]An unidentified by-product was present in our crude reaction mixture. When the condensation was carried out under the original Helferich conditions (17), namely in nitromethane as solvent, a substantial amount of what appeared to be an α-glycoside was formed along with **5***a*.

For the reason of alkali lability of the glycosidic bond referred to earlier, the customary de-*O*-acetylation procedure using sodium methoxide could be employed with **6***a* only, to which this limitation does not apply and which readily gave the deacetylated glycoside **6** in high yield. As far as the remaining tetraacetates were concerned, the facile cleavability by methoxide of β-nitroalkyl glycosides, earlier observed in 2-nitroethyl β-D-glucopyranoside (10), was confirmed on the example of **2***a*: deacetylation was accompanied by rapid cleavage of the glycosidic bond so that, after a few minutes, no **2** survived. Consequently, we had to resort to acid-catalyzed deacetylation as we had done in related cases (20) where the problem was deacetylation of hexopyranosides that possessed an activating nitro group at C-6 (*i.e.*, also in β-position to an acetal oxygen atom). The mild conditions of methanolysis in the presence of methyl *p*-toluenesulfonate permitted the removal of the acetyl groups with only a tolerable degree of concurrent transglycosylation. The minor by-product, methyl α-D-glucopyranoside, as well as traces of incompletely deacetylated materials, if present, were separated chromatographically, and the glycosides **2**–**5** were isolated in good yields (Table 1). They had retained the β-configuration as was indicated by spectral and polarimetric data.

No evidence was obtained for the isolated, crystalline product **2** to contain aglycon epimers although its acetate **2***a* had been found to be an epimeric mixture. One must assume either that the n.m.r. spectrum did not reveal epimers although they were present, or that in fact a single species had crystallized. The 1-methyl-2-nitroethyl glycoside **3**, which was obtained as a chromatographically pure syrup, was clearly demonstrated to consist of diastereoisomers. Its high-field signal, centered at δ 1.30 and attributable to the aglycon *C*—CH_3 group, was a pair of overlapping doublets (J = 6.5 Hz in each), and the same was true for the anomeric proton signal near δ 4.4 ($J_{1,2}$ = 7.5 Hz in each). In the spectrum of the crystalline 2-nitrobutyl glycoside **4**, on the other hand, no signal multiplicities that could be ascribed to different epimers were detected, and it is recalled that the tetraacetate **4***a* had appeared uniform also. The deacetylated glycoside **5** was a syrup. Its n.m.r. signal at highest field (centered near δ 1.0), which was assigned to the methyl portion of the aglycon ethyl group, consisted of two overlapping triplets indicating the presence of epimers.

The glycosides **2**–**6** were submitted to toxicological tests in chickens where, in comparison with miserotoxin, **3** and **5** showed similar and **2** and **4** showed enhanced toxicity while **6** had no effect.[3]

Experimental

General Methods

Melting points were taken in capillaries in an electrically heated aluminum block equipped with a calibrated thermometer. Evaporations were carried out under reduced pressure at about 35° (bath temperature). All reactions were monitored by t.l.c. on silica gel G; the spots were made visible by heating the plates sprayed with 1% ceric sulfate in 10% sulfuric acid. For column chromatography, silica gel 7734 (70–325 mesh) of E. Merck AG, Darmstadt, was used. In addition to solvent combinations mentioned in the text, the following systems (volume ratios) were frequently employed for chromatography: A, carbon tetrachloride – ethyl acetate (2:1); B, ethyl acetate – methanol (5:1); C, 10% acetone in benzene; D, 15% acetone in benzene; E, 20% acetone in benzene; F, 10% ethanol in benzene; G, 20% ethanol in benzene; H, 30% ethanol in benzene.

I.r. spectra were routinely taken from all starting materials and reaction products, and were in every respect compatible with the constitutions. All primary and secondary nitro compounds exhibited strong bands at 1550 ± 5 cm^{-1} (asymmetric NO_2 stretching vibration); in the tertiary nitro compounds **6**, **6***a*, and 2-methyl-2-nitro-1-propanol this band occurred at 1535 cm^{-1}.

Optical rotations were measured at room temperature in a Perkin-Elmer 141 automatic polarimeter.

N.m.r. data were obtained on a Varian HA-100 instrument except for those of the starting nitro alcohols which were recorded on a T-60 instrument. Unless otherwise stated, tetramethylsilane was used as internal standard.

Materials

3-Nitro-1-propanol

This compound was obtained in 71% yield from redistilled, commercial 3-bromo-1-propanol (Eastman Kodak Co., Rochester, N.Y.) and silver nitrite in anhydrous ether by the Victor Meyer reaction (21). The n.m.r. data (in $CDCl_3$) of the distilled, colorless liquid: δ 2.23 (2H, quintet); 2.52 (singlet, OH); 3.74 (2H, triplet); 4.53 (2H, triplet).

2-Nitro-1-propanol

This compound was prepared by Henry addition of formaldehyde (37% aqueous solution) to nitroethane in ethanol, in the presence of strongly basic anion exchange resin Amberlite IRA-401(OH^-), essentially according to the procedure of Astle and Abbot (22). The yield of distilled product was 61%. The n.m.r. data (in $CDCl_3$): δ 1.37 (3H, doublet, *C*—CH_3); 3.07 (1H, singlet, exchangeable with D_2O, OH); 3.95 (2H, doublet, O—CH_2—); 4.69 (1H, sextet, —$CH(NO_2)$—).

1-Nitro-2-propanol

This compound was obtained in similar manner from acetaldehyde and nitromethane in 45% yield (22). The

n.m.r. data (in $CDCl_3$); δ 1.35 (3H, doublet, *C*—CH_3); 3.20 (1H, doublet, exchangeable with D_2O, OH); 4.30–4.80 (3H, overlapping multiplets, O_2N—CH_2— and —*CH*(OH)—).

2-Nitro-1-butanol

The commercial product of J. T. Baker Chemical Co. was used after redistillation *in vacuo*.

2-Nitro-3-pentanol

This compound was prepared in 59% yield from propionaldehyde and nitroethane (22). The n.m.r. data (in $CDCl_3$): δ 1.00 (3H, triplet, C-5 methyl group), 1.50–1.70 (5H, overlapping multiplets, C-1 methyl and C-4 methylene groups); 2.90 (1H, broad doublet, exchangeable with D_2O, OH); 3.90 (1H, broad multiplet, C-3 proton); 4.60 (1H, multiplet, C-2 proton).

2-Methyl-2-nitro-1-propanol

Obtained in 24% yield from formaldehyde and 2-nitropropane (22), this nitro alcohol crystallized from benzene in colorless needles, m.p. 87–89.5°. The n.m.r. data (in $CDCl_3$): δ 1.58 (6H, singlet, $C(CH_3)_2$); 2.47 (1H, triplet, exchangeable with D_2O, OH); 3.90 (2H, doublet, collapsing to singlet upon D_2O addition, O—CH_2—).

2,3,4,6-Tetra-O-acetyl-α-D-glucopyranosyl Bromide (7)

The glycosyl halide 7, m.p. 88–89° and $[\alpha]_D$ +198°(*c*, 2, chloroform), was prepared according to the literature (23).

Other Reagents, and General Reaction Conditions

Chloroform used as solvent in Koenigs–Knorr reactions was freed from ethanol and dried shortly before use (24). Reactive silver oxide (25) and silver carbonate (26) were freshly prepared. Anhydrous calcium sulfate (Drierite) was powdered and activated by heating in the oven at 240° for 2 h. Anhydrous silver perchlorate was used as commercially supplied. Although no untoward incidents occurred in this laboratory, a note of caution regarding a potential explosion hazard of this chemical (14) is here repeated. The condensation reactions of **7** with nitro alcohols were carried out at about 25° with vigorous magnetic stirring. The reaction mixture was protected from light and from access of atmospheric moisture. In spite of the use of Drierite as an internal desiccant, a certain amount of **7** inevitably suffered hydrolysis to produce tetra-*O*-acetyl-D-glucose (TAG). The presence of this by-product (which is common in such syntheses) was revealed by the t.l.c. using an authentic sample for comparison. In one case, the identity of TAG was ascertained following its isolation. Similarly, methyl α-D-glucopyranoside, which arose as a side-product in the acid-catalyzed methanolyses of **2***a*–**5***a*, was detected by its mobility on t.l.c. and was identified in one example following its chromatographic isolation.

3-Nitropropyl 2,3,4,6-Tetra-O-acetyl-β-D-glucopyranoside (1a)

3-Nitropropanol (1.65 g), silver oxide (7.0 g), and Drierite (8 g) were first stirred in chloroform (50 ml) for 30 min under a pure nitrogen atmosphere, and a solution of **7** (5.84 g) in chloroform (30 ml) was then added dropwise during the course of 2 h. Stirring was continued for 1 h. The reaction mixture was filtered through sintered glass, the residue washed well with chloroform, and the filtrate evaporated to yield a pale-yellow oil (7.1 g). The oil, which showed two major spots (the slower one corresponding to TAG) as well as several minor spots on t.l.c. with solvent A, was applied to a silica gel column (500 g). Elution with carbon tetrachloride – ethyl acetate (7:4) and evaporation of the fractions that contained only the faster-moving main product furnished virtually pure **1***a* as a colorless substance (2.86 g, 46%, based on **7**). Crystallization from ethanol gave beautiful leaflets, m.p. 116°, $[\alpha]_D$ −4.8° (*c*, 0.5, chloroform). The n.m.r. data (in $CDCl_3$): δ 1.99, 2.01, 2.06, 2.08 (12H, singlets, *O*-acetyl); 2.26 (2H, quintet, aglycon C-2 methylene); 3.7 and 4.0 (2H and 1H multiplets due to H-5 and aglycon O—CH_2); 4.2 (2H, H-6,6′); 4.46 (2H, symmetric triplet, J = 6.5 Hz, aglycon C-3 methylene); 4.49 (1H, doublet, $J_{1,2}$ = 8 Hz, H-1. The lower-field line nearly coincided with the lower-field line of the nitromethylene triplet, and the higher-field line was 1.5 Hz beside the center line of the latter, as seen at 250 Hz sweep width); δ 5-region (3H, partially overlapping signals with large splittings, H-2, -3, -4).

Anal. Calcd. for $C_{17}H_{25}NO_{12}$ (435.4): C, 46.89; H, 5.79; N, 3.22. Found: C, 46.77; H, 5.93; N, 3.12.

3-Nitropropyl β-D-Glucopyranoside (1)

To **1***a* (1.63 g) in anhydrous methanol (25 ml) was added 0.1 *N* sodium methoxide solution (10 ml). After 5 h at room temperature the solution was deionized with cation exchanges and evaporated to give a slightly yellow gel (1.1 g) which on t.l.c. with solvent B showed one major spot (**1**) and a more slowly moving minor spot. Separation on a silica gel column (100 g) using solvent B furnished pure **1** which failed to crystallize. Upon drying *in vacuo* it was a cream-colored powder (900 mg, 90%); $[\alpha]_D$ −24.0° (*c*, 2, water). Reported for miserotoxin (8), $[\alpha]_D$ −22.0° (water). I.r. bands were at 3350 (broad, OH), 2880 (broad), 1545 and 1380 (strong, asymmetric and symmetric NO_2 vibrations), 1425, 1350, 1160, 1050, 890 cm^{-1}. The n.m.r. spectrum in acetone-d_6 showed at lowest field a 2-proton triplet (δ 4.65, J = 7 Hz) and at highest field (δ 2.27) a 2-proton quintet, which were due to the aglycon C-3 and -2 methylene groups, respectively. Upon addition of D_2O, these signals were slightly shifted (δ 4.68 and 2.32). The DOH peak, which partially obscured the anomeric proton signal, could be displaced downfield by addition of DCl, and the H-1 signal was then revealed as a clear doublet ($J_{1,2}$ = 7.5 Hz) at δ 4.44. The remaining protons all resonated in the range δ 3.1–4.2 and were not amenable to ready analysis. Data (60 MHz) reported for miserotoxin (8) were in essential agreement with those given here.

Anal. Calcd. for $C_9H_{17}NO_8$ (267.2): C, 40.45; H, 6.41; N, 5.24. Found: C, 40.50; H, 6.47; N, 5.25.

2-Nitropropyl 2,3,4,6-Tetra-O-acetyl-β-D-glucopyranoside (2a)

A mixture of 2-nitro-1-propanol (1.49 g), silver carbonate (3.26 g), silver perchlorate (2.46 g), powdered Drierite (8 g), and chloroform (50 ml) was stirred for 30 min, and solid **7** (8.7 g) was then introduced in 3 portions in 10 min intervals. After 30 min, further quantities of silver carbonate (0.4 g) and silver perchlorate (0.1 g) were added, and after another 30 min an extra amount of **7** (0.8 g) was added. The reaction mixture was worked up 2 h after the introduction of the first portion of **7**. T.l.c. with solvent E indicated the presence of **2***a* (R_f 0.70) and TAG (R_f 0.48) in the pale-yellow syrup (9.85 g) obtained upon evaporation of the solvent. Chromatography as

described for **1***a* but with benzene (100 ml), solvent C (200 ml), and solvent E (1500 ml) as eluants furnished **2***a* (2.65 g, 42.8%) as a syrup that crystallized (m.p. 124–127°) on trituration with absolute ethanol. Recrystallization from absolute ethanol – petroleum ether gave colorless prisms, m.p. 135–137°, $[\alpha]_D$ −18.4° (*c*, 1, chloroform), ν_{max} 1750 and 1550 cm^{-1}. The n.m.r. data (in $CDCl_3$): δ 1.46, 1.50 (3H, two overlapping doublets, J = 7 Hz, aglycon *C*—CH_3); 1.97, 1.99, 1.99, 2.06 (12H, s, *O*-acetyl); 3.7 (1H, m, H-5); 3.85–4.30 (4H, partially overlapping quartets of aglycon *O*—CH_2 and H-6,6′); 4.48, 4.53 (1H, two doublets, J = 7.5 Hz, H-1), 4.75 (1H, broad multiplet, aglycon —$CHNO_2$); δ 5-region (3H, m, H-2, -3, -4).

Anal. Calcd. for $C_{17}H_{25}NO_{12}$ (435.4): C, 46.89; H, 5.79; N, 3.22. Found: C, 47.03; H, 5.97; N, 3.03.

From subsequent fractions the less mobile product was isolated in crystalline form and identified as TAG by its m.p. (129–131°) and n.m.r. spectrum.

2-Nitropropyl β-D-*Glucopyranoside (2)*

Anhydrous methanol (30 ml) containing **2***a* (1.67 g) and freshly distilled methyl *p*-toluenesulfonate (55 mg) was refluxed with exclusion of atmospheric moisture. The progress of methanolysis was monitored by t.l.c. (solvent H), and the reaction was stopped after 29 h when the major product (R_f 0.35) gave a strong spot and the spot of a by-product (R_f 0.25) still was quite faint. (Pilot runs had shown that the latter tends to increase with time.) The syrup (1.15 g) obtained upon solvent evaporation was chromatographed on a silica gel column (60 g) by use of solvent G. Good separation was achieved, the fractions showing the spot of R_f 0.35 yielding a pure syrup of **2** (668 mg, 65%). Crystallization occurred from a minimal volume of dry methanol upon careful addition of ether and prolonged cooling. The rosette-shaped crystals exhibited m.p. 115–117°, $[\alpha]_D$ −12.3° (*c*, 1, methanol). The n.m.r. data (in acetone-d_6 + D_2O): δ 1.49 (3H, doublet, J = 7 Hz, aglycon *C*—CH_3); 3.2–4 (unresolved signals of sugar ring protons and DOH); 4.12 (center of 2H multiplet, aglycon OCH_2); 4.36 (1H, doublet, J = 7.5 Hz, H-1); 4.94 (1H, multiplet, aglycon $CHNO_2$).

Anal. Calcd. for $C_9H_{17}NO_8$ (267.2): C, 40.45; H, 6.41; N, 5.24. Found: C, 40.26; H, 6.58; N, 5.09.

From subsequent fractions of the column the minor product of R_f 0.25 was isolated. It crystallized readily (m.p. 163–165°) and was identified as methyl α-D-glucopyranoside by spectral and polarimetric comparison with an authentic sample.

*1-Methyl-2-nitroethyl 2,3,4,6-Tetra-O-acetyl-*β-D-*glucopyranoside (3a)*

Lower-melting Product (3a₁)

1-Nitro-2-propanol (1.01 g), silver carbonate (1.51 g), silver perchlorate (0.31 g), Drierite (14 g), and chloroform (50 ml) were stirred together for 30 min. A solution of **7** (3.76 g) in chloroform (50 ml) was then added dropwise in the course of 15 min, and another 0.50 g of **7** in chloroform was added after 2 h. The reaction was allowed to proceed for another 2 h. The inorganic material was filtered off and washed with chloroform, and the filtrate was evaporated to give a yellow syrup (4.8 g). Relatively rapid passage of this syrup through a silica gel column (150 g) with solvent E accomplished a partial separation of the nitro glycoside from more slowly moving TAG. The combined fractions containing the glycoside gave a syrup (3.93 g) which was still strongly contaminated by TAG. A second, similar chromatography was therefore performed, and this resulted in isolation of nearly pure **3***a*₁ (1.464 g, 35%) which crystallized on evaporation of the solvent, m.p. 123–129°. The m.p. was 127–128° after one, and 128–129° after a second, recrystallization from 99% ethanol. The melt was always turbid, clearing only above 130°. The specific rotation of the analytical sample was $[\alpha]_D$ −14.6° (*c*, 1, chloroform). The n.m.r. data (in $CDCl_3$): δ 1.27, 1.33 (3H, two doublets with J = 6 Hz (apparent triplet), aglycon *C*—CH_3); 1.96, 1.98, 1.98, 2.06 (12H, singlets, *O*-acetyl); 3.7 (1H, multiplet, H-5); 4.1–4.25 (2H, multiplet, H-6,6′); 4.34, 4.36 (two doublets, J = 7.5 Hz (apparent unsymmetric quartet), H-1; superimposed on broad multiplet of aglycon O—CH); 4.58 (midpoint of two quartets, aglycon CH_2NO_2); δ 5-region (3H, multiplets with large splittings, H-2, -3, -4).

Anal. Calcd. for $C_{17}H_{25}NO_{12}$ (435.4): C, 46.89; H, 5.79; N, 3.22. Found: C, 46.84; H, 5.73; N, 3.40.

A similar experiment was performed with 1-nitro-2-propanol (1.73 g), silver carbonate (3.5 g), silver perchlorate (2.73 g; note the relative increase), Drierite (15 g), and **7** (9.1 g) which was introduced as the solid in 5 portions in the course of 1.5 h. The total reaction time was 5.5 h. Chromatography on a 500-g silica gel column which was eluted with benzene (50 ml) followed by benzene–acetone – ethyl acetate (15:4:1) (1l) furnished a total of 3.78 g (52.7%) crude crystalline **3***a* in four fractions. Recrystallization from absolute ethanol gave 472 mg of **3***a*₂ (m.p. 137–140°; identified by n.m.r., see the next paragraph) from the first fraction and 1.47 g of **3***a*₁ (m.p. 123–130°) from the subsequent fractions (total 27%).

Higher-melting Product (3a₂)

1-Nitro-2-propanol (416 mg), silver perchlorate (810 mg), and Drierite (5 g) were stirred in dry nitromethane (35 ml) for 30 min, and **7** (1.63 g) was then added. After 3 h an additional 300 mg of silver perchlorate was added, and stirring was continued for 1 h. Solvent evaporation from the filtered reaction mixture gave a brown liquid (2.2 g) which was chromatographed on silica gel (115 g) with benzene (100 ml) and solvent E (600 ml). Early effluent fractions (35 ml) contained unreacted nitro alcohol (250 mg). Later fractions showing a single spot on t.l.c. were combined and gave syrupy **3***a*₂ which crystallized on trituration with ethanol. The yield was 307 mg (18%). Recrystallized from ethanol, the product showed m.p. 139–142° and $[\alpha]_D$ −17.2° (*c*, 0.7, chloroform). The n.m.r. data (in $CDCl_3$): similar to those of **3***a*₁ except that the aglycon *C*—CH_3 signal appeared as a strong doublet at δ 1.33 superimposed by a weak doublet at δ 1.27; furthermore, the multiplets in the δ 4.1–4.7 region contained fewer but broadened peaks.

Anal. Calcd. for $C_{17}H_{25}NO_{12}$ (435.4): C, 46.89; H, 5.79; N, 3.22. Found: C, 46.78; H, 5.78; N, 3.29.

1-Methyl-2-nitroethyl β-D-*Glucopyranoside (3)*

The tetraacetate **3***a*₁ (1.90 g) was refluxed for 20 h in anhydrous methanol (45 ml) containing methyl *p*-toluenesulfonate (65 mg). The reaction mixture was revealed by t.l.c. (solvent G) to contain a major product (R_f 0.35) as well as minor products that migrated faster (presumably incompletely deacetylated compounds) and more slowly (presumably methyl glucoside). Chromatographically

pure but syrupy **3** (0.49 g) was isolated by fractionation on a silica gel column (30 g) using solvents F, G, and H. Incompletely deacetylated material collected from fore-fractions was subjected to a second, similar methanolysis followed by chromatography, to give another crop of **3** (0.16 g). Thus, the total yield was 0.65 g (56%). The colorless syrup, $[\alpha]_D$ −18.3° (*c*, 1.1, methanol), could not be induced to crystallize. The n.m.r. data (in acetone-d_6): δ 1.3 (3H, overlapping doublets, J = 6.5 Hz, aglycon *C*—CH_3); 4.41, 4.44 (1H, two doublets, J = 7.5 Hz, H-1); 4.60 (2H, multiplet, aglycon CH_2NO_2).

Anal. Calcd. for $C_9H_{17}NO_8$ (267.2); C, 40.45; H, 6.41. Found: C, 40.84, H, 6.39.

2-Nitrobutyl 2,3,4,6-Tetra-O-acetyl-β-D-glucopyranoside (4a)

2-Nitro-1-butanol (1.15 g), silver carbonate (3.68 g), silver perchlorate (2.82 g), and Drierite (8 g) in chloroform (50 ml) were allowed to react with **7** (5.75 g) which was added in three portions in the course of 20 min. Stirring was then continued for another 90 min. The colorless oil (6.2 g) obtained on work-up was chromatographed on silica gel (250 g) by elution with benzene (100 ml) followed by benzene containing 8% acetone (100 ml), solvents C and D (100 ml each), and solvent E (500 ml). The fractions showing a single spot of the fastest moving product were combined and gave colorless **4***a* which solidified on trituration with absolute ethanol; yield, 1.852 g (42.6%). An analytical sample was recrystallized from ethanol, m.p. 86–88°, $[\alpha]_D$ −18.8° (*c*, 1.06, chloroform). The n.m.r. data (in $CDCl_3$): δ 0.97 (3H, triplet, J = 7 Hz, aglycon *C*—CH_3); 1.70 (2H, multiplet, aglycon C—CH_2—C); 1.97, 1.98, 2.02, 2.07 (12H, s, *O*-acetyl); 3.7 (1H, multiplet, H-5); 3.8–4.3 (4H, multiplets, aglycon *O*—CH_2 and H-6,6′); *ca.* 4.4 (1H, multiplet, aglycon $CHNO_2$); 4.53 (1H, doublet, J = 7.5 Hz, H-1); δ 5-region (3H, multiplets, H-2, -3, -4).

Anal. Calcd. for $C_{18}H_{27}NO_{12}$ (449.4): C, 48.10; H, 6.06; N, 3.12. Found: C, 48.05; H, 5.90; N, 3.04.

2-Nitrobutyl β-D-Glucopyranoside (4)

The tetraacetate **4***a* (1.30 g) was refluxed for 24 h in methanol (26 ml) containing methyl *p*-toluenesulfonate (52 mg). The solution, which then showed one major spot (R_f 0.35, compound **4**) and a faint spot (R_f 0.28 methyl glucoside) on t.l.c. with solvent H, was evaporated to give a colorless syrup. Purification of the syrup on a column of silica gel (80 g) by sequential elution with benzene (50 ml) and benzene containing increasing proportions (8–20%) of ethanol furnished chromatographically pure, partially crystalline **4** (660 mg, 81%). Recrystallization from a minimum volume of anhydrous methanol with addition of a few drops of ethyl acetate and ether gave colorless crystals of m.p. 130–132°, raised to 144–145° by further recrystallization; $[\alpha]_D$ −22° (*c*, 0.33, water). The n.m.r. data (in acetone-d_6 + D_2O): δ 0.91 (3H, triplet, aglycon *C*—CH_3); 1.86 (2H, quintet, aglycon C—CH_2—C); 4.1 (2H, multiplet, aglycon *O*—CH_2); 4.36 (1H, doublet J = 7.5 Hz, H-1); 4.80 (1H, multiplet, aglycon $CHNO_2$). The ring proton signals in the δ 3–4 region were not resolved.

Anal. Calcd. for $C_{10}H_{19}NO_8$ (281.3): C, 42.70; H, 6.81; N, 4.98. Found: C, 42.81; H, 6.63; N, 4.94.

1-Ethyl-2-nitropropyl 2,3,4,6-Tetra-O-acetyl-β-D-glucopyranoside (5a)

Lower-melting Product (5a$_1$)

2-Nitro-3-pentanol (2.03 g), silver carbonate (3.04 g), silver perchlorate (4.55 g), and Drierite (12 g) in chloroform (150 ml) were allowed to react with **7** (9.76 g) which was added to the mixture in 3 portions in 15 min intervals. After the addition, stirring was continued for 1 h. Work-up gave a pale-yellow oil (11 g) which was chromatographed on silica gel (500 g) using benzene (100 ml) and solvent G (1.6 l) as eluants. The fractions that showed a single spot (R_f 0.7) on t.l.c. were combined (250 ml) and afforded a pure syrup of **5***a*$_1$ that crystallized partially on drying (3.5 g, 50%). Additional nitro glycoside was contained along with TAG in subsequent fractions. Upon recrystallization from ethanol, **5***a*$_1$ melted at 125–126° and showed $[\alpha]_D$ −19.6° (*c*, 1, chloroform). The n.m.r. data (in $CDCl_3$): δ 0.92, 0.96 (3H, two overlapping triplets, J = 7 Hz, CH_3 of aglycon ethyl group); δ 1.5-region (5H, multiplet, CH_3 of aglycon nitropropyl and CH_2 of ethyl groups); 1.96–2.06 (12H, *O*-acetyl signals); 3.7 (1H, multiplet, H-5); 4.0–4.7 (5H, poorly resolved signals due to aglycon *O*—CH, H-6,6′ (δ 4.18), aglycon $CHNO_2$, H-1); δ 5-region (3H, multiplets, H-2, -3, -4).

Anal. Calcd. for $C_{19}H_{29}NO_{12}$ (463.4): C, 49.24; H, 6.31; N, 3.02. Found: C, 49.02; H, 6.20; N, 3.10.

Higher-melting Product (5a$_2$)

A mixture of 2-nitro-3-pentanol (0.55 g), powdered mercuric cyanide (2.07 g), Drierite (3 g), and **7** (3.38 g) in 1,2-dichloroethane (40 ml; dried by distillation from P_2O_5) was vigorously stirred for 30 h. The vessel was periodically flushed with nitrogen to remove accumulated hydrogen cyanide. The reaction mixture exhibited three spots on t.l.c. (benzene – ethyl acetate – ethanol, 15:4:1); the fastest and strongest spot (R_f 0.8) corresponded to **5***a*$_2$, the slowest to TAG, and the middle spot was not identified. The solution was diluted with chloroform and washed three times with water. The organic phase was dried (Na_2SO_4) and evaporated to give a yellow liquid (3.42 g). Column chromatography on silica gel (130 g) with the above solvent system, and rechromatography of mixed fractions on a smaller column, afforded about 0.80 g (42%) of nitro glycoside as a chromatographically uniform syrup of which 0.3 g crystallized from ethanol, m.p. 133–139°. An analytical sample was recrystallized from ethanol and then melted at 136–139°, the turbid melt clearing at 142°. $[\alpha]_D$ −21.6° (*c*, 1.2, chloroform). The i.r. spectrum was nearly identical with that of **5***a*$_1$. The n.m.r. data in $CDCl_3$ were very similar to those of **5***a*$_1$, with a pair of triplets at δ 0.92 and 0.95; *O*-acetyl signals at 1.95, 1.98, 2.02, and 2.03; and the H-1 signal as two nearly coinciding doublets centered at δ 4.47.

Anal. Calcd. for $C_{19}H_{29}NO_{12}$ (463.4): C, 49.24; H, 6.31; N, 3.02. Found: C, 49.08; H, 6.14; N, 3.28.

1-Ethyl-2-nitropropyl β-D-Glucopyranoside (5)

The tetraacetate **5***a*$_1$ (1.46 g) was refluxed for 45 h in methanol (30 ml) containing methyl *p*-toluenesulfonate (45 mg). The presence of one major spot (R_f 0.4) and 3 faint spots (R_f 0.7, 0.5, and 0.15) was then indicated by t.l.c. (solvent G). Upon removal of the methanol, the material was chromatographed on silica gel (60 g) with

solvent G. The fractions containing only main product, or main product contaminated by the less mobile by-product (methyl glucoside), were combined and rechromatographed in the same way. This resulted in isolation of **5** as a pure syrup (565 mg, 61%), $[\alpha]_D$ −28.6° (*c*, 1.9, methanol). The n.m.r. data (in acetone-d_6): δ 1.0 (3H, overlapping triplets, aglycon CH_3 of ethyl group); 1.4–1.7 (5H, multiplets, CH_3 of aglycon nitropropyl and CH_2 of ethyl groups); 4.8 (1H, multiplet, aglycon $CHNO_2$). The remaining protons resonated from δ 2.85–4.50 and their signals were not resolved.

Anal. Calcd. for $C_{11}H_{21}NO_8$ (295.3): C, 44.74; H, 7.17. Found: C, 44.51; H, 7.39.

2-Methyl-2-nitropropyl 2,3,4,6-Tetra-O-acetyl-β-D-glucopyranoside (6a)

2-Methyl-2-nitro-1-propanol (2.38 g), silver carbonate (13.65 g), silver perchlorate (1.00 g), Drierite (20 g), and **7** (15.4 g) were stirred in chloroform (100 ml) for 15 h, with half of **7** being admitted 30 min after the start. The filtered reaction solution and chloroform washing of the inorganic residue were evaporated to give a yellow oil (14.6 g) which for chromatographic purification was divided in two parts. Each part was applied to a 500 g silica gel column to be eluted with solvent D. The fractions containing a single product spot (R_f 0.55 on t.l.c. with the same solvent system), or the same together with a trace of impurity (R_f 0.35; TAG), furnished syrups (total 4.85 g) from which crops of chromatographically pure prisms totalling 3.60 g (40%) were obtained upon trituration with 99% ethanol; m.p. 153–157°. A recrystallized sample showed m.p. 158–159° and $[\alpha]_D$ −20.1° (*c*, 1, chloroform). The n.m.r. data (in $CDCl_3$): δ 1.50, 1.56 (two 3H singlets, aglycon CH_3 groups); 1.96, 1.98, 1.98, 2.06 (12H, singlets, *O*-acetyl); 3.7 (1H, multiplet, H-5); 3.98 (2H, singlet, aglycon *O*—CH_2); 4.20 (2H, multiplet, H-6,6′); 4.49 (1H, doublet, J = 7.5 Hz, H-1); δ 5-region (3H, overlapping multiplets, H-2, -3, -4).

Anal. Calcd. for $C_{18}H_{27}NO_{12}$ (449.4): C, 48.10; H, 6.06; N, 3.12. Found: C, 48.03; H, 5.98; N, 3.30.

2-Methyl-2-nitropropyl β-D-Glucopyranoside (6)

To a vigorously stirred suspension of **6a** (1.00 g) in anhydrous methanol (12 ml) was added 3.5 ml of a sodium methoxide solution (containing 17.5 mg of Na). The suspension cleared within 5 min and, after 20 min, was deionized with cation exchanger and evaporated. The white residue (0.60 g, 96%) gave a single spot on t.l.c. (solvent G). By recrystallization from methanol–benzene–ether mixture, large colorless prisms of **6** (509 mg, 81%) were obtained; m.p. 141–142°, $[\alpha]_D$ −23.3° (*c*, 1.1, methanol). The n.m.r. spectrum (in D_2O, with acetone as lock signal): upfield, 0.60 (6H, singlet, aglycon CH_3 groups); downfield, 1.90 (midpoint of AB quartet, 2H, aglycon *O*—CH_2); 2.20 p.p.m. (1H, doublet, J = 7.5 Hz, H-1). The ring proton signals (0.9–1.7 p.p.m. downfield) were poorly resolved.

Anal. Calcd. for $C_{10}H_{19}NO_8$ (281.3): C, 42.70; H, 6.81; N, 4.98. Found: C, 42.89; H, 6.80; N, 5.10.

This work was supported by the Defence Research Board of Canada.

1. H. H. Nicholson. Can. J. Anim. Sci. **43**, 237 (1963).
2. E. H. Cronin and M. C. Williams. Weeds, **12**, 177 (1964).
3. M. C. Williams and W. Binns. Weeds, **15**, 359 (1967).
4. M. C. Williams and F. A. Norris. Weed Sci. **17**, 236 (1969).
5. K. R. Van Kampen and L. F. James. Pathol. Vet. **6**, 413 (1969).
6. M. C. Williams. J. Range Manage. **23**, 400 (1970).
7. G. A. Mosher, C. R. Krishnamurti, and W. D. Kitts. Can. J. Anim. Sci. **51**, 475 (1971).
8. F. R. Stermitz, F. A. Norris, and M. C. Williams. J. Am. Chem. Soc. **91**, 4599 (1969).
9. H. H. Baer, W. Rank, and F. Kienzle. Can. J. Chem. **48**, 1302 (1970).
10. B. Helferich and M. Hase. Ann. **554**, 261 (1943).
11. J. Conchie, G. A. Levvy, and C. A. Marsh. Advan. Carbohydr. Chem. **12**, 157 (1957).
12. H. H. Baer. Advan. Carbohydr. Chem. Biochem. **24**, 67 (1969).
13. H. H. Baer and L. Urbas. *In* The chemistry of the nitro and nitroso groups. Part 2. *Edited by* H. Feuer. Interscience Publishers, New York, New York. 1970. p. 75.
14. M. L. Wolfrom, A. O. Pittet, and I. C. Gillam. Proc. Natl. Acad. Sci. (U.S.A.), **47**, 700 (1961).
15. P. W. Austin, F. E. Hardy, J. G. Buchanan, and J. Baddiley. J. Chem. Soc. **1964**, 2128. K. Kum. Carbohydr. Res. **11**, 269 (1969).
16. H. Bredereck, A. Wagner, G. Faber, H. Ott, and J. Rauther. Ber. **92**, 1135 (1959).
17. B. Helferich and K. F. Wedemeyer. Ann. **563**, 139 (1949). B. Helferich and K. Weis. Ber. **89**, 314 (1956).
18. H. M. Flowers. Methods Carbohydr. Chem. **6**, 474 (1972).
19. B. Coxon and H. G. Fletcher, Jr. J. Am. Chem. Soc. **85**, 2637 (1963); **86**, 922 (1964). B. Coxon and L. D. Hall. Tetrahedron, **20**, 1685 (1964).
20. H. H. Baer and I. Furić. J. Org. Chem. **33**, 3731 (1968). H. H. Baer and M. Bayer. Can. J. Chem. **49**, 568 (1971). See also Z. Eckstein, E. Grochowski, R. Kowalik, and T. Urbański. Bull. Acad. Pol. Sci. Ser. Sci. Chim. **11**, 687 (1963).
21. W. F. Baitinger, P. von R. Schleyer, T. S. S. R. Murty, and L. Robinson. Tetrahedron, **20**, 1635 (1964).
22. M. J. Astle and F. P. Abbott. J. Org. Chem. **21**, 1228 (1956).
23. R. U. Lemieux. Methods Carbohydr. Chem. **2**, 221 (1963).
24. A. I. Vogel. Practical organic chemistry. 3rd ed. Longmans, Green and Co., London. 1962. p. 176.
25. B. Helferich and W. Klein. Ann. **450**, 219 (1926).
26. M. L. Wolfrom and D. R. Lineback. Methods Carbohydr. Chem. **2**, 342 (1963).

A Study on the Kinetically Controlled Cyclization of 6-Deoxy-3-*O*-methyl-6-nitro-D-glucose and -L-idose, and the Preparation of Optically Active Nitroinositol Derivatives[1]

JAN KOVÁŘ AND HANS H. BAER

Department of Chemistry, University of Ottawa, Ottawa, Canada K1N 6N5

Received March 12, 1973

The cyclization (internal Henry addition) of 6-deoxy-3-*O*-methyl-6-nitro-D-glucose (**1**) and -L-idose (**2**) was investigated with respect to the sequence in which stereoisomeric deoxynitroinositol methyl ethers are formed from each. It was found that, under conditions of kinetic control, the primary products generated from **1** are the nitronate **4'** (that corresponds to the epimeric deoxynitroinositols **4** and **5** having the *epi*-3 and *muco*-3 configurations, respectively) and the nitronate L-**6'** of optically active 1-deoxy-4-*O*-methyl-1-nitro-L-*myo*-inositol (L-**6**). They are formed in approximately equal proportions. Ensuing thermodynamically controlled processes lead to racemization of L-**6** and formation of the *scyllo* isomer **3** at a relatively slow rate. The cyclization of **2**, found to be faster than that of **1**, gave as primary products the enantiomeric nitronate D-**6'** and the nitronate **3'** in a ratio of about 4:1. The nitronate **4'** arose by subsequent epimerization. The optically active compounds D-**6** and L-**6** were isolated in pure, crystalline form.

La cyclisation (addition interne selon Henry) du déoxy-6 *O*-méthyl-3 nitro-6 D-glucose (**1**) et -L-idose (**2**) a été étudiée plus particulièrement du point de vue de la formation d'éthers méthyliques de déoxynitroinositols stéréoisomèrs à partir de chacun d'eux. Il a été prouvé que, dans des conditions de contrôle cinétique, les produits principaux obtenus à partir de **1** sont le nitronate **4'** (qui correspond aux déoxynitroinositols épimères **4** et **5** ayant les configurations *épi*-3 et *muco*-3, respectivement) et le nitronate L-**6'** du déoxy-1 *O*-méthyl-4 nitro-1 L-*myo*-inositol (L-**6**) optiquement actif. Ceux-ci sont formés dans des proportions approximativement égales. Le processus contrôlé thermodynamiquement qui suit, a conduit à la racémisation de L-**6** et à la formation de l'isomère *scyllo* **3** avec une vitesse relativement lente. La cyclisation de **2**, plus rapide que celle de **1**, a conduit, comme produits principaux, au nitronate énantiomère D-**6'** et au nitronate **3'** dans des proportions 4:1. Le nitronate **4'** est obtenu par épimérisation subséquente. Les composés optiquement actifs D-**6** et L-**6** ont été isolés pure, sous forme cristalline.

[Traduit par le journal]

Can. J. Chem., **51**, 2836 (1973)

In the preceding article of this series (1) we described the synthesis of 6-deoxy-3-*O*-methyl-6-nitro-D-glucose (**1**) and -L-idose (**2**), and the cyclization of these sugars to deoxynitroinositol monomethyl ethers. Four crystalline cyclization products were obtained in that preparative work. They were three meso compounds, namely, 1-deoxy-4-*O*-methyl-1-nitro-*scyllo*-inositol (**3**), 3-deoxy-6-*O*-methyl-3-nitro-*epi*-inositol (**4**), and 3-deoxy-6-*O*-methyl-3-nitro-*muco*-inositol (**5**), and one racemic compound, 1-deoxy-4-*O*-methyl-1-nitro-DL-*myo*-inositol (DL-**6**). The results conformed to a fair degree to those recorded by Grosheintz and Fischer (2) for the cyclization of the analogous, nonmethylated nitro hexoses. There were, however, certain apparent incongruities calling for an explanation, and some questions regarding the stereochemical course of these reactions remained open, so that a more detailed investigation seemed indicated. Thus, we obtained different yields of four individual stereoisomers depending on whether pure **1** or mixtures of **1** and **2** served as starting materials,[2] whereas the earlier authors (2) had obtained, under a given set of conditions, identical mixtures of three (nonmethylated) deoxynitroinositols regardless of the configuration (D-*gluco* or L-*ido*) of the nitro hexose employed.[3] Evidently, thermodynamic equilibration of stereoisomers took place in the course of their operations. This was supported by experiments performed by the authors themselves (2) and later by Lichtenthaler (4), demonstrating that the three individual deoxynitroinositols do indeed epimerize readily in the presence of alkali; each of

[1]Cyclizations of dialdehydes with nitromethane. XVI. For part XV in this series see ref. 1.

[2]Pure **2** was not available (1).

[3]The products were later shown to possess the *scyllo*, DL-*myo*-1, and *muco*-3 configurations (3, 4). The *epi*-3 isomer corresponding to **4** was not encountered.

Can. J. Chem. Downloaded from www.nrcresearchpress.com by 210.87.254.42 on 09/05/12
For personal use only.

Can. J. Chem. Downloaded from www.nrcresearchpress.com by 210.87.254.42 on 09/05/12
For personal use only.

the compounds appeared to give a similar mixture of the *scyllo* and DL-*myo*-1 isomers. It was subsequently found (5) that 6-deoxy-6-nitro-D-glucose and -L-idose differ in the rates at which they cyclize at given p*H* values. This observation would seem to preclude significant epimerization at C-5 in the nitro hexoses themselves prior to cyclization, and one might infer that different kinetic products should be obtainable from the two sugars provided that subsequent epimerization on the inositol stage is slow enough. However, no attempts have thus far been made to determine whether this proviso does hold, and if so, what is the precise composition of the kinetically favored products arising from individual 6-nitro hexoses and what are the conditions best suited for isolation of such products. We herein report the results of an examination of these questions as regards the cyclization of the 3-*O*-methyl sugars **1** and **2**, and we expect to discuss the thermodynamically controlled epimerization of the products in a subsequent paper (6).

Methods

In order to identify, and possibly isolate, primary cyclization products arising from the nitro hexoses **1** and **2** it was necessary to provide conditions that were mild enough to minimize epimerization yet sufficiently effective to ensure reasonable reaction times. It was found that the course of the cyclization could be conveniently monitored when it was performed at 0° in aqueous barium hydroxide solution, with either an approximately equivalent amount (1.1 equiv) or a catalytic amount (0.1 equiv) of base present. The former conditions, resulting initially in a reaction medium of about p*H* 12, and the latter ones, where the p*H* was near 7, produced comparable inositol mixtures from a given sugar although, naturally, the reaction was faster in the strongly alkaline medium. The weakly basic conditions were advantageous for the isolation of kinetic products.

Analysis of the reaction mixtures at specified time intervals was performed by deionization followed by trimethylsilylation and v.p.c. of the products. To this end, compounds **1**–**6** were first trimethylsilylated and chromatographed singly and also as mixtures of known composition, and retention times (Table 1) and detector responses were determined. It was ascertained that the procedure gave reproducible results, reliably reflecting the composition of mixtures with sufficient accuracy (see Experimental). The crystalline β-anomer of **1** gave a main peak accompanied by a minor peak that was attributable to an admixture of the α-anomer. (The latter may have been present before, or arisen during, trimethylsilylation.) Brief exposure of the β-anomer to the weakly alkaline conditions referred to earlier (p*H* ~ 7) resulted in formation of these two peaks in approximately equal strength, due to anomeric equilibration, before any nitroinositol peaks were generated. The syrupy mixture of **1** and **2** gave rise to both of the peaks mentioned, and to two peaks attributed to anomers of the L-*ido* isomer **2**. The *scyllo* nitroinositol **3** produced a single peak requiring no further comment. The *epi*-3 and *muco*-3 isomers (**4** and **5**) gave one and the same peak upon trimethylsilylation and therefore could not be distinguished by this method. However, this fact was of no consequence for the present work since they both are derived from the same nitronate. Nitronates are the actual primary products in the cyclization, and the peak corresponding to **4** and (or) **5** could thus be taken as a direct measure for their common nitronate.[4] The DL-*myo*-1 isomer DL-**6** produced a strong peak that was always accompanied by a minor peak of 1/10 its intensity. In mixtures

TABLE 1. Relative retention times of trimethylsilyl derivatives in v.p.c.

Compound	T_R
1[a]	1.56
1[b]	1.18
2[c]	1.08
2[d]	1.02
3	1.45
4	0.73
5	0.73
6[c,e]	1.00
6[d]	0.39

[a]β-Anomer.
[b]α-Anomer.
[c]Main peak.
[d]Minor peak.
[e]Reference standard.

[4]In fact, if **4** and **5** had given separate peaks it would have been necessary to use the sum of these for the purpose at hand. Whether the trimethylsilyl derivatives fortuitously have an identical retention time or whether one of the isomers was converted into the other in the process cannot be stated. However it is recalled that **4**, upon acetonation, yielded the di-*O*-isopropylidene derivative of **5** (1).

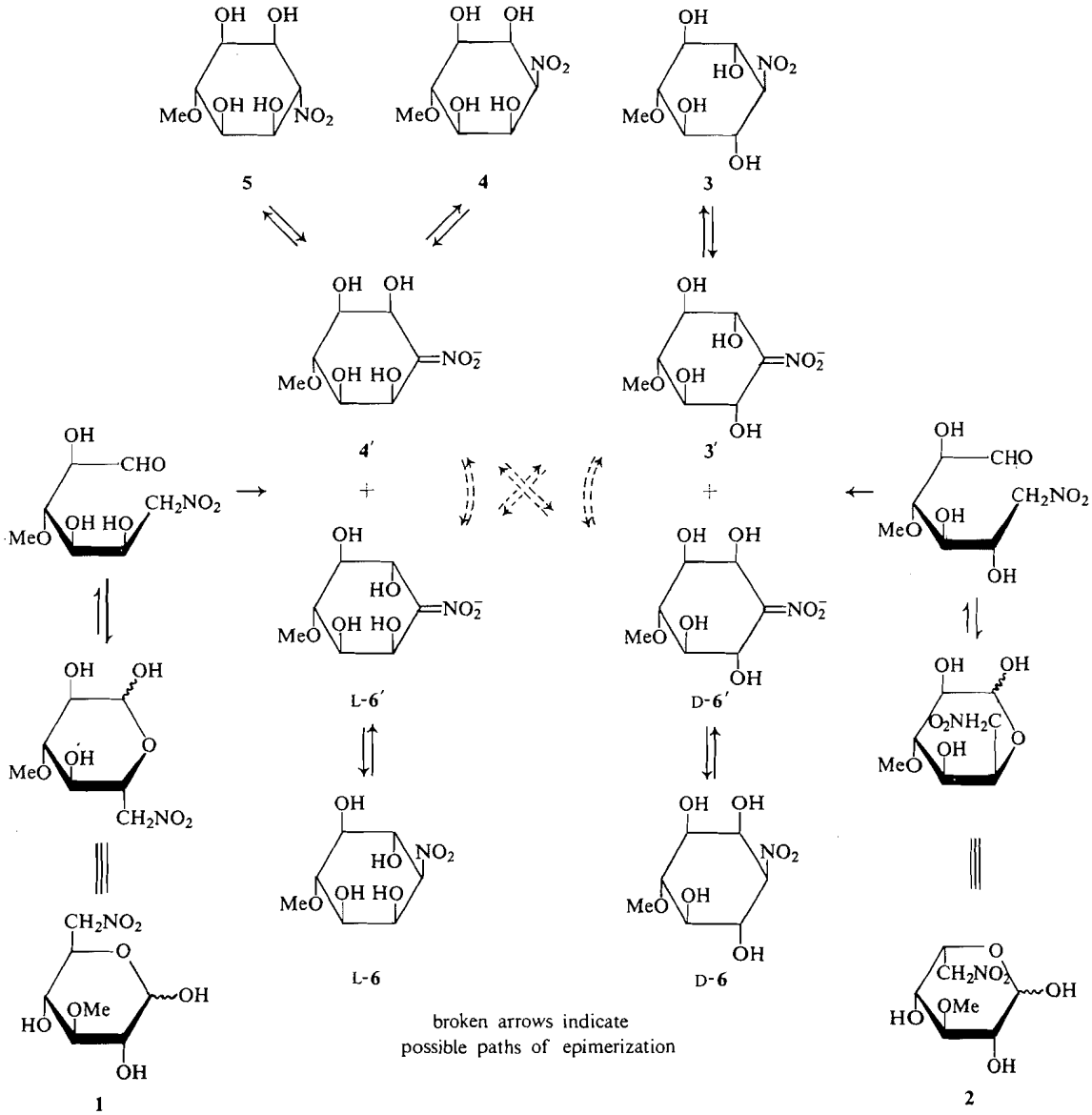

of various kinds this minor peak was never seen unless the main peak corresponding to **6** was present also, and although its significance remained obscure it was considered to originate in some way from **6**; the sum of the two peaks was therefore taken as representing the proportion of this isomer. One difficulty to be faced in assays of mixtures containing both **2** and **6** was the fact that the major peak of **6** coincided with that of the lesser anomer of **2**. It will be seen in the discussion of results that this circumstance was relevant only to a few measurements and did not impair interpretations.

Results and Discussion

In the aldol-type addition reaction between a primary nitroalkane and an aldehyde, the nitro alcohol produced arises as its nitronate salt in the first instance. In the case of the cyclization of any given 6-deoxy-6-nitrohexose one can expect the formation of two diastereoisomeric deoxynitroinositol salts due to the creation of a new

Can. J. Chem. Downloaded from www.nrcresearchpress.com by 210.87.254.42 on 09/05/12
For personal use only.

TABLE 2. Time-dependent formation of products from **1**

Time	Composition of reaction mixture (%)[a]						
	1-β	**1**-α	**3**	**4**, **5**	**6**	U[b]	
A. With 1.1 equiv of base (p*H* 12)							
1.7 min	24	18		29	29		
5.0 min	9	8		42	41		
16.6 min	4	3		47	46		
50.0 min	1			50	49		
166.6 min			1	54	45		
5.7 h			4	43	51	2	
22.4 h			7	46	47		
29 h			10	49	41		
96 h			14	54	30	2	
168 h			20	52	26	2	(p*H* 11–12)
264 h			26	50	22	2	(p*H* 10)
432 h			34	48	16	2	(p*H* 9–10)
B. With 0.1 equiv of base (p*H* ~ 7)							Rotation[c] (°)
1.7 min	50	48				2	
5.0 min	52	45		tr[d]	tr	2	−0.623
16.6 min	54	43		tr	1	2	−0.580
50.0 min	51	43		2	2	2	−0.448
166.6 min	46	42		4	6	2	−0.370
23.5 h	7	6		42	45		−0.598
45.5 h				42	58		−0.659
119 h				44	56		
168 h			tr	46	54		−0.228
288 h			1	45	54		−0.268
456 h			2	36	62		
624 h			3	36	61		−0.220

[a]As determined by v.p.c. after acidification. In the reaction medium itself, the nitro compounds exist in p*H*-dependent equilibrium with their nitronates. At p*H* 12, the equilibrium lies far on the side of the latter, and at p*H* 7, on the side of the former.
[b]Unidentified product.
[c]Absolute rotation at 365 nm of an aliquot of the reaction solution, measured in a 1 dm tube after deionization. See Experimental.
[d]Trace (< 1%).

chiral center at the carbon atom that was formerly C-1 in the hexose.[5] Thus, the D-*gluco* derivative **1** should give the nitronate **4′** (= **5′**), the salt common to the *epi*-3 (**4**) and *muco*-3 (**5**) nitroinositol derivatives, and secondly the nitronate L-**6′**, the salt of the L-*myo*-1 isomer L-**6**. The L-*ido* hexose **2** should form the nitronate **3′** derived from the *scyllo* isomer **3**, and the nitronate D-**6′** belonging to the D-*myo*-1 isomer D-**6**. If, under the prevailing reaction conditions, epimerization should occur at C-5 of the starting hexose before, during, or after the cyclization, all four nitronates would be formed from either hexose, with D-**6′** and L-**6′** emerging as the racemate. This is what has been observed in preparative work with these particular compounds (1) and their nonmethylated analogs (2, 4).

Table 2 summarizes the progress of the cyclization of **1** at 0°. It is seen that in the presence of a slight excess of base (A) the sugar anomerizes practically at once and disappears within 1 h. During this period of time two nitronates arise in a ratio of approximately 1:1, with the ratio remaining constant for about 1 day. Similarly, in the presence of a catalytic amount of base (B) there occurs instant anomerization followed by gradual disappearance of **1** with concomitant formation of the two nitro compounds in similar proportions, although the reaction expectedly is slower and complete consumption of **1** requires more than a day. V.p.c. of the products confirmed that one of the

[5]The reaction proceeds through the open-chain form of the sugar, in which C-1 is achiral, and the anomeric configuration of the cyclic form is therefore irrelevant.

Can. J. Chem. Downloaded from www.nrcresearchpress.com by 210.87.254.42 on 09/05/12
For personal use only.

TABLE 3. Time-dependent formation of products from **2** and **1**

Time	Composition of reaction mixture (%)[a] 1-β	1-α	2	3	4, 5	6	U[b]	
	A. With 1.1 equiv of base (p*H* 12)							
1.7 min	10	9	0	11	13	57		
5.0 min	7	8		10	17	58		
16.6 min	3	4		9	23	61		
50.0 min				9	28	64		
166.6 min				8	30	62		
5.6 h				10	23	64	4	
22.8 h				13	28	55	**4**	
46 h				13	33	51	3	
96 h				16	31	49	4	
168 h				14	41	42	3	(p*H* 11)
336 h[e]				18	49	31	2	(p*H* 9–10)
	B. With 0.1 equiv of base (p*H* ~ 7)							Rotations[c] (°)
1.7 min	30	7	49[f]			(14)[g]		+0.085
5.0 min	29	7	49			(15)		+0.086
16.6 min	28	7	47	tr[d]	tr	(17)		+0.101
60.0 min	26	7	41	2	tr	(24)		+0.132
166.8 min	23	10	20	7	2	38		+0.160
5.9 h	23	10	10	9	5	43		+0.178
25.2 h	11	9	0	11	11	58		+0.155
50 h	4	3		12	18	63		+0.117
120 h	tr	tr		12	27	60		+0.107
291 h				11	20	69		
460 h				10	17	73		+0.081

[a]–[d]See footnotes to Table 2.

[e]At this time a strong deposit had occurred in the reaction mixture, and the aliquot that was withdrawn for analysis was a suspension of the solid in the supernatant.

[f]The values given in this column refer to the main anomer of 2. The minor anomer, whose percentage would have to be added for an estimate of the total proportion of 2 present, is chromatographically indistinguishable from 6 (see Table 1 and text) and is represented by (decreasing) fractions of the values listed for the latter. The starting material analyzed as follows: 1-β, 27%, 1-α, 7%, 2 (main peak), 54%, 2 (minor peak), 12%; α_{365} +0.050°.

[g]It follows from [f] that for the first hour or two, *i.e.* so long as there is still a large amount of 2 present, the actual proportion of 6 is represented by (increasing) fractions of the values in this column.

nitronates was **4′** and the other **6′**. Since the solution had retained optical activity at the time of complete disappearance of **1**, one of the enantiomers of **6** must have been present predominantly if not exclusively. Owing to its origin from the D-*gluco* compound **1** it must have been the enantiomer L-**6**. Further inspection of Table 2 shows that a third nitronate (**3′**) arises very slowly and only after the cyclization of **1** is complete. Consequently, **3′** cannot be a primary product but owes its formation to epimerization of **6′**.

In summary, then, the results discussed thus far prove clearly that the products of kinetic control in the cyclization of **1** are the nitronates **4′** and L-**6′** (with no significant preference for either), that cyclization is much faster than epimerization, and that epimerization leads relatively rapidly to racemic DL-**6′** and more slowly to **3′**. The ultimate thermodynamic equilibrium, which is not recorded in Table 2, will be the subject of a later communication (6).[6]

A like set of experiments was performed with a 2:1 mixture[2] of **2** and **1**. Naturally the data (Table 3) presented a more complex picture, but they nevertheless confirmed the results disclosed

[6]The reader will note in Table 2, B that the reaction was not monitored until equilibrium was reached, as the last entry shows optical activity still persisting. In the experiment recorded in Table 2, A, the p*H* value of the solution was found to decrease after some time (see the last three entries). It is to be discussed (6) in what way the p*H* influences the nitronate distribution at equilibrium.

Can. J. Chem. Downloaded from www.nrcresearchpress.com by 210.87.254.42 on 09/05/12
For personal use only.

Can. J. Chem. Downloaded from www.nrcresearchpress.com by 210.87.254.42 on 09/05/12
For personal use only.

above and revealed the behavior of **2**. First of all, it is seen that **2** cyclizes more rapidly than **1**. In the presence of excess base (Table 3, A), all of **2** was consumed after 1.6 min while nearly half of **1** remained at that time, in accordance with the data of Table 2, A. The nitronate **3′** was present at that time as one of the primary products expected to arise from **2**, and so was the nitronate **4′** that stemmed from **1**. The preponderant product at this point, however, was the nitronate **6′**. It must have contained the L-enantiomer (from **1**) and the D-enantiomer (from **2**), with the latter predominating because of the given ratio and observed relative reaction speeds of the precursors. That this was true was demonstrated by the dextrorotation that was recorded when a comparable point in the experiment listed in Table 3, B was reached (1 day). It is to be noted that **1**, which constituted 20% of the mixture at that point, is levorotatory (1) whereas D-**6** is dextrorotatory as was ascertained later on. A maximum of positive rotation is reached when all of **2** (also dextrorotatory but less strongly so than D-**6**) has reacted, and from then on the rotation decreases due to production of L-**6** by cyclization of **1** and, concurrently but more slowly, by racemization of D-**6′**. Further analysis of the data in Table 3, A and B, reveals that four times as much D-**6′** as **3′** is generated from **2** in the cyclization step, which contrasts with the 1:1 ratio of kinetic products arising from **1** (Table 2). With time progressing, the amount of **4′** in the mixture is seen to increase slowly at the expense of **6′** (Table 3, A), which must be ascribed to thermodynamically controlled epimerization.

An interesting difference exists in the behavior of **1** in the two sets of reaction conditions of Table 3. Under the strongly basic conditions (A), **1** begins to cyclize immediately albeit more slowly than **2**. In the absence of a stoichiometric amount of base (B), **1** does not appear to react appreciably until most of **2** is consumed after several hours. About half of **1** was still left after 24 h whereas in the cyclization of pure **1** (Table 2, B) the proportion surviving that period amounted to 13% only. The phenomenon may perhaps be explained by assuming that a greater nitromethylene acidity of **2** results in setting up buffer conditions which delay the cyclization of **1**.

In conclusion it can be stated that the products of kinetic control in the cyclization of **2** are the nitronates **3′** and D-**6′** (with the latter being favored about fourfold), and that **4′** is formed by ensuing epimerization. The reaction of **2** was found to be faster than that of **1** under both sets of conditions which were employed. A difference in nitromethylene acidity might partly be responsible for this. However, another factor is probably also important in this regard, namely, the conformational instability of idopyranose derivatives which facilitates reactions that require mutual approach of C-1 and -6. The same explanation has been suggested previously for the marked difference in rate of cyclization of 6-deoxy-6-nitro-D-glucose and -L-idose in the p*H* range 5–7 (5).

On the basis of the above results we were able to elaborate conditions under which maximum accumulation of kinetic products was obtained, and we succeeded in isolating the optically active L-*myo*-1 derivative L-**6** from the reaction mixture of **1**. A crystalline, crude product of 80% purity was obtained in 54% yield, and recrystallization furnished the optically pure enantiomer in 33% yield. The *muco*-3 isomer **5** was isolated in 28% yield from the mother liquor; it corresponded to the second kinetic nitronate (**4′**) produced in this reaction. The D-*myo*-1 enantiomer D-**6** was isolated in optically pure form in a yield of 19% upon cyclization of the mixture of **1** and **2**. Considering that the starting mixture contained only 60–65% of **2**, the yield of D-**6** based on **2** corresponded to about 30%.

Experimental

The preparation of the nitro sugars **1** and **2** and of the nitro inositol derivatives **3**, **4**, **5**, and DL-**6** has been described (1); the crystalline β-anomer of **1** and a syrupy mixture containing 60–65% of **2** were used for the present work. Optical rotations were measured in a 1 dm tube in a Perkin-Elmer 141 automatic polarimeter using a mercury lamp as the light source. V.p.c. was performed in a Varian Aerograph, Series 1200, with a hydrogen flame detector and a recorder equipped with a 224 Disc. Mod. integrator. The aluminum column (length, 5 ft; diameter, $\frac{1}{8}$ in.) was packed with 10% Carbowax 20M on Chromosorb W and was operated isothermally at 155–165°. The carrier gas was helium applied at a pressure of 80–90 p.s.i.

Analytical Procedure

The relative retention times (Table 1) and detector response values for the trimethylsilyl derivatives of **1–6** were determined as follows (7). The reagent for trimethylsilylation was prepared by mixing dry pyridine (2 ml), hexamethyldisilazane (1.8 ml), and trifluoroacetic

Can. J. Chem. Downloaded from www.nrcresearchpress.com by 210.87.254.42 on 09/05/12
For personal use only.

acid (0.2 ml). The reagent could be stored in a refrigerator for several weeks without deteriorating. An accurately weighed test sample (6.0 mg) was dissolved in 0.30 ml of the reagent by brief shaking, and the solution was then allowed to stand overnight at room temperature before 2–3 μl of it was injected into the chromatograph by means of a microsyringe. The solution was kept in a tightly stoppered vial in a refrigerator for later repeat analyses. Various test mixtures of known composition were assayed several times each, and the percentage values found deviated from the mean values no more than 2–3% and often less. The main peak of compound DL-**6** served as the retention time standard (1.00); its actual retention time under the conditions employed was approximately 10 min. As standard for calculating detector response values, the sum of the main and minor peaks given by DL-**6** was used. (see Discussion).

Cyclizations

A sample (100–200 mg) of the nitro hexose (mol. wt. 223) was dissolved in 0.0025 *N* acetic acid (0.45–0.9 ml) so that an *M* solution was obtained. (The purpose of the acid was to guard against premature commencement of cyclization, especially of **2**; compare ref. 5). The solution was cooled to 0°, and the calculated amount of 0.485 *N* barium hydroxide solution that would provide 1.1 equiv of base was added in the experiments of sections A, Tables 2 and 3. For example, 205.2 mg of **1** dissolved in 0.92 ml of said acid was rendered alkaline by the addition of 2.09 ml of hydroxide solution. For the experiments referred to in sections B of Tables 2 and 3, a 0.053 *N* barium hydroxide solution was used so as to provide 0.1 equiv of base. Samples of 0.10 ml were withdrawn from the reaction mixture at time intervals as stated (Tables 2 and 3), and the reaction was quenched by introducing the sample into 0.1 *N* acetic acid (1.0 ml). The solution was then passed through a bed (0.3 ml) of Dowex-1X2 (acetate form) and thereafter through a bed (0.6 ml) of Rexyn-101 (H^+) contained in a small column (disposable pipette) which was subsequently eluted with water (1.5–2.0 ml). The column could be re-used several times, after washing with more water. In cases where the optical rotation of the product was to be determined, the effluent volume was adjusted to 2.5 ml and the measurement was made in a 1 dm tube. The solution was then evaporated to dryness, and the residue was further dried in an oil pump vacuum at room temperature. It was subjected to trimethylsilylation and v.p.c. as described above.

*1-Deoxy-4-O-methyl-1-nitro-*L*-myo-inositol (*L*-**6**)*

A suspension of the crystalline nitro sugar **1** (583 mg, 2.61 mmol) in 0.0025 *N* acetic acid (2.61 ml) was stirred in an ice-water bath under a nitrogen atmosphere, and a chilled, 0.0533 *N* barium hydroxide solution (5.03 ml, 0.1 equiv) was added. The resulting solution was stored in a stoppered flask for 48 h at 0°. It was then poured into ice-cold 0.1 *N* acetic acid (10 ml), and the mixture was passed sequentially through 1 ml of Dowex-1X2 (acetate form) and 5 ml of Rexyn-101 (H^+) which were washed with water to give a total effluent volume of 24 ml. Evaporation of the effluent followed by coevaporation with added ethanol and drying *in vacuo* furnished a residue that was triturated with absolute ethanol and benzene (1 ml each). There was obtained a crystalline material (314 mg, 54%) showing m.p. 166–170° and $[\alpha]_{365}$ −147°. Recrystallization from 99% ethanol gave pure L-**6**, m.p. 178.5–179.5°; $[\alpha]_{578}$ +16.2°, $[\alpha]_{546}$ +15.0°, $[\alpha]_{436}$ +2.5°, $[\alpha]_{365}$ −184° (*c*, 0.4 in 0.0025 *N* CH_3CO_2H). M.p. and rotation remained unchanged on further recrystallization, and an n.m.r. spectrum in 2.1 *N* CF_3CO_2D in D_2O was identical with that described for DL-**6** (1).

Anal. Calcd. for $C_7H_{13}NO_7$ (223.2): C, 37.66; H, 5.87; N, 6.28. Found: C, 37.87; H, 6.01; N, 6.22.

The first mother liquor (from the trituration with ethanol–benzene) was evaporated and the residue crystallized from ethyl acetate to give an optically inactive material (164 mg) that melted at 151–152° and proved to be virtually pure *muco*-3 isomer (**5**).

*1-Deoxy-4-O-methyl-1-nitro-*D*-myo-inositol (*D*-**6**)*

A solution of the syrupy mixture of **2** and **1** (509 mg) in 0.0025 *N* acetic acid (2.28 ml) was treated with 0.0533 *N* barium hydroxide (4.38 ml) exactly as described above for **1**, except that the reaction time was 22 h only. Work-up as before afforded a partially crystalline syrup (536 mg) which upon trituration with 99% ethanol and benzene (1 ml each) and cooling overnight at 0° furnished crude D-**6** (213 mg), m.p. 172–174°, $[\alpha]_{365}$ +121°. Recrystallization from ethanol gave 97 mg (19%) of D-**6** melting at 176–177° and exhibiting $[\alpha]_{578}$ −15°, $[\alpha]_{546}$ −18°, $[\alpha]_{436}$ −4.7°, $[\alpha]_{365}$ +190° (*c*, 0.2 in 0.0025 *N* CH_3CO_2H). An n.m.r. spectrum of the product was identical with that of the enantiomer.

Anal. Calcd. for $C_7H_{13}NO_7$: N, 6.28. Found: N, 6.08.

The mother liquor was shown to contain unreacted **1**.

Support of this work by the National Research Council of Canada is gratefully acknowledged. Mrs. Ursula Williams is thanked for preparing the starting compounds.

1. J. KOVÁŘ and H. H. BAER. Can. J. Chem. **51**, 1801 (1973).
2. J. M. GROSHEINTZ and H. O. L. FISCHER. J. Am.Chem. Soc. **70**, 1479 (1948).
3. T. POSTERNAK. Helv. Chim. Acta, **34**, 1600 (1951). T. POSTERNAK, W. H. SCHOPFER, and R. HUGUENIN. Helv. Chim. Acta, **40**, 1875 (1957).
4. F. W. LICHTENTHALER. Chem. Ber. **94**, 3071 (1961).
5. H. H. BAER and W. RANK. Can. J. Chem. **43**, 3462 (1965).
6. J. KOVÁŘ and H. H. BAER. Can. J. Chem. In press.
7. K. M. BROBST. Methods Carbohydr. Chem. **6**, 3 (1972).

Some Synthetic Interconversions in the Nitrocyclohexane System[1]

HANS H. BAER, DOUGLAS C. SHIELDS, AND GEOFFREY G. DAWSON[2]
Department of Chemistry, University of Ottawa, Ottawa, Canada K1N 6N5

Received April 2, 1973

Several transformations starting from *trans,trans*-2-nitrocyclohexane-1,3-diol (**1**) and its diacetate (**2**) were carried out as model reactions for synthetic work on nitro sugars. They included methylation with diazomethane, dehydration, dehydroacetylation, nucleophilic elimination–additions with alcohols, and bromination. The monomethyl ether of **1** (**3**), the monomethyl ether acetate (**5**), the dimethyl and dibenzyl ethers (**4** and **9**), bromonitro compounds derived from **1** and **4** (**13** and **14**), and four 3-substituted 2-nitrocyclohexenes with methoxyl, ethoxyl, acetoxyl, and hydroxyl groups as substituents (**6**, **8**, **7**, and **11**, respectively) were obtained in these studies. The nitronate formation of **1** and **4** and attendant production of nitroolefins was investigated by u.v. spectroscopy.

Plusieurs transformations portant sur le *trans,trans* nitro-2 cyclohexane diol-1,3 (**1**) et son diacétate (**2**) ont été effectuées pour servir de modèles de réaction à un travail de synthèse sur les nitrosucres. Elles comprennent des méthylations par le diazométhane, des déshydratations, des déshydroacétylations, des élimination–additions nucléophiles avec les alcools et des bromations. Au cours de cette étude, l'éther monométhylique de **1** (**3**), l'acétate de l'éther monométhylique (**5**), les éthers diméthylique et dibenzylique (**4** et **9**), les composés bromonitros dérivés de **1** et **4** (**13** et **14**) et quatre nitro-2 cyclohexènes substitués en 3 par les groupes méthoxyle, éthoxyle, acétoxyle et hydroxyle (respectivement **6**, **8**, **7** et **11**) ont été obtenus. La formation du nitronate de **1** et **4** et la production subséquente de nitrooléfines ont été étudiées par spectroscopie ultraviolette. [Traduit par le journal]

Can. J. Chem., 51, 2843 (1973)

2*t*-Nitrocyclohexane-1*r*,3*c*-diol (**1**), a compound that is readily prepared (1, 2) by cyclization of glutaraldehyde with nitromethane, represents a useful point of departure for model studies of synthetic and stereochemical problems which are relevant to the more complex chemistry of nitro sugars. For example, treatment of its diacetate **2** with ammonia afforded (3) in a single operation 1*r*,3*c*-diamino-2*t*-nitrocyclohexane, which was isolated upon *N*-acetylation. The diamination was explained (3) as a sequence of two elimination–addition reactions, and it has since been applied to acetylated deoxynitroinositols (3–6) and nitro glycosides including nucleosides (6–8). Treatment of **1** itself with various aliphatic amines furnished analogous, *N*,*N*′-disubstituted diaminonitrocyclohexanes (2), and similar reactions with thiols led to bisthioethers (9). A study (10) on the stereochemistry of protonation of the sodium nitronate of **1** was of interest in connection with related investigations in nitro glycosides (11). It was therefore considered worthwhile to perform, in the nitrocyclohexane system, a number of additional reactions that would complement current research in nitro carbohydrates.

The reactions that were carried out successfully are delineated in Scheme 1. Boron trifluoride-catalyzed methylation of **1** with diazomethane furnished the monomethyl ether **3** and the dimethyl ether **4**. So far as we know, this technique for methylation of aliphatic hydroxyl groups (12) had not previously been tried on nitro alcohols, and the question was whether the reagent is compatible with the nitro function in **1** and related nitro glycols. Diazomethane does not react with simple, weakly acidic nitroalkanes ($pK_a^{nitro} > ca.$ 8), but with negatively substituted nitroalkanes having a pK_a^{nitro} of less than *ca.* 8 it reacts, even without boron trifluoride catalysis, to give nitronic esters that may subsequently undergo various kinds of irreversible transformations (13*a*). For nitro sugars, pK_a values of 8–11 have been reported (11, 14), suggesting that some of them might be borderline cases in this respect. The selective methylation of hydroxyl groups in **1** placed confidence in possible applications of diazomethane to nitro sugars for which the customary base-promoted alkylation methods, although never actually tried, *prima facie* do not recommend themselves, both because they would

[1]Taken in part from the M.Sc. Thesis of D. C. Shields, University of Ottawa, 1970.
[2]Postdoctoral Fellow, 1968–1970.

Can. J. Chem. Downloaded from www.nrcresearchpress.com by 210.87.254.5 on 09/05/12
For personal use only.

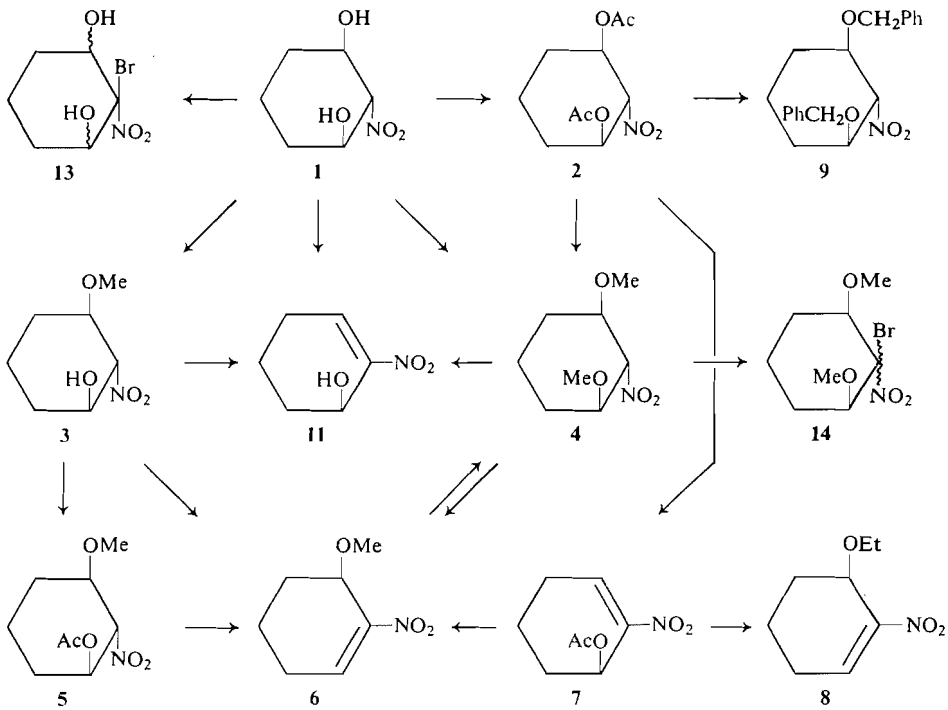

SCHEME 1

likely effect *O*- and (or) *C*-alkylation involving the nitro function (13*a*), and because of the proclivity of many nitro sugar derivatives to incur configurational and structural changes in basic media (11, 13*b*, 14–17). In the meantime, the diazomethane method has, in fact, been utilized in the synthesis of methyl 3,6-dideoxy-2,4-di-*O*-methyl-3-nitro-α-D-glucopyranoside (18).

Boron trifluoride-catalyzed acetylation (19), which is now routinely used in nitro sugars and has also served (3) for preparing the diacetate **2** from **1**, readily afforded the acetate **5** from **3**. Next, 3-methoxy-2-nitrocyclohexene (**6**) was made by dehydration of **3** as well as by dehydroacetylation of **5**. The former conversion was accomplished by treatment of the alcohol with aluminum oxide in toluene at 75°, following earlier observations (20) that certain nitro sugar derivatives can be dehydrated in a similar way.[3] The dehydroacetylation of **5** was carried out by Schmidt–Rutz reaction with sodium bicarbonate in refluxing benzene (13*b*); the yield was only moderate (22%). The same process proved more efficient with the diacetate **2**, giving 3-acetoxy-2-nitrocyclohexene (**7**) in 46% yield. There was no evidence for elimination of a second molecule of acetic acid, which would have resulted in a diene as was the case in the dehydroacetylation of methyl 3-deoxy-3-nitrohexopyranoside 2,4,6-triacetates (21).

Treatment of **2** with sodium methoxide in methanol at 0° led to the dimethyl ether **4**, no doubt by way of a double elimination–addition process through the steps **2** → **7** → **6** → **4** (Scheme 2). There is ample precedent in the literature for alkoxylation of α-nitroalkenes generated *in situ* from β-acyloxynitroalkanes (13*b*, 20, 22), and the twofold sequence clearly parallels the diaminations cited above. In agreement with this scheme, the methoxy olefin **6**, independently prepared as mentioned before, added methanol to give **4** under the same conditions of base catalysis. Furthermore, the acetoxy olefin **7**, obtained from **2** as stated in the preceding paragraph, was found to react with methanol to furnish **6** even in the absence of base; quantitative conversion took place at 65° within 12 h. Refluxing of **7** in ethanol quantitatively produced 3-ethoxy-2-nitrocyclohexene (**8**). It is proposed

[3]In the examples studied (20), the reaction temperature was 110°, and nitroolefinic derivatives were generated as intermediates that underwent further transformations in line with their particular structural features and by virtue of other reagents present.

Can. J. Chem. Downloaded from www.nrcresearchpress.com by 210.87.254.5 on 09/05/12
For personal use only.

Can. J. Chem. Downloaded from www.nrcresearchpress.com by 210.87.254.5 on 09/05/12
For personal use only.

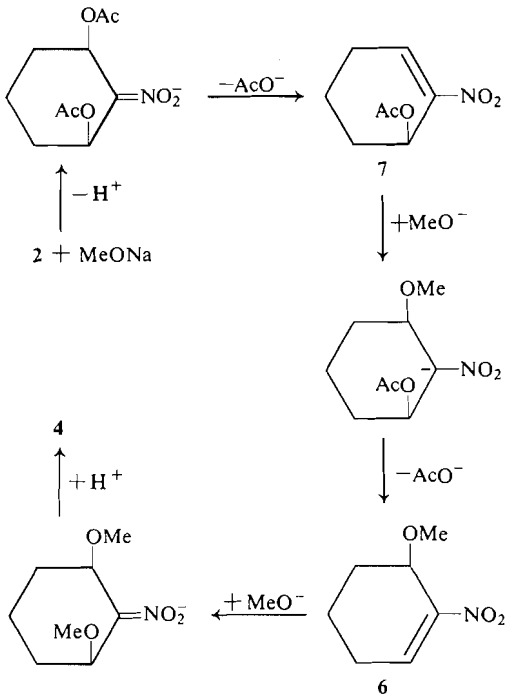

SCHEME 2

that these noncatalyzed substituent exchanges occur in a concerted manner, with the acetoxy bond breaking as the alkoxy bond is being formed (Scheme 3). For if one were to assume two distinct steps instead, namely (for **7** → **6**), methanol addition independent from subsequent elimination of acetic acid, then it would be difficult to explain why the product (**6**), in its turn, altogether resists adding methanol so that,

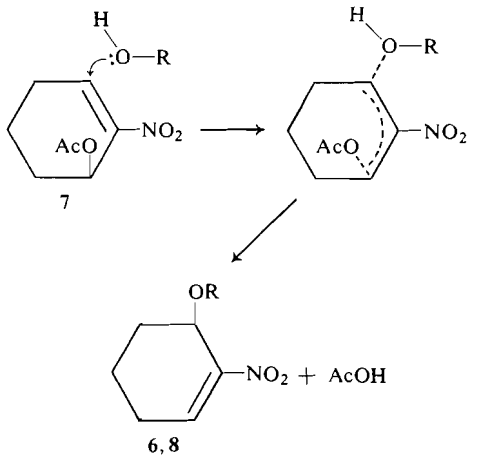

SCHEME 3

in the absence of base, the process stops at this stage instead of proceeding to **4**.

In order to explore further the synthetic utility of elimination–addition reactions of this kind, the diacetate **2** was allowed to react with benzyl alcohol and sodium benzoxide in tetrahydrofuran. Although the oily product that was isolated in 53% yield was not submitted to elemental analysis, spectral evidence showed it to be the dibenzoxy compound **9**. T.l.c. indicated that further products arise in the reaction (for which variously modified conditions were tried), and it seemed that olefins such as **7** and the benzoxy analog of **6** were among them. All attempts to react **2** with isopropoxide failed to give the corresponding bis-isopropyl ether, and a small amount of the olefin **7** was the only product that could be isolated.

Further studies were devoted to the behavior of the diol **1** and the dimethyl ether **4** towards alkali. It had previously been shown (10) that **1** undergoes partial epimerization when it is dissolved in *M* sodium borate solution; upon acidification after 20 h, mainly the starting diol **1** was recovered but small proportions of its *cis,trans* and *cis,cis* isomers were found to be present also. Undoubtedly the isomers also exist, as minor products, in the reaction mixture of the nitromethane cyclization of glutaral-

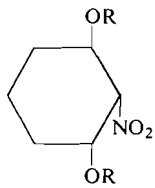

10 R = H
10*a* R = Ac

dehyde (2), and we have in fact been able to isolate the *cis,trans* isomer **10** by column chromatography in 15% yield besides the main product **1** which was obtained in 66% yield. However, a reaction hitherto apparently unrecognized, though not unexpected, was found to be brought about in **1** by strong base. Figure 1*a* shows u.v. spectra indicating the formation of nitronate in aqueous sodium hydroxide solutions of different normalities. In *N* and 0.1 *N* solutions, the characteristic anion peak at 246 nm is generated instantly and in full strength, or nearly so. The absorbance in *N* NaOH solution, corresponding to an ε value of 11 000 which is reasonable for

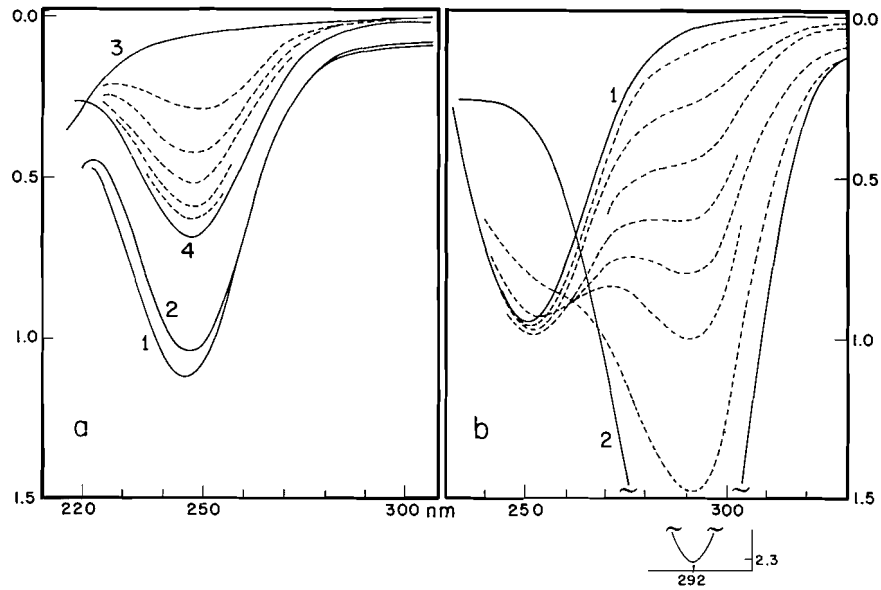

FIG. 1. (*a*) Nitronate u.v. absorption generated in 10^{-4} *M* solutions of **1** in aqueous sodium hydroxide. Curves 1 and 2, in 1 *N* and 0.1 *N* NaOH, respectively, after 1 min and essentially unchanged after 10 min. Curve 3, in 0.001 *N* NaOH (p*H ca.*10), constant for 1 h. Curve 4, in 0.01 *N* NaOH (p*H* 11.1) after 40 and 75 min; broken tracings, after 2, 4, 6, 12, and 24 min (increasing absorbance). (*b*) The same in 1 *N* ethanolic potassium hydroxide. Curve 1, after 4 min. Broken tracings, increasing absorbances after 0.25, 1, 1.5, 2, 2.5, 3, and 4.5 h. Curve 2, after 24 h.

such compounds, suggests that far-reaching ionization is attained. In 0.01 *N* NaOH, the nitro–nitronate equilibrium lies markedly less far on the nitronate side and is approached only after about 30 min, the half-time of equilibration being about 3 min at 26°. The nitronate proportion present in 0.001 *N* NaOH is too small to cause an absorption peak. Now it was observed that the anion peak of **1** in ethanolic, *N* potassium hydroxide solution (λ_{max} 250 nm) slowly decreased with time and completely disappeared within 20 h; concurrently a new, and more intense, peak arose at 292 nm (Fig. 1*b*). The dimethyl ether **4** behaved in a qualitatively similar manner although its nitronate was formed less rapidly. Even in 0.1 *N* sodium hydroxide solution, maximum absorption intensity at 248 nm was attained only after about 2 h (with a half-time of 22 min). This is depicted in Fig. 2*a* which also shows the beginning of the subsequent decline in the peak with concomitant appearance of long wavelength absorption. Figure 2*b* shows the change that occurred in ethanolic *N* potassium hydroxide solution where the new peak at 293 nm was fully established after 5 h.

The spectral phenomena just described are familiar from the chemistry of 3-deoxy-3-nitroaldopyranosides and need to be explained in the same terms as the analogous processes encountered there (15). The absorption in the 290 nm region is due to β,γ-unsaturated (allylic) nitronates (**12***a*, **12***b*) which arise by slow proton abstraction from intermediate α-nitroalkenes (Scheme 4). The latter are formed by β-elimination of a hydroxide (**11** from **1**) or methoxide ion (**6** from **4**) and are considered to be the same intermediates that are involved in the epimerizations and elimination–additions referred to before. Upon acidification of the allylic nitronates **12**, the nitronic acids liberated tautomerize rapidly.[4] *C*-Protonation in cyclohexene 3-nitronate (23) and other conjugated nitronates usually favors the terminal carbon atom of the system (13*a*), and in the present cases we were indeed able to isolate **6**, which was identified by i.r. and n.m.r. spectroscopic comparison, and **11**, which was characterized by its spectra and, further, by borohydride reduction giving known *trans*-

[4]In the analogous work in 3-nitro pyranosides (15), the corresponding nitronic acids incurred other transformations which were not elucidated in detail but were thought to involve hydrolysis of the enol ether linkage present in those structures.

Can. J. Chem. Downloaded from www.nrcresearchpress.com by 210.87.254.5 on 09/05/12
For personal use only.

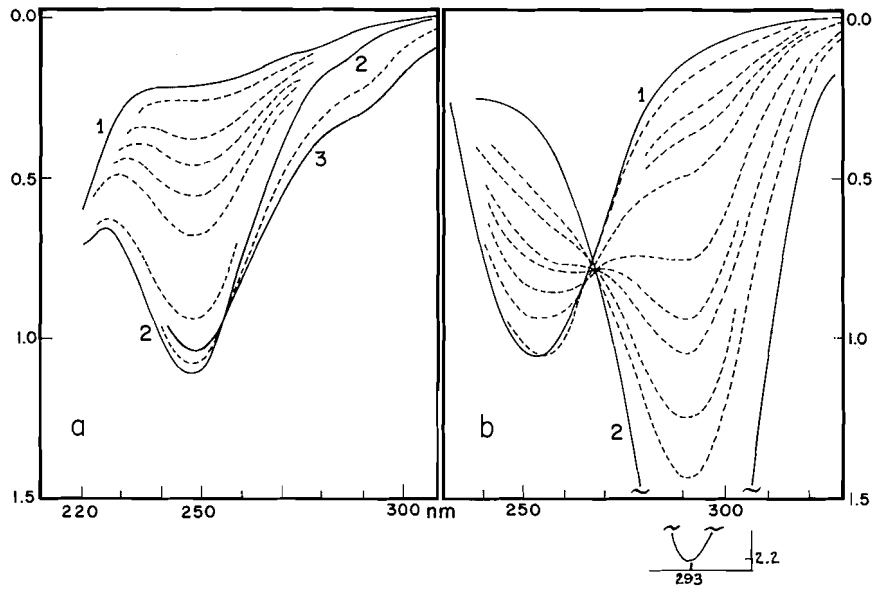

FIG. 2. (*a*) Nitronate u.v. absorption generated in a 10^{-4} *M* solution of **4** in 0.1 *N* aqueous sodium hydroxide. Curve 1, after 2 min. Curves 2 and 3, after 2 and 5 h, respectively. Broken tracings, increasing absorbances after 5, 10, 15, 22, 30, 60, and 165 min. (*b*) The same in 1 *N* ethanolic potassium hydroxide. Curve 1, after 3 min. Curve 2, after 5 h. Broken tracings, increasing absorbances after 6, 12, 17, 24, 42, 56, 65, 85, and 106 min.

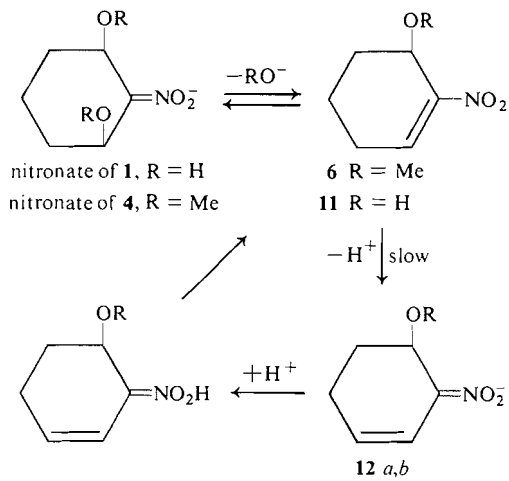

SCHEME 4

2-nitrocyclohexanol. Compound **11** arose not only from **1** but also, along with **6**, from **4**. The reaction was performed in an aqueous medium; it was therefore not surprising in light of the mechanism discussed, that part of the material underwent exchange of a methoxyl substituent. Conversely, exchange of hydroxyl for alkoxyl groups by the action of alcohols has been observed in nitro sugars and formulated as proceeding through intermediary α-nitroolefins (20, 24, 25).

Finally, compounds **1** and **4** were subjected to bromination by means of bromine and alkali according to the method concurrently applied to nitro sugars and published in detail (26). It had been found, in sugars, that formation of bromonitro derivatives is strongly dependent on stereochemical features. In rigid pyranosides where an equatorial nitro group was flanked by two equatorial substituents, bromination of the nitromethine carbon did not occur under standard conditions that afforded smooth bromination in sterically more favorable isomers. The conditions provided an equivalent amount of sodium hydroxide, in dilute solution at 0–20°, for the purpose of generating the requisite nitronate salt, and failure of bromination was attributed to sterically impeded nitronate formation. Under the conditions stated, **1** and **4** were resistant likewise, which is in harmony with their low acidity as reflected in Figs. 1 and 2 (absence of nitronate peak at p*H* 10). When nitronate formation was enforced by a strongly alkaline medium, bromination did proceed and bromonitro derivatives (**13** and **14**, respectively) were obtained in good yields. Each was accom-

Can. J. Chem. Downloaded from www.nrcresearchpress.com by 210.87.254.5 on 09/05/12
For personal use only.

Can. J. Chem. Downloaded from www.nrcresearchpress.com by 210.87.254.5 on 09/05/12
For personal use only.

panied by a small amount of second product, presumably a stereoisomer.

The new trisubstituted cyclohexane derivatives **3**, **4**, **5**, and **9** were shown by n.m.r. spectroscopy to possess the *trans,trans* configuration like their known precursors **1** and **2**. Thus, in **3**, the signal at lowest field (δ 4.28) was a one-proton triplet attributable to the nitromethine proton, and its splitting of 9.5 Hz indicated a 1,2,3-triaxial proton arrangement and therefore equatorial orientation of the three substituents. Compounds **4**, **5**, and **9** exhibited the same kind of nitromethylene triplet, with splittings of 9–10 Hz. The symmetrically substituted compounds **4** and **9** showed single signals for their magnetically equivalent substituents, *i.e.*, one six-proton methoxyl singlet was given by **4**, and one 10-proton phenyl singlet as well as one four-proton benzylic methylene singlet was given by **9**. The spectrum of the bromonitro diol **13** was not readily interpretable in terms of configuration, but that of the dimethyl ether **14** revealed the methoxyl groups to be magnetically equivalent and therefore *cis*-oriented to each other. The configuration with respect to the bromonitro carbon remained unknown.

The n.m.r. spectra of the unsaturated derivatives **6**, **7**, **8**, and **11** all exhibited in mid-field (δ 4.42, 6.03, 4.53, and 4.85, respectively) a narrow quartet or triplet for H-3 containing couplings of 2–4 Hz. This indicated that the dihedral angles between H-3 and either proton at C-4 were both small, and on this basis the $^5H_4$ half-chair conformation, with pseudo-equatorial hydrogen and pseudo-axial substituent at C-3, could be assigned to these compounds. (The alternate $^4H_6$ conformation would call for a large and a small vicinal coupling in the H-3 signal). The conformation adopted is that which is predicted on grounds of the $A^{(1,2)}$ effect, the unfavorable nonbonded interaction between the nitro group, situated on an endocyclic double bond in a six-membered ring, and a neighboring pseudo-equatorial substituent (27). A case of precedence for the operation of this effect in an unsaturated nitro pyranose derivative has been reported (28).

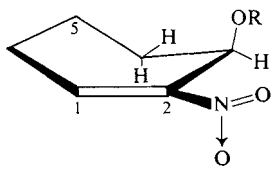

$^5H_4$ conformation

6, 7, 8, 11

Experimental

T.l.c. was performed on silica gel G plates and routinely used for monitoring separations by column chromatography. Spots were made visible by heating the plates sprayed with ceric sulfate in 10% sulfuric acid. Unless otherwise indicated, the following combinations of carbon tetrachloride – ethyl acetate were used as chromatographic solvents: A, 1:1; B, 3:2; C, 2:1; D, 7:3; E, 3:1; F, 4:1; G, 6:1.

Unless specified otherwise, the n.m.r. data refer to 100 MHz spectra obtained from $CDCl_3$ solutions (lock signal, tetramethylsilane). I.r. spectra were obtained on a Beckman IR-20 instrument form Nujol mulls (or neat oils if so indicated). U.v. spectra were measured on a Perkin-Elmer 202 spectrophotometer.

2t-Nitrocyclohexane-1r,3c-diol (1) and Racemic 1r,2c,3t-Stereoisomer (10), and Their Diacetates 2 and 10a

Commercial glutaraldehyde (25% aqueous solution) was cyclized with nitromethane both by the original (1) and the modified (2) procedure. Yields of **1** (m.p. *ca.* 160°) were approximately 50–65%. Further recrystallization of **1** from benzene–ethanol (4:1) raised the melting point to 165–166°. Reported: m.p. 159–161° (1), 154° (2). Crude preparations, and especially the mother liquors thereof, showed a spot that moved slightly faster than that of **1** (t.l.c. with solvent A). A run starting from 9.5 g of dialdehyde (= 38 ml of solution) and performed according to the literature (2) gave a first crop of **1** (9.0 g). The remainder of the material was chromatographed on a column of silica gel (490 g) using solvent C as eluant. Initial fractions furnished a very small amount (74 mg) of an oil that appeared to be spectroscopically identical with the nitroolefin **11**. Subsequent fractions yielded an oil which solidified on standing (2.35 g, 15.3%). It showed only the faster t.l.c. spot and was judged to be identical with the *cis,trans* isomer of **1** (*i.e.* **10**, the racemic 1*r*,2*c*,3*t*-isomer) previously obtained (10) as an amorphous solid in 3% yield by base-catalyzed epimerization of **1**. Confirmation was obtained by acetylation with acetic anhydride and boron trifluoride (19) which gave the crystalline diacetate **10***a* in 63% yield; m.p. 87° after recrystallization from ethanol – petroleum ether. Reported: m.p. 88–89°. The n.m.r. spectrum of **10***a* in $CDCl_3$ was in agreement with the reported data (10) except that we noted slightly different chemical shifts for the acetoxy singlets (δ 1.99 and 2.02 rather than 2.05 and 2.08) and the H-2 quartet (δ 4.54 rather than 4.65); $J_{1,2}$ = 3.5 Hz, $J_{2,3}$ = 10.5 Hz.

Further elution of the column produced another 1.15 g of **1** (total yield, 66%). The diacetate **2**, m.p. 90–91.5°, was prepared as described (3) (lit. (1) m.p. 89–90°). N.m.r. data (in $CDCl_3$): δ 2.00 (s, 6H, OAc); 4.58 (t, 1H, $J_{1,2} = J_{2,3}$ = 10.5 Hz, H-2); 5.2 (sextet, 2H, H-1 and -3); 1.3–2.5 (m, 6H).

Can. J. Chem. Downloaded from www.nrcresearchpress.com by 210.87.254.5 on 09/05/12
For personal use only.

1-O-Methyl-2t-nitrocyclohexane-1r,3c-diol (3) and 1,3-Di-O-methyl-2t-nitrocyclohexane-1r,3c-diol (4)

From 1 by Diazomethane

An ethereal solution of diazomethane was prepared from nitrosomethylurea (50 g) and stored over Dry Ice. A suspension of the diol **1** (4.0 g) and freshly activated (150°) Drierite (3 g) in dry ether (40 ml) was stirred at 0°, and a few drops of boron trifluoride etherate followed by 3–4 ml of the diazomethane solution were added. As the yellow color of the reaction mixture began to fade, further small portions of diazomethane solutions were added, and when the color persisted for several minutes, additional small quantities of BF_3 were introduced. This alternating addition was continued for 3 h or longer, until the entire diazomethane solution and about 5 ml of catalyst had been consumed. Production of light, flocculent polymethylene was observed during the process. The reaction mixture was then treated briefly with some activated charcoal, filtered, and evaporated to give a colorless or faintly yellow oil. The oil contained **3** (R_f 0.6), **4** (R_f 0.4), and starting material **1** (R_f 0.3) according to t.l.c. with solvent **B**, in a visually estimated ratio of about 5:1:5. The components could be separated, and most of the unreacted **1** recovered, as is described below. Alternatively, the methylation was allowed to continue, using a correspondingly larger quantity of diazomethane, until t.l.c. revealed the presence of **3** (major product) and **4** (minor product) together with only a small proportion of **1**.

In order to remove the bulk of unreacted **1**, if present, the oily reaction product was triturated with chloroform (200 ml) whereby insoluble **1** (*e.g.* 1.5 g) separated as a white solid. The filtrate was evaporated to give a residue which was chromatographed on silica gel (300 g) by means of solvent **C**. The fractions (15 ml) were monitored by t.l.c. There was obtained, in turn, 420 mg of **4**, 1.62 g of **3**, and 230 mg of **1** (43% recovery, together with the 1.5 g, above). The yield of **3** was 37%, and that of **4** was 9% (65 and 15.5%, respectively, if the recovered **1** is taken into account). Similar chromatography of a reaction mixture from a more exhaustive methylation (see above) afforded 2.45 g (52%) of **3** and 890 mg (20%) of **4**.

The dimethyl ether **4** was found to be the major product when the reaction was carried out under cooling with Dry Ice, rather than at 0°, possibly because competing decomposition of diazomethane is less severe. Thus, from 2.0 g of **1** and diazomethane generated from 50 g of nitrosomethylurea there was obtained, upon eventual solvent evaporation, an oil that contained only a trace of **3** and that crystallized on cooling. Recrystallization from benzene – petroleum ether furnished **4** (2.03 g, 87%) as colorless platelets, m.p. 79–80°.

Compound **3** crystallized as colorless tablets from carbon tetrachloride, m.p. 80–81.5°; ν_{max} 3420 (sharp; OH), 1545 (NO_2), 1050–1075 cm^{-1} (strong; C—O—C). N.m.r. data: δ 4.28 (t, 1H, $J_{1,2} = J_{2,3} = 9.5$ Hz, H-2); 4.0 (broad peak, resolved to multiplet on adding D_2O, H-3); 3.6 (m, H-1); 3.32 (s, 3H, OCH_3); 2.35 (d, 1H, OH); 1.1–2.3 (unresolved signals, 6H, methylene groups).

Anal. Calcd. for $C_7H_{13}NO_4$ (175.2): C, 47.99; H, 7.48; N, 8.00. Found: C, 47.83; H, 7.59; N, 7.86.

Compound **4**, which after a second recrystallization also melted at 81° (compare **3**!), lacked hydroxyl absorption in the i.r.; ν_{max} 1550 (NO_2), 1090–1065 cm^{-1} (strong, C—O—C). N.m.r. data: δ 4.30 (t, 1H, $J_{1,2} = J_{2,3} = 10$ Hz, H-2); 3.6 (sextet, 2H, H-1 and -3); 3.31 (s, 6H, OCH_3); 1.0–2.5 (unresolved methylene signals, 6H).

Anal. Calcd. for $C_8H_{15}NO_4$ (189.2): C, 50.78; H, 7.99; N, 7.40. Found: C, 50.98; H, 7.83; N, 7.25.

Compound 4 from 2

To a chilled (0°) solution of **2** (40 mg) in anhydrous methanol (40 ml) was added, with stirring, a 0.037 *N* solution of sodium methoxide (1 ml; 0.23 mol equiv). After 7 min, carbon dioxide was passed through the solution for 0.5 h. (It had been found in numerous similar experiments that treatment of **2** with increased amounts of base and (or) for extended periods of time favored the formation of by-products and decreased the yield in **4**.) The reaction mixture was evaporated, and the residue was taken up in ethyl acetate which was treated with charcoal, filtered, and evaporated to yield a pale-yellow oil. The t.l.c. (solvent **C**) showed a trace of remnant **2**, a major spot of **4**, and a minor spot that had the mobility of **3**. (Presumably, some **3** could have arisen owing to de-*O*-acetylation competing with acetoxy elimination.) The oil was chromatographed on a small column of silica gel (4 g) with benzene–ether (4:1). The fractions containing pure **4** were treated with charcoal and then furnished a colorless oil that was crystallized from benzene – petroleum ether. The crystals (17 mg, 55%) melted at 79–80° and gave an i.r. spectrum identical with that of **4** obtained previously.

1-O-Methyl-2t-nitrocyclohexane-1r,3c-diol 3-Acetate (5)

Compound **3** (350 mg) was acetylated with acetic anhydride (6 ml) and boron trifluoride etherate (8 drops) at ambient temperature (40 min). The mixture was poured into ice water which was stirred until the excess anhydride was decomposed, and then extracted with several portions of ether. Evaporation of the dried ($MgSO_4$) extract with added toluene, and treatment of the residue with activated carbon, afforded **5** as a colorless oil that crystallized on cooling. Recrystallization from carbon tetrachloride – petroleum ether afforded 390 mg (90%) of white platelets, m.p. 92–93°; ν_{max} 1740 (C=O), 1550 (NO_2), 1235, 1200, 1100, 1040 cm^{-1} (all strong, C—O—C). N.m.r. data: δ 5.14 (m, 1H, H-3); 4.43 (t, 1H, $J_{1,2} = J_{2,3} = 10.3$ Hz, H-2); 3.68 (m, 1H, H-1); 3.32 (s, 3H, OCH_3); 1.99 (s, 3H, OAc); 1.3–2.4 (unresolved methylene signals).

Anal. Calcd. for $C_9H_{15}NO_5$ (217.2): C, 49.77; H, 6.96; N, 6.45. Found: C, 49.73; H, 7.04; N, 6.47.

3-Methoxy-2-nitrocyclohexene (6)

From 7

The acetoxy olefin **7** (47 mg) was refluxed in anhydrous methanol (4 ml) for 12 h, after which a single spot slightly faster moving than **7** was seen on t.l.c. (solvent **F**). Evaporation gave **6** in quantitative yield as a colorless oil. Crystals that formed on cooling to −10° melted at room temperature. I.r. data (neat oil): ν_{max} 2940, 2825 (C—H); 1670 (C=C); 1515 and 1340 (NO_2); 1450; 1090 and 1070 cm^{-1} (C—O—C). N.m.r. data: δ 7.40 (q, 1H, J = 3–4 Hz, H-1); 4.44 (q, 1H, half-height width *ca.* 5 Hz, H-3); 3.44 (s, 3H, OCH_3); 1.1–2.5 (methylene signals, 6H).

Can. J. Chem. Downloaded from www.nrcresearchpress.com by 210.87.254.5 on 09/05/12
For personal use only.

Anal. Calcd. for $C_7H_{11}NO_3$ (157.2): C, 53.49; H, 7.05; N, 8.91. Found: C, 53.64; H, 7.23; N, 8.71.

From 5

Compound **5** (217 mg) and dry sodium bicarbonate (3.34 g) were heated with magnetic stirring in refluxing benzene (15 ml, dried over and distilled from sodium). After 10 h the reaction solution was cooled, filtered, and evaporated to give a yellow oil. Crystallization from carbon tetrachloride – petroleum ether returned 110 mg of unreacted **5**. The mother liquor showed two major t.l.c. spots corresponding to **5** and **6**. Separation on a silica gel column (10 g) using solvent G yielded another 20 mg of **5**, and 35 mg of **6** that was identified by its i.r. spectrum.

From 3

Compound **3** (183 mg) and dry, basic (20) aluminum oxide were stirred in toluene (15 ml, dried over sodium) at 70–75° for 90 min. The pale-yellow reaction mixture was treated with activated carbon, filtered, and evaporated to give a brown oil which, according to t.l.c. (solvent G), contained **6** as the major component. Chromatographic purification on silica gel (15 g) using solvent G yielded 69 mg (42%) of **6** whose i.r. spectrum was identical with that of the previous sample.

From 4

See later on.

3-Acetoxy-2-nitrocyclohexene (7)

The diacetate **2** (1.01 g) and sodium bicarbonate (6.8 g; dried at 120°) were stirred in refluxing dioxane (40 ml, dried over sodium) for 2.5 h. Work-up furnished a yellow oil that showed two major spots (7 and unreacted **2**) and several minor spots on t.l.c. (solvent G). Separation on silica gel (70 g) gave **7** (350 mg, 46%) and **2** (300 mg). The former crystallized from benzene – petroleum ether; m.p. 65–66°. I.r. data (neat oil before crystallization): ν_{max} 3000–2800 (C—H), 1730 (C=O), 1660 (C=C), 1515 and 1340 (NO_2), 1225 (C—O—C), 1155, 1005–900 cm^{-1}. N.m.r. data: δ 7.58 (q, 1H, J = 3 and 5 Hz, H-1); 6.03 (symm. t, 1H, J = 3 Hz, H-3); 2.00 (s, 3H, OAc); 1.6–2.6 (methylene multiplets).

Anal. Calcd. for $C_8H_{11}NO_4$ (185.2): C, 51.89; H, 5.99; N, 7.56. Found: C, 52.03; H, 5.79; N, 7.50.

3-Ethoxy-2-nitrocyclohexene (8)

The acetoxy olefin **7** (90 mg) was refluxed in 99% ethanol (5 ml) for 15 h, after which time t.l.c. (solvent F) showed essentially a single, new spot. Evaporation gave **8** as a nearly colorless oil; ν_{max} (neat): 3000–2800 (C—H), 1665 (C=C), 1510 and 1340 (NO_2), 1090 and 1070 cm^{-1} (C—O—C). N.m.r. data: δ 7.37 (q, 1H, J = 3-4 Hz, H-1); 4.53 (t, 1H, J *ca.* 3 Hz); 3.64 (q, 2H, ethyl CH_2); 1.16 (t, 3H, ethyl CH_3); 1.4–2.6 (methylene multiplets, 6H).

Anal. Calcd. for $C_8H_{13}NO_3$ (171.2): C, 56.12, H, 7.65; N, 8.18. Found: C, 56.06; H, 7.57; N, 8.32.

1,3-Di-O-benzyl-2t-nitrocyclohexane-1r,3c-diol (9)

A 2 *N* solution of sodium benzoxide in benzyl alcohol (0.60 ml, 4 mol equiv) was added dropwise, with stirring at room temperature, to a solution of **2** (70 mg) in anhydrous tetrahydrofuran (5 ml). A white precipitate was produced. Stirring was continued for 8 min, and carbon dioxide was then passed through the mixture for 30 min. Dilution of the mixture with ethyl acetate (20 ml), treatment with activated carbon, filtration, and evaporation gave an oil that contained benzyl alcohol and, according to t.l.c. in solvent E, a major reaction product (**9**), along with two minor, more slowly moving products. No **2** remained. Chromatography on a 50 g silica gel column with benzene–ether (4:1) furnished a total of 52 mg (53%) of a colorless oil from the fractions containing pure or nearly pure **9**. Crystallization could not be achieved. I.r. data of a chromatographically pure fraction (neat oil): 3100–3000 and 2940, 2860 (C—H); 2000–1670 (weak, aromatic combination bands); 1600, 1490, 1450 (arom. C=C); 1550, 1360 (NO_2); 1090 (broad; C—O—C); 1025, 730, 690 cm^{-1}. N.m.r. data: δ 7.35 (s, 10 H, phenyl), 4.67 (s, 4H, benzylic CH_2); 4.45 (t, 1H, $J_{1,2} = J_{2,3}$ = 9 Hz, H-2); 3.52 (m, 2H, H-1 and -3); 2.3–1.2 (methylene multiplets, 6H).

When less than the proportion of benzoxide specified above was used, *e.g.*, only 0.7–2 mol equiv, the crude products obtained after 5 min and even after a prolonged reaction time of 30 min apparently contained much nitroolefinic material, as suggested by i.r. bands occurring at 1660 and 1515 cm^{-1}.

Reaction of 2 with Sodium Isopropoxide

To a solution of **2** (245 mg) in dry benzene (50 ml) was added dropwise, with stirring at room temperature, a suspension of sodium isopropoxide (164 mg, 2 mol equiv) in benzene (20 ml). Stirring was continued for 1 h during which time a flocculent precipitate was formed. The mixture was treated with 5 ml of cation exchange resin, filtered, and evaporated to give a pale-yellow oil which t.l.c. (solvent B) showed to contain two major and several minor components. Of the former, one appeared to be starting **2**, and the other proved to be the acetoxy olefin **7** upon chromatographic isolation (yield, 42 mg) using solvent E, and identification by i.r. and n.m.r. spectra.

Similar experiments, in which tetrahydrofuran or isopropyl alcohol were employed as solvents and varying reaction times were tried, also seemed to produce chiefly **7** and (or) unidentified products as revealed by t.l.c.

Reaction of 1 with Sodium Hydroxide

Exploratory Experiments

Samples of **1** (20 mg) were dissolved in aqueous, 4 *N* sodium hydroxide (1 ml) at room temperature. After certain periods of time, the solutions were diluted with water and neutralized or acidified, by use of Amberlite IR-120 (H^+) or *N* hydrochloric acid (which did not appear to make a difference), and concentrated *in vacuo* for t.l.c. with solvent A. After alkali treatment for 10 min, 0.5, 1, 2, and 4 h there was seen a very strong spot (R_f 0.65) attributed to **11**, and a weak spot of starting **1** (R_f 0.3) together with a slightly faster trace spot (R_f 0.35–0.4). No significant change during 4 h was observed. On the other hand, use of 1 *N* NaOH produced, after 10 min, considerably less of the product R_f 0.65. An even slower reaction was observed with methanolic 1 *N* sodium methoxide which produced, however, *two* fast-moving spots (R_f 0.65 and 0.6; traces after 5 min, and fair spots after 1 h).

3-Hydroxy-2-nitrocyclohexene (11)

A solution of the diol **1** (0.50 g) in 4 *N* NaOH (50 ml)

Can. J. Chem. Downloaded from www.nrcresearchpress.com by 210.87.254.5 on 09/05/12
For personal use only.

was allowed to stand at 25° for 1 h and then diluted with water, cooled with ice, and deionized with Amberlite IR-120 (H^+). The resin was subsequently washed well with water followed by ethanol, and the combined solution was evaporated *in vacuo* to give a syrup. This was chromatographed on silica gel (40 g) with solvent A, fractions of 8 ml size being collected. Fraction Nos. 5–10 yielded 140 mg of the major reaction product **11** (R_f 0.65) in pure form. Fraction Nos. 11–19 (dry weight, 40 mg) were mixtures of **11** and the two slow-moving compounds. Fraction Nos. 20–40 contained small amounts of material presumed to be **1**.

Compound **11** was an oil that distilled at 0.2 mm Hg at *ca.* 140° (bath temperature), with partial decomposition. I.r. data (neat film of dried but undistilled substance): 3400 cm^{-1} (broad; OH); 2950, 2870 (C—H); 1660 (C=C); 1515 (strong; nitroalkene); 1340 (strong); 1250, 1180, 1165, 1085 (weak); 1060 and 985 (strong); 950–800 (6 weak bands); 750, 730 (medium). N.m.r. data (60 MHz): δ 7.45 (t, 1H, J = 4 Hz, H-1); 4.85 (narrow q, 1H, J = 2–3 Hz, H-3); 3.17 (s, 1H, removable by adding D_2O; OH); 1.6–2.6 (m, 6H, methylene).

In another experiment, the crude oil obtained on similar alkali treatment of **1** (400 mg) was dissolved in ethanol (15 ml), and $NaBH_4$ (250 mg) was added. After 20 min the mixture was deionized with cation exchange resin and evaporated. In the oil obtained, the t.l.c. spot corresponding to **11** was considerably weaker than previously, and a new and slightly faster spot was visible. Separation was achieved on a column of silica gel (40 g) using solvent D as eluant; the fraction size was 3 ml. Fraction Nos. 38–56 gave a single spot on t.l.c. and yielded 100 mg of an oil that did not show any olefinic signal (n.m.r.) or nitroalkene absorption (i.r.). It crystallized on cooling, and recrystallization from carbon tetrachloride – petroleum ether gave 40 mg of *trans-2-nitrocyclohexanol*, m.p. 46–47° (lit. (29) m.p. 47–48°). I.r. and n.m.r. spectra established identity with an authentic sample synthesized by oxidation (30) of *trans*-2-aminocyclohexanol.

Reactions of 3 and 4 with Sodium Hydroxide

Exploratory Experiments

These were carried out as described for **1** in the preceding section, except that, for **4**, small amounts of dioxane and methanol were added to the alkaline reaction mixture to assist in dissolving the compound. After 10–30 min in 4 N NaOH, compounds **3** (R_f 0.4) and **4** (R_f 0.6) both gave two product spots, apparently the same (R_f 0.5 and 0.7), on t.l.c. with solvent D. The R_f 0.5 spot corresponded to **11** (R_f 0.65 in solvent A), and the R_f 0.7 spot was attributed to **6**.

Isolation of 6 and 11

The diether **4** (0.40 g) was added to aqueous 4 N NaOH (20 ml). Stirring for 30 min at room temperature failed to effect complete solution. Dioxane was therefore added dropwise to dissolve all remnant **4**, and sufficient methanol was added to produce a homogeneous phase. Stirring was continued for 30 min. Work-up and column chromatography was performed as described for **11** in a preceding section, except that solvent D was employed and 6 ml fractions were collected. Fraction Nos. 13–20 gave **6** (40 mg) and fraction Nos. 24–40 gave **11** (50 mg). Both products were identified by their i.r. and n.m.r. spectra.

2-Bromo-2-nitrocyclohexane-1,3-diol (13)

The diol **1** (0.50 g) was dissolved in 1 N sodium hydroxide (3.1 ml, 1 mol equiv), and after 2 min bromine was added in small drops until its color persisted. A precipitate was formed. The mixture was evaporated, and added portions of ethanol followed by ethyl acetate were evaporated from the residue. The t.l.c. with benzene–ether (3:2) showed remnant **1** (R_f 0.3) and two products, R_f 0.4 and 0.5. Fractionation was achieved on silica gel (50 g) with the same solvent mixture. The product of R_f 0.4 was obtained as a colorless oil which crystallized on scratching. Recrystallization from benzene–ethanol gave **13** (310 mg, 41%), m.p. 188–189°. I.r. bands were at 3480, 3400 (OH), 1545 with shoulder at 1560 (NO_2), 1190, 1080, 1060, 945, 860, 735 cm^{-1}. N.m.r. data (in acetone-d_6): δ 4.15 (2H, complex multiplet, H-1 and -3); 1.5–2.0 (6H, methylene multiplets).

Anal. Calcd. for $C_6H_{10}BrNO_4$ (240.1): C, 30.02; H, 4.20; N, 5.84; Br, 33.29. Found: C, 30.07; H, 4.53; N, 5.64; Br, 33.44.

The faster-moving component was also isolated from the column as a solidifying oil, but only a small part (12 mg) was obtained crystalline, m.p. 132–134° (from carbon tetrachloride). The i.r. spectrum was very similar to that of the main product, with slight differences in band positions and relative intensities. Mass spectra were nearly identical, revealing the presence of bromine.

2-Bromo-1,3-di-O-methyl-2-nitrocyclohexane-1,3-diol (14)

To a mixture of the diether **4** (1.0 g) and 2.5 N sodium hydroxide (20 ml) was added some tetrahydrofuran followed by methanol as required to produce a homogeneous solution. Bromine was then added dropwise until the solution stayed yellow. The excess base was removed by means of cation exchange, and the solution was evaporated to dryness. The material contained a product (R_f 0.4) besides unreacted **4** (R_f 0.25) (t.l.c. with benzene–ether 3:2). Separation was achieved on a silica gel column (100 g) using the same solvent. The faster-moving product (**14**) was obtained as a solid that was recrystallized from carbon tetrachloride – petroleum ether; m.p. 92–93°. The yield was 0.68 g (48%). I.r. bands: 1555 (strong, NO_2); 1090 cm^{-1} (strong, C—O—C). N.m.r. data: δ 4.10 (m, 2H, H-1 and -3); 3.45 (s, 6H, OCH_3); δ 2.0 (m, 6H, methylene). The mass spectrum exhibited molecular ion peaks at *m/e* 269 and 267.

Anal. Calcd. for $C_8H_{14}BrNO_4$ (268.1): C, 35.84; H, 5.26; N, 5.22. Found: C, 35.76; H, 5.43; N, 5.02.

Starting **4** (185 mg) was recovered from later fractions.

Support of this work by the National Research Council of Canada is acknowledged.

1. F. W. LICHTENTHALER. Chem. Ber. **96**, 945 (1963).
2. F. W. LICHTENTHALER, T. NAKAGAWA, and A. EL-SCHERBINEY. Chem. Ber. **101**, 1837 (1968).
3. H. H. BAER and M. T. C. WANG. Can. J. Chem. **46**, 2793 (1968).
4. F. J. M. RAJABALEE. Ph.D. Thesis. University of Ottawa, Ottawa, Ontario. 1969.
5. F. W. LICHTENTHALER and P. VOSS. Tetrahedron Lett. 2297 (1969).

6. F. W. LICHTENTHALER, P. VOSS, and N. MAJER. Angew. Chem. **81**, 221 (1969).
7. F. W. LICHTENTHALER, G. TRUMMLITZ, and H. ZINKE. Tetrahedron Lett. 1213 (1969).
8. T. NAKAGAWA, Y. SATO, T. TAKAMOTO, N. MAJER, and F. W. LICHTENTHALER. Bull. Soc. Chem. Japan, **43**, 3866 (1970); F. W. LICHTENTHALER and W. FISCHER. Chem. Commun. 1081 (1970).
9. F. W. LICHTENTHALER and P. Voss. Ann. Chem. **724**, 81 (1969).
10. S. J. ANGYAL and B. M. LUTTRELL. Aust. J. Chem. **23**, 1485 (1970).
11. H. H. BAER and J. KOVÁŘ. Can. J. Chem. **49**, 1940 (1971).
12. E. MÜLLER and W. RUNDEL. Angew. Chem. **70**, 105 (1958). E. MÜLLER, M. BAUER, and W. RUNDEL. Z. Naturforsch. **14b**, 209 (1959). E. G. GROS and E. M. GRUNIERO. Carbohydr. Res. **14**, 409 (1970), and earlier work cited there.
13. H. FEUER (*Editor*). The chemistry of the nitro and nitroso groups. Interscience Publishers, New York, N.Y. 1969–1970. (*a*) A. T. NIELSEN. Part 1, pp. 349–486. (*b*) H. H. BAER and L. URBAS. Part 2, pp. 75–200.
14. H. H. BAER and W. RANK. Can. J. Chem. **49**, 3197 (1971).
15. H. H. BAER and F. KIENZLE. Ann. Chem. **695**, 192 (1966).
16. H. H. BAER, S. H. L. CHIU, and D. C. SHIELDS. Can. J. Chem. This issue.
17. H. H. BAER. Adv. Carbohydr. Chem. Biochem. **24**, 67 (1969).
18. H. H. BAER and C. W. CHIU. Carbohydr. Res. In press.
19. H. H. BAER, F. KIENZLE, and F. RAJABALEE. Can. J. Chem. **46**, 80 (1968).
20. H. H. BAER, T. NEILSON, and W. RANK. Can. J. Chem. **45**, 991 (1967). H. H. BAER and W. RANK. Can. J. Chem. **47**, 2811 (1969).
21. H. H. BAER and F. KIENZLE. J. Org. Chem. **33**, 1823 (1968).
22. H. FEUER and S. MARKOFSKY. J. Org. Chem. **29**, 929 (1964). H. H. BAER and F. KIENZLE. Can. J. Chem. **43**, 190 (1965).
23. A. T. NIELSEN. J. Org. Chem. **27**, 2001 (1962).
24. H. H. BAER and F. KIENZLE. Can. J. Chem. **45**, 983 (1967).
25. M. L. WOLFROM, U. G. NAYAK, and T. RADFORD. Proc. Natl. Acad. Sci. USA, **58**, 1848 (1967).
26. H. H. BAER and W. RANK. Can. J. Chem. **51**, 2001 (1973).
27. F. JOHNSON and S. K. MALHOTRA. J. Am. Chem. Soc. **87**, 5492 (1965).
28. R. U. LEMIEUX, T. L. NAGABHUSHAN, and S. W. GUNNER. Can. J. Chem. **46**, 405 (1968).
29. T. E. STEVENS and W. D. EMMONS. J. Am. Chem. Soc. **79**, 6008 (1957).
30. H. H. BAER and S. H. L. CHIU. Can. J. Chem. **51**, 1812 (1973).

Can. J. Chem. Downloaded from www.nrcresearchpress.com by 210.87.254.5 on 09/05/12
For personal use only.

Photolyse du butène-1 dans l'ultraviolet à vide

GUY J. COLLIN[1]

Radiation Chemistry Section, National Bureau of Standards, Washington, D.C. 20234

Reçu le 5 mars 1973

Le butène-1 est photolysé dans l'ultraviolet à vide (147–105 nm) et les produits principaux de la fragmentation de la molécule sont l'allène, les butadiènes, l'éthylène et l'acétylène. L'addition de l'atome d'hydrogène sur la double liaison forme le radical butyle secondaire et le radical butyle primaire (9% à 147 nm). Aux plus courtes longueurs d'onde, cette proportion passe à 18% à 123.6 nm montrant aussi que certains atomes d'hydrogène possèdent une énergie cinétique supérieure à l'énergie thermique tout au moins à 10 et à 11.6–11.8 eV.

The vacuum u.v. photolysis of 1-butene was studied in the 147–105 nm region. The main products formed from the fragmentation of excited molecules are allene, 1,3- and 1,2-butadienes, ethylene, and acetylene. The addition of a hydrogen atom to the double bond produces mainly secondary butyl radicals (91%) at 147 nm. At 123.6 nm, this proportion becomes 82%. Thus at shorter wavelengths (10 and 11.6–11.8 eV), hydrogen atoms are produced with a kinetic energy higher than the thermal energy.

Can. J. Chem., 51, 2853 (1973)

Introduction

La photolyse du butène-1 est bien connue en ce qui concerne le domaine de l'ultraviolet lointain: région de 185 nm et de 202–206 nm (1). Dans ce domaine de l'énergie, la principale réaction de décomposition de la molécule butène-1 est la réaction de scission de la liaison carbone–carbone située en position β de la double liaison. Nous avons étendu cette étude à la région comprise entre 147 et 104.8 nm. En outre, nous avons essayé de déterminer quelle peut-être l'importance de l'énergie cinétique que contiennent les atomes d'hydrogène libérés. Une étude semblable sur l'isobutène a déjà été publiée (2).

Procédure Expérimentale

La procédure expérimentale, ainsi que les lampes d'irradiation, ont déjà été décrites (3).

Le butène-1 a été purifié par c.p.g. puis dégasé avant d'être utilisé. Le butène-1,1-d_2 est un produit Merck, Sharp and Dohme of Canada et contient 1.2% de butène-1-d_1. Les résultats rapportés ont été corrigés pour cette impureté.

L'actinométrie a été faite en admettant que le rendement quantique M/N (nombre de molécules M produites par rapport au nombre N de molécules excitées formées par absorption d'un photon) de l'acétylène dans l'irradiation de l'éthylène est égale à l'unité entre 147 et 123.6 nm (4). Aux lignes d'argon, l'actinométrie est faite en mesurant le courant ionique libéré dans la cellule irradiée. Le rendement quantique d'ionisation du butène-1 est connu et est 0.32_1 (3).

Le taux de conversion est généralement inférieur à 0.1%, sauf dans de rares cas où il peut atteindre 0.5%.

Résultats

Ceux-ci sont rapportés dans les tableaux et figures de ce texte. Les rendements rapportés sont les rendements quantiques Φ ou les rendements par rapport au rendement des molécules excitées M/N(ex.); ces deux rendements étant liés par la relation $M/N(\text{ex.}) = \Phi/\Phi(\text{ex.})$. A ces résultats, il convient d'ajouter les résultats des analyses par spectrométrie de masse des produits formés dans l'irradiation du $CH_3CH_2CH{=}CD_2$.

La composition de l'éthylène varie de façon importante avec la pression de l'échantillon (tableau 1). La composition isotopique de l'acétylène est indépendante de la pression et de la lampe utilisée et de la présence ou de l'absence de l'oxygène. Il en est de même de l'allène et du propène:

$$C_2{-}D_2/{-}D_1/{-}D_0: 21.5 \pm 1.5/55 \pm 2/24 \pm 2$$

$$C_3H_2{-}D_2/{-}D_1/{-}D_0: 87 \pm 2/12 \pm 1/2 \pm 2$$

$$C_3H_3{-}D_3/{-}D_2: 15.5 \pm 1.5/84.5 \pm 1.5$$

En l'absence d'oxygène, l'éthane produit à 147 nm est

$$C_2H_4{-}D_2/{-}D_1/{-}D_0: 10/5/85$$

[1]Chercheur invité de la NBS en 1968–69; travail subventionnér en partie par la U.S. Atomic Energy Commission. Adresse actuelle: Département des Sciences Pures, Université du Québec à Chicoutimi, Chicoutimi, Québec, Canada G7H 2B1.

Can. J. Chem. Downloaded from www.nrcresearchpress.com by 210.87.254.40 on 09/05/12
For personal use only.

TABLEAU 1. Photolyse du $CH_3CH_2CH_2CD_2$: analyse de l'éthylène

Réactifs (Torr)							
Butène-1	Oxygène	Additif	λ (nm)	C_2H_4	C_2H_3D	$C_2H_2D_2$	C_2HD_3
2.00	0.10	—	147.0	50	3.0	42.7	4.3
2.00	0.09	Krypton: 86	147.0	65.0	4.8	29.0	1.2
2.00	—	Hélium: 215	147.0	66.5	1.6	30.1	1.7
1.00	—	—	123.7	53.7	1.9	39.0	5.3
1.00	—	Hélium: 67	123.7	71.8	1.4	25.2	1.6
4.00	0.2	—	104.8 106.7	55.4	7.1	33.0	4.0

Discussion

Caractéristiques générales

Dans la région de l'ultraviolet à vide considérée ici, c'est-à-dire entre 104.8 et 147 nm, le spectre d'absorption du butène-1 est connu (5). A l'énergie émise par la raie de résonnance du xénon, 8.4 eV, l'absorption d'un photon conduit à une molécule neutre excitée. Aux raies de résonnance du krypton et de l'argon, 10.0 et 11.6–11.8 eV, une fraction des molécules ayant absorbé un photon sont ionisées:

[1] $C_4H_8\text{-}1 + h\nu \rightarrow (C_4H_8)^{**}$

[2] $C_4H_8\text{-}1 + h\nu \rightarrow [C_4H_8^+]^* + e^-$

L'importance relative des réactions 1 et 2 est connue (3, 6). Puisqu'à 8.4 eV, il n'y a pas d'ion formé (Φ(ion) = 0.00), le rendement M/N(ex.) est égal au rendement quantique. Au cours de ce qui suit, rien ne sera dit des réactions de l'ion excité $[C_4H_8^+]^*$. A 10.0 eV, cet ion ne contient pas assez d'énergie pour se fragmenter. Il ne contribue donc probablement pas aux produits analysés ici. En fait, il est connu que cet ion initie la polymérisation du monomère (7).

Toutes le valeurs des rendements sont donc rapportées au nombre de molécules excitées formées en phase gazeuse et seront donc de la forme M/N(ex.). On supposera donc que la formation de tous les produits mesurés ne proviennent que des réactions qui succèdent à la réaction 1.

Décomposition de la molécule excitée

La molécule excitée formée par absorption d'un photon contient au minimum 194.5 kcal mol^{-1}. C'est une énergie beaucoup plus grande que l'énergie requise pour briser l'une quelconque des liaisons de la molécule: environ 100 kcal mol^{-1}. Il est donc raisonnable d'admettre que l'espèce excitée a un temps de vie inférieur au temps disponible entre deux collisions dans le domaine de pression étudié ici:

[3] $(C_4H_8\text{-}1)^{**} \rightarrow H, R, R_1R_2$

où H et R sont respectivement l'atome d'hydrogène et un radical libre et R_1R_2 est un produit moléculaire stable. Le rendement de ces produits est donc, en principe, indépendant de la pression dans le présent domaine d'étude. Des résultats (voir plus loin), il ressort que plusieurs produits ont des rendements qui sont en première approximation indépendants de la pression (fig. 1). Il en est ainsi des rendements en allène et propyne (tableaux 2 et 3).

[4] $(C_4H_8\text{-}1)^{**} \rightarrow C_3H_4 + CH_4 \quad \Delta H =$ 27.7 kcal mol^{-1}

[5] $(C_4H_8\text{-}1)^{**} \rightarrow C_3H_4 + CH_3 + H \quad \Delta H =$ 132 kcal mol^{-1}

Cette réaction est précisée par l'analyse isotopique de l'allène formé dans l'irradiation du $CH_3CH_2CH{=}CD_2$:

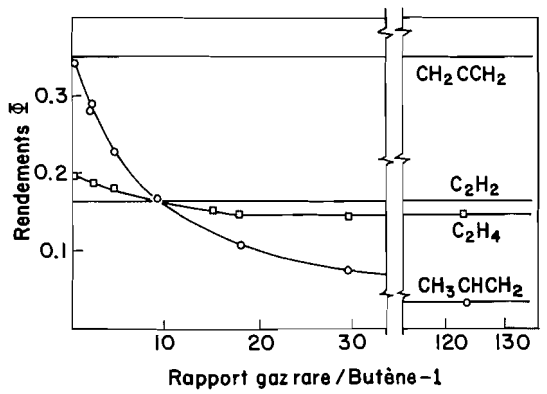

FIG. 1. Photolyse à 8.4 eV. Effet de la pression totale (additif: hélium ou krypton) sur les rendements; butène-1: 2 Torr.

Can. J. Chem. Downloaded from www.nrcresearchpress.com by 210.87.254.40 on 09/05/12
For personal use only.

TABLEAU 2. Photolyse du butène-1: rendements du M/N(ex)

	8.4 eV			10.0 eV			11.6–11.8 eV		
Butène-1[a]	2.00	2.00	2.00	1.00	2.00	2.00	1.00	4.00	2.00
Oxygène[a]	—	0.09	0.09	—	0.10	0.10	0.15	0.16	0.16
Hélium[a]	—	—	274	—	—	195	—	—	360
CH_4	0.05_3	0.01_9	0.01_5	0.05_5	0.01_4	0.01_8	0.02_5	0.04_3	0.02_9
C_2H_2	0.17	0.16	0.20	0.15_9	0.18	0.18_4	0.33	0.33	0.27
C_2H_4	0.19_8	0.23	0.15_4	0.26_4	0.30	0.19	0.48	0.42	0.26_3
C_2H_6	0.27_8	0.03_5	0.03_5	0.18	0.01_4	0.02	0.01	0.00_9	0.01_3
C_3H_6	0.34_2	0.35	0.03_4	0.47	0.35	0.04_5	0.66	0.54	0.04
C_3H_4[b]	0.03_2	0.03_9	0.03_5	0.04_3	0.02_2	0.03_3	0.02_4	0.02_8	0.04_2
C_3H_4[c]	0.35	0.35	0.35	0.20	0.20	0.20	0.13_2	0.13_2	0.13_2
C_4H_6-1,2	0.02_6	0.03	0.03_6	0.03_2	0.02_2	0.02_2	0.03_5	n.d.	0.03_8
C_4H_6-1,3	n.d.[d]	0.29	n.d.	n.d.	0.33_6	n.d.	n.d.	0.13_3	n.d.

[a]Torr. [b]Propyne. [c]Allène. [d]Non déterminé.

TABLEAU 3. Photolyse du butène-1: rendements M/N(ex.) en présence d'H_2S

Butène-1	10.0	10.0	2.0	10.0	10.0	2.0
H_2S	1.0	0.5	—	1.0	0.5	—
He	—	—	7.4	—	—	7.3
O_2	—	—	0.1	—	—	0.1
λ (eV)	8.4	8.4	8.4	10.0	10.0	10.0
CH_4	0.70	n.d.[b]	0.015	0.43_7	0.38_5	0.01_1
C_2H_4	0.24_8	0.22_9	0.18_4	0.30	0.30_4	0.27_5
C_2H_6	0.20_8	0.19_4	0.03	n.d.	0.16_3	0.01_1
C_3H_6	0.15_4	0.18_4	0.22_4	0.23_4	0.22_7	0.24_5
C_3H_8	0.00_7	0.00_2	0.00	$\}0.03_4$	$\}0.04_3$	0.00
C_3H_4[a]	0.02_9	0.04_7	0.04_2			0.01_9
n-C_4H_{10}	0.79	0.70 ± 0.05	0.00	0.69	0.58	0.00

[a]Propyne. [b]Non determiné.

[6] $(CH_3CH_2CH{=}CD_2)^{**} \rightarrow CH_3 + CH_2{=}C{=}CD_2 + H$

Puisque 87% de l'allène est de l'allène-d_2, cela est l'indication que la liaison carbone–carbone scindée se trouve en position β de la double liaison. Cependant, 12% de l'allène est de l'allène -d_1, indiquant ainsi qu'il peut y avoir une redistribution partielle des atomes d'hydrogène soit dans la molécule excitée, soit dans le radical C_3H_5 s'il est formé temporairement ou encore y avoir une mauvaise deutération partielle du butène-1 utilisé en ce qui regarde la situation des deux atomes de deutérium.

L'endothermicité des réactions 4 et 5 est compatible avec l'énergie des photons incidents. Etant donné le faible rendement en méthane "moléculaire", plus précisément de celui formé en présence d'oxygène, le rapport des constantes Φ_4/Φ_5 est inférieur ou égal à 0.04, 0.07, et 0.14 respectivement aux raies de résonnances du xénon, du krypton et de l'argon. Cette situation a déjà été remarquée dans la photolyse de l'isobutylène (2) et des *cis*- et *trans*-butènes-2 (8*a*). De la même manière, on peut admettre en l'absence de toute preuve que le radical CH_2—CH—CH_2 est formé temporairement et qu'il se décompose en perdant son atome d'hydrogène central pour former l'allène alors que la formation de propyne requiert la perte d'atome d'hydrogène terminal avec la migration de l'atome d'hydrogène central vers l'autre carbone terminal. Cette formation est donc peu favorable en accord avec les résultats expérimentaux.

La formation de l'acétylène est, elle aussi, en majorité issue d'une ou de plusieurs réactions de décomposition du monomère excité (fig. 1):

[7] $(C_4H_8\text{-}1)^{**} \rightarrow C_2H_2 + C_2H_6 \quad \Delta H =$ 34 kcal mol^{-1}

[8] $(C_4H_8\text{-}1)^{**} \rightarrow C_2H_2 +$ autres produits que C_2H_6

A partir des résultats obtenus, la valeur maximum du rapport Φ_7/Φ_8 est de 0.08 avec les trois

Can. J. Chem. Downloaded from www.nrcresearchpress.com by 210.87.254.40 on 09/05/12
For personal use only.

types de lampes utilisées. En fait, il serait plus judicieux de considérer la formation de l'éthylène et de l'acétylène dans le système suivant:

[9] $(C_4H_8\text{-}1)^{**} \rightarrow C_2H_5 + C_2H_3 \quad \Delta H =$ 89.5 kcal mol^{-1}

Les deux fragments radicalaires ont au minimum 105 kcal mol^{-1} d'énergie à se partager de telle sorte qu'au moins l'un des deux radicaux se décompose:

[10*a*] $(C_2H_5)^{*} \rightarrow C_2H_4 + H \quad \Delta H = 39$ kcal mol^{-1}

[10*b*] $(C_2H_3)^{*} \rightarrow C_2H_2 + H \quad \Delta H = 42$ kcal mol^{-1}

Il se peut même, thermodynamiquement cela est possible, que les deux radicaux éthyle et vinyle se décomposent, donnant lieu globalement à la réaction suivante:

[11] $(C_4H_8\text{-}1)^{**} \rightarrow C_2H_2 + C_2H_4 + 2H \quad \Delta H =$ 170 kcal mol^{-1}

Afin d'apprécier l'importance des réactions 9 + 10*a* et 9 + 10*b*, il faut pouvoir évaluer le rendement des radicaux éthyles et vinyles stables. Dans un système insaturé comme le butène-1 et en présence d'hydrogène sulfuré, les radicaux libres réagissent avec l'hydrogène sulfuré pour former le composé moléculaire supérieur (8*b*):

[12] $R + H_2S \rightarrow RH + HS$

Dans ces conditions, l'accroissement des rendements en éthylène et en éthane, en présence d'hydrogène sulfuré indique l'importance des rendements des radicaux vinyles et éthyles à la condition, bien sûr, que la réaction 12 soit bien la seule à être efficace dans le processus de capture des radicaux libres. On obtient ainsi les rendements maximum pour les réactions 9 + 10*a* et 9 + 10*b* (tableaux 3). Il en est de même pour les autres radicaux. Alors que les rendements en acétylène et allène sont inchangés, la présence de l'hydrogène sulfuré augmente aussi et considérablement les rendements en méthane et butane, montrant ainsi les rendements importants en radicaux méthyles et butyles.

L'analyse isotopique de l'acétylène produit dans l'irradiation du $CH_3CH_2CH{=}CD_2$ montre que 76% de l'acétylène est formé par décomposition de l'espèce $CH{=}CD_2$:

[13] $(CH{=}CD_2)^{*} \rightarrow C_2D_2(\text{ou } C_2HD) + H(\text{ou D})$

Cependant, 25% de l'acétylène est perhydrogéné montrant la possibilité d'au moins un autre processus de fragmentation conduisant à l'acétylène. Dans la photochimie des butènes-2, une réaction importante est la fragmentation en acétylène et deux radicaux méthyles (8*a*). Il est alors facile d'imaginer que cette fragmentation est précédée d'un transfert interne d'un atome d'hydrogène. Un tel transfert a été observé dans la photochimie de l'isobutène (2) (voir la composition isotopique de l'éthane). De la même

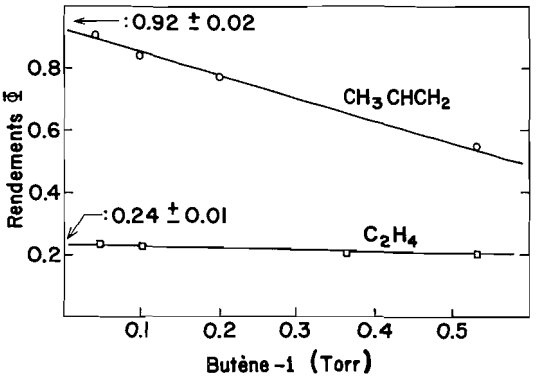

FIG. 2. Photolyse à 8.4 eV. Rendements à basse pression.

[14] $(CH_3CH_2CH{=}CD_2)^{**} \rightarrow$
$(CH_3CH{=}CHCD_2H)^{**} \rightarrow C_2H_2 + CH_3 + CD_2H$

façon, l'éthylène formé est en majorité perhydrogéné, démontrant ainsi la validité du mécanisme. A hautes pressions, 70% de l'éthylène est -d_0; cependant, 30% sont de l'éthylène-d_2. Là encore, il existe au moins un autre processus de formation de l'éthylène comme:

[15] $(C_4H_8\text{-}1)^{**} \rightarrow 2C_2H_4$

Etant donné les rendements des radicaux éthyles et vinyles, il s'en suit que la réaction 15 pourrait très bien rendre compte d'une part de la formation de l'éthylène. Cette éventualité rappelle un résultat déjà obtenu dans la photochimie du cyclobutane (9) et du méthylcyclopropane (10) qui se décomposent essentiellement dans une réaction similaire à la réaction 15. D'autres réactions de décomposition de la molécule butène-1 excitée sont responsables de la formation des butadiènes:

[16] $(C_4H_8\text{-}1)^{**} \rightarrow C_4H_6\text{-}1,3 + H_2(\text{ou } 2H)$

[17] $(C_4H_8\text{-}1)^{**} \rightarrow C_4H_6\text{-}1,2 + H_2(\text{ou } 2H)$

Enfin la formation du propène résiduel à haute pression est sans doute attribuable à la décomposition du monomère excité en radical méthylène et en propène comme cela a déjà été

Can. J. Chem. Downloaded from www.nrcresearchpress.com by 210.87.254.40 on 09/05/12
For personal use only.

Can. J. Chem. Downloaded from www.nrcresearchpress.com by 210.87.254.40 on 09/05/12
For personal use only.

démontré dans le cas de l'isobutène et des butènes-2 (2, 8*a*). Les rendements quantiques d'une telle réaction sont faibles: 0.03 et 0.05 aux raies de résonnance du xénon et du krypton.

Réactions radicalaires

Même en présence d'oxygène, les atomes d'hydrogène s'additionnent sur la double liaison pour former un radical butyle excité:

[18] $H + C_4H_8\text{-}1 \rightarrow (s\text{-}C_4H_9)^* \quad \Delta H = -41 \text{ kcal mol}^{-1}$

[19] $H + C_4H_8\text{-}1 \rightarrow (n\text{-}C_4H_9)^* \quad \Delta H = -37 \text{ kcal mol}^{-1}$

Le radical butyle formé contient plus d'énergie qu'il ne lui en faut pour se décomposer (11):

[20] $(s\text{-}C_4H_9)^* \rightarrow C_3H_6 + CH_3 \quad \Delta H = 26 \text{ kcal mol}^{-1}$

[21] $(n\text{-}C_4H_9)^* \rightarrow C_2H_4 + C_2H_5 \quad \Delta H = 23 \text{ kcal mol}^{-1}$

[22] $(s\text{- ou } n\text{-}C_4H_9)^* + M \rightarrow C_4H_9 + M$

Les réactions de décomposition des radicaux butyles sont en compétition avec la réaction de stabilisation par collision dans le domaine de pression étudié ici. Ces réactions sont en accord avec les analyses par spectrométrie de masse des propènes et éthylènes (figs. 1 et 2).

[23] $H(D) + C_2H_5CH{=}CD_2 \rightarrow (C_2H_5CHCD_2H(D))^* \rightarrow CH_3 + CH_2{=}CHCD_2H \text{ (ou } CH_2{=}CHCD_3)$

[24] $H(D) + C_2H_5CH{=}CD_2 \rightarrow (C_2H_5CH_2(D)CD_2)^* \rightarrow C_2H_5 + CH_2{=}CD_2 \text{ (ou } CHD{=}CD_2)$

Le propène formé est en majorité du propène-d_2 et un pourcentage relativement faible est du propène-d_3. Après déduction de l'éthylène formé par décomposition du monomère excité, l'analyse de l'éthylène par spectrométrie de masse montre une variété d'éthylène-d_2 et -d_3 dont la formation décroît avec la pression. Dans le cas de l'éthylène et du propène, le rapport des espèces -d_3/-d_2 est voisin de 0.18 aux trois longueurs d'ondes (voir résultats). Ce rapport est à comparer avec le rapport D/H contenu dans le monomère, rapport qui est égal à 0.33.

Il est intéressant de comparer ici les rendements des réactions 20 et 21 à basses pressions. La décroissance relative du rendement en éthylène comparée à celle du propène croît lorsque l'énergie incidente utilisée croît de 8.4 à 11.6–11.8 eV. Il apparaît que l'addition des atomes d'hydrogène sur la double liaison ne produit essentiellement que des radicaux butyles secondaires à 8.4 eV (91%). Récemment il a été démontré que 94.3% de l'addition des atomes d'hydrogènes thermiques se fait sur le carbone terminal (12). A la précision expérimentale près, les atomes d'hydrogène libérés dans la photolyse à 8.4 eV peuvent donc être assimilés à des atomes thermiques. A 10.0 eV, seulement 82% de l'addition conduit au radical butyle secondaire. Il faut donc conclure que les atomes d'hydrogène formés à 10.0 eV possèdent en moyenne une énergie cinétique supérieure à l'énergie thermique. L'addition de l'atome d'hydrogène sur la double liaison est alors moins sélective. A 11.6–11.8 eV, cette proportion n'est plus que de 63%.

Il existe enfin une autre possibilité de réaction de l'atome d'hydrogène:

[25] $H + C_4H_8\text{-}1 \rightarrow C_4H_7 + H_2$

L'importance de cette réaction est mineure.

TABLEAU 4. Photolyse du butène-1: rendements des produits en l'absence d'oxygène[a]

Butène-1	2.00	2.00	1.00
Hélium	—	215	—
λ (eV)	8.4	8.4	10.00
Propane	0.09_5	0.05_1	0.05_0
cis-Butène-2	0.00_8	0.01_5	n.d.
trans-Butène-2	0.02_2	0.03_2	n.d.
n-Butane	0.04_2	0.08	n.d.
Méthyl-3-butène-1	0.01_4	0.01_5	0.01_4
Cyclobutane	0.00_2	0.00_6	0.00_2
Isopentane	0.17_5	0.24_6	0.14_5
Pentène-1	0.01_1	0.00_2	0.00_2
n-Pentane	0.01_6	0.02_7	0.02_6
Pentène-2	0.01_8	n.d.	0.01_1
Méthyl-3-pentane	0.01_1	0.05_1	0.02_9

[a]Tous les rendements de ces produits sont égaux à 0.00 en présence d'oxygène (0.09 Torr).

TABLEAU 5. Rendements radicalaires: Photolyse du butène-1

λ (eV)	8.4	10.0
CH_3[a]	0.50 ± 0.03	0.32 ± 0.04
C_2H_5[b]	0.16 ± 0.02	0.14_5 ± 0.02
C_2H_3	0.08 ± 0.02	0.12 ± 0.02
$n\text{-}C_4H_9$	0.08 ± 0.01	0.14_5 ± 0.01
$s\text{-}C_4H_9$	0.89 ± 0.02	0.91 ± 0.02
C_4H_7	0.12 ± 0.03	0.13 ± 0.03
CH_2	0.03 ± 0.01	0.05 ± 0.02
	1.86 ± 0.14	1.85 ± 0.16

[a,b]A l'exclusion de ceux provenant de la fragmentation des radicaux *n*-butyles et *s*-butyles respectivement.

TABLEAU 6. Fragmentation de la molécule butène-1 photochimiquement excitée

$(C_4H_8\text{-}1)^{**} \rightarrow$	184.9[a]	147	123.7	104.8–106.4
$C_3H_4 + CH_3 + H\ (CH_4)$	0.04[b]	0.38	0.23	0.16
$C_4H_6 + 2H\ (H_2)$	—	0.32	0.36	0.17
$2C_2H_4$	0.09	0.04	0.05	}
$C_2H_3 + C_2H_4 + H$	—	0.07	0.09	}0.20
$C_2H_2 + C_2H_5 + H$	—	0.16	0.12	}
$C_2H_2 + C_2H_6$	0.01	0.03	0.02	}
$C_2H_2 + 2CH_3$	—	0.04	0.05	}0.33
$C_3H_6 + CH_2$	—	0.03	0.04_5	0.05
$C_4H_7 + H$	0.12	$\leqslant 0.05$	$\leqslant 0.05$	$\leqslant 0.05$
$C_3H_5 + CH_3$	0.71	0.0	0.0	0.0
Total	0.97	1.12	1.01	0.96

[a]Référence 1. [b]Formation de méthane moléculaire surtout.

Le rapport $k_{25}/k_{18} + k_{19}$ est de 1.6×10^{-2} (13). Cette faible participation de la réaction 25 est confirmée par le fait que les réactions de combinaison possible entre les radicaux C_4H_7 et le radical méthyle est faible (tableau 4). La somme des rendements des méthylbutènes et des pentènes correspondants est en effet inférieure à 0.03 ce qui, compte tenu de l'importance des radicaux méthyles, entraîne un rendement en radicaux butènyles de l'ordre de 0.12 à 8.4 eV. Ce rendement est cependant supérieur à celui attendu par la seule réaction 25. En conséquence, il se peut que d'autres radicaux réagissent avec le monomère dans une réaction similaire à la réaction 25. Il se peut également que l'absorption directe d'énergie conduise à la formation d'un radical C_4H_7. Cependant, étant donné l'énergie initiale de la molécule excitée, on peut en limiter le rendement quantique à 0.05 (8*a*). Tenant compte du rapport k_{18}/k_{19}, il est donc facile d'estimer le rendement en atomes d'hydrogène aux trois lampes utilisées (tableau 5). Il est en particulier intéressant de noter qu'à 8.4 eV, le rendement $\Phi(H)$ est de l'ordre de l'unité comme cela a déjà été démontré dans le cas des butènes-2 (8*a*).

Les autres radicaux les plus importants sont les radicaux méthyles, éthyles et vinyles. La formation de l'isopentane, du pentane normal et du méthyl-3-pentane est d'origine radicalaire et ceux-ci sont formés dans les réactions de combinaison des radicaux méthyles et éthyles avec les radicaux butyles. Il en est de même de l'éthane, du propane et du butane normal à partir des radicaux méthyles et éthyles alors que le méthane, les *trans*- et *cis*-butènes-2 le sont par dismutation des radicaux correspondants. En supposant que les radicaux libres réagissent entre eux de façon statistique et en connaissant les rapports des constantes de vitesse des réactions de dismutation et de combinaison des différentes paires de radicaux, on peut ainsi calculer les rendements des différents produits d'origine radicalaire (8*a*). Les résultats sont en accord avec ceux obtenus par l'utilisation de H_2S (tableau 5). Il faut enfin noter que les rendements des radicaux butyles secondaires et primaires sont connus à partir de la décroissance des rendements en propylène et éthylène en fonction de la pression.

Conclusion

Il est enfin possible d'établir de façon simplifiée l'importance relative des principaux processus de fragmentation de la molécule butène-1 excitée mis en évidence (tableau 6). Ces résultats sont comparés avec ceux obtenus à plus longue longueur d'onde (1). Il faut enfin dire que, dans la région de l'ultraviolet à vide et à des pressions relativement faibles, la fragmentation de la molécule photochimiquement excitée conduit essentiellement à un produit moléculaire stable et à deux fragments radicalaires.

Nous tenons à exprimer notre gratitude au professeur P. Ausloos qui, non seulement a bien voulu commenter ce travail, mais également nous a permis d'utiliser certains résultats inédits de son laboratoire.

1. P. BORRELL et P. CASHMORE. Ber. Bunsenges. Phys. Chem. 72, 182 (1968). P. BORRELL, P. CASHMORE, A. CERVENKA, et F. C. JAMES. J. Chim. Phys. 229 (1970).
2. J. HERMAN, K. HERMAN, et P. AUSLOOS. J. Chem. Phys. 52, 28 (1970).
3. R. GORDEN, JR., R. E. REBBERT, et P. AUSLOOS. NBS–NSRDS, note technique 496 (1969).
4. J. G. CALVERT et J. N. PITTS, JR. Photochemistry. J. Wiley and Sons, Inc., New York. 1967. p. 504.

Can. J. Chem. Downloaded from www.nrcresearchpress.com by 210.87.254.40 on 09/05/12
For personal use only.

5. J. A. R. SAMSON, F. F. MARMO, et K. WATANABE. J. Chem. Phys. **36**, 783 (1962).
6. A. A. SIDDIQI, C. T. CHEN, G. G. MEISELS, et R. GORDEN, JR. J. Chem. Phys. **57**, 4506 (1972).
7. L. W. SIECK, S. G. LIAS, L. HELLNER, et P. AUSLOOS. J. Res. Nat. Bur. Stand. A, **76**, 115 (1972).
8. (*a*) G. J. COLLIN et P. M. PERRIN. Can. J. Chem. **50**, 2823 (1972). (*b*) G. J. COLLIN, P. M. PERRIN, et C. M. GAUCHER. Can. J. Chem. **50**, 2391 (1972).
9. R. D. DOEPKER et P. AUSLOOS. J. Chem. Phys. **43**, 3814 (1965).
10. R. D. DOEPKER. J. Phys. Chem. **73**, 3219 (1969).
11. B. S. RABINOVITCH, R. F. KUBIN, et R. E. HARRINGTON. J. Chem. Phys. **38**, 405 (1963).
12. W. E. FALCONER et W. A. SUNDER. Int. J. Chem. Kinet. **3**, 395 (1971).
13. W. E. FALCONER et W. A. SUNDER. Int. J. Chem. Kinet. **4**, 315 (1972).

Can. J. Chem. Downloaded from www.nrcresearchpress.com by 210.87.254.40 on 09/05/12
For personal use only.

Estimation of Phenols by the 4-Aminoantipyrine Method: Identification of the Colored Reaction Products by Proton Magnetic Resonance Spectroscopy

PETER F. JONES AND K. E. JOHNSON

Regina Water Research Institute, University of Saskatchewan, Regina, Saskatchewan S4S 0A2

Received April 10, 1973

The products from the oxidation of several phenols in the presence of 4-aminoantipyrine have been isolated and their p.m.r. spectra examined. The results confirm the proposed formation of *p*-quinoneimide adducts and the elimination of the para-group in the case of reactive *p*-substituted phenols. Data from ortho-substituted phenols reveal the formation of *syn* and *anti* geometrical isomers of the quinoneimide. In contrast, when the starting phenol has a meta-substituent, only a single isomer, the less hindered *anti* form, is obtained. An unusually large anisotropic effect of the antipyryl group, causing a deshielding of the closest proton on the quinoneimide ring, has been found. In the reaction between *p*-benzoquinone and 4-aminoantipyrine, the color obtained is due to the formation of the *p*-quinoneimide, and not to a charge-transfer complex.

Les produits d'oxydation de plusieurs phénols en présence d'amino-4 antipyrine ont été isolés et leurs spectres de r.m.n. examinés. Les résultats confirment la formation proposée d'adduits de la *p*-quinone imide et l'élimination du groupe para dans le cas des phénols *p*-substitués réactifs. Les données sur les phénols ortho substitués révèlent la formation d'isomères géométriques *syn* et *anti* de la quinoneimide. Au contraire, lorsque le phénol de départ possède un substituant méta, la forme *anti* la moins encombrée est le seul isomère obtenu. On a constaté un effet d'anisotropie inhabituellement fort du groupe antipyryle provoquant un déblindage du proton le plus proche sur le cycle quinone imide. Dans la réaction entre la *p*-benzoquinone et l'amino-4 antipyrine, la couleur observée est due à la formation de la *p*-quinoneimide et non au complexe de transfert de charge. [Traduit par le journal]

Can. J. Chem., 51, 2860 (1973)

Can. J. Chem. Downloaded from www.nrcresearchpress.com by 210.87.254.105 on 09/05/12
For personal use only.

Introduction

The presence of phenols at very low (p.p.b.) concentrations in potable water supplies may cause taste and odor problems on chlorination. The standard procedure (1) for the estimation of phenols at such levels involves the photometric measurement of the dye formed on oxidation of the phenol-containing sample in the presence of excess 4-aminoantipyrine (4-amino-2,3-dimethyl-1-phenyl-3-pyrazolin-5-one), **1** (4-AAP). Our

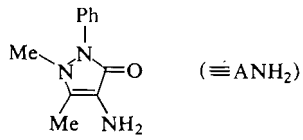

(≡ANH_2)

1

interest in and use of this method have led us to investigate the chemical basis of the test.

The method was introduced by Emerson (2) in 1943; he suggested on the basis of analogy with other aromatic amines that the reaction led to the formation of a *p*-quinoneimide adduct (see Scheme 1).

Para-coupling was proposed to explain the failure of the reaction with those phenols having

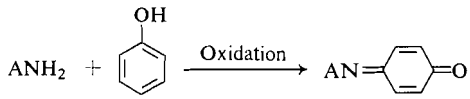

SCHEME 1

alkyl, aryl, nitroso, nitro, benzoyl, ester, and aldehyde groups in the para-position. However, certain *p*-substituted phenols did show a positive response and these groups (halo, carboxyl, alkoxyl, and sulfonic acid) were said to be expelled. No explanation of the nature of the "expulsion" was advanced.

Emerson and Sagal (3) later reported degradative evidence to support the proposed *p*-quinoneimide structure. *p*-Toluquinone was isolated following the hydrolysis, under diazotization conditions, of the dye obtained from *m*-cresol

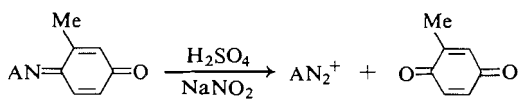

SCHEME 2

Müller *et al.* (4) have since questioned the proposed expulsion of groups from the para-position. They were unable to detect the removal

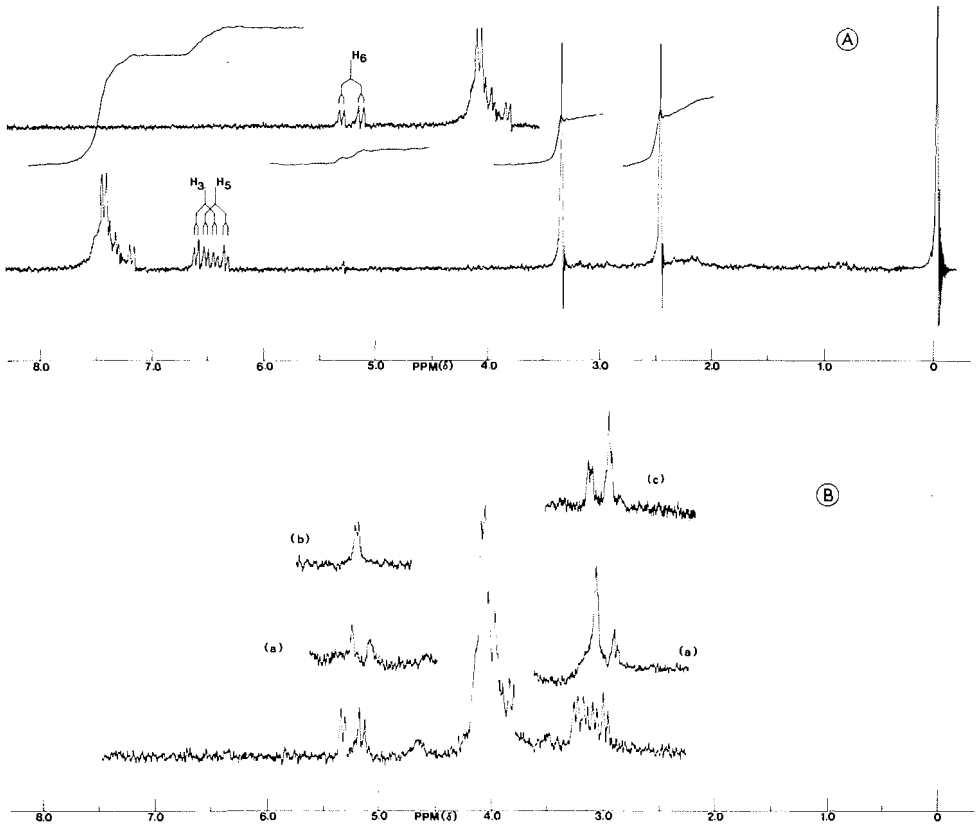

FIG. 1. (A) P.m.r. spectrum of phenol adduct, **2**. Upper trace offset 200 Hz. (B) Decoupled vinylic signals in **2**: (*a*) H_2 irradiated, (*b*) H_5 irradiated, (*c*) H_6 irradiated.

of carboxyl or alkoxyl substituents and consequently suggested that ortho-coupling had occurred. However, more recent studies (5–7) appear to confirm Emerson's original hypothesis. Dyes were isolated from the reactions of *p*-halophenols and the corresponding unsubstituted compounds. The products were found to be identical, confirming the elimination of the halogen atom. On the basis of visible spectra it was concluded that expulsion of *p*-alkoxyl and *p*-carboxyl groups also occurred. Elemental analyses on the isolated dyes gave empirical formulas corresponding to the structure of the expected *p*-quinoneimide adduct. Unfortunately, however, no other physical proof of structure was examined.

Thielemann (8) has recently shown that *p*-benzoquinone forms a dye with 4-AAP, which on chromatographic evidence is identical to that obtained from the oxidation of phenol. This might be taken as further proof of the *p*-quinoneimide structure. However, Okano and Uekama (9) reported that *p*-quinones gave colored products not only with 4-AAP, but also with other antipyrine derivatives where imide formation is impossible. They suggested that the formation of charge-transfer complexes was responsible for the color. Such complexes would, of course, also show the hydrolytic behavior quoted by Emerson as proof of the quinoneimide structure.

Thus there is no conclusive evidence for the structure of the dye products, and since such knowledge is essential for a fundamental understanding of the reaction pathway, we have consequently reinvestigated the Emerson reaction using modern spectroscopic techniques. The method chosen was to carry out the reaction with model phenols and to examine the p.m.r. spectra of the isolated dyes. As a result we have been able to assign the structure of the adducts unambiguously and further to reveal hitherto unobserved structural details.

Can. J. Chem. Downloaded from www.nrcresearchpress.com by 210.87.254.105 on 09/05/12
For personal use only.

Can. J. Chem. Downloaded from www.nrcresearchpress.com by 210.87.254.105 on 09/05/12
For personal use only.

Results and Discussion

Phenol and Reactive Para-substituted Phenols

Phenol and its *p*-chloro, -carboxyl, and -methoxy derivatives were found to react to each give a dye having a similar m.p. and an identical p.m.r. spectrum. This confirms the elimination of the latter two groups, previously proposed (6) on the basis of visible spectroscopy. The p.m.r. spectrum, shown in Fig. 1A, confirms the *p*-quinoneimide structure of the product **2**.

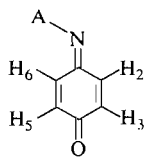

2

Apart from the aromatic multiplet and the two methyl singlets arising from the antipyryl group, two vinylic multiplets can be seen. The doublet of doublets, which is at remarkably low field, is assigned (see later) to the proton H_6 which is *syn* to the antipyryl group and is coupled to both H_5 and H_2. The higher field signal, an eight line multiplet, must arise from the overlapping of the two doublets of doublets expected from the protons adjacent to the carbonyl group, H_3 and H_5. Integration of the spectrum suggested that the remaining signals due to H_2, the proton *anti* to the antipyryl group, are buried under the aromatic multiplet (in fact a portion of this signal appears to be visible).

The position of H_2 was confirmed by spin-decoupling experiments, as shown in Fig. 1B. When the suspected H_2 region was irradiated, the signal due to H_6 collapsed to the expected doublet. Similarly the high field vinylic signal now appeared as a mixture of a doublet (one-half of the unchanged doublet of doublets due to H_5) and an unresolved multiplet (assumed to arise from superposition of the other half of the H_5 signal on the collapsed H_3 signal, predicted to be a doublet). A similar, but mirror image, situation was found in this region when H_6 was irradiated. Here H_5 is decoupled while H_3 is unchanged. Finally, the expected narrow doublet for H_6 was observed when H_5 was irradiated. These decoupling experiments reveal that the most deshielded of the protons adjacent to the imino group, H_6, is coupled to the most shielded of the protons adjacent to the carbonyl group, and the reverse. Thus, knowing the identity of H_6, it is possible to assign the identities of all the other ring protons.

The values observed for the vicinal coupling (J_{56}, $J_{23} \simeq 10$ Hz) and for the long-range cross-ring coupling (J_{26}, $J_{35} \simeq 2$ Hz) are of the magnitude reported for other quinone derivatives (10*a*). While the positions of the protons adjacent to the carbonyl group, H_3 and H_5, are very similar, those adjacent to the imino bond, H_2 and H_6, are separated by approximately 1.5 p.p.m., revealing that the antipyryl group has an extremely large anisotropic effect. A similar, but smaller, effect has been reported (11) in the spectra of quinonemonooximes and their anions.

The product from the reaction of *p*-benzoquinone with 4-AAP was identical to that obtained from the oxidation of phenol. Therefore the colors formed from *p*-quinones and 4-AAP are due to the formation of *p*-quinoneimides, and not to charge-transfer complexes, as previously suggested (9).

Symmetrical Ortho-disubstituted Phenols

Adducts **3** and **4** were obtained from 2,4,6-trichlorophenol and 2,6-dimethylphenol respectively. Their p.m.r. spectra are shown in Fig. 2.

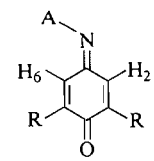

3 R = Cl
4 R = Me

With the dichloro compound **3**, which provides a further example of the elimination of a *p*-chlorine atom, the low field doublet assigned to H_6, the proton *syn* to the antipyryl group, is the only visible vinylic signal. It is again assumed that the signal of the *anti* proton, H_2, is buried under the aromatic multiplet. Unfortunately, the low solubility of this compound prevented confirmation by accurate integration.

The p.m.r. spectrum of the dimethyl derivative **4** was unique among the compounds studied in that it revealed the signals of both the *syn* and *anti* proton. Both appeared as identical multiplets due to the additional long-range coupling with the allylic protons of the vicinal methyl group. This coupling, $J_{HCCMe} = 1.4$ Hz, of similar magnitude to those reported (10*b*) for analogous compounds, is also, as expected, shown in the six proton doublet due to these methyl groups.

Can. J. Chem. Downloaded from www.nrcresearchpress.com by 210.87.254.105 on 09/05/12
For personal use only.

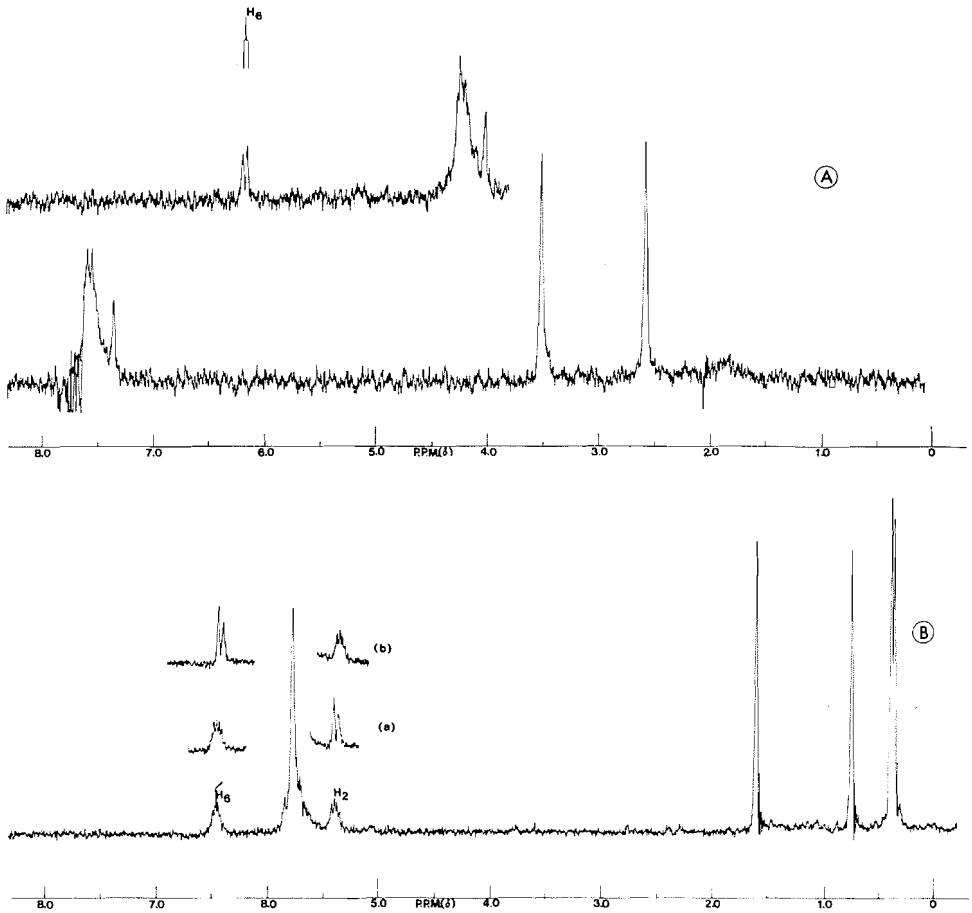

FIG. 2. (A) P.m.r. spectrum of 2,4,6-trichlorophenol adduct, **3**. Upper trace offset 200 Hz. (B) P.m.r. spectrum of 2,6-dimethylphenol adduct, **4**. Complete spectrum offset 100 Hz. Insert: (*a*) H_2 decoupled and (*b*) H_6 decoupled from vicinal methyl group.

When this doublet was irradiated and the H_2 and H_6 signals were examined, each was found to have collapsed to the expected doublet. Similarly, on irradiation of either H_2 or H_6 the methyl doublet collapsed to a broadened singlet.

The absence of signals in the δ 6.5 p.p.m. region in both compounds confirms the previous assignment of signals in this region of the phenol adduct **2** to the protons adjacent to the carbonyl group, H_3 and H_5.

Ortho-monosubstituted Phenols

The identical chloro compound **5** was obtained from both 2-chlorophenol and 2,4-dichlorophenol, confirming the report of Svobodova and Gasparic (6), while *o*-cresol gave the adduct **6**. Their p.m.r. spectra are shown in Fig. 3. Both compounds have a single proton H_5 adjacent to the carbonyl group and one might expect to find in each case a doublet for H_5, which is coupled only with H_6. However, both compounds show four lines in the appropriate region. This result suggests the formation of a mixture of *syn* and *anti* isomers in both cases, a doublet being obtained from each isomer. The presence of geometrical isomers is clearly shown in the appearance of the lowest field signals,

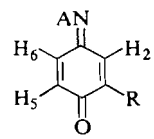

5 R = Cl
6 R = Me

Can. J. Chem. Downloaded from www.nrcresearchpress.com by 210.87.254.105 on 09/05/12
For personal use only.

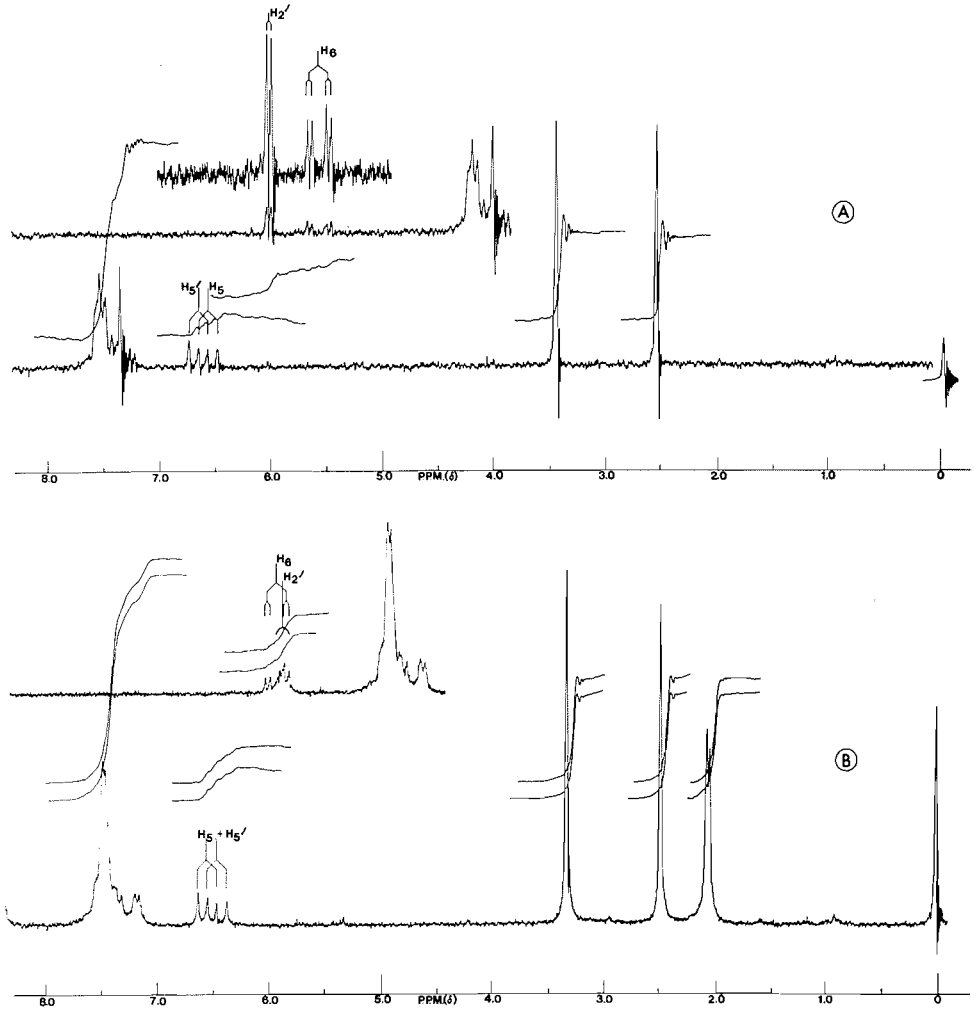

FIG. 3. (A) P.m.r. spectrum of 2-chlorophenol adducts, **5***a* and *b*. Upper trace offset 200 Hz. (B) P.m.r. spectrum of *o*-cresol adducts, **6***a* and *b*. Upper trace offset 150 Hz.

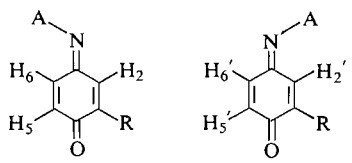

5 R = Cl
6 R = Me

which arise from a proton adjacent to the C=N bond and *syn* to the antipyryl group. Inspection of the chloro compounds, **5***a* and *b*, shows that these protons, H_6 and H_2', are not identical chemically. In the *anti* isomer **5***a* the proton H_6, coupled to both H_2 and H_5, should appear as a doublet of doublets, whereas in the *syn* isomer **5***b* this proton H_2' is only coupled to H_6' and should therefore be a doublet. Examination of Fig. 3A reveals the predicted splitting pattern. Spin-decoupling experiments confirm the proposed coupling assignments, and also reveal that in the four line high field vinylic signal due to H_5 and H_5', the former is the more shielded of the two protons. Again the protons adjacent to the C=N bond and *anti* to the antipyryl group, H_2 and H_6', appear to be hidden under the phenyl multiplet.

The lowest field signals of the *o*-cresol adducts, **6***a* and *b*, are more complex than those of the chloro analog, due to the additional long-range

Can. J. Chem. Downloaded from www.nrcresearchpress.com by 210.87.254.105 on 09/05/12
For personal use only.

coupling of H_2' with the allylic protons of the vicinal methyl group. While one-half of the doublet of doublets due to H_6 is clearly visible, the other half is superimposed on the multiplet arising from H_2'. As with the chloro compounds the *anti* protons, H_2 and H_6', are not visible.

Comparison of the lowest field signals of **5** and **6** shows that in the chloro compound **5**, H_2' (adjacent to chlorine) is at lower field than H_6 (adjacent to hydrogen), while the reverse is true for the methyl analog **6**. Therefore the vinylic proton is deshielded by a vicinal chlorine atom and shielded by a vicinal methyl group. This follows the expected trend for substituted alkenes (10*c*).

In both cases approximately equal amounts of the *syn* and *anti* isomer appear to have been formed. This might have been anticipated, since there should be little interaction between the substituent and the remote antipyryl group, and consequently both isomers should be of similar energy.

Meta-monosubstituted Phenols

In all of the previous adducts **2**–**6**, the ring positions ortho to the C=N bond are unsubstituted. Although the signals of these protons, H_2 and H_6, are widely separated because of the anisotropy of the antipyryl group, it is not possible *a priori* to distinguish the identity of each signal. Accordingly the adducts **7** and **8** were prepared from 3-chlorophenol and *m*-cresol respectively. Here it might be anticipated

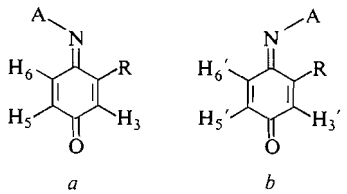

a *b*

7 R = Cl
8 R = Me

that unequal amounts of the *syn* and *anti* isomers would be produced, with the *anti* isomer *a* predominating in each case, because of unfavorable steric interaction between the substituent and antipyryl groups in the *syn* configuration. Examination of Fisher–Hirschfelder–Taylor models confirms that there is severe crowding in the *syn* isomer *b*.

The p.m.r. spectra illustrated in Fig. 4 clearly show in both cases a low field doublet. With the chloro compound **7**, integration of this doublet indicates that a single isomer, which from the above argument must be the *anti* isomer **7***a*, has been formed. Thus the lowest field signal must be due to H_6, the proton *syn* to the antipyryl group in the *anti* isomer. The presence of a single isomer appears to be confirmed by the high field vinylic signal, since only one doublet, due to coupling of H_3 with H_5, and one doublet of doublets, arising from the coupling of H_5 with both H_3 and H_6, are apparent.

A similar situation is found with the *m*-cresol adduct where again only a single isomer, **8***a*, appears to have been formed. The high field vinylic region is more complex than for the chloro compound due to additional long-range coupling of H_3 with the vicinal methyl group. The H_3 multiplet is superimposed upon one-half of the doublet of doublets due to H_5.

The formation of a single isomer, presumed to be *anti*, has also been noted (11) from the p.m.r. spectra of appropriately substituted quinone-oximes. The results allow us therefore to unambiguously assign signals for H_2 and H_6 in the previous compounds **2**–**6**.

The antipyryl group consequently can be seen to exert a substantial anisotropic effect, causing deshielding of a proton *syn* to it and adjacent to the C=N bond. While differences in the chemical shifts of *syn* and *anti* protons have been noted (10*d*) in the spectra of several classes of compounds having a C=N bond, the anisotropic effect of the antipyryl group is unusually large. The effect may be due to a conformation in which the *syn* proton may lie in the plane of the antipyryl carbonyl group and close to the oxygen atom, since large deshieldings have been noted (10*e*) in such cases. Examination of Fisher–Hirschfelder–Taylor models indicates that steric crowding may prevent free rotation of the antipyryl group around its external C—N bond and that in the resulting fixed conformation the *syn* hydrogen may in fact lie close to the antipyryl carbonyl oxygen.

In addition, the antipyryl group appears to have an opposite, but greatly reduced, effect on the *syn* proton meta to the C=N bond. Thus, in the phenol adduct **2** the *syn* proton H_5 is more shielded than the *anti* proton H_3. An identical result is found with the products from the ortho-substituted phenols **5** and **6**. In both cases, the *syn* proton H_5 in the *syn* isomer resonates at higher field than the corresponding *anti* proton H_5' of the *anti* isomer.

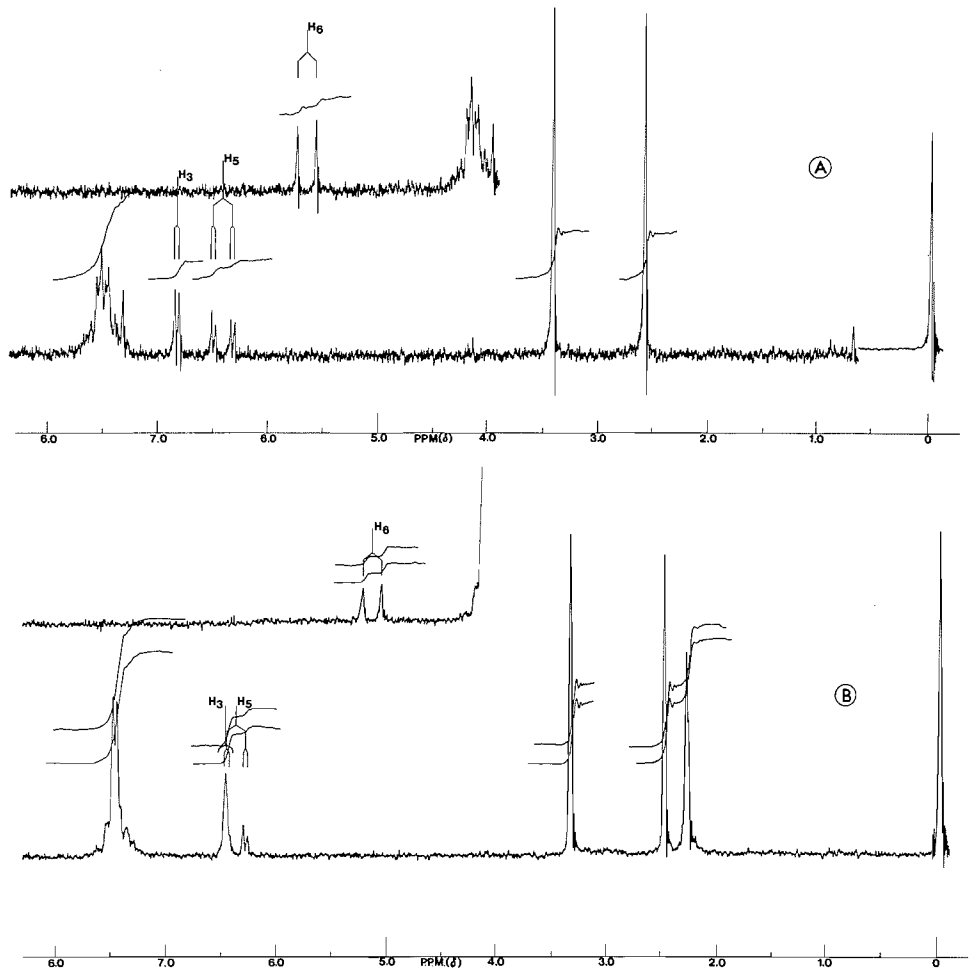

FIG. 4. (A) P.m.r. spectrum of 3-chlorophenol adduct, **7***a*. Upper trace offset 200 Hz. (B) P.m.r. spectrum of *m*-cresol adduct, **8***a*. Upper trace offset 200 Hz.

Experimental

P.m.r. spectra were recorded on a Varian A-60 spectrometer in deuterochloroform solvent and with tetramethylsilane as an internal standard. Spin-decoupling experiments were carried out using a Model V-6058 spin-decoupler.

Buffer solutions of p*H* 10.4 and 6.86 were prepared by dissolving dry buffer salt (Fisher) in distilled water. Buffer solutions for the p*H* 8 region were prepared by adjusting the latter, using a p*H* meter, to the appropriate p*H* by addition of dilute ammonia. 4-Aminoantipyrine (Aldrich) and the starting phenols were purchased from commercial suppliers and were used without further purification.

Melting points were taken on a hot stage apparatus and are uncorrected. Microanalyses were performed by Galbraith Laboratories Inc., Knoxville, Tennessee.

Preparation of Dyes

To a stirred mixture of 1 mmol of the given phenol and 0.35 g (1.5 mmol) of 4-aminoantipyrine in 75 ml of the appropriate buffer solution was added 2.7 g (10 mmol) of potassium persulfate dissolved in 50 ml of the same buffer solution. On mixing, a red color formed instantaneously and precipitation commenced rapidly. The reaction mixture was stirred for 30–60 min and the precipitate was then filtered off and washed several times with distilled water. The solid was then dried in air.

The yield and m.p. of purified samples are recorded in Table 1. P.m.r. spectral data are reported in Tables 2 and 3 (see text for interpretation). In those cases where formation of geometrical isomers was possible, comparison with the p.m.r. spectrum of the crude product indicated that recrystallization had not markedly effected the isomer ratio.

With potassium persulfate as oxidizing agent, only in the case of 2- and 3-chlorophenol was there any indication of the formation of significant amounts of any side-product(s). The unidentified side-product(s) showed several peaks in the δ 2.0–3.5 p.p.m. region. In the case of 3-chlorophenol it was not possible to obtain

Can. J. Chem. Downloaded from www.nrcresearchpress.com by 210.87.254.105 on 09/05/12
For personal use only.

TABLE 1. Preparation of *p*-quinoneimide dyes

Starting phenol	Product	p*H*	Yield (%)	M.p. (°C)
Phenol	**2**	10.4	69	165–168[a,e]
4-Hydroxybenzoic acid	**2**	10.4	68	163–167[b,e]
4-Chlorophenol	**2**	8.1	76	163–167[a,e]
4-Methoxyphenol	**2**	8.2	25	165–169[c,e]
2,4,6-Trichlorophenol	**3**	8.1	55	182–184[d,f]
2,6-Dimethylphenol	**4**	8.8	57	168–174[d,g]
2,4-Dichlorophenol	**5**	8.1	68	168–171[b,h]
2-Chlorophenol	**5**	10.4	56	162–167[b,h]
o-Cresol	**6**	8.0	72	159–164[c,i]
3-Chlorophenol	**7**	10.4	43	169–172[b,j]
m-Cresol	**8**	8.2	75	164–168[a,k]

[a]Recrystallized from dichloromethane – 100–120° petroleum ether.
[b]Recrystallized from chloroform – 100–120° petroleum ether.
[c]Recrystallized from benzene.
[d]Recrystallized from benzene – 100–120° petroleum ether.
[e]Literature (6) m.p. 168–170°.
[f]Anal. Calcd. for $C_{17}H_{13}Cl_2N_3O_2$: C, 56.37; H, 3.62; N, 11.60. Found: C, 56.59; H, 3.64; N, 11.45.
[g]Anal. Calcd. for $C_{19}H_{19}N_3O_2$: C, 71.01; H, 5.96; N, 13.08. Found: C, 71.23; H, 6.04; N, 12.94.
[h]Literature (6) m.p. 172–174°.
[i]Literature (5) m.p. 162–165°.
[j]Literature (7) m.p. 179–183°.
[k]Anal. Calcd. for $C_{18}H_{17}N_3O_2$: C, 70.34; H, 5.58; N, 13.67. Found: C, 70.34; H, 5.50; N, 13.04.

TABLE 2. Chemical shift data for *p*-quinoneimide adducts[a]

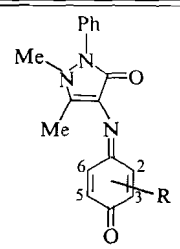

Compound	H_2	H_3	H_5	H_6	Ph	NMe	CMe	Other
2	Buried under phenyl	6.54 (d of d)	6.45 (d of d)	8.51 (d of d)	7.2–7.7 (m)	3.35 (s)	2.49 (s)	—
3 ($R_3 = R_5 = Cl$)	Buried under phenyl	—	—	9.52 (d)	7.3–7.7 (m)	3.51 (s)	2.59 (s)	—
4 ($R_3 = R_5 = Me$)	7.08 (m)	—	—	8.13 (m)	7.2–7.6 (m)	3.25 (s)	2.43 (s)	2.02 (d)(3,5-diMe)
5[b] ($R_3 = Cl$)	Buried under phenyl (H_2)	—	6.60 (d)(H_5)	8.94 (d of d) (H_6)	7.2–7.8 (m)	3.47 (s)	2.55 (s)	—
	9.42 (d)(H_2')		6.69 (d)(H_5')	Buried under phenyl (H_6')				
6[b] ($R_3 = Me$)	Buried under phenyl (H_2)	—	6.45 (d)(H_5)	8.48 (d of d)(H_6)	7.1–7.8 (m)	3.30 (s)	2.45 (s)	2.05 (d)(3-Me)
	8.41 (m)(H_2')		6.52 (d)(H_5')	Buried under phenyl (H_6')				
7 ($R_2 = Cl$)	—	6.85 (d)	6.44 (d of d)	9.03 (d)	7.2–7.8 (m)	3.42 (s)	2.60 (s)	—
8 ($R_2 = Me$)	—	6.49 (m)	6.39 (d of d)	8.51 (d)	7.2–7.7 (m)	3.34 (s)	2.49 (s)	2.28 (d)(2-Me)

[a]Chemical shifts are given as δ values followed by the multiplicity (m = multiplet, s = singlet, d = doublet, d of d = doublet of doublets).
[b]Mixture of *syn* and *anti* isomers. Primed values are those for the *anti* isomer (see text).

Can. J. Chem. Downloaded from www.nrcresearchpress.com by 210.87.254.105 on 09/05/12
For personal use only.

TABLE 3. Spin–spin coupling constants (Hz) of *p*-quinoneimide adducts assuming first-order splitting

Compound	
2	$J_{26} = 2.5, J_{35} = 2.1, J_{23} = 10.5, J_{56} = 10.3$
3	$J_{26} \simeq 2$
4	$J_{26} = 2.5, J_{HCCMe} = 1.4$
5	$J_{26} = J_{2'6'} = 2.6, J_{56} = 10.4, J_{5'6'} = 10.0$
6	$J_{26} = 2.8, J_{56} = 10.4, J_{5'6'} = 10.1$
7	$J_{35} = 2.4, J_{56} = 10.3$
8	$J_{35} = 2.4, J_{56} = 10.2, J_{HCCMe} = 1.2$

a pure sample of **7** by recrystallization, although the p.m.r. spectrum showed that it was present and only in the *anti* form **7***a*. This difficulty was overcome by the substitution of 6.6 g (20 mmol) of potassium ferricyanide as oxidizing agent. In this case there was no impurity formation and **7***a* was the sole product. Similar difficulties with these and other halophenols have been noted (7).

Reaction Between p-Benzoquinone and 4-Aminoantipyrine

Addition of 0.108 g (1 mmol) of *p*-benzoquinone (yellow) and 0.203 g (1 mmol) of 4-aminoantipyrine (cream) to 10 ml of chloroform gave a red solution. This was allowed to stand in the dark for 70 h. Addition of 100–120° petroleum ether caused the precipitation of a reddish brown solid. This was filtered off to give 0.262 g (89%) of **2**, m.p. 162–167°. Recrystallization from benzene – 100–120° petroleum ether gave 0.215 g (73%) of red crystals, m.p 166–169°. The p.m.r. spectrum of the product was identical to that of the compound from the oxidation of phenol.

Grateful acknowledgment is made to the National Research Council of Canada for its generous support of this work.

1. Standard methods for the examination of water and wastewater. 13th Ed. American Public Health Association, Washington. 1971. p. 504.
2. E. EMERSON. J. Org. Chem. **8**, 417 (1943).
3. E. EMERSON and J. SAGAL. J. Org. Chem. **13**, 535 (1948).
4. K. H. MÜLLER, B. CHRIST, and M. SCHNEIDER. Arch. Pharm. **293**, 567 (1960).
5. D. SVOBODOVA and J. GASPARIC. Coll. Czech. Chem. Commun. **33**, 42 (1968).
6. D. SVOBODOVA and J. GASPARIC. Coll. Czech. Chem. Commun. **35**, 1567 (1970).
7. D. SVOBODOVA, J. GASPARIC, and L. NOVAKOVA. Coll. Czech. Chem. Commun. **35**, 31 (1970).
8. H. THIELEMANN. Pharmazie, **24**, 483 (1969).
9. T. OKANO and K. UEKAMA. Yakugaki Zasshi, **87**, 1231 (1967); Chem. Abstr. **68**, 95182b (1968).
10. L. M. JACKMAN and S. STERNHELL. Applications of nuclear magnetic resonance spectroscopy in organic chemistry. 2nd Ed. Pergamon Press, London. 1969. (*a*) p. 340; (*b*) p. 318; (*c*) p. 185; (*d*) p. 226; (*e*) p. 91.
11. R. K. NORRIS and S. STERNHELL. Aus. J. Chem. **19**, 841 (1966).

Can. J. Chem. Downloaded from www.nrcresearchpress.com by 210.87.254.105 on 09/05/12
For personal use only.

Photoisomerization of Acylsilanes to Siloxycarbenes, and Their Reactions with Polar Reagents[1]

J. M. DUFF AND A. G. BROOK
Department of Chemistry, University of Toronto, Toronto 181, Ontario

Received February 1, 1973

The photolysis of acylsilanes in a variety of polar reagents (alcohols, acetic acid, HCN, pyrrole, etc.) is shown to involve formation of isomeric siloxycarbenes which act as nucleophiles and insert into the polar H—X bonds present in the reagents. With alcohols as solvents, mixed acetals of an aldehyde with 1 mol each of silanol and alcohol are formed, but these subsequently undergo dark, acid-catalyzed reactions, by one of two mechanisms which involve either carbon–oxygen or silicon–oxygen bond cleavage. The acid catalyst appears to be a by-product of the photolysis reaction. Kinetic and stereochemical evidence is presented in support of the proposed reaction pathways.

On a montré que la photolyse d'acylsilanes dans une série de réactifs polaires (alcools, acide acétique, HCN, pyrrole, etc.) implique la formation de siloxycarbènes isomériques qui agissent comme un nucléophile afin de s'insérer dans les liens polaires H—X que l'on trouve dans les réactifs. En se servant d'alcool comme solvant, des mélanges d'acétales d'une aldéhyde possédant 1 mol de silanol et 1 mol d'alcool sont formés bien que ces produits subissent par la suite des réactions (dans l'obscurité) catalysées par de l'acide, en suivant un des deux mécanismes impliquant soit un clivage du lien carbone–oxygène soit un clivage du lien silicium–oxygène. Le catalyseur acide a semblé être un produit secondaire de la réaction de photolyse. De même on apporte des preuves cinétiques et stéréochimiques afin d'appuyer le mécanisme réactionnel proposé. [Traduit par le journal]

Can. J. Chem., **51**, 2869 (1973)

Since their first synthesis in 1957 (1) acylsilanes (R_3SiCOR') have been of considerable interest to chemists because of their extremely long-wavelength carbonyl absorption both in the infrared ($R' = Me$, $\lambda_{max} = 6.08\ \mu$; $R' = Ph$, $\lambda_{max} = 6.18\ \mu$) and ultraviolet $n \rightarrow \pi^*$ region ($R' = Me$, $\lambda_{max} = 380$–390 nm (ε 100–400); $R' = Ph$, $\lambda_{max} = 415$–440 nm (ε 200–300)). Various explanations for these bathochromic shifts have been summarized (2). Following the early discoveries (3, 4) that acylsilanes, particularly in alcohol solution, were unstable to light (*i.e.* normal room illumination) the study of the photochemistry of acylsilanes has been a subject of continuing interest in these laboratories (5–11). A preliminary report (5) dealing with photolyses of a variety of acylsilanes in alcohol solution indicated that two types of processes appeared to be occurring depending on whether or not traces of base were present in the solvent. We describe here a mechanistic and stereochemical study of these processes and the results of photolyses in related protic solvents.

[1]From the Ph.D. Thesis of J. M. Duff, University of Toronto, 1970.

Photolyses in Protic Reagents in the Presence of Added Base

The photolyses of almost all acylsilanes in alcohols to which a trace of weak base (usually pyridine) has been added are relatively clean, rapid reactions giving as the single major product a mixed acetal of an aldehyde with silanol and the alcohol solvent.

These acetals are isolable as such only when base is present and, as will be described later, are very sensitive towards acid-catalyzed solvolysis. Typical results are shown in Table 1. The structures were established by normal spectroscopic methods and in some cases by alternative syntheses. For example, the product from the photolysis of acetyltriphenylsilane in ethanol was also readily synthesized by the addition of triphenylsilanol to ethyl vinyl ether using the procedure of Shostakovskii *et al.* (12). This product, like the other mixed acetals, showed an

Can. J. Chem. Downloaded from www.nrcresearchpress.com by 210.87.254.6 on 09/05/12
For personal use only.

TABLE 1. Photolysis products of acylsilanes in alcohol containing pyridine

Compound	Alcohol	Time	Product	% yield[a]
$Ph_3SiCOPh$	EtOH	7 min	$Ph_3SiOCHPh(OEt)$	100
$Ph_3SiCOC_6H_4$—X-*p* (X = H, *t*-Bu, Cl, Br)	MeOH	~8 "	$Ph_3SiOCHAr(OMe)$	94[b]
$Ph_3SiCOPh$	*i*-PrOH	25 "	$Ph_3SiOCHPh(O$*i*-$Pr)$	~99
$Ph_3SiCOMe$	EtOH	12 "	$Ph_3SiOCHMe(OEt)$	84[c]
"	MeOH	15 "	$Ph_3SiOCHMe(OMe)$	77[b,c]
R_3Si^*COPh[d]	EtOH	8 "	$R_3Si^*OCHPh(OEt)$	100
"	MeOH	10 "	$R_3Si^*OCHPh(OMe)$	94[b]
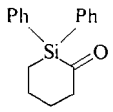	MeOH	30 "	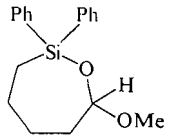	~90[e]
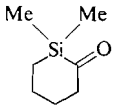	*i*-PrOH	6 h	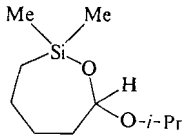	80[e]
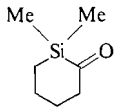	*t*-BuOH	15 h	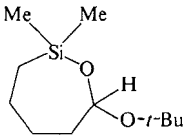	60[e]

[a]Unless specified otherwise, yields were determined by n.m.r. analysis of the photolyzate. See Experimental for the photolysis conditions.
[b]Minor amounts of alkoxysilane also formed.
[c]Minor products unidentified but presumably formed in competing radical processes.
[d]R_3Si^* ≡ chiral 1-NpPhMeSi.
[e]Products isolated by distillation.

i.r. absorption (typical of Si—O—C) from 9–10 μ, and the characteristic 1-proton n.m.r. signal (a quartet here) at about δ 5 p.p.m. of a hydrogen attached to an acetal carbon.

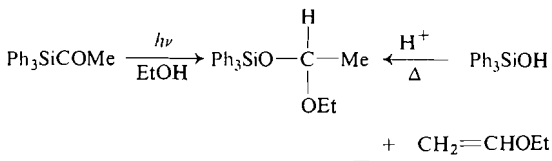

+ $CH_2{=}CHOEt$

Degradative studies also confirmed the mixed acetal structures. Thus reduction with lithium aluminum hydride under conditions known to reduce alkoxysilanes gave the corresponding silanes in good yield and acid- or base-catalyzed hydrolysis gave the expected silanol and aldehyde.

As has been proposed earlier (5) the formation of these mixed acetal products can be interpreted as arising from the insertion of a photochemically generated siloxycarbene into the polar O—H bond of the various alcohols.

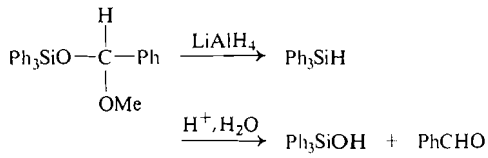

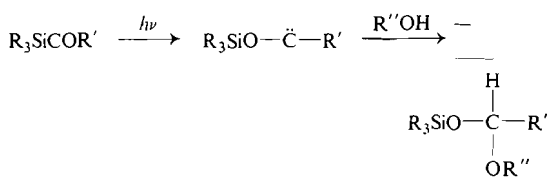

In order to determine the scope of these insertion reactions the photolysis of benzoyltriphenylsilane in other polar solvents was investigated. Products corresponding to the

Can. J. Chem. Downloaded from www.nrcresearchpress.com by 210.87.254.6 on 09/05/12
For personal use only.

Can. J. Chem. Downloaded from www.nrcresearchpress.com by 210.87.254.6 on 09/05/12
For personal use only.

"insertion" of the siloxycarbene into the polar bonds of acetic acid hydrogen cyanide, hydrogen chloride, pyrrole, thiophenol, and malononitrile have been characterized. Though not essential in these reactions, the addition of base (pyridine for hydrogen cyanide and sodium acetate for acetic acid) sometimes afforded higher yields of the insertion products.

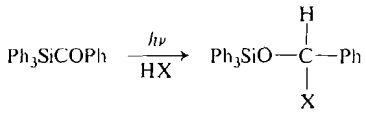

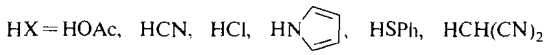

The acetic acid, pyrrole, and hydrogen cyanide products were relatively stable solids and could be crystallized in pure form. Others were too unstable to isolate analytically pure. Photolysis in aqueous dioxane gave triphenylsilanol and benzaldehyde, the products expected from decomposition of the intermediate H—OH insertion product (the hemiacetal $Ph_3SiOCHPh(OH)$). Related products were formed with acetyltriphenylsilane in acetic acid, hydrogen cyanide, or hydrogen chloride and with cyclic acylsilanes such as 1,1-diphenylsilacyclohexan-2-one in acetic acid, the other reagents not being tested. The above reagents, and alcohols, are related in that they possess reasonably acidic hydrogens ($pK_a < \sim 16$). However, no similar insertions were observed when acylsilanes were irradiated in the similarly acidic solvents, nitromethane or cyclopentadiene. The significance of these results will be discussed later.

The Stereochemistry of the Photolyses in Alcohol

When optically active benzoyl-1-naphthylphenylmethylsilane, $[\alpha]_D$ 6.2°, was photolyzed in methanol containing a trace of pyridine an optically active mixed acetal, $[\alpha]_D$ −8.2°, containing about 6% of 1-naphthylphenylmethylmethoxysilane was obtained. This mixture was reduced with lithium aluminum hydride under conditions known to reduce alkoxysilanes with retention of configuration (13), and the configuration (14) of the 1-naphthylphenylmethylsilane isolated ($[\alpha]_D$ −25°, *ca.* 75% optically pure) was identical to that of the starting benzoylsilane (15). Hence it is evident that the mixed acetal was formed from the acylsilane with at least 75% net retention of configuration.

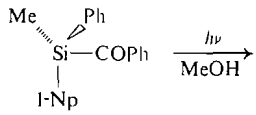

6.2°

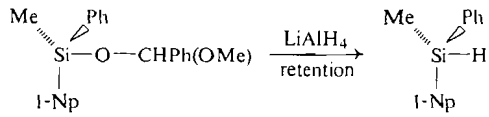

−8.2° −25°

Small amounts of methoxysilane, which probably arose from solvolysis of the mixed acetal, a reaction which occurs with inversion of configuration at silicon (13), would effectively reduce the optical purity of the hydride so the value of 75% represents a minimum optical purity for the mixed acetal.

Photolyses of Acylsilanes in Alcohols

When the acylsilanes were irradiated in purified methanol or ethanol the products usually obtained were "solvolysis" products, a mixture of alkoxysilane, silanol, aldehyde, and aldehyde dialkyl acetal. The products were identified and their yields determined by a combination of i.r., n.m.r., g.l.c. analyses and, in some cases, isolation. Some typical results are shown in Table 2.

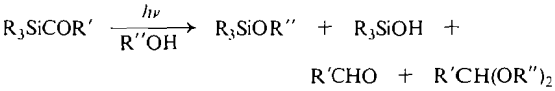

One exception was benzoyl-1-naphthylphenylmethylsilane, which, when irradiated in purified methanol, gave the mixed acetal previously found in basic alcohol as the major reaction product. When the composition of this solution was subsequently followed with time, in the dark, using n.m.r. analysis of aliquots, it was observed that the mixed acetal concentration slowly fell while at the same time the concentration of methoxysilane, silanol, benzaldehyde, and benzaldehyde dimethyl acetal grew at a similar rate to eventually become the sole components in the system. This process could be inhibited by adding a few drops of pyridine which stabilized the mixed acetal. Hence it is evident that the solvolysis products were being

TABLE 2. Yields of photolysis products of acylsilanes in purified alcohols[a]

Compound	Alcohol	Products			
		R_3SiOH	R_3SiOR''	$R'CHO$	$R'CH(OR'')_2$
$Ph_3SiCOPh$	EtOH	68–75	25–32	10	90
"	MeOH	20–25	75–80	15	85
$Ph_3SiCOMe$	EtOH	25[b]	75[b]	[c]	20[d]
"	MeOH	21[b]	79[b]	[c]	40[d]
1-NpPhMeSiCOPh	EtOH	[e]	[e]	10	90

[a]R_3SiOH and R_3SiOR'' determined by n.m.r.; $R'CHO$ and $R'CH(OR'')_2$ determined by g.l.c.
[b]Relative yields. Minor by-products also present.
[c]Acetaldehyde not measurable.
[d]Amount of acetaldehyde dialkyl acetal increases with time.
[e]Total $R_3SiOH + R_3SiOEt = 100\%$. Silanol could not be measured.

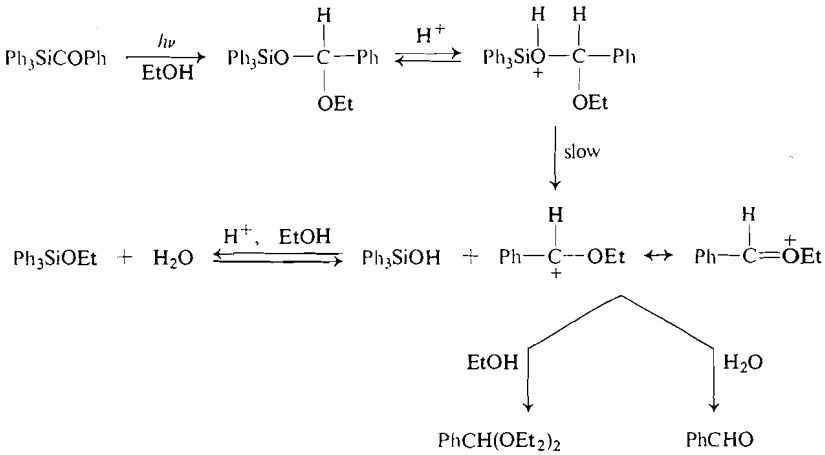

SCHEME 1

formed in the dark from the mixed acetal, a finding shown to be true for other acylsilanes under a variety of conditions.

By cooling the solution being photolyzed it was possible to slow down the rate of solvolysis while not significantly altering the rate of photolysis. A further differentiation in rates was effected by using two lamps, thereby doubling the rate of photolysis. Using these conditions and by removing aliquots of the photosolution and stabilizing these solutions by addition of pyridine it was possible, using a combination of n.m.r. and g.l.c. analysis, to determine with reasonable accuracy and reproducibility the concentrations of most of the species in the system.

The resulting kinetic data indicated that there were two different modes of acid-catalyzed decomposition of the mixed acetals, one predominating with benzoylsilanes and the other with acetyltriphenylsilane.

The behavior of benzoyltriphenylsilane in ethanol is illustrated in Scheme 1. Photolysis gives the mixed acetal initially but in the presence of acid (to be documented later) protonation on the siloxy-oxygen followed by slow, rate-determining dissociation gives silanol (which can be isolated in good yield) and a resonance-stabilized carbonium ion. The silanol, in the acidic alcohol, is fairly rapidly converted to ethoxysilane, this being a known reaction (16). The carbonium ion (which may never be truly free) suffers attack at carbon by ethanol to yield primarily benzaldehyde diethyl acetal but, with traces of water present, may also yield some free aldehyde via the hemiacetal.

This mechanism is supported by the kinetic data of Fig. 1. The benzoylsilane concentration rapidly fell to zero over about 20 min, at which time the light was shut off. While less obvious in this case, due to its instability, the concentra-

Can. J. Chem. Downloaded from www.nrcresearchpress.com by 210.87.254.6 on 09/05/12
For personal use only.

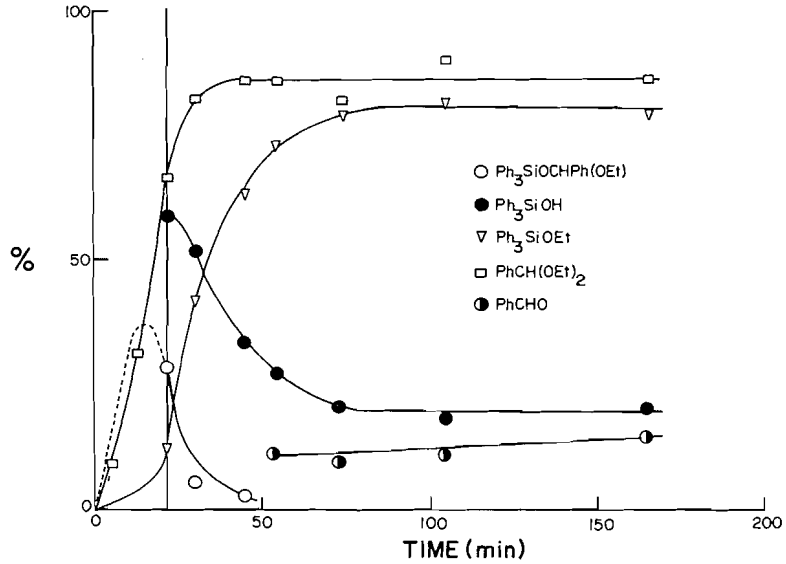

FIG. 1. Plot of the product yields *vs.* time for the photolysis of benzoyltriphenylsilane in ethanol at 0°.

tion of mixed acetal, shown by the dotted curve, initially rose rapidly, paralleling the decay of acylsilane, but it then began to decompose, giving rise to triphenylsilanol and benzaldehyde diethyl acetal. The silanol concentration also diminished as triphenylethoxysilane was formed, until an equilibrium mixture was reached.

The photolysis of benzoyltriphenylsilane in methanol was similar but in this case the rate of decomposition of the mixed acetal was relatively slow and the silanol concentration did not build up to the same extent, being present in about 30% yield at the most during the reaction.

Three additional pieces of information support this mechanism involving acid-catalyzed displacement at carbon. Firstly, the kinetics of decomposition of $Ph_3SiOCHPh(OMe)$ could be determined at 0° and the log concentration *vs.* time plot was a good straight line (Fig. 2) in accord with the *pseudo* first-order kinetics required by Scheme 1. Secondly, a series of para-substituted benzoyltriphenylsilanes were photolyzed in methanol and the rates of decomposition of the mixed acetals were followed by n.m.r. spectroscopy. The acetals derived from *p*-methoxy- and *p*-*t*-butyl-benzoyltriphenylsilane decomposed too rapidly to measure quantitatively and had disappeared by the time the photolyses were completed. The *p*-chloro and *p*-bromo mixed acetals were less reactive than the unsubstituted compound, the *pseudo* first-

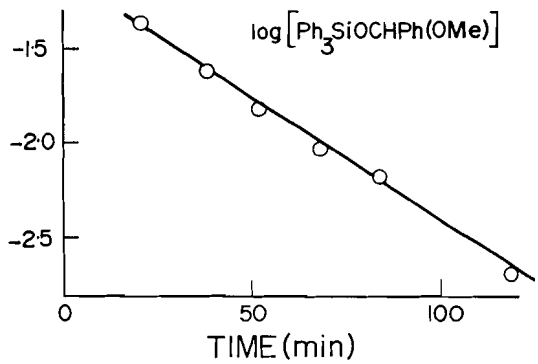

FIG. 2. Plot of log [$Ph_3SiOCHPh(OMe)$] *vs.* time for the photolysis of benzoyltriphenylsilane in methanol at 0°.

order rate constants being 4.56×10^{-2}, 3.07×10^{-2}, and 3.75×10^{-2} min^{-1} for the unsubstituted *p*-chloro and *p*-bromo compounds, respectively. This behavior is that expected from a reaction involving rate-determining formation of a benzyl-type carbonium ion stabilized by resonance interaction with a *p*-substituent.

Finally, the stereochemistry of the decomposition of the mixed acetal from (+)-benzoyl-1-naphthylphenylmethylsilane has been established. As shown above, the mixed acetal was formed in methanol with a high degree of retention of configuration. If the proposed mechanism were valid the silanol would also be formed with retention of configuration because the C—O bond breaking during solvolysis does not

Can. J. Chem. Downloaded from www.nrcresearchpress.com by 210.87.254.6 on 09/05/12
For personal use only.

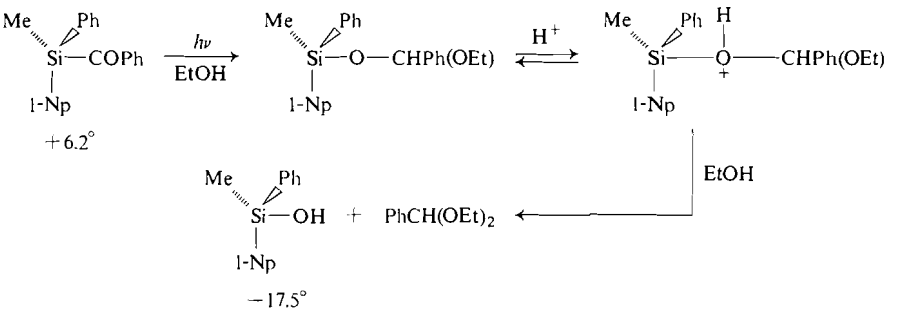

involve the asymmetric silicon center. The chiral benzoylsilane was photolyzed in ethanol at 0° and small amounts of the photolysis solution were removed and examined by infrared spectroscopy. When a maximum amount of silanol was indicated, the reaction mixture was worked up to give a 40% yield of (−)-1-napthylphenylmethylsilanol, $[\alpha]_D$ −17.5° (isolated by chromatography under conditions where the accompanying mixed acetal and methoxysilane were stable), which corresponds to an optical purity of at least 85% and to retention of configuration at silicon.

Hence it is clear that the decomposition of the mixed acetal from a benzoylsilane involves cleavage of the carbon–oxygen bond, the same process as is known to occur in general acid-catalyzed acetal formation or decomposition (17).

When the optically active (+)-benzoylsilane was irradiated in methanol the resultant methoxysilane, the major product present in the solution after *ca.* 1 h at room temperature (which arose through the acid-catalyzed methanolysis of the silanol), was found to be virtually racemic. This finding was not unexpected since it is known that the rate of racemization of 1-naphthylphenylmethylmethoxysilane in methanol is considerably accelerated by traces of acid (18). A previous report (5) that the methoxysilane thus obtained was significantly levorotatory is now believed to be erroneous (the product was levorotatory due to the presence of (−)-mixed acetal and (−)-silanol in the photolyzate).

A second mode of decomposition of the mixed acetals, believed to predominate in the photolysis of acetyltriphenylsilane in ethanol, is shown in Scheme 2. Here, protonation of the mixed acetal (either on the siloxy or ethoxy oxygen) followed by nucleophilic attack at silicon by ethanol yields ethoxysilane and the hemiacetal of acetaldehyde or, by what is essentially a β-elimination mechanism, acetaldehyde plus ethanol. These two alternatives have not been distinguished.

The data in Fig. 3 confirms the general features

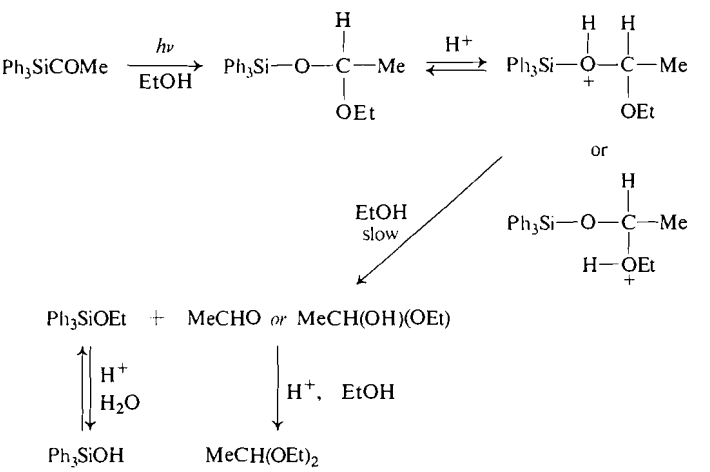

SCHEME 2

Can. J. Chem. Downloaded from www.nrcresearchpress.com by 210.87.254.6 on 09/05/12
For personal use only.

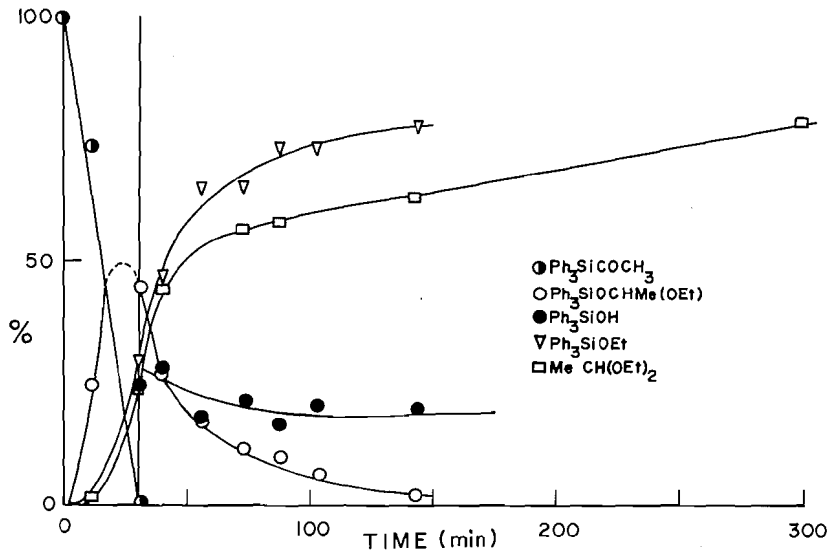

FIG. 3. Plot of the product yields *vs.* time for the photolysis of acetyltriphenylsilane in ethanol at 0°.

expected of this mechanism. Again acetylsilane rapidly decreased in concentration during the photolysis time (*ca.* 30 min) and the mixed acetal concentration rapidly increased initially and then fell off as it suffered solvolysis. The log concentration *vs.* time plot for the decomposition of $Ph_3SiOCHMe(OEt)$ was linear (Fig. 4) in accord with the proposed mechanism. Unlike the previous case, when silanol was formed initially, here ethoxysilane appears to be formed directly from the mixed acetal, there being no evidence for major amounts of silanol. (This was even more evident in the data for the solvolysis in methanol where by the time the acetylsilane concentration was down to 20% the methoxysilane concentration had reached 70%). What is equally important is that, as expected from the mechanism of Scheme 2, the amount of acetaldehyde diethyl acetal builds up at a rate which is much slower than the rate of decomposition of the mixed acetal; this is consistent with the independent formation of acetaldehyde diethyl acetal from acetaldehyde or its hemiacetal. The silanol could have arisen from hydrolysis of the mixed acetal or ethoxysilane due to the traces of water in the system.

In summary, it appears that there are two distinct mechanisms for the acid-catalyzed decomposition of the (photochemically formed) mixed acetals. The mixed acetals from benzoyltriphenylsilane preferentially undergo acetal carbon–oxygen bond cleavage (cf. conventional

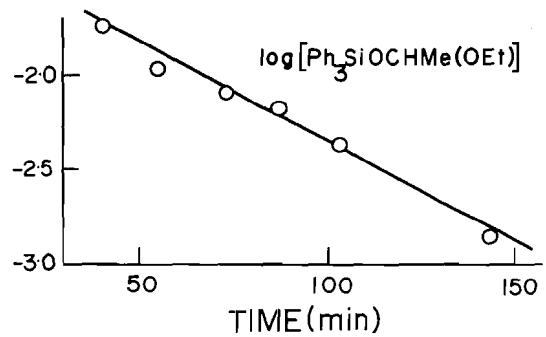

FIG. 4 Plot of log [$Ph_3SiOCHMe(OEt)$] *vs.* time for the photolysis of acetyltriphenylsilane in ethanol at 0°.

acetal hydrolysis), while those from acetylsilanes preferentially undergo silicon–oxygen bond cleavage (cf. solvolysis of alkoxysilanes or β-elimination).

Evidence for the Presence of Acid

It was indicated above that the solvolyses reaction were acid-catalyzed but we have deferred until now evidence that acids were involved and what their source was. It appears that the acid present is photochemically generated. Thus, solutions of benzoyltriphenylsilane in carefully purified methanol, on titration immediately after photolysis, shown an increased acid concentration of the order of 1/100 of a mole per mole of benzoylsilane photolyzed. Great precautions were taken to avoid the possibility that

Can. J. Chem. Downloaded from www.nrcresearchpress.com by 210.87.254.6 on 09/05/12
For personal use only.

Can. J. Chem. Downloaded from www.nrcresearchpress.com by 210.87.254.6 on 09/05/12
For personal use only.

the acid was introduced as an impurity on the surface of the glassware by using a variety of treatments of the glassware or by using polyethylene flasks, neither of which altered the observed phenomena.

Further evidence that acid was formed during the photolysis was provided by showing that although benzaldehyde was indefinitely stable in the methanol or ethanol used in the experiments or in solutions of acylsilane in the dark, if it was added to any photolysis solution it was relatively rapidly converted, in the dark, to benzaldehyde dialkyl acetal. Acid is the only effective catalyst known for this conversion (19, 20) and the rate of the process, under standard conditions, could be used to establish the relative acidity of various photosolutions. From observed rates it was deduced that the acetyltriphenylsilane–methanol photosolution was markedly more acidic than the photosolution from benzoyltriphenylsilane in methanol which in turn was slightly more acidic than that from benzoyl-1-napthylphenylmethylsilane in ethanol.

This acetal formation could be duplicated by adding comparable amounts (*ca.* 0.01 mol. equiv.) of relatively strong acids (sulfanilic, hydrochloric, oxalic) to solutions of benzaldehyde in alcohol but comparable rates of conversion could not be effected by addition of formic or acetic acid in similar (or even markedly greater) concentration. This suggests that the latter acids, which might conceivably have arisen from oxidation of the alcohols, cannot be the species responsible for the catalysis. Benzoic acid (conceivably formed by oxidation of benzaldehyde, although precautions were taken to avoid oxidation by working under nitrogen) was more effective as a catalyst than formic or acetic acid, but only at much higher concentrations than had been indicated by titration did it duplicate the rate of acetal formation in the photosolutions. The phenomenon of acid-catalyzed processes occurring during photolyses in alcohols is not unique to acylsilanes (21–23).

The Mechanism of Formation of the Mixed Acetals and Related Products

There is now compelling evidence in the literature that some ketones can be photoisomerized to oxacarbenes (21). The results described above are readily explained by similar photoisomerizations of acylsilanes to siloxycarbenes which

$$R_3SiCOR' \xrightarrow{h\nu} R_3SiO-\ddot{C}-R' \xrightarrow{HX} R_3SiO-\underset{X}{\overset{H}{C}}-R'$$

insert into polar bonds giving rise to mixed acetals and related products.

In principle the siloxycarbene could be nucleophilic or electrophilic in character, *i.e.* the effectiveness of trapping agents would depend either on their proton donating or electron donating ability. Evidence has already been published which demonstrated that cyclic siloxycarbenes from silacyclohexanones were strongly nucleophilic in nature, forming a cyclopropane adduct with the electron-deficient olefin, diethyl fumarate (9), or oxiranes via nucleophilic attack of the carbonyl group of aldehydes and ketones (10). The photochemistry of the acyclic acylsilanes (none of which were found to form related cyclopropanes or oxiranes in detectable amounts) is also most readily interpreted on the basis of the siloxycarbene being markedly nucleophilic. Thus the reagents which effectively trapped the siloxycarbene were in general acidic (ROH, HOAc, HCN, HCl, pyrrole, etc.). The fact that acetonitrile ($pK_a \sim 25$) failed to react with siloxycarbenes while malononitrile ($pK_a \sim 12$) did so readily demonstrates that it is the acidity of a substance rather than the availability of a site for electrophilic attack (*e.g.* the CN group) which governs whether reaction will occur. Furthermore pyrole ($pK_a \sim 15$) was the only amine of those investigated which was found to trap the carbene from benzoyltriphenylsilane; benzoyltriphenylsilane reacted slowly in the dark with diethylamine ($pK_a \sim 33$) but gave no evidence of undergoing photolysis in this solvent.

However, besides the noticeable nucleophilicity, there is a second property that must be ascribed to siloxycarbenes before the photochemistry of acylsilanes may be fully rationalized. It appears that siloxycarbene formation is a fast, reversible reaction and that if the siloxycarbene is not trapped by a suitable reagent it reverts to acylsilane. (An analogy of this process, involving isomerization of an alkoxycarbene to a ketone, has appeared recently (24).) Scheme 3 illustrates our preferred general mechanism for acylsilane photochemistry in which reversible carbene formation competes with an alternative radical cleavage process (11).

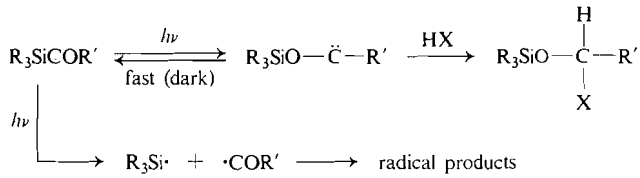

SCHEME 3. Proposed general mechanism for acylsilane photochemistry.

Of the acylsilanes studied to date, benzoyltriphenylsilane appears to undergo carbene formation almost exclusively since it reacts only very slowly when irradiated in nonpolar solvents (25), while phenylacetyltriphenylsilane (even in alcohol solutions) gives only radical-derived products (11). All other acylsilanes investigated show dual behavior, giving carbene products in the presence of suitable reagents, but otherwise forming radical products. In general the radical cleavage appears to be slower than the photoisomerization to siloxycarbene. The isolation of minor amounts of radical-derived product from the photolysis of acetyltriphenylsilane in methanol (11) is in accord with this scheme. This concept of the siloxycarbene as a short-lived nucleophilic intermediate also explains the relative inertness of benzoyltriphenylsilane to irradiation in nitromethane and cyclopentadiene.[2] Although these reagents are moderately acidic (pK_a's *ca.* 10 and 15, respectively) they are known to have a low kinetic acidity (26) (k_1 10^{-8} and 10^{-2}, respectively) in contrast to the reagents which did trap siloxycarbenes ($k_1 \sim 10^9$). With reagents of low kinetic acidity it is probable that the rate of isomerization of siloxycarbene back to acylsilane is more rapid than its rate of proton abstraction from the reagent to give the insertion product.

Finally, it is pertinent to comment on the demonstrated greater tendency of cyclic acylsilanes to react via siloxycarbenes relative to their acyclic analogs. It is apparent from a study of models that the approach of the carbene-carbon to the silicon atom, which is required for their isomerization back to acylsilane, is opposed by ring strain in the cyclic siloxycarbenes. Thus the apparently greater reactivity of the cyclic siloxycarbenes, relative to their acyclic analogs, may be due more to an increased lifetime than to real differences in their reactivities.

Further studies of a photophysical nature, designed to establish the validity of our proposed general mechanism for photolyses (Scheme 3), are in progress.

[2]Cyclopentadiene does not appear to quench the photolysis of benzoyltriphenylsilane in other solvents.

Experimental

General

All photolyses were carried out using a 100 W PAR 38 clear mercury lamp, ASA code H34-4GS (available from Westinghouse); the lamp has intense emission bands at 366, 405, and 436 mμ, reasonably matched with the u.v. absorption maxima of acetyl- and benzoyl-silanes at about 380 and 420 mμ, respectively. Irradiations were carried out in Pyrex flasks under nitrogen. In the case of benzoylsilanes, completion of a photolysis was indicated by the disappearance of the yellow color. For alkanoylsilanes the progress of the irradiation could be followed by observing the disappearance of the i.r. carbonyl band at *ca.* 6.08 μ in small, worked-up samples. Control experiments were carried out to ensure that the acylsilanes did not undergo dark reactions with the solvents and reagents used.

The instruments used in the experiments are as follows: Perkin-Elmer 237B Infrared Spectrophotometer; Varian A60, A56/60, T60 and, occasionally, HA100 n.m.r. spectrometers; AEI MS 902 mass spectrometer, operated at 70 eV.; Galileo-type MN 602 manual polarimeter, using a 1 dm micro-cell; Varian-Aerograph Series 200 dual column g.c. instrument with a thermal conductivity detector. Microanalyses were performed by A. B. Gygli of Toronto.

Photolyses in Alcohol Containing Pyridine

In the experiments described here commercial grade absolute ethanol or reagent grade methanol were used without further purification. Pyridine, 50 μl per 10 ml of solution, was generally used but similar amounts of piperidine or triethylamine gave the same results. Sodium carbonate could also be used for photolyses in ethanol. The standard conditions for an experiment involved irradiation of 0.00069 mol of acylsilane in 10 ml of solvent containing 50 μl of pyridine. The required reaction times and yields of the mixed acetals are given in Table 1. The major products from the acyclic acylsilanes all proved to be unstable oils which partially decomposed on standing at room temperature for several hours, or on attempted distillation. Although some mixed acetals were moderately stable to chromatography on silica gel, this procedure failed to separate them from accompanying alkoxysilane. All products had a characteristic i.r. spectral pattern from 9–10 μ; the n.m.r. spectra of the mixed acetals from the acyclic acylsilanes are given in Table 3.

Confirming evidence for the mixed acetal structures

Can. J. Chem. Downloaded from www.nrcresearchpress.com by 210.87.254.6 on 09/05/12
For personal use only.

TABLE 3. N.M.R. spectral data for acyclic mixed acetals[a]

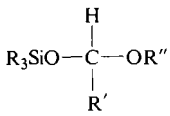

Compound	R_3Si	H	R′	R″
$Ph_3SiOCHPh(OEt)$	7.1–7.8 m	5.90 s	7.1–7.8 m	3.38 q (J = 7 Hz) 0.90 t (J = 7 Hz)
$Ph_3SiOCHPh(OMe)$	7.1–7.7 m	5.85 s	7.1–7.7 m	3.01 s
$Ph_3SiOCHPh(O\textit{i}\text{-}Pr)$	7.1–7.8 m	5.88 s	7.1–7.8 m	3.81 septet (J = 6 Hz)[b] 0.90, 1.03 2d (J = 6 Hz)
$Ph_3SiOCHMe(OEt)$	7.1–7.8 m	5.03 q (J = 5 Hz)	1.31 d (J = 5 Hz)	3.33 complex[c] 0.96 t (J = 7 Hz)
$Ph_3SiOCHMe(OMe)$	7.2–7.8 m	4.92 q (J = 5 Hz)	1.30 d (J = 5 Hz)	3.12 s
1-NpPhMeSiOCHPh(OEt)	7.1–8.2 m 0.73 s (SiMe)	5.73 s	[d]	3.42 complex[c] 0.99 t (J = 7 Hz)
1-NpPhMeSiOCHPh(OMe)	7.1–8.3 m 0.68 s (SiMe)	5.82 s	[d]	3.05 s

[a]Carbon tetrachloride solution, internal tetramethylsilane standard.
[b]Nonequivalent methyl groups.
[c]Nonequivalent methylene protons.
[d]Buried in aromatic multiplet.

was obtained from the following mass spectra of crude photolyzates:

(*a*) Benzaldehyde methyl triphenylsilyl acetal (M = $Ph_3SiOCHPh(OMe)$); *m/e* (relative intensity, proposed origin): 396 (3, M), 365 (2, M—OMe), 319 (5, M—Ph), 290 (9, Ph_3SiOMe), 259 (18, Ph_3Si), 213 (29, Ph_2SiOMe), 161 (100, unidentified), 121 (81, PhCH(OMe)).

(*b*) Acetaldehyde ethyl triphenylsilyl acetal (M = $Ph_3SiOCHMe(OEt)$); *m/e* (relative intensity, proposed origin): 348 (5, M), 333 (4, M—Me), 319 (4, M—Et), 303 (10, M—OEt), 271 (21, M—Ph), 259 (100, Ph_3Si), 161 (75, unidentified), 77 (78, Ph), 73 (75, MeCH(OEt)).

(*c*) Benzaldehyde ethyl 1-naphthylphenylmethylsilyl acetal (M = 1-NpPhMeSiOCHPh(OEt)); *m/e* (relative intensity, proposed origin): 398 (1, M), 369 (0.5, M—Et), 292 (10, 1-NpPhMeSiOEt), 277 (13, 1-NpPhSiOEt), 264 (50, 1-NpPhMeSiOH), 249 (90, 1-NpPhSiOH), 135 (100, PhCH(OEt)), 127 (18, Np), 105 (43, PhCO), 77 (70, Ph).

Several cyclic mixed acetals were more stable than their acyclic counterparts and could be purified by distillation. These experiments are described in full.

1,1-Diphenyl-1-sila-2-oxa-3-methoxycycloheptane

A solution of 0.323 g of 1,1-diphenyl-1-silacyclohexanone-2 in magnesium-dried methanol (35 ml) containing 20 μl of pyridine was irradiated for 30 min. Removal of solvent at reduced pressure gave the mixed acetal as an oil contaminated with a small amount of what is believed to be the isomeric open chain aldehyde, 5-(diphenylhydroxysilyl)pentanal (4). The product was chromatographed on silica gel (eluting with benzene) and then was distilled to give the pure mixed acetal, b.p. 130–132°/0.04 mm; i.r. (CCl_4): 9–10 μ (complex, Si—O—C); n.m.r. (CCl_4): δ 7.10–7.75 (m, 10H, aryl-H), 4.90 (broad t, 1H, acetal H), 3.23 (s, 3H, O*Me*), 0.91–2.15 p.p.m. (m, 8H, $(CH_2)_4$).

Anal. Calcd. for $C_{18}H_{22}O_2Si$: C, 72.46; H, 7.43. Found: C, 72.93; H 7.48.

1,1-Dimethyl-1-sila-2-oxa-3-isopropoxycycloheptane

A solution of 1,1-dimethyl-1-silacyclohexanone-2 (1.0 g) in magnesium-dried 2-propanol containing 2 drops of pyridine, at 0°, was irradiated for 6 h. Removal of solvent at reduced pressure, followed by distillation, gave 0.9 g (80%) of the cyclic acetal as clear liquid, b.p. 44–46°/1.0 mm; n_D^{20} 1.4362; i.r. (CCl_4): 9–10 μ (complex, SiOC); n.m.r. (CCl_4): δ 4.83 (broad t, 1H, acetal *H*), 3.83 (septet, J = 6 Hz, 1H, OC*H*Me_2), 1.11, 1.04 (2d, J = 6 Hz, 6H, CH*Me*$_2$), 1.8–0.4 (complex, 8H, $(CH_2)_4$), 0.11, 0.03 p.p.m. (2s, each 3H, $SiMe_2$).

Anal. Calcd. for $C_{10}H_{22}O_2Si$: C, 59.35; H, 10.96. Found: C, 59.18; H, 11.42.

1,1-Dimethyl-1-sila-2-oxa-3-t-butoxycycloheptane

A solution of 2.0 g of 1,1-dimethyl-1-silacyclohexanone-2 in 20 ml of dry *t*-butanol containing 1 drop of pyridine was irradiated for 15 h. Removal of solvent on a rotary evaporator gave a yellow liquid which was distilled (44–45°/0.9 mm) to give 1.8 g (60%) of the cyclic acetal as a colorless liquid, n_D^{20} = 1.4376; i.r. (CCl_4): 9–10 μ (complex, Si—O—C); n.m.r. (CCl_4): δ 5.10 (broad t, 1H, acetal H), 1.15 (s, 9H, Bu^t), 1.8–0.4 (complex, 8H, $(CH_2)_4$), 0.07–0.03 (2s, each 3H, Me_2Si).

Anal. Calcd. for $C_{11}H_{24}O_2Si$: C, 61.16; H, 11.18. Found: C, 61.57; H, 11.51.

Hydrolysis of Benzaldehyde Ethyl Triphenylsilyl Acetal

The photolyzate obtained from 2.3 g of benzoyltriphenylsilane in ethanol (essentially pure mixed acetal), dissolved in 10% aqueous acetone, was treated with 4 drops of concentrated hydrochloric acid. After 30 min, workup using ether–water and distillation of the product

Can. J. Chem. Downloaded from www.nrcresearchpress.com by 210.87.254.6 on 09/05/12
For personal use only.

Can. J. Chem. Downloaded from www.nrcresearchpress.com by 210.87.254.6 on 09/05/12
For personal use only.

(200°; Kugelrohr) pure benzaldehyde (0.56 g, 84%), identified by its i.r. spectrum was obtained. Recrystallization of the solid residue from carbon tetrachloride – pentane gave pure triphenylsilanol (1.54 g, 88%), m.p. 154–156°, m.m.p. 154–156°. Similar degradations were carried out with other acyclic acetals.

Hydrolysis of 1,1-Diphenyl-1-sila-2-oxa-3-methoxycycloheptane

A sample of 0.41 g of the cyclic acetal in 20 ml of THF was treated with 2 ml of 1% potassium hydroxide. After 15 min the acidified solution was extracted with ether. The product was chromatographed on silica gel, eluting with 1:1 benzene–chloroform, to give 0.25 g (68%) of 5-(diphenylhydroxysilyl)pentanal (4).

Reduction with Lithium Aluminum Hydride

Qualitative degradative tests were carried out by stirring small samples of the triphenylsilyl mixed acetals with excess lithium aluminum hydride in diethyl ether solvent for about 24 h at room temperature. Spectra of the worked-up product showed that triphenylsilane (strong i.r. absorption at 4.70 μ and n.m.r. singlet at δ 5.45 p.p.m.) was the major product.

Alternative Synthesis of Acetaldehyde Triphenylsilyl Ethyl Acetal

A solution of 1.38 g (0.005 mol) of triphenylsilanol in 4.0 g (0.055 mol) of ethyl vinyl ether containing 4 μl of concentrated hydrochloric acid was sealed under nitrogen in a Pyrex tube and was heated at 67° for 21 h. After cooling, removal of the solvent gave a thick, clear, odorless oil, whose spectra were identical to those of the photochemically obtained acetal, $Ph_3SiOCHMe(OEt)$.

Reduction of Optically Active Benzaldehyde 1-Naphthylphenylmethylsilyl Methyl Acetal

The photolyzate from benzoyl-1-naphthylphenylmethylsilane (0.35 g, 0.001 mol), $[\alpha]_D$ +6.2°, in methanol containing pyridine was refluxed for 19 h in di-*n*-butyl ether (30 ml) containing 0.18 g (0.005 mol) of lithium aluminum hydride. Workup gave a thick oil (0.22 g) which was chromatographed on silica gel, eluting with 1:10 petroleum ether (60–70°) – carbon tetrachloride, to give pure 1-naphthylphenylmethylsilane, m.p. 40–51°, $[\alpha]_D$ −25.1° (*c*, 7.65, cyclohexane) (lit. (13) $[\alpha]_D$ 34°, cyclohexane).

Photolysis of Benzoyltriphenylsilane in Aqueous Dioxane

A solution of 0.50 g of benzoyltriphenylsilane in 10 ml of 20% aqueous dioxane was irradiated for 35 min until the color disappeared. Removal of solvent at the rotary evaporator gave an oil; an i.r. spectrum indicated that triphenylsilanol and benzaldehyde were the only products present. Crystallization from carbon tetrachloride – pentane gave 0.34 g (90%) of triphenylsilanol.

Photolysis of Benzoyltriphenylsilane in Acetic Acid

The photolysis of 1.0 g of benzoyltriphenylsilane in glacial acetic acid gave as the major product acetoxytriphenylsilane (along with about 5% of the expected carbene insertion product (see below)). Crystallization from dry hexane gave 0.76 g (91%) of acetoxytriphenylsilane (m.p. 95.5–97°; lit (27) m.p. 97°).

When the photolysis of 1.0 g of the benzoylsilane was carried out in a well-stirred suspension of 1.0 g of sodium acetate in glacial acetic acid (25 ml) it was completed in 25 min. Removal of solvent and extraction of the residue with dry ether gave a mixture of acetoxytriphenylsilane and α-triphenylsiloxybenzyl acetate (*ca.* 21:79 respectively by n.m.r.). After several recrystallizations from hexane had failed to yield pure siloxybenzyl acetate the product was rapidly chromatographed on silica gel, eluting with benzene. Early fractions (0.25 g) were recrystallized from pentane to give pure α-triphenylsiloxybenzyl acetate, m.p. 65–67°.

The results of similar photolyses of acyclic acylsilanes in polar solvents are summarized in Table 4.

Alternative Synthesis of (Triphenylsiloxy)phenylacetonitrile

Benzaldehyde cyanohydrin (29) (1.0 g, 0.0075 mol) was added to a solution of 1.47 g (0.005 mol) of triphenylchlorosilane in 80 ml of hexane–toluene (3:1) containing 0.79 g (0.01 mol) of pyridine. The solution was refluxed for 5 h and then the solvent was removed at reduced pressure. The residue was boiled with 60 ml of hexane and the solution, decanted from insoluble tar, was filtered over charcoal. The product (0.90 g, 46%) was obtained as large clear crystals, m.p. 87.5–89°, the spectra of which were identical to those of the photochemically prepared material (Table 4). Treatment of the nitrile with dilute hydrochloric acid in acetone gave triphenylsilanol (85%) and benzaldehyde cyanohydrin (spectroscopically identified). Concentrated hydrochloric acid (in dioxane) converted the nitrile to triphenylsilanol (80% after recrystallization) and *dl*-mandelic acid (62%), identified by m.m.p.

Degradation of α-Triphenylsiloxybenzylmalononitrile

A sample of 0.80 g of the benzoyltriphenylsilane–malononitrile photolyzate (containing about 15% of triphenylsilanol) was stirred in methanol at 20° for 26 h. Removal of the solvent followed by distillation (150°/10 mm; Kugelrohr) gave 0.18 g (63%) of benzalmalononitrile (i.r. 4.44 μ), m.p. 83–84°; lit. (30) 83.5–84°. The nonvolatile product was recrystallized from carbon tetrachloride – pentane to give 0.48 g (94%) of triphenylsilanol.

Photolysis of 1,1-Diphenyl-1-silacyclohexanone-2 in Acetic Acid

A solution of the acylsilane (0.132 g) in 10 ml of glacial acetic acid was irradiated for 20 min. The solvent was then removed and the residue was distilled to give a clear oil, b.p. *ca.* 170°/0.01 mm, which appeared to be almost pure 1,1-diphenyl-1-sila-2-oxa-3-acetoxycycloheptane; i.r. (CCl_4): 5.71 μ (C=O of acetate); n.m.r. (CCl_4): δ 7.1–7.7 (m, 10H, aromatic H), 6.28 (broad, 1H $OCHOAc$), 1.76 (s, 3H, $COMe$), 1.1–2.1 (complex, 8.2H, $(CH_2)_4$) p.p.m.

A small sample of the above material was hydrolyzed in dilute aqueous acidic acetone at room temperature for 20 h. Workup gave an oil, the spectra of which were identical to those of 5-(diphenylhydroxysilyl)pentanal (4).

Photolyses of Acylsilanes in Purified Alcohols

Pure dry methanol and ethanol were prepared by standard procedures. The glassware used was thoroughly cleaned and dried. Immediately prior to its use a flask was rinsed several times with the same purified alcohol to be used in the photolysis. Following the irradiation of

Can. J. Chem. Downloaded from www.nrcresearchpress.com by 210.87.254.6 on 09/05/12
For personal use only.

TABLE 4. Photolyses of acylsilanes in protic solvents

$$Ph_3SiCOR' \xrightarrow[HX]{h\nu} Ph_3SiO-\underset{X}{\overset{H}{C}}-R'$$

Acylsilane(g)	Reagent	Photolysis conditions	Product	Yield[a]	N.m.r. data[b] H	R′	X
$Ph_3SiCOPh$ (1.0)	HOAc	25 ml; 20 min	$Ph_3SiOCHPh(OAc)$[c]	5	7.02 s (1H)	Aryl m	1.61 s (3H)
$Ph_3SiCOPh$ (1.0)	HOAc	25 ml + 1.0 g NaOAc; 40 min	$Ph_3SiOCHPh(OAc)$[c,d]	79	7.02 s (1H)	Aryl m	1.61 s (3H)
$Ph_3SiCOPh$ (1.0)	HCN	Saturated solution in benzene (40 ml); 45 min	$Ph_3SiOCHPh(CN)$[e,f]	80	5.45 s (1H)	Aryl m	—
$Ph_3SiCOPh$ (1.0)	Pyrrole	12 ml; 2 h	$Ph_3SiOCHPh(N\text{-pyrryl})$[g]	>90	*ca.* 6.5 (1H)	Aryl m	6.5 m (2H) 6.0 m (2H)
$Ph_3SiCOPh$ (0.25)	HSPh	1 ml in 9 ml CH_3CN; 13 min	$Ph_3SiOCHPh(SPh)$	90	6.18 s	Aryl m	Aryl m
$Ph_3SiCOPh$ (0.50)	HCl	Saturated solution in cyclohexane (20 ml); 40 min	$Ph_3SiOCHPhCl$[h]	>90	6.84 s	Aryl m	—
$Ph_3SiCOPh$ (2.0)	$HCH(CN)_2$	5 g in 50 ml CH_3CN; 16 h	$Ph_3SiOCHPh(CH(CN)_2)$[i]	75	4.80 d (1H, J = 6)	Aryl m	5.08 d (1H, J = 6)
$Ph_3SiCOMe$ (1.0)	HOAc	25 ml; 55 min	$Ph_3SiOCHMe(OAc)$[j]	~80	6.22 q (1H, J = 5)	1.44 d (3H, J = 5)	1.62 s (3H)
$Ph_3SiCOMe$ (0.30)	HCN	Saturated solution in benzene (25 ml); 28 min	$Ph_3SiOCHMe(CN)$[k]	~60	4.47 q (1H, J = 6.5)	1.36 d (3H, J = 6.5)	—

[a]Yields estimated from n.m.r. spectra of crude photolyzates.
[b]δ values from internal TMS in CCl_4.
[c]Other product Ph_3SiOAc.
[d]Pure material isolated by chromatography and crystallization from hexane, m.p. 65–67°; i.r. (CCl_4) 5.74 μ.
Anal. Calcd. for $C_{27}H_{24}O_3Si$: C, 76.38; H, 5.70. Found: C, 76.39; H, 5.65.
[e]Other products are believed to be the isomeric isonitrile (i.r. 4.70 μ; n.m.r. δ 5.94) and traces of silanol and benzaldehyde.
[f]Pure material isolated by chromatography and crystallization from hexane, m.p. 88–89°.
Anal. Calcd. for $C_{26}H_{21}NOSi$: C, 79.75; H, 5.41; N, 3.58. Found: C, 79.80; H, 5.37; N, 3.64.
[g]Pure product (28%) isolated by crystallization from pentane m.p. 68–70°; i.r. (CCl_4) 7.86 μ (*N*-substituted pyrrole (28)).
Anal. Calcd. for $C_{29}H_{25}NOSi$: C, 80.70; H, 5.84; N, 3.25. Found: C, 80.75; H, 5.90; N, 3.40.
[h]The compound fumes in the air; accompanying products identified were Ph_3SiOH and PhCHO.
[i]Accompanying product, Ph_3SiOH; see degradation experiment.
[j]I.r. (CCl_4) 5.72 μ.
[k]Accompanying product, Ph_3SiOH; i.r. 4.49 μ (weak).

TABLE 5. Conditions for analysis of the volatile photolysis products in methanol and ethanol[a]

Photolysis	Injection (μl)	Column temperature (°)	Flow (ml/min)	Filaments (mA)	Retention times (min)[b]		
					C_5H_5N	R'CHO	R'CH(OR'')$_2$
$Ph_3SiCOPh$–EtOH[c]	50	241	150	100	5.1	8.8	12.4
$Ph_3SiCOPh$–MeOH[c]	50	231	150	100	5.2	8.9	16.4
$Ph_3SiCOMe$–EtOH[d]	100	150	155	120	8.3	—[e]	6.8
$Ph_3SiCOMe$–MeOH[d]	100	144	155	120	11.8	—[e]	5.9

[a]Varian Series 200 dual column instrument, injector 275°, detector block 300°.
[b]Following a run, the nonvolatile products were slowly removed with the column at 300°.
[c]Samples contained 10 μl pyridine/ml.
[d]Samples contained 5 μl pyridine/ml.
[e]Acetaldehyde not detectable.

samples of acylsilane in alcohol, the solvent was removed under reduced pressure and the residue was examined by n.m.r. spectroscopy. Peaks due to the nonvolatile products, silanol, alkoxysilane, and mixed acetal (if present), were generally sufficiently separated to allow determination of the yields by integration. The silanol peak, if it overlapped with any other peak, could generally be shifted to a clear region of the spectrum by diluting the solution.

The yields of the volatile photolysis products, aldehyde and dialkyl acetal, formed in alcohol solution, were determined by direct g.l.c. analysis of the photolysis solutions using a specially prepared 20 ft × 3/8 in. column of 30% SE-30 silicone gum on acid-washed dimethyldichlorosilane-treated Chromosorb W. This column was used in all the work described below. Unfortunately, conditions could not be found, using this or any other column, for the determination of small amounts of acetaldehyde in alcohol since its peak was buried under the solvent peak. Pyridine, which was also used in the kinetic runs to quench further acid-catalyzed reactions, was found to be a convenient internal standard for the yield determinations. The conditions used are shown in Table 5. Calibration curves were prepared for each compound determined.

Representative yields of the volatile products formed in irradiations at room temperature are given in Table 2.

Isolation of the Major Silicon-containing Photolysis Products: Benzoyltriphenylsilane–Ethanol; Isolation of Triphenylsilanol

The photolysis of 0.50 g (0.0014 mol) of benzoyltriphenylsilane in 10 ml of ethanol was complete in 24 min. Removal of the solvent followed by recrystallization of the residue from carbon tetrachloride – hexane gave 0.28 g (74%) of pure triphenylsilanol, m.p. 155–156°, identified by m.m.p.

Similar procedures gave triphenylmethoxysilane from the photolysis of actyltriphenylsilane in methanol and triphenylethoxysilane from acetyltriphenylsilane in ethanol, the products being isolated by crystallization and identified by m.m.p.

A Kinetic Study of the Photolyses in Ethanol and Methanol

In the kinetic runs 0.0069 mol of acylsilane was irradiated in 100 ml of purified alcohol at 0°. Samples were withdrawn using a 10 ml pipette and were mixed with an accurately measured volume of pyridine (50 or 100 μl depending on the run) which served to quench further reaction of the mixed acetal. Small samples of the resulting solution were used for determination of the volatile products by g.l.c., as previously described. The solvent was then removed and the resulting oil, in deuterochloroform, was analyzed by n.m.r. for mixed acetal, silanol, and alkoxysilane. The results of kinetic measurements for two representative runs are represented in Figs. 1 and 3. In most cases at least two runs were carried out; the results were found to be closely reproducible.

The Photolyses of p-Substituted Benzoyltriphenylsilanes in Methanol

The photolyses of *p*-methoxy-, *p*-*t*-butyl-, *p*-bromo-, and *p*-chloro-benzoyltriphenylsilane in methanol containing pyridine were found to proceed at about the same rate as that of benzoyltriphenylsilane and gave analogous products. Table 6 lists the yields of the mixed acetals and the important n.m.r. spectral features of the mixed acetals and solvolysis products (which were later observed in purified alcohol). The corresponding values for benzoyltriphenylsilane are included for comparison. Like the unsubstituted compounds the *p*-substituted mixed acetals were unstable and decomposed readily on standing to (spectroscopically identified) *p*-substituted benzaldehyde, triphenylmethoxysilane, and triphenylsilanol.

The procedure used for the kinetic investigations of the photolyses of *p*-bromo- and *p*-chloro-benzoylsilane was identical to that described above for the unsubstituted compound, but only nonvolatile products were determined.

Isolation of 1-Naphthylphenylmethylsilanol from the Photolysis of (+)-Benzoylsilane in Ethanol

A suspension of 2.43 g (0.0069) of (+)-benzoyl-1-naphthylphenylmethylsilane, $[\alpha]_D$ +6.2°, in 100 ml of purified ethanol at 0°, was irradiated with two lamps for 12 min. Small samples of the photosolution were withdrawn and investigated by i.r. spectroscopy. At the 95 min mark when silanol (2.70 μ) appeared to be at a maximum concentration, a 40 ml sample (equivalent to 0.00276 mol of the starting acylsilane) was withdrawn and was worked up. An n.m.r. spectrum of the resulting product showed that about 40% of 1-naphthylphenylmethylsilanol was present.

The oil was chromatographed on silica gel. Elution with 1:1 benzene – carbon tetrachloride gave, in the first five fractions, 0.51 g of a mixture of the mixed acetal and

Can. J. Chem. Downloaded from www.nrcresearchpress.com by 210.87.254.6 on 09/05/12
For personal use only.

TABLE 6. Yields of the mixed acetals and n.m.r. spectral features[a] of the products from the photolysis of *p*-substituted benzoylsilanes in methanol

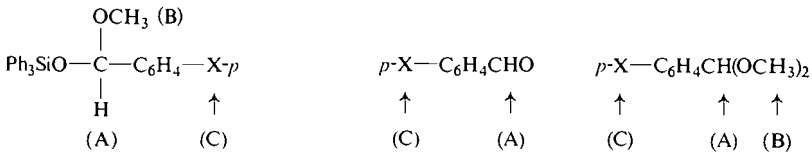

X	% yield[b]	H_A	H_B	H_C	H_A	H_C	H_A	H_B	H_C
OMe	50[c]	5.81	3.12	3.73	9.80	3.78	5.33	3.27	3.73
$C(Me)_3$	94	5.85	3.11	1.27	9.87	1.28	5.32	3.26	1.28
H	94	5.85	3.09	—	9.80	—	5.32	3.21	—
Cl	94	5.81	3.10	—	9.80	—	5.31	3.21	—
Br	94	5.79	3.09	—	9.81	—	5.30	3.21	—

[a]In deuterochloroform.
[b]The other products were triphenylmethoxysilane and free aldehyde.
[c]This mixed acetal was very unstable and decomposed in the solution used for n.m.r. spectroscopy.

1-naphthylphenylmethylethoxysilane along with traces of benzaldehyde and benzaldehyde diethyl acetal. The balance of the material eluted with this solvent mixture contained 1-naphthylphenylmethylsilanol along with benzaldehyde and benzaldehyde diethyl acetal. This fraction after being pumped on at 125°/0.1 mm to remove the volatile compounds gave 0.29 g (40%) of oil, $[\alpha]_D$ −17.5° (*c*, 14.3, diethyl ether), judged by n.m.r. to be pure 1-naphthylphenylmethylsilanol (lit. (13) $[\alpha]_D$ 20°, diethyl ether).

1-Naphthylphenylmethylmethoxysilane from the Photolysis of (+)-Benzoyl-1-naphthylphenylmethylsilane in Methanol

A suspension of 0.50 g (0.0014 mol) of (+)-benzoyl-1-naphthylphenylmethylsilane, $[\alpha]_D$ +5.7°, in 25 ml of methanol was irradiated for 26 min. The solution was held at room temperature for 1 h to allow conversion of mixed acetal to silanol and methoxysilane. Workup, followed by pumping on the resulting oil at 60°/0.5 mm for 5 min to remove volatile contaminants, gave 1-naphthylphenylmethylmethoxysilane along with a small amount of 1-naphthylphenylmethylsilanol. This material had $[\alpha]_D^{24}$ −1.5° (*c*, 10.0, cyclohexane).

A repetition of this procedure on a slightly larger scale (0.70 g of the benzoylsilane) gave a similar product having $[\alpha]_D$ −0.5°. In a third run, the crude product was optically inactive. The low negative rotation is not really meaningful since traces of silanol (maximum $[\alpha]_D$ −20°) may have been present in the samples.

Investigations of the Catalyst in the Photosolutions

Titration of the Benzoyltriphenylsilane–Methanol Photosolution (29)

A 10 ml sample of purified methanol containing 1 drop of a 1% solution of thymol blue indicator in methanol was titrated with a 0.102 *N* solution of sodium methoxide in methanol. In five separate titrations 0.05–0.07 ml was required to change the indicator color from red to yellow.

Following this, 0.25 g (0.00069 mol) samples of benzoyltriphenylsilane were irradiated in 10 ml of the same purified methanol until the solutions were bleached.

TABLE 7. The conversion of benzaldehyde to benzaldehyde dimethyl acetal in the benzoyltriphenylsilane–methanol photosolution[a] at 0°

Time (min)	% yield[b] PhCHO	% yield[b] $PhCH(OMe)_2$
0[c]	10	90
6	112	88
19	105	95
42	99	101
86	95	105
130	84	116

[a]At 0.00069 mol in 10 ml of methanol.
[b]Normalized yield; 100% = 0.00069 mol.
[c]Sample taken prior to addition of PhCHO.

Similar titration of two such photosolutions required 0.14 and 0.13 ml of titrant corresponding to about 7×10^{-6} mol of acid.

Determination of the Rate of Conversion of Benzaldehyde to its Dialkyl Acetal in Various Photosolutions

The general procedure involved the photolysis of 0.00069 mol of acylsilane in 10 ml of purified alcohol under nitrogen. Benzaldehyde (0.00069 mol) was then added to the solution and 1 ml samples were withdrawn at various times and, following addition of 10.0 μl of pyridine, were analyzed by g.l.c. Results of a typical experiment are shown in Table 7. A similar procedure was used to determine the rate of conversion of benzaldehyde to its dimethyl acetal in methanol containing acetic, formic, benzoic, hydrochloric, oxalic, and sulfanilic acids. Details of a typical experiment may be found in Table 8.

Experiments which were carried out in duplicate gave

Can. J. Chem. Downloaded from www.nrcresearchpress.com by 210.87.254.6 on 09/05/12
For personal use only.

TABLE 8. The conversion of benzaldehyde to benzaldehyde dimethyl acetal in methanol containing oxalic acid[a] at 25°

Time (min)	Relative proportions	
	PhCHO	$PhCH(OMe)_2$
0.5	96	4
7	46	54
21	22	78

[a]Concentration 0.0006 *M*; 0.54 mg acid in 10 ml MeOH.

excellent reproducibility. In addition, it was found that the use of different samples of alcohol (Fisher Certified ACS methanol, unpurified, dried by distillation from magnesium or purified by conventional procedures) had little effect on the results. Also, in each of the three acylsilane–alcohol photosolutions studied it was shown that results did not depend on the glassware used for the photolyses. Thus the use of previously unused flasks, direct from the manufacturer, gave similar results and when the flask used for a run was immediately rinsed several times with pure alcohol and was then reused for the same experiment, identical results were obtained.

This research was supported by the National Research Council of Canada.

1. A. G. BROOK. J. Am. Chem. Soc. **79**, 4373 (1957).
2. A. G. BROOK. Adv. Organomet. Chem. **7**, 95 (1968).
3. A. G. BROOK, R. KIVISIKK, and G. E. LEGROW. Can. J. Chem. **43**, 1175 (1965).
4. A. G. BROOK and J. B. PIERCE. J. Org. Chem. **30**, 2566 (1965).
5. A. G. BROOK and J. M. DUFF. J. Am. Chem. Soc. **89**, 454 (1967).
6. A. G. BROOK and J. M. DUFF. J. Am. Chem. Soc. **91**, 2118 (1969).
7. A. G. BROOK. Intra-Sci. Chem. Rep. In press.
8. A. G. BROOK, P. J. DILLON, and R. PEARCE. Can. J. Chem. **49**, 133 (1971).
9. A. G. BROOK, H. W. KUCERA, and R. PEARCE. Can. J. Chem. **49**, 1618 (1971).
10. A. G. BROOK, R. PEARCE, and J. B. PIERCE. Can. J. Chem. **49**, 1622 (1971).
11. A. G. BROOK and J. M. DUFF. Can. J. Chem. **51**, 2024 (1973).
12. M. F. SHOSTAKOVSKII, D. A. KOCHKIN, I. A. SHIKHIEV, and V. M. VLASOV. J. Gen. Chem. USSR, **25**, 593 (1955).
13. L. H. SOMMER. Stereochemistry, mechanism and silicon. McGraw–Hill, New York. 1956.
14. T. ASHIDA, R. PEPINSKY, and Y. OKAYA. Abstr. Int. Union Crystallogr. Congr. Rome, 1963.
15. A. G. BROOK and W. W. LIMBURG. J. Am. Chem. Soc. **85**, 832 (1963).
16. C. EABORN. Organosilicon compounds. Butterworth's Scientific Publications, London. 1962. p. 297.
17. E. H. CORTES. Prog. Phys. Org. Chem. **4**, 1 (1967).
18. R. W. BAKER, R. W. BOTT, C. EABORN, and P. W. JONES. J. Organomet. Chem. **1**, 37 (1963).
19. J. HINE. Phys. organic chemistry. McGraw–Hill, New York. 1956. p. 244.
20. J. D. ROBERTS and M. C. CASERIO. Basic principles of organic chemistry. Benjamin, New York. 1964. p. 445.
21. P. YATES. Pure Appl. Chem. **16**, 93 (1968).
22. P. YATES and L. KILMURRY. J. Am. Chem. Soc. **88**, 1563 (1966).
23. P. YATES and L. KILMURRY. Tetrahedron Lett. 1739 (1964).
24. A. M. FOSTER and W. G. AGOSTA. J. Am. Chem. Soc. **94**, 5777 (1972).
25. A. G. BROOK, A. R. BASSINDALE, and P. B. BULKOWSKY. Unpublished studies.
26. D. J. CRAM. Fundamentals of carbanion chemistry. Academic Press, New York. 1965. Chap. 1.
27. V. BAZANT, V. CHVALOVSKY, and J. RATHOUSKY. Organosilicon compounds. Czech. Acad. Sci. Publ. 1965. Part II.
28. A. KREUTZBERGER and P. A. KALTER. J. Chem. Phys. **65**, 624 (1961).
29. H. BUCHERER and A. GROLEE. Ber. **39**, 1224 (1906).
30. B. B. CORSON and P. A. KALTER. J. Am. Chem. Soc. **50**, 2825 (1928).

Can. J. Chem. Downloaded from www.nrcresearchpress.com by 210.87.254.6 on 09/05/12
For personal use only.

Aryl Carbanions. A ^{13}C Nuclear Magnetic Resonance Study of Deuterium Exchange in Acenaphthenes and Related Aromatic Hydrocarbons[1]

D. H. HUNTER AND J. B. STOTHERS
Department of Chemistry, University of Western Ontario, London, Ontario
Received March 9, 1973

The base-catalyzed hydrogen–deuterium exchange rates for the aromatic and benzylic centers in acenaphthene, 2,3-dihydrophenalene, 1,8-dimethylnaphthalene, 1,1,2,2,-tetramethylacenaphthene, and diphenylmethane have been determined using ^{13}C n.m.r. The exchange rates serve as a probe of carbanion stability and reactivity, clearly indicating the importance of ring strain effects on carbanion stability.

Les vitesses d'échange hydrogène–deutérium catalysé par une base pour les centres aromatiques et benzyliques de l'acénaphthène, dihydro-2,3 phénalène, diméthyl-1,8 naphtène, tétraméthyl-1,1,2,2 acénaphthène et diphényl méthane, ont été mesurées par la r.m.n. du ^{13}C. Ces vitesses d'échange qui apportent des informations sur la stabilité et la réactivité du carbanion, montrent de façon claire l'importance des effets de tension de cycle sur la stabilité du carbanion. [Traduit par le journal]

Can. J. Chem., **51**, 2884 (1973)

Can. J. Chem. Downloaded from www.nrcresearchpress.com by 210.87.254.6 on 09/05/12
For personal use only.

Introduction

Base-catalyzed hydrogen, deuterium, or tritium exchange is a commonly used probe for kinetic acidity and perhaps then for thermodynamic acidity. Several experimental approaches have been used for determining the kinetic acidities of hydrogens in a molecule. Where a molecule has a single reactive site either by symmetry or by large differences in reactivity, kinetic acidities have been monitored by measuring the rate of appearance or disappearance of deuterium by proton n.m.r., mass spectrometry, and combustion analysis. Tritium exchange rates have been followed by scintillation techniques.

For molecules having several different hydrogens of similar kinetic acidity, the usual techniques become inappropriate and the synthesis of specifically labelled materials becomes essential. The use of ^{13}C n.m.r. to monitor deuterium incorporation (1) provides a satisfactory alternative solution to this problem. Provided the individual carbon signals are separate and assignable, the extent of deuterium incorporation at a given carbon can be determined directly by integration of the ^{13}C n.m.r. spectrum.

The kinetic acidities of the aryl protons in a series of specifically labelled aromatic hydrocarbons have been investigated using an amide–amine catalyst (2). These studies have allowed assessment of some of the factors which affect aryl anion stability. We wished to extend these studies to systems in which aryl proton exchange may occur through benzyl-like anionic intermediates to assess the importance of this exchange pathway. Thus the kinetic acidities of some 1,8-disubstituted naphthalenes have been determined by observing base-catalyzed deuterium incorporation from *t*-butyl alcohol-O-*d*–potassium *t*-butoxide.

[1]Part 30 in the series ^{13}C NMR Studies (Pt. 29, ref. 24).

Results and Discussion

Synthesis of Substrates

Of the substrates, acenaphthene (**1**), 1,8-dimethylnaphthalene (**3**), and diphenylmethane (**5**) were obtained commercially and 2,3-dihydrophenalene (**2**) (3) and 1,1,2,2-tetradeuterioacenaphthene (**1**-d_4) (4) were prepared by previously reported procedures. A new procedure was developed for 1,1,2,2-tetramethylacenaphthene (**4**) since the published method is long (5) and methylation of the anion from acenaphthene proved to be unexpectedly complicated (6). The synthetic scheme is summarized in Fig. 1.

The last step in the preparation of 1,1,2,2-tetramethylacenaphthene (**4**), the thermolysis of sulfone **9**, requires comment. First, significantly better yields of product were obtained by refluxing **9** as a neat liquid (~400°) rather than by using a flow system. The flow technique was only partially successful since the temperatures (650–1000°) required to convert **9** → **4** resulted in decomposition of **4**. Under such conditions **4** gave significant amounts of 1,2-dimethylacenaphthylene. Second, significantly higher temperatures

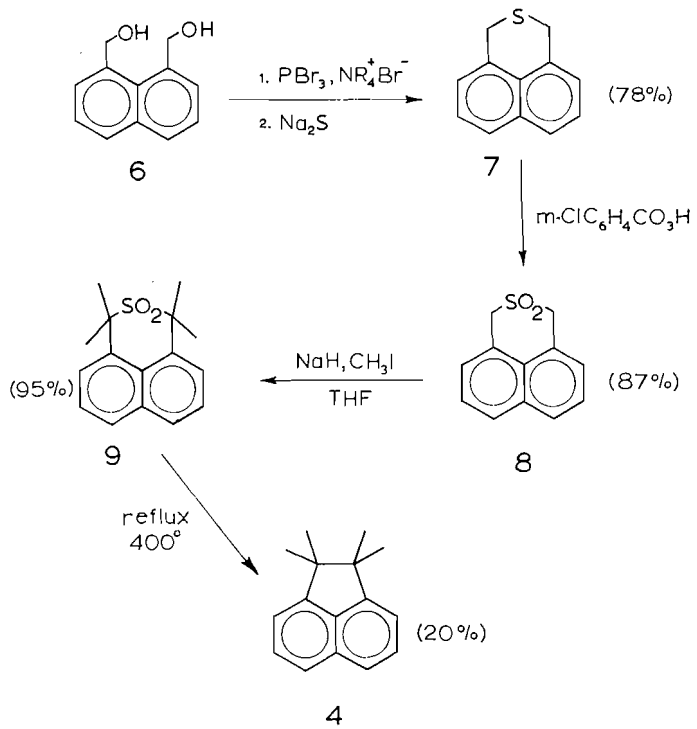

FIG. 1. Sequence employed for the preparation of **4**.

are needed for the conversion of **9** to **4** than for pyrolysis of allylsulfones and those sulfones which can yield orthoquinoidal methanes, but are somewhat milder than those necessary for simple alkyl sulfones (7). Thus it would appear that such intramolecular desulfonylation reactions can be synthetically useful even if a stepwise rather than concerted decomposition of the sulfone is likely.

^{13}C *Spectra*

The use of ^{13}C n.m.r. spectra seemed attractive for monitoring the incorporation of deuterium into these systems since the aryl carbons exhibit appreciably different chemical shifts and quantitative assessments of deuterium content at individual sites are readily accomplished by integration (8). The ^{13}C spectrum of acenaphthene has been described and unequivocal assignments established (9) as shown in Fig. 2*a*. Upon replacement of hydrogen by deuterium at a specific carbon, the shielding of that carbon is increased by the deuterium isotope effect and its absorption is a triplet since $I_D = 1$. Because the isotope shift is 0.3–0.5 p.p.m. (8–12 Hz at 25.2 MHz) and $J_{CD} \sim 25$ Hz, the C—H singlet (^{13}C bearing H) and C—D triplet (^{13}C bearing D) do not overlap; thus, the relative intensities of the ortho, meta, and para C—H signals can be determined readily by integration yielding the relative extents of deuteration. Since deuterium incorporation, however, occurs at all three positions, it was necessary to include an additional signal in the spectra for calibration purposes. We selected *p*-dichlorobenzene and a known amount was added to each sample for analysis. Thus, the deuterium content at each position was determined by careful integration of four signals, three for each substrate and the CH signal of *p*-ClC_6H_4Cl.

Since deuterium nuclei are unaffected by proton decoupling, the effects of ^{13}C–D coupling are manifest in these spectra; this feature is particularly helpful as an assignment aid because geminal and vicinal aryl ^{13}C–D coupling constants differ appreciably. From the data for benzene (10) and the fact that $J_{CD} = J_{CH}$ (6.51), the geminal couplings are ~ 0.2 Hz while $J_{CD}^{vic} \sim 1$ Hz. Thus, in the present systems, deuterium exchange at an ortho position is

Can. J. Chem. Downloaded from www.nrcresearchpress.com by 210.87.254.6 on 09/05/12
For personal use only.

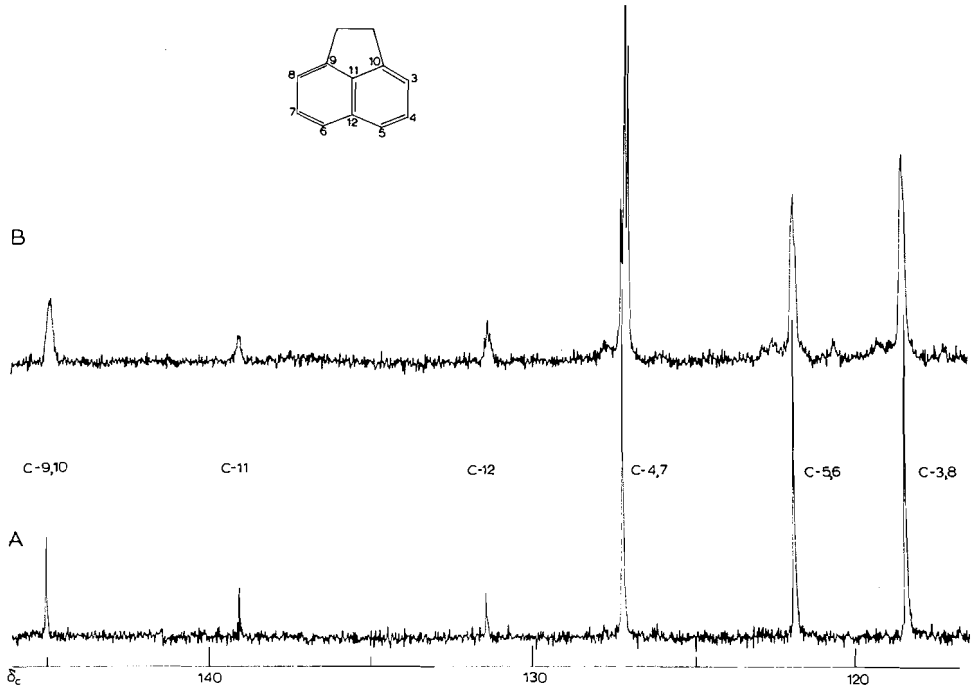

FIG. 2. Aromatic regions of the ^{13}C spectra of **1** (A) normal material, (B) after treatment with *t*-BuO$^-$ – *t*-BuOD at 204° (run 3).

evident from the marked broadening of the para carbon signal by coupling, while the meta signal is essentially unaffected by coupling but still exhibits characteristic changes because there are measurable geminal isotope shifts of 0.1 p.p.m. (2.5 Hz at 25 MHz). Consequently, a portion of the meta C—H absorption is shifted upfield, *i.e.* the meta band consists of two signals with the higher field component indicating the presence of deuterium at a geminal position. In these spectra, therefore, the ortho and para C—H signals are broadened by respective deuteration at the para and ortho positions, while the meta C—H absorption splits into two and then three signals upon mono- and di-deuteration at the ortho and para positions. These effects are illustrated in Fig. 2*b* for acenaphthene. Exclusive deuteration at the meta position would, of course, split the ortho and para C—H signals but this splitting is masked if deuteration also occurs at the other positions. Thus, as the extent of deuteration increases the meta band is readily distinguished from the ortho and para absorptions.

Although the ^{13}C assignments for acenaphthene have been unequivocally established by selective proton-decoupling experiments, the reported assignments (9) for 1,8-dimethylnaphthalene appeared to be incorrect on the basis of the spectra obtained in this study and the characteristic effects produced by deuteration. To confirm our suspicions, samples of partially deuterated 1,8-dimethylnaphthalene were converted to acenaphthene and the ^{13}C spectra of the latter recorded. From integrations of each pair of samples, unequivocal assignments for 1,8-dimethylnaphthalene follow directly. The spectra for one such pair are shown in Fig. 3. The ^{13}C shielding data for the hydrocarbons employed in this study are collected in Table 1.

Exchange Studies

The relative kinetic acidities of the various hydrogens in the aromatic hydrocarbons studied were determined from the rates of deuterium incorporation using 0.24 *M* potassium *t*-butoxide in *t*-butyl alcohol-O-*d* as the exchange medium. The exchange rates were followed at two temperatures, 120 and 204 °. At the lower temperature only exchange of benzylic hydrogens was observed whereas exchange of aromatic hydrogens required 204°. This temperature difference cor-

Can. J. Chem. Downloaded from www.nrcresearchpress.com by 210.87.254.6 on 09/05/12
For personal use only.

Can. J. Chem. Downloaded from www.nrcresearchpress.com by 210.87.254.6 on 09/05/12
For personal use only.

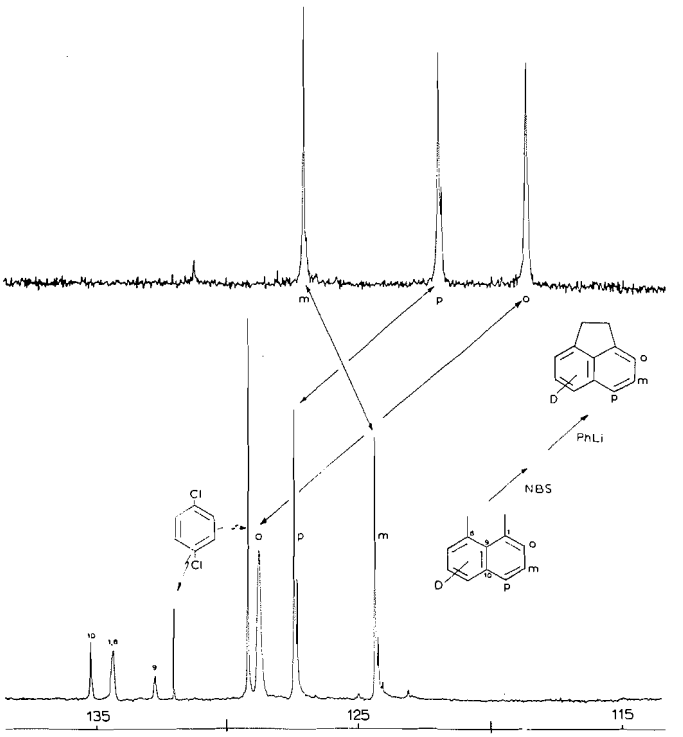

FIG. 3. A comparison of the aryl absorption for partially deuterated **3** and **1**, the latter prepared as indicated. The lower spectrum also included *p*-dichlorobenzene as a calibration standard for integration.

TABLE 1. ^{13}C shieldings for the aryl hydrocarbons (δ_C, p.p.m. from TMS, in CCl_4 solutions)

Carbon	**1**	**2**	**3**	**4**	**5**
1	30.1	31.1	134.4	49.4	41.7
2	30.1	22.9	128.8 (ortho)	49.4	140.4
3	118.6 (ortho)	31.1	124.3 (meta)	116.9 (ortho)	128.4 (ortho)
4	127.1 (meta)	123.3 (ortho)	127.5 (para)	122.5 (meta)	127.9 (meta)
5	121.9 (para)	124.8 (meta)	127.5	127.5 (para)	125.6 (para)
6	121.9	125.6 (para)	124.3	127.5	
7	127.1	125.6	128.8	122.5	
8	118.6	124.8	134.4	116.9	
9	145.0	123.3	132.8	152.6	
10	145.0	135.3	135.2	152.6	
11	139.1	035.3	—	134.6	
12	131.4	129.8	—	131.2	
13	—	133.5	—		
Me			25.6	25.8	

responds to a rate difference of about 10^3, assuming $\Delta H \approx 25$ kcal/mol (11).

Internal Return

The observed rates of deuterium incorporation can be related to kinetic acidities if internal return (carbanion formation without exchange) is minor or constant. As has been observed for some systems (*e.g.* fluorenyl, triphenylmethyl, and allyl derivatives), internal return contributes to varying extents (12).

$$\text{R—H} + {}^{-}\text{OR} \underset{k_{-1}}{\overset{k_1}{\rightleftharpoons}} [\text{R}^{-}\text{HOR}] \xrightarrow[k_2]{\text{DOR}} \text{exchange}$$

Using the extent of intramolecular isomerization (isomerization without exchange) in 1,3- and 1,5-proton shifts as a gauge for internal return, some generalizations are possible. With alkoxides in alcohol, potassium *t*-butoxide in *t*-butyl alcohol in particular, the intramolecular component is small and is usually less than 50%, suggesting that the rate of carbanion formation is at most a factor of two larger than the exchange rate. The contribution due to intramolecularity also seems to decrease with increasing temperature (13) and is not very sensitive to the structure of the carbon acid. Thus the observed exchange rates should be close to the actual rates of carbanion formation.

Although the ambiguity introduced by internal return remains for the molecules examined, the high temperature required (especially for aromatic exchange) and the structural similarity between the various carbanionic intermediates help to mollify the doubts.

Benzyl Exchange

The extent of base-catalyzed hydrogen–deuterium exchange at 120° as a function of time was determined using proton n.m.r. These data were converted to pseudo first-order rate constants for exchange on a per hydrogen basis. These rate constants for the substituted naphthalenes, shown in Fig. 4, cover a 20-fold range with acenaphthene the most acidic kinetically and 1,8-dimethylnaphthalene the least.

The similar kinetic acidities of 1,8-dimethylnaphthalene and 2,3-dihydrophenalene suggest that neither steric nor conformational effects are of major importance. The enhanced acidity of acenaphthene would thus appear to reflect hybridization changes at the benzyl carbon which becomes more electronegative towards the

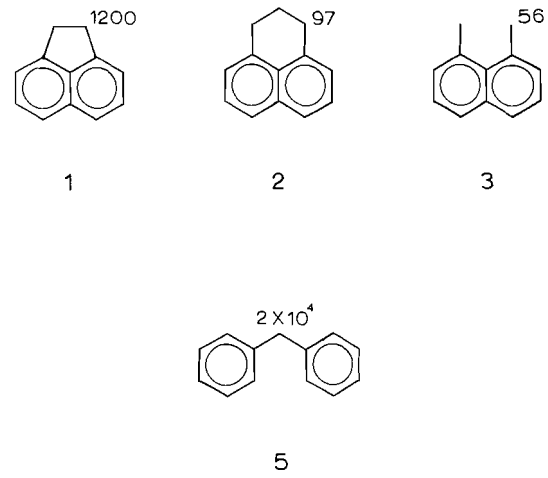

FIG. 4. Rate constants ($k_1 \times 10^7$ s^{-1}) for benzyl exchange at 120.4° for **1**, **2**, **3**, and **5**. For the latter the value was estimated from measurements at 60° assuming $\Delta H^{\ddagger} = 25$ kcal/mol.

bonded hydrogens as a result of the reduced C—C—C bond angle of 105° (14).

Aromatic Exchange

The extent and position of hydrogen–deuterium exchange at 204° at various times was determined using carbon-13 n.m.r. The results are reported in Table 2. This data has been used not only to interpret the mechanism of the exchange processes but also for ^{13}C signal assignments as discussed earlier.

Mechanism of Exchange

A qualitative picture of the relative kinetic acidities within any particular hydrocarbon can be obtained upon inspection of Table 2. To facilitate comparisons, these data were also converted to pseudo first-order rate constants for exchange on a per hydrogen basis. Reasonable plots were obtained from the rates of approach to equilibrium and rate constants were derived as given in Fig. 5.

The reactivity of the aromatic hydrogens varies by a factor of $\sim 10^2$ with the most acidic $\sim 10^4$ slower than the benzylic hydrogens. This should be compared with the results for toluene in cyclohexylamine–cyclohexylamide where the reactivity difference is about 10^2 (2*c*). For most of the compounds (except **4**) the benzyl anion is formed most frequently since, as mentioned earlier, the 84° temperature difference corresponds to a rate difference of about 10^3.

Except for acenaphthene and 1,1,2,2-tetra-

Can. J. Chem. Downloaded from www.nrcresearchpress.com by 210.87.254.6 on 09/05/12
For personal use only.

TABLE 2. Exchange reactions in *t*-BuOK – *t*-BuOD at 204 °C

Run	Substrate		Time (min)	% H remaining		
	Nature	Concentration (*M*)		Ortho	Meta	Para
1	**1**-d_4	0.37	291	0.83	1.00	0.77
2	**1**-d_4	0.37	720	0.73	0.96	0.58
3	**1**-d_4	0.48	1410	0.61	0.88	0.38
4	**1**-d_4	0.35	1490	0.61	0.87	0.45
5	**1**	0.39	7170	0.54	0.74	0.51
6	**2**	0.34	643	1.00	0.86	0.90
7	**2**	0.28	1440	0.94	0.63	0.71
8	**2**	0.34	3000	0.89	0.50	0.60
9	**3**	0.38	600	1.00	0.73	0.88
10	**3**	0.37	1500	1.00	0.46	0.72
11	**3**	0.32	9960	0.81	0.37	0.42
12	**4**	0.24	300	1.00	1.00	0.92
13	**4**	0.24	725	1.00	0.96	0.84
14	**4**	0.24	7844	0.98	0.61	0.46
15	**5**	0.41	720	0.99	0.86	0.88
16	**5**	0.41	3101	0.94	0.52	0.66
17	**5**	0.40	13102	0.87	0.42	0.47

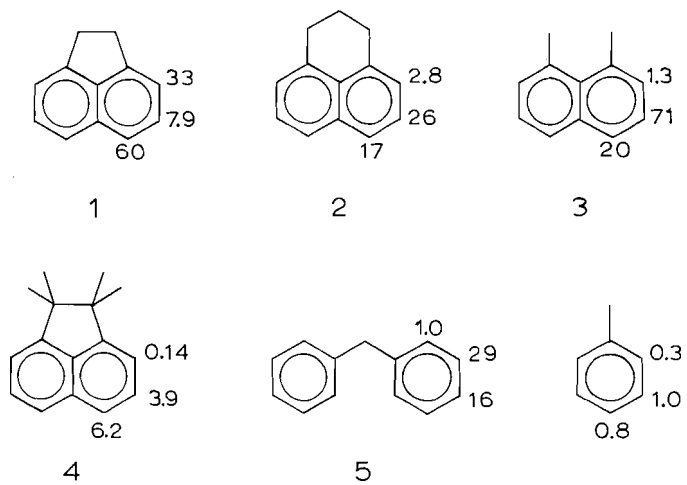

FIG. 5. Rate constants ($k_1 \times 10^7$ s^{-1}) for aryl exchange at 204° for **1**–**5**. Relative rate constants for toluene averaged from ref. 2*c*.

methylacenaphthene, the compounds studied show a very similar pattern of reactivity in the aromatic ring ($m > p > o$). This is the same pattern observed for toluene in which the meta[2] position is the most acidic (2*c*). Acenaphthene stands in marked contrast with the *meta* position, the *least* reactive. This unique behavior suggests either a change in mechanism or the presence of a significant perturbing influence on phenyl anion stabilities.

In the study of exchange of aromatic hydrocarbons in an amine–amide medium (2*b*) two mechanisms were considered: (*a*) direct exchange through aryl anions and (*b*) exchange via an addition–elimination process. The authors provided evidence favoring the aryl anion mechanism. With the introduction of benzyl hydrogens an additional mechanism is possible; aromatic

[2]The designation of ortho, meta, and para for monosubstituted benzenes will be used also for the naphthalene systems with 2,7 as ortho; 3,6 as meta; and 4,5 as para.

Can. J. Chem. Downloaded from www.nrcresearchpress.com by 210.87.254.6 on 09/05/12
For personal use only.

Can. J. Chem. Downloaded from www.nrcresearchpress.com by 210.87.254.6 on 09/05/12
For personal use only.

exchange at specific positions through deuteration in the ring of the preferentially formed benzyl anion followed by rearrangement. However, on the basis of the evidence obtained (2*c*), the aryl anion mechanism is favored for both toluene and benzene. The introduction of the methyl group on the benzene ring resulted in reduced reactivity at all ring positions with the meta position the least deactivated. Thus, rather than providing a more facile alternative route for ring exchange, the methyl group destabilizes the phenyl anions, presumably through a polar effect.

Similarly diphenylmethane, 1,8-dimethylnaphthalene, and 2,3-dihydrophenalene behave in a manner analogous to toluene in spite of the enhanced reactivity of the benzyl position. This suggests that aromatic exchange in these molecules is through the aryl anions rather than benzyl anions. This must certainly be so for exchange at the meta position.

The preferential exchange of acenaphthene in the para and ortho positions as well as the enhanced reactivity of the benzyl position are consistent with a change in mechanism to aromatic exchange through the benzyl anion or perhaps the dianion (6). However, the results obtained with 1,1,2,2-tetramethylacenaphthene mitigate against these possibilities; except for the ortho position, which should be susceptible to steric effects, both acenaphthenes show the same reactivity pattern. This suggests that some other structural features of acenaphthene are responsible for the changes in relative reactivity of the ring positions.

Ring strain in the aromatic ring and the concomitant changes in hybridization seem to provide a satisfactory alternative picture. An X-ray analysis of acenaphthene (14) has provided the bond angles shown in Fig. 6. From these, orbital hybridizations for the carbons at the ring fusions can be calculated (15) and are indicated in Fig. 6. The directed electronegativity of the carbons at the ring fusions should serve to enhance the acidity of the ortho and para positions more than the meta. Such effects have also been invoked to rationalize the kinetic acidities of the ring protons in biphenylene, benzcyclobutene, and triptycene (2*a*).

For the hydrocarbons examined in this study, ring protonation of benzyl anions does not seem to play a competitive role in aromatic exchange even though the benzyl anions form up to 10^6 times faster than aryl anions. This selectivity for

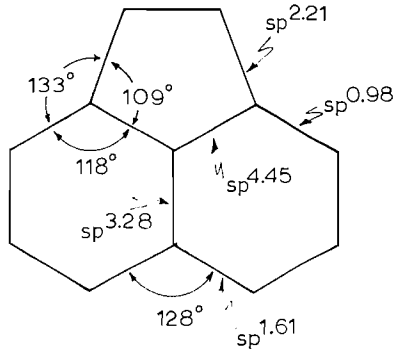

FIG. 6. Bond angles and calculated orbital hybridization in **1**.

the benzyl position establishes much higher limits for hydrocarbons than that previously estimated from the neutralization of 2-phenyl-2-propylpotassium (16). Apparently for the hydrocarbons the acidity of the benzyl proton must be further enhanced before selective ortho–para exchange will be observed. For example, both phenol (17) and aniline (18) exchange selectively at the ortho and para positions.

The ^{13}C shieldings of the ortho and para carbons in acenaphthene (**1**) are significantly shielded relative to these centers in 1,8-dimethylnaphthalene (**3**), perhaps because of ring strain. The corresponding ortho carbons in biphenylene absorb at essentially the same position as those in **1** (19). Ring strain effects have recently been observed in the e.s.r. spectra of anion radicals of substituted benzenes and naphthalenes (20). The basicities of some quinoxalines have also been interpreted in terms of ring strain (21).

Experimental

Bases and Solvents

The *t*-butyl alcohol-O-*d* was prepared by the procedure of Young and Guthrie (22) and analyzed for 0.98 atoms D/molecule. The base solution was prepared by adding freshly cut and cleaned potassium metal to the alcohol. The same base solution (0.24 *N*; <0.002 *M* in D_2O) was used for all reactions and reanalyzed after the final reaction was run. The pentane was distilled before use.

Substrates

The acenaphthene, 1,8-dimethylnaphthalene, and diphenylmethane were purified commercial samples. The sample of 1,1,2,2-tetradeuterioacenaphthene was prepared according to the procedure of Trost (4). The sample of 2,3-dihydrophenalene was obtained as a side product of the reaction of β-(1-naphthyl)-propionic acid in anhydrous hydrogen fluoride (3). The 1,1,2,2-tetramethylacenaphthene was prepared according to the following procedure.

Can. J. Chem. Downloaded from www.nrcresearchpress.com by 210.87.254.6 on 09/05/12
For personal use only.

1,1,2,2-Tetramethylacenaphthene

(a) 1,8-Di(bromomethyl)naphthalene

To a well-stirred solution of 27.7 g (0.15 mol) of 1,8-di(hydroxymethyl)naphthalene (**6**) (4) and 25 g (0.074 mol) of tetrabutylammonium bromide in 500 ml of methylene chloride at 0° was added rapidly 90.7 g (0.33 mol) of phosphorus tribromide. The reaction mixture was stirred 24 h at ambient temperature and then poured into ice and water. The methylene chloride was washed once with water, once with saturated sodium bicarbonate, dried, and evaporated to yield 63.4 g of crude material.

The added ammonium bromide serves to eliminate the otherwise significant amounts of cyclic ether (1H,3H-naphtho[1,8-*c*-*d*]-pyran) that are formed.

(b) 1H,3H-Naphtho[1,8-c,d]-thiopyran (7)

To 40.8 g (0.17 mmol) of sodium sulfide (.9H_2O) in 150 ml of water and 300 ml of 95% ethanol was added dropwise the 63.4 g of previously prepared crude 1,8-di(bromomethyl)naphthalene in 120 ml of tetrahydrofuran. After refluxing for 12 h, the solvent was removed using a rotary evaporator and the residue was dissolved in ether and water. Both the layers were re-extracted. The organic layers were combined, dried, and evaporated. Recrystallization from methanol (carbon treatment) yielded 21.8 g of **7** (78% based upon **6**) of m.p. 95–96°, lit. 96–97° (23).

(c) 1H,3H-Naphtho[1,8-c,d]-thiopyran-2,2-dioxide (8)

To a stirred solution of *m*-chloroperbenzoic acid (51 g; 0.25 mol) in 400 ml of methylene chloride was added slowly a solution of **7** (21.8 g; 0.12 mol) in 50 ml of methylene chloride. After the initial exothermic reaction, the reaction solution was refluxed for 12 h, cooled, filtered, and washed with saturated sodium bicarbonate, dilute sodium sulfite, and then dried. Crystallization from 300 ml of methylene chloride yielded 9.8 g (37%) of material m.p. 235–236°. A second crop, 2.1 g (m.p. 234–236°), was obtained from 75 ml of methylene chloride.

The precipitate from the filtration proved to contain much **8**. It was treated with excess dilute sodium hydroxide and extracted twice with methylene chloride to dissolve all solids. The methylene chloride was washed, dried, and evaporated to yield an additional 9.0 g of material m.p. 236–239°. This raised the yield to 87%.

Anal. Calcd. for $C_{12}H_{10}SO_2$: C, 66.03; H, 4.62; S, 14.66. Found: C, 66.00; H, 4.50; S, 14.74.

The n.m.r. spectrum ($CDCl_3$) showed the methylene protons as a singlet (δ = 4.7; 4H) and the aromatics as a multiplet (δ = 7.4–8.1; 6H). The i.r. spectrum (chloroform) showed the characteristic sulfone absorptions at 1115 and 1320 cm^{-1}.

(d) 1,1,3,3-Tetramethylnaphtho[1,8-c,d]-thiopyran-2,2-dioxide (9)

To a cooled, stirred suspension of sodium hydride (27 g; 0.6 mol; 54% washed three times with pentane) and **8** (16.3 g; 75 mmol) in 175 ml of tetrahydrofuran was added a solution of 37.5 ml (0.6 mol) of methyl iodide in 50 ml of tetrahydrofuran. Bubbling occurred for 6 h as the reaction mixture warmed to room temperature and was then stirred for 50 h total. The excess sodium hydride was destroyed with water.

The reaction mixture was extracted using methylene chloride and water. After drying, the product was crystallized from methylene chloride – hexane to yield 14 g of material m.p. 258–260° and 5.7 g (m.p. 256–258°) with an overall yield of 95%.

Anal. Calcd. for $C_{16}H_{18}SO_2$: C, 70.04; H, 6.61; S, 11.66. Found: C, 70.20; H, 6.60; S, 11.62.

The n.m.r. spectrum ($CDCl_3$) showed the methyl singlet at δ = 1.9 (12H) and the aromatics as a multiplet at δ = 7.5–8.0 (6H).

(e) 1,1,2,2-Tetramethylacenaphthene (4)

A 10 g (36 mmol) sample of **9** was heated to reflux (~400°) under an argon atmosphere using a sand bath. The reflux temperature was maintained by collecting the lower boiling material (260–300°) as it formed. Heating was continued until reaction was nearly complete (~6 h) as judged by the pot residue and by monitoring the sulfur dioxide evolved. The distillate and pot residues were combined using methylene chloride to yield about 5 g of crude material.

The pentane soluble material was chromatographed on silica gel using pentane. The first major fraction (a complex mixture by v.p.c.) was distilled and the middle fraction (2.7 g; b.p. 71–73° at 0.05 mm) was recrystallized from ethanol to yield 1.1 g (15%) of material m.p. 53–55°, lit. 57–58° (5). Analysis by v.p.c. indicated 95% purity.

The pentane insolubles were sublimed at 0.05 mm to yield 1 g (10%) of unreacted **9**.

Procedures for the Exchange Reactions

(a) At 120.4°

Typically, a 30 mg sample of substrate in 1 ml of 0.24 *N* potassium *t*-butoxide – *t*-butyl alcohol-O-*d* was evacuated, degassed, and sealed in a 5 mm n.m.r. tube. The reaction was monitored by integrating the aromatic hydrogens, the benzyl hydrogens, and the hydroxyl hydrogens at selected times. After the final point the tube was opened and the sample isolated by extraction with pentane and water, followed by sublimation. N.m.r. analysis was then made on this material. In all cases there was good agreement between the two analyses.

At least five points were obtained to define the rate constant for each case. The enhanced reactivity of **5** required a lower temperature for exchange (60°) and the rate constant at 120° was estimated by assuming $\Delta H^{\ddagger}$ = 25 kcal/mol (11).

(b) At 204°

A 250–300 mg sample of substrate and 5 ml of 0.24 *N* potassium *t*-butoxide – *t*-butyl alcohol were twice degassed and sealed in a Carius tube. After heating for the specified time in a thermoregulated Wood's metal bath, the tube was opened and the substrate isolated using pentane and water for extraction. The substrate was normally chromatographed using silica gel and pentane and then sublimed or distilled. Recoveries were usually greater than 90%.

Samples for ^{13}C analysis were prepared by mixing weighed amounts of substrate and *p*-dichlorobenzene which was used as an internal standard for integration.

The individual analyses were converted to pseudo first-order rate constants from plots of the rate of approach to isotopic equilibrium. Runs 3, 4, 5, 11, and 17 provided estimates for isotopic equilibrium positions with **1**, **3**, and **5**. The corresponding equilibrium percentages were then estimated for **2** and **4** by taking account of the

substrate concentration and the number of exchangeable protons. The rate of approach to equilibrium provides the sum of the forward and reverse rate constants and the equilibrium constant provides the ratio, thus allowing calculation of each rate constant.

Conversion of 1,8-Dimethylnaphthalene (3) to Acenaphthene (1)

The sample of partially exchanged **3** (242 mg; 1.5 mmol) and *N*-bromosuccinimide (531 mg; 3.0 mmol) with 5 ml of carbon tetrachloride was refluxed for 90 min using a 275 W white sun lamp. After cooling and filtering, the filtrate was evaporated to dryness to yield 472 mg of crude material. This product was used without further purification. Following the procedure of Trost (4) the crude 1,8-di(bromomethyl)naphthalene was dissolved in 10 ml of benzene and 5 ml of ether and this solution was degassed and placed under an argon atmosphere. Commercial phenyllithium solution (1.25 ml; 2.25 mmol) was added dropwise to the reactant at −15°. After stirring and warming to ambient temperature over about 1 h, the solution was poured into water, which was extracted three times with an ether–pentane mixture. The organic layers were washed with water, dried, solvent evaporated, and the residue was chromatographed on silica gel using pentane. After sublimation the crystalline product (167 mg; 68%) was shown by ^{13}C n.m.r. and v.p.c. to contain considerable biphenyl which was removed by preparative v.p.c. to yield 101 mg (41%) of **1**.

^{13}C Spectra

Noise-decoupled ^{13}C spectra were obtained with a Varian XL-100-15 spectrometer operating in the Fourier transform mode. All samples were examined as 20–25% (w/v) solutions in CCl_4 containing a known amount of *p*-dichlorobenzene as a calibration standard for integrations. Initially, operating conditions were adjusted to give signals of equal intensity for the aryl C—H nuclei. Using these conditions, the partially deuterated samples were run, in duplicate or triplicate, and the C—H signals carefully integrated to determine the extent of deuteration for each center.

We wish to thank the National Research Council of Canada for financial support.

1. D. H. HUNTER, A. L. JOHNSON, J. B. STOTHERS, A. NICKON, J. L. LAMBERT, and D. F. COVEY, J. Am. Chem. Soc. **94**, 8582 (1972).
2. (*a*) A. STREITWIESER JR., G. R. ZIEGLER, P. C. MOWREY, A. LEWIS, and R. G. LAWLER. J. Am. Chem. Soc. **90**, 1357 (1968). (*b*) A. STREITWIESER JR., R. G. LAWLER, and C. PERRIN. J. Am. Chem. Soc. **87**, 5383 (1965). (*c*) A. STREITWIESER JR., R. A. CALDWELL, R. G. LAWLER, and G. R. ZIEGLER. J. Am. Chem. Soc. **87**, 5399 (1965). (*d*) A. STREITWIESER JR. and R. A. CALDWELL. J. Am. Chem. Soc. **87**, 5394 (1965). (*e*) A. STREITWIESER JR. and G. R. ZIEGLER. Tetrahedron Lett. 415 (1971). (*f*) A. L. SHATENSHTEIN. Adv. Phys. Org. Chem. **1**, 184 (1963).
3. L. F. FIESER and M. D. GATES JR. J. Am. Chem. Soc. **62**, 2335 (1940).
4. B. M. TROST. J. Am. Chem. Soc. **89**, 1847 (1967).
5. A. BOSCH and R. K. BROWN. Can. J. Chem. **46**, 715 (1968).
6. L. D. KERSHNER, J. M. GAIDIS, and H. H. FREEDMAN. J. Am. Chem. Soc. **94**, 985 (1972).
7. J. L. KICE. *In* The chemistry of organic sulfur compounds. Vol. 2. *Edited by* N. A. KHARASCH. Pergamon Press, New York. 1966. pp. 116–120.
8. J. B. STOTHERS, C. T. TAN, A. NICKON, F. HUANG, R. SRIDHAR, and R. WEGLEIN. J. Am. Chem. Soc. **94**, 8581 (1972).
9. A.J. JONES, T. D. ALGER, D. M. GRANT, and W. M. LITCHMAN. J. Am. Chem. Soc. **92**, 2386 (1970).
10. F. J. WEIGERT and J. D. ROBERTS. J. Am. Chem. Soc. **89**, 2967 (1967).
11. D. H. HUNTER and D. J. CRAM. J. Am. Chem. Soc. **86**, 5478 (1964).
12. D. J. CRAM. Fundamentals of carbanion chemistry. Academic Press, Inc., New York. 1965. pp. 98–102, 176–193.
13. D. H. HUNTER and R. W. MAIR. Can. J. Chem. **47**, 2361 (1969).
14. H. W. W. EHRLICH. Acta Cryst. **10**, 699 (1957).
15. K. MISLOW. Introduction to stereochemistry. W. A. Benjamin, New York. 1965. Section 1–3.
16. G. A. RUSSELL. J. Am. Chem. Soc. **81**, 2017 (1959).
17. B. ERICSSON, B. NIST, and K. V. SARKANEN. Chim. Biochim. Lignine, Cellulose, Hemicelluloses, Actes Symp. Int. Grenoble, France, 59 (1964).
18. F. LAUGENBUCHER, R. MECKE, and E. D. SCHMID. Liebigs Ann. Chem. **669**, 11 (1963).
19. A. J. JONES and D. M. GRANT. Chem. Commun. 1670 (1968).
20. S. E. BALES and R. D. RIEKE. J. Org. Chem. **37**, 3866 (1972).
21. J. H. MARKGRAF and R. J. KATT. J. Org. Chem. **37**, 717 (1972).
22. A. T. YOUNG and R. D. GUTHRIE. J. Org. Chem. **35**, 853 (1970).
23. M. P. CAVA, N. M. POLLACK, and D. A. REPELLA. J. Am. Chem. Soc. **89**, 3640 (1967).
24. M. GORDON, S. H. GROVER, and J. B. STOTHERS. Can. J. Chem. **51**, 2092 (1973).

Can. J. Chem. Downloaded from www.nrcresearchpress.com by 210.87.254.6 on 09/05/12
For personal use only.

^{13}C Nuclear Magnetic Resonance Studies. 32. The ^{13}C Spectra of Several Norbornyl Derivatives[1]

J. B. STOTHERS, C. T. TAN, AND K. C. TEO

Department of Chemistry, University of Western Ontario, London, Ontario N6A 3K7

Received March 28, 1973

The ^{13}C n.m.r. spectra of several norbornyl derivatives have been recorded to examine the variation of ^{13}C shieldings with molecular geometry. Since it is well established that nonbonded interactions between vicinal carbon nuclei lead to pronounced upfield shifts, the so-called γ effects, series of methyl-substituted norbornanes, norbornenes, norbornan-2-ones (norcamphors), and norborn-5-en-2-ones were prepared as model systems having a variety of γ interactions between vicinal methyl groups. The observed shifts of these methyl carbons are considered in terms of the dihedral angle relating the vicinal nuclei. The use of specific deuteration for unequivocal signal assignments of carbons geminal and vicinal to the site of deuteration is illustrated.

Les spectres r.m.n. ^{13}C de plusieurs dérivés du norbornyle ont été enregistrés afin d'étudier la variation de l'effet de blindage du ^{13}C en fonction de la géométrie moléculaire. Puisqu'il est bien connu que des interactions non-liées entre des carbones vicinaux entraînent des déplacements du signal vers des champs élevés, relation connue sous le nom effets-γ plusieurs norbornanes, norbornènes, norbornanones-2 (norcamphres) et norbornène-5 ones-2 substitués par des groupes méthyles ont été préparés afin de servir de modèles possédant différentes interactions γ entre des groupes méthyles vicinaux. On a utilisé la deutération spécifique pour attribuer sans ambiguité les signaux se rattachant aux carbones géminés et vicinaux au site de deutération. [Traduit par le journal]

Can. J. Chem., 51, 2893 (1973)

Introduction

From the results of some of the earliest systematic studies of ^{13}C shielding trends within various families of compounds it was established that ^{13}C shieldings are remarkably sensitive to molecular geometry (1). In particular, the relative orientation of vicinal carbons, or of a carbon vicinal to a hetero atom, has a marked effect on their observed shieldings which has been attributed to 1,4-nonbonded interactions. These shifts, termed γ effects, are consistently to higher field with increased steric crowding and, consequently, provide a new method for the assignment of stereochemistry in a variety of systems. The relative magnitudes of the shifts are well characterized for cyclohexane derivatives (2, 3) in which, for example, an axial methyl carbon absorbs *ca.* 6 p.p.m. upfield from its equatorial counterpart. The axial methyl experiences γ *gauche* interactions with C-3 and -5 while the equatorial methyl is *anti* to these ring carbons. An even larger difference ($\sim$12 p.p.m.) is found (4) for the C-19 angular methyl carbons in 5α- and 5β-steroids for which there is also a difference of two γ *gauche* interactions (with C-2 and -4 in the 5α-series). Clearly the shielding of these methyl carbons depends strikingly on the dihedral angle relating the γ nuclei but these alicyclic derivatives provide examples for only two such angles, the *gauche* and *anti* arrangements. The relatively rigid and well-defined norbornyl skeleton, however, offers a framework with which a variety of dihedral angles between γ nuclei can be examined. We have prepared a series of methyl-substituted norbornyl derivatives primarily to investigate the effect of different vicinal orientations on the observed shieldings. While the ^{13}C spectra of a number of the compounds included in this series have been reported previously (5–9), these were reexamined to obtain data for the entire series under comparable conditions, namely 10–20% solutions in deuteriochloroform, for internal consistency. The earlier results were determined by steady-state operation which necessitated the use of highly concentrated solutions. Furthermore, a variety of referencing methods were employed which renders difficult detailed comparison of the results from different laboratories. In the present study, all data were measured relative to internal tetramethylsilane (TMS) which appears to be the reference of general choice.

In most instances the assignment of signals to specific carbons was straightforward on the basis

[1]Part 31, ref. 32; Part 30, ref. 33.

Can. J. Chem. Downloaded from www.nrcresearchpress.com by 210.87.254.40 on 09/05/12
For personal use only.

TABLE 1. ^{13}C shieldings for some methyl- and dimethyl-norbornanes and -norbornenes[a]

Parent	Substitution	C-1	C-2	C-3	C-4	C-5	C-6	C-7	Me
Norbornane	Nil	36.3	29.6	29.6	36.3	29.6	29.6	38.3	
	exo-2-Me	43.0	36.4	39.8	36.9	30.0	28.7	34.8	22.3
	endo-2-Me	41.7	34.0	40.2	37.7	30.2	22.1	38.4	17.4
	exo-2-*exo*-3-Me_2	44.5	39.9	39.9	44.5	29.7	29.7	31.9	15.7
	endo-2-*exo*-3-Me_2	42.4	44.0	45.2	44.4	30.3	21.2	36.9	15.9(2-Me); 21.1(3-Me)
	endo-2-*endo*-3-Me_2	43.1	34.8	34.8	43.1	21.8	21.8	39.7	11.8
Norbornene	Nil	41.8	135.2	135.2	41.8	24.6	24.6	48.5	
	exo-5-Me	42.3	135.9	137.0	48.3	32.5	34.6	44.8	21.6
	endo-5-Me	43.1	136.7	132.1	47.2	32.5	33.7	50.1	19.3
	exo-5-*exo*-6-Me_2	49.5	136.8	136.8	49.5	34.5	34.5	41.8	16.7
	endo-5-*exo*-6-Me_2	49.4	137.9	133.0	48.1	42.5	41.5	46.6	18.6(5-Me); 20.2(6-Me)
	endo-5-*endo*-6-Me_2	49.1	135.0	135.0	49.1	35.7	35.7	49.3	14.4

[a]In p.p.m. from internal TMS in $CDCl_3$ solutions.

of the earlier results, together with off-resonance decoupled spectra and the general additivity of substituent effects on shieldings. For four of the derivatives, however, an unambiguous assignment was only achieved through the examination of specifically deuterated materials. With Fourier transform operation and proton decoupling, the effects of a single deuterium atom are readily detected in the absorptions of the carbons geminal and vicinal to the deuterated center (10); consequently, the unequivocal identification of a few signals results from a single substitution. The utility of this technique is illustrated for the four 5,6-dimethylnorcamphors.

Results

The ^{13}C shieldings for the norbornanes and norbornenes examined in this study are listed in Table 1. Each of the parent compounds and their monomethyl derivatives had been examined previously (6, 7) and, in general, the agreement between the various sets of data is reasonable in view of the different referencing methods employed. For comparison with our results, those reported relative to CS_2 (6) were converted to the TMS scale using the factor 192.8 p.p.m. (*1b*). Although the present results tend toward higher field than the earlier data by approximately 0.5 p.p.m., the observed shieldings for the methyl carbons differ by only 0.0–0.2 p.p.m. in the three sets of results, indicating the existence of small but significant solvent effects rather than arising from calibration differences. With the single exception of the olefinic carbons in norbornene, the differences between our data and those of the Roberts' group (6) are <0.5 p.p.m. while comparisons with the results of Lippmaa *et al.* (7) reveal substantial differences (1.5–2.0 p.p.m.) for C-6 in *exo*-2-methylnorbornane, C-7 in *endo*-2-methylnorbornane, as well as C-4 and -6 in *endo*-5-methylnorborn-2-ene.

From the methyl results for the *exo*- and *endo*-monomethyl derivatives in each series it is apparent that the *endo*-methyl carbons are shielded relative to their *exo*- counterparts. On this basis the assignment of the methyl signals in the *trans*-dimethyl derivatives is straightforward. The remaining signals for the *trans*-dimethyl compounds were assigned by comparison of the observed shieldings with those expected on the basis of additivity of the individual substituent effects of each methyl group. Apart from the consistent upfield shift of each skeletal carbon (0.3–0.6 p.p.m.), our assignments agree well with those of Lippmaa *et al.* (7) except for the reversal of the C-5 and -6 signals for *trans*-5,6-dimethylnorbornene. The assignments for each of the four *cis*-dimethyl derivatives were readily accomplished, again by comparison of the observed shieldings with those predicted assuming additivity of methyl substituent effects. Major deviations occur only for the methine carbons bearing methyl groups as expected from the general behavior of carbon nuclei in fragments having appreciable γ interactions. In these cases, the methyl groups are eclipsed, or nearly so, and the pronounced upfield shifts found for the methyl and methine carbons seem unexceptional. These shifts are considered in more detail in the Discussion.

Our results for the norcamphors are collected in Table 2. The assignments for the carbonyl, bridgehead, α-carbon (C-3), and methyl signals presented no problems on the basis of the ob-

Can. J. Chem. Downloaded from www.nrcresearchpress.com by 210.87.254.40 on 09/05/12
For personal use only.

TABLE 2. ^{13}C shieldings for some methyl-substituted norcamphors[a]

Substitution	C-1	C-2	C-3	C-4	C-5	C-6	C-7	Me
Nil	49.7	217.4	45.1	35.3	27.1	24.2	37.6	
1-Me	53.6	218.4	45.5	34.3	28.9	31.5	44.1	13.8
exo-3-Me	49.4	220.0	48.2	41.5	28.0	23.8	34.4	14.1
endo-3-Me	50.2	219.8	48.2	40.4	20.9	25.4	37.2	10.7
exo-5-Me	50.5	216.1	45.5	41.8	34.5	33.3	34.2	22.0
endo-5-Me	51.1	217.6	39.0	40.3	32.4	33.1	38.7	17.1
exo-6-Me	56.6	216.4	44.2	36.0	37.3	31.0	34.2	20.8
endo-6-Me	55.8	216.7	45.8	35.5	35.8	32.3	38.7	18.7
1-*anti*-7-Me_2	55.6	218.5	46.1	39.0	26.4	27.8	46.6	11.5(1-Me), 10.5(7-Me)
1-*syn*-7-Me_2	56.0	218.7	41.0	38.7	28.2	31.9	47.7	11.8(1-Me), 10.9(7-Me)
exo-5-*exo*-6-Me_2	57.9	217.6	45.5	43.2	38.1	33.9	31.6	14.9(6-Me), 15.7(5-Me)
exo-5-*endo*-6-Me_2	56.8	216.8	46.1	42.0	43.4	41.8	35.6	17.2(6-Me), 21.0(5-Me)
endo-5-*exo*-6-Me_2	57.7	217.2	38.1	41.2	42.9	40.2	36.0	15.9(5-Me), 19.7(6-Me)
endo-5-*endo*-6-Me_2	57.4	216.9	39.4	41.2	34.4	33.9	37.9	11.9(5-Me), 13.6(6-Me)
7,7-Me_2	58.1	217.5	44.1	43.3	27.6	22.7	45.2	20.7(*anti*), 21.6(*syn*)
3,3-Me_2	50.0	222.0	46.8	46.1	23.3	24.5	34.9	21.4(*endo*), 23.2(*exo*)
6,6-Me_2	61.7	216.6	44.1	35.9	43.8	35.8	36.8	28.2(*endo*), 29.7(*exo*)
1,3,3-Me_3	53.8	222.6	43.1	45.3	24.9	31.8	41.5	14.6(1-Me), 21.6(*endo*), 23.3(*exo*)
3,3-*exo*-6-Me_3	57.0	220.0	46.0	46.9	33.5	31.5	31.7	21.0(6-Me), 21.3(*endo*), 23.2(*exo*)
3,3-*endo*-6-Me_3	56.3	219.3	47.7	46.6	30.6	33.4	36.3	18.1(6-Me), 20.0(*endo*), 23.9(*exo*)
1,7,7-Me_3	57.5	218.7	43.2	43.1	27.1	29.9	46.6	9.2(1-Me), 19.1(*anti*), 19.8(*syn*)
1-*endo*-3,7,7-Me_4	58.3	221.4	43.9	48.2	19.9	31.0	45.8	9.6(1-Me), 11.7(3-Me), 19.3, 19.4

[a]In p.p.m. from internal TMS in $CDCl_3$ solutions.

served shieldings and the off-resonance decoupled spectra. For the 5- and 6-methyl derivatives, the methine carbon bearing methyl was readily identified by off-resonance decoupling. The remaining methylene signals were assigned by comparison of the observed shieldings with those predicted assuming that introduction of a methyl group causes changes similar to those found for norbornane, using the values for norcamphor as the base. For an unequivocal assignment of the C-5 and -6 signals in norcamphor, the spectrum of norcamphor-3-*exo*-d_1 was recorded. The methylene signal at 27.1 p.p.m. showed the characteristic broadening caused by vicinal coupling with the *exo*-deuterium (10) while that at 24.2 p.p.m. was unaffected; thus these signals arise from C-5 and -6, respectively. The opposite assignment had been reported by one group (5). Although, from additivity, C-5 and -7 in *endo*-6-methylnorcamphor are predicted to be equivalent, the lower field signal of the two remaining methylene signals (38.7 and 35.8 p.p.m.) was assigned to C-7 since there is no precedent for an *endo*-methyl to shield C-7 by 2 p.p.m.; our assignment for these positions is reversed from that given earlier (6). Our assignments for C-5 and -6 are also reversed from those in an earlier report (6) but off-resonance decoupling supports the present identification.

Of the remaining ketones in Table 2, the 3,3- and 6,6-dimethyl as well as the 1,3,3- and 1,7,7-trimethyl derivatives have been reported previously (5–9) and the agreement between the various sets of results is satisfactory. It may be noted that our assignment for the 7-methyl carbons in camphor followed from the spectrum of the *endo*-3,9,9,9-tetradeuterio derivative (11).[2] An earlier report using a similar test surprisingly reached the opposite conclusion (5) while results of selective-decoupling experiments (7) agree with the present assignment.

While most of the assignments for the four 5,6-dimethylnorcamphors are straightforward, the C-4, -5, and -6 signals cannot be unambiguously assigned without additional information. For this purpose, the ketones were subjected to base-catalyzed deuterium exchange of the 3-proton and the spectra of the deuterated

[2]A sample of camphor-3,9,9,9-d_4 was kindly supplied by Prof. E. W. Warnhoff. It may be noted that the C-5 signal in its spectrum was essentially unchanged from its appearance in the spectrum of camphor indicating that the 3-deuterium is *endo* and, thus, only weakly coupled with C-5. Earlier results for camphor-3-*exo*-d_1 established that an *exo*-3-deuterium is strongly coupled with C-5 (10).

Can. J. Chem. Downloaded from www.nrcresearchpress.com by 210.87.254.40 on 09/05/12
For personal use only.

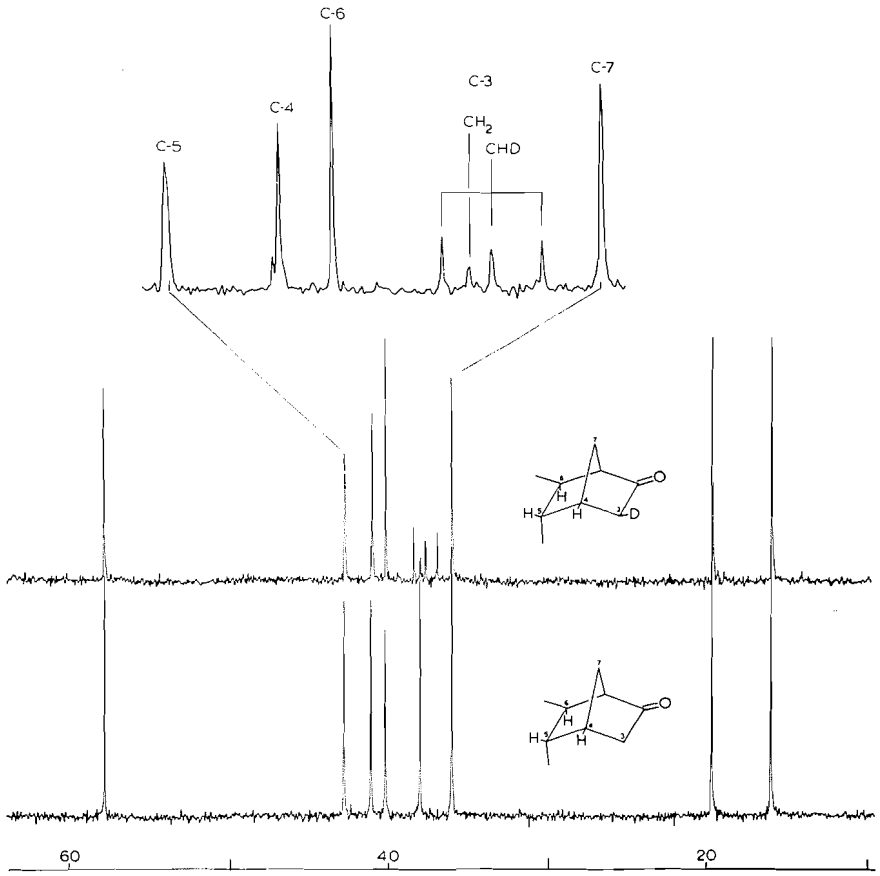

FIG. 1. High field region of the ^{13}C spectra of *endo*-5-*exo*-6-dimethylnorcamphor (lower spectrum) and its *exo*-3-d_1-derivative (upper spectrum). The upper inset is a fourfold expansion of the central portion to illustrate the effects of deuterium substitution.

ketones compared with those of the normal materials. In each case, the monodeuterated ketones exhibited a 0.1 p.p.m. upfield shift for one of the unassigned methine signals, a significantly broadened band for another, while the third was unaffected. Thus, the assignments for C-4, -5, and -6, respectively, were completed unequivocally. To illustrate these characteristic effects the spectra for *endo*-5-*exo*-6-dimethylnorcamphor and its *exo*-3-d_1-derivative are reproduced in Fig. 1. In the expanded spectrum shown at the top of this figure, the differences in the C-4, -5, and -6 absorptions are apparent. The small spike on the low field side of the main C-4 absorption corresponds exactly to the C-4 absorption in the normal material indicating that deuteration was not complete. Clearer evidence of this is given by the pattern for C-3 which consists of a triplet arising from ^{13}C–D coupling which is shifted upfield from the residual CH_2 signal by *ca.* 0.5 p.p.m. The marked broadening of the C-5 signal relative to the C-6 peak readily identifies each.

The assignments for the 1,7-dimethylnorcamphors follow directly from the available data for the corresponding hydrocarbons (7) and monomethyl ketones (6). Since the 1- and 7-methyl carbons are *gauche* the upfield shift relative to their positions in the monomethyl ketones is expected to be comparable for both. On this basis, the more shielded methyl signal was assigned to the 7-methyl carbon in each case. The methyl assignments for 7,7-dimethylnorcamphor were based on the relative shieldings for the corresponding carbons in camphor discussed above. The comparison of the data for *endo*-3-methylcamphor with those for camphor leads readily to the assignments listed.

Can. J. Chem. Downloaded from www.nrcresearchpress.com by 210.87.254.40 on 09/05/12
For personal use only.

TABLE 3. ^{13}C shieldings[a] of some norborn-5-en-2-ones

Substitution	C-1	C-2	C 3	C-4	C-5	C-6	C-7	Me
Nil	55.8	214.7	37.1	40.0	142.7	130.4	50.8	
exo-3-Me	55.6	217.8	40.0	46.0	143.7	131.4	46.9	15.7
endo-3-Me	56.3	215.8	42.5	45.0	140.7	130.1	49.8	16.5
3,3-Me_2	56.4	219.1	42.9	50.6	143.1	130.3	47.9	24.4(*exo*) 26.8(*endo*)
5-Me	56.2	214.4	36.7	44.4	153.5	121.9	49.4	16.2
6-Me	60.6	215.3	38.1	39.9	135.3	141.2	50.5	15.7

[a]In p.p.m. from internal TMS in $CDCl_3$ solutions.

The 3,3,6-trimethylnorcamphors were isolated as the minor rearrangement products arising from homoenolization of fenchone (12). The assignments given in Table 2 were obtained by a comparison of the observed shieldings with those estimated by combining the data for the 6-methylnorcamphors and camphenilone. For each carbon in 3,3-*exo*-6-trimethylnorcamphor, the agreement is <0.2 p.p.m., while the deviations for the *endo*-isomer are larger, especially for the C-5, -6, and methyl carbons. An interpretation of these deviations is considered in the next section.

The shielding results for the norborn-5-en-2-ones are given in Table 3. Of these compounds, only the parent has been reported earlier (7) and the present data agree well with the published values. The olefinic carbons were distinguished by selective decoupling experiments and the remaining assignments were readily completed with off-resonance decoupling results. The methylnorbornenones similarly presented no assignment problems but the olefinic assignments were confirmed for the 3-methyl derivatives by selective decoupling. The expected variation in the olefinic shieldings upon methyl substitution of an olefinic hydrogen (1) gives these assignments directly for the last two entries in Table 3.

Of the norbornenones, 3,3-dimethylnorborn-5-en-2-one is the only previously unreported compound and its proton spectrum was analyzed completely by a variety of double resonance experiments. The parameters for the skeletal protons are listed in Table 4. The methyl groups absorb at δ 1.039 (*endo*) and 1.143 (*exo*) and simultaneous irradiation at the latter enhanced the intensity of the 7-proton at 2.227 p.p.m. by 7.9%, thereby distinguishing the *anti*-proton. The tabulated values seem unexceptional for this structure. The molecular weight was determined by high resolution mass spectrometry to be 136.0889; calculated for $C_9H_{12}O$: 136.0888.

TABLE 4. Proton parameters[a] for skeletal protons of 3,3-dimethylnorborn-5-en-2-one

	1	4	5	6	*syn*-7[b]	*anti*-7[b]
1	2.013	1.7_2	~0.1	3.2_4	1.4_4	1.5_6
4		2.746	2.80	1.1_0	2.2_4	1.5_6
5			6.559	5.5_8	~0	0.4_4
6				6.068	0.3	0.65
7*s*					2.083	9.6_0
7*a*						2.227

[a]The values on the diagonal are the chemical shifts in p.p.m. from internal TMS, ±0.005 p.p.m., while the off-diagonal values are the coupling constants in Hz, ±0.05 Hz.
[b]*syn* and *anti* with respect to the olefinic bond.

Discussion

Since the shielding trends exhibited by the skeletal carbons in many of these compounds have been considered in detail previously (1, 6, 7), the following discussion is centered primarily on the methyl and carbonyl absorptions and their variation with structure and substituent orientation. As noted in the Introduction, the marked γ effects associated with 1,4-nonbonded interactions are particularly striking in ^{13}C spectra and the present series afford a number of comparisons of these interactions as a function of the dihedral angle relating the γ nuclei. The dihedral angle offers, at the least, a relative measure of the degree of steric crowding, the factor which is currently thought to dominate these γ effects (1, 13). Although a detailed analysis will require a more complete description of molecular geometry, relatively little geometric information is available for these systems but it has been shown that the norbornyl skeleton may be twisted from C_{2v} symmetry by as much as 14° (14). Because of this flexibility, albeit limited, complete force-field calculations are required to obtain the most probable geometry for each compound. While we have begun work in this direction, it seems reasonable, at present, to consider the ^{13}C shielding data qualitatively in terms of the estimated dihedral angles.

Can. J. Chem. Downloaded from www.nrcresearchpress.com by 210.87.254.40 on 09/05/12
For personal use only.

Can. J. Chem. Downloaded from www.nrcresearchpress.com by 210.87.254.40 on 09/05/12
For personal use only.

As a reference point for considering the methyl shieldings in these systems, the data for *exo*-2-methylnorbornane, *exo*-5-methylnorborn-2-ene, and *exo*-5-methylnorcamphor have been selected because the latter may be expected to be least affected by the carbonyl and olefinic functions. This gives a base value of 22.0 ± 0.4 p.p.m. It is interesting that this lies midway between the methyl shieldings for methylcyclohexane (2) and methylcyclopentane (15) but it is difficult to rationalize the trend. The *endo*-2-methylnorbornane and *endo*-5-methylnorcamphor have comparable methyl shieldings, 17.4 and 17.1 p.p.m., respectively. The upfield shift of *ca.* 4.7 p.p.m. is consistent with a decreased dihedral angle (ϕ) between these *endo*-methyl carbons and the γ-carbons (C-6 and -3, respectively). For the latter, $\phi \sim 45°$ whereas $\phi \sim 90°$ for the *exo*-methyl groups relative to C-7 since the *synchro* twist occurring in *exo*-2-methylnorbornane (14) tends to increase ϕ from the value of $\sim 85°$ for a symmetric skeleton. It is interesting that $\phi \sim 65°$ for a 7-methyl carbon relative to *both* carbons in the nearer ethano bridge and the observed shielding of 12.7 p.p.m. (6) represents a shift of 9.3 p.p.m. upfield from the base value which is essentially twice the shift exhibited by the *endo*-methyl as one would expect. These may be compared with the 1.3 ± 0.2 p.p.m. upfield shifts found for the 2- and 5-methyl carbons upon *trans*-vicinal methyl substitution, *i.e. trans*-2,3-dimethylnorbornane, and the *trans*-5,6-dimethylnorcamphors, for which $\phi \sim 120°$. Although the 6-methyl shieldings in the monomethylnorcamphors differ from those found for the 5-methyl derivatives the effect of a *trans*-vicinal methyl group is comparable for both. While the orientation of the *endo*-6-methyl group relative to C-2 is similar to that of the *endo*-5-methyl and C-3, the smaller shift of −2.1 p.p.m. for the former presumably results from the absence of an *endo*-2-hydrogen. Similarly, the methyl carbon in *endo*-5-methylnorborn-2-ene is only 2.3 p.p.m. more shielded than its *exo*-counterpart. The increased shielding for the *exo*-6-methyl relative to the *exo*-5-methyl may be due in part to a long-range shielding effect of the carbonyl group (C-4 in cyclohexanone is shielded relative to cyclohexane) or may result from a difference in the degree of twist of the skeleton. An indication that the latter feature may contribute is the fact that the 5- and 6-methyl carbons in the norbornenones are nearly equivalent (0.5 p.p.m.) and this skeleton is less flexible (14).

The 1-methyl shieldings for the α- and β-santenones (1,7-dimethylnorcamphors) compared with that for 1-methylnorcamphor show an upfield shift of 2.2 ± 0.2 p.p.m. Although this seems smaller than may have been anticipated since $\phi \sim 60°$, the methyl carbons in the santenones are further separated because of the small bridge angle of *ca.* 96° (16). A comparable shift is found for the 7-methyl carbons by comparison with the data for the 7-methylnorcamphors (6).

For the *cis*-vicinal dimethyl groups, ϕ lies in the range 0–15° and as expected the upfield shifts relative to the monomethyl derivatives are largest. For the norbornanes and norcamphors the *cis-exo*-methyls are shielded by −6.3 ± 0.3 p.p.m. while the *cis-endo*-methyls are shifted −5.3 ± 0.3 p.p.m. Perhaps the difference is indicative of different degrees of twisting since the shifts for both *exo*- and *endo*-dimethyl carbons in the less flexible 5,6-dimethylnorborn-2-enes are equal, −4.9 p.p.m.

The remaining monomethyl ketones are those with methyl carbons vicinal to the carbonyl oxygen and it is apparent that these are substantially shielded. Since the *exo*-3-methyl is shifted by −8.2 p.p.m. and the *endo*-3-methyl by −6.7 p.p.m., it can be suggested that the dihedral angle between the C—Me and C=O bonds is smaller for the former because of skeletal twist. Interestingly, the α-*endo*-methyl carbon in *endo*-3-methylnorborn-5-en-2-one is only shielded by −2.8 p.p.m. relative to the corresponding hydrocarbon while the α-*exo*-methyl is shifted −5.9 p.p.m. in the ketone. From these data one might anticipate a relatively large shielding difference for the methyl carbons in the 3,3-dimethyl derivative but the observed difference is 2.4 p.p.m. With one exception, the remaining 3,3-dimethyl derivatives exhibit comparable differences between the 3-methyl carbon shieldings, 1.8 ± 0.1 p.p.m., indicating presumably that the relative geometries of these carbons are similar in each case. Interestingly, the difference between the methyl carbons in 6,6-dimethylnorcamphor is comparable, 1.6 p.p.m. For 3,3-*endo*-6-trimethylnorcamphor, however, the 3-methyl carbons differ by 3.9 p.p.m. with the *endo*-carbon substantially shielded relative to the other 3,3-dimethyl derivatives. Since the *endo*-6-methyl is not nearly so greatly affected, it follows the difference for the α-methyls may arise from a change in their orientation relative to the carbonyl bond such that the *endo*-methyl is closer to the carbonyl oxygen and the *exo*-methyl

Can. J. Chem. Downloaded from www.nrcresearchpress.com by 210.87.254.40 on 09/05/12
For personal use only.

farther from it than is the case for the other 3,3-dimethyl derivatives.

It is interesting that the nonequivalence of 0.8 ± 0.1 p.p.m. for the 7-methyl carbons in 7,7-dimethylnorcamphor and camphor is essentially the same as that for the 7-methylnorcamphors (6) while these carbons differ by 0.4 p.p.m. in the santenones and by only 0.1 p.p.m. in *endo*-3-methylcamphor. Perhaps these variations arise from slight differences in skeletal twist, a notion which is supported by the 1 p.p.m. downfield shift found for the 3-methyl group in the latter derivative relative to the methyl shielding in *endo*-3-methylnorcamphor.

As mentioned earlier, the shielding variations for the skeletal sp^3-hybridized carbons have been discussed in detail previously (6, 7) and the present data are entirely consistent with the expected trends. It may be noted that, while attention has been focussed on the methyl shieldings, each carbon nucleus in the four-carbon fragment involved in a *gauche* γ interaction, *e.g.* C-1, -2, and -6, and CH_3 in *endo*-2-methylnorbornane, etc., are shielded relative to their positions in an *anti* arrangement. Thus C-6 is shielded by an *endo*-2-methyl group, C-7 by an *exo*-methyl, etc. Thus, it is hardly surprising that the C-5 and -6 nuclei in the *cis*-5,6-dimethylnorcamphors and C-2 (C-3) in the *cis*-2,3-dimethylnorbornanes are upfield from their positions predicted by assuming that the substituent effects of each methyl group are additive, *i.e.* the eclipsing interaction of the vicinal methyls increases the shieldings of the ethano-bridge carbons.

Previously it had been pointed out (7, 17) that these 1,4-interactions are not reciprocal in that the skeletal carbons exhibit larger shifts with crowding than the methyl carbons. This comparison, however, may not be valid because different sorts of nuclei are affected. The present results permit comparisons of methyl with methyl and it is apparent that these are similarly affected. It seems hardly surprising that methyl, methylene, and methine nuclei exhibit different sensitivities to γ *gauche* interactions and it emphasizes one of the difficulties in developing a satisfactory theoretical basis for these shifts. The problems associated with deriving a simple prescription to account for the effects of steric crowding of γ nuclei have been discussed by Dalling and Grant (2).

In the spectra of the ketones, the most readily identified signal is undoubtedly the carbonyl peak and its variations with structure are interesting. In general, the present carbonyl data are approximately 2 p.p.m. downfield from the earlier results presumably because of hydrogen bonding with chloroform. It is established that hydrogen bonding tends to decrease carbonyl shieldings (18). An examination of Table 2 shows that in the absence of α-methyl substitution the carbonyl carbons in the norcamphors absorb at δ_c 217.0 ± 0.5 (standard deviation). As expected, α-methylation shifts the carbonyl absorption downfield but the magnitude of the shift depends on the position of substitution. The 3-methyl groups cause somewhat larger shifts (2.5 p.p.m.) than a 1-methyl group (~1 p.p.m.). Since methyl substitution of an α-hydrogen places the methyl carbon γ to the carbonyl oxygen it is conceivable that the normal β-effect of the methyl group at the carbonyl carbon (1) is reduced by the γ interaction with the oxygen. Since the dihedral angle between the C—Me and C=O bonds is less for a bridgehead methyl than for a 3-methyl group, the differences in the observed shifts may be rationalized. The effects of *exo*- and *endo*-3-methyl groups appear to be comparable in the monomethyl derivatives and additive in the 3,3-dimethyl compounds. For the norbornenones, however, an *exo*-3-methyl group has a substantially greater effect than its *endo*-counterpart (3.1 *vs.* 1.1 p.p.m.). The upfield shift exhibited by each of the norbornenones relative to the similarly substituted methylnorcamphor has been noted previously and attributed to homoconjugation (19). Support for this interpretation is given by the 12.3 p.p.m. difference observed for the olefinic carbons in norbornenone consistent with polarization of the double bond toward the carbonyl group. Although, as Lippmaa *et al.* (7) have pointed out C-2 (C-3) is shielded in norbornene relative to norbornane by 5.0 p.p.m. and, consequently, attributing the 2.7 p.p.m. shielding of the carbonyl carbon in norbornenone entirely to homoconjugation may be an oversimplification. It may be noted, however, that the downfield shift of C-3 in these ketones is more pronounced for norcamphor indicating a reduced inductive effect of the carbonyl bond in norbornenone which is consistent with some degree of homoconjugation in the latter compound.

Experimental

Materials

Apart from norbornane and norbornene, which are commercially available, the hydrocarbons were prepared

Can. J. Chem. Downloaded from www.nrcresearchpress.com by 210.87.254.40 on 09/05/12
For personal use only.

by published procedures. The 5,6-dimethylnorbornenes, obtained by the methods of Miller and Greenlee (20) were hydrogenated over platinum oxide to yield the corresponding dimethylnorbornanes. The monomethyl derivatives were prepared by a similar sequence from the carboxylic acids formed by Diels–Alder addition of cyclopentadiene with acrylonitrile followed by hydrolysis (21). The *exo*- and *endo*-acids were separated by the iodolactonization procedure.

1-Methylnorcamphor (22), the santenones (23), and the 3-methylnorcamphors (24) were prepared from commercial norcamphor while the remaining monomethyl- and 5,6-dimethyl-norcamphors were obtained by hydroboration (25) of the olefins to the *exo*-alcohols followed by oxidation with CrO_3–pyridine in CH_2Cl_2 (26) to the required ketones. In those cases in which mixtures of two ketones were obtained, the individual isomers were isolated by gas chromatography (g.c.) using a 20% SE30 column. Camphenilone was prepared from camphene by ozonolysis (27) and 7,7-dimethylnorcamphor was obtained from 10-camphorsulfonic acid via ketopinic acid (28) which was decarboxylated by the silver salt degradation (29) and the ketone obtained by reduction of the bromoketone with sodium in alcohol followed by Jones oxidation. The 3,3,6-trimethylnorcamphors were isolated as the minor products in the homoenolization of fenchone (12). Professor N. H. Werstiuk and E. W. Warnhoff kindly provided samples of 6,6-dimethylnorcamphor and *endo*-3-methylcamphor, respectively.

The 5- and 6-methylnorborn-5-en-2-ones were obtained by the following sequence. The Diels–Alder addition of methylcyclopentadiene and vinyl acetate furnished a mixture of acetates from which 5- and 6-methylnorborn-5-enyl acetate were separated by g.c. Treatment of the individual esters with lithium aluminum hydride followed by oxidation with CrO_3–pyridine in CH_2Cl_2 gave the required ketones. This procedure is analogous to that recently reported by Krieger and Masar (30). The 3-methylnorborn-5-en-2-ones were prepared by the Diels–Alder reaction of cyclopentadiene and the enol acetate of propanal (31). The mixture of acetates was hydrolyzed and oxidized to afford a mixture of the *exo*- and *endo*-3-methylnorborn-5-en-2-ones which was separable by g.c. In a similar manner a small sample of the 3,3-dimethyl ketone was obtained from the enol acetate of isobutyraldehyde.

In all cases the i.r. and proton spectra of ketones were consistent with the expected structures and with those reported previously. The physical data for the new compounds encountered in these preparations are listed below.

exo,exo-5,6-Dimethylnorcamphor: ν_{max} ($CDCl_3$) 1725 cm^{-1}; δ_H ($CDCl_3$) 0.97 (d), methyl protons.

Anal. Calcd. for $C_9H_{14}O$: C, 78.21; H, 10.20. Found: C, 78.67; H, 10.30.

endo-5-*exo*-6-Dimethylnorcamphor: ν_{max} ($CDCl_3$) 1720 cm^{-1}; δ_H (CCl_4) 0.93 (d), 1.12 (d), methyl protons.

Anal. Calcd. for $C_9H_{14}O$: C, 78.21; H, 10.20. Found: C, 78.74; H, 10.45.

exo-5-*endo*-6-Dimethylnorcamphor: ν_{max} ($CDCl_3$) 1720 cm^{-1}; δ_H ($CDCl_3$) 1.30 (d), 1.34 (d), methyl protons.

Anal. Calcd. for $C_9H_{14}O$: C, 78.21; H, 10.20. Found: C, 78.44; H, 10.16.

N.m.r. Spectra

Proton spectral data were obtained with a Varian HA-100 instrument. ^{13}C spectra were recorded with a Varian XL-100-15 system operating in the Fourier transform mode. Solutions (10–15% w/v) in deuteriochloroform containing a few drops of TMS were examined in 5 mm tubes using a 5 mm receiver insert. With spectral widths of 2000 Hz, or less, and the available memory core (4K) all peak positions were determined to ± 1 Hz. In general, 2000 transients were accumulated for each sample. Off-resonance decoupling was employed to confirm the assignments for methyl, methylene, methine, and quaternary carbons, and specifically deuterated materials were examined in a few cases to distinguish between methine resonances as described in the Results section.

We wish to thank the National Research Council of Canada for financial support of this study. We are grateful to Professors E. W. Warnhoff and N. H. Werstiuk for kindly providing samples of *endo*-3-methylcamphor and 6,6-dimethylnorcamphor respectively, and to M. Gordon, J. L. Gough, S. H. Grover, and P. M. Pellitt for technical assistance.

1. (*a*) G. C. Levy and G. L. Nelson. ^{13}C Nuclear magnetic resonance for organic chemists. Wiley-Interscience, New York. 1972. (*b*) J. B. Stothers. Carbon-13 NMR spectroscopy. Academic Press, New York. 1972. (*c*) N. K. Wilson and J. B. Stothers. *In* Topics in stereochemistry. Vol. 8. *Edited by* E. L. Eliel and N. L. Allinger. Wiley-Interscience, New York. 1973.
2. D K. Dalling and D. M. Grant. J. Am. Chem. Soc. **89**, 6612 (1967); **94**, 5318 (1972).
3. F. A. L. Anet, C. H. Bradley, and G. W. Buchanan. J. Am. Chem. Soc. **93**, 258 (1971).
4. B. Balogh, D. M. Wilson, and A. L. Burlingame. Nature, **233**, 261 (1971). J. L. Gough, J. P. Guthrie, and J. B. Stothers. J. Chem. Soc. Chem. Commun. 979 (1972).
5. E. Wenkert, A. O. Clouse, D. W. Cochran, and D. Doddrell.Chem. Commun. 1433 (1969).
6. J. B. Grutzner, M. Jautelat, J. B. Dence, R. A. Smith, and J. D. Roberts. J. Am. Chem. Soc. **92**, 7107 (1970).
7. E. Lippmaa, T. Pehk, J. Paasivirta, N. Belikova, and A. Plate. Org. Mag. Res. **2**, 581 (1970).
8. N. H. Werstiuk, R. Taillefer, R. A. Bell, and B. G. Sayer. Can. J. Chem. **50**, 2146 (1972).
9. L. F. Johnson and W. C. Jankowski. Carbon-13 NMR spectra. Wiley-Interscience, New York. 1972.
10. J. B. Stothers, C. T. Tan, A. Nickon, F. Huang, R. Sridhar, and R. Weglein. J. Am. Chem. Soc. **94**, 8581 (1972).
11. G. C. Joshi and E. W. Warnhoff. J. Org. Chem. **37**, 2383 (1972).
12. D. H. Hunter, A. L. Johnson, J. B. Stothers, A. Nickon, J. L. Lambert, and D. F. Covey. J. Am. Chem. Soc. **94**, 8582 (1972).
13. D. M. Grant and B. V. Cheney. J. Am. Chem. Soc. **89**, 5315 (1967).
14. C. Altona and M. Sundaralingam. J. Am. Chem. Soc. **92**, 1995 (1970).
15. M. Christl, H. J. Reich, and J. D. Roberts. J. Am. Chem. Soc. **93**, 3463 (1971).
16. J. F. Chiang, C. F. Wilcox, and S. H. Bauer. J. Am. Chem. Soc. **90**, 3149 (1968).

17. G. VAN BINST and D. TOURWE. Org. Mag. Res. **4**, 625 (1972).
18. P. C. LAUTERBUR. Ann. N.Y. Acad. Sci. **70**, 841 (1958). G. E. MACIEL and G. C. RUBEN. J. Am. Chem. Soc. **85**, 3903 (1963). G. E. MACIEL and D. D. TRAFICANTE. J. Phys. Chem. **69**, 1030 (1965). G. E. MACIEL and J. J. NATTERSTAD. J. Chem. Phys. **42**, 2752 (1965).
19. N. GURUDATA and J. B. STOTHERS. Can. J. Chem. **47**, 3601 (1969).
20. H. N. MILLER and K. W. GREENLEE. J. Org. Chem. **26**, 3734 (1961).
21. W. R. BOEHME, E. SCHIPPER, W. G. SCHARPF, and J. NICHOLS. J. Am. Chem. Soc. **80**, 5488 (1958).
22. J. A. BERSON, J. S. WALIA, A. REMANICK, S. SUZAKI, P. REYNOLDS-WARNHOFF, and D. WILLNER. J. Am. Chem. Soc. **83**, 3986 (1961).
23. L. D. HATFIELD and W. D. HUNTSMAN. J. Org. Chem. **32**, 844 (1967).
24. E. J. COREY, R. HARTMANN, and R. A. VATAKENCHERRY. J. Am. Chem. Soc. **84**, 2611 (1962).
25. E. L. ALLRED, C. L. ANDERSON, and R. L. SMITH. J. Org. Chem. **31**, 3493 (1966).
26. R. RATCLIFFE and R. RODEHORST. J. Org. Chem. **35**, 4000 (1970).
27. R. CRIEGEE and P. GUNTHER. Chem. Ber. **96**, 1564 (1963).
28. P. D. BARTLETT and L. H. KNOX. Org. Syn. **45**, 55 (1965).
29. P. WILDER and A. WINSTON. J. Am. Chem. Soc. **75**, 5370 (1953).
30. H. KRIEGER and S-E. MASAR. Suom. Kemi. B, **43**, 318 (1970).
31. P. Z. BEDONKIAN. J. Am. Chem. Soc. **66**, 1325 (1944).
32. S. H. GROVER, J. P. GUTHRIE, J. B. STOTHERS, and C. T. TAN. J. Mag. Res. **10**, 227 (1973).
33. D. H. HUNTER and J. B. STOTHERS. Can. J. Chem. This issue.

Can. J. Chem. Downloaded from www.nrcresearchpress.com by 210.87.254.40 on 09/05/12
For personal use only.

In situ Generation and Electrophilic Addition Reactions of the Elements of 'XF'[1]

L. D. HALL AND D. L. JONES

Department of Chemistry, The University of British Columbia, Vancouver 8, British Columbia

Received November 1, 1971[2]

Addition of the elements of 'IF' and of 'BrF' to alkenes can be effected by the *in situ* generation of these electrophiles from the halogen-AgF. For cyclohexene, 3,3,6,6-tetradeuterocyclohexene, methylenecyclohexane, styrene, and indene, these reactions are simple. However, for acenaphthylene, halogen–fluorine exchange and other reactions make the overall reaction quite complex. Electrophilic addition reactions for 1-fluoro-acenaphthylene are also described. The n.m.r. spectra of many of the products are given and discussed in some detail.

L'addition des éléments 'IF' et 'BrF' aux alcènes peut être effectuée par réaction in situ de ces électrophiles à partir de AgF-halogène. Pour le cyclohexène, tétradeutero-3,3,6,6 cyclohexène, méthylcyclohexane, styrène et indène, les réactions sont simples. Cependant pour l'acénaphtylène, l'échange halogène–fluor et d'autres réactions rendent la réaction globale complexe. Les réactions d'addition électrophile pour le fluoro-1 acénaphtylène ont été également décrites. Les spectres r.m.n. de plusieurs de ces produits ont été donnés et discutés de façon détaillée. [Traduit par le journal]

Can. J. Chem., **51**, 2902 (1973)

A crucial aspect of our programme to develop fluorine as a structural probe has always been the synthesis of specifically fluorinated substrates. One of the methods which was found to be successful in the carbohydrate area involved the addition of the elements 'XF', where X = Cl, Br, or I, to an unsaturated sugar (2); the preferable source of the 'XF' electrophile was shown to be the generation *in situ* from halogen and silver monofluoride. In the present paper we describe the reaction of a variety of alkenes with the above source of the elements of 'XF'. As will be seen, the initial addition reaction may be followed by further halogen exchange reactions which are sometimes so fast that the initially formed adduct cannot be isolated.

It is appropriate to comment here that there had previously been some controversy in the literature concerning the efficacy of the X_2–AgF method for generating 'XF'. Schmidt and Meinert (3) reported that in acetonitrile solvent the elements of iodine monofluoride could be added across the double bond of cyclohexene, to form *trans*-1-fluoro-2-iodocyclohexane in 60% yield. However, Andreatta and Robertson (4), attempting to repeat this reaction, isolated only *N*-acetyl-2-iodocyclohexylamine in 17% yield; this work will show that the 'IF' addition reaction to cyclohexene is indeed a viable reaction, and can be extended to a variety of other alkenes, and also to 'BrF' additions.

Results and Discussion

The compounds described in the first section of the following discussion were for the most part isolable in pure form and were fully characterized. In constrast, the acenaphthyl fluorides discussed subsequently were generally unstable and hence could only be characterized by their ^1H and ^{19}F n.m.r. spectra.

The reactions summarized in Scheme 1 are typical of those of aliphatic alkenes. Slow addition of a dilute solution of iodine in benzene to a stirred suspension of AgF in cyclohexene and benzene afforded as sole product 1-fluoro-2-iodocyclohexane (**1**). The stereochemistry of the product was shown to be *trans* by examination of the ^1H n.m.r. spectrum of the product (**1**-d_4) obtained from 3,3,6,6-tetradeuterocyclohexene: it is noteworthy that neither the ^1H nor the ^{19}F n.m.r. spectra of the *crude* product arising from that reaction showed any detectable impurities.[3]

The addition of 'BrF' to cyclohexene was also successful, again producing a *trans*-product (2).

[1]For a preliminary communication see ref. 1. Presented in part at the 51st Canadian Chemical Conference of the Chemical Institute of Canada, Vancouver, British Columbia, June 3–5, 1968.

[2]Revision received February 23, 1973.

[3]The ^1H n.m.r. spectrum of this deuterated compound is shown in the accompanying paper (5).

Can. J. Chem. Downloaded from www.nrcresearchpress.com by 210.87.254.6 on 09/05/12
For personal use only.

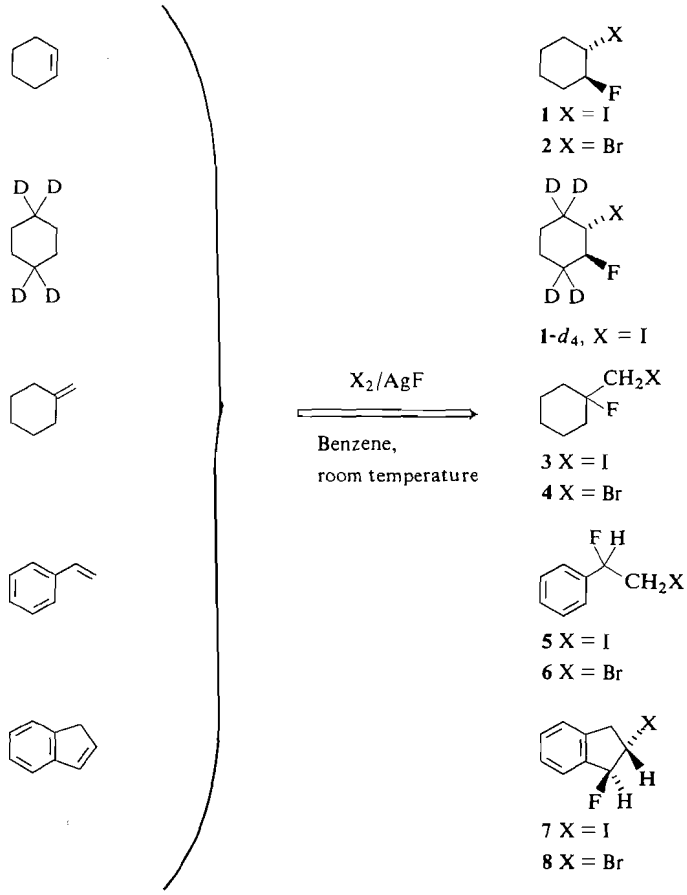

SCHEME 1

This reaction was more difficult to carry out and the AgF had to be absolutely dry, otherwise the 1,2-dibromide was formed.

Direct extension of the 'IF' and 'BrF' addition reactions to methylene-cyclohexane, styrene, and indene produced in each instance the reaction product having the structure anticipated for the reaction of X^+F^-.

In marked contrast to the ease of the above addition reactions, attempts with acenaphthylene were at first unsuccessful. 'BrF' addition in benzene solution produced no 'BrF' adduct, but gave instead a low yield of the *cis*- and *trans*-difluorides (**9**, **10**) (see Scheme 2). The major product of the reaction contained no fluorine and was high melting. In addition to these products, there were also two others, both in trace quantities, which were observed in the ^{19}F n.m.r. spectrum of the crude product; one was later shown to be 1-fluoro-acenaphthylene (**11**) and the other 1-bromo-2,2-difluoro-acenaphthene (**12**) designated hereafter as the 'BrF_2 adduct'.

If, however, the solvent was 50/50 benzene–acetonitrile,[4] the *trans*-'BrF' product (**13**) resulted. Increasing proportions of benzene in the solvent produced a mixture of all three products; *trans*-'BrF', *cis*- and *trans*-difluorides, as well as "polymeric" material; altering the time of the reaction seemed to have some effect on the relative amounts. Interestingly, it was not possible to convert the 'BrF' product to difluoride using AgF, with either benzene or acetonitrile as solvent. However, addition of Br_2 to acenaphthylene produced only *trans*-dibromide, confirming Cristols' result (6) and subsequent shaking with AgF yielded only *trans*-BrF (**13**).

[4]Acenaphthylene was dissolved in benzene–acetonitrile, but Br_2 added as a benzene solution.

Can. J. Chem. Downloaded from www.nrcresearchpress.com by 210.87.254.6 on 09/05/12
For personal use only.

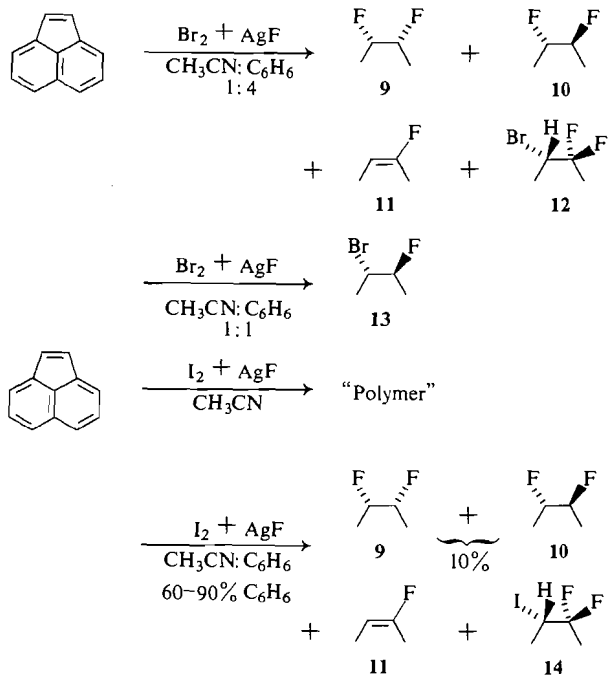

SCHEME 2

Reactions of I_2 + AgF with acenaphthylene were performed as for the Br_2 + AgF reactions; however the experimental results were significantly different. Any 'IF' product, if it ever existed, was too unstable to be isolated and led to further products. In benzene, the major fluorinated products were once again the *cis*- and *trans*-difluorides (**9**, **12**) but in low yield. Trace quantities of fluoro-acenaphthylene (**11**) and the 'IF_2' adduct (**14**) were also observed and isolated.

With increasing quantities of acetonitrile in the solvent, less of the above products were observed, and the best yields were obtained in 80–90% benzene.[5] Below 50% benzene none of these compounds were formed in substantial quantities but other fluorinated products were observed in the ^{19}F n.m.r. spectrum; however, they decomposed with every attempted isolation (such as column chromatography). From the chemical shift and multiplicity of the ^{19}F resonance it was evident that the unknown products could well contain a *trans*-'IF' adduct which would be expected to be very unstable indeed. The ratio of *cis*:*trans* difluorides was found to be close to 1:2, and essentially independent of solvent, in the range benzene–acetonitrile (40:60) to pure benzene. Finally it was observed that a number of other compounds were formed in trace quantities, and from the pattern of their ^{19}F resonances they appeared very similar in structure to the *trans*-difluoride.

The unexpected results obtained with 'XF' additions to acenaphthylene can be attributed to the increased reactivity of the halogen 'X' of the 'XF' adduct. This reactivity is well illustrated by the effect of AgF on 1-bromo-acenaphthene, 1-bromo-indan and bromo-cyclohexane respectively. The acenaphthene derivative is converted to the fluoride in minutes; in contrast, the indan compound requires 24 h for the same reaction, and bromo-cyclohexane is unreactive.

The products obtained from the 'XF' reactions with acenaphthylene suggested that many acenaphthyl fluorides might be obtained by a series of simple reactions, chiefly utilizing 1-fluoro-acenaphthylene (**11**); such compounds would provide the necessary data to determine the effect of electronegativity on $^3J_{HF}$ couplings.

1-fluoro-acenaphthylene (**11**) was prepared by the method described by Merritt and Johnson (7), *i.e.*, elimination of HF, using a refluxing

[5]Volume measurement.

Can. J. Chem. Downloaded from www.nrcresearchpress.com by 210.87.254.6 on 09/05/12
For personal use only.

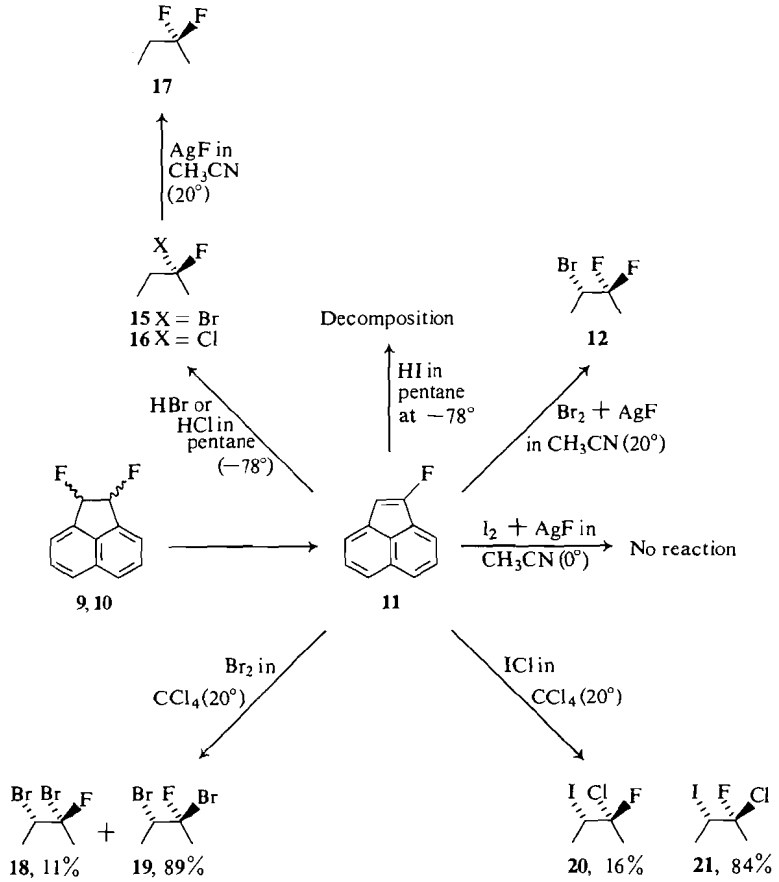

SCHEME 3

solution of KOH in ethanol, from either the *cis*- or the *trans*-1,2-difluoride of acenaphthene. The conversion obtained from this reaction was never quantitative, and it was necessary to recycle the recovered starting material. The reactions performed with **11** are summarized in Scheme 3. For convenience each of these reactions is listed separately below.

(a) Addition of HCl or HBr, Followed by AgF Exchange

Addition of HBr or HCl gas to a solution of 1-fluoro-acenaphthylene (at −78°) yielded the corresponding '*gem*-BrF' (**15**) and '*gem*-ClF' (**16**) adducts; in neither case was any vicinal product observed. Shaking either of these compounds with AgF powder in acetonitrile solution at room temperature produced the *gem*-difluoride (**17**). Addition of HI, instead of HCl or HBr, produced only decomposition even at −78°.

(b) 'BrF' Addition

Conditions identical with those used for acenaphthylene itself afforded as major product the expected 'BrF_2' adduct spectroscopically identical with the trace material found in the reaction of acenaphthylene; two minor components were also formed, but these were not identified.

(c) 'IF' Addition

The analogous reaction between I_2, AgF, and 1-fluoro-acenaphthylene did not proceed.

(d) Br_2 Addition

When elemental bromine was added to fluoro-acenaphthylene in either CCl_4 or CH_3CN solution, both *cis*- and *trans*-products (**18, 19**) were observed; the ratio of *cis*–*trans* was 1:8.

(e) ICl Addition

Analogous treatment of 1-fluoro-acenaphthylene with an ICl solution in CCl_4 gave similar

Can. J. Chem. Downloaded from www.nrcresearchpress.com by 210.87.254.6 on 09/05/12
For personal use only.

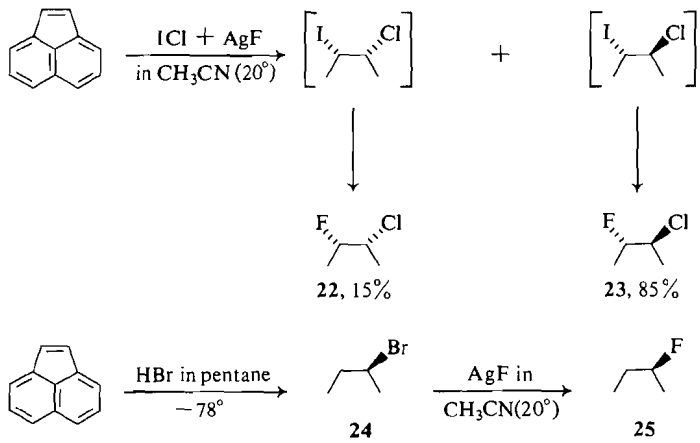

SCHEME 4

results, *i.e. cis-* and *trans*-products (**20**, **21**) in the ratio 1:5.

Some apparently anomalous additions have been previously observed with acenaphthylene by several other workers; thus Cl_2 addition can be made to add *cis* or *trans*, depending on reagents whereas only a *trans*-dibromide is known (6). Furthermore, HBr and HCl addition has been shown to go 75–90% *cis* (8). However, it is possible that earlier workers (6) might have missed a small quantity of a minor product, such as a *cis*-dibromide, for example.

The *cis-* and *trans*-'ClF' adducts (**22**, **23**) shown in Scheme 4 were prepared by 'XF' addition to acenaphthylene using ICl and AgF in CH_3CN solution. Once again, the *trans*-adduct predominated (85%).

Following the procedure of Dewar and Fahey, 1-bromo-acenaphthene (**24**) was synthesized from acenaphthylene and HBr (8); this compound readily exchanged its bromine atom for a fluorine of AgF, in acetonitrile solution at room temperature. Unfortunately, this resulting fluoride was extremely unstable, and all attempts at purification or isolation resulted in decomposition; thus it was found impossible to run the compound on any available chromatographic apparatus (*i.e.* acid, neutral, or basic silica gel or alimina on either columns or plates). Additionally, it was decomposed by washing with a weakly basic aqueous solution, and also by warm chloroform.

Summary

The reactions discussed above indicate that electrophilic addition of the elements of 'IF' and 'BrF' to alkene can be accomplished using the halogen-AgF reagent. Addition of 'IF' is more facile than that of 'BrF' and for aliphatic alkenes both are simple reactions. However, if the 'XF'-product has the bromine or iodine substituent in a benzylic position then further reactions can follow the initial addition and the overall reaction sequence is then extremely complex.

The reactions discussed here afforded a range of interesting substrates for n.m.r. studies and these are described in three accompanying papers (5, 10, 11).

Experimental

All solutions were concentrated under reduced pressure. Benzene and acetonitrile were dried over calcium sulfate and light petroleum and dichloro-methane were fractionally distilled before use. Silver fluoride[6] was stored in a vacuum dessicator and ground to a fine powder just prior to a reaction. Cyclohexene was distilled before a reaction, but all other reagents were used as received.

Silica gel used for chromatographic columns was Mallinckrodt CC-7, a neutral high-purity grade.

trans-2-Iodocyclohexylfluoride (1)

Cyclohexene (3.1 ml, 2.5 g) and silver monofluoride (12 g) were added to benzene (50 ml) and the resulting mixture stirred vigorously and cooled in an ice–bath. A solution of iodine (8 g) in benzene (80 ml) was then added over 0.5 h with continued stirring.

The reaction mixture was filtered and the filtrate washed successively with aqueous sodium bicarbonate, sodium thiosulfate, sodium bicarbonate, and finally with water. The organic layer was separated, dried ($MgSO_4$), and concentrated to a clear liquid whose ^1H n.m.r. spectrum was virtually indistinguishable from the distilled material. Distillation under reduced pressure gave **1** (4.4 g, 63%), b.p. 50° (2 mm) (lit. (9), 64° (9 mm)), n_D^{23}

[6]From Harshaw Chemical Co.

Can. J. Chem. Downloaded from www.nrcresearchpress.com by 210.87.254.6 on 09/05/12
For personal use only.

Can. J. Chem. Downloaded from www.nrcresearchpress.com by 210.87.254.6 on 09/05/12
For personal use only.

1.5310 (lit. (9), n_D^{20} 1.5318). The ^{19}F chemical shift in $CHCl_3$ solution was +159.9 p.p.m. with respect to $CFCl_3$ as a reference.

Anal. Calcd. for $C_6H_{10}IF$: C, 31.59; H, 4.42; I, 8.32. Found: C, 31.76; H, 4.63; I, 8.11.

trans-1-Bromo-2-fluoro-cyclohexane (2)

The same procedure as for preparation of **1** was used except that bromine was substituted for iodine, and no thiosulfate washing was necessary in the work-up. Bromine (6.0 g) in benzene (25 ml) was added dropwise, and all other procedures and quantities remained the same. The n.m.r. spectra of crude and distilled material again were very similar, and also matched that of the product of the Bowers reaction (9). The product had a b.p. 58° (9 mm) (lit. (9), 30° (13 mm)[7]), n_D^{25} 1.4825 (lit. (9) n_D^{20} 1.4830).

Anal. Calcd. for $C_6H_{10}BrF$: C, 39.78; H, 5.56; F, 10.49. Found: C, 39.90; H, 5.65; F, 10.61.

1-Iodomethyl-cyclohexyl Fluoride (3)

Prepared in a similar procedure as used for **1**. Quantities used were; AgF (10 g); methylene cyclohexane (2.5 g) dissolved in benzene (35 ml); iodine (8.5 g) dissolved in benzene (85 ml). Reaction time was 90 min. Crude yield 6.0 g; distilled yield 4.4 g (70%), b.p. 61° (1 mm), n_D^{25} 9.5175, ϕ_c 151.2 p.p.m.

Anal. Calcd. for $C_7H_{12}IF$: C, 34.73; H, 4.97. Found: C, 34.88; H, 5.02.

1-Bromomethyl-cyclohexyl Fluoride (4)

Similar procedure as for **2**; to methylene cyclohexane (2.5 g) and AgF (10 g) in benzene (40 ml) was added bromine (8 g) in benzene (40 ml) over 1 h at 0°. Distillation afforded 3.0 g of 4 (yield 59%), b.p. 47° (1 mm), n_D^{25} 1.4825, ϕ_c 156.3 p.p.m.

Anal. Calcd. for $C_7H_{12}BrF$: C, 43.12; H, 6.15. Found: C, 42.89; H, 6.25.

The position of the substituents is obtained from the n.m.r. spectrum; the lack of an identifiable $^2J_{HF}$ coupling (characteristically about 50 Hz) located the fluorine at the tertiary position.

2-Iodo-1-fluoro-1-phenylethane (5)

Identical procedure as for preparation of **1**, except that styrene (2.5 g) was used as starting material. Distillation *in vacuo*, however, resulted in decomposition. Crude yield (after work-up and removal of solvent), 4.7 g (78%). The n.m.r. spectrum showed that the product was substantially pure and its similarity to that of the bromo-derivative **6**, which is discussed below; ϕ_c +166.8 p.p.m.

2-Bromo-1-fluoro-1-phenylethane (6)

Same procedure as for **2**, except that styrene (2.5 g) and bromine (5.0 g) in benzene (40 ml) were used; time of addition was 105 min.

Distillation under reduced pressure produced a clear liquid, 3.5 g (71%), b.p. 69° (1 mm), n_D^{25} 1.5409, ϕ_c +174.5 p.p.m.

The n.m.r. spectra demonstrated the position of the substituents: the partial ^1H spectrum has two identifiable regions, an AB and M region of an ABMX spectra (where X = ^{19}F). The 50 Hz J_{MX} positions the fluorine in the secondary position.

2-Iodo-1-fluoro-indan (7)

Again, the same procedure was used as for **1**, (indene (2.8 g) was reacted with iodine (9.0 g) and AgF (13.0 g)). Although the product could not be distilled without decomposition, the crude product after work-up was a clear liquid, whose n.m.r. spectra showed no impurities. Crude yield was 4.8 g (66%), ϕ_c +155.2 p.p.m., $^2J_{HF}$ 5.6 Hz, $^3J_{HF}$ 18 Hz. The structure is derived from the n.m.r. spectra which are similar to those of the bromo-compound discussed below.

This compound was extremely unstable and the pure liquid, obtained by eluting off a neutral silica gel column with light petroleum at low temperatures, decomposed at room temperature in seconds. Elution down an alumina column produced indene. Solid $NaCO_3$ was effective in preventing decomposition.

2-Bromo-1-fluoro-indan (8)

Indene (2.8 g) was reacted with bromine (6.0 g) and AgF (13.0 g) over 90 min and worked-up in the usual way. Crude yield was 5.1 g (88%), ϕ_c 160.4 p.p.m., $^2J_{HF}$ 55 Hz, $^3J_{HF}$ 17 Hz. Distillation was not possible, but (in contrast to **7**) the material could be purified by elution down an alumina column with light petroleum.

In the ^1H spectra the proton next to the fluorine (identified by the characteristic $^2J_{HF}$ 55 Hz) has only one other coupling into it. Hence the fluorine must be in the 1-position. Furthermore, the proton to slightly higher field, which must be *geminal* to the bromine atom, is split into 16 lines (thus four couplings) and must be in the 2-position. The n.m.r. spectra and conformation of **8** are discussed more fully in the accompanying paper (10).

cis- and trans-1,2-Difluoro-acenaphthene (9, 10)

Acenaphthylene (2.0 g) was dissolved in a stirred mixture of benzene (40 ml), acetonitrile (10 ml), and AgF (10 g). Iodine (4.0 g) was also dissolved in the same solvent mixture (40 ml) and this solution was then added dropwise to the acenaphthylene–AgF mixture over 1 h, with cooling (ice-bath) and stirring. The mixture was then poured into a larger volume of a saturated $NaHCO_3$ aqueous solution, mixed thoroughly, filtered, and the organic layer separated from the filtrate and washed with more water. Drying over Na_2SO_4 and Na_2CO_3 and removal of solvent produced a dark red viscous liquid, whose ^{19}F n.m.r. spectrum revealed the presence of at least two compounds.

This crude product mixture was then separated chromatographically by eluting down a neutral silica gel column with light petroleum (b.p. 37°). The column fractions were monitored by t.l.c., ^1H and ^{19}F n.m.r. First off the column was a small amount of starting material, quickly followed by fluoro-acenaphthylene (**11**) and 1-iodo-2,2-difluoro-acenaphthene (**14**), both in trace quantities; then came a major product, *trans*-1,2-difluoro-acenaphthene (**10**). Further elution with 20% CH_2Cl_2 in light petroleum produced *cis*-1,2-difluoro-acenaphthene (**9**), contaminated with some highly colored material. The fractions containing **9** and **10** were then purified by twice eluting them down silica gel columns as above.

[7]The literature value of the boiling point of **2** appears to be in error; a sample of **2** prepared by the literature method (9) had a boiling point in agreement with that reported here.

Can. J. Chem. Downloaded from www.nrcresearchpress.com by 210.87.254.6 on 09/05/12
For personal use only.

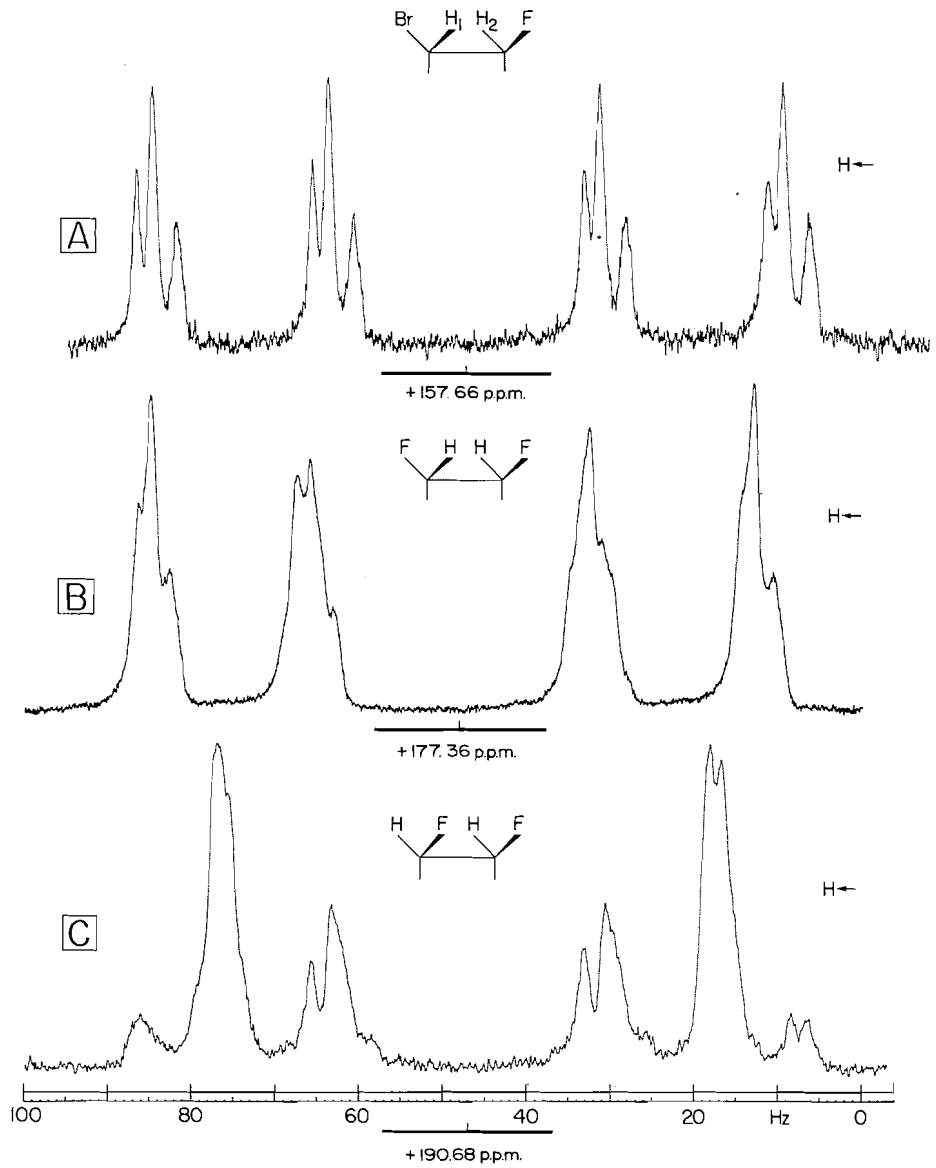

FIG. 1. ^{19}F n.m.r. (94.07 MHz) of the three major products of the 'XF' addition to acenaphthylene. A, *trans*-bromofluoride (**13**); B, *trans*-difluoride (**10**); C, *cis*-difluoride (**9**).

The ^1H spectrum of each is identical with its ^{19}F spectrum, which is a characteristic of A_2X_2 systems such as **9** and **10**; the ^{19}F spectra of each is shown in Figs. 1B and 1C and the ^1H spectra[8] in Figs. 2A and 2C. Decoupling of the aromatic protons of **10** produced a marked sharpening of the lines, as shown in Fig. 2B, but a similar decoupling experiment on **9** was a failure.

Crystalline samples of **9** and **10**, which were obtained by slow cooling of an ethanol–water solution, gave satisfactory elemental analyses.

Anal. Calcd. for $C_{12}H_{10}F_2$: C, 75.79; H, 4.21; F, 20.00. Found (*cis*): C, 75.95; H, 4.20; F, 19.80. Found (*trans*): C, 75.55; H, 4.00; F, 20.30.

Other physical data are:

	cis (**9**)	*trans* (**10**)
M.p. (°C)	113	47
$^3J_{HF}$ (Hz)	5.2	19.13
$^3J_{HH}$ (Hz)	5.1	1.23
$^3J_{FF}$ (Hz)	16.4	1.23
ϕ_c (p.p.m.)	190.68	177.36
τ_H	3.24	4.32

[8]Actually they are *partial* ^1H spectra, since the aromatic region is not shown.

Can. J. Chem. Downloaded from www.nrcresearchpress.com by 210.87.254.6 on 09/05/12
For personal use only.

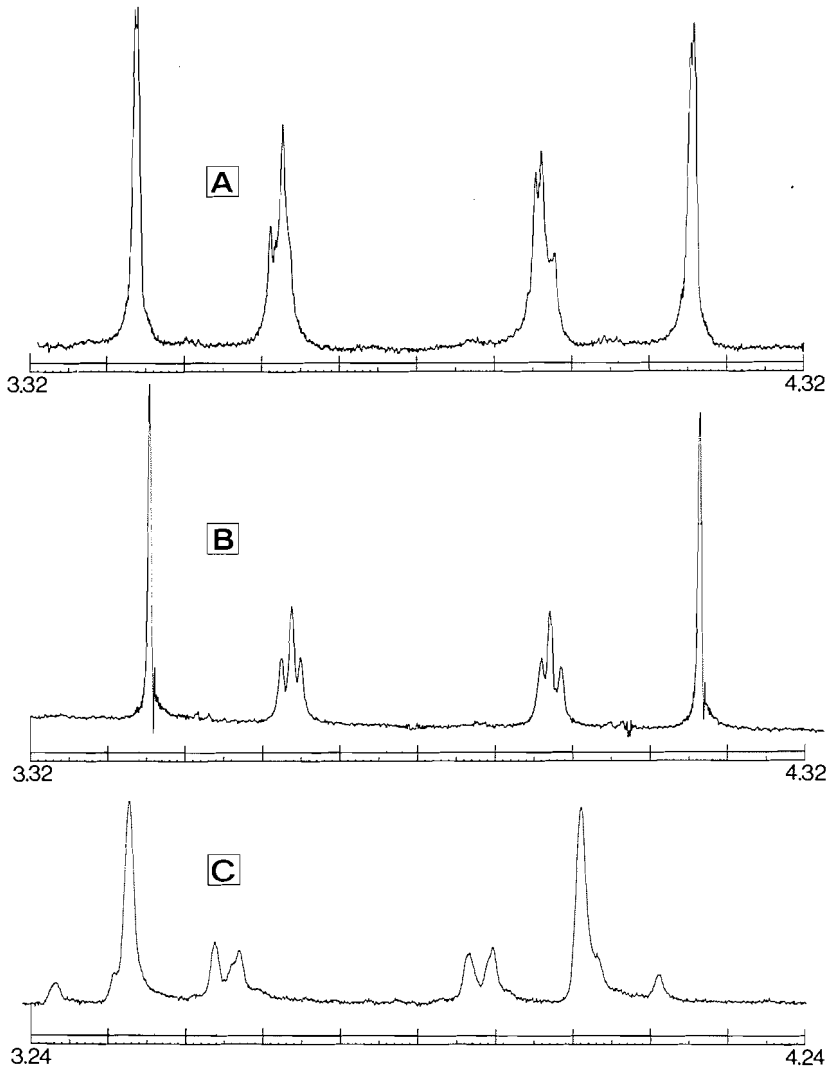

FIG. 2. Partial ^{1}H n.m.r. spectra (100 MHz) of the difluorides of acenaphthylene. A, the normal spectrum of the *trans*-difluoride (**10**); B, the same spectrum but measured with simultaneous irradiation of the aromatic protons; C, the normal spectrum of the *cis*-difluoride (**9**).

Although quantitative values for the yields could not be obtained, subjective estimates are 10% for the *trans*-isomer (**10**) and 5% for the *cis* (**9**). A series of experiments were carried out to optimize the yield; the percentage of benzene in the solvent was varied from 50–100% and an optimum yield was obtained in the range 80–90% benzene. However, the ratio of *trans*–*cis* was constant at 2:1. The analysis of the A_2X_2 n.m.r. spectra was done by hand;[9] agreement with Merritt and Johnsons' values (7) is good for the *cis*-isomer but rather poorer for the *trans*. This is understandable since the previous analysis would have been carried out on a spectrum such as Fig. 2A rather than 2B.

[9]A_2X_2 spectra consist of two unconnected sub-spectra and as such cannot be analyzed by an iterative computer procedure.

*trans-1-Bromo-2-fluoro-acenaphthene (**13**)*

A solution containing Br_2 (2.5 g) and benzene (25 ml) was added dropwise to a vigorously stirred suspension of finely powdered AgF in 50:50 benzene–acetonitrile at 0°. Simultaneously, another solution containing acenaphthylene (2.0 g) in benzene (25 ml) was also added.

This addition was carried out over a period of 20 min, after which the reaction mixture was immediately filtered, washed with $NaHCO_3$ solution, and then dried over Na_2SO_4–$CaSO_4$. The resulting light yellow solution was evaporated under vacuum to 5–10 ml[10] and then eluted down an alumina column with light petroleum. Apart from a small quantity of starting material (which runs very fast) the only product was **13**; the ^{19}F spectrum is

[10]Further concentration increases the possibility of decomposition.

Can. J. Chem. Downloaded from www.nrcresearchpress.com by 210.87.254.6 on 09/05/12
For personal use only.

shown in Fig. 1A and a partial ^1H spectrum in Fig. 3B. Decoupling of the aromatic protons revealed that this latter spectrum was the AB part of an ABX; this is shown above in Fig. 3A. Selective decoupling, not shown, of the left-hand doublet of H_2 collapsed the corresponding left-hand doublet in H_1. This confirms the analysis of spectra, and indicates that $^3J_{1F}$ has the same sign as $^2J_{2F}$. The small $^3J_{12}$, 1.0 Hz also indicates a *trans* relationship between Br and F.

The product **13** is very unstable and has to be kept well below 0° unless stabilized by solid $NaCO_3$. A concentrated pentane solution, cooled in Dry Ice deposited yellow crystals; however, they proved to have some solvent in them. A similar experiment with ethanol had the same result; however, the material deposited from this solution when warmed to −25° and pumped on for 4 h produced a crop of white–yellow crystals which had a sharp m.p. of 35° and whose ^1H n.m.r. showed no solvent present; they also gave satisfactory elemental analysis. The crystals were extremely unstable, being decomposed within minutes at room temperature.

Anal. Calcd. for $C_{12}H_{10}BrF$: C, 57.39; Br, 31.85; F, 7.57. Found: C, 57.16; Br, 31.59; F, 7.43.

τ_{H_1} 4.32; τ_{H_2} 3.52; ϕ_c 157.66 p.p.m.; $^3J_{HF}$ 21.4 Hz; $^3J_{HH}$ 1.0 Hz.

The product **13** could be distinguished from acenaphthylene with t.l.c.; the two compounds ran very close together (**13** last) but upon charring with concentrated H_2SO_4, acenaphthylene gives a green color whereas **13** turns brown.

1-Fluoro-acenaphthylene (11)

Following the procedure of Merritt and Johnson (7), *cis*-difluoroacenaphthene (**9**) (1.0 g) was heated under reflux with KOH (3 g) in ethanol (50 ml) for 5 h. The ^{19}F n.m.r. spectrum of the crude product indicated that most of the starting material had reacted. The product mixture was worked-up by removing most of the ethanol *in vacuo*, dissolving in petroleum ether and washing with water. The organic layer was dried, filtered, and concentrated again, prior to separation on a neutral silica gel column with pentane–benzene (70:30). The product **11** ran ahead of the starting material (**9**) and gave a characteristic yellow color to the solution.

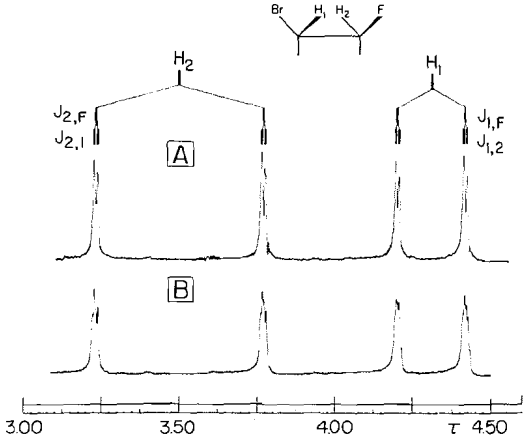

FIG. 3. Partial ^1H n.m.r. (100 Hz) of 1-bromo-2 fluoro-acenaphthene (**13**). A, the spectra measured with simultaneous irradiation of the aromatic protons; B, the normal spectrum.

Spectroscopically (^1H and ^{19}F n.m.r.), this material appeared to be free of impurities; however, small amounts of acenaphthylene itself which were undetected in the n.m.r. spectrum were picked out on a t.l.c. plate (very slightly ahead of **11**). Therefore the material was rerun down an extra long column (60 in.) of neutral silica gel with pentane; this removed the residual acenaphthylene. The two compounds could be distinguished on a t.l.c. plate by the fact that fluoro-acenaphthylene (**11**) fluoresces under u.v. light whereas acenaphthylene does not.

A crystalline sample of **11** was obtained by cooling a pentane solution to −78°; m.p. 37°, yellow plates (previously reported as oil). ^1H n.m.r. singlet at τ 4.00 (besides aromatic region), ^{19}F n.m.r. singlet at ϕ_c 99.4 p.p.m.; no impurity peaks were detected.

The reaction yield was high (from ^{19}F n.m.r.) but not quantitative. Significant amounts of starting material remained even with long reaction times (24 h) or high alkalinity of the solution. Use of *trans*-difluoro-acenaphthene (**10**) lowered the yield somewhat.

1-Bromo-2,2-difluoroacenaphthylene (12)

Bromine (0.4 g) in benzene (5 ml) was added over 20 min to a stirred solution of fluoro-acenaphthylene (**11**) (0.20 g) in acetonitrile (50 ml), containing powdered AgF (4.0 g). After the reaction, bicarbonate solution was added and the whole mixture filtered; the organic layer was separated, dried, filtered, and concentrated. ^{19}F n.m.r. of this material showed strong resonance which was evidently the AB-part of an ABX spectrum, and identified the main product as **12**; this was the same spectrum as that picked up weakly in the 'BrF' addition to acenaphthylene. This was analyzed (with TWOSUM) to give the following parameters: J_{AB} 253.65 Hz ($^2J_{H_1F_2}$ (*gem*)), J_{AX} 15.28 Hz ($^3J_{HF_1}$ (*cis*)), J_{BX} 3.72 Hz ($^3J_{HF_2}$ (*trans*)), ν_{AB} = 237.14 Hz (2.52 p.p.m.), τ_H 4.23, $\phi_c(F_1)$ 88.3 p.p.m.; $\phi_c(F_2)$ 85.8 p.p.m.

1-Iodo-2,2-difluoroacenaphthene (14)

'IF' did not react with 1-fluoro-acenaphthylene (**11**) under a variety of conditions, including as solvent acetonitrile, 60:40 benzene–acetonitrile, and benzene.

A small quantity of the desired product (**14**) was retrieved from the 'IF' reaction with acenaphthylene; after two chromatographic separations a spectroscopically pure sample was obtained, with a yield of only 0.2%. The large geminal F–F coupling (252 Hz) and the presence of only one other spin coupling into each ^{19}F resonance identified the product. The quartet in the ^1H spectrum confirmed this; $\phi_c(F_1)$ 75.8 p.p.m., $\phi_c(F_2)$ 87.5 p.p.m., τ_H = 4.24, $^2J_{FF}$ 252 Hz, $^3J_{HF_2}$ (*cis*) 16.26 Hz, $^3J_{HF_1}$ (*trans*) 4.24 Hz.

1-Bromo-1-fluoro-acenaphthene (15)

Fluoro-acenaphthylene (**11**) (0.30 g) was dissolved in dichloromethane and cooled to −78°; HBr gas was then bubbled in slowly until the characteristic yellow color of **11** had disappeared (15 min), leaving a cream-colored solution. The solvent and excess HBr were then removed *in vacuo*, leaving a light brown solid. All chromatographic treatment of this material ended in decomposition.

Can. J. Chem. Downloaded from www.nrcresearchpress.com by 210.87.254.6 on 09/05/12
For personal use only.

The ^1H spectrum showed only a single ABX spectrum (AB-part) in the methylene region; the ^{19}F spectrum contained only a quartet at low field, with total width of 33 Hz, thus ruling out any *geminal* H–F coupling.The product must then be 15: τ_{H_1} 6.14, τ_{H_2} 6.00, ϕ_c 79.8 p.p.m., $^2J_{HH}$ 18.3 Hz, $^3J_{HF}$ (*cis*) 22.8 Hz, $^3J_{HF}$ (*trans*) 10.3 Hz.

1-Chloro-1-fluoro-acenaphthene (16)

The same reaction was performed as above, substituting HCl for HBr, with similar results; again no vicinal products were observed. Pentane was an equally good solvent for the reaction, which appeared (spectroscopically) to be quantitative: $\tau_{H_1} \simeq \tau_{H_2}$ 5.775, ϕ_c 81.3 p.p.m. ($^3J_{HF}$ (*cis*) + $^3J_{HF}$ (*trans*)) 32.8 Hz.

1,1-Difluoroacenaphthene (17)

A solution of **15** (40 mg) in acetonitrile was shaken with AgF (0.20 g) at 20° for 20 min. The solid matter was filtered off and the acetonitrile removed *in vacuo*; t.l.c. showed two compounds both running fast, on silica gel. ^{19}F n.m.r. of this material indicated two resonances; the weaker one was fluoro-acenaphthylene (**11**) and the other a triplet resonating at somewhat higher field than either **15** or **16**. ^1H n.m.r. again showed the singlet at low field, characteristic of **11** and also a triplet at lower field than that for either **15** or **16**. Integration of this region showed it to contain two protons (by comparison with aromatic region). Integration of the ^{19}F resonances gave the product ratio of 17:11 as 81%:19% (allowing for two fluorines in **17**).

Substituting **16** for **15** in this reaction and allowing 1 h reaction time gave substantially the same result, thus confirming that the new product **17** is the *gem*-difluoride. The identical triplets observed in both the ^1H and ^{19}F spectra are again characteristic of an AA′XX′ system; this time the large $J_{AA'}$ ($^2J_{FF}$ 250 Hz) effectively reduces the spectra to a true A_2X_2 (in which $J_{AX} = J_{A'X'}$ etc). This feature, which was verified by generating a theoretical spectrum using a reasonable set of parameters, is rather unfortunate since only the *sum* of the *vicinal* couplings may be extracted. The *geminal* couplings cannot be measured at all.

An attempt was made to get around this problem by selective deuteration; DBr was synthesized from PBr_3 (15 ml) according to the procedure in Shoemaker and Garland (12). This was then reacted with **11** in the same way as before to produce **15**-d_1, and exchanged with AgF to give **17**-d_1. This product was purified successfully by eluting down neutral silica gel with petroleum ether, but the ^1H spectrum again showed a broad[11] triplet with shoulders which could not be decoupled from the aromatic region; the latter region itself was very broad (> 75 Hz). The only parameters which can be extracted therefore are: ϕ_c 84.5 p.p.m.; τ_H 6.52, ($^3J_{HF}$ (*cis*) + $^3J_{HF}$(*trans*)) 26.4 Hz.

[11]The spectrum of a deuterated compound such as **17**-d_1 has been thoroughly investigated by Kanazawa and Baldeschewieler (13) and as such is capable of analysis, provided that a reasonably well-resolved spectrum can be obtained. However, the extreme broadness of the lines prevents one from observing the weak transitions which are necessary to obtain the full analysis of the spectrum.

cis-1,2-Dibromo-1-fluoro-acenaphthene (18) and trans-1,2-Dibromo-1-fluoro-acenaphthene (19)

To fluoro-acenaphthylene (**11**) (0.20 g) was added Br_2 (0.20 g) as a CCl_4 solution, over 15 min at 20°. ^1H and ^{19}F n.m.r. showed that there were two products, of which the predominant one (89%) had a small $^3J_{HF}$ and was therefore assigned as the *trans* adduct. *cis* (**18**) (11%) ϕ_c 83.8 p.p.m., τ_H 4.30, $^3J_{HF}$ (*cis*) 18.9 Hz. *trans* (**19**) (89%) ϕ_c 89.7 p.p.m., τ_H 3.94, $^3J_{HF}$ (*trans*) 3.1 Hz (all in benzene solution). The reaction was performed in CH_3CN with the same result.

cis-1,2-Iodochloro-1-fluoro-acenaphthene (20) and trans-1,2-Iodochloro-1-fluoro-acenaphthene (21)

ICl (220 mg) was added to fluoro-acenaphthylene (**11**) in the same way as above. ^1H and ^{19}F n.m.r. again revealed two products; the predominant one having the smallest $^3J_{HF}$ was assigned the configuration with iodine and chlorine *trans*. The product ratio was also similar, 5:1 in favor of the *trans* (ICl) adduct. *cis* (**20**) (16%) ϕ_c 82.2 p.p.m., τ_H 3.67, $^3J_{HF}$ 19.7 Hz. *trans* (**21**) (84%) ϕ_c 74.9 p.p.m., τ_H 3.68, $^3J_{HF}$ 6.0 Hz (both in CCl_4 solution).

cis-1-Chloro-2-fluoro-acenaphthene (22) and trans-1-Chloro-2-fluoro-acenaphthene (23)

Powdered AgF (8 g) was added to an acetonitrile solution (50 ml) of acenaphthylene (2.0 g) and the mixture cooled with an ice-bath. ICl (2.0 g), dissolved in acetonitrile (30 ml), was then added over 20 min to this mixture, with stirring. At the end of this period, the reaction was worked-up in the usual way. ^{19}F n.m.r. of this crude product revealed two resonances in the ratio 85:15, and it was immediately eluted down a neutral silica gel column with petroleum ether – benzene.

Three compounds were separated; the first and major component contained no fluorine and showed a sharp singlet at τ 4.45, indicating that it was the *trans*-dichloride of acenaphthene; the mass spectrum, melting point and elemental analysis confirmed this.

The second compound, running close behind, gave ^{19}F and ^1H n.m.r. spectra almost identical with that of **13** (see Figs. 1A and 3A) and was assigned as the *trans*-chlorofluoride (**23**). The last component, a minor one, was evidently the *cis*-chlorofluoride (**22**), since there were two low-field protons with a coupling between them of 6.0 Hz (expected for $^3J_{HH}$, $\phi = 0°$), which were coupled to fluorine. The n.m.r. parameters in benzene solution are:

	cis (**22**)	*trans* (**23**)
$^3J_{HF}$ (Hz)	10.0	21.0
$^2J_{HF}$ (Hz)	53.7	53.5
$^3J_{HH}$ (Hz)	6.0	1.0
τ_{H_1}	4.87	4.53
τ_{H_2}	4.36	3.77
ϕ_c (p.p.m.)	173.3	162.5

1-Fluoro-acenaphthene (25)

One gram of **24** was shaken with powdered AgF (2.0 g) for 20 min in acetonitrile at room temperature. The grey precipitate and excess AgF was filtered off and water and chloroform added to the solution. The organic layer was separated, dried, and concentrated down carefully without heating. The ^1H spectrum showed a set of broad lines

Can. J. Chem. Downloaded from www.nrcresearchpress.com by 210.87.254.6 on 09/05/12
For personal use only.

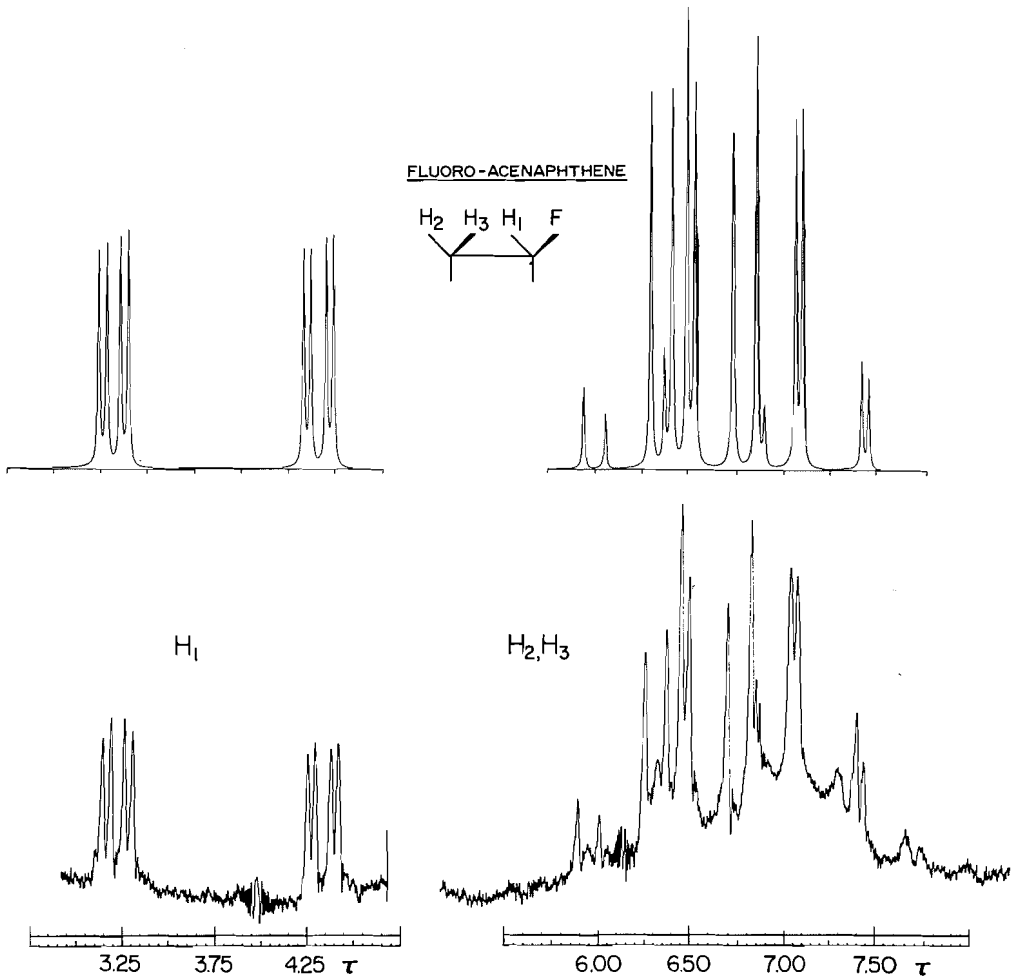

FIG. 4. Partial ^1H n.m.r. spectra of 1-fluoro-acenaphthene. The lower trace shows the spectrum measured with simultaneous irradiation of the aromatic protons. The upper trace is the computer simulation using the parameters listed in the text. The sample used could not be purified and hence contained some impurities.

in the methylene region and an octet at low field. By careful adjustment of the solvent, the complexity of the spectrum was reduced as much as possible (with 60% chloroform, 40% acetone). The lines were further sharpened by decoupling of the aromatic protons, and this double resonance (^1H) spectrum is shown in Fig. 4, bottom.

The spectrum was then analyzed by hand as an ABMX system; values from this analysis were used as the input numbers for an iterative computer analysis of the spectrum using TWOSUM. The final computer spectrum, which is shown above in Fig. 4, top, had an average deviation of only 0.028 Hz from the experimental.

Some impurity lines are visible in Fig. 4; it was found impossible to purify **25** in any way at all, since it decomposed on alumina and silica gel, and with gentle heat, weak acid or base. N.m.r. parameters: $^3J_{H_3F}$ (*cis*) 29.52 Hz, $^3J_{H_1H_2}$ (*cis*) 6.68 Hz, $^3J_{H_2F}$ (*trans*) 21.39 Hz, $^3J_{H_1H_3}$ (*trans*) 1.485 Hz, $^2J_{H_2H_3}$ (*gem*) 18.30 Hz, $^2J_{H_1F}$ (*gem*) 55.59 Hz, τ_{H_1} 3.665, τ_{H_2} 6.458, τ_{H_3} 6.661, ϕ_c 158.8 p.p.m.

Nuclear Magnetic Resonance Measurements

All n.m.r. measurements were made with a modified Varian HA-100 instrument (14) operating in the locked modes of operation, using appropriate reference substances; all proton chemical shifts are given with respect to tetramethylsilane and fluorine shifts (ϕ_c values) are with respect to fluorotrichloromethane (freon 11).

Spectra for analysis purposes were run on appropriate sweep widths, usually 100 Hz, and were fully calibrated.

Analyses of the n.m.r. spectra were often performed by long-hand methods. Computer based analyses used the programme TWOSUM, kindly provided by Dr. John Martin of the University of Alberta, Edmonton, and the

IBM 7040 computer at the University of British Columbia Computer Centre. A plotting routine SMASH was written by Mr. John Coulthard of the U.B.C. Computer Centre and was used in conjunction with a Calcomp plotter.

It is a pleasure to thank the National Research Council of Canada and Imperial Oil Ltd. for their financial support of this work.

1. L. D. HALL, D. L. JONES, and J. F. MANVILLE. Chem. and Ind. (London), 991 (1965).
2. (*a*) L. D. HALL and J. F. MANVILLE. Chem. Commun. 35 (1968). (*b*) L. D. HALL and J. F. MANVILLE. Can. J. Chem. **47**, 361 (1969).
3. H. SCHMIDT and H. MEINERT. Angew. Chem. **71**, 126 (1959); **72**, 109 (1960); **72**, 493 (1960).
4. R. H. ANDREATTA and A. N. ROBERTSON. Aust. J. Chem. **19**, 1961 (1966).
5. L. D. HALL and D. L. JONES. Can. J. Chem. **51**, 2915 (1973).
6. S. J. CRISTOL, F. R. STERNITZ, and P. S. RAMEY. J. Am. Chem. Soc. **78**, 4939 (1956).
7. R. F. MERRITT and F. A. JOHNSON. J. Org. Chem. **31**, 1859 (1966).
8. M. J. S. DEWAR and R. C. FAHEY. J. Am. Chem. Soc. **85**, 2245 (1963).
9. A. BOWERS, L. C. IBANEZ, E. DENOT, and R. BECERRA. J. Am. Chem. Soc. **82**, 4001 (1960).
10. L. D. HALL and D. L. JONES. Can. J. Chem. **51**, 2925 (1973).
11. L. D. HALL and D. L. JONES. Can. J. Chem. **51**, 2930 (1973).
12. D. P. SHOEMAKER and C. W. GARLAND. Experiments in physical chemistry. McGraw-Hill, New York. 1963.
13. Y. KANAZAWA and J. D. BALDESCHWIELER. J. Mol. Spectrosc. **16**, 325 (1965).
14. R. BURTON and L. D. HALL. Can. J. Chem. **48**, 59 (1970).

Can. J. Chem. Downloaded from www.nrcresearchpress.com by 210.87.254.6 on 09/05/12
For personal use only.

Conformational Analysis of *trans*-1-Fluoro-2-iodocyclohexane: a Nuclear Magnetic Resonance Study[1]

L. D. HALL AND D. L. JONES

Department of Chemistry, The University of British Columbia, Vancouver 8, British Columbia

Received November 1, 1971[2]

The ^1H and ^{19}F n.m.r. spectra of the title compound and its 3,3,6,6-tetradeutero analog have been measured in a variety of solvents and over a wide range of temperatures. These measurements have been used as the basis of calculations of the thermodynamic and kinetic parameters for the chair–chair conformational equilibrium of this substance. The poor agreement between the different methods of evaluating ΔG is discussed.

Les spectres r.m.n. du proton et du fluor des composés-titres et de leurs analogues 3,3,6,6-tétradeutériés ont été mesurés dans plusieurs solvants et des températures très variés. Ces mesures ont été utilisées pour calculer les paramètres thermodynamiques et cinétiques de l'équilibre conformationel chaise–chaise de ces substances. La corrélation très faible qui existe entre les différentes méthodes d'évaluation du ΔG est discutée. [Traduit par le journal]

Can. J. Chem., **51**, 2914 (1973)

Introduction

We have been concerned for a number of years with the development of methods for synthesizing specifically fluorinated organic substances and with the evaluation of the stereospecific dependencies of ^{19}F n.m.r. parameters (2). An important stage of these continuing studies was to be an intercomparison of the effectiveness of different proton and fluorine n.m.r. parameters for studying chemical equilibria: the unsymmetrically fluorinated derivative, *trans*-1-fluoro-2-iodocyclohexane (1) which had become available as the result of work described in an accompanying paper (3) was ideally suited for this purpose.

Prior to this study Bovey and his coworkers (4) had made a detailed n.m.r. study of cyclohexyl fluoride and we shall refer to their work later in this paper. Roberts and his group (5) had extensively used fluorine as a conformational probe: their approach differs somewhat from our own insofar as they chose deliberately to retain the internal symmetry of the six-membered ring by using a CF_2 group and for this reason alone we shall make no further reference to their many excellent studies.

Results and Discussion

The derivatives chosen for this study were *trans*-1-fluoro-2-iodocyclohexane (**1**) and the corresponding 3,3,6,6-tetradeutero analog (**1**-d_4). Both substances were conveniently synthesized (3) by the stereospecific addition of the elements of "IF" (generated *in situ* from I_2 and AgF) to the corresponding cyclohexene. At room temperature, the ^1H spectrum of the IF adduct of cyclohexene (**1**) consists of two regions;

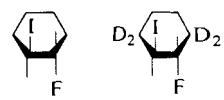

1 **1**-d_4

(*i*) 5–6 τ showing resolvable fine structure and assignable to the methine protons; and (*ii*) a high field region, of poorer resolution, which integrates to four times the area of *i*. This spectrum will not be considered further, owing to the greater simplicity of the spectrum of **1**-d_4.

Part of the ^1H n.m.r. spectrum of **1**-d_4 is shown in the lower trace of Fig. 1; the upper trace shows the same spectrum with irradiation of the deuterium nuclei. This spectrum is clearly the AB part of an ABX-system[3] and

[1]This paper forms Part IV of a series entitled, "The Conformations of Cyclic Compounds in Solution". For Part III see ref. 1. An account of this work was given at the 51st Canadian Chemical Conference of the Chemical Institute of Canada, Vancouver, British Columbia, June 3–5, 1968. Full details were published in the M.Sc. Thesis of D. L. Jones, University of British Columbia, 1970.

[2]Revision received February 23, 1973.

[3]Two small, long-range couplings are also present; their source is unknown.

Can. J. Chem. Downloaded from www.nrcresearchpress.com by 210.87.254.40 on 09/05/12
For personal use only.

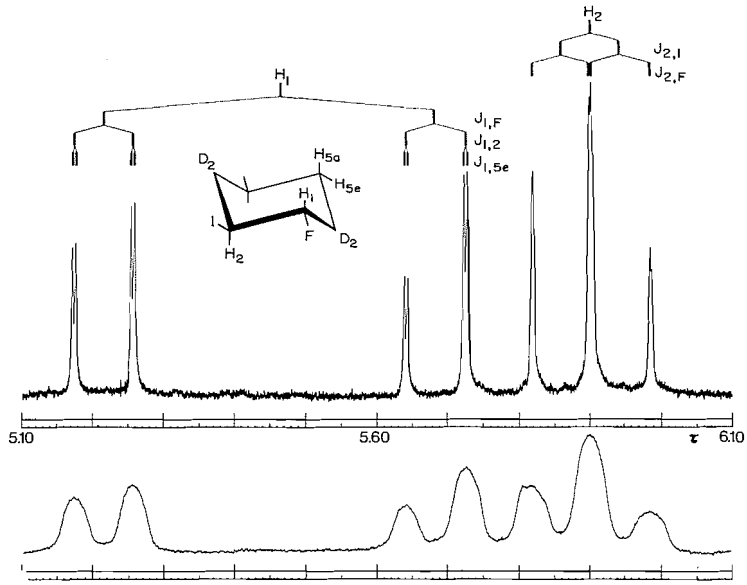

FIG. 1. Partial ^{1}H n.m.r. spectra (100 MHz) of 1-fluoro-2-iodo-cyclohexane-3,3,6,6-d_4 (**1**-d_4) in CS_2 solution at room temperature. The lower trace shows the normal resonances of the H_1 and H_2 protons. The upper trace shows the same resonances with simultaneous irradiation at the deuterium resonance frequency. The two traces were run at different gains. Note the additional long-range couplings in each of the resonances: that in H_1 is *ca.* 0.3 Hz.

the 8 Hz coupling indicates that H_1 and H_2 are *diaxial*, and hence *trans* to one another. This identifies the primary conformation of the molecule as that having both the I and F substituents equatorially oriented, as in **B**, and also confirms the stereospecificity of the addition reaction.

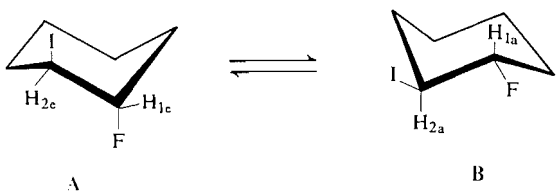

A B

The room temperature ^{19}F spectra of both **1** and **1**-d_4 consist of broad doublets spacing approximately 50 Hz, corresponding to $^2J_{HF}$, and little information can be gained from them alone.

It is convenient to divide the remainder of the discussion into two separate sections. The first will deal with various evaluations of the free energy differences between the two conformers and the second with the determination of the activation parameters of the chair–chair equilibrium (**A** $\rightleftarrows$ **B**).

Evaluation of the Conformation Equilibrium

In this section we shall first describe the measurements which were made and then give a brief discussion of their significance.

(*a*) ^{1}*H Spectra*

The ^{1}H spectrum (with ^{2}H-decoupling) of **1**-d_4 in CS_2 solution at $-100°$ is shown in Fig. 2A; here the two chair conformations of the molecule (**A**, **B**) have been 'frozen out' and *two* ABX spectra are observed.

Each of these two ABX spectra were analyzed without using the X part;[4] this analysis yields the values of the various coupling constants in each conformer at $-100°$, in CS_2 solution. A calculated composite spectrum, based on this analysis is shown in Fig. 2B. Using these values, the position of the conformational equilibrium at room temperature may be calculated from

[4]It is possible to analyze an ABX spectrum purely from the AB part providing one has some prior knowledge of J_{AX} and J_{BX}. In this case, the geminal ^{1}H–^{19}F coupling, $^2J_{HF}$ (= J_{AX}), can be safely assumed to be of the same sign as $^2J_{HF}$, but considerably smaller (6).

All these partial ABX spectra were subjected to iterative computer analysis. In order to link up the energy levels, it is necessary to put in a 'false' X-transition, the frequency of which may be calculated from the AB part, with the above considerations in mind.

Can. J. Chem. Downloaded from www.nrcresearchpress.com by 210.87.254.40 on 09/05/12
For personal use only.

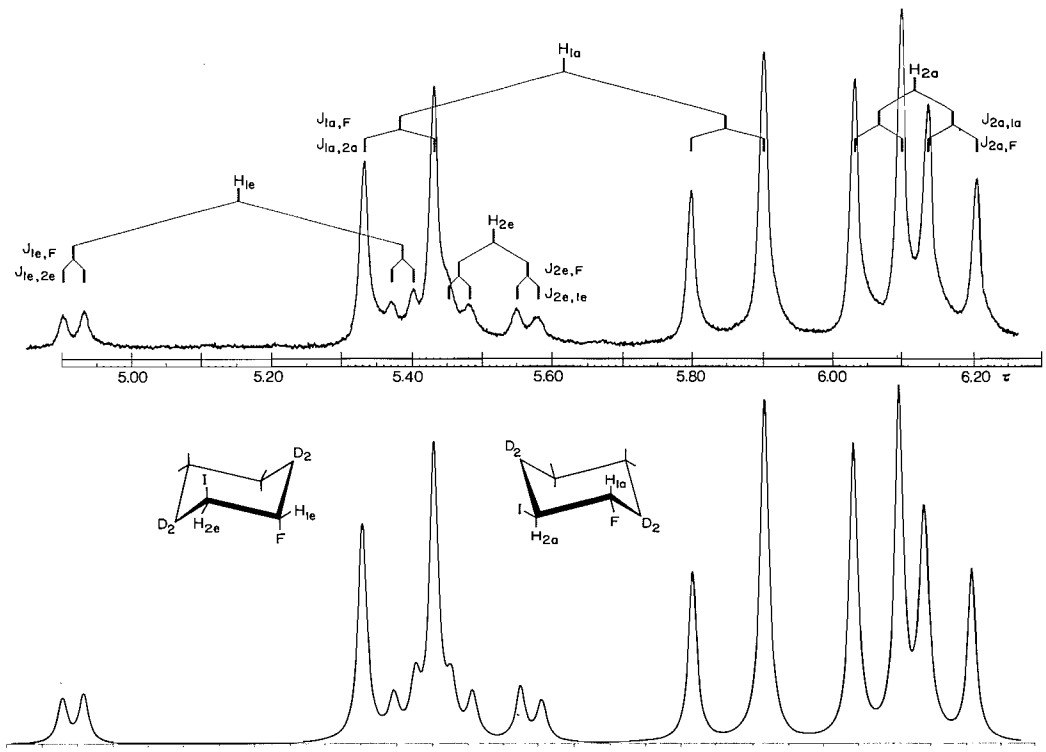

FIG. 2. Partial ^{1}H n.m.r. spectra (100 MHz) of 1-fluoro-2-iodo-cyclohexane-3,3,6,6-d_4 (**1**-d_4) in CS_2 solution at $-100°$ with deuterium decoupling. The upper trace shows the experimental spectrum and the lower a line-plot of the calculated spectrum.

the value of the coupling constants in the time-averaged spectrum (obtained at room temperature), Fig. 1.

Furthermore, the position of the equilibrium may also be determined[5] in other solvents by use of these low temperature values; the spectrum of **1**-d_4 in benzene, chloroform, acetone, and pentane were therefore obtained, and the results are summarized in Table 1. Also shown are equilibrium calculations based on the ^{1}H chemical shifts.

(b) ^{19}F Spectra

The ^{19}F spectrum of **1** in CS_2 solution at $-100°$ is shown in Fig. 3B; the expanded spectrum of the minor conformer (Fig. 3C) exhibits a second large splitting (*ca.* 43 Hz) which is conformatory evidence that the minor conformer is **A**.

Using ^{1}H-decoupling, the ^{19}F spectra of **1** was recorded in CS_2 solution at various temperatures between 0 and $-85°$. With ^{1}H couplings removed, the major contribution to the linewidth in this region is the exchange broadening. The widths and positions of various resonances from these spectra are given in Table 2A. It can be seen that at either end of the temperature scale, the peak positions are not static; since this was contrary to results already in the literature, the low temperature spectra were later retaken, but without ^{1}H-decoupling. These data are also included in Table 2A; there is a difference in the absolute value of the peak positions of the two sets of data (decoupled and normal spectra). This is because different samples were used, the original one having decomposed.

Calculation of the Free Energy Value

The experiments described above provide five different sets of parameters which were used as the basis of separate evaluations of the conformational free energy difference, ΔG^0.

[5]All of these calculations assume temperature independence of the respective parameters; this is discussed further later on.

Can. J. Chem. Downloaded from www.nrcresearchpress.com by 210.87.254.40 on 09/05/12
For personal use only.

TABLE 1. N.m.r. parameters of **1**-d_4 in various solvents and percentage population of the diaxial conformer **A**

	Solvent						
Parameter	$CDCl_3$	Pentane	Benzene	Acetone	CS_2 at room temperature	CS_2 at −100°*	CS_2 at −100°†
J_{AB}	8.3_2	7.7_6	8.4_2	8.8_5	7.8_5	10.0_6	3.0_3
J_{AX}	47.5_6	47.5_0	47.6_6	47.8_3	47.6_4	47.6_0	47.4_6
J_{BX}	7.5_8	7.6_0	7.3_5	7.1_6	7.4_2	6.0_9	9.9_2
ν_A	547.0_5	550.1_5	571.2_2	548.4_2	554.4_4	565.3_5	518.4_2
ν_B	591.1_0	591.9_3	620.8_7	585.6_9	594.7_3	613.8_7	555.0_8
Average deviation	0.098	0.059	0.012	0.014	0.022	0.019	0.046
	% diaxial conformer (**A**)						
By $^3J_{HH}$	25.0	32.8	23.4	17.3	31.4		
$^3J_{HF}$	38.9	34.3	28.5	27.8	34.8		
ν_A					23.2		
ν_B					27.2		

*Parameters for diequatorial conformer **B**.
†Parameters for diaxial conformer **A**.

(a) Vicinal Coupling Constants ($^3J_{HH}$ and $^3J_{HF}$)

Using $^3J_{HH}$ from Table 1 the fraction of **1**-d_4 existing in the diaxial conformation is calculated to be 0.314; from values of $^3J_{HF}$ the fraction is 0.348. These values correspond to $\Delta G^0 =$ 0.478 and $= 0.397$ kcal/mol respectively. The difference between these numbers may represent a systematic error in the method, in particular a temperature dependence of the coupling constants, or it may just reflect the inaccuracy of experimental data; it is worth noting that an error of only 0.4 Hz in the value of $^3J_{HF}$ in either conformer would account for the difference, and the spectrum of the diaxial conformer is rather difficult to measure accurately (see Fig. 2A).

To be more specific, the first-order value of $^3J_{HF}$ taken from the low-temperature ^{19}F spectrum of **1** (Fig. 3C) is actually 11 Hz, 1.1 Hz more than the value calculated from the low temperature ^1H spectrum (Fig. 3A). Thus this inaccuracy of measurement appears to be a most likely source of error.

It is interesting at this point to consider some similar work by Anet (7) who used a specifically-deuterated cyclohexanol and its associated reference compounds (*cis*- and *trans*-4-*t*-butyl derivatives). From the various observed coupling constants, two independent calculations of the position of the equilibrium can be made; the fraction of the minor conformer is respectively calculated as 0.16 and 0.29. The reason for this discrepancy was not given; however, it seems possible that there is an appreciable *temperature dependence* of the coupling constants involved in both Anet's work and the present study.

Turning to solvents other than CS_2, the data in Table 1 indicate that for solvents which are non-polar like CS_2 (*i.e.* pentane, benzene) the agreement between $^3J_{HH}$ and $^3J_{HF}$ calculations is reasonable, whereas for the polar solvents acetone and chloroform, the agreement is quite poor. In fact, the gap between $^3J_{HH}$ and $^3J_{HF}$ calculations is too large to be attributable to experimental error (14% for chloroform) and this seems to indicate that the coupling constants are subject to a *solvent dependence* (8). There is certainly some precedent for this phenomenon; thus Stothers (9) determined the equilibria of 2-halocyclohexanones by comparison with the *cis*- and *trans*-4-*t*-butyl derivatives and used $J_{AX} + J_{BX}$ as well as chemical shifts. A variety of solvents were tried, and $J_{AX} + J_{BX}$ in the *cis* compound was found to vary from 5.7 (in cyclohexane) to 7.1 Hz (in acetonitrile).

(b) Areas

By integrating the individual peaks of the low temperature ^{19}F spectrum (*e.g.* Fig. 3B), the fraction of **1** in diaxial form was calculated as 0.153 at −90°; this corresponds to $\Delta G^0 =$ 0.625 kcal/mol.

Can. J. Chem. Downloaded from www.nrcresearchpress.com by 210.87.254.40 on 09/05/12
For personal use only.

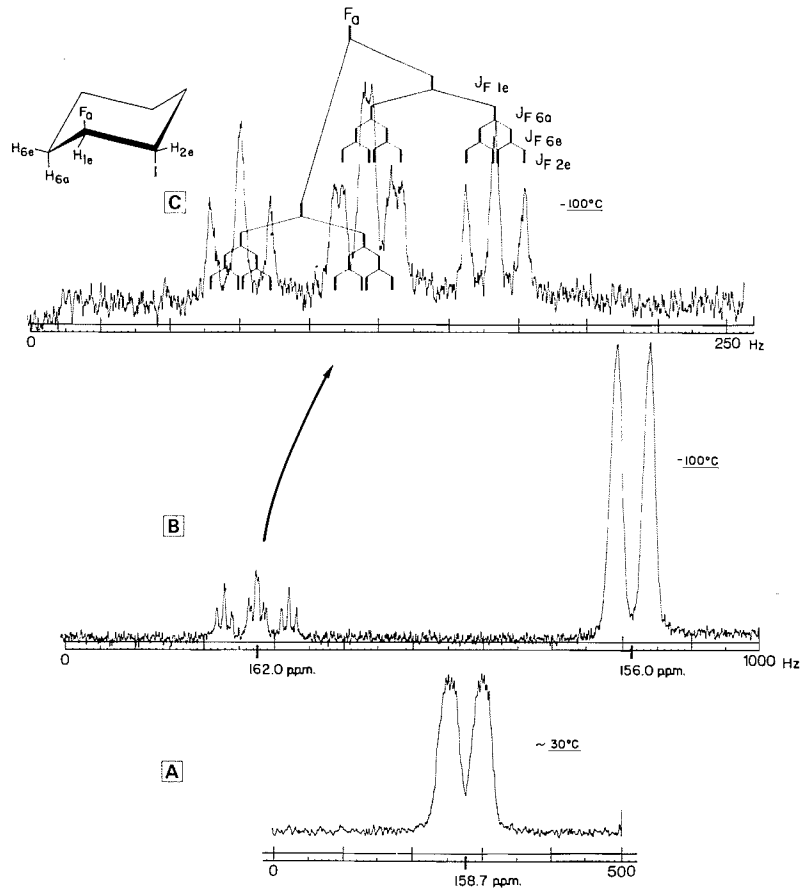

FIG. 3. ^{19}F n.m.r. spectra of 1-fluoro-2-iodo-cyclohexane (**1**) in CS_2 solution. A, shows the spectrum measured at room temperature; B, shows the spectrum measured at $-100°$, and C is an expansion of the low-field component of B. The first order assignment of this resonance, which corresponds to the axial fluorine substituent of conformer **A**, is also given. All chemical shifts are with respect to internal $CFCl_3$.

The areas of the equatorial and axial ^{19}F peaks were also measured under conditions of ^1H-decoupling. The intensities of both peaks were increased by about a factor of two, but the ratio stayed approximately constant (fraction diaxial = 0.150, Table 2B). Thus there appears to be a general (and favorable) *Overhauser effect* with ^1H-decoupling, but in this case it is not stereospecific.

(c) ^{19}F Chemical Shifts

The ^{19}F peak positions of **1** listed in Table 2A show that from $-65°$ to $-95°$ there is a fairly regular decrease[6] of 0.9 Hz per degree and from 0 to $-30°$ there is an average decrease of 1.2 Hz per degree. In the next section it will be shown that, from exchange considerations alone, the peak position is essentially invariant of temperature, approximately 20° on either side of the coalescence point; in this case the coalescence point can readily be seen to be approximately $-45°$. These calculations of when the peak positions are independent of temperature are not in accord with the statement in ref. 4: "Approximate calculations of the ^{19}F peak shift *versus* temperature ... showed that at temperatures of about 15–20° and above, the shift has become independent of the rate of conformational change ...." The input parameters for their calculation are of course different from the present one, but it can be shown that this does not significantly alter the conclusion. Examination of Table II in ref. 4

[6]This refers to the major, diequatorial, conformer.

Can. J. Chem. Downloaded from www.nrcresearchpress.com by 210.87.254.40 on 09/05/12
For personal use only.

TABLE 2A. ^{19}F Spectra of **1** as a function of temperature

	^1H-Decoupled spectra*			Normal spectra*	
	Major peak				
Temperature (°K)	Position	Width	Minor peak Position	Major peak position	Minor peak position
273	14 920.0	5.0			
263	908.0	9.5			
258	902.6	13.5			
253	896.2	20			
248	889.5	29			
243	882.5	36			
238	871.0	55			
233	858.0	89			
228	825.5	114			
223	792.5	86			
218	764.0	69.5			
213				14 711	15 213
208	746.5	21.4	15 264	14 704	15 221
203				14 701	15 227
198	736.5	5.6	15 265.5	14 695	15 227
193				14 693	15 224
188	14 727.5		15 260.5	14 689	15 222
183				14 684	15 219
178	(Frozen sample)		15 253.5	14 678	15 215

TABLE 2B. Area measurements

	Decoupled (%)		Normal (%)	
Temperature (°K)	Diequatorial	Diaxal	Diequatorial	Diaxal
183	85.0	15.0	84.7	15.3

*Two different samples were used, one for the data on the left hand side of Table 2A (*i.e.* ^1H-decoupled spectra) and the data in Table 2B, and the other for the data on the right-hand side of Table 2A (simple spectra). The first was approximately 20% in CS_2 solution (by volume), but the second one was more dilute, to permit more lengthy low-temperature measurements.
Peak positions are in Hz upfield of $CFCl_3$ resonance (internal).

shows the same kind of behavior as that described here, *i.e.* the peak positions continue to move to low field far away from the coalescence point. Evidently, either the individual chemical shifts of the two conformers are temperature dependent, or else the chemical shift of $CFCl_3$ is temperature dependent, or both.

The larger temperature dependence above the coalescence point is expected because the peak position now depends on the value of K, the equilibrium constant, which in turn depends on the temperature, ΔG^0 being constant. Thus supposing a ΔG^0 value of 0.625 kcal/mol[7] one may calculate the rate at which K is changing the temperature: at 273 °K, % (diaxial) = 24.1 and at 263 °K, % (diaxial) = 23.3.

If the chemical shift between conformers is 515 Hz (obtained by extrapolating low temperature data), then the time-averaged positions at 273 and 263 °K are 124.2 and 120.1 Hz respectively. Thus the peak position increases at a rate 0.4 Hz/°K in this temperature region, given the above assumptions.

Using the data in Table 2 to estimate the position of equilibrium requires a quantitative value for the temperature dependence of each conformer. For the diaxial conformer this quantity is not so well defined, because it is slower to recover from the exchange effects (hence the necessity for the extra data in Table 2). However, it does appear that the temperature dependence of the diaxial conformer is less than that of the diequatorial; from Table 2, value of 0.7 and 0.9 Hz/°K can be taken.

Extrapolating the peak positions of each conformer at −85 to 0° by these amounts then, the

[7]Fortunately this value is not critical.

Can. J. Chem. Downloaded from www.nrcresearchpress.com by 210.87.254.40 on 09/05/12
For personal use only.

Can. J. Chem. Downloaded from www.nrcresearchpress.com by 210.87.254.40 on 09/05/12
For personal use only.

averaged peak position at 0° is 116 Hz from the diequatorial resonance and 400 Hz from the diaxial. This leads to values of 22.5% diaxial and $\Delta G^0 = 0.672$ kcal/mol (at 0°). Now combining this value for % diaxial along with temperature dependence of the individual conformers (0.9 and 0.7 Hz/°K), and the temperature dependence of K itself (0.4 Hz/°K, above) we may calculate the net change in the averaged peak position = ((0.775)0.9 + (0.225)0.7 + 0.4) = 1.25 Hz/°K; the observed increase with temperature is 1.2 Hz/°K, which is reasonable agreement.

(d) ^1H Chemical Shifts

Using the chemical shifts of H_1 and H_2 derived from the low temperature (−100°) spectra of **1**-d_4 yields values of 23.2 and 29.2% diaxial respectively at ambient temperature (*ca.* 35°). This corresponds to ΔG^0 values of 0.544 and 0.735 kcal/mol respectively (at 35°). Variable temperature ^1H spectra were not run, so no correction for temperature dependence of the chemical shifts could be made, as was done for the ^{19}F spectra; this undoubtedly introduces significant errors (10), and could well account for most of the difference in values from H_1 and H_2.

(e) ^{19}F Linewidths

Using the general lineshape expression of Gutowsky and Holm (11) a set of theoretical spectra may be generated, in which the residence time τ, and the equilibrium constant K may be varied. For any given value of K, there is a unique value of τ which gives rise to the largest linewidth; this is the coalescence point for that value of K. Thus the linewidth at the coalescence point is a function of K, and from the experimental linewidth, a value of K may be deduced.

The ^{19}F spectra of **1**, with ^1H-decoupling, were treated in this way and the maximum experimental linewidth was 114 Hz (at 228 °K, see Table 2); from the calculated spectra (*vide infra*), this implies that $K = 4.26$, which corresponds to $\Delta G^0 = 0.659$ kcal/mol.

A criticism of this method of deducing K might be that, in fact, the maximum may not be obtained, since the spectra were recorded at intervals of 5 °K, and the linewidth is a rapidly varying function of temperature. However, this criticism may be countered as follows: with a typical kinetic barrier to inversion (say 10 kcal/mol) a temperature increase of 5 °K decreases the residence time τ, by a factor of approximately 1.7 (see next part on rate calculations). Near coalescence, the linewidth is a more slowly varying function of temperature and a factor of 1.7 in τ is not enough to allow a significantly larger linewidth to come between 89 and 114 Hz (at 233 and 228 °K). This can be seen from the tables of calculated linewidths.

In the above discussions the value of ΔG^0 has been calculated in four different ways, and different values obtained. It seems sensible to adopt as the "best" values those derived from the methods having the fewest assumptions. On this basis, the coupling constant results and the ^1H chemical shift calculations must be classed as less reliable than the ^{19}F shift calculations, since no temperature dependence was accounted for. The preferred values are therefore: (20% solution in CS_2 solution). $\Delta G^0 = 0.625$ kcal/mol (−90°), areas of ^{19}F resonance; $\Delta G^0 = 0.672$ kcal/mol (0°), extrapolated ^{19}F shifts; $\Delta G^0 = 0.659$ kcal/mol (−45°), linewidth of ^{19}F resonance. The other values are: $\Delta G^0 = 0.397$ kcal/mol (35°) $^3J_{HF}$; $\Delta G^0 = 0.478$ kcal/mol (35°), $^3J_{HH}$; $\Delta G^0 = 0.735$ kcal/mol (35°), chemical shift of H_1; $\Delta G^0 = 0.544$ kcal/mol (35°), chemical shift of H_2.

Taking the three 'preferred' values together, it appears that ΔG^0 is nearly independent of temperature, if we state reasonable experimental limits, say ±0.025 kcal/mol. This implies a zero or significantly small entropy ($\Delta S^0 = -0.5$ e.u or lower).

Bovey *et al.* (4), examing cyclohexyl fluoride, arrived at ΔG^0 values of 0.242 (at 218 °K, from ^{19}F area measurements) and 0.153 kcal/mol (at 302 °K, from ^{19}F chemical shifts). This implies a positive entropy, $\Delta S^0 = 1.05$ e.u. However, there was no allowance made in that work for temperature dependence of ^{19}F chemical shifts, and it can be seen from the published data (Table II, ref. 4) that both the averaged resonance at high temperatures, and the equatorial resonance at low temperatures are strongly dependent on temperature; however, the axial resonance appears to be temperature independent. A quantitative estimate is hard to make because of the comparatively large amount of scatter in the points, but the equatorial resonance data is fitted quite well by 0.0095 p.p.m./°K (*i.e.* same as above for (1)). If a zero temperature dependence is assumed for the axial resonance, one can calculate that the ΔG^0 value is now 0.231

TABLE 3. Repulsion between substituents in the diequatorial form of some 1,2-dihalo-cyclohexanes*

Substituent(s)	*A* value† (kcal/mol)	Reference	Sum of *A* values† of substituents (kcal/mol)	Repulsion between halogens (kcal/mol)
F	0.276	10		
Cl	0.528	10		
Br	0.476	10		
I	0.468	10		
IF	0.650	This work	0.744	0.1
ICl	−0.250	12	0.996	1.2
Cl–Cl	0.200	13	1.056	0.8
Br–Br	−0.300	13	0.952	1.2
I–I	−1.000	14	0.936	1.9

*Measurements were all taken in CS_2 solution except for the last compound (di-iodide), for which benzene was used. This may be expected to make a significant difference to the *A* value of the di-iodide (see Table 1), and lower the calculated repulsion from 1.9 kcal/mol to approximately 1.6–1.7 kcal/mol.
†Free energy difference between the substituent(s) in the equatorial and axial orientation(s).

kcal/mol at 302 °K which is very close to the low temperature value given by Bovey. This would imply that ΔS^0 for this system is also close to zero. For **1**, the results are: (20% in CS_2) $\Delta G^0 = 0.650 \pm 0.025$ kcal/mol (183–273 °K); $\Delta H^0 = \Delta G^0$; $\Delta S = 0 \pm 0.5$ e.u.

This value of ΔG^0 is close to the sum of (0.744 kcal/mol) of the individual ΔG^0 values reported for iodine and fluorine in the literature (10). This sum is expected to be somewhat higher than the observed ΔG^0 for "cyclohexane IF", since the repulsions between the halogen atoms (in the diequatorial conformer) would be expected to reduce the latter value. The rather small reduction, 0.1 kcal/mol indicates, however, that this repulsion is quite small. This is in contrast to the case of "cyclohexane ICl" (12), in which the *diaxial* form predominates and $\Delta G^0 = 0.24$ kcal/mol. The sum of the *A* values for 'I' and 'Cl' in the diequatorial form must be contributing approximately 1.2 kcal/mol, or 12 times that between 'I' and 'F'. The repulsion between two bromine atoms or between two chlorine atoms can be similarly calculated, and both are found to be large (Table 3).

Rate Calculations

The activation free energy ΔF^f, enthalpy ΔH^f and entropy ΔS^f, associated with the chair-to-chair inversion of a cyclohexane derivative may readily be determined from a plot of rate, *k*, *vs.* inverse temperature, $1/T$ (4).

Using the Gutowsky–Holm equation (11) a computer programme GUTHO was written which calculates the width, height, and position of all resonances in a one-spin system undergoing chemical exchange. Input data required are the fractional population difference *PD*, the chemical shifts of both resonances in the slow exchange limit *SA* and *SB*, and the residence time *T*. This programme was then applied to the ^{19}F spectra of **1**, in which ^1H couplings had been removed by irradiation. *SA* and *SB* were fixed and then *PD* and *T* were varied in integral steps. Since, in our case, $(SA - SB)$ only varies about 4% (from 188 to 273 °K), this is not a bad approximation. However, *PD* varies considerably due to the temperature dependence of the equilibrium constant, throughout the range of experimental spectra.

Using the value $\Delta G^0 = 0.650$ kcal/mol, values of *PD* were calculated for each of the experimental spectra, and then the residence time *T* ($= \tau$) picked which most closely fitted the experimental peak width (4). The data are shown in Table 4. The plot of ln τ *vs.* $10^3/T$ is shown in Fig. 4, and has a slope which corresponds to an activation energy of 10.72 kcal/mol.

From this plot ΔF^f, ΔH^f, and ΔS^f may be calculated. However, these calculations contain the inherent assumption that the chair-to-chair inversion involves only one barrier; it has been pointed out (15), that in the event of there being *two* barriers to the process then the observed rate constant *k* is actually equal to one-half of the actual rate constant for passing over each barrier. For a cyclohexane derivative, it seems likely that a boat form is an intermediate in the process, and k_{cb}, the rate constant for the chair-to-boat process is equal to twice the observed rate constant. Hence the activation parameters for the chair-to-boat equilibrium are as follows:

Can. J. Chem. Downloaded from www.nrcresearchpress.com by 210.87.254.40 on 09/05/12
For personal use only.

TABLE 4. Kinetic data for conformational inversion of **1**

Temperature (°K)	$10^3/T$ (°K)	$PD = P_A - P_B$	^{19}F Linewidth (^1H-decoupled) (Hz)	Residence time τ (s)
273	3.66	0.536	5.0	6.6×10^{-6}
263	3.80	0.552	9.5	1.3×10^{-5}
258	3.88	0.560	13.5	2.0×10^{-5}
253	3.96	0.568	20	3.1×10^{-5}
248	4.03	0.578	29	4.7×10^{-5}
243	4.115	0.586	36	5.9×10^{-5}
238	4.20	0.595	55	9.5×10^{-5}
233	4.295	0.604	89	1.7×10^{-4}
228	4.39	0.614	114	2.8×10^{-4}
223	4.49	0.623	86	6.4×10^{-4}
218	4.59	0.634	69.5	8.0×10^{-4}
208	4.81	0.655	21.4	2.7×10^{-3}
198	5.05	0.677	5.6	1.2×10^{-2}

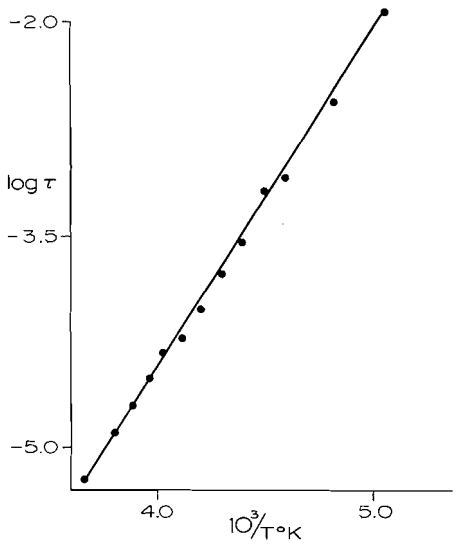

FIG. 4. Arrhenius plot for the conformational inversion of **1**.

At 216.5 °K (−56.5°): $\Delta F_{cb}^{f} = 9.65$ kcal/mol, $\Delta H^{f} = 10.27$ kcal/mol, $\Delta S_{cb}^{f} = 3.0$ e.u. At 266 °K (−7°): $\Delta F_{cb}^{f} = 9.45$ kcal/mol; $\Delta H^{f} = 9.99$ kcal/mol; $\Delta S^{f} = 2.0$ e.u.

Bovey *et al.* (4) have pointed out that activation parameters such as these are actually composite values of the forward and backward reactions, and they have given a set of equations to find the individual parameters. Using these parameters we obtain then the activation parameters for the chair–chair inversion process of **1** in CS_2 solution; these data are summarized in Table 5.

TABLE 5. Activation parameters for **1** in CS_2 solution

Parameter	Temperature (°K) 216.5	266
ΔF_{ca}^{f}(cb) (kcal/mol)	10.38	10.23
ΔF_{ac}^{f}(cb) (kcal/mol)	9.74	9.59
ΔH_{ca}^{f} (kcal/mol)	10.83	10.49
ΔH_{ac}^{f} (kcal/mol)	10.17	9.84
ΔS_{ca}^{f}(cb) (e.u.)	2.1	0.9
ΔS_{ca}^{f}(cb) (e.u.)	2.1	0.9

The most reliable work on the conformational inversion of cyclohexane systems appears to be that of Anet and Bourn (15), who studied cyclohexane-d_{11}. Their values for ΔF_{cb}, ΔH, and ΔS_{cb} are respectively 10.22 kcal/mol, 10.8 kcal/mol, and 2.8 e.u. (all at −67°). The comparable values in this study are (for diequatorial chair-to-boat process, since this has the lowest ground state) 10.38 kcal/mol, 10.83 kcal/mol, and 2.1 e.u. This is remarkably close agreement.

The small positive value of ΔS_{eq}^{f}(cb) is, as has been pointed out, (4, 15) exactly as expected, on the basis of symmetry grounds, *e.g.* for cyclohexane, there are six possible paths for reaching a cyclohexene-like transition state (16), and thus $\Delta S_{cb}^{f} = R \ln 6 = 3.6$ e.u. (neglecting vibrational and rotational entropy contributions).

Can. J. Chem. Downloaded from www.nrcresearchpress.com by 210.87.254.40 on 09/05/12
For personal use only.

Can. J. Chem. Downloaded from www.nrcresearchpress.com by 210.87.254.40 on 09/05/12
For personal use only.

Summary

The most interesting part of the above results appear not to be the final values obtained, but the appraisal of the various methods. Thus we conclude that the chemical shifts and vicinal coupling constants are *all* temperature dependent, those involving ^{19}F being particularly susceptible; there is no reason to suppose that this is a unique case, and instead it is likely that these phenomena are general.

It can be calculated that in order to bring the ΔG^0 values obtained from coupling constants into line with the above value, temperature coefficients of $+3 \times 10^{-3}$ Hz/°K (for $^3J_{HF}$) and -3×10^{-3} Hz/°K (for $^3J_{HH}$) are required. A recent review by Laszlo (17) presents some other evidence of temperature dependence of various coupling constants.

ΔG^0, calculated from the chemical shift of H_1 is 'high', whereas that from H_2 is 'low'; however, a shift of only 2.5 Hz in ν_{H_2}, of 1 Hz in ν_{H_1}, would account for the difference. Jensen and co-workers (10) have shown that this phenomenon is in fact general. Bovey *et al.* (4) noted that the conformer ratio of cyclohexyl fluoride as determined by ^1H chemical shifts differed from the value obtained from area measurements. This discrepancy is now explained.

Error limits on activation parameters have in most investigations apparently been determined by the authors' estimate of the accuracy of the measurement, rather than their evaluation of the validity of the method. This can be seen by considering the disagreement between workers using different methods. Anet and Bourn (15), in a refreshing departure, have taken the opposite view, *i.e.* systemmatic error is not so small as to allow the random error to become dominant, and this appears to be far more logical. Thus subjective estimates for errors in ΔH^f and ΔF_{cb}^f might be ± 0.2 kcal/mol, and ± 1.0 e.u. for ΔS_{cb}^f.

Experimental

*trans-1-Fluoro-2-iodo-cyclohexane-3,3,6,6-d_4 (**1**-d_4)*

The reaction described previously for cyclohexene (*3a*, *d*) was repeated on 3,3,6,6-tetradeutero-cyclohexene[8] on a somewhat smaller scale (0.25 g of deuterated material). To avoid possible decomposition on heating the product was not purified by distillation; the ^1H and ^{19}F n.m.r. spectra showed no detectable impurities.

All n.m.r. measurements were made with an extensively modified Varian HA-100 spectrometer operating in the locked, frequency-swept mode of operation. The equipment used for the heteronuclear decoupling experiments has since been described elsewhere (18).

Spectral analyses were performed using a slightly modified version of the programme TWOSUM,[9] and a plot-routine, SMASH, using an I.B.M. 7040 computer at the University of British Columbia Computing Centre.

The analysis of the chemical exchange spectra of **1** was carried out empirically; based on the Gutowsky–Holm equation (11) a simple programme GUTHO was written which calculated all the peak heights, widths, and positions for a two-site exchange, with certain parameters fixed. First the chemical shifts of each resonance were determined (from low temperature work) and the population ratio of the conformers calculated (from area measurements, etc.). Then the peak positions, etc. were calculated by Gutho for a given residence time, τ; τ was varied over a range of 10^6 and the calculated spectrum which most closely matched the experimental could then easily be selected. Thus a τ value was readily obtained for each experimental spectra, and allowed the calculation of activation parameters. This method, while not as rigorous as the line-fitting approach, has the important advantage of speed; the loss of accuracy is believed to be small, if at all, on the basis of the excellent Arrhenius plot obtained. Anet and Bourn (15), in a study of cyclohexane-d_{11}, came to the same conclusion.

It is a pleasure to thank the National Research Council of Canada for their generous financial assistance. This study was also supported by a grant from Imperial Oil Ltd.

1. L. D. HALL. Carbohydr. Res. **4**, 429 (1967).
2. (*a*) L. D. HALL, J. F. MANVILLE, and N. S. BHACCA. Can. J. Chem. **47**, 1 (1969); (*b*) A. B. FOSTER, R. HEMS, L. D. HALL, and J. F. MANVILLE. Chem. Commun. 158 (1968); (*c*) L. D. HALL, R. N. JOHNSON, J. ADAMSON, and A. B. FOSTER. Chem. Commun. 463 (1970).
3. (*a*) L. D. HALL, D. L. JONES, and J. F. MANVILLE. Chem. Ind. (London), 1787 (1967); (*b*) L. D. HALL and J. F. MANVILLE. Chem. Commun. 35 (1968); (*c*) L. D. HALL and J. F. MANVILLE. Can. J. Chem. **47**, 361 (1969); (*d*) L. D. HALL and D. L. JONES. Can. J. Chem. **51**, 2902 (1973).
4. F. A. BOVEY, E. W. ANDERSON, F. P. HOOD, and R. L. KORNEGAY. J. Chem. Phys. **40**, 3099 (1964).
5. J. D. ROBERTS. Chem. Brit. 529 (1968) and refs. therein.
6. L. D. HALL and J. F. MANVILLE. Carbohydr. Res. **9**, 11 (1969) and refs. therein.
7. F. A. L. ANET. J. Am. Chem. Soc. **84**, 1053 (1962).
8. F. HRUSKA, D. W. MCBRIDE, and T. SCHAFFER. Can. J. Chem. **45**, 1081 (1967) and refs. therein.
9. J. B. STOTHERS. Can. J. Chem. **45**, 2943 (1967).

[8]Purchased from Merk, Sharp and Dohme.

[9]We are indebted to Dr. John Martin of the University of Alberta, Edmonton, for providing us with a copy of this programme.

10. (*a*) F. R. JENSEN and B. H. BECK. J. Am. Chem. Soc. **90**, 3251 (1968); (*b*) F. R. JENSEN, C. H. BUSHWELLER, and B. H. BECK. J. Am. Chem. Soc. **91**, 344 (1969).
11. H. S. GUTOWSKY and C. H. HOLM. J. Chem. Phys. **25**, 1228 (1956).
12. E. PREMUZIC and L. W. REEVES. Can. J. Chem. **45**, 2943 (1967).
13. L. W. REEVES and K. O. STROMME. Trans. Faraday Soc. **57**, 390 (1961).
14. R. U. LEMIEUX and J. W. LOWN. Can. J. Chem. **42**, 893 (1964).
15. F. A. L. ANET and A. J. R. BOURN. J. Am. Chem. Soc. **89**, 760 (1967).
16. J. B. HENDRICKSON. J. Am. Chem. Soc. **83**, 4537 (1961).
17. P. LASZLO. *In* Progress in nuclear magnetic resonance spectroscopy. Vol. 11. *Edited by* J. W. Emsley, J. Feeney, and L. H. Sutcliffe. Pergamon Press. 1967.
18. L. D. HALL and R. BURTON. Can. J. Chem. **48**, 59 (1970).

Can. J. Chem. Downloaded from www.nrcresearchpress.com by 210.87.254.40 on 09/05/12
For personal use only.

Observations on the Electronegativity Dependence of Vicinal ^{19}F–^{1}H Coupling Constants

L. D. HALL AND D. L. JONES

Department of Chemistry, The University of British Columbia, Vancouver 8, British Columbia

Received November 1, 1971[1]

The *vicinal* ^{19}F–^{1}H couplings of 16 1,2-disubstituted derivatives of acenaphthene are reported. A plot of these couplings against substituent electronegativity shows a better agreement with an *exponential* relationship than with a conventional *linear* relationship.

Les constantes de couplage vicinal ^{19}F–^{1}H de 16 dérivés disubstitués-1,2 de l'acénaphtène sont rapportées. Une courbe reliant ces constantes avec l'électronégativité des substituants montre une meilleure relation si une fonction *exponentielle* est utilisée plutôt qu'une fonction *linéaire*.

[Traduit par le journal]

Can. J. Chem., **51**, 2925 (1973)

Introduction

It is well known that *vicinal* (^{3}J) ^{1}H–^{1}H couplings have a marked dependence on the dihedral angle separating the two C—H bonds (1) and also on the electronegativity (2) of nearby substituents: this latter variation also has a configurational dependence (3). Although *vicinal* ^{19}F–^{1}H couplings have received less attention it is clear that they also show all three of these dependencies (2*e*, 4). A fundamental assumption of all these studies of variations of coupling constants as a function of substituent electronegativity has been that a *linear* relationship should exist. In the present paper we shall question the validity of this tenet and shall demonstrate that for dihedral angles of *ca.* 0 and *ca.* 100° the relationship is non-linear, and *may* be exponential.

Any *experimental* evaluation of the effect of electronegativity changes on coupling constants requires a range of derivatives having essentially the same geometry but with substituents of differing electronegativity. The acenaphthene system was chosen as fulfilling this geometric requirement and fortunately it possessed the requisite chemical reactivity whereby a variety of halogen substituents could be introduced (5).

Results and Discussion

The syntheses of the specifically fluorinated derivatives **1**–**16** of the acenaphthene system were given in an accompanying paper (5), as also were full details of the analysis of their n.m.r. spectra: these were generally straightforward, and gave the data listed in Table 1. Included in that Table is the sum of the substituent electronegativities; Huggins' values (6) were used.

In assembling the data of Table 1 it has been assumed that an orientation effect of the type previously postulated (4*d*, *g*) for 60° dihedral angles is either very small or non-existent. That this assumption is reasonable is shown as follows: in compounds **3** and **2** (*trans-* and *gem*-acenaphthene BrF) $^{3}J_{HF}$ (0°) is 21.5 and 23.0 Hz respectively. In **4** (*gem*-acenaphthene ClF) the sum of the two couplings is 32.8, whereas in the *trans-* and *cis*-ClF compounds **6** and **5** the couplings are 21.0 and 10.0 respectively, a sum of 31.0. Similarly, in **11** (*gem*-difluoro-acenaphthene) the sum of the two couplings is 26.4, and from the individual *trans-* and *cis*-difluorides (**12**, **13**) the couplings are 18.8 and 5.2 respectively, a sum of 24.0.

Inspection of the data shown in Table 1 indicates that there is a monotonic relationship between the total electronegativity and the ^{19}F–^{1}H coupling: as the electronegativity increases so the coupling decreases.

All previous investigations of the relationship between electronegativity and coupling constants have concluded that it was a linear relationship.[2] This may seem logical at first sight, since a

[1]Revision received February 23, 1973

[2]A referee kindly drew our attention to a publication by Schaefer and Sutton (11) that had previously documented a non-linear electronegativity dependence for the ^{2}J and ^{3}J proton–proton couplings of a series of substituted ethylenes.

Can. J. Chem. Downloaded from www.nrcresearchpress.com by 210.87.254.5 on 09/05/12
For personal use only.

TABLE 1. Vicinal coupling constants for 1,2-substituted, fluoro-halo derivatives of acenaphthene

Derivative	Substituents* A	B	C	Sum of substituent electronegativities†	Coupling constant J_{cis}	J_{trans}
1	H	H	F	4.4	29.5	21.4
2	H	Br	F	5.15	23.0	10.0
3	Br	F	H	5.15	21.5	—
4	H	Cl	F	5.25	(Sum = 32.8)	
5	Cl	H	F	5.35	—	10.0
6	Cl	F	H	5.35	21.0	—
7	I	Cl	F	5.80	—	6.0
8	I	F	Cl	5.80	19.7	—
9	Br	Br	F	5.90	—	3.1
10	Br	F	Br	5.90	18.9	—
11	H	F	F	6.10	(Sum = 26.4)	
12	F	F	H	6.10	18.8	—
13	F	H	F	6.10	—	5.2
14	I	F	F	6.55	16.0	4.8
15	Br	F	F	6.85	15.3	3.7
16	F	F	F	7.80	12.8	1.2

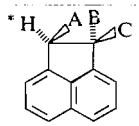

†Huggins values (6) for the two additional substituents; *i.e.* not including one H and one F substituent.

strongly electronegative substituent, X, should 'pull' the electron density out of the neighboring bonds and thus decrease the coupling constants which are transmitted along them. This effect may reasonably be supposed to be proportional to the 'electronegative strength' of X. However, there is a basic fault with this reasoning, for it supposes that the source of electron density in the neighboring bonds is *infinite* and has no 'electronegative strength' of its own.

If one substituent X with electronegativity ε reduces the coupling constant J from J_0 to $(J_0 - Y)$, then a second (similar) substituent would not have the same effect (*i.e.* reduce J to $(J_0 - 2Y)$ as in the linear case), but rather it should reduce J *by the same fraction*, *i.e.* from $(J_0 - Y)$ to $(J_0 - Y)/J_0 \cdot (J_0 - Y)$. To put it another way, the rate of decrease with electronegativity is proportional to the remaining electron density and thus, coupling constant:

$$dJ/d\varepsilon = -kJ$$

or

$$dJ/J = kd\varepsilon$$

Hence:

$$lnJ = -k\varepsilon + \text{constant}$$

$$J = ae^{-k\varepsilon}$$

where 'a' is some constant.

Thus a negative exponential decay of coupling constant with electronegativity is a more logical relationship to expect than a linear one.[3] The data from Table 1 was fitted by a computer programme[4] to both exponential and linear relationships, and the results are shown in Table 2. It can be seen that the exponential fit is decidedly better especially for $J(trans)$ and a graph of the data is shown in Fig. 1. From this graph it is evident that the most important point is the size of $^3J_{HF}$ (*trans*) for the compound with the least electronegative substituents, *i.e.* acenaphthene fluoride itself (**1**). To further support this result the corresponding 1-fluoro-indan was synthesized.

The extremely complex ^{1}H n.m.r. spectrum of this compound (an ABCDMX with long range couplings) is not amenable to analysis within the lifetime of even a graduate student, but the ^{19}F spectrum is composed of two broad overlapping triplets, the bandwidth of which is the sum of the vicinal couplings into fluorine, *ca.*

[3]In both cases, coupling constants are assumed to be directly related to electron density.

[4]LQF, a library programme of the University of British Columbia Computing Centre, utilizes a least squares procedure.

Can. J. Chem. Downloaded from www.nrcresearchpress.com by 210.87.254.5 on 09/05/12
For personal use only.

TABLE 2. Vicinal ^{19}F–^{1}H coupling constant dependence on electronegativity; a comparison of exponential and linear fits to the data

	Exponential fit	Deviation*	Linear fit	Deviation*
$^3J_{HF}(cis)$	$J = 87.75e - 0.2522$	0.87	$J = -4.52 + 46.37$	1.32
$^3J_{HF}(trans)$	$J = 985.68e - 0.8749$	1.18	$J = -5.15 + 38.13$	3.35

*Deviation is the root mean square of the differences between calculated and experimental points.

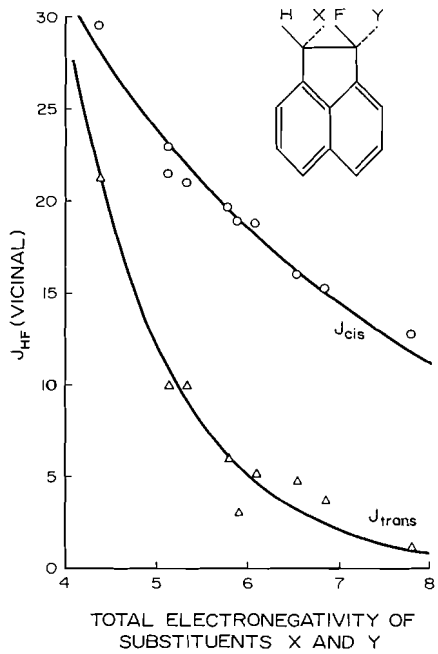

FIG. 1. Plot showing variation of vicinal ^{19}F–^{1}H couplings *vs.* total substituent electronegativity for 1,2-disubstituted-1-fluoro-acenaphthenes.

55 Hz. The largest $^3J_{HF}$ (*cis*) that may be expected is about 30 Hz, even if the five-membered ring is planar (4*f*), thus leaving a value of about 25 Hz for $^3J_{HF}$ (*trans*); this certainly supports the value obtained from acenaphthyl fluoride.

The reasons for the linear plots arrived at experimentally by previous workers can now be seen:

(*a*) The dependence of $^3J_{HH}$ on electronegativity is much less than for $^3J_{HF}$, thus leading to a shallower curve which is quite easily approximated by a straight line. A recalculation of some original data published for $^3J_{HH}$ couplings (2*h*, *i*) shows that they too give a slightly better fit for an exponential rather than a linear relationship.

(*b*) The ranges of electronegativity considered previously were not very wide, again leading to an effectively shallower curve.

(*c*) The $^3J_{HF}$ values considered previously had dihedral angles of 60 and 180°, which may well have less of an electronegativity dependence than at 100°, where it is really evident that a linear relationship is inadequate.

Since $^3J_{HF}$ couplings have such a large dependence on electronegativity, a general Karplus-type curve which is usually drawn, showing dihedral angle dependence, is not practical. However, one can plot several curves, each for a given electronegativity, and thus describe the three dimensional surface. In Table 3 there is listed a set of data collected from various references and this work; it can be seen that there are still some gaps to be filled but enough data are available for it to be useful, *i.e.* one should be able to make reasonable deductions concerning structure in most cases.

It is appropriate to comment here that the whole concept of substituent electronegativity, as applied to any molecule consisting of more than two atoms, is a nebulous one, and is essentially unsuitable for any incisive quantitation. With this in mind it is really questionable how far one can pursue the concept of electronegativity dependence of spin coupling constants: nevertheless, if one is to attempt to evaluate any such dependence it seems mandatory to recognize that it will be intrinsically non-linear, even if the experimental data *appear* to support a linear dependence.

Experimental

The syntheses of the compounds studied have been given elsewhere (5) together with details of the analyses of their n.m.r. spectra; the reader is referred to that paper for further details; all assignments and analyses were quite straightforward. Figures showing the spectra of some derivatives were included.

It was decided to determine the relative signs of a *cis*- and *trans*-pair of *vicinal* ^{19}F–^{1}H couplings. This was performed by the double resonance experiments described below, which were themselves confirmed by the use of a

Can. J. Chem. Downloaded from www.nrcresearchpress.com by 210.87.254.5 on 09/05/12
For personal use only.

TABLE 3. Vicinal ^{19}F–^{1}H coupling constants as a function of electronegativity* and dihedral angle (from various references as well as this work)

	Nominal dihedral angle (degree)				
Electronegativity*	0	60	100	120	180
4.4	29.5	11.5†	21.4		43.5†
4.85	25.1‡			12.8‡	
5.15	23.0		10.0		
	21.5				
6.1	19.1	10, 11§	5.1		35§
6.55	16.0		4.8		
6.7		5, 11‖			23–25‖
6.85	15.3		3.7		
7.8	12.8		1.2		

*'Electronegativity' is the sum of the individual electronegativities of two substituents X_1 and X_2 in the fragment:

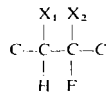

†See ref. 4*b*.
‡See ref. 4*f*.
§See ref. 4*a*.
‖See ref. 4*h*.

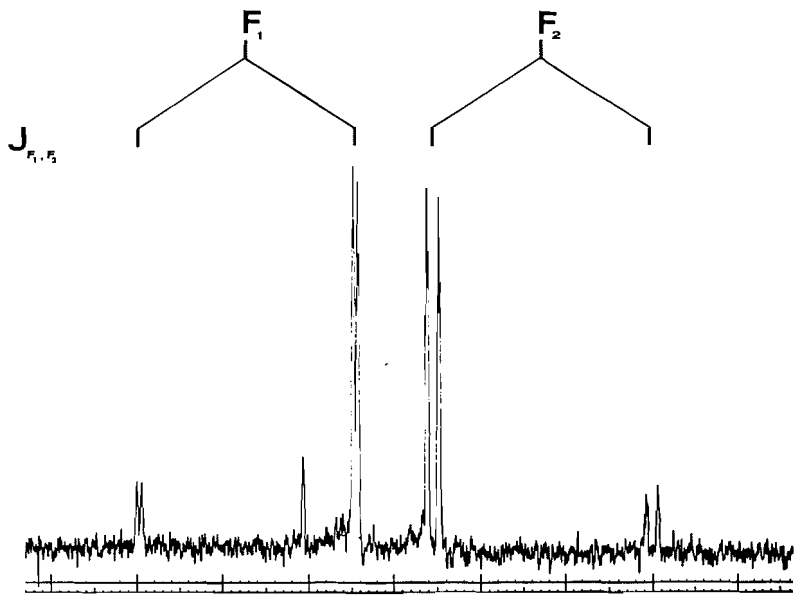

FIG. 2. Fluorine n.m.r. spectrum (94.07 MHz) for 2-bromo-1,1-difluoro-acenaphthene (**15**).

computer programme[5] which simulates the *approximate* effect of such an experiment.

A plotting routine, SMASH, for n.m.r. spectra was written by John Coulthard of the University of British Columbia Computing Centre; it enabled the binary output of LAØCØØN, TWOSUM, or NMDRS to be matched directly with experimental spectra. This was particularly useful with NMDRS where the linewidths within a given spectrum are not constant.

The ^{19}F spectrum of 1-bromo-2,2-difluoroacenaphthene (**15**) is shown in Fig. 2 and is basically an ABX spectrum, with each fluorine further coupled to two of the ring hydrogens, yielding a triplet for each AB resonance (Fig. 3A, B). Irradiation of one triplet in the weak

[5]The original listing of the programme NMDRS (7) was obtained from the National Physical Laboratory, Teddington, U.K.; this programme was in ALGOL, and the necessary translation to FORTRAN was kindly carried out by Susan Boyd of the University of British Columbia Computing Centre.

Can. J. Chem. Downloaded from www.nrcresearchpress.com by 210.87.254.5 on 09/05/12
For personal use only.

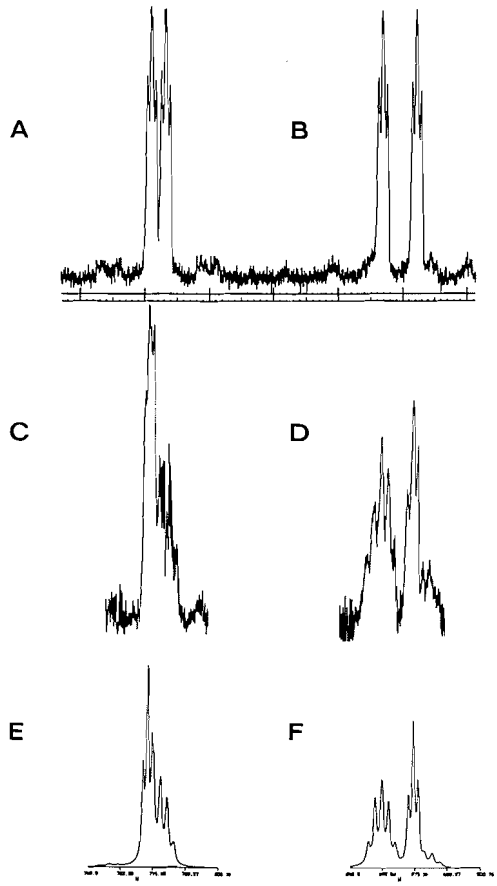

FIG. 3. Partial ^{19}F n.m.r. spectra of 2-bromo-1,1-difluoro-acenaphthene (**15**). The peaks shown in A and B are the normal resonances of the center components of the fluorine "quartet", A being the high field transitions of F_1 and B being the low field transitions of F_2 (see Fig. 2). The spectra shown in C and D are the same components measured in the presence of a second radiofrequency field; in C this has been centered on the highest field transitions of the fluorine "quartet" whereas for D it was centered on the lowest field transitions. The spectra given in E and F are the calculated spectra corresponding to C and D respectively.

resonance of F_2 affects the connected triplet in the strong resonance of F_1; had there been no extra 'tripletting' (*i.e.* if it had been a simple ABX, instead of ABM_2X), this 'spin tickling' would cause the two connected resonances to split into two new resonances, whose splitting equals the strength of the irradiating field (8).

However, the extra coupling into F_1 and F_2 causes the transfer of half the splitting of the irradiated resonance (F_2) to F_1; this new splitting, $\frac{1}{2}J_{MF_2}$, is added or subtracted from J_{MF_1} depending on how the resonances are connected (regressively or progressively) (9). The results of two such experiments are shown in Fig. 3C, D. It can be seen that in one case the triplet splitting has increased (from 1.7 to 2.5 Hz) and in the other it has decreased.

Shown below are the spectra calculated by NMDRS; the agreement is very satisfactory. These experiments confirm that the two *vicinal* ^{19}F–^{1}H couplings have the same *relative* signs; presumably both are *absolutely* positive (10).

It is a pleasure to thank the National Research Council of Canada and Imperial Oil Ltd. for their financial support of this work.

1. M. KARPLUS. J. Chem. Phys. **30**, 11 (1959); J. Am. Chem. Soc. **85**, 2870 (1963).
2. (*a*) R. E. GLICK and A. A. BOTHNER-BY. J. Chem. Phys. **25**, 362 (1956); (*b*) N. SHEPPARD, C. N. BANWELL, and J. J. TURNER. Spectrochim. Acta, **16**, 794 (1960); (*c*) C. N. BANWELL and N. SHEPPARD. Mol. Phys. **3**, 350 (1960); (*d*) J. R. CAVANAUGH and B. P. DAILEY. J. Chem. Phys. **34**, 1099 (1961); (*e*) H. S. GUTOWSKY, G. G. BELFORD, and P. E. MCMAHON. J. Chem. Phys. **36**, 3353 (1962); (*f*) C. N. BANWELL and N. SHEPPARD. Disc. Faraday Soc. **34**, 115 (1962); (*g*) T. SCHAEFER. Can. J. Chem. **40**, 1 (1962); (*h*) K. L. WILLIAMSON. J. Am. Chem. Soc. **85**, 516 (1963); (*i*) P. LASZLO and P. SCHLEYER. J. Am. Chem. Soc. **85**, 2709 (1963); (*j*) R. J. ABRAHAM and K. G. R. PACHLER. Mol. Phys. 166 (1964).
3. (*a*) N. S. BHACCA and D. H. WILLIAMS. *In* Applications of N.M.R. spectroscopy in chemistry. Holden Day, San Francisco. 1964; (*b*) H. BOOTH. Tetrahedron Lett. 411 (1965).
4. (*a*) J. D. ROBERTS. Angew. Chem. **75**, 20 (1963); (*b*) F. A. BOVEY, E. W. ANDERSON, F. P. HOOD, and R. L. KORNEGAY. J. Chem. Phys. **40**, 3099 (1964); (*c*) L. D. HALL and J. F. MANVILLE. Chem. & Ind. (London), 991 (1965); (*d*) R. J. ABRAHAM and L. CAVALLI. Mol. Phys. **9**, 67 (1965); (*e*) R. J. ABRAHAM, L. CAVALLI, and K. G. R. PACHLER. Mol. Phys. **11**, 471 (1966); (*f*) K. L. WILLIAMSON, YUAN-FANG LI, F. H. HALL, and SUSAN SWAGER. J. Am. Chem. Soc. **88**, 5678 (1966); (*g*) L. D. HALL and J. F. MANVILLE. Chem. Commun. 37 (1968); (*h*) L. D. HALL, J. F. MANVILLE, and N. S. BHACCA. Can. J. Chem. **47**, 1 (1969).
5. L. D. HALL and D. L. JONES. Can. J. Chem. **51**, 2902 (1973).
6. M. L. HUGGINS. J. Am. Chem. Soc. **75**, 4123 (1953).
7. G. GOVIL and D. H. WHIFFEN. Mol. Phys. **12**, 449 (1967).
8. R. FREEMAN and W. ANDERSON. J. Chem. Phys. **37**, 2053 (1962).
9. R. FREEMAN and B. GESTBLOM. J. Chem. Phys. **47**, 1472 (1967).
10. (*a*) E. L. MACKOR and D. MACLEAN. J. Chem. Phys. **44**, 64 (1966); (*b*) R. A. BERNHEIM and B. J. LAVERY. J. Am. Chem. Soc. **89**, 1279 (1967).
11. T. SCHAEFFER and H. M. SUTTON. Can. J. Chem. **45**, 3153 (1967).

Can. J. Chem. Downloaded from www.nrcresearchpress.com by 210.87.254.5 on 09/05/12
For personal use only.

Conformational Studies of 1,2-Disubstituted Indan Derivatives by Nuclear Magnetic Resonance Spectroscopy[1]

L. D. HALL AND D. L. JONES

Department of Chemistry, The University of British Columbia, Vancouver 8, British Columbia

Received November 1, 1971[2]

The n.m.r. spectra of *trans*-2-bromo-1-fluoro-indan (**2**) have been analyzed, and the n.m.r. data used as the basis for a conformational assignment.

Le spectre r.m.n. du bromo-2 fluoro-1 indane-*trans* (**2**) a été analysé et ces données ont été utilisées pour établir la conformation. [Traduit par le journal]

Can. J. Chem., **51**, 2930 (1973)

Can. J. Chem. Downloaded from www.nrcresearchpress.com by 210.87.254.105 on 09/05/12
For personal use only.

Introduction

Nuclear magnetic resonance spectroscopy has proven to be a powerful tool for studying configurational and conformational problems associated with six-membered ring systems: to a large degree, this success is associated with well-defined stereospecificities of *vicinal* ^1H–^1H (2) and ^{19}F–^1H (3) coupling constants for the ranges of dihedral angles found for chair conformations. Unfortunately the *vicinal* couplings of saturated five-membered rings do not fall into separate, well defined categories and as a result it is often difficult to use them to assign a configuration, let alone a conformation. Various subterfuges can be adopted whereby "selection-rules" may be used as the basis for more objective evaluations, but these are empirical as, for example in the CYCLOPS treatment (4), and may have their own particular limitations.

The conformational problems associated with the indan (**1**) system are simpler than those commonly encountered in saturated five-membered rings since the ring either exists in the envelope conformation having C-2 above (the ^2V-conformation in **A**) or below (as in the V_2-conformation in **B**) the plane defined by the rest of the ring.

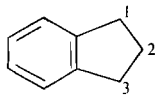

1

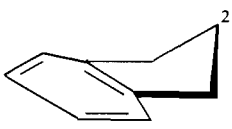

A

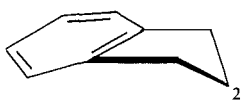

B

The indane system has previously been the subject of several ^1H n.m.r. studies. Buys and Havinga (5) considered *trans*-1,2-dichloro-, *trans*-1,2-dibromo-, and *trans*-2-bromo-1-chloro-indan; combining dipole moment data with ^1H n.m.r. spectra they were able to arrive at the constant J_0 in the Karplus equation. To do this they needed to assume (*a*) that the pucker of the ring for all three molecules was 25° (in both conformations); (*b*) that the different molecules would have the same coupling constant in each conformer (*i.e.* the increased electronegativity of chlorine over bromine would have negligible effect); (*c*) that the Karplus equation could be strictly applied; and (*d*) some parameters for relating dipole moments and coupling constants (*e.g.* the partial moment along the C—X bond, the valency angle C—C—X, and others). From the observed *vicinal* ^1H–^1H couplings and the calculated value of J_0, the position of the conformational equilibrium could be calculated; the mole fraction of diaxial conformer increased from 0.67 in the dichloride to >0.95 in the dibromide.

In the second work, Austin and Lillya (6) measured the ^1H n.m.r. spectra of 22 1,2-disubstituted indans (both *cis* and *trans*) and extracted the three vicinal ^1H–^1H couplings from each. They assumed that these couplings were subject to a *linear* attenuation due to the electronegativity of the substituents which they allowed for by using reference data from the literature (7);

[1]Part VI of a series "The Conformations of Cyclic Compounds in Solution." For Part IV see ref. 1.

[2]Revision received February 23, 1973.

Can. J. Chem. Downloaded from www.nrcresearchpress.com by 210.87.254.105 on 09/05/12
For personal use only.

their own data show that this particular procedure was incorrect. No conclusions were drawn regarding the degree of pucker of the five-membered ring.

The synthesis (8) of *trans*-2-bromo-1-fluoroindan (**2**) provided an ideal model compound for a conformational study. With the known (9) dependence of $^3J_{HF}$ upon electronegativity and dihedral angle the degree of pucker was determined with fair accuracy. Values of $^3J_{HH}$ were then used to estimate the position of the conformational equilibrium.

Results and Discussion

The ^{1}H n.m.r. spectrum of **2**, run as the neat liquid, was reasonably straightforward to assign. Irradiation of the aromatic protons sharpened

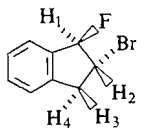

2

the transitions due to H_1, H_3, and H_4 and enabled a far more accurate analysis to be made, as also did ^{1}H–[^{19}F] decoupling experiments. The resonances of H_3 and H_4 shown in Fig. 1A are typical; see also experimental section. The ^{19}F spectrum is a broad band; however, ^{19}F–[^{1}H] double resonance spectra helped confirm the spectral assignments.

The signs of the various coupling constants were determined by a series of spin-tickling experiments; since both the spectra and the experiments were reasonably complex, a computer programme (NMDRS, see Experimental) was used to check their outcome. Irradiation of the lowest field transition of the H_2 resonance (at τ 5.5263) produced the spectrum shown in Fig. 1B; the computer-simulated spectrum is shown in Fig. 1C. It can be seen that transitions 5 and 7 (counting from low field) of both H_3 and H_4 are split; this indicates that $^3J_{2F}$ has the same sign as both $^4J_{3F}$ and $^4J_{4F}$, but $^3J_{24}$ and $^3J_{23}$ have opposite signs to $^2J_{34}$. Since *vicinal* ^{1}H–^{19}F couplings ($^3J_{HF}$) are positive (10) this indicates that both long-range ^{1}H–^{19}F couplings in this molecule ($^4J_{3F}$ and $^4J_{4F}$) are positive. The agreement between theoretical and experimental spectra is reasonably good. Each transition is

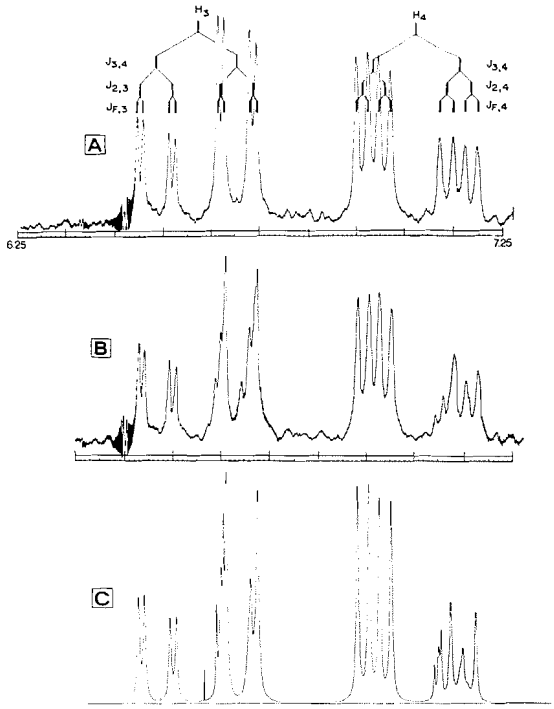

FIG. 1. The H_3 and H_4 resonances (100 MHz) of **2**. A, the spectrum measured with simultaneous irradiation of the aromatic protons; B, as for A, but with irradiation of the lowest field transition of the H_2 resonance; C, the computer simulation of the spectrum given in B.

now split into three lines rather than the usual two for spin-tickling, since the original transition in the H_3 (or H_4) spectrum is actually an unresolved doublet (due to the coupling of H_1) and only one line of each doublet is split in the spin-tickling experiment.

In a separate experiment a transition of the H_3 resonance was irradiated and the effect observed in the H_2 resonance; this indicated the $^4J_{3F}$ and $^3J_{2F}$ have the same sign, but $^2J_{24}$ and $^3J_{34}$ have opposite signs.

With the results of these experiments on hand, the normal spectra of **2** were subject to iterative computer analysis using TWOSUM (see Experimental section); the fit between the calculated and experimental spectra (^{1}H only) was satisfactory with an average deviation of only 0.049 Hz.[3] The final calculated coupling constants (Hz) are:

[3]One imaginary ^{19}F transition was put into the experimental set in order to link the energy levels together.

$^3J_{12} = 3.15$	$^3J_{23} = 6.74$	$^2J_{34} = -17.06$
$^4J_{13} = 0.0$	$^3J_{24} = 4.56$	$^4J_{3F} = 1.20$
$^4J_{14} = 0.0$	$^3J_{2F} = 17.27$	$^4J_{4F} = 2.45$
$^2J_{1F} = 55.73$		

It now remains to decide the shape adopted by the five-membered ring of **2**. Consideration of the size of $^3J_{2F}$ (17.3 Hz) in comparison with data for systems with similar electronegative (ε 5.15) substituents (9) indicates that the dihedral angle between H_2 and F is either 10–25° or about 110–125°. However, the second possibility is ruled out since the five-membered ring would have to bend an absurd amount to achieve such a large dihedral angle between *cis*-atoms. Hence the bend of the ring is determined to be in the region 10–25°, but this does not decide which way the ring is bent. Since $^3J_{24}$ and $^3J_{12}$ must be nearly equal, by symmetry, we can

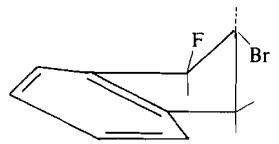

C

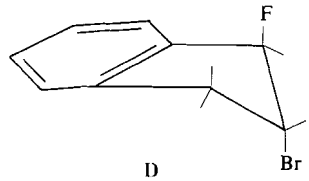

D

assign the larger coupling (6.7 Hz) to $^3J_{23}$. For 1-bromo-acenapthene (11), with similar electronegativity, $^3J_{HH}$ (0°) = 6.8 Hz, and for the vinyl fluoride adduct of hexachlorocyclopentadiene (12), $^3J_{HH}$ (0°) = 7.0 Hz. Hence a small bend of the five-membered ring is also to be expected from this piece of information. However, $^3J_{23}$ also has approximately the same value with either conformation **C** or **D**.

The relative amounts of each conformer may, however, be deduced by comparison of $^3J_{12}$ with other data in this study. $^3J_{HH}$ ($\phi = 180°$) is obtained from the analysis of *trans*-1-bromo-2-fluoro-cyclohexane-3,3,6,6-d_4 (1) (10.1 Hz) and $^3J_{HH}$ ($\phi = 100°$) from *trans*-1-bromo-2-fluoro-acenapthene (9) (1.0 Hz). Thus for $\phi = 145°$ a value of 7.0 Hz is reasonable, and the experimental value of 3.15 Hz indicates that the *diaxial* conformer **D** predominates to the extent of *ca.* 60%.

The values of $^3J_{12}$ and $^3J_{24}$ may be compared with those in other *trans*-1,2-dihalides (5, 6).

	$^3J_{12}$	$^3J_{24}$
Br–F	3.15	4.56
Br–Br	1.2	1.3
Br–Cl	2.7	3.1
Cl–Cl	3.3	3.8
Cl–I	2.9	3.2

Since the bromo-fluoride has the highest electronegativity, there appears to be more diequatorial conformer present in this compound than in the other dihalides, once again indicating the small amount of halogen–halogen repulsion when fluoride is involved (1).

Experimental

The synthesis of *trans*-2-bromo-1-fluoro-indan (**2**) is described in an accompanying paper (8).

All n.m.r. measurements were made with an extensively modified (13) Varian HA-100 instrument operating in the locked frequency-sweep mode.

The computer-based analysis of the spectra of **2** used a version of the TWOSUM programme, kindly provided by Dr. J. Martin (University of Alberta, Edmonton) in conjunction with a plot-routine, SMASH, written by John Coulthard of the University of British Columbia Computing Centre.

The spin-tickling experiments used to determine the relative signs of the coupling constants were checked by using as double-resonance simulation programme, NMDRS[4] in conjunction with SMASH.

Although this programme is extraordinarily useful, it remains that *sometimes* the theoretical line shapes are rather poor reproductions of the experimental. This may reflect the inadequacy of the double resonance programme (NMDRS), which neglects all *relaxation effects* in calculating the line shapes; the programme frequently predicted extremely sharp lines which are virtually never observed in practice. Whether or not this was the fault of NMDRS as noted above or simply an instrumental problem (*e.g.* the saturation level of a very sharp line may be much lower than normal) was not determined.

Several figures have been submitted to the Depository for Unpublished Data.[5] Since we feel that some of these

[4]The original listing of the programme NMDRS (14) was obtained from the National Physical Laboratory, Teddington, U.K.; this programme was in ALGOL, and the necessary translation to FORTRAN was kindly carried out by Susan Boyd of the University of British Columbia Computing Centre.

[5]These figures may be obtained at a nominal charge, from the Depository of Unpublished Data, National Science Library, National Research Council of Canada, Ottawa, Canada K1A 0S2.

Can. J. Chem. Downloaded from www.nrcresearchpress.com by 210.87.254.105 on 09/05/12
For personal use only.

Figures may be of interest, we have appended below their Figure captions.

FIG. 1. Partial ^1H n.m.r. spectra (100 MHz) of 2-bromo-1-fluoro-indan (**2**). A, the spectrum of H_1, measured with simultaneous irradiation of the aromatic protons; B, the computer simulation of A; C, as for A, but with simultaneous irradiation at the ^{19}F resonance frequency.

FIG. 2. Partial ^1H n.m.r. spectra (100 MHz) of **2**. A, the spectrum of H_2, measured with simultaneous irradiation of the aromatic protons; B, the computer simulation of A; C as for A, but with simultaneous irradiation at the ^{19}F resonance frequency.

FIG. 3. Partial ^1H n.m.r. spectra of **2**. A, the resonances of H_3 and H_4 with simultaneous irradiation of the aromatic protons; B, the computer simulation of A.

FIG. 4. Partial ^1H n.m.r. spectra (100 MHz) of **2**. A, the resonances of H_3 and H_4 measured with simultaneous irradiation of the aromatic protons; B, as for A, but with irradiation at the fluorine resonance frequency.

FIG. 5. Partial ^1H n.m.r. spectra (100 MHz) of **2**. A, the spectrum measured with simultaneous irradiation of the aromatic protons and of the third transition from low field of the H_3 resonance; B, computer simulation of A; C, the spectrum measured with simultaneous irradiation of the fourth, lowest field transition of the H_3 resonance; D, computer simulation of C.

This work was supported by operating grants from the National Research Council of Canada (A-1905) and by funds from Imperial Oil Ltd.

1. L. D. HALL and D. L. JONES. Can. J. Chem. **51**, 2915 (1973).
2. M. KARPLUS. J. Chem. Phys. **30**, 11 (1959); J. Am. Chem. Soc. **85**, 2870 (1963).
3. A. D. BARFORD, A. B. FOSTER, J. H. WESTWOOD, L. D. HALL, and R. N. JOHNSON. Carbohydr. Res. **19**, 49 (1971) and refs. therein.
4. L. D. HALL, P. R. STEINER, and C. PEDERSON. Can. J. Chem. **48**, 1155 (1970).
5. H. R. BUYS and E. HAVINGA. Tetrahedron, **24**, 4967 (1967).
6. R. A. AUSTIN and C. P. LILLYA. J. Org. Chem. **34**, 1327 (1967).
7. S. L. SMITH and R. H. COX. J. Phys. Chem. **72**, 198 (1968).
8. L. D. HALL and D. L. JONES. Can. J. Chem. **51**, 2903 (1973).
9. L. D. HALL and D. L. JONES. Can. J. Chem. **51**, 2925 (1973).
10. L. D. HALL and J. F. MANVILLE. Carbohydr. Res. **9**, 11 (1969).
11. M. J. S. DEWAR and R. C. FAHEY. J. Am. Chem. Soc. **85**, 2245 (1963).
12. K. L. WILLIAMSON, Y. F. LI, F. H. HALL, and S. SWAGER. J. Am. Chem. Soc. **88**, 5678 (1966).
13. R. BURTON and L. D. HALL. Can. J. Chem. **48**, 59 (1970).
14. G. GOVIL and D. H. WHIFFEN. Mol. Phys. **12**, 449 (1967).

Can. J. Chem. Downloaded from www.nrcresearchpress.com by 210.87.254.105 on 09/05/12
For personal use only.

The Kinetics of the Reaction $2C_3H_6 \rightarrow C_3H_5 + C_3H_7$

M. SIMON AND M. H. BACK
Chemistry Department, University of Ottawa, Ottawa, Canada, K1N 6N5

Received December 19, 1972

An attempt has been made to measure the rate constant for the bimolecular process

$$2C_3H_6 \rightarrow C_3H_5 + i\text{-}C_3H_7$$

using acetaldehyde as a radical scavenger. The rate constant obtained may be expressed as follows:

$$\log k \text{ (l mol}^{-1}\text{ s}^{-1}) = 10.4 - 43\,500/2.3RT$$

This activation energy corresponds to a value of 36 kcal/mol for ΔH_f(allyl).

On a essayé de mesurer la constante de vitesse du processus bimoléculaire

$$2C_3H_6 \rightarrow C_3H_5 + i\text{-}C_3H_7$$

en utilisant l'acétaldéhyde pour piéger le radical. La constante de vitesse obtenue peut être exprimée comme suit:

$$\log k \text{ (l mol}^{-1}\text{ s}^{-1}) = 10.4 - 43\,500/2.3RT$$

Cette énergie d'activation correspond à une valeur de 36 kcal/mol pour le ΔH_f(allyle).

[Traduit par le journal]

Can. J. Chem., **51**, 2934 (1973)

Introduction

In a recent study of the kinetics of the decomposition of propylene in the region of 750 °K (1) it was suggested that the initiation step in the chain reaction was the bimolecular reaction of propylene to give an allyl and a propyl radical.

[1] $$2C_3H_6 \rightarrow C_3H_5 + i\text{-}C_3H_7$$

The present work describes an attempt to measure the rate constant for this process. The method involved the pyrolysis of propylene in the presence of a suitable scavenger to convert propyl radicals to propane. The scavenger chosen was acetaldehyde so that reaction 1 would be followed by

[2] $$C_3H_7 + CH_3CHO \rightarrow C_3H_8 + CH_3CO$$

If all the propyl radicals formed in reaction 1 react by reaction 2 the rate of formation of propane may be equated to the rate of reaction 1, provided other sources of propane are not important.

Experimental

Materials

Research grade propylene was obtained from Matheson of Canada, Whitby, Ontario. Analysis by gas chromatography showed a propane impurity of 0.007 mol%. This correction to the yield of propane was usually about 5% and never more than 10%. Acetaldehyde was prepared from research grade paraldehyde by distillation under nitrogen. Acetaldehyde was stored under vacuum at temperatures below 20 °C.

Apparatus and Procedure

The apparatus, a conventional static pyrolysis system, has been described (2). Two reaction vessels were used, each 200 cc, with S/V ratios of 1.0 and 8.5 cm^{-1}. The reactants were mixed in a one-liter flask with an internal cold finger. Various mixing procedures were tried; the most efficient involved inducing convection currents in the gases with a 100 W light bulb placed at one side of the flask. Whether the reactants were condensed together or not had no effect on the results. The reactants were introduced directly from the mixing flask into the reaction vessel through a Hoke diaphragm seal stainless steel valve. The products and reactant were condensed together and analyzed on an F and M temperature-programed gas chromatograph using a 3 ft column of silica gel and alumina. Rates of formation of products were measured at four temperatures, 743, 763, 783, and 803 °K, and over a range of pressures.

Results

The main products from the pyrolysis of propylene in the presence of acetaldehyde were methane, carbon monoxide, ethane, ethylene, butane, butene, and propane. Higher hydrocarbon products were not measured because their appearance on the gas chromatographic analysis was obscured by the large quantities of acetaldehyde. The present paper reports only the results of the measurement of the rate of formation of propane. Measurements of the other products are reported in the following paper. Initial rates of formation of propane were measured as a function of acetaldehyde pressure for several pressures of propylene at each temperature.

Can. J. Chem. Downloaded from www.nrcresearchpress.com by 210.87.254.42 on 09/05/12
For personal use only.

Can. J. Chem. Downloaded from www.nrcresearchpress.com by 210.87.254.42 on 09/05/12
For personal use only.

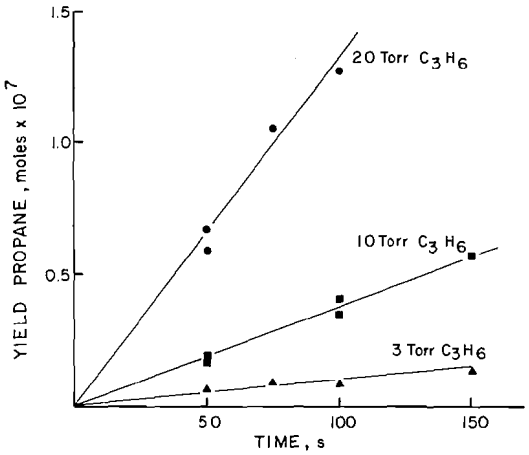

FIG. 1. Yield of propane as a function of time.

Typical results for the yield as a function of time are shown in Fig. 1.

There are two important kinetic features of the present system which enable the rate of formation of propane to be equated to the rate of reaction 1. As acetaldehyde is added to propylene, the rate of formation of propane should increase until a limiting value is obtained, which indicates that all the propyl radicals produced in reaction 1 are converted to propane by reaction with acetaldehyde. This behavior is illustrated in Figs. 2, 3, and 4. The yield of propane remained constant for ratios of propylene to acetaldehyde between 1:10 and 1:15 and most of the experiments were done with a ratio of about 1:14. Average values of the rate in the plateau region are given in Table 1. At 783 and 803 °K rates were measured in both the packed and unpacked reaction vessels. The rates were the same in each vessel and the values given in

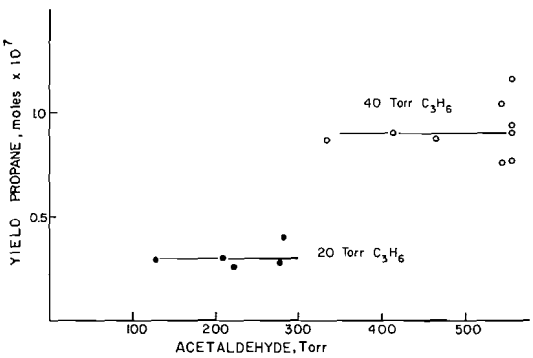

FIG. 2. Yield of propane as a function of acetaldehyde pressure, 743 °K.

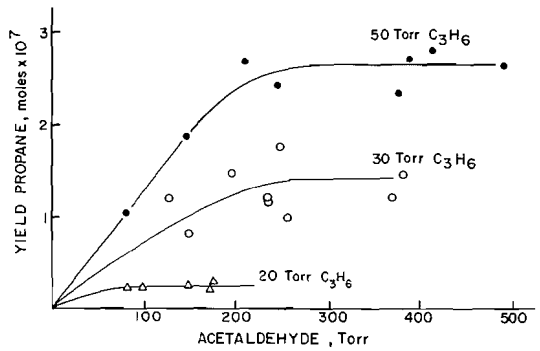

FIG. 3. Yield of propane as a function of acetaldehyde pressure, 783 °K.

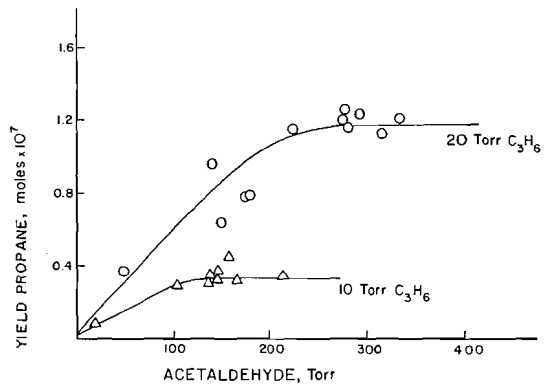

FIG. 4. Yield of propane as a function of acetaldehyde pressure, 803 °K.

TABLE 1. Rates of formation of propane in the plateau region

	Rate of formation (mol l^{-1} s^{-1} × 10^9)			
$P_{C_3H_6}$(Torr)	743 °K	763 °K	783 °K	803 °K
40	4.54	7.63	12.9*	22.7
35	3.18	5.40	10.7*	
30	2.58	4.14	8.24*	13.4
25	1.97	2.63	6.06*	9.8
20	1.46	2.22	3.61*	6.1*
15			2.42*	3.5*
10	0.66	0.859	1.13*	1.8*
5	0.30	0.470	0.62*	0.5
	Rate constant k_1 (l mol^{-1} s^{-1} × 10^3)			
Equation	743 °K	763 °K	783 °K	803 °K
3	6.1	13.0	23.8	40.0
4	4.9	8.7	20.6	38.8

*Denotes average value obtained from experiments in the packed and unpacked reaction vessels.

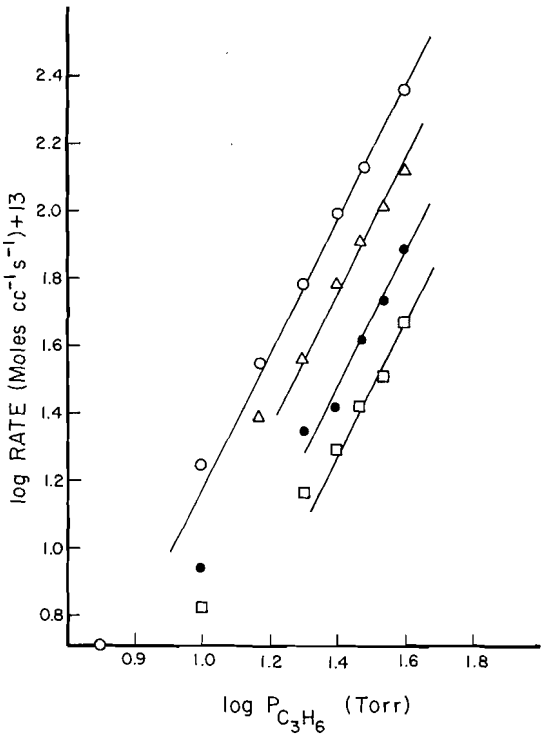

FIG. 5. Logarithm of the rate of formation of propane at the plateau against the logarithm of the propylene pressure. ○, 803 °K; △, 783 °K, ●, 763 °K; □, 743 °K.

Table 1 represent the average obtained from both sets of experiments.

The rate of formation of propane in the plateau region should be second order with respect to propylene. In Fig. 5 the log of the rate is plotted against the log of the propylene pressure. At each temperature, the line has been drawn to correspond to an order of 2.0. At pressures above 20 Torr the rate is second order with respect to propylene, but below about 20 Torr some propane appears to be formed by a lower order process, particularly at the lower temperatures.

A second-order rate constant was calculated from the relation

$$[3]\quad k_1 = \frac{\text{Rate of propane formation at plateau}}{[C_3H_6]^2}$$

where the rate was taken in the region of pressure where it was second order with respect to propylene. These values are shown in Table 1 as k_1 calculated from eq. 3.

In an attempt to correct k_1 for the occurrence of a lower order process giving propane, the data were analyzed according to the following equation:

$$\text{Rate of propane} = k_x[C_3H_6]^n + k_1[C_3H_6]^2$$

where k_x may be a composite rate constant. Linear plots of the following form were obtained only for $n = 1/2$.

$$[4]\quad \frac{\text{Rate}(C_3H_8)}{[C_3H_6]^{1/2}} = k_x + k_1[C_3H_6]^{3/2}$$

The data at 743 °K are shown in Fig. 6. The mechanism whereby propane is formed with a square-root dependence on the concentration of propylene is probably complex. In fact in these experiments this dependence represents an overall dependence of the rate on both reactants, since a constant ratio of acetaldehyde and propane was maintained. The separate dependence of the rate on each reactant cannot be determined. Furthermore, the value of k_x changed very little over the temperature range, indicating an activation energy of the order of 10 kcal/mol. Such a low value suggests the rate may be a complex sum of competing reactions or that surface reactions may be important.

Values of k_1 obtained from plots of eq. 4 are included in Table 1 as k_1 calculated from eq. 4. The two values of k_1 are essentially the same at the two higher temperatures where the rate was second order over a wide range of pressures. At

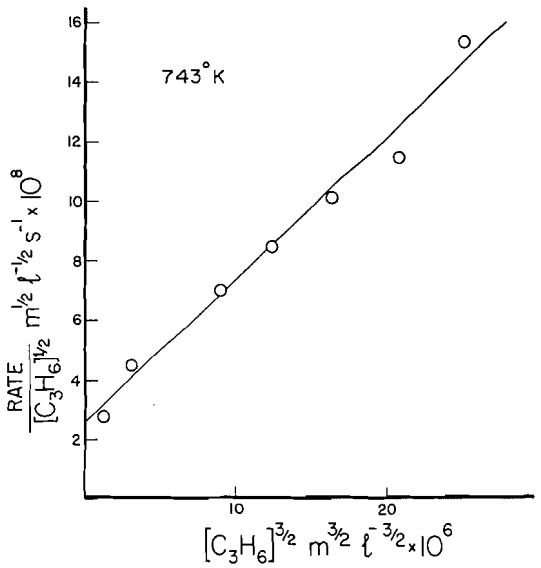

FIG. 6. Plot of eq. 4 with $n = 1/2$ for data obtained at 743 °K.

Can. J. Chem. Downloaded from www.nrcresearchpress.com by 210.87.254.42 on 09/05/12
For personal use only.

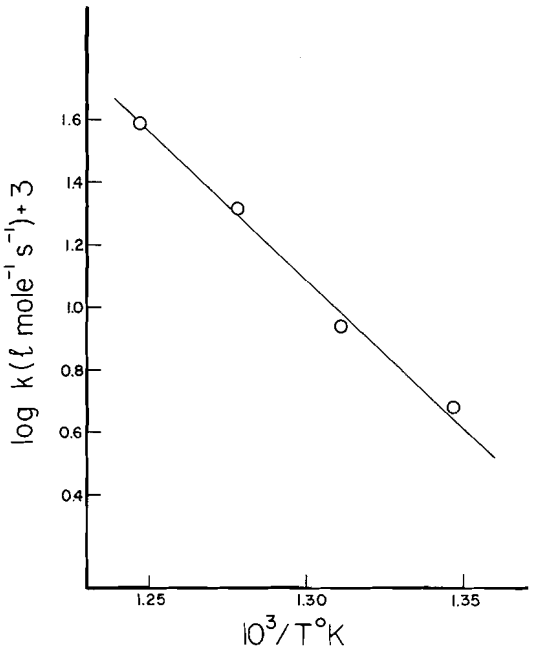

FIG. 7. Arrhenius plot of k_1.

the two lower temperatures, where more curvature in the order plot was observed the correction was as much as 30%.

An Arrhenius plot of the corrected values of k_1 is shown in Fig. 7. From this plot the following expression was obtained for k_1:

$$\log k_1(\text{l mol}^{-1}\ \text{s}^{-1}) = 10.4 - \frac{43\,500}{2.3RT}$$

The frequency factor for reaction 1 may be calculated from the entropy change of the reaction and the rate constant for the reverse disproportionation of allyl and propyl radicals. If the rate constant for combination of allyl and propyl radicals is assumed to be the same as that for two methyl radicals and the ratio of disproportionation to combination is taken as 0.20, the frequency factor for reaction 1 is 1.6×10^{10} l mol^{-1} s^{-1}. Although this ratio of disproportionation to combination has not been measured it may be estimated from the relation between k_d/k_c and $S_d^0 - S_c^0$ (3). The value of 0.20 obtained from this procedure is very similar to the value of 0.18 measured for the reaction of allyl and ethyl radicals (4). The calculated and measured values for the frequency factor are in excellent agreement.

The activation energy of k_1 represents the endothermicity of reaction 1 if the activation energy for the reverse process is assumed to be zero. Thus a value of 36 kcal/mol may be derived for ΔH_f(allyl) at temperatures in the region of 750 °K. The change in ΔH from 750 °K to 298 °K is less than 0.5 kcal/mol and this correction may be neglected. The limits of error are probably larger than indicated by the scatter of the data and a reasonable estimate is ± 2 kcal/mol.

An attempt was made to measure the rate of formation of propyl radicals using H_2S as scavenger. Although under some conditions, a plateau in the rate of formation of propane was observed as the concentration of H_2S was increased, the rate in the plateau region was approximately first order with respect to propylene, not second order. The rate was increased by about a factor of four in the packed reaction vessel and a given set of experiments was not reproducible over a period of time. The kinetics in this system were too complex to permit a straightforward measurement of the rate of reaction 1.

Discussion

The observed frequency factor for reaction 1 is in very good agreement with the value predicted from a simple consideration of the entropy change in the reaction and a comparison of the reverse disproportionation reaction with others of a similar type. The bimolecular reaction may therefore be described as a hydrogen atom transfer process similar to such reactions involving radicals but requiring a higher energy barrier. If excited electronic states of propylene were important, the frequency factor would likely be much lower.

Some recent measurements of ΔH_f(allyl) are summarized in Table 2. The low value obtained in the present experiments may be the result of an erroneously high rate of formation of propane. Several sources of propane, other than the sequence of reactions 1 and 2, might be suggested in the present system.

Hydrogen is a minor product in the pyrolysis of mixtures of acetaldehyde and propylene and is probably formed by the reaction of hydrogen atoms with acetaldehyde or propylene.

[5] $\quad H + CH_3CHO \rightarrow H_2 + CH_3CO$

[6] $\quad H + C_3H_6 \rightarrow H_2 + C_3H_5$

Addition of hydrogen atoms to propylene would

Can. J. Chem. Downloaded from www.nrcresearchpress.com by 210.87.254.42 on 09/05/12
For personal use only.

TABLE 2. Recent measurements of ΔH_f(allyl)

Authors	Reference	Method	$\Delta H_f(C_3H_5)$ at 298 °K
Busfield and Ivin (1961)	5	Kinetics of pyrolysis	34 0 ± 2 8
Golden, Rodgers, and Benson (1966)	6	Addition of I_2	40.6 ± 1
Homer and Lossing (1966)	7	Kinetics of pyrolysis	33
Akers and Throssell (1967)	8	Kinetics of pyrolysis	38
Tsang (1967)	9	Kinetics of pyrolysis	39 ± 2
Trenwith (1967)	10	Kinetics of pyrolysis	38.4 ± 1.5
Field and Abell (1969)	11	Photoaddition of HBr	41.5
Golden, Gac, and Benson (1969)	12	Low pressure pyrolysis	41.2 ± 2
Lossing (1971)	13	Ionization potential	40 ± 2
Present work		Kinetics of pyrolysis	36 ± 2

lead to formation of propyl radicals and hence to propane.

[7] $$H + C_3H_6 \rightarrow C_3H_7$$

Absolute values for k_5, k_6, and k_7 are not well established in the temperature range of 800 °K. Nevertheless if k_5 is taken as approximately equal to k_6 the following expression may be obtained (14):

$$\log \frac{k_7}{k_5} \approx + \frac{2000}{2.3RT} \approx 0.5$$

Under the present conditions the ratio of the rate of addition to propylene to the rate of abstraction from acetaldehyde in the plateau region will be about 0.2. These estimates are, however, not very reliable, and a better assessment of the importance of reaction 7 may be obtained from a consideration of the kinetics of hydrogen formation.

There are several possible sources of hydrogen atoms in the present system.

[8] $$CH_3CHO \rightarrow CH_3 + CHO$$

[9] $$CHO \rightarrow CO + H$$

[10] $$C_3H_6 \rightarrow C_3H_5 + H$$

[11] $$CH_3 + CH_3CHO \rightarrow CH_2CHO + CH_4$$

[12] $$C_3H_5 + CH_3CHO \rightarrow CH_2CHO + C_3H_6$$

[13] $$CH_2CHO \rightarrow CH_2CO + H$$

[14] $$CH_3 + C_3H_6 \rightarrow C_4H_9$$

[15] $$C_4H_9 \rightarrow C_4H_8 + H$$

[16] $$C_3H_5 + C_3H_6 \rightarrow C_6H_{11}$$

[17] $$C_6H_{11} \rightarrow C_6H_{10} + H$$

None of these reactions forming hydrogen atoms lead to a rate of formation of propane which is comparable to the rate observed or which is second order with respect to propylene and independent of the concentration of acetaldehyde. For example, the rate of reaction 10 is much slower than the rate of formation of propane in the present system. The rate of formation of hydrogen atoms by reactions 8 and 9 will be a function of the concentration of acetaldehyde and would not give the plateaus observed for the rate of formation of propane. The rates of reactions 11 and 14 depend on the concentration of methyl radicals and would likewise not be independent of the concentration of acetaldehyde. The concentration of allyl radicals may become independent of the concentration of acetaldehyde but in the present experiments, reactions 12 and 16 must be small relative to reactions 11 and 14, respectively. Furthermore, in the plateau region $k_5(CH_3CHO)$ should be greater than $(k_6 + k_7)(C_3H_6)$ and addition should not be an important process. Nevertheless, because the yield of hydrogen could not be measured with certainty and might be as much as five times the yield of propane under some conditions, the rate of formation of propane may be in error due to hydrogen atom addition to propylene by as much as a factor of two. Even this error has a small effect on the activation energy, provided the frequency factor for reaction 1 is not greater than the calculated value.

A second source of propane in this system might be the reaction, similar to reaction 1, of acetaldehyde and propylene.

[18] $$C_3H_6 + CH_3CHO \rightarrow C_3H_7 + CH_3CO$$

The rate of formation of propane from this reaction would be linearly dependent on the acetaldehyde concentration and a plateau would

Can. J. Chem. Downloaded from www.nrcresearchpress.com by 210.87.254.42 on 09/05/12
For personal use only.

not be observed. Reaction 18 must not be important in this system. A corollary to this conclusion is that the rate of this process must be about fifty times slower than the measured rate of reaction 1 in order that a plateau be observed with the ratio of acetaldehyde to propylene in the present experiments. If the frequency factors for reactions 1 and 18 are the same, as appears likely from the similarity of the entropy change of the reactions, this restriction implies an activation energy of about 48 kcal/mol for reaction 18. Using the heats of formation of the radicals given in ref. 15 the endothermicity of reaction 18 is 47 kcal/mol. The restriction is thus well within the uncertainty of the estimation.

The kinetics of the formation of propane in the present system is consistent with its formation by the sequence of reactions 1 and 2. This interpretation, however, leads to a value for the heat of formation of the allyl radical lower than the most recent measurements but in agreement with values obtained from studies of the kinetics of pyrolysis reactions. Probably the most troublesome error in kinetic studies is the uncertainty in the mechanism of the reaction, which to a large extent determines the confidence with which the measured activation energy may be identified with the endothermicity of the reaction. Such errors have, however, not been identified in the present or the previous kinetic studies and it must be concluded that the reason for the range of values obtained for ΔH_f(allyl) remains uncertain.

The dissociation energy of the allyl radical was given an upper limit of 70 kcal/mol from measurements of the electronic absorption spectrum of the radical (16). This implies a lower limit of 28 kcal/mol for ΔH_f(allyl). The present results are well within this limitation.

The authors thank the National Research Council of Canada for continued financial support.

1. M. Simon and M. H. Back. Can. J. Chem. **48**, 317 (1970).
2. M. L. Boyd, T. M. Wu, and M. H. Back. Can. J. Chem. **46**, 2415 (1968).
3. R. A. Holroyd and G. W. Klein. J. Phys. Chem. **67**, 2275 (1963).
4. D. G. L. James and G. E. Troughton. Trans. Faraday Soc. **62**, 145 (1966).
5. W. K. Busfield and K. J. Ivin. Trans. Faraday Soc. **57**, 1044 (1961).
6. D. M. Golden, A. S. Rodgers, and S. W. Benson. J. Am. Chem. Soc. **88**, 3196 (1966).
7. J. B. Homer and F. P. Lossing. Can. J. Chem. **44**, 2211 (1966).
8. R. J. Akers and J. J. Throssell. Trans. Faraday Soc. **63**, 124 (1967).
9. W. Tsang. J. Chem. Phys. **46**, 2817 (1967).
10. A. B. Trenwith. Trans. Faraday Soc. **63**, 124 (1967).
11. R. J. Field and P. I. Abell. J. Am. Chem. Soc. **91**, 7226 (1969).
12. D. M. Golden, N. A. Gac, and S. W. Benson. J. Am. Chem. Soc. **91**, 2136 (1969).
13. F. P. Lossing. Can. J. Chem. **49**, 357 (1971).
14. A. F. Trotman-Dickenson and G. S. Milne. Tables of bimolecular gas reactions. National Bureau of Standards Reference Data Series 9, 1967.
15. S. W. Benson. Thermochemical kinetics. Wiley, New York. 1968.
16. C. L. Currie and D. A. Ramsay. J. Chem. Phys. **45**, 488 (1966).

Can. J. Chem. Downloaded from www.nrcresearchpress.com by 210.87.254.42 on 09/05/12
For personal use only.

The Co-Pyrolysis of Acetaldehyde and Propylene

M. SIMON AND M. H. BACK
Chemistry Department, University of Ottawa, Ottawa, Canada, K1N 6N5

Received December 19, 1972

Analysis of both major and minor products of the thermal reaction of mixtures of propylene and acetaldehyde over the temperature range 750–800 °K and at pressures below atmospheric show that both reactants initiate radical chains and that both addition and abstraction reactions of radicals with propylene are important. The relation to general mechanisms of the inhibiting effect of propylene in pyrolysis reactions is discussed.

L'analyse des produits mineurs et majeurs, issus de la réaction thermique d'un mélange propylène–acétaldéhyde entre 750 et 800 °K à des pressions inférieures à la pression atmosphérique, a montré premièrement que les deux réactifs sont capables d'initier des chaînes radicalaires et deuxièmement que les réactions d'addition et d'élimination, des radicaux avec le propylène, sont importantes. Dans le cas des réactions de pyrolyse, on discute de la relation entre l'effet inhibiteur du propylène et les mécanismes généraux de ces réactions. [Traduit par le journal]

Can. J. Chem., **51**, 2940 (1973)

Can. J. Chem. Downloaded from www.nrcresearchpress.com by 210.87.254.6 on 09/05/12
For personal use only.

Introduction

Propylene has long been known to inhibit the decomposition of many organic compounds (1–4). The inhibition has been explained by both addition and abstraction reactions of radicals with propylene. Both reactions reduce the apparent rate of reaction, the former by the formation of higher molecular weight products which lowers the rate of pressure increase, and the latter by the substitution of the relatively non-reactive allyl radical for the more reactive chain-carrying radical. A general mechanism has been formulated for such systems by Niclause *et al.* (5), who developed equations describing the rate of decomposition of an organic compound as a function of the concentration of additive for various types of chain mechanisms. With propylene they assumed that the predominant effect is the substitution of the allyl radical for the normal propagating radical, and for simplicity neglected addition reactions, as had been done by other authors (6, 7), although it was acknowledged that they could have some importance. Addition reactions were considered by Quinn (8) and by Marta *et al.* (9) in their studies of the effect of propylene on the pyrolysis of butane and of propionaldehyde, respectively, but their importance could not be assessed with any certainty because of incomplete product analysis. The relative importance of addition and abstraction reactions is a basic question in the mechanism of inhibition by propylene and in the related effect of self-inhibition of the pyrolysis of paraffins by the product olefins. The self-inhibition of neopentane, for example, has been explained by the ease of abstraction from the product isobutene (10), while the self-inhibition of propane (11) and isobutane (12) has been accounted for by addition processes.

Initiation of chains by unimolecular dissociation of propylene in propylene-inhibited reactions has been suggested (7) but it has generally been recognized that this dissociation would be slow compared to initiation by the original reactant. The bimolecular reaction of propylene to give radicals, either with itself or with the reactant, has not been considered in inhibition studies, but may under some conditions be faster than the unimolecular dissociation (13).

In spite of the considerable attention that has been given to the mechanism of inhibition by propylene the relative importance of abstraction, addition, and initiation reactions of propylene remains in some doubt. Previous studies have reported only the measurement of the rate of pressure change (14, 15) or of formation of major products (16–18), whereas a detailed examination of the products, both major and minor, is necessary to clarify these questions. In a recent study of the acetaldehyde–propylene system undertaken to measure the rate of bimolecular initiation by disproportionation of propylene (19) product data were obtained which showed the importance of addition to and initiation by propylene in this system. The present paper describes these results and their application to the mechanism of inhibition by propylene in general.

Can. J. Chem. Downloaded from www.nrcresearchpress.com by 210.87.254.6 on 09/05/12
For personal use only.

Experimental

Mixtures of propylene and acetaldehyde were pyrolyzed in a conventional static system which has been described (20). The purification of the reagents, the technique of mixing, and the analysis procedure for condensable products were given in the preceding paper. Methane and carbon monoxide were collected with a Toepler pump into a gas burette, where the total quantity was measured. The proportion of methane, carbon monoxide, and hydrogen was determined by combustion on a copper oxide furnace maintained at 420 °C. Because the yield of hydrogen was small (< 1% of CH_4 + CO), reliable values could not be obtained by this technique. The yield of hydrogen was estimated as roughly equivalent to the yield of propane.

Results and Discussion

Measurements were made at total pressures ranging from 20 to 600 Torr, usually with a ratio of propylene to acetaldehyde of 0.07, and at temperatures of 743, 763, 783, and 803 °K.

The main products were methane and carbon monoxide and their rates of formation were 100 times greater than the rates of formation of the other products. The decomposition was thus primarily that of acetaldehyde. The other products analyzed were, in order of importance, ethylene, ethane, butane, butene, propane, and hydrogen. Initial rates of formation of these products, except hydrogen, were measured, and, except for butane, yield–time plots were linear through the origin. Typical examples are shown in Fig. 1 and the measured rates, obtained from similar plots, are given in Table 1. At each temperature some experiments were done in the packed reaction vessel and in each case, no change in the rates of formation of products was observed. The rates in Table 1 are average values obtained using data from experiments in the packed and unpacked vessels.

In Table 2, the rates of formation of the main products from mixtures of propylene and acetaldehyde in the ratio 0.07 are compared with the rates of formation of each of these products from the pyrolysis of acetaldehyde (21) and propylene (13) separately. The rates of formation of products from the pyrolysis of 40 Torr of propylene were not measured directly, but were obtained by extrapolation of rates measured at higher pressures (100–600 Torr). They should therefore be regarded as approximate. In the two previous studies of the inhibition of acetaldehyde by propylene at 823 °K (14) and at 798 °K (16), where a minimum in the rate was observed at a ratio of propylene to acetaldehyde of 0.25, a ratio of 0.07 decreased the rate by a factor of 0.6, in good agreement with the present results.

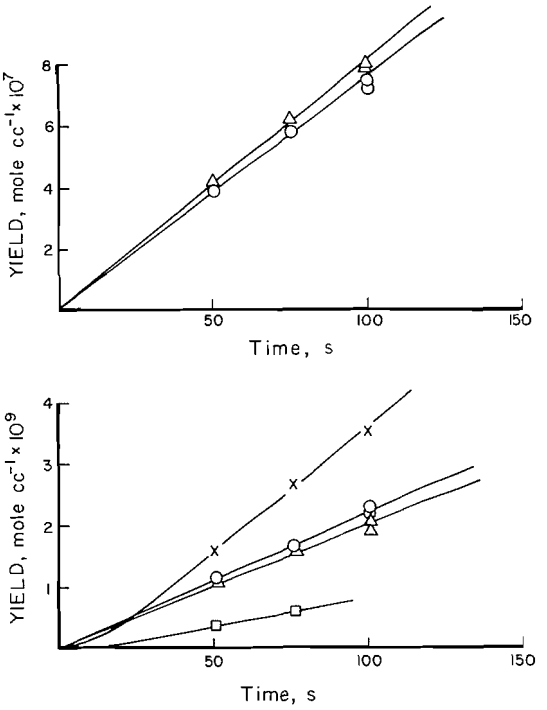

FIG. 1. Yields of products as a function of time. Temperature, 763 °K; pressure of propylene, 40 Torr; pressure of acetaldehyde, 550 Torr. Upper curve: △, CO; ○, CH_4. Lower curve: ×, butane; ○, ethylene; △, ethane; □, butene.

The product distribution from the mixture is quite different from that of either reactant by itself. In pure acetaldehyde, hydrocarbon products other than ethane were not observed. In pure propylene saturated hydrocarbon products other than methane were in very low yield, but higher molecular weight compounds, particularly C_6 hydrocarbons (not listed), were important products. In the pyrolysis of propylene addition to the double bond is a dominant feature of the mechanism, while in the pyrolysis of acetaldehyde abstraction of the aldehydic hydrogen is by far the most important chain-propagation process. In the mixture the availability of both types of reaction gives a new product distribution which illustrates the effect of the mutually interacting chain-propagation processes.

The following mechanism is a modification of the general mechanism proposed by Niclause *et al.* (5) to include initiation by propylene and addition of radicals to propylene.

[1] $$CH_3CHO \rightarrow CH_3 + CHO$$

TABLE 1. Initial rate of formation

T (°K)	$[C_3H_6]$ (Torr)	$[CH_3CHO]$ (Torr)	Rate (mol cc^{-1} s^{-1}) × 10^9 CO	× 10^9 CH_4	× 10^{12} C_2H_6	× 10^{12} C_2H_4	× 10^{12} C_4H_{10}	× 10^{12} C_4H_8
743	40	550	4.68	4.14	12.1	15.0	27.5	
	35	490	3.58	3.64			14.1	
	30	420	3.36	3.02		14.0		
	25	350	2.80	2.58		10.7	6.01	
	20	280	1.83	1.85	5.35	5.30	4.24	
	10	140	0.813	0.845	2.42	3.43	1.52	
	5	70	0.35	0.35	0.88	1.31	1.01	
763	40	550	8.08	7.78	21.9	23.2		
	35	490	6.79	6.57	16.3	14.7		
	30	420	4.81	5.05		12.2		
	25	350	4.00	3.74				
	20	280	2.97	2.70		7.98		
	10	140	1.16	1.10	3.53	3.38		
	5	70	0.47	0.465	1.52	2.07		
783	60	510	12.2	8.48	42.7	40.1	59.6	
	50	420	8.59	8.08	31.8	32.3	44.2	
	40	340	6.26	5.81	24.1	24.5	24.2	
	40	550	16.4	13.5	43.8	50.5	59.3	26.0
	35	490	14.4	10.8	33.8	40.2	33.4	
	30	250	4.80	3.74	15.7	15.0	11.9	
	30	420	11.5	9.29		23.7	23.5	17.3
	25	350	8.18	6.92	20.6	17.5	14.0	10.7
	20	280	6.62	5.76	15.8	13.8	8.48	8.81
	15	210	5.05	3.61	11.7	9.5	3.28	5.46
	10	140	3.03	2.58	8.08	7.47	1.16	3.6
	5	70	1.31	0.92	4.44	5.35		1.5
803	60	510			113	111	75.8	
	50	420			83.4		41.4	
	40	340			73.2	74.2	28.3	
	40	550	25.1	23.2		101	50.5	
	35	490	21.1	19.8	64.1	87.3	41.2	
	30	250			47.5	57.1	20.2	
	30	420	17.6	15.9	44.4		25.9	
	25	350	14.0	12.5			19.7	
	20	280	10.9	9.43	29.9	26.3	18.4	
	15	210	8.40	6.06	20.6	16.5	10.3	
	10	140	4.95	3.92	11.3	8.05	5.66	
	5	70	1.86	1.62	4.8	6.06	2.52	
	3	40	1.11	0.91	2.8	4.4	1.0	
	2	30	0.61	0.40	2.1	2.5	0.58	
	1	15	0.23	0.14	0.6	1.2	0.40	

[2] $2C_3H_6 \rightarrow C_3H_5 + C_3H_7$

[3] $CH_3 + CH_3CHO \rightarrow CH_4 + CH_3CO$

[4] $CH_3CO \rightarrow CH_3 + CO$

[5] $CH_3 + C_3H_6 \rightarrow CH_4 + C_3H_5$

[6] $C_3H_5 + CH_3CHO \rightarrow C_3H_6 + CH_3CO$

[7] $CH_3 + C_3H_6 \rightarrow C_4H_9$

[8] $C_3H_5 + C_3H_6 \rightarrow C_6H_{11}$

[9] $2CH_3 \rightarrow C_2H_6$

[10] $2C_3H_5 \rightarrow C_6H_{10}$

[11] $CH_3 + C_3H_5 \rightarrow C_4H_8$

[12] $C_4H_9 + CH_3CHO \rightarrow C_4H_{10} + CH_3CO$

[13] $C_4H_9 + C_3H_6 \rightarrow C_4H_{10} + C_3H_5$

[14] $C_4H_9 \rightarrow C_4H_8 + H$

[15] $C_4H_9 \rightarrow C_2H_5 + C_2H_4$

Can. J. Chem. Downloaded from www.nrcresearchpress.com by 210.87.254.6 on 09/05/12
For personal use only.

TABLE 2. Comparison of rates of formation of products from acetaldehyde, propylene, and propylene + acetaldehyde mixtures at $T = 796$ °K

Product	Rate of formation (mol cc^{-1} s^{-1} × 10^{11})		
	Acetaldehyde (550 Torr)	Propylene (40 Torr)	Propylene (40 Torr) + acetaldehyde (550 Torr)
CO	3600	—	2140
CH_4	3600	0.115	1950
C_2H_6	0.307	—	4.90
C_2H_4	—	0.1	6.45
C_3H_8	—	0.024	1.82
C_4H_{10}	—	—	5.13
C_4H_8	—	0.008	4.07
H_2	5.55	0.02	<10

The importance of addition reactions is evident from the relative rates of formation of methane and carbon monoxide, (Fig. 1) and from the rates of formation of C_4 products. The yields of methane are 10–20% lower than the yields of carbon monoxide over the range of temperature and pressure studied, whereas in the pyrolysis of acetaldehyde itself the yields of methane and carbon monoxide are identical to within 0.5% (22). Methyl radicals therefore react by a process which does not give methane and which can only be reaction 7.

The relative importance of abstraction and addition reactions in the inhibition process may be roughly estimated by a comparison of the yields of carbon monoxide and methane. Assuming as a first approximation, that the chain-propagation process gives an acetyl radical and that all acetyl radicals decompose to give carbon monoxide, then the yield of carbon monoxide in the mixture is a measure of the inhibition caused by the substitution of the methyl radical by the allyl radical. The yield of methane from the mixture is reduced not only by this effect but also by addition of methyl radicals to propylene. From Table 2 it may be seen that in this study the addition of propylene reduced the rate of formation of carbon monoxide by a factor of 0.59 and the rate of formation of methane by 0.53. About 10% of the inhibition can therefore be attributed to addition of methyl radicals to propylene. The rate as measured by the pressure increase will be further reduced by subsequent addition of higher molecular weight radicals to propylene.

The formation of butane and butene may be accounted for by the sequence of reactions 7, 12, 13, and 14. Since the addition of methyl radical to propylene gives a secondary butyl radical, isomerization must occur either before or after decomposition. In either case the activation energies for reactions 14 and 15 may be expected to be similar. Alternatively, further addition of the butyl radical may occur, followed by isomerization and decomposition of the C_7 radical, giving C_2H_5, C_2H_4, or C_4H_8. Indeed, the sum of the yields of butane + butene + ethane or ethylene accounts for only about 10% of the difference between methane and carbon monoxide and suggests that higher molecular weight compounds, formed by successive addition of radicals to propylene and not detected by the analysis, may be important products. The rates of formation of butane, ethane, and ethylene as a function of acetaldehyde pressure are shown in Fig. 2.

The occurrence of the bimolecular initiation reaction of propylene, reaction 2, is demonstrated by the formation of propane as a primary product, reported in the preceding paper. The importance of this initiation compared to initiation by acetaldehyde may be estimated using the value for k_2 obtained in the preceding paper and the previously measured value of $k_1 = 10^{15.7}e^{80000/RT}$ (22). With a ratio of propylene to acetaldehyde of 0.07 and at a pressure of propylene of about 25 Torr at 783 °K,

$$\frac{\text{Rate [1]}}{\text{Rate [2]}} = \frac{k_1[CH_3CHO]}{k_2[C_3H_6]^2} = 0.3$$

Taking into account the uncertainty in these rate

Can. J. Chem. Downloaded from www.nrcresearchpress.com by 210.87.254.6 on 09/05/12
For personal use only.

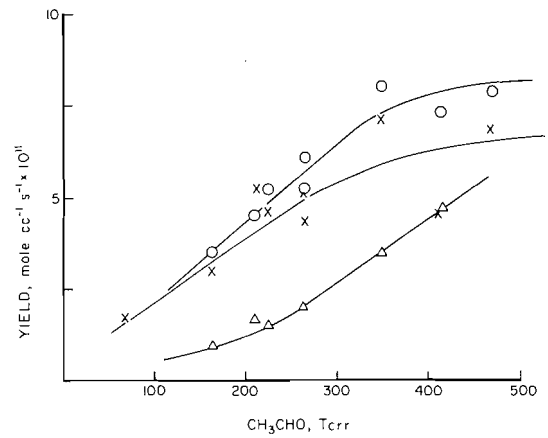

FIG. 2. Rate of formation of products as a function of acetaldehyde pressure. Temperature, 803 °K; pressure of propylene, 30 Torr. ○, ethylene; ×, ethane; △, butane.

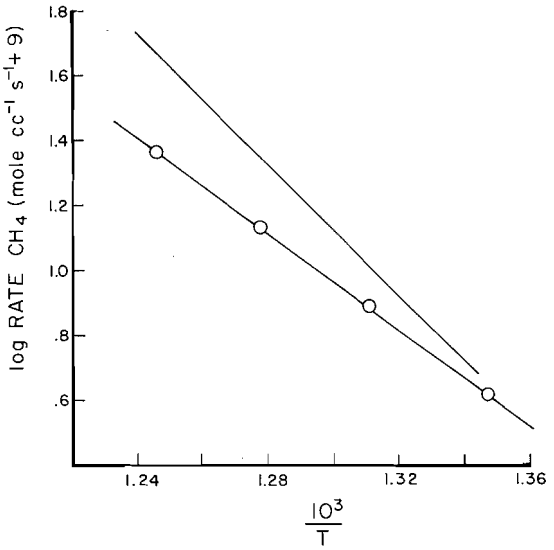

FIG. 3. Arrhenius plot of the rate of formation of methane. ○, 40 Torr C_3H_6 + 550 Torr CH_3CHO; solid line, 550 Torr CH_3CHO.

constants, the two rates may be considered to be roughly equal. With a ratio of propylene to acetaldehyde of 0.25, where the minimum in the rate was observed (14), initiation by reaction 2 would be at least three times as fast as by reaction 1 and would become increasingly important as the pressure of propylene was increased. The activation energy of the rate, obtained from the Arrhenius plot shown in Fig. 3, was 34 kcal/mol. This value is considerably lower than the value of 49 kcal/mol for the decomposition of acetaldehyde itself and is consistent with the occurrence of an additional initiation step of lower activation energy than the dissociation of acetaldehyde.

The analysis of inhibition mechanisms by Niclause *et al.* (5) showed that in the case where reaction with the additive forms a radical less reactive than the original chain-propagating radical, as is the case with propylene, the rate of reaction of the mixture will decrease with addition of inhibitor to a limit which represents the complete conversion of the original chain-propagating radical to the less reactive allyl radical. The rate of reaction of the mixture will increase only if propylene contributes to the initiation of radicals. Thus the subsequent increase in rate beyond the minimum value observed with mixtures of propylene and acetaldehyde (14) may quite reasonably be attributed to the initiation by propylene by the bimolecular disproportionation reaction. In mixtures of propylene with propionaldehyde (9) and with butane (23), where the rate was also observed to increase after passing through a minimum value, initiation by propylene may also be important. The ratio of propylene to reactant at which this secondary increase in rate is observed is a function of several competing rates, not only the rates of initiation, and cannot easily be predicted for any particular system.

The authors thank the National Research Council of Canada for generous financial assistance and Dr. R. A. Back for helpful discussions.

1. P. G. ASHMORE. Catalysis and inhibition of chemical reactions. Butterworths, London. 1963.
2. Z. G. SZABO. Advances in the kinetics of homogeneous gas reactions. Methuen, London. 1964.
3. B. G. GOWENLOCK. The inhibition of gaseous free radical chain reactions. Progress in reaction kinetics, Pergammon. **3**, 171 (1965).
4. J. H. PURNELL and C. P. QUINN. The pyrolyses of paraffins, photochemistry and reactions kinetics. *Edited by* P. G. Ashmore, F. S. Dainton, and T. M. Sugden. Cambridge University Press. 1967.
5. M. NICLAUSE, R. MARTIN, F. BARONNET, and G. SCACCHI. Rev. Inst. Fr. Pet. **21**, 1724 (1966).
6. F. O. RICE, and O. L. POLLY. J. Chem. Phys. **6**, 273 (1938).
7. D. J. MCKENNEY, B. W. WOJCIECHOWSKI, and K. J. LAIDLER. Can J. Chem. **41**, 1993 (1963).
8. C. P. QUINN. Symposium on the kinetics of pyrolytic reactions, Chemical Institute of Canada, Ottawa. 1964.

Can. J. Chem. Downloaded from www.nrcresearchpress.com by 210.87.254.6 on 09/05/12
For personal use only.

9. F. MARTA, G. ACS, and Z. G. SZABO. Acta Chim. Acad. Sci. Hung. **50**, 263 (1966).
10. G. M. CÔME and F. BARONNET. C. R. Acad. Sc. **268**C, 1917 (1969).
11. D. A. LEATHARD and J. H. PURNELL. Proc. R. Soc. A **305**, 517 (1968).
12. R. S. KONAR, J. H. PURNELL, and C. P. QUINN. Trans. Faraday Soc. **64**, 1319 (1968).
13. M. SIMON and M. H. BACK. Can. J. Chem. **48**, 317 (1970).
14. J. R. E. SMITH and C. N. HINSHELWOOD. Proc. R. Soc. A **180**, 237 (1942).
15. F. J. STUBBS and C. N. HINSHELWOOD. Proc. R. Soc. A **200**, 455 (1950).
16. G. R. FREEMAN, C. J. DANBY, and C. N. HINSHELWOOD. Proc. R. Soc. A **245**, 456 (1958).
17. S. K. Ho. Proc. R. Soc. A **276**, 278 (1963).
18. F. BARONNET, M. DZIERZYNSKI, R. MARTIN, and M. NICLAUSE. C. R. Acad. Sc. **267**C, 355 (1968). F. BARONNET, R. MARTIN, and M. NICLAUSE. J. Chim. Phys. **69**, 236 (1972).
19. M. SIMON and M. H. BACK. Can. J. Chem. This issue.
20. M. L. BOYD, T.-M. WU, and M. H. BACK. Can. J. Chem. **46**, 2415 (1968).
21. K. J. LAIDLER and M. T. H. LIU. Proc. R. Soc. A **297**, 365 (1967).
22. M. T. H. LIU and K. J. LAIDLER. Can. J. Chem. **46**, 479 (1968).
23. J. H. PURNELL and C. P. QUINN. Nature, **189**, 656 (1961).

Can. J. Chem. Downloaded from www.nrcresearchpress.com by 210.87.254.6 on 09/05/12
For personal use only.

Photolyse de l'ammoniac et de l'ammoniac perdeuterié à 185, 147, et 123.6 nm

JEANNINE MASANET, JANINE FOURNIER, ET CATHERINE VERMEIL

Equipe de Recherche du CNRS, associée à l'ESPCI, 10, rue Vauquelin, 75231 PARIS CEDEX 05 France

Reçu le 24 janvier 1973

La photolyse de l'ammoniac et de l'ammoniac perdeutérié a mis en évidence les faits suivants:

A 147 et à 123.6 nm, il existe un effet isotopique très important sur le rapport des rendements en hydrogène moléculaire et en hydrogène atomique $\phi_{H_2}/\phi_H > \phi_{D_2}/\phi_D$ tandis qu'à 185 nm $\phi_{H_2}/\phi_H = \phi_{D_2}/\phi_D$. La dissociation selon NH $(X^3\Sigma^-)$ + H + H apparaît à $\lambda = 147$ nm, ce qui implique $D_{NH-H} \leqslant 90$ kcal mol^{-1}.

On a pu évaluer la vitesse de la réaction D + $ND_3 \rightarrow D_2 + ND_2$, $k_{D+ND_3} = 3.5 \times 10^{13} \exp(-14400/RT)$ cm^3 mol^{-1} s^{-1}.

A very important isotopic effect for the ratio of molecular and atomic hydrogen yield in the photolysis of ammonia at 147 and 123.6 nm has been found $\phi_{H_2}/\phi_H > \phi_{D_2}/\phi_D$ while at 185 nm $\phi_{H_2}/\phi_H = \phi_{D_2}/\phi_D$.

The dissociation $NH_3 + h\nu \rightarrow$ NH $(X^3\Sigma^-)$ + H + H occurs for wavelengths as high as 147 nm which implies that $D_{NH-H} \leqslant 90$ kcal mol^{-1}.

The rate constant of the reaction D + $ND_3 \rightarrow D_2 + ND_2$ has been evaluated $k_{D+ND_3} = 3.5 \times 10^{13}$ exp $(-14\,400/RT)$ cm^3 mol^{-1} s^{-1}.

Can. J. Chem., 51, 2946 (1973)

Introduction

La photolyse de l'ammoniac dans son premier état excité $\tilde{A}\,^1A_2''$ est relativement bien connue (1,2); on considère généralement que la dissociation a lieu exclusivement en NH_2 + H. La photodissociation des autres états électroniques a été principalement suivie par spectroscopie d'absorption ou d'émission des radicaux NH et NH_2, formés soit par photolyse continue (3–5), soit par photolyse éclair (6). Ces travaux ne permettent pas de connaître les probabilités relatives des différents modes de dissociation. La présente étude a pour objet cette détermination dans trois régions différentes du spectre d'absorption en appliquant à l'ammoniac la méthode précédemment utilisée pour l'étude de la photolyse de l'eau (7,8), du méthane (9) et de leurs composés perdeutériés.

Principe de la methode

Selon l'état dissociatif atteint par absorption photonique, une molécule hydrogénée RH_2 peut en général se dissocier selon les trois modes suivants:

$$RH_2 + h\nu \rightarrow RH + H \quad \phi_a$$
$$\rightarrow R + H + H \quad \phi_b$$
$$\rightarrow R + H_2 \quad \phi_{H_2}$$
$$\phi_H = \phi_a + 2\phi_b$$

Si les atomes H sont interceptés par du deutérium, le schéma cinétique suivant rend compte des réactions secondaires des atomes H (en négligeant les réactions des radicaux R et RH et pour des taux de conversion faibles).

H (+M)	$\rightarrow \frac{1}{2}H_2$	k_d
H + RH_2	$\rightarrow H_2$ + RH	k_e
H + D_2	$\rightarrow$ HD + D	k_f
H + D (+M)	$\rightarrow$ HD	k_g
D (+ M)	$\rightarrow \frac{1}{2}D_2$	k_h
D + RH_2	$\rightarrow$ HD + RH	k_l

La mesure des concentrations relatives en H_2 et HD dans D_2 permet de déterminer pour des conditions d'irradiation variées, le rapport $[H_2]/[HD]$ en fonction du rapport $[RH_2]/[D_2]$. En appliquant le principe des états stationnaires et en négligeant k_g devant $k_f\,[D_2]$, on obtient:

$$\frac{[H_2]}{[HD]} = \frac{\phi_{H_2}}{\phi_H}\left(\frac{1}{1 + \frac{k_i[D][RH_2]}{\phi_H}\left(1 + \frac{k_d + k_e[RH_2]}{k_f[D_2]}\right)}\right) + \frac{k_d(\frac{1}{2} + \phi_{H_2}\phi_H^{-1}) + k_e[RH_2](1 + \phi_{H_2}\phi_H^{-1})}{k_f[D_2]\left[1 + \frac{k_i[D][RH_2]}{\phi_H}\left(1 + \frac{k_d + k_e[RH_2]}{k_f[D_2]}\right)\right]}$$

Can. J. Chem. Downloaded from www.nrcresearchpress.com by 210.87.254.6 on 09/05/12
For personal use only.

Can. J. Chem. Downloaded from www.nrcresearchpress.com by 210.87.254.6 on 09/05/12
For personal use only.

On obtient évidemment une expression analogue pour la photolyse de mélanges $RD_2 + H_2$.

Les rendements relatifs $[H_2]/[HD]$ (ou $[D_2]/[HD]$) sont exprimés graphiquement en fonction des rapports $[RH_2]/[D_2]$ (ou $[RD_2]/[H_2]$). Dans un domaine de concentration suffisante en RH_2, on obtient ainsi des droites qu'on peut extrapoler pour $[RH_2]/[D_2] \rightarrow 0$. *L'ordonnée à l'origine ainsi obtenue représente* $\phi_{H_2}/2\phi_H$, $(\phi_{D_2}/2\phi_D)$; on a alors en effet:

$$k_e\,[RH_2]/k_f[D_2] \ll 1$$

et

$$k_i[D][RH_2] \rightarrow \phi_H$$

Pour $[RH_2]$ constant, l'expression de $[H_2]/[HD]$ devient, avec une bonne approximation

$$\frac{[H_2]}{[HD]} - \left(\frac{[H_2]}{[HD]}\right)_{\text{limite}} = \frac{\alpha}{[D_2]} = \frac{1}{[D_2]}(A + B[RH_2])$$

avec

$$A \simeq (\phi_{H_2}/\phi_H + 0.5)k_{H+M}/k_{H+D_2}$$

et

$$B \simeq (\phi_{H_2}/\phi_H + 1)\,k_{H+RH_2}/k_{H+D_2}$$

Pour le système $RD_2 + H_2$, on a de même

$$A' \simeq (\phi_{D_2}/\phi_D + 0.5)k_{D+M}/k_{D+H_2}$$

$$B' \simeq (\phi_{D_2}/\phi_D + 1)k_{D+RD_2}/k_{D+H_2}$$

On a alors les rapports suivants

$$A/A' = (k_{D+H_2}/k_{H+D_2})(k_{H+M}/k_{D+M})(\phi_{H_2}/\phi_H + 0.5)(\phi_{D_2}/\phi_D + 1)^{-1}$$

$$B/B' = (k_{D+H_2}/k_{H+D_2})(k_{H+RH_2}/k_{D+RD_2}) \times (\phi_{H_2}/\phi_H + 1)(\phi_{D_2}/\phi_D + 1)^{-1}$$

Pour un composé RH_2 donné, on observe une variation importante des rapports ϕ_{H_2}/ϕ_H, ϕ_{D_2}/ϕ_D, A/A', B/B' en fonction de l'énergie du rayonnement photonique. *Les variations de* ϕ_{H_2}/ϕ_H, ϕ_{D_2}/ϕ_D, *tiennent à l'ouverture de nouvelles vallées dissociatives au fur et à mesure que l'on atteint de nouvelles hypersurfaces de potentiel; les variations de* A/A' *et* B/B' *sont essentiellement dues à celle du rapport* R *des constantes de vitesse d'échange isotopique* k_{D+H_2}/k_{H+D_2} *avec l'énergie cinétique des atomes H ou D.*

A partir des valeurs expérimentales de A/A', ϕ_{H_2}/ϕ_H, ϕ_{D_2}/ϕ_D et en prenant pour k_{H+M}/k_{D+M} la valeur de 1.35 (11,12) (atomes thermalisés), on peut calculer le rapport R. Par comparaison avec la valeur de R mesuré par Westenberg et de Haas (10) pour des mélanges en équilibre thermique $R = 0.9 \exp 900/T$, ($R = 18$ pour $T = 300$ K), on calcule une température fictive T_λ, variable avec $h\nu$, qui est reliée de façon statistique à l'énergie cinétique moyenne des atomes H ou D, de la même façon que leur concentration est supposée stationnaire. Tout se passe comme si le milieu réactionnel était porté à la température T_λ. Ce procédé de calcul n'a de sens que si les atomes H et D sont, pour une énergie photonique donnée, formés avec des énergies cinétiques voisines, hypothèse de travail vraisemblable étant donné l'identité des surfaces de potentiel de RH_2 et de RD_2 et la faible différence des énergies de dissociation de ces deux molécules.

En portant la valeur de R dans le rapport B/B', on obtient pour k_{H+RH_2}/k_{D+RD_2} une valeur expérimentale relative à des atomes "chauds". On ne dispose pas en général de mesures expérimentales de ces deux constantes de vitesse (pour des milieux en équilibre thermique) mais si k_{H+RH_2} est connue, on peut évaluer k_{D+RD_2} et, à l'aide de la température T_λ calculée plus haut, la valeur de $\Delta E^* = E^*_{H+RH_2} - E^*_{D+RD_2}$, différence des énergies d'activation de deux réactions e et e'. E^* doit en principe rester constant quand $h\nu$ varie. On peut ainsi contrôler la validité des résultats obtenus.

Les rapports ϕ_{H_2}/ϕ_H, ϕ_{D_2}/ϕ_D, ne dépendent pas de l'intensité de la source, qu'il n'est donc pas nécessaire de connaître. Cependant l'erreur due à l'extrapolation est loin d'être négligeable, de l'ordre de 20%. La connaissance de T_λ ne permet pas de connaître l'énergie cinétique des atomes H ou D au moment de leur formation. Cependant cette évaluation moyenne permet d'éliminer certains modes dissociatifs ou, au contraire, d'accorder une probabilité importante à d'autres.

C'est ainsi que pour H_2O, photolysé à 185, 147, 123.6 nm, le rapport R était toujours bien inférieur à 18, indiquant que les atomes d'hydrogène formés possédaient de l'énergie cinétique, cette énergie étant d'autant plus élevée que l'énergie des photons incidents était plus grande. Ce résultat a été attribué au fait qu'aux trois longueurs d'onde on observe la même dissociation en $H + OH(X^2\Pi)$ et que l'énergie excédentaire, croissant avec l'énergie incidente des photons, était emportée essentiellement sous forme d'énergie cinétique par les atomes d'hydrogène. Ce résultat est en accord avec les résultats de Welge et Stuhl (13) qui, à 147 nm, ont observé

TABLEAU 1. Tableau récapitulatif des résultats expérimentaux concernant la photolyse de $NH_3(ND_3)$, $H_2O(D_2O)$ et $CH_4(CD_4)$ à diverses longueurs d'onde

		$\lambda = 185$ nm	$\lambda = 147$ nm	$\lambda = 123.6$ nm
NH_3	ϕ_{H_2}/ϕ_H	0.04	0.4	1.5
	ϕ_{D_2}/ϕ_D	0.04	0.06	0.08
	A/A'	5	10	7.5
	B/B'	6.25	23	8
	R	3.5	5.3	2.4
	T °K	750	500	950
	$E_{cin\ max}$ (kcal mol^{-1})	47.5	86–0	119–24
		réaction 1	réactions 1 et 6	réactions 1 et 6
H_2O	ϕ_{H_2}/ϕ_H	0	0	0.40
	ϕ_{D_2}/ϕ_D	0	0	0.20
	R	3.5	2.5	1.5
	T °K	750	950	1500
	$E_{cin\ max}$ (kcal mol^{-1})	35.5	72	106–9.2
CH_4	ϕ_{H_2}/ϕ_H			1.5
	ϕ_{D_2}/ϕ_D			1.5
	R			18
	T °K			300
	$E_{cin\ max}$ (kcal mol^{-1})			120–20–3

que le radical hydroxyle était en équilibre avec le milieu et que l'atome d'hydrogène emportait toute l'énergie excédentaire.

Dans le cas du méthane au contraire, à 123.6 nm, on a trouvé $R = 18$, indiquant que les atomes d'hydrogène sont dans leur quasi totalité thermiques. La probabilité de la photodissociation en CH_3 ($\tilde{X}^2A_2''$) + H, qui aurait laissé à l'atome d'hydrogène une énergie cinétique importante, est ainsi relativement faible, en accord avec les travaux théoriques de Lindholm (14).

Les résultats obtenus par cette méthode pour H_2O et CH_4 sont portés dans le tableau 1.

Données spectrales et thermodynamiques concernant la molécule d'ammoniac

Le spectre de l'ammoniac a été étudié par de nombreux auteurs (15–21). Il se compose principalement d'un continuum et de séries de bandes. Le premier continuum s'étend de 220 à 160 nm avec un maximum vers 187 nm. Les bandes ont été étudiées par Duncan pour NH_3 (18) et pour NH_2D, NHD_2, et ND_3 (19); il a mis en évidence quatre progressions dans le spectre de NH_3: 1ère de 168 à 217 nm; 2ème de 139 à 167 nm; 3ème de 122 à 144 nm; 4ème de 116 à 121 nm.

Les bandes de la première série sont diffuses, les trois autres, par contre, sont fines. L'étude approfondie de Douglas (22) révèle une prédissociation importante du premier état $\tilde{A}^1A_2$. Pour ND_3 l'état $\tilde{A}^1A_2$ possède une structure fine, ce qui le différencie de NH_3.

Les données thermodynamiques concernant la molécule d'ammoniac dans le domaine spectral considéré ont été récapitulées par Okabe et Lenzi (5); le tableau 2 est tiré de la référence (5) mais les seuils d'énergie correspondant aux réactions 2 et 8 ont été corrigés d'après les données de Stedman (23) relatives à la différence d'énergie entre les états X ($^3\Sigma^-$) et a ($^1\Delta$) de NH.

Conditions expérimentales

L'ammoniac de pureté 99.96%, l'hydrogène de pureté 99.995%, le deutérium de pureté 99.4% proviennent d'Air Liquide. L'ammoniac perdeutérié est un produit Merck, Sharp, and Dohm. Tous ces gaz ont été utilisés sans purification préalable. Le système d'irradiation lumineuse a été décrit précédemment (7). La cellule d'irradiation qui contient les mélanges $NH_3 + D_2$ et $ND_3 + H_2$ de concentrations connues, est un cylindre de pyrex de 160 cm^3 de volume, de 4 cm de diamètre recouvert intérieurement d'une couche d'or brillant de provenance Degussa 46 E/10%; elle est séparée du système d'irradiation par une fenêtre de fluorure de lithium Harshaw clivée.

Les pressions d'ammoniac ont varié entre 10 et 40

Can. J. Chem. Downloaded from www.nrcresearchpress.com by 210.87.254.6 on 09/05/12
For personal use only.

TABLEAU 2.* Seuils thermodynamiques des différents modes de dissociation de NH_3

Réaction			E(eV)	(nm)
[0]	$NH_3 \rightarrow NH$	$(X^3\Sigma^-) + H_2$	3.91	317
[1]	$\rightarrow NH_2$	$(\tilde{X}^2B_1) + H$	4.43	279.8
[2]	$\rightarrow NH$	$(a^1\Delta) + H_2$	4.54	275.3
[3]	$\rightarrow NH_2$	$(\tilde{A}^2A_1) + H$	5.70	217.5
[4]	$\rightarrow NH$	$(b^1\Sigma^+) + H_2$	6.61	187.5
[5]	$\rightarrow NH$	$(A^3\Pi) + H_2$	7.62	162.7
[6]	$\rightarrow NH$	$(X^3\Sigma^-) + H + H$	8.44	146.8
[7]	$\rightarrow NH$	$(c^1\Pi) + H_2$	8.35	142.5
[8]	$\rightarrow NH$	$(a^1\Delta) + H + H$	9.07	126.7

*Les réactions 0, 5, 8 sont interdites par les règles de corrélation.

Torrs; celles de deutérium ou d'hydrogène entre 10 et 400 Torrs.

Les mesures de pression sont effectuées à l'aide d'une jauge de pression absolue à capsule AEI. Le rapport des concentrations des deux hydrogènes isotopiques H_2/HD (ou D_2/HD) formés par irradiation à la température ambiante dans un mélange de composition connue, est mesuré à l'aide d'un spectromètre de masse Thomson-Houston THN 205 (7–8). Dans le cas des irradiations de ND_3, la cellule était conditionnée pendant plusieurs jours afin d'éviter les échanges spontanés aux parois.

Resultats expérimentaux

Les résultats obtenus avec NH_3 et ND_3 sont portés dans le tableau 1, avec ceux obtenus précédemment pour l'eau et le méthane. A titre indicatif, on a calculé l'énergie cinétique maximum susceptible d'être emportée par l'atome d'hydrogène si, pour chaque type de dissociation, toute l'énergie excédentaire est transformée en énergie cinétique des fragments. Lorsque plusieurs modes de dissociation sont possibles, l'énergie cinétique de H peut avoir plusieurs valeurs pour une énergie photonique donnée; en conséquence on trouve dans certains cas plusieurs valeurs de l'énergie cinétique des atomes H.

On a porté sur la fig. 1 toutes les valeurs expérimentales de R dont on dispose en fonction de l'énergie cinétique maximum des atomes d'hydrogène. Si on veut bien considérer la courbe tracée comme un simple repère, on peut conclure qu'à 185 nm la production d'atomes d'hydrogène n'a lieu que selon la dissociation (1); qu'à 147 nm la production d'atomes d'hydrogène a lieu en grande partie selon la réaction 6, tandis qu'à 123.6 nm, les réactions 6 et 3 ont des probabilités vraisemblablement voisines.

Si on porte les diverses valeurs de T_λ calculées

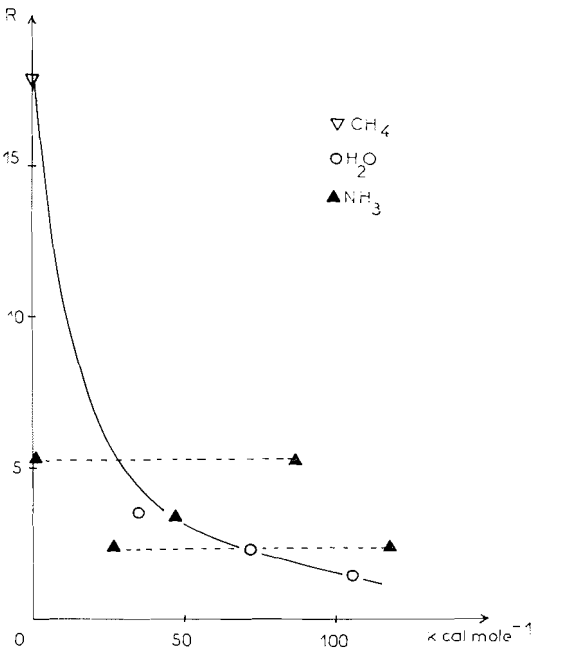

FIG. 1. Variation du rapport $R = k_{D+H_2}/k_{H+D_2}$ en fonction de l'énergie cinétique maximum des atomes d'hydrogène pour CH_4, H_2O, et NH_3.

pour NH_3 et ND_3 à partir des rapports A/A' dans les rapports B/B' on obtient: $E^*_{D+ND_3} - E^*_{H+NH_3} = 800 \pm 300$ cal/mol^{-1}. Cette valeur est en accord raisonnable avec la différence d'énergie de zéro des deux molécules, vraisemblablement comprise entre 500 et 1000 cal.

A partir de la constante de vitesse k_{H+NH_3} mesurée par Oganesyan et Nalbadayan (24):

$$k_{H+NH_3} = 5 \times 10^{13} \exp(-13610/RT) \text{ cm}^3 \text{ mol}^{-1} \text{ s}^{-1}$$

et en admettant un rapport de 1.35 pour les

Can. J. Chem. Downloaded from www.nrcresearchpress.com by 210.87.254.6 on 09/05/12
For personal use only.

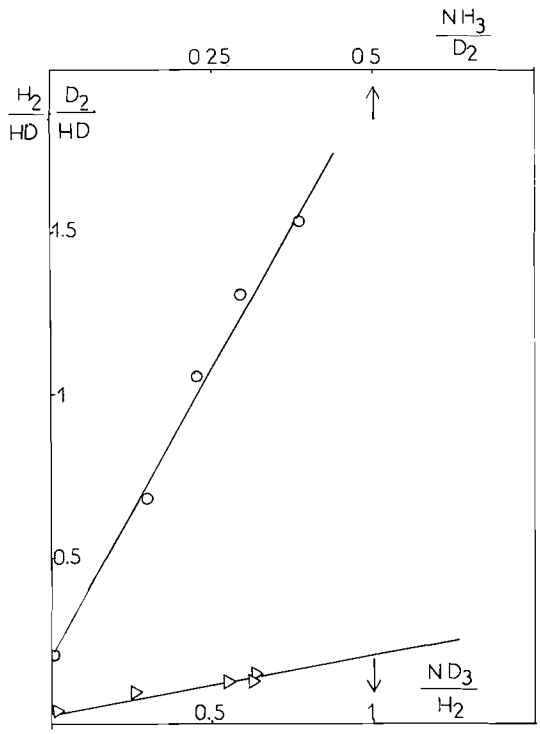

FIG. 2. Photolyse des mélanges $NH_3 + D_2$ et $ND_3 + H_2$ à 147 nm: ○, NH_3 6.4×10^{17} cm^3 mol^{-1}; △, ND_3 4.8×10^{17} cm^3 mol^{-1}.

facteurs préexponentiels, on obtient donc

$$k_{D+ND_3} = 3.5 \times 10^{13} \exp(-14\,400/RT) \text{ cm}^3 \text{ mol}^{-1} \text{ s}^{-1}$$

A titre d'exemple, les résultats expérimentaux obtenus par photolyse de $NH_3 + D_2$ et de $ND_3 + H_2$ à 147 nm sont portés sur la fig. 2.

Discussion

L'examen des résultats de la photolyse de l'ammoniac et de l'ammoniac perdeutérié permet les remarques suivantes:

(1) A 185 nm

Seuls les processus 1, 2, 3, 4 sont possibles énergétiquement. On trouve $\phi_{H_2}/\phi_H = \phi_{D_2}/\phi_D = 0.04$; par conséquent, les processus 2 et 4 n'interviennent que très faiblement dans la décomposition. Dans le permier continuum Schurath, Tiedman, et Schindler (1) à 204.2 nm et Mc Nesby, Tanaka et Okabe (2) à 185 nm n'ont pas mis en évidence la formation d'hydrogène moléculaire; les rendements trouvés ici n'étant que de 4%, nos résultats ne sont pas incompatibles avec ceux des auteurs précédents.

L'émission de NH_2 ($\tilde{A}^2A_1 \rightarrow \tilde{X}^2B_1$) n'a été observée par Okabe et Lenzi que pour $\lambda \leqslant 164$ nm. A 185 nm, NH_2 est donc formé dans son état fondamental et la réaction 1 rend compte de la quasi totalité de la photodissociation. Le premier continuum $\tilde{A}^1A_2''$ peut donc être corrélé totalement ou presque totalement aux fragments NH_2 ($\tilde{X}^2B_1$) + H aussi bien dans le cas de NH_3 que dans le cas de ND_3, malgré l'aspect différent des spectres de ces deux molécules.

Puisque tous les atomes d'hydrogène proviennent de la dissociation 1, on peut évaluer à 47.5 kcal l'énergie maximale que possèderait ces atomes si toute l'énergie était transformée en énergie cinétique. Il est assez vraisemblable en conséquence que le radical NH_2 ($\tilde{X}^2B_1$) formé par ce processus n'a pas une énergie interne considérable.

(2) A 147 nm

Le rendement quantique en NH_2 ($\tilde{A}^2A_1$) a été estimé par Okabe et Lenzi (5) dans cette région spectrale à moins de 10^{-3}. De plus, Bayes, Becker, et Welge (6) observent NH ($X^3\Sigma^-$) produit par photolyse éclair de NH_3 dès $\lambda < 155$ nm et considèrent que NH ($X^3\Sigma^-$) est un produit primaire de la photolyse. Nous observons $T_{147} < T_{185}$, ce qui conduit à attribuer aux atomes d'hydrogène formés à 147 nm une énergie cinétique moyenne inférieure à celle qu'ils acquièrent à 185 nm. Deux interprétations peuvent rendre compte de cet ensemble de résultats: la dissociation 6 a lieu directement en trois fragments ou la formation de NH passe par une prédissociation de $NH_2(\tilde{A}^2A_1)$ en NH ($X^3\Sigma^-$) + H.

On observe un effet isotopique important ($\phi_{H_2}/\phi_H = 0.4$; $\phi_{D_2}/\phi_D = 0.06$). Si la dissociation 6 a lieu, l'effet observé serait dû au fait que NH_3 et ND_3 seraient portés par le rayonnement de 147 nm dans des états vibroniques différents. Si NH_2 ($\tilde{A}^2A_1$) est prédissocié, sa section efficace de prédissociation serait inférieure à celle de ND_2 ($\tilde{A}^2A_1$).

L'observation de la dissociation 6 (directe ou par prédissociation) à 147 nm implique pour l'énergie de liaison D_{NH-H} une valeur inférieure ou égale à 90 kcal/mol, en meilleur accord avec la détermination d'Altshuler (25) de 88 ± 4

Can. J. Chem. Downloaded from www.nrcresearchpress.com by 210.87.254.6 on 09/05/12
For personal use only.

kcal/mol qu'avec une valeur plus récente donnée par Clyne et Thrush (26) de 95 ± 4 kcal/mol.

(3) A 123.6 nm

On obtient $T_{123.6} > T_{185} > T_{147}$; il s'ensuit que l'énergie cinétique des atomes H est plus élevée qu'aux autres longueurs d'onde. Ceci s'explique par l'absence de nouvelles vallées dissociatives susceptibles de former des atomes H.

Par ailleurs, outre un important effet isotopique, on note une augmentation du rapport ϕ_{H_2}/ϕ_H par rapport aux valeurs obtenues aux autres longueurs d'onde. Ceci peut correspondre à l'intervention de la réaction 7 en accord avec l'observation (3–5) de l'émission de NH $c^1\Pi \rightarrow a^1\Delta$. D'après Duncan l'absorption à 123.6 nm porte NH_3 (18) dans un niveau vibronique discret de la troisième série de bandes, tandis que ND_3 (19) est porté dans une zone diffuse. L'effet isotopique observé s'expliquerait par une prédissociation de ND_3 (et non de NH_3) conduisant aux réactions 1, 3 ou 6. Comme dans le cas précédent, l'effet isotopique peut aussi s'expliquer par une section efficace de prédissociation plus grande pour ND_2 ($\tilde{A}^2A_1$) que pour NH_2 ($\tilde{A}^2A_1$).

1. SCHURATH, P. TIEDMAN, et R. N. SCHINDLER. J. Phys. Chem. **73**, 457 (1969).
2. J. R. MCNESBY, I. TANAKA, et H. OKABE. J. Chem. Phys. **36**, 605 (1962).
3. K. H. BECKER et K. H. WELGE. Z. Naturforsch. **18a**, 600 (1963).
4. K. H. BECKER et K. H. WELGE. Z. Naturforsch. **19a**, 1006 (1964).
5. H. OKABE et M. LENZI. J. Chem. Phys. **47**, 5241 (1967).
6. K. D. BAYES, K. H. BECKER, et K. H. WELGE. Z. Naturforsch. **17a**, 676 (1962).
7. M. COTTIN, J. MASANET, et C. VERMEIL. J. Chim. Phys. **63**, 959 (1966).
8. J. MASANET et C. VERMEIL. J. Chim. Phys. **66**, 1248 (1969).
9. L. HELLNER, J. MASANET, et C. VERMEIL. J. Chem. Phys. **55**, 1022 (1971).
10. A. A. WESTENBERG et N. G. DE HAAS. J. Chem. Phys. **47**, 1391 (1961).
11. D. O. HAM, D. W. TRAINOR, et F. KAUFMAN. J. Chem. Phys. **53**, 4395 (1970).
12. R. E. ROBERT, R. B. BERNSTEIN, et L. F. CURTISS. J. Chem. Phys. **50**, 5163 (1969).
13. K. H. WELGE et F. S. STHUL. J. Chem. Phys. **46**, 2240 (1967).
14. E. LINDHOLM. Arkiv. Fis. **37**, 37 (1968); J. Chem. Phys. **52**, 4921 (1970).
15. K. WATANABE. J. Chem. Phys. **22**, 1564 (1954).
16. K. WATANABE et S. P. SOOD. Sci. of Light, **14**, 36 (1965).
17. J. K. DIXON. Phys. Rev. **47**, 711 (1935).
18. A. F. B. DUNCAN. Phys. Rev. **47**, 822 (1935).
19. A. F. B. DUNCAN. Phys. Rev. **50**, 700 (1936).
20. A. D. WALSH et P. A. WARSOP. Trans. Faraday Soc. **57**, 345 (1961).
21. A. E. DOUGLAS et J. M. HOLLAS. Can. J. Phys. **39**, 479 (1961).
22. A. E. DOUGLAS. Disc. Faraday Soc. **35**, 158 (1963).
23. D. H. STEDMAN. J. Chem. Phys. **52**, 3966 (1970).
24. OGANESYAN et NALBADAYAN. Dokl. Akad. Nauk SSSR, **160**, 162 (1965).
25. A. ALTSHULER. J. Chem. Phys. **22**, 1947 (1954).
26. M. A. A. CLYNE et B. A. THRUSH. Proc. Roy. Soc. 227 (1962).

Can. J. Chem. Downloaded from www.nrcresearchpress.com by 210.87.254.6 on 09/05/12
For personal use only.

The Crystal and Molecular Structure of Penta-*p*-tolylantimony, $(p\text{-}CH_3C_6H_4)_5Sb$

C. BRABANT, J. HUBERT, AND A. L. BEAUCHAMP

Department of Chemistry, University of Montreal, Montreal, Quebec

Received March 12, 1973

Penta-*p*-tolylantimony crystals are monoclinic, space group $P2_1/c$, with a = 14.545(5), b = 4(6), c = 19.754(8) Å, β = 122.88(4)°, and Z = 4. The structure was solved by the standard heavy-atom method and anisotropic refinement on 1677 independent observed reflections led to a conventional R factor of 0.051. Unlike pentaphenylantimony, which is known to exist as square pyramidal molecules in the crystal, the corresponding penta-*p*-tolyl derivative exhibits the more common trigonal bipyramid structure. The Sb—C equatorial bond length average, 2.16 Å, is significantly shorter than the axial average, 2.26Å. Two of the C—Sb—C bond angles in the equatorial plane (113, 130°) differ considerably from 120°, but the other angles around antimony are normal. Packing forces appear to play a determining role in the structures observed for penta-aryl derivatives of antimony in the solid state.

Le penta-*p*-tolylantimoine cristallise dans le groupe monoclinique $P2_1/c$, a = 14.545(5), b = 12.134(6), c = 19.754(8) Å, β = 122.88(4)°, et Z = 4. L'affinement effectué sur 1677 réflexions observées indépendantes a conduit à un facteur résiduel R de 0.051. Contrairement au pentaphénylantimoine, dont la structure pyramidale carrée est connue, le dérivé penta-*p*-tolyl possède la structure d'une bipyramide triangulaire. La longueur moyenne des liaisons Sb—C équatoriales (2.16 Å) est significativement plus courte que celle des liaisons axiales (2.26 Å). On observe des écarts importants à la valeur prévue de 120° pour deux des angles C—Sb—C du plan équatorial (113 et 130°). Tous les autres angles impliquant l'antimoine sont normaux. Les interactions intermoléculaires dans le cristal jouent vraisemblablement un rôle déterminant dans la structure qu'adoptent les dérivés penta-arylés de l'antimoine à l'état solide.

Can. J. Chem., **51**, 2952 (1973)

Can. J. Chem. Downloaded from www.nrcresearchpress.com by 210.87.254.42 on 09/05/12
For personal use only.

It is known from X-ray work that in the solid state, $(C_6H_5)_5P$ and $(C_6H_5)_5As$ have the trigonal bipyramid structure (1), whereas $(C_6H_5)_5Sb$ exists as distorted square pyramidal molecules (2). This structure of pentaphenylantimony has recently been confirmed from three-dimensional X-ray data (3) and the pattern of Sb—C bond lengths (4 long, 1 short) observed in the latter study favors the view that the molecule is basically square pyramidal.

In order to determine the role played by intermolecular forces in this compound, a crystallographic study of some penta-aryl antimony compounds was undertaken. Penta-*p*-tolylantimony $(p\text{-}CH_3C_6H_4)_5Sb$ was selected first. It was felt that additional methyl groups on the rings would have little electronic effect on antimony, but would necessarily lead to a completely different molecular packing in the crystal.

Experimental Section

Crystal data

$C_{35}H_{35}Sb$ f.w. = 577.42

Monoclinic, $P2_1/c$, a = 14.545(5), b = 12.134(6), c = 19.754(8) Å, β = 122.88(4)°, V = 2927.8 Å^3, ρ_m = 1.30(1) g cm^{-3} (flotation in aqueous KI solution), Z = 4, ρ_c = 1.310 g cm^{-3}, t = 22 °C. λMoK$\bar{\alpha}$ = 0.71068 Å, λMoKβ = 0.63225 Å, μMoKα = 9.3 cm^{-1}.

Preparation

The starting stibine $(p\text{-}CH_3C_6H_4)_3Sb$ was obtained by reaction of $SbCl_3$ with $p\text{-}CH_3C_6H_4MgBr$ (4). It was dissolved in petroleum ether and converted to $(p\text{-}CH_3C_6H_4)_3SbCl_2$ by bubbling chlorine gas into the solution. Finally, the dichloride was reacted with an excess of $p\text{-}CH_3C_6H_4Li$ in ether, as described by Wittig and Clauss (5). The compound $(p\text{-}CH_3C_6H_4)_5Sb$ was isolated as a white powder and recrystallized from *n*-hexane (m.p. 189°).

The colorless crystals obtained from *n*-hexane are general parallelepipeds elongated along the *b* axis. The crystals, mounted on glass fibers, were left exposed to the atmosphere throughout this work. They are not affected by air, but decompose slowly in the X-ray beam.

Crystallographic Measurements

The cell parameters reported above with their e.s.d.'s were calculated by refinement (6) of the 2θ, ω, and χ angles for 12 independent MoKβ peaks centered on a Picker FACS-1 automatic diffractometer.

A fresh crystal with dimensions 0.10 × 0.37 × 0.15 mm^3 was used for data collection. A total of 4191 measurements within a sphere $2\theta \leqslant 45°$ were collected using Zr-filtered MoK$\bar{\alpha}$ radiation. The θ/2θ scan technique was used at a scan rate of 1°(2θ)/min. A scan range of 1.5° was selected and increased with 2θ to allow for the $\alpha_1\alpha_2$ doublet separation. Background counts B_1 and B_2 of 20 s were taken at each limit of the scan range. The three standard reflections all fell to 36% of their initial intensity during data collection.

The net intensities I were obtained from $I = P - T(B_1 + B_2)/40$, where T is the total scan time and P is the

Can. J. Chem. Downloaded from www.nrcresearchpress.com by 210.87.254.42 on 09/05/12
For personal use only.

total scan count. A measurement was considered as statistically significant when $I \geqslant 300$ counts and $\geqslant 10\%$ of the total background count. By these criteria, approximately 2000 measurements (including the systematically absent reflections and most of the measurements in the 35–45° 2θ range) were rejected. After averaging the equivalent measurements, 1677 independent observed reflections remained. Absorption corrections based on the equations of the crystal faces was applied (NRC-3 program) and the data were finally corrected for the Lorentz and polarization effects.

Refinement

The scattering factors for carbon and antimony were those of Cromer and Waber (7); for hydrogen, those of Mason and Robertson (8) were used. The anomalous dispersion terms $\Delta f'$ (−0.75) and $\Delta f''$ (1.86) of antimony (7) were included in the calculations.

The structure was solved by the conventional heavy-atom method and refined by full-matrix least squares. The position of antimony was obvious from the three-dimensional Patterson map. Refinement of the coordinates and isotropic temperature factors of antimony led to $R = \Sigma(|F_o| - |F_c|)/\Sigma|F_o| = 0.27$. A difference Fourier map phased on antimony revealed the positions of the 35 carbon atoms. The coordinates and isotropic temperature factors of the 36 non-hydrogen atoms converged to $R = 0.086$. At this point, anisotropic temperature factors were defined for each atom. Individual weights $w = 1/\sigma_F^2$ based on counting statistics (9) were applied. The resulting distribution of $w|\Delta F|^2$ *vs.* $|F_o|$ showed that the weights were too large for strong reflections and too small for weak ones. Subsequently, the weights for medium reflections were left unchanged, but those assigned to the remaining reflections were calculated from $w = 1/\sigma_F^2$ $(1 + 0.77(|F_o| - 15.6))$ for $|F_o| > 15.6$ or $w = 1/\sigma_F^2$ $(1 - 0.13\ (10.5 - |F_o|))$ for $|F_o| < 10.5$. The constants in the equations were adjusted to make the distribution of $w|\Delta F|^2$ practically constant with respect to $|F_o|$. A slight increase remained as a function of $\sin\theta/\lambda$.

The hydrogen atoms of the rings were fixed at the calculated positions (C—H distance of 1.08 Å) and assigned isotropic temperature factors of 6. The hydrogen parameters were not refined in subsequent cycles, but they were given the same shifts as the corresponding carbon atoms. Refinement of the coordinates and anisotropic temperature factors of the 36 non-hydrogen atoms converged to $R = 0.051$ and $R_w = \{\Sigma w(|F_o| - |F_c|)^2/\Sigma w|F_o|^2\}^{1/2} = 0.054$. The final difference Fourier map did not show peaks higher than ± 0.4 e/Å^3. The surrounding of the methyl carbon atoms was carefully searched, but no hydrogens were found.

In addition to the conventional independent atom treatment described above, the structure was also refined with the six-membered rings defined as idealized hexagons (C—C distance fixed at 1.397 Å), according to the method described previously (3). For each carbon ring, the x, y, and z coordinates of the center, the three angles describing the orientation of the hexagon, and the six isotropic temperature factors of the carbon atoms were refined. Antimony and the methyl carbon atoms were treated as independent atoms and refined anisotropically. This treatment resulted in $R = 0.058$ and $R_w = 0.063$, a value slightly higher than for the independent atom model. On the basis of the Hamilton test (10), the independent atom model should be preferred, but the use of the idealized model to describe librating aromatic rings has already been justified (3).

The results reported here were those obtained with the independent atom model, except for the Sb—C bond lengths and angles, for which the values obtained with both models are given. The calculations were carried out with a CDC 6600 computer and the programs used are described elsewhere (3, 11)[1].

Results and Discussion

The atom parameters derived from the independent atom model are listed in Table 1. The carbon atoms are identified with labels of the type C(ij), where i is the ring number and j corresponds to sequential numbering of the ring vertices with $j = 1$ for the atom bound to antimony. Index $j = 7$ refers to the methyl group. Hydrogen atoms are referred to with the same pair of indices as the carbon atom to which they are attached.

Description of the Structure

The penta-*p*-tolylantimony molecule is shown in Fig. 1. The bond lengths and angles involving antimony are given in Table 2. Unlike pentaphenylantimony, the *p*-tolyl compound is trigonal bipyramidal. Rings 1 and 2 are axial, while rings 3, 4, and 5 occupy the equatorial positions. As usual, the axial Sb—C bonds are significantly longer (2.24–2.29 Å) than the equatorial (2.15–2.18 Å). The C(11)—Sb—C(21) segment is practically linear (177–178°), and the C_{ax}—Sb—C_{eq} angles are all in the 87–92° range. The equatorial Sb—C bonds are coplanar within experimental errors, but considerable departure from 120° is observed for two of the angles. The C(31)—Sb—C(51) angle is normal (117°), but the small C(31)—Sb—C(41) (113°) and the large C(41)—Sb—C(51) (130°) angles suggest a displacement of ring 4 towards ring 3. In spite of some distortion, a description of the molecule in terms of a trigonal bipyramid is fully justified.

The geometry of the *p*-tolyl groups is normal. The bond lengths and angles in the rings average 1.39 Å and 120° respectively.[1] The C(i4)—C(i7) distances involving methyl carbon atoms (1.54–1.60 Å) are all larger than normal, possibly due to neglect of hydrogen atoms. The six-membered rings are planar within 0.03 Å and the maximum distance of a methyl carbon atom from its ring

[1]The structure factor table and the list of bond lengths and angles in the tolyl rings are available, at a nominal charge, from the Depository of Unpublished Data, National Science Library, National Research Council of Canada, Ottawa, Canada K1A 0S2.

TABLE 1. Refined fractional coordinates ($\times 10^4$) and anisotropic temperature factors ($\times 10^4$) derived from the independent atom model; t.f. = exp $[-(\beta_{11}h^2 + \beta_{22}k^2 + \beta_{33}l^2 + 2\beta_{12}hk + 2\beta_{13}hl + 2\beta_{23}kl)]$

Atom	x	y	z	β_{11}	β_{22}	β_{33}	β_{12}	β_{13}	β_{23}
Sb	2987.2(8)	398.0(9)	1604.4(6)	76.9(9)	88.8(10)	45.6(5)	−0.8(11)	34.4(6)	2.1(9)
C(11)	4460(12)	−21(13)	1571(10)	93(15)	99(19)	64(9)	6(12)	55(11)	13(9)
C(12)	4666(13)	428(14)	1012(9)	106(16)	146(19)	57(8)	40(16)	44(10)	28(11)
C(13)	5616(19)	100(20)	1008(13)	170(24)	179(27)	86(12)	−27(21)	96(15)	0(15)
C(14)	6280(18)	−726(16)	1493(13)	184(26)	92(23)	70(12)	−10(17)	76(15)	9(11)
C(15)	6086(14)	−1168(13)	2042(11)	117(18)	82(16)	98(12)	50(14)	65(13)	36(12)
C(16)	5188(16)	−801(13)	2062(11)	118(18)	90(18)	93(11)	32(14)	74(13)	32(11)
C(17)	7282(13)	−1137(14)	1472(10)	134(18)	190(22)	120(22)	27(16)	105(13)	−7(13)
C(21)	1466(12)	806(14)	1592(9)	103(16)	80(18)	71(9)	−7(13)	61(10)	−10(10)
C(22)	803(13)	66(13)	1655(9)	78(14)	136(23)	67(9)	−6(13)	48(10)	−8(9)
C(23)	−49(13)	377(18)	1741(10)	92(17)	133(21)	88(11)	−9(18)	59(11)	−7(14)
C(24)	−272(13)	1477(21)	1778(9)	65(15)	165(26)	53(8)	8(18)	22(9)	0(13)
C(25)	359(16)	2267(14)	1685(10)	113(19)	91(9)	80(10)	29(15)	44(12)	4(11)
C(26)	1227(13)	1937(16)	1610(9)	85(16)	111(20)	69(10)	−20(15)	41(11)	−17(11)
C(27)	−1190(13)	1852(15)	1913(11)	114(17)	226(24)	130(13)	28(17)	98(13)	−1(15)
C(31)	4018(14)	822(11)	2856(8)	89(16)	80(16)	52(8)	2(12)	41(11)	−5(8)
C(32)	5065(14)	1196(14)	3180(11)	59(15)	132(19)	59(10)	−5(13)	30(11)	8(11)
C(33)	5689(11)	1537(13)	3987(13)	40(13)	97(17)	76(11)	−15(12)	1(11)	−8(11)
C(34)	5320(16)	1522(14)	4517(13)	119(22)	122(20)	130(15)	21(16)	95(17)	13(14)
C(35)	4267(17)	1092(15)	4159(11)	131(19)	205(23)	66(11)	−11(18)	72(13)	−21(13)
C(36)	3611(11)	767(13)	3341(10)	72(13)	190(25)	46(8)	−16(13)	29(10)	−6(11)
C(37)	6005(13)	1940(15)	5390(9)	157(21)	230(26)	32(8)	−6(17)	−4(11)	−59(12)
C(41)	2462(13)	−1319(12)	1388(13)	65(14)	64(16)	66(10)	−21(13)	32(10)	−16(12)
C(42)	1736(14)	−1737(16)	678(10)	78(16)	115(20)	45(9)	−24(15)	17(10)	−21(12)
C(43)	1393(11)	−2832(19)	595(11)	50(14)	151(23)	55(10)	−25(16)	13(10)	−60(14)
C(44)	1839(15)	−3528(16)	1258(13)	90(17)	176(26)	47(10)	84(18)	41(12)	40(15)
C(45)	2587(13)	−3103(16)	1987(10)	80(15)	139(22)	24(8)	13(15)	18(9)	11(11)
C(46)	2916(11)	−1993(17)	2058(10)	65(14)	84(18)	47(9)	−9(14)	17(10)	−14(11)
C(47)	1405(13)	−4772(12)	1123(10)	180(20)	29(15)	136(14)	−14(13)	98(14)	−9(11)
C(51)	2577(14)	1724(13)	763(9)	75(15)	112(19)	34(8)	1(14)	24(10)	19(10)
C(52)	1566(14)	1738(14)	55(12)	96(18)	114(19)	57(10)	6(15	30(12)	32(12)
C(53)	1241(13)	2587(20)	−488(10)	85(17)	181(25)	49(10)	−27(18)	32(11)	−1(13)
C(54)	1919(19)	3497(19)	−323(12)	114(20)	172(27)	62(11)	54(21)	62(14)	19(15)
C(55)	2955(17)	3473(15)	410(14)	148(23)	76(18)	86(12)	−23(17)	85(15)	−9(13)
C(56)	3256(12)	2614(17)	928(10)	90(16)	106(18)	60(9)	−8(15)	56(10)	17(12)
C(57)	1611(14)	4575(15)	−877(10)	209(22)	175(21)	91(11)	76(19)	103(13)	98(14)

plane is 0.09 Å. For antimony, the distances to the same planes (0.10–0.14 Å) are of the same magnitude as observed in pentaphenylantimony (3), except for ring 2, where the distance is 0.27 Å. This corresponds to a relatively large angle of 6.7° between the Sb—C(21) bond and the plane of ring 2. This deformation will be discussed below.

Molecular Packing

All the intramolecular contacts are larger than the sum of the van der Waals radii (12). The shortest intermolecular contacts are listed in Table 3.

The strongest interaction (full line, Fig. 2) involves axial type 1 rings belonging to neighboring molecules. Values considerably less than normal are found for C(31)—C′(31) (3.25 Å) and for H(13)—C′(13) (or H′(13)—C(13)) (2.78 Å). Nevertheless, these short contacts do not result in any obvious distortions.

Some other intermolecular distances are less, though only slightly, than the sum of the van der Waals radii. For example, H′(32) and H′(33) on one molecule interact with several carbon atoms of ring 4 on another molecule (dotted line, Fig. 2). From their relative orientations, one would expect ring 3 and/or ring 4 to be displaced from the equatorial plane, but this is not the case.

There is little doubt that the abnormal C—Sb—C angles in the equatorial plane are the result of packing effects. A careful survey of the region between ring 4 and ring 5, where strain is expected, shows (Fig. 2) that the space is filled by ring 2′ from a centrosymmetrically related molecule. However, the H(43)—C′(25) contacts

Can. J. Chem. Downloaded from www.nrcresearchpress.com by 210.87.254.42 on 09/05/12
For personal use only.

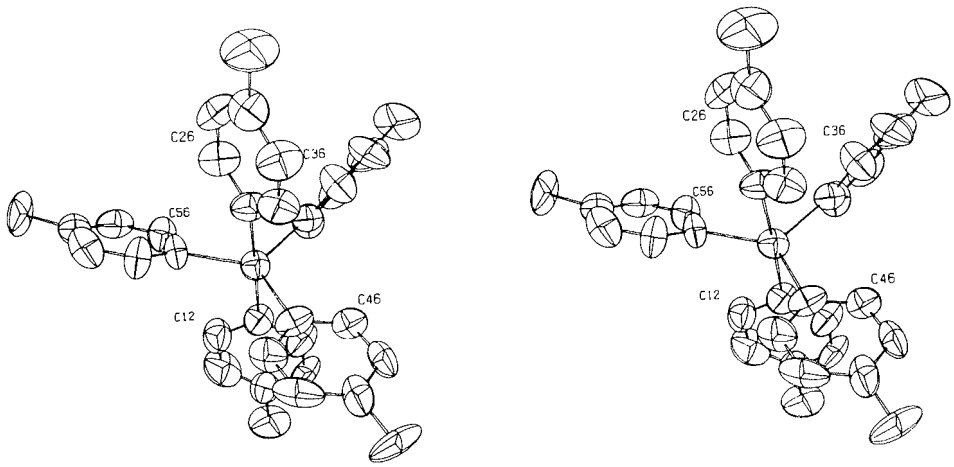

FIG. 1. Stereoscopic view of the trigonal bipyramidal penta-*p*-tolylantimony molecule. One of the atoms on each ring is labeled according to the convention given in the text. Rings 1 and 2 are axial, rings 3, 4, and 5 are equatorial. The ellipsoids correspond to 50% probability.

TABLE 2. (*a*) Bond lengths involving the antimony atom

Bond	Lengths (Å) Independent atom model	Idealized hexagon model
Sb—C(11)	2.238(17)	2.274(13)
Sb—C(21)	2.254(14)	2.291(11)
Sb—C(31)	2.145(12)	2.149(7)
Sb—C(41)	2.180(14)	2.165(8)
Sb—C(51)	2.151(15)	2.174(10)

(*b*) Bond angles involving the antimony atom

Bonds	Angle (deg.) Independent atom model	Idealized hexagon model
C(11)—Sb—C(21)	178.0(6)	177.2(4)
C(11)—Sb—C(31)	90.4(6)	91.0(4)
C(11)—Sb—C(41)	91.0(7)	90.9(4)
C(11)—Sb—C(51)	90.9(7)	90.6(4)
C(21)—Sb—C(31)	91.5(6)	91.5(4)
C(21)—Sb—C(41)	88.3(7)	89.2(4)
C(21)—Sb—C(51)	88.2(7)	87.2(4)
C(31)—Sb—C(41)	114.0(7)	112.5(4)
C(31)—Sb—C(51)	116.0(7)	117.2(4)
C(41)—Sb—C(51)	130.0(7)	130.2(4)

(dashed lines) are normal (2.98 Å), although they would certainly become abnormally short if ring 4 were displaced towards ring 5 to restore the normal C(41)—Sb—C(51) angle of 120°.

In connection with the 10° distortion in the equatorial plane, a 7.6° angle is found between the Sb—C′(21) bond and the plane through ring 2′. This ring seems to be tilted in a suitable direction to avoid the approach of H(43) and H(42). The reason that steric strain shows up as bending at C′(21) appears to be the presence of H′(36) which would oppose any displacement of C′(21) in its own direction.

Structure of R_5Sb Molecules

Although by no means abundant, some structural information is now available on penta-organo derivatives of antimony. For instance, square pyramidal molecules are known to exist in crystals of pentaphenylantimony (2, 3) and it was concluded from the vibrational spectra (13) that the same structure is maintained in CH_2Cl_2 and CH_2Br_2 solutions. In the case of pentacyclopropylantimony, the vibrational spectra were also interpreted in terms of square pyramidal

TABLE 3. Intermolecular contacts

Atoms	Transformation*	(Å)†
C(13)—C′(13)	$1-x, \bar{y}, \bar{z}$	3.25
H(13)—C′(13)	$1-x, \bar{y}, \bar{z}$	2.78
C(45)—H′(32)	$\bar{x}, 1/2+y, 1/2-z$	2.82
C(45)—H′(33)	$\bar{x}, 1/2+y, 1/2-z$	2.99
C(43)—H′(33)	$\bar{x}, 1/2+y, 1/2-z$	2.85
C(42)—H′(33)	$\bar{x}, 1/2+y, 1/2-z$	2.96
H(35)—C′(55)	$x, 1/2-y, 1/2+z$	2.82
H(16)—H′(56)	$1-x, -1/2+y, 1/2-z$	2.21
C(25)—H′(43)	$\bar{x}, \bar{y}, \bar{z}$	2.98

*To generate the coordinates of the primed atom from those of Table 1 (unprimed atoms).
†E.s.d.'s are 0.03 Å.

Can. J. Chem. Downloaded from www.nrcresearchpress.com by 210.87.254.42 on 09/05/12
For personal use only.

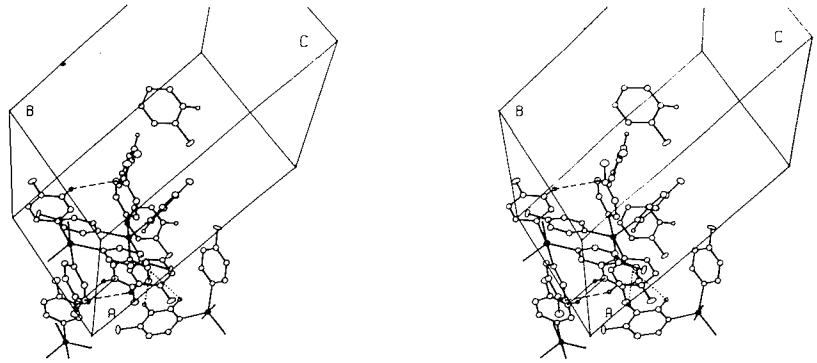

FIG. 2. Packing diagram for penta-*p*-tolylantimony. The antimony atoms are represented by dark spheres. The hydrogen atoms have been omitted, except for those discussed in the text. The complete molecule in the center of the diagram has the same orientation as in Fig. 1 and the rings can be identified by comparison.

molecules (14). On the other hand, a trigonal bipyramid structure has been established by infrared spectroscopy for pentamethylantimony (15) and by X-ray diffraction for phenylbis-2,2′-biphenyl-enylantimony (16) and penta-*p*-tolylantimony. Furthermore, preliminary results obtained in this laboratory on $(C_6H_5)_5Sb\cdot\frac{1}{2}C_6H_{12}$ indicate that the pentaphenylantimony molecule *in this crystal* has a trigonal bipyramid structure with virtually no distortion. Therefore, two examples of square pyramidal compounds are known, whereas a trigonal bipyramid structure has been observed in four cases. This suggests that antimony, like phosphorus and arsenic, shows a certain preference for a trigonal bipyramid structure, even in its organic derivatives.

Five-coordinate molecules frequently exhibit stereochemical non-rigidity and the intramolecular exchange of axial and equatorial positions in phosphorus compounds has been thoroughly investigated (17). Less is known on antimony compounds, but the room temperature n.m.r. spectrum of penta-*p*-tolylantimony in CS_2 has been interpreted in terms of trigonal bipyramid molecules undergoing fast intramolecular exchange (18). We have recorded the n.m.r. spectrum down to -100 °C in the same solvent and found that the exchange is fast even at that temperature.

In agreement with the above evidence for a low energy barrier in the exchange process, the crystal structures of $(C_6H_5)_5Sb$ and $(p\text{-}CH_3C_6H_4)_5Sb$ afford indications for highly flexible molecules. For example, in the *p*-tolyl derivative, two equatorial C—Sb—C angles show large (10°) distortions. In the case of pentaphenylantimony, departure from trigonal bipyramid geometry is so large that the resulting molecule must be considered as a distorted square pyramid. If extra energy is needed to stabilize the "distorted" structures in the crystals, it must be supplied by intermolecular interactions. The penta-aryl compounds discussed here are so similar in weight, size, bond polarity, chemical properties, etc., that the crystals are not expected to differ considerably in packing energy. Therefore, although the ground state structure of penta-arylantimony molecules appears to be the trigonal bipyramid, we may reasonably assume that the square pyramid or any similar structure would not be considerably higher in energy. This would explain that relatively small variations in packing energy result in important structural change.

We wish to thank the National Research Council of Canada for a research grant and scholarships.

1. P. J. WHEATLEY. J. Chem. Soc. 2206 (1964).
2. P. J. WHEATLEY. J. Chem. Soc. 3718 (1964).
3. A. L. BEAUCHAMP, M. J. BENNETT, and F. A. COTTON. J. Am. Chem. Soc. **90**, 6675 (1968).
4. G. S. HIERS. Organ. Synth. **I**, 550 (1941).
5. G. WITTIG and K. CLAUSS. Ann. **577**, 26 (1952).
6. W. R. BUSING and H. A. LEVY. Acta Cryst. **22**, 457 (1967).
7. D. T. CROMER and J. T. WABER. Acta Cryst. **18**, 104 (1965); D. T. CROMER. Acta Cryst. **18**, 17 (1965).
8. R. MASON and G. B. ROBERTSON. Advances in structure research by diffraction methods. Vol. 2. *Edited by* R. Brill and R. Mason. Interscience, New York. 1966. p. 57.
9. G. H. STOUT and L. H. JENSEN. X-ray structure determination. Macmillan Co., New York. 1969. p. 457.
10. W. C. HAMILTON. Acta Cryst. **18**, 502 (1965).

Can. J. Chem. Downloaded from www.nrcresearchpress.com by 210.87.254.42 on 09/05/12
For personal use only.

11. A. L. BEAUCHAMP and D. GOUTIER. Can. J. Chem. **50**, 977 (1972).
12. F. A. COTTON and G. WILKINSON. Advanced inorganic chemistry. Interscience. 2nd ed. New York. 1966. p. 115.
13. I. R. BEATTIE, K. M. S. LIVINGSTON, G. A. OZIN, and R. SABINE. J. Chem. Soc. Dalton Trans. 784 (1972).
14. A. H. COWLEY, J. L. MILLS, T. M. LEOHR, and T. V. LONG II. J. Am. Chem. Soc. **93**, 2150 (1971).
15. A. J. DOWNS, R. SCHMUTZLER, and I. A. STEIR. Chem. Commun. 221 (1966).
16. D. HELLWINKEL and M. BACH. Naturwissen **56**, 214 (1969).
17. E. L. MUETTERTIES. Acc. Chem. Res. **3**, 266 (1970).
18. D. HELLWINKEL. Angew. Chem. Int. Ed. **5**, 725 (1966).

Can. J. Chem. Downloaded from www.nrcresearchpress.com by 210.87.254.42 on 09/05/12
For personal use only.

Pseudo-thermodynamic Parameters and Isotope Effects for Hydrolysis of a Series of Benzyl Chlorides in Water

K. M. KOSHY, R. E. ROBERTSON, AND W. M. J. STRACHAN
Department of Chemistry, University of Calgary, Calgary, Alberta T2N 1N4

Received February 12, 1973

The temperature coefficient of the enthalpy of activation ($\Delta C_p^{\ddagger}$) for the hydrolysis of *p*-methyl, *p*-chloro and *p*-nitro benzyl chlorides have been determined, as well as α-deuterium isotope effects and kinetic solvent isotope effects. These results are discussed in terms of probable mechanism of hydrolysis in water.

On a déterminé le coefficient de température de l'enthalpie d'activation ($\Delta C_p^{\ddagger}$) lors de l'hydrolyse des chlorures de *p*-méthyl, *p*-chloro et *p*-nitro benzyle. De même, les effets isotopiques de l'α-deutérium et les effets isotopiques du solvant, d'ordre cinétique, ont été déterminés. On discute de ces résultats en fonction d'un mécanisme possible de l'hydrolyse dans l'eau. [Traduit par le journal]

Can. J. Chem., **51**, 2958 (1973)

Can. J. Chem. Downloaded from www.nrcresearchpress.com by 210.87.254.5 on 09/05/12
For personal use only.

The extensive work on the effect of substitution on the rate of solvolysis in the benzyl series has been adequately summarized by several authors (1–7). A recurrent observation has been that the rates resulting from *p*-substitution through a series of such compounds fail to give a linear Hammett correlation (8–11). This less usual consequence of substitution has been attributed variously to a change in mechanism, mixed mechanism, or to the possible involvement of varying degrees of nucleophilic interaction, the weight of evidence appearing to favor the latter possibility (3, 6, 12). This would imply corresponding changes in charge development in the transition state. We were interested in correlating such changes with possible changes in the heat capacity of activation ($\Delta C_p^{\ddagger}$) and other indicators of mechanistic differences for hydrolysis of a series of *p*-substituted benzyl chlorides in water. No previous work of this kind existed save for the unsubstituted member (13) and some extrapolated data from work in alcohol-water mixtures by Hyne and co-workers (7).

In such a series *p*-methoxybenzyl chloride probably reacts by a limiting mechanism in water but the reaction is too fast to be studied by our methods. It is less certain that the *p*-methyl member approximates to a limiting mechanism though support for either possibility can be found. The other members were expected to provide examples of S_N2 behavior but the exact differentiation in terms of $\Delta C_p^{\ddagger}$-values and the α-deuterium isotope effect could only be guessed at.

Experimental

The kinetic rate data given here were obtained with the same equipment used in previous studies reported from this laboratory (14).

The *p*-methylbenzyl chloride was obtained after the lithium aluminum hydride reduction of the ethyl ester of a purified sample of toluic acid. Preliminary kinetic studies with reagent grade *p*-methylbenzyl chloride even after distillation, proved unsatisfactory. Fractional distillation of the product obtained from the reduced ester by treatment with $SOCl_2$ gave a pure compound as found by g.l.c.: b.p., 48° (1 mm), n.m.r.$_{TMS}^{CCl4}$ δ 7.15 (m,4,aryl), 4.45(s,2,methylene), 2.32(s,3,methyl). On hydrolysis this compound gave strictly first order rates. The corresponding α-deuterated compound was obtained by the same method but using lithium aluminum deuteride as the reducing agent.

p-Chlorobenzyl chloride, practical grade, was fractionally distilled through a glass bead column. The middle one-third was collected, b.p. 99–99.5 °C at 12 mm. *p*-Nitrobenzyl chloride, reagent grade, was recrystallized from petroleum ether, absolute ethanol, and dried in a vacuum pistol at 2 mm pressure, m.p. 72.5–73 °C.

In the kinetic studies, doubly distilled water or heavy water (better than 99.75% D_2O) was adjusted with KCl

TABLE 1. Rate constants for the solvolysis of *p*-methylbenzyl chloride in water

Temperature (°C)	Rate constant ($\times 10^{-5}$ s^{-1})
17.17	15.85 ± 0.05
19.70	22.58 ± 0.04
21.79	30.14 ± 0.08
24.71	44.31 ± 0.06
28.79	74.36 ± 0.09
30.99	97.85 ± 0.11
35.12	160.8 ± 0.3
36.99	200.1 ± 0.3
41.98	351.6 ± 0.7

TABLE 2. Rate constants for the solvolysis of *p*-chlorobenzyl chloride in water

Temperature (°C)	Rate constant ($\times 10^{-5}$ s^{-1})	Temperature (°C)	Rate constant ($\times 10^{-5}$ s^{-1})
51.22	13.75±0.02	59.88	32.10±0.07
53.27	16.89±0.10	61.79	38.48±0.15
53.27	16.96±0.02	63.83	46.42±0.02
55.77	21.39±0.02	66.01	56.28±0.23
57.86	26.32±0.08	68.64	71.30±0.20
59.87	32.01±0.15	70.75	85.38±0.12

TABLE 3. Rate constants for the solvolysis of *p*-nitrobenzyl chloride in water

Temperature (°C)	Rate constant ($\times 10^{-5}$ s^{-1})	Temperature (°C)	Rate constant ($\times 10^{-5}$ s^{-1})
55.15	0.9258±0.0012	64.1	2.238±0.008
57.42	1.157 ±0.007	66.08	2.726±0.013
59.54	1.435 ±0.007	68.05	3.250±0.008
60.14	1.519 ±0.005	71.60	4.488±0.019
62.06	1.851 ±0.002	72.94	5.040±0.012

to give a specific conductance of approximately 10^{-5} ohm^{-1} cm^{-1}. The solvent was degassed and 25–30 ml were added to each of four Queen-type stirred conductivity cells (15) (cell constants *ca.* 0.3). These, plus an additional 20 ml of the degassed solvent were placed in a stable thermostat. At each temperature, the substrate with the exception of *p*-nitrobenzyl chloride, was added from a Hamilton microsyringe (2–3 μl) to the 20 ml of solvent and 2–3 ml of the resulting solution was added to each of the cells yielding a reaction solution of approximately 10^{-4} *M* in substrate. In the case of *p*-nitrobenzyl chloride, the sample was added to the solvent as *ca.* 10 mg of a 3:1 Kieselguhr–chloride mixture (to aid rapid solution), and, after vigorous shaking, 2–3 ml of the solution filtered under nitrogen pressure directly into the stirred cells. Conductivity–time measurements obtained on the Auto-RAM and their computational treatment have been described elsewhere (14). Temperature control was maintained in the thermostats by Tronac controllers to ±0.005 °C or better and temperature measurements were made with a platinum resistance thermometer.

Results and Discussion

The kinetic rate constants so determined are recorded in Tables 1 to 3. The specific rate constant of hydrolysis for *p*-bromobenzyl chloride at 62.07 °C was 38.7 ± 0.3 × 10^{-5} s^{-1}. Since there was no reason to suspect that the $\Delta C_p^{\ddagger}$ value for this substituent would differ significantly from the *p*-chloro analogue, no extensive study was undertaken. The temperature dependence of the rate was expressed in the usual fashion by an empirical equation of the form $\log_{10} k = A_1 + A_2/T + A_3 \log_{10} T$ and values of the constants, A_1, A_2, and A_3 are given in Table 4. By applying transition state considerations, values of $\Delta H^{\ddagger}$, $\Delta S^{\ddagger}$, and $\Delta C_p^{\ddagger}$ can be derived. These values are collected in Table 5. Since the value of $\Delta C_p^{\ddagger}$ for *t*-butyl chloride hydrolyzing in water is about the same as the value found for the *p*-methylbenzyl chloride under similar conditions, it is easy to argue that the degree of charge development is similar and from this approximation draw mechanistic conclusions.

This is probably valid. For these weakly polar and relatively insoluble halides the uncertainties relating to differences in initial state solvation are probably small compared to the much larger differences relating to charge development and separation, at the transition state. Thus the fact

TABLE 4. Empirical constants for the three parameter temperature–rate equation* for the hydrolysis of para-substituted benzyl chlorides in water

Substituent	A_1	$-A_2$	$-A_3$
p-Methyl	126.1948	10035.52	38.74531
Hydrogen†	67.4044	7306.02	19.3092
p-Chloro	79.3558	7934.30	23.3995
p-Nitro	79.0380	8164.51	23.5285

*$\log_{10} k = A_1 + A_2/T + A_3 \log_{10} T$.
†Reference 13.

Can. J. Chem. Downloaded from www.nrcresearchpress.com by 210.87.254.5 on 09/05/12
For personal use only.

TABLE 5. Pseudo-thermodynamic parameters of activation for the solvolysis of para-substituted benzyl chlorides in water at 40 °C*

Substituent	$\Delta H^{\neq}$ (kcal mol^{-1})	$-\Delta S^{\neq}$ (cal deg^{-1} mol^{-1})	$-\Delta C_p^{\neq}$ (cal deg^{-1} mol^{-1})
p-Methyl	21.19±0.03	2.6±0.1	79±3
Hydrogen†	20.83±0.01	11.0±0.0	41±2
p-Chloro	21.12±0.19	11.2±0.6	48±9
p-Nitro	22.09±0.42	14.4±1.3	49±17
t-Butyl-Cl‡	23.80	14.4 (10°)	83
Methyl-Cl§	24.00	12.3 (75°)	49

*For the *p*-nitro and *p*-chloro substrates, this temperature is considerably outside of the experimentally observed range and results in a higher degree of error in the parameters.
†Reference 13.
‡Reference 14.
§Reference 30.

TABLE 6. Rate constants, k.s.i.e.'s and activation parameters for the solvolysis of para-substituted benzyl chlorides in heavy water

Substituent	Temperature (°C)	k_{D_2O} ($\times 10^{-5}$ s^{-1})	k_{H_2O}* ($\times 10^{-5}$ s^{-1})	k_{H_2O}/k_{D_2O}	$\Delta H_{D_2O}^{\neq}$	$\Delta S_{D_2O}^{\neq}$
p-Methyl	24.965	30.96 ±0.10	45.80	1.48	22.42±0.06	+ 0.6±0.2
	34.449	102.6 ±0.3	148.6	1.45		
Hydrogen	32.520	2.512†	3.27	1.30		
	49.963	17.28†	21.8	1.26	20.79±0.24	−11.6±0.8
	60.00	45.8‡	58.1	1.27		
p-Nitro	55.273	0.6782±0.0029	0.987	1.45	22.32±0.11	−14.4±0.3
	65.774	2.019 ±0.010	2.63	1.30		

*Rate constants in water were calculated from the three parameter equations, the constants of which are given in Table 4.
†Reference 30.
‡Reference 31.

that $\Delta C_p^{\neq}$ values for the *p*-methylbenzyl and *t*-butyl chlorides are about the same points to a similarity in solvent reorganization. The fact that adamantyl nitrate (16) has a much larger temperature coefficient of $\Delta H^{\neq}$ probably indicates that none of the above halides hydrolyse in water by a limiting mechanism. That they tend to this limit is acceptable, but how close to the limit is difficult to estimate on the basis of $\Delta C_p^{\neq}$ values as a mechanistic criterion. In both the above examples, the ion-pair mechanism may be acceptable (17). By the same reasoning, it is doubtful whether the degree of charge development indicated by our $\Delta C_p^{\neq}$ values would justify a similar conclusion for the other members reported in Table 5, unless the term "ion-pair" is to include every degree of charge development. For example, the $\Delta C_p^{\neq}$ value calculated for the benzyl *p*-Cl and *p*-NO_2 compounds are seen to be of about the same magnitude as that found for the hydrolysis of other primary halides. In contrast to an earlier implication (17), Sneen now appears to accept such a broadening of the term "ion-pair intermediate" (18). When that term is taken to include any "extended covalent bond" it is, in our view, equivalent to saying that only activated molecules react. If such an all inclusive definition is needed, then the hypothesis has little additional value as a practical criterion on which to base mechanistic discussions.[1]

Two other sources of information relating to the transition state and thus indirectly to solvent disruption were explored: the kinetic solvent isotope effect and the α-deuterium isotope effect. Rate data for solvolysis in D_2O are summarized in Table 6 and it will be apparent that the value of k_{H_2O}/k_{D_2O} for the *p*-methyl and the *p*-nitro compounds are about the same. Since there is other evidence which suggests that it is unlikely that these two compounds react by the same mechanism, or more correctly, with the same

[1]For other criticism of the original claims see refs. 19–21. In citing these critical appreciations of this proposal, we do not overlook the value of a re-examination and elaboration of mechanistic concepts in S_N reactions.

Can. J. Chem. Downloaded from www.nrcresearchpress.com by 210.87.254.5 on 09/05/12
For personal use only.

Can. J. Chem. Downloaded from www.nrcresearchpress.com by 210.87.254.5 on 09/05/12
For personal use only.

degree of charge development, this similarity in k_{H_2O}/k_{D_2O} values is not helpful. We may go further and say that in general this rate ratio does not provide a basis for clear mechanistic distinction for S_N reactions in water even though reasonable expectations would seem to require an observable correlation. We have noted previously a failure of this ratio to correlate with values of $\Delta C_p^{\ddagger}$ in the halide series though the systematic differences which are found in the $\Delta C_p^{\ddagger}$ values between the sulfonates and the halides is paralleled by a systematic difference in k_{H_2O}/k_{D_2O} values. However where large differences exist in $\Delta C_p^{\ddagger}$ values in the displacement of halides which on the basis of other evidence point to mechanistic differences, no corresponding differences are found in the k.s.i.e. This failure to respond to mechanistic differences in the halide series has not been explained satisfactorily and we can only guess that because of the complexity of the effects which are incorporated into the ratio there is a compensation of opposed terms. By way of contrast, the α-deuterium isotope effect, though having about the same absolute values as the k.s.i.e. is less complex and can be correlated with the $\Delta C_p^{\ddagger}$ values and with mechanistic shifts.

Rate data for the α-deuterated benzyl chlorides and corresponding isotope effects are summarized in Table 7. Originally it was thought that a k_H/k_D values close to 1.15/D-atom at 25 °C was characteristic of an S_N1 mechanism. With the accumulation of further data it has been found that each leaving group has a characteristic maximum value of k_H/k_D. Thus 1.15 is the maximum for chloride as a leaving group while Br^- and I^- give smaller values. When the leaving group is a fluoride or groups such as tosylate, trifluromethanesulfonate or nitrate (groups which are attached to the α-carbon through an oxygen atom) values markedly higher than 1.15 are observed in the limit (15, 25). If allowance is made for these characteristic differences, the α-deuterium isotope effect can be used as a good indicator of the extent of bond breaking at the transition state. Where bond making is important the effect becomes small and may even be inverse (23). α-Deuterium isotope effects for three benzyl chlorides are compared with corresponding values for three other compounds in Table 7. The value of k_H/k_D for the *p*-methylbenzyl chloride is seen to be much higher than for the other compounds cited and is but slightly less than the postulated limiting value and in accord with the indications derived from the $\Delta C_p^{\ddagger}$ value. Since the k_H/k_D values reflect differences in bond breaking, solvolysis in other solvents would be expected to alter this ratio. This inference is illustrated by a comparison of our data (24) and that due to Shiner (25) (Table 8). A conclusion to be drawn from this comparison is that since k_H/k_D for the *p*-methyl compound is slightly higher for solvolysis in 70% and 97% trifluroethanol than we found in water, while the value in 50% ethanol is much lower, the mechanism in water for this compound is not limiting. In a strict sense (26) and in the absence of other data to the contrary this would imply an S_N2 mechanism. Further the similarity between the $\Delta C_p^{\ddagger}$ values for the *p*-methylbenzyl chloride and *t*-butyl chloride noted above and the "normal values" obtained for the other members of the series may be taken as strong evidence (27–29) against "mixed kinetics" for hydrolysis of members of this series (3). These conclusions are close to those of Kochi and Hammond for the solvolysis of a series of benzyl tosylates (1) while the more complex hypothesis advanced by Shiner (22) is unnecessary, at least for hydrolysis in water.

TABLE 7. α-Deuterium isotope effects for hydrolysis in water

Chloride	k_H/k_D	Reference
p-Methylbenzyl	1.279 (30°)	This work
Benzyl	1.095 (65°)	This work
p-Chlorobenzyl	1.061 (65°)	This work
Methyl chloride	0.92 (80°)	23
Ethyl bromide	0.98 (80°)	24
Isopropyl bromide	1.07 (60°)	24

TABLE 8. α-Deuterium effect for the solvolysis of *p*-methylbenzyl chloride in various solvent (25 °C)

Solvent	k_H/k_D for one deuterium atom	Reference
97% TFE	1.143	25
70% TFE	1.140	25
Water	1.132	This work
50% Ethanol	1.086	25

1. J. K. KOCHI and G. S. HAMMOND. J. Am. Chem. Soc. 75, 3445 (1953).
2. R. FUCHS and D. M. CARLTON. J. Am. Chem. Soc. **85**, 104 (1963).
3. Y. OKAMOTO and H. C. BROWN. J. Org. Chem. **22**, 485 (1957).

4. B. BENSLEY and G. KOHNSTAM. J. Chem. Soc. 4747 (1957).
5. E. TOMMILA and E. PAAKKALA, U. K. VIRTANEN, A. ERVA, and S. VARILA. Ann. Acad. Sci. Fenn. **A11**, (91) 1 (1959).
6. E. TOMMILA. Acta Chem. Scand. **20**, 923 (1966).
7. J. B. HYNE, R. WILLS, and R. E. WONKA. J. Am. Chem. Soc. **84**, 2914 (1962).
8. R. FUCHS and D. M. CARLTON. J. Org. Chem. **27**, 1520 (1962).
9. H. H. JAFFÉ. Chem. Rev. **55**, 191 (1953).
10. J. W. HILL and A. FRY. J. Am. Chem. Soc. **84**, 2763 (1962).
11. E. GRUNWALD and J. LEFFLER. Rates and equilibria of organic reactions, John Wiley and Sons, Inc., New York. 1963.
12. C. G. SWAIN and W. P. LANGSDORF. J. Am. Chem. Soc. **73**, 2813 (1951).
13. J. M. W. SCOTT and R. E. ROBERTSON. J. Chem. Soc. 1596 (1961).
14. S. E. SUGAMORI and R. E. ROBERTSON. J. Am. Chem. Soc. **91**, 7254 (1969).
15. K. M. KOSHY. Ph.D. Thesis, University of Calgary, Calgary, Alberta. 1973.
16. K. M. KOSHY and R. E. ROBERTSON. Unpublished data.
17. R. A. SNEEN and J. W. LARSEN. J. Am. Chem. Soc. **91**, 362 (1969); **91**, 6031 (1969).
18. R. A. SNEEN. Accounts Chem. Res. **6**, 46 (1973).
19. B. J. GREGORY, G. KOHNSTAM, M. PADDON-ROW, and A. QUEEN. Chem. Commun. 1032 (1970).
20. J. KURZ and J. C. HARRIS. J. Am. Chem. Soc. **92**, 4117 (1970).
21. D. J. ROBERTS, J. H. HARRIS, R. E. HOLLAND, P. v. R. SCHLEYER. J. Am. Chem. Soc. **941**, 7868 (1972).
22. V. J. SHINER, JR. Isotope effects in chemical reactions. ACS Monograph 167. *Edited by* C. J. Collins and N. S. Bowman. Van Nostrand Reinhold Co. New York, 1970. p. 90.
23. J. A. LLEWELLYN, R. E. ROBERTSON, and J. M. W. SCOTT. Can. J. Chem. **38**, 222 (1960).
24. K. T. LEFFEK, J. A. LLEWELLYN, and R. E. ROBERTSON. Can. J. Chem. **38**, 1505 (1960).
25. V. J. SHINER, JR., M. RAPP, and H. R. PINNICK, JR. J. Am. Chem. Soc. **92**, 232 (1970).
26. V. GOLD. J. Chem. Soc. 4633 (1956).
27. G. KOHNSTAM. Adv. Phys. Org. Chem. **5**, 121 (1967).
28. J. M. W. SCOTT and R. E. ROBERTSON. Can. J. Chem. **50**, 167 (1972).
29. D. J. BARNES, M. COLE, S. LOBO, J. G. WINTER, and J. M. W. SCOTT. Can. J. Chem. **50**, 2175 (1972).
30. R. L. HEPPOLETTE and R. E. ROBERTSON. Proc. Roy. Soc. **A252**, 273–285 (1959).
31. L. TREINDL, R. E. ROBERTSON, and S. E. SUGAMORI. Can. J. Chem. **47**, 3397 (1969).

Can. J. Chem. Downloaded from www.nrcresearchpress.com by 210.87.254.5 on 09/05/12
For personal use only.

Etude du succinate de chrome(II) dihydraté, $[Cr(C_4H_4O_4).H_2O]_2.2H_2O$

PATRICK SHARROCK, THÉOPHILE THÉOPHANIDES, ET FRANÇOIS BRISSE
Département de Chimie, Université de Montréal, Montréal, Québec

Reçu le 2 avril 1973

Le succinate de chrome(II) dihydraté, $[Cr(II)(C_4H_4O_4).H_2O]_2.2H_2O$ a été synthétisé pour la première fois. Ce sel a été caractérisé par son spectre infrarouge et par diffraction des rayons-X. Il cristallise dans le système triclinique et la maille a pour dimensions: $a = 6.522(10)$, $b = 7.596(3)$, $c = 8.154(4)$ Å, $\alpha = 103.2(1)$, $\beta = 73.4(1)$, et $\gamma = 98.7(1)°$. Il est isostructural du succinate de cuivre(II) dihydraté. Le succinate de chrome(II), rouge, s'oxyde très rapidement à l'air en un produit bleu-vert de composition $Cr(III)(C_4H_4O_4)(OH).H_2O$.

Chromium(II) succinate dihydrate $[Cr(II)(C_4H_4O_4).H_2O]_2.2H_2O$ has been synthesized for the first time. It has been characterized by its infrared spectrum and by X-ray diffraction. The triclinic unit cell has for dimensions: $a = 6.522(10)$, $b = 7.596(3)$, $c = 8.154(4)$ Å, $\alpha = 103.2(1)$, $\beta = 73.4(1)$, and $\gamma = 98.7(1)°$. This salt is isostructural with copper(II) succinate dihydrate. The red chromium(II) succinate is quickly oxidized in air and the blue oxidation product has composition $Cr(III)(C_4H_4O_4)(OH).H_2O$.

Can. J. Chem., 51, 2963 (1973)

Introduction

Les acides carboxyliques forment avec le cuivre des complexes de structures variées dans lesquels le ligand est mono-, bi- ou tridentate (1–5). Parmi tous ces complexes les carboxylates dinucléaires à structure cage ont été les plus étudiés, car pour ces composés il existe une possibilité de liaison métal–métal (6). Cependant, il semble que les structures cage soient imposées aux molécules dinucléaires par la géométrie particulière du groupement carboxylate plutôt que par la présence d'un lien métal–métal. Autrement dit, dans le cas des complexes cuivriques, l'interaction Cu–Cu est la conséquence et non pas le prérequis à la structure cage. Par contre, une étude récente (7) de l'acétate de chrome(II) révèle qu'une liaison multiple métal–métal est possible. En effet, l'acétate de chrome(II) est diamagnétique (8) et la distance Cr–Cr a pour longueur seulement 2.362(1) Å.

Les complexes du cuivre(II) avec les acides α,ω-dicarboxyliques ont aussi été étudiés (9–11). Le succinate de cuivre, à structure cage, est un exemple typique: son moment magnétique de 1.34 MB, à 16 °C, est en dessous de la valeur de 1.73 MB attendue en ne tenant compte que du spin (9). La distance Cu–Cu (12) est de 2.610(1) Å. Comme les acétates de Cu(II) et de Cr(II) sont isostructuraux (13) nous avons recherché si cette similitude se retrouvait entre les sels des acides dicarboxyliques et en particulier entre les succinates de Cu(II) et de Cr(II).

Partie expérimentale

Le succinate de chrome(II) a été synthétisé par une méthode analogue à celle utilisée pour la préparation de l'acétate de chrome(II) (14). Les manipulations ont été faites dans une boîte à gants, sous atmosphère d'azote purifié; les solvants utilisés ont été préalablement purgés à l'azote. On dissout 10 g de $CrCl_3.6H_2O$ (0.0376 mol) dans 30 ml d'eau. On ajoute 10 ml d'une solution aqueuse contenant 0.054 mole d'acide chlorhydrique. A cette solution verte on ajoute 3 g (0.05 mol) de poudre de zinc et on recouvre le bécher d'un verre de montre pour éviter les pertes par projection. Après une demi-heure la solution est devenue bleu-turquoise. Au bout de trois-quarts d'heure la réduction est terminée. La solution est filtrée pour enlever l'excès de poudre de zinc. Le filtrat est recueilli directement dans une solution de 6.5 g (0.0402 mol) de succinate de sodium anhydre dans 20 ml d'eau. Il se forme un précipité abondant de couleur rouge sienne-brûlée. Sept lavages, de 20 ml d'eau chacun, suffisent pour éliminer toutes traces d'ions chlorures de 2 g de précipité. Le produit est finalement lavé trois fois avec du méthanol puis est conservé sous éther pour le protéger des traces résiduelles d'oxygène dans la boîte à gants. Le succinate de chrome(II) s'oxyde très facilement à l'air en un produit bleu-gris.

Seule la forme oxydée du succinate de chrome a été analysée, après avoir été séchée à 100 °C. Le carbone et l'hydrogène ont été dosés par microanalyse élémentaire par Chemalytics Inc., Tempe, Arizona. Le chrome a été dosé par gravimétrie sous forme de chromate de baryum (15).

Les spectres infrarouges ont été enregistrés entre 4000 et 250 cm^{-1} sur un spectrophotomètre Perkin–Elmer 621. Les échantillons ont été broyés et comprimés sous forme de pastilles de bromure de potassium. Dans le cas du succinate de chrome(II) la pastille comprenait deux zones protectrices extérieures en KBr pur.

Tous les films de poudre ont été pris dans une caméra Debye–Scherrer de 114.5 mm de diamètre en utilisant les radiations filtrées du cuivre et du chrome (λ $CuK_{\bar{\alpha}}$ =

Can. J. Chem. Downloaded from www.nrcresearchpress.com by 210.87.254.6 on 09/05/12
For personal use only.

Can. J. Chem. Downloaded from www.nrcresearchpress.com by 210.87.254.6 on 09/05/12
For personal use only.

1.54178 Å et λ $CrK_{\bar{\alpha}}$ = 2.2909 Å). Les échantillons finement broyés dans la boîte à gants ont été introduits dans des capillaires de Lindemann (0.3 mm de diamètre) et scellés sous azote. Les intensités des raies ont été estimées visuellement.

Résultats et discussion

L'augmentation de poids au cours de l'oxydation du succinate de chrome(II) a été mesurée de la façon suivante: On renferme 2 g de succinate de chrome(II) rouge dans un tube de Schlenk (14) préalablement pesé et on place le tout sur une balance analytique. Dans une première expérience, on entrouvre les deux robinets pour laisser l'air pénétrer lentement dans le tube de Schlenk. On enregistre les changements de poids en fonction du temps. Le gain maximum de poids observé est de 3.99 %.[1] On déduit de cela que le produit de départ est bien le succinate de chrome(II) dihydraté car pour la réaction:

$$2\,[Cr(succinate).2H_2O] + \tfrac{1}{2}O_2 \rightarrow 2\,[Cr(succinate)(OH).H_2O] + H_2O$$

on s'attend à un gain de poids théorique de 3.95 % à condition que la molécule d'eau libérée reste emprisonnée dans le tube de Schlenk. On reprend cette expérience en faisant passer dans le tube de Schlenk un courant d'oxygène bien sec pendant 24 h. On note tout d'abord une augmentation de poids de 3.75%. Par la suite le poids de l'échantillon diminue régulièrement et très lentement. Au bout de 24 h, le poids reste constant. La diminution de poids est de 0.37% du poids initial. Cette baisse de poids s'explique bien par la perte lente d'une molécule d'eau entraînée hors du tube de Schlenk par le courant d'oxygène. En effet, le gain de poids dû à l'oxydation et la perte de poids due à l'élimination d'une molécule d'eau se combinent pour donner une diminution théorique de 0.49%, en accord avec la mesure expérimentale. Dans une troisième expérience on chauffe l'échantillon à 130 °C pendant 12 h. La perte de poids observée, 9.43%, coïncide avec le changement de poids théorique résultant de la perte de trois molécules d'eau, 9.37%.

Les résultats des analyses élémentaires confirment que la composition du succinate de chrome(III), forme oxydée, est bien: $Cr(III)(C_4H_4O_4)(OH).H_2O$.

Anal. calc. pour $CrC_4H_7O_6$: Cr, 25.61; C, 23.60; H, 3.45. Trouvé: Cr, 25.05; C, 23.09; H, 2.56.

Diffraction des rayons-X

Le diagramme de poudre du succinate de chrome(II) a été pris et comparé à celui du succinate de cuivre(II). Les diagrammes des deux succinates sont pratiquement identiques, tant du point de vue de la position des raies que de leurs intensités. Ces deux composés sont donc isostructuraux. Les diagrammes de poudre de ces deux composés ont été indexés par comparaison des distances réticulaires et des intensités observées aux valeurs correspondantes calculées[2] à partir des coordonnées fractionnaires et des facteurs thermiques des atomes et des paramètres de la maille élémentaire du succinate de cuivre(II) publiés par O'Connor et Maslen (12). Les paramètres de maille des succinates de cuivre(II) et de chrome(II) affinés selon la méthode de Cohen (16), sont présentés Tableau 1. En ce qui concerne les dimensions de la maille du succinate de cuivre(II), nos résultats sont en bon accord avec ceux publiés (12). Le volume de la maille du succinate de chrome(II) est légèrement, mais significativement, supérieur à celui du sel de cuivre. Les distances réticulaires et les intensités observées et calculées pour les deux succinates sont présentées Tableau 2. Les intensités du diagramme de poudre du succinate de chrome(II) ont été calculées en conservant les coordonnées atomiques fractionnaires du succinate de cuivre(II) mais en remplaçant l'atome de cuivre par un atome de chrome. Ce calcul des intensités permet de vérifier qu'aucune bande de forte

TABLEAU 1. Dimensions des mailles*

	$Cu(C_4H_4O_4).2H_2O$		$Cr(C_4H_4O_4).2H_2O$
	Référence 12	Ce travail	ce travail
a	6.437(11) Å	6.420(10) Å	6.522(10) Å
b	7.623(4)	7.618(5)	7.596(3)
c	8.081(5)	8.087(5)	8.145(4)
α	103.90(13)°	103.8(2)°	103.2(1)°
β	73.50(35)	73.4(3)	73.4(1)
γ	98.62(22)	98.6(2)	98.7(1)

*Il est possible de calculer les dimensions des mailles réduites conventionnelles correspondantes, en se servant de la matrice de transformation α = /100/010/00$\bar{1}$/ (23).

[1]Les résultats indiqués ont été corrigés pour tenir compte de la poussée d'Archimède qui varie selon la nature du gaz contenu dans le tube de Schlenk.

[2]Les intensités calculées tiennent compte des facteurs de Lorentz et de polarisation de sorte que ces intensités sont directement comparables aux intensités observées.

TABLEAU 2. Distances réticulaires et intensités pour les succinates de Cu(II) et de Cr(II)

			$Cu(C_4H_4O_4).2H_2O$ $CuK\bar{\alpha}$				$Cr(C_4H_4O_4).2H_2O$ $CrK\bar{\alpha}$			
h	k	l	d_{obs}	d_{cal}	I_{obs}	I_{cal}*	d_{obs}	d_{cal}	I_{obs}	I_{cal}*
0	0	1	7.58	7.58	100	100	7.71	7.65	100	100
0	1	0	7.36	7.39	50	68	7.31	7.36	40	76
1	0	0	6.15	6.14	20	19	6.23	6.21	20	14
0	1	1	5.92	5.92	10	15	5.92	5.92	15	16
1	0	1	5.52	5.54	25	39	5.59	5.59	50	36
1	1	0	4.931	4.931	20	25	4.997	4.980	30	23
0	1	1	4.799	4.823	5	1	—	4.851	—	0
1	1	0	4.514	4.539	5	1	4.551	4.546	5	2
1	0	1	4.246	4.256	20	22	4.302	4.306	40	23
1	1	1	4.006	4.020	5	4	4.054	4.034	15	3
0	0	2	3.792	3.789	5	3	3.827	3.827	10	6
1	0	2	3.681	3.688	30	25	3.719	3.721	50	24
1	1	1	3.597	3.602	10	14	3.633	3.644	10	12
1	2	1	3.451	3.450	10	9	3.454	3.454	20	11
1	2	0	3.286	3.289	5	3	3.305	3.303	10	3
2	0	0	3.064	3.072	10	5	3.113	3.107	20	8
1	2	0		3.053		5	3.043	3.046	5	4
0	2	2	2.969	2.962	5	5	2.956	2.959	10	4
2	1	0	2.928	2.924	5	4		2.962		3
1	2	1	2.867	2.869	10	7	2.868	2.864	5	6
2	0	2	2.764	2.770	10	8	2.795	2.795	15	7
2	2	1	2.591	2.628	10	2	2.648	2.649	5	2
1	0	3		2.589		3	2.615	2.612	5	2
0	3	1	2.496	2.495	15	9	2.505	2.482	20	8
2	1	1	2.466	2.468	15	10		2.501		10
1	2	2	2.425	2.422	5	4	2.426	2.424	5	3
2	1	3	2.327	2.331	10	5	2.351	2.351	10	4
0	3	2	2.290	2.287	10	7	2.285	2.278	25	6
2	0	3	2.262	2.265	15	14		2.286		14
1	3	0	2.216	2.221	5	4	2.214	2.213	5	3
2	2	1	2.137	2.137	20	11	2.162	2.161	20	11
2	1	2	2.076	2.076	5	1	2.099	2.093	5	1
1	3	2	1.993	1.995	5	4	1.990	1.990	10	3
3	1	3	1.892	1.894	5	3	1.916	1.912	5	3

*Intensités calculées à partir des données de la réf. 12. Voir le texte pour les détails.

intensité n'a été omise de l'indexation. Les distances réticulaires groupées par une accolade étaient trop rapprochées pour être mesurables individuellement.

La distance Cr–Cr, obtenue à partir des coordonnées fractionnaires du succinate de Cu(II) et des dimensions de la maille du sel de Cr(II), est de 2.60 Å. La distance Cr–Cr ainsi calculée n'est pas significativement plus courte que la distance Cu–Cu dans le succinate de Cu(II) et reste bien loin de 2.362 Å observé dans le cas de l'acétate de Cr(II) monohydraté (7).

Pour tenter de confirmer "l'effet métal–métal *trans*" proposé par Cotton (17), les intensités qu'auraient les lignes de diffraction d'un diagramme de poudre de succinate de chrome(II) ont été calculées pour différentes valeurs de la distance Cr–Cr, de 2.60 Å jusqu'à un minimum de 2.36 Å. Seules les six premières raies présentaient des changements notables d'intensités. Ces variations étaient cependant insuffisamment marquées pour permettre un choix, compte tenu de la méthode d'évaluation des intensités observées. Seulement des données tridimensionnelles à partir d'un cristal unique de succinate de chrome(II) permettraient de calculer avec précision la distance Cr–Cr. Nous n'avons malheureusement pas encore réussi à obtenir un tel cristal.

Spectres infrarouges

Les spectres infrarouges de l'acide succinique et de divers succinates sont représentés fig. 1. Les attributions ont déjà été faites pour toutes les

Can. J. Chem. Downloaded from www.nrcresearchpress.com by 210.87.254.6 on 09/05/12
For personal use only.

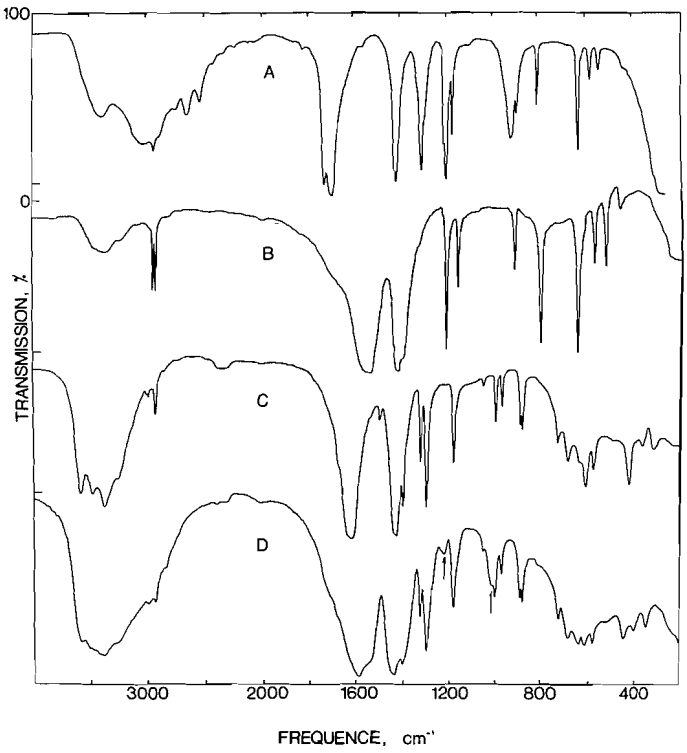

FIG. 1. Spectres infrarouges: *A*, acide succinique; *B*, succinate de sodium; *C*, succinate de cuivre(II) dihydraté; *D*, succinate de chrome(II) dihydraté. Les flèches indiquent des bandes dues à des traces résiduelles de méthanol.

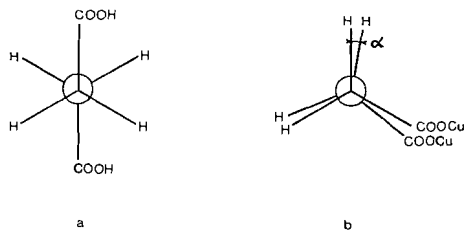

FIG. 2. Représentations de Newman: *a*, forme alternée *trans* dans l'acide succinique; *b*, forme éclipsée *cis* dans le succinate de cuivre(II) dihydraté. L'angle dièdre α est de 4.2°.

bandes observées (18, 19). Les spectres des succinates de cuivre(II) et de chrome(II) sont remarquablement identiques et ceci confirme l'isostructuralisme de ces deux complexes. Les spectres infrarouges des succinates de cuivre(II) et de chrome(II) sont distincts des spectres de la forme alternée *trans* trouvée dans l'acide succinique (18) ou dans les succinates des métaux alcalins (19). Il est reconnu que les différentes fréquences ν_{CH_2} sont sensibles à la conformation des chaînes linéaires (19). La fig. 2 représente les projections de Newman pour l'acide succinique et pour le succinate de cuivre(II); l'angle dièdre α de 4.2° a été calculé à partir des données de la réf. 12. Comme les spectres infrarouges des succinates de cuivre(II) et de chrome(II) sont identiques en dessous de 1400 cm^{-1}, il est raisonnable de conclure que les fréquences observées sont caractéristiques de la forme éclipsée *cis*.

En ce qui concerne la région du carbonyle, la validité de la spectroscopie vibrationnelle dans l'élucidation de la structure des carboxylates a déjà été mise en doute par de nombreux auteurs (20, 21). L'examen de la forme et de la position de la bande ν_{asym} CO seule permettrait de distinguer entre deux types de structures. En effet, les sels alcalins des acides carboxyliques ont une bande assez large vers 1550–1575 cm^{-1} tandis que les complexes à structure cage ont une bande fine à des fréquences généralement plus élevées (21, 22).

Cependant en ce qui concerne le succinate de chrome(II), la bande ν_{asym} CO à 1585 cm^{-1} est relativement large et présente un épaulement.

Can. J. Chem. Downloaded from www.nrcresearchpress.com by 210.87.254.6 on 09/05/12
For personal use only.

Une raison probable de cette différence serait due à une légère oxydation de l'échantillon, puisque la bande ν_{asym} CO de la forme oxydée du succinate de chrome coïncide avec l'épaulement observé à 1540 cm^{-1}.

Nous remercions le Conseil National des Recherches du Canada pour l'aide financière apportée à ce travail.

1. C. K. PROUT, J. R. CARRUTHERS et F. J. C. ROSSOTTI. J. Chem. Soc. (A), 3342 (1971).
2. R. C. KOMSON, A. T. MCPHAIL, F. E. MABBS, et J. K. PORTER. J. Chem. Soc. (A). 3447 (1971).
3. D. B. W. YAWNEY et R. J. DOEDENS. Inorg. Chem. **9**, 1626 (1970).
4. B. W. SKELTON et T. N. WATERS. J. Chem. Soc. Dalton, 2133 (1972).
5. M. B. CINGI, C. GUASTINI, A. MUSATTI, et M. NARDELLI. Acta Cryst. **B25**, 1833 (1969).
6. R. W. JOTHAM, S. F. A. KETTLE, et J. A. MARKS. J. Chem. Soc. Dalton, 428 (1972).
7. F. A. COTTON, B. G. DEBOER, M. D. LAPRADE, J. R. PIPAL, et D. A. UCKO. Acta Cryst. **B27**, 1664 (1971).
8. A. EARNSHAW, L. F. LARKWORTHY, et K. S. PATEL. Proc. Chem. Soc. 281 (1963).
9. L. DUBICKI, C. M. HARRIS, E. KOKOT, et R. L. MARTIN. Inorg. Chem. **5**, 93 (1966).
10. B. N. FIGGIS et D. J. MARTIN. Inorg. Chem. **5**, 100 (1966).
11. O. ASAI, M. KISHITA, et M. KUBO. J. Phys. Chem. **63**, 96 (1959).
12. B. H. O'CONNOR et E. N. MASLEN. Acta Cryst. **20**, 824 (1966).
13. J. N. VAN NIEKERK, F. R. L. SHOENING, and J. F. DE WET. Acta Cryst. **6**, 501 (1953).
14. W. L. JOLLY. The synthesis and characterization of inorganic compounds. Prentice Hall, Englewood Cliffs, New Jersey. 1970.
15. A. I. VOGEL. Quantitative inorganic analysis. 2nd ed. Longmans, London. 1955. p. 453.
16. M. U. COHEN. Rev. Sci. Instr. **6**, 68 (1935).
17. F. A. COTTON et J. G. NORMAN, JR. J. Am. Chem. Soc. **94**, 5697 (1972).
18. M. SUZUKI et T. SHIMANOUCHI. J. Mol. Spectrosc. **28**, 394 (1968).
19. Y. KURODA et M. KUBO. J. Phys. Chem. **64**, 759 (1960).
20. C. OLDHAM. Progress in inorganic chemistry. **10**, 223 (1968).
21. K. NAKAMOTO. Infrared spectra of inorganic and coordination compounds. J. Wiley, New York. 1963. p. 198.
22. G. COSTA, E. PAULUZZI, et A. PUXEDDU. Gazz. Chim. Ital. **87**, 885 (1957).
23. International tables for X-ray crystallography. Vol. I. Kynoch Press, Birmingham. 1969. p. 530.

Can. J. Chem. Downloaded from www.nrcresearchpress.com by 210.87.254.6 on 09/05/12
For personal use only.

An Investigation into σ and π Contributions to Long Range ^1H–^1H Coupling Constants in Conjugated Dienes and Diynes Using CNDO and INDO Molecular Orbital Calculations[1]

IAN R. PEAT[2] AND WILLIAM F. REYNOLDS[3]

Department of Chemistry, University of Toronto, Toronto, Ontario, Canada M5S 1A1

Received March 29, 1973

Molecular orbital calculations based on finite perturbation theory in the CNDO/2 and INDO approximations are carried out for fourteen conjugated dienes and diynes for which experimental results are available. There is generally very good agreement between experimental and calculated (INDO) coupling constants. Comparison of results of CNDO/2 and INDO calculations elucidates the relative importance of σ and π pathways for the various long-range coupling constants.

Des calculs d'orbitales moléculaires basés sur la théorie des perturbations dans les approximations CNDO/2 et INDO, ont été effectués sur quatorze dièns et diynes conjugués qui peuvent être reliés à des résultats expérimentaux. Dans la majorité des cas, un excellent accord fut noté entre les constantes de couplage (INDO) calculées et expérimentales. La comparaison des résultats obtenus par des calculs CNDO/2 et INDO a permis d'établir l'importance relative des contributions σ et π en ce qui a trait aux différentes constantes de couplage à longue-distance. [Traduit par le journal]

Can. J. Chem., 51, 2968 (1973)

Introduction

Molecular orbital calculations based on finite perturbation theory (1) in the INDO (2) and CNDO/2 (3) approximations have proved to be a powerful method for investigating mechanisms of transmission of long range ^1H–^1H coupling constants and, in particular, for determining the relative importance of σ and π contributions to these coupling constants (4–11).

While there have been a number of experimental investigations of coupling constants in conjugated dienes and diynes (4, 7, 12–21), there have been relatively few theoretical calculations of these coupling constants. Harris and coworkers calculated π contributions to coupling constants in 1,3-butadiene, 1,3-butadiyne, and 1,3,5-hexatriyne by several π molecular orbital methods (22). Bacon and Maciel calculated several of the coupling constants in 1,3-butadiene and a limited number of coupling constants in pentadiene and hexadiene isomers, using INDO finite perturbation calculations (4). They also investigated the effect of neglecting some of the one-center exchange integrals (to separate σ and π effects) and of distorting the molecular framework. Finally, Schaefer *et al.* have used both INDO and CNDO/2 calculations to estimate σ and π contributions to coupling constants in 1-penten-3-yne (7). Consequently it seemed appropriate to carry out a systematic theoretical investigation of coupling constants in conjugated dienes and diynes using CNDO/2 and INDO finite perturbation calculations. The results of this investigation are reported below.

Details of Calculations

CNDO/2 and INDO finite perturbation calculations were carried out using a modified version of the Quantum Chemistry Program Exchange Program 141. The modified program reproduced previously published results for several compounds (1). Standard bond lengths and angles (23) were used for the calculations on linear dienes and diynes. For cyclopentadiene, bond lengths and angles were taken from the microwave structure (24). Calculations were carried out on an IBM 370 computer.

Results and Discussion

Calculations were performed for s-*trans*- (**1***a*) and s-*cis*-1,3-butadiene (**2**), *trans*- and *cis*-1,3-pentadiene (respectively **1***b* and **1***c*) cyclopentadiene (**3**) and its 1-methyl and 2-methyl derivatives (for which experimental results have recently been reported (25)); acetylene and 1,3-butadiyne and their methyl and dimethyl derivatives. Results are summarized in Tables 1 to 3.

[1]Taken in part from the Ph.D. thesis of I.R. Peat, University of Toronto, Toronto, Ontario, 1973.

[2]Gulf Oil Fellowship Holder 1971–1973.

[3]On leave during 1973 at the C.N.R.S. Centre de Recherches sur les Macromolecules, Strasbourg, France.

Can. J. Chem. Downloaded from www.nrcresearchpress.com by 210.87.254.105 on 09/05/12
For personal use only.

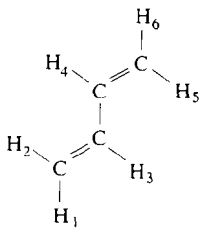

1*a*

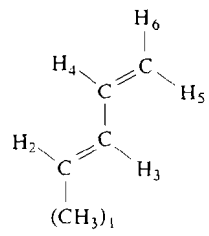

1*b*

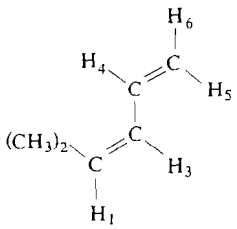

1*c*

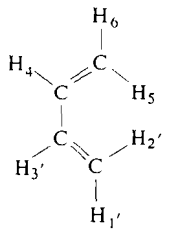

2

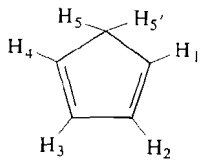

3

In cases where Bacon and Maciel (4) had also determined the coupling constants by INDO calculations, there is very close agreement between the two results.

(a) Conjugated Dienes

As a result of the neglect of one-center exchange integrals in the CNDO/2 approximation, these calculations do not predict the contribution from π coupling pathways arising from McConnell's spin polarization mechanism, *i.e.* they only measure σ coupling contributions (23). By comparison, the INDO calculations include one-center exchange integrals and consequently estimate both σ and π contributions. While it is tempting to take J(INDO) − J(CNDO) as a measure of π contributions (7), this is not strictly valid. A comparison of CNDO and INDO calculations of coupling constants in saturated systems (23) demonstrates that σ contributions are not equally estimated by the two methods. It appears that J(INDO) is alternately more positive, then more negative, than J(CNDO) as the number of intervening bonds increases. Consequently J(INDO) − J(CNDO) is not an exact measure of π contributions. However, for small J(CNDO), if J(INDO) − J(CNDO) is significantly different from zero, then this can be attributed to the presence of π contributions.

The results of the CNDO and INDO calculations for the butadienes (see Table 1) are in very good agreement with the available experimental data for these or closely related compounds (12, 16) although there is a persistent tendency to overestimate the magnitudes of the coupling constants. The agreement is generally significantly better than that noted by Harris *et al.* for π electron calculations (22). The calculations wholly support the conclusions of Bothner-By and Harris concerning the relative importance of σ and π contributions for these derivatives (14). For example, the INDO calculations correctly predict the relative magnitudes of the three non-equivalent ^5J values in **1***a*, $^5J_{16}(J_{tt}) > {}^5J_{15} = {}^5J_{26}(J_{ct}) \gtrsim {}^5J_{25}(J_{cc})$. Furthermore, the CNDO/2 calculations suggest small σ contributions to $^5J_{15}$, $^5J_{25}$, and $^5J_{26}$ but a significant σ contribution to $^5J_{16}$. The corresponding coupling constant for the s-*cis* isomer, $^5J_{1'6}$, is predicted to have a negligible σ contribution, confirming that $^5J_{16}$ is transmitted stereospecifically through the all-*trans* or zig-zag pathway. However, the calculations appear to overestimate the magnitude of this contribution. This appears to be a general problem associated with CN/INDO finite perturbation calculations. A similar overestimation of the stereospecific *meta–alpha* coupling constant was noted for styrene, with the error being greater for the INDO than for the CNDO calculations (5, 26).

The calculations are also in good agreement with all of the ^4J values for which experimental data are available. There are minor discrepancies for the values of $^4J_{14}$ and $^4J_{24}$ in the s-*trans* configuration (**1***a*). The calculations suggest $|J_{24}| > |J_{14}|$ when in fact they are equal in value (12, 16). The CNDO/2 calculations indicate that the calculated difference arises from a negative σ contribution to $^4J_{24}$. This is likely due to a direct interaction between H_2 and H_4 similar to that in *o*-xylene (9) and *cis*-2-butene (11). The failure to observe this experimentally may be a result of molecular distortions which increase the distance between H_2 and H_4 (17). The results for $^4J_{1'4}$ in the s-*cis* conformation (**2**) are partic-

Can. J. Chem. Downloaded from www.nrcresearchpress.com by 210.87.254.105 on 09/05/12
For personal use only.

Can. J. Chem. Downloaded from www.nrcresearchpress.com by 210.87.254.105 on 09/05/12
For personal use only.

TABLE 1. Comparison of experimental and calculated coupling constants (Hz) for conjugated dienes

	1,3-Butadiene						1,3-Pentadiene					
	s-*trans* conformation (**1***a*)			s-*cis* conformation (**2**)			*trans* isomer (**1***b*)			*cis* isomer (**1***c*)		
		Calculated			Calculated			Calculated			Calculated	
	Experimental*	CNDO	INDO	Experimental*	CNDO	INDO	Experimental†	CNDO	INDO	Experimental†	CNDO	INDO
$J_{12} = J_{56}$	1.74	10.15	4.85		10.18	4.78	J_{12} 6.69	5.17	7.75	7.10	5.26	7.79
$J_{13} = J_{46}$	10.17	7.86	9.21	9.42	8.28	9.68	J_{13} −1.70	−0.12	−2.25	10.86	8.40	9.86
$J_{14} = J_{36}$	−0.86	−0.07	−1.26	1.06	1.85	1.87	J_{14} 0.45	0.01	0.75	−1.14	−0.23	−1.43
$J_{15} = J_{26}$	0.69	0.18	1.00		−0.14	0.62	J_{15} −0.76	0.02	−1.05	0.81	0.28	1.13
J_{16}	1.30	1.03	2.42	0.91	−0.03	0.84	J_{16} −0.74	0.06	−1.04	1.53	1.17	2.62
$J_{23} = J_{45}$	17.05	19.67	25.71		20.28	26.52	J_{23} 15.06	20.04	26.38	−1.83	0.34	−1.69
$J_{24} = J_{35}$	−0.83	−0.42	−1.46		−0.18	−1.16	J_{24} −0.78	−0.42	−1.50	0.21	−0.23	0.41
J_{25}	0.60	0.03	0.87		−0.35	0.53	J_{25} 0.61	0.03	0.89	−0.54	0.03	−0.93
J_{34}	10.41	13.75	17.65	5.14	6.35	6.78	J_{26} 0.74	0.19	1.03	−0.64	0.00	−0.99
							J_{34} 10.30	13.73	17.65	10.95	13.81	17.82
							J_{35} −0.79	−0.41	−1.49	−0.85	−0.43	−1.50
							J_{36} −0.81	−0.09	−1.32	−0.81	−0.08	−1.30
							J_{45} 16.93	19.74	25.78	16.89	20.11	26.33
							J_{46} 10.22	7.90	9.23	10.24	8.04	9.42
							J_{56} 1.89	10.19	4.86	2.12	10.18	4.82

	Cyclopentadiene			Methyl cyclopentadienes: 1-Methyl isomer			Methyl cyclopentadienes: 2-Methyl isomer		
		Calculated			Calculated			Calculated	
	Experimental‡	CNDO	INDO	Experimental‡	CNDO	INDO	Experimental‡	CNDO	INDO
J_{12}	5.05	3.84	4.54	−1.6	0.00	−1.75	−1.5	0.01	−1.77
J_{13}	1.09	1.98	2.18	0.4	0.10	0.69	1.4	1.92	2.07
J_{14}	1.98	1.21	2.18	−0.4	0.18	−0.66	1.8	1.20	2.18
J_{15}	1.33	0.79	1.21	−0.2	−0.23	−0.66	1.8	0.73	1.39
J_{23}	1.93	2.04	1.71	1.9	1.99	1.64	−0.4	0.08	−0.48
J_{24}	1.09	1.98	2.18	1.4	1.92	2.06	0.4	0.23	0.86
J_{25}	−1.51	0.72	−0.58	−1.3	0.71	−0.48	2.0	1.76	2.28
J_{34}	5.05	3.84	4.54	5.4	3.87	4.45	5.4	3.78	4.43
J_{35}	−1.51	0.72	−0.58	−1.5	0.81	−0.55	−1.5	0.77	−0.49
J_{45}	1.33	0.79	1.21	1.4	0.69	1.18	1.4	0.74	1.07

*Experimental values from ref. 12. The s-*cis* values were considered to be those for 1,3-cyclohexadiene.
†Experimental values from ref. 17.
‡Experimental values from ref. 25.

TABLE 2. Comparison of corresponding coupling constants (Hz) in 1,3-butadiene and styrene

	s-*trans*-1,3-butadiene		Styrene			s-*cis*-1,3-butadiene		Styrene	
	Exp	Calcd (INDO)	Exp*	Calcd (INDO)		Exp	Calcd (INDO)	Exp†	Calcd (INDO)
J_{24}	−0.83	−1.46	−0.50	−0.28	$J_{2'4}$	—	−1.16	−0.50	−0.77
J_{25}	0.60	0.87	<0.07	0.40	$J_{2'5}$	—	0.53	−0.15	−0.05
J_{26}	0.69	1.00	0.18	0.50	$J_{2'6}$	—	0.62	<0.07	0.20

*Values for 3,4-dichlorostyrene (average of two planar conformations) (5).
†Values for 2,5-dichlorostyrene (5).

TABLE 3. Experimental and calculated coupling constants (Hz) for acetylene and conjugated diynes

	J value		
		Calculated	
Compound	Experimental*	CNDO	INDO
Acetylene	|9.1|	6.54	10.99
Propyne	|2.9| − |3.6|	0.06	−2.29
2-Butyne	|2.7|	2.34	3.29
1,3-Butadiyne	|2.2|	0.18	1.04†
1,3-Pentadiyne	|1.27|	0.00	−0.97
2,4-Hexadiyne	|1.3|	0.87	1.38
2,4,6-Octatriyne	|0.4|	0.00	0.58

*Experimental values from ref. 30.
†Did not converge after 100 iterations.

ularly interesting. They reproduce the experimental change in sign from $^4J_{14}$ and confirm that this is due to a stereospecific σ contribution. They also provide a striking demonstration of the fallacy of taking J(INDO) − J(CNDO) as a measure of π contributions. In this case, J(INDO) − J(CNDO) ≈ 0. Since the corresponding value for $^4J_{14}$ is −1.2 Hz, this would imply a strongly stereospecific π coupling mechanism. However, there is no experimental evidence for strongly stereospecific π effects. In actual fact, the INDO calculations must overestimate the stereospecific σ contribution (relative to the CNDO/2 calculations) by an amount equal in magnitude but opposite in sign to the calculated π contributions.

It is probable that performing INDO calculations with and without one-center exchange integrals corresponding to σ–π exchange interactions (4) may provide a more reliable estimate of π contributions. For example, this approach does yield approximately equal π contributions for $^4J_{14}$ in **1***a* (−0.52 Hz) and $^4J_{1'4}$ in **2** (−0.29 Hz) (4). However, it is probably less reliable for estimating σ contributions since, as discussed above, the INDO calculations often overestimate these contributions. Thus it would appear that neither approach gives precise values for both σ and π contributions.

The ^2J and ^3J values are also in reasonable agreement with experiment. Probably the most significant result in this case is the correct prediction of the relative magnitudes of J_{34} and $J_{3'4}$ for the two derivatives with the difference again arising from a stereospecific σ effect.

It is instructive to compare the experimental and calculated ^4J and ^5J values for butadienes with the corresponding values for styrenes (see Table 2). The two sets of values show very similar patterns, with the values for styrene being consistently lower. This is the expected result since the C_1—C_2 π bond order in styrene is lower. The CNDO calculations for $^5J_{2'5}$ in both cases provide evidence for a direct interaction leading to a negative value for $^5J_{2'5}$. This has been observed experimentally for 2,5-dichlorostyrene (5). Support for the existence of this direct interaction follows from a comparison of the INDO and CNDO values for $J_{2'5}$ when the C_1—C_α—C_β bond angle is opened up to 130°, thus separating the proximate protons. $J_{2'5}$(CNDO) becomes less negative, approaching zero, while the INDO value becomes more positive, approaching the J_{25}(INDO) value (26).

The calculations for **1***b* demonstrate that the stereospecific σ effect for $^5J_{16}$ in s-*trans* 1,3-butadiene (**1***a*) has been almost completely removed by replacing H_1 by a methyl group. Experimental values for $^6J_{15}$ and $^6J_{16}$ in **1***b* and $^6J_{25}$ and $^6J_{26}$ in **1***c* are nearly identical and are equal in magnitude and opposite in sign to $^5J_{15}$, $^5J_{25}$, and $^5J_{26}$ in **1***a*. These observations are consistent with the predictions of the methyl group replacement technique (27) for a system with a dominant π electron coupling pathway.

Can. J. Chem. Downloaded from www.nrcresearchpress.com by 210.87.254.105 on 09/05/12
For personal use only.

Can. J. Chem. Downloaded from www.nrcresearchpress.com by 210.87.254.105 on 09/05/12
For personal use only.

The calculations closely reproduce these trends, even reproducing the relative magnitude of the six bond coupling constants.

By contrast, $^4J_{14}$ and $^4J_{24}$ in **1***a* are significantly larger than the corresponding 5-bond methyl proton coupling constants in **1***b* ($^5J_{14}$) and **1***c* ($^5J_{24}$). The INDO calculations reproduce both trends. In the former case, the apparent failure of the methyl group replacement technique could be due to a σ contribution to $^4J_{14}$ in **1***a* (4, 17), although the CNDO calculations do not support this assumption. In the latter case the difference may be due to both a direct interaction in **1***c*, since $^5J_{24}$ has a minimum positive value (maximum negative value by CNDO) when one of the methyl protons is proximate to H_4, and to a σ contribution in **1***a*. Finally, the difference could, in part, be due to in-plane distortions of the molecular framework of the pentadiene isomers (4, 17).

$^5J_{14}$ in **1***b* (as calculated by INDO) varies from 0.07 Hz for the C—H bond of the methyl group coplanar to the carbon skeleton to 1.42 Hz for a perpendicular C—H bond with an approximate $\sin^2\phi$ dependence (maximum deviation 0.09 Hz). A similar angular dependence is noted for other long range methyl proton coupling constants. This is analogous to the previously noted behavior of long range coupling constants to the α protons of styrene (5), toluene (9), and benzaldehyde (28). This type of behavior has been attributed to an allylic π mechanism (29).

There is a persistent tendency for couplings involving H_1 to increase on going from **1***a* to **1***c* but H_2 couplings remain essentially constant on going from **1***a* to **1***b* (17). These trends are reproduced almost quantitatively by the INDO calculations. Similarly, INDO calculations qualitatively reproduce the general increase in coupling constants on going from **1***a* to *cis,cis*-2,4-hexadiene (4). This suggests that the observed increases in coupling constants are due to electronic effects rather than molecular distortions, as previously suggested (17). However, the latter possibility cannot be totally ruled out, since INDO calculations predict that in-plane distortions will also cause increases in coupling constants (4). The observed increase in J_{56} for **1***b* and **1***c* relative to **1***a* is not predicted by our calculations, suggesting that it might arise from molecular distortions. Geminal coupling constants are particularly sensitive to small angle changes.

In general, our calculations for 1,3-butadiene and related compounds have provided more mechanistic information than the π electron calculations of Harris and co-workers (22) and have extended the conclusions of Bacon and Maciel (4) concerning the relative importance of σ and π mechanisms in these compounds.

In the case of cyclopentadiene (**3**), there is generally very good agreement between experimental and calculated (INDO) coupling constants. The worst agreement is for $^4J_{25}$ ($^4J_{35}$). Here the INDO calculations indicate a negative contribution, presumably due to an allylic coupling mechanism (29) while CNDO suggests a positive contribution, presumably a σ contribution through the pseudo zig-zag arrangement. It appears that the calculations again overestimate this contribution. All other coupling constants appear to be transmitted through the σ system. The calculations also appear to overestimate the stereospecific σ contribution to $^4J_{13}$.

The calculations closely reproduce the experimental trends on going from 1,3-cyclohexadiene (calculations for **2**) to cyclopentadiene (**3**), *i.e.* the large decrease for $J_{1'3}$ (J_{12}) and $J_{3'4}$ (J_{23}), the near constancy of $J_{1'4}$ (J_{13}) and the significant increase for $J_{1'6}$ (J_{14}). The latter increase is clearly due to the additional σ pathway through C_5.

The calculations also closely reproduce the experimental coupling constants for 1-methyl- and 2-methylcyclopentadiene. The CNDO calculations suggest that the coupling constants of the methyl group to the olefinic protons are dominated by a π mechanism, as previously suggested (25). $^4J_{15}$ for 1-methylcyclopentadiene is apparently transmitted through the σ system while $^5J_{25}$ for 2-methylcyclopentadiene is an example of homoallylic coupling (29) involving the π electron system. The CNDO calculations reproduce this coupling since, in this case, there is a direct interaction of both C—H bonds with the π bond.

(b) Acetylenes and Conjugated Diynes

The results of the calculations for these derivatives indicate that the coupling constant in acetylene is dominated by a σ mechanism but those for propyne and 1,3-butadiyne ("diacetylene") are dominated by π mechanisms. This should also hold for the more extended coupling paths for the other derivatives. The significant CNDO values in 2-butyne and 2,4-hexadiyne

Can. J. Chem. Downloaded from www.nrcresearchpress.com by 210.87.254.105 on 09/05/12
For personal use only.

can again be attributed to the direct interaction of the C—H bonds with the π electron system, *i.e.* a type of homoallylic interaction.

The overall agreement between experimental and calculated (INDO) results is good. The only surprising result is for 1,3-butadiyne. For the pairs propyne,2-butyne and 1,3-pentadiyne, 2,4-hexadiyne replacement of a proton by a methyl group is predicted and observed to leave the magnitude of the coupling constant almost unchanged. A similar theoretical prediction is made for the pair 1,3-butadiyne, 1,3-pentadiyne. Although the coupling constant for the former compound did not converge (after 100 iterations), its magnitude changed by less than 0.001 Hz over the last 60 iterations. Therefore, it is improbable that the failure to converge introduced any significant error. In the light of the above discussion, it is surprising to note that the magnitude of the experimental coupling constant for 1,3-butadiyne is almost twice that for its mono- and dimethyl derivatives. The origin of this discrepancy between experiment and calculation is unclear, particularly since the CNDO calculations suggest that there is no unexpected σ effect present.

Calculations were also performed for 2,4,6-octatriyne. There is again good agreement with experiment (30), supporting our earlier conclusions that INDO calculations give nearly quantitative predictions of coupling constants transmitted through extended π pathways (8).

Summary and Conclusions

This investigation has further demonstrated the great usefulness of molecular orbital calculations based upon finite perturbation theory in the CNDO/2 and INDO approximations for investigating mechanisms of transmission of long-range ^1H–^1H coupling constants and, in particular, for separating σ and π effects. In all cases the INDO calculations have reproduced the signs of the coupling constants and in most cases they have accurately predicted the magnitudes of the J values. Fortunately the CNDO calculations have largely fallen into two classes; those where the calculated coupling constants were nearly zero (negligible σ contribution) and those where the calculated coupling constants were similar to the experimental value. Except in systems where a homoallylic pathway is present, the latter results suggest dominant σ contributions.

The calculations for the 1,3-butadiene derivatives indicate that all long range coupling constants except $^5J_{16}$ in the s-*trans* conformation and $^4J_{14}$ in the s-*cis* isomer are dominated by π contributions. In the latter two cases, there is a significant σ contribution through the all-*trans* or zig-zag pathway. In the case of *cis*- and *trans*-1,3-pentadiene, all long-range coupling constants to the methyl group are dominated by π contributions. In the case of cyclopentadiene and its 1-methyl and 2-methyl derivatives, the couplings between olefin protons are dominated by σ interactions while the methyl proton – olefin proton couplings arise almost exclusively from π interactions. Finally all coupling constants in a series of acetylene and 1,3-butadiyne derivatives except that for acetylene are transmitted through the π system.

Financial support from the National Research Council of Canada is gratefully acknowledged. I.R.P. thanks Gulf Oil Canada Ltd for a Fellowship. W.F.R. expresses his gratitude to Professors H. Benoit and G. Weill of the C.N.R.S. Centre de Recherches sur les Macromolecules for their hospitality since this manuscript was written during a visit to that Institute.

1. J. A. Pople, J. W. McIver, Jr., and N. S. Ostlund. J. Chem. Phys. **49**, 2960 (1968); **49**, 2965 (1968).
2. J. A. Pople and G. A. Segal. J. Chem. Phys. **43**, 5136 (1965).
3. J. A. Pople, D. L. Beveridge, and P. A. Dobosh. J. Chem. Phys. **47**, 2026 (1967).
4. M. Bacon and G. E. Maciel. Mol. Phys. **21**, 257 (1971).
5. M. Barfield, C. J. Macdonald, I. R. Peat, and W. F. Reynolds. J. Am. Chem. Soc. **93**, 4195 (1971).
6. R. Wasylishen and T. Schaefer. Can. J. Chem. **49**, 3316 (1971).
7. L. Ernst, W. M. Hutton, and T. Schaefer. Can. J. Chem. **50**, 1863 (1972).
8. C. J. Macdonald, G. K. Hamer, I. R. Peat, and W. F. Reynolds. Can. J. Chem. **50**, 2035 (1972).
9. R. Wasylishen and T. Schaefer. Can. J. Chem. **50**, 1852 (1972).
10. R. Wasylishen and T. Schaefer. Can. J. Chem. **50**, 274 (1972).
11. M. Barfield and S. Sternhell. J. Am. Chem. Soc. **94**, 1905 (1972).
12. R. T. Hobgood and J. H. Goldstein. J. Mol. Spectrosc. **12**, 76 (1964).
13. A. A. Bothner-By and R. K. Harris. J. Am. Chem. Soc. **87**, 3445 (1965).
14. A. A. Bothner-By and R. K. Harris. J. Am. Chem. Soc. **87**, 3451 (1965).
15. A. V. Cunliffe and R. K. Harris. Mol. Phys. **13**, 269 (1967).
16. A. L. Segre, L. Zetta, and A. di Corato. J. Mol. Spectrosc. **32**, 296 (1969).

17. A. ALBRIKTSEN, A. V. CUNLIFFE, and R. K. HARRIS. J. Magn. Res. **2**, 150 (1970).
18. E. I. SNYDER, L. J. ALTMAN, and J. D. ROBERTS. J. Am. Chem. Soc. **84**, 2004 (1962).
19. J. C. HIRST and D. M. GRANT. J. Am. Chem. Soc. **84**, 2009 (1962).
20. H. M. HUTTON and T. SCHAEFER. Can. J. Chem. **45**, 1165 (1967).
21. R. M. LEQUAN and M. P. SIMONNIN. Compt. rend. Acad. Sci. Paris (C) 266 (1968); 825 (1968).
22. A. V. CUNLIFFE, R. GRINTER, and R. K. HARRIS. J. Magn. Res. **3**, 299 (1970).
23. D. L. BEVERIDGE and J. A. POPLE. Approximate molecular orbital theory. McGraw-Hill Book Company. New York, N.Y. 1970.
24. L. H. SCHARPEN and V. W. LAURIE. J. Chem. Phys. **43**, 2765 (1965).
25. V. A. KORENEVSKY and N. M. SERGEYEV. J. Am. Chem. Soc. **94**, 8586 (1972).
26. I. R. PEAT. Ph.D. Thesis, University of Toronto, Toronto, Ontario. 1973.
27. R. HOFFMAN. Ark. Kem. **17**, 1 (1961).
28. C. L. BELL, S. S. DANYLUK, and T. SCHAEFER. Can. J. Chem. **47**, 3592 (1969).
29. M. BARFIELD and B. CHAKRABARTI. Chem. Rev. **69**, 759 (1969).
30. E. I. SNYDER and J. D. ROBERTS. J. Am. Chem. Soc. **84**, 1582 (1962).

Can. J. Chem. Downloaded from www.nrcresearchpress.com by 210.87.254.105 on 09/05/12
For personal use only.

Pulse Radiolysis of Alkali Metal Solutions in Ethylamine[1]

J. W. FLETCHER, W. A. SEDDON, AND F. C. SOPCHYSHYN

Physical Chemistry Branch, Atomic Energy of Canada Limited, Chalk River Nuclear Laboratories, Chalk River, Ontario

Received March 21, 1973

Pulse radiolysis of solutions of alkali metal ethylamides in ethylamine shows the formation of three distinct species; the solvated electron e_s^-, the alkali metal anion M^-, and a species considered to be the cation–electron pair with stoichiometry M. The three species coexist in equilibrium in accord with the equations

$$e_s^- + M^+ \rightleftharpoons (M^+—e_s^-) \text{ or } M$$

$$M + e_s^- \rightleftharpoons M^-$$

Studies of these solutions as a function of temperature, alkali metal concentration, and added complexing agents ("crown" compounds) show that e_s^- and M have distinct absorption spectra with the former having a maximum $\geqslant$1800 nm. The latter exhibit maxima at 1400 nm for Na and K, ~1400 nm for Cs, and 1600–1700 nm for Li. The corresponding M^- species were observed in sodium, potassium, and cesium solutions with absorption maxima at 680, 890, and 1100 nm, respectively.

Rate and equilibrium constants for the formation of M and M^- vary markedly with the nature of the alkali metal. Estimates for these constants along with the extinction coefficients for the various species are summarized and compared with data obtained in alkali metal solutions.

La radiolyse pulsée de solutions d'éthylamidures de métaux alcalins dans l'éthylamine conduit à la formation de trois espèces distinctes: l'électron solvaté e_s^-, l'anion métallique M^- et une espèce considérée comme étant une paire de cation-électron de stoechiométrie M. Les trois espèces coexistent en équilibre selon:

$$e_s^- + M^+ \rightleftharpoons (M^+ - e_s^-) \text{ ou } M$$

$$M + e_s^- \rightleftharpoons M^-$$

Les études de ces solutions en fonction de la température, concentration en métal alcalin et addition d'agents complexants (composés "couronne") montrent que e_s^- et M possèdent des spectres d'absorption distincts, le premier avec un maximum $\geqslant$1800 nm et pour le second, un maximum à 1400 nm pour Na et K, ~1400 nm pour Cs et 1600–1700 nm pour Li. Les espèces M^- correspondantes ont été observées pour les solutions de sodium, potassium et césium avec respectivement un maximum d'absorption à 680, 890 et 1100 nm. Les constantes de vitesse et d'équilibre pour la formation de M et M^- varient de façon notable avec la nature du métal. Des valeurs sur ces constantes de même que celles des coefficients d'extinction pour les diverses espèces ont été rapportées et comparées aux données obtenues pour les solutions de métal alcalin. [Traduit par le journal]

Can. J. Chem., 51, 2975 (1973)

Introduction

It is well known that alkali metals dissolve in liquid amines and liquid ammonia to give intensely colored solutions. Such solutions are generally very stable but can be catalytically decomposed to give the corresponding alkali metal alkylamides of general formula RCH_2NHM_s

$$RCH_2NH_2 + M_s \rightarrow RCH_2NHM_s + \tfrac{1}{2}H_2$$

Numerous investigations (refs. 1 and 2 and references therein) on the optical, magnetic, and conductance properties of alkali-metal solutions have indicated that intermediate species of stoichiometry e_s^-, M, and M^- are produced in equilibrium according to the equations

$$[1] \qquad e_s^- + M^+ \underset{k_{-1}}{\overset{k_1}{\rightleftharpoons}} (M^+—e_s^-) \text{ or } M$$

$$[2] \qquad M + e_s^- \underset{k_{-2}}{\overset{k_2}{\rightleftharpoons}} M^-$$

However, little is known about the equilibrium constants or the rate at which these equilibria are established. Interconversion of all three species has been observed in the flash photolysis of ethereal solutions (3–5) but prior to our earlier communication (6), no similar kinetic or optical evidence for the species M has been reported in amines.

[1]AECL No. 4545.

Can. J. Chem. Downloaded from www.nrcresearchpress.com by 210.87.254.5 on 09/05/12
For personal use only.

Can. J. Chem. Downloaded from www.nrcresearchpress.com by 210.87.254.5 on 09/05/12
For personal use only.

With the development of fast infrared detectors pulse radiolysis can now be increasingly useful in the study of alkali metal solutions (7–9). This paper describes our results on the optical spectra and kinetics of the species, e_s^-, M, and M^- generated from the corresponding alkali metal ethylamides in Li, Na, K, and Cs solutions in ethylamine.

Experimental

Details of our pulse radiolysis facilities have been described elsewhere (10–12). Briefly, solutions were irradiated at room temperature with 0.5–2.0 μs pulses from a 2.5 MeV electron Van de Graaff accelerator. Rectangular quartz irradiation cells with an optical path length of 0.5–2.0 cm were mounted in a specially designed Pyrex or quartz flow system (Fig. 1). Samples were changed between pulses by a magnetically operated float valve which allows solution to flow from the reservoir B, through the cell C, to the drain D.

Ethylamine (Eastman Organic Chemicals) was dried and, to avoid cross contamination, purified under vacuum by fractional distillation from the appropriate alkali metal solutions. Alkali metals were stored and handled in a Dry Box. Metal ethylamide solutions were prepared in the following manner. Sodium (Baker reagent), potassium, and lithium (Fisher Chemicals) were pressed in the form of 0.1–1 mm diameter wire and transferred in calibrated weights per unit length to 2–3 mm diameter Pyrex or quartz tubing. These in turn were transferred, under vacuum, to the flow system, bulb D, via a modified (line of sight) greaseless stopcock, A (J. Young Ltd.). To aid dissolution it was found necessary to mirror the sodium samples. Aliquots of cesium (Alfa Inorganics Inc.) were "pipetted" in 0.5 mm diameter tubing and transferred to the flow system in a similar fashion. When necessary, analyses for Li, Na, or K were performed by absorption flame spectroscopy. Ethylamine was then fractionally distilled on to the metal and the resulting blue solutions catalytically bleached with electrolyzed Pt gauze to form the corresponding metal ethylamide (13). These solutions were then poured into bulb B to commence the experiment.

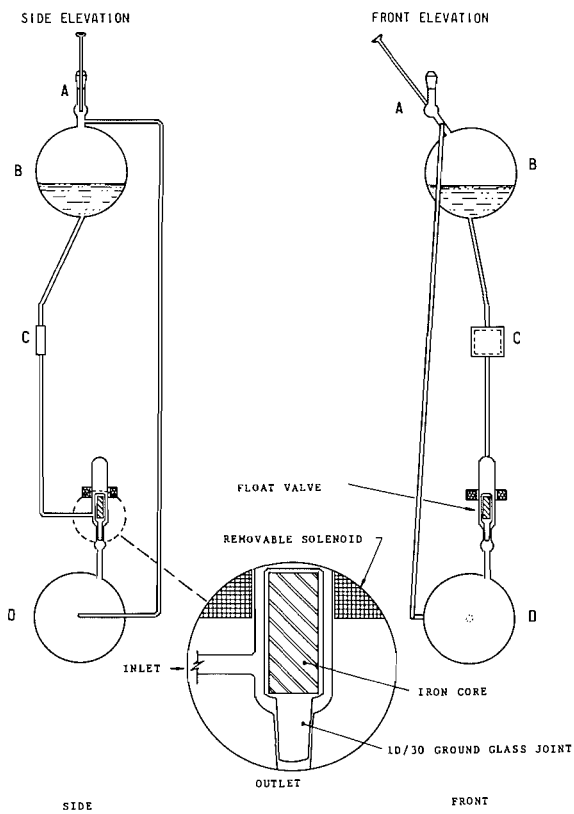

FIG. 1. Pulse radiolysis flow system. *A*, "line of sight" greaseless stopcock; *B*, 200 ml reservoir with solution under investigation; *C*, optical cell; *D*, drain (200 ml).

Fast infrared detection techniques were used throughout and great care taken to avoid misinterpretation of the data due to inherent features of the detector (14). A silicon photodiode SDG-100A, E.G. and G. Incorporated, covering the wavelength region 350–1100 nm and a liquid nitrogen cooled indium antimonide detector, Spectronics, SD-8721-2 with a nominal range of 1000–5500 nm were found to be excellent for our purposes. Under our operating conditions the former had a response time (0–98%) ≤80 ns and the latter (0–100%) ≤200 ns (14). A Corning 7-56 glass filter and long pass interference filters at 1500 and 1800 nm (Type LP sapphire substrate, Infrared Industries, Inc.) were used in conjunction with a Bausch and Lomb f 3.5 high intensity grating monochromator to eliminate second order wavelengths.

For most of the experiments three oscilloscope traces were recorded on a single Polaroid photograph. Examples are given in Figs. 3 to 9 where curve A shows the output profile of the analyzing light flash on a time scale of 500 μs/division. Curve B shows the transient signal recorded simultaneously with A, but at a higher gain, while curve C represents the analyzing light baseline on the

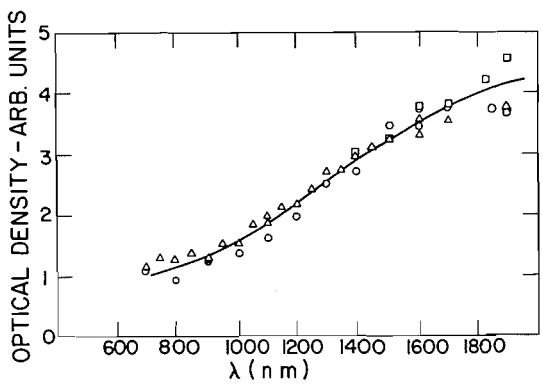

FIG. 2 Transient absorption spectrum observed immediately after an 0.5 μs pulse, spectrum is normalized to a dose/pulse ≤2 × 10^{19} eV/l; ○, pure ethylamine; △, □, separate experiments in ~1 × 10^{-3} *M* lithium ethylamide.

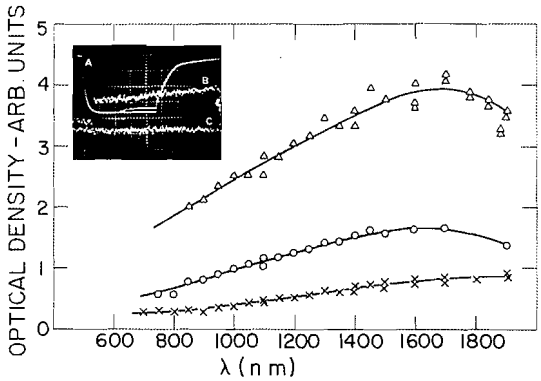

FIG. 3. Absorption spectrum observed in $\sim 1 \times 10^{-3}$ *M* lithium ethylamide solutions as a function of time, spectra are normalized to a dose/pulse $\leqslant 2 \times 10^{19}$ eV/l; ×, immediately after the pulse; ○, 150 μs after the pulse; △, 400 μs after the pulse. The inset shows the transient absorption, curve *B*, monitored at 1400 nm, dose 8.8×10^{19} eV/*l*, ordinate 1.1% absorption/div., abscissa 5 μs/div. See Experimental section for relevance of traces *A* and *C*.

same amplification and time scale as B. The transient signal at lower gain is superimposed on curve A.

Results

Pure Ethylamine and Lithium Ethylamide Solutions

Figure 2 shows the absorption spectrum observed at room temperature immediately after a 0.5 μs pulse in pure ethylamine and in solutions containing $\sim 1 \times 10^{-3}$ *M* lithium ethylamide. In both cases the absorption maximum lies at $\geqslant 1800$ nm but no peak could be clearly resolved due to the large solvent absorption at the longer wavelengths. In pure ethylamine, the absorption decays completely with a half-life $t_{1/2} \leqslant 1$ μs, whereas in lithium ethylamide solutions a slow growth in absorption is observed after the pulse.

Figure 3 shows the spectrum observed in $\sim 1 \times 10^{-3}$ *M* lithium ethylamide solutions as a function of time, the maximum gradually shifting to 1600–1700 nm with a corresponding increase in intensity over a period of about 400 μs (inset Fig. 3). The overall transient signal is however markedly dose dependent and this is illustrated in Fig. 4. At large doses per pulse ($\geqslant 10^{20}$ eV/l) the initial absorption partially decays on a μs time scale, a feature not observed at lower pulse intensities. This effect can be seen by comparing the inset traces in Figs. 3 and 4.

Sodium and Potassium Ethylamide Solutions

Figure 5 shows the optical spectra obtained in

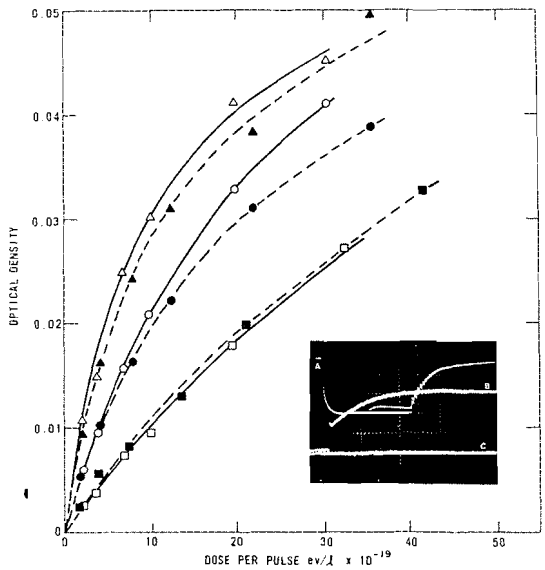

FIG. 4. Dose dependence of the transient absorption observed in $\sim 1 \times 10^{-3}$ *M* lithium ethylamide in a 1 cm cell. Open symbols, monitored at 1700 nm; closed symbols, 1900 nm. □, ■, 1 μs after the pulse; ○, ●, 150 μs after the pulse; △, ▲, 400 μs after the pulse. The inset curve *B* shows the transient absorption monitored at 1700 nm, dose 30.5×10^{19} eV/l, ordinate 3.3%/div., abscissa 50 μs/div. See Experimental section for relevance of traces *A* and *C*.

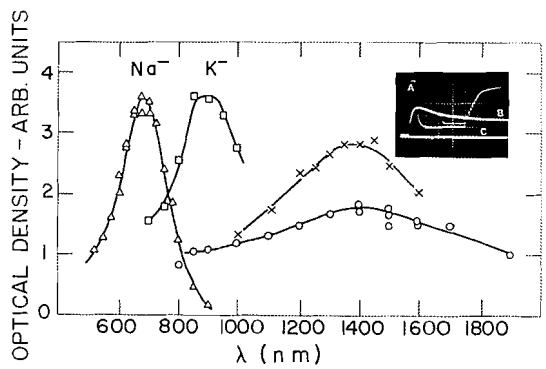

FIG. 5. Absorption spectra observed in 2.5×10^{-4} *M* sodium ethylamide and 4.5×10^{-4} *M* potassium ethylamide in ethylamine. ○, sodium solutions 5–14 μs after the pulse; △, sodium solutions 400 μs after the pulse; ×, potassium solutions 5–14 μs after the pulse; □, potassium solutions 400 μs after the pulse. For clarity the optical densities of the shorter time scale spectra are arbitrarily displaced with respect to each other and the long time scale spectra. The spectrum observed immediately after the pulse (not shown) is identical to that shown in Figs. 2 and 3. The inset curve *B* shows the transient absorption observed in 4.5×10^{-4} *M* potassium solutions at 1400 nm. Dose 15.3×10^{19} eV/l, ordinate 5.0%/div., abscissa 20 μs/div. Traces *A* and *C* are discussed in the Experimental section.

Can. J. Chem. Downloaded from www.nrcresearchpress.com by 210.87.254.5 on 09/05/12
For personal use only.

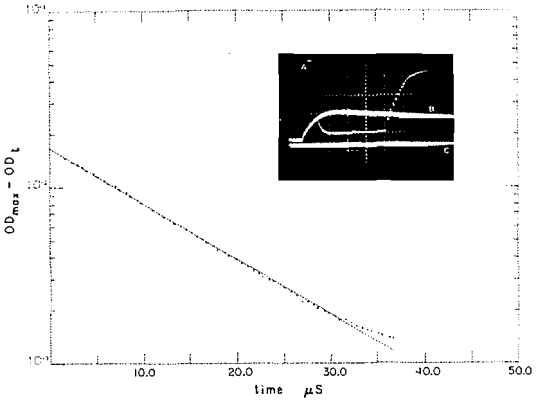

FIG. 6. First order analysis of an oscilloscope trace showing the build up, curve *B*, of the transient species observed in 4.5×10^{-4} *M* potassium ethylamide solutions at 1400 nm in a 1.0 cm cell. Dose 1.2×10^{19} eV/l, ordinate 2.4% absorption/div., abscissa 20 μs/div. Traces *A* and *C* are discussed in the Experimental section.

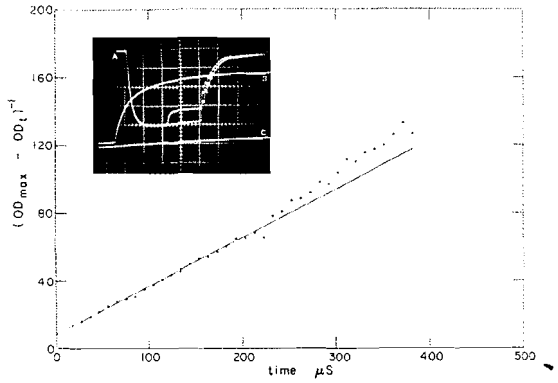

FIG. 7. Second order analysis of an oscilloscope trace showing the formation of Na^-, curve *B*, monitored at 700 nm in 2.5×10^{-4} *M* solutions of sodium ethylamide in a 1.0 cm cell. Dose 2.2×10^{19} eV/l, ordinate 5.0% absorption/div., abscissa 50 μs/div. Traces *A* and *C* are discussed in the Experimental section.

2.5×10^{-4} *M* solutions of sodium ethylamide and 4.5×10^{-4} *M* potassium ethylamide. Once again the spectrum observed immediately after the pulse (not shown) exhibits a maximum at $\geqslant$1800 nm and is very similar to those presented in Figs. 2 and 3. During the next 10–14 μs the absorption continues to increase in intensity and at the same time the spectrum shows a distinct change with the maximum shifted to 1400 nm. This absorption eventually decays to form a long-lived species with well characterized bands at 680 and 890 nm assigned to the metal–electron dimer species Na^- and K^-, respectively (1). The inset in Fig. 5 shows the formation and decay of the transient species in potassium solutions.

As in the case of lithium solutions the yield and rate of formation of the transient signals are a function of dose/pulse.

Studies at low dose ($\sim 1 \times 10^{19}$ eV/l) in 2.5×10^{-4} *M* solutions of sodium ethylamide and 4.5×10^{-4} *M* potassium ethylamide show the rate of formation of the absorption at

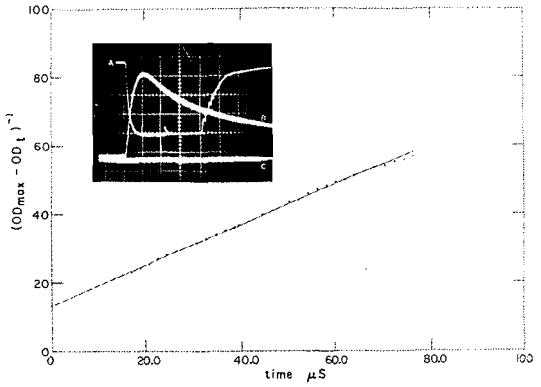

FIG. 8. Second order analysis of the decay portion of an oscilloscope trace showing the growth and decay, curve *B*, of the transient species observed in 2.5×10^{-4} *M* sodium ethylamide solutions at 1400 nm in a 1.0 cm cell. Dose 2.6×10^{19} eV/l, ordinate 2.4% absorption/div., abscissa 10 μs/div. Traces *A* and *C* are discussed in the Experimental section.

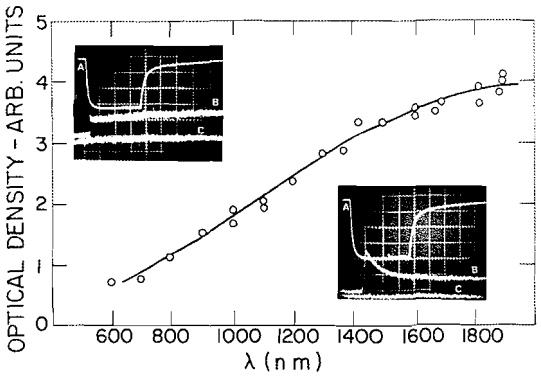

FIG. 9. Optical spectra and transient signals observed in solutions containing $\sim 2 \times 10^{-3}$ *M* potassium ethylamide, $\sim 2 \times 10^{-3}$ *M* lithium ethylamide, and 4×10^{-3} *M* "crown" compound. Upper left, curve *B* monitored at 1500 nm; dose 1.6×10^{19} eV/l, ordinate 1.25% absorption/div., abscissa 50 μs/div. Lower right, curve *B* monitored at 1500 nm; dose 12.1×10^{19} eV/l, ordinate 2.5% absorption/div., abscissa 5 μs/div. Optical path lengths, 1.0 cm. Traces *A* and *C* are discussed in the Experimental section.

Can. J. Chem. Downloaded from www.nrcresearchpress.com by 210.87.254.5 on 09/05/12
For personal use only.

Can. J. Chem. Downloaded from www.nrcresearchpress.com by 210.87.254.5 on 09/05/12
For personal use only.

1400 nm to be first order and dependent on the nature of the alkali metal. Figure 6 shows an example of an oscilloscope trace and its kinetic analysis corresponding to the build up in the potassium solution. For both sodium and potassium solutions the 1400 nm band decays by a second order process with the concomitant formation of the 675 or 890 nm bands, respectively. Figures 7 and 8 illustrate this situation using examples chosen from the sodium solution.

Effect of Added "Crown" Compound

Previous studies (2, 15, 16) have shown that the addition of a cyclic polyether such as dicyclohexyl-18-crown-6[2], ("crown" compound) complexes alkali metal cations and enhances their solubility in a variety of amines and ethers. Figure 9 shows the optical spectra and transient signals observed from a solution prepared in a Pyrex flow system containing $\sim 2 \times 10^{-3}\ M$ potassium ethylamide, $\sim 2 \times 10^{-3}\ M$ lithium ethylamide, and $4 \times 10^{-3}\ M$ "crown" compound. At doses of about 2×10^{19} eV/l the transient absorption shows virtually no sign of decay or growth over a period of $\geqslant 500$ μs (upper inset). At higher doses per pulse the absorption consists of two parts; an initial rapid decay followed by a long lived residual component (lower inset). Both the initial and long lived absorptions have identical spectra with a maximum at >1800 nm. There is no evidence for the formation of either Na^- (via Na^+ contamination from the vessel) or K^-.

Cesium Ethylamide Solutions

Figure 10 shows the spectra obtained in $\sim 6 \times 10^{-5}\ M$ solutions of cesium ethylamide. The spectrum observed immediately after the pulse is relatively weak with an apparent maximum around 1800 nm. During the next 2–3 μs the intensity increases rapidly giving a strong absorption with a broad maximum from 1200–1500 nm. This spectrum changes again over the following 5 μs resulting in a final spectrum with a maximum at 1100 nm and a shoulder at ~ 1400 nm. Oscilloscope traces showing the formation of the transient species are presented in Fig. 11.

The rate of formation of the cesium species is significantly faster and, for equivalent concentrations, the least dose dependent, of the series Li, Na, and K. Figure 12 shows the effect of increasing the dose/pulse in a solution containing $2 \times 10^{-3}\ M$ cesium ethylamide.

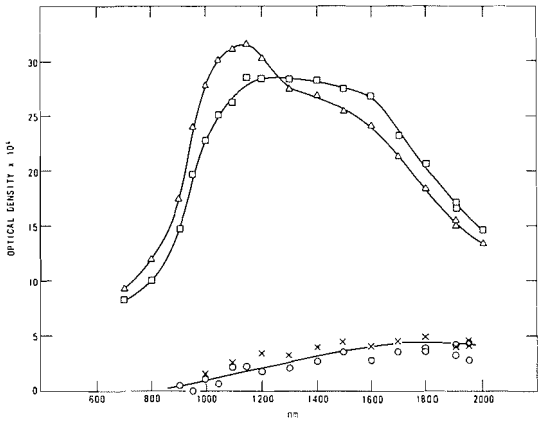

FIG. 10. Absorption spectra observed in $\sim 6 \times 10^{-5}\ M$ cesium ethylamide solutions in an 0.5 cm cell. ○, ×, spectrum observed in separate experiments at the end of an 0.5 μs pulse (dose per pulse $\sim 4.6 \times 10^{19}$ eV/l); □, spectrum observed 2.5 μs after the pulse; △, spectrum observed 7.0 μs after the pulse (dose per pulse $\sim 10^{20}$ eV/l). All spectra are normalized to a dose per pulse of $2.7_5 \times 10^{18}$ eV/l.

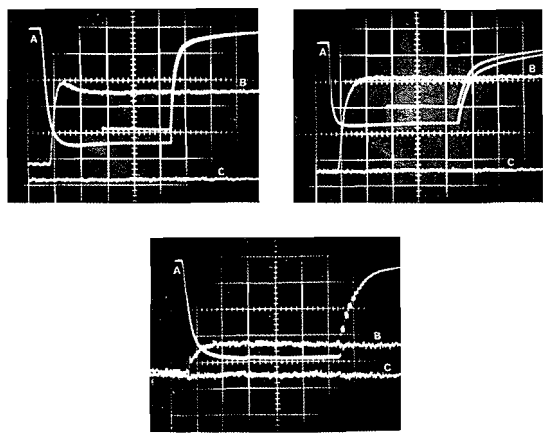

FIG. 11. Oscilloscope traces showing the formation of the transient species in $\sim 1.2 \times 10^{-5}\ M$ solutions of cesium ethylamide in an 0.5 cm cell. Upper left curve *B*, wavelength 1900 nm, dose 10.7×10^{19} eV/l, ordinate 4.5% absorption/div, abscissa 5 μs/div., Upper right curve *B*, wavelength 1000 nm, dose 10.2×10^{19} eV/l, ordinate 5.5% absorption/div., abscissa 5 μs/div.; Lower trace curve *B*, wavelength 1900 nm, dose 4.5×10^{19} eV/l, ordinate 2.6% absorption/div., abscissa 10 μs/div. Traces *A* and *C* are discussed in the Experimental section.

[2]Complimentary sample, courtesy of H. K. Frensdorff, E. I. DuPont de Nemours and Co. Inc., Elastomer Chemical Dept., Research Division, Wilmington, Delaware 19898.

Can. J. Chem. Downloaded from www.nrcresearchpress.com by 210.87.254.5 on 09/05/12
For personal use only.

TABLE 1. Rate and equilibrium constant data for alkali metals dissolved in ethylamine

Alkali metal	Ethylamide concentration (M)	$k_1(M^{-1}\,s^{-1})$	$\lambda = 1400$ nm		$OD_{1400}{}^2/OD_{M^-}$	$K_{-5}[M^+] = \frac{[M^2]}{[M^-]}$
			$2k_4/\varepsilon$	$k_4(M^{-1}\,s^{-1}) \times 10^{-10}$		
Li	$\sim 1 \times 10^{-3}$	4×10^6				
Na	2.5×10^{-4}	1.2×10^9	6×10^5	2.4 ± 0.1*	$< 0.8 \times 10^{-5}$	$< 1 \times 10^{-9}$
K	4.5×10^{-4}	1.6×10^8	1.5×10^5	0.62 ± 0.08	$\sim 7 \times 10^{-3}$	$\sim 2 \times 10^{-7}$
	2.3×10^{-3}		4×10^5	1.6 ± 0.4	†	
Cs	$\sim 3.5 \times 10^{-6}$	2×10^{10}				‡

*From rate of build up of Na^- at 700 nm; $k_4 \sim 1.6 \times 10^{10}\ M^{-1}\,s^{-1}$.
†For the more concentrated solution the reaction order appears to decrease to ~1.6.
‡Difficult to estimate. It appears that $K_{-5}(Cs^+) > K_{-5}(Na^+)$ but $\leqslant K_{-5}(K^+)$.

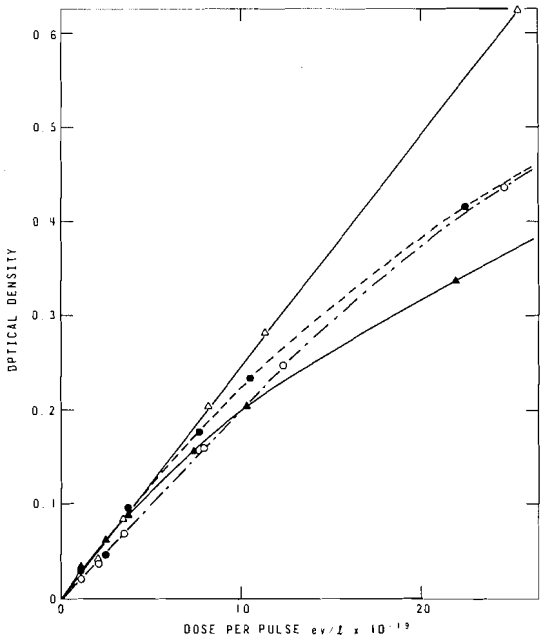

FIG. 12. Effect of increasing dose per pulse on the transient absorptions observed in 2×10^{-3} *M* cesium ethylamide solutions in a 1.0 cm cell. Open symbols monitored at 1050 nm; closed symbols, 1500 nm; ○, ●, 2 μs after the pulse; △, ▲, 400 μs after the pulse.

Discussion

Spectral Assignments

Optical spectra of alkali metal solutions in amines and or ethers have been studied extensively (1, 2, 16). In general such spectra are composed of at least two absorption bands ascribed to metal-dependent and metal-independent species. The former band occurs at relatively short wavelengths, $\leqslant 1000$ nm, whereas the latter is often much broader and extends further into the infrared with a pronounced solvent dependence on both the maxima and band shape (2).

In sodium and potassium solutions in a variety of amine and ether solvents it is now generally accepted that the metal-dependent bands at 675 and 890 nm, can be assigned to a species of stoichiometry M^-, *i.e.* Na^- and K^-, respectively (1, 17, 18). Similarly, the band observed at 1050 nm in cesium solutions in tetrahydrofuran and ethylamine–ammonia is assigned to Cs^- (2, 16, 17).

Hitherto it has been common to assign the longer wavelength infrared absorptions to the solvated electron (19–21). This is supported in a number of amine and ether solvents where a good correlation exists between the absorption maxima (ranging from 1300–2200 nm) found by pulse radiolysis and flash photolysis and those observed in alkali metal solutions (2, 3, 7). However the agreement is not exact and Lok *et al.* (2), note that the metal solution bands are in general broader and at slightly higher energies than those found by pulse radiolysis. These authors suggest that such variations in band shape might arise from the interaction of e_s^- with the cation. It has also been pointed out for lithium solutions in ethylamine (1), that the single absorption band observed at 1400 nm at −17 °C, may be a composite of at least two paramagnetic species, namely e_s^- and possibly a neutral monomeric species (M or $M^+ - e_s^-$).

Cyclic polyethers ("crown" compounds) have been used by Dye and co-workers (2, 15, 16), to complex the alkali metal cation and, under the appropriate conditions, shift the equilibria 1 and 2, in favor of e_s^-. In ethylamine these workers observe a maximum at 1800 nm for e_s^- at room temperature (2). This peak position is consistent with our pulse radiolysis spectra observed immediately after the pulse in pure ethylamine, Li, Na, K, or Cs ethylamide solutions, and mixtures containing an excess of "crown" compound (Figs. 2, 3, 9, and 10). We suggest therefore that in ethylamine the true e_s^- absorption has a maximum at $\geqslant 1800$ nm, a wavelength significantly different from the infrared band maxima of 1400–1600 nm normally attributed to e_s^- in alkali metal solutions (19–21).

The rate of formation of the 1400 nm band is metal dependent (Table 1) and for 2.5×10^{-4} *M* sodium and 4.5×10^{-4} *M* potassium solutions the species is present in significant concentration 5 μs after the pulse (Fig. 5). In $\sim 1 \times 10^{-3}$ *M* lithium ethylamide solutions its formation is much slower and the shift in wavelength from 1800 nm is not as pronounced (Fig. 3).

We therefore propose that the bands formerly assigned to the solvated electron in ethylamine solutions are in fact due to a metal electron species of stoichiometry M. In sodium and potassium solutions at room temperature this species has a maximum at 1400 nm. In lithium solutions it is shifted towards 1600–1700 nm. It is conceivable that this latter absorption contains an appreciable equilibrium concentration of e_s^- which artificially displaces the maximum beyond

Can. J. Chem. Downloaded from www.nrcresearchpress.com by 210.87.254.5 on 09/05/12
For personal use only.

Can. J. Chem. Downloaded from www.nrcresearchpress.com by 210.87.254.5 on 09/05/12
For personal use only.

the 1400 nm obtained in sodium and potassium solutions. The 1600–1700 nm peak position correlates well with the band maxima of 1400 nm reported for lithium solutions at -17 °C and the temperature coefficient of ~ 6 nm per degree (1).

In $\sim 6 \times 10^{-5}$ *M* cesium ethylamide solutions (Fig. 10) the pulse radiolysis spectrum observed on a long time scale ($\geqslant 7$ μs) very closely resembles the steady state spectrum observed in cesium ethylamide solutions (1). However, the intermediate spectrum observed after 2.5 μs is clearly different and much more intense than the absorption obtained immediately after the pulse. Again our results show that in dilute cesium ethylamide solutions three species can clearly be distinguished. On the basis of the previous discussion we therefore conclude that (*a*) the initial species with a maxima at $\geqslant 1800$ nm is due to e_s^-; (*b*) the maxima at 1100 nm is due to Cs^-; and (*c*) the broad long wavelength shoulder with a maximum ~ 1400 nm is largely due to the monomer species, Cs, with equilibrium contributions from Cs^- and possibly e_s^-.

Kinetics and Dose Dependence

Formation of M

Studies of dilute solutions of Li, Na, K, and Cs ($\leqslant 1 \times 10^{-3}$ *M*) indicate that the rate of formation of M is first order and consistent with reaction 1, for example see Fig. 6. However we make no attempt in this paper to differentiate between reactions involving the cation M^+ and those possibly involving the undissociated metal

[3] $CH_3CH_2NHM + e_s^- \rightleftharpoons CH_3CH_2NH^- + M$

alkylamide CH_3CH_2NHM. Data from methylamine at -62.2 °C show that the potassium salt is only weakly dissociated (22), with $<2\%$ present as K^+ in 10^{-3} *M* solution. Even in liquid ammonia the corresponding sodium, potassium, and cesium amides are $<10\%$ dissociated (23). It is likely therefore that 10^{-3} *M* ethylamides are largely associated in ethylamine at room temperature. For simplicity our ensuing discussion assumes that the total concentration of the metal ethylamide is relevant to the overall rate of reaction involving M^+. Observed differences in the series lithium–cesium may in part be due to different degrees of dissociation of the alkyl ethylamides but such conjecture is outside the scope of this work.

Experimentally the dose per pulse and/or solute concentration must be chosen to minimize side reactions arising from radiolysis. For example, we believe the initial rapid decay illustrated in the oscilloscope trace in Fig. 4 is due to the reaction of e_s^- with other radical species produced during the pulse. The analysis is complicated further in that the decay of M to produce M^- is a second order process (Figs. 7 and 8), the rate of which becomes relatively more significant at higher doses. Any such contribution increases the error in determining OD_{max}, the optical density corresponding to the complete formation of M, although corrections can be made in the computer analysis of such build-ups (24). Furthermore, since the absorption spectra of e_s^- and M overlap, the buildup of M should strictly be corrected for equilibrium concentrations of e_s^-. However, in view of the much lower extinction coefficient for e_s^- (see below) and with equilibrium 1 clearly in favor of M, such corrections ($\leqslant 5\%$) were not considered significant. At low doses where the rate of decay of M is minimized we estimate from plots such as shown in Fig. 6 that $k_1 = 4 \times 10^6$, 1.6×10^8, 1.2×10^9, and 2.0×10^{10} M^{-1} s^{-1} for Li^+, K^+, Na^+, and Cs^+, respectively (Table 1).

Formation of M^-

In sodium and potassium solutions the spectrum of M^- is well established and distinctly separated from that of e_s^- and M. Sodium solutions represent the simplest case and here the decay of e_s^- and M to M^- is virtually complete indicating that the overall equilibria is largely in favor of Na^-.

The formation of M^- is second order, dependent on the nature of the alkali metal, and consistent with an overall pseudo-second order reaction 4,

[4] $$e_s^- + e_s^- \overset{M^+}{\rightleftharpoons} M^-$$

The overall rate of formation of M^- can be measured either by observing the decay of M at 1400 nm or via the build up of M^- at 675, or 890 nm, for Na^- and K^-, respectively. Figure 7 shows a kinetic plot corresponding to the formation of Na^- with a pseudo second order rate constant $4k_4 \sim 0.3 \times 10^6 \varepsilon_{M^-}$ $M^{-1}s^{-1}$. Since the equilibrium for reaction 1 appears to lie well to the right we can simplify the overall kinetics by neglecting reaction 2 and assume that M^- is formed by reaction 5

TABLE 2. Relative extinction coefficient data, expressed as $G\varepsilon$, for e_s^-, M, and M^- in Li, Na, K, and Cs solutions in ethylamine*

Metal	Ethylamide concentration ($\times 10^4$ M)	λ (nm)	$G\varepsilon(\times 10^{-5})$ e_s^-	M	M^-
Li (Pyrex)	5	1400	0.17	0.70†	—
Li (quartz)	10	1600	0.13	~0.5	—
Na	2.5	1400	≤0.20	1.6	
	2.5	680–700			1.8, 2.3
K	4.5	1400	0.13	0.9	
	23	1400		1.7	
	4.5	850			1.4
	23				1.9(2.3)‡
K(+ "crown")		1600	0.20		
Cs	0.7	1950	0.20		
	~0.4	1100			1.3
	0.08	1900	0.23		
	0.01	1500	0.23	1.3	
	21	1500		1.6	

*Values obtained from dose studies. Extinction coefficients can be estimated assuming $G_{e_s^-} = 2$, $G_M = 2$, and $G_{M^-} = 1$.
†Solution contains Na^+ contamination from the Pyrex, value probably high.
‡Corrected assuming $K_{-5}[M^+] \sim 2 \times 10^{-7}$.

[5] $$M + M \rightleftharpoons M^- + M^+$$

On this basis we deduce $2k_5$ is equivalent to $2k_4 = 6 \times 10^5 \varepsilon_M M^{-1} s^{-1}$ (Fig. 8). Since Na^- is the final species, errors in OD_{max} are not as significant as those discussed previously concerning the formation of M. Combination of the above "k_4" values with the appropriate extinction coefficients (see Table 2 below) for Na and Na^- gives $k_4 = 2.0 \pm 0.4 \times 10^{10} M^{-1} s^{-1}$. However, this rate constant is strictly a measure of the overall stoichiometry composed in detail of the equilibria 1–3 and probably equilibrium 5. Consequently k_4 represents the value in $2.5 \times 10^{-4} M$ sodium ethylamide and will be concentration dependent as M^+ changes the equilibrium concentrations of e_s^-, M, and M^-.

It should be noted here that from similar studies in ethylenediamine, Dye *et al.* (8), suggest the formation of Na^- occurs via the intermediate e_2^{2-}

[6] $$e_s^- + e_s^- \rightleftharpoons e_2^{2-}$$

[7] $$e_2^{2-} + Na^+ \rightarrow Na^-$$

Further kinetic studies in methylamine (25) indicate that a mechanism consisting of reactions 1, 2, and 5 fits Dye's data on the effect of cation concentration, equally as well as reactions 6 and 7.

In potassium solutions similar kinetic treatment to that described for sodium gives the corresponding value $k_4 = 1.1 \pm 0.5 \times 10^{10} M^{-1} s^{-1}$. However, only the initial portions of the build-up and decay curves can be utilized since there is an additional complication in that the decay of M to M^- does not go to completion. On a long time scale the concentration of M reaches a finite steady state indicating that the equilibrium constant for the dissociation of M^- is greater than the analogous case for sodium solutions. As such, the equilibrium concentrations of M and M^- can be estimated from the residual optical densities observed after ~200 μs at 1400 (OD_{1400}), and 890 nm (OD_{890}), respectively. Figure 13 shows such steady state values for $4.5 \times 10^{-4} M$ solutions of potassium ethylamide as a function of dose per pulse.

On the basis of reaction 5, the equilibrium constant for the potassium solution $K_{-5} = [M]^2/[M^-][M^+]$. As a first approximation $K_{-5}[M^+] \propto OD^2_{1400}/OD_{890} = 7 \times 10^{-3}$. Using the appropriate extinction coefficients, deduced from Table 2, $K_{-5}[M^+]$ is then estimated as $\sim 2 \times 10^{-7} M$. The curve (Fig. 13) drawn through the OD_{1400} points represents the calculated fit to these data on the basis of K_{-5} and the best line drawn through points at 890 nm. The agreement is quite good and supports the second order formation of M^- in equilibrium with M. However in $2.3 \times 10^{-3} M$

Can. J. Chem. Downloaded from www.nrcresearchpress.com by 210.87.254.5 on 09/05/12
For personal use only.

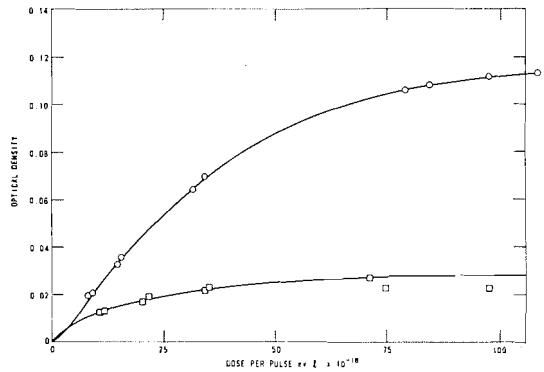

FIG. 13. Optical density of the transient species observed ~200 μs after the pulse in 4.5×10^{-4} *M* potassium ethylamide solutions as a function of dose per pulse in a 1.0 cm cell. □, 1400 nm; ○, 890 nm. Curves are calculated as described in the text.

potassium ethylamide solutions the relationship is not as satisfactory since to fit the data

$$K_{-5} \propto \frac{OD_{1400}{}^{1.6}}{OD_{890}}$$

implying the overall formation of M^- is of mixed order. Whether this is real, due to changes in the degree of dissociation of the ethylamide (22), or simply experimental error, is not known.

As mentioned earlier, Na^- is the predominant stable species in sodium solutions. From a similar analysis we estimate $K_{-5}[Na^+] < 1 \times 10^{-9}$ M. In cesium solutions the spectra of M and M^- overlap considerably so a reliable estimate for $K_{-5}(Cs^+)$ is not possible. However since both Cs^- and Cs are observed as stable species this indicates that $K_{-5}(Cs^+) > K_{-5}(Na^+) \leqslant K_{-5}(K^+)$. In common with the chemistry of alkali metal solutions no evidence was obtained in this work for Li^-.

Table 1 summarizes our rate and equilibrium constant data.

Decay Characteristics in the Presence of "Crown"

As mentioned previously, the addition of "crown" compound to ethylamine solutions containing K^+, Li^+, and presumably Na^+ from the vessel walls, displaces the equilibria 1 and 2 and prevents the formation of the M and M^- species. The solvated electron thus becomes the predominant reactive species and such solutions might be expected to be more characteristic of liquid ammonia than of amines. Although we have not attempted any detailed kinetic study of the "crown" mixtures the decay characteristics of e_s^- are qualitatively very similar to those observed on the pulse radiolysis of alkali metal amide solutions in liquid ammonia. The latter are characterized by an initial rapid reaction, principally between e_s^- and NH_2 radicals, followed by a long-lived residual absorption attributed to a stable e_s^- species (26 and 9 for earlier references).

In "crown" solutions, at low doses/pulse, the initial e_s^- absorption is stable for $\geqslant 500$ μs and shows no sign of an additional build up due to the formation of an M species. At higher doses the e_s^- absorption partially decays leaving a long lived residual component, again due to e_s^- (Fig. 9 and text). By analogy with ammonia we attribute the partial decay to the reaction of e_s^- with other radical species produced during the pulse. The addition of "crown" does therefore impart more "ammonia-like" properties to the ethylamine solutions.

Yields and Extinction Coefficients

Figures 4 and 12 show the formation of the various species as a function of dose per pulse in lithium and cesium solutions. It should be noted that at fixed times, but different wavelengths, there is a difference in relative intensity as a function of dose per pulse. This provides additional evidence that the overall absorption is a composite of more than one species. Similar plots (not shown), intermediate in character, were obtained for sodium and potassium solutions. These dose effects can be correlated with the measured values of k_1 (Table 1) where it might be expected that competing processes for e_s^- would be less significant with Cs^+ than for Li^+.

In view of this dose dependence we have estimated the initial yield for the various species from the linear portion of such curves and then in turn calculated the corresponding $G\varepsilon$ values.

Comparison with extinction coefficients measured in alkali metal solutions is difficult for two reasons. First, there is some uncertainty in the radiolytic yield of e_s^- in liquid amines and as an extension of this work we are attempting to deduce better values. Steady state data from γ radiolysis of liquid methylamine (27), and ethylamine (28), give $G_{e^-} = 3.2 \pm 0.2$ and 2.1 ± 0.1 molecules/100 eV, respectively. This large difference between very similar amines may or may not be real. Secondly, with the possible exception of e_s^- and Na^- our $G\varepsilon$

Can. J. Chem. Downloaded from www.nrcresearchpress.com by 210.87.254.5 on 09/05/12
For personal use only.

Can. J. Chem. Downloaded from www.nrcresearchpress.com by 210.87.254.5 on 09/05/12
For personal use only.

determinations represent minimum values since all three species are in equilibrium with each other. Since the respective equilibrium constants are as yet poorly defined, no attempt has been made to correct the basic experimental data. However, in sodium solutions the equilibria appear to be predominantly in favour of Na^-. The value for ε_{Na^-} ought then to provide some check on the consistency of our pulse radiolysis data with results obtained previously.

Assuming that $G_{e_s^-} = 2.1$ (28), then from Table 2 we deduce an extinction coefficient for e_s^- of $\sim 10^4\ M^{-1}\ cm^{-1}$ at 1800 nm. This is less than the value of 2×10^4 established for e_s^- in ethylenediamine (8, 29). In ethylenediamine it is possible that the e_s^- absorption contains a contribution from the sodium ion-pair species M, since our results indicate this reaction to be extremely fast. Unfortunately, in recent work using "crown" compounds (2), no estimates were made for the extinction coefficients of e_s^- and therefore we cannot ascertain the significance, if any, of our lower value.

On the other hand, again assuming $G_{e_s^-} = 2.1$, we find $\varepsilon_{Na^-} = 2 \pm 0.2 \times 10^5\ M^{-1}\ cm^{-1}$, based on a stoichiometry of two solvated electrons per Na^-. This extinction coefficient is some 3–4 times greater than previous estimates of 4.9 ± 0.7 to $6 \pm 2 \times 10^4\ M^{-1}\ cm^{-1}$, deduced from flash photolysis experiments in potassium ethylamide solutions (13). However, the latter work was done before it was realized that the species in question was in fact Na^- (due to Na^+ contamination from the glass) with the equivalent of two, and not one, electrons per mole. The quoted extinction coefficients should therefore be doubled to have the correct stoichiometry and hence give a value $\varepsilon_{Na^-} = 1.2 \pm 0.4 \times 10^5\ M^{-1}\ cm^{-1}$. In ethylenediamine the corresponding extinction coefficient is $8.2 \pm 0.3 \times 10^4\ M^{-1}\ cm^{-1}$ giving a calculated oscillator strength of 1.9 ± 0.2 consistent with the stoichiometry Na^- (29). Assuming $\varepsilon_{Na^-} = 2 \times 10^5\ M^{-1}\ cm^{-1}$ our spectra indicate an oscillator strength of at least four. This suggests that $G_{Na^-} \sim 2$ and hence in basic solutions $G_{e_s^-} \sim 4$, a factor of two higher than in pure ethylamine (28). Further studies on this point are in progress.

Finally Fig. 14 represents a reproduction of the various oscilloscope traces at doses $\leqslant 2 \times 10^{19}\ eV\ l^{-1}$, showing the comparative rate of increase and magnitude of $G\varepsilon$ (corresponding to the formation of M) as a function of time for different Li, Na, K, and Cs solutions. An interesting comparison is the apparent difference between two similar lithium solutions contained in Pyrex and quartz flow systems. In the Pyrex system both the $G\varepsilon$ value and the rate of formation of M appear greater than in quartz. This we believe is a further illustration of sodium contamination from the Pyrex (1, 29, 30) since the sodium species has a much faster rate of formation (Table 1). This, coupled with its higher extinction coefficient (Table 2), results in an apparently enhanced rate and growth of the "lithium" species.

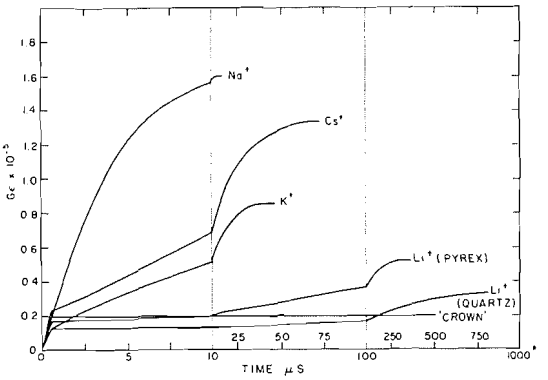

FIG. 14. Rate of formation of the species monitored at 1400–1500 nm in solutions of Li, Na, K, and Cs ethylamide. Dose per pulse $\leqslant 2 \times 10^{19}$ eV/l. Li (Pyrex), $5 \times 10^{-4}\ M$, Li (quartz), $\sim 1 \times 10^{-3}\ M$; Na, $2.5 \times 10^{-4}\ M$; K, $4.5 \times 10^{-4}\ M$; Cs, $1 \times 10^{-6}\ M$; "crown", $4 \times 10^{-3}\ M$ plus $\sim 2 \times 10^{-3}\ M$ K ethylamide and $\sim 2 \times 10^{-3}\ M$ Li ethylamide.

Conclusion

Pulse radiolysis of alkali metal ethylamide solutions demonstrates the existence of three distinct optical bands corresponding to the species of stoichiometry e_s^-, M, and M^-. Both e_s^- and M absorb in the infrared region of the spectrum but with a significant difference in the absorption maximum and magnitude of the extinction coefficient. The rate and equilibrium constants for the formation of the species M and M^- are markedly dependent on the nature of the alkali metal.

1. I. HURLEY, T. R. TUTTLE, JR., and S. GOLDEN. Metal ammonia solutions. I.U.P.A.C., Colloque Weyl II, 449 (1969).
2. M. T. LOK, F. J. TEHAN, and J. L. DYE. J. Phys. Chem. **76**, 2975 (1972).
3. L. J. GILING, J. G. KLOOSTERBOER, R. P. H.

RETTSCHNICK, and J. D. W. VAN VOORST. Chem. Phys. Lett. **8**, 457 (1971).
4. J. G. KLOOSTERBOER, L. J. GILING, R. P. H. RETTSCHNICK, and J. D. W. VAN VOORST. Chem. Phys. Lett. **8**, 462 (1971).
5. M. FISHER, G. RAMME, S. CLAESSON, and M. SZWARC. Chem. Phys. Lett. **9**, 309 (1971).
6. J. W. FLETCHER, W. A. SEDDON, J. JEVCAK, and F. C. SOPCHYSHYN. Chem. Phys. Lett. **18**, 592 (1973).
7. L. M. DORFMAN, F. Y. JOU, and R. WAGEMEN. Ber. Bunsenges. Phys. Chem. **75**, 681 (1971).
8. J. L. DYE, M. G. DEBACKER, J. A. EYRE, and L. M. DORFMAN. J. Phys. Chem. **76**, 839 (1972).
9. J. L. DYE, M. G. DEBACKER, and L. M. DORFMAN. J. Chem. Phys. **52**, 6251 (1970).
10. W. A. SEDDON, C. WILLIS, M. J. YOUNG, and E. B. SELKIRK. Atomic Energy of Canada Limited report No. AECL-3853.
11. W. A. SEDDON, J. W. FLETCHER, and F. SOPCHYSHYN. Can. J. Chem. **51**, 1123 (1973).
12. E. B. SELKIRK and W. A. SEDDON. Atomic Energy of Canada Limited report No. AECL-4134.
13. M. OTTOLENGHI and H. LINSCHITZ. Adv. Chem. Ser. **50**, 149 (1965).
14. W. A. SEDDON, E. B. SELKIRK, and J. W. FLETCHER. Int. J. Radiat. Phys. Chem. **5**, 323 (1973).
15. J. L. DYE, M. T. LOK, F. J. TEHAN, R. B. COOLEN, N. PAPADAKIS, J. M. CERASO, and M. G. DEBACKER. Ber. Bunsenges Phy. Chem. **75**, 659 (1971).
16. J. L. DYE. Presented at Colloque Weyl III, Hanita, Upper Gallilee, June, 1972. To be published.
17. S. MATALON, S. GOLDEN, and M. OTTOLENGHI. J. Phys. Chem. **73**, 3098 (1969).
18. S. H. GLARUM and J. H. MARSHALL. J. Chem. Phys. **52**, 5555 (1970).
19. H. BLADES and J. W. HODGINS. Can. J. Chem. **33**, 411 (1955).
20. M. OTTOLENGHI, K. BAR-ELI, and H. LINSCHITZ. J. Chem. Phys. **43**, 206 (1965).
21. J. L. DYE and R. R. DEWALD. J. Phys. Chem. **68**, 135 (1964).
22. E. ROCHARD and J. RAVOIRE. J. Chim. Phys. **68**, 1183 (1971).
23. R. DELMAS, P. COURVOISIER, and J. RAVOIRE. Adv. Chem. Ser. **89**, 25 (1969).
24. J. W. FLETCHER and N. BURNHAM. Atomic Energy of Canada Limited AECL report. In preparation.
25. W. A. SEDDON, J. W. FLETCHER, and J. JEVCAK. Atomic Energy of Canada Ltd. report AECL-4259. p. 60.
26. D. M. J. COMPTON, J. F. BRYANT, R. A. CESENA, and B. L. GEHMAN. Pulse radiolysis. Academic Press, New York, 1965. p. 43.
27. D. SMITHIES and A. J. WHITWORTH. J. Chem. Soc. A, 1987 (1969).
28. A. HABERSBERGEROVÁ, I. JANOVSKÝ, and J. TEPLY. Chem. Commun. 1678 (1970).
29. M. G. DEBACKER and J. L. DYE. J. Phys. Chem. **75**, 3092 (1971).
30. I. HURLEY, T. R. TUTTLE, JR., and S. GOLDEN. J. Chem. Phys. **48**, 2818 (1968).

Can. J. Chem. Downloaded from www.nrcresearchpress.com by 210.87.254.5 on 09/05/12
For personal use only.

Synthesis and Structural Studies of the Metal(II) Mercury Tetrathiocyanate Complexes with Lewis Bases[1]

R. MAKHIJA,[2] L. PAZDERNIK,[3] AND R. RIVEST

Département de chimie, Université de Montréal, Montréal, Québec

Received January 8, 1973

Complexes of the type $MHg(SCN)_4.2L$, where M = Mn^{2+} to Zn^{2+} and Cd^{2+} and L = THF or Py, have been synthesized and characterized by spectroscopic methods. The thiocyanato groups are bridging between M^{2+} and Hg^{2+} whereas the donor atom of the ligand is coordinated to M^{2+} which now attains octahedral configuration. Definite shifts in certain absorption bands of the ligands upon coordination to M^{2+} are correlated to the formation constant of the metal atom involved in coordination. Electronic spectral data as well as magnetic measurements show that the M^{2+} is a high spin species in an octahedral environment. The X-ray powder photographs indicate that Co^{2+} and Zn^{2+} complexes are isostructural and also most probably are Mn^{2+} and Fe^{2+}. Tentative assignments for metal–NCS, M–ligand, Hg—S, and L—M—L absorption bands are discussed.

Les complexes du type $MHg(SCN)_4.2L$ où M = Mn^{2+} à Zn^{2+}, Cd^{2+}, et L = THF ou Py, ont été synthétisés et caractérisés à l'aide de méthodes spectroscopiques. Les groupes thiocyanato forment un pont entre le M^{2+} et le Hg^{2+} alors que l'atome donneur du coordinat est relié au Mn^{2+} qui possède alors une configuration octaédrique. Les déplacements obtenus pour certaines bandes d'absorption des coordinats lors de la coordination au M^{2+} ont été reliés à la constante de formation des complexes impliqués lors de la coordination. Des données obtenues des spectres électroniques aussi bien que magnétiques ont montré que le M^{2+} a un spin élevé et est dans un environnement octaédrique. Les photographies tirées des rayons-X (poudre) ont montré que les complexes du Co^{2+} et du Zn^{2+} sont isostructuraux de même que, fort probablement, ceux du Mn^{2+} et Fe^{2+}. Des attributions hypothétiques pour les bandes d'absorption métal—NCS, M—coordinat, Hg—S et L—M—L sont discutées. [Traduit par le journal]

Can. J. Chem., **51**, 2987 (1973)

Introduction

In our previous paper (1) we have reported the syntheses and structures of cobalt(II) mercury tetrathiocyanate complexes with Lewis bases. Related compounds like $MHg(SCN)_4$ with M = Mn^{2+}, Fe^{2+}, Co^{2+}, Ni^{2+}, Cu^{2+}, and Zn^{2+} have been known to be quite stable and their infrared, reflectance spectra, and X-ray powder patterns for some salts are reported (2–7). The X-ray structure (8) shows that the blue salt $HgCo(NCS)_4$ contains Co(II) in almost regular tetrahedral sites surrounded by four nitrogen atoms, while there is essentially tetrahedral coordination of the mercury by sulfur atoms. The corresponding zinc salt is isomorphous with cobalt salt (9). In the green salt $CuHg(SCN)_4$, the Cu atom is surrounded by an approximate square plane of nitrogen atoms, with bridging sulfur atoms above and below the plane (10). To understand the coordinating ability of the acidic metal site, we have prepared complexes $MHg(SCN)_4 \cdot 2L$, with M = Mn^{2+} to Zn^{2+} or Cd^{2+}, L = THF or py and have characterized them by an elemental analysis infrared, electronic, magnetic, and X-ray powder photographs. The probable structures are discussed.

Experimental

Materials and Manipulations

Anhydrous metal(II) chlorides from Alfa Inorganics Inc., and mercuric thiocyanate from B.D.H. were used without further purification.

Tetrahydrofuran and pyridine Fisher analytical grade were purified by standard methods (11) and stored on molecular sieves (4A B.D.H.). Absolute alcohol was distilled and dried over molecular sieves (4A B.D.H.). All these chemicals were stored in a Dry Box flushed with dry nitrogen.

The physical measurements, *e.g.*, infrared, ultraviolet, visible spectra, magnetic susceptibility, and X-ray powder patterns were made as discussed in our earlier paper (1).

The microanalyses were done by Galbraith Laboratories, Inc., Knoxville, Tenn., U.S.A..

Synthesis of the THF Complexes

Metal(II) chlorides were dissolved in dry tetrahydro-

[1]Presented in part at the 56th Canadian Chemical Conference of the Chemical Institute of Canada, Montreal, Quebec, June 1973.

[2]Present address: Department of Chemistry, McGill University, Montreal, Quebec.

[3]Present address: Département de chimie, Université du Québec à Trois-Rivières, Trois-Rivières, Québec.

Can. J. Chem. Downloaded from www.nrcresearchpress.com by 210.87.254.105 on 09/05/12
For personal use only.

Can. J. Chem. Downloaded from www.nrcresearchpress.com by 210.87.254.105 on 09/05/12
For personal use only.

TABLE 1. Analytical results of $MHg(SCN)_4 \cdot 2L$ (L = THF or py) complexes

Complex	% Analysis											
	Hg		M		Carbon		Hydrogen		Nitrogen		Sulfur	
	Found	Calcd.	Found	Calcd.	Found	Calcd.	Found	Calcd.	Found	Calcd.	Found	Calcd.
$MnHg(SCN)_4 \cdot 2THF$	31.11	31.74	8.27	8.69	22.57	22.81	2.55	2.55	8.87	8.87	20.76	20.29
$FeHg(SCN)_4 \cdot 2THF$	31.38	31.77		8.84	22.08	22.77	2.86	2.54	8.49	8.85	19.43	20.26
$CoHgHg(SCN)_4 \cdot 2THF$	31.56	31.56	8.85	9.28	22.50	22.67	2.50	2.52	8.70	8.82	20.00	20.16
$NiHg(SCN)_4 \cdot 2THF$	30.63	31.59		9.23	22.60	22.67	2.15	2.53	7.97	8.81	20.01	20.17
$CuHg(SCN)_4 \cdot 2THF$	31.10	31.31	9.85	9.92	22.23	22.50	2.35	2.52	8.66	8.74	19.65	20.02
$CdHg(SCN)_4 \cdot 2THF$	30.84	29.10		16.30	19.12	20.91	2.04	2.32	7.74	8.12	17.82	18.58
$ZnHg(SCN)_4$	40.80	40.26		10.17	9.40	9.63	0.10	—	11.09	11.24	25.02	25.69
$MnHg(SCN)_4 \cdot 2py$		31.05	8.23	8.56	25.89	26.03	1.38	1.56	12.92	13.01	19.82	19.85
$FeHg(SCN)_4 \cdot 2py$		31.00	7.89	8.63	24.08	25.99	1.48	1.56	11.91	12.99	18.27	19.82
$CoHg(SCN)_4 \cdot 2py$	31.66	30.86	8.83	9.06	24.49	25.86	1.42	1.55	12.32	12.93	19.76	19.73
$NiHg(SCN)_4 \cdot 2py$		30.86	8.93	9.03	25.26	25.88	1.74	1.55	11.66	12.93	19.62	19.74
$CuHg(SCN)_4 \cdot 2py$		30.64	9.71	9.70	25.47	25.68	1.71	1.53	12.59	12.84	19.21	19.59
$ZnHg(SCN)_4 \cdot 2py$	30.42	30.55	9.77	9.96	25.57	25.61	1.74	1.54	12.76	12.86	19.08	19.54
$CdHg(SCN)_4 \cdot 2py$	28.37	28.52	15.06	15.98	24.21	23.90	1.78	1.43	11.20	11.95	18.54	18.23

Can. J. Chem. Downloaded from www.nrcresearchpress.com by 210.87.254.105 on 09/05/12
For personal use only.

furan and to this added ~2% solution of mercuric thiocyanate in tetrahydrofuran slowly with constant stirring. The solutions added were exactly in the mole ratio of 1:2. The reactants were stirred for 3 d, the resulting precipitates were filtered, washed with the solvent, and dried in vacuum at room temperature. The following reaction took place

$$2Hg(SCN)_2 + MCl_2 \xrightarrow{THF} MHg(SCN)_4 \cdot 2THF + HgCl_2$$

From the filtrate mercuric chloride was obtained along with small amounts of thiocyanates. $ZnCl_2$ or even $Zn(SCN)_2$ failed to form an adduct with THF, but only gave $ZnHg(SCN)_4$.

Synthesis of the Pyridine Complexes

The THF complexes of the type $MHg(SCN)_4 \cdot 2THF$ except for the zinc complex were treated with approximately 2% solution of pyridine in absolute alcohol. The reactants were stirred for 2–3 d, the resulting solids were filtered, washed and dried in vacuum. An alternate method for preparing the pyridine complexes was by reacting 1 mol of metal thiocyanate with 1 mol of mercuric thiocyanate in 2% pyridine solution either in absolute alcohol or tetrahydrofuran. Using this method, the pyridine adduct of $ZnHg(SCN)_4$ was isolated.

These complexes are insoluble in water and in most of the organic solvents except for the pyridine complexes which are slightly soluble in pyridine. Solution spectra, molar conductance or molecular weight measurements could not be made on them. They are non-melting but do decompose above 250 °C. The analytical results are given in Table 1.

Results and Discussion

Near Infrared Spectra

The infrared frequencies of the fundamental vibrations of the complexes studied are given in Tables 2 and 3.[4] The infrared absorption bands related to the pyridine and the THF vibrations of bis-pyridine and bis-tetrahydrofuran complexes of $MHg(SCN)_4$ can easily be assigned except the very weak overtone bands. The assignment of the absorption bands due to the C—N, C—S, Hg—S stretching and S—C≡N deformation are also made by comparing the spectra of complexes with those of the simple salts, KSCN(12) and $MHg(SCN)_4$ (13). For those bands which do not occur in the free ligand, namely, M—L stretching and L—M—L bending modes which occur in the far infrared region, tentative assignments have been made using the available literature (6, 14, 15).

[4]Complete set of tables and figures (Tables 2, 3, 6, 7; Figs. 1 and 2) is available, at a nominal charge, from the Depository of Unpublished Data, National Science Library, National Research Council of Canada, Ottawa, Canada K1A 0S2.

The bis-Pyridine Complexes

The lowest ring vibrations of pyridine (16) at 405 cm^{-1} and 604 cm^{-1}, due to out-of-plane and in-plane vibrations, respectively, are significantly shifted to higher frequencies 420–38 cm^{-1} and 625–45 cm^{-1} in our complexes, which is due to coordination of pyridine to a metal. Similar shifts have been observed by other workers also (17–19). In our complexes they both follow the Irving–Williams order of Mn^{2+} (420, 625), Fe^{2+} (420, 625), Co^{2+} (425, 631), Ni^{2+} (435, 632), Cu^{2+} (438, 640), Zn^{2+} (427, 645) which is directly related to the equilibrium constants for the formation of complexes with nitrogen donating ligands (20). We can conclude that these bands shift to higher frequencies as much as 35 cm^{-1} on coordination to a transition metal of the first row. In addition to these, we do find small shifts of other pyridine bands.

The THF Complexes

In THF complexes, the strong band associated with the C—O—C antisymmetric stretching shows the expected frequency decrease (21, 22), the strong 1070 cm^{-1} band in tetrahydrofuran moves to 1035–1040 cm^{-1}, similarly, the 908 cm^{-1} C—O—C symmetric stretching band moves to 876–890 cm^{-1}. These are typical features of tetrahydrofuran being coordinated to a metal atom, which are observed in our complexes. The infrared spectrum of $CoHg(SCN)_4$ shows a carbon–nitrogen and carbon–sulfur stretching frequencies at 2137 cm^{-1} and 793 cm^{-1} respectively. In the analogous compounds in which cobalt(II) is replaced by other divalent metals, these vibrations occur at approximately the same frequencies with the same intensities indicating no effect of changing M^{2+} on ν(C≡N) and ν(C—S) bands. The position of these bands in our complexes is comparable to the position of the same bands in $MHg(SCN)_4$ (13) since they appear at 2116–60 cm^{-1} and 716–70 cm^{-1}, respectively.

The S—C≡N deformation bands occur as a pair at *ca.* 465 cm^{-1} and *ca.* 445 cm^{-1} in our complexes, which are in good agreement with the values of 461 cm^{-1} and 448 cm^{-1} for $MHg(SCN)_4$ (15).

Far Infrared Spectra

The far infrared spectra of the complexes are shown in Figs. 1 and 2 and assignments of the important bands in the region 300–33 cm^{-1} are

TABLE 4. Far infrared spectra of the complexes (cm^{-1})*

Complex	ν_{M-NCS}†	ν_{M-L}†	ν_{Hg-S}	δ_{L-M-L}	Unassigned
$MnHg(SCN)_4 \cdot 2THF$	230–385 br		200–125 br	174–80 s br	
$FeHg(SCN)_4 \cdot 2THF$	240–48 s br		206–14 s br	188 m	166 sh, 132w, 128w, 78m
$CoHg(SCN)_4 \cdot 2THF$	260 s	236 s	215 s	196 s	
$NiHg(SCN)_4 \cdot 2THF$	258–68 s br	220–26 s br	198–202 s br	182 sh	
$CuHg(SCN)_4 \cdot 2THF$	262–266 s br	223–226 s br	196–204 s br	182 sh	
$CdHg(SCN)_4 \cdot 2THF$	230–365 s br		206–14 s br	144–48 s br	106–14 mbr, 84w, 78s, 58s
$MnHg(SCN)_4 \cdot 2py$	210 s br		196 s br	159 m	150 m
$FeHg(SCN)_4 \cdot 2py$	224–30 s br		206–12 s br	200 sh	165 m
$CoHg(SCN)_4 \cdot 2py$	226–38 vs br		204–18 s br	188 sh	70 m, 50 w
$NiHg(SCN)_4 \cdot 2py$	260–4 s br 246–50 m w	225 s	198–208 s br	182 s	164 w
$CuHg(SCN)_4 \cdot 2py$	280 sh 268 s	216–20 s br	184–94 m br	—	150 m, 100 m br
$ZnHg(SCN)_4 \cdot 2py$	270 vs br		220 ms	173 s 155 m	88 m, 77 s, 66 s
$CdHg(SCN)_4 \cdot 2py$	—	164–68 s br	190–98 s br	144–148 s	125 m, 75 w
$K_2Hg(SCN)_4 \cdot$			204–18 m br		155 s br 94–88 s, 65 m, 45 w

*vs = very strong, s = strong, m = medium, w = weak, br = broad.
†The missing M—NCS or M—L stretching bands are most probably hidden under the assigned bands.

summarized in Table 4.[4] In this region we should expect stretching vibrations of M—NCS, M—Ligand and Hg—S. We have assigned the strong absorption bands at 250–280 cm^{-1} as shown in Table 4, to M—NCS stretching. Clark and Williams (19) have shown that M—NCS stretching frequency decreases approximately by 65 cm^{-1} when changing the environment from tetrahedral to polymeric octahedral around metal atom. Since M—NCS stretching vibrations in tetrahedral complexes $MHg(SCN)_4$ appear *ca.* 320–278 as reported by Forster and Goodgame (6). Our results show a decrease in frequency, and are in good agreement with available data.

The metal—ligand and Hg—S stretching vibrations are assigned on the assumption that for a series of compounds $MHg(SCN)_4 \cdot 2L$, of the same stereochemistry, the ν(M—L) and ν(Hg—S) vibrations will have approximately the same frequencies. In some cases, overlapping can take place, hance making it difficult to assign a particular band with certainty. We have assigned absorption bands located at 220–240 cm^{-1} to asymmetric ν(M—O) (THF) or ν(M—N) (pyridine) stretching vibrations (23). ν(M—N) asymmetric vibrations are strongly dependent on the ligand to which the nitrogen atom is attached and their frequencies fall off in the order metal—ammonia(24) (420–500 cm^{-1}) metal—hydrazine(25) (306–440 cm^{-1}), metal—glycine (26) (275–423 cm^{-1}), metal—pyridine (200–287 cm^{-1}) (27), metal—α′α′-dipyridyl(23), metal—*o*-phenanthroline(1, 27), *i.e.*, among other factors, they are function of the mass of the ligand.

Hg—S stretching bands have been assigned by many workers (13) around 200 cm^{-1}. We have assigned the strong absorption bands in the 198–220 cm^{-1} region to Hg—S stretching modes as shown in Figs. 1 and 2. We do observe a number of bands below 200 cm^{-1} which may be due to symmetric M—L stretching, and L—M—L bending modes. These are not assigned due to uncertainty.

Electronic Spectra and Magnetic Susceptibilities

The corrected magnetic moments of our complexes at room temperatures are shown in Table 5, which are indicative of M^{2+} being in a weak crystal field, hence high spin state. The extensive orbital contribution (*i.e.* ~0.9 for Co^{2+}, 0.6 for Fe^{2+}, and 0.5 for Ni^{2+}) over spin only moment also implies an octahedral environment around M^{2+}. The values of the electronic absorption in the u.v.–visible region are in good agreement with those reported for M^{2+} in an octahedral configuration.

The electronic, the magnetic spectra, and the internal consistency of the infrared results lead us to conclude that in these complexes: (*i*) THF and pyridine are coordinated to a transition metal, (*ii*) the bridged structure M—SCN—M is

Can. J. Chem. Downloaded from www.nrcresearchpress.com by 210.87.254.105 on 09/05/12
For personal use only.

Can. J. Chem. Downloaded from www.nrcresearchpress.com by 210.87.254.105 on 09/05/12
For personal use only.

TABLE 5. Magnetic moments and electronic spectra of complexes taken in Nujol mulls in kK

Complex	Color	$\mu_{eff.}$(B.M.)	Ultraviolet	Visible	Near infrared
$MnHg(SCN)_4 \cdot 2THF$	White	5.89	39.06; 36.50; 29.85		8.59; 7.58; 6.80
$FeHg(SCN)_4 \cdot 2THF$	Yellow	5.45	39.37; 36.36; 30.49; 27.03		11.56; 9.09; 7.19
$CoHg(SCN)_4 \cdot 2THF$	Pink	4.80	40.00; 36.50; 30.49; 27.93	21.14; 20.00; 16.67	9.30
$NiHg(SCN)_4 \cdot 2THF$	Green	3.52	39.06; 36.50; 29.85	16.00	10.58; 8.69
$CuHg(SCN)_4 \cdot 2THF$	Bluish Green	1.89	39.68; 37.04; 29.85	14.82	—
$CdHg(SCN)_4 \cdot 2THF$	White	0.00	39.68; 36.36; 30.30		—
$MnHg(SCN)_4 \cdot 2py$	White	5.90	40.00; 36.76; 29.85	—	—
$FeHg(SCN)_4 \cdot 2py$	Yellow	5.62	40.00; 36.76; 29.67; 24.69	—	—
$CoHg(SCN)_4 \cdot 2py$	Pink	5.01	40.00; 36.76; 32.78; 29.23	21.05; 19.05	9.34
$NiHg(SCN)_4 \cdot 2py$	Green	3.18	40.00; 36.63; 29.41	17.24	10.64
$CuHg(SCN)_4 \cdot 2py$	Light Green	2.00	39.68; 36.76; 34.48; 26.67	15.27	—
$CdHg(SCN)_4 \cdot 2py$	White	0.00	40.00; 36.76; 30.77	—	—

maintained, (*iii*) M^{2+} is in a high spin state within octahedral environment.

X-Ray Powder Patterns and Probable Space Group

Compounds of the type $MHg(SCN)_4$ (1–3) are known for many years. The X-ray single crystal studies of $CoHg(SCN)_4$ (28) have shown that both cobalt and mercury are tetrahedrally attached by thiocyanato bridging, and $ZnHg(SCN)_4$ is isomorphous with the cobalt compound (1).

The strong lines in the powder photograph of our compounds (THF series) are identical, but because of the large number of lines it is hard to conclude that they are isomorphous. The powder patterns of Co-pyridine and Zn-pyridine complexes are superimposable, which demonstrates their isomorphic structure.[4]

Financial support from the National Research Council of Canada is greatly appreciated. We thank Professor A. L. Beauchamp for helpful discussions. Authors are very thankful to Dr. R. N. Jones, National Research Council of Canada for running the far infrared spectra in his laboratory.

1. R. MAKHIJA, L. PAZDERNIK, and R. RIVEST. Can. J. Chem. **51**, 438 (1973).
2. D. FORSTER and D. M. L. GOODGAME. J. Chem. Soc. (A), 262 (1965).
3. D. FORSTER and D. M. L. GOODGAME. Inorg. Chem. **4**, 823 (1965).
4. F. A. COTTON, D. M. L. GOODGAME, M. GOODGAME, and A. SACCO. J. Am. Chem. Soc. **83**, 4157 (1961).
5. A. L. BEAUCHAMP. Personal communication.
6. D. FORSTER and D. M. L. GOODGAME. Inorg. Chem. **4**, 715 (1965).
7. D. E. SCAIFE. Inorg. Chem. **6**, 625 (1967).
8. J. W. JEFFERY. Acta. Cryst. Supp. **6**, A66 (1963).
9. W. STAHL and M. STRAUMANIS. Z. Physik. Chem. **193**, 121 (1944).
10. A. KORCZYNSKI. Roczniki Chem. **36**, 1539 (1962).
11. D. D. PERRIN, W. L. F. ARMAREGO, and DAWN R. PERRIN. Purification of laboratory chemicals. Pergamon Press. 1966. pp. 248–249, 262.
12. A. TRAMER. J. Chim. Phys. **59**, 232 (1962).
13. R. A. BAILEY, S. L. KOZAK, T. W. MICHELSEN, and W. N. MILLS. Coord. Chem. Rev. **6**, 407 (1971).
14. A. SABATINI and I. BERTINI. Inorg. Chem. **4**, 959 (1965).
15. R. J. MUREINIK and W. ROBB. Spectrochim. Acta, **24A**, 837 (1968).
16. (*a*) C. H. KLINE and J. TURKEVICH. J. Chem. Phys. **12**, 300 (1944). (*b*) G. ZERBI, J. OVEREND, and B. CRAWFORD. J. Chem. Phys. **38**, 122 (1963).
17. N. S. GILL, R. H. NUTTALL, D. E. SCAIFE, and D. W. A. SHARP. J. Inorg. Nucl. Chem. **18**, 79 (1961).
18. R. J. H. CLARK and C. S. WILLIAMS. Inorg. Chem. **4**, 350 (1965).
19. R. J. H. CLARK and C. S. WILLIAMS. Spectrochim. Acta, **22**, 1081 (1966).
20. F. A. COTTON and G. WILKINSON. Advance inorganic chemistry. 2nd ed. Interscience Publication, New York. 1966. pp. 690.
21. R. J. KERN. J. Inorg. Nucl. Chem. **24**, 1105 (1962).
22. R. C. MAKHIJA and R. A. STAIRS. Can. J. Chem. **47**, 2293 (1969).
23. K. NAKAMOTO. Personal communication.
24. K. NAKAMOTO. Infrared spectra of inorganic and coordination compounds. John Wiley and Sons, Inc., New York, N.Y. 1963. p. 150.
25. L. SACCONI and A. SABATINI. J. Inorg. Nucl. Chem. **25**, 1389 (1963).
26. T. J. LANE, J. A. DURKIN, and R. J. HOOPER. Spectrochim. Acta, **20**, 1013 (1964).
27. R. J. H. CLARK. J. Chem. Soc. 1377 (1962).
28. J. W. JEFFERY and K. M. ROSE. Acta Cryst. **B24**, 653 (1968).

Can. J. Chem. Downloaded from www.nrcresearchpress.com by 210.87.254.105 on 09/05/12
For personal use only.

Apparent Molal Heat Capacities and Volumes of Tetrabutylammonium Carboxylates and Related Solutes in Water at 25 °C

PAUL-ANDRÉ LEDUC AND JACQUES E. DESNOYERS
Department of Chemistry, Université de Sherbrooke, Sherbrooke, Quebec
Received March 6, 1973

The apparent molal volumes and heat capacities were measured in water at 25 °C with a flow digital densimeter and a flow microcalorimeter for the following salts: tetrabutylammonium octanoate, tetrabutylammonium butanoate, tetrabutylammonium bromide, ammonium acetate, ammonium chloride, ammonium bromide, sodium octanoate, and sodium acetate. The tetrabutylammonium octanoate and butanoate and sodium octanoate form micelles at 0.13, 0.6, and 0.35 *M*, respectively. The concentration dependence of the apparent molal volumes of the carboxylate salts is similar to that of typical hydrophobic or hydrophilic electrolytes. On the other hand, in the submicellar region, the concentration dependence of their apparent molal heat capacities is abnormal when compared with model electrolytes. It seems that the heat capacities may be reflecting interactions involving a hydrogen bonding of the carboxylate group with water.

Les capacités calorifiques et les volumes apparents molaires ont été mesurés dans l'eau à 25 °C au moyen d'un microcalorimètre dynamique et d'un densimètre digital à écoulement pour les sels suivants: les octanoate, butanoate et bromure de tétrabutylammonium, les octanoate et acétate de sodium et les acétate, chlorure et bromure d'ammonium. Les octanoate et butanoate de tétrabutylammonium et l'octanoate de sodium forment des micelles aux concentrations suivantes: 0.13, 0.6, et 0.35 *M*. La dépendance sur la concentration des volumes apparents molaires des carboxylates est semblable à celle des électrolytes hydrophobes ou hydrophiles typiques. Par contre, dans la région sous-micellaire, la dépendance sur la concentration des capacités calorifiques apparentes molaires est anormale par rapport aux électrolytes modèles. Il semble que les capacités calorifiques font ressortir des interactions du type pont hydrogène entre les groupements carboxylate et les molécules d'eau.

Can. J. Chem., **51**, 2993 (1973)

Introduction

Recently, Lindenbaum (1) has measured the enthalpies of dilution of some tetrabutylammonium carboxylates in water. These salts formed by two hydrophobic ions, one symmetrical and one linear, are quite soluble in water and are characterized by very large exothermic enthalpies of dilution. The nature of the interactions giving rise to these large solubilities and enthalpies are still somewhat obscure, but they are of fundamental importance to the understanding of structural interactions and hydrophobic bonding in water. We have felt that the knowledge of the apparent molal volumes, ϕ_v, and heat capacities, ϕ_c, of tetrabutylammonium butanoate (TBABu) and octanoate (TBAOc) in water at 25 °C would be useful in this respect since these properties have proven to be very informative on hydrophobic interactions (2, 3). The negative concentration dependence of ϕ_v and ϕ_c has been attributed to hydrophobic interactions (non-contact ion pairing). It was also shown that micelle formation causes a large increase in ϕ_v and a large decrease in ϕ_c. We were also led in this study to measure ϕ_v and ϕ_c of ammonium acetate (NH_4Ac), NH_4Cl, NH_4Br, sodium acetate (NaAc), and sodium octanoate (NaOc). The ϕ_c of n-Bu_4NBr (TBABr) (4) have also been extended to higher concentrations.

Experimental

The preparation and purification of TBABu and TBAOc were essentially the same as was described by Lindenbaum (1). The origin and purity of the required chemicals are: TBABr (Eastman Kodak) recrystallized twice from ethyl acetate (5), silver nitrate 99.98% (Engelhard), butanoic acid (Baker), and octanoic acid (Baker). Both acids were distilled under vacuum from a fractionating column and the distillates were shown to be chromatographically pure.

The salt NaOc was prepared as described by Campbell *et al.* (6) and dried under vacuum at 120 °C for 48 h. All other salts (ACS Fisher certified reagent) were used without further purification and, except for NH_4Ac which is highly hygroscopic, dried in the same manner. The latter salt was freeze-dried under vacuum in a rotating flask containing stainless steel balls which helped to remove traces of water by crushing the crystals. The finely powdered salt was then transferred and weighed, all under dry nitrogen atmosphere.

All solutions, except those of TBAOc and TBABu,

Can. J. Chem. Downloaded from www.nrcresearchpress.com by 210.87.254.6 on 09/05/12
For personal use only.

TABLE 1. Apparent molal volumes and heat capacities in water at 25 °C; parameters of eqs. 4 and 5 from least-squares fitting*

Electrolyte	ϕ_v^0 (cm^3 mol^{-1})	B_v'	c_{max} (mol l^{-1})	ϕ_c^0 (J K^{-1} mol^{-1})	B_c'	c_{max} (mol l^{-1})
TBABu	346.2	−18.4	0.2	1548.4	42	0.35
TBAOc	411.3	−25	0.1	1906	744	0.1
TBABr	300.59(13)	−11.85(13)	0.3	1205.9	−22	0.35
NH_4Ac	58.55	0.15	1.8	105.4	−12.7	0.7
NH_4Cl	35.79	−0.25	0.8	−52.6	−2.2	0.8
NH_4Br	42.57(2)	−0.55(2)	0.9	−60.8	5.2	1.0
NaOc	132.14	0.1_6	0.3	592.8	44	0.3
NaAc	39.18	0.24	2.6	69.7	10.7	2.5
NaCl	16.63(14)	−0.03(14)	1.0	−81.4(11)	15.6(11)	1.0
NaBr	23.47(11)	−0.08(11)	1.0	−84.5(11)	16.4(11)	1.0

*Reference numbers in parentheses.

were freshly prepared by weight with water redistilled from an alkaline permanganate solution. TBABu and TBAOc solution were obtained from a weight dilution of a 2.110_7 and 1.020_8 m stock solution. The molalities were converted to molarities whenever necessary using the measured densities of the solutions.

The apparent molal volumes and heat capacities are obtained from the following equations

$$[1] \qquad \phi_v = \frac{M}{d_0} - 1000\frac{(d - d_0)}{cd_0}$$

$$[2] \qquad \phi_c = Mc_p + 1000\frac{(c_p - c_p^0)}{m}$$

or

$$[3] \qquad \phi_c = \phi_v\sigma_0 + 1000\frac{(\sigma - \sigma_0)}{c}$$

where M is the salt molecular weight, c the molarity, m the molality, d the density (in g cm^{-3}), c_p the weight specific heat (in J K^{-1} g^{-1}) and $\sigma(= c_p d)$ the volumetric specific heat (in J K^{-1} cm^{-3}). For pure water at 25 °C, d_0, c_p^0 and $\sigma_0 = c_p^0 d_0$ were taken respectively as 0.997047 g cm^{-3} (7), 4.1793 J K^{-1} g^{-1} (8) and 4.1670 J K^{-1} cm^{-3}.

The differences in densities were measured to $\pm 3 \times 10^{-6}$ g cm^{-3} with a flow digital densimeter (9) and $(\sigma - \sigma_0)/\sigma_0$ with a flow microcalorimeter (10). The $\Delta\sigma/\sigma_0$ is obtained to $\pm 0.3\%$ (11) up to the limit of the sensitivity on $\Delta\sigma$ which is 7×10^{-5} J K^{-1} cm^{-3}. The general procedures for the density and heat capacity measurements were described in the original references.

Results

The experimental densities and volumetric specific heats and derived ϕ_v and ϕ_c are available elsewhere.[1] The data at low concentrations were fitted to the equations

$$[4] \qquad \phi_v = \phi_v^0 + A_v c^{1/2} + B_v' c$$

$$[5] \qquad \phi_c = \phi_c^0 + A_c c^{1/2} + B_c' c$$

where ϕ_v^0 and ϕ_c^0 are the standard apparent molal quantities (infinite dilution), A_v and A_c are the limiting Debye–Hückel slopes (A_v = 1.867 and A_c = 28.99 for 1:1 electrolytes in water at 25 °C) and the parameters B_v' and B_c' give the deviations from the Debye–Hückel law (B_v' and B_c' should be distinguished from B_v and B_c which correspond to eqs. 4 and 5 expressed in m). These parameters are obtained by a weighted least-squares method and are given in Table 1; those for NaBr and NaCl are also included for comparison. The densities of TBABr (12) and NH_4Br (2) were taken from the literature.

The accuracy of the present measurements may best be checked from the additivity of ϕ_c^0 and ϕ_v^0 and, whenever possible, from a comparison with literature data.

[1a] ϕ_c^0(NaOc) + ϕ_c^0(TBABr) − ϕ_c^0(NaBr) = 1883 J K^{-1} mol^{-1}
ϕ_c^0(TBAOc) = 1906 J K^{-1} mol^{-1}

[1b] ϕ_v^0(NaOc) + ϕ_v^0(TBABr) − ϕ_v^0(NaBr) = 409.3 cm^3 mol^{-1}
ϕ_v^0(TBAOc) = 411.3 cm^3 mol^{-1}

[2a] $\phi_c^0(NH_4Br)$ + ϕ_c^0(NaAc) − ϕ_c^0(NaBr) = 93.4 J K^{-1} mol^{-1}
$\phi_c^0(NH_4Ac)$ = 105.4 J K^{-1} mol^{-1}

[2b] $\phi_v^0(NH_4Br)$ + ϕ_v^0(NaAc) − ϕ_v^0(NaBr) = 58.2 cm^3 mol^{-1}
$\phi_v^0(NH_4Ac)$ = 58.6 cm^3 mol^{-1}

[1] Photocopies of the actual experimental data may be obtained at a nominal charge, upon request, from: Depository of Unpublished Data, National Research Council of Canada, Ottawa, Canada K1A 0S2.

Can. J. Chem. Downloaded from www.nrcresearchpress.com by 210.87.254.6 on 09/05/12
For personal use only.

Can. J. Chem. Downloaded from www.nrcresearchpress.com by 210.87.254.6 on 09/05/12
For personal use only.

[3a] $\phi_c^0(NH_4Br) - \phi_c^0(NH_4Cl) = -8\ J\ K^{-1}\ mol^{-1}$

$\phi_c^0(NaBr) - \phi_c^0(NaCl) = -3\ J\ K^{-1}\ mol^{-1}$

[3b] $\phi_v^0(NH_4Br) - \phi_v^0(NH_4Cl) = 6.7\ cm^3\ mol^{-1}$

$\phi_v^0(NaBr) - \phi_v^0(NaCl) = 6.8\ cm^3\ mol^{-1}$

[4a] $\phi_c^0(TBAOc) - \phi_c^0(TBABu) = 358\ J\ K^{-1}\ mol^{-1}$

$\phi_c^0(HeptNH_3Br) - \phi_c^0(PrNH_3Br) = 343\ J\ K^{-1}\ mol^{-1}$ (ref. 3)

[4b] $\phi_v^0(TBAOc) - \phi_v^0(TBABu) = 65.1\ cm^3\ mol^{-1}$

$\phi_v^0(HeptNH_3Br) - \phi_v^0(PrNH_3Br) = 63.8\ cm^3\ mol^{-1}$ (ref. 2)

For alkali halides, ϕ_c can usually be obtained to $\pm 0.5\ J\ K^{-1}\ mol^{-1}$ above 0.1 *m* (8). Since eq. 5 is usually obeyed over a fairly wide concentration range, ϕ_c^0 can often be determined to better than $1\ J\ K^{-1}\ mol^{-1}$ with alkali halides (11). With the carboxylate salts, the limited concentration regions where eq. 5 can be used, errors in the determination of the initial stock solutions (with TBAOc and TBABu) and the possibility of a small degree of hydrolysis probably increase the uncertainty on ϕ_c^0 to about $\pm 10\ J\ K^{-1}\ mol^{-1}$. The only ϕ_c^0 of carboxylate salts that can be compared with literature data is NaOc; KOc was studied in 0.04 *N* KOH by Goddard *et al.* (15) and their ϕ_c^0, after correction for the difference between Na^+ and K^+, is $621\ J\ K^{-1}\ mol^{-1}$, compared with our $594\ J\ K^{-1}\ mol^{-1}$.

The ϕ_v^0 all appear to be precise to better than $1\ cm^3\ mol^{-1}$ from the additivity tests. Also ϕ_v^0 of NaAc ($39.18\ cm^3\ mol^{-1}$) can be compared with Millero's recommended value ($39.25\ cm^3\ mol^{-1}$) (16) and ϕ_v of NaOc, derived from Campbell's densities (6), agree inside the experimental uncertainty with ours.

The accuracy on ϕ_v and ϕ_c is sufficiently good to insure that any trends we will observe when comparing B_v' and B_c' for different electrolytes could not be due to experimental uncertainty.

Discussion

Ion–Solvent Interactions

The standard ϕ_v^0 of hydrophobic solutes are rather insensitive to ion–solvent interactions due to the compensation between the cavity effect and the increase in ice-likeness (2, 17). On the other hand, ϕ_c^0 of structure makers are usually much larger than their intrinsic heat capacities (18), *i.e.* the molar heat capacity of the solute itself. These latter values are not known for the present organic ions but their order of magnitude can be estimated from the specific heats of related organic liquids or solids (1.8 to $2\ J\ K^{-1}\ g^{-1}$ in general) and the solute molecular weight. With this test, TBAOc, TBABu, TBABr, and NaOc all appear as strong hydrophobic structure makers, while all the other salts are structure breakers ($\phi_c^0 < C_p(in)$). This is in agreement with the B_η viscosity coefficients which indicate that NH_4Br is a structure breaker (19) and with the enthalpies of transfer from H_2O to D_2O which suggest that sodium acetate is a structure breaker (20). Finally, ϕ_c^0 and ϕ_v^0 of NaOc are comparable with those of octylamine hydrobromide (2, 3), if allowance is made for the difference between Na^+ and Br^-. Therefore, the ϕ_v^0 and ϕ_c^0 of the present salts are all normal when compared with other similar solutes, or at least the anomalies are not obvious from their signs and orders of magnitude.

Solute–Solute Interactions

The concentration dependence of ϕ_v of the long chain carboxylate salts are compared with TBABr on Fig. 1. The excess apparent molal volumes, $\phi_v^{EX} = \phi_v - \phi_v^0 - A_v c^{1/2}$,[2] all show

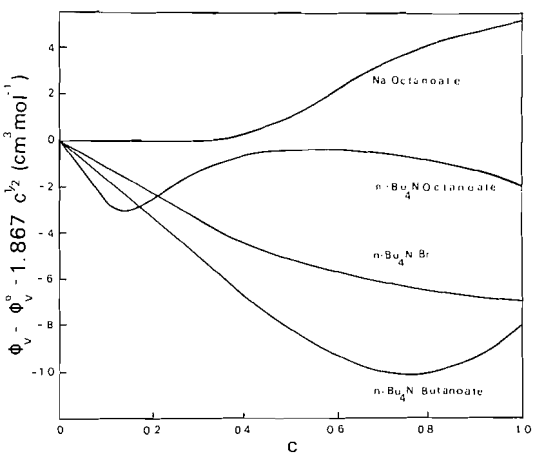

FIG. 1. Excess apparent molal volumes of carboxylate salts and tetrabutylammonium bromide in water at 25 °C.

[2]In defining these excess functions, we have assumed the Debye–Hückel limiting law to be part of the ideal function.

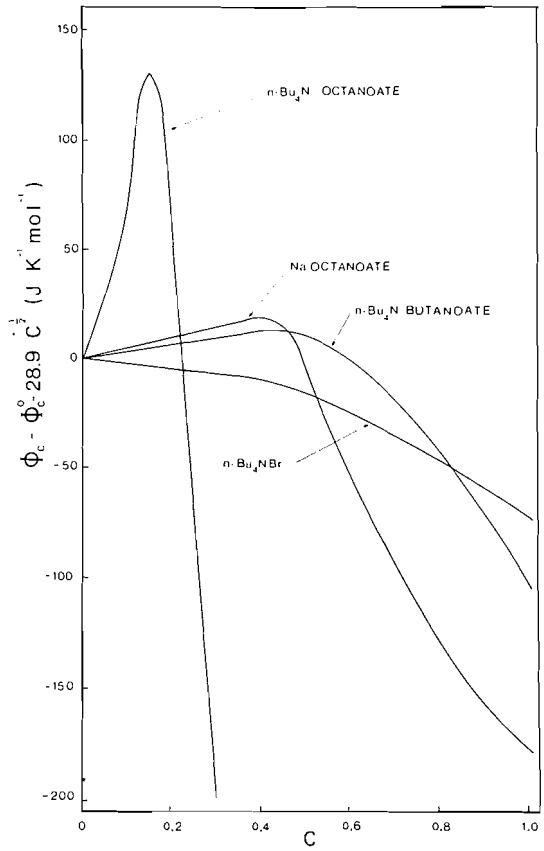

FIG. 2. Excess apparent molal heat capacities of carboxylate salts and tetrabutylammonium bromide in water at 25 °C.

an initial decrease and, with the carboxylate salts, eventually an increase with concentration. Micelle formation has been shown to be accompanied by a sharp increase in ϕ_v (2, 21). Therefore some hydrophobic association occurs with the carboxylate salts, but the lack of sharpness in the increase suggests that micelles are formed over a wide range of concentration. The critical micelle concentration (CMC) was taken as the minimum in ϕ_v^{EX} which probably corresponds to the region where micelles begin to form. The estimated critical micelle concentrations of these systems are summarized in Table 2. There are also signs of hydrophobic bonding with TBABr beyond 0.3 *M* although this association cannot really be qualified as micelle formation. The most interesting feature of Fig. 1 is probably the large decrease in the CMC when Na^+ is substituted for TBA^+. This is a general observation that

TABLE 2. CMC of carboxylate salts in water at 25 °C

	CMC (mol l^{-1})		
Electrolyte	from ϕ_v*	from ϕ_c†	Average
TBAOc	0.13	0.14	0.13
NaOc	0.32	0.38	0.35
TBABu	0.7	0.4	0.6

*CMC taken as the minima in Fig. 1.
†CMC taken as the maxima in Fig. 2.

larger counter ions reduce the CMC of surfactants (22). The explanation often given is that adsorption of the counter ions increases with their size.

A negative B_v' is usually interpreted through the overlap of hydrophobic co-spheres (5, 12, 23, 24) with typical hydrophobic salts such as the tetraalkylammonium halides (5, 12, 13) and long-chain alkylamine hydrobromides (2) in the sub-micellar region. Corresponding to the large positive apparent molal relative enthalpies ϕ_L of TBABu and TBAOc (1), a large negative B_v' is observed, and B_v' of TBAOc is more negative than either TBABr or NaOc. This suggests strong hydrophobic–hydrophobic structural interactions either of the cation–cation or cation–anion type. The only unexpected result is with NaOc, which has a slightly positive B_v' while a negative one would have been predicted. No explanation for this can be given.

With the present surfactants we can assume some kind of cooperative effect between the cationic–anionic and anionic–anionic hydrophobic interactions leading to stronger overall attractive forces (lower ΔG and CMC). This can be considered a triplet interaction; the attractive forces between two hydrophobic anions is larger in the presence of TBA^+. Therefore, the ϕ_v data, in agreement with the heats of dilution (1), seem to indicate that hydrophobic pair or triplet interactions increase in the order TBABr < TBABu < TBAOc, which is what we would expect.

The excess heat capacities, $\phi_c^{EX} = \phi_c - \phi_c^0 - A_c c^{1/2}$ (see footnote 2), for the carboxylate salts and TBABr are compared in Fig. 2. The large decrease in ϕ_c usually accompanying micelle formation (3, 15) is again observed for the long-chain carboxylate salts. The CMC, taken as the maximum in ϕ_c^{EX}, are given in

Can. J. Chem. Downloaded from www.nrcresearchpress.com by 210.87.254.6 on 09/05/12
For personal use only.

Can. J. Chem. Downloaded from www.nrcresearchpress.com by 210.87.254.6 on 09/05/12
For personal use only.

Table 2 and appear in reasonable agreement with those obtained from ϕ_v.

The parameters B_c' of most tetraalkylammonium halides (4, 25) and alkylamine hydrobromides (3) are all negative at 25 °C. This negative excess heat capacity has been attributed to hydrophobic–hydrophobic interactions (4); if hydrophobic hydration is responsible for the large positive $\phi_c^0 - C_p$ (in), then overlap of the hydrophobic co-spheres should decrease the structural effect per mole of solute. If this explanation is correct we would expect the excess ϕ_c in the submicellar region, or B_c' to become more negative in the order TBABr < TBABu < TBAOc. The exact opposite is observed. This apparent contradiction either means that the interpretation of B_c' previously given was wrong or that extra solute–solute interactions occur with the hydrophobic carboxylate salts.

Studies presently underway in this laboratory on the temperature dependence of B_c' of hydrophobic solutes indicate that dB_c'/dT is quite often positive. This means that B_c' of salts such as TBABr become less negative as the temperature decreases. As a matter of fact, with nonyl trimethyl ammonium bromide, B_c' actually becomes positive at 5 °C. Therefore, the previous interpretation of B_c' (4) might well have been wrong and the long-chain carboxylate salts might be behaving like typical hydrophobic solutes at very low temperatures. This explanation might account for ϕ_c^{EX} of TBABu and TBAOc, but the positive ϕ_c^{EX} of NaOc in the submicellar region is still intriguing since B_c' of octylamine hydrobromide (2) is negative and that of sodium octylsulfate (26) is approximately zero. The carboxylate group could therefore be partially responsible for the positive B_c'. It has been shown (27) that the addition of an —OH or —COONa group on a benzene ring causes a negative contribution to ϕ_c^0 and a positive ϕ_c^{EX}. The decrease in ϕ_c^0 was attributed to solute–solvent hydrogen bonding which was a weak interaction compared with the $H_2O...H_2O$ hydrogen bond but which increased in relative strength as the temperature was raised. This small but very temperature-dependent hydrogen-bonding interaction could account for the large contribution of these groups to ϕ_c^0. With the present solutes, it is not possible to compare ϕ_c^0 of the ions with the corresponding alkanes to determine the effect of the —COONa group since the data on these alkanes are not available. On the other hand, the ϕ_c^{EX} may very well be related to the hydrogen-bonding capacity of these electrolytes.

If hydrogen bonding interactions are involved with ϕ_c^{EX} of hydrophobic solutes, they should also show up with hydrophilic electrolytes such as NH_4Ac and NaAc. Alkali halides have small positive or negative B_v' and B_c' parameters. An examination of Table 1 indicates that B_v' of NH_4Ac and NaAc are normal when compared with NaCl and NaBr. For B_c' NaAc seems normal but NH_4Ac is more negative than expected. However, a systematic study of simple protic solutes in water would be necessary to establish the importance of hydrogen-bonding interactions on ϕ_c^{EX}.

We are grateful to Dr. S. Lindenbaum for making available to us, prior to publication, the preparation and purification procedure of the tetrabutylammonium carboxylates and to G. Perron and J. P. Savard for their assistance with some of the measurements. Grateful acknowledgment is also made to the National Research Council of Canada and to Environment Canada for financial assistance.

1. S. Lindenbaum. J. Phys. Chem. **75**, 3733 (1971).
2. J. E. Desnoyers and M. Arel. Can. J. Chem. **45**, 359 (1967).
3. P. A. Leduc, J.-L. Fortier, and J. E. Desnoyers. In preparation.
4. P. R. Philip and J. E. Desnoyers. J. Solution Chem. **1**, 353 (1972).
5. B. E. Conway, R. E. Verrall, and J. E. Desnoyers. Trans. Faraday Soc. **62**, 2738 (1966).
6. A. N. Campbell, E. N. Kartzmark, and G. R. Lakshminarayanan. Can. J. Chem. **40**, 839 (1962).
7. G. S. Kell. J. Chem. Eng. Data, **12**, 66 (1967).
8. H. F. Stimson. Am. J. Phys. **23**, 614 (1955).
9. P. Picker, E. Tremblay, and C. Jolicoeur. J. Solution Chem. Submitted.
10. P. Picker, P.-A. Leduc, P. R. Philip, and J. E. Desnoyers. J. Chem. Thermodyn. **3**, 631 (1971).
11. J.-L. Fortier, P. A. Leduc, and J. E. Desnoyers. J. Solution Chem. Submitted.
12. W.-Y. Wen and S. Saito. J. Phys. Chem. **68**, 2639 (1964).
13. G. Perron and J. E. Desnoyers. J. Chem. Eng. Data, **17**, 136 (1972).
14. F. Vaslow. J. Phys. Chem. **70**, 2286 (1966).
15. E. D. Goddard, C. A. J. Hoeve, and G. C. Benson. J. Phys. Chem. **61**, 593 (1957); P. White and G. C. Benson. J. Phys. Chem. **64**, 599 (1960).
16. F. J. Millero. Water and aqueous solutions. *Edited by* R. A. Horne. Wiley. 1972. Chapt. 13.
17. M. E. Friedman and H. A. Scheraga. J. Phys. Chem. **69**, 3795 (1965).

18. H. S. FRANK and W.-Y. WEN. Discuss. Faraday Soc. **24**, 133 (1957).
19. M. KAMINSKY. Z. Phys. Chem. (Frankfurt), **12**, 206 (1957).
20. H. SNELL and J. GREYSON. J. Phys. Chem. **74**, 2148 (1970).
21. F. FRANKS and H. T. SMITH. J. Phys. Chem. **68**, 3581 (1964).
22. K. SHINODA, T. NAKAGOWA, B. TAMAMASKI, and T. ISEMURA. Colloïdal surfactants. Academic Press. 1963. Chapt. 1.
23. H. S. FRANK. J. Phys. Chem. **67**, 1554 (1963).
24. J. E. DESNOYERS, M. AREL, G. PERRON, and C. JOLICOEUR. J. Phys. Chem. **73**, 3346 (1969).
25. G. PERRON and J. E. DESNOYERS. To be published.
26. G. M. MUSBALLY, G. PERRON, and J. E. DESNOYERS. To be published.
27. J. E. DESNOYERS, R. PAGÉ, G. PERRON, J.-L. FORTIER, P. A. LEDUC, and R. F. PLATFORD. Can. J. Chem. In press.

Can. J. Chem. Downloaded from www.nrcresearchpress.com by 210.87.254.6 on 09/05/12
For personal use only.

Mass Spectral Studies of Binuclear Metal Complexes: Copper(I) Carboxylates

DENIS C. K. LIN AND JOHN B. WESTMORE
Department of Chemistry, University of Manitoba, Winnipeg, Manitoba R3T 2N2
Received March 22, 1973

The thermal decomposition of twenty-five cupric carboxylates was studied by mass spectrometry. In eleven cases volatile cuprous carboxylates (many of which have not been previously reported) were detected amongst the decomposition products. The cuprous carboxylates from acetic, propionic, *n*-butyric, isobutyric, difluoroacetic, trifluoroacetic, benzoic, *p*-fluorobenzoic, *p*-chlorobenzoic, *o*-chlorobenzoic, and pentafluorobenzoic acids were all found to be dimeric in the vapor phase. Two basically different fragmentation pathways can be proposed depending upon whether the copper salt is formed from an alkyl- or aryl-carboxylic acid. For the former, the spectra are dominated by even-electron fragment ions formed by initial loss of $RCO_2\cdot$ from the molecular ion. For the latter, a parallel fragmentation pathway initiated by loss of CO_2 from the molecular ion and migration of the aryl group to the metal is also present.

La décomposition thermique de 25 carboxylates cupriques a été étudiée à l'aide de la spectrométrie de masse. Dans 11 cas, on a pu détecter la présence de carboxylates cuivreux volatils (plusieurs de ceux-ci n'ont pas déjà été décrits) parmi les produits de décomposition. Les carboxylates cuivreux des acides acétique, propionique, *n*-butyrique, iso-butyrique, difluoroacétique, trifluoroacétique, benzoïque, *p*-fluorobenzoïque, *p*-chlorobenzoïque, *o*-chlorobenzoïque et pentafluorobenzoïque, se présentent tous sous forme dimérique en phase vapeur. Deux processus fondamentalement différents de fragmentation peuvent être proposés selon que le sel de cuivre est formé à partir d'un acide carboxylique alcoyle ou aryle. Pour le premier cas, les spectres se composent surtout de fragments ioniques comportant un nombre pair d'électrons qui proviennent de la perte initiale de $RCO_2\cdot$ de l'ion moléculaire. Pour le second cas, un processus de fragmentation parallèle issu de la perte de CO_2 de l'ion moléculaire et de la migration du groupe aryle au métal est aussi présent. [Traduit par le journal]

Can. J. Chem., 51, 2999 (1973)

Introduction

Since the reports of the synthesis of copper(I) formate and acetate near the beginning of this century (1–3) the structures and chemistry of copper(I) carboxylates have, until recently, been largely ignored. It is now apparent that compounds of this class may be useful reagents, particularly for organic synthesis. For example, synthesis of thiolbenzoate esters can be achieved with copper(I) thiobenzoate (4). Some copper(I) carboxylates can be decarboxylated giving organocopper intermediates which may then be coupled with aryl halides to give unsymmetrical biaryls, oxidized or pyrolyzed to give symmetrical biaryls, or hydrolyzed to arenes (5–8). Knowledge as to the relative stabilities and properties of copper(I) carboxylates would be useful in their synthesis and characterization.

Our primary interest in these complexes was to study the competing effects of metal and ligand in the mass spectra of metal-containing compounds, an area of theoretical and practical importance. Only a few copper(I) carboxylates have been prepared by simple methods (9, 10). However, our initial observations (11) that copper(I) acetate and benzoate could be produced thermally from the corresponding copper(II) complexes prompted a search for other copper(I) carboxylates that could be detected in a similar way. Consequently, we prepared twenty-five copper(II) carboxylates and in eleven cases were able to detect volatile copper(I) carboxylates among the products of decomposition of a sample of the copper(II) compound heated on the sample probe of a mass spectrometer.

Of importance in an interpretation of the mass spectra of the copper-containing compounds is a knowledge of their probable structure. Important conclusions can be drawn from structural information obtained for the solid state. Copper(II) carboxylates have been widely studied. Of particular interest have been measurements of antiferromagnetic interactions between neighboring copper(II) ions in the dimeric or polymeric systems by structural and magnetic susceptibility determinations, and by optical, infrared, or electron paramagnetic resonance spectroscopy. Much of this work has been reviewed (12–14). Usually the carboxylate anions serve as bridging groups between copper ions. On the other hand, for copper(I) only the structure of copper(I) acetate has been reported (15, 16). It contained chains of

Can. J. Chem. Downloaded from www.nrcresearchpress.com by 210.87.254.6 on 09/05/12
For personal use only.

TABLE 1. Decomposition of copper(II) carboxylates, $Cu(CO_2R)_2$, on the mass spectrometer sample probe indicating the major decomposition products identified, for those compounds which did not give detectable amounts of volatile copper(I) carboxylates

Copper(II) carboxylate	R	Major decomposition products identified*
Formate†	H	RCO_2H (100°)
Chloroacetate	CH_2Cl	RCO_2H (95°), HCl, CH_3Cl, followed at ~300° by Cu_3Cl_3, Cu_4Cl_4
Dichloroacetate	$CHCl_2$	RCO_2H (120°), HCl, CH_2Cl_2, followed at ~300° by Cu_3Cl_3, Cu_4Cl_4
Phenylacetate	$CH_2C_6H_5$	RCO_2H (110°), $C_6H_5CO_2H$
o-Toluate	*o*-$CH_3C_6H_4$	RCO_2H (115°)
p-Toluate	*p*-$CH_3C_6H_4$	RCO_2H (115°), $(RCO)_2O$ (195°)
o-Fluorobenzoate	*o*-FC_6H_4	RCO_2H (160°), $(RCO)_2O$ (190°), RCO_2R, R_2CO
o-Methoxybenzoate	*o*-$CH_3OC_6H_4$	RCO_2H (105°), C_2H_6, HCO_2H, H_2CO?
p-Ethoxybenzoate	*p*-$C_2H_5OC_6H_4$	RCO_2H (75°), $(RCO)_2O$ (245°), RCO_2R, R_2CO, R_2O, R_2
o-Hydroxybenzoate	*o*-HOC_6H_4	RCO_2H (100°), RH (220°), HCO_2H, H_2CO
p-Hydroxybenzoate	*p*-HOC_6H_4	RCO_2H (90°)
o-Nitrobenzoate	*o*-$NO_2C_6H_4$	RCO_2H (165°)
p-Nitrobenzoate	*p*-$NO_2C_6H_4$	RCO_2H (175°), $(RCO)_2O$ (300°)
β-Naphthoate	β-$C_{10}H_7$	RCO_2H (130°), $(RCO)_2O$ (225°), RCO_2R

*H_2O, CO_2, and possibly CO were always detected. In some cases positive identification was not obtained because a significant ion could arise either from the suspected compound or as a fragment ion from a compound of higher mass. The sample temperature (± 10°) at which the acid and anhydride were first detected is given in parentheses.

†Other workers (18) obtained a mass spectrum, but with considerable difficulty, containing the copper(I) salt.

dimeric units linked together by copper(I)–oxygen interactions. In the dimeric units each carboxylate group bridges the two cuprous ions to form an eight-membered ring in which, although the copper–copper separation was identical to that in copper metal, there was believed to be only a small interaction between the copper ions. The dimeric units bear a formal resemblance to the dimeric silver(I) perfluorobutyrate complex (17). This structure supports our original claim (11) that the major copper-containing species in the vapor was dimeric since, in view of the long separations between the dimeric units in the solid, the interactions between them would be quite weak. Nevertheless, very low intensity ions containing three or four copper atoms have been detected in the mass spectra of subliming copper(I) formate, acetate, trifluoroacetate, and benzoate (18) indicating that small quantities of a more highly associated species, probably the tetramer, also sublime, in addition to large quantities of dimer. (A similar observation has been made for metal acetylacetonates. Although the major subliming species was the monomer, more highly associated species were observed at low intensity (19).)

Experimental

The mass spectra were obtained on a Hitachi Perkin–Elmer RMU-6D single focussing mass spectrometer. About 0.5 mg of the copper(II) carboxylate sample was packed into a sample tube and inserted into the mass spectrometer via the solids inlet system. While monitoring the mass spectra at frequent intervals the sample temperature was raised slowly from ~40° until copper-containing species could be detected in the spectra or until a maximum temperature of~ 300° had been reached. The ionization chamber temperature was ~200° and the electron energy was 50 V.

The copper(II) carboxylates were prepared using published procedures (12, 20, 21) and were dried under a diffusion pump vacuum for 24 h before use.

Results and Discussion

Thermal Decompositions

The compounds studied are listed in Tables 1 and 2. In all cases, as the temperature of the sample was raised, the first decomposition products detected were CO_2, H_2O, and the carboxylic acid. Many of the aromatic carboxylates also gave the acid anhydride, but at higher temperatures. The compounds which did not give detectable amounts of copper(I) carboxylates are given in Table 1, while those that did are listed in Table 2. Apart from this difference, the nature of the decomposition products in the two tables seems very similar and we have not been able to find any simple parameter upon which to make a distinction between the compounds in the two tables. In fact, the differences between the decompositions of the isomers *o*- and *p*- CH_3, OH, NO_2, and Cl benzoates indicates that if electronic and steric factors control the course of decomposition they must be very subtle.

Thermogravimetric analysis of all compounds in air, and in vacuo, also failed to establish a classification for the compounds of Tables 1 and

Can. J. Chem. Downloaded from www.nrcresearchpress.com by 210.87.254.6 on 09/05/12
For personal use only.

TABLE 2. Decomposition of copper(II) carboxylates, $Cu(CO_2R)_2$, on the mass spectrometer sample probe, indicating major decomposition products identified for those compounds which gave readily detectable amounts of volatile copper(I) carboxylates

Copper(II) carboxylate	R	Major decomposition products identified*
Acetate	CH_3	RCO_2H (115°)
Acetate-d_3	CD_3	RCO_2D (115°)
Propionate	C_2H_5	RCO_2H (130°), C_2H_4?, C_2H_2?
n-Butyrate	*n*-C_3H_7	RCO_2H (45°), C_3H_6, C_2H_6, C_2H_4?, C_2H_2?
iso-Butyrate	iso-C_3H_7	RCO_2H (40°), HCO_2H, C_2H_6, C_3H_6, CH_4, C_2H_4?, C_2H_2?
Difluoroacetate	CHF_2	RCO_2H (175°), H_2CO
Trifluoroacetate	CF_3	RCO_2H (135°)
Benzoate	C_6H_5	RCO_2H (175°), $(RCO)_2O$ (200°), RCO_2R
p-Fluorobenzoate	*p*-FC_6H_4	RCO_2H (130°), $(RCO)_2O$ (245°)
p-Chlorobenzoate	*p*-ClC_6H_4	RCO_2H (75°), $(RCO)_2O$ (130°), ROH?
o-Chlorobenzoate	*o*-ClC_6H_4	RCO_2H (175°), $(RCO)_2O$ (250°)
Pentafluorobenzoate	C_6F_5	RCO_2H (145°), R_2

*See footnote to Table 1.

(22). We obtained residues in all cases (except for the chloroacetates for which volatile copper(I) chlorides can be formed (Table 1)) indicating, at best, only partial conversion to copper(I) carboxylates for the compounds of Table 2. Residues of metal or metal oxide were reported in the thermogravimetric analysis of copper(II) acetate (23, 24), trifluoroacetate (25), *n*-butyrate (26), and halobenzoates (27), and metal bromide from copper(II) bromoacetate (28), though some differences in reported decomposition products probably reflect different experimental conditions and procedures. In Angel's early study (2) the yield of cuprous acetate was 3–4%. These observations are all in direct contrast to a recent report that copper(II) acetate can be sublimed unchanged in vacuo (29).

The Mass Spectra

Two basic types of fragmentation can be identified in the mass spectra of the copper-containing vapor species depending upon whether the carboxylate is derived from an aliphatic or an aromatic carboxylic acid. It is thus convenient to separate the data into Tables 3 and 4, where ion assignments, and the odd or even character of the ions, are also indicated in the conventional way. Only the relative intensities of copper-containing ions are shown since the origin (*i.e.* copper complex or other decomposition product) of other ions is ambiguous. The decompositions of the copper(II) carboxylates were apparently quite smooth since reproducible spectra could readily be obtained. We contend that only the dimer is present in significant amounts. Appreciable concentrations of monomer are considered unlikely since the relative intensities of mono-copper containing ions remained sensibly constant with variations of sample temperature indicating that mono- and di- copper-containing ions have a common parent molecular ion. This is to be expected if the copper(I) carboxylates have similar structures to the previously discussed structure for the acetate.

The atomic compositions of the ions in the spectra can be unambiguously assigned. Observed peak intensities within a given ion type agreed well with calculated intensities based on relative abundances of copper and chlorine isotopes (Cu_1, 63:65, 0.691:0.309; Cu_2, 126:128:130, 0.477:0.427:0.096; Cu_2Cl, 161:163:165:167, 0.362:0.439:0.176:0.013; Cu_2Cl_2, 196:198:200:202, 0.274:0.421:0.235:0.060). So that, in future investigations, spectra can more readily be compared, the relative intensities presented in Tables 3 and 4 are for the highest peak in the group of peaks, but if desired, the relative intensities for each ion type can be calculated by using the multipliers given in the footnote to Table 4.

Our previously reported (11) mass spectra of copper(I) acetate and benzoate have subsequently been confirmed by others (18, 29). Our mass spectrum of copper(I) trifluoroacetate is in substantial agreement with a reported spectrum (18).

In view of the structural information cited earlier, the only acceptable structure for the dimers is **1** in which the C—O bonds are of equal length and normal for a carboxyl group, the copper–copper separation is similar to that in the metal, and the O—Cu—O bond angle is

Can. J. Chem. Downloaded from www.nrcresearchpress.com by 210.87.254.6 on 09/05/12
For personal use only.

TABLE 3. Relative intensities of copper-containing ions in the mass spectra of aliphatic carboxylates, $Cu_2(CO_2R)_2$*

Ion	m/e:r.i. for R = CH_3† [150°]	C_2H_5 [180°]	n-C_3H_7 [95°]	iso-C_3H_7 [115°]	CHF_2 [195°]	CF_3 [180°]
$Cu_2(CO_2R)_2^{+\cdot}$	244(250):62	272:28	300:39	300:30	316:20	352:13
$Cu_2(CO_2R)CO_2^+$	229(232):13	—	—	—	265:4	283:8
$[Cu_2(CO_2R)_2 - 28]^{+\cdot}$	—	—	272:2‡	—	—	—
$Cu_2CO_2R^+$	185(188):100	199:100	213:100	213:100	221:100	239:100
$[Cu_2CO_2R - 28]^+$	—	—	185:3‡	—	—	—
Cu_2R^+	141(144):21	155:5	169:9	169:17	—	—
Cu_2F^+	—	—	—	—	145:58	145:65
$Cu_2O^{+\cdot}$	142(142):14	142:7	—	—	142:21	142:21
Cu_2H^+	—	127:11	127:10	127:16	—	—
$Cu_2^{+\cdot}$	126(126):11	126:9	126:6	126:9	126:37	126:27
$Cu(CO_2R)R^+$	—	—	193:3	—	—	—
$Cu(CO_2R)H^+$	—	—	151:3	—	—	—
$CuCO_2^+$	107(107):19	107:7	107:9	107:12	107:9	107:23
$CuCO^+$	—	91:14	—	—	91:5	—
Cu^+	63(63):27	63:10	63:9	63:12	63:93	63:95

*See footnote to Table 4. Sample temperatures in square brackets.
†*m/e* values in parentheses are for R = CD_3.
‡In the formation of these low intensity ions the loss of 28 a.m.u. could correspond to losses of CO or C_2H_4. The former is considered unlikely, and this peak is only observed when C_2H_4 can be eliminated from the R group.

TABLE 4. Relative intensities of copper-containing ions in the mass spectra of aromatic carboxylates, $Cu_2(CO_2R)_2$*

Ion	m/e:r.i. for R = C_6H_5 (220°)	p-F—C_6H_4 (225°)	p-Cl—C_6H_4 (175°)	o-ClC_6H_4† (260°)	C_6F_5† (245°)
$Cu_2(CO_2R)_2^{+\cdot}$	368:76	404:85	436:53	436:100	548:100
$Cu_2(CO_2R)R^{+\cdot}$	324:27	360:26	392:27		
$Cu_2CO_2R^+$	247:11	265:21	281:16		
$Cu_2R_2^{+\cdot}$	280:28	316:17	348:19		
Cu_2R^+	203:100	221:100	237:100	237:~20	293:~90
Cu_2F^+	—	145:24	—		
Cu_2H^+	127:4	—	127:21		
$Cu_2^{+\cdot}$	126:4	126:7	126:15		
CuR_2^+	217:52	253:20	—		
$CuR^{+\cdot}$	140:18	—	—		
Cu^+	63:52	63:95	63:74		

**m/e* values given are based on ^{63}Cu and ^{35}Cl. Except for R = C_6H_4Cl this gives the most abundant ion in the group. Relative intensities are given for the most abundant isotopic combination in the ion type and are not corrected to give relative total ion currents for the ion type. If desired these could be calculated by using the multipliers: Cu_1, ×1.45; Cu_2, ×2.10; Cu_2Cl, ×2.28; Cu_2Cl_2, ×2.38. (See text.) Sample temperatures in parentheses.
†Copper-containing ions were detected only at very low intensities and only the molecular ion and Cu_2R^+ could be measured.

only slightly smaller than 180°. This structure is in accord with the known preference for Cu(I) to form digonal bonds, a preference which has been interpreted in terms of formation of copper $d_{z^2}s$ hybrid orbitals (30).

The molecular ions are of high abundance in most of the spectra, indicating high stability. This can be understood from the following considerations. The molecular ions can be formally

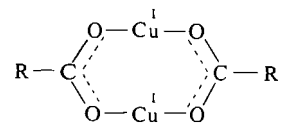

1

represented by either of the canonical structures **2** or **3**. In **2** one of the copper ions is formally in its +2 oxidation state, a state known to be stable

Can. J. Chem. Downloaded from www.nrcresearchpress.com by 210.87.254.6 on 09/05/12
For personal use only.

Can. J. Chem. Downloaded from www.nrcresearchpress.com by 210.87.254.6 on 09/05/12
For personal use only.

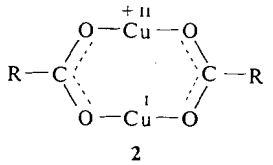

2

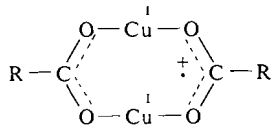

3

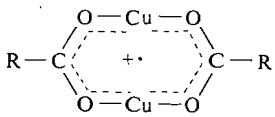

4

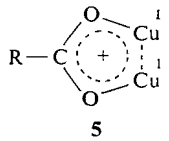

5

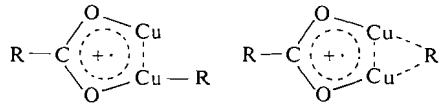

6*a* or 6*b*

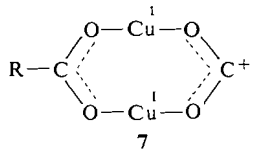

7

in the aqueous solution chemistry of copper. Since the pioneering work of Shannon and coworkers (19, 31), many correlations between mass spectral fragmentation patterns and the relative stabilities of metal oxidation states have been made (ref. 32 and references therein). In molecular orbital terms the relative stability of Cu(II) can be regarded as a ready donation of copper d_π electron density into ligand π orbitals (there is a vacancy in the bonding π orbital of **3**) and it seems preferable to regard the molecular ion by **4** in which the positive charge and unpaired electron are delocalized over π orbitals of both ligands and both copper atoms. Thus **4** should have high stability. Assignment of formal oxidation states in **4** is not useful since extensive mixing of the metal and ligand π orbitals is implied.

It has been possible to obtain a number of copper(I) carboxylate dimers to study the effect of the R group on the mass spectra. It is to be expected that electron withdrawing R groups would destabilize, while electron releasing R groups would stabilize the molecular ion. Thus, the relative intensities of the molecular ions are lowest when R = CF_3 and CHF_2.

Important fragment ions derived from the molecular ion can be represented by **5** and, when R is an aryl group, by **6**. **5** is formed from M^+ by elimination of $RCO_2^{\cdot}$, likely as $R^{\cdot}$ and CO_2. Whether these latter are lost sequentially or simultaneously cannot be determined unequivocally though intensities of the intermediate **7** are low, or not detectable, and when R = n-C_3H_7 a metastable peak was detected for the fragmentation $M^+ \rightarrow$ **5**. Certainly, if **7** was formed, elimination of CO_2 should occur readily. The ion $Cu_2(CO_2R)^+$ is evidently a very stable species since it is the base peak when R is an alkyl group. It is to explain this high stability that the structure **5** is suggested. The structure shown involves bonding interactions between the copper atoms (to be discussed later). Additional evidence for bond formation between the copper atoms is given by the presence in the spectra of other di-copper containing ions and in which copper–copper bonds cannot be denied. Furthermore, except when R = CF_3 or CHF_2, the total intensities of monocopper containing ions are relatively low. The lowered stability of **5** for these latter two cases can be understood by lower copper–oxygen bond strengths caused by the electronegative CF_3 or CHF_2 groups, an effect which is well-known. (For example, compare the stability constants of the copper(II) β-diketonate complexes: $Cu(acac)_2$, log $\beta_2 = 22.6$; $Cu(tfacac)_2$, log $\beta_2 = 17.2$; $Cu(hfacac)_2$, log $\beta_2 = 8$ (estimated), all in 75 volume % dioxane (33).) In addition, copper–fluorine bond formation can occur readily, a process which reflects the greater stability of these bonds compared with copper–hydrogen or copper–alkyl bonds.

When R is an aryl group, fragment ions which involve loss of CO_2 and rearrangement of R to the metal are prominent. The fragmentations are supported by metastable peaks as indicated below in the conventional way:

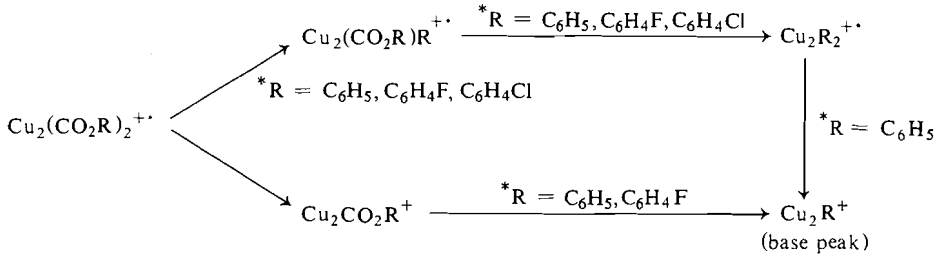

It can be noted that $Cu_2(CO_2R)R^{+\cdot}$ and $Cu_2R_2^{+\cdot}$ are radical ions (normally of lower stability than even-electron ions) and the only analogous rearrangement observed when R is an alkyl group gives the even-electron Cu_2R^+. Their presence reflects the higher stability of copper–aryl compared to copper–alkyl bonds, as evidenced by the relatively greater stability of arylcopper(I) (6, 7, 34) to alkylcopper(I) compounds (ref. 35 and references therein). Phenyl migration to copper in the mass spectra of other copper compounds (36, 37) and to other metals (37) has also been reported. The enhanced stability of the aryl-containing ions and radical ions evidently arises from π-electron delocalization between copper and aryl moieties, but we make no suggestion as to whether the aryl group occupies terminal or bridging sites with respect to the copper atoms. Bridging groups may not be essential for stability since copper(I) has a marked tendency to form copper clusters. Thus, some organocopper(I) compounds are polynuclear with octamers and tetramers apparently preferred (6, 7, ref. 35 and references therein). Copper clusters based on the cube and tetrahedron respectively were believed present (6, 7) in *m*-(trifluoromethyl)phenylcopper and *o*-(trifluoromethyl)phenylcopper.

Other noteworthy ions in the spectra include the even-electron species Cu_2F^+ and Cu_2H^+. Their precursor is probably $Cu_2(CO_2R)^+$ though only when R = CHF_2 was a metastable peak detected for the formation of Cu_2F^+ from this ion. Whenever fluorine is present in the ligand, Cu_2F^+ is formed, to the exclusion of Cu_2H^+, probably reflecting the greater strength of fluorine–copper compared to hydrogen–copper bonds. The Cu_2H^+ ion was observed in all other cases except for the acetate, reflecting the high energy required for formation of $CO_2 + CH_2$ compared to CO_2 + olefin (or aryne?) for the other complexes.

The major points of the spectra have been discussed. Further details of the fragmentations are obscured by absence of metastable transitions. Ions containing two copper atoms are noticeably persistent in the spectra and the only monocopper ion of consistently significant intensity is Cu^+.

The stability of the $Cu_2(CO_2R)^+$ ion is of interest. Assuming its point group to be C_{2v} and with axes as represented in **8** it is readily shown that the ligand σ orbitals transform as $A_1 + B_1$

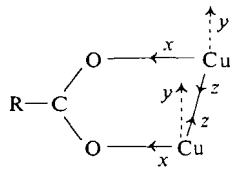

8

and the out-of-plane π orbitals as $A_2 + B_2$. Pairs of equivalent copper orbitals transform as follows: $A_1 + B_1$, s, p_x, p_z, d_{z^2}, d_{xz}, $d_{x^2-y^2}$; $A_2 + B_2$, p_y, d_{xy}, d_{yz}. If **8** is regarded as formed from RCO_2^- and two d^{10} Cu(I) ions, hybrid orbitals on each copper atom, having substantial p_x character would act as acceptors for the ligand σ electrons. However, if in-plane bonds between the copper atoms are to be formed then mixing of $4p_z$, 4s, $3d_{z^2}$, and $3d_{xz}$ orbitals (as major contributors) and promotion of a d electron are required. A σ bond (d_{z^2}, p_z major contributors) and/or π bond (d_{xz}) *might* be formed in this way but we are unable to estimate their importance.

The metal orbitals which could contribute to out-of-plane π-bonding are the p_y, d_{xy}, and d_{yz} orbitals. If mixing of these orbitals and d electron promotion occur then π and/or δ bond formation between the copper atoms is possible. Furthermore, delocalization of charge between ligand and metal out-of-plane orbitals is possible. This may account possibly for the stability of the ion, $Cu_2(CO_2R)^+$.

Can. J. Chem. Downloaded from www.nrcresearchpress.com by 210.87.254.6 on 09/05/12
For personal use only.

Can. J. Chem. Downloaded from www.nrcresearchpress.com by 210.87.254.6 on 09/05/12
For personal use only.

Our rationalization of the stability of $Cu_2(CO_2R)^+$ is regarded as speculative. On the one hand, the existence of the organocopper(I) cluster compounds suggests the possibility of direct copper–copper bonding. Furthermore, weak copper–copper δ bonding interactions have been postulated in some copper(II) carboxylates (38). On the other hand, on the basis of promotion energy considerations, direct copper–copper bonding was not considered likely in (4-methyl-2-cupriobenzyl)dimethylamine in spite of the short Cu—Cu distances of 2.377 and 2.389 Å (39). In a positive ion, however, this latter objection may well be outweighed by the opportunity provided to delocalize the positive charge.

Conclusions

Two basic types of fragmentation pathway can be identified in the mass spectra of dimeric cuprous carboxylates. For aliphatic carboxylates the spectra are dominated by even-electron ions formed by initial loss of $RCO_2\cdot$ from the molecular ion. For aromatic carboxylates a parallel fragmentation pathway initiated by loss of CO_2 from the molecular ion and migration of the aryl group to the metal is also present.

We thank the National Research Council of Canada for financial support of this work.

1. A. Angel. Trans. Chem. Soc. 345 (1906).
2. A. Angel and A. V. Harcourt. J. Chem. Soc. 1385 (1902).
3. A. Pechard. C. R. Acad. Sci. **136**, 504 (1903).
4. A. Ferretti. Can. J. Chem. **50**, 4056 (1972).
5. A. Cairncross, J. R. Roland, R. M. Henderson, and W. A. Sheppard. J. Am. Chem. Soc. **92**, 3187 (1970).
6. A. Cairncross and W. A. Sheppard. J. Am. Chem. Soc. **93**, 247 (1971).
7. A. Cairncross, H. Omura, and W. A. Sheppard. J. Am. Chem. Soc. **93**, 248 (1971).
8. J. Chodowska-Palicka and M. Nilsson. Acta Chem. Scand. **25**, 3451 (1971).
9. M. Calvin. J. Am. Chem. Soc. **61**, 2230 (1939).
10. H. D. de Ahne and H. D. Hardt. Z. Anorg. Allg. Chem. **383**, 263 (1971).
11. C. Reichert, D. K. C. Fung, D. C. K. Lin, and J. B. Westmore. Chem. Commun. 1094 (1968).
12. M. Kato, H. B. Jonassen, and J. C. Fanning. Chem. Rev. **64**, 99 (1964).
13. J. Lewis. Pure Appl. Chem. **10**, 27 (1965).
14. C. Oldham. Prog. Inorg. Chem. **10**, 225 (1968).
15. T. Ogura, R. D. Mounts, and Q. Fernando. J. Am. Chem. Soc. **95**, 949 (1973).
16. M. G. B. Drew, D. A. Edwards, and R. Richards. J. Chem. Soc. D, 124 (1973).
17. A. E. Blakeslee and J. L. Hoard. J. Am. Chem. Soc. **78**, 3029 (1956).
18. D. A. Edwards and R. Richards. Inorg. Nucl. Chem. Lett. **8**, 783 (1972).
19. C. G. MacDonald and J. S. Shannon. Aust. J. Chem. **19**, 1545 (1966).
20. M. C. Sneed, J. L. Maynard, and R. C. Brasted. Comprehensive inorganic chemistry. 2nd ed. Van Nostrand, New York. 1954. p. 106.
21. J. Lewis and F. Mabbs. J. Chem. Soc. 3894 (1965).
22. D. C. K. Lin and J. B. Westmore. Unpublished results.
23. D. A. Edwards and R. N. Hayward. Can. J. Chem. **46**, 3443 (1968).
24. K. C. Patil, G. V. Chandrashekhar, M. V. George, and C. N. R. Rao. Can. J. Chem. **46**, 257 (1968).
25. M. J. Baillie, D. H. Brown, K. C. Moss, and D. W. A. Sharpe. J. Chem. Soc. A, 3110 (1968).
26. L. Van My, G. Périnet, and P. Bianco. Bull. Soc. Chim. Fr. 3104 (1966).
27. F. Charbonnier, J. Gazet, and J. Gauthier. C. R. Acad. Sci. C, **266**, 373 (1968).
28. M. F. Obier and Y. Dartiguenave. C. R. Acad. Sci. C, **266**, 1694 (1968).
29. Kh. Sh. Khariton, A. V. Ablov, and G. A. Popovich. Dokl. Acad. Nauk SSSR, **204**, 1374 (1972).
30. L. E. Orgel. J. Chem. Soc. 4186 (1958).
31. J. S. Shannon and J. M. Swan. Chem. Commun. 33 (1965).
32. M. J. Lacey and J. S. Shannon. Org. Mass Spectrom. **6**, 931 (1972).
33. L. G. Van Uitert, W. C. Fernelius, and B. E. Douglas. J. Am. Chem. Soc. **75**, 457 (1953).
34. A. Camus and N. Marsich. J. Organomet. Chem. **14**, 441 (1968).
35. M. F. Lappert and R. Pearce. J. Chem. Soc. D, 24 (1973).
36. C. Reichert and J. B. Westmore. Can. J. Chem. **48**, 3213 (1970).
37. M. J. Lacey, C. G. MacDonald, and J. S. Shannon. Org. Mass Spectrom. **1**, 115 (1968).
38. B. N. Figgis and R. L. Martin. J. Chem. Soc. 3837 (1956).
39. J. M. Guss, R. Mason, I. Søtofte, G. van Koten, and J. G. Noltes. J. Chem. Soc. D 446 (1972).

The Limiting Conductance of $^1/_3In^{3+}$ Ion and the Conductances of Aqueous Solutions of Indium Trichloride

A. N. CAMPBELL

Department of Chemistry, University of Manitoba, Winnipeg, Manitoba R3T 2N2

Received March 19, 1973

The direct determination of the limiting conductance of $^1/_3In^{3+}$ ion is not possible because of hydrolysis. This figure has been obtained by a method which may be open to criticism as 56.3 mhos, at 25°. If anything, this figure is too high.

La détermination directe de la conductance limite de l'ion $^1/_3In^{3+}$ n'est pas possible à cause de l'hydrolyse. Le chiffre de 56.3 mhos à 25° a été obtenu par une méthode qui peut être ouverte à la critique. Quoiqu'il en soit, cette valeur est trop élevée. [Traduit par le journal]

Can. J. Chem., **51**, 3006 (1973)

The only investigation to be found in the literature of the conductances of aqueous solutions of indium trichloride is that of Thiel (1), who found a rapid increase in conductance, with dilution, in the dilute range ($\Lambda = 225$ mhos, for $c = 0.0003$ equiv/l), which he correctly attributed to hydrolysis. It occurred to me that it might be possible to measure the limiting conductance of $\frac{1}{3}In^{3+}$ experimentally, if the hydrolysis were suppressed by having excess of HCl present.

Some rough work with a p*H* meter gave the impression that 0.001 *N* HCl would be sufficiently strong to suppress the hydrolysis. Work was therefore undertaken on the conductance of indium trichloride in (*a*) conductance water, (*b*) HCl of strength 0.001 *N*. When pure water is the solvent, it is sufficient to subtract from the specific conductance of the solution that of the solvent by way of correction, but this is not sufficient when HCl solution is the solvent, because the ionic strength has a fixed minimum value, even when no indium salt is present. I know no way of calculating this effect theoretically, and therefore I made the assumption that the effect would be the same in an electrolyte of similar type, *viz.* lanthanum trichloride, a salt which does not undergo hydrolysis. The method I have adopted, therefore, was to determine the specific conductances of the solution in HCl and of the HCl solvent, and subtract one from the other. The final step was to plot the equivalent conductance against the square root of the ionic strength ($\sqrt{6c + 0.001}$), and to extrapolate the straight line plots which resulted to $\sqrt{6c + 0.001} = 0.0316$ ($c = 0$). This value of the limiting conductance ($\Lambda^{0\prime}$) when subtracted from the value of Λ^0 in pure water (known for lanthanum chloride) gave, it is to be hoped, the correction factor to be added to the limiting conductance of indium trichloride in 0.001 *N* HCl. The argument assumes that because La^{3+} and In^{3+} have the same charge, this is the only factor affecting the speed of the ion, at comparable ionic strength. The argument assumes, for instance, that the hydration of the ions is the same. As for the formation of complex ions, which undoubtedly occurs with In^{3+}, this is hardly likely to affect the conductance at limiting dilution. For the sake of completeness, I also determined the conductances of KCl and of $BaCl_2$ in 0.001 *N* HCl, since the conductances of these salts in water are well known. As expected, the differences between $\Lambda^{0\prime}$ and Λ^0 became less with decreasing valence (3:1, 2:1, 1:1).

All measurements were made at 25°. The conductances of barium chloride and of potassium chloride were plotted against $\sqrt{3c + 0.001}$ and $\sqrt{c + 0.001}$ respectively.

Experimental

Solid indium trichloride trihydrate was purchased from British Drug Houses but no attempt was made to obtain the anhydrous salt.[1] Lanthanum chloride heptahydrate was obtained from the Kerr-McGee Chemical Corporation. It was generally used in this form but was occasionally dehydrated by heating at 150°. Analysis of the solutions in the transport number work was done by precipitation as the hydrate and ignition to the oxide. Conductance water was obtained from a Haereus quartz still, using

[1]The author is indebted to Cominco Ltd. of Trail, British Columbia, for a concentrated solution (13.37 *N*) of pure indium chloride and a supply of indium metal.

Can. J. Chem. Downloaded from www.nrcresearchpress.com by 210.87.254.5 on 09/05/12
For personal use only.

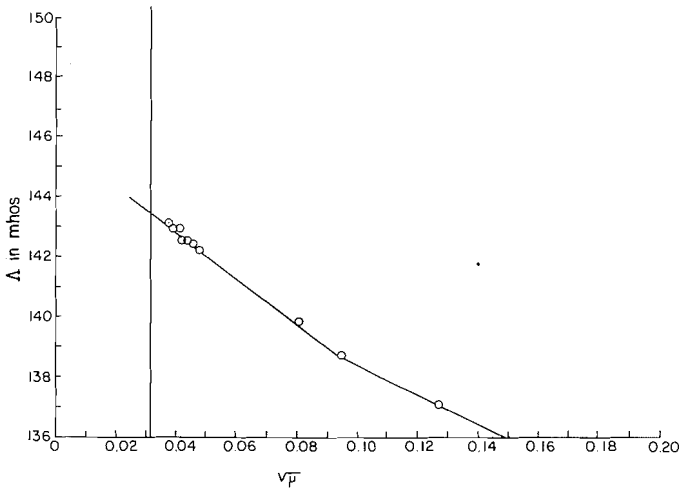

FIG. 1. Equivalent conductance of KCl in the presence of 0.001 *N* HCl, *vs.* (ionic strength)$^{1/2}$ ($\sqrt{c}$).

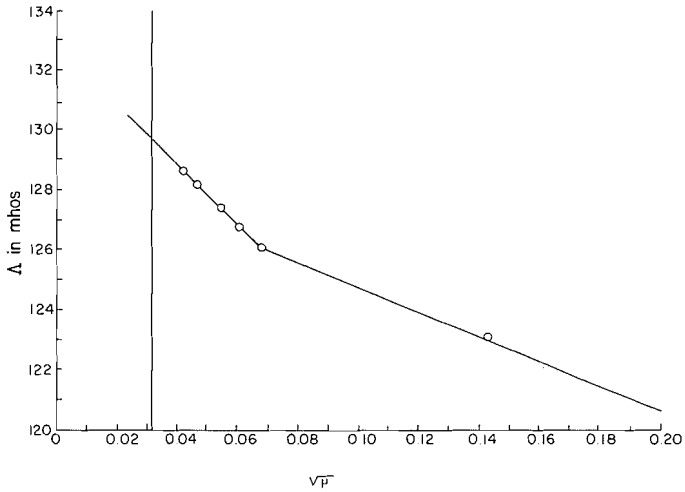

FIG. 2. Equivalent conductance of $BaCl_2$ in the presence of 0.001 *N* HCl *vs.* (ionic strength)$^{1/2}$ ($\sqrt{3c}$).

water which had previously been passed through an ion exchange column. No attempt was made to remove carbon dioxide from the water, so the specific conductance usually ran about 1×10^{-6} mho.

Conductance measurements were made on a Beckmann conductance bridge, model RC—18A, using, when necessary, a Shedlovsky quartz cell. In short, the technique was modern and accurate. The transference number was measured by the Hittorf method, using a silver anode and a silver/silver chloride cathode. In order to avoid passivity, the current was kept low, sometimes as low as 1.5 mA, with a correspondingly long run time, on one occasion as long as 72 h. Despite popular belief, this does not cause any change in the concentration of the intermediate compartment. Quantity of electricity was measured as the product of current by time. Absolutely constant current was supplied from an apparatus built by the National Research Council of Canada.

The results varied rather widely between 0.426 and 0.485 for the transport number of the cation. On the supposition that these limits are valid, the limiting conductance of $\frac{1}{3}In^{3+}$ ion must lie between 57 and 72 mho.

The numerical data are to be found in the Depository of Unpublished Data.[2] Figure 1 gives the equivalent conductance of potassium chloride in 0.001 *N* HCl, versus $\sqrt{c + 0.001}$. Extrapolated to $\sqrt{0.001} = 0.0316$, the limiting conductance appears to be 143.50, against a

[2]Photocopies may be obtained at a nominal charge, from the Depository of Unpublished Data, National Science Library, National Research Council of Canada, Ottawa, Canada K1A 0S2.

Can. J. Chem. Downloaded from www.nrcresearchpress.com by 210.87.254.5 on 09/05/12
For personal use only.

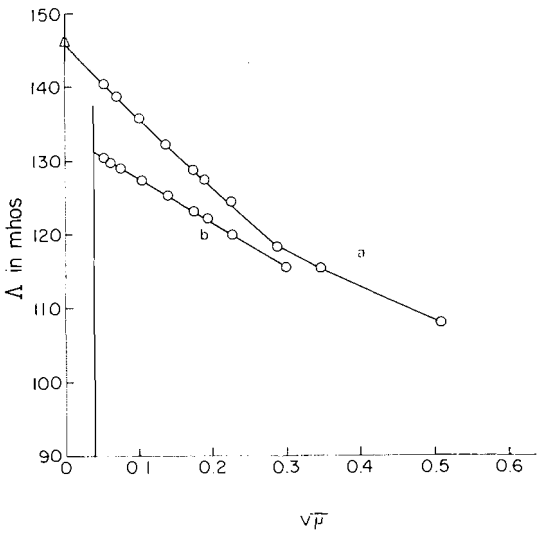

FIG. 3. Equivalent conductance of $LaCl_3$ in water (a) and in 0.001 *N* HCl (b) *vs.* $\sqrt{6c}$ and $\sqrt{6c + 0.001}$.

limiting conductance in pure water of 149.86. This indicates that the limiting conductance of a 1:1 electrolyte is reduced by 6.36 mhos, in the presence of 0.001 *N* HCl.

To show the effect of valence on the reduction in Λ^0, the conductance of $BaCl_2$ in 0.001 N HCl was measured.

Figure 2 shows the results for barium chloride; Λ is plotted *vs.* $\sqrt{3c + 0.001}$. The limiting conductance in acid appears to be 129.7 against a water value of 139.98. For a 2:1 electrolyte, the limiting conductance is reduced by 10.3 mhos.

Figure 3 gives the corresponding data for lanthanum trichloride, plotting Λ *vs.* $\sqrt{6c + 0.001}$. The limiting conductance appears to be 131.7, as against a value in pure water of 146.0. This would imply that the limiting conductance is reduced by 14.3 mhos, for a 1:3 electrolyte.

It appears that the effect of 0.001 *N* HCl in reducing conductance increases with the valence of the ion.

The corresponding data for indium chloride are given in Fig. 4.

Conclusion

The figures for the most dilute solutions of indium chloride in water are not shown, but the steep ascent of the curve is sufficiently obvious, indicating the hydrolysis of indium chloride in water. The sudden rise of the curve appears to commence at $\sqrt{6c + 0.001} = 0.3$, *i.e.* at $c = 0.015$ *N*, suggesting that hydrolysis is not appreciable above this concentration. The (large scale) extrapolation of Λ in the presence of acid gives a limiting value of 118.3 mhos. If to this is added 14.3 for a 1:3 electrolyte, the figure of 132.6 is arrived at for the limiting conductance of indium trichloride in water. From this the limiting transference number of indium in indium trichloride would appear to be 0.425 and the limiting conductance of $\frac{1}{3}In^{3+}$ ion, 56.3. This figure is lower than those of most ternary ions but higher than those of many binary ions. Since the effective diameter of an ion is largely a question of the degree of solvation, this would imply that the In^{3+} ion is more highly hydrated than say, the Al^{3+} ion.

The form of the curve expressing the conductance of indium chloride against the ionic strength in the presence of an acid shows that the limiting

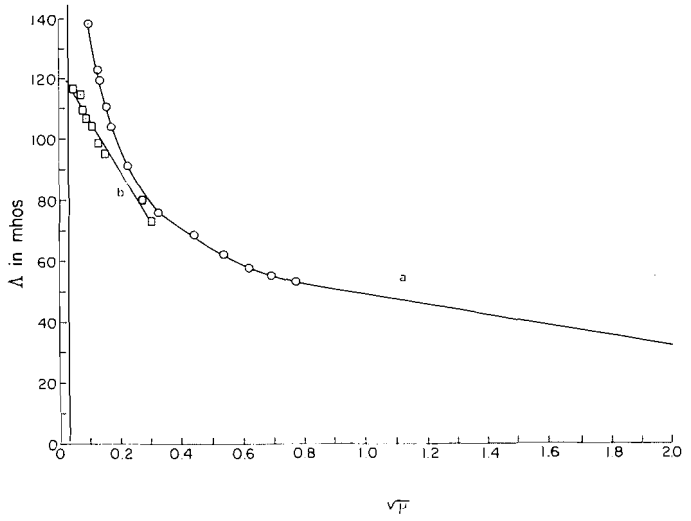

FIG. 4. Equivalent conductance of $InCl_3$ in water (a) and in the presence of 0.001 *N* HCl (b) *vs.* $\sqrt{6c}$ and $\sqrt{6c + 0.001}$.

Can. J. Chem. Downloaded from www.nrcresearchpress.com by 210.87.254.5 on 09/05/12
For personal use only.

slope is greater than the Onsager slope. The obvious conclusion is that hydrochloric acid of strength 0.001 *N* is not sufficient entirely to suppress hydrolysis. Incidentally, if this were the case, my figure for the limiting conductance of $\frac{1}{3}In^{3+}$ would be still lower and this seems, on the face of it, improbable. Against this explanation of incomplete suppression of hydrolysis, I advance the following facts. (*1*) The conductance of a strong (13.37 *N*) solution of indium chloride in pure water is almost negligible ($\Lambda = 1.04$ mhos) and (*2*) the transport number indicates a lowest possible value of 56.6 for the ionic conductance. To explain the anomalous slope, I suggest that the ionization of indium trichloride takes place in stages

$$\rightarrow InCl_2 \rightleftarrows InCl_2 + Cl'$$
$$\rightleftarrows InCl^{2+} + 2\ Cl' \rightleftarrows In^{3+} + 3\ Cl'$$

The actual mechanism may be much more complicated, but the scheme is sufficient for its purpose. The final stage of the ionization, preponderating only in very dilute solutions would account for the steep slope of the graph.

1. A. THIEL. Z. Anorg. Chem. **40**, 332 (1904).

Can. J. Chem. Downloaded from www.nrcresearchpress.com by 210.87.254.5 on 09/05/12
For personal use only.

^{13}C–H Coupling Constants in Cyclic Systems; a Probe for Hyperconjugation and Homoconjugation?

NICK H. WERSTIUK, ROLAND TAILLEFER, RUSSELL A. BELL, AND BRIAN SAYER

Department of Chemistry, McMaster University, Hamilton, Ontario

Received September 25, 1972[1]

^{13}C–H coupling constants have been determined for bicyclic and tricyclic carbonyl compounds. In comparison to acyclic and monocyclic ketones these systems show an increase in the coupling constant at the bridgehead alpha to the carbonyl group.

Les constantes de couplage ^{13}C–H ont été déterminées dans le cas de composés bicycliques et tricycliques comportant une fonction carbonyle. Par comparaison avec des cétones acycliques ou monocycliques, ces systèmes ont montré une augmentation de la constante de couplage pour la position en tête de pont alpha du groupe carbonyle. [Traduit par le journal]

Can. J. Chem., **51**, 3010 (1973)

Can. J. Chem. Downloaded from www.nrcresearchpress.com by 210.87.254.6 on 09/05/12
For personal use only.

Introduction

The correlation between hybridization and coupling constant for directly bonded ^{13}C—H and ^{13}C—^{13}C nuclei has provided an experimental tool for the estimation of s character in a carbon–hydrogen or carbon–carbon bond (1–10). In this area experimental and theoretical studies (11–13) have centered mainly on alicyclic hydrocarbons to avoid substituent effect problems.

Our study of the chemistry of bicyclic diones (14) has necessitated that we obtain hybridizational and conformational information on these systems. To that end a study of ^{13}C–H and ^{13}C–^{13}C coupling constants in bicyclic and tricyclic systems has been undertaken to ascertain whether or not the coupling constants are hybridizational probes in the presence of polar groups.

Results and Discussion

This communication reports the coupling constants for C_1—H, C_3—H, and C_4—H in **1**–**16**. The data are listed in Table 1.

That the difference between J_{C_1-H} and J_{C_4-H} in ketones **2** and **8**, and the thione **11** as well as J_{C_4-H} in **8** and **9** is not accountable directly in terms of an inductive effect is established by the following facts. The J_{C-H} values (CH_3-) for ethane, acetone, and acetophenone are 126, 127, and 127 Hz, respectively (12). Also, Ellis and Maciel (8) have shown that J_{C-H} alpha to the carbonyl group in 2,2-dimethylcyclopropanone (160), cyclobutanone (134.8), and cyclopentanone (129.5), respectively, is identical to J_{C-H} for the corresponding precursor hydrocarbon (cyclopropane, 161; cyclobutane, 134.6; cyclopentane, 128.5). Interestingly, a correlation, which utilizes the Swain–Lupton F (field effect) values (18) for $-I^+$ and $-I^-$ groups (12), provides information about the influence of inductive effects on J_{C-H}. The plot of J_{C-H} *vs.* the F values (Fig. 1) for a series of substituted methanes CH_3—X, where X is a $-I^+$ or $-I^-$ group, establishes that distinct correlations exist for the two types of substituents. The plot for the latter is located at a constant 15–20 Hz below the $-I^+$ plot. Thus, although the same sensitivity to $-I^+$ and $-I^-$ substituents is indicated, there must be either an attenuation of the inductive effect or there are

TABLE 1. ^{13}C–H coupling constants*

Substrate	C-1	C-3	C-4
1	142 ± 1	130 ± 2	142 ± 1
2	152 ± 1	134 ± 1	142 ± 2
3	157 ± 1		157 ± 1
4	142 ± 1		142 ± 1
5	153 ± 1	138 ± 1	155 ± 1
6	155 ± 1	130 ± 2	144 ± 2
7	144 ± 2		139 ± 2
8	152 ± 1		142 ± 2
9			150 ± 2
10	159 ± 1		158 ± 1
11	155 ± 1		143 ± 2
12		134 ± 2	143 ± 1
13			159 ± 1
14	152 ± 1		152 ± 1
15	144 ± 1		144 ± 1
16	141 ± 1		133 ± 2

*The ^{13}C shift assignments for a majority of the substrates have been reported previously (15–17).

[1]Revision received April 26, 1973.

Can. J. Chem. Downloaded from www.nrcresearchpress.com by 210.87.254.6 on 09/05/12
For personal use only.

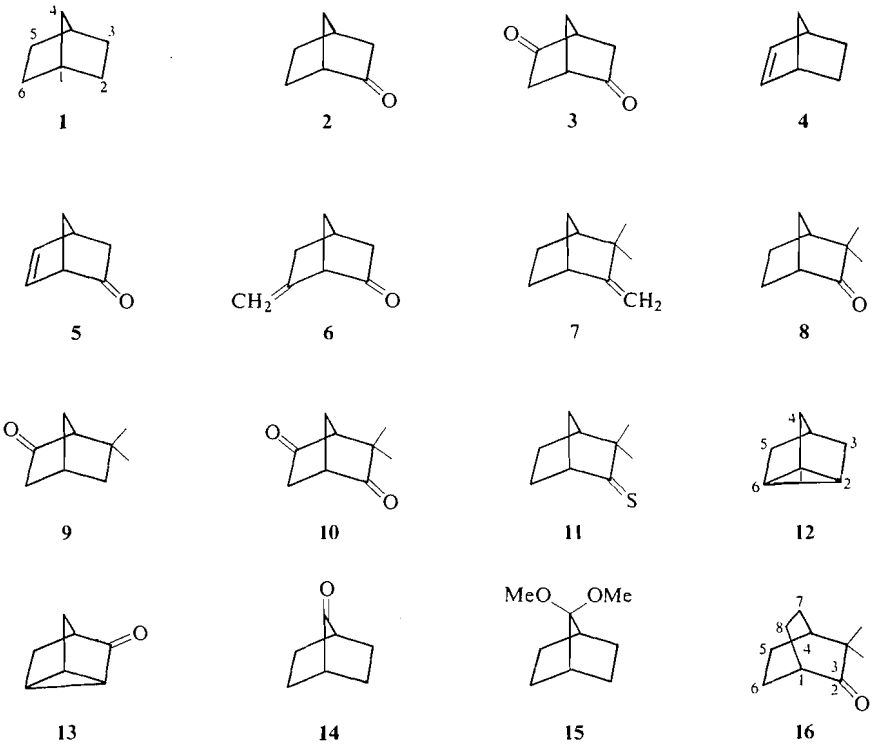

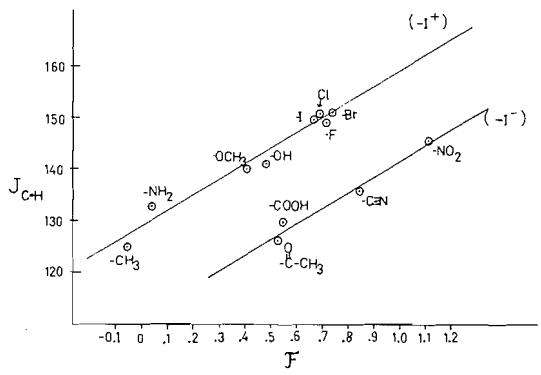

FIG. 1. Plot of J_{C-H} (H—CH_2—X) *vs.* the field effect values *F*.

other unknown factors which operate by a constant factor to decrease J_{C-H}. Conceivably, hyperconjugative interaction between C—H bonds and the π system of the $-I^-$ substituent (19) could contribute to the attenuation constant. Nevertheless, the correlations support the contention that $-I^+$ and $-I^-$ substituents interact differently with C—H bonds.

Strain effects also do not account adequately for the increase in J_{C-H} at the bridgehead since J_{C_4-H} and J_{C_3-H} in the [2.2.1]-system are insensitive to the total strain energy.[2] That is, while the strain energy (20) increases through the series **1**, **4**, and **12** (18.4, 22.8, 42.9 kcal/mol, respectively) the change in J_{C_4-H} is minimal. Compare also J_{C_3-H} for **1** and **12**. Furthermore, a comparison of the C–H coupling constants (alpha to the carbonyl) and strain energies (SE) (21) for cyclobutanone, cyclopentanone, and norcamphor with those of the parent hydrocarbons establishes that there is no correlation between ΔJ and Δ(SE).

Several factors may contribute to the unexpected increase in J_{C_1-H} in **2**, **3**, **8**, **9**, **10**, **11**, and **14** and J_{C_4-H} in **13**. Conceivably, hyperconjugative interaction between the appropriate strained σ bond and the carbonyl or thiocarbonyl is important and alters the hybridization at C-1 and C-4. Interestingly, Olah *et al.* (22) have reported a J_{C_1-H} value of 152 ± 5 Hz for the 2-phenylnorbornyl cation. Also, while the effect of a benzoyl group on J_{C-H} in a methyl group is minimal (*vide supra*) there is an increase of 11 Hz

[2]It is understood that not all the "strain" in each case is located in the bridgehead bonds.

TABLE 2. Coupling constant and strain energy differences

Substrate	SE		Δ(SE)	ΔJ*
	Ketone	Hydrocarbon		
Cyclobutyl	29.03	27.17	1.86	0
Cyclopentyl	6.40	7.53	—1.13	0
Bicyclo[2.2.1]heptyl	18.54	17.90	0.64	10±2†

*Alpha to the carbonyl group.
†At C-1.

TABLE 3. ^{1}H chemical shifts (p.p.m.)

Substrate	H-1	H-4	H-5	H-6	Reference
Norcamphor	2.39	2.54			26
Nortricyclane		1.91			23
Nortricyclanone		1.80			
Norbornene	2.81	2.81	5.93	5.93	27
Norbornenone	2.87	3.14	6.54	6.09	27

in $J_{\alpha C-H}$ and $J_{\beta C-H}$ in the conjugated system benzoylcyclopropane (173 Hz) over cyclopropane (162 Hz) (23). Possibly, the attenuating hyperconjugation component (*vide supra*) is removed in the [2.2.1]-systems because the bridgehead C—H bond is aligned perpendicular to the π system, thereby unmasking the inductive effect of the carbonyl group. Conceivably, the alignment of the lone pairs on the oxygen or sulfur with respect to the C—H bond is critical in the norbornyl systems and in benzoylcyclopropane.

Nevertheless, the J_{C-H} values for 7-norbornanone (152 ± 1), nortricyclanone (159 ± 1), and the ketal **15** (144 ± 1) account for the reactivity order observed in the KO-*t*-Bu-catalyzed exchange studies carried out by Gassman and Zalar (24). While 25% of C-1,C-4 hydrogen in 7-norbornanone is exchanged for deuterium after 48 h at 200°, exchange is 75% complete at C-4 in nortricyclanone after only 29 h. The dimethyl ketal of nortricyclanone does not exchange at C-4.

Therefore, since J_{C_1-H} for camphenilone (**8**) is 152 ± 1 Hz, it is likely that some of the deuterium incorporated into **8** at C-1 and -6 via homoenolization (25) is actually introduced through exchange at the bridgehead. We are currently studying base-catalyzed exchange in 6,6-dimethylcamphenilone to check this.

We propose therefore that the upfield shift of C_1—H over C_4—H in norcamphor and C_4—H in nortricyclanone (Table 3) over nortricyclane, is in each case primarily a consequence of "sp-like" hybridization rather than shielding by the carbonyl in the former and the cyclopropyl ring in the latter (23). ^{13}C chemical shift data for nortricyclanone and nortricyclane (Table 4) further support this proposal. That is, while C-1 experiences a downfield shift of 12.1 p.p.m. in norcamphor over norbornane the downfield shift of C-4 in nortricyclanone relative to nortricyclane is only 6.8 p.p.m. and is consistent with more "sp-like" hybridization at C-4, as established by J_{C_4-H}.

The data for norbornenone (**5**) are of interest. While the effect of the introduction of a double bond into norcamphor on J_{C_1-H} is minimal, J_{C_3-H} and J_{C_4-H} (155 ± 1) show dramatic increases. Therefore, in a valence bond description, **17** contributes significantly to the ground state of norbornenone and affects J_{C_4-H}. That **17** must be considered is further supported by ^{1}H and ^{13}C chemical shift data listed in Tables 3 and 4 respectively.

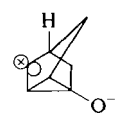

17

Possibly, cyclic conjugation, resulting from conjugation (through space) between C-6 and the carbonyl group at C-2 and hyperconjugation through three σ bonds (28, 29, 30, 31), operates

Can. J. Chem. Downloaded from www.nrcresearchpress.com by 210.87.254.6 on 09/05/12
For personal use only.

TABLE 4. ^{13}C chemical shifts*

Substrate	C-1	C-2	C-3	C-4	C-5	C-6	C-7	Reference
Norbornane	37.3	30.6	30.6	37.3	30.6	30.6	39.2	16
Norcamphor	49.4	216.1	44.6	35.1	27.0	23.6	37.2	This work
Nortricyclane	11.7	11.7	34.1	30.6	34.1	11.7	34.1	9
Nortricyclanone	18.5	16.3	214.1	37.4	31.2	18.5	31.2	This work
Norbornene	42.0	24.8	24.8	42.0	135.8	135.8	48.8	16
Norbornenone	55.8	212.8	36.7	40.0	143.0	130.8	50.8	16

*Downfield from TMS.

in **5**. The cyclic conjugation could alter J_{C-H} by changing the molecular orbital description of the carbon framework and ΔE for the C—H bond. Several σ-coupled systems, namely diazabicyclooctane (29, 32), *exo*- and *endo*-dicyclopentadienones (28), diazaadamantone (28), tricyclo[4.4.2.0^{1,6}]dodeca-3,8-diene-11,12-dione (33), and *exo*- and *endo*-polycyclic cyclobutanones (34) warrant study to determine whether or not the C–H coupling constants on the σ framework are influenced by this hyperconjugation. The bridgehead coupling constants in diones **3** and **10** are 157–159 Hz. The unexpected increase in J_{C-H} over norcamphor may be due to improved hyperconjugative alignment of the C_1—C_6 and C_4—C_5 bonds as a result of a synchro-twist (35) as indicated by models and/or the interaction of the carbonyl groups via three σ-bond conjugation.

Although the contribution of each of the factors which determines the magnitude of J_{C-H} cannot be described precisely at present, the bridgehead coupling constants for the diones **3** (C-1, C-4; 157 ± 1) and **11** (C-1, C-4; 159 ± 1) and norbornenone (**5**) (C-4; 155 ± 1) establish that enhanced rates of base-catalyzed exchange should be expected at these sites. Studies on 3,3-dimethylnorbornenone and 3,3,6,6-tetramethylnorbornane-2,5-dione are presently underway.

Experimental

The ^{13}C–H spin–spin coupling constants were obtained on a Varian HA-100 spectrometer at 23.5 kG and 25.1 MHz. The operating probe temperature was +55 °C. Field frequency stabilization was achieved by use of an external (1.5 mm capillary) $^{13}CS_2$ lock and chemical shift measurements required for the location of appropriate carbons were made initially relative to internal dioxane and then to tetramethylsilane. A sample volume of 0.2–0.3 ml was used in a 5 mm o.d. sample tube with dioxane or CCl_4 as solvent where necessary. A signal accumulation of 300–500 scans on a Varian Associates C-1024 time averaging computer was required. J_{C-H} was obtained from the doublets and triplets by drawing an envelope for each absorption (broadened by long range coupling) and using the center (at half the peak width at half height) of the Gaussian curves. Each value quoted is the mean of 3–4 determinations. Our value of 142 ± 1 for J_{C_1-H} in norbornane is identical to that obtained from satellite studies (36). Furthermore, our value of J_{C_1-H} for **6** was identical to that obtained on an XL-100 FT system.[3] The comparisons provide a calibration for our values.

The ketones and diones used in this study were prepared in conjunction with base-catalyzed exchange studies (14) and the syntheses will be described in subsequent publications.

*Thiocamphenilone (**11**)*

Camphenilone (1.0 g, > 98% purity) was dissolved in absolute ethanol (25 ml), and HCl and H_2S were bubbled through the reaction mixture (37) for 2h. The reaction was monitored by withdrawing and quenching aliquots with solid sodium bicarbonate under pentane and analyzing the pentane solutions by g.l.p.c. on a 10 ft × ¼ in. 10% Carbowax on a Chromosorb W column maintained at 150° with He as the carrier gas. When the reaction was 85–95% complete the mixture was quenched by adding it to a slurry of solid $NaHCO_3$ and purified pentane that was cooled in ice. The pentane solution that was obtained after filtration was concentrated by distillation through a 6 in. helix-packed column until two layers separated. The pentane layer was removed, dried, and concentrated further (2–3 ml). The thione (0.30 g), an orange glassy solid, was isolated by preparative g.l.p.c. utilizing the conditions described above.

Financial support by the National Research Council of Canada is gratefully acknowledged. We thank Professor Warkentin for generous samples of **14** and **15** and Professor Stothers for a generous sample of **16**.

1. N. MULLER and D. E. PRITCHARD. J. Chem. Phys. **31**, 768, 1471 (1959).
2. J. N. SHOOLERY. J. Chem. Phys. **31**, 1427 (1959).
3. J. RANFT. Ann. Phys. Leipzig, **8**, 322 (1961).
4. R. M. LYNDEN-BELL and N. SHEPPARD. Proc. R. Soc. Ser. A, **269**, 385 (1962).
5. K. FREI and H. J. BERNSTEIN. J. Chem. Phys. **38**, 1216 (1963).
6. F. J. WEIGERT and J. D. ROBERTS. J. Am. Chem. Soc. **89**, 5962 (1967).

[3]We thank Dr. I. C. P. Smith of the National Research Council of Canada for a spectrum of **6**.

Can. J. Chem. Downloaded from www.nrcresearchpress.com by 210.87.254.6 on 09/05/12
For personal use only.

7. F. J. WEIGERT, M. WINOKUR, and J. D. ROBERTS. J. Am. Chem. Soc. **90**, 1566 (1968).
8. P. D. ELLIS and G. E. MACIEL. J. Am. Chem. Soc. **92**, 5829 (1970).
9. J. B. GUNTZNER, M. JAUTELAT, J. B. DENCE, R. A. SMITH, and J. D. ROBERTS. J. Am. Chem. Soc. **92**, 7107 (1970).
10. R. D. BERTRAND, D. M. GRANT, E. L. ALLRED, J. C. HENSHAW, and A. B. STRONG. J. Am. Chem. Soc. **94**, 997 (1972).
11. J. A. POPLE and D. P. SANTRY. Mol. Phys. **8**, 1 (1964).
12. G. E. MACIEL, J. W. MCIVER, JR., N. S. OSTLUND, and J. A. POPLE. J. Am. Chem. Soc. **92**, 1, 11, 4151, 4497, 4506 (1970).
13. M. RANDIC, Z. MEIĆ, and A. RUBČIĆ. Tetrahedron, **28**, 565 (1972).
14. N. H. WERSTIUK and R. TAILLEFER. Can. J. Chem. **48**, 3966 (1970).
15. E. WENKERT, A. O. CLOUSE, D. W. COCHRAN, and D. DODDRELL. Chem. Commun. 1433 (1969).
16. E. LIPPMAA, T. PEHK, J. PAASIVIKTA, N. BELIKOVA, and A. PLATÉ. Org. Mag. Res. 581 (1970).
17. N. H. WERSTIUK, R. TAILLEFER, R. A. BELL, and B. SAYER. Can. J. Chem. **50**, 2146 (1972).
18. C. G. SWAIN and E. C. LUPTON, JR. J. Am. Chem. Soc. **90**, 4328 (1968).
19. A. LIBERLES, B. O. LEARY, J. E. EILERS, and D. R. WHITMAN. J. Am. Chem. Soc. **94**, 6894 (1972).
20. R. B. TURNER, P. GOEBEL, B. J. MALLON, W. VON E. DOERING, J. F. COBURN, JR., and M. POMERANTZ. J. Am. Chem. Soc. **90**, 4315 (1968).
21. N. L. ALLINGER, M. T. TRIBBLE, and M. A. MILLER. Tétrahedron, **28**, 1173 (1972).
22. G. A. OLAH, A. M. WHITE, J. R. DEMEMBER, A. COMMEYRAS, and C. Y. LUI. J. Am. Chem. Soc. **92**, 4627 (1970).
23. P. H. WEINER and E. R. MALINOWSKI. J. Phys. Chem. **71**, 2791 (1967).
24. P. G. GASSMAN and F. V. ZALAR. J. Am. Chem. Soc. **88**, 3070 (1966).
25. A. NICKON, J. L. LAMBERT, S. J., and J. E. OLIVER. J. Am. Chem. Soc. **88**, 2787 (1966).
26. D. G. FARNUM and G. MEHTA. J. Am. Chem. Soc. **91**, 3526 (1969).
27. S. E. MASAR and H. KRIEGER. Soumen Kemistil. B, **42**, 3 (1969).
28. R. C. COOKSON, J. HENSTOCK, and J. HUDEC. J. Am. Chem. Soc. **88**, 1059, 1060 (1966).
29. R. HOFFMAN, A. IMAMIERA, and W. J. HEBRE. J. Am. Chem. Soc. **90**, 1499 (1968).
30. R. HOFFMANN, E. HEILBRONNER, and R. GLEITER. J. Am. Chem. Soc. **92**, 706 (1970).
31. R. HOFFMANN. Accs. Chem. Res. **4**, 1 (1971).
32. E. HEILBRONNER and K. A. MUSZKAT. J. Am. Chem. Soc. **92**, 3818 (1970).
33. S. C. NEELY, R. FINK, D. VAN DER HELM, and J. J. BLOOMFIELD. J. Am. Chem. Soc. **93**, 4903 (1971).
34. R. D. MILLER and V. Y. ABRAITYS. J. Am. Chem. Soc. **94**, 663 (1972).
35. C. ALTONA and M. SUNDARALINGAM. J. Am. Chem. Soc. **92**, 1995 (1970).
36. K. TORI, R. MUNEYUKI, and H. TANIDA. Can. J. Chem. **41**, 3142 (1963).
37. R. H. ABELES, R. F. HATTON, and F. H. WESTHEIMER. J. Am. Chem. Soc. **79**, 712 (1957).

Can. J. Chem. Downloaded from www.nrcresearchpress.com by 210.87.254.6 on 09/05/12
For personal use only.

Can. J. Chem. Downloaded from www.nrcresearchpress.com by 210.87.254.105 on 09/05/12
For personal use only.

Canadian Journal of Chemistry

Published by
THE NATIONAL RESEARCH COUNCIL OF CANADA

Journal canadien de chimie

Publié par
LE CONSEIL NATIONAL DE RECHERCHES DU CANADA

Volume 51 Number 18 September 15, 1973 Volume 51 numéro 18 15 septembre 1973

Structure of the Capsular Polysaccharide of *Klebsiella* K-type 20[1]

YUEN-MIN CHOY AND GUY G. S. DUTTON

Department of Chemistry, University of British Columbia, Vancouver, British Columbia

Received March 5, 1973

Methylation, periodate oxidation, and partial hydrolysis studies on the capsular polysaccharide, and on the carboxyl reduced polymer, of *Klebsiella* K20 show the structure to consist of a repeating unit

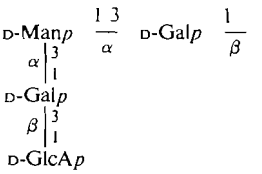

The anomeric linkages were determined by p.m.r. spectroscopy of the carboxyl reduced polysaccharide, and periodate degraded polysaccharides. The p.m.r. spectroscopy of the original polysaccharide also showed the presence in the polysaccharide of one *O*-acetyl group per eight sugar residues.

Des réactions de méthylation, d'oxydation au périodate et d'hydrolyse partielle, sur le polysaccharide capsulaire ainsi que sur le polymère avec le groupe carboxyle réduit, de *Klebsiella* K20 ont démontré que la structure se compose d'une unité fondamentale qui se répète à savoir:

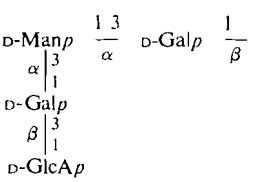

On a donc démontré que la chaîne principale comporte un acide aldobiouronique comme ramification latérale. La *Klebsiella K20* est le premier exemple de ce type de structure.

Les liaisons anomériques ont été identifiées à l'aide de la spectroscopie r.m.n. en ce qui a trait au polysaccharide avec le groupe carboxyle réduit et aux polyosides apparentés obtenus par dégradations successives selon la méthode de Smith.

Le spectre r.m.n. du polysaccharide original a aussi révélé la présence d'un groupe *O*-acétyle par rapport à huit sucres. Cependant la position de liaison de ce groupe n'a pu être déterminée.

[Traduit par le journal]

Can. J. Chem., **51**, 3015 (1973)

Qualitative analyses of the capsular polysaccharides of the 80 serotypes of *Klebsiella* bacteria have been provided by Nimmich (1, 2) who has shown that the great majority contain D-glucuronic acid in combination with hexose and deoxyhexose sugars. Despite the amount of qualitative information available on *Klebsiella* polysaccharides at the start of our work detailed structures were only known for types K2, K8, and K54, (3, and references therein) to which

[1]Presented in part at the 56th Canadian Chemical Conference of the Chemical Institute of Canada, Montreal, Quebec, June, 1973.

Can. J. Chem. Downloaded from www.nrcresearchpress.com by 210.87.254.105 on 09/05/12
For personal use only.

must now be added K9 (4), K21 (5), and K24 (6). Each of these structures is composed of a repeat unit involving a single sugar side chain. In addition, the type K5 is distinguished by the lack of carbohydrate side chain (7) and K56 by the lack of uronic acid (8). The structure of K-type 20 is the first of these capsular polysaccharides to be encountered with an aldobiouronic acid side chain. A preliminary report has appeared (9) which showed that the aldobiouronic acid is 3-*O*-(β-D-glucopyranosyluronic acid)-D-galactose and the nature of the repeat unit is now discussed.

The polysaccharide after purification by Cetavlon, deionization, and freeze drying had $[\alpha]_D^{20}$ +94° and a neutralization equivalent (by titration) of 701. The p.m.r. spectrum, run at room temperature, of a 2% solution of the sodium salt of the polysaccharide in D_2O showed a singlet at τ 7.8 characteristic of *O*-acetyl and the absence of pyruvate. Determination of the acetyl:sugar ratio was hampered by the presence of the large HOD peak which overlapped the region associated with the signals due to the anomeric protons. However, integration of the ring protons and the acetate signal indicated one acetyl group to approximately eight sugar units. The presence of the *O*-acetyl group was also confirmed by formation of the hydroxamic ester. An attempt to locate the position of the *O*-acetyl group using the procedure of de Belder and Norrman (10) was unsuccessful due to the very low yield, probably because of the high molecular weight (5–9 × 10^5) of the *Klebsiella* capsular polysaccharide. Similar difficulties have been encountered in other cases (6, 7).

Acid hydrolysis of the polysaccharide showed the rapid liberation of an aldobiouronic acid and complete hydrolysis gave D-mannose, D-galactose, and the aldobiouronic acid in equal amounts (9). Partial hydrolysis using the apparatus of Galanos *et al.* (11) gave a dialyzate containing an aldobiouronic acid as the major component together with an aldotetrauronic acid in addition to neutral sugars. The acidic compounds were separated on paper and partial hydrolysis of the aldotetrauronic acid, after borohydride reduction, gave galactitol, mannose, and aldotri- and aldobiouronic acids. The last named and the aldobiouronic acid isolated from the total hydrolysis were identical with that already described (9).

On methylation and hydrolysis, the original capsular polysaccharide gave the neutral sugars shown in Table 1A and when the uronic acid in the methylated polymer was reduced before hydrolysis the compounds in Table 1B were obtained. Methylation of the residual polysaccharide recovered from the partial hydrolysis gave the results shown in Table 1C which show that 4,6-di-*O*-methyl-D-mannose has largely been replaced by 3,4,6-tri-*O*-methyl-D-mannose thus demonstrating that the aldobiouronic acid is joined to position 3 of the mannose unit which in turn is linked through position 2. The small quantities of tetramethyl sugar arose from some fragmentation of the main chain.

TABLE 1. Methyl ethers from the hydrolyzates of methylated *Klebsiella* K20 polysaccharides

Sugars	Sample* A†	B	C	D	E
2,3,4,6-Tetra-*O*-methyl-D-mannose			2		
2,3,4,6-Tetra-*O*-methyl-D-galactose			3	1	
3,4,6-Tri-*O*-methyl-D-mannose			9		1
2,4,6-Tri-*O*-methyl-D-galactose	+	2	12	1	1
2,3,4-Tri-*O*-methyl-D-glucose		1			
4,6-Di-*O*-methyl-D-mannose	+	1	1	1	

*A, neutral sugars from methylated original K20 polysaccharide; B, reduced methylated K20 polysaccharide; C, methylated residual polysaccharide after partial hydrolysis; D, methylated polysaccharide (S1) recovered from first Smith degradation; E, methylated S2.
†Approximate molar ratios; (+) signifies present.

The methylation results in conjunction with the oligosaccharides isolated indicate the general nature of the polysaccharide. Confirmation of the proposed structure and definitive assignment of each anomeric configuration were obtained by successive Smith periodate degradations (12, 13), conveniently carried out on the carboxyl reduced polymer.

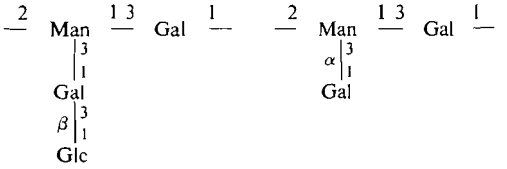

Carboxyl reduced K20 Polysaccharide S1

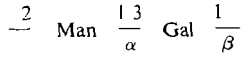

Polysaccharide S2

Carboxyl reduced polysaccharide (5, 14, 15) on hydrolysis gave D-galactose, D-glucose, and D-mannose in the ratio 2:1:1. The p.m.r. spectrum run in D_2O at 95° indicated the presence of two α-D- and two β-D-linkages (Table 2).

TABLE 2. P.m.r. data on *Klebsiella* K20 capsular polysaccharide and derived polysaccharides and oligosaccharides

Repeating unit of compound	τ value* (coupling constant, Hz)	Ratio of integral	Proton† assignment
$\frac{2}{-}$ Man $\frac{1\ 3}{\alpha}$ Gal $\frac{1}{\beta}$ $\alpha\vert^{3}_{1}$ Gal $\beta\vert^{3}_{1}$ Glc	4.78 + 4.86	2	α-Gal $\frac{1\ 3}{-}$ Man α-Man $\frac{1\ 3}{-}$ Gal
	5.00 (*ca.* 6)	1	β-Glc $\frac{1\ 3}{-}$ Gal
	5.45(7)	1	β-Gal $\frac{1\ 2}{-}$ Man
$\frac{2}{-}$ Man $\frac{1\ 3}{\alpha}$ Gal $\frac{1}{\beta}$ $\alpha\vert^{3}_{1}$ Gal	4.63	1	α-Gal $\frac{1\ 3}{-}$ Man
	4.73	1	α-Man $\frac{1\ 3}{-}$ Gal
	5.40(7)	1	β-Gal $\frac{1\ 2}{-}$ Man
$\frac{2}{-}$ Man $\frac{1\ 3}{\alpha}$ Gal $\frac{1}{\beta}$	4.80	1	α-Man $\frac{1\ 3}{-}$ Gal
	5.48(6)	1	β-Gal $\frac{1\ 2}{-}$ Man
	4.75	0.5	α-Gal—OH
GlcA $\frac{1\ 3}{\beta}$ Gal—OH	5.40(7)	1.4	β-Gal—OH
			β-GlcA $\frac{1\ 3}{-}$ Gal

*Spectra run in D_2O with external tetramethylsilane (τ = 10 at 100 MHz).
†All sugars have D-configuration and are pyranose.

These signals may be assigned as a result of the periodate oxidations described below.

On the basis of the proposed structure the terminal D-glucose unit (from D-glucuronic acid) is the only periodate susceptible residue in the carboxyl reduced polysaccharide and it was found that 0.57 mol of periodate per hexose was reduced. Smith degradation gave glycerol and a degraded polysaccharide (S1) with $[\alpha]_D$ +129° and in the p.m.r. spectrum of which the signal at τ 5.00 had disappeared (Table 2). This is consistent with the loss of one sugar residue with a β-D-glycosidic bond. The signal at τ 5.00 had a width of about 6 Hz but no clearly distinguishable doublet. Hydrolysis of methylated S1 gave the compounds shown in Table 1D.

In S1 the terminal galactose may now be oxidized by periodate (consumption 0.8 mol/hexose) and degradation gave glycerol and a new polysaccharide (S2). This polymer had $[\alpha]_D$ +57° and the p.m.r. spectrum showed the presence of one α-D- and one β-D-linkage, in contrast to two α-D- and one β-D-linkages in S1, thus demonstrating that the lateral D-galactose is joined to the main chain by an α-glycosidic bond. Furthermore, since the signal at τ 5.48 exhibited a splitting of 6 Hz this must be due to the galactose unit in the main chain which therefore has a β-D-linkage. The methylation results on S2 are given in Table 1E.

All the evidence so far adduced is consistent with the proposed structure but the results do not exclude the possibility that the main chain is composed of blocks of D-mannose and of D-galactose units. That this is not the case is clearly demonstrated by subjecting polysaccharide S2 to one further Smith degradation. Examination on paper of the hydrolysis products, after reduction with borohydride, showed only glycerol and a compound with R_{Gal} 1.05; no slower moving compounds were observed. Hydrolysis of the latter compound gave only glycerol and D-galactose. This experiment thus provides convincing proof that the main chain, and hence the side chains, have a regular alternating structure. The structure of the capsular polysaccharide of *Klebsiella* K-type 20 may therefore be written

$$\frac{2}{-}\ \text{D-Man}p\ \frac{1\ 3}{\alpha}\ \text{D-Gal}p\ \frac{1}{\beta}$$
$$\alpha\vert^{3}_{1}\ \text{D-Gal}p$$
$$\beta\vert^{3}_{1}\ \text{D-GlcA}p$$

Can. J. Chem. Downloaded from www.nrcresearchpress.com by 210.87.254.105 on 09/05/12
For personal use only.

Can. J. Chem. Downloaded from www.nrcresearchpress.com by 210.87.254.105 on 09/05/12
For personal use only.

Experimental

General methods are as previously described (5).

Isolation and Properties of Capsular Polysaccharide

A culture of *Klebsiella* K-type 20 (889/50) was grown as for K21 (5) and after 3 days the cells were diluted with 1% phenol and centrifuged for 30 min at 60 000 × gravity. The clear supernatant was poured into ethanol and the product was redissolved in water. The acidic polysaccharide was precipitated with Cetavlon, redissolved in the minimum volume of 4 *M* sodium chloride, and isolated by precipitation into ethanol. The yield of pure polysaccharide was approximately 3 g per 4 l of medium and two such batches were pooled for the structure investigations.

The purified polysaccharide was dissolved in distilled water, deionized with Amberlite IR 120 resin, dialyzed, and freeze-dried. The product had $[\alpha]_D^{20}$ +94° (*c* 0.21, water), N, 0%. The equivalent weight of the polysaccharide was found to be 701 (theory 680) by titration with 0.03 *M* sodium hydroxide.

The above neutralized polysaccharide was lyophilized. The residue was dissolved in D_2O and exchanged twice by lyophilization. The p.m.r. spectrum of a 2% solution of D_2O showed a peak at τ 7.8 indicating the presence of *O*-acetyl. Due to the high viscosity of this solution, the magnitude of the HOD peak was so great that difficulty was encountered in obtaining quantitative information between the anomeric protons and the acetyl group. However, integration of the ring protons and the acetyl group showed there is approximately one acetyl per eight sugar units (5).

The presence of acetate was also confirmed by methanolysis of the polysaccharide and identification of the methyl acetate using the hydroxylamine – ferric chloride reagent (7). Attempted location of the *O*-acetyl group using the procedure of de Belder and Norrman (10) was unsuccessful due to the extremely low yield in the reaction with methyl vinyl ether.

Hydrolysis of the Polysaccharide

Polysaccharide (150 mg) was hydrolyzed with 2 *M* trifluoroacetic acid (TFA) at 100° for 2 h. After evaporation, the hydrolyzate was found by paper chromatography in solvent A to contain D-mannose, D-galactose, and a component with the mobility of an aldobiouronic acid (R_{Gal} 0.26). The hydrolyzate was separated into neutral and acidic fractions using ion-exchange resins (Amberlite IR 120 and Duolite A-4). The neutral fraction contained D-mannose and D-galactose in a 1 : 1 ratio as determined by the g.l.c. of the alditol acetates (column a) which permitted recovery of the individual compounds and identification of D-mannitol hexaacetate, m.p. 118–120°, and galactitol hexaacetate, m.p. 162–164°.

The D-configuration of galactose was shown by a positive reaction on part of the hydrolyzate with D-Galactostat reagent and of mannose by the positive circular dichroism (c.d.) curve of mannitol hexaacetate (16). The acidic component (60 mg, R_f 0.16, solvent C) was found to have $[\alpha]_D^{20}$ +17° (*c* 0.75, water) and an equivalent weight of 349 when titrated with 0.03 *M* sodium hydroxide ($C_{12}H_{20}O_{12}$ requires 356). A portion (20 mg) of the aldobiouronic acid was dissolved in 3 ml of 0.3 *M* acetate buffer (p*H* 4.8), 3 mg of β-D-glucosidase was added, and the solution was incubated at 38° for 6 h. D-Galactose was found by paper chromatography in solvent B to be the only neutral sugar present, whereas the presence of D-galactose, D-glucuronic acid, and D-glucuronolactone was demonstrated in solvent A. The same results were obtained by hydrolysis of the aldobiouronic acid (10 mg) using 3.5 *M* hydrochloric acid at 100° for 2.5 h.

The aldobiouronic acid (20 mg) was methylated and hydrolyzed with 3 *M* hydrochloric acid at 95° for 3.5 h. Paper chromatography in solvent E showed the presence of 2,4,6-tri-*O*-methyl-D-galactose (R_f 0.66) and 2,3,4-tri-*O*-methyl-D-glucuronic acid (R_f 0.22). The identity of 2,4,6-tri-*O*-methyl-D-galactose was confirmed by g.l.c.–m.s. of the alditol acetate. Another portion of the capsular polysaccharide (20 mg) was hydrolyzed (0.4 *M* TFA, 95°, 2 h) and the aldobiouronic acid was found as the only mobile component on paper chromatography in solvent A.

Partial Hydrolysis of Polysaccharide

K20 polysaccharide (1 g) was partially hydrolyzed (0.4 *M* TFA, 30 h, 95°) using the apparatus described by Galanos, Lüderitz, and Himmelspach (11). The degraded polysaccharide in the dialysis sac was kept for subsequent methylation. The dialyzate was evaporated and separated into neutral and acidic fractions by ion-exchange resin. On paper chromatography (solvent C) the acidic fraction was shown to contain an aldobiouronic acid (R_{Gal} 0.45) as the major component together with aldotetrauronic acid (R_{Gal} 0.08) and trace amounts of aldotriuronic acid (R_{Gal} 0.30). The acids were separated by paper chromatography (solvent C) and analyzed as follows.

The aldobiouronic acid (80 mg) was found to have identical characteristics as the aldobiouronic acid isolated previously. P.m.r. data: τ 4.75 (0.5H); 5.4, J = 7 Hz (1.4H).

The aldotetrauronic acid (50 mg) had an equivalent weight of 650. The acid (10 mg) was partially hydrolyzed (1 *M* TFA, 95°, 1 h) and paper chromatography (solvent A) showed the presence of D-galactose as the principal monosaccharide with traces of D-mannose and a series of aldobiouronic, aldotriuronic, and aldotetrauronic acids which had the same mobilities as the components of the original mixtures. The aldotetrauronic acid (10 mg) was reduced with sodium borohydride and, after removal of the borate, the product was hydrolyzed with 2 *M* TFA for 1/2 h. On paper chromatography (solvents A and B), the neutral compound found was galactitol, which was confirmed by g.l.c. of the alditol acetate, m.p. 162–164°. Also produced were the same aldobio-, aldotrio-, and aldotetrauronic acids (solvent C) described above.

Methylation Analysis of the Polysaccharide

Capsular polysaccharide (90 mg) was methylated by the method of Hakomori to give a product which showed no absorption at 3600 cm^{-1}. A portion (20 mg) was hydrolyzed (2 *M* TFA, 100°, 2 h). Analysis of hydrolyzate by paper chromatography (solvent E) showed the presence of 2,4,6-tri-*O*-methyl-D-galactose (R_f 0.66), 4,6-di-*O*-methyl-D-mannose (R_f 0.59), a methylated aldobiouronic acid (R_f 0.35), and a small quantity of 2,3,4-tri-O-methyl-D-glucuronic acid. The hydrolyzate was separated into neutral and acidic fractions using ion-exchange resin (Duolite A-4). On paper chromatography, the neutral

Can. J. Chem. Downloaded from www.nrcresearchpress.com by 210.87.254.105 on 09/05/12
For personal use only.

fraction was shown to contain 2,4,6-tri-*O*-methyl-D-galactose (R_f 0.4, solvent D) and 4,6-di-*O*-methyl-D-mannose (R_f 0.29, solvent D). Reduction ($NaBH_4$), removal of borate, acetylation in a sealed tube (pyridine and acetic anhydride 1:1, 1 ml, 95°, 15 min), and injection (in ethyl acetate) onto column b at 200° showed two peaks.

The component eluted first had a retention time (6.9 min) and mass spectrum identical to authentic 2,4,6-tri-*O*-methyl-D-galactitol triacetate. The second component was similarly identical in retention time (9.9 min) and mass spectrum to authentic 4,6-di-*O*-methyl-D-mannitol tetraacetate (Table 1A). Demethylation and reacetylation of the partially methylated alditol acetate gave the corresponding galactitol hexaacetate, m.p. 166–169° and D-mannitol hexaacetate, m.p. 119–122°.

A portion (4 mg) of the acidic fraction was hydrolyzed (3.5 *M* HCl, 100°, 2 h) and the hydrolyzate was found to contain 2,4,6-tri-*O*-methyl-D-galactose (analyzed by g.l.c.–m.s. of the alditol acetate) as the only neutral sugar, and 2,3,4-tri-*O*-methyl-D-glucuronic acid (R_f 0.22, solvent E). Another portion (5 mg) was methanolyzed with 2% methanolic – hydrogen chloride and reduced with lithium borohydride. After removal of the borate the product was hydrolyzed (0.5 *M* H_2SO_4, 4 h). Paper chromatography showed the presence of 2,3,4-tri-*O*-methyl-D-glucose (R_f 0.62, solvent D) and 2,4,6-tri-*O*-methyl-D-galactose (R_f 0.40, solvent D). G.l.c. of the alditol acetates showed two peaks at 9.5 and 8.7 min (column b, 200°, flow rate 60 ml/min) which were identical in retention time and mass spectrum to the corresponding authentic alditol acetates.

Another sample of methylated polysaccharide (20 mg) was reduced with lithium borohydride and hydrolyzed. Quantitative analysis of the derived alditol acetates by g.l.c. (column a, 180–217° at 2°/min) showed the presence of 2,4,6-tri-*O*-methyl-D-galactose (24.5 min), 2,3,4-tri-*O*-methyl-D-glucose (26 min), and 4,6-tri-*O*-methyl-D-mannose (29.8 min) in a molar ratio of 2:1:1 (Table 1B). The identity of the methylated sugars was again confirmed by m.s. of the derived alditol acetates.

Methylation of Degraded Polysaccharide

A portion of the degraded polysaccharide (120 mg) recovered from the partial hydrolysis was methylated and the product was hydrolyzed (2 *M* TFA, 100°, 4 h) to give (paper chromatography) 3,4,6-tri-*O*-methyl-D-mannose (R_f 0.58, solvent D) and 2,4,6-tri-*O*-methyl-D-galactose (R_f 0.38, solvent D) as the major components, together with minor components of 2,3,4,6-tetra-*O*-methyl-D-galactose and D-mannose, and faint traces of methylated aldobiouronic acid (solvent E). The hydrolyzate was reduced with sodium borohydride, acetylated, and injected onto column b at 190°. 2,3,4,6-Tetra-*O*-methyl-D-mannose (6.5 min), 2,3,4,6-tetra-*O*-methyl-D-galactose (8.0), 3,4,6-tri-*O*-methyl-D-mannose (12.0), 2,4,6-tri-*O*-methyl-D-galactose (16.0), and 4,6-di-*O*-methyl-D-mannose (18.0) were found in a ratio of 2:3:9:12:1 (Table 1C). The mass spectrum of 3,4,6-tri-*O*-methyl-D-mannose was identical to an authentic sample.

Reduction of the Capsular Polysaccharide

Capsular polysaccharide (0.5 g) was converted into the methyl ester propionate and reduced with lithium borohydride to give the reduced polysaccharide (0.4 g), $[\alpha]_D^{24}$ +95.5° (*c* 2, water). The reduced polysaccharide (20 mg) was hydrolyzed (2 *M* TFA, 100°, 4 h) and analysis of the hydrolyzate by paper chromatography and g.l.c. showed D-galactose, D-glucose, and D-mannose in a ratio of 2:1:1.

Galactitol hexaacetate had m.p. 166–169°, D-glucitol hexaacetate had m.p. 96–98°, and D-mannitol hexaacetate had m.p. 119–122°. The hydrolyzate gave a positive test with D-Glucostat reagent, thus confirming the D-configuration of glucuronic acid. The p.m.r. spectrum of the reduced K20 polysaccharide was run in D_2O at 95° and was shown to give anomeric signals at τ (4.78 + 4.86), 5.00, and 5.45 in the ratio of 2:1:1 (Table 1). The signals at τ 5.45 showed a distinct doublet with a coupling constant of 7 Hz.

Smith Periodate Degradations and Methylation Studies of the Degraded Polysaccharides

The carboxyl reduced polysaccharide (66 mg) was dissolved in 10 ml water and 20 ml 0.05 *M* sodium metaperiodate was added. After 66 h, 0.57 mol of periodate per hexose unit was consumed. Ethylene glycol (1.5 ml) was added and the product was then dialyzed overnight against running water. Sodium borohydride (0.5 g) was added and the solution was left overnight. The solution was deionized with Amberlite IR 120, freeze-dried, and the product was distilled with several portions of methanol. The derived polyalcohol was dissolved in 5 ml 0.5 *M* TFA and left at room temperature overnight. On paper chromatography (solvent A) only glycerol was identified (R_f 0.45). The product was dialyzed against 2 l of distilled water. The dialyzate when evaporated was found to contain glycerol by paper chromatography and g.l.c. (glycerol triacetate 6.4 min, column b at 150°). The degraded polysaccharide (S1) remaining in the dialysis sac was freeze-dried. It has $[\alpha]_D^{20}$ +129°. P.m.r. spectrum of the degraded polysaccharide in D_2O showed signals at τ 4.6, 4.78, and 5.4 in a ratio of 1:1:1. The signals at τ 5.4 showed a doublet with coupling constant of 7 Hz, all other coupling constants being small. The degraded polysaccharide was then methylated by the Hakomori method and hydrolyzed. Paper chromatography showed the presence of 2,3,4,6-tetra-*O*-methyl-D-galactose (R_f 0.70, solvent D), 2,4,6-tri-*O*-methyl-D-galactose (R_f 0.38, solvent D), and 4,6-di-*O*-methyl-D-mannose (R_f 0.29, solvent D). The ratio was found to be 1.05:0.9:1 by g.l.c. of the alditol acetates (Table 1D). 2,3,4,6-Tetra-*O*-methyl-D-galactitol acetate had a retention time of 13 min (column b, 160–200° at 2°/min) and had a mass spectrum identical to an authentic sample.

Another portion of the carboxyl reduced polysaccharide (0.3 g) was oxidized by periodate as described previously to yield 0.2 g of the degraded polysaccharide (S1). To this degraded polysaccharide S1 (0.2 g) 50 ml of 0.04 *M* sodium periodate was added. Periodate consumption was found to be 0.8 mol per hexose unit after 2 days. The derived polyaldehyde after reduction with sodium borohydride was partially hydrolyzed with 0.4 *M* TFA at room temperature overnight. Glycerol was found to be the only component mobile on paper chromatography in solvent A (R_f 0.44). The product was dissolved in 5 ml of water and dialyzed against 1 l of distilled water. The substance that remained in the dialyzing sac was freeze-dried to yield 0.1 g of a new degraded polysaccharide (S2). The degraded polysaccharide S2

had $[\alpha]_D^{20}$ +57° (*c* 0.35, water). P.m.r. of this polysaccharide was run in D_2O at 95° and showed signals at τ 4.8 and 5.48 in a ratio of 1:1. The signals at τ 5.48 consisted of a doublet with coupling constant of 6 Hz while that at τ 4.8 had a very small coupling constant.

A portion (27 mg) of the degraded polysaccharide S2 was methylated by the Hakomori method and hydrolyzed (2 *M* TFA, 100°, 4 h). Paper chromatography (solvent D) showed the presence of 3,4,6-tri-*O*-methyl-D-mannose (R_f 0.57) and 2,4,6-tri-*O*-methyl-D-galactose (R_f 0.38). The ratio was found to be 1:1 by g.l.c. of the alditol acetate when 3,4,6-tri-*O*-methyl-D-mannose had a retention time (22 min, column b, 180–200° at 2°/min) and a mass spectrum identical to an authentic sample.

The degraded polysaccharide (S2, 43 mg) was further degraded by periodate. After the usual work-up the derived polyalcohol was hydrolyzed with 0.5 *M* TFA at room temperature for 6 h. The product was then reduced with sodium borohydride. After removal of the borate, paper chromatography in solvents B and C showed the presence of glycerol (R_{Gal} 4.3, solvent B; R_{Gal} 2.1, solvent C) and an unknown component (R_{Gal} 1.05, solvent B; R_{Gal} 1.2, solvent C).

The unknown component was separated by paper chromatography in solvent B, and then hydrolyzed with 2 *M* TFA for 2 h. On paper chromatography in solvents A and B, D-galactose and glycerol (R_{Gal} 4.6, solvent A; R_{Gal} 2.4, solvent B) were identified. The product was reduced with sodium borohydride and acetylated. On g.l.c., glycerol triacetate (retention time 8 min, column a, 140–200°) and galactitol hexaacetate (retention time 58 min) were found in equimolar amounts.

We are grateful to Dr. I. Ørskov for a culture of *Klebsiella* K20 (889/50), to Dr. P. J. Salisbury for growing the bacteria and to Dr. J. J. R. Campbell and Dr. J. B. Hudson for the use of their centrifuges.

We appreciate the continued financial support of the National Research Council and Y.M.C. acknowledges with thanks the award of a Killam Fellowship.

1. W. NIMMICH. Z. Med. Mikrobiol. Immunol. **154**, 117 (1968).
2. W. NIMMICH. Acta Biol. Med. Germ. **26**, 397 (1971).
3. G. G. S. DUTTON and Y. M. CHOY. Carbohydr. Res. **21**, 169 (1972).
4. B. LINDBERG, J. LONNGREN, J. L. THOMPSON, and W. NIMMICH. Carbohydr. Res. **25**, 49 (1972).
5. Y. M. CHOY and G. G. S. DUTTON. Can. J. Chem. **51**, 198 (1973).
6. Y. M. CHOY, G. G. S. DUTTON, and A. M. ZANLUNGO, Can. J. Chem. **51**, 1819 (1973).
7. G. G. S. DUTTON and M. T. YANG. Can. J. Chem. **51**, 1826 (1973).
8. Y. M. CHOY and G. G. S. DUTTON. Can. J. Chem. This issue.
9. Y. M. CHOY and G. G. S. DUTTON. J. Bacteriol. **112**, 635 (1972).
10. A. N. DE BELDER and B. NORRMAN. Carbohydr. Res. **8**, 1 (1968).
11. C. GALANOS, O. LÜDERITZ, and K. HIMMELSPACH. Eur. J. Biochem. **8**, 332 (1969).
12. I. J. GOLDSTEIN, G. W. HAY, B. A. LEWIS, and F. SMITH. Methods Carbohydr. Chem. **5**, 361 (1965).
13. G. G. S. DUTTON and K. B. GIBNEY. Carbohydr. Res. **25**, 99 (1972).
14. G. G. S. DUTTON and S. KABIR. Anal. Lett. **4**, 95 (1971).
15. G. G. S. DUTTON and S. KABIR. Carbohydr. Res. **28**, 187 (1973).
16. G. M. BEBAULT, J. M. BERRY, Y. M. CHOY, G. G. S. DUTTON, N. FUNNELL, L. D. HAYWARD, and A. M. STEPHEN. Can. J. Chem. **51**, 324 (1973).

Can. J. Chem. Downloaded from www.nrcresearchpress.com by 210.87.254.105 on 09/05/12
For personal use only.

Structure of the Capsular Polysaccharide of *Klebsiella* K-type 56[1]

YUEN-MIN CHOY AND GUY G. S. DUTTON
Department of Chemistry, University of British Columbia, Vancouver, British Columbia

Received March 5, 1973

Methylation, periodate oxidation, and partial hydrolysis studies on the capsular polysaccharide of *Klebsiella* K-type 56 show the structure to be a repeating unit consisting of

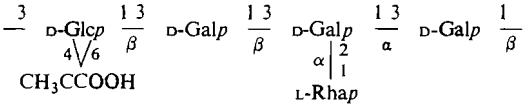

The nature of the anomeric linkages was determined by p.m.r. spectroscopy of isolated oligosaccharides. The position of the L-rhamnose side chain was defined by characterization of the di- and tetrasaccharides obtained by partial hydrolysis of the fully methylated polysaccharide.

This structure represents the first capsular polysaccharide lacking uronic acid to be studied in the genus *Klebsiella*.

Les méthodes de méthylation, oxydation périodique et hydrolyse partielle ont démontré que la structure de *Klebsiella* K-type 56 se compose d'une unité qui se répète:

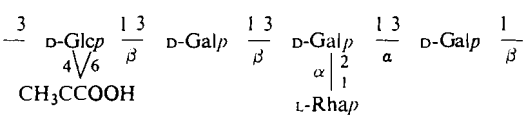

Les liaisons anomères ont été distinguées par la spectroscopie r.m.n. des oligosaccharides isolés. La position de la chaîne latérale du L-rhamnose était décidée par la caractérisation des di- et tetrasaccharides obtenus par l'hydrolyse partielle du polysaccharide complètement méthylé.

Cette capsule de *Klebsiella* est la première d'être trouvée sans un reste de l'acide uronique.

Can. J. Chem., **51**, 3021 (1973)

The majority of the capsular polysaccharides of *Klebsiella* owe their acidic properties to the presence of D-glucuronic acid but in a few instances the acidity is due entirely to the presence of pyruvic acid (1, 2) in a ketal linkage (3). We now report the structure of the capsular polysaccharide from *Klebsiella* K-type 56 which represents the first example to be investigated of those *Klebsiella* capsules lacking uronic acid.

The capsular polysaccharide, after purification through Cetavlon precipitation, had $[\alpha]_D^{24}$ $+79°$ and an equivalent weight of 908. The p.m.r. spectrum of the polysaccharide, run in D_2O at 95° on the sodium salt, indicated the presence of one pyruvic acid ketal and one 6-deoxyhexose to five anomeric protons the chemical shifts of which (Table 1) corresponded to two α-glycosidic linkages and three β-links (4, 5).

Reaction of the polysaccharide with acid rapidly liberated L-rhamnose and total hydrolysis gave L-rhamnose, D-galactose, and D-glucose in the ratio of 1.1:3:1. The configurations of the first- and last-named were determined by measurements of the circular dichroism (c.d.) of the alditol acetates; that of D-galactose was proved by measurement of the c.d. spectrum of a methylated derivative isolated subsequently (6). Since L-rhamnitol acetate does not crystallize readily this sugar was identified as methyl α-L-rhamnopyranoside.

Partial hydrolysis of the polysaccharide gave a series of neutral oligosaccharides which were separated from monosaccharides by charcoal column chromatography and individual components were obtained by gel filtration on Sephadex G-15. These were shown to be a glucosyl-galactose disaccharide together with related tri- and tetrasaccharides. The structures of these oligosaccharides are given in Table 1 together with the chemical shift of the anomeric protons which enables the nature of the gly-

[1]Presented in part at the 56th Canadian Chemical Conference of the Chemical Institute of Canada, Montreal, Quebec, June, 1973.

Can. J. Chem. Downloaded from www.nrcresearchpress.com by 210.87.254.42 on 09/05/12
For personal use only.

TABLE 1. P.m.r. data on *Klebsiella* K56 capsular polysaccharide and derived oligosaccharides

Repeating unit of compound	τ value* (coupling constant, Hz)	Ratio of integrals	Proton† assignment
Glc $\frac{1\ 3}{\beta}$ Gal—OH	4.64	0.5	α-Gal—OH
	5.28(7)	1.5	β-Gal—OH
			β-Glc $\frac{1\ 3}{}$ Gal
Glc $\frac{1\ 3}{\beta}$ Gal $\frac{1\ 3}{\beta}$ Gal—OH	4.63	0.5	α-Gal—OH
	5.29(7)	2.5	β-Gal—OH
			β-Glc $\frac{1\ 3}{}$ Gal
			β-Gal $\frac{1\ 3}{}$ Gal
Glc $\frac{1\ 3}{\beta}$ Gal $\frac{1\ 3}{\beta}$ Gal $\frac{1\ 3}{\alpha}$ Gal—OH	4.63	0.5	α-Gal—OH
	4.75	1	α-Gal $\frac{1\ 3}{}$ Gal
	5.28(7)	2.6	β-Gal—OH
			β-Gal $\frac{1\ 3}{}$ Gal
			β-Gal $\frac{1\ 3}{}$ Gal
$CH_3CCOONa$ $\frac{3}{}$ Glc (4/6) $\frac{1\ 3}{\beta}$ Gal $\frac{1\ 3}{\beta}$ Gal (2/1 α L-Rha) $\frac{1\ 3}{\alpha}$ Gal $\frac{1}{\beta}$	4.76	2	α-Rha $\frac{1\ 2}{}$ Gal
			α-Gal $\frac{1\ 3}{}$ Gal
	5.08‡	2	β-Glc $\frac{1\ 3}{}$ Gal
			β-Gal $\frac{1\ 3}{}$ Glc
	5.28‡	1	β-Gal $\frac{1\ 3}{}$ Gal
	8.57	3	CH_3 of pyruvate ketal
	8.73(5)	3	CH_3 of Rha
$CH_3CCOONa$ $\frac{3}{}$ Glc (4/6) $\frac{1\ 3}{\beta}$ Gal $\frac{1\ 3}{\beta}$ Gal $\frac{1\ 3}{\alpha}$ Gal $\frac{1}{\beta}$	4.75	1	α-Gal $\frac{1\ 3}{}$ Gal
	5.09‡	1	β-Gal $\frac{1\ 3}{}$ Glc
	5.21‡	2	β-Glc $\frac{1\ 3}{}$ Gal
			β-Gal $\frac{1\ 3}{}$ Gal
$\frac{3}{}$ Glc $\frac{1\ 3}{\beta}$ Gal $\frac{1\ 3}{\beta}$ Gal $\frac{1\ 3}{\alpha}$ Gal $\frac{1}{\beta}$	8.57	3	CH_3 of pyruvate ketal
	4.75(3)	1	α-Gal $\frac{1\ 3}{}$ Gal
	5.24(5–7)	3	β-Glc $\frac{1\ 3}{}$ Glc
			β-Gal $\frac{1\ 3}{}$ Glc
			β-Gal $\frac{1\ 3}{}$ Gal

*Spectra run in D_2O with external tetramethylsilane (τ = 10) at 100 MHz.
†All sugars have D-configuration except L-rhamnose and all are pyranose.
‡Signals *ca.* 6 Hz wide but no distinct splitting presumably on account of the viscosity of the solution.

cosidic linkage to be determined. The structures given were determined by (a) hydrolysis with acid and enzyme, (b) partial hydrolysis, and (c) methylation, as described in the Experimental.

A sample of pure capsular polysaccharide was methylated and hydrolyzed to give the sugars shown in Table 2A. The identity of the individual partially methylated sugars was determined by comparison with standards using (a) paper chromatography, (b) gas–liquid chromatography and mass spectrometry (g.l.c.–m.s.) of the alditol acetate, and (c) demethylation to the parent alditol acetate.

These results indicate that two of the D-galac-

Can. J. Chem. Downloaded from www.nrcresearchpress.com by 210.87.254.42 on 09/05/12
For personal use only.

Can. J. Chem. Downloaded from www.nrcresearchpress.com by 210.87.254.42 on 09/05/12
For personal use only.

TABLE 2. Methyl ethers from the hydrolyzates of methylated *Klebsiella* K56 oligo- and polysaccharides

	Sample*						
	R_f	A	B	C	D	E	F
Fraction 1	0.78†			+			
2,3,4-Tri-*O*-methyl-L-rhamnose	0.72	1		+	+		
Fraction 2	0.66			+			
2,4,6-Tri-*O*-methyl-D-galactose	0.47	2	3	+	+	1.5	1
4,6-Di-*O*-methyl-D-galactose	0.30	1		+	+	0.8	1
2-*O*-Methyl-D-glucose	to 0.25	1	1	+	+	1.0	1

*A, methylated original K56 polysaccharide; B, polysaccharide recovered from elimination of L-rhamnose by Smith degradation; C, partial hydrolysis with formic acid of sample A; D, reduced fraction 1; E, fraction 2; F, component 2b. The numbers indicate approximate molar amounts (see Experimental for details); (+) signifies present, no quantitative implication.
†T.l.c. silica gel, solvent D.

tose units are linked through position 3 and that the third carries a terminal L-rhamnose residue linked at position 2 or 3. Isolation of 2-*O*-methyl-D-glucose is consistent with the presence of a 4,6-*O*-(1-carboxyethylidene)-D-glucose unit linked in the chain through position 3.

The single unit side chain of L-rhamnose was most conveniently removed by Smith degradation (7) and the p.m.r. spectrum of the recovered polysaccharide demonstrated the retention of the pyruvic acid, the elimination of the deoxy sugar unit, and the loss of one α-glycosidic linkage per repeat unit. This is in agreement with the change in optical rotation ($[\alpha]_D$ $+79° \rightarrow +97°$) in the initial stages of the acid hydrolysis of the original polysaccharide on the assumption that L-rhamnose is the most acid labile residue. Hydrolysis of the recovered, methylated polysaccharide gave 2,4,6-tri-*O*-methyl-D-galactose in place of the 4,6-dimethyl ether (Table 2B) indicating that the L-rhamnose unit is joined to position 2.

The methylation data in conjunction with the analysis of the oligosaccharides enable the repeat unit of *Klebsiella* K56 capsular polysaccharide to be written thus

$$\overset{3}{-}\ \mathrm{Glc}\ \overset{1\,3}{-}\ \mathrm{Gal}\ \overset{1\,3}{-}\ \mathrm{Gal}\ \overset{1\,3}{-}\mathrm{Gal}- \quad \text{and} \quad \left|\begin{matrix}2\\1\\\mathrm{Rha}\end{matrix}\right.$$

but they provide no information as to which D-galactose unit carries the L-rhamnose substituent. Partial hydrolysis of the original polysaccharide is not applicable here since the L-rhamnose is preferentially eliminated and each of the D-galactose units is similarly linked ($1 \rightarrow 3$). Partial hydrolysis of the methylated polysaccharide using formic acid, however, enabled this problem to be solved in the following manner.

Examination of the hydrolyzate (C) by t.l.c. showed the formation of products in addition to the expected methylated sugars. One of these (fraction 1) moved faster than 2,3,4-tri-*O*-methyl-L-rhamnose and the other (fraction 2) had a mobility between this sugar and 2,4,6-tri-*O*-methyl-D-galactose (Table 2C). Fractions 1 and 2 were separated from a portion of the hydrolyzate (C) and the former, after reduction and hydrolysis, gave the methylated sugars shown in Table 2D together with an alditol assumed to be 2,4,6-tri-*O*-methyl-D-galactitol. This fraction presumably corresponds to one complete pentasaccharide repeating unit.

Fraction 2 was obtained in greater amount and was investigated as follows. The p.m.r. spectrum showed the presence of pyruvate and the ratio of the sugars obtained on total hydrolysis of this fraction suggested it was a mixture (Table 2E). When this fraction was reduced with sodium borohydride and examined by t.l.c. there was a marked reduction in mobility and two components were observed with R_f values 0.14 (component 2a) and 0.07 (component 2b). Complete hydrolysis of component 2b gave the sugars shown in Table 2F together with 2,4,6-tri-*O*-methyl-D-galactitol, thus demonstrating that this component is a tetrasaccharide terminated by a 2,4,6-tri-*O*-methyl-D-galactose unit. Therefore, the rhamnose side chain cannot be attached to this terminal galactose residue. When component 2b was methylated and hydrolyzed 2,3-di-*O*-methyl-D-glucose was obtained but no 2,3,4,6-tetra- or 2-*O*-methylglucoses thus confirming the position of attachment of the pyruvate ketal and showing the glucose unit to be the nonreducing end. Component 2a was obtained in small quantity and hydrolysis gave 2-*O*-methyl-D-glucose and 2,4,6-tri-*O*-methyl-D-galactitol in approximately equal amounts.

The free disaccharide corresponding to component 2a was more readily obtained when the remainder of the formic acid hydrolyzate (C) was further hydrolyzed with trifluoroacetic acid at 95° for 4 h. Separation by t.l.c. of this hydrolyzate gave the disaccharide (R_f 0.60) in addition to methylated monosaccharides. Total hydrolysis of the disaccharide gave 2-*O*-methyl-D-glucose and 2,4,6-tri-*O*-methyl-D-galactose and

Can. J. Chem. Downloaded from www.nrcresearchpress.com by 210.87.254.42 on 09/05/12
For personal use only.

hydrolysis of the reduced disaccharide gave the same products as component 2a. These results demonstrate that the rhamnose side chain is not joined to the galactose which is linked directly to glucose and hence, by elimination, must be joined to the central galactose unit.

Partially methylated disaccharides have been obtained fortuitously through incomplete hydrolysis (*e.g.* 8,9) and use has been made of the acid lability of furanosidic linkages in fully methylated polysaccharides to study acetate distribution (10), but we believe this is the first occasion that methylated oligosaccharides have been deliberately isolated as part of a structural investigation. The success of this approach in the present instance is no doubt aided by the known acid lability of 1 → 3-linked D-galactose units (11). The inability to isolate a methylated trisaccharide terminated by the 4,6-di-*O*-methyl-D-galactose residue is presumably due to the greater stability of the α-D- compared to the β-D-galactosidic linkage (12). In using this method clearly care must be exercised since methylated pentasaccharides may have very high mobilities and di- and tetrasaccharide units may migrate at the same rate.

The structure of the capsular polysaccharide of *Klebsiella* K56, the first representative of the type where pyruvic acid is the only acidic constituent, may thus be written

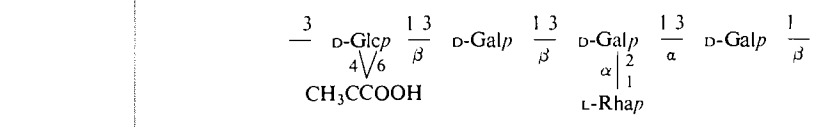

Experimental

General methods are as previously described (3).

Isolation and Properties of Klebsiella K56 Capsular Polysaccharide

Klebsiella K56 was grown on the medium as for K21 and the harvested capsular polysaccharide and cells (~2 l) were diluted two-fold with water and centrifuged at 27 000 r.p.m. at 4° for 30 min. The supernatant was collected and poured with stirring into ethanol (5 vol). The polysaccharide was collected, dissolved in distilled water, and purified through precipitation with Cetavlon giving 8 g of pure acidic polysaccharide having $[\alpha]_D^{24}$ +79° (*c* 0.43, water) as Na^+ salt. After deionization with Amberlite IR120 and dialysis, the equivalent weight was found by titration with 0.01 *M* sodium hydroxide (phenolphthalein) to be 908.

A sample of the Na^+ salt of the polysaccharide was dissolved in D_2O and exchanged twice by lyophilization. The p.m.r. spectrum of the solution (2% in D_2O) was run at 95° and showed a sharp singlet at τ 8.57, a doublet at 8.73, and five protons in the range 4.6–5.3 (Table 1). Integration showed the ratio between the singlet at τ 8.57 and the doublet at 8.73 to be 1:1 and the presence of five anomeric protons.

The existence of pyruvic acid was also confirmed by hydrolysis of the polysaccharide and identification of the pyruvic acid by paper chromatography (solvent A) using *o*-phenylenediamine spray which gave a characteristic fluorescence when examined by u.v. (13).

Hydrolysis of the Polysaccharide

Polysaccharide (50 mg) was hydrolyzed with 2 *M* trifluoroacetic acid at 95° for periods of 0.5, 1, 2, and 4 h. The liberation of L-rhamnose was found (paper chromatography) to be maximum at 0.5 h with no increase on longer hydrolysis. After 4 h, the hydrolyzate was evaporated and the ratio of L-rhamnose, D-galactose, and D-glucose was found to be 1.1:3:1 by g.l.c. of the alditol acetates (column a). Galactitol hexaacetate had m.p. and mixed m.p. 162–164° and D-glucitol hexaacetate had m.p. and mixed m.p. 98–99°. The configuration of L-rhamnose and D-glucose was determined by measuring the c.d. curves of the alditol acetates (6).

A sample of the polysaccharide was methanolyzed (3% MeOH–HCl, 2 h) and the methyl glycosides separated by t.l.c. using solvent D. Only the component having R_f 0.4 was extracted and after recrystallization from ethyl acetate it was identified as methyl α-L-rhamnopyranoside m.p. and mixed m.p. 108–109°.

Partial Hydrolysis of the Polysaccharide

K56 polysaccharide (1 g) was dissolved in trifluoroacetic acid (50 ml, 0.5 *M*) and the solution was heated on a steam bath for 1 h. The solution was evaporated and fractionated using a charcoal column (Darco G60, 10 × 3 cm). Monosaccharides were eluted by distilled water (2 l) and a series of oligosaccharides (mainly di-, tri-, and tetrasaccharides) was eluted with 20% aqueous ethanol (1 l); yield of oligosaccharides about 0.3 g. The mixture of oligosaccharides (100 mg) was applied to a Sephadex G15 column (110 × 2 cm) which was irrigated with water at a flow rate of 4–6 ml/h. The oligosaccharides (R_{Gal} values 0.52, 0.23, 0.16, solvent C) were separated into di- (40 mg), tri- (20 mg), and tetrasaccharides (25 mg) and analyzed as follows.

Analysis of Disaccharide

The p.m.r. spectrum (Table 1) of the disaccharide, run in D_2O at 95°, showed it to be β-linked. Hydrolysis (10 mg, 2 *M* TFA, 4 h, 95°) showed D-galactose and D-glucose as the only two sugars present in the ratio of approximately 1:1 (g.l.c. of the alditol acetates). The same ratio was obtained when another portion (10 mg) was dissolved in 5 ml 0.3 *M* acetate buffer (p*H* 5.5) to which β-D-glucosidase (10 mg) was added and the solution was incubated at 38° for 16 h. The disaccharide (10 mg) was methylated and hydrolyzed to give 2,3,4,6-tetra-*O*-methyl-D-glucose and 2,4,6-tri-*O*-methyl-D-galactose (paper chromatography, solvent D, R_f 0.80 and 0.40 respectively) together with small amounts of tri-*O*-methyl-D-galactofuranose (R_f 0.59, solvent D). The ratio of 2,3,4,6-tetra-*O*-methyl-D-glucose to 2,4,6-tri-*O*-methyl-D-galactose was found to be approximately 1:0.9 as determined by g.l.c. of the alditol acetates.

Can. J. Chem. Downloaded from www.nrcresearchpress.com by 210.87.254.42 on 09/05/12
For personal use only.

Trisaccharide

The p.m.r. spectrum showed both anomeric protons to be at τ 5.29. Partial hydrolysis (5 mg, 0.5 *M* TFA, 95°, 30 min) showed (solvent C) the formation of D-galactose and the disaccharide described above. Partial hydrolysis of a reduced sample gave the same disaccharide and galactitol (R_G 0.88, solvent B), hexaacetate m.p. 164–166° (isolated by g.l.c.).

Tetrasaccharide

The p.m.r. spectrum showed the anomeric protons at τ 4.75 (1H) and 5.28 (2H). Partial hydrolysis gave D-galactose and the above di- and trisaccharides. A portion (10 mg) was methylated and hydrolyzed to give a minor component corresponding to 2,3,4,6-tetra-*O*-methyl-D-glucose (R_f 0.79) and a major component equivalent to 2,4,6-tri-*O*-methyl-D-galactose (R_f 0.37, solvent D). Lack of material precluded further identification.

Methylation of the Polysaccharide

Capsular polysaccharide (1 g) was methylated by the Hakomori procedure and, after dialysis and chloroform extraction, the product was fractionated by extraction with petroleum ether – chloroform. The fraction soluble in the 70:30 mixture showed no hydroxyl absorption in the i.r. and was used for analysis.

The fully methylated polysaccharide (85 mg) was hydrolyzed with 2 *M* trifluoroacetic acid at 100° for 2 h and then at 95° for 16 h. The acid was evaporated and the syrup was shown by paper chromatography (solvent D) to contain the four components (R_f values 0.88, 0.42, 0.16, 0.07) given in Table 2A. The ratio was found to be 0.85:2.2:1:1 as determined by g.l.c. of the alditol acetates which permitted isolation of 2-*O*-methyl-D-glucitol pentaacetate as a crystalline derivative having m.p. and mixed m.p. 54–56° (13). The identity of the other three components was confirmed by m.s. of the individual alditol acetates, demethylation (BCl_3), and reacetylation to the parent alditol acetate, m.p. of galactitol hexaacetate 164–167°, m.p. of D-glucitol hexaacetate 99°.

The c.d. spectrum of 2,4,6-tri-*O*-methyl-D-galactitol acetate was identical to that of a standard sample thus confirming the configuration of D-galactose.

Smith Degradation

Capsular polysaccharide (220 mg) was dissolved in sodium metaperiodate (100 ml, 0.025 *M*). After 64 h in the dark at 4°, 0.45 mol of periodate had been consumed per sugar unit. Following the addition of ethylene glycol, dialysis, reduction with sodium borohydride, dialysis, deionization, lyophilization, and removal of borate, the product was hydrolyzed (TFA, 0.5 *M*) at room temperature for 8 h. Paper chromatography in solvent A showed the presence of one mobile compound identified, by comparison with a standard, as 1-deoxyglycerol (1,2-propanediol) having R_f 0.80 and retention time 4.2 min on column a at 90°.

The polymeric product in 5 ml of water was dialyzed against 2 l of distilled water and the residue was freeze dried to yield a degraded polymer (150 mg). The degraded polysaccharide (70 mg) was methylated (Hakomori procedure) and then hydrolyzed. Paper chromatography (solvents D and E) showed only the presence of 2,4,6-tri-*O*-methyl-D-galactose and 2-*O*-methyl-D-glucose in the ratio of 3:1 (g.l.c. of the alditol acetates). The identity of the two compounds was again confirmed by m.s. of the alditol acetates and by the isolation of crystalline 2-*O*-methyl-D-glucitol pentaacetate, m.p. 54–56°.

The degraded polysaccharide had $[\alpha]_D^{20}$ +97° (*c* 1.0, water) and a portion (40 mg) of the sodium salt was exchanged twice with D_2O by lyophilization. The p.m.r. spectrum was run at 95° in D_2O (100%) and showed a singlet at τ 8.57 while the doublet at 8.73 was completely absent. The anomeric signals (Table 1) at τ 4.75, 5.09, and 5.21 were found to be in a ratio of 1:1:2. Integration showed one pyruvic acid per four sugar units. The anomeric signal at τ 5.09 was shifted upfield to 5.24 when the pyruvate ketal group was removed by hydrolysis with 0.1 *M* trifluoroacetic acid at 95° for 1 h.

Partial Hydrolysis of Methylated Capsular Polysaccharide

Methylated polysaccharide (200 mg) was hydrolyzed with 90% formic acid at 70° for 45 min. The hydrolyzate (C) was shown to contain products in addition to the expected methylated monosaccharides (Table 2C). The majority (150 mg) of the hydrolyzate (C) was resolved by t.l.c. (solvent D) and fraction 1 (R_f 0.78), obtained in only small quantity, on borohydride reduction and hydrolysis gave the sugars shown in Table 2D and an alditol assumed to be 2,4.6-tri-*O*-methyl-D-galactitol acetate.

Fraction 2 (R_f 0.66) was obtained in larger amount (40 mg) and total hydrolysis of a portion (7 mg) gave the results shown in Table 2E. Reduction of fraction 2 with sodium borohydride gave (t.l.c., solvent D) two components with R_f values 0.14 (component 2a) and 0.07 (component 2b). Isolation and hydrolysis of component 2a (12 mg) showed, on paper, only 2-*O*-methyl-D-glucose and on acetylation and g.l.c. 2-*O*-methyl-D-glucose acetates and 2,4,6-tri-*O*-methyl-D-galactitol acetate in a ratio of 1:1.25 (column a 170–220° at 2°/min, retention times 36 and 38 min and 22 min respectively).

When component 2b was isolated and hydrolyzed (10 mg) paper chromatography showed the presence of 2,4,6-tri-*O*-methyl-D-galactose (R_f 0.39, solvent D; 0.61, solvent E), 4,6-di-*O*-methyl-D-galactose (0.14, 0.46) and 2-*O*-methyl-D-glucose (0.06, 0.35). Acetylation of the hydrolyzate and g.l.c. showed these components (retention times 18, 23; 26, 32; 37, 38 min) and 2,4,6-tri-*O*-methyl-D-galactitol (25 min) in the ratio 1.1:1:1:1.3. Methylation and hydrolysis of component 2b (5 mg) gave only 2,4,6-tri-*O*-methyl-D-galactose (R_f 0.38, solvent D) and 2,3-di-*O*-methyl-D-glucose (0.27). The identity of the latter was confirmed by g.l.c.–m.s. of the derived alditol acetate.

The smaller part (50 mg) of the original hydrolyzate (C) was further hydrolyzed (0.5 *M* TFA, 95°, 4 h) and paper chromatography showed the presence of a compound (R_f 0.79, solvent E) moving slower than 2,3,4-tri-*O*-methyl-L-rhamnose (R_f 0.88). This compound (15 mg) was isolated by t.l.c. (R_f 0.6, solvent D). Complete hydrolysis (2 *M* TFA, 95°, 16 h) of a portion (5 mg) gave 2,4,6-tri-*O*-methyl-D-galactose and 2-*O*-methyl-D-glucose in the ratio of 1:1. Reduction and hydrolysis of the remainder showed on paper only 2-*O*-methyl-D-glucose and, after acetylation, 2,4,6-tri-*O*-methyl-D-galactitol acetate (22 min, column a 170–220° at 2°/min) and 2-*O*-methyl-D-glucose acetates (36 and 38 min) in the ratio of 1.2:1.

We are grateful to Dr. I. Ørskov for a culture of *Klebsiella* K56 (3534/51), to Dr. P. J. Salisbury for growing the bacteria, and to Dr. J. J. R. Campbell and Dr. J. B. Hudson for the use of their centrifuges.

We appreciate the continued financial support of the National Research Council and Y.M.C. acknowledges with thanks the award of a Killam Fellowship.

1. W. NIMMICH. Z. Med. Mikrobiol. Immunol. **154**, 117 (1968).
2. W. NIMMICH. Acta Biol. Med. Germ. **26**, 397 (1971).
3. G. G. S. DUTTON and Y. M. CHOY. Can. J. Chem. **51**, 198 (1973).
4. Y. M. CHOY, G. G. S. DUTTON, A. M. STEPHEN, and M. T. YANG. Anal. Lett. **5**, 675 (1972).
5. G. M. BEBAULT, Y. M. CHOY, G. G. S. DUTTON, N. FUNNELL, A. M. STEPHEN, and M. T. YANG. J. Bacteriol. **113**, 1345 (1973).
6. G. M. BEBAULT, J. M. BERRY, Y. M. CHOY, G. G. S. DUTTON, N. FUNNELL, L. D. HAYWARD, and A. M. STEPHEN. Can. J. Chem. **51**, 324 (1973).
7. I. J. GOLDSTEIN, G. W. HAY, B. A. LEWIS, and F. SMITH. Methods Carbohydr. Chem. **5**, 361 (1965).
8. (*a*) G. G. S. DUTTON and T. G. MURATA. Can. J. Chem. **39**, 1955 (1961). (*b*) G. G. S. DUTTON and S. A. MCKELVEY. Can. J. Chem. **39**, 2582 (1961).
9. G. G. S. DUTTON and S. KABIR. Carbohydr. Res. **28**, 187 (1973).
10. B. LINDBERG, J. LÖNNGREN, and W. NIMMICH. Carbohydr. Res. **23**, 47 (1972).
11. C. J. LAWSON ad D. A. REES. J. Chem. Soc. C, 1301 (1968).
12. B. CAPON. Chem. Rev. **69**, 407 (1969).
13. M. DUCKWORTH and W. YAPHE. Chem. Ind. Lond. 747 (1970).

Can. J. Chem. Downloaded from www.nrcresearchpress.com by 210.87.254.42 on 09/05/12
For personal use only.

Structure cristalline et moléculaire du cyclopentadiényle dicarbonyle triphénylphosphine manganèse, $MnC_5H_5(CO)_2P(C_6H_5)_3$

CLAUDE BARBEAU, KLAUS SORRENTO DICHMANN ET LOUIS RICARD

Département de Chimie, Université Laval, Québec, Québec

Reçu le 14 juin 1972[1]

La structure cristalline du cyclopentadiényle dicarbonyle triphénylphosphine manganèse a été déterminée à partir de données tridimentionnelles obtenues de clichés de chambre à précession de Buerger. 2931 intensités indépendantes ont été utilisées dans l'affinement de la structure effectuée selon la méthode des moindres carrés. Le facteur de désaccord final est 0.11. $MnC_5H_5(CO)_2P(C_6H_5)_3$ cristallise dans le groupe spatial triclinique

$P\bar{1}$, $a = 9.41(2)$, $b = 10.60(2)$, $c = 11.36(2)$ Å,

$\alpha = 103.47(16)$, $\beta = 79.47(16)$, $\gamma = 101.72(16)°$, $V = 1068$ Å^3

La molécule présente des paramètres atomiques presque identiques à ceux de la molécule $MnC_5H_5(CO)_3$ sauf pour les distances des liaisons Mn—C qui passent de 1.80 Å à 1.75 Å. La distance Mn—P (2.236 Å) et les paramètres inchangés du groupement Mn—C_5H_5 confirment le pouvoir donneur élevé du cyclopentadiényle.

The crystalano molecular structure of cyclopentadienyl manganese dicarbonyl-triphenyl phosphine has been determined by means of three dimensional data obtained by a Buerger precession camera. 2931 independent intensities were utilized in the refinement of the structure using the least-squares method. The final disagreement factor is 0.11. $MnC_5H_5(CO)_2P(C_6H_5)_3$ crystallizes in the triclinic space group.

$p\bar{1}$, $a = 9.41(2)$, $b = 10.60(2)$, $c = 11.36(2)$ Å,

$\alpha = 103.47(16)$, $\beta = 79.47(16)$, $\gamma = 101.72(16)°$, $V = 1078$ Å^3

The molecule shows atomic parameter almost identical to those of $MnC_5H_5(CO)_3$ except for the Mn—C bond lengths which change from 1.80 to 1.73 Å. The Mn—P distance (2.236 Å) and the unchanged parameters for the Mn—C_5H_5 group confirm the strong donating power of the cyclopentadienyl group. [Journal translation]

Can. J. Chem., **51**, 3027 (1973)

Introduction

Dans le but de mieux connaître les effets du remplacement d'un groupe CO d'un métal carbonyle par un donneur D sur les paramètres structuraux tel que longueurs de liaison métal–ligand et angles de liaison, nous présentons le premier d'une série d'articles traitant de la structure cristalline et moléculaire de dérivés substitués de métaux carbonyle. $MnC_5H_5(CO)_3$ présente l'avantage de contenir un petit nombre de groupements carbonyles et de former des composés substitués stables. Puisque le remplacement d'un groupement CO entraîne ordinairement des changements importants, tant dans les fréquences de vibration C—O que dans les moments dipolaires (1), les composés $MnC_5H_5(CO)_2P(C_6H_5)_3$ et $MnC_5H_5(CO)(P(C_6H_5)_3)_2$ pourraient présenter des modifications structurales. Nous présentons ici la structure cristalline et moléculaire du composé monosubstitué $MnC_5H_5(CO)_2P(C_6H_5)_3$.

[1]Revision recue le 2 mai 1973.

Partie expérimentale

$MnC_5H_5(CO)_2P(C_6H_5)_3$ précipite sous la forme de poudre lors de l'illumination, par une lampe à vapeur de mercure du type General Electric H-100 A4/T, d'une solution de 1 mmol de $MnC_5H_5(CO)_3$ de 3 mmol de $P(C_6H_5)_3$ dans 70 ml de méthanol (2). Le solide jaunâtre est dissous dans une solution (1:1) benzène–éthanol d'où on obtient, par lent refroidissement, des cristaux de taille moyenne de 0.5 × 0.3 × 0.1 mm.

Données cristallines: $C_{25}H_{20}MnO_2P$ m.m. 438.3

triclinique[2] $P\bar{1}$, $a = 9.41(2)$, $b = 10.60(2)$, $c = 11.36(2)$Å

$\alpha = 103.47(16)$, $\beta = 79.47(16)$,

$\gamma = 101.72(16)°$

$V = 1068$ Å^3, $\rho_o = 1.36(1)$, $z = 2$, $\rho_c = 1.362$

(20 °C, Mo K$\bar{\alpha}$, $\lambda = 0.71069$ Å)

La densité a été mesurée selon la méthode de flottaison dans une solution de chlorure de césium. La détermination du groupe spatial et les mesures des paramètres cristallins ont été effectuées sur des clichés de chambre à précession de Buerger. Le cristal prélevé pour la cueillette

[2]Les dimensions de la maille réduite selon Delaunay (3) sont: $a = 9.41$ Å, $b = 11.36$ Å, $c = 12.66$ Å, $\alpha = 93.39°$, $\beta = 124.96°$, et $\gamma = 100.53°$.

Can. J. Chem. Downloaded from www.nrcresearchpress.com by 210.87.254.40 on 09/05/12
For personal use only.

Can. J. Chem. Downloaded from www.nrcresearchpress.com by 210.87.254.40 on 09/05/12
For personal use only.

TABLEAU I. Coordonnées atomiques ($\times 10^4$) et coefficients d'agitation thermique[a]

Atome	x	y	z	B (Å^2)
Mn	2277(2)	3450(1)	1561(1)	[b]
P	1497(2)	2045(2)	2829(2)	[b]
O(1)	5385(9)	3414(8)	1557(7)	[b]
O(2)	2248(10)	5672(7)	3626(7)	[b]
C(1)	4138(12)	3407(8)	1579(7)	[b]
C(2)	2246(11)	4777(8)	2795(9)	[b]
C(4)	2339(21)	2585(16)	−0356(10)	[b]
C(5)	2697(27)	3985(19)	−0185(14)	[b]
C(6)	1537(27)	4551(17)	0524(17)	[b]
C(7)	0368(18)	3535(17)	0794(14)	[b]
C(8)	0870(19)	2333(15)	0248(12)	[b]
C(9)	2218(9)	0486(8)	2435(7)	3.9(1)
C(10)	2762(13)	0035(12)	1226(11)	6.4(2)
C(11)	3306(16)	−1195(14)	0914(13)	8.1(3)
C(12)	3320(14)	−1849(13)	1833(12)	7.2(3)
C(13)	2806(13)	−1377(12)	3024(11)	6.6(2)
C(14)	2235(11)	−0203(10)	3354(9)	5.1(2)
C(15)	1929(8)	2692(7)	4392(6)	3.4(1)
C(16)	0852(11)	2817(10)	5395(9)	5.5(2)
C(17)	1279(14)	3400(12)	6551(12)	6.9(3)
C(18)	2696(13)	3826(11)	6686(10)	6.2(2)
C(19)	3811(12)	3679(11)	5683(10)	6.3(2)
C(20)	3403(10)	3106(9)	4530(9)	4.9(2)
C(21)	−0488(9)	1531(8)	3076(8)	4.3(1)
C(22)	−1174(11)	0234(9)	2992(9)	5.2(2)
C(23)	−2721(13)	−0092(12)	3204(11)	6.6(2)
C(24)	−3532(16)	0915(14)	3491(13)	7.8(3)
C(25)	−2881(16)	2214(14)	3582(13)	8.0(3)
C(26)	−1328(13)	2542(11)	3412(11)	6.4(2)

Atome	U_{11}	U_{22}	U_{33}	U_{12}	U_{13}	U_{23}
Mn	80(1)	49(1)	47(1)	−2(0)	−21(1)	19(1)
P	47(1)	38(1)	45(1)	7(1)	−8(1)	9(1)
O(1)	71(5)	96(6)	86(5)	11(4)	13(4)	12(5)
O(2)	130(7)	52(4)	89(5)	25(4)	−24(5)	2(4)
C(1)	87(7)	46(4)	41(4)	1(4)	2(4)	11(3)
C(2)	78(6)	39(4)	81(6)	15(4)	−23(5)	23(4)
C(4)	180(16)	122(12)	44(5)	−11(10)	−38(8)	25(6)
C(5)	239(22)	117(13)	70(8)	−43(13)	−62(11)	55(9)
C(6)	212(20)	99(12)	104(12)	5(12)	−89(13)	53(10)
C(7)	143(13)	116(12)	110(10)	7(9)	−84(10)	43(9)
C(8)	140(13)	109(9)	76(7)	−20(8)	−60(8)	24(7)

[a]Les écarts-types sont donnés entre parenthèses.
[b]Le facteur de température de chacun de ces atomes est de la forme

$$\exp\{-2\pi^2(a^{*2}h^2U_{11} + b^{*2}k^2U_{22} + c^{*2}l^2U_{33} + 2a^*b^*hkU_{12} + 2a^*c^*hlU_{13} + 2b^*c^*klU_{23})\}$$

Chaque coefficient U est multiplié par 10^3.

des intensités mesurait 0.40 × 0.30 × 0.20 mm. Trois expositions de durée variable (5 min – 16 h) ont été prises pour chacune des 19 strates (4 le long de b, 4 le long de c, 6 le long de [011] et 5 le long de [01$\bar{1}$]) en utilisant la chambre à précession de Buerger. Les intensités ont été mesurées à l'aide d'un microdensitomètre du type Wooster Mark IV. Le coefficient d'absorption linéaire ayant comme valeur $\mu = 7.4$ cm^{-1}, aucune correction d'absorption n'a été apportée sur les intensités qui ont cependant été corrigées pour les facteurs de Lorentz et ceux de polarisation. La mise sur échelle absolue a été réalisée en utilisant la méthode statistique de Wilson (4). Un total de 2931 réflexions indépendantes ont été mesurées et ont servi aux calculs. Les programmes utilisés ont été tirés du système X-RAY-70 de Stewart et coll. (5).

Determination de la structure

Les coordonnées des atomes Mn et P ont été obtenues à partir de la fonction de Patterson tridimensionnelle. Deux synthèses de Fourier ont permis de localiser 27 autres atomes de la molécule et d'abaisser l'indice résiduel

$$R = \frac{\Sigma(\big||F_o| - |F_c|\big|)}{\Sigma|F_o|} \text{ à } 0.27$$

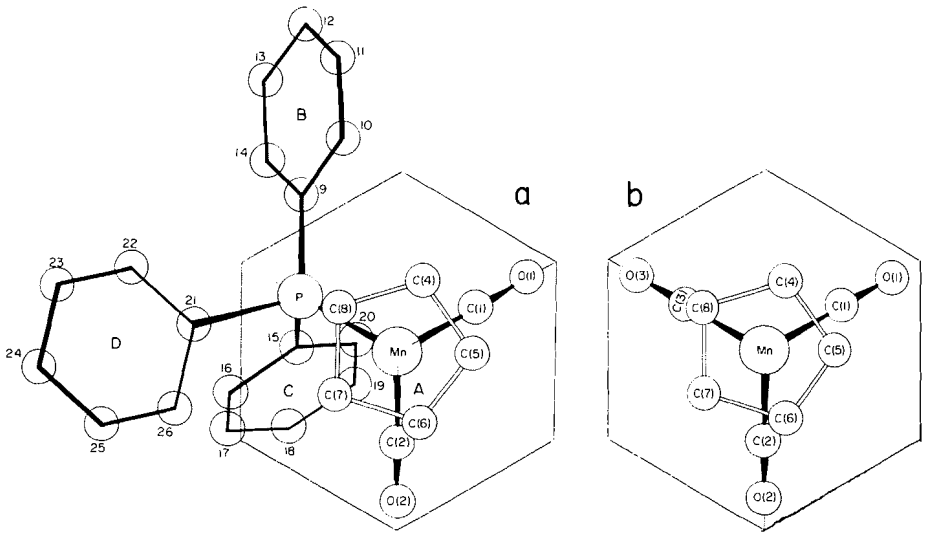

FIG. 1. Projection orthogonale dans un plan parallèle à celui du cycle C_5H_5 des composés: (*a*) $MnC_5H_5(CO)_2P(C_6H_5)_3$; (*b*) $MnC_5H_5(CO)_3$.

L'affinement des paramètres atomiques et des coefficients d'agitation thermique a été réalisé par la méthode des moindres carrés (matrice complète) en minimisant la fonction $S = \Sigma w(|F_o| - |F_c|)^2$. Quatre cycles en isotropie thermique avec des poids w unitaires ont réduit R à 0.17. Deux itérations subséquentes en anisotropie thermique pour les atomes directement reliés au manganèse et en isotropie pour les carbones des phényles ont abaissé R à 0.12. L'introduction à ce stade de poids w ($=1/\sigma^2$), exprimés en termes de $\sigma = 0.120F_o + 0.255 + 3.114/F_o$, et le rejet de 33 réflexions montrant des écarts ΔF supérieurs à 3σ, ont amené le facteur de désaccord à 0.108 en deux itérations.

Ni les coefficients d'agitation thermique ni les coordonnées atomiques n'ont subi de déplacement supérieur à 0.1σ lors de ces deux derniers cycles. Une synthèse de Fourier-différence n'a dévoilé aucun pic significatif (<0.9 $e/Å^3$).

Les facteurs de forme atomique utilisés sont tirés de la référence 6. Les valeurs définitives des coordonnées atomiques, des coefficients d'agitation thermique et de leurs écarts-types sont consignés dans le tableau 1. L'ensemble des facteurs de structure observés et calculés a été versé au dépôt des données non publiées.[3]

Description de la structure

La fig. 1*a* schématise une molécule de $MnC_5H_5(CO)_2P(C_6H_5)_3$ dans une projection orthogonale sur un plan parallèle à celui du cycle C_5H_5. La numérotation utilisée est celle employée pour la molécule non-substituée $MnC_5H_5(CO)_3$ (7) présentée à la fig. 1*b* selon la même projection. Les positions relatives des atomes communs des deux composés sont demeurés inchangés.

Les distances et les angles de valence sont présentés dans le tableau 2. Le tableau 3 donne les coefficients des plans moyens des cycles phényles et du cycle cyclopentadiényle ainsi que les écarts à ces plans. L'empilement des deux molécules dans la maille laisse une distance minimale de 2.5 Å de contact intermoléculaire tandis que les distances de contact intramoléculaire sont supérieures à 3.5 Å (incluant les atomes H).

Le groupement $P(C_6H_5)_3$ présente des paramètres semblables à ceux de la triphénylphosphine libre (8) et sa position dans la molécule, relative aux autres groupements, indique que le remplacement d'un groupe CO par un donneur aussi volumineux n'introduit pas de contrainte stérique ou des perturbations majeures dans le complexe. La distance Mn—P (2.236(3) Å) est plus courte que la somme des rayons covalents de Mn et P (2.48 Å) (9) et légèrement inférieure à la valeur moyenne de 2.30 Å observée dans les composés substitués de $Mn_2(CO)_{10}$ (10). La présence d'un donneur tel que cyclopentadiényle devrait contribuer à apporter une charge négative sur le métal, charge qui devrait être retournée en partie sur le groupement $P(C_6H_5)_3$ par l'intermédiaire d'un recouvrement d'orbitales de caractère π. Une liaison Mn—P à caractère

[3]On peut obtenir la série complète des tableaux à un prix nominal, en s'adressant au Dépôt des données non publiées, Bibliothèque scientifique nationale, Conseil national de recherches du Canada, Ottawa, Canada K1A 0S2.

Can. J. Chem. Downloaded from www.nrcresearchpress.com by 210.87.254.40 on 09/05/12
For personal use only.

TABLEAU 2. Distances interatomiques et angles de valence[a]

Liaison	Distance (Å)	Liaison	Angle (°)
Mn—C(1)	1.766(12)	C(1)—Mn—C(2)	92.42(41)
Mn—C(2)	1.740(10)	C(1)—Mn—P	92.65(27)
Mn—P	2.236(3)	C(2)—Mn—P	90.52(32)
		O(1)—Mn—O(2)	92.04(24)
C(1)—O(1)	1.168(12)	O(1)—Mn—P	93.80(18)
C(2)—O(2)	1.173(11)	O(2)—Mn—P	90.58(21)
Mn—C(4)	2.152(12)	Mn—C(1)—O(1)	177(1)
Mn—C(5)	2.135(13)	Mn—C(2)—O(2)	179(1)
Mn—C(6)	2.123(12)		
Mn—C(7)	2.161(13)	C(4)—C(5)—C(6)	110(2)
Mn—C(8)	2.155(11)	C(5)—C(6)—C(7)	109(2)
		C(6)—C(7)—C(8)	106(2)
C(4)—C(5)	1.428(23)	C(7)—C(8)—C(4)	110(1)
C(5)—C(6)	1.386(27)	C(8)—C(4)—C(5)	105(2)
C(6)—C(7)	1.419(24)		
C(7)—C(8)	1.416(21)	C(9)—P—C(15)	101.41(34)
C(8)—C(4)	1.429(22)	C(15)—P—C(21)	102.65(35)
		C(21)—P—C(9)	103.88(37)
P—C(9)	1.842(8)		
P—C(15)	1.837(8)		
P—C(21)	1.825(9)		
C(9)—C(10)	1.383(14)		
C(10)—C(11)	1.441(18)		
C(11)—C(12)	1.386(18)		
C(12)—C(13)	1.363(16)		
C(13)—C(14)	1.400(15)		
C(14)—C(9)	1.410(13)		
C(15)—C(16)	1.380(12)		
C(16)—C(17)	1.408(16)		
C(17)—C(18)	1.343(16)		
C(18)—C(19)	1.403(15)		
C(19)—C(20)	1.397(14)		
C(20)—C(15)	1.393(12)		
C(21)—C(22)	1.385(13)		
C(22)—C(23)	1.415(15)		
C(23)—C(24)	1.380(17)		
C(24)—C(25)	1.377(19)		
C(25)—C(26)	1.419(18)		
C(26)—C(21)	1.400(14)		

[a]Les écarts-types sont donnés entre parenthèses.

double se traduirait par cette "contraction" de l'ordre de 0.24 Å.

Le cycle cyclopentadiényle, considéré comme un donneur tridenté, présente les même caractéristiques dans les composés $MnC_5H_5(CO)_3$ et $MnC_5H_5(CO)_2P(C_6H_5)_3$ tant au point de vue des distances $Mn—C_{C_5H_5}$ et $C_{C_5H_5}—C_{C_5H_5}$ qu'au point de vue plan du cycle et agitation thermique des carbones. On retrouve aussi les mêmes paramètres structuraux dans $MnC_5H_5(CO)_2$-C_7H_8 (11). Ainsi $Mn—C_{C_5H_5}$ se situe à 2.16 ± 0.01 Å dans les trois composés tandis que $C_{C_5H_5}—C_{C_5H_5}$ présente une distance moyenne de 1.41 ± 0.02 Å. Il apparaît donc que le remplacement d'un CO par un ligand à caractère donneur n'affecte pas la liaison $Mn—C_5H_5$ de façon appréciable. De façon indirecte, il s'ensuit que C_5H_5 est un bon donneur dont le pouvoir accepteur est fort probablement assez faible pour que le groupement ne subisse pas de variations tant dans les paramètres atomiques que dans la fréquence de vibration de valence $Mn—C_5H_5$ (1).

L'introduction du donneur $P(C_6H_5)_3$ apporte des changements au niveau des liaisons Mn—CO.

Can. J. Chem. Downloaded from www.nrcresearchpress.com by 210.87.254.40 on 09/05/12
For personal use only.

TABLEAU 3. Plans moyens

(*a*) Coefficients des équations des plans: $lX + mY + nZ - p = 0$

Plan	l	m	n	p	χ^2
A	−0.5227	0.1545	−0.8384	0.0589	1.4
B	−0.8599	−0.4884	−0.1482	2.5142	2.6
C	−0.2787	0.9501	−0.1403	−0.4274	3.1
D	−0.2022	0.1357	−0.9699	3.1217	8.4

(*b*) Distances (Å) de chacun des atomes à leur plan

Plan A		Plan B		Plan C		Plan D	
C(4)	−0.0091	C(9)	0.0039	C(15)	0.0065	C(21)	0.0105
C(5)	0.0159	C(10)	−0.0138	C(16)	−0.0088	C(22)	−0.0030
C(6)	−0.0102	C(11)	0.0133	C(17)	−0.0041	C(23)	−0.0084
C(7)	0.0003	C(12)	0.0018	C(18)	0.0117	C(24)	0.0062
C(8)	0.0049	C(13)	−0.0074	C(19)	−0.0056	C(25)	0.0183
		C(14)	0.0013	C(20)	−0.0056	C(26)	−0.0244

NOTE: Le système orthonormé des axes de référence comprend X le long de a, Y dans le plan ab et Z le long de c^*.

Comparativement à $MnC_5H_5(CO)_3$ (1.80 ± 0.02 Å) et à $MnC_5H_5(CO)_2C_7H_8$ (1.79 ± 0.01 Å) la distance moyenne Mn—CO est plus courte de 0.04 Å (1.75 ± 0.01 Å). Lors du remplacement d'un groupe CO d'un métal carbonyle par la triphénylphosphine, la fréquence de vibration de valence M—C augmente alors que celle de vibration de valence C—O diminue (1). Le mécanisme accepté de transfert de la charge nette supplémentaire introduite par $P(C_6H_5)_3$ implique un renforcement de la liaison M—C et un affaiblissement du lien C—O par retour π dans l'orbitale moléculaire antiliante du monoxyde de carbone. On devrait donc observer, à la suite de la diminution de distance Mn—CO, un accroissement de la longueur de liaison C—O. Quoique l'écart ne soit pas statistiquement très significatif, on peut cependant noter que les valeurs moyennes de 1.14 et 1.17 Å pour les distances C—O dans les composés non-substitué et monosubstitué sont en accord avec un affaiblissement des liaisons C—O par suite de l'introduction de $P(C_6H_5)_3$.

Conclusion

Sauf pour une tendance marquée vers un changement des paramètres de liaison Mn—CO, le remplacement d'un groupe CO de $MnC_5H_5(CO)_3$ par le groupe donneur $P(C_6H_5)_3$ n'affecte ni la liaison Mn—C_5H_5 ni l'arrangement géométrique autour de l'atome central.

Nous remercions le Conseil national de recherches du Canada pour l'aide technique et une bourse d'études (L.R.). Le Ministère de l'Education du Québec nous a octroyé une aide financière pour laquelle nous lui sommes reconnaissants.

1. C. BARBEAU. Can. J. Chem. **45**, 161 (1967).
2. W. STROHMEIER et C. BARBEAU. Z. Naturforsch. **17b**, 848 (1962).
3. INTERNATIONAL TABLES FOR X-RAY CRYSTALLOGRAPHY. Vol. I. Kynoch Press, Birmingham, England. 1965. p. 530.
4. A. J. C. WILSON. Nature, **150**, 152 (1942).
5. J. M. STEWART, F. A. KUNDELL, et J. C. BALDWIN. The X-RAY-70 System. University of Maryland, College Park, Maryland. 1970.
6. INTERNATIONAL TABLES FOR X-RAY CRYSTALLOGRAPHY. Vol. III. Kynoch Press, Birmingham, England. 1965.
7. A. F. BERNDT et R. E. MARSH. Acta Cryst. **16**, 118 (1963).
8. J. J. DALY. J. Chem. Soc. 3799 (1964).
9. M. R. CHURCHILL. *Dans* Perspectives in structural chemistry. Vol. III. *Edité par* J. D. Dunitz et J. A. Ibers. Wiley, N.Y. 1970. p. 126.
10. J. H. ENEMARK et J. A. IBERS. Inorg. Chem. **6**, 1575 (1967). M. A. BENNETT, G. B. ROBERTSON, R. WATT, et P. O. WHIMP. Chem. Commun. 752 (1971).
11. B. GRANOFF et R. A. JACOBSON. Inorg. Chem. **7**, 2328 (1968).

Can. J. Chem. Downloaded from www.nrcresearchpress.com by 210.87.254.40 on 09/05/12
For personal use only.

Photochemistry of Pivalaldehyde in Solution Studied by CIDNP

HOLGER E. C. CHEN, AREND GROEN, AND MICHAEL COCIVERA
Department of Chemistry, University of Guelph, Guelph, Ontario

Received April 18, 1973

The n.m.r. spectrum observed during irradiation of pivalaldehyde dissolved in perfluoromethylcyclohexane indicates the formation of several compounds whose hydrogens are spin polarized. These compounds are 2-methylpropane, 2-methylpropene, and pivalaldehyde. A mechanism involving radical reactions which is consistent with these results is presented. According to this mechanism, the primary photochemical step is cleavage of the bond between the carbonyl carbon and the tertiary carbon of the *t*-butyl group. In contrast, this step does not appear to be important for acetaldehyde. As a test of the proposed mechanism CCl_4 is added to trap free radicals. In this case, one of the products is CCl_3COH. A mechanism for the formation of this and the other products having nuclear spin polarization is presented.

Le spectre r.m.n. obtenu lors de l'irradiation de la pivalaldéhyde dissoute dans du perfluorométhylcyclohexane, a montré qu'il se formait plusieurs produits. Ces composés sont le méthyl-2 propane, le méthyl-2 propène et la pivalaldéhyde. On propose un mécanisme impliquant des réactions radicalaires qui serait en accord avec les résultats obtenus. Selon ce mécanisme, l'étape photochimique fondamentale est la clivage de la liaison entre le carbone du carbonyle et le carbone tertiaire du groupe *t*-butyle. Au contraire, cette étape ne semble pas importante en ce qui a trait à l'acétaldéhyde. Afin de prouver le mécanisme proposé, on ajouta du CCl_4 au mélange réactionnel pour isoler les radicaux libres; dans ce cas, l'un des produits isolés fut le CCl_3COH. Un mécanisme est proposé afin d'expliquer la formation de ce produit ainsi que des autres. [Traduit par le journal]

Can. J. Chem., 51, 3032 (1973)

Introduction

Chemically induced dynamic nuclear polarization (CIDNP) has proven to be very useful in the study of the mechanisms of radical reactions. In addition to providing information concerning the nature of the radicals involved, CIDNP has proven useful in the detection of compounds which are unstable under the experimental conditions employed. For example, while pivalaldehyde has been detected by CIDNP as one of the products arising from the photolysis of di-*t*-butyl ketone (*1*), this aldehyde was not detected by means of conventional product studies (2), presumably because the prolonged irradiation used for product studies decomposed the compound. More recently, CIDNP has been used to detect short-lived enols arising during the radiation-induced reaction of acetaldehyde (3) and acetophenone with phenol (4). The results of the acetaldehyde study are consistent with the conclusion that the main reaction path involves the transfer of the carbonyl hydrogen from one aldehyde molecule to a second one to give a radical pair consisting of an acetyl radical and an α-hydroxyethyl radical. A similar reaction has been observed for benzaldehyde (5, 6). Since in the di-*t*-butyl ketone study, we obtained no evidence that pivalaldehyde undergoes a similar reaction, we have undertaken a study of the photolysis of pivalaldehyde. In this paper we report the results of this study. Our results indicate that pivalaldehyde does not react in the same manner as acetaldehyde or benzaldehyde. Instead the photolysis appears to involve α-cleavage similar to that suggested for α-aryl aldehyde (7) to give a radical pair consisting of the *t*-butyl radical and the formyl radical. Analysis of the resulting n.m.r. spectra indicates that an excited triplet electronic state is the precursor for this radical pair.

Experimental

Pivalaldehyde (Canadian Laboratories) contained a small amount of impurity. This compound was purified by fraction distillation, checked by n.m.r. and g.l.c., and used in the photochemical studies. The distillation reduced the impurity to about 1% of pivalaldehyde. Carbon tetrachloride (Baker reagent, spectrograde), perfluoromethylcyclohexane (Pierce Chemical), and trichloroacetaldehyde (Aldrich) were checked by n.m.r. and used without purification.

Formyl chloride was synthesized by reaction of thionyl chloride with formic acid. It was trapped in CCl_4 and used without further purification.

The proton n.m.r. spectra at 100 MHz were obtained at 15 °C using a Varian HA-100-15 spectrometer which we have modified to operate on a time-sharing mode. In this mode, we are able to use a quartz probe which allowed direct irradiation of the sample while the

n.m.r. spectrum was being obtained. This probe was built in our laboratory and the details are given elsewhere (1). The n.m.r. spectra were obtained before, during, and after irradiation. The radiation source is a 1000 W Hanovia mercury xenon lamp. A filter was employed to allow transmission of radiation having wavelengths greater than 310 nm.

Results

A n.m.r. spectrum obtained during irradiation of a solution of 0.2 *M* pivalaldehyde in perfluoromethylcyclohexane is illustrated in Fig. 1*A*. As indicated in this figure, the spectra of three compounds are observed: pivalaldehyde **1**, methyl hydrogen singlet at 0.85 p.p.m., carbonyl hydrogen singlet at 9.22 p.p.m.; 2-methylpropane **2**, methyl hydrogen doublet at 0.73 p.p.m., and methine hydrogen decuplet at 1.56 p.p.m.; 2-methylpropene **3**, methyl hydrogen triplet at 1.53 p.p.m. and methylene hydrogen septet at 4.48 p.p.m. This spectrum was obtained using a 500 Hz sweep range, and the chemical shifts are given relative to the tetramethylsilane resonance. As illustrated in this figure, both absorption and emission resonances occur, indicating the CIDNP effect. Because the lines at 1.50 and 4.48 p.p.m. are rather weak at the gain used for Fig. 1*A*, these lines are illustrated at higher gain in Fig. 1*B*. In addition, the lines at 4.48 p.p.m. in *B* were obtained at half the sweep width used in *A*. The spectrum obtained after the sample has been irradiated for about 250 s consists of **1** and a small amount of **2** and what might be tetramethylbutane. Furthermore at higher gain the weak resonance of the methyl hydrogen of 2-methylpropene can be observed. In addition, the intensity of the methyl hydrogen line of **1** does not differ significantly during and after irradiation. Thus all of the lines in Fig. 1*A* except the methyl hydrogen line of **1** are enhanced absorption and/or emission lines.

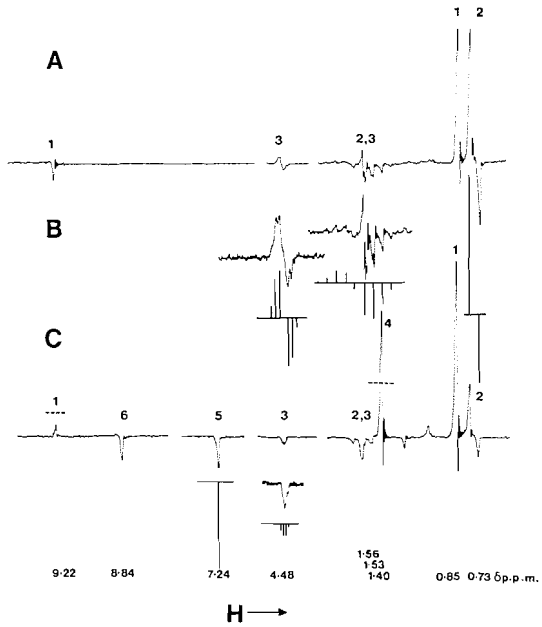

FIG. 1. 100 MHz n.m.r. spectra obtained during irradiation with wavelength greater than 310 nm. *A*, solution containing 0.2 *M* pivalaldehyde in perfluoromethylcyclohexane at 15 °C temperature. All resonance lines were obtained using 500 Hz sweepwidth. *B*, same solution at higher gain. In addition the lines at δ 4.48 p.p.m. were obtained using 250 Hz sweepwidth. *C*, solution containing 0.2 *M* pivalaldehyde and 0.2 *M* CCl_4 in perfluoromethylcyclohexane at 15 °C. All signals were obtained using 500 Hz sweepwidth. In addition, the resonance at δ 4.48 is illustrated at higher gain. The stick figures illustrate calculated relative intensities.

This experiment has been repeated for pivalaldehyde concentrations ranging from 0.1 to 1 mol/l. While the overall intensity of the spectrum depends on the concentration, the relative intensities of the individual lines do not appear to be altered significantly. Furthermore no new lines were observed at higher concentrations. When the experiment was repeated using a degassed sample, only a slight increase in the overall intensity of the spectrum was observed. Similar spectra were obtained when perfluorobenzene and deuteroacetonitrile were each used as the solvent. On the other hand, when a perfluoromethylcyclohexane solution containing 0.2 *M* pivalaldehyde and 0.2 *M* CCl_4 is irradiated under the same conditions, the spectrum (Fig. 1*C*) differs significantly from the one given in Fig. 1*A*. First, in addition to the lines observed in *A*, five new lines are observed. Three of these five have been definitely assigned to *t*-butyl chloride **4** at 1.40 p.p.m., chloroform **5** at 7.24 p.p.m., and trichloroacetaldehyde **6** at 8.94 p.p.m. We have ruled out the possibility that formyl chloride is responsible for any of these lines because we have determined its chemical shift as 8.04 p.p.m. The remaining two lines are unidentified. Second, the relative intensities and/or directions of lines in *C* differ from corresponding lines in *A*. These differences will be discussed in the next section.

Discussion

As in the case of di-*t*-butyl ketone (1), the observed spectra can be explained in terms of radical reactions occurring via radical pairs.

$$(CH_3)_3CCOH \xrightarrow{h\nu} [(CH_3)_3C\cdot\cdot COH]^T$$

1

[1] $\longrightarrow$ 1

[2] $[(CH_3)_3C\cdot\cdot COH]^{T,F} \longrightarrow (CH_3)_3CH + CO$ (2)

[3] $\longrightarrow (CH_3)_3C\cdot + \cdot COH$

[4] $(CH_3)_3C\cdot + \cdot COH \longrightarrow [(CH_3)_3C\cdot\cdot COH]^F$

[5] $2(CH_3)_3C\cdot \longrightarrow [(CH_3)_3C\cdot\cdot C(CH_3)_3]^F$

[6] $[(CH_3)_3C\cdot\cdot C(CH_3)_3]^F \longrightarrow 2 + (CH_3)_2C = CH_2$ (3)

[7] $\longrightarrow$ tetramethylbutane

SCHEME 1

Before discussing the simulation of these spectra, it is convenient to present in Schemes 1 and 2 the mechanism proposed to explain our results.

According to Scheme 1, **1** absorbs a quantum of light and via intersystem crossing from an excited electronic singlet state eventually ends up in an electronic triplet state from which the $[(CH_3)_3C\cdot\cdot COH]^T$ radical pair is formed. The superscript T indicates that the radical pair precursor is a triplet state. This radical pair has several reaction paths available to it such as recombination (eq. 1), disproportionation (eq. 2), and dissociation (eq. 3). If the radical pair dissociates to free radicals (*i.e.* no spin correlation between the unpaired electrons), the *t*-butyl radical and the formyl radical may reassociate to form the radical pair $[(CH_3)_3C\cdot\cdot COH]^F$ which can react via eqs. 1 and 2 or dissociate according to eq. 3. Likewise two *t*-butyl radicals may associate to form the radical pair $[(CH_3)_3C\cdot\cdot C(CH_3)]^F$ which may react according to eqs. 6 and 7 or dissociate. Finally, two formyl radicals may associate to form the radical pair $[HOC\cdot\cdot COH]^F$; however, because Δg is zero, no net nuclear spin polarization would be observed for the products derived from this radical pair. Similarly, tetramethylbutane obtained according to eq. 8 would exhibit no nuclear spin polarization (1), and no enhanced resonance is observed for this compound.

The CIDNP spectrum observed in the presence of carbon tetrachloride supports this scheme and provides additional information. The mechanism proposed to explain the spectrum in Fig. 1*C* is given in Scheme 2.

In this scheme, the initial radical pair $[(CH_3)_3C\cdot\cdot COH]^T$ formed from the triplet precursor reacts to give **1** and **2** with nuclear spin polarization in the same manner as Scheme 1. However, once this radical pair dissociates to the free *t*-butyl radical and the free formyl radical, reassociation of these radicals is prevented by the reactions given by eqs. 8–12. That is, the presence of CCl_4 reduces the formation of $[(CH_3)_3C\cdot\cdot COH]^F$ and $[(CH_3)_3C\cdot\cdot C(CH_3)]^F$ to the point that nuclear spin polarization resulting from these radical pairs is minor compared to the reaction paths given in Scheme 2.

These conclusions are based on the calculation of the nuclear spin polarization which results from each radical pair given in Schemes 1 and 2. Details of the theory used to calculate the nuclear spin polarization have been given previously (1), and only the final equations are given here. The nuclear spin polarization in a diamagnetic product is proportional to $(\rho_{ss}^m - \rho_{ss}^j)$ where m and j indicate nuclear spin states and ρ_{ss}, which is the diagonal density matrix element for the singlet spin state of the radical pair, is given by the expression

$$[13] \quad \rho_{ss}^j = \frac{(\alpha_{ss} + \mu_j(2 + \gamma)\alpha_{TT})/k_{-2}}{1 + \gamma + \mu_j(2 + \gamma)}$$

In this equation, α_{ss} and α_{TT} depend on the nature of precursor for the radical pair: for singlet precursor $\alpha_{ss} = r$ and $\alpha_{TT} = 0$; for triplet precursor $\alpha_{TT} = r'/3$ and $\alpha_{ss} = 0$; and if two separate free radicals combine to form the radical pair, $\alpha_{TT} = \alpha_{ss} = r''/4$ where r, r', and r'' are the rates for formation of the radical pair. In addition in eq. 13, $\gamma = k_1/k_{-2}$ where k_1 is the rate constant for product formation from the radical pair and k_{-2} is the rate constant for dissociation of the radical pair; and μ_j is given by the expression

$$[14] \quad \mu_j = \frac{H_{ST}^2/k_{-2}^2}{(1 + \gamma/2)^2 + 4J^2/k_{-2}^2 + (2 + \gamma)H_{ST}^2/k_{-2}^2}$$

In eq. 14, J is the electron exchange integral, and H_{ST} is the off-diagonal matrix element of the spin-Hamiltonian which mixes the singlet with the $M = 0$ state of the triplet manifold, and is obtained from the expression

$$[15] \quad H_{ST} = \tfrac{1}{2}\beta H_0(g_1 - g_2) + \tfrac{1}{2}\sum_l (A_1^l - A_2^l) < M_1|I_z^l|M_1>$$

In this expression β is the electron Bohr magneton, H_0 is the strength of the external magnetic

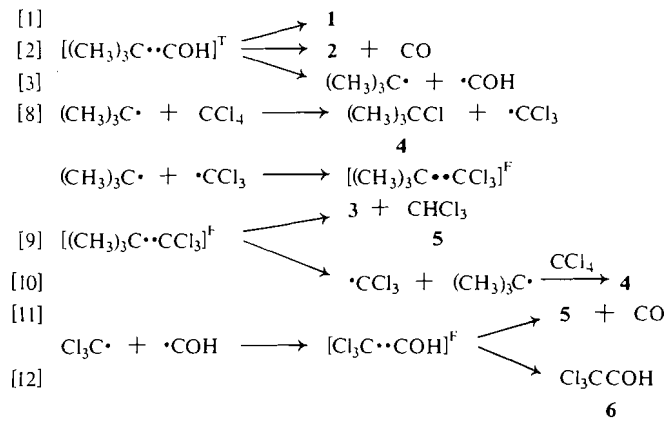

SCHEME 2

field, g is the isotropic electronic g factor, A is the electron-nuclear coupling constant, M_I is the nuclear spin state, I_z is z component of the nuclear spin operator, and the subscript and superscript label the electron and nucleus, respectively.

For the calculations, the g and A values for each radical are taken from e.s.r. data. The values used for J, k_{-2}, and γ are 10^8 Hz, 10^9 s^{-1}, and 0.2, respectively; and although they are reasonable (1), they are somewhat arbitrary. Consequently, absolute values for nuclear spin polarization could not be calculated. However, since the e.s.r. data are known, the calculated relative values are meaningful and very useful in understanding the photochemical reaction of pivalaldehyde.

Consider first the formation of **2** and its spectra in Figs. 1*A* and 1*C*. According to Scheme 1, this compound can be formed from three different radical pairs: $[(CH_3)_3C\cdot\cdot COH]^T$, $[(CH_3)_3C\cdot\cdot COH]^F$, and $[(CH_3)_3C\cdot\cdot C(CH_3)_3]^F$. On the basis of the fit of calculated spectrum with the observed spectrum and the effect of CCl_4, one can determine that the polarization observed for **1** in Fig. 1*A* probably results from all three radical pairs. Furthermore, the radical pair $[(CH_3)_3C\cdot\cdot COH]^S$ derived from a singlet precursor cannot be responsible for the observed polarization because calculations show that it would give the opposite polarization. For the calculations based on these radical pairs, the values used for A and g are +22.7 G (1, 8) and 2.0025 for $(CH_3)_3C\cdot$, and +137 G (9) and 2.0009 (9) for ·COH. The value of g for $(CH_3)_3C\cdot$ is based on the values obtained for alkyl radicals (10). In addition, as was done previously, the following values were used for the indirect nuclear spin coupling constants: +6.4 Hz, vicinal coupling for **2**; and −1.1 Hz, allylic coupling for **3**.

As mentioned above, the spectrum of **2** can result from three different radical pairs. To arrive at this conclusion, it is necessary to compare Fig. 1*A* with 1*C* because Scheme 2 indicates that the formation of **2** is derived solely from $[(CH_3)_3C\cdot\cdot COH]^T$. Based on this radical pair, the calculated resonance lines for the methyl and methine hydrogens are given under Figs. 1*A* and 1*B*. Comparison of the calculated lines of the methyl hydrogens with the observed ones in Fig. 1*C* indicates a good fit. Unfortunately it is not possible to make the same comparison for the methine hydrogen because of the superposition of the *t*-butyl chloride and the methyl hydrogen lines of 2-methylpropene. We will return to the methine hydrogen below.

Thus, because of the fit between the calculated and observed intensities for the lines of the methyl hydrogen of **2**, we conclude that **2** is formed via the radical pair $[(CH_3)_3C\cdot\cdot COH]^T$ when **1** is irradiated in the presence of CCl_4. Furthermore, since the observed intensity pattern is similar in Fig. 1*A*, also, part of the polarization for **2** when CCl_4 is not present probably occurs via $[(CH_3)_3C\cdot\cdot COH]^T$. Reaction via the radical pair $[(CH_3)_3C\cdot\cdot COH]^S$ does not fit because the sign of the polarization calculated on this basis is opposite to the one observed. The importance of $[(CH_3)_3C\cdot\cdot C(CH_3)_3]^F$ to the polarization observed in Fig. 1*A* is determined in the following manner. The intensity of the methyl absorption

line divided by the intensity of the methyl emission line is 2.6 in Fig. 1*A* and 3.2 in Fig. 1*B*. If only $[(CH_3)_3C\cdot\cdot COH]^T$ were responsible for the polarization, the ratio in Fig. 1*A* should be 3.2. If only $[(CH_3)_3C\cdot\cdot C(CH_3)_3]^F$ were responsible for the polarization, the ratio based on a previous calculation (1) should be 1. Thus, $[(CH_3)_3C\cdot\cdot C(CH_3)_3]^F$ contributes to part of the polarization of the methyl hydrogen of **2** observed in Fig. 1*A*. Additional evidence for this conclusion is obtained from the spectrum for 2-methylpropene as described below.

The contribution of $[(CH_3)C\cdot\cdot COH]^F$ to the polarization of **2** in the absence of CCl_4 cannot be determined with any degree of certainty. Although the intensity of the absorption and emission lines of the methyl hydrogen decrease in the presence of CCl_4 (Fig. 1*A vs.* Fig. 1*C*), we cannot rule out the possibility that the decrease is due mainly to the absence of any appreciable reaction via $[(CH_3)_3C..C(CH_3)_3]^F$ and to singlet or triplet energy transfer from pivalaldehyde to CCl_4.

For the methine hydrogen of **2**, the calculated intensities should be compared with intensities observed in the presence of CCl_4 since the intensities were calculated on the basis of $[(CH_3)_3C\cdot\cdot COH]^T$. Unfortunately, these lines are masked by the methyl hydrogen lines (emission) of **3** and the methyl hydrogen line (absorption) of **4**. For comparison with the methine lines in Figs. 1*A* and 1*B*, the calculated intensities should include the values based on $[(CH_3)_3C\cdot\cdot COH]^T$, $[(CH_3)_3C\cdot\cdot COH]^F$, and $[(CH_3)_3C\cdot\cdot C(CH_3)_3]^F$. However, since the relative contributions of each of these radical pairs is not known, such a simulation would be arbitrary. Instead, the relative intensities calculated only on the basis of $[(CH_3)_3C\cdot\cdot COH]^F$ and $[(CH_3)_3C\cdot\cdot COH]^T$ (since they give identical results) have been included in Fig. 1 to illustrate that the polarization for **2** is consistent with F and T precursors rather than the S precursor.

As indicated earlier, while the carbonyl hydrogen line of **1** appears as emission during irradiation, the methyl hydrogen does not appear to be polarized. This result is consistent with the formation of **1** via $[(CH_3)_3C\cdot\cdot COH]^{T,F}$. The calculated relative intensity of the carbonyl hydrogen of **1** is about four times the value for the methyl hydrogen. Consequently, when the calculated intensity of the carbonyl hydrogen is normalized to the observed value in Fig. 1, the calculated intensity of the methyl hydrogen is a small fraction of the observed intensity, and no effect is expected.

In Fig. 1*C*, the carbonyl hydrogen line of **1** no longer appears as emission; however, its intensity is decreased compared to its intensity after irradiation (indicated by the dashed line). Thus, the polarization of this hydrogen in the presence of CCl_4 is decreased. A possible explanation for this decrease might be that polarization occurs via $[(CH_3)_3C..COH]^{T,F}$ in the absence of CCl_4 whereas it occurs only via $[(CH_3)_3C\cdot\cdot COH]^T$ in the presence of CCl_4 (Scheme 2). However, as mentioned above, we cannot rule out the possibility that the decrease is due to quenching of the excited state of pivalaldehyde by CCl_4.

As mentioned above, the spectrum for 2-methylpropene **3** provides additional evidence for the occurrence of the radical pair $[(CH_3)_3C\cdot\cdot C(CH_3)_3]^F$ in the absence of CCl_4. As indicated in Scheme 1, **3** may be formed via a disproportionation reaction involving this radical pair. The calculated line intensities for the methylene hydrogens of **3** are illustrated under the observed intensities in Fig. 1*B*. Unfortunately, a similar comparison cannot be made for the methyl hydrogen of **3** because its lines are masked by the lines of the methine hydrogen of **2**. Another possible path for the formation of olefin is a disproportionation reaction involving $[(CH_3)_3C\cdot\cdot COH]^{T,F}$ to give olefin plus HCOH. However, no enhanced HCOH line is observed, and in this case the calculated intensity pattern for the methylene hydrogen differs from the observed one. Consequently, in the absence of CCl_4, our results are consistent with the formation of **3** mainly via $[(CH_3)_3C\cdot\cdot C(CH_3)_3]^F$.

In the presence of CCl_4, the intensity pattern for the lines of **3** change markedly as can be seen in Fig. 1*C*. The net emission observed for both the methylene and the methyl hydrogens of **3** is consistent with the formation of olefin via $[(CH_3)_3C\cdot\cdot CCl_3]^F$. The intensity pattern calculated for the methylene hydrogen lines is given under the corresponding observed lines in Fig. 1*C*. The calculated pattern for the methyl hydrogen is not presented since comparison with the observed pattern is not possible because of overlap with other lines. For this calculation, a value of 2.0091 was used for the *g* factor of $\cdot CCl_3$ (11).

The other product which results from this

radical pair is $CHCl_3$, and in agreement with observation, the calculation indicates emission for this line. Another source for this compound is the radical pair $[Cl_3C\cdot\cdot COH]^F$. As indicated in Scheme 2 this radical pair can give either $CHCl_3$ or Cl_3CCOH, both of which are observed. Again in agreement with observation, the calculation based on this radical pair indicates emission for the resonance lines for these compounds. The calculated intensity for Cl_3CCOH has not been included in Fig. 1 because it cannot be compared directly with the calculated intensities of the other products. Thus, both $[(CH_3)_3C\cdot\cdot CCl_3]^F$ and $[Cl_3C\cdot\cdot COH]^F$ can provide $CHCl_3$ having its hydrogen spin polarized. Our results do not allow us to determine the relative contribution of these two radical pairs to the formation of $CHCl_3$.

As indicated in Fig. 1*C*, the intensity of the *t*-butyl chloride line decreases to the dashed lines when the irradiation is stopped, indicating polarization of its hydrogens. This enhanced absorption can be rationalized as indicated in eq. 10 of Scheme 2. When the radical pair $[(CH_3)_3C\cdot\cdot CCl_3]^F$ dissociates, the hydrogens of $(CH_3)_3C\cdot$ are initially polarized. This radical then reacts with CCl_4 to form *t*-butyl chloride and $\cdot CCl_3$ at a rate fast enough to make the lifetime of $(CH_3)_3C\cdot$ shorter than the spin–lattice relaxation time of its hydrogens. Consequently, the polarization is retained in *t*-butyl chloride. Calculation of the polarization according to this mechanism gives the proper sign for the polarization. The calculated intensity of *t*-butyl chloride has not been included in Fig. 1 because it cannot be compared directly with the calculated intensities of the other product lines.

Finally, in addition to the reactions given by eqs. 8–12, it is probable that CCl_4 reacts with pivalaldehyde via a chain mechanism. A chain reaction between isovaleraldehyde and CCl_4 to give $CHCl_3$ and isovaleryl chloride as the main products has been reported (12). In the case of pivalaldehyde, we observe *t*-butyl chloride and $CHCl_3$ as the major products when pivalaldehyde is irradiated in the presence of CCl_4. A possible mechanism is

$$RCOH + \cdot CCl_3 \rightarrow RCO\cdot + CHCl_3$$

$$RCO\cdot \rightarrow R\cdot + CO$$

$$R\cdot + CCl_4 \rightarrow RCl + \cdot CCl_3$$

where R signifies the *t*-butyl group. This chain mechanism is similar to the one proposed earlier for isovaleraldehyde (12) except that a step for the loss of CO by $RCO\cdot$ is included and $R\cdot$ rather than $RCO\cdot$ reacts with CCl_4. While this chain mechanism can explain the formation of *t*-butyl chloride and $CHCl_3$, it cannot account for the nuclear spin polarization observed for these products during irradiation because it does not involve the formation of radical pairs. Consequently, Scheme 2 must also be included to explain the n.m.r. spectrum. Some idea of the importance of the chain mechanism compared with Scheme 2 can be obtained by comparing the intensities of the $CHCl_3$ and *t*-butyl chloride lines after irradiation. The ratio of *t*-butyl chloride intensity to the $CHCl_3$ intensity is about 25. This ratio is an average of runs on four identical samples. If only the chain mechanism suggested above were occurring, this ratio should be 9.

In summary, our CIDNP results are consistent with a mechanism in which the primary photochemical step in the photolysis of pivalaldehyde in perfluoromethylcyclohexane is the cleavage of the bond between the carbonyl carbon and the tertiary carbon of the *t*-butyl group. This step appears to occur predominantly via an excited electronic triplet state of pivalaldehyde. In contrast, this mechanism does not appear to be the main route responsible for the CIDNP effects observed in the photochemical reaction of acetaldehyde in solution (3). Finally, as indicated by the chain mechanism discussed above, the occurrence of CIDNP effects does not preclude the possibility of other reaction steps which may be more important in product formation (see also ref. 7).

The authors thank Dr. D. R. Arnold for indicating the possibility of a chain reaction. This research was supported in part by the Petroleum Research Fund administered by the American Chemical Society and by the National Research Council of Canada.

1. M. Tomkiewicz, A. Groen, and M. Cocivera. J. Chem. Phys. **56**, 5850 (1972).
2. N. Yang, E. Feit, M. Hui, N. Turro, and J. Dalton. J. Am. Chem. Soc. **92**, 6974 (1970).
3. B. Blank and H. Fischer. Helv. Chim. Acta, **56**, 506 (1973).
4. S. Rosenfeld, R. Lawler, and H. Ward. J. Am. Chem. Soc. **95**, 946 (1973).
5. M. Cocivera and A. Trozzolo. J. Am. Chem. Soc. **92**, 1772 (1970).

6. G. CLOSS and D. PAULSON. J. Am. Chem. Soc. **92**, 7229 (1970).
7. K. SCHAFFNER, H. WOLF, S. M. ROSENFELD, R. LAWLER, and H. WARD. J. Am. Chem. Soc. **94**, 6553 (1972).
8. H. FISCHER. J. Phys. Chem. **73**, 3834 (1969).
9. F. ADRIAN, E. COCHRAN, and V. BOWERS. J. Chem. Phys. **36**, 1661 (1962).
10. H. FISCHER. Magnetic properties of free radicals, Landalt-Bornstein. *Edited by* K. Hellwege and A. Hellwege. Springer-Verlag, Berlin. 1965. pp. 22–38.
11. A. HUDSON and H. HUSSAIN. Mol. Phys. **16**, 199 (1969).
12. S. WINSTEIN and F. SEUBOLD. J. Am. Chem. Soc. **69**, 2916 (1947).

A Synthesis of 2-Acetamido-2,6-dideoxy-D-gulose, 2-Acetamido-2,6-dideoxy-D-idose, and 2,6-Dideoxy-D-*xylo*-hexose (Boivinose)[1]

MALCOLM B. PERRY AND VIRGINIA DAOUST

Division of Biological Sciences, National Research Council of Canada, Ottawa, Canada K1A 0R6

Received February 27, 1973

The base-catalyzed addition of nitromethane to 5-deoxy-D-xylose gave a mixture of 1,6-dideoxy-1-nitro-D-gulitol (**2**) and 1,6-dideoxy-1-nitro-D-iditol (**3**) (*ca.* 1 :1) which underwent the Nef reaction to give 6-deoxy-D-gulose and 6-deoxy-D-idose. Acetylation of mixed **2** and **3** afforded the corresponding 2,3,4,5-tetra-*O*-acetyl-1,6-dideoxy-1-nitro-D-gulitol (**4**) and 2,3,4,5-tetra-*O*-acetyl-1,6-dideoxy-1-nitro-D-iditol (**5**) derivatives which on treatment with methanolic ammonia yielded 2-acetamido-1,2,6-trideoxy-1-nitro-D-gulitol (**11**) and 2-acetamido-1,2,6-trideoxy-1-nitro-D-iditol (**12**) (*ca.* 6 :1). Compounds **11** and **12** underwent the modified Nef reaction to give 2-acetamido-2,6-dideoxy-D-gulose (**13**) and 2-acetamido-2,6-dideoxy-D-idose (**14**) which were separated by cellulose column chromatography.

Compound **4** was converted to 3,4,5-tri-*O*-acetyl-1,2,6-trideoxy-1-nitro-D-*xylo*-hex-1-enitol (**6**) which on catalytic reduction gave 3,4,5-tri-*O*-acetyl-1,2,6-trideoxy-1-nitro-D-*xylo*-hexitol (**7**). Compound **7** underwent the Nef reaction to yield 2,6-dideoxy-D-*xylo*-hexose (**8**) (D-boivinose).

L'addition, catalysée par une base, du nitrométhane au déoxy-5 D-xylose a conduit au mélange (*ca.* 1 :1) de didéoxy-1,6 nitro-1 D-gulitol (**2**) et de didéoxy-1,6 nitro-1 D-iditol (**3**) qui, soumis à la réaction de Nef, a conduit au déoxy-6 D-gulose et déoxy-6 D-idose. L'acétylation du mélange **2** et **3** a conduit aux dérivés correspondants tétra-*O*-acétyl-2,3,4,5 didéoxy-1,6 nitro-1 D-gulitol (**4**) et tétra-*O*-acétyl-2,3,4,5 didéoxy-1,6 nitro-1 D-iditol (**5**) qui, à l'aide d'un traitement avec une solution d'ammoniaque dans du méthanol, ont produit un mélange (*ca.* 6 :1) d'acétamido-2 tridéoxy-1,2,6 nitro-1 D-gulitol (**11**) et d'acétamido-2 tridéoxy-1,2,6 nitro-1 D-iditol (**12**). Les composés **11** et **12**, lorsque soumis à la réaction modifiée de Nef, ont conduit à l'acétamido-2 didéoxy-2,6 D-gulose (**13**) et à l'acétamido-2 didéoxy-2,6 D-idose (**14**) lesquels ont pu être séparés par chromatographie sur colonne de cellulose.

Le composé **4** a été transformé en tri-*O*-acétyl-3,4,5 tridéoxy-1,2,6 nitro-1 D-*xylo*-hexène-1 itol (**6**) qui, par réduction catalytique, a donné le tri-*O*-acétyl-3,4,5 tridéoxy-1,2,6 nitro-1 D-*xylo* hexitol (**7**). Le composé **7** soumis à la réaction de Nef a conduit au didéoxy-2,6 D-*xylo*-hexose (**8**) (D-boivinose).

[Traduit par le journal]

Can. J. Chem., **51**, 3039 (1973)

5-Deoxy-D-xylose (**1**) (1) underwent base-catalyzed addition of nitromethane to give approximately equal amounts of the expected 1,6-dideoxy-1-nitro-D-gulitol (**2**) and 1,6-dideoxy-1-nitro-D-iditol (**3**) derivatives. A portion of this product treated under the Nef reaction conditions (2, 3) gave 6-deoxy-D-gulose (**9**) and 6-deoxy-D-idose (**10**) which were separated by cellulose column chromatography. Both sugars had properties in agreement with those previously recorded and each on treatment with phenylhydrazine gave 6-deoxy-D-*xylo*-hexose phenylosazone. Kovár and Baer (4) and Baer (5) have shown that the nitromethane addition to aldoses is subject to kinetic control and that the epimeric product ratio is mainly influenced by the configuration at C-3 leading to the predominant production of the derivative with 2,4-*threo* hydroxyl groups. On these stereochemical considerations, hexitol **2** would have been expected as the major product. The equal yields of hexitols **2** and **3** may, however, represent thermodynamic products considering the extended reaction time (20 h) used.

Acetylation of mixed **2** and **3** afforded their corresponding 2,3,4,5-tetra-*O*-acetyl derivatives **4** and **5** from which 2,3,4,5-tetra-*O*-acetyl-1,6-dideoxy-1-nitro-D-gulitol (**4**) (identified by Nef reaction product) was obtained crystalline. The compound **4** on treatment with sodium bicarbonate in boiling benzene solution gave 3,4,5-tri-*O*-acetyl-1,2,6-trideoxy-1-nitro-D-*xylo*-hex-1-enitol (**6**) and reduction of this compound with hydrogen in the presence of palladium black afforded 3,4,5-tri-*O*-acetyl-1,2,6-trideoxy-1-nitro-D-*xylo*-hexitol (**7**) which underwent the Nef reaction to yield 2,6-dideoxy-D-*xylo*-hexose (**8**) (D-boivinose). The 2,6-dideoxy-D-*xylo*-hexose

[1]NRCC No. 13290.

Can. J. Chem. Downloaded from www.nrcresearchpress.com by 210.87.254.6 on 09/05/12
For personal use only.

Can. J. Chem. Downloaded from www.nrcresearchpress.com by 210.87.254.6 on 09/05/12
For personal use only.

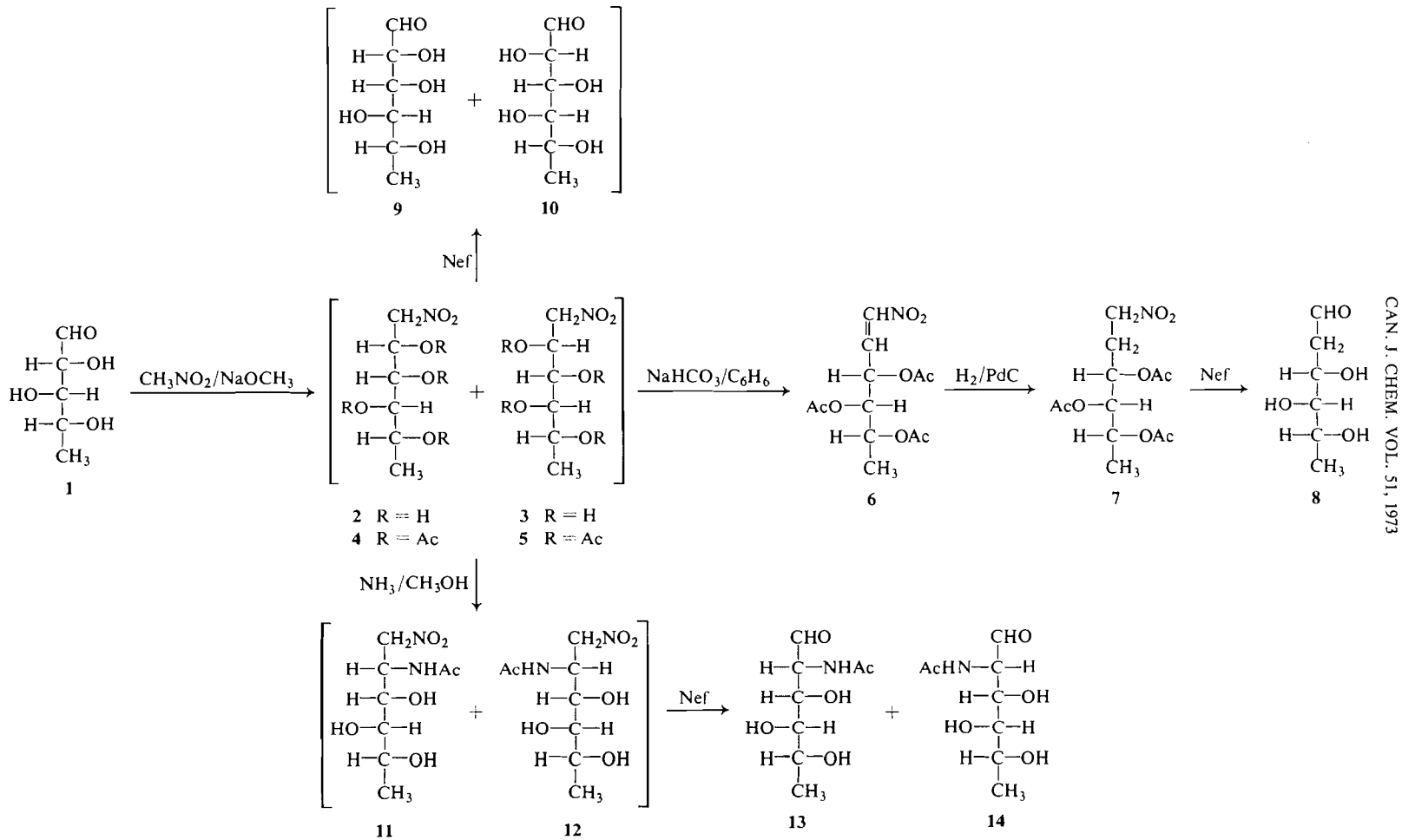

Can. J. Chem. Downloaded from www.nrcresearchpress.com by 210.87.254.6 on 09/05/12
For personal use only.

had physical properties in agreement with those recorded for the compounds isolated from natural glycosides (6) and with the compound synthesized from methyl 2,3-anhydro-α-D-alloside (7).

The mixed 2,3,4,5-tetra-*O*-acetyl-1,6-dideoxy-1-nitro-D-hexitols **4** and **5** on treatment with methanolic ammonia afforded a mixture of 2-acetamido-1,2,6-trideoxy-1-nitro-D-gulitol (**11**) and 2-acetamido-1,2,6-trideoxy-1-nitro-D-iditol (**12**) which underwent the modified Nef reaction (3) to yield 2-acetamido-2,6-dideoxy-D-gulose (**13**) and 2-acetamido-2,6-dideoxy-D-idose (**14**) (*ca.* 6:1) which were separated by cellulose column chromatography. The 2-acetamido-2,6-dideoxy-D-idose was obtained crystalline but the 2-acetamido-2,6-dideoxy-D-gulose, which could not be induced to crystallize, was hydrolyzed with hydrochloric acid to give crystalline 2-amino-2,6-dideoxy-D-gulose hydrochloride which had physical properties in agreement with those recorded for the sugar synthesized from 2-amino-2-deoxy-D-gulose (8). It is interesting to note that the amination of 3,4,5,6-tetra-*O*-acetyl-1,2-dideoxy-1-nitro-D-*xylo*-hex-1-enitol (9) followed by treatment of the products under the modified Nef reaction conditions afforded 2-acetamido-2-deoxy-D-gulose and 2-acetamido-2-deoxy-D-idose in the ratio 8.1 : 1.

Experimental

Paper chromatography was performed by the descending method (10) on Whatman No. 1 filter paper using either (A) pyridine – ethyl acetate – water (2 : 5 : 5 v/v, top layer) or (B) 1-butanol – ethanol – water (4 : 1 : 5 v/v, top layer) as the mobile phase. Glycoses were detected with either (a) 2% silver nitrate in acetone followed by 3% sodium hydroxide in ethanol (11), (b) 2% *p*-anisidine hydrochloride in ethanol (12) or 2% ninhydrin in acetone. The rates of movement of the glycoses are quoted relative to D-galactose (R_{Gal}) or to 2-amino-2-deoxy-D-glucose hydrochloride (R_{GN}).

G.l.p.c. was carried out using a Hewlett-Packard model 402 chromatograph with a hydrogen flame detector and fitted with glass U-tubes (4 ft × 6 mm × 3 mm internal diameter) packed with either (A) 10% neopentylglycol sebacate polyester on 80–100 mesh acid washed Chromosorb W or (B) 3% ECNSS-M on 100–120 mesh Gas-Chrom Q (Applied Science Labs., State College, Pa.). Retention times of the compounds are quoted relative to penta-*O*-acetyl-L-arabinitol (T_A) or 2-acetamido-1,3,4,5,6-penta-*O*-acetyl-2-deoxy-D-glucitol (T_{GNo1Ac}).

Melting points were determined on a Fisher-Johns apparatus and are corrected. Solutions were concentrated under reduced pressure and below 40 °C. Optical rotations were determined at 20 °C using a Perkin–Elmer 141 polarimeter. I.r. spectra were obtained by the potassium bromide disc technique using a Perkin-Elmer 237B Infracord.

A. Addition of Nitromethane to 5-Deoxy-D-xylose

To a solution of 5-deoxy-D-xylose (**1**) (1) (10 g) in a mixture of methanol (120 ml) and nitromethane (50 ml) was added 1.7 *N* sodium methoxide in methanol (54 ml) and the stirred reaction mixture was kept at 20 °C for 20 h. Following the addition of ether (1 l), the precipitated product was collected by filtration, washed with a little cold methanol, ether, light petroleum (b.p. 30–60 °C), and dried *in vacuo* (12.9 g). The product (12.5 g) in water (200 ml) was passed down a column of Rexyn 101(H^+) ion-exchange resin (280 ml) and the eluate and water washings were concentrated to a syrup (10.3 g) containing 1,6-dideoxy-1-nitro-D-gulitol (**2**) and 1,6-dideoxy-1-nitro-D-iditol (**3**).

B. Synthesis of 6-Deoxy-D-gulose (9) and 6-Deoxy-D-idose (10)

A portion of mixed **2** and **3** (from experiment A) (1 g) dissolved in a solution of $Ba(OH)_2.8H_2O$ (1.23 g) in water (20 ml) was added dropwise with stirring to a solution of concentrated sulfuric acid (1.13 ml) in water (10 ml). After 16 h at room temperature, the reaction mixture was neutralized ($BaCO_3$), filtered, and the filtrate after deionization with mixed Rexyn 101(H^+) and RG6(OH^-) ion-exchange resins (10 ml) was concentrated to a syrup (0.52 g). Paper chromatographic examination of the syrup (solvent A) revealed two components having R_{Gal} 3.98 and 2.82 corresponding in mobility and color reactions with authentic **10** and **9** respectively.

A portion of the mixed **9** and **10** (5 mg) was reduced ($NaBH_4$) and acetylated (13) and g.l.p.c. (column B, 180 °C) of the product gave two peaks corresponding in retention times with 1,2,3,4,5-penta-*O*-acetyl-6-deoxy-D-gulitol (T_A 0.83, 51%) and 1,2,3,4,5-penta-*O*-acetyl-6-deoxy-D-iditol (T_A 1.08, 49%).

Separation of **9** and **10** by cellulose column (4 × 60 cm) chromatography using 1-butanol – water (10 : 1 v/v) as the mobile phase gave the following compounds.

(1) 6-Deoxy-D-idose (10)

10 (170 mg) was eluted first from the column and remained a chromatographically pure syrup having $[\alpha]_D$ +14.7° (*c*, 0.7 in water) and R_{Gal} 3.98 (solvent A). The reduced ($NaBH_4$) and acetylated sugar on g.l.p.c. examination (column B, 180 °C) gave a single peak with T_A 1.08, and treatment with phenylhydrazine afforded 6-deoxy-D-*xylo*-hexose phenylosazone having m.p. and mixture m.p. 175–177 °C (lit. (14) m.p. 168–172 °C, (15) 182–184 °C dec.) and giving an i.r. spectrum identical with an authentic derivative.

(2) 6-Deoxy-D-gulose (9)

9 (188 mg) had $[\alpha]_D$ −41° (*c*, 0.5 in water) (lit. 1, 16) $[\alpha]_D$ −38° (water), gave a single spot on paper chromatography (R_{Gal} 2.82 (solvent A)), and the reduced ($NaBH_4$) and acetylated derivative gave a single peak on g.l.p.c. (column B, 180 °C) with T_A 0.83. **9** on treatment with phenylhydrazine afforded 6-deoxy-D-*xylo*-hexose phenylosazone with m.p. and mixture m.p. 175–177 °C.

C. 2,6-Dideoxy-D-xylo-hexose (8)

(1) Acetylation of 1,6-Dideoxy-1-nitro-D-gulitol (2) and 1,6-Dideoxy-1-nitro-D-iditol (3)

The mixture of **2** and **3** (experiment *A*) (9 g) in acetic anhydride (80 ml) was treated with a drop of concentrated sulfuric acid and the mixture was heated on a boiling

Can. J. Chem. Downloaded from www.nrcresearchpress.com by 210.87.254.6 on 09/05/12
For personal use only.

water bath for 30 min. The cooled mixture was poured into an ice–water mixture (700 ml) and after 1 h the acetylated derivatives, which had separated as an oil, were collected, taken up in chloroform (200 ml), washed with water (3 × 50 ml), dried (anhydrous Na_2SO_4), and concentrated to a syrup (13.4 g). An ethanol solution of the product afforded crystalline 2,3,4,5-tetra-*O*-acetyl-1,6-dideoxy-1-nitro-D-gulitol (**4**) (4.2 g) which after two recrystallizations from ethanol had m.p. 158–159 °C and $[\alpha]_D$ +14.4° (*c*, 0.4 in chloroform).

Anal. Calcd. for $C_{14}H_{21}NO_{10}$: C, 46.28; H, 5.83; N, 3.86. Found: C, 46.47; H, 5.79; N, 3.70.

*(2) 3,4,5-Tri-O-acetyl-1,2,6-trideoxy-1-nitro-*D*-xylo-hex-1-enitol (6)*

Compound **4** (3.5 g) in dry benzene (45 ml) was boiled under reflux for 2.5 h with sodium bicarbonate (6 g). The cooled reaction mixture was filtered and the filtrate was concentrated to a syrup (3.3 g). An ethanol solution of the product kept at 2 °C afforded crystalline **6** (2.1 g) which had m.p. 126–127 °C and $[\alpha]_D$ +6.5° (*c*, 0.4 in chloroform).

Anal. Calcd. for $C_{12}H_{17}NO_8$: C, 47.52; H, 5.65; N, 4.62. Found: C, 47.45; H, 5.63; N, 4.59.

*(3) 3,4,5-Tri-O-acetyl-1,2,6-trideoxy-1-nitro-*D*-xylo-hexitol (7)*

Compound **6** (1.5 g) in ethanol (50 ml) was shaken with hydrogen at room temperature and pressure in the presence of palladium black (0.15 g). One mol equiv of hydrogen was absorbed in 30 min and the rate of reduction then became very slow. At this point, the reaction mixture was filtered and the filtrate was concentrated to a syrup (1.4 g). A methanol solution of the product gave crystalline **7** (0.92 g) which had m.p. 82–83 °C and $[\alpha]_D$ −16.6° (*c*, 0.3 in chloroform) unchanged on further recrystallization from methanol.

Anal. Calcd. for $C_{12}H_{19}NO_8$: C, 47.21; H, 6.27; N, 4.59. Found: C, 47.35; H, 6.40; N, 4.49.

*(4) 2,6-Dideoxy-*D*-xylo-hexose (8)*

Compound **7** (0.5 g) was dissolved in *N* sodium hydroxide solution (9 ml) at 37 °C and after 2 h the solution was added dropwise with stirring to a solution of concentrated sulfuric acid (3 ml) in water (20 ml) and the mixture was kept at 20 °C for 18 h. Following neutralization ($BaCO_3$) and filtration, the filtrate was passed down columns of Rexyn 101(H^+) (20 ml) and RG6(OH^-) (15 ml) ion-exchange resins and the eluate and washings were concentrated to a syrup (0.36 g). Crystalline **8** (0.27 g), obtained from acetone solution, gave a single spot on paper chromatography (R_{Gal} 5.22, solvent A) and had m.p. 98–99 °C and $[\alpha]_D$ −14° (*c*, 1 in acetone) (lit. (6, 7) m.p. 100–103 °C and $[\alpha]_D$ −15° (acetone)).

Anal. Calcd. for $C_6H_{12}O_4 \cdot \frac{1}{2}H_2O$: C, 45.85; H, 8.34. Found: C, 46.03; H, 8.47.

*D. 2-Acetamido-2,6-dideoxy-*D*-gulose (13) and 2-Acetamido-2,6-dideoxy-*D*-idose (14)*

The mixture of **4** and **5** (remaining from experiment C(1)) (9.2 g) in dry methanol (100 ml) was cooled to 0 °C and ammonia gas was passed into the solution over 30 min to saturation, and the mixture was kept at 20 °C for 18 h. The concentrated mixture was triturated with hot chloroform (3 × 60 ml) to remove acetamide and the residual syrup (4.6 g) dissolved in a solution of $Ba(OH)_2 \cdot 8H_2O$ (5.7 g) in water (90 ml) was added dropwise with stirring to a solution of concentrated sulfuric acid (5.3 ml) in water (50 ml). After 18 h at room temperature, the reaction mixture was neutralized ($BaCO_3$), filtered, and the filtrate was passed down a column of mixed Rexyn 101(H^+) and RG6(OH^-) ion-exchange resins (25 ml). Concentration of the column eluate and water washings afforded a syrup (1.94 g) which on paper chromatographic examination (solvent A) revealed two spots with R_{Gal} 4.74 and 4.04 (visual ratio 1 :10) corresponding in mobility with **14** and **13** respectively. A portion of the product (5 mg) after reduction ($NaBH_4$) and acetylation (17) on g.l.p.c. analysis (210 °C) gave two peaks corresponding in retention times with 2-acetamido-1,3,4,5-tetra-*O*-acetyl-2,6-dideoxy-D-iditol (T_{GNo1Ac} 0.37 (columns A and B), 15%) and 2-acetamido-1,3,4,5-tetra-*O*-acetyl-2,6-dideoxy-D-gulitol (T_{GNo1Ac}0.47 (column A), 0.43 (column B), 85%).

The mixture of **13** and **14** (1.75 g) was fractionated by cellulose column (4 × 60 cm) chromatography using 1-butanol–water (10 :1 v/v) as the mobile phase to give the following compounds.

*(1) 2-Acetamido-2,6-dideoxy-*D*-idose (14)*

The first pure fraction from the column was concentrated to a syrup (0.22 g) and the fraction, moistened with ethanol, afforded crystalline **14** which had m.p. 145–147 °C and $[\alpha]_D$ −11.5° (*c*, 0.6 in water) unchanged on further recrystallization.

Anal. Calcd. for $C_8H_{15}NO_5$: C, 46.82; H, 7.37; N, 6.83. Found: C, 46.55; H, 7.40; N, 6.90.

14 gave a single spot on paper chromatography (R_{Gal} 4.74 (solvent A)) and following reduction ($NaBH_4$) and acetylation (17) the product gave a single peak on g.l.p.c. (210 °C) with T_{GNo1Ac}0.37 (columns A and B).

*(2) 2-Acetamido-2,6-dideoxy-*D*-gulose (13)*

The second fraction from the column was **13** (1.32 g) which remained a syrup and had $[\alpha]_D$ −75° (*c*, 0.5 in water). On paper chromatographic examination, **13** gave a single spot with R_{Gal} 4.04 (solvent A) and after reduction ($NaBH_4$) and acetylation (17) it gave 2-acetamido-1,3,4,5-tetra-*O*-acetyl 2,6-dideoxy-D-gulitol which on g.l.p.c. (210 °C) gave a single peak with T_{GNo1Ac}0.47 (column A) and 0.43 (column B).

*(3) 2-Amino-2,6-dideoxy-*D*-gulose Hydrochloride*

Compound **13** (from experiment *D*(2)) (1.1 g) was hydrolyzed with 3 *N* hydrochloric acid (25 ml) at 100 °C for 3 h and, following concentration, the resulting syrup was dissolved in a methanol–2-propanol mixture. On keeping at 2 °C, crystalline 2-amino-2,6-dideoxy-D-gulose hydrochloride (0.89 g) was obtained which had m.p. 171 °C (dec.) and $[\alpha]_D$ −36.4° (*c*, 1.2 in water) (lit. (8) m.p. >170 °C and $[\alpha]_D$ −35° (water)), and gave a single ninhydrin positive spot on paper chromatography (solvent B) with R_{GN} 1.67.

Anal. Calcd. for $C_6H_{14}NO_4Cl$: C, 36.10; H, 7.07; N, 7.02. Found: C, 36.05; H, 7.27; N, 6.84.

1. P. A. Levene and J. Compton. J. Biol. Chem. **111**, 325 (1935).
2. J. U. Nef. Ann. **280**, 263 (1894).
3. C. Satoh and A. Kiyomoto. Chem. Pharm. Bull. Tokyo, **12**, 615 (1964).
4. J. Kovář and H. H. Baer. Can. J. Chem. **48**, 2377 (1970).

5. H. H. BAER. Adv. Carbohydr. Chem. Biochem. **24**, 67 (1969).
6. O. SCHINDLER and T. REICHSTEIN. Helv. Chim. Acta, **35**, 730 (1952).
7. H. R. BOLLIGER and T. REICHSTEIN. Helv. Chim. Acta, **36**, 302 (1953).
8. K. BRENDEL, P. H. GROSS, and H. K. ZIMMERMAN. Ann. **691**, 192 (1966).
9. M. B. PERRY and A. C. WEBB. Can. J. Chem. **47**, 1245 (1969).
10. S. M. PARTRIDGE. Biochem. J. **42**, 238 (1948).
11. W. E. TREVELYAN, D. D. PROCTER, and J. S. HARRISON. Nature, **166**, 444 (1950).
12. L. HOUGH, J. K. N. JONES, and W. H. WADMAN. J. Chem. Soc. 1702 (1950).
13. S. W. GUNNER, J. K. N. JONES, and M. B. PERRY. Can. J. Chem. **39**, 1892 (1961).
14. A. C. ARCUS and N. L. EDSON. Biochem. J. **64**, 385 (1956).
15. M. L. WOLFROM and S. HANESSIAN. J. Org. Chem. **27**, 1800 (1962).
16. K. DOEBEL, E. SCHITTLER, and T. REICHSTEIN. Helv. Chim. Acta, **31**, 688 (1948).
17. M. B. PERRY and A. C. WEBB. Can. J. Biochem. **46**, 1163 (1968).

Can. J. Chem. Downloaded from www.nrcresearchpress.com by 210.87.254.6 on 09/05/12
For personal use only.

Organic Sulfur Mechanisms. 13. Sulfene Formation by a Reverse Diels–Alder Reaction

JAMES FREDERICK KING AND ERROL GEORGE LEWARS
Department of Chemistry, University of Western Ontario, London, Ontario

Received April 4, 1973

Dimethyl 2,2-dioxido-4-phenyl-2-thiabicyclo[2.2.2]octa-5,7-diene-5,6-dicarboxylate (**5**), a molecule purposely designed to undergo a thermal reverse Diels–Alder reaction to form sulfene and an aromatic co-fragment, has been synthesized. Thermolysis of **5** gave dimethyl biphenyl-2,3-dicarboxylate (7) and, in addition, (*a*) in the presence of an enamine (**6**) gave the appropriate sulfene–enamine adduct (**8**), and (*b*) with an excess of *p*-toluidine gave methanesulfon-*p*-toluidide (**10**), in agreement with the above expectation. In the absence of sulfene traps the only product identified, in addition to **7**, was sulfur dioxide; further experiments failed to determine the fate of the methylene group but serve to exclude certain possibilities, including fragmentation of sulfene to sulfur dioxide and a trappable carbenoid species.

On a synthétisé le dioxydo-2,2 phényl-4 thia-2 bicyclo[2.2.2] octadiène-5,7 dicarboxylate-5,6 de diméthyle (**5**), afin d'étudier spécifiquement sa transformation thermique, selon une réaction inverse de Diels–Alder, en sulfène et en un fragment aromatique. La thermolyse de **5** a conduit au biphényl dicarboxylate-2,3 de diméthyle (**7**) et a conduit, en plus, (*a*) en présence d'une énamine (**6**) au composé d'addition prévu sulfène–énamine (**8**) et (*b*) en présence d'un excès de *p*-toluidine au méthanesulfon-*p*-toluidine (**10**) ce qui est en accord avec les prévisions énoncées antérieurement. En absence de sulfène, le seul produit identifié, en plus de **7**, a été l'anhydride sulfureux (SO_2); d'autres expériences n'ont pas réussi à montrer ce qu'il advient du groupe méthylène mais ont cependant permis de rejeter certaines hypothèses, en particulier celle qui impliquerait la fragmentation du sulfène en anhydride sulfureux et en une espèce carbènoide isolable. [Traduit par le journal]

Can. J. Chem., **51**, 3044 (1973)

Introduction

For some time we have been engaged in the study of the formation of sulfenes by thermolysis (1–3). Our goal in continuing this work has been to find a particularly mild, general route to sulfenes in which by-products or co-products would be either absent or unreactive toward the sulfene. This paper presents the details of one of our recent approaches to the problem which has employed the reverse Diels–Alder reaction (4); a preliminary report has already appeared (5).

The simplest reaction leading to formation of a sulfene by a reverse Diels–Alder reaction would be **1** → **2** + **3**. A rough thermochemical estimate indicates that the reaction **1** → **2** + **3** would be endothermic by about 40 to 50 kcal/mol,[1] but a molecule so constituted that the diene is part of an incipient aromatic system (*e.g.* **5**) would be

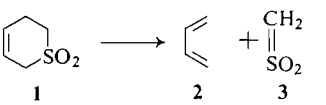

1 **2** **3**

expected to react more readily. Using essentially the method of Benson *et al.* (8), we estimate that for the fragmentation of bicyclo[2.2.2]octadiene into benzene and ethylene $\Delta H^0 \approx +1$ kcal/mol or lower,[2] whereas $\Delta H^0 = +39.7$ kcal/mol for the conversion of cyclohexene into butadiene and

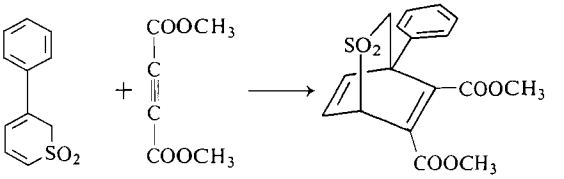

4 **5**

[1]In simple average bond energy terms ΔH for the reaction **1** → **2** + **3** would be given by $E(C{-}C) + E(C{-}SO_2) - E_\pi(C{=}C) - E_\pi(C{=}SO_2)$, where $E_\pi(C{=}C) = E(C{=}C) - E(C{-}C)$ and $E_\pi(C{=}SO_2) = E(C{=}SO_2) - E(C{-}SO_2)$. We take $E(C{-}C) = 82.6$ kcal/mol and $E(C{=}C) = 145.8$ kcal/mol (6) (and so $E_\pi(C{=}C) = 63.2$ kcal/mol), $E(C{-}SO_2) = 62$ kcal/mol (average of the values deduced by Mackle (7)), and estimate (see Appendix) a value for $E_\pi(C{=}SO_2)$ of $\sim 35 \pm 5$ kcal/mol.

[2]Without correcting for steric strain we estimate $\Delta H^0 = +10.5$ kcal/mol. No estimate of the steric strain in the bicyclic diene itself is at hand but the corresponding correction for bicyclo[2.2.2]octane may be obtained by comparing the experimental $\Delta H_f = -24.09$ kcal/mol (9) with the value -33.5 kcal/mol derived by addition of Benson's group energies. The value so obtained, 9.4 kcal/mol, may be regarded as a lower limit for bicyclo[2.2.2]octadiene since the latter is almost certainly more strained than its saturated analog.

Can. J. Chem. Downloaded from www.nrcresearchpress.com by 210.87.254.42 on 09/05/12
For personal use only.

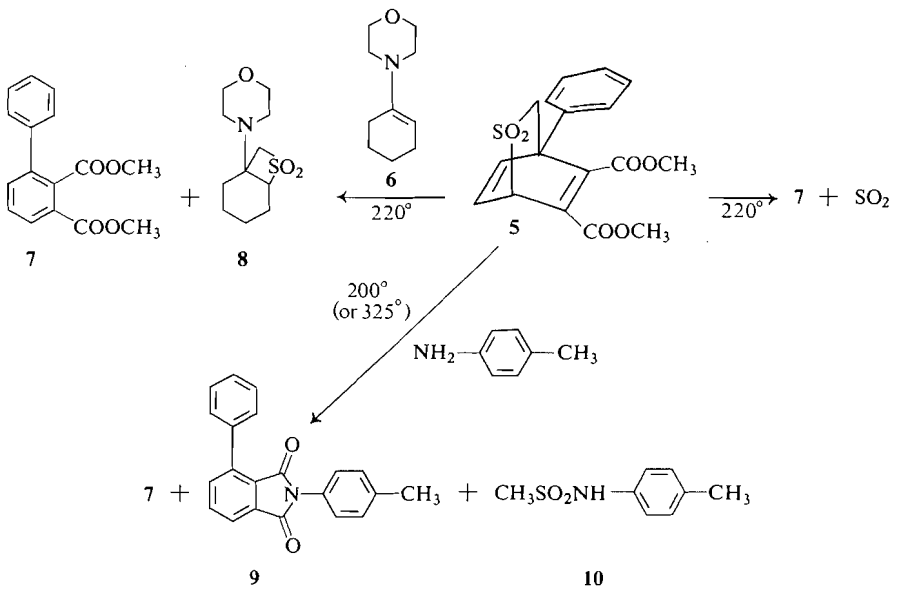

SCHEME 1

ethylene. In addition, as has been pointed out by Kwart and King (4), such a fragmentation process would be expected to be accompanied by an increase in entropy and hence be favored by an increase in temperature.

Results and Discussion

Synthesis of the Material to be Thermolyzed

The simplest bicyclic sulfone that would give sulfene and an aromatic co-product is 2-thiabicyclo[2.2.2]octa-5,7-diene 2,2-dioxide, but our attempts to obtain it from the monocyclic sulfide 1-thiacyclohexa-2,4-diene (10) having proved fruitless we explored the formation of the [2.2.2]bicyclo system using the substituted cyclohexadienic sulfone **4** (11). Dimethyl acetylenedicarboxylate with the sulfone **4** under mild conditions gave no reaction, but a 46% yield of **5** was obtained by heating the reagents at 140° for 68 h; small amounts of both starting material and thermolysis product were detectable in the reaction mixture. The product (**5**) was a solid melting at 210–211° for which the structure is established by the full agreement of the mode of synthesis and analytical and spectroscopic data. The n.m.r. spectrum is particularly indicative: in addition to phenyl hydrogens at 7.1 to 7.5 and two methyl groups 3.34 and 3.80, there is an AB quartet at 3.01 and 3.40 (J = 11.0) due to the methylene group and an ABX pattern, δ_A 6.84, δ_B 6.64, δ_X 5.30 p.p.m., J_{AB} 7.6, J_{AX} 6.6, and J_{BX} 1.6 Hz, arising from the olefinic plus bridgehead hydrogens.

Thermolysis of 5 in the Presence of Sulfene Traps

The thermolyses of **5** are summarized in Scheme 1. At 220° in the presence of the enamine **6** the biphenyldicarboxylic ester **7** and the enamine adduct **8** were obtained in 80% and 38% yields, respectively. The products were identical with authentic specimens synthesized essentially as described respectively by Heilbron and coworkers (12) and by Borowitz (13). An improvement in one step of the synthesis of the biphenyl diester (**7**) seems worth noting. Conventional esterification of 3-nitrophthalic acid stops at the monoester and whereas the earlier workers used a silver salt procedure to effect complete esterification, we found that sodium hydride in dimethylformamide followed by treatment with methyl iodide gave the diester in good yield.

The formation of **7** and **8** is clearly in agreement with a reverse Diels–Alder process as originally expected. Confirmation of this was obtained by the finding that methanesulfon-*p*-toluidide is the principal product (52% yield) when **5** is heated at 325° for 1.5 min with excess *p*-toluidine; a slightly lower yield of the sulfonamide (39%) was obtained when the reaction was carried out at 200° for 15 min. The biphenyl diester (**7**) was obtained in 49% yield at 325° (45% at 200°); some of the biphenyl portion ap-

Can. J. Chem. Downloaded from www.nrcresearchpress.com by 210.87.254.42 on 09/05/12
For personal use only.

peared as the imide **9** (17% yield at 325°, 30% at 200°). The imide (**9**) can be prepared by heating the biphenyl ester (**7**) with *p*-toluidine, and presumably some of the imide in the reaction product from **5** is so formed or else arises from a precursor derived from reaction of **5** with *p*-toluidine before the reverse Diels–Alder reaction takes place.

Thermolysis of 5 in the Absence of Sulfene Traps: The Fate of the Sulfene

One of the aims of this study, as pointed out in the Introduction, was to find a general method of making a sulfene in which neither the starting material nor the co-products would react with sulfene.[3] Such a reaction might make it possible to perform certain experiments on sulfenes not hitherto feasible, for example, performance of direct observations on sulfenes under conditions rather more convenient than the -196 to $< -160°$ range to which such experiments have been restricted to date (2). Since the results described above strongly indicated that sulfene was formed in at least 50% yield from **5**, it was felt that its thermolysis in the absence of the usual sulfene traps should be looked at.

An attempt at flash thermolysis (cf. refs. 2 and 3) at 700° and < 1 μ, carried out by Dr. R. A. Marty of this department, proved disappointing because the sulfone **5** proved almost involatile in the flash thermolysis apparatus and was induced to sublime into the hot tube only with great difficulty. The result is that it is unclear whether thermal decomposition actually takes place in the hot tube in the gas phase or merely during the heating of the material to induce sublimation. The infrared spectrum of the product on the cold finger at $-196°$ showed very weak bands of 1230 and 1330 cm^{-1} corresponding to the strongest bands previously observed for sulfene (2), but the weakness of the spectrum of the material from **5** precludes an unambiguous conclusion.

Simply heating **5** in the melt at 220° gave **7** in 95% yield. The only co-product that we have identified is sulfur dioxide which is formed in about 80% yield; the fate of the methylene carbon is unclear. The formation of sulfur dioxide would seem to point to the fragmentation of sulfene into methylene and sulfur dioxide, but when the thermolysis was carried out in the presence of a large excess of cyclooctene, there was no sign of the methylene adduct, bicyclo[6.1.0]nonane, even though an estimated 5% conversion to the methylene adduct would have been clearly detectable. It is noteworthy that a number of authors (one of us included) have suggested and looked for fragmentation of a sulfene to carbene and sulfur dioxide, and in no instance has any evidence for such a reaction been obtained (14). A simple estimate suggests that the reaction $CH_2{=}SO_2 \rightarrow CH_2 + SO_2$ is endothermic by 55 to 60 kcal/mol.[4]

Two other possibilities for the decomposition of the sulfene were explored and discarded. Under flash thermolysis conditions above 700—800°, sulfenes undergo desulfinylation, *i.e.* loss of sulfur monoxide with formation of the aldehyde or ketone (3). Even though the nearly quantitative conversion of sulfur monoxide to sulfur dioxide under these conditions seemed improbable, we made attempts to detect formation of formaldehyde. None was observed; control experiments indicated that a 10% yield would have been readily detectable. Another possibility was that the sulfene had dimerized to form Opitz' sulfene dimer, 1,3-dithietane 1,1,3,3-tetroxide. Under conditions of flash thermolysis this compound gives some sulfur dioxide, ethylene, and formaldehyde (16). No sign of ethylene was found in the gaseous products from **5**, thereby rendering it unlikely that the sulfur dioxide observed arises via Opitz' sulfene dimer.

Having excluded the above possibilities the question remains: where does the CH_2 go? With the comparatively modest supplies of **5** that were available the thermolyses were normally carried out on quantities of the order of 50 mg and the actual mass represented by the methylene group is thus only 2 mg. A small quantity of intractable, apparently polymeric material remained on the wall of the Carius tube after these reactions and

[3]It should perhaps be specifically pointed out that no such method was known at the outset of this study. The present work and the recently discovered sulfo-Cope rearrangement (1) come closest at present, and these are not ideal owing to the relatively high temperatures required.

[4]Using average bond energies $\Delta H = E_\pi(C{=}SO_2) + E(\dot{C}{-}\dot{S}O_2)$. We used for the former 35 kcal/mol (see Appendix) and for the latter the average of the estimated bond dissociation energies of a number of radicals of the type $R{-}\dot{S}O_2$, *viz.* 22 kcal/mol (7). Approximate similarity of $D(\dot{C}H_2{-}\dot{S}O_2)$ and $D(CH_3{-}\dot{S}O_2)$ is to be expected in view of the similarity of $D(CH_3{-}H)$ and $D(\dot{C}H_2{-}H)$, which are reported to be 104 and 106 kcal/mol, respectively (15).

Can. J. Chem. Downloaded from www.nrcresearchpress.com by 210.87.254.42 on 09/05/12
For personal use only.

Can. J. Chem. Downloaded from www.nrcresearchpress.com by 210.87.254.42 on 09/05/12
For personal use only.

small amounts of unidentified materials were seen in the crude products; either (or both) of these materials could perhaps originate from the "lost" methylene. It would appear that **5**, though it has proved very useful in demonstrating the possibility of generating sulfenes by such a reverse Diels–Alder reaction, is not the ideal substrate either for flash thermolysis or determining what happens to the sulfene fragment in the absence of added traps. We intend to continue study of the latter points with another substrate when the opportunity presents itself.

Experimental

Melting points were taken in capillary tubes with a Gallenkamp apparatus and are uncorrected. Unless stated otherwise recrystallizations were effected from CH_2Cl_2–hexane, analytical t.l.c. was performed with microscope slides coated with silica gel, and preparative t.l.c. with 20 × 20 cm or 10 × 20 cm glass plates bearing 20 or 10 g of silica gel, respectively. T.l.c. plates were developed with CH_2Cl_2, analytical plates being visualized with iodine vapor and preparative plates by means of the u.v. phosphor in the silica gel; compounds were extracted from preparative plates using CH_2Cl_2–MeOH (100:15, v/v). In aqueous work-ups, dichloromethane solutions were run through a small plug of cotton wool (previously washed with dichloromethane to remove fats) before evaporation, which simultaneously removed the remaining trace of water azeotropically. I.r. spectra were measured with a Beckman IR20A, and n.m.r. spectra with Varian T-60 or HA-100 spectrometers.

Synthesis of Dimethyl 2,2-Dioxido-4-phenyl-2-thiabicyclo-[2.2.2]octa-5,7-diene-5,6-dicarboxylate (5)

A solution of sulfone **4** (11) (80 mg, 0.39 mmol) and dimethyl acetylenedicarboxylate (77 mg, 0.54 mmol) in xylene (5 ml) in a 10 ml round-bottomed flask was flushed with nitrogen for 10 min. The flask was then sealed with a wired-on serum cap and heated at 140° for 68 h. The bright-yellow solution was evaporated (rotary evaporator connected to an oil pump) to give a mixture of oil and crystalline solid, 153 mg. T.l.c. indicated that starting **4** was only a minor component of this reaction mixture. Recrystallization readily gave the adduct **5** as very pale-yellow, elongated prisms, m.p. 203–206°, 52 mg; a second crop of 10 mg was obtained (total yield 62 mg, 46%). Examination by n.m.r. of the material remaining in the mother liquors showed them to contain virtually no adduct. (The biphenyl **7** was a major component.) Similar results were obtained when the reaction was scaled up by a factor of about 10. Recrystallization gave an analytical sample as rosettes of colorless, elongated prisms, m.p. 210–211.5°, darkening right after melting.

I.r.: 1731, 1316, 1125 cm^{-1}; n.m.r.: 7.1–7.5 (m, 5H); an ABX pattern (3H, δ_A 6.84, δ_B 6.64, δ_X 5.30, J_{AB} 7.6, J_{AX} 6.6, J_{BX} 1.6), an AB quartet (2H, δ_A 3.40, δ_B 3.01, J 11.0 Hz), 3.34 (3H), 3.30 p.p.m. (3H).

Anal. Calcd. for $C_{17}H_{16}O_6S$: C, 58.60; H, 4.63; S, 9.20. Found: C, 58.83; H, 4.68; S, 9.06.

Thermolysis of 5

(a) In the Absence of Added Reagents

The adduct **5** (50 mg) was sealed under nitrogen in a 10 × 150 mm Pyrex tube, and the tube was immersed in an oil bath at 220° for 7 min; the compound melted, went brown, and effervesced. The tube was cooled under tapwater and opened; it was noted that the colorless gas in the tube smelled like sulfur dioxide and was acidic to moist p*H* test paper. The thermolyzate was an orange-brown gum, 48 mg, readily soluble in $CDCl_3$, the n.m.r. spectrum of which solution showed it to be essentially the biphenyl diester **7**; there was some absorption at δ 3.0–3.4. T.l.c. showed, besides the biphenyl **7**, a spot corresponding to less mobile material which was not further studied.

A dichloromethane solution of the thermolyzate was passed through a 5 × 15 mm column of neutral alumina (Woelm, activity I) and evaporated to give **7** as a clear, light-brown oil, 37 mg (95% yield), estimated by n.m.r. to be 95–99% pure. Two recrystallizations gave colorless rosettes, m.p. 95–95.5°; with authentic **7** (12) of m.p. 95–96°, the mixed m.p. was 95–96°. The two materials were indistinguishable by t.l.c., and their i.r. spectra were identical.

The yield of sulfur dioxide was found by thermolyzing the adduct **5** (50 mg) in a 12 × 100 mm Pyrex tube connected to a 45 × 110 mm gas cell, the apparatus having been previously evacuated and closed off. The thermolysis tube was almost completely immersed in an oil bath at 220° for 7 min; a little of the **5** appeared to distil rather than decompose. I.r. examination of the material in the gas cell showed it to be virtually only sulfur dioxide. The yield of sulfur dioxide and the upper limit to possible ethylene formation were found by comparing the i.r. spectrum of the gaseous thermolysis products with a series of spectra of known amounts of sulfur dioxide and of ethylene. These standard spectra were obtained by injecting through a serum cap from a syringe known volumes of the gases (at atmospheric pressure and room temperature) into the evacuated thermolysis tube – i.r. cell apparatus. The yield of sulfur dioxide was 82 ± 10%, and the yield of ethylene (of which there was no definite indication) was < 5%. The spectrum showed only very weak bands which might be ascribed to C—H or C=O groups. Sulfur dioxide was also identified by thermolyzing the adduct under a slow stream of nitrogen and sweeping the gaseous products into a trap cooled in Dry Ice. Dichloromethane was added and the u.v. spectrum of the solution was taken: there was no indication of anything besides sulfur dioxide (λ_{max} (CH_2Cl_2) 287 mμ).

Preparative t.l.c. of the thermolyzate residue (brownish solid) led to the recovery of 8% starting adduct **5** and the isolation of 81% of the biphenyl **7** (the yields of sulfur dioxide and the biphenyl were calculated taking into account the recovered adduct).

(b) Attempt to Detect a Carbenoid Species in the Thermolysis of 5

The adduct **5** (50 mg) and cyclooctene (1.0 ml) were heated under nitrogen in a sealed tube for *ca.* 10 min at 220°. The reaction mixture was filtered and the filtrate was distilled in an evacuated L-shaped tube (one arm heated in a waterbath, the other cooled in Dry Ice). The distillate was checked by v.p.c. (10% SE-30 on Chromo-

Can. J. Chem. Downloaded from www.nrcresearchpress.com by 210.87.254.42 on 09/05/12
For personal use only.

sorp W, 6 ft × 1/4 in. copper column, 92°, helium flow *ca.* 60 ml/min); only a peak corresponding to cyclooctene was seen. By injecting known mixtures of cyclooctene and bicyclo[6.1.0]nonane it was shown that a 5% yield of bicyclo[6.1.0]nonane would have been detectable.

(c) Attempt to Detect Formaldehyde from the Thermolysis of 5

In one arm of an L-shaped tube was placed a solution of dimedone (20 mg) in about 0.5 ml of methanol, and a micro stirring bar. In the other arm was placed the adduct **5** (25 mg). The tube was sealed and the arm holding the adduct was heated at 220° for 7 min while the dimedone solution was stirred and cooled in ice. The whole length of the apparatus above the solution was then warmed with a flame to drive any formaldehyde (which might have condensed as paraformaldehyde) into the dimedone solution. The solution was then checked by t.l.c.: there was no trace of the dimedone adduct. A control experiment treating paraformaldehyde in the same way as the adduct **5** indicated that a 10% yield of formaldehyde would have been readily detectable.

Thermolysis of 5 in the Presence of Enamine 6

The adduct **5** (100 mg, 0.29 mmol) and the enamine (1.0 ml; 6.0 mmol) from cyclohexanone and morpholine (**6**) (24) were sealed under nitrogen in a 10 × 140 mm Pyrex tube holding a micro stirring bar. The mixture was stirred and heated at 200° for 25 min. The clear solution was evaporated and thoroughly evacuated to give an oil, 157 mg. The oil was dissolved in 10 ml of dichloromethane, extracted with 3 × 5 ml of 1 *N* HCl, and the HCl was then basified (*ca.* 25 ml of 10% NaOH) and extracted with 3 × 5 ml of dichloromethane, evaporation of which gave the sulfene–enamine adduct **8**, 32.6 mg (47%); this was estimated by n.m.r. to be *ca.* 80% pure, making the yield of adduct about 38%. A control experiment showed that this procedure for isolating the sulfene–enamine adduct led to its recovery in 97% yield. The crude **8** was recrystallized twice to give colorless prisms, m.p. 136–138°; with authentic **8** (11) of m.p. 138–140°, the mixed m.p. was 136–138°. The two materials were indistinguishable on t.l.c. (CH_2Cl_2–MeOH, 100:2 and 100:3, v/v) and showed identical i.r. spectra.

The acid-insoluble materials were obtained by evaporating the dichloromethane solution from which **8** had been removed as described. Preparative t.l.c. gave the biphenyl **7**, 62 mg (80%), identified by direct comparison with authentic material (mixed m.p., t.l.c., and i.r. spectra). In addition, a more polar material (19 mg), showing ν_{max} (CH_2Cl_2) 1729, 1315, 1128 cm^{-1}, was isolated but not further investigated.

Thermolysis of 5 in p-Toluidine

The adduct **5** (50 mg) and *p*-toluidine (200 mg) were sealed under nitrogen in a 10 × 150 mm Pyrex tube. The tube was briefly warmed on the steambath and agitated to produce a solution which was then allowed to cool and set to a solid mass. The reaction mixture was immersed for 1.5 min in an oil bath at 325°, then quickly cooled under the tap. The contents of the tube were dissolved in 10 ml of CH_2Cl_2, washed with 10 ml of 1 *N* HCl and then 4 × 10 ml of water and evaporated to give a yellow oil, 53 mg. This was dissolved in 10 ml of CH_2Cl_2 and extracted with 4 × 5 ml of 5% NaOH. The NaOH extracts were acidified (*ca.* 2 ml of concentrated HCl), extracted with 4 × 5 ml of CH_2Cl_2, and the CH_2Cl_2 was evaporated to give the sulfonamide **10** as a colorless solid, 12.5 mg (52%, taking into account recovered **5**). A control experiment showed that this procedure led to virtually quantitative recovery of the sulfonamide. Two recrystallizations gave colorless platelets, m.p. 100–101°; with authentic sulfonamide **10** (25) of m.p. 101–102.5°, the mixed m.p. was 101–102°. The two materials were indistinguishable on t.l.c. (CH_2Cl_2–MeOH, 100:2, v/v; both silica gel and neutral alumina), and their i.r. spectra were identical.

Evaporation of the CH_2Cl_2 solution from which the sulfonamide had been extracted gave the base-insoluble material as a yellow oil, 39.4 mg. Preparative t.l.c. (plate run three times) gave five bands. The two minor bands, 1.8 mg and 3.1 mg, were not investigated. The least mobile band (4.7 mg) was indistinguishable from starting adduct **5** on t.l.c. (analytical plate run four times). The next most mobile band (21.1 mg) was shown by n.m.r. to be *ca.* 90% pure biphenyl **7** (49% yield, if 90% pure). The most mobile band, 7.7 mg, was shown by n.m.r. to be *ca.* 95% pure biphenyl imide derivative **9** (17% yield, if 95% pure). The combined yield of biphenyl products was thus 66%.

That the material designated as the biphenyl 7 was in fact this compound was rigorously shown in another experiment in which the analogous band gave, after further purification (again subjected to preparative t.l.c., treated with decolorizing charcoal, and run through a 5 × 10 mm column of Woelm activity I neutral alumina with CH_2Cl_2, then recrystallized twice), colorless rosettes, m.p. 95–96°; with authentic biphenyl diester of m.p. 95–96°, the mixed m.p. was 95–96°. The two materials were indistinguishable on t.l.c., and their i.r. spectra were identical.

The material designated as the imide **9** was assigned this structure by comparison with authentic imide (*vide infra*) of the analogous band in another experiment: two recrystallizations (ethyl acetate – hexane) gave colorless needles, m.p. 175–176.5°; with authentic imide of m.p. 175–176°, the mixed m.p. was 175.5–176.5°. The two materials were indistinguishable on t.l.c., and their i.r. spectra were identical.

Thermolysis of the adduct **5** with *p*-toluidine at lower temperatures (200°/15 min) gave somewhat lower yields of sulfonamide (39%) and higher yields of the imide **9** (30%); the yield of biphenyl diester was about the same (45%).

Preparation of Dimethyl Biphenyl-2,3-dicarboxylate (7): a Simple Method for Esterification of 3-Nitrophthalic Acid

The synthesis of the biphenyl diester **7** by reaction of benzene with diazotized dimethyl 3-aminophthalate was carried out essentially as described by Heilbron and coworkers (12). One step in this synthesis, namely the formation of dimethyl 3-nitrophthalic acid, was modified as follows.

In a 100 ml round-bottomed flask was placed sodium hydride (57% dispersion in mineral oil, 406 mg, 9.7 mmol). The flask was flushed with nitrogen, fitted with a stirring bar and a serum cap, and the sodium hydride dispersion was washed twice with pentane by stirring briefly, letting the NaH settle, and removing the supernatant pentane

Can. J. Chem. Downloaded from www.nrcresearchpress.com by 210.87.254.42 on 09/05/12
For personal use only.

(syringe technique). Dimethylformamide (DMF, 50 ml) was then added, and a solution of 3-nitrophthalic acid (1.0 g, 4.17 mmol) in DMF (4.0 ml) was added fairly quickly (brisk effervescence, the H_2 was allowed to escape through a syringe needle); the syringe was rinsed with 2 × 2 ml of DMF. After stirring for 20 min at 25°, methyl iodide (2.0 ml, 4.55 g, 32 mmol) was added to the suspension over 30 s, and stirring was continued for 23 h. The light-yellow suspension was poured into 300 ml of water, extracted with 3 × 50 ml of CH_2Cl_2, and the CH_2Cl_2 extracts were washed with 4 × 150 ml of water and evaporated to give an oil which on evacuation overnight crystallized to a light-yellow solid, m.p. 66–68° (lit. (12) 67–68°), 0.92 g (81%); one spot on t.l.c. Recrystallization (CH_2Cl_2 : CCl_4 : hexane) gave colorless prisms, m.p. 69–70°. The structure was confirmed by the infrared (ν_{max} (CH_2Cl_2) *no* OH, 1737, 1538, 1350, 1280 cm^{-1}) and n.m.r. (δ 8.32, d, J=8.0 Hz, 2H; 7.67, t, J=8.0 Hz, 1H; 4.03, s, 3H; 3.97, s, 3H) spectra.

Attempts at esterification of 3-nitrophthalic acid using acidic catalysts (HCl, concentrated H_2SO_4, or BF_3-etherate (26)) gave the monoester alone or a mixture of the mono- and diesters.

Preparation of Authentic Biphenyl Imide **9**

The biphenyl diester **7** (51 mg) and *p*-toluidine (298 mg) were heated at 200° for 20 min under nitrogen in a sealed 10 × 150 mm Pyrex tube. The reaction mixture was dissolved in 10 ml of CH_2Cl_2, washed with 10 ml of 1 *N* HCl, then with 4 × 10 ml of water, and evaporated to give a pale-yellow oil, 50 mg. The n.m.r. spectrum showed this material to consist of diester : imide in the molar ratio 4.2 : 1.0. This reaction mixture was treated with *p*-toluidine (429 mg) and methanesulfonic acid (2.2 mg) at 200° for 20 min, as before. Workup gave a light-yellow oil, 47 mg, the n.m.r. spectrum of which showed it to consist of diester **7** and imide **9** in the molar ratio 1.3 : 1.0. Preparative t.l.c. led to the isolation of the biphenyl diester **7** (24 mg) and the imide **9** (white solid, m.p. 172–173°, 21 mg, 68% on the basis of reacted diester). The assigned structure **9** is supported by spectra and microanalysis. ν_{max} (CH_2Cl_2) 1778 w, 1721, 1515 m, 1381 cm^{-1}; this compares well with the i.r. spectrum of *N*-methyl phthalimide (prepared from phthalimide, sodium hydride, and methyl iodide in DMF), ν_{max} (CH_2Cl_2) 1773 w–m, 1713 cm^{-1}. The n.m.r. spectrum showed δ ($CDCl_3$) 8.1–7.2 (m, 12H), 2.38 (s, 3H). Recrystallization (ethyl acetate – hexane) gave colorless needles, m.p. 175–176°.

Anal. Calcd. for $C_{21}H_{15}NO_2$: C, 80.49; H, 4.82; N, 4.47. Found: C, 80.42; H, 4.72; N, 4.60.

We thank the National Research Council of Canada for financial assistance and Dr. R. A. Marty for carrying out the flash thermolysis experiments.

1. J. F. King and D. R. K. Harding. Chem. Commun. 959 (1971).
2. J. F. King, R. A. Marty, P. de Mayo, and D. L. Verdun. J. Am. Chem. Soc. **93**, 6304 (1971).
3. J. F. King, P. de Mayo, C. L. McIntosh, K. Piers, and D. J. H. Smith. Can. J. Chem. **48**, 3704 (1970).
4. H. Kwart and K. King. Chem. Rev. **68**, 415 (1968).
5. J. F. King and E. G. Lewars. Chem. Commun. 700 (1972).
6. T. L. Cottrell. The strengths of chemical bonds. 2nd ed. Butterworths, London. 1958.
7. H. Mackle. Tetrahedron, **19**, 1159 (1963).
8. S. W. Benson, F. R. Cruickshank, D. M. Golden, G. R. Haugen, H. E. O'Neal, A. S. Rodgers, R. Shaw, and R. Walsh. Chem. Rev. **69**, 279 (1969).
9. P. v. R. Schleyer, J. E. Williams, and K. R. Blanchard. J. Am. Chem. Soc. **92**, 2377 (1970).
10. L. Brandsma and P. J. W. Schuijl. Rec. Trav. Chim. **88**, 513 (1969).
11. G. Pagani. Gazzetta, **97**, 1518 (1967).
12. E. C. Butterworth, I. M. Heilbron, D. H. Hey, and R. Wilkinson. J. Chem. Soc. 1386 (1938).
13. I. J. Borowitz. J. Am. Chem. Soc. **86**, 1146 (1964).
14. G. Opitz. Angew. Chem. Int. Ed. **6**, 107 (1967).
15. S. W. Benson. J. Chem. Ed. **42**, 502 (1965).
16. D. R. K. Harding. Ph.D. Thesis. University of Western Ontario, London, Ontario. 1973.
17. G. Geiseler and R. Kuschmiers. Z. Phys. Chem. N.F. **28**, 33 (1961).
18. E. J. Forman and D. N. Hume. Talanta, **11**, 129 (1964).
19. J. W. Bayles and A. F. Taylor. J. Chem. Soc. 417 (1961).
20. T. W. S. Lee. Ph.D. Thesis. University of Western Ontario, London, Ontario. 1969.
21. J. F. King, E. A. Luinstra, and D. R. K. Harding. Chem. Commun. 1313 (1972).
22. E. A. Luinstra. Ph.D. Thesis. University of Western Ontario, London, Ontario. 1971.
23. C. S. Rondestvedt. J. Am. Chem. Soc. **76**, 1926 (1954).
24. S. Hünig, E. Lücke, and W. Brenninger. Org. Synth. **41**, 65 (1961).
25. I. B. Douglass and B. S. Farah. J. Org. Chem. **24**, 973 (1959).
26. J. L. Marshall, K. C. Erickson, T. K. Folsom. Tetrahedron Lett. 4011 (1970).

Appendix

Estimate of the "π-Bond Energy" of Sulfene

Our estimate of the "π-bond energy" of sulfene, $E_\pi(C{=}SO_2)$ (defined as $E(C{=}SO_2) - E(C{-}SO_2)$ was obtained by averaging an upper and a lower limit for $E_\pi(C{=}SO_2)$, each obtained by a slightly roundabout argument as follows.

It is evident from eqs. 1 to 3 that $\Delta H_1 + \Delta H_2 = \Delta H_3$ and $\Delta H_3 = E(C{-}H) + E(SO_2{-}Cl) - E_\pi(C{=}SO_2) - E(HCl)$, and so $E_\pi(C{=}SO_2) = E(C{-}H) + E(SO_2{-}Cl) - E(HCl) - \Delta H_1 - \Delta H_2$.

[1] CH_3SO_2Cl + 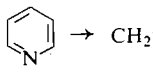 → $CH_2{=}SO_2$ + 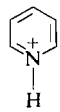 Cl^- + ΔH_1

[2] 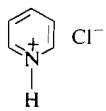 Cl^- → + HCl + ΔH_2

[3] $CH_3SO_2Cl \rightarrow CH_2{=}SO_2 + HCl + \Delta H_3$

E(C—H) and E(HCl), respectively 98.7 and 103.1 kcal/mol, are readily available (6) but $E(SO_2—Cl)$ is surprisingly uncertain; we use the value 58 ± 6 kcal/mol (17). An estimate of the heat of neutralization of pyridine with hydrogen chloride ($-\Delta H_2$) in acetonitrile of -19 kcal/mol may be made from data on the reaction of pyridine and hydrogen bromide taken with a comparison of the values of ΔH for the reactions of hydrogen bromide and hydrogen chloride with 1,3-diphenylguanidine (18). The corresponding data are not available for the reaction in 1,2-dimethoxyethane, the solvent for which we make an estimate of ΔH_1, but it seems probable that the variation in heat of neutralization on changing from one not very polar solvent to another is less than the uncertainties in the other parameters employed here. (With tributylamine and 2,4-dinitrophenol, for example, the variation in ΔH has been found to be <3 kcal/mol over a range of solvents including dibutyl ether, benzene, and fluorobenzene (19).)

The value of ΔH_1 is not known but a rough limit of <4 kcal/mol may be set as follows: (*a*) One may estimate $\Delta H_1^{\ddagger} = 8.7$ kcal/mol from the rate constants for reaction 1 in dimethoxyethane at 20.0 and 40.0° (20), and obviously ΔH_1 must be $<\Delta H_1^{\ddagger}$. (*b*) The magnitude of $\Delta H_1^{\ddagger} - \Delta H_1$ is unknown but a lower limit may be found from the following: (i) The amount of reversal of [1] in D_2O must be very small since the amount of $CH_2DSO_3^-$ that is formed is $<0.5\%$ (and that can be formed by other mechanisms than reversal of [1]) (21). (ii) In the reaction of methanesulfonyl chloride, piperidine, and water (molar ratio 1:2:30) in dimethoxyethane, a 98% yield of the piperidine was obtained (22). In order to account for the selectivities of water trapping *vs.* reversal of [1] and piperidine *vs.* water trapping, the activation barrier to reversal must be at least 5 kcal/mol greater than that for piperidine. Even if the latter barrier were zero (which is unlikely), ΔH_1 must therefore be <4 kcal/mol. Inserting all of these values in the expression above we obtain $E_\pi(C{=}SO_2) > 31$ kcal/mol.

An *upper* limit to $E_\pi(C{=}SO_2)$ may be deduced from the observation (23) that of the two ways of removing HCl from β-chloroethanesulfonyl chloride, that which gives the carbon–carbon double bond predominates, probably by a large amount, but at least by enough to lead to a 72% isolated yield of ethenesulfonyl chloride under one set of conditions (23); at the very least $\Delta G_5^{\ddagger} - \Delta G_4^{\ddagger} > 0$ kcal/mol.

[4] $ClCH_2CH_2SO_2Cl + R_3N \rightarrow CH_2{=}CHSO_2Cl + R_3\overset{+}{N}H\ Cl^- + \Delta H_4$

[5] $ClCH_2CH_2SO_2Cl + R_3N \rightarrow Cl—CH_2—CH{=}SO_2 + R_3\overset{+}{N}H\ Cl^- + \Delta H_5$

The two reactions involve a common attack of base on an α-hydrogen, and the (developing) charge in the α-carbon at some point proceeds to displace one of the chlorine atoms, either the one on the sulfur or the one on the carbon. In view of the probable similarity of the energy profiles it seems highly likely that the difference $\Delta G_5^{\ddagger} - \Delta G_4^{\ddagger}$ is a reflection of the difference $\Delta H_5 - \Delta H_4$, and also that $\Delta G_5^{\ddagger} - \Delta G_4^{\ddagger}$ is smaller than $\Delta H_5 - \Delta H_4$ because the bonds that lead to the energy difference are not fully formed and would not show the energy difference in full at the transition state stage. Since $\Delta H_5 - \Delta H_4 = E_\pi(C{=}C) + E(SO_2—Cl) - E_\pi(C{=}SO_2) - E(C—Cl)$, and $E_\pi(C{=}C) = E(C{=}C) - E(C—C) = 63.2$ kcal/mol (6), $E(C—Cl) = 81$ kcal/mol (6), and $E(SO_2—Cl) = 58$ kcal/mol (16), $\Delta H_5 - \Delta H_4 > \Delta G_5^{\ddagger} - \Delta G_4^{\ddagger} > 0$, then $E_\pi(C{=}SO_2) < 40$ kcal/mol.

Taking a number between the upper and lower limits, we obtain $E_\pi(C{=}SO_2) = 35 \pm 5$ kcal/mol. This number depends on a highly uncertain value for $E(SO_2—Cl)$ and a change in the latter would similarly change $E_\pi(C{=}SO_2)$. The value is clearly only rough but we believe that until a better one is obtained it can be useful in constructing energy diagrams for the reactions of sulfenes, and for the approximate thermochemical estimates of the kind made in this paper.

Can. J. Chem. Downloaded from www.nrcresearchpress.com by 210.87.254.42 on 09/05/12
For personal use only.

Thermodynamic Properties of Aqueous Organic Solutes in Relation to Their Structure. Part I. Free Energy of Transfer from H_2O to D_2O for a Series of Isomeric Ketones

CARMEL JOLICOEUR AND GHISLAIN LACROIX
Department of Chemistry, Université de Sherbrooke, Sherbrooke, Quebec

Received April 5, 1973

The solubilities of 18 decanones have been measured in H_2O and D_2O at 25 °C from their u.v. absorption spectra. The data were used to calculate ΔG_t^0, the standard free energy of transfer of these solutes from H_2O to D_2O. ΔG_t^0 was found negative for the saturated ketones, but positive for most of the unsaturated and polycyclic isomers. A rough correlation was observed between ΔG_t^0 and the degree of branching in the hydrocarbon chains of the ketones: ΔG_t^0 increases with the degree of branching. From the temperature dependence of ΔG_t^0 obtained at 10, 25, and 40 °C, heats of transfer ΔH_t^0 were determined for typical ketones, namely 2-decanone and adamantanone. ΔH_t^0 was found as -2.1 kcal mol^{-1} for 2-decanone and $\sim 0 \pm 0.5$ kcal mol^{-1} for adamantanone.

The results are discussed in terms of two main contributions: (1) an isotope effect in the free energy of cavity formation and (2) perturbation of solvent structure by the solutes, differing in H_2O and D_2O. Using the scaled-particle theory to evaluate the former, the variations in the observed ΔG_t^0 are assigned to the structural part of ΔG_t^0.

Nous avons mesuré, par spectroscopie d'absorbtion dans l'u.v., la solubilité d'une série de 18 décanones dans H_2O et D_2O à 25 °C. L'enthalpie libre standard pour le transfert ($H_2O \rightarrow D_2O$) des cétones, ΔG_t^0, s'avère négative pour les cétones saturées alors que pour la plupart des cétones insaturées on trouve des valeurs positives. Nous pouvons mettre en évidence une corrélation qualitative entre la grandeur de ΔG_t^0 et le degré d'embranchement des substituants alcoyles des cétones: ΔG_t^0 augmente avec le nombre d'embranchements dans les chaines alcoyles. Pour quelques systèmes types, notamment la décanone-2 et l'adamantanone, la chaleur du transfert $H_2O \rightarrow D_2O$, ΔH_t^0, a également été obtenue à partir des mesures de solubilité à 10, 25 et 40 °C. Pour la décanone-2, ΔH_t^0 est évaluée à -2.1 kcal mol^{-1} et à 0 ± 0.5 kcal mol^{-1} pour l'adamantanone.

L'interprétation des résultats est donnée selon deux contributions principales aux fonctions de transfert: (1) différence dans l'énergitique de la formation d'une cavité dans les deux solvants et (2) différence dans les effets que les solutés exercent sur la structure des solvants. La première contribution est évaluée à l'aide de la théorie "scaled-particle", et la spécificité observée dans le ΔG_t^0 des différents solutés est attribuée à la partie structurale de la fonction de transfert.

Can. J. Chem., 51, 3051 (1973)

Introduction

Studies on the properties of nonpolar or hydrophobic solutes in water commonly lead to the inference that the hydrogen-bonded structure of this solvent is stabilized in the neighborhood of the solute particle. The earlier evidence came from thermodynamic data, namely the observation of unusually large entropy losses upon dissolution of inert gases in water (1, 2). Confirmation of the concept of solvent structural enhancement was later found in other thermodynamic studies and kinetic investigations of large organic ions (*e.g.* tetraalkylammonium ions) for which anomalously large molar heat capacity and *B*-viscosity coefficients were found (3, 4). Further investigations of aqueous solutions of hydrophobic solutes using a variety of thermodynamic, kinetic, and spectral methods (5, these recent reviews deal with one or more aspects of this field) also helped to strengthen the idea that hydrocarbon-like solutes can promote *some* hydrogen-bonded structure in the surrounding solvent.

This concept is attractive, particularly in view of the formation of clathrate hydrates by hydrocarbon gases (see, for example, 6*b*) and several hydrophobic salts (6*a*), though it should be stressed that no long-lived (*i.e.* $> 10^{-10}$ s) clathrate structure has been observed in solutions of hydrophobic ions or molecules. Only indications of time-averaged structures have been assessed (5*a*, 7–9), often using the analogy between the effects produced by a hydrophobic solute and by a decrease in temperature. It should also be recognized that questions raised on some of the evidence for the structure

Can. J. Chem. Downloaded from www.nrcresearchpress.com by 210.87.254.42 on 09/05/12
For personal use only.

promoting effects of hydrophobic solutes have not yet found satisfactory answers. In particular, Everett (10) judiciously pointed out that the large partial molal heat capacity $\bar{C}_p^0$ of inert molecules in water need not necessarily result from an increase of the amount or the stability of hydrogen-bonded structures in the solution. In fact, the explanation of $\bar{C}_p^0$ would only require that the water–water bonds which are perturbed by the hydrophobic particles become more sensitive towards temperature changes. Alternate explanations of other observations have been offered recently (11, 12), indicating that the molecular phenomena associated with the solvation of aqueous hydrophobic solutes have by no means found a unique or adequate description.

If, as we believe, some time-averaged structure is promoted around hydrophobic groups (at least near and below room temperature (13)), one might expect that the internal structure or geometry of the solute could play a role in determining the overall structural perturbation in the solvent. In other words, the solute geometry which is best accommodated in the solvent structure might have a feedback effect in inducing further stabilization of the water structure. The finding of such a correlation between the solute structure and its effect on the water structure could thus serve to confirm the initial concept of water structure stabilization by inert molecules.

Some attempts to relate the properties of aqueous solutes with their intrinsic structural features can be found, namely for acids (14), alcohols and sugars (15–18), and various other solutes (19–21). These investigations were concerned primarily with different arrangements of hydrophilic groups on solute molecules rather than with the structural features of their hydrophobic groups. In studies involving different isomers on the hydrophobic portion, noticeable differences are found among the properties of the isomers; for example the partial molal volumes of the isomeric butanols in water are measurably different (15, 16). Little can be gained from this information, however, since the solvation of the polar group of these small molecules could make an important contribution to their thermodynamic properties, and since similar differences are found in the thermodynamic properties of the isomeric butanols in methanol (22).

The purpose of this and following studies is to establish whether the geometry of hydrophobic solutes has a significant influence on their thermodynamic properties in water, and more specifically on the part of these properties which is commonly assigned to structural effects in the solvent. The work was initiated with a series of 18 decanones for which the free energy of transfer from $H_2O \rightarrow D_2O$ was measured at 25 °C. This transfer process is generally thought to emphasize the structural influences of the solutes (23–25) and therefore seems appropriate for the problem at hand.

Experimental

The origin and properties of the decanones used in the present work are summarized in Table 1. The specified purity was estimated from g.c. analysis carried out with a Hewlett Packard (Model HP-5750) chromatograph, using a Carbowax 20-M on Chromosorb-W column. The criteria for stating the purity as >99.5% was that no shoulder peak could be observed with a detector sensitivity such that the intensity of the main peak was ~5 full scales. The water used in preparing saturated solutions was doubly distilled over alkaline $KMnO_4$ in an all-glass still and equilibrated with atmospheric CO_2. D_2O (99.8%) was purchased from two different sources (Stohler Isotope Chemicals and Merck, Sharp and Dohme) and was used as such; the results of experiments carried out with both materials were identical. The cyclohexane used in some extraction experiments was Fisher Spectranalyzed grade.

Saturated solutions of the ketones in H_2O and D_2O were prepared by adding an excess of the ketone (~0.5 g) to ~15 cm^3 of solvent. The mixture was mechanically shaken in a constant temperature bath (±0.05 °C) for 3–4 h and allowed to equilibrate overnight. Aliquots were then sampled for absorbance measurements, using a transfer tube fitted with a small sintered glass filter and applying a light pressure over the solution. The mother solution was agitated again for several hours, allowed to equilibrate, and the absorbance of a second aliquot was recorded. If any discrepancy was found between the two results, the procedure was repeated a third time. For each ketone, at least three pairs of H_2O and D_2O saturated solutions were prepared, giving a minimum of six measurements for each compound.

The absorbance of the saturated solutions were recorded in the range (2200–4000 Å) using either a Perkin-Elmer (Model DB-G) or a Cary-14 Spectrophotometer, with stoppered cells of various path-lengths ranging between 5 and 50 mm. The absorbance of the saturated solution in water was first recorded directly. The absorbance of the solution in heavy water was then measured relative to that of the aqueous solution at the same λ_{max}, *i.e.*, H_2O (sat'd) in the reference compartment and D_2O (sat'd) in the sample compartment. The absolute solubility of the ketones in H_2O was calculated from their absorbance and that of dilute solutions prepared quantitatively. The latter measurements were, however, very difficult and only the magnitude of the saturation concentrations obtained is significant.

Can. J. Chem. Downloaded from www.nrcresearchpress.com by 210.87.254.42 on 09/05/12
For personal use only.

TABLE 1. Properties of isomeric ketones

Compound No.	Name	Formula	Supplier*	Purity†	λ_{max}‡
1	2-Decanone	$C_{10}H_{20}O$	PB	>98%	2420
2	3-Decanone	"	PB	>99.5%	2380
3	4-Decanone	"	PB	>99	2340
4	2-Me-3-nonanone	"	KK	>99	2340
5	2-Me-4-nonanone	"	KK	>99.5	2760
6	2-Me-5-nonanone	"	KK	>99.5	2660
7	4-Me-5-nonanone	"	KK	>99	2740
8	3-Me-2-nonanone	"	KK	>97	2380
9	2,2-Di-Me-3-octanone	"	KK	>99	2700
10	3-*i*-Pr-2-heptanone	"	A	>95	2290
11	4-*t*-Bu-cyclohexanone	$C_{10}H_{18}O$	A	>99.5	2780
12	2-Bu-cyclohexanone	"	PB	>99	2380
13	3,3,5,5-Tetra-Me-cyclohexanone	"	A	>98	2420
14	Menthone	"	A	>98	2890
15	Camphor (*dl*)	$C_{10}H_{16}O$	A	>99.5	2840
16	Adamantanone	$C_{10}H_{14}O$	A	>99.5	2800
17	8-Ketricyclo-5.2.1.$0^{2,6}$ decanone	"	A	>99	2820
18	4-Phenyl-2-butanone	$C_{10}H_{12}O$	A	>99.5	2800

*PB: PFALTZ and Bauer; KK: K and K; A: Aldrich Chemicals.
†Estimated by g.l.c. as described in Experimental.
‡Position of peak at which absorbances were measured.

Throughout this work, thorough cleaning procedures of all laboratory glassware and spectrophotometer cells were followed. Also, great care was exercised to avoid evaporation of the organic solutes while handling the solutions. To assert the validity of this method in measuring relative solubilities, a number of tests were carried out, with respect to the following points.

(a) Keto–Enol Equilibrium and Partial Deuteration of the Ketone

While this known exchange could affect the solubility of the ketones in D_2O, it was verified that the solubilities of either 2-decanone or 4-phenyl-2-butanone in D_2O containing 0.01 *M* NaOD were time independent over a period of 48 h.

(b) By-products and Impurities in the Ketones

Impurities, particularly if they are water soluble, could significantly change the solubility of the ketones. To verify the possibility of solubilizing effects, each pair of saturated solutions of a given compound was prepared using different excess amounts of ketone (*e.g.* from 0.1 to 1 g). This produced no significant changes in the measured solubilities, except for 3-Me-2-nonanone and 3-decanone, of which the first was already known to be of lower purity (Table 1).

(c) Solvent Effects on Extinction Coefficients

In these experiments, the extinction coefficient of the ketones are assumed independent of the media, H_2O or D_2O. This was established by taking aliquots of D_2O saturated with 2-decanone and diluting 20-fold in H_2O and D_2O respectively. Both λ_{max} and the absorbance of the dilute solutions (95% D_2O and 95% H_2O) were found identical.

(d) Applicability of Beer's Law

The solubility measurements rely on the applicability of Beer's law to these mixtures. This could be demonstrated by showing that the relative absorbance of saturated solutions of 2-decanone in H_2O and D_2O was the same, whether the measurement was taken directly on these solutions or on cyclohexane extracts of the aqueous solutions. In the latter method an aliquot of each saturated solution was extracted quantitatively with cyclohexane and diluted 10-fold.

Results

The standard free energy of transfer from H_2O to D_2O was calculated from the usual equation (25):

$$[1] \quad \Delta G_t^0 \equiv \Delta G^0_{H_2O \rightarrow D_2O} = -RT \ln(X_{D_2O}/X_{H_2O})$$

where X is the mole fraction of the solute. As is commonly done for such dilute solutions, the solute activity coefficients are assumed to be identical in both solutions. Since the absorbance measurements are related to molar concentrations, M, these are converted to mole fractions (25):[1]

[1]In the molarity – mole fraction conversion it is assumed that the partial molal volume of the ketones is the same in H_2O and D_2O. For R_4N^+ ions, this is true within ~1% (26) and, thus, for the concentrations used here (<0.05 *M*) the error introduced is easily shown to be negligible.

Can. J. Chem. Downloaded from www.nrcresearchpress.com by 210.87.254.42 on 09/05/12
For personal use only.

TABLE 2. Results of differential solubility measurements of decanones in H_2O and D_2O at 25 °C

Compound No. (see Table 1)	Structure	$S^0(H_2O)$* (mol l^{-1})	$\Delta G^0(H_2O \rightarrow D_2O)$ (cal mol^{-1})	$\Delta H^0(H_2O \rightarrow D_2O)$‡ (kcal mol^{-1})
1	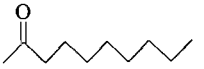	0.02	−180±43†	−2.1±0.5
2	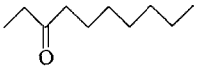	0.04	−270±36	
3	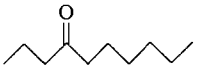	0.009	−330±68	
4	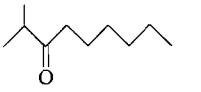	0.02	−145±8	
5	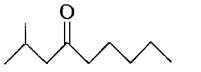	0.0006	−130±5	
6	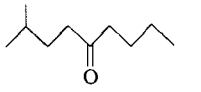	0.003	−90±15	
7	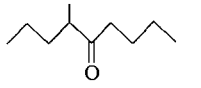	0.001	−182±25	
8	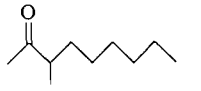	0.01	−300±100	
9	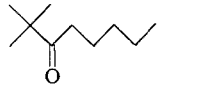	0.0006	−67±5	
10	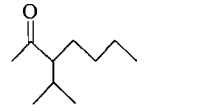	0.007	−196±19	
11	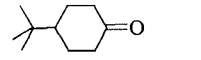	0.003	−86±15	
12	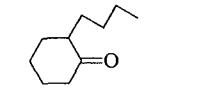	0.02	−232±27	
13	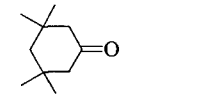	0.05	−204±27	−3.3±0.5
14	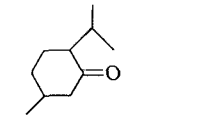	0.01	+18±5	

Can. J. Chem. Downloaded from www.nrcresearchpress.com by 210.87.254.42 on 09/05/12
For personal use only.

TABLE 2. *(Concluded)*

Compound No. (see Table 1)	Structure	$S^0(H_2O)$* (mol l^{-1})	$\Delta G^0(H_2O \rightarrow D_2O)$ (cal mol^{-1})	$\Delta H^0(H_2O \rightarrow D_2O)$‡ (kcal mol^{-1})
15	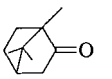	0.009	+32±5	
16	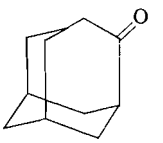	0.002	+55±12	0±0.5
17	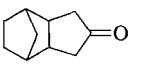	0.02	+60±10	0±0.5
18	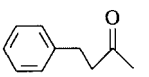	0.01	+120±20	

*Estimated as described in Experimental.
†Standard deviation (see Results).
‡From measurements at 10, 25, and 40 °C; the uncertainty was estimated graphically.

[2] $$\frac{X_{D_2O}}{X_{H_2O}} = \frac{M_{D_2O}}{M_{H_2O}} \times F$$

The factor F includes molecular weights W and densities d of the two solvents:

$$F = \frac{W_{D_2O}}{W_{H_2O}} \times \frac{d_{H_2O}}{d_{D_2O}}$$

at 25 °C: $F = 1.00361$ (25). In terms of the measured absorbances, we then have

[3] $$\Delta G_t^0 = -RT \ln \left\{ \left[1 + \frac{\Delta A}{A(H_2O)} \right] \times F \right\}$$

where $A(H_2O)$ is the absorbance of the saturated solution in H_2O and ΔA is the differential absorbance of the saturated solutions in H_2O and D_2O (D_2O against H_2O). The heat of transfer $\Delta H^0_{H_2O \rightarrow D_2O} \equiv \Delta H_t^0$ obtained for a few ketones was determined graphically from van't Hoff plots:

[4] $$d(\Delta G_t^0/T)/d(1/T) = \Delta H_t^0$$

ΔG_t^0 values for all the ketones investigated are reported in Table 2, with the estimated solubility of the ketones in H_2O (*cf.* Experimental). ΔH_t^0 is also given in four cases which are believed to be representative of their structural categories. The uncertainty quoted on ΔG_t^0 values is the standard deviation on a minimum of five measurements. The accuracy of ΔH_t^0 was estimated graphically.

In attempts to establish a correlation between ΔG_t^0 and the structural features of the solutes, the results have been plotted against several parameters which relate to their molecular structures and properties. The parameters chosen were: the position of the carbonyl group on linear ketones (Fig. 1), the degree of unsaturation of the alkyl substituents (Fig. 2), and the number of branching centers on the alkyl groups (Fig. 3). In the evaluation of the latter, we counted the

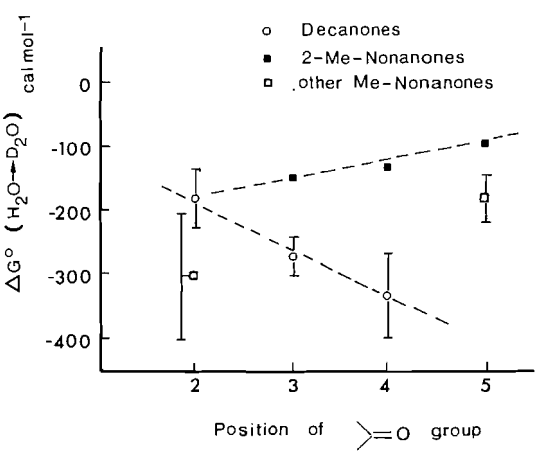

FIG. 1. Standard free energy of transfer from H_2O to D_2O of several decanones and methylnonanones at 25 °C (Table 2) correlated with position of the carbonyl on the linear alkyl chain.

Can. J. Chem. Downloaded from www.nrcresearchpress.com by 210.87.254.42 on 09/05/12
For personal use only.

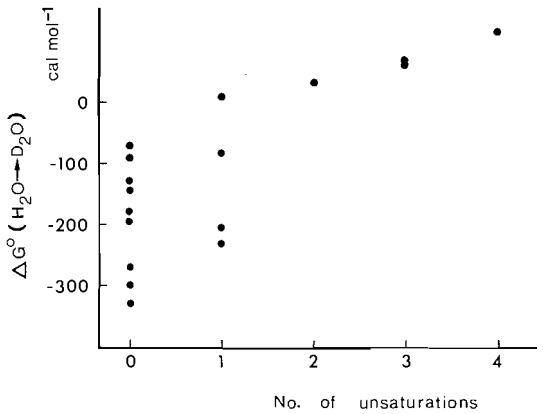

FIG. 2. ΔG_t^0 data from Table 2 correlated with the number of unsaturations in the hydrocarbon substituents.

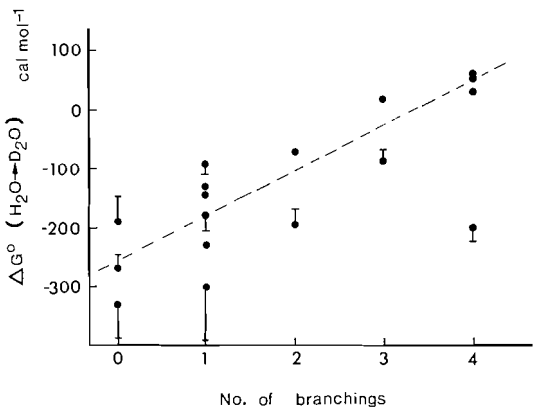

FIG. 3. ΔG_t^0 data from Table 2 correlated with the number of branching centers on the alkyl substituents: ΔG_t^0 for 4-phenyl-2-butanone was not included, and only one half of each error bar has been drawn.

number of carbon atoms bearing three substituents other than hydrogen, counting as two branchings a tetrasubstituted carbon. The best correlation, apparent from these data, is found with the degree of branching in the hydrocarbon chains of the solute.

Discussion

The results shown in Table 2 clearly indicate some specificity among the various isomeric ketones of same chemical composition. In addition, ΔG_t^0 which is negative for the linear saturated ketones becomes positive with most of the unsaturated homologs, particularly with the polycyclic compounds. ΔH_t^0 values apparently make a similar distinction between the two categories of ketones.

As is indicated by the larger solubilities of these ketones compared to similar hydrocarbons (27, 28), the solvation of the carbonyl group probably contributes to the thermodynamic properties of these solutes in aqueous media, and a solvent isotope effect on this contribution might be expected; in fact, this and two other contributions must be examined before the observed differences in ΔG_t^0 or ΔH_t^0 can be assigned to specific structural effects.

The free energy of transfer can conveniently be broken down into several contributions, by analogy with a similar procedure used in discussing heats of transfer (29):

$$[5]\quad \Delta G_t^0 = \Delta G_t^0(\mathrm{CAV}) + \Delta G_t^0(\mathrm{SOL}) + \Delta G_t^0(\mathrm{STR}) + \Delta G_t^{\mathrm{Ex}}(\mathrm{HI})$$

where the terms represent respectively the solvent isotope effect on the free energy, due to:

CAV: process of cavity formation in the solvent; SOL: solvation of the polar group of the molecule (dipole–dipole interactions, hydrogen bonding); STR: structural rearrangement of the solvent around the cavity enclosing the solute; (HI): solute–solute interactions (hydrophobic interaction) which must be considered since these measurements are carried out at finite concentrations. (This term obviously relates to the assumption of equal activity coefficients in H_2O and D_2O, *cf.* Results.)

Of course the contribution which would reflect specific influences due to different structures of hydrophobic groups would be ΔG_t^0(STR). The latter is intimately connected with ΔG_t^0(CAV), and it is by no means clear that these can be separated (29).

(a) ΔG_t^0(SOL)

Carbonyl groups are known to act as proton acceptors in hydrogen bonding with various donors (30). Because of the zero point energy difference (23), a solvent isotope effect can be expected on the free energy of solvation of the $\diagdown\!\!\diagup C{=}O$ group, probably in the direction of a lower chemical potential for the ketone in D_2O compared to H_2O. If the various ketones have different basicity or steric hindrance at the $\diagdown\!\!\diagup C{=}O$ group, the magnitude of ΔG_t^0(SOL) could differ for each of the compounds investigated here. Several experimental findings strongly indicate, however, that ΔG_t^0(SOL), and its

Can. J. Chem. Downloaded from www.nrcresearchpress.com by 210.87.254.42 on 09/05/12
For personal use only.

Can. J. Chem. Downloaded from www.nrcresearchpress.com by 210.87.254.42 on 09/05/12
For personal use only.

variation throughout the series of ketones, must be small compared to the variations observed in ΔG_t^0.

This is first suggested by the fact that ΔG_t^0 of acetone is $\simeq 0 \pm 15$ cal mol^{-1} (31). Thus ΔG_t^0(SOL) could only be as large as the contribution from two methyl groups, and of opposite sign. Also, we see from Fig. 1 that changing the position of the $\rangle C{=}O$ group has a significant consequence on ΔG_t^0, but the effect is opposite in the two series of saturated ketones. This again indicates that the solvation of the $\rangle C{=}O$ group does not make a dominant contribution to ΔG_t^0.[2]

Evidence in support of the similar basicity of the various ketones is supplied by proton chemical shift measurements δ of protonated ketones (32). The observed δ for, *e.g.*, adamantanone and di-*t*-butylketone are large and very similar (respectively −13.85 and −13.51 p.p.m.) indicating similar basicity, in spite of drastically different molecular properties. As a further check of the similar proton accepting ability of the ketones studied here, we measured the shift induced in the fundamental —OH stretching frequency of CH_3OH upon hydrogen bonding to several ketones. The red shifts, measured in mixtures of 2 *M* ketones and 1 *M* CH_3OH in CCl_4, for compounds **1**, **10**, **16**, and **18** (See Table 1 or 2) were found respectively as 110, 160, 165, and 185 cm^{-1} relative to 1 *M* CH_3OH in CCl_4. These data indicate a noticeable degree of specificity, but at least for the last three compounds, the variations are small compared to the magnitude of the observed shifts. Since —OH stretching frequencies are very sensitive towards hydrogen bonding and usually well correlated with the hydrogen-bond energies (30), it appears that the basicity of the ketones studied here must be quite similar.

From the above considerations it thus seems justified to conclude that ΔG_t^0(SOL) is not the dominant contribution to ΔG_t^0, and that specific solvation effects cannot explain the variance observed in ΔG_t^0 for the ketones under investigation.

(b) ΔG_t^{Ex} *(HI)*

Some of the linear ketones studied here have the general structure of nonionic surfactants, hence hydrophobic interactions (perhaps even micelle formation) might occur in solutions of these compounds. The excess free energy arising from these interactions also exhibits a solvent isotope effect which was found as ~ -50 cal mol^{-1} for micellar *n*-dodecyltrimethylammonium bromide (34).

To demonstrate the absence of micellar aggregates in saturated solutions of 2-decanone and 4-decanone, we used a method based on changes in the e.s.r. spectrum of stable nitroxide radicals (13). This procedure was shown to be very effective in detecting the onset of aggregation of surfactant molecules with solutes bearing an alkyl chain longer than *n*-hexyl (13). In the present case, the e.s.r. spectra of di-tert-butylnitroxide (DTBNO) (5×10^{-5} *M*) in saturated solutions of either 2- or 4-decanone were identical to the DTBNO spectrum in water.[3] The presence of a significant concentration of micellar clusters in the solutions examined can thus be excluded. Remaining possible contributions from pairwise hydrophobic interactions are not expected to be significant for ΔG_t^0, on the basis of the following arguments.

(1) The isotope effect on the excess free energy of hydrophobic solutes such as Bu_4NBr is negative, but barely detectable up to concentrations of 2–3 *m* (35).

(2) Comparing the $(H_2O \rightarrow D_2O)$ transfer functions of small hydrocarbons, Ben-Naim (36) recently concluded that the solvent isotope effect on the hydrophobic interaction leads to a *positive* free energy contribution, *i.e.* ΔG_t^{Ex}(HI) > 0; the latter is less than 5% of the total free energy change due to the hydrophobic interaction (at 25 °C).

(c) ΔG_t^0*(CAV)*

As mentioned earlier, the solvent isotope effect on G^0(CAV) and G^0(STR) may not be truly separable. Still, it is interesting to inquire about the anticipated sign and magnitude of ΔG_t^0(CAV), using available means of estimating free energies of cavity formation.

The recent correlation established between the solubility of hydrocarbons and their estimated surface area (37) have been taken as evidence for the importance of the G^0(CAV) term in the free energy of solution. If the latter can be assumed

[2]In heats of transfer (33), the isotope effect due to hydrogen bonding is clearly evidenced only with such strong acceptors as F^-.

[3]For details on the experimental conditions see ref. 13.

Can. J. Chem. Downloaded from www.nrcresearchpress.com by 210.87.254.42 on 09/05/12
For personal use only.

as (37)

$$G^0(\mathrm{CAV}) = 4\pi r^2\sigma_0$$

where r and σ_0 are respectively the radius of a spherical cavity and the bulk surface tension of the solvent, then one would expect small negative values of ΔG_t^0(CAV) because $\sigma_0(D_2O)$ is less than $\sigma_0(H_2O)$ by approximately 0.05% (25).[4] Since, for a given volume, the surface area of a cylindrical cavity is greater than that of a spherical cavity, we would predict ΔG_t^0 to be somewhat more negative for, *e.g.*, 2-decanone than for adamantanone.[5] Though for these two solutes, the relative order is correct, clearly, the free energy of cavity formation cannot be large enough to account for the magnitude of ΔG_t^0 on the basis of the surface tensions of H_2O and D_2O.

The free energy of cavity formation can also be computed from the scaled-particle theory which has been applied with remarkable results to solutions of nonpolar compounds in aqueous and nonaqueous solvents (38, 39). The theory envisages the solvent as a hard sphere fluid in which the reversible work required to create a cavity depends on particle density (number of particles per unit volume), pressure, temperature, and solvent and cavity diameters, a_1 and a_2. We used this theory to compute ΔG_t^0(CAV) assuming that the hard sphere diameters of H_2O and D_2O are identical (2.76 Å) and calculating the particle density from the molar volumes of H_2O and D_2O (40). ΔG_t^0(CAV) values were computed for several temperatures and cavity diameters, and the results are given in Fig. 4. The near linear dependence of ΔG_t^0(CAV) with a_2^2 shows that the theory emphasizes surface effects. Since the particle density is lower in D_2O than in H_2O, the prediction of a negative ΔG_t^0(CAV) is not surprising, but even the magnitude of the calculated ΔG_t^0(CAV) is in reasonable agreement. For example, for a spherical cavity having a volume equal to the partial molal volume of propane in H_2O (41), ΔG_t^0(CAV) is calculated as ~ -80 cal mol^{-1}, whereas ΔG_t^0 has been reported as -17.4 cal mol^{-1} (24). A similar estimate for *n*-decane[6] leads to ΔG_t^0(CAV) ~ -150 cal mol^{-1} which can be compared to our ΔG_t^0 for the *n*-decanones ~ -275 cal mol^{-1} (average). Thus the scaled-particle theory apparently accounts for much of the negative ΔG_t^0 without recourse to structural changes induced in the solvent by the solute.

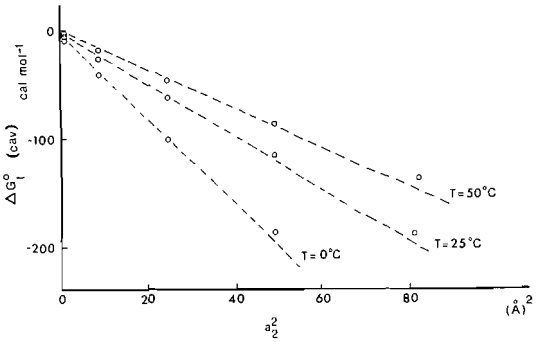

FIG. 4. Isotope effect on the free energy of cavity formation computed for several cavity diameters (a) and temperatures using the scaled-particle theory (see part c of Results). The hard sphere diameter of the water molecule was taken as 2.76 Å.

Calculations of ΔH_t^0(CAV) from the scaled-particle theory, with the assumptions given above, also lead to striking results: both ΔH_t^0-(CAV) and ΔS_t^0(CAV) are large and negative as is observed experimentally for a number of inert gases and hydrocarbons (24, 25, 36).[7] For a cavity the size of *n*-decane, we compute ΔH_t^0-(CAV) and ΔS_t^0(CAV) as respectively -0.9 kcal mol^{-1} and -2.4 e.u., which can be compared with -2.1 kcal mol^{-1} and -6.4 e.u. found for 2-decanone.

The observed positive ΔG_t^0 for a number of ketones, however, remains to be explained and require a more physical examination of the calculations of ΔG_t^0(CAV). The assumption that H_2O and D_2O only differ by their amount of free volume does not completely describe these peculiar liquids: while the particle density decreases in going from H_2O to D_2O, the cohesive energy density is greater in D_2O than in H_2O, *i.e.* zero point energy effect on the hydrogen bond (25). The intermolecular attraction potential, which is absent in the scaled-particle theory,

[4]More appropriate data for such a comparison would be hydrocarbon $-H_2O$ and hydrocarbon $-D_2O$ interfacial tensions, but there appear to be no data on the latter. On the other hand, scaling of these quantities for small curvature radii still remains a problem.

[5]The assumption on the relative surface area is contrary to other estimates (37) in which the surface area was calculated to increase with branching of a molecule.

[6]The partial molal volume ϕ_v of *n*-decane was estimated from ϕ_v(propane) assuming additive methylene group contributions (42).

[7]Other aspects of these calculations will be discussed in more detail elsewhere.

Can. J. Chem. Downloaded from www.nrcresearchpress.com by 210.87.254.42 on 09/05/12
For personal use only.

would thus lead to additional work required to expand a cavity in D_2O compared to H_2O. A simple explanation of some of our experimental results follows immediately. Since the amount of void space is greater in D_2O than in H_2O, solutes which can occupy this void space without excessive disruption of hydrogen bonds in the solvent will be best accommodated in D_2O (negative ΔG_t^0). This reasoning is a straightforward extension of Eley's proposition to account for the properties of inert gases in water (2), and possibly would apply to the linear ketones studied here.[8] On the other hand, bulky molecules such as adamantanone require cavities much larger than those existing in the solvent; for these, a significant number of hydrogen bonds must then be broken, a process which will require more work in D_2O than in H_2O. If the latter contribution is dominant, ΔG_t^0 would then be positive, with ΔH_t^0 and ΔS_t^0 also more positive.

The interpretation nicely accounts for the observed ΔG_t^0 which is negative for the linear ketones and increases with the degree of branching in the hydrocarbon groups, finally becoming positive for the bulky polycyclic molecules. Within the available ΔH_t^0 and ΔS_t^0 data, the explanation is consistent, except with a few cyclohexanone derivatives. In particular, tetramethylcyclohexanone stands out, as a bulky molecule, having a large *negative* ΔG_t^0 and ΔH_t^0. If these effects are real, they might, however, point out to other interesting specific behaviors which are presently being investigated through other thermodynamic measurements.

It may be added that the interpretation given here also accounts for other experimental findings, namely the positive ΔG_t^0 for benzene (36) and substituted benzenes (31). Likewise, the negative ΔH_t^0 for Bu_4N^+, compared to the positive ΔH_t^0 for Ph_4As^+ (33), may find a suitable explanation in the geometry of their respective hydrocarbon substituents.

(d) ΔG_t^0(STR)

As mentioned earlier, the thermodynamic quantities for the transfer of inert solutes from H_2O to D_2O are usually interpreted in terms of solvent structural perturbation by the solutes (24–26, 31, 33, 43). This follows from the assumption that molecular or liquid H_2O and D_2O are negligibly different (*e.g.* similar dipole moments, polarizabilities, and dielectric constants), except in the extent of hydrogen bonding responsible for the structure in the two liquids. Quantitatively, the extent of hydrogen bonding can only be defined as |(number of bonds) × (ΔH^0 per bond)|, but this quantity is larger for D_2O than for H_2O. The rationale underlying this postulate was well summarized by Arnett and McKelvey (25). A second widely used assumption is that whatever perturbation the solute exerts on the solvent structure (structure breaking or structure stabilizing), it will be more extensive in D_2O (25).

In a case of particular interest here, the $H_2O \rightarrow D_2O$ transfer of hydrocarbons, the negative ΔH_t^0 and ΔS_t^0 have been attributed to greater solvent ordering in the hydrocarbon solutions in D_2O compared to H_2O (24). However, if a significant part of the negative ΔG_t^0 (also of ΔH_t^0 and ΔS_t^0) can be explained from the hard sphere model, which invokes only the properties of the pure solvents, then only the difference between ΔG_t^0 and ΔG_t^0(CAV) can be assigned to structural effects. While relying on the scaled-particle theory for the (CAV) contribution to the transfer function may be questionable (44), it must be pointed out that ΔG_t^0(CAV) is much less dependent than G^0(CAV) on the choice of computation parameters (*e.g.* solvent hard sphere diameter). If we adopt ΔG_t^0(STR) as

$$\Delta G_t^0(\text{STR}) = \Delta G_t^0 - \Delta G_t^0(\text{CAV})$$

and again using the comparison between *n*-decane and 2-decanone, we find for the latter $\Delta G_t^0(\text{STR}) \simeq -30$ cal mol^{-1}, $\Delta H_t^0(\text{STR}) \simeq -1.2$ kcal mol^{-1}, and $\Delta S_t^0(\text{STR}) \simeq -4$. e.u. From the sign of these transfer functions we could then conclude, as in the earlier interpretation (24), that the linear 2-decanone induces more solvent ordering (structure) in D_2O than in H_2O. Presumably, the opposite would be true in cases where $\Delta G_t^0(\text{STR}) > 0$, *i.e.* adamantanone, but this could only be confirmed with more accurate data on ΔH_t^0.

The limited data on ΔH_t^0 preclude a more detailed interpretation of the ΔG_t^0. Still, within the validity of the present calculation of the cavity contribution, it can be concluded that the differences in the observed ΔG_t^0 for the different

[8]The effective diameter of the methylene group in water can be estimated from partial molal volume data (42) as 3.1 Å, somewhat less than for Ar (3.5 Å).

ketones originate in the structural part of ΔG_t^0.[9] From this and the present measurements, we can only infer that the linear ketones induce more structure in D_2O than in H_2O, while the reverse appears probable for the rigid polycyclic molecules. This is, in part, the connection we sought between the structure of a solute and the perturbation it exerts on the water structure. Now, if the structural part of the $H_2O \rightarrow D_2O$ transfer functions truly reflect the solvent structural perturbation by the solute, we must then ask: do the polycyclic molecules studied here exert *any* stabilizing influence on the water structure? The prominence of such solutes in natural chemical systems makes worthy further attempts to answer this question.

Conclusion

The magnitudes of the free energy and heat of transfer ($H_2O \rightarrow D_2O$) of large hydrophobic solutes are strongly influenced by the structure of these solutes. However, the solvent isotope effect on the thermodynamic quantities for the process of cavity formation in the solvent appears to be an important contribution to ΔG_t^0 and ΔH_t^0. Using the scaled-particle theory to compute the cavity contribution, the remainder is assigned to structural perturbations in the solvent, and is interpreted in terms of a better stabilization of the solvent structure by the linear molecules compared to those which are highly branched.

Financial support of this work by the National Research Council of Canada is gratefully acknowledged. We thank Dr. P. R. Philip for assistance with some of the calculations and Mr. Eric Firkins for i.r. spectral measurements. We also thank these people and Prof. J. E. Desnoyers for helpful discussions.

1. H. S. FRANK and M. W. EVANS. J. Phys. Chem. **13**, 507 (1945).
2. D. D. ELEY. Trans. Faraday Soc. **40**, 184 (1944).
3. H. S. FRANK and W. Y. WEN. Discuss. Faraday Soc. **24**, 133 (1957).
4. R. L. KAY and D. F. EVANS. J. Phys. Chem. **70**, 2325 (1966).
5. (*a*) W. Y. WEN. *In* Water and aqueous solutions. *Edited by* R. A. Horne. John Wiley and Sons Inc., New York, 1972, Chapt. 15. p. 613. (*b*) F. FRANKS. *In* Physico-chemical processes in mixed aqueous solvents. *Edited by* F. Franks. Heinemann Educational Books Ltd., London. 1967. p. 50 (*c*) J. E. DESNOYERS and C. JOLICOEUR. *In* Modern aspects of electrochemistry. Vol. 5. *Edited by* J. O'M. Bockris and B. E. Conway. Plenum Press. N.Y. 1969. p. 1. (*d*) M. J. BLANDAMER. Q. Rev. Lond. **24**, 1969 (1970). (*e*) F. FRANKS. *In* Hydrogen-bonded solvent systems. *Edited by* A. K. Covington and P. Jones. Taylor and Francis Ltd., London. 1968. p. 196.
6. (*a*) R. MCMULLAN and G. A. JEFFREY. J. Chem. Phys. **31**, 1231 (1959). (*b*) H. D. NELSON and C. L. DE LIGNY. Rec. Trav. Chim. **87**, 623 (1968).
7. G. E. WALRAFEN. J. Chem. Phys. **55**, 768 (1971).
8. C. JOLICOEUR, N. D. THE, and A. CABANA. Can. J. Chem. **49**, 2008 (1971).
9. H. G. HERTZ, B. LINDMAN, and V. SIEPE. Ber. Bunsenges. Phys. Chem. **73**, 542 (1969).
10. D. H. EVERETT. Discuss. Faraday Soc. **24**, 217 (1957).
11. A. HOLTZER and M. F. EMMERSON. J. Phys. Chem. **73**, 26 (1969).
12. M. LUCAS. J. Phys. Chem. **76**, 4030 (1972).
13. C. JOLICOEUR and H. L. FRIEDMAN. J. Soln. Chem. In press. C. JOLICOEUR and H. L. FRIEDMAN. Ber. Bunsenges. Phys. Chem. **75**, 248 (1971).
14. D. H. EVERETT and W. F. K. WYNNE-JONES. Trans. Faraday Soc. **35**, 1421 (1939).
15. M. E. FRIEDMAN and H. A. SCHERAGA. J. Phys. Chem. **69**, 3795 (1965).
16. F. FRANKS and H. T. SMITH. J. Chem. Eng. Data, **13**, 538 (1968).
17. J. L. NEAL and D. A. GORING. J. Phys. Chem. **74**, 658 (1970).
18. G. G. MALENKOV. J. Struct. Chem. **7**, 321 (1966).
19. D. N. GLEW, H. D. MAK, and N. S. RATH. *In* Hydrogen-bonded solvent systems. *Edited by* A. K. Covington and P. Jones. Taylor and Francis Ltd., London. 1968. p. 196.
20. J. E. DESNOYERS, R. PAGÉ, G. PERRON, P. A. LEDUC, J.-L. FORTIER, and R. E. PLATFORD. Can. J. Chem. **51**, 2129 (1973).
21. F. FRANKS, M. A. S. QUICKENDEN, D. S. REID, and B. WATSON. Trans. Faraday Soc. **66**, 582 (1970).
22. J. POLAK, S. MURAKAMI, V. T. LAM, H. D. PFLUG, and G. C. BENSON. Can. J. Chem. **48**, 2457 (1970).
23. C. G. SWAIN and R. F. W. BADER. Tetrahedron, **10**, 183 (1960).
24. G. NEMETHY and H. A. SCHERAGA. J. Chem. Phys. **41**, 689 (1964).
25. E. M. ARNETT and D. R. MCKELVEY. *In* Solute–solvent interactions. *Edited by* J. F. Coetzee and C. D. Ritchie. Interscience Publishers, New York. 1969. p. 344.
26. B. E. CONWAY and L. H. LALIBERTÉ. Trans. Faraday Soc. **66**, 3032 (1970). G. PERRON and J. E. DESNOYERS. J. Chem. Eng. Data, **17**, 136 (1972).
27. C. MCAULIFFE. J. Phys. Chem. **70**, 1267 (1966).
28. F. FRANKS. Nature, **210**, 87 (1966).

[9]Variations of ΔG_t^0(CAV) corresponding to differences in the intrinsic volumes should be small, particularly for the series of ketones of same chemical composition (*cf.* Table 2, compounds **1–10**). For instance, the molal volumes of the isomeric butanols differ by less than 2% (16).

Can. J. Chem. Downloaded from www.nrcresearchpress.com by 210.87.254.42 on 09/05/12
For personal use only.

29. C. V. KRISHNAN and H. L. FRIEDMAN. J. Phys. Chem. **73**, 1572 (1969).
30. A. S. N. MURTHY and C. N. R. RAO. Appl. Spectr. Rev. **2**, 69 (1968).
31. D. B. DAHLBERG. J. Phys. Chem. **76**, 2045 (1972).
32. G. A. OLAH and M. CALIN. J. Am. Chem. Soc. **90**, 938 (1968). G. A. OLAH, M. CALIN, and D. H. O'BRIEN. J. Am. Chem. Soc. **89**, 3586 (1970).
33. C. V. KRISHNAN and H. L. FRIEDMAN. J. Phys. Chem. **74**, 2356 (1970).
34. M. F. EMMERSON and A. HOLTZER. J. Phys. Chem. **71**, 3320 (1970).
35. C. M. L. CHEN. Ph.D. Thesis. Clark University, Pittsburgh, Pa. 1968.
36. A. BEN-NAIM, J. WILT, and M. YAACOBI. J. Phys. Chem. **77**, 95 (1973).
37. R. B. HERMANN. J. Chem. Phys. **75**, 363 (1971).
38. R. A. PIEROTTI. J. Chem. Phys. **69**, 281 (1965).
39. A. FEILLOLAY and M. LUCAS. J. Phys. Chem. **76**, 3068 (1972).
40. G. S. KELL. J. Chem. Eng. Data, **12**, 66 (1967).
41. W. L. MASTERTON. J. Chem. Phys. **22**, 1830 (1954).
42. J. E. DESNOYERS and M. AREL. Can. J. Chem. **45**, 359 (1967).
43. J. E. DESNOYERS, R. FRANCESCON, P. PICKER, and C. JOLICOEUR. Can. J. Chem. **49**, 3460 (1971). P. R. PHILIP and J. E. DESNOYERS. J. Solution Chem. **1**, 353 (1972).
44. A. BEN-NAIM and H. L. FRIEDMAN. J. Phys. Chem. **71**, 449 (1967).

Can. J. Chem. Downloaded from www.nrcresearchpress.com by 210.87.254.42 on 09/05/12
For personal use only.

La décomposition du tétraméthylgermane par les atomes Hg $6(^3P_1)$

JOCELYN DUVAL ET YVES ROUSSEAU
Université de Montréal, Département de Chimie, Montréal, Québec

Reçu le 14 mars 1973

Le seul processus primaire de la décomposition photosensibilisée au mercure à 2537 Å du tétraméthylgermane est la rupture d'une liaison C—H puisque le rendement quantique en hydrogène tend vers l'unité. Pour des conditions modérées, l'hydrogène moléculaire et le di(triméthylgermyl)-1,2 éthane sont les seuls produits de la réaction. La recombinaison des deux radicaux primaires conduit, surtout à basse pression, à des radicaux méthyles qui, par arrachement d'un atome d'hydrogène sur le substrat, produisent du méthane.

The primary process in the mercury photosensitized decomposition of tetramethylgermane is a C—H bond cleavage. The hydrogen quantum yield, extrapolated at infinite pressure, is close to unity. Under mild conditions, hydrogen and 1,2-di(trimethylgermyl)ethane are the only products observed. At high intensities and low substrate pressures, atomic cracking occurs yielding methyl radicals which lead to the formation of methane.

Can. J. Chem., 51, 3062 (1973)

Le parellélisme réactionnel entre les alcanes et les silanes ou germanes avec les atomes de mercure dans leur état $6(^3P_1)$ est apparent à la suite des travaux de Gunning et de ses collaborateurs (1). Même le tétraméthylsilane semble se comporter comme le néopentane vis-à-vis des atomes de mercure excités; sa décomposition est amorcée par le bris d'une liaison C—H. Cependant aucun travail n'a été effectué sur le tétraméthylgermane et, étant donné l'augmentation de dimensions en passant du silane au germane, on peut se demander si ce parallélisme sera conservé dans le cas des dérivés alkylés du germanium. On peut supposer que la liaison Ge—C est plus vulnérable et peut être plus facilement rompue qu'une liaison C—C ou Si—C. Nous avons donc entrepris d'étudier le comportement du tétraméthylgermane lors de sa réaction avec les atomes de mercure dans leur état excité $6(^3P_1)$. Puisqu'il n'y a pas de possibilité de formation de doubles liaisons entre deux atomes de germanium, on peut supposer que la cinétique de décomposition sera simple.

Section expérimentale

Le tétraméthylgermane (TMG) utilisé provient de la compagnie K + K et n'est pur qu'à 95%. On le purifie par chromatographie en phase gazeuse en utilisant une colonne de 24 pieds contenant de l'huile de silicone D C 200 à 30% sur chromosorb. La fraction collectée à la sortie du chromatographe est ensuite distillée pour y enlever les traces d'eau et de dioxyde de carbone. Le TMG ainsi purifié contient moins de 0.01% d'impuretés tel que déterminé par spectrométrie de masse et chromatographie. Le composé pur est gardé à une température de −64 °C. Les trois intensités lumineuses utilisées furent déterminées par la méthode de Hatchard et Parker (2) et confirmées par l'actinomètre N_2O–*n*-butane (3). Les produits sont analysés par chromatographie en phase gazeuse et par spectrométrie de masse. Les photolyses sont effectuées à température ambiante en utilisant une lampe au mercure à basse pression de Hanovia Lamp Division, type SC 2537. La radiation émise à 1849 Å est filtrée en se servant d'une cellule réactionnelle en Vycor 7910. Cette cellule est cylindrique. Son diamètre est de 5 cm et elle a 10 cm de longueur. Pour les études à 46.2 μeinstein/min une cellule de 3 cm de diamètre et de 22 cm de longueur est placée à l'intérieur de l'hélice de la lampe.

Resultats et discussion

Les principaux produits de la réaction sont: H_2, CH_4, et $[(CH_3)_3Ge—CH_2]_2$. A basse intensité lumineuse, le rendement en méthane est faible par rapport a celui des deux autres produits (~1%). Le di(triméthylgermyl)-1,2 éthane donne un spectre de masse caractéristique à cause des cinq isotopes stables du germanium. Les résultats rapportés au tableau 1 indiquent

TABLEAU 1. Rendements quantiques en hydrogène et en méthane en fonction de la pression de TMG*

P_{TMG} (Torr)	Φ_{H_2}	Φ_{CH_4}
10.5	0.17	0.003
51.5	0.38	0.004
150	0.60	0.005
250	0.76	0.008
295	0.76	0.008

*Intensité lumineuse: 0.02 μeinstein/min; temps de photolyse: 90 min.

Can. J. Chem. Downloaded from www.nrcresearchpress.com by 210.87.254.105 on 09/05/12
For personal use only.

Can. J. Chem. Downloaded from www.nrcresearchpress.com by 210.87.254.105 on 09/05/12
For personal use only.

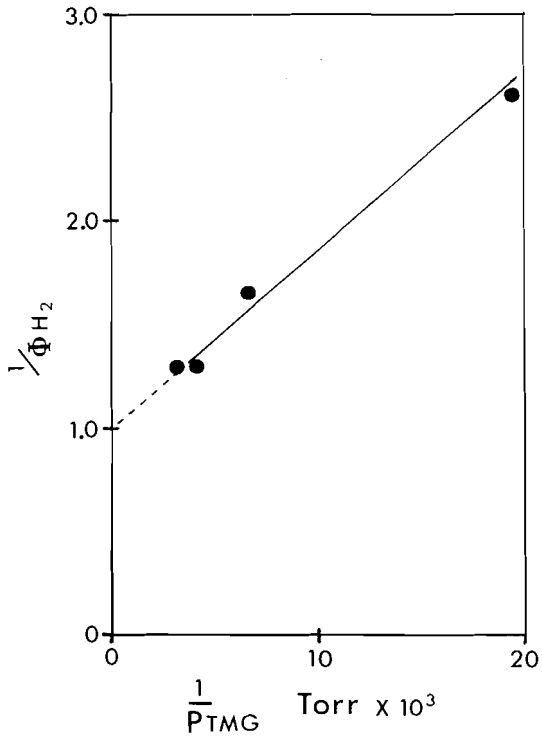

FIG. 1. Inverse du rendement quantique d'hydrogène en fonction de l'inverse de la pression de tétraméthylgermane.

une augmentation du rendement quantique en hydrogène en fonction de la pression de substrat. Il est donc peu probable que l'hydrogène soit formé par l'intermédiaire d'une molécule de tétraméthylgermane excitée à temps de vie assez long pour être désactivée par collisions. D'autre part on peut constater à la fig. 1, que la valeur de l'inverse du rendement quantique en hydrogène devient 1, lorsqu'extrapolée à pression infinie, ce qui est compatible avec un processus primaire impliquant une rupture C—H, *i.e.*

[1] $Hg\ 6(^3P_1) + TMG \rightarrow H^{\cdot} + H_2C{-}Ge(CH_3)_3 + Hg(^1S_0)$

[2] $Hg\ 6(^3P_1) + TMG \rightarrow HgH + H_2C{-}Ge(CH_3)_3$

L'intervention d'atomes métastables Hg $6(^3P_0)$, si elle a lieu, doit être suivie d'une réaction de décomposition du tétraméthylgermane afin d'être compatible avec le rendement quantique unitaire.

[3] $Hg\ 6(^3P_1) + TMG \rightarrow Hg\ 6(^3P_0) + TMG$

[4] $Hg\ 6(^3P_0) + TMG \rightarrow H^{\cdot} + H_2C{-}Ge(CH_3)_3 + Hg(^1S_0)$

La réaction 4 est peu probable, compte tenu du fait que le rendement quantique de décomposition du propane par les atomes Hg $6(^3P_0)$ est seulement de 0.57 à 63 °C. (4). L'hydrogène moléculaire et le di(triméthylgermyl)-1,2 éthane sont possiblement formés par les réactions suivantes:

[5] $H^{\cdot} + TMG \rightarrow H_2 + H_2C{-}Ge(CH_3)_3$

[6] $2\ H_2C{-}Ge(CH_3)_3 \rightarrow (CH_3)_3\ Ge{-}CH_2{-}CH_2{-}Ge(CH_3)_3$

Bien qu'un rendement quantique du di(triméthylgermyl)-1,2 éthane n'ait pu être mesuré à cause de l'absence de standard, ce produit est le seul produit lourd observé à faible intensité lumineuse et, dans tous les cas, constitue près de 99% de la fraction des produits plus lourd que le TMG. Les résultats obtenus à une pression de substrat de 250 Torr et mis en graphique à la fig. 2 sont compatibles avec le mécanisme proposé. En effet on peut y constater que l'hydrogène est un produit primaire alors que le méthane, dont le rendement augmente en fonction du temps de photolyse, est un produit secondaire.

Si on considère sous un autre angle les résultats du tableau 1, on peut attribuer l'augmentation observé dans les rendements quantiques à une désactivation incomplète des atomes Hg $6(^3P_1)$ à basse pression. Ceci n'est d'ailleurs pas particulier au TMG, mais a aussi été noté pour le tétraméthylsilane (1). D'autre part on peut voir au tableau 2 que, même à pression élevée, l'intensité lumineuse incidente a une influence mar-

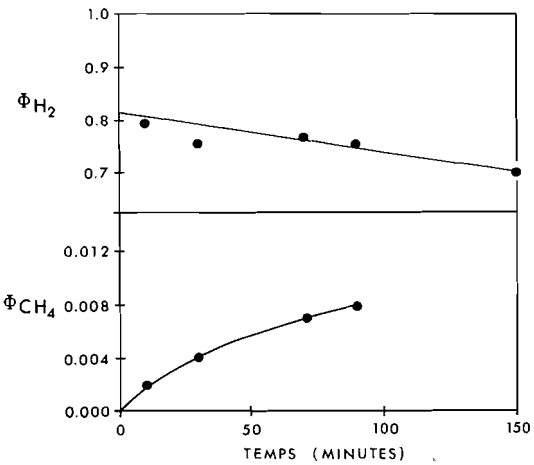

FIG. 2. Rendements quantiques de méthane et d'hydrogène en fonction du temps d'irradiation.

TABLEAU 2. Rendements quantiques en hydrogène en fonction de l'intensité lumineuse absorbée

I_a (μeinstein/min)	P_{TMG} (Torr)	Φ_{H_2}	% décomposition
46.2	100	0.002	0.6
10.1	100	0.058	0.8
0.02	100	0.48	0.2
46.2	225	0.003	0.2
10.1	230	0.13	0.5
0.02	230	0.73	0.1

quée sur le rendement quantique en hydrogène. Un certain nombre de réactions entre radicaux, en particulier celle impliquant les deux radicaux formés dans l'acte primaire, peuvent être responsable de ce phénomène:

[7*a*] $H^{\cdot} + {}^{\cdot}CH_2—Ge(CH_3)_3 \rightarrow (TMG)^*$

[7*b*] $(TMG)^* \rightarrow TMG$

L'intermédiaire (TMG)* peut être la principale source de radicaux méthyles.

[8] $(TMG)^* \rightarrow CH_3^{\cdot} + {}^{\cdot}Ge(CH_3)_3$

En effet, la formation d'une liaison C—H libère quelques 100 kcal/mol et la rupture du lien Ge—C n'en requiert que 65. Cependant puisque le nombre de degrés de liberté de la molécule TMG est grand, on peut supposer que 7*b* est prédominante. Toutefois si la réaction 8 est la principale source des radicaux méthyles, le méthane étant formé par 9,

TABLEAU 3. Rapport hydrogène/méthane en fonction de la pression de TMG*

P_{TMG} (Torr)	$[H_2]/[CH_4]$	% CH_4
7.0	4.5	18
13.5	8.5	10
45.5	24.5	4.5
90.0	27.0	3.8

*Intensité lumineuse absorbée: 46.2 μeinstein/min.

[9] $CH_3^{\cdot} + TMG \rightarrow CH_4 + {}^{\cdot}CH_2—Ge(CH_3)_3$

une augmentation de la pression doit être accompagnée d'un accroissement du rapport H_2/CH_4. Ceci est confirmé au tableau 3. A des taux de conversion plus élevés d'autres produits sont formés. Entre autres, on a pu identifier les produits suivants: C_2H_6, C_3H_8, C_2H_4, $(CH_3)_3Ge—CH_2—Ge(CH_3)_3$, et $(CH_3)_3Ge—Ge(CH_3)_3$.

1. M. A. NAY, G. N. G. WOODALL, O. P. STRAUSZ, and H. E. GUNNING. Can. J. Chem. **42**, 2140 (1964).
2. C. A. PARKER. Proc. Roy. Soc. (Lond.), A **220**, 104 (1953); C. G. HATCHARD and C. A. PARKER. Proc. Roy. Soc. (Lond.), A **235**, 518 (1956).
3. Y. ROUSSEAU and H. E. GUNNING. Can. J. Chem. **41**, 465 (1963).
4. J. M. CAMPBELL, O. P. STRAUSZ, and H. E. GUNNING. J. Am. Chem. Soc. **95**, 740 (1973).

Can. J. Chem. Downloaded from www.nrcresearchpress.com by 210.87.254.105 on 09/05/12
For personal use only.

Correlation of Ionization Potentials and the Sums of Substituent Constants for Substituted Benzenes

HARRY W. GIBSON

Xerox Corporation, Rochester Research Center, 800 Phillips Road, Webster, New York 14580

Received January 23, 1973

Previously reported experimentally determined ionization potentials of substituted benzenes are well correlated by the sum of the para substituent constants, regardless of the orientation of the substituents. σ^+ is better than σ for this purpose. Tri- through hexasubstituted benzenes are also correlated, but the slope and intercept are higher in accord with electrostatic theory. These results in support of recent MO calculations indicate that substituent constants are good measures of the energy of the highest occupied orbital.

Les potentiels d'ionisation expérimentaux précédemment rapportés pour les benzènes substitués sont en bonne corrélation avec la somme des constantes de substituant para. A cet effet, σ^+ est meilleur que σ. La corrélation pour les benzènes tri à hexa substitués a été également faite, la pente et l'ordonnée à l'origine sont plus élevées ce qui est en accord avec la théorie électrostatique. Ces résultats, qui concordent avec les récents calculs des OM, montrent que les constantes de substituants sont une bonne mesure de l'énergie de l'orbitale occupée la plus haute. [Traduit par le journal]

Can. J. Chem., 51, 3065 (1973)

Can. J. Chem. Downloaded from www.nrcresearchpress.com by 210.87.254.105 on 09/05/12
For personal use only.

The wide applicability of the Hammett and related equations to reaction kinetics and a variety of spectral and physical properties (1) has attracted the attention of molecular orbital theorists (2–6). These studies seem to place linear free energy equations of the Hammett type on a very sound theoretical basis.

Ionization potentials have long been recognized as absolute measures of energies of the highest occupied molecular orbitals (7). The ionization potential is defined as the energy necessary to remove an electron completely from a molecule or atom in the ground state to produce a positively charged ion and a free electron. In a few instances ionization potentials (IP) for homologous series, *e.g.*, *p*-substituted acetophenones (8), substituted toluenes (9) and monosubstituted benzenes (9), were correlated with the Hammett constants.

No one, however, appears to have correlated all values for substituted benzenes with the Hammett equation. Such a correlation would demonstrate on an experimental basis the link between orbital energies and substituent constants. For such a correlation to exist the electron being removed must be from a π orbital involved in the aromatic ring. If a substituent itself contains localized electrons of comparable or lower ionization potential, the compound will not fit the general correlation. On this basis the substituent is affecting the reactive site, *i.e.*, the π cloud, both by its resonance and inductive contributions. This would mean that σ_{para} values should be used since they include contributions from both effects, whereas σ_{meta} values do not include resonance contributions. To a first approximation the effect of the disposition of substituents with regard to one another is expected to be small.[1] Indeed, for disubstituted benzenes the difference in ionization potentials of the three isomers is less than 0.2 eV (9–11) (see Table 1), which is less than the deviation between the various methods used to obtain the data used herein.[2] As shown in Table 2, para substituent constants do give better fits of the data (10, 11). Brown's σ^+ values (12), which were derived for electrophilic reactions, *i.e.*, those involving generation of a positive charge on the aromatic nucleus as the result of attack by an electrophile, *e.g.*, NO_2^+, Br^+, seem to give slightly better correlations as previously noted (8, 9).

Figure 1 is a plot of ionization potential *vs.* $\sum\sigma^+_{para}$ for 49 mono- and disubstituted benzenes (10, 11) excluding phenols, bromides, and

[1]One rather obvious exception is the case where steric interference of the two (or more) substituents causes non-coplanarity of the substituent and ring, leading to loss of resonance contribution.

[2]All substituted benzenes for which ionization potentials were available from refs. 10 and 11 were used. The former are the "best" values from ref. 15. In many cases σ^+_{para} values are not available.

TABLE 1. Summary of data

(*a*) Mono- and disubstituted benzenes

X	Y	$\Sigma\sigma_{para}$	$\Sigma\sigma^{+}_{para}$	IP (eV)*	Calculated IP (eV) Eq. 1	Eq. 2
H	H	0.00	0.00	9.25	9.11	8.80
H	CH_3	−0.17	−0.31	8.82†‡	8.84	8.55
H	C_2H_5	−0.15	−0.30	8.77†‡	8.85	8.58
H	*t*-C_4H_9	−0.20	−0.26	8.68	8.88	8.51
H	C_6H_5	0.01	—	8.27	—	8.81
H	CH_2Cl	0.18	−0.01	9.19‡	9.10	9.06
H	CHO	0.22	—	9.52	—	9.12
H	COOH	0.41	—	9.73‡	—	9.40
H	$COOCH_3$	0.39	0.48	9.35	9.54	9.37
H	$COCH_3$	0.50	—	9.77†	—	9.51
H	CN	0.63	0.66	9.95†	9.70	9.72
H	Cl	0.23	0.11	9.07	9.21	9.13
H	Br	0.23	0.15	8.98	8.98	9.13
H	I	0.28	0.13	8.73	8.99	9.21
H	OH	−0.37	−0.92	8.51	8.30	8.26
H	OCH_3	−0.27	−0.78	8.20†	8.42	8.41
H	OC_2H_5	−0.24	—	8.13	—	8.45
H	SH	0.15	—	8.32	—	9.02
H	NO_2	0.78	0.79	9.92	9.81	9.93
H	NH_2	−0.66	−1.3	7.70	7.96	7.84
H	$N(CH_3)_2$	−0.60	−1.7	7.30‖	7.61	7.92
H	$NHCOCH_3$	0.00	—	8.39‡	—	8.80
CH_3	*m*-CH_3	−0.34	−0.62	8.58	8.56	8.31
CH_3	*p*-CH_3	−0.34	−0.62	8.44	8.56	8.31
CH_3	*o*-CH_3	−0.34	−0.62	8.56	8.56	8.31
CH_3	*p*-CHO	0.05	—	9.33‡	—	8.87
CH_3	*p*-$COOCH_3$	0.22	0.17	8.94‡	9.26	9.12
CH_3	*m*-$COCH_3$	0.33	—	9.15‡	—	9.28
CH_3	*m*-CN	0.49	0.35	9.66‡	9.42	9.51
CH_3	*p*-CN	0.49	0.35	9.76‡	9.42	9.51
CH_3	*o*-Cl	0.06	−0.20	8.83	8.93	8.89
CH_3	*m*-Cl	0.06	−0.20	8.83	8.93	8.89
CH_3	*p*-Cl	0.06	−0.20	8.69	8.93	8.89
CH_3	*m*-OH	−0.44	−1.23	8.52‡	8.02	8.16
CH_3	*o*-Br	0.06	−0.16	8.78	8.97	8.89
CH_3	*m*-Br	0.06	−0.16	8.81	8.97	8.89
CH_3	*p*-Br	0.06	−0.16	8.67	8.97	8.89
CH_3	*o*-I	0.11	−0.18	8.62	8.95	8.96
CH_3	*m*-I	0.11	−0.18	8.61	8.95	8.96
CH_3	*p*-I	0.11	−0.18	8.50	8.95	9.69
CH_3	*m*-NO_2	0.61	0.47	9.65‡	9.53	9.69
CH_3	*p*-NO_2	0.61	0.47	9.82‡	9.53	9.69
CH_3	*m*-NH_2	−0.83	−1.61	7.50†	7.69	7.60
CH_3	*p*-NH_2	−0.83	−1.61	7.50‖	7.69	7.60
CH_3	*o*-$N(CH_3)_2$	−1.00	−2.01	7.37‖	7.33	7.35
CH_3	*m*-$N(CH_3)_2$	−1.00	−2.01	7.35‖	7.33	7.35
CH_3	*p*-$N(CH_3)_2$	−1.00	−2.01	7.33‖	7.33	7.35
F	H	0.06	−0.07	9.20†	9.05	8.89
F	*o*-CH_3	−0.11	−0.38	8.90†	8.66	8.64
F	*m*-CH_3	−0.11	−0.38	8.92†	8.66	8.64
F	*p*-CH_3	−0.11	−0.38	8.78†	8.66	8.64
F	*p*-CF_3	0.60	—	9.69†	—	9.67
F	*o*-Cl	0.29	0.04	9.16†	9.15	9.22
F	*m*-Cl	0.29	0.04	9.21	9.15	9.22
F	*p*-Cl	0.29	0.04	9.43‡	9.15	9.22
F	*p*-Br	0.29	0.08	8.99	9.15	9.22

Can. J. Chem. Downloaded from www.nrcresearchpress.com by 210.87.254.105 on 09/05/12
For personal use only.

TABLE 1. (*Concluded*)

X	Y	$\Sigma\sigma_{para}$	$\Sigma\sigma^{+}_{para}$	IP (eV)*	Calculated IP (eV) Eq. 1	Eq. 2
F	*o*-F	0.12	−0.14	9.31	8.99	8.98
F	*p*-F	0.12	−0.14	9.25	8.99	8.98
F	*o*-NH_2	−0.60	−1.37	7.95†	7.90	7.93
F	*m*-NH_2	−0.60	−1.37	7.90†	7.90	7.93
F	*p*-NH_2	−0.60	−1.37	7.82	7.90	7.93
NH_2	CHO	−0.44	—	8.25‡	—	8.16
NH_2	*o*-Cl	−0.43	−1.5	7.90†‖	7.78	8.17
NH_2	*m*-$COCH_3$	−0.16	—	8.09‡	—	8.57
NH_2	*p*-$COCH_3$	−0.16	—	8.17‡	—	8.57
NH_2	*o*-NO_2	0.12	−0.51	8.66‡	8.66	8.98
NH_2	*m*-NO_2	0.12	−0.51	8.7‡	8.66	8.98
NH_2	*p*-NO_2	0.12	−0.51	8.85‡	8.66	8.98
$COCH_3$	*p*-Cl	0.73	—	9.47‡	—	9.86
$COCH_3$	*m*-OCH_3	0.23	—	8.53‡	—	9.13
$COCH_3$	*p*-OCH_3	0.23	—	8.62‡	—	9.13
$COCH_3$	*m*-NO_2	1.28	—	9.89‡	—	10.66
$COCH_3$	*p*-NO_2	1.28	—	10.07	—	10.66
Cl	*m*-Cl	0.46	0.22	9.12	9.31	9.47
Cl	*p*-Cl	0.46	0.22	8.95	9.31	9.47
Cl	*o*-Cl	0.46	0.22	9.06	9.31	9.47
Cl	*p*-OH	−0.14	−0.82	9.07	8.38	8.60
$COOCH_3$	*p*-NO_2	1.17	1.47	10.20	10.41	10.50
$COOCH_3$	*p*-OCH_3	0.12	−0.30	8.43	8.85	8.98
$N(CH_3)_2$	*p*-$N(CH_3)_2$	−1.66	−3.4	6.6‖	6.10	6.39
CHO	*p*-NO_2	1.00	—	10.27‡	—	10.25
CHO	*p*-Cl	0.45	—	9.61‡	—	9.45
CHO	*m*-OH	0.01	—	9.32‡	—	8.95
$COCH_3$	*m*-OH	0.13	—	8.67‡	—	8.99
$COCH_3$	*p*-OH	0.13	—	8.70‡	—	8.99
COC_6H_5	*p*-OH	0.09	—	8.59	—	8.93
Br	*p*-OH	−0.14	−0.77	9.04‡	8.43	8.60
NO_2	*p*-OH	0.41	0.32	9.52‡	9.39	9.39

(*b*) Tri-, tetra-, penta- and hexasubstituted benzenes

Compound	$\Sigma\sigma_{para}$	$\Sigma\sigma^{+}_{para}$	IP (eV)*	Calculated IP (eV) Eq. 3	Eq. 4
1,2,3-$(CH_3)_3C_6H_3$	−0.51	−0.93	8.48†	8.71	8.31
1,2,4-$(CH_3)_3C_6H_3$	−0.51	−0.93	8.27†	8.71	8.31
1,3,5-$(CH_3)_3C_6H_3$	−0.51	−0.93	8.39†	8.71	8.31
1,2,4,5-$(CH_3)_4C_6H_2$	−0.68	−1.24	8.03†	8.37	8.01
1,2,3,4-$F_4C_6H_2$	0.24	−0.28	9.61†	9.42	9.60
1,2,4,6-$NH_2(CH_3)_3C_6H_2$	−1.17	−2.23	7.45†	7.28	7.16
1,2,4,5-$NH_2(CH_3)_3C_6H_2$	−1.17	−2.23	7.45†	7.28	7.16
C_6F_5H	0.30	−0.35	9.55†	9.34	9.71
$(CH_3)_5C_6H$	−0.85	−1.55	7.92†	8.03	7.71
$CH_3C_6F_5$	0.13	−0.66	9.6†	9.00	9.41
1,2,4-$[(CH_3)_2N](CH_3)_2C_6H_3$	−0.94	−2.32	7.17‖	7.18	7.56
1,2,6-$[(CH_3)_2N](CH_3)_2C_6H_3$	−0.94	−2.32	7.22‖	7.18	7.56
1,3,5-$[(CH_3)_2N](CH_3)_2C_6H_3$	−0.94	−2.32	7.25‖	7.18	7.56

*From ref. 10 unless otherwise specified; by photoionization unless otherwise specified.
†From ref. 11.
‡By electron impact.
‖By charge transfer spectroscopy.

Can. J. Chem. Downloaded from www.nrcresearchpress.com by 210.87.254.105 on 09/05/12
For personal use only.

TABLE 2. Linear least squares correlation of IP* and $\Sigma\sigma$ using various combinations of substituent constants (σ)

Series (number of points)	Method†	Slope	Intercept	r‡
Monosubstituted acetophenones (10)	1	1.38	8.27	0.895
	2	1.27	8.43	0.974
Monosubstituted fluorobenzenes (8)	1	1.67	8.80	0.829
	2	1.72	8.93	0.982
	3	1.05	9.29	0.990
Monosubstituted toluenes (16)	1	1.59	8.76	0.862
	2	1.47	8.88	0.981
	3	0.950	9.16	0.977

*Meta and para-disubstituted compounds only; ortho compounds are not considered in this table. Phenols, iodides, and bromides are excluded. Data from Table 1.

†*Method 1*: σ_{meta} for both substituents used for meta compounds; σ_{para} for both substituents used for para compounds, *e.g.*, for *m*-nitroacetophenone: $\Sigma\sigma = \sigma_{meta\,(COCH_3)} + \sigma_{meta\,(NO_2)} = 0.38 + 0.71 = 1.09$. *Method 2*: σ_{para} used regardless of substitution pattern, *e.g.*, for either *m*- or *p*-nitroacetophenone: $\Sigma\sigma = \sigma_{para\,(COCH_3)} + \sigma_{para\,(NO_2)} = 0.50 + 0.78 = 1.28$. *Method 3*: σ^+_{para} used regardless of substitution pattern.

‡Correlation coefficient $r = 1$ for perfect fit.

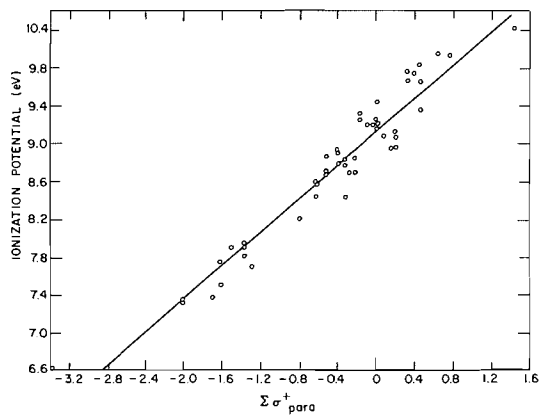

FIG. 1. Plot of experimental ionization potential *vs.* sum of para electrophilic substituent constants ($\Sigma\sigma^+_{para}$) for 49 mono and ortho-, meta- and para-disubstituted benzenes. Slope 0.885, intercept 9.11, correlation coefficient 0.967.

iodides. The correlation coefficient is 0.967. The standard deviation of the points from eq. 1 is 0.20 eV.

$$[1] \qquad IP = 0.885\Sigma\sigma^+ + 9.11$$

Use of 28 values from the same data set obtained by photoionization gives a correlation coefficient of 0.958; electron impact data gives a correlation coefficient of 0.890 for 18 points. While precisions of 0.05 eV or less are often quoted, inspection of literature data (10, 11) reveals that differences from laboratory to laboratory and method to method are at least 0.1 eV and quite often 0.2 eV. Therefore, this correlation is considered good in view of the fact that the ionization potentials were obtained by a variety of techniques and by a variety of investigators. No effort was made here to select "favorable" values.

It is significant that nine ortho-disubstituted compounds are well correlated by use of $\Sigma\sigma^+_{para}$. For the ten such compounds included in the correlation, the standard deviation is 0.16 eV. This upholds the original premise that orientation effects in disubstituted benzenes, at least, are within the scatter of points from eq. 1 (see below, however).

As one might anticipate bromo and iodo substituted aromatics do not always correlate; they have noticeably lower ionization potentials than expected from the Hammett constant values. If bromo and iodo compounds are included in the $\Sigma\sigma^+_{para}$ correlation (total of 58 points) the correlation coefficient drops to 0.953. The lower ionization potentials of the bromides and iodides may be due in part to their high polarizability, which could affect their electronic contribution more in solution than in the gas phase. The slopes are much lower than the other aromatics, that of the iodides being lower than bromides (slopes 0.495 *vs.* 0.816, respectively; intercepts 8.89 *vs.* 8.67, respectively).

Ionization potential *vs.* $\Sigma\sigma_{para}$ for 59 mono- and disubstituted benzenes (excluding phenols, thiophenol, acetophenones, bromides, and iodides), yields a correlation that can be expressed as eq. 2.

Can. J. Chem. Downloaded from www.nrcresearchpress.com by 210.87.254.105 on 09/05/12
For personal use only.

Can. J. Chem. Downloaded from www.nrcresearchpress.com by 210.87.254.105 on 09/05/12
For personal use only.

[2] $$IP = 1.45\sum\sigma + 8.80$$

The standard deviation of the 59 points from this line is 0.26 eV and the correlation coefficient is 0.943. Again the nine ortho-disubstituted benzenes correlate equally well with a standard deviation of 0.24 eV.

Use of all data except that for thiophenol, phenols, and acetophenones (71 points) gives a slope of 1.42 and an intercept of 8.77, an equation only slightly different from eq. 2, but the correlation coefficient drops to 0.933. Again this is partly due to the fact that bromides and iodides have lower than expected ionization potentials.

Phenols (from examination of nine examples) seem to ionize at higher potentials than anticipated (13). This could be related to the unusual problems involved in the assignment of substituent constants in these systems (1). Or it may be that the ionization occurs from either a π orbital of the benzene ring or a localized electron on the oxygen depending on the substituent, *i.e.*, that the ionization potentials of the two orbitals are close. In contrast phenolic ethers are well correlated.

Acetophenones seem to lose an electron from a different orbital than most of the aromatics since their ease of ionization (Table 1) is lower than expected from eq. 2 (8); the orbital involved could be on the carbonyl oxygen. We note, however, that the slope, *i.e.*, sensitivity to substituent effect, is the same for acetophenones as for the other aromatics. (Acetophenones were not correlated by $\sum\sigma^+$ since σ^+ for $COCH_3$ is not available (1).) The $NHCOCH_3$ group also appears to lead to lower ionization potentials. The sulfhydryl group also falls in this category.

A more rigorous test of the correlation of IP and $\sum\sigma$ is provided by data for more highly substituted benzenes, although a limited number of such data are available (Table 1). The σ^+_{para} correlation for tri-through hexasubstituted benzenes is given by eq. 3 and is shown in Fig. 2.

[3] $$IP = 1.10\sum\sigma^+ + 9.73$$

The standard deviation for the 13 points is 0.23 eV and the correlation coefficient is 0.951. The slope and intercept are appreciably higher than for the mono- and disubstituted benzenes (eq. 1). This is in accord with the electrostatic model (9, 14) which predicts that placing groups with the same sign of σ ortho to one another will result in a higher ionization potential than if

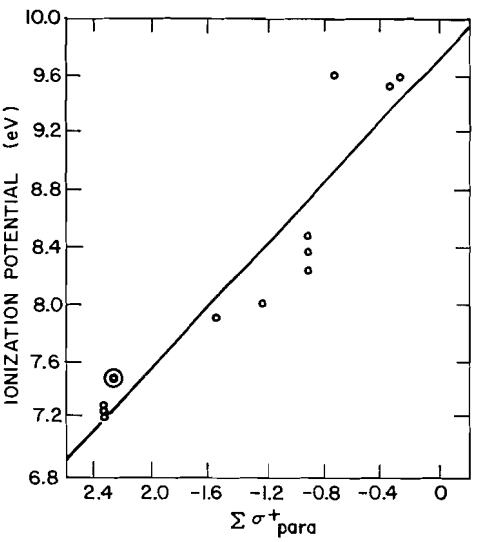

FIG. 2. Plot of experimental ionization potentials *vs.* sum of para electrophilic substituent constants ($\sum\sigma^+_{para}$) for tri- through hexasubstituted benzenes. Slope 1.10, intercept 9.73, correlation coefficient 0.951.

they are meta or para. Conversely, if the groups have oppositely signed σ's, the ionization potential of the ortho isomer will be lower. This leads to a greater slope and intercept. The tri- through hexasubstituted benzenes are better fit by $\sum\sigma_{para}$ giving eq. 4; the standard deviation is 0.23 eV and the correlation coefficient 0.966.

[4] $$IP = 1.73\sum\sigma + 9.19$$

These correlations of multi-substituted benzenes corroborate the linear relationship found in mono- and disubstituted benzenes, substantiate the general additivity of substituent effects even though the influence of dipolar effects modulates it and indicate a fundamental relationship between energies of highest occupied molecular orbitals and Hammett substituent constants.

This correlation offers the possibility of assigning σ and/or σ^+ values of substituents from the ionization potentials of a series of derivatives. For example σ^+ for CHO is not known (1); from 5 points it is estimated to be 0.50 ± 0.07. Preferably, all data would be gathered by the same technique on the same calibrated instrument.

In conclusion a good general correlation between ionization potential and the sum of substituent constants exists. This substantiates molecular orbital theory calculations which reveal the fundamental character of the Hammett

and related equations. Thus, substituent constants seem to provide a useful and convenient guide for prediction of ionization potentials for substituted aromatic systems. Conversely ionization potentials may be used to calculate substituent constants, especially σ^+, which may not otherwise be available.

1. C. D. RITCHIE and W. F. SAGER. Prog. Phys. Org. Chem. **2**, 323 (1964).
2. H. H. JAFFE. J. Am. Chem. Soc. **76**, 5843 (1954); **77**, 274 (1955).
3. D. PETERS. J. Chem. Soc. 2654 (1957).
4. D. HOROWITZ. Stud. Cercet. Chem. **15**, 927 (1967); Chem. Abstr. **68**, 117210p (1968).
5. J. KUTHAN and V. SKOLA. Z. Chem. 340 (1968); Chem. Abstr. **70**, 14594d (1969).
6. M. GODFREY. J. Chem. Soc. (B), 1540 (1971); Tetrahedron Lett. 753 (1972).
7. J. C. LORQUET. Rev. Mod. Phys. **32**, 312 (1960).
8. A. BUCHS, G. P. ROSETTI, and B. P. SUSZ. Helv. Chem. Acta, **47**, 1563 (1964).
9. G. T. CRABLE and G. L. KEARNS. J. Phys. Chem. **66**, 436 (1962).
10. Handbook of Chemistry and Physics. Chemical Rubber Co., 54th ed. 1971–1972. p. E-62*ff*.
11. V. I. VEDENEYEV, L. V. GURVICH, V. N. KONDRAT'YEV, V. A. MEDVEDEV, and YE. L. FRANKURICH. Bond energies, ionization potentials and electron affinities. St. Martins Press, New York. 1966.
12. H. C. BROWN. Adv. Phys. Org. Chem. **1**, 35 (1963).
13. S. PIGNATARO, A. FOFFANI, G. INNORTA, and G. DISTEFANO. Z. Phys. Chem. (Frankfurt am Main), **49**, 20 (1966).
14. N. D. COGGESHALL. J. Chem. Phys. **32**,1265 (1960).
15. Ionization potentials, appearance potentials and heats of formation of gaseous positive ions. U.S. Department of Commerce, National Bureau of Standards. NSRDS-NBS 26, June 1969.

Can. J. Chem. Downloaded from www.nrcresearchpress.com by 210.87.254.105 on 09/05/12
For personal use only.

Combinatorial Entropy of Mixing for Molecules Differing in Size and Shape

RÜDIGER N. LICHTENTHALER, DENIS S. ABRAMS, AND JOHN M. PRAUSNITZ
Chemical Engineering Department, University of California, Berkeley

Received March 6, 1973

In reducing experimental vapor–liquid equilibrium data it is common to calculate the Gibbs energy of mixing in excess of that for a solution whose entropy of mixing is given by one of two expressions: ideal entropy or Flory–Huggins entropy. The first of these is proper for a mixture of small molecules of similar size and the second one is proper for a mixture of monomer and chain polymer. This paper considers intermediate cases where there are significant differences in molecular shape as well as size. An expression is derived for the combinatorial entropy of mixing; this expression has Flory's result as the leading term but also contains corrections for molecular bulkiness. The combinatorial entropy of mixing depends on characteristic parameters reflecting both molecular size and shape. Methods are given for simple evaluation of these parameters and illustrations for representative mixtures are presented. In some case, the corrections for bulkiness can be very large.

En réduisant les données sur l'équilibre expérimental vapeur liquide, il est commun de calculer l'énergie de mélange de Gibbs en excès de celle d'une solution dont l'entropie de mélange est donnée par l'une des deux expressions: entropie idéale ou entropie Flory–Huggins. La première est propre au mélange de petites molécules aux dimensions semblables et la seconde est relative à un mélange de monomère ou polymère en chaine. Cette note traite des cas intermédiaires où il n'existe pas de différences significatives aussi bien dans la forme que dans la taille de la molécule. Une expression a été déduite pour l'entropie combinatoire de mélange cette expression contient le résultat de Flory comme terme dominant et aussi des termes correctifs pour l'encombrement moléculaire. L'entropie combinatoire de mélange dépend des paramètres caractéristiques reflétant à la fois la forme et la dimension de la molécule. Des méthodes simples d'évaluation de ces paramètres et des illustrations par des mélanges représentatifs ont été présentées. Dans certains cas les corrections apportées à l'encombrement peuvent être très élevées.

[Traduit par le journal]

Can. J. Chem., 51, 3071 (1973)

Can. J. Chem. Downloaded from www.nrcresearchpress.com by 210.87.254.40 on 09/05/12
For personal use only.

In recent years much effort has been devoted toward developing the statistical thermodynamics of liquid mixtures (1). While most of this effort has been directed at mixtures of simple fluids containing small, spherical molecules, considerable progress has also been achieved in mixtures containing both large and small molecules as in polymer solutions (2); this progress follows primarily from work by Flory (3) and by Patterson and Delmas (4) based on a partition function proposed by Prigogine (5). These recent developments, however, are concerned with residual thermodynamic properties, determined by differences in free volumes and in intermolecular forces. In the last twenty years very little attention has been given to the configurational properties of solutions as determined by the combinatorial factor. In this work we reconsider the problem of calculating the combinatorial entropy of mixing fluids whose molecules differ in size and shape. We have derived an expression similar to that of Tompa (6) using arguments different from those used previously. Our main concern, however, is directed at application of Tompa's result which appears to have been forgotten by contemporary workers in solution thermodynamics. We make some specific suggestions toward quantitative calculations of the combinatorial entropy of mixing which, in turn, are useful for reduction and subsequent interpretation of experimental data for real solutions.

We consider a binary mixture of two fluids indicated by subscripts 1 and 2. The entropy of mixing is defined as the change in entropy when N_1 molecules of 1 and N_2 molecules of 2 are mixed at constant temperature and pressure to form a homogeneous solution. It is convenient to write this entropy of mixing as the sum of two parts:

$$\Delta S = \Delta S^{C} + \Delta S^{R} \qquad [1]$$

where superscript C stands for combinatorial and superscript R stands for residual. While the recent work of Flory, Patterson and others has been directed at ΔS^{R}, we are here concerned only with ΔS^{C}. The mixing process considered here is one where the molecules of fluids 1 and 2 have finite size but no forces of attraction and where the isothermal, isobaric mixing process occurs also at constant volume.

Can. J. Chem. Downloaded from www.nrcresearchpress.com by 210.87.254.40 on 09/05/12
For personal use only.

Let molecule 1 consist of one segment and molecule 2 of r segments. As discussed in numerous textbooks, two expressions are commonly used for ΔS^C:

$$[2] \qquad \frac{\Delta S^C}{k} = -[N_1 \ln x_1 + N_2 \ln x_2]$$

$$[3] \qquad \frac{\Delta S^C}{k} = -[N_1 \ln \Phi_1 + N_2 \ln \Phi_2]$$

where x is the mole fraction

$$[x_1 = N_1/(N_1 + N_2) \quad x_2 = N_2/(N_1 + N_2)]$$

and Φ is the segment fraction

$$[\Phi_1 = N_1/(N_1 + rN_2) \quad \Phi_2 = rN_2/(N_1 + rN_2)].$$

Equation 2 gives the ideal entropy of mixing as used in the theory of regular solutions (7) and eq. 3, due to Flory, is used, almost without exception, in the polymer-solution literature. Equation 3 follows from well-defined assumptions (8) including the assumption that molecule 2 (the polymer) is a long, flexible chain; eq. 3, then, was not intended to apply to large bulky molecules. Using an approach different from Flory's, eq. 3 has also been derived by Longuet-Higgins (9) and by Silberberg (10).

In 1947 Hildebrand (11) presented a phenomenological, free-volume derivation of the combinatorial entropy of mixing. While that derivation is *ad hoc* and difficult to justify theoretically, it points to an important conclusion (later verified by Tompa (12)), *viz.*, the entropy of combinatorial mixing has a lower bound given by eq. 2 and an upper bound given by eq. 3; the "true" combinatorial entropy of mixing lies between these limits. Just where the "true" combinatorial entropy lies between these limits depends on the size and shape of the molecules. Tompa has shown that for mixtures of bulky molecules, eq. 2 provides a better approximation than eq. 3.

While eqs. 2 and 3 are quoted in all textbooks on liquid-mixture thermodynamics, it will be useful to have an expression which, taking molecular size and shape into consideration, is capable of covering the domain bounded by eqs. 2 and 3. We have derived such an expression here; it is

$$[4] \qquad \frac{\Delta S^C}{k} = -[N_1 \ln \Phi_1 + N_2 \ln \Phi_2] + \sum_{t=1}^{z} \alpha^{(t)} \left(1 - \left(\frac{q}{r}\right)^t\right) r \left\{\left[N_1 + \left(\frac{q}{r}\right)^t rN_2\right] \times \left[\ln\left(N_1 + \left(\frac{q}{r}\right)^t rN_2\right) - \ln(N_1 + N_2)\right] - rN_2\left(\frac{q}{r}\right)^t \ln\left(\frac{q}{t}\right)^t\right\}$$

A derivation of eq 4 is given in the Appendix. A similar equation, based on a different derivation, was given by Tompa (6).

In eq. 4, r is the number of segments of molecule 2 divided by that of molecule 1 and q is the surface (contact) area of molecule 2 divided by that of molecule 1. The coordination number z is the number of nearest neighbors of a molecular segment.

The parameters $\alpha^{(t)}$ depend on molecular size and shape. They obey the relations

$$[5] \qquad \sum_{t=1}^{z} \alpha^{(t)} = r - 1$$

$$[6] \qquad \sum_{t=1}^{z} t\alpha^{(t)} = \frac{z}{2}(r - q)$$

The quantity on the right side of eq. 6 is the number of contacts made by segments of molecule 2 with other segments in the same molecule.

Before discussing particular applications of eq. 4, it is instructive to point out some general properties of that equation.

(*a*) The first two terms in eq. 4 are identical to eq. 3; in other words, the summation term in eq. 4 is essentially a correction to Flory's equation.

(*b*) If molecules 1 and 2 are identical in shape and size, then $q = r = 1$. In that event, all $\alpha^{(t)}$'s are zero and eq. 4 reduces to eq. 2.

(*c*) If the coordination number z becomes very large, $q/r \to 1$ and it can be shown that the summation term in eq. 4 vanishes.

(*d*) The first two terms in eq. 4 are always positive and for $r > 1$, eq. 3 always gives an entropy of mixing that is larger than that given by eq. 2. Therefore, if eq. 4 is to give a result intermediate between eqs. 2 and 3, it is necessary that the summation term in eq. 4 be negative for $q/r < 1$ ($q/r > 1$ is physically impossible). The

summation term in eq. 4 is essentially always negative and increasingly so as $q/r \to 0$. For mixtures of bulky molecules of different size ($q/r \ll 1$), eq. 4 approaches eq. 2 as suggested by Monte Carlo studies of mixtures of different-sized spheres (1, 13). For mixtures where q/r is slightly less than unity, eq. 4 gives an entropy of mixing which is very slightly less than that given by eq. 2. In such a case therefore, eq. 4 is, strictly speaking, not valid although the error is negligibly small. For such mixtures and for mixtures where $r \approx 2$ or less, eq. 2 should be used.

(*e*) For mixtures of chain molecules, eq. 4 reduces to the result obtained by Huggins (14) and discussed by Guggenheim (15).

Determination of Parameters

To apply eq. 4, it is necessary to devise a consistent and physically reasonable method for evaluating the parameters r, q, and $\alpha^{(i)}$. We present such a method below.

To evaluate r, we use the van der Waals volumes calculated by Bondi (16). Using the group contributions of Chapt. 14 in Bondi's book it is simple to calculate the van der Waals volume v^* of a large variety of molecules. Then

$$[7] \qquad r = v_2^*/v_1^*$$

For typical mixtures, we find that r is nearly equal to the ratio of molar volumes.

To evaluate q, it is tempting to use Bondi's calculations of van der Waals surface areas. However, the surface areas given by Bondi are too large for our purposes; Bondi calculates the total surface area whereas we require that part of the total surface area which is available for interaction with neighboring molecules. Because of steric requirements, not all of the total surface area is available for interaction with nearest neighbors.

To establish a consistent method for evaluating both q and $\alpha^{(i)}$, we use a simple lattice model with $z = 6$. We assume that the dimensions of a molecule can be represented by three mutually perpendicular, characteristic lengths (l_x, l_y, l_z), whose product is equal to the van der Waals volume:

$$[8] \qquad v^* = l_x l_y l_z$$

As indicated in the Appendix for this simple lattice $\alpha^{(4)} = \alpha^{(5)} = \alpha^{(6)} = 0$. Therefore the three parameters $\alpha^{(1)}$, $\alpha^{(2)}$, and $\alpha^{(3)}$ suffice to describe the bulkiness of the molecule. It can then be shown that

$$[9] \qquad r = \frac{(l_x l_y l_z)_2}{(l_x l_y l_z)_1}$$

$$[10] \qquad q = \frac{(l_x l_y + l_x l_z + l_y l_z)_2}{(l_x l_y + l_x l_z + l_y l_z)_1}$$

$$[11] \qquad \alpha^{(1)} = 2(r - 1) - 3(r - q) + \alpha^{(3)}$$

$$[12] \qquad \alpha^{(2)} = 3(r - q) - (r - 1) - 2\alpha^{(3)}$$

$$[13] \qquad \alpha^{(3)} = (r - 1) - 3q + 3\frac{(l_x + l_y + l_z)_2}{(l_x + l_y + l_z)_1}$$

For a given molecule, the parameters l_x, l_y, l_z must be determined by the size and shape of that molecule, subject to the boundary condition given by eq. 8. To find these parameters, we utilize data for bond angles and bond lengths. To illustrate, Table 1 gives parameters for some representative molecules. These parameters were obtained primarily from van der Waals radii given by Bondi. For silicon-containing compounds Bondi's method of calculation was used with bond parameters taken from Handbook of Chemistry and Physics.

Combinatorial Entropies of Mixing for Some Representative Binary Mixtures

To illustrate the use of eqs. 4 and 9–13, we present calculations for a few typical binary mixtures. These are shown in Figs. 1–4. Parameters used to prepare these figures can easily be calculated with eqs. 9 to 13 using the numbers given in Table 1.

Our main interest is to compare results obtained from eq. 4 with those obtained from Flory's equation (eq. 3). The essential difference between these equations is related to the largest possible number of connections (bonds) which a segment, upon being placed in the lattice, may have with already placed segments of the same molecule. In Flory's equation, suitable for chain molecules, that maximum number is one. We therefore designate results obtained from Flory's equation by the letters SCSM which stand for Single-Connected Segment Model. By contrast, eq. 4 permits a segment of a large molecule to be connected to as many as $z - 1$ other segments of the same molecule which have already been placed on the lattice. Therefore we designate results obtained from eq. 4 by the letters MCSM

Can. J. Chem. Downloaded from www.nrcresearchpress.com by 210.87.254.40 on 09/05/12
For personal use only.

TABLE 1. Molecular parameters for combinatorial entropy of mixing

Fluid	(Å) l_x	l_y	l_z	v^* In cm³/mol	v^* In Å³/molecule
n-Alkanes					
CH_4	3.05	3.05	3.05	17.1	28.4
C_2H_6	4.12	3.32	3.32	27.3	45.4
C_3H_8	5.66	3.32	3.32	37.6	62.4
C_4H_{10}	7.20	3.32	3.32	47.8	79.4
C_5H_{12}	8.74	3.32	3.32	58.0	96.3
C_6H_{14}	10.3	3.32	3.32	68.3	114
C_7H_{16}	11.8	3.32	3.32	78.5	130
C_8H_{18}†	13.3	3.32	3.32	88.7	147
n-Alkenes					
C_2H_4	3.60	3.32	3.32	23.9	39.7
C_3H_6	5.13	3.32	3.32	34.1	56.5
C_4H_8	6.68	3.32	3.32	44.3	73.6
C_6H_{12}	9.71	3.32	3.32	64.7	107
C_8H_{16}	12.8	3.32	3.32	85.2	141
n-Alkynes					
C_2H_2	3.48	3.32	3.32	23.1	38.4
C_4H_6	6.55	3.32	3.32	43.5	72.2
C_8H_{14}	12.7	3.32	3.32	84.4	140
Cycloalkanes					
C_5H_{10}	5.31	5.31	2.90	49.2	81.8
C_6H_{12}	5.67	5.67	3.03	58.7	97.4
Aromatics					
C_6H_6	5.81	5.81	2.38	48.4	80.3
Naphthalene	8.88	5.81	2.38	74.0	123
Anthracene	11.9	5.81	2.38	99.6	165
Spherical Molecules					
CF_4	3.57	3.57	3.57	27.3	45.5
CCl_4	4.43	4.43	4.43	52.3	86.9
CBr_4	4.68	4.68	4.68	61.7	103
CI_4	5.20	5.20	5.20	84.7	141
$C(CH_3)_4$	4.58	4.58	4.58	58.0	96.1
$Si(CH_3)_4$	4.76	4.76	4.76	65.3	108
$(CH_3)_8(SiO)_4$	6.52	6.52	6.52	167	277

†For *n*-alkanes $C_{N_c}H_{2N_c}$($N_c > 1$) the following equations are valid: $l_x = 1.54N_c + 1.04$ Å; $l_y = l_z = 3.32$ Å. $v^* = 10.23N_c + 6.88$ cm³/mol $= 16.98N_c + 11.42$ Å³/molecule.

which stand for Multiple-Connected Segment Model.

Figures 1–4 give excess combinatorial entropies per mole of sites. The excess entropy is defined, as usual, as the entropy of mixing in excess of that found for an ideal system (eq. 2). While eqs. 2, 3, and 4 give entropies per mole of mixture, we can easily convert to entropies per mole of sites by writing

$$[14] \quad \frac{S^E(\text{per mole of sites})}{S^E(\text{per mole of mixture})} = 1 - \left(1 - \frac{1}{r}\right)\Phi_2$$

where Φ_2 is the site fraction of polymer.

Figure 1 gives results for the system *n*-hexane–*n*-hexadecane. Since both components are chain molecules, results from eq. 3 are essentially identical to those from eq. 4.

Figure 2 gives results for the system methane–*n*-hexadecane. Because of the larger size difference, entropies shown in Fig. 2 are appreciably larger than those shown in Fig. 1. Again, there is not much difference between SCSM and MCSM results. However, the relative difference in Fig. 2 is larger than that shown in Fig. 1 because the width of methane is smaller than that of hexadecane while the width of hexane is the same as that of hexadecane. The lower entropy for MCSM is in agreement with computer calculations reported by Bellemans (17).

Can. J. Chem. Downloaded from www.nrcresearchpress.com by 210.87.254.40 on 09/05/12
For personal use only.

Can. J. Chem. Downloaded from www.nrcresearchpress.com by 210.87.254.40 on 09/05/12
For personal use only.

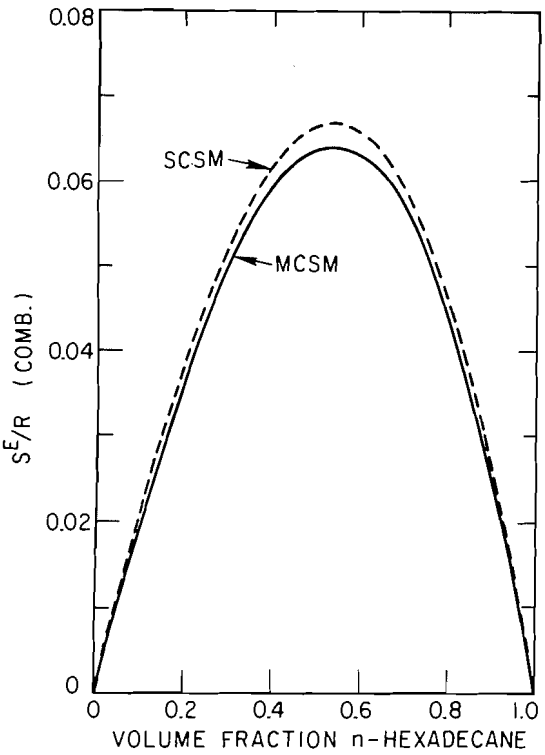

FIG. 1. Excess combinatorial entropy per mole of sites for *n*-hexane–*n*-hexadecane.

Figure 3 gives results for the system carbon tetrachloride – octamethylcyclotetrasiloxane (OMCTS). Both components consist of spherical molecules and therefore we expect a significant difference between SCSM and MCSM results. While the magnitude of the excess entropy is small, Fig. 3 shows that Flory's equation gives an excess entropy nearly twice as large as that found from eq. 4.

Figure 4 gives results for mixtures of benzene and polyethylene of carbon number 8022. All calculations shown are obtained from eq. 4 with parameters given in Table 1. The purpose of Fig. 4 is to show how the degree of bulkiness of the polyethylene affects the excess combinatorial entropy. Curve A refers to linear (straight-chain) polyethylene with $l_x = 12354$ and $l_y = l_z = 3.32$ (See Table 1 where all distances are given in Angstroms.) Curve B refers to a flat ribbon, *i.e.* to a double-strand linear polyethylene with $l_x = 6177$, $l_y = 6.64$, and $l_z = 3.32$. Curve C is also for a flat ribbon, but now the polyethylene is a quadruple-strand chain with $l_x = 3089$, $l_y = 13.28$, and $l_z = 3.32$. Curve D is for polyethylene in a rod-like shape with $l_x = 3089$, $l_y = l_z = 6.64$. Curve E is for a similar rod-shaped polyethylene but with shorter axis and larger cross-section; in this case $l_x = 154$, $l_y = 66.4$, and $l_z = 13.28$. Finally curve F is for polyethylene in the shape of a cube with $l_x = l_y = l_z = 51.4$.

Figure 4 clearly shows that the entropy is strongly affected by the bulkiness of the large molecule, *i.e.* by the extent to which the segments in the large molecule are multiple-connected rather than single-connected when placed onto the lattice. Flory's formula (eq. 3) cannot distinguish between the six cases shown in Fig. 4. Since Flory's formula depends only on the volume ratio, it gives results which are the same for all six cases, independent of molecular shape. Excess combinatorial entropies from eq. 3 are essentially identical to those shown by curve A.

Residual Excess Gibbs Energy

To interpret and correlate experimental data for liquid mixtures, it is desirable to calculate residual thermodynamic functions which, in turn, can be related to a suitable partition function. Following Flory (18), ΔG^R, the residual

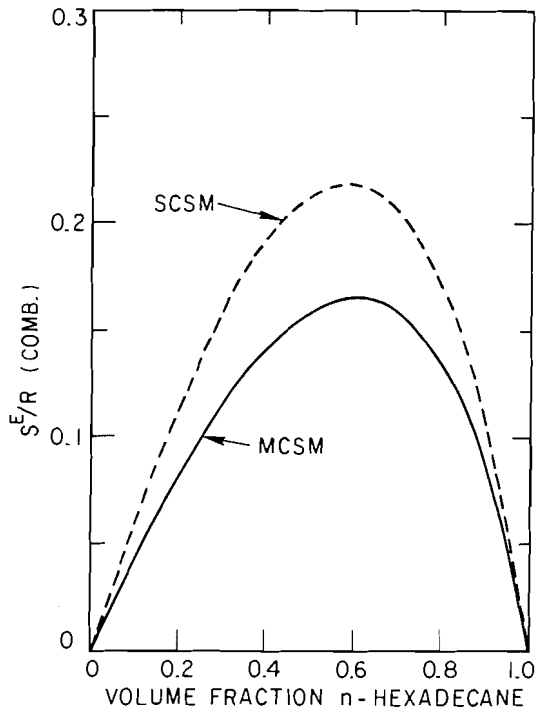

FIG. 2. Excess combinatorial entropy per mole of sites for methane–*n*-hexadecane.

Can. J. Chem. Downloaded from www.nrcresearchpress.com by 210.87.254.40 on 09/05/12
For personal use only.

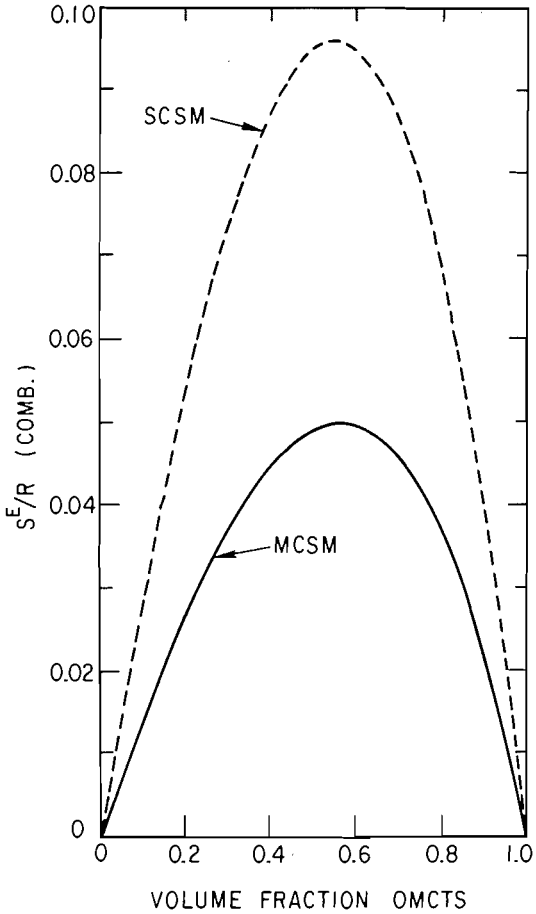

FIG. 3. Excess combinatorial entropy per mole of sites for carbon tetrachloride – OMCTS.

Gibbs energy of mixing is found from the experimental excess Gibbs energy of mixing by

$$[15]\quad \Delta G^R = G^E(\text{experimental}) - G^E(\text{combinatorial})$$

Since H^E(combinatorial) is zero, eq. 15 becomes

$$[16]\quad \Delta G^R = G^E(\text{experimental}) + TS^E(\text{combinatorial})$$

In some cases the residual Gibbs energy of mixing is sensitive to the model chosen for calculating S^E(combinatorial). To illustrate, Fig. 5 gives results for the system carbon tetrachloride – OMCTS and Fig. 6 for the system benzene – OMCTS; experimental data are from Marsh (19). For both systems the excess combinatorial entropy was calculated twice, once with eq. 3 and once with eq. 4. Since OMCTS is a large spherical molecule, many of its segments are multiple rather than single connected when placed onto the lattice. The excess combinatorial entropy calculated from Flory's equation is, therefore, too large and in both binary systems the residual Gibbs energy of mixing based on SCSM is more than twice that calculated from MCSM.

The results shown in Figs. 5 and 6 indicate that in some mixtures the residual Gibbs energy of mixing is a strong function of the method used to calculate the combinatorial entropy of mixing. Thus details in the calculation of the combinatorial entropy of mixing may affect interpretation and subsequent correlation of residual excess functions in mixtures.

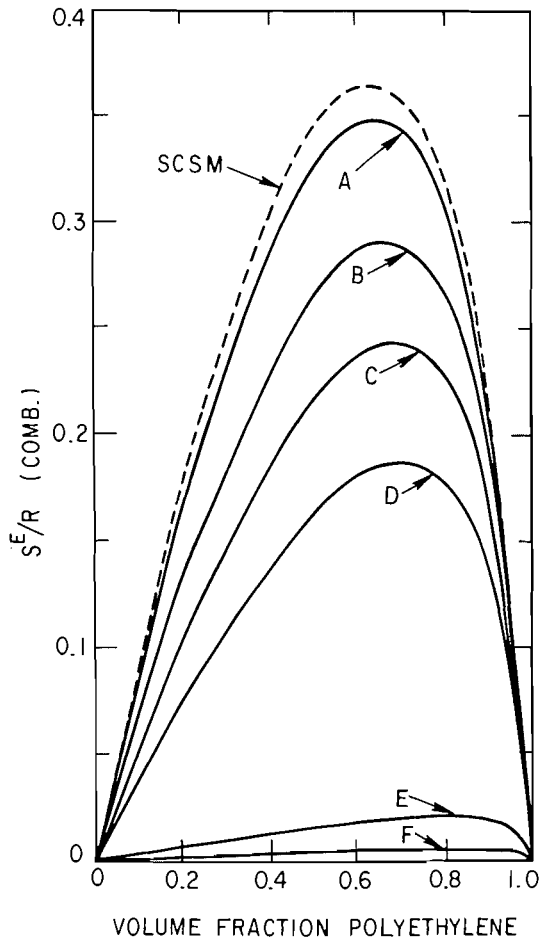

FIG. 4. Excess combinatorial entropy per mole of sites for benzene–polyethylene.

Can. J. Chem. Downloaded from www.nrcresearchpress.com by 210.87.254.40 on 09/05/12
For personal use only.

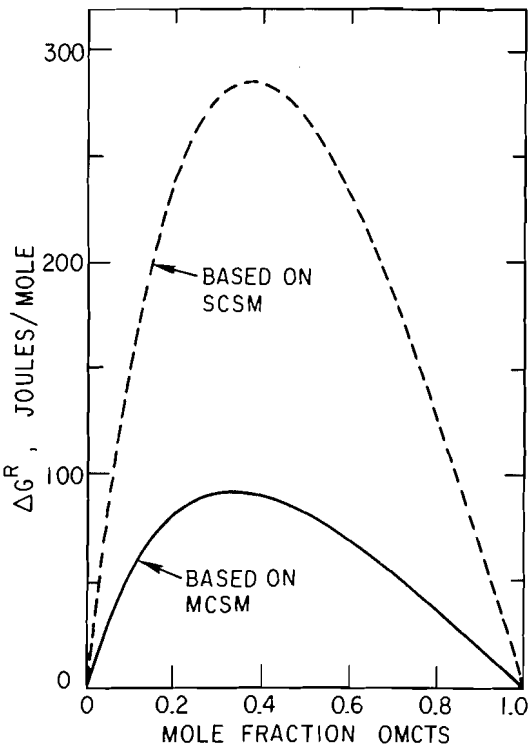

FIG. 5. Residual Gibbs energy of mixing for carbon tetrachloride – OMCTS at 25 °C.

Appendix

Derivation of Eq. 4

We consider a three-dimensional lattice with N sites. We want to fill the lattice with N_2 (large) solute molecules and N_1 (small) solvent molecules. Each solute molecule occupies r lattice sites and each solvent molecule occupies one site, such that $N = N_1 + rN_2$. We assume that all configurations have the same energy.

We proceed in the usual way by placing the N_2 solute molecules onto the lattice, one after another. The remaining sites are then filled with solvent molecules. Suppose j solute molecules have already been placed; we now want to compute $\gamma_{j+1,i}$ which is the number of ways we can place the ith segment of the $(j + 1)$th solute molecule.

Consider the first segment of a solute molecule and let Y_1 be the number of ways we can place that segment in the lattice if that lattice were empty. Now for the case where j solute molecules have already been placed previously, $\gamma_{j+1,1}$ is given by

$$[A1] \qquad \nu_{j+1,1} = \left(\frac{N - rj}{N}\right) Y_1$$

Equation $A1$ says that $\gamma_{j+1,1}$ is smaller than Y_1 by a factor which is the fraction of unoccupied sites.

It is tempting to generalize eq. $A1$ by assuming that the reducing factor, *viz.* the fraction of unoccupied sites, can also be used to calculate the number of ways of placing the ith segment, that is, to assume

$$[A2] \qquad \nu_{j+1,i} = \left(\frac{N - rj - (i - 1)}{N}\right) Y_i \approx \left(\frac{N - rj}{N}\right) Y_i$$

where Y_i is the number of ways of placing the ith segment of the $(j + 1)$th molecule when the lattice is nearly empty, containing only $i - 1$ segments of the $(j + 1)$th molecule. Since rj is generally much larger than $(i - 1)$, the equation can be simplified as shown.

Equation $A2$ was used by Flory. We do not use it here, however, because the reducing factor

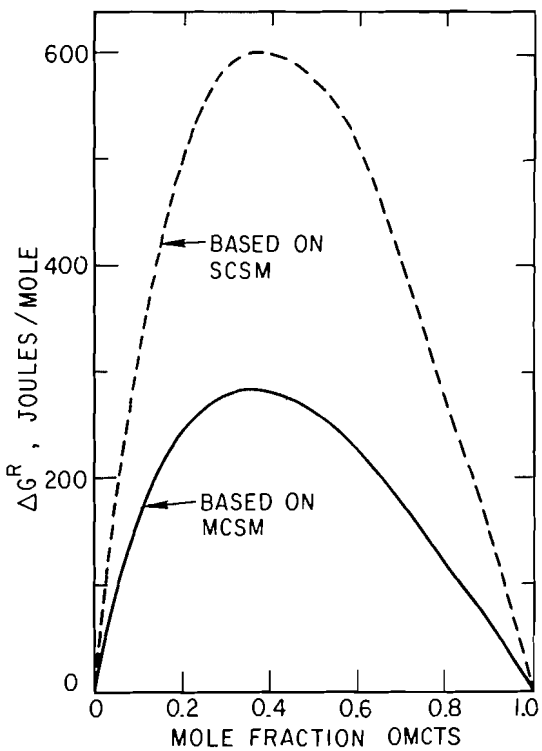

FIG. 6. Residual Gibbs energy of mixing for benzene–OMCTS at 25 °C.

Can. J. Chem. Downloaded from www.nrcresearchpress.com by 210.87.254.40 on 09/05/12
For personal use only.

$(N - rj)/N$, while valid for the first segment, is too low for subsequent segments. Once the first segment of a solute molecule has been placed on a particular site, the probability that an adjacent site is empty, is larger than $(N - rj)/N$. Stated in more general terms, if $i - 1$ sites of a solute molecule have been placed on the lattice, the probability that a fixed site adjacent to the $(i - 1)$th segment is empty, is larger than $(N - rj)/N$. The probability is larger because if we know that $i - 1$ segments have already been placed in the region where we want now to place the ith segment, we know that this region is less concentrated in solute molecules than the lattice as a whole.

To obtain an improved expression for $\gamma_{j+1,i}$, we must first introduce the parameters z and q. The coordination number of the lattice is z; each solvent molecule has z nearest neighbors. Each solute molecule has a number of nearest neighbors equal to qz, which is less than rz, because some of the nearest neighbors of a segment within a solute molecule belong to the same molecule. Whereas the total number of segment–segment contacts for a molecule is rz, only qz contacts are external. For a bulky solute molecule, where many of the segments are internal (*i.e.* completely or primarily surrounded by segments of the same molecule), q/r is well below unity. For a linear chain molecule with no rings, q and r do not differ very much; they are related by

$$[A3] \qquad qz = rz - 2r + 2$$

Equation *A*3 is valid also for branched chain molecules. However, this equation assumes that a molecule does not bend back on itself, *i.e.* a segment of a molecule is never placed such that one of its immediate neighbors is a segment of that same molecule more than two links removed.

In Flory's equation (eq. *A*2) the reduction factor $(N - rj)/N$ is too low. If it is known that a given site (arbitrarily labeled A) is the neighbor of one site already occupied by a segment of the $(j + 1)$th molecule, then, the probability that site A is occupied by another segment of that same $(j + 1)$th molecule is $(1 - q/r)$, not zero as assumed in eq. *A*2. Further, if site A is such that t of its neighbors are occupied by segments of the $(j + 1)$th molecule, then the probability that site A is occupied by another segment of that same $(j + 1)$th molecule is even higher; it is $1 - (q/r)^t$. We therefore replace eq. *A*2 by writing

$$[A4] \quad \nu_{\substack{j+1,i \\ i>1}} = \left(\frac{N - rj}{N}\right) \times \left[1 - \left(1 - \left(\frac{q}{r}\right)^t\right)\frac{rj}{N}\right]^{-1} Y_i$$

The factor in parentheses in eq. *A*4 is always less than unity and since it is in the denominator, the number of ways of placing the ith segment of the $(j + 1)$th molecule as given by eq. *A*4 is larger than that given by eq. *A*2.

As the coordination number rises, the difference between r and q falls; when $z \to \infty$, $q/r \to 1$. In that case eq. *A*4 reduces to eq. *A*2.

Omitting symmetry numbers, we can now write the number of configurations, *i.e.* the number of ways of arranging N_1 solvent molecules and N_2 solute molecules

$$[A5] \quad \Omega(N_1,N_2) = \frac{1}{N_2!}\prod_{j=1}^{N_2}\prod_{i=1}^{r}\nu_{j,i}$$

$$= \frac{1}{N_2!}\prod_{j=1}^{N_2}\left\{[N - r(j-1)] \times \frac{[N - r(j-1)]^{r-1}\rho}{\prod_{t=1}^{z}\left[N - \left(1 - \left(\frac{q}{r}\right)^t\right)r(j-1)\right]^{\alpha^{(t)}}}\right\}$$

where ρ is the product of all Y_i values of one solute molecules (for $i > 1$) and $\alpha^{(t)}$ is the number of segments of a solute molecule which, when placed on the lattice, have already t neighbors occupied by segments of that same solute molecule. The sequence of placing segments on the lattice must be such that preference is always given to that segment which, when placed on the lattice, has the largest number of neighbors which are previously-placed segments. Two conservation equations relate the parameters $\alpha^{(t)}$ to the parameters q and t. These are eqs. 5 and 6 in the text.

We can now calculate the combinatorial entropy of mixing from

$$[A6] \qquad \frac{\Delta S^C}{k} = \ln\frac{\Omega(N_1,N_2)}{\Omega(0,N_2)\Omega(N_1,0)}$$

where k is Boltzmann's constant. To do so we first apply Stirling's approximation for large N to eq. *A*5 and obtain

Can. J. Chem. Downloaded from www.nrcresearchpress.com by 210.87.254.40 on 09/05/12
For personal use only.

$$[A7]\quad \ln\Omega(N_1,N_2) = N_2 \ln \rho - N_2 \ln N_2 - N_1 \ln N_1 + N \ln N + \sum_{t=1}^{z} \frac{\alpha^{(t)}}{\left(1 - \left(\frac{q}{r}\right)^t\right) r} \times \left\{ \left[N - \left(1 - \left(\frac{q}{r}\right)^t\right) r N_2 \right] \times \ln \left[N - \left(1 - \left(\frac{q}{r}\right)^t\right) r N_2 \right] - N \ln N \right\}$$

Substitution of *A*7 into eq. *A*6 gives eq. 4 in the text.

The parameter $\alpha^{(t)}$ represents the number of segments of a solute molecule which, upon being placed in the lattice, have t nearest neighbors occupied by other segments of the same molecule. The integer t varies from unity to z.

To illustrate the calculation of $\alpha^{(t)}$, we consider a two-dimensional example. Suppose we have a two-dimensional molecule of 20 sites; the molecule is a rectangle 4 sites wide and 5 sites long, as shown in Fig. 7. We assume that for a two-dimensional lattice $z = 4$; thus, for example, site 8 has four nearest neighbors (3, 7, 9, and 13). The rectangular molecule has $r = 20$ and qz, the number of nearest-neighbor external contacts, is 18 (one external contact each for sites 2, 3, 4, 10, 15, 19, 18, 17, 11, and 6; two external contacts for sites 1, 5, 20, and 16).

We place the segments on the lattice such that each segment placed must have the largest possible number of previously placed segments as neighbors. First we place segment 1. Then we place segments 2, 3, 4, and 5, and then segment 6. In each of these five placements, the segment placed has one nearest neighbor. Next we could place segment 11 or 10 or 7 or 8 or 9. We must choose segment 7 because it will be placed with two neighbors while the others would be placed with only one neighbor. After 7, comes 8, 9, and 10, each with two neighbors. Next comes 11 (with one neighbor) followed by 12, 13, 14, and 15 (with two neighbors). Finally, we place 16 (one neighbor) followed by 17, 18, 19, and 20 (two neighbors).

1	2	3	4	5
6	7	8	9	10
11	12	13	14	15
16	17	18	19	20

FIG. 7. Two dimensional molecule occupying 20 sites.

All placements (for $i > 1$) have either one or two neighbors. Thus $\alpha^{(3)} = \alpha^{(4)} = 0$. As indicated by the sequence of the previous paragraph

$\alpha^{(1)} = 7$ (Segments 2, 3, 4, 5, 6, 11, and 16)

$\alpha^{(2)} = 12$ (Segments 7, 8, 9, 10, 12, 13, 14, 15, 17, 18, 19, and 20)

It can readily be shown that these values for $\alpha^{(t)}$ satisfy eqs. 5 and 6 in the text:

$$\sum_{t=1}^{z} \alpha^{(t)} = r - 1 = 19$$

$$\sum_{t=1}^{z} t\alpha^{(t)} = \frac{z}{2}(r - q) = 31$$

Extension to Multicomponent Mixtures

Unfortunately there is no unambiguous way to generalize eq. 4 in the text to mixtures containing more than two components. For a mixture of n components the value of $\Omega(N_1,N_2,...N_n)$ depends upon the sequence 1, 2, ...n used for placing the molecules on the lattice, as pointed out long ago by Miller (20). Generalization can be achieved only in the special case where $\alpha^{(t)}r^{-1}[1 - (q/r)^{(t)}]^{-1}$ is the same for all molecules.

For financial support the authors are grateful to the National Science Foundation, to the donors of the Petroleum Research Fund, to the Paint Research Institute and to Gulf Research and Development Co. During the course of this work R. N. Lichtenthaler was a Deutsche Forschungsgemeinschaft fellow and D. S. Abrams was the recipient of a National Scholarship of the University of the Witwatersrand.

1. D. HENDERSON and P. J. LEONARD. Physical chemistry in advanced treatise. Vol. VIII B. Academic Press. 1971. Chapt. 7.
2. Discuss. Faraday Soc. **49**; Polymer solutions. 1970.
3. P. J. FLORY. Discuss. Faraday Soc. **49**, 7 (1970).
4. D. PATTERSON and G. DELMAS. Discuss. Faraday Soc. **49**, 98 (1970).

5. I. PRIGOGINE. The molecular theory of solutions. North Holland Press. 1957.
6. H. TOMPA. Trans. Faraday Soc. **48**, 363 (1952).
7. J. H. HILDEBRAND, J. M. PRAUSNITZ, and R. L. SCOTT. Regular and related solutions. Van Nostrand Reinhold Company. 1970.
8. P. J. FLORY. Principles of polymer chemistry. Cornell University Press. 1953.
9. H. C. LONGUET-HIGGINS. Discuss. Faraday Soc. **15**, 73 (1953).
10. A. SILBERBERG. J. Chem. Phys. **48**, 2835 (1968).
11. J. H. HILDEBRAND. J. Chem. Phys. **15**, 225 (1947).
12. H. TOMPA. Polymer solutions. Butterworth Publ. Ltd., London. 1956.
13. J. S. ROWLINSON. Discuss. Faraday Soc. **49**, 30 (1970).
14. M. L. HUGGINS. Ann. N.Y. Acad. Sci. **43**, 1 (1942).
15. E. A. GUGGENHEIM. Proc. Roy. Soc. A183, 203 (1944).
16. A. BONDI. Physical properties of molecular crystals, liquids and glasses. John Wiley and Sons, Inc., New York. 1968.
17. A. BELLEMANS. International Symposium on Macromolecular Chemistry, Helsinki. 1972.
18. P. J. FLORY. J. Am. Chem. Soc. **87**, 1833 (1965).
19. K. N. MARSH. Trans. Faraday Soc. **64**, 883 (1968).
20. A. R. MILLER. Proc. Camb. Phil. Soc. **43**, 422 (1947).

Can. J. Chem. Downloaded from www.nrcresearchpress.com by 210.87.254.40 on 09/05/12
For personal use only.

Nucleophilic Attack on Some Isothiazolium Salts

DAVID M. MCKINNON AND MOHAMED E. HASSAN
Chemistry Department, University of Manitoba, Winnipeg, Manitoba

Received February 19, 1973

A variety of isothiazolium salts has been prepared and allowed to react with sodium benzoylacetate. 2-Benzoylthiophenes are obtained, suggesting that the position of initial nucleophilic attack is at the sulfur atom of the heterocyclic cation. Reaction with hydrogen sulfide gave acyclic reduction products, or 1,2-dithiole derivatives, depending on the type of substituent on nitrogen in the isothiazolium salts.

Une série de sels d'isothiazolium a été préparée et mise en réaction avec le benzoylacétate de sodium. Des benzoyl-2 thiophènes ont été obtenus laissant penser que l'attaque nucléophile initiale se faisait sur l'atome de soufre du cation hétérocyclique. La réaction avec l'hydrogène sulfuré conduit aux produits de réduction acyclique ou aux dérivés dithiole-1,2, en fonction du type de substituant sur l'azote dans les sels d'isothiazolium. [Traduit par le journal]

Can. J. Chem., **51**, 3081 (1973)

Can. J. Chem. Downloaded from www.nrcresearchpress.com by 210.87.254.5 on 09/05/12
For personal use only.

While studies of nucleophilic attack on isothiazoles (1) and isothiazolones (2–5) indicate that the attack takes place at the ring sulfur atom, the situation with isothiazolium salts is by no means as clear. Various reactions of isothiazolium salts **1** with nucleophiles have been interpreted as occurring at carbon atom 3 (1, 6, 7), but in these reactions the products obtained could also have been formed by initial attack at sulfur. The reaction of certain 5-methylthioisothiazolium salts with hydrosulfide (8) has been suggested to occur at ring sulfur and recently (9) attack at carbon atom 3 by nitrogen nucleophiles, and at sulfur by hydrogen sulfide, has been demonstrated. In this work we wish to report some of our studies on the isothiazolium system which provide evidence on the position of nucleophilic attack.

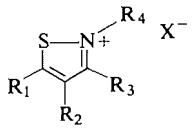

1

	R_1	R_2	R_3	R_4	X
a	H	H	H	Me	ClO_4
b	Ph	H	H	Me	ClO_4
c	Ph	H	H	Ph	ClO_4
d	Ph	Ph	H	Me	ClO_4
e	Ph	H	Ph	Ph	ClO_4
f	Ph	H	SMe	Me	I
g	SMe	Ph	H	Ph	ClO_4
h	SMe	H	Ph	Me	ClO_4
i	H	Ph	H	Ph	ClO_4
j	Ph	Ph	H	Ph	ClO_4
k	H	Ph	H	Me	ClO_4

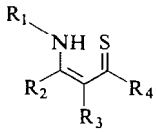

2

	R_1	R_2	R_3	R_4
a	Ph	H	H	Ph
b	Ph	Ph	H	Ph
c	Ph	H	Ph	SMe
d	Me	Ph	H	SMe
e	Ph	H	Ph	Ph
f	Me	Ph	H	NHMe
g	Me	SMe	H	Ph

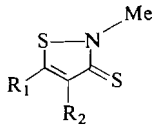

3

a R_1 = Ph, R_2 = H
b R_1 = R_2 = Ph

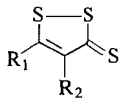

4

a R_1 = H, R_2 = Ph
b R_1 = Ph, R_2 = H

A variety of isothiazolium salts **1**(*a–k*) was used in the investigation. Most of these except **1***h* had been made before. Compound **1***a* had been isolated as its iodide (10), but we found it simpler to alkylate isothiazole by dimethyl sulfate and isolate the salt as its perchlorate. **1***g* was prepared by alkylation of 2,4-diphenylisothiazoline-3-thione, the reverse of a reaction previously described (8). Compound **1***h*, which was new, was prepared by iodine oxidation of methyl 3-methylaminodithiocinnamate (**2***d*) similarly to known methods (8, 11). The dithioester was prepared by treatment of 3-methylthio-5-phenyl-1,2-

Can. J. Chem. Downloaded from www.nrcresearchpress.com by 210.87.254.5 on 09/05/12
For personal use only.

dithiolium iodide with methylamine according to known methods (12). It is reported to be accompanied by 2-methyl-5-phenylisothiazoline-3-thione (**3***a*) and by 5-phenyl-1,2-dithiole-3-thione (**4***b*). In our investigation we found that the former compound was accompanied by greater or lesser amounts of *N*-methyl 3-methylaminothiocinnanamide (**2***f*), depending on the quantity of methylamine used, and in fact when a large excess of methylamine was used, the isothiazolinethione was not found and the amide was obtained instead. Treatment of the thione with methylamine gave no reaction, suggesting that the thione is not a precursor of the thioamide, and that the latter arises instead via some mechanistic change in the reaction of the dithiolium salt with the amine.

The isothiazoline-3-thione from the above reaction was smoothly converted by hydrogen peroxide in acetic acid into the 2-methyl-5-phenylisothiazolium cation, isolated as its perchlorate (**1***b*). Likewise, 2-methyl-4,5-diphenylisothiazoline-3-thione (**3***b*), prepared by reaction of 3-methylthio-4,5-diphenyl-1,2-dithiolium iodide with methylamine, was converted to 2-methyl-4,5-diphenylisothiazolium perchlorate (**1***d*). These oxidations by hydrogen peroxide in acetic acid are related to reactions of isothiazoline-5-thiones (8), and dithiolethiones (13, 14). Since *N*-alkylisothiazolium salts can be dealkylated to isothiazoles (15), the reaction represents another synthesis of these from dithiolium salts. These salts were identical to ones prepared (8) by methylation of isothiazoles, and by another method, the treatment of 1,2-dithiolium salts with methylamine to form β-methylaminopropenethiones **2** (16), which oxidized by iodine to form the *N*-methylisothiazolium salts **1***b* and *d*, isolated as the perchlorates. Yields by this method were rather poor, comparable to one such reaction previously studied (11), but it does at least represent a quick synthesis of *N*-alkylisothiazolium salts from the readily accessible (13, 14) 1,2-dithiolium salts.

Treatment of the isothiazolium salts **1** with sodium benzoylacetate yielded 2-benzoylthiophenes **5** in all cases. The formation of these can be explained by nucleophilic attack of a phenacyl ion (actual or potential) on ring sulfur, to give ring opening, followed by attack of the activated methylene group on the imine function to give recyclization to the thiophenes. The results from the 3- or 5-alkylthioisothiazolium salts **1***f*, *g*, and *h* are especially striking. By analogy with other related heterocyclic systems (16), had nucleophilic attack occurred at carbon, 3- or 5-acylmethleneisothiazoles would have been expected. For all cases except **1***f* cyclization occurs by loss of amine, but in that case, methanethiolate anion, a better leaving group, is lost instead, with formation of a 3-amino-2-benzoylthiophene (**5***e*). This reaction also afforded the acyclic reduction product **2***g*, which could have arisen by reaction of eliminated methanethiolate ion with another molecule of starting isothiazolium salt, either by reduction, or by nucleophilic attack. Similar results have been obtained for the attack of benzenethiol (**9**) or benzenethiolate anion (below) on isothiazolium salts. Likewise, the attack of hydrosulfide ion on two alkylthioisothiazolium salts in ethanol (8) may be rationalized as occurring by a similar route.

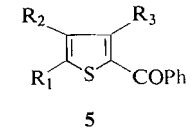

5

	R_1	R_2	R_3
a	H	H	H
b	Ph	H	H
c	Ph	Ph	H
d	Ph	H	Ph
e	Ph	H	NHMe
f	SMe	Ph	H
g	SMe	H	Ph
h	H	Ph	H

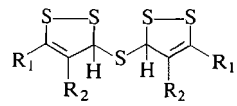

6

a $R_1 = R_2 = Ph$
b $R_1 = H, R_2 = Ph$

Sykes and Ullah (9) found that attack of hydrogen sulfide on the isothiazolium system in aqueous solution gave bis-1,2-dithiol-3-yl sulfides **6** instead of reduction products. Accordingly, we treated a number of the isothiazolium salts with hydrosulfide ion in ethanol, or hydrogen sulfide in water, and examined the products. Little difference if any was found in the reaction products derived from either method, and the course of the reaction appears to depend mainly on whether the original isothiazolium salt is *N*-aryl or *N*-alkyl substituted. The former give mainly reduction products, β-aminopropenethiones or derivatives **2**, while the latter give reduction, bis-1,2-dithiol-3-yl sulfides **6**, or 1,2-dithiole-3-thione **4** products.

The differences in the products obtained probably arise from changes in the mechanism shown in Scheme 1.

The intermediate disulfide imine A could either

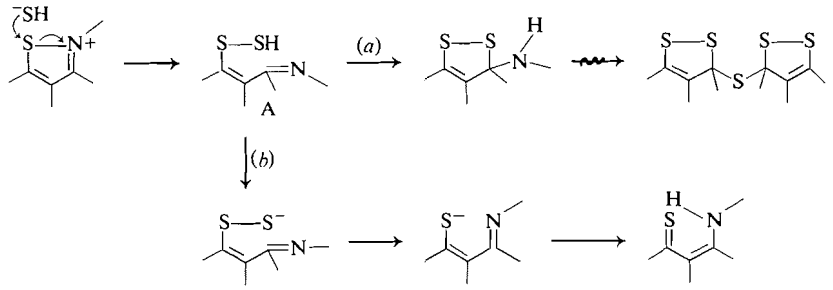

SCHEME 1

add to the imine group (path a), to give an aminodithiole, with eventual formation of a bis-dithiolyl sulfide, or extrude sulfur (path b) to give a β-aminothione derivative. For aliphatic imines A the former would be the preferred route, but where the imine is stabilized by conjugation with an aromatic ring, the latter would be preferred, leading to an acyclic reduction product. Path a is analogous to a step in the formation of 1,2-dithiolium salts from 1,3-diketones with hydrogen disulfide in acidic media (14), while path b is analogous to steps in the known reactions of 1,2-dithiolium salts with bases, particularly with primary aromatic amines (17). In path a, the conversion of the aminodithiole to the sulfide could be accomplished by nucleophilic exchange between the aminodithiole and hydrogen sulfide, as has been suggested (17) for reactions of 1,3-dithioles. Intermediate formation of a 1,2-dithiolium cation (9) may be involved.

With one compound, 2-methyl-5-methylthio-3-phenylisothiazolium perchlorate (**1***h*) the acyclic reduction product **2***d* was obtained. The other product isolated was not a bis-dithiolyl sulfide, but was 5-phenyl-1,2-dithiole-3-thione (**4***b*). While the exact mechanism leading to this is unknown, it is not unreasonable that it could be derived from a compound of the type

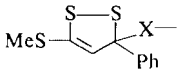

X = S or NHMe

formed by cyclization of the intermediate disulfide suggested in Scheme 1. The reactions leading to the formation of **2***d* and **5***b* from isothiazolium salt **1***h* and of **2***g* and **4***b* from **1***f* likely follow a similar scheme.

The isolation of only the thione **4***a* from reaction of the isothiazolium salt **1***k*, instead of a sulfide **6***b*, presents some difficulty. However, the thione does appear to be derived from the sulfide since prolonged treatment of the latter with hydrogen sulfide or sodium hydrosulfide gave thione. The necessary oxidation could be accomplished by unreacted isothiazolium salt, intermediate dithiolium cation as suggested above, or by sulfur arising from decomposition of either of these.

Treatment of two isothiazolium salts **1***e* and **1***b* with sodium benzenethiolate in ethanol gave reduction products **2***b* and **2***d* respectively, and diphenyldisulfide. These results are comparable to other such studies made (9).

Experimental

The i.r. spectra were obtained on a Perkin–Elmer model 337 spectrophotometer in liquid paraffin mulls. The n.m.r. spectra were obtained on a Varian Model 56/60A spectrometer and, unless otherwise stated, in deuterochloroform at 40°, using tetramethylsilane as an internal standard. Mass spectra were obtained on a Finnegan 1015 quadrupole mass spectrometer. T.l.c. was performed using "Camag" silica gel D.S.F.5, and column chromatography on alumina 506-C-1, Brockman activity 1, both supplied by Mondray Ltd. Development of both, unless otherwise stated, was by benzene. Melting points were obtained on a Fisher–Johns melting point apparatus.

*Preparation of 2-Methylisothiazolium Perchlorate (**1***a*)*

Isothiazole (0.85 g, 0.01 mol) and dimethyl sulfate (1 ml) were heated at 100° for 1 h. The mixture was treated with ether and the precipitated oil dissolved in acetic acid, and treated with 70% perchloric acid (0.5 ml). Colorless needles, m.p. 145°, were obtained (61%). A sample of the perchlorate treated with aqueous sodium iodide gave the iodide identical (mixed m.p. and i.r.) with an authentic sample (10).

Reaction of 3-Methylthio-5-phenyl-1,2-dithiolium Iodide with Methylamine

This reaction was performed as described (12) except that the equivalent quantity of 40% ethanolic methylamine solution was used. Work-up gave 5-phenyl-1,2-dithiole-3-thione, methyl β-methylaminodithiocinnamate, and 2-methyl-5-phenylisothiazoline-3-thione as described. When the reaction was performed with a fourfold excess of the

Can. J. Chem. Downloaded from www.nrcresearchpress.com by 210.87.254.5 on 09/05/12
For personal use only.

Can. J. Chem. Downloaded from www.nrcresearchpress.com by 210.87.254.5 on 09/05/12
For personal use only.

TABLE 1. Reactions of isothiazolium salts with sodium benzoylacetate

Isothiazolium salt **1**	Source	Product **5**	Yield %	M.p. °C	Analysis							
					Calculated (%)				Found (%)			
					C	H	N	S	C	H	N	S
a	*	*a*	71	57†								
b	*	*b*	68	132‡								
c	§	*b*	63	132								
d	*	*c*	68	150–152	81.13	4.71	—	9.41	81.17	4.84	—	9.51
e	§	*d*	42	101‖								
f	¶	*e*	38	108–109	73.51	5.12	4.76	10.95	73.45	5.25	4.67	10.91
g	*	*f*	77	89–91	69.75	4.52	—	20.65	70.07	4.62	—	20.88
h	*	*g*	74	82–83	69.75	4.52	—	20.65	70.04	4.69	—	20.85
i	**	*h*	40	96	77.35	4.54	—	12.12	77.07	4.69	—	12.24

*This work.
†Literature (19) 57°.
‡Literature (20) 132°.
§Reference 11.
‖Reference 21 m.p. 101°.
¶Reference 12.
**Reference 8.

Can. J. Chem. Downloaded from www.nrcresearchpress.com by 210.87.254.5 on 09/05/12
For personal use only.

amine solution, and the mixture worked up as above, chromatography on 5% deactivated alumina gave initially 5-phenyl-1,2-dithiole-3-thione and methyl β-methylaminodithiocinnamate. Extraction of a broad strongly adsorbed band with acetone gave a yellow oil which crystallized on scratching. Recrystallization from ethanol gave pale-yellow prisms, m.p. 96–98° (35%).

Anal. Calcd. for $C_{11}H_{14}N_2S$: C, 64.21; H, 6.83; N, 13.59; S, 15.55. Found: C, 63.92; H, 6.89; N, 13.52; S, 15.64.

N.m.r. τ 7.28 (3H doublet, $J = 3.2$ Hz, the amidic methyl), 7.00 (3H doublet, $J = 3.2$ Hz, the amine methyl), 5.02 (1H singlet, vinylic proton), 3.40 (1H band, the amidic NH), 2.68 (5H multiplet, the aromatic protons), −1.20 (1H band, the amine NH, hydrogen bonded to C=S).

The mass spectrum: M^+ 206, calcd. 206, 173 (M—SH)

*Preparation of 2-Methyl-5-methylthio-3-phenylisothiazolium Perchlorate (**1h**)*

Methyl β-methylaminodithiocinnamate (446 mg, 2 mmol) in ethanol (5 ml) was treated with saturated iodine solution until there was a slight permanent cloudiness. 70% perchloric acid (1 ml) was added, and dilution with ether produced yellow crystals. The product was recrystallized from acetic acid containing perchloric acid as yellow needles, m.p. 184–186 (83%).

Anal. Calcd. for $C_{11}H_{12}NS_2ClO_4$: C, 41.05; H, 3.73; N, 4.35; S, 20.55; Cl, 11.05. Found: C, 41.07; H, 3.86; N, 4.23; S, 20.08; Cl, 10.92.

N.m.r. (dimethylsulfoxide-d_6) τ 7.21 (3H singlet, the S—CH_3 group), 5.99 (3H singlet, the N—CH_3 group), 2.51–2.15 (5H bands, the aromatic protons).

Treatment of 2-Methyl-5-phenylisothiazoline-3-thione with Methylamine

The thione (50 mg) and 40% methylamine solution in ethanol (1 ml) were refluxed together 1 h. The starting material was recovered on work-up.

*Reaction of 3-Methylthio-4,5-diphenyl-1,2-dithiolium Iodide with Methylamine, 2-Methyl-4,5-diphenylisothiazoline-3-thione (**3b**)*

The salt (4.28 g, 0.01 mol) in tetrahydrofuran (70 ml) was treated with 60% methylamine solution in ethanol (6 ml) at room temperature and stirred until homogeneous. The solution was evaporated, and the residue chromatographed in benzene on 5% deactivated alumina. Two bands were obtained. A red band gave 4,5-diphenyl-1,2-dithiole-3-thione (31%), and a strongly adsorbed yellow band was extracted with acetone. Evaporation gave a yellow solid which was recrystallized from ethanol as pale-yellow needles, m.p. 133° (28%).

Anal. Calcd. for $C_{16}H_{13}NS_2$: C, 67.85; H, 4.59; N, 4.94; S, 22.62. Found: C, 67.82; H, 4.45; N, 5.01; S, 22.81.

N.m.r. τ 6.21 (3H singlet, the methyl protons), 2.53–2.87 (10H bands, the aromatic protons).

The mass spectrum: calcd. M^+ 283. Found, 283.

*Preparation of 2-Methyl-5-phenylisothiazolium Perchlorate (**1b**)*

(a) From 2-Methyl-5-phenylisothiazoline-3-thione

Powdered thione (103.5 mg, 0.5 mmol) in acetic acid (4 ml) was treated with 30% hydrogen peroxide (0.15 ml). The solid dissolved almost immediately and the solution became dark yellow. After 1 h, the solution was treated with ether, and the precipitated oil treated with 70% perchloric acid (0.1 ml). The oil solidified and was recrystallized from acetic acid as pale-yellow plates, m.p. 144–145° (80%). Identical mixed m.p. and i.r. with an authentic specimen (11).

(b) From 3-Phenyl-1,2-dithiolium Perchlorate

The perchlorate (1.035 g, 5 mmol) in ethanol (10 ml) was treated with 40% ethanolic methylamine solution (2 ml) and warmed gently with stirring until homogeneous. The red solution was treated with saturated ethanolic iodine solution (2 ml), and 70% perchloric acid (1 ml) added. Dilution with ether and scratching gave a brown precipitate which was recrystallized from acetic acid containing perchloric acid as yellow plates, identical (mixed m.p. and i.r.) with the above (20%).

*Preparation of 2-Methyl-4,5-diphenylisothiazolium Perchlorate (**1d**)*

(a) From 2-Methyl-4,5-diphenylisothiazoline-3-thione

This reaction was performed as for the previous synthesis. Pale-yellow needles, m.p. 99°, were obtained (75%). Identical (mixed m.p. and i.r.) with an authentic specimen (8).

(b) From 3,4-Diphenyl-1,2-dithiolium Perchlorate

This reaction was carried out as described for the previous compound, except that recrystallization was effected from acetone containing perchloric acid. Pale-yellow needles of the salt were obtained (25%), identical (mixed m.p. and i.r.) to an authentic specimen.

*Preparation of 5-Methylthio-2,4-diphenylisothiazolium Perchlorate (**1g**)*

2,4-Diphenylisothiazoline-5-thione (8) (0.566 g, 2 mmol) in *n*-butyl acetate (10 ml) was treated with methyl iodide (2 ml) and allowed to stand. An oily precipitate which was deposited initially crystallized on further standing. The mixture was diluted with ether, filtered, and the salt converted to the perchlorate in acetic acid containing perchloric acid. Recrystallization from acetic acid gave pale-yellow prisms, m.p. 158°, identical (mixed m.p. and i.r.) with an authentic specimen (8).

Reaction of Isothiazolium Salts with Sodium Benzoylacetate: General Method

The isothiazolium salts (~1 mmol) were added to a suspension in ethanol of sodium benzoylacetate (~1.5 mmol) (prepared by addition of benzoylacetic acid (18) to a molar solution of sodium ethoxide in ethanol). The mixture was stirred and gently warmed until homogeneous. The mixture was diluted with water and the ether extract dried. Evaporation gave either crystalline material directly or oils which were purified by t.l.c. prior to crystallization. Products were recrystallized from ethanol or ethanol–benzene, 1:1, mixture. Reactions and products are summarized in Table 1.

Treatment of salt **1*f*** with sodium benzoylacetate gave an oily product which on examination by t.l.c. gave the thiophene **5*e***. The first band on elution gave 30 mg of an orange oil, whose n.m.r. had a broad band at −4.5 τ, typical of β-aminoenethiones (9, 22). This was not analyzed, but an iodine oxidation in the presence of perchloric acid gave back salt **1*f***, confirming its structure as **2*g***.

TABLE 2. Reactions of isothiazolium salts with sodium hydrosulfide (method a) or hydrogen sulfide (method b)

Isothiazolium salt **1**	Source	Method	Products in order of elution (yields %)
c	*	a	**2***a*(52)
c	*	b	**2***a*(56)
d	*	b	**6***a*(40)†
e	*	b	**2***b*(45)
f	*	a	**2***g*(32)‡, **4***b*(28)
g	*	b	**2***c*(45), **4***a*(49)
h	*	b	**2***d*(43), **4***b*(45)
j	§	b	**2***e*(20)
k	‖	b	**4***a*(21)

*See Table 1.
†This could not be isolated sufficiently pure for analysis, and was converted by treatment with perchloric acid into 3,4-diphenyl-1,2-dithiolium perchlorate (11), similarly to known methods (17).
‡Identified by conversion (I_2, $HClO_4$) to 1*f*.
§Reference 11.
‖Reference 8.

Reactions of Isothiazolium Salts with Hydrogen Sulfide or Sodium Hydrogen Sulfide

(a) The isothiazolium salts (~1 mmol) in ethanol (10 ml) were treated with equivalent quantities of ethanolic molar sodium hydrosulfide solution, and stirred until homogeneous. The solutions were diluted with water and ether-extracted.

(b) The salts (~1 mmol) in water suspension were treated with hydrogen sulfide and boiled 10 min. The mixtures were cooled and ether-extracted.

The ether extracts from *a* or *b* were dried, evaporated, and examined by t.l.c. The results are summarized in Table 2. There was little to choose between the two methods, and yields and products by each were comparable when performed on identical compounds.

*Reaction of 2,3,5-Triphenylisothiazolium Perchlorate (**1e**) with Sodium Benzenethiolate*

The isothiazolium salt (613.5 mg, 1 mmol) in ethanol (20 ml) was treated with the equivalent quantity of sodium benzenethiolate in ethanol (1 ml), and stirred until homogeneous. The dark-red solution was diluted with water and extracted with ether. Chromatography afforded 1-anilino-1,3-diphenylprop-1-ene-3-thione (81%) identical (mixed m.p. and i.r.) with an authentic sample (17). Diphenyl disulfide (89 mg) was also isolated from the reaction mixture.

*Reaction of 2-Methyl-5-methylthio-3-phenylisothiazolium Perchlorate (**1h**) with Sodium Benzenethiolate*

The reaction, performed as above, gave methyl β-methylaminodithiocinnamate (59%), identical with an authentic specimen (12).

Reaction of Bis-4-phenyl-1,2-dithiol-3-yl Sulfide with Hydrogen Sulfide

The sulfide (0.2 g) (23) in water (10 ml) was boiled and a stream of hydrogen sulfide passed through. After 10 min the mixture was cooled and ether-extracted. The extract on examination by t.l.c. gave unreacted material, and 4-phenyl-1,2-dithiole-3-thione **4***a* (30%). Boiling of the sulfide with sodium hydrogen sulfide gave similar results.

The authors are very grateful to the National Research Council of Canada for financial support of this research. We also wish to thank Mr. M. Arneson for the preparation of mass spectra and Mr. R. Dickenson for the preparation of n.m.r. spectra.

1. K. R. H. WOOLDRIDGE. The chemistry of mononuclear isothiazoles. *In* Advances in heterocyclic chemistry. Academic Press, New York. 1972.
2. W. D. CROW and I. GOSNEY. Aust. J. Chem. **19**, 1693 (1966).
3. W. D. CROW and I. GOSNEY. Aust. J. Chem. **20**, 2729 (1967).
4. W. D. CROW and I. GOSNEY. Aust. J. Chem. **22**, 765 (1969).
5. W. D. CROW and I. GOSNEY. Tetrahedron, **26**, 1463 (1970).
6. J. M. LANDESBERG and R. A. OLOFSON. Tetrahedron, **22**, 2135 (1966).
7. F. T. LEE and G. P. VOLPP. J. Heterocycl. Chem. **7**, 415 (1970).
8. G. E. BACHERS, D. M. MCKINNON, and J. M. BUCHSHRIBER. Can. J. Chem. **50**, 2568 (1972).
9. P. SYKES and H. ULLAH. J. Chem. Soc. Perkin Trans. I, 2305 (1972).
10. P. CHAPLEN, R. SLACK, and K. R. H. WOOLDRIDGE. J. Chem. Soc. 4577 (1965).
11. D. M. MCKINNON and E. A. ROBAK. Can. J. Chem. **46**, 1885 (1968).
12. G. LE COUSTUMER and Y. MOLLIER. Bull. Soc. Chim. Fr. 3076 (1970).
13. E. KLINGSBERG and A. SCHREIBER. J. Am. Chem. Soc. **83**, 2934 (1961).
14. D. LEAVER, W. A. H. ROBERTSON, and D. M. MCKINNON. J. Chem. Soc. 5106 (1962).
15. J. Faust. Z. Chem. **8**, 170 (1968).
16. E. BROWN, D. LEAVER, and D. M. MCKINNON J. Chem. Soc. C, 1202 (1970).
17. D. LEAVER, D. M. MCKINNON, and W. A. H. ROBERTSON. J. Chem. Soc. 32 (1965).
18. R. MEYER and K. TOGEL. Ann. **79**, 367 (1906).
19. W. MINNIS. Org. Synth. **12**, 62 (1932).
20. G. PFISTER-GUILLOUZO and N. LOSAC'H. Bull. Soc. Chim. Fr. 153 (1963).
21. D. LEAVER. Personal communication.
22. C. PAULMIER, Y. MOLLIER, and N. LOSAC'H. Bull. Soc. Chim. Fr. 2463 (1965).
23. H. NEWMAN and R. B. ANGIER. Chem. Commun. 353 (1967).

Can. J. Chem. Downloaded from www.nrcresearchpress.com by 210.87.254.5 on 09/05/12
For personal use only.

The Geometrical Dependence of Experimental and Theoretical Nuclear Spin–Spin Coupling Constants in the $^{15}NH_2$ Fragment

RODERICK E. WASYLISHEN[1]

National Institute of Arthritis, Metabolism, and Digestive Diseases, National Institutes of Health, Bethesda, Maryland 20014

AND

T. SCHAEFER

Department of Chemistry, University of Manitoba, Winnipeg, Manitoba R3T 2N2

Received April 6, 1973

Approximate molecular orbital theory at the INDO level of approximation has been used to examine $^1J(^{15}N,H)$ and $^2J(HNH)$ in ammonia as a function of the HNH angle. The couplings are very sensitive to the value of the HNH angle in the range from 110 to 120°. The computed trends are compared with those observed in other compounds containing the $^{15}NH_2$ fragment. The signs and magnitudes of $^1J(^{15}N,H)$ and $^2J(HNH)$ have been measured for 2-aminoacetophenone at temperatures where the amino protons are nonequivalent. The observed and calculated results suggest that the amino group lies in the plane of the benzene ring. In aniline the magnitude of $^2J(HNH)$ lies between 1 and 2 Hz and on the basis of the trends in the calculated and experimental values the sign can be confidently taken as negative.

La théorie approchée de l'orbitale moléculaire au niveau d'approximation INDO a été utilisée pour examiner $^1J(^{15}N,H)$ et $^2J(HNH)$ dans l'ammoniac en fonction de l'angle HNH. Les couplages sont très sensibles à la valeur de l'angle HNH dans l'intervalle 110–120°. Les tendances calculées ont été comparées à celles observées pour d'autres composés contenant le fragment $^{15}NH_2$. Les signes et amplitudes de $^1J(^{15}NH)$ et $^2J(HNH)$ ont été mesurés pour l'amino-2 acétophénone aux températures où les protons de l'amine ne sont pas équivalents. Les résultats observés et calculés suggèrent que le groupe amino est dans le plan du cycle benzènique. Dans l'aniline l'amplitude de $^2J(HNH)$ vaut 1 à 2 Hz et sur la base des valeurs calculées et expérimentales prévues, le signe peut être pris négatif en toute confiance.

[Traduit par le journal]

Can. J. Chem., 51, 3087 (1973)

Can. J. Chem. Downloaded from www.nrcresearchpress.com by 210.87.254.6 on 09/05/12
For personal use only.

Introduction

Experimental data on one-bond $^{15}N,H$ spin–spin coupling constants, $^1J(^{15}N,H)$, in the $^{15}NH_2$ fragment (1–3) vary from −61.2 Hz in ammonia (4) to −92.6 Hz in $(C_6H_5)_2C{=}\overset{+}{N}H_2$ (5). The variations have been interpreted on the basis that $^1J(^{15}N,H)$ is linearly related to the % 2s character of the N—H bonding orbitals. By taking $\overset{+}{N}H_4$ as an sp^3 hybridized system and $(C_6H_5)_2C{=}\overset{+}{N}H_2$ as an sp^2 hybridized system, Binsch and co-workers (5) deduced the empirical relationship

$$[1]\quad \%\ 2s\ \text{character} = 0.43\ ^1J(^{15}N{-}H) - 6$$

Recently Axenrod *et al.* (6) used this relationship to interpret $^1J(^{15}N,H)$ values observed in a large number of substituted anilines. $^1J(^{15}N,H)$ values varied from −74.8 Hz (4-$N(Me)_2$ in $CDCl_3$) to −92.6 Hz (2,4-$(NO_2)_2$ in DMSO). On the basis of eq. 1 the authors suggested that the nitrogen hybridization state changes from essentially sp^3 in the presence of strongly electron-donating substituents such as 4-$N(Me)_2$, to sp^2 in the presence of strongly electron-withdrawing substituents.

Similar conclusions had earlier been reached by Randall and co-workers (6*b*, 6*c*). *Ab initio* molecular orbital (MO) calculations indicate that para substitution by π electron acceptors flattens the nitrogen pyramid and that π electron donors have the opposite effect (6*d*).

Equation 1 and similar relationships (7–12), including those which relate $^1J(^{13}C,H)$ to "carbon 2s character", can be rationalized either by localized MO theory (11) or by valence bond theory (12). McConnell's (13) MO formulation gives

$$[2]\quad J_{XH} = (4/3)^2 h\beta^2\gamma_X\gamma_H(\Delta E)^{-1}s_X^2(0)s_H^2(0)P^2_{s_Xs_H}$$

In this expression β is the Bohr magneton, $s_X^2(0)$ is the 2s orbital density at the nucleus,

[1]NRCC Postdoctorate Fellow, 1972–73.

Can. J. Chem. Downloaded from www.nrcresearchpress.com by 210.87.254.6 on 09/05/12
For personal use only.

X (where X = ^{13}C or ^{15}N), $s_H^2(0)$ is the orbital density at the proton, ΔE is a mean "excitation energy", and $P_{s_X s_H}$ is the s_X,s_H element of the bond-order matrix.

If the factor $s_X^2(0)\ s_H^2(0)\ (\Delta E)^{-1}$ does not vary from one molecule to another then ^1J(X,H) is linearly related to $P^2_{s_X s_H}$, assuming that the Fermi contact mechanism dominates. The use of simple relationships between $^1J(^{13}C,H)$ and carbon hybridization or "% 2s character" has been criticized (10, 11, 14–16).[2] In some cases variations in $^1J(^{13}C,H)$ have been accounted for in terms of changes in effective nuclear charge, $s_c^2(0)$ (16).

The more general MO theory of Pople and Santry (17) does not make the average energy approximation, but there are other problems (18). Valence bond methods share some of the problems encountered by the MO methods (19).

Recently Pople and co-workers (18, 20, 21) have developed a finite perturbation technique which allows the calculation of coupling constants without making some of the approximations inherent in the earlier MO methods. The application of this technique using unrestricted INDO MO wave functions in an approximate SCF framework has been described (22–24). Briefly, the Fermi contact contribution to nuclear spin–spin coupling between two nuclei, A and B, is given by the equation

$$[3]\quad J_{AB} = h/2\pi[(8\pi/3)\beta]^2\gamma_A\gamma_B s_A^2(0)s_B^2(0) \times [(\partial/\partial h_B)\rho^{spin}_{s_A s_A}(h_B)]_{h_B=0}$$

The parameter h_B is the perturbation due to the nuclear moment μ_B and has the form, $h_B = 8/3\pi\beta\mu_B s_B^2(0)$. The valence s-orbital densities at the nucleus, s_A^2 (0) and $s_B^2(0)$, are assumed to be invariant from molecule to molecule, depending only on the nature of atoms A and B. All other terms in eq. 3 have their usual meaning.

Using this technique, Maciel *et al.* (22) have shown that calculated $^1J(^{13}C,H)$ values are closely related to *calculated* $P^2_{C(2s),H(s)}$ values in the absence of $-I^-$ substituents ($-CF_3$, $-C(O)X$, $-NO_2$, $-CN$, etc.).

In this paper we use this approach to examine the relationship between $^1J(^{15}N,H)$ in the NH_2 fragment and parameters such as bond order and nitrogen pyramidalization. Calculated results are reported for ammonia, formamide, aniline, and 2-aminoacetophenone. The possible application of $^2J(HNH)$ values to the determination of the geometry of the amino group is also discussed. The results of low-temperature proton n.m.r. studies on 2-aminoacetophenone-^{15}N are reported.

[2]Similar criticisms would also apply to the interpretation of $^1J(^{15}N,H)$ values.

Results and Discussion

Computational Results

All coupling constants were calculated using eq. 3 with the same parameterization as used previously by Pople *et al.* (18, 21, 22). The convergence criterion used here was previously described (24).

Ammonia

Spin–spin coupling constants in ammonia were calculated as a function of θ, the HNH

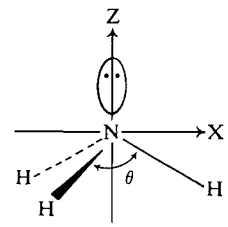

1

angle. The N—H bond length was taken as 1.0136 Å (25) in all calculations, and θ was varied from 90 to 120° in steps of 2°. Calculated values of $^1J(^{15}N,H)$, $^2J(HNH)$, $P^2_{N(s),H(s)}$, and the nitrogen and hydrogen charge densities (q) are given in Table 1. In Figs. 1 and 2, $^1J(^{15}N,H)$ and $^2J(HNH)$ are plotted against θ. Notice that as θ increases $^1J(^{15}N,H)$ increases in magnitude and $^2J(HNH)$ becomes more positive. In Fig. 3, $^1J(^{15}N,H)$ is plotted against $P^2_{N(s)H(s)}$.

In order to assess the importance of variations in the effective nuclear charges on calculated $^1J(^{15}N,H)$ values, a procedure analogous to that used by Maciel *et al.* (22) was applied. The correction factor for ^{15}N—H coupling constants is given by

$$[4]\quad \frac{s_H^2(0)s_N^2(0)}{[s_H^2(0)s_N^2(0)]_0} = \frac{(1.0 - 0.30q_H)^3(3.90 - 0.35q_N)^3}{(3.90)^3}$$

where the denominator $[s_H^2(0)s_N^2(0)]_0$ corresponds to the nonpolar neutral case. q_H and q_N refer to the net electron charge densities on hydrogen and nitrogen respectively. On going

TABLE 1. Calculated spin–spin coupling constants, bond orders, and net charge densities as a function of nitrogen pyramidalization in ammonia

θ°, ∠HNH	$^1J(^{15}N,H)$* (Hz)	$^2J(HNH)$ (Hz)	$P^2_{N(s)H(s)}$	q_N	q_H
90	−13.85	−14.00	0.1364	−0.2253	0.0751
92	−15.26	−13.17	0.1425	−0.2257	0.0752
94	−16.85	−12.41	0.1490	−0.2268	0.0756
96	−18.69	−11.70	0.1559	−0.2287	0.0762
98	−20.81	−11.02	0.1635	−0.2314	0.0771
100	−23.27	−10.39	0.1716	−0.2350	0.0783
102	−26.16	−9.66	0.1805	−0.2393	0.0798
104	−29.56	−8.95	0.1902	−0.2445	0.0815
106	−33.60	−8.16	0.2007	−0.2506	0.0835
108	−38.42	−7.25	0.2122	−0.2576	0.0859
110	−44.27	−6.14	0.2248	−0.2654	0.0885
112	−51.27	−4.80	0.2386	−0.2740	0.0913
114	−59.87	−3.07	0.2537	−0.2835	0.0945
116	−70.48	−0.82	0.2703	−0.2937	0.0979
118	−83.69	2.16	0.2883	−0.3046	0.1015
120	−100.33	6.14	0.3076	−0.3159	0.1053
107.05	−36.02	−7.70	0.2066	−0.2541	0.0847
109.4712	−42.58	−6.47	0.2214	−0.2632	0.0877

*The authors of ref. 2 report on page 154 that Pople, McIver, and Ostlund calculate −42.7 Hz for a pyramidal situation and −99.4 Hz for a hypothetical planar form.

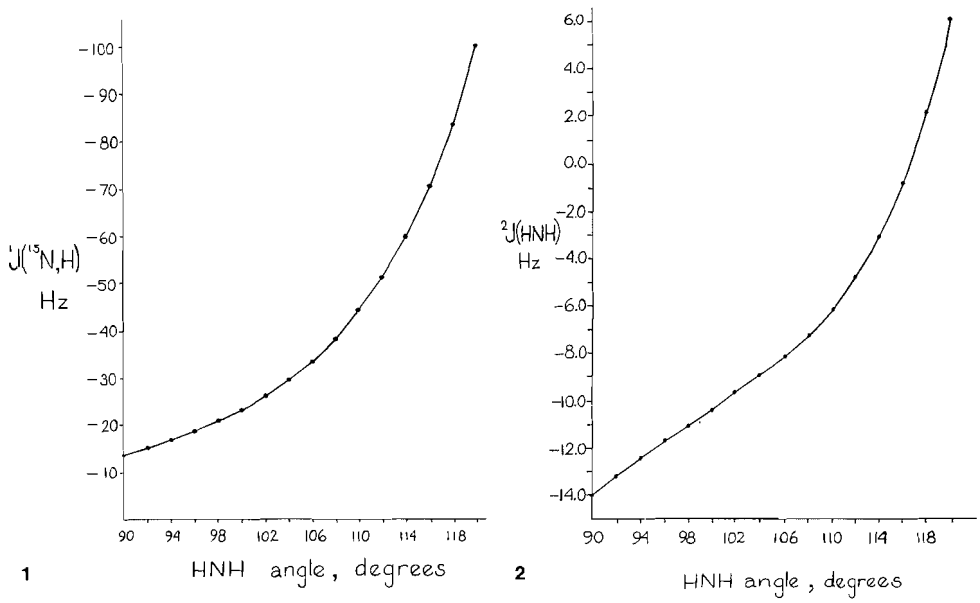

FIG. 1. A plot of the calculated $^1J(^{15}N,H)$ values in Hz *vs.* the HNH bond angle for ammonia.
FIG. 2. A plot of the calculated $^2J(HNH)$ values in Hz *vs.* the HNH angle in ammonia.

from θ = 90 to 120°, the correction factor given by eq. 4 changed from 0.9917 to 0.9877. Thus the adjusted $^1J(^{15}N,H)$ values varied by less than 1 Hz from those given in Table 1.

Calculated $^2J(HNH)$ values were also adjusted in order to account for variations in $s_H^2(0)s_N^2(0)$. Using eq. 2 in ref. 22 the correction factor varied from 0.8722 for θ = 90° to 0.8248 for θ = 120°, thus giving rise to significant adjustments in $^2J(H,H)$. For θ = 90, 100, 110, and 120°, $^2J(HNH)_{adj}$ = −12.21 Hz, −9.01 Hz, −5.22 Hz, and 5.06 Hz, respectively. The calculations

Can. J. Chem. Downloaded from www.nrcresearchpress.com by 210.87.254.6 on 09/05/12
For personal use only.

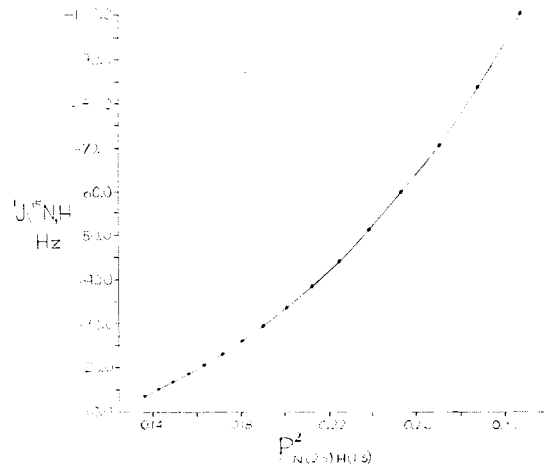

FIG. 3. A plot of the calculated $^1J(^{15}N,H)$ values in Hz *vs.* $P^2_{N(2s)H(1s)}$ for ammonia.

yield a steep dependence of both $^2J(HNH)$ and $^1J(^{15}N,H)$ on the HNH angle in the range from 110 to 120° and suggest the measurement of both coupling constants in attempts to determine the geometry of the NH_2 fragment in molecules in solution.

Other Molecules

Approximate MO calculations of $^1J(^{15}N,H)$ and $^2J(HNH)$ at the INDO level of approximation for aniline and 2-aminoacetophenone have been presented (9). For aniline the geometry of the amino group was taken from the microwave results of Lister and Tyler (26), which give the angle θ between the extension of the C—N bond and the bisector of the HNH angle as 37.7°.

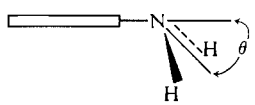

2

Another calculation on aniline assumed complete planarity of the molecule with C—N and N—H bond lengths equal to those given (26) for the nonplanar molecule. Standard geometries were used in a planar (apart from the methyl protons) model of 2-aminoacetophenone. INDO calculations of $^2J(HNH)$ in the ammonium ion and formamide were also carried out. For the ammonium ion the N—H bond length was taken as 1.03 Å. Two calculations were made for formamide, one using Pople's standard geometries (a planar geometry), the other using a slightly nonplanar geometry derived from microwave studies. The results of these calculations are presented in Table 2 together with available experimental data. Notice that for the compounds in Table 2, $^2J(HNH)_{calcd}$ is slightly more positive than $^2J(HNH)_{obs}$. Similar problems are encountered in the case of calculated $^2J(HCH)$ values (18, 22, 23).

Of particular interest are the calculated $^1J(^{15}N,H)$ values for formamide. The use of atomic coordinates obtained from a microwave study (27) results in $|^1J(^{15}N,H_A)| > |^1J(^{15}N,H_M)|$, in agreement with experiment. However, for standard geometries, but using 1.40 Å for the C—N bond length, the calculated absolute value of $^1J(^{15}N,H_M)$ is greater than that of $^1J(^{15}N,H_A)$. It should be pointed out that the microwave results (27) indicate that the N—H_M bond is slightly longer than the N—H_A bond. Also, using the microwave data, INDO gives $P_{N(2s),H(1s)_A} = 0.5333$ while $P_{N(2s),H(1s)_M} = 0.5186$. When one assumes equal N—H bond lengths, INDO calculates $P_{N(2s),H(1s)_A} < P_{N(2s),H(1s)_M}$.

The agreement between calculated and observed $^2J(HNH)$ values in Table 2 is tolerably good for those molecules in which the HNH angle is expected to be considerably larger than 109.5°.

Experimental Results and Discussion

General Problems in Measuring $^2J(HNH)$

While experimental values of $^1J(^{15}N,H)$ are fairly readily available, values for $^2J(HNH)$ are scarce. Reasons for this scarcity are: 1, amino protons are usually chemically equivalent due to rapid rotation (on the n.m.r. time scale) about the X—N bond in the X—NH_2 fragment; exceptions are formamide and some of its derivatives; 2, ^{14}N(99.635% natural abundance) causes substantial broadening of the amino proton resonance; 3, amino protons are often undergoing rapid intermolecular exchange on the n.m.r. time scale (9).

Deuterium substitution yields $^2J(H,D)$ but $g_H = 6.55g_D$ and the accurate deduction of small $^2J(H,H)$ values becomes difficult. Also, since deuterium has a quadrupole moment, the rate of deuterium spin–lattice relaxation must be small in order to observe a well-resolved triplet in the proton spectrum. This should not be a problem if the amino group is free to rotate (*i.e.*, has a short correlation time, see ref. 29). Tritium ($I = \frac{1}{2}$, $g_T/g_H = 1.067$) substitution would be the most sensible method of eliminating

Can. J. Chem. Downloaded from www.nrcresearchpress.com by 210.87.254.6 on 09/05/12
For personal use only.

TABLE 2. Some calculated and observed $^1J(^{15}N,H)$ and $^2J(HNH)$ values in Hz

Compound		$^1J(^{15}N,H)$ Calcd.	$^1J(^{15}N,H)$ Obs.	$^2J(HNH)$ Calcd.	$^2J(HNH)$ Obs.	Experimental references
$^+NH_4$		−73.52	−73.2	−7.47	−12.4	28
NH_3 107.05°		−36.02	−61.2	−7.70	−10.35	4
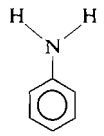		−59.53*	−78.875	−0.04*	(−)1 to (−)2	9
		−92.20†		+9.23†		
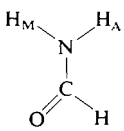	N—H_A	−86.09‡	−89.7	+3.80‡	+2.8	7
	N—H_M	−80.89‡	−86.4			
	N—H_A	−88.10§†		+4.93§†		
	N—H_M	−92.48§†				
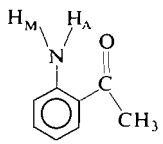	N—H_A	−99.25†	−90.8 ± 0.2	+7.61†	+4.9 ± 0.2	‖
	N—H_M	−87.76†	−89.5 ± 0.2			

*Microwave data used. See ref. 26.
†Planar amino group.
‡Microwave data used. See ref. 27.
§Standard geometries used; ref. 18, p. 110, 1.40 Å for C—N (24).
‖Present study.

problem 1 if it were not for its radioactivity. Some applications have been reported (30, 31). The second problem can of course be overcome by using ^{15}N enriched compounds ($I = \frac{1}{2}$). The third problem can be removed by drying samples with basic alumina (8, 9, 32) and NaOH (8, 9) or Na–K metal alloys (33).

2-Aminoacetophenone-^{15}N, (3)

At low temperatures (~ −70 °C) rotation about the C—N bond in **3** is slow on the n.m.r. time scale (34) and one observes an AMX type of

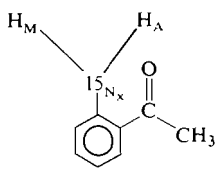

3

spectrum for the $^{15}NH_2$ moiety. For a 15 mol % sample of **3** in diethylether at approximately −90 °C, ν_A = 8.31 p.p.m. and ν_M = 6.21 p.p.m. from internal TMS, J_{AM} = 4.9 ± 0.2 Hz, J_{AX} = −90.8 ± 0.2 Hz, and J_{MX} = −89.5 ± 0.2 Hz. The sign of $^2J(H_A,H_M)$ relative to $^1J(^{15}N,H_A)$ and $^1J(^{15}N,H_A)$ was determined by standard heteronuclear tickling experiments (35). Irradiation of the highest frequency nitrogen transitions (10, 133, 937.1 Hz) perturbed the highest frequency peaks of the H_A and H_M doublets. The doublets referred to here are those due to the coupling $^2J(H_A,H_M)$. Irradiation of the lowest frequency nitrogen transitions (10, 133, 755.2 Hz) perturbed the lowest frequency peaks of the H_A and H_M doublets. These results indicate a positive ratio of the reduced couplings, $^1K(N,H)/^2K(H_A,H_M)$. Because $^1J(^{15}N,H)$ is negative, $^2J(H_A,H_M)$ is positive.

It is of interest to compare the chemical shifts of the amino protons in **3** at 20 °C with those observed at −90 °C. At 20 °C the amino protons resonate at approximately 6.75 p.p.m. to low field of TMS. This is 0.51 p.p.m. upfield from the average shift [(6.21 + 8.31)/2 = 7.26 p.p.m.] observed at −90 °C. Assuming that the chemical shift of the amino proton, H_M, is approximately temperature independent, then the chemical shift of H_A at 20 °C must be [6.75 + (6.75 − 6.21)] = 7.29 p.p.m. Thus proton H_A experiences a low-field shift of approximately 1.01

Can. J. Chem. Downloaded from www.nrcresearchpress.com by 210.87.254.6 on 09/05/12
For personal use only.

TABLE 3. Some compounds for which rotation of the $-NH_2$ group is slow

Compound	Solvent	$-{}^1J(^{15}N,H)$		$^2J(HNH)$	References
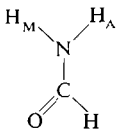	Acetone	$^{15}N-H_A$	89.7 Hz	+2.8 Hz	7
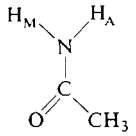	Acetone	$^{15}N-H_A$	89.2 87.6	2.5	41
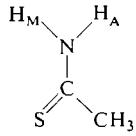	$CDCl_3$	$^{15}N-H_A$ $^{15}N-H_M$	91 94	5	42
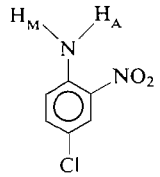	$CDCl_3$	$^{15}N-H_{av}$	91.1*	2.8	1
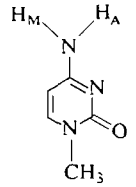	DMF-d_8	$^{15}N-H_{av}$	90*	2.8	43

*Only average $^1J(^{15}N,H)$ values were reported.

p.p.m./110 °C or 0.009 p.p.m./°C. Calculations by Muller and Reiter (36) predict a temperature dependence of the chemical shift of 0.002 to 0.008 p.p.m./°C for hydroxyl protons involved in hydrogen bonding to oxygen. These calculations have been experimentally confirmed by Schaefer and Kotowycz (37) and by Gramstad and Becker (38).[3] In **3** part of the apparent observed temperature dependence of the $N-H_A$ proton shift may arise from hydrogen bonding to ether by the $N-H_M$ proton and/or from changes in the conformation of the methyl–keto group and/or the amino group with temperature. Notice that at room temperature $^1J(^{15}N,H) = -89.0 \pm 0.5$ Hz, while at low temperature $^1J(^{15}N,H)_{av} = -90.1 \pm 0.4$ Hz.

[3]Gramstad and Becker (38) have observed values between 0.01 and 0.018 p.p.m./°C.

Our experimental results for **3** are similar to the ones recently observed for **4** by Negrebetskii, Bogdanov, and Kessenikh (39). For a solution of **4** in dimethylsulfoxide, $\nu_A - \nu_M = 1.56$ p.p.m., $^1J(^{15}N,H_A) = -91.0$ Hz, $^1J(^{15}N,H_M) = -92.3$ Hz, and $^2J(H_A,H_M) = +5.0$ Hz. It is

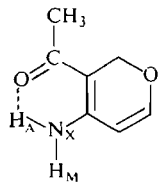

4

interesting that we observe $|^1J(^{15}N,H_A)| > |^1J(^{15}N,H_M)|$ in **3**, however, in qualitative agreement with theory. Solvent effects are probably responsible for this apparent discrepancy, the

Can. J. Chem. Downloaded from www.nrcresearchpress.com by 210.87.254.6 on 09/05/12
For personal use only.

Can. J. Chem. Downloaded from www.nrcresearchpress.com by 210.87.254.6 on 09/05/12
For personal use only.

dimethylsulfoxide molecule being a strong proton acceptor in hydrogen bonding (47).

Other examples where rotation of the amino group is slow and $^2J(HNH)$ values have been measured are formamide (7, 40), acetamide (41), thioacetamide (42), 4-chloro-2-nitroaniline (1), and 1-methylcytosine (43). The results are summarized in Table 3. The sign of $^2J(HNH)$ in formamide is positive. On the basis of the calculations described above for ammonia, aniline, and 2-aminoacetophenone, the relatively large and negative $^1J(^{15}N,H)$ values observed for the compounds in Table 3 indicate positive $^2J(HNH)$ values for these molecules.

Aniline and 2-Chloroaniline

By using deuterium substitution we had shown at 100 MHz that $^2J(HNH) \leq |1\text{ Hz}|$ in 2-chloroaniline (8) and ± 2 Hz in aniline (9). These results were confirmed by the 220 MHz proton spectra of the $^{15}NH_2$ and ^{15}NHD fragments of these compounds. Considering this result and the observed $^1J(^{15}N,H)$ values for aniline (−78.88 Hz, 17 mol % in benzene-d_6), and for 2-chloroaniline (−82.3 Hz, 10 mol % in benzene-d_6), it is reasonable to suggest $^2J(HNH)$ as negative in aniline.

$^2J(HXH)$ in Other Systems

It has been reported that $^2J(HPH)$ becomes more positive as the H—P—H bond angle increases (44). For example in PH_3 (H—P—H bond angle 93.9°), $^2J(HPH) = -13.3$ while in $^+PH_4$ (H—P—H bond angle 109.47°), $^2J(HPH) \leq |1.3|$ (44). Two-bond H—C—H fragments show a similar trend (45). In methane $^2J(HCH) = -12.5$ Hz, while in ethylene $^2J(HCH) = +2.4$ Hz.

Other Factors Affecting $^1J(^{15}N,H)$ and $^2J(HNH)$

Intrinsic Substituent Effects—Although changes in geometry probably account for most of the observed variations in these couplings, intrinsic substituent effects may be present. For example, in *p*-substituted toluenes where changes in the methyl group geometry are probably small, $^1J(^{13}C,H)$ varies from 127.2 Hz in *p*-nitrotoluene to 125.4 Hz in *p*-*t*-butyltoluene (46). The total variation of 1.4% is much less than that of 13.3% in $^1J(^{15}N,H)$ for the analogous anilines (6). On this basis intrinsic substituent effects could probably account for as much as 10% of the observed variation in $^1J(^{15}N,H)$ in a closely related set of molecules such as ring-substituted anilines.

Turning to $^2J(HNH)$, the calculated values for *planar* aniline and *o*-aminoacetophenone (Table 2) differ by less than 10%; while the experimental values differ widely, clearly reflecting the predominant effect on $^2J(HNH)$of the different geometry of the amino group in the two molecules. In 4-chloro-2-nitroaniline (Table 3) $^2J(HNH)$ is 2.8 Hz (assumed positive), rather less than the +5.2 Hz observed for *o*-aminoacetophenone. Rather than interpreting this as an intrinsic substituent effect, we prefer to assume that the amino group in the nitro compound is not completely planar. Indeed, i.r. data (47) on *o*-nitroaniline and *o*-acetophenone indicate substantially stronger hydrogen bonding in the latter compound (an HNH angle difference of 12° being implied).

Solvent Effects—$^1J(^{15}N,H)$ increases in magnitude in anilines as the polarity of the solvent rises (32) in a manner similar to $^1J(^{13}C,H)$ in chloroform (48), and is probably explained by the perturbations caused by intermolecular electric fields (49, 50). In fact, Axenrod and Wieder (51) propose the use of solvent effects on $^1J(^{15}N,H)$ in measuring the relative strengths of intramolecular hydrogen bonds in ortho-substituted anilines.

Similarly, in *o*-aminoacetophenone the internal electric field arising from the lone pair electrons of the carbonyl group could account for the larger magnitude of $^1J(^{15}N,H_A)$ for the intramolecularly hydrogen bonded proton than of $^1J(^{15}N,H_M)$ (Table 2). The opposite order of the magnitudes of these couplings (39) in **4** must then be caused by the strong intermolecular hydrogen bond to the dimethylsulfoxide solvent molecule.

In both **3** and **4** the intramolecular hydrogen bond involves the carbonyl group, but in **4** the solvent is the very polar dimethyl sulfoxide. Yet $^2J(HNH)$ has the same magnitude in **3** and **4**, suggesting a relatively small solvent effect on this coupling constant. But $^2J(HCH)$ is sensitive to solvent polarity (50) and due care should therefore be exercised when comparing $^2J(HNH)$ in different solvents.

Conclusions

In a series of closely related molecules, *e.g.*, substituted anilines, it is probably safe to use

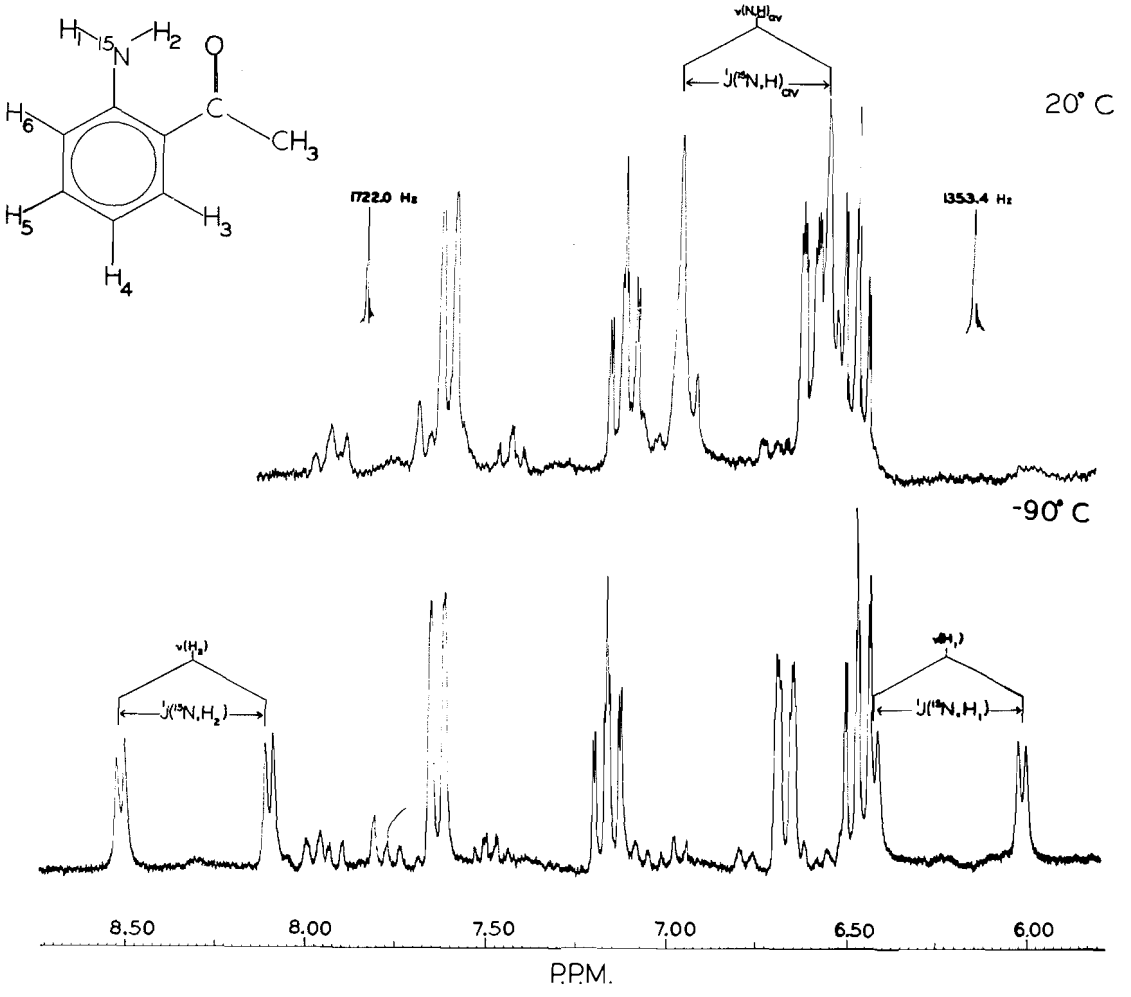

FIG. 4. The p.m.r. spectrum at 220 MHz of 2-aminoacetophenone-^{15}N as a 15 mol % solution in ether, the shift scale being relative to internal tetramethylsilane. At −90 °C the amino proton spectrum displays the 5.2 Hz coupling constant between these protons. The ring proton spectrum has been fully analyzed in ref. 9. The many small peaks arise from impurities introduced during the synthesis of the compound from aniline-^{15}N (9), enriched to 95 at. % in ^{15}N.

observed values of $^1J(^{15}N,H)$ and $^2J(HNH)$ in estimating the planarity of the $—NH_2$ fragment. Because of possible substituent and solvent effects the estimates of nitrogen planarity are at best semiquantitative, *i.e.* the calculation of HNH angles to the nearest 1° on the basis of observed $^1J(^{15}N,H)$ and $^2J(HNH)$ values is not recommended.

Ideally, all measurements should be carried out in a solvent which does not compete with substituents for hydrogen bonding to the N—H protons. In addition, the temperature of measurement should be low enough so that the amino group does not rapidly rotate about the C—N bond on the n.m.r. time scale.

The observed values of $^2J(HNH) = +4.9 \pm 0.2$ Hz and $^1J(^{15}N,H) = -90.8 \pm 0.2, -89.5 \pm 0.2$ Hz in 2-aminoacetophenone, together with previous estimates (9) of $^6J_p(NH,H) < |0.06|$ Hz, indicate that the amino group in 2-aminoacetophenone is very nearly coplanar with the aromatic ring.

On the basis of a comparison of experimental measurements with present calculations we predict that $^2J(HNH)$ is probably small and negative (−1.5 Hz) in aniline, while in 2-chloro-

Can. J. Chem. Downloaded from www.nrcresearchpress.com by 210.87.254.6 on 09/05/12
For personal use only.

Can. J. Chem. Downloaded from www.nrcresearchpress.com by 210.87.254.6 on 09/05/12
For personal use only.

aniline the coupling is probably very close to zero. The use of tritium substitution for the deduction of $^2J(HNH)$ values is suggested.

Experimental

The synthesis of 2-aminoacetophenone-^{15}N has been described (9). The diethylether solution, approximately 15 mol %, was degassed by the freeze–pump–thaw technique. Figure 4 displays the p.m.r. spectrum at 220 MHz at 20 °C and at −90 °C. The preparation of aniline-^{15}N and 2-chloroaniline -^{15}N samples containing the ^{15}NHD group has been given (9). Coupling constant measurements were made with either Varian HA-100 or Varian HR-220 spectrometers by methods similar to those described in detail before (9). The double resonance experiments were carried out on the HA-100 spectrometer. Computations were carried out using an IBM 360/65 computer.

We thank Dr. Ludger Ernst for preparing the sample of 2-aminoacetophenone-^{15}N, Dr. Herman J. C. Yeh for his assistance in measuring the sign of ^2J(H,H) in 2-aminoacetophenone, and Dr. Edwin Becker for several helpful comments concerning this manuscript. We are grateful to the National Research Council for financial assistance.

1. T. Axenrod. *In* Nitrogen NMR. G. Webb and M. Witanowski, *Editors*. Plenum Publishing Co., New York, N.Y. In press.
2. E. W. Randall and D. G. Gillies. *In* Progress in nuclear magnetic resonance spectroscopy. Vol. 6. J. W. Emsley, J. Feeney, and L. H. Sutcliffe (*Editors*). Pergamon Press, Oxford. 1971. p. 119.
3. R. L. Lichter. *In* Determination of organic structures by physical methods. Vol. 4. F. C. Nachod and J. J. Zucherman (*Editors*). Academic Press. 1971. p. 195.
4. R. A. Bernheim and H. Batiz-Hernandez. J. Chem. Phys. **40**, 3446 (1964).
5. G. Binsch, J. B. Lambert, B. W. Roberts, and J. D. Roberts. J. Am. Chem. Soc. **86**, 5564 (1964).
6. (*a*) T. Axenrod, P. S. Pregosin, M. J. Wieder, E. D. Becker, R. B. Bradley, and G. W. A. Milne. J. Am. Chem. Soc. **93**, 6536 (1971). (*b*) E. W. Randall and J. J. Zuckerman. Chem. Commun. **732**, 1966. (*c*) M. R. Bramwell and E. W. Randall. Chem. Commun. **250**, 1969. (*d*) W. J. Hehre, L. Radom, and J. A. Pople. Chem. Commun. **669**, 1972.
7. A. J. R. Bourn and E. W. Randall. Mol. Phys. **8**, 567 (1964).
8. R. Wasylishen and T. Schaefer. Can. J. Chem. **49**, 3627 (1971).
9. R. Wasylishen, J. B. Rowbotham, L. Ernst, and T. Schaefer. Can. J. Chem. **50**, 2575 (1972).
10. J. B. Stothers. Carbon-13 NMR spectroscopy. Academic Press, New York. 1972. Chapts. 9 and 10, and references therein.
11. (*a*) N. Muller and D. E. Pritchard. J. Chem. Phys. **31**, 768, 1471 (1959). (*b*) J. M. Shoolery. J. Chem. Phys. **31**, 1427 (1959).
12. H. S. Gutowsky and C. Juan. J. Chem. Phys. **37**, 2198 (1962).
13. H. M. McConnell. J. Chem. Phys. **24**, 460 (1956).
14. A. Saika. J. Chem. Phys. **45**, 2715 (1966).
15. V. M. S. Gil and J. J. C. Teixeira-Dias. Mol. Phys. **15**, 47 (1968).
16. D. M. Grant and W. M. Litchman. J. Am. Chem. Soc. **87**, 3994 (1965).
17. J. A. Pople and D. P. Santry. Mol. Phys. **8**, 1 (1963).
18. J. A. Pople and D. L. Beveridge. Approximate molecular orbital theory. McGraw–Hill Book Company, New York, N.Y. 1970.
19. M. Barfield. J. Chem. Phys. **48**, 4458, 4468 (1968).
20. J. A. Pople, J. W. McIver, Jr., and N. S. Ostlund. Chem. Phys. Lett. **1**, 465 (1967).
21. J. A. Pople, J. W. McIver, Jr., and N. S. Ostlund. J. Chem. Phys. **49**, 2960, 2965 (1968).
22. G. E. Maciel, J. W. McIver, Jr., N. S. Ostlund, and J. A. Pople. J. Am. Chem. Soc. **92**, 1, 11, 4151, 4497, 4506 (1970).
23. K. D. Summerhays and G. E. Maciel. Mol. Phys. **24**, 913 (1972).
24. R. Wasylishen and T. Schaefer. Can. J. Chem. **50**, 2989 (1972).
25. P. A. Helminger and W. Gordy. Phys. Rev. **188**, 100 (1969).
26. D. G. Lister and J. K. Tyler. Chem. Commun. 152 (1966).
27. C. C. Costain and J. M. Dowling. J. Chem. Phys. **32**, 158 (1960).
28. W. McFarlane and R. R. Dean. J. Chem. Soc. A, 1535 (1968).
29. Ch. Brevard, J. P. Kintzinger, and J. M. Lehn. Tetrahedron, **28**, 2429, 2447 (1972).
30. J. Bloxsidge, J. A. Elvidge, J. R. Jones, and E. A. Evans. Org. Magn. Resonance, **3**, 127 (1971).
31. D. E. Caddy, J. A. Elvidge, J. R. Jones, E. A. Evans, and J. C. Turner. Abstracts, 2nd. International Symposium on NMR Spectroscopy. Organized by the Chemical Society at the University of Surrey. July 3–7, 1972.
32. L. Paolillo and E. D. Becker. J. Magn. Resonance, **2**, 168 (1970).
33. K. L. Henold. Chem. Commun. 1340 (1970).
34. R. Wasylishen and T. Schaefer. Can. J. Chem. **49**, 3575 (1971).
35. W. McFarlane. *In* Determination of organic structures by physical methods. Vol. 4. F. C. Nachod and J. J. Zuckerman (*Editors*). Academic Press. 1971. p. 139.
36. N. Muller and R. C. Reiter. J. Chem. Phys. **42**, 3265 (1965).
37. T. Schaefer and G. Kotowycz. Can. J. Chem. **46**, 2865 (1968).
38. T. Gramstad and E. D. Becker. J. Mol. Struct. **5**, 253 (1970).

39. V. V. NEGREBETSKII, V. S. BOGDANOV, and A. V. KESSENIKH. J. Struct. Chem. (USSR), **12**, 649 (1972). English translation.
40. T. DRAKENBERG and S. FORSÉN. J. Phys. Chem. **74**, 1 (1970).
41. M. LILER. J. Magn. Resonance, **5**, 333 (1971).
42. W. WALTER, H. P. KUBERSKY, E. SCHAUMANN, and K.-J. REUBKE. Liebigs Ann. Chem. **719**, 210 (1968).
43. R. R. SHOUP, E. D. BECKER, and H. T. MILES. Biochem. Biophys. Res. Commun. **43**, 1350 (1971).
44. S. L. MANATT, E. A. COHEN, and A. H. COWLEY. J. Am. Chem. Soc. **91**, 5919 (1969).
45. J. A. POPLE and A. A. BOTHNER-BY. J. Chem. Phys. **42**, 1339 (1965).
46. C. H. YODER, R. H. TUCK, and R. E. HESS. J. Am. Chem. Soc. **91**, 539 (1969).
47. P. J. KRUEGER. Can. J. Chem. **40**, 2300 (1962).
48. D. F. EVANS. J. Chem. Soc. 5575 (1963).
49. M. BARFIELD and M. D. JOHNSTON, JR. Chem. Rev. **73**, 53 (1973).
50. S. L. SMITH. Top. Current Chem. **27**, 119 (1972).
51. T. AXENROD and M. J. WIEDER. J. Am. Chem. Soc. **93**, 3541 (1971).

Can. J. Chem. Downloaded from www.nrcresearchpress.com by 210.87.254.6 on 09/05/12
For personal use only.

Quantum Organic Photochemistry. IV. The Photoisomerization of Diimide and Azoalkanes[1]

N. Colin Baird and Jerrald R. Swenson

Photochemistry Unit, Department of Chemistry, University of Western Ontario, London, Ontario

Received April 10, 1973

Potential energy surfaces for the isomerization of diimide and azomethane in the ground, $^1(n,\pi^*)$, $^3(n,\pi^*)$, and $^3(\pi,\pi^*)$ states have been calculated by *ab initio* molecular orbital methods. Two mechanisms are considered in detail, the first involving in-plane motion of the substituent group and the second involving twisting about the N—N bond. The first mechanism is preferred for the ground and $^3(\pi,\pi^*)$ states, whereas the second mechanism is preferred for the (n,π^*) states. A significant barrier to rotation is predicted for the $^3(\pi,\pi^*)$ state. The vibrationally-relaxed (twisted) lowest triplet of diimide is predicted to lie 36 kcal mol^{-1} above the ground state.

Les surfaces d'énergie potentielle pour l'isomération de la diimide et de l'azométhane, dans les états fondamentaux $^1(n,\pi^*)$,^{3} (n,π^*) et $^3(\pi,\pi^*)$, ont été déterminées par les méthodes des orbitales moléculaires *ab initio*. Deux mécanismes ont été considérés en détail, le premier impliquant un mouvement dans le plan du substituant et le second, une torsion autour de la liaison N—N. On a préféré le premier mécanisme pour les états fondamentaux et $^3(\pi,\pi^*)$ tandis que le second mécanisme répond mieux aux états (n,π^*). Une barrière de rotation notable a été prévue pour l'état $^3(\pi,\pi^*)$. Le triplet de relaxation vibrationnelle (torsion) la plus basse est de 36 kcal mol^{-1} au-dessus de l'état fondamental selon nos prévisions.

[Traduit par le journal]

Can. J. Chem., **51**, 3097 (1973)

Introduction

cis–trans Isomerization is frequently observed in photochemical studies of azoalkanes. Using diimide, HNNH, as a model system for such compounds, one can imagine two simple mechanisms by which the isomerization can occur. In mechanism **I**, the affected hydrogen atom moves in the plane defined by the remaining atoms throughout the reaction; the transition state presumably occurs when the hydrogen atom lies approximately on the N—N axis. In

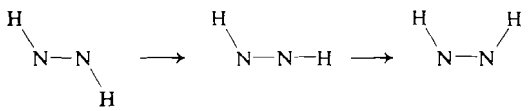

I

mechanism **II** the affected hydrogen atom rotates about the N—N bond such that the transition state corresponds to a conformation with equal HNN angles and a dihedral angle between the N—H bonds of approximately 90°.

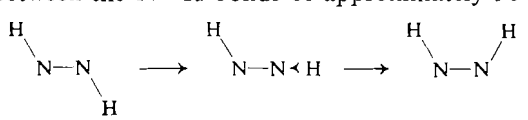

II

(A third possible mechanism, which involves a linear HNNH conformation in the transition state, can be eliminated from consideration on the basis of our own and previous (2, 3) *ab initio* calculations.)

Since a C_2 axis is preserved throughout mechanism **II**, orbital symmetry considerations (4) can be applied to predict the existence or absence of symmetry-imposed barriers in the isomerization. The important molecular orbitals to be considered are the N—N π and π^* orbitals and the lone pair orbitals on each nitrogen atom. The lone pairs will interact to yield a symmetric combination n_+, and an antisymmetric combination n_-. Since the through space interaction of the lone pairs in azo compounds is considerable, the two resulting MOs are well separated in energy; the n_+ combination lies above n_- for the *trans* isomer whereas n_- lies above n_+ for the *cis* (5) (see Fig. 1). Although the position of the π-bonding MO relative to n_+ and n_- is not intuitively obvious, both our calculations for HNNH and azomethane and the analysis of the photoelectron spectrum of *trans*-azomethane (6) place the π MO *between* the two "nonbonding" lone pair MO's. The completed orbital correlation diagram with the MOs labelled according to their behavior under C_2 is shown in Fig. 1.

[1]Publication No. 81 of the Photochemistry Unit. Research supported by the National Research Council of Canada. For Part III, see ref. 1.

Can. J. Chem. Downloaded from www.nrcresearchpress.com by 210.87.254.105 on 09/05/12
For personal use only.

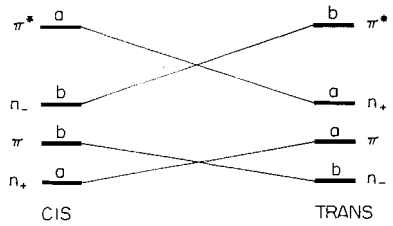

FIG. 1. Orbital correlation diagram for diimide.

Since the electron configuration $(n_-)^2(\pi)^2(n_+)^2$ for the *trans* ground state correlates with a doubly excited configuration of the *cis* isomer, rotation about the double bond is symmetry-forbidden in the ground state. In contrast, isomerization via twisting is an allowed reaction in the lowest (n,π^*) singlet and triplet states, since the configuration $(n_-)^2(\pi)^2(n_+)^1(\pi^*)^1$ of the *trans* isomer correlates with the $(n_+)^2(\pi)^2(n_-)^1(\pi^*)^1$ configuration of the *cis* isomer. Finally, the electron configuration for (π,π^*) states of the *trans* isomer, namely $(n_-)^2(\pi)^1(n_+)^2(\pi^*)^1$ correlates with the *doubly excited* configuration $(n_+)^1(\pi)^2(n_-)^1(\pi^*)^2$ of the *cis* isomer. Thus isomerization by twisting is a symmetry-forbidden process in the (π,π^*) states of diimide, in complete contrast to the situation in ethylene for which there should not only be no barrier to rotation, but in which the conformation with the methylene groups twisted 90° should represent a minimum in the (π,π^*) energy surfaces (7).

To test the predictions made above, and to determine the relative energetic and geometric demands for isomerization by mechanisms **I** and **II**, we have carried out *ab initio* molecular orbital calculations for the ground, $^1(n,\pi^*)$, $^3(n,\pi^*)$, and $^3(\pi,\pi^*)$ states of diimide and, to a lesser extent, of azomethane.

Method of Calculation

The wavefunctions have been determined by the closed shell SCF-LCAO-MO method of Roothaan (8). A minimal basis set of Slater type orbitals (STO's) was used to expand the molecular orbitals. Each s and p type STO was simulated by a linear combination of three Gaussian type orbitals using the STO-3G expansions of Pople and co-workers (9). Unless otherwise indicated, the energies of the excited states were evaluated from the ground state wavefunction with no configuration interaction (CI). Standard molecular exponents (9) were employed throughout except for the nitrogen $2p_\sigma$ STO exponent which was assumed to be 2.20 by analogy with optimized exponents for N_2 (10).

Results and Discussion

Ground-state Geometries and Isomerization Surfaces for Diimide and Azomethane

The potential energy surface for HNNH was explored with respect to the N—N distance, the H—N—N bond angle, and the dihedral angle between the two N—H bonds. (For simplicity, all N—H bond lengths were taken as 1.01 Å and the two H—N—N angles were assumed to be equal.) The absolute minimum in the surface occurs at the *trans* conformation (*i.e.* dihedral angle of 180°) with an H—N—N angle of 109° and a N—N bond length of 1.21 Å. The calculated geometry agrees very well with that deduced from an analysis of the i.r. spectrum of *trans* diimide, R_{N-N} = 1.238 Å, angle H—N—N = 109° (11). In parallel with our observations regarding the C—C distance in ethylene,[2] the agreement between the calculated and observed N—N distance is improved further if configuration interaction between the ground electronic configuration and the $(\pi)^0(\pi^*)^2$ configuration is included (R_{N-N} = 1.25 Å with CI).

Although the N—N bond length in *trans* diimide is close to that expected by analogy with the isoelectronic hydrocarbons (since the central bond distance increases by ~0.13 Å in going from a triple to a double bond in both cases), the H—N—N angle of 109° is much smaller than the H—C—C angle of 121° observed for ethylene. Our calculations predict, however, that the H—N—N angle opens appreciably to 115° at the second minimum in the potential surface which corresponds to an exactly planar *cis* conformation (R_{N-N} = 1.21 Å). The *cis* isomer is predicted to be less stable than the *trans* by 5 kcal mol^{-1}, in reasonable agreement with other calculations (2, 12). An even larger increase in bond angle in going from the *trans* to the *cis* geometry is predicted by a limited search of the potential surface for CH_3NNCH_3; using assumed values of 1.09 and 1.47 Å for the C—H and C—N bond distances, respectively, the optimum C—N—N angle for *trans* azomethane is predicted to be 113° (in excellent agreement with the experimental value (13) of 112°), whereas that for the *cis* conformation is predicted to be 122°. Presumably, relief of steric interactions between the alkyl groups in *cis* azo compounds provides the driving force for the greater *cis–trans* angle increase. Indeed, an

[2]N. C. Baird and R. F. Barr, unpublished calculations.

Can. J. Chem. Downloaded from www.nrcresearchpress.com by 210.87.254.105 on 09/05/12
For personal use only.

Can. J. Chem. Downloaded from www.nrcresearchpress.com by 210.87.254.105 on 09/05/12
For personal use only.

empirical correlation between the R—N—N bond angle and the predicted $^1(n,\pi^*)$ excitation energy of *cis* azo compounds suggests that the C—N—N angle in *cis*-azo-2-methyl-2-propane is approximately 131° (14). Unfortunately, there is no structural information available for any *cis* azoalkane with which to test this prediction of large C—N—N angles.

In order to evaluate activation energies for isomerization in the ground state of diimide, optimum geometries were obtained for the "idealized" transition states of mechanisms **I** and **II** (*i.e.* angle $N_A—N_B—H = 180°$ for **I**, dihedral angle = 90° for **II**). In agreement with the intuitive expectation that mechanism **I** requires only rehybridization at N_B but does not significantly affect either the N—N or the N_A—H bond, the optimum $H—N_A—N_B$ angle of 110° and the optimum N—N distance of 1.21 Å predicted for the type **I** transition state are very similar to those for the *trans* conformation. A plot of energy *vs.* $N_A—N_B—H$ angle yields a value of 182° (*i.e.* a quasi *trans* conformation) rather than 180° for the transition state, the point for 182° lying only 0.1 kcal mol^{-1} higher than for the idealized geometry.

The optimized geometry for the idealized transition state of mechanism **II** occurs for an H—N—N angle of 124° and an N—N distance of 1.24 Å; although the N—N bond distance is slightly longer than for the planar ground state, the increase is much less than in ethylene for reasons which will be discussed later. Using the "idealized" bond angle and bond length quoted above, the energy maximum in the potential energy curve for twisting (see curve *a* of Fig. 2) is found to occur at a dihedral angle between the N—H bonds of 98°; the energy at this angle is 9 kcal mol^{-1} more positive than at 90°. Since a level crossing occurs for the ground state in going from *trans* to *cis*, configuration interaction between the ground configuration and the $(n)^0(\pi^*)^2$ and $(\pi)^0(\pi^*)^2$ doubly excited configurations has been included in the determination of the potential energy curve for the ground state illustrated in Fig. 2.

The activation energy for isomerization via mechanism **I** is predicted to be significantly smaller than by mechanism **II** for both diimide and azomethane. The calculated activation energy for the *trans* to *cis* isomerization of diimide is 60 kcal mol^{-1} for mechanism **I** and 84 kcal mol^{-1} for mechanism **II**. These values are in reasonable agreement with the 50 and

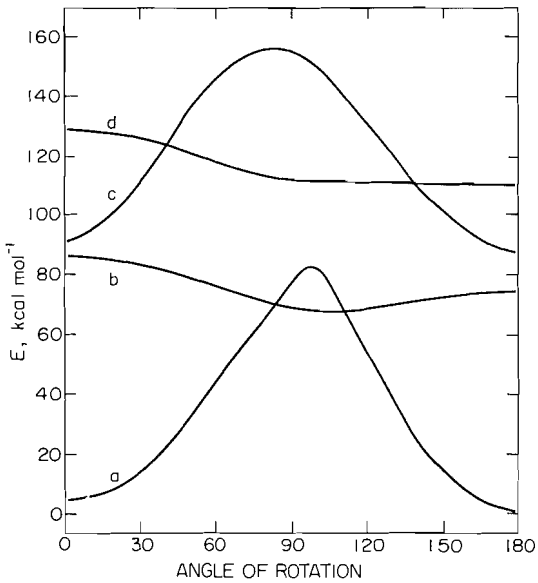

FIG. 2. Calculated potential energy curves for rotation about the N—N bond in diimide: (*a*) the ground state; (*b*) the $^3(n,\pi^*)$ state; (*c*) the $^3(\pi,\pi^*)$ state; (*d*) the $^1(n,\pi^*)$ state. The zero of the energy scale is the *trans* ground state.

84 kcal mol^{-1} values computed by Lehn and Munsch (3), especially considering their use of an idealized transition state for mechanism **II**. Dimethyl substitution is predicted to lower barriers to ~58 and ~78 kcal mol^{-1} for mechanisms **I** and **II**, respectively, according to prototype calculations on azomethane (using N—N distances appropriate to diimide). Unfortunately, there exist no experimental data for either diimide or azoalkanes with which to compare these predictions, since simple azoalkanes appear to decompose rather than isomerize thermally.[3] Our calculated activation energy of 60 kcal mol^{-1} for isomerization of diimide is consistent with this result, since the experimental activation energy for azomethane decomposition is only 50.2 kcal mol^{-1} (16).

Excited State Geometries, Energies, and Isomerization Pathways

The optimum H—N—N angles and N—N distances calculated for the lowest $^1(n,\pi^*)$, $^3(n,\pi^*)$, and $^3(\pi,\pi^*)$ states of diimide are listed in Table I for the *cis*, *trans*, idealized bent, and

[3]Difluorodiimide is known to isomerize thermally with an activation energy of 33.2 kcal mol^{-1} (15). However, since fluorine as a substituent may well act differently than hydrogen or methyl, it is difficult to compare our predictions with this result.

TABLE 1. Calculated geometries for diimide[a]

State	*trans*		*cis*		Bent		Twisted	
	R_{N-N}	Angle H—N—N	R_{N-N}	Angle H—N—N	R_{N-N}	Angle H—N—N	R_{N-N}	Angle H—N—N
Ground	1.21 (1.25)	109	1.21	115	1.21	110	1.24 (1.26)	124
$^1(n,\pi^*)$	1.26	121	1.22	133	1.24	116	1.22	127
$^3(n,\pi^*)$	1.26	120	1.22	132	1.24	118	1.26	117
$^3(\pi,\pi^*)$	1.42	105	1.42	114	1.38	108	1.36	128

[a]Bond distances in Å; bond angles in degrees. Values in parentheses refer to calculations which include Cl (see text).

idealized twisted conformations. The effect of (n,π^*) excitation upon the N—N bond distance in the planar geometries is rather small compared to the C—O bond elongation found for the (n,π^*) states of formaldehyde (17). The difference is due to the fact that whereas the highest occupied molecular orbital (HOMO) in formaldehyde is essentially C—O nonbonding, the HOMO in both *cis* and *trans* diimide is N—N *antibonding*. Thus, removal of an electron from the n_- MO of *cis* diimide increases the N—N overlap population by 0.21, an amount which almost compensates for the decrease of 0.29 due to single occupancy of the π^* MO. A greater increase in N—N distance is predicted for the *trans* conformation, since the HOMO of the ground state is less antibonding (−0.11) than for the *cis* conformation.[4] The large increase in the N—N distance predicted for the $^3(\pi,\pi^*)$ excitation is not unexpected, since the π bond is destroyed in the process.

Potential energy curves obtained from closed-shell calculations for isomerization by twisting (mechanism **II**) in these three excited states are shown in Fig. 2. In all cases the shape of the curves agrees qualitatively with that expected from the orbital symmetry arguments above and with that obtained by Kearns (18) from Huckel-like calculations. For the $^3(n,\pi^*)$ state the calculations predict no barrier to isomerization by twisting; indeed the minimum for this lowest triplet state occurs at a dihedral angle of 103°, at which point the energy is 7 kcal mol^{-1} lower than for the *trans* conformation according to calculations which employ ground state eigenvectors. Recalculation of this curve using the Roothaan open-shell method (19) leads to an even deeper minimum (of 14 kcal mol^{-1}) at 97° relative to the *trans* conformation; this value is very similar to the energy gain of 16 kcal mol^{-1} predicted for twisting ethylene by 90° in its $^3(\pi,\pi^*)$ state.[5] Note that the triplet curve crosses that for the singlet ground state for dihedral angles in this region. The existence of this crossing provides a rationalization for the failure to observe phosphorescence in simple azoalkanes (20). As the excited triplet molecule relaxes from the planar to the optimum twisted conformation, its energy approaches and eventually crosses that for the ground state. Such a situation should be particularly favorable for a T_1–S_0 radiationless transition.

In contrast to the behavior in the ground state, isomerization by the "allowed" twisting process (mechanism **II**) is much preferred energetically to mechanism **I** for both the $^3(n,\pi^*)$ and $^1(n,\pi^*)$ states of diimide. The energies required to reach the type **I** transition state are 25 and 23 kcal mol^{-1}, respectively, compared to the zero to reach the twisted conformation in both the triplet and singlet (n,π^*) states. Note, however, that *trans* to *cis* isomerization by mechanism **II** in the $^1(n,\pi^*)$ state should require a significant activation energy if the *trans* conformer is vibrationally relaxed, since the *cis* conformer is predicted to be significantly less stable than the *trans* in the $^1(n,\pi^*)$ state (see curve *d* of Fig. 2). As noted by Kearns (18) this effect should be accentuated in azo compounds due to additional destabilization of the *cis* conformation by steric effects.

The prediction that twisting in the $^3(\pi,\pi^*)$ state is a forbidden process is indeed substan-

[4]Ionization of the least tightly bound electron should result in a *decrease* in the central bond distance for diimide and azo compounds (particularly the *cis* conformations), an effect which is rare in polyatomic molecules.

[5]The value for ethylene is obtained using the same open-shell procedure.

Can. J. Chem. Downloaded from www.nrcresearchpress.com by 210.87.254.105 on 09/05/12
For personal use only.

Can. J. Chem. Downloaded from www.nrcresearchpress.com by 210.87.254.105 on 09/05/12
For personal use only.

tiated by the *ab initio* calculations; the *trans* to *cis* barrier is predicted to be 71 kcal mol^{-1} by mechanism **II** compared to 65 kcal mol^{-1} for mechanism **I**. Although no configuration interaction is included in the calculation of these values, it is most unlikely that the barriers would be altered substantially by CI since there exists no other low-lying triplet which is strongly coupled to the π,π^* triplet.

In summary, *ab initio* calculations confirm the orbital symmetry prediction that isomerization by twisting about a N=N bond is forbidden in the ground and $^3(\pi,\pi^*)$ states; in both cases isomerization via in-plane motion requires a lesser amount of activation energy. The orbital symmetry prediction that twisting is an allowed process in (n,π^*) states is also confirmed by the calculations; for such states isomerization via the in-plane motion requires a substantial amount of activation energy.

Finally, we have made an attempt to estimate the triplet energy of diimide. Since the calculation of a triplet energy involves comparing the energies of two different states, care must be taken to allow for the unequal correlation energies of the different states. The procedure followed here is the CI(PCMO) method developed by Buenker and Peyerimhoff (21). The ground state energy is that obtained after a limited configuration interaction with the two lowest doubly excited configurations, using eigenvectors appropriate to the ground state. The energy for the 90° twisted $^3(n,\pi^*)$ state is that obtained after configuration interaction with the three other configurations of the same symmetry obtained by single and double excitations among the four MO's shown in Fig. 1 and using an open-shell wavefunction for the $^3(n,\pi^*)$ state.[6] The O—O band S_0–T_1 transition energy deduced in this manner for *trans* diimide is 36 kcal mol^{-1}, a value which lies between those for the isoelectronic species O_2 and C_2H_4, but at an energy somewhat greater than the 14–18 kcal mol^{-1} range estimated by Kosower (22).

[6]The total energies for the planar ground state and twisted triplet are −108.6199 and −108.5627 a.u., respectively, which correspond to improvements of 0.0521 and 0.0316 a.u., respectively, due to the inclusion of CI.

1. N. C. Baird and R. M. West. Mol. Photochem. **5**, 209 (1973).
2. L. J. Schaad and H. B. Kinser. J. Phys. Chem. **73**, 1901 (1969).
3. J. M. Lehn and B. Munsch. Theor. Chim. Acta, **12**, 91 (1968).
4. R. B. Woodward and R. Hoffmann. Agnew. Chem. **81**, 797 (1969).
5. R. Hoffmann. Acc. Chem. Res. **4**, 1 (1971).
6. E. Haselbach and E. Heilbronner. Helv. Chim. Acta, **53**, 684 (1970).
7. A. J. Merer and R. S. Mulliken. Chem. Rev. **69**, 639 (1969).
8. C. C. J. Roothaan. Rev. Mod. Phys. **23**, 69 (1951).
9. W. J. Hehre, R. F. Stewart, and J. A. Pople. J. Chem. Phys. **51**, 2657 (1969).
10. B. J. Ransil. Rev. Mod. Phys. **32**, 245 (1960).
11. A. Trombetti. Can. J. Phys. **46**, 1005 (1968).
12. D. P. Wong, W. H. Fink, and L. C. Allen. J. Chem. Phys. **52**, 6291 (1970).
13. A. Almenningen, I. M. Anfinsen, and A. Haaland. Acta Chem. Scand. **24**, 1230 (1970).
14. N. C. Baird, P. de Mayo, J. R. Swenson, and M. C. Usselman. Chem. Commun. 314 (1973).
15. J. Binenboym, A. Burcat, A. Lifshitz, and J. Shamir. J. Am. Chem. Soc. **88**, 5039 (1966).
16. O. K. Rice and D. V. Sickman. J. Chem. Phys. **4**, 242 (1936).
17. G. Herzberg. Molecular spectra and molecular structure. Vol. III. Van Nostrand, Princeton, N.J. 1967. p. 612.
18. D. R. Kearns. J. Phys. Chem. **69**, 1062 (1965).
19. C. C. J. Roothaan. Rev. Mod. Phys. **32**, 179 (1960).
20. R. E. Rebbert and P. Ausloos. J. Am. Chem. Soc. **87**, 1847 (1965).
21. R. J. Buenker and S. D. Peyerimhoff. J. Chem. Phys. **53**, 1368 (1970).
22. E. M. Kosower. Acc. Chem. Res. **4**, 193 (1971).

Cimicine and Cimicidine, Lactonic Alkaloids from *Haplophyton cimicidum*

M. P. CAVA, M. V. LAKSHMIKANTHAM, AND S. K. TALAPATRA
Department of Chemistry, University of Pennsylvania, Philadelphia, Pa. 19174

AND

PETER YATES, I. D. RAE, M. ROSENBERGER, AND A. G. SZABO
Lash Miller Chemical Laboratories, University of Toronto, Toronto 5, Ontario

AND

B. DOUGLAS AND J. A. WEISBACH
Smith Kline and French Laboratories, Philadelphia, Pa. 19101

Received April 9, 1973

Evidence is presented in support of the stereostructures **4** and **5** for cimicine and cimicidine, respectively. Alkaloids **4** and **5**, as well as the lactonic bases aspidophytine (**23**) and haplophytine (**1**), are converted by alkaline hydrogen peroxide to the corresponding 10-oxo derivatives.

On présente des preuves qui justifient l'attribution des stéréostructures **4** et **5** à la cimicine et à la cimicidine, respectivement. Les alcaloïdes **4** et **5**, de même que les bases lactoniques aspidophytine (**23**) et haplophytine (**1**), sont transformés par l'action de péroxyde d'hydrogène alcalin en dérivés oxo-10.
[Traduit par le journal]

Can. J. Chem., **51**, 3102 (1973)

Can. J. Chem. Downloaded from www.nrcresearchpress.com by 210.87.254.42 on 09/05/12
For personal use only.

Haplophyton cimicidum (Apocynaceae) has been shown to contain a number of alkaloids of the aspidospermine type. Among these are the novel binuclear indole base haplophytine (**1**) (1–5), the carbinolamine-ether bases haplocine (**2**) and haplocidine (**3**) (6), and the carbinolamine-lactone bases cimicine (7) and cimicidine (1, 2, 7).[1] In this paper, evidence is presented in support of the stereostructures **4** and **5** for cimicine and cimicidine, respectively, and some additional chemistry of these alkaloids is discussed.

Cimicine, m.p. 229–231°, $[\alpha]_D$ +113° ($CHCl_3$), has the molecular formula $C_{22}H_{26}N_2O_4$. Its p.m.r. spectrum shows a number of points of similarity to that of its companion alkaloid haplocine (**2**) (6). Thus, neither base shows a peak attributable to either a methoxyl or an *N*-methyl group. Cimicine shows a strongly hydrogen-bonded hydroxyl at δ 10.70, analogous to that (δ 10.80) shown by haplocine. Furthermore, a three-proton triplet at δ 1.32 coupled to a two-proton quartet at δ 2.64 (J = 8 Hz) strongly suggested the presence in cimicine of an *N*-propionyl function similar to that found in haplocine. Both bases give a complex three-proton signal in the aromatic region. The u.v. spectra of cimicine and haplocine (Table 1) are very similar, both in neutral and in basic solution, suggesting the presence of the same chromophoric system in both compounds.

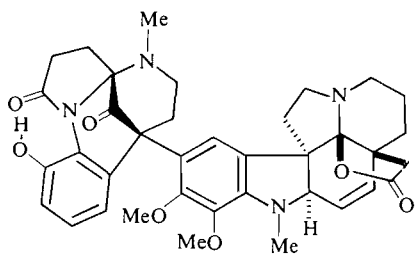

1

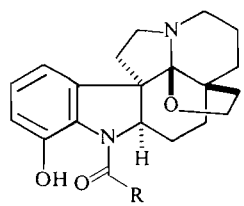

2 R = Et
3 R = Me

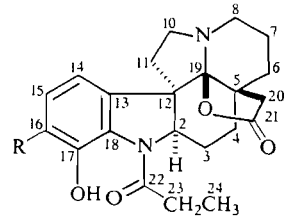

4 R = H
5 R = OMe

The KBr i.r. spectrum of haplocine shows a set of three bands attributable to the 7-hydroxy-

[1] A preliminary communication of part of this work has appeared (7).

TABLE 1. Ultraviolet spectra of cimicine and haplocine

	λ_{max}(EtOH)	ε_{max}
Cimicine (neutral)	221; 257; 295	31 700; 8630; 4600
(basic)	235; 260 (infl.); 311	23 000; 5750; 5180
Haplocine (neutral)	220; 260; 292	34 000; 8340; 4000
(basic)	235; 262 (infl.); 311	29 000; 6090; 5900

TABLE 2. The c.m.r. spectra of cimicine, cimicidine, and 10-oxocimicine[a]

Carbon[b]	δ[c,d] Cimicine	Cimicidine	10-Oxocimicine
2	67.0 (d)	67.7 (d)	66.9 (d)
3, 4, 7	20.0 (t), 24.6 (t)[e]	20.0 (t), 25.6 (t)[e]	18.7 (t), 23.5 (t) 24.4 (t)
5	40.2 (s)	40.3 (s)	40.6 (s)
6, 11	33.6 (t), 34.3 (t)	33.7 (t), 34.8 (t)	34.1 (t), 37.0 (t)
8, 20	42.2 (t), 43.3 (t)	42.3 (t), 43.5 (t)	41.4 (t), 42.3 (t)
10	48.1 (t)	48.3 (t)	172.5 (s)
12	58.5 (s)	58.0 (s)	53.0 (s)
13	137.8 (s)	137.2 (s)	134.4 (s)
14	118.2 (d)	114.5 (d)	119.8 (d)
15	128.3 (d)	110.3 (d)	129.1 (d)
16	115.0 (d)	149.9 (s)	115.4 (d)
17	146.9 (s)	129.6 (s)	147.5 (s)
18	127.2 (s)	128.0 (s)	127.4 (s)
19	106.1 (s)	106.3 (s)	100.1 (s)
21	175.4 (s)	175.6 (s)	172.8 (s)
22	172.2 (s)	172.2 (s)	172.1 (s)
23	28.0 (t)	28.2 (t)	28.4 (t)
24	9.4 (q)	9.5 (q)	9.5 (q)
OCH_3	—	56.2 (q)	—

[a]The c.m.r. spectra were recorded in deuteriochloroform at 25.16 MHz with a Varian XL-100-15 instrument operating in the pulsed Fourier transform mode.
[b]See structures 4 and 5 for the numbering system.
[c]Chemical shift values (δ) are reported in p.p.m. downfield from tetramethylsilane as internal standard. The multiplicities of the signals, determined by comparison of random noise-decoupled spectra with off-resonance partially decoupled spectra, represent coupling between the carbon atom and the protons that are directly bonded to it.
[d]*Cf.* second and third footnotes.
[e]Superimposed signals.

N-acyldihydroindole chromophore, at 6.15, 6.24, and 6.37 μ; the corresponding spectrum of cimicine shows the same three bands at identical positions, as well as a split carbonyl band at 5.63 and 5.71 μ. In chloroform solution, the latter band appears at 5.65 (sh) and 5.72 μ.

The spectral relationships between haplocine and cimicine, combined with a consideration of their molecular formulas, suggested that cimicine is an oxo derivative of haplocine. The position of the shorter-wavelength carbonyl band of cimicine and the fact that cimicine, but not haplocine, is soluble in dilute aqueous alkali, led to the γ-lactone formulation **4** for cimicine. Direct confirmation of this structure was obtained by chromic oxide – pyridine oxidation of (+)-haplocine, which gave (+)-cimicine, albeit in low yield.

The stereostructure **2** has been established for haplocine by direct chemical correlation with the alkaloids limaspermine, palosine, and aspidospermine (8). The conversion of (+)-haplocine to (+)-cimicine thus establishes the stereostructure **4** for natural cimicine.

The c.m.r. spectrum of cimicine (Table 2) is in good accord with this structural assignment. Low-field singlets at δ 172.2 and 175.4 can be assigned to the *N*-propionyl and lactone carbonyl carbon atoms, respectively,[2] and six signals in

[2]The individual assignment of the carbonyl carbon signals are based on comparison with the spectrum of 10-oxocimicine (*vide infra*).

Can. J. Chem. Downloaded from www.nrcresearchpress.com by 210.87.254.42 on 09/05/12
For personal use only.

Can. J. Chem. Downloaded from www.nrcresearchpress.com by 210.87.254.42 on 09/05/12
For personal use only.

the δ 115–150 region are assignable to the aromatic carbon atoms. A singlet at δ 106.1 can be assigned to C-19, the sp^3-carbon atom of the carbinolamine lactone function; a similar signal is present in the spectrum of haplophytine. Two signals in the δ 50–100 region at δ 67.0 and 58.5 are assignable on the basis of their chemical shifts and multiplicities to C-2 and -12, respectively. The remaining signals can be assigned on a like basis as shown in Table 2.[3]

The molecular formula $C_{23}H_{28}N_2O_5$, proposed earlier for cimicidine (1), has now been confirmed by mass spectrometry (m.s.). The i.r. spectrum of cimicidine in KBr shows carbonyl bands at 5.65, 5.70, and 6.15 μ corresponding to those of cimicine; in chloroform solution, the short-wavelength doublet appears at 5.64 and 5.72 μ. The p.m.r. spectrum of cimicidine resembles that of cimicine in that it shows the absence of an *N*-methyl signal, and the presence of signals attributable to a hydrogen-bonded hydroxyl (at δ 10.75) and an *N*-propionyl group (a three-proton triplet at δ 1.32 (J = 8 Hz) and a two-proton quartet at δ 2.64 (J = 8 Hz). In contrast to the p.m.r. spectrum of cimicine, however, that of cimicidine shows a methoxyl signal at δ 3.87. The δ 3.87 peak represents four protons, the fourth proton corresponding to the C-2 hydrogen, whose signal is discernible at δ 3.98 in the spectrum of cimicine. Finally, the p.m.r. spectrum of cimicidine shows only two aromatic proton signals in the form of an AB quartet at δ 6.73 and δ 7.02 (J = 8 Hz). All of the above data are in accord with the assignment of either a 14- or a 16-methoxycimicine structure to cimicidine. The latter structure, **5**, is strongly favored because of the frequent occurrence of 16-oxygenated aspidospermine-type alkaloids, *e.g.*, aspidocarpine (9), aspidolimidine (10), aspidoalbine (11), and pyrifolidine (12), and the absence of reports of the occurrence in nature of 14-oxygenated alkaloids of this type. Also, the appreciable chemical shift between the aromatic proton signals is in better accord with the 16-methoxycimicine formulation. The above data, together with the dextrorotatory nature of both cimicine and cimicidine, lead to the stereostructure **5** for cimicidine.

As expected, the c.m.r. spectrum of cimicidine closely resembles that of cimicine (Table 2), except for the presence of a quartet at δ 56.2, arising from the methoxyl carbon, and changes in the aromatic carbon region associated with the introduction of the methoxyl substituent.

In the course of the original investigation of cimicidine, catalytic hydrogenation of the alkaloid was reported to give a dihydrocimicidine (2). We have confirmed this observation, and we formulate dihydrocimicidine as the zwitterionic structure **7**. The carboxylate anion of **7** gives rise to an i.r. band at 6.13 μ. As expected, the hydrochloride (**10**) of **7** contains an unionized carboxyl group, which gives rise to a band at 5.83 μ that shifts to shorter wavelength (5.78 μ) on conversion to the methyl ester **11**. The closely related cimicine is reduced either catalytically or by sodium borohydride to the analogous dihydro derivative **6**. Dihydrocimicine (**6**), its hydrochloride (**8**), and its methyl ester (**9**) show carbonyl bands at the same positions as those of the corresponding cimicidine derivatives. The hydrogenolysis of the carbinolamine lactone system of cimicine and cimicidine is analogous to the reduction of carbinolamine ethers, *e.g.*, the reductive cleavage of haplocine (**2**) to limaspermine (6, 8); the assignment of configuration at C-19 is based on this analogy.

Snyder *et al.* have reported that both haplophytine and cimicidine react with alkaline hydrogen peroxide to give transformation products containing an additional oxygen and two fewer hydrogen atoms (2). We now propose that these compounds are 10-oxohaplophytine (**12**) and 10-oxocimicidine (**13**), respectively.

In view of the relative abundance of cimicine as compared to cimicidine, the alkaline hydrogen peroxide oxidation of cimicine was chosen by us for detailed study. A solution of cimicine (**4**) in dilute aqueous base reacted slowly with hydrogen peroxide to give a precipitate of a new, neutral compound, 10-oxocimicine (**14**). In accord with this formulation, **14** showed carbonyl absorptions at 5.56 μ (γ-lactone), 5.82 μ (γ-lactam), and 6.14 μ (*N*-propionyl group). The γ-lactam carbonyl band of the closely related *O*-methyl-N_a-acetyl-10-oxoaspidoalbine (**17**) appears at 5.88 μ (11). Proof that the phenolic hydroxyl of cimicine is intact in the hydrogen peroxide oxidation product was obtained by converting the latter into its *O*-methyl derivative (**15**) and into its *O*-acetyl derivative (**16**).

The p.m.r. spectrum of **14** resembles that of cimicine, but shows a two-proton multiplet in

[3]There are ambiguities in the assignment of some close-lying signals.

Can. J. Chem. Downloaded from www.nrcresearchpress.com by 210.87.254.42 on 09/05/12
For personal use only.

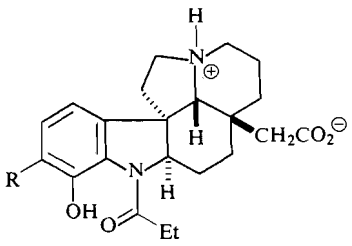

6 R = H
7 R = OMe

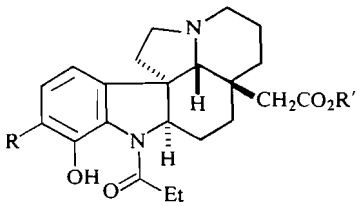

8 R = R′ = H (HCl salt)
9 R = H, R′ = Me
10 R = OMe, R′ = H (HCl salt)
11 R = OMe, R′ = Me

the δ 3.8–4.3 region in contrast to the one-proton multiplet at δ 4.0 in the latter spectrum attributed to the proton at C-2. The additional signal in the spectrum of **14** is assigned to one of the C-8 protons, which lies in the plane of the carbonyl group at C-10.[4] The c.m.r. spectrum of **14** (Table 2) resembles that of cimicine, except for the replacement of the C-10 methylene carbon triplet at δ 48.1 by a lactam carbonyl carbon singlet at δ 172.5. There are also significant upfield shifts of the signals assignable to C-12, -19, -21; these shifts can be accounted for in terms of the interpretation given below of the effect engendered by introduction of the 10-oxo group on the i.r. spectrum of cimicine.

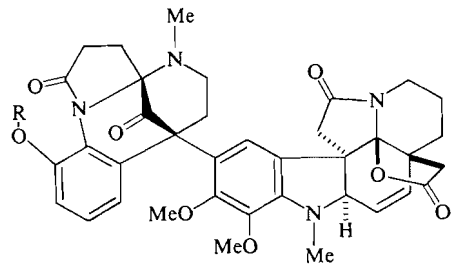

12 R = H
23 R = Me
24 R = Ac

[4]Analogous signals are present in the spectra of **15**, **16**, 10-oxohaplophytine and its derivatives, and 10-oxoaspidophytine (*vide infra*).

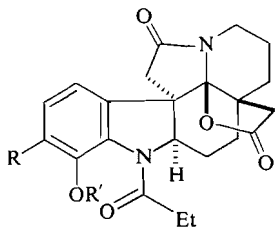

13 R = OMe, R′ = H
14 R = R′ = H
15 R = H, R′ = Me
16 R = H, R′ = Ac

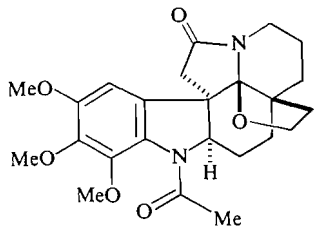

17

Brief comment may be made concerning the relative positions of the γ-lactone carbonyl bands of cimicine and 10-oxocimicine. The lactone band of 10-oxocimicine (**14**) appears at 5.56 μ, or at somewhat shorter wavelength than the usual γ-lactone range (5.62–5.68 μ) (13). The corresponding lactone carbonyl band of cimicine by contrast appears at the abnormally long wavelength value of 5.72 μ, despite the fact that the inductive effect of the adjacent carbinolamine nitrogen might be expected to *shorten* the lactone carbonyl wavelength. We suggest, therefore, that the position of the cimicine lactone carbonyl reflects a contribution from the open-chain dipolar canonical form **18**, as shown below. Resonance of this type would be expected to be inhibited in the case of 10-oxocimicine, since the positive nitrogen of the dipolar form (**19**) would be adjacent to a carbonyl carbon.

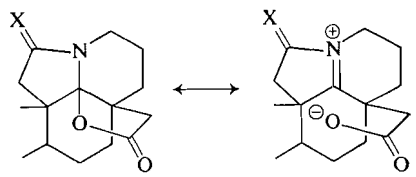

18 X = H_2
19 X = O

A plausible mechanism for the conversion of

cimicine (**4**) to 10-oxocimicine (**14**) is outlined below:

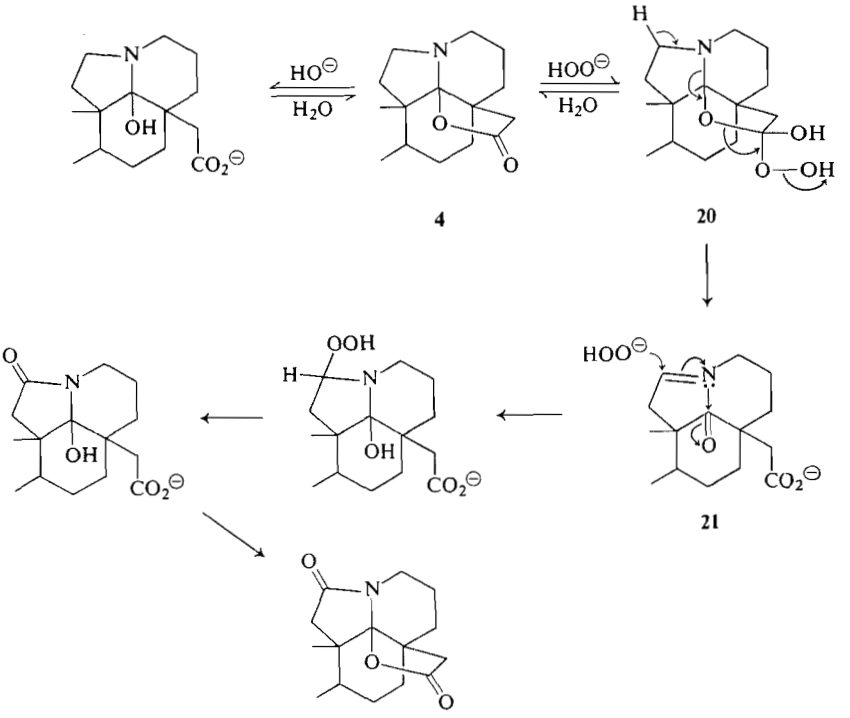

The initial steps involve addition of hydroperoxide anion to the lactone carbonyl giving **20** and fragmentation of the pyrrolizidine system. Addition of hydroperoxide anion to the resulting imine **21** can take place with transannular attack on the ketonic carbonyl. Elimination of water from the α-hydroperoxy amine and lactonization complete the reaction sequence.

Two features of this mechanism require comment. First, the selective elimination of the proton from C-10 in intermediate **20**, rather than from C-8, is in accord with the fact that Dreiding models show that only the former elimination process can take place via a coplanar transition state. Second, the initial hydroperoxide attack is pictured as taking place on the lactone system in an alkaline solution, a medium in which no free lactone might be expected to survive. The presence of a small amount of cimicine in equilibrium with the ring-opened carboxylate form in aqueous base can be proven experimentally, however, by the slow extraction of cimicine by organic solvent from an aqueous alkaline solution. Precedent exists for the closure of a γ-lactone ring in an aqueous basic medium (14).[5]

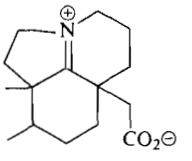

22

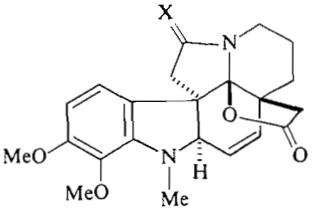

25 X = H_2
26 X = O

The hydrogen peroxide oxidation product of haplophytine (**1**) may be assigned the structure 10-oxohaplophytine (**12**) on the assumption that, as in the case of cimicine, oxidation takes place in the neighborhood of the carbinolamine lac-

[5]The imine **21** might also arise by attack of hydroperoxide anion on a small amount of the immonium ion **22** in equilibrium with **4**, followed by fragmentation.

Can. J. Chem. Downloaded from www.nrcresearchpress.com by 210.87.254.42 on 09/05/12
For personal use only.

Can. J. Chem. Downloaded from www.nrcresearchpress.com by 210.87.254.42 on 09/05/12
For personal use only.

tone system. In confirmation of this assignment, oxohaplophytine gives a methyl ether (**23**) and an acetyl derivative (**24**), showing that the phenolic function of haplophytine has survived the oxidation. Furthermore, acid cleavage of oxohaplophytine does not yield aspidophytine (**25**) (4, 5) as does haplophytine, but rather a compound assigned the structure 10-oxoaspidophytine (**26**). As expected, alkaline peroxide oxidation of aspidophytine also afforded 10-oxoaspidophytine, the spectral properties of which showed it to be closely analogous to 10-oxocimicine (**14**).

Experimental

Cimicine (4) and Cimicidine (5)

The alkaloid mixture (1) (100 g) from *Haplophyton cimicidum* was stirred twice with distilled water (1500 ml) for 6 h at room temperature, and the mixture was filtered (5). The combined aqueous filtrates were extracted with chloroform (5 × 200 ml), and the extract was dried and evaporated to give a semi-crystalline residue (60–70 g). This was dissolved in absolute ethanol (2 l), and the material that crystallized was recrystallized five times from absolute ethanol to give cimicine (**4**; *ca.* 10 g), m.p. 229–231°; $[\alpha]_D$ +113° ($CHCl_3$); λ_{max} (KBr) 5.63, 5.71, 6.15 μ; λ_{max} (EtOH) (ε) 221 (31 700), 257 (8630), 295 (4600) nm; λ_{max} (EtOH–NaOH) (ε) 235 (23 000), 260 (infl., 5750), 311 (5180) nm; δ 1.32 (t, J = 8 Hz, 3 H), 2.64 (q, J = 8 Hz), 3.98 (m, 1 H), 6.8–7.2 (m, 3 H), 10.70 (s, 1 H); *m/e* 382, 338.

Anal. Calcd. for $C_{22}H_{26}N_2O_4$: C, 69.09; H, 6.85; N, 7.33. Found: C, 69.30; H, 6.58; N, 7.45.

The mother liquor from the first crop of cimicine was concentrated to two-thirds volume; on standing the solution deposited a mixture of cimicine and cimicidine (7:3, as estimated by p.m.r. spectroscopy). This was fractionally crystallized from acetone followed by final crystallization from ethanol to give cimicidine (**5**; *ca.* 1.0 g), m.p. 266–268° dec. (lit. (1) m.p. 268–270° dec.); λ_{max} (Nujol) 5.65 (sh), 5.70, 6.15 μ; λ_{max} (EtOH) (ε) 228 (23 900), 262 (7300), 293 (infl., 1500) nm; λ_{max} (EtOH–NaOH) (ε) 234 (21 900), 308 (4900) nm; δ ($CDCl_3$) 1.32 (t, J = 8 Hz, 3 H), 2.64 (q, J = 8 Hz), 3.87 (s, 3 H), 3.8–4.2 (m, 1 H), 6.73 (d, J = 8 Hz, 1 H), 7.02 (d, J = 8 Hz, 1 H), 10.75 (s, 1 H); *m/e* 412, 368.

Anal. Calcd. for $C_{23}H_{28}N_2O_5$: C, 66.97; H, 6.84; N, 6.79. Found: C, 66.61 H, 6.84; N, 6.87.

Oxidation of Haplocine to Cimicine

To a solution of haplocine (65 mg) in dichloromethane (10 ml) was added a solution of Collins' reagent (15) (700 mg) in dichloromethane. A red-brown solid precipitated at once. After 10 min the mixture was treated with ammonia, and the organic layer was separated after filtration through a Celite pad. The residue (42 mg) from evaporation of the organic layer was treated with aqueous 10% sodium hydroxide and the mixture was shaken with ether to remove non-lactonic material; the aqueous layer was made just acid, then basified with ammonia, and extracted with dichloromethane. The residue (28 mg) was subjected to t.l.c. on basic silica with development with chloroform – 10% methanol. Extraction of the band with the same R_f as that of cimicine yielded 6 mg of cimicine, m.p. 228–230° (identified by spectral comparison); $[\alpha]_D$ +82° ($CHCl_3$).

Reduction of Cimicine: Formation of Dihydrocimicine (6)

Cimicine (564 mg) in absolute ethanol (30 ml) was hydrogenated over prereduced platinum oxide (50 mg) at room temperature and atmospheric pressure. After 40 min 1.1 mol. equiv. of hydrogen had been taken up, and a fluffy solid had separated from solution. The solid was filtered and dissolved in methanol. The solution was filtered to remove the catalyst and concentrated to give dihydrocimicine (**6**). Two recrystallizations from methanol yielded the pure compound (140 mg), m.p. 266–270° dec.; λ_{max} (Nujol) 3.8 (br), 6.13 μ.

Anal Calcd. for $C_{22}H_{28}N_2O_4$: C, 68.72; H, 7.34; N, 7.29. Found: C, 68.31; H, 7.59; N, 7.64.

The *hydrochloride* was obtained as a glass; λ_{max} (Nujol) 3.8 (br), 5.82, 6.15 μ. The *methyl ester*, prepared by treatment of the hydrochloride with ethereal diazomethane, had m.p. 193–197°; λ_{max} ($CHCl_3$) 5.78, 6.14 μ; *m/e* 398, 168.

Dihydrocimicine was also obtained by reduction of cimicine (100 mg) in methanol (10 ml) with sodium borohydride (100 mg) for 10 h at room temperature. Addition of water (10 ml) and acetic acid (2 drops), extraction with chloroform (3 × 25 ml), and evaporation of the extract gave a semi-crystalline residue. Crystallization from methanol gave dihydrocimicine as a microcrystalline solid, m.p. 265–267° dec., identical with the hydrogenation product from cimicine.

Hydrogenation of Cimicidine: Formation of Dihydrocimicidine (7)

Cimicidine was hydrogenated by the method of Snyder *et al.* (2) to give the dihydrate of dihydrocimicidine, m.p. 265–267° dec. (lit. (2) m.p. 262–264° dec.); λ_{max} (Nujol) 3.0 (br), 3.7 (br), 6.13, 6.30 μ. The *hydrochloride*, m.p. *ca.* 255° dec. (lit. (2) m.p. 245–260° dec.), had λ_{max} (Nujol) 3.9 (br), 5.83, 6.13 μ. The *methyl ester* was obtained as an amorphous solid; λ_{max} ($CHCl_3$) 5.78, 6.14 μ; *m/e* 428, 168.

Oxidation of Cimicine with Alkaline Hydrogen Peroxide: Formation of 10-Oxocimicine (14)

Cimicine (1.00 g) was dissolved in aqueous 1% sodium hydroxide (50 ml) and treated with 30% hydrogen peroxide (20 ml). The mixture was stirred at 0° for 1 h and at room temperature for a further 2 h. The solid that separated was filtered, and a further 20 ml of 30% hydrogen peroxide was added to the filtrate. The mixture was stirred for 5 h at room temperature, and the additional solid that separated was filtered and combined with the first crop (total: 520 mg). The crude product was crystallized from ethanol to give 10-oxocimicine (480 mg) as needles, m.p. 297–299°, λ_{max} (Nujol) 5.56, 5.82, 6.14 μ; λ_{max} (EtOH) (ε) 220 (20 500), 256 (5900), 294 (1800) nm; λ_{max} (EtOH–NaOH) (ε) 234 (19 400), 259 (infl., 5100), 315 (4700) nm; δ ($CDCl_3$) 1.23 (t, J = 8 Hz, 3 H), 3.8–4.3 (m, 2 H), 6.8–7.2 (m, 3 H), 10.55 (s, 1 H); *m/e* (relative abundance) 396 (50), 340 (100).

Can. J. Chem. Downloaded from www.nrcresearchpress.com by 210.87.254.42 on 09/05/12
For personal use only.

Anal. Calcd. for $C_{22}H_{24}N_2O_5$: C, 66.65; H, 6.10; N, 7.07. Found: C, 66.35; H, 6.12; N, 7.13.

The aqueous filtrate was concentrated to 10 ml, cooled in an ice bath, and acidified with concentrated hydrochloric acid. The precipitate thus obtained was dried to yield a white granular solid; λ_{max} (Nujol) 2.85, 2.96, 3.9 (br), 5.9, 6.2 μ. Crystallization of this product from ethanol converted it to 10-oxocimicine (188 mg).

*O-Methyl-10-oxocimicine (**15**)*

10-Oxocimicine was methylated with ethereal diazomethane; the product was crystallized from ethanol to give the *O*-methyl derivative, m.p. 243–245°; λ_{max} (Nujol) 5.59, 5.82, 6.06 μ; δ ($CDCl_3$) 1.15 (t, J = 8 Hz, 3 H), 3.87 (s, 3 H), 3.8–4.6 (m, 2 H), 6.8–7.3 (m, 3 H).

Anal Calcd. for $C_{23}H_{26}N_2O_5$: C, 67.30; H, 6.39; N, 6.83. Found: C, 67.33; H, 6.38; N, 6.97.

*O-Acetyl-10-oxocimicine (**16**)*

Acetylation of 10-oxocimicine with acetic anhydride and pyridine for 6 h at room temperature followed by crystallization of the product from ethanol gave the *O*-acetyl derivative, m.p. 257–260°; λ_{max} (Nujol) 5.56 (sh), 5.64, 5.80, 5.97 μ; δ ($CDCl_3$) 1.17 (t, J = 8 Hz, 3 H), 2.25 (s, 3 H), 3.9–4.3 (m, 2 H), 7.0–7.6 (m, 3 H); *m/e* 438.

*Oxidation of Haplophytine with Alkaline Hydrogen Peroxide: Formation of 10-Oxohaplophytine (**12**)*

Haplophytine (1.00 g was dissolved in aqueous 1% sodium hydroxide (50 ml) and treated with 30% hydrogen peroxide (50 ml). The temperature of the solution was maintained at 15° throughout the course of the reaction. The solid that separated was filtered after 1, 2, 4, 7, and 24 h and air dried (total: 410 mg). The crude product was recrystallized from ethanol to give 10-oxohaplophytine, m.p. 220–222° and 268° dec. (lit. (16) m.p. 216–219° and 250–260° dec.); λ_{max} ($CHCl_3$) 5.62, 5.72, 5.88, and 6.05 μ; λ_{max} (EtOH) (ε) 220 (51 200), 268 (15 500), 307 (4000) nm; δ ($CDCl_3$) 2.43 (s, 3 H), 2.98 (s, 3 H), 3.17 (s, 3 H); 3.65 (s, 3 H), 4.02 (d of d, J = 10, 2 Hz, 1 H), 5.60 (d, J = 11 Hz, 1 H), 5.97 (d of d, J = 11, 2 Hz, 1 H), 6.27 (d of d, J = 8, 2 Hz, 1 H), 6.9–7.2 (m, 3 H), 8.94 (s, 1 H)[6] (together with peaks arising from ethanol of solvation); *m/e* (relative abundance) 666.2659 (13; M^+ = 666.2690), 638.2802 (100; M − CO = 638.2741).

Anal. Calcd. for $C_{37}H_{38}N_4O_8.2C_2H_5OH$: C, 64.91; H, 6.60; N, 7.39. Found: C, 65.02; H, 6.37; N, 7.61.

A sample, m.p. 222–224° and 255° dec., crystallized from benzene also tenaciously retained solvent.

Anal. Calcd. for $C_{37}H_{38}N_4O_8.0.75\ C_6H_6$: C, 68.72; H, 5.91; N, 7.73. Found: C, 68.73; H, 5.99; N, 7.43.

*O-Methyl-10-oxohaplophytine (**23**)*

10-Oxohaplophytine in benzene–methanol was methylated with excess of ethereal diazomethane for 7 days with additions of fresh ethereal diazomethane after 2, 4, and 5 days. The crude product obtained after removal of the solvents was crystallized from ethanol to give the *O*-methyl derivative, m.p. 252–255° dec.; λ_{max} ($CHCl_3$) 5.61, 5.73 (sh), 5.85 μ; δ ($CDCl_3$) 2.47 (s, 3 H), 3.08 (s, 3 H), 3.18 (s, 3 H), 3.65 (s, 3 H), 3.75 (m, 1 H), 3.95 (s, 3 H), 4.15 (m, 1 H), 5.68 (d of d, J = 11, 1 Hz, 1 H), 6.02 (d of d, J = 11, 2 Hz, 1 H), 6.28 (d of d, J = 7, 2 Hz, 1 H), 6.8–7.3 (m, 3 H); *m/e* 680.

Anal. Calcd. for $C_{38}H_{40}N_4O_8.1.5\ H_2O$: C, 64.48; H, 6.12; N, 7.92. Found: C, 64.56; H, 6.06; N, 8.02.

*O-Acetyl-10-oxohaplophytine (**24**)*

10-Oxohaplophytine was acetylated with acetic anhydride and pyridine at reflux for 40 min. The crude product obtained after dilution with water, adjustment of the p*H* to 8 with aqueous 10% sodium bicarbonate, and extraction with dichloromethane was crystallized from aqueous ethanol to give the *O*-acetyl derivative, m.p. 287–289° dec.; λ_{max} ($CHCl_3$) 5.64, 5.72, 5.85 μ; λ_{max} (EtOH) (ε) 219 (54 000), 263 (13 900), 304 (3800) nm; δ 2.27 (s, 3 H), 2.47 (s, 3 H), 2.98 (s, 3 H), 3.14 (s, 3 H), 3.60 (s, 3 H), 3.7 (m, 1 H), 4.0 (br d, J = 12 Hz, 1 H), 5.60 (br d, J = 11 Hz, 1 H), 5.95 (d of d, J = 11, 2 Hz, 1 H), 6.55 (m, 1 H), 7.0–7.3 (m, 3 H).

Anal. Calcd. for $C_{39}H_{40}N_4O_9$: C, 66.10; H, 5.65; N, 7.91. Found: C, 65.79; H, 5.76; N, 7.87.

*Acid Cleavage of 10-Oxohaplophytine: Formation of 10-Oxoaspidophytine (**26**)*

A solution of 10-oxohaplophytine (320 mg) in 6 *N* hydrochloric acid (10 ml) was heated on the steam bath for 1 h under nitrogen. The solution was then cooled and basified with ammonia. The precipitated solid was extracted into chloroform. The extract was dried and evaporated to give a dark residue (89 mg), which was dissolved in ether; the solution was filtered to remove some dark insoluble solid and evaporated. The residue (69 mg) was crystallized from ether–hexane to give 55 mg of unchanged 10-oxohaplophytine, m.p. 220°. The pale-yellow solid (14 mg) from the mother-liquor of crystallization was chromatographed on alumina (Neutral, Grade II) in chloroform solution to yield 9 mg of 10-oxoaspidophytine in the 4 × 10 ml fraction, m.p. 236–237° after one crystallization from ethanol, *m/e* 396. This was identified as **26** by i.r., p.m.r., and t.l.c. comparison.

*Oxidation of Aspidophytine with Alkaline Hydrogen Peroxide: Formation of 10-Oxoaspidophytine (**26**)*

Aspidophytine (200 mg) was dissolved in ice-cold aqueous 2% sodium hydroxide (10 ml) and 30% hydrogen peroxide (10 ml) was added with stirring at 0°. After 2 h 6 *N* hydrochloric acid was added to bring the solution to p*H* 6, and the latter was rapidly extracted with dichloromethane (2 × 15 ml). The extract was dried and evaporated, and the residue was sublimed at 200° (0.05 mm) to give colorless needles (55 mg), m.p. 242–243°; λ_{max} ($CHCl_3$) 5.65, 5.63, 5.85 μ; λ_{max} (EtOH) (ε) 222 (28 700), 259 (4800), 306 (1550) nm; δ ($CDCl_3$) 3.17 (s, 3 H), 3.68 (m, 1 H), 3.77 (s, 3 H), 3.80 (s, 3 H), 4.03 (br d, J = 12 Hz, 1 H), 5.57 (d of d, J = 10, ~1 Hz, 1 H), 6.01 (d of d, J = 10, 2.5 Hz, 1 H), 6.25 (d, J = 8.5 Hz, 1 H), 7.03 (d, J = 8.5 Hz, 1 H); *m/e* 396.

Anal. Calcd. for $C_{22}H_{24}N_2O_5$: C, 66.65; H, 6.10; N, 7.07. Found: C, 66.98; H, 6.52; N, 7.20.

This work was supported in part by grants from the National Institutes of Health (HE-12961) and the National Research Council of Canada.

[6]In this and subsequent p.m.r. spectra the methyl proton signals are frequently superimposed on multiplet signals of other protons and the relative areas assigned to them represent approximate estimates.

1. E. F. ROGERS, H. R. SNYDER, and R. F. FISCHER. J. Am. Chem. Soc. **74**, 1987 (1952).
2. H. R. SNYDER, R. F. FISCHER, J. F. WALKER, H. E. ELS, and G. A. NUSSBERGER. J. Am. Chem. Soc. **76**, 4601 (1954).
3. H. R. SNYDER, H. F. STROHMAYER, and R. A. MOONEY. J. Am. Chem. Soc. **80**, 3708 (1958).
4. I. D. RAE, M. ROSENBERGER, A. G. SZABO, C. R. WILLIS, P. YATES, D. E. ZACHARIAS, G. A. JEFFREY, B. DOUGLAS, J. L. KIRKPATRICK, and J. A. WEISBACH. J. Am. Chem. Soc. **89**, 3061 (1967).
5. P. YATES, F. N. MACLACHLAN, I. D. RAE, M. ROSENBERGER, A. G. SZABO, M. P. CAVA, M. BEHFOROUZ, M. V. LAKSHMIKANTHAM, and W. ZEIGER. Submitted for publication.
6. M. P. CAVA, S. K. TALAPATRA, K. NOMURA, J. A. WEISBACH, B. DOUGLAS, and E. C. SHOOP. Chem. Ind. Lond. 1242 (1963).
7. M. P. CAVA, S. K. TALAPATRA, P. YATES, M. ROSENBERGER, A. G. SZABO, B. DOUGLAS, R. F. RAFFAUF, E. C. SHOOP, and J. A. WEISBACH. Chem. Ind. Lond. 1875 (1963).
8. M. P. CAVA, K. NOMURA, and S. K. TALAPATRA. Tetrahedron, **20**, 581 (1964).
9. S. MCLEAN, K. PALMER, and L. MARION. Can. J. Chem. **38**, 1547 (1960).
10. B. GILBERT, J. A. BRISSOLESE, J. M. WILSON, H. BUDZIKIEWICZ, L. J. DURHAM, and C. DJERASSI. Chem. Ind. Lond. 1949 (1962).
11. C. DJERASSI, L. D. ANTONACCIO, H. BUDZIKIEWICZ, J. M. WILSON, and B. GILBERT. Tetrahedron Lett. 1001 (1962).
12. C. DJERASSI, A. A. P. G. ARCHER, T. GEORGE, B. GILBERT, and L. D. ANTONACCIO. Tetrahedron, **16**, 212 (1961).
13. L. J. BELLAMY. The infrared spectra of complex molecules. 2nd. ed. Wiley. N.Y. 1958. p. 179.
14. H. STOBBE. Justus Liebigs Ann. Chem. **308**, 89 (1899).
15. J. C. COLLINS, W. W. HESS, and F. J. FRANK. Tetrahedron Lett. 3363 (1968).
16. H. R. SNYDER, R. F. FISCHER, J. F. WALKER, H. E. ELS, and G. A. NUSSBERGER. J. Am. Chem. Soc. **76**, 2819 (1954).

Can. J. Chem. Downloaded from www.nrcresearchpress.com by 210.87.254.42 on 09/05/12
For personal use only.

Reactions of Ozonides. XI. A ^{14}C Tracer Study of the Ozonolysis of Ethylidenecyclohexane in Cyclohexanone

DUNDAPPA R. KERUR AND DENNIS G. M. DIAPER
Department of Chemistry, Royal Military College of Canada, Kingston, Ontario

Received March 19, 1973

Using ^{14}C labelling of cyclohexanone or ethylidenecyclohexane, examination of the products of ozonolysis of the alkene in the presence of the ketone reveal 6-hexanolide to be initially formed in $< 1\%$ yield. Cyclohexanone peroxides are the major products from ethylidenecyclohexane ozonized in cyclohexanone. Carbonyl-modified alkene ozonolysis is therefore suggested to be explicable by the Criegee mechanism, and it is unnecessary to invoke Baeyer–Villiger interactions. Ozonide formation is not totally suppressed by cyclohexanone.

L'utilisation du marquage au ^{14}C de la cyclohexanone ou de l'éthylidènecyclohexane pour examiner les produits d'ozonolyse de l'alcène en présence d'une cétone, montre que la formation initiale d'hexanolide-6 est $< 1\%$ de rendement. Les peroxydes de la cyclohexanone sont les produits majeurs de l'éthylidènecyclohexane et l'ozone dans la cyclohexanone. L'ozonolyse de l'alcène modifié par un carbonyle peut donc être expliquée par le mécanisme de Criegee sans qu'il sont nécessaire d'invoquer les interactions de Baeyer–Villiger. La formation d'ozonide n'est pas totalement supprimée par la cyclohexanone.
[Traduit par le journal]

Can. J. Chem., **51**, 3110 (1973)

Can. J. Chem. Downloaded from www.nrcresearchpress.com by 210.87.254.40 on 09/05/12
For personal use only.

Introduction

Story and co-workers (1, 2, 3) have recently studied the ozonolysis of certain alkenes in the presence of carbonyl compounds and find that surprisingly the yield of ozonide is very small, although previous theories of ozonolysis mechanisms require the same carbonyl compound to be a precursor in ozonide formation. In *n*-pentane, for example, ozonolysis of ethylidenecyclohexane (**1**) gives good yields of the expected ozonide **3**; however, in the presence of excess of cyclohexanone, the reaction produced "no" ozonide, but only cyclohexanone, acetaldehyde, and 6-hexanolide (**5**) were found. These authors accordingly proposed a mechanism involving reduction of the initially produced Staudinger molozonide (**4**) by cyclohexanone to give an intermediate dioxetane (**6**), the cyclohexanone producing, in a Baeyer–Villiger type of reaction, 6-hexanolide. Subsequent decomposition of the dioxetane would then produce cyclohexanone and acetaldehyde (Scheme 1). Since the ozonolysis solution, after solvent removal, was reported to be viscous, it seemed desirable to consider polymeric reactions as alternative explanations. If, for example, alternating cyclohexane ring units in a polymer chain were derived from cyclohexanone and the zwitterion from ethylidenecyclohexane with subsequent random decomposition to 6-hexanolide, valuable information on the course of the reaction mechanisms could be obtained from specific activities using one or the other starting material labelled with ^{14}C. Other possible explanations of 6-hexanolide formation, such as zwitterion–carbonyl reactions of an unusual type, as well as the side-products of ozonolysis, could also be studied in a labelling experiment. Accordingly we examined the ozonolysis of ethylidenecyclohexane labelled with ^{14}C in the ring using unlabelled cyclohexanone as solvent; also we studied the ozonolysis of unlabelled ethylidenecyclohexane using labelled cyclohexanone as a solvent. These experiments made possible the examination of the reaction products by the isotopic dilution technique in a reliable quantitative fashion.

Experimental

Materials and Reference Compounds

6-Hexanolide, b.p. 118–120°/15 mm (lit. 118–119°/15 mm (4)) was prepared in 77% yield by the Baeyer–Villiger reaction of peroxytrifluoroacetic acid with cyclohexanone (cf. 5). Its n.m.r. spectrum (Varian A-60-A; all spectra measured undiluted or in CCl_4 with tetramethylsilane internal standard) had peaks at δ 4.13–4.26 ($COOCH_2$), 2.51–2.68 (CH_2COO), and 1.78–1.80 p.p.m. (ring CH_2). Attempts to convert it to 6-hydroxyhexanoic acid by saponification using NaOH gave a syrup which polymerized readily to $HO((CH_2)_5CO)_nH$, m.p. 52–54° (6). The lactone was readily converted to 6-hydroxyhexanoic acid hydrazide, m.p. 112–113°, in 82% yield (6).

"Cyclohexanone peroxides" (**7**, **8**, and **9**) were obtained by known procedures (7). 1,1′-Dihydroxycyclohexyl

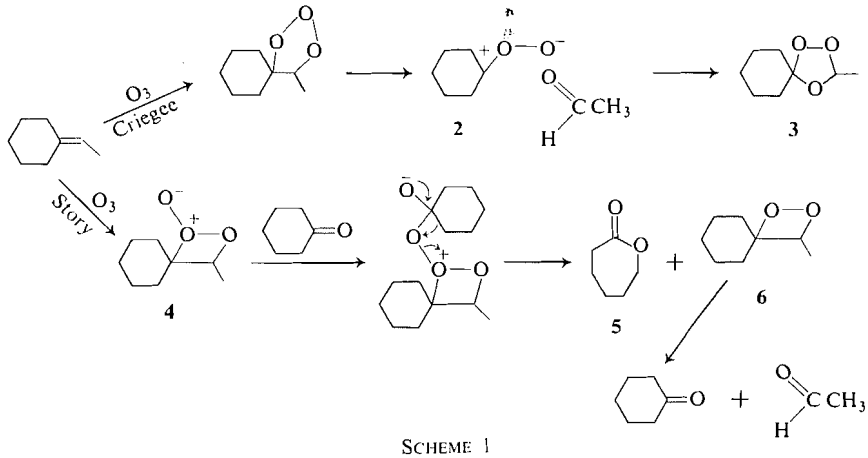

SCHEME 1

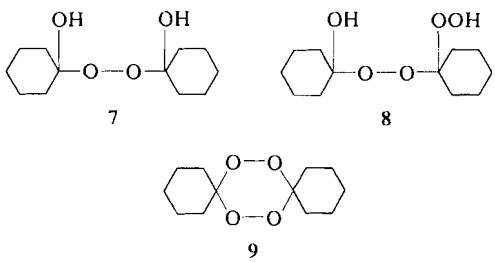

peroxide (**7**), m.p. 71–73°, was prepared in 67% yield by the action of 30% hydrogen peroxide on cyclohexanone in the molar ratio of 1:2. 1-Hydroxy-1′-hydroperoxydicyclohexyl peroxide (**8**), m.p. 76–77°, was obtained in 75.2% yield by reaction of 30% hydrogen peroxide on **7** in the presence of dilute HCl. Its n.m.r. spectrum showed peaks at δ 1.78 and 1.58 p.p.m. and structureless absorption between 2.56–2.83 and 2.21–2.47 p.p.m. **8** reacted vigorously with 85% hydrazine hydrate, but **9** did not. Dicyclohexyl diperoxide (**9**), m.p. 130–131°, was prepared in 3.7% yield by the action of 30% hydrogen peroxide on cyclohexanone (1:1) in the presence of perchloric acid. Its n.m.r. spectrum had a strong peak at 1.55 p.p.m. and broad peaks at 2.60–2.77 and 1.78–1.93 p.p.m. **8** slowly changed into **9** on standing; accordingly purification to constant specific activity in the labelling experiments was not tried.

Ethylidenecyclohexane ozonide (**3**) was prepared in 87% yield by ozonation of the alkene in *n*-pentane at −30°. This reaction also gave **9** in 9.7% yield. An undiluted sample of the ozonide had an n.m.r. spectrum with a well-defined quartet at 5.28 (J = 5 Hz, CH), a broad peak at 1.65 (ring CH_2), and a doublet at 1.32 p.p.m. (J = 5 Hz, CH_3).

Cyclohexanol-^{14}C was obtained in 96% yield by hydrogenation of phenol containing some ring-labelled phenol (Amersham-Searle Corp., Arlington Heights, Ill., 32 mCi/mmol) over Raney nickel at 1200 p.s.i. and 175–200°. Dichromate oxidation in acid gave cyclohexanone-^{14}C in 50% yield, b.p. 154–158° (lit. 155° (8)), 2,4-dinitrophenylhydrazone, m.p. 161–162° (lit. 162° (8)). The i.r. and n.m.r. spectra of the labelled and unlabelled samples were identical. Specific activity of the labelled ketone was 538.3 ± 2.4 c.p.m./mg. Samples were spread on planchets and counted using a Nuclear Chicago end-window counter. Corrections were made for self-absorption. The statistical error is recorded.

Ring-labelled ethylidenecyclohexane was obtained from the ketone by a Wittig synthesis as follows: triphenylethylphosphonium bromide, m.p. 206–208° (lit. 205–207° (9)), was prepared in 67% yield, based on triphenylphosphine, by boiling the latter with an excess of ethyl bromide in dry benzene. Phenyllithium reacted with the bromide and labelled cyclohexanone to give ethylidenecyclohexane-^{14}C, b.p. 134–138° (lit. 135–136° (10)), 597.4 ± 8.9 c.p.m./mg, having n.m.r. and i.r. spectra identical with those of an authentic sample (Aldrich).

Ozonation of Unlabelled Ethylidenecyclohexane in Unlabelled Cyclohexanone

An ozone–oxygen stream was passed into a solution of 1.40 g of the alkene in 50 ml of cyclohexanone at −15°. Removal of excess cyclohexanone with the aid of a high vacuum pump and a cold trap at −78° gave 1.75 g of a colorless viscous residue (dioxetanes are frequently yellow). This residue liberated iodine immediately and copiously from a solution of potassium iodide in acetic acid. A broad band, attributed to OH, was observed in the i.r. spectrum at 2.9–3.0 μ and there was a strong carbonyl peak at 5.9 μ. The n.m.r. spectrum showed peaks at δ 2.21–2.31, 1.75–1.78, and 1.63 p.p.m. Minor unstructured absorption was also noted at δ 5.0–5.3, 4.1–4.3, and 2.7–3.1 p.p.m. When 85% hydrazine hydrate was added, effervescence and evolution of heat occurred, but on boiling with ethanol and subsequent evaporation no 6-hydroxyhexanoic acid hydrazide crystals were formed.

Analysis of the syrupy residue by t.l.c. on Eastman "Chromagram" sheets gave inadequate separation in most single or mixed solvents. Almost complete resolution into four components was obtained in butyl acetate; their R_f values were respectively 0.90, 0.70, 0.44, and 0.25. Authentic **9**, **8**, and **3** had R_f values respectively of 0.96, 0.74, and 0.49. **7** was absent. The other spot, attributed to peroxy polymers, showed considerable "tailing".

Can. J. Chem. Downloaded from www.nrcresearchpress.com by 210.87.254.40 on 09/05/12
For personal use only.

Can. J. Chem. Downloaded from www.nrcresearchpress.com by 210.87.254.40 on 09/05/12
For personal use only.

Spray reagents used for t.l.c. spot visualization were 3% KI in 5% aqueous acetic acid and concentrated H_2SO_4.

Ozonation of Ethylidenecyclohexane in Labelled Cyclohexanone

The above experiment was repeated except that 241.8 mg of cyclohexanone-^{14}C (totalling 1.3×10^5 c.p.m.) was added as well as 50 g of unlabelled cyclohexanone. The residue after solvent removal had 4.03 ± 0.1 c.p.m./mg and therefore contained only about 0.5% of the added tracer. The recovered cyclohexanone had specific activity 2.7–3.0 ± 0.2 c.p.m./mg (at least 98% recovery based on the weight of recovered ketone).

T.l.c. failed to isolate the 6-hexanolide present in this residue, therefore a dilution analysis as the hydrazide was attempted as follows. To the residue was added 0.5 g of authentic 6-hexanolide. After adding 5 ml of 85% hydrazine hydrate and 25 ml of 95% ethanol, the reaction mixture was boiled for 1 h. Evaporation gave the semi-solid hydrazide, which was recrystallized twice from ethyl acetate, m.p. 113–115°. No radioactivity could be detected in the recovered 6-hydroxyhexanoic acid hydrazide.

Ozonation of Labelled Ethylidenecyclohexane in Unlabelled Cyclohexanone

The alkene (704.6 mg, specific activity 114.4 ± 1.7 c.p.m./mg) in 25 ml of cyclohexanone was treated with ozone as above. The residue after solvent removal (889.1 mg, 57.5 ± 0.5 c.p.m./mg, radiochemical yield in this experiment 63.4%) was divided into several portions. The recovered cyclohexanone was divided into several portions. The recovered cyclohexanone registered 0.3–1.2 ± 0.3 c.p.m./mg.

To 259.5 mg of the residue, 255.5 mg of authentic 6-hexanolide, 3 ml of 85% hydrazine hydrate, and 10 ml of 95% ethanol were added. After boiling for 1 h, the reaction product was recovered and recrystallized as before, giving 312.3 mg of 6-hydroxyhexanoic acid hydrazide, m.p. 114–116°, specific activity 1.5 ± 0.3 c.p.m./mg. After four successive recrystallizations of a portion, radioactivity became undetectable. Another portion after seven recrystallizations had a constant residual activity of 0.6 ± 0.1 c.p.m./mg. This experiment, together with the preceding experiment, shows a yield of not more than 0.25% of 6-hexanolide in the residue as determined by radioactive assay.

To 33.1 mg of the residue in 1 ml of ether, 51.6 mg of authentic purified ozonide was added and the components of the mixture were separated by t.l.c. Ozonide recovered by ether extraction of the silica gel (9.6 mg) had a specific activity of 1.2 ± 0.5 c.p.m./mg. Authentic cyclohexanone peroxides **3**, **8**, and **9** were chromatographed with the sample for comparison. **9** was visualized by sulfuric acid spray; it liberates iodine from acid KI only slowly. **9** separated as crystals from the ozonation residue on long standing at room temperature. Although **8** was not obtained crystalline from the ozonation residue, its presence was detected by t.l.c. and its concentration, from intensity of t.l.c. spots, appeared similar to that of **9**; **3** was present in smaller quantity and polymeric peroxides were also detected. Some cyclohexanone was also present in the residue (i.r.).

Discussion

The major products of ethylidenecyclohexane ozonolysis in cyclohexanone are "cyclohexanone peroxides" **8** and **9**. The latter crystallizes well, and may in fact be more conveniently prepared by carbonyl-modified ozonolysis of this and other alkylidenecyclohexanes (11) than by published procedures. The former does not crystallize so well. Both are known to decompose under a variety of conditions, including thermolysis in the presence or absence of acids, to 6-hexanolide and related products (12–14). Isolation of 6-hexanolide by gas chromatography of a mixture containing cyclohexanone peroxides is unreliable evidence of its initial presence.

Isotopic dilution analysis enables an accurate upper limit to be set for the concentration of the substance analyzed. 6-Hexanolide was below detection limits (<0.04%) in the labelled cyclohexanone experiment and <0.25% in the experiment using labelled alkene in unlabelled cyclohexanone. Story's proposed mechanism (Scheme 1) (1, 2, 3) would require labelled 6-hexanolide from the former but not the latter experiment. The isotopic dilution study rules out significant formation of 6-hexanolide by Scheme 1 and also by other routes such as Scheme 2 which are in agreement with the Criegee mechanism. Formation of small quantity of 6-hexanolide from the ethylidenecyclohexane moiety argues its origin from zwitterion **2**, possibly through dimeric forms **8** and **9**.

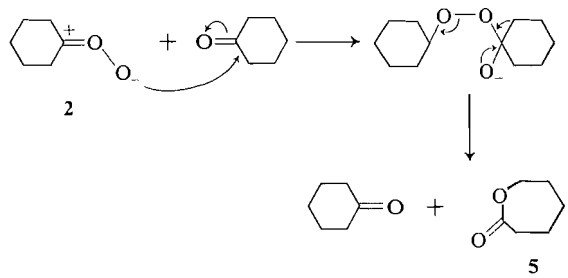

SCHEME 2

Ozonide (**3**) formation was not suppressed completely by the cyclohexanone but the yield was diminished from 86.6% in pentane to 2.9% in cyclohexanone as solvent. In the competition between ozonide formation and other reactions a difference of a few kilocalories in activation energies would account for this difference in yield; such an energy difference may be explained

by solvent polarity effects. Kopecky *et al.* (15) incline to this view, which they support by demonstrating the absence of dioxetane **6** when ethylidenecyclohexane is ozonized in pinacolone. In cyclohexanone **5** and **6** should be produced in equimolecular proportions according to Scheme 1.

Formation of labelled cyclohexanone from ethylidenecyclohexane is explicable in a number of ways. Direct formation by the Criegee mechanism and bimolecular loss of O_2 from the zwitterion (16, 17) or zwitterion – carbonyl redox reaction (18) are all plausible. Formation of labelled cyclohexanone by Scheme 1 would require production of an equimolecular quantity of 6-hexanolide **5**; this was not observed. Cyclohexanone itself is only slowly attacked by ozone, giving adipic acid (19).

We wish to thank Professor S. N. Naldrett for the use of a Nuclear-Chicago counter. Financial support from Defence Research Board of Canada under Grant 9530-17 is gratefully acknowledged.

1. P. R. Story, J. A. Alford, J. R. Burgess, and W. C. Ray. J. Am. Chem. Soc. **93**, 3042 (1971).
2. P. R. Story, J. A. Alford, W. C. Ray, and J. R. Burgess. J. Am. Chem. Soc. **93**, 3044 (1971).
3. P. R. Story, E. A. Whited, and J. A. Alford. J. Am. Chem. Soc. **94**, 243 (1972).
4. Eastman organic chemicals catalog. Eastman Kodak Company, Rochester, N.Y. 1971. p. 109.
5. E. E. Smissman, J. F. Murren, and N. A. Dahle. J. Org. Chem. **29**, 3517 (1964).
6. F. J. Van Natta, J. W. Hill, and W. H. Carothers. J. Am. Chem. Soc. **56**, 455 (1934).
7. M. S. Kharasch and G. Sosnovsky. J. Org. Chem. **23**, 1322 (1958).
8. R. L. Shriner, R. C. Fuson, and D. Y. Curtin. The systematic identification of organic compounds. John Wiley & Sons, Inc., New York. 1965. p. 362.
9. U. H. M. Fagerlund and D. R. Idler. J. Fisheries Res. Bd. Can. **17**, 597 (1960); Chem. Abstr. **55**, 2730*h* (1961).
10. G. Gelli, A. Maccioni, and M. Secci. Ann. Chim. Rome, **53**, 1379 (1963).
11. D. R. Kerur and D. G. M. Diaper. Unpublished results.
12. W. Dilthey, M. Inckel, and H. Stephan. J. Prakt. Chem. **154**, 219 (1940).
13. M. Stoll and W. Scherrer. Helv. Chim. Acta, **13**, 142 (1930).
14. E. G. E. Hawkins, J. Chem. Soc. **19**, 2691 (1969).
15. K. R. Kopecky, P. A. Lockwood, J. E. Filby, and R. W. Reid. Can. J. Chem. **51**, 468 (1973).
16. S. Fliszar and J. B. Chylinska. Can. J. Chem. **46**, 783 (1968).
17. P. S. Bailey, J. A. Thompson, and B. A. Shoulders. J. Am. Chem. Soc. **88**, 4098 (1966).
18. D. G. M. Diaper. Can. J. Chem. **44**, 2819 (1966).
19. P. S. Bailey. Chem. Rev. **58**, 925 (1958).

Can. J. Chem. Downloaded from www.nrcresearchpress.com by 210.87.254.40 on 09/05/12
For personal use only.

Thermodynamic Properties of Zinc Chloride in Alkali Chloride Melts by Electromotive Force Measurements

RON J. ROBERTSON[1] AND ALFRED S. KUCHARSKI
Department of Chemical Engineering, University of Waterloo, Waterloo, Ontario

Received January 5, 1973

Electromotive force measurements on the $ZnCl_2$–ACl systems where A = K, Rb, and Cs were made using cells of the type

$$Zn_{(l)}|ZnCl_2\text{–}ACl_{(l)}|\text{graphite, } Cl_{2(g,\ 1\ atm)}$$

in the temperature range 450° to 800 °C. The partial molar free energies, enthalpies, and excess entropies have been determined from the temperature dependence of the emf results. These thermodynamic properties exhibit increasing negative departure from ideality as the basicity of the alkali metal salt increases. The results are interpreted in terms of an acid–base reaction and are discussed in relation to current models.

On a évalué la force électromotrice des système $ZnCl_2$–ACl où A = K, Rb et Cs en utilisant des piles du type

$$Zn_{(l)}|ZnCl_2\text{–}ACl_{(l)}|\text{graphite, } Cl_{2(g,\ 1\ atm)}$$

pour des températures de 450 à 800 °C. Les énergies libres molaires partielles, les enthalpies ainsi que les entropies en excès ont été déterminées à partir de la dépendance des résultats fem par rapport à la température. Pour ces propriétés thermodynamiques, on a trouvé un écart négatif par rapport au cas idéal qui va en augmentant à mesure que la basicité du sel métallique alcalin augmente. Les résultats sont interprétés en fonction d'une réaction acide–base et sont comparés aux modèles classiques.

[Traduit par le journal]

Can. J. Chem., 51, 3114 (1973)

Introduction

Acid–base reactions at high temperatures are important in many metallurgical processes. For example, in the smelting and the converting of copper–nickel sulfide ores, iron is eliminated as an iron oxide by reacting it with silica to form a fluid slag. In this type of reaction, silica acts as an acid by accepting oxygen from other basic oxides to break down the three dimensional network structure of liquid silica. In this manner, highly viscous slags can be made more fluid by the addition of basic oxides. The basicity of a particular metallic oxide can be simply related (1) to the coulombic force of attraction that a metal cation exerts on an oxygen anion.

The theoretical interpretation of this phenomena has been hampered by the lack of accurate thermodynamic data. In particular there is a lack of data reported for the enthalpy and entropy of mixing for metallic oxide – silica molten systems. The inherent difficulties encountered at the very high temperatures required to study these molten oxide systems accounts for this fact. However, the free energies (2–4) and the enthalpy of mixing (5) for the PbO–SiO_2 have been reported in the literature excluding the silica-rich compositions.

A plot of the interaction parameter, $\Delta H/(X_{PbO})(X_{SiO_2})$ *vs.* X_{SiO_2} by the latter authors for the PbO–SiO_2 system exhibits a minimum in the composition range $X_{SiO_2} = 1/3$. Also, the partial excess entropy of mixing of SiO_2 calculated from the combination of the electrochemical free energies and calorimetric enthalpies of mixing indicate a similar discontinuity at approximately $X_{SiO_2} = 1/3$. The formation of the orthosilicate via the reaction

$$[1] \qquad 2PbO + SiO_2 \rightarrow Pb_2SiO_4$$

is postulated to account for this unusual behavior. The binary phase diagrams for other MO–SiO_2 systems (6) exhibit immiscibility gaps; however, with increasing basicity of the metal oxide, MO, the gap diminishes and even disappears as in the alkali metal oxide – SiO_2 binary systems. Thus heats of mixing for such partially miscible systems should be positive in the region of the miscibility gap. Heats of mixing for systems of this type have not been reported

[1]Technical Assistant, Gaspe Copper Mines Ltd., Murdochville, Quebec.

Can. J. Chem. Downloaded from www.nrcresearchpress.com by 210.87.254.40 on 09/05/12
For personal use only.

Can. J. Chem. Downloaded from www.nrcresearchpress.com by 210.87.254.40 on 09/05/12
For personal use only.

in the literature in spite of their technical and theoretical importance.

To understand the acid–base behavior of molten oxide systems, molten fluoride systems have been considered by Holm and Kleppa (7) to be "weak oxide" analogs. The ionic radius of the fluoride ion ($r_{F^-} = 1.36$ Å) is approximately equal to the ionic radius of oxygen ($r_{O^{2-}} = 1.40$ Å). Both BeF_2 and SiO_2 are highly viscous and poor conductors in the liquid state and thus reflect the polymeric nature of their liquid state.

The enthalpies of mixing for the BeF_2–LiF and BeF_2–KF systems reported by these authors indicate that the BeF_2–LiF system exhibits both negative and positive deviations. But this immiscibility tendency is not reflected in the BeF_2–KF system since the enthalpy of mixing for this system is totally negative with a maximum occurring approximately at the composition $X_{BeF_2} = 1/3$. If the ionic radii for the alkali metal ions are considered, the immiscibility tendencies in the BeF_2–LiF system and the lack of it in the BeF_2–KF system can be understood. The small lithium ion ($r = 0.60$ Å) makes LiF a poor base since it is able to form strong electrostatic bonds with the surrounding F^- ions and approaches the Be^{2+}—F^- bond strength. In contrast, the larger potassium ion ($r = 1.33$ Å) is able to donate F^- ions to the acidic Be^{2+} ion to form the tetrahedral complex, BeF_4^{2-} in the basic composition range. The partial entropy of mixing for BeF_2 was computed from the free energies of mixing determined from both phase diagrams and emf measurements. The results indicate large negative deviations in the LiF rich range.

The analogy between the BeF_2–LiF and SiO_2–alkaline earth oxide systems has been suggested by Cantor *et al.* (8) in their viscosity and density measurements in the BeF_2–LiF system. The calculated activation energy for viscous flow decreases with LiF concentrations similar to the analogous SiO_2 – alkaline earth oxide systems.

The enthalpies of mixing of metallic chloride – alkali chloride measured by Kleppa and coworkers (9–12) also exhibit this type of acid–base behavior in varying degrees. A discrete complex anion model has been developed by Pelton (13) to establish a semi-quantitative basicity scale for MY_2–AY halide systems where M is a divalent metal cation and A is an alkali metal cation.

The similarities of the liquid structures for $ZnCl_2$ and SiO_2 have been proposed by Angell and Wong (14) and indicate that a $ZnCl_2$-based analog could be used to elucidate the behavior of the baulky oxide systems. Spectroscopic investigation (15, 16) of zinc chloride – alkali chloride systems indicate that these systems exhibit extreme acid–base behavior. This behavior is quite similar to the oxide systems in that the polymeric species are broken down by the ligands from the donating base. In addition, viscosity (17), density (18), and electrical conductivity (19) support this view. However, the enthalpies and entropies of mixing of these binary systems has not been determined (20).

From the temperature dependence of the free energy it has been demonstrated for the $MnCl_2$–ACl systems (A = Li, Na, K, Cs) (21) that enthalpies and entropies can be accurately determined. The acidic solution properties of $ZnCl_2$ can be investigated in the reaction

$$[2] \qquad Zn_{(l)} + Cl_{2(g,\ 1\ atm)} \rightarrow ZnCl_{2(l,\ soln)}$$

by means of an electrolytic cell of the type

$$Zn_{(l)}|ZnCl_2\text{–}ACl_{(l)}|\text{graphite},\ Cl_{2(g,\ 1\ atm)}$$

This type of cell has been used by Takahashi (22) to determine the thermodynamic properties of $ZnCl_2$ in a solvent consisting of a LiCl–KCl eutectic. The activity of $ZnCl_2$ is low in the alkali chloride-rich concentrations reflecting the tendency of the acidic character of Zn^{2+} cation to coordinate four Cl^- anions to form the tetrahedral complex, $ZnCl_4^{2-}$. This result is substantiated by Flengas and Ingraham (23) in the e.m.f. measurements of dilute solutions of $ZnCl_2$ in a solvent of equimolar NaCl–KCl. In addition Markov and Chernov (24) have calculated the liquidi in the alkali chloride-rich concentrations for the $ZnCl_2$–RbCl and $ZnCl_2$–CsCl phase diagrams by postulating the formation of the tetrahedral complex. The thermodynamic properties of $ZnCl_2$–ACl (A = Li, Na, K, Rb, Cs, Ba) have been reviewed by Dijkhuis *et al.* (20), however; the free energies of mixing for the $ZnCl_2$–KCl, $ZnCl_2$–RbCl, and $ZnCl_2$–CsCl systems were measured by Markov and Volkov (25, 26) using a non-equilibrium technique. It was not possible to determine accurately the enthalpies and entropies of mixing for these systems. Thus, the aim of the present investigation is to determine electrochemically the free energies of mixing and thereby be able to cal-

culate the enthalpies and entropies of mixing to elucidate the thermodynamic properties of acid–base reactions at high temperatures.

Experimental

Anhydrous zinc chloride and alkali chloride were prepared by heating slowly reagent grade material under vacuum to 200 °C and 400 °C respectively for a period of several hours. To insure final dehydration, the zinc chloride salt was fused under a stream of anhydrous hydrogen chloride gas. This gas was bubbled through the melt for approximately 20 min followed by flushing with argon gas to remove the dissolved hydrogen chloride gas. In a similar manner, the alkali chlorides were dehydrated in the solid state using anhydrous hydrogen chloride gas or chlorine. After the salts were cooled under an argon atmosphere, the zinc chloride or alkali chloride salts were transferred to a dry box and stored in sealed containers.

The design of the electrochemical cell used in this series of measurements is given in Fig. 1. This cell differs slightly from the one that was employed previously (21). To minimize the volatility of $ZnCl_2$, each half cell had a diameter of approximately 10 mm. This small cross-sectional area limited the loss of $ZnCl_2$ through volatilization and the area was further reduced by insertion of the graphite electrodes. The effectiveness of this design was verified by the facts that very little $ZnCl_2$ was observed on the colder walls of the cell even in the pure $ZnCl_2$ and $ZnCl_2$-rich compositions and that the cell potentials could be reproduced in a heating and cooling cycle. The latter would not be feasible if there was an excessive $ZnCl_2$ loss.

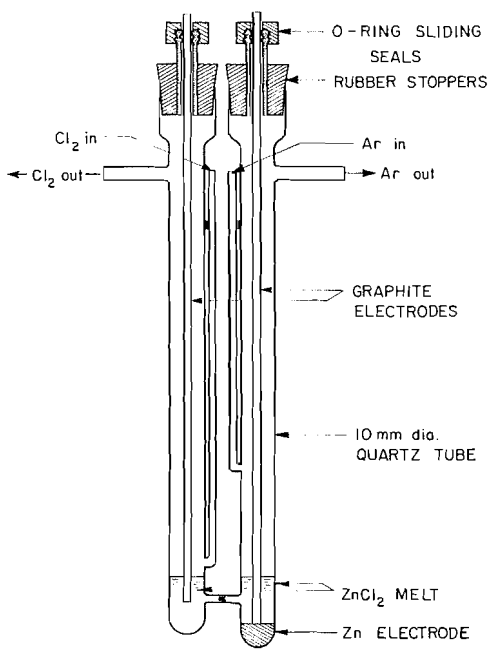

FIG. 1. EMF formation cell.

The zinc metal half-cell compartment was extended to accommodate a liquid zinc electrode. The zinc metal used in this work had a purity of 99.9%.

The graphite electrodes were treated in the usual manner (20) by heating to 1000 °C under vacuum and then passing chlorine gas over the electrodes. No attack or swelling of the graphite was observed as reported previously for the $CdCl_2$–NaCl (27) and the $MnCl_2$–ACl (A = Li, Na, K, and Cs) systems (21).

A period of approximately 1 day was required for chlorine saturation in pure $ZnCl_2$ and $ZnCl_2$-rich concentrations especially at low temperatures. However, once the melts were saturated with chlorine, the cell potentials were stable and reproducible. Only a short time was necessary to saturate the alkali chloride-rich concentrations. The reversibility of the cell potentials was verified by polarization tests in which a current from an external source was passed through the cell. The cell potential always returned to the former unpolarized value within a minute upon removal of the external polarizing source.

In order to correct for the lowering of the chlorine pressure in the chlorine half-cell by the $ZnCl_2$ vapor at high temperatures, the vapor pressure was measured by a transportation method. Chlorine gas was passed over a boat of the molten salt and the volume of chlorine gas was determined by a displacement method. This correction is appreciable in the pure $ZnCl_2$ and $ZnCl_2$-rich concentrations.

Results

As indicated, the vapor pressure of the $ZnCl_2$ becomes appreciable in the pure state or in the $ZnCl_2$-rich compositions. The vapor pressure of pure $ZnCl_2$ was measured at 569 °C and found to be 54 mm Hg. This result agrees to within 4 mm Hg of the measurements made by Bloom *et al.* (28) and George *et al.* (29). Thus the emf data for the pure $ZnCl_2$ were corrected for the vapor pressure of $ZnCl_2$ using the equation determined by Bloom and is given in Table 1.

The vapor pressure of $ZnCl_2$ for several $ZnCl_2$-rich compositions is also given in Table 1. The vapor pressure in the $ZnCl_2$–RbCl and the $ZnCl_2$–CsCl systems is expected to be much

TABLE 1. Vapor pressure of the pure $ZnCl_2$, $ZnCl_2$–KCl, and $ZnCl_2$–CsCl systems; $\log P = A + B/T$ (mm Hg)

	X_{ZnCl_2}	A	B	Standard deviation
$ZnCl_2$ (Bloom (28))	1.0	9.574	−6639.5	
$ZnCl_2$–KCl (this work)	0.52	10.559	−8275.5	±1.4 mm Hg
	0.72	10.049	−7290.0	±1.0 mm Hg
$ZnCl_2$–CsCl (this work)	0.72	6.674	−4477.7	±1.3 mm Hg

Can. J. Chem. Downloaded from www.nrcresearchpress.com by 210.87.254.40 on 09/05/12
For personal use only.

Can. J. Chem. Downloaded from www.nrcresearchpress.com by 210.87.254.40 on 09/05/12
For personal use only.

lower than the $ZnCl_2$–KCl system following the trends reported for the $MnCl_2$–ACl (A = K, Rb, and Cs) systems (21). Therefore, no correction was applied to the compositions greater than $X_{ACl} = 0.48$ where A = Rb, Cs. The maximum correction applied to the solutions was only approximately 3 mV and 10 mV in pure $ZnCl_2$ in the temperature range studied. The corrected E^0 emf values for two separate experimental runs were fitted by least square analysis to give the linear equation

$$E^0 = 1927.5 - 0.45472T$$

The standard deviation for the fit was found to be 1.7 mV.

In Table 2, the standard potential is compared at various temperatures with those calculated from the available standard free energy data. Also, the standard potentials are compared with the new values obtained when the lower heat of fusion (2450 cal) measured by Cubicciotti *et al.* (30) is combined with the tabulated thermochemical data of Wicks and Block (36).

The solution properties were measured using the cell shown in Fig. 1 representing reaction 2. The partial free energy of mixing for $ZnCl_2$, $\Delta\bar{G}_{ZnCl_2}$, is given as

$$[3] \qquad \Delta\bar{G}_{ZnCl_2} = -ZF(E - E^0)$$

The partial molar free energies are related to partial enthalpies and entropies of mixing by the equation

$$[4] \qquad \Delta\bar{G}_{ZnCl_2} = \Delta\bar{H}_{ZnCl_2} - T\Delta\bar{S}_{ZnCl_2}$$

If the enthalpy and entropy of mixing are taken to be temperature independent the quantity $(E - E^0)$ can be expressed as a linear function of temperature over a narrow temperature range. Thus, the partial enthalpies and entropies of mixing for $ZnCl_2$ were obtained from the intercepts and the slope of the linear functions $(E - E^0)$ plotted *vs.* temperature. The plots of $(E - E^0)$ *vs.* temperature for the three binary systems are given in Figs. 2, 3, and 4. It is seen that the data are well represented by the least square lines shown. The maximum deviation in all three binary systems is 2 mV and the largest deviation of an individual experimental point is approximately 4 mV. The equations are given in Table 3 along with the standard and maximum deviations for each line. The partial molar excess free energies of mixing of $ZnCl_2$, $\Delta\bar{G}^{XS}_{ZnCl_2}$ at 600 °C are also listed in Table 3 along with the partial molar enthalpies and excess entropies of mixing for $ZnCl_2$. These two properties are temperature independent as shown by the linearity of the plots. The partial molar heats of mixing for KCl, RbCl, and CsCl were calculated using the Gibbs–Duhem equation. These calculations are shown in Figs. 5, 6, and 7. Also, the partial molar heats of mixing for $ZnCl_2$ and the integral heats for each binary system are given in the figures.

TABLE 2. Comparison of the thermochemical and electrochemical standard potential (mV) for the formation of $ZnCl_2$

Parameter	Value at (°C) 450	500	550	600	Reference
E_T^0	1629	1603	1577	1552	34
E_T^0	1608	1578	1549	1520	35
E_T^0	1596	1561	1525	1490	36, 30
E_E^0	1600	1573	1555	1532	This work

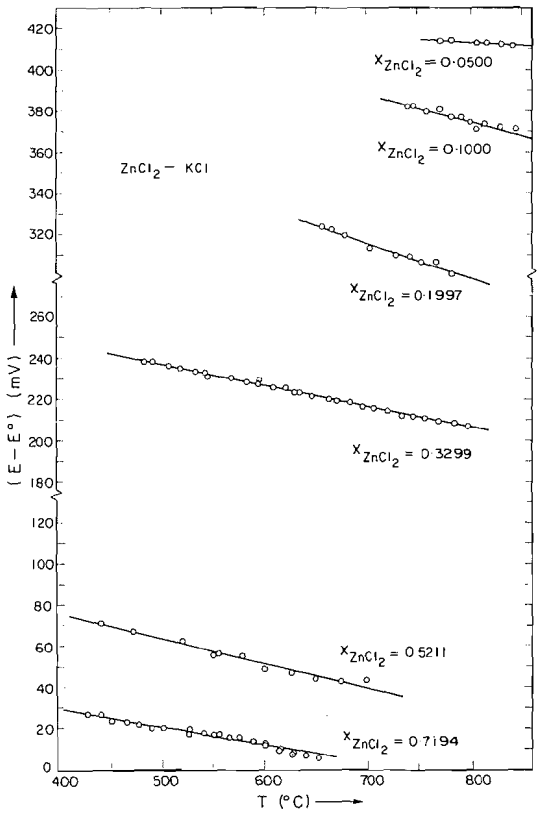

FIG. 2. Plots of $E - E^0$ *vs.* temperature for the $ZnCl_2$–KCl system.

Can. J. Chem. Downloaded from www.nrcresearchpress.com by 210.87.254.40 on 09/05/12
For personal use only.

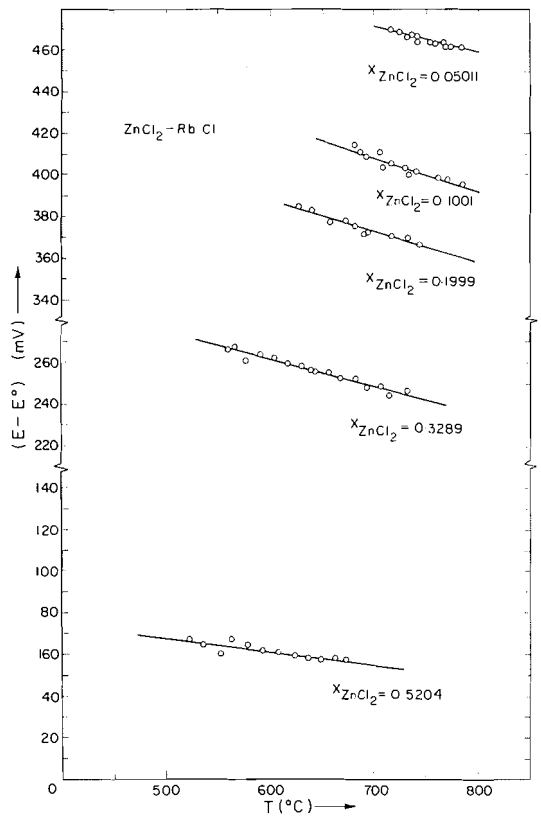

FIG. 3. Plots of $E - E^0$ *vs.* temperature for the $ZnCl_2$–RbCl system.

The integral heats of mixing were calculated from the well known expression

$$[5] \quad \Delta H_M = X_{ACl}\Delta\bar{H}_{ACl} + X_{ZnCl_2}\Delta\bar{H}_{ZnCl_2}$$

By using the standard deviations given in Table 3, the uncertainty in calculating integral heat of mixing is estimated to lie in the range of 150 to 350 cal per g-mol. This uncertainty limit is not significant in these systems with a large exothermic heat of mixing.

The partial excess free energy of mixing of $ZnCl_2$ at 600 °C for the three systems is plotted in Fig. 8. The dashed lines indicate that the partial excess free energies of $ZnCl_2$ have been extrapolated below the liquidus temperature. Also, the results of Markov and Volkov (25) have been plotted as solid circles for the $ZnCl_2$–KCl and the $ZnCl_2$–RbCl systems. These results were obtained using a nonequilibrium technique. The values of $\Delta\bar{G}^{XS}_{ZnCl_2}$ at infinite dilution are seen to be approximately −20, −23, and −25 kcal/mol for the KCl, RbCl, and CsCl systems. This increasing negative departure from ideality parallels the increasing basicity of the alkali chloride from KCl through to CsCl.

Discussion

In previous publications (21, 31) a model has been tested to account for the enthalpies of mixing for reactive charge asymmetrical systems of the type MCl_2–ACl where M represents a transition metal divalent cation and A an alkali metal cation. In this model the enthalpy of mixing is divided into two effects; the heat of mixing arising from the reaction to form the tetrahedral complex according to the reaction

$$[6] \quad 2ACl + ZnCl_2 \rightarrow A_2ZnCl_4$$

and the mixing of the products with remaining reactants to form a solution. Hence, the enthalpy of mixing is given as

$$[7] \quad \Delta H_M = \Delta H_R + \Delta H_m$$

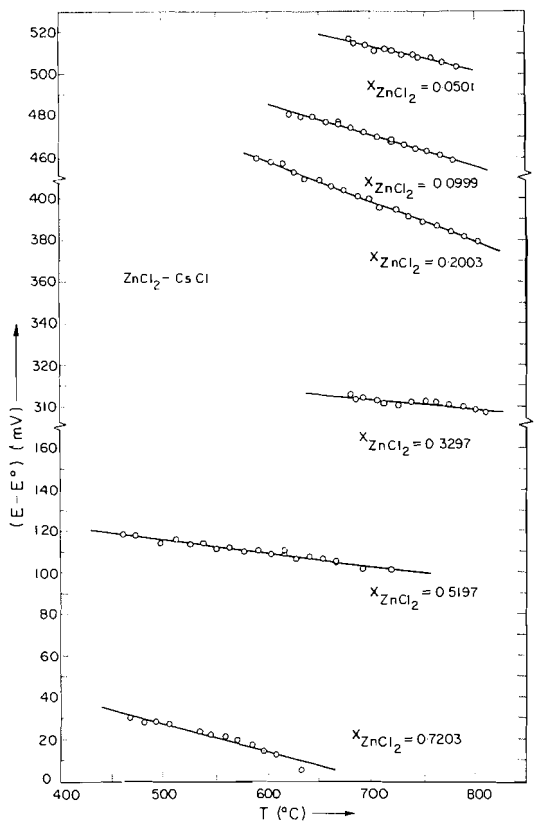

FIG. 4. Plots of $E - E^0$ *vs.* temperature for the $ZnCl_2$–CsCl system.

TABLE 3. Linear least square fits for $E - E^0$ *vs.* temperature at compositions in $ZnCl_2$–ACl systems

X_{ZnCl_2}	A^*	B^*	Deviation (mV) Standard	Deviation (mV) Maximum	$\Delta\bar{G}^{XS}_{ZnCl_2}$ 600 °C (cal/mol)	$\Delta\bar{H}_{ZnCl_2}$ (cal/mol)	$\Delta\bar{S}^{XS}_{ZnCl_2}$ (e.u.)
			$ZnCl_2$–KCl				
0.0500	455.0	−0.0388	0.1	0.2	(−19340)	−20990	−7.74
0.1000	510.3	−0.1261	1.7	3.8	(−18170)	−23580	−10.4
0.1997	479.3	−0.1683	1.4	2.3	(−14950)	−22120	−10.9
0.3299	317.6	−0.1038	0.6	1.8	−10230	−14650	−7.0
0.5211	154.7	−0.1181	1.9	3.4	−2100	−7135	−6.7
0.7194	91.4	−0.0916	1.2	2.0	−320	−4220	−4.9
			$ZnCl_2$–RbCl				
0.0501	592.0	−0.1244	1.1	1.9	−22030	−27320	−11.7
0.1001	562.4	−0.1584	1.8	3.6	−19190	−15940	−11.9
0.1999	517.6	−0.1484	1.7	2.8	−17560	−23870	−10.0
0.3289	376.3	−0.1309	1.5	3.8	−11780	−17360	−8.2
0.5204	116.3	−0.0628	1.8	3.9	−2690	−5370	−4.2
			$ZnCl_2$–CsCl				
0.0501	620.1	−0.1100	0.7	1.3	−23920	−28600	−11.0
0.0999	613.4	−0.1467	0.7	1.4	−22040	−28290	−11.3
0.2003	585.2	−0.1915	0.8	1.6	−18840	−26990	−12.0
0.3297	356.0	−0.0438	1.3	2.0	−14560	−16420	−4.2
0.5197	166.7	−0.0656	1.1	1.9	−4900	−7690	−4.3
0.7203	132.5	−0.1360	1.8	4.3	−320	−6110	−6.9

$^*E - E^0$ (mV) $= A + BT$.

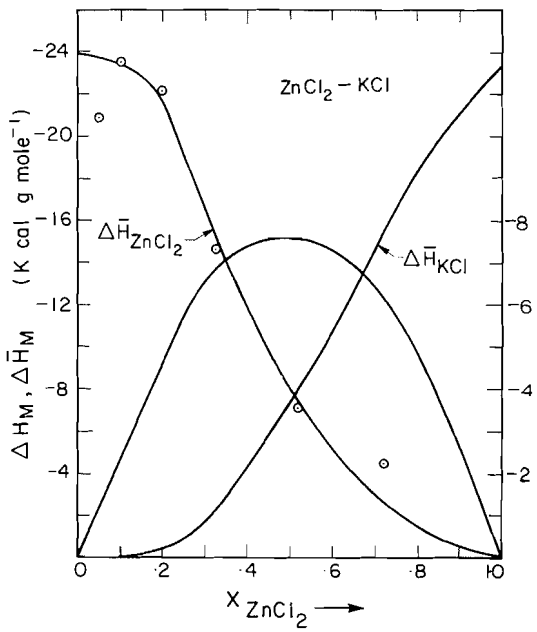

FIG. 5. Partial and integral enthalpies of mixing in the $ZnCl_2$–KCl system.

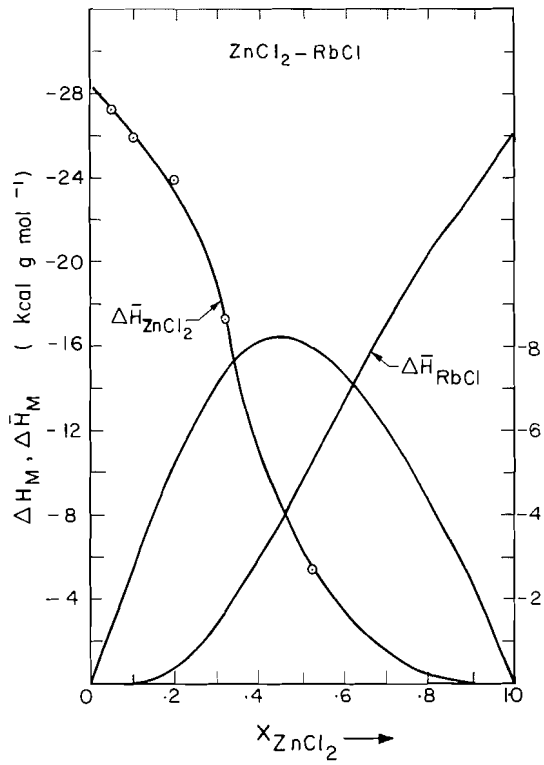

FIG. 6. Partial and integral enthalpies of mixing in the $ZnCl_2$–RbCl system.

where ΔH_R represents the "reaction part" and ΔH_m represents the "mixing part" of the enthalpy of mixing.

In this model ΔH_R is considered to be the

Can. J. Chem. Downloaded from www.nrcresearchpress.com by 210.87.254.40 on 09/05/12
For personal use only.

Can. J. Chem. Downloaded from www.nrcresearchpress.com by 210.87.254.40 on 09/05/12
For personal use only.

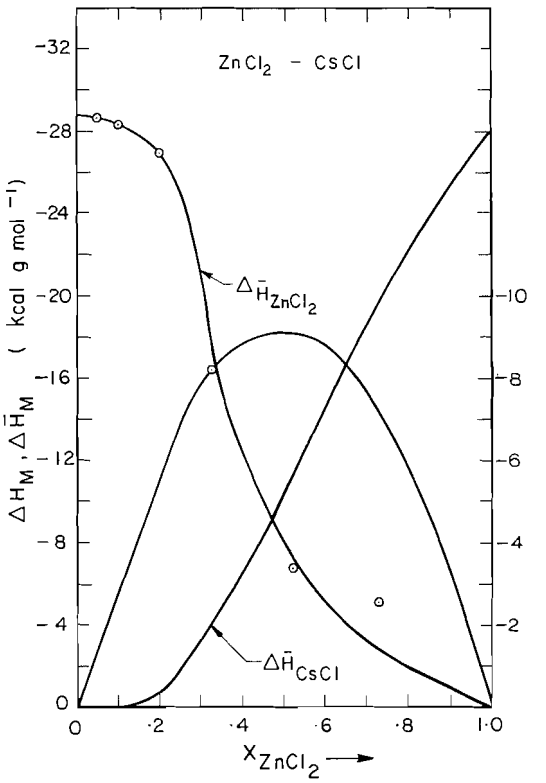

FIG. 7. Partial and integral enthalpies of mixing in the $ZnCl_2$–CsCl system.

major contributor to the enthalpy of mixing and is proportional to the amount of complex formed. The "reaction heat" is calculated in the composition range $X_{ZnCl_2} > 1/3$ as

$$\Delta H_R = 0.5 X_{ACl} b_R \quad [8]$$

and in the range $X_{ZnCl_2} < 1/3$ as

$$\Delta H_R = X_{ZnCl_2} b_R \quad [9]$$

The parameter, b_R can be simply determined at the composition $X_{ZnCl_2} = 1/3$ since the "mixing" contribution vanishes and thus the total heat of mixing becomes

$$\Delta H_M = b_R/3 \quad [10]$$

The values for b_R that were determined for the systems $ZnCl_2$–KCl, $ZnCl_2$–RbCl, and $ZnCl_2$–CsCl are listed in Table 4 along with the Pauling ionic radius and "polarizing power" of the alkali cation. It is evident that as the polarizing power of the alkali metal cation decreases the "reaction part" of the enthalpy becomes more pronounced, reflecting the increasing basicity of the alkali metal salt.

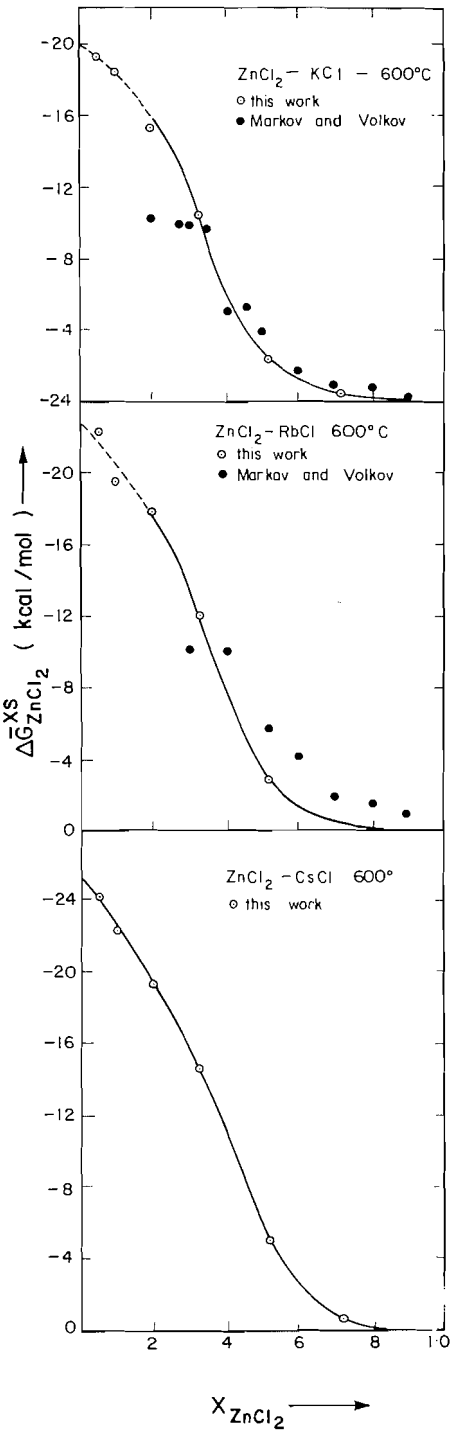

FIG. 8. Partial excess free energy of mixing of $ZnCl_2$ at 600 °C for the systems $ZnCl_2$–KCl, $ZnCl_2$–RbCl, and $ZnCl_2$–CsCl. The solid circles represent the results Markov and Volkov for the $ZnCl_2$–KCl and the $ZnCl_2$–RbCl systems.

Can. J. Chem. Downloaded from www.nrcresearchpress.com by 210.87.254.40 on 09/05/12
For personal use only.

TABLE 4. Enthalpy and entropy parameter for the $ZnCl_2$–ACl system

Parameter	Value KCl	RbCl	CsCl	Unit
b_R	−21.0	−22.8	−24.6	kcal/mol
ε	−9	−9	−10	kcal/K mol
r_{A+}	1.33	1.48	1.69	Å
$1/(r_{A+} + 1.80)^2$	0.102	0.093	0.082	$(Å)^{-2}$

This tendency also becomes more apparent when the model is applied to the entropies of mixing. The entropy of mixing is determined by considering a vibrational and a configurational contribution. The partial entropy of mixing for $ZnCl_2$ is calculated from the model as

$$[11]\quad \Delta\bar{S}_{ZnCl_2} = -R \ln \frac{4(2X_{ZnCl_2} - X_{ACl})^3}{(1 + X_{ZnCl_2})(4X_{ZnCl_2} - X_{ACl})^2}$$

in the composition range $X_{ZnCl_2} > 1/3$ and in the composition range $X_{ZnCl_2} < 1/3$

$$[12]\quad \Delta\bar{S}_{ZnCl_2} = \varepsilon - R \ln \frac{X_{ZnCl_2}(X_{ACl} - X_{ZnCl_2})}{(X_{ACl} - 2X_{ZnCl_2})^2}$$

The vibration contribution, ε, is associated with reaction 6 and can be calculated from eq. 12 and the experimental results. The corresponding average values that were determined are shown in Table 4. However, eq. 11 indicates that there is no vibrational contribution from the formation of the tetrahedral complex since the addition of $ZnCl_2$ to compositions in this range would not result in the formation of more tetrahedral complexes of the type $ZnCl_4^{2-}$. In addition, the partial entropy of mixing given by eq. 11 is positive in this composition range and thus the partial excess entropy of $ZnCl_2$ should not have a negative value in this range. This prediction of the model for the entropy is not substantiated by the large negative partial excess entropies for $ZnCl_2$ in the acidic range reported in Table 3. For acidic compositions ($X_{ZnCl_2} > 1/3$) it would appear that other complexes become possible to satisfy Zn^{2+} cation desire for a tetrahedral chloride environment through sharing arrangements.

In the treatment by Pelton (13) only two parameters are used in the model to account for the acid–base behavior of MY_2–AY halide systems. One of the parameters (b_1) used in the model reflects the inherent appetite of M^{2+} ion to form the tetrahedral complex ion. For example, the values of b_1 parameter found for BeF_2, $CoCl_2$, and $MnCl_2$ systems are −50, −22, and 0.0 kcal per mol indicating the decreasing acidity of the M^{2+} ion. The average value of −27 kcal per mol for the b_1 parameter that was estimated from the present enthalpy results indicate that $ZnCl_2$ is highly associated in the pure state. Hence, the application of the discrete complex anion model in the highly acidic composition becomes doubtful as with the previous model. It would appear that polymeric models developed by Masson *et al.* (32) and Baes (33) would be more applicable in the acidic regions. However, these polymeric models would have to be modified to include vibrational entropy effects.

The authors wish to acknowledge the use of the facilities and equipment at the Department of Chemical Engineering, University of Waterloo, Waterloo, Ontario and especially Dr. J. Wynnyckyj for the use of some of the equipment used in this work. The financial support by the National Research Council of Canada is also gratefully acknowledged.

1. R. G. WARD. An introduction to the physical chemistry of iron and steel making. Edward Arnold Publishers Ltd., London. 1962. p. 18.
2. F. D. RICHARDSON and L. E. WEBB. Bull. Inst. Min. Metal. **584**, 529 (1955).
3. R. SRIDHAR and J. H. E. JEFFES. Trans. Inst. of Min. and Metall. **76**, C44 (1967).
4. G. G. CHARETTE and S. N. FLENGAS. Can. Metal. Q. **7** (4), 191 (1968).
5. T. OSTVOLD and O. J. KLEPPA. Inorg. Chem. **8**, 78 (1969).
6. C. BODSWORTH. Physical chemistry of iron and steel manufacture. Longmans, London. 1963. p. 85.
7. J. L. HOLM and O. J. KLEPPA. Inorg. Chem. **6**, 645 (1967).
8. S. CANTOR, W. T. WARD, and T. MOYNIHAN. J. Chem. Phy. **50**, 2874 (1968).
9. O. J. KLEPPA and F. G. MCCARTY. J. Phys. Chem. **70**, 1249 (1966).
10. G. N. PAPATHEODOROU and O. J. KLEPPA. J. Inorg. Nucl. Chem. **32**, 889 (1970).
11. G. N. PAPATHEODOROU and O. J. KLEPPA. J. Inorg. Nucl. Chem. **33**, 1249 (1971).
12. G. N. PAPATHEODOROU and O. J. KLEPPA. Inorg. Chem. **10**, 872 (1971).
13. A. D. PELTON. Can. J. Chem. **49**, 3919 (1971).
14. C. A. ANGELL and J. WONG. J. Chem. Phys. **53**, 2053 (1970).
15. W. BUES. Z. anorg. allgem Chem. **279**, 104 (1970).
16. J. R. MOYER, J. C. EVANS, and G. Y. S. LO. J. Electrochem. Soc. **113**, 158 (1966).

17. H. BLOOM and I. A. WEEKS. Trans. Faraday Soc. **67**, 1421 (1971).
18. H. BLOOM and I. A. WEEKS. Trans. Faraday Soc. **67**, 1411 (1971).
19. H. BLOOM and I. A. WEEKS. Trans. Faraday Soc. **67**, 1416 (1971).
20. C. DIJKHUIS, R. DIJKHUIS, and G. JANZ. Chem. Rev. **68**, 253 (1968).
21. A. S. KUCHARSKI and S. N. FLENGAS. J. Electrochem. Soc. **119**, 1170 (1972).
22. M. TAKAHASHI. J. Electrochem. Soc. of Jap. **28**, 313 (1960).
23. S. N. FLENGAS and T. R. INGRAHAM. Can. J. Chem. **35**, 1254 (1957).
24. B. F. MARKOV and R. V. CHERNOV. Ukr. Khim Zh. **24**, 139 (1958).
25. B. F. MARKOV and S. V. VOLKOV. Ukr. Khim Zh. **30**, 545 (1964).
26. B. F. MARKOV and S. V. VOLKOV. Ukr. Khim Zh. **30**, 906 (1964).
27. C. G. M. DIJKHUIS and J. A. H. KETELAAR. Electrochem. Acta, **11**, 1622 (1953).
28. H. BLOOM, T. H. SPURLING, and J. WONG. Austr. J. Chem. **23**, 501 (1970).
29. L. C. GEORGE, A. VISNAPUIE, B. C. MAREK, and R. M. DOERR. U.S. Dept. of Interior, Bur. of Mines. 969, #7307.
30. D. CUBICCIOTTI and H. EDING. J. Chem. Phy. **40**, 978 (1965).
31. S. N. FLENGAS and A. S. KUCHARSKI. Can. J. Chem. **49**, 3971 (1971).
32. C. R. MASSON, I. B. SMITH, and S. S. WHITEWAY. Can. J. Chem. **48**, 1456 (1970).
33. C. F. BAES JR. J. Solid State Chem. **1**, 159 (1970).
34. W. J. HAMER, M. S. MALMBERG and B. RUBIN. J. Electrochem. Soc. **103**, 8 (1965).
35. O. KUBASCHEWSKI, E. EVANS, and C. B. ALCOCK. Metallurgical thermochemistry. Pergamon Press, Toronto. 1971.
36. C. E. WICKS and F. E. BLOCK. U.S. Bur. Mines Bull. 605 (1963).

Can. J. Chem. Downloaded from www.nrcresearchpress.com by 210.87.254.40 on 09/05/12
For personal use only.

The Effects of Potassium Fluoride and Potassium Iodide on the Expansivity of Water

NOEL M. BURNS

Canada Centre for Inland Waters, Department of the Environment, Burlington, Ontario

Received October 18, 1972

An examination of the specific volumes of KF and KI solutions over the concentration range 0.1 to 2.0 *m* and over the temperature range 0° to 95° has led to the conclusion that the partial molal expansivity of the salts is due almost entirely to changes in the electrostrictive processes in water with temperature and are not due to changes in the structural effects of the salts on the bulk water with changing temperature. However, structural effects are considered to be of significant magnitude below 70°.

Un examen des volumes spécifiques des solutions de KF et KI dans l'intervalle de concentration de 0.1 à 2.0 *m* et de température de 0° à 95°, a permis de conclure que l'expansion partielle molaire des sels est presqu'entièrement due aux changements dans les processus électrostrictifs de l'eau avec la température et non aux changements des effets structuraux des sels sur la masse d'eau. On considère cependant qu'au dessous de 70° des effets de structure peuvent avoir une amplitude significative.

[Traduit par le journal]

Can. J. Chem., 51, 3123 (1973)

Can. J. Chem. Downloaded from www.nrcresearchpress.com by 210.87.254.42 on 09/05/12
For personal use only.

Introduction

In a recent discussion (1) of ion–water interactions, the partial molal volume of an ion at infinite dilution, $\bar{V}^0_{ion}$ has been attributed to the following components:

$$[1] \quad \bar{V}^0_{ion} = \bar{V}^0_{cryst} + \bar{V}^0_{elect} + \bar{V}^0_{disord} + \bar{V}^0_{caged}$$

where $\bar{V}^0_{cryst}$ is the crystal partial molal volume, $\bar{V}^0_{elect}$ is the electrostriction partial molal volume, $\bar{V}^0_{disord}$ is the disordered or void-space molal volume, and $\bar{V}^0_{caged}$ is the caged or structural partial molal volume.

The crystal volume of the ion $\bar{V}^0_{cryst}$ is usually considered to be temperature independent (2, 3) so that eq. 1 can be simplified by differentiating with respect to temperature, giving

$$[2] \quad \bar{E}^0_{ion} = \bar{E}^0_{elect} + \bar{E}^0_{disord} + \bar{E}^0_{caged}$$

where $\bar{E}^0_{ion}$ represents the partial molal expansivity of the ion and the other symbols represent the appropriate partial molal expansivity contributions. If a study is made of the partial molal expansivities over a range of temperatures, it is possible to learn about the magnitude of the different effects, since $\bar{E}^0_{elect}$ would have a large effect at high temperatures and $\bar{E}^0_{caged}$ would have a more obvious effect at low temperatures. The partial molal expansivity of a salt would represent the sum of the effects of the positive and negative ions.

In order that the relative magnitudes of the above mentioned quantities could be estimated, an investigation of the expansivities of potassium fluoride and potassium iodide solutions over an extended concentration range and temperature range was carried out.

Experimental

Eleven solutions each of KI and of KF were made up having molal concentrations: 0.1 *m*; 0.2 *m*, and thereafter with increments of 0.2 *m* up to 2.0 *m*. Shawinigan analytical grade KI was dried for 2 days at 180° and then used to make up the iodide solutions with distilled, deionized water. It was found that prolonged heating of KF caused the production of some insoluble material; thus, Allied Chemical analytical grade, anhydrous KF was placed in a vacuum desiccator for 2 weeks and the fluoride solutions were made up from this salt.

Specific gravities were measured using 25 ml Fisher density bottles, filled with deaerated solution, and then placed in a thermostated water bath controlled to ±0.005°. When the bottles had equilibrated, they were removed from the bath and dried. After equilibration to room temperature, the bottles were weighed to within 0.0001 g. The procedure was then repeated at a higher temperature. This was done at 5° intervals from 0° to 95°. The volumes of the density bottles were determined at each temperature by carrying out the same experimental procedure with pure water as was done with the solutions and using the values given in the literature (4) for the specific volume of water.

Results

The values reported for the specific volumes, V (V = volume of 1 g of solution), of the solutions at the different temperatures are the average of three experimentally determined values. The

Can. J. Chem. Downloaded from www.nrcresearchpress.com by 210.87.254.42 on 09/05/12
For personal use only.

TABLE 1. Coefficients a_i for eq. 3 for aqueous KI solutions; the resultant polynomials fit the specific volume (ml g^{-1}) data within the experimental error between 0° and 95°

[KI] (m)	a_0	$a_1 \times 10^{-5}$	$a_2 \times 10^{-6}$	$a_3 \times 10^{-8}$	$a_4 \times 10^{-10}$
0.0	1.00010	−5.2243	7.5547	−4.1832	1.4922
0.1005	0.98766	−3.9511	7.8736	−5.4118	2.2917
0.2002	0.97594	−1.0362	7.2388	−4.7552	1.9720
0.4010	0.95348	2.9504	6.5050	−4.2551	1.8109
0.5877	0.93573	5.7603	6.2326	−4.5771	2.0988
0.7995	0.91319	8.6590	5.6030	−3.9422	1.7843
0.9985	0.89479	10.6230	5.4990	−4.2956	2.0236
1.2123	0.87769	15.4045	3.5644	−1.1231	0.2931
1.4025	0.86068	17.1394	3.2042	−0.9040	0.2641
1.5995	0.84528	19.0750	2.6191	−0.1008	−0.1822
1.8015	0.83069	17.9971	3.6055	−2.0062	0.8133
1.9935	0.81728	21.8776	2.3126	−0.4672	0.1959

TABLE 2. Coefficients a_i for eq. 3 for aqueous KF solutions; the resultant polynomials fit the specific volume (ml g^{-1}) data within the experimental error between 0° and 95°

[KF] (m)	a_0	$a_1 \times 10^{-5}$	$a_2 \times 10^{-6}$	$a_3 \times 10^{-8}$	$a_4 \times 10^{-10}$
0.0	1.00010	−5.2243	7.5547	−4.1832	1.4922
0.1021	0.99470	−2.6055	6.7765	−3.0658	0.8166
0.1922	0.99006	−1.3789	6.8560	−3.7857	1.4018
0.3880	0.98053	1.1346	6.5225	−3.8325	1.5248
0.4965	0.97525	3.5296	5.7760	−2.7798	0.9176
0.8066	0.96086	7.1722	5.0420	−2.2864	0.7750
1.0031	0.95209	9.7770	4.5457	−1.9850	0.6769
1.2633	0.94127	12.0276	4.0266	−1.5485	0.4942
1.3894	0.93598	13.5931	3.3503	−0.5556	0.0074
1.6030	0.92749	14.9364	3.3393	−1.0111	0.3022
1.8019	0.91989	16.1456	3.1260	−0.9860	0.3503
1.9980	0.91256	16.7888	3.1137	−1.2313	0.5088

average deviation from the mean for each density determination was 4×10^{-5} g ml^{-1} for 0.1 to 1.0 m solutions of both salts and 7×10^{-5} g ml^{-1} for 1.2 to 2.0 m solutions. These errors are sufficiently large to throw doubt on the fifth decimal figure in the values reported below and lead to an uncertainty of about ±2.5% of the volume difference observed due to a 5° temperature change in a solution; and a ±0.5% uncertainty in the specific volume change associated with an increase of 0.2 m in KF concentration. The twenty values for the specific volume of each solution were fitted to a polynomial of the form,

$$[3] \qquad V = \sum_{i=0}^{4} a_i t^i$$

where a_i are adjustable coefficients (i refers to the different terms in the expression) and t is the temperature in degrees Celsius. The coefficients of eq. 3 for each of the KI solutions are shown in Table 1 and those for the KF solutions are given in Table 2. The average difference between the observed value of V and those calculated by means of eq. 3 for the same conditions of temperature and concentration, was $\pm 5 \times 10^{-5}$ ml g^{-1}.

Table 3 shows a comparison of expansivities of 0.1 m KI at different temperatures determined from the volume measurements of Millero and Drost-Hansen (5) who used a magnetic float densitometer, with the results obtained in this study by using density bottles.

The partial molal volumes obtained for each solution at the different temperatures were fitted to a polynomial expression of the form

$$[4] \qquad \bar{V} = \sum_{i=0}^{3} a_i t^i$$

TABLE 3. Comparison of expansivities of 0.1 *m* KI

Temperature	Calculated*	This work
20	2.17×10^{-4} deg^{-1}	2.20×10^{-4} deg^{-1}
25	2.66	2.69
30	3.10	3.14
35	3.52	3.54
40	3.92	3.91

*From values listed in ref. 5.

These expressions were then differentiated with respect to temperature so that values were obtained for the partial molal expansivities of all the solutions at the different temperatures. The results of these calculations are shown in Fig. 1. The values obtained by the above calculations for the partial molal expansivity of KI at 25° are: infinite dilution, 0.121 ml mol^{-1} deg^{-1}; 0.1005 *m*, 0.117 ml mol^{-1} deg^{-1}. These values compare with the value obtained by Noyes (6) for KI at 25° at infinite dilution of 0.127 ml mol^{-1} deg^{-1} and the value obtained by Millero and Drost-Hansen (5) for 0.10153 *m* KI at 25° of 0.092 ml mol^{-1} deg^{-1}. Millero (1) has calculated the partial molal expansivity of KF solutions at infinite dilution between 25° and 40° and the values calculated from his expression are 0.06 ml mol^{-1} deg^{-1} at 25° and 0.0 ml mol^{-1} deg^{-1} at 40° which compare with values calculated in this work of 0.07 ml mol^{-1} deg^{-1} at 25° and 0.03 ml mol^{-1} deg^{-1} at 40 °C.

Expansivities of the individual solutions were obtained from the expression

$$[5] \qquad E = \frac{1}{V}\frac{dV}{dt}$$

where the values for dV/dt were obtained by differentiating eq. 3 with respect to temperature. The use of expansivities enables a comparison to be made of the behavior of solutions having different densities. The expansivity data were smoothed by being fitted to an equation of the form

$$[6] \qquad E = \sum_{i=0}^{3} B_i m_i$$

at each temperature, where B_i are adjustable coefficients and m is molality. The values for E calculated by means of eq. 6 varied from the unsmoothed values by 0.5% on average.

Figures 2 *a*, *b*, *c*, *d*, and 3 *a*, *b*, *c*, *d*, show plots of the expansivities, E *vs.* temperature for water and for the KF and KI solutions. The trends are

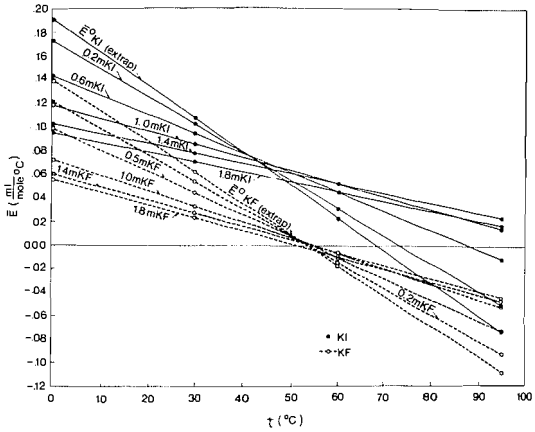

FIG. 1. Partial molal expansivities of KI and KF solutions *vs.* temperature. The calculated uncertainty for E for the KF solutions is ±0.01 ml mol^{-1} and for the KF solutions is ±0.02 ml mol^{-1}.

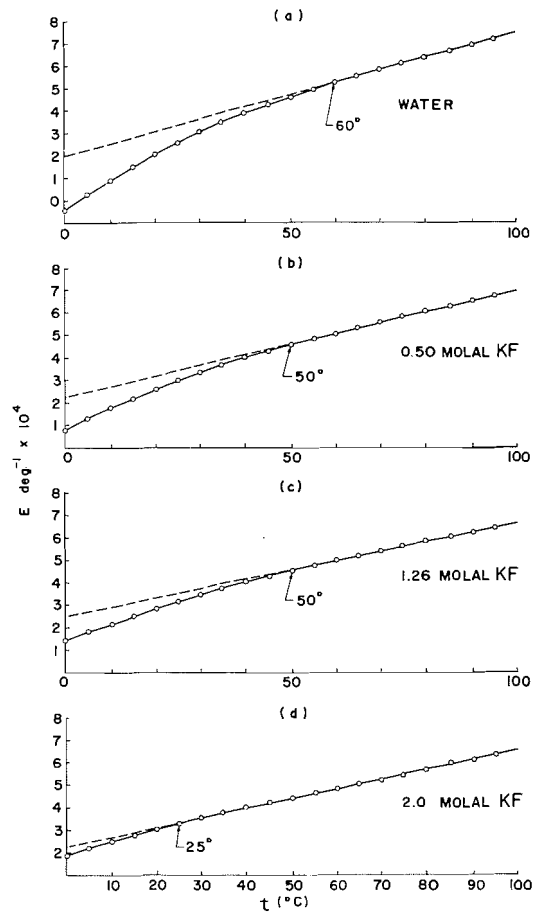

FIG. 2. Expansivities of pure water and KF solutions between 0° and 95°.

Can. J. Chem. Downloaded from www.nrcresearchpress.com by 210.87.254.42 on 09/05/12
For personal use only.

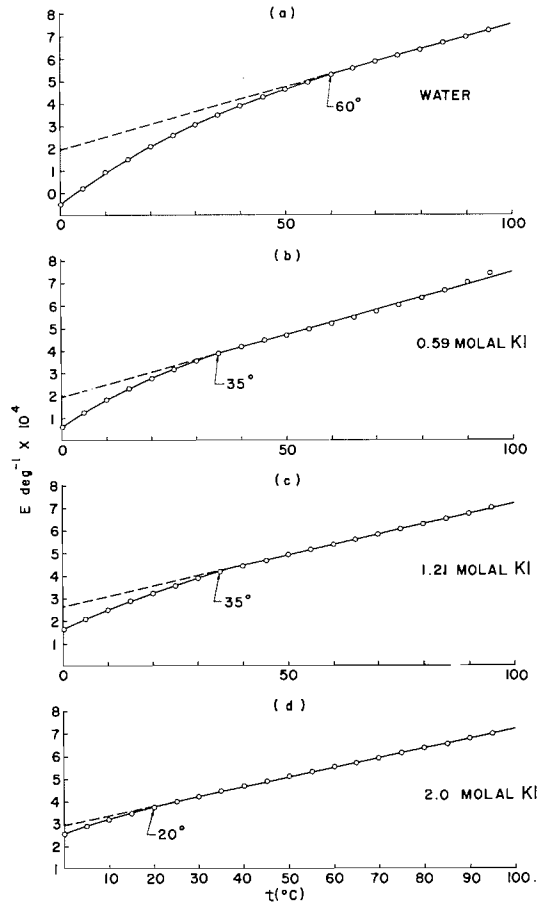

FIG. 3. Expansivities of pure water and KI solutions between 0° and 95°.

gradual and only part of the calculated data is shown.

Discussion

Part I

As an ion is introduced into water, the segment of water which is affected by the ion changes from having normal water structure to being subject to incorporation as water of hydration or structure modification outside of the hydrated ion or void space effects as the hydrated ion is fitted into the surrounding fluid. Because of these processes, the partial molal expansivity gives information relative to change in the expansivity of the water which has been effected by the introduction of the ion into the solvent.

The predominant feature of the data (Fig. 1) is that the partial molal expansivities of KF and KI solutions are concentration independent at about 53° and 50°, respectively. This means that in this temperature range there is an effect of the salt on the expansivity of water which either disappears or is constant for all concentrations, whereas at other temperatures this effect is significant and variable. It is of interest to examine the various terms of eq. 2 to find which effect causes the observed predominant feature.

The quantity, $\bar{V}^0_{disord}$, is the volume taken up when the hydrated ion does not fit exactly into the surrounding fluid and a commonly used expression for evaluating this quantity is given by Millero (1),

$$[7] \qquad \bar{V}^0_{disord} = Ar^2$$

where A is a proportionality constant having the values 4.09 (6) and 4.03 (2). Also, Millero (7) has estimated the value of $\bar{V}^0_{disord}$ over the temperature range 0° to 200° for an ion having a diameter of 1.0 Å and found $\bar{V}^0_{disord}$ increased slightly with temperature. Consequently, $\bar{E}^0_{disord}$ would probably be small and fairly constant over a wide temperature range and would increase with increasing ion size with no major change in $\bar{E}^0_{disord}$ at 50°.

The term, $\bar{V}^0_{caged}$ refers to the effect of the hydrated ion on the bulk liquid. Simple monovalent ions are considered (8) to decrease structure in the adjacent bulk liquid and this would cause $\bar{V}^0_{caged}$ to have a negative value. Since the amount of structure in the bulk liquid decreases with increasing temperature, $\bar{V}^0_{caged}$ would become less negative with increasing temperature. This reasoning would lead to the conclusion that a structure breaking solute would cause the value for $\bar{E}^0_{caged}$ to be positive but there is no reason to believe that there would be any major change in the value of $\bar{E}^0_{caged}$ about 50°.

Hepler (9) has developed an expression for $\bar{V}^0_{elect}$ of an ion

$$[8] \qquad \bar{V}^0_{elect} = -\int_r^\infty \int_p^0 \beta dP 4\pi r^2 dr$$

where r = Goldschmidt crystal radius of the ion (10), β = isothermal compressibility of the solvent, P = internal pressure due to the charge on the ion = KZ^2/r^4 where Z is the charge on the ion. Taking P and r to be independent of temperature, differentiation of eq. 8 leads to

$$[9] \qquad \bar{E}^0_{elect} = -\frac{\partial \beta}{\partial t_{p,r}} \int_r^\infty \int_p^0 dP 4\pi r^2 dr$$

Can. J. Chem. Downloaded from www.nrcresearchpress.com by 210.87.254.42 on 09/05/12
For personal use only.

Can. J. Chem. Downloaded from www.nrcresearchpress.com by 210.87.254.42 on 09/05/12
For personal use only.

The isothermal compressibility of water has a significant temperature dependence (Fig. 5) so $\bar{E}^0_{elect}$ could be expected to be temperature sensitive; being positive below 47° since in this temperature range $d\beta/dt$ is negative; being equal to zero at 47° since at this temperature $d\beta/dt = 0$ (11), and being negative above 47° where $d\beta/dt$ is positive. The magnitude of the term $\bar{E}_{elect}$ depends on the temperature of the water which is taken from its normal state in the bulk liquid into the compressed state of water of hydration since it is dependent on the value of $\partial\beta/\partial t$ of water, although in its final state the water of hydration would be dissimilar from that in normal water. However, the temperature of minimum isothermal compressibility of water as calculated from the data of Kell and Whalley (12) does not appear to be significantly affected by moderate pressure changes ($\beta_{min} = 44.17$ bar^{-1} at 47° at 1 bar; $\beta_{min} = 28.56$ bar^{-1} at 57° at 2000 bar). The argument outlined above would suggest that $\bar{E}_{elect} \approx 0.0$ at about 50° for most hydrated ions.

It would seem that the pattern of observed values for $\bar{E}_{(KF)}$ follow the pattern which would be predicted for $\bar{E}_{(elect)}(KF)$ on the basis of eq. 9. This fact, together with eqs. 10, 11, and 12 which are proposed below, would make it possible to explain the observed values for $\bar{E}_{(KF)}$.

$$[10]\quad \bar{E}_{elect}(KF) \gg \bar{E}_{disord}(KF) + \bar{E}_{caged}(KF)$$

$$[11]\quad \bar{E}_{disord}(KF) + \bar{E}_{caged}(KF) \approx 0.0 \text{ ml mol}^{-1} \text{ deg}^{-1}$$

$$[12]\quad \frac{\partial E_{elect}}{\partial t}(KF) \gg \frac{\partial}{\partial t}(\bar{E}_{disord}(KF) + \bar{E}_{caged}(KF))$$

It is to be expected that eq. 10 would hold because the fluoride ion is small causing $\bar{V}_{elect}(F^-)$ to be large and $\bar{V}_{disord}(F^-)$ to be small.

The observation that the plots of $\bar{E}$ *vs.* temperature for different concentrations of KI have a common value of 0.6 ± 0.1 ml mol^{-1} deg^{-1} at about 53° can be similarly explained by proposing that the processes which are described by eqs. 13 and 14 operate simultaneously with the electrostrictive effects of KI in water.

$$[13]\quad (\bar{E}_{disord}(KI) + \bar{E}_{caged}(KI)) \approx 0.6 \pm 0.1 \text{ ml mol}^{-1} \text{ deg}^{-1}$$

and

$$[14]\quad \frac{\partial \bar{E}_{elect}}{\partial t}(KI) \gg \frac{\partial}{\partial t}(\bar{E}_{disord}(KI) + \bar{E}_{caged}(KI))$$

The value given in eq. 13 is probably due to $\bar{V}_{disord}(I^-)$ being large in this case as is demonstrated by eq. 7 because (I^-) is a relatively large ion.

Figure 1 shows that the value dE/dt decreases with increasing concentrations for both KF and KI to 1.4 *m* and thereafter appears to remain constant. This is to be expected since the amount of free water for the salt to interact with diminishes with each addition of salt due to ion hydration. An alternative explanation is that at concentrations greater than 1.4 *m*, the ionic spheres of influence begin to overlap as suggested by Gurney (13) causing dE/dm to be small. Thus the generalized statement can be made that in the case of KF solutions the electrostrictive effects of the ions on the water predominate over the structure modifying and the void space effects but in the case of KI solutions the electrostrictive effects are of the same order of magnitude as the other two effects.

In the foregoing discussion the assumption has been made that the ionic radius, *r*, is temperature independent. This assumption is probably not entirely correct but if the temperature dependence of *r* is small, the arguments above will remain valid.

Part II

It would seem from the discussion above that the volume effects of salts on the structure in liquid water outside of the hydrated ion are very small or non-existent. The question then arises as to whether there are significant volume effects of structure in water and whether salts affect this structure in an observable manner, *i.e.*, is $\bar{V}_{caged}$ of significant magnitude. In this regard, data from the literature on specific volume, isothermal compressibility, excess acoustic absorbance of water, the specific volume of heavy water, and the expansivities of KF and KI solutions have been examined.

Figure 4 shows a plot of the data published by Kell (11) for the thermal expansivity, $E = (1/V)(dV/dt)$, of water against temperature. The thermal expansivities are estimated to be accurate to 2×10^{-6} deg^{-1} near 100 °C and it is possible to draw a straight line from 70° to 100° within the limits of this error.

Kell (14) has also published an equation for

Can. J. Chem. Downloaded from www.nrcresearchpress.com by 210.87.254.42 on 09/05/12
For personal use only.

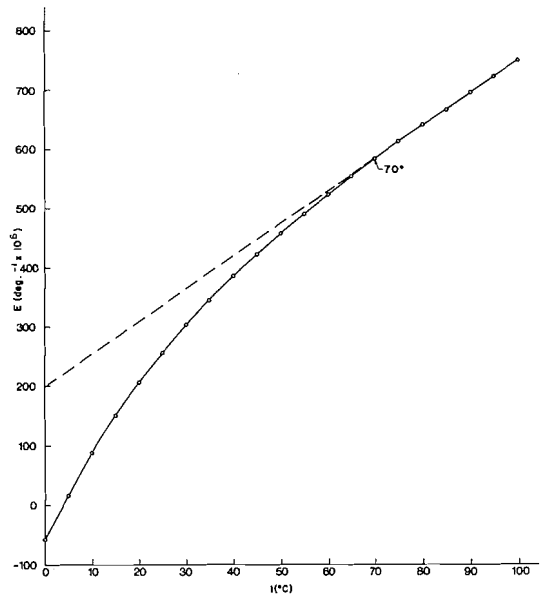

FIG. 4. Expansivity of water between 0° and 100°.

the calculation of the isothermal compressibility of water from 0° to 110° with a standard error of 0.002×10^{-6} bar^{-1}. This expression was differentiated with respect to temperature, t, and Fig. 5 shows a plot of $d\beta/dt$ *vs.* t. Again, there appears to be a straight-line section between 70° and 100°.

In addition, the excess acoustic absorbance data as reported by Hall were plotted. The values for 90° and 100° were calculated by extrapolation of Hall's expression (15). Hall's theory has been seriously questioned (16, 17) but the expression may be regarded as correct from the empirical standpoint and as such is useful for the extrapolation of data (17). The plot of the excess acoustic absorbance of water *vs.* temperature, Fig. 6, shows a straight-line section between 60°–70° and 100° with a large increase in absorption as the temperature drops below 60°–70°.

There is no special significance to the straight-line sections discussed above except in that they are curves of significantly reduced curvature when compared to the more obvious curves at the lower temperatures. In reality, what has been demonstrated is that the pattern of change with temperature is significantly different below 70° to that above 70° in the three properties discussed here.

The patterns observed in the data above can be explained in terms of either the mixture model of liquid water (18–23) or the continuum model (24–26). If the mixture model is considered, then it is necessary to postulate the existence of a bulky species of water which increases in concentration in liquid water as the temperature is lowered below 70°. This type of species has frequently been discussed in the literature (18–20, 23). If the continuum model is considered, then it is necessary to postulate that there is a significant increase in the number of molecules in the

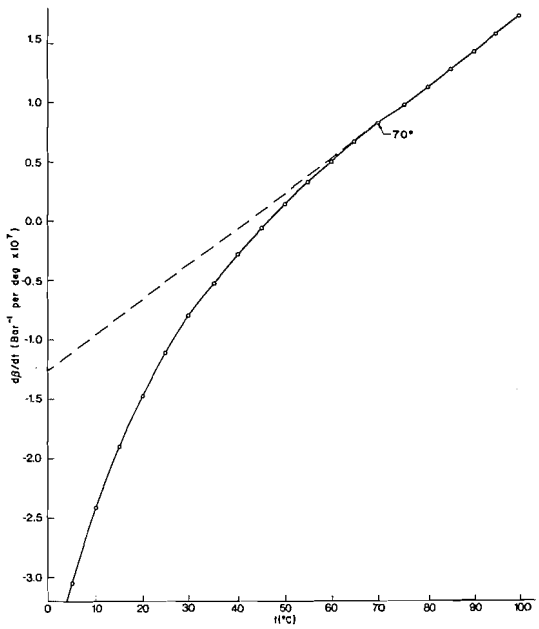

FIG. 5. The variation of isothermal compressibility of water with temperature between 0° and 100°.

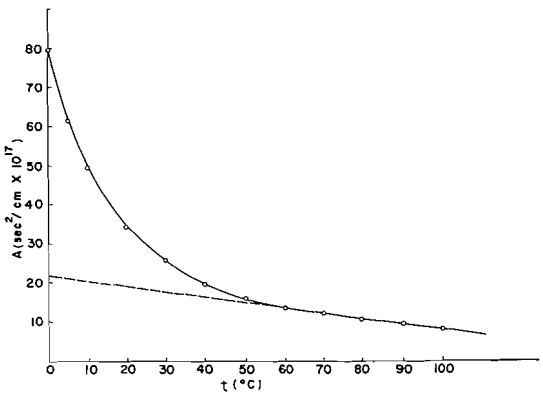

FIG. 6. Variation of excess acoustic absorbance of water between 0° and 100°.

higher volume states as the temperature is lowered below 70°.

The lowered value of the observed expansivity of water below 70° (Fig. 4) E_{obs} can be explained by the disappearance of water in a bulky state with increasing temperature.

In general terms, the experimental compressibility of a liquid, β_{obs} can be expressed by,

$$[15] \qquad \beta_{obs} = \beta_\infty + \beta_r$$

$$[16] \qquad \frac{d\beta_{obs}}{dt} = \frac{d\beta_\infty}{dt} + \frac{d\beta_r}{dt}$$

where β_∞ is the instantaneous compressibility and is a measure only of the decrease in the average distance between molecules with pressure and is independent of molecular rearrangement. β_∞ increases with increasing temperature as the average distance between molecules increases due to expansion; that is, $d\beta_\infty/dt$ is positive. β_r is the relaxational compressibility due to volume decrease as a bulky arrangement transforms into a denser arrangement with increased pressure, in accord with the Le Chatelier principle. In the case of water, β_r would decrease with increasing temperature as a result of the decreasing concentration of bulky species, that is $d\beta_r/dt$ is negative. Thus, it can be seen from eq. 16 that $d\beta_{obs}/dt$ is lowered by the presence of a bulky compressible species below 70°.

The excess acoustical absorbance of ultrasound is the sound energy absorbed due to bulk viscosity, *i.e.*, the energy absorbed by friction as a structure collapses under the compression of a sound wave and reforms again. Figure 6 shows a high absorbance at low temperatures which decreases markedly as the temperature increases to 60°–70° and thereafter decreases linearly with temperature. The marked increase in excess acoustic absorbance below 70° can be attributed to the presence of some molecules in an arrangement which is significantly more bulky than the molecular arrangements which exist above that temperature and that these bulky structures absorb energy as they collapse and reform under the pressures and rarefactions of a sound wave.

The data presented above would appear to support the postulate that there are a number of water molecules present in water in a bulky-structured arrangement and that the number of such molecules increases significantly as the temperature decreases below 70°.

Both KF and KI are what would be termed "structure-breakers" with KI being the strongest "structure-breaker". Thus, if the effect of these two salts on water structure is observable, they should affect the three structure-sensitive properties discussed above. The data shown in Figs. 2 and 3 demonstrate that the curvature below 70° in the *E vs.* temperature plot of water is definitely diminished by the addition of KF and KI to the water. However, it would appear that even at 2.0 *m*, there is structure present in water at the lower temperatures. There does not seem to be any significant difference in the structure-removing ability of the different salts. It would then seem that the effect of monovalent ions on structure in water outside of the hydrated ion is not large but is nevertheless significant.

The data of Kell and Whalley (12) provide the opportunity of checking whether the removal of bulky structure by increased pressure causes a decrease in the curvature in the $d\beta/dt$ *vs.* t plot below 70°. The plot of $d\beta/dt$ *vs.* t (Fig. 5) is very similar to the dV/dt *vs.* t (Fig. 4) and the curvature below 70° in the $d\beta/dt$ *vs.* t plot has been attributed to the presence of bulky structure in water at these temperatures. Since increased pressure should decrease the amount of bulky structure in water, increased pressure should diminish the curvature in the $d\beta/dt$ *vs.* t plot if the postulate is correct that the presence of bulky structure in water lowers the value of $d\beta/dt$ and dV/dt below 70°. In Fig. 7 the change in the specific volume V with temperature and pressure is studied and it is quite obvious that the feature attributed to the presence of bulky structure in water is diminished by increased external pressure in a similar manner to the changes produced on *E vs.* t by additions of halide salts to water.

As a final check on the above reasoning, it was considered that an increase in the amount of bulky structure present in water should cause a decrease in the expansivity at the lower temperatures. D_2O is considered to be more structured than H_2O (27–29); for example, the temperature of maximum density of D_2O, $t_{max}(D_2O) = 11.18°$ whereas for water $t_{max}(H_2O) = 3.98°$. A comparative plot of the expansivities of H_2O and D_2O is shown in Fig. 8. It is not possible to state in terms of the data available (11) whether there is in reality a straight-line segment above 80°. Nevertheless, it can be seen that D_2O has a lower expansivity than H_2O below 70° in accord with the suggested hypothesis.

Can. J. Chem. Downloaded from www.nrcresearchpress.com by 210.87.254.42 on 09/05/12
For personal use only.

Can. J. Chem. Downloaded from www.nrcresearchpress.com by 210.87.254.42 on 09/05/12
For personal use only.

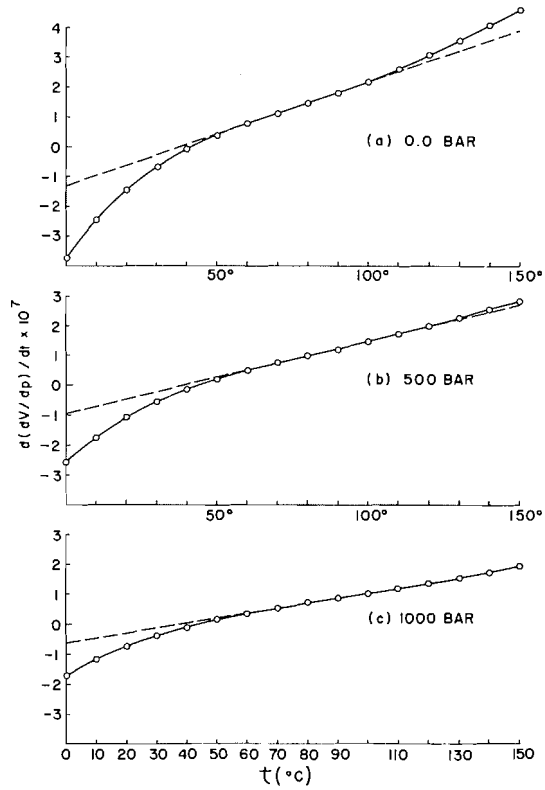

FIG. 7. Variation of specific volume of water with pressure and temperature.

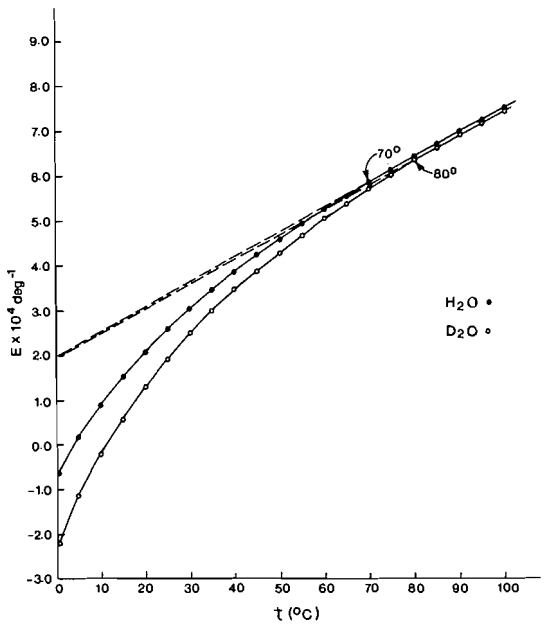

FIG. 8. A comparison of the expansivities of H_2O and D_2O at different temperatures.

Conclusions

Data on the partial molal expansivity of KF and KI solutions have been presented which can be explained simply by assuming that the temperature of minimum isothermal compressibility of water which has undergone electrostriction is similar to that of normal water at atmospheric pressure. It would appear that the effect of temperature on $\overline{V}_{elect}$ is much greater than on $\overline{V}_{disord}$ or $\overline{V}_{caged}$.

Literature data on the expansivity, compressibility, and excess acoustical absorbance of sound in pure water have been examined along with data on the expansivity of heavy water. This data led to the formulation of the hypothesis that water structured in a bulky arrangement exists in pure water at temperatures below 70°. An examination of the data on the expansivity of KF and KI solutions showed that the proposed bulky structure in water is significantly removed by the addition of the halide salts to pure water.

The author is grateful to the University of Alberta and the Province of Alberta for financial assistance while measurements were carried out at the Department of Chemistry, University of Alberta, Edmonton, and also to H. B. Dunford, J. E. Desnoyers, and W. A. Adams for helpful discussions.

1. F. J. MILLERO. *In* Water and aqueous solutions: structure thermodynamics and transport processes. *Edited by* R. A. Horne. Wiley-Interscience, N.Y. 1972. Chapt. 13.
2. M. H. PANCKHURST. Rev. Pure Appl. Chem. **19**, 45 (1969).
3. B. S. GOURARY and F. J. ADRIAN. Solid-State Phys. **10**, 127 (1960).
4. Smithsonian Institute Tables. *Quoted in* Handbook of chemistry and physics. 47th ed. Chemical Rubber Publishing Co. 1966–67. p. F-4.
5. F. J. MILLERO and W. DROST-HANSEN. J. Chem. Eng. Data, **13**, 331 (1968).
6. R. M. NOYES. J. Am. Chem. Soc. **86**, 971 (1964).
7. F. J. MILLERO. Chem. Rev. **71**, 147 (1971).
8. H. S. FRANK and W. Y. WEN. Discuss. Faraday Soc. **24**, 133 (1957).
9. L. G. HEPLER. J. Phys. Chem. **61**, 1426 (1957).
10. V. W. GOLDSCHMIDT. Skr. Norske Videnskap-Adad. Oslo. I. Mat-Naturv. Klasse, 1 (1926).
11. G. S. KELL. J. Chem. Eng. Data, **12**, 66 (1967).
12. G. S. KELL and E. WHALLEY. Phil. Trans. Roy. Soc. Lond. **A258**, 565 (1965).
13. R. W. GURNEY. Ionic processes in solution. Dover N.Y. 1962.
14. G. S. KELL. J. Chem. Eng. Data, **15**, 119 (1970).
15. L. HALL. Phys. Rev. **73**, 775 (1948).
16. T. A. LITOVITZ and E. H. CARNEVALE. J. Appl. Phys. **26**, 816 (1955).

17. J. J. MARKHAM, R. T. BEYER, and R. B. LINDSAY. Rev. of Mod. Phys. **23**, 252 (1951).
18. J. D. BERNAL and R. H. FOWLER. J. Chem. Phys. **1**, 515 (1933).
19. H. S. FRANK and A. S. QUIST. J. Chem. Phys. **34**, 604 (1961).
20. S. NEMETHY and H. A. SCHERAGA. J. Chem. Phys. **36**, 3382 (1962).
21. K. BUIJS and G. R. CHOPPIN. J. Chem. Phys. **39**, 2035 (1963).
22. G. E. WALRAFEN. J. Chem. Phys. **40**, 3249 (1964).
23. G. M. DAVIES and T. A. LITOVITZ. *In* Water and aqueous solutions: structure thermodynamics and transport processes. *Edited by* R. A. Horne. Wiley–Interscience, N.Y. 1972. Chapt. 10.
24. J. POPLE. Proc. Roy. Soc. (Lond.), **205A**, 163 (1951).
25. G. S. KELL. *In* Water and aqueous solutions: structure thermodynamics and transport processes. *Edited by* R. A. Horne. Wiley–Interscience, N.Y. 1972. Chapt. 9.
26. M. FALK and T. A. FORD. Can. J. Chem. **44**, 1699 (1966).
27. E. WHALLEY. Trans. Faraday Soc. **53**, 1578 (1957).
28. C. G. SWAIN and R. F. W. BADER. Tetrahedron, **10**, 183 (1960).
29. G. NEMETHY and H. A. SCHERAGA. J. Chem. Phys. **41**, 680 (1964).

Can. J. Chem. Downloaded from www.nrcresearchpress.com by 210.87.254.42 on 09/05/12
For personal use only.

The Pulse Radiolysis of Penicillamine and Penicillamine Disulfide in Aqueous Solution[1]

JOHN W. PURDIE[2]
Division of Biological Sciences, National Research Council of Canada, Ottawa, Canada K1A 0R6

AND

HUGH A. GILLIS AND NORMAN V. KLASSEN
Division of Physics, National Research Council of Canada, Ottawa, Canada K1A 0S1

Received March 16, 1973

Aqueous solutions of penicillamine (RSH) and penicillamine disulfide (RSSR) have been pulse irradiated at several pH's and the ensuing reactions studied. The rate constant for the reaction of solvated electrons with penicillamine disulfide decreases from $7.3 \times 10^9\ M^{-1}\ s^{-1}$ at pH 7 to $0.8 \times 10^9\ M^{-1}\ s^{-1}$ at pH 10. The first-order rate constant for the decomposition of the resulting radical anion, $RSSR^-$, increases from $1.77 \times 10^6\ s^{-1}$ at pH 7 to $6.5 \times 10^6\ s^{-1}$ at pH 10. Both of these pH effects are attributed to deprotonation of the two amino groups of the disulfide which have microscopic pK values of 7.9 and 8.5. The equilibrium constant for the reaction

[2] $$RS\cdot + RS^- \rightleftharpoons RSSR^-$$

is $(2.31 \pm 0.2) \times 10^2\ M^{-1}$ at pH 8 but increases to $3.04 \times 10^2\ M^{-1}$ at pH 7 and decreases to $0.96 \times 10^2\ M^{-1}$ at pH 9. Measured from the kinetics of the build-up of $RSSR^-$, $k_{-2} = 1.83 \times 10^6\ s^{-1}$ at pH 8.

Decay of $RSSR^-$ in the presence of RSH follows second-order kinetics at high dose rates and first-order kinetics at low dose rates. At high dose rates two second-order reactions

$$RS\cdot + RS\cdot \rightarrow RSSR$$

$$RS\cdot + RSSR^- \rightarrow RSSR + RS^-$$

appear to be involved with rate constants of $1.7 \times 10^9\ M^{-1}\ s^{-1}$ and $6.4 \times 10^9\ M^{-1}\ s^{-1}$ respectively at pH 8. At low dose rates the decay appears to be due to a pseudo first-order reaction between $RSSR^-$ and H_2O, $k \sim 2 \times 10^3\ s^{-1}$, with valine (RH) and penicillamine trisulfide (RSSSR) as principal products. These products are obtained in similar yields by gamma radiolysis of penicillamine solutions. At pH 5, the thiyl radical decays by second-order kinetics, $2k = (2.85 \pm 0.15) \times 10^9\ M^{-1}\ s^{-1}$.

Studies of solutions containing penicillamine and methanol showed that penicillamine repairs methanol radicals very efficiently by hydrogen transfer, $k = (1.1 \pm 0.1) \times 10^8\ M^{-1}\ s^{-1}$. The implications of the results for chemical radioprotection are discussed.

Des solutions aqueuses de penicillamine (RSH) et du disulfide de penicillamine (RSSR) ont été soumises à des irradiations pulsées à plusieurs pH et on a étudié les réactions suivantes. La constante de la vitesse de la réaction entre l'électron solvaté et le disulfide de penicillamine a diminué de $7.3 \times 10^9\ M^{-1}\ s^{-1}$ à pH 7.0 jusqu'à $0.8 \times 10^9\ M^{-1}\ s^{-1}$ à pH 10.0. La constante de vitesse de premier ordre pour la décomposition du produit radical ($RSSR^-$) augmente de $1.77 \times 10^6\ s^{-1}$ à pH 7 jusqu'à $6.5 \times 10^6\ s^{-1}$ à pH 10. On attribue ces deux effets de pH à la déprotonation des deux groupes amino du disulfide qui ont des pK microscopiques de 7.9 et 8.5. La constante d'équilibre de la réaction

[2] $$RS\cdot + RS^- \rightleftharpoons RSSR^-$$

est $(2.31 \pm 0.2) \times 10^2\ M^{-1}$ à pH 8.0 mais augmente jusqu'à $3.04 \times 10^2\ M^{-1}$ à pH 7.0 et diminue jusqu'à $0.96 \times 10^2\ M^{-1}$ à pH 9.0. La cinétique obtenue par la mesure de la formation de $RSSR^-$ à pH 8.0 fournit une constante de vitesse de $k_{-2} = 1.83 \times 10^6\ s^{-1}$.

En présence de RSH, la décomposition suit une cinétique du deuxième ordre à fortes intensités d'exposition et du premier ordre à faibles intensités d'exposition. Dans le cas des fortes intensités d'exposition il semble que deux réactions du deuxième ordre soient à considérer

$$RS\cdot + RS\cdot \rightarrow RSSR$$

$$RS\cdot + RSSR^- \rightarrow RSSR + RS^-$$

[1]Issued as DREO Report No. 683 and NRCC No. 13318.
[2]Attached staff from Defence Research Establishment Ottawa.

Can. J. Chem. Downloaded from www.nrcresearchpress.com by 210.87.254.42 on 09/05/12
For personal use only.

dont les constantes de vitesse respectives sont $1.7 \times 10^9\ M^{-1}\ s^{-1}$ et $6.4 \times 10^9\ M^{-1}\ s^{-1}$ à pH 8.0. Aux faibles intensités il semble que la décomposition soit dûe à une réaction entre $RSSR^-$ et H_2O, $k \sim 2 \times 10^3\ s^{-1}$, dont les produits de réaction sont la valine (RH) et le trisulfide de penicillamine (RSSR). Ces mêmes produits sont obtenus avec des rendements semblables par irradiation des solutions de penicillamine à l'aide des rayons gammas. A pH 5.0, le radical RS· se décompose selon une cinétique du deuxième ordre, $2k = (2.85 \pm 0.15) \times 10^9\ M^{-1}\ s^{-1}$.

Par étude des solutions contenant de la penicillamine et du méthanol, on a montré que la penicillamine peut reconstituer efficacement les radicaux du méthanol par transfert de l'hydrogène avec une vitesse de réaction, $k = (1.1 \pm 0.1) \times 10^8\ M^{-1}\ s^{-1}$. Les résultats obtenus sont discutés au point de vue de la protection chimique contre les rayonnements.

Can. J. Chem. Downloaded from www.nrcresearchpress.com by 210.87.254.42 on 09/05/12
For personal use only.

Introduction

The effect of ionizing radiation on aqueous solutions of thiols and disulfides has been studied extensively and in recent years the pulse radiolysis technique has been applied to this problem. A major reason for the interest in these compounds is that many thiols and some of the corresponding disulfides protect mammals from the damaging effects of ionizing radiation (1). Although cysteamine (2-mercaptoethylamine), cysteine, and many closely related compounds are protective *in vivo*, penicillamine (β,β-dimethylcysteine) has no protective property (2). This lack of protective ability bears no obvious relationship to the reaction rates of penicillamine with free radicals from water as it reacts rapidly with both hydrated electrons (3) and hydroxyl radicals (4). However, it was observed earlier that the radiation chemistry of penicillamine disulfide differs considerably from that of disulfides of radioprotective thiols (see ref. 5 and references therein) but the difference was difficult to relate to radioprotective efficiency. Thus it is important to study the initial reactions and the free radicals involved in the radiolysis of penicillamine. A detailed knowledge of the differences between penicillamine and radioprotective thiols may provide an insight into the chemical processes involved in radioprotection.

Pulse radiolysis of aqueous solutions of cysteamine was studied by Adams *et al.* (6) and they concluded that the thiyl radical (RS·) produced initially combines with the sulfhydryl anion to give a radical anion ($RSSR^-$) in an equilibrium process

$$[1] \qquad OH\cdot + RSH \rightarrow H_2O + RS\cdot$$

$$[2] \qquad RS\cdot + RS^- \rightleftharpoons RSSR^-$$

The same transient is produced when a solvated electron reacts with a disulfide:

$$[3] \qquad RSSR + e_{aq}^- \rightarrow RSSR^-$$

Analogous radical anions have been reported for such compounds as hydrogen sulfide (7), cysteine (8), glutathione (9, 10), several alkyl mercaptans (11), selenourea (12), and enzymes containing disulfide bonds (13).

As reported previously (14), we have identified both the thiyl radical and the radical anion of penicillamine and we now describe further details including the kinetics of the formation and decay of these radicals and related product analysis.

Experimental

Penicillamine was purchased from Calbiochem and the disulfide was obtained from Wateree Chemical Co., Lugoff, S.C. Solutions, prepared in cleaned glassware with triply distilled water, were buffered with 8 mM phosphate and the final pH was adjusted by using NaOH or H_2SO_4 when necessary. The solutions were deaerated by bubbling with N_2O or argon as required. *t*-Butanol (Fisher Certified) was added as a hydroxyl radical scavenger in some cases.

For steady-state radiolysis a ^{60}Co "Gammacell 220" (Atomic Energy of Canada Ltd.) with a dose rate of 130 rad/s was employed.

In the pulse experiments the radiation source was the National Research Council linac. Pulse widths between 10 ns and 1 μs were used, and the dose per pulse was varied between 70 rad and 6 krad. Solutions were contained in a single-pass cell 2 cm long. Spectral measurements were made with a split light-beam system which included a Xe arc lamp, Bausch and Lomb high intensity monochromators, suitable filters to reduce scattered light, and either Phillips XP1003 photomultipliers or EG & G YAG-100 Si photodiodes as detectors. A Pyrex filter was always placed between the lamp and sample in measurements above 320 nm to prevent photolysis. For some kinetic measurements, in which the analyzing light was not split, a tungsten lamp replaced the Xe arc and an interference filter centered at 450 nm with a bandpass of 50 nm was used instead of the monochromator. Small variations in dose from pulse to pulse were monitored by a secondary emission chamber behind the cell, and dosimetry was done with $5 \times 10^{-3}\ M$ KSCN solutions saturated with N_2O, for which $G\varepsilon_{500}(CNS)_2^- = 4.2 \times 10^4\ M^{-1}\ cm^{-1}$ (100 eV)$^{-1}$ (15).

Samples for product analysis were acidified and run as soon as possible on a Technicon amino acid analyzer, with care being taken to exclude air (16).

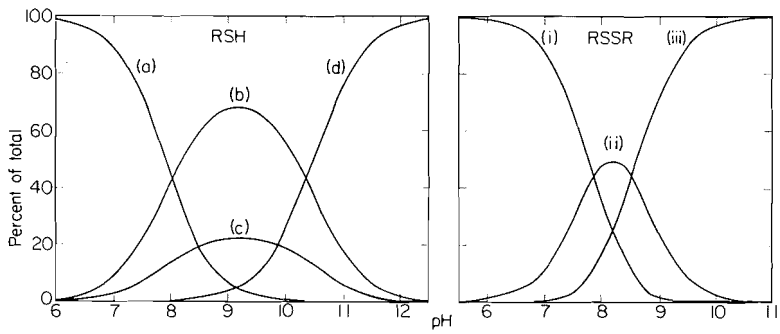

FIG. 1. Percentages calculated for the different ionic forms of penicillamine (Scheme 1) and penicillamine disulfide (Scheme 2).

Results and Discussion

Titration of Penicillamine and Penicillamine Disulfide

The carboxyl, amino, and sulfhydryl groups of penicillamine are deprotonated as the pH is increased. Between pH 5 and 10, the range used in this work, the carboxyl group is completely deprotonated. The deprotonation of the amino and sulfhydryl groups may be represented schematically (Scheme 1). Titration of *a* with alkali leads to a mixture of *b* and *c*. The ratio of *b* to *c* was determined as 3:1 for penicillamine from measurements of the absorption due to the deprotonated sulfhydryl at the λ_{max} of 230 nm; this method has been described by Benesch and Benesch (17). This ratio was combined with literature (18) values of the dissociation constants, $pK_1 = 1.8$, $pK_2 = 7.9$, and $pK_3 = 10.5$, to obtain the micro-ionization constants: $pK_A = 8.02$, $pK_B = 8.50$, $pK_C = 10.33$, and $pK_D = 9.90$. The percentages of the different forms were calculated as a function of pH and are illustrated in Fig. 1.

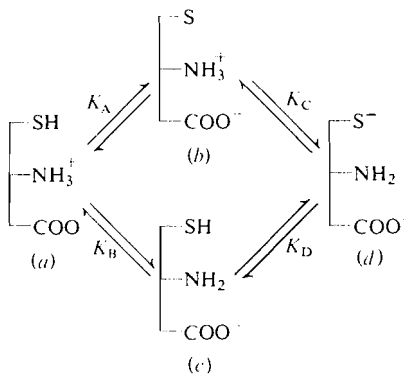

SCHEME 1

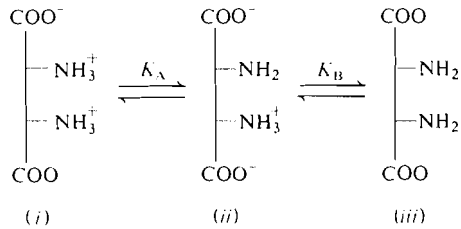

SCHEME 2

Deprotonation in penicillamine disulfide, represented in Scheme 2, is simpler since the two amino groups are indistinguishable due to the symmetry of the molecule. Nevertheless, as in the case of cystine (19), removal of one proton makes the second one more difficult to remove. The experimental pK values for the amino groups were determined by titration of the disulfide with alkali to be $pK_3 = 7.6$ and $pK_4 = 8.8$. Then by following the procedure described for cystine (19), the microscopic pK values were found to be $pK_A = 7.9$ and $pK_B = 8.5$ and the dissociation curves shown in Fig. 1 were calculated.

e_{aq}^- + *Penicillamine Disulfide*

Argon saturated solutions of RSSR were irradiated for the purpose of determining the extinction coefficient for $RSSR^-$ at 450 nm (λ_{max}) as a function of pH. The solutions also contained *t*-butanol at 100 times the concentration of RSSR in order to remove OH radicals. The rate of reaction 3 was measured as a function of pH by observing the decay of the electron at 700 nm. As seen in Table 1, the observed k_3 decreases considerably as the pH is increased, and this decrease is probably associated with the change in the net charge on penicillamine disulfide from 0 at pH 7 to −2 at pH 10.

The ionic strength of the solutions was not

Can. J. Chem. Downloaded from www.nrcresearchpress.com by 210.87.254.42 on 09/05/12
For personal use only.

TABLE 1. Rate constants for reaction of e_{aq}^- with penicillamine disulfide

	$k_3 \times 10^{-9}$ (M^{-1} s^{-1})	
p*H*	Obs.	Corr.
6.0	7.3	7.3
7.0	7.3	7.3
8.0	4.5	3.7
9.0	2.3	1.6
10.0	1.4	0.8

negligible because of the 8 m*M* phosphate buffer and the disulfide itself. This should have no effect at p*H* 6 but should increase the rate of reaction at the higher p*H* values. The rate constants corrected to zero ionic strength were obtained from the equation (20)

$$\log (k_{corr}/k_{obs}) = 1.02\, Z\, \mu^{1/2}/(1 + a\mu^{1/2})$$

where μ is the ionic strength of the solution, $a = R/3$ where R is the sum of the radii of the two reactants, taken as 6.5 Å and Z is the charge on the disulfide. The corrected k's are also given in Table 1.

The rate of a diffusion-controlled reaction between two solute molecules, at least one of which is uncharged, is given by the Smoluchowski equation (20)

$$k = \frac{4\pi DRN_0}{10^3}\, M^{-1}\, s^{-1}$$

where D is the sum of the diffusion coefficients of the two species, R is the sum of their radii, and N_0 is Avogadro's number. This equation may be applied to the reaction of e_{aq}^- with the disulfide at p*H* 7. At p*H* 10 where the charge on the disulfide is -2, the Debye equation should be used (20):

$$k = \frac{-4\pi DZ_AZ_Br_0N_0}{10^3[1 - \exp(Z_AZ_Br_0/R)]}\, M^{-1}\, s^{-1}$$

where Z_A is the charge on species A, $r_0 = e^2/\varepsilon kT$ where e is the charge on the electron and ε is the dielectric constant. The radius of the electron is about 2.5 Å (21) and we estimate the effective radius of the disulfide at 4 Å so that R is taken as 6.5 Å. The diffusion coefficient of the electron is 4.7×10^{-5} cm^2 s^{-1} (22), that of the disulfide is probably about 0.7×10^{-5} cm^2 s^{-1}, so that we assume D is 5.4×10^{-5} cm^2 s^{-1}. The calculated rate constants, in M^{-1} s^{-1}, at p*H* 7 and 10 for diffusion-controlled reaction, are 2.7×10^{10} and 0.7×10^{10}, respectively, as compared to our corrected experimental values of 0.7×10^{10} and 0.08×10^{10}. Thus the values calculated for a diffusion-controlled reaction are somewhat greater than the corrected values in Table 1. It should be noted that the rate constant calculated at p*H* 10 is quite sensitive to the choice of R. Also the assumption that the net charge on the molecule should be used in the Debye equation may not be valid. We conclude that although the decrease in rate constants in going from p*H* 7 to 10 is qualitatively in accord with the effect of the change in charge on diffusion-controlled reactions, other effects would seem to be involved as well. Hoffman and Hayon found values for k_3 of 1.2×10^{10} M^{-1} s^{-1} and 0.35×10^{10} M^{-1} s^{-1} at p*H* 7.0 and 12.4, respectively (23). They concluded from their measurements of the rates of reaction of e_{aq}^- with several disulfides over a range of p*H* that the effect of net charge on the rate constant is relatively small.

Rate of Decomposition of RSSR⁻

The decay of $RSSR^-$ in the absence of RSH was followed at its λ_{max} of 450 nm at p*H* 6–10, and the results are shown in Fig. 2 and Table 2. Electron decay was greater than 90% by the time of the first point for each of the curves of Fig. 2. At p*H* 6 (not shown in Fig. 2) and 7 the decay obeys good first-order kinetics over the three half-lives, and comparison with Fig. 1 shows that the decay is due to splitting of the radical anion of species *i* of Scheme 2. It is likely that the p*K* values of the amino groups of the radical anion are higher than those of the disulfide due to the additional negative charge. However, protonation should not influence the observed decay since the decay is very fast in all cases. For example, if protonation is rapid with a rate constant about 10^{10} M^{-1} s^{-1}, then the first-order rate constant at p*H* 8 is 10^2 s^{-1} which is too slow to compete with the decay ($k_{-2} = 1.75 \times 10^6$ s^{-1}). At p*H* 10 the decay is much faster, again obeys good first-order kinetics, and is the dissociation of the radical anion of species *iii* of Scheme 2 which has a net charge of -3. Presumably the decay is faster because of the repulsion of the negative charges on both halves of the anion. At p*H* 8 the decay is fast initially but after about 50% decay obeys first-order kinetics with a rate constant approximately equal to that at p*H* 6 and 7. The decay curve at

Can. J. Chem. Downloaded from www.nrcresearchpress.com by 210.87.254.42 on 09/05/12
For personal use only.

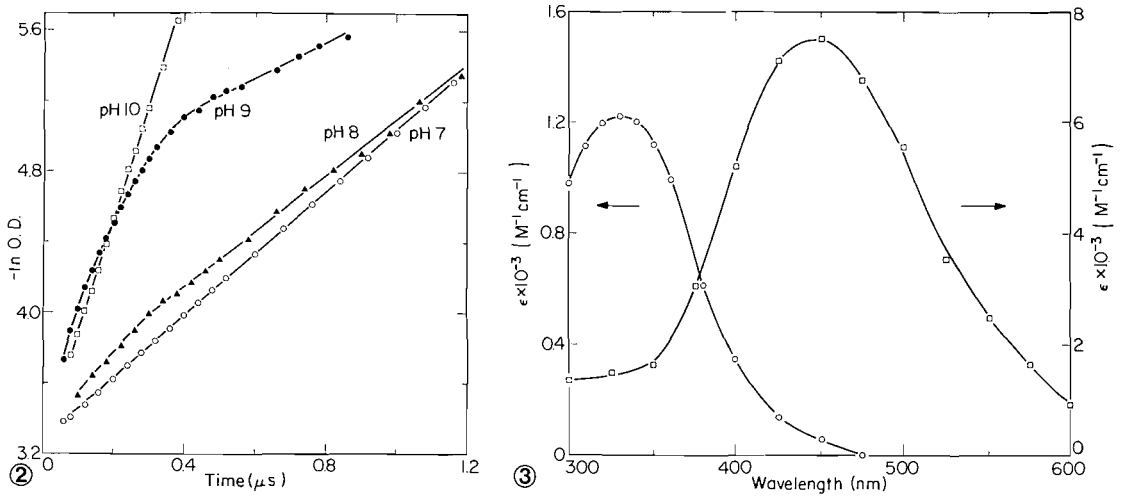

FIG. 2. First-order plots of the decay of $RSSR^-$ formed by reaction 3 in the absence of thiol: ○, p*H* 7.0, 5 m*M* RSSR; ▲, p*H* 8.0, 5 m*M* RSSR; ●, p*H* 9.0, 20 m*M* RSSR; □, p*H* 10.0, 20 m*M* RSSR.

FIG. 3. Absorption spectra of the RS· radical (○, left hand scale) and the $RSSR^-$ radical anion (□, right hand scale).

TABLE 2. Rate constants and extinction coefficients for $RSSR^-$ at 450 nm

p*H*	[RSSR] (m*M*)	$k_{-2} \times 10^{-6}$ (s^{-1})	$\varepsilon_{450} \times 10^{-3}$ ($M^{-1}\,cm^{-1}$)
6.0	5	1.74	7.5
7.0	5	1.77	7.5
8.0	1	1.55*	
	2.5	1.59*	
	5	1.48*	
	20	1.03*	7.6
9.0	20	6.5†	7.4
10.0	20	6.5	7.7

*From the later straight-line portion of the first-order decay plot, see Fig. 2.
†Initial fast decay, see Fig. 2.

p*H* 8 suggests that the anion of species *ii* of Scheme 2 dissociates at about the same rate as the anion of species *i*; the faster rate initially is due to the faster dissociation of a small amount of anion of species *iii*. At p*H* 9 the decay curve shows a fast initial rate, due to the dissociation of the anion of species *iii*, followed by a slower rate which is approximately the same as the rate at p*H* 7 and due to the dissociation of the anion of species *ii*.

The effect of concentration of disulfide was studied only at p*H* 8, and as seen in Table 2 the rate decreases as the concentration is increased. This is similar to the observation of Shafferman that the rate constant for the decay of the electron adduct of glutathione decreases with glutathione concentration (10). Possibly it is simply a salt effect, that is, repulsion between negative charges on the two halves of the anion is decreased at higher ionic strength.

Spectra of $RSSR^-$ and RS

As reported previously (14), the absorption spectrum of $RSSR^-$, produced by reaction 3, was measured at p*H* 6. The spectrum has now been measured at p*H* 7 and 8 and found to be identical within experimental error. At p*H* 9 it was difficult to measure precisely due to the rapid initial decay of the absorption as discussed above, but λ_{max} was found to be still at 450 nm. As described previously (14) the thiyl radical, produced at p*H* 5 by reaction 1, has $\lambda_{max} = 330$ nm and $\varepsilon_{330} = 1.22 \times 10^3\ M^{-1}\ cm^{-1}$. The spectra of RS· and $RSSR^-$ are redrawn in Fig. 3 to illustrate that of the RS· more clearly. No correction was necessary for the absorption of the parent compounds. Only the disulfide absorbs above 300 nm. Its extinction coefficient is 1.3% of that of the radical anion at 300 nm and less at higher wavelengths.

Extinction Coefficients of $RSSR^-$

Extinction coefficients of $RSSR^-$ at 450 nm were obtained from dosimetry and by extrapolating decay curves such as those in Fig. 2 back to the time of formation of half the maximum [$RSSR^-$]. In all cases this time was about 20 ns after the start of the 10 ns wide pulses used in these experi-

Can. J. Chem. Downloaded from www.nrcresearchpress.com by 210.87.254.42 on 09/05/12
For personal use only.

Can. J. Chem. Downloaded from www.nrcresearchpress.com by 210.87.254.42 on 09/05/12
For personal use only.

ments. The values found at different pH values are shown in Table 2. Because the initial portions of the decay plots at pH 8 and 9 are far from being straight lines, the extrapolations and therefore estimates of the extinction coefficient are rather uncertain at these pH values. From the data of Table 2 we conclude that ε_{450} for $RSSR^-$ is 7.5×10^3, with little pH dependence between 6 and 10.

Determination of K_2

The equilibrium constant for reaction 2 is defined as

$$K_2 = [RSSR^-]_{eq}/[RS\cdot]_{eq}[RS^-]$$

where $[RSSR^-]_{eq}$ and $[RS\cdot]_{eq}$ are the concentrations of RS· and $RSSR^-$ under equilibrium conditions. K_2 was determined by irradiating N_2O saturated solutions of penicillamine at pH 7, 8, and 9, and following the transient absorption at 450 nm. We calculated $[RS\cdot]_{eq}$ from the stoichiometric relationship $[RS\cdot]_{eq} = [RS\cdot]_0 - [RSSR^-]_{eq}$, where $[RS\cdot]_0$ is the total production of RS·.

$[RS\cdot]_0$ results from the production of RS· in several ways. The major source of RS· is reaction 1 and $G(OH) = 5.95$ in N_2O saturated solutions (15). It has been reported that 31% of hydrogen atoms react with penicillamine to give H_2 and RS·, and the remainder give H_2S and R· (24). The R· radicals might eventually give RS· by the reaction

$$R\cdot + RSH \rightarrow RH + RS\cdot$$

However, the rate constant for this reaction is only $1.1 \times 10^8\ M^{-1}\ s^{-1}$ when R· is $\cdot CH_2OH$ (see below). This reaction could not yield any RS· radicals until after the maximum absorption is reached, at least at the lower concentrations of penicillamine. Since $G(H) = 0.6$, the G of RS· from reactions of hydrogen atoms is 0.2. This is added to $G(OH)$ to give $G(RS\cdot)_0 = 6.15$. Another factor is important only at high concentrations of RSH where some of the e_{aq}^- is captured by RSH rather than by N_2O to give OH, and by analogy to the reaction between e_{aq}^- and cysteine (25), this reaction does not give RS·. The rate of e_{aq}^- + penicillamine has been measured as 5.1×10^9 at pH 6.5 (3). It was assumed that this reaction applies only to reaction with RSH, and that reaction with RS^- is very much slower by analogy with the effect of deprotonation on the rate of e_{aq}^- + RSSR. By using this rate constant and the known rate constant for e_{aq}^- + N_2O it was calculated that $G(OH)$ in N_2O saturated 10 mM penicillamine solution at pH 8.0 is 94% of its value in very dilute solutions.

$[RSSR^-]$ extrapolated to mid pulse was taken as a first approximation to $[RSSR^-]_{eq}$. The extrapolated value was never more than 9% greater than $[RSSR^-]$ at the maximum. However, the absorption at 450 nm is due to both $RSSR^-$ and RS· (see Fig. 3). A first approximation to $[RS\cdot]_{eq}$ was made by assuming that the absorbance at 450 nm represented only $RSSR^-$ and subtracting the value of $[RSSR^-]_{eq}$, obtained by extrapolation, from $[RS\cdot]_0$. A first approximation of the absorbance at 450 nm by $[RS\cdot]_{eq}$ could then be made. Repetition of this mathematical procedure converged to the results that absorbance at 450 nm due to RS· was 16 and 1.6% of that due to $RSSR^-$ for 0.5 and 5 mM solutions, respectively, at pH 8, and 27 and 11% for 1 and 2.5 mM solutions, respectively, at pH 7. Values of K_2 calculated from $[RS\cdot]_{eq}$, $[RS\cdot]_0$, and $[RSSR^-]_{eq}$ determined as described above are shown in Table 3.

It is seen that at pH 8 K_2 remains constant over a 20-fold range in concentration; the fraction of RS· radicals combined with RS^- in the complex at equilibrium varies from 5 to 44% over this concentration range. It is also seen that as the pH increases, K_2 decreases. This is quite reasonable since as the pH increases, the rate of decomposition of $RSSR^-$ increases as seen above. In general because of the difference in dissociation constants of the NH_3^+ groups in penicillamine and penicillamine disulfide, and the differences between the effect of charge of both species on k_2 and the charge on RSSR on k_3, the average charge on $RSSR^-$ might be different depending on whether it is formed by reaction 2 or 3. How-

TABLE 3. Equilibrium constants and rate constants from build-up of $RSSR^-$ in RSH solutions

pH	[Penicillamine] (mM)	$K_2 \times 10^{-2}$ (M^{-1})	$k_{-2} \times 10^{-6}$ (s^{-1})
8.0	0.5	2.44	
	1	2.43	1.89
	2.5	2.11	1.77
	5	2.29	1.79
	10	2.26	1.86
		Average 2.31	
7.0	1	3.04	
	2.5	3.00	
9.0	2.5	0.96	

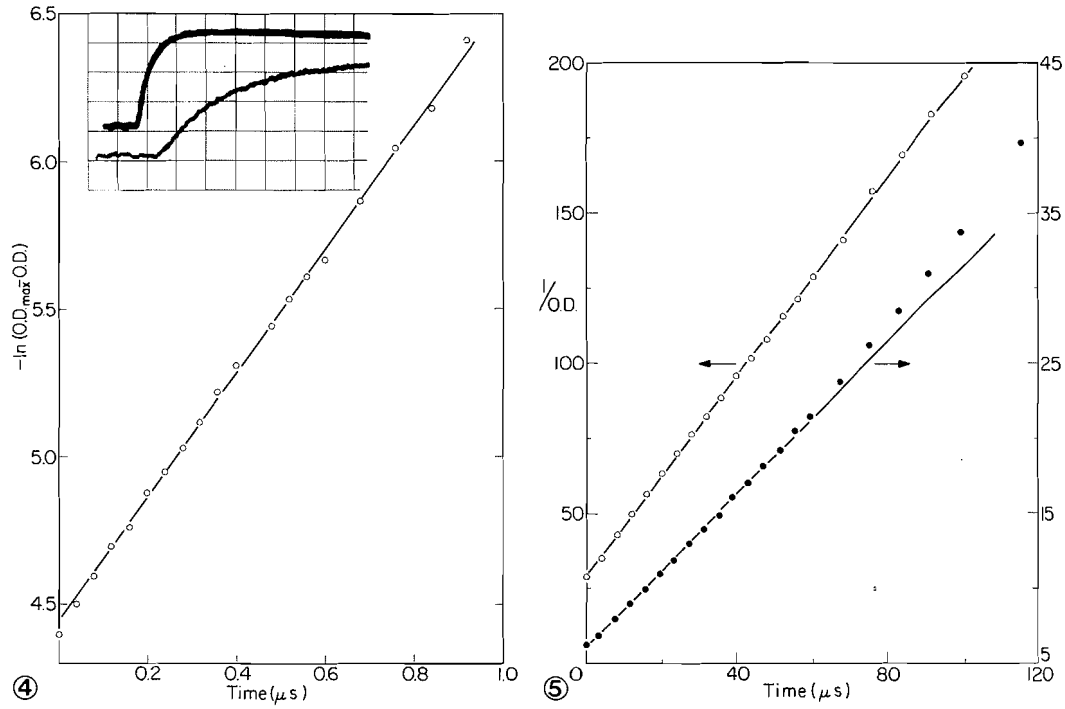

FIG. 4. Pseudo first-order plot of $RSSR^-$ formation in 2.5 mM penicillamine solution at pH 8.0. Inset: oscilloscope trace; sweep speeds 0.2 and 1 μs per division; absorption at maximum, 3.3%; pulse width 20 ns.

FIG. 5. Second-order plots of the decay of $RSSR^-$ in penicillamine solutions irradiated with high doses: ○, 1 mM RSH, pH 8.0, left hand scale; ●, 10 mM RSH, pH 8.0, right hand scale.

ever, at pH 7 both amino groups on $RSSR^-$ are protonated regardless of how it is formed, and we can combine the equilibrium constant with the value of k_{-2} given in Table 2 to calculate $k_2 = 5.3 \times 10^8\ M^{-1}\ s^{-1}$.

Our equilibrium constant K_2 for penicillamine of $2.3 \times 10^2\ M^{-1}$ at pH 8 may be compared to that of $6 \times 10^3\ M^{-1}$ found for cysteamine ($NH_2CH_2CH_2SH$) at pH 8.5 by Adams *et al.* (6), and that of $9.5 \times 10^3\ M^{-1}$ found for cysteine at pH 8.2 by Barton and Packer (26). Comparison with K found in the cysteine system is particularly interesting since the only difference is substitution of the two hydrogens on the α-carbon in cysteine by methyl groups in penicillamine. The much smaller K for penicillamine could be due to steric hindrance by the methyls, and/or extra stability of RS· due to the electron-donating properties of the methyl groups.

Growth of $RSSR^-$ in N_2O Saturated Penicillamine Solutions

Under our experimental conditions the production of RS· by reaction 1 in N_2O saturated solutions of penicillamine is much faster than the formation of $RSSR^-$ by reaction 2. For example, the formation of $RSSR^-$, as evidenced by its absorption at 450 nm, is shown in inset of Fig. 4 for a 2.5 mM solution of penicillamine at pH 8.0. The $t_{1/2}$ for formation of $RSSR^-$ is about 0.3 μs. On the other hand, Armstrong measured k_1 as $4.7 \times 10^9\ M^{-1}\ s^{-1}$ at pH 1 (4), so that $t_{1/2}$ for the formation of RS· should be only 0.06 μs at 2.5 mM if k_1 is independent of pH. Adams and co-workers found k_1 was independent of pH for cysteamine (6) and we measured $k_1 = 4.3 \times 10^9\ M^{-1}\ s^{-1}$ for penicillamine at pH 11 by competition experiments using carbonate ions. It can also be seen from the inset to Fig. 4 that the decay of $RSSR^-$ is negligible during its formation. Under such conditions the formation of $RSSR^-$ should be described by the first-order kinetics expression

$$\ln \frac{[RSSR^-]_{max}}{[RSSR^-]_{max} - [RSSR^-]} = k_{-2}(1 + K_2[RS^-])t$$

where $[RSSR^-]_{max}$ and $[RSSR^-]$ are the maxi-

Can. J. Chem. Downloaded from www.nrcresearchpress.com by 210.87.254.42 on 09/05/12
For personal use only.

Can. J. Chem. Downloaded from www.nrcresearchpress.com by 210.87.254.42 on 09/05/12
For personal use only.

mum concentration of $RSSR^-$ and its concentration at time t respectively. Hence a plot of $-\ln [O.D._{max} - O.D.]$ *vs.* time should give a straight line from the slope of which k_{-2} may be calculated. Figure 4 shows such a plot for the 2.5 m*M* solution at p*H* 8.0 illustrated in the inset and Table 3 contains the values of k_{-2} calculated from such plots. The average value of k_{-2} at p*H* 8.0 is 1.8×10^6 s^{-1}. The predominant formation reaction at p*H* 8.0 should be the radical of species *a* of Scheme 1 reacting with species *b* to give the radical anion identical to that produced from the disulfide at p*H* 6 and 7. From Table 2 it is seen that the value of k_{-2} at these p*H* values is about 1.7×10^6 s^{-1}. Thus we obtain good agreement for the value of k_{-2} by two quite different methods.

Decay Kinetics of $RSSR^-$ in RSH Solutions

With high-dose pulses, $RSSR^-$ decayed by second-order kinetics, especially at the lower concentrations of penicillamine. This is illustrated in Fig. 5, where it is seen that second-order kinetics are obeyed to at least 85% decay in a 1 m*M* penicillamine solution at p*H* 8.0. These decay reactions are expected to be the same as those found previously in cysteamine and cysteine solutions (6, 27).

[4] $$RS\cdot + RS\cdot \rightarrow RSSR$$

[5] $$RS\cdot + RSSR^- \rightarrow RSSR + RS^-$$

We have already seen that the rate of build-up of absorption due to $RSSR^-$ is much faster than its decay, so that $RS\cdot$ and $RSSR^-$ are in equilibrium during decay of $RSSR^-$. Hence the following expression for decay of $RSSR^-$:

$$-\frac{d}{dt}[RSSR^-] = k_{obs}[RSSR^-]^2$$

$$k_{obs} = \frac{1}{K_2[RS^-] + 1}\left(\frac{2k_4}{K_2[RS^-]} + k_5\right)$$

The values for k_{obs} determined from second-order plots at concentrations from 0.5 to 10 m*M* at p*H* 8.0 are listed in Table 4. The values at 0.5 and 5 m*M* were used to solve for k_4 and k_5 by simultaneous equations. It was calculated that $2k_4 = 1.73 \times 10^9$ M^{-1} s^{-1} and $k_5 = 6.4 \times 10^9$ M^{-1} s^{-1}. These values of k_4 and k_5 were then used to calculate the values of k to be expected at the other concentrations, and it is seen in Table 4 that these are in good agreement with the experimental k_{obs} values. This agreement

TABLE 4. Second-order rate constants for decay of $RSSR^-$

p*H*	[RSH] (*mM*)	$k \times 10^{-10}$ (M^{-1} s^{-1}) Obs.	Calcd.
8.0	0.5	4.05	—
	1	2.50	2.23
	2.5	1.13	1.10
	5	0.68	—
	10	0.36	0.42
7.0	1	10.0	—
	2.5	3.5	—

constitutes good evidence that no other decay reactions are important at high initial concentrations of $RSSR^-$; more specifically the reaction

$$2\ RSSR^- \rightarrow \text{Products}$$

does not seem to be important. These rate constants indicate that for p*H* 8.0 solutions at 0.5 m*M* the rate of reaction 4 is 5.7 times that of reaction 5, whereas at 10 m*M* it is only 0.28 times that of reaction 5.

Our second-order rate constants are rather similar to those reported for aqueous solutions of cysteamine; for the reaction corresponding to reaction 4, $2k = 1 \times 10^9$ M^{-1} s^{-1} and for the reaction corresponding to 5, $k = 5 \times 10^9$ M^{-1} s^{-1} in the cysteamine system (27).

At p*H* 7.0 reaction 5 is not very important at the two concentrations at which the decay rate was measured. If it is assumed that $k_5 = 6.4 \times 10^9$ M^{-1} s^{-1} at p*H* 7.0 also, then $2k_4$ is calculated to be 2.4×10^9 M^{-1} s^{-1} at 1 m*M* and 2.0×10^9 M^{-1} s^{-1} at 2.5 m*M*. We previously reported that $2k_4 = 2.6 \times 10^9$ M^{-1} s^{-1} (14); this measurement was made at p*H* 5 by observing the decay of absorption due to the $RS\cdot$ radical directly. By the same technique we have now redetermined k_4 more accurately and find $2k_4 = (2.85 \pm 0.15) \times 10^9$ M^{-1} s^{-1} over a range of penicillamine concentration from 0.5 to 5 m*M*. We attribute the slight increase in $2k_4$ with decrease in p*H* to protonation of the amino group so that at p*H* 5 all $RS\cdot$ radicals have a net charge of 0.

At lower concentrations of $RSSR^-$ and higher initial concentrations of penicillamine, the decay of $RSSR^-$ was found to deviate from second-order kinetics and approach first-order behavior. Figure 5 shows that a 10 m*M* p*H* 8.0 solution deviates more from second-order

Can. J. Chem. Downloaded from www.nrcresearchpress.com by 210.87.254.42 on 09/05/12
For personal use only.

kinetics than a 1 mM pH 8.0 solution irradiated with a pulse of the same dose. When pulses of smaller dose were used to irradiate 10 mM solutions, they showed deviations at smaller percent decay. Thus $RSSR^-$ appears to decay by a reaction in addition to reactions -2, 4, and 5 discussed above. We propose that this additional reaction is a pseudo first-order reaction of the type,

[6] $$RSSR^- + H_2O \rightarrow RSS\cdot + RH + OH^-$$

Obviously this reaction is favored at low $[RSSR^-]$ as compared to reactions 4 and 5, and it is also favored at high concentrations of penicillamine where k_{obs} is smaller. However, we were not able to work at a low enough $[RSSR^-]$ such that reaction 6 is the only mode of decay, because of the necessity of having enough absorption to follow $RSSR^-$ with reasonable precision. Under conditions such that reactions 2, -2, 4, 5, and 6 are important, the total rate expression for decay of $[RSSR^-]$ is

$$-\frac{d}{dt}[RSSR^-] = k_{obs}[RSSR^-]^2 + k_6[RSSR^-]$$

This expression is readily integrated to give

$$\ln \frac{[RSSR^-]_0\ (k_6 + k_{obs}[RSSR^-])}{[RSSR^-]\ (k_6 + k_{obs}[RSSR^-]_0)} = kt$$

where $[RSSR^-]_0$ is the initial $[RSSR^-]$. From this expression k_6 was determined by obtaining the best computer fit to data obtained in experiments with small $[RSSR^-]_0$. The values used for k_{obs} were the experimental values of Table 4, obtained at much higher $[RSSR^-]_0$. In Fig. 6 we compare the experimental points and computed curve for the best value of k_6 of $(2.3 \pm 0.2) \times 10^3\ s^{-1}$ for a 10 mM pH 8.0 solution of penicillamine, and the agreement is quite good. In this case the kinetics are very close to first order; $[RSSR^-]_0$ for the experiment of Fig. 6 is only 1.8% of that of the 10 mM experiment of Fig. 5.

We find values of k_6 of $(1.7 \pm 0.2) \times 10^3\ s^{-1}$ and $(1.5 \pm 0.1) \times 10^3\ s^{-1}$ for 5 and 2.5 mM solutions, respectively, at pH 8.0, and $k_6 = (2.8 \pm 0.5) \times 10^3\ s^{-1}$ for a 2.5 mM solution at pH 7.0. We favor the interpretation of these data that the pseudo first-order rate constant is independent of pH and concentration of penicillamine, but the data are not extensive enough to eliminate the possibility that the following reactions are also important:

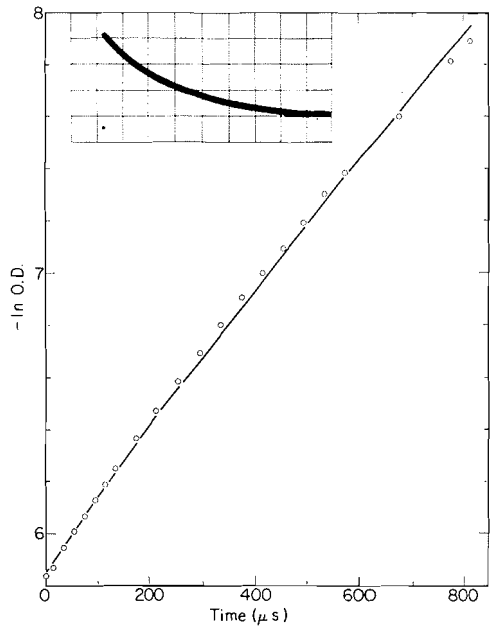

FIG. 6. First-order plot of the decay of $RSSR^-$ in penicillamine solution, 10 mM, pH 8.0. ○, Experimental points; solid line computed from first- and second-order rate constants. Inset: oscilloscope trace; sweep speed 100 μs per division; absorption at maximum, 0.67%.

[7] $$RSSR^- + RSH \rightarrow \text{Products}$$

[8] $$RSSR^- + H^+ \rightarrow \text{Products}$$

However, Hoffman and Hayon (23) have measured the second-order rate constant of [8] as $(3.3 \pm 1.0) \times 10^9\ M^{-1}\ s^{-1}$, which is a pseudo first-order rate constant of $33 \pm 10\ s^{-1}$ at pH 8.0. Therefore reaction 8 does not seem to be important under our conditions.

Product Yields

Table 5 presents the yields of the main products found in the radiolysis of solutions of

TABLE 5. Yields (G values) of major products obtained by gamma or pulse radiolysis of 10 mM penicillamine solutions saturated with N_2O

Irradiation	pH	RSSR	RSSSR*	RH	H_2S
Gamma	5.0	2.4	0.6	1.15	0.7
Gamma	8.0	1.4	2.2	2.4	0.5
Pulse (low dose rate)	5.0	1.9	0.7	0.9	—
	8.0	0.9	1.8	2.4	—
Pulse (high dose rate)	8.0	2.0	0.4	0.3	—

*D. A. Armstrong and G. C. Goyal have independently obtained penicillamine trisulfide by γ-radiolysis of penicillamine in aqueous solution (personal communication).

Can. J. Chem. Downloaded from www.nrcresearchpress.com by 210.87.254.42 on 09/05/12
For personal use only.

penicillamine under a variety of conditions. The G values were reproducible with a maximum deviation of ± 0.2 except for the disulfide where the results were less reproducible (± 0.4). We confine our attention first to 10 mM pH 8.0 solutions. Each solution was analyzed after an absorbed dose of about 20 krad. In the pulse experiments a sequence of high or low dose-rate pulses was used. In the high dose-rate pulse experiments the dose per pulse was about 5 krad, comparable to that used in the experiments of Fig. 5. Under these conditions reactions 4 and 5 are most important in the decay of $RSSR^-$, and therefore penicillamine disulfide should be the most important product. Table 5 shows that this expectation is borne out. In the low-dose experiments the dose per pulse was about 34 rad, less than that used in the experiment of Fig. 6. By our kinetic scheme, reaction 6 should be the only important decay reaction of $RSSR^-$ for both γ and low dose-rate pulse irradiation at pH 8. Table 5 shows that under these conditions the yields of penicillamine trisulfide (RSSSR) and valine (RH) are somewhat higher than those of the disulfide. We suggest that these products result from the reactions

[6] $RSSR^- + H_2O \rightarrow RSS\cdot + RH + OH^-$

[9] $RSS\cdot + RS\cdot \rightarrow RSSSR$

One expects, along with reaction 9, the reactions

[4] $RS\cdot + RS\cdot \rightarrow RSSR$

[10] $RSS\cdot + RSS\cdot \rightarrow RSSSSR$

We looked carefully for product tetrasulfide and found only a trace, but discovered that it reacts with penicillamine, possibly in a disproportionation reaction

[11] $RSSSSR + RSH \rightarrow RSSSR + RSSH$

The rate of this reaction is such that any tetrasulfide produced by irradiation would have mostly disappeared in the interval of about an hour between the times of irradiation and product analysis.

Thus product yields provide evidence for the formation of RSS· in reaction 6, although this reaction may not be general for disulfide radical anions. Hoffman and Hayon (23) have observed the RS· radical as a product of reaction 8 for the radical anions of several disulfides, and also as a product of the reaction of hydrogen atoms with the disulfides. Both reactions are presumed to involve the short-lived radical RSSHR as intermediate. However, they did not observe the RS· radical as a product of the reaction of H atoms with penicillamine disulfide. Reaction 6 might be expected to involve the same intermediate and it appears to dissociate by breaking a C—S rather than an S—S bond. The C—S bond of penicillamine may be weaker because the carbon is tertiary. The same reason accounts for the difference between cysteine and penicillamine in the competition

$$RSH + H \rightarrow H_2 + RS\cdot$$

$$RSH + H \rightarrow H_2S + R\cdot$$

In cysteine (α carbon is primary) the reaction to give H_2 is favored by 3.5:1 (28), whereas with penicillamine the reaction to give H_2S is favored by 2.5:1 (24). Similarly in the photosensitized decomposition of disulfides, C—S cleavage is an important process for t-butyl disulfide, but not important for cyclohexyl and hexyl disulfides (29).

Trisulfide must be produced by one or more reactions other than 6 and 9 in order to explain the formation of trisulfide at pH 5 where no $RSSR^-$ is formed.

Repair of Free Radicals by Hydrogen Transfer

Adams *et al.* (30) found that the hydrogen transfer reaction

[12] $R'\cdot + RSH \rightarrow R'H + RS\cdot$

could be followed by measuring the rate of formation of the radical anion by reaction 2 at a suitable pH. We investigated this by using 2.5 and 5 mM penicillamine solutions containing 0.5 or 1 M methanol. The results were analogous to those of Adams *et al.*; at the low dose used (70 rad/pulse) the maximum absorption observed at 450 nm in the presence of methanol was equal to the maximum absorption in the absence of methanol. The build-up of the absorption was slower in solutions containing methanol and followed good first-order kinetics. From the kinetic plot $k_{12} = (1.1 \pm 0.1) \times 10^8\ M^{-1}\ s^{-1}$ was calculated. This rate constant is a little faster than that reported for cysteamine (30), $6.8 \times 10^7\ M^{-1}\ s^{-1}$. Thus the lack of radioprotective properties in penicillamine cannot be related to the hydrogen transfer reaction.

Implications for Radioprotection

It is clear that penicillamine differs signifi-

cantly in its radiation chemistry from other sulfhydryl compounds which have been studied. However, it requires some extrapolation to relate the unusual behavior to the absence of radioprotective properties. As reported above, penicillamine transfers hydrogen efficiently to repair other radicals so this reaction does not explain the difference. It is possible that radical anions are less harmful than thiyl radicals in biological systems and the low K_2 discussed above indicates fewer RS· radicals of penicillamine will combine with ionized thiols to form $RSSR^-$ complexes. However, at physiological p*H* (about 7) the concentration of RS^- will be very low and hence a large fraction of RS· radicals of, for example, cysteamine, will also remain uncomplexed.

The ready formation of trisulfide may be important as it indicates a relatively weak carbon-sulfur bond in penicillamine. It appears that trisulfides are formed by more than one pathway. Trisulfides were also obtained in high yield by radiolysis of penicillamine disulfide and cysteine – penicillamine disulfide (16). If RS· radicals of penicillamine react with protein disulfide bridges with resultant formation of trisulfides, irreversible damage may be done. This may occur by a simple sulfur exchange reaction

$$RS\cdot + R'SSR' \rightarrow R\cdot + R'SSSR'$$

or by a sequence of reactions. Trisulfide formation in proteins will change the tertiary structure and, in many cases, would be harmful. Thus, although penicillamine scavenges free radicals efficiently and repairs alkyl radicals rapidly, the thiyl radicals formed may not be harmless.

We are grateful to Mr. G. G. Teather and Mrs. D. E. Hanafi for excellent technical assistance, and to Dr. K. Lokan for assistance with computer programming.

1. (*a*) D. G. DOHERTY. *In* Radiation protection and recovery. *Edited by* A. Hollaender. Pergamon Press, New York, N.Y. 1960. p. 45. (*b*) A. HOLLAENDER and D. G. DOHERTY. *In* Radiation damage and sulfhydryl compounds. International Atomic Energy Agency, Vienna. 1969. p. 1.
2. J. F. THOMSON. Radiation protection in mammals. Reinhold Publishing Corp., New York, N.Y. 1962. p. 53.
3. R. BRAAMS. Radiat. Res. **27**, 319 (1966).
4. W. A. ARMSTRONG. Can. J. Chem. **47**, 3737 (1969).
5. J. W. PURDIE. Can. J. Chem. **49**, 725 (1971).
6. G. E. ADAMS, G. S. MCNAUGHTON, and D. B. MICHAEL. *In* The chemistry of ionization and excitation. *Edited by* G. R. A. Johnson and G. Scholes. Taylor and Francis, London. 1967. p. 281.
7. W. KARMANN, G. MEISSNER, and A. HENGLEIN. Z. Naturforsch. **226**, 273 (1967).
8. G. E. ADAMS. *In* Current topics in radiation research. Vol. 3. *Edited by* M. Ebert and A. Howard. North Holland Publishing Co., Amsterdam. 1967. p. 83.
9. M. SIMIC and M. Z. HOFFMAN. J. Am. Chem. Soc. **92**, 6096 (1970).
10. A. SHAFFERMAN. Israel J. Chem. **10**, 725 (1972).
11. W. KARMANN, A. GRANZOW, G. MEISSNER, and A. HENGLEIN. Int. J. Radiat. Phys. Chem. **1**, 395 (1969).
12. R. BADIELLO and E. M. FIELDEN. Int. J. Radiat. Biol. **17**, 1 (1970).
13. J. V. DAVIES, M. EBERT, and R. J. SHALEK. Int. J. Radiat. Biol. **14**, 19 (1968).
14. J. W. PURDIE, H. A. GILLIS, and N. V. KLASSEN. Chem. Commun. 1163 (1971).
15. G. E. ADAMS, J. W. BOAG, J. CURRANT, and B. D. MICHAEL. *In* Pulse radiolysis. *Edited by* M. Ebert, J. P. Keene, A. J. Swallow, and J. H. Baxendale. Academic Press, London. 1965. p. 117.
16. J. W. PURDIE. Can. J. Chem. **47**, 1029, 1037 (1969).
17. R. E. BENESCH, and R. BENESCH. J. Am. Chem. Soc. **77**, 5877 (1955).
18. The Merck Index, 8th Edition. *Edited by* P. G. Stercher. Merck Co., Rahway, N.J. 1968.
19. J. P. GREENSTEIN and M. WINITZ. Chemistry of the amino acids. Vol. 1. Wiley, New York, N.Y. 1961. p. 506.
20. R. E. WESTON, JR. and H. A. SCHWARZ. Chemical kinetics. Prentice-Hall, Englewood Cliffs, N.J. 1972.
21. E. J. HART and M. ANBAR. The hydrated electron. Wiley-Interscience, New York. 1970. p. 61.
22. K. H. SCHMIDT and W. L. BUCK. Science, **151**, 70 (1966).
23. M. Z. HOFFMAN and E. HAYON. J. Am. Chem. Soc. **94**, 7950 (1972).
24. (*a*) T.-L. TUNG. Ph.D. thesis, University of Missouri, Columbia, Mo. 1971; (*b*) T.-L. TUNG and R. R. KUNTZ. Private communication.
25. V. G. WILKENING, M. LAL, M. ARENDS, and D. A. ARMSTRONG. J. Phys. Chem. **73**, 185 (1968).
26. J. P. BARTON and J. E. PACKER. Int. J. Radiat. Phys. Chem. **2**, 159 (1970).
27. G. E. ADAMS, R. C. ARMSTRONG, A. CHARLESBY, B. D. MICHAEL, and R. L. WILLSON. Trans. Faraday Soc. **65**, 732 (1969).
28. V. G. WILKENING, M. LAL, M. ARENDS, and D. A. ARMSTRONG. Can. J. Chem. **45**, 1209 (1967).
29. G. W. BYERS, H. GRUEN, H. G. GILES, H. N. SCHOTT, and J. A. KAMPMEIER. J. Am. Chem. Soc. **94**, 1016 (1972).
30. G. E. ADAMS, G. S. MCNAUGHTON, and B. D. MICHAEL. Trans. Faraday Soc. **64**, 902 (1968).

Can. J. Chem. Downloaded from www.nrcresearchpress.com by 210.87.254.42 on 09/05/12
For personal use only.

Hexamethylazoxybenzene. Structure, Basicity, and Rearrangement[1]

ROBIN A. COX[2] AND ERWIN BUNCEL
Department of Chemistry, Queen's University, Kingston, Ontario

Received March 14, 1973

2,2′,4,4′,6,6′-Hexamethylazoxybenzene (**1**) has been prepared and characterized. The u.v. spectrum is indicative of large distortion from coplanarity. **1** is only slightly more basic than azoxybenzene despite expectations due to electronic effect of the methyl substituents. Two factors are considered responsible for this: steric inhibition of resonance in the unprotonated species and steric hindrance to hydration in the conjugate acid.

Rearrangement of **1** in moderately concentrated sulfuric acid gives rise to the alcohol 4-hydroxymethyl-2,2′,4′,6,6′-pentamethylazobenzene (**6**). A Bamberger type phenolic product which would result from methyl migration is not observed. Possible reaction mechanisms are given.

L'hexaméthyl-2,2′,4,4′,6,6′-azoxybenzène (**1**) a été préparé et caractérisé. Le spectre u.v. indique une forte distorsion par rapport au plan. **1** n'est que légèrement plus basique que l'azoxybenzène malgré l'effet électronique attendu des substituants méthyles. Deux facteurs ont été considérés comme responsables de cet état: l'inhibition stérique à la résonance dans l'espèce non protonée et l'empêchement stérique à l'hydratation dans l'acide conjugué.

Le réarrangement de **1** dans l'acide sulfurique de concentration moyenne conduit à l'alcool hydroxyméthyl-4 pentaméthyl-2,2′,4′,6,6′ azobenzène (**6**). Un produit phénolique de type Bamberger résultant de la migration de méthyle n'a pas été observé. Des mécanismes possibles pour la réaction ont été donnés.
[Traduit par le journal]

Can. J. Chem., **51**, 3143 (1973)

As part of a continuing study on structure and reactivity of azoxy compounds (1, 2), we have prepared for the first time the symmetrically polysubstituted derivative 2,2′,4,4′,6,6′-hexamethylazoxybenzene, **1**. We report in this paper on the spectral characteristics of **1**, on its basicity as defined by eq. 1, and on its rearrangement.

[1] 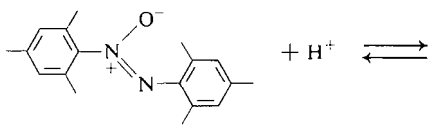 + H^+ ⇌

1

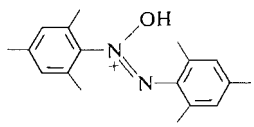

2

Spectral Characterization

The compound **1**, prepared by oxidation of the hexamethylazobenzene, has the u.v.-visible spectral characteristics given in Table 1. The assignments of the bands are similar to previous designations (3–5). The E_1 band is an electronic transition of the benzene rings, the E_2 band probably involves the azoxy function and one of the benzene rings, while the K band represents a $\pi \rightarrow \pi^*$ transition involving the entire conjugated system. For purposes of comparison Table 1 also contains the K-band data for azoxybenzene, and for some dialkyl derivatives.

It is seen that the K band in **1** is shifted to shorter wavelength, relative to azoxybenzene, and the extinction coefficient is considerably smaller. This effect is also observed with the 2,2′-dialkyl azoxybenzenes, though to a lesser extent, but it is reversed with the 4,4′-dialkyl azoxybenzenes. The bathochromic shift in the K band for the 4,4′-azoxybenzenes has been attributed in the past to operation of the inductive effect (6) and the hyperconjugative effect (3). On the other hand, the hypsochromic shift and the diminution in absorption intensity of the K band which is observed with the 2,2′-dialkyl azoxybenzenes has been generally attributed to steric hindrance to coplanarity, since steric inhibition of resonance would raise the energy level of the excited state relative to the ground state, and to reduced overlap between the π and π^* orbitals.

The distortion from coplanarity (deformation

[1]Part XI in a series on the Wallach rearrangement. For Part X see ref. 1.

[2]Present address: Department of Chemistry, University of British Columbia, Vancouver 8, B.C.

Can. J. Chem. Downloaded from www.nrcresearchpress.com by 210.87.254.42 on 09/05/12
For personal use only.

TABLE 1. Spectral characteristics of substituted azoxybenzenes

Azoxybenzenes[a]	λ (nm)	ε	Band	Δλ	Δε	θ(°)
2,2′,4,4′,6,6′-Hexamethyl	214(s)	18 300	E_1			
	240(s)	7 500	E_2			
	307	3 800	K	−16	−10 700	67
4,4′-Dimethyl	330	18 100	K	+7	+3 600	—
2,2′-Dimethyl	312	11 100	K	−11	−3 400	38
4,4′-Diethyl	334	20 700	K	+11	+6 200	—
2,2′-Diethyl	309	9 300	K	−14	−5 200	48
Unsubstituted	323	14 500	K	0	0	—

[a]Data for 2,2′,4,4′,6,6′-hexamethylazoxybenzene are from the present work and refer to methanol solvent. The rest of the data are taken from the literature (3, 6).

angle, θ) may be calculated from the diminution in the molar extinction of the K band, according to the relationship[3] (7), $\cos^2\theta = \varepsilon/\varepsilon_0$. In this equation ε is the molar extinction coefficient for the ortho-substituted derivative while ε_0 is the value for the para-substituted analog; this assumes that the electronic effect of the substituent(s) is independent of the position of substitution (ortho or para) and that in the absence of steric effects the extinction coefficients for the two isomers should be the same. Application of this relationship to the dimethyl- and diethylazoxybenzenes leads to deformation angles of 38 and 48°, respectively (3, 6).

The choice of a reference model in the present study provides a difficulty. If one assumes, as has been done previously (6), that the contribution of each alkyl group is additive, then the theoretical decrease in intensity would be given by $+3600 \times 3 = +10\,800$, so that in the absence of steric effects the extinction coefficient for **1** should be $14\,500 + 10\,800 = 25\,300$. Hence θ is calculated from the relationship $\cos^2\theta = 3800/25\,300$ which yields θ = 67°. Though the absolute value is somewhat in doubt, it is clear that **1** has the largest distortion so far observed in the azoxybenzene series. It may be noted that X-ray structure data give an angle of twist of 22.6° for 4,4′-dimethoxyazoxybenzene (9) so that the calculated deformation angles shown in Table 1 should all be augmented correspondingly.

Basicity

The pK_a of **1** was determined by the spectrophotometric method employed previously (10).

[3]The alternative relationship $\cos\theta = \varepsilon/\varepsilon_0$ has also been proposed (8) and leads to somewhat larger values of the deformation angle θ. For consistency with previous work (3, 6) we use the relationship given in the body of the text.

TABLE 2. Spectral data for pK_a measurements

H_2SO_4[a] (*M*)	H_0[b]	A_{BH^+}[c]	A_B[d]	*I*[e]
6.57	−3.14	0.110	0.275	—
7.34	−3.63	0.210	0.542	0.092
8.25	−4.20	0.187	0.412	0.058
8.92	−4.60	0.288	0.458	0.228
9.24	−4.77	0.381	0.492	0.441
9.52	−4.93	0.470	0.465	0.728
10.20	−5.27	0.682	0.412	2.29
10.73	−5.51	0.789	0.345	5.07
11.35	−5.80	0.868	0.310	15.1
11.61	−5.90	0.885	0.305	23.8
12.32	−6.21	0.903	0.290	58.3

[a]Contains 5% dioxane.
[b]Data from ref. 11.
[c]Absorbance at 378 nm.
[d]Absorbance at 306 nm.
[e]Ionization ratio, $I = (A - A_B/A_{BH^+} - A)$, calculated at 378 nm, using $A_B = 0.145$ and $A_{BH^+} = 0.916$ (see text).

The acidic medium used was aqueous sulfuric acid containing 5% dioxane, the organic co-solvent being required in order to enhance solubility of the substrate. An H_0 scale applicable to this medium is available (11).

Protonation of **1** is characterized by appearance of an absorption maximum in the 387 nm region due to species **2**. Measurements over a range of acid concentrations give a typical sigmoid curve when A_{387} is plotted against H_0 (data of Table 2). One thus obtains a pK_a of −5.02 corresponding to the H_0 value at the inflection point.[4] Absorbances at 307 nm corresponding to the unprotonated species did not show a consistent decrease with increased acidity, possibly due to a selective medium effect since isosbestic point behavior was not observed. The Davis–Geissman (12) procedure was therefore not deemed applicable. However,

[4]The measured pK_a refers to the H_0 value at 50% protonation rather than to the thermodynamic dissociation constant.

Can. J. Chem. Downloaded from www.nrcresearchpress.com by 210.87.254.42 on 09/05/12
For personal use only.

Can. J. Chem. Downloaded from www.nrcresearchpress.com by 210.87.254.42 on 09/05/12
For personal use only.

the smooth sigmoid curve of A_{387} *vs.* H_0 yielded values of ε_B and ε_{BH^+} which were then used to calculate ionization ratios over the acidity region examined. The log I *vs.* H_0 plot is linear with a slope of 1.51. A pK_a value of -5.02 is obtained from this plot corresponding to log $I = 0$, in good agreement with the value derived from the A_{387} *vs.* H_0 plot. The "Hammett slope" of 1.51 is considerably higher than the value 1.0 recorded for azoxybenzene and 0.9–1.0 for the naphthyl azoxy series (10), though it is well within the range of slope values compiled by Bunnett and Olsen for a variety of organic bases (13). Apparently **1** is a poor Hammett base, which could be due to the abnormal amount of twist in this molecule. The different acidity response of **1** compared to azoxybenzene, as reflected in the dependence of log I on H_0, is thus not too surprising.

It is of interest to discuss the basicity of **1** in terms of structural and electronic effects and to compare the pK_a value with that of the parent azoxybenzene. For that purpose the measured pK_a of **1** may be reduced to the value applicable to aqueous medium by means of an appropriate correction factor (11), which then yields pK_a (aq) $= -4.85$. It follows that **1** is a stronger base than azoxybenzene, pK_a (aq) $= -5.15$, but only moderately so. Qualitatively, one can account for the increased basicity of **1** by examining the possibility of delocalization of charge due to contribution by canonical structures such as the following:

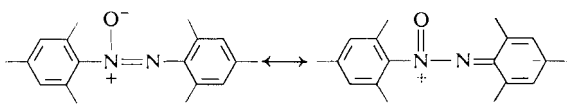

1a *1b*

The electron-releasing effect of methyl will result in diminished importance of structures such as **1***b*. The consequent increased charge density on the azoxy oxygen relative to that of azoxybenzene should lead to **1** being more basic than azoxybenzene, which is as observed. A more complete treatment should also consider inductive and steric effects.

However, quantitatively, the increased basicity of **1** over that of azoxybenzene is far less than might have been anticipated. The data of Hahn and Jaffé (14) on the pK_a of substituted azoxybenzenes show that 4,4′-dimethylazoxybenzene has increased basicity by almost 1 pK unit over that of azoxybenzene. If one assumes the effect of the methyl substituents to be additive then the calculated pK_a of **1** would be around -2.

It is probable that the variance between the anticipated and the actual pK_a value of **1** is due, in part, to steric inhibition of resonance. Thus to the extent that the methyl groups cause distortion from planarity in the molecule, the hyperconjugative capability of these methyls will become diminished. The second factor to be considered is steric hindrance to hydration (15). Since the protonated form of the base will be more hydrated by solvent molecules than the neutral form, the presence of the ortho methyl groups in **1** will interfere with solvation of the protonated azoxy function and hence destabilize the protonated form. This factor will also result in decreased basicity relative to the situation in azoxybenzene. Corroboration of the role of this factor in the present system is indicated by a negative ϕ value (-0.55) when the data are plotted according to the procedure of Bunnett and Olsen (13), which is indicative of less than optimum hydration of the BH^+ species. The hydration factor may well weigh the most heavily in reducing the basicity of **1** (cf. ref. 16).

Acid Catalyzed Rearrangement

Investigation of the Wallach rearrangement of **1** in acidic media promised to be of particular interest since a "normal" type rearrangement (2), whereby hydroxyl enters a vacant ortho or para position, is precluded in this system. It appeared possible, however, that an alternative pathway would prevail, with a methyl group migrating from a para to a meta position, as indicated in Scheme 1. This pathway is based on a presumed analogy with the Bamberger rearrangement of substituted phenyl hydroxylamines in acid media where methyl migration follows nucleophilic attack thus leading to a rearranged phenolic product (17, 18). The proposal of initial formation of the dication **3** is by analogy with our previous hypothesis of the intervention of such a metastable intermediate in the reaction of azoxybenzene (19, 20).

If the overall process shown in Scheme 1 were in fact to occur this would constitute the first example of alkyl migration in the Wallach rearrangement. On the other hand it was tempting to conceive of the possibility that, in the absence of group migration, **3** would be stabilized in these media and thus become spectrally observable or otherwise lead to some product characteristic of that species.

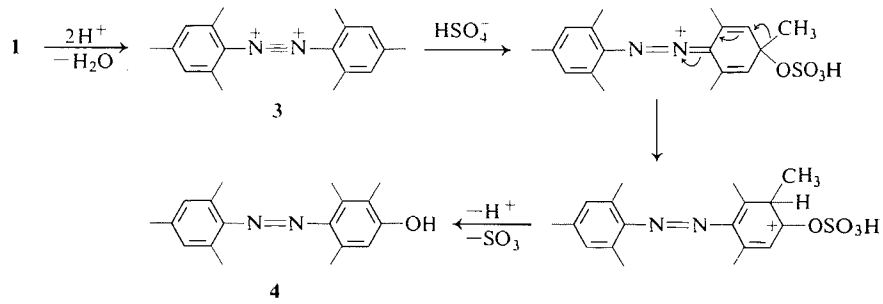

SCHEME 1

Examination of **1** in strong sulfuric acid solutions (75–95% H_2SO_4) shows rather quickly that some kind of reaction does occur, since the spectrum characteristic of the protonated reactant disappears with time and is replaced by a new absorption which is stable in these reaction media (21). However, it was apparent that the reaction product was not phenolic since the spectrum of the base-quenched reaction mixture was qualitatively quite similar to the spectrum of the neutral or slightly acidic solution of the reaction product. This contrasts with the situation for azoxybenzene where the azophenolate ion was found to have its principal absorption displaced to longer wavelengths compared to the azophenol (19). To remove any possible doubt that **4** could have been formed from **1**, the authentic **4** was examined spectrally and found to have different characteristics in acidic and basic media. Similarly, 2,2′,4,4′,6,6′-hexamethylazobenzene, **5**, which could conceivably have been formed from **1** by reduction (by analogy with the reported (22) reduction of hexabromoazoxybenzene in strong acid) was found to have different spectral properties than the reaction product.

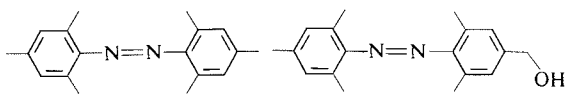

5 **6**

Since the reaction product did not appear to be a known compound, its isolation and physical characterization was deemed necessary. Product isolation was effected by treatment of a 6×10^{-4} *M* solution in 85.6% H_2SO_4 at 44.4° for 1 h (a concurrent spectral examination showed reaction to be complete) and work-up. A red crystalline solid was obtained whose u.v.-visible spectral characteristics corresponded to those of the species produced in the reaction as followed spectrophotometrically. The complete u.v. spectral data for the product as well as the reference compounds **1**, **4**, and **5** are given in Table 3, in neutral, acidic, and basic media. Some spectra in acid medium are shown in Fig. 1.

Elemental analysis of the reaction product showed it to be an isomer of the reactant. The i.r. spectrum showed pronounced absorption due to OH, pointing to an alcoholic material, since it is known not to be a phenol. In the n.m.r. spectrum, a 2-proton signal at 4.52 p.p.m. was indicative of the $ArCH_2OH$ grouping, in accord with structure **6**, and the rest of the n.m.r. spectrum was in complete agreement with that assignment. The presence of two distinct 2-proton peaks in the aromatic region shows that the CH_2OH function could not be present in an

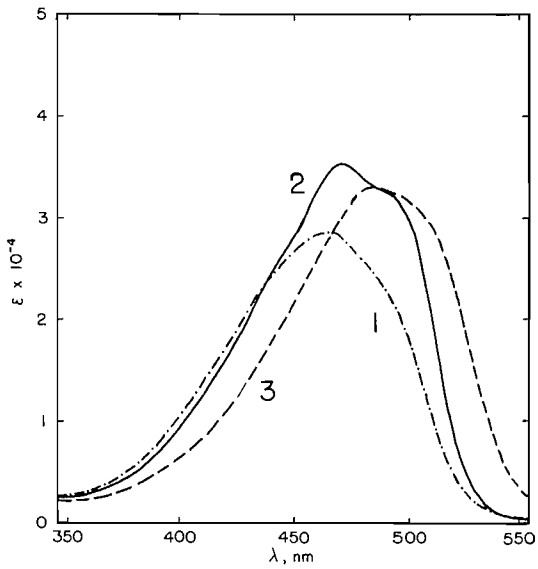

FIG. 1. Visible spectra in 87% H_2SO_4 of the reaction product **6** (curve 1), the azo-compound **5** (curve 2), and the phenol **4** (curve 3).

Can. J. Chem. Downloaded from www.nrcresearchpress.com by 210.87.254.42 on 09/05/12
For personal use only.

TABLE 3. Spectral data of the reaction product (**6**) and of the compounds **1**, **4**, and **5** in neutral, acidic, and basic media

Compound	Neutral[a,b]		Acidic[a,c]		Basic[a,d]	
1	240	(7 500)	—		240	(7 500)
	306.5	(3 800)	387	(4 700)	307	(3 800)
5	237	(9 250)	252	(4 200)	237	(8 900)
	324	(14 800)	315	(2 500)	324	(14 400)
	462	(950)	475	(35 100)	462	(950)
4	249	(9 800)	258	(5 600)	264	(8 700)
	340	(15 200)	312	(2 800)	379	(18 800)
	463	(1 340)	488	(32 900)		—
6	235	(8 500)	245	(4 200)	236	(7 900)
	321.5	(12 800)	312	(3 000)	320.5	(11 500)
	461	(1 050)	462.5	(28 400)	~450	(~850)

[a] λ in nm, (ε).
[b] In methanol, 8.00×10^{-5} *M*, in 1 cm cells.
[c] In 85.58% H_2SO_4, 4.00×10^{-5} *M*, in 1 cm cells.
[d] In 0.05 *M* KOH in methanol, 8.00×10^{-5} *M*, in 1 cm cells.

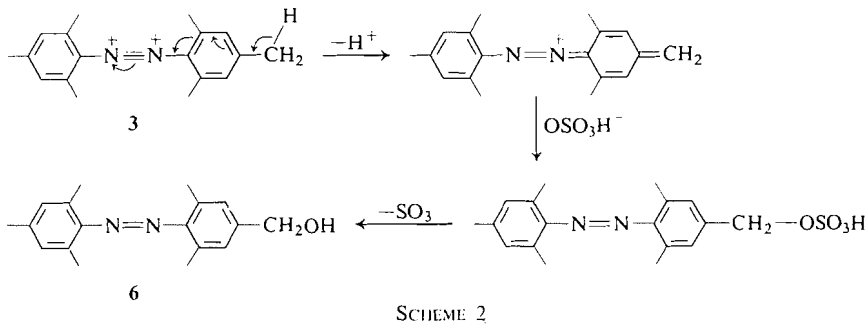

SCHEME 2

ortho position since in that case three aromatic signals should have been present in the ratio 2:1:1. Acetylation of the product resulted in loss of the O—H absorption and the appearance of a C=O peak in the i.r., while the n.m.r. spectrum showed the presence of a CH_3CO signal as well as a shift of the $ArCH_2O$ signal down-field by 0.4 p.p.m. from that of the reactant. The mass spectra of the reaction product and of the acetyl derivative were fully characteristic of the structural assignment given, *viz.* **6** for the reaction product and **6**-acetate for the derivative.

The unusual course of rearrangement of the substrate **1** could arise as a result of the reaction pathway indicated in Scheme 2, starting from the dicationic intermediate **3** which would be formed as previously (20). It should be pointed out that other pathways leading to product **6** are possible, for instance by direct nucleophilic attack by H_2O or HSO_4^- on a proton of the para methyl group of the conjugate acid **2**. However, the recent demonstration by Olah *et al.* that a dicationic species is formed from azoxybenzene in superacid (23) tends to lend support to the dicationic intermediate postulated in Scheme 2. Finally, we wish to draw attention to the synthetic potential of this reaction since nucleophilic substitution on methyls attached to aromatic rings is quite uncommon (24, 25).

Experimental

2,2′,4,4′,6,6′-Hexamethylazoxybenzene (1)

This compound was prepared by the peracid oxidation of 2,2′,4,4′,6,6′-hexamethylazobenzene (26). The azobenzene (6.66 g, 0.025 mol) was dissolved in chloroform (50 ml) in a 100 ml flask fitted with a reflux condenser and drying tube. *m*-Chloroperbenzoic acid (5.33 g, 0.026 mol, 85% Aldrich technical grade) was then added, and the solution refluxed on a steam-bath until it was a clear lemon-yellow color (4 h). The solution was cooled, washed with bicarbonate and water, and dried over calcium chloride. Rotary evaporation of the chloroform gave the product as a yellow oil which slowly crystallized into an amorphous yellow solid. Two recrystallizations

Can. J. Chem. Downloaded from www.nrcresearchpress.com by 210.87.254.42 on 09/05/12
For personal use only.

Can. J. Chem. Downloaded from www.nrcresearchpress.com by 210.87.254.42 on 09/05/12
For personal use only.

from ethanol resulted in a crystalline solid (yellow plates); yield 84%, m.p. 63–64°.

Anal. Calcd. for $C_{18}H_{22}N_2O$: C, 76.56; H, 7.85; N, 9.92. Found: C, 76.87; H, 7.65; N, 10.07.

U.v. spectrum, see Table 1; n.m.r. δ 2.19 (s, 6, 2′- and 6′-CH_3); 2.30 (s, 3, 4-CH_3); 2.32 (s, 3, 4′-CH_3); 2.36 (s, 6, 2- and 6-CH_3); 6.79 (s, 2, 3- and 5-H); 6.84 (s, 2, 3′- and 5′-H).

4-Hydroxy-2,2′3,4′,6,6′-hexamethylazobenzene (4)

This substance was prepared by a standard diazo-coupling procedure (27), from 2,4,6-trimethylaniline and 2,3,5-trimethylphenol. Recrystallization from 60–80 petroleum ether gave the product as small red needles, m.p. 117–118°.

Anal. Calcd. for $C_{18}H_{22}N_2O$: C, 76.56; H, 7.85; N, 9.92. Found: C, 76.16; H, 7.68; N, 9.73.

U.v. spectrum, see Table 3; n.m.r. δ 2.16 (s, ~3, 3-CH_3); 2.28 (s, ~3, 4′-CH_3); 2.33 (s, ~6, 2′- and 6′-CH_3); 2.36 (s, ~6, 2- and 6-CH_3); 4.80 (broad, 1, OH); 6.26 (s, 1, 5-H); 6.78 (s, 2, 3′- and 5′-H).

4-Hydroxymethyl-2,2′,4′,6,6′-pentamethylazobenzene (6): Reaction Product Isolation

Hexamethylazoxybenzene (103.5 mg) was dissolved in 85.6% sulfuric acid (600 ml) in a 1 l flask which was heated in an oil-bath at 44.4° while stirring. A small portion of this solution was continuously scanned in the SP 800 spectrophotometer, using a 1 mm cell in a thermostatted cell block. When the scanned sample indicated that reaction was complete (1 h, 10 half-lives) the main reaction solution was cooled in ice. A portion of the reaction solution was quenched in 1 *M* NaOH in EtOH–H_2O (20:80) for spectral examination. The acidic reaction solution was then carefully diluted to 1200 ml with cold water and cooled again. The diluted acid solution was added slowly with continuous stirring and cooling to a solution of 750 g NaOH in 2 l water in a 20 l flask. Additional water had to be added to keep the Na_2SO_4 in solution and the final volume was about 10 l. This solution, which was cloudy with precipitated product, was extracted with small portions of ether until the aqueous layer was quite clear. The combined ether extracts were washed with water and dried over calcium chloride. Rotary evaporation of the ether left a red solid; the yield at this stage was 94.7 mg, or 91.5% of starting material. Purification was achieved by chromatography over neutral alumina, eluting with ether, and recrystallization from CCl_4. A mat of very fine red needles was obtained, m.p. 94–95°.

Anal. Calcd. for $C_{18}H_{22}N_2O$: C, 76.56; H, 7.85; N, 9.92. Found: C, 76.56; H, 7.85; N, 10.01.

U.v. spectrum, see Table 3; n.m.r. δ 2.32 (s, ~3, 4′-CH_3); 2.39 (s, ~12, 2-, 2′-, 6-, and 6′-CH_3); ~3.4 (broad, 1, OH); 4.52 (s, 2, Ar-CH_2-O); 6.83 (s, 2, 3′- and 5′-H); 6.98 (s, 2, 3- and 5-H). I.r. (cm^{-1}) 3445 (broad, bonded OH); 3618 (sharp, free OH). Mass spectrum, *m/e* (relative intensity) 282 (48), molecular ion; 135 (59), $C_6H_2(CH_3)_2CH_2OH^{\cdot+}$; 119 (100), $C_6H_2(CH_3)_3^{\cdot+}$; otherwise characteristic of an azo-compound (28).

4-Acetoxymethyl-2,2′,4′,6,6′-pentamethylazobenzene

The reaction product **6** was acetylated by refluxing it overnight in acetic acid – acetic anhydride (50:50). Rotary evaporation gave a red solid which was purified by column chromatography over acid-washed alumina, eluting with benzene – 60–80 petroleum ether (50:50), and recrystallization from ethanol. The product was a red crystalline solid, m.p. 65–66°.

Anal. Calcd. for $C_{20}H_{24}N_2O_2$: C, 74.05; H, 7.46; N, 8.63. Found: C, 74.27; H, 7.58; N, 8.63.

U.v. (CH_3OH) λ 239 nm (ε 8700); 317 (12 400); 458 (1040). N.m.r. δ 2.01 (s, 3, CH_3—C═O); 2.27 (s, 3, 4′-CH_3); 2.40 (s, 12, 2-, 2′-, 6-, and 6′-CH_3); 4.94 (s, 2, Ar-CH_2-O); 6.82 (s, 2, 3′- and 5′-H); 7.00 (s, 2, 3- and 5-H). I.r. (cm^{-1}) 1730 (C═O). Mass spectrum, *m/e* (relative intensity) 324 (52), molecular ion; 177 (19), $C_6H_2(CH_3)_2CH_2OCOCH_3^{\cdot+}$; 119 (100), $C_6H_2(CH_3)_3^{\cdot+}$; 220 (23); otherwise typical of an azo-compound (28).

Spectral Measurements

The u.v.-visible spectral measurements were performed by the method previously described (10). The n.m.r. spectra were taken on a Varian T60 instrument, in CCl_4 solution, and the data are quoted as p.p.m. relative to TMS internal standard. The i.r. spectra were obtained in $CHCl_3$ solution using a Unicam SP 1000 spectrophotometer.

We gratefully acknowledge financial support from the National Research Council of Canada in the form of an operating grant.

1. E. Buncel and A. Dolenko. Tetrahedron Lett. 113 (1971).
2. E. Buncel. *In* Mechanisms of molecular migrations. Vol. 1. *Edited by* B. S. Thyagarajan. Wiley, N.Y. 1968.
3. P. H. Gore and O. H. Wheeler. J. Am. Chem. Soc. **78**, 2160 (1956).
4. H. H. Jaffé and M. Orchin. Theory and applications of ultraviolet spectroscopy. Wiley, New York. 1962.
5. C. Tosi. Spectrochim. Acta, **22**, 1701 (1966).
6. B. T. Newbold and D. Tong. Can. J. Chem. **42**, 836 (1964).
7. H. B. Klevens and J. R. Platt. J. Am. Chem. Soc. **71**, 1714 (1949).
8. E. A. Braude, W. F. Forbes, and F. Sondheimer. Nature, **173**, 117 (1954).
9. W. R. Kringbaum, Y. Chatani, and P. G. Barber. Acta Crystallogr. Sect. B, **26**, 97 (1970).
10. A. Dolenko, K. Mahendran, and E. Buncel. Can. J. Chem. **48**, 1736 (1970).
11. D. S. Noyce and M. J. Jorgensen. J. Am. Chem. Soc. **83**, 2525 (1961).
12. C. T. Davis and T. A. Geissman. J. Am. Chem. Soc. **76**, 3507 (1954).
13. J. F. Bunnett and F. P. Olsen. Can. J. Chem. **44**, 1899 (1966).
14. C-S. Hahn and H. H. Jaffé. J. Am. Chem. Soc. **84**, 949 (1962).
15. F. E. Condon. J. Am. Chem. Soc. **87**, 4494 (1965).
16. J. Burgers, M. A. Hoefnagel, P. E. Verkade, H. Visser, and B. M. Wepster. Rec. Trav. Chim. **76**, 357 (1957).
17. E. Bamberger and F. Brady. Chem. Ber. **33**, 3642 (1900).

18. H. J. SHINE. Aromatic rearrangements. Elsevier, New York. 1967. pp. 182, 279.
19. E. BUNCEL and B. T. LAWTON. Can. J. Chem. **43**, 862 (1965).
20. E. BUNCEL and W. M. J. STRACHAN. Can. J. Chem. **48**, 377 (1970).
21. E. BUNCEL and R. A. COX. Chem. Commun. 1259 (1972).
22. P. H. GORE and O. H. WHEELER. J. Org. Chem. **26**, 3295 (1961).
23. G. A. OLAH, K. DUNNE, D. P. KELLY, and Y. K. MO. J. Am. Chem. Soc. **94**, 7438 (1972).
24. T. PARSONS, JR. and J. C. BAILAR, JR. J. Am. Chem. Soc. **58**, 268 (1936).
25. P. B. BAKER, V. R. HOLLAND, and B. C. SAUNDERS. Tetrahedron, **29**, 85 (1973).
26. E. HASELBACH. Helv. Chim. Acta, **53**, 1526 (1970).
27. F. G. MANN and B. C. SAUNDERS. Practical organic chemistry. 4th Ed. Longmans, London. 1960. p. 208.
28. J. H. BOWIE, G. E. LEWIS, and R. G. COOKS. J. Chem. Soc. B, 621 (1967).

Can. J. Chem. Downloaded from www.nrcresearchpress.com by 210.87.254.42 on 09/05/12
For personal use only.

Can. J. Chem. Downloaded from www.nrcresearchpress.com by 210.87.254.105 on 09/05/12
For personal use only.

Synthetic Approaches to a Novel Carbohydrate Conjugated Diene: 4,6-*O*-Benzylidene-1,2,3-trideoxy-3-*C*-methylene-D-*erythro*-hex-1-enopyranose[1]

STEVE Y-K. TAM, DAVID E. ILEY,[2] NEVILLE L. HOLDER,[3] DAVID R. HICKS, AND BERT FRASER-REID
Chemistry Department, University of Waterloo, Waterloo, Ontario

Received January 16, 1973

Four routes to the title compound **1** are outlined, three of which (i), (ii), and (iv) are simple one-step processes from readily available carbohydrate precursors. In the third route (iii) the α-keto benzoate **6***a* is methylenated and the benzoate group replaced by methanesulfonate. The product (**6***d*) rearranges upon iodinolysis giving the primary allylic iodide (**2***b*) which undergoes 1,4-elimination with methyl lithium to give the title compound (**1**). All reaction intermediates are readily crystallizable and with the exception of (**6***b*) obtainable in > 80% yield.

Quatre voies de synthèse menant au composé **1** sont décrites; trois (i), (ii) et (iii) sont des processus simples n'impliquant qu'une réaction à partir de sucres précurseurs facilement disponibles. Dans la troisième voie (iii) l'α-cétobenzoate **6***a* est méthylé et le groupe benzoate remplacé par un méthanesulfonate. Le produit **6***d* se réarrange par iodolyse pour donner l'iodure allylique primaire (**2***d*) qui subit une élimination-1,4 en présence de méthyl-lithium pour fournir le composé 1. Tous les intermédiaires de ces réactions sont facilement cristallisables et à l'exception de **6***b* sont obtenus avec des rendements > 80%. [Traduit par le journal]

Can. J. Chem., **51**, 3150 (1973)

Alkoxyhalogenation of the novel diene **1** proceeds in a highly stereoselective manner to give α-D-hex-2-enopyranosides of type **2**, in which the aglycon may be a simple alcohol residue (1) or another monosaccharide (2). These structures (**2**) are remarkably equipped for diverse structural manipulation and are therefore of value for the preparation of highly modified mono- and disaccharides. However, prosecution of these interests requires better avenues to **1** than presently exist (3). Accordingly we now report four additional routes, three (i, ii, and iv) being one-step processes from known materials, and the fourth a more elaborate process in which the intermediates are synthetically interesting in their own right.

(i) The most direct route conceivable is Wittig methylenation (4) of the known enone **3** (5). However, in practice the reaction proceeded in less than 10% yield owing, undoubtedly, to **3** being a vinylogous lactone.[4]

(ii) The methyl olefin **4** may be prepared from **2***a* by LAH reduction (1) or from the 3-*C*-methyl

[1]Pyranosiduloses. Part VII. For Part VI see N. L. Holder and B. Fraser-Reid, Tetrahedron, in press.

[2]Undergraduate Summer Research Participant (1972).

[3]Taken in part from the Ph.D. Thesis of N.L.H., University of Waterloo, Waterloo, Ontario, Canada, 1972. Present address: Gillette Research Institute, Rockville, Maryland, U.S.A.

[4]The positive charge required at carbon-3 for methylenation of enone **3** to occur (4) is dissipated to the ring oxygen as in **g**. Accordingly other arrangements of the

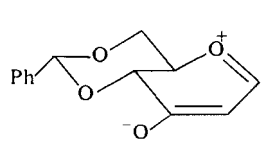

g

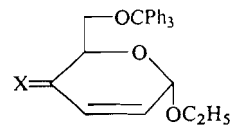

h X = 0
j X = CH_2

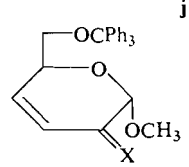

i X = 0
k X = CH_2

chromophore in **h** (6) and **i** (7) in which the lactol oxygen is δ-located, undergo methylenation to **j** and **k**, respectively, in greater than 60% yield (8).

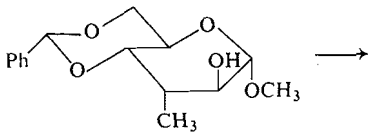

5

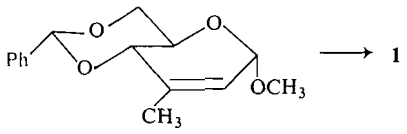

4

alcohol, **5** (9). Brief (0.25 h) pyrolysis of the xanthate ester of **5** in biphenyl gives **4** but prolonged (0.5 h) pyrolysis of **5** gives diene **1** in about 25% yield (10).

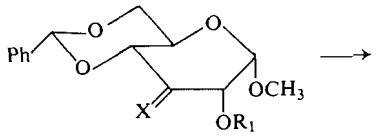

6

	X	R_1
a	O	COPh
b	CH_2	COPh
c	CH_2	H
d	CH_2	SO_2CH_3
e	O_2	$SO_2C_6H_4$-*p*-CH_3

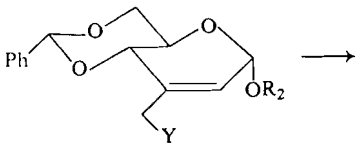

2

	Y	R_2
a	Br	CH_3
b	I	CH_3
c	halogen	monosaccharide

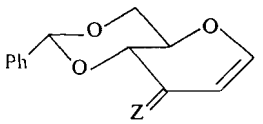

1 Z = CH_2
3 Z = O

(iii) The keto benzoate **6***a* (11) reacted with methylene phosphorane (4) to give a plethora of products; however, with the Cainelli reagent (12) at room temperature, the desired substance **6***b* (m.p. 152–154°), was obtained along with some readily separated debenzoylated material **6***c*[5] (m.p. 192.5–194°. Anal. Calcd.: C, 64.74; H, 6.52. Found: C, 64.87; H, 6.66). Complete debenzoylation of the reaction mixture and methanesulfonylation afforded **6***d* (m.p. 174–174.5°. Anal. Calcd.: C, 53.95; H, 5.61; S, 9.00. Found: C, 53.51; H, 5.86; S, 9.27). When **6***d* was treated with a 15-fold excess of lithium iodide in refluxing diethyl ether for 1 h it was converted to the allyl iodide **2***b*, so recognized because of the similarity of its n.m.r. spectrum to that of **2***a* (1). 1,4-Elimination of methyl hypoiodite from **2***b* was effected in 2 h by use of a 5 *M* excess of methyl lithium in refluxing ether, whereupon diene **1** was the sole product, isolable in >85% yield. The conversion of **6***a* → **1** can be executed without isolation of intermediates in an overall yield of ~40%.

(iv) The fourth route arises from the gratifying discovery that the tosyl ketone **6***e* (13) when treated in benzene–ether with an excess of the Cainelli reagent (12) for 3 h at room temperature,[5] gave **1** directly. The yield after silica column chromatography using 1:4 ethyl acetate – petroleum ether (35–60) mixture was usually ~50%.

The reaction in route iv undoubtedly passes through stages akin to those in iii, iodinolysis being effected by iodide ion produced *in situ*. The superiority of the tosylate as a leaving group precludes the need for the vast excess of iodide and refluxing temperatures required to convert **6***d* to **2***b*. In iv the Grignard reagent is evidently sufficiently basic to cause 1,4-elimination of $IOCH_3$.

We are indebted to the National Research Council and Bristol Laboratories for financial support. In addition

[5]Magnesium turnings (445 mg) previously washed successively with dilute HCl, water, absolute ethanol, and anhydrous ether, and then thoroughly dried in an oven, are added to pre-distilled mercury (150 g) and stirred at room temperature for 2 h in a nitrogen atmosphere. The amalgam is then covered with 1:1 benzene–ether (16 ml) and cooled to −10°. Methylene iodide (1.75 g) dissolved in 1:1 benzene–ether (30 ml) is added during 20 min and stirring continued for 5 min. At this point the supernatant liquid should be translucent and devoid of colour. Ketone **6***a* (1.0 g) dissolved in 1:1 benzene–ether (160 ml) is added as rapidly as possible and stirred at room temperature for 5 h. (A nitrogen atmosphere must be rigorously maintained in the reaction vessel throughout these operations). After quenching with ammonium chloride solution, the mixture is poured into a separatory funnel and the mercury is drawn off. The organic layer is then isolated and worked up in the usual way.

Can. J. Chem. Downloaded from www.nrcresearchpress.com by 210.87.254.105 on 09/05/12
For personal use only.

one of us (S. Y-K. T.) is grateful to the University of Waterloo for a bursary.

1. B. FRASER-REID and B. RADATUS. Chem. Commun. 779 (1970); B. FRASER-REID and B. RADATUS. Can. J. Chem. **50**, 2919 (1972).
2. D. E. ILEY. Unpublished results.
3. B. FRASER-REID and B. RADATUS. Can. J. Chem. **50**, 2909 (1972).
4. G. WITTIG and U. SCHÖLLKOPF. Org. Syn. **40**, 66 (1960).
5. P. M. COLLINS. Carbohydr. Res. **11**, 125 (1969).
6. B. FRASER-REID, A. MCLEAN, E. W. USHERWOOD, and M. YUNKER. Can. J. Chem. **48**, 2877 (1970).
7. B. FRASER-REID and N. L. HOLDER. Chem. Commun. 31 (1972).
8. N. L. HOLDER, Ph.D. Thesis. University of Waterloo, Waterloo, Ontario. 1972.
9. T. D. INCH and G. J. LEWIS. Carbohydr. Res. **15**, 1 (1970).
10. D. R. HICKS, R. AMBROSE, and B. FRASER-REID. Tetrahedron. Lett. 2507 (1973).
11. F. A. CAREY and K. O. HODGSON. Carbohydr. Res. **12**, 463 (1970).
12. F. BERTINI, P. GRASSELLI, G. ZUBIANI, and G. CAINELLI. Tetrahedron, **26**, 1281 (1970).
13. K. ONODERA and N. KASHIMURA. Meth. Carbohydr. Chem. **6**, 331 (1966).

The Master Equation for the Dissociation of a Dilute Diatomic Gas. X. How Rotation Causes Low Arrhenius Temperature Coefficients

HUW O. PRITCHARD

Chemistry Department, University of Manchester Institute of Science and Technology, Manchester 1, England[1] *and Centre for Research in Experimental Space Science, York University, Downsview, Ontario*[2]

Received June 4, 1973

It is shown that previously calculated nonequilibrium rate constants for the dissociation of H_2 and D_2 appear to approach a rotationally averaged equilibrium expression at low temperature. This equilibrium form of the rate expression *itself* has an Arrhenius temperature coefficient for dissociation which is significantly less than the dissociation energy, and the corresponding recombination rate constant has a negative temperature coefficient. The reasons for this are explained.

On a montré que les constantes de vitesse de non équilibre pour la dissociation de H_2 et D_2 précédemment calculées semblaient tendre vers une expression d'équilibre de rotation moyennée à basse température. Cette forme d'équilibre pour l'expression de vitesse en elle-même possède un coefficient de température d'Arrhénius pour la dissociation qui est inférieur de façon notable à l'énergie de dissociation et la constante de vitesse de recombinaison correspondante possède un coefficient de température négatif; une explication a été donnée. [Traduit par le jurnal]

Can. J. Chem., **51**, 3152 (1973)

In an earlier paper in this series (1) we calculated approximate theoretical rate constants for the dissociation of H_2 and D_2 by the third body He over the temperature range 700–5000 °K. Pursuing our previous assertion (2) that low Arrhenius temperature coefficients in diatomic dissociations reflect increasing departures from a Boltzmann distribution among bound states with increasing temperature, we examine here the possibility that at low temperatures, the rate constants may tend to some equilibrium form of the rate expression; for reasons already explained (1), 700 °K is the lowest temperature at which nonequilibrium calculations are feasible with existing computing facilities.

One may formulate a rotationally averaged form of the standard collision-theory rate constant for dissociation as

$$[1] \qquad \tilde{k}_d = \frac{Z(T)}{\mathrm{pf}_{\mathrm{total}}} \sum_J \mathrm{pf}(J) e^{-D(J)/kT}$$

where $Z(T)$ is a collision number (assumed at the

[1]Visiting Professor January–June 1973.
[2]Permanent address.

Can. J. Chem. Downloaded from www.nrcresearchpress.com by 210.87.254.105 on 09/05/12
For personal use only.

one of us (S. Y-K. T.) is grateful to the University of Waterloo for a bursary.

1. B. FRASER-REID and B. RADATUS. Chem. Commun. 779 (1970); B. FRASER-REID and B. RADATUS. Can. J. Chem. **50**, 2919 (1972).
2. D. E. ILEY. Unpublished results.
3. B. FRASER-REID and B. RADATUS. Can. J. Chem. **50**, 2909 (1972).
4. G. WITTIG and U. SCHÖLLKOPF. Org. Syn. **40**, 66 (1960).
5. P. M. COLLINS. Carbohydr. Res. **11**, 125 (1969).
6. B. FRASER-REID, A. MCLEAN, E. W. USHERWOOD, and M. YUNKER. Can. J. Chem. **48**, 2877 (1970).
7. B. FRASER-REID and N. L. HOLDER. Chem. Commun. 31 (1972).
8. N. L. HOLDER, Ph.D. Thesis. University of Waterloo, Waterloo, Ontario. 1972.
9. T. D. INCH and G. J. LEWIS. Carbohydr. Res. **15**, 1 (1970).
10. D. R. HICKS, R. AMBROSE, and B. FRASER-REID. Tetrahedron. Lett. 2507 (1973).
11. F. A. CAREY and K. O. HODGSON. Carbohydr. Res. **12**, 463 (1970).
12. F. BERTINI, P. GRASSELLI, G. ZUBIANI, and G. CAINELLI. Tetrahedron, **26**, 1281 (1970).
13. K. ONODERA and N. KASHIMURA. Meth. Carbohydr. Chem. **6**, 331 (1966).

The Master Equation for the Dissociation of a Dilute Diatomic Gas. X. How Rotation Causes Low Arrhenius Temperature Coefficients

HUW O. PRITCHARD

Chemistry Department, University of Manchester Institute of Science and Technology, Manchester 1, England[1] *and Centre for Research in Experimental Space Science, York University, Downsview, Ontario*[2]

Received June 4, 1973

It is shown that previously calculated nonequilibrium rate constants for the dissociation of H_2 and D_2 appear to approach a rotationally averaged equilibrium expression at low temperature. This equilibrium form of the rate expression *itself* has an Arrhenius temperature coefficient for dissociation which is significantly less than the dissociation energy, and the corresponding recombination rate constant has a negative temperature coefficient. The reasons for this are explained.

On a montré que les constantes de vitesse de non équilibre pour la dissociation de H_2 et D_2 précédemment calculées semblaient tendre vers une expression d'équilibre de rotation moyennée à basse température. Cette forme d'équilibre pour l'expression de vitesse en elle-même possède un coefficient de température d'Arrhénius pour la dissociation qui est inférieur de façon notable à l'énergie de dissociation et la constante de vitesse de recombinaison correspondante possède un coefficient de température négatif; une explication a été donnée. [Traduit par le jurnal]

Can. J. Chem., **51**, 3152 (1973)

In an earlier paper in this series (1) we calculated approximate theoretical rate constants for the dissociation of H_2 and D_2 by the third body He over the temperature range 700–5000 °K. Pursuing our previous assertion (2) that low Arrhenius temperature coefficients in diatomic dissociations reflect increasing departures from a Boltzmann distribution among bound states with increasing temperature, we examine here the possibility that at low temperatures, the rate constants may tend to some equilibrium form of the rate expression; for reasons already explained (1), 700 °K is the lowest temperature at which nonequilibrium calculations are feasible with existing computing facilities.

One may formulate a rotationally averaged form of the standard collision-theory rate constant for dissociation as

$$[1] \qquad \tilde{k}_d = \frac{Z(T)}{\mathrm{pf}_{\mathrm{total}}} \sum_J \mathrm{pf}(J) e^{-D(J)/kT}$$

where $Z(T)$ is a collision number (assumed at the

[1]Visiting Professor January–June 1973.
[2]Permanent address.

Can. J. Chem. Downloaded from www.nrcresearchpress.com by 210.87.254.5 on 09/05/12
For personal use only.

TABLE 1. Comparison of nonequilibrium and rotationally averaged equilibrium rate constants for dissociation of H_2 and D_2; k_d = nonequilibrium rate constant, $\tilde{k}_d$ = equilibrium rate constant, both in units of cm^3 $molecule^{-1}$ s^{-1}

	H_2			D_2		
T	$\tilde{k}_d$	k_d	$\tilde{k}_d/k_d$	$\tilde{k}_d$	k_d	$\tilde{k}_d/k_d$
5000	5.54×10^{-13}	3.5×10^{-14}	16	3.09×10^{-13}	4.5×10^{-14}	6.9
4000	4.68×10^{-14}	—	—	2.57×10^{-14}	—	—
3000	6.81×10^{-16}	(6.8×10^{-17})	(10)	3.60×10^{-16}	—	—
2000	1.28×10^{-19}	1.9×10^{-20}	6.8	5.91×10^{-20}	2.1×10^{-20}	2.9
1500	2.07×10^{-23}	4.2×10^{-24}	4.9	8.89×10^{-24}	4.0×10^{-24}	2.2
1000	5.72×10^{-31}	1.7×10^{-31}	3.4	1.88×10^{-31}	$\sim1.1\times10^{-31}$	1.7
700	1.11×10^{-40}	4.3×10^{-41}	2.6	2.49×10^{-41}	$\sim1.7\times10^{-41}$	1.5
500	1.28×10^{-53}	—	—	1.71×10^{-54}	—	—
300	8.75×10^{-84}	—	—	3.51×10^{-85}	—	—

moment to be independent of J for consistency with the earlier work), $pf(J)$ and pf_{total} are rotation–vibration partition functions as before (1), and $D(J)$ is the effective dissociation energy of the J'th rotational state; this expression can be cast in other useful equivalent forms, *e.g.*

$$[2] \quad \tilde{k}_d = \frac{Z(T)}{pf_{total}} \sum_J (2J+1) e^{-[D_0 + U_{max}(J)]/kT}$$

or

$$[3] \quad \tilde{k}_d = Z(T) e^{-D_0/kT} \sum_J \frac{(2J+1) e^{-U_{max}(J)/kT}}{pf_{total}}$$

Using the same collision numbers as were used previously (1), Table 1 compares the calculated nonequilibrium rate constants (Table 12 of ref. 1) for H_2 and D_2 with the rotationally averaged equilibrium rate constants. The summation in [2] was taken over all J (both odd and even) and $U_{max}(J)$ was taken to be *either* the maximum rotational barrier height, as tabulated by LeRoy (3), *or* the topmost quasi-bound level if the resonance width was greater than 1 cm^{-1}, again as tabulated by LeRoy; we have already discussed in detail the justification for cutting off the top of the rotational barrier for those quasi-bound rotation–vibration states having short lifetimes (1). As expected, the equilibrium rate constant always exceeds the nonequilibrium rate constant, but by a factor which decreases rapidly with decreasing temperature: the data are compared graphically in Fig. 1 and, although the nonequilibrium results for D_2 are much less extensive, it seems entirely reasonable to continue both curves towards an intercept at $T = 0$ where the equilibrium and nonequilibrium rate constants would coincide. Furthermore, the disparity between the equilibrium and nonequilibrium rates is less for D_2 than for H_2, consistent with the fact that D_2 has more rotation–vibration levels than does H_2, and therefore more pathways in the network (1); unlike the nonequilibrium rates, however, the equilibrium dissociation rate for D_2 is always less than it is for H_2.

TABLE 2. Equilibrium and nonequilibrium Arrhenius temperature coefficients ($\tilde{E}$ and E respectively) for dissociation, in kcal mol^{-1}; values of E taken from ref. 1

	H_2		D_2	
T	$\tilde{E}$	E	$\tilde{E}$	E
4000–5000	98.2	92	98.9	(94)
3000–4000	100.9	94	101.7	(96)
2000–3000	102.8	97	103.9	(99)
1500–2000	103.6	100	104.9	102
1000–1500	103.7	101.5	105.3	103.5
700–1000	103.7	102.5	105.4	104.5
2000–5000	101.5	96	102.5	97

NOTE: $D_0^{H_2}$ = 103.3 kcal mol^{-1}; $D_0^{D_2}$ = 105.1 kcal mol^{-1}.

Table 2 shows the Arrhenius temperature coefficients of the equilibrium and nonequilibrium rates: it will be seen that, although the effect is not as marked as in the nonequilibrium case, even the equilibrium Arrhenius temperature coefficients fall progressively below the respective dissociation energies at high temperatures. The reason for this is simple. Rotation has always been discounted in the past as a cause of low Arrhenius temperature coefficients because it was assumed that the dissociation paths for molecules with high J quantum numbers must be high-energy paths, and are therefore discriminated against (2, 4, 5). However, if we *insist* that the

Can. J. Chem. Downloaded from www.nrcresearchpress.com by 210.87.254.5 on 09/05/12
For personal use only.

Can. J. Chem. Downloaded from www.nrcresearchpress.com by 210.87.254.5 on 09/05/12
For personal use only.

molecules are rotationally equilibrated, then the higher the temperature, the more molecules are forced to take these high-energy paths. In effect, the critical energy for dissociation is temperature dependent, and rises slowly with temperature: simple differentiation of the expression $k =$ const. exp $[-D(T)/kT]$ with respect to temperature shows that dk/dT is *less* than it would be for constant D if $dD(T)/dT$ is positive, and therefore the Arrhenius temperature coefficient will also be less than expected.

Inspection of either expression 2 or 3 reveals that at very low temperatures the equilibrium rate constant for dissociation will tend to the standard collision theory result of $Z(T)$ exp $[-D_0/kT]$, whence it follows that the rate constant for recombination (*i.e.*, $\tilde{k}_d/K$) will also tend to a very simple form. The rotationally averaged equilibrium rate constants for recombination, calculated using the equilibrium constants (1) and the corresponding dissociation rate constants, are shown in Table 3. It will be noticed, rather surprisingly, that they decrease monotonically throughout the whole range 300–5000 °K (despite the fact that $Z(T)$ increases with temperature).[3]

It is often the case that it is possible to rationalize the occurrence of unexpected Arrhenius temperature coefficients from the point of view of one of the two processes, *i.e.*, *either* dissociation *or* recombination, but quite difficult to visualize the complementary effect on the reverse process: a complete understanding of such effects requires that we can visualize *both* processes *equally* satisfactorily. We have accounted for the dissociation case very simply by saying that as the temperature rises, the assumption of rotational equilibration forces more and more molecules to dissociate via high-energy paths, and therefore the rate of dissociation does not rise as rapidly as it otherwise would. Likewise in recombination, an increase in the approach velocity of a pair of atoms means that, except for a head-on collision, the encounter has more angular momentum. Hence, as the temperature rises and gas-kinetic velocities increase, more and more encounters possess high angular momenta, and are therefore forced to take recombination paths which have higher and higher centrifugal barriers: in other words, more and more pairs of atoms face higher and higher activation energy barriers, at the expense of those low-J encounters which face no barrier, and the total rate of recombination actually falls.

It had been tentatively concluded, both by us (1) and by Dove and Jones (7), that rotational

TABLE 3. Rotationally averaged equilibrium recombination rate constants in cm^6 molecule^{-2} s^{-1}

T	H_2	D_2
5000	9.23×10^{-33}	5.28×10^{-33}
4000	1.02×10^{-32}	5.80×10^{-33}
3000	1.13×10^{-32}	6.43×10^{-33}
2000	1.28×10^{-32}	7.27×10^{-33}
1500	1.38×10^{-32}	7.85×10^{-33}
1000	1.53×10^{-32}	8.67×10^{-33}
700	1.67×10^{-32}	9.45×10^{-33}
500	1.82×10^{-32}	1.02×10^{-32}
300	2.05×10^{-32}	1.13×10^{-32}

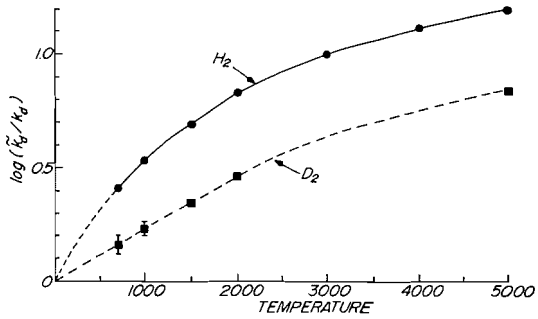

FIG. 1. Comparison of nonequilibrium and rotationally averaged equilibrium rate constants for dissociation of H_2 and D_2; k_d = nonequilibrium rate constant, $\tilde{k}_d$ = equilibrium rate constant.

[3]Again, the rotationally averaged equilibrium recombination rate for D_2 is always less than that for H_2, by a factor of about 0.57–0.58 at most temperatures. The figure 0.57_7 is $0.8165\times(\frac{1}{2})^{3/2}\times2$ where 0.8165 is the ratio of the two collision numbers used (1) and the other two factors arise in the ratio of the standard statistical mechanical expressions for the two equilibrium constants (6): the term $(\frac{1}{2})^{3/2}$ comes from translational partition function terms, and the factor of 2 comes from rotational partition function terms. Thus as $T\rightarrow0$ and the rotational partition function no longer has its classical form, the ratio of the rotationally averaged equilibrium recombination rates for D_2 and H_2 will be

$$(\tfrac{1}{2})^{3/2}\,(pf_{rot}^{D2}/pf_{rot}^{H2})\,(Z_{M,D_2}/Z_{M,H_2})$$

In the absence of nuclear spin effects the rotational partition function ratio would eventually drop out, but for H_2 and D_2 this will not happen; on top of this, nonequilibrium (network) effects will introduce approximately another factor of between 1 and 2 (cf. Fig. 1).

effects *may* have something to do with the observation of low Arrhenius temperature coefficients in diatomic dissociation reactions, because of the fact that theoretically computed temperature coefficients were much more in line with experimental observation if rotational disequilibrium was explicitly considered in the model calculations. It seems clear from the present examination that, in fact, an equilibrium model including rotational effects can account (at least in the energy-transfer dominated regime) for negative temperature coefficients in diatomic recombination, or for "low" temperature coefficients of the dissociation rate: however, it is also clear from Fig. 1 that nonequilibrium effects must be superimposed and that although these nonequilibrium effects decrease in importance with decreasing temperature, they are likely to be present even down to the lowest temperatures where recombination has yet been studied (8).

The author would like to thank the National Research Council of Canada and the Nuffield Foundation for travel assistance, and the University of Manchester Regional Computer Centre for the use of its facilities.

1. T. ASHTON, D. L. S. MCELWAIN, and H. O. PRITCHARD. Can. J. Chem. **51**, 237 (1973).
2. H. O. PRITCHARD. J. Phys. Chem. **65**, 504 (1961).
3. R. J. LEROY. J. Chem. Phys. **54**, 5433 (1971); Report No. WIS-TCI-387, University of Wisconsin Theoretical Institute, 1971.
4. S. H. BAUER and S. C. TSANG. Phys. Fluids, **6**, 182 (1963).
5. E. E. NIKITIN. Theory of thermally induced gas phase reactions, transl. E. W. Schlag, Indiana University Press, Bloomington, Indiana, 1966.
6. R. H. FOWLER and E. A. GUGGENHEIM. Statistical thermodynamics. Cambridge University Press, Cambridge. 1939.
7. J. E. DOVE and D. G. JONES. Chem. Phys. Lett. **17**, 134 (1972).
8. D. O. HAM, D. W. TRAINOR, and F. KAUFMAN. J. Chem. Phys. **53**, 4395 (1970).

Can. J. Chem. Downloaded from www.nrcresearchpress.com by 210.87.254.5 on 09/05/12
For personal use only.

Can. J. Chem. Downloaded from www.nrcresearchpress.com by 210.87.254.6 on 09/05/12
For personal use only.

Canadian Journal of Chemistry

Published by
THE NATIONAL RESEARCH COUNCIL OF CANADA

Journal canadien de chimie

Publié par
LE CONSEIL NATIONAL DE RECHERCHES DU CANADA

Volume 51 Number 19 October 1, 1973 Volume 51 numéro 19 1 octobre 1973

Diterpenoid Metabolites of *Cyathus helenae*. Cyathin B_3 and Cyathin C_3

WILLIAM A. AYER AND LESLIE L. CARSTENS

Chemistry Department, University of Alberta, Edmonton, Alberta T6G 2E1

Received April 9, 1973

Cyathin B_3, a metabolite of *Cyathus helenae* is shown to possess structure **3***a*. Cyathin C_3 is 1,2-dehydrocyathin B_3 (**4***a*). Cyathin B_3 has been correlated with cyathin A_3 (**1**) and cyathin C_3 with allocyathin B_3 (**2**).

On a montré que la cyathine B_3, métabolite du *Cyathus helenae* possède la structure **3***a*. La cyathine C_3 correspond au déhydro-1,2 cyathine B_3 (**4***a*). Une corrélation entre la cyathine B_3 et la cyathine A_3 (**1**), la cyathine C_3 avec l'allocyathine B_3 (**2**), a été rapportée.

[Traduit par le journal]

Can. J. Chem., 51, 3157 (1973)

The bird's nest fungus *Cyathus helenae* Brodie (Gasteromycetes) when grown on liquid culture produces a mixture of substances showing antibiotic activity (1). Our initial report on the separation of the components describes six components of the mixture, including 2,4,5-trihydroxybenzaldehyde and five C_{20} compounds (1). Recently (2) we have shown that one of these C_{20} compounds, cyathin A_3, possesses the novel diterpenoid structure **1**, and that an additional component of the mixture, allocyathin B_3, possesses structure **2**. The stereochemistry shown in **1** and **2**, including the absolute configuration, has been established by X-ray crystallography (3). We now wish to report the structure of cyathin B_3 (1) and that of a newly detected component of the cyathin mixture, cyathin C_3.[1]

Crude cyathin B_3 was isolated by column chromatography (silicic acid) of an ethyl acetate extract of the culture broth of *Cyathus helenae* grown on a defined (1) medium, and crystallized from ether–pentane (m.p. 131–133°). The mass spectrum shows an apparent molecular ion at *m/e* 316 ($C_{20}H_{28}O_3$, h.r.m.s.).[2] However, the appearance of a strong peak at *m/e* 314 in the mass spectrum and the complexity and nature of the n.m.r. spectrum (see Experimental) suggested that the crystalline material is a mixture of cyathin B_3 and a dehydro analog (cyathin C_3). T.l.c. over silica gel and over alumina and with several solvent systems showed a single spot, but t.l.c. over silica gel impregnated with 10% silver nitrate revealed two overlapping spots at higher R_f values along with apparent decomposition products near the origin (no decomposition was observed in the absence of silver nitrate). Preparative t.l.c. (silica gel – $AgNO_3$) afforded only partial separation and was accompanied by extensive loss of material. Since the n.m.r. and i.r. spectra indicated that the material was a mixture of unsaturated aldehydes

[1]The C_{20} compounds are named in the following way (1): compounds containing 30 hydrogens are placed in the A series of cyathins; those with 28 hydrogens in the B series; those with 26 hydrogens in the C series. The subscript after the letter denotes the number of oxygens. Isomers of the first isolated cyathins are designated allocyathins, *e.g.*, cyathin B_3 is $C_{20}H_{28}O_3$ and isomeric with allocyathin B_3.

[2]Because of the small quantities of pure material available, all molecular formulas have been established by high resolution mass spectrometry (h.r.m.s.). Eventual correlation with compounds of established molecular formula validates the deductions made in this manner.

Can. J. Chem. Downloaded from www.nrcresearchpress.com by 210.87.254.6 on 09/05/12
For personal use only.

(n.m.r. signals at δ 9.91 and 9.61, i.r. bands at 2810, 2710, 1692 cm^{-1}), it seemed possible that the two components of the mixture were the aldehydes **3***a* (cyathin B_3) and **4***a* (cyathin C_3), C-15 dehydro analogs of cyathin A_3 (**1**) and allocyathin B_3 (**2**), respectively. The correctness of this supposition is supported by the experiments described below.

Cyathin A_3 (**1**) and allocyathin B_3 (**2**) are readily transformed into the internal methyl ketals **5** and **6**, respectively, by treatment with methanolic HCl (2). Similar treatment of the cyathin B_3 – cyathin C_3 mixture gave a mixture of cyathin B_3 methyl ketal (**7***a*) and cyathin C_3 methyl ketal (**8***a*) which was separable, without extensive decomposition, by p.t.l.c. on silica gel – 10% silver nitrate. As expected (4) the more highly unsaturated ketal **8** displayed the lower R_f value.

Cyathin B_3 methyl ketal (**7***a*) absorbs at 233 nm (ε 5300) in the u.v. (α,β-unsaturated aldehyde (5)) and shows characteristic α,β-unsaturated aldehyde absorption in the i.r. The n.m.r. spectrum displays an aldehydic proton at δ 9.88, a one-proton signal at δ 7.00 (β-proton of α,β-unsaturated carbonyl system), a multiplet at δ 4.97 (C-11 proton), a methoxyl signal at δ 3.26, as well as the appropriate *C*-methyl signals. The mass spectrum shows the appropriate parent peak at *m/e* 330 and no $M^+ - 2$ peak.

The spectroscopic properties of cyathin C_3 methyl ketal (**8***a*) are similar to those of **7** except for those attributable to the cyclopentadiene moiety. Thus, the u.v. spectrum shows a shoulder (257 nm) due to the cyclopentadiene chromophore (2, 6) superimposed on the unsaturated aldehyde chromophore (236 nm). This absorption band is clearly resolved in the circular dichroism (c.d.) spectrum. The olefinic protons at C-1 and -2 in **8***a* appear as an AB quartet (J = 5.5 Hz) centered at δ 6.15 in the n.m.r. Characteristic olefinic C—H stretching bands appear at 3050 cm^{-1} in the i.r.

Acetylation of the cyathin B_3 – cyathin C_3 mixture with acetic anhydride – pyridine led to the formation of at least three products (t.l.c.), separable by p.t.l.c. Besides *O*-acetylcyathin B_3 (**3***b*) and *O*-acetylcyathin C_3 (**4***b*), a compound of higher R_f value showing u.v. absorption at 325 nm (β 10 600) and 260 nm (ε 6200) was obtained. This latter compound showed an apparent molecular ion at *m/e* 298 ($C_{20}H_{26}O_2$) and is assigned structure **9** (anhydrocyathin B_3).

In order to prove rigorously the structure assigned to cyathin B_3, a direct correlation with cyathin A_3 (**1**), the structure and absolute stereo-

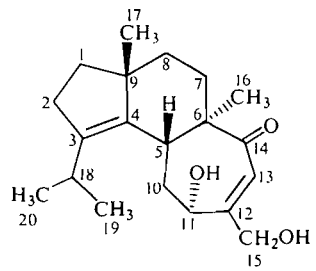

1

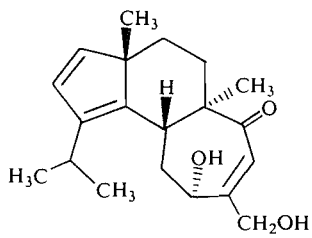

2

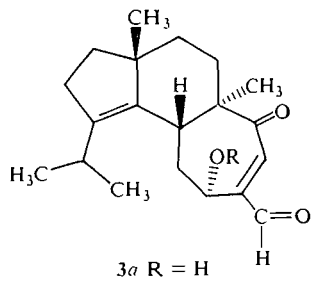

3*a* R = H
3*b* R = Ac

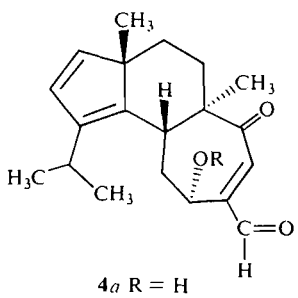

4*a* R = H
4*b* R = Ac

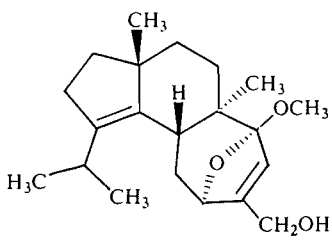

5

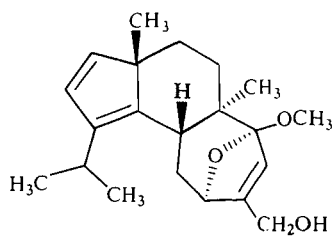

6

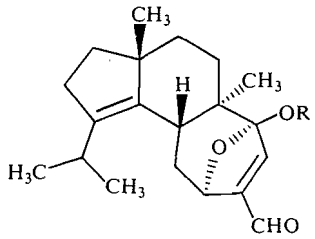

7*a* R = CH_3
7*b* R = H

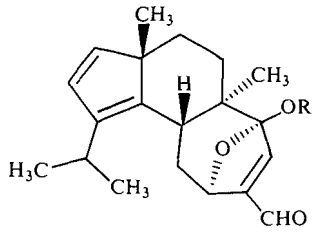

8*a* R = CH_3
8*b* R = H

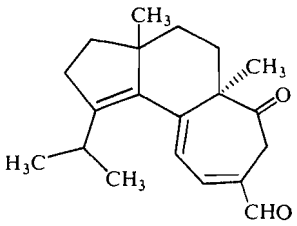

9

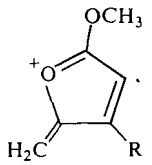

10 R = CH_2OH
11 R = CHO

chemistry of which is known with certainty (2, 3), was established. Reduction of cyathin B_3 methyl ketal (**7**) with sodium borohydride in ethanol gave cyathin A_3 methyl ketal (**5**) identical in all respects (t.l.c. behavior, m.s., i.r., n.m.r., optical rotation, c.d. spectrum) with an authentic sample. Similarly, reduction of cyathin C_3 methyl ketal (**8**) gave allocyathin B_3 methyl ketal (**6**). Thus cyathin B_3 has the structure and stereochemistry depicted in **3***a*, and cyathin C_3 is **4***a*.[3]

The mass spectra of cyathin A_3 methyl ketal (**5**) and allocyathin B_3 (**6**) are both completely dominated by an intense peak at *m/e* 141, presumed to have structure **10** (2). It is noteworthy that the mass spectra of ketals **7** and **8** *do not* show an appreciable peak at *m/e* 139 for the corresponding ion **11**. It appears that the electron-withdrawing formyl group markedly destabilizes an ion of this type.

Experimental

Mass spectra including high resolution mass spectra were recorded on an A.E.I. model MS-9 mass spectrometer, i.r. spectra on a Perkin-Elmer model 421 dual grating spectrometer or on a Unicam SP 1000 dual grating spectrometer, u.v. spectra on a Cary model 14M spectrophotometer, and c.d. spectra on a Jasco model 5 spectropolarimeter. N.m.r. spectra were measured on a Varian HA-100 spectrometer, tetramethylsilane being used as an internal standard. In the description of n.m.r. spectra s = singlet, d = doublet, t = triplet, q = quartet, m = multiplet. Silica gel thin-layer chromatograms were carried out using 0.5 mm layers of Silica Gel G (E. Merck, Darmstadt) containing *ca.* 1% Electronic Phosphor (General Electric, Cleveland); materials were detected by viewing under u.v. light or by spraying with 30% sulfuric acid and charring. Argentated silica gel plates were prepared by slurrying 45 g Silica Gel G with 100 ml of an aqueous solution containing 5 g silver nitrate; the adsorbent layers were activated at 120° for 2 h, protected from light as much as possible, and used within 24 h. For preparative separations, layers of 0.5–0.7 mm were employed. Unless otherwise specified the solvent system used to develop chromatograms was benzene–acetone – acetic acid (75:25:1). All solvents were distilled before use.

Isolation of Cyathin B_3 – Cyathin C_3 Mixture

Total ethyl acetate soluble metabolites of *Cyathus helenae* (1) (2.7 g) were chromatographed in a quartz column (50 mm diameter) over silicic acid (220 g, Mallinckrodt 100 mesh) containing Electronic Phosphor (1 g) using chloroform (0.75% ethanol) as eluent. The progress of the separation was monitored with a short wavelength u.v. lamp. The thirteenth 125 ml fraction (0.33 g) was crystallized from ether–pentane and gave colorless needles (0.13 g), m.p. 131–133°, which proved to be a mixture of cyathin B_3 and cyathin C_3 showing the following properties: mass spectrum (70 eV) *m/e* (relative intensity) 316 (23), 314 (11), 301 (22), 299 (5), 273 (11), 255 (12), 204 (23), 203 (23), 201 (21), 189 (58), 187 (21), 175 (14), 173 (10), 161 (28), 159 (17), 119 (37), 105 (39), 91 (46), 55 (57),

[3]The similarity between the u.v. spectra of the ketalized and unketalized forms of cyathin B_3 and cyathin C_3 and the fact that their i.r. spectra in solution show only one carbonyl band suggests that these compounds, like cyathin A_3 and allocyathin B_3, exist substantially in the hemiketal forms **7***b* and **8***b*, at least in the solvents used for the spectral measurements.

Can. J. Chem. Downloaded from www.nrcresearchpress.com by 210.87.254.6 on 09/05/12
For personal use only.

Can. J. Chem. Downloaded from www.nrcresearchpress.com by 210.87.254.6 on 09/05/12
For personal use only.

41 (100); exact mass measurement, 316.2037 (calcd. for $C_{20}H_{28}O_3$, 316.2038); i.r. (CCl_4) 3585, 3350 (br) 3050 (w), 2810, 2710, 1692 (v.s.), 1625 cm^{-1} (w); u.v. (dioxane) 233 nm (ε 6800); n.m.r. ($CDCl_3$) δ 9.91 (s), 9.61 (s), 7.01 (s), 6.6–6.2 (complex), 5.01 (m), methyl region complex.

Attempted Separation of Cyathin B_3 – Cyathin C_3 Mixture

The crystalline material described above (100 mg) was applied to four 10 × 20 cm plates coated with silica gel – 10% $AgNO_3$ and these were developed with Skellysolve B – acetone (3:2). Two overlapping bands were detected by u.v. These were removed in 3 fractions, and the top and bottom fractions rechromatographed on silica gel. In this way it was possible to obtain cyathin B_3 (47 mg), m.p. 130–132°, only slightly contaminated with cyathin C_3 (as judged by n.m.r. and m.s.) Cyathin B_3 showed the following properties: mass spectrum (70 eV) *m/e* (relative intensity) 316 (68), 301 (57), 273 (28), 255 (27), 204 (42), 203 (39), 189 (100), 175 (28), 161 (42), 105 (41), 91 (45), 55 (54), 41 (84); n.m.r. ($CDCl_3$) δ 9.91 (1H, s), 7.06 (1H, s), 5.08 (1H, m), 1.08 (3H, s), 1.03 (6H, d, J = 6.5 Hz), 0.94 (3H, s).

Preparation and Separation of Cyathin B_3, Cyathin C_3 Methyl Ketals (7a and 8a)

The mixture of cyathin B_3 and cyathin C_3 (77 mg) was dissolved in anhydrous methanol (2 ml) and a saturated solution of hydrogen chloride in methanol (1.5 ml) was added at room temperature. After 48 h, t.l.c. indicated complete reaction and the solvent was removed at the pump. Preparative t.l.c. over silica gel – 10% $AgNO_3$ (solvent system, Skellysolve B – acetone (3:1), R_f values 0.58 (*7a*) and 0.51 (**8***a*)) was used to separate the two components, neither of which could be induced to crystallize.

Cyathin B_3 methyl ketal shows the following properties: $[\alpha]_D^{24}$ −105° (*c* 0.1, isooctane); mass spectrum (70 eV) *m/e* (relative intensity) 330 (24), 315 (14), 301 (20), 299 (23), 255 (21), 227 (23), 204 (21), 199 (21), 189 (100), 175 (31), 161 (33), 133 (35), 119 (47), 105 (63), 91 (65), 55 (67), 41 (86); exact mass measurement 330.2184 (calcd. for $C_{21}H_{30}O_3$, 330.2195); i.r. (CCl_4) 2850, 2720, 1692 (s), 1625 cm^{-1}; u.v. (isooctane) 233 nm (ε 5300); n.m.r. (CCL_4) δ 9.88 (s, H-15), 7.00 (s, *H*-13), 4.97 (br s, *H*-11), 3.26 (s, methoxyl), 2.93 (septet, *H*-18, J = 7 Hz), 2.3–1.1 (complex), 0.98 (d, J = 7 Hz, one isopropyl methyl), 0.94 (s, 3H, *H*-16 or -17), 0.90 (s, 3H, *H*-17 or -16), 0.89 (d, J = 7 Hz, one isopropyl methyl); c.d. (*c* 0.1 in isooctane) $\Delta\varepsilon_{346}$ − 0.97, $\Delta\varepsilon_{235}$ − 2.78.

Cyathin C_3 methyl ketal shows the following properties: $[\alpha]_D^{24}$ − 89° (*c* 0.043, isooctane); mass spectrum (70 eV) *m/e* (relative intensity) 328 (39), 313 (13), 299 (25), 295 (21), 253 (25), 225 (20), 202 (27), 187 (100), 173 (28), 159 (23), 145 (32), 133 (20), 119 (24), 105 (22), 101 (45), 91 (25), 75 (77), 55 (16), 41 (29); exact mass measurement 328.2042 (calcd. for $C_{21}H_{28}O_3$, 328.2039); i.r. (CCl_4) 3050, 2850, 2810, 2720, 1693 (s), 1625 cm^{-1}; u.v. (isooctane) 236 nm (ε 7400), 257 (sh) nm (ε 4300); n.m.r. (CCl_4) δ 9.92 (s, *H*-15), 7.03 (s, *H*-13), 6.20 and 6.10 (AB quartet, *H*-1 and -2, J = 5.5 Hz), 5.05 (m, *H*-11), 3.29 (s, methoxyl), 2.95 (septet, *H*-18, J = 7 Hz), 2.5–2.1 (complex, 2H), 1.8–1.1 (complex), 1.09 and 1.03 (two nonequivalent isopropyl methyls, *J*'s 7 Hz), 0.88 (s, 3H, *H*-16 or -17), 0.77 (s, 3H, *H*-17 or -16): c.d. (*c* 0.043 in isooctane) $\Delta\varepsilon_{356}$ −1.23, $\Delta\varepsilon_{258}$ −4.31, $\Delta\varepsilon_{235}$ −9.23.

Acetylation of Cyathin B_3 – Cyathin C_3 Mixture

Cyathin B_3 – cyathin C_3 mixture (20 mg) was acetylated for 8 h at 40° in methylene chloride (1 ml) containing pyridine (0.16 ml) and acetic anhydride (0.08 ml). The crude product (21 mg) showed three spots on t.l.c. and was separated into its components by p.t.l.c. on silica gel (solvent system, Skellysolve B – acetone (3:1), double development). The least polar compound (5 mg), assigned structure **9**, showed an apparent molecular ion at *m/e* 298 in the mass spectrum (base peak at *m/e* 283) corresponding to $C_{20}H_{26}O_2$. The u.v. spectrum of this material had $\lambda_{max}^{(dioxane)}$ 260 mm (ε 6300) and 325 nm (ε 10 600) and the i.r. spectrum (CCl_4) showed aldehyde C—H stretch at 2810 and 2710 cm^{-1}, carbonyl absorption at 1710 and 1680 cm^{-1}, and C=C stretch at 1615 and 1580 cm^{-1}, and active methylene at 1421 cm^{-1}.

The compound of intermediate R_f value (7 mg) showed properties consistent with those expected for *O*-acetylcyathin B_3 (**3***b*): mass spectrum (70 eV) *m/e* 358, 343,316, 298, 283; i.r. (CCl_4) 2810, 2710, 1745, 1710, 1680 cm^{-1}.

The compound of lowest R_f value was obtained in very small quantity (2 mg). The mass spectrum (M^+ 356) and i.r. (1750, 1705, 1690 cm^{-1}) suggest that it is *O*-acetylcyathin C_3 (**4***b*).

Sodium Borohydride Reduction of Cyathin B_3 Methyl Ketal

Cyathin B_3 methyl ketal (*7a*, 14 mg) was dissolved in 95% ethanol (0.5 ml) and 0.5 ml of a solution of sodium borohydride in ethanol (1 mg/ml) was added. After 15 min, t.l.c. indicated complete reduction. The solvent was removed, water added, and the solution extracted with carbon tetrachloride. Purification by p.t.l.c. on silica gel G provided cyathin A_3 methyl ketal (**5**, 4 mg) as a gum, identical in t.l.c. behavior, mass spectrum, i.r. spectrum, and optical rotation ($[\alpha_D^{24}$ −158° (isooctane), authentic cyathin A_3 methyl ketal shows $[\alpha]_D^{25}$ − 154° (7)) with an authentic sample (2).

Sodium Borohydride Reduction of Cyathin C_3 Methyl Ketal

Cyathin C_3 methyl ketal (**8***a*, 22 mg) was reduced as described above for **7***a*. Isolation and purification afforded allocyathin B_3 methyl ketal (14 mg), identical (t.l.c., m.s., i.r., u.v. (λ_{max} 255 nm), c.d. ($\Delta\varepsilon_{253}$ −3.46)) with an authentic sample (2).

We wish to thank the National Research Council of Canada for financial support, Dr. H. Taube for valuable advice and assistance, and J. Ball for technical assistance.

1. A. D. Allbutt, W. A. Ayer, H. J. Brodie, B. N. Johri, and H. Taube. Can. J. Microbiol. **17**, 1401 (1971).
2. W. A. Ayer and H. Taube. Tetrahedron Lett. 1917 (1972).
3. M. J. Bennett and R. M. Tuggle. Submitted for publication.
4. A. S. Gupta and S. Dev. J. Chromatogr. **12**, 189 (1963).
5. A. I. Scott. Interpretation of the ultraviolet spectra of natural products. Pergamon Press, New York. 1964. p. 77.
6. S. McLean and P. Haynes. Tetrahedron, **21**, 2313, 2343 (1965).
7. H. Taube. Ph.D. Thesis, University of Alberta, Edmonton, Alberta. 1972. p. 132.

Nucleic Acid Related Compounds. 8. Direct Conversion of 2′-Deoxyinosine to 6-Chloropurine 2′-Deoxyriboside and Selected 6-Substituted Deoxynucleosides and Their Evaluation As Substrates of Adenosine Deaminase[1,2]

MORRIS J. ROBINS AND GERALD L. BASOM

Department of Chemistry, The University of Alberta, Edmonton, Alberta T6G 2G2

Received April 9, 1973

Trifluoroacetylation of 2′-deoxyinosine (**2**), obtained by enzymatic deamination of 2′-deoxyadenosine (**1**), gave the 3′,5′-bis-*O*-trifluoroacetate (**3**). Reaction of the electronegatively substituted deoxynucleoside, **3**, with DMF – thionyl chloride complex in refluxing methylene chloride gave a high yield of 6-chloropurine 2′-deoxyriboside (**4**) after deblocking.

Displacement of chloride of **4** by hydrosulfide to give 6-mercaptopurine 2′-deoxyriboside (**5**) followed by sulfur alkylation with *p*-nitrobenzyl bromide gave 6-*S*-(*p*-nitrobenzyl) thiopurine 2′-deoxyriboside (**6**) which was alternatively prepared by displacement of chloride from **4** by *p*-nitrobenzyl mercaptide, generated *in situ* from the isothiouronium salt. Methyl mercaptide reaction with **4** gave 6-methylthiopurine 2′-deoxyriboside (**7**). Treatment of **4** with trimethylamine gave the corresponding quaternary ammonium chloride (**8**) which was allowed to react with potassium fluoride to give 6-fluoropurine 2′-deoxyriboside (**9**). Respective amine displacements on **4** gave 6-benzylaminopurine 2′-deoxyriboside (**10**), and 6-hydroxylaminopurine 2′-deoxyriboside (**11**). Reaction of **4** with liquid ammonia completed the first reported transformation of 2′-deoxyinosine (**2**) to 2′-deoxyadenosine (**1**).

Biological rationale for the synthesis of these 2′-deoxynucleosides and their evaluation as substrates of adenosine deaminase are discussed. Major mass spectral fragmentations are tabulated.

La trifluoroacétylation du déoxy-2′ inosine (**2**), obtenu par désamination enzymatique du déoxy-2′ adénosine (**1**), conduit au bis-*O*-trifluoroacétate-3′,5′ (**3**). La réaction du déoxy nucléoside substitué par un groupe électronégatif **3**, avec le complexe DMF – chlorure de thionyle dans le chlorure de méthylène à reflux conduit au chloro-6 purine déoxy-2′ riboside (**4**) après déblocage.

Le déplacement du chlorure dans **4** par l'hydrogénosulfure pour donner le mercapto-6 purine déoxy-2′ riboside (**5**), suivi d'une S-alkylation par le bromure de *p*-nitrobenzyle conduit au *S*-(*p*-nitrobenzyl)-6 thiopurine déoxy-2′ riboside (**6**) qui peut être préparé d'une autre façon par déplacement du chlorure dans **4** par le *p*-nitrobenzylsulfure engendré *in situ* à partir de sel d'isothiouronium. La réaction du méthylsulfure sur **4** conduit au méthyl-6 thiopurine déoxy-2′ riboside (**7**). Le traitement de **4** par la triméthylamine conduit au chlorure d'ammonium quaternaire correspondant (**8**) qui, mis en présence de fluorure de potassium, conduit au fluoro-6 purine déoxy-2′ riboside (**9**). Les déplacements respectifs sur l'amine dans **4** conduisent au benzylamino-6 purine déoxy-2′ riboside (**10**) et à l'hydroxylamino-6 purine déoxy-2′ riboside (**11**). La réaction de **4** sur l'ammoniac liquide complète la transformation déoxy-2′ inosine (**2**) en déoxy-2′ adénosine (**1**), rapporté pour la première fois.

La justification biologique pour la synthèse de ces déoxy-2′ nucléosides et leur évaluation comme substrats pour l'adénosine déaminase ont été discutées. Un tableau sur les fragments majeurs en spectrométrie de masse a été rapporté. [Traduit par le journal]

Can. J. Chem., **51**, 3161 (1973)

We wish to report the conversion of 2′-deoxyinosine (**2**) into 6-chloro-9-(2-deoxy-β-D-*erythro*-pentofuranosyl)purine (**4**) as the first such successful functionalization of a purine 2′-deoxynucleoside.

A large number of 6-substituted purines and their nucleosides have been prepared and biologically evaluated (for reviews see ref. 1). Some nucleoside derivatives of this type show significant activity and are useful in cancer chemotherapy and other biochemical applications (2).

The syntheses of 6-substituted purine ribosides have been effected by several routes including coupling of suitable purine and sugar derivatives (3–5) but most conveniently by the direct chlorination of a tri-*O*-acylated inosine (6–8). Due to the acid and heat lability of purine 2′-deoxynucleosides, however, analogous attempts with di-*O*-

[1]Generous financial support from the National Cancer Institute of Canada, the National Research Council of Canada (A 5890), and The University of Alberta is gratefully acknowledged.

[2]For the previous paper in this series see ref. 30.

Can. J. Chem. Downloaded from www.nrcresearchpress.com by 210.87.254.5 on 09/05/12
For personal use only.

Can. J. Chem. Downloaded from www.nrcresearchpress.com by 210.87.254.5 on 09/05/12
For personal use only.

acylated 2′-deoxyinosine have failed. The useful synthetic intermediate 6-chloro-9-(2-deoxy-β-D-*erythro*-pentofuranosyl)purine (6-chloropurine deoxyriboside) (**4**) has been prepared previously by base–sugar coupling using the chloromercuri procedure (9) or the fusion method (10). Each of these routes gives **4** in only about 6% yield.

We had observed some time ago (11) that 3′-*O*-*p*-toluenesulfonyl-2′-deoxyadenosine survived intact during hot 80% acetic acid removal of a trityl function. Several groups have recently concluded that nucleosides are acid hydrolyzed by an A-1 mechanism resulting in dissociation of protonated base from positively charged glycosyl ion (12). Thus, substitution of strongly electronegative groups on the sugar moiety would be expected to destabilize glycosyl carbonium ion formation and thus retard sugar–base cleavage.

Reaction of 2′-deoxyinosine (**2**) with trifluoroacetic anhydride gave amorphous 3′,5′-di-*O*-acylate (**3**) (see Scheme 1) as evaluated by t.l.c. and spectroscopic methods. Treatment of this unisolated intermediate (**3**) with thionyl chloride – DMF (7, 8) in refluxing methylene chloride with constant nitrogen purging, followed by methanol treatment and chromatography gave **4** in greater than 80% overall yield from **2** with only about 8% cleavage to hypoxanthine. As observed by others using various conditions (A.D. Broom, private communication and J. Žemlička, private communication), attempted analogous reaction of 3′,5′-di-*O*-acetyl-2′-deoxyinosine resulted in quantitative cleavage of the glycosidic bond.

Paterson and co-workers have found that certain 6-*p*-nitrobenzylthiopurine-9-β-D-ribofuranosides inhibit mediated nucleoside transport across cell membranes (13, and other papers from that laboratory). The 2′-deoxy analog (**6**) was prepared by two routes. Reaction of *p*-nitrobenzyl bromide with thiourea followed by addition of **4** and potassium hydroxide (*in situ* generation of benzyl mercaptide from the isothiouronium salt) gave **6** contaminated with an unidentified product which was removed by chromatography. Alternatively, treatment of **4** with hydrosulfide produced 6-mercaptopurine deoxyriboside (**5**) (9, 14) in 86% yield, and sulfur alkylation of **5** with benzyl bromide gave pure **6** in 87% yield.

Since 6-methylthiopurine riboside has been shown to be active against tumor cell lines resistant toward 6-mercaptopurine riboside and to be phosphorylated by and resistant to different enzymes (15, 16), its 2′-deoxy analog is of interest. When **4** was treated with methyl mercaptide, 6-methylthio-9-(2-deoxy-β-D-*erythro*-pentofuranosyl)purine (**7**) was obtained in 90% yield. The enzymic preparation of **5** and its methylation to **7** are recorded in abstract form (14) with a comparable m.p. for characterization.

Kiburis and Lister (17) succeeded in synthesizing the elusive (18) 6-fluoropurines and their nucleosides employing fluoride displacement on 6-purinyl-trimethylammonium salts. They prepared 6-fluoropurine riboside in some 30% yield by this procedure (17). Reaction of **4** proceeded quantitatively with trimethylamine to give the quaternary salt **8** which was treated with potassium fluoride to provide **9** in 66% yield.

The 2′-deoxynucleoside (**10**) of the potent plant cytokinin (19) 6-benzylaminopurine was prepared in 93% yield by stirring **4** with benzylamine. The properties of **10** are identical to those of a sample prepared by alkylation–rearrangement of 2′-deoxyadenosine (**1**) with benzyl bromide (20).

Treatment of **4** with hydroxylamine gave 6-hydroxylamino-9-(2-deoxy-β-D-*erythro*-pentofuranosyl)purine (**11**) whose 9-riboside analog has been reported to be a potent anti-leukemic agent (21).

Finally, reaction of **4** with liquid ammonia proceeded cleanly to give a 96% yield of 2′-deoxyadenosine (**1**). Alcoholic ammonia (9) was not as satisfactory and alkoxy attack may lead to additional products (22). Adenosine deaminase (adenosine aminohydrolase) cleanly and quantitatively converts 2′-deoxyadenosine (**1**) to 2′-deoxyinosine (**2**). However, this enzymatic reaction is apparently irreversible (23). The present chemical sequence of trifluoracetylation of **2** to give **3**, chlorination to give **4**, and ammonolysis to **1** represents the first recorded reversal of the overall enzymatic process (*i.e.* conversion of 2′-deoxyinosine to 2′-deoxyadenosine).

The mass spectra of these compounds (see Table 1) are for the most part readily interpreted following the fragmentation scheme of McCloskey and co-workers (24). This is summarized in Scheme 2, path 1. However, there are several interesting exceptions.

The mass spectral base peak occurs at *m/e* 81 (relative intensity 100%) for 6-mercaptopurine deoxyriboside (**5**). There is also a significant

Can. J. Chem. Downloaded from www.nrcresearchpress.com by 210.87.254.5 on 09/05/12
For personal use only.

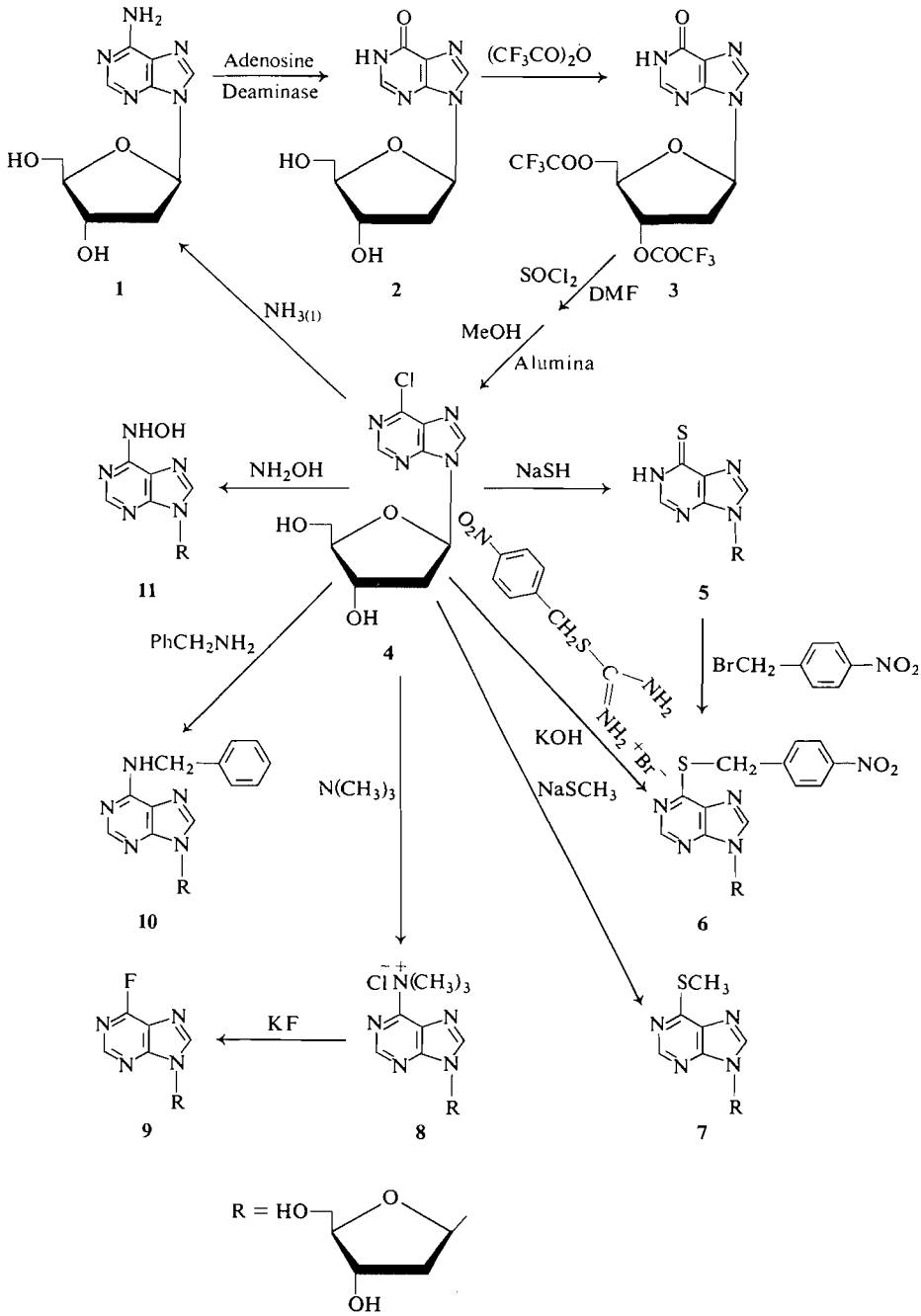

SCHEME 1

Can. J. Chem. Downloaded from www.nrcresearchpress.com by 210.87.254.5 on 09/05/12
For personal use only.

TABLE 1. Mass spectral fragmentations

Compound (probe temperature)		Characteristic ions (*m/e*/relative intensity)						Selected diagnostic ions (*m/e*/relative intensity)
		M	*c*	*d*	*h*	*b* + H	*b* + 2H	
1	(185°)	251/9	221/11	162/44	164/15	135/100	136/33	117(*s*)/9; 108(*b* − CN)/22
4	(200°)	270/3	240/6	181/30	183/12	154/100	155/30	119(*b* + H − Cl)/65; 117(*s*)/20
5	(200°)	268/0.2	238/0.3	179/0.7	181/0.3	152/70	153/8	232(*M* − $2H_2O$)/4; 125(*b* − CN)/15; 119(*b* − S)/15; 117(*s*)/24; 98(*b* − HCN − CN)/56; 81(*s'*)/100
6	(210°)	403/4	373/0.5	314/4	316/1	287/100	288/16	240(*b* − NO_2)/4; 208(*b* − NO_2 − S)/25; 120(*b* + 2H − $SCH_2C_6H_5NO_2$)/28; 117(*s*)/12
7	(175°)	282/10	252/5	193/30	195/10	166/100	167/33	120(*b* + 2H − SCH_3)/20
8	(160°)[a]	279/8[a]	249/4[a]	190/27[a]	192/8[a]	163/54[a]	164/17[a]	148(*b* + H − CH_3)/42[a]; 134(*b* + H − $2CH_3$)/100[a]
9	(175°)	254/1	224/25	165/87	167/12	138/31	139/75	255(*M* + H)/1; 117(*s*)/100
10	(200°)	341/14	311/4	252/24	254/10	225/91	226/20	106($[H_2N{=}CHC_6H_5]^{+\cdot}$)/100; 91($[C_7H_7]^{+\cdot}$ tropylium)/50
11	(175°)	267/1	221/5[b]	162/16[b]	164/5[b]	151/20	152/4	251(*M* − O)/3; 215(*M* − O − $2H_2O$)/1; 136(*b* + 2H − O)/20; 135(*b* + H − O)/80; 117(*s*)/18; 108(*b* − O − CN)/32; 98(*b* − 2CN)/90; 97(*b* − HCN − CN)/74; 81(*s'*)/100
11	(225°)	267/1.5						215(*M* − O − $2H_2O$)/13; 136(*b* + 2H − O)/13; 135(*b* + H − O)/100; 108(*b* − O − CN)/36; 81(*s'*)/34

[a]Nomenclature is for ions formed *after* loss of CH_3Cl from **8**.
[b]Nomenclature is for ions formed *after* loss of O.

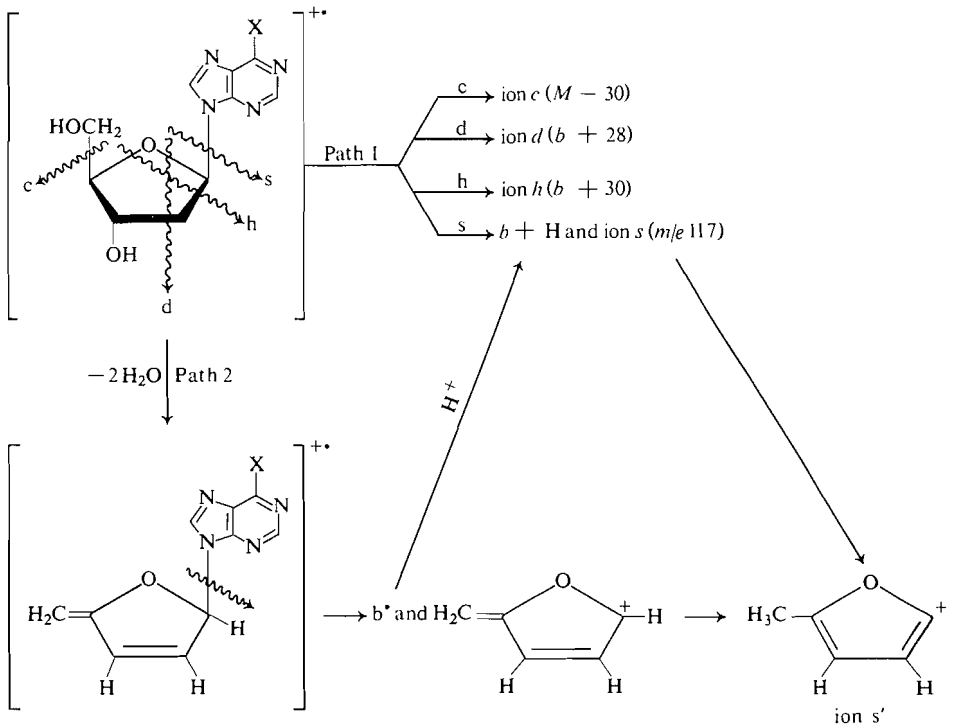

SCHEME 2

peak at *m/e* 232 corresponding to $M - 36$. The *m/e* 81 peak is compatible with a methylfuran ion (ion *s'*) which may arise as shown in Scheme 2. However, an ion of *m/e* 81 has been reported in the fragmentation of several purines (25, 26) to which the following structure was assigned:

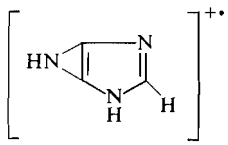

High resolution peak matching for the peak observed in the mass spectrum of **5** gave the value *m/e* 81.0341 as an apparent singlet. The calculated value for ion *s'* (C_5H_5O) is 81.0340 whereas that for $C_3H_3N_3$ is 81.0327. Thus, while ion *s'* is favored, the theoretical masses for the two possible ions are too close to allow conclusive assignment. Therefore, a mass spectrum of 6-thioinosine (probe temperature 200°) was obtained for comparison. The peak at *m/e* 81 was observed at a relative intensity of only 6% (*m/e* 152 (*b* + H), relative intensity 100%), which indicates that the peak at *m/e* 81 in the deoxynucleoside **5** arises primarily from the sugar moiety. Although a significant *m/e* 81 peak has not been reported for free 2'-deoxynucleosides previously, this peak was found to be significant for 3',5'-bistrifluoracetates (27). Thus structural features in 2'-deoxynucleosides may alter the relative importance of paths 1 and 2 which will affect the intensities of ions *c*, *d*, *h*, etc.

Path 2 apparently contributes strongly in the fragmentation of **11**. A further complication occurs by initial extrusion of the hydroxylamino oxygen atom. This loss of oxygen was found to occur also in the spectrum of the riboside analog.[3] The mass spectra of **11** varied markedly with changes in probe temperature.

The spectrum of the 6-fluoro compound **9** is interesting in that the relative intensities of the fragment ions differ significantly from those of the other compounds studied. The most intense peak is due to ion *s*, normally a relatively weak peak. Ions *d* and *b* + 2H are more than twice as abundant as the *b* + H ion which normally gives the most intense peak. An

[3] N^6-Hydroxyadenosine (6-*N*-hydroxylaminopurine riboside) prepared by the procedure of Giner-Sorolla *et al.* (21).

Can. J. Chem. Downloaded from www.nrcresearchpress.com by 210.87.254.5 on 09/05/12
For personal use only.

TABLE 2[a]. Enzyme substrate activity

Compound	$K_m(\times 10^5)$	$V_{max}(\%)$	Substrate activity[b]
1	2.4	100	+
4	16.7	15	+
5	—	—	−
6	—	—	−[c]
7	—	—	+[d]
9	22	100	+
10	—	—	−
11	6.3	44	+

[a]K_m and V_{max} values were obtained from plots of $1/C_0$ *vs.* $1/V_0$. V_0 values were determined by measuring the decrease in absorption between substrate and product (**2**) at 265 nm (**1**, $\Delta\varepsilon = 7500$; **11**, $\Delta\varepsilon = 7000$) or the corresponding increase in absorption at 250 nm **4**, $\Delta\varepsilon = 6000$; **9**, $\Delta\varepsilon = 6000$) for the 5–65 s period following addition of substrate to enzyme. The changes in absorption were recorded on a Cary 15 spectrophotometer using a moving chart to verify the linear $\Delta A/\Delta t$ relationship. V_0 values were determined for at least five initial substrate concentrations from $1\text{–}10 \times 10^{-5}$ *M*. Enzyme solutions were freshly prepared for each substrate and maintained at 0° in 0.05 *M* tris-HCl buffer (p*H* 8 at 0°) and varied from $1\text{–}10 \times 10^{-4}$ mg/0.1 ml. Each determination was initiated by the rapid addition of 1.4 ml of substrate solution in 0.05 *M* KH_2PO_4 buffer (p*H* 7 at 25°) to 0.1 ml of enzyme solution.

[b]Substrate activity was evaluated by treating 5×10^{-4} *M* substrate in 0.05 *M* KH_2PO_4 buffer (p*H* 7 at 25°) with 100 times the normal amount of enzyme. After 30 h, an aliquot was diluted tenfold and the u.v. spectrum compared to control solutions.

[c]Tested in DMSO–buffer (1:1).

[d]Relative rate compared to 1 *ca.* 0.00005.

unusually abundant $M + H$ peak is also present, with approximately the same intensity as the M peak. Decomposition of the $M + H$ ion to form ion *s* due to the enhanced ease of glycosidic bond cleavage (12) offers a possible explanation for the observed anomalous fragment ion intensities.

Adenosine Deaminase Substrate Activity

A number of 6-substituted-purine ribosides have been found to be substrates of adenosine aminohydrolase; chloro, iodo, methylamino, etc., functions are hydrolyzed to yield inosine (28). Deoxyadenosine (**1**) is also a well-known substrate which is deaminated with efficiency comparable to that of adenosine (29).

The deoxynucleosides prepared in this study were subjected to the enzyme, and kinetic parameters were determined for those which were hydrolyzed with reasonable velocity (see Table 2).

The present facile preparation of **4** makes the synthesis of any 6-substituted-purine-9-(2-deoxy-β-D-*erythro*-pentofuranoside), obtainable by nucleophilic displacement, readily available. Analogous studies on 2′-deoxyguanosine are in progress in this laboratory.

Experimental

Melting points were determined on a Fisher-Johns apparatus and are uncorrected. N.m.r. spectra were recorded on a Varian 56/60 spectrometer with TMS or DSS as reference for proton spectra. U.v. spectra were recorded on Cary 14 or 15 spectrometers. Optical rotations were determined on a Perkin-Elmer model 141 polarimeter using a 10 cm, 1 ml micro cell. Mass spectra were determined by the mass spectrometry laboratory of this department on AEI MS-2 and MS-9 instruments at 70 eV. Sample introduction was via direct probe at temperatures specified. Micro analyses were obtained by the microanalytical laboratory of this department and by Schwarzkopf Microanylitical Laboratory, Woodside, N.Y. Evaporations were effected using a Büchler rotating evaporator under aspirator or mechanical oil pump vacuum at 40° or less.

Types I and II adenosine deaminase were purchased from Sigma Chemical Company.

Enzymatic Preparation of 2′-Deoxyinosine (2)

To a suspension of 20 g (0.08 mol) of **1** in 1.1 l of 0.02*M* KH_2PO_4 aqueous buffer (p*H* 7) was added 0.1 g of Type II adenosine deaminase and the mixture was stirred for 20 h at room temperature. The resulting clear solution was evaporated (40°) to about 800 ml and the suspension produced was filtered. The filtrate was similarly concentrated to 200 ml and again filtered. Ethanol (200 ml) was added to the filtrate and this mixture was concentrated to 20 ml and filtered. The combined filter cakes were dissolved in 1 l of hot 80% ethanol, filtered, and the filtrate cooled at 5° for 18 h. Crystalline **2** (16.4 g, 82%) was collected by filtration. This product had m.p. 216–217° (a commercial sample had m.p. 216–218°) and was of adequate purity to use in the following reaction. Further material of lower purity could be obtained from the above filtrates. Mixed m.p., t.l.c., u.v., n.m.r., and mass spectral comparison verified the identity of this material and a commercial sample of 2′-deoxyinosine.

6-Chloro-9-(2-deoxy-β-D-erythro-pentofuranosyl)purine [6-Chloropurine 2′-Deoxyriboside] (4)

A suspension of 10.1 g (0.04 mol) of anhydrous **2**

Can. J. Chem. Downloaded from www.nrcresearchpress.com by 210.87.254.5 on 09/05/12
For personal use only.

Can. J. Chem. Downloaded from www.nrcresearchpress.com by 210.87.254.5 on 09/05/12
For personal use only.

(dried at 75°/0.5 mm Hg for 15 h) in 200 ml of anhydrous CH_2Cl_2 in a dried 5 l three-necked flask protected by drying tubes was flushed well with dry nitrogen and cooled in an ice bath. Trifluoroacetic anhydride (90 g (0.43 mol) freshly distilled from P_2O_5) was added and the mixture stirred for 2 h while the temperature was allowed to rise to 15°. An aspirator with a drying tube in the line was attached and the cooling bath was removed. The mixture was stirred *in vacuo* at room temperature until a white solid foam remained and then a mechanical oil pump (1 mm Hg) was attached for 20 min. This product (**3**) migrated with $R_F \sim 0.42$ (t.l.c. Eastman silica gel No. 6060; $ClCH_2CH_2Cl$–acetone 10:7; **2**, $R_F \sim 0.03$). The ^1H n.m.r. spectrum of **3** in DMSO-d_6 had peaks at δ 2.6–3.3 (m, 2, $H_{2',2''}$), 4.65 (m, 3, $H_{4'}$, $H_{5',5''}$), 5.80 (m, 1, $H_{3'}$), 6.40 ("t", $J_{H_1'-H_2',2''} = 7.0$ Hz, 1, $H_{1'}$), 8.00 and 8.30 (s and s, 1 and 1, H_2 and H_8). These positions correspond to downfield Δδ shifts of approximately 0.1, 0.6, 1.4, 0.8, and 1.0 p.p.m. for the 1′, 2′-2″, 3′, 4′, and 5′-5″ protons, respectively, compared to the resonance positions for 2′-deoxyinosine (**2**) in the same solvent. There was essentially no change in the heterocyclic 2 and 8 proton peak positions of **3** compared to **2** which confirmed that no reaction of the highly electronegative trifluoroacetyl groups with the hypoxanthine moiety of **3** had occurred. The ^{19}F n.m.r. spectrum of **3** had a doublet at δ 74.5 and a singlet at 75.8 (DMSO-d_6, $CFCl_3$ internal) of equal intensity, corresponding to the two trifluoroacetyl groups. The mass spectrum of **3** corresponded to published values (27). The flask was fitted with a dropping funnel, an efficient condenser, and a gas purging tube, and 1 l of dry CH_2Cl_2 was added. A solution of 32 ml (53 g, 0.45 mol) of freshly distilled $SOCl_2$ and 16 ml of DMF (distilled from P_2O_5 and stored over Linde 5A molecular sieves) in 400 ml of dry CH_2Cl_2 was added dropwise over a 2 h period while the reaction was maintained at gentle reflux in an oil bath at 55° and a steady stream of dry nitrogen was bubbled through the stirred solution. The reaction was allowed to proceed an additional 5 h under these conditions and the mixture was cooled. Filtration gave 0.38 g (0.003 mol, 7.5%) of hypoxanthine. The filtrate was slowly poured into an ice-cold solution of 60 g (0.71 mol) of $NaHCO_3$ in 1 l of H_2O with vigorous stirring. Stirring was continued for 15 min, the phases were separated, the aqueous layer was extracted with two 250 ml portions of CH_2Cl_2, and the combined organic phase was dried over Na_2SO_4. Drying agent was removed by filtration, washed with dry CH_2Cl_2, and the combined filtrate was evaporated. The resulting thin syrup was dissolved in 10 ml of cold MeOH and this solution was applied to a column (2.5 × 40 cm, 150 g) of neutral alumina packed in MeOH. The column was developed with MeOH. The first 50 ml contained no product and was discarded. The following 400 ml of eluate was combined and evaporated to give a white solid foam which was crystallized from EtOAc–MeOH (6:1) to give 8.77 g (81%) of **4**, m.p. 139–143°; $[\alpha]_D^{22}$ −12.7° (*c* 1, MeOH) u.v. max (H_2O) 264 nm (ε 10 400); n.m.r.[4] (D_2O) δ 6.64 (t, 1, $J_{H_1'-H_2',H_2''} =$ 6.7 Hz, H_1'), 8.76 and 8.84 (s and s, 1 and 1, H_2 and H_8); lit. m.p. 142–145°, $[\alpha]_D^{26}$ −11.0 ± 0.5° (MeOH) (9); m.p. 144–145°, $[\alpha]_D^{25}$ −10.8° (*c* 1.04, MeOH) (10).

Anal. Calcd. for $C_{10}H_{11}ClN_4O_3$: C, 44.37; H, 4.09; Cl, 13.10; N, 20.70. Found: C, 44.44; H, 3.83; Cl, 13.05; N, 20.50.

9-(2-Deoxy-β-D-erythro-pentofuranosyl)purine-6-thione [6-Mercaptopurine 2′-deoxyribofuranoside] (5)

Hydrogen sulfide was slowly bubbled for 1 h through an ice-cold solution prepared by adding 0.12 g (0.005 mol) of sodium to 15 ml of anhydrous MeOH. A solution of 0.54 g (0.002 mol) of **4** in 15 ml of MeOH was then added, the ice-bath removed, and the solution stirred at room temperature while maintaining slow introduction of H_2S. Crystallization of product from the reaction solution began after about 1 h. After 4 h, H_2S introduction was terminated and the flask was stoppered and allowed to stand for 18 h. The resulting product was collected by filtration and recrystallized from 40 ml of MeOH–H_2O (3:2) to give 0.46 g (86%) of **5**, m.p. 184–186°; $[\alpha]_D^{22}$ −22.5° (*c* 1, 0.1 *N* NaOH), −14.0° (*c* 1, 1.0 *N* NaOH); u.v. max (0.1 *N* HCl) 324; 224 nm (ε 20 900; 9700) (0.1 *N* NaOH) 311; 231 nm (ε 20 700; 14 500); n.m.r.[4] (DMSO-d_6) δ 6.32 (t, 1, $J_{H_1'-H_2',H_2''} = 7.0$ Hz, $H_{1'}$), 8.20 and 8.50 (s and s, 1 and 1, H_2 and H_8); lit. m.p. 180–185° (9), 193–197° (9), 180–181° (14); $[\alpha]_D^{26}$ −23.5 ± 1° (1 *M* NaOH) (9), $[\alpha]_D^{22}$ −13.6° (1.0 *N* NaOH) (14).

Anal. Calcd. for $C_{10}H_{12}N_4O_3S$: C, 44.78; H, 4.51; N, 20.89; S, 11.93. Found: C, 44.55; H, 4.43; N, 20.95; S, 12.21.

6-S-(p-Nitrobenzyl)thio-9-(2-deoxy-β-D-erythro-pentofuranosyl)purine (6)

Method A

A solution of 0.86 g (0.004 mol) of *p*-nitrobenzyl bromide and 0.30 g (0.004 mol) of thiourea in 20 ml of absolute EtOH was stirred at room temperature for 1 h. A solution of 1.08 g (0.004 mol) of **4** in 30 ml of absolute EtOH was then added and the combined reaction was purged well with dry nitrogen. A solution of 0.45 g (0.008 mol) of KOH in 20 ml of absolute EtOH was added dropwise over a period of 30 min while stirring and slow nitrogen purging was continued. The resulting mixture was then refluxed for 3 h on a steam-bath and allowed to stand under nitrogen at room temperature for 15 h. H_2O (150 ml) was added and the mixture was filtered. The filter cake was washed with two 25 ml portions of H_2O and then recrystallized from 500 ml of MeOH–H_2O (4:1) to give 1.1 g of white crystals. This material was composed of 6 plus a minor impurity migrating about 20% faster on t.l.c. (upper phase of EtOAc–*n*-PrOH–H_2O 4:1:2, silica gel). It was dissolved in 200 ml of hot 1,2-dimethoxyethane (glyme) and 10 g of silica gel was added. This mixture was evaporated to dryness and the resulting impregnated powder was added to the top of a column (1.5 × 60 cm, 60 g) of dry-packed silica gel. The column was developed with 5% MeOH in $CHCl_3$ and 20 ml fractions were collected. T.l.c. homogeneous fractions were combined and evaporated to give a white solid which was crystallized from 400 ml of MeOH–H_2O (7:1) to afford 0.81 g (50%) of **6**, m.p. 174–176°; $[\alpha]_D^{22}$ −19.5° (*c* 1, DMF); u.v. max (MeOH) 284 nm (ε 31 300), Sh 290 nm (ε 30 400); n.m.r.[4] (DMSO-d_6) δ 4.83 (s, 2, —SCH_2—), 6.52 (t, 1, $J_{H_1'-H_2',H_2''} =$ 7.0 Hz, H_1'), 7.6–8.4 (A_2B_2 m, 4, *phenyl H's*) 8.76 and 8.80 (s and s, 1 and 1, H_2 and H_8).

[4]The sugar moiety of all these 2′-deoxynucleosides gives rise to a similar n.m.r. pattern: δ ~2.1–3.1 (br m, 2, $H_{2'},H_{2''}$), ~3.7 (m, 2, $H_{5'},H_{5''}$), ~4.0 (m, 1, $H_{4'}$), ~4.5 (m, 1, $H_{3'}$). For actual n.m.r. spectra see ref. 10.

Can. J. Chem. Downloaded from www.nrcresearchpress.com by 210.87.254.5 on 09/05/12
For personal use only.

Anal. Calcd. for $C_{17}H_{17}N_5O_5S$: C, 50.62; H, 4.25; N, 17.36; S, 7.95. Found: C, 50.76; H, 4.24; N, 17.14; S, 8.25.

Method B

To a stirred suspension of 0.28 g (0.002 mol) of anhydrous potassium carbonate and 0.27 g (0.001 mol) of **5** in 10 ml of DMF (distilled from P_2O_5 and stored over Linde 5A molecular sieves) was added a solution of 0.22 g (0.001 mol) of *p*-nitrobenzyl bromide in 5 ml of dry glyme dropwise over a period of 5 min. The resulting mixture was stirred for 2 h at room temperature and filtered. The pink filtrate was evaporated to a thin syrup which was coevaporated with two 10 ml portions of xylene. The resulting white solid was crystallized from MeOH to give 0.35 g (87%) of **6**, m.p. 173–176°. A 1:1 mixture with product from method A had m.p. 174–176° and spectral properties and t.l.c. behavior of the samples were identical.

6-Methylthio-9-(2-deoxy-β-D-erythro-pentofuranosyl)-purine (7)

To an ice-cold solution prepared by adding 1 ml (0.86 g, 0.018 mol) of methanethiol to a solution of 0.14 g (0.006 mol) of sodium metal in 20 ml of absolute EtOH was added a solution of 0.54 g (0.002 mol) of **4** in 15 ml of absolute EtOH. The resulting mixture was stirred for 90 min (the ice-bath was removed after 30 min) and then filtered. The filtrate was evaporated to 20 ml and 20 ml of EtOAc was added. This mixture was evaporated to 10 ml and 30 ml of EtOAc was added. The mixture was briefly cooled at −15° and filtered. The filtrate was evaporated and the resulting solid was crystallized from MeOH–EtOAc (1:1) to afford 0.51 g (90%) of **7**, m.p. 157–158° (lit. (14) m.p. 155–156°); $[\alpha]_D^{22}$ −16.3° (*c* 1, H_2O); u.v. max (H_2O) 282 nm (ε 22 400), Sh 290 nm (ε 20 700); n.m.r.[4] (D_2O) δ 2.50 (s, 3, $-SCH_3$), 6.40 (t, 1, $J_{H_1'-H_2',H_2''}$ = 6.7 Hz, H_1'), 8.25 and 8.40 (s and s, 1 and 1, H_2 and H_8).

Anal. Calcd. for $C_{11}H_{14}N_4O_3S$: C, 46.81; H, 5.00; N, 19.85; S, 11.34. Found: C, 46.62; H, 5.07; N, 20.08; S, 11.05.

9-(2-Deoxy-β-D-erythro-pentofuranosyl)purin-6-yltrimethylammonium Chloride (8)

To a solution of 1.0 g (0.0037 mol) of **4** in 250 ml of dry 1,2-dimethoxyethane (glyme) was added 10 ml (6.1 g, 0.10 mol) of trimethylamine and the mixture was stirred at room temperature for 30 min while protected from moisture by a drying tube. The white solid product was collected by filtration and the filter cake immediately washed with 40 ml of anhydrous ethyl ether and transferred to a vacuum desiccator. The dried salt, **8**, 1.14 g (93%), had m.p. 154–155°; u.v. max (MeOH) 266 nm (ε 9000); n.m.r.[4] (DMSO-d_6) δ 3.90 (s, 9, $-N(CH_3)_3$), 6.58 (t, 1, $J_{H_1'-H_2',H_2''}$ = 6.5 Hz, H_1'), 9.06 and 9.13 (s and s, 1 and 1, H_2 and H_8).

Anal. Calcd. for $C_{13}H_{20}ClN_5O_3$: C, 47.34; H, 6.11; Cl, 10.75; N, 21.24. Found: C, 47.13; H, 6.07; Cl, 10.87; N, 20.81.

6-Fluoro-9-(2-deoxy-β-D-erythro-pentofuranosyl)purine (9)

To a stirred suspension of 1.75 g (0.03 mol) of KF (dried at 170° for 15 h) in 20 ml of dry DMF maintained at 40° in an oil bath was added 1.0 g (0.003 mol) of **8**. The reaction was allowed to proceed for 40 min, cooled, and filtered. The filtrate was added to 6 g of neutral silica gel and the slurry was evaporated (25°, mechanical oil pump). The resulting impregnated powder was added to the top of a column (1.5 × 40 cm, 30 g) of dry-packed neutral silica gel. The column was developed with EtOAc and after a 20 ml forerun, the following 900 ml of eluate was combined and evaporated to 50 ml. This was allowed to stand at −15° for 20 h and 0.51 g (66%) of crystalline **9** was collected by filtration. This product, **9**, had m.p. 148–150°; $[\alpha]_D^{22}$ −20.5° (*c* 1, H_2O); u.v. max (H_2O) 249 nm (ε 7000); n.m.r.[4] (DMSO-d_6) δ 6.53 (t, 1, $J_{H_1'-H_2',H_2''}$ = 6.7 Hz, H_1'), 8.70 and 8.87 (s and s, 1 and 1, H_2 and H_8); ^{19}F n.m.r. (DMSO-d_6, $CFCl_3$ internal reference) δ 72.5 (s, 1, 6-*F*).

Anal. Calcd. for $C_{10}H_{11}FN_4O_3$: C, 47.24; H, 4.36; F, 7.47; N, 22.04 Found: C, 47.30; H, 4.44; F, 7.67; N, 21.82.

6-N-Benzylamino-9-(2-deoxy-β-D-erythro-pentofuranosyl)purine [N⁶-Benzyl-2′-deoxyadenosine] (10)

To 3 ml of benzylamine was added 0.27 g (0.001 mol) of **4** and the mixture was stirred for 1 h at room temperature. Et_2O (20 ml) was added and the resulting mixture was filtered. The solid was discarded and the filtrate was evaporated. The residue was treated with 20 ml of Et_2O, filtered, and the filtrate was evaporated. A mechanical oil pump was attached and most of the remaining benzylamine was evaporated *in vacuo*. The resulting thin syrup was triturated with Et_2O while cooling in ice to give crystalline **10**, m.p. 167–174°, in quantitative yield. This material was recrystallized from MeOH to afford 0.32 g (93%) of **10**, m.p. 174–176°; $[\alpha]_D^{22}$ −20.4° (*c* 1, MeOH); u.v. max (MeOH) 269 nm (ε 22 600); n.m.r.[4] (DMSO-d_6) δ 4.75 (br d, 2, NH—CH_2—Ph), 6.36 (t, 1, $J_{H_1'-H_2',H_2''}$ = 7.0 Hz, H_1'), 7.1–7.4 (m, 5, *Ph*), 8.20 and 8.34 (s and s, 1 and 1, H_2 and H_8). This product was identical to **10** prepared by an alternative procedure (20).

Anal. Calcd. for $C_{17}H_{19}N_5O_3$: C, 59.81; H, 5.61; N, 20.52. Found: C, 59.56; H, 5.58; N, 20.37.

6-N-Hydroxylamino-9-(2-deoxy-β-D-erythro-pentofuranosyl)purine [6-Hydroxylaminopurine 2′-Deoxyriboside] (11)

To a hot solution of 1.51 g (0.027 mol) of KOH in 60 ml of absolute EtOH was added a hot solution of 1.67 g (0.024 mol) of hydroxylamine hydrochloride in 75 ml of absolute EtOH. This was allowed to cool, finally in an ice-bath, and was filtered. To the clear filtrate was added 0.65 g (0.0024 mol) of **4** and the resulting solution was refluxed for 3 h by heating in an oil bath at 100°. The reflux condenser was removed and the solution concentrated to about 50 ml. A solution of 0.15 g (0.0027 mol) of KOH in 15 ml of absolute EtOH was added and the volume was again reduced to about 50 ml by open distillation. The mixture was cooled, filtered, and the filtrate evaporated to a white gum. This material was dissolved in 30 ml of hot absolute EtOH, the solution was treated with 100 ml of hot EtOAc, and allowed to stand for 5 days at −15°. Crystalline **11** (0.40 g) was collected by filtration and another 0.16 g of product was obtained from the mother liquor by concentration and cooling. Total yield of **11**, 0.56 g (87%), m.p. 139–140°, softening at 110–115° and 130–135°; $[\alpha]_D^{22}$ −21.8° (*c* 1, MeOH);

u.v. max (MeOH) 266 nm (ε 12 500); n.m.r.[4] (DMSO-d_6) δ 6.29 (t, 1, $J_{H_1'-H_2',H_2''}$ = 7.0 Hz, H_1'), 7.88 and 8.18 (s and s, 1 and 1, H_2 and H_8), 8.2–10.4 (br s, 2, 6-*NHOH*).

Anal. Calcd. for $C_{10}H_{13}N_5O_4$: C, 44.94; H, 4.90; N, 26.21. Found: C, 45.08; H, 5.19; N, 25.57.

6-Amino-9-(2-deoxy-β-D-erythro-pentofuranosyl)purine [2′-Deoxyadenosine] (1)

A solution of 0.27 g (0.001 mol) of **4** in about 2 ml of liquid ammonia was sealed in a stainless steel pressure reactor and allowed to stand for 20 h at room temperature. The ammonia was allowed to evaporate and a solution of 0.04 g (0.001 mol) of NaOH in 20 ml of H_2O was added. T.l.c. showed only one product with migration identical to naturally occurring 2′-deoxyadenosine. The solution was evaporated, 20 ml of absolute EtOH was added, and the resulting mixture was filtered. The filtrate was evaporated and this process was repeated using 10 ml of warm absolute EtOH to remove NaCl. Recrystallization of the resulting solid from EtOH gave 0.24 g (96%) of **1**, m.p. 189–190°; $[\alpha]_D^{22}$ −24.5° (*c* 1, H_2O); u.v. max (H_2O) 259 nm (ε 14 000). These constants and other physical data compare well with those of naturally occurring 2′-deoxyadenosine.

Anal. Calcd. for $C_{10}H_{13}N_5O_3$: C, 47.80; H, 5.21; N, 27.87. Found: C, 47.58; H, 5.32; N, 27.96.

1. (*a*) J. A. Montgomery and H. J. Thomas. Adv. Carbohydr. Chem. **17**, 301 (1962); (*b*) R. K. Robins. J. Med. Chem. **7**, 186 (1964); (*c*) R. K. Robins. *In* Heterocyclic compounds. Vol. 8. *Edited by* R. C. Elderfield. John Wiley & Sons, Inc., New York, N.Y. 1967. Chapt. 3.
2. A. Goldin, H. B. Wood, Jr., and R. R. Engle. Cancer Chemother. Rep. Part 2, **1**, 1 (1968).
3. J. Davoll and B. A. Lowy. J. Am. Chem. Soc. **74**, 1563 (1952).
4. T. Sato, T. Simadate, and Y. Ishido. Nippon Kagaku Zasshi, **81**, 1440 (1960); Y. Ishido and T. Sato. Bull. Chem. Soc. Jap. **34**, 347 (1961).
5. T. Nishimura and I. Iwai. Chem. Pharm. Bull. Tokyo, **12**, 352 (1964).
6. J. F. Gerster, J. W. Jones, and R. K. Robins. J. Org. Chem. **28**, 945 (1963).
7. M. Ikehara and H. Uno. Chem. Pharm. Bull. Tokyo, **13**, 221 (1965).
8. J. Žemlička and F. Šorm. Collect. Czech. Chem. Commun. **30**, 1880 (1965).
9. R. H. Iwamoto, E. M. Acton, and L. Goodman. J. Org. Chem. **27**, 3949 (1962).
10. M. J. Robins and R. K. Robins. J. Am. Chem. Soc. **87**, 4934 (1965).
11. M. J. Robins and R. K. Robins. J. Am. Chem. Soc. **86**, 3585 (1964).
12. J. A. Zoltewicz, D. F. Clark, T. W. Sharpless, and G. Grahe. J. Am. Chem. Soc. **92**, 1741 (1970); R. P. Panzica, R. J. Rousseau, R. K. Robins, and L. B. Townsend. J. Am. Chem. Soc. **94**, 4708 (1972); L. Hevesi, E. Wolfson-Davidson, J. B. Nagy, O. B. Nagy, and A. Bruylants. J. Am. Chem. Soc. **94**, 4715 (1972); E. R. Garrett and P. J. Mehta. J. Am. Chem. Soc. **94**, 8532 (1972); R. Shapiro and M. Danzig. Biochemistry, **11**, 23 (1972).
13. J. M. Oliver and A. R. P. Paterson. Can. J. Biochem. **49**, 262 (1971); A. R. P. Paterson and J. M. Oliver. Can. J. Biochem. **49**, 271 (1971).
14. M. Honjo, Y. Furukawa, Y. Yoshioka, A. Imada, S. Fujii, K. Ootsu, T. Kimura, T. Komeda, and T. Matsumoto. Ann. Rep. Takeda Res. Lab. 271 (1968); Chem. Abst. **70**, 97105*u* (1969).
15. L. L. Bennett, Jr., R. W. Brockman, H. P. Schnebli, S. Chumley, G. J. Dixon, F. M. Schabel, Jr., E. A. Dulmadge, H. E. Skipper, J. A. Montgomery, and H. J. Thomas. Nature, **205**, 1276 (1965).
16. A. R. P. Paterson and A. Sutherland. Can. J. Biochem. **42**, 1415 (1964).
17. J. Kiburis and J. H. Lister. J. Chem. Soc. C, 3942 (1971).
18. R. K. Robins. *In* Heterocyclic compounds. Vol. 8. *Edited by* R. C. Elderfield. John Wiley & Sons, Inc., New York, N.Y. 1967. pp. 307–308.
19. W. J. Burrows, F. Skoog, and N. J. Leonard. Biochemistry, **10**, 2189 (1971).
20. M. J. Robins and E. M. Trip. Biochemistry, **12**, 2179 (1973).
21. A. Giner-Sorolla, L. Medrek, and A. Bendich. J. Med. Chem. **9**, 143 (1966).
22. L. F. Christensen, A. D. Broom, M. J. Robins, and A. Bloch. J. Med. Chem. **15**, 735 (1972).
23. H. M. Kalckar, J. Biol. Chem. **167**, 462 (1947).
24. S. J. Shaw, D. M. Desiderio, K. Tsuboyama, and J. A. McCloskey. J. Am. Chem. Soc. **92**, 2510 (1970).
25. J. S. Shannon and D. S. Letham. New Zealand J. Sci. **9**, 833 (1966).
26. J. Heiss, K.-P. Zeller, and W. Voelter. Org. Mass Spectrom. **3**, 181 (1970).
27. W. A. Koenig, L. C. Smith, P. F. Crain, and J. A. McCloskey. Biochemistry, **10**, 3968 (1971).
28. B. M. Chassy and R. J. Suhadolnik. J. Biol. Chem. **242**, 3655 (1967).
29. A. Bloch, M. J. Robins, and J. R. McCarthy, Jr. J. Med. Chem. **10**, 908 (1967); S. Frederiksen. Arch. Biochem. Biophys. **113**, 383 (1966).
30. M. J. Robins, R. Mengel, and R. A. Jones. J. Am. Chem. Soc. **95**, 4074 (1973).

Can. J. Chem. Downloaded from www.nrcresearchpress.com by 210.87.254.5 on 09/05/12
For personal use only.

Nuclear Magnetic Resonance Experiments on Acetals. 43. Reversal of Previous Conformational Assignment in 5-Fluoromethylated-5′-Me-1,3-dioxanes

M. ANTEUNIS AND F. BORREMANS

State University of Gent, Department of Organic Chemistry, Laboratory for NMR Spectroscopy, Krijgslaan, 271 (S.4B) Gent; Belgium B-9000

Received September 13, 1972[1]

Additional n.m.r. investigations on 5-fluoromethylated-5′-Me-1,3-dioxanes have made it necessary for us to reverse the spectral assignments which were forwarded recently (1) in this journal. Thus, the 5-CF_2H group prefers the *axial* position to the extent of *ca.* 900 cal/mol, whereas the 5-CFH_2 group displays a similar preference for the axial position to the extent of *ca.* 200 cal/mol. An explanation for these unexpected results is advanced. Final structural assignments have been made possible by homo- and heteronuclear double resonance experiments and by ASIS-studies. The observed relative shifts for 5-CF_nH_{3-n} and 5-CH_3 signals are shown to be normal (*e.g.* δ(5e) < δ(5a)). Also, the previously reported ^4J(F,H) long range couplings follow a classical M-path.

Une étude r.m.n. (assistée d'irridiations multiples) sur les CHF_2-5 CH_3-5′ CH_3-2 dioxannes-1,3 dans C_6D_6 a démontré que l'assignation de configurations proposée récemment pour ces dérivés est erronnée. Il en découle qu'en faite les groupements CF_nH_{3-n}-5 (n = 1,2) préfèrent vis à vis de CH_3-5 la position axiale (*ca.* 900 cal/mol pour CF_2H-5 et *ca.* 200 cal/mol pour CFH_2-5). Ceci est inattendu en vue des moments dipolaires macroscopiques. Une explication est avancée. Comme pour tout autre dioxanne on trouve que δ(5e) < δ(5a).

Can. J. Chem., 51, 3170 (1973)

We wish to focus attention upon the pitfall we encountered with respect to the conformational aspects of 5-CF_nH_{3-n}-1,3-dioxanes,[2] published recently (1) in this journal.

We attributed the n.m.r. spectrum shown in Fig. 1 (ref. 1) to a,e-5-difluoromethyl-5′-Me-2-Me-1,3-dioxane, and we assigned the n.m.r. spectrum shown in Fig. 2 (ref. 1) to the corresponding e,a-isomer. Consequently, the conformational equilibrium **1***b* ⇌ **2***b* was believed to favor the conformer with the equatorial CF_2H group. The same situation was also accepted for the case of 5-fluoromethyl-1,3-dioxane (**1***a* ⇌ **2***a*). These conclusions seemed logical considering the group dipole moments in the system. Moreover, they were strengthened by the observation of a small equilibrium shift when switching from CS_2 to $CHFCl_2$ as solvent.

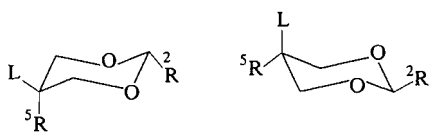

1 **2**

a L = CFH_2; ^{5}R = Me; ^{2}R = H
b L = CF_2H; ^{5}R = Me; ^{2}R = H

We had at that time tacitly accepted (see tables and figures in ref. 1) that the chemical shift (δ) values in these 5,5′-geminally disubstituted derivatives would fall in the order δ(Me-5e) > δ(Me-5a), δ(CF_2H-5e) > δ(CF_2H-5a), and δ(CFH_2-5e) > δ(CFH_2-5a). This situation would then be of opposite trend to that observed in mono-alkyl- and 5,5′-*gem*-dialkyl substituted dioxanes (3). Although we noted this discrepancy, quantitative treatment was precluded by the highly polar, nonspherical nature of the CH_2X or CHX_2 groups, each of which might present nonidentical rotameric distributions in the 5-axial *vs.* 5-equatorial positions, respectively.

We have now obtained convincing evidence that our original structure attributions are incorrect. Thus, the n.m.r. spectrum shown in Fig. 2 (ref. 1), corresponds to *r*-2,*trans*-5-dimethyl-*cis*-5′-CF_2H-1,3-dioxane (**3**), the most stable isomer with lowest GC retention time, while the n.m.r. spectrum displayed in Fig. 1 (1) belongs to *r*-2,*cis*-5-dimethyl-*trans*-5′-CF_2H-1,3-dioxane (**4**). This conclusion follows from the following new evidence.

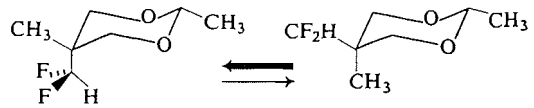

3 **4**

[1]Revision received May 30, 1973.
[2]For synthesis of these derivatives see ref. 2.

Can. J. Chem. Downloaded from www.nrcresearchpress.com by 210.87.254.5 on 09/05/12
For personal use only.

Table 1. ^{1}H n.m.r. shifts (in p.p.m.) in C_6D_6 of compounds **3** and **4**

	H-2	H-4,6e	H-4,6a	Me-5	Me-2	CHF_2
3	4.25	3.8	2.9	0.4	1.22	6.38
4	4.18	3.48	3.35	1.19	1.25	4.73

TABLE 2. ASIS for 2-Me-5-Me-5′-CHF_2-1,3-dioxanes in p.p.m.

$\Delta\delta^{CS_2}_{C_6C_6}$	5-CH_3	2-CH_3	H-4,6a	H-4,6e	H-2	CHF_2
3	0.30	0.01	0.38	0.05	0.25	−0.25
4	0.05	−0.02	0.25	0.12	0.25	0.58

(*a*) Double and triple irradiations in C_6D_6 solutions clearly demonstrate the existence of a nonzero $^4J(CHF_2, H\text{-}4,6a)$ for **3** (3.7 Hz), whereas the corresponding long range $^4J(F,H)$ is *not* observed in **4**. The magnitude of this observed long range coupling requires that the CHF_2 substituent occupy the axial position in 3. Additionally, in C_6D_6 solution the signals due to H-4,6 and due to Me-2 and Me-5 in **4** are found to be well differentiated (Table 1), and one can observe a long range coupling ^4J(Me-5, H-4,6a) in **4** (~0.7 Hz) but *not* in **3**. This corresponds to the classical planar zig-zag patterns (M-mode) observed earlier (4) in these derivatives. The occurrence of this long range coupling in **4** requires that the Me-5 group be axial in this compound. These observations alone unequivocally permit our assigning the n.m.r. spectra of compounds **3** and **4**.[3]

(*b*) ASIS values for **3** and **4** are gathered in Table 2. ASIS data obtained by Anderson (5) on 5,5′-diMe-2-alkyl-1,3-dioxanes reveal the 5-equatorial position to be particularly shielded (0.3 to 0.4 p.p.m. with respect to the 5-axial position), while H-4,6 axial is shielded 0.1 to 0.15 p.p.m. more than is H-4,6 equatorial. Thus, the ASIS (Table 2) on 5-Me and 5-CHF_2, (+0.3 and +0.58 p.p.m. for an equatorial position in **3** and **4** respectively) and the pronounced positive ASIS values for H-4,6 axial, also conform to the assignments of H-4,6 as pointed out under (*a*), and are strongly indicative and consistent with the newly proposed assignments of structures **3** and **4**.

(*c*) The axial 5-Me in **4** and the axial 5-CF_2H signals in **3** appear at lower field relative to the corresponding equatorial signals in **3** and **4** respectively, in agreement with what is observed in all other 5,5′-disubstituted-1,3-dioxanes (3).

Heteronuclear ^{19}F–^1H decoupling on both **3** and **4** discloses a more pronounced long range interaction 5-CF_2H/5-CH_3 in **4** (~1 Hz) than in **3** (<0.5 Hz). This may be the result of a preferred orientation in the latter compound for the CF_2H group, as depicted in structure **3**, which excludes a classical M-path.[4] The rotamers pointing the C—F bond over the ring seemingly are disfavored, presumably for electrostatic and steric reasons.

Consequently, as a result of the new reversed assignment, the estimations for the conformational preferences of CF_2H and CFH_2 groups (as deduced from naïve additive contributions for geminal substitution) now become ΔG_{200} (CFH_2) ≃ +200 cal/mol (in $CHFCl_2$) $\Delta G_{300}(CF_2H)$ ≃ +980 cal/mol (in CS_2), and $\Delta G_{300}(CF_2H)$ ≃ +800 cal/mol (in $CHFCl_2$), respectively. These results clearly illustrate the unexpected behavior of CH_2X groups, in general, *for which the axial position is preferred.* This situation is paralleled by the behavior of the 5-Me-5′-CH_2OH-1,3-dioxane (7 and references therein). Typically, the 5-CH_2OMe group has almost no conformational preference, as $\Delta G°$(CH_2OMe-5) was found to be close to zero

[3]Similar proof by multiple irradiation n.m.r. experiments could not be obtained in CS_2 for the CF_2H derivative **2***h* in ref. 1 (now structure **4**), since the 5-Me and 2-Me signals overlap and the 4,6 protons are isochronous. This has been, in fact, the origin of our entanglement.

[4]It should be pointed out that the conformation pictured in **3** might in principle also show a long range 5-CF_2H/5-CH_3 interaction, to be compared with the syn-axial $^4J(F,H)$ interactions observed in some but not all fluorinated hexopyranosyl fluorides (6). Obviously, ^4J couplings obtained in these derivatives "indicate that some caution may be necessary before such syn–axial couplings are used for configurational assignments" (6).

Can. J. Chem. Downloaded from www.nrcresearchpress.com by 210.87.254.5 on 09/05/12
For personal use only.

(8). Our present results disclose an unexpected behavior for which no satisfactory explanation has been offered previously.[5] We believe that the phenomenon may find its origin in the fact that the electronegative substituent causes an increase in % s character of the carbon atom in the CH_2X and CHX_2 moieties, with the result that successive polarization of the hydrogen atoms in the C—H bonds involved confers a high degree of positive character upon them. The hydrogen atom which is situated above the dioxane ring then experiences an attractive force from (the axial p orbitals of) the ring oxygen atoms. Thus, a microscopic, highly localized dipole–dipole interaction, and *not* an overall molecular dipole, must be considered to understand the conformational behavior of multi-site polar molecules.[6] It is interesting to observe, however, that hetero atoms directly bonded on C-5 in 1,3-dioxanes do follow the general trend expected from separated dipole–vector considerations (with the possible exception of F-5 (12) and OH-5 (13), for which in the latter hydrogen bonding effects might be anticipated (13)). Work on the conformational behavior of other 5-Me-5′-CH_2X-1,3-dioxanes (X = Cl, Br, I) is in progress, and preliminary results of ^1H n.m.r. measurements at $T < T_c$ do indicate a similar axial preference for the CH_2X group. We plan to report the results of these shortly.

The Ministry of Scientific Programmation is thanked for the funds allowing the acquisition of a 300 MHz machine. The National Fonds voor Wetenschappelijk Onderzoek (N.F.W.O.) has provided valuable financial support of the research program.

1. M. ANTEUNIS and P. DIRINCK. Can. J. Chem. **50**, 423 (1972).
2. P. DIRINCK, M. ANTEUNIS, and C. BECU. J. Fluorine Chem. **2**, 339 (1973).
3. E. L. ELIEL and R. J. L. MARTIN. J. Am. Chem. Soc. **90**, 682 (1968); M. C. KNOEBER, Ph.D. Dissertation, University of Notre Dame, Notre Dame, Ind. 1967; *cf.* M. ANTEUNIS, D. TAVERNIER, and F. BORREMANS. Bull. Soc. Chim. Belges, **75**, 407 (1966) and J. L. JUNGNICHEL and C. A. REILLY. J. Mol. Spectrosc. **16**, 135 (1965).
4. M. ANTEUNIS, W. VANDENBROUCKE, and N. SCHAMP. Bull. Soc. Chim. Belges, **76**, 522 (1967).
5. J. E. ANDERSON. Tetrahedron Lett. **51**, 4713 (1965).
6. L. D. HALL, R. N. JOHNSON, J. ADAMSON, and A. B. FOSTER. Can. J. Chem. **49**, 122 (1971).
7. E. L. ELIEL and H. D. BANKS. J. Am. Chem. Soc. **94**, 172 (1972).
8. E. L. ELIEL. Personal communication; Aspects of conformational analysis of small molecules. Abstr. No. 588, XXIIIrd International Congress of Pure and Applied Chemistry, Boston, Mass. July 1971.
9. E. L. ELIEL and S. A. EVANS JR. J. Am. Chem. Soc. **94**, 8587 (1972).
10. R. J. ABRAHAM and Z. L. ROSSETTI. Tetrahedron Lett. 4965 (1972).
11. P. DIRINCK and M. ANTEUNIS. Can. J. Chem. **50**, 412 (1972).
12. L. D. HALL and R. N. JOHNSON. Org. Magn. Res. **4**, 369 (1972).
13. E. L. ELIEL and K. KALOUSTIAN. Chem. Commun. **290** (1970).

[5]Recently Eliel *et al.* (private communication, September 15 1972; see ref. 9) have found axial preferences for positively charged 5-substituents (*e.g.* $MeS^+—O^-$ and $MeSO_2$). This was considered to result from an electrostatic attraction involving the syn-axial O-p lobes and S^+.

[6]Very recently, after the first draft of our paper was submitted for publication, Abraham and Rossetti (10) found that the anomalous stabilization of the diaxial form of *trans*-1,4-dichlorocyclohexane may be explained in terms of syn–axial H:Cl interactions as the result of the enhanced acidities of the H atoms involved. Such inductive polarization, caused by the presence of the second halogen atom, was found by CNDO/2 calculation to even be important for the geminal H atom. Thus, our picture of attractive forces existing between an axial CF_nH_{3-n} and the oxygen p-lobes may indeed substantially favor this conformer relative to the equatorial form. Furthermore, such attractions would be impossible in the related 4-fluoromethylated-6-Me-1,3-dioxanes, where indeed it was found (11) that the behavior of such systems more or less follows the predictions made on the basis of simple dipole–dipole explanations.

Can. J. Chem. Downloaded from www.nrcresearchpress.com by 210.87.254.5 on 09/05/12
For personal use only.

Thermal Isomerization of α,β-Epoxyketones

PRABHAKER G. KHAZANIE AND EDWARD LEE-RUFF
Department of Chemistry, York University, Downsview 463, *Ontario*

Received March 8, 1973

Pyrolysis of α,β-epoxyketones at 260° resulted in the formation of β-diketones derived from a 1,2 shift of a β hydrogen or alkyl substituent to the α carbon. Hydrogen migrates in preference to methyl in the case of 2-ethylidenecyclopentanone and 2-ethylidenecyclohexanone oxides. Thermal conversion of 2-cyclopentylidenecyclopentanone oxide to the spiro β-diketone **4** was quantitative.

La pyrolyse d'α,β-époxycétones à 260° a conduit à la formation de β-dicétones via la migration 1,2 d'un hydrogène β ou d'un substituant alcoyle vers le carbone α. Dans le cas des oxydes d'éthylidène-2 cyclopentanone et d'éthylidène-2 cyclohexanone, le groupe hydrogène migre de préférence au groupe méthyle. La conversion thermique de l'oxyde de cyclopentylidène-2 cyclopentanone en β-dicétone spiro **4** a été quantitative. [Traduit par le journal]

Can. J. Chem., **51**, 3173 (1973)

Photochemical transformations of α,β-epoxyketones are known to give β-diketones in low yields (1–3). Johnson and co-workers (2) have shown that irradiation of ether solutions of α or β pulegone oxides resulted in their interconversion and also in the formation of stereoisomeric 2-acetyl-2,5-dimethylcyclohexanones. A similar mixture was obtained on pyrolysis of either the α- or β-pulegone oxide. It was suspected that the formation of the photoproducts was the result of decomposition of vibrationally excited α,β-pulegone oxide. In order to establish the generality of such thermal transformations of α,β-epoxyketones we undertook a study of the thermal chemistry of various spiro α,β-epoxyketones. Furthermore, since it was reported (1) that 2-cyclopentylidenecyclopentanone oxide upon irradiation resulted in the formation of spiro[4·5]decane-1,6-dione in 25% yield, it was of interest to us to see if the thermolysis of 2-cycloalkylidenecycloalkanone oxides would undergo similar transformations to give spiro β-diketones. These could serve as important synthetic intermediates in the synthesis of natural products possessing the spirobicyclic ring system.

Results and Discussion

The syntheses of epoxyketones **1***b–d* and **3** were accomplished by direct treatment of the corresponding 2-alkylidenecycloalkanones with either *m*-chloroperbenzoic acid or hydrogen peroxide. Attempted synthesis of **1***a* by treatment of 2-ethylidenecyclopentanone with hydrogen peroxide or *m*-chloroperbenzoic acid was unsuccessful, with only trace amounts of the

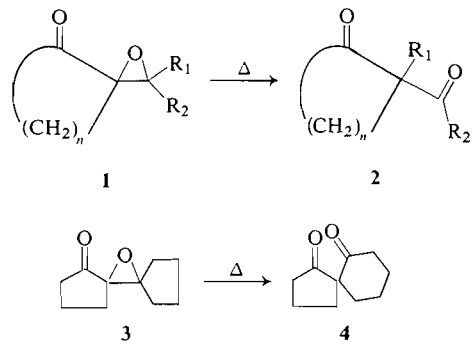

a $R_1 = H$, $R_2 = CH_3$, $n = 3$
b $R_1 = R_2 = CH_3$, $n = 3$
c $R_1 = H$, $R_2 = CH_3$, $n = 4$
d $R_1 = R_2 = CH3$, $n = 4$

SCHEME 1

epoxide detectable. The synthesis of epoxide **1***a* was accomplished by epoxidation of the 2-ethylidenecyclopentanol and subsequent oxidation of the epoxy-alcohol with chromium trioxide in acetic acid. The structures of **1***a–d* and **3** (Scheme 1) were established from spectral data and comparison with data reported in literature. The stereochemistry of **1***a* and **1***c* could not be ascertained; however, the n.m.r. spectra of these indicated the presence of one stereoisomer.

Samples (50–250 mg) of pure epoxyketone were pyrolyzed in sealed pyrex tubes at 260° for 65–80 min. The reactants were degassed by six freeze–thaw cycles and evacuated to 10^{-3} mm pressure. The products were analyzed and collected by v.p.c. In all cases only the major product was identified (Table 1). The structures of

Can. J. Chem. Downloaded from www.nrcresearchpress.com by 210.87.254.105 on 09/05/12
For personal use only.

TABLE 1. % formation of β-diketones from pyrolysis of epoxyketones

Pyrolysis of	Time of pyrolysis (min)	% formation of major product	% unreacted starting material
1*a*	75	68	9
1*b*	80	56	10
1*c*	80	79	3
1*d*	80	59	8
3	65	100	0

pyrolysis products **2***a–d* and **4** were established from their spectral data as well as independent synthesis by known routes. The major products in all cases are the result of an alkyl or hydrogen shift from the β to α carbon with initial bond fission occurring between the α-carbon–oxygen bond. Such a process would give rise to a stable delocalized diradical of the type

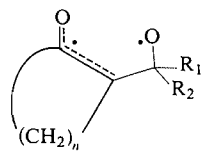

The preferred migration of hydrogen to methyl in the case of epoxyketones **1***a* and *c* is analogous to the reported greater migratory aptitude of hydrogen compared to an alkyl group in carbonium ion rearrangements (4). The quantitative thermal conversion of epoxyketone **3** to **4** suggests that its reported photochemical conversion in low yields proceeds by vibrationally excited levels of the electronic ground state of the epoxyketone. The high yield in the thermal conversion of **3** to **4** suggests that spiro β-diketones of similar type can be obtained by pyrolysis of the appropriate 2-cycloalkylidenecycloalkanone oxides. We are currently investigating the generality of such transformations as a synthetic route in the preparation of spirobicyclic β-diketones.

Experimental

Melting points and boiling points were uncorrected. The i.r. spectra were recorded with a Unicam SP 1000 instrument. The n.m.r. spectra were measured with a Varian A-60 and a Varian HA-100 instrument. Samples were dissolved in CCl_4 and $CDCl_3$ solvents using tetramethylsilane as the internal standard. V.p.c. was performed on a Varian Aerograph Series 1700 instrument using the following columns: (*a*) 3% SE-30 on Varaport 30 (0.25 in., 5 ft 4 in.); (*b*) 10% FFAP on chromosorb P (0.25 in., 6 ft); (*c*) 6% SE-30 + 4% QF 1 on chromosorb W AW, DMCS treated (0.25 in., 6 ft). Microanalyses were performed by Gygli Microanalytical laboratory, Toronto, Ontario.

Pyrolysis of Epoxides (General Procedure)

The pyrolysis of epoxides was carried out in a steel oven at 260°. The temperature gauge of the oven was calibrated using a thermocouple. Samples were placed in pyrex tubes, 1 cm diameter, 1 mm thick glass, and 6–7 cm long. The samples were degassed by five or six freeze–pump–thaw cycles at 10^{-3} mm pressure, sealed, wrapped in an aluminum foil, and heated for varying lengths of time. The samples were then cooled, opened, and the pyrolytic mixtures were analyzed by v.p.c., i.r., and n.m.r. spectroscopy.

Lithium Aluminum Hydride Reduction of 2-Ethylidenecyclopentanone

2-Ethylidenecyclopentanone (5) (11 g, 0.1 mol) dissolved in absolute ether (50 ml) was added dropwise with stirring to a slurry of lithium aluminum hydride (1.6 g, 0.04 mol) in ether (50 ml) at room temperature. Upon completion of addition, the reaction mixture was refluxed at 40° for an additional hour. Excess hydride was then decomposed by addition of moistened ether, and 10% Na–K-tartarate. The organic layer was separated, filtered, washed with brine, and dried over anhydrous sodium sulfate. Removal of ether gave alcohol, 2-ethylidenecyclopentanol (10.3 g, 92%). The alcohol was obtained pure by distillation, b.p. 74°/15 mm: i.r. 3420 cm^{-1} (OH stretch); n.m.r. δ 5.3–5.82 (1H, m) 4.75 (1H, disappeared with D_2O), 4.28 (1H), 1.45–2.5 (9H, m).

2-Ethylidenecyclopentanol Oxide

To an ice-cold solution of 72% *m*-Cl-perbenzoic acid (16.4 g) in chloroform (175 ml) was added 8.5 g of 2-ethylidenecyclopentanol in 20 ml chloroform. The reaction mixture was kept at 0° for 2 h and then at room temperature for 6 h. It was then washed with 10% sodium sulfate, 5% sodium carbonate, and brine, and dried over anhydrous sodium sulfate. Removal of chloroform under reduced pressure gave a thick liquid which upon distillation afforded pure epoxy alcohol (6.3 g): i.r. 3475 cm^{-1} (OH stretch), 862, 910, 1100, 1250 cm^{-1}; n.m.r. δ 3.55–3.9 (1H, m), 2.8–3.2 (1H, q), 2.25 (OH, disappeared with D_2O), 1.45–2.05 (6H, m), 1.23 (3H, d, J = 5 Hz).

2-Ethylidenecyclopentanone Oxide (1a)

Chrominum trioxide (1.1 g) was dissolved in 15 ml glacial acetic acid and frozen in an ice bath. To this was added 1.1 g of above epoxy alcohol in 5 ml acetic acid. The mixture was allowed to thaw. After complete thawing the reaction mixture was stirred for 5 min. The solution gave a greenish color and the temperature increased. The flask was again cooled in an ice bath for 2 min, allowed to thaw, and stirred for an additional 20 min. The mixture was transferred to a 250 ml Erlenmeyer flask and 150 ml of diethyl ether was added. A precipitate formed and was filtered off. The filtrate was neutralized with saturated sodium bicarbonate solution, washed with brine, and dried over anhydrous sodium sulfate. Removal of ether under reduced pressure gave a crude mixture (0.5 g),

Can. J. Chem. Downloaded from www.nrcresearchpress.com by 210.87.254.105 on 09/05/12
For personal use only.

Can. J. Chem. Downloaded from www.nrcresearchpress.com by 210.87.254.105 on 09/05/12
For personal use only.

which was purified by v.p.c. (6% SE-30 + 4% QF 1 column at 100 °C; rate of He flow, 46 cc/min: i.r. (CCl_4) 1752 cm^{-1} (C=O stretch), 880, 1060, 1255, 1290, 1420 cm^{-1}; n.m.r. δ 3–3.3 (1H, q), 1.28 (3H, d, J = 5Hz), 1.95–2.38 (6H, m); M^+: *m/e* 126.

Anal. Calcd. for $C_7H_{10}O_2$: C, 66.68; H, 7.93. Found: C, 66.50; H, 8.01.

2-Isopropylidenecyclopentanone Oxide (1b)

To an ice-cold solution of 10.68 g of 72% *m*-Cl-perbenzoic acid in 125 ml chloroform was added 6.2 g (0.05 mol) 2-isopropylidenecyclopentanone (6) in 20 ml chloroform. The reaction mixture was stirred between 0–5° for 8 h. The reaction mixture was then washed with 10% sodium sulfite, 5% sodium carbonate, brine, and dried over anhydrous magnesium sulfate. Removal of solvent under reduced pressure gave a mixture of two products (5.3 g). The mixture was distilled over a short path at 0.03 mm pressure to give 2.05 g of epoxide (30%): i.r. 1746 cm^{-1} (C=O stretch), 820, 930, 1030, 1250 cm^{-1}; n.m.r. δ 1.34 (6H, d, J = 2Hz), 1.85–2.4 (6H, m); u.v. max (EtOH) 209 mm (ε 2280); M^+: *m/e* 140.

Anal. Calcd. for $C_8H_{12}O_2$: C, 68.57; H, 8.57. Found: C, 68.49; H, 8.85.

2-Ethylidenecyclohexanone Oxide (1c)

A mixture of 2-ethylidenecyclohexanone (7) (7.44 g, 0.06 mol), methanol (60 ml), and 30% hydrogen peroxide (17.22 ml, 0.18 mol), in a 200 ml three-necked flask equipped with a stirrer, a dropping funnel, and a thermometer was cooled to 15–20°. A solution of 6 *N* sodium hydroxide (5.1 ml, 0.03 mol) was added dropwise with stirring over a period of 20 min. Stirring was continued for 4 h with the temperature being maintained at 25°. The reaction mixture was then poured into 150 ml brine and extracted with two 200-ml portions of ether. After the combined ether extracts were washed and dried, the solvent was removed under reduced pressure and the residual liquid analyzed by v.p.c. The crude product (7 g) which consisted principally of only one compound was distilled, b.p. 75°/0.5 mm, to give 4.5 g (58%) of pure **1***c*: i.r. 1720 cm^{-1} (C=O stretch), 790, 890, 990, 1275, 1410, 1450, cm^{-1}; n.m.r. δ 2.85–3.28 (1H, q), 1.25 (3H, d, J = 5Hz), 1.7–2.6 (8H, m); u.v. max (EtOH) 207 nm; (ε 600); M^+ *m/e* 140.

Anal. Calcd. for $C_8H_{12}O_2$: C, 68.57; H, 8.57. Found: C, 68.66; H, 8.54.

2-Isopropylidenecyclohexanone Oxide (1d)

(*A*). Using the method described for the preparation of 2-ethylidenecyclohexanone oxide, from 6.9 g (0.05 mol) of 2-isopropylidenecyclohexanone (8), 14.5 ml hydrogen peroxide (30%) and 4.1 ml of 6 *N* aqueous sodium hydroxide in 35 ml methanol was obtained 6.5 g crude product. The crude product was distilled over a short path at 0.03 mm to give 5.34 g of **1***d*: i.r. 1720 cm^{-1} (C=O stretch), 790, 890, 1120, 1235, 1275 cm^{-1}; n.m.r. δ 1.55–2.6 (8H, m), 1.12 (3H, s) 1.36 (3H, s); M^+: *m/e* 154.

(*B*) Using the procedure described for the preparation of 2-isopropylidenecyclopentanone oxide, from 2.76 g (0.02 mol) of 2-isopropylidenecyclohexanone and 4 g of 72% *m*-Cl-perbenzoic acid in 40 ml chloroform was obtained 1.9 g of **1***d*.

Anal. Calcd. for $C_9H_{14}O_2$: C, 70.13; H, 9.09. Found: C, 70.08; H, 9.30.

2-Cyclopentylidenecyclopentanone Oxide (3)

Using the method described for the preparation of 2-isopropylidenecyclopentanone oxide, from 6 g of 2-cyclopentylidenecyclopentanone (9) and 8.96 g of 72% *m*-Cl-perbenzoic acid in 120 ml chloroform was obtained 5.8 g of a crude mixture. This was chromatographed on 100 g silica gel, activity III–IV (50 × 3 cm) with 8:2 benzene – diethyl ether. The epoxide was then crystallized from *n*-hexane (39%), m.p. 39–40° (lit. (1) m.p. 38–40°): i.r. 1743, 1160, 960 cm^{-1}; n.m.r. ($CDCl_3$) δ 2.6–1.4 (m); u.v. max (EtOH) 305 nm.

Pyrolysis of 2-Ethylidenecyclopentanone Oxide (1a)

The epoxide **1***a* (55 mg) was pyrolyzed at 260° and 10^{-3} mm pressure for 75 min. The pyrolyzed sample gave six peaks on v.p.c. (3% SE-30, 100°, He flow 44 cc/min). The major component **2***a* was collected by freezing the vapors in a U-shaped glass tube dipped in ice – salt water mixture. The structure of β-diketone was deduced from analytical and spectroscopic data as well as independent synthesis[1] (10): i.r. 1240, 1615, 1660, 1710, and 1740 cm^{-1}; n.m.r. (CCl_4) δ 1.85–2.65 (10H, m, containing sharp singlets at 1.92 and 2.23).

Pyrolysis of 2-Isopropylidenecyclopentanone Oxide (1b)

A sample of 150 mg of **1***b* was pyrolyzed as above for 80 min. The pyrolyzed sample gave eight peaks on v.p.c. (column *c*, 100°, gas flow 46 cc/min). The major compound was identified to be the diketone **2***b* by spectral data and independent synthesis (11): i.r. 1705, 1743 cm^{-1}; n.m.r. δ 1.3 (3H, 5), 1.5–2.75 (9H, m, with a sharp singlet at 2.12).

Pyrolysis of 2-Ethylidenecyclohexanone Oxide (1c)

The above procedure was followed. The pyrolyzed sample when analyzed on column a at 90° (He flow rate 42 cc/min) showed nine peaks. The major component (79%) was identified as β-diketone **2***c* by independent synthesis (11), and spectroscopic data: i.r. 1612, 1710 cm^{-1}; n.m.r. δ 1.6–2.5 (12H, m, with sharp singlet at 2.06).

Pyrolysis of 2-Isopropylidenecyclohexanone Oxide (1d)

The procedure used for the pyrolysis of **1***b* was followed. The major product (59%) was identified as β-diketone **2***d* by independent synthesis (11) and spectroscopic data: 1700 cm^{-1} (C=O stretch, broad); n.m.r. δ 1.17 (3H, s), 1.98 (3H, s), and 1.4–2.7 (8H, m).

Pyrolysis of 2-Cyclopentylidenecyclopentanone Oxide (3)

A sample of 250 mg of **3** was heated to 260° at 10^{-3} mm pressure for 65 min. V.p.c. analysis of the pyrolyzed sample showed a 100% yield of spiro β-diketone (4). The spectra of this β-diketone were identical to those of the compound obtained by photolysis (1) of 2-cyclopentylidenecyclopentanone oxide (3): u.v. max (EtOH) 287 nm; i.r. 1732, 1698 cm^{-1}; n.m.r. ($CDCl_3$) δ 2.9–1.1 (m).

The authors wish to acknowledge the support of the National Research Council of Canada by a grant in aid of this research.

[1]From the pyrrolidine enamine of cyclopentanone by analogy with compound **2***c*.

1. J. R. WILLIAMS and G. M. SARKISIAN. J. Org. Chem. **37**, 4463 (1972).
2. C. K. JOHNSON, B. DOMINY, and W. REUSCH. J. Am. Chem. Soc. **85**, 3894 (1963).
3. H. E. ZIMMERMAN, B. R. COWLEY, C.-Y. TSENG, and J. W. WILSON. J. Am. Chem. Soc. **86**, 947 (1964).
4. W. E. BACHMAN and J. W. FERGUSON. J. Am. Chem. Soc. **56**, 2081 (1934).
5. R. MAYER, Chem. Ber. **88**, 1853 (1955).
6. Y. POIRIER, L. LEGRAND, and N. LOZAC'H. Bull. Soc. Chim. France, **3**, 1054 (1966).
7. N. BASBULESCU and A. QUILCO. Gazz. Chim. Ital. **91**, 326 (1961).
8. S. M. MUKHERJI, R. P. GANDHI, and O. P. VIG. J. Indian Chem. Soc. **33**, 853 (1956).
9. O. WALLACH. Ber. **29**, 2955 (1896).
10. P. J. HAMRICK JR., C. F. HAUSER, and C. R. HAUSER. J. Org. Chem. **24**, 583 (1959).
11. G. STORK, A. BRIZZOLARA, H. LANDESMAN, J. SZMUSZKOVICZ, and R. TERRELL. J. Am. Chem. Soc. **85**, 207 (1963).

Can. J. Chem. Downloaded from www.nrcresearchpress.com by 210.87.254.105 on 09/05/12
For personal use only.

Nuclear Magnetic Resonance Study of Hydrogen Bonding in 1,1,1-Trifluoro-2-hydroxy-4-alkanones

EBERHARD KIEHLMANN, B. C. MENON, AND NORA MCGILLIVRAY
Department of Chemistry, Simon Fraser University Burnaby 2, British Columbia

Received April 24, 1973

Addition of fluoral at the α-carbon of 3-pentanone, cyclohexanone, 4-methyl-2-pentanone, and acetone gives 1,1,1-trifluoro-2-hydroxy-3-methyl-4-hexanone (**1***a* and *b*, diastereomers), 2-(1-hydroxy-2,2,2-trifluoroethyl)cyclohexanone (**2***a* and *b*, diastereomers), 1,1,1-trifluoro-2-hydroxy-6-methyl-4-heptanone (**3**), and 1,1,1-trifluoro-2-hydroxy-4-pentanone (**4**), respectively. Hydrogen-bonding studies, based on proton and fluorine n.m.r. measurements, show strong intramolecular >C=O···H—O bonding with relatively weak intermolecular interactions in **1***a* and **2***a*, and intermolecular F···H—O bonding in **1***b*, **2***b*, **3**, and **4**.

L'addition de fluoral sur le carbone α de la pentanone-3, cyclohexanone,méthyl-4 pentanone-2 et acétone conduit au trifluoro-1,1,1 hydroxy-2 méthyl-3 hexanone-4 (**1***a* et **1***b*, diastéréoisomères), (hydroxy-1 trifluoroéthyl-2,2,2)-2 cyclohexanone (**2***a* et **2***b*, diastéréoisomères), trifluoro-1,1,1 hydroxy-2 méthyl-4 heptanone-2 (**3**) et trifluoro-1,1,1 hydroxy-2 pentanone (**4**) respectivement. Les études sur les liaisons hydrogène, effectuées par résonance magnétique nucléaire du proton et du fluor, montrent une liaison intramoléculaire >C=O···H—O forte et des interactions intermoléculaires relativement faibles pour **1***a* et **2***a*; et une liaison intermoléculaire F···H—O pour **1***b*, **2***b*, **3** et **4**. [Traduit par le journal]

Can. J. Chem., **51**, 3177 (1973)

In an earlier paper (1), we have characterized several diastereomeric pairs of 1,1,1-trichloro-2-hydroxy-4-alkanones, including 1,1,1-trichloro-2-hydroxy-3-methyl-4-hexanone (Cl analogs of **1***a* and *b*) and 2-(1-hydroxy-2,2,2-trichloroethyl)-cyclohexanone (Cl analogs of **2***a* and *b*), and made configurational assignments on the basis of p.m.r. and i.r. spectral studies of hydrogen-bonding interactions and dihedral —CHOH—CHR— bond angles. The low-melting isomer of each pair was found to exhibit strong intramolecular hydrogen bonding, attributable mainly to >C=O···H—O rather than Cl···H—O interaction, and was assigned the *threo* structure while the high-melting isomer was assigned the *erythro* structure (Fig. 1).

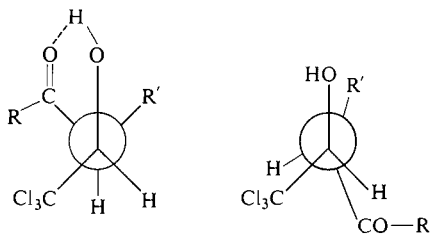

threo (low m.p.) *erythro* (high m.p.)

FIG. 1. Structure assignments for RCO—CHR'—CHOH—CCl_3.

If, instead of chloroketols (Fig. 1), the corresponding fluoroketols are used for the spectroscopic studies, the presence of F···H—O hydrogen bonds should be discernible from their F-19 n.m.r. spectra and hence should settle the question whether halogen or the carbonyl oxygen is the preferred proton acceptor site in intramolecularly hydrogen-bonded 1,1,1-trihalo-2-hydroxy-4-alkanones. With this goal in mind, we have synthesized a series of fluoroketols and recorded their proton and fluorine n.m.r. spectra as a function of their concentrations in chloroform-*d* at room temperature.

Results and Discussion

Reaction of Fluoral with Ketones

The fluoroketols were prepared by crossed aldol condensation of fluoral with the respective aliphatic ketones in glacial acetic acid – sodium acetate medium using a modification of the procedure described previously (2) for chloral–ketone condensations (eq. 1). Cyclohexanone and 3-pentanone gave two diastereomeric products, respectively, while only one ketol was obtained from the reaction of acetone with fluoral. In the case of 4-methyl-2-pentanone, only the ketol (**3**) resulting from fluoral addition

[1] $RCOCH_2R' + CF_3CHO \rightarrow RCOCHR'—CHOHCF_3$

1*a* and *b* R = Et, R' = CH_3 **3** R = *i*-Bu, R' = H
2*a* and *b* R—R' = —$(CH_2)_4$— **4** R = CH_3, R' = H

Can. J. Chem. Downloaded from www.nrcresearchpress.com by 210.87.254.5 on 09/05/12
For personal use only.

Can. J. Chem. Downloaded from www.nrcresearchpress.com by 210.87.254.5 on 09/05/12
For personal use only.

at the α-methyl carbon could be isolated from the product mixture although the F-19 n.m.r. spectrum of the crude product showed the presence of traces of the isomeric methylene condensation product, 1,1,1-trifluoro-2-hydroxy-3-isopropyl-4-pentanone. In contrast, no 1,1,1-trichloro-2-hydroxy-3-isopropyl-4-pentanone was detected in the reaction mixture formed from chloral and 4-methyl-2-pentanone (2). Thus, addition at the methylene carbon is sterically inhibited by the bulky isopropyl substituent but, with the relatively small fluoral molecule as electrophile, this steric hindrance is less pronounced than with chloral.

Anhydrous fluoral (b.p. −19°) was obtained by treatment of commercial fluoral hydrate with concentrated sulfuric acid and phosphorus pentoxide (3) and trapping at −78°. The gas was then bubbled into a mixture of ketone, acetic acid, and sodium acetate at the desired reaction temperature (70–100°) using a slow stream of nitrogen to prevent oxidation. Although anhydrous fluoral appears to interact strongly with the solvent (acetic acid) and react fairly rapidly with the ketone, evaporation losses during its preparation and low fluoral hydrate reagent purity are believed to be the main reasons for the low product yields. Diastereomeric fluoroketols were separated and purified by adsorption chromatography on silicic acid and elution with chloroform.

Hydrogen Bonding Studies by Nuclear Magnetic Resonance

Proton magnetic resonance measurements on alcohols and amines have shown that hydrogen bond formation is accompanied by a displacement of the chemical shift of the protons involved toward lower magnetic field strength (4, 5). When the OH group of a molecule forms a hydrogen bond to a donor atom X, the electronic structure and hence the magnetic susceptibility of that OH bond are altered leading to a change in the magnetic shielding. Thus it is the generation of a strong electric field in the vicinity of the OH bond which causes the observed downfield shift (6).

Trifluoromethylcarbinols which are structurally closely related to the fluoroketols under discussion have been studied spectroscopically to establish conformational preferences as a function of hydrogen bonding interactions. Cannon and Stace (7) have reported a "free" OH stretching band for trifluoroethanol in carbon tetrachloride solution (3617 cm^{-1}) which persisted even in the pure liquid state (3628 cm^{-1}). They have interpreted this observation as evidence for the absence of intramolecular F···HO bonding. Oki and Iwamura (8) found an OH band for trifluoroethanol in 0.003 *M* carbon tetrachloride solution which was asymmetric on the high-frequency side and explained it in terms of an unresolved doublet due to *trans* ⇆ *gauche* isomerism and restricted rotation about the carbon–oxygen single bond (eq. 2). They

[2] 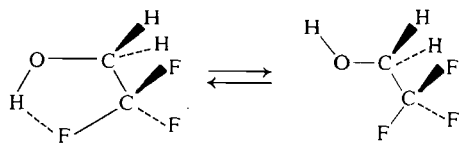

gauche *trans*

concluded from a mathematical resolution of the doublet that trifluoroethanol exists predominantly in the intramolecularly hydrogen-bonded *gauche* form. A temperature-dependent *trans* ⇆ *gauche* equilibrium (eq. 2), with a relatively small population in the *trans* form, was also observed by Krueger and Mettee (9).

Because of their structural similarity to the fluoroketols (**1***a* and *b*, **2***a* and *b*, **3**, and **4**) under investigation, we have included 1,1,1-trifluoro-2-propanol (**5**) and 2,2,2-trifluoroethanol (**6**) as part of our hydrogen-bonding studies. The chemical shift data are summarized in Table 1. The upfield shift of the hydroxyl proton on dilution observed for all eight compounds is typical for the behavior of intermolecularly hydrogen-bonded aggregates of solute molecules being broken up into monomeric species. The dilution shifts measured for the fluoroketols **1***b*, **2***b*, **3**, and **4** are similar to those for the trifluoromethylcarbinols **5** and **6**, with relatively steep slopes at lower concentrations, suggesting similar hydrogen-bonding interactions for all six compounds. Since the monomeric species of **5** have already been shown to exist predominantly in the intramolecularly hydrogen-bonded *gauche* form (7–9), it is reasonable to assume that the hydroxyl protons of the monomeric species of **1***b*, **2***b*, **3**, and **4** are also hydrogen-bonded to fluorine (Fig. 2).

The i.r. spectra of **1***b*, **2***b*, **3**, and **4**, taken in carbon tetrachloride solution at as low a concentration as 0.005 *M*, show a broad peak at 3520 cm^{-1} with a small shoulder at 3600 cm^{-1}

TABLE 1. Fluorine and hydroxyl proton chemical shifts for $RCOCHR'CHOHCF_3$ and CF_3CHROH

Compound	Mol fraction	Chemical shift OH*	Chemical shift CF_3†	Compound	Mol fraction	Chemical shift OH*	Chemical shift CF_3†
1*a*	0.29	261	−4332	**3**	0.23	255	−4494
	0.14	260	−4332		0.11	243	−4484
	0.07	256	−4333		0.05	232	−4483
	0.03	255	−4334		0.02	223	−4477
1*b*	0.29	245	−4346	**4**	0.28	261	−4503
	0.14	230	−4336		0.14	249	−4495
	0.07	215	−4329		0.07	237	−4488
	0.03	204	−4323		0.03	224	−4485
2*a*	0.23	273	−4254	**5**	0.41	257	−4614
	0.11	268	−4254		0.20	230	−4601
	0.05	262	−4254		0.10	191	−4593
	0.02	259	−4254		0.05	161	−4587
2*b*	0.23	235	−4296	**6**	0.38	239	−4398
	0.11	221	−4282		0.19	218	−4381
	0.05	210	−4277		0.09	198	−4368
	0.02	196	−4270		0.04	176	−4360

*In Hz downfield from TMS in $CDCl_3$ at 60 MHz (accuracy ± 1 Hz).
†In Hz downfield from $CFCl_3$ in $CDCl_3$ at 56.4 MHz (accuracy ± 1 Hz).

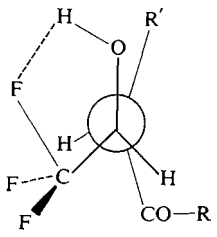

erythro

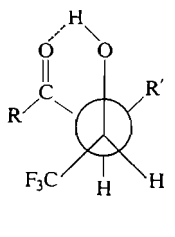

threo

1*b* R′ = CH_3, R = Et
2*b* R—R′ = —$(CH_2)_4$—
3 R = *i*-Bu, R′ = H
4 R = CH_3, R′ = H

1*a* R′ = CH_3, R = Et
2*a* R—R′ = —$(CH_2)_4$—

FIG. 2. Conformational assignments for $RCOCHR'CHOHCF_3$.[1]

pointing to a preponderance of hydrogen-bonded OH groups in the monomeric species. Finally, the downfield dilution shift observed in the fluorine n.m.r. spectra (Table 1) shows clearly that the halogen atoms are involved in intermolecular hydrogen-bond formation to the hydroxyl groups of these compounds. The larger proton dilution shifts reported earlier for the chlorine analogs of **1***b* and **2***b* may be taken as evidence for the larger chlorine atom being a somewhat better hydrogen bond acceptor site than fluorine.

In sharp contrast to the behavior of **1***b*, **2***b*, **3**, and **4**, dilution results in a very small upfield shift in the absorption position for the hydroxylic protons of the *threo*-fluoroketols **1***a* and **2***a*. Huggins, Pimentel, and Shoolery (10) have interpreted this flattening of the dilution shift curve as being due to the intrusion of intramolecularly hydrogen-bonded species even at relatively high concentrations. Since the position of the hydroxylic proton relative to the fluorine atoms has not been changed in going from one diastereomer (**1***b* or **2***b*) to the other (**1***a* or **2***a*) and the shape of the dilution shift curves now is drastically different from that observed for the carbonyl-free trifluoromethylcarbinols **5** and **6**, we must conclude that in **1***a* and **2***a* intramolecular hydrogen bonding occurs to the carbonyl group rather than to the halogen atom. This conclusion is further supported by the following experimental observations: (*a*) the F-19 n.m.r. spectra of **1***a* and **2***a* show negligible dilution shifts (Table 1) pointing to the non-involvement of fluorine in hydrogen-bond formation, and (*b*) the i.r. spectra of **1***a* and **2***a* at high dilution exhibit a broad absorption peak at 3520 cm^{-1} with a weak shoulder at 3600 cm^{-1} indicating the presence of hydrogen-bonded hydroxyl groups.

[1]The H—C—C—H dihedral angles for the *erythro* (140°) and *threo* (60°) forms of the fluoroketols have been assumed to be similar to the values reported for the corresponding chlorine analogs.

Can. J. Chem. Downloaded from www.nrcresearchpress.com by 210.87.254.5 on 09/05/12
For personal use only.

Can. J. Chem. Downloaded from www.nrcresearchpress.com by 210.87.254.5 on 09/05/12
For personal use only.

A comparison of hydroxyl proton chemical shifts ($\delta_{OH}°$) at infinite dilution, obtained by extrapolation of the data listed in Table 1, is informative and shows that **1***a* and **2***a* absorb at approximately the same magnetic field strength (250 Hz downfield from TMS); the same relationship applies to the pairs **1***b* and **2***b* (185 Hz), and **3** and **4** (210 Hz), respectively. Thus, the structure of the alkyl groups R and R′ has a negligible effect on $\delta_{OH}°$ while the nature of specific intramolecular hydrogen-bonding interactions causes considerable chemical shift differences. The higher $\delta_{OH}°$ values for **1***a* and **2***a* relative to **1***b* and **2***b*, respectively, indicate that the hydroxyl proton is deshielded more by hydrogen bonding to carbonyl oxygen than by hydrogen bonding to fluorine. It is also noteworthy that the F-19 absorption of **1***b*, **2***b*, **3**, **4**, **5**, and **6** is shifted *downfield* on dilution while the H-1 absorption is shifted *upfield*. These opposite trends are to be expected since hydrogen-bonding interactions cause a decrease in the symmetry of the fluorine p-orbital which overlaps with the hydroxyl proton 1s-orbital, and the resulting increase in the fluorine paramagnetic screening term shifts the CF_3 resonance peak to lower magnetic field (11, 12). The $\delta_{OH}°$ values for the chlorine analogs of **1***b*, **2***b*, and **3** are approximately 190, 190, and 200 Hz, respectively (extrapolation of data reported in ref. 1), *i.e.*, substitution of fluorine by chlorine has only a small effect on the OH proton chemical shift. This is in agreement with $\delta_{OH}°$ values reported in the literature (3) for trichloro- and trifluoroethanol and has been attributed to similar bond polarities for trichloro- and trifluoromethyl groups.

In conclusion, a strongly concentration-dependent equilibrium between monomeric and intermolecularly hydrogen-bonded species prevails in fluoroketols **1***b*, **2***b*, **3**, and **4** while **1***a* and **2***a* form strong intramolecular hydrogen bonds even at low concentrations.

Experimental

Melting points are uncorrected. I.r. spectra were run in CCl_4 solution on a Perkin–Elmer 457 or Beckman IR-12 spectrometer, u.v. spectra in 95% ethanol on a Unicam SP-200 instrument. N.m.r. spectra were recorded in $CDCl_3$ on a Varian A56/60 spectrometer, using TMS as internal standard for proton spectra (60 MHz) and $CFCl_3$ as external standard for F-19 spectra (56.4 MHz). Analytical-scale separations of diastereomeric 1,1,1-trifluoro-2-hydroxy-4-alkanones and other v.p.c. analyses were performed on a Varian Aerograph Model 1200-1 HY-FI III gas chromatograph using a 5 ft × 1/8 in. column packed with 5% SE-52 or 1% OV-17 on Aeropak 30 (column temperature 50–85°) and nitrogen as carrier gas (30 ml/min). Trifluoroethanol (Aldrich) and 1,1,1-trifluoro-2-propanol (Aldrich) were purified by fractional distillation.

Preparation of Anhydrous Fluoral

Using a modification of the procedure described in the literature (3), 53 g (0.45 mol) of fluoral hydrate (practical, Columbia Organic Chemicals) was added dropwise (2 h) to a stirred, preheated (90–95°) mixture of 83 ml concentrated sulfuric acid and 22 g of phosphorus pentoxide, and the fluoral (b.p. −19°) was swept with nitrogen into a cold trap (−78°). After completion of the addition, heating and stirring was continued for another hour. The anhydrous product (27 g = 61% yield) was used for the aldol condensations (see below) without further purification. The formation of small amounts of an unidentified, white polymeric material in the glass tubing leading to the trap was noticed in all experiments.

Reaction of Fluoral with 3-Pentanone

A mixture of 56.5 g (0.66 mol) of freshly distilled 3-pentanone, 39.6 g (0.66 mol) of glacial acetic acid, and 1.55 g (0.019 mol) of anhydrous sodium acetate was placed in a 500-ml three-necked flask fitted with condenser, thermometer, and gas inlet tube. Using a slow stream of nitrogen, anhydrous fluoral gas, prepared from 0.45 mol of commercial fluoral hydrate (see before), was evaporated slowly from a condensing trap by removing the cooling bath and bubbled into the magnetically stirred reaction mixture over a 1-h period. The temperature rose to 34° and some unreacted fluoral was collected in a second trap (−78°) connected to the condenser. The mixture was then heated in an oil bath at 84° for 17½ h, allowed to cool, filtered (NaOAc), and distilled (aspirator) to leave a yellow liquid residue which, on fractional high-vacuum distillation, gave 8.3 g (10% yield) of a mixture of *erythro-* and *threo*-1,1,1-trifluoro-2-hydroxy-3-methyl-4-hexanone (**1***a* and *b*). The diastereomers were separated by column chromatography on silicic acid (Mallinckrodt, Analytical Reagent, 100 mesh).

1*a*: b.p. 55–58°/1.0 mm; n.m.r. ($CDCl_3$) τ 8.95 (t, 3H, CH_3CH_2), 8.75 (d, 3H, CH_3CH), 7.43 (q, 2H, CH_3CH_2), 7.00 (m, 1H, CH_3CH), and 5.97 (broad peak, 1H, CHOH); i.r. (0.1 *M* CCl_4) 3450 cm^{-1} (OH; shoulders at 3530 and 3600) and 1710 (CO; shoulder at 1720).

1*b*: b.p. 60–63°/1.0 mm; n.m.r. ($CDCl_3$) τ 8.95 (t, 3H, CH_3CH_2), 8.73 (d, 3H, CH_3CH), 7.42 (q, 2H, CH_3CH_2), 7.02 (m, 1H, CH_3CH), and 5.58 (broad m, 1H, CHOH); i.r. (0.05 *M* in CCl_4) 3520 cm^{-1} (OH; shoulder at 3600) and 1715 (CO; shoulder at 1720); u.v. (EtOH) λ_{max} 216 nm (ε 80) and 273 nm (ε 35).

Reaction of Fluoral with Cyclohexanone

Anhydrous fluoral prepared from 0.45 mol of fluoral hydrate was bubbled into a mixture of 84.3 g (0.86 mol) of cyclohexanone, 51.6 g (0.86 mol) of acetic acid, and 2.03 g (0.025 mol) of sodium acetate as described before and the reagents were heated at 95° for 17 h. The normal work-up procedure yielded 63.7 g of crude product from which 30.3 g (35% yield) of a mixture (ratio 3:7 by v.p.c.) of the two fluoroketols **2***a* and *b* was obtained by frac-

Can. J. Chem. Downloaded from www.nrcresearchpress.com by 210.87.254.5 on 09/05/12
For personal use only.

tional distillation under high vacuum (68–76°/0.05 mm). The diastereomers were separated by adsorption chromatography (see before).

2*a*: b.p. 68–70°/0.05 mm; n.m.r. ($CDCl_3$) τ 7.0–8.5 (broad multiplet, 9H), and 5.90 (broad multiplet, 1H, C*H*OH); i.r. 3462 cm^{-1} (OH; shoulders at 3550 and 3620; 0.005 *M* in CCl_4) and 1705 (CO; 0.1 *M* in CCl_4); u.v. (EtOH) λ_{max} 223 nm (ε 88) and 280 nm (ε 38).

2*b*: m.p. 35–37°, b.p. 74–76°/0.05 nm; n.m.r. ($CDCl_3$) τ 7.0–8.5 (broad multiplet, 9H) and 5.28 (sharp quartet of doublets, 1H, C*H*OH); i.r. 3628 cm^{-1} (OH; 0.005 *M* in CCl_4) and 1710 (CO; 0.1 *M* in CCl_4); u.v. (EtOH) λ_{max} 204 nm (ε 35) and 281 nm (ε 31).

*Preparation of 1,1,1-Trifluoro-2-hydroxy-6-methyl-4-heptanone (**3**)*

Anhydrous fluoral prepared from 0.425 mol of fluoral hydrate was bubbled into a mixture of 70.0 g (0.70 mol) of 4-methyl-2-pentanone, 32.0 g (0.53 mol) of acetic acid, and 6.0 g (0.073 mol) of sodium acetate as described before and the reagents were heated at 110° for 3 h. Work-up and fractional distillation gave 12.0 g (14% yield) of **3**, m.p. 13–15°, b.p. 77–80°/1.25 mm, which was further purified by column chromatography. The fluorine n.m.r. spectrum revealed the presence of small amounts of the two diastereomeric 1,1,1-trifluoro-2-hydroxy-3-isopropyl-4-pentanones (doublets at 4368 and 4386 Hz upfield from $CFCl_3$). Characterization of **3**: n.m.r. ($CDCl_3$) τ 9.07 (d, 6H, $(CH_3)_2C$), 7.65 (m, 3H, $CHCH_2CO$), 7.22 (m, 2 diastereotopic protons, CH_2CHOH) and 5.48 (m, 1H, C*H*OH); i.r. (0.1 *M* in CCl_4) 3520 cm^{-1} (OH; broad, with shoulder at 3620) and 1715 (CO); u.v. (EtOH) λ_{max} 212 nm (ε 400) and 269 nm (ε 180).

*Preparation of 1,1,1-Trifluoro-2-hydroxy-4-pentanone (**4**)*

Fluoral was generated from 0.43 mol of fluoral hydrate (see before) and admitted into a mixture of 49.9 g (0.86 mol) of acetone, 51.6 g (0.86 mol) of acetic acid, and 2.03 g (0.025 mol) of sodium acetate over a 45 min period. The reagents were heated at 70° (oil bath temperature) for 72 h. after which time most of the solvent and unreacted ketone were removed at aspirator vacuum (oil bath below 60°). The remaining yellow-green liquid was taken up in methylene dichloride, washed with aqueous $NaHCO_3$ solution and water, dried ($MgSO_4$), and distilled (after CH_2Cl_2 evaporation) to give 18 g (27% yield) of 1,1,1-trifluoro-2-hydroxy-4-pentanone (**4**), b.p. 45–50°/0.7 nm. Removal of the last traces of acetic acid by extraction and distillation proved to be difficult in this case due to the high volatility (sublimation) of this compound. A pure product sample was obtained by adsorption chromatography (see before). Characterization of **4**: n.m.r. ($CDCl_3$) τ 7.75 (s, 3H, CH_3CO), 7.17 (m, 2 diastereotopic protons, CH_2) and 5.48 (m, 1H, C*H*OH); i.r. (0.1 *M* in CCl_4) 3520 cm^{-1} (OH; broad, with shoulder at 3620) and 1725 (CO).

The authors wish to thank the National Research Council of Canada for the financial support of this work and Messrs. M. Pudek and D. Sabourin for technical assistance.

1. E. Kiehlmann and P. W. Loo. Can. J. Chem. **47**, 2029 (1969).
2. E. Kiehlmann and P. W. Loo. Can. J. Chem. **49**, 1588 (1971).
3. M. Braid, H. Iserson, and F. E. Lawlor. J. Am. Chem. Soc. **76**, 4027 (1965); D. E. McGeer, R. Stewart, and M. M. Mocek. Can. J. Chem. **41**, 1024 (1963).
4. W. Liddel and N. F. Ramsey. J. Chem. Phys. **19**, 1608 (1951).
5. H. S. Gutowsky and A. Saika. J. Chem. Phys. **21**, 1688 (1953).
6. J. A. Pople, W. G. Schneider, and H. J. Bernstein. High-resolution nuclear magnetic resonance. McGraw-Hill Book Co., Inc., New York, N.Y. 1959.
7. C. G. Cannon and B. C. Stace. Spectrochim. Acta, **13**, 253 (1958).
8. M. Oki and H. Iwamura. Bull. Chem. Soc. Jap. **35**, 1744 (1962).
9. P. J. Krueger and H. D. Mettee. Can. J. Chem. **42**, 340 (1964).
10. C. M. Huggins, G. C. Pimentel, and J. N. Shoolery. J. Phys. Chem. **60**, 1311 (1956).
11. W. Doddrell, E. Wenkert, and P. V. Demarco. J. Mol. Spectrosc. **32**, 162 (1969).
12. J. W. Emsley, J. Feeney, and L. H. Sutcliffe, editors. Progress in nuclear magnetic resonance spectroscopy. MacMillan (Pergamon), New York, N.Y. Vol. 7. 1971. p. 34f.

Kinetic Study of the Epimerization of 1,1,1-Trichloro-2-hydroxy-3-methyl-4-hexanone

EBERHARD KIEHLMANN, FRED MASARO, AND FREDERICK J. SLAWSON
Department of Chemistry, Simon Fraser University, Burnaby 2, British Columbia

Received April 13, 1973

The acetate-catalyzed epimerization of 1,1,1-trichloro-2-hydroxy-3-methyl-4-hexanone has been studied in glacial acetic acid as solvent at five different temperatures. The reaction follows pseudo first-order, reversible kinetics and is associated with an activation energy of 24.0 ± 0.4 kcal/mol. Rate and product studies have shown that epimerization occurs by an enolization–ketonization pathway rather than dehydration–rehydration or retroaldol–aldolization. The ratio of diastereomeric ketols formed by condensation of 2-pentanone and 2-heptanone with chloral does not change as a function of time while the stereochemistry of the chloral addition to cyclohexanone is kinetically controlled during the initial reaction period.

L'épimérisation catalysée par l'entité acétate de la trichloro-1,1,1 hydroxy-2 méthyl-3 hexanone-4 a été étudiée à cinq différentes températures en utilisant comme solvant l'acide acétique glacial. La réaction se définit comme étant une réaction de pseudo premier ordre àcaractère réversible et possédant une énergie d'activation de 24.0 ± 0.4 kcal/mol. Des études de la vitesse ainsi que des produits obtenus ont montré que l'épimérisation se produit à la suite d'un processus d'énolisation–cétonisation plutôt qu'à la suite d'une déshydratation–réhydratation ou d'une rétroaldolisation–aldolisation. Le rapport des cétols diastéréoisomériques formés par condensation de la pentanone-2 avec l'heptanone-2 en présence de chloral ne change pas en fonction du temps alors que la stéréochimie de l'addition du chloral sur le clyclohexanone est controlée cinétiquement durant la période initiale de la réaction.

[Traduit par le journal]

Can. J. Chem., 51, 3182 (1973)

The crossed aldol condensation of an aldehyde with a symmetrical aliphatic ketone of the general structure RCH_2COCH_2R leads to the creation of two asymmetric centers in the β-hydroxycarbonyl product of the addition step. Thus, if the reaction can be stopped at the ketol stage, the product mixture will consist of two diastereomers each composed of a *dl*-pair of enantiomers (eq. 1). Under conditions permitting equilibration (epimerization) of the two diastereomers, the product ratio is said to be thermodynamically controlled and the product of greater thermodynamic stability will predominate. On the other hand, if equilibration does not occur or if the rate of epimerization is much slower than the rate of the preceding condensation reaction, the observed ratio of diastereomers is said to be kinetically controlled, *i.e.*, it reflects the relative rates of their formation and therefore permits conclusions to be drawn about the preferred transition state geometry in the aldol addition step.

As a continuation of our interest in the regio- and stereochemistry of the crossed aldol condensation of trihaloacetaldehydes with aliphatic ketones (1, 2), we have now carried out a kinetic study of the epimerization of 1,1,1-trichloro-2-hydroxy-3-methyl-4-hexanone (**1**) in glacial acetic acid – acetate medium in order to elucidate its mechanism. Three pathways may be postulated for this reaction which has been observed (1) for several diastereomeric 1,1,1-trichloro-2-hydroxy-4-alkanones (eq. 2): dissociation of **1** into chloral and diethyl ketone followed by re-con-

[1]

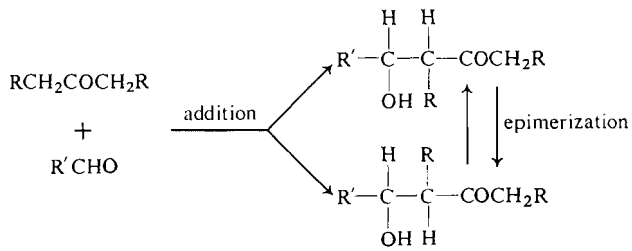

Can. J. Chem. Downloaded from www.nrcresearchpress.com by 210.87.254.42 on 09/05/12
For personal use only.

[2] 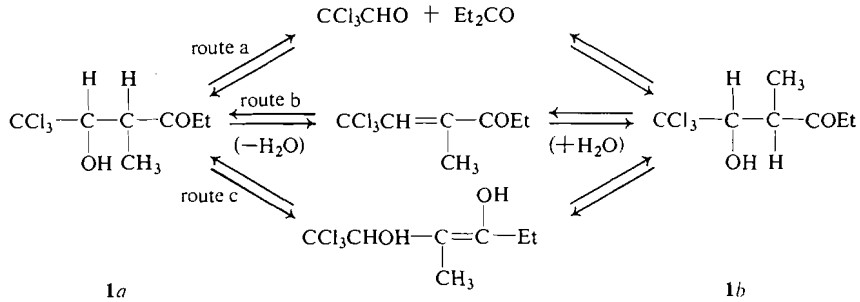

densation to form the ketol with opposite configuration at one of the two asymmetric carbons (retro-aldol reaction, route a), elimination of water followed by rehydration (route b), or an enolization–ketonization sequence (route c). It was hoped that a comparison of the epimerization rate with previously measured rate constants for hydrogen–deuterium exchange and aldol condensation under similar reaction conditions (2) would not only permit determination of the epimerization pathway but also, indirectly, conclusions about the rate-determining step in the formation of **1** from chloral and diethyl ketone.

The two diastereomers of **1** were selected as model compounds because they give well-separated peaks on the gas chromatogram, the preparative reaction does not yield any other, structurally isomeric ketols (as would be the case for the condensation of chloral with unsymmetrical dialkyl ketones), and the preparative separation of the high-melting component (**1***b*) from the diastereomeric product mixture can be readily accomplished by fractional distillation and crystallization. Also, the relative configurations of the *threo* (**1***a*) and *erythro* (**1***b*) isomer are known from previous spectroscopic studies (3).

Experimental

Reagents

Pure anhydrous chloral (b.p. 97°) was obtained by distillation of commercially available material (Chloral, Practical, Stabilized, MCB) from phosphorus pentoxide. Commercial diethyl ketone (b.p. 102°) was purified by fractional distillation while glacial acetic acid (Baker and Adamson, U.S.P.) and sodium acetate (Baker and Adamson, anhydrous reagent) were used without further purification in the preparative experiments. For the kinetic studies, 'Baker Analyzed' reagent-grade acetic acid was used and the anhydrous sodium acetate was purified by heating at 160° for 2 h and storing in a desiccator.

*Preparation of erythro-1,1,1-Trichloro-2-hydroxy-3-methyl-4-hexanone (**1***b*)*

In a 1-l flask, fitted with Friedrich condenser and $CaCl_2$ drying tube, were placed 86 g (1 mol) of diethyl ketone, 119 g (0.81 mol) of anhydrous chloral, 16.7 g (0.20 mol) of anhydrous sodium acetate, and 96.6 g (1.61 mol) of glacial acetic acid. After heating the mixture at 100–105° for 52 h, solvent and unreacted starting materials were removed by vacuum distillation (25–30°/0.9 mm). Ether (500 ml) and water (200 ml) were added to the residue, the ether layer was separated, washed (H_2O and aqueous $NaHCO_3$), and dried ($MgSO_4$), and the solvent was evaporated. High-vacuum distillation of the remaining oily product mixture gave six fractions (b.p. 89–115°/0.05–0.26 mm) the last of which (16.3 g, b.p. 105–115°/0.05–0.09 mm) contained more than 80% (by v.p.c.) of the desired diastereomer and solidified on cooling. Filtration and two recrystallizations from cyclohexane gave pure **1***b*, m.p. 58–58.5° (lit. (4) 58.5°).

Epimerization Rate Measurements

Into a long-neck, pear-shaped 10-ml flask were placed 6.00 g (0.10 mol) of reagent-grade acetic acid and 0.30 g (0.00365 mol) of anhydrous sodium acetate; the sodium acetate was allowed to dissolve and 1.50 g (0.00643 mol) of **1***b* was added to the cooled solution. The flask was fitted with a reflux condenser (using a Teflon sleeve), drying tube, and mercury valve and lowered into a thermostatted oil bath (paraffin oil, Saybolt viscosity 335/350) which had been equilibrated overnight at the desired temperature (±0.03°). Timing was started 1 min after immersion and 25-μl samples were withdrawn at various time intervals using a specially adapted micropipette. The fraction of **1***b* remaining at time *t* was determined by injection of each sample, dissolved in chloroform (0.2 ml), into a gas chromatograph (Varian Aerograph Model 1200-1 HY-FI III with 1% OV-17 on 80/100 Chromosorb G column at 117°) and by several planimetric integrations of the peak areas for the two epimers. The v.p.c. peak area ratios were shown to correspond to concentration ratios by repeated injections of samples of known concentrations (standard deviation $\sigma = \pm 0.015$ for 10 injections of $[\mathbf{1}b]/([\mathbf{1}a] + [\mathbf{1}b]) = 0.536$). Heating of the reaction mixture (>90°) for prolonged time periods (>5 days) resulted in the formation of small quantities of a white crystalline substance which was identified as sodium chloride.

Aldol Condensation Product Ratios as Function of Time

To obtain an approximate measure of the variation of the product ratio as a function of time when cyclohexa-

Can. J. Chem. Downloaded from www.nrcresearchpress.com by 210.87.254.42 on 09/05/12
For personal use only.

[3] 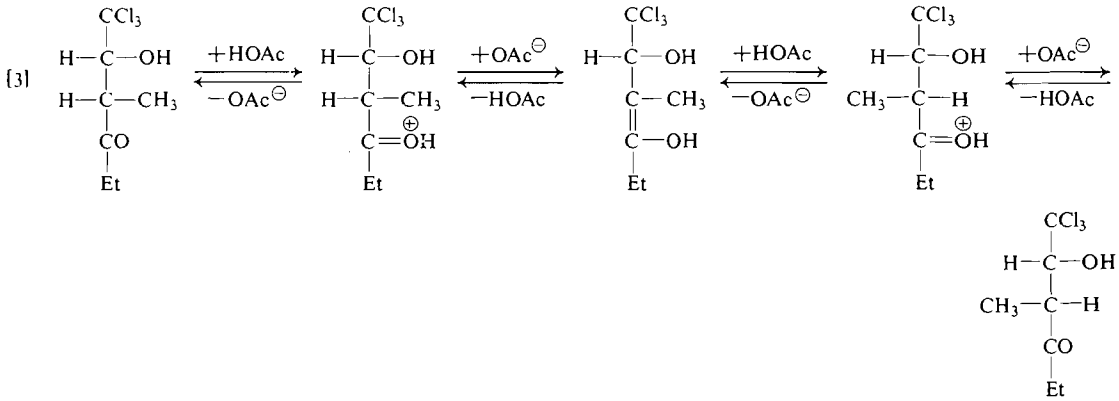

none, 2-pentanone, and 2-heptanone react with chloral under typical aldol condensation conditions, mixtures of sodium acetate, dimethoxyethane (DME), chloral, and the respective ketone (molar ratio 1:8:4:5) were heated at 100 ± 2° for 48 h and kinetically assayed (by v.p.c.) at various time intervals. For 2-pentanone and 2-heptanone, the ketol product ratio was found to remain essentially constant (based on eight assays) at A:B:C = 22:18:60 and 23:21:56 (average relative deviation ± 15%), respectively, where A and B represent the two diastereomeric methylene condensation products and C is the ketol resulting from condensation at the α-CH_3 carbon. The same constancy was observed for the reaction of diethyl ketone with chloral in acetic acid (**1***a*:**1***b* = 50:50) while the composition of the ketol mixture formed from cyclohexanone and chloral in DME changed drastically from 63:37 (after ½ h) to 50:50 (1 h), 37:63 (2 h), and 23:77 (8 h), remaining constant thereafter.

Results and Discussion

The epimerization mechanism was first investigated by several types of product studies under conditions similar to those of the kinetic experiments. Heating a mixture of the two diastereomeric 1,1,1-trichloro-2-hydroxy-3-methyl-4-hexanones (**1***a* and *b*) at 100° for 20 h, using glacial acetic acid as solvent and sodium acetate as catalyst, gave no diethyl ketone detectable by v.p.c. of the reaction mixture on a Reoplex-400 column at 60°. Also, admixture of acetone did not result in the formation of 1,1,1-trichloro-2-hydroxy-4-pentanone as would be expected if chloral was formed as intermediate. These findings are in agreement with the previously reported observation that the condensation products of chloral with *unsymmetrical* ketones do not undergo structural isomerization under the preparative reaction conditions (1) and rule out the retroaldol reaction pathway (eq. 2, route a) for the epimerization. Independent preparation of an authentic sample of 1,1,1-trichloro-3-methyl-2-hexen-4-one (5), determination of its v.p.c. retention time (5% SE-52 column at 120°), and injection of a sample of the reaction product obtained by heating **1***b* at 100° for 96 h demonstrated that the epimerization reaction was not accompanied by dehydration[1] (eq. 2, route b) thus leading us to the conclusion that the epimerization of **1***b* proceeds via the enolization pathway (eq. 3). Furthermore, the ratios of the diastereomeric ketols formed from chloral and various acyclic aliphatic ketones were found to remain constant over the entire reaction period indicating that the epimerization rate is much faster than the rate of chloral–ketone addition, *i.e.*, the stereochemistry of the aldol condensation under these conditions is thermodynamically controlled while the regiochemistry (1) is kinetically controlled. The stereochemistry of the aldol addition of cyclohexanone to chloral, on the other hand, is subject to kinetic control as evidenced by the observed change in the diastereomeric product composition from 63:37 to 23:77 over the initial 8-h period. In this case, the enol double bond is locked into *cis* configuration due to its confinement in a six-membered ring leading to a preferred transition state geometry for the reaction with chloral. Stiles and co-workers (6) have reported similar results for the condensation of *p*-nitrobenzaldehyde with cyclohexanone. It is noteworthy that both 3-(*p*-nitrophenyl)-1,2-diphenyl-3-hy-

[1]The remote possibility that reversible elimination occurs to an undetectable extent has been ruled out by treating the solution of a typical 1,1,1-trichloro-2-alken-4-one in acetic acid with an equimolar amount of water and testing (by v.p.c.) for the presence of the expected hydration product. After 72 h at 80°, no 1,1,1-trichloro-2-hydroxy-4-pentanone was formed from 1,1,1-trichloro-2-penten-4-one under these conditions. We are grateful to one of the referees for suggesting this experiment.

Can. J. Chem. Downloaded from www.nrcresearchpress.com by 210.87.254.42 on 09/05/12
For personal use only.

TABLE 1. Rate and equilibrium constants for the epimerization of 1,1,1-trichloro-2-hydroxy-3-methyl-4-hexanone in HOAc†

Temperature* (°)	$k_f + k_r$ ($\times 10^3$ h^{-1})	k_f ($\times 10^3$ h^{-1})	k_r ($\times 10^3$ h^{-1})	K_{eq}
70.29	7.02±0.16	3.45	3.56	0.97
75.29	11.05±0.22	5.50	5.55	0.99
80.32	17.42±0.38	8.81	8.61	1.02
85.34	29.72±0.95	15.2	14.6	1.04
90.37	46.09±2.34	23.5	22.6	1.04

*Including stem correction.
†[NaOAc] = 0.639 *M*.

droxy-1-propanone (**2**) in basic medium (aqueous dioxane) and 2-hydroxybicyclo[3.3.1]-nonan-9-one (**3**) in basic (KOH – acetone-d_6) and acidic medium (aqueous HCl) have been found to epimerize by the reverse aldolization readdition mechanism as evidenced by the lack of deuterium incorporation required for the alternative dehydration–rehydration and enolization pathways (7, 8).

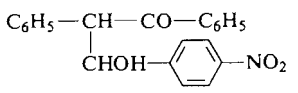

2

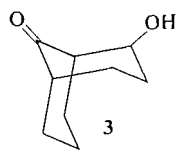

3

Our rate studies have confirmed the enolization route (eq. 3) for the epimerization of **1***b*. The reaction follows pseudo first-order, reversible kinetics and is associated with an equilibrium constant of approximately one. If B, B_0 and B_e represent the concentrations of **1***b* at time t, time zero, and at equilibrium, respectively, k_f and k_r the rate constants for the forward and reverse reaction, and K_{eq} the equilibrium constant for the reaction, then the expressions summarized in eqs. 4–6 permit calculation of the individual rate constants (Table 1).

[4] $$\mathbf{1}b \underset{k_r}{\overset{k_f}{\rightleftharpoons}} \mathbf{1}a$$

[5] $$\ln \frac{B_0 - B_e}{B - B_e} = (k_f + k_r) \cdot t$$

[6] $$K_{eq} = \frac{B_0 - B_e}{B_e} = \frac{k_f}{k_r}$$

Experimental values were fitted to eq. 5 by means of a linear, least-squares computer program giving the ($k_f + k_r$) values listed in Table 1. The equilibrium constants were calculated from several concentration measurements after at least 322 h at the respective temperatures (eq. 6). Approximate rate constants for the forward reaction were also determined graphically by measuring the initial slope of a plot of ln B_0/B *vs.* time giving values of 3.06, 4.97, 7.68, 13.53, and 22.74 ($k_f \times 10^3$ h^{-1}) at 70, 75, 80, 85, and 90°, respectively. In this approach, the reverse reaction (**1***a* → **1***b*) is neglected during the initial period which has the predictable effect of retarding the forward rate thus leading to smaller k_f values than obtained from eqs. 5 and 6. The data of Table 1 were found to agree well with those of two other runs and the activation energy was calculated to be 24.0 kcal/mol (Fig. 1) with an estimated root-mean-square error of ±0.4 kcal/mol.

A comparison of these kinetic results with those reported for the hydrogen–deuterium

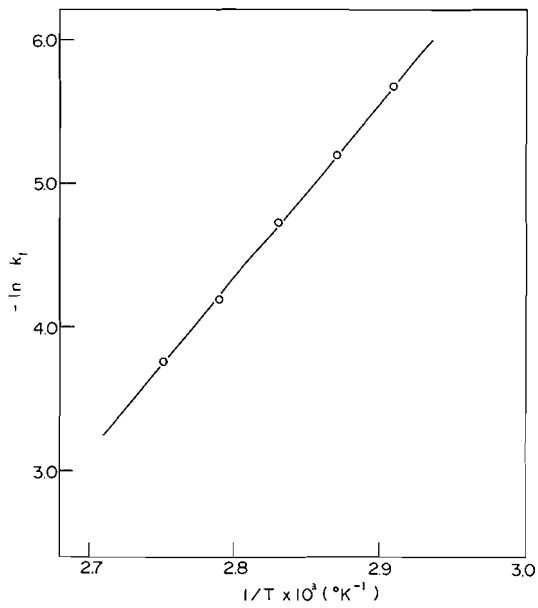

FIG. 1. Effect of temperature on epimerization rate.

Can. J. Chem. Downloaded from www.nrcresearchpress.com by 210.87.254.42 on 09/05/12
For personal use only.

exchange and the crossed aldol reaction of chloral at the methylene carbon of 2-heptanone and butanone under similar reaction conditions (2) confirms our earlier conclusions based on product studies, namely that the epimerization rate is of the same order of magnitude as the enolization rate of structurally similar ketones but much faster than the rate of the aldol addition step. This is to be expected on the basis of a common enolization–ketonization mechanism for both isotope exchange and epimerization and agrees with the observation by Rappe and Sachs (9) that the rates of acid-catalyzed deuteration of butanone and 3-methyl-2-butanone are approximately equal, *i.e.*, very little affected by additional branching at the α-carbon. The ratio of the diastereomeric ketols formed from diethyl ketone and chloral in glacial acetic acid with sodium acetate as catalyst is, therefore, thermodynamically controlled so that it is impossible to draw conclusions about the transition state geometry of the aldol addition on the basis of rate and/or product studies with this and other acyclic, aliphatic ketones. Saturated cyclic ketones, however, appear to be suitable model compounds for an investigation of the stereochemistry of the aldol condensation (10, 11) since they permit a systematic study of diastereomer ratios and configurations before equilibration has occurred. We are presently pursuing research along these lines.

The authors wish to thank Miss N. McGillivray for technical assistance and the National Research Council of Canada for the financial support of these investigations.

1. E. Kiehlmann and P. W. Loo. Can. J. Chem. **49**, 1588 (1971).
2. B. C. Menon and E. Kiehlmann. Can. J. Chem. **49**, 3648 (1971).
3. E. Kiehlmann and P. W. Loo. Can. J. Chem. **47**, 2029 (1969).
4. F. Caujolle, P. Couturier, and C. Dulaurans. Bull. Soc. Chim. Fr. **17**, 19 (1950).
5. E. Kiehlmann, P. W. Loo, B. C. Menon, and N. McGillivray. Can. J. Chem. **49**, 2964 (1971).
6. M. Stiles, R. R. Winkler, Y. Chang, and L. Traynor. J. Am. Chem. Soc. **86**, 3337 (1964).
7. L. Traynor. Ph.D. Thesis, University of Michigan, Ann Arbor, Mich. 1964. p. 12.
8. P. B. Condit. Ph.D. Thesis, University of Michigan, Ann Arbor, Mich. 1970. p. 41.
9. C. Rappe and W. H. Sachs. J. Org. Chem. **32**, 3700 (1967).
10. J. E. Dubois and M. Dubois. Tetrahedron Lett. 4215 (1967).
11. J. E. Dubois and M. Dubois. J. Chem. Soc. Chem. Commun. 1567 (1968).

Can. J. Chem. Downloaded from www.nrcresearchpress.com by 210.87.254.42 on 09/05/12
For personal use only.

Further Studies in the Reactions of Triethylaluminum with Bis-(diphenylphosphino) amines

DONALD F. CLEMENS, ROBERT B. SMITH, JR., AND JOHN G. DICKINSON
The Chemistry Department, East Carolina University, Greenville, North Carolina 27834

Received January 8, 1973

Triethylaluminum reacts with bis(diphenylphosphino)-*n*-propylamine and bis(diphenylphosphino)-*n*-butylamine to form the 1:1 adducts in which the aluminum atom is pentacoordinate. Triethylaluminum does not react with other bis(diphenylphosphino)amines in which the third substituent on the nitrogen atom is α-methylbenzyl, benzyl, or 1,1-dimethylamine. The formation of adducts from straight-chain hydrocarbons and the total lack of reactivity for the Lewis bases containing bulky groups leads to the postulation that steric hindrance prevents the free pair of electrons on the phosphorus atoms from being available to the triethylaluminum.

Le triéthylaluminium réagit sur la bis(diphénylphosphino)-*n*-propylamine et la bis(diphénylphosphino)-*n*-butylamine pour former des adduits 1:1 dans lesquels l'atome d'aluminium est pentacoordiné. Le triéthylaluminium ne réagit pas sur les autres bis(diphénylphosphino) amines dans lesquelles le troisième substituant sur l'azote est l'α-méthylbenzyle, benzyle ou diméthyl-1,1 amine. La formation d'adduits à partir des chaînes droites hydrocarbonées et le manque total de réactivité pour les bases de Lewis contenant des groupes volumineux conduisent à postuler que l'encombrement stérique empêche la disponibilité des paires d'électrons libres du phosphore au triéthylaluminium.

[Traduit par le journal]

Can. J. Chem., **51**, 3187 (1973)

Can. J. Chem. Downloaded from www.nrcresearchpress.com by 210.87.254.42 on 09/05/12
For personal use only.

It has been shown that triethylaluminum reacts with hydrazines (1), biphosphines (2), and aminophosphines (2) to form adducts in which the aluminum atom is pentacoordinate by virtue of being symmetrically located with respect to two adjacent electron donor atoms. A recent study of the reactions of triethylaluminum with hydrazinophosphorus compounds (3), such as $P[(CH_3)NN(CH_3)]_3P$, indicated that, although reaction did occur, the aluminum atom was tetracoordinate, not pentacoordinate as in the above cases. In the course of extending this work it was decided to examine the reactions of triethylaluminum with a variety of bis(diphenylphosphino)amines similar to some of the P—N—P compounds reported previously (2). The purpose of this study was to determine whether the third substituent on the nitrogen atom may, through steric hindrance, prevent the formation of the Lewis acid–base adduct or allow compounds to be formed in which only one of the phosphorus atoms interacts with the aluminum. Reactions were attempted with molecules such as $RN[P(C_6H_5)_2]_2$ in which the R groups were *n*-propyl, *n*-butyl, α-methylbenzyl, benzyl, and 1,1-dimethylamine. Pentacoordinate aluminum complexes were formed only in the reactions where R represented a straight chain hydrocarbon. The other compounds failed to react indicating no tendency to form a complex involving the bonding of only one of the phosphorus atoms to triethylaluminum.

Experimental

Materials

Solvents used in these experiments were distilled and stored over calcium hydride. Diphenylchlorophosphine, obtained as a gift from Stauffer Chemical Co., was vacuum distilled under nitrogen at 113° (0.14 mm). Triethylaluminum, obtained as a gift from Texas Alkyls, was distilled under nitrogen at 48° (0.045 mm). 1,1-Bis-(diphenylphosphino)-2,2-dimethylhydrazine was prepared by the method of Nielsen and Sisler (4). The bis(diphenylphosphino)amines were synthesized by the reaction of diphenylchlorophosphine with the appropriate amine according to standard procedures (5–7).

General Methods

All manipulations were done either in an inert atmosphere chamber filled with dry nitrogen or in a typical high-vacuum line. I.r. spectra were obtained from KBr pellets using a Beckman IR-12 spectrophotometer. The proton n.m.r. spectra were recorded using a Perkin–Elmer Model R-20 spectrometer operated at 60 MHz. The shift values were obtained using TMS as an internal reference. ^{31}P n.m.r. spectra were obtained by Charles Moreland, University of North Carolina at Raleigh, at 40.5 MHz using P_4O_6 as an internal reference on a Varian HA-100 spectrometer. Elemental analyses were done by Galbraith Laboratories, Inc., Knoxville, Tenn.

The Interaction of Bis(diphenylphosphino)-n-propylamine with Triethylaluminum

$$2\ C_3H_7N[P(C_6H_5)_2]_2 + Al_2(C_2H_5)_6 \rightarrow 2\ C_3H_7N[P(C_6H_5)_2]_2 \cdot Al(C_2H_5)_3$$

Can. J. Chem. Downloaded from www.nrcresearchpress.com by 210.87.254.42 on 09/05/12
For personal use only.

A 0.545 g (0.0048 mol) sample of triethylaluminum was dissolved in a mixture of 3 ml of benzene and 3 ml of hexane in a 200 ml, two-necked reaction flask containing a Teflon-coated magnetic stirring bar. Bis-(diphenylphosphino)-*n*-propylamine (2.00 g, 0.0047 mol) was placed in a tipping tube and attached to the reaction flask. A vacuum stopcock was fitted into the other neck of the reaction flask and the entire apparatus was attached to the vacuum line. After degassing the reactants, a small portion of the bis(diphenylphosphino)-*n*-propylamine was added to the reaction flask which was cooled with a Dry Ice – acetone bath. The mixture was then stirred as it was allowed to warm to room temperature. After coming to room temperature, the mixture was again chilled and the addition process repeated. This procedure was continued until all of the solid had been added. The reaction was allowed to proceed for 2 h at room temperature after which the solvent was removed leaving a white crystalline reaction product. The reaction flask was then transferred, still under vacuum, to the inert atmosphere chamber where the crude product was washed with six small portions of hexane and recrystallized from hot hexane. The crystals were dried by passing nitrogen through the solid on a glass frit, m.p. 106–108°.

Anal. Calcd. for $C_3H_7N[P(C_6H_5)_2]_2 \cdot Al(C_2H_5)_3$: C, 73.17; H, 7.83; N, 2.59; P, 11.43; Al, 4.98. Found: C, 72.90; H, 7.72; N, 2.50; P, 11.29; Al, 5.04.

The i.r. spectrum contained peaks at 3000 (m), 2900 (m), 1963 (w), 1820 (w), 1670 (vw, b), 1590 (m), 1470 (s), 1375 (w, b), 1325 (sh, w), 1305 (m), 1270 (w, b), 1215 (w), 1180 (m), 1165 (m), 1125 (m), 1090 (s), 1060 (s), 1020 (m), 995 (w), 925 (sh, m), 912 (s), 885 (vw), 850 (sh, w), 838 (sh, w), 825 (s, b), 740 (s, b), 692 (s, b).

The ^1H spectrum obtained using $CDCl_3$ as a solvent consists of a peak at τ 2.57 assigned to phenyl protons, and a multiplet at τ 6.80 (average) assigned to the NCH_2 group, a broad multiplet at about τ 8.9 (average) assigned to the CH_3CH_2 methylene group, a triplet at τ 9.00 (J = 8.0 Hz) assigned to the methyl protons of the ethyl group bonded to aluminum, a triplet at τ 9.62 (J = 6.0 Hz) assigned to the CH_3 signal in the *n*-propyl group, and a quartet at τ 9.99 (J = 8.0 Hz) assigned to the methylene protons adjacent to the aluminum atom.

The ^{31}P n.m.r. spectrum obtained from a benzene solution consists of a single peak at +51 p.p.m. from P_4O_6 or −62 p.p.m. from H_3PO_4.

Increasing the ratio of triethylaluminum to aminophosphine in subsequent reactions had no effect on the composition of the product.

The Interaction of Bis(diphenylphosphino)-n-butylamine with Triethylaluminum

$$2\ C_4H_9N[P(C_6H_5)_2]_2 + Al_2(C_2H_5)_6 \rightarrow 2\ C_4H_9N[P(C_6H_5)_2]_2 \cdot Al(C_2H_5)_3$$

By the same procedure described previously 2.00 g (0.00453 mol) of bis(diphenylphosphino)-*n*-butylamine was allowed to react with 0.516 g (0.0452 mol) of triethylaluminum to give a quantitative yield of a white crystalline solid which had a melting point range of 91–93° after recrystallization from hot hexane.

The i.r. spectrum contained peaks at 3000 (m), 2850 (s), 1970 (w), 1900 (w), 1825 (vw), 1775 (vw), 1670 (w), 1600 (m), 1590 (sh, w), 1475 (s), 1455 (m), 1435 (s), 1410 (w), 1465 (w), 1300 (m), 1260 (w), 1230 (m), 1200 (sh, w), 1175 (m), 1155 (m), 1125 (vw), 1115 (sh, vw), 1080 (s, b), 1065 (s, b), 1050 (sh, w), 1025 (w), 975 (s, vb), 925 (w), 885 (sh, w), 855 (s), 795 (sh, m), 775 (s), 750 (sh, s), 740 (vs, b), 695 (vs, b).

The ^1H n.m.r. spectrum obtained using $CDCl_3$ as a solvent consists of a peak τ 2.60 assigned to phenyl protons, a multiplet at τ 6.77 (average) assigned to the NCH_2 group, a triplet at τ 9.02 (J = 8.0 Hz) assigned to the methyl protons of the ethyl group bonded to aluminum, a very broad multiplet at τ 9.1 (average) assigned to the methyl and methylene protons of the butyl group, and a quartet at τ 9.97 (J = 8.0 Hz) assigned to the protons of the methylene group bonded to aluminum. (The $AlCH_2CH_3$ triplet rises well above the broad signal at τ 9.1 and can be reasonably accurately assigned; however, the CH_3 signal of the *n*-butyl group, which is at about τ 9.5 cannot be accurately assigned because it merges into the broad τ 9.09 peak.) This spectrum is consistent with the 1:1 adduct that has been shown to form in other cases such as the *n*-propyl compound described above.

The ^{31}P n.m.r. spectrum obtained from a benzene solution consists of a single peak at +51 p.p.m. from P_4O_6 or −62 p.p.m. from H_3PO_4.

The reaction was repeated with increased concentrations of triethylaluminum but in each case the 1:1 reaction product was isolated.

The following compounds were mixed with triethylaluminum but no reaction was observed regardless of stoichiometry or temperature: 1,1-bis(diphenylphosphino)-2,2-dimethylhydrazine, $(CH_3)_2NN[P(C_6H_5)_2]_2$; bis(diphenylphosphino)-α-methylbenzylamine, $(C_6H_5)CH(CH_3)N[P(C_6H_5)_2]_2$; and bis(diphenylphosphino)-benzylamine, $C_6H_5CH_2N[P(C_6H_5)_2]_2$.

Discussion

The reactions of triethylaluminum with bis-(diphenylphosphino)-*n*-propylamine and with bis(diphenylphosphino)-*n*-butylamine to produce the new compounds $C_3H_7N[P(C_6H_5)_2]_2 \cdot Al(C_2H_5)_3$ and $C_4H_9N[P(C_6H_5)_2]_2 \cdot Al(C_2H_5)_3$ are in accord with published data and the products are the expected results of these reactions. These two new compounds have structures in which the aluminum atom is symmetrically located with respect to the two phosphorus atoms and thus can be considered to be pentacoordinated.

The ^{31}P n.m.r. spectra indicate that the two phosphorus atoms have the same environment since a single sharp peak is observed in both compounds. These results obviate the possibility of only one phosphorus atom being bonded to aluminum. The possibility of the aluminum being bonded to nitrogen can be discounted by the fact that the NCH_2 signals in the ^1H n.m.r. spectra fall at the same location in the parent phosphorus compounds as they do in the aluminum complexes. A change in the electron density on the

Can. J. Chem. Downloaded from www.nrcresearchpress.com by 210.87.254.42 on 09/05/12
For personal use only.

nitrogen atom would be expected if there was an Al—N bond and this would cause an upfield shift in the NCH_2 protons.

The i.r. spectra of these compounds have many absorption bands which may be readily assigned from i.r. data in the literature. Among the more readily identified bands are those in the 3120 to 2860 cm^{-1} region which are characteristic of the phenyl C—H, the methyl C—H, and the methylene C—H stretching vibrations. Three weak absorptions attributed to monosubstituted benzene are found between 1975 and 1820 cm^{-1}. A strong sharp band at 1440 to 1430 cm^{-1} is assigned to the *P*-phenyl vibration (8). The P—N bands are known to vary and have generally been assigned the 1000–800 cm^{-1} (5, 9, 10) and 773–743 cm^{-1} regions (8). Phenyl peaks characteristic of monosubstituted benzene are also found at 760–720 and at 700–690 cm^{-1}.

Steric hindrance problems due to the bulk of the group bonded to the bridging nitrogen atom were first encountered during the attempted synthesis of bis(diphenylphosphino)-*t*-butylamine, $(CH_3)_3CN[P(C_6H_5)_2]_2$. In this case the only compound that could be obtained was diphenylphosphino-*t*-butylamine, $(CH_3)_3CNHP(C_6H_5)_2$. Hirschfelder models of these compounds indicated that the bulk of the *t*-butyl group would not permit synthesis of the bis(diphenylphosphino)-*t*-butylamine.

Models of the bis(diphenylphosphino)amines containing -1,1-dimethylamine, α-methylbenzyl, or benzyl groups on the bridging nitrogen atom were compared to models of the bases that formed stable adducts $(CH_3(CH_2)_2N[P(C_6H_5)_2]_2$ and $CH_3(CH_2)_3N[P(C_6H_5)_2]_2)$. These comparisons indicated that the bulky groups bonded to the bridging nitrogen atom in the unreactive bases do cause the phenyl rings to be rotated in such a manner as to cover or shield the phosphorus atoms. The only orientation of the phenyl rings that exposed the phosphorus atoms sufficiently for attack would be unlikely because the rings had face-to-face orientations. These face-to-face orientations would result in considerable repulsions brought about by the interpenetrations of π electron clouds.

The results of this study indicate that the steric nature of the group bonded to the bridging nitrogen atom in bis(diphenylphosphino)amines is the determining factor that governs whether adduct formation will take place. It is interesting to note that there appears to be no tendency for the aluminum atom to react with just one of the phosphorus atoms. If the aluminum can get into position to form a bond with phosphorus it bonds with both phosphorus atoms.

1. D. F. Clemens, W. S. Brey, Jr., and H. H. Sisler. Inorg. Chem. **2**, 1251 (1963).
2. D. F. Clemens, H. H. Sisler, and W. S. Brey, Jr. Inorg. Chem. **5**, 527 (1966).
3. S. F. Spangenberg and H. H. Sisler. Inorg. Chem. **8**, 1004 (1969).
4. R. P. Nielsen and H. H. Sisler. Inorg. Chem. **2**, 753 (1963).
5. G. Ewart, A. P. Lane, J. McKechnie, and D. S. Payne. J. Chem. Soc. 1543 (1964).
6. D. F. Clemens, M. L. Caspar, D. Rosenthal, and R. Peluso. Inorg. Chem. **9**, 960 (1970).
7. D. F. Clemens, W. Perkinson, A. Crain, and G. Locko. Unpublished results.
8. J. B. Class, J. G. Aston, and J. S. Oakwood. J. Am. Chem. Soc. **75**, 2937 (1953).
9. R. P. Nielsen, J. F. Vincent, and H. H. Sisler. Inorg. Chem. **2**, 760 (1963).
10. D. S. Payne and A. P. Walker. J. Chem. Soc. (C), 498 (1966).

The Hemicelluloses of Western Red Cedar (*Thuja plicata* (Donn))

GUY G. S. DUTTON AND NORMAN A. FUNNELL
Department of Chemistry, University of British Columbia, Vancouver 8, British Columbia

Received December 27, 1972[1]

The hemicelluloses of *Thuja plicata* (Donn) of the family Cupressaceae have been examined as part of a chemotaxonomic study. Little difference has been found from other Coniferales except that the xylan contains a percentage of L-arabinose lower than for many Pinaceae. Although 2- and 3-*O*-methylxylitol acetates are not separable by g.l.c. the composition of such a mixture may be determined by circular dichroism (c.d.) or by proton magnetic resonance (p.m.r.) spectroscopy.

Une étude chemotaxonomique a été faite sur les hémicelluloses de *Thuja plicata* (Donn) de la famille des Cupressacées. Une différence minime a été constatée comparativement à d'autres Conifères, à part que le xylane renferme un pourcentage d'arabinose inférieur à celui normalement trouvé chez des Pinacées. Bien que les acétates de méthylxylitol-2 et 3 ne soient pas séparés par la c.p.g., la composition d'un tel mélange peut être dosée par le dichroisme circulaire (d.c.) ou par la spectroscopie de résonance magnétique nucléaire (r.m.n.).

Can. J. Chem., **51**, 3190 (1973)

Trees may be classified as angiosperms (hardwoods) or gymnosperms (softwoods) and the hemicelluloses of these two groups are different in that the former consist mainly of the xylan type whereas the latter contain substantial quantities of mannose rich polysaccharides in addition to xylans. The literature pertaining to wood hemicelluloses has been reviewed extensively by Timell (1). The gymnosperm group, however, contains at least 6 main families which comprise 50 genera and about 600 species (2, 3). Of these families that of the Pinaceae (Abietaceae) contains the genera more commonly encountered commercially *e.g.* Pinus and Picea, and reference to the review by Timell (1) shows that it is almost exclusively members of this family whose hemicelluloses have been examined in detail. In continuation of previous work on the hemicelluloses of west coast trees we now report a study on *Thuja plicata* (Donn), a member of the family Cupressaceae and will, in due course, discuss the non-cellulosic polysaccharides of *Sequoia sempervirens* of the family Taxodiaceae. It is hoped that these structural studies may be useful in establishing a chemotaxonomic classification amongst the order Coniferales since it is considered (2) that the family Cupressaceae is more highly evolved than the Pinaceae. Certain aspects of the hemicelluloses of western red cedar have been examined previously (4) but no complete study has been made of these polysaccharides.

Western red cedar sawdust was solvent extracted, delignified (5), and extracted sequentially with potassium and sodium hydroxides (6) to give a mixture of xylan and galactoglucomannan (GGM) and a substantially pure glucomannan (GM). Each fraction was delignified at room temperature with buffered sodium chlorite (7) and precipitation with barium hydroxide was used to separate the xylan and GGM and to purify the GM (6, 8). The yields, on an ash-free basis, of xylan, GGM, and GM were 4.0, 1.5, and 6.4% of the wood. An attempt was made to separate the xylan and GGM on a column of DEAE-cellulose in the carbonate form (9) with several different eluents but no resolution was obtained except for a small quantity of degraded cellulose. The use of an ion-exchange column (10, 11) was similarly unproductive.

The arabino-4-*O*-methylglucuronoxylan had an equivalent weight of 775 and a molecular weight (12) of about 17 000, corresponding to a d.p. of 110, $[\alpha]_D$ $-36°$ (*c* 1.5, water), and the neutral sugars comprised 91% xylose and 5% arabinose with the balance being hexoses. The relatively high proportion of uronic acid was confirmed by analysis of the carboxyl reduced polymer (13) which gave the ratio of xylose:4-*O*-methylglucose as 4.5:1. An equivalent weight of 775 corresponds to approximately 27% uronic acid. The acidic component was characterized by the isolation of the crystalline aldotriouronic acid (14) 2-*O*-(4-*O*-methyl-α-D-glucopyranosyluronic acid)-β-D-xylopyranosyl-D-xylose after partial hydrolysis.

[1]Revised manuscript received June 13, 1973.

Can. J. Chem. Downloaded from www.nrcresearchpress.com by 210.87.254.6 on 09/05/12
For personal use only.

TABLE 1. Methylated sugars from xylan and carboxyl-reduced xylan

Component	Retention times (min)*		Molar ratio	
	Column a	Column b	Xylan	Reduced xylan
2,3,5-Me_3-Ara†	15	12	0.03	trace
2,3,4-Me_3-Xyl	20	15	0.06	0.07
2,3,4,6-Me_4-Glc		20		0.20
2,3-Me_2-Xyl	31	23	1.00	1.00
2- and 3-Me-Xyl	43	30	0.15	0.31

*As alditol acetates; column a, 3% ECNSS-M, 170° for 10 min, then to 220° at 2°/min; column b, 5% BDS, 145–210° at 2°/min.
†2,3,5-Me_3-Ara = 2,3,5-tri-*O*-methyl-L-arabinose, etc.

TABLE 2. Methylated sugars from galactoglucomannan and glucomannan

Component	Compound	Retention times (min)		Molar ratio	
		Alditol acetates*	Aldose acetates†	GGM	GM
1*a*	2,3,4,6-Me_4-Glc‡	27	10, 13	0.10 (G:M = 1:2)	0.16 (G:M = 8:1)
1*b*	2,3,4,6-Me_4-Man	27	20		
2	2,3,4,6-Me_4-Gal	31	17	0.26	0.03
3	2,3,6-Me_3-Man	47	26	2.6	4.2
4	2,3,6-Me_3-Glc	49	21, 22	1.0	1.0
5	2,3-Me_2-Man	59	30	0.34	0.15
6	2,3-Me_2-Glc	62	—	0.23	0.04

*3% ECNSS-M, 170° 10 min, then to 220° at 2°/min.
†3% ECNSS-M, 150–210° at 2°/min.
‡2,3,4,6-Me_4-Glc = 2,3,4,6-tetra-*O*-methyl-D-glucose, etc.

Fractionation of the fully methylated (15, 16) xylan gave a main fraction having 38.6% methoxyl and which, on hydrolysis, gave the components shown in Table 1. These figures suggest a chain length of 20 while the data (Table 1) on the reduced methylated xylan indicate a value of about 15. This xylan must therefore have a small degree of chain branching in addition to the single unit pendant groups. This was substantiated by periodate oxidation of the xylan when a significant amount of ethylene glycol was obtained in addition to glycerol and xylose.

The separation of the methylated sugars shown in Table 1 is conveniently made by g.l.c. using alditol acetates but since the 2- and 3-*O*-methylxylitol acetates are inseparable it has been necessary to use some other system to resolve this pair of compounds. We have drawn attention (17) to the fact that 3-*O*-methylxylitol is achiral and the percentage in a mixture with the 2-isomer may be determined by measurement of the $\Delta\varepsilon$ value of the c.d. spectrum of the mixture of alditol acetates. Alternatively, the chemical shift in p.m.r. spectroscopy of the *O*-methyl group is different for the two alditols: 2-methylxylitol tetraacetate, τ 6.55; 3-isomer, τ 6.40. Thus integration of the signals permits a quantitative analysis. In this manner the monomethylxylitol tetraacetate fraction isolated by g.l.c. was shown by both c.d. and p.m.r. to contain the 2- and 3-methyl derivatives in the ratio of 1:2.

Purified galactoglucomannan (GGM_5) had $[\alpha]_D$ −3.8° (*c* 1, water), mol. wt. 9000 (d.p. 55), and a hexose content of 90%. The mannose:glucose:galactose ratio was 8:2:1 and from the methylated polysaccharide the sugars shown in Table 2 were obtained. The small proportion of tetramethyl sugars indicates the essential linearity of this polysaccharide, a result confirmed by periodate oxidation which yielded mainly glycerol and erythritol.

The glucomannan had $[\alpha]_D$ −38° (*c* 0.4, 2 *N* sodium hydroxide) and on hydrolysis the ratio of mannose:glucose:galactose was approximately 4:1:0.1. The components shown in Table 2 were obtained from the methylated polysaccharide. The results confirm the small amount of D-galactose in the GM and show that

Can. J. Chem. Downloaded from www.nrcresearchpress.com by 210.87.254.6 on 09/05/12
For personal use only.

Can. J. Chem. Downloaded from www.nrcresearchpress.com by 210.87.254.6 on 09/05/12
For personal use only.

little branching is possible, a conclusion substantiated by the fact that periodate degradation gave almost exclusively erythritol. The poor solubility of the GM in methyl sulfoxide, and hence the failure of the initial Hakomori methylation, is almost certainly due to incomplete removal of barium ions (6).

The advantages of separating certain methylated sugars as their acetates has been discussed elsewhere (18) but it may be noted that this technique, when employed here, permits the demonstration that the chains of GGM are terminated preferentially by D-mannose units whereas the chains of GM are primarily terminated with D-glucose residues. In the analysis of each of the methylated polysaccharides the amount of di- (or mono-) methyl sugars always greatly exceeded that required by the amount of tetra- (or tri-) methyl sugars isolated. It has been shown (19) that undermethylation by only 0.5% will result in 3.9% higher dimethylhexose content in the hydrolyzate but also, and perhaps less obviously, that hydrolysis under different conditions of the same methylated polysaccharide gives widely different ratios of tetra- to dimethyl (tri- to mono-) sugars (20). The advent of g.l.c. has facilitated the determination of minor components in a mixture but has also thrown into sharp focus the dangers of attempting to distinguish between n and $n + 1$ branch points.

When the data of Table 2 are used to deduce the ratio of the three hexoses present in each of the GM and GGM and these values are compared to those obtained from the original polysaccharides it will be noted that fair agreement is obtained in the case of the GM but that there is a significant difference in the case of the GGM. It has been pointed out elsewhere (20) that the conventional solvent extraction of a methylated polysaccharide may give fractions in which the sugar ratio differs greatly. This suggests that these fractions which, for convenience, are called xylans, GGM's, and GM's are, in fact, mixtures of related polysaccharides.

It has been shown (21), in the case of bacterial polysaccharides, that p.m.r. spectroscopy is most useful in determining the relative number of α and β linkages in such materials. The accepted (1) structures for galactoglucomannans have the glucose and mannose joined by β-D-linkages with the galactose linked in an α-configuration. Similarly, in xylans the xylose units have β-D-linkages with the arabinose and 4-*O*-methylglucuronic acid joined by α-glycosidic bonds. It should therefore be possible to distinguish the relative number of such linkages as in the case of the bacterial polysaccharides. However, when this p.m.r. technique was applied to such hemicelluloses no discrete peaks were obtained in the spectral region associated with anomeric protons. In like manner, gel filtration of hemicelluloses does not give sharp peaks but diffuse bands. All of the present evidence, and particularly that obtained from p.m.r. spectroscopy, suggests that these hemicelluloses are indeed mixtures of related polysaccharides. It seems likely that in the area of hemicellulose chemistry no one has yet studied a pure polysaccharide in the true sense of the word.

In so far as one is entitled to draw conclusions from the above results it would seem that the general nature of the hemicelluloses of western red cedar is similar to that of other conifers. The amount of xylan appears to be relatively high and that of GM to be on the low side but the figures cited (1) for other genera are sufficiently varied that generalization is difficult. In the xylan the percentage of uronic acid is on the high side while that of arabinose is definitely lower than for many of the Pinaceae (1) and these observations may prove to be characteristic of the Cupressaceae.

Experimental

General Methods

Melting points were taken between glass slides on a Fisher–Johns apparatus and are uncorrected. Optical rotations were measured with a Perkin-Elmer model 141 polarimeter at 23 ± 1°. Gas–liquid partition chromatography was carried out using an F & M 720 instrument equipped with a thermal conductivity detector. Peak areas were determined with an Infotronics CRS-100 electronic integrator. The following column and operating conditions were used: 8 ft × 1/4 in. 3% ECNSS-M on 60–70 mesh Chromosorb W (non-acid washed) with a helium flow rate of 75 ml/min. For alditol acetates the program was 170° for 10 min, then to 220° at 2°/min; for aldose acetates 150 to 210° at 2°/min; for periodate oxidation products 130 to 180° at 2°/min. All sugar analyses were by g.l.c. of alditol acetates. Paper chromatographic separations were carried out on Whatman No. 1 paper using the following solvent systems: *A*, ethyl acetate – pyridine – water (8:2:2) for 24 h; *B*, butanone–water azeotrope for 5–8 h; *C*, butanol–ethanol–water (4:1:5) for 24 h; *D*, ethyl acetate – acetic acid – formic acid – water (18:3:1:4) for 24 h. Separations were visualized using silver nitrate in acetone for non-reducing compounds (22) and *p*-anisidine hydrochloride spray for reducing sugars (23); R_G indicates with respect to 2,3,4,6-tetra-*O*-methyl-D-glucose. All evaporations were carried

Can. J. Chem. Downloaded from www.nrcresearchpress.com by 210.87.254.6 on 09/05/12
For personal use only.

out under reduced pressure below 40°. I.r. spectra were run in carbon tetrachloride solution at a concentration of about 10%. All hydrolyses were done with trifluoroacetic acid (2 *M*) at 100° for 4 h unless otherwise noted (24). Samples for mass spectral analysis were collected in capillary tubes from the gas chromatograph (25). Demethylations were carried out using boron trichloride (26). Solutions of dimethylsulfinyl anion used for methylations (15, 16) were assayed as described for the methylation of the glucomannan.

Molecular Weight Determinations

Molecular weight determinations were carried out using gel permeation chromatography (12). A polyethylene column (1.15 × 86 cm) of Bio-Gel P-300 (Bio-Rad Laboratories), treated with dichlorodimethylsilane and equipped with a suction pump, was used. Sodium chloride (*M*) was used as eluant. Carbohydrate material was assayed by the phenol – sulfuric acid method (27). Both xylan and galactoglucomannan samples gave broad maxima, indicating a wide distribution in molecular weights. The figures quoted are weight averaged molecular weights but these values should only be considered approximate since the column was calibrated with a series of dextrans (12) which have different exclusion volumes to hemicelluloses.

Circular Dichroism Measurements

Circular dichroism (c.d.) measurements were carried out using a JASCO J-20 instrument as described elsewhere (17) by observing the acetoxy chromophore of alditol acetates. By this means, it was shown that all mannose and glucose residues are of the D series, while all arabinose residues are of the L series. Galactose and xylose were also shown to be of the D series, since their partially methylated derivatives gave c.d. curves corresponding to authentic 1,5-di-*O*-acetyl-2,3,4,6-tetra-*O*-methyl-D-galactitol and 1,3,4,5-tetra-*O*-acetyl-2-*O*-methyl-D-xylitol, respectively.

Isolation of Western Red Cedar Holocellulose

Samples of western red cedar were ground to sawdust in a Wiley mill and extracted batchwise (750 g) with methanol (2 l) in a Soxhlet extractor for 12 h. Extracted sawdust (225 g, moisture 5%) was delignified by treatment with sodium chlorite and acetic acid (5); 2-octanol was used to suppress foaming. After air drying the yield of holocellulose was 154 g (72%, residual Klason lignin 3%).

Extraction of Western Red Cedar Holocellulose with Alkali

Holocellulose (140 g) was extracted with potassium hydroxide (24%, 1500 ml) under nitrogen (28). The mixture was shaken for 6 h and allowed to stand overnight. Filtration and washing, followed by precipitation into ethanol (6 l) containing an excess of glacial acetic acid (1 l) and drying by solvent exchange (ethanol – acetone – petroleum ether), yielded the potassium hydroxide extract (19.7 g, 10.2% of wood, ash 12.5%). G.l.c. gave xylose 75%, mannose 12.8%, arabinose 5.4%, galactose 3.8%, and glucose 3.0%.

The solids remaining after potassium hydroxide extraction were similarly extracted with sodium hydroxide (17.5%) containing boric acid (4%) (1500 ml) (29). After precipitation into ethanol – acetic acid and drying by solvent exchange, the hemicellulose was obtained (14.1 g, 7.3% of wood, ash 8.6%). G.l.c. gave mannose 71.5%, glucose 19%, xylose 4.1%, galactose 2.8%, and arabinose 2.6%.

Fractionation of the Potassium Hydroxide Extract

The potassium hydroxide extract (18.1 g) was suspended (7) in sodium chlorite (100 g/l, 150 ml) buffered with sodium acetate (5 g) and glacial acetic acid (10 ml). After stirring for 22 h the solution was centrifuged to remove a small amount of insoluble material, precipitated into 4 volumes of ethanol acidified with glacial acetic acid, recovered, and dried by solvent exchange (16.3 g). The material was then dissolved in water (150 ml), potassium hydroxide (20%, 150 ml) was added, and barium hydroxide (5%, 1100 ml) was added over 2 h with vigorous stirring. The precipitate was recovered by centrifugation, dissolved in acetic acid (50%, 50 ml), and reprecipitated into ethanol (200 ml). After drying by solvent exchange, polysaccharide GGM_1 was obtained (4.4 g, ash 44.2%). The supernatant remaining after barium hydroxide addition was concentrated to 500 ml, then precipitated into ethanol (2 l) containing an excess of glacial acetic acid (200 ml). After drying, polysaccharide X_1 was obtained (11.2 g, ash 29.2%).

Purification of Arabinoglucuronoxylan

A portion of X_1 (10.1 g) was suspended in water (200 ml), then sodium hydroxide (17.5%) and boric acid (4%) (200 ml) were added. A small amount of insoluble material was removed by centrifugation. Barium hydroxide (5%, 800 ml) was then added dropwise with stirring. The precipitate formed was recovered by centrifugation to yield X_2 (0.40 g). Paper chromatography in solvent *A* of this fraction showed the presence of substantial amounts of hexose and the fraction was not further examined. The supernatant was poured into 3 volumes of ethanol, the precipitate was recovered by centrifugation, dissolved in ice-cold acetic acid (50%, 50 ml), then reprecipitated into 2 volumes of ethanol, and recovered by centrifugation to yield X_3 (7.85 g, $[\alpha]_D$ −36° (*c* 1.5, water), ash 0.4%, equiv. wt. 775 by titration, mol. wt. 17 000). Paper chromatography of X_3 hydrolyzate indicated a high pentose to hexose ratio. G.l.c. gave xylose 91%, arabinose 5.1%, mannose 1.7%, glucose 1.2%, and galactose 1%.

Methylation of Arabinoglucuronoxylan

A sample of X_3 (1.50 g) after dialysis overnight, deionization, freeze drying, and drying *in vacuo* for 24 h at 40°, was methylated in dry dimethyl sulfoxide (30 ml) with methylsulfinyl anion (1.5 *M*, 30 ml) and methyl iodide (6.5 ml). After 1½ h reaction time the solution was poured into water and the precipitate formed was removed by spatula, dissolved in chloroform (50 ml), extracted three times with water (25 ml), then evaporated to dryness (1.1 g). Fractionation with petroleum ether (30–60°) and chloroform (v/v) gave: fraction 1 (90:10), 56 mg; fraction 2 (80:20), 316 mg; fraction 3 (75:25), 600 mg, $[\alpha]_D$ −22.2° (*c* 1, chloroform), OMe 38.6%, no i.r. absorption at 3400 cm^{-1}.

Characterization of Component Sugars

Paper chromatography of the hydrolyzate of fraction 3 in solvents *B* and *C* showed five components which were tentatively identified by comparison with standards.

Can. J. Chem. Downloaded from www.nrcresearchpress.com by 210.87.254.6 on 09/05/12
For personal use only.

More positive identification and quantitative determination were achieved by g.l.c. of the alditol acetates (30), including co-chromatography with standards, and by mass spectrometry (31, 32).

Component **1** (15 min) was identified as 2,3,5-tri-*O*-methyl-L-arabinose (0.03 mol) and component **2** (20 min) as 2,3,4-tri-*O*-methyl-D-xylose (0.12). The principal constituent was component **3** (31 min) characterized as 2,3-di-*O*-methyl-D-xylose (1.0). The mass spectrum of components **4***a* and *b* (43 min, 0.15 mol) was consistent with that to be expected from a mixture of the alditol acetates of 2- and 3-monomethylpentitols. Collection (25) of this fraction from the g.l.c. and solution of 7 mg in 0.4 ml of 99.8% D_2O gave a p.m.r. spectrum (60 MHz) showing $-OCH_3$ signals at τ 6.40 (3-*O*-methylxylitol) and τ 6.55 (2-*O*-methylxylitol) in the approximate proportion of 2:1. The c.d. spectrum of pure 2-*O*-methyl-D-xylitol tetraacetate gives $\Delta\varepsilon_{212}^{MeCN}$ +0.37 whereas the 3-methyl derivatives has $\Delta\varepsilon = 0$. A solution of components **4***a* and *b* (1.1 mg) in acetonitrile (0.12 ml) had $\Delta\varepsilon_{212}^{MeCN}$ +0.13 hence the mixture contains 35% of 2-*O*-methyl-D-xylitol tetraacetate.

Periodate Oxidation of Arabinoglucuronoxylan

X_3 (157.3 mg) was reacted with sodium metaperiodate (0.0488 *M*, 50 ml) at 5° in the dark. The periodate uptake was initially rapid becoming essentially constant (1.10 mol/sugar unit) after 1 week. Iodate and excess periodate were destroyed by the addition of ethylene glycol (0.5 ml); the solution was dialyzed overnight, then reduced with sodium borohydride (130 mg). After neutralization with glacial acetic acid, hydrolysis with trifluoroacetic acid (2 *N*, 10 ml, 6 h) at room temperature, and distillation four times with methanol, paper chromatography in solvents *A* and *D* showed the presence of a large amount of xylose. After a further reduction with sodium borohydride (20 mg), g.l.c. of the alditol acetates showed the presence of three major components, which cochromatographed with the peracetates of ethylene glycol, glycerol, and xylitol, together with a small peak due to an unidentified component.

Isolation and Identification of the Aldotriouronic Acid

A sample of X_3 (0.5 g) was hydrolyzed for 1 h by refluxing in trifluoroacetic acid (2 *N*). After centrifugation, evaporation, and passage through columns of Amberlite IR 120 (H^+) resin and Duolite A-4 (OH^-) resin, the acidic fraction was eluted with 10% formic acid. Paper chromatography (solvent *D*) showed the presence of five spots with R_{xylose} 1.17, 0.87, 0.60, 0.48, and 0.24. The fraction with R_{xylose} 0.48 corresponded to that of the genuine aldotriouronic acid *O*-(4-*O*-methyl-α-D-glucopyranosyluronic acid)-(1 → 2)-*O*-β-D-xylopyranosyl-(1 → 4)-D-xylopyranose. Preparative paper chromatography in solvent *D* was used to isolate the acid (60 mg). The crystalline material had m.p. 175–177° (14) and $[\alpha]_D$ +50° (*c* 0.60, water). P.m.r. data (D_2O) of sodium salt: singlet τ 6.55 (OMe); 1 proton broad singlet τ 4.74 (H-1 of 4-*O*-methyl-α-D-glucopyranosyluronic acid); 1.5 proton doublets τ 5.43 and 5.40 (J = 7 and 8 Hz) (H-1 of non-reducing xylose and H-1 (β) of reducing xylose); 0.5 proton doublet τ 4.85 (J = 3 Hz) (H-1 (α) of reducing xylose).

Reduction of the Xylan

A portion of the xylan (200 mg) was reduced by the method of Dutton and Kabir (13). After freeze drying (yield 131 mg), the material showed no i.r. absorption in the carbonyl region. Paper chromatographic analysis (solvent *A*) of the hydrolyzate showed the presence of 4-*O*-methyl-D-glucose. G.l.c. examination of the hydrolyzate as alditol acetates on a column of 5% butanediol succinate (13) gave a pentose to 4-*O*-methyl-glucose ratio of 4.5–5:1.

The reduced xylan was methylated (16, 17) and on hydrolysis gave the components shown in Table 1.

Purification of Galactoglucomannan

Western red cedar GGM (18 g) was suspended in water (150 ml), potassium hydroxide (20%, 150 ml) added, and the mixture stirred for 0.5 h. The insoluble material was removed by centrifugation, dissolved in acetic acid (50%, 10 ml), precipitated into ethanol (50 ml), and dried by solvent exchange to yield GGM_4 (1.28 g). This fraction, as indicated by g.l.c., was enriched in pentoses and was not examined further. To the material soluble in potassium hydroxide, barium hydroxide (5%, 1 l) was added dropwise with stirring. The precipitate formed was centrifuged, redissolved in acetic acid (50%, 50 ml), precipitated into ethanol (200 ml), and dried by solvent exchange to yield GGM_2 (3.70 g). G.l.c. of the alditol acetates of this fraction showed a hexose to pentose ratio of 7:1. To the barium hydroxide supernatant, ethanol was added to give a flocculent precipitate (8) which was recovered by centrifugation and dried by solvent exchange to yield GGM_3 (3.78 g, $[\alpha]_D$ −15.8° (*c* 1.5, water). This fraction was shown by g.l.c. to have a pentose to hexose ratio of 3.5:1 and was not further examined.

GGM_2 (3.5 g) was suspended in water (125 ml), potassium hydroxide (20%, 125 ml) was added, and barium hydroxide (5%, 500 ml) was added dropwise with stirring. The precipitate was recovered by centrifugation to yield GGM_5 (2.50 g, $[\alpha]_D$ −3.8° (*c* 1, water), ash 0.75%, mol. wt. 8850). Further addition of ethanol yielded a flocculent precipitate GGM_6 (1.05 g), which was shown by paper chromatography in solvent *A* to be enriched in pentoses with respect to GGM_5. This fraction was not further examined.

Paper chromatography of GGM_5 hydrolyzate indicated a high hexose to pentose ratio. G.l.c. gave mannose 66%, glucose 16%, xylose 8.4%, galactose 8.0%, and arabinose 1.6%.

Methylation of Galactoglucomannan

A sample of GGM_5 (0.4 g) after deionization, freeze drying, and drying *in vacuo* at 50° for 24 h, was methylated in dry dimethyl sulfoxide (10 ml) with methylsulfinyl anion (1.5 *M*, 10 ml) and methyl iodide (5 ml). After 6 h reaction time, the solution was poured into water, dialyzed for 36 h against running tap water, and freeze dried (yield 380 mg). Fractionation, as for the methylated xylan gave a product (fraction 3, 80:20, 125 mg) having $[\alpha]_D$ −4.3° (*c* 1, chloroform) and showing no i.r. absorption at 3400 cm^{-1}.

Characterization of Component Sugars

Paper chromatography of the hydrolyzate of fraction 3 in solvents *B* and *C* showed the presence of six major components, the molar ratios of which are given in Table 2. Component **1** was resolved into **1***a* and *b* in the ratio 1:2 by chromatography of the aldose acetates (18) at 170°. All components co-chromatographed with authentic alditol acetate samples and had mass spectra

Can. J. Chem. Downloaded from www.nrcresearchpress.com by 210.87.254.6 on 09/05/12
For personal use only.

consistent with the assigned structures. In addition **3** and **4** were demethylated (26) and acetylated to give (g.l.c.) D-mannitol hexaacetate, m.p. 115–117° and D-glucitol hexaacetate, m.p. 95–97°. Other minor components, investigated only by mass spectrometry, were tentatively identified as two 2,6-di-*O*-methylhexitols and a 2,3,4-tri- and 2,3-di-*O*-methylpentitol, presumably from contaminating xylan.

Periodate Oxidation of Galactoglucomannan

Western red cedar GGM_5 (148.9 mg) was reacted with sodium metaperiodate (0.0488 *M*, 50 ml) at 5° in the dark. The periodate uptake was initially very rapid, becoming constant (1.28 mol/sugar unit) after 1 week. Iodate and excess periodate were destroyed by the addition of ethylene glycol (0.5 ml), the solution was dialyzed overnight, then reduced with sodium borohydride (150 mg). After neutralization with glacial acetic acid, deionization, hydrolysis with trifluoroacetic acid (2 *M*, 10 ml, 6 h) at room temperature, and distillation four times with methanol, paper chromatography in solvents *A* and *D* showed the presence of erythritol and glycerol. G.l.c. of the alditol acetates showed two major peaks, the faster co-chromatographing with glycerol triacetate (18 min), the slower with erythritol tetraacetate (36 min), m.p. 85°.

Purification of Glucomannan

Crude sodium hydroxide extract (9.0 g) was suspended in sodium chloride (100 g/l, 75 ml) buffered with sodium acetate (2.5 g) in glacial acetic acid (5 ml). After stirring for 18 h, the mixture was poured into ethanol (500 ml), washed three times with water (20 ml), then partially dried by solvent exchange. While still moist the solid was redissolved in sodium hydroxide (10%) and boric acid (4%) (250 ml) and a small amount of insoluble material was removed by centrifugation. Barium hydroxide (5%, 300 ml) was added dropwise with vigorous stirring. The precipitate was collected by centrifugation, washed twice with sodium hydroxide (5%, 20 ml), redissolved in ice-cold acetic acid (50%, 150 ml), precipitated into ethanol (500 ml), and recovered. Repetition of this procedure yielded GM_2 (5.80 g, $[\alpha]_D$ −38° (*c* 0.4, 2 *N* sodium hydroxide), ash 2.2%) (4). G.l.c. gave: mannose 77%, glucose 18.5%, galactose 1.6%, xylose 2.9%, and a trace of arabinose.

Methylation of Glucomannan

Purified GM_2 (1.5 g), after dialysis overnight, freeze drying, passage through a 200 mesh screen, and drying *in vacuo* at 55° for 17 h, was dispersed in dry dimethyl sulfoxide (50 ml) under dry nitrogen. Sodium hydride (57% oil dispersion, 3 g) was washed free of oil with dry petroleum ether (30–60°), then reacted with dry dimethyl sulfoxide (30 ml) for 4 h at 50–60°. Titration of this reagent with sulfuric acid (0.5 *M*) showed a strength of 2.6 *M*; however, titration with formanilide using triphenylmethane as indicator gave a strength of only 1.2 *M*. The methylsulfinyl ion (25 ml) was then added at room temperature to the polysaccharide suspension. Little gel formation occurred; the reaction mixture was stirred overnight under nitrogen. Methyl iodide (4 ml) was added over 10 min at 10°, the reaction allowed to proceed for 3 h, then poured into water, dialyzed for 48 h, and recovered by freeze drying. The material was insoluble in chloroform and thus a Haworth methylation was carried out using sodium hydroxide (30%, 125 ml) and methyl sulfate (60 ml) with addition of sodium hydroxide (5 g) and methyl sulfate (5 ml) hourly for 7 h. After stirring overnight at 0°, the mixture was neutralized with sulfuric acid (*M*), dialyzed, and the polysaccharide (1.4 g) recovered by freeze drying. A second Hakomori methylation was then carried out to yield fully methylated polysaccharide (1.1 g).

Fractionation with petroleum ether (30–60°) and chloroform (v/v) gave: fraction 1 (90:10), 0.128 g, $[\alpha]_D$ −17.5° (*c* 1, chloroform); fraction 2 (80:20), 0.657 g, $[\alpha]_D$ −23.8°, OMe 44.6%; fraction 3 (75:25), 0.344 g, $[\alpha]_D$ −23.1°, OMe 43.0%. Fractions 2 and 3 did not show any i.r. absorption at 3400 cm^{-1}.

Characterization of Component Sugars

Paper chromatography in solvents *B* and *C* of the hydrolyzate of fraction 2 showed the presence of six major components, the molar ratios of which, as determined by g.l.c. of the alditol acetates, are given in Table 2.

Component **1** (30 min) was readily shown to be a mixture of the derivatives of 2,3,4,6-tetra-*O*-methyl-D-glucose (**1***a*) and 2,3,4,6-tetra-*O*-methyl-D-mannose (**1***b*) in the ratio of 8.1:1 by chromatography of the aldose acetates (18) isothermally at 170°.

All components, as their alditol acetates, co-chromatographed with authentic samples and gave mass spectra consistent with their assigned structure. In addition **3** and **4** were demethylated (26) and acetylated to give (g.l.c.) D-mannitol hexaacetate, m.p. 119–121° and D-glucitol hexaacetate, m.p. 95–96°, respectively. Several very minor components were also detected as noted for the methylated GGM.

Periodate Oxidation of Glucomannan

Purified GM_2 (149.2 mg) was reacted with sodium metaperiodate (0.0483 *M*, 100 ml) at 5° in the dark. The periodate uptake was initially very rapid, becoming constant (0.81 mol/sugar unit) after 1 week. Iodate and excess periodate were destroyed with ethylene glycol (0.5 ml), the solution was dialyzed overnight, and reduced with sodium borohydride (150 mg). After neutralization with glacial acetic acid, hydrolysis with trifluoroacetic acid (2 *M*, 20 ml, 7 h) at room temperature, distillation four times with methanol, and deionization, paper chromatography in solvents *A* and *B* showed the presence of erythritol and faint spots corresponding to mannitol and glycerol.

Periodate oxidation products (50 mg) were acetylated with acetic anhydride (1 ml) and sodium acetate (10 mg) for 1 h at 100°. G.l.c. gave two major peaks which co-chromatographed with glycerol triacetate (12 min) and erythritol tetraacetate (27 min), m.p. 85°.

The authors thank the National Research Council of Canada for financial support and for the award of a scholarship to N.A.F. We appreciate the assistance of Mr. G. M. Barton in obtaining the wood and preparing the sawdust.

1. T. E. TIMELL. Adv. Carbohydr. Chem. **19**, 247 (1964); **20**, 409 (1965).
2. C. J. CHAMBERLAIN. Gymnsperms, structure and evolution. Univ. Chicago, Chicago, Ill. 1935.
3. H. J. DITTMER. Phylogeny and form in the plant kingdom. van Nostrand, Princeton, N.J. 1964.

4. J. K. HAMILTON and E. V. PARTLOW. J. Am. Chem. Soc. **80**, 4880 (1958).
5. E. L. WISE, M. MURPHY, A. A. D'ADDIECO. Paper Trade J. **122**, 35 (1946).
6. T. E. TIMELL. Tappi, **44**, 88 (1961).
7. D. W. CLAYTON. Svensk papperstidn. **66**, 115 (1963).
8. G. G. S. DUTTON, B. I. JOSELEAU, and P. E. REID. Tappi, **56**, 168 (1973).
9. I. R. SIDDIQUI and P. J. WOOD. Carbohydr. Res. **16**, 452 (1971).
10. D. A. APPLEGARTH and G. G. S. DUTTON. J. Chromatogr. **15**, 246 (1964).
11. D. A. APPLEGARTH and G. G. S. DUTTON. Tappi, **48**, 204 (1965).
12. S. C. CHURMS. Adv. Carbohydr. Chem. Biochem. **25**, 13 (1970).
13. G. G. S. DUTTON and S. KABIR. Anal. Lett. **4**, 95 (1971).
14. J. K. HAMILTON and N. S. THOMPSON. J. Am. Chem. Soc. **79**, 6464 (1957).
15. S. HAKOMORI. J. Biochem. (Tokyo), **55**, 205 (1964).
16. P. A. SANDFORD and H. E. CONRAD. Biochemistry, **5**, 1508 (1966).
17. G. M. BEBAULT, J. M. BERRY, Y. M. CHOY, G. G. S. DUTTON, N. FUNNELL, L. D. HAYWARD, and A. M. STEPHEN. Can. J. Chem. **51**, 324 (1973).
18. G. M. BEBAULT, G. G. S. DUTTON, and R. H. WALKER. Carbohydr. Res. **23**, 430 (1972).
19. K. WALLENFELS, G. BECHTLER, R. KUHN, H. TRISCHMANN, and H. EGGE. Angew Chem. Int. Ed. **2**, 515 (1963).
20. G. G. S. DUTTON and R. H. WALKER. Cellul. Chem. Tech. **6**, 295 (1972).
21. G. M. BEBAULT, Y. M. CHOY, G. G. S. DUTTON, N. FUNNELL, A. M. STEPHEN, and M. T. YANG. J. Bacteriol. **113**, 1345 (1973).
22. W. E. TREVELYAN, D. P. PROCTER, and J. S. HARRISON. Methods Carbohydr. Chem. **1**, 21 (1962).
23. L. HOUGH, J. K. N. JONES, and W. H. WADMAN. J. Chem. Soc. 1702 (1950).
24. P. ALBERSHEIM, D. J. NEVINS, P. D. ENGLISH, and A. KARR. Carbohydr. Res. **5**, 340 (1967).
25. G. G. S. DUTTON and K. B. GIBNEY. J. Chromatogr. **72**, 179 (1972).
26. T. G. BONNER, E. J. BOURNE, and S. MCNALLY. J. Chem. Soc. 2929 (1960).
27. M. DUBOIS, K. A. GILLES, J. K. HAMILTON, G. A. REBERS, and F. SMITH. Anal. Chem. **28**, 350 (1956).
28. J. K. HAMILTON and G. R. QUIMBY. Tappi, **40**, 781 (1957).
29. J. K. N. JONES, L. E. WISE, and J. P. JAPPE. Tappi, **39**, 139 (1956).
30. H. BJÖRNDAL, B. LINDBERG, and S. SVENSSON. Acta Chem. Scand. **21**, 1801 (1967).
31. H. BJÖRNDAL, B. LINDBERG, and S. SVENSSON. Carbohydr. Res. **5**, 433 (1967).
32. H. BJÖRNDAL, C. G. HELLERQVIST, B. LINDBERG, and S. SVENSSON. Angew. Chem. Int. Ed. **9**, 610 (1970).

Can. J. Chem. Downloaded from www.nrcresearchpress.com by 210.87.254.6 on 09/05/12
For personal use only.

Gas–Liquid Chromatography – Mass Spectrometry of Permethylated Aldosyl Aldonates

JOHN N. C. WHYTE

Fisheries Research Board of Canada, 6640 N.W. Marine Drive, Vancouver 8, British Columbia

Received April 30, 1973

Oxidation of neutral disaccharides yielded aldosyl aldonic acids which were methylated and separated by g.l.c. and subjected to mass spectrometry. The electron-impact fragmentation patterns afforded by these derivatives discriminated between (1 → 3), (1 → 4), and (1 → 6) linked residues and differed from that postulated for (1 → 2) intermolecular bonds. Primary scission of the aldonate moieties provided for the ionized hexosyl containing fragments which formed the high mass diagnostic peaks in these spectra. The mass spectra exhibited by the oxidized products could be correlated to those obtained from reduced, permethylated pseudoaldobiouronic acids.

L'oxydation de disaccharides neutres a conduit aux acides aldosyl aldoniques qui furent méthylés et séparés par c.g.l. pour ensuite être analysés par spectrométrie de masse. Les pics de fragmentation obtenus à l'aide de l'impact électronique de ces dérivés ont permis de choisir entre les résidus liés de manière (1 → 3), (1 → 4) et (1 → 6) et sont différents de ceux appartenant aux liens intermoléculaires (1 → 2). La première cassure des unités aldonates explique la présence de fragments renfermant des unités hexosyles ionisées qui forment la région des pics d'identification de ces spectres. Les spectres de masse obtenus des produits oxydés peuvent être reliés à ceux obtenus à partir des formes réduites des acides pseudoaldobiouroniques perméthylés. [Traduit par le journal]

Can. J. Chem., 51, 3197 (1973)

Can. J. Chem. Downloaded from www.nrcresearchpress.com by 210.87.254.42 on 09/05/12
For personal use only.

Introduction

In the determination of the structural features of oligosaccharides by mass spectrometry a variety of derivatives have been employed. The spectral analyses of the derived peracetates (1), *N*-arylamine peracetates (2), *N*-phenylosotriazole peracetates (3), and 1-phenylflavazole peracetates (4) have been used to assess the molecular weight, the sequence of monosaccharide units, and in some cases the position of the glycosidic linkages in the parent oligomers. Similarly the derived pertrimethylsilyl ethers (5, 6) and corresponding alditol pertrimethylsilylates (7) of oligosaccharides have provided fragmentation patterns which, when coupled with analyses of peak intensity ratios, established most of the glycosidic linkages in the molecules (8). In contrast to the above derivatives which provided spectra with diagnostic peaks of low intensity and high mass, the permethylated derivatives offered fragmentation patterns of much lower mass units, thus facilitating the use of lower resolution instruments. The mass spectra of permethylated disaccharides have discriminated between (1 → 2), (1 → 4), and (1 → 6) linked residues (9). To distinguish between (1 → 3) and (1 → 4) linked moieties the corresponding permethylated alditols were investigated (10) employing sodium borodeuteride for the reduction stage, since without deuterium labelling the derivatives were too symmetrical for the electron-impact fragmentation pattern to be meaningful. In our studies (11), however, we have found that the relatively low abundance of the few diagnostic peaks in these spectra, together with the incomplete shift to one higher mass unit of those ions incorporating deuterium, do not allow for unequivocal assignment of the (1 → 3) and (1 → 4) glycosidic linkages in disaccharides.

This study on the mass spectrometry of permethylated aldosyl aldonates, where oxidation of the neutral disaccharides afforded nonsymmetrical structures, was an attempt to obviate the identical fragmentation patterns associated with those previously cited derivatives. In addition, the results of this study could also be correlated to the mass fragmentation patterns provided by the permethylated derivatives of reduced pseudoaldobiouronic acids.

Experimental

Commercial samples of maltose, cellobiose, lactose, isomaltose, and melibiose were used. Laminaribiose was obtained from the partial hydrolysate of laminaran (12) by separation on a charcoal column (13) and sodium

TABLE 1. Relative retention times of permethylated disaccharide alditols and aldonates on g.l.c.

Compound	Stationary phase			
	10% SE30 (250°)	1.5% XE60 1.5% EGS (195°)	3% QF1 (200°)	1% OV17 (210°)
Laminaribiitol	1.07	0.95	1.00	1.10
Cellobiitol	1.02	0.92	1.04	0.96
Maltitol*	1.00	1.00	1.00	1.00
Lactitol	1.01	1.20	1.10	1.18
Isomaltitol	1.29	1.48	1.38	1.43
Melibiitol	1.36	1.82	1.55	1.79
Mannoglycerate	0.38	0.44	0.45	0.29
Laminaribionate	1.21	1.55	1.65	1.13
Cellobionate	1.26	1.98	1.84	1.46
Maltonate	1.21	2.06	1.83	1.60
Lactobionate	1.22	2.56	2.00	1.79
Isomaltonate	1.55	2.98	2.54	2.10
Melibionate	1.64	3.76	2.87	2.50

*Reference standard.

2-*O*-α-D-mannopyranosyl-D-glycerate was isolated from the red seaweed *Rhodomela larix* (14).

G.l.p.c. was carried out using a Hewlett-Packard 5750 gas chromatograph with hydrogen flame detectors and fitted with columns (180 × 0.45 cm) packed with (*a*) 10% SE30 (w/w) on DMCS treated Chromosorb W (60–80 mesh), (*b*) 1.5% XE60, 1.5% EGS (w/w) on DMCS treated Chromosorb W (60–80 mesh), (*c*) 3% QF1 (w/w) on Gas Chrom Q, and (*d*) 1% OV-17 (w/w) on Gas Chrom Q. Development was made with nitrogen at a flow rate of 60 ml/min at the column temperature specified and retention times are quoted relative to permethylated maltitol. The mass spectrometer, Nuclide 12-90G, was operated at a source temperature of 240° and an ionization potential of 70 eV.

To the disaccharide (20 mg) in water (20 ml, 0°) containing barium carbonate (100 mg) was added bromine (0.1 ml) and the mixture shaken, then stored 24 h in the dark at room temperature. Excess bromine was removed by aeration and the mixture reduced to half volume by evaporation in a round bottom flask on a rotary evaporator. Neutral red indicator was added to the mixture at 0° followed by the dropwise addition of aqueous barium hydroxide at 0° to maintain an orange coloration (p*H* 8.0) for a period of 2.5 h. Carbon dioxide was then passed into the mixture to p*H* 7.0 and the barium salts dried by evaporation with the last traces of water being removed on a high vacuum pump. Dry distilled methyl sulfoxide (10 ml) was introduced into the nitrogen-flushed flask through a rubber septum (15) followed by a solution of methylsulfinyl carbanion in methyl sulfoxide (2 *M*, 10 ml) and the mixture ultrasonicated for 1 h. The resultant mixture after a further 1 h was solidified by cooling and methyl iodide (5 ml) added to complete the methylation. The reaction solution was poured into cold dilute aqueous acetic acid to minimize possible high alkalinity and the resultant mixture extracted with chloroform. The combined extracts were water washed, dried over anhydrous magnesium sulfate, and evaporated to yield the permethylated aldosyl aldonate which was dissolved in distilled ethyl acetate prior to injection on the g.l.c. using column *b*. Occasionally, in addition to the major component peak, some minor peaks were evident in the g.l.c. of these preparations.

Samples for spectroscopic analysis were collected at the exit port of the gas chromatograph by condensation in glass capillary tubes which were then inserted directly into the mass spectrometer.

Results and Discussion

Oxidation of the disaccharides with buffered bromine water yielded the barium salts of the aldonic acids together with the corresponding lactones. The latter were converted into the aldonic acid salts by mild treatment with dilute barium hydroxide and after thorough desiccation the combined oxidation mixture was methylated with the Hakomori procedure (16) to furnish the methyl esters and methyl ethers of the derived aldosyl aldonates.

The relative retention times on g.l.c. for these derivatives, together with the corresponding permethylated aldosyl alditols, are presented in Table 1. The aldonate derivatives had retention times significantly greater than the respective alditols, yet only the column with 3% QF1 as the stationary phase proved effective in separating discretely these two groups of derivatives. Thus, this would be the most versatile column for the separation and mass spectrometric study of pseudoaldobiouronic acid components present in the reduced, permethylated, partial hydrolysate of an acidic polysaccharide. The best separation within the group of alditols and

Can. J. Chem. Downloaded from www.nrcresearchpress.com by 210.87.254.42 on 09/05/12
For personal use only.

TABLE 2. Partial mass spectra of permethylated disaccharide aldonates

m/e	Maltonate	Cellobionate	Lactobionate	Isomaltonate	Melibionate	Laminaribionate
45	35	36	43	37	35	46
59	15	17	18	12	10	14
71	26	26	33	33	34	23
73	13	13	15	38	15	11
75	42	37	40	56	45	37
88	100	100	100	100	100	100
89	27	26	30	20	20	22
101	57	54	61	80	74	63
103	2	26	5	13	11	5
111	45	38	37	43	37	26
115	7	11	10	10	8	6
119	11	12	15	13	16	3
127	12	11	13	11	11	8
129	5	5	9	18	18	26
155	14	11	12	1	6	9
159	3	4	8	36	29	6
185	16	20	22	21	24	10
187	48	50	33	59	38	31
191	—	—	—	12	11	—
217	8	8	11	4	5	3
219	7	7	12	11	14	6
249	33	38	37	53	60	29
293	—	—	—	1.76	1.40	—
309	17	19	18	20	24	8
319	0.60	1.00	1.00	0.65	0.8	0.39
322	0.57	—	0.33	—	—	—
331	—	—	—	—	—	0.79
337	—	—	—	1.08	1.63	—
349	0.72	1.89	2.83	—	—	—
351	0.51	1.21	1.46	0.54	0.56	0.73
363	—	—	—	—	—	1.24
381	1.20	2.43	2.00	—	—	—
395	—	—	—	—	—	1.47
407	0.90	0.81	1.33	—	—	0.53
425	—	—	—	—	—	0.65
439	0.45	0.48	0.46	—	—	0.50
453	0.27	—	—	—	—	—

aldonates was provided by the mixed stationary phase 1.5% XE60 and 1.5% EGS and would be the obvious choice when dealing specifically with either of these groups of derivatives; the aldonate derivatives separated on this column provided the mass spectra presented in Table 2.

The electron-impact fragmentation pattern of a permethylated aldosyl aldonate can be considered to originate from the molecular ion (odd-electron ion radical) formed by abstraction of an electron from the oxygen atom in the pyranose ring or from an oxygen atom in one of the methoxyl groups of the acyclic moiety, then principally by subsequent homolytic fission of the adjacent bonds or by rearrangements involving conjugated electronic shifts in the pyranose ring to furnish even-electron carbonium ions.

The spectra of these aldosyl aldonate derivatives were devoid of molecular ions but had common ion fragments originating from scission at the glycosidic linkages. The ion of mass 219 for the hexose unit also provided, by subsequent elimination of one or two molecules of methanol, for the ions at *m/e* 187 (m* = 159.7) and 155. Further elimination and rearrangement mechanisms for this hexose moiety as outlined by Kochetkov and Chizhov (17) provided for the common ions at *m/e* 71, 73, 88 (base peak of all spectra), 101, and 111. The corresponding ion fragment at *m/e* 249 for the ionized aldonate moiety provided for the ions at *m/e* 217 and 185 by progressive loss of methanol.

Most of the high mass ions arose from the primary cleavage of the bonds in the aldonate

Can. J. Chem. Downloaded from www.nrcresearchpress.com by 210.87.254.42 on 09/05/12
For personal use only.

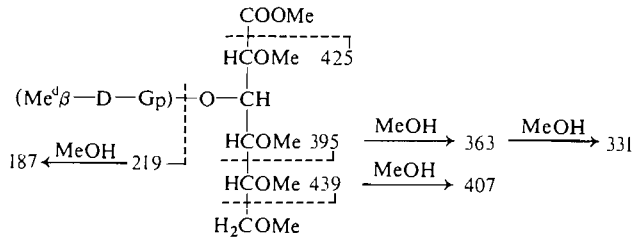

SCHEME 1

residues. As illustrated in Scheme 1, scission of the (1 → 3) linked permethylated laminaribionate allowed for the ions of mass 439[$M^{\ddagger}$ – $^{\bullet}CH_2OMe$], 425[$M^{\ddagger}$ – $^{\bullet}COOMe$], and 395[$M^{\ddagger}$ – $^{\bullet}CH(OMe).CH_2OMe$] which also provided, by progressive loss of the methanol molecules, for the ions at mass 407, 363, and 331.

By similar bond cleavage in the acyclic moiety of the (1 → 4) linked permethylated cellobionate derivative, the diagnostic ions at *m/e* 381[$M^{\ddagger}$ – $^{\bullet}CH(OMe).COOMe$] and 349[$M^{\ddagger}$ – $^{\bullet}CH(OMe).COOMe$-MeOH] were formed from cleavage of the C_2—C_3 bond, as illustrated in Scheme 2. The ions at mass 439 and 407 which

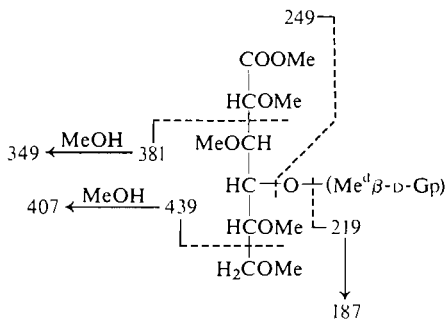

SCHEME 2

are common to the spectra of (1 → 4) and (1 → 3) linked molecules were totally absent in the spectrum of the (1 → 6) linked derivatives and of the major diagnostic ions of mass 337 and 293, 191 and 159(191 – MeOH) were formed respectively by scission of the C_3—C_4 and C_4—C_5 bonds of the acyclic moiety of permethylated isomaltonate as shown in Scheme 3.

Common to all these spectra were the ions at *m/e* 351, 319, and 309 which were associated with rearrangement processes involving the hexose residue. Proof for the formation of these ions was presented by considering the simplified spectrum afforded by permethylated 2-*O*-α-D-mannopyranosyl-D-glyceric acid, Fig. 1. As out-

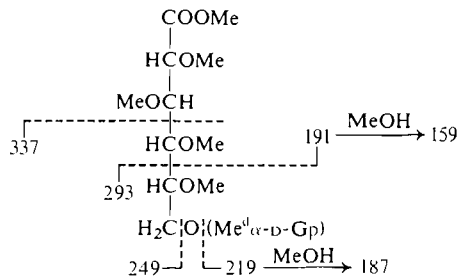

SCHEME 3

lined in Fig. 1, the sequence of conjugated electronic shifts gave rise to the ions of mass 177 and 251 which corresponded in the aldosyl hexonic acid series to the ions at 309 and 383 respectively, the latter ion by elimination of methanol providing the observable ion fragments in the spectra at *m/e* 351 and 319. Evidence that the ion at mass 309 originated from the fragment at *m/e* 383 was demonstrated by the presence of the metastable peak at *m/e* 249.3. The intense metastable peak at *m/e* 200.7 corresponded to the transition of the fragment of mass 309 affording by heterolytic bond cleavage,

MeO—CH=O—aldonate, the aldonate carbonium ion at *m/e* 249. This fragmentation pattern was corroborated by studying the mass spectra of permethylated aldosyl alditols where the metastable peak at *m/e* 187.2 confirmed the transition of the corresponding ion at *m/e* 295,

MeO—CH=O—alditol to the ionized alditol moiety at *m/e* 235.

It is evident from the fragmentation pattern of these derivatives that the hexosyl glycosidic linkage prevents cleavage of the adjacent carbon bonds in the aldonate residue and that this effect is negated progressively through the β and γ bond positions especially when the carbon atoms forming these bonds bear the electron donating methyl groups (18). It has been observed from

Can. J. Chem. Downloaded from www.nrcresearchpress.com by 210.87.254.42 on 09/05/12
For personal use only.

Can. J. Chem. Downloaded from www.nrcresearchpress.com by 210.87.254.42 on 09/05/12
For personal use only.

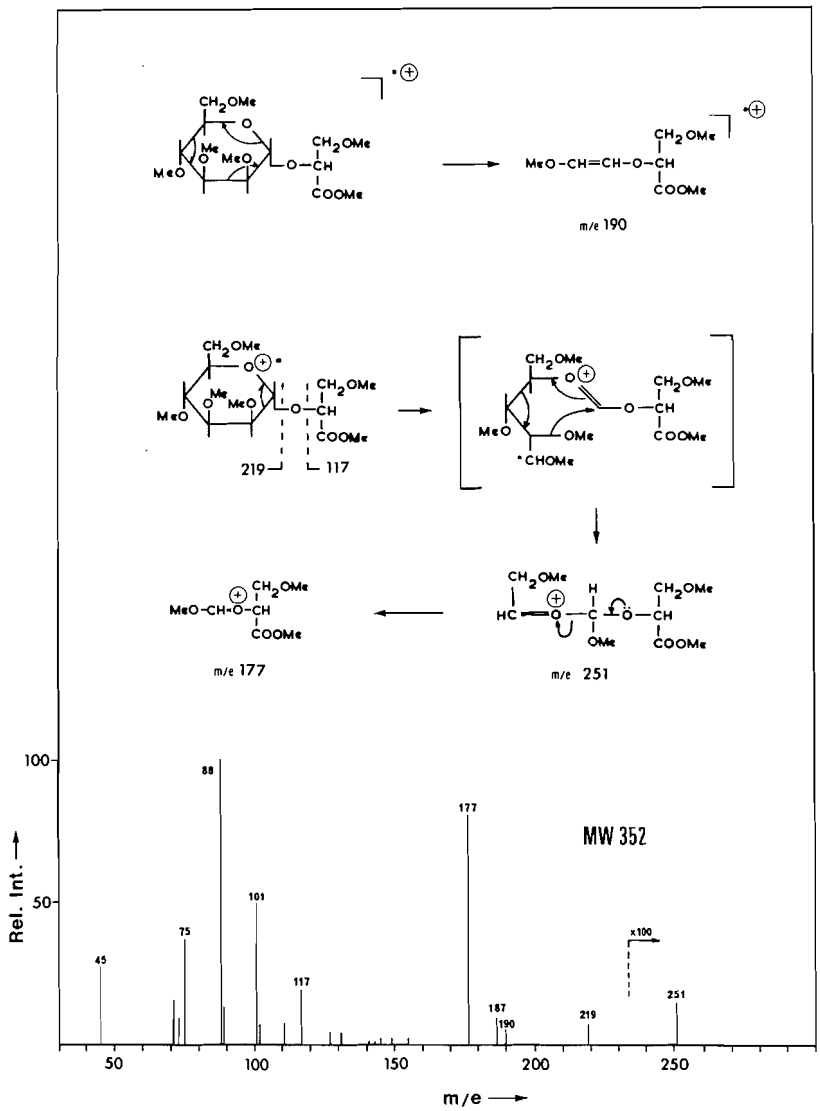

FIG. 1. Mass spectrum (70 eV) and mode of fragmentation of permethylated 2-*O*-α-D-mannopyranosyl-D-glyceric acid.

the fragmentation of permethylated aldonic acids (19) that the bonds adjacent to the ester group are more stable to electron impact than those adjacent to methoxyl groups. Thus it can be postulated that the mass spectra of (1 → 2) linked permethylated aldosyl hexonic acids would exhibit intense peaks at *m/e* 351 and 133 formed by the cleavage of the susceptible C_3—C_4 aldonate bond and minor peaks at *m/e* 395, 363(395 – MeOH), and 331(363 – MeOH) due to the cleavage of the extremely susceptible C_4—C_5 bond. Consequently it can be concluded that the mass spectra of (1 → 2), (1 → 3), (1 → 4), and (1 → 6) linked residues in permethylated aldosyl aldonates exhibit ions at *m/e* (395, 363, 331, and 133), (439, 425, 407, 395, 363, and 331), (439, 407, 381, and 349), and (337, 293, 191, and 159) respectively, which offer when collated diagnostic analyses of these derivatives.

These results indicated the utility of the oxidized permethylated derivatives of neutral disaccharides as eminently suitable derivatives for the mass spectrometric determination of the

position of the intermolecular bonds. As the mass spectra of stereoisomeric sugars are practically indistinguishable, the above results might be correlated to the linkage analyses by mass spectrometry of reduced permethylated pseudoaldobiouronic acids. Thus it is reasonable to assume that the (1 → 4) and (1 → 3) linked pseudoaldobiouronic acid derivatives would exhibit spectra identical to those provided by the (1 → 3) and (1 → 4) linked neutral disaccharide derivatives respectively.

The author is indebted to Mr. J. Love for mass spectral determinations.

1. J. KARLINER. Tetrahedron Lett. 3545 (1968).
2. O. S. CHIZHOV, N. K. KOCHETKOV, N. N. MALYSHEVA, A. I. SHIYONOK, and V. L. CHASHCHIN. Org. Mass Spectrom. **5**, 1157 (1971).
3. O. S. CHIZHOV, N. K. KOCHETKOV, N. N. MALYSHEVA, A. I. SHIYONOK, and V. L. CHASHCHIN. Org. Mass Spectrom. **5**, 1145 (1971).
4. G. S. JOHNSON, W. S. RULIFFSON, and R. G. COOKS. Carbohydr. Res. **18**, 233 (1971).
5. N. K. KOCHETKOV, O. S. CHIZHOV, and N. V. MOLODTSOV. Tetrahedron, **24**, 5587 (1968).
6. J. VINK, J. J. DE RIDDER, J. P. KAMERLING, and J. F. G. VLIEGENTHART. Biochem. Biophys. Res. Commun. **42**, 1050 (1971).
7. J. KÄRKKÄINEN. Carbohydr. Res. **11**, 247 (1969).
8. J. P. KAMERLING, J. F. G. VLIEGENTHART, J. VINK, and J. J. DE RIDDER. Tetrahedron, **27**, 4275 (1971).
9. O. S. CHIZHOV, L. A. POLTAKOVA, and N. K. KOCHETKOV. Dokl. Akad. Nauk SSSR, **158**, 685 (1964).
10. J. KÄRKKÄINEN. Carbohydr. Res. **14**, 27 (1970).
11. J. N. C. WHYTE and G. A. STRASDINE. Carbohydr. Res. **25**, 435 (1972).
12. V. C. BARRY and J. E. MCCORMICK. Methods in carbohydrate chemistry, I. Academic Press, New York, N.Y. 1962. p. 328.
13. P. ANDREWS, L. HOUGH, and D. B. POWELL. Chem. and Ind. 658 (1956).
14. J. N. C. WHYTE. Can. J. Chem. **47**, 4083 (1969).
15. P. A. SANDFORD and H. E. CONRAD. Biochemistry, **5**, 1508 (1966).
16. S. HAKOMORI. J. Biochem. Tokyo, **55**, 205 (1964).
17. N. K. KOCHETKOV and O. S. CHIZHOV. Adv. Carbohydr. Chem. **21**, 39 (1966).
18. H. BJÖRNDAL, C. G. HELLERQUIST, B. LINDBERG, and S. SVENSSON. Angew. Chem. Int. Ed. **9**, 610 (1970).
19. J. N. C. WHYTE. Unpublished results.

Can. J. Chem. Downloaded from www.nrcresearchpress.com by 210.87.254.42 on 09/05/12
For personal use only.

Fluorine N.M.R. Spectra of Sulfur, Phosphorus, and Silicon Fluorides: Hydrolysis and Intra- and Intermolecular Mechanisms of Fluorine Exchange

JAMES ANDREW GIBSON, DAVID GEORGE IBBOTT, AND ALEXANDER F. JANZEN

Department of Chemistry, University of Manitoba, Winnipeg, Manitoba, R3T 2N2

Received February 15, 1973

The fluorine n.m.r. spectra of SF_4, $[(CH_3)_2CH]_2NSF_3$, $PF_5{:}O(C_2H_5)_2$, SiF_5^-, $SiF_5{:}NH_3^-$, and $SiF_5{:}HN(C_2H_5)_2^-$ have been recorded after treatment of glassware and reagents with $[(CH_3)_3Si]_2NH$ to remove H_2O and HF impurities. A mechanism of intramolecular and intermolecular fluorine exchange, involving Lewis acid – Lewis base interaction and rapid equilibration of five and six coordinate geometries, is proposed.

Les spectres r.m.n. du fluor pour le SF_4, $[(CH_3)_2CH]_2NSF_3$, $PF_5{:}O(C_2H_5)_2$, SiF_5^-, $SiF_5{:}NH_3^-$ et $SiF_5{:}HN(C_2H_5)_2^-$ ont éte enregistrés, après avoir traité la verrerie ainsi que les réactifs avec du $[(CH_3)_3Si]_2NH$ afin d'éliminer les impuretés attribuables à l'H_2O et au HF. On propose un mécanisme se rattachant à l'échange intramoléculaire et intermoléculaire du fluor, qui impliquerait une interaction acide de Lewis – base de Lewis ainsi qu'une équilibration rapide des géométries à cinq et six coordinats. [Traduit par le journal]

Can. J. Chem., **51**, 3203 (1973)

The stereochemistry and "rigidity" of trigonal bipyramidal molecules has received much attention in recent years and the rapid exchange of axial and equatorial fluorines in phosphorus, sulfur, and silicon fluorides has been explained by various mechanisms, in particular, Berry pseudorotation (1–3), as well as turnstile rotation (4), bimolecular exchange (5–7), collision activated exchange (8), solvent assisted exchange (9), impurity catalyzed exchange (*vide infra*) and others (10).

We have re-emphasized the role of trace amounts of water or hydrogen fluoride in exchange phenomena and demonstrated that the rate of fluorine exchange in $(CH_3)_3SiF$, $(CH_3)_2NSF_3$, and $(C_2H_5)_2NSF_3$ may be reduced by adding silicon–nitrogen compounds such as $(CH_3)_3SiNR_2$ or $[(CH_3)_3Si]_2NH$ which may reduce the concentration of H_2O and HF by chemical reaction (11–13). Additional evidence of the effect of these impurities on the n.m.r. spectra of sulfur, phosphorus, and silicon fluorides is now presented. The results are consistent with Lewis acid – Lewis base interactions and rapid equilibration of five and six coordinate geometries. The proposed mechanism distinguishes between inter- and intramolecular exchange of fluorine atoms.

Results and Discussion

Sulfur Fluorides

The fluorine n.m.r. spectrum of SF_4 has been reported previously by Cotton, George, and Waugh (14), Muetterties and Phillips (7), and Bacon, Gillespie, and Quail (15). The spectra were resolved at different temperatures, suggesting that impurities might be the cause of this discrepancy. The sensitivity of the n.m.r. spectrum of SF_4 to trace catalysts and the possibility of impurity catalyzed exchange was pointed out by Muetterties and Phillips (16). If these impurities are H_2O and HF, then treatment of SF_4 sample with silicon–nitrogen compounds should reduce the concentration of these impurities and further raise the temperature at which resolution is possible.

Silicon–nitrogen compounds react with SF_4, however, if a 2:1 molar ratio of SF_4 and $[(CH_3)_3Si]_2NH$ was used, about 30–40% unreacted SF_4 remained for n.m.r. studies. The volatile components of this reaction, consisting of unreacted SF_4, $(CH_3)_3SiF$, and SOF_2, along with solvent $CFCl_3$, were not separated since this led to loss of resolution, but were condensed into an n.m.r. tube which was sealed and kept at $-196°$ until required for n.m.r. studies. This method was repeated on at least four occasions

Can. J. Chem. Downloaded from www.nrcresearchpress.com by 210.87.254.40 on 09/05/12
For personal use only.

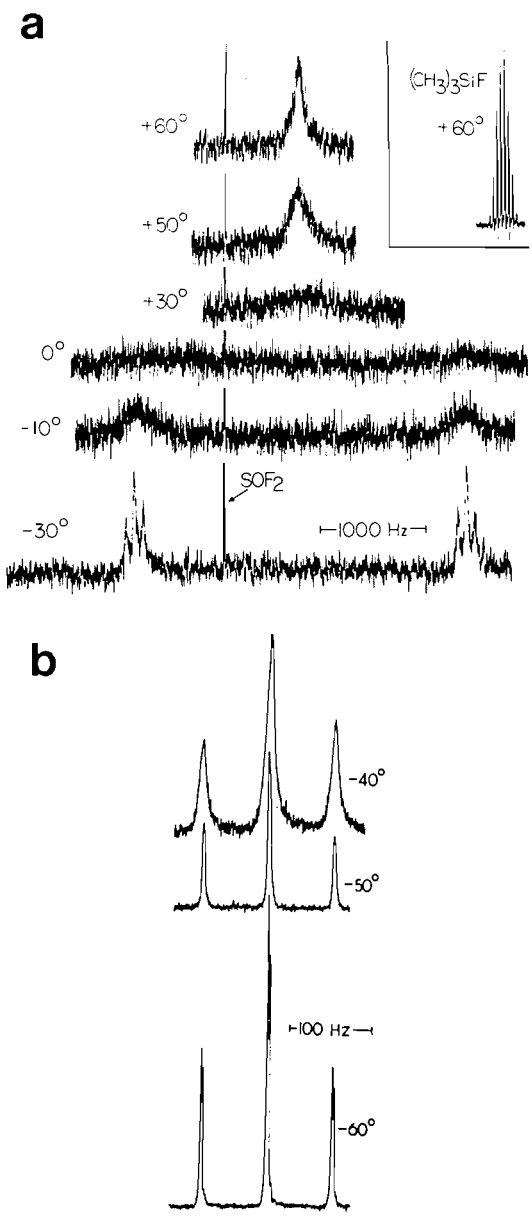

FIG. 1(*a*). Temperature dependent fluorine n.m.r. spectrum of SF_4 in $CFCl_3$ solvent. Sample contained SOF_2 (sharp singlet) and $(CH_3)_3SiF$ (dectet at upper right of figure). (*b*) Low temperature n.m.r. spectrum of SF_4 showing only high field multiplet of symmetrical spectrum, on expanded scale.

and in each case the temperature dependent spectra shown in Fig. 1*a* and 1*b* could be reproduced. Other techniques were unsuccessful. For example, repeating the above procedure with $(CH_3)_3SiN(C_2H_5)_2$ instead of $[(CH_3)_3Si]_2NH$, or treating glassware with $[(CH_3)_3Si]_2NH$ but omitting direct addition to SF_4, gave only poorly resolved spectra.

Once the sample is heated to $+60°$, then resolution is lost on re-cooling. Thus the triplets seen at $-30°$ in Fig. 1*a* do not re-appear until $-60°$, and the resolution seen at $-60°$ in Fig. 1*b* cannot be attained again. On the other hand, if SF_4 is treated with $[(CH_3)_3Si]_2NH$ and gaseous products stored in sealed n.m.r. tube, then after one month at room temperature the spectra of Fig. 1*a* and 1*b* may be reproduced. These results suggest strongly that only *in situ* reaction of $[(CH_3)_3Si]_2NH$ with trace amounts of H_2O and HF is sufficient to remove these contaminants, while transferring SF_4 in vacuum line or heating sample re-introduces contaminants.

The spectra of Fig. 1*a* and *b* may be compared with spectra published previously. The spectrum seen at $-60°$ (Fig. 1*b*) was observed by Gillespie and co-workers at $-90°$ and explained on the basis of an A_2B_2 system. The triplets seen at $-30°$ (Fig. 1*a*) were previously seen at $-60°$ (15), $-85°$ (7), and $-94°$ (14). The half-height width at $+60°$ is about 90 Hz, the same as reported by Muetterties and Phillips at $+23°$ (7). The half-height width increases slightly on raising the temperature to $+70°$, presumably due to more rapid introduction of contaminants. The coupling constants at $-60°$ are identical to those reported by Gillespie and co-workers at $-101°$, while the chemical shift is 3125 Hz, compared to 2935 ± 10 Hz for the neat sample (15).

An activation energy may be estimated from Fig. 1. By inspection, the temperature at which the axial and equatorial fluorines merge into a single peak occurs at about $+15 \pm 5°$, and the collapse of the triplets at about $-18 \pm 5°$. Calculation of τ at the two temperatures (17) gives $\tau = \sqrt{2}/2\pi(3125)$ and $\sqrt{2}/2\pi(78)$ and plot of $-\ln 1/\tau$ *vs.* $1/T$ gives $E_a = 16.3 \pm 5$ kcal/mol. This value for the activation energy may be compared with previous estimates of 4 ± 1 kcal/mol (14) and 4.5 ± 0.8 kcal/mol (17).[1] That a higher activation energy is observed after treatment of SF_4 sample with $[(CH_3)_3Si]_2NH$ supports our assumption that the concentration of H_2O and HF has been reduced and therefore the low energy impurity catalyzed pathway of fluorine exchange is no longer available. The value of E_a

[1]The results of Bacon, Gillespie, and Quail (15) imply an activation energy greater than 4 kcal/mol.

Can. J. Chem. Downloaded from www.nrcresearchpress.com by 210.87.254.40 on 09/05/12
For personal use only.

Can. J. Chem. Downloaded from www.nrcresearchpress.com by 210.87.254.40 on 09/05/12
For personal use only.

may represent only a lower limit to the uncatalyzed exchange process, since we cannot claim that all impurities have been removed, furthermore, the removal of H_2O and HF probably involves equilibrium processes for which the equilibrium constants have not been determined.

The mechanism of the uncatalyzed exchange reaction was not investigated, however, the n.m.r. spectra of Fig. 1*a* and 1*b* appear to rule out fluorine exchange of SF_4 with either SOF_2 or $(CH_3)_3SiF$ up to at least $+60°$ since, during the entire temperature run, the SOF_2 remained as a sharp singlet and $(CH_3)_3SiF$ as a well resolved dectet (J_{FH} = 7.5 Hz).

Previously, we reported the n.m.r. spectra of *N,N*-dialkylaminosulfur trifluorides, R_2NSF_3 where R = CH_3 and C_2H_5 (11). The analogous *N,N*-diisopropylamino derivative was prepared by eq. 1 and the n.m.r. spectrum recorded at

[1] $(CH_3)_3SiN[CH(CH_3)_2]_2 + SF_4 \rightarrow [(CH_3)_2CH]_2NSF_3 + (CH_3)_3SiF$

$-68°$, as shown in Fig. 2. A doublet, $J_{F^aSF^e}$ = 53 Hz, at -61.9 p.p.m. is assigned to the axial fluorines and the triplet, $J_{F^eSF^a}$ = 53 Hz, at -18.3 p.p.m. is assigned to the equatorial fluorine. Each component of the triplet appears to have triplet fine structure, with $J_{F^eSNCH} \sim 4$ Hz. Because of the similarity of chemical shifts and coupling constants to those of the *N,N*-dimethyl- and *N,N*-diethyl-analogs, the synthesis of $[(CH_3)_2CH]_2NSF_3$ was carried out only once and no attempt was made to improve the resolution of Fig. 2.

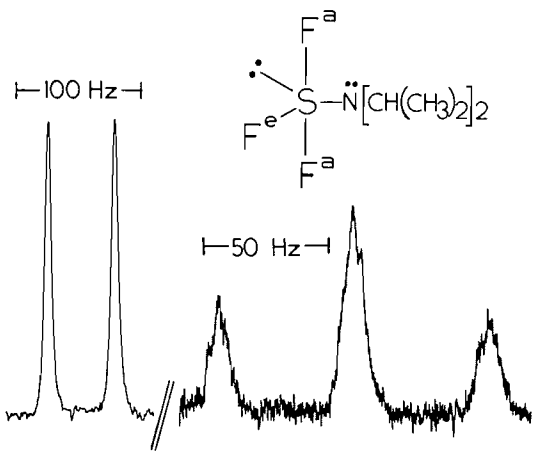

FIG. 2. Fluorine n.m.r. spectrum of $[(CH_3)_2CH]_2NSF_3$ at $-68°$.

Phosphorus and Silicon Fluorides

Since ^{31}P and ^{29}Si (natural abundance 4.67%) have spin 1/2, n.m.r. may distinguish between intermolecular and intramolecular fluorine exchange. Intermolecular exchange involves bond breaking and loss of P—F or Si—F coupling, whereas intramolecular exchange retains bonding and coupling. In the case of sulfur fluorides it is difficult to establish whether exchange is inter- or intramolecular since sulfur lacks a convenient spin.

An n.m.r. study of the diethylamine catalyzed hydrolysis of trimethylfluorosilane established that fluorine exchange occurs via an intermolecular mechanism with loss of ^{29}Si—F coupling

[2] $(CH_3)_3SiF + H_2O \rightleftarrows (CH_3)_3SiOH + HF$

(12). On the basis of the kinetics and rate expression, it appeared that one or two H_2O molecules may coordinate to $(CH_3)_3SiF$ in the transition state, prior to Si—F bond breaking. Therefore, depending on the symmetry of the molecule, a rapid pre-equilibrium involving water coordinated to the central atom may result in an observable intramolecular averaging of fluorine environments. If intramolecular exchange involving H_2O is too rapid on the n.m.r. time scale, perhaps other Lewis bases such as amines or ethers may slow down intramolecular exchange.

Phosphorus pentafluoride is known to form 1:1 complexes with a variety of Lewis bases such as ethers, sulfoxides, amines, amides, and esters (18–20). The structure of the PF_5:base complex was shown to be octahedral on the basis of the doublet–quintuplet fine structure observed in the ^{19}F n.m.r. In the case of $PF_5:O(C_2H_5)_2$, only a pair of doublets, but not the pair of quintuplets, was resolved at $-78°$, while on warming the pair of doublets merged into single peaks. Loss of fine structure, but retention of P—F coupling, as required for intramolecular fluorine exchange, was attributed to the rapid equilibrium (18).

[3] $PF_5 + \text{base} \rightleftarrows PF_5\text{:base}$

A re-investigation of the ^{19}F n.m.r. spectrum of $PF_5:O(C_2H_5)_2$ in excess diethyl ether (molar ratio 1:4) showed some improvement in resolution. As seen in Fig. 3, the pair of quintuplets assigned to F^a may be observed at $-65°$. On warming to $-40°$, the quintuplets become two broad peaks while at $-20°$ only a broadened doublet (P—F coupling) remains. The coupling constants at $-65°$ are J_{F^aP} = 745 Hz, J_{F^bP} = 790

Can. J. Chem. Downloaded from www.nrcresearchpress.com by 210.87.254.40 on 09/05/12
For personal use only.

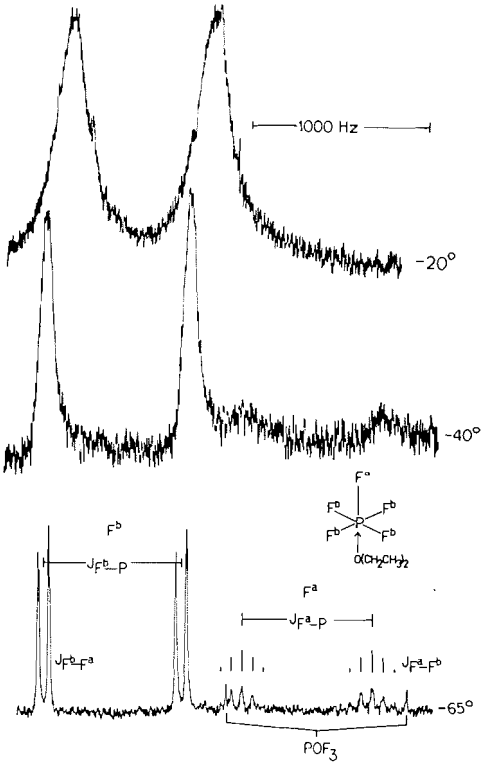

FIG. 3. Temperature dependent fluorine n.m.r. spectrum of PF_5:$O(C_2H_5)_2$ adduct. Sample contained some POF_3.

Hz, and $J_{F^aF^b}$ = 62 Hz, and the chemical shifts of F^b and F^a are +66.3 and +86.0 p.p.m., respectively. At −20° the averaged chemical shift is +69.6 p.p.m. and the averaged coupling constant J_{FP} = 820 Hz, The averaged values of the chemical shift and coupling constant at −20° are between the values of the weighted averages at −65° and free PF_5,[2] as required if the equilibrium of eq. 3 shifts to the left with increasing temperature.

An activation energy may be estimated from Fig. 3 (and other spectra not shown). The temperature at which axial and basal fluorines merge into a doublet occurs at about −30 ± 5°, and the loss of axial to basal fluorine coupling occurs at about −55 ± 5°, hence $\tau = \sqrt{2}/2\pi(1111)$ and $\sqrt{2}/2\pi(62)$ and E_a = 12.2 ± 5 kcal/mol.

In addition to the intramolecular fluorine exchange process of eq. 3, the spectrum shown in Fig. 3 provides evidence for an intermolecular process, in which P—F bond breaking occurs. This is demonstrated by the significant line broadening above −20°, which is most likely due to more rapid hydrolysis or decomposition of the PF_5 – diethyl ether solution at higher temperatures. Consistent with this view, it was found that line broadening is a function of time, for example, the half-height width increased from 55 to 150 Hz over a period of 85 min at +38°. This result would argue against self-ionization or bimolecular exchange as the mechanism of intermolecular fluorine exchange in these PF_5 – diethyl ether solutions.

The fluorine n.m.r. spectra of pentafluorosilicates have been reported by Klanberg and Muetterties (22) who found that SiF_5^-, $RSiF_4^-$, and $R_2SiF_3^-$ showed spectroscopic equivalence of fluorine atoms at room temperature, while $(C_6H_5)_2SiF_3^-$ showed axial and equatorial fluorines at lower temperature. It was suggested that the dominant exchange process for the equilibration of fluorine atom environments in SiF_5^- probably is intramolecular Berry pseudorotation; in addition the loss of F—^{29}Si coupling above −60° suggested an intermolecular mechanism, due either to a dissociative or associative (fluorine bridging) process. At the same time, Klanberg and Muetterties noted the influence of impurities on the n.m.r. spectra and, interestingly, proposed the existence of $CH_3SiF_4(H_2O)^-$.

Conclusive evidence that intermolecular fluorine exchange in SiF_5^- is due to hydrolysis is presented in Fig. 4. Figure 4*a* shows the fluorine n.m.r. spectrum of re-crystallized $(n\text{-}C_3H_7)_4N^+SiF_5^-$ in CH_2Cl_2 solvent at +38°. Since no F—^{29}Si coupling is observed, SiF_5^- must be undergoing rapid intermolecular fluorine exchange. Figure 4*b* shows the n.m.r. spectrum of the same sample after addition of $[(CH_3)_3Si]_2$-

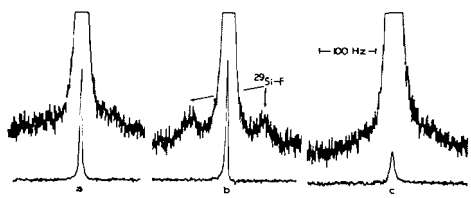

FIG. 4. Fluorine n.m.r. spectra at +38° of $(n\text{-}C_3H_7)_4N^+SiF_5^-$ in CH_2Cl_2 solution (*a*) untreated; (*b*) after addition of $[(CH_3)_3Si]_2NH$ (0.0062 g); (*c*) after addition of H_2O (0.001 g). The high amplitude spectra were obtained with fast sweep (4 Hz/s), high Rf power and high bandwidth (4 Hz) and without spinning of sample. Chemical shift of centre singlet peak is +136.7 p.p.m.

[2]The chemical shift of PF_5 is reported as +75.87 p.p.m. and J_{FP} = 916 Hz (7, 21).

Can. J. Chem. Downloaded from www.nrcresearchpress.com by 210.87.254.40 on 09/05/12
For personal use only.

NH. Now F—^{29}Si coupling (140 Hz) is clearly evident, hence intermolecular exchange has been slowed down. Introduction of H_2O results once more in loss of F—^{29}Si coupling, as seen in Fig. 4*c*. These results are entirely consistent with hydrolysis as the mechanism of intermolecular fluorine exchange.

[4] $$SiF_5^- + H_2O \rightleftarrows SiF_4OH^- + HF$$

While the evidence based on F—^{29}Si coupling shows that intermolecular exchange may be slowed down, the fact that all five fluorine atoms give a single peak at $+38°$ (and also at $-90°$) is proof that a lower energy intramolecular mechanism of exchange is still equilibrating axial and equatorial fluorines. If intramolecular exchange is due to Lewis acid – Lewis base interactions, then a variable temperature n.m.r. study of SiF_5^- and a suitable base might provide experimental evidence on this point.

Adducts of SiF_5^- are known. The enthalpies of dissociation of ammonia and amine adducts of tetraalkylammonium pentafluorosilicates have been determined by Wharf and Onyszchuk (23). Clark and co-workers concluded from infrared studies that a variety of Lewis bases form adducts SiF_5:base$^-$, where base is $(C_2H_5)_2NH$, $(C_2H_5)_3N$, $(n\text{-}C_3H_7)_3N$, C_5H_5N, and $(C_2H_5)_3P$ (24).

Ammonia was added to a solution of $(n\text{-}C_3H_7)_4N^+SiF_5^-$ in CH_2Cl_2 which was treated with $[(CH_3)_3Si]_2NH$. The molar ratio of NH_3 to SiF_5^- was 14:1.0. As seen in Fig. 5, the variable temperature n.m.r. spectrum shows a sharp single peak at $+123.6$ p.p.m. at $+24°$ which broadens on cooling and eventually splits into two components, a low field peak at $+118.6$ p.p.m. assigned to the four basal fluorines, F^b, and a peak at $+136.6$ p.p.m. assigned to the apical fluorine, F^a. The spectrum is reversible on warming the sample and the results are consistent with rapid equilibrium:

[5] $$SiF_5^- + NH_3 \rightleftarrows SiF_5{:}NH_3^-$$

This behavior is very similar to that of the PF_5 and $(C_2H_5)_2O$ system.

The equilibrium of reaction 5 involves intramolecular fluorine exchange and requires retention of F—^{29}Si coupling. This coupling could be observed at $+24°$ ($J_{F^{29}Si} = 120 \pm 5$ Hz), as well as at $-83°$ ($J_{F^a{}^{29}Si} = 120 \pm 10$ Hz and $J_{F^b{}^{29}Si} = 125 \pm 5$ Hz). Coupling between axial and basal fluorines is small, probably $J_{F^aF^b} \sim 3$ Hz. Klanberg and Muetterties found previously

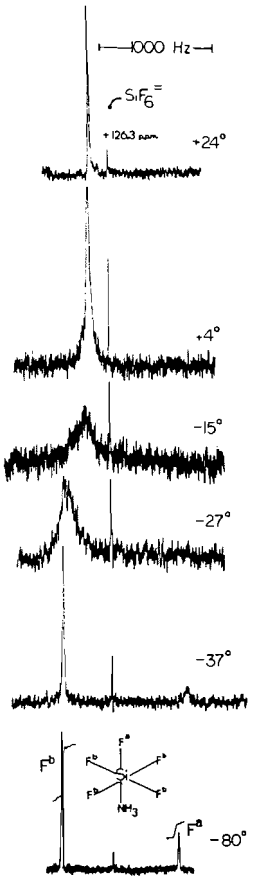

FIG. 5. Temperature dependent fluorine n.m.r. spectrum of $(n\text{-}C_3H_7)_4N^+SiF_5^-$ (0.11 g) and NH_3 (0.09 g) in CH_2Cl_2 solution (0.5 ml).

that coupling between axial and equatorial fluorines in $(C_6H_5)_2SiF_3^-$ is probably <5 Hz (22).

The temperature at which axial and basal fluorines merge into a single averaged peak is estimated, by inspection of Fig. 5, as $-20 \pm 5°$. Unfortunately, the temperature at which F^a—F^b coupling is lost could not be estimated because of the small coupling constant. In an attempt to observe coupling to nitrogen, the complex $SiF_5{:}^{15}NH_3^-$ was prepared, but the FSi—^{15}N coupling at low temperature was also small (<15 Hz) and partly obscured by FSi—^{15}NH coupling, hence an activation energy could not be calculated for the exchange process of reaction 5.

The behavior of the diethylamine adduct of SiF_5^- was studied and found to be similar to that of the ammonia adduct. The variable temperature n.m.r. spectrum of a solution containing 5.8:1.0 molar ratio of $(C_2H_5)_2NH$ to SiF_5^- is

Can. J. Chem. Downloaded from www.nrcresearchpress.com by 210.87.254.40 on 09/05/12
For personal use only.

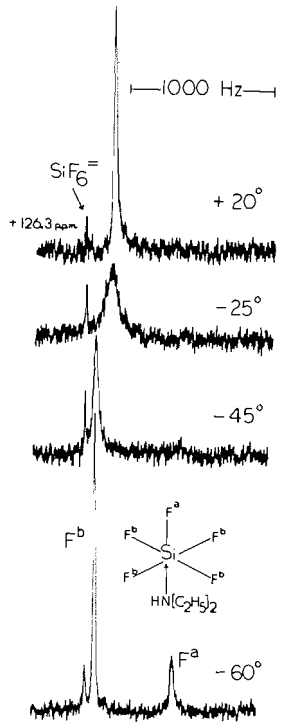

FIG. 6. Temperature dependent fluorine n.m.r. spectrum of $(n\text{-}C_3H_7)_4N^+SiF_5^-$ (0.077 g) and $(C_2H_5)_2NH$ (0.11 g) in CH_2Cl_2 solution (0.5 ml).

shown in Fig. 6. At +20° a single peak is observed at +129.8 p.p.m. which broadens and, on further cooling to −60°, splits into two components, a low field peak at +127.5 p.p.m. assigned to the basal fluorines and an upfield peak at +136.9 p.p.m. assigned to the apical fluorine. By inspection of Fig. 6, the temperature at which axial and basal fluorines merge is estimated as $-35 \pm 5°$.

Comparison of the chemical shifts of ammonia and diethylamine adducts at low temperature shows that the apical fluorines are in nearly identical positions, however, the basal fluorines vary, going from +118.6 p.p.m. for the ammonia adduct to +127.5 p.p.m. for the diethylamine adduct. In both cases, the chemical shift at room temperature is the weighted average of the low temperature spectrum, therefore the equilibrium involving SiF_5^- and base must be essentially to

[6] $$SiF_5^- + \text{base} \rightleftarrows SiF_5\text{:base}^-$$

the right, consistent with the large excess of base used, and changes in the position of equilibrium are not detected by changes in chemical shift.

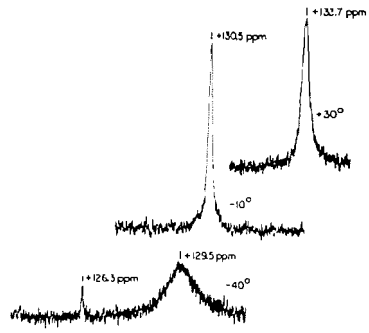

FIG. 7. Temperature dependent fluorine n.m.r. spectrum of $(n\text{-}C_3H_7)_4N^+SiF_5^-$ (0.11 g) and $(C_2H_5)_2NH$ (0.083 g) in CH_2Cl_2 solution (0.5 ml). Spectrum below −40° is identical to that of Fig. 6.

Such changes may be detected by reducing the molar ratio of $(C_2H_5)_2NH$ to SiF_5^- to 3.1:1.0. As seen in Fig. 7, the chemical shift varies from +133.7 p.p.m. at +30° to +129.5 p.p.m. at −40°. Below −40° the spectrum is identical to the low temperature region of Fig. 6. The equilibrium of reaction 6 therefore shifts to the left with increasing temperature, consistent with the behavior observed for the PF_5 and diethyl ether system.

Mechanism of Fluorine Exchange

A mechanism of fluorine exchange which describes the effect of trace amounts of H_2O and HF and distinguishes clearly between intermolecular and intramolecular fluorine exchange is summarized in reactions 7 and 8.

[7] $$R_xM\text{—}F + H_2O \rightleftarrows R_xM\text{—}OH + HF$$

[8]

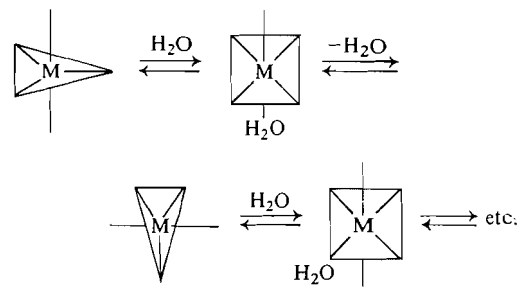

Reaction 7 illustrates an equilibrium leading to intermolecular fluorine exchange with loss of coupling as the bond between fluorine and the central atom is broken.

Reaction 8 illustrates intramolecular exchange. Lewis bases such as H_2O, NH_3, $(C_2H_5)_2NH$, or $(C_2H_5)_2O$ may interact with Lewis acids such as

Can. J. Chem. Downloaded from www.nrcresearchpress.com by 210.87.254.40 on 09/05/12
For personal use only.

PF_5, SiF_5^- etc., resulting in rapid interconversion between five and six coordinate geometries. The positions of the fluorine atoms are therefore averaged, but coupling of fluorine to the central atom is retained.

In the case of hydrolysis of reactive fluorides. Reaction 8 may be viewed as the first step of the reaction; a rapid pre-equilibrium involving coordination of water to the central atom, followed by elimination of HF, as in reaction 7.

Experimental

General procedures have been described previously (11, 12). SF_4 (Matheson Co.), PF_5 (PCR, Gainesville), and $[(CH_3)_3Si]_2NH$ (Alfa) were purified by trap-to-trap distillation and stored in a metal vacuum system. Ammonia-^{15}N (99% isotopic purity) was purchased from Stohler Isotope Chemicals, Montreal. $(n\text{-}C_3H_7)_4NSiF_5$ was prepared and purified by the method of Clark and co-workers and characterized by its m.p. and i.r. spectrum (24). Diisopropylamine (6.0 g, 60 mmol) was dried over sodium and condensed onto $(CH_3)_3SiCl$ (2.5 g, 250 mmol); reaction occurred on warming to room temperature to give $(CH_3)_3SiN[CH(CH_3)_2]_2$, which was purified by distillation at $50°/10^{-3}$ cm and identified by ^1H n.m.r.: septet(H), $J = 6.7$ Hz at -2.9 p.p.m.; doublet(CH_3), $J = 6.7$ Hz at -0.7 p.p.m.; and singlet($(CH_3)_3Si$) at $+0.2$ p.p.m. Chemical shifts are relative to external tetramethylsilane.

N.m.r. spectra were recorded on a Varian A-56/60A spectrometer equipped with variable temperature probe, using 56.4 and 60 MHz for fluorine and proton, respectively. Temperatures were calibrated with the aid of a variable temperature *vs.* chemical shift chart (25). Fluorine chemical shifts are relative to internal $CFCl_3$.

Sulfur Tetrafluoride

The Pyrex U-tube, shown below, was treated with $[(CH_3)_3Si]_2NH$ by gently refluxing for several hours, then evacuated at 10^{-4} mm and flamed out. $[(CH_3)_3Si]_2NH$ (0.19 g, 1.2 mmol) and SF_4 (0.26 g, 2.4 mmol) were condensed into the U-tube at $-196°$. A vigorous

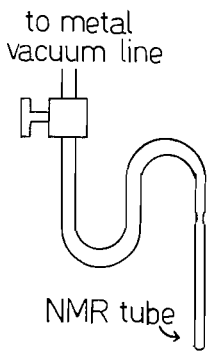

reaction occurred on warming to 25°. Only the volatile components of the reaction mixture, consisting of about 30–40% unreacted SF_4 as well as $(CH_3)_3SiF$ and SOF_2, identified by n.m.r. and mass spectral investigation, were condensed into the n.m.r. tube, along with solvent $CFCl_3$ (0.5 ml) and the n.m.r. tube sealed and kept at $-196°$ until required for n.m.r. study. Gaseous products were not separated since this led to loss of resolution. At the completion of the n.m.r. studies the n.m.r. tube was opened and SF_4 separated by trap-to-trap distillation and identified by i.r. and mass spectrometry.

N,N-Diisopropylaminosulfur Trifluoride

SF_4 (0.26 g, 2.4 mmol) was condensed onto $(CH_3)_3SiN[CH(CH_3)_2]_2$ (0.42 g, 2.4 mmol) in a U-tube at $-196°$ and allowed to react on warming to 25°, according to the procedure described previously for the analogous *N,N*-dimethyl- and *N,N*-diethyl- derivatives (11). The product, $[(CH_3)_2CH]_2NSF_3$, as well as $(CH_3)_3SiF$ and some SOF_2, were condensed into the n.m.r. tube along with solvent $CFCl_3$ (0.5 ml) and the spectrum recorded at $-68°$. $[(CH_3)_2CH]_2NSF_3$ was identified on the basis of the similarity of its ^{19}F n.m.r. spectrum to that of the *N,N*-dimethyl- and *N,N*-diethyl- analogs.

Phosphorus Pentafluoride – Diethyl Ether Complex

The $PF_5{:}O(C_2H_5)_2$ complex was prepared by condensing PF_5 (0.15 g, 1.3 mmol) and $(C_2H_5)_2O$ (0.43 g, 5.8 mmol) into a silylated (with $[(CH_3)_3Si]_2NH$) and flamed out n.m.r. tube, which was sealed and kept at $-196°$ until required for n.m.r. studies. The variable temperature n.m.r. spectrum of the complex is shown in Fig. 3. Attempts to slow down the rate of exchange in uncomplexed PF_5 have, so far, been unsuccessful.

Pentafluorosilicate Ammonia and Diethylamine Adducts

Solutions of $(n\text{-}C_3H_7)_4NSiF_5$ were made up by weighing out suitable amounts into dry n.m.r. tubes and adding CH_2Cl_2 as solvent through silicone septum cap. A small amount of $[(CH_3)_3Si]_2NH$ was added through cap to assist in "drying" solution. The ^{19}F n.m.r. spectrum at $+38°$ gave a sharp singlet at $+136.7$ p.p.m., with $J_{F^{29}Si} = 140 \pm 5$ Hz (lit. $+136.0$ p.p.m. and $J_{F^{29}Si} = 148 \pm 2$ Hz at $-66°$ (22). Ammonia and diethylamine were condensed onto these solutions and the n.m.r. tube sealed. The ^{19}F n.m.r. spectra of the adducts are shown in Figs. 5, 6, and 7.

The financial assistance of the National Research Council of Canada and the Petroleum Research Fund, administered by the American Chemical Society, is gratefully acknowledged. We also thank NRCC for a post graduate scholarship (to J.A.G.).

1. R. S. Berry. J. Chem. Phys. **32**, 933 (1960); W. Mahler and E. L. Muetterties. Inorg. Chem. **4**, 1520 (1965); R. Schmutzler. Angew. Chem. Int. Ed. **4**, 496 (1965).
2. G. M. Whitesides and H. L. Mitchell. J. Am. Chem. Soc. **91**, 5384 (1969).
3. R. R. Holmes. Acc. Chem. Res. **5**, 296 (1972); L. C. Hoskin and R. C. Lord. J. Chem. Phys. **46**, 2402 (1967; R. S. Berry, M. Tamres, C. J. Ballhausen, and H. Johansen. Acta Chem. Scand. **22**, 231 (1968); J. B. Florey and L. C. Cusachs. J. Am. Chem. Soc. **94**, 3040 (1972); R. Hoffmann, J. M. Howell and E. L. Muetterties. J. Am. Chem. Soc. **94**, 3047 (1972); A. Rauk, L. C. Allen, and K. Mislow. J. Am.

Chem. Soc. **94**, 3035 (1972); J. I. MUSHER. J. Am. Chem. Soc. **94**, 5662 (1972).
4. P. GILLESPIE, P. HOFFMAN, H. KLUSACEK, D. MARQUARRDING, S. PFOHL, F. RAMIREZ, E. A. TSOLIS, and I. UGI. Angew. Chem. Int. Ed. **10**, 687 (1971); and other papers by Ramirez and co-workers.
5. R. L. REDINGTON and C. V. BERNEY. J. Chem. Phys. **43**, 2020 (1965); R. A. FREY, R. L. REDINGTON, and A. L. K. ALJIBURY. J. Chem. Phys. **54**, 344 (1971).
6. T. A. FURTSCH, D. S. DIERDORF, and A. H. COWLEY. J. Am. Chem. Soc. **92**, 5759 (1970).
7. E. L. MUETTERTIES and W. D. PHILLIPS. J. Am. Chem. Soc. **81**, 1084 (1959).
8. S. BROWNSTEIN. Can. J. Chem. **45**, 1711 (1967).
9. J. D. MACOMBER. J. Magn. Resonance, **1**, 677 (1969).
10. W. MAHLER and E. L. MUETTERTIES. J. Chem. Phys. **33**, 636 (1960); J. H. LETCHER and J. R. VAN WAZER. J. Chem. Phys. **45**, 2926 (1966); E. L. MUETTERTIES. J. Am. Chem. Soc. **91**, 4115 (1969); J. I. MUSHER. Angew. Chem. Int. Ed. **8**, 54 (1969).
11. D. G. IBBOTT and A. F. JANZEN. Can. J. Chem. **50**, 2428 (1972).
12. J. A. GIBSON and A. F. JANZEN. Can. J. Chem. **50**, 3087 (1972).
13. A. F. JANZEN, J. A. GIBSON, and D. G. IBBOTT. Inorg. Chem. **11**, 2853 (1972).
14. F. A. COTTON, J. W. GEORGE, and J. S. WAUGH. J. Chem. Phys. **28**, 994 (1958).
15. J. BACON, R. J. GILLESPIE, and J. W. QUAIL. Can. J. Chem. **41**, 1016 (1963).
16. E. L. MUETTERTIES and W. D. PHILLIPS. J. Chem. Phys. **46**, 2861 (1967).
17. J. A. POPLE, W. G. SCHNEIDER and H. J. BERNSTEIN. High-resolution nuclear magnetic resonance. McGraw–Hill, New York, N.Y. 1959. p. 223.
18. E. L. MUETTERTIES, T. A. BITHER, M. W. FARLOW, and D. D. COFFMAN. J. Inorg. Nucl. Chem. **16**, 52 (1960).
19. A. A. WOOLF. J. Inorg. Nucl. Chem. **3**, 285 (1956).; D. H. BROWN, G. W. FRASER, and D. W. A. SHARP. J. Chem. Soc. (A), 171 (1966); I. K. GREGOR. Aust. J. Chem. **18**, 1485, 2035 (1965).
20. L. LUNAZZI and S. BROWNSTEIN. J. Magn. Resonance, **1**, 119 (1969).
21. C. H. DUNGAN and J. R. VAN WAZER. Compilation of reported ^{19}F n.m.r. chemical shifts. Wiley–Interscience, New York, N.Y. 1970. no. 532.
22. F. KLANBERG and E. L. MUETTERTIES. Inorg. Chem. **7**, 155 (1968).
23. I. WHARF and M. ONYSZCHUK. Can. J. Chem. **50**, 3450 (1972); I. WHARF and M. ONYSZCHUK. Can. J. Chem. **48**, 2250 (1970).
24. H. C. CLARK, K. R. DIXON, and J. G. NICOLSON. Inorg. Chem. **8**, 450 (1970).
25. A. L. VAN GEET. Anal. Chem. **42**, 679 (1970).

Can. J. Chem. Downloaded from www.nrcresearchpress.com by 210.87.254.40 on 09/05/12
For personal use only.

The Photochemically Produced Ketyl of Perfluorobenzophenone: Electron Spin Resonance Studies of Solvent Effects[1]

FREDERICK PETER SARGENT AND MARSHALL GRANT BAILEY

Research Chemistry Branch, Whiteshell Nuclear Research Establishment, Atomic Energy of Canada Limited, Pinawa, Manitoba, R0E 1L0

Received April 5, 1973

The ketyl radical is formed when solutions of perfluorobenzophenone are photolyzed with u.v. light. The radical was identified by electron spin resonance (e.s.r.) studies of the effects of solvent, temperature, chemical exchange, and deuteration on the spectra. Solvent mixtures of cyclohexane and ethanol gave spectra which were very sensitive to the mole fraction of alcohol in the range 0–1%. An equilibrium constant for solvent molecule exchange has been deduced.

Le radical cétyle est produit lorsque des solutions de perfluorobenzophénone sont photolysées avec de la lumière ultraviolette. Le radical a pu être identifié grâce à la résonance de spin électronique impliquant des effets de solvant, de température, d'échange chimique et de deutération. Des mélanges de solvant, cyclohexane-éthanol, ont conduit à des spectres où l'on a dénoté une très grande sensibilité vis-à-vis la fraction molaire d'alcool dans l'intervalle allant de 0–1%. De même, on a déduit une constante d'équilibre pour l'échange solvant–molécule. [Traduit par le journal]

Can. J. Chem., 51, 3211 (1973)

Introduction

In an earlier publication we reported the e.s.r. spectrum observed during the photolysis of perfluorobenzophenone, $(C_6F_6)_2CO$, in 2-propanol (1). This was assigned to the perfluorobenzophenone ketyl $(C_6F_6)_2\dot{C}OH$. Our studies have now been extended to other solvents to show that the observed spectra are indeed due to the ketyl, and not to radicals derived from the addition of solvent radicals to the keto group or the aromatic rings of perfluorobenzophenone (PFB). It will be shown that the spectra are very similar in all the solvents, and the identity of the radical is established as the ketyl.

Experimental

E.s.r. spectra were recorded with a Varian V4500 spectrometer. Aqueous alkaline solutions of Fremy's salt were used for magnetic field sweep calibrations, taking $a_N = 13.0$ G.

Solutions of perfluorobenzophenone (PFB) in various solvents were photolyzed *in situ* with a 100 W compact mercury arc lamp. The samples were held in 4 mm o.d. quartz tubes or in flat cells, depending on the dielectric properties of the solvent. All chemical reagents were used as received, with the exception of cyclohexane, which was dried with sodium wire.

Theoretical e.s.r. spectra were computer-simulated, and plotted with appropriate scaling, to permit direct comparison with the experimental charts. When the line positions and intensities agreed, it was assumed that the interpretation was correct.

[1]AECL No. 4561.

Molecular orbital calculations of the coupling constants and spin densities were of the McLachlan type (2), using the heteroatom method (3).

Results and Discussion

Spectra in Alcohols and Other Solvents

Photolysis of PFB in methanol, ethanol, and 2-propanol gave different spectra, but only because of differences in the value of one hyperfine splitting (h.f.s.). The spectrum in 2-propanol was poorly resolved at room temperature, but was much improved at +80 °C; a typical spectrum at +80 °C is shown in Fig. 1*a*. The more obvious features were interpreted visually, but it was necessary to use computer simulation of the spectrum to arrive at a complete interpretation. The simulated 2-propanol spectrum of Fig. 1*b* was computed by assuming that the unpaired electron interacts as follows:

(*i*) A Lorentzian line shape with peak to peak line width of 0.25 G.

(*ii*) Two equivalent nuclei of spin $\frac{1}{2}$ and h.f.s. of 8.23 G.

(*iii*) Four equivalent nuclei of spin $\frac{1}{2}$ and h.f.s. of 4.66 G.

(*iv*) Four equivalent nuclei of spin $\frac{1}{2}$ and h.f.s. of 1.77 G.

(*v*) One nucleus of spin $\frac{1}{2}$ and h.f.s. of 2.42 G.

The agreement between the experimental and the simulated spectra of Fig. 1*a* and *b* is good, and was shown to be almost perfect for expanded

Can. J. Chem. Downloaded from www.nrcresearchpress.com by 210.87.254.5 on 09/05/12
For personal use only.

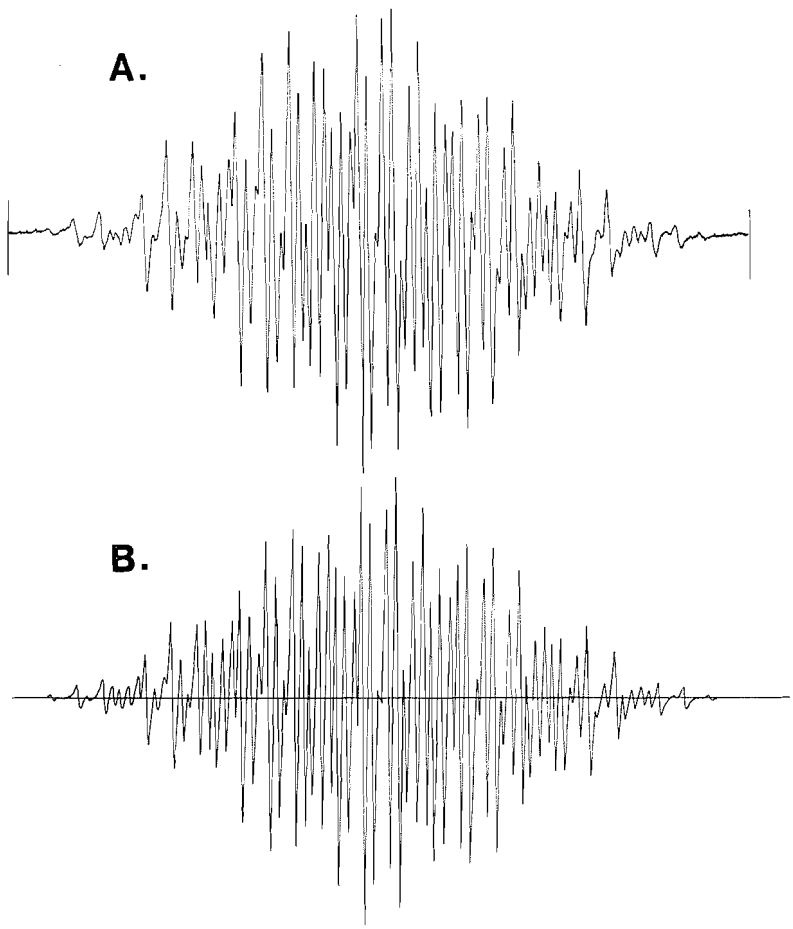

FIG. 1. (*a*) E.s.r. spectrum observed during the photolysis of perfluorobenzophenone in 2-propanol at 80 °C. Sweep width 50 G. (*b*) Simulated spectrum using values of Table 1.

charts recorded at slower magnetic-field sweep speeds. We have identified the radical as the ketyl of PFB, $(C_6F_6)_2\dot{C}OH$, for reasons explained in the next section. The h.f.s. are assigned to the positions in the radical listed in Table 1, on the basis of symmetry and simple molecular orbital calculations. The h.f.s. of 2.42 G is due to the ketyl hydroxyl proton, and the others to fluorine nuclei. No line width variations were observed in the ketyl spectra in contrast to those of partly fluorinated nitrobenzene anions (4, 5) and the cations of perfluorinated hydrocarbons (6).

The spectra in methanol and ethanol, although different in appearance, have similar h.f.s. to those in 2-propanol. The main difference is in the magnitude of the hydroxyl proton coupling, a_{OH}^{H}.

Photolysis of PFB in the other solvents of Table 1, with the exception of cyclohexane, gave very similar spectra, which were all assigned to the ketyl radical.

Identity and Mechanism of Formation of the Observed Radicals

The motive for this study was to substantiate our previous assignment (1) of the e.s.r. spectra to the PFB ketyl. There is always the possibility of an adduct radicals being formed from the addition of a solvent radical to the PFB. The similarity of the spectra, apart from the magnitude of a_{OH}^{H}, in methanol, ethanol, and 2-pro-

Can. J. Chem. Downloaded from www.nrcresearchpress.com by 210.87.254.5 on 09/05/12
For personal use only.

TABLE 1. Nuclear hyperfine coupling constants (G) for the PFB ketyl in various solvents

Solvent	T(°C)	a_{OH}^{H}	a_{ortho}^{F}	a_{meta}^{F}	a_{para}^{F}	$W_{pp}^{(a)}$
CH_3OH	10	1.89	4.47	1.89	8.25	0.32
CD_3OD	20	—	4.48	1.83	8.04	0.70
CD_3OD[e]	70	0.30[d]	—	—	—	—
C_2H_5OH	80	2.22	4.68	1.75	8.20	0.23
2-PrOH	80	2.42	4.66	1.77	8.23	0.25
Perdeutero 2-PrOH[e]	80	0.33[d]	4.61	1.75	8.17	0.18
MTHF[b]	90	2.37	4.55	1.76	8.13	0.29
TEA[c]	20	1.47	4.37	1.47	8.06	0.40
Cyclohexane	40	0.0	4.92	1.99	8.58	0.36
Cyclohexane + 1 vol of EtOH	40	1.86	4.61	1.84	8.32	0.37
Cyclohexane + 1 vol of CD_3OD	40	0.00	4.54	1.83	8.24	0.70

[a]Full peak to peak first derivative line width.
[b]MTHF is 2-methyltetrahydrofuran.
[c]TEA is triethylamine.
[d]Deuterium coupling.
[e]High resolution.

panol, discounts this possibility. The adduct radicals would be

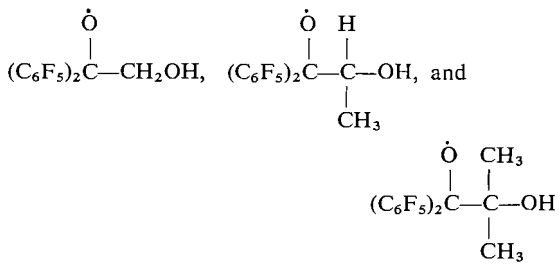

respectively. These would be expected to give vastly different spectra, as would also radicals derived from addition to the aromatic rings. Therefore we are confident that the species observed during the photolysis of PFB in all the solvents of Table 1 is the ketyl. In addition, the magnitudes of a_{OH}^{H} for the hydroxyl proton h.f.s. are in approximate agreement with values for the unfluorinated benzophenone ketyl (7).

The mechanism for the formation of the ketyl radical is probably similar to that generally accepted for benzophenone itself, *i.e.* reactions 1–3, where superscript *S and *T refer to electronically excited singlet and triplet states respectively. In the case of alcohols, R· may further reduce PFB to the ketyl.[2]

[1] $$(C_6F_5)_2CO \rightarrow (C_6F_5)_2CO^{*S}$$

[2] $$(C_6F_5)_2CO^{*S} \rightarrow (C_6F_5)_2CO^{*T}$$

[3] $$(C_6F_5)_2CO^{*T} + RH \rightarrow (C_6F_5)_2\dot{C}OH + R\cdot$$

[2]See reference 18.

To provide evidence for the existence of triplet PFB, we performed photosensitization experiments in the glassy state at 77 °K similar to those reported by Farmer *et al.* (8) for benzophenone. Solutions of PFB and naphthalene in a mixed solvent consisting of two volumes of absolute ethanol and one volume of diethyl ether were frozen in liquid nitrogen to give clear glasses. When the samples were photolyzed *in situ* at 77 °C with light of wavelength greater than 340 nm (Corning Filter 4-76/9780) the ($\Delta M = 2$) half-field e.s.r. absorption of naphthalene triplet was easily detected. No triplet naphthalene e.s.r. absorption was found when PFB was not present. We interpret these observations in the same way as those for benzophenone (8, 9). The exciting light is only absorbed by the PFB, therefore it must generate the triplet of naphthalene indirectly by energy transfer from the PFB triplet. We assume that the triplet state of PFB is also formed in the photolysis of liquid solutions. Recent flash photolysis experiments support this conclusion (10).

In our experiments we observed that, after prolonged photolysis of the solutions, some ketyl remained when the u.v. light had been extinguished. This suggests that a thermal equilibrium exists, between PFB, the ketyl radical, and the products. This point should be borne in mind if the system is adopted as an actinometer, as has been proposed (11).

The presence of a hydroxyl proton in the radical was further substantiated by studies of temperature and exchange effects.

Can. J. Chem. Downloaded from www.nrcresearchpress.com by 210.87.254.5 on 09/05/12
For personal use only.

Can. J. Chem. Downloaded from www.nrcresearchpress.com by 210.87.254.5 on 09/05/12
For personal use only.

Temperature Effects

The hydroxyl proton h.f.s. of the ketyl radical was shown to increase with increasing temperature, and was similar to that reported for the unfluorinated ketyl (7) and other OH containing radicals.

Proton Exchange Effects

The assignment of the 2.42 G h.f.s. in 2-propanol to a hydroxyl proton was also confirmed by the observation of acid-catalyzed exchange effects on the spectrum. Samples containing 0.1 *M* PFB with varying amounts of hydrochloric acid were examined during photolysis at 80 °C. Care was taken to maintain a constant proportion of water in these, since its presence decreases the value of a_{OH}^{H}. We found that a_{OH}^{H} decreased with increasing concentration of acid and the line width increased. We attribute these changes to the exchange reaction 4.

[4] $$(C_6F_5)_2COH + H^+ \leftrightarrows (C_6F_5)_2COH_2^+$$

This decreases the lifetime of the spin states of the hydroxyl proton and therefore broadens the e.s.r. lines. Such effects are well known (12, 13), and the theory has been given elsewhere (14, 15).

Therefore the proton h.f.s. observed for spectra in all the solvents of Table 1 is due to hydroxyl proton. This is further substantiated by the results in deuterated solvents.

Deuterated Solvents

Reactions 1–3 show that the ketyl radical of PFB is formed during photolysis by abstraction of a hydrogen atom from a solvent molecule. Therefore, in a deuterated solvent a deuterium atom will be abstracted and the ketyl radical $(C_6F_5)_2\dot{C}OD$ formed. The spectrum in perdeuterated 2-propanol should only differ from that in the protiated solvent in that the hydroxyl doublet of 2.42 G should be replaced by a triplet of about 0.37 G.[3] The spectrum taken at 80 °C gave a_{OD}^{D} equal to 0.33 G. The line width of 0.18 G was the smallest found in these studies.

Spectra in Cyclohexane–Ethanol Mixtures

The spectrum observed during the photolysis of PFB in cyclohexane did not give a hydroxyl proton h.f.s. This could mean that a different radical was formed, or that a_{OH}^{H} for the ketyl in cyclohexane is zero. The latter seemed the most likely, and it implies that in mixtures of cyclohexane and ethanol a_{OH}^{H} should increase with increasing alcohol content. Photolysis of such solutions gave the expected variation, as shown in Table 2 and Fig. 2. The rapidly changing portion of the curve of Fig. 2 was not very reproducible for different stock solutions. This was shown to be due to small variations in the water content of the alcohol used.

The variation of a_{OH}^{H} with alcohol content follows a smooth curve which can be extrapolated to zero for pure cyclohexane. Therefore we conclude that the radical observed in cyclohexane is the same as in the other solvents, namely the ketyl.

This variation may be analyzed to yield a solvent exchange equilibrium constant. The theory (16, 17) assumes that relatively stable one-to-one complexes are formed between the radical and the solvents S_A and S_B. In the mixed solvent the equilibrium 5 exists

[5] $$RS_A + S_B \rightleftarrows RS_B + S_A$$

and the rate of solvent exchange is so rapid that the spectra of RS_A and RS_B are time-averaged to give only one spectrum. The relationship

TABLE 2. Nuclear hyperfine coupling constants (G) for the PFB ketyl in cyclohexane–ethanol mixtures at 40 °C

Volume % EtOH	a_{OH}^{H}	a_{ortho}	a_{meta}	a_{para}	ΔW_{pp}[a]
Nil	—	4.90	1.96	8.59	0.43
0.04	—	4.87	2.01	8.58	0.44
0.08	0.43				0.37
0.2	0.89	4.70	1.89	8.47	0.36
0.2	1.00	4.63	1.84	8.40	0.37
0.4	1.41	4.65	1.86	8.38	0.27
0.5	1.44	4.63	1.87	8.35	0.27
1.0	1.86	4.61	1.84	8.32	0.37
100	2.16				
0.15	0.37				
0.2	0.51				
0.3	0.80				
0.4	1.04				
0.5	1.09				
		Different stock solution			
0.6	1.28				
0.8	1.46				
1.0	1.61				
10	1.98				
80	2.10				
100	2.16				
0.4	1.18				

[a]Peak to peak first derivative full line width.

[3]The value of a_{OD}^{D} is computed from the ratio of the proton and deuteron nuclear magnetic moments and spin.

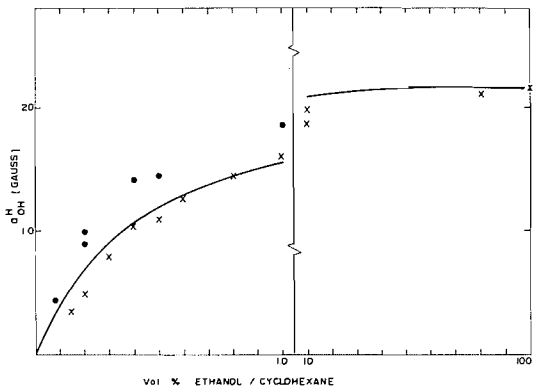

FIG. 2. The variation of a_{OH}^{H} in cyclohexane–ethanol mixtures.

between the observed h.f.s., a_{OH}^{H}, the equilibrium constant K, and the ratio of the solvent concentration α is given in eq. 6.

$$[6] \qquad a_{OH}^{H} = 2.16K\alpha/(K\alpha + 1)$$

where 2.16 is the OH coupling constant (h.f.s.) in pure ethanol. Analysis of our data leads to K values in the range 200–300. The curve for K equal to 250 is shown in Fig. 2. This very simple model implies that in a 0.5 volume % solution of ethanol in cyclohexane the PFB ketyl will be half solvated by ethanol. Such specific solvation is quite common for anion radicals such as those of nitro compounds, but is comparatively rare for neutral radicals.

The Variation of the Hyperfine Splittings

Temperature Effects

We interpret the variation of a_{OH}^{H} with temperature in much the same way that Wilson did for the unfluorinated ketyl (7). This h.f.s. arises from two effects, one direct and the other indirect. If the $>\dot{C}OH$ group is planar, then a_{OH}^{H} only arises from spin density on the oxygen atom. This is the indirect effect, since it involves spin polarization of the OH bond to give spin density at the hydrogen nucleus. If the OH group is rotated out of the plane the hydrogen 1s orbital can overlap with the carbonyl carbon 2p orbital leading to spin density at the hydrogen nucleus. This is the direct effect. The total interaction is expressed in eq. 7 where Q_I and

$$[7] \qquad a_{OH}^{H} = Q_I\rho_O + Q_D\rho_C$$

Q_D are constants and ρ_O and ρ_C are the spin densities at the oxygen and carbonyl carbon atoms respectively. To account for the increase of a_{OH}^{H} with increasing temperature and its zero value in cyclohexane, we assume Q_I and Q_D to be of opposite sign and Q_D to be positive. Increasing the temperature increases the proportion of those torsional isomers which permit direct overlap, so a_{OH}^{H} increases.

Solvent Effects

The data presented in Tables 1 and 2 show that as the hydroxylic-proton coupling increases that of the aromatic ring fluorine decreases. These differences are most marked between cyclohexane and the alcohols. The cyclohexane–ethanol mixtures of Table 2 show a smooth change from one solvent to the other. We assign these changes to differences in the solvent–ketyl radical interactions, and note that increasing the solvent polarity increases the value of a_{OH}^{H} at the expense of the aromatic-ring fluorine couplings.

The temperature variation of the OH proton coupling shows that a_{OH}^{H} has a positive sign, and that the direct overlap of the hydrogen 1s orbital with the adjacent carbon 2p orbital is the dominant interaction. In the case of cyclohexane a_{OH}^{H} is zero, and we conclude that the direct overlap is equal and opposite to the contribution from spin polarization of the OH bond due to spin density resident on the oxygen. Therefore the increase in a_{OH}^{H} when the solvent is changed from cyclohexane to an alcohol is due to an increase in the proportion of the OH coupling arising from direct overlap. Since this change in solvent also decreases the fluorine couplings, we conclude that spin density has shifted from the aromatic rings to the $>\dot{C}OH$ group.

Simple molecular orbital calculations of the effect of solvent on the e.s.r. spectra of radical anions have been described by Gendell *et al.* (16) and successfully applied to the benzophenone ketyl by Wilson (7). We have extended these to the PFB ketyl, and find that the theory accounts for the general direction of the effects. For example, increasing the polarity of the solvent from cyclohexane to ethanol is accounted for by merely increasing the electronegativity of the carbonyl oxygen atom. This has the effect of decreasing the spin density on the aromatic rings and on the oxygen, but increasing it on the carbonyl carbon. It leads to a decrease in the fluorine h.f.s. and an increase in a_{OH}^{H} from direct overlap. Hence the theory is in agreement

Can. J. Chem. Downloaded from www.nrcresearchpress.com by 210.87.254.5 on 09/05/12
For personal use only.

with the experimental observations summarized in Tables 1 and 2

Conclusions

The radical observed during the photolysis of solutions of perfluorobenzophenone has been shown to be the ketyl $(C_6F_5)_2\dot{C}OH$ This assignment has been substantiated by deuteration, proton exchange, and effects of temperature and solvent, together with simple molecular orbital calculations.

The assistance of Dr. R. E. D. McClung of the University of Alberta and K. H. Witzke of W.N.R.E. with development of the computer simulation program is gratefully acknowledged. We wish to thank Dr. A. Singh of W.N.R.E. for interesting discussions and for suggesting the project.

1. F. P. SARGENT and M. G. BAILEY. Can. J. Chem. **49**, 2350 (1971).
2. A. D. MCLACHLAN. Mol. Phys. **3**, 233 (1960).
3. A. STREITWIESER. Molecular orbital theory for organic chemists. John Wiley and Sons, Inc., New York. 1961.
4. A. CARRINGTON, A. HUDSON, and G. R. LUCKHURST. Proc. Roy. Soc. London, A, **284**, 582 (1965).
5. P. B. AYSCOUGH, F. P. SARGENT, and R. WILSON. J. Chem. Soc. 5418 (1963).
6. C. THOMSON and W. J. MACCULLOCH. Mol. Phys. **19**, 817 (1970).
7. R. WILSON. J. Chem. Soc. (B), 84 (1968).
8. J. B. FARMER, C. L. GARDNER, and C. A. MCDOWELL. J. Chem. Phys. **34**, 1058 (1961).
9. A. TERENIN and V. ERMOLAEV. Trans. Faraday Soc. **52**, 1042 (1956).
10. A. SINGH, M. G. JONASSON, F. C. SOPCHYSHYN, and F. P. SARGENT. 23rd International Congress of Pure and Applied Chemistry, Boston, 1971. p. 99. Abst. No. 235.
11. N. FILIPESCU, J. P. PINION, and F. L. MINN. Chem. Commun. 1413 (1970).
12. H. FISHER. Mol. Phys. **9**, 149 (1965).
13. H. ZELDES and R. LIVINGSTON. J. Chem. Phys. **45**, 1946 (1966).
14. J. A. POPLE, W. G. SCHNEIDER, and H. S. BERSTEIN. High resolutions nuclear magnetic resonance. McGraw-Hill Book Co., Inc., New York. 1959. pp. 218–224.
15. H. S. GUTOWSKY, D. W. MCCALL, and P. SLICHTER. J. Chem. Phys. **21**, 279 (1953).
16. J. GENDELL, J. H. FREED, and G. K. FRAENKEL. J. Chem. Phys. **37**, 2832 (1962).
17. J. PANELL. Mol. Phys. **7**, 317 (1963–4).
18. G. E. ADAMS and R. L. WILLSON. J. Chem. Soc. FARADAY II, **69**, 719 (1973).

Can. J. Chem. Downloaded from www.nrcresearchpress.com by 210.87.254.5 on 09/05/12
For personal use only.

Na^+ and K^+ Binding by Fulvic Acid[1]

DONALD S. GAMBLE
Soil Research Institute, Canada Agriculture, Ottawa, Canada K1A 0C6

Received May 8, 1973

The electrostatic binding of Na^+ and K^+ by fulvic acid in aqueous solution has been measured with cation electrodes at 25.00 °C ± 0.05. The binding equilibria were followed during the course of acid–base titrations, and have revealed distinct binding regions in the titration curves. In one of these regions Na^+ is more strongly bound than is K^+. The standard free energies of binding were 11.7×10^3 to 20.5×10^3 J/mol ± 2% for Na^+, and 11.5×10^3 to 17.8×10^3 J/mol ± 1%, for K^+.

La combinaison électrostatique de Na^+ et de K^+ par l'acide fulvique en solution aqueuse a été mesurée à l'aide d'électrodes sensibles aux cations à 25.00 C ± 0.05. Les états d'équilibre lors de la combinaison ont été évalués lors de titrations acide–base et ont mis en relief différentes régions de combinaison existant dans les courbes de titrations. Dans une de ces régions, le Na^+ est lié plus fortement que le K^+. Les énergies libres standards de liaison sont comprises dans l'intervalle allant de 11.7×10^3 jusqu'à 20.5×10^3 J/mol ± 2% pour le Na^+ et dans l'intervalle allant de 11.5×10^3 jusqu'à 17.8×10^3 J/mol ± 1% pour le K^+. [Traduit par le journal]

Can. J. Chem., 51, 3217 (1973)

Introduction

The literature gives various indications of the electrostatic binding of cations by humic polyelectrolytes. Among these are the electrical conductance measurements of Mukherjee and Lahiri in 1958 (1). Posner observed that alkali chlorides make humic acid more strongly acidic, and has used acid–base titrations to measure these changes in the acid dissociation equilibrium (2, 3).

More recently, KCl was found not only to have this same effect on fulvic acid, but also to displace the first titration equivalence point to a higher value (4, 5). Reporting fulvic acid – metal ion complexing stabilities in 1970, Schnitzer and Hansen demonstrated that generally log K was a decreasing linear function of KCl concentration in the ionic strength range 0.0 to 0.15 (6).

The only direct measurements of alkali ion binding by humic materials were those previously reported in 1953 by Marshall and Patnaik (7, 8). They found stronger binding for Na^+ than for K^+. The purpose of the present work is to check this unexpected result and obtain detailed chemical information by making direct potentiometric measurements with metal ion electrodes.

[1]Presented in part at the 56th Canadian Chemical Conference of the Chemical Institute of Canada, Montreal, Quebec June 4–6, 1973. Contribution No. 460.

Theory

It is assumed that the alkali metal ions are electrostatically held in the neighborhood of ionized functional groups, and that conceptually they can be assigned to these functional groups. Any prior assumptions as to which functional groups or fulvic acid fractions bind the metal ions would be difficult to justify. Such assumptions are, however, unnecessary. Instead, the binding equilibrium is defined in terms of all of the ionized functional groups, according to eq. 1.

$$T^- + M^+ \overset{\bar{K}_5}{\rightleftharpoons} (T^-M^+) \qquad \bar{K}_5 = m_{TM}/(m_T m_M) \qquad [1]$$

$\bar{K}_5$ is found to be a weighted average function, in just the same way as has been described previously for the H^+ dissociation and Cu^{2+} complexing equilibrium quotients of fulvic acid (9, 4, 5, 10). Equation 2 gives the result for the present case.

$$\bar{K}_5 = \frac{1}{\chi_T} \int_0^{\chi_T} K_5(\chi_T) d\chi_T \qquad \chi_T = m_T/C_T \qquad [2]$$

m_T and χ_T are the molality and mole fraction, respectively, of acid functional groups free from both H^+ and metal ions. C_T is the molality of functional groups titrated up to the second

Can. J. Chem. Downloaded from www.nrcresearchpress.com by 210.87.254.105 on 09/05/12
For personal use only.

Can. J. Chem. Downloaded from www.nrcresearchpress.com by 210.87.254.105 on 09/05/12
For personal use only.

acid–base equivalence point. K_5 is defined by eq. 3 for the infinitesimal increment of functional groups $\delta c_T = \delta m_T + \delta m_{TM}$.

$$[3] \quad K_5 = \frac{\delta m_{TM}}{m_M \delta m_T} = \left(\frac{\gamma_M \gamma_T}{\gamma_{TM}}\right) \kappa_5{}^0 \exp\left(-\Delta G_5{}^e/RT\right)$$

Assuming that no covalent bonding exists for alkali ion binding, then $\kappa_5{}^0 \equiv 1$. $K_5 = K_5(\chi_T)$ may be calculated from experimental data by differentiating along the path described by a titration, according to eq. 4.

$$[4] \quad K_5 = \mathrm{d}(\chi_T \bar{K}_5)/\mathrm{d}\chi_T$$

If the functional groups in a particular region of the titration curve, χ_T' to χ_T'', do not bind metal ions, then this will be reflected in the $\bar{K}_5$ curve. The calculation with eq. 4 will accordingly give $K_5 = 0$ for $\chi_T' \leqslant \chi_T \leqslant \chi_T''$. This formulation of the problem is therefore perfectly general.

Rigorous numerical values for the activity coefficients in eq. 3 are unavailable. Experimental results are therefore presented as values of $\Delta G_5{}^b$, which is defined by eq. 5.

$$[5] \quad \Delta G_5{}^b \equiv \Delta G_5{}^e - 2.303\, RT \log \frac{\gamma_M \gamma_T}{\gamma_{TM}}$$

Experimental

Chemicals

The fulvic acid used was the Batch FA1, which has been previously described (4). H_2O redistilled under N_2 and 0.1 *N* standard bases were also used. The other chemicals were all of Reagent Grade quality.

Equipment

Orion Na^+ Specific Ion combination electrode Model No. 96-11, and Metrohm combination glass/AgCl micro electrodes, p*H* range 0 to 11, temperature range 10 to 100 °C were used with a Beckman Research Model p*H* meter. The Na^+ electrode cable was covered with a grounded shield before use.

Corning Monovalent Cation electrode and a Fisher calomel reference electrode were used with a Fisher Accumet Model 520 digital p*H*/ion meter. A 5.000 ml calibrated microburett, ±0.005 ml was also used.

Thermostats and calibrated thermometers were used to maintain the temperature at 25.00 °C ± 0.05.

Cation Molality Standards

The H^+ standards were prepared essentially as previously described (4), with NaOH or KOH being used as appropriate.

Each Na^+ standard curve was constructed with 12 to 15 standard solutions prepared gravimetrically to cover the NaCl concentration range 2. × 10^{-3} *m* to 12. × 10^{-3} *m*. The molality *vs.* Volts data points were fitted to polynomials by the method of least squares.

K^+ standards were prepared gravimetrically in sets of 8 or 9 to cover the KCl concentration range 3. × 10^{-3} *m* to 11. × 10^{-3} *m*. Because biases among these sets of standards were not observable outside the extent of scatter within a set, all of the data from these standards were fitted by least squares to a single standard curve.

Experimental Methods

Four independent experiments, from which CO_2 was excluded, were carried out at 25.00 °C ± 0.05. Each experiment consisted of at least six independent but identical titrations. Each titration used 100. g of sample solution having 0.1 g of fulvic acid dissolved in H_2O. There were generally about 70 data points per titration. For each experiment an average titration curve was calculated by least squares fitting. Random scatter and random biases were thus averaged out. The first two experiments were done by NaOH titration, with free Na^+ molality being measured in one and free H^+ molality being measured in the other. A pair of K^+ binding experiments was done in the same way. The last of these four experiments was previously published work (4). The potentiometric measurements were conducted essentially as previously described (4).

Results

Data from the four experiments are given in Fig. 1 and Tables 1 and 2. The Na^+ curve of Fig. 1 and the H^+ molalities of Table 1 represent the average titration curves of Experiments 1 and 2, respectively. Likewise the K^+ curve of Fig. 1 and the H^+ molalities of Table 2 represent the average titration curves of Experiments 3 and 4. The significant points are:

(*a*) For both cations, binding evidently begins at 4. mequiv./g and then increases steeply.

(*b*) Na^+ shows stronger binding than does K^+ up to about 11.0 mequiv./g. This is in qualitative accord with the results reported by Marshall and Patnaik (7).

(*c*) The Na^+ binding curve of Fig. 1 goes through a maximum of 2.880 × 10^{-3} *m* at 8.6 mequiv./g, after which some of the bound Na^+ is released.

(*d*) The K^+ binding curve of Fig. 1 has a drastic change of slope at just about 8.0 mequiv./g, and then apparently approaches as a limit the same value of 2.880 × 10^{-3} *m* attained by the Na^+ binding maximum.

The K_5 curves of Fig. 2 reveal very distinct ion binding regions in the NaOH and KOH titrations. Each curve has a peak standing on a 1.5 mequiv./g base, and a plateau also 1.5 mequiv./g wide. These regions are, however, interchanged in the two titration curves. Except

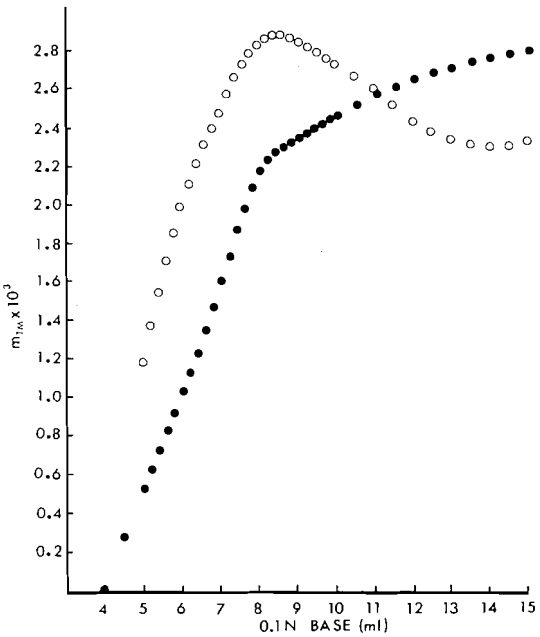

FIG. 1. Alkali metal ion bound during the acid–base titration of fulvic acid at 25.00 °C ± 0.05: ○, Na^+, standard error ±0.66% to ±1.7%; ●, K^+, standard error ±1.2% to ±1.8%.

in the plateau regions, the Na^+ binding is clearly seen to be somewhat stronger here than is the K^+ binding.

An examination of Tables 1 and 2 shows that in the 5.000 ml to 6.000 ml region, the NaOH titration curve has H^+ concentrations greater than those of the KOH titration curve, by a factor of more than 10^3. This difference is in exactly the same region as the Na^+ peak and K^+ plateau of Fig. 2. The corresponding effect for the K^+ binding peak is shown in Fig. 3. Δm_H is the change in H^+ molality resulting from the replacement of Na^+ with K^+. Although the H^+ displacement effect of Fig. 3 is almost obscured by experimental error, Δm_H changes sign in just the right region. In addition, the Δm_H peak occurs at 7.4 mequiv./g. This is the exact location of the K^+ binding peak in Fig. 2. The K_5 peaks of Fig. 2 thus have corroboration from independent experiments.

Numerical values for the free energy function of eq. 5 are listed in Table 3. Assuming that $(\gamma_{T\,Na}/\gamma_T) \approx 1$, and using the data of Robinson and Stokes (11) for 0.01 *m* NaCl, one obtains for the corresponding standard free energies,

$$[6] \qquad \Delta G_5^{e} \approx \Delta G_5^{b} + 0.3 \times 10^3 \text{ J/mol}$$

TABLE 1. Na^+ binding by fulvic acid at 25.00 °C ± 0.05 calculated for 0.10020 g fulvic acid in 100.0000 g of solution

0.1 *N* NaOH (ml)	H^+ molality	$\bar{K}_5$	χ_T (±6.1%)
5.000	$1.53\times10^{-5}\pm9.8\%$	$100.8\pm7.8\%$	0.445
5.200	9.48×10^{-6}	106.9	0.488
5.400	5.78×10^{-6}	120.1	0.489
5.600	4.17×10^{-6}	131.2	0.492
5.800	4.17×10^{-6}	140.1	0.498
6.000	1.00×10^{-9}	147.3	0.503
6.200	8.62×10^{-10}	151.6	0.511
6.400	7.28×10^{-10}	153.8	0.521
6.600	5.99×10^{-10}	153.9	0.533
6.800	4.77×10^{-10}	152.1	0.546
7.000	3.62×10^{-10}	149.7	0.560
7.200	$2.41\times10^{-10}\pm4.4\%$	$151.3\pm5.7\%$	0.569
7.400	1.41×10^{-10}	150.6	0.579
7.600	8.46×10^{-11}	148.9	0.587
7.800	5.13×10^{-11}	147.2	0.592
8.000	3.47×10^{-11}	145.7	0.591
8.200	2.47×10^{-11}	143.4	0.590
8.400	1.85×10^{-11}	140.1	0.590
8.600	$1.55\times10^{-11}\pm2.1\%$	$135.9\pm5.4\%$	0.590
8.800	1.30×10^{-11}	130.7	0.591
9.000	1.09×10^{-11}	124.8	0.594
9.200	9.22×10^{-12}	119.2	0.597
9.400	7.88×10^{-12}	113.9	0.600
9.600	6.86×10^{-12}	109.0	0.603
9.800	6.10×10^{-12}	104.4	0.606
10.000	5.57×10^{-12}	100.1	0.609
10.500	4.98×10^{-12}	90.1	0.617
11.000	$4.91\times10^{-12}\pm7.5\%$	$81.4\pm5.4\%$	0.625
11.500	4.73×10^{-12}	72.9	0.636
12.000	3.57×10^{-12}	65.6	0.646
12.500	3.04×10^{-12}	60.6	0.653
13.000	2.76×10^{-12}	56.5	0.658
13.500	2.51×10^{-12}	53.5	0.660
14.000	2.31×10^{-12}	51.3	0.660
14.500	2.14×10^{-12}	49.9	0.658
15.000	$2.02\times10^{-12}\pm1.7\%$	$49.1\pm6.0\%$	0.654

The magnitudes of these values in Table 3 are very similar to those reported in the literature for theoretical and experimental work on polyelectrolytes (12–15).

Experimental Errors

The errors in the H^+ measurements have been discussed previously (4, 5). In the same way, potentiometric measurements were the chief source of error in the determination of Na^+ and K^+ concentrations. The errors in the answers were estimated from the standard deviations of the least squares fit computer printouts, and from the errors in the published equivalence point values (4).

Can. J. Chem. Downloaded from www.nrcresearchpress.com by 210.87.254.105 on 09/05/12
For personal use only.

TABLE 2. K^+ binding by fulvic acid at 25.00 °C ± 0.05 calculated for 0.10015 g fulvic acid in 100.0000 g of solution

0.1 *N* KOH (ml)	H^+ molality	$\bar{K}_5$	χ_T (±1.0%)
5.000	$4.53\times10^{-6}\pm28\%$	29.3±3.4%	0.577
5.200	9.15×10^{-9}	33.5	0.588
5.400	5.92×10^{-9}	37.4	0.600
5.600	3.66×10^{-9}	40.9	0.613
5.800	2.15×10^{-9}	44.1	0.625
6.000	1.21×10^{-9}	47.7	0.635
6.200	6.82×10^{-10}	50.4	0.647
6.400	4.23×10^{-10}	53.4	0.657
6.600	3.27×10^{-10}	57.2	0.666
6.800	3.08×10^{-10}	61.3	0.673
7.000	3.05×10^{-10}	65.7	0.681
7.200	$2.81\times10^{-10}\pm23\%$	70.0±4.4%	0.687
7.400	2.24×10^{-10}	73.9	0.694
7.600	1.05×10^{-10}	77.8	0.695
7.800	5.43×10^{-11}	81.6	0.690
8.000	4.49×10^{-11}	84.9	0.681
8.200	3.65×10^{-11}	86.5	0.674
8.400	2.90×10^{-11}	86.2	0.671
8.600	$2.24\times10^{-11}\pm15\%$	85.4±2.9%	0.670
8.800	1.68×10^{-11}	84.5	0.668
9.000	1.21×10^{-11}	83.6	0.666
9.200	7.75×10^{-12}	82.9	0.663
9.400	6.84×10^{-12}	82.2	0.660
9.600	6.52×10^{-12}	81.7	0.656
9.800	6.19×10^{-12}	81.1	0.653
10.000	5.87×10^{-12}	80.6	0.650
10.500	5.08×10^{-12}	80.0	0.640
11.000	$4.36\times10^{-12}\pm3.0\%$	79.5±2.7%	0.630
11.500	3.73×10^{-12}	78.2	0.623
12.000	3.21×10^{-12}	76.9	0.616
12.500	2.78×10^{-12}	75.6	0.610
13.000	2.47×10^{-12}	74.3	0.604
13.500	2.24×10^{-12}	73.1	0.598
14.000	2.09×10^{-12}	71.8	0.593
14.500	2.00×10^{-12}	70.5	0.588
15.000	$1.94\times10^{-12}\pm6.7\%$	69.2±2.5%	0.584

Error estimates are not available for the published work of Marshall and Patnaik (7).

Discussion

The very distinct binding and nonbinding regions of the titration curves seen in Fig. 1 suggest the possibility that the fulvic acid has discrete binding and nonbinding fractions. Figure 2 in turn indicates that the binding region has two distinct parts. Although the peaks and plateaus are interchanged in the two curves of Fig. 2, the peak in each curve may nonetheless represent the same fulvic acid fraction or set of functional groups. One cannot assume that the

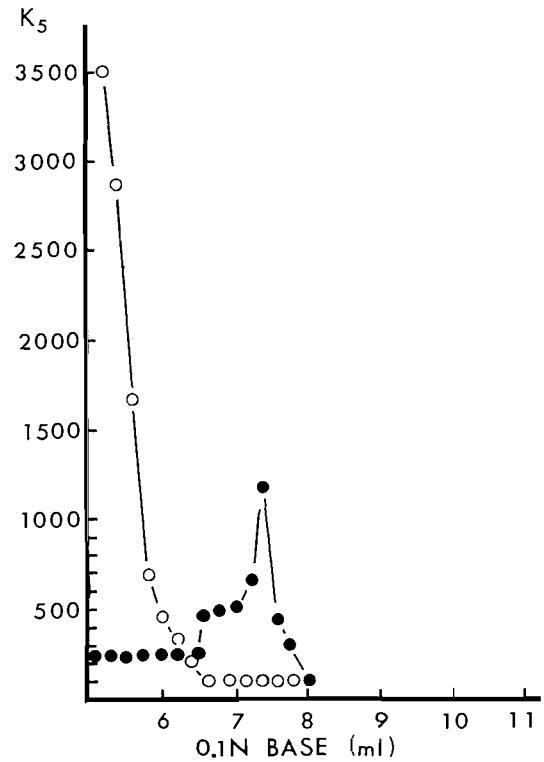

FIG. 2. Alkali ion binding equilibria at 25.00 °C ± 0.05: ○, Na^+, standard error ±11.%; ●, K^+, standard error ±6.0%.

TABLE 3. Electrostatic binding by fulvic acid. Standard free energies at 25.00 °C uncorrected for activity coefficients (0.1000 g fulvic acid/100 g of solution)

0.1 *N* base (ml)	$-\Delta G_5^b$ (J/mol) × 10^{-3}	
	Na^+ ± 2%	K^+ ± 1%
5.200	20.2	
5.400	19.7	
5.600	18.4	
5.800	16.2	13.4
6.000	15.2	
6.200	14.4	
6.400	13.2	
6.600		15.1
6.800		15.1
7.000		15.2
7.200	11.4	16.1
7.400		17.5
7.600		14.9
7.800		14.2
8.000		11.3

Can. J. Chem. Downloaded from www.nrcresearchpress.com by 210.87.254.105 on 09/05/12
For personal use only.

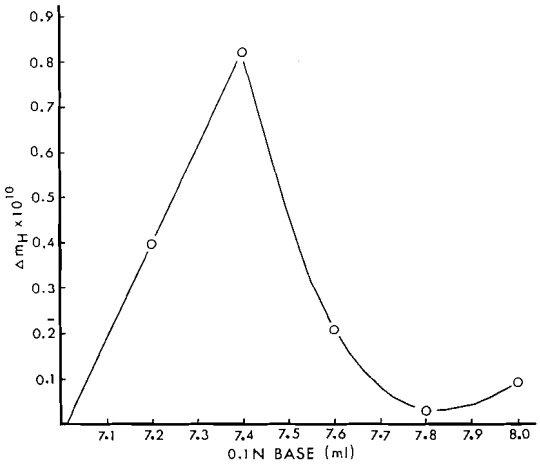

FIG. 3. H^+ displacement by metal ions. Effect of K^+ relative to that of Na^+.

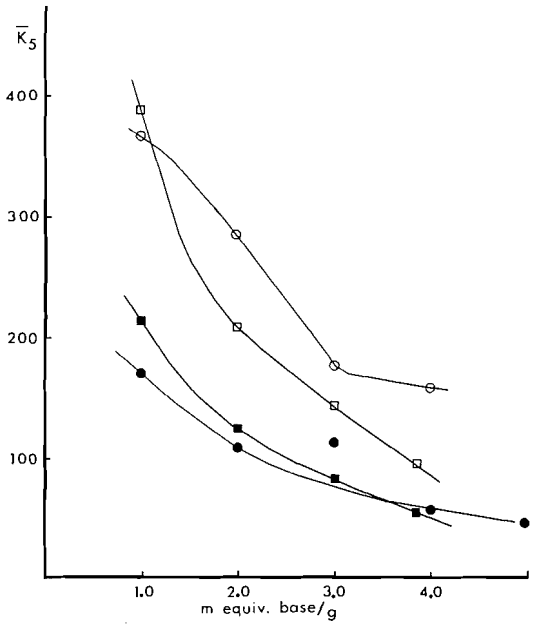

FIG. 4. Alkali ion binding equilibria for Wisconsin peat fractions; from Marshall and Patnaik (7). $\bar{K}_5$ calculated assuming from their titrations $\approx$ 5.0 mequiv./g of acidic functional groups, and $\alpha_T \approx$ (mequiv. of base)/5.0/g. Hymatomelanic acid: ⊙, Na^+; ●, K^+. Humic acid: ⊡, Na^+; ■, K^+.

acidic functional groups will be ionized in the same order during titration with the two standard bases.

The two humic fractions extracted from a Wisconsin peat by Marshall and Patnaik differed in both the geographical source and the preparation method from the fulvic acid used here. Despite this, the curves in Fig. 4 are quite comparable to the present results. This raises the question, therefore, of whether the binding preference for Na^+ over K^+ is common or widespread.

Structural causes are suspected for this binding preference, especially since it is so closely identified with a particular region of the titration curve. Structure is known to affect the binding of alkali ions by such neutral molecules as the crown ethers and certain antibiotics (16–19). The metal ions are held within rings or cages lined with oxygen atoms.

In aqueous systems such complexing usually requires removal of some or all of the cation's solvating water molecules. The usual preference for K^+ over Na^+ resulting from this is reversed for special cases in which the enclosure is too small for the K^+. The standard free energies for such complexes are evidently characteristic of ion–dipole interactions (17).

The fulvic acid – alkali metal ion "complexes" probably differ from the above complexes in two ways. Firstly, the standard free energies of Table 3 are more characteristic of ion–polyion interactions. Secondly, there is evidence (9) to suggest that fulvic acid has an open structure consisting of a two or three dimensional array of poorly condensed aromatic rings. These are highly substituted with functional groups and side chains. Such a structure is unlikely to possess the rigidity or uniformity of size required to selectively bind Na^+ rather than K^+. The experimental results may, however, be explained by postulating that fulvic acid in aqueous solution possesses cages lined by solvated carboxylate groups. If the incoming cation is able to share solvating water molecules with the carboxylate groups, then the smaller bare-ion diameter of Na^+ could be favored over that of K^+.

Mr. D. A. Hindle carried out the large number of careful measurements and assisted with the calculations. The author is indebted to Professor J. A. Marinsky of the Department of Chemistry, State University of New York at Buffalo, for valuable discussions.

1. P. N. MUKHERJEE and A. LAHIRI. Fuel, **37**, 220 (1958).
2. A. M. POSNER. 8th Int. Congr. of Soil Sci. Bucharest, Romania. Publishing House of the

Can. J. Chem. Downloaded from www.nrcresearchpress.com by 210.87.254.105 on 09/05/12
For personal use only.

Academy of the Socialist Republic of Romania. 1964. p. 161.
3. A. M. POSNER. J. Soil Sci. **17**, 65 (1966).
4. DONALD S. GAMBLE. Can. J. Chem. **50**, 2680 (1972).
5. DONALD S. GAMBLE. Can. J. Chem. **48**, 2662 (1970).
6. M. SCHNITZER and E. H. HANSEN. Soil Sci. **109**, 333 (1970).
7. C. E. MARSHALL and N. PATNAIK. Soil Sci. **75**, 153 (1953).
8. F. SCHEFFER and B. ULRICH. Lehrbuch der Agrikulturchemie und Bodenkunde. III. Teil. Humus and Humusdüngung. Band I. Ferdinand Enke Verlag Stuttgart. p. 75.
9. DONALD S. GAMBLE and MORRIS SCHNITZER. The chemistry of fulvic acid and its reactions with metal ions. *In* Trace metals and metal–organic interactions in natural waters. *Edited by* Philip C. Singer. Ann Arbor Science Publishers, Inc. 1973.
10. DONALD S. GAMBLE, M. SCHNITZER, and I. HOFFMAN. Can. J. Chem. **48**, 3197 (1970).
11. R. A. ROBINSON and R. H. STOKES. Electrolyte solutions. 2nd ed. Butterworths, London. 1959.
12. JACOB A. MARINSKY. Interpretation of ion-exchange phenomena. *In* Ion exchange. Vol. 1. *Edited by* Jacob A. Marinsky. Marcel Dekker, Inc., New York. 1966. Chapt. 9.
13. S. LIFSON and A. KATCHALSKY. J. Polym. Sci. **13**, 43 (1954).
14. R. ARNOLD and J. TH. G. OVERBEEK. Rec. Trav. Chim. **69**, 192 (1950).
15. TURNER ALFREY, JR., PAUL W. BERG, and HERBERT MORAWETZ. J. Polym. Sci. **7**, 543 (1951).
16. C. J. PEDERSEN. J. Am. Chem. Soc. **92**, 391 (1970).
17. H. K. FRENSDORFF. J. Am. Chem. Soc. **93**, 600 (1971).
18. C. J. PEDERSEN. J. Am. Chem. Soc. **89**, 7017 (1967).
19. C. J. PEDERSEN. J. Am. Chem. Soc. **92**, 386 (1970).

Can. J. Chem. Downloaded from www.nrcresearchpress.com by 210.87.254.105 on 09/05/12
For personal use only.

Some New Iron Carbonyl Cluster Complexes of Di(tertiary arsines)

L. S. CHIA, W. R. CULLEN, J. R. SAMS, AND J. E. H. WARD
Department of Chemistry, University of British Columbia, Vancouver 8, British Columbia

Received April 5, 1973

New polynuclear iron carbonyl complexes having the stoichiometry $LFe_3(CO)_{10}$ have been obtained from the reactions of $Fe_3(CO)_{12}$ with the di(tertiary arsine) ligands $(CH_3)_2AsC(X)(Y)CF_2As(CH_3)_2$ (X = Y = H; X = H, Y = F; X = F, Y = CF_3). The structures of the new cluster complexes have been investigated using i.r., n.m.r., and Mössbauer spectroscopies. Mössbauer data are also reported for $LFe_3(CO)_{10}$ and $LFe_3(CO)_9$ derivatives of the mixed ligand $(CH_3)_2AsC{=}CP(C_6H_5)_2CF_2CF_2$.

De nouveaux complexes polynucléaires fer-carbonyle ayant la stoechiométrie $LFe_3(CO)_{10}$ ont été obtenus à partir de réactions du $Fe_3(CO)_{12}$ avec des coordinats di(arsine tertiaire) $(CH_3)_2AsC(X)(Y)CF_2As(CH_3)_2$ (X = Y = H; X = H, Y = F; X = F, Y = CF_3). Les structures des nouveaux complexes d'agrégat ont été étudiées à l'aide des spectroscopies infra-rouge, r.m.n. et Mössbauer. Les résultats tirés de la spectroscopie Mössbauer sont aussi présentés pour les dérivés $LFe_3(CO)_{10}$ et $LF_3(CO)_9$ du coordinat mélangé $(CH_3)_2AsC{=}CP(C_6H_5)_2CF_2CF_2$. [Traduit par le journal]

Can. J. Chem., 51, 3223 (1973)

Introduction

The fluorocarbon-bridged di(tertiary arsine) $f_4$fars (**1***a*) forms the interesting complex $f_4farsFe_3(CO)_{10}$ (**2***a*)(1, 2) in which the ligand has replaced one terminal carbonyl group from each of the equivalent iron atoms (B and C) of $Fe_3(CO)_{12}$. However, no such $Fe_3(CO)_{10}$ derivative is formed by the related di(tertiary phosphine) $f_4$fos (**1***b*), nor by the hydrocarbon-

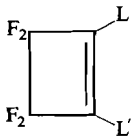

1

a L = $(CH_3)_2As$ = L′, $f_4$fars
b L = $(C_6H_5)_2P$ = L′, $f_4$fos
c L = $(CH_3)_2As$, L′ = $(C_6H_5)_2P$, f_4AsP

bridged ligands diphos and diars (diphos = 1,2-bis(diphenylphosphino)ethane and diars = 1,2-bis(dimethylarsino)benzene) (3). On the other hand the reaction of the mixed ligand f_4AsP (**1***c*) with $Fe_3(CO)_{12}$ does result in the formation of an $Fe_3(CO)_{10}$ complex (4), believed to have structure **2***b*.

It appears that the bite of the ligand is probably more important than electronic factors in determining its ability to form an (L—L′)-$Fe_3(CO)_{10}$ derivative. Thus the ligand **3**, which is electronically similar to $f_4$fars but should have a smaller As...As separation because of the

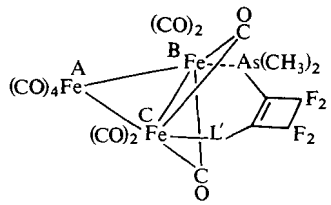

2

a L′ = $(CH_3)_2As$
b L′ = $(C_6H_5)_2P$

acyclic bridging group, does not form an $Fe_3(CO)_{10}$ complex (5). The importance of

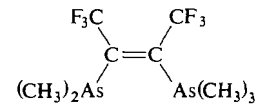

3

ligand bite is also evident in the tendency of these and related ligands to act as chelating groups (4–9).

In view of the difference in properties between **1***a* and **3** it was of interest to examine the reactions of the related di(tertiary arsines) **4** with $Fe_3(CO)_{12}$. The longer C—C distances compared to **3** and free rotation about the C—C bond, should provide a slightly bigger bite for the ligands **4**, and hence favor the formation of $Fe_3(CO)_{10}$ complexes. We find in all three cases that (L—L′)$Fe_3(CO)_{10}$ derivatives are in fact obtained but spectroscopic evidence indicates they do not all have structures analogous to **2**.

TABLE 1. Analytical, i.r. and ^{1}H n.m.r. data for new (L—L′)$Fe_3(CO)_{10}$ complexes

(L—L′)	Calcd. (found) (%) C	H	ν(CO)[a](cm^{-1})	^{1}H n.m.r.[b] (p.p.m.)
$(CH_3)_2AsCH_2CF_2As(CH_3)_2$	26.63(26.40)	1.96(2.09)	2074 s 2021 s 2011 m,sh 2001 vs,br 1987 m,sh 1972 m	2 singlets, 0.48 (area 3), 0.27 (area 3), and a triplet (J = 19 Hz) centered at 0.70 (area 1).
$(CH_3)_2AsCHFCF_2As(CH_3)_2$	25.98(25.10)	1.77(1.89)	2074 s 2024 s 2005 vs,br 1988 m,sh 1974 m	3 singlets, 0.55, 0.42, 0.34 (areas 1:2:1)[c]
$(CH_3)_2AsCF(CF_3)CF_2As(CH_3)_2$	25.28(25.32)	1.50(1.73)	2072 s 2022 vs 2006 s 1994 m 1987 m 1973 m 1770 w,br	3 singlets, 0.70, 0.67, 0.28 (areas 1:1:2)

[a]Cyclohexane solution.
[b]Benzene solution.
[c]Not sufficiently soluble to detect a signal from the —C(H)F— proton.

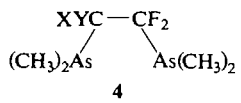

4

a X = H = Y
b X = H, Y = F
c X = F, Y = CF_3

A preliminary report on these compounds has appeared (5).

We also report here ^{57}Fe Mössbauer data for $f_4AsPFe_3(CO)_{10}$ (4) and a complex of formula $f_4AsPFe_3(CO)_9$ in which the ligand has undergone rearrangement and the $Fe_3(CO)_{12}$ skeleton is no longer present (4, 10).

Experimental

The Mössbauer spectrometer and attendant experimental details have been described previously (8). I.r. spectra were recorded on a Perkin–Elmer 457 instrument, mass spectra on an AEI MS-9 spectrometer, and ^{1}H n.m.r. spectra (C_6H_6 solution) on a Varian HA-100 spectrometer. Chemical shifts are given in p.p.m. downfield from external TMS. The ligands **4** were prepared as reported elsewhere (11–13).

Preparation of [(CH$_3$)$_2$AsCF(CF$_3$)CF$_2$As(CH$_3$)$_2$]-Fe$_3$(CO)$_{10}$

A mixture of triiron dodecacarbonyl (1.25 g, 2.48 mmol) and 1,2-bis(dimethylarsino)hexafluoropropane (0.75 g, 2.08 mmol) was refluxed in 30 ml of 40–60° petroleum ether under a nitrogen atmosphere for 13 h. The solvent was removed under reduced pressure and the resulting products were chromatographed on Florisil while eluting with petroleum ether – diethyl ether mixtures. The $Fe_3(CO)_{10}$ complex eluted as a dark red band, second last off the column (0.063 g, 4%). Other products obtained were $[(CH_3)_2AsCF(CF_3)CF_2As(CH_3)_2]Fe(CO)_3$ identified only by i.r. spectroscopy and the previously known $[(CH_3)_2AsFe(CO)_3]_2$ (14).

The $Fe_3(CO)_{10}$ derivatives of **4***a* and *b* were prepared in a manner identical to the above, yields of 27 and 38%, respectively, being obtained. In the former case other products identified were (L—L′)$Fe(CO)_4$ (42%) and (L—L′)$Fe_2(CO)_8$ (10%), although neither was characterized further.

Results and Discussion

Analytical and spectroscopic data for the new cluster complexes are given in Tables 1 and 2. The mass spectra of the three new $Fe_3(CO)_{10}$ derivatives formed by the ligands **4** all show a parent ion followed by the loss of 10 carbonyl groups. The remainder of the cracking patterns are of little help in determining the structures and will not be considered further here.

The spectroscopic properties of $[(CH_3)_2AsCHFCF_2As(CH_3)_2]Fe_3(CO)_{10}$ (**5**) are very similar to those of **2***a* (1), although due to the ligand asymmetry the ^{1}H n.m.r. spectrum of **5** is more complicated, showing three methyl proton singlets of relative areas 1:2:1. There are only four terminal carbonyl bands in the i.r. spectrum of **5**, indicating a fairly symmet-

TABLE 2. Mössbauer isomer shifts δ, quadrupole splittings ΔE_Q, and linewidths Γ for polynuclear iron carbonyl complexes at 80 °K

Compound	Iron atom	$\delta^{a,b}$	$\Delta E_Q{}^a$	$\Gamma_1{}^a$	$\Gamma_2{}^a$
$Fe_3(CO)_{12}$	A	0.29	0.12	0.28	0.29
	B,C	0.37	1.13	0.27	0.26
$f_4farsFe_3(CO)_{10}$	A	0.27	0.14	0.23	0.23
	B,C	0.42	1.52	0.23	0.25
$[(CH_3)_2AsCHFCF_2As(CH_3)_2]Fe_3(CO)_{10}$	A	0.28	0.13	0.26	0.25
	B,C	0.40	1.59	0.27	0.32
$[(CH_3)_2AsCF(CF_3)CF_2As(CH_3)_2]Fe_3(CO)_{10}$	A	0.24	0.59	0.44	0.28
	B	0.36	1.43	0.22	0.28
	C	0.51	1.12	0.44	0.28
$[(CH_3)_2AsCH_2CF_2As(CH_3)_2]Fe_3(CO)_{10}$	A	0.28	0.56	0.27	0.30
	B,C	0.45	1.21	0.35	0.33
$f_4AsPFe_3(CO)_{10}$	A	0.33	0.32	0.28	0.25
	B,C	0.39	1.15	0.32	0.40
$f_4farsFe_3(CO)_9$	A	0.22	1.00	0.27	0.29
	B	0.39	0.67	0.28	0.29
	C	0.29	0.23	0.23	0.21
$f_4AsPFe_3(CO)_9$	A	0.23	0.88	0.26	0.30
	B	0.38	0.58	0.33	0.30
	C	0.27	0.36	0.33	0.21

[a] In mm s^{-1}. ± 0.02 mm s^{-1}. [b] Relative to sodium nitroprusside.

rical structure. The ^{57}Fe Mössbauer spectra of **2***a* and **5** are virtually identical, the only significant differences being that the outer lines in the latter are slightly broadened and show a somewhat greater splitting (Table 2). Both these effects may arise from the small asymmetry of the ligand structure, which could make the two dimethylarsino groups slightly different in σ-donor and π-acceptor properties resulting in a very slight inequivalence of Fe^B and Fe^C. However, the spectroscopic evidence leaves little doubt that in **5** the ligand is bonded to the $Fe_3(CO)_{10}$ moiety in an identical way to **2***a*.

On the other hand the Mössbauer spectrum of $[(CH_3)_2AsCF(CF_3)CF_2As(CH_3)_2]Fe_3(CO)_{10}$ (**6**) derived from ligand **4***c* is very different in appearance, consisting of four lines of approximate relative areas 1:2:1:2. For a compound containing three iron atoms and giving rise to a four-line Mössbauer spectrum with the relative areas of two lines being twice those of the other two, there are six possible combinations of lines. For each of these combinations there are 3! permutations of the iron atoms making a total of 36 possible ways of assigning the spectral lines. In trying to rule out as many of these assignments as we can, we shall rely on data we have collected for more than 40 iron carbonyl derivatives of related di(tertiary arsines and phosphines) in which the iron atoms are formally in the zero oxidation state (1, 4, 6, 8, 15). Although the quadrupole splittings in such complexes can vary widely depending on details of the stereochemistry about the iron atom, isomer shift values have invariably been found to lie within the range $+0.16 \leqslant \delta \leqslant +0.51$ mm s^{-1}. It therefore seems best to base conclusions on isomer shift data where possible, and to eliminate those assignments for which δ values fall well outside the above range.

The possible line combinations in the Mössbauer spectrum of **6** and the values of isomer shifts and quadrupole splittings derived therefrom are shown in Scheme 1. Combinations i–iv can be ruled out at once, since in every case at least two of the three isomer shift values are unreasonable, one being negative and the other at either +0.80 or +1.07 mm s^{-1}. Neither of the remaining combinations can be discarded solely on the basis of the magnitudes of the δ values, although the +0.09 mm s^{-1} value from combination v seems suspect. Therefore we shall examine both these combinations in terms of the possible structures for **6** shown in Fig. 1. In struc-

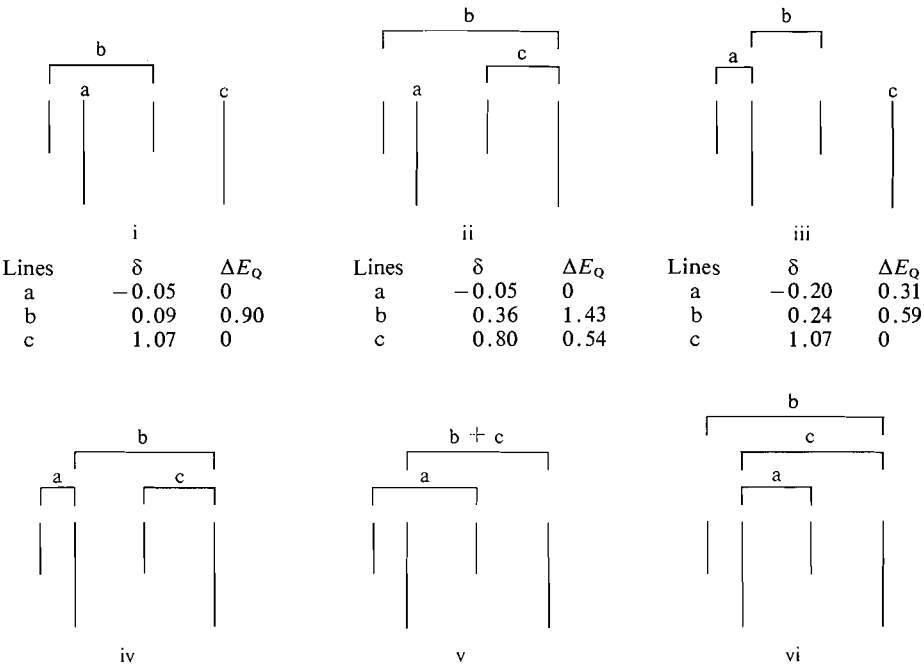

Lines	δ	ΔE_Q
a	−0.05	0
b	0.09	0.90
c	1.07	0

Lines	δ	ΔE_Q
a	−0.05	0
b	0.36	1.43
c	0.80	0.54

Lines	δ	ΔE_Q
a	−0.20	0.31
b	0.24	0.59
c	1.07	0

Lines	δ	ΔE_Q
a	−0.20	0.31
b	0.51	1.12
c	0.80	0.54

Lines	δ	ΔE_Q
a	0.09	0.89
b,c	0.51	1.12

Lines	δ	ΔE_Q
a	0.24	0.59
b	0.36	1.43
c	0.51	1.12

SCHEME 1. Possible line combinations and corresponding parameters in the Mössbauer spectrum of $[(CH_3)_2AsCF(CF_3)CF_2As(CH_3)_2]Fe_3(CO)_{10}$.

tures **I** and **II** the ligand is acting as a bridging group, having replaced one carbonyl group from each of two different iron atoms, while in structures **III** and **IV** the ligand is chelating.

Since combination v requires degeneracy of two of the iron atoms, the only possible structures consistent with this combination are **I** and **III**. For the former we would clearly expect the Mössbauer parameters for **6** to be very nearly the same as those for **2***a* and **5**, which they are not. In particular it would be very difficult to explain the large changes in both δ and ΔE_Q for Fe^A (lines a), since for this structure these parameters should be little altered. Moreover, the δ values for the two equivalent iron atoms are greater than anticipated, since our experience has been that replacement of one carbonyl group by an arsine or phosphine ligand raises the isomer shift of that iron atom by about 0.04–0.08 mm s^{-1}. The chelate structure **III** is similarly subject to objections regarding the isomer shift values, in that δ_A should increase rather than decrease compared to $Fe_3(CO)_{12}$, while $\delta_B(=\delta_C)$ should be approximately unchanged. We therefore consider that both these structures, and hence combination v, can be eliminated as highly unlikely on the basis of the Mössbauer data.

Only structures **II** and **IV**, each with three inequivalent iron atoms, are consistent with the sole remaining combination vi. For the bridged structure **II** we would expect both δ_A and δ_C to increase slightly compared to their values in $Fe_3(CO)_{12}$, while δ_B should be nearly constant. From the data in Table 2 we must associate the value $\delta_b = 0.36$ mm s^{-1} with Fe^B, neither of the other δ values being at all reasonable for this iron atom. This immediately leads to the difficulty that δ_a is slightly lower than δ_A in $Fe_3(CO)_{12}$ while δ_c has increased markedly, both effects being contrary to expectations. For structure **IV**, we would expect the δ values for Fe^A and Fe^B to be essentially unchanged from their values in $Fe_3(CO)_{12}$ while δ_c is expected to increase by about 0.08–0.16 mm s^{-1}. If we assign the isomer shifts of 0.24, 0.36, and 0.51 mm s^{-1}

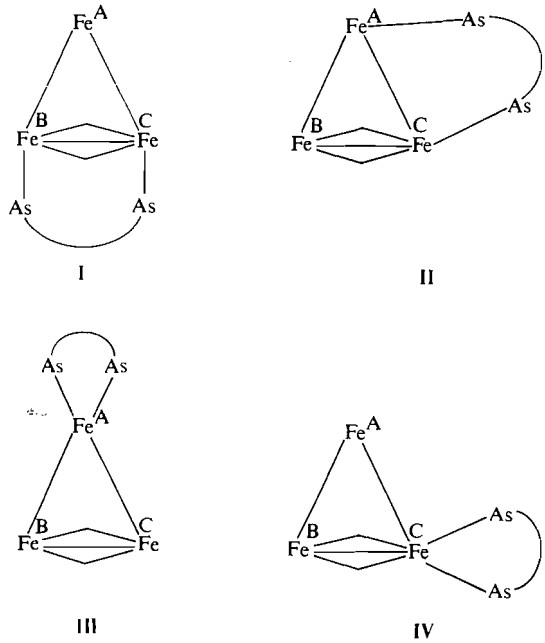

FIG. 1. Possible structures for $(As–As)Fe_3(CO)_{10}$ complexes. To avoid complicating the figure all terminal CO groups have been omitted and the ligand is symbolized simply as As As. Bridging carbonyl groups between iron atoms B and C (equivalent in the parent $Fe_3(CO)_{12}$) are denoted by "bent" bonds.

to iron atoms A, B, and C, respectively, all the δ values are in good agreement with our predictions. The only point about the Mössbauer parameters which seems slightly unusual for structure **IV** is the increase in ΔE_Q for Fe^B, which one might have expected to be unaffected by chelation of the ligand at Fe^C. However, this could presumably be caused by the bulkiness of the ligand or solid state packing effects, and the assignment of structure **IV** to compound **6** seems most consistent with the available data.

The Mössbauer spectrum of $[(CH_3)_2AsCH_2CF_2As(CH_3)_2]Fe_3(CO)_{10}$ (**7**) consists of lines at −0.15, −0.01, +0.55, and +1.05 mm s^{-1} with relative areas of approximately 2:1:1:2. While the line positions are quite similar to those of **6**, the area ratios are like those of ***2a***. Again there are six possible combinations of lines, and again four of these can be ruled out on the grounds that they all lead to unreasonable isomer shift values for at least two of the iron atoms. The remaining possibilities vii and viii are shown in Scheme 2 together with the parameters derived from these combinations. By arguments entirely

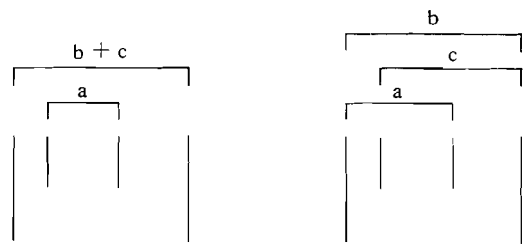

Line	δ	ΔE_Q
a	0.28	0.56
b	0.45	1.21
c	0.45	1.21

Line	δ	ΔE_Q
a	0.20	0.71
b	0.45	1.21
c	0.52	1.06

SCHEME 2. Line combinations in the Mössbauer spectrum of $[(CH_3)_2AsCH_2CF_2As(CH_3)_2]Fe_3(CO)_{10}$ having acceptable isomer shift values.

analogous to those employed above it can be shown that only structures **II** and **IV** of Fig. 1 are compatible with vii while only **I** and **III** are consistent with viii.

First consider combination vii. In going from $Fe_3(CO)_{12}$ to structure **II** one would expect the δ values for Fe^A and Fe^C to each increase by about 0.04–0.08 mm s^{-1}, with δ for Fe^B remaining nearly constant. However, there is no way of permuting the three isomer shifts and three iron atoms so as to satisfy these requirements and we conclude that **II** is not the correct structure. Although structure **IV** is less objectionable on the basis of Mössbauer data and was tentatively suggested as a possible structure for this complex (5), there are certain difficulties associated with the δ values since two of the three should be essentially the same as in $Fe_3(CO)_{12}$.

The n.m.r. spectrum of **7** provides additional evidence. With this particular ligand (***4a***) structure **IV** should lead to inequivalence of all four methyl groups, but only two equal-area singlets due to the methyl protons are observed. By comparison we note that the compound

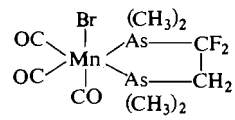

which has approximately the same symmetry as **IV** shows methyl proton resonances (C_6H_6 solution) at τ = 8.530, 8.660, 8.806, and 8.959 p.p.m. (13). On the other hand, the more symmetrical

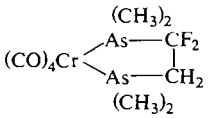

shows only two methyl proton singlets at τ 9.42 and 9.52 p.p.m. (C_6H_6 solution) (13). Thus the n.m.r. data for **7** would seem to favor the symmetrical structures **I** or **III**.

For combination viii of the Mössbauer lines, structure **III** seems highly unlikely in view of the δ values, since replacement of two CO groups on Fe^A should give a substantial increase in δ_A while having little or no effect on δ_B and δ_C. It therefore appears that **7** has structure **I**, analogous to **2***a* and **5**, but different from **6**.

It is possible that the bulky CF_3 group restricts rotation about the C—C bond in the ligand to such an extent that only the chelate complex **IV** is possible for ligand **4***c*. In the other two ligands **4***a* and *b*, which have smaller groups (H, F) attached to the bridging carbon atoms, the rotational barrier could be small enough to allow the bite of the ligand to become sufficient to complex as in **I**.

Complex **2***b*, the $Fe_3(CO)_{10}$ derivative of the mixed ligand f_4AsP(**1***c*) (4), has spectroscopic properties which are quite similar to those of $f_4$fars complex **2***a*. The highest peak in the mass spectrum of **2***b* corresponds to $f_4AsPFe_3(CO)_{10}$ and there is a stepwise loss of 10 carbonyl groups. The ^1H n.m.r. spectrum indicates that both the $(CH_3)_2As$ and $(C_6H_5)_2P$ groups are coordinated (4, 6). The ^{19}F n.m.r. spectrum, which is very similar to that of f_4AsP, suggests that both arsenic and phosphorus are bonded to the triiron fragment in such a way that the original symmetry of the ligand is preserved. The i.r. spectrum shows the presence of both terminal and bridging carbonyl groups.

These data are all consistent with the proposed (4) structure **2***b*, but rather surprisingly the Mössbauer spectrum of this complex is more like that of the parent $Fe_3(CO)_{12}$ than that of **2***a* (see Table 2). The most significant difference between the spectra of $Fe_3(CO)_{12}$ and $f_4AsPFe_3(CO)_{10}$ is a small increase in the splitting of the central doublet in the latter. However, the outer pair of lines is substantially and unsymmetrically broadened, an effect which could easily result from the slight inequivalence of Fe^B and Fe^C in the bridged structure **2***b*, but is difficult to rationalize for the only other structure compatible with the i.r. and n.m.r. data, *i.e.*, a chelated structure analogous to **III**. The general chemical behavior of f_4AsP towards the iron carbonyls $Fe(CO)_5$, $Fe_2(CO)_9$, and $Fe_3(CO)_{12}$ (4) also suggests that a chelate $Fe_3(CO)_{10}$ species is unlikely. Whereas $f_4AsPFe(CO)_4$ in which the ligand is monodentate is produced in all the reactions of f_4AsP with the iron carbonyls so far investigated and is indeed the most characteristic product, $f_4AsPFe(CO)_3$ can only be obtained in low yield under forcing conditions. The apparent ease with which f_4AsP substitutes just one carbonyl group from an iron carbonyl moiety is illustrated by the isolation and characterization of such derivatives as $f_4AsPFe_2(CO)_8$ in which the ligand is bridging two $Fe(CO)_4$ fragments, $(f_4AsP)_2Fe(CO)_3$ in which both ligands are monodentate and P-bonded, and $(f_4AsP)_2Fe_2(CO)_4$ in which one ligand is terdentate and the second is bridging the two iron atoms (4).

The similarity in chemical properties of $f_4farsFe_3(CO)_{10}$ and $f_4AsPFe_3(CO)_{10}$ also suggests they have similar structures. Both compounds are readily converted to $(L—L')Fe_3(CO)_9$ derivatives when refluxed in cyclohexane for $\sim$1 h(1, 4), and both $Fe_3(CO)_9$ products have been shown by X-ray diffraction studies to have structure **8** (10, 16). Thus the conversion to the

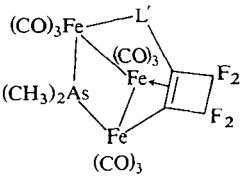

8

a L′ = $(CH_3)_2As$, $f_4farsFe_3(CO)_9$
b L′ = $(C_6H_5)_2P$, $f_4AsPFe_3(CO)_9$

$Fe(CO)_9$ complexes results in ligand fragmentation and involves breaking a bond between arsenic and the fluorocarbon bridging group, with the formation of Fe—As and Fe—C σ-bonds.

Whereas the Mössbauer spectrum of **8***a* can be fitted by five independent Lorentzian lines of approximate relative areas 1:1:1:1:2 consistent with the presence of three inequivalent iron atoms (1), we are able to resolve only four independent lines in the case of **8***b* with areas in the approximate ratios 1:2:1:2. In overall appearance, however, the two spectra are very

similar, with the second line in the spectrum of the f_4AsP derivative corresponding to a superposition of lines two and three in the spectrum of the f_4fars complex. Detailed arguments have been given (1) concerning the assignment of the Mössbauer spectral lines for $f_4farsFe_3(CO)_9$. On the same basis the assignments for $f_4AsPFe_3(CO)_9$ given in Table 2 have been obtained. It should be noted that in both compounds corresponding iron atoms have almost identical isomer shifts as expected. Differences in corresponding ΔE_Q values are not large ($\sim$0.1 mm s^{-1}) and presumably reflect primarily slight differences in bond angles at the various iron atoms.

We thank the National Research Council of Canada for financial support and Mrs. A. Sallos for technical assistance.

1. W. R. CULLEN, D. A. HARBOURNE, B. V. LIENGME, and J. R. SAMS. Inorg. Chem. **9**, 702 (1970).
2. P. J. ROBERTS, B. R. PENFOLD, and J. TROTTER. Inorg. Chem. **9**, 2137 (1970).
3. W. R. CULLEN and D. A. HARBOURNE. Can. J. Chem. **47**, 3371 (1969).
4. L. S. CHIA, W. R. CULLEN, and D. A. HARBOURNE. Can. J. Chem. **50**, 2182 (1972).
5. J. P. CROW, W. R. CULLEN, J. R. SAMS, and J. E. H. WARD. J. Organomet. Chem. **22**, C29 (1970).
6. W. R. CULLEN, D. A. HARBOURNE, B. V. LIENGME, and J. R. SAMS. Inorg. Chem. **8**, 1464 (1969).
7. J. P. CROW, W. R. CULLEN, F. G. HERRING, J. R. SAMS, and R. L. TAPPING. Inorg. Chem. **10**, 1616 (1971).
8. W. R. CULLEN, D. A. HARBOURNE, B. V. LIENGME, and J. R. SAMS. Inorg. Chem. **8**, 95 (1969).
9. F. W. B. EINSTEIN and J. TROTTER. J. Chem. Soc. A, 824 (1967).
10. F. W. B. EINSTEIN and R. D. G. JONES. J. Chem. Soc. Dalton, 2563 (1972).
11. W. R. CULLEN and N. K. HOTA. Can. J. Chem. **42**, 1123 (1964).
12. W. R. CULLEN and G. E. STYAN. J. Organomet. Chem. **4**, 151 (1965).
13. J. E. H. WARD. Ph.D. Thesis, University of British Columbia, Vancouver, B.C. (1972).
14. W. R. CULLEN and L. M. MIHICHUK. Can. J. Chem. **51**, 936 (1973).
15. L. S. CHIA, W. R. CULLEN, J. R. SAMS, and J. C. SCOTT. Unpublished results.
16. F. W. B. EINSTEIN, A. M. PILOTTI, and R. RESTIVO. Inorg. Chem. **10**, 1947 (1971).

Terpenes and Terpenoids. IV.[1] Some Esters and Amides of Thujic Acid

V. HACH[2] AND ELIZABETH C. MCDONALD
MacMillan Bloedel Research Limited, Vancouver 12, British Columbia

Received October 16, 1972[3]

Representatively substituted esters (**3***c–h*) and amides (**4***a–l*) of thujic acid (**3***a*) were prepared using the acid chloride as intermediate and were screened for their insect repellent and attractant potential. *N,N*-Diethyl thujamide (**4***d*) was found to be a highly active repellent of the yellow fever mosquito (*Aedes aegypti*) as well as of other insect species.

Des amides (**4***a–l*) ainsi que des esters (**3***c–h*) dérivés de l'acide thujique **3***a* et substitués de manière caractéristique ont été préparés en utilisant comme intermédiaire le chlorure d'acide. Ces composés furent par la suite étudiés en fonction de leur potentiel répulsif ou attracteur vis-à-vis des insectes. La *N,N*-diéthyl thujamide (**4***d*) s'est révélée être un produit à caractère répulsif très efficace contre les moustiques responsables de la fièvre jaune (*Aedes aegypti*) aussi bien que contre les autres espèces d'insectes.
[Traduit par le journal]

Can. J. Chem., **51**, 3230 (1973)

Can. J. Chem. Downloaded from www.nrcresearchpress.com by 210.87.254.105 on 09/05/12
For personal use only.

The wood of western red cedar (*Thuja plicata Donn*) is renowned for its resistance to bacterial and mycotic decay and for its ability to withstand insect attack both in timber stands and sawmill products (1, 3). The antibacterial and antimycotic properties of this wood have been studied in detail and are generally attributed to the low molecular weight extractives (1–3), particularly the three thujaplicins (**1***a–c*). On the other hand investigations of these extractives for possible insect control agents have been few and consequently our present interest is concentrated in this area.

The major cedar wood extractives are the thujaplicins (**1***a–c*), plicatic acid (**2**), thujic acid (**3***a*), and its methyl ester (**3***b*). β-Thujaplicin (**1***b*) was tested by Becker (4) against larvae of *Hylotrupes bajulus* (Crambycidae)[4] and was found to be a highly active insecticide. Experiments (2) with larvae of *Reticulothermes flavipes* showed a very low degree of termicidal activity in either β- or γ-thujaplicin (**1***b* and *c*) and in plicatic acid (**2**). The methyl ester of thujic acid (**3***b*) showed toxicity to larvae of the black carpet beetle, the furniture carpet beetle, and the case-making moth. Unfortunately, detailed quantitative results of these experiments have not been published (1). Recently Arndt (2) examined the so called "neutral fraction" of the wood extract

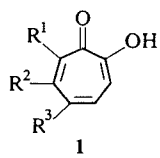

1

a (α) R^1 = *i*-Pr; R^2 = R^3 = H
b (β) R^2 = *i*-Pr; R^1 = R^3 = H
c (γ) R^3 = *i*-Pr; R^1 = R^2 = H

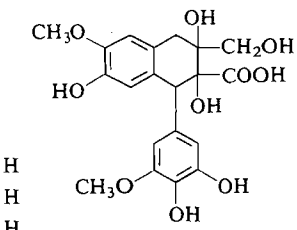

2

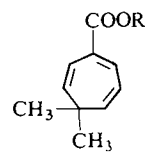

3

R
a —H
b —CH_3
c —$CH(CH_3)_2$
d —$(CH_2)_3CH_3$
e —$CH{\cdot}CH_2{\cdot}CH{\cdot}CH_3$ (CH_3, CH_3)
f —$(CH_2)_7CH_3$
g — 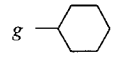
h —CH_2CH_2— 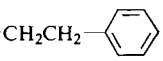

which consists essentially of the methyl ester **3***b* and found a striking degree of termicidal activity against *Reticulotermes flavipes*.

These promising reports concerning methyl thujate (**3***b*) prompted us to investigate in more

[1]For papers I–III of this series see refs. 14 and 18.
[2]Present address: Department of Chemistry, University of British Columbia, Vancouver 8, British Columbia.
[3]Revision received June 11, 1973.
[4]A common pest of structural timber in Europe.

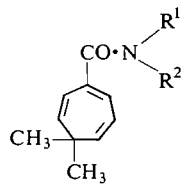

4

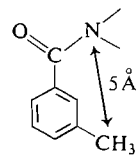

5

	R^1	R^2
a	$-CH_3$	$-H$
b	$-CH_3$	$-CH_3$
c	$-C_2H_5$	$-H$
d	$-C_2H_5$	$-C_2H_5$
e	$-(CH_2)_3CH_3$	$-H$
f	$-(CH_2)_3CH_3$	$-(CH_2)_3CH_3$
g		$-H$
h	$-CH_2-C_6H_5$	$-H$
i	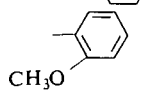	$-H$
j	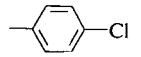	$-H$
k		$-H$
l	$-CH_2 \cdot CH_2 \cdot CH_2 \cdot CH_2 \cdot CH_2-$	

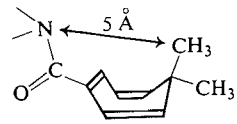

6

detail two classes of derivatives of thujic acid (**3***a*). The series of esters **3***c–h* was an obvious choice. The second series, substituted amides of thujic acid (**4***a–l*), was conceived on the basis of analogy with *N,N*-diethyl-*m*-toluamide (**5**). This amide, developed in 1954 by systematic testing of various synthetic compounds (5, 6), is an extremely potent repellent commonly used against various species of insects. Surprisingly, Jones and Jacobson (7) recently discovered that amide **5** also is a key component of the female sex attractant of the pink bollworm moth and thus a natural compound.[5] Further pertinent support for the projected exploration of the amide function came from recent work on insect juvenile hormone and juvabione analogs (9). This had shown that replacement of an ester group by an alkylamido function leads to profound enhancement of several types of insect controlling activity in both series of compounds.

We isolated thujic acid (**3***a*) from the viscous oil obtained by steam distillation of western red cedar wood (12, 15). This oil contained as main components the above mentioned extractives **1***a–c*, **3***a*, and methyl thujate (**3***b*). The acid was extracted by a solution of $NaHCO_3$, precipitated by acidification, and purified by crystallization. The acid chloride used as intermediate for the preparation of both the esters and the amides was obtained in excellent yield by the dimethylformamide catalyzed reaction (10) of thujic acid with $SOCl_2$ at room temperature. However, it was not possible to purify the crude liquid acid chloride by distillation due to ensuing decomposition of the product. Thus, the crude acid chloride was used directly.[6] It is known that under acidic

[5]It is important to note that there is a high degree of structural specificity associated with this amide in regard to its repellent and sex attractant activity. None of the isomers derived from *o*- or *p*-toluic acid showed any appreciable degree of activity. Consequently, the activity of amide **5** will perhaps be, apart from other necessary conditions, closely associated with the distance between the ring-positioned CH_3 group and the nitrogen of the amide group. Inspection of Dreiding models revealed that in diethyl-*m*-toluamide (**5**) and in contemplated amide structures (*e.g.* in **4***d* = **6**), the distance between the ring-positioned methyl group and the N of the amide group could be almost identical, averaging about 5 Å. Thujic acid was assumed to be in the well established (8) trough-like conformation. In both cases the amide nitrogen was projected into the center of a circle circumscribed by this atom in a freely rotating carboxamido group. However, we do not make any claims as to the conclusiveness of this assumption and accept it merely as a working hypothesis.

[6]Hurd and Edwards (13) prepared this chloride by a pyridine catalyzed reaction between the acid and $SOCl_2$. However, as in our case, they were unable to purify the crude chloride. Action of $SOCl_2$ without a catalyst led to a product which after hydrolysis gave a mixture of acids, presumably cumic and thujic. Apparently, the elevated temperature necessary for the acid chloride formation without catalyst was sufficient to bring about isomerization of thujic to cumic acid by action of HCl evolved in the reaction mixture.

Can. J. Chem. Downloaded from www.nrcresearchpress.com by 210.87.254.105 on 09/05/12
For personal use only.

Can. J. Chem. Downloaded from www.nrcresearchpress.com by 210.87.254.105 on 09/05/12
For personal use only.

TABLE 1. Esters of thujic acid

Ester	B.p. (°C/mm Hg)	Mol. formula	Mol. wt.	Elemental analysis C % calcd.	C % found	H % calcd.	H % found	O % calcd.	O % found
3*c* Isopropyl	78/0.4	$C_{13}H_{18}O_2$	206.27	75.69	75.85	8.80	8.70	15.51	15.47
3*d* *n*-Butyl	99/0.8	$C_{14}H_{20}O_2$	220.30	76.32	76.38	9.15	9.20	14.53	14.67
3*e* 2(4-Methylpentyl)	104/0.5	$C_{16}H_{24}O_2$	248.35	77.37	77.61	9.74	9.66	12.89	12.80
3*f* *n*-Octyl	140/0.6	$C_{18}H_{28}O_2$	276.40	78.21	78.27	10.21	10.31	11.59	11.42
3*g* Cyclohexyl	129/0.7	$C_{16}H_{22}O_2$	246.34	78.01	78.12	9.00	8.92	12.99	12.86
3*h* 2-Phenethyl	153/0.5	$C_{18}H_{20}O_2$	268.34	80.56	80.46	7.51	7.60	11.93	11.86

TABLE 2. Amides of thujic acid

Amide	B.p. (°C/mm Hg)	M.p. (°C)	Recrystallization solvent and crystal appearance	Mol. formula	Mol. wt.	Elemental analysis C % calcd.	C % found	H % calcd.	H % found	N % calcd.	N % found	Method of preparation
4*a* *N*-Methyl	138/0.6	90	MeOH rhomboids	$C_{11}H_{15}NO$	177.24	74.54	74.75	8.53	8.61	7.90	7.80	B
4*b* *N*,*N*-Dimethyl	116/0.6	47	MeOH plates	$C_{12}H_{17}NO$	191.26	75.35	75.42	8.76	9.06	7.32	7.23	B
4*c* *N*-Ethyl	129/0.4	—		$C_{12}H_{17}NO$	191.26	75.35	75.15	8.76	8.86	7.32	7.10	B
4*d* *N*,*N*-Diethyl	99/0.3	—		$C_{14}H_{21}NO$	219.32	76.67	76.51	9.65	9.80	6.39	6.52	A, B
4*e* *N*-*n*-Butyl	131/0.2	—		$C_{14}H_{21}NO$	219.32	76.67	76.41	9.65	9.68	6.39	6.31	A
4*f* *N*,*N*-Di-*n*-butyl	131/0.5	—		$C_{18}H_{29}NO$	275.43	78.47	78.43	10.61	10.65	5.07	5.04	A
4*g* *N*-Cyclohexyl	—	128	75% EtOH prisms	$C_{16}H_{23}NO$	245.35	78.32	78.22	9.45	9.51	5.71	5.67	A
4*h* *N*-Benzyl	170/0.3	—		$C_{17}H_{19}NO$	253.34	80.60	80.86	7.56	7.60	5.53	5.60	A, B
4*i* *N*-*o*-Methoxyphenyl	—	65	95% EtOH needles	$C_{17}H_{19}NO_2$	269.32	75.81	75.64	7.11	7.16	5.20	5.17	C
4*j* *N*-*p*-Chlorophenyl	—	89	75% *i*-PrOH plates	$C_{16}H_{16}ClNO$*	273.75	70.20	69.93	5.89	5.88	5.11	5.04	C
4*k* *N*-2-Thiazolyl	—	139	*i*-PrOH plates	$C_{13}H_{14}N_2O_3S$†	246.32	63.37	63.18	5.73	5.86	11.37	11.19	A
4*l* *N*-1-Piperidyl	128/0.5	35	Hexane needles	$C_{15}H_{21}NO$	231.33	77.88	78.00	9.15	9.29	6.06	6.02	A

*Calcd.: Cl, 12.95; Found: 12.72.
†Calcd.: S, 13.02; Found: 12.94.

Can. J. Chem. Downloaded from www.nrcresearchpress.com by 210.87.254.105 on 09/05/12
For personal use only.

conditions thujic acid easily rearranges into cumic acid (11, 12), eq. 1.

[1] 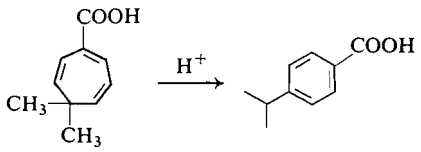

We assured ourselves that under the present reaction conditions the thujic acid chloride formed did not contain any cumoyl chloride.[7]

The desired esters were prepared by reacting a slight excess of the crude thujic acid chloride with the appropriate alcohol in pyridine solution at 50° for 6 h. The crude esters were purified by distillation indicating that up to 150° the cycloheptatriene ring is thermally stable. The esters are summarized in Table 1. Three modifications of the common reaction between acid chloride and amine were used[8] to prepare amides **4***a–l* summarized in Table 2.

Methyl thujate (**3***b*) accompanying the free acid in the steam distillate of cedar wood appeared to be a potential starting material for the preparation of these amides. Indeed, it was possible to obtain several of them by reaction of **3***b* with aliphatic amines at elevated temperature. Unfortunately, the yields were low and products obtained contained considerable amounts of by-products. Most probably the α,β-unsaturated ester grouping of methyl thujate (**3***b*) was sufficiently reactive and a Michael-type addition took place parallel with the expected amide formation; eq. 2 exemplifies this point for the reaction with diethylamine. Although analytical and spectral properties of these products were in accord with this formulation we did not pursue this line to conclusive evidence.

[2] 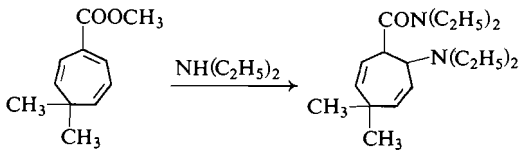

Only the unsubstituted amide and anilide of thujic acid and the ethyl and *p*-bromphenacyl esters were prepared previously (8, 13). None of these compounds has been reported to possess any type of biological activity.

[7]See Experimental.

[8]See Experimental for details.

We presented details of methods applied in evaluating the insect-controlling potential of our compounds, as well as discussion regarding structure–activity relationships in a separate paper (14). Therefore here we confine ourselves to outlining the most pertinent results in Table 3. In summary, the diethylamide of thujic acid (**4***d*) has been shown to be an extremely potent repellent of several insect species. Of particular interest is its activity against the blood-sucking yellow fever transmitter, *Aedes aegypti*. In contrast, thujic acid esters showed only traces of activity against species represented in Table 3. This again emphasizes the potential of the alkylamido group as a modifying substructure for various types of insect-controlling compounds of natural origin, as has already been exemplified in the case of juvenile hormone and juvabione analogs (9).

Finally, we may note that representative compounds of both series were screened[9] against several leaf eating insects. However, as yet, no distinct ovicidal, attractant or repellent activity has been observed. This testing program is continuing.

Experimental

General

Alcohols and amines used in the preparation of the respective esters and amides were of commercial origin, mostly reagent grade, and were used without further purification. G.l.c. analyses[10] were carried out using a 5 ft × 1/8 in. column packed with 5% OV-17 on 100–120 mesh GasChrom Q with a gas flow rate of 25 ml N_2/min and an appropriate temperature in the 100–250° range depending on the mol. wt. and type of compound tested. I.r. spectra of all compounds prepared were taken on a Perkin-Elmer 521 instrument and were in agreement with the expected structures. Melting points determined on a Kofler hot stage microscope and boiling points were not corrected. Elemental analyses were made by Galbraith Laboratories, Knoxville, Tennessee.

Isolation of Thujic Acid 3a

One hundred and twenty grams of a dark tarry oil obtained by steam distillation of cedar wood[11] was stirred with 500 ml of cyclohexane for 2 h at 25° until most of the oil dissolved. The solution was filtered to remove a small amount of undissolved material and the

[9]We appreciate the co-operation of Dr. I. Weatherston, Insect Pathology Research Institute, Sault St. Marie, Ontario.

[10]The analyses were kindly provided by Dr. W. G. Howells and Mr. K. L. McDonald and their staff. Their assistance in this regard is gratefully acknowledged.

[11]Our thanks are due to Mr. R. J. Rocchini and his staff for providing us with the steam distilled material.

TABLE 3. Summary of repellent and attractant activity of selected amides of thujic acid*

	Repellent activity			Attractant activity
	Yellow fever mosquito (*Aedes aegypti*)	German cockroach (*Blatella germanica*)	American cockroach (*Periplaneta americana*)	Yellow fever mosquito (*Aedes aegypti*)
Amide tested				
4*b*	6	—†	—†	
4*c*	—†			Active‡
4*d*	312	133	102	
4*f*	—†	25		
4*g*				Active‡
4*i*				Active‡
4*k*				Active‡
Standards tested§				
Dimethyl phthalate	100			
3,3-bis(Hydroxymethyl)heptane	1220			
Fencholic acid		100	100	

*We thank Dr. M. Beroza, Dr. C. H. Schmidt, Mr. E. S. Hall, and Dr. D. E. Weidhaas, and their collaborators at the United States Department of Agriculture, Entomology Research Division, for screening our samples and for permission to use the resultant data for publication.

†Inactive.

‡Showed a distinct degree of attractancy. Extreme difference in volatility between these compounds and the standard attractant L-(+)-lactic acid does not allow for a more quantitative comparison. In specific terms, the screened compounds showed activity in the 0.1–1.0% range of the standard attractant.

§The activity of standards is arbitrarily set at 100. Consequently, numerical values given for specific compounds represent percentage points of activity relative to standard.

Can. J. Chem. Downloaded from www.nrcresearchpress.com by 210.87.254.105 on 09/05/12
For personal use only.

filtrate was stirred with 900 ml of a saturated $NaHCO_3$ solution until gas evolution ceased. The two phases were separated and another 200 ml of the $NaHCO_3$ solution was added to the cyclohexane layer and stirred for 1 h. Upon separation the aqueous phases were combined and carefully acidified with 10% HCl. The resulting yellow precipitate was filtered off and dried *in vacuo*. The thujic acid thus obtained was about 80% pure by g.l.c. The crude acid was effectively purified by recrystallization from 80% acetic acid and was then better than 95% pure by g.l.c., m.p. 86–89°, lit. (12, 13, 15) m.p. 88–89°. For the purpose of further identification the acid was converted by the method described below into its methyl ester, m.p. 35°, lit. (12, 16) 34–35°. The n.m.r. spectrum (60 MHz) of this methyl ester was identical with those published in the literature (15, 17).

Thujic Acid Chloride

Thujic acid (16.4 g, 0.1 mol) was slowly (1 h) added to a mixture of 17.8 g (0.15 mol) thionyl chloride and 0.73 g (0.01 mol) dimethylformamide. The mixture was left for 2 h at 25° and subsequently the excess of $SOCl_2$ was evaporated *in vacuo* at 40°. The crude chloride, a straw-colored oil, was used in subsequent esterifications and amidations directly.

The chloride (1 g) was stirred (1 h, 25°) with 20 ml of a 10% $NaHCO_3$ solution. Then the mixture was acidified with concentrated HCl and extracted with 1,2-dichloroethane; the extract was evaporated and the residue was tested for the presence of cumic acid by g.l.c. and i.r. None was detected.

Esters of Thujic Acid (3c–h)

The respective alcohol (0.08 mol) was dissolved in 20 ml of pyridine and 0.1 mol of the above acid chloride was added with stirring. The reaction mixture was kept at 60° for 6 h, left overnight at 25°, and then poured into water. The ester was extracted with ethyl ether and the extract was washed consecutively with water, 5% HCl, 10% $NaHCO_3$, and water. The dried ether solution was evaporated and the crude ester was purified by fractional distillation. All distilled esters showed only one peak on g.l.c. analysis with impurities estimated at less than 1%. Yields obtained were mostly better than 75% and no effort was made to optimize them. Using a similar procedure, the isopropyl ester of cumic acid was prepared and used as standard in a search (g.l.c.) for any traces of it in isopropyl thujate. Thus an additional proof was obtained that the thujic – cumic acid rearrangement did not take place during the acid chloride formation.

Amides of Thujic Acid (4a–l)

Method A. N,N-Di-n-butyl Thujamide (4f)

A benzene solution of di-*n*-butylamine (20%, 0.3 mol) was placed in an ice–water bath and 0.1 mol thujic acid chloride was added with stirring over 30 min so that the temperature did not exceed 40°. The mixture was stirred for 2 h and then left overnight. Water (150 ml) was added and the benzene layer which formed was separated. The aqueous phase was extracted with benzene, the original benzene phase and extracts were then combined, washed consecutively with H_2O, 10% HCl, 10% aqueous

$NaHCO_3$, and H_2O, and evaporated. The crude amide was purified by fractional distillation. See Table 2.

Method B. N,N-Diethyl Thujamide (4d)

An aqueous solution (20%) of diethylamine (0.3 mol) was stirred in an ice–water bath and 0.1 mol acid chloride was added over 30 min so that the temperature did not exceed 25°. Stirring was continued for 2 h and the mixture was then left overnight. The amide was extracted with benzene. Subsequent treatment of the extract and isolation procedure were similar to those in method A.

Method C. N-p-Chlorophenyl Thujamide (4j)

p-Chloroaniline (2.1 g, 0.016 mol) was dissolved in 15 ml pyridine and 3 g (0.016 mol) of thujic acid chloride was added over 10 min at 10°. After 2 h at 25° the mixture was quenched with ice and the subsequent work-up was similar to that of methods A and B.

This work was supported, in part, by a grant from the National Research Council of Canada, Industrial Research Assistance Program (IRAP). The skillful experimental collaboration of Mrs. E. C. Fryberg is appreciated.

1. J. A. F. GARDNER. The chemistry and utilization of western red cedar. Department of Forestry Publication No. 1023. 1963.
2. U. ARNDT. Holzforschung, **22**, 104 (1968).
3. H. McLEAN. For. Prod. J. **20**, 48 (1970).
4. G. BECKER. Holzforschung, **17**, 19 (1965).
5. R. L. METCALFE. *In* Encyclopedia of chemical technology. Vol. 11. 2nd ed. *Edited by* A. Standen. Interscience, New York, N.Y. 1966. pp. 723–738.
6. E. T. McCABE, W. F. BARTHEL, S. I. GERTLER, and S. A. HALL. J. Org. Chem. **19**, 493 (1954).
7. W. A. JONES and M. JACOBSON. Science, **159**, 99 (1968).
8. R. E. DAVIS and A. TULINSKY. Tetrahedron Lett. 839 (1962).
9. P. A. CRUICKSHANK and R. M. PALMERE. Nature, **233**, 438 (1971).
10. H. H. BOSSHARD, R. MORY, M. SCHMID, and H. ZOLLINGER. Helv. Chim. Acta, **42**, 1653 (1959).
11. J. HOWARD. U.S. Patent 3 361 800 (1968).
12. A. B. ANDERSON and E. C. SHERRARD. J. Am. Chem. Soc. **55**, 3831 (1933).
13. C. D. HURD and O. E. EDWARDS. J. Am. Chem. Soc. **71**, 1016 (1949).
14. V. HACH and E. C. McDONALD. Science, **174**, 144 (1971).
15. J. GRIPENBERG. Acta Chem. Scand. **3**, 1137 (1949); **10**, 487 (1956).
16. E. F. KURTH. J. Am. Chem. Soc. **72**, 5178 (1950).
17. M. WILLCOTT III. Ph.D. Thesis, Yale University, New Haven, Conn. 1963.
18. V. HACH and E. C. McDONALD. Tetrahedron Lett. 3175 (1970); Can. J. Chem. **49**, 1762 (1971).

Can. J. Chem. Downloaded from www.nrcresearchpress.com by 210.87.254.105 on 09/05/12
For personal use only.

Hot-Tube Reactions of Dehydroabietic Acid with Ketene-Producing Reagents. Pyrolysis of the Acid Chloride and Symmetrical and Mixed Anhydride Derivatives of Dehydroabietic Acid

RAY F. SEVERSON AND WALTER H. SCHULLER
Naval Stores Laboratory,[1] *Olustee, Florida 32072*

Received March 26, 1973

Dehydroabietic acid (**1***a*) was reacted with diketene, acetic acid, acetic anhydride, isopropenyl acetate, acetyl chloride, and acetone on Vycor rod at 450 °C in a hot tube. Dehydroabietic anhydride (**1***b*) and acetyl dehydroabietate (**1***c*) were pyrolyzed at 450 °C and dehydroabietyl chloride (**1***d*) was pyrolyzed over a temperature range of 290–500 °C. The major olefin products resulting from decarboxylation of the various derivatives were 19-norabieta-4,8,11,13-tetraene (**2**), 19-norabieta-4(18),8,11,13-tetraene (**3**), 19-norabieta-3,8,11,13-tetraene (**4**), and *cis*-1,10a-dimethyl-7-isopropyl-1,2,3,9,10,10a-hexahydrophenanthrene (**5**). High conversions to these compounds were obtained. In the presence of the ketene-producing reagents the olefins were oxidized to yield substantial amounts of retene (**6**), compounds **2** and **5** being the most readily dehydrogenated. The acid isomerization of **2**, **3**, **4**, and **5** was studied using *p*-toluenesulfonic acid in toluene at 110 °C.

On a fait réagir l'acide déhydroabiétique (**1***a*) avec le dicétène, l'acide acétique, l'anhydridre acétique, l'acétate d'isopropényle, le chlorure d'acétyle et l'acétone sur une tige Vycor à 450 °C dans un tube chaud. L'anhydride déhydroabiétique (**1***b*), le déhydroabiétate d'acétyle (**1***c*) ont été pyrolysés à 450 °C et le chlorure de déhydroabiétyle (**1***d*) dans l'intervalle de température 290–500 °C. Les produits oléfiniques majeurs qui résultent de la décarboxylation des divers dérivés sont le norabiéta-19 tétraène-4,8,11,13 (**2**), le norabiéta-19 tétraène-4(18),8,11,13 (**3**) le norabiéta-19 tétraène-3,8,11,13 (**4**) et le *cis*-diméthyl-1,10a isopropyl-7 hexahydro-1,2,3,9,10,10a phénanthrène (**5**). Les conversions en ces composés sont élevées. En présence de réactifs producteurs de cétène, les oléfines ont été oxydées en des quantités substantielles de rétène (**6**), les composés **2** et **5** étant deshydrogénés le plus rapidement. L'isomérisation acide de **2**, **3**, **4** et **5** a été étudiée en utilisant l'acide *p*-toluène sulfonique dans le toluène à 110 °C.
[Traduit par le journal]

Can. J. Chem., 51, 3236 (1973)

Introduction

Our previously described work has illustrated that under certain conditions (400–500 °C) hot-tube pyrolysis of certain resin acids, in particular dehydroabietic acid (**1***a*), yields isolable A-ring olefins (19-norabieta-4,8,11,13-tetraene (**2**), 19-norabieta-4(18),8,11,13-tetraene (**3**), and 19-norabieta-3,8,11,13-tetraene (**4**)) (1, 2). Those conditions, however, which minimized further decomposition of the initial decarboxylation products, resulted in only about a 7% conversion of the acids to olefins.

It seemed feasible that the pyrolysis of some of the more thermally labile carboxylate derivatives of **1***a*, such as anhydrides and acid halides (3), would result in a much improved route to the A-ring olefins. Because of the increased reactivity of these derivatives it was considered possible to substantially decrease secondary decomposition products, while still maintaining desirable conversion levels, by reducing the reaction temperatures. The increased bulk of the derivatives made it seem probable that the carbonyl moiety would be eliminated more selectively and the yield of the vinylidine compound **3** would be improved. Recent interest in a facile transformation of **1***a* to **3**, to be used as a possible precursor in steroid synthesis (4), makes an increase in the relative amount of **3** in the olefin product highly desirable.

Since ketene can be produced from a variety of reagents under hot-tube conditions (3, 5), **1***a* might be reacted with these materials in the pyrolysis tube to form mixed anhydrides which then would decompose to yield the desired olefins, thus eliminating a prior synthetic step.

In this paper, work designed to verify these assumptions will be reported. The acid isomerization of the olefins obtained also was studied.

Experimental

Dehydroabietic Anhydride (1b)

This previously reported compound (6) was prepared by heating, under nitrogen, 5 g of **1***a* and 75 ml acetic

[1]One of the laboratories of the Southern Region, Florida/Antilles Area, Agricultural Research Service, U.S. Department of Agriculture.

Can. J. Chem. Downloaded from www.nrcresearchpress.com by 210.87.254.6 on 09/05/12
For personal use only.

Can. J. Chem. Downloaded from www.nrcresearchpress.com by 210.87.254.6 on 09/05/12
For personal use only.

anhydride and allowing the acetic acid which formed to distill out at a rate which maintained the pot temperature at 140 °C. Heating was stopped when the pot temperature reached 200 °C. The residue was dissolved in 20 ml of anhydrous acetone and the solid which formed upon cooling was collected and dried to yield 4.7 g, m.p. 137–40 °C (lit. (6) 142 °C). Recrystallization from hot heptane yielded 3.2 g of product, m.p. 140.5–142 °C; i.r. (KBr): ν_{max} 1810 and 1740 cm^{-1} (C=O, $Ab_{1740}/Ab_{1810} = 0.89$, $Ab_{2920(CH)}/Ab_{1805(CO)} \simeq 1.0$).

Acetyl Dehydroabietate (1c)

Ketene (prepared in a ketene generator from acetone (5)) was bubbled through a cold solution of 5 g of **1***a* in acetone until all the acid was consumed. The solvent was removed to yield an oil which solidified upon standing. The product was recrystallized from hot heptane to yield 3.2 g; m.p. 68–70 °C; i.r. (KBr): ν_{max} 1800 and 1735 cm^{-1} (C=O), $Ab_{1735}/Ab_{1805} = 0.9$, $Ab_{2920(CH)}/Ab_{1805(CO)} \simeq 0.5$); u.v. (heptane): λ_{max} 275.5 (ε 600) and 267.0 nm (ε 580); $[\alpha]_D^{25}$ +57.2° (*c*, 2.0 EtOH, no change in 2 h), +56.6° (*c*, 2.0 heptane).

Anal. Calcd. for $C_{22}H_{30}O_2$: C, 77.15; H, 8.82; O, 14.02. Found: C, 76.93; H, 8.93; O, 13.79.

Dehydroabietyl Chloride (1d)

This compound was prepared as described by Jeger and Durst (7). The previously uncharacterized crude product was distilled at 140 °C and 0.1 mm Hg in a molecular still to yield a colorless sirup with a neutralization equivalent of 319.7 (theory 318.9); i.r. (neat): ν_{max} 1800 cm^{-1} (C=O); u.v.: λ_{max} (isooctane) 275 (ε 735) and 267 nm (ε 740); $[\alpha]_D^{25}$ +125° (*c*, 3.2 isooctane).

Anal. Calcd. for $C_{20}H_{27}ClO$: C, 75.35; H, 8.56; Cl, 11.12. Found: C, 75.37; H, 8.60; Cl, 10.90.

Pyrolysis

The pyrolysis apparatus used has been described (2). Typically, 4 g of **1***a* in 20 ml of acetic acid was added dropwise into the Vycor rod pyrolysis column over a 60-min period (N_2 flow 20 ml/min). When addition was complete, the pyrolyzate was removed quantitatively with acetone and stripped on a rotoevaporator at 40 °C under water jet vacuum. Similar runs were made with acetic anhydride, isopropenyl acetate, acetyl chloride, and acetone. In the diketene experiment, a solution of 4 g of **1***a* and 4 ml of diketene in 16 ml of acetone was used. Compounds **1***b*, *c*, and *d* were pyrolyzed as 10% solutions in benzene (2 g in 20 ml). The pyrolyzates from the acid chloride runs were trapped over aqueous Na_2CO_3. The solvent was removed under reduced pressure on a rotoevaporator. Ether was added to the residue and the p*H* of the aqueous layer was adjusted to about 7 with dilute HCl. The ether extracts were washed with water until neutral, dried over Na_2SO_4, filtered, and the solvent was removed to yield oils. All pyrolyzates were protected from the atmosphere until they were analyzed for product composition.

Determination of Percent Yield

A weighed portion of each pyrolyzate was treated with an ethyl ether – diazomethane solution, a known amount of hexacosane (internal standard) was added, and the resulting solution was analyzed by g.l.c. using a 15 ft × 3/16 in. 10%-Dexsil 300 GC column (80/100 mesh NAW Chromosorb W, 100 ml/min He and temperature program 220–280 °C at 2 °C/min). The peak area for each component was corrected for differences in response, before percent yield data was calculated. All unidentified products were assumed to have the same response as the olefins. Response factors were determined from a solution containing known amounts by weight of the olefins, retene (1-methyl-7-isopropylphenanthrene (**6**)), **1***e*, and hexacosane.

Identification of Products

The products identified were collected from the Dexsil 300 column at 250 °C and rechromatographed and collected. Compounds **2**, **3**, **4**, **6**, and methyl dehydroabietate (**1***e*) were identified by g.l.c. retention data and i.r. and u.v. spectra (1).[2]

cis-1,10a-Dimethyl-7-isopropyl-1,2,3,9,10,10a-hexahydrophenanthrene (5)[3] was collected as a colorless oil which solidified upon standing, m.p. 34–35 °C; i.r. (neat): 1650 (R_1R_2C=CHR) (8), 1616 and 1500 (C=C, Ar), 884 (isolated ArH), 825 (two adjacent ArH), and 805 cm^{-1} (R_1R_2C=CHR) (8); n.m.r. (CCl_4): δ 0.84 (s, 3, C_{10a}—Me), 0.96 (d, 3, J = 6.0 Hz, C_1—Me), 1.21 (d, 6, J = 6.8 Hz, isopropylmethyls), 6.01 (t, 1, $J \simeq 3$ Hz, C_4—H), 6.79 (s, 1, C_8—H), 6.85 (d, 1, J = 7.5 Hz, C_6—H) and 7.29 p.p.m. (d, 1, J = 7.5 Hz, C_5—H); λ_{max} (95% EtOH) 296 (ε 1500), 287 (ε 1900), and 255 (ε 16 300) nm; $[\alpha]_D^{25}$ −93.4° (*c*, 1.3 95% EtOH). Mass spectrum *m/e* (relative intensity) 254.2049 ($C_{19}H_{26}$ requires 254.2034) (100), 239 (43.6), 212 (6.4), and 213 (18.3).

Anal. Calcd. for $C_{19}H_{26}$: C, 89.70; H, 10.30. Found: C, 89.40; H, 10.29.

Olefin Acid Isomerization

A stock acid solution containing 0.58 mg/ml of *p*-toluenesulfonic acid (*p*-TSA) in toluene was prepared (water of hydration was removed by azeotropic distillation). Several glass Carius tubes were placed on Dry-Ice and charged with 1-ml portions of the stock *p*-TSA solution and 1 ml of an anhydrous toluene solution containing 1.24 mg/ml of the A-ring olefin mixture consisting of 42% of **2**, 21% of **3**, and 37% of **4**. The tubes were flushed with argon, sealed under vacuum, and placed in an oil-bath at 110 °C. The tubes were removed at intervals, placed on Dry-Ice, opened, hexacosane internal standard added, and the *p*-TSA removed by washing with Na_2CO_3. The samples were analyzed by g.l.c.

The initial isomerization of **5** was run under identical conditions. After 48 h reaction time, the remaining tubes were opened and an additional 0.5 ml of a solution containing 1.33 mg/ml of *p*-TSA was added. The tubes were

---

[2]The n.m.r. data for compounds **2** and **3** given in ref. 1 were reported incorrectly. The C_{10}—Me resonance for **2** was at δ 1.33 instead of 1.24 and the C_4—Me at 1.66 instead of 1.33. The value for the C_4—Me for compound **3** was at 1.72 instead of 1.27. We thank Professor J. W. Huffman, Clemson University, for bringing these errors to our attention.

[3]The abietane nomenclature cannot be used for olefin **5** since it no longer has the β-C_4—methyl. In all discussions centered around **5**, the numbering system used for phenanthrene derivatives, as shown in structure **5** in Scheme 1, will be used. The term "A-ring olefins" will only be used in discussing those compounds with the normal abietane stereochemistry (β-C_4—Me), *i.e.* compounds **2**, **3** and **4**.

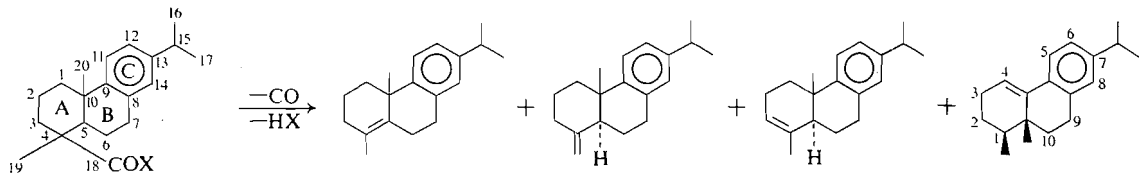

1 2 3 4 5

a X = OH
b X = dehydroabietate
c X = $OCOCH_3$
d X = Cl
e X = OCH_3

SCHEME 1

resealed and replaced in the oil-bath at 110 °C. The samples were analyzed at intervals as given above. Mass balances (from g.l.c. internal standard) were excellent (97–103%) at all intervals monitored.

Results and Discussion

Solutions of **1***a* in ketene-producing reagents, *i.e.* diketene–acetone, acetic acid, acetic anhydride, isopropenyl acetate, acetyl chloride, and acetone, were reacted in a hot tube under nitrogen at 450 °C on Vycor rod. Compounds **1***b* and *c* were pyrolyzed in benzene solutions under the same conditions. The compositions of the pyrolyzates obtained are shown in Table 1.

In order to study the effect of temperature on the pyrolyzate composition, the acid chloride **1***d* was pyrolyzed at 290 °C over Na_2CO_3 in the g.l.c. injection port and at 350–500 °C in the hot tube. Product analysis of these runs is given in Table 2.

Compounds **2**, **3**, **4**, **6**, and **1***a* were identified by comparison of their g.l.c. retention data and i.r. and u.v. spectra with the authentic compounds. The mass spectrum of **5** showed that it was isomeric with **2**, **3**, and **4** (molecular ion, *m/e* 254). Unlike the other olefins, the u.v. spectrum of **5** showed strong absorption at 255 nm (ε 16 300), indicating the presence of an aromatic conjugated double bond (9). Since Δ^5-dehydrohomodehydroabietic acid (**7**) has the normal **1***a* u.v. maxima (λ_{max} 267 and 275.5 nm (10)), the only compounds consistent with the spectral data are the *cis*- or *trans*-1,10a-dimethyl-7-isopropyl-1,2,3,9,10,10a-hexahydrophenanthrene. Comparison of the methyl and vinyl n.m.r. resonances of **5** with the n.m.r. data of the known *cis*- and *trans*-deisopropyl analogs **8** and **9** (11) clearly showed that **5** is the *cis*-dimethyl compound.

Inspection of Table 1 shows that, as anticipated, **1***a* did react directly with the reagents or with ketene produced by thermal decomposition of the various reagents in the hot tube to form a mixed anhydride which then decomposed to yield olefins. The fact that **1***c* gave essentially the same spectrum of products substantiates this conclusion. In contrast to the mixed anhydride pyrolyzates, only a trace of **6** was found when the symmetrical anhydride **1***b* was pyrolyzed.

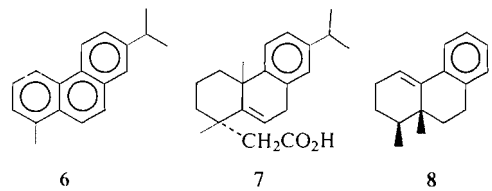

6 7 8

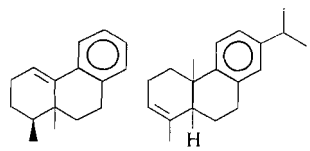

9 16

Also, a much higher relative yield of the new olefin, **5**, was found. This observation indicates that ketene or radicals formed during ketene formation are behaving as dehydrogenation agents and are oxidizing the olefins to **6**, compounds **2** and **5** being most readily dehydrogenated. The percent recovery data show that decomposition of **1***b* is essentially complete under these conditions. Amounts of g.l.c. volatile material were considerably lower in some of the other runs, probably due to the reaction of **1***a* with ketene in the pyrolyzate-trapping system. (The i.r. spectrum of the crude pyrolyzate from

Can. J. Chem. Downloaded from www.nrcresearchpress.com by 210.87.254.6 on 09/05/12
For personal use only.

TABLE 1. Percent composition of anhydride pyrolyzates at 450 °C

	Dehydroabietic anhydride[a]	Acetyl dehydroabietate[a]	Dehydroabietic acid in the presence of: Diketene[b]	Acetic anhydride[c]	Isopropenyl acetate[c]	Acetic acid[c]	Acetyl chloride[c]	Acetone[c]
	Mol % of hydrocarbon fraction[d]							
Δ^4-Alkene (**2**)	14	17	15	8	7	13	27	16
$\Delta^4(18)$-Alkene (**3**)	20	12	22	13	21	13	11	23
Δ^3-Alkene (**4**)	26	30	32	25	34	34	27	27
cis-Dimethylalkene (**5**)	23	10	6	4	8	4	11	34
Retene (**6**)	>1	9	13	26	13	29	9	—
Unidentified	17	22	12	24	17	7	15	—
	Mol % dehydroabietic acid recovered[e]							
	74	23	23	12	45	52	2	83
	Mol % g.l.c. volatile material recovered[e]							
	199	98	90	43	98	73	58	89

[a]Pyrolyzed as 10% solutions in benzene.
[b]Reacted as a 20% solution in diketene–acetone.
[c]Pyrolyzed as 20% solution of 1*a* in 20 ml of other reagent.
[d]Based on total mol of g.l.c. volatile material in hydrocarbon fraction.
[e]Based on initial amount of compound pyrolyzed.

TABLE 2. Percent composition of dehydroabietyl chloride pyrolyzate

	Pyrolysis temperature (°C) 290[b]	350[c]	400[c]	450[c]	500[c]	Relative[a] retention time
	Mol % composition of products[d]					
Δ^4-Alkene (**2**)	17	27	25	25	7	0.42
$\Delta^4(18)$-Alkene (**3**)	10	16	16	22	17	0.44
Δ^3-Alkene (**4**)	19	26	28	29	21	0.46
cis-Dimethylalkene (**5**)	46	24	16	12	7	0.50
Retene (**6**)	—	>1	>1	1	4	0.75
Unidentified	7	6	15	11	44	—
	Mol % dehydroabietyl chloride unreacted[e]					
	—	29	3	1	0	
	Mol % g.l.c. volatile material recovered[f]					
	30	103	100	100	63	

[a]Relative to hexacosane (on Dexsil 300, temperature program 220–280 °C at 2°/min).
[b]Pyrolyzed in Na_2CO_3 coated injected port.
[c]Pyrolyzed as 10% solutions in benzene on Vycor rod.
[d]Based on total mol of g.l.c. volatile products in hydrocarbon fraction
[e]Hydrolyzed to 1*a* and converted to 1*e* (relative retention time 0.80) before analysis; based on amount of 1*c* pyrolyzed.
[f]Based on the amount of 1*c* pyrolyzed.

the diketene run showed anhydride carbonyl absorption.) The mixed anhydride (**1***c*), which was not volatile under the g.l.c. conditions used, would decrease the amount of g.l.c. volatile material recovered. Unlike **1***d*, **1***b* and *c* did not spontaneously decompose in the g.l.c. injection port at 290 °C.

The product compositions of the pyrolyzates obtained from **1***d* as a function of temperature are given in Table 2. Above 400 °C, essentially

Can. J. Chem. Downloaded from www.nrcresearchpress.com by 210.87.254.6 on 09/05/12
For personal use only.

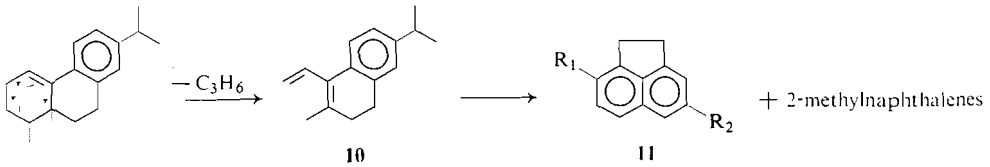

10 11

SCHEME 2

all the acid chloride decomposed to yield hydrocarbon products. A theoretical recovery of g.l.c. volatile products was obtained over the 350–450 °C range. The extremely low conversion to **6** at 450 °C and below substantiates our previous rationalization for the high yields of this material observed in the presence of ketene. As with the resin acids (1), a large decrease in recovered material and increase in multi lower molecular weight unidentified hydrocarbons were observed at 500 °C. These lower molecular weight materials and **6** appear to be formed predominantly by secondary decompositions of **2** and **5**. Both of these olefins have the structural requirements to readily undergo the thermal retro Diels–Alder reaction (12) resulting in the loss of ethylene from **2** (1) and propylene from **5** as shown in Scheme 2. This is substantiated by the fact that compounds **8** and **9** undergo a retro Diels–Alder reaction to lose propylene in the mass spectrometer (11). The loss of the isopropyl group to yield an ion at *m/e* 213 somewhat complicates this observation of the retro Diels–Alder reaction in the mass spectrum of **5**. However, after correction for higher isotopes resulting from isopropyl fragmentation, one-half of the intensity of the ion at *m/e* 212 can be attributed to retro Diels–Alder fragmentation. The formation of **10** at higher temperatures readily explains the formation of the various 2-methylnaphthalenes and substituted acenaphthenes (**11**) formed during the pyrolysis of **1***e* at 600–800 °C (2).[4]

In contrast to the other olefins, **5** was produced from **1***d* in decreasing relative amounts with increasing reaction temperature. The recovery rate at 450 °C and below clearly indicates that the retro Diels–Alder reaction does not occur to any appreciable extent at these temperatures. A possible explanation for the decreasing yield of **5** could be gas-phase acid isomerization of the primary decomposition olefin products. It has been reported that the normal A-ring olefins

[4]Although not previously identified, the neutral fraction of the 450 °C pyrolyzate from **1***a* contained 2.5% of **5** (1).

TABLE 3. Course of the acid isomerization of the A-ring olefins[a]

	% composition[b]				
Time, h	**16**	**2**	**3**	**4**	**5**
0	—	42	21	37	—
1	—	51	14	35	—
2	1	55	10	34	—
4	5	64	6	25	—
20	16	73	3	8	—
28	27	67	2	4	—
46.5	40	54	2	3	1
90.5	47	49	1	2	1
162.5	52	43	1	2	2
252.5	52	43	1	2	2
299.5	52	43	1	2	2

[a]Data obtained using *p*-TSA in toluene at 110 °C.
[b]Assignments were made by g.l.c. retention and u.v. data.

(**2**, **3**, and **4**) are readily isomerized by *p*-TSA in refluxing toluene to yield an olefin mixture containing predominantly **4** and a new compound, 19-nor-5-β-abieta-3,8,11,14-tetraene (**16**), in which the latter predominates (13). Since no effort was made to carry this reaction to completion, the isomerization was repeated.

An olefin mixture consisting of 42% of **2**, 21% of **3**, and 37% of **4** was heated at 110 °C with *p*-TSA in toluene under an inert atmosphere. The course of the isomerization was monitored by g.l.c. at various intervals (Table 3). After 160 h a steady-state composition of 52% of **1***b*, 43% of **2**, 2% of **4**, and 1% of **3** was obtained.[5] The normal A-ring olefins reached an equilibrium condition in 40 h consisting of 93% of **2**, 5% of **4**, and 2% of **3**. A very slow conversion to **5** also had occurred, with 2% of the mixture being **5** after 300 h. Pure **5** was treated under the same conditions and no change was observed after heating for 90 h. The fact that **5** is stable to acid is consistent with its proposed structure,

[5]The plot of percent composition *vs.* time (Fig. 1) for the acid isomerization of the 19-norabieta-tetraenes (**2**, **3**, and **4**) using *p*-TSA in toluene at 110 °C is available at a nominal charge, from the Depository of Unpublished Data, National Science Library, National Research Council of Canada, Ottawa, Canada K1A 0S2.

Can. J. Chem. Downloaded from www.nrcresearchpress.com by 210.87.254.6 on 09/05/12
For personal use only.

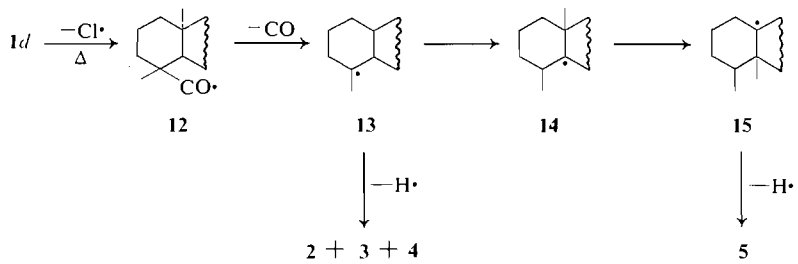

SCHEME 3

since the phenyl-conjugated double bond system should result in the most stable system.

From the isomerization data it should be safe to conclude that little if any acid-catalyzed rearrangement of the initially formed **5** had occurred in the hot tube. The absence of **16** and the constant A-ring olefin ratios below 450 °C on the **1***d* pyrolyzate indicate that acid induced rearrangement does not readily take place during pyrolysis. The constant relative A-ring olefin ratios in the pyrolyzates of **1***d* below 450 °C also indicate that thermally induced isomerization is not important at the lower temperatures. If thermal double bond rearrangements were occurring, a relative increase would be expected in the yield of **2** and **5** with increasing pyrolysis temperatures.

A possible rationale for the decreasing yield of **5** with increasing temperature may be the mechanism by which the various products are formed. From other pyrolysis work on acid halides (14), the first step in the decomposition of **1***d* may be assumed to be the loss of a chlorine radical, followed by decarbonylation to yield intermediate **13**, as shown in Scheme 3. The lower temperatures favor rearrangement to the most stable radical (**15**) and therefore the formation of **5**. As the temperature increases, the concentration of radicals increases, making hydrogen abstraction more probable. Thus, radical stability becomes less important and an increased yield of **2**, **3**, and **4** results.

The authors wish to thank Dr. Bernard A. Parkin, Jr. and Mr. Gordon S. Fisher of the Naval Stores Laboratory for many helpful discussions; Miss Lynn Griffin, Dept. of Chem., Florida State University, for the mass spectral analysis; and Mr. Richard Rosanski, Dept. of Chem., Florida State University, for obtaining the n.m.r. data.

1. R. F. SEVERSON and W. H. SCHULLER. Can. J. Chem. **50**, 2224 (1972).
2. R. F. SEVERSON, W. H. SCHULLER, and R. V. LAWRENCE. Can. J. Chem. **49**, 4027 (1971).
3. C. A. BUEHLER and D. E. PEARSON. Survey of organic synthesis. Wiley-Interscience, New York, N.Y. 1970. p. 886.
4. J. W. HUFFMAN. J. Org. Chem. **35**, 478 (1970).
5. L. FIESER and M. FIESER. Reagents for organic synthesis. John Wiley and Sons, Inc., New York, N.Y. 1967. p. 528.
6. LE-VAN-THOI. Peintures, Pigments, Vernis, **29**, 125 (1953).
7. D. JEGER and O. DURST. Helv. Chem. Acta, **30**, 1853 (1947).
8. A. WEISSBERGER. Chemical applications of spectroscopy. Interscience Publishers, Inc., New York, N.Y. 1956. pp. 372 and 382.
9. H. W. WHITLOCK, JR., P. B. REICHARDT, and F. M. SILVER. J. Am. Chem. Soc. **93**, 485 (1971).
10. G. STORK and J. W. SCHULENBERG. J. Am. Chem. Soc. **84**, 284 (1962).
11. H. W. WHITLOCK, JR. and L. E. OVERMAN. J. Am. Chem. Soc. **93**, 2247 (1970).
12. F. O. RICE and M. T. MURPHY. J. Am. Chem. Soc. **66**, 765 (1944).
13. J. W. Huffman. J. Org. Chem. **37**, 17 (1972).
14. M. LADASKI, C. H. LEIGH, and M. SZWARC. Proc. Roy. Soc. (London), A, **214**, 273 (1952).

Can. J. Chem. Downloaded from www.nrcresearchpress.com by 210.87.254.6 on 09/05/12
For personal use only.

Gas Phase Solvation of the Ammonium Ion by NH_3 and H_2O and Stabilities of Mixed Clusters $NH_4^+(NH_3)_n(H_2O)_w$

J. D. PAYZANT, A. J. CUNNINGHAM, AND P. KEBARLE
Chemistry Department, University of Alberta, Edmonton, Alberta T6G 2G2

Received March 28, 1973

Can. J. Chem. Downloaded from www.nrcresearchpress.com by 210.87.254.6 on 09/05/12
For personal use only.

The gas phase equilibria

$(n,n-1)$ $\quad NH_4^+(NH_3)_n = NH_4^+(NH_3)_{n-1} + NH_3$

$(w,w-1)$ $\quad NH_4^+(H_2O)_w = NH_4^+(H_2O)_{w-1} + H_2O$

and those leading to mixed clusters like

$$NH_4^+(NH_3)_{n-1}(H_2O)_w + NH_3 = NH_4^+(NH_3)_n(H_2O)_w$$

were measured with a pulsed electron beam high pressure ion source mass spectrometer. The ion source contained pure ammonia or mixtures of ammonia and water vapor at pressures in the Torr range. Determination of the temperature dependence of the equilibrium constants led to the evaluation of ΔG^0, ΔH^0, and ΔS^0 values for the equilibria from $n = 1$ to 4 and $w = 1$ to 5. The ΔG^0 values for the $NH_4^+(NH_3)_n$ equilibria were in good agreement with previous determinations from this laboratory. Fair agreement was observed for the ΔH^0 and ΔS^0 values. Comparison with the corresponding results for $NH_4^+(H_2O)_w$ showed that the $\Delta H_{n,n-1}$ and $\Delta G^0_{n,n-1}$ were larger than $\Delta H_{w,w-1}$ and $\Delta G^0_{w,w-1}$. The difference was largest for the first step (1,0) and decreased progressively until a reversal with water values becoming larger occurred at the (5,4) step. The stronger hydrogen bonds of NH_3 to NH_4^+ for low ligand numbers is explained by the greater basicity of NH_3. As the ionic charge becomes dispersed and more distant stronger interactions are obtained with water which gives stronger H bonds in the absence of positive ionic charge. Breaks in the $\Delta H_{n,n-1}$ values indicate existence of a relatively stable $NH_4^+(NH_3)_4$ symmetric ion. A much smaller and less distinct break is observed with pure water ligands.

The mixed ammonia–water clusters show similar effects. The addition of a NH_3 molecule to a pure water ligand complex gives the strongest interaction. The addition of H_2O to a pure ammonia cluster gives the weakest interaction. The above effect is strongest at lowest ligand numbers. The difference decreases gradually and becomes reversed for more than four ligands.

Les équilibres en phase gazeuse

$(n,n-1)$ $\quad NH_4^+(NH_3)_n = NH_4^+(NH_3)_{n-1} + NH_3$

$(w,w-1)$ $\quad NH_4^+(H_2O)_w = NH_4^+(H_2O)_{w-1} + H_2O$

et ceux qui conduisant aux mélanges d'association du type

$$NH_4^+(NH_3)_{n-1}(H_2O)_w + NH_3 = NH_4^+(NH_3)_n(H_2O)_w$$

ont été étudiés par la mesure du rayon électronique pulsé à haute pression dans une source d'ion d'un spectromètre de masse. La source ionique contient de l'ammoniac pur ou des mélanges d'ammoniac–vapeur d'eau à des pressions de l'ordre du Torr. L'étude de l'influence de la température sur les constantes d'équilibre conduit aux valeurs ΔG^0, ΔH^0 et ΔS^0 des équilibres pour $n = 1$ à 4 et $w = 1$ à 5. Les valeurs de ΔG^0 obtenues pour les équilibres de $NH_4^+(NH_3)_n$ sont en bon accord avec les déterminations antérieures faites au laboratoire. Les valeurs de ΔH^0 et ΔS^0 concordent également. La comparaison avec les résultats correspondant pour $NH_4^+(H_2O)$ montre que $\Delta H_{n,n-1}$ et $\Delta G^0_{n,n-1}$ sont supérieurs à $\Delta H_{w,w-1}$ et $\Delta G^0_{w,w-1}$. La différence est la plus forte dans la première étape (1,0) et décroît progressivement jusqu'à une situation inversée c'est à dire des valeurs supérieures pour l'eau dans l'étape (5,4). Les liaisons hydrogènes plus fortes entre NH_3 et NH_4^+ pour des nombres de ligands faibles s'expliquent par une plus forte basicité de NH_3. A mesure que la charge ionique se disperse et que les interactions lointaines deviennent plus fortes avec l'eau, celle-ci donne des liaisons H plus fortes en l'absence de charge positive ionique. La coupure dans les valeurs $\Delta H_{n,n-1}$ indique l'existence d'un ion relativement stable $NH_4^+(NH_3)_4$ symétrique. Avec les ligands eau pure, cette coupure est plus faible et moins distincte. Les associations mixtes ammoniac-eau donnent des effets similaires. L'addition d'une molécule d'ammoniac au ligand eau pure complexée conduit à l'interaction la plus forte. L'addition d'eau à l'ammoniac associé donne l'interaction la plus faible. L'effet ci-dessus est le plus prononcé lorsque les nombres de ligands sont les plus bas. La différence décroît graduellement pour devenir inversée pour plus de quatre ligands.

[Traduit par le journal]

Can. J. Chem. Downloaded from www.nrcresearchpress.com by 210.87.254.6 on 09/05/12
For personal use only.

Introduction

Some of the earliest measurements of gas phase clustering equilibria done in this laboratory dealt with the ammonium ion.

$$(n,n-1) \quad NH_4^+(NH_3)_n = NH_4^+(NH_3)_{n-1} + NH_3$$

Studies of the equilibria $(n,n-1)$ at different temperatures led to values (1) for $\Delta H_{n,n-1}$ and $\Delta S_{n,n-1}$ for $n = 1$ to $n = 5$. The ΔH values obtained were 27 kcal/mol for the (1,0) step followed by a much decreased 17 kcal for the second step (2,1) then slower decreases for the (3,2) and (4,3) steps and again a somewhat larger decrease to the (5,4) step. These results were interpreted (1*a*) as an indication of a particularly stable $NH_3H^+NH_3$ with a symmetrically shared proton followed by the "normal" ammonium ion clusters $NH_4^+(NH_3)_n$ from $n = 3$ to $n = 4$ and then a change over to an "outer shell" position for the fifth ligand molecule. The existence of a symmetric four ammonia species $NH_4^+(NH_3)_4$ was supported by the findings of an earlier study (2) in which the mixed clusters $NH_4^+(NH_3)_n(H_2O)_w$ had been observed. These experiments were done with mixtures of water and ammonia vapor at a single temperature. The relative abundances of the clusters showed that when $n + w$ was less than four (*i.e.* inner shell) ammonia was taken into the cluster in preference to water. For clusters where $n + w$ was bigger than four the data could be interpreted by assuming preference of NH_3 in the inner shell of four molecules and preference for water in the outer shell (2).

The present work is intended as an improvement and extension of the earlier findings. More complete measurements were made this time, including the study of the ammonium ion solvated by water molecules alone, *i.e.* the species $NH_4^+(H_2O)_w$. Furthermore the mixed cluster stabilities were studied as a function of temperature so that enthalpy changes and entropy changes for the NH_3, H_2O exchange and addition to given mixed clusters could be obtained. We believe that these new results give a more accurate and consistent picture of ammonia ion solvation by ammonia and water molecules and the importance of hydrogen bonding. Furthermore, these results also connect to recent gas phase studies of the proton held alkyl amine dimers (3) and to the hydrogen bonded species obtained in protonated water, methanol, and dimethyl ether (4).

Experimental

The measurements were done with a pulsed electron beam high pressure mass spectrometer which was described earlier (5). Some specific details in procedures relating to the systems treated are shown below.

(a) The $NH_4^+(NH_3)_n$ Equilibria

These measurements were made with pure NH_3 at pressures between 2–7 Torr and temperatures between 25–450 °C. The ammonium clusters were the only ions observed. Pulsing of the electron beam allowed detection of the time dependent intensities of the ions extending over a few ms. The observed relative concentrations became constant in less than 100 μs after the electron pulse indicating rapid achievement of clustering equilibrium. A rapid establishment of the equilibrium for the conditions used is expected since the rate constants for the clustering reactions should be similar to those measured for the $H^+(H_2O)_n$ system (5).

(b) The $NH_4^+(H_2O)_w$ Equilibria

To observe the $NH_4^+(H_2O)_w$ equilibria one must use a very large H_2O:NH_3 pressure ratio. In such a system primary ionization leads to H_2O^+ and OH^+ ions which are rapidly converted to H_3O^+ and higher water clusters. The NH_4^+ and $NH_4^+(H_2O)_w$ ions are produced by bimolecular reactions of H_3O^+ and $H^+(H_2O)_n$ with NH_3. The rate constants for these reactions should be in the $k = 10^{-9}$ cm^3 molecule^{-1} s^{-1} range. The half life for formation of NH_4^+ should thus be in the $t_{1/2} = 0.7\ (10^{-9}n)^{-1}$ range where n represents the number of NH_3 molecules per cm^3. At a pressure of NH_3 equal to 10 mTorr, $n \approx 10^{14}$ and $t_{1/2} \approx 10^{-5}$ s. Thus only 10 mTorr NH_3 are sufficient for a rapid conversion to ammonium ion clusters. Typically 2–7 Torr of water vapor containing 1–10 mTorr of NH_3 were used in the experiments. No H_3O^+ or $H^+(H_2O)_n$ clusters were observed under these conditions. The equilibrium concentrations of the proton hydrates are expected to be very small since the proton affinities of NH_3 and H_2O differ by some 40 kcal.

(c) The Mixed Cluster Equilibria $NH_4^+(NH_3)_n(H_2O)_w$

The mixed clusters were observed with water vapor at pressures 2–8 Torr containing a few percent of ammonia vapor. These small concentrations of ammonia were found generally sufficient to produce all mixed clusters. This is possible since NH_3 is strongly preferred in the inner shell. The water pressure was determined directly by the ion source manometer reading. The partial pressure of ammonia was determined by observing the ions $NH_4^+(NH_3)_n$ and $NH_4^+(NH_3)_{n-1}$ and using the $K_{n-1,n}$ determined in the experiments with pure ammonia

$$(n,n-1) \quad NH_4^+(NH_3)_n = NH_4^+(NH_3)_{n-1} + NH_3$$

In the mixed solvent system the number of positive ions coexistent at equilibrium was often very large, some 12 mixed clusters being present in some experiments. It was found difficult to record the time dependent ion intensities of all these ions in a given experiment. The time required for this was very long (2–3 h) and it was difficult to maintain constant reaction conditions over such a period. To overcome this problem a gated single channel scaler was used instead of the multichannel analyzer. The master pulse generator, triggering the electron pulse, activated a

TABLE 1. Thermodynamic values[a] for the gas phase reactions $(n,n-1)$

	$NH_4^+(NH_3)_n = NH_4^+(NH_3)_{n-1} + NH_3$				$NH_4^+(H_2O)_n = NH_4^+(H_2O)_{n-1} + H_2O$		
		ΔG^0_{298}					
$n,n-1$	ΔH^{0a}	This work	Literature	ΔS^0	ΔH^0	ΔG^0_{298}	ΔS^0
1,0	24.8±0.4[b](27)[c]	17.1(17.5)[c]		26(32)[c]	17.3±0.4[b]	11.4	19.7
2,1	17.5±0.2(17)	8.9(9.0)	9.6[d],10.6[e]	23(26.8)	14.7±0.2	8.2	21.9
3,2	13.8±0.2(16.5)	6.1(6.4)	6.5[d]	26(34)	13.4±0.2	5.9	25.1
4,3	12.5±0.5(14.5)	3.7(3.8)	3.4[d]	30(36)	12.2±0.3	4.1	27.3
5,4	— (7.5)	(0.2)	—	(25)	9.7±0.3	3.0	22.4

[a]All ΔH and ΔG values in kcal/mol, ΔS values in e.u., standard state 1 atm.
[b]Standard deviation given only for ΔH, similar deviations found for ΔG and ΔS.
[c]Values in parentheses are results from earlier determinations of ref. 1*a*.
[d]Reference 6.
[e]Reference 2.

second pulse generator which kept the gate of the scaler closed for the first 100 μs after the electron pulse. In this manner all ions with reaction times greater than 100 μs were collected together. The achieved increase in signal intensity allowed direct, slow, mass scanning of the cluster ion intensities. Spot checks with the multiscaler were made. No differences in the equilibrium constants determined by the two methods were found which was to be expected since equilibria should have become established in less than 100 μs.

In all runs, described in parts *a*, *b*, and *c* above, a slow gas flow through the flow type ion source (3) was maintained. The flow rate through the ion source corresponded to some 70 cm^3/s which leads to a gas residence time of 50 ms in the ionization region.

Results

The $NH_4^+(NH_3)_n$ results are summarized in Table 1. Figure 1 gives an illustration of the temperature and pressure range used for the (0,1) equilibrium. The equilibrium constant is seen to be independent of the ammonia pressure used. Similar results were obtained for the pressure dependence of the other equilibrium constants. Figure 2 gives the van't Hoff plots from which $\Delta H_{n,n-1}$ and $\Delta S_{n,n-1}$ for the pure ammonia system were determined. Included in the table are the results from the earlier determination (1*a*). The ΔG^0 values are seen to be very close to those of the earlier determination. The new ΔH values and consequently also the ΔS values are somewhat lower. The reason for the differences is not too well understood. The earlier determination (1*a*) was done with a proton beam high pressure ion source at significantly lower pressures and no time dependence measurement. The earlier temperature measurement in the high temperature range was also suspected to be somewhat inaccurate, since somewhat similar differences were observed between recent (5) and

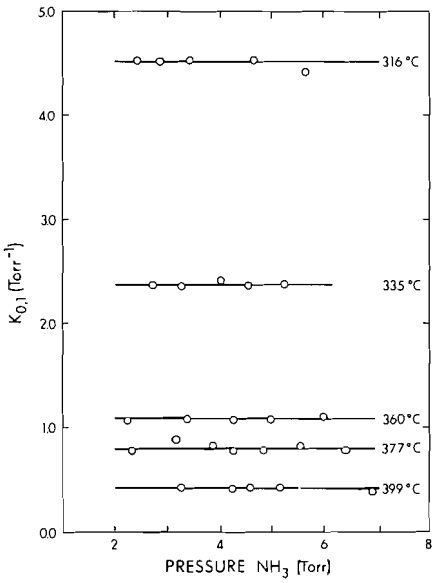

FIG. 1. Dependence of equilibrium constant $K_{0,1}$ for reaction $NH_4^+ + NH_3 = NH_4^+NH_3$ on pressure of NH_3 at different reaction temperatures. Standard state 1 Torr.

older determinations of the $H^+(H_2O)_n$ equilibria. Table 1 also includes some recent ΔG^0 determinations by Fehsenfeld and Ferguson (6) based on measurements with the flowing afterglow (7) method. The afterglow results were obtained by measurement of the forward and reverse rates of the reactions with O_2 and CO_2 as buffer gases. Since the measurements were done at a single temperature only $K = k_f/k_r$ and ΔG^0_{296} were obtained by Fehsenfeld and Ferguson. The agreement with the present results for $\Delta G^0_{4,3}$ and $\Delta G^0_{3,2}$ is seen to within 0.3 and 0.4 kcal. A difference of 0.7 kcal or larger

Can. J. Chem. Downloaded from www.nrcresearchpress.com by 210.87.254.6 on 09/05/12
For personal use only.

Can. J. Chem. Downloaded from www.nrcresearchpress.com by 210.87.254.6 on 09/05/12
For personal use only.

exists for the $\Delta G^0{}_{2,1}$ value. Probably, the Fehsenfeld–Ferguson determination is more accurate since it deals with a ΔG^0 determination at the quoted temperature, while the present $\Delta G^0{}_{298}$ is based on equilibria measurements obtained at considerably higher temperature. On the whole the agreement between the ΔG^0 values is quite good considering the difference of experimental technique and the experimental difficulties.

The results for the $NH_4{}^+(H_2O)_w$ clusters are also given in Table 1. The van't Hoff plots of the equilibrium constants from which the data were derived are shown in Fig. 2. The van't Hoff plots for the mixed cluster equilibria are given in Figs. 3, 4, and 5 and the resulting thermodynamic values in Tables 2 and 3. In order to shorten the designations an abbreviated notation was used. A clustering reaction like

$$NH_4{}^+(NH_3)_2(H_2O)_1 + H_2O = NH_4{}^+(NH_3)_2(H_2O)_2$$

was replaced by n_2w_1,n_2w_2, and an exchange reaction like

$$NH_4{}^+(NH_3)_3(H_2O)_1 + H_2O = NH_4{}^+(NH_3)_2(H_2O)_2 + NH_3$$

was replaced by n_3w_1,n_2w_2, etc.

As evident from the van't Hoff plots in Figs. 3, 4, and 5, in general the mixed cluster determinations were carried out over a fairly narrow temperature range. The ΔH and ΔS values are therefore of correspondingly reduced accuracy.

The exchange reaction data in Table 3 were derived from the clustering reaction data in Table 2, since ΔG for a reaction like (n_3w_1,n_2w_2) is equal to ΔG^0 for (n_2w_1,n_2w_2) minus ΔG^0 for (n_2w_1,n_3w_1). The ΔG^0 values for several exchange reactions observed in the early work (2) from this laboratory on mixed ammonia–water clusters are also given in Table 3. These values

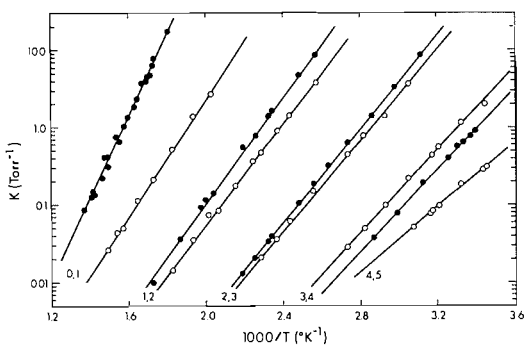

FIG. 2. Van't Hoff plots for reactions $NH_4{}^+(NH_3)_{n-1} + NH_3 = NH_4{}^+(NH_3)_n$, ●; and $NH_4{}^+(H_2O)_{n-1} + H_2O = NH_4{}^+(H_2O)_n$, ○. Results show very clearly the much greater stability of $NH_3H^+NH_3$ over $NH_4{}^+OH_2$. However, the interaction with water becomes progressively less unfavorable and at the (3,4) equilibrium the water cluster has become more stable. Standard state 1 Torr.

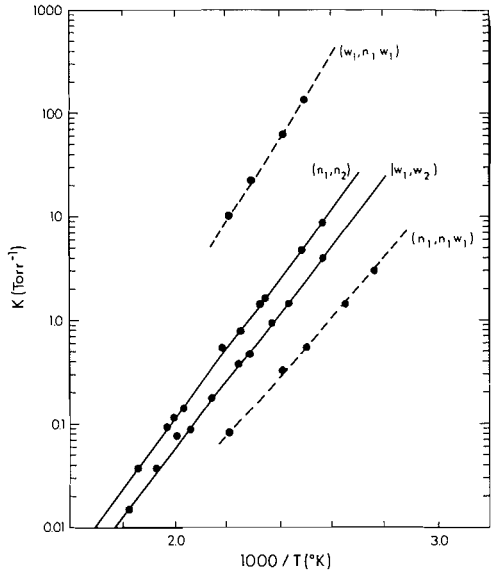

FIG. 3. Van't Hoff plots for equilibria: $NH_4{}^+ + H_2O = NH_4{}^+NH_3H_2O$ (n_1,n_1w_1); $NH_4{}^+H_2O + H_2O = NH_4{}^+(H_2O)_2$ (w_1,w_2); $NH_4{}^+NH_3 + NH_3 = NH_4{}^+(NH_3)_2$ (n_1,n_2); and $NH_4{}^+H_2O + NH_3 = NH_4{}^+NH_3H_2O$ (w_1,n_1w_1). Standard state 1 Torr.

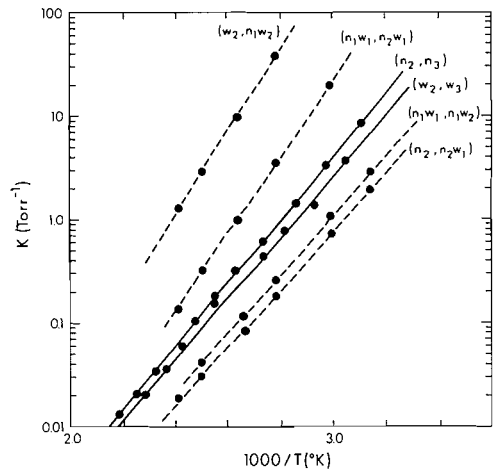

FIG. 4. Van't Hoff plots for mixed ammonia–water clusters equilibria involving the addition of one ligand (H_2O or NH_3) to a cluster containing two ligands. For notation see Fig. 3 and text. Strongest interaction is obtained by adding NH_3 to a pure water ligand cluster, weakest by adding H_2O to a pure ammonia cluster. Standard state 1 Torr.

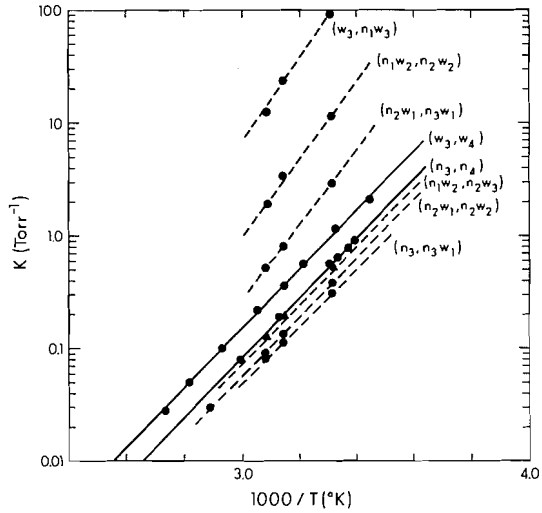

FIG. 5. Van't Hoff plots for mixed ammonia–water cluster equilibria involving the addition of one ligand (H_2O or NH_3) to a cluster containing three ligands. For notation see Fig. 3 or text. Strongest interaction is obtained when adding one NH_3 to a pure water ligand cluster, weakest interaction on adding H_2O to a pure water ligand cluster. Notable are also the much bigger intervals (ΔG decreases) between the upper plots, *i.e.* addition of NH_3 compared with the lower plots, *i.e.* addition of H_2O. Standard state 1 Torr.

TABLE 2. Thermodynamic parameters for the addition of successive ligands to NH_4^+

Reaction[a]	$-\Delta H$[b]	$-\Delta S$[c,d]	$-\Delta G$[b,d]
$0,n_1$	24.8±0.4[e]	25.9±0.7	17.1±0.5
$0,w_1$	17.3±0.4	19.7±0.7	11.4±0.4
n_1,n_2	17.5±0.2	22.9±0.5	8.9±0.3
n_1,n_1w_1	12.9±0.3	20.3±0.7	6.9±0.4
w_1,n_1w_1	18.4±0.5	23.0±1.2	11.6±0.6
w_1,w_2	14.7±0.2	21.9±0.3	8.2±0.2
n_2,n_3	13.8±0.2	25.7±0.4	6.1±0.2
n_2,n_2w_1	12.4±0.2	24.6±0.6	5.0±0.3
n_1w_1,n_2w_1	17.1±0.3	31.8±0.7	7.6±0.3
n_1w_1,n_1w_2	12.7±0.3	25.0±0.9	5.3±0.4
w_2,n_1w_2	18.2±0.4	30.3±1.0	9.2±0.5
w_2,w_3	13.4±0.2	25.1±0.6	5.9±0.3
n_3,n_4	12.5±0.4	29.4±1.2	3.7±0.5
n_3,n_3w_1	11.7±0.3	27.9±1.1	3.4±0.5
n_2w_1,n_3w_1	15.0±0.4	34.3±1.0	4.7±0.5
n_2w_1,n_2w_2	11.7±0.3	27.8±0.9	3.5±0.4
n_1w_2,n_2w_2	15.7±0.6	33.9±1.9	5.6±0.8
n_1w_2,n_1w_3	12.2±0.3	28.5±0.9	3.7±0.4
w_3,n_1w_3	17.3±1.0	35.1±3.3	6.9±1.4
w_3,w_4	12.2±0.3	27.3±0.8	4.1±0.4
n_4,n_5	7.5	25	0.2[f]
w_4,w_5	9.7±0.3	22.4±0.8	3.0±0.4

[a]Notation used for reaction $NH_4^+ + NH_3 = NH_4^+(NH_3)_1$, $(0,n_1)$; for reaction $NH_4^+(NH_3)_1 + NH_3 = NH_4^+(NH_3)_2$, (n_1,n_2); for $NH_4^+(NH_3) + H_2O = NH_4^+(NH_3)(H_2O)$, (n_1,n_1w_1); etc.
[b]In kcal/mol.
[c]In entropy units.
[d]Standard state 1 atm, $T = 300$ °K.
[e]Quoted errors are one standard deviation.
[f]Reference 1*a*.

were obtained from the intensities given in Table 2 of ref. 2. ΔG^0 values measured by Fehsenfeld and Ferguson (6) for the exchange reactions are also included in Table 3. On the whole there is fair to good agreement between these three sets of ΔG^0 values.

Discussion

The new data support the conclusions from the earlier work which were outlined in the introduction. The availability of the new $NH_4^+(H_2O)_w$ and extensive mixed cluster data permit some new insights. Figure 6 shows the enthalpy changes $\Delta H_{n,n-1}$ of Table 1 plotted *vs.* n. The enthalpy changes for the formation of $NH_4^+(NH_3)_n$ species are seen to be generally larger than those for $NH_4^+(H_2O)_w$. The difference is largest for the $\Delta H_{1,0}$ step and decreases progressively. In the earlier work this effect was explained on basis of the higher polarizability of ammonia. An alternate description used in more recent, related work (3, 8) is to consider the hydrogen bond, formed between NH_4^+ and the incoming NH_3 or HOH as a partial acid base reaction where NH_4^+ is the acid and NH_3 or HOH the base. From this viewpoint the stronger gas phase base (3) NH_3 should lead to the stronger hydrogen bond, *i.e.* larger $\Delta H_{1,0}$ and $\Delta G_{1,0}$ values. The partial proton transfer, *i.e.* partial acid–base reaction concept, was shown to be valid for Cl^-–HR complexes (8) and the alkyl amine proton held dimers (3).

Recently Peyerimhoff and co-workers (10) have published a theoretical study of the $[H_3N—H—NH_3]^+$ species based on *ab initio* s.c.f. calculations. The binding energy for dissociation to $NH_4^+ + NH_3$ calculated by these authors is 36 kcal, which is considerably higher than the present experimental value of ~25 kcal for $\Delta H_{1,0}$. Allowing for a couple of kcal correction for the zero point energy one still must conclude that the difference is considerable beyond the experimental error of the present determination and that the theoretical value is probably incorrect. More interesting are the theoretical results on the geometry of the complex and the charge distribution. Peyerimhoff and co-workers

Can. J. Chem. Downloaded from www.nrcresearchpress.com by 210.87.254.6 on 09/05/12
For personal use only.

Can. J. Chem. Downloaded from www.nrcresearchpress.com by 210.87.254.6 on 09/05/12
For personal use only.

TABLE 3. Changes of ΔG^0, ΔH, and ΔS for successive replacement of ammonia by water in a cluster with fixed total number of ligands[a]

Reaction[a]	ΔG^0_{298} (kcal/mol) This work	ΔG^0_{298} (kcal/mol) Literature	ΔH (kcal/mol)	ΔS (e.u.)
n_1,w_1	5.7	4.97[b]	7.5	6.2
n_2,n_1w_1	2.0	2.7[b] 1.7[c]	4.6[d]	2.6[d]
n_1w_1,w_2	3.4	4.1[b]	3.7[d]	1.1[d]
n_3,n_2w_1	1.1	1.44[b] 1.2[c]	1.4	1.1
n_2w_1,n_1w_2	2.3	2.49[b] 1.7[c]	4.4	6.8
n_1w_2,w_3	3.3	3.48[b]	4.8	5.2
n_4,n_3w_1	0.3	0.4[c]	0.8	1.5
n_3w_1,n_2w_2	1.2		3.3	6.5
n_2w_2,n_1w_3	1.9		3.5	5.4
n_1w_3,w_4	2.8		5.1	7.8

[a]Values calculated from data of Table 2. For explanation of notation used in designation of reactions see Table 2 or text.
[b]Private communication (6), after present experimental work was completed.
[c]Reference 2.
[d]These values show reversed change from that expected. This is probably due to experimental error. $\Delta H(n_2,n_1w_1)$ is expected to be smaller than $\Delta H(n_1w_1,w_2)$.

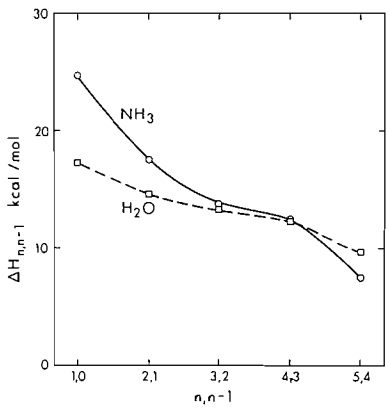

FIG. 6. Plot of $\Delta H_{n,n-1}$ for reactions: $NH_4^+(NH_3)_n = NH_4^+(NH_3)_{n-1} + NH_3$ and $NH_4^+(H_2O)_n = NH_4^+(H_2O)_{n-1} + H_2O$ *vs.* $n,n-1$. Gradual change to more favorable interactions with water is indicated for n larger than 4.

(10) find that the lowest energy configuration is not symmetric but that the proton is closer to one of the N atoms. The barrier for proton transfer was found to be ~3.5 kcal for a fixed N—N distance but became only ~2 kcal when the N—N distance was allowed to adjust (decrease) to give minimum energy while the proton was transferred. This low energy barrier indicates very nearly free exchange of the proton at room temperature. The authors also found significant electron density decrease in the N—H bonds on formation of the dimer showing that considerable positive charge dispersal occurs in that species. It is interesting to note that theoretical (11) and experimental (12) findings for the isoelectronics species $[H_2OHOH_2]_2^+$ predict a symmetric equilibrium position of the proton between the two O atoms. However, the potential minimum for motion of the proton along the line of O centers is very broad (11) which shows that the ammonia and water proton dimers are not totally devoid of similarity.

The present results (Table 1 and Fig. 6) show that with increasing number of ligands the NH_4^+ interactions with water molecules become progressively closer in magnitude to those with ammonia. A crossover occurs with the $\Delta H_{5,4}$ value for water becoming larger than that for ammonia (see Fig. 6). It is interesting to note that the ΔG values cross over even earlier, *i.e.* $\Delta G^0_{4,3}$ for water is larger than that for ammonia. This gradual change and reversal is also seen very directly in the van't Hoff plots of Fig. 2. One may understand these results by considering that the positive charge becomes progressively dispersed and less important to the bonding with increase of the number of ligand molecules. Therefore, gradually, the greater hydrogen bonding ability of HOH (in the absence of an ionic charge) becomes more and more important.

The mixed clusters show the operation of similar principles. The data in Table 2 show that for a total of up to four ligands the addition of an ammonia molecule is always favored over the addition of a water molecule. The effect is larger the smaller the total number of ligands and the smaller the number of NH_3 molecules initially present in the cluster. Again this effect is most directly observed in the van't Hoff plots of Figs. 3, 4, and 5. The straight lines corresponding to the different equilibria are spread out like a fan. The center of the fan falls between the two lines for the pure ammonia or pure water clusters. The top line, *i.e.* the most favorable interaction, is always that for the addition of NH_3 to a pure water cluster while the bottom line is that for the addition of a water molecule to a pure ammonia cluster.

The same trends are expressed in the exchange or switching reactions shown in Table 3. For example the exchange reaction

$NH_4^+(H_2O)_4 + NH_3 = NH_4^+(NH_3)_1(H_2O)_3 + H_2O$

is strongly exothermic while the reaction

$NH_4^+(NH_3)_3H_2O + NH_3 = NH_4^+(NH_4)_4 + H_2O$

is almost thermoneutral. The entropy changes for the exchange reactions (Table 3) are generally small as is to be expected for reactions of this type. The data show that ΔS becomes more positive the more unfavorable the exchange. For example the exchange n_3,n_2w_1 has a ΔH of 1.4 kcal and a ΔS of 1.1 e.u. The less favorable exchange n_1w_2,w_3 in which the last ammonia molecule is lost has a larger ΔH of 4.8 kcal and a larger ΔS of 5.2 e.u. Such a relationship between ΔH and ΔS is often observed. It should be noted that on grounds of probability only, the first reaction should have the larger ΔS since the number of ammonia molecules that can be replaced is larger.

The treatment of the data in the earlier work (2) on mixed ammonia and water clusters utilized a factor γ for the preferential intake of ammonia over water molecules in a cluster. γ was obtained by a statistical fit of the relative intensities of mixed clusters with a fixed total number of ligands. The data indicated that γ does not change much with the number of ammonia molecules present in the cluster. It is evident from the present work and the present treatment of the data that this is not so. We realize now that the early set of experimental results was not sufficiently extensive to show that the preference factor approach was not useful and that it leads to a somewhat misleading averaging of the changing preference for ammonia in a cluster with a fixed total number of ligands.

Unfortunately the present results do not include measurements with a low temperature source which would have permitted good measurements for the equilibria involving more than five molecules. Such a source was constructed and is in use (4) but has not yet been applied to the ammonium ion. The available data in Table 1 show that there is a break in the ΔH values between $\Delta H_{4,3}$ and $\Delta H_{5,4}$ for the pure ammonia clusters but a considerably smaller break for the NH_4^+–water system. A small but still distinct break occurs between the $\Delta G^0_{4,3}$ and $\Delta G^0_{5,4}$ values for pure ammonia, while there is no noticeable break for the NH_4^+–water system. This difference of behavior between ammonia and water should be caused by factors similar to those outlined in the discussion of the one to four molecule results. Since ammonia is a stronger base than water, it hydrogen bonds more strongly when H atoms with appreciable positive charge are available. The dispersal of positive charge increases from $NH_4^+NH_3$ to $NH_4^+(NH_3)_4$ and the strength of the H bonding decreases. In $NH_4^+(NH_3)_4NH_3$ an additional bonding decrease occurs since no more "ammonium" hydrogens are available. The decrease is smaller than one might have expected since charge was dispersed all along during the growth of the cluster. HOH, on the other hand, is a strong hydrogen bonding species even in the absence of ionic charge and can be expected to show an even less distinct transition from "inner" to "outer" shell. This result is in line with observations in the $H_3O^+(H_2O)_w$ system (13) where only a very indistinct break between $\Delta H_{3,2}$ and $\Delta H_{4,3}$ was observed. Similarly no distinct breaks were observed in the hydration of the alkali and halide ions (14). Very large and distinct breaks can be observed in the gas phase with systems in which hydrogen bonding is restricted by the presence of other substituents. For example recent work (4) has shown that the ΔH and ΔG^0 for the dissociation of the proton held dimethyl ether dimer $(CH_3)_2OH^+O(CH_3)_2$ are large and comparable to those for $H_2OH^+OH_2$ species. However, the stability of the $(CH_3OCH_3)_3H^+$ species is found to be very much lower than that of the corresponding proton trihydrate.

The authors wish to acknowledge the support of the National Research Council of Canada.

1. (*a*) S. K. SEARLES and P. KEBARLE. J. Phys. Chem. **72**, 742 (1968). (*b*) A. M. HOGG, R. M. HAYNES, and P. KEBARLE. J. Am. Chem. Soc. **88**, 28 (1966).
2. A. M. HOGG and P. KEBARLE. J. Chem. Phys. **43**, 449 (1965).
3. R. YAMDAGNI and P. KEBARLE. J. Am. Chem. Soc. **95**, 3504 (1973).
4. E. GRIMSRUD and P. KEBARLE. J. Am. Chem. Soc. To be published.
5. A. J. CUNNINGHAM, J. D. PAYZANT, and P. KEBARLE. J. Am. Chem. Soc. **94**, 7627 (1972).
6. F. C. FEHSENFELD and E. E. FERGUSON. Thermal energy positive ion reactions in a wet atmosphere containing ammonia. To be published.
7. E. E. FERGUSON, F. C. FEHSENFELD, and A. L. SCHMELTEKOPF. Adv. Atomic Mol. Phys. **5**, 1 (1969).

Can. J. Chem. Downloaded from www.nrcresearchpress.com by 210.87.254.6 on 09/05/12
For personal use only.

8. R. YAMDAGNI and P. KEBARLE. J. Am. Chem. Soc. **93**, 7139 (1971).
9. J. P. BRIGGS, R. YAMDAGNI, and P. KEBARLE. J. Am. Chem. Soc. **94**, 5128 (1972).
10. P. MULET, S. D. PEYERIMHOFF, and R. J. BUENKER. J. Am. Chem. Soc. **94**, 8301 (1972).
11. (*a*) W. P. KRAEMER and G. H. F. DIERCKSEN. Chem. Phys. Lett. **5**, 463 (1970). (*b*) P. A. KOLLMAN and L. C. ALLEN. J. Am. Chem. Soc. **92**, 6101 (1970). (*c*) M. D. NEWTON and S. EHRENSON. J. Am. Chem. Soc. **93**, 4971 (1971).
12. J. WILLIAMS and S. W. PETERSON. Spectroscopy in inorganic chemistry. Vol. 2. Academic Press Inc., New York and London. 1971. p. 1.
13. P. KEBARLE, S. K. SEARLES, A. ZOLLA, J. SCARBOROUGH, and M. ARSHADI. J. Am. Chem. Soc. **89**, 6393 (1967).
14. M. ARSHADI, R. YAMDAGNI, and P. KEBARLE. J. Phys. Chem. **74**, 1475 (1970).

Can. J. Chem. Downloaded from www.nrcresearchpress.com by 210.87.254.6 on 09/05/12
For personal use only.

Infrared Absorption Band Shape Studies: Fundamental OH Stretching Vibration of Benzyl Alcohol Conformers in Dilute Carbon Tetrachloride Solution[1, 2]

P. J. KRUEGER AND B. F. HAWKINS
Department of Chemistry, University of Calgary, Calgary, Alberta T2N 1N4

Received April 24, 1973

The fundamental OH stretching doublet in the i.r. spectra of a series of monomeric *p*-X-benzyl alcohols (X = OCH_3, CH_3, H, Cl, NO_2) observed in dilute CCl_4 solution over the temperature range −5 to +40 °C is resolved into two components corresponding to different molecular conformers, using digital computing techniques and a Cauchy–Gauss sum band model. The temperature and substituent dependence of frequencies, band shape indices, and band widths are discussed in terms of intramolecular (electronic displacements and OH···π hydrogen bonds) and intermolecular (OH···Cl_4C and π–σ electron donor–acceptor) interactions. The OH band shapes, which range from 60–98% Cauchy character, reflect variations in the intermolecular interactions which impede molecular re-orientation, and can be correlated with the electronic nature of X and the molecular conformation. The formation of an intramolecular OH···π hydrogen bond results in significantly slower rotational relaxation of the alcohol molecule. The enthalpy differences between the two conformers are found to be 1.52 ± 0.13, 1.57 ± 0.15, 1.53 ± 0.08, 1.06 ± 0.13, and 1.15 ± 0.11 kcal/mol for the compounds in the order stated above.

Le doublet de la vibration fondamentale d'élongation du OH dans les spectres i.r. d'une série d'alcools *p*-X-benzyliques monomères (X = OCH_3, CH_3, H, Cl, NO_2) observé en solution diluée dans CCl_4, dans l'intervalle de température −5 à +40 °C, a été résolu en deux composantes correspondant aux différentes conformations moléculaires par les techniques de calcul digital et sur un modèle de sommation de bande selon Cauchy–Gauss. Les variations des fréquences en fonction de la température, substituant, indices de forme et largeurs de bande, ont été discutées par rapport aux interactions intramoléculaires (déplacement électronique et liaisons hydrogène OH···π) et intermoléculaires (OH···Cl_4C et π–σ donneur–accepteur d'électron). Les formes des bandes OH qui ont un caractère de Cauchy de 60 à 98%, reflètent les variations des interactions intermoléculaires qui gênent la réorientation moléculaire et peuvent être en corrélation avec la nature électronique de X et la conformation moléculaire. La formation d'une liaison hydrogène intramoléculaire OH···π a pour résultat une relaxation rotationnelle nettement plus lente pour la molécule alcool. Les différences d'enthalpie entre les deux conformères sont de 1.52 ± 0.13, 1.57 ± 0.15, 1.53 ± 0.08, 1.06 ± 0.13 et 1.15 ± 0.11 kcal/mol pour les composés dans l'ordre cité ci-dessus.
[Traduit par le journal]

Can. J. Chem., 51, 3250 (1973)

Can. J. Chem. Downloaded from www.nrcresearchpress.com by 210.87.254.40 on 09/05/12
For personal use only.

Introduction

Mathematical Models

The quantitative measurement of band shapes in condensed phase i.r. absorption spectra and their physical interpretation have remained rather elusive objectives until recently. The statistical approach to such measurements has recently been reviewed by Young and Jones (1), while Gordon (2) and Shimizu (3) independently developed a detailed kinetic picture using the time correlation function. The two methods are clearly related (1), and this paper attempts to show how, using one particular model, the analog spectrophotometer record with which the chemist is familiar can be correlated with solute/solvent perturbations at the molecular level, and on the picosecond time scale.

A comprehensive review of the experimental and theoretical factors influencing the measurement of profiles and intensities of i.r. absorption bands for materials in condensed states is available (4). The shape of an isolated vibrational absorption band arising in a molecule which rotates in an undamped fashion in a solvent medium may be expressed by a Gaussian function

$$[1] \quad A(\nu)_g = ab_g^{-2} \exp\{-(\nu - \nu_0)^2 \times \ln 2b_g^{-2}\}$$

and the corresponding band shape where strong

[1]Taken in part from the M.Sc. Thesis of B. F. Hawkins.
[2]Presented at the 24th Conference on Analytical Chemistry and Applied Spectroscopy, Cleveland, Ohio, March 5–9, 1973.

Can. J. Chem. Downloaded from www.nrcresearchpress.com by 210.87.254.40 on 09/05/12
For personal use only.

solute/solvent perturbations exist may be given by a Cauchy function

$$[2] \qquad A(\nu)_c = a\{b_c^2 + (\nu - \nu_0)^2\}^{-1}$$

where ν_0 is the position of the band center, $2b$ is the width of the band at one-half the maximal intensity, and a/b^2 is the peak height. For a computer-oriented least squares analysis the variables can be generalized as X_1, X_2, X_3,..., etc. (1) and eqs. 1 and 2 can then be written as

$$[3] \qquad A(\nu)_g = X_5 \exp\{-X_4^2(\nu - X_2)^2\}$$

and

$$[4] \qquad A(\nu)_c = X_1\{1 + X_3^2(\nu - X_2)^2\}^{-1}$$

respectively. Here X_1 and X_5 are the Cauchy and Gauss peak heights (a/b^2), respectively, X_2 is the position of the band center, $X_3 = 1/b_c$, and $X_4^2 = \ln 2/b_g^2$.

While several functions can be used to describe absorption bands which have shapes that are intermediate between those of the limiting pure Cauchy and pure Gaussian types,[3] the sum function

$$[5] \qquad A(\nu)_s = X_1\{1 + X_3^2(\nu - X_2)^2\}^{-1} + X_5 \exp\{-X_4^2(\nu - X_2)^2\}$$

was employed as a model in these studies (1). Pitha and Jones have shown (5) that the sum function is much better than the product function in describing the absorption band profile. For an overlapping band system composed of M bands, and where an adjustable absorption baseline parameter is allowed for, a total of $(3M + 1)$ parameters require minimization when using a Cauchy function to represent the absorption profile, and $(5M + 1)$ parameters when using the sum function for each component. It has been shown (6) that the sum function with the restraint that $(X_4/X_3) = 0.8$ is successful in fitting simulated absorption profiles convoluted with a triangular slit function. This mathematical convenience was adhered to in this investigation; it means that the half-band width of the Cauchy part of the sum function is held nearly equal to the half-band width of the Gaussian part.[4]

Band areas can be determined by simple integration once observed profiles have been fitted mathematically, and for the Cauchy curve

$$[6] \quad \text{Area} = \int_{-\infty}^{+\infty} A(\nu)_c = (X_1/X_3)\tan^{-1}\{X_3(\nu - X_2)\}\Big|_{-\infty}^{+\infty} = \pi(X_1/X_3)$$

for the Gaussian curve

$$[7] \quad \text{Area} = \int_{-\infty}^{+\infty} A(\nu)_g = (\pi)^{1/2}(X_5/X_4)$$

and for the sum function

$$[8] \quad \text{Area} = [6] + [7] = \pi(X_1/X_3) + (\pi)^{1/2}(X_5/X_4)$$

For bands fitted with the sum function, the amount of Cauchy character, expressed as a fraction, can be determined from the ratio

$$[9] \quad \text{Band shape index} = \text{Area [6]}/\text{Area [8]}$$

A schematic representation of this band shape model is found in Fig. 1.

Computer programs using the method of damped least squares to fit spectra with Cauchy, and Cauchy–Gauss sum and product functions are available (7) and will not be discussed further here. The convergence between the observed and calculated band envelope may be evaluated through the minimization function

$$[10] \qquad \phi = \sum_{i=1}^{M} [(I_i)_{obs} - (I_i)_{calcd}]^2$$

where the I's are transmittance values and M is

[3]These include the Voigt profile and the Cauchy–Gauss product function (4).

[4]Actually $(X_4/X_3) = (\ln 2)^{1/2} = 0.83$ for the two half-band widths to be exactly equal. While a shallow minimum in the maximal error in the curve fitting process has been noted previously for synthetic singlet bands when $(X_4/X_3) = 0.8$ (5), this could not be duplicated in our study of overlapped doublets. Fraser and Suzuki (6) claim that the improvement in fit when this ratio is held at 0.8 is marginal, and that equal half-band widths for the two components of the hybrid sum function are preferred. Our computer resolution studies on *p*-methoxybenzyl alcohol OH bands, where the greatest differences in half-band widths and shape indices are observed for the two conformers, show that for (X_4/X_3) values chosen in the range 0.6–1.0 the conclusions drawn subsequently in this paper are not affected significantly.

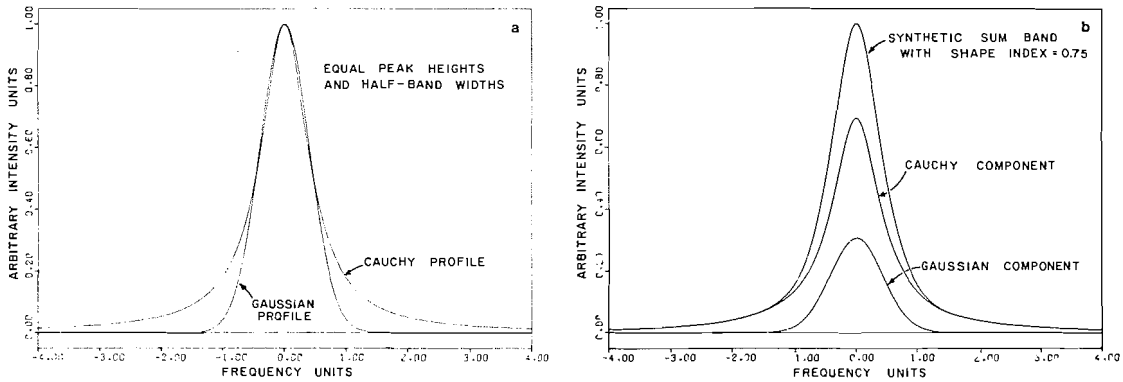

FIG. 1. Schematic representation of i.r. absorption band shape model. (*a*) Limiting Gaussian and Cauchy profiles, normalized to the same peak height and half-band width. (*b*) Synthetic sum band with shape index 0.75, showing Cauchy and Gaussian components ($X_4/X_3 = 0.8$).

the number of ordinate measurements. Two other criteria used to determine the significance of the final solution are the maximum transmittance difference between the observed and the calculated envelope (ΔT_{max}), and the standard error

$$[11] \qquad S = [\phi/(M - N)]^{1/2}$$

where N is the number of band indices X_1, X_2, X_3,..., X_N which are varied to obtain a minimum value of ϕ.

Benzyl Alcohol Conformers

The doublet absorption in the 3600 cm^{-1} region of benzyl alcohol was first noted by Fox and Martin (8), who assigned the high frequency component to a conformer in which the OH was well removed from the phenyl group and the low frequency component to a conformer with an intramolecular OH···π bond. While Flynn *et al.* (9) and Pitha and Horak (10) ascribed the doublet to rotational isomerism about the C—O bond, as observed in aliphatic alcohols, the intramolecular hydrogen bond was confirmed by Oki and Iwamura (11) who noted that the relative intensity of the low frequency band increased with respect to the intensity of the high frequency band when electron donating substituents were attached to the phenyl ring.[5]

[5]While Oki and Iwamura (11) concluded that the substituent dependence of the relative intensities of the doublet implies an intramolecular OH···π hydrogen bond involving the π-electrons on C_1, their band resolution procedure assumed a Cauchy band shape for all components. In the light of band shape variations observed in the present study, this conclusion should be treated with caution.

The essential features of the conformational equilibrium in benzyl alcohols can be expressed by

[12] 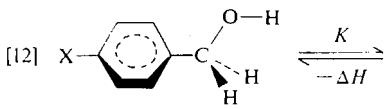

(I) "free" OH

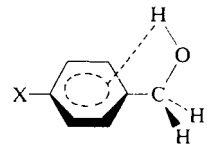

(II) intramolecular OH···π bonded OH

where, in dilute solution in a solvent like CCl_4 the "free" OH group in **I** is interacting with the solvent, and no specific orientation of the OH is implied in **II**, other than that it be engaged in an OH···π hydrogen bond. For purposes of band resolution in this investigation, it was assumed that the observed envelope consisted of two symmetrical overlapped component bands of unknown shape ranging somewhere between the pure Cauchy and pure Gaussian forms.

The equilibrium constant (K) can be obtained as a function of temperature by measuring the relative areas (A) of the absorption bands corresponding to each conformer, and, provided that the ratio of intrinsic molar absorbances for the two bands is temperature independent, the enthalpy difference (ΔH) between the two conformers, under the measurement conditions, follows directly from the integrated form of the

Can. J. Chem. Downloaded from www.nrcresearchpress.com by 210.87.254.40 on 09/05/12
For personal use only.

Can. J. Chem. Downloaded from www.nrcresearchpress.com by 210.87.254.40 on 09/05/12
For personal use only.

Van't Hoff equation. Experimentally, this is the slope of the log (A_I/A_{II}) *vs.* $1/T$ plot. The entropy difference (ΔS) between the two conformers can only be obtained if the ratio of the intrinsic molar absorptivities for the two bands is equal to unity (or some other known value).

The benzyl alcohol OH bands are strongly overlapped, and thus typical of many i.r. absorption spectra in which separate band areas cannot readily be determined directly. Graphical and other analog procedures to resolve the component bands have been applied with varying degrees of success, but normally some assumption has to be made about the basic band shape(s), and this may strongly bias the "solution".[6]

This investigation was designed to see if computer resolution of the OH bands in benzyl alcohol spectra could give some information about band shapes, within the limits imposed by the Cauchy–Gauss sum function model, and whether the shape indices could be interpreted in terms of molecular dynamics and the general chemical behavior of the system. Since the band resolution process employed cannot guarantee a unique solution in view of the large number of variables minimized, particularly for Cauchy–Gauss hybrid functions, interpretations of the model are largely based on general trends with changes in temperature and in the ring substituent, which emerge from the collective evaluation of a large number of independent spectra and computing runs.

Experimental

Apparatus

Spectra were recorded on a Perkin–Elmer Model 621 double beam grating spectrophotometer, and both the frequencies and transmittance readings were simultaneously encoded digitally on eight track paper tape using a Perkin–Elmer DDR-1 digital data recorder. A constant encoding interval of 0.5 cm^{-1} was used, leading to some 800 pairs of data points over the range 3830 to 3430 cm^{-1}. Contact points on the transmittance encoder were at intervals of 0.001 transmittance units, and the encoder was calibrated with a set of standard rotating sector disks with transmittance values of 0.710, 0.501, 0.251, 0.126, and 0.063 supplied by Research and Industrial Instruments Co. The scanning rate was 7 cm^{-1}/min and the spectral slit width was 5 cm^{-1}. The experimental procedure was essentially the same as that described by Jones (12).

Alcohol solutions ($\sim 3.0 \times 10^{-3}$ *M*) were made up volumetrically in Fisher "spectral quality" CCl_4 which had been doubly dried over Linde 4A molecular sieves. Matched 2.0 cm "Infrasil" quartz cells were used, with pure solvent in the reference beam. The quartz cells were both enclosed in brass holders through which methanol was circulated, in parallel, using a Lauda TK-30D Ultra Kryomat capable of maintaining a cell temperature stability of ± 0.1 °C over the temperature range employed (-5 to $+45$ °C). The temperature of the solution in the sample cell was monitored continuously with an Atkins calibrated thermistor probe inserted into the solution through a Teflon stopper in the filling port. The absolute accuracy of the temperatures measured is ± 0.2 °C. Spectra were recorded only after temperature stability had been achieved. The sample compartment and the spectrophotometer itself were purged with dry air.

Data Collection

Transmittance values encoded at 10 cm^{-1} intervals with the rotating sectors (5000–7000 r.p.m.) were the basis of the transmittance scale, and a parabolic function was used to obtain true transmittance values by interpolation. Transmittance values at frequencies other than those where sector values had been encoded were also obtained by interpolation. An encoded background spectrum (solvent *vs.* solvent) was subtracted from the sample spectrum to eliminate any baseline irregularities.

The frequency scale of the spectrophotometer was calibrated using water vapor as a standard (13), and the reported frequencies are considered to be accurate to ± 0.5 cm^{-1}. Calibration spectra indicated that deviations of the frequency drive from linearity were insignificant in the range in question.

Data Analysis

All calculations were performed on an IBM 360/50 computer initially, and later on a CDC 6400 computer using the Fortran IV programs developed by Jones *et al.* (7).

Initial values of X_1, X_2, and X_3 were estimated from the analog version of the spectra, and the digital spectrum (doublet OH peak) resolved into two optimized pure Cauchy components. For the Cauchy–Gauss hybrid (sum function) band fitting process, the optimized indices of the Cauchy fit were used as input values. The Gaussian contribution (X_5) was restricted to zero or positive values, and (X_4/X_3) was held at 0.8.

After each iteration the calculated band envelope (undistorted) was convoluted with a symmetrical triangular spectrophotometer slit function before comparison with the experimentally observed envelope. Synthesized curves were computed at 0.5 cm^{-1} intervals and transmittance values rounded to the nearest 0.001. Iteration was continued until there was little change in the minimization function (ϕ) over several cycles. Computation was also set to end if the maximal transmittance difference became less than 0.001 or the standard error became less than 0.002.

The spectra were typically recorded at noise levels of 0.005 to 0.010 transmittance units. From eq. 11, since $N \ll M$, it follows that a "fit" of the calculated band envelope would have been achieved when $\phi \leq S^2M$. Thus, for noise levels of 0.005 to 0.010 transmittance units ϕ should be equal to or less than 2.0×10^{-2} or 8.0×10^{-2}, respectively.

[6]Spectrophotometer slit distortion must also be taken into consideration.

Can. J. Chem. Downloaded from www.nrcresearchpress.com by 210.87.254.40 on 09/05/12
For personal use only.

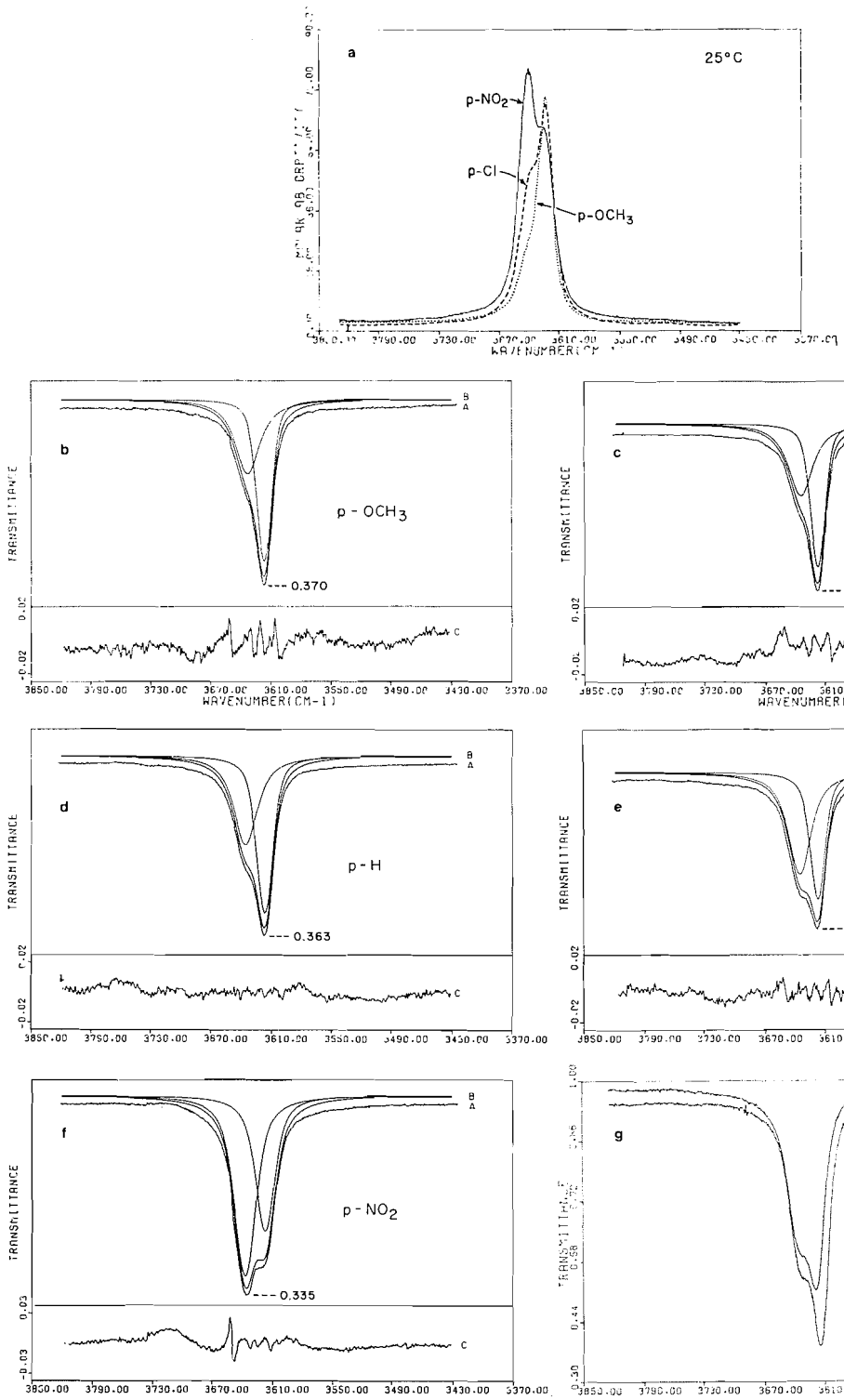

Can. J. Chem. Downloaded from www.nrcresearchpress.com by 210.87.254.40 on 09/05/12
For personal use only.

Materials

The benzyl alcohols used were commercial materials. Spectral grade benzyl alcohol and anisyl alcohol were dried over anhydrous $CaSO_4$ and $MgSO_4$ and then distilled through a spinning band column. *p*-Chloro-, *p*-nitro-, and *p*-methylbenzyl alcohol were recrystallized from water and dried over P_2O_5 in a vacuum desiccator. The samples used had physical constants in acceptable agreement with literature values.

Results and Discussion

Test of Band Resolution Procedures

Jones *et al.* (14) have shown that the method of pseudodeconvolution to correct for spectral slit distortion leads to incomplete recovery of half-band widths and areas for bands with true peak absorbances of less than 0.2. For bands of Cauchy profile, the errors involved approached 5% for half-band widths and 10% for areas even at $s/\Delta\nu_{1/2}$ ratios near 0.1. The alternative method of accounting for spectral slit distortion used here, that of convoluting the synthesized curve with a slit function before fitting it to the experimentally observed envelope after each iteration in the least squares minimization process, has only been tested on a synthetic doublet composed of two bands of the same peak height, half-band width, and shape (15). It was felt desirable to determine the ability of this method to recover true band parameters under conditions more analogous to the system under investigation. Two tests were applied.

Test spectra simulating two overlapped Cauchy profiles with wide variations in peak height and half-band width, and with the approximate spacing of the doublet in the benzyl alcohols, were generated and convoluted with a symmetrical triangular slit function of 5.0 cm^{-1} half-width. For a fixed Cauchy band shape the recovery of true peak heights and band-widths was extremely efficient, with errors of less than 0.1%. For *p*-nitrobenzyl alcohol spectra of the same solution obtained at slit widths of 5.0, 3.5, and 2.2 cm^{-1}, Cauchy–Gauss sum band fitting led to variations of the order of 2–5% in recovered "true" peak heights, half-band widths, band areas, and shape indices. For duplicate spectra on the same solution at the same slit-width, the recovered band indices showed variations up to 2.5%. The recovered frequencies of the band centers lay well within 0.5 cm^{-1} for this series.

Resolved Spectra

A comparative view of the spectra is found in Fig. 2*a*. Figure 2*b–f* shows Calcomp plots of the experimentally observed OH doublets for the five benzyl alcohols, as regenerated from the digital data, as well as the corresponding fitted synthetic spectra based on convoluted Cauchy–Gauss sum bands, and the error curves showing the deviation between the experimental spectra and the calculated spectra.[7] For the 75 spectra reported here (60 000 data points) the "goodness of fit" criteria used had the following mean values: minimization function (ϕ) = 0.0162 (transmittance units)^2; standard error (S) = 0.0043 transmittance units; maximum deviation (ΔT_{max}) = 0.0142 transmittance units. Figure 2*g* shows the typical temperature dependence observed in the experimental spectra.

Table 1 summarizes and compares all the relevant data for the resolved OH band components at 25 °C.

Without exception, the resolution of the doublet into two pure Cauchy components led to a poorer fit; for all 75 spectra mean values of ϕ = 0.0337 (transmittance units)^2, S = 0.0063 transmittance units, and ΔT_{max} = 0.0235 transmittance units were obtained. Furthermore, the statistical validity of the Cauchy fit decreased with decreasing temperature, a result of the temperature dependence of the shape index, which is discussed later.

[7]As noted by one of the referees, the presence of ^{13}C, and the possibility of hot bands and weak overtones may contribute to the inability to fit i.r. spectra precisely to an equation like [5].

FIG. 2. (*a*) Comparative view of *p*-X-benzyl alcohol spectra in dilute CCl_4 solution, with absorbance expressed per mol of alcohol. Spectra for *p*-CH_3 and *p*-H compounds omitted since they are qualitatively similar to the *p*-OCH_3 spectrum. See Table 2 for intensity data. (*b*)–(*f*) Curve A: experimentally observed OH bands for benzyl alcohols in dilute CCl_4 solution, as regenerated from normalized digital data with a Calcomp plotter. Concentrations ~3 × 10^{-3} *M*. Temperatures ~28 °C. Path length = 2.0 cm. Peak transmittance values indicated. Curves B: resolved OH band components, using Cauchy–Gauss sum profiles, and calculated doublet (all displaced with respect to curve A for display purposes). Components convoluted with a triangular slit function of 5 cm^{-1} half-width to match spectrophotometer distortion of curve A. Curve C: deviations between experimental and convoluted calculated spectra. Transmittance scale expanded relative to curve A. (*g*) Experimentally observed temperature dependence of OH bands in *p*-chlorobenzyl alcohol in dilute CCl_4 solution. Curves displaced for display purposes.

TABLE 1. Characteristics of computer resolved band components[a] for "free" OH (conformer **I**) and intramolecularly OH···π bonded (conformer **II**) absorption bands in *p*-X-benzyl alcohols in dilute CCl_4 solution

Substituent	Conformer	ν_{OH} (cm^{-1}) at 25 °C[b,c]	$(\nu_{OH}^{I} - \nu_{OH}^{II})$ (cm^{-1}) at 25 °C	$d\nu_{OH}/dT^{c}$ (cm^{-1}/°C)	Band shape index at 25 °C[c,d]	Half-band widths at 25 °C[c] (cm^{-1})	$-\Delta H^{c,e}$ (kcal/mol)
p-OCH_3	**I**	3632.5	16.8	0.058	0.982	25.3	1.52 ± 0.13
	II	3615.7		0.080	0.624	14.4	
p-CH_3	**I**	3634.1	16.6	0.079	0.988	27.0	1.57 ± 0.15
	II	3617.5		0.097	0.615	14.7	
p-H	**I**	3634.3	18.2	0.069	0.926	24.9	1.53 ± 0.08
	II	3616.1		0.086	0.698	15.1	
p-Cl	**I**	3634.7	18.1	0.056	0.937	23.5	1.06 ± 0.13
	II	3616.6		0.093	0.657	16.0	
p-NO_2	**I**	3636.2	19.6	0.041	0.867	19.6	1.15 ± 0.11
	II	3616.6		0.064	0.805	18.9	

[a]Cauchy–Gauss sum bands; see text for details of model used.
[b]See refs. 11 and 16 for previously reported values not derived from a computer refined curve fitting process.
[c]Based on plots *vs.* temperature, and the collective assessment of data by least squares technique.
[d]Band area of Cauchy component divided by total band area under doublet. Pure Cauchy band = 1.000; pure Gaussian band = 0.000.
[e] ± standard deviation.

Frequencies

The OH frequencies reported in Table 1 for both conformers are based on the frequency *vs.* temperature plots in Fig. 3 which smooth out small irregularities which arise in the curve fitting process. Figure 3 approximates the temperature dependence of the frequencies as being linear, although in some cases a tendency toward regular curvature is apparent. Frequency increases for the "free" OH range from 0.04–0.08 cm^{-1}/°C, while those for the intramolecularly hydrogen bonded OH range from 0.06–0.10 cm^{-1}/°C (Table 1). For each compound the intramolecularly hydrogen bonded OH is more temperature sensitive than the free OH, which may be related to the greater (induced) polarity of the former ($O^{\delta-}$—$H^{\delta+}$···π). Solvent dependent shifts of inter- and intramolecular hydrogen bonded XH frequencies have been noted previously (17).

The polarity of the OH bond and the OH frequency in **I** increase only slightly as the electron withdrawing character of the ring substituent increases,[8] due to the insulating methylene group. The frequency displacement on intramolecular hydrogen bond formation ranges from 16.6 cm^{-1} in *p*-methylbenzyl alcohol to 19.6 cm^{-1} in *p*-nitrobenzyl alcohol.

Intensities

The integrated molar absorption for the OH doublet increases by 65% from *p*-methoxy- to *p*-nitrobenzyl alcohol, and parallels the Hammett σ values of the *p*-substituent, while the corresponding ratio of band intensities A_{II}/A_{I} drops from 1.48 to 0.60 (Table 2). Absolute A_{I} and A_{II} values cannot be determined since the absolute population of the two conformers is not known. The ratio A_{II}/A_{I} only gives this if the intrinsic molar absorptions of **I** and **II** are identical; that is unlikely to be the case here. Since the high frequency OH component moves from being the minor component of the doublet in *p*-methoxybenzyl alcohol to the major component in *p*-nitrobenzyl alcohol (Fig. 2*a*), the overall intensity increase of the doublet referred to above can be related to increasing polarity of the OH bond.

For bands established to be of near-Cauchy shape, *e.g.* the high frequency band of *p*-methoxybenzyl alcohol, the band areas reported by Oki and Iwamura (11) are within

[8]On intermolecular OH···O hydrogen bond formation to tetrahydrofuran as a common base in dilute CCl_4 solutions, the OH frequency displacement increases with increasing Hammett σ values of the *p*-substituent (18).

Can. J. Chem. Downloaded from www.nrcresearchpress.com by 210.87.254.40 on 09/05/12
For personal use only.

Can. J. Chem. Downloaded from www.nrcresearchpress.com by 210.87.254.40 on 09/05/12
For personal use only.

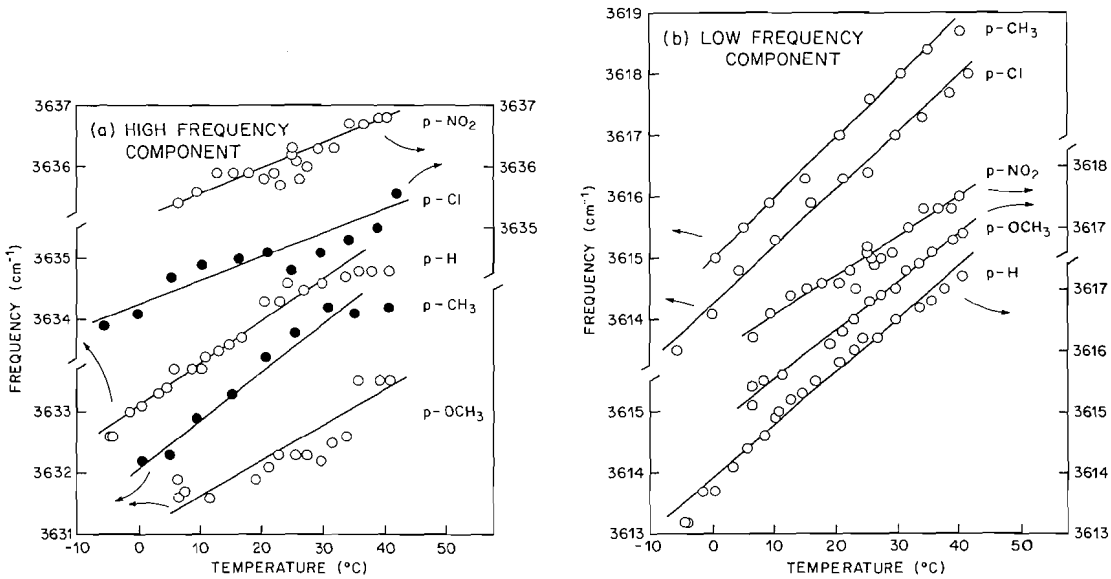

FIG. 3. Temperature dependence of frequency of component OH bands in benzyl alcohols in dilute CCl_4 solution: (*a*) "free" OH bands, (*b*) intramolecularly OH···π bonded band.

TABLE 2. OH band intensities in *p*-X-benzyl alcohols[a] (dilute CCl_4 solution; 25 °C)

Substituent	σ[b]	*A* (cm mol^{-1}; $\log_{10}$)[c] × 10^{-3} I[d]	II[d]	I + II	A_{II}/A_I
p-OCH_3	−0.27	0.80	1.19	1.99	1.48
p-CH_3	−0.17	1.10	1.27	2.37	1.16
p-H	0.00	1.06	1.37	2.43	1.30
p-Cl	+0.23	1.48	1.25	2.73	0.84
p-NO_2	+0.78	2.05	1.24	3.29	0.60

[a]Integrated band areas of deconvoluted components based on Cauchy–Gauss sum function model.
[b]Hammett substituent constants, from ref. 19.
[c]IUPAC practical intensity unit (4). These values have to be multiplied by 2.303 to make them comparable to those in ref. 11.
[d]Apparent intensities only, per mol of alcohol, since the individual concentrations of I and II are not known.

5% of our values, but for those now shown to have a hybrid shape, the inflexible Cauchy model used by them without an iterative curve-fitting procedure leads to differences in excess of 55%, *e.g.* in the low frequency band of *p*-methoxybenzyl alcohol.

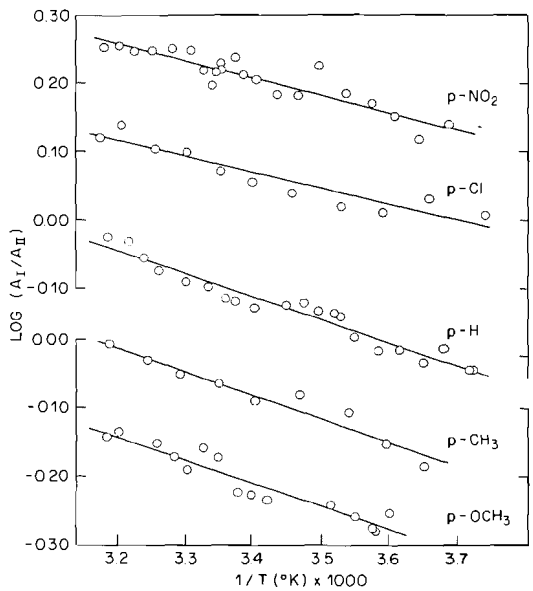

FIG. 4. Temperature dependence of the logarithm of the OH band area ratios for the conformational equilibrium in *p*-X-benzyl alcohols in dilute CCl_4 solution.

Thermodynamics

From the least squares treatment of the log (A_I/A_{II}) *vs.* $1/T$ plots in Fig. 4, the enthalpy difference between conformers **I** and **II** may be established, assuming that the intrinsic molar absorbance ratio for these two conformers is temperature independent over this temperature range. These thermodynamic quantities are summarized in Table 1, together with their deviations, and their substituent dependence is illustrated in Fig. 5. The low frequency band clearly belongs to the thermodynamically more stable conformer. Conformer **I** is stabilized by interactions of the OH with the solvent (favored

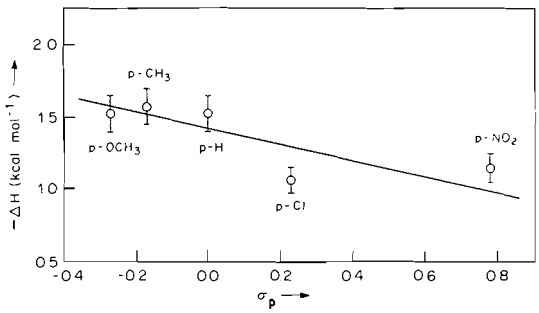

FIG. 5. Dependence of $-\Delta H$ for intramolecular OH···π hydrogen bond formation in *p*-X-benzyl alcohols in dilute CCl_4 solution, on the Hammett substituent constant of X.

as σ increases) and by π-electron/solvent interactions (favored as σ decreases). The stability of conformer **II** is related to the strength of the OH···π interaction, and this depends on the OH acidity (hydrogen bond favored as σ increases) and, more importantly, the basicity of the aromatic ring (hydrogen bond favored as σ decreases). Furthermore, some π-electron/solvent interactions will also exist in **II**.

The enthalpy differences found are similar to those reported for other intramolecular OH···π bonds (20). For benzyl alcohol itself in dilute CCl_4 solution, $-\Delta H$ for the conformational equilibrium was reported to be 2.34 kcal/mol (21), based on graphical resolution of the OH doublet, and using spectra uncorrected for slit distortion. This is substantially higher than our present value of 1.53 ± 0.08 kcal/mol.

The intercepts of the lines in Fig. 4 are not significantly different, suggesting similar entropy differences between conformers **I** and **II** for these compounds. No evaluation of ΔS was attempted since the intrinsic molar absorptions for the OH bands in the two conformers are not known.

Band Shape Index

The computed shape indices for both conformers are plotted as a function of temperature in Figs. 6 and 7. Least squares lines were fitted to the points. The "free" OH bands of *p*-methoxy and *p*-methyl benzyl alcohol are almost pure Cauchy in character, and their shape is temperature independent, since the slight slope shown for these compounds in Fig. 6 is not deemed to be significant in view of the lack of precision in the determination of this parameter. For the remaining compounds the "free" OH

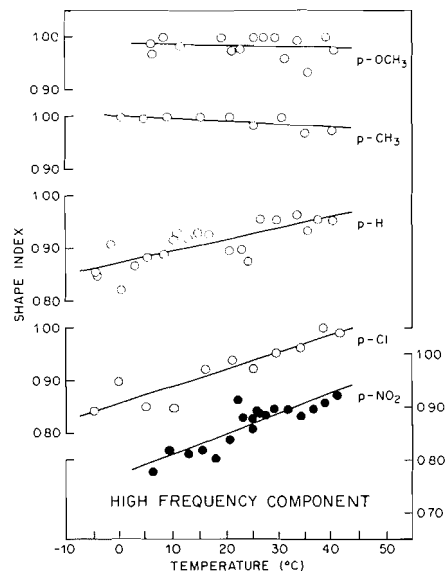

FIG. 6. "Free" OH band shape index dependence on temperature for benzyl alcohols in dilute CCl_4 solution. Pure Cauchy band = 1.00; pure Gaussian band = 0.00.

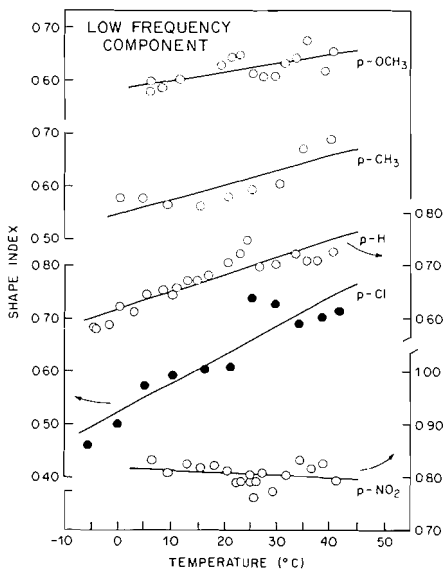

FIG. 7. Intramolecularly hydrogen bonded OH band shape index dependence on temperature for benzyl alcohols in dilute CCl_4 solution.

band is more Gaussian, and the Gaussian character increases as the temperature decreases.

For a given *p*-substituent the intramolecularly hydrogen bonded OH band is always much more Gaussian than the corresponding "free" OH band. Further, the intramolecularly hydrogen

Can. J. Chem. Downloaded from www.nrcresearchpress.com by 210.87.254.40 on 09/05/12
For personal use only.

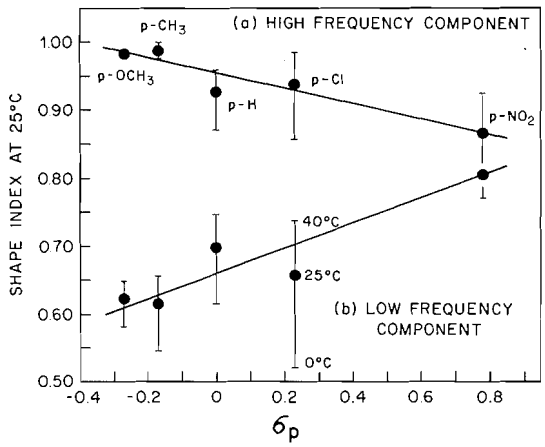

FIG. 8. Dependence of OH band shape index in *p*-X-benzyl alcohols on the Hammett substituent constant of X. Circles refer to values at 25 °C; ranges indicate spread of values between 0 and +40 °C. (*a*) "Free" OH band, (*b*) intramolecularly OH···π bonded band.

bonded OH band again becomes more Gaussian as the temperature is lowered, except in *p*-nitrobenzyl alcohol, where its shape is temperature independent (Fig. 7).

Figure 8 shows that the shape indices for both components are linearly related to the electron donating or withdrawing ability of the ring substituent, as measured by the Hammett substituent constant, but that the two conformers have an *opposite* dependence, leading to a situation in which anisyl alcohol has an almost pure Cauchy "free" OH band and an intramolecularly hydrogen bonded OH band which is approximately 40% Gaussian, whereas in *p*-nitrobenzyl alcohol the corresponding bands are about 10 and 20% Gaussian, respectively (figures cited at 25 °C; see also Table 1). The points in Fig. 8 are based on values at 25 °C derived from the least squares lines in Figs. 6 and 7, in order to minimize the reliance on any individual spectrum.

These band shape measurements can be rationalized in terms of two basic types of solute–solvent interactions which impede molecular re-orientation in these solutions, an OH···Cl_4C hydrogen bond and a π–σ electron donor–acceptor (charge transfer) type of interaction between the aromatic π-electrons and CCl_4. Both are well known. Alcohol OH frequencies in CCl_4 are displaced to lower values from their position in hexane, and such shifts correspond to specific intermolecular interactions, with general dielectric effects playing a secondary role (22). Charge transfer complexes between aromatic π-electrons and CCl_4 are also well documented (23). The following solid compounds have been identified in freezing point diagrams (24): CCl_4·benzene; $(CCl_4)_2$·benzene; CCl_4·toluene; CCl_4·1,2,4-trimethylbenzene; $(CCl_4)_2$·anisole. These same authors found no solid complexes of CCl_4 with *o*-xylene, *m*-xylene, chlorobenzene, bromobenzene, or nitrobenzene (24, 25). The heats of dissociation of the 1:1 complexes of CCl_4 with benzene and *p*-xylene are 3.5 and 6.3 kcal/mol, respectively (24). Other workers have reported the equilibrium constants for complex formation between CCl_4 and benzene, mesitylene, and hexamethylbenzene, based on ultraviolet measurements in *n*-hexane at 25 °C, to be 0.009 ± 0.004, 0.113 ± 0.044, and 0.64 ± 0.12 l mol^{-1} (26, 27). Other evidence for such π–σ interactions between aromatic compounds and CCl_4 comes from enthalpies of mixing (28), far i.r. spectra (29), and submillimeter dielectric absorption of mixtures (30), among many other measurements.

These concepts can now be applied as follows, with a substituent dependence of interactions (*a*)–(*e*) as discussed below in terms of the order of X = *p*-OCH_3, *p*-CH_3, *p*-H, *p*-Cl, and *p*-NO_2:

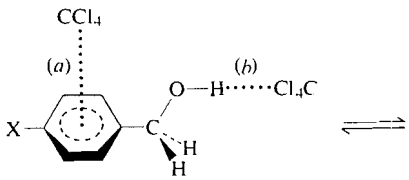

(I)

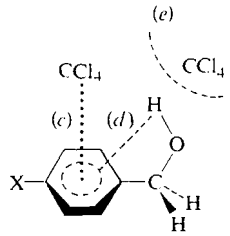

(II)

(1) A pure Gaussian profile implies unhindered molecular rotation; increasing Cauchy character corresponds to increasing intermolecular interactions which impede molecular re-orientation.

(2) Interaction (*a*) decreases as the π-electron

Can. J. Chem. Downloaded from www.nrcresearchpress.com by 210.87.254.40 on 09/05/12
For personal use only.

Can. J. Chem. Downloaded from www.nrcresearchpress.com by 210.87.254.40 on 09/05/12
For personal use only.

density falls, and (*b*) increases slightly as the OH polarity increases, but (*a*) dominates in conformer **I**. The molecular re-orientation of **I** is thus most hindered when X = *p*-OCH_3 (near Cauchy band shape), and somewhat less hindered when X = *p*-NO_2 (decreased Cauchy band character).

(3) For a given X, interaction (*c*) < interaction (*a*) because the aromatic π-electrons in **II** are at least to some degree tied up in an intramolecular OH···π hydrogen bond. This accounts for the fact that for a given X, conformer **II** is always freer to rotate (more Gaussian band shape) than conformer **I**.

(4) In conformer **II** the intramolecular OH···π hydrogen bond (*d*) strength decreases as the π-electron density falls. Whereas hydrogen bond strength in general is controlled by both the acidity of the proton donor and the acceptor power of the base, the latter appears to be the dominant factor here, masking the small intrinsic increase in OH polarity due to X. Geometric restrictions prohibiting proper access of the hydroxyl proton to the π-electrons may play an important role here.

(5) The reduction in intramolecular OH···π interaction in **II** as the π-electron density falls leaves the residual π-electrons more available for π–σ donor–acceptor interaction with CCl_4. Interaction (*c*) thus increases with X in the order given, because this is the order of increasing *availability* of π-electrons as far as the solvent is concerned. Of all the species studied, conformer **II** of *p*-methoxybenzyl alcohol is least perturbed by the solvent since its OH group and π-electrons are largely tied up internally (most Gaussian band), whereas *p*-nitrobenzyl alcohol (**II**) experiences more rotational damping, leading to a greater Cauchy band character (almost equivalent to that of **I** for this compound, as the OH···π interaction is weak).

(6) Interaction (*e*) in **II** plays a minor role, with an undetermined substituent dependence. While the intrinsic polarity of the OH bond would increase with X in the order given, the OH···π interaction decreases in this order, with an accompanying decrease in the OH polarity induced by hydrogen bond formation. The substituent dependence of the net OH polarity can, therefore, not be predicted. Furthermore, it appears reasonable to suggest considerable shielding of the hydroxyl proton in **II**, reducing OH···Cl_4C interaction, particularly when (*d*) is strong.

(7) In general, increasing Gaussian character as temperature decreases implies a longer period of unperturbed rotation of the solute molecule before solvent molecules interfere kinetically. In conformer **I**, when X = *p*-OCH_3 or *p*-CH_3 the ring electron density is large enough to provide for sufficient interaction with CCl_4 over the entire temperature range investigated to lead to an almost pure Cauchy and temperature independent band shape, *i.e.* these are near limiting cases. For *p*-nitrobenzyl alcohol, conformer **I** shows the normal temperature dependence which may reflect the polar OH group and OH···Cl_4C interaction, but in conformer **II** the combination of π-electron withdrawal by the substituent plus the intramolecular OH···π bond appear to leave this species less sensitive to changes in the interaction with CCl_4 over this temperature range.

Band Widths

Half-band widths for both component OH bands are shown to increase with increasing temperature, in general, in Fig. 9. Values extracted for 25 °C from the least squares lines in this figure are found in Table 1. Band widths are normally very sensitive to slight band shape changes, and to the degree of misfit in the curve fitting process. Hence the apparent decrease in the width of the intramolecularly OH···π bonded band in *p*-chlorobenzyl alcohol with increasing temperature may be anomalous; the data may only warrant an interpretation that this band width is relatively temperature independent.

The temperature dependence of the OH band width in conformer **II** is smaller than that of the OH band width in conformer **I**, with the exception of *p*-nitrobenzyl alcohol, where not only the absolute values of the half-band widths but also their temperature dependencies are nearly identical. The fact that the band shapes and the half-widths for both conformers of *p*-nitrobenzyl alcohol are nearly identical supports the view that π–σ electron–donor acceptor interaction with the solvent is the dominant factor hindering molecular re-orientation.

While half-band widths have been related directly to mean re-orientation times and their temperature dependence to mean reorientational potential barriers (31), such approximations rest on an assumed Cauchy band shape, which does not apply to most of the bands studied here. On the other hand, our observations are qualitatively consistent with the relative magnitudes of

Can. J. Chem. Downloaded from www.nrcresearchpress.com by 210.87.254.40 on 09/05/12
For personal use only.

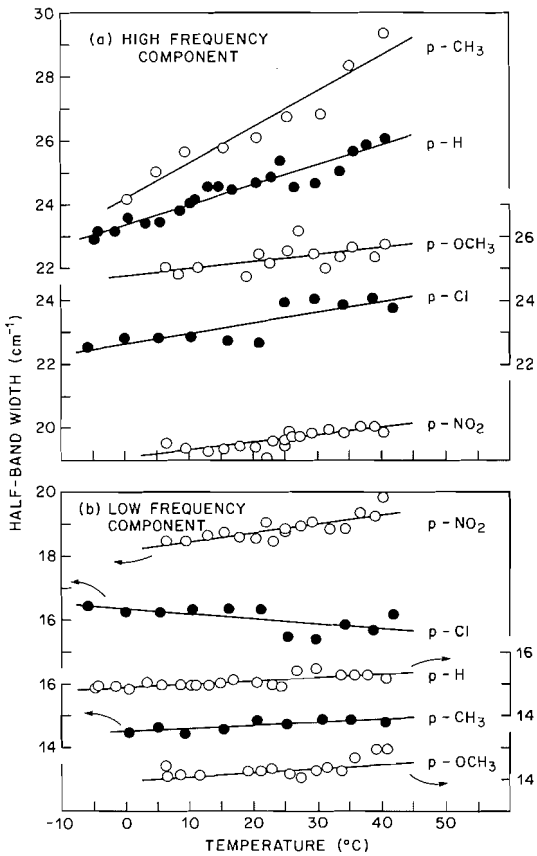

FIG. 9. Temperature dependence of half-band widths of OH bands in benzyl alcohols in dilute CCl_4 solution. (*a*) "Free" OH band, (*b*) intramolecularly OH···π bonded band.

the rotational diffusion constant (β), which, for the Cauchy–Gauss sum function, is defined by the half-band width of the Cauchy component; this corresponds to the slope of the linear portion of the logarithmic time correlation plot (1) after rotational diffusion is the principal factor, and can be obtained from

$$[13] \qquad \beta = 2\pi c b_c = 2\pi c / X_3$$

For a given ring substituent, β for conformer **I** is expected to be greater than for conformer **II**, since the latter interacts less with neighboring solvent molecules. By the same token β (and b_c, or the band width of the sum band in this model) is expected to be less temperature dependent in **II** than in **I**, as observed.

The general relationship between half-band widths at 25 °C with σ (Fig. 10) is similar to that observed for the band shape index (Fig. 8). These figures also summarize the temperature dependence of these two parameters, indicating that (*a*) for the high frequency component, the temperature dependence of the shape index increases with σ, while the corresponding temperature dependence of the half-band width decreases with σ (the only exception being the *p*-OCH_3 compound), and (*b*) for the low frequency component, the temperature dependence of the shape index also increases with σ, but here the temperature independent exception is the *p*-NO_2 compound, while the corresponding temperature dependence of the half-band widths is relatively small and increases slightly with σ (the exception being the *p*-OCH_3 compound).

The symmetry of molecular vibrations and the direction of the transition moment relative to the axis about which molecular orientation takes place have also been shown to affect the temperature dependence of i.r. band widths in liquids (31–33). For liquid toluene, molecular re-orientation about an axis perpendicular to the phenyl ring is indicated (33). In conformer **I** of the benzyl alcohols the OH bond is approximately perpendicular to the sixfold axis of the phenyl ring, while in conformer **II** it is at an angle of about 51° to this axis. Assuming the OH transition moments to lie parallel to the OH bonds, and π–σ electron donor–acceptor interaction as being the dominant solvent perturbation, then a higher temperature dependence would be expected for conformer **I** than for **II**, as observed.

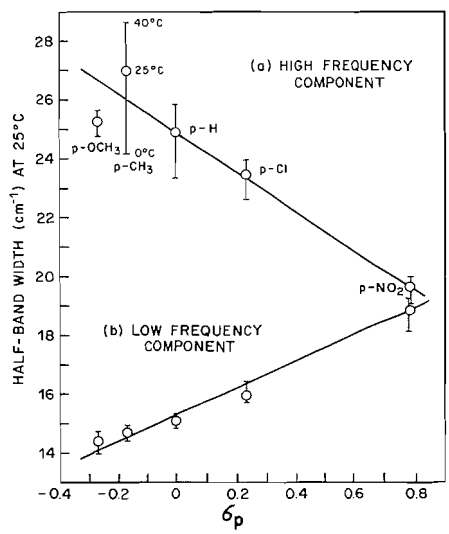

FIG. 10. Dependence of OH half-band widths in *p*-X-benzyl alcohols on the Hammett substituent constant of X. Circles refer to values at 25 °C; ranges indicate spread of values between 0 and +40 °C. (*a*) "Free" OH band, (*b*) intramolecularly OH···π bonded band.

Can. J. Chem. Downloaded from www.nrcresearchpress.com by 210.87.254.40 on 09/05/12
For personal use only.

Concluding Remarks

The general assumption that i.r. absorption bands in liquids and solutions have a Cauchy profile is unwarranted in the absence of a rigorous assessment of the experimentally observed contour (corrected for slit width effects). The Cauchy–Gauss sum function appears to be an adequate and convenient model for the quantitative evaluation of the shapes of symmetrical bands. Band shape and band width changes may be induced by conformational changes in the molecule as well as by intramolecular electronic effects. Band shapes may thus eventually provide information about the nature of molecular conformations. Furthermore, the temperature dependence of band shapes and band widths can act as probes of solute/solvent interaction, particularly rotational re-orientation. Further details of the mechanisms involved should become apparent as other carefully selected chemical systems are investigated; in particular the extent to which band shapes and widths independently reflect different facets of molecular dynamics in the condensed state requires further experimental study.

This project was supported by the National Research Council of Canada. The computer programs referred to in ref. 7 were kindly supplied by Dr. R. N. Jones.

1. R. P. Young and R. N. Jones. Chem. Rev. **71**, 219 (1971).
2. R. G. Gordon. J. Chem. Phys. **39**, 2788 (1963); **41**, 1819 (1964); **43**, 1307 (1965).
3. H. Shimizu. J. Chem. Phys. **43**, 2453 (1965).
4. K. S. Seshadri and R. N. Jones. Spectrochim. Acta, **19**, 1013 (1963).
5. J. Pitha and R. N. Jones. Can. J. Chem. **45**, 2347 (1967).
6. R. D. B. Fraser and E. Suzuki. Anal. Chem. **41**, 37 (1969).
7. R. N. Jones, T. E. Bach, H. Fuhrer, V. B. Kartha, J. Pitha, K. S. Seshadri, R. Venkataraghavan, and R. P. Young. Computer programs for absorption spectrophotometry. NRCC Bull. No. 11. Ottawa. 1968. J. Pitha and R. N. Jones. Optimization methods for fitting curves to infrared band envelopes: computer programs. NRCC Bull. No. 12. Ottawa. 1968. R. N. Jones and R. P. Young. Additional computer programs for absorption spectrophotometry and band fitting. NRCC Bull. No. 13. Ottawa. 1969.
8. J. T. Fox and A. E. Martin. Trans. Faraday Soc. **36**, 897 (1940).
9. T. D. Flynn, R. L. Werner, and B. M. Graham. Aust. J. Chem. **12**, 575 (1959).
10. J. Pitha and M. Horak. Coll. Czech. Chem. Commun. **25**, 1586 (1960).
11. M. Oki and H. Iwamura. Bull. Chem. Soc. Jap. **32**, 955 (1959).
12. R. N. Jones. Pure Appl. Chem. **18**, 303 (1969).
13. Tables of wavenumbers for the calibration of infrared spectrometers. I.U.P.A.C., Butterworths, London. 1961.
14. R. N. Jones, R. Venkataraghavan, and J. W. Hopkins. Spectrochim. Acta, **23A**, 925 (1967); **23A**, 941 (1967).
15. J. Pitha and R. N. Jones. Can J. Chem. **44**, 3031 (1966).
16. J. Brandmueller and K. Seevogel. Spectrochim. Acta, **20**, 453 (1964).
17. A. Allerhand and P. von R. Schleyer. J. Am. Chem. Soc. **85**, 371 (1963).
18. P. J. Krueger and B. F. Hawkins. Unpublished results.
19. D. H. McDaniel and H. C. Brown. J. Org. Chem. **23**, 420 (1958).
20. A. S. N. Murthy and C. N. R. Rao. Appl. Spec. Rev. **2**, 69 (1968).
21. J. Fruwert, G. Giesler, W. Geyer, and S. Sieber. Z. Phys. Chim. (Leipzig), **241**, 74 (1969).
22. L. J. Bellamy, H. E. Hallam, and R. L. Williams. Trans. Faraday Soc. **54**, 1120 (1958).
23. C. N. R. Rao, S. N. Bhat, and P. C. Divivedi. Appl. Spec. Rev. **5**, 1 (1971).
24. J. B. Ott, J. R. Goates, and A. H. Budge. J. Phys. Chem. **66**, 1387 (1962).
25. J. R. Goates, R. J. Sullivan, and J. B. Ott. J. Phys. Chem. **63**, 589 (1959).
26. R. Anderson and J. M. Prausnitz. J. Chem. Phys. **39**, 1225 (1963).
27. R. F. Weimer and J. M. Prausnitz. J. Chem. Phys. **42**, 3643 (1965).
28. M. L. McGlashan, D. Stubley, and H. Watts. J. Chem. Soc. A, 673 (1969).
29. G. W. Chantry, H. A. Gebbie, and H. N. Mirza. Spectrochim. Acta, **23A**, 2749 (1967).
30. A. M. North and T. G. Parker. Trans. Faraday Soc. **67**, 2234 (1971).
31. S. Higuchi, S. Tanaka, and H. Kamada. Spectrochim. Acta, **28A**, 1721 (1972).
32. M. A. Moharram. Z. Phys. Chem. (Leipzig), **251**, 33 (1972).
33. A. V. Rakov. Opt. Spectrosc. **13**, 203 (1962).

α-Pyrones. II.[1] The Synthesis of α-Pyrones From α,β-Unsaturated Aldehydes. Part II[1,2]

CH. R. ENGEL, A. F. DE KRASSNY, A. BÉLANGER,[3] AND G. DIONNE[4]

Department of Chemistry, Laval University, Quebec, Quebec G1K 7P4

Received April 17, 1973

It is shown that the reaction of acrolein with bromomalonate in the presence of an alkali alkoxide, leading to a 2-formylcyclopropane-1,1-dicarboxylate, may be applied to the steroid series; thus, a 20-methylene 21-aldehyde gives in excellent yield the corresponding cyclopropane derivative. The possibility of converting such systems to α-pyrones was investigated in the case of the acrolein adduct, diethyl 2-formylcyclopropane-1,1-dicarboxylate. While its cyclopropane ring could not be isomerized to an olefin with aluminum chloride or by reactions catalyzed by transition metals and while photolysis led to a dihydrofuran derivative, pyrolysis in high vacuum at 550–575° afforded directly an α-pyrone, ethyl coumalate. Evidence is put forward for the intermediacy of 3-ethoxycarbonyl-α-pyrone in this reaction.

La réaction de l'acroléine avec un bromomalonate en présence d'un alcoolate alcalin, qui conduit à un formyl-2 cyclopropanedicarboxylate-1,1, peut être appliquée à la série stéroïde, un 21-aldéhyde 20-méthylénique donnant en excellent rendement le dérivé cyclopropanique correspondant. Nous avons étudié la possibilité de convertir de tels systèmes en α-pyrones dans le cas du formyl-2 cyclopropanedicarboxylate-1,1 de diéthyle, dérivé de l'acroléine. Tandis que son cycle à trois chaînons ne put être isomérisé en oléfine avec le chlorure d'aluminium ou par des réactions catalysées par des métaux de transition et tandis que sa photolyse conduisit à un dérivé dihydrofurannique, sa pyrolyse, à 550–575° et sous haut vide, donna directement une α-pyrone, le coumalate d'éthyle. Nous suggérons l'α-pyrone 3-éthoxycarbonylée comme intermédiaire dans cette réaction.

Can. J. Chem., **51**, 3263 (1973)

In 1969 our laboratory reported one of the first syntheses of bufadienolides, a class of steroids comprising highly active cardiotonics, which are characterized by an α-pyrone ring whose position 5 is linked to the 17β-position of the steroid nucleus. The salient feature of our synthesis (1, cf. also 2) (compare Scheme 1, pathway *a*) consisted in a Michael addition of diethyl malonate to a 20-methylene 21-aldehyde, the hydrolysis product of the resulting adduct being subsequently subjected to enol-lactonization with concomitant decarboxylation, and the still required double bond, in conjugation with the carbonyl function of the lactone, being then introduced by a variety of methods. This pathway to bufadienolides (and generally to α-pyrones) suffers only from the relatively low yield of the dehydrogenation step which, in our experiments, did not exceed 35% of *pure* product; Pettit *et al.* (3) report yields of 43–60% of *crude* product when the dehydrogenation is carried out with sulfur.

The attempt to "prefigure" the desired double bond in the form of a suitable substituent of the malonate employed (cf. Scheme 1, pathway *b*) is obviously problematic. The olefin-forming elimination from the addition product, involving a leaving group (X in adduct **iii** of Scheme 1) which is α and not β to the ester groups, could hardly be expected to compete successfully with a 1,3-elimination resulting in a cyclopropane; indeed, the hydrogens β to the ester functions show no particular mobility, in contradistinction to the hydrogen α to the aldehyde group. Not surprisingly therefore, Warner and Moe obtained (cf. 4 also 5, 6), by the reaction of acrolein with diethyl bromomalonate not, as they first surmised (7), diethyl 3-formyl-1-propene-1,1-dicarboxylate (cf. **vi** in Scheme 1), but the 2-formylcyclopropane-1,1-dicarboxylate (cf. **v** in Scheme 1). In spite of this, the potential for an α-pyrone synthesis of the addition of a substituted

[1]Paper XXX in our series on Steroids and Related Products (1) has to be considered the first communication of the present series.

[2]The main results of this paper were the subject of a communication presented before the 55th Annual Conference and Exhibition of the Chemical Institute of Canada, Quebec, June 1972.

[3]Some of the results reported here are contained in the B.Sc. thesis of A. Bélanger, presented to the Department of Chemistry, Laval University, April 1970.

[4]Abbreviated from part of the doctoral thesis of G. Dionne, to be presented to the School of Graduate Studies of Laval University.

Can. J. Chem. Downloaded from www.nrcresearchpress.com by 210.87.254.42 on 09/05/12
For personal use only.

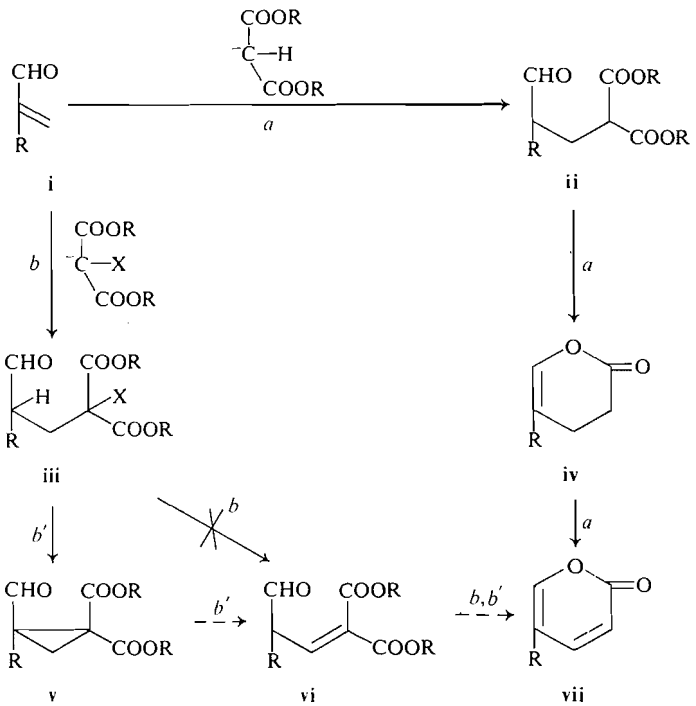

SCHEME 1

malonate such as bromomalonate to an α,β-unsaturated aldehyde still seemed worth exploring since the resulting cyclopropane derivatives (cf. **v**) are valence isomers of 4-formyl 2-butenoic esters (cf. **vi**), the immediate precursors of α-pyrones. If an isomerization of cyclopropanes of type **v** to olefins of type **vi** could be effected, an attractive modification of our first α-pyrone synthesis would be realized.

We at first attempted to apply Warner and Moe's synthesis of cyclopropane derivatives of type **v** (Scheme 1) to steroids, in particular to the 20-methylene 21-aldehyde **1** (1) from which our original bufadienolide synthesis had originated. Treatment of aldehyde **1** with an excess of diethyl bromomalonate in the presence of tertiary sodium butoxide in tertiary butanol afforded in 74% yield the desired cyclopropane derivative **2**. This product gave a marked reaction with tetranitromethane, showed an u.v. absorption maximum (in cyclohexane) at 205 nm (log ε 3.5), attributable to a carbonyl-conjugated cyclopropane, and exhibits in the i.r. (in KBr), apart from the peaks characteristic of the aldehyde, ester, and hydroxyl functions, a band at 1020 cm^{-1} which we assign to the cyclopropyl moiety. In the n.m.r. one proton of the cyclopropyl–methylene group appears as a doublet at 2.20 δ with a coupling constant of 5 Hz. The structure was confirmed by elemental analysis.

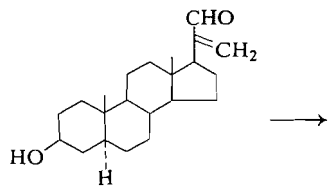

1

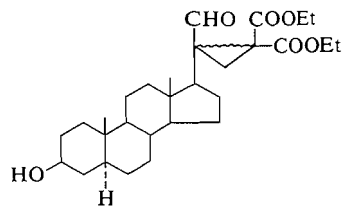

2

Since, in preliminary experiments, we were unable to isomerize the cyclopropane ring of the aldehydo ester **2** and even encountered difficulties in hydrolyzing its ester functions, we decided to investigate the valence isomerization

Can. J. Chem. Downloaded from www.nrcresearchpress.com by 210.87.254.42 on 09/05/12
For personal use only.

Can. J. Chem. Downloaded from www.nrcresearchpress.com by 210.87.254.42 on 09/05/12
For personal use only.

of such systems in the series originally studied by Warner and Moe. Using the American authors' procedure (7), we realized a 64% yield of diethyl 2-formylcyclopropane-1,1-dicarboxylate (**3**). We record in the Experimental its spectroscopic data since the product has not yet been fully characterized in this respect (cf. 4–7). Attention is drawn to the u.v. absorption maximum at 207 nm (log ε 3.3) and to the fact that the n.m.r. signals closely parallel those of cyclopropane-1,1,2-tricarboxylic acid (8): the protons of the cyclopropyl–methylene group form with the cyclopropyl proton of the formyl-substituted carbon atom 2 an ABX system, the C_2-proton being, of course, also coupled with the aldehydic proton.[5]

In view of the great ease of the reductive opening of the cyclopropane ring of the 2,4-dinitrophenylhydrazone of compound **3** with a 5% palladium-on-charcoal catalyst at room temperature and 1.8 atm (7), the inertness of the system to isomerization to an olefinic derivative is noteworthy. Treatment with aluminum chloride, even at temperatures exceeding those reported in the literature (cf. 10) gave no results. Neither were reactions catalyzed by transition metals successful. When the cyclopropane derivative was heated in benzene with bis(triphenylphosphine)iridium carbonyl chloride to 130°, following the procedure of Volger *et al.* (11) or when it was treated with *trans*-dichlorobis(tri-*n*-butylphosphine)nickel(II) (12)[6] and diisobutylaluminum chloride according to the method of Miller and Pinke (13), the starting material was recovered unchanged.[7]

Numerous examples of photolytic valence isomerizations to olefins of cyclopropanes conjugated with carbonyl functions (cf. 15–18) or with phenyl or nitro groups (19, 20) have been reported. We therefore irradiated the cyclopropane derivative **3** in benzene solution using a Pyrex filter, according to the method of Beugelmans (18). Instead of obtaining an aliphatic olefin we isolated the dihydrofuran **5**. Its structure was evident from its elemental composition and from its spectral characteristics. In the i.r. the aldehyde band had disappeared, the ester bands were visible at 1750 and 1275 cm^{-1} (in KBr), and the 4,5-double bond at 3122 and 1630 cm^{-1}, the latter band having the intensity characteristic of a vinyl ether; the maximum at 1065 cm^{-1} corroborated this structural feature. The n.m.r. spectrum confirmed the absence of the aldehyde group and of the cyclopropane ring and the presence of the ester groups; the two olefinic protons together with the methylene protons of carbon atom 3 form an AMX_2-system comprising a multiplet centered at 6.33 δ corresponding to one proton ($H_A = H_5$), a multiplet centered at 4.95 δ also corresponding to one proton ($H_M = H_4$), and finally a multiplet corresponding to two protons centered at 3.18 δ ($2H_X = 2H_3$). The chemical shifts agree well with those reported in the literature for dihydrofuran (21*a*), if one takes into consideration that the deshielding by the neighboring ester groups should result in a downfield shift of the 3-protons (which amounts to 0.65 p.p.m.). The coupling constants (cf. Experimental) correspond well to the expected values (21*b*).

A plausible mechanism for the formation of the dihydrofuran derivative **5** is formally represented in Scheme 2. The participation of the aldehyde carbonyl group in the ring opening is substantiated by the fact that no photolytic ring opening occurs in the case of the ethylenedioxy

[5]The formation of the three-membered ring by a Perkin cyclization seems perfectly plausible and far more probable than by a reaction involving a carbene, formed by the action of the alcoholate on the bromomalonate. Indeed, while the carbanion formed by proton abstraction from a haloform is only stabilized by inductive effects and converts readily to a carbene, the anion formed from bromomalonate is also significantly stabilized by conjugative effects. We were able to establish the non-intermediacy of a carbene by subjecting a steroid with an unhindered isolated double bond, 5α-androst-2-en-17β-ol (**I**) (9) to the action of excess bromomalonate and sodium *t*-butoxide in *t*-butanol. Even after prolonged reaction periods and at elevated temperatures, the starting material was recovered in almost quantitative yield.

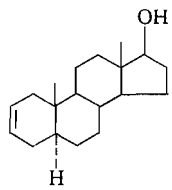

I

[6]We sincerely thank Professor Ray G. Miller for very kindly providing us with the description of the preparation of this reagent.

[7]The fact that certain cyclopropane systems cannot be opened by transition metal-catalyzed reactions is, however, not novel; it was discussed in the quoted paper by Volger *et al.* (11) and was recently again demonstrated by Gassman *et al.* (14).

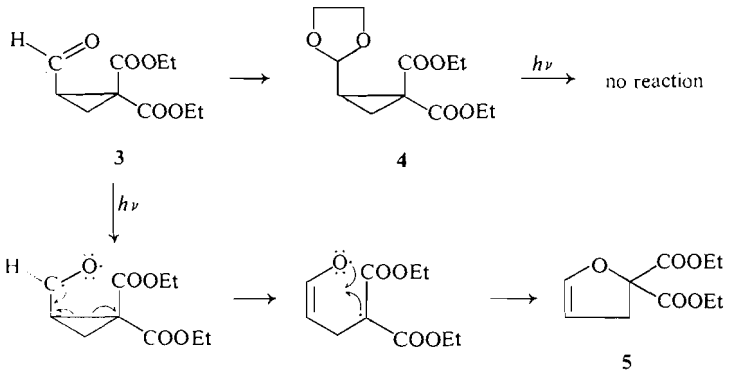

SCHEME 2

derivative **4**. We refer for the preparation of ketal **4** to the Experimental.

We finally succeeded in opening the cyclopropane ring of the diethoxycarbonyl aldehyde **3** by pyrolysis under nitrogen at 0.1 mm Hg at 550–575°. The remarkable feature of this reaction resides in the fact that it is accompanied by cyclization to an α-pyrone and by an apparent 1,3-migration of the remaining ethoxycarbonyl substituent (cf. below), pure ethyl coumalate (**6***a*) being isolated in 20% yield. At 500°, a temperature sufficient for the opening of most cyclopropanes (for instance, for the transformation of cyclopropyl ketones into cyclopentenones (22)), no reaction occurred.

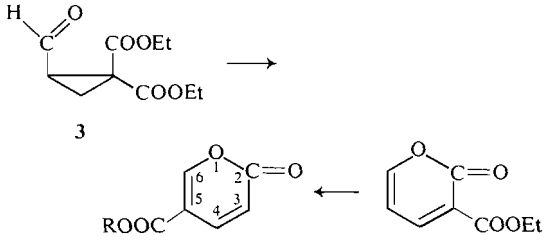

The structure of the coumalic ester was proved by elemental analysis and by its spectral characteristics. In the u.v. it showed maxima at 245 and 288 nm ($\log \varepsilon_{245}$ 3.83, $\log \varepsilon_{288}$ 3.45), in the i.r. (in KBr) maxima at 1760, 1650, and 1565 cm^{-1}, typical of the α-pyrone ring, and at 1730 and 1300 cm^{-1}, attributable to the ester group. These data agree well with those reported in the literature (23). The n.m.r. spectrum revealed, apart from the signals of the ethyl ester, the 3-, 4-, and 6-protons as three distinct multiplets representing an AMX system. The signal of the 6-proton (H_X), centered at 8.35 δ, shows small coupling constants with the vinylic protons 4 (H_A) and 3 (H_M) ($J_{4,6}$ = 3 Hz, $J_{3,6}$ = 1 Hz), whereas the coupling constant of the 3- and 4-protons (the signals of which are centered respectively at 6.28 and 7.8 δ) amounts to 10 Hz. The identity of the compound was confirmed by its hydrolysis with aqueous sulfuric acid to coumalic acid **6**, an authentic sample of which was prepared according to the method of Wiley and Smith (24, cf. also 25) from malic acid. Conversely, authentic coumalic acid was transformed according to the method of Pechmann (25) into its ethyl ester **6***a* which was found identical to the product arising from the pyrolysis of the cyclopropyl aldehyde **3**.[8]

It seems logical to assume that 3-ethoxycarbonyl-α-pyrone (**7**) is an intermediate in the formation of ethyl coumalate (**6***a*) from the formyl cyclopropane dicarboxylate **3**. While no plausible mechanism for the direct formation of the 5-substituted α-pyrone **6***a* can be advanced, the transformation of the cyclopropane derivative **3** to 3-ethoxycarbonyl-α-pyrone (**7**) can be rationalized readily (cf. Scheme 3);[9] furthermore, Pirkle *et al.* (27) have shown that apparent methyl and bromine 5 → 3 migrations occur upon pyrolytic decarboxylation of 5-methyl and 5-bromo 6-carb-

[8]We recall that coumalic acid may be decarboxylated in excellent yield (cf. 25, 26).

[9]In Scheme 3 the conversion of diethyl 2-formylcyclopropane-1,1-dicarboxylate (**3**) to 3-ethoxycarbonyl-α-pyrone (**7**) is *formally* represented as involving a concerted transformation of the cyclopropane system to an α-pyrone derivative. Naturally, one can also consider that the valence isomerization of the cyclopropane into an olefin precedes the formation of the heterocycle (cf. Scheme 1). Furthermore, while the symbolism employed in Scheme 3 implies ionic reactions, one has to consider that under pyrolytic conditions the reaction may well involve free radicals.

Can. J. Chem. Downloaded from www.nrcresearchpress.com by 210.87.254.42 on 09/05/12
For personal use only.

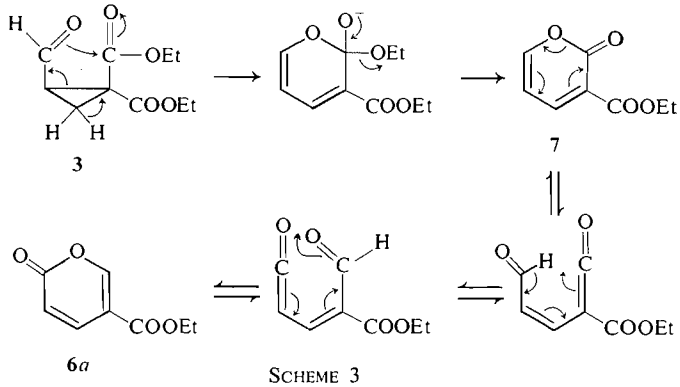

SCHEME 3

oxy-α-pyrones. The American authors explain these apparent migrations by the assumption of a ring opening to a ketene,[10] followed by a 1,5-sigmatropic hydrogen shift and ring closure to an isomeric α-pyrone. Since these transformations have to be regarded as reversible (cf. 27), the formation at high temperatures of ethyl coumalate (**6***a*) from 3-ethoxycarbonyl-α-pyrone (**7**) may be explained as summarily depicted in Scheme 3. In the case of 3- and 5-ethoxycarbonyl-α-pyrones, in contradistinction to the case of 3- and 5-methyl-α-pyrones, the equilibrium is displaced towards the 5-substituted product.

In order to substantiate the intermediacy of 3-ethoxycarbonyl-α-pyrone (**7**) in the formation of ethyl coumalate (**6***a*) from the formylcyclopropane dicarboxylate **3**, we synthesized 3-ethoxycarbonyl-α-pyrone (**7**) from 1,1,3,3-tetraethoxypropane and diethyl malonate (cf. 29) and subjected it to pyrolysis under the conditions used for the preparation of ethyl coumalate (**6***a*) from the cyclopropane derivative **3**. This resulted in a high yield of ethyl coumalate (**6***a*).

Further studies are required and are in progress in our laboratory in order to determine whether or not the two-step synthesis of ethyl coumalate from acrolein can be applied to the synthesis of other α-pyrones.

Experimental[11]

Ethyl 3β-Hydroxy-21-oxo-23-ethoxycarbonyl-20,23-cyclo-5α,20ξ-cholanate (2)

Sodium (80 mg) was dissolved in *t*-butanol (40 ml). To an aliquot of 10 ml of this solution, 790 mg of diethyl bromomalonate was added in a nitrogen atmosphere and, subsequently, 960 mg of 3β-hydroxy-20-methylene-5α-pregnan-21-al (**1**) (1), dissolved in 30 ml of *t*-butanol. A white precipitate formed and the mixture became acidic. The remainder of the sodium *t*-butoxide solution was added slowly and the mixture was stirred for 1 day. Another 15 ml of a sodium *t*-butoxide solution (prepared from 30 mg of sodium) was added, followed by 0.1 ml of diethyl bromomalonate, and the mixture was heated to 30–35° for 3 h. According to thin-layer analysis, the reaction was complete and the mixture was poured into ice water, the precipitate was extracted with dichloromethane, the organic solution was washed with water, and was dried over sodium sulfate. Evaporation of the solvent gave 1.469 g of a product which was chromatographed on 150 g of silica gel. Elutions with benzene – ethyl acetate (90:10) gave 1.029 (74% yield) of the formyl dicarboxylate **2**, m.p. 158–165°. A sample was recrystallized three times from dichloromethane–hexane and sublimed twice in high vacuum at 150–168° for analysis. Fine needles, m.p. 180–180.5°; $[\alpha]_D^{25}$ −36.6° (*c*, 1.000 in $CHCl_3$); λ_{max} (cyclohexane) 205 nm (log ε 3.47); ν_{max} (KBr) 3450 (OH), 2750 (aldehyde), 1740 and 1720 (ester groups), 1712 (aldehyde), 1240 (esters), 1082 and 1050 (hydroxyl), 1020 cm^{-1} (cyclopropyl); δ ($CDCl_3$)[12] 0.69 (s) (18-CH_3), 0.81 (s) (19-CH_3), 1.22 (t, J = 7 Hz), and 1.29 (t, J = 7 Hz) (ester-CH_3), 1.57 (s) (OH, exchanged with D_2O), 2.20 (1 H, d, J = 5 Hz) (1 H of cyclopropyl-CH_2), 3.68 (1 H, m) (3α-H), 4.10 (q, J = 7 Hz), and 4.22 (q, J = 7 Hz) (CH_2 of esters), 9.95 (1 H, s) (aldehyde).

Anal. Calcd. for $C_{29}H_{44}O_6$: C, 71.28; H, 9.08. Found: C, 70.98; H, 8.98.

[10]For the photolytic formation of ketenes from α-pyrones cf. ref. 28.

[11]The melting points were taken in evacuated capillaries and the temperatures were corrected. For elution column chromatography, neutral aluminum oxide Woelm, activity III, and Davison's silica gel no. 923 were employed. Dry-column chromatography was performed with Woelm dry-column chromatography silica gel, activity III; t.l.c. with Merck-Darmstadt silica gel. The i.r. spectra were recorded on Beckman IR-4 and IR-12 spectrophotometers and the u.v. spectra on a Beckman DK-1A instrument. The n.m.r. spectra were taken on a Varian A-60 spectrometer, tetramethylsilane serving as internal standard, if not otherwise stated. The microanalyses were performed by Dr. F. Pascher, Bonn, Germany, and Ayerst Laboratories, Montreal (Director of the Analytical Division: Dr. G. Schilling), to whom we express our sincere appreciation.

[12]Recorded on a Varian HA-100 spectrometer by Prof. G. Just, McGill University, Montreal, to whom we express our sincere appreciation.

Can. J. Chem. Downloaded from www.nrcresearchpress.com by 210.87.254.42 on 09/05/12
For personal use only.

Can. J. Chem. Downloaded from www.nrcresearchpress.com by 210.87.254.42 on 09/05/12
For personal use only.

Diethyl 2-Formylcyclopropane-1,1-dicarboxylate (3)

According to the procedure of Warner and Moe (7), 23 g of acrolein and 95.2 g of diethyl bromomalonate were transformed into 54.2 g (64.1% yield) of purified diethyl 2-formylcyclopropane-1,1-dicarboxylate (3), b.p. 79.5–82°/0.25–0.3 mm Hg; the crude product (70.675 g, 84%) had been purified by fractional vacuum distillation using a Vigreux column. The analytical sample was prepared by two further vacuum distillations; b.p. 78–80°/0.08 mm Hg (lit. (4): 88–90°/0.01 mm Hg); n^{25} 1.4490 (lit. (4), n^{25} 1.4509); λ_{max} (cyclohexane) 207 nm (log ε 3.29); ν_{max} (film) 3120 (cyclopropyl-CH_2), 2720 (aldehyde), 1747 and 1732 (esters), 1720 (aldehyde), 1270 and 1205 (esters), 1025 cm^{-1} (cyclopropyl); δ (CCl_4) 1.3 (t, J = 7 Hz) (ester-CH_3), 1.50–2.10 (m) (cyclopropyl-CH_2), 2.45–2.82 (m) (cyclopropyl-CH), 4.12 (q, J = 7 Hz) (ester-CH_2), 9.25 (d, J = 5 Hz) (aldehyde).

Anal. Calcd. for $C_{10}H_{14}O_5$: C, 56.07; H, 6.59. Found: C, 55.94; H, 6.57.

2,4-Dinitrophenylhydrazone

This derivative was prepared in the usual fashion (30); m.p. 146–146.5° (lit. (7): 141.7–142.7°); λ_{max} (EtOH) 355 nm (log ε 4.31); ν_{max} (KBr) 3305 (NH), 3120 (cyclopropyl), 3100 (aromatic C—H), 1730 (esters), 1638 (C=N), 1620 and 1595 (aromatic C=C), 1525 and 1340 (nitro), 1270 and 1210 (esters), 825 cm^{-1} (aromatic C—H deformation); δ($CDCl_3$) 1.28 (t, J = 7 Hz) and 1.32 (t, J = 7 Hz) (ester-CH_3), 1.6–2.2 (m) (cyclopropyl-CH_2), 2.6–3.1 (cyclopropyl-CH), 4.26 (q, J = 7 Hz) and 4.28 (q, J = 7 Hz) (ester-CH_2), 7.32 (s) (C*H*=N), 7.45 (d, J = 10 Hz), 8.20–8.60 (m), and 9.12 (d, J = 2.5 Hz) (aromatic protons), 11.2 (broad s) (NH).

Anal. Calcd. for $C_{16}H_{18}N_4O_8$: C, 48.73; H, 4.60; N, 14.21. Found: C, 48.68; H, 4.65; N, 14.18.

Diethyl 2-Ethylenedioxymethylcyclopropane-1,1-dicarboxylate (4)

From a solution of 1.5 g of diethyl 2-formylcyclopropane-1,1-dicarboxylate (3) in 230 ml of absolute benzene, 40 ml of solvent was removed by distillation and 20 ml of freshly distilled ethylene glycol and 93 mg of *p*-toluenesulfonic acid were added. The mixture was refluxed for 10 h and then poured into an iced saturated sodium bicarbonate solution. The product was extracted with ether, the organic solution was washed with a 2 *N* sodium carbonate solution and with water, and was dried over sodium sulfate. Evaporation of the solvent gave 1.6 g (89% yield) of ketal **4**. The product was purified by fractional vacuum distillation, giving 1.32 g (73.5%) of pure material; b.p. 100–103°/0.04 mm Hg. For analysis the product was redistilled *in vacuo*; b.p. 102°/0.04 mm Hg; n^{25} 1.4565; ν_{max} (film) 3120 (cyclopropyl), 1740 and 1270 (esters), 1140 cm^{-1} (ketal); δ (CCl_4) 1.25 (t, J = 7 Hz) (ester-CH_3), 3.88 (m) (ketal-CH_2), 4.18 (q, J = 7 Hz) (ester-CH_2), 4.7 (d, J = 5 Hz) (H on ethylenedioxy-substituted C).

Anal. Calcd. for $C_{12}H_{18}O_6$: C, 55.80; H, 7.03. Found: C, 55.45; H, 7.02.

Unsuccessful Attempts at Valence Isomerization of Diethyl 2-Formylcyclopropane-1,1-dicarboxylate (3)

(a) With Aluminum Chloride

For 90 min, 1 g of the formyl cyclopropane dicarboxylate **3** was treated with 1.6 g of aluminum chloride at 100–110°. The usual work-up gave 852 mg of a yellow oil, the u.v., i.r., n.m.r., and thin-layer analyses of which clearly indicated that it consisted of slightly decomposed starting material. There was no evidence for the formation of an olefinic derivative. When the reaction was carried out at 150° for a period of 3 h, a far less pure product was obtained which again showed the characteristics of the starting material but which also indicated the formation of other (in part hydroxylated) products which were not further investigated and which did not contain appreciable amounts of olefins.

(b) With Bis(triphenylphosphine)iridium Carbonyl Chloride

A solution of 1 g of the formyl cyclopropane dicarboxylate **3** in 25 ml of absolute benzene was heated with 78 mg of bis(triphenylphosphine)iridium carbonyl chloride to 130° for 18 h. The solution was filtered, washed with water, dried and taken to dryness to give 888 mg of a brownish oil, identified as impure starting material. The same result was obtained when the reaction was carried out at 160° for 24 h.

(c) With trans-Dichlorobis(tri-n-butylphosphine)-nickel(II) and Diisobutylaluminum Chloride

A solution of 1 g of the formyl cyclopropane dicarboxylate **3** in 20 ml of absolute toluene was treated with 210 mg of diisobutylaluminum chloride and 87 mg of *trans*-dichlorobis(tri-*n*-butylphosphine)nickel(II) for 3 h. Ice was added and the product was extracted with ether. The ethereal solution was washed with water and dried over sodium sulfate, and the solvent was evaporated. The remaining yellow oil was identified as the starting material. The reaction was repeated at reflux temperature for 5 h with the same result.

Photolysis of Diethyl 2-Formylcyclopropane-1,1-dicarboxylate (3)

A solution of 4.429 g of the formyl cyclopropane dicarboxylate **3** in 500 ml of absolute benzene was irradiated under nitrogen with an immersed 450 W Hanovia mercury lamp, using a Pyrex filter and a quartz vessel, cooled by a cold-water jacket. After 30 h the reaction was interrupted and the solvent was removed under reduced pressure. A portion of 3.4 g of the residue (4.435 g of a brownish oil) was subjected to dry-column chromatography (31) on 1 kg of silica gel, using petroleum ether – ether (2:1) as solvent system. Thus 2.039 g (60% yield) of pure diethyl *2,3-dihydrofurane-2,2-dicarboxylate* (**5**) was obtained. Vacuum distillation gave the analytical sample; b.p. 79–80°/0.1 mm Hg; n^{25} 1.4452; λ_{max} (cyclohexane) 203 nm (log ε 3.2), λ_{max} (EtOH) 203 nm (log ε 3.45); ν_{max} (film) 3122 (double bond), 1750 (esters), 1635 (strong band of enolic double bond), 1270 cm^{-1} (esters); δ (CCl_4) 1.32 (6 H, t, J = 7 Hz) (ester-CH_3), 4.30 (4 H, q, J = 7 Hz) (ester-CH_2), 3.18 (2 H, d of d, $J_{3,4}$ = 2.5 Hz, $J_{3,5}$ = 2.0 Hz) (H_2 of C-3 = 2 H_X of AMX_2 system), 4.95 (1 H, d of t, $J_{4,3}$ = 2.5 Hz, $J_{4,5}$ = 2.5 Hz) (H_4 = H_M of AMX_2 system), 6.32 (1 H, d of t, $J_{5,3}$ = 2.0 Hz, $J_{5,4}$ = 2.5 Hz) (H_5 = H_A of AMX_2 system).

Anal. Calcd. for $C_{10}H_{14}O_5$: C, 56.07; H, 6.59. Found: C, 55.57; H, 6.68.

Can. J. Chem. Downloaded from www.nrcresearchpress.com by 210.87.254.42 on 09/05/12
For personal use only.

Photolysis of Diethyl 2-Ethylenedioxymethylcyclopropane-1,1-dicarboxylate (4)

A quantity of 1.6 g of the ketal derivative **4** of the aldehydo ester **3** was irradiated as described for the photolysis of the free aldehyde **3**. The work-up gave 1.6 g (quantitative crude yield) of a yellow oil, the i.r. and n.m.r. spectra of which revealed that it only contained the starting material, the cyclopropane derivative **4**. A portion of this product (1.5 g) was dissolved in 300 ml of absolute benzene and was again irradiated, this time without a Pyrex filter and for 17 h. Evaporation of the solvent gave 1.5 g (quantitative crude yield) of a yellowish oil which was again identified by i.r., n.m.r., and thin-layer analyses as unchanged starting material **4**.

Ethyl Coumalate (6a)

(a) By Pyrolysis of Diethyl 2-Formylcyclopropane-1,1-dicarboxylate (3)

A quantity of 9 g of diethyl 2-formylcyclopropane-1,1-dicarboxylate (**3**) was slowly distilled, in the course of 10 h, under nitrogen at 0.1 mm Hg, and the vapors were passed through a Vycor tube, filled with crushed Vycor glass, preheated to 550–575°. The distillate was collected in a Dry-Ice trap, the dark-brown product (3.728 g) was diluted with ether, the solution was washed with a saturated sodium bicarbonate solution and with water and was dried over sodium sulfate. Evaporation of the solvent gave 3.126 g of a brown oil. A portion of 2 g of this product was purified by dry-column chromatography on 600 g of silica gel, using petroleum ether – ether (1 : 1) as solvent system. Thus, 903 mg (corresponding to an overall yield of 20.2%) of ethyl coumalate (ethyl 2-pyrone-5-carboxylate) (**6a**) was obtained. For analysis, the product was redistilled under vacuum; b.p. 82–83°/0.1 mm Hg; m.p. 35–35.5° (lit. (25): 36°); n^{25} 1.4782; λ_{max} (EtOH) 245 (log ε 3.8) and 288 nm (log ε 3.4); ν_{max} (film) 3100 (double bond), 1760 (lactone), 1730 (ester), 1665 and 1650 (double bonds), 1300 cm^{-1} (ester); δ (CCl_4) 1.38 (3 H, t, J = 7 Hz) (ester-CH_3), 4.35 (2 H, t, J = 7 Hz) (ester-CH_2), 6.28 (1 H, d of d, $J_{3,4}$ = 10 Hz, $J_{3,6}$ = 1 Hz) (H_3 = H_A of AMX system), 7.80 (1 H, d of d, $J_{4,3}$ = 10 Hz, $J_{4,6}$ = 3 Hz) (H_4 = H_M of AMX system), 8.35 (1 H, d of d, $J_{6,4}$ = 3 Hz, $J_{6,3}$ = 1 Hz) (H_6 = H_X of AMX system).

Anal. Calcd. for $C_8H_8O_4$: C, 57.14; H, 4.80. Found: C, 56.69; H, 4.84.

(b) From Coumalic Acid (6)

A solution of 10.2 g of coumalic acid (**6**), prepared as described below (cf. 24), in 150 ml of absolute ethanol was refluxed for 1.5 h with 60 ml of concentrated sulfuric acid. The cooled solution was poured onto 100 g of ice and the product was extracted with ether. The organic solution was washed with a saturated sodium bicarbonate solution and with water and was dried over sodium sulfate. Evaporation of the solvent gave 11.9 g of a brown oil which was purified by fractional vacuum distillation. The product (b.p. 72–74°/0.04 mm Hg, m.p. 34–35°) was found identical to a sample prepared as described under (*a*), by the comparison of the u.v., i.r., and n.m.r. spectra.

(c) By Pyrolysis of Ethyl α-Pyrone-3-carboxylate (7)

Pyrolysis of 10.2 g of ethyl α-pyrone-3-carboxylate (7) (cf. below), under the conditions described under (*a*), led to 7.8 g (76.5%) of a dark-brown oil, the u.v., i.r., and n.m.r. spectra of which established its identity with ethyl coumalate (**6a**). Vacuum distillation gave 7.05 g (69%) of pure ethyl coumalate (**6a**), b.p. 79–81°/0.08 mm Hg, the spectra of which were superimposable on those of the products described under (*a*) and (*b*).

Coumalic Acid (6)

(a) From Ethyl Coumalate (6a), Obtained by Pyrolysis of the Cyclopropane Derivative 3

To a solution of 3.36 g of ethyl coumalate (**6a**), prepared from the formyl cyclopropane dicarboxylate **3**, in 40 ml of 95.5% sulfuric acid, 25 cc of water was added slowly. The solution was left for 20 h at room temperature and was then precipitated on 150 g of ice. The product was extracted with ether–chloroform (3 : 1), the organic solution was washed with water and was then extracted with a saturated sodium bicarbonate solution. The alkaline, aqueous extract was acidified to the Congo-blue reaction with concentrated hydrochloric acid and the product was extracted with ether–chloroform (3 : 1). The organic layer was washed with water and dried over sodium sulfate. Removal of the solvent gave 2.41 g (81%) of a light-brown solid, m.p. 190–195°. The product was dissolved in 20 ml of hot methanol and this solution was treated with 250 mg of Norit-A. The hot mixture was filtered and the volume of the filtrate was reduced to approximately 15 ml and cooled in an ice bath. The precipitate was filtered, washed with cold methanol and dried. Thus 1.505 g (50.5% yield) of light yellow crystals, m.p. 208–210°, were obtained. Recrystallization from methanol raised the melting point to 210–212°. A sample was sublimed twice in high vacuum between 120 and 130° for analysis. Almost colorless powder, m.p. 214.5–215° (lit. (24) 209–210°); λ_{max} (EtOH) 243 (log ε 3.7) and 288 nm (log ε 3.5); ν_{max} (KBr) 3200–2500 (acid), 1720 (lactone), 1680 (acid), 1630 and 1550 (double bonds), 1405 and 1230 cm^{-1} (acid); δ (CF_3COOH) 6.78 (1 H, d of d, $J_{3,4}$ = 10 Hz, $J_{3,6}$ = 1 Hz) (H_3 = H_A of AMX system), 8.25 (1 H, d of d, $J_{4,3}$ = 10 Hz, $J_{4,6}$ = 3 Hz) (H_4 = H_M of AMX system), 8.70 (1 H, d of d, $J_{6,4}$ = 3 Hz, $J_{6,3}$ = 1 Hz) (H_6 = H_X of AMX system).

Anal. Calcd. for $C_6H_4O_4$: C, 51.44; H, 2.88. Found: C, 51.42; H, 2.97.

(b) From Malic Acid

A quantity of 50 g of malic acid was transformed, as described by Wiley and Smith (24), into 21.2 g (80.5% yield) of crude coumalic acid (**6**), m.p. 196–203°. The product was purified in hot methanol with Norit-A and recrystallized twice from methanol to give 16.4 g (62.5% yield) of pure coumalic acid (**6**), m.p. 208–211°, which was found identical with the one prepared as described under (*a*), by the comparison of the u.v., i.r., and n.m.r. spectra, and by the determination of a mixture melting point.

Ethyl 2-Pyrone-3-carboxylate (7)

A quantity of 55 g of 1,1,3,3-tetraethoxypropane was transformed, according to the procedure of Windholz *et al.* (29), with 40 g of diethyl malonate, 100 ml of acetic anhydride, and catalytic amounts of zinc chloride, to 58.4 g of *diethyl 3-ethoxyallylidenemalonate*; b.p. 114°/0.08 mm Hg (lit. (29): b.p. 128°/0.2 mm Hg); ν_{max} (CH_3OH) 300 nm (log ε 4.32) (lit. (29): 300 nm (log ε 4.39)); ν_{max} (film) 1720 (esters), 1630 (double bond), 1245 cm^{-1} (esters); δ (CCl_4) 1.28 (3 H, t, J = 7 Hz) (enol ether-CH_3), 1.32 (6 H, t, J = 7 Hz) (ester-CH_3), 4.22

(2 H, q, J = 7 Hz) (enol ether-CH_2), 4.26 (4 H, q, J = 7 Hz) (ester-CH_2), 6.20 (1 H, t, J = 12 Hz) (olefinic proton), 7.18 (1 H, d, J = 12 Hz) (olefinic proton), 7.38 (1 H, d, J = 12 Hz) (olefinic proton).

As described by Windholz *et al.* (29), a quantity of 12.6 g of diethyl 3-ethoxyallylidenemalonate was heated in 140 ml of 99% formic acid for 1 h to give 6.1 g (72.7% yield) of *ethyl 2-pyrone-3-carboxylate* (**7**); b.p. 95–97°/0.08 mm Hg (lit. (29): b.p. 122–123°/0.2 mm Hg), λ_{max} (CH_3OH) 308 nm (log ε 3.72) (lit. (29): 309 nm (log ε 3.87)); ν_{max} (film) 3110 (double bonds), 1760 (lactone), 1745 (ester), 1630 and 1555 (double bonds), 1270 cm^{-1} (ester); δ (CCl_4) 1.37 (3 H, t, J = 7 Hz) (ester-CH_3), 4.4 (2 H, q, J = 7 Hz) (ester-CH_2), 6.62 (1 H, d of d, $J_{5,4}$ = 7 Hz, $J_{5,6}$ = 5 Hz) (H_5 = H_A of AMX system), 7.95 (1 H, d of d, $J_{6,5}$ = 5 Hz, $J_{6,4}$ = 2.5 Hz) (H_6 = H_M of AMX system), 8.35 (1 H, d of d, $J_{4,5}$ = 7 Hz, $J_{4,6}$ = 2.5 Hz) (H_4 = H_X of AMX system).

Anal. Calcd. for $C_8H_8O_4$: C, 57.14; H, 4.80. Found: C, 57.21; H, 4.73.

Treatment of 5α-Androst-2-en-17β-ol (I) with Diethyl Bromomalonate

To 10 ml of a solution prepared from 140 mg of sodium and 100 ml of *t*-butanol, 1.2 ml of diethyl bromomalonate was added and, subsequently, 1 g of 5α-androst-2-en-17β-ol (I) (9), dissolved in 50 ml of *t*-butanol. The rest of the sodium *t*-butoxide solution was added and the mixture was kept for 3 h at room temperature and subsequently at 90° for 5 h. No reaction was observed by thin-layer analysis. The product was poured into ice water and the precipitate was extracted with dichloromethane. The organic solution was washed with water and dried over sodium sulfate. Evaporation of the solvent gave 991 mg of the starting material. The result was analogous when the diethyl bromomalonate was added to a solution containing the steroid and sodium *t*-butoxide. Variations of the reaction conditions did not alter the results.

Sincere thanks are extended to Mrs. J. Capitaine for her assistance in some of the experiments and to Professor G. Just, McGill University, for kindly subjecting one of our products to an n.m.r. analysis at 100 MHz. We gratefully acknowledge the technical cooperation of the late Mr. D. Capitaine and of Mrs. G. Pelletier. Our appreciation is expressed to the National Research Council of Canada, the Ministère de l'Education du Gouvernement du Québec, to Ayerst Laboratories, Montreal, Quebec, and to the Schering Corporation, Bloomfield, New Jersey, for financial assistance. One of us (G. D.) sincerely thanks the National Research Council of Canada for the award of a scholarship.

1. Ch. R. Engel, R. Bouchard, A. F. de Krassny, L. Ruest, and J. Lessard. Steroids, **14**, 637 (1969).
2. W. Haede, W. Fritsch, K. Radscheidt, U. Stache, and H. Ruschig. Justus Liebigs Ann. Chem. **741**, 92 (1970).
3. (*a*) G. R. Pettit, D. C. Fessler, K. D. Pauli, P. Hofer, and J. C. Knight. J. Org. Chem. **35**, 1398 (1970); (*b*) G. R. Pettit and J. R. Dias. J. Org. Chem. **36**, 3207 (1971).
4. D. T. Warner, J. Org. Chem. **24**, 1536 (1959).
5. M. Mousseron, R. Fraisse, R. Jacquier, and G. Bonavent. C. R. Acad. Sci. **248**, 1465 (1959).
6. G. Bonavent, M. Causse, and R. Fraisse-Julien. Bull. Soc. Chim. Fr. 2462 (1964).
7. D. T. Warner and O. A. Moe. J. Am. Chem. Soc. **70**, 3470 (1948).
8. J. D. Graham and M. T. Rogers. J. Am. Chem. Soc. **84**, 2249 (1962).
9. M. M. Janot, A. Khuong-Huu, and R. Goutarel. Bull. Soc. Chim. Fr. 1640 (1960).
10. G. Combaut et L. Giral. Bull. Soc. Chim. Fr. 3258 (1969).
11. H. C. Volger, H. Hogeveen, and M. M. P. Gaasbeek. J. Am. Chem. Soc. **91**, 2137 (1969).
12. K. A. Jensen. Z. Anorg. Chem. **229**, 265 (1936).
13. R. G. Miller and P. A. Pinke. J. Am. Chem. Soc. **90**, 4500 (1968).
14. (*a*) P. G. Gassman and F. J. Williams. J. Am. Chem. Soc. **94**, 7733 (1972); (*b*) P. G. Gassman, G. R. Meyer, and F. J. Williams. J. Am. Chem. Soc. **94**, 7741 (1972); (*c*) P. G. Gassman, T. J. Atkins, and J. T. Lumb. J. Am. Chem. Soc. **94**, 7757 (1972).
15. W. G. Dauben, L. Schutte, and R. E. Wolf. J. Org. Chem. **34**, 1849 (1969).
16. W. G. Dauben, L. Schutte, R. E. Wolf, and E. J. Deviny. J. Org. Chem. **34**, 2512 (1969).
17. C. H. Robinson, O. Gnoj, and F. E. Carlon. Tetrahedron Lett. 2515 (1965).
18. R. Beugelmans. Bull. Soc. Chim. Fr. 3087 (1965).
19. G. W. Griffin, J. Covell, R. C. Petterson, R. M. Dodson, and G. Klose. J. Am. Chem. Soc. **87**, 1410 (1965).
20. G. Brown. U.S. Govt. Res. Rept. **38** [22], 25 (1963).
21. L. M. Jackman and S. Sternhell. *In* Applications of nuclear magnetic resonance spectroscopy in organic chemistry. 2nd Ed. Pergamon Press, Oxford, London, Edinburgh, New York, Toronto, Sydney, Paris, Braunschweig. 1969; (*a*) p. 188; (*b*) pp. 316–317.
22. W. F. Berkowitz and A. A. Ozirio. J. Org. Chem. **36**, 3787 (1971).
23. F. Stitt, G. F. Bailey, G. B. Coppinger, and T. W. Campbell. J. Am. Chem. Soc. **76**, 3642 (1954).
24. R. H. Wiley and N. R. Smith. *In* Organic syntheses, Coll. Vol. IV. John Wiley and Sons Inc., New York. 1963, pp. 201–202.
25. H. von Pechmann. Justus Liebigs Ann. Chem. **264**, 261 (1891).
26. H. E. Zimmerman, G. L. Grunewald, and R. M. Doufler. Org. Synth. **46**, 101 (1966).
27. W. H. Pirkle, H. Seto, and W. V. Turner. J. Am. Chem. Soc. **92**, 6984 (1970).
28. (*a*) P. de Mayo. *In* Advances in organic chemistry. *Edited by* R. A. Raphael. E. C. Taylor, and H. Wynberg. Interscience Publishers, Inc. New York. 1960, p. 394; (*b*) J. P. Guthrie,

Can. J. Chem. Downloaded from www.nrcresearchpress.com by 210.87.254.42 on 09/05/12
For personal use only.

C. L. McINTOSH, and P. DE MAYO. Can. J. Chem. **48**, 237 (1970); (*c*) W. H. PIRKLE and L. H. McKENDY. J. Am. Chem. Soc. **91**, 1175 (1969); (*d*) O. L. CHAPMAN, C. L. McINTOSH, and J. PACANSKY. J. Am. Chem. Soc. **95**, 244 (1973); (*e*) C. L. McINTOSH and O. L. CHAPMAN. J. Am. Chem. Soc. **95**, 247 (1973); (*f*) R. G. S. PONG and J. S. SHIRK. J. Am. Chem. Soc. **95**, 248 (1973).

29. T. B. WINDHOLZ, L. H. PETERSON, and G. J. KENT. J. Org. Chem. **28**, 1443 (1963).
30. R. L. SHRINER, R. C. FUSON, and D. Y. CURTIN. *In* The systematic identification of organic compounds. 5th Ed. John Wiley and Sons Inc., New York. 1967. p. 253.
31. (*a*) B. L. LOEV and K. M. SNADER. Chem. Ind. 15 (1965); (*b*) B. LOEV and M. M. GOODMAN. Chem. and Ind. 2026 (1967).

Can. J. Chem. Downloaded from www.nrcresearchpress.com by 210.87.254.42 on 09/05/12
For personal use only.

Selective Benzoylation of Methyl 6-Deoxy-α- and β-D-glucopyranosides

YÔTARO KONDO, KIYOSHI MIYAHARA, AND NAOKI KASHIMURA
Department of Agricultural Chemistry, Kyoto University, Kyoto, Japan

Received February 28, 1973

Selective dimolar benzoylation of methyl 6-deoxy-α- and β-D-glucopyranosides yielded the 2,3-di-*O*-benzoate of the respective glucopyranoside as the major product in 61 and 29% yields. The orders of the reactivity of the secondary hydroxyl groups in α- and β-anomers were different, *i.e.*, the order was 2-OH > 3-OH > 4-OH for the former and 3-OH > 2-OH > 4-OH for the latter.

La benzoylation bimolaire sélective des méthyls déoxy-6 α- et β-D-glucopyranosides a conduit au dérivé di-*O*-benzoate-2,3 des glucopyranosides comme produit majeur avec des rendements de 61 et de 29% respectivement. L'ordre de réactivité des groupes hydroxyles secondaires dans les anomères α et β s'est révélé être différent, *i.e.*, l'ordre était dans le premier cas OH-2 > OH-3 > OH-4 et dans le second cas OH-3 > OH-2 > OH-4. [Traduit par le journal]

Can. J. Chem., 51, 3272 (1973)

Introduction

Selective benzoylation of hexopyranosides (1–9) is of theoretical interest in relation to the relative reactivity of primary and secondary hydroxyl groups and provides a facile route for the preparation of important synthetic intermediates (3, 6–8). There are few comparative studies on selective benzoylation of α- and β-hexopyranosides. This communication describes the selective benzoylation of methyl 6-deoxy-α- and β-D-glucopyranosides and factors determining the reactivity of the hydroxyl groups are discussed.

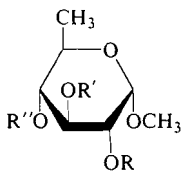

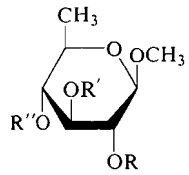

1 R = R′ = R″ = H
2 R = R″ = Bz, R′ = H
3 R = R″ = Bz, R′ = Ts
4 R = R′ = Bz, R″ = H
5 R = R′ = Bz, R″ = Ts
6 R = R′ = R″ = Bz

7 R = R′ = R″ = H
8 R = R″ = Bz, R′ = H
9 R = R′ = Bz, R″ = H
10 R = R′ = Bz, R″ = Ts
11 R′ = R″ = Bz, R = H
12 R = R′ = R″ = Bz

Results and Discussion

Treatment of methyl 6-deoxy-α-D-glucopyranoside (**1**) with 2 mol. equiv. of benzoyl chloride in pyridine at −40 °C gave the syrupy 2,3-di-*O*-benzoate **4** as the major product in 61% yield after column chromatography on silicic acid. Its structure was established by tosylation,[1] giving methyl 2,3-di-*O*-benzoyl-6-deoxy-4-*O*-*p*-tolylsulfonyl-α-D-glucopyranoside (**5**), previously described by Jary and Capek (10). The sulfonate **5** undergoes bimolecular displacement with sodium azide in *N*,*N*-dimethylformamide to yield methyl 4-azido-2,3-di-*O*-benzoyl-4,6-dideoxy-α-D-galactopyranoside, which exhibited absorption of the azido group at 2110 cm^{-1} in the i.r. spectrum.

The chromatographic fractionation further afforded a syrupy dibenzoate **2** on the basis that tosylation of the dibenzoate gave methyl 2,4-di-*O*-benzoyl-6-deoxy-3-*O*-*p*-tolylsulfonyl-α-D-glucopyranoside (**3**), which was readily distinguishable from the known 2- and 4-*O*-*p*-tolylsulfonyl isomers by comparison of their physical properties.

Assignment of the position of *p*-tolylsulfonyl group in **3** and **5** was further confirmed by p.m.r. spectroscopy. The signals of H-3 of **3** and H-4 of **5** appeared respectively 0.69 and 0.64 p.p.m. to higher field than those of the corresponding hydrogens of tribenzoate **6** (Table 1). The *p*-tolylsulfonyl groups of **3** and **5** are therefore attached to C-3 and C-4 respectively. Because of the powerful deshielding effect of benzoyloxy group, the signal of ring proton attached to the same carbon atom as the ester group occurs to low field of the other protons with exception of the anomeric proton (4, 11).

By similar treatment of methyl 6-deoxy-β-D-glucopyranoside (**7**) with 2 mol. equiv. of benzoyl chloride, methyl 2,3-di-*O*-benzoyl-6-deoxy-β-D-glucopyranoside (**9**) was obtained as the major product in 29% yield after column chromatography. The structure of the dibenzoate

[1] Migration of the benzoyl ester group is unlikely to occur under tosylating conditions (4, 5).

Can. J. Chem. Downloaded from www.nrcresearchpress.com by 210.87.254.6 on 09/05/12
For personal use only.

Can. J. Chem. Downloaded from www.nrcresearchpress.com by 210.87.254.6 on 09/05/12
For personal use only.

TABLE 1. Chemical shifts (τ) and coupling constants (Hz) of benzoylated methyl 6-deoxy-α- and β-D-glucopyranosides in C_6D_6 at 90 MHz

	6	**3**	**5**	**12**	**10**	**11**	**8**
C—CH_3	8.78(d)	8.92(d)(+0.14)*	8.57(d)(−0.27)	8.81(d)	8.41(d)(−0.33)	8.83(d)(+0.02)	8.83(d)(+0.02)
Ph—CH_3		8.46(s)	8.41(s)		8.47(s)		
O—CH_3	6.94(s)	7.06(s)(+0.12)	7.09(s)(+0.15)	6.89(s)	6.87(s)(−0.02)	6.72(s)(−0.17)	6.71(s)(−0.18)
H-1	4.79(d)	4.97(d)(+0.18)	4.98(d)(+0.19)	5.51(d)	5.74(d)(+0.22)	5.84(d)(+0.33)	5.62(d)(+0.11)
H-2	4.47(q)	4.53(q)(+0.06)	4.67(q)(+0.20)	4.13(q)	4.34(q)(+0.21)	6.21(q)(+1.09)	4.52(q)(+0.39)
H-3	3.38(t)	4.07(t)(+0.69)	3.64(t)(+0.26)	3.86(t)	4.11(t)(+0.25)	4.17(t)(+0.31)	6.07(t)(+2.21)
H-4	4.39(t)	4.57(t)(+0.20)	5.13(t)(+0.64)	4.49(t)	5.21(t)(+0.73)	4.67(t)(+0.18)	4.86(t)(+0.37)
H-5	5.87(o)	6.07(o)(+0.20)	6.07(o)(+0.20)	6.49(o)	6.63(o)(+0.14)	6.59(o)(+0.10)	6.61(o)(+0.12)
$J_{1,2}$	3.8	3.8	3.5	7.8	7.7	7.7	8.0
$J_{2,3}$	10.3	9.8	10.0	9.5	9.3	9.5	9.8
$J_{3,4}$	10.3	9.8	10.0	9.5	9.3	9.5	9.8
$J_{4,5}$	10.3	9.8	10.0	9.5	9.3	9.5	9.8
$J_{CH_3,H}$	6.2	6.5	6.1	5.9	5.7	6.0	6.3

*The values in the parentheses of compounds **3** and **5**, and those of **10**, **11** and **8**, indicate the increments of the chemical shifts relative to those of **6** and **12**, respectively; s = singlet; d = doublet; t = triplet; q = quartet; o = octet.

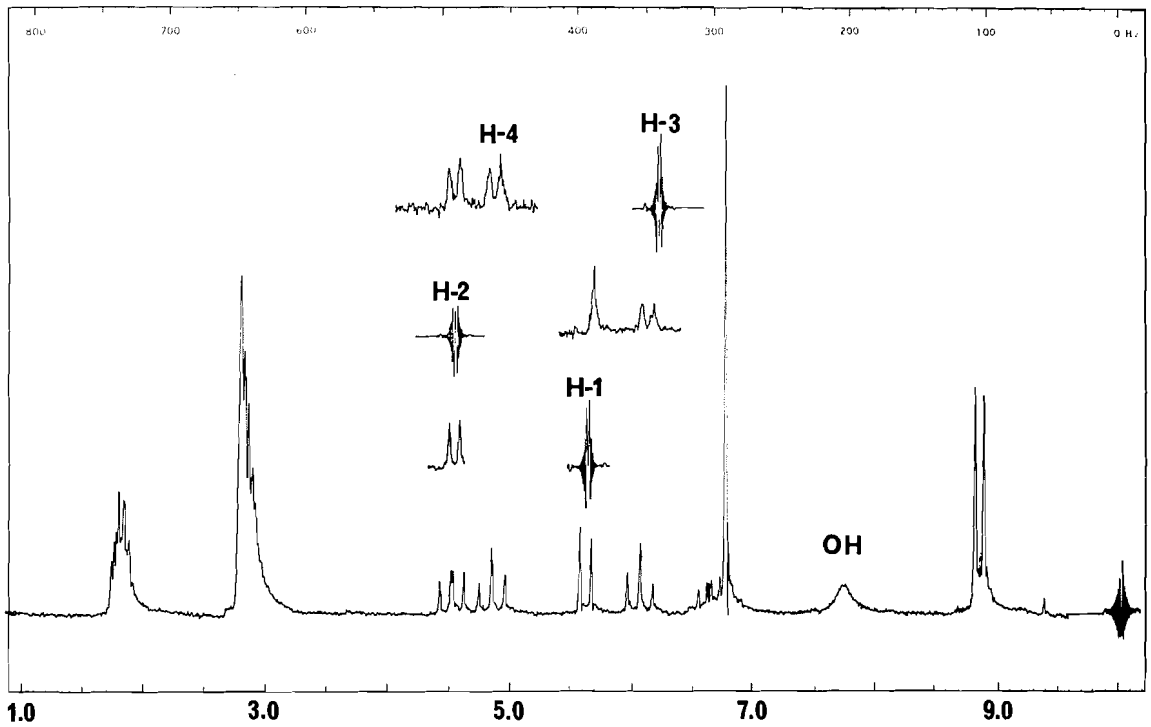

FIG. 1. The 90 MHz p.m.r. spectrum of 2,4-di-*O*-benzoate **8** in C_6D_6 (τ).

was established by tosylation, giving methyl 2,3-di-*O*-benzoyl-4-*O*-*p*-tolylsulfonyl-β-D-glucopyranoside (**10**) of which physical constants were in good agreement with those of an authentic sample reported by Kaufmann (12).

Two dibenzoates were further isolated in 1 and 4% yields which were shown to be the 2,4- and 3,4-di-*O*-benzoates (**8** and **11**) by p.m.r. spectroscopy. The spectrum of **8** shown in Fig. 1 exhibited at the lowest field (τ 4.52) a quartet (J = 8.0 and 9.8 Hz) characteristic of H-2 of the β-anomer, and in the p.m.r. spectra of tribenzoates **6** and **12** their H-3 signals appeared at the lowest field. Accordingly, the high field triplet at τ 6.07 (J = 9.8 Hz) must correspond to H-3 attached to the same carbon atom as free hydroxyl rather than benzoyl group. The H-4 signal appeared as a triplet at τ 4.86 (J = 9.8 Hz) and the H-1 signal as a doublet at τ 5.62 (J = 8.0 Hz). In the dibenzoate **11** (Fig. 2), the H-3 signal occurred as a triplet at the lowest field (τ 4.17, J = 9.5 Hz) and therefore the triplet at high field (τ 4.67) must be attributed to H-4. The H-2 signal appeared as a quartet characteristic of the β-anomer (J = 7.7 and 9.5 Hz) at 1.09 p.p.m. higher field (τ 6.21) compared with that of **12**, indicating that C-2 is unsubstituted. The H-1 signal was observed as a doublet at τ 5.74 (J = 7.7 Hz). These assignments were in good agreement with the decoupling experiments (Figs. 1 and 2).

In dibenzoylation of methyl 6-deoxy-α-D-glucopyranoside (**1**), the preponderance of the 2,3-di-*O*-benzoate (61%) over the 2,4-di-*O*-benzoate (17%) shows that the relative reactivity (judged by the yield of reaction products) of the secondary hydroxyl groups in **1** is in the order, 2-OH > 3-OH > 4-OH, which is consistent with that obtained by Williams and Richardson (4) for methyl α-D-glucopyranoside. This result suggests that the substituted groups at C-5, methyl and hydroxymethyl (or benzoyloxymethyl) groups, do not affect the order of reactivity in benzoylation. On the other hand, the yield of dibenzoates in dibenzoylation of methyl 6-deoxy-β-D-glucopyranoside (**7**) was in the order of the 2,3- (29%), 3,4- (4%), and 2,4-di-*O*-benzoates (1%). Therefore, the order of reactivity of the secondary hydroxyl groups in **7** is 3-OH > 2-OH > 4-OH.

Can. J. Chem. Downloaded from www.nrcresearchpress.com by 210.87.254.6 on 09/05/12
For personal use only.

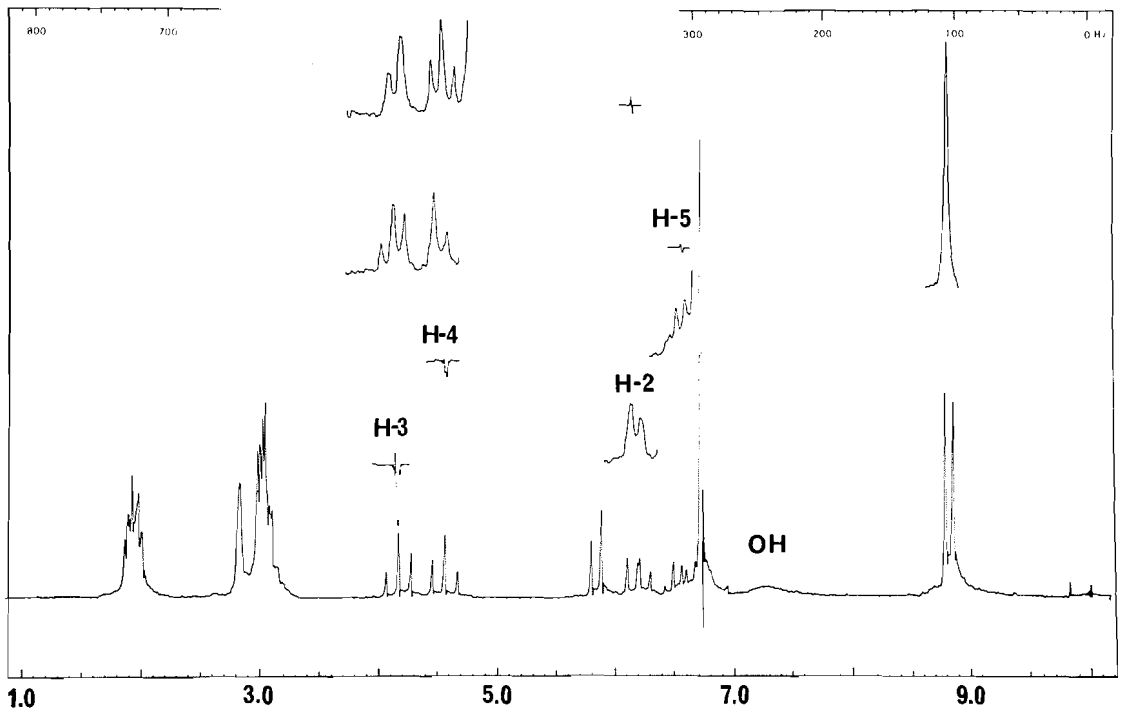

FIG. 2. The 90 MHz p.m.r. spectrum of 3,4-di-*O*-benzoate **11** in C_6D_6 (τ).

The higher total yield of the reaction products of the α-anomer (77.7%) compared with that of the β-anomer (57.1%) indicates that the former is more rapidly benzoylated than the latter. In the β-anomer the 3-OH group is more reactive than the 2-OH group while the reverse is true for the α-anomer. The high reactivity of the 2-OH group in the α-anomer may be due to intramolecular hydrogen bonding between the 2-OH group and the axial C-1 methoxyl group (8, 9, 13, 14), and the lower reactivity of the 2-OH group in the β-anomer may be attributed to lack of hydrogen bond formation (13, 15, 16). It is of interest to note that the 4-OH group in methyl 6-deoxy-α- and β-D-glucopyranosides is the least reactive towards benzoylation while it is more reactive than the other secondary hydroxyl groups in selective disulfonylation of methyl β-D-glucopyranoside (17).

Experimental

Melting points were determined with a Yanagimoto micro hot-stage apparatus and are uncorrected. Optical rotations were measured with a Yanagimoto OR-20 polarimeter. T.l.c. was carried out on silica gel G (Merck) with benzene–ether (4:1, v/v) as mobile phase and column chromatography was performed using silicic acid (Mallinkrodt, 100 mesh). The i.r. spectra were recorded with a Hitachi EPI-G3 and the p.m.r. spectra with a Hitachi–Perkin–Elmer 90 MHz instrument using benzene-d_6 solution with tetramethylsilane as an internal standard. Benzoyl chloride used was purified by distillation from its benzene solution.

Selective Dimolar Benzoylation of Methyl 6-Deoxy-α-D-glucopyranoside (1)

Benzoyl chloride (0.61 ml, 2.1 equiv.) was added dropwise over a period of 15 min to a stirred solution of compound **1** (18) (0.0025 mol, 445 mg) in anhydrous pyridine (17.8 ml) at −40 °C. The bath temperature was kept below −20 °C for 3 h, at 0 °C for 24 h, and then stirred at room temperature for 2 days and extracted with chloroform. The extract was washed with dilute sulfuric acid, saturated sodium bicarbonate, and water, and dried over Na_2SO_4. The crude syrupy product after evaporation of the solution was shown to contain two major and one minor components by t.l.c. Fractionation of the mixture on a silicic acid column (300 g) using benzene–ethyl acetate mixture yielded two syrupy fractions, 2,4-di-*O*-benzoate **2** (160 mg, 16.6%) and 2,3-di-*O*-benzoate **4** (590 mg, 61.1%), that could not be crystallized. The minor component appears to be tri-*O*-benzoate **6** from the result of t.l.c.

Methyl 2,3-Di-O-benzoyl-6-deoxy-4-O-p-tolylsulfonyl-α-D-glucopyranoside (5)

The dibenzoate **4** (240 mg) in pyridine (2.5 ml) was treated with toluene-*p*-sulfonyl chloride (600 mg) for 5 days at room temperature with stirring. The mixture

Can. J. Chem. Downloaded from www.nrcresearchpress.com by 210.87.254.6 on 09/05/12
For personal use only.

Can. J. Chem. Downloaded from www.nrcresearchpress.com by 210.87.254.6 on 09/05/12
For personal use only.

was extracted and purified as described above to give the crystalline product. Recrystallization from ethanol gave the title compound (260 mg, 77.4%), m.p. 141–142 °C, $[\alpha]_D^{24}$ +95.8° (*c* 0.5, $CHCl_3$), lit. (10) m.p. 140–142 °C, $[\alpha]_D^{24}$ +98.6° (*c* 0.55, $CHCl_3$).

The sulfonate **5** (100 mg) in *N*,*N*-dimethylformamide (3 ml) was further heated with sodium azide (100 mg) for 3 days at 65 °C with stirring to yield a syrupy methyl 4-azido-2,3-di-*O*-benzoyl-4,6-dideoxy-α-D-galactopyranoside which could not be crystallized. The i.r. spectrum showed the absorption of the azido group (ν_{max} film 2110 cm^{-1}) but the sulfonyl group was absent. The product was not further investigated.

Methyl 2,4-Di-O-benzoyl-6-deoxy-3-O-p-tolylsulfonyl-α-D-glucopyranoside (3)

The dibenzoate **2** (160 mg) in pyridine (1.7 ml) was treated with toluene-*p*-sulfonyl chloride (400 mg) for 4 days to give the sulfonate **3** (115 mg, 51.4%), m.p. 140–141 °C, $[\alpha]_D^{24}$ +69.0° (*c* 0.5, $CHCl_3$), cf. methyl 3,4-di-*O*-benzoyl-6-deoxy-2-*O*-*p*-tolylsulfonyl-α-D-glucopyranoside (19), m.p. 120–122.5 °C, $[\alpha]_D^{21}$ +15.78° (*c* 0.5, $CHCl_3$).

Anal. Calcd. for $C_{28}H_{28}O_9S$: C, 62.21; H, 5.23; S, 5.93. Found: C, 61.96; H, 5.04; S, 5.95.

Selective Dimolar Benzoylation of Methyl 6-Deoxy-β-D-glucopyranoside (7)

Methyl 6-deoxy-β-D-glucopyranoside (18) (7, 0.005 mol, 890 mg) in pyridine (35.6 ml) was treated with benzoyl chloride (1.22 ml, 2.1 equiv.) as described for the α-anomer. T.l.c. examination of the crude product indicated the presence of several components. Chromatographic separation of the components on a silicic acid column gave five fractions. The first eluted syrupy compound was identified as the tri-*O*-benzoate **12** (50 mg, 2.1%) by comparison of the R_f value with that of an authentic sample. The syrupy 2,4-di-*O*-benzoate **8** (20 mg, 1.1%) was crystallized from ether, m.p. 160–161 °C, $[\alpha]_D^{30}$ −24.6° (*c* 0.3, $CHCl_3$).

Anal. Calcd. for $C_{21}H_{22}O_7$: C, 65.27; H, 5.74. Found: C, 65.11; H, 5.67.

The 2,3-di-*O*-benzoate **9** was obtained as a syrup (550 mg, 28.5%), and the 3,4-di-*O*-benzoate **11** (80 mg, 4.1%) was crystallized from ether, m.p. 164–165 °C, $[\alpha]_D^{30}$ −82.4° (*c* 0.5, $CHCl_3$).

Anal. Calcd. for $C_{21}H_{22}O_7$: C, 65.27; H, 5.74. Found: C, 64.89; H, 5.74.

The syrupy monobenzoates (300 mg, 21.3%) were shown to be composed of three components by t.l.c.

Methyl 2,3-Di-O-benzoyl-6-deoxy-4-O-p-tolylsulfonyl-β-D-glucopyranoside (10)

Treatment of the dibenzoate **9** (240 mg) in pyridine (2.5 ml) with toluene-*p*-sulfonyl chloride (600 mg) for 6 days gave the sulfonate **10** (224 mg, 66.7%), m.p. 158–159 °C, $[\alpha]_D^{24.5}$ +20.0° (*c* 0.2, MeOH), lit. (13) m.p. 162 °C, $[\alpha]_D^{19}$ +19.9 ± 2° (*c* 0.99, MeOH).

Methyl 2,3,4-Tri-O-benzoyl-6-deoxy-β-D-glucopyranoside (12)

A solution of **7** (100 mg) in pyridine (3.5 ml) was stirred with benzoyl chloride (0.5 ml) for 4 days at room temperature. It was worked-up in the usual manner to give a syrup which was crystallized from ethanol (190 mg, 69.0%), m.p. 251–252 °C, $[\alpha]_D^{17}$ −42.9° (*c* 0.28, pyridine).

Anal. Calcd. for $C_{28}H_{26}O_8$: C, 68.6; H, 5.35. Found: C, 68.55; H, 5.37.

1. T. Lieser and R. Schweizer. Ann. **519**, 271 (1935).
2. R. W. Jeanloz and D. A. Jeanloz. J. Am. Chem. Soc. **79**, 2579 (1957).
3. A. F. Krasso and P. A. Seib. J. Chem. Soc. (C), 314 (1971).
4. J. M. Williams and A. C. Richardson. Tetrahedron, **23**, 1369 (1967).
5. A. C. Richardson and J. M. Williams. Tetrahedron, **23**, 1641 (1967).
6. M. W. Horner, L. Hough, and A. C. Richardson. J. Chem. Soc. (C), 1336 (1970).
7. M. W. Horner, L. Hough, and A. C. Richardson. Carbohydr. Res. **17**, 209 (1971).
8. G. J. F. Chittenden and J. G. Buchanan. Carbohydr. Res. **11**, 379 (1969).
9. P. C. Wollwage and P. A. Seib. J. Chem. Soc. (C), 3143 (1971).
10. J. Jary and K. Capek. Collect. Czech. Chem. Commun. **31**, 315 (1966).
11. L. M. Jackman and S. Sternhell. Application of nuclear magnetic resonance spectroscopy in organic chemistry. 2nd Ed. Pergamon, Braunschweig, 1969. p. 176.
12. H. Kaufmann. Helv. **48**, 769 (1965).
13. R. D. Guthrie, A. M. Prior, and S. E. Creasey. J. Chem. Soc. (C), 1961 (1970).
14. K. W. Buck, J. M. Duxbury, A. B. Foster, A. R. Perry, and J. M. Webber. Carbohydr. Res. **2**, 122 (1966).
15. A. J. Michell and H. G. Higgins. Tetrahedron, **21**, 1109 (1965).
16. H. Spedding. J. Chem. Soc. 3617 (1961).
17. R. C. Chalk, D. H. Ball, and L. Long, Jr. J. Org. Chem. **31**, 1509 (1966).
18. M. E. Evans, L. Long, Jr., and F. W. Parrish. J. Org. Chem. **33**, 1074 (1968).
19. J. Jary, K. Capek, and J. Kovar. Collect. Czech. Chem. Commun. **29**, 930 (1964).

Carbon-13 Resonance Spectroscopic Studies on the Formation of Borate and Diphenylborinate Complexes of Polyhydroxy Compounds[1]

PHILIP A. J. GORIN AND MYTOSK MAZUREK

Prairie Regional Laboratory, National Research Council of Canada, Saskatoon, Saskatchewan

Received February 22, 1973

On complexing with sodium tetraborate the ^{13}C magnetic resonance (c.m.r.) spectra of certain sugars contain considerably broadened signals. Replacement of the reagent with sodium diphenylborinate resulted in spectra with sharp singlets corresponding to the diphenylborinate complex, indicating that ^{13}C–^{11}B coupling likely does not occur. Most of the broadening is due rather to either the presence of more than one conformer of the borate complex or the rapid interconversion of the compound with borate complexes of types II and III. In one group of experiments the complexing of diphenylborinate with several low molecular weight sugars and polysaccharides was followed through c.m.r. spectroscopy. In another, complexing was observed with pyranosides having 1,3-hydroxyl groups with orientations that were almost diaxial. In the equilibrium reactions the approximate extent of complexing was estimated and with compounds that can form more than one complex, such as glycerol, the number and structures of the complexes were determined.

Par complexation avec le tétraborate de sodium les spectres de résonance magnétique du ^{13}C de certains sucres comportent un élargissement des signaux considérable. Le remplacement de ce réactif par le diphénylborinate de sodium a pour résultat spectral des singulets fins correspondant au complexe avec le diphénylborinate, montrant que le couplage ^{13}C-^{11}B n'existe probablement pas. La majeure partie de cet élargissement est due plutôt soit à la présence de plus d'un conformère du complexe borate ou à l'interconversion rapide du composé dans les complexes borates de type II et III. Dans une série d'expériences, la complexation du diphénylborinate avec plusieurs sucres de bas poids moléculaire et polysaccharides a été suivie par r.m.n. du ^{13}C. Dans d'autres, cette complexation a été observée avec des pyranosides comportant des groupes hydroxyle-1,3 dont les orientations sont presque diaxiales. Dans les réactions d'équilibration, le pourcentage approximatif de complexation a été évalué; avec des composés pouvant former plus d'un complexe, tel le glycérol, le nombre et les structures des complexes ont été déterminés. [Traduit par le journal]

Can. J. Chem., 51, 3277 (1973)

Introduction

It was shown in a previous publication (1) that following addition of sodium tetraborate to solutions of carbohydrates in D_2O the formation of borate complexes could be followed by changes in the carbon-13 magnetic resonance (c.m.r.) spectra of the parent compounds. Two types of spectral effects were observed. In one type the signals remain sharp and changes in chemical shift take place and in the other the resonances of the signals remain the same, but broadening of signals of ^{13}C nuclei in the vicinity of the complex occurs[2] (Fig. 3 in ref. 1). Three possible explanations for the latter phenomenon were considered, two of which involve conformational factors. One is that the ring containing the boron atom interconverts rapidly between two or more conformations thus giving an average c.m.r. spectrum. It is more likely that the borate complexes of type II and one or two stereoisomeric type III complexes (Fig. 1) are in equilibrium with the sugar but their interconversion is so fast that they cannot be detected individually by c.m.r. spectroscopy. No change in resonance of the ^{13}C signals was observed since presumably the conformations of the carbon skeletons of sugar and its type II or III complexes were not appreciably different and the carbons were not deshielded to any extent in the borate forms. The other possible explanation is that the signals of ^{13}C nuclei are coupled to ^{11}B nuclei of spin $\frac{3}{2}$ and that quadrupole type broadening occurs.

The latter is now shown to be likely incorrect, however, by the following experiment. In the previous study addition of borax to a D_2O solution of methyl 2,3-di-*O*-methyl-α-D-mannopy-

[1]NRCC No. 13302.

[2]These signals are very stunted and have a line width of 40 Hz. This compares with 5–7 Hz for the other signals. All of the latter were also broadened (to 8–12 Hz) in accord with the finding that a general slight line broadening occurs on addition of sodium diphenylborinate or borate to sugar solutions.

Can. J. Chem. Downloaded from www.nrcresearchpress.com by 210.87.254.6 on 09/05/12
For personal use only.

Can. J. Chem. Downloaded from www.nrcresearchpress.com by 210.87.254.6 on 09/05/12
For personal use only.

TABLE 1. Chemical shifts of c.m.r. signals of polyhydroxy compounds and diphenylborinate complexes, formed on addition of 1 and 3 mol equiv. of sodium diphenylborinate: estimated percentages of unchanged compounds in the equilibria

	Compound and system examined	% of compound in equilibrium with diphenylborinate ester	Relative downfield differences of resonances of signals from that of external TMS in coaxial capillary (δ_C) in p.p.m.																			
1	(*a*) 1,2:5,6-Di-*O*-isopropylidene-D-mannitol	—	110.5	—	—	75.8 (C-2)	70.8 (C-3)	—	67.1* (C-1)	38.9	37.3											
	(*b*) 1:1 S–DPB†	11	110.4	78.0	77.3	75.8	70.8	67.5	67.1	39.2	37.8											
2	(*a*) Methyl 4,6-di-*O*-methyl-α-D-mannopyranoside	—	101.4 (C-1)	—	—	77.6* (C-4)	—	—	—	71.7 (C-5)	70.8 (C-3)	70.6 (C-4, -6)		—	60.7	—	59.0	55.4				
	(*b*) 1:1 S–DPB	55	101.4	100.9	79.0	77.6	75.4	74.8	71.9	71.7	70.8	70.6		69.0	60.7	60.4	59.0	55.3				
	(*c*) 1:3 S–DPB	26	101.4	100.9	79.0	77.6	75.4	74.8	71.9	71.7	70.8	70.6		69.0	60.7	60.4	59.0	55.3				
3	(*a*) Methyl 2,3-di-*O*-methyl-α-D-mannopyranoside	—	—	98.2 (C-1)	80.4 (C-2)	—	77.1 (C-3)	—	73.1* (C-5)	—	—	66.7 (C-4)		61.5 (C-6)	59.0 (OCH_3)	—	57.4 (OCH_3-3)	55.4 (OCH_3-1)				
	(*b*) 1:1 S–DPB	80	98.7	98.2	80.4	79.6	77.1	76.2	73.1	71.6	68.8	66.7	63.4	61.5	59.1	—	57.4	55.5				
	(*c*) 1:3 S–DPB	36	98.7	98.2	80.4	79.6	77.1	76.2	73.1	71.6	68.8	66.7	63.4	61.5	59.1	—	57.3	55.5				
4	(*a*) *myo*-Inositol	—	—	75.0	—	—	—	73.0	72.8	71.7*												
	(*b*) 1:1 ratio of sugar to diphenylborinate	38	75.7	75.0	74.8	74.1	—	73.1	72.8	71.8												
	(*c*) 1:3 S–DPB	25	75.8	75.1	74.8	74.1	73.2	—	72.8	71.8												
5	(*a*) 1,4,5,6-Tetra-*O*-methyl-*myo*-inositol	—	—	84.2*	82.7	82.1	—	80.4	—	—	70.9	68.3	60.5	—	—	—	57.3					
	(*b*) 1:1 S–DPB	38	84.9	84.1	82.7	82.0	—	80.4	76.3	71.4	70.8	68.3	60.5	60.3	60.0	59.0	57.4					
	(*c*) 1:3 S–DPB	28	84.9	84.0	82.6	82.0	81.8	80.4	76.3	71.5	70.8	68.3	60.6	60.3	59.9	—	57.4					
6	(*a*) 1,2:3,4-Di-*O*-isopropylidene-L-*chiro*-inositol	—	110.9	79.2 (C-1)	76.7	—	72.1* (C-3)	27.3	25.1													
	(*b*) 1:1 S–DPB	32	110.9	79.2	76.7	76.4	72.1	27.3	25.1													
	(*c*) 1:3 S–DPB	10	111.2	79.2	76.8	76.5	72.0	27.3	25.0													
7	(*a*) 1,2-*O*-isopropylidene-α-D-glucofuranose	—	113.0*	—	—	105.2 (C-1)	—	84.9 (C-2)	80.2 (C-4)	—	74.1 (C-3)	—	68.9 (C-5)	—	64.1 (C-6)	26.2	25.7					
	(*b*) 1:1 S–DPB	9	112.9	112.7	106.4	105.2	85.7	85.1	80.2	74.6	—	71.3	—	64.6	—	26.0	25.6					
	(*c*) 1:3 S–DPB	0	—	112.8	106.4	—	85.7	—	80.2	74.6	—	71.4	—	64.6	—	26.7	26.1					
8	(*a*) 1,2-*O*-Isopropylidene-3-*O*-methyl-α-D-glucofuranose		113.0	105.2 (C-1)	—	83.7 (C-2)	—	81.3 (C-3)	80.0 (C-4)	—	68.7* (C-5)	—	—	64.0 (C-6)	58.0	26.1	25.7					
	(*b*) 1:1 S–DPB	34	112.8	105.2	105.0	83.7	82.6	81.3	80.0	69.9	68.7	66.2		64.1	58.1	26.2	25.9					
	(*c*) 1:3 S–DPB	10	113.0	—	105.0	83.7	82.6	81.4	—	69.9	—	66.2	—	—	58.1	26.2	25.9					
9	(*a*) 6-*O*-Isopropyl-1,2-*O*-isopropylidene-α-D-glucofuranose	—	113.0	—	105.2 (C-1)	—	84.9 (C-2)	—	80.4* (C-4)	—	74.2 (C-3	73.6 or $CH.Me_2$)	—		—	—	70.2	67.9	26.3	25.8	21.8	
	(*b*) 1:1 S–DPB		113.4	113.0	106.2	105.2	85.5	85.0	82.8	80.4	75.1	74.2	73.7	73.0		71.1	70.7	70.2	68.1	26.8	26.4	26.1	21.8
	(*c*) 1:3 S–DPB	0	113.4	—	106.2	—	85.5	—	82.7	—	75.1	74.3	—	73.0	71.1	70.2	—	—	26.8	26.5	26.2	21.9	
10	(*a*) Methyl α-D-glucopyranoside	—	99.8* (C-1)	—	73.7 (C-2)	—	—	—	72.2 (C-3	or	71.8 C-5)	70.2 (C-4)	—	—	61.2 (C-6)	55.5 (OCH_3)						
	(*b*) 1:1 S–DPB	40	100.3	99.9	75.5	73.7	73.3	—	—	72.2	71.9	70.2	67.9	—	63.3	61.3	55.6					
	(*c*) 1:3 S–DPB	22	100.4	99.9	75.6	73.8	73.4	72.8	—	72.2	71.9	70.3	67.9	—	63.3	61.3	55.8					
11	(*a*) Methyl α-D-mannopyranoside	—	101.5 (C-1)	—	—	—	73.2 (C-5)	71.2 (C-2)	70.6 (C-3)	—	67.5 (C-4)	—	61.6 (C-6)	55.4 (OCH_3)								
	(*b*) 1:1 S–DPB	30	101.5	101.0	76.4	75.0	73.2	71.6	71.3	70.6	69.7	67.5	62.0	61.6	55.5							
12	(*a*) Methyl β-D-glucopyranoside	—	—	103.8 (C-1)	76.4 (C-3 and	C-5)	—	—	73.7 (C-2)	—	70.2* (C-4)	—	61.5 (C-6)	57.7 (OCH_3)								
	(*b*) 1:1 S–DPB	30	104.2	103.8	76.5	75.9	75.3	74.5	73.8	71.6	70.3	63.1	61.4	57.8								
13	(*a*) Methyl 3,6-anhydro-α-D-glucopyranoside	—	—	99.5	—	76.4	—	72.0	71.8	—	70.4	69.8	—	58.5								
	(*b*) 1:1 S–DPB	70	101.6	99.5	77.4	76.4	72.4	72.0	71.8	71.2	70.4	69.8	69.6	58.5								
	(*c*) 1:3 S–DPB	30	101.6	99.6	77.4	76.8	72.4	71.9	—	71.3	70.4	69.8	—	58.5								
	(*d*) 4:1 S–B†	50	100.7	99.5	76.9	76.4	71.8	71.0	70.6	70.0	69.0	58.3										
	(*e*) 2:1 S–B	0	100.7	—	76.9	—	—	71.2	70.8	70.0	69.1	58.3										
14	(*a*) Methyl 3,6-anhydro-β-D-glucopyranoside	—	—	104.1	—	75.3	72.8	72.5	71.8	—	—	70.2	56.5									
	(*b*) 1:1 S–DPB	45	106.1	104.2	77.6	75.4	72.8	72.4	71.8	71.4	71.0	70.4	56.5									
	(*c*) 1:3 S–DPB	10	106.2	—	77.6	—	—	—	—	71.5	71.2	70.6	56.5									
	(*d*) 4:1 S–B	0	104.5	76.5	71.4	70.4	70.0	56.5														
	(*e*) 2:1 S–B	0	104.7	76.6	71.4	70.4	69.8	56.5														
15	1,6-Anhydro-β-D-glucopyranose	—	102.6	77.4	73.7	72.0	71.4	66.4	31.5													
16	2,4-Di-*O*-methyl-α,β-L-rhannose	—	94.8	91.7	83.9	83.5	82.9	82.1	74.0	72.2	70.6	68.3	63.0	61.2	59.8	18.2						
17	(*a*) 1,2-*O*-Isopropylidene-6-*O*-methyl-α-D-glucofuranose	—	113.1 (CO)	—	—	105.2 (C-1)	—	88.9 (C-2)	—	80.4* (C-4)	—	—	74.6 (C-3 and	74.0 -6)	—	67.3 (C-5)	59.2	—	—	—		
	(*b*) 1:1 S–DPB	50	113.1	112.9	106.3	105.2	85.4	88.9	83.2	80.4	75.7	75.5	74.6	74.0	70.3	26.2 67.3	— 59.2	25.7 58.9	26.2	26.0	25.8	

*Percentage of unchanged compound was estimated by comparison of this signal with that of the MeOH standard.
†S–DPB = ratio of sugar to diphenylborinate and S–B = molar ratio of sugar to sodium tetraborate.

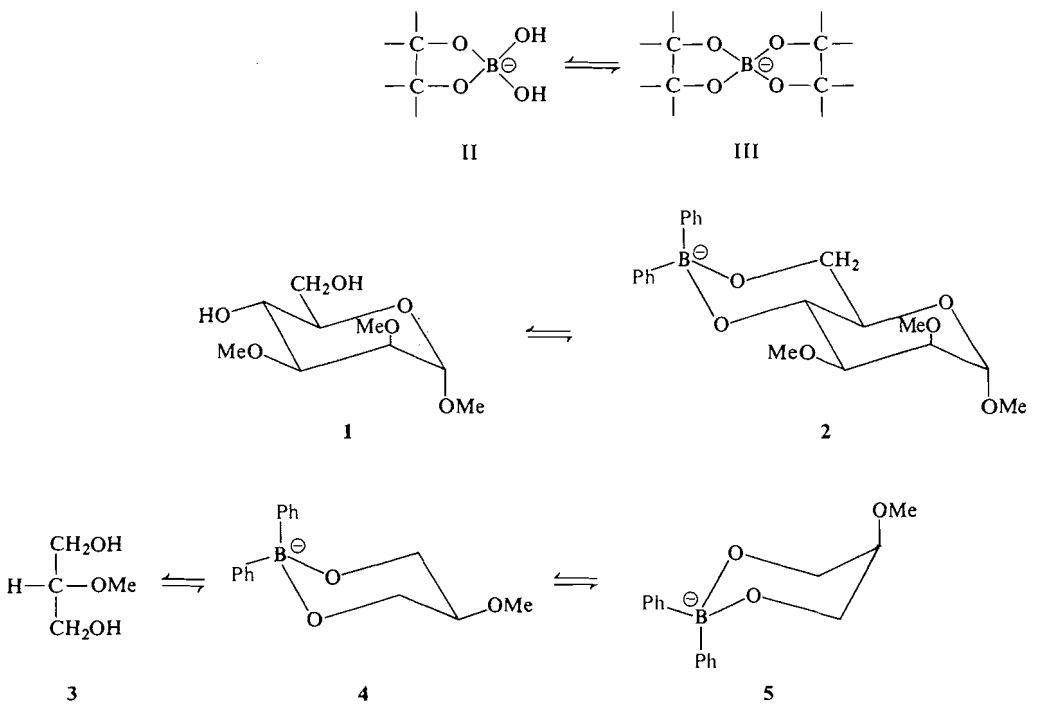

FIG. 1. Equilibria of polyhydroxy compounds with borates and diphenylborinates.

ranoside (Fig. 1; **1**) resulted in marked broadening of the C-4, -5, and -6 signals of the c.m.r. spectrum (Fig. 3 in ref. 1). However, when borax was replaced with 3 mol equiv. of sodium diphenylborinate six new signals appeared (Fig. 3, compare spectra A and B) which corresponded to C-1 to -6 of the diphenylborinate complex (Fig. 1; **2**). No ^{13}C–^{11}B splitting was observed in the ^{13}C signals of carbons in the sugar ring or the aromatic rings of the complex. Their line widths were comparable with those of unreacted sugar.

Two other compounds, *myo*-inositol and 1,4,5,6-tetra-*O*-methyl-*myo*-inositol both gave c.m.r. spectra which contained broadened signals following addition of sodium tetraborate (1). They also complexed with diphenylborinate as indicated by the appearance of new c.m.r. signals (Table 1). This finding is in accord with that of Garegg and Lindström (2) who showed that the p.m.r. spectrum of *epi*-inositol was modified on addition of sodium diphenylborinate. The cyclitol contains several *cis*-1,2-diol groups capable of complexing in addition to 1,3-diaxial hydroxyls which may also possibly react (see later discussion). However, *cis*-cyclohexane-1,2-diol does not form a diphenylborinate complex in appreciable amount since the c.m.r. spectrum remains unchanged on addition of the reagent. The glycol group evidently lacks the inductive effect of adjacent hydroxyls which would favor complex formation. Such an explanation was used by Angyal and McHugh (3) when it was found that on paper electrophoresis in aqueous borax *cis*-cyclohexane-1,2-diol is less mobile than a structurally related compound having an additional *trans*-hydroxyl adjacent to the glycol group.

The degree of complexing of polyhydroxy compounds with diphenylborinate in deuterium oxide cannot be estimated directly on the basis of the signal size of carbons in the complex because of the possibly different nuclear Overhauser effect and the difference of relaxation times of the various nuclei. However, the proportion of uncomplexed material can be estimated by comparing the size of a suitable signal with that of the methyl resonance of methanol (δ_C 49.5), which is used as an internal standard during graded addition of sodium diphenylborinate. Since there are insufficient data points to completely define any given signal the accuracy of the measurements is not great and

Can. J. Chem. Downloaded from www.nrcresearchpress.com by 210.87.254.6 on 09/05/12
For personal use only.

Can. J. Chem. Downloaded from www.nrcresearchpress.com by 210.87.254.6 on 09/05/12
For personal use only.

the percentages quoted for uncomplexed material should be regarded as accurate to only ±10%. The chemical shifts of certain polyhydroxy compounds, those of the diphenylborinate compounds, and the percentage of complex formed on addition of 1 and 3 mol equiv. of sodium diphenylborinate are recorded in Table 1.

Many of the diphenylborinate complexes known to be formed on the basis of c.m.r. spectroscopy were previously found to give borate complexes (ref. 1 and references contained therein) and should have structures analogous to the type II (Fig. 1) complex. Compounds containing only two hydroxyl groups with suitable stereochemistry complex on these positions and hexopyranosides should give rise to a 4,6-complex (4). C.m.r. spectral evidence was obtained for complexing of the OH-2 and OH-4 hydroxyl groups of methyl 3,6-anhydro-α-D-glucopyranoside (**6**, Fig. 2) with sodium diphenylborinate since five new c.m.r. signals were obtained (Table 1). With 1 and 3 mol equiv. of reagent 30% and 70% of the complex was formed, respectively. The pyranoid ring of **6** should be in the 1C conformation or a close approximation to it by analogy with 3,6-anhydro-α,α-trehalose hexaacetate (5) and 3,6:3′,6′-dianhydro-α,α-trehalose tetraacetate (6), which had their bicyclic portions assigned this conformation on the basis of p.m.r. spectral evidence. Furthermore, the H-1 signal of **6** had J = 3 Hz, which is very close to the splitting of the H-1 signals of the bicyclic portions of the above derivatives. Examination of Büchi molecular models of **6** show that the restriction of a 3,6-anhydro group distorts the 1C conformation so that the *syn*-axial oxygen atoms on C-2 and -4 are closer than in an unstrained 1C-pyranoid ring.

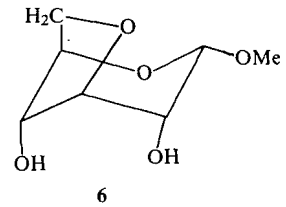

6

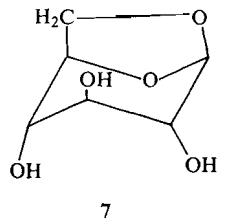

7

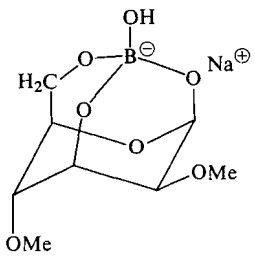

8

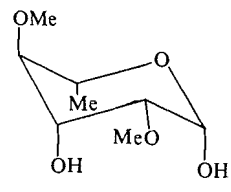

9

FIG. 2. Compounds connected with the reaction of borate with 1,3-*syn*-hydroxyl groups.

The β-anomer of methyl 3,6-anhydro-D-glucopyranoside reacts to a greater extent with sodium diphenylborinate (Table 1). In this case p.m.r. spectral examination showed that, in contrast to the α-anomer, the H-1 signals of the free sugar had different chemical shifts. Quantitation showed that 55% and 90% of the complex was formed on addition of 1 and 3 mol equiv. of reagent, respectively. The coupling constants of H-1 of the anhydride and its complex were both 0 Hz, indicating that the dihedral angles of H-1 and -2 of each compound are similar and that the conformation of the anhydride is close to that of its complex, which can only exist in a slightly distorted 1C form. Moreover, the other possibility, that a conformation of the anhydride is a skew-boat form is precluded since the dihedral angle of H-1 and -2 would approach 180°. This would give rise to a large H-1 coupling constant since values of 8–11 Hz are obtained when two vicinal hydrogen atoms on a six-membered ring are *trans* (7). As noted above β-anomer complexes to a higher extent than the α-anomer. This is probably due to non-bonded interactions in the latter between one of the phenyl groups on the borinate ring (in a chair form) and the equatorial OCH_3-1 group.

In a related anhydride, 1,6-anhydro-β-D-glucopyranose (**7**, Fig. 2), c.m.r. spectral examination showed that it does not form a diphenylborinate complex. This is perhaps not surprising since X-ray crystal-structure analysis showed that the *syn*-axial oxygen atoms on C-2 and -4 are separated by 3.30 Å whereas in an unstrained pyranoid system they would be ~2.5 Å apart (8). Although Garegg and Lindström (2) suggested that this type of complexing is possible in *epi*-inositol, which is unstrained and contains 1,3-diaxial hydroxyl groups, the p.m.r. spectrum of the mixed diphenylborinates could not be completely rationalized. It would be of interest to investigate compounds such as this, which can only form complexes between the 1,3-diaxial

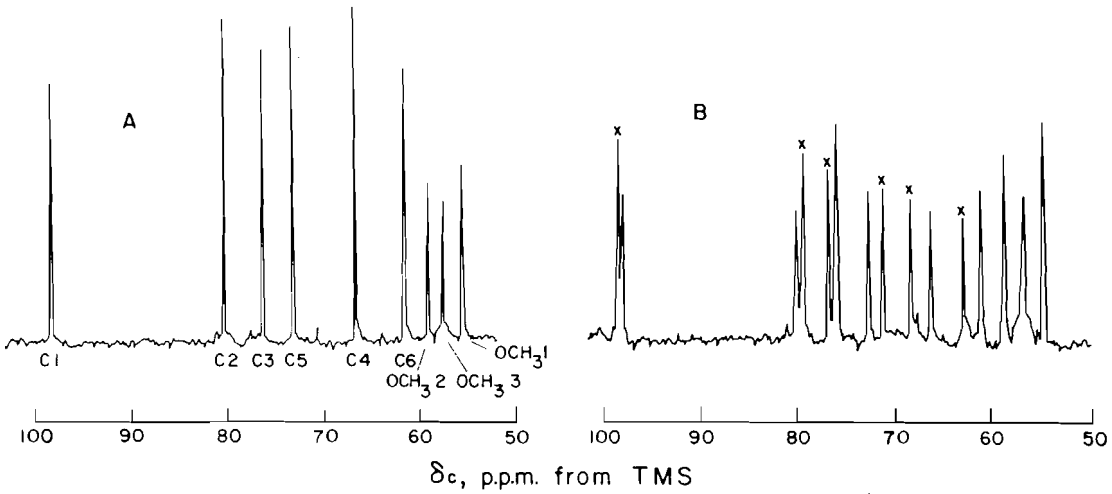

FIG. 3. C.m.r. spectra of methyl 2,3-di-*O*-methyl α-D-mannopyranoside (A) and the equilibrium mixture formed on addition of 3 mol equiv. of sodium diphenylborinate (B) (the new signals of the complex are marked with a cross).

hydroxyl groups. Related compounds, as represented by the 2,4-benzeneboronate of methyl α-D-xylopyranoside (9) and *N*-(*p*-bromophenyl)-α-D-ribopyranosylamine (10), have been prepared, but under kinetically controlled conditions.

The experiments with the anhydrides were parallelled using sodium tetraborate as reagent. C.m.r. spectroscopy showed that whereas the α- and β-anomers[3] of methyl 3,6-anhydro-D-glucopyranoside complex readily, 1,6-anhydro-β-D-glucopyranose does not. On addition of 0.25 mol equiv. of sodium tetraborate (0.5 mol equiv. of "available borate") to methyl 3,6-anhydro-α-D-glucopyranose in D_2O the c.m.r. spectrum showed that approximately 50% of the sugar did not react whereas when the amount of reagent was increased to 0.5 mol equiv. unchanged sugar could not be detected (Table 1). This is suggestive of formation of a type II complex (Fig. 1) in which the ratio of sugar to boron is 1:1. This contrasts with the reaction of tetraborate with methyl 3,6-anhydro-β-D-glucopyranoside since the sugar reacted completely after addition of 0.25 mol equiv. of reagent (Table 1) thus indicating formation of a type III spirane complex (Fig. 1). The c.m.r. spectrum was not altered on addition of a further 0.25 mol equiv. of sodium tetraborate. The difference between the type of borate complex formed suggests that the distance between the *syn*-O-2 and -4 atoms in the α-anomer differs from that of the β-anomer, and that the conformations of the 1C rings are therefore somewhat different.

In a previous publication (*1*) it was shown by c.m.r. spectroscopy that 2,4-di-*O*-methyl-D-mannose reacts in D_2O with sodium tetraborate to form a borate and a tridentate structure involving O-1, -3, and -6 (**8**, Fig. 2) was proposed. In order to show whether O-6 had a role in complex formation the action of sodium tetraborate and diphenylborinate on 2,4-di-*O*-methyl-α,β-L-rhamnose was determined. Participation was demonstrated since c.m.r. and p.m.r. spectroscopy showed that no reaction occurred with OH-1 and -3 alone in the $1C_\beta$ form (**9**, Fig. 2).

Certain polyhydroxy compounds have a stereochemistry suitable for formation of more than one diphenylborinate complex and c.m.r. spectroscopy can be used for analysis of the mixtures. For example, the c.m.r. spectrum of glycerol in D_2O (Fig. 4, spectrum C) is modified on addition of 3 mol equiv. of sodium diphenylborinate to spectrum F (Fig. 3), which can be rationalized in terms of complexes with five- and six-membered rings. The more prominent features of spectrum F are a broad complex signal centered on δ_C 65.4 and a sharp signal at δ_C 74.2, the latter being assigned to C-2 since it was absent from the c.m.r. spectrum of a solution of DL-glycerol-2-*d* containing diphenylborinate in D_2O. The signal was shown to arise from C-2 of a glycerol 1,2-diphenylborinate anion by consideration of the spectra obtained from 1-*O*-

[3]Electrophoretic mobility of the borate complex of the β-anomer was noted by Theander (34).

Can. J. Chem. Downloaded from www.nrcresearchpress.com by 210.87.254.6 on 09/05/12
For personal use only.

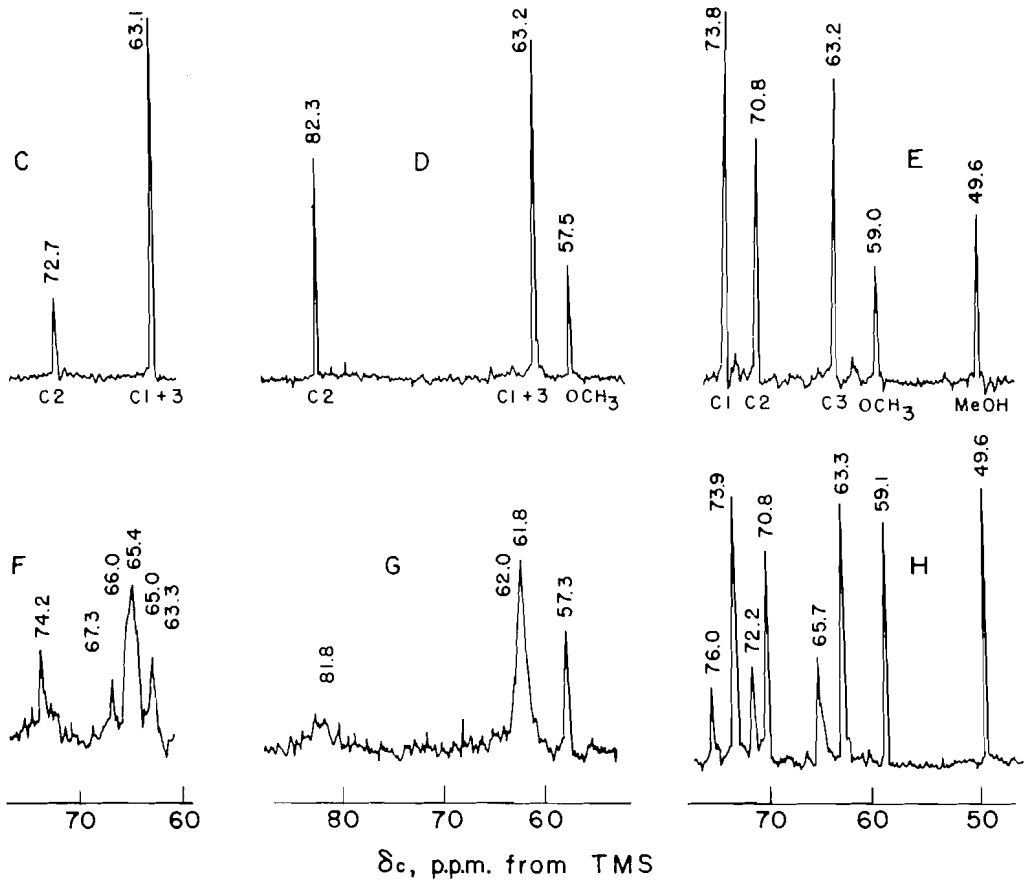

FIG. 4. C.m.r. spectra of glycerol (C) (with 3 mol/mol of sodium diphenylborinate (F)), 2-*O*-methylglycerol (D) (with 1 mol/mol of sodium diphenylborinate (G)), and 1-*O*-methyl-D-glycerol (E) (with 1 mol/mol of sodium diphenylborinate).

methyl-D-glycerol. The spectrum of the polyol contains c.m.r. signals (Fig. 4, spectrum E) which can be assigned as δ_C 73.8 (C-1), δ_C 70.8 (C-2), δ_C 63.2 (C-3), δ_C 59.0 (OCH_3) by taking into account the downfield shift of a CHOH group of a compound when it is converted to a $CHOCH_3$ group (11). Following addition of 1 mol equiv. of sodium diphenylborinate the signals of C-1, -3, and -2 apparently undergo downfield displacements of 2.1, 2.4, and 1.4 p.p.m., respectively (Fig. 4, spectrum H), the last value being close to that of 1.5 p.p.m.observed for the downfield shift of the C-2 signal of glycerol on complexing (Fig. 4; compare spectra C and F). The remaining broad signal centered at δ_C 65.4 (Fig. 4, spectrum F) of the glycerol–diphenylborinate system can be assigned to a 1,3-complex by comparison with the c.m.r. spectrum of the 1,3-diphenylborinate complex of 2-*O*-methylglycerol in D_2O. When an equivalent proportion of reagent was added the C-1 + C-3 signal in spectrum D (Fig. 4) was broadened and shifted downfield by about 1.6 p.p.m. and the C-2 signal was broadened to a line width of 2.8 p.p.m. (Fig. 4, spectrum G). This likely is due to a time averaging effect caused by rapid interconversion of conformers **4** and **5** (Fig. 1). The c.m.r. spectra D and G show that in the 2-*O*-methylglycerol system the equilibrium greatly favors the phenylborinate complex, whereas in the 1-*O*-methylglycerol system the complex is the minor component. This suggests that the diphenylborinate complexes of glycerol are mainly in the six-membered ring form.

Although 1,2-*O*-isopropylidene-α-D-glucofuranose should be able to form two diphenylborinate complexes, it was found that on addition of excess sodium diphenylborinate the c.m.r. spectrum contained only nine signals, which corresponded to formation of only one complex. The

Can. J. Chem. Downloaded from www.nrcresearchpress.com by 210.87.254.6 on 09/05/12
For personal use only.

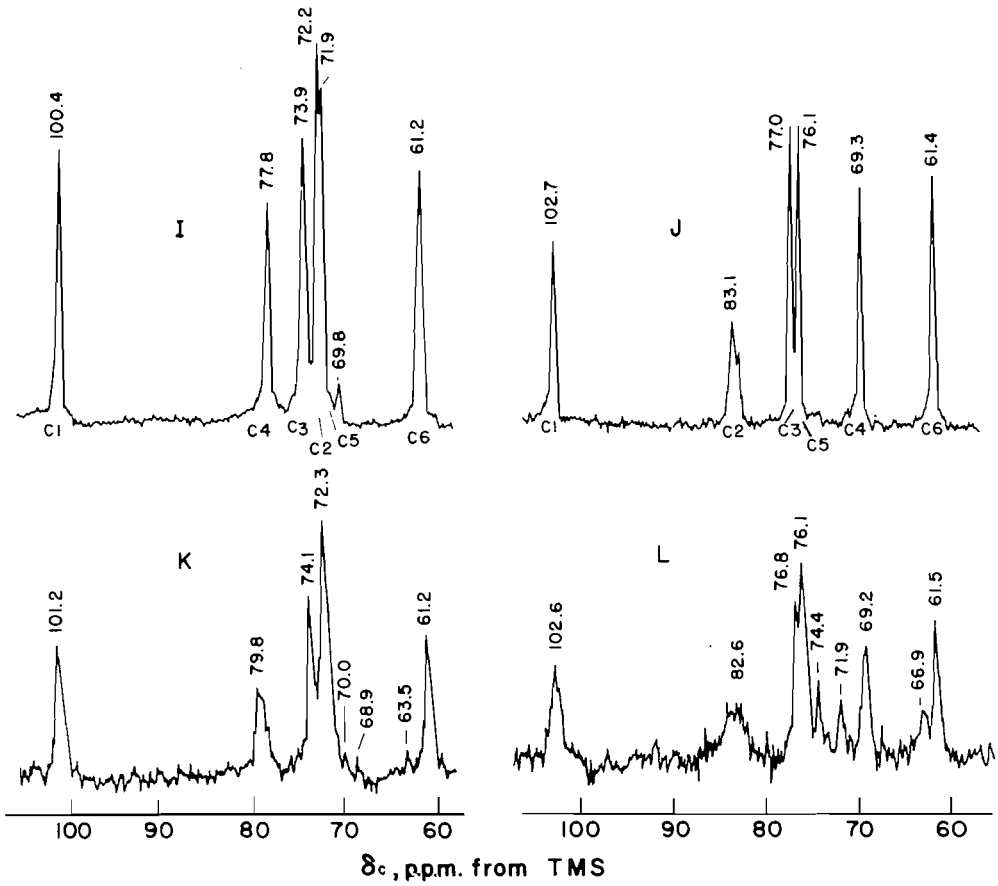

FIG. 5. C.m.r. spectra of soluble potato starch (I) (with 1 mol/mol of sodium diphenylborinate (K)) and a (1→2)-linked β-D-glucopyranan (J) (with mol equiv. of sodium diphenylborinate (L)). The minor signal in *I* is absent in the spectrum of amylose.

equilibrium was on the side of the complex since the new signals greatly predominated in the spectrum following addition of 1 mol equiv. of reagent. In order to determine whether a 5,6- or 3,5-complex was formed the degree of complexing of model compounds was determined following addition of 1 mol equiv. of reagent. Unfortunately 1,2-*O*-isopropylidene-3-*O*-methyl-α-D-glucofuranose on one hand and the 6-*O*-methyl and 6-*O*-isopropyl derivatives of 1,2-*O*-isopropylidene-α-D-glucofuranose on the other, complexed to approximately the same degree and an assignment could not be made (Table 1).

C.m.r. spectroscopy of the borate complexes of polysaccharides is impractical by virtue of the general line broadening phenomenon described above and elsewhere (1) and the ability of borate to form intermolecular complexes which are highly viscous in solution. As sodium diphenylborinate should not give rise to either of these effects a number of polysaccharides of known chemical structure were tested.

The spectral properties of potato starch, which contains mainly (1→4)-linked α-D-glucopyranose units and only relatively few non-reducing end-units that can complex with diphenylborinate, were compared with those of a (1→2)-linked β-D-glucopyranan from *Arthrobacter radiobacter* (12), in which each unit has the potential to complex at the 4 and 6 hydroxyls. After 1 mol equiv. of the reagent was added to potato starch in D_2O, all the signals in the c.m.r. spectrum were broadened, likely due to the presence of sodium ion, and two new very small signals at δ_C 68.9 and δ_C 63.5 appeared. Since two new signals with similar chemical shift appeared when diphenylborinate was added to methyl α-D-glucopyranoside it would appear that they form on a non-reducing end-unit carbon (Table 1; Fig. 5; spectra I and K). On addition of sodium di-

Can. J. Chem. Downloaded from www.nrcresearchpress.com by 210.87.254.6 on 09/05/12
For personal use only.

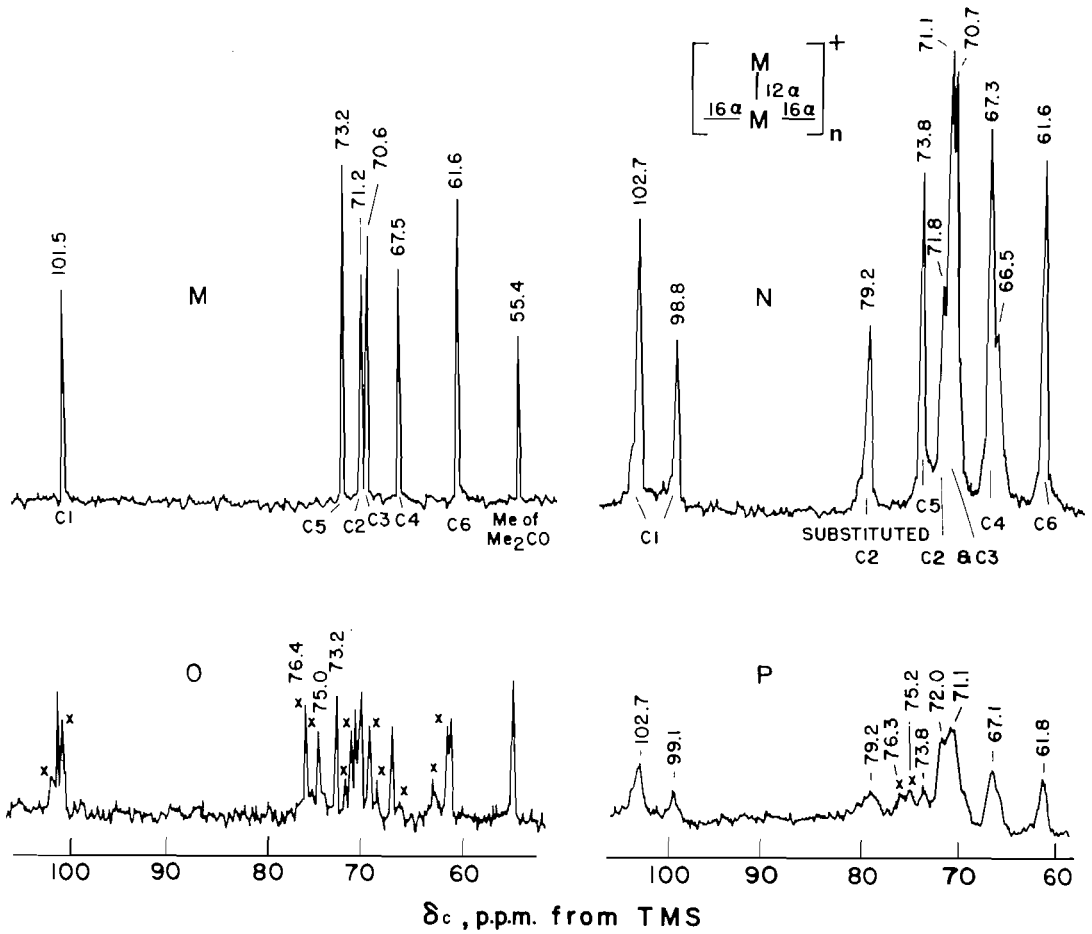

FIG. 6. C.m.r. spectra of methyl-α-D-mannopyranoside (M) and mannan from *E. fibuliger* (N) and those obtained on addition of 1 mol equiv. of sodium diphenylborinate (O and P, respectively) (+structure of mannan; ×signals of complexes).

phenylborinate to a D_2O solution of the (1→2)-linked β-D-glucopyranan the c.m.r. spectrum became less well-resolved and several new signals were formed. In this case two new signals at δ_C 66.9 and δ_C 71.9 appeared, which compares with signals at δ_C 63.1 and δ_C 71.6 in the c.m.r. spectrum of the diphenylborinate of methyl β-D-glucopyranoside. The signal of the glucan diphenylborinate at δ_C 82.6 is much broader than the others.[4] It should arise from C-2 because of its proximity to C-2 in the glucan, which was assigned by its downfield displacement (13) from the C-2 region of β-D-glucose (11). Apparently its resonance is more sensitive to whether the substituted unit contains a diphenylborinate group and whether the glucosyl group at C-2 is diphenylborinated or not.

Interpretation of the c.m.r. spectra of the diphenylborinate derivatives of more complex polysaccharides is more difficult since they contain a larger number of relatively broad signals. However, certain c.m.r. spectra could be partly rationalized. For example, the mannan from *Endomycopsis fibuliger* consists of a (1→6)-linked α-D-mannopyranose main chain with each unit substituted in the 2-position predominantly with single α-D-mannopyranose units (14; see insert in spectrum N, Fig. 6). After addition of 1 mol equiv. of diphenylborinate the c.m.r.

[4]The line widths of the signals of the polysaccharides were broad (20 Hz) compared with those of monosaccharides (5–7 Hz). Even those of starch, which was not complexed to any degree, broadened to about 30 Hz on addition of sodium diphenylborinate.

Can. J. Chem. Downloaded from www.nrcresearchpress.com by 210.87.254.6 on 09/05/12
For personal use only.

Can. J. Chem. Downloaded from www.nrcresearchpress.com by 210.87.254.6 on 09/05/12
For personal use only.

spectrum developed two new signals at δ_C 76.3 and δ_C 75.2. These could arise from C-2 and -3 of a non-reducing end-unit substituted in the 2- and 3-positions by diphenylborinate, since on complexing the c.m.r. spectrum of methyl α-D-mannopyranoside contained new signals at δ_C 76.4 and δ_C 75.0. When a similar approach was used on the mannans from *Saccharomyces rouxii* (15, 16) and *Saccharomyces cerevisiae* (17), which contain longer side-chains and therefore a lower proportion of non-reducing end-units, comparable new signals of a relatively smaller magnitude were detected. These mannans have (1→6)-linked α-D-mannopyranose main chains with the units substituted in the 2-positions. The mannan from *S. rouxii* contains mainly *O*-α-D-mannopyranosyl-(1→2)-*O*-α-D-mannopyranosyl side-chains and the one from *S. cerevisiae* contains a high proportion of *O*-α-D-mannopyranosyl-(1→3)-*O*-α-D-mannopyranosyl-(1→2)-*O*-α-D-mannopyranosyl side-chains.

Experimental

Carbon-13 Magnetic Resonance Spectroscopy

C.m.r. spectra were obtained using a Varian XL-100-15 n.m.r. spectrometer with Fourier transform on approximately 1 mmol of carbohydrate in deuterium oxide (2 ml) at 27° contained in a n.m.r. tube (12 mm diameter) incorporating a Teflon plug which prevented vortex formation on spinning. Under these conditions approximately 5000 transients were used. The spectra incorporated 4096 data points when a sweep width of 5000 Hz (198.4 p.p.m.) was used. Quantitative estimation of complexing was carried out by comparison of the size of a given signal with that of the methyl resonance of methanol, used as internal standard. The sweep width was then 2500 Hz (94.2 p.p.m.) and the number of transients correspondingly greater. In the former runs the acquisition time was 0.4 s, the pulse width 50 μs, and the maximum decoupling power (10 W) was used, and was centered on 500 Hz downfield from the ^1H resonance of TMS, corresponding to the approximate center of the p.m.r. spectra. The hetero-noise bandwidth was 2000 Hz.

Chemical shifts are in p.p.m., the term δ_C describing the downfield difference of the signal resonance and that of external TMS contained in a coaxial capillary. Under these conditions the methyl signal of methanol is at δ_C 49.5.

Diphenylborinic acid was prepared by the method of Coates and Livingstone (18) from the ethanolamine complex of diphenylboric acid (supplied by Aldrich Chemical Company) and converted to its sodium salt by the procedure of Garegg and Lindström (2). Starting from the complex (5 g) an aqueous solution (20 ml) of the acid was prepared and adjusted to p*H* 10 with aqueous sodium hydroxide. The solution was evaporated, weighed, and then made up to 20 ml in deuterium oxide. In each experiment involving c.m.r. spectroscopy of sugars and their diphenylborinates 1 mmol of polyhydroxy compound was dissolved in deuterium oxide (2 ml) and immediately after preparation of the spectrum 1 mol equiv. of sodium diphenylborinate in deuterium oxide (1.1 ml) was added, the spectra determined, and then a third spectrum was obtained following addition of a further 2 mol equiv. of reagent in deuterium oxide (2.2 ml). The percentage of complexing was estimated by comparing the size of unchanged material with the CH_3 resonance of methanol.

The compounds tested for diphenylborinate complex formation are as follows: 1,2:5,6-di-*O*-isopropylidene-D-mannitol (19), methyl 4,6-di-*O*-methyl-α-D-mannopyranoside (20), methyl 2,3-di-*O*-methyl-α-D-mannopyranoside (21), 1,4,5,6-tetra-*O*-methyl-*myo*-inositol (22), 1,2:3,4-di-*O*-isopropylidene-L-*chiro*-inositol (23), 1,2-*O*-isopropylidene-α-D-glucofuranose (24), 6-*O*-isopropyl-1,2-*O*-isopropylidene-α-D-glucofuranose (25), 1,2-*O*-isopropylidene-3-*O*-methyl-α-D-glucofuranose (26), 2-*O*-methylglycerol (27), methyl 3,6-anhydro-α-D-glucopyranoside (28), *S. cerevisiae* mannan (17), *S. rouxii* mannan (15, 16), *E. fibuliger* mannan (14), *A. radiobacter* glucan (12), glycerol (Nichols Chemical Co.), methyl α-D-glucopyranoside (Calbiochem), methyl α-D-mannopyranoside (Sigma Chemical Co.), soluble potato starch (Fischer Scientific Co.), *cis*-cyclohexane-1,2-diol (K. and K. Laboratories Inc.), ethylene glycol (Fischer Scientific Co.), and *myo*-inositol (H. M. Chemical Co.).

1-*O*-Methyl-D-glycerol was prepared by methylation of 1,2-*O*-isopropylidene-L-glycerol (29) with silver oxide – methyl iodide followed by hydrolysis of the product with 80% acetic acid at 100°.

Glycerol-2-*d* was obtained by the reduction of dihydroxyacetone with sodium borodeuteride in deuterium oxide.

1,2-*O*-isopropylidene-6-*O*-methyl-α-D-glucofuranose was obtained by methylation of 3,5-*O*-benzylidene-1,2-*O*-isopropylidene-α-D-glucofuranose (30) with silver oxide – methyl iodide followed by removal of the *O*-benzylidene group with 80% acetic acid at 35° for 18 h.

Proton Magnetic Resonance Spectroscopy

The p.m.r. spectra of compounds were obtained using an XL-100-15 Varian n.m.r. spectrometer on a continuous wave mode on the same D_2O solutions as used above. The temperature was 27° and chemical shifts are expressed in δ (p.p.m.) based on the CH_3 resonance of tetramethylsilane contained in a coaxial capillary.

The p.m.r. (and c.m.r.) spectra of 1,6-anhydro-β-D-glucopyranose (31) and 2,4-di-*O*-methyl-L-rhamnose (32) were not changed on addition of sodium tetraborate in one series of experiments and sodium diphenylborinate in another. The percentage of complex formed on addition of sodium diphenylborinate to methyl 3,6-anhydro-β-D-glucopyranoside (33) was measured by comparison of the size of the H-1 signal of the sugar at δ 5.30 (J = 0 Hz) with that of H-1 of the complex at δ 5.37 (J = 0 Hz). The H-1 signal of methyl 3,6-anhydro-α-D-glucopyranoside was at δ 5.47 (J = 3 Hz) and was indistinguishable from that of its diphenylborinate.

1. P. A. J. Gorin and M. Mazurek. Carbohydr. Res. **27**, 325 (1973).
2. P. J. Garegg and K Lindström. Acta Chem. Scand. **25**, 1559 (1971).

3. S. J. ANGYAL and D. J. MCHUGH. J. Chem. Soc. 1423 (1957).
4. A. B. FOSTER. Adv. Carbohydr. Chem. **12**, 81 (1957).
5. E. R. GUILLOUX, F. PERCHERON, and J. DEFAYE. Carbohydr. Res. **10**, 267 (1969).
6. G. BIRCH, C. K. LEE, and A. C. RICHARDSON. Carbohydr. Res. **10**, 235 (1971).
7. P. L. DURETTE and D. HORTON. Adv. Carbohydr. Chem. **26**, 49 (1971).
8. Y. J. PARK, H. S. KIM, and G. A. JEFFREY. Acta Crystallogr. B, **27**, 220 (1971).
9. B. LINDBERG and K. N. SLESSOR. Acta. Chem. Scand. **21**, 910 (1967).
10. H. SHIMANOUCHI, N. SAITO, and Y. SASATA. Bull. Chem. Soc. Jap. **42**, 1239 (1969).
11. D. E. DORMAN and J. D. ROBERTS. J. Am. Chem. Soc. **92**, 1355 (1970).
12. P. A. J. GORIN, J. F. T. SPENCER, and D. W. S. WESTLAKE. Can. J. Chem. **39**, 1067 (1961).
13. N. YAMAOKA, T. USUI, Z MATSUDA, K. TUZIMURA, H. SUGIYAMA, and S. SETO. Tetrahedron Lett. 2047 (1971).
14. P. A. J. GORIN, J. F. T. SPENCER, and R. J. MAGUS. Can. J. Chem. **47**, 3569 (1969).
15. P. A. J. GORIN and A. S. PERLIN. Can. J. Chem. **34**, 1796 (1956).
16. P. A. J. GORIN, J. F. T. SPENCER, and D. E. EVELEIGH. Carbohydr. Res. **11**, 387 (1969).
17. Y. C. LEE and C. E. BALLOU. Biochemistry, **4**, 257 (1965).
18. G. E. COATES and J. G. LIVINGSTONE. J. Chem. Soc. 4909 (1961).
19. E. BAER and H. O. L. FISCHER. J. Am. Chem. Soc. **61**, 761 (1939).
20. R. G. AULT, W. N. HAWORTH, and E. L. HIRST. J. Chem. Soc. 1012 (1935).
21. G. J. ROBERTSON. J. Chem. Soc. 330 (1934).
22. Y. C. LEE and C. E. BALLOU. J. Biol. Chem. **239**, 1316 (1964).
23. S. J. ANGYAL and C. G. MACDONALD. J. Chem. Soc. 686 (1952).
24. O. T. SCHMIDT. Methods Carbohydr. Chem. **2**, 318 (1963).
25. S. S. BHATTARCHARJEE and P. A. J. GORIN. Can. J. Chem. **47**, 1195 (1969).
26. K. FREUDENBERG, W. DÜRR, H. VON HOCHSTETTER, H. VON HAVE, W. JACOBI, A. NÖE, and E. GARTNER. Chem. Ber. **61B**, 1735 (1928).
27. H. S. HILL, M. S. WHELEN, and H. HIBBERT. J. Am. Chem. Soc. **50**, 2235 (1928).
28. B. HELFERICH, W. KLEIN, and W. SCHAFER. Chem. Ber. **59B**, 79 (1926).
29. E. BAER and H. O. L. FISCHER. J. Biol. Chem. **128**, 463 (1939).
30. S. AKIYA and T. WATANABE. J. Pharm. Soc. Jap. **67**, 97 (1947).
31. E. MONTGOMERY, N. K. RICHTMYER, and C. S. HUDSON. J. Am. Chem. Soc. **65**, 3 (1943).
32. K. BUTLER, P. F. LLOYD, and M. STACEY. J. Chem. Soc. 1531 (1955).
33. W. N. HAWORTH, L. N. OWEN, and F. SMITH. J. Chem. Soc. 88 (1941).
34. O. THEANDER. Acta Chem. Scand. **18**, 1297 (1964).

Can. J. Chem. Downloaded from www.nrcresearchpress.com by 210.87.254.6 on 09/05/12
For personal use only.

The Synthesis of (±)-Cordrastine. A New Route to the Phthalideisoquinoline System

V. SMULA, N. E. CUNDASAWMY, H. L. HOLLAND, AND D. B. MACLEAN
Department of Chemistry, McMaster University, Hamilton, Ontario

Received April 27, 1973

The phthalideisoquinoline system has been synthesized from substituted 2-phenyl-1,3-indandiones as starting materials. The key step in the synthesis is the rearrangement of the spirobenzylisoquinoline ring system to the phthalideisoquinoline system. The diastereomeric cordrastines, I and II, have been synthesized by this method and their relative configurations have been established by comparison of their p.m.r. spectra with those of phthalideisoquinoline alkaloids of known configuration.

Le système phtalideisoquinoléine a été synthétisé à partir des phényl-2 indanediones-1,3 substituées comme composés de départ. L'étape clé dans la synthèse correspond au réarrangement du système cyclique spirobenzylisoquinoléine en système phtalidéisoquinoléine. Les cordrastines diastéréoisomères I et II ont été synthétisées par cette méthode et leurs configurations relatives établies par comparaison des spectres r.m.n. avec ceux d'alcaloides phtalideisoquinoléine de configuration connue.
[Traduit par le journal]

Can. J. Chem., **51**, 3287 (1973)

The alkaloid cordrastine, a member of the phthalideisoquinoline group, was isolated by Manske in 1936 from *Corydalis aurea* Willd (1, 2). It was originally assigned its structure on the basis of an exceptionally good correspondence of the analytical figures with the formula $C_{18}H_{13}NO_2(OCH_3)_4$ and similarities in chemical behavior between it and the known phthalideisoquinoline alkaloid, hydrastine. A synthesis of cordrastine, reported in 1950 by Haworth and Pinder (3), yielded two racemic modifications of the alkaloid, designated cordrastine I and cordrastine II. Their synthetic route, outlined in Scheme 1, involved the cyclization of a substituted phenylethylamide of a phthalidecarboxylic acid followed by reduction of the intermediate dehydrophthalideisoquinoline (Scheme 1). This method was also used to synthesize hydrastine.

Earlier syntheses of phthalideisoquinoline alkaloids, such as that of narcotine (4, 5), hydrastine (6), bicuculline (7), and adlumine (7) have all involved the condensation of a substituted 7-nitrophthalide with a 1-hydroxytetrahydroisoquinoline as shown in Scheme 2. In the absence of the activating nitro group, condensations between hemiaminals of the type shown and a dialkoxyphthalide gave only poor yields of phthalideisoquinolines (4). This synthetic method suffers both from the lack of readily available starting materials and from the formation of side products arising from coupling

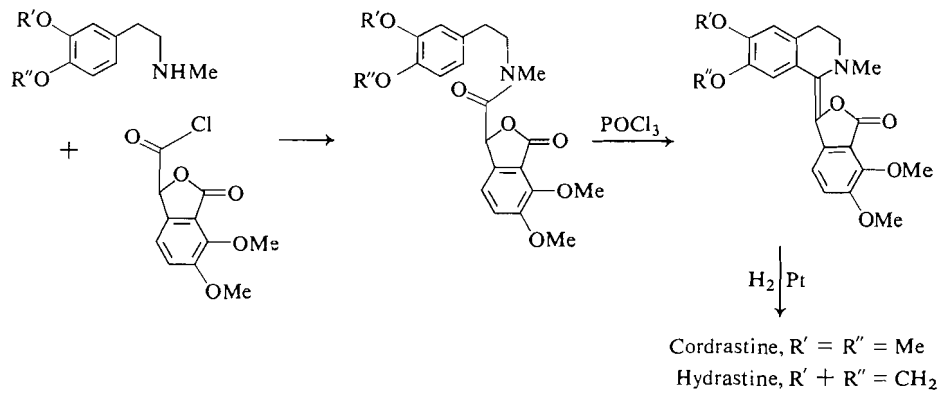

SCHEME 1

Can. J. Chem. Downloaded from www.nrcresearchpress.com by 210.87.254.42 on 09/05/12
For personal use only.

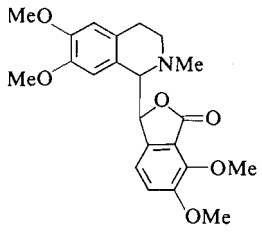

Cordrastine

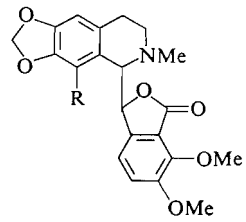

Narcotine, R = OMe
Hydrastine, R = H

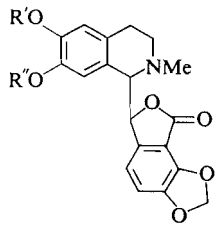

Bicuculline, R′ + R″ = CH_2
Adlumine R′ = R″ = OMe

of the two benzene rings in the steps required for the removal of the nitro group. The synthetic route of Haworth and Pinder mentioned above, although it is potentially one of general applicability, has not been extended beyond the preparation of cordrastine and hydrastine. We report here a new approach to the phthalideisoquinoline system, exemplified by a synthesis of the diastereomers, cordrastine I and cordrastine II, which is outlined in Scheme 3.

The key step in our synthesis, the rearrangement of a spirobenzylisoquinoline to a phthalideisoquinoline, is shown in Scheme 4. In a previous publication (8), the preparation of 2-acetyl-6,7-dimethoxy-1,2-dihydroisoquinoline-1-spiro-2′-(1′,3′-indandione) (**10**) as an intermediate in a model synthesis of (±)-ochrobirine was described.

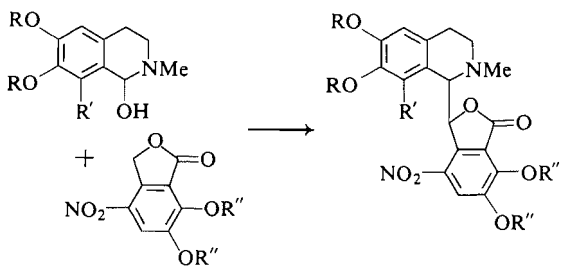

SCHEME 2

It has been found that the spirobenzylisoquinoline **10**, if treated under vigorous conditions with 6 *M* HCl in aqueous ethanol, rearranges to the phthalideisoquinoline **11** in high yield.

The i.r. spectrum of **10** shows absorption in the carbonyl region at 1715 and 1750 cm^{-1} typical of 1,3-indandiones reported in this and a previous paper (8); it also shows amide absorption at 1642 cm^{-1}. In the i.r. spectrum of **11** the absorptions attributed to the indandione system and the amide have disappeared but a new absorption at 1772 cm^{-1} typical of a γ-lactone is present. The aromatic region of the p.m.r. spectra of **10** and **11** is complex but the p.m.r. spectra reported for **5**, **6**, and **7** below are easily interpreted and are in accord with rearrangement of the spirobenzyl- to the phthalideisoquinoline system.

To evaluate the usefulness of this approach in the synthesis of the phthalideisoquinoline alkaloids, the spirobenzylisoquinoline **5**, in which both benzene rings carry two methoxyl substituents, was prepared by a method directly analogous to that used for the preparation of **10** (8). The reactions leading to spirobenzylisoquinolines such as **5** and **10** have been discussed fully (8) and the synthesis of **5** through the sequence **1** → **2** → **3** → **4** → **5** outlined in Scheme 3 presents no novel features.

Treatment of **5** with 6 *M* HCl in aqueous ethanol at the reflux temperature led, as expected, to the phthalideisoquinolines **6** and **7**. This reaction is thought to proceed by the mechanism outlined in Scheme 5, in which the ammonium salt formed by hydrolysis of the acetamide suffers attack by water at one of the carbonyl groups. Ring opening of the indanedione system then gives an intermediate which, in the presence of acid, cyclizes to the phthalideisoquinoline system. Attack occurs either at C-1′ or -3′ leading to an approximately equimolar mixture of two phthalideisoquinolines, one with the methoxy groups at C-4′ and -5′ (**6**) and the other with the methoxy substituents at C-6′ and -7′ (**7**). For the sake of clarity only the steps leading to the desired product **6** have been shown in Scheme 5. The driving force for this rearrangement is apparently the formation of the aromatic system. It is noteworthy that analogous tetrahydroisoquinolines (8) do not rearrange under similar reaction conditions.

The spectral properties of **6** and **7** agree with the structure assigned and are very different

Can. J. Chem. Downloaded from www.nrcresearchpress.com by 210.87.254.42 on 09/05/12
For personal use only.

Can. J. Chem. Downloaded from www.nrcresearchpress.com by 210.87.254.42 on 09/05/12
For personal use only.

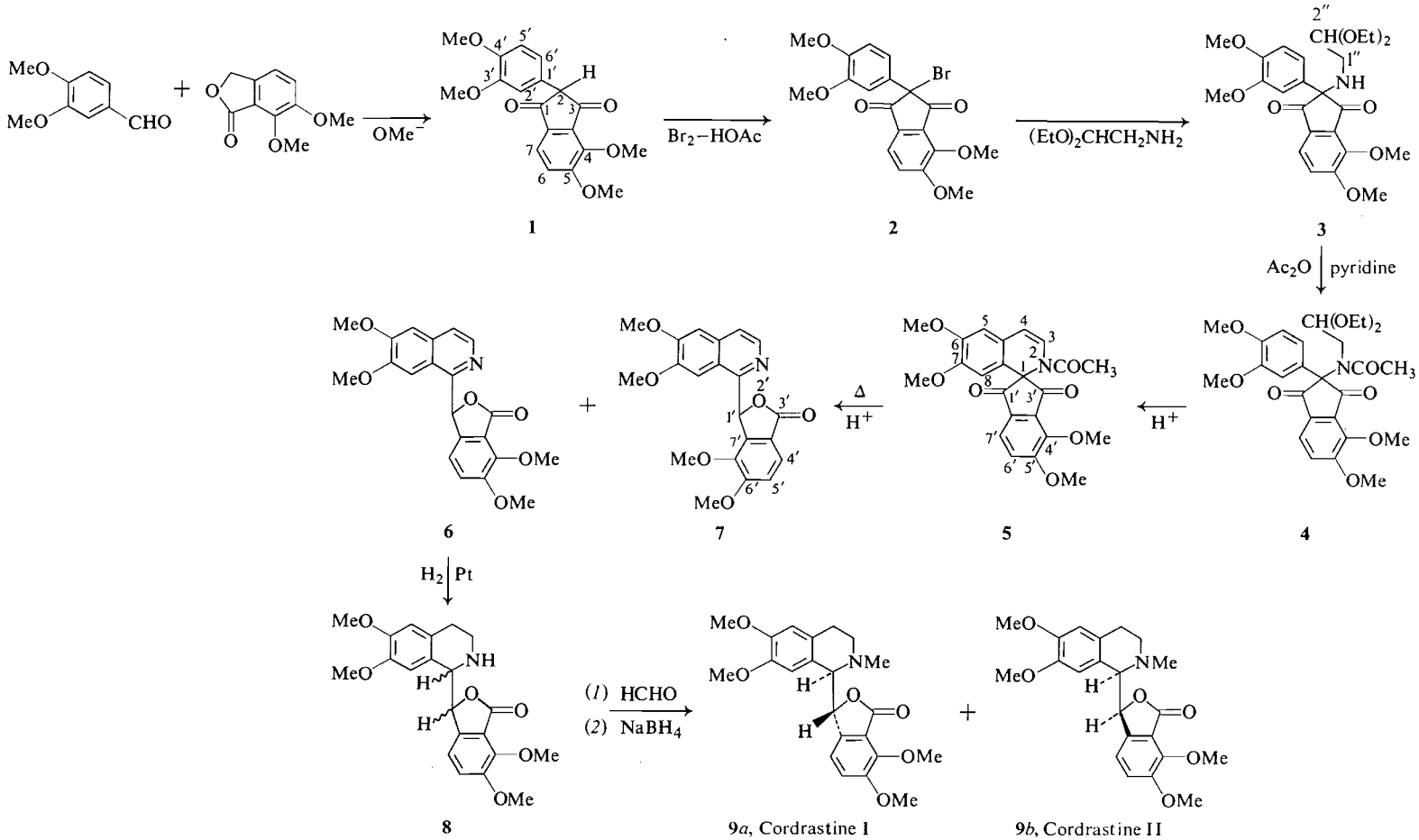

SCHEME 3

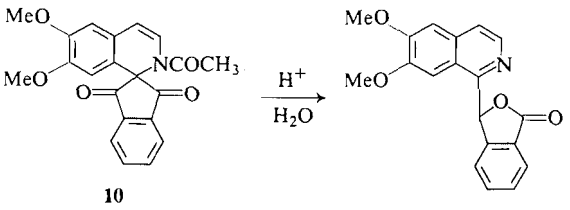

10 11

SCHEME 4

from those of **5**. Compound **5** has carbonyl absorption at 1710 and 1745 cm^{-1} typical of 1,3-indandione, and amide absorption at 1640 cm^{-1}. These absorptions are absent in **6** and **7** and are replaced by a single absorption in the carbonyl region at 1760 cm^{-1} in each compound. The p.m.r. spectra also agree with the structural assignment. Thus in **5** the protons of the double bond at the 3,4 position of the dihydroisoquinoline appear as an AB quartet at δ 5.65 and 6.86 whereas the same protons appear in **6** as an AB quartet at δ 7.48 and 8.33 and in **7** at δ 7.48 and 8.30. The downfield shift exhibited by this pair of protons would be expected in the transformation of the dihydroisoquinoline system of **5** to the aromatic isoquinoline system in **6** and **7**. On the other hand the AB system found for the C-6′ and -7′ protons at δ 7.45 and 7.85 in **5** has moved upfield as expected, in **6** to δ 7.02 and 7.20.

The phthalideisoquinolines **6** and **7** may be distinguished readily by their p.m.r. spectra. Thus **6** shows an AB quartet assignable to the C-6′ and -7′ protons at δ 7.02 and 7.20, whereas **7**, in which the proton at C-4′ is adjacent to the carbonyl group of the phthalide moiety, shows signals due to the C-4′ and -5′ protons as an AB quartet at δ 7.10 and 7.71. One half of the AB quartet of **7** (that due to the proton at C-4′) appears at considerably lower field than does the corresponding signal in **6** because of deshielding by the adjacent carbonyl.

Having obtained the phthalideisoquinoline **6**, it was subjected to mild hydrogenation over Adam's catalyst to yield a diastereomeric mixture of two phthalidetetrahydroisoquinolines (**8**) which was difficult to separate. Accordingly the mixture was treated directly with formaldehyde and sodium borohydride (8) to give, in good yield, a mixture of two products readily separable by preparative layer chromatography. These compounds had melting points similar to those reported for cordrastine I and II (3).

The p.m.r. spectra of the cordrastines are in accord with the structure proposed for natural cordrastine (2). Cordrastine I has absorptions at δ 4.01 (J = 3.4 Hz) and at δ 5.33 (J = 3.4 Hz) assigned to the protons at C-1 and -1′, respectively. These assignments are made by analogy with other phthalideisoquinoline alkaloids (9) and follow also from the decoupling experiments

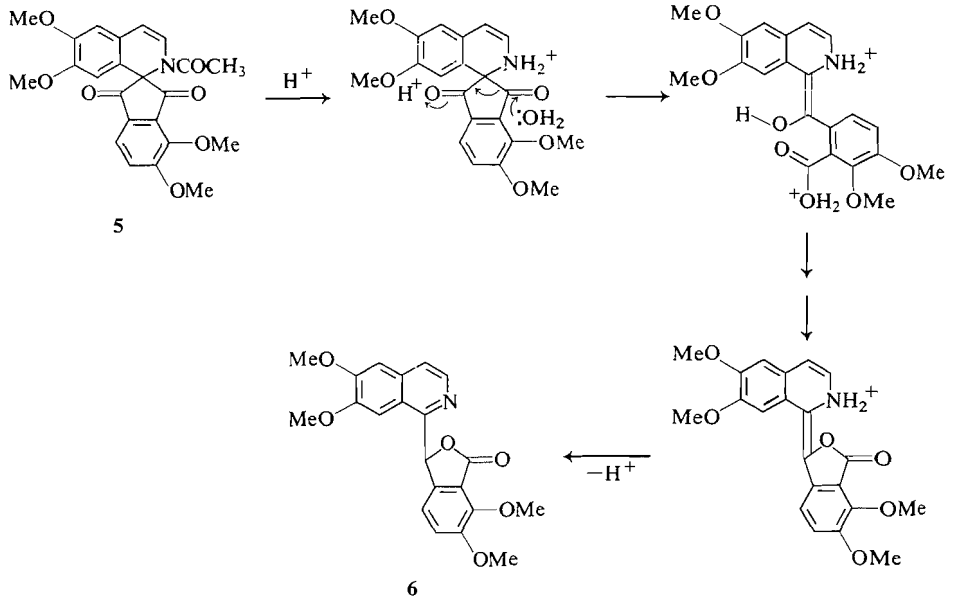

5 6

SCHEME 5

Can. J. Chem. Downloaded from www.nrcresearchpress.com by 210.87.254.42 on 09/05/12
For personal use only.

TABLE 1. Aromatic signals of the phthalide ring of the cordrastines, adlumine, and hydrastine

	δ value			
Proton	Cordrastine I	Adlumine (9)	Cordrastine II	Hydrastine (9)
C-6′	6.90	6.87	7.06	7.09
C-7′	7.23	7.19	6.54	6.50

reported below. Irradiation at δ 4.01 collapses the doublet at δ 5.33 to a singlet and also sharpens the aromatic singlet at δ 6.62 ($w_{\frac{1}{2}}$ = 2.0 Hz before irradiation and $w_{\frac{1}{2}}$ = 1.4 Hz during irradiation) which may now be assigned to the proton at C-8. The second aromatic singlet was virtually unaffected. Irradiation at δ 5.33 collapses the doublet at δ 4.01 and also affects the low field half of the AB quartet arising from the ortho aromatic protons at C-6′ and -7′ at δ 6.90 and 7.23, respectively. Thus the signal at δ 7.23 sharpened during irradiation from $w_{\frac{1}{2}}$ = 2.0 Hz to $w_{\frac{1}{2}}$ = 1.0 Hz. Similar observations have been made in related systems (9). Assignment of the resonance at δ 6.29 to the C-5 proton was confirmed by another double irradiation experiment in which the signal at δ 6.29 sharpened from $w_{\frac{1}{2}}$ = 2.0 Hz to $w_{\frac{1}{2}}$ = 1.4 Hz when the sample was irradiated at δ 2.52, presumably at a C-4 proton.

A similar series of double irradiation experiments confirms the assignment of the p.m.r. spectrum of cordrastine II. Thus irradiation at the C-1 proton resonance at δ 4.00 collapses the C-1′ proton doublet at δ 5.54 and sharpens the signal of the C-8 proton at δ 6.19 from $w_{\frac{1}{2}}$ = 2.8 Hz to $w_{\frac{1}{2}}$ = 1.9 Hz. Irradiation of the C-1′ proton resonance at δ 5.54 collapses the C-1 proton doublet at δ 4.00 and sharpens that half of the AB quartet at δ 6.54, assigned to the C-7′ proton, from $w_{\frac{1}{2}}$ = 2.8 Hz to $w_{\frac{1}{2}}$ = 1.8 Hz. In addition, irradiation at δ 2.70 causes a sharpening of the C-5 proton resonance at δ 6.54 from $w_{\frac{1}{2}}$ = 2.0 Hz to $w_{\frac{1}{2}}$ = 1.5 Hz.

P.m.r. studies (9, 10), along with other studies using physical methods such as o.r.d. (11) have been used to establish the relative and absolute configuration at C-1 and -1′ of many of the phthalideisoquinoline alkaloids. Thus hydrastine and adlumine differ in the relative configuration at C-1 and -1′ (11) and this difference is reflected characteristically in the phthalide aromatic region of their p.m.r. spectra (9). The relevant proton absorptions, together with those of cordrastine I and cordrastine II, are listed in Table 1.

The p.m.r. data strongly suggest that cordrastine I has the same relative configuration at C-1 and -1′ as does adlumine, and is therefore represented by structure *9a* in Scheme 3. Cordrastine II ought to have the relative configuration *9b*, corresponding to that of hydrastine, and indeed a close correlation is observed between the phthalide aromatic region of the p.m.r. spectra of cordrastine II and hydrastine. The assignment of the relative configuration at C-1 and -1′ of cordrastines I and II is therefore in accord with the results of Teitel and coworkers (12).

Haworth and Pinder were unsuccessful in their attempts to achieve a resolution of cordrastine I or cordrastine II and no attempt has been made to resolve the cordrastines produced in this synthesis. The synthesis, however, does provide a new route to the phthalideisoquinoline system which requires only readily available starting materials and which should prove to be of general applicability.

Experimental

Apparatus, Methods, and Materials

Melting points were determined on a Kofler block and are uncorrected. I.r. spectra were recorded on a Beckman IR5 or a Perkin–Elmer 337 spectrophotometer in chloroform solution unless otherwise stated. The p.m.r. spectra were obtained at 100 MHz on a Varian HA100 instrument or at 60 MHz on a Varian A60, using deuteriochloform as solvent and tetramethylsilane as internal standard. Chemical shifts are reported in p.p.m. (δ) from TMS, the symbols s (singlet), d (doublet), t (triplet), q (quartet), and m (multiplet) being used in reporting the spectra. Mass spectra were routinely run on all samples using a C.E.C. 21-110B double-focusing instrument. High resolution mass spectrometry was performed by the described methods (13). Column chromatography was carried out on basic alumina (Fisher) and t.l.c. employed Merck silica gel, F-254.

The microanalyses were performed by Gygli Microanalytical Laboratory, Toronto, Ontario.

*1-(1′-Phthalide)-6,7-dimethoxyisoquinoline (**11**)*

A solution of 2-acetyl-6,7-dimethoxy-1,2-dihydro-

Can. J. Chem. Downloaded from www.nrcresearchpress.com by 210.87.254.42 on 09/05/12
For personal use only.

Can. J. Chem. Downloaded from www.nrcresearchpress.com by 210.87.254.42 on 09/05/12
For personal use only.

isoquinoline-1-spiro-2′-(1′,3′-indandione) (**10**) (8) (0.182 g, 0.0005 mol) in ethanol (12 ml, absolute) and hydrochloric acid (12 ml, 12 *M*) was heated under reflux for 12 h. The mixture was taken to dryness, water added, the solution basified with ammonia and extracted with chloroform.

The extract was washed, dried, and evaporated to give a residue which on crystallization from ether gave a sample (0.133 g, 83%) melting at 175–177°.

Anal. Calcd. for $C_{19}H_{15}NO_4$: C, 71.03; H, 4.67; N, 4.36. Found: C, 70.84; H, 4.58; N, 4.44.

I.r.: ν_{max} 1772 cm^{-1}; p.m.r.: 3.77 (3H, s, $—OCH_3$), 4.03 (3H, s, $—OCH_3$), 7.07 (1H, s, benzylic H), 7.32–8.27 (8H, m, aromatic H's).

2-(3′,4′-Dimethoxyphenyl)-4,5-dimethoxy-1,3-indandione (1)

A mixture of meconin (45 g, 0.23 mol), 3,4-dimethoxybenzaldehyde (38.6 g, 0.23 mol), and ethyl propionate (112 ml) was dissolved in a solution of sodium methoxide (37.7 g, 0.7 mol) in methanol (140 ml), and the resulting solution was heated to reflux under a nitrogen atmosphere. After 10 min the solution solidified to give a red solid which was dissolved in 1 l of water and extracted with ether. The aqueous phase was then acidified with concentrated hydrochloric acid to p*H* 2 and cooled in ice. The white solid that separated was filtered, washed with ice-water and dried at 50° to yield the crude product **1** in almost quantitative yield. Recrystallization from chloroform–methanol afforded an analytically pure sample melting at 187–189° (lit. 190–191° (14)).

Anal. Calcd. for $C_{19}H_{18}O_6$: C, 66.65; H, 5.29. Found: C, 66.63; H, 5.53.

I.r.: ν_{max} 1710, 1745 cm^{-1}; p.m.r.: 3.88 (s, 6H, 2—OCH_3), 4.03 (s, 3H, $—OCH_3$), 4.13 (s, 3H, $—OCH_3$), 4.20 (s, 1H, benzylic H), 6.81 (broad s, 3H, aromatic H's), 7.44 and 7.84 (2H, ABq, J = 9.0 Hz, C-6 and C-7 H's).

2-Bromo-2-(3′,4′-dimethoxyphenyl)-4,5-dimethoxy-1,3-indandione (2)

The indandione **1** (14.9 g, 0.044 mol) was suspended in acetic acid (150 ml) and the stirred suspension treated with a solution of bromine (7 g, 0.044 mol) in acetic acid (200 ml) at room temperature under a nitrogen atmosphere. After the addition was complete (10–15 min) the solution was stirred for a further 5 min and then the solvent was removed under reduced pressure without heating above 30 °C. The green oily residue so obtained (19.4 g) was homogeneous by t.l.c. (2% methanol–chloroform, R_f 0.6) and was used directly in the next stage. Compound **2** decomposed on storage and when attempts were made to purify it.

2-(2″,2″-Diethoxyethylamino)-2-(3′,4′-dimethoxyphenyl)-4,5-dimethoxy-1,3-indandione (3)

Compound **2** prepared as above (19.4 g) was dissolved in dry ether (500 ml) and the solution stirred under nitrogen at room temperature during the addition of aminoacetaldehyde diethyl acetal (13.2 ml, 0.1 mol). Stirring was continued at room temperature for a further 40 h and then water (500 ml) was added to the solution and the mixture was transferred to a separatory funnel. The aqueous layer was discarded and the ethereal layer washed twice with further 500-ml portions of water, dried over sodium sulfate, and evaporated to yield 19.9 g of solid material. Crystallization from ether–ligroin (b.p. 110–115°) then afforded **3** (15.1 g, 72% from **1**), melting at 95–97°. Anal. Calcd. for $C_{25}H_{31}NO_8$: mol. wt. 473.2049; C, 63.40; H, 6.60; N, 2.96. Found: mol. wt. 473.2060; C, 63.40; H, 7.06; N, 2.96.

I.r.: ν_{max} 1710, 1745 cm^{-1}; p.m.r.: 1.19 (6H, t, J = 6.5 Hz, $—CH_2CH_3$), 2.33 (1H, broad s, N—H), 2.73 (2H, d, J = 6.0 Hz, $N—CH_2—$), 3.30–3.80 (4H, m, $—CH_2CH_3$), 3.84 (3H, s, $—OCH_3$), 3.90 (3H, s, $—OCH_3$), 4.01 (3H, s, $—OCH_3$), 4.22 (3H, s, $—OCH_3$), 4.65 (1H, t, J = 6.0 Hz, $—CH_2—CH(OEt)_2$), 6.74 (1H, ABd, J = 9.0 Hz, C-5′ H), 6.88 (1H, ABXq, J = 9.0, 2.1 Hz, C-6′ H), 7.18 (1H, d, J = 2.1 Hz, C-2′ H), 7.36 and 7.76 (2H, ABq, J = 8.2 Hz, C-6 and C-7 H's).

N-Acetyl-2-(2″,2″-diethoxyethylamino)-2-(3′,4′-dimethoxyphenyl)-4,5-dimethoxy-1,3-indandione (4)

A solution of the amine **3** (15.0 g, 0.032 mol) in pyridine (40 ml) and acetic anhydride (70 ml) was stirred at room temperature for 40 h. The solvent was then removed under reduced pressure and the residue dissolved in benzene and applied to a column of basic alumina. Elution from benzene to chloroform in 5% steps afforded **4** as a pale green oil (14.9 g 74%) which crystallized in contact with petroleum ether (b.p. 80–100°). Recrystallization from the same solvent gave a pale yellow product, m.p. 67–68°.

Anal. Calcd. for $C_{27}H_{33}NO_9$: C, 62.90; H, 6.45. Found: C, 63.13; H, 6.50.

I.r.: 1645 cm^{-1} (amide carbonyl), 1710, 1745 cm^{-1}; p.m.r.: 1.10 (6H, t, J = 6.5 Hz, $—OCH_2CH_3$), 2.25 (3H, s, $—NCOCH_3$), 3.20–3.70 (6H, m, methylene H's), 3.77 (3H, s, $—OCH_3$), 3.82 (3H, s, $—OCH_3$), 3.83 (3H, s, $—OCH_3$), 4.05 (3H, s, $—OCH_3$), 4.48 (1H, t, J = 6.0 Hz, $—CH_2CH(OEt)_2$), 6.81 (1H, ABd, J = 8.0 Hz, C-5′ H), 7.13 (1H, ABXq, J = 8.0, 2.1 Hz, C-6′ H), 7.17 (1H, d, J = 2.1 Hz, C-2′ H), 7.22 and 7.64 (2H, ABq, J = 8.0 Hz, C-6 and C-7 H's).

2-Acetyl-6,7-dimethoxy-1,2-dihydroisoquinoline-1-spiro-2′-(4′,5′-dimethoxy-1′,3′-indandione) (5)

A solution of the amide **4** (14 g, 0.026 mol) in ethanol (100 ml, absolute) and hydrochloric acid (100 ml, 12 *M*) was stirred at room temperature for 20 h. The mixture was then poured onto ice (300 g) and the resulting solution basified with ammonia and extracted with chloroform. The chloroform extract was dried and evaporated to give a residue (13.2 g) that was chromatographed on basic alumina. A 5% stepwise elution from benzene to chloroform yielded **5** (7.9 g) which was recrystallized from ethanol to give a sample (7.4 g, 67%) melting at 210–211°.

Anal. Calcd. for $C_{23}H_{21}NO_7$: C, 65.24; H, 5.00; N, 3.31. Found: C, 65.53; H, 5.22; N, 3.35.

I.r.: ν_{max} 1640 cm^{-1} (amide), 1710, 1745 cm^{-1}; p.m.r.: 2.21 (3H, s, $N—COCH_3$), 3.40 (3H, s, $—OCH_3$), 3.77 (3H, s, $—OCH_3$), 3.95 (3H, s, $—OCH_3$), 4.01 (3H, s, $—OCH_3$), 5.65 and 6.86 (2H, ABq, J = 8.0 Hz, C-3 and C-4 H's), 6.13 (1H, s, C-8 H), 6.68 (1H, s, C-5 H), 7.45 and 7.85 (2H, Abq, J = 8 Hz, C-6′ and C-7′ H's).

1-[1′-(4′,5′-Dimethoxyphthalide)]-6,7-dimethoxyisoquinoline (6) and 1-[1′-(6′,7′-Dimethoxyphthalide)]-6,7-dimethoxyisoquinoline (7)

A solution of the amide **5** (2.60 g, 0.006 mol) in ethanol (80 ml, absolute) and hydrochloric acid (80 ml, 12 *M*), was heated under reflux for 2 h. After cooling the solution it was diluted with water (50 ml) and extracted with dichloromethane. The aqueous portion was then basified

Can. J. Chem. Downloaded from www.nrcresearchpress.com by 210.87.254.42 on 09/05/12
For personal use only.

with ammonia and reextracted with dichloromethane and the basic extract dried and evaporated to give a residue (1.7 g) which on crystallization from ethanol gave the phthalideisoquinoline **6**. Recrystallization of crude **6** from dichloromethane – petroleum ether (60–80°) gave a sample (0.9 g, 40%) melting at 179–181° with decomposition.

Anal. Calcd. for $C_{21}H_{19}NO_6$: C, 66.13; H, 5.02; N, 3.67. Found: C, 66.08; H, 4.84; N, 3.71.

I.r.: ν_{max} 1760 cm^{-1}; p.m.r.: 3.89 (3H, s, —OCH_3), 3.92 (3H, s, —OCH_3), 3.99 (3H, s, —OCH_3), 4.14 (3H, s, —OCH_3), 6.93 (1H, s, aromatic or methine H), 7.02 and 7.20 (2H, ABq, J = 8.0 Hz, C-6′ and C-7′ H's) 7.16 (1H, s, aromatic or methine H), 7.30 (1H, s, aromatic or methine H), 7.48 and 8.33 (2H, ABq, J = 6.0 Hz, C-4 and C-3 H's).

Evaporation of the ethanolic mother liquor after the removal of **6** gave a residue (0.74 g) from which the phthalideisoquinoline 7 was isolated by crystallization from aqueous methanol. Recrystallization from the same solvent gave a sample of 7 (0.6 g, 27%) melting at 198–200° with decomposition.

Anal. Calcd. for $C_{21}H_{19}NO_6$; C, 66.13; H, 5.02; N, 3.67. Found: C, 66.17; H, 5.15; N, 3.81.

I.r.: ν_{max} 1760 cm^{-1}; p.m.r.: 3.35 (3H, s, —OCH_3), 3.92 (3H, s, —OCH_3), 3.94 (3H, s, —OCH_3), 4.00 (3H, s, —OCH_3), 7.10 and 7.71 (2H, ABq, J = 7.5 Hz, C-4′ and C-5′ H's), 7.08 (1H, s, aromatic or methine H), 7.13 (1H, s, aromatic or methine H), 7.38 (1H, s, aromatic or methine H), 7.48 and 8.30 (2H, ABq, J = 6.0 Hz, C-4 and C-3 H's).

The phthalideisoquinolines **6** and **7** were separable by t.l.c. Elution with ethyl acetate showed **6** at R_f 0.42 and **7** at R_f 0.35.

*1-[1′-(4′,5′-Dimethoxyphthalide)]-6,7-dimethoxy-1,2,3,4-tetrahydroisoquinoline (**8**)*

A solution of the amine **6** (0.38 g, 0.001 mol) in ethanol (25 ml, absolute) and 70% perchloric acid (0.25 ml) was hydrogenated over a platinum oxide catalyst (0.1 g) at 50 p.s.i. pressure and room temperature for 3 h. After the catalyst had been removed by filtration, evaporation of the solvent yielded a solid residue which was dissolved in dilute ammonia. This solution was extracted with dichloromethane and the extract dried over sodium sulfate and evaporated to give an oil (0.29 g) which upon examination by t.l.c. was found to consist of two components (R_f 0.5 and 0.37, with 10% methanolic chloroform). This oil was used in the next stage without further purification.

*1-[1′-(4′5′-Dimethoxyphthalide)]-2-methyl-6,7-dimethoxy-1,2,3,4-tetrahydroisoquinoline (Cordrastine, **9**)*

The amine **8** (0.2 g, 0.00052 mol), without purification, was dissolved in 37% aqueous formalin (2 ml) and the solution heated under reflux for 2 h. After this time, the solution was evaporated *in vacuo* and the resulting solid dissolved in methanol (10 ml) and the solution then cooled in an ice bath. An excess of sodium borohydride (*ca.* 0.04 g) was added cautiously to this solution, with rapid stirring, and after the addition was complete the stirring was continued for a further 15 min. The solution was then poured into water and the aqueous mixture extracted with dichloromethane. The extract was dried over sodium sulfate and evaporated to give a residue which was applied to a 2 mm preparative layer plate (Merck Silica Gel F-254). Elution with 5% methanolic chloroform afforded two major components corresponding to cordrastine I (0.096 g, 46%) and cordrastine II (0.089 g, 43%) at R_f's 0.6 and 0.3 respectively. Cordrastine I was purified by crystallization from methanol, m.p. 156–157° (lit. 155–156° (3)).

Anal. Calcd. for $C_{22}H_{25}NO_6$; C, 66.14; H, 6.31; N, 3.50. Found: C, 66.21; H, 6.50; N, 3.53.

I.r.: ν_{max} 1760 cm^{-1}; p.m.r.: 2.61 (3H, s, N—CH_3), 2.0–3.2 (4H, m, C-3 and C-4 H's), 3.67 (3H, s, —OCH_3), 3.76 (6H, s, 2—OCH_3's), 3.84 (3H, s, —OCH_3), 4.01 (1H, d, J = 3.4 Hz, C-1 H), 5.53 (1H, d, J = 3.4 Hz, C-1′ H), 6.29 (1H, s, C-5 H), 6.62 (1H, s, C-8 H), 6.90 and 7.24 (2H, ABq, J = 8.5 Hz, C-6′ and C-7′ H's, respectively).

Cordrastine II was converted into the picrate salt which was recrystallized from methanol–acetone, m.p. 208° (dec.) (lit. m.p. 202°, dec. (3)).

Anal. Calcd. for $C_{28}H_{28}N_4O_{13}$; C, 53.50; H, 4.49; N, 8.91. Found: C, 53.42; H, 4.61; N, 8.76.

Decomposition of the picrate on an alumina column by elution with methanol gave the free base, m.p. 117–118° (lit. m.p. 118–119° (3)). I.r.: ν_{max} 1755 cm^{-1}; p.m.r.: 2.54 (3H, s, N—CH_3), 2.40–3.20 (4H, m, C-3 and C-4 H's), 3.60 (3H, s, —OCH_3), 3.80 (3H, s, —OCH_3), 3.83 (3H, s, —OCH_3), 3.96 (3H, s, —OCH_3), 4.00 (1H, d, J = 3.5 Hz, C-1 H), 5.54 (1H, d, J = 3.5 Hz, C-1′ H), 6.19 (1H, s, C-8 H), 6.54 (1H, s, C-5 H), 6.54 and 7.06 (2H, ABq, J = 8.0 Hz, C-7′ and C-6′ H's respectively).

We thank the National Research Council of Canada for financial support of this work.

1. R. H. F. Manske. Can. J. Res. **14B**, 325 (1936).
2. R. H. F. Manske. Can. J. Res. **16B**, 81 (1938).
3. R. D. Haworth and A. R. Pinder. J. Chem. Soc. 1776 (1950).
4. W. H. Perkin and R. Robinson. J. Chem. Soc. **99**, 775 (1911).
5. M. A. Marshall, F. L. Pyman, and R. Robinson. J. Chem. Soc. 1315 (1934).
6. E. Hope, F. L. Pyman, F. G. P. Remfry, and R. Robinson. J. Chem. Soc. 236 (1931).
7. P. W. G. Groenewoud and R. Robinson. J. Chem. Soc. 199 (1936).
8. N. E. Cundasawmy and D. B. MacLean. Can. J. Chem. **50**, 3028 (1972).
9. S. Safe and R. Y. Moir. Can. J. Chem. **42**, 160 (1964).
10. A. R. Battersby and H. Spencer. J. Chem. Soc. 1087 (1965).
11. G. Snatzke, G. Wollenberg, J. Hrbek, F. Santavy, K. Blaha, W. Klyne, and R. J. Swan. Tetrahedron, **25**, 5059 (1969).
12. S. Teitel, J. O'Brien, and A. Brossi. J. Org. Chem. **37**, 1879 (1972).
13. C. K. Yu and D. B. MacLean. Can. J. Chem. **49**, 3025 (1971).
14. O. Oskaja and G. Vanags. Latvijas PSR Zinatnu Akad. Vestis, Kim. Ser. 87 (1962); Chem. Abstr. **59**, 7439h.

Identification by Combined Gas–Liquid Chromatography – Mass Spectrometry of Sterols Isolated from *Scenedesmus obliquus* Grown in Light and Heavy Water

P. BÉLANGER AND J. A. ZINTEL

Merck Sharp & Dohme Canada Limited, P.O. Box 899, Pointe Claire – Dorval 700, Québec

AND

W. J. A. VANDEN HEUVEL AND J. L. SMITH

Merck Sharp & Dohme Research Laboratories, Rahway, New Jersey 07065

Received December 18, 1972[1]

The sterol fraction from *Scenedesmus obliquus*, grown in heavy water, has been shown by combined g.l.c. – mass spectrometry to contain $\Delta^{7,22}$-ergostadiene-3β-ol, Δ^{7}-ergostenol, chondrillasterol, and Δ^{7}-chondrillastenol. The same algae, grown in light water, contain these four sterols and, in addition, ergosterol and corbisterol.

La fraction des stérols obtenus de *Scenedesmus obliquus*, une álgue croissant dans l'eau lourde, a été analysée par la combinaison c.p.v. et spectrométrie de masse. Il est montrée que les stérols isolés sont le $\Delta^{7,22}$-ergostadiene-3β-ol, le Δ^{7}-ergostenol, le chondrillasterol et le Δ^{7}-chondrillastenol. La même algue croissant dans l'eau ordinaire contient aussi l'ergostérol et le corbistérol en plus des quatres autres stérols déjà mentionnés.

Can. J. Chem., **51**, 3294 (1973)

Introduction

The identification of the components in a mixture from a biological source is a recurring challenge to the natural products chemist. Among the recently developed methods for the characterization of compounds on the microgram scale, probably none surpasses combined gas–liquid chromatography (g.l.c.)–mass spectrometry (m.s.) in success for the analysis of multicomponent samples. The steroid field has been a particularly active area for the application of this method (1).

We now wish to report on the use of combined g.l.c.–m.s. in the identification of the sterols found in the algae *Scenedesmus obliquus* grown in both light and heavy water.

Experimental

Isolation of the Sterol Fraction

Scenedesmus obliquus algae were grown following the methods of Williams *et al.* (2) in heavy water having a deuterium content greater than 99%. The harvested cells (5 g) were placed in a 500-ml flask and saponified by refluxing for 2 h in 250 ml 2 *M* potassium hydroxide (1:1 aqueous ethanol). The resulting solution was cooled and extracted twice with an equal volume of petroleum ether (b.p. 30–60 °C). The aqueous layer containing the fatty acids was set aside. The organic layer containing the unsaponifiables was dried over sodium sulfate after two washings with water and was concentrated to a syrup at reduced pressure. The residue (410 mg) was then dissolved in 20 ml acetone–ethanol (1:1) and 500 mg of digitonin added as a 0.5% solution in the same solvent mixture. The solution was left at room temperature overnight.

The resulting digitonide was collected by filtration, washed first with a 1:1 mixture of ether–acetone and then with ether. The solid was taken up in 10 ml dimethylsulfoxide, heated on a steam bath for 10 min, cooled, and extracted four times with hexane. A white solid (42 mg) was obtained when the hexane solution was evaporated to dryness.

The light cells (5 g) obtained from *Scenedesmus obliquus* that grew in ordinary water yielded by a similar treatment 65 mg of the light sterol fraction.

G.l.c.–m.s.

Combined g.l.c.–m.s. was carried out with an LKB Model 9000 instrument. A 7 ft × 3 mm i.d. glass column was employed. It was packed with 1% SE-30 on 80–100 mesh acid-washed and silanized Gas-Chrom P. The column was operated isothermally at 250 °C with the helium carrier gas flow set at 30 ml/min. Spectrometer conditions: source temperature, 270 °C; electron energy, 70 eV; accelerating potential, 3.5 kV; trap current, 60 μA.

Trimethylsilylation was effected by dissolving the sample (~100 μg) in 100 μl bis(trimethylsilyl)acetamide (BSA) and allowing the mixture to stand at room temperature for 2 h.

Results and Discussion

The chromatograms resulting from the isothermal analysis of the light and deuterated

[1]Revised manuscript received June 15, 1973.

Can. J. Chem. Downloaded from www.nrcresearchpress.com by 210.87.254.5 on 09/05/12
For personal use only.

Can. J. Chem. Downloaded from www.nrcresearchpress.com by 210.87.254.5 on 09/05/12
For personal use only.

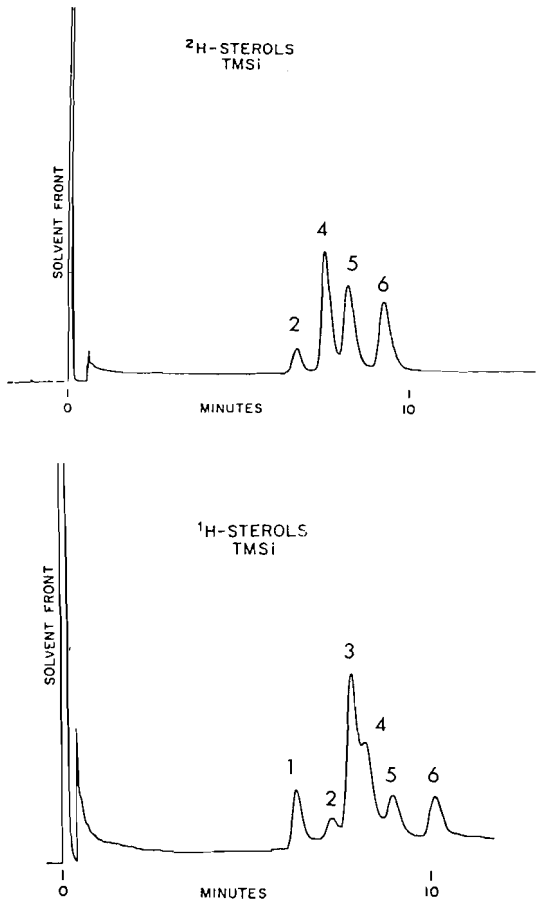

FIG. 1. Elution pattern of heavy sterols (upper chromatogram) and light sterols (lower chromatogram) as their TMSi derivatives.

sterol fractions are presented in Fig. 1. Changes in relative retention times are often observed with related hydroxy steroids which differ in the stereochemistry or position of the hydroxyl group following TMSi derivative formation. No change in relative retention time relationships was observed following trimethylsilylation of the sterol fraction, suggesting that the sterols possess similarly situated hydroxyl groups and differ in positions remote from the hydroxyl function.

It is clear from the mass spectra presented in Fig. 2 that the deuterium content of the sterols is less than that of heavy water in which the algae were grown (99%). A measure of the level of label in these sterols was obtained by comparing the weight average molecular weight (3) taken from these spectra together with that of unlabelled sterol and that calculated for 100% ^{2}H sterol, the isotope correction being made only for carbon-13. The results of this calculation are close to 96% ^{2}H and this method provides a rough but convenient measure of the extent of labelling. The more precise computation, described by Wendt and McCloskey (4), yielded values that are lower by a few percent and are reported in Table 1.

The reason for such a low deuterium content is obscure at present as the water used in growing the *Scenedesmus obliquus* was never less than 99% ^{2}H. A possible source of this apparent dilution may be the residual amount of light isotope in the cells, an amount which can be slow to disappear completely as the rate of multiplication of cells in heavy water is 2.5–3.5 times slower than the rate in ordinary water. Another source of hydrogen contamination could be an isotope effect which would tend to concentrate the lighter isotope in the cells, resulting in deuterium content somewhat lower than expected.

The mass spectra of the TMSi sterols were also obtained and the molecular ion values for these derivatives and the free sterols are reported in Table 2. The difference between the TMSi deriva-

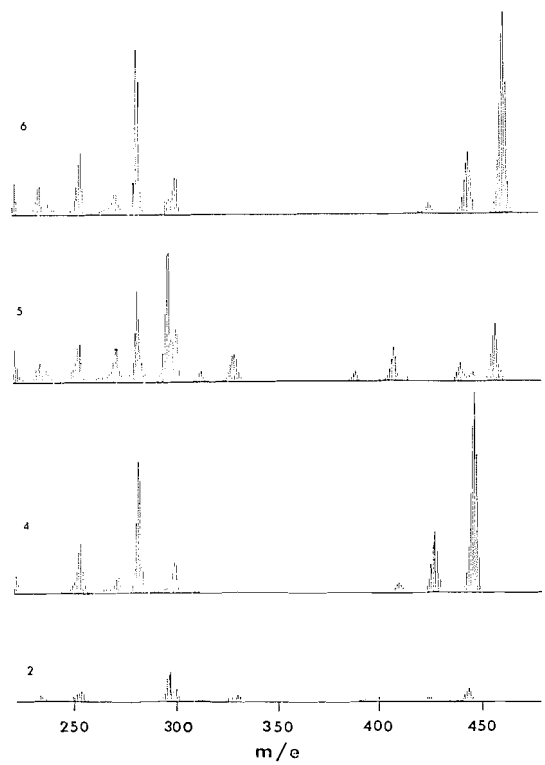

FIG. 2. Normalized mass spectra of ^{2}H-sterols.

TABLE 1. Elution time for the light and heavy TMSi sterols

Sterol	Isotope content	Retention time* Heavy	Light	Isotope effect
2	94.6	6.7	7.4	1.10
4	93.9	7.5	8.2	1.09
5	94.4	8.2	9.0	1.10
6	95.2	9.3	10.1	1.09

*Retention times are reported in minutes away from the solvent front. Isothermal —250 °C.

TABLE 2. Molecular ions and empirical formulae for deuterosterols and TMSi ethers

Sterol	Free sterols *m/e*	Empirical formula	TMSi ethers *m/e*	Empirical formula
2	443	$C_{28}D_{45}OH$	515	$C_{28}D_{45}OTMSi$
4	447	$C_{28}D_{47}OH$	519	$C_{28}D_{47}OTMSi$
5	459	$C_{29}D_{47}OH$	531	$C_{29}D_{47}OTMSi$
6	463	$C_{29}D_{49}OH$	535	$C_{29}D_{49}OTMSi$

tive and the free sterol is 72 a.m.u. in each case, the hydroxyl group being —OH rather than —O^{2}H. This is not unexpected as the isolation of the sterols is carried out in light water and ethanol. On the basis of the resulting empirical formulae, the mixture contains two C_{28} sterols (mono- and diene) and two C_{29} sterols (also mono- and diene).

Examination of the fragmentation patterns of the deuterated derivatives demonstrates the position of the double bonds. It is known from the work of Knights (5) and Brooks *et al.* (1, 6) that TMSi derivatives of Δ^5-3β-ol sterols are easily recognized in mass spectrometry by the presence of an intense (often base) peak at *m/e* 129 which corresponds to the ion $Me_3SiO^+=\!\!/\!\!-\!\!-$. There is no analogous signal at *m/e* 133 in the mass spectra of the deuterated TMSi sterols. All four spectra of Fig. 2, however, contain ions centered at *m/e* 301 and 282, which can be attributed to fragmentation typical of a Δ^7-containing 3β-ol sterol. The ions M − (side chain) and M − (side chain + HDO) are explained by a mechanism proposed by Brooks (1).

According to Knights (5) the presence of a 22:23 double bond results in intense peaks arising from loss of the side chain with the additional extrusion of two hydrogen atoms in addition to the ions M − (side chain). In Fig. 2, spectra of **2** and **5** exhibit distributions centered at 301 and also 297 a.m.u., strongly suggesting that the corresponding sterols possess a 22:23 double bond. This deuterium transfer from the nucleus does not occur with a saturated side chain, and spectra of **4** and **6** do not exhibit it. A process of this type has been postulated by Wyllie and Djerassi (7) to explain the fragment centered at 297 a.m.u., whereas the fragment around 301 is a simple side chain elimination.

Δ^7-Ergostenol (**4**), chondrillasterol (**5**), and Δ^7-chondrillastenol (**6**) have been identified in the sterol fraction from *Scenedesmus obliquus* grown in light water (8). The molecular formulae of the three sterols correspond to those of deuterated sterols **4**, **5**, and **6**, respectively (Fig. 1). Chondrillasterol would be expected to exhibit a shorter retention time with SE-30 than Δ^7-chondrillastenol, as stigmasterol ($\Delta^{22,23}$ double bond) is eluted prior to β-sitosterol (saturated side chain) (9). A possible structure for sterol **2** is $\Delta^{7,22}$-ergostadiene-3β-ol, which possesses the appropriate molecular formula, M − (side chain + D_2) fragmentation, and is eluted faster than the C_{28}-monoene. As the two C_{29} sterols differ by a $\Delta^{22,23}$ double bond, an analogous difference between the C_{28} sterols would not be surprising.

The sterol fraction from *Scenedesmus obliquus* grown in light water was also analyzed by combined g.l.c.–m.s. The chromatogram resulting from the analysis of this fraction as the TMSi ethers is presented in Fig. 1.

The mixture of light sterols appears to be composed of six compounds. Components **2**, **4**, **5**, and **6** in the light sterol fraction were found, on the basis of combined g.l.c.–m.s. data, to correspond respectively to the four components of the heavy sterol fraction. The relative amounts of the sterols were estimated from the TMSi ether peak areas and are contained in Table 3.

The molecular ion *m/e* 396 found for component **1** from light water suggested that it was a C_{28} sterol with three double bonds. Comparison of the mass spectra for this compound and its TMSi ether with those of ergosterol (free and TMSi ether) demonstrated conclusively the equivalence of these two compounds.

Sterol **3** was found to exhibit a molecular ion of *m/e* 410, indicating it to be a C_{29} sterol with three double bonds. The low mass (up to *m/e* 250) portion of the spectrum for sterol **3** is virtually identical to that of ergosterol. At higher

Can. J. Chem. Downloaded from www.nrcresearchpress.com by 210.87.254.5 on 09/05/12
For personal use only.

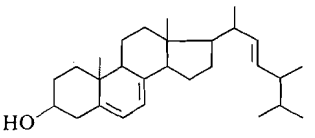

1
Ergosterol

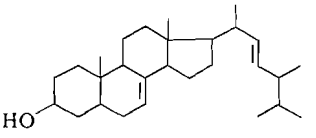

2
$\Delta^{7,22}$-Ergostadiene-3β-ol

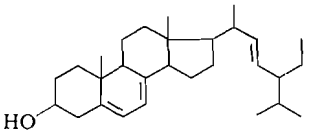

3
Corbisterol

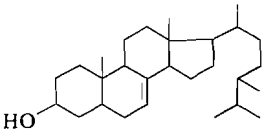

4
Δ^{7}-Ergosten-3β-ol

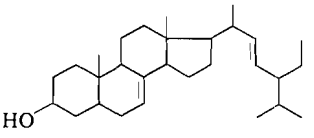

5
Chondrillasterol

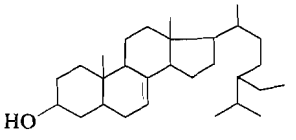

6
Δ^{7}-Chondrillastenol

TABLE 3. Composition of the sterol mixtures as TMSi ethers

Sterol	Light*		Heavy
1	11		
2	6	11	7
3	35		
4	23	43	36
5	13	24	32
6	12	22	25

*First column gives relative percent; second column gives relative percent for the four steroids in common.

masses the fragmentation pattern is also very similar to that of ergosterol, but with the signals increased by 14 a.m.u. *e.g.* *m/e* 395 and 381 (M − 15), *m/e* 392 and 378 (M − 18), *m/e* 377 and 363 (M − (15 + 18)), *m/e* 351 and 337 (M − 59); this last fragment is held by Brooks *et al.* (1, 6) to be characteristic of the ergosterol nucleus, requiring that the additional methyl group in sterol **3** be placed on the side chain.

A likely candidate for sterol **3** is thus corbisterol (10), both on the basis of its fragmentation pattern and also by analogy with the C_{28} series where the three sterols are well characterized.

The retention times for the light and perdeuterated sterols are presented in Table 1. It can be readily observed that the heavy sterols are eluted faster than the analogous light sterols. This isotope effect has been reported in a large number of cases (4, 11–13) and has been discussed by Saha and Sweeley (14). It is of greater magnitude and more easily detected when the molecules under study contain a large number of hydrogen atoms.

As both the light and heavy sterol fractions were obtained from the same type of algae, the absence of two sterols in the deuterium oxide derived sample is somewhat surprising. Several possibilities can account for this absence. This difference may be attributable to the occurrence of a mutation during the growth of the organism in heavy water. It has been shown in yeast (*Saccharomyces cerevisiae*) (15) that ergosterol is produced by successive dehydrogenation with insertion of the 5:6 double bond as the final step. A second explanation for the difference in composition may be the result of an isotope effect upon this key step. The most reasonable explanation, however, is that growth of the algae in deuterium oxide is conducive to the selection of

Can. J. Chem. Downloaded from www.nrcresearchpress.com by 210.87.254.5 on 09/05/12
For personal use only.

recessive cell types not capable of producing the third double bond.

Conclusion

The sterol fraction from *Scenedesmus obliquus* grown in heavy water has been shown by combined g.l.c.–m.s. to contain $\Delta^{7,22}$-ergostadiene-3β-ol, Δ^{7}-ergostenol, chondrillasterol, and Δ^{7}-chondrillastenol. The same algae grown in light water contain these four sterols and, in addition, ergosterol and corbisterol.

1. C. J. W. Brooks and B. S. Middleditch. *In* Modern methods of steroid analysis. *Edited by* E. Heftmann. Academic Press, New York. In press.
2. A. J. Williams, A. T. Morse, and R. S. Stuart. Can. J. Microbiol. **12**, 1167 (1966).
3. W. J. A. Vanden Heuvel, J. L. Smith, G. Albers-Schonberg, B. Plazonnet, and P. Bélanger. *In* Modern methods of steroid analysis. *Edited by* E. Heftmann. Academic Press, New York. In press.
4. G. Wendt and J. A. McCloskey. Biochemistry, **9**, 4854 (1970).
5. B. A. Knights. J. Gas Chromatogr. **5**, 273 (1967).
6. C. J. W. Brooks, E. C. Horning, and J. S. Young. Lipids, **3**, 391 (1968).
7. S. G. Wyllie and C. Djerassi. J. Org. Chem. **33**, 305 (1968).
8. G. W. Patterson. Lipids, **6**, 120 (1971).
9. E. C. Horning, C. J. W. Brooks, and W. J. A. Vanden Heuvel. *In* Advances in lipid research. Vol. 6. *Edited by* R. Paoletti and D. Kritchevsky. Academic Press, New York. 1968.
10. T. Tamura, K. Kokuma, and T. Matsumoto. Nippon Kagaku Zasshi, **77**, 987 (1956); C.A. **51**, 18357b.
11. J. G. Atkinson, A. A. Russell, and R. S. Stuart. Can. J. Chem. **45**, 1963 (1967).
12. W. J. A. Vanden Heuvel, J. L. Smith, and J. S. Cohen. J. Chromatogr. Sci. **8**, 567 (1970).
13. J. A. McCloskey, A. M. Lawson, and F. A. J. M. Leemans. Chem. Commun. 285 (1967).
14. N. C. Saha and C. C. Sweeley. Anal. Chem. **40**, 1628 (1968).
15. M. Fryberg, A. C. Oehlschlager, and A. M. Unrau. Biochem. Biophys. Res. Commun. **48**, 593 (1972).

Can. J. Chem. Downloaded from www.nrcresearchpress.com by 210.87.254.5 on 09/05/12
For personal use only.

Metabolites from a *Scytalidium* Species

JOHN A. FINDLAY AND DAVID KWAN

Department of Chemistry, University of New Brunswick, Fredericton, New Brunswick

Received April 11, 1973

The structure **1**, 3,6,8-trihydroxytetralone, proposed (1) earlier for scytalone is corroborated by synthesis of an aromatization product 1,3,8-trimethoxynaphthalene. A new minor metabolite of the same *Scytalidium* species is shown to be 4,8-dihydroxytetralone (**6**).

La structure **1**, trihydroxy-3,6,8 tétralone, qui a été proposée auparavant (1) pour la scytalone est corroborée par la synthèse d'un produit d'aromatisation soit le triméthoxy-1,3,8 naphtalène. On démontre qu'un nouveau métabolite mineur de la même espèce *Scytalidium* est la dihydroxy-4,8 tétralone, **6**. [Traduit par le journal]

Can. J. Chem., 51, 3299 (1973)

Recently we proposed (1) the structure **1**, 3,6,8-trihydroxytetralone, for a new metabolite isolated from culture filtrates which had supported growth of a species of *Scytalidium*. The juxtaposition of the oxygen substituents in **1** was deduced, in part, from its transformation into tri-oxygen substituted naphthalene derivatives whose substitution patterns were determined to be 1,3,8 by analysis of n.m.r. data. One of these derivatives, namely the triacetate **2***a* (m.p. 120–123°), has been reported by Stetter and Heidel (2) to have a melting point of 111°.[1] These authors prepared their material by acetylation of the product of dehydrogenation of 1,3,8-decalintrione. This discrepancy in physical characteristic prompted us to seek synthetic corroboration of our conclusions about the oxygen substitution pattern. Accordingly we have now transformed scytalone into 1,3,8-trimethoxynaphthalene in 76% yield by treatment with dimethylsulfate and potassium carbonate in anhydrous acetone and confirmed the structure of this aromatization product by independent synthesis.

Treatment of 3-bromopropionic acid with triphenylphosphine in boiling benzene provided the corresponding triphenylphosphonium salt from which the ylid **3** was generated and condensed with commercially available 3,5-dimethoxybenzaldehyde (**4**) to furnish 4-(3′,5′-dimethoxyphenyl)-3-butenoic acid (**5**) in 60% yield. Attempts to cyclize **5** to 8-hydroxy-1,3-dimethoxynaphthalene (**2***c*) under a variety of conditions gave poor yields and it was tentatively concluded that product **5** must be largely the *trans* isomer. Since in the n.m.r. spectrum of **5** the signals for the olefinic protons are superimposed on those arising from the aromatic protons it was not possible to make any firm conclusions about *cis–trans* isomer ratios. Conversion of the cyclization product **2***c* to 1,3,8-trimethoxynaphthalene was accomplished using the same reagents employed for the trimethylation of scytalone. The product **2***b* proved to be identical in all respects with the scytalone aromatization product.

It should be noted that attempts to bring

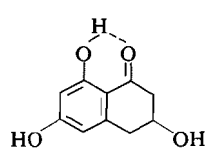

1

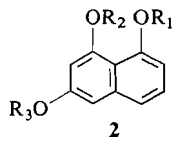

2

a $R_1, R_2, R_3 = COCH_3$
b $R_1, R_2, R_3 = CH_3$
c $R_1 = H; R_2, R_3 = CH_3$

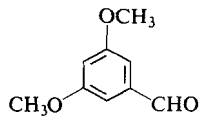

4

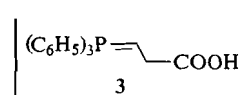

3

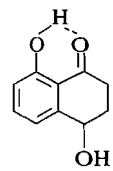

6

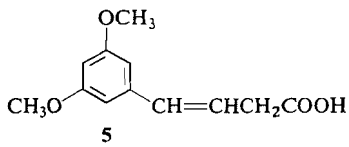

5

[1]A sample (m.p. 111°) supplied later by Dr. H. Stetter proved to be non-identical with our material and appeared to be 6,8-diacetoxytetralone from spectral data.

Can. J. Chem. Downloaded from www.nrcresearchpress.com by 210.87.254.105 on 09/05/12
For personal use only.

Can. J. Chem. Downloaded from www.nrcresearchpress.com by 210.87.254.105 on 09/05/12
For personal use only.

about a substantial degree of isomerization or possible migration of the double bond in **5** by treatment with strong base were ineffective.

From the same culture filtrates which afforded scytalone we have now isolated a minor metabolite whose structure **6**, 4,8-dihydroxytetralone, was tentatively assigned on the basis of spectroscopic data and confirmed by synthesis of its racemate from juglone. The mass spectrum of this new metabolite shows a molecular ion *m/e* 178 ($C_{10}H_{10}O_3$) and a base peak at *m/e* 160 ($M^+ - H_2O$). As in the case of scytalone the presence of an orthohydroxyphenone system is indicated by the u.v. spectrum chromophore (3) and supported by i.r. data. The n.m.r. spectrum ($CDCl_3$) shows a one-proton singlet at δ 12.4 p.p.m. typical of a bonded hydroxyl proton of such orthohydroxyphenone systems (1) while the presence of a 1,2,3-trisubstituted aromatic ring is apparent from the three single proton signals centered at δ 6.9, 7.0, and 7.5 p.p.m. whose mutual couplings (*vide infra*) can only be interpreted in terms of an aromatic AMX system (4). A one-proton triplet at δ 5.9 (J = 5 Hz) is assigned to the C-4 hydrogen of **6** while a pair of two-proton multiplets centered at δ 2.2 and 2.7 p.p.m. are accounted for by the C-3 and -2 methylenes, respectively. The remaining hydroxyl proton gives rise to a broad signal centered at δ 1.9 p.p.m. Thus the features of the n.m.r. spectrum are adequately explained in terms of structure **6**.

To confirm this conclusion racemic 4,8-dihydroxytetralone was prepared by reduction of β-hydrojuglone obtained from juglone (5). The n.m.r., u.v., and solution ($CHCl_3$) i.r. spectra are identical with those recorded from the new metabolite. Minor differences in the solid state (KBr) i.r. spectra and melting point characteristics indicate that the material from the natural source occurs in optically active form. Insufficient material was available to make optical rotation measurements.

In contrast to syctalidin (6) neither scytalone nor 4,8-dihydroxytetralone proved to have significant antifungal activity against selected test organisms.

Experimental

The i.r. spectra were recorded on a Perkin-Elmer model 237B instrument. Mass spectra were obtained with an Hitachi Perkin-Elmer RMU-6D spectrometer. The u.v. spectra were determined on a Perkin-Elmer model 467 spectrophotometer. N.m.r. spectra were recorded with a Varian T-60 instrument employing tetramethylsilane as internal standard. A Kofler hot stage apparatus was employed to determine melting points which are uncorrected.

Methylation of Scytalone (1)

A mixture of scytalone (**1**) (27 mg), dimethylsulfate (0.5 ml), and anhydrous potassium carbonate (0.96 g) in dry acetone (8 ml) was refluxed for 36 h. Evaporation of acetone, dilution with water, and extraction with chloroform afforded a brown oil which was purified by preparative t.l.c. to furnish a yellowish crystalline product (20 mg, 76%): m.p. 74–76°; ν_{max} (KBr) 2930, 2830, 1620, 1580, 1450, 1410, 1385, 1350, 1290, 1250, 1215, 1200, 1155, 1125, 1100, 1040, 995, 940, 960, 845, 795, 745, 725 cm^{-1}; δ ($CDCl_3$) 3.9 (3H, s), 3.95 (6H, s), 6.4–6.8 (4H, complex multiplet), 7.2–7.4 (1H, m); λ_{max} (95% C_2H_5OH) 235, 285, 296, 320, 335 (log ε 4.69, 3.73, 3.73, 3.4, 3.6) nm; *m/e* 218 (M^+, $C_{13}H_{14}O_3$, 100%), 203 ($M - CH_3$), 189, 175, 160, 145, 130, 115.

3-Triphenylphosphonium Propanoic Acid Bromide

A mixture of triphenylphosphine (28.8 g), 3-bromopropanoic acid (15.3 g), and dry benzene (50 ml) was refluxed for 18 h. The benzene layer was decanted and the yellow oily residue was triturated with acetone affording 3-triphenylphosphonium propanoic acid bromide (33.1 g, 80%) as white crystals: m.p. 196–197°; ν_{max} ($CHCl_3$) 3100 (broad), 2940, 1740, 1590, 1480, 1440, 1385, 1320, 1110, 1000 cm^{-1}; δ ($CDCl_3$) 2.96 (2H, m), 3.8 (2H, m), 7.8 (15 H, bd) p.p.m.

4-(3′,5′-Dimethoxyphenyl)-3-butenoic Acid (5)

A mixture of 3,5-dimethoxybenzaldehyde (8.3 g) and 3-triphenylphosphonium propanoic acid bromide (20.8 g) in dimethylsulfoxide and tetrahydrofuran (50 ml each) was dropped slowly into a flask containing sodium hydride (2.4 g) at 0° under nitrogen. The mixture was stirred overnight at room temperature and then water was added and the solution washed three times with ether. The aqueous layer was acidified with dilute hydrochloric acid and extracted with three portions of ether. After washing with water and drying ($MgSO_4$) the ether was evaporated yielding a brown viscous oil (11.9 g) which was chromatographed on a silica gel column. From ether eluates the white solid (6.7 g, 60%) was recovered and recrystallized from benzene–*n*-hexane yielding compound **5**: m.p. 56–64°; ν_{max} ($CHCl_3$) 3060 (broad), 2940, 2820, 1720, 1590, 1460, 1280, 1150 cm^{-1}; δ ($CDCl_3$) 3.25 (2H, d, J = 5 Hz), 3.75 (6H, s), 6.5 (5H, m) and 11.4 (1H, s) p.p.m.; λ_{max} (95% C_2H_5OH) 227, 260, 298 (log ε 4.58, 4.35, 3.78) nm; M (mass spectrometry) 222.

6,8-Dimethoxy-1-naphthol (2c)

A mixture of 4-(3′,5′-dimethoxyphenyl)-3-butenoic acid (**5**) (0.44 g) and polyphosphoric acid (22 g) was stirred at 90–100° for 4 h. The resulting black viscous liquid was dissolved in ice cold water and extracted with chloroform. Evaporation of the chloroform layer afforded a brown paste (0.38 g) which was subjected to preparative t.l.c. White crystalline solid **5** (0.028 g, 7%) m.p. 57–63° was thus recovered: ν_{max} (KBr) 3360 (broad), 2920, 1610, 1590, 1450, 1430, 1405, 1370, 1320, 1240, 1195, 1160, 1125, 1070, 1060, 1025, 980, 935, 830, 815, 750, 710 cm^{-1}; δ ($CDCl_3$) 3.9 (3H, s), 4.0 (3H, s), 6.45 (1H, d, J = 2 Hz),

6.6–6.8 (2H, m), 7.2–7.5 (2H, m), 9.1 (1H, s) p.p.m.; λ_{max} (95% C_2H_5OH) 232, 288, 300, 323, 337.5 (log ε 4.38, 3.55, 3.55, 3.36, 3.38); *m/e* 204 ($C_{12}H_{12}O_3^+$, 100%), 189 ($M^+ - CH_3$), 175, 161.

1,3,8-Trimethoxynaphthalene (2b) from 6,8-Dimethoxy-1-naphthol (2c)

A mixture of 6,8-dimethoxy-1-naphthol (**2***c*) (30 mg), dimethylsulfate (0.5 ml), and anhydrous potassium carbonate (0.96 g) in dry acetone (8 ml) was refluxed for 16 h. Evaporation of acetone, dilution with water, and chloroform extraction afforded a brown oil (0.45 mg) which was purified by preparative t.l.c. giving crystalline 1,3,8-trimethoxynaphthalene (**2***b*) (28 mg, 92%), m.p. 74–76° identical in spectroscopic characteristics with material obtained from scytalone (**1**) and giving no melting point depression on admixture.

Isolation of 4,8-Dihydroxytetralone from Scytalidium FY Strain Culture Medium

The crude chloroform extract (0.55 g) from the culture filtrate medium which had supported growth of *Scytalidium* FY strain (2) was chromatographed on a silica gel column. The ether–benzene (1.4) eluates were combined, evaporated, and rechromatographed on a preparative t.l.c. silica gel plate developed with acetone–benzene 1:4. The metabolite (R_f 0.46) showed green phosphorescence under long u.v. light and was recovered as a yellowish white solid (12 mg) and recrystallized from *n*-hexane to furnish crystals: m.p. 70–72°; ν_{max} ($CHCl_3$) 3600, 2925, 1640, 1580, 1450, 1365, 1335, 1260, 1100, 985, 930, 890 cm^{-1}; ν_{max} (KBr) 3320, 2920, 2850, 1630, 1615, 1570, 1450, 1405, 1365, 1336, 1325, 1308, 1260, 1216, 1200, 1160, 1100, 1075, 1065, 1046, 1030, 973, 890, 845, 820, 806, 770, 746, 703, 615 cm^{-1}; λ_{max} (95% C_2H_5OH) 220, 260, 332 (log ε 4.1, 3.8, 3.5); λ_{max} (95% C_2H_5OH + OH^-) 223, 230, 263, 372 (log ε 4.2, 4.1, 3.7, 3.7); *m/e* 178 (M^+, $C_{10}H_{10}O_3$), 160 ($M - H_2O$), 150 (100%, $M - C_2H_4$); δ ($CDCl_3$) 1.9 (1H, broad, exchanges with D_2O), 2.2 (2H, m), 2.75 (2H, m), 5.9 (1H, t, J = 5 Hz), 6.9 (1H, dd, J = 8 Hz, J = 1 Hz), 7.0 (1H, bd, J = 8 Hz), 7.5 (1H, t, J = 8 Hz), 12.4 (1H, s, exchanges with D_2O) p.p.m.

Reduction of β-Hydrojuglone to 4,8-Dihydroxytetralone

A solution of β-hydrojuglone (5) (0.55 g) in dry tetrahydrofuran (10 ml) was dropped slowly into a flask containing lithium aluminum hydride (38 mg) in dry tetrahydrofuran (10 ml) immersed in a Dry Ice – acetone bath. The mixture was stirred for 7 h at −40°. Water was added and the aqueous suspension treated with dilute hydrochloric acid and extracted with ether until the aqueous layer remained clear. The green ethereal extract was washed with water, dried ($MgSO_4$), and evaporated. Purification of the crude product by preparative t.l.c. gave yellowish white crystalline **6** (0.25 g, 38%): m.p. 99–100°; ν_{max} (KBr) 3270, 2980, 2870, 1630, 1610, 1570, 1450, 1410, 1360, 1345, 1330, 1310, 1290, 1250, 1215, 1200, 1160, 1095, 1075, 1045, 1030, 982, 925, 895, 845, 815, 780, 746, 705, 610 cm^{-1}. Other spectral data are identical with those of material isolated from the natural source (*vide supra*).

The authors are grateful to Dr. G. M. Strunz, M. A. Stillwell, and M. Kakushima, Canadian Forestry Service, Fredericton, New Brunswick for providing material for this study. This work was supported in part by a grant from the National Research Council of Canada. The authors thank Dr. H. Stetter, Institut für Organische Chemie, Aachen, Germany for providing a sample for comparison purposes.

1. J. A. FINDLAY and D. KWAN. Can. J. Chem. **51**, 1617 (1973).
2. H. STETTER and H. HEIDEL. Chem. Ber. **99**, 2172 (1966).
3. R. A. MORTON and A. L. STUBBS. J. Chem. Soc. 1347 (1940).
4. M. ZANGER. Org. Mag. Res. **4**, 1 (1972).
5. Y. P. VOLKOV, M. N. KOLOSOV, V. G. KOROBKO, and M. M. SHEMYAKIN. Izv. Akad. Nauk SSSR, Ser. Khim. No. 3, 492 (1964).
6. G. M. STRUNZ, M. KAKUSHIMA, and M. A. STILLWELL. J. Chem. Soc. Perkin I, 2280 (1972).

Can. J. Chem. Downloaded from www.nrcresearchpress.com by 210.87.254.105 on 09/05/12
For personal use only.

Can. J. Chem. Downloaded from www.nrcresearchpress.com by 210.87.254.6 on 09/05/12
For personal use only.

Canadian Journal of Chemistry

Published by
THE NATIONAL RESEARCH COUNCIL OF CANADA

Journal canadien de chimie

Publié par
LE CONSEIL NATIONAL DE RECHERCHES DU CANADA

Volume 51 Number 20 October 15, 1973

Volume 51 numéro 20 15 octobre 1973

Singlet and Triplet States of Aminonitrenes: An *Ab Initio* Molecular Orbital Study[1]

N. C. BAIRD AND R. F. BARR[2]

Photochemistry Unit, Department of Chemistry, University of Western Ontario, London, Ontario

Received April 13, 1973

Ab initio STO-3G molecular orbital calculations are reported for the lowest singlet and the lowest triplet state of the aminonitrenes H_2NN, $CH_3(H)NN$, F(H)NN, and HCO(H)NN. The optimum geometry calculated for the H_2NN triplet is nonplanar (C_s symmetry), with N—N and N—H bond distances of 1.436 and 1.034 Å, and HNN and HNH angles both of 107.5°. The optimum singlet is predicted to be planar (C_{2v} symmetry), with N—N and N—H distances of 1.276 and 1.041 Å respectively, and an HNN angle of 124°. An analysis of the calculated geometries and electron density distributions indicates that the "idealized" representations **3** and **5** are adequate to explain the bonding in the triplet and singlet respectively. The effects of methyl, fluoro, and carbonyl substitution upon the singlet–triplet splitting and upon the charge distribution are discussed. The optimum-geometry triplet is predicted to be slightly more stable than the optimum-geometry singlet in all cases.

On présente les calculs d'orbitales moléculaires, *ab initio* STO-3G, pour l'état singulet de plus basse énergie et pour l'état triplet de plus basse énergie des aminonitrènes H_2NN, $CH_3(H)NN$, F(H)NN et HCO(H)NN. La géométrie optimum calculée pour le triplet du H_2NN est non planaire (symétrie C_s), avec des longueurs de liaison N—N et N—H égales à 1.436 et 1.034 Å et avec des angles HNN et HNH égaux tous les deux à 107.5°. On prédit que la géométrie optimum du singulet est planaire (symétrie C_{2v}) avec des longueurs de liaison N—N et N—H égales à 1.276 et 1.041 Å et avec un angle HNN égal à 124°. Une analyse des géométries calculées ainsi que des ditributions de densité électronique a montré que les représentations "idéalisées" **3** et **5** sont suffisantes pour expliquer les liaisons dans l'état triplet et dans l'état singulet respectivement. On discute des effets de la substitution par les groupes méthyle, fluoro et carbonyle sur la séparation singulet–triplet et sur la distribution des charges. On prédit que, dans tous les cas, la géométrie optimum de l'état triplet sera légèrement plus stable que la géométrie optimum de l'état singulet. [Traduit par le journal]

Can. J. Chem., 51, 3303 (1973)

Introduction

The chemistry of aminonitrenes (1,1-diazenes) has received some attention recently (1), due to the synthetic utility of these species in the preparation of aziridines. A considerable amount of information concerning the reactivity of the "nitrene nitrogen" has been collected by Rees and co-workers (2, see also ref. 3) via experiments using phthalimido nitrene **1** and related compounds. In particular, these compounds are found to add stereospecifically to olefins, and this addition occurs exclusively in a 1,2-manner even at low olefin concentrations.

Yields of the aziridine **2** are found to increase if olefins substituted by electron-withdrawing groups are employed. These observations have led to the conclusion that the reacting species is a singlet, and that this singlet corresponds to the ground state of aminonitrenes. In contrast, the

[1]Publication No. 87 of the Photochemistry Unit. Research supported by the National Research Council of Canada.

[2]Holder of NRCC Studentships, 1970–74.

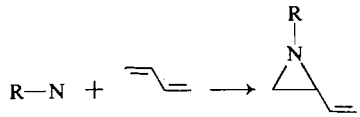

1 2

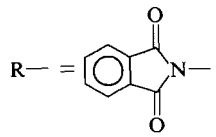

ground state of most other types of nitrenes (which, unlike aminonitrene, do not possess a substituent which can stabilize the singlet state by donation of a lone pair of π electrons) is known to be a triplet (1).

Unfortunately there exists, at present, very little information from either physical measurements or accurate quantum-mechanical calculations concerning the relative stabilities, geometries, and bonding of the low-lying states of either the (unknown) parent compound H_2NN or its derivatives. Although semiempirical calculations by the CNDO/2, (4 *cf.* ref. 1) and INDO (5) methods for H_2NN have been reported recently, their reliability in this context is questionable, especially since the singlet–triplet splitting predicted (5) of more than 1 a.u. (*i.e.* >630 kcal mol^{-1}) is obviously much too large. For these reasons, we have undertaken *ab initio* calculations for H_2NN and some of its simple derivatives in order to obtain a better estimate of the relative energies of the singlet and triplet states, to find the effect of substituents on this splitting, and to determine the optimum geometry for the parent molecule.

Method of Calculation

The wave functions and energies reported herein are the result of nonempirical ("*ab initio*") calculations using the SCF–LCAO–MO theories of Roothaan (6). For the triplet states, open shell theory was employed to determine the best single-configuration energy and wave function, while for the closed shell singlet, the best single-configuration wave function was impoved by including configuration interaction with the doubly excited state corresponding to a $(\pi)^2 \rightarrow (\pi^*)^2$ excitation.

A minimal basis set of Slater-type orbitals was employed to expand the molecular orbitals; the STO exponents used were the standard molecular values suggested by Pople and co-workers (7). All integrals over STO's were expanded in terms of integrals over Gaussian-type orbitals using the STO-3G technique of Pople and co-workers (7); integrals over GTO's were evaluated using subroutines from the IBMOL package.[3] All calculations were executed on the CDC Cyber 73 computer at the University of Western Ontario.

All orbital and electron densities and overlap populations were computed from single-determinant wave functions using the Mulliken population analysis scheme.

Results and Discussion

The Lowest Triplet State

Simultaneous optimization of the geometric variables for the lowest triplet state of H_2NN yields a *nonplanar*, almost tetrahedral, structure of C_s symmetry with a relatively long nitrogen–nitrogen bond:

$$R_{NN} = 1.43_6 \text{ Å} \qquad HNN = 107.5°$$
$$R_{NH} = 1.03_4 \text{ Å} \qquad HNH = 107.5°$$

The total energy of -108.5889 a.u. for this pyramidal shape is 7.6 kcal mol^{-1} more negative than for the optimum planar triplet (in which the N—N distance contracts to 1.40 Å); this inversion barrier should probably be regarded as an upper limit, given that Pople and co-workers have found that the NH_3 barrier is greatly overestimated using an STO-3G basis set (8). Both the quasi-tetrahedral shape and the Mulliken population analysis for triplet aminonitrene are consistent with the valence-bond representation

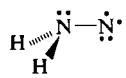

3

3. In particular, the unpaired spin is almost completely localized (96%) on the nitrene nitrogen atom, and the symmetry-allowed delocalization of the amino lone pair into the quasi-π $2p_z$ orbital of the nitrene nitrogen occurs only to the extent of 0.06*e*. Similarly, the population of 1.01*e* (Table 1) for the nitrene N $2p_y$ orbital is very close to the idealized value expected from **3**. Thus the nitrogen–nitrogen linkage in the triplet is almost exactly that of a single σ bond.

[3]The IBMOL program used was the modification by W. A. Saunders (Catholic University of America) of the original version by E. Clementi and D. R. Davis.

Can. J. Chem. Downloaded from www.nrcresearchpress.com by 210.87.254.6 on 09/05/12
For personal use only.

Can. J. Chem. Downloaded from www.nrcresearchpress.com by 210.87.254.6 on 09/05/12
For personal use only.

TABLE 1. Gross orbital populations for singlet and triplet H_2NN

Atom	Orbital[a]	Population (in *e*) Singlet	Triplet
N_{amino}	1s	1.995	1.996
	2s	1.441	1.591
	$2p_x$	1.639	1.629
	$2p_y$	1.114	1.068
	$2p_z$	1.092	1.066
	Total atomic	7.281	7.350
$N_{nitrene}$	1s	1.998	1.999
	2s	1.833	1.894
	$2p_x$	0.361	1.061
	$2p_y$	1.927	1.010
	$2p_z$	0.985	1.034
	Total atomic	7.104	6.998
H	1s	0.808	0.826

[a]The origin of the coordinate system was chosen at the amino nitrogen with the *z* axis coincident with the N—N bond, the *y* axis lying in the plane of the H_2N unit, and the *x* axis mutually perpendicular to *y* and *z*. The optimum molecular geometry for the state in question is used in both cases.

The Lowest Singlet State

The "idealized" distribution of the nonbonding and π electrons among atomic orbitals of planar aminonitrene is illustrated in Scheme 1. Since the triplet **4** correlates with the $^3(n,\pi^*)$ state of the isoelectronic molecule formaldehyde, and since the splitting between singlet and triplet (n,π^*) states in H_2CO is rather small (9), one might anticipate that the singlet state **5** in H_2NN would not lie far above the triplet. The *ab initio* calculations predict, however, that the splitting between **4** and **5** is rather large—approximately 46 and 48 kcal mol^{-1} for planar and pyramidal geometries, respectively, compared to ~13 kcal mol^{-1} calculated for H_2CO.[4] The difference between H_2NN and H_2CO is due to the fact that the "odd" π electron in H_2NN is localized heavily on the "nitrene nitrogen", and thus the nπ* exchange integral and the singlet–triplet splitting is rather substantial, whereas the corresponding odd π electron density in H_2CO is localized largely on the carbon atom, thus yielding a much smaller nπ* exchange integral and singlet–triplet split.

Thus, although the triplet **4** is predicted to correspond to the ground state of aminonitrene (*vide infra*), the most stable singlet is the closed-shell species **6** rather than the open-shell configuration **5**. Simultaneous optimization of all geometrical variables for the closed-shell configuration **6** yields a planar C_{2v} structure with a nitrogen–nitrogen bond length similar to the double-bond value of 1.25 Å predicted for diimide (10):

$$R_{NN} = 1.27_6 \text{ Å} \qquad HNN = 124°$$
$$R_{NH} = 1.04_1 \text{ Å}$$

These values are in good agreement with those in an earlier *ab initio* calculation for planar singlet H_2NN by Allen and co-workers (1.282 Å, 1.003 Å, 122° respectively) (11) and with the semiempirical CNDO/2 (4) and INDO (5) calculations. Both the short NN distance and the requirement for a planar geometry are indicative of a relatively strong coordinate π bond between the nitrogens, even though the transfer of charge from the amino lone pair to the vacant $2p_\pi$ orbital of the nitrene nitrogen amounts to only 0.36*e*. As discussed elsewhere (12), the existence of a strong coordinate π bond does *not* require near-equal sharing of the electron pair; thus, the 0.36*e* transfer here yields a π overlap population which is 73% of the maximum "covalent" value (*i.e.* the value which would be achieved if the electron pair was shared equally). The π bonding in singlet H_2NN is sufficient that the π bonding MO (predicted ionization potential 12.3 eV) is *not* the highest-occupied orbital but rather it is the second highest; the HOMO (predicted

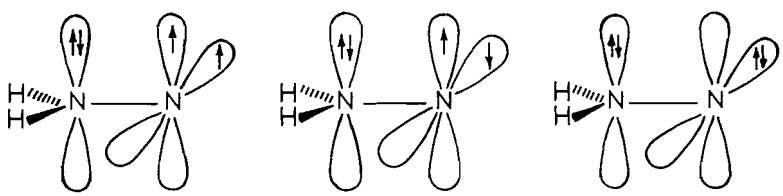

4 5 6

SCHEME 1

[4]N. C. Baird and R. F. Barr. Unpublished STO-3G calculations.

Can. J. Chem. Downloaded from www.nrcresearchpress.com by 210.87.254.6 on 09/05/12
For personal use only.

ionization potential 7.6 eV) corresponds to an in-plane orbital of *b* symmetry which is almost completely localized on the nitrene nitrogen. The energetic stability of this "nitrene lone pair orbital" is significantly lower than that in ammonia (predicted ionization potential 9.7 eV for NH_3).[4]

Overall, the polarity of the nitrogen–nitrogen multiple linkage agrees qualitatively with that anticipated from resonance between the two important valence-bond structures **7***a* and **7***b* for the singlet, since the transfer of π electron density from the amino to the nitrene nitrogen exceeds the back transfer of σ electron density in the opposite direction.

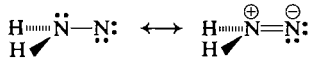

7a *7b*

The *overall* charge distribution (Fig. 1) is in *apparent* disagreement with this resonance since the amino nitrogen is more negatively charged than is the nitrene nitrogen; however the high electron density at the amino N is due primarily to the polarity of the N—H bonds.

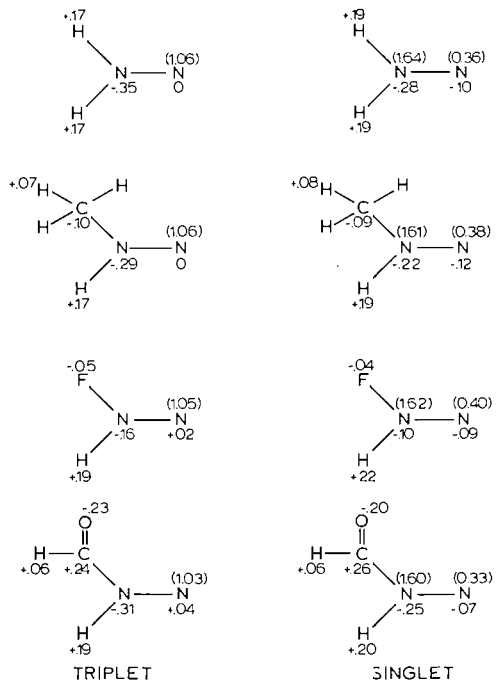

FIG. 1. Gross atom net charges (signed quantities) and selected gross π orbital populations (in parentheses) for the lowest triplet and singlet states of aminonitrenes. All quantities are in electron units.

Finally, it should be noted that the total energy of −108.5470 a.u. calculated for singlet aminonitrene corresponds to a structure which is some 36.4 kcal mol^{-1} *less* stable than for the isomeric *trans*-diimide (calculated using 2 × 2 CI with the same doubly excited configurations in both cases). In contrast, the lowest *triplet* state of H_2NN is predicted to be 46.2 kcal mol^{-1} more stable than is the lowest (twisted) triplet of diimide (10).

Aminonitrene Derivatives

Ab initio calculations for the monomethyl (**8**), monofluoro (**9**), and monocarbonyl (**10**) derivatives of aminonitrene were carried out for both singlet and triplet states. In all cases, nitrogen–nitrogen bond lengths and amino nitrogen bond angles which are optimum for H_2NN were assumed in the derivatives. All remaining distances and angles in **10** were assumed equal to the experimental values established for formamide (13).

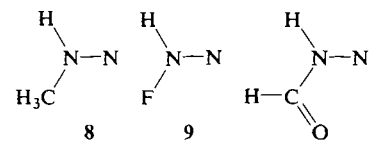

8 **9** **10**

The N—C and N—F distances of 1.47 and 1.37 Å respectively assumed in **8** and **9** were taken by analogy with $(CH_3)_3N$ and N_2F_4 (14); C—H distances of 1.089 Å and exactly tetrahedral HCH angles were assumed for the methyl group.

Gross atomic partial charges and selected gross π orbital populations for these derivatives are compared to those for the parent aminonitrene in Fig. 1. Note that the overall effect of each substituent considered, including methyl, is to withdraw electron density from the HNN framework relative to the values for singlet and triplet H_2NN.

The net charge of the nitrene nitrogen is approximately −0.1*e* in the parent aminonitrene singlet and in all the singlet derivatives considered. Although this amounts to less than half the negative charge predicted by semiempirical calculations, the conclusion by the authors of the latter calculations (4, 5) that the nitrene nitrogen should be nucleophilic is not altered. For both the methyl and carbonyl derivatives, the changes due to substitution in the net charges on the

TABLE 2. Calculated energies for aminonitrene triplets relative to the singlet at its optimum geometry

Geometry used for triplet	Relative energy (kcal mol^{-1})			
	H_2NN	$CH_3(H)NN$	F(H)NN	HCO(H)NN[a]
Optimum triplet geometry	−26.3	−25.7	−24.3	−28.6
Optimum singlet geometry	−5.3	−6.0	+3.3	−16.9

[a]The C=O and N=N bonds in HCO(H)NN are assumed to be *cis* with respect to each other.

nitrene nitrogen are almost entirely due to changes in the $2p_\pi$ orbital population (given in parentheses in the diagrams of Fig. 1), whereas both the σ and π orbital populations of the amino nitrogen are altered. The fluorine atom in **9** donates 0.02*e* to the NN π electron system, whereas the carbonyl group in **10** withdraws 0.07*e*; both effects agree qualitatively with intuitive expectations for such substituents. Note, however, that the sum of the π electron density associated with the two nitrogen atoms remains close to 2.0*e* in all cases.

The changes in the atomic charges due to substitution in the aminonitrene triplets closely parallel those established for the singlets. The total electron density at the amino nitrogen is about 0.07*e greater*, and that for the nitrene nitrogen is about 0.11*e less* in the triplet compared to the singlet in all cases. Note that the nitrene nitrogen is predicted to be electrically neutral in the parent compound.

Singlet–Triplet Splitting and the Ground State of Aminonitrenes

The calculated singlet–triplet splittings for each aminonitrene are listed in Table 2; all values are relative to the singlet in its optimum geometry. The calculated energy splittings are interesting in several respects. First, the singlet–triplet separation is quite low and is nowhere near the >600 kcal mol^{-1} estimate for H_2NN from INDO calculations (5). Second, the triplet at its optimum molecular geometry is predicted to be more stable than the optimum singlet, again in contrast to the semiempirical calculations. Note, however, that the separation is almost zero at the optimum singlet geometry. Third, the singlet–triplet splitting is relatively unaffected (within ±3 kcal mol^{-1} when optimum geometries are compared) by substitution.

Although we believe the present *ab initio* calculations on H_2NN to yield much more realistic energy separations than can be obtained from semiempirical calculations, previous experience with calculations of the S_0–T_1 splitting in CH_2 (15, 16) suggests that the values listed in Table 2 are somewhat too negative. In particular, the methylene triplet is predicted to be ~29 kcal mol^{-1} more stable than the singlet by STO-3G calculations using 2 × 2 CI for the singlet, whereas calculations using a much larger basis set and a much greater degree of configuration interaction lowers this value to ~12 kcal mol^{-1} (16), which agrees well with the most recent experimental determinations (17). Because CH_2 is isoelectronic with the parent nitrene NH, the "error" in the present calculations is probably in the same direction and of the same magnitude as for CH_2. One would anticipate that more refined calculations would predict that the optimum triplets for aminonitrenes are ~10 kcal mol^{-1} more stable than the optimum singlets, and that in most cases the singlet lies below the triplet *at the optimum singlet geometry*. Thus the observed chemical reactions of aminonitrenes, all of which have been interpreted as arising from a singlet ground state, may be explicable in terms of a singlet state which undergoes intersystem crossing very slowly to the ground state triplet; *i.e.* the initially formed aminonitrene becomes "trapped" in the singlet well. Obviously, more refined calculations are indicated to settle this important question.

1. (*a*) B. V. IOFFE and M. A. KUZNETSOV. Russ. Chem. Rev. **41**, 131 (1972); (*b*) W. LWOWSKI. Nitrenes. John Wiley, New York. 1970. Chapt. 10.
2. R. S. ATKINSON and C. W. REES. Chem Commun. 1230 (1967); D. J. ANDERSON, T. L. GILCHRIST, D. C. HORWELL, and C. W. REES. Chem Commun. 146 (1969); D. J. ANDERSON, T. L. GILCHRIST, and C. W. REES. Chem Commun. 147 (1969); R. S. ATKINSON and C. W. REES. J. Chem. Soc. (C), 772 (1969); D. J. ANDERSON, T. L. GILCHRIST, D. C. HORWELL, and C. W. REES. J. Chem Soc. (C), 576 (1970).

Can. J. Chem. Downloaded from www.nrcresearchpress.com by 210.87.254.6 on 09/05/12
For personal use only.

3. M. BAUDRU and A. FOUCAUD. C. R. **270**, 104 (1970).
4. V. YA. BESPALOV, L. A. KARTSOVA, V. I. BARANOVSKII, and B. V. IOFFE. Dokl. Akad. Nauk. SSSR, **200**, 99 (1971).
5. L. J. HAYES, F. P. BILLINGSLEY II, and C. TRINDLE. J. Org. Chem. **37**, 3924 (1972).
6. C. C. J. ROOTHAAN. Rev. Mod. Phys. **23**, 69 (1951); **32**, 179 (1960).
7. W. J. HEHRE, R. F. STEWART, and J. A. POPLE. J. Chem. Phys. **51**, 2657 (1969).
8. W. A. LATHAN, W. J. HEHRE, L. A. CURTISS, and J. A. POPLE J. Am. Chem. Soc. **93**, 6377 (1971).
9. G. HERZBERG. Molecular spectra and molecular structure. Vol. III. Van Nostrand, Princeton, N.J. 1967. p. 612.
10. N. C. BAIRD and J. R. SWENSON. Can. J. Chem. In press.
11. D. PAN WONG, W. H. FINK, and L. C. ALLEN. J. Chem. Phys. **52**, 6291 (1970).
12. N. C. BAIRD and R. K. DATTA. Inorg. Chem. **11**, 17 (1972).
13. C. C. COSTAIN and J. M. DOWLING. J. Chem. Phys. **32**, 158 (1960).
14. L. E. SUTTON, *editor*. Tables of interatomic distances and configurations in molecules and ions. Special Publications 11 and 18. The Chemical Society, London. 1959 and 1965.
15. H. F. SCHAEFFER III. The electronic structure of atoms and molecules. Addison–Wesley. 1972. p. 309–316.
16. C. F. BENDER, H. F. SCHAEFFER III, D. R. FRANCESCHETTI, and L. C. ALLEN. J. Am. Chem. Soc. **94**, 6888 (1972).
17. H. M. FREY. J. Chem. Soc. Chem. Commun. 1024 (1972).

Can. J. Chem. Downloaded from www.nrcresearchpress.com by 210.87.254.6 on 09/05/12
For personal use only.

The Effect of Refractive Index of the Medium on the Position of the Camera Lens in Schlieren Optics

L. Ivan Epstein and Percival Nixon

Department of Biophysics, Medical College of Virginia, Health Sciences Division, Virginia Commonwealth University, Richmond, Virginia 23219

AND

Alfred J. Richard

Department of Chemistry and Pharmaceutical Chemistry, Medical College of Virginia, Health Sciences Division, Virginia Commonwealth University, Richmond, Virginia 23219

Received April 9, 1973

A linear relation has been established between the plane of focus for schlieren optics in the ultracentrifuge cell along the optic axis, and the refractive index of the liquid contained in the cell. Such a relation shows that there occurs a defocussing effect when a large change in refractive index is generated in the liquid column during centrifugation of multi-component systems.

Une relation linéaire est établie entre le niveau focale pour les optiques schlieren dans la cellule de l'ultracentrifugeuse le long de l'axe optique, et de l'indice de réfraction du liquide contenue dans la cellule. Une telle relation montre qu'il existe un effet sur les optiques si l'indice de réfraction change beaucoup durant la centrifugation des liquides avec de plusieurs composants.

Can. J. Chem., **51**, 3309 (1973)

Introduction

The need has become apparent for focussing of the camera lens of schlieren and interferometric optical systems of the analytical ultracentrifuge on different levels of the centrifuge cell along the optic axis (1–6). For macromolecular solutions, the 1/2 plane, the 2/3 plane, even the 5/6 plane have been recommended, depending upon experimental conditions. Richards *et al.* (1) mentioned the need for refocussing every time a solvent of different refractive index was used. The method for focussing on any chosen plane in the cell was given clearly and in great detail. The authors showed a linear relation between the position of the camera lens of their ultracentrifuge and the position in the rotor of the ruled disk upon which the lens was focussed. The position of the ruled disk was varied by spacers placed beneath it in the rotor. This paper suggests a simple relation for choosing the plane of focus when the centrifuge cell is filled with pure liquids, rather than with solutions.

Measurements of the isothermal compressibilities of organic liquids by ultracentrifugation in the Beckman Model E ultracentrifuge have thus far been done with the camera lens of the schlieren optical system presumably focussed at the mid plane of the cell (7–9). When the calculations of Richards *et al.* (1) were applied to centrifuge cells filled with organic liquids, it was found that the camera lenses had, in fact, been focussed on various planes within the cell, depending upon the refractive indexes of the liquids studied. It would appear, however, that all compressibility experiments should be performed with the camera lens focussed on a level of the cell along the optic axis such that the emerging ray would be recorded on the photograph at its entrance coordinate along the centrifugal axis. The optic and centrifugal axes are at 90° to each other.

Experimental

As an aid in focussing the camera lens on any level in the cell, a simple device was fabricated to hold the ruled quartz disk in the rotor. The new disk holder had the same exterior dimensions as a centrifuge cell housing, but with an interior thread (40/in) which allowed a threaded, o-shaped, cap to be driven down the entire length of the holder. A 2 mm wide slot was cut in the side of the holder, leaving 3 mm of metal at each end for strength. The disk was placed upon the cap, its position accurately measured through the slot, on a microcomparator, and the unit then placed in the rotor for the focussing procedure. A tool of this nature should be of some usefulness if refocussing were at least necessary for every change of drive in the ultracentrifuge (1).

Can. J. Chem. Downloaded from www.nrcresearchpress.com by 210.87.254.5 on 09/05/12
For personal use only.

Can. J. Chem. Downloaded from www.nrcresearchpress.com by 210.87.254.5 on 09/05/12
For personal use only.

Results

The level of choice for focussing in the cell filled with pure liquids was determined by the method of Wiener (10) which states that if the velocity of light (v) is a linearly decreasing function of distance (r) from the center of rotation, then the path of the light ray in the cell would be an arc of a circle whose center is located on r at that point where $v = 0$. Therefore, since $v = c/n$

$$[1] \qquad dv/dr = \text{constant} = \frac{d(c/n)}{dr} = -(c/n^2)(dn/dr)$$

where c is the speed of light in a vacuum and n is the refractive index of the medium. After integration of

$$[2] \qquad \int_{v_m}^{v=0} dv = (\text{constant}) \int_{r_m}^{r_{v=0}} dr$$

and substitution for the constant and for v_m, it follows that

$$[3] \qquad r_{v=0} = r_m + \frac{n_m}{(dn/dr)_m}$$

where the subscript m refers to the entrance plane of the light into the cell. Next, as illustrated in Fig. 1, the arc of a circle of radius $(r_{v=0} - r_m)$ was drawn across the thickness of the cell with center at the point $r_{v=0}$. The cell thickness was 1.2 cm. A chord equal to twice the cell thickness would give

$$[4] \quad \text{chord} = (2)(1.2) = 2(r_{v=0} - r_m)\sin a$$

where by geometry it can be shown that a is the angle of incidence of the light ray at the side of energence of the cell. Snell's law gave the exit angle a',

$$[5] \qquad \sin a'/\sin a = n/n'$$

where $n' = 1$ (refractive index in the vacuum chamber) and n was the refractive index of the medium, assumed equal to the refractive index at the entrance plane of the light.

Reference to Fig. 1 shows that (1.2) (tan $a/2$) gave the depth (dr) below the entrance plane, at which the light ray emerged from the cell. Similarly, (1.2) (tan a') gave the height (dr') above the exit depth at which the back extrapolation of the exit ray struck the back of the cell. The point where the back extrapolated line crossed the entrance plane of the light determined

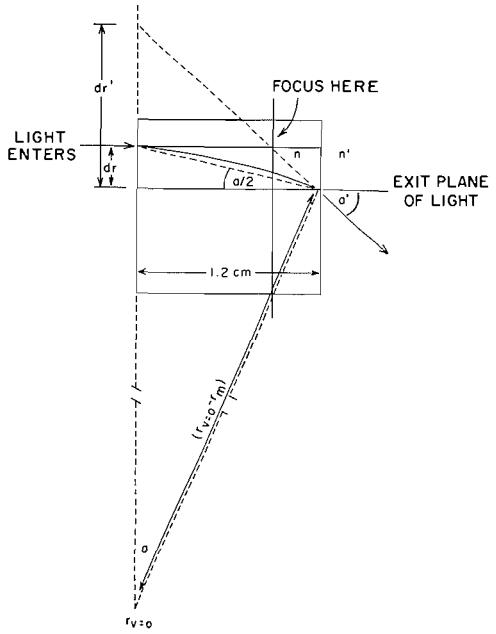

FIG. 1. Curved path (solid line) followed by light passing through a centrifuge cell. The values of dr and of dr' are greatly exaggerated for the purpose of illustration. The camera lens should be focussed on that plane in the cell where the back extrapolated line crosses the entrance plane of the light.

the plane (along the optic axis) upon which the camera lens was focussed. It was then possible to determine the exact position of the camera and cylinder lenses as described by Richards *et al.* (1). In Fig. 2, the back extrapolated lines are shown for benzene at two speeds of the centrifuge, two temperatures at each speed, and at two values of r_m. For the meniscus (r_m was arbitrarily set at 6.0 cm) the refractive index and density data for benzene at 20 °C and 1 atm were available (11, 13), but $(dn/dr)_m$ was calculated from the equation of Dayantis (7, 8).

$$[6] \qquad dn/dr = \frac{\beta(n^2 + 2)(n^2 - 1)\rho w^2 r}{6n}$$

where β was the isothermal compressibility of the medium in bars^{-1}; w was the angular velocity; ρ was the density of the medium. For benzene, the compressibility data of Holder and Whalley (12) was used. When an entrance plane for the light was chosen somewhere below the meniscus, for instance, at 7.0 cm, the pressure dependence of the refractive index, of the density, of the refractive index gradient, and of the isothermal

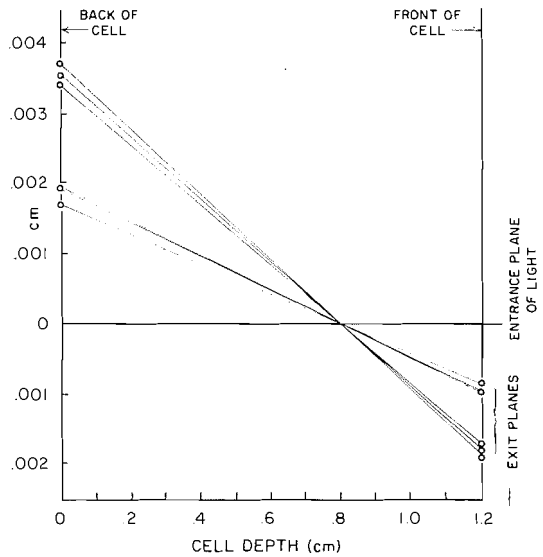

FIG. 2. Back extrapolated lines for benzene. Beginning with the upper line on the left the conditions are: 33 450 r.p.m., 20 °C, entrance plane 7.0 cm; 33 450 r.p.m., 25 °C, entrance plane 6.0 cm; 33 450 r.p.m., 20 °C, entrance plane 6.0 cm; 23 150 r.p.m., 25 °C, entrance plane 7.0 cm; 23 150 r.p.m., 25 °C, entrance plane 6.0 cm; 23 150 r.p.m., 20 °C, entrance plane 6.0 cm. All lines cross the entrance plane of light at 0.8 cm, or the 2/3 level of the cell.

compressibility of benzene had to be considered (8) before introduction of these terms into the equation of Dayantis. In the region up to about 200 bars, normally encountered in the centrifuge (15) plots of the data of Waxler *et al.* (13) showed that for benzene at several temperatures and wavelengths, $dn/dp \cong 5 \times 10^{-5}$ refractive index units per bar; from which the refractive index of benzene could be approximated at the pressures found in the centrifuge cell. Specific volumes were also given by Waxler *et al.* for benzene at several pressures and temperatures. The pressure dependency of the isothermal compressibility of benzene was given by Holder and Whalley (12) at several temperatures, and was extrapolated to 20 °C. The six lines of Fig. 2 cross the entrance plane at a common point, 0.8 cm from the back of the cell. Similar graphs were obtained for water (14) and for carbon tetrachloride (12). Again each of these compounds had a single crossing point, whose position, however, was determined by the refractive index of the compound at 1 atm, 20 °C, and 5461 Å.

Figure 3 shows the plane of focus for 6 liquids measured from the back of the 1.2 cm centrifuge cell, for 20 °C and utilizing the refractive index at the green line of mercury, 5461 Å. Least squares analysis gave the relation

$$[7] \qquad y(\text{cm}) = 0.243\, n_{5461}{}^{20^\circ} + 0.436 \qquad r = 0.997$$

The regression coefficient (r) measures the fit of experimental points to the equation. A value of 1.00 for r would indicate a perfect fit. With the refractive index at 25°, similar analysis would result in the expression

$$[8] \qquad y(\text{cm}) = 0.2726\, n_{5461}{}^{25^\circ} + 0.3914 \qquad r = 0.999$$

It should be noted that eqs. 7 and 8 apply only for cells of 1.2 cm thickness. The focal plane in a 3.0 cm cell is readily obtained for any liquid by the ratio

$$[9] \qquad y_{3.0\text{ cm}} = (y_{1.2\text{ cm}})\,(3.0/1.2)$$

Similar relations may be written to calculate the focal plane in cells of any thickness.

Discussion

In this laboratory (9), with the camera lens presumably focussed on the middle of a cell with sapphire windows, isothermal compressibilities were obtained at 1 atm and 20 °C from meniscus readings of dn/dr on schlieren patterns at 23 150

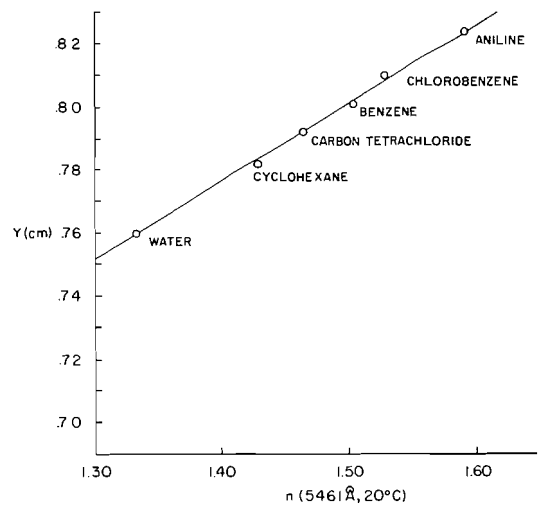

FIG. 3. Focal plane distance (cm) from the back of the cell, plotted against the refractive index of the liquid contained in the cell. Refractive index measured at 20 °C and 5451 Å.

Can. J. Chem. Downloaded from www.nrcresearchpress.com by 210.87.254.5 on 09/05/12
For personal use only.

r.p.m. for seven liquids, in good agreement with published values obtained by different methods (12). When an attempt was made to study the pressure dependence of isothermal compressibilities, by taking schlieren pictures at several rotor speeds, and measuring dn/dr along the liquid column (8) it was observed that the meniscus values of compressibility for all the liquids studied dropped 4 to 5% as the rotor speed increased up to 39 000 r.p.m. Since it was assumed that the pressure at the meniscus remained at 1 atm regardless of rotor speed, the compressibilities should have stayed constant. This effect was presumably due to the errors described by Wiener (10) at high values of dn/dr. In fact, it was completely eliminated by correct focussing for each liquid according to eq. 7. Fortunately, as shown in Fig. 2, the plane of focus did not vary with rotor speed, temperature, or position along the centrifugal axis for pure liquids. It should be stressed, however, that such is not necessarily the case when multicomponent systems are centrifuged (1, 6). A fundamental assumption in this work is that the refractive index gradient be essentially constant from the top to the bottom of the cell. It is not possible to justify this assumption in solutions where the solute sediments appreciably, except perhaps in the plateau region, as was done by Dayantis (7, 16). With low molecular weight solutes, however, sedimentation may be negligible at rotor speeds that give measurable values of dn/dr, and thus the focal plane in the cell would be determined by the refractive index of the mixture at 1 atm.

1. E. G. RICHARDS, D. TELLER, and H. K. SCHACHMAN. Anal. Biochem. **41**, 189 (1971).
2. L. GROPPER. Anal. Biochem. **7**, 401 (1964).
3. F. E. LABAR and R. L. BALDWIN. J. Phys. Chem. **66**, 1952 (1962).
4. H. SVENSSON. Opt. Acta, **1**, 25 (1954).
5. H. SVENSSON. Opt. Acta. **3**, 164 (1956).
6. D. A. YPHANTIS. Biochem. **3**, 297 (1964).
7. J. DAYANTIS. C. R. Acad. Sci. Paris Ser. C, **267**, 223 (1968).
8. A. J. RICHARD, J. GLICK, and R. BURKAT. Anal. Biochem. **37**, 378 (1970).
9. A. J. RICHARD and K. S. ROGERS. Can. J. Chem. **49**, 3956 (1971).
10. O. WIENER. Ann. Phys. Chem. **49**, 105 (1893).
11. E. W. WASHBURN. *Editor*. International critical tables. McGraw-Hill Co., Inc. New York. 1962.
12. G. A. HOLDER and E. WHALLEY. Trans. Faraday Soc. **58**, 2095 (1962).
13. R. M. WAXLER, C. E. WEIR, and H. W. SCHAMP. J. Res. Nat. Bur. Std. **68A**, 489 (1964).
14. R. VEDAM and G. HOLTON. J. Acoust. Soc. Am. **43**, 108 (1968).
15. T. SVEDBERG and K. O. PEDERSEN. The ultracentrifuge. Clarendon Press, Oxford. 1940. p. 267.
16. J. DAYANTIS, C. REISS, and H. BENOIT. Makromol. Chem. **120**, 113 (1968).

Can. J. Chem. Downloaded from www.nrcresearchpress.com by 210.87.254.5 on 09/05/12
For personal use only.

Pyrolyses and Mass Spectra of 2-Benzoxazolinone, 2-Benzimidazolinone, and 2-Benzothiazolinone

MICHAEL L. THOMSON AND DON C. DEJONGH[1]

Department of Chemistry, University of Montreal, P.O. Box 6128, Montreal 101, Quebec

Received March 22, 1973

The electron-impact and chemical-ionization mass spectra of 2-benzoxazolinone (**5**), 2-benzimidazolinone (**6**), and 2-benzothiazolinone (**7**) have been compared with their pyrolysis products and parallels have been found. In each case, loss of CO occurs from M^+, followed by loss of CO for **5** and by HCN for **6** and **7**. At 950° in a stream of N_2, **5** gave 17% of C_5H_5N isomers, related to the loss of 2CO, along with 5.6% of quinoline. Compound **6** gave 14% of $C_6H_4N_2$ isomers, related to the loss of CO. At 950°, **7** gave 2-thiophenecarbonitrile (1.1%), cyanonaphthalenes (4.5%), aniline (3%), cyanobenzene (2.5%), naphthalene (1.5%), and phenylisocyanate (2.5%). From **5**–**7** 20–70% of the starting material was recovered or accounted for by isolation and identification of products in each case. G.c./m.s. was used to study pyrolysis mixtures.

On rapporte les spectres de masse de la benzoxazolinone-2 (**5**), de la benzimidazolinone-2 (**6**) et de la benzothiazolinone-2 (**7**), tels qu'obtenus par impact électronique et par ionisation chimique en utilisant l'isobutane. On compare ces spectres avec les produits de pyrolyse des composés **5**–**7**. Dans chaque cas, l'ion moléculaire élimine une molécule de CO. Pour les composés **6** et **7**, ce processus est suivi d'une élimination de HCN, alors que pour le composé **5**, il est suivi de la perte d'une deuxième molécule de CO. La pyrolyse du composé **5** à 950° dans un courant d'azote conduit à la formation de quinoline (5.6%) et d'isomères répondant à la formule C_5H_5N, ces derniers à la suite de l'élimination de deux molécules de CO. Parallèlement, le composé **6** donne des isomères répondant à la formule C_5H_5N, ces derniers à la suite de l'élimination de deux molécules de CO. Parallèlement, le composé **6** donne des isomères répondant à la formule $C_6H_4N_2$ par élimination d'une molécule de CO et d'une molécule de H_2. Les produits de la pyrolyse du composé **7** à 950° sont le thiophènecarbonitrile-2 (1.1%), les cyanonaphthalènes (4.5%), l'aniline (3%), le cyanobenzène (2.5%), le naphthalène (1.5%) et l'isocyanate de phényle (2.5%). Les produits formés ainsi que les produits originaux récupérés représentent de 20 à 70% des produits de départ. La combinaison de la chromatographie en phase gazeuse avec la spectrométrie de masse était employée pour étudier les mélanges obtenus des pyrolyses.

Can. J. Chem., **51**, 3313 (1973)

Introduction

We have compared the electron-impact (e.i.) and chemical-ionization (c.i.) mass spectra of 2-benzothiazolinethione (**1**), 2-benzimidazolinethione (**2**), and 2-benzoxazolinethione (**3**) with their pyrolysis products, and parallels have been found (1). The loss of S from the molecular ions

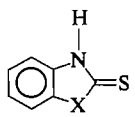

1 X = S
2 X = NH
3 X = O

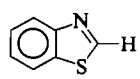

4

is the lowest energy fragmentation observed at low voltages. Also, the loss of S is the only fragmentation observed from their (M + H) ions in the chemical-ionization mass spectra. The loss of S is also observed upon pyrolysis. For example, 2-benzothiazolinethione (**1**) gives a 23% yield of benzothiazole (**4**) and a 13% yield of cyanobenzene at 800°. The formation of **4** can be accounted for by the loss of S from **1**; cyanobenzene forms by loss of S_2 from the 2-thione and by loss of S from **4**. This one-step loss of S_2 is also observed in the mass spectrum of **1**.

This study has now been extended to 2-benzoxazolinone (**5**), 2-benzimidazolinone (**6**), and 2-benzothiazolinone (**7**). U.v. and i.r. spectra indicate that **5** exists predominantly in the lactam form (2), so we will use this structure in the schemes even though we don't know the structure of the molecular ions. Likewise, i.r. spectra and dipole moments provide evidence for the presence of the keto structure of **6**, (3) and

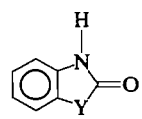

5 Y = O
6 Y = NH
7 Y = S

[1]To whom correspondence should be addressed at Case postale 6128, Montréal 101, Québec.

Can. J. Chem. Downloaded from www.nrcresearchpress.com by 210.87.254.105 on 09/05/12
For personal use only.

Can. J. Chem. Downloaded from www.nrcresearchpress.com by 210.87.254.105 on 09/05/12
For personal use only.

measured ^{14}N chemical shifts have shown that **7** exists exclusively in the thiazolinone form (4).

In each case, the 2-ones **5**–**7** have been pyrolyzed several times at a variety of temperatures. Their mass spectra have been obtained under conditions of electron impact (e.i.) at 70 and lower eV. Exact-mass measurements have been made in order to determine the elemental compositions of the ions. Also, the chemical ionization (c.i.) mass spectra have been obtained for comparison with the e.i. spectra and with the products of pyrolysis.

Millard and Temple have briefly described the e.i. mass spectrum of 2-benzothiazolinone (**7**) (5), and the e.i. mass spectrum of 2-benzoxazolinone (**5**) has been reported but not discussed (6). The 70 eV e.i. mass spectrum of 2-benzimidazolinone (**6**) is given in Fig. 1. Even though the mass spectrum of **6** has not been published, the e.i. mass spectra of 11 substituted 2-benzimidazolinones have been studied (7).

Our samples were pyrolyzed by sublimation into a stream of N_2 which passed through a hollow quartz tube surrounded by a 12 in. furnace (1,8). In general, a N_2 flow rate of 0.25 l/min and a system pressure of 2.5 Torr were used. Pyrolysis products have been identified by isolation and characterization. Combined gas chromatography – mass spectrometry (g.c.–m.s.) was also used.

Experimental

Melting points were determined by the open capillary method using a Mel-Temp apparatus and were corrected.

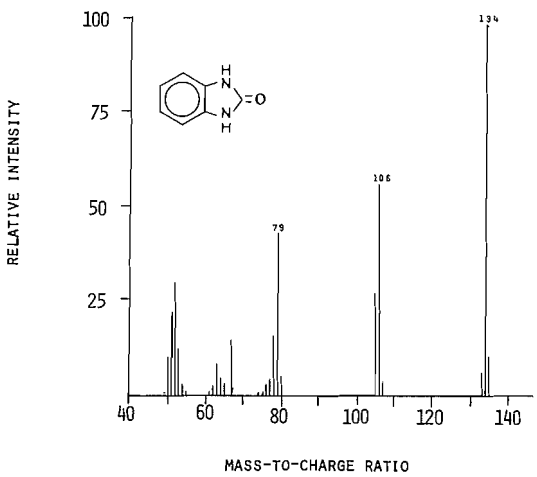

FIG. 1. The e.i. mass spectrum (70 eV) of 2-benzimidazolinone.

I.r. spectra were recorded with a Beckman IR8 and a Perkin-Elmer Infracord. N.m.r. spectra were taken on a Varian T-60 spectrometer using 1% TMS as an internal standard. U.v. spectra (1 cm path) were determined on a Bausch and Lomb Spectronic 505. Low resolution mass spectra were obtained from a Hitachi RMU-6D mass spectrometer. Electron voltage readings were taken directly from the dial since more precise values were not needed. Combined g.c.–m.s. data were determined with a LKB 9000 instrument.

Exact-mass data were obtained from an AEI MS 902 mass spectrometer linked to a PDP 8 computer. All experimental values agreed with the calculated values within ± 0.0015 mass units. The c.i. mass spectra were taken from a Dupont 21/491 mass spectrometer at a source temperature of 250° and a probe temperature of 80°, using isobutane.

The g.l.p.c. work was carried out using a Hewlett-Packard 5752B Research Chromatograph with a thermal conductivity detector. Columns were prepared with 0.25 in. copper tubing and 60/80 mesh Chromosorb W as a solid support, unless otherwise stated. A total of 13 columns was used; during the initial stages of analysis of the pyrolysis mixtures most of the columns were tried. However, only the column that gave the best separations is reported for each analysis. Comparison of the areas under the peaks of the pyrolysis products with the areas under the peaks of solutions of known concentrations of the same compound was used to determine yields.

Chemicals

2-Benzoxazolinone (**5**) was purchased from Eastman Organic Chemicals, m.p. 138–139° (lit. (9) m.p., 137–138°). 2-Benzimidazolinone (**6**) was obtained from Aldrich Chemical Co., m.p. 316–317° (lit. (10) m.p., 313–316°). Their purities were also checked by g.l.p.c., t.l.c., and mass spectrometry. 2-Cyanoaniline, 2-cyanopyridine, 3-cyanopyridine, and 4-cyanopyridine were also purchased from Aldrich. 1- and 2-cyanonaphthalene were purchased from Eastman.

2-Benzothiazolinone (7)

2-Benzothiazolinone (**7**) was prepared from 2-benzothiazolinethione (**1**) by the procedure of Efros and Davidenkov (11). Yield 6.5 g (36%), m.p. 136–137° (lit. (11) m.p. 136°), i.r. ($HCCl_3$) 3350 and 1675 cm^{-1}.

Anal. Calcd. for C_7H_5NOS: C, 55.63; H, 3.31. Found: C, 55.77; H, 3.40.

cis,cis-2,4-Hexadienedinitrile

A mixture of *o*-phenylenediamine (2.4 g, Aldrich), lead tetraacetate (27.9 g), and 130 ml of ether was stirred under N_2 for 3 h. The solution turned dark brown, was filtered and washed with aqueous $NaHCO_3$ until neutral, and then washed with water. The ether layer was dried ($MgSO_4$) and evaporated under vacuum. The brown residue was sublimed at 66°, 0.5 Torr, giving a white solid, m.p. 124–126° (lit. (12) m.p. 128–129°). G.l.p.c. traces and u.v. spectra showed no trace of the diamine.

Pyrolysis Apparatus and Procedure

The pyrolysis apparatus and procedure have been described previously (1). The sample in a stream of nitrogen passes through a quartz tube heated by an electric furnace 12 in. long. The flow rate is 0.25 l/min at 2.5 Torr. A series of traps is placed between the quartz

TABLE 1. Temperatures used in the pyrolyses of 2-benzoxazolinone (**5**) and results[a]

Quantity (g) and temperature (°)	% recovered								
	5	**8**	**9**	**10**	**11**	**12**	**13**	**14**	Total[b]
1.933 900	9.0	3.5	6.2	5.5	3.4	2.1	0.7	2.5	32.9
			15.2						
1.733 950	2.9	3.5	7.0	6.3	5.6	2.8	0.7	1.6	30.4
			16.8						
1.444 1000	0.0	2.4	5.6	5.1	3.6	2.0	0.1	1.4	20.2
			13.1						

[a]Compounds **8**–**10** are isomeric; product **8** is pyridine; **9** and **10** are *cis* and *trans* isomers of 2,4-pentadienenitrile; **11** is quinoline; **12** is cyanobenzene; **13** is aniline; and **14** is phenol.
[b]It was assumed that one molecule of **5** is needed to produce one molecule of all products except **11**, in which case two molecules of **5** are needed.

tube and the pump. A solution is made of the material in the traps. G.l.p.c. and t.l.c. are used to separate the compounds in this solution.

Pyrolysis of 2-Benzoxazolinone (5)

The temperatures used in the pyrolyses of 2-benzoxazolinone (**5**) and the results are summarized in Table 1. A N_2 flow rate of 0.25 l/min was used. The initial pressure of the system was 0.8–1.2 Torr; it increased to a maximum of 6.0 Torr as **5** was sublimed into the N_2 stream and returned to its original value when all starting material had passed through. The products were collected in three traps, each cooled with liquid nitrogen. These traps were eluted with CH_3OH, acetone, and $CHCl_3$, and the combined washings were analyzed by g.l.p.c. The best separation of lower molecular weight components was achieved with a 12 ft 10% Carbowax 20M column held at 100° for 10 min, then programmed to 230° at 8°/min, and then held at 230° for 10 min. The other components were studied with a 6 ft 3% OV-225 CHROM HP 80/100 mesh column held at 100° for 2 min, then programmed to 250° at 8°/min, and then held at 250° for 4 min.

The mass spectra of products **8**–**10** show molecular-ion peaks at *m/e* 79 and a loss of HCN, giving *m/e* 52. Product **8** was identified as pyridine by comparison of its u.v. spectrum and g.l.p.c. retention time with those of a commercial sample. Products **9** and **10** were identified as the *cis* and *trans* isomers of 2,4-pentadienenitrile on the basis of their mass, n.m.r., i.r., and u.v. spectra. For example, absorption at 2220 cm^{-1} is characteristic of the cyano group; also, absorptions at 1570 and 665 cm^{-1} are characteristic of the *cis* form whereas 1592 and 950 cm^{-1} are characteristic of the *trans* form (13). It is interesting to note that approximately equal amounts of the two isomers were formed via equilibration at 575° of the *cis* form to the *cis,trans* mixture (14). We also obtain nearly equal amounts of each isomer.

Product **11** was shown to be quinoline on the basis of its u.v. spectrum and retention time, compared to those of a commercial sample. Likewise, product **12** was found to be cyanobenzene; **13** was found to be aniline; and **14** was found to be phenol by comparison of their retention times and spectra with those of commercial samples.

Pyrolysis of 2-Benzimidazolinone (6)

The temperatures used in the pyrolyses of 2-benzimidazolinone (**6**) and the results are given in Table 2. A flow of N_2 of 0.23 l/min and a system pressure of 1–3 Torr were used. The air-cooled trap and the two liquid nitrogen-cooled traps were eluted with EtOH, MeOH, acetone, and CH_2Cl_2. The solutions were combined and concentrated.

Mass spectra of the products were obtained from a LKB 9000 g.c.–m.s. combination using a 6 ft 3% OV-210 CHROM HP 80/100 mesh column programmed between 100 and 200° at 4°/min. The products were collected from a 6 ft 10% QF-1 CHROM HP 80/100 mesh column programmed in the same manner. Since starting material (**6**) does not elute from either column, it was recovered from a 6 ft 3% OV-1 CHROM HP 80/100 mesh column programmed between 100 and 250° at 15°/min and then held at 250° for 5 min.

Products **15**–**20** are isomeric; their mass spectra contain molecular ions at *m/e* 104 and intense fragment peaks at *m/e* 77. Compounds **15**–**17** are the isomeric cyanopyridines and **18**–**20** are the isomeric 2,4-hexadienedinitriles. 2-Cyanopyridine (**15**) and its 3-cyano (**16**) and 4-cyano (**17**) isomers and 2-aminocyanobenzene (**21**) were identified by g.l.p.c. retention times compared with those of commercial samples, g.l.p.c. peak enhancement, and comparison of their mass, i.r., and u.v. spectra with those of the known materials. The product *cis,cis*-2,4-hexadienedinitrile (**18**) was identified by retention time, peak enhancement, and mass and u.v. spectra, compared with the sample prepared as described above. Aniline (**13**) and cyanobenzene (**12**) were likewise characterized by comparison.

The three hexadienedinitriles gave identical mass spectra and very similar u.v. spectra with maxima at 261 nm. All three have been reported to have maxima near 260 nm (15). The *cis,cis* isomer (**18**) was identified on the g.l.p.c. trace by comparison and peak enhancement. For the two remaining isomeric hexadienedinitriles,

Can. J. Chem. Downloaded from www.nrcresearchpress.com by 210.87.254.105 on 09/05/12
For personal use only.

TABLE 2. Temperatures used in the pyrolyses of 2-benzimidazolinone (**6**) and results[a]

Quantity (g) and temperature (°)	% recovered						
	6	Cyanopyridines **15–17**	Hexadienedinitriles **18–20**	**21**	**13**	**12**	Total
2.259 950	56.5	2-, 2.3 3-, 3.0 4-, 1.3 6.6	*cis,cis-*, 0.7 *cis,trans-*, 1.1 *trans,trans-*, 0.4 2.2	0.4	2.3	0.8	68.8
		8.8 ($C_6H_4N_2$)					
2.572 1000	10.2	2-, 3.9 3-, 4.6 4-, 1.8 10.3	*cis,cis-*, 1.0 *cis,trans-*, 1.8 *trans,trans-*, 0.8 3.6	2.0	1.5	2.1	29.7
		13.9 ($C_6H_4N_2$)					

[a]Compound **21** is 2-aminocyanobenzene, **13** is aniline, and **12** is cyanobenzene.

TABLE 3. Temperatures used in the pyrolyses of 2-benzothiazolinone (**7**) and results[a]

Quantity (g) and temperature (°)	% recovered								
	7	**25**	**23**	**24**	**12**	**13**	**22**	**26**	Total
2.959 950	8.7	1.1	2.4	1.8	2.6	2.7	1.3	2.5	23.1
			4.2						
2.605 1000	1.3	1.4	2.4	4.0	5.4	1.8	1.7	3.7	21.7
			6.4						

[a]Compound **25** is 2-thiophenecarbonitrile; **23** and **24** are 1- and 2-cyanonaphthalene; **12** is cyanobenzene; **13** is aniline; **22** is naphthalene; and **26** is methyl carbanilate.

the one which eluted first was assigned the *cis,trans* structure (**19**) and the other one, the *trans,trans* structure (**20**). Our experience with the isomeric 2,4-pentadienenitriles (**9** and **10**) showed that the *cis* isomer (**9**) eluted before the *trans* isomer (**10**).

Pyrolysis of 2-Benzothiazolinone (7)

The temperatures used in the pyrolyses of 2-benzothiazolinone (**7**) and the results obtained are given in Table 3. A N_2 flow rate of 0.25 l/min was used, and the system pressure varied between 1.5 and 3.0 Torr during the pyrolyses. The traps were eluted with methanol, acetone, and CH_2Cl_2; the solutions were combined, concentrated, and analyzed. The 6 ft 3% OV-210 CHROM HP 80/100 mesh column was held at 100° for 4 min, and then programmed to 200° at 4°/min. After reaching 200°, the oven was held there for 10 min.

Cyanobenzene (**12**), aniline (**13**), naphthalene (**22**), 1- and 2-cyanonaphthalene (**23** and **24**), and starting material (**7**) were identified by comparison of their retention times and u.v. and mass spectra with those of commercial samples, and by g.l.p.c. peak enhancement.

Product **25** was identified as 2-thiophenecarbonitrile on the basis of its mass (M+, *m/e* 109), i.r. (2250 cm^{-1}), and u.v. (λ_{max} in CH_2Cl_2, 241.5 nm) spectra. The u.v. spectrum of 2-thiophenecarbonitrile has been observed at λ_{max} 242 nm (16) whereas the 3-isomer absorbs at λ_{max} 236 nm (17).

Another product (**26**) was identified as methyl carbanilate by comparison of its u.v., i.r., and mass spectra with those of a sample prepared by addition of phenylisocyanate to methanol.

Discussion

2-Benzoxazolinone (5)

The 70 eV e.i. mass spectrum of 2-benzoxazolinone (**5**) is summarized in Scheme 1. Intense metastable peaks are found for losses of CO_2 and 2CO from the molecular ions. The loss of CO from the molecular ions, followed by CO, is also observed in the metastable peaks, al-

Can. J. Chem. Downloaded from www.nrcresearchpress.com by 210.87.254.105 on 09/05/12
For personal use only.

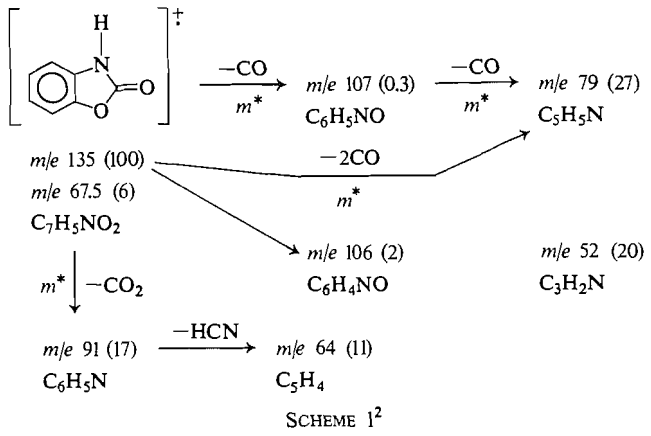

SCHEME 1[2]

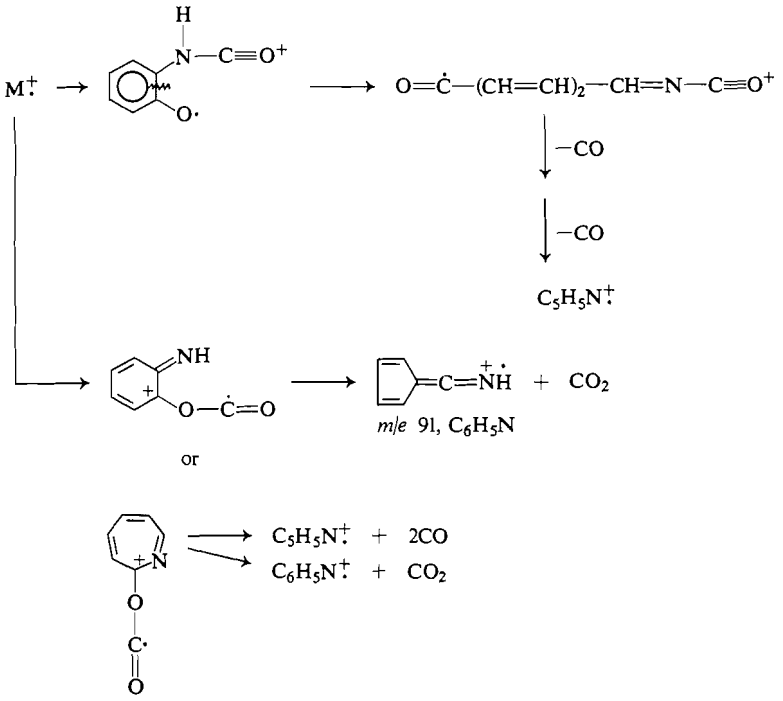

SCHEME 2

though the metastable peak for the loss of 2CO is much more intense. The width and shape of the small metastable peak for the loss of CO indicates that internal energy is being released as translational energy of the fragments. For a discussion of the significance of the shapes of metastable peaks see ref. 18. At 15 eV, *m/e* 91 and 79 are approximately equally abundant, ~2%. The (M + H) ion is present in the c.i. mass spectrum but there are no appreciable fragment ions present.

One can attempt to rationalize these data as shown in Scheme 2, as well as with other speculative ion structures. The loss of 2CO from the open-chain ion would require the two molecules to be lost from opposite ends of the chain. Previously, examples have been cited where a loss of two molecules from different parts of an ion

[2]The elemental compositions are the result of the exact-mass measurements; the values in parentheses are relative intensities; *m** denotes a metastable peak found in the mass spectrum.

Can. J. Chem. Downloaded from www.nrcresearchpress.com by 210.87.254.105 on 09/05/12
For personal use only.

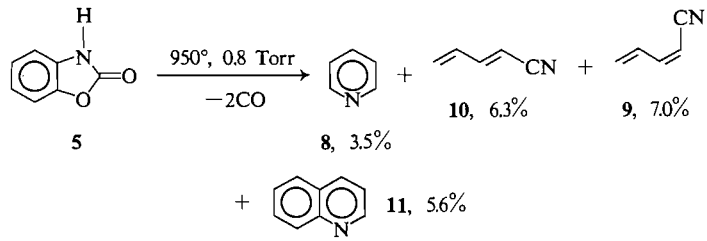

[I]

5 8, 3.5% 10, 6.3% 9, 7.0%

+ 11, 5.6%

gives rise to a metastable peak for the combined loss (Scheme 1, ref. 19). In comparison, the low energy fragmentations of the molecular ions of 2-benzoxazolinethione (**3**) are losses of S and COS (1). The only fragmentation in the c.i. spectrum of **3** is loss of S from the (M + H) ions (1).

The major products in the pyrolyses of **5** are three C_5H_5N isomers. When 1.9 g of **5** was pyrolyzed at 950° with a N_2 flow rate of 0.23 l/min and an initial system pressure of 0.8 Torr, 2.9% of **5** was recovered and 16.8% of C_5H_5N (**8–10**) was isolated, as shown in eq. 1.

Other products isolated were quinoline (**11**, 5.6%), cyanobenzene (2.8%), phenol (1.6%), and aniline (0.7%), for a total of 30.4% of the starting material accounted for. The formula of quinoline, C_9H_7N, corresponds to the dimerization of C_5H_5N, followed by loss of HCN and H_2.

Aniline could form by loss of CO_2 from **5** followed by abstraction of 2H· and phenol by loss of HNCO followed by addition of 2H·. However, aniline, phenol, and/or cyanobenzene, which are common pyrolysis products from this type of heterocyclic compound (1), could form by a degradation–recombination mechanism.

If, indeed, **8–11** arise from C_5H_5N via initial loss of 2CO from the molecule, they, along with the 2.9% of recovered **5**, account for 25.2 of the 30.4% of products isolated. Thus the major fragmentations observed in the mass spectrum of **5** can be used to rationalize the products formed upon pyrolysis.

2-Benzimidazolinone (6)

The 70 eV e.i. mass spectrum of 2-benzimidazolinone (**6**) is given in Fig. 1. In the c.i. spectrum of **6**, the (M + H) ion at *m/e* 135 is present, but there are no abundant fragment ions. The major fragmentation pathway of **6** is the consecutive losses of CO and 2HCN, as summarized in Scheme 3. At 15 eV, the peaks which remain are *m/e* 134 (100), 106(5), and 105(3). The metastable peak for the loss of CO is broad and concave (18).

The structures given in eq. 2 can account for the major fragmentation path. In comparison, oxidation of 2-iminobenzotriazole (**27**) with lead tetraacetate gives 2,4-hexadienedinitrile in good yield (eq. 3) (20). The intermediate in brackets in eq. 3 could not be trapped with acetylene dicarboxylate. Also, the decomposition of aromatic *o*-diazides at 160–170° to 2,4-hexadienedinitriles via the same intermediate seems to be a general reaction (21).

At 1000°, we recovered 10.2% of the starting material (**6**), and we isolated 13.9% of $C_6H_4N_2$ isomers, as shown in eq. 4. In addition, 2.0% of 2-aminocyanobenzene, 2.1% of cyanobenzene, and 1.5% of aniline were isolated. Thus, in all, 29.7% of the starting material has been accounted for. The percentages of the isomeric

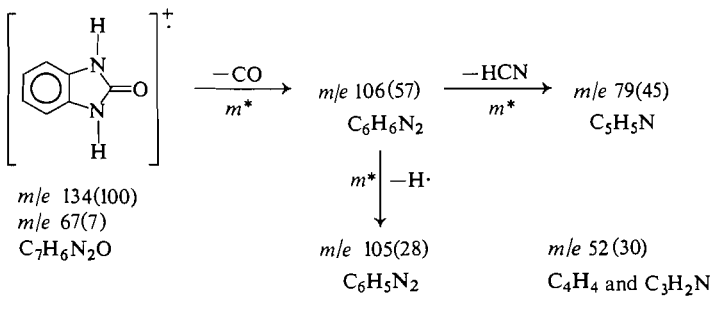

SCHEME 3

Can. J. Chem. Downloaded from www.nrcresearchpress.com by 210.87.254.105 on 09/05/12
For personal use only.

Can. J. Chem. Downloaded from www.nrcresearchpress.com by 210.87.254.105 on 09/05/12
For personal use only.

[2] $M^{+\cdot} \xrightarrow[m^*]{-CO}$ 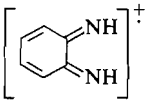 or 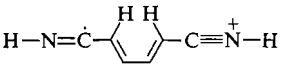 $\xrightarrow{-HCN}$ $C_5H_5N^{+\cdot}$ *m/e* 79

m/e 134 *m/e* 106

$m^* \downarrow -H\cdot$

$N{\equiv}C{-}(CH{=}CH)_2{-}C{\equiv}\overset{+}{N}{-}H$

m/e 105

[3] 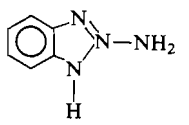 $\xrightarrow{Pb(OAc)_4}$ 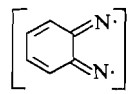 $\longrightarrow$ $N{\equiv}C{-}(CH{=}CH)_2{-}C{\equiv}N$

27

[4] **6** $\xrightarrow[1000°]{-CO}$ 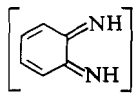 $\xrightarrow{-H_2}$ 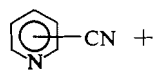 + $N{\equiv}C{-}(CH{=}CH)_2{-}C{\equiv}N$

15–17 10.3% **18–20** 3.6%

cyanopyridines were 3.9% of the 2-isomer (**15**), 4.6% of the 3-isomer (**16**), and 1.8% of the 4-isomer (**17**). The 2,4-hexadienedinitriles were present as the *cis,cis* isomer (**18**, 1%), the *cis,trans* isomer (**19**, 1.8%) and the *trans,trans* isomer (**20**, 0.8%).

We have pyrolyzed benzimidazole (**28**) at 1000° and isolated 2-aminocyanobenzene (**21**), eq. 5 (1). It is possible that **6**, in a high energy path, loses H_2O or HO· to give an intermediate,

[5] 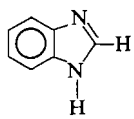 $\xrightarrow{1000°}$ 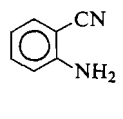

28 **21**

similar to the intermediate from **28**, which leads to formation of **21**. The pyrolysis of **21** at 1000° gave aniline (1). Thus the formation of **21** and of aniline in the pyrolysis of **6** may be related.

Once again, the resemblance of the fragmentation in the e.i. mass spectrum to its pyrolytic paths is striking.

2-Benzothiazolinone (7)

In the c.i. mass spectrum of 2-benzothiazolinone (**7**), the (M + H) peak is present and there are no abundant fragment ions. In contrast, the peak for loss of S in the c.i. spectrum of the isomeric 2-benzoxazolinethione (**3**) is 6% of the intensity of the (M + H) peak (1).

In the 70 eV e.i. spectrum of **7** there is one major fragmentation path (eq. 6). As was the

[6] 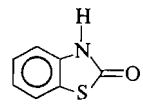 $\xrightarrow[m^*]{-CO}$

m/e 151(100)
m/e 75.5(7)
C_7H_5NOS

m/e 123(40) $\xrightarrow[m^*]{HCN}$ *m/e* 96(41)

C_6H_5NS C_5H_4S

case with the molecular ions of **5** and **6**, the metastable peak for the loss of CO is broad and concave, indicating a release of internal energy. The peaks at *m/e* 123 and 96 persist as the electron voltage is lowered, with *m/e* 96 disappearing before *m/e* 123.

In the 70 eV e.i. mass spectrum of **3**, the major fragmentations are losses of S and COS (1). However, there are small peaks at *m/e* 123(4%) for loss of CO and at *m/e* 96(7%) for loss of CO followed by HCN. Thus, it is possible that some of the molecular ions of **3** rearrange to the molecular ions of **7** before fragmenting. There are no substantial peaks at (M − S) or (M −

COS) in the mass spectrum of **7**. Dimethylthioncarbamates have been found to rearrange to dimethylthiolcarbamates upon heating and also upon electron impact (eq. 7) (22).

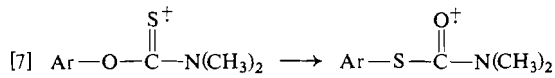

[7] $Ar-O-\overset{S^+}{\overset{\|}{C}}-N(CH_3)_2 \longrightarrow Ar-S-\overset{O^+}{\overset{\|}{C}}-N(CH_3)_2$

No products were isolated from the pyrolyses of **7** which could be directly related to the fragmentations in its mass spectrum. This is probably due to the fact that the sulfur atom is retained and gives products such as cyclopentadienethione (C_5H_4S) which polymerize. At 950°, 8.7% of starting material was recovered and 14.4% of products was isolated and identified.

The major products are 1-cyanonaphthalene (**23**, 2.4%), 2-cyanonaphthalene (**24**, 1.8%), naphthalene (1.3%), aniline (2.7%), and cyanobenzene (2.6%). One can speculate that naphthalene and the cyanonaphthalenes are formed by the loss of COS and/or CO and S from **3** and **7**, perhaps through the intermediacy of cyanocyclopentadiene (eq. 8). For example, dimerization

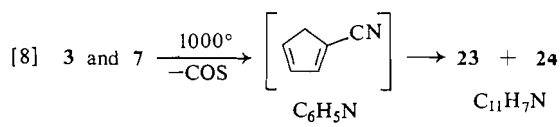

[8] **3** and **7** $\xrightarrow[-COS]{1000°}$ [C_6H_5N] $\longrightarrow$ **23** + **24** ($C_{11}H_7N$)

of C_6H_5N gives $C_{12}H_{10}N_2$ which can yield $C_{11}H_7N$ (**23** and **24**) by losses of HCN and H_2, and naphthalene ($C_{10}H_8$), by loss of 2HCN. We considered a similar possibility for the formation of quinoline from the pyrolysis of **5**. Naphthalene (6.7%), **23** (12.3%), and **24** (14.9%) have also been obtained from the pyrolysis of **3**, in addition to benzoxazole (**4**, O in place of S, 1.3%), and 2-cyanophenol (37.7%) (1). The possible intermediacy of cyanocyclopentadiene is being investigated.

Two other products were isolated in small yields at 950°, 2-thiophenecarbonitrile (**25**, 1.1%) and phenylisocyanate (**29**), isolated as its methyl carbanilate derivative (2.5%). Compound **29** can be formed from **7** by the loss of S and is trapped

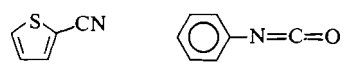

25 **29**

by methanol when the traps which are cooled by liquid N_2 are washed out after the pyrolysis is terminated. The origin of the small amount of **25** is more obscure.

The overall yields obtained from the pyrolysis of the 2-ones **5**–**7** are substantially lower than the yields obtained from the corresponding 2-thiones **1**–**3** (1). The 2-thiones expel an atom of S, leaving a stable aromatic azole **30**. On the other hand, the 2-ones expel CO, leaving an

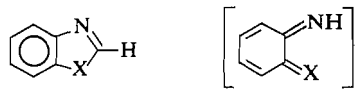

30 X = S, NH, O **31** X = O, NH, S

ortho-quinoid intermediate (**31**), or a rearranged isomer which is unstable and polymerizes or degrades further.

Nevertheless, the C_5H_5N isomers (17% yield) and the quinoline (5.6% yield) obtained from the pyrolysis of **5** can be associated with the loss of CO from **31** (X = O). The loss of 2CO is also the major fragmentation in the mass spectrum of **5**. Similarly, the formation of the $C_6H_4N_2$ isomers (14% yield) from the pyrolysis of **6** can be associated with the loss of H_2 from **31** (X = NH) and with the loss of CO from **6**, followed by H·, observed in the mass spectrum.

If compound **7** indeed forms **31** (X = S) upon pyrolysis, the loss of HCN would give C_5H_4S, cyclopentadienethione, which would not be expected to be stable and would polymerize. Loss of CS from **31** would give C_5H_5N which could react with S and lose H_2 to give thiophenecarbonitrile (**25**). On the other hand, loss of S from **31** (X = S) would give C_6H_5N which could lead to **23** and **24**. The loss of CO followed by HCN is the major fragmentation observed in the mass spectrum of **7**, whereas the loss of S from the (M − CO) ions is minor. It seems that the formation of **23** and **24** in the pyrolyses of **3** and **7** are likely related. In summary, the relationship between the pyrolysis and mass spectrum of **7** is ambiguous possibly because of the instability of sulfur containing products.

In conclusion, it has been possible to interpret the mass spectra and pyrolyses of **1**–**7** in terms of the extrusion of small species such as HCN, CO, and S, demonstrating another series of compounds which show similarity between the two processes. Upon pyrolysis, it is possible that major products do not survive to be isolated. If a large percentage of the starting material is not accounted for, this factor must be considered when the comparison is made between mass spectra and pyrolysis. If most of the starting material can be accounted for, on the other hand,

Can. J. Chem. Downloaded from www.nrcresearchpress.com by 210.87.254.105 on 09/05/12
For personal use only.

it is evident that a major pyrolytic path has not been obscured.

This investigation was supported by a grant from the National Research Council of Canada. We wish to thank Dr. O. A. Mamer, Royal Victoria Hospital, Montreal, for use of the LKB 9000 GC/MS combination and Drs. O. M. Colvin and C. Fenseleau, Johns Hopkins University School of Medicine, for use of the Dupont 21/491 mass spectrometer from which chemical ionization mass spectra were obtained.

1. D. C. DeJongh and M. L. Thomson. J. Org. Chem. **38**, 1356 (1973).
2. N. L. Aryutkina, A. F. Vasil'ev, N. A. Poznanskaya, N. I. Shvetsov-Shilovskii, S. N. Ivanova, and N. N. Mel'nikov. Zh. Obshch. Khim. **40**, 1872 (1970).
3. V. V. Kalmykov, V. E. Blokhin, and K. V. Aglitskaya. Tr. Voronezh. Gos. Univ. **73**, 67 (1969); Chem. Abstr. **74**, 47608 (1971).
4. A. Mathias. Mol. Phys. **12**, 381 (1967).
5. B. J. Millard and A. F. Temple. Org. Mass Spectrom. **1**, 285 (1968).
6. F. M. Hershenson, L. Bauer, and K. F. King. J. Org. Chem. **33**, 2543 (1968).
7. T. Kametani, S. Hirata, S. Shibuya, and M. Shio. Org. Mass Spectrom. **4**, 395 (1970).
8. D. C. DeJongh and G. N. Evenson. J. Org. Chem. **37**, 2152 (1972) and references therein.
9. H. R. Snyder, C. T. Elston, and D. B. Kellom. J. Am. Chem. Soc. **75**, 2014 (1953).
10. D. Harrison and A. C. B. Smith. J. Chem. Soc. 3157 (1959).
11. L. S. Efros and L. R. Davidenkov. J. Gen. Chem. USSR **21**, 2289 (1951).
12. K. Nakagawa and H. Onoue. Chem. Commun. 396 (1965).
13. J. G. Grasselli, B. L. Ross, H. F. Huber, and J. M. Augl. Chem. Ind. (London), 162 (1963).
14. H. R. Snyder, K. C. Murdock, and C. S. Marvel. J. Am. Chem. Soc. **75**, 4742 (1953).
15. J. A. Elvidge and P. Sims. J. Chem. Soc. (C), 385 (1966).
16. G. H. Jeffrey, R. Parker, and A. I. Vogel. J. Chem. Soc. 570 (1961).
17. Y. Sugimoto, S. Nishimura, and E. Inoto. Bull. Univ. Osaka, Prefecture Ser. A, **8**, 71 (1959). Chem. Abstr. **55**, 12029 (1961).
18. K. R. Jennings. *In* Mass spectrometry: techniques and applications. *Edited by* G. W. A. Milne. Wiley Interscience, New York. 1971.
19. D. C. DeJongh, S. C. Perricone, M. L. Gay, and W. Korytnyk. Org. Mass Spectrom. **1**, 151 (1968).
20. C. D. Campbell and C. W. Rees. Chem. Commun. 192 (1965).
21. J. H. Hall. J. Am. Chem. Soc. **87**, 1147 (1965).
22. J. C. Tou and R. M. Rodia. Org. Mass Spectrom. **6**, 493 (1972).

Can. J. Chem. Downloaded from www.nrcresearchpress.com by 210.87.254.105 on 09/05/12
For personal use only.

Etude cinétique du système Cu(II)–adénine

G. Boivin et M. Zador

Département de Chimie, Université de Montréal, c.p. 6128, Montréal 101, Québec

Reçu le 16 mars 1973

La cinétique de la formation et de la dissociation de divers complexes Cu(II)–adénine a été étudiée par les méthodes de la relaxation thermique et du "flux stoppé".

Entre p*H* 3.5 et 5 la formation de Cu(II)·aH est très rapide; celle de Cu(II)·$(aH)_2$ a été étudiée et les constantes de vitesse ont été déterminées. A pH < 3 les formes protonées ont une contribution importante à la vitesse de réaction. En milieu basique deux complexes différents ont été étudiés; la réaction d'échange avec l'EDTA se fait par deux voies parallèles.

Le mécanisme des diverses réactions est discuté et comparé au système Cu(II)–adénosine.

The kinetics of formation and dissociation of Cu(II)–adenine complexes have been studied by stopped flow and relaxation methods.

Between pH 3.5 and 5 the formation of Cu(II)·aH is too fast to be measured; formation of Cu(II)·$(aH)_2$ has been studied and rate parameters have been determined. At pH < 3 protonated species make an important contribution to measured reaction rates. In basic media two different complexes have been investigated. The exchange reaction with EDTA proceeds by two parallel reaction paths.

The mechanism of these reactions is discussed and compared with that proposed for the Cu(II)–adenosine system.

Can. J. Chem., 51, 3322 (1973)

L'adénine est une des quatre bases constituantes de l'ARN et de l'ADN; on la retrouve aussi dans certains coenzymes comme l'ATP et le NAD. Les métaux de transition bivalents forment des complexes avec l'adénine. Le Cu(II) en particulier forme des complexes très stables qui ont fait l'objet de nombreux travaux tant au point de vue de leur nature qu'au point de vue de leur stabilité en solution aqueuse (1–12). Ces études ont montré l'existence de plusieurs complexes dont la nature dépend de l'acidité du milieu réactionnel. En effet, en milieu acide, les complexes Cu(II)·aH et Cu(II)·$(aH)_2$ (aH = adénine) prédominent, tandis qu'en milieu basique, les espèces Cu(II)·$(OH^-)_n$·(a^-) et Cu(II)·$(OH^-)_m$·$(a^-)_2$ ont été mises en évidence (5).

Nous nous proposons dans ce travail d'étudier la cinétique de formation et de dissociation des divers complexes du Cu(II) avec l'adénine en solution aqueuse.

Partie expérimentale

Les réactifs

L'adénine est un produit de Aldrich Chemical Co. Le perchlorate cuivrique a été obtenu en dissolvant l'oxyde cuivrique dans l'acide perchlorique. La solution stock a été dosée par iodométrie et par absorption atomique. L'EDTA est un produit Fisher Scientific Co. Le pyrophosphate et le tripolyphosphate de sodium sont de Alfa Inorganics. Les solutions d'adénine ont été fraîchement préparées avant chaque série d'expériences. La force ionique des solutions a été maintenue constante à l'aide du perchlorate de sodium. Le pH des solutions est ajusté en utilisant de l'acide perchlorique ou de l'hydroxyde de sodium.

Appareillage

La cinétique des réactions a été étudiée par les méthodes de la relaxation thermique et du "flux stoppé", dont les principes sont décrits dans la littérature (13).

L'appareil de relaxation provient de Messenlagen Studiengesselschaft m.b.H., Göttingen, Allemagne. L'appareil du "flux stoppé" est constitué d'un système à mélange rapide Durrum–Gibson et d'un monochromateur Jarrel–Ash 0.25 m. Dans chaque cas, les variations de densité optique ou de transmission des solutions sont enregistrées sur un oscillographe cathodique et le signal obtenu est photographié. Les spectres visibles ont été obtenus sur un spectrophotomètre Cary–14. Les cellules réactionnelles sont thermostatées et, dans le cas de la relaxation, la température est mesurée avant chaque expérience à l'intérieur de la cellule, à l'aide d'un thermocouple cuivre–constantan.

Méthodes cinétiques

La cinétique de relaxation du système Cu(II)·adénine, en milieu acide, peut être suivie par la diminution de l'absorption sur une des extrémités de la bande d'absorption du complexe Cu(II)·$(aH)_2$ à 570 nm ou du cuivre vers 715 nm. La cinétique de formation et de dissociation du complexe Cu(II)·$(aH)_2$, en milieu acide, peut également être étudiée par "flux stoppé" aux mêmes longueurs d'onde. La dissociation des complexes, en milieu basique, est étudiée par la méthode du "flux stoppé". Les solutions à mélanger sont ajustées au même pH. On suit la cinétique de disparition des complexes aux longueurs d'onde appropriées.

Les solutions ont été dégazées pour empêcher la forma-

Can. J. Chem. Downloaded from www.nrcresearchpress.com by 210.87.254.6 on 09/05/12
For personal use only.

Can. J. Chem. Downloaded from www.nrcresearchpress.com by 210.87.254.6 on 09/05/12
For personal use only.

tion de bulles. Les solutions à mélanger ont la même force ionique pour éviter des phénomènes provoqués par une chaleur de mélange. Dans chaque cas, des vérifications ont été faites pour s'assurer qu'un des réactifs seul ne présentait pas de relaxation.

Résultats et discussion

(1) Etude cinétique du système Cu(II)·adénine entre pH 3.5 et pH 5

L'étude spectrophotométrique du système a été effectuée en vue de déterminer les conditions expérimentales optimales pour l'étude cinétique.

L'examen des spectres d'absorption dans le visible permet de mettre en évidence deux complexes. L'addition du Cu(II) à l'adénine est accompagnée d'abord d'une augmentation d'absorption de la bande de l'adénine à $\lambda < 400$ nm et de l'apparition d'une nouvelle bande à $\lambda =$ 570 nm. Simultanément, un épaulement de la bande de l'adénine se manifeste de $\lambda \simeq 350$ à 450 nm. L'augmentation de la concentration en Cu(II) entraîne originalement l'augmentation de ces deux bandes; elles passent ensuite par un maximum, ce qui est suivi d'une diminution d'intensité. Les bandes finissent par s'atténuer et disparaître à très haute concentration en Cu(II). Il ne demeure finalement que la bande à $\lambda < 400$ nm, dont l'intensité n'est plus modifiée significativement par une augmentation de la concentration en Cu(II).

Il est raisonnable d'admettre que dans ce dernier cas, l'augmentation d'absorption de la bande de l'adénine correspond à la formation complexe Cu(II)·aH, d'après l'éq. 2, qui serait favorisé en excès de cuivre.

$$[1]\quad aH_2^+ \rightleftharpoons aH + H^+ \qquad K_a = [aH][H^+]/[aH_2^+]$$

$$[2]\quad Cu(II) + aH \underset{k_{-1}}{\overset{k_1}{\rightleftharpoons}} Cu(II)\cdot aH \qquad K_1 = \frac{[Cu(II)\cdot aH]}{[Cu(II)][aH]}$$

L'existence du complexe Cu(II)·aH a déjà fait l'objet d'une étude spectrophotométrique et sa constante d'équilibre de formation fut déterminée ($K_1 = 500\ M^{-1}$ à 25 °C) (5).

La bande à $\lambda \simeq 570$ nm et l'épaulement de $\lambda \simeq 350$ nm à 450 nm dénotent la formation du complexe Cu(II)·$(aH)_2$, d'après l'éq. 3.

$$[3]\quad Cu(II)\cdot aH + aH \underset{k_{-2}}{\overset{k_2}{\rightleftharpoons}} Cu(II)\cdot(aH)_2,$$

$$K_2 = \frac{[Cu(II)\cdot(aH)_2]}{[\overline{Cu(II)\cdot aH}][\overline{aH}]}$$

Le complexe Cu(II)·$(aH)_2$ serait prépondérant à grande concentration en adénine.

En étudiant la relaxation de ce système dans diverses conditions expérimentales, c'est-à-dire à plusieurs concentrations en réactifs, à des pH, des températures et des longueurs d'onde différents, on observe une seule relaxation, avec des temps de l'ordre de 1–100 ms, attribuée à la formation du complexe Cu(II)·$(aH)_2$.

Les résultats ont été interprétés en admettant que la relaxation est due à la réaction [3] et que la réaction [2] est très rapide. Le temps de relaxation τ est donné par l'éq. 4.

$$[4]\quad \tau^{-1} = k_2([\overline{Cu(II)\cdot aH}] + [\overline{aH}]) + k_{-2}$$

où les concentrations sont celles à l'équilibre.

Les concentrations à l'équilibre ont d'abord été calculées en utilisant les valeurs de K_a et de K_1 de la littérature. On détermine ensuite les paramètres k_2 et k_{-2} ainsi que K_2. On effectue alors un nouveau calcul en tenant compte de cette dernière valeur. Ainsi, par approximations successives, on arrive au meilleur accord entre résultats expérimentaux et calculés. Ces calculs ont été effectués par ordinateur. L'ensemble des résultats est présenté dans le tableau 1. L'éq. 4 a pu être vérifiée et les valeurs de k_2 et de k_{-2} ainsi que les énergies d'activation ont été déterminées et les valeurs correspondantes sont groupées au tableau 2. On remarque que la valeur de K_2 obtenue est supérieure à celle de K_1, ce qui est contraire à ce que l'on observe généralement. Il est hasardeux de tirer une conclusion de cette observation étant donné que les deux constantes ont été obtenues par des méthodes très différentes.

Nous avons pu également étudier ce système par la méthode du "flux stoppé". En effectuant

TABLEAU 1. Temps de relaxation du système Cu(II)·adénine à pH = 4.5*

T = 17 °C		T = 26 °C		T = 36 °C	
$\Sigma\bar{c} \times 10^3$† ($M$)	τ (a) (ms)	$\Sigma\bar{c} \times 10^3$ (M)	τ (b) (ms)	$\Sigma\bar{c} \times 10^3$ (M)	τ (c) (ms)
3.78	7.5	4.21	5	4.88	2.8
2.30	12	2.67	7.5	3.21	4
0.97	26	1.30	14	1.64	6
0.51	50	0.70	20	0.86	8

*Chaque temps de relaxation est une moyenne de plusieurs expériences et la reproductibilité est meilleure que 5%.

† $\Sigma\bar{c} = ([\overline{Cu(II)\cdot aH}] + [\overline{aH}])$, force ionique = 0.5 M, [Cu(II)] = 7.2×10^{-4} M, [aH] = 7.5×10^{-3} à 1.25×10^{-3} M. (a) $K_1 = 1400\ M^{-1}$, (b) $K_1 = 500\ M^{-1}$, (c) $K_1 = 230\ M^{-1}$. pK_a = 4.18.

TABLEAU 2. Constantes de vitesse de formation et de dissociation du complexe Cu(II)·$(aH)_2$. ainsi que les énergies d'activation correspondantes*

T (°C)	$k_2 \times 10^{-4}$ (M^{-1} s^{-1})	k_{-2} (s^{-1})	$K_2 \times 10^{-3}$ (M^{-1})
36	5.7 ± 0.5	72 ± 10	0.8 ± 0.2
26	4.2 ± 0.4	22 ± 4	1.9 ± 0.6
17	3.3 ± 0.3	6 ± 2	5.6 ± 2

*E_2 = 5 ± 1.5 kcal/mol, E_{-2} = 25 ± 3 kcal/mol.

le mélange, on constate initialement une variation brusque de densité optique (à λ = 340 nm) avec une constante de temps plus petite que 1 ms qui est probablement due à la formation du complexe Cu(II)·aH. Ce phénomène est suivi d'une réaction plus lente due à la formation du complexe Cu(II)·$(aH)_2$, d'après l'équation de vitesse de deux réactions opposées d'ordre un. Les valeurs de k_2 et k_{-2} ainsi déterminées sont identiques à celles du tableau 2 obtenues par relaxation.

Il est intéressant de constater que les constantes de vitesse de formation du complexe Cu(II)·$(aH)_2$ sont d'un facteur de plus de dix plus grandes que celles pour le complexe Cu(II)·adénosine (14). Dans ce dernier cas une des sites de coordination (N_9) est altérée dû à la présence du groupe ribose; ceci cause également une diminution de basicité. Il est à noter également que la vitesse de formation de Cu(II)·aH est nettement plus grande que celle du complexe 1:2, contrairement à ce que l'on a constaté, *e.g.* dans le cas de l'éthylènediamine (15) où l'introduction de la deuxième molécule se fait avec une vitesse deux fois plus lente que celle de la première molécule. Cet effet a déjà été noté dans le cas de certains complexes avec les acides aminés (16).

Il faut souligner aussi que la valeur de la constante k_2 est de plusieurs ordres de grandeur inférieure à celle observée par exemple pour l'éthylènediamine (15). Bien que l'on pourrait parler ici d'effet stérique ou de basicité moindre du ligand, les résultats sont difficilement compatibles avec un mécanisme impliquant comme étape lente le départ d'une molécule d'eau de coordination du Cu(II). Le mécanisme intime de formation de complexes du Cu(II) reste donc relativement peu compris.

L'influence du pH sur la vitesse de réaction a été étudiée à concentration d'adénine constante, et prise en excès par rapport au Cu(II). Les résultats ont montré une augmentation de τ avec une diminution du pH entre pH 4.9 et 3.5. Toutefois, l'influence du pH peut être interprétée en tenant compte de l'éq. 1 impliquant une diminution de [aH] avec l'augmentation de l'acidité. En introduisant les concentrations à l'équilibre dans l'équation de vitesse 4, on obtient des valeurs convenables pour les constantes de vitesse k_2 et k_{-2}.

(2) Influence de l'acidité sur la cinétique de relaxation à pH < 3

Le mécanisme simple représenté par les éq. 1 à 3 ne laisse prévoir qu'une influence indirecte de l'acidité sur la vitesse de réaction, tel que confirmé par les résultats à pH ⩾ 3.5. A pH < 3 par contre, quand le cuivre est pris en excès par rapport à l'adénine, l'augmentation de l'acidité entraîne l'augmentation de la vitesse de réaction.

Les temps de relaxation en fonction de l'acidité du milieu dans différentes conditions figurent dans le tableau 3. D'après ces résultats, l'inverse du temps de relaxation augmente linéairement avec la concentration en acide à l'équilibre (fig. 1). Pour expliquer cette catalyse acide, il faut ajouter deux étapes supplémentaires au mécanisme correspondant aux éq. 1–3.

[5] $$Cu(II)\cdot(aH)_2 + H^+ \rightleftharpoons Cu(II)\cdot(aH)_2H^+, \qquad K_3 = \frac{[Cu(II)\cdot(aH)_2H^+]}{[Cu(II)\cdot(aH)_2][H^+]}$$

[6] $$Cu(II)\cdot aH + aH_2^+ \underset{k_{-4}}{\overset{k_4}{\rightleftharpoons}} Cu(II)\cdot(aH)_2H^+$$

Les réactions 3 et 6 se feraient parallèlement et les réactions 1, 2 et 5 seraient à l'équilibre.

L'éq. 5 implique la protonation rapide de l'adénine à un site différent du site de coordination du métal, et l'éq. 6 la formation et la dissociation de ce complexe. La vitesse totale est donnée par la contribution des éq. 3 et 6. L'éq. 7

[7] $$d[Cu(II)\cdot aH]/dt = -k_2[Cu(II)\cdot aH][aH] + k_{-2}[Cu(II)\cdot(aH)_2] - k_4[Cu(II)\cdot aH][aH_2^+] + k_{-4}[Cu(II)\cdot(aH)_2H^+]$$

peut être résolue linéairement. Bien qu'il soit possible d'obtenir une solution exacte, elle contient trop de termes pour être vérifiée quantitativement. Il faut accomplir une série d'approximations en éliminant les termes très petits pour ce cas particulier, en tenant compte: (*i*) de la valeur calculée des concentrations à l'équilibre, (*ii*) des constantes d'équilibres et (*iii*) en admettant que $k_2 > k_4$, $k_{-2} < k_{-4}$ et $K_3 < K_n^{-1}$. On obtient alors l'éq. 8.

Can. J. Chem. Downloaded from www.nrcresearchpress.com by 210.87.254.6 on 09/05/12
For personal use only.

TABLEAU 3. Influence de l'acidité sur les temps de relaxation du système Cu(II)·adénine en excès de Cu(II)*

T = 21 °C		T = 30 °C		T = 31 °C	
$[H^+] \times 10^3$ (M)	τ (ms)	$[H^+] \times 10^3$ (M)	τ (ms)	$[H^+] \times 10^3$ (M)	τ (ms)
1.4	50	1.8	21	1.4	20
2.6	40	3.4	18	2.0	18
4.6	30	7.1	11	3.0	15
8.0	22	10.0	8	4.2	13
13.0	17	13.0	7	6.5	10
15.0	16	—	—	9.2	8
18.0	14	18.0	5.5	16.0	5.5

*[Cu(II)] = 0.144 M, [aH] = 5.0×10^{-3} M, force ionique = 0.5 M, λ = 340 nm.

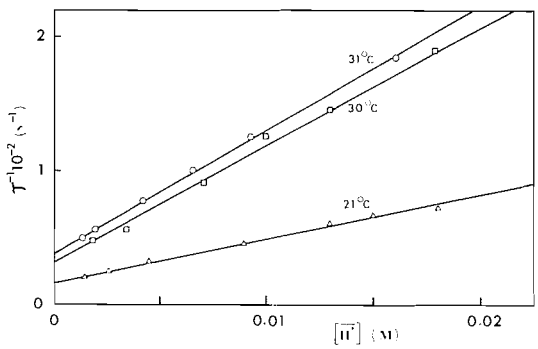

FIG. 1. Influence de l'acidité sur les temps de relaxation. [Cu(II)] = 0.144 M, [adénine] = 5.0×10^{-3} M, force ionique = 0.5 M, λ = 340 nm.

$$[8]\quad \tau^{-1} = k_{-2} + k_4([\overline{Cu(II)\cdot aH}] + [\overline{aH_2}^+]) + 2k_2K_3K_a[\overline{Cu(II)\cdot aH}] + (k_{-4} + 2k_4[\overline{Cu(II)\cdot aH}])\,K_3[\overline{H^+}] + 2k_2K_a[\overline{Cu(II)\cdot aH}]/[\overline{H^+}].$$

La comparaison de cette dernière équation avec les résultats expérimentaux permet de dégager les conclusions suivantes: (*i*) La droite expérimentale de la fig. 1 implique que le terme $2k_2K_a[\overline{Cu(II)\cdot aH}]/[\overline{H^+}]$ est négligeable, ce qui est confirmé à partir des résultats obtenus en excès d'adénine. (*ii*) L'ordonnée à l'origine, correspondant aux termes qui ne contiennent pas $[H^+]$, est égale à k_{-2} compte tenu de l'erreur expérimentale, ce qui implique que la contribution des autres termes ne dépasse pas 10% (voir tableau 4). (*iii*) A des acidités s'approchant de 0.01 M, la contribution des éqs. 5 et 6 est prépondérante et la catalyse acide observée est due à la dissociation rapide de $Cu(II)(aH)_2H^+$.

La pente de la droite obtenue ne permet pas de connaitre les valeurs exactes de k_4, k_{-4} et de K_3.

TABLEAU 4. Paramètres des droites de la Fig. 1.

T (°C)	Ordonnée à l'origine (s^{-1})	Pente $\times 10^{-3}$ ($M^{-1}\,s^{-1}$)	k_{-2}* (s^{-1})
21	17	3.2	19
30	32	8.7	36
31	38	9.5	40

*Valeurs tirées du tableau 2 pour la température de l'expérience.

On peut estimer à 21 °C, la limite inférieure de $k_{-4} \sim 10^2\ s^{-1}$, pour une limite supérieure de $K_3 \sim 10^2\ M^{-1}$; la limite supérieure de k_4 compatible avec les résultats est d'environ $10^3\ M^{-1}\ s^{-1}$. Ceci est fait en tenant compte en première approximation, uniquement des équilibres 1–3 pour calculer les concentrations à l'équilibre, ce qui est raisonnable étant donné que $K_3 \ll K_a^{-1}$.

La concentration en Cu(II) en *excès* n'a pas d'influence sur les temps de relaxation à acidité constante. Entre 0.072 et 0.43 M les temps de relaxation restent constants. Ceci est en accord avec le mécanisme proposé, puisque dans la solution exacte de l'éq. 8 les termes contenant le Cu(II) sont négligeables. Il faut souligner que l'influence de la concentration en Cu(II) serait tout autre si la réaction enregistrée était la formation de Cu(II)·aH; alors on devrait obtenir une variation linéaire de τ^{-1} en fonction de la concentration en Cu(II).

La mécanisme proposé n'est pas le seul à être compatible avec les résultats expérimentaux. Dans divers cas étudiés, impliquant des ligands protonés (15, 17), on admet plutôt une déprotonation du ligand, tel l'éthylènediamine, avant la formation du complexe, due au fait que les

Can. J. Chem. Downloaded from www.nrcresearchpress.com by 210.87.254.6 on 09/05/12
For personal use only.

sites de protonation et de complexation sont les mêmes (15). Dans le cas de l'adénine ceci n'est pas le cas, étant donné que le site de protonation est l'azote N_1, tandis que la complexation avec le Cu(II) se fait en positions N_3 et N_9 et l'existence du complexe protoné tel $Cu(II)\cdot(aH)_2H^+$ est possible. Toutefois, un mécanisme semblable à celui proposé pour l'éthylènediamine (15) ne peut pas être exclu, ni un transfert de proton lent conduisant à une catalyse acide générale qui fut mise en évidence dans les réactions d'échange de ligand de complexes Cu(II)·peptides (18).

(3) Dissociation du complexe $Cu(II)\cdot(aH)_2$ par le pyrophosphate et le tripolyphosphate

Il est connu que les ions pyrophosphates et tripolyphosphates forment divers complexes avec le Cu(II). Ces anions complexent très fortement le cuivre en milieu faiblement acide (19); en présence de polyphosphate, les complexes entre le Cu(II) et l'adénine se trouvent donc complètement dissociés.

La dissociation du complexe $Cu(II)\cdot(aH)_2$ a été étudiée en mélangeant une solution contenant le Cu(II) et l'adénine à l'équilibre avec une solution de polyphosphate en grand excès par rapport au complexe $Cu(II)\cdot(aH)_2$ à acidité constante (l'excès de polyphosphate servant de tampon). Une seule courbe de dissociation est observée avec une cinétique d'ordre un. Les constantes de vitesse expérimentales sont données au tableau 5. La fig. 2 montre que la constante varie linéairement avec la concentration en polyphosphate (ph). Ceci indique que la réaction s'effectue par deux voies parallèles: (*i*) l'une, indépendante du

TABLEAU 5. Variation de la constante expérimentale de dissociation du complexe $Cu(II)\cdot(aH)_2$ en fonction de la concentration en polyphosphate*

	Pyrophosphate		Tripolyphosphate	
	$pH = 4.5$	$pH = 3.5$	$pH = 4.0$	$pH = 3.5$
$[ph] \times 10^3$ (M)	k_{exp} (s^{-1})	k_{exp} (s^{-1})	k_{exp} (s^{-1})	k_{exp} (s^{-1})
50	62.7	46.0	76.0	53.0
30			53.0	43.0
25	43.0	36.0		
20			43.0	34.4
10			31.4	26.6
0.5	23.0	23.0		
0.3	21.6	19.2	21.6	19.7
0.15	19.2	19.2		

*$k_{-2} = 19.5\ s^{-1}$, $k_{-2} = 18\ s^{-1}$, force ionique = 0.5 M, $\lambda = 570$ nm, $[Cu(II)] = 2.13 \times 10^{-3}$ M, $[aH] = 5 \times 10^{-3}$ M, $T = 25$ °C.

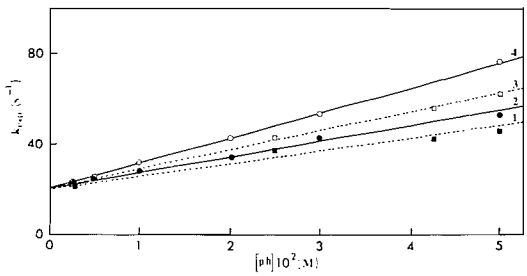

FIG. 2. Variation de la constante de vitesse de dissociation de $Cu(II)\cdot(aH)_2$ avec la concentration en polyphosphate. (1) pyrophosphate, $pH = 3.5$; (2) tripolyphosphate, $pH = 3.5$; (3) pyrophosphate, $pH = 4.5$; (4) tripolyphosphate, $pH = 4.0$. $T = 25$ °C; $[Cu(II)] = 2.13 \times 10^{-3}$ M; [adénine] $= 5.0 \times 10^{-3}$ M; force ionique = 0.5 M; $\lambda = 570$ nm.

polyphosphate, correspond au déplacement des éqs. 2 et 3 vers la gauche, avec la réaction 3 comme étape lente, suivi de la réaction rapide du Cu(II) avec le polyphosphate et (*ii*) l'autre, qui est d'ordre un en polyphosphate, serait la réaction d'échange d'après l'éq. 9.

$$[9] \qquad Cu(II)\cdot(aH)_2 + ph \xrightarrow{k_5} Cu(II)\cdot ph + 2aH$$

La constante expérimentale correspondant à ce mécanisme est donnée par l'éq. 10.

$$[10] \qquad k\ exp = k_{-2} + k_5\,[ph]$$

La pente des droites de la fig. 2 donne k_5, qui, comme attendu, varie avec le pH du milieu. Bien que le mécanisme de cette réaction nécessiterait une étude plus approfondie, l'on peut déjà conclure que k_5 augmente avec la basicité du ligand entrant. En effet, l'augmentation du pH favorisant les espèces les moins protonées, donc les plus basiques, entraîne l'augmentation de k_5. Ceci permet aussi de suggérer qu'une catalyse acide générale est à exclure dans ce cas.

Le fait que toutes les droites ont la même ordonnée à l'origine, soit environ $20\ s^{-1}$ correspondant à k_{-2}, montre que l'éq. 10 est bien vérifiée.

(4) Etude du système Cu(II)·adénine en milieu basique

L'existence de complexes du Cu(II) avec l'adénine ayant perdu un proton a été mise en évidence par des mesures potentiométriques (2, 3). On a pu montrer par une étude potentiométrique la formation de deux types de complexes, ayant des constantes de stabilité assez

Can. J. Chem. Downloaded from www.nrcresearchpress.com by 210.87.254.6 on 09/05/12
For personal use only.

élevées, soit: $Cu(II)(OH)_n\cdot(a^-)(\log K_1 = 6.99)$ et $Cu(II)(OH)_m\cdot(a^-)_2(\log K_2 = 6.3)$ (5).

L'étude spectrophotométrique de ce système montre que ces deux complexes peuvent être différenciés et que leur importance varie avec les conditions expérimentales. A pH = 8.8 avec un rapport [aH]/[Cu(II)] = 4, on a le complexe $Cu(II)(OH)_m\cdot(a^-)_2$, de couleur violette, qui absorbe à λ_{max} = 570 nm. Une augmentation du pH jusqu'à pH = 11.5 entraîne le déplacement de la bande vers les plus grandes longueurs d'onde (λ_{max} = 630 nm), correspondant à la formation de $Cu(II)\cdot(OH)^-_n\cdot(a^-)$, de couleur bleu qui est le seul complexe observé pour un rapport Cu(II)/aH = 1. Les deux complexes semblent contenir un nombre d'ions hydroxyles différent ($n > m$) ce qui explique le changement observé avec l'augmentation du pH. Comme ce comportement n'est pas prévu d'après les résultats de Reinert et Weiss (5), il est clair qu'une étude plus approfondie de ce système est encore nécessaire.

L'étude cinétique a révélé que la formation des complexes était trop rapide pour être étudiée par "flux stoppé"; la très grande stabilité des complexes rend la méthode de relaxation inutilisable. Les constantes de vitesse de dissociation ont, néanmoins, pu être déterminées en étudiant la réaction d'échange avec l'EDTA.

Pour simplifier l'étude, on a choisi tout d'abord des conditions expérimentales où $Cu(II)\cdot(OH^-)_n\cdot(a^-)$ prédomine. En mélangeant une solution du complexe avec une solution d'EDTA au même pH, on observe une seule réaction dont la vitesse expérimentale d'ordre un varie linéairement avec la concentration en EDTA et un mécanisme par deux voies parallèles est en accord avec les résultats:

$$[11]\quad Cu(II)\cdot(OH^-)_n(a^-) \xrightarrow{k_6} Cu(II)\cdot(OH^-)_n + a^-$$

$$[12]\quad Cu(II)\cdot(OH^-)_n + EDTA \xrightarrow{\text{rapide}} Cu(II)\cdot EDTA$$

$$[13]\quad Cu(II)\cdot(OH^-)_n(a^-) + EDTA \xrightarrow{k_7} Cu(II)\cdot EDTA + a^-$$

Les éqs. 11 et 12 correspondent à la dissociation du complexe suivie de la formation rapide de Cu(II)·EDTA. L'éq. 13 correspond à la réaction d'échange dont le mécanisme détaillé reste encore à élucider. La constante de vitesse expérimentale est donnée par:

$$[14]\quad k_{exp} = k_6 + k_7\,[EDTA]$$

Par voie graphique, on obtient à 25 °C: k_6 = 0.05 s^{-1} et k_7 = 7.5 $M^{-1}\,s^{-1}$. On peut aussi estimer la constante de vitesse de formation du complexe, en utilisant la valeur de la constante d'équilibre, à environ $5 \times 10^5\ M^{-1}\,s^{-1}$.

TABLEAU 6. Variation de la constante expérimentale de dissociation en fonction de la concentration en EDTA pour les complexes $Cu(II)(OH^-)_n\cdot(a^-)$ et $Cu(II)(OH^-)_m\cdot(a^-)_2$*

[EDTA] (M)	k_{exp} (a) (s^{-1})	k_{exp} (b) (s^{-1})	k_{exp} (c) (s^{-1})
0.085	0.64	0.63	173
0.075	0.58	0.53	173
0.050	0.40	0.38	173
0.0375	0.34	0.29	173
0.025	0.23	0.20	153
0.010	0.11	0.12	115

*k_{-6} = 0.05 s^{-1}, pour le complexe $Cu(II)(OH^-)_n\cdot(a^-)$ [Cu(II)] = 3.6×10^{-3} M, force ionique = 0.5 M, T = 25 °C; (a) pH = 11.0, [aH] = 0.02 M, λ = 290 nm; (b) réaction lente, pH = 9.0, [aH] = 0.01 M, λ = 570 nm; (c) réaction rapide, pH = 9.0, [aH] = 0.01 M, λ = 570 nm.

Quand on étudie la réaction à pH = 9 où $Cu(II)\cdot(OH^-)_m(a^-)_2$ prédomine, deux réactions sont observées. La réaction la plus rapide ($\tau_{\frac{1}{2}} \sim 4$ ms) est attribuée à la dissociation de $Cu(II)\cdot(OH^-)_m(a^-)_2$; dans le domaine de concentration accessible expérimentalement, la constante de vitesse de cette réaction semble être indépendante de la concentration en EDTA, bien qu'à faible concentration on observe une diminution (voir tableau 6), ce qui indiquerait qu'il s'agit de la dissociation de $Cu(II)\cdot(OH^-)_m(a^-)_2$. Malheureusement, le signal faible ne permet pas une étude quantitative plus poussée.

La réaction lente correspond à celle étudiée à pH = 11 et les constantes de vitesse correspondent à celle obtenue a ce pH.

Il est à noter que ces réactions sont de type différent de celles observées dans le cas du système Cu(II)·adénosine en milieu basique; dans ce dernier cas la coordination s'effectue au moyen des groupes hydroxyles du ribose. Ceci se reflète dans la valeur des constantes de vitesse de dissociation de complexes et les constantes de vitesse d'échange avec l'EDTA (14).

Conclusion

L'adénine et le Cu(II) forment en solution divers complexes, suivant le domaine de leur concentration et le pH de la solution, qui ont été étudiés au point de vue cinétique.

En milieu acide, les constantes de vitesse de formation et de dissociation du complex Cu(II)·

Can. J. Chem. Downloaded from www.nrcresearchpress.com by 210.87.254.6 on 09/05/12
For personal use only.

$(aH)_2$ ont pu être mesurées; la formation de ce complexe se fait d'un facteur de dix plus rapidement que celle de Cu(II)·adénosine, mais nettement plus lentement que celle de Cu(II)·aH.

A pH < 3 les formes protonées jouent un rôle prépondérant; le temps de relaxation diminue avec la diminution du pH, ce qui est attribué à la décomposition rapide du complexe protoné $Cu(II)\cdot(aH)_2H^+$.

Les complexes existant en milieu basique ont pu être étudiés grâce à leurs réactions d'échange avec l'EDTA. A pH 11 la dissociation du complexe $Cu(II)\cdot(OH^-)_n(a^-)$ se fait parallèlement à la réaction d'échange. Ceci est analogue aux réactions des complexes Cu(II)–adénosine avec l'EDTA en milieu basique (14).

A pH 9 deux réactions successives ont pu être mises en évidence; la premiére, la plus rapide, correspond à la dissociation de $Cu(II)\cdot(OH^-)_m(a^-)_2$ et la deuxième est la réaction observée à pH 11.

Bien que nos résultats aient été obtenus en milieu acide ou basique à cause de limitations expérimentales, ils permettent néanmoins d'élucider la complexité de la cinétique de l'interaction Cu(II)–adénine aux pH physiologiques où plusieurs de ces complexes coexistent.

Les auteurs remercient le Ministère de l'Education du Québec pour l'octroi qui a rendu possible la réalisation de ce travail et le Conseil national de recherches du Canada pour la bourse d'entretien accordée (G.B.).

1. A. ALBERT. Biochem. J. **54**, 646 (1953).
2. T. HARKINS et H. FREISER. J. Am. Chem. Soc. **80**, 1132 (1958).
3. M. M. TAQUI KHAN et C. R. KRISHNAMORTHY. J. Inorg. Nucl. Chem. **33**, 1417 (1971).
4. E. E. KRISS et K. B. YATSIMIRSKII. Russ. J. Inorg. Chem. **13**, (9), 1223 (1968).
5. H. REINERT et R. WEISS. Hoppe-Seyler's Z. Phys. Chem. **350**, 1310 (1969).
6. R. WEISS et H. VENNER. Hoppe-Seyler's Z. Phys. Chem. **333**, 169 (1963).
7. H. REINERT et R. WEISS. Z. Chem. **9**, 381 (1969).
8. R. WEISS et H. VENNER. Hoppe-Seyler's Z. Phys. Chem. **341**, 229 (1965).
9. R. WEISS et H. VENNER. Hoppe-Seyler's Z. Phys. Chem. **345**, 122 (1966).
10. E. SLETTEN. Acta Cryst. **B25**, 1480 (1969).
11. P. MEESTER, D. M. L. GOODGAME, K. A. PRICE et A. C. SKAPSKI. Nature, **229**, 191 (1971).
12. P. MEESTER, D. M. L. GOODGAME, K. A. PRICE et A. C. SKAPSKI. Chem. Commun. 1573 (1970).
13. M. EIGEN et L. DE MAEYER. *Dans* "Technique of organic chemistry". Vol. VIII. *Edité par* L. Weissberger. P. II. 1963. p. 895; F. CALDIN. Fast reactions in solution. Oxford Blackwell Scient. Publ. (1964).
14. G. BOIVIN et M. ZADOR. Can. J. Chem. **50**, 3117 (1972).
15. L. J. KIRSCHENBAUM et K. KUSTIN. J. Chem. Soc(A), 684 (1970).
16. R. F. PASTERNACK, P. R. HUBER, U. M. HUBER et H. SIGEL. Inorg. Chem. **11**, 276 (1972).
17. V. S. SHARMA et D. L. LEUSSING. Inorg. Chem. **11**, 138 (1972); **11**, 1955 (1972).
18. G. K. PAGENKOPF et D. W. MARGERUM. J. Am. Chem. Soc. **90**, 501 (1968).
19. P. E. STURRUCK. Dissert. Abstr. **21**, 2090 (1960).

Can. J. Chem. Downloaded from www.nrcresearchpress.com by 210.87.254.6 on 09/05/12
For personal use only.

4-Chlorothiane 1-Oxide Conformations: a Large 1,4-Dipolar Effect

GORDON WOOD, C. C. BARKER[1], AND ANNE KLIGERMAN
Department of Chemistry, University of Windsor, Windsor 11, Ontario

Received May 24, 1973

Conformational ratios of *cis*- and *trans*-4-chlorothiane 1-oxide were obtained through low temperature n.m.r. studies. The former compound exists predominantly in the S—O axial form (74:26) and the latter almost exclusively in the S—O axial form (at least 96:4). The *cis* compound approximates additive behavior; the large discrepancy in the *trans* compound is consistent with a 1,4-dipolar interaction.

Les rapports conformationnels des oxydes des chloro-4-thiane-1 *cis* et *trans* ont été obtenus par études r.m.n. à basse température. Le premier composé existe principalement (74:26) dans la forme avec le groupe S—O axial alors que le deuxième existe presqu'exclusivement (au moins 96:4) avec le S—O axial. Les caractéristiques du produit *cis* sont approximativement celles que l'on peut évaluer sur la base de propriétés additives; le fait que cette propriété soit loin d'être vérifiée avec l'isomère *trans* indiquerait qu'une forte interaction dépolarisée 1,4 est présente.

[Traduit par le journal]

Can. J. Chem., 51, 3329 (1973)

Introduction

In the past five years numerous conformational studies on six-membered ring compounds have suggested that 1,4-interactions of polar substituents are important (1–3). The 4-chlorothiane 1-oxides are particularly interesting in this connection because of the unusual preference of the S=O group for the axial position.

The only attempt to assign conformations to these compounds to date (4) was based on i.r. studies which required an assumption about the relative extinction coefficients of axial and equatorial C—Cl bonds. The approximate result for the *cis* compound obtained in this work (1:1 ratio) was not in strict agreement with additivity of ΔG° values (additivity is expected since electrostatic interactions are equal in both chair conformations). The result for the *trans* compound deviated significantly from additivity in a direction consistent with a 1,4 electrostatic effect. (The estimate of 8:1 in favor of the diaxial form implies a 1.2 kcal/mol preference, whereas additivity would predict −0.2 kcal/mol.)

We undertook to determine the conformational ratios for these compounds through the more direct low temperature n.m.r. procedure by measurement of integrated intensities of the methine proton at C-4 (below coalescence).

[1]Taken in part from the M.Sc. Thesis of C. C. Barker, University of Windsor, October, 1971.

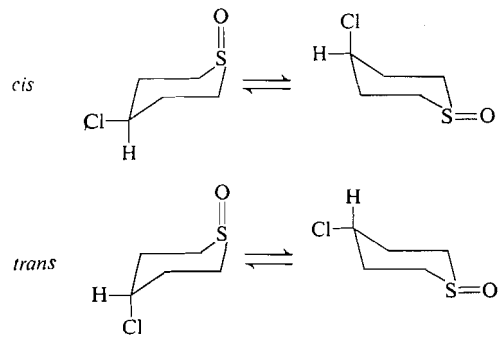

Results and Discussion

The isomeric 4-chlorothiane 1-oxides were prepared by oxidation of the corresponding sulfides and separated by fractional crystallization and sublimation.

A solution (10% in CD_2Cl_2) of *cis*-4-chlorothiane 1-oxide had a methine signal at $\delta = 4.1$ which showed coalescence between −50 and −55° and clean separation of two peaks below −70°. Several scans of the spectrum at −75° and integration yielded a ratio of 26:74 for the methine signals. The former was downfield by 28 Hz and had a $w_{1/2}$ of 8.5 Hz and was therefore assigned to equatorial hydrogen. The larger signal had $w_{1/2}$ of 21.3 Hz centered at 241 Hz and was assigned to axial hydrogen. The weighted average of the half-widths of the two signals at low temperature is 18 Hz, which agrees reasonably well with 15 Hz found at room temperature.

Can. J. Chem. Downloaded from www.nrcresearchpress.com by 210.87.254.5 on 09/05/12
For personal use only.

Can. J. Chem. Downloaded from www.nrcresearchpress.com by 210.87.254.5 on 09/05/12
For personal use only.

The discrepancy could be caused in part by an entropy factor, although reduced resolution (0.6 Hz) at the lower temperature may also be a factor.

A solution (3% in CD_2Cl_2) of the *trans* compound showed a methine proton signal with $w_{1/2} = 10$ Hz at $\delta = 4.5$ which underwent no observable change on cooling to $-84°$. The methine signal was predominantly equatorial ($w_{1/2} = 9$ Hz at $-65°$). Since the limit of detection was estimated at 4% (see Experimental), we conclude that the *trans* isomer is at least 96% in the diaxial form. The low temperature experiment on this compound was repeated in CD_2Cl_2–$ClCD_2CD_2Cl$ solution. No change in the signal with temperature was noted but interference from solvent absorption could perhaps have obscured a small signal. The fact that the $w_{1/2}$ observed at $-65°$ is less than at room temperature suggests that a small amount of axial proton may be present at room temperature, so that the estimate of 96% equatorial proton should be fairly close to the true value.

Comparison of these results with the previous work (4) shows some disagreement and, in particular, the new results are more consistent with additivity of conformational free energies for the *cis* compound. Using the "best value" (5) for chlorine and for S=O, the value determined for thiane oxide (6), additivity would give $\Delta G° = +0.4\,(Cl) - (-0.2)\,(S{=}O) = 0.6$ kcal/mol. (The sign convention emphasizes that S=O prefers the axial position.) This rough calculation agrees reasonably well with the present experimental result of 0.4 kcal/mol favoring the S=O axial, Cl equatorial form.

The n.m.r. result for the *trans* compound corresponds to a minimum value of 1.3 kcal/mol of preference for the diaxial form at $-65°$. Additivity would give a 0.2 kcal/mol preference for the diequatorial form and the discrepancy is thus 1.5 kcal/mol. We attribute this discrepancy to a 1,4-dipolar effect; to our knowledge this is the largest deviation from additivity of this kind yet observed. Some perspective on the magnitude of this effect may be gained by comparison with related systems.

It should be pointed out that while the i.r. method suffers from the lack of verifiable extinction coefficients, our low temperature work was done in different solvents and part of the disagreement with the earlier work may result from this fact.

Rationalization of 1,4-dipolar effects by resort to calculation has not been very productive so far (3*a*). The result presented here is particularly difficult to understand in terms of simple electrostatic interactions, because the positive charge on the ring atom (sulfur) is partial, whereas in the piperidinium system it is approximately unity. It is possible that the partial negative charge on oxygen increases the diaxial preference. The related cyclic sulfone was synthesized for comparison, but gave no evidence for the presence of a form with equatorial chlorine (methine $w_{1/2} = 7.5$ Hz, unchanged except for some loss of resolution between $+30$ and $-120°$).[2]

Experimental

All melting points were determined on a Fisher–Johns melting point block and are uncorrected. G.l.c. was conducted on an F. and M. Model 720 instrument using a 6 ft × 1/2 in. silicone gum rubber column (GE XE-60). The i.r. spectra were recorded on a Beckman Model IR-12 spectrometer. Ambient n.m.r. spectra were recorded on a JEOLCO JNM-C60S spectrometer in CD_2Cl_2 solution. Low temperature n.m.r. spectra were taken on a JNM-C60HL spectrometer with a JRA-1 accumulator using solutions in CD_2Cl_2. Saturation was shown to have a negligible effect on the area ratio for the *cis* compound by increasing the r.f. level.

3-Carbomethoxy-4-oxothiacyclohexane

Cyclization of dimethyl 3,3-thiodipropionate (Aldrich) followed the procedure of Onesta and Castelfranchi (7).

4-Chlorothiopyrane

The three-step procedure of Adlerova and Protiva (8) was used to convert the cyclization product to 4-chlorothiopyrane.

4-Chlorothiane-1-oxide

The oxide (mixed isomers) was prepared by periodate oxidation (9) of 4-chlorothiopyrane. Overall yield for the five steps was 15%.

Separation of cis- and trans-4-Chlorothiane 1-Oxide

A crude sample of the mixed isomers (2.2 g) was recrystallized from CCl_4. The needle-like crystals (0.8 g), after repeated crystallization, yielded a pure (98% by g.l.c.) sample of *cis*-4-chlorothiane 1-oxide, m.p. 119–123° (lit. 120–121° (4)). The n.m.r. spectrum had a single methine proton band at 4.1 p.p.m. (246 Hz, previously reported (4) 251 Hz). The i.r. spectrum showed sulfoxide (S=O) absorption at 1000–1100 cm^{-1} and C—Cl stretching at 760 cm^{-1} (KBr) and in CS_2, 729, 756 cm^{-1} (lit. 719, 748 (4)).

Anal. Calcd. for C_5H_9ClOS: C, 39.3; H, 5.9; Cl, 23.2. Found: C, 39.8; H, 6.2; Cl, 22.9.

The residue from initial CCl_4 crystallization was alternately sublimed and the sublimate crystallized from

[2]This experiment was suggested by Prof. Robert Stolow in a private communication.

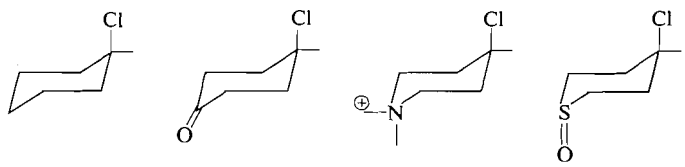

$-\Delta G^\circ_{Cl}$	+0.4	−0.2 to −0.5	0.0 to −0.7	−1.1*†
Deviation	—	0.6–0.9	0.4–1.1	1.5†
Ref.	5	2	3	This work

*Obtained by subtracting $-\Delta G^\circ_{S=O} = -0.2$ from the observed $-\Delta G^\circ = -1.3$. This procedure arbitrarily places all the deviation in the $-\Delta G^\circ_{Cl}$ value.
†Minimum values, see text.

CCl_4 to remove the last trace of *cis* isomer. Finally, the residue was crystallized from petroleum ether to a purity of 98% (g.l.c.). The n.m.r. spectrum showed a single methine band at 4.5 p.p.m. (270 Hz, previously reported (4) at 271 Hz). The i.r. spectrum had sulfoxide (S=O) absorption at 1000–1100 cm^{-1} and C—Cl stretching bands (CS_2 solution) at 765 and 719 cm^{-1} (lit. 747, 714 cm^{-1} (4)).

Anal. Calcd. for C_5H_9ClOS: C, 39.3; H, 5.9; Cl, 23.2. Found: C, 39.6; H, 6.1; Cl, 23.1.

Estimation of Detection Limit in trans-1-Chlorothiane 1-Oxide

Two attempts were made to estimate the concentration of minor conformer (equatorial Cl, equatorial S=O) present in the *trans* compound. Accumulation of 36 scans of the low temperature spectrum showed no sign of an additional signal in the appropriate region. Finally, addition of small amounts of the *cis* isomer to the 3% CD_2Cl_2 solution of the *trans* compound demonstrated that at a *trans*:*cis* ratio of 98:2, the minor signal was not detected, but at 96:4 it was.

We wish to acknowledge the technical assistance of Mr. D. Hill and Dr. M. H. Miskow in obtaining n.m.r. spectra, and of Mr. Brian Adlam for the 4-chlorothiane 1,1-dioxide experiment.

The financial assistance of the National Research Council of Canada is gratefully acknowledged.

1. Gordon Wood, E. P. Woo, and M. H. Miskow. Can. J. Chem. **47**, 429 (1969) and references therein.
2. R. D. Stolow and T. W. Giants. Chem. Commun. 528 (1971) and references therein.
3. (*a*) R. D. Stolow, D. I. Lewis, and P. A. D'Angelo. Tetrahedron, **26**, 5831 (1970). (*b*) M.-L. Stein, G. Chiurdoglu, R. Ottinger, J. Reisse, and H. Christol. Tetrahedron, **27**, 411 (1971).
4. J. C. Martin and J. J. Uebel. J. Am. Chem. Soc. **86**, 2936 (1964).
5. J. A. Hirsch. *In* Topics in stereochemistry. Vol. 1. *Edited by* N. A. Allinger and E. L. Eliel. Wiley-Interscience, New York. 1967. p. 202.
6. J. B. Lambert and R. G. Keske. J. Org. Chem. **31**, 3429 (1966).
7. R. Onesta and G. Castelfranchi. Gazz. Chim. Ital. **89**, 1127 (1959). Chem. Abstr. **54**, 22618c (1960).
8. E. Adlerova and M. Protiva. Czech. Chem. Commun. **24**, 1268 (1959).
9. C. R. Johnson and N. J. Leonard. J. Org. Chem. **27**, 282 (1962).

Can. J. Chem. Downloaded from www.nrcresearchpress.com by 210.87.254.5 on 09/05/12
For personal use only.

Binary Dinitrogen Complexes of Rhodium, $Rh(N_2)_n$ (where n = 1–4), in Low Temperature Matrices

GEOFFREY A. OZIN AND ANTHONY VANDER VOET

Lash Miller Chemical Laboratories and Erindale College, University of Toronto, Toronto, Ontario M5S 1A1

Received March 19, 1973

The products of the cocondensation reactions of Rh atoms with N_2 and N_2/Ar mixtures at 10 °K are investigated by matrix isolation infrared spectroscopy and are shown to be binary dinitrogen complexes of the form $Rh(N_2)_n$. Examination of the reaction products in pure $^{14}N_2$, $^{15}N_2$, $^{14}N_2/^{15}N_2$, and in dilute $Ar/^{14}N_2$, $Ar/^{14}N_2/^{15}N_2$, and $Ar/^{14}N_2/^{14}N^{15}N/^{15}N_2$ matrices establish the values of n to be 1-4. Isotopic frequencies are computed for the NN stretching modes of the individual dinitrogen complexes on the basis of the Cotton–Kraihanzel (C.K.) force field approximation and are found to be in close agreement with observed values. Trends in the best fit C.K. force constants for $Rh(N_2)_n$ (n = 1-4) and the thermodynamic stabilities of the individual complexes as indicated by the function ΔH_c^n, a measure of the enthalpy of decomposition, are discussed. Comparisons are made between $Ni(N_2)_n$ and $Rh(N_2)_n$ (where n = 1–4). The structure of $Rh(N_2)_4$ in solid nitrogen is shown to be that of a distorted tetrahedron. Calculations show that a site symmetry of D_{2d} for $Rh(N_2)_4$ satisfactorily accounts for all of the spectral lines observed for the complex in nitrogen. In solid argon, $Rh(N_2)_4$ appears to have an approximately regular tetrahedral structure. The relationship between RhN_2 and N_2 chemisorbed on Rh metal is discussed and compared with the analogous Ni–, Pd–, and Pt–nitrogen systems.

Les produits de réactions de cocondensation des atomes Rh sur N_2 et sur des mélanges N_2/Ar à 10 °K, ont été étudiés par spectroscopie infrarouge sur des matrices isolées. Les produits formés sont des complexes binaires diazotés du type $Rh(N_2)_n$. L'examen des produits de réaction dans des matrices pures de $^{14}N_2$, $^{15}N_2$, $^{14}N_2/^{15}N_2$ et diluées de $Ar/^{14}N_2$, $Ar/^{14}N_2/^{15}N_2$ et $Ar/^{14}N_2/^{14}N^{15}N/^{15}N_2$, permet d'établir les valeurs de n de 1 à 4. Les fréquences isotopiques ont été calculées pour les vibrations d'élongation NN dans les complexes diazotés individuels sur la base de l'approximation du champ de force de Cotton–Kraihanzel (C.K.); un accord proche des valeurs observées a été trouvé. Les tendances dans les meilleures constantes de force C.K. pour $Rh(N_2)_n$ (n = 1 à 4) et les stabilités thermodynamiques des complexes individuels indiquées par ΔH_c^n (qui mesure l'enthalpie de décomposition) ont été discutées. Des comparaisons entre $Ni(N_2)_4$ et $Rh(N_2)_4$ ont été faites (où n = 1 à 4). La structure de $Rh(N_2)_4$ dans l'azote solide est celle d'un tétraèdre distordu. Les calculs montrent qu'un site de symétrie D_{2d} pour $Rh(N_2)_4$ tient compte de façon satisfaisante de toutes les raies spectrales observées pour ce complexe dans l'azote. Dans l'argon solide, $Rh(N_2)_4$ apparaît sous forme de tétraèdre approximativement régulier. La relation entre RhN_2 et N_2 chimisorbé sur Rh métal a été discutée et comparée avec les systèmes analogues Ni–, Pd–, Pt– azote. [Traduit par le journal]

Can. J. Chem., **51**, 3332 (1973)

Introduction

Because of their relationship to biological nitrogen fixation problems and transition metal carbonyl complexes, inorganic compounds containing molecular dinitrogen as a ligand have been of considerable interest to both synthetic and structural chemists. Many of the transition metals have been shown to form stable complexes (1, 2) with one or two dinitrogen groups coordinated to the metal atom.

Recently, matrix isolation vibrational spectroscopy of metal atom vapors cocondensed with molecular nitrogen have shown the existence of binary transition metal dinitrogen compounds $M(N_2)_n$, with as many as four dinitrogen molecules coordinated to a single metal atom (3, 4). One of the obvious benefits of the study of these matrix isolated species (as well as the analogous $M(CO)_n$ (5, 6) and $M(O_2)_m$ (7) complexes) is the ability to study the effect of increased coordination on the strengths of the ligand and metal–ligand bonds, without the necessity of including other stabilizing ligands. This, in conjunction with the ability to prepare mixed ligand species such as $Ni(CO)_n(N_2)_{4-n}$ (8) and $Ni(O_2)(N_2)_m$ (9) (n = 1–3, m = 1, 2) also enables direct comparison of the sigma and pi bonding characteristics of different ligands when bonded to the same metal atom and competing for the same bonding electrons.

In the majority of these binary dinitrogen complexes the molecular ligand was shown by

Can. J. Chem. Downloaded from www.nrcresearchpress.com by 210.87.254.42 on 09/05/12
For personal use only.

Can. J. Chem. Downloaded from www.nrcresearchpress.com by 210.87.254.42 on 09/05/12
For personal use only.

$^{14}N^{15}N$ isotopic substitution to be bonded in an "end-on" fashion, and in the unmixed species to have molecular structures analogous to the metal carbonyls, for example, tetrahedral $Ni(N_2)_4$ and $Ni(CO)_4$ (3), trigonal planar $Pd(N_2)_3$ and $Pd(CO)_3$ (3, 6), linear symmetrical $Pd(N_2)_2$ and $Pd(CO)_2$ (3, 6), etc.

An exception to this mode of bonding was observed in the products of the cocondensation of cobalt atoms and dilute N_2/Ar matrices where the $Co(N_2)$ species was shown to have the N_2 ligand bonded in a dihapto or side-on manner (10). Moreover, the products of co-condensing Co atoms with pure nitrogen gave rise to a (as yet unassigned (11)) four line spectrum in the NN stretching region, belonging to a single species, an unusual result when compared to the Ni, Pd, and Pt systems. The investigation of the rhodium/dinitrogen system is therefore an important next step in the understanding and identification of the cobalt dinitrogen compounds and indeed of all members of the group. Accordingly, cocondensation reactions of rhodium atoms with pure nitrogen and nitrogen–argon mixtures were undertaken. The results are reported in the following sections.

Experimental

Monatomic Rh vapor was generated by directly heating a thin (0.005 in.) ribbon filament of Rh with AC. The rhodium (99.99%) was supplied by McKay Inc., New York. Research grade $^{14}N_2$ (99.99%) and Ar (99.99%) were supplied by Matheson. Isotopically enriched $^{15}N_2$ (99.5%) was supplied by Prochem.

The furnace used for the evaporation of the metals has been described previously (12). The rate of metal atom depositions was continuously monitored using a quartz crystal microbalance (13). In the infrared experiments matrices were deposited on a cryotip cooled to 10 °K by means of an Air Products Displex closed cycle helium refrigerator. Spectra were recorded on a Beckmann IR 12 spectrophotometer.

Results and Discussion

Rhodium Monodinitrogen, $Rh(N_2)$

Cocondensation of rhodium atoms with very dilute nitrogen–argon mixtures ($^{14}N_2$:Ar < 1:250) at 10 °K gave rise to an intense infrared absorption band at 2154 cm^{-1}. When slightly higher concentration matrices were used, for example, $^{14}N_2$:Ar = 1:250 to 1:100 (see Fig. 1*A*), the most intense absorption band was still at 2154 cm^{-1} but was accompanied by a very weak shoulder at 2159 cm^{-1} (shown below to be a matrix splitting of the 2154 cm^{-1} band) and another weak band at 2188 cm^{-1} which under high resolution was also a closely spaced doublet, 2189/2186.5 cm^{-1} (Fig. 1*A*), also attributed to a matrix splitting. Warm-up experiments performed on these dilute $^{14}N_2$/Ar matrices indicated the gradual disappearance of the band at 2154 cm^{-1}, the increase in intensity of the 2188 cm^{-1} band, and the appearance of a new band at 2195 cm^{-1} and a stronger doublet at 2179.5/2175 cm^{-1}. The spectrum obtained after warm-up of the $^{14}N_2$:Ar = 1:100 matrix to 30–35 °K is shown in Fig. 1*B*, where it is seen that the 2159/2154 cm^{-1} doublet has almost completely disappeared and the bands at 2195, 2188, and 2179.5/2175 cm^{-1} predominate. These four main lines grew and decayed at different rates during warm-up experiments and appeared with markedly different relative intensities in experiments in which the $^{14}N_2$:Ar ratio was varied. This behavior suggested the formation of at least *four* different dinitrogen species from the Rh/N_2 matrix cocondensation reaction. *A priori* the complex of lowest coordination number could be associated with the main absorption band at 2154 cm^{-1} observed in very dilute mixtures. The stoichiometry of this species was defined by examining the products

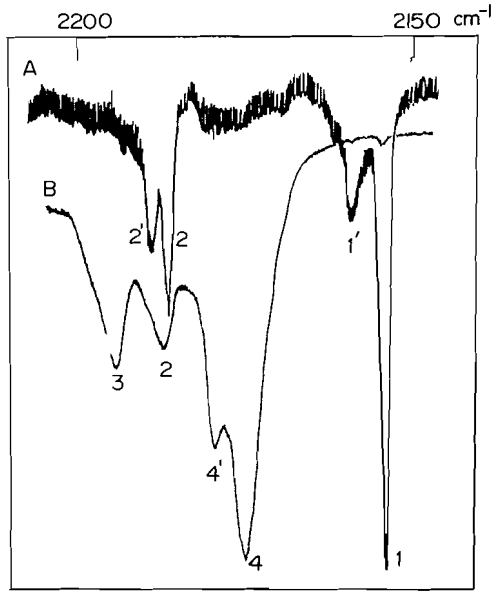

FIG. 1. The matrix infrared spectrum of the products of the cocondensation reaction of Rh atoms with $^{14}N_2$:Ar = 1:100 (*A*) after deposition at 10 °K and (*B*) after warm-up to 30–35 °K.

Can. J. Chem. Downloaded from www.nrcresearchpress.com by 210.87.254.42 on 09/05/12
For personal use only.

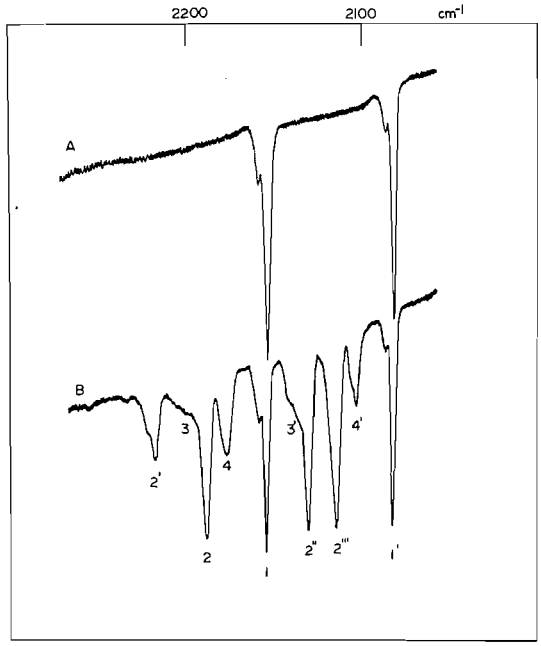

FIG. 2. The matrix infrared spectrum of the products of the cocondensation reaction of Rh atoms with $^{14}N_2$:$^{15}N_2$:Ar ≅ 1:1:500 (*A*) after deposition at 10 °K and (*B*) after warm-up to 20–25 °K.

of the cocondensation reaction of Rh atoms with $^{14}N_2$:$^{15}N_2$:Ar ≅ 1:1:500 at 10 °K. The spectrum, given in Fig. 2*A*, shows that the 2159/2154 cm^{-1} absorption has a *single* nitrogen-15 counterpart absorption at 2088/2083 cm^{-1}. This doublet isotope pattern is characteristic of a monodinitrogen species where the lines at 2159/2154 and 2088/2083 cm^{-1} are assigned to Rh$^{14}N_2$ and Rh$^{15}N_2$, respectively. Cocondensation of Rh atoms with a statistically scrambled isotopic mixture $^{14}N_2$:$^{14}N^{15}N$:$^{15}N_2$:Ar = 1:2:1:2000 resulted in a spectrum containing *four* lines of almost *equal* intensity (Fig. 3) at 2154.1, 2119.7, 2118.0, and 2082.5 cm^{-1}. The equality of the band intensities, the similar band widths at half height (≃1.0 cm^{-1}), and the 1.7 cm^{-1} separation observed for the central Rh($^{14}N^{15}N$)/Rh($^{15}N^{14}N$) doublet prove unequivocally that the dinitrogen ligand in Rh(N_2) is bonded in an "end-on" fashion to the rhodium atom.

Rhodium Tetradinitrogen, Rh(N_2)$_4$

When Rh atoms were cocondensed with a 1:10 mixture of $^{14}N_2$ in Ar at 10 °K the matrix infrared spectrum shown in Fig. 4*A* was obtained. Intense absorptions were observed at 2196, 2188, 2177.5, and 2154.5 cm^{-1} with very weak bands at approximately 2232 and 2136 cm^{-1}. Upon warm-up in the range 10–40 °K the *four* main bands grew and decayed in intensity at different rates (see Fig. 4(*B–D*)) yielding finally a strong line at 2177.5 cm^{-1} with a weaker line at 2196 and a shoulder at 2187 cm^{-1}. Prolonged warm-ups at 35–40 °K gave a final spectrum showing the bands at 2196 cm^{-1} and 2177.5 cm^{-1}. The very weak lines observed at about 2232 and 2136 cm^{-1} on deposition grew in intensity on warm-up to 40 °K and were assigned to aggregate species (see later). The results of more dilute $^{14}N_2$/Ar experiments (1/100 and 1/250, see, for example, Fig. 1) initially showed absorptions at 2159/2154 cm^{-1} (RhN_2) and at 2188 cm^{-1}. However, the warm-up characteristics of these matrices paralleled the behavior of the $^{14}N_2$/Ar = 1/10 experiments. A *prima facie* interpretation suggests, therefore, that all four Rh/N_2 species were formed in the concentrated N_2/Ar matrices when initially deposited at 10 °K and that the band at 2177.5 cm^{-1} (2179.5/2175 cm^{-1} in more dilute matrices) probably corresponds to the highest coordinated species.

Rh atoms were cocondensed with pure $^{14}N_2$ at 10 °K and yielded the infrared spectrum shown

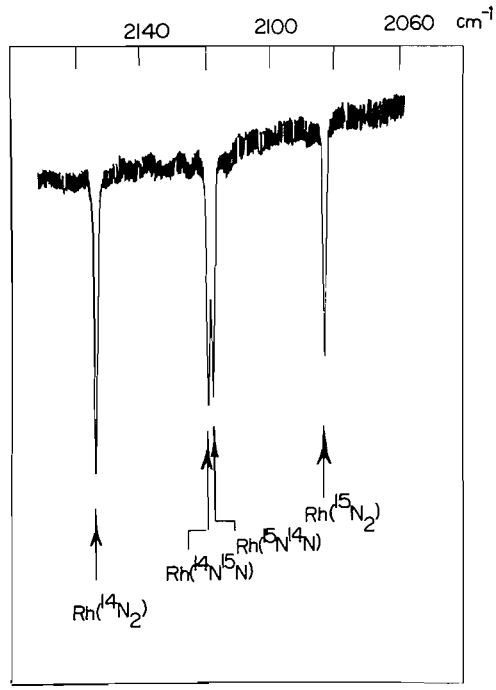

FIG. 3. The matrix infrared spectrum of the products of the cocondensation reaction of Rh atoms with $^{14}N_2$:$^{14}N^{15}N$:$^{15}N_2$:Ar ≅ 1:2:1:2000 at 10 °K.

Can. J. Chem. Downloaded from www.nrcresearchpress.com by 210.87.254.42 on 09/05/12
For personal use only.

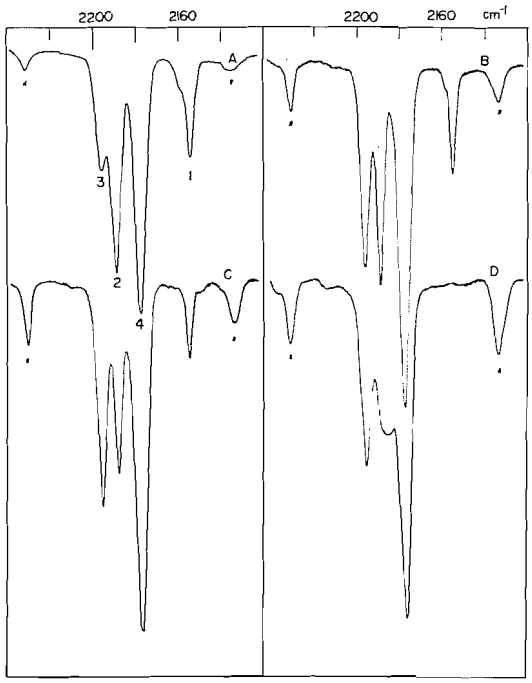

FIG. 4. The matrix infrared spectrum of the products of the cocondensation reaction of Rh atoms and $^{14}N_2$:Ar = 1:10 (*A*) after deposition at 10 °K, (*B–D*) after successive warm-up experiments at 20, 30, and 35–40 °K, respectively. The asterisks indicate aggregate species (see text).

in Fig. 5*A*. The spectrum showed a very intense absorption at 2179 cm^{-1}, an absorption of medium intensity at 2203 cm^{-1}, and two extremely weak absorptions at about 2238 and 2218 cm^{-1}. The relative intensities of the two bands at 2179 and 2203 cm^{-1} were essentially invariant to changes in the rate of deposition of Rh atoms. In addition it was observed that in matrix warm-ups to 35–40 °K the intensities of the main lines at 2203/2179 cm^{-1} gradually *decreased* retaining approximately equal relative intensities (Fig. 5*B*). The very weak lines originally at 2238 and 2218 cm^{-1} grew in intensity during warm-up to yield lines at 2242/2238 and 2218/2215 cm^{-1} (Fig. 5*B*) as well as another very weak line at about 2113 cm^{-1} and are assigned to rhodium–nitrogen aggregate species (see later for details). The frequencies observed after the cocondensation of Rh atoms with $^{14}N_2$:$^{15}N_2$ = 1:1 are listed in Table 1. These and the intensity pattern are reminiscent of the results obtained in the analogous $Ni(^{14}N_2)_n$-$(^{15}N_2)_{4-n}$ system (where n = 0–4) in solid N_2 (3).

Since the principal band at 2179 cm^{-1} appears to correspond to the 2177.5 cm^{-1} line in N_2/Ar matrices,[1] and since one must conclude that the 2203 cm^{-1} line derives from the same species as the 2179 cm^{-1} line, both bands can be assigned to $Rh(N_2)_4$. The two lines must arise therefore from the *partial* or complete removal of the degeneracy of either the T_2 (tetrahedral) or E_u (square planar) NN stretching mode in the lattice of α-$^{14}N_2$ (the low temperature phase of solid N_2 (14)).

An attempt to obtain isotopic frequencies of $Rh(N_2)_4$ and to avoid the distortion problem by deposition of Rh atoms with a $^{14}N_2/^{15}N_2$/Ar = 1/1/20 mixture and warming the matrix to 35–40 °K was considered. However, since after warm-up of $^{14}N_2$/Ar = 1/10 matrices over a prolonged period of time the 2196 cm^{-1} band persists with medium intensity, it was felt that the intermediate responsible for this line would be present as well in the isotopic experiment with bands of intensity sufficient to obscure some of the isotopic components of $Rh(^{14}N_2)_n$-

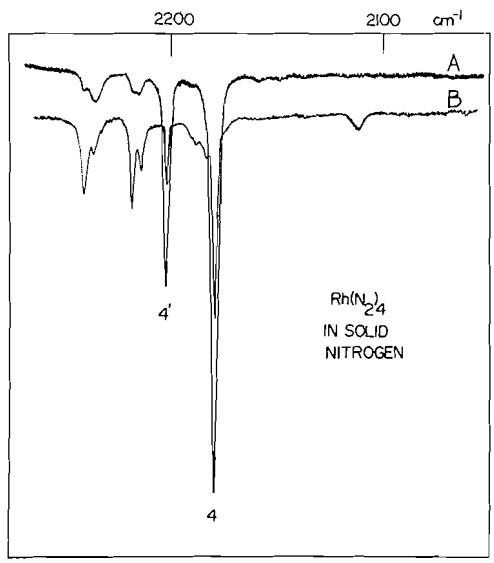

FIG. 5. The matrix infrared spectrum of the products of the cocondensation reaction of Rh atoms with pure $^{14}N_2$ (*A*) after deposition at 10 °K and (*B–C*) after warm-up to 25 and 35 °K, respectively.

[1]The much smaller doublet splitting for the T_2 or E_u mode of $Rh(N_2)_4$ in dilute N_2/Ar (1/250, 1/100) matrices observed at 2179.5/2175 cm^{-1} may also reflect a "slight" lattice perturbation of the regular symmetry but is a very much less serious effect than is observed in solid α-N_2.

Can. J. Chem. Downloaded from www.nrcresearchpress.com by 210.87.254.42 on 09/05/12
For personal use only.

$(^{15}N_2)_{4-n}$ (n = 0–4) and complicate the assignments. Thus this isotopic experiment was not thought to be worthwhile.

In order to clarify the structure of $Rh(N_2)_4$ in solid nitrogen and consequently in N_2/Ar matrices, one first assumes the perturbation to be caused by the coordinated dinitrogen molecules attempting to adopt, as much as possible, orientations similar to those they would have had in the pure unsubstituted nitrogen lattice. As in the $Ni(N_2)_4$ system (3), the rhodium atom would probably choose to reside in the more spacious substitutional site of the f.c.c. lattice of α-N_2. If the preferred interaction of the rhodium were with four tetrahedrally disposed nearest neighbor N_2 molecules, then the "distortion" of the end-on bonded N_2 molecules would be toward the substitutional site symmetry of N_2 in the unsubstituted lattice, *i.e.* C_2. Whether in actual fact the lattice affects the N—Rh—N skeletal angles or causes deviation of the Rh—N≡N angle away from linearity (which seems more likely), as shown below, cannot be determined. If the preferred interaction with four N_2 molecules in $Rh(N_2)_4$ were square planar (D_{4h}), the α-nitrogen lattice would favor the site symmetry C_{2h} with the C_2 axis in the square plane.

Therefore the 2203/2179 cm^{-1} doublet may arise from (*i*) a regular tetrahedral molecule whose symmetry is very *slightly* distorted towards D_{2d}, (*ii*) the same as (*i*) but with a considerable angular distortion towards D_{2d} ("squashed" tetrahedral molecule), or (*iii*) a regular square planar D_{4h} molecule whose symmetry is reduced to C_{2h} in the nitrogen lattice. A resumé of the splittings expected for the two possible $Rh(N_2)_4$ symmetries and the respective intensity relationships expected are compared with the observed data below.

	T_d	D_{2d}	ν_{NN}	I_E/I_{B_2} Calculated	I_E/I_{B_2} Observed
(*i*)	T_2	B_2	2203	$\tan^2(\theta/2) \cong 2(\theta = 109°28')$	3.59–3.89
		E	2179		
(*ii*)	T_2	B_2	2203	$\tan^2(\theta/2)$*	3.59–3.89
		E	2179		

	D_{4h}	C_{2h}	ν_{NN}	I_{B_u}/I_{A_u} Calculated	I_{B_u}/I_{A_u} Observed
(*iii*)	E_u	A_u	2203	1	3.59–3.89
		B_u	2179		

*Best fit for calculated value $\theta = 124°21' \rightarrow 126°21'$.

The results clearly indicate that the lattice distortion is to a D_{2d} configuration with an "effective" N_2—Rh—N_2 angle of $126°14' \rightarrow 124°21'$. The two intensity ratios and postulated angles given are compatible with the observed spectra on deposition at 10 °K and after diffusion controlled warm-up to 35 °K, respectively.

Frequency and C.K. Force Constant Calculations for $Rh(N_2)_4$ in Solid N_2

On the basis of the D_{2d} symmetry model, the C.K. force constants (15) were calculated by applying a least squares analysis of the observed isotopic frequencies for the six molecules $Rh(^{14}N_2)_n(^{15}N_2)_{4-n}$ (n = 0–4) shown below ($k_{NN,NN}$ is associated with θ and $k'_{NN,NN}$ with β).

The calculated and observed frequencies are compared in Table 1. (Included in the table are the best fit C.K. k_{NN} and $k_{NN,NN}$ force constants.) The agreement is within 3 cm^{-1} for all observed lines and provides convincing support for our vibrational assignment of these lines to $Rh(N_2)_4$ having distorted tetrahedral D_{2d} symmetry in solid α-N_2.

Rhodium Bisdinitrogen, $Rh(N_2)_2$, and Rhodium Trisdinitrogen, $Rh(N_2)_3$

The species giving rise to the two major bands at 2196 and 2188 cm^{-1}, observed on deposition of concentrated $^{14}N_2$/Ar = 1/10 matrices and during warm-up of dilute $^{14}N_2$/Ar matrices, have not as yet been characterized. A *prima*

TABLE 1. Isotopic frequency calculations* for the NN stretching modes of $Rh(^{14}N_2)_n(^{15}N_2)_{4-n}$ (where n = 0–4) in solid nitrogen†

Frequency (cm^{-1})		
Calculated	Observed	Assignment
2106.5	2106.5	ν_E(VI), ν_{B_2}(III) $\nu_{A''}$(V)
2117.9	2115.0	$\nu_{A'}$(V)
2118.2	2116.5	ν_B(IV)
2120.8	2121.0	$\nu_{A'}$(II)
2125.3	2122.0	ν_A(IV)
2129.7	2129.5	ν_{B_2}(VI)
2143.1	2146.0	ν_{A_1}(III)
2147.1	2148.5	ν_{A_1}(V)
2180.5	2179.5	ν_E(I), ν_{B_2}(III) $\nu_{A''}$(II)
2192.5	2193.0	ν_B(IV)
2197.2	2198.0	$\nu_{A'}$(II)
2203.2	2203.0	ν_{B_2}(I)
2210.2	2208.0	$\nu_{A'}$(V)
2220.6	—	ν_A(IV)
2226.4	2227.5	ν_{A_1}(III)
2232.7	2231.0	$\nu_{A'}$(II)

*The best fit NN C.K. force constants were k_{NN} = 19.989, $k_{NN,NN}$ = 0.382, and $k'_{NN,NN}$ = 0.165 mdyn/Å (see text for notation).
†Calculations for $Rh(N_2)_4$ with D_{2d} symmetry.

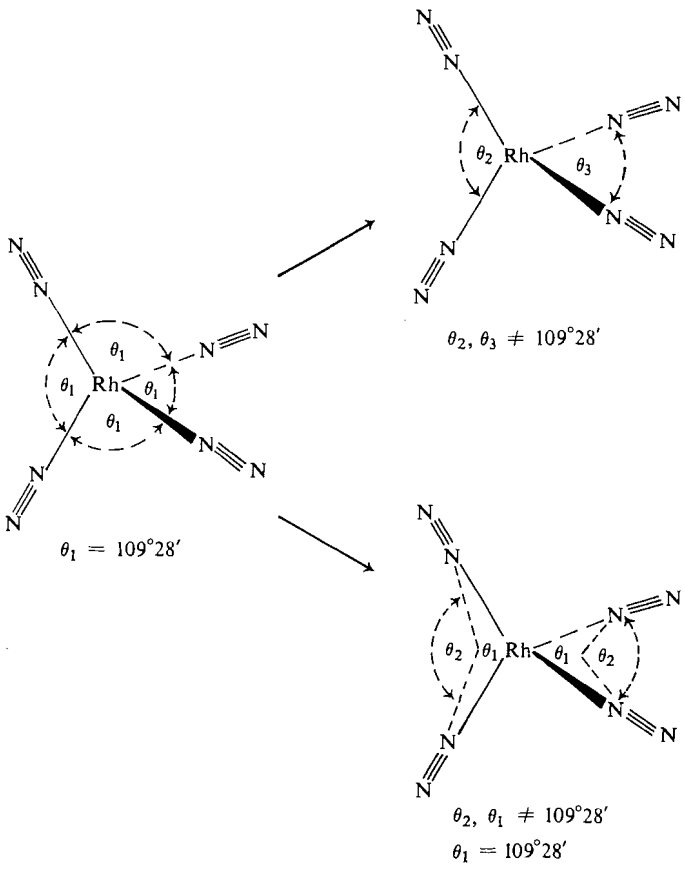

Can. J. Chem. Downloaded from www.nrcresearchpress.com by 210.87.254.42 on 09/05/12
For personal use only.

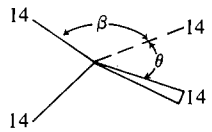

D_{2d} (I)

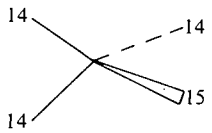

C_s (II)

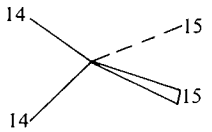

C_{2v} (III)

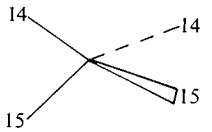

C_2 (IV)

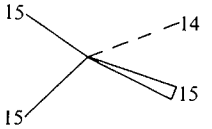

C_s (V)

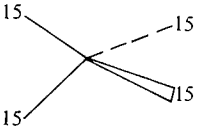

D_{2d} (VI)

facie assignment of these two lines, in light of the foregoing discussions, is to a bis- and trisdinitrogen dinitrogen complex.

$Rh(N_2)_2$

The 2188 cm^{-1} absorber was the *first* to appear on warm-up of very dilute N_2/Ar matrices initially showing only $Rh(N_2)$, and often accompanied $Rh(N_2)$ in more concentrated matrices, upon cocondensation at 10 °K. Warm-up studies indicated that as the 2188 cm^{-1} line intensity began to decrease, that of the band at 2179.5/2175 cm^{-1} assigned to $Rh(N_2)_4$ increased. At 35–40 °K the band assigned to $Rh(N_2)$ at 2159/2154 cm^{-1} had disappeared and a new band at 2196 cm^{-1} appeared. It is significant that in very dilute matrices this 2196 cm^{-1} line *only* appeared at the end of the warm-up experiments, whereas the $Rh(N_2)_4$ species (2179.5/2175 cm^{-1}) was already present. Only in more concentrated matrices ($^{14}N_2$/Ar = 1:10) did the 2196 cm^{-1} line appear with any appreciable intensity (see Fig. 4 and section on warm-up characteristics and stabilities).

When Rh atoms were cocondensed with an isotopic mixture $^{14}N_2$:$^{15}N_2$:Ar = 1:1:500 at 10 °K and warmed up to 20–25 °K, the isotopic counterparts of the band at 2188 cm^{-1} were observed. The spectrum is shown in Fig. 2*B* and in addition to the lines at 2159/2154 and 2088/2083 cm^{-1} assignable to $Rh(^{14}N_2)$ and $Rh(^{15}N_2)$, a *doublet of doublets* isotope pattern is observed at 2218, 2188 and 2130, 2115 cm^{-1}. Further warm-up studies of this matrix showed that these four bands behaved in a similar manner and could be assigned to the four expected NN stretching modes of the mixed isotopic bisdinitrogen molecules, $Rh(^{14}N_2)_n(^{15}N_2)_{2-n}$ (where n = 0–2). The observation of only one line at 2188 cm^{-1} in $^{14}N_2$/Ar matrices[2] assignable to a bisdinitrogen species, suggests that the $Rh(N_2)_2$ molecule is probably linear, with $D_{\infty h}$ symmetry (analogous to other transition metal binary carbonyl and dinitrogen compounds, observed thus far, *e.g.* $Ni(N_2)_2$, $Ni(CO)_2$, $Pd(CO)_2$, $Pd(N_2)_2$) (3, 5, 6). The C.K. force constants for $Rh(N_2)_2$ were calculated for a linear $D_{\infty h}$ molecule in the manner outlined for $Rh(N_2)_4$. Table 2 shows the results of the frequency calculation and lists the best fit C.K. k_{NN} and $k_{NN,NN}$ force constants. The agreement between the observed and calculated frequencies is within 1.7 cm^{-1} for all observed lines, indicating the assignment of these bands to a linear bisdinitrogen molecule to be compatible with the observed data.

$Rh(N_2)_3$

The characterization of a trisdinitrogen complex of rhodium proved to be difficult in part, because it was only when concentrated $^{14}N_2$/Ar matrices were used that the remaining unassigned band at 2196 cm^{-1} was observed with any appreciable intensity. Unfortunately, at these concentrations, mixed $^{14}N_2/^{15}N_2$/Ar experiments are complicated by the presence of the isotopic components of the bis- and tetradinitrogen molecules. Careful examination of

[2]The small splitting of this line (2.5 cm^{-1}) is ascribed to a matrix site splitting.

Can. J. Chem. Downloaded from www.nrcresearchpress.com by 210.87.254.42 on 09/05/12
For personal use only.

TABLE 2. Isotopic frequency calculations for the NN stretching modes of $Rh(^{14}N_2)_n(^{15}N_2)_{2-n}$ (where $n = 0$–2)*

Frequency (cm^{-1})		
Calculated	Observed	Assignment
2115.0	2113.3	Σ_u^+ $Rh(^{15}N_2)_2$
2131.0	2130.0	Σ^+ $Rh(^{15}N_2)(^{14}N_2)$
2187.5	2187.5	Σ_u^+ $Rh(^{14}N_2)_2$
2218.0	2219.2	Σ^+ $Rh(^{14}N_2)(^{15}N_2)$

*The best fit NN C.K. force constants were $k_{NN} = 20.183$, $k_{NN} = 0.449$ mdyn/Å.

TABLE 3. Isotopic frequency calculations for $Rh(^{14}N_2)_n(^{15}N_2)_{3-n}$* (where $n = 0$–3)†

Frequency (cm^{-1})		
Calculated	Observed	Assignment
2233.2	Not obsvd.‡,§	$Rh(^{14}N_2)_2(^{15}N_2)$
2219.2	Not obsvd.‡,‖	$Rh(^{14}N_2)(^{15}N_2)_2$
2194.8	2196	$Rh(^{14}N_2)_3$
2144.4	2145	$Rh(^{14}N_2)(^{15}N_2)_2$
2130.9	‖	$Rh(^{14}N_2)_2(^{15}N_2)$
2120.4	2118	$Rh(^{15}N_2)_3$

*Assuming trigonal planar structure.
†Best fit NN C.K. force constants were $k_{NN} = 20.168$ and $k_{NN,NN} = 0.302$ mdyn/Å. Least squares analyses were performed with the assignment of the 2145 cm^{-1} band to both $Rh(^{14}N_2)_2(^{15}N_2)$ and $Rh(^{14}N_2)(^{15}N_2)_2$, the latter giving the best fit.
‡These two lines are expected to have low intensities compared to the corresponding isotopic line at 2145 cm^{-1}.
§Probably obscured by aggregate lines in this region (see text).
‖Expected to be overlapped by the stretching modes of $Rh(^{14}N_2)(^{15}N_2)$ at 2219.2 and 2130.0 cm^{-1} (see Table 3).

the spectra resulting from Rh atoms cocondensed with $^{14}N_2:^{15}N_2:Ar = 1:1:500$ at 10 °K and warm-up at 40 °K, resulted in the identification of two isotopic lines in the nitrogen-15 region at 2145 cm^{-1} and 2118 cm^{-1} which were not observed in any of the other runs and which are *not* assignable to $Rh(N_2)$, $Rh(N_2)_2$, or $Rh(N_2)_4$. These are associated with the expected $^{15}N_2$ modes of two of the isotopic trisdinitrogen molecules $Rh(^{14}N_2)_2(^{15}N_2)$, $Rh(^{14}N_2)(^{15}N_2)_2$, and $Rh(^{15}N_2)_3$, respectively. As the infrared absorption at 2196 cm^{-1} is the only major band which can be associated with $Rh(^{14}N_2)_3$ in $^{14}N_2$/Ar matrices, it is not unreasonable to assume a trigonal planar D_{3h} structure for the trisdinitrogen rhodium complex (similar to the known tris-complexes $Ni(CO)_3$, $Ni(N_2)_3$, $Pd(CO)_3$, $Pd(N_2)_3$, $Pt(CO)_3$, and $Pt(N_2)_3$) (3–6). The best fit C.K. force constants k_{NN} and $k_{NN,NN}$, were determined for planar $Rh(N_2)_3$, using the observed isotopic lines at 2196, 2145, and 2118 cm^{-1}. The calculated frequencies are listed in Table 3 and are in reasonably close agreement for the three observed lines and lend some support to the assignment.

The Observation of Low Frequency Skeletal Modes in $Rh(N_2)_n$ and the Nature of the Rh—N Band

The detection of low frequency modes for matrix isolated binary dinitrogen and carbonyl complexes has proven difficult on a number of previous occasions generally because of (*i*) the low matrix concentrations required for efficient isolation, (*ii*) the low absorptivities associated with these vibrations and the corresponding low intensities of the bands, and (*iii*) the occurrence of those modes below the low frequency limit of the infrared spectrometer.

In the case of $Rh(^{14}N_2)$ in pure $^{14}N_2$, only when the NN stretching mode at 2179.5 cm^{-1} was arranged to be fully absorbing was it possible to observe very weak broad infrared absorptions at 392–412, 532, and 543 cm^{-1} and a weak line at 345 cm^{-1}.

The mode in $Rh(^{14}N_2)_4$ at 345 cm^{-1} showed

Can. J. Chem. Downloaded from www.nrcresearchpress.com by 210.87.254.42 on 09/05/12
For personal use only.

a band width at half height of about 6.4 cm^{-1}. This mode in the $Rh(^{14}N_2)_n(^{15}N_2)_{4-n}$ spectrum was observed at about 343 cm^{-1} but with a corresponding band width of 11.0 cm^{-1} and could represent an envelope of all the νRh—N stretching modes of the isotopic molecules n = 0–4.[3] Molecular $Rh(^{14}N_2)_4$ has four infrared active vibrations of T_2 symmetry: νNN, stretching; δRh—N—N, bending; νRh—N, stretching; δNRhN, bending.

By analogy with $Ni(^{12}C^{16}O)_4$ which shows the δC—Ni—C mode at 80 cm^{-1}, it is unlikely that the δNRhN bending mode would be observed for $Rh(^{14}N_2)_4$, as the range of the spectrometer was 4000–200 cm^{-1}. The NN stretching mode (T_2) of $Rh(^{14}N_2)_4$ has been assigned, therefore it remains to identify the low frequency mode at 345 cm^{-1} as either the νRhN stretching or δRh—N—N deformational mode. In $Ni(^{12}C^{16}O)_4$ the corresponding νNiC and δNi—C—O vibrations lie at 423.1 and 458.9 cm^{-1}, where it is noteworthy that the νNiC stretching mode is by far the most intense. It thus seems reasonable to deduce that the band observed at 345 cm^{-1} for $Rh(^{14}N_2)_4$ is the T_2 νRhN metal–ligand stretching mode.[4] For the purpose of comparison we have listed below the observed metal–ligand infrared active stretching modes for a selection of binary dinitrogen and carbonyl complexes of Ni, Pd, and Pt.

Compound	νMN (cm^{-1})	k_{MN} (mdyn/Å)	Symmetry type	Reference
$Ni(N_2)_4$	283	0.81	T_2	3
$Rh(N_2)_4$	345	1.44	T_2*	This study
$Ni(CO)_4$	422	1.80	T_2	17
$Pd(CO)_4$	256	0.82	T_2	16
$Pt(CO)_4$	304	1.28	T_2	16
$Pd(N_2)_2$	340	1.25†	Σ_u^+	16

*Assumed to be approximately tetrahedral for the purpose of this discussion.
†Obtained using the approximation that $Pd(N_2)_2$ is PdX_2(X = 28 a.m.u.) and $\lambda = k_{PdN}(\mu_X + 2\mu_{Pd})$.

Clearly there is insufficient data for $Rh(^{14}N_2)_4$ to permit a complete vibrational analysis. However, it is interesting that a full analysis of $Ni(^{12}C^{16}O)_4$ (23) yielded potential energy distributions which indicated that there was very little coupling between the νNiC stretching and δNi—C—O deformational modes. Therefore, a reasonable estimate of the Rh—N bond stretching force constants may be obtained using a simple analysis, in which $Rh(^{14}N_2)_4$ is considered to be RhX_4, where X is treated as a point mass of 28 a.u. and $\lambda = k_{M-C}(\mu_X + \frac{4}{3}\mu_M)$ where μ_X and μ_M are the reciprocal masses of X and M respectively, k_{MC} is the M—C bond stretching force constant, and $\lambda = 0.58915\ (\nu/1000)^2$ where ν is the metal–ligand stretching frequency. The values obtained for various M—N and M—C bond stretching force constants using this approximation are shown in the above table. It is reassuring to note that the full analysis for $Ni(^{12}C^{16}O)_4$ based on all vibrations (23) yields a k_{NiC} of 1.98 mdyn/Å to be compared with 1.80 mdyn/Å obtained from the simple analysis.

[3]Low frequency modes associated with the molecules $Rh(N_2)_n$ (where n = 1–3) were too weak to observe.

Rhodium Dinitrogen Aggregate Species

When Rh atoms were cocondensed with pure N_2 matrices, in addition to the strong lines assigned to $Rh(N_2)_4$, very weak lines were observed at about 2238 and 2218 cm^{-1} (Fig. 5*A*) which grew in intensity upon warm-up to 35 °K to yield lines at 2242/2238, 2218/2215 with a new weak line at about 2213 cm^{-1}. By decreasing the rate of Rh atom deposition these weak lines became vanishingly small compared to the lines of $Rh(N_2)_4$. Warm-up of these nitrogen matrices containing low concentrations of Rh atoms caused the very weak lines at 2242, 2218, and 2113 cm^{-1} to grow in intensity (the 2113 cm^{-1} being now more intense than the other two bands) while the $Rh(N_2)_4$ lines gradually disappeared. These observations together with the close proximity of these weak high frequency lines to the frequency reported for N_2 chemisorbed on Rh metal (18) indicate that aggregate species $Rh_x(N_2)_y$ are probably being formed in the Rh/N_2 experiments. Weak lines at similar frequencies are also formed in

[4]This assignment must be regarded as tentative. However, this does not in any way change the conclusions reached in the remainder of the paper.

Can. J. Chem. Downloaded from www.nrcresearchpress.com by 210.87.254.42 on 09/05/12
For personal use only.

Can. J. Chem. Downloaded from www.nrcresearchpress.com by 210.87.254.42 on 09/05/12
For personal use only.

$N_2/Ar = 1:10$ experiments and upon warm-up of more dilute N_2/Ar matrices. Intuitively one might relate the presence of terminal NN stretching modes of the aggregate formed with high rates of Rh atom deposition (at 2238, 2215 cm^{-1}), the absence of bridging (low frequency) NN stretching modes of the aggregate, and the analogy with the Co—Co bonded form of $Co_2(CO)_8$ to the formation of $Rh_2(N_2)_8$ containing a Rh—Rh bond. However, when low rates of Rh atom deposition are employed and the matrices warmed, both terminal and bridge NN stretching modes appear for the aggregate species (2242, 2218 cm^{-1} (terminal) and 2113 cm^{-1} (bridge)).

One can speculate as to the formation of an aggregate (which by analogy with $Co_2(CO)_8$ will be referred to as $Rh_2(N_2)_8$) by one or both of the following reaction schemes.

(*i*) Reaction of diatomic rhodium (Rh_2) (formed in the matrix on cocondensation at 10 °K, using high rates of Rh atom deposition) with N_2,

$$Rh_2 + 8N_2 \rightarrow Rh_2(N_2)_8 \quad \text{(A)}$$

(*ii*) Dimerization of $Rh(N_2)_4$ during matrix warm-up experiments,

$$2Rh(N_2)_4 \rightarrow Rh_2(N_2)_8 \quad \text{(B)}$$

where

$$A = (N_2)_4Rh—Rh(N_2)_4$$

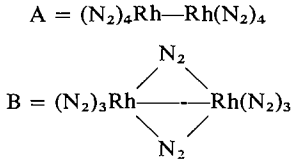

These two reaction schemes are compatible with the spectral changes and lend support to the idea of two forms of $Rh_2(N_2)_8$ analogous to $Co_2(CO)_8$.

It is interesting to note that although these discussions regarding the formation and presence of $Rh_2(N_2)_8$ must be regarded as purely speculative, the formation of both isomers of $Co_2(CO)_8$ (16) has been observed in a series of analogous Co/CO matrix infrared experiments. In these, $Co(CO)_4$ was synthesized and $Co_2(CO)_8$ was observed after warm-up experiments of the tetracarbonyl as well as directly after depositions at 10 °K employing high metal atom deposition rates.

Warm-Up Characteristics and Stabilities of the Binary Dinitrogen Complexes of Rhodium

From our experiences with the binary carbonyl and dinitrogen complexes of Ni, Pd, and Pt, it has proven possible to relate qualitatively the difference between the force constant of the free ligand and the respective C.K. force constant in a series of closely related compounds to their relative thermodynamic stabilities (3, 4).

The assumption that was made was that ΔH_{ML}, the average metal–ligand bond energy, is given by

$$\Delta H_{ML} \propto k^L - k^L_{C.K.}$$

where k^L and $k^L_{C.K.}$ are the free ligand and C.K. bond stretching force constants respectively, and that ΔH_c, the enthalpy of decomposition of the compound to the metal and free ligand, is given by

$$\Delta H_c \propto n\Delta H_{ML}$$

where n is the coordination number of the complex.

The results for Ni and Pd paralleled their warm-up behavior and confirmed that the most stable complexes were those with the highest stoichiometries, that is $Ni(N_2)_4$ and $Pd(N_2)_3$.

The values of ΔH_c for $Ni(N_2)_n$, and $Rh(N_2)_n$ are shown below.

	ΔH_c	
n	Ni	Rh
4	11.00	9.76
3	9.66	6.78
2	7.68	4.50
1	4.63	3.28

The order for Rh is that expected from the warm-up behavior of $Rh(N_2)_n$ ($n = 1$–4) but also seems to indicate the considerably *greater* stability of $Rh(N_2)_4$ as compared to $Rh(N_2)_3$ or $Rh(N_2)_2$. It will be recalled that warm-up of dilute matrices yielded bands assigned to $Rh(N_2)_4$ before any bands due to $Rh(N_2)_3$ appeared. One can appreciate these relative stabilities more easily by reference to the graphical plot of ΔH_c^n *vs.* n (Fig. 6), where ΔH_c^n is the enthalpy of decomposition of $M(N_2)_n$. Particularly noteworthy is the large difference between ΔH_c^4 and ΔH_c^3 for $Rh(N_2)_4/Rh(N_2)_3$ as compared to the much smaller difference between $Ni(N_2)_4/Ni(N_2)_3$.

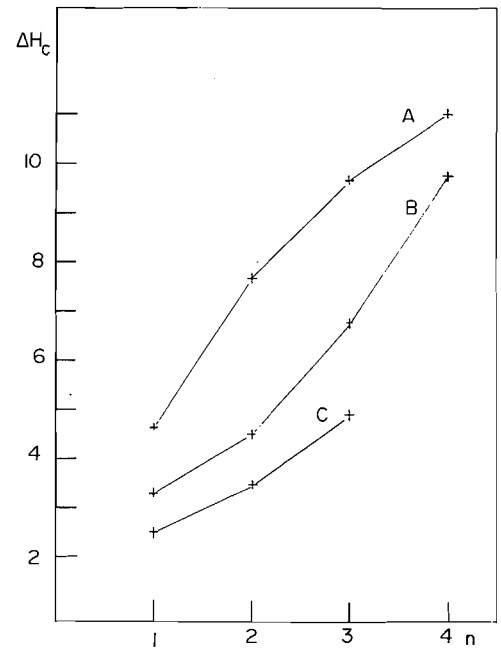

FIG. 6. Graphical plot of ΔH_c^n *vs.* n for (*A*) $Ni(N_2)_n$, (*B*) $Rh(N_2)_n$, and (*C*) $Pd(N_2)_n$ (see text for notation).

Relationship between RhN_2 and N_2 Chemisorbed on Rh

We have recently reported data for MN_2 (where M = Ni, Pd, and Pt) and have compared it with N_2 chemisorbed onto M (3, 4). It was found that the extent of metal–ligand bond weakening was approximately the same for the three metals when going from MN_2 to the chemisorbed ligand which suggested that the forces which bind molecules to surfaces upon chemisorption might be similar in many ways to those operating in more conventional metal–ligand coordination complexes (19).

Data for chemisorbed N_2 on Rh metal indicates the NN stretching frequency to lie at 2236 cm^{-1} (18) (note that lines at about this frequency appeared at the final warm-up stages of the matrices at 40 °K and were considered to belong to higher aggregate species). As with Ni, Pd, and Pt dinitrogen systems, the NN stretching frequency for chemisorbed N_2 lies above that of the respective monodinitrogen compound, indicative of a lower M—N_2 bond strength. As discussed previously (3, 4) this may arise from the fact that a surface metal atom releases some of its electrons into the conduction band of the metal. This formally raises the oxidation state of the metal, thereby decreasing the extent of back bonding below that which takes place when a single metal atom is bonded to a nitrogen molecule. It is interesting to note that the ratio $(\Delta\nu_{RhN_2}/\Delta\nu_{Rh.ChemiN_2}) = 1.9$ compared to 1.9, 1.7, and 1.6 for the Ni, Pd, and Pt nitrogen systems respectively, indicating that the extent of bond weakening in dinitrogen is approximately the same for the four metals when going from MN_2 to chemisorbed N_2.

Summary of Structure and Bonding in Binary Dinitrogen Complexes of Rhodium

Matrix cocondensation reactions of rhodium with N_2 and dilute N_2/Ar mixtures have resulted in the identification of the dinitrogen species $Rh(N_2)_n$ (where n = 1–4). Assignments are made for the $Rh(N_2)_n$ complexes on the basis of variable concentration experiments, isotopic substitutions, and diffusion warm-up experiments. Cotton–Kraihanzel force constants were obtained for all molecules using least squares analysis of the isotopic frequencies (Table 4). $Rh(N_2)_4$ in solid α-nitrogen appears to have a squashed tetrahedral structure (D_{2d}) but an approximately regular tetrahedral configuration (T_d) in solid argon.

The bonding of the dinitrogen molecule(s) in $Rh(N_2)_n$ appear in many respects to be similar to the coordinated dinitrogen molecule in the few stable rhodium dinitrogen complexes that have been prepared (see Table 5) as well as coordinated dinitrogen in $Ni(N_2)_n$ and $Pd(N_2)_m$. The structures of $Rh(N_2)_n$ appear to be similar to those found for the corresponding binary carbonyl and dinitrogen complexes of Ni and Pd although we cannot eliminate totally the possibility of $Rh(N_2)_2$ being non-linear and $Rh(N_2)_3$ being non-planar with this data alone.

In conclusion one should perhaps comment on the fact that the electronic configuration of ground state atomic rhodium is $5s^14d^8$ and the

TABLE 4. Cotton–Kraihanzel k_{NN} and $k_{NN.NN}$ force constants* for $Rh(N_2)_n$ (where n = 1–4)

	k_{NN}	$k_{NN.NN}$	$k'_{NN.NN}$†
$Rh(N_2)_4$	19.99	0.382	0.165
$Rh(N_2)_3$	20.17	0.300	
$Rh(N_2)_2$	20.18	0.450	
$Rh(N_2)$	19.15		
N_2	22.43		

*Units in mdyn/Å.
†See text for notation.

Can. J. Chem. Downloaded from www.nrcresearchpress.com by 210.87.254.42 on 09/05/12
For personal use only.

TABLE 5. Some known dinitrogen compounds containing rhodium

Compound	$\nu_{N\equiv N}$ (cm^{-1})	Reference
$Rh(PPh_3)_2(N_2)(Cl)$	$2152(^{14}N_2)$	20
$K_2[Rh(OH)_2(NO_2)_6(NH_3)_2(N_2)]$ containing skeletal Rh—N≡N—Rh group	$2070^*(^{14}N_2)$	21
Cyclic binuclear complexes of structure type 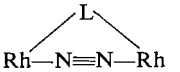	—	22
RhN_2 chemisorbed species	$2236(^{14}N_2)$ $2200(^{14}N^{15}N)$ $2162(^{15}N_2)$	18

*Raman spectrum.

configuration of Rh(0) in $Rh(N_2)_4$ is expected to be d^9 and a Jahn–Teller distortion from regular tetrahedral symmetry is predicted. Under circumstances where lattice sites effects are minimal (*i.e.* in dilute N_2/Ar matrices) only a very small splitting (4.5 cm^{-1}) of the T_2 NN stretching mode was observed. Whether this splitting is indicative of a matrix site effect or a genuine Jahn–Teller distortion cannot be decided upon with the available data. Whatever the cause of the perturbation of $Rh(N_2)_4$ in argon may be, it is clearly very small.

We wish to thank Mr. Ted Huber and Mr. Peter Kündig for helpful discussion and technical assistance, Dr. Martin Moskovits for his assistance with the frequency and intensity calculations of $Rh(N_2)_4$, and the National Research Council of Canada, the Research Corporation, and Erindale College for financial assistance.

1. J. CHATT. Proc. R. Soc. Ser. B, **172**, 327 (1969).
2. A. D. ALLEN, R. O. HARRIS, B. R. LOESCHER, J. R. STEVENS, and R. N. WHITELY. Chem. Rev. **73**, 11 (1973).
3. H. HUBER, E. P. KÜNDIG, M. MOSKOVITS, and G. A. OZIN. J. Am. Chem. Soc. **95**, 332 (1973).
4. E. P. KÜNDIG, M. MOSKOVITS, and G. A. OZIN. Can. J. Chem. In press.
5. R. L. DEKOCK. Inorg. Chem. **10**, 1205 (1971).
6. E. P. KÜNDIG, M. MOSKOVITS, and G. A. OZIN. Can. J. Chem. **50**, 3587 (1972).
7. H. HUBER and G. A. OZIN. Can. J. Chem. **50**, 3746 (1972); H. HUBER, W. KLOTZBÜCHER, G. A. OZIN, and A. VANDER VOET. Can. J. Chem. In press.
8. E. P. KÜNDIG, M. MOSKOVITS, and G. A. OZIN. Can. J. Chem. In press.
9. W. KLOTZBÜCHER and G. A. OZIN. J. Am. Chem. Soc. **95**, 3790 (1973).
10. G. A. OZIN and A. VANDER VOET. Can. J. Chem. **51**, 637 (1973).
11. G. A. OZIN and A. VANDER VOET. Unpublished results.
12. E. P. KÜNDIG, M. MOSKOVITS, and G. A. OZIN. J. Mol. Struct. **14**, 137 (1972).
13. M. MOSKOVITS and G. A. OZIN. J. Appl. Spectrosc. **26**, 481 (1972).
14. R. W. G. WYCKOFF. Crystal structures. Vol. 7. Interscience, New York, N.Y. p. 29.
15. F. A. COTTON and C. S. KRAIHANZEL. J. Am. Chem. Soc. **84**, 4432 (1962).
16. E. P. KÜNDIG and G. A. OZIN. Unpublished results.
17. L. H. JONES, R. S. MCDOWELL, and M. GOLDBLATT. J. Chem. Phys. **48**, 2663 (1968).
18. YU. G. BOROD'KO and V. S. LYUTOV. Kinet. Catal. **12**, 202 (1971).
19. R. P. EISCHENS. Acc. Chem. Res. **5**, 74 (1972).
20. L. YU UKHIN, YU. A. SHVETSOV, and M. L. KHIDEKEL. Akad. Nauk. S.S.S.R. 957 (1967).
21. L. S. VOLKOVN, V. M. VOLKOV, and S. S. CHERNIKOV. Russ. J. Inorg. Chem. **16**, 1383 (1971).
22. G. I. KOZUB and V. V. KARPOV. Bull. Acad. Sci. U.S.S.R. Div. Chem. Sci. **21**, 638 (1972).
23. L. H. JONES, R. S. MCDOWELL, and M. GOLDBLATT. J. Chem. Phys. **48**, 2663 (1968).

Can. J. Chem. Downloaded from www.nrcresearchpress.com by 210.87.254.42 on 09/05/12
For personal use only.

The Infrared and Raman Spectra and Vibrational Assignment of *t*-Butyl Bromide-h_9 and -d_9

JOHN E. BERTIE AND SHAM SUNDER
Department of Chemistry, The University of Alberta, Edmonton, Alberta

Received January 11, 1973

The infrared spectra between 4000 and 10 cm^{-1} of *t*-butyl bromide-h_9 and -d_9 in the gas and liquid states, and the Raman spectra between 3500 and 10 cm^{-1} of the liquids under parallel and perpendicular polarizations, have been recorded and assigned. The compatibility of the assignments for the light and heavy molecules has been checked by normal coordinate calculations, in which 14 valence force constants have reproduced 40 fundamental frequencies with an average error of 1.5%. The calculated thermodynamic properties of both molecules are presented for temperatures between 50 and 500 °K.

Les spectres infra-rouges dans la région de 4000 à 10 cm^{-1} des bromures de *t*-butyle-h_9 et -d_9 à l'état gazeux et liquide ainsi que les spectres Raman dans la région de 3500 à 10 cm^{-1} des liquides à l'aide de lumière polarisée parallèlement et perpendiculairement, ont été enregistrés et interprétés. La concordance des attributions pour les molécules légères et lourdes a été vérifiée à l'aide de calculs en coordonnées normales lesquels ont permis de relier 40 fréquences fondamentales à 14 constantes de force valentielle avec une erreur moyenne de 1.5%. De même on présente les propriétés thermodynamiques calculées des deux molécules pour des températures allant de 50 à 500 °K. [Traduit par le journal]

Can. J. Chem., 51, 3344 (1973)

Introduction

As part of a study of the infrared and Raman spectra of *t*-butyl bromide in its three solid phases, we have recorded the infrared spectrum of the gas and liquid between 4000 and about 10 cm^{-1}, and the Raman spectrum of the liquid to 3500 cm^{-1} away from the exciting line, for both C_4H_9Br and C_4D_9Br at room temperature. With this data we have assigned the intramolecular modes of these molecules, and have checked the consistency of the assignments for the h_9 and d_9 molecules by a normal coordinate calculation.

The vibrational spectrum of C_4H_9Br has been discussed many times in the literature (1–15). However, no paper exists which reports the entire infrared spectrum of the liquid, aside from simply citing the fundamental frequencies, and neither the infrared nor the Raman spectrum of the vapor has been published. The most complete published infrared spectrum of the liquid covers the region from 3500 to 450 cm^{-1} (5) and suffers only from the rather low resolution available in 1950. Other workers (13–15) have extended the range to below 100 cm^{-1}, and Zeil and co-workers (10, 11) have recorded the infrared spectrum of the liquid and gas between 600 and 4000 cm^{-1} but only report a partial spectrum of the liquid and a list of fundamental frequencies drawn from both spectra. The only Raman polarization data for the liquid was published (3) in 1940, and only a partial Raman spectrum has been published (11) since.

With the exception of the methyl torsional modes, which have only recently been assigned (14, 15), the assignment of the spectrum of C_4H_9Br below 800 cm^{-1} has not been seriously challenged since Sheppard (5) assigned it using his own infrared data and Wagner's (3) Raman data. Various assignments for the remainder of the bands have been based on the same data (5, 6, 9, 12), and Huttner and Zeil (11) used their own data and assigned the fundamentals with the aid of a normal coordinate calculation.

The only report of the spectrum of C_4D_9Br is that of Zeil and co-workers (10) who published the infrared spectrum of the liquid between 950 and 1350 cm^{-1} and listed and assigned the fundamental frequencies above 700 cm^{-1}. Their assignment suffers from a misunderstanding over the probable frequencies of the CD_3 stretching and CD_3 deformation modes. The error in the assignment of the deformation modes was subsequently recognized (11), but the spectrum of C_4D_9Br was not reassigned.

Experimental

The *t*-butyl bromide-h_9 was Matheson, Coleman and Bell's research grade. To remove isobutene and hydrogen bromide impurities it was washed with 10% aqueous sodium bicarbonate followed by water. After drying over

Can. J. Chem. Downloaded from www.nrcresearchpress.com by 210.87.254.105 on 09/05/12
For personal use only.

Can. J. Chem. Downloaded from www.nrcresearchpress.com by 210.87.254.105 on 09/05/12
For personal use only.

anhydrous calcium chloride it was fractionated on a Teflon, spinning-band column and collected at 73.0 ± 0.5 °C.

t-Butyl bromide-d_9 was prepared from *t*-butyl alcohol-d_9, purchased from Merck, Sharp, and Dohme of Canada, by reaction with DBr in heavy water. It was purified as described above, collecting the fraction distilling at 72.5 ± 1 °C. Mass spectrometric analysis indicated about 7% of C_4D_8HBr and less than 1% $C_4D_7H_2Br$ in the product. No other impurities were detected.

The mid-infrared spectra were recorded on a Beckman I.R. 12 spectrophotometer calibrated, to ± 0.5 cm^{-1} below 2000 cm^{-1} and ± 1 cm^{-1} above 2000 cm^{-1}, using standard gases (16) and the Beckman fiducial marker accessory. The resolution was better than 1 cm^{-1} above 650 cm^{-1} and better than 2 cm^{-1} below 650 cm^{-1}. Individual gas-phase bands were studied at 0.5 cm^{-1} resolution.

Far-infrared spectra, up to about 380 cm^{-1}, were recorded using a Beckman-RIIC interferometer at a resolution of 1 cm^{-1}. The details of this instrument have been described elsewhere (17).

Raman spectra were recorded at 1 or 1.5 cm^{-1} resolution, using a Carson's lab 10SP Ar^+, Kr^+ laser, a SPEX 1401 monochromator, an ITT FW-130 photomultiplier cooled to −30 °C and photon-counting electronics. To excite the spectra, the 6471 and 5682 Å lines were used at a power of about 50 mW at the sample, after filtering to remove emission lines. Calibration to ± 1 cm^{-1} was achieved using the 459 cm^{-1} band of carbon tetrachloride (18), the spectrum of indene (19), and the manufacturer's statement of scale linearity to within ± 1 cm^{-1}; no evidence which contradicted this statement was found in this work. Ninety-degree excitation was used, the polarizations were selected by a polaroid analyzer, and a polarization scrambler was used in front of the entrance slit.

The Raman samples were held in melting-point capillary tubes. The infrared samples were contained in standard 10 cm path gas cells, or standard liquid cells, fitted with cesium iodide or polyethylene windows. The liquid cells were fitted with spacers 0.2 mm or less thick, but the film thicknesses are not known with certainty.

Results

The infrared spectra of *t*-butyl bromide-h_9 in the gas and liquid states at room temperature are shown in Figs. 1 and 2. The Raman spectrum of liquid *t*-butyl bromide-h_9 at room temperature is shown in Fig. 3 along with that of *t*-butyl bromide-d_9; no features were detected in the region omitted from Fig. 3. Figure 4 shows the more intense bands in the infrared spectrum of *t*-butyl bromide-h_9 on a scale which shows the band contours clearly. The frequencies of the features observed are listed in Table 1 to an accuracy of ± 1 cm^{-1}.

The infrared spectra of *t*-butyl bromide-d_9 are shown in Fig. 5 for the gas and liquid phases at room temperature. The intense bands in the spectrum of the gas are shown in Fig. 6 and the frequencies of the features observed in the infrared and Raman (Fig. 3) spectra are listed in Table 2 to an accuracy of ± 1 cm^{-1}.

For both compounds the frequencies of corresponding features in the infrared and Raman spectra of the liquid coincided within the combined errors of measurement. All of the weaker features in the spectra presented have been confirmed from spectra in which they are more intense, except for certain bands in the Raman spectrum of C_4D_9Br. A significant fluorescence problem was encountered with C_4D_9Br and its Raman lines appear to be weaker than those of C_4H_9Br. Both of these factors contributed to the following uncertainties in the Raman data for C_4D_9Br: the existence, frequency, and polarization of the features at 207 and 904 cm^{-1}; the details of the perpendicular spectrum between 2050 and 2200 cm^{-1}; whether the bands at 2221 cm^{-1}, 2238 cm^{-1}, and between 1150 and 1300 cm^{-1} are depolarized or partly polarized.

Discussion

The molecule was assumed to have C_{3v} symmetry with the unique hydrogen atom on each methyl group *anti* to the bromine. The detailed molecular structure is not known and the following parameters were used: $r_{C-H} = 1.093$ Å (assumed all equal); $r_{C-C} = 1.54$ Å; $r_{C-Br} = 1.96$ Å; all angles tetrahedral (20). The moments of inertia calculated from these parameters are: for C_4H_9Br, $I_a = 183 \times 10^{-40}$, $I_b = 416 \times 10^{-40}$; for C_4D_9Br, $I_a = 241 \times 10^{-40}$, $I_b = 488 \times 10^{-40}$; where the units are g cm^2, and bromine-79 is the assumed isotope. In the simplest approximation for gas-phase band contours, one expects (21, 22) an A_1 transition to yield a parallel band with well-defined PQR structure and a degenerate, *E*, transition to yield a perpendicular band which is a smooth peak showing no fine structure under our resolution. In fact, very few of the bands in the spectra of the gases could be classified with certainty in this way (Figs. 4 and 6), presumably due to complicating factors such as Coriolis interaction, hot bands, and the change in rotational constants with vibrational state. In most cases, therefore, the bands were assigned to parallel or perpendicular transitions on the basis of the Raman polarization data. The only assignments that are totally, or heavily, based on the shapes of the bands in the spectrum of the gas are those of ν_3 of C_4H_9Br (Fig. 4 and Table 1) and ν_1, ν_{13}, and ν_{15} of C_4D_9Br (Fig. 6 and Table 2).

TABLE 1. Infrared and Raman spectra of *t*-butyl bromide-h_9 at room temperature

Infrared		Raman, liquid			
Gas, ν (cm^{-1})	Liquid, ν (cm^{-1})	ν (cm^{-1})	Polarization[a]	Assignment	
3496 w	3483 vw			$\nu_7 + \nu_{14}$	
3390 w	3382 w			$\nu_{13} + \nu_{22}$	
3256 w	3251 w			$\nu_8 + \nu_{15}$	
3217 w	3205 w			$\nu_2 + \nu_{23}$	
2992 vs	2985 vs	2983 m	dP	$\nu_{13}(E)$	as.CH_3 str.
2977 vs	2970 vs	2971 s	PP	$\nu_{14}(E)$	as.CH_3 str.
				$\nu_1(A_1)$	as.CH_3 str.
2953 s	2945 m	2944 m	dP	$\nu_{15}(E)$	s.CH_3 str.
2934 s	2925 s	2924 vs	P	$\nu_2(A_1)$	s.CH_3 str.
2910 s					
	2903 m	2902 s	P	$2\nu_{16}$	
		2890 s	P	$2\nu_{17}$	
2875 sh	2870 sh			$\nu_3 + \nu_4$	
		2850 sh		$\nu_4 + \nu_{16}$	
	2827 w			$\nu_{16} + \nu_{18}$	
2800 w				$\nu_{17} + \nu_{18}$	
2790 w	2782 w	2783 w	P	$2\nu_4$	
	2754 vw			$\nu_4 + \nu_{18}$	
2733 w	2726 m	2726 m	P	$2\nu_{18}$	
2695 vw	2689 vw			$\nu_{17} + \nu_{19}$	
2634 vw	2629 w			$\nu_4 + \nu_{19}$	
	2604 vw			$\nu_{18} + \nu_{19}$	
	2471 vw			$2\nu_{19}$	
2404 w	2399 w			$\nu_{18} + \nu_{20}$	
2302 w	2298 w			$2\nu_5$, $\nu_{18} + \nu_{21}$	
2182 w	2171 w			$\nu_6 + \nu_{18}$	
	1911 vw			$\nu_4 + \nu_7$	
1859 w	1859 w			$\nu_3 + \nu_{22}$	
	1791 vw			$\nu_3 + \nu_8$	
1734 w	1731 w			$\nu_6 + \nu_{21}$	
1480 s	1475 s			$\nu_3(A_1)$	as.CH_3 def.
1457 s	1457 s	1459 m	dP	$\nu_{16}(E)$	as.CH_3 def.
	1449 sh	1447 sh	dP	$\nu_{17}(E)$	as.CH_3 def.
1423 w	1423 w	1425 sh	dP	$\nu_{20} + \nu_{22}$	
1406 w				$\nu_6 + 2\nu_8$	
1397 sh	1393 w	1395 w	P	$\nu_4(A_1)$	s.CH_3 def.
1375 vs	1371 vs	1372 w	dP	$\nu_{18}(E)$	s.CH_3 def.
	1324 sh			$\nu_6 + \nu_7$, $\nu_8 + \nu_{20}$	
1238 s	1238 s	1236 w	dP	$\nu_{19}(E)$	CC str.
1203 w	1198 w	1200 vw	P	$\nu_{21} + \nu_{24}$	
1153 vs	1144 vs	1142 vs	P	$\nu_5(A_1)$	CH_3 rock
	1059 w			$\nu_6 + \nu_{12}$	
1033 w	1031 w	1031 w	dP	$\nu_{20}(E)$	CH_3 rock
	930 vw	931 w	dP	$\nu_{21}(E)$	CH_3 rock
	813 sh	815 sh	PP	$\nu_7 + \nu_8$	
808 s	804 s	805 s	PP	$\nu_6(A_1)$	CC str.
		643 w	P	$\nu_{22} + \nu_{24}$	
608 w	604 w	604 w	P	$2\nu_8$	
571 w	571 sh	571 sh	P	$2\nu_{23}$	
524 s	518 s	516 vs	P	$\nu_7(A_1)$	CBr str.
396 w	394 w	395 w	dP	$\nu_{22}(E)$	CCC def.
304 s	303 s	301 vs	P	$\nu_8(A_1)$	CCC def.
	285 sh	285 sh	dP	$\nu_{23}(E)$	CH_3 torsion
	272 sh	271 sh	dP	$\nu_{24}(E)$	CCBr def.
	214 vw	215 w	P	$\nu_7 - \nu_8$	
		187 w	P		

[a]dP, P, and PP mean depolarized, polarized, and partly polarized ($0.4 < \rho_l < 0.75$), respectively.

Can. J. Chem. Downloaded from www.nrcresearchpress.com by 210.87.254.105 on 09/05/12
For personal use only.

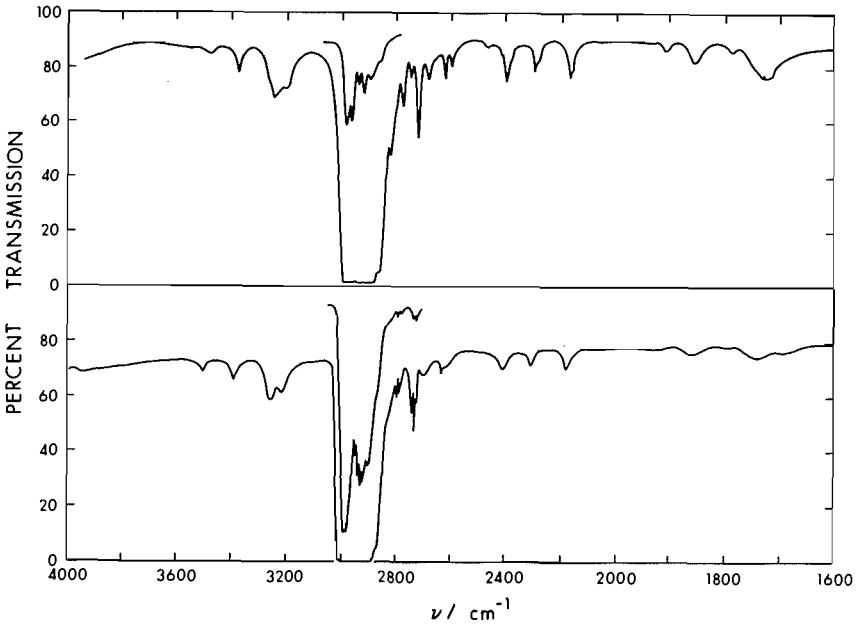

FIG. 1. The infrared spectra of *t*-butyl bromide-h_9 in the gas (lower box) and liquid (upper box) states at room temperature. The gas pressures were 80 and 10 Torr and the pathlength was 10 cm. The liquid pathlengths were nominally 0.02 and 0.2 mm. The resolution was 1 cm^{-1}.

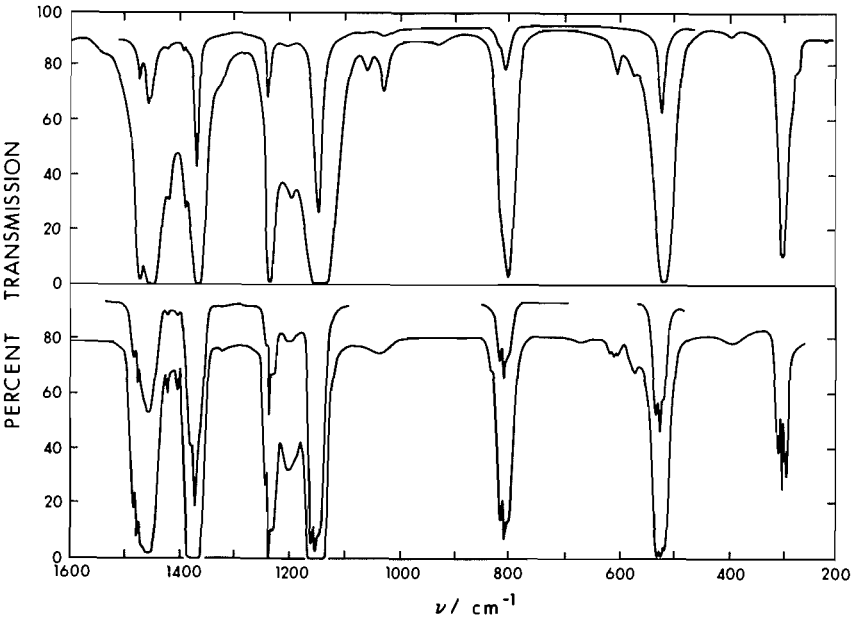

FIG. 2. The infrared spectra of *t*-butyl bromide-h_9 in the gas (lower box) and liquid (upper box) states at room temperature. The gas pressures were 80 and 10 Torr and the pathlength was 10 cm. The liquid pathlengths were nominally 0.02 and 0.2 mm. The resolution was 1 cm^{-1} above 650 cm^{-1} and about 2 cm^{-1} below 650 cm^{-1}.

Can. J. Chem. Downloaded from www.nrcresearchpress.com by 210.87.254.105 on 09/05/12
For personal use only.

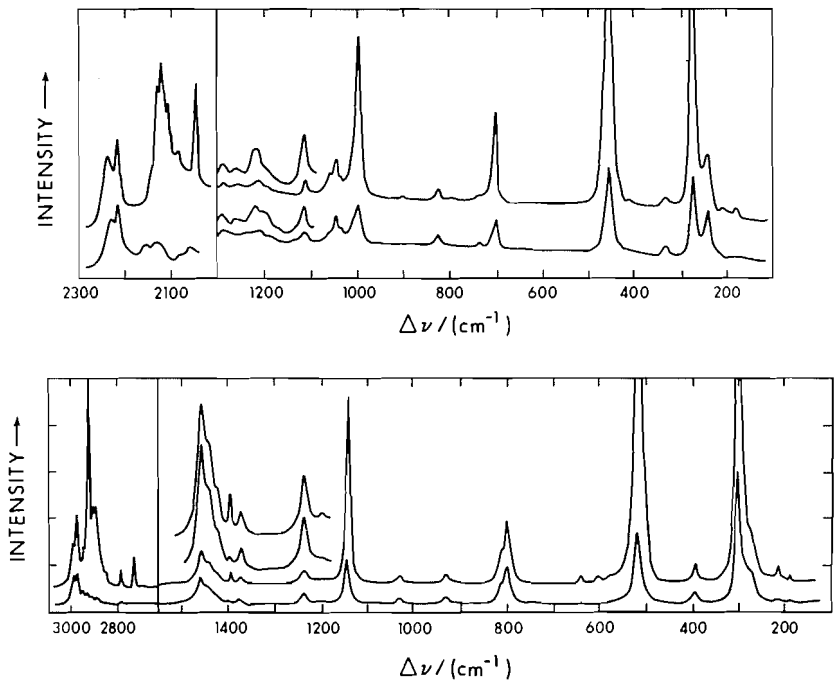

FIG. 3. Raman spectra of liquid *t*-butyl bromide-h_9 (lower box) and -d_9 (upper box) at room temperature, uncorrected for photomultiplier sensitivity. The resolution was 1 cm^{-1} and 1.5 cm^{-1} for *t*-butyl bromide-h_9 and -d_9, respectively. In each box the upper full curve shows the spectrum under parallel polarization and the lower full curve shows that under perpendicular polarization. The partial spectra near to 1200 cm^{-1} show the weaker features under higher gain settings, again with the parallel-polarized spectrum above the perpendicular-polarized one.

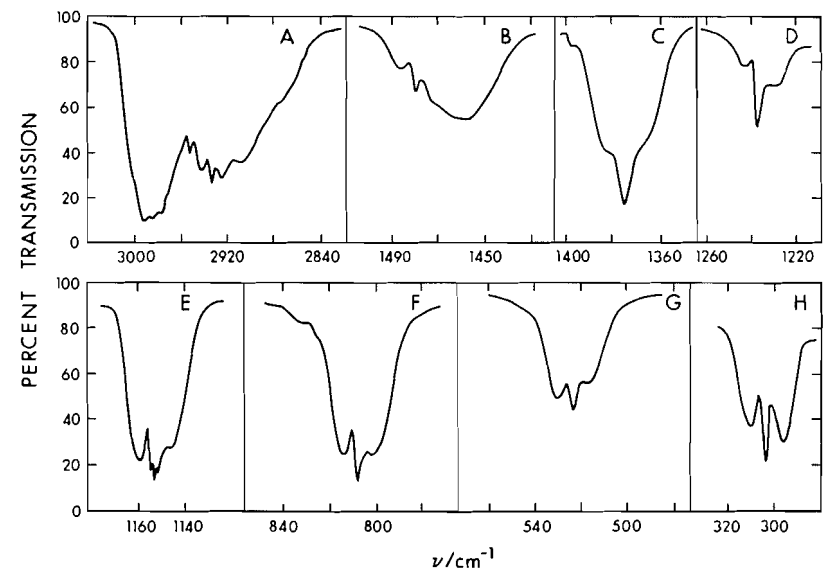

FIG. 4. Intense bands in the infrared spectrum of gaseous *t*-butyl bromide-h_9. The resolution was 0.5 cm^{-1}.

Can. J. Chem. Downloaded from www.nrcresearchpress.com by 210.87.254.105 on 09/05/12
For personal use only.

TABLE 2. Infrared and Raman spectra of *t*-butyl bromide-d_9 at room temperature

Infrared		Raman, liquid			
Gas, ν (cm^{-1})	Liquid, ν (cm^{-1})	ν (cm^{-1})	Polarization[a]	Assignment	
	3271 vw			$\nu_1 + \nu_{17}$	
	3243 vw			$\nu_2 + \nu_3$	
2971 w	2963 w			C_4D_8HBr	
2925 w	2922 w			C_4D_8HBr	
2570 vw	2561 vw			$\nu_{13} + \nu_{22}$	
	2460 vw			$\nu_2 + \nu_{22}$	
2246 s	2240 s	2240 ms	dP	$\nu_{13}(E)$	as.CD_3 str.
2229 s, 2221 s	2217 s	2216 ms	PP	$\nu_{14}(E)$, $\nu_1(A_1)$	as.CD_3 str.
2145 sh	2150 m	2148 sh	dP	$\nu_3 + \nu_{17}$, ν_{18}, or ν_{19}	
	2131 sh	2130 s	P	$2\nu_4$	
2124 ms				$\nu_{15}(E)$	s.CD_3 str.
	2117 ms	2118 s	P	$\nu_2(A_1)$	s.CD_3 str.
2104 m		2107 s	P	$2\nu_{17}$	
2084 m	2084 m	2086 m	P	$\nu_{17} + \nu_{18}$ or ν_{19}	
2076 m	2070 m			$2\nu_{18}$, $2\nu_{19}$	
2060 m				$\nu_5 + \nu_{17}$	
2053 m	2048 m	2046 s	P	$\nu_4 + \nu_5$	
1742 w	1734 w			$\nu_5 + \nu_{21}$	
1447 w	1443 w			$\nu_3 + \nu_{22}$	
1307 w	1303 w			$\nu_3 + \nu_{24}$	
1291 m	1285 m	1287 vw	dP	$\nu_4 + \nu_{23}$	
		1257 vw	dP	$\nu_5 + \nu_{23}$	
1214 ms	1214 s	1215 w	dP	$\nu_{16}(E)$	CC str.
		1200 sh w	dP	$\nu_5 + \nu_{24}$	
	1190 sh			$\nu_{21} + \nu_7$	
1175 sh				$\nu_6 + \nu_7$	
1168 sh	1158 w			$\nu_{20} + \nu_{22}$	
1118 ms	1114 s	1115 w	P	$\nu_3(A_1)$	as.CD_3 def.
1097 w	1092 w			$\nu_8 + \nu_{20}$	
1072 sh	1071 sh			$\nu_{21} + \nu_{22}$	
	1062 w	1062 w	PP	$\nu_4(A_1)$	s.CD_3 def.
1052 s	1049 s	1048 m	dP	$\nu_{17}(E)$	CD_3 def.
1040 w	1038 sh	1038 w	dP	$\nu_{18}(E)$, $\nu_{19}(E)$	CD_3 def.
1011 vs	1000 vs	1001 s	P	$\nu_5(A_1)$	CD_3 rock
940 sh	939 vw			$\nu_6 + \nu_{23}$	
923 w	903 w	904 vw	dP	$\nu_6 + \nu_{24}$, $2\nu_7$	
	880 vw			$\nu_6 + \nu_{12}$	
	837 vw			$\nu_8 + \nu_{22} + \nu_{23}$	
824 w	822 w	823 w	dP	$\nu_{20}(E)$	CD_3 rock
	758 vw			$\nu_{11}(A_2)$, $\nu_7 + \nu_{22}$	
742 vw	738 vw	739 vw	dP	$\nu_{21}(E)$	CD_3 rock
706 m	703 ms	705 ms	P	$\nu_6(A_1)$	CC str.
537 m	521 m			$2\nu_8$	
484 sh	480 sh			$\nu_8 + \nu_{24}$	
463 ms	454 s	454 vs	P	$\nu_7(A_1)$	CBr str.
		411 vw	P	$2\nu_{24}$	
335 w	335 w	337 w	dP	$\nu_{22}(E)$	CCC def.
274 m	273 ms	274 vs	P	$\nu_8(A_1)$	CCC def.
239 w	241 w	243 m	dP	$\nu_{23}(E)$	CCBr def.
	206 vw	~207 vw	dP	$\nu_{24}(E)$	CD_3 torsion
	181 vw	181 w	P	$\nu_7 - \nu_8$	

[a]dP, P, and PP mean depolarized, polarized, and partly polarized ($0.4 < \rho_t < 0.75$), respectively.

Can. J. Chem. Downloaded from www.nrcresearchpress.com by 210.87.254.105 on 09/05/12
For personal use only.

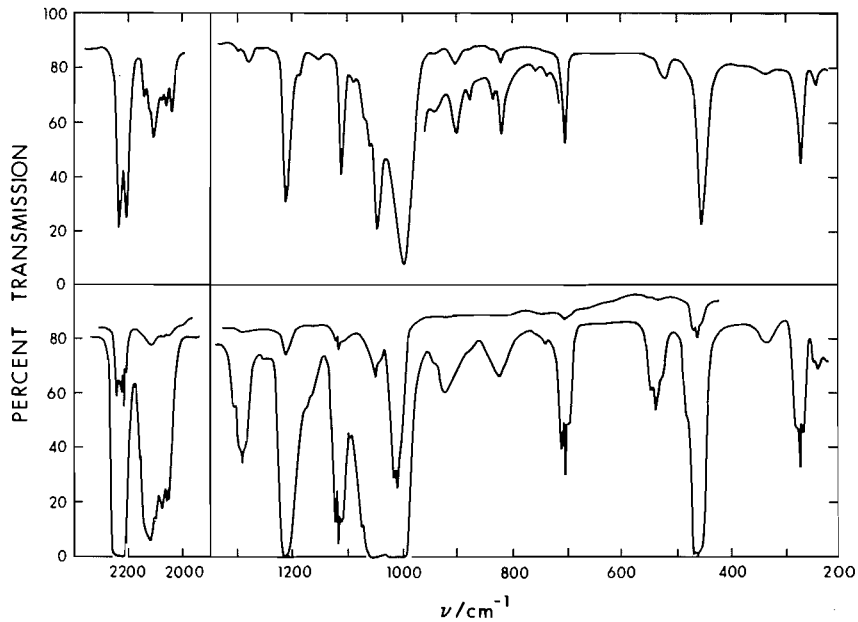

FIG. 5. The infrared spectra of *t*-butyl bromide-d_9 in the gas (lower box) and liquid (upper box) phases at room temperature. The gas pressures were 50 and 5 Torr and the pathlength was 10 cm. The liquid pathlength was nominally 0.1 mm but is uncertain. The resolution was 1 cm^{-1} above, and about 2 cm^{-1} below, 650 cm^{-1}.

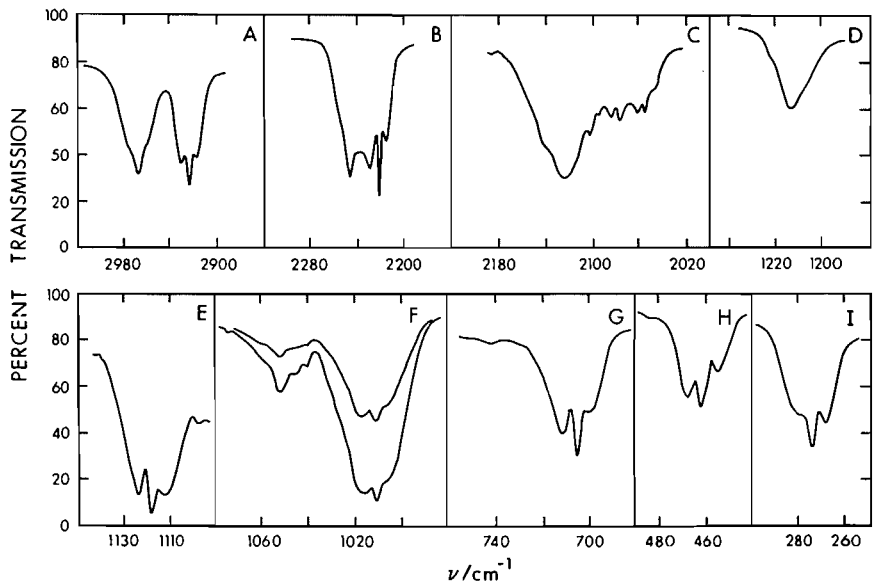

FIG. 6. The intense bands in the infrared spectrum of gaseous *t*-butyl bromide-d_9. The resolution was 0.5 cm^{-1}. The bands in box A are due to *t*-butyl bromide-d_8.

Can. J. Chem. Downloaded from www.nrcresearchpress.com by 210.87.254.105 on 09/05/12
For personal use only.

TABLE 3. Fundamental frequencies and assignments for *t*-butyl bromide-h_9 and -d_9

		C_4H_9Br			C_4D_9Br		
		Frequency (cm^{-1})			Frequency (cm^{-1})		
	Mode	Observed	Calculated[a]	Description	Observed	Calculated[a]	Description
A_1	ν_1	2977	2981	as.CH_3 str.	2221	2227	as.CD_3 str.
	ν_2	2934	2947	s.CH_3 str.	2118[b]	2125	s.CD_3 str.
	ν_3	1480	1464	as.CH_3 def.	1118	1123	s.CD_3 def. + CD_3 rock + CC str.
	ν_4	1397	1394	s.CH_3 def.	1062[b,c]	1054	as.CD_3 def.
	ν_5	1153	1169	CH_3 rock	1011	1002	CD_3 rock + as.CD_3 def.
	ν_6	808	809	CC str.	706	687	CC str. + CD_3 rock
	ν_7	524	527	CBr str.	463	467	CBr str.
	ν_8	304	300	+ CCC def.	274	274	+ CCC def.
A_2	ν_9		2978	as.CH_3 str.		2221	as.CD_3 str.
	ν_{10}		1456	as.CH_3 def.		1045	as.CD_3 def.
	ν_{11}		1021	CH_3 rock		772	CD_3 rock
	ν_{12}		267	CH_3 torsion		189	CD_3 torsion
E	ν_{13}	2992	2982	as.CH_3 str.	2246	2230	as.CD_3 str.
	ν_{14}	2977	2979	as.CH_3 str.	2229[c]	2223	as.CD_3 str.
	ν_{15}	2953[c]	2946	s.CH_3 str.	2124	2122	s.CD_3 str.
	ν_{16}	1457	1462	as.CH_3 def.	1214	1215	CC str. + CD_3 rock
	ν_{17}	1449[b]	1457	as.CH_3 def.	1052	1051	as.CD_3 def.
	ν_{18}	1375	1378	s.CH_3 def.	1040[c]	1047	as.CD_3 def.
	ν_{19}	1238	1257	CC str. + CH_3 rock	1040[c]	1035	s.CD_3 def. + CD_3 rock
	ν_{20}	1033	1031	CH_3 rock	824	788	CD_3 rock
	ν_{21}	930[b]	930	CH_3 rock + CC str.	742	736	CD_3 rock + CC str.
	ν_{22}	396	396	CCC def.	335	339	CCC def.
	ν_{23}	285[b]	283	CH_3 torsion	239	242	CCBr def.
	ν_{24}	272[b]	244	+ CCBr def.	206[b]	182	CD_3 torsion

[a]For C-12 and Br-79. The frequencies calculated for Br-81 are within 0.2 cm^{-1} of these.
[b]Frequencies for the liquid state. All others are for the gas.
[c]These frequencies were given half-weight during the refinement.

The $8A_1 + 12E$ active fundamentals were assigned (Tables 1 and 2), using the approximate symmetry coordinate descriptions of the modes, to the more intense transitions of the correct symmetry in the frequency ranges which are known to be appropriate from the spectra of other molecules. Only two points require further comment. The degenerate methyl torsion of C_4H_9Br is assigned (Table 1) to a feature at 285 cm^{-1}, instead of at 272 cm^{-1} (15), to place it closer to its frequencies in *t*-butyl fluoride, 298 cm^{-1} (9), and *t*-butyl chloride, 290 cm^{-1} (23). The stretching and deformation modes of the methyl groups are assigned in terms of the symmetric (s.) and asymmetric (as.) displacements within the individual methyl groups, even though these have only C_s local (site) symmetry. For the stretching modes this can be shown to be useful by making use of the bands at 2925 and 2971 cm^{-1} in the infrared spectrum of gaseous C_4D_9Br which are assigned to the C_4D_8HBr impurity. Similar bands have been observed in other systems (23, 24). From the moments of inertia of C_4D_8HBr, calculated from the parameters presented above, one expects (22) that the band due to the stretching vibration of a C—H bond *anti* to the CBr bond closely resembles a parallel band, and can be assigned at 2925 cm^{-1}, while that of a C—H bond *gauche* to the C—Br bond resembles a perpendicular band and can be assigned at 2971 cm^{-1}. The force constants derived from these frequencies can be

Can. J. Chem. Downloaded from www.nrcresearchpress.com by 210.87.254.105 on 09/05/12
For personal use only.

Can. J. Chem. Downloaded from www.nrcresearchpress.com by 210.87.254.105 on 09/05/12
For personal use only.

used, without an interaction constant, to calculate the frequencies and eigenvectors of the C_s methyl group. These approximate those of a C_{3v} methyl group although, of course, the two higher frequencies differ by about 20 cm^{-1} in the C_s model and are degenerate in the C_{3v} model. Therefore one can expect that, in *t*-butyl bromide, the $A_1 + A_2 + 2E$ asymmetric CH_3 stretching modes occur approximately 50 cm^{-1} (about 100 cm^{-1} for CD_3) to high frequency of the $A_1 + E$ symmetric CH_3 stretching modes.

The assignment for C_4H_9Br presented in Table 1 agrees with that of Huttner and Zeil (11) except for the CH_3 stretching and deformation modes, for which the present data differs significantly from 'heirs. The only assignments which we regard as very uncertain are those of ν_{14} and ν_{15}. No obvious alternative assignment exists for ν_{14}, but ν_{15} could be assigned to the broad maximum at 2910 cm^{-1} in the spectrum of the gas. The assignment for C_4D_9Br is presented in Table 2. The evidence for the assignment of ν_4, ν_{14}, ν_{15}, ν_{18}, ν_{19}, and ν_{24} is less convincing than that for the remaining modes, but no alternatives are clear except that ν_{15} could be assigned at 2149 cm^{-1} in the liquid.

The frequencies of the fundamental vibrations of both molecules are presented in Table 3, along with the results of a normal coordinate calculation which was done to check the compatibility of the assignments for the two molecules and to obtain more detailed descriptions of the vibrational modes. The calculations used Wilson's GF method (25) through the programs GMAT (26) and FPERT (27), and are reported in detail elsewhere (28). One set of initial values of the diagonal valence force constants was taken from *t*-butyl chloride (23) and a different set was taken from a previous study of *t*-butyl bromide (11). These two quite different sets of force constants converged to the same values, when refined to fit the frequencies of C_4H_9Br with the methyl torsional force constant set to zero. The methyl torsional force constant and selected interaction constants were then added to the diagonal force constants so obtained, and the force field was refined to fit the frequencies of both molecules. The calculated frequencies and assignments (based on the eigenvectors and the potential energy distribution) are shown in Table 3 and the force constants are listed in Table 4. The 40 frequencies were fitted by the 14 force constants with an average error of 8 cm^{-1} or 1.2%. One feature of this calculation is that the potential energy of ν_7 and ν_8 contained large (25–50%) contributions from the CBr, CCBr interaction constant (28). The force field of Huttner and Zeil (11) also yields this feature, which could only be avoided by constraining many of the force constants about the central carbon atom during the refinement. The frequencies so obtained (28) are not quite so close to the observed ones as are those presented here, but the calculated assignments are essentially the same.

TABLE 4. Valence force constants for *t*-butyl bromide[a]

Co-ordinate	Value
C—Br	2.560[b]
C—C	4.0546
C—H[c]	4.8097
C—C—Br	0.8800
H—C—H[c]	0.5336
C—C—H[c]	0.6823
C—C—C	1.1390
CH_3 torsion	0.0148[b]
C—Br C—C	0.7396
C—C C—C′	0.5284
C—H C—H′[c]	0.0946
C—Br C—C—Br	0.4753
C—C—H C—C—H′[c]	−0.0347
C—C C—C—H[c]	0.2196

[a]The units are mdyn Å^{-1}, mdyn, and mdyn Å for bond stretching, stretch–bend interaction, and angle deformation constants, respectively.
[b]During refinement these constants were constrained to the values shown, which were selected from many trials.
[c]All of the force constants of this type were assumed to be equivalent.

The calculated assignments (Table 3) confirmed the empirical assignments (Tables 1 and 2) except that ν_3 of C_4D_9Br was calculated to be the symmetric CD_3 deformation, with some admixture of CD_3 rock and C—C stretch, rather than the asymmetric deformation which was calculated to be ν_4 and to contribute somewhat to ν_5. The calculations also showed (Table 3) that several other modes must be described in terms of more than one symmetry coordinate. The full potential energy distribution and eigenvectors, as well as the **U**, **G**, and **F** matrices used in these calculations, are given in ref. 28.

Table 5 presents the thermodynamic functions of *t*-butyl bromide-h_9 and -d_9 (in parentheses). These were calculated from the observed fre-

TABLE 5. Thermodynamic properties of *t*-butyl bromide-h_9 and -d_9 (in parenthesis) at 1 atm pressure and for the ideal gaseous state[a]

T(°K)	$(H_0 - E_0^0)/T$	$(G_0 - E_0^0)/T$	S_0	C_p
50	7.98 (8.09)	43.53 (44.33)	51.51 (52.42)	8.20 (8.83)
100	8.90 (9.74)	49.26 (50.36)	58.16 (60.10)	12.00 (14.17)
150	10.71 (12.04)	53.20 (54.74)	63.91 (66.78)	16.48 (18.89)
200	12.61 (14.27)	56.54 (58.51)	69.16 (72.79)	20.06 (23.02)
250	14.43 (16.44)	59.56 (61.93)	73.99 (78.37)	23.30 (27.19)
300	16.18 (18.58)	62.34 (65.12)	78.52 (83.70)	26.52 (31.37)
350	17.88 (20.70)	64.96 (68.14)	82.85 (88.84)	29.75 (35.37)
400	19.57 (22.77)	67.46 (71.04)	87.03 (93.81)	32.90 (39.07)
450	21.22 (24.77)	69.86 (73.84)	91.08 (98.61)	35.90 (42.45)
500	22.83 (26.69)	72.18 (76.55)	95.01 (103.24)	38.71 (45.52)

[a]Units are cal mol^{-1} deg^{-1}.

quencies of the A_1 and E modes, the calculated frequencies of the A_2 modes, and the moments of inertia given above; they are, thus, appropriate to the bromine-79 isotope.

The National Research Council of Canada is thanked for their support of this work. Sham Sunder thanks the Killam Estate (Ottawa) for the award of a fellowship. We are grateful to Dr. Hirschmann for help in obtaining a copy of ref. 12.

1. W. D. HARKINS and H. E. BOWERS. Phys. Rev. **38**, 1845 (1931).
2. A. DADIEU, A. PONGRATZ, and K. W. F. KOHLRAUSCH. Monatsh. **61**, 369 (1932).
3. J. WAGNER. Z. Phys. Chem. Part B, **45**, 341 (1940).
4. F. S. MORTIMER, R. B. BLODGETT, and F. DANIELS. J. Am. Chem. Soc. **69**, 822 (1947).
5. N. SHEPPARD. Trans. Faraday Soc. **46**, 527 (1950).
6. M. C. TOBIN. J. Am. Chem. Soc. **75**, 1788 (1953).
7. I. NAKAGAWA. J.C.S. Jap. Pure Chem. Sect. **77**, 602 (1956).
8. M. HAYASHI. Nippon Kagaku Zasshi, **78**, 1743 (1957).
9. D. E. MANN, N. ACQUISTA, and D. R. LIDE, JR. J. Mol. Spectrosc. **2**, 575 (1958).
10. W. ZEIL, H. BUCHERT, H. HEEL, and H. PFÖRTNER. Z. f. Elektr. **64**, 769 (1960).
11. W. HUTTNER and W. ZEIL. Spectrochim. Acta, **22**, 1007 (1966).
12. ROBERT P. HIRSCHMANN. U.S. Atomic Energy Commission IS-641 (1963).
13. F. F. BENTLEY, N. T. MCDEVITT, and A. L. ROZEK. Spectrochim. Acta, **20**, 105 (1964).
14. N. T. MCDEVITT, A. L. ROZEK, F. F. BENTLEY, and A. D. DAVIDSON. J. Chem. Phys. **42**, 1173 (1965).
15. J. R. DURIG, S. M. CRAVEN, and J. BRAGIN. J. Chem. Phys. **51**, 5663 (1969).
16. Tables of wavenumbers for the calibration of infrared spectrophotometers. I.U.P.A.C. Butterworths Scientific Publications, London. 1961.
17. J. E. BERTIE and D. A. OTHEN. Can. J. Chem. **50**, 3443 (1972).
18. G. HERZBERG. Infrared and Raman spectra. D. Van Nostrand, Co. Inc., New Jersey. 1945.
19. J. LOADER. Basic laser Raman spectroscopy. Heyden and Son Ltd., London. 1970. p. 27.
20. J. Q. WILLIAMS and W. GORDY. J. Chem. Phys. **18**, 994 (1950).
21. S. L. GERHARD and D. M. DENNISON. Phys. Rev. **43**, 197 (1933).
22. T. UEDA and T. SHIMANOUCHI. J. Mol. Spectrosc. **28**, 350 (1968).
23. J. C. EVANS and G. Y. S. LO. J. Am. Chem. Soc. **88**, 2118 (1966).
24. D. C. MCKEAN. Chem. Commun. 1373 (1971).
25. E. B. WILSON, J. C. DECIUS, and P. C. CROSS. Molecular vibrations. McGraw–Hill Book Co. Inc., New York. 1955.
26. J. H. SCHACHTSCHNEIDER. Technical Report No. 231-64, Project Number 31450, Shell Development Co., Emeryville, California.
27. J. H. SCHACHTSCHNEIDER. Technical Report No. 57-65, Project Number 31450, Shell Development Co., Emeryville, California.
28. S. SUNDER. Ph.D. Thesis. University of Alberta, Edmonton, Alberta. 1972.[1]

[1]Photocopies are available at a nominal charge, upon request, from the National Science Library, National Research Council of Canada, Ottawa, Canada K1A 0S2.

Can. J. Chem. Downloaded from www.nrcresearchpress.com by 210.87.254.105 on 09/05/12
For personal use only.

Preparation of 2-Methoxytetrahydropyran-3-one from Halogenated Dihydro- and Tetrahydropyran Precursors

J. E. ROFF[1] AND R. K. BROWN

The Department of Chemistry, University of Alberta, Edmonton, Alberta

Received December 4, 1972[2]

The reaction of 5-halo-3,4-dihydro-2*H*-pyran with halogen and sodium methoxide gives in good yield the corresponding 3,3-dihalo-2-methoxytetrahydropyran. The latter, upon treatment with aqueous sodium hydroxide or sodium methoxide in methanol failed to provide 2-methoxytetrahydropyran-3-one but instead gave the 3-halo-2-methoxy-5,6-dihydro-2*H*-pyran. The ketone, 2-methoxytetrahydropyran-3-one was obtained by the treatment of 5-chloro-3,4-dihydro-2*H*-pyran with *m*-chloroperoxybenzoic acid followed by the addition of sodium methoxide.

Attempts to prepare the 3,3-dibromo-2-methoxytetrahydropyran by the reaction of 3-bromo-2-methoxytetrahydropyran with bromine were unsuccessful, but gave the ring cleavage product, methyl 2,5-dibromopentanoate.

La réaction d'un halo-5 dihydro-3,4-2*H*-pyrane sur un halogène et du méthoxyde de sodium conduit au dihalo-3,3 méthoxy-2 tétrahydropyrane avec un bon rendement. Ce dernier, après traitement avec de la soude aqueuse ou du méthoxyde de sodium dans le méthanol, conduit au halo-3 méthoxy-2 dihydro-5,6-2*H*-pyrane au lieu du méthoxy-2 tétrahydropyranone-3. La cétone méthoxy-2 tétrahydropyranone-3 a été obtenue par traitement du chloro-5 dihydro-3,4-2*H* pyrane à l'acide *m*-chloroperoxybenzoique suivi d'une addition de méthoxyde de sodium. Des tentatives de préparation du dibromo-3,3 méthoxy-2 tétrahydropyrane par réaction du bromo-3 méthoxy-2 tétrahydropyrane sur le brome ont échoué et ont conduit au dibromo-2,5 pentanoate de méthyle, produit de rupture de cycle.

[Traduit par le journal]

Can. J. Chem., **51**, 3354 (1973)

As part of a program exploring avenues leading to the total synthesis of monosaccharides, the preparation of 2-methoxytetrahydropyran-3-one from halogenated dihydro- and tetrahydropyran precursors was undertaken, since the ketone might be a useful intermediate for some monosaccharide syntheses. This note describes the results obtained.

The reaction of 5-chloro-3,4-dihydro-2*H*-pyran (**1**, X = Cl (1)) or its bromo analog, (**1**, X = Br (2)) with chlorine in the presence of methyl alcohol and sodium methoxide gave 3,3 - dichloro - 2 - methoxytetrahydropyran, (**2**, X = Y = Cl) and 3-bromo-3-chloro-2-methoxytetrahydropyran, (**2**, X = Cl, Y = Br) respectively, in very good yield (Scheme 1). Similarly, **2**, X = Y = Br, was obtained by bromination of **1**, X = Br. Attempts to prepare **2**, X = Y = Br, by direct bromination of the acetal 3-bromo-2-methoxytetrahydropyran failed, but instead provided the acyclic compound methyl 2,5-dibromopentanoate.

Base catalyzed hydrolysis of **2**, X = Y = Cl or Br, or X = Cl, Y = Br, failed to produce the desired ketone **4** but instead gave **3** in 2% yield along with 90% of unchanged **2** when X = Y = Cl in **2**, in 74% yield when X = Y = Br in **2**, and in 95% yield when X = Cl, Y = Br in **2**. Similarly, the reaction of **2**, X = Cl, Y = Br, with sodium methoxide in methanol gave **3**, X = Cl, in excellent yield while **3**, Y = Br, was obtained in 62% yield by the same reaction with **2**, X = Y = Br. In contrast, the methanolic sodium methoxide reaction with **2**, X = Y = Cl, proved to be much more difficult, as with the hydrolysis reaction above, and provided **3**, Y = Cl, in 5% yield along with 90% of unchanged **2**, X = Y = Cl.

The ketone **4** was made available by the reaction of **1**, X = Cl, with *m*-chloroperoxybenzoic acid in methylene chloride followed by addition of sodium methoxide (as shown in Scheme 2). There was obtained a mixture of six compounds (as shown by g.l.c.) in which **4** predominated in the relative proportion of 70% accompanied by unchanged **1**, X = Cl (8%), 3-chloro-2-methoxytetrahydropyran (10%), 3,3-dichloro-2-methoxytetrahydropyran (~1%), and two unidentified substances (each about 5%). Identifi-

[1]Postdoctoral Fellow, 1967–1969; now with the Toxicology Laboratory, Edmonton, Alberta.

[2]Revision received July 9, 1973.

Can. J. Chem. Downloaded from www.nrcresearchpress.com by 210.87.254.105 on 09/05/12
For personal use only.

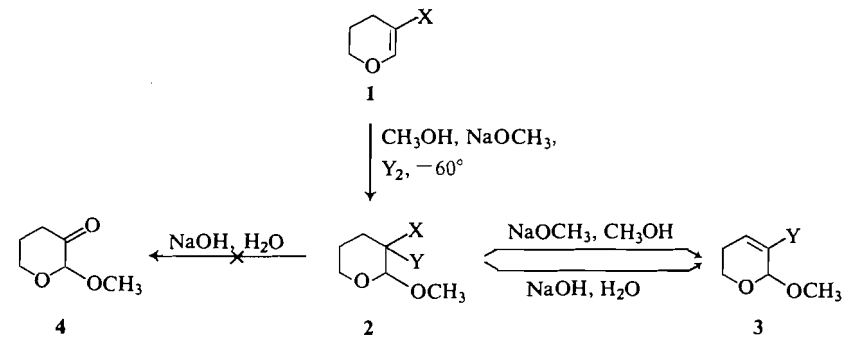

SCHEME 1

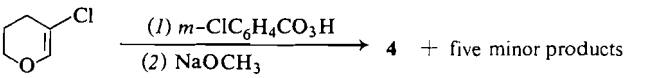

SCHEME 2

cation was made by both isolation of small samples by g.l.c. and by comparison of g.l.c. retention times with those of known compounds. It was possible to isolate **4** by fractional distillation from the mixture but decomposition and polymerization reduced the isolated yield to 20–25%.

Experimental

All melting points and boiling points are uncorrected. The elemental analyses were performed by Mrs. D. Mahlow of this Department. The p.m.r. spectra were obtained by Mr. R. N. Swindlehurst using a Varian Associates A60 spectrometer and by Mr. Glen Bigam using a Varian Associates HR100 spectrometer in this Department. Tetramethylsilane was used as reference. G.l.c. analyses were made with an F and M model 700 chromatograph using a column, 1/8 in. × 12 ft, containing 20% butanediol succinate on Gas-Chrom P (60–80 mesh) with a helium flow-rate of 40 ml/min. The i.r. spectra were obtained with Perkin-Elmer instruments, models 21 and 421. Solvents were removed by rotary evaporator under reduced pressure unless otherwise stated.

Halogenation of 3,4-Dihydro-2H-pyrans

By use of the reported procedure (5) for the bromination of 2-methoxymethyl-3,4-dihydro-2*H*-pyran, the following compounds were obtained.

3,3-Dichloro-2-methoxytetrahydropyran

This was obtained from the addition of 0.5 mol of chlorine in 300 ml of carbon tetrachloride to 0.5 mol of 5-chloro-3,4-dihydro-2*H*-pyran (1) in 1 l of methanol containing 0.5 mol of sodium methoxide. Yield 83%; b.p. 54° at 1.6 mm; n_D^{25} 1.4752 (lit. (3) b.p. 40–42° at 2 mm).

3-Bromo-3-chloro-2-methoxytetrahydropyran

This was obtained from the addition of 0.5 mol of bromine in carbon tetrachloride to 0.5 mol of 5-chloro-3,4-dihydro-2*H*-pyran (1) in methanol (1 l) containing sodium methoxide (0.5 mol). Yield 78%; b.p. 56° at 0.9 mm; n_D^{25} 1.5027.

Anal. Calcd. for $C_6H_{10}BrClO_2$: C, 31.39; H, 4.39; halogen determined as chloride, 30.90. Found: C, 31.29; H, 4.14; halogen (as chloride) 30.88.

Both the p.m.r. and i.r. spectra agreed with the structure proposed.

In addition there was obtained an 8% yield of *cis-trans*-3-chloro-2-methoxytetrahydropyran, b.p. 60° at 8 mm, n_D^{23} 1.4583 (lit. (1) b.p. 74° at 18 mm, n_D^{12} 1.4646).

3,3-Dibromo-2-methoxytetrahydropyran

The addition of bromine to 5-bromo-3,4-dihydro-2*H*-pyran (2) in methanolic sodium methoxide as described above gave 3,3-dibromo-2-methoxytetrahydropyran in 91% yield: b.p. 63° at 0.6 mm; n_D^{25} 1.5305.

Anal. Calcd. for $C_6H_{10}Br_2O$: C, 26.29; H, 3.68; Br, 58.33. Found: C, 26.47; H, 3.91; Br, 58.49.

Both the p.m.r. and i.r. spectra agreed with the structure proposed.

3-Chloro-2-methoxy-5,6-dihydro-2H-pyran

(a) From 3-bromo-3-chloro-2-methoxytetrahydropyran

The dehydrohalogenation procedure reported for the preparation of *trans*-2-methoxy-6-methoxymethyl-5,6-dihydro-2*H*-pyran (5) was followed. From 22.9 g (0.1 mol) of the bromo-chloro compound there was obtained, by distillation under reduced pressure, 14.1 g (95%) of 3-chloro-2-methoxy-5,6-dihydro-2*H*-pyran; b.p. 64° at 12 mm; n_D^{25} 1.4706.

Anal. Calcd. for $C_6H_9ClO_2$: C, 48.49; H, 6.10; Cl, 23.85. Found: C, 48.39; H, 6.09; Cl, 23.80.

The p.m.r. spectrum obtained in $CDCl_3$ agreed with the structure and showed a quartet centered at 6.05 p.p.m. (1H) J ~3 and 6 Hz; a singlet at 4.68, $w_{1/2}$ ~2.5 Hz; a multiplet at 4.20–3.65 (2H); a singlet at 3.42 (3H); a multiplet at 2.80–1.50 (2H). The i.r. spectrum (neat) showed weak absorption at 1660 cm^{-1} (C=C).

The reaction of 3-bromo-3-chloro-2-methoxytetrahydropyran with aqueous sodium hydroxide gave a 93% yield of 3-chloro-2-methoxy-5,6-dihydro-2*H*-pyran.

Can. J. Chem. Downloaded from www.nrcresearchpress.com by 210.87.254.105 on 09/05/12
For personal use only.

(b) From 3,3-dichloro-2-methoxytetrahydropyran

The reaction of 18.5 g (0.1 mol) of 3,3-dichloro-2-methoxytetrahydropyran with 0.2 mol of sodium methoxide in methanol, following the procedure used in (*a*) above gave 0.7 g (5%) of 3-chloro-2-methoxy-5,6-dihydro-2*H*-pyran and 16.6 g (90%) of unchanged 3,3-dichloro-2-methoxytetrahydropyran.

A similar reaction, using aqueous sodium hydroxide gave a 2% yield of the olefin and 90% recovered unchanged dichloro compound.

3-Bromo-2-methoxy-5,6-dihydro-2H-pyran

Following the above procedure to prepare 3-chloro-2-methoxy-5,6-dihydro-2*H*-pyran, 27.4 g (0.1 mol) of 3,3-dibromo-2-methoxytetrahydropyran heated with methanol and sodium methoxide, gave 4.4 g (16%) of unchanged dibromo compound and 12.0 g (62%) of 3-bromo-2-methoxy-5,6-dihydro-2*H*-pyran: b.p. 52° at 2.2 mm; n_D^{25} 1.4970 (lit. (4) b.p. 92–94° at 14 mm; n_D^{27} 1.4960).

The p.m.r. spectrum in $CDCl_3$ agreed with the structure and showed a quartet at 6.28 p.p.m., J ~2.5 and 5.5 Hz (1H); a singlet at 4.75, $w_{1/2}$ ~2.5 Hz (1H); a multiplet at 4.10–3.65 (2H); a singlet at 3.42 (3H); a multiplet at 2.90–1.65 (2H). The i.r. spectrum (film) showed a weak band at 1648 cm^{-1} (C=C).

When heated with aqueous sodium hydroxide at 65° for 18 h, 3,3-dibromo-2-methoxytetrahydropyran gave 3-bromo-2-methoxy-5,6-dihydro-2*H*-pyran in 74% yield. Higher temperatures resulted in lower yields.

3-Bromo-2-methoxytetrahydropyran

The reaction of 3,4-dihydro-2*H*-pyran with bromine and methanol was carried out by the procedure reported for the preparation of 3-bromo-2-methoxy-6-methoxymethyltetrahydropyran (5).

From 84 g (1 mol) of the dihydropyran there was obtained 165 g (85%) of 3-bromo-2-methoxytetrahydropyran which from previous experience with the bromomethoxylation of similar compounds (5) is considered to be nearly completely the *trans* isomer. B.p. 87° at 12 mm (lit. (6) b.p. 88–89° at 18 mm).

Methyl 2,5-Dibromopentanoate

To a well-stirred mixture of 3-bromo-2-methoxytetrahydropyran (9.75 g, 0.1 mol) and 15.9 g of anhydrous sodium carbonate in 150 ml of carbon tetrachloride, kept at 35°, was added dropwise a solution of bromine (16.0 g, 0.1 mol) in 50 ml of carbon tetrachloride. The mixture was then stirred overnight and allowed to reach room temperature. The solids were then removed and the solution was shaken several times with saturated aqueous sodium bicarbonate. The organic solution was dried (Na_2SO_4), freed from solvent and the residue was distilled under reduced pressure yielding 9.6 g (35%) of methyl 2,5-dibromopentanoate: b.p. 63° at 0.6 mm; $n_D^{26.5}$ 1.5090 (lit. (7) b.p. 93–95° at 1.5 mm; n_D^{25} (1.5099).

2-Methoxytetrahydropyran-3-one

To a stirred solution of 35.5 g (0.3 mol) of 5-chloro-3,4-dihydro-2*H*-pyran in 250 ml of dichloromethane kept between 0 and 10°, was added slowly a solution of 64.8 g (0.3 mol) of 80% *m*-chloroperoxybenzoic acid in dichloromethane. The mixture was then stirred overnight and allowed to reach room temperature. The precipitated *m*-chlorobenzoic acid was removed and to the residual solution, kept cool with an ice bath, was added 32.4 g (0.6 mol) of sodium methoxide. The mixture was then stirred overnight (room temperature), following which the solids were separated and the solvent removed under reduced pressure. The residual oil (24 g, ~60%) was found by g.l.c. to consist of 2-methoxytetrahydropyran-3-one (70%), unchanged 5-chloro-3,4-dihydro-2*H*-pyran (8%), 3-chloro-2-methoxytetrahydropyran (9%), 3,3-dichloro-2-methoxytetrahydropyran (1–2%), and two unidentified substances (each about 5%).

The crude mixture, when subjected to fractional distillation under reduced pressure, decomposed with polymerization and provided only a relatively small amount (20–25%) of pure 2-methoxytetrahydropyran-3-one: b.p. 44° at 2 mm; $n_D^{26.5}$ 1.4611.

Anal. Calcd. for $C_6H_{10}O_3$: C, 55.37; H, 7.74. Found: C, 54.60; H, 7.72.

The p.m.r. spectrum in $CDCl_3$ agreed with the structure proposed, showing a singlet at 4.54 mm (1H); broad multiplet, 4.4–3.7 (2H); singlet, 3.49 (3H); broad multiplet, 2.9–2.0 (4H). The i.r. spectrum (film) showed strong absorption at 1730 cm (C=O) and at 1100 cm^{-1} (C—O—C).

The authors wish to thank the National Research Council of Canada for financial assistance for a part of this work.

1. O. Riobe. Bull. Soc. Chim. Fr. 829 (1951).
2. R. Paul. Bull Soc. Chim. Fr. 1397 (1934).
3. D. G. Jones and J. G. M. Bremner. Brit. pat. 598 080, Feb. 10, 1948; Chem. Abstr. **42**, 4614c (1948).
4. P. Paul and S. Tchelitcheff. Bull. Soc. Chim. Fr. 869 (1956).
5. F. Sweet and R. K. Brown. Can. J. Chem. **46**, 2283 (1968).
6. G. F. Woods and H. Sanders. J. Am. Chem. Soc. **68**, 2483 (1946).
7. N. Isenberg, I. Barkocy, and S. R. Parker. Angew. Chem. Int. Ed. **3**, 63 (1964).

Can. J. Chem. Downloaded from www.nrcresearchpress.com by 210.87.254.105 on 09/05/12
For personal use only.

The Synthesis of Some Alkyl Hex-3-enopyranosiduloses[1,2]

N. L. HOLDER[3] AND B. FRASER-REID
Chemistry Department, University of Waterloo, Waterloo, Ontario

Received February 13, 1973

Routes to methyl 3,4-dideoxy-α-D-*glycero*-hex-3-enopyranosidulose **1***a* have been developed which use cheap readily-available chemicals, which are operable on a large scale and which have readily crystallizable materials as key intermediates (Scheme 4). Extensive use is made of reductive elimination of vicinal sulfonyloxy groups which is shown to operate equally well whether these groups on the pyranoside ring are in *cis* or *trans* relationship. Contrary to other reported cases, it is found that the carbon-2 allylic hydroxyl goup is oxidized with manganese dioxide whether it is in pseudoaxial or equatorial orientation.

Différentes méthodes utilisant des produits chimiques peu coûteux et facilement disponibles, pouvant facilement être rentables à grande échelle et impliquant des produits intermédiaires facilement cristallisables, on été développées afin d'obtenir le méthyl didéoxy-3,4 α-D-*glycéro* hexèno-3 pyranosidulose **1***a* (schéma **4**). Dans ces méthodes, on a très souvent utilisé la réaction d'élimination réductive des groupes sulfonyloxy vicinaux qui fonctionne bien, indépendamment de la relation *cis* ou *trans* pouvant exister entre ces groupes sur l'anneau pyranosyde. Contrairement à ce qui a déjà été rapporté dans d'autres cas, on a trouvé que le groupe hydroxyle allylique sur le carbone-2 est oxydé à l'aide du bioxyde de manganèse sans tenir compte de son orientation pseudoaxiale ou équatoriale.

[Traduit par le journal]

Can. J. Chem., **51**, 3357 (1973)

Introduction

Carbohydrate molecules possessing ketonic (1) and/or olefinic (2) unsaturation are currently the preferred precursors for the synthesis of branched-chain, amino, and rare sugars as may be evinced by a number of recent reviews (3). In recent years, major advances have been made in the study of molecules possessing both types of unsaturation in conjugation (4), these molecules being of interest in view of the array of synthetic techniques available to them (5). We wish to report the synthesis of some alkyl 3,4-dideoxy-hex-3-enopyranosiduloses from readily available starting materials by way of simple laboratory processes.

At the inception of this project, there existed confirmatory evidence for the structures and conformations of some methyl 3,4-dideoxy-α- and β-D-*glycero*-hex-3-enopyranosiduloses **1** (6, 7). These compounds were obtained as syrups in low yields by acid-catalyzed elimination from enolic precursors **2** having the appropriate anomeric configurations (6), or by way of their anomeric fluorides **3** (7). However, there existed no synthetic methods by which these seemingly

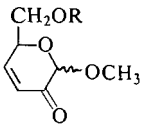

1

a α-OCH_3; R = H
b α-OCH_3; R = CH_3
c β-OCH_3; R = CH_3
d α-OCH_3; R = COPh
e α-OCH_3; R = *p*-$NO_2C_6H_4$
f α-OCH_3; R = Ac
g α-OCH_3; R = CPh_3

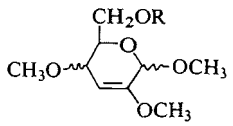

2

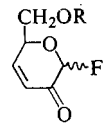

3

valuable precursors could be obtained in large quantities from readily available and cheap starting materials. Because of their synthetic utility and the success in this laboratory in synthesizing some alkyl 2,3-dideoxy-α-D-*glycero*-hex-2-enopyranosid-4-uloses (4*g*, *h*) we addressed ourselves to the synthesis of **1***a*.

Results and Discussion

One conceivable route to **1***a* has as its final step the selective oxidation of the corresponding allylic alcohol. This was of additional interest in view of the recently observed failure of certain allylic alcohols to respond to manganese dioxide oxidation (4*c* and *i*). Hence we were prompted to investigate this effect on the C-2 epimeric allylic alcohols **4***a* and **5***a* whose syntheses there-

[1]Pyranosiduloses Part V, for Part IV see reference 4*a*.
[2]Portions of this work have appeared in preliminary communications (4*b*, 18).
[3]Taken from the Ph.D. thesis of N.L.H., University of Waterloo, Waterloo, Ontario, 1972. Present address: Gillette Research Institute, Rockville, Maryland, U.S.A.

Can. J. Chem. Downloaded from www.nrcresearchpress.com by 210.87.254.6 on 09/05/12
For personal use only.

TABLE 1. 60 MHz n.m.r. parameters for some methyl 3,4-dideoxy-α-D-*erythro*-hex-3-enopyranosides (**4**) and the related pyranosiduloses **1** ($CDCl_3$, TMS)

Compound	Chemical shifts (τ) H-1	H-2	H-3,H-4	H-5	H-6,H-6′	OCH_3	Coupling constants (Hz)*
4*a*	5.1	5.7–6.0	4.27	5.7–6.0	6.41	6.5	Except as indicated
4*b*	5.1	5.6–5.9	4.2	5.6–5.9	5.8	6.5	$J_{12} \sim 4.0$
4*c*	4.7	4.45	4.05	5.3–5.7	5.5	6.5	$J_{56} = J_{56'} = 5.0$
4*d*	4.7	4.4	4.0	~5.4	5.4	6.5	H-3 and H-4 appear as an over-
4*e*	5.14	5.8	4.27	5.8	6.7	6.57	lapping singlet and H-2 and H-5 as overlapping multiplets
5*b*	5.34	6.34	4.14	5.8	6.8	6.6	$J_{12} < 1$
1*a*	5.2	—	3.80,2.9	~5.2	5.2	6.41	In all cases except as indicated
1*d*	5.19	—	3.80,2.94	~5.15	5.39,5.5	6.44	$J_{13} \sim 1.0$
1*e*	5.12	—	3.80,2.87	~5.1	5.34	6.4	$J_{34} = 10.7$
							$J_{35} = 2.6$–2.7
							$J_{45} = 1.0$–1.5
							$J_{56} = J_{56'} = 5.0$
1*f*	5.2	—	3.80,2.94	~5.15	5.67	6.44	In **1***e* and **1***f* H-1 and H-5 unresolved
1*g*	5.44	—	3.94,2.95	5.5	6.7	6.54	$J_{34} = 11.0$; $J_{35} = 2.5$;
							$J_{45} = 1.7$; $J_{56} = J_{56'} = 5.0$

*Spacings read directly from the spectrum.

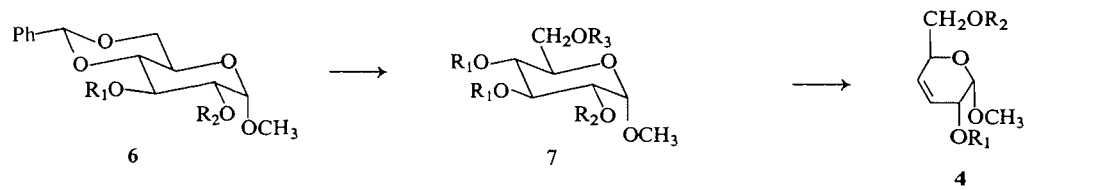

6

a $R_1 = R_2 = H$
b $R_1 = H$; $R_2 = COPh$
c $R_1 = R_2 = SO_2CH_3$
d $R_1 = R_2 = SO_2C_6H_4$-*p*-CH_3
e $R_1 = COPh$; $R_2 = H$

7

a $R_1 = H$; $R_2 = R_3 = COPh$
b $R_1 = R_3 = H$; $R_2 = COPh$
c $R_1 = SO_2CH_3$; $R_2 = R_3 = COPh$
d $R_1 = H$; $R_2 = COPh$; $R_3 = CPh_3$
e $R_1 = SO_2CH_3$; $R_2 = COPh$; $R_3 = CPh_3$

4

a $R_1 = R_2 = H$
b $R_1 = H$; $R_2 = COPh$
c $R_1 = R_2 = COPh$
d $R_1 = R_2 = COC_6H_4$-*p*-NO_2
e $R_1 = H$; $R_2 = CPh_3$
f $R_1 = SO_2CH_3$; $R_2 = CPh_3$
g $R_1 = COPh$; $R_2 = CPh_3$

SCHEME 1

fore became our initial objective (Schemes 1 and 2).

One synthetic approach to **4***a* is summarized in Scheme 1. Obtainment of starting material **6***a* was greatly simplified by treating methyl α-D-glycopyranoside with α,α-dimethoxytoluene according to the method described by Evans (8). The selective benzoylation of **6***a* → **6***b* developed by Carey and Hodgson (9) paved the way to the key intermediate, the dibenzoate **7***a*, via debenzylidination of **6***b* and then selective benzoylation of the derived monobenzoate **7***b*. This three step route to **7***a* was better in overall yield and easier in execution than direct dibenzoylation of methyl α-D-glucopyranoside reported earlier (10). Compound **7***a* was di-*O*-methanesulfonylated and reductive elimination (11) of the resulting 3,4-dimesylate (**7***c*) gave a mixture of **4***b* and *c*. The configurational relationship of **4***b* and **4***c* follows from the fact that the mixture upon benzoylation gave only **4***c* and upon deesterification gave only **4***a* as a mobile oil. The compound **4***a* was characterized as its di-*O*-*p*-nitrobenzoate **4***d* and its 6-*O*-trityl ether **4***e*; the n.m.r. parameters of **4***a* and its benzoate esters are recorded in Table 1.

It is now clear that an ester adjacent to a vicinal dimesylate grouping is usually lost during reductive elimination (11*a*). However the deesterification is not complete and there is no change in configuration.

For reasons of completeness, we desired to determine whether *cis*-di-*O*-methanesulfonyl groups in a pyranoside molecule as in **10***a* would

Can. J. Chem. Downloaded from www.nrcresearchpress.com by 210.87.254.6 on 09/05/12
For personal use only.

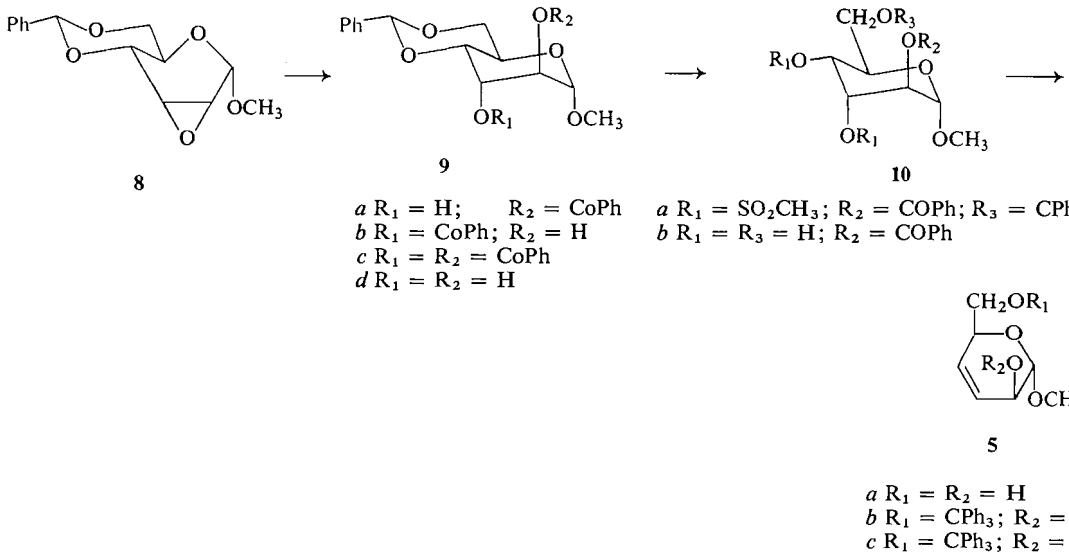

8

9

a R_1 = H; R_2 = CoPh
b R_1 = CoPh; R_2 = H
c R_1 = R_2 = CoPh
d R_1 = R_2 = H

10

a R_1 = SO_2CH_3; R_2 = COPh; R_3 = CPh_3
b R_1 = R_3 = H; R_2 = COPh

5

a R_1 = R_2 = H
b R_1 = CPh_3; R_2 = H
c R_1 = CPh_3; R_2 = COPh

SCHEME 2

also undergo ready reductive elimination. Although this reaction had been applied successfully to *cis*- and *trans*-sulfonyl esters of cyclohexanes (12), iodide displacement of the *cis*-groups may be influenced by steric effects of other groups present on the pyranoside ring. The pathway to **10***a*, as outlined in Scheme 2, requires **9***a*, the reported synthesis of which is bedevilled by the production of variable quantities of the unwanted isomer **9***b*, and the dibenzoate **9***c* (13). In an alternative approach to **9***a*, based upon ample precedent (14), the oxirane **8** obtained from **6***c* was treated with sodium benzoate in DMF, a highly nucleophilic medium (15), in the hope that the *trans*-diaxial product **9***a* would be favored. However, the ratio of **9***a* to the 3-*O*-benzoyl glucopyranoside **6***e*, arising from diequatorial scission of **8** was discouragingly small. All modifications of the above method failed to give the desired compound in acceptable yields (16).

In view of the ready availability of **9***d* (17), the selective benzoylation method of Carey and Hodgson (9) was applied. In the event, **9***a* was obtained in only 50% yield; however, it was the only benzoylated product formed (18). Catalytic hydrogenolysis of **9***a* afforded **10***b* but attempted C-6 selective benzoylation of this latter compound resulted in a complex mixture. Accordingly, a solution of **10***b* and trityl chloride in anhydrous pyridine was allowed to stand at room temperature (19, 20) until the reaction was complete (t.l.c.), whereupon excess methanesulfonyl chloride was added to esterify the secondary hydroxyl groups leading to **10***a*.

Elimination of the methanesulfonyl groups from **10***a* with concomitant introduction of 3,4-unsaturation was readily achieved under the usual experimental conditions (11*a*). Here too, as in earlier examples, the reductive elimination was accompanied by some debenzoylation at carbon-2. The mixture **5***b* and **5***c* was debenzoylated to give the alcohol **5***b* as a crystalline material.

The successful reductive eliminations of **7***c* and **10***a* indicate that this process may be applied to carbohydrate molecules bearing either *cis*- or *trans*-dimethanesulfonate groups. The presence or the orientation of acid or base labile groups does not effect the outcome of the reaction. Therefore, the reaction pathway opined by one of us in 1969 (11*a*) and reproduced here probably holds.

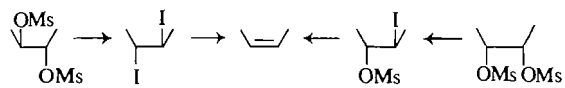

The spacing (J_{12} = ~1 Hz) in **5***b* and **10***a* indicates that the carbon-2 retained its configuration during the reductive elimination **10***a* → **5***b* + **5***c*. In the light of earlier results **7***c* → **4***b* + **4***c* (*vide supra*) and the results

Can. J. Chem. Downloaded from www.nrcresearchpress.com by 210.87.254.6 on 09/05/12
For personal use only.

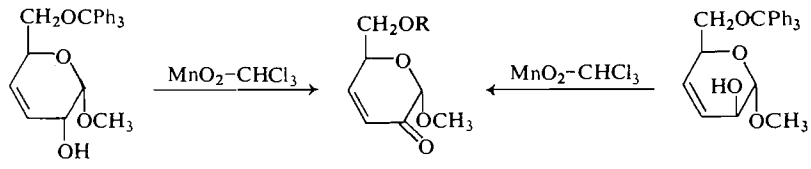

SCHEME 3

recorded earlier by Fraser-Reid and Boctor (11*a*) this process may now be regarded as normal. In **4***a* H-3 and H-4 give overlapping signals ~4τ and show very little fine structure. This is to be expected since the dihedral angles between H-2 and H-3 on the one hand, and H-4 and H-5 on the other, are approximately 90° in each case, which according to the observations of Garbish (21) correlates with very small coupling constants.

It is commonly observed that a sulfonate situated at C-2 of a pyranoside ring is loathe to displacement by a charged nucleophile (22, 23). However in the light of the success of Ferrier and co-workers (24) in displacing a C-4 allylic sulfonyloxy group, we undertook to treat the mesylate **4***f* with sodium benzoate in refluxing DMF. The experiment was successful yielding a single substance which upon debenzoylation gave **5***b*. This salutary result (*a*) strongly supports the hypothesis that the enhanced reactivity of the secondary allylic esters at C-2 is attributable to resonance stabilization of the transition state (25) and (*b*) shows unequivocally that there was no inversion of stereochemistry at C-2 during debenzoylation which accompanied the reductive eliminations in Schemes 1 and 2.

The final stage in the synthesis of the methyl 3,4-dideoxy-α-D-hex-3-enopyranosiduloses **1**, is the selective oxidation of the allylic alcohol at C-2. In the preliminary experiments it was found that the diol **4***a* was oxidized by manganese dioxide to a crystalline hydroxy-ketone **1***a* without affecting the primary alcohol (*Cf.* 4*g*). However on a preparative scale, **1***a* was obtained as a brown syrup and consequently the 6-*O*-trityl ether **4***e* was oxidized to a crystalline enone **1***g* (Scheme 3) in 94% yield; n.m.r. parameters are tabulated (Table 1). Similarly, the pseudoaxial alcohol **5***b* was oxidized to the same ketone **1***g* in comparable yields and purity. Therefore, contrary to the observations that the pseudoaxial allylic alcohols at C-4 (4*c*) and at C-3[4] (4*i*) are not oxidized with manganese dioxide, both epimeric C-2 allylic alcohols **4***e* and **5***b* are oxidized to the hex-3-enopyranosidulose. It is instructive to note that oxidation of **4***e* could also be achieved with chromium trioxide in pyridine (4*i*); however the yield of the enone **11** was only 64%. Removal of the protective group of **1***g* with hydrogen chloride in chloroform (26) was readily accomplished, whereby **1***a* was isolated in about 83% yield in crystalline form.

The elegance of the synthetic route summarized in Scheme 1 is vitiated by the necessity for chromatographic separations and the isolation of several non-crystalline intermediates. In view of this and in light of the knowledge gained from Schemes 2 and 3 the most economical route to **1***a* is outlined in Scheme 4. This path originates with the previously described monobenzoate **6***b* and the key intermediates **7***e* and **4***e* were isolated as crystalline derivatives in high yields. The overall yield of **1***a* from **6***b* is about 50%.

The hydroxy-ketone **1***a* could be esterified to give the benzoate **1***d*, *p*-nitrobenzoate **1***e*, and acetate **1***f*. Methyl 6-*O*-benzoyl-3,4-dideoxy-α-D-hex-3-enopyranosidulose **1***d* was also obtained by manganese dioxide oxidation of the monobenzoate **4***b*. The benzoate esters **1***d* and **1***e* are crystalline compounds and gave satisfactory analytical and spectroscopic data. On the other hand, the acetate **1***f* is non-crystalline and its structure was based on its n.m.r. and i.r. spectra. Some 60 MHz n.m.r. data for these esters are given in Table 1. The physical data are in complete agreement with the parameters recorded by

[4]By contrast the C-3 equatorial alcohol in 1,2-dideoxy-4,6-*O*-isopropylidine-D-*arabino*-hex-1-enopyranose was oxidized by activated manganese dioxide (16).

Can. J. Chem. Downloaded from www.nrcresearchpress.com by 210.87.254.6 on 09/05/12
For personal use only.

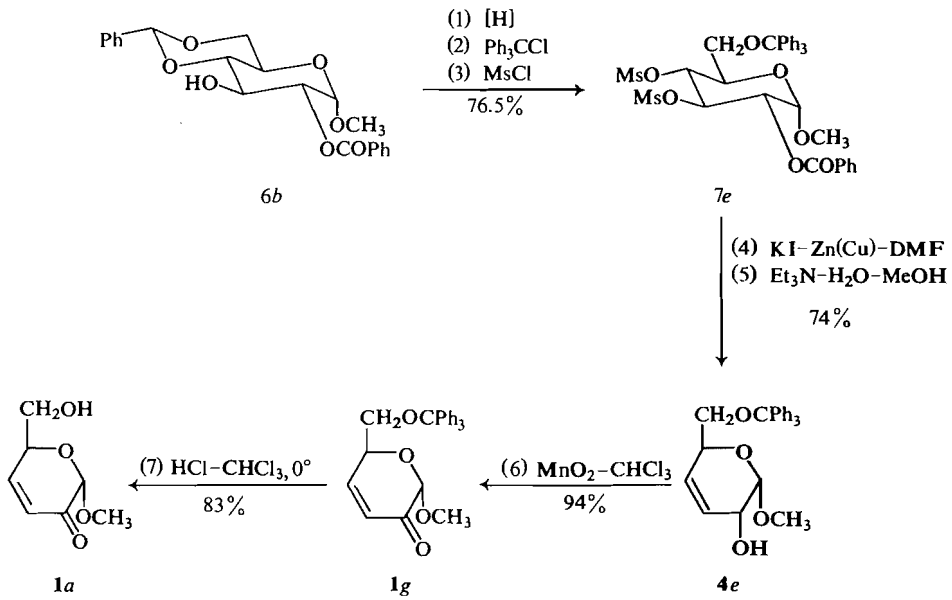

SCHEME 4

Anet (6) for the 6-*O*-methyl derivative and by Bock and Pedersen (7) for the 6-*O*-benzoyl and 6-*O*-acetyl compounds.

Experimental

Melting points were determined on a Fisher-Johns heating stage and are uncorrected. Elemental analyses were performed by Chemalytics Inc., Tempe, Arizona 85281. The n.m.r. spectra ($CDCl_3$, TMS) were determined on a Varian T-60 spectrometer, the *J* values quoted in the table being the spacings measured directly from the spectra. I.r. spectra were determined on a Beckman model I.R. 10 spectrometer using 0.1 mm sodium chloride solution cells (chloroform as solvent). U.v. spectra were obtained from a Beckman DBG Grating Spectrophotometer and a Cary Recording Spectrophotometer model 14 (methanol as solvent). Mass spectra were measured with a CEC model 21-110B double focusing instrument at an i.p. of 70 eV. Optical rotations were determined on a Carl Zeiss model LEP nür 370740 Lichtelektusches Praizision-polarimeter at 23 °C.

T.l.c. was performed on glass plates coated with silica gel (HF-254, E. Merck) to a thickness of 0.3 mm. The chromatograms were first viewed under u.v. light and then sprayed with concentrated sulfuric acid. For column chromatography E. Merck Silica Gel (0.063–0.20 mm 70–230 mesh, A.S.T.M.) was used.

The procedures for reductive elimination (11) and manganese dioxide oxidation (4*g*) were as described previously.

Methyl 4,6-O-Benzylidene-α-D-glucopyranoside **6***a*

The following modification of Evans' recently reported synthesis (8) is recommended.

Methyl-α-D-glucopyranoside (97 g, 0.5 mol), 76 ml of α,α-dimethoxytoluene, and 10.0 g of *p*-toluenesulfonic acid in 400 ml of dry DMF were refluxed on a steam bath under water-aspirator vacuum for 1 h. The solvent was removed from the reaction mixture and the final traces of DMF evaporated under high vacuum. The white crystalline residue was heated with saturated sodium bicarbonate until the product was finely dispersed. The mixture was cooled to room temperature and the product filtered off and washed thoroughly with water and then petroleum ether (30–60°) or hexane until free of benzaldehyde. The product was dried at normal pressure and then under high vacuum at ~70 °C for about 12–18 h. Yield: 127 g (90%); m.p. 162–164° (*cf.* lit. (17) value 163–164°).

Methyl 2-O-Benzoyl-α-D-glucopyranoside 7b

Compound **6***b* (9) was debenzylidinated by atmospheric hydrogenolysis in methanol containing a few drops of H_2SO_4, platinum oxide being the catalyst. The title compound **7***b* was obtained in 95% yield after crystallization from chloroform; m.p. 181–182°; $[\alpha]_D^{23}$ +152.3 (*c*, 1 in ethanol).

Anal. Calcd. for $C_{14}H_{18}O_7$: C, 56.37; H, 6.08. Found: C, 55.69; H, 6.25.

Methyl 2,6-Di-O-benzoyl-α-D-glucopyranoside **7***a*

Method (a)

Methylene chloride (100 ml) was cooled to −78 °C and a solution of **7***b* (6.0 g, 20.13 mmol) in pyridine (50 ml) added. Benzoyl chloride (2.7 ml, 23.4 mmol) was added dropwise over a period of 0.5 h. The solution was maintained at this temperature for a further 0.5 h and then placed in a refrigerator (*ca.* 8 °C) for an additional 48 h. The reaction mixture was poured into an ice–water mixture (about 700 ml), the solution acidified with dilute hydrochloric acid, and the product extracted with methylene chloride (4 × 100 ml). After washing

Can. J. Chem. Downloaded from www.nrcresearchpress.com by 210.87.254.6 on 09/05/12
For personal use only.

Can. J. Chem. Downloaded from www.nrcresearchpress.com by 210.87.254.6 on 09/05/12
For personal use only.

with saturated sodium bicarbonate, water, and drying with sodium sulfate, the methylene chloride was removed leaving a residue which crystallized from benzene – petroleum ether (60–80 °C), affording 5.0 g (61% yield) of **7***a*; m.p. 138–140° (*cf.* lit. (10*b*) value 141–142°).

Method (b)

This is a modified version of the method reported by Lieser and Schweizer (10*b*). A solution of methyl-α-D-glucopyranoside (200 g, 1.03 mol) in methylene chloride (1.0 l) and pyridine (2.0 l) was cooled to ~ −30 °C. Benzoyl chloride (258 ml, 2.234 mol) was added over a period of 3 h and the benzoylation conducted as described above. The desired product, **7***a* 242.5 g was obtained in 59% yield.

Methyl 2,6-Di-O-benzoyl-3,4-di-O-methanesulfonyl-α-D-glucopyranoside **7***c*

The di-*O*-benzoyl glucopyranoside **7***a* (10.0 g, 24.8 mmol) was dissolved in pyridine (66 ml) and the solution cooled to −10 °C with an ice–salt bath. Methanesulfonyl chloride (10 ml, 128.5 mmol) was added slowly over a period of 2.5 h. Work-up procedure (as for **7***a* above) gave an amorphous solid, **7***c*, 13.0 g (93% yield); $[\alpha]_D^{23}$ +125.22 (*c*, 6.0 in $CHCl_3$); i.r. ν_{max} 1730 (benzoate ester), 1180, 1453 (CH_3—SO_2—) cm^{-1}. A satisfactory elemental analysis could not be obtained for this compound. In the mass spectrum the molecular ion was very weak; however for M − C_6H_5COOH($C_{16}H_{20}O_{10}S_2$) calculated mass 436.050, observed 436.047.

When the preparation was operated on a 20 times larger scale, the product failed to crystallize although from the t.l.c. it was homogeneous and had the proper R_f value. It could be used in the reductive elimination step directly.

Methyl 2-O-Benzoyl-3,4-di-O-methanesulfonyl-6-O-trityl-α-D-glucopyranoside **7***e*

The 2-*O*-benzoate **7***b* (9.0 g, 0.03 mol) was treated with trityl chloride (15.0 g, 0.054 mol) in 50 ml dry pyridine at room temperature for 48 h. T.l.c. indicated the absence of **7***b* and a substance presumed to be **7***d*. Without isolation, more pyridine (50 ml) was added, the solution cooled to −10 °C, and 50 ml methanesulfonyl chloride added. Work-up as for **7***a* above gave a gummy residue which crystallized readily from ether–methanol and yielded 14.0 g (76.5%) of **7***e*; m.p. 169–170°; $[\alpha]_D^{23}$ +103.57 (*c*, 5 in $CHCl_3$). I.r. ν_{max} 1730 (aromatic ester); 1365, 1180 (CH_3—SO_2—); 1605 (aromatic) cm^{-1}.

Anal. Calcd. for $C_{35}H_{36}S_2O_{11}$: C, 60.33; H, 5.21; S, 9.20. Found: C, 60.12; H, 5.19; S, 9.30.

Reductive Elimination of Methyl 2,6-Di-O-benzoyl-3,4-di-O-methanesulfonyl-α-D-glycopyranoside **7***c*. *Methyl 3,4-dideoxy-α-D-erythro-hex-3-enopyranoside* **4***a*, *its 6-O-benzoyl (***4***b) and 2,6-Di-O-benzoyl (***4***c) Derivatives*

To a solution of **7***c* (250 g, 0.436 mol) in 1.7 l of dry DMF was added sodium iodide (312.5 g, 2.180 mol) and zinc–copper couple (134 g, 2.180 mol). The rapidly-stirred solution was refluxed for 3 h, this time having been determined previously in a small-scale experiment. Isolation as previously described (11*a*) afforded an oily residue (90 g) which showed two spots on t.l.c. with R_f values 0.6 and 0.27 ($CHCl_3$–EtOAc, 1:1). A portion (7 g) of the mixture was chromatographed on a silica column. Elution with chloroform – ethyl acetate (1:1) gave a gum (4.0 g) which was homogeneous on t.l.c. (R_f 0.6). The n.m.r. parameters (Table 1) provide strong evidence for the dibenzoate **4***c*.

Further elution of the column afforded 2.5 g of material which was also chromatographically pure (R_f 0.27). The chemical shifts and coupling constants of the protons compiled in Table 1 are consistent with the proposed structure **4***b*. Independent proof of structure was provided by oxidation to the known ketone **1***d* (*vide infra*).

A 2% solution of **4***b* and **4***c* (separately or as a mixture) in methanol–water–triethylamine mixture (5:2:1) was kept at room temperature for 18 h. The solvent was evaporated leaving a mobile oil which was washed twice with petroleum ether (30–60°). T.l.c. showed the diol **4***a*, R_f 0.1 in ethyl acetate. A mixture of **4***b* and **4***c* (90 g) yielded 35 g of **4***a* (~35%) from **7***a*. The diol was characterized as its di-*O*-*p*-nitrobenzoate **4***d*; m.p. 152–153; $[\alpha]_D^{23}$ −57.7 (*c*, 5.0 in $CHCl_3$).

Anal. Calcd. for $C_{21}H_{18}N_2O_{10}$: C, 55.03; H, 3.96; N, 6.11. Found: C, 55.13; H, 3.99; N, 6.15.

N.m.r. parameters for **4***a*, *b*, *c*, and *d* are given in Table 1.

Methyl 3,4-Dideoxy-6-O-trityl-α-D-erythro-hex-3-enopyranoside **4***e*

Method (a)

A solution of syrupy **4***a* (6.0 g) and chlorotriphenylmethane (12.0 g) in dry pyridine (30 ml) was kept at room temperature for 72 h. The reaction mixture was poured into ice–water and the solid was triturated with saturated sodium bicarbonate, washed with water, and dried. The product was chromatographed on a silica column. Elution with 2 l of methylene chloride removed triphenyl carbinol (6.2 g). Further elution with 2 l chloroform – ethyl acetate (9:1) gave 8.0 g of **4***e* which crystallized from diethyl ether – ethanol.

Method (b)

The tritylated dimesylate prepared above **7***e* (2.32 g) was subjected to reductive elimination as described for **7***c*. After 3 h t.l.c. indicated a mixture presumed to be **4***e* and **4***g*. Debenzoylation was effected with the methanol–water–triethylamine system (*cf.* **4***a*) for 36 h. Purification by column chromatography gave **4***e* which crystallized from methanol (1.0 g, 74% from **7***e*).

Compound **4***e* had m.p. 122–123°; $[\alpha]_D^{23}$ −11.34 (*c*, 6.05 in $CHCl_3$); i.r. ν_{max} 3490 (hydroxyl) and 1595 (aromatic) cm^{-1}. Its n.m.r. spectrum, summarized in Table 1, is in agreement with the structure **4***e* assigned.

Anal. Calcd. for $C_{26}H_{26}O_4$: C, 77.59; H, 6.51. Found: C, 77.75; H, 6.46.

Methyl-2-O-benzoyl-4,6-O-benzylidene-α-D-glucopyranoside **9***a*

Methyl 2,3-anhydro-4,6-*O*-benzylidene-α-D-allopyranoside (**8**) (17) (1.0 g, 3.78 mol) and sodium benzoate (4.0 g) in *N*,*N*-dimethylformamide (100 ml) was refluxed for 12 h. The solution was diluted with water and extracted with ether. Drying and evaporation of the organic phase yielded a product which was chromatographed on a silica column using chloroform – ethyl acetate (1:3) for elution. The fractions collected yielded methyl 3-*O*-benzoyl-4,6-*O*-benzylidene-α-D-glucopyranoside **6***e* (~20%) (27), starting epoxide **8** (~20%), and monobenzoate **9***a* (~45%).

Can. J. Chem. Downloaded from www.nrcresearchpress.com by 210.87.254.6 on 09/05/12
For personal use only.

Monobenzoate **9***a* crystallized from methanol as long needles; m.p. 139–140° (lit. (13) m.p. 138–139°); $[\alpha]_D^{23}$ +9.75 (*c*, 5.5 in $CHCl_3$).

Anal. Calcd. for $C_{21}H_{22}O_7$: C, 65.28; H, 5.74. Found: C, 65.25; H, 5.72.

Methyl 2-O-Benzoyl-3,4-di-O-methanesulfonyl-6-O-trityl-α-D-altropyranoside **10***a*

A solution of **9***a* (2.9 g, 8.925 mmol) in methanol (200 ml) was hydrogenolyzed as described above for **6***b*. The product **10***b* (2.0 g) was treated with trityl chloride (3.5 g) in anhydrous pyridine (15 ml) for 12 h when t.l.c. indicated that the reaction was complete. A further 14 ml of pyridine was added, the mixture cooled to ~ 10 °C, and treated with methanesulfonyl chloride (10 ml). The usual work-up afforded an oil which crystallized readily from ether to give 3.16 g (58.5%) of **10***a*; m.p. 194 °C (dec.); $[\alpha]_D^{23}$ −13.88 (*c*, 6.0 in $CHCl_3$); i.r. ν_{max} 1745 (ester), 1425, and 1188 (CH_3—SO_2—) cm^{-1}.

Anal. Calcd. for $C_{35}H_{36}S_2O_{11}$: C, 60.33; H, 5.21; S, 9.20. Found: C, 60.22; H, 5.08; S, 8.90.

Methyl 3,4-Dideoxy-6-O-trityl-α-D-threo-hex-3-enopyranoside **5***b*

Method (a)

The tritylated altroside **10***a* (232 mg, 0.333 mmol) was dissolved in 3 ml of dry dimethylformamide and to this solution was added sodium iodide (249.6 mg, 1.6665 mmol) and zinc–copper couple (108.9 mg, 1.6665 mmol) and the mixture refluxed for 6 h after which time t.l.c. indicated the presence of two new compounds. The reaction products were isolated in the usual way and the n.m.r. spectrum of the residue (129 mg) showed a composition of 60% benzoate **5***c* and 40% alcohol **5***b*. Debenzoylation was completed by treating the product mixture with methanol–water–triethylamine (5:1:1) for 13 h. The resulting **5***b* crystallized from methanol; m.p. 152–153°; $[\alpha]_D^{23}$ +37.98 (*c*, 5.0 in $CHCl_3$); i.r. ν_{max} 3490 (hydroxyl) and 1595 (aromatic) cm^{-1}. The n.m.r. parameters are tabulated in Table 1.

Anal. Calcd. for $C_{26}H_{26}O_4$: C, 77.59; H, 6.51. Found: C, 77.69; H, 6.58.

Method (b)

Compound **4***e* (5.0 g, 12.4 mmol) was converted to the methenesulfonate in the usual way (*vide supra*). Crystallization from ethyl acetate – ethanol gave **4***f*, 5.0 g (83.75%); m.p. 69–70°; $[\alpha]_D^{23}$ −28.48 (*c*, 5.0 in $CHCl_3$); i.r. ν_{max} 1350, 1170, 850, 890 (CH_3SO_2—) cm^{-1}; n.m.r. τ 6.95 (s, 3, —SO_2—CH_3), 6.77 (d, 2, $J_{5,6'} = J_{5,6'} =$ 5.0 Hz, H-6, H-6′), 6.5 (s, 3, —OCH_3), 5.5–5.9 (m, 1, H-5), 4.9 (d, 1, $J_{1,2} = 4$ Hz, H-1), 4.75 (m, 1, H-2), 3.9–4.4 (AB quartet, 2, $J_{3,4} = 10$ Hz, H-3, H-4), 2.3–2.9 (m, aromatic protons).

Anal. Calcd. for $C_{27}H_{28}SO_6$: C, 67.49; H, 5.87; S, 6.66. Found: C, 67.30; H, 5.83; S, 6.57.

A mixture of **4***f* (4.0 g, 8.3 mmol) and sodium benzoate (20.0 g) in 300 ml of dry DMF was refluxed for 24 h. The product, isolated in the usual way, showed a single spot on a t.l.c. plate. However the product was placed on a silica column and eluted with chloroform. This afforded a light straw-colored foam, 3.5 g (83.5%) whose n.m.r. spectrum was consistent with the *threo* benzoate **5***c*.

Debenzoylation as in method *a* afforded 1.9 g (82.6%) of the title compound **5***b*.

Methyl 3,4-Dideoxy-6-O-trityl-α-D-glycero-hex-3-enopyranosidulose **1***g*

Method (a)

The tritylate **4***e* (7.0 g, 17.4 mmol) in chloroform (3.5 l) was stirred with activated manganese dioxide (84.0 g) for 48 h. The solids were filtered and the filtrate evaporated to give compound **1***g* (6.5 g, 94% yield) which readily crystallized from diethyl ether – ethanol (or ethanol) as long needles; m.p. 127.5–128°; $[\alpha]_D^{23}$ −15.86 (*c*, 5.75 in chloroform); u.v. λ_{max} 228.2 nm (ε 20 100); i.r. ν_{max} 1706, 1613 (α,β-unsaturated ketone) cm^{-1}. The n.m.r. parameters are given in Table 1.

Anal. Calcd. for $C_{26}H_{24}O_4$: C, 77.98; H, 6.04. Found: C, 78.14; H, 5.87.

Method (b)

Compound **5***b* (300 mg; 0.746 mmol) was oxidized with manganese dioxide as in method *a* for 40 h. Ketone **1***g* was isolated in 93.8% yield.

Method (c)

The oxidant was prepared (*cf.* 4*i*) by adding 15.0 g of CrO_3 to pyridine (500 ml) which was previously cooled to ~ −5 °C. The mixture was then allowed to come to room temperature and compound **4***e* (8.8 g, 21.88 mmol) dissolved in 30 ml of pyridine was added and the mixture stirred at room temperature. A chromatogram, in chloroform – ethyl acetate (3:1), taken after 12 h showed that the reaction had gone to completion. Ether (~800 ml) was then added and the mixture filtered. The filtrate was evaporated to a low volume, methylene chloride (200 ml) was added followed by 400 ml of ether, and the mixture filtered. The filtrate was treated twice again in a similar manner. Evaporation of solvent left a residue which crystallized from ethanol to give 6.0 g (67.8%) of **11**.

Methyl 3,4-Dideoxy-α-D-glycero-hex-3-enopyranosidulose **1***a*

Method (a)

Methyl 3,4-dideoxy-α-D-*erythro*-hex-3-enopyranoside **4***a* (oil, 1.32 g) was oxidized with manganese dioxide as described above for compound **4***e*. After 24 h the residue (870 mg) showed two spots on t.l.c. in ethyl acetate. The mixture (870 mg) was separated on a silica gel column and eluted with ethyl acetate (250 ml). The first fraction yielded **1***a* which crystallized as long needles from diethyl ether – petroleum ether (30–60°) and yielded 600 mg; m.p. 60.5–61°; $[\alpha]_D^{23}$ +54.65 (*c*, 5.0 in $CHCl_3$); u.v. λ_{max} 225.2 nm (ε 9521); i.r. ν_{max} 3571 (hydroxyl), 1700, 1653 (α,β-unsaturated ketone) cm^{-1}. The n.m.r. parameters are shown in Table 1.

Anal. Calcd. for $C_7H_{10}O_4$: C, 53.16; H, 6.37. Found: C, 53.12; H, 5.88.

Further elution of the column with ethyl acetate (100 ml) afforded unchanged starting material **4***a* (150 mg).

Method (b)

Chloroform was cooled down to about −5 °C and hydrogen chloride gas bubbled through for 5 s. The ice-cold HCl–chloroform solution (10 ml) was then added to the compound **1***g* (1.0 g, 2.5 mmol) dissolved in 5 ml of cold chloroform and the resulting solution kept at 0 °C with an ice bath. After 0.5 h, t.l.c. indicated that the reaction had gone to completion. The acid was neutralized

Can. J. Chem. Downloaded from www.nrcresearchpress.com by 210.87.254.6 on 09/05/12
For personal use only.

after 1 h with solid sodium carbonate and after filtration, the solvent evaporated by blowing a stream of nitrogen over the solution. The solid residue was chromatographed on a silica gel column. Elution with 1000 ml of chloroform gave triphenylcarbinol and further elution with chloroform – ethyl acetate (9:1) afforded 350 mg (85%) of **1***a*.

Methyl 6-O-Benzoyl-3,4-dideoxy-α-D-glycero-hex-3-enopyranosidulose **1***d*

Method (a)

The 6-*O*-benzoate **4***b* was oxidized with manganese dioxide in the usual way to the keto-benzoate **1***d* (90%); m.p. 87–88° (lit. (7) 85.5–86°).

Method (b)

Alternatively, ketone **1***a* (0.474 g; 3.0 mmol) was dissolved in methylene chloride (6 ml) and cooled to −30 °C with Dry-Ice – acetone before adding dry pyridine (3 ml). Benzoyl chloride (0.61 ml, 5.0 mmol) was added dropwise during 0.5 h and the mixture maintained for an additional 0.5 h at −30 °C. The usual work-up gave a gum which crystallized from ethanol giving 0.600 g (76.3% yield) of the benzoate **1***d*.

Methyl 3,4-Dideoxy-6-O-p-nitrobenzoyl-α-D-glycero-hex-3-enopyranosidulose **1***e*

p-Nitrobenzoylation of ketol **1***a* in the usual way (28) gave the title compound **1***e*; m.p. 138.5–139°; $[\alpha]_D^{23}$ −47.64 (*c*, 5.0 in $CHCl_3$). N.m.r. parameters are in Table 1.

Anal. Calcd. for $C_{14}H_{13}NO_7$: C, 54.73; H, 4.26; N, 4.56. Found: C, 54.71; H, 4.24; N, 4.55.

Methyl 6-O-Acetyl-3,4-dideoxy-α-D-glycero-hex-3-enopyranosidulose **1***f*

Ketol **1***a* (0.237 g, 1.5 mmol) was dissolved in dry pyridine and the solution cooled in an ice–salt bath. Acetic anhydride (3 ml) was added slowly to the cold solution which was well stirred during the addition. The reaction flask was placed in the refrigerator and left overnight. Methanol was added to the solution in order to destroy the excess acetic anhydride after which the solution was evaporated under reduced pressure at about 40 °C. Toluene was evaporated from the residue a number of times to remove the last traces of pyridine. The residue (homogeneous on t.l.c.) had a red color and was filtered on a short silica column using ethyl acetate – chloroform (1:3) as solvent. The residue **1***f* 0.273 g (90% yield) was an oil and its n.m.r. parameters are given in Table 1.

We are grateful to the National Research Council of Canada and Bristol Laboratories for financial support.

1. (*a*) K. G. A. Jackson and J. K. N. Jones. Can. J. Chem. **47**, 2498 (1969); (*b*) P. T. Beynon, P. M. Collins, D. Gardiner, and W. G. Overend. Carbohydr. Res. **6**, 431 (1968); (*c*) D. Horton, M. Nakadate, and J. M. J. Tronchet. Carbohydr. Res. **7**, 56 (1968); (*d*) V. M. Parikh and J. K. N. Jones. Can. J. Chem. **43**, 3452 (1965); (*e*) W. G. Overend. Chem. Ind. (London), 342 (1963); (*f*) J. M. Sugihara and G. U. Yuen. J. Am. Chem. Soc. **79**, 5780 (1957).
2. (*a*) R. J. Ferrier. Advan. Carbohydr. Chem. and Biochem. **24**, 199 (1969); (*b*) R. J. Ferrier. Advan. Carbohydr. Chem. **20**, 67 (1965).
3. (*a*) H. Grisebach and R. Schmid. Angew. Chem. Int. Ed. **11**, 159 (1972; (*b*) J. S. Brimacombe. Angew. Chem. Int. Ed. **10**, 236 (1971); (*c*) J. S. Brimacombe. Angew. Chem. Int. Ed. **8**, 401 (1969).
4. (*a*) B. Fraser-Reid, N. L. Holder, and M. B. Yunker. Chem. Commun. 1286 (1972); (*b*) B. Fraser-Reid and N. L. Holder. Chem. Commun. 31, (1972); (*c*) B. Fraser-Reid, B. J. Carthy, N. L. Holder, and M. Yunker. Can. J. Chem. **49**, 3038 (1971); (*d*) E. H. Williams, W. A. Szarek, and J. K. N. Jones. Carbohydr. Res. **20**, 49 (1971); (*e*) O. Achmatowicz Jr., P. Bukowski, B. Szechner, Z. Zwiezchowska, and A. Zamojski. Tetrahedron, **22**, 1973 (1971); (*f*) W. Meyer Zu Reckendorf. Chem. Ber. **103**, 2418 (1970); (*g*) B. Fraser-Reid, A. McLean, E. W. Usherwood, and M. Yunker, Can. J. Chem. **48**, 2877 (1970); (*h*) B. Fraser-Reid, A. McLean, and E. W. Usherwood. J. Am. Chem. Soc. **91**, 5392 (1969); (*i*) P. M. Collins. Carbohydr. Res. **11**, 125 (1969); (*j*) P. J. Benyon, P. M. Collins, P. T. Doganges, and W. G. Overend. J. Chem. Soc. (C), 1131 (1966); (*k*) K. Heyns and H. Gottschalck. Ber. **99**, 3718 (1966).
5. (*a*) H. O. House and W. F. Fischer, Jr. J. Org. Chem. **34**, 3615 (1969), and references cited therein. (*b*) D. H. R. Barton, E. F. Lier, and J. F. McGhie. J. Chem. Soc. (C), 1031 (1968); (*c*) E. J. Corey and D. Crouse. J. Org. Chem. **33**, 298 (1968); (*d*) E. D. Bergmann, D. Ginsburg, and R. Pappo. *In* Organic reactions. Vol. 10. *Edited by* R. Adams. John Wiley and Sons, Inc., New York. 1959. p. 179.
6. E. F. L. J. Anet. Carbohydr. Res. **1**, 348 (1966).
7. K. Bock and C. Pedersen. Tetrahedron Lett. 2983 (1969).
8. M. E. Evans. Carbohydr. Res. **21**, 473 (1972).
9. F. A. Carey and K. O. Hodgson. Carbohydr. Res. **12**, 463 (1970).
10. (*a*) J. M. Williams and A. C. Richardson. Tetrahedron, **23**, 1369 (1967); (*b*) T. Lieser and R. Schweizer. Ann. **519**, 291 (1935).
11. (*a*) B. Fraser-Reid and B. Boctor. Can. J. Chem. **47**, 393 (1969); (*b*) R. S. Tipson and A. Cohen. Carbohydr. Res. **1**, 338 (1965).
12. S. J. Angyal and R. J. Young. Aust. J. Chem. **14**, 8 (1961).
13. R. W. Jeanloz and D. A. Jeanloz. J. Am. Chem. Soc. **80**, 5692 (1958).
14. (*a*) S. J. Angyal and T. S. Stewart. Aust. J. Chem. **20**, 2117 (1967); (*b*) E. J. Reist, A. Berutez, L. Goodman, B. R. Baker, and W. W. Lee. J. Org. Chem. **27**, 3274 (1962); (*c*) W. W. Lee, A. Berutez, L. Goodman, and B. R. Baker. J. Am. Chem. Soc. **82**, 2648 (1960); (*d*) R. Jeanloz, D. A. Prins, and T. Reichstein. Helv. Chim. Acta, **29**, 371 (1946); (*e*) S. Peat and L. F. Wiggins. J. Chem. Soc. 1810 (1938); (*f*) N. K. Richtmyer and C. S. Hudson. J. Am.

Chem. Soc. **63**, 1727 (1941); (*g*) G. J. ROBERTSON and W. WHITEHEAD. J. Chem. Soc. 319 (1940).
15. (*a*) E. J. REIST, R. R. SPENCER, and B. R. BAKER. J. Org. Chem. **24**, 1618 (1959); (*b*) E. J. REIST, L. GOODMAN, and B. R. BAKER. J. Am. Chem. Soc. **80**, 5775 (1958).
16. N. L. HOLDER. Ph.D. Thesis, University of Waterloo, Waterloo, Ontario, 1972.
17. N. R. RICHTMYER. Meth. Carbohydr. Chem. **1**, 107 (1962).
18. N. L. HOLDER and B. FRASER-REID. Synthesis, 83, 1972.
19. B. HELFERICH. Adv. Carbohydr. Chem. **3**, 79 (1948).
20. (*a*) I. R. SIDDIQUI and B. URBAS. Carbohydr. Res. **5**, 210 (1967);(*b*) I. R. SIDDIQUI and V. L. MURTY. Carbohydr. Res. **8**, 477 (1968).
21. E. W. GARBISH. J. Am. Chem. Soc. **86**, 5561 (1964).
22. D. H. BALL and F. W. PARRISH. Adv. Carbohydr. Chem. **24**, 139 (1969); A. C. RICHARDSON. Carbohydr. Res. **10**, 395 (1969).
23. A. DYMTRACZENKO, W. A. SZAREK, and J. K. N. JONES. Chem. Commun. 1220 (1971); W. A. SZAREK, B. T. LAWTON, and J. K. N. JONES. Tetrahedron Lett. 4867 (1969).
24. D. M. CIMENT, R. J. FERRIER, and W. G. OVEREND. J. Chem. Soc. (C), 446 (1966).
25. A. STREITWIESER. Chem. Rev. **56**, 585 (1956).
26. Y. M. CHOY and A. M. UNRAU. Carbohydr. Res. **17**, 439 (1971).
27. R. W. JEANLOZ and D. A. JEANLOZ. J. Am. Chem. Soc. **79**, 2579 (1957).
28. R. L. SHRINER, R. C. FUSON, and D. Y. CURTIN. The systematic identification of organic compounds. 4th Ed. John Wiley and Sons, Inc. New York. 1956. p. 212.

Can. J. Chem. Downloaded from www.nrcresearchpress.com by 210.87.254.6 on 09/05/12
For personal use only.

Free Radical Substitution Reactions of Sulfur Monochloride. A Limited Synthesis of Mercaptans[1]

DENNIS D. TANNER AND BRIAN G. BROWNLEE
The Department of Chemistry, University of Alberta, Edmonton, Alberta

Received May 8, 1973

The photolysis of sulfur monochloride with a series of saturated aliphatic hydrocarbons yielded alkyl chlorides, di- and polysulfides, hydrogen chloride, and elemental sulfur. The free radical substitution reactions leading to the production of alkyl chloride and the di- and polysulfides were shown to proceed via a chlorine atom abstraction reaction. The major products, the di- and polysulfides could be transformed quantitatively, by lithium aluminum hydride reduction into their corresponding mercaptans. The reaction describes a simple free radical route to the synthesis of a variety of alkyl mercaptans.

La photolyse du monochlorure de soufre avec une série d'hydrocarbures aliphatiques saturés conduit aux chlorures d'alkyles, di- et polysulfures, acide chlorhydrique et au soufre élémentaire. On a montré que les réactions de substitution par radicaux libres conduisant à la formation de chlorure d'alkyde etaux di- et polysulfures procèdent par une réaction d'abstraction d'un atome de chlore. Les produits majeurs, les di- et polysulfures peuvent être transformés quantitativement par réduction à l'hydrure de lithium et aluminium en leurs mercaptans correspondants. La réaction constitue une voie d'accès simple par radicaux libres à une variètè d'alkylmercaptans.

[Traduit par le journal]

Can. J. Chem., 51, 3366 (1973)

Introduction

Although sulfur monochloride is a widely used substance for a large variety of industrial processes little has been published on the free radical reactions of this reagent (1). The photo-induced reaction of sulfur monochloride with a number of hydrocarbon substrates has been carried out in a continuous flow reactor in order to obtain as the desired substitution products, alkylthiosulfenyl chlorides (2). The products were characterized by converting them to their derivative thiocyanates, and dimethylamino disulfides.

$$RSSCl + 2KCN \rightarrow RSCN + KSCN + KCl$$

$$RSSCl + 2HN(CH_3)_2 \rightarrow RSSN(CH_3)_2 + H_2N(CH_3)_2Cl$$

The main side reaction reported was the formation of elemental sulfur. Alkyl chlorides were obtained, but were not quantitated.

Müller and Schmidt (2) suggested that the initial step in the reaction was the photo-initiated homolysis of the S—Cl bond, eq. 1.

$$[1] \qquad S_2Cl_2 \xrightarrow{h\nu} Cl\cdot + \cdot S_2Cl$$

Hydrogen abstraction was suggested to be by chlorine atoms, eq. 2.

$$[2] \qquad RH + Cl\cdot \rightarrow R\cdot + HCl$$

Two possibilities were proposed for the formation of the alkyl thiosulfenyl chlorides, eqs. 3 and 4.

$$[3] \qquad R\cdot + S_2Cl_2 \rightarrow RS_2Cl + Cl\cdot$$

$$[4] \qquad R\cdot + \cdot S_2Cl \rightarrow RS_2Cl$$

Alkyl chlorides were suggested as arising from coupling reactions, eq. 5.

$$[5] \qquad R\cdot + Cl\cdot \rightarrow RCl$$

In order to explore the synthetic utility of sulfur monochloride as a reagent to form carbon sulfur bonds free radically, the photolysis was investigated in a static system and the reactions were carried out until all of the active halogen was consumed.

Results and Discussion

The photolysis of sulfur monochloride with a selected series of saturated hydrocarbons each yielded a similar mixture of products. The composition of these mixtures can best be illustrated by the major products (>1%) obtained from the reaction of cyclohexane (Table 1). It was determined that, under the reaction conditions, for each mol of sulfur monochloride that was used approximately 1 mol (±10%) of cyclohexane was consumed.

The mechanism of the reaction is apparently complex and could not be written as a chain reaction since, although it was photo-initiated,

[1]Taken from the M.Sc. dissertation in chemistry of B. G. Brownlee, University of Alberta, 1968.

Can. J. Chem. Downloaded from www.nrcresearchpress.com by 210.87.254.105 on 09/05/12
For personal use only.

TABLE 1. The products from the photolysis of carbon tetrachloride solutions of S_2Cl_2 (0.28 *M*) and cyclohexane (2.8 *M*)

Product	Yield (mol per mol of S_2Cl_2)[a]
$C_6H_{11}Cl$	0.29±0.01
$C_6H_{11}S_2C_6H_{11}$	0.08±0.004
$C_6H_{11}(S)_nC_6H_{11}$[b]	0.30±0.01
S	0.30–0.35
HCl	1.47±0.01

[a]Errors indicate reproducibility limits for two or three independent experiments.
[b]$n > 2$.

it could not be induced by benzoyl peroxide (80°) or AIBN (40°) and comparable photochemical reactions were not retarded by molecular oxygen or nitric oxide. The lack of an appreciable chain length for the photo-induced reaction is undoubtedly due to the presence of molecular sulfur, an effective radical scavenger (3), which is formed during the reaction.

In the reactions of the hydrocarbons studied, the hydrocarbon material that was consumed during the reaction appeared as (>90%) monosubstituted alkyl chlorides or di- and polysulfides. An analysis of the products from the reaction of butane and isobutane is given in Table 2. The primary:secondary:tertiary selectivities per hydrogen of sulfur monochloride with butane and isobutane could be calculated from the product yields given in Table 2 by comparing the ratios of the primary chlorides plus sulfides with those of the secondary and tertiary isomers. The values obtained, 1:3.1:4.6, are quite comparable to those reported for molecular chlorine with these substrates, 1:3.5:4.8 (vapor phase, 40°) (4).

The substitution pattern for the sulfur containing compounds was determined by n.m.r. spectral analysis. The validity of this analysis was confirmed by carrying out a lithium aluminum hydride reduction of the reaction mixture, quantitatively transforming the di- and polysulfides into mercaptans, and comparing the g.l.p.c. analysis of the mercaptans obtained with those of the di- and polysulfides analyzed by n.m.r.

The selectivities obtained for the reactions of sulfur monochloride with the two isomeric butanes suggested that the hydrogen abstracting species in the reaction was the chlorine atom. This suggestion was further substantiated by determining the relative rates of reaction of sulfur monochloride with a number of substrates and comparing these rates with those previously obtained for the reactions of molecular chlorine (see Table 3).

If one assumes that the di- and polysulfides, which are the major products of the substitution reaction, are formed by alkyl radical displacement on sulfur and that the alkyl chlorides are

$$R\cdot + Y-(S)_n-R \rightarrow R-(S)_n-R + Y\cdot \qquad \begin{matrix} n \geq 2 \\ Y = Cl, RS, SCl \end{matrix}$$

formed by displacement on a terminal chlorine, then the partition of the products between chlorides and sulfides would be subject to steric interactions. From these assumptions the generalization follows that the primary alkyl radicals would most likely favor displacement on sulfur while tertiary radicals would give lower values of the ratio of sulfides to chlorides (S ratios). Values of these ratios calculated from the distribution of products found in the reaction of the appropriate substrates are listed in Table 4 for a number of radicals, and can be of use in predicting the product distribution of sulfides and chlorides produced in the reaction.

The synthetic limitations of the reagent are that it gives the distribution of products determined by the nonselective chlorine atoms and that it gives a mixture, although easily separable after reduction, of mercaptans and chlorides.

A number of model substrates were subjected to the photochemical reactions of sulfur monochloride and reduced to their mixtures of alkyl chloride and mercaptans. The yields of mercaptans, although not outstanding (see Table 5), provide a simple free radical route to alkyl mercaptans, and may possibly be useful in the synthesis of otherwise difficultly obtainable compounds.

Experimental

Materials

Sulfur monochloride was supplied by Hooker Electrochemical Co. (highest purity grade) and was purified by the Method of Brauer (6). It was distilled from elemental sulfur (4% by weight) at atmospheric pressure, b.p. 126° (680 mm), lit. (6) b.p. 138°. A further distillation from elemental sulfur (2% by weight) under reduced pressure gave pure material, b.p. 71° (70 mm).

Anal. Calcd. for S_2Cl_2: Cl, 52.51. Found: Cl, 52.39, 52.45.

The u.v. spectrum (C_6H_{12}) showed maxima at 201 (log ε 3.71) and 265 mμ (log ε 3.83). Literature values (2, 7) are 265 and 266 mμ (log ε 3.80). The absorbance went to zero above 510 mμ for a concentrated solution

Can. J. Chem. Downloaded from www.nrcresearchpress.com by 210.87.254.105 on 09/05/12
For personal use only.

TABLE 2. The substitution products and yields from the photo-initiated reactions of sulfur monochloride with butane and isobutane

	Product yields (mol per mol S_2Cl_2)[a]			
Isobutane	*tert*-C_4H_9Cl	iso-C_4H_9Cl	iso-$C_4H_9S_x$—[b]	*tert*-$C_4H_9S_x$—[b]
	0.18 ± 0.01	0.15 ± 0.01	0.50 ± 0.02	0.20 ± 0.01
Butane	*n*-C_4H_9Cl	*sec*-C_4H_9Cl	*n*-$C_4H_9S_x$—[b]	*sec*-$C_4H_9S_x$—[b]
	0.08 ± 0.01	0.20 ± 0.01	0.26 ± 0.03	0.47 ± 0.03

[a]The errors given are the deviations from the average of three or more independent experiments.
[b]Analysis of these products was carried out by n.m.r. and the values recorded were verified within the error limits given, by g.l.p.c. analysis of the mercaptans produced upon their reduction with lithium aluminum hydride.

TABLE 3. Relative reactivities of various hydrocarbons toward sulfur monochloride at 40° compared with relative reactivities of the same hydrocarbons toward chlorine atoms

	Relative reactivity per molecule		
Hydrocarbon	This work[a]	Ref. 4[b]	Ref. 5[c]
	S_2Cl_2	Cl_2	Cl_2
Cyclohexane	1.00	1.00	1.00
Cyclopentane	0.82 ± 0.05	0.86	0.75 ± 0.01
2,3-Dimethylbutane	0.69 ± 0.03	0.61	0.86
Toluene	0.135 ± 0.015	0.13	—
Norbornane	0.70 ± 0.06	—	0.75 ± 0.05

[a]Values obtained at 40°, Freon 112 as solvent (3 *M*). Experimental uncertainties are standard deviations for two reactions.
[b]Values obtained at 40°, reactants as solvent.
[c]Values obtained at 68°, carbon tetrachloride as solvent (5 *M*).

TABLE 4. *S* values for various alkyl radicals in the photo-initiated reactions of sulfur monochloride with hydrocarbons

Radical	*S* value[a] (RSH/RCl)
$CH_3CH_2CH_2CH_2\cdot$	2.9
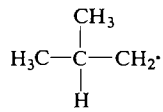	2.4
$CH_3CH_2\dot{C}HCH_3$	2.1
	2.1
	1.8
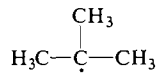	1.3

[a]All values are for reactions carried out at 40°.

TABLE 5. The yields of mercaptans from the reaction of sulfur monochloride with saturated hydrocarbons

Hydrocarbon	Product	Yield (%)
C_6H_{12}	$C_6H_{11}SH$	61
C_5H_{10}	C_5H_9SH	45
n-C_4H_{10}	*n*-C_4H_9SH	23
	sec-C_4H_9SH	45
iso-C_4H_{10}	iso-C_4H_9SH	46
	tert-C_4H_9SH	18
neo-C_5H_{12}	neo-$C_5H_{11}SH$	46
Adamantane	1-Adamantyl mercaptan	9
	2-Adamantyl mercaptan	21

(1.1×10^{-2} *M*). For 1% of contaminating sulfur dichloride the absorbance would have been 0.01 at 520 mμ (7). This absence of absorption above 510 mμ, the excellent agreement of the extinction coefficient at 265 mμ with the literature value (7), and the elemental analysis were taken as proof of the absence of sulfur dichloride in the purified sulfur monochloride. After purification the sulfur monochloride was stored at room temperature protected from light and atmospheric moisture.

Cyclohexane was Phillips Petroleum Co. pure grade material. Cyclopentane was Matheson, Coleman and Bell practical grade material. It was purified by treating with concentrated sulfuric acid, followed by dilute potassium permanganate solution. After drying and distillation it had b.p. 46.5° (700 mm) and was > 99.5% pure by g.l.p.c. analysis. Butane, isobutane, and neopentane were Phillips Petroleum Co. research grade gases. Toluene was purified by distilling from phosphorus pentoxide and had b.p. 107.5° (700 mm). 2,3-Dimethylbutane was Phillips Petroleum Co. research grade. Adamantane was *puriss* grade material supplied by Aldrich Chemical Co. Freon 112 (1,1-difluoro-1,2,2,2-tetrachloroethane) had b.p. 89.5–90.0° (700 mm); Freon 113 (1,1,2-trichloro-1,2,2-trifluoroethane) had b.p. 45.5° (704 mm). The carbon tetrachloride solvent used in reactions of sulfur monochloride with hydrocarbons was Fisher Scientific Spectranalyzed Reagent and it was distilled before use.

Can. J. Chem. Downloaded from www.nrcresearchpress.com by 210.87.254.105 on 09/05/12
For personal use only.

Can. J. Chem. Downloaded from www.nrcresearchpress.com by 210.87.254.105 on 09/05/12
For personal use only.

Reactions of Sulfur Monochloride with Hydrocarbon Substrates

A carbon tetrachloride solution of sulfur monochloride (0.3 *M*) and the desired hydrocarbon (3 *M*) were placed in Pyrex ampoules, degassed, and sealed under vacuum. After equilibration in a Pyrex water bath at 40.0 ± 0.1°, the ampoules were irradiated with two 200 W tungsten lamps. Irradiation times were 20–80 h depending on the size of sample and initial concentration of reactants. The reactions could be followed visually. After several h, the original pale yellow color of the sulfur monochloride had deepened. As the reactions progressed this yellow color faded until, at complete reaction, the reaction mixtures were nearly colorless. Reaction mixtures were tested at this point with moist potassium iodide – starch paper and found to be free from active chlorine.

Preparative reactions were carried out either in large sealed ampoules for the reactions of the more volatile hydrocarbon substrates or in a three-necked flask equipped with a magnetic stirrer and reflux condenser. The condenser outlet was connected to a gas bubbler filled with KEL-F oil so that a positive pressure was maintained in the reaction vessel. After flushing the system with nitrogen irradiation was begun, at ambient temperatures, with two 200 W incandescent lamps. In these reactions the heat from the lamps caused the temperature to rise to approximately 50–60°.

Reaction of Cyclohexane with Sulfur Monochloride

When reaction ampoules were opened the sharp smell of hydrogen chloride was apparent. When the escaping gas was bubbled through water, the aqueous portion acidified, and silver nitrate solution added, a precipitate of silver chloride was observed. Hydrogen chloride yields were determined by breaking ampoules under water and titrating the hydrogen chloride with standard 0.1 *M* sodium hydroxide solution using phenolphthalein as the indicator. The amount of hydrogen chloride per mol of S_2Cl_2 was found to vary from 1.39–1.46 for reactions 0.094–0.300 *M* in S_2Cl_2 and 2.8 *M* in cyclohexane.

The absence of hydrogen sulfide was confirmed by a negative test with lead acetate and acetic acid.

Elemental sulfur could conveniently be isolated from the reaction mixtures by column chromatography. Four reaction mixtures (20 ml each) from sulfur monochloride (0.111 *M*, 0.009 mol) and cyclohexane (2.8 *M*, 0.22 mol) were combined and the solvent was removed by distillation. Treatment of the residue with Skellysolve B left 0.097 g of undissolved elemental sulfur. Chromatography of the soluble portion on silica gel (70 g) gave a further 0.104 g of elemental sulfur eluted with Skellysolve B. The total yield of sulfur (0.201 g) represented 35% of the sulfur originally present as sulfur monochloride. A duplicate experiment yielded 30% of elemental sulfur. The sulfur isolated was identical to elemental sulfur in melting point (116–118°), mixture melting point, R_f upon analysis by t.l.c. on silica gel, and color test with pyridine – sodium hydroxide reagent (8).

Cyclohexyl chloride was determined by analyzing reaction mixtures by g.l.p.c. (5 ft × ¼ in., 20% SE-30 at 100°) after addition of chlorobenzene as the external standard. Fractional distillation of a reaction mixture yielded pure cyclohexyl chloride, whose identity and purity was established by a comparison of its identical g.l.p.c. retention time, i.r. spectrum, and refraction index (n_D^{20} 1.464; lit. (9) n_D^{20} 1.462) with those of an authentic sample.

Dicyclohexyl disulfide was estimated for one reaction mixture (sulfur monochloride 0.31 *M*, cyclohexane 3 *M* in carbon tetrachloride) by g.l.p.c. (5 ft × ¼ in., 20% SE-30 column programmed from 115–200°) after addition of naphthalene as the external standard. A yield of 0.084 mol of dicyclohexyl disulfide/mol of sulfur monochloride was determined. Its identity was established by the comparison of its g.l.p.c. retention time, its t.l.c. R_f (silica gel), and mass and i.r. spectra, with those of an authentic sample.

The dicyclohexyl polysulfides were analyzed by n.m.r. or by reduction with lithium aluminum hydride to cyclohexyl mercaptan.

Nuclear Magnetic Resonance Analysis of the Polysulfides

A 10-ml portion of a reaction mixture (sulfur monochloride 0.306 *M*, cyclohexane 3.0 *M* in carbon tetrachloride) was evaporated and benzyl chloride (0.062 g, 0.49 mmol) was added to the residue. From the n.m.r. spectrum (benzene) the ratio of the methylene protons of the standard (τ 5.9) to the α-protons of the dicyclohexyl polysulfides (τ 6.7–7.7) was 1:1.9. From this, a yield of 0.30 mol of dicyclohexyl polysulfides (including the disulfide) per mol of sulfur monochloride was calculated. Resonances for the α-proton of residual cyclohexyl chloride and the ring protons were observed at τ 6.1–6.5 and τ 7.7–9.4. The analysis was calibrated by using known mixtures of di- and tetrasulfides made from authentic materials.

Lithium Aluminum Hydride Reduction of the Polysulfide

The residue obtained after the distillation of the volatile materials (cyclohexane, carbon tetrachloride, and cyclohexyl chloride) from the reaction mixture was dissolved in THF and added dropwise to a stirred solution of lithium aluminum hydride in THF (0°). The reaction mixture was stirred at room temperature for 0.5 h and then heated under reflux for 3 h. Excess hydride was decomposed by dropwise addition of water to the cooled solution (0°). Toluene was added as the standard. After addition of concentrated hydrochloric acid (2 ml) and stirring for 10–15 min the reaction mixture was analyzed for cyclohexyl mercaptan by g.l.p.c. (10 ft × ¼ in., 10% SE-30 column programmed from 40–150°). The yield of cyclohexyl mercaptan was 0.608 ± 0.020 mol per mol of sulfur monochloride for the two reactions analyzed. The method of analysis was found to be quantitative by carrying it out on known mixtures of di- and tetrasulfides. The mercaptan was further characterized by converting it to cyclohexyl 2,4-dinitrophenyl disulfide, m.p. 114.5–115.5 and comparing its m.p., mixture m.p., and i.r. with those of authentic materials.

Competitive Reactions

For the competition experiments, 2-ml portions of a solution of cyclohexane (2.8 *M*, 5.6 mmol), the second hydrocarbon (2.7–2.9 *M*, 5.4–5.8 mmol) and Freon 112 (3 *M*) were placed in ampoules containing sulfur monochloride (0.42 g, 3.1 mmol). The ampoules were degassed

Can. J. Chem. Downloaded from www.nrcresearchpress.com by 210.87.254.105 on 09/05/12
For personal use only.

and sealed under vacuum. The original solution, without sulfur monochloride, was analyzed by g.l.p.c., using a 10 ft × ¼ in., 10% SE-30 on 60/80 Chromosorb W AW column, to give the initial peak area ratio of Freon 112 to cyclohexane and to the second hydrocarbon. The ampoules containing sulfur monochloride were irradiated at 40° for 60–85 h. The reaction mixtures were then analyzed by g.l.p.c. to give the final peak area ratios. Relative reactivities ($k_{RH}/k_{C_6H_{12}}$) were calculated in the usual manner (10). The results of these calculations are listed in Table 3.

Reaction of Sulfur Monochloride with n-Butane and Isobutane

The desired amount of hydrocarbon (5 ml, 50 mmol) was transferred into an ampoule cooled in Dry Ice. An aliquot (10.0 ml) of a standard solution of sulfur monochloride (0.3 *M*, 3.0 mmol) and Freon 112 (0.2 *M*, 2.0 mmol) in carbon tetrachloride was then pipetted into the ampoule. The ampoule was degassed, sealed under vacuum and irradiated at 40° for 80–100 h.

The reactions with *n*-butane when analyzed by g.l.p.c. (20 ft × ⅛ in., 5% SF-96 on Chromosorb W AW-DMCS column) gave (four reactions) 0.08 ± 0.01 mol per mol S_2Cl_2 of 1-chlorobutane and 0.20 ± 0.01 mol per mol S_2Cl_2 of 2-chlorobutane. The reactions with isobutane when analyzed by g.l.p.c. (SF-96 column) gave for four reactions 0.18 ± 0.01 mol per mol of S_2Cl_2 of *tert*-butyl chloride. The chlorides were quantitated using standard calibration curves determined for Freon 112 and the authentic materials.

The polysulfides produced in the reaction were collected, after the removal of solvent and alkyl chlorides, by distillation, and were analyzed directly by n.m.r. spectroscopy, and also by analysis of the mercaptans formed upon lithium aluminum hydride reduction of the mixture of polysulfide.

To the mixture of mercaptans isolated after reduction was added an external standard (Freon 113). The mixture was analyzed by g.l.p.c. (20 ft × ⅛ in., SF-96 column). *n*-Butane yielded 0.23 mol per mol of S_2Cl_2 of 1-butyl mercaptan and 0.45 mol per mol of S_2Cl_2 of. 2-butyl mercaptan. Isobutane yielded 0.45 ± 0.01 mol per mol of S_2Cl_2 of isobutyl mercaptan and 0.18 ± 0.01 mol per mol of S_2Cl_2 of *tert*-butyl mercaptan.

The mercaptans were identified and characterized by their n.m.r. spectra and the spectra of their 2,4-dinitrophenyl disulfide derivatives. The n.m.r. analysis of the polysulfides of *n*-butane was carried out by adding a known amount of anisole as a standard to the polysulfide residue and the n.m.r. spectrum of the mixture was obtained using carbon tetrachloride as the solvent. In preparing the samples undissolved elemental sulfur was removed by filtration. The spectrum was assigned by comparison with di-*n*-butyl and di-*sec*-butyl disulfides as model compounds by peak enhancement. Terminal methyl groups appeared as overlapping signals at τ 8.8–9.3, the doublet for the —S—CH—CH_3 methyl group was at τ 8.63, methylene protons were from τ 8.0–8.8, and the α-protons were unresolved from τ 6.8–7.6 in good agreement with literature values (11) for the chemical shifts of the α-protons of di-*n*-butyl and di-*sec*-butyl and di-, tri-, and tetrasulfides. The isomer distribution, determined from the integrated spectra, agreed within the experimental limits determined by the analysis of the mercaptan mixtures.

The analysis of the n.m.r. spectra of the polysulfides of isobutane was carried out by assigning the absorption peaks, using di-*tert*-butyl disulfide, di-*tert*-butyl tetrasulfide, and di-isobutyl disulfide as model compounds. Singlets for *tert*-butyl protons were present at τ 8.71 (disulfide) and τ 8.62 (polysulfides). The *gem*-dimethyl doublet was at τ 9.0, a multiplet for the tertiary hydrogens was at τ 7.4–8.2 and a multiplet for the α-protons was at τ 7.05–7.35 for the isobutyl groups. The chemical shifts of the α-protons and the *tert*-butyl singlets were in agreement with literature values (11, 12). The isomer ratios were determined by comparing the integrated area for the *gem*-dimethyl doublet to that for the *tert*-butyl singlets. The total yield of butyl groups was determined by comparing their nine proton signals to the eight proton signals of an added standard, anisole. The results agreed within the experimental limits given by the reduction method.

Reaction of Sulfur Monochloride with Cyclopentane

In the vessel described for preparative reactions cyclopentane and sulfur monochloride were reacted to 75% completion in 5 days (iodometric titration). The deep amber reaction mixture was stirred with excess potassium iodide in 10% aqueous acetic acid. The aqueous portion was separated and the organic layer was washed with aqueous sodium thiosulfate solution, water, and then dried over anhydrous sodium sulfate. The reaction mixture was analyzed as was that for cyclohexane and yielded after reduction 0.42 ± 0.03 mol per mol S_2Cl_2 of cyclopentyl mercaptan and 0.24 mol per mol S_2Cl_2 of cyclopentyl chloride.

Reaction of Sulfur Monochloride with Neopentane

Neopentane (6 ml) and a carbon tetrachloride solution (10 ml) of sulfur monochloride (0.29 *M*, 2.9 mmol) were placed into five large ampoules. One of these ampoules contained Freon 112 (0.133 g, 0.65 mmol) as the internal standard. The ampoules were degassed, sealed, and irradiated at 40° for 3 days after which time the reaction mixtures were nearly colorless.

The reaction mixture containing Freon 112 was analyzed by g.l.p.c. (25 ft × ¼ in., 10% UCON POLAR or Firebrick column) in order to estimate the yield of neopentyl chloride. Using calibration data for Freon 112 *vs.* isobutyl chloride, a yield of 36% (0.11 g, 1.05 mmol) of neopentyl chloride was estimated.

The solvent was removed from all five reaction mixtures and the combined polysulfides were reduced with lithium aluminum hydride (1.0 g, 0.026 mol) in ether (75 ml, heated under reflux for 24 h). After decomposition of excess hydride the ether solution was poured into ice–water (100 ml) containing hydrochloric acid (10 ml). The layers were separated, the aqueous portion was extracted with ether (50 ml), and the combined ether extracts were washed with water (50 ml) and saturated sodium chloride solution (50 ml) and dried over anhydrous sodium sulfate. The ether was removed by distillation through a short Vigreux column. Distillation of the residue gave 0.70 g (46%) of neopentyl mercaptan: b.p. 95–100° (688 mm);

Can. J. Chem. Downloaded from www.nrcresearchpress.com by 210.87.254.105 on 09/05/12
For personal use only.

n_D^{20} 1.4689; i.r. (CS_2) 2950, 2920, 2905, 2855, 1380, and 1355 cm^{-1}; n.m.r. (CCl_4) τ 7.63 (d, 2, J = 9 Hz, —S—CH_2—), τ 8.88 (t, 1, J = 9 Hz, S—H), and τ 9.03 (s, 9, *tert*-butyl).

The 2,4-dinitrobenzenesulfenyl derivative was prepared from the mercaptan (0.19 g, 1.8 mmol) and 2,4-dinitrobenzenesulfenyl chloride (0.445 g, 1.9 mmol) by the usual method (13). After crystallization of the crude product from methanol, 0.35 g (69%) of neopentyl 2,4-dinitrophenyl disulfide, m.p. 85–88° was obtained. Two further crystallizations from methanol gave an analytically pure sample, m.p. 91–92°.

Anal. Calcd. for $C_{11}H_{14}N_2O_4S_2$: C, 43.69; H, 4.67; N, 9.27. Found: C, 43.46; H, 4.81; N, 9.28.

Reaction of Sulfur Monochloride with Adamantane

The reaction was carried out in a three-necked flask. Adamantane (20 g, 0.147 mol) was reacted for 4 days with sulfur monochloride (2.00 g, 0.0148 mol) in carbon tetrachloride (100 ml). The solvent was removed from the reaction mixture and the residue was subjected to column chromatography using an alumina column packed in Skellysolve B. Elution with Skellysolve B gave 15.3 g of recovered adamantane and 2.05 g of a misture of elemental sulfur and chloroadamantane. The sulfur was isolated by dissolving the chlorides in acetone. The soluble portion (1.61 g) was shown to possess an n.m.r. spectrum ($CDCl_3$) consistent with a 60:40 mixture of 1-chloroadamantane and 2-chloroadamantane by comparison with published spectral data for these two compounds (14, 15). The yields of 1-chloroadamantane and 2-chloroadamantane calculated were therefore 38% (5.6 mmol) and 26% (3.8 mmol) respectively based on sulfur monochloride. The isomers could be separated by preparative g.l.p.c. 1-Chloroadamantane had m.p. 168–169°, lit. (16) m.p. 168.5–169.5°. The n.m.r. spectrum ($CDCl_3$) of the material was identical to that reported in the literature (14). 2-Chloroadamantane had m.p. 196–197°, lit. (17) m.p. 196°. The n.m.r. spectrum of this material was identical to that reported in the literature (15).

Lithium Aluminum Hydride Reduction of the Polysulfides of 1-Adamantyl Mercaptan and 2-Adamantyl Mercaptan

A portion (1.32 g) of the polysulfides previously obtained by column chromatography was reduced with lithium aluminum hydride (1.0 g, 0.026 mol) in THF (50 ml, heated under reflux for 3 h). After decomposition of excess hydride, the reaction mixture was poured into ice–water (300 ml) containing sulfuric acid (10 ml). After extraction with chloroform (2 × 150 ml) the combined extracts were washed with water (2 × 150 ml) and dried over anhydrous sodium sulfate. Removal of the solvent gave 1.04 g of a pale yellow semisolid. This material was subjected to column chromatography on a column of 30 g of alumina packed in Skellysolve B. Elution with Skellysolve B gave 0.585 g of material consisting of two components by g.l.p.c. analysis (5 ft × ¼ in., SE-30 column). The isomer of shorter retention time was the 1-isomer (30%) and the isomer of longer retention time was the 2-isomer (70%). Using the yield of isolated material and the isomer ratio from g.l.p.c. analysis the yield of 1-adamantyl mercaptan was 9% (1.3 mmol) and the yield of 2-adamantyl mercaptan was 21% (3.1 mmol) based on sulfur monochloride and corrected for the reduction of all of the polysulfide residue.

Pure samples of the two mercaptans were isolated by preparative g.l.p.c. 1-Adamantyl mercaptan had m.p. 95–97°, lit. (18) m.p. 100–102°; i.r. (CCl_4) 2910, 2850, 1450, and 2565 cm^{-1} (S—H, weak); n.m.r. (CCl_4) τ 8.06 (s, 9, β and γ hydrogens), τ 8.29 (s, 6, δ hydrogens), and τ 8.57 (s, 1, S—H); mass spectrum *m/e* (relative intensity) 168 (14), 136 (12), 135 (100), 93 (15), 79 (17).

Mol. Wt. Calcd. for $C_{10}H_{16}S$: 168.0973. Found (exact mass): 168.0970.

2-Adamantyl mercaptan had m.p. 146–148°; i.r. (CCl_4) 2910, 2850, 1465, 1455, and 2580 cm^{-1} (S—H, very weak); n.m.r. (CCl_4) τ 6.65 (d broad, 1, J = 7 Hz, —S—C—H), τ 7.77 and 8.48 (q broad, 4, J_{gem} = 13 Hz, A_2B_2 quartet) τ 8.15 (s, broad, 10) and τ 8.54 (d, 1, J = 7 Hz, S—H); mass spectrum *m/e* (relative intensity) 168 (33), 136 (15), 135 (100), 93 (20), 91 (11), 81 (10), 79 (21).

Mol. Wt. Calcd. for $C_{10}H_{16}S$: 168.0973. Found (exact mass). 168.0974.

1-Adamantyl 2,4-dinitrophenyl Disulfide and 2-Adamantyl 2,4-dinitrophenyl Disulfide

1-Adamantyl mercaptan (0.011 g, 0.06 mmol) was reacted with 2,4-dinitrobenzenesulfenyl chloride (0.015 g, 0.06 mmol) in the usual manner. After crystallization of the product from methanol 0.013 g (59%) of 1-adamantyl 2,4-dinitrophenyl disulfide was obtained as yellow needles, m.p. 159–160°.

Anal. Calcd. for $C_{16}H_{18}N_2O_4S_2$: C, 52.44; H, 4.95; N, 7.65. Found: C, 52.23; H, 4.94; N, 8.10.

2-Adamantyl mercaptan (0.025 g, 0.15 mmol) was reacted with 2,4-dinitrobenzenesulfenyl chloride (0.038 g, 0.16 mmol). The crude product was crystallized from ethyl acetate – cyclohexane. After a further crystallization from methanol 0.018 g (33%) of analytically pure 2-adamantyl 2,4-dinitrophenyl disulfide, m.p. 144–145° was obtained.

Anal. Calcd. for $C_{16}H_{18}N_2O_4S_2$: C, 52.44; H, 4.95; N, 7.65. Found: C, 52.78; H, 5.26; N, 7.33.

The authors wish to thank the National Research Council of Canada and the University of Alberta for their generous support of this work.

1. L. A. WILES and Z. S. ARIYAN. Chem. Ind. 2102 (1962).
2. E. MÜLLER and E. W. SCHMIDT. Chem. Ber. **97**, 2622 (1964).
3. (*a*) C. WALLING. Free radicals in solution. John Wiley and Sons, Inc., New York, N.Y. 1957. p. 170; (*b*) W. A. PRYER. *In* Free radicals. McGraw-Hill Inc., New York, N.Y. 1966. p. 216.
4. G. A. RUSSELL, A. ITO, and D. G. HENDRY. J. Am. Chem. Soc. **85**, 2976 (1963).
5. C. WALLING and M. F. MAYAHI. J. Am. Chem. Soc. **81**, 1485 (1959).
6. Handbook of preparative inorganic chemistry. Vol. I. *Edited by* I. G. Brauer. Academic Press Inc., New York, N.Y. 1963. p. 372.
7. T. M. LOWRY and G. JESSOP. J. Chem. Soc. 1421 (1929).

8. F. J. WELCHER. Organic analytical reagents. Vol. III. D. Van Nostrand Co. Inc., Toronto, Ontario. 1947. p. 39.
9. A. I. VOGEL. A textbook of practical organic chemistry. 3rd Ed. Longmans Green and Co. Ltd., London, England. 1956. p. 293.
10. C. WALLING, A. L. RIEGER, and D. D. TANNER. J. Am. Chem. Soc. **85**, 3142 (1963).
11. B. D. VINEYARD. J. Org. Chem. **31**, 601 (1966).
12. D. GRANT and J. R. VAN WAZER. J. Am. Chem. Soc. **86**, 3012 (1964).
13. R. B. LANGFORD and D. D. LAWSON. J. Chem. Soc. **34**, 510 (1957).
14. R. C. FORT, JR. and P. VON R. SCHLEYER. J. Org. Chem. **30**, 789 (1965).
15. F. W. VAN DEURSEN and P. K. KORVER. Tetrahedron Lett. 3923 (1967).
16. G. W. SMITH and H. D. WILLIAMS. J. Org. Chem. **26**, 2207 (1961).
17. J. PIRSCH. Monatsch. Chem. **97**, 260 (1966).
18. J. R. GEIGY, A.-G., Belgian Patent 629 370 (1963); Chem. Abstr. **60**, 9167c (1964).

Can. J. Chem. Downloaded from www.nrcresearchpress.com by 210.87.254.105 on 09/05/12
For personal use only.

On the Thermodynamically Controlled Epimerization of Deoxynitroinositol Monomethyl Ethers[1]

JAN KOVÁŘ AND HANS H. BAER
Department of Chemistry, University of Ottawa, Ottawa, Canada K1N 6N5

Received June 8, 1973

1-Deoxy-4-*O*-methyl-1-nitro-*scyllo*-inositol (**1**), its *myo*-1 epimer (**2**), 3-deoxy-6-*O*-methyl-3-nitro-*epi*-inositol (**3**), and its *muco*-3 epimer (**4**) in the presence of excess base give nitronates (**1′** from **1**, **2′** from **2**, and **3′** from **3** and **4**) which are mutually interconverted by epimerization. The equilibrium constants were determined, revealing the order of thermodynamic stabilities of the nitronates to be **3′** > **2′** > **1′**. In the presence of a catalytic amount of base, the nitro inositols epimerize also, and the order of stability of the free nitro compounds is **1** > **2** ≫ **4** > **3**. The connection between these epimerization equilibria and the pK_a values of the compounds is discussed. The results are explained in terms of conformational analysis, whereby the importance of the $A^{(1,3)}$ strain is reasserted and good agreement with calculated conformational energy data is obtained.

Le déoxy-1-*O*-méthyl-4 nitro-1 *scyllo* inositol (**1**), son épimère *myo*-1 (**2**), le déoxy-3-*O*-méthyl-6 nitro-3 *épi*-inositol (**3**) et son épimère *muco*-3 (**4**), en présence d'un excès de base conduisent aux nitronates (**1′** à partir de **1**, **2′** à partir de **2**, et **3′** à partir de **3** et **4**) qui s'interconvertissent mutuellement par épimérisation. Les constantes d'équilibre ont été déterminées et indiquent l'ordre de stabilité thermodynamique suivant pour les nitronates **3′** > **2′** > **1′**. En présence de quantité catalytique de base, les inositols nitro s'épimérisent également et l'ordre de stabilité des composés nitro libres est **1** > **2** ≫ **4** > **3**. La relation entre les équilibres d'épimérisation et les valeurs des pK_a des composés a été discutée. Les résultats ont été interprétés par l'analyse conformationnelle et l'importance de la tension $A^{(1,3)}$ a été confirmée; un bon accord avec les données d'énergie conformationnelle calculée a été obtenu.
[Traduit par le journal]

Can. J. Chem., **51**, 3373 (1973)

In recent articles we have described the synthesis (2) of the four stereoisomeric deoxynitroinositol monomethyl ethers (**1–4**) having the *scyllo*, *myo*-1, *epi*-3, and *muco*-3 configurations, and have discussed the formation of these products by cyclization of 6-deoxy-6-nitro-D-glucose and -L-idose from the viewpoint of kinetic control (3). We now report on the results of base-catalyzed epimerizations that lead to equilibria of **1–4**, and discuss the factors by which these are governed.

Results

It is seen in n.m.r. spectra that addition of excess sodium deuteroxide to solutions of the nitro inositols in D_2O leads to rapid conversion of the compounds into their nitronates. This is also revealed in u.v. spectra by the generation of strong nitronate absorption peaks at 250–253 nm. The nitronates **1′** and **2′** (derived from **1** and **2**, respectively) and **3′** (derived from **3** and **4**) then undergo epimerization so that, within 24 h at ambient temperature, mixtures of **1′**, **2′**, and **3′** showing nearly identical n.m.r. spectra are produced from each of the four individual nitro compounds. The percentage compositions given in Table 1 were obtained by integration of the methoxyl signals. Mainly because of overlap of ring proton signals with the methoxyl signal of **3′**, and to a lesser extent of **2′** (Table 2), these data cannot claim great accuracy. Nevertheless, the mean ratio of approximately 1:3:7 for **1′**, **2′**, and **3′** at equilibrium, as derived from Table 1, is in fair agreement with results obtained by another, more accurate mode of analysis, namely v.p.c. For such analysis the nitroinositols **1–4** were allowed to epimerize in the presence of excess barium hydroxide at room temperature and the equilibrated mixtures were acidified, deionized, and subjected to v.p.c. after trimethylsilylation in the manner detailed earlier (3). The results show excellent agreement in the equilibrium compositions arrived at from **1**, **2**, and **3** while the values obtained starting with **4** deviated slightly (Table 3). Excluding the latter set of values, the mean ratio of nitronates **1′**:**2′**:**3′** at equilibrium was found to be 1:4.5:9.1; with inclusion of the set, it was 1:4.6:9.7.

[1]Part XXIX in a series on reactions of nitro sugars. For part XXVIII see ref. 1.

Can. J. Chem. Downloaded from www.nrcresearchpress.com by 210.87.254.5 on 09/05/12
For personal use only.

TABLE 1. Approximate ratios of **1′**, **2′**, and **3′** in alkaline solutions* of **1–4**

Starting compound															
1				**2**				**3**				**4**			
Time (h)	% composition			Time (h)	% composition			Time (h)	% composition			Time (h)	% composition		
	1′	**2′**	**3′**		**1′**	**2′**	**3′**		**1′**	**2′**	**3′**		**1′**	**2′**	**3′**
0.17	47	53	0	0.17	11	89	0	0.17	0	0	100	0.17	0	0	95†
2.7	15	51	34	2.4	19	54	27	4.0	9	28	63	1.0	0	0	100
23	7	20	73	23	10	31	59	22	10	24	66	4.0	0	27	73
								45	12	22	66	21	8	29	63
												49	10	29	61
Equilibrium ratio from **1**: 1:2.9:10.2															
from **2**: 1:3.1:5.9															
from **3**: 1:1.8:5.5															
from **4**: 1:2.9:6.1															
mean: 1:2.68:6.93															

*Solutions in D_2O containing 1.1 equiv of NaOD, at 35 °C.
†There was 5% of free **4** still present at that time.

TABLE 2. Proton chemical shifts (δ)* and coupling constants (Hz)†

Compound	Chemical shifts							Coupling constants			
	H-1	H-2	H-3	H-4	H-5	H-6	OCH_3	$J_{2,3}$	$J_{3,4}$	$J_{4,5}$	$J_{5,6}$
1′	‡	2.48(d)	1.72(q)	0.90(t)	1.72(q)	2.48(d)	1.33(s)	6	8	8	6
2′	‡	2.83(d)	[	1.43–1.63(m)	]	2.60(d)	1.37(s)	3	§	§	8
3′	= H-5	2.96(d)		‡ 2.96(d)		[1.35–1.40(m)]	1.40(s)	‡	‡	3	§

*In NaOD–D_2O solution with acetone as internal reference, measured on 60 MHz instrument. Signal multiplicities are in parentheses.
†Obtained by first-order analysis.
‡Not applicable.
§Could not be measured.

When any one of the nitroinositols was allowed to epimerize, not in strongly alkaline medium but at p*H* 7 in the presence of only a catalytic amount of barium hydroxide, an equilibrium of the free nitro compounds (**1** ⇌ **2** ⇌ **3** ⇌ **4**) was established. Under these conditions, the equilibrations of both **1** and **2** required 3 days[2] and led to identical mixtures containing **1**, **2**, and **3** + **4** in the % ratio **74**:**23**:**3** (Table 4). Compounds **3** and **4** cannot be distinguished by the v.p.c. method (3); however, it was possible to estimate from n.m.r. spectra that they exist at equilibrium in a ratio of about 2:3. The ratio of **1**:**2**:**3**:**4** can therefore be expressed as 74:23:1.2:1.8. It was found that equilibrium between **3** and **4** (as distinct from the final equilibrium between all four isomers) was reached in 2.5 h departing from **4** and in about 2 days departing from **3**.

TABLE 3. Epimerization of nitronates in excess barium hydroxide

Starting compound	% nitronate in equilibrium*		
	3′	**2′**	**1′**
1	62.1	31.3	6.6
2	61.9	31.6	6.4
3	62.6	30.0	7.4
4	67.0	27.3	5.7
Mean, **1–3**	62.2	31.0	6.8
Mean, **1–4**	63.4	30.05	6.5

*After 42 h at *ca.* 28 °C in the presence of a 6–8 fold molar excess of 0.05 *N* $Ba(OH)_2$.

When the *muco*-3 isomer **4** was completely converted (as ascertained by the n.m.r. spectrum) into its nitronate **3′** by the action of excess alkali and the nitronate solution was then acidified, a

[2]Experiments with **4** showed that this compound epimerizes too slowly under these conditions to permit observation of the final equilibrium within a reasonable period of time.

Can. J. Chem. Downloaded from www.nrcresearchpress.com by 210.87.254.5 on 09/05/12
For personal use only.

Can. J. Chem. Downloaded from www.nrcresearchpress.com by 210.87.254.5 on 09/05/12
For personal use only.

TABLE 4. Epimerization of nitro compounds near neutrality*

Starting compound	Time (h)	Products formed (%) 1	2	3 + 4	U†
1	1	82	14	0	4
	69	71	22	3	4
2	1	11	84	5	
	68	72	22	3	3

*In the presence of 0.1 equiv. of $Ba(OH)_2$ at 27 °C; measured p*H* *ca.* 7.
†Unidentified product, possibly 6-deoxy-3-*O*-methyl-6-nitro-L-idose arising by ring-opening of **1** (2).

mixture of nitroinositols was quantitatively recovered. This mixture consisted to at least 80% of the *epi*-3 isomer **3** and 18–19% of the *myo*-1 isomer **2**, but no **4** was regenerated as far as could be detected by n.m.r. spectroscopy. Formation of **3** was thus revealed to be very strongly favored kinetically over formation of **4** from their common nitronate.

Discussion

From the nitronate equilibrium **1′** ⇌ **2′** ⇌ **3′**, the free energy differences of epimeric pairs were calculated (Table 5). The order of nitronate stability is seen to be **3′** > **2′** > **1′**. This result is in full accord with expectations considering the calculated conformational stabilities of these molecules. Using the parameters for nonbonded substituent interactions previously employed in similar systems (4–6) and, in particular, taking for the $A^{(1,3)}$ interaction (7) between the nitronate grouping and an adjacent equatorial hydroxyl group a value (5, 6) of 2.0 kcal/mol, one arrives at conformational enthalpies ΔH for each of the two chair conformations of each nitronate (Table 6). On the basis of these values, the conformational free energies ΔG of compounds **1′**, **2′**, and **3′** were calculated and it follows from the data that the calculated free energy differences between **1′** and **2′**, **1′** and **3′**, and **2′** and **3′** are 0.80, 1.30, and 0.50 kcal/mol, respectively. These differences show good agreement with those found experimentally (see Table 5), which lends support to the premise on which the calculations were based, namely, the existence and magnitude of the $A^{(1,3)}$ effect.

TABLE 5. Free energy differences of nitronates as calculated from equilibrium constants

Epimer pair	$\Delta G°$ (kcal/mol) based on n.m.r.	v.p.c.
1′/2′	0.7	0.90
1′/3′	1.2	1.34
2′/3′	0.5	0.44

For the nitronates **1′** and **2′**, the preponderance of the conformer with an equatorial methoxyl group was borne out by the ring proton coupling constants. In the spectrum of **3′** the corresponding signals, which should have afforded proof of conformation, unfortunately were not resolved. However, in view of the large energy difference which conformational theory allocates to the two chair forms of **3′**, there can be no doubt that the one having an equatorial methoxyl group is vastly preferred.

From the composition ratio 74:23:1.2:1.8 of the free nitro compounds **1**–**4** at equilibrium, the free energy differences (in kcal/mol) of epimeric pairs were derived as 2.43 (for **1** and **3**), 1.74 (for **2** and **3**), and 0.24 (for **4** and **3**). Let us now compare these values with conformational free energy data derived for the compounds from the calculation of their nonbonded substituent interactions. Inspection of the conformational formulas in Table 7 shows that in **1**, **2**, and **3** the conformer having an axial nitro group is encumbered by a *syn*-triaxial interaction between that group and two hydroxyl groups. A numerical value for the energy of this type of arrangement is not available. However, one can safely assume that it is at least as large as (and probably larger than) the interaction energy of three *syn*-axial hydroxyl or methoxyl groups. A rough estimate then leads readily to the conclusion that these conformers are highly disfavored so that one need consider only the alternate, equatorial nitro conformations. In the *muco*-3 isomer **4**, the same problem does not arise since, in the axial nitro conformer, the nitro group does not interact with hydroxyls but with two hydrogen atoms instead, and for the latter interaction a value of 1.05 kcal/mol may be used (8). Another unknown parameter is the *gauche* interaction between an equatorial nitro group and a vicinal hydroxyl. However, we are here concerned only with energy *differences* between given conformations which mostly contain two such nitro–hydroxyl *gauche* arrangements each, and the

Can. J. Chem. Downloaded from www.nrcresearchpress.com by 210.87.254.5 on 09/05/12
For personal use only.

TABLE 6. Conformational energy data of nitronates calculated from nonbonded substituent interactions*

Compound	Conformations	$\Delta H°$ (kcal/mol) *a*	$\Delta H°$ (kcal/mol) *b*	$\Delta G°$ (kcal/mol)
1′	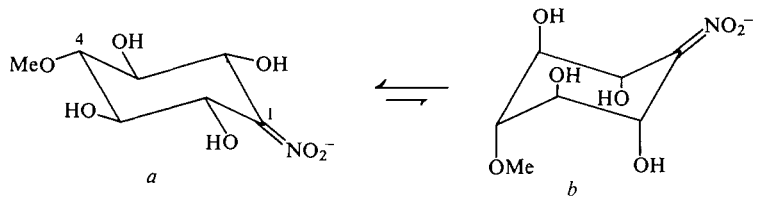 *a* ⇌ *b*	5.40	6.00	5.10†
2′	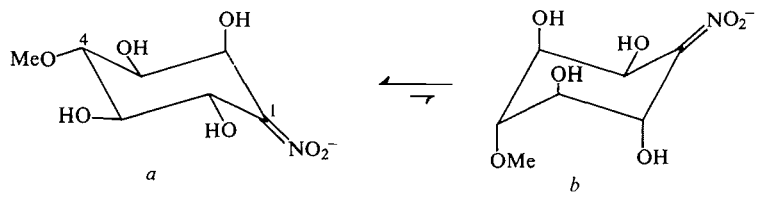 *a* ⇌ *b*	4.30	6.25	4.30‡
3′	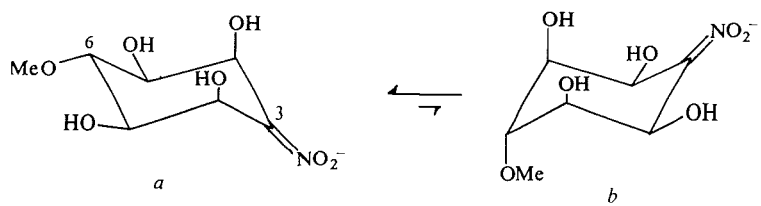 *a* ⇌ *b*	3.80	7.10	3.80‡

*The following values (4) were employed (kcal/mol): interaction between an axial OH or OCH_3 group and one *syn*-axial H atom, 0.45; between two *syn*-axial OH groups or an axial OCH_3 and one *syn*-axial OH group, 1.5; between two adjacent OH or OCH_3 groups in *gauche* arrangement (e–e or e–a), 0.35; between the nitronate group and one adjacent, equatorial OH, 2.0 (*5*, *6*).
†From the $\Delta H°$ values of the two conformers, taking into account the entropy of mixing.
‡Due to the large difference in enthalpy of the two conformers, the more stable one must predominate strongly so that the entropy of mixing term becomes negligible.

Can. J. Chem. Downloaded from www.nrcresearchpress.com by 210.87.254.5 on 09/05/12
For personal use only.

TABLE 7. Conformational energy data of **1–4** calculated from nonbonded substituent interactions*

Compound (configuration)	Conformations	$\Delta H°$ (kcal/mol)		$\Delta G°$ (kcal/mol)
		a	*b*	
1 (*scyllo*)	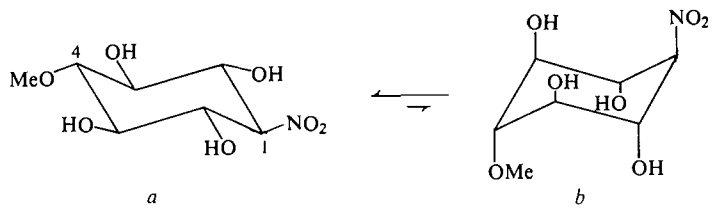 *a* ⇌ *b*	1.40 + 2B	≫ *a*	1.40 + 2*B*
2 (DL-*myo*-1)	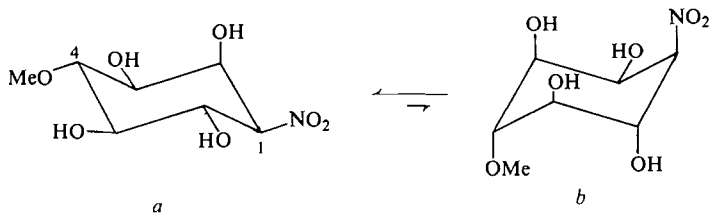 *a* ⇌ *b*	2.30 + 2B	≫ *a*	2.30 + 2*B*
3 (*epi*-3)	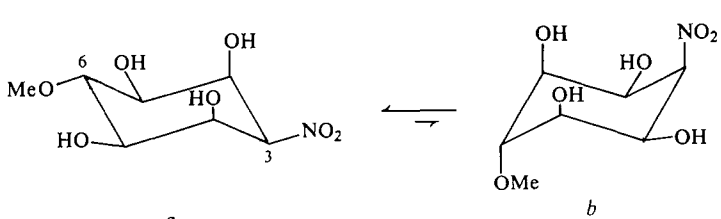 *a* ⇌ *b*	3.80 + 2B	≫ *a*	3.80 + 2*B*
4 (*muco*-3)	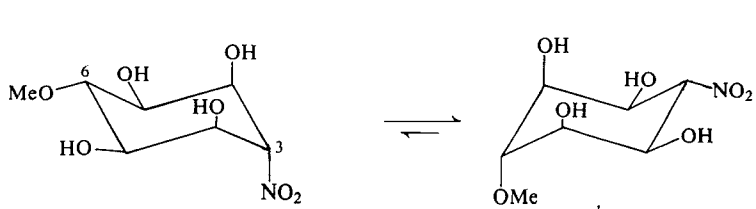 *a* ⇌ *b*	4.85	4.00 + 2B	3.6 + 2*B* to† 3.7 + 2*B*

*For the basis of calculations see the footnotes to Table 6 and the text.
†Range resulting from use of an estimated range of 0.3–0.4 kcal/mol for B.

numerical value (B) of the unknown factor will therefore cancel in these cases. An exception occurs in the assessment of the conformational equilibrium in **4**. The n.m.r. spectrum of **4** suggests that the equatorial-nitro conformer predominates (although the extent of this predominance may be small), and one is therefore led to conclude that the B-value does not exceed, and could possibly be less than, a *gauche* hydroxyl–hydroxyl interaction of 0.35 kcal/mol. Table 7 lists conformational energies calculated in this manner. The free energy differences (kcal/mol) are 2.40 (between **1** and **3**), 1.50 (between **2** and **3**), and 0.1–0.2 (between **4** and **3**). Comparison of these values with the aforementioned experimental values shows good agreement.

Further, it is interesting to correlate with each other the epimeric equilibria of the free nitro compounds and those of their nitronates. Since the base-catalyzed equilibrium of the free nitro compounds must proceed through anion formation, the acidity constants should determine these correlations. Thus, it follows from Scheme 1, in which HA and HB represent a pair of epimeric nitro compounds and A^- and B^- their respective anions, that the ratio of equilibrium constants for the epimerizations equals the ratio of acidity constants (eq. 1).[3]

$$\begin{array}{ccc} HA & \overset{K_1}{\rightleftharpoons} & H^+ + A^- \\ {\scriptstyle K_{HA/HB}}\Big\uparrow\Big\downarrow & & \Big\uparrow\Big\downarrow{\scriptstyle K_{A^-/B^-}} \\ HB & \overset{K_2}{\rightleftharpoons} & H^+ + B^- \end{array}$$

SCHEME 1

$$[1] \qquad K_{A^-/B^-}/K_{HA/HB} = K_1/K_2$$

We have measured the pK_a values of **1–4** by half-titration and found 10.7 and 9.9 for **1** and **2**, respectively. For **3** and **4** in equilibrium with **3′**, a pH value of 8.75 at half-titration was determined. It follows from Scheme 2 that "K", the apparent acidity constant of this system, is given by eq. 2.[4]

$$HC_1 \underset{K_4}{\overset{K_3}{\rightleftharpoons}} H^+ + C^- \rightleftharpoons HC_2$$

(where HC_1 = **3**, HC_2 = **4**, and C^- = **3′**)

SCHEME 2

$$[2] \qquad \text{"}K\text{"} = K_3K_4/(K_3 + K_4)$$

Furthermore, it is seen[4] that

$$[3] \qquad K_3/K_4 = HC_2/HC_1$$

Since we have found the equilibrium ratio of **3** and **4** to be 2:3, the pK_a values of **3** and **4** may be calculated from eqs. 2 and 3 to be 8.35 and 8.52, respectively. Table 8 allows a comparison of the experimentally determined ratios of epimerization constants with those of the acidity constants, both expressed as differences of their logarithms.[5] Reasonable agreement with the equality of ratios anticipated from eq. 1 is observed.

Experimental

The preparation (2) of compounds **1–4** and the analytical procedures (3) have been described previously. N.m.r. spectra were recorded on a Varian T60 instrument. The pH measurements were made using a glass electrode and a Philips pH-meter.

Epimerizations

The epimerization reactions were carried out essentially like the cyclizations of nitro hexoses earlier described in detail (3), with the following modifications.

All the reactions that were monitored by v.p.c. were performed at room temperature (25–27°). The epimeriza-

[3]Equation 1 is derived as follows.

$K_1 = [H^+][A^-]/[HA]$ and $K_2 = [H^+][B^-]/[HB]$

Further,

$K_{A^-/B^-} = [A^-]/[B^-]$ and $K_{HA/HB} = [HA]/[HB]$

Consequently,

$$K_1/K_2 = \frac{[H^+][A^-]/[HA]}{[H^+][B^-]/[HB]} = \frac{[A^-]}{[B^-]} \times \frac{[HB]}{[HA]} = K_{A^-/B^-} \times \frac{1}{K_{HA/HB}}$$

[4]Equation 2 is derived as follows.

$K_3 = [H^+][C^-]/[HC_1]$ and $K_4 = [H^+][C^-]/[HC_2]$

Since at half-titration,

$[HC_1] + [HC_2] = [C^-]$ and "K" $\equiv [H^+]$,

it follows

$$K_4 = \frac{[H^+][C^-]}{[C^-] - [HC_1]}$$

and further, from

$$[HC_1] = \frac{[H^+][C^-]}{K_3}, \quad K_4 = \frac{[H^+][C^-]}{[C^-] - [H^+][C^-]/K_3} = \frac{[H^+]}{1 - [H^+]/K_3}$$

which can be rearranged to $[H^+] \equiv \text{"}K\text{"} = \frac{K_3K_4}{K_3 + K_4}$.

[5]In terms of free energies $\Delta\Delta G^\circ = 2.3\ RT\Delta \log K = 2.3\ RT\Delta pK_a$[kcal/mol].

Can. J. Chem. Downloaded from www.nrcresearchpress.com by 210.87.254.5 on 09/05/12
For personal use only.

TABLE 8. Comparison of ratios of equilibrium constants of epimerization with differences in pK_a values

Constants	Epimer pairs		
	1 and **3**	**2** and **3**	**4** and **3**
$K_{HA/HB}$	61.67	19.17	1.50
log $K_{HA/HB}$	1.79	1.28	0.18
$K_{A-/B-}$	0.103	0.474	1.00
log $K_{A-/B-}$	−0.99	−0.32	0.00
Δ log K	2.78	1.60	0.18
Δ pK_a	2.35	1.55	0.18

tions at about pH 7 were done at 0.25 M in inositol and 0.025 N in barium hydroxide. The epimerizations in strongly alkaline medium (Table 3) were carried out in the presence of a larger excess of base than previously (3). Thus, the nitroinositol (2–3 mg) was dissolved in 2.0 ml of 0.053 N $Ba(OH)_2$ and the solution was allowed to stand in a closed vial protected from atmospheric carbon dioxide.

The reactions monitored by n.m.r. spectroscopy were performed at the temperature of the probe (35°). For example, 18.0 mg of the nitroinositol was dissolved in deuterium oxide (0.32 ml) and rendered alkaline by the addition of 0.08 ml of 1.22 N NaOD solution (1.2 mol equiv.). A solution of **3′** obtained in this way from **4** was acidified, after 40 min, by pouring it into 0.1 N acetic acid (2 ml). The solution was then passed consecutively through layers of Dowex-1 × 2 (acetate form; 0.3 ml) and Rexyn 101 (H^+; 0.6 ml) which were washed with water. Evaporation followed by two coevaporations with added ethanol, and drying of the residue *in vacuo*, gave a material (20 mg) that, according to v.p.c. analysis, consisted of **3** or **4** (80%), **2** (19%), and **1** (trace). According to n.m.r. analysis, the main product must have been **3** since the readily distinguishable OCH_3 signal of **4** was not observed so that only a very small proportion of **4** could have been present. Crystallization from ethanol gave 6 mg of **3** as colorless, lustrous crystals, m.p. 160–162°.

This work was supported by the National Research Council of Canada.

1. H. H. BAER and W. RANK. Can. J. Chem. **51**, 2001 (1973).
2. J. KOVÁŘ and H. H. BAER. Can. J. Chem. **51**, 1801 (1973).
3. J. KOVÁŘ and H. H. BAER. Can. J. Chem. **51**, 2836 (1973).
4. S. J. ANGYAL. Aust. J. Chem. **21**, 2737 (1968).
5. H. H. BAER and J. KOVÁŘ. Can. J. Chem. **49**, 1940 (1971).
6. J. KOVÁŘ, K. ČAPEK, and H. H. BAER. Can. J. Chem. **49**, 3960 (1971).
7. F. JOHNSON and S. K. MALHOTRA. J. Am. Chem. Soc. **87**, 5492 (1965); F. JOHNSON. Chem. Rev. **68**, 375 (1968); F. JOHNSON and D. T. DIX. J. Am. Chem. Soc. **93**, 5931 (1971).
8. H. FELTKAMP and N. C. FRANKLIN. J. Am. Chem. Soc. **87**, 1616 (1965); F. R. JENSEN, C. H. BUSHWELLER, and B. H. BECK. J. Am. Chem. Soc. **91**, 344 (1969).

Can. J. Chem. Downloaded from www.nrcresearchpress.com by 210.87.254.5 on 09/05/12
For personal use only.

Conformational Study of *N*-Methyl-5,6-dihydro-7*H*,12*H*-dibenz[*c*,*f*]-azocine by Nuclear Magnetic Resonance Spectroscopy[1]

ROGER N. RENAUD AND ROBERT B. LAYTON[2]
National Research Council of Canada, Ottawa, Canada

AND

ROBERT R. FRASER
Department of Chemistry, University of Ottawa, Ottawa, Canada

Received May 10, 1973

A study of the n.m.r. spectra of *N*-methyl-5,6-dihydro-7*H*,12*H*-dibenz[*c*,*f*]azocine, its deuterated derivative, and its conjugate acid in deuteriochloroform and in trifluoracetic acid at 27 and at −62° has shown that the molecule prefers the rigid "crown" conformation. From the equilibrium constant for the equilibrium flexible ⇄ crown at 27 and at −62°, ΔH and ΔS values of -3.2 ± 0.5 kcal/mol and -7 ± 3 e.u. respectively were determined, indicating the preference for the crown conformer. A barrier to interconversion of the flexible to crown form at −62° was determined to be 15.3 ± 0.3 kcal/mol.

These parameters provide the first experimental data pertinent to the conformational properties of the 1,4-cyclooctadiene system.

Une étude des spectres de résonance magnétique nucléaire du *N*-méthyl dihydro-5,6-7*H*,12*H* dibenz-[*c*,*f*] azocine, de son dérivé deutérié et de son acide conjugué dans le deutériochloroforme et dans l'acide trifluoroacétique, à 27 et −60°, montre que la molécule adopte préférentiellement la conformation rigide en couronne. A partir de la constante de l'équilibre forme flexible ⇄ couronne à 27 et −62°, les valeurs de ΔH et ΔS de -3.2 ± 0.5 kcal/mol et -7 ± 3 u.e. ont été déterminées, respectivement, indiquant une préférence pour le conformère couronne. Une barrière d'interconversion de la forme flexible à la forme couronne a été déterminée à −62° et vaut 15.3 ± 0.3 kcal/mol. Ces paramètres fournissent les premières données expérimentales pertinentes sur les propriétés conformationnelles du système cyclooctadiène-1,4.
[Traduit par le journal]

Can. J. Chem., 51, 3380 (1973)

Introduction

In the last decade, eight-membered ring compounds have been the object of extensive investigation, including molecular orbital calculations (3), dipole moment studies (4), X-ray crystallography (5–7), and n.m.r. spectroscopy (8–11). By far, n.m.r. has proved to be the most powerful tool in the conformational determination of cyclic molecules in solution (10, 12, 13). Among the eight-membered rings, the cyclooctanes and cyclooctatetraenes are the two classes on which the majority of conformational analyses have been conducted (10, 14). The conformations of the cyclooctenes (6, 10, 15), cyclooctadienes (16), and cyclooctatrienes (17), on the other hand, have been less extensively investigated.

Of the three cyclooctadiene isomers only the 1,5-diene has been the object of experimental study (18). The cycloocta-1,4-diene has, however, been recently discussed from the point of view of possible conformations. Dunitz and Waser (16) have proposed that this compound should exist as flexible **1** and crown **2** isomers. Experimental efforts to examine this claim by n.m.r. would undoubtedly be hampered by the spectral complexity of such multi-spin systems. Spectral simplification, though, can be achieved by a number of current techniques such as substitution of one or more protons on the ring by deuterium (9), fluorine (11), heteroatoms (19, 20), and/or aromatic rings (14).

We have undertaken an n.m.r. study of the conformational properties of an hetero analogue of cycloocta-1,4-diene, namely *N*-methyl-5,6-dihydro-7*H*,12*H*-dibenz[*c*,*f*]azocine (**3**) (21, 22), with a view to determining its most favorable ground state. The presence of the aromatic rings and nitrogen in the molecule provides a simple n.m.r. spectrum[3] from which its conformational properties ought to be determinable.

[1]NRCC No. 13350.
[2]NRCC Postdoctorate Fellow, 1972 to present.

[3]A qualitative description of the n.m.r. spectrum of **3** was reported earlier (21).

Can. J. Chem. Downloaded from www.nrcresearchpress.com by 210.87.254.6 on 09/05/12
For personal use only.

Can. J. Chem. Downloaded from www.nrcresearchpress.com by 210.87.254.6 on 09/05/12
For personal use only.

1 2

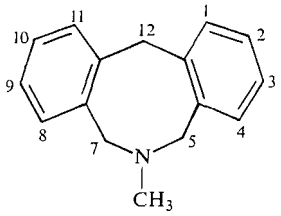

3

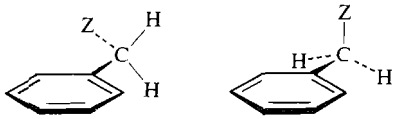

$\phi = 0°$ $\phi = 90°$

5 6

The parent compound **3** has been prepared by Pala and co-workers (22) utilizing an intermediate previously prepared by Bergmann and Pelchowicz (23), 2,2′-bis(bromomethyl)-diphenylmethane. It was our belief that their yield of this compound (22% after eight steps) could be improved by the choice of a better synthon (38) for its generation. Consequently, we utilized the readily available dibenzsuberone **4** (Scheme 1) as starting material and, after a sequence of five steps, obtained the desired intermediate in a yield of 53%. Treatment of 2,2′-bis(bromomethyl)-diphenylmethane with methylamine gave **3** in 57% yield.

Experimental

All melting points are uncorrected. All i.r. spectra were recorded on a Perkin–Elmer 237 Grating Spectrometer. Only the characteristic bands are reported (cm^{-1}). Routine n.m.r. spectra were measured using a Varian A-60 spectrometer. Precise studies on the title compound were carried out using a Varian HA-100 spectrometer. All coupling constants were determined with an accuracy of ± 0.1 Hz. The n.m.r. spectra were measured in deuteriochloroform unless otherwise specified and the chemical shifts are reported on the scale.

For the kinetic measurements at $-62\,°C$ intergrals were taken every 150 s and the rate constant obtained by a least squares analysis of the data. The standard deviation (1.5×10^{-5}) in the rate constant and the possible error in measurement of the probe temperature (2°) lead to an uncertainty in ΔG^{+} of 0.3 kcal/mol. The above relatively accurate integral measurements are possible as we are monitoring the intensity of a sharp singlet as a function of time. Thus, systematic errors are minimized and only random errors produce scatter in the data.

Benzophenone-2,2′-dicarboxylic Acid

An acetone solution of dibenzsuberone (5 g) was oxidized with potassium permanganate (14 g) in the presence of sodium bicarbonate, according to the method of Smith and Rouault (24). Work-up and recrystallization from ethanol afforded 4.7 g (72%) of product: m.p. 213.5–2.4° (lit. (25) 212°); i.r. (Nujol) 3300–2200, 1700, 1670; n.m.r. (DMSO-d_6) 7.15–8.40 (8H, multiplet, aromatic), 10.15 (2H, broad singlet, OH).

Diphenylmethane-2,2′-dicarboxylic Acid

Benzophenone-2,2′-dicarboxylic acid (6.0 g) in ammonia was treated with zinc dust (19.0 g) over 20 h in a manner similar to that described by Bergmann and Pelchowicz (23). The yield of the diacid, m.p. 259–261° (lit. (23) 254.5°) was 5.4 g (94%): i.r. (Nujol) 3300–2200, 1720; n.m.r. (DMSO-d_6) 7.00–8.20 (10H, multiplet, aromatic and OH; elimination of 2H by exchange with D_2O), 4.88 (2H, singlet, methylene).

Dimethyl-diphenylmethane-2,2′-dicarboxylate

Diphenylmethane-2,2′-dicarboxylic acid (4.6 g) was esterified with methanol (240 ml) in presence of concentrated sulfuric acid (1 ml) under reflux for 36 h. Then, the product was freed from excess methanol and collected in ether. The ethereal solution was washed with a cold solution of sodium bicarbonate, dried over $MgSO_4$, filtered and the solvent removed to give 4.8 g (95%) of an oily residue which solidified on standing: m.p. 42–44° (lit. (23) 44°); i.r. ($CHCl_3$) 1725; n.m.r. (DMSO-d_6) 7.00–8.10 (8H, multiplet, aromatic), 4.82 (2H, singlet, methylene), 3.79 (6H, singlet, methyl).

2,2′-Bis(hydroxymethyl)-diphenylmethane

Dimethyl-diphenylmethane-2,2′-dicarboxylate (4.8 g)

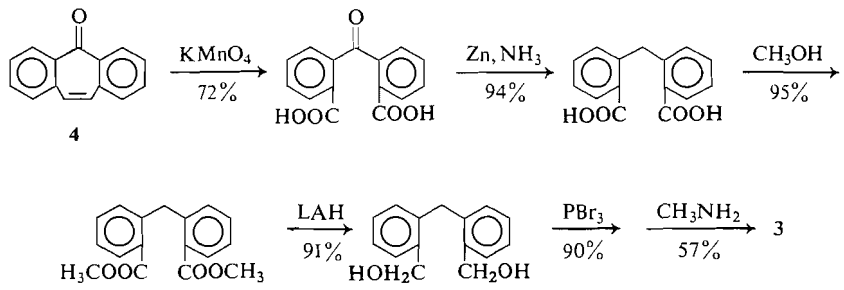

SCHEME 1

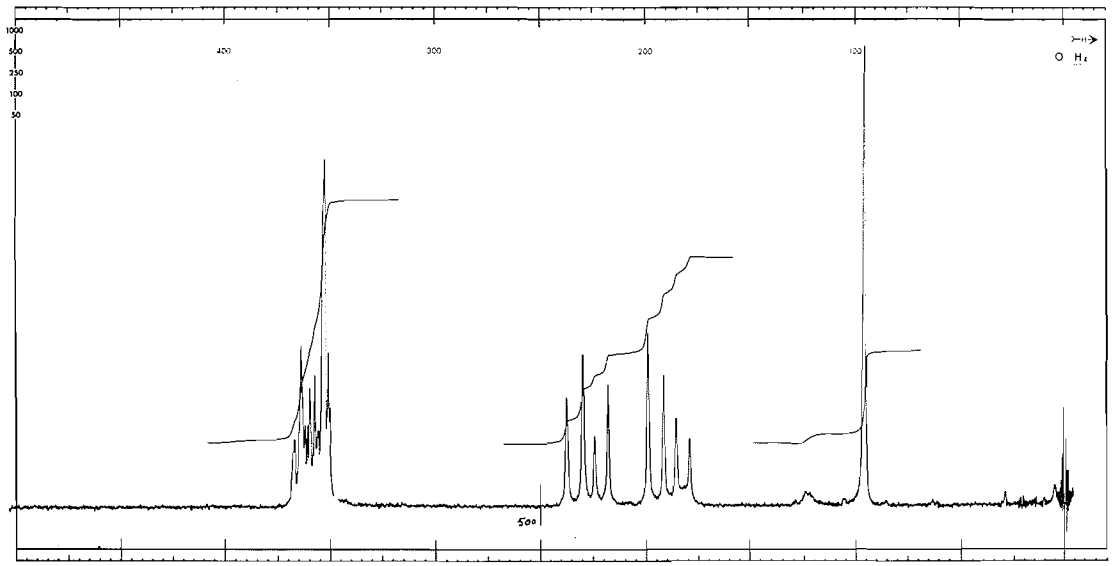

FIG. 1. The ^1H n.m.r. spectrum of *N*-methyl-5,6-dihydro-7*H*,12*H*-dibenz[*c*,*f*]azocine (**3**) in deuteriochloroform.

was reduced to 2,2′-bis(hydroxymethyl)-diphenylmethane as described in the literature (23) in 91% yield: m.p. 162–162.5° (lit. (23) 158–158.5°); i.r. (Nujol) 3350–2800; n.m.r. (DMSO-d_6) 6.8–7.8 (8H, multiplet, aromatic), 4.56 (4H, singlet, methylene), 4.10 (2H, singlet, methylene), 3.42 (2H, broad singlet, hydroxyl).

2,2′-Bis(bromomethyl)-diphenylmethane

2,2′-Bis(hydroxymethyl)-diphenylmethane (1.5 g) was reacted with phosphorous tribromide according to Bergmann and Pelchowicz (23). The pale yellow crystalline product was recrystallized from benzene to afford 2.1 g (90%) of solid melting at 92° (lit. (23) 93–94°): n.m.r. 7.0–7.7 (8H, multiplet, aromatic), 4.54 (4H, singlet, methylene), 4.37 (2H, singlet, methylene).

N-Methyl-5,6-dihydro-7H,12H-dibenz[c,f]azocine

2,2′-Bis(bromomethyl)-diphenylmethane (1.5 g was reacted with methylamine according to the procedure of Casadio *et al.* (22). There was obtained after sublimation of the crude product, 1.0 g (57%) of *N*-methyl-5,6-dihydro-7*H*,12*H*-dibenz-[*c*,*f*]azocine: m.p. 92° (lit. (22) 93°); n.m.r. 6.98–7.40 (8H, multiplet, aromatic), 4.26 (4H, quartet, methylene adjacent to N), 4.00 (2H, quartet, methylene), 1.90 (3H, singlet, methyl).

5,5,7,7-Tetradeuterio-N-methyl-5,6-dihydro-7H,12H-dibenz[c,f]azocine

Using a procedure analogous to that quoted above, dimethyl-diphenylmethane-2,2′-dicarboxylate was reduced with lithium aluminum deuteride. The tetradeuterated product of that reaction was converted in an identical manner to that described above into 5,5,7,7-tetradeuterio-*N*-methyl-5,6-dihydro-7*H*,12*H*-dibenz-[*c*,*f*]azocine. The isotopic purity was estimated by n.m.r. spectroscopy to be better than 95%.

Results and Discussion

A. Nuclear Magnetic Resonance Spectral Parameters

The n.m.r. spectrum of **3** in deuteriochloroform exhibits two well-defined AB quartets in a ratio of 2:1 (Fig. 1). These quartets, centered at δ 4.30 (J = 14.9 Hz)[4] and δ 4.09 (J = 12.7 Hz), correspond to the protons on C-5 and C-7, and on C-12 respectively. The *N*-methyl region of the spectrum shows that more than one isomer is present. At room temperature a sharp singlet at δ 1.94 represents the major isomer (91.7% of methyl absorption) and a small broad peak at δ 2.44 represents the minor isomer (8.3% of methyl absorption). Absorptions due to the methylene protons of the minor isomer were too weak to be observed.

When trifluoroacetic acid (TFA) is added gradually to the sample in deuteriochloroform, the low field protons of the quartet, centered at δ 4.30, shift slowly downfield and finally appear at δ 5.26 (J = 14.0 Hz) in pure TFA. This shift to low field is typical of protons α to nitrogen because of a decreasing shielding of the adjacent protons by the positively charged nitrogen in the

[4]All the geminal coupling constants discussed herein are assumed to be negative as has been found for the benzylic methylene protons of 2,3-diphenylpropionic acid (27).

Can. J. Chem. Downloaded from www.nrcresearchpress.com by 210.87.254.6 on 09/05/12
For personal use only.

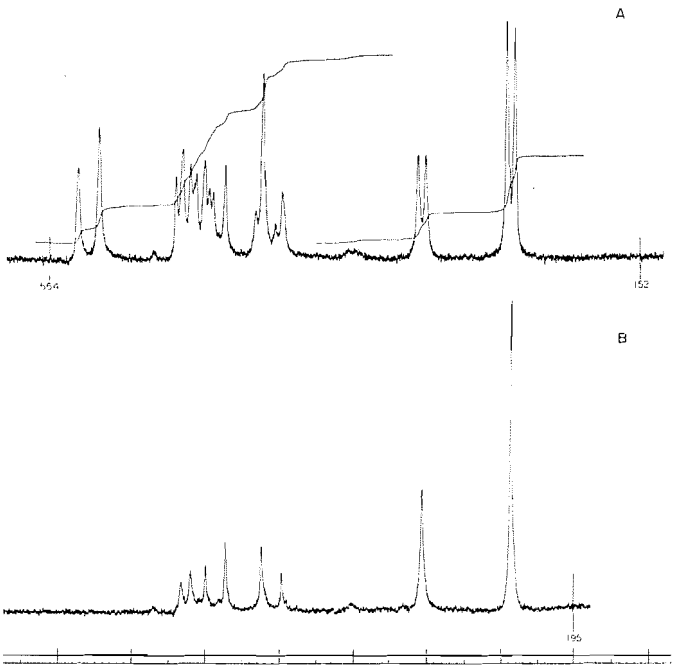

FIG. 2. The ^1H n.m.r. spectrum of (A) **3**-H^+ in TFA and (B) **3**-H^+ (5,5,7,7-d_4) in TFA-d_1.

conjugate acid **3**-H^+ (26). Of particular significance is the fact that in pure TFA this signal is still a doublet, *i.e.* $J_{H-\overset{+}{N}-C-H}$ must be less than 1 Hz since all the other protons α to nitrogen show vicinal (H—$\overset{+}{N}$—C—H) splittings that indicate the exchange of the $\overset{+}{N}$—H proton with solvent is slow on the n.m.r. time scale. We have previously established the presence of a Karplus relationship between the magnitude of vicinal H—H coupling for the H—N—C—H fragment of amines in TFA (28) and the dihedral angle between the vicinal protons. The lack of vicinal coupling in the low field absorption of **3** in TFA shows, therefore, that the angle between the proton on nitrogen and these protons on the α carbons is ≈90°.

Examination of Dreiding models shows that the geometry of the flexible conformer permits both of the H—$\overset{+}{N}$—C—H bond angles[5] to vary between 0 and 120°. Thus, for the flexible form, one must expect, on the average, a coupling of some magnitude between the proton on nitrogen and both of the adjacent methylene protons. In the rigid crown conformer, however, the H—$\overset{+}{N}$—C—H bond angles are fixed at 90 and 30° for the non-equivalent protons. As a result, the absence of observable H—$\overset{+}{N}$—C—H splitting indicates a 90° dihedral angle and is consistent only with assignment of the crown conformation[6] to the major isomer.

The relative intensities of the two methyl peaks are also affected by the presence of acid. The addition of TFA to the sample in deuteriochloroform causes a downfield shift of both *N*-methyl groups (26). Concomitantly, the smaller peak increases in intensity as the concentration of TFA increases until, in pure TFA, it accounts for 28% of the total methyl absorption and appears at δ 2.98. The other *N*-methyl peak has

[5]In general, the Dreiding models are too rigid and estimated bond angles are only accurate to within 5°. Bond angles reported in this paper are to be considered within this range.

[6]An X-ray crystallographic examination of the azocine **3** (37) has since shown that the preferred conformer in the crystal state is also the crown form.

Can. J. Chem. Downloaded from www.nrcresearchpress.com by 210.87.254.6 on 09/05/12
For personal use only.

Can. J. Chem. Downloaded from www.nrcresearchpress.com by 210.87.254.6 on 09/05/12
For personal use only.

shifted to δ 2.39. Both peaks are doublets and display the characteristic $H-\overset{+}{N}-C-H$ coupling of 5.3 Hz (26).[7]

The remainder of the methylene proton absorption of the two isomers of **3** in TFA is not sufficiently resolved to allow individual assignments to be made (Fig. 2A). However, the assignment of the methylene bridge protons of the two isomers is made possible by the examination of the deuterated derivative of **3** in which the hydrogens at C-5 and C-7 have been replaced by deuterium.

The spectrum of **3**-H^+ (5,5,7,7-d_4) in TFA-d_1 shows a quartet for the major isomer centered at δ 4.08 (J = 13.5 Hz) and a second isomer centered at δ 4.60 (J = 19.0 Hz) (Fig. 2B). The magnitudes of these two geminal coupling constants allow assignment of crown and flexible conformations to the major and minor isomers respectively. It is recognized that a benzene ring on a methylene group causes a negative shift on the geminal proton–proton coupling constant and that this shift varies with conformation. Empirical (29, 30) and theoretical (31, 32) evidence support this correlation and estimate the effect to be at least 4 Hz in the most favorable conformation **5** and zero in the conformation **6**, achieved by a rotation of 90° about the phenyl—CH_2 bond. A Dreiding model of the crown form of **3** shows φ to be very close to 90° for both benzene rings, leading to the expectation that they should have a negligible influence on ^2J. On the other hand, a model of the flexible form allows one of the two methylene groups to be oriented at φ = 30° and the other at φ = 90° in either of two equivalent "twist-boat" types of conformation. Thus, an appreciable negative shift of the geminal coupling constant ought to be caused by the hyperconjugative effect of the benzene rings in the flexible conformation. The observed value ^2J of −13.5 Hz for the major isomer represents a normal value for a diphenylmethane-type methylene group possessing φ = 90° for both benzenes to CH_2 bonds (33). The 5.6 Hz more negative value of ^2J in the minor isomer is only consistent with a flexible conformation for this isomer.

B. Temperature Dependence of Equilibrium Constant

From integration of the peaks for the N-CH_3 groups of the two isomers at room temperature and −62°, the equilibrium constants K_{eq} (minor ⇄ major) were found to be 11.0 and 124 respectively. From such a temperature dependence, ΔS_{eq} is calculated to be -7 ± 3 e.u. and $\Delta H_{eq} = -3.2 \pm 0.5$ kcal/mol.[8] The much greater entropy for the minor isomer is corroborative evidence that it possesses a flexible conformation. A comparable difference in entropy between the "crown" and "boat-chair" forms of tetroxocane has been found by Anet and Degen (20).

C. Barrier to Inversion

While it should be possible to determine the barrier to interconversion of the crown and flexible forms by DNMR (34), the strongly biased equilibrium makes line-shape measurements difficult and relatively less accurate. Since the two N-CH_3 peaks were observed to coalesce at about 40°, thus indicating a barrier of the order of 15 kcal/mol, we have undertaken a direct measurement of this interconversion by a "temperature-jump" experiment. A deuteriochloroform solution of **3** was plunged into liquid nitrogen. The sample after 5 min was warmed quickly to −62° and placed in the proble of the HA-100 spectrometer which was also held at −62°. Integration showed the proportion of isomers to be 96.5 and 3.5. The rate of relaxation to the equilibrium position of 99.2 to 0.8 at −62°, determined by repeated integrations, was found to be $6 \pm 1.2 \times 10^{-4}$ s^{-1}. This corresponds to a free energy of activation of 15.3 ± 0.3 kcal/mol for conversion of the flexible to crown forms.

In conclusion, we have established the presence

[7]A point to be noted here is that protonation of a crown–flexible conformer mixture could give rise to four different conjugate acids and thus four sets of methyl doublets. However, only two doublets are observed, indicating the presence of only two isomeric conjugate acids. The other two isomers (having the opposite but undetermined configuration at nitrogen) are presumably too unstable to populate the mixture in measurable quantity. Interconversion of all isomers occurs readily via the following equilibria: $\text{crown}_1 \rightleftarrows \text{flexible}_1 \rightleftarrows \text{flexible}_2 \rightleftarrows \text{crown}_2$ (the subscripts indicating the configuration at nitrogen).

[8]The rather large uncertainty in ΔS results from the limits of accuracy in integration which we estimate to be ±0.5% for the measurement of well-resolved sharp singlets. There can be no doubt that there is a large entropy difference between conformers for, if ΔS were zero, the concentration of flexible form at −62 °C ought to have been 3.2%.

of two conformations of the azocine **3** whose n.m.r. and thermodynamic properties allow assignment of a "crown" conformation to the energetically favored isomer and a "flexible" conformation to the less abundant isomer. Both the thermodynamic and kinetic parameters for this conformational equilibrium have been determined. It is tempting to propose the data for **3** as providing reasonable estimates of the conformational equilibrium in *cis*-1,4-cyclooctadiene. Indeed, substitution of aromatic rings in the place of double bonds does not appear to alter conformations significantly (18) nor alter the barrier to interconversion appreciably (35) unless the rings are adjacent to one another (14). Similarly, replacement of a CH_2 group by a nitrogen atom causes little change in bond length and resultant geometry (36). We can, therefore, propose that the conformational properties exhibited by **3** constitute a reasonable estimate of the analogous properties of 1,4-cyclooctadiene.

Finally, the predominant isomer, the crown conformation of **3**, possesses some unique geometric features that should prove helpful in the study of other phenomena, in particular the study of substituent effects on geminal coupling constants (30) since the projected angle ϕ is 90°.

Further work related to azocines having different alkyl groups on nitrogen is in progress. Hopefully, such studies will provide information on steric effects in these eight-membered rings.

One of us (R.R.F.) acknowledges the financial support of the National Research Council of Canada.

1. G. AHLERS and J. F. HORNING. J. Phys. Chem. **65**, 2102 (1961).
2. O. BASTIANSON, L. HEDBERG, and K. HEDBERG. J. Chem. Phys. **27**, 1311 (1957).
3. K. MISLOW and H. D. PERLMUTTER. J. Am. Chem. Soc. **84**, 3591 (1962).
4. J. D. ROBERTS. J. Am. Chem. Soc. **72**, 3300 (1950).
5. R. SRINIVASAN and T. SRIKRISHNAN. Tetrahedron, **27**, 1009 (1971).
6. R. D. BACH, U. MAZUR, I. HAMANA, and S. K. LAUDERBACK. Tetrahedron, **28**, 1955 (1972).
7. J. D. DUNITZ and V. PRELOG. Angew. Chem. **72**, 896 (1960).
8. F. A. L. ANET and J. S. HARTMAN. J. Am. Chem. Soc. **85**, 1204 (1963).
9. F. A. L. ANET and M. ST-JACQUES. J. Am. Chem. Soc. **88**, 2585 (1966).
10. F. A. L. ANET. Conformational analysis. *Edited by* G. Chiurdogly. Academic Press, New York. 1965. p. 15.
11. J. E. ANDERSON, E. S. GLAZER, D. L. GRIFFITH, R. KNORR, and J. D. ROBERTS. J. Am. Chem. Soc. **91**, 1386 (1969).
12. E. L. ELIEL, N. L. ALLINGER, S. J. ANGYAL, and G. A. MORRISON. Conformational analysis. Wiley (Interscience), New York, N.Y. 1965.
13. M. HANACK. Conformational theory. Academic Press, New York, N.Y. 1965.
14. G. H. SENKLER, JR., D. GUST, P. X. RICCOBONO, and K. MISLOW. J. Am. Chem. Soc. **94**, 8626 (1972).
15. P. C. MANOV, D. P. SHOEMAKER, and A. S. PARKES. J. Am. Chem. Soc. **92**, 5260 (1970).
16. J. D. DUNITZ and J. WASER. J. Am. Chem. Soc. **94**, 5645 (1972); F. A. L. ANET and L. KOZERSKI. J. Am. Chem. Soc. **95**, 3407 (1973).
17. R. M. HUISGEN and G. BOSCHE. Tetrahedron Lett. 1769 (1965). M. ST-JACQUES and R. PRUD'HOMME. Tetrahedron Lett. 4833 (1970).
18. D. MONTECALVO, M. ST-JACQUES, and R. WASYLISHEN. J. Am. Chem. Soc. **95**, 2023 (1973).
19. J. DALE, T. EKELAND, and J. KRANE. J. Am. Chem. Soc. **94**, 1389 (1972).
20. F. A. L. ANET and P. J. DEGEN. J. Am. Chem. Soc. **94**, 1390 (1972).
21. G. PALA, A. MANTEGANI, and E. ZUGNA. Tetrahedron, **26**, 1275 (1970).
22. S. CASADIO, G. PALA, E. CRESCENZI, E. MARAZZI-UBERTI, G. COPPI, and C. TURBA. J. Med. Chem. **11**, 97 (1968).
23. E. D. BERGMANN and Z. PELCHOWICZ. J. Am. Chem. Soc. **75**, 4281 (1953).
24. L. I. SMITH and G. F. ROUAULT. J. Am. Chem. Soc. **65**, 745 (1943).
25. J. V. BRAUN, G. MANY, and E. REINSCH. Ann. **468**, 277 (1929).
26. J. C. N. MA and E. W. WARNHOFF. Can. J. Chem. **43**, 1849 (1965).
27. R. R. FRASER. Can. J. Chem. **40**, 1483 (1962).
28. R. R. FRASER, R. N. RENAUD, J. K. SAUNDERS, and Y. Y. WIGFIELD. Can. J. Chem. **51**, 2433 (1973).
29. R. CAHILL, R. C. COOKSON, and T. A. CRABBE. Tetrahedron, **25**, 4711 (1969).
30. R. R. FRASER and R. N. RENAUD. Can. J. Chem. **49**, 755 (1971).
31. M. BARFIELD and D. M. GRANT. J. Am. Chem. Soc. **85**, 1899 (1963).
32. J. A. POPLE and A. A. BOTHNER-BY. J. Chem. Phys. **42**, 1339 (1965); G. E. MACIEL, J. W. MCIVER, N. S. OSTLUND, and J. A. POPLE. J. Am. Chem. Soc. **92**, 4151 (1970).
33. R. R. FRASER and A. JURAYDINI. Can. J. Chem. **48**, 3591 (1970).
34. G. BINSCH. Top. Stereochem. **3**, 164 (1968).
35. G. W. BUCHANAN. Tetrahedron Lett. 665 (1972).
36. J. B. LAMBERT. J. Am. Chem. Soc. **89**, 1836 (1967); J. B. LAMBERT, R. G. KESKE, and D. K. WEARY. J. Am. Chem. Soc. **89**, 5921 (1967).
37. F. R. AHMED and A. D. HARDY. Acta Cryst. B. To be published.
38. E. J. COREY. Pure Appl. Chem. **14**, 19 (1967).

Can. J. Chem. Downloaded from www.nrcresearchpress.com by 210.87.254.6 on 09/05/12
For personal use only.

Arrhenius *A* Factors of Unimolecular Decomposition of Alcohols Formed by Insertion of $O(^1D_2)$ Atoms into the CH Bonds of Paraffins[1]

K. J. MINTZ[2] AND R. J. CVETANOVIĆ

Division of Chemistry, National Research Council of Canada, Ottawa, Canada K1A 0R9

Received December 21, 1972

The Arrhenius *A* factors of unimolecular decomposition of alcohols have been calculated approximately by a simple formula from the experimental rate constants of decomposition of "chemically activated" alcohols (formed by insertion of $O(^1D_2)$ atoms into the CH bonds of paraffins) and the structural and thermochemical properties of the alcohols. The more exact R.R.K.M. method of calculation is shown to be in reasonable agreement with the simpler method for CH_3OH decomposition. The resultant large positive entropies of activation are consistent only with involvement of "loose" activated complexes in the unimolecular decomposition of alcohols.

Les facteurs Arrhénius *A* pour la décomposition monomoléculaire des alcools ont été calculés approximativement à l'aide d'une simple formule tirée des constantes de vitesses pour la décomposition d'alcools chimiquement activés (formés par insertion d'atomes $O(^1D_2)$ à l'intérieur des liens CH des paraffines) ainsi que des propriétés structurales et thermochimiques des alcools. La méthode de calcul R.R.K.M., plus exacte, est en accord avec la méthode plus simple utilisée, comme il est démontré dans le cas de la décomposition du CH_3OH. Les entropies élevées et positives d'activation résultantes sont en accord seulement avec la présence de complexes activés "instables" lors de la décomposition monomoléculaire des alcools. [Traduit par le journal]

Can. J. Chem., **51**, 3386 (1973)

Introduction

In recent studies in this laboratory (1–4), it has been shown that $O(^1D_2)$ atoms insert into the CH bonds of hydrocarbons to form alcohols. The alcohol molecules formed are, however, vibrationally excited ("hot", "chemically activated") and decompose if not stabilized by collisions with other molecules. The experimental values of the rate constants (k_a) of their unimolecular decomposition show qualitatively the expected dependence on the exothermicity of the insertion reaction, the number of degrees of freedom, and the bond dissociation energy of the weakest bond in the molecule. Furthermore, approximate calculations based on Kassel's classical expression (5) for k_a indicate (3, 4) that the Arrhenius pre-exponential factors (A) of decomposition are likely to be high (considerably in excess of the "normal" values of about 10^{13} s^{-1}), *i.e.*, that these reactions have large positive entropies of activation ($\Delta S^{\neq}$). The latter are a common feature of unimolecular decomposition of polyatomic molecules into two free radicals (6) and are in principle explainable by the R.R.K.M. quantum mechanical theory of unimolecular reactions by postulating formation of "loose" activated complexes (7).

For the unimolecular decomposition of the hot alcohols formed by insertion of $O(^1D_2)$ atoms into the CH bonds of hydrocarbons, no meaningful R.R.K.M. calculations could be carried out since experimental values of the Arrhenius *A* factors are not available. Conversely, *a priori* R.R.K.M. calculations of the *A* factors require arbitrary assumptions about the structure of the activated complexes. This latter procedure has been the usual method (8) for the interpretation of experimental data from both chemical and thermal activation studies. An example particularly relevant to the present work is the recent study of Growcock, Hase, and Simons (9) on the unimolecular decomposition of chemically activated alkanes formed by insertion of singlet methylene into CH bonds of alkanes. For the reactions of $O(^1D_2)$ with some paraffins, the *A* factors were calculated (3, 4) from Kassel's expression, but, as will be mentioned later, this required the use of an adjustable ("empirical") parameter and the values obtained are only very approximate. The above conclusions regarding the activation entropies and structure of the

[1]NRCC No. 13301.

[2]NRCC Postdoctorate Fellow 1972–1973.

Can. J. Chem. Downloaded from www.nrcresearchpress.com by 210.87.254.6 on 09/05/12
For personal use only.

Can. J. Chem. Downloaded from www.nrcresearchpress.com by 210.87.254.6 on 09/05/12
For personal use only.

activated complexes for these reactions remained therefore doubtful. In fact, it remained uncertain whether these reactions do involve "chemically activated" alcohol molecules in the ground electronic state and conform to the general pattern. In the present note, we show that approximate values of A (and hence of $\Delta S^{\ddagger}$) can be easily calculated directly from the experimental k_a values using only knowledge of the properties of the reactant molecules (and not of the activated complexes).

Forst (10) has recently derived the following expression for the specific probability of unimolecular decomposition in thermal systems at an energy E:

$$k(E) = AN(E - E_\infty)/N(E) \quad E > E_\infty \qquad [1]$$
$$= 0 \quad E < E_\infty$$

where E_∞ is the high pressure activation energy for reaction and $N(E)$ is the density of states of the reactant molecule at energy E. Equation 1 assumes implicitly that A and E_∞ are temperature independent quantities. In chemical activation studies, the reactant can frequently be regarded as being monoenergetic because of the large exothermicity of the activating reaction relative to the thermal energy distribution at room temperature. Under such conditions, $k(E)$ can be set equal to k_a and [1] can be used directly to obtain the Arrhenius A factor.[3]

Procedure

The following basic assumptions of the R.R.K.M. theory are used throughout this work: there is fast energy flow among the vibrations but none between the vibrations and external rotations, *viz.*, all of the vibrational modes are treated as "active" and the external rotations as "adiabatic". The torsions are treated as free internal rotations. The "strong collision" assumption is made; the experimental justification for these reactions has been given (2).

If the classical density of states is used, [1] reduces to eq. 2, which is of a form somewhat similar to Kassel's expression (5)

$$k(E) = A((E - E_\infty)/E)^{v-1+r/2} \qquad [2]$$

[3]The theoretical rate constant, $k(E)$, in [1] should be increased by the appropriate factor to account for centrifugal effects (11, 12). However, in this work, the experimental value, *viz.* k_a, is used; hence, it is not necessary to make this correction.

where v is the number of vibrations excluding the torsional modes and r is the number of internal rotations. In the application of Kassel's theory, the exponent in [2] is $(s - 1)$, where s represents the total number of vibrations, and it is usually regarded as a fitting parameter. Also, E_∞ is replaced by E_0, the "critical" energy.

In this work the densities of states are calculated by a semi-classical method due to Whitten and Rabinovitch (12) as modified by Forst (13). At the fairly high energies involved, this approximation is quite acceptable. The effects of anharmonicity (13) should not be important for the size of molecules involved in the present study and are not considered. The formula for the rate constant is

$$k(E) = A\left(\frac{E - E_\infty + a'E_z}{E + aE_z}\right)^{v-1+r/2} \qquad [3]$$

where E_z is the zero-point energy of the molecule and a' and a are functions of E, E_z, and the vibrational frequencies, having values between zero and unity (13).

Since the reactions of $O(^1D_2)$ with paraffins

$$RH + O(^1D_2) \rightarrow ROH^* \qquad [4]$$

occur at approximately each collision, their activation energies must be very close to zero (14). The average values of the energy, E, of the alcohols formed (ROH*) are therefore given by

$$E = -\Delta H_{f_0}^0(ROH) + \Delta H_{f_0}^0(RH) + \Delta H_{f_0}^0(O(^1D_2)) + E_{th} \qquad [5]$$

where E_{th} is the average thermal energy of the reactants. It should be noted that the translational energy of ROH* is unavailable for decomposing the molecule since translation–vibration energy transfer can occur only during a collision, in which case the molecule becomes de-excited (from the "strong collision" assumption). Similarly, the external rotations have been assumed to be adiabatic. Assuming that the translations and external rotations are both classically excited, a value of $3RT$ should be subtracted from the value of E calculated by [5]. This correction is included in the values of E used here which were calculated from thermochemical data (15, 16) and are shown in Table 1. However, it must be noted that this correction is only very approximate because of the improbability that the reaction of $O(^1D_2)$ with paraffins yields vibrationally excited alcohols with transla-

TABLE 1. Results of calculations based on eq. 1 and 3

	E_z[a]	ΔH°_{298}[a]	E^a	k_a[b]	A^b	$\Delta S_{1000}{}^{\ddagger}$[c]
CH_3—OH	30.8 ± 0.1	92.3 ± 0.7	136.0	1.25×10^{12}[e]	7.8×10^{15}	9.8
CH_3—CH_2OH	47.7 ± 0.7	82 ± 3	143.5	$<2.5 \times 10^{11}$[e]	$<1.8 \times 10^{16}$	<11.4
C_2H_5—CH_2OH	64.8 ± 1.0	80 ± 3	146.2	$\sim 10^{11}$[f]	$\sim 1.2 \times 10^{17}$	~15
CH_3—$CH(CH_3)OH$	64.7 ± 1.7	81 ± 3	149.8	$\sim 10^{11}$[f]	$\sim 1.2 \times 10^{17}$	~15
$(CH_3)_2CH$—CH_2OH	82.0 ± 2.0	78 ± 3	147.0	2.2×10^{9}[g]	3.1×10^{16}	12.5
CH_3—$C(CH_3)_2OH$	81.0 ± 2.2	80 ± 3	154.0	3.8×10^{9}[g]	5.1×10^{16}	13.5
$(CH_3)_3C$—CH_2OH	98.3 ± 2.5	74 ± 3	147.2	2.4×10^{8}[h]	1.4×10^{16}	10.9
$CH_2CH_2CH_2CH_2CHOH$	88.9 ± 3.4	72[d]	153.2	5.9×10^{8}[i]	2.5×10^{15}	7.5

[a] In kcal/mol.
[b] In s^{-1}.
[c] In cal/deg mol.
[d] Estimated by Michaud and Cvetanović from group additivity rules.
[e] Reference 24.
[f] Reference 1.
[g] Reference 2.
[h] Reference 3.
[i] Reference 4.

tions and rotations in a Boltzmann distribution. Although, fortunately, this problem does not create any significant uncertainty in this study, in chemical activation studies in which E is much smaller, this effect may be important.

Calculation of E_z and a requires knowledge of all the vibrational frequencies. Methanol is the only alcohol for which a complete vibrational analysis has been done (17). The frequencies of the other alcohols in Table 1 were estimated by analogy with CH_3OH and alkanes or cycloalkanes of similar structure (17, 18). The values of E_z are listed in Table 1 together with their estimated uncertainties.

The Arrhenius activation energy, E_∞, for the forward step of the unimolecular process

$$\text{Reactant} \rightleftharpoons (^*) \rightleftharpoons \text{Products}$$

can be related (6), using transition state theory, to the enthalpy of the reaction, $\Delta H_T{}^0$, *viz*,

$$E_\infty = \Delta H_T{}^*(\text{f}) + RT$$

or

$$[6] \quad E_\infty = \Delta H_T{}^0 + \Delta H_0{}^*(r) + T\langle \Delta C_V{}^* \rangle(\text{r}) + (1 - \Delta n)RT$$

where (f) and (r) refer to the forward and reverse steps, respectively. $\langle \Delta C_V{}^* \rangle(\text{r})$ is the average heat capacity change in the formation of the activated complex from the products.

In the particular case of a bond scission reaction, $\Delta H_0{}^*(\text{r})$, *i.e.* $\Delta H_0{}^*$ for recombination of two free radicals, is usually assumed to be zero and the same assumption will be made in the present work. Also in this case $\Delta n = 1$ so that:

$$[7] \quad E_\infty = \Delta H_T{}^0 + T\langle \Delta C_V{}^* \rangle(\text{r})$$

For recombination of two free radicals, $\langle \Delta C_V{}^* \rangle(\text{r})$ is at most a relatively small quantity (6). By taking extremes of "loose" and "tight" activated complexes, it can be shown that $|\Delta C_V{}^*(\text{r})| < \frac{3}{2}R$. Benson and O'Neal (6) have pointed out that the usual assumption of zero activation energy of radical recombination at all temperatures implies that $\langle \Delta C_V{}^* \rangle(\text{r}) = 0$, in which case $E_\infty = \Delta H_T{}^0$. For the present case, the error due to neglecting $\langle \Delta C_V{}^* \rangle(\text{r})$ in eq. 7 is considerably less than that due to uncertainty in $\Delta H_T{}^0$ (*i.e.*, the room temperature bond dissociation enthalpies of the critical bonds in the alcohols).

The $\Delta H_T{}^0$ values were calculated from the heats of formation (at 298 °K) of the two radical fragments (15, 19), *viz.* (in kcal/mol) CH_3, 34.8 ± .3; OH, 9.4 ± .2; C_2H_5, 25.7 ± 1; *i*-C_3H_7, 17.6 ± 1; *t*-C_4H_9, 6.8 ± 1; CH_2OH, −8 ± 3; CH_3CHOH, −18 ± 3; $(CH_3)_2COH$, −29 ± 3. The last value was obtained by assuming for the $(CH_3)_2C(OH)$—H bond dissociation energy 88–89 kcal/mol, from the extrapolation of the $CH_2(OH)$—H and $CH_3CH(OH)$—H bond dissociation energies of 92 and 90 kcal/mol (19), respectively. The resultant C—C bond dissociation energies shown in Table 1 appear to be internally consistent.

Obviously, since $\Delta H_T{}^0$ is a (weak) function of T, the value of A calculated by [1] will depend to some extent on the temperature chosen. For CH_3OH decomposition, $\Delta H_T{}^0$ (kcal/mol) is 90.35 at 0 °K, 92.30 at 298, 94.03 at 1000, and 92.84 at 2000 °K, with an uncertainty of 0.7 at 0° and 298° and probably larger uncertainties at higher temperatures. The corresponding values are not available for the other reactions, though

Can. J. Chem. Downloaded from www.nrcresearchpress.com by 210.87.254.6 on 09/05/12
For personal use only.

Can. J. Chem. Downloaded from www.nrcresearchpress.com by 210.87.254.6 on 09/05/12
For personal use only.

similar variation with temperature would be expected.

Results and Discussion

The calculated values of A, obtained by matching eq. 3 to the experimental rate constants, are shown in Table 1 together with their corresponding entropies of activation for a temperature of 1000 °K, which were calculated from the expression:

$$[8] \qquad A = (ekT/h) \exp (\Delta S^{\ddagger}/R)$$

The reason for choosing this particular temperature will be evident from the discussion further below. The uncertainties in E_z and E cause about 10–20% uncertainty in the values of A; this is of the same magnitude as the likely uncertainty in the experimental rate constant, k_a. On the other hand, the uncertainty in ΔH_T^0 causes A to be uncertain to about a factor of two. Although most bond-dissociation energies cannot be estimated much more precisely than 3 kcal/mol, the relative values in a given series should be somewhat more accurate; therefore, the relative A factors have smaller uncertainties. The value for CH_3OH appears to be subject to considerably less uncertainty. The uncertainty regarding $\langle \Delta C_V^{\ddagger} \rangle$(r) discussed above introduces at most an uncertainty of ± 0.6 kcal/mol in the values of E_∞ and therefore errors in A of not more than 15%.

In principle, the distribution of the energy of the activated species should be taken into account, as has been done by Rabinovitch and Setser (8). Fortunately, the calculated A is very nearly a linear function of E over the rather narrow range of energies in this distribution; hence considering the system as monoenergetic with an average E does not create any significant increase in uncertainty in these calculations. Moreover, as discussed above, there is some question about the appropriate distribution to be used in the general equations of Rabinovitch and Setser. In any case, the uncertainty in A due to this problem is certainly much smaller than that due to uncertainty in the bond-dissociation energy.

The large positive $\Delta S^{\ddagger}$ values in Table 1 have been derived directly from the experimental rate constants of unimolecular decomposition of the chemically activated alcohols without assuming structures for the activated complexes. In principle they could be used to determine the structure of the activated complex. Unfortunately, as is shown below, the calculation of $\Delta S^{\ddagger}$ from an Arrhenius A factor is not very useful for distinguishing details of activated complexes. However, in general terms, it has been shown (7) that large positive $\Delta S^{\ddagger}$ in unimolecular decompositions requires the postulate of loose activated complexes. In fact, the A factors in Table 1 are quite similar in magnitude, for example, to the A factors observed experimentally in thermal dissociation of alkanes (6) (10^{16}–10^{17} s^{-1}) which are generally rationalized by postulating formation of "loose" activated complexes.

The methanol decomposition has an A factor about half of the other acyclic alcohol decompositions. This can be attributed to a different type of bond being broken. The cyclopentanol decomposition has an A factor which is very much smaller than that of the other alcohols. This difference, no doubt, is caused by the former case involving a ring opening which does not allow complete separation of the fragments. In this connection, it is interesting to note that Michaud and Cvetanović (4), by assuming that the entropy of the activated complex could be approximated by that of n-pentanol, had estimated $\Delta S^{\ddagger} = 12$ cal/deg mol, which is somewhat higher than the value in Table 1. The decomposition of t-C_4H_9OH has a reaction path degeneracy of 3; hence its A factor for a single reaction path is 1.7×10^{16} s^{-1}, in close agreement with those for the other acyclic compounds.[4]

It is of interest to compare the A factors calculated by the method proposed in this paper with those calculated by the usual application of R.R.K.M. theory. This calculation was done only for the CH_3OH decomposition, the only case for which sufficiently accurate data are available. According to the R.R.K.M. theory (7)

$$[9] \qquad k(E) = \frac{1}{h} \frac{Q^{\ddagger}}{Q} \frac{G^{\ddagger}(E - E_0)}{N(E)}$$

where $Q^{\ddagger}/Q$ is the ratio of the product of the adiabatic partition functions in the activated complex to that in the molecule; $G^{\ddagger}(E - E_0)$ is

[4]Similarly the decomposition of i-C_3H_7OH has a reaction path degeneracy of 2. Unfortunately, k_a for i-C_3H_7OH as well as n-C_3H_7OH could not be determined very accurately (1). However, if the relative k_a values for these decompositions are assumed to be more reliable, then the A factor for i-C_3H_7OH is about 40% greater than that for n-C_3H_7OH.

Can. J. Chem. Downloaded from www.nrcresearchpress.com by 210.87.254.6 on 09/05/12
For personal use only.

the sum of states of the active degrees of freedom in the activated complex up to energy $E - E_0$. E_0, the critical energy, was assumed to be equal to ΔH_0^0, *i.e.*, it was assumed that there is no energy barrier for the reverse reaction.

The structure of the activated complex was assumed to be identical to that of the molecule except that the C—O distance was increased to 2 Å (models I and I*a*), 3 Å (model II), or 5 Å (model III). Since the activated complex is "loose", it should resemble the products more than the reactants. Hence, in model I*a* the vibrational frequencies of CH_3 and OH are used rather than those of CH_3OH. The method used for determining the frequencies of the activated complex is the same as used by other workers (9): the frequencies of the normal modes in CH_3OH that change into translations or rotations in the products are reduced by a constant factor (while holding all other frequencies constant) until the theoretical rate constant calculated by [9] becomes equal to the experimental value. This procedure is obviously rather arbitrary.[5] The resultant frequencies are shown in Table 2 and the values of $\Delta S^{\ddagger}$ calculated by standard statistical-thermodynamic methods, assuming the ideal-gas, rigid-rotator, simple-harmonic oscillator approximation, are listed in Table 3.[6] As can be seen from Table 3, $\Delta S^{\ddagger}$ is most sensitive to the structure of the activated complex at low temperatures. At 1000 °K, the R.R.K.M. calculations predict values of A (using eq. 8) similar to that calculated by eq. 1.

It is of some interest to test the validity of the assumption of constant A factors implicit in eq. 1. The theoretical thermal rate constant calculated by the standard transition state theory expression

$$[10] \qquad k_{\text{theor}} = \frac{kT}{h} e^{\Delta S_T^{\ddagger}/R} e^{-\Delta H_T^{\ddagger}/RT}$$

was plotted in Arrhenius form for model I*a* as shown in Fig. 1. This plot shows that the Arrhenius equation should provide an excellent empirical approximation over the temperature range of interest (298 °K and above). A least-squares determination of the slope and intercept using the points marked on the graph yields Arrhenius parameters: $E_\infty = 93.5 \pm 0.2$ kcal/mol; $A = 5 \pm 1 \times 10^{15}$ s^{-1}. On the other hand, using [8] to calculate A from $\Delta S^{\ddagger}$ (as is usually done) apparently predicts that A should change rather rapidly with temperature. This apparent anomaly is due to the compensating effect of the temperature variation of A and E_∞ when plotted in the Arrhenius form. (If the plot in Fig. 1 is broken into a series of Arrhenius plots for small temperature intervals, a series of A and E_∞ values varying slightly with temperature may be obtained.)

TABLE 2. Frequencies and C—O bond lengths (r_{C-O}) used in the R.R.K.M. calculations for CH_3OH decomposition

		Value			
		Transition state model			
Parameter	Molecule	I	II	III	I*a*
r_{C-O} (Å)	1.427	2.0	3.0	5.0	2.0
ν (cm^{-1})					
CH_3 rocks	1060	168.5	216.6	311.0	216.6
	1165	185.2	238.1	341.8	238.1
OH bend	1345	213.8	274.8	394.7	274.8

The values of the decomposition rate constant (k_f) for methanol in the temperature range of potential experimental interest (1000–2000 °K) derived from eq. 1 and the R.R.K.M. calculations are compared in Table 3. The eq. 1 values

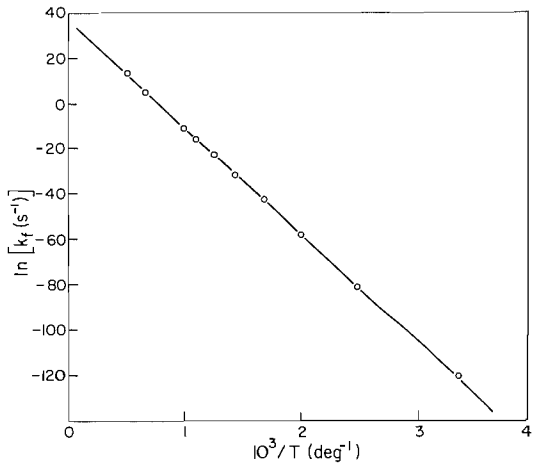

FIG. 1. Theoretical Arrhenius plot for the unimolecular decomposition $CH_3OH \rightarrow CH_3 + OH$.

[5]In the extreme case, if the CH_3 rocks in the activated complex were assumed to be the same as in the molecule and only OH bond was adjusted, $\Delta S_{298}^{\ddagger}$ would be 9.6 cal deg^{-1} mol^{-1} (model I).

[6]The barrier height of the restricted internal rotation (torsion) in the activated complex was assumed, for lack of further information, to be the same as in the molecule (1070 cal/mol).

TABLE 3. Results of the R.R.K.M. and eq. 1 calculations on CH_3OH decomposition

Temperature (°K)	R.R.K.M. values for the transition state models of table 2				Values based on eq. 1
	I	II	III	Ia	
			$\Delta S^{\ddagger}$ (cal deg^{-1} mol^{-1})		
2000	9.3	9.3	9.1	9.5	
1500	9.7	9.7	9.5	9.9	
1000	10.0	10.0	9.9	10.2	9.8
500	10.4	10.4	9.5	9.1	
298	7.6	7.7	7.9	6.7	
			A_f (10^{-15} s^{-1})		
1000	8.7	8.7	8.3	9.6	7.8
			k_f (s^{-1})		
2000	4.8×10^5	5.2×10^5	5.5×10^5	4.6×10^5	6.4×10^5
1500	1.7×10^2	1.8×10^2	1.9×10^2	1.5×10^2	2.8×10^2
1000	2.1×10^{-5}	2.3×10^{-5}	2.7×10^{-5}	1.8×10^{-5}	5.2×10^{-5}
			k_r (10^{-13} cm^3 mol^{-1} s^{-1})		
2000	1.5	1.6	1.6	1.3	1.9
1500	0.97	1.04	1.08	0.65	1.5
1000	0.58	0.64	0.74	0.36	1.4
500	0.49	0.59	0.78	0.16	1.5
298	0.22	0.30	0.51	0.11	1.2

have been calculated from the Arrhenius equation using the A and E_∞ values (7.8×10^{15} s^{-1} and 92.3 kcal/mol, respectively) obtained in our calculations based on eq. 1. The R.R.K.M. values have been calculated from eq. 10 using the activation parameters obtained in our calculations for the four transition state models. Evidently, the two approaches predict very similar values of k_f. (Even better agreement is obtained if in the calculation of the eq. 1 values the actual values of ΔH_T^0 at the three temperatures are used for E_∞ instead of the uniform value of 92.3 kcal/mol. However, in view of the simplifying assumptions implicit in the present treatment and the uncertainties in the data, this correction would be difficult to justify and has not been incorporated into the k_f values in Table 3.)

It is evident that eq. 1 can be used to obtain the "empirical" values of the Arrhenius parameters and thus to predict the experimental values of the decomposition rate constants from a single $k(E)$ value and the structural properties of the reactant. However, information on the transition state and on the finer details of energy dependence of $k(E)$ requires a more exact theoretical treatment. For example, the ratio $k(E)_{\text{R.R.K.M}}/k(E)_{\text{eq. 1}}$ for methanol varies for our transition state model I from 0.88 to 1.09 as E is increased from 120 to 150 kcal/mol.

A useful check on the present method of determining A would be to calculate rate constants of the reverse radical combinations from our A-factors and compare them with experimental values. (This procedure has been used by Simons and co-workers (9), who found, in fact, that their A factors for the unimolecular decomposition of alkanes, determined from chemical activation rate constants through R.R.K.M. theory, could not be correlated with the known rate constants for the reverse alkyl radical combinations.) Since reasonably accurate entropies of the reaction and the rates of the reverse reaction are known only for the methanol reaction, only one comparison can be made. For this reaction, $CH_3 + OH \rightarrow CH_3OH$, Fenimore (20) obtained a rate constant of $4 \pm 2 \times 10^{12}$ cm^3 mol^{-1} s^{-1}, independent of temperature between 1970 and 2190 °K. The predicted rate constant (k_r) for the radical combination reaction is given by

$$[11] \qquad k_r = k_f \, e^{\Delta H_T^\circ/RT} \, e^{-\Delta S_T^\circ/R}(RT)$$

The k_r values obtained, based on the k_f derived from eq. 1 and from the R.R.K.M. calculations, are shown in Table 3. They are in good mutual agreement at 2000 °K but appear to be significantly higher than the experimental value. It is of interest to note that the R.R.K.M. calculations predict a significant variation of the free

Can. J. Chem. Downloaded from www.nrcresearchpress.com by 210.87.254.6 on 09/05/12
For personal use only.

Can. J. Chem. Downloaded from www.nrcresearchpress.com by 210.87.254.6 on 09/05/12
For personal use only.

radical combination rate constant with temperature, which, when plotted in Arrhenius form, yields an activation energy of about 1.5 kcal/mol for model I*a*. On the other hand, the calculations based on eq. 1, which implicitly assumes temperature independent Arrhenius parameters for k_f, predict that k_r should be virtually independent of temperature.

Simons and co-workers (9) carried out an extensive study of the decomposition of chemically activated alkanes produced by methylene insertion into paraffinic CH bonds. They found that the rate constants of the reverse (radical combination) reactions, predicted by R.R.K.M. theory in the same manner as was used here, were substantially lower than the experimental values at 298 °K. They suggested that there exists a dilemma of theoretical importance. It is clear from our calculations (see Table 3) that the "dilemma" is that the absolute rate theory calculations with loose transition states predict a marked increase of the rate constant with temperature, so that it is smaller than experimental at low temperatures and larger at high temperatures. Most experimental evidence (in particular, on methyl radical combination) indicates that the rate constant changes only slightly with temperature and, if anything, decreases with increasing temperature. Hase (21) has recently proposed that adoption of a negative critical energy (of -2.0 kcal/mol) for CH_3 radical recombination will eliminate the discrepancy between the forward and reverse rates for ethane decomposition. However, his model predicts that the CH_3 recombination rate constant should change from 2.4×10^{13} at 400 °K to 1.2×10^{14} cm^3 mol^{-1} s^{-1} at 298 °K. The predicted large change appears to be inconsistent with the experimental evidence so that the dilemma does not seem to be resolved.

The results of the present calculation show that the trends in the experimental values of the rate constants of unimolecular decomposition of the hot alcohols formed by insertion of $O(^1D_2)$ atoms into the CH bonds of different alkanes are consistent with the postulate that the decomposition into free radicals involves highly vibrationally excited ("chemically activated") alcohol molecules in their ground electronic state and that it proceeds through "loose" activated complexes, as anticipated. In this connection, it is necessary to point out that in thermal systems the primary step in the unimolecular decomposition of *t*-butanol has been shown (22, 23) to be

[12] $$t\text{-}C_4H_9OH \rightarrow i\text{-}C_4H_8 + H_2O$$

which clearly involves a four-center activated complex. This may appear to contradict the assumption in the present work that the unimolecular decompositions of alcohols in chemical activation systems involve bond scissions, *e.g.*

[13] $$t\text{-}C_4H_9OH \rightarrow CH_3 + (CH_3)_2\dot{C}OH$$

However, the products observed in the chemical activation studies and behavior in the presence of free radical scavenger (O_2) are compatible only with bond scissions leading to formation of free radicals. This apparent anomaly can be easily resolved by comparing the Arrhenius parameters of reactions 12 and 13.

For *chemically* activated *t*-butanol formed by insertion of $O(^1D_2)$ into the tertiary CH bond of isobutane (*i.e.* for $E = 154$ kcal/mol, as listed in Table 1), and with Tsang's (23) $A_{12}(2.5 \times 10^{13}$ s$^{-1})$ and $E_{\infty 12}$ (61.6 kcal/mol), eq. 3 gives $k_{12}(E) = 1.8 \times 10^8$ s^{-1}. This is much smaller than the experimental value of 3.8×10^9 s^{-1}. Therefore, even if reaction 12 were occurring, it would amount to less than about 4% of total reaction and would be difficult to observe, in agreement with the experiment.

On the other hand, for *thermally* activated *t*-butanol, say at 1000 °K, fission into free radicals (reaction 13) should be relatively small. For thermal activation, the ratio of the integrated rate constants, k_a, is

[14] $$\frac{k_a(13)}{k_a(12)} = \frac{\int_{E_{0(13)}}^{\infty} k_{13}(E)N(E)\exp(-E/RT)\,dE}{\int_{E_{0(12)}}^{\infty} k_{12}(E)N(E)\exp(-E/RT)\,dE}$$

For simplicity, all $k(E)N(E)$ values in eq. 14 were calculated from eq. 3, although the latter is strictly valid only at larger E, and the respective E_0 values were equated to E_∞. The computed ratios of $k_a(13)/(k_a(12) + k_a(13))$ are 0.003 at 700 °K, 0.16 at 1000 °K, 0.62 at 1300 °K, and 0.95 at 2000 °K. Although these computations are approximate and are based on a particular choice of Arrhenius parameters for reactions 12 and 13, an appreciable contribution from the

bond fission reaction 13 may be expected at temperatures in excess of about 1000 °K. In fact, Tsang, who worked in the range 1050–1300 °K, did observe some "side products" (*i.e.* products other than isobutene) at 1300 °K, though he suggested that they might be due to decomposition of *i*-butene. It is evident that thermal and chemical activation do not necessarily follow the same mechanism; chemical activation makes it possible to study a reaction which would be difficult or impossible to study thermally.

1. H. YAMAZAKI and R. J. CVETANOVIĆ. J. Chem. Phys. **41**, 3703 (1964).
2. G. PARASKEVOPOULOS and R. J. CVETANOVIĆ. J. Chem. Phys. **50**, 590 (1969).
3. G. PARASKEVOPOULOS and R. J. CVETANOVIĆ. J. Chem. Phys. **52**, 5821 (1970).
4. P. MICHAUD and R. J. CVETANOVIĆ. J. Phys. Chem. **76**, 1375 (1972).
5. L. S. KASSEL. The kinetics of homogeneous gas reactions. Chemical Catalogue, New York, N.Y. 1932. p. 103.
6. S. W. BENSON and H. E. O'NEAL. Kinetic data on gas-phase unimolecular reactions. NSRDS-NBS 21. Washington, D.C. 1970.
7. R. A. MARCUS and O. K. RICE. J. Phys. Chem. **55**, 894 (1951); G. M. WIEDER and R. A. MARCUS. J. Chem. Phys. **37**, 1835 (1962).
8. B. S. RABINOVITCH and D. W. SETSER. Adv. Photochem. **3**, 1 (1964).
9. F. B. GROWCOCK, W. L. HASE, and J. W. SIMONS. J. Phys. Chem. **76**, 607 (1972); In. J. Chem. Kinet. **5**, 77 (1973).
10. W. FORST. J. Phys. Chem. **76**, 342 (1972).
11. E. V. WAAGE and B. S. RABINOVITCH. Chem. Rev. **70**, 377 (1970).
12. G. Z. WHITTEN and B. S. RABINOVITCH. J. Chem. Phys. **38**, 2466 (1963).
13. W. FORST. Chem. Rev. **71**, 339 (1971).
14. R. J. CVETANOVIĆ. Reactions of $O(^1D_2)$ atoms *In* The natural stratosphere. CIAP Vol. I. To be published.
15. JANAF thermochemical tables. NSRDS-NBS 37. Washington, D.C. 1970.
16. Selected values of thermodynamic properties of hydrocarbons and related compounds. American Petroleum Institute.
17. T. SHIMANOUCHI. Tables of molecular vibrational frequencies. NSRDS-NBS 39. Washington, D.C. 1972.
18. V. SCHETTINO, M. P. MARZOCCHI, and S. CALIFARO. J. Chem. Phys. **51**, 5264 (1969).
19. J. A. KERR. Chem. Rev. **66**, 465 (1966).
20. C. P. FENIMORE. Twelfth symposium (International) on combustion. Combustion Institute, 1969. p. 463.
21. W. L. HASE. J. Chem. Phys. **57**, 730 (1972).
22. J. A. BARNARD. Trans. Faraday Soc. **55**, 947 (1959).
23. W. TSANG. J. Chem. Phys. **40**, 1498 (1964).
24. C. L. LIN and W. B. DEMORE. J. Phys. Chem. **77**, 863 (1973).

Can. J. Chem. Downloaded from www.nrcresearchpress.com by 210.87.254.6 on 09/05/12
For personal use only.

Recombination of Iodine Atoms by Flash Photolysis over a Wide Temperature Range. V. I_2 in CF_4, SF_6, CO_2, Ne, Kr[1]

HEN WON CHANG AND GEORGE BURNS

Lash Miller Chemical Laboratories, University of Toronto, Toronto, Ontario M5S 1A1

Received April 30, 1973

Recombination rate constants for iodine atoms in CF_4, SF_6, CO_2, Ne, and Kr were studied by flash photolysis. The results can be summarized as follows:

$$\log k_r^{CF_4} = 10.247 - 2.627 \log (T/300) \text{ (between 300 and 810 °K)}$$
$$\log k_r^{SF_6} = 10.315 - 2.590 \log (T/300) \text{ (between 300 and 810 °K)}$$
$$\log k_r^{CO_2} = 10.224 - 3.274 \log (T/300) + 1.867 \log^2 (T/300) \text{ (between 300 and 980 °K)}$$
$$\log k_r^{Ne} = 9.190 - 1.898 \log (T/300) + 1.294 \log^2 (T/300) \text{ (between 300 and 960 °K)}$$
$$\log k_r^{Kr} = 9.572 - 2.654 \log (T/300) + 1.850 \log^2 (T/300) \text{ (between 300 and 1000 °K)}$$

These rate constants are compared with those available in the literature, and analyzed, qualitatively, in terms of current theories of recombination reactions.

Les constantes de vitesse pour la recombinaison des atomes d'iode dans le CF_4, SF_6, CO_2, Ne et Kr ont été évaluées à l'aide de la photolyse (éclair). Les résultats peuvent être résumés ainsi:

$$\log k_r^{CF_4} = 10.247 - 2.627 \log (T/300) \text{ (entre 300 et 810 °K)}$$
$$\log k_r^{SF_6} = 10.315 - 2.590 \log (T/300) \text{ (entre 300 et 810 °K)}$$
$$\log k_r^{CO_2} = 10.224 - 3.274 \log (T/300) + 1.867 \log^2 (T/300) \text{ (entre 300 et 980 °K)}$$
$$\log k_r^{Ne} = 9.190 - 1.898 \log (T/300) + 1.294 \log^2 (T/300) \text{ (entre 300 et 960 °K)}$$
$$\log k_r^{Kr} = 9.572 - 2.654 \log (T/300) + 1.850 \log^2 (T/300) \text{ (entre 300 et 1000 °K)}$$

Ces constantes de vitesse ont été comparées avec celles existant dans la littérature et ont été analysées, qualitativement, en fonction des théories modernes des réactions de recombinaison.

[Traduit par le journal]

Can. J. Chem., 51, 3394 (1973)

Can. J. Chem. Downloaded from www.nrcresearchpress.com by 210.87.254.6 on 09/05/12
For personal use only.

Recently, it became possible to measure the recombination rates of iodine (1–4) and bromine (5–6) atoms by flash photolysis over a wide temperature range. When these data were interpreted in terms of classical trajectory calculations (7–11), it was determined that two mechanisms are responsible for the recombination: the energy transfer (e.t.) mechanism

$$[1] \qquad X + X \rightleftarrows X_2^*$$

$$[2] \qquad X_2^* + M \rightarrow X_2 + M$$

and the radical molecule complex mechanism (r.m.c.)

$$[3] \qquad X + M \rightleftarrows XM$$

$$[4] \qquad XM + X \rightarrow X_2 + M,$$

where X is Br or I atom, X_2^* is an unstable orbiting pair produced via two body collision, XM is a weakly bound dimer, and M is the third body.

The trajectory calculations suggest that, if the third body is inert and light, the e.t. mechanism predominates. On the other hand, if the molecule M is either large or heavy, or is chemically active, it would be the r.m.c. mechanism that would determine the overall rate of the reaction. In most cases studied so far (7–11), both mechanisms contributed to the reaction. However, the interpretation of the experimental results would have been simpler if only one of these mechanisms would have been predominant.

In the present work, recombination of iodine in CF_4, SF_6, CO_2, Ne, and Kr is studied over a wide temperature range. Since Ne is inert and is a relatively light third body, it is probable that the recombination would proceed via the e.t. mechanism. On the other hand, one can deduce qualitatively from earlier work (7–11) that the recombination in CF_4, SF_6, and CO_2 would most likely proceed via the r.m.c.

[1]Research sponsored, in part, by the Air Force Office of Scientific Research, Air Force Systems Command, USAF, under grant No. AROSR-71-2016. The United States Government is entitled to reproduce and distribute reprints for Government purposes notwithstanding any copyright notation hereon.

Can. J. Chem. Downloaded from www.nrcresearchpress.com by 210.87.254.6 on 09/05/12
For personal use only.

mechanism. Recombination of I atoms in Kr is of special interest, because the interaction between I and Kr is presently being investigated by the cross molecular beam technique (12). It will be possible to employ data obtained (12) in order to calculate the recombination rate constant using a minimum number of assumptions. We were also interested in CO_2 as a third body because we wanted to compare the recombination rate to the rate of dissociation of I_2 in CO_2, which is available in the literature (13*a*). All these measurements were done in hope that interactions between iodine and the third body used could be described by a sufficiently reasonable and simple potential energy surface, so that meaningful comparison between experiments and trajectory calculations would be possible.

The apparatus used in this work, and the data analysis, were previously described (1, 2). B.D.H. reagent iodine was used and the diluent gases were obtained from the Matheson Company with the following specification: CF_4, 99.7% pure; SF_6, 99.8% pure; CO_2, 99.8% pure; Ne, 99.995% pure; Kr, 99.995% pure.

The experimental results are shown in Figs. 1 and 2. Here k_r^M is defined via the expression $d[I_2]/dt = k_r[I]^2[M]$ and is given in $l^2\ mol^{-2}\ s^{-1}$. The rate constants were fitted to the following relationship as a function of temperature.

$$\log k_r^{CF_4} = 10.247 - 2.627 \log (T/300) \quad \text{(between 300 and 810 °K)}$$

$$\log k_r^{SF_6} = 10.315 - 2.590 \log (T/300) \quad \text{(between 300 and 810 °K)}$$

$$\log k_r^{CO_2} = 10.224 - 3.274 \log (T/300) + 1.867 \log^2 (T/300) \quad \text{(between 300 and 980 °K)}$$

$$\log k_r^{Ne} = 9.190 - 1.898 \log (T/300) + 1.294 \log^2 (T/300) \quad \text{(between 300 and 960 °K)}$$

$$\log k_r^{Kr} = 9.572 - 2.654 \log (T/300) + 1.850 \log^2 (T/300) \quad \text{(between 300 and 1000 °K)}$$

CF_4, SF_6, and CO_2 are more efficient third bodies than any of the inert gases (1, 2). It appears that for these three gases the r.m.c. mechanism may be even more important than in the case of xenon (10). A similar result was obtained in the study of bromine atom recombination in the presence of an excess of CF_4 and SF_6 (5). Recombination of either iodine or bromine atoms proceeds at the same rate in CF_4; the same is true for SF_6. However, earlier measurements (13*b*) of $k_r^{SF_6}$ for Br are about 2.5 times smaller than $k_r^{SF_6}$ for Br reported more recently (5). We are unable to account for this discrepancy, especially because k_r^{He}, k_r^{Ar},

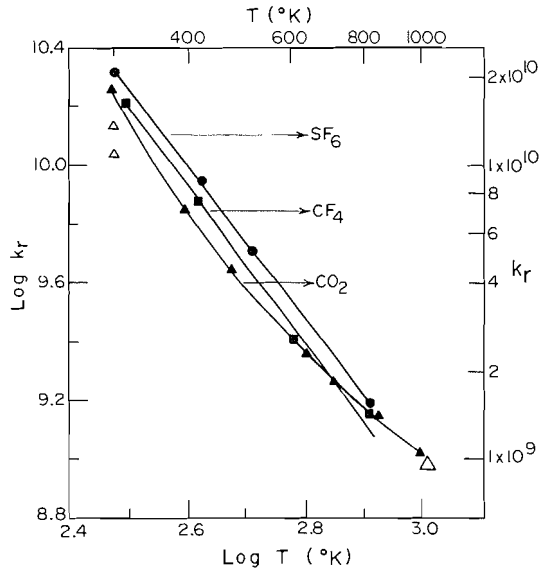

FIG. 1. Recombination rate constants of iodine atoms, k_r, as a function of temperature. Circles, $k_r^{SF_6}$, present work; squares, $k_r^{CF_4}$, present work; solid triangles, $k_r^{CO_2}$, present work; open triangles at 293 °K, $k_r^{CO_2}$, refs. 15, 16 and 17; open triangle at 1120 °K, $k_r^{CO_2}$, ref. 13*a*.

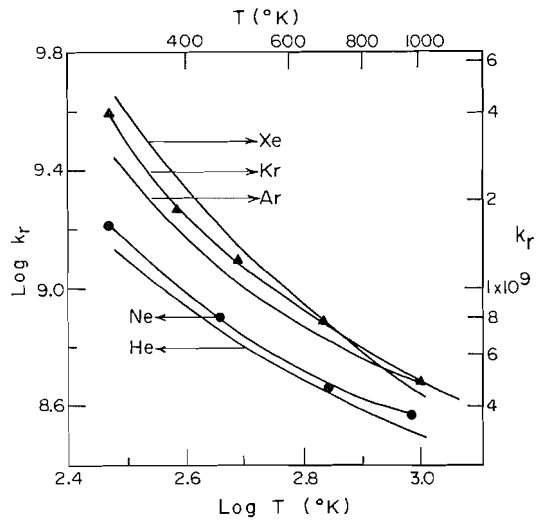

FIG. 2. Recombination rate constants of iodine atoms, k_r, as a function of temperature. Triangles, k_r^{Kr}, present work; circles, k_r^{Ne}, present work; k_r^{Xe}, k_r^{Ar}, and k_r^{He}, ref. 2.

TABLE 1. Recombination rate constants for $2I + CO_2 \rightarrow I_2 + CO_2$ reaction

Reference	$k_r^{CO_2}$ (293 °K)	$k_r^{CO_2}$ (1120 °K)	$k_r^{CO_2}(400\ °K)/k_r^{CO_2}(293\ °K)$
Rabinowitch and Wood (14)	3.3×10^{10}		
Russell and Simons (15)	1.35×10^{10}		0.4
Porter and Smith (16)	1.35×10^{10}		
Bunker and Davidson (17)	1.1×10^{10}		
Britton *et al.* (13*a*)		9.3×10^{8}	
This work	$1.8^4 \times 10^{10}$	9.2×10^{8}*	0.4

*Extrapolated from data at lower temperature.

TABLE 2. Recombination rate constants for $2I + Ne$ (or Kr) $\rightarrow I_2 + Ne$ (or Kr) reaction

Reference	k_r^{Ne}(293 °K)	k_r^{Kr}(293 °K)
Christie *et al.* (36)	1.65×10^{9}	4.08×10^{9}
Bunker and Davidson (17)	1.49×10^{9}	
This work	1.62×10^{9}	3.97×10^{9}

$k_r^{N_2}$, and k_r^{Ne} for Br, reported in ref. (13*b*) agree very well with those obtained previously in our laboratory (6). The recombination rate constant of iodine atoms in CO_2, obtained in this work at 300 °K, is considerably smaller than that obtained by Rabinowitch and Wood (14), but agrees well with that measured by Russell and Simons (15), and by Porter and Smith (16) (Table 1). Russell and Simons reported one ratio of rate constants, $k_r^{CO_2}(400\ °K)/k_r^{CO_2}(293\ °K) = 0.4$ which agrees well with that obtained in the present work. Britton and co-workers (13*a*) calculated $k_r^{CO_2}$ at 1120 °K from the dissociation rate constant obtained in shock wave experiments and the equilibrium rate constant. As can be seen from Fig. 1 and Table 1, their $k_r^{CO_2}$ value is in good agreement with $k_r^{CO_2}$ (1120 °K) obtained by extrapolation of our data. There has been a great deal of controversy in the literature regarding the validity of the rate quotient law ($k_{forward}/k_{reverse} = K_{eq}$) as applied to recombination–dissociation (18,19). There is a large body of experimental data (20–25) which suggest that the law may not be valid for these particular reactions. Unfortunately, these data were obtained in shock wave experiments, which, in general, may be susceptible to large, and sometimes unpredictable, errors. On the other hand, theoretical investigations (26–35) strongly suggest that the rate quotient law should be valid under the experimental conditions (20–25). Present work supports theoretical conclusions (26–35), as far as $2I + CO_2 \rightarrow I_2 + CO_2$ reaction is concerned.

Christie and co-workers (36) and Bunker and Davidson (17) measured k_r^{Ne} and k_r^{Kr} at 293 °K, and their values all agree well with our values (Table 2). The rate constant of iodine recombination in the presence of inert gases increases as the atomic number of the inert gas increases, as shown in Fig. 2 except at highest temperatures, where k_r^{Ar}, k_r^{Kr}, and k_r^{Xe} are nearly equal to each other. This trend was also found in the recombination of bromine atoms (6).

We would like to acknowledge the support of the Air Force Office of Scientific Research, U.S.A. This work was also supported in part by the National Research Council of Canada and the Defence Research Board of Canada, Grant No. 9530-54.

1. J. A. BLAKE and G. BURNS. J. Chem. Phys. **54**, 1480 (1971).
2. J. K. K. IP and G. BURNS. J. Chem. Phys. **56**, 3155 (1972).
3. J. BROWN and G. BURNS. Can. J. Chem. **48**, 2133 (1970).
4. H. W. CHANG and G. BURNS. J. Chem. Phys. To be published.
5. S. K. CHANG, A. G. CLARKE, and G. BURNS. J. Chem. Phys. **54**, 1835 (1971).
6. J. K. K. IP and G. BURNS. J. Chem. Phys. **51**, 3414 (1969).
7. A. G. CLARKE and G. BURNS. J. Chem. Phys. **55**, 4717 (1971).
8. A. G. CLARKE and G. BURNS. J. Chem. Phys. **56**, 4636 (1972).

Can. J. Chem. Downloaded from www.nrcresearchpress.com by 210.87.254.6 on 09/05/12
For personal use only.

9. A. G. CLARKE and G. BURNS. J. Chem. Phys. **58**, 1908 (1973).
10. W. H. WONG and G. BURNS. J. Chem. Phys. **59**, 4459 (1973).
11. W. H. WONG and G. BURNS. J. Chem. Phys. To be published.
12. M. J. CARDILLO, M. S. CHOW, and E. F. GREENE. Div. of Phys. Chem. 163rd ACS National Meeting. April, 1972. Paper 77.
13. (*a*) D. BRITTON, N. DAVIDSON, W. GEHMAN, and G. SCHOTT. J. Chem. Phys. **25**, 804 (1956); (*b*) B. A. DEGRAFF and K. J. LANG. J. Phys. Chem. **74**, 4181 (1970).
14. E. RABINOWITCH and W. G. WOOD. J. Chem. Phys. **4**, 497 (1936).
15. K. E. RUSSELL and J. SIMONS. Proc. Roy. Soc. London, A**271**, 271 (1953).
16. G. PORTER and J. A. SMITH. Nature, **184**, 446 (1959).
17. D. L. BUNKER and N. DAVIDSON. J. Am. Chem. Soc. **80**, 5090 (1958).
18. O. K. RICE. J. Phys. Chem. **65**, 1972 (1961).
19. H. O. PRITCHARD. J. Phys. Chem. **66**, 2111 (1962).
20. H. B. PALMER and D. F. HORNIG. J. Chem. Phys. **26**, 98 (1957).
21. D. BRITTON. J. Phys. Chem. **64**, 742 (1960).
22. M. WARSHAY. J. Chem. Phys. **54**, 4060 (1971).
23. H. HIRAOKA and R. HARDWICK. J. Chem. Phys. **36**, 1715 (1962).
24. R. W. DIESEN and W. J. FELMLEE. J. Chem. Phys. **39**, 2115 (1963).
25. M. VAN THIEL, D. J. SEERY, and D. BRITTON. J. Phys. Chem. **69**, 834 (1965).
26. J. C. KECK and G. F. CARRIER. J. Chem. Phys. **43**, 2284 (1965).
27. B. WIDOM. J. Chem. Phys. **55**, 44 (1971).
28. O. K. RICE. J. Phys. Chem. **67**, 1733 (1963).
29. (*a*) H. J. KOLKER. Z. Naturforsch. **23**a, 1102 (1968); (*b*) H. J. KOLKER. J. Chem. Phys. **44**, 582 (1966).
30. D. L. S. MCELWAIN and H. O. PRITCHARD. J. Am. Chem. Soc., **91**, 7693 (1969).
31. N. S. SNIDER. J. Chem. Phys. **42**, 548 (1965).
32. B. WIDOM. Science, **148**, 1555 (1965).
33. N. S. SNIDER. J. Chem. Phys. **45**, 3299 (1966).
34. C. A. BRAU. J. Chem. Phys. **47**, 1153 (1967); **47**, 3076 (1967).
35. N. S. SNIDER and J. ROSS. J. Chem. Phys. **44**, 1087 (1966).
36. M. I. CHRISTIE, A. J. HARRISON, R. G. W. NORRISH, and G. PORTER. Proc. Roy. Soc. London, A**231**, 446 (1955).

Can. J. Chem. Downloaded from www.nrcresearchpress.com by 210.87.254.6 on 09/05/12
For personal use only.

A Quantitative Investigation of the Ozonolysis Reaction. XVIII. A Kinetic Study of the Ozone Attack on Phenylethylenes

H. HENRY, M. ZADOR, AND S. FLISZÁR
Département de Chimie, Université de Montréal, Montréal, Québec

Received April 18, 1973

Absolute reaction rates for the ozonolysis of phenylethylenes in the liquid phase indicate: (*i*) a Hammett dependence, with $\rho \simeq -1$, for the ring-substituted *trans* stilbenes, (*ii*) a solvent effect, whereby the ozone attack is promoted by polar solvents, and (*iii*) no temperature effect between 15 and 35 °C, thus indicating $\Delta H^{\neq} \simeq 0$.

L'étude des constantes de vitesse pour l'ozonolyse de phényléthylènes en solution montre: (*i*) une relation de Hammett pour les stilbènes *trans* substitués dans le noyau, avec $\rho \simeq -1$, (*ii*) un effet de solvant, l'attaque de l'ozone étant promue en milieu polaire et (*iii*) l'absence d'un effet de température entre 15 et 35 °C, conduisant à $\Delta H^{\neq} \simeq 0$.

Can. J. Chem., **51**, 3398 (1973)

Early kinetic measurements of the reaction between ozone and organic compounds were made on benzene and derivatives thereof, *e.g.* the halogen- and alkyl-substituted benzenes (1–5). On the basis of these results, as well as from the observation that catalysts (such as aluminum chloride and boron trifluoride) which promote attack by electrophiles enhance the rate of reaction between ozone and the benzene derivatives (2, 3), it was concluded that the ozone attack on unsaturated organic compounds is electrophilic in nature. This is not at variance with the evidence that the ozone–olefin reaction is usually a 1,3-dipolar cycloaddition (6).

The rate constants for the reaction of ozone with substituted benzenes are relatively small, ranging (at 25 °C in CCl_4) from 0.028 to 245 $l\ mol^{-1}\ s^{-1}$ for benzene and hexamethylbenzene respectively (5). Hence, conventional techniques for "slow" reactions are adequate for these studies. This, however, is no longer the case for the study of the ozone reaction with ethylenic carbon–carbon double bonds, both in the gas and in the liquid phase. Fast reaction techniques are required in order to measure the rate constants which are of the order of $10^4 - 10^5\ l\ mol^{-1}\ s^{-1}$ (7–9).

The investigations by Cvetanović and coworkers using stopped-flow techniques (8, 9), have confirmed the electrophilic nature of the ozone attack on ethylenic carbon–carbon double bonds in a variety of cases. Ozone, due to its dipolar character, exhibits both an electrophilic and a nucleophilic tendency in the cycloaddition to give the 1,2,3-trioxolane (primary ozonide) (9–11). The observed trends in reactivity cannot be explained simply in terms of an electrophilic attack. It is now recognized that predictions on the ordering of rate constants according to the substituents on the ethylenic carbon atoms may well be in error if they are based *only* on the acceptance of an electrophilic tendency of the ozone attack. In fact, present results indicate that in some cases, *e.g.* the phenylethylenes (12, 13), the initial electrophilic attack proceeds rapidly via an irreversible 1,3-dipolar cycloaddition to give the final product, the primary ozonide. A different pathway, however, implying the reversible formation of a π or σ complex is also considered likely (9, 10, 12, 13).

These two aspects have been investigated recently in a systematic study of series of closely related compounds, such as alkyl-substituted ethylenes (13) and substituted phenylethylenes (12), in order to gain a better knowledge of the substituent effects governing the rate constants. Competitive kinetic techniques were used; these have the advantage over absolute rate measurements of being easier from the experimental point of view and, hence, less susceptible to possible errors.[1]

[1]Previous kinetic results (14) concerning the ozonolysis of ring-substituted styrenes are in error. Slowly decomposing products (probably open-chain benzaldehyde peroxides (15)) arising from the cleavage of the primary ozonides have interfered with the u.v. measurements of the ozone concentrations. By coincidence, the erroneous results also agreed in their comparison with relative reaction rates, as determined from the consumption of olefin in competitive experiments.

Can. J. Chem. Downloaded from www.nrcresearchpress.com by 210.87.254.5 on 09/05/12
For personal use only.

Can. J. Chem. Downloaded from www.nrcresearchpress.com by 210.87.254.5 on 09/05/12
For personal use only.

The interest in kinetic data is twofold. Firstly, in the ozonolysis of molecules containing several carbon–carbon double bonds relatively little is known about the preferential site of ozone attack. A better knowledge of kinetic data and of both electronic and steric factors of the substituents may prove helpful in discussing the preferential sites of ozone attack. Secondly, such knowledge proves helpful in elucidating the modes of attack from a mechanistic point of view.

The object of the present paper is a study of the specific reaction rates for the ozonolysis in liquid phase of selected phenylethylenes, covering electronic, solvent, and temperature effects. These ethylenes present the advantage that their reactions with ozone as far as final reaction products resulting from the cleavage of the primary ozonides are concerned have already been studied in some detail (15). The ozonolysis of these ethylenes in inert and in participating (ROH) solvents has been shown to be in complete agreement with Criegee's mechanism (16). In particular, the 1:1 olefin–ozone stoichiometry is clearly established and no reaction path other than that described by Criegee's mechanism has ever been observed for these compounds (15).

Experimental

The ring-substituted stilbenes were prepared by Dr. M. Granger, using standard methods; the other olefins are commercial products. Their purity was verified by g.l.c. Spectrograde solvents were used. The solvents were treated to prevent the rapid decomposition of ozone by impurities. A stream of ozonized oxygen was bubbled through the solvent at a rate of about 15 mmol of O_3 per h at room temperature for 45 min. The solution was then flushed with a stream of dry nitrogen for 2–3 h until the emergent N_2 gas contained no ozone. The pretreated solvents were used for preparing the olefin solutions. Ozone was delivered to the pretreated solvents at a flow rate of 15 mmol/h to give the ozone solutions. These are stable for several hours when CCl_4 and CH_2Cl_2 are used as solvents. In $CHCl_3$ the stability is somewhat reduced. In CH_3CN, however, special care must be taken to prepare the solutions immediately before use as the decomposition of the O_3 solution becomes quite noticeable within a few minutes. This decomposition is, however, of no kinetic importance because these reactions take place in about 100 ms.

A Durrum–Gibson stopped-flow apparatus with a Kel-F mixing chamber was used, together with a Jarrel–Ash 0.25 meter monochromator. The reaction was followed by means of a Tektronix 535A oscilloscope and photographs were taken of the signals.

The kinetics were followed by the measurement of the decrease in olefin absorbance (D) with time. The wave length was chosen in such a manner that no absorption from the ozone or from the reaction products could interfere. This was controlled by experiments indicating no residual absorbance at the particular wave length used, after a complete reaction of the olefin with excess amounts of ozone.

The rate constants were calculated from eq. 1,

$$[1]\quad \log([Ol]/[O_3]) - \log([Ol]_0/[O_3]_0) = ([Ol]_0 - [O_3]_0)kt/2.3$$

representing the ozone–olefin reaction assuming first order kinetics with respect to each reactant. Assuming the validity of the Beer–Lambert law, it follows, that

$$[2]\quad \log[D_t/(D_t - D_\infty)] - \log[D_0/(D_0 - D_\infty)] = D_\infty[Ol]_0 kt/2.3\ D_0$$

where D_0 is the absorbance at $t = 0$, and D_t the corresponding value at $t = t$. The absorption D_∞ at $t = \infty$ is a measure of the unreacted olefin and, hence, $D_0 - D_\infty$ a measure of the olefin consumed at $t = \infty$. All the kinetic runs were made using an excess of olefin with respect to ozone. Hence, the olefin consumed at $t = \infty$ is also equal to the initial amount of ozone. Consequently, the latter quantity need not be determined separately and, indeed, does not appear as such in eq. 2. Therefore, no error is introduced by the uncertainty of the initial ozone concentration and, thus, by any instability of the ozone solutions used for the experiments. In addition, it must be remembered that on the time scale of the kinetic runs the decomposition of the ozone solution is negligible.

The results of a typical run for the ozonolysis of *trans*-stilbene in CCl_4 at 25 °C are given in Table 1. As indicated by the kinetic plot (Fig. 1) obtained from these results, eq. 2 is obeyed satisfactorily, thus supporting the assumptions made in its derivation.

Results and Discussion

Most of the hitherto reported kinetic measurements have been based on ozone consumption relative to time (8, 9, 17), as determined by u.v. spectroscopy. In the present work the measurements are based on the rate of consumption of olefin. As indicated below for the case of styrene, a cross-checking of values obtained by these alternative methods confirms their adequacy.

Previous reports indicate a certain possibility of a dependence of measured rate constants on the concentrations of the reactants, when the concentrations were changed over several orders of magnitude (8). The results for *trans*-stilbene in CCl_4 at 25° reported in Table 2 indicate, however, a satisfactory constancy of the rate constants over a reasonable range of concentrations. The value $k = 3.8 \pm 0.2 \times 10^5\ M^{-1}\ s^{-1}$ thus obtained for *trans*-stilbene at 25° from the measurement of the rate of olefin consumption

TABLE 1. Ozonolysis of *trans*-stilbene in CCl_4 solution, at 25°

Reaction time (ms)	[Ol] × 10^5 (M)[a]	[O_3] × 10^5 (M)[b]	k × 10^{-5} (M^{-1} s^{-1})
0	5.0	4.0	
20	4.0	3.0	3.75
40	3.2	2.2	3.80
60	2.8	1.8	3.65
70	2.6	1.6	3.74
100	2.2	1.2	3.83
125	2.0	1.0	3.76
160	1.8	0.8	3.67
200	1.6	0.6	3.79
∞	1.0	0	

[a]Calculated from the observed optical density.
[b]Calculated from the consumption of olefin, assuming a 1:1 stoichiometry.

TABLE 2. Effect of the ozone and olefin initial concentrations on the rate constant for *trans*-stilbene in CCl_4, at 25°

[Ol]$_0$ × 10^5 (M)	[O_3]$_0$ × 10^5 (M)	k × 10^{-5} (M^{-1} s^{-1})
2.5	0.8	3.90 ± 0.2
5.0	2.4	3.81
7.5	5.0	3.76
10.0	9.0	3.92

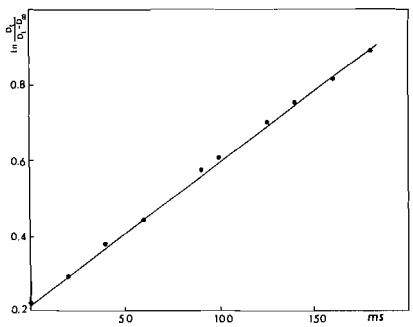

FIG. 1. A verification of eq. 2: ln $[D_t/(D_t - D_\infty)]$ *vs.* time, in ms.

can be used for a comparison with results previously reported (8) obtained from measurements of ozone consumption with time. From this k value for *trans*-stilbene and from the relative rate constant k(*trans*-stilbene)/k(styrene) = 3.48 ± 0.07 (12), the calculated rate constant for styrene is 1.09 × 10^5 M^{-1} s^{-1}. This value compares favorably with the value 1.03 × 10^5 M^{-1} s^{-1} reported by Cvetanović and co-worker (9), which is based on the determination of k for 1-hexene (from the measurement of ozone consumption) and on k(styrene)/k(1-hexene).

The effect of ring substitution was examined in the case of the stilbenes at 25°. The results are reported in Table 3, together with a comparison of the relative rate constants with respect to *trans*-stilbene obtained from (*i*) the present direct measurements of k and (*ii*) from relative rate constants determined with respect to styrene (12). The over-all agreement appears to be reasonable, within experimental limits.

The Hammett plot (Fig. 2) obtained from the present k values appears to be satisfactory. The negative slope ($\rho \simeq -1.0$) compares favorably with that determined from competitive measurements ($\rho = -0.9$). This result is thus in line with previous results (12) which had been interpreted in terms of an electrophilic attack of ozone on the ethylenic carbon–carbon double bond, proceeding by an "irreversible" 1,3-dipolar cycloaddition to give the primary ozonide.[2]

The effect of solvent on k was examined for *trans*- and *cis*-stilbene and for triphenylethylene at 25° (Table 4). The results consistently indicate

[2]In the present work, we have no experimental indication for any appreciable formation of π or σ complex intermediates which have been discussed in other cases (9, 13, 18, 19). The addition of ozone to olefin proceeds without an initial abrupt change in the optical density which would be expected to occur if a complex with different u.v. absorption were rapidly formed.

Can. J. Chem. Downloaded from www.nrcresearchpress.com by 210.87.254.5 on 09/05/12
For personal use only.

TABLE 3. Rate constants for the ozonolysis of *p*-substituted stilbenes in CCl_4 solution, at 25 °C

Substituent X	$k \times 10^{-5}$ (M^{-1} s^{-1})[a]	k_X/k_H	k_X/k_H (lit. 12)
p-CH_3	7.3 ± 0.2	1.92	1.48
H	3.8 ± 0.2	1	1
p-Cl	2.9 ± 0.1	0.76	0.64
p-NO_2	0.71 ± 0.02	0.19	0.22

[a]These *k* values are determined from 6–10 independent experiments, with a confidence limit of 95%.

TABLE 4. Effect of solvent on the rate constant (25 °C)

	$k \times 10^{-4}$ (M^{-1} s^{-1})		
Solvent	*trans*-Stilbene	*cis*-Stilbene	Triphenylethylene
CCl_4	38 ± 2	1.77 ± 0.1	1.69 ± 0.1
$CHCl_3$	60 ± 2		
CH_2Cl_2	91 ± 2		
CH_3CN	140 ± 9	4.77 ± 0.1	5.86 ± 0.2

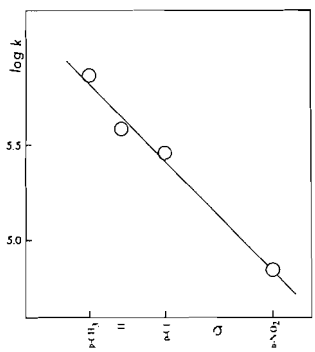

FIG. 2. Hammett plot of log *k* for the ring-substituted *trans* stilbenes, in CCl_4 solution at 25°, *vs.* the substituent constants σ.

that the rate constant increases as the dielectric constant of the solvent is increased. This can be regarded as an indication that the transition state is more polar than the reactants in their ground states.

The effect of α-substitution on 1,3-dipolar cycloadditions is described by Huisgen as "dramatic" (6). This effect can be recognized from the comparison of the results obtained with α-substituted stilbenes at 25° in CCl_4 (Table 5). With respect to *trans*-stilbene, both phenyl and methyl substitutions in the α position result in a significant decrease in the rate constant. A similar though less pronounced substitution effect is observed for α-methylstyrene relative to styrene, indicated by *k*(α-methylstyrene)/*k*(styrene) = 0.86. A better insight into

TABLE 5. Rate constants for the ozonolysis of α-substituted *trans* stilbenes and of *cis*-stilbene, in CCl_4 at 25°

Olefin	$k \times 10^{-4}$ (M^{-1} s^{-1})
trans-Stilbene	38 ± 2
α-Methyl-*trans*-stilbene	10 ± 1
Triphenylethylene	1.69 ± 0.10
cis-Stilbene	1.77 ± 0.10

the effect of methyl substitution on the kinetics is obtained from the consideration that, in principle, replacement of an ethylenic H by CH_3 results in an increase of the rate constant. From competitive kinetic studies (12) it follows that *k*(β-methylstyrene)/*k*(styrene) = 5.1 ± 0.15. In the case of the triphenylethylene, the significant decrease in the rate constant with respect to *trans*-stilbene can be attributed *in part* to a steric effect by which the geminal phenyl groups are no longer in the plane of the remainder of the molecule. The resulting decrease in polarizability of the ethylenic carbon–carbon double bond could be invoked to explain the decrease in the rate constant. This result would be in line with previous assumptions (6), *i.e.* that any increase of the polarizability of the ethylenic C—C double bond should enhance its dipolarophilic nature, and conversely. However, it must also be considered that the steric hindrance to ozone attack contributed by the geminal substituents may be largely

Can. J. Chem. Downloaded from www.nrcresearchpress.com by 210.87.254.5 on 09/05/12
For personal use only.

TABLE 6. Effect of temperature on the rate of ozonolysis of selected phenylethylenes, in CCl_4 solution

Olefin	$k \times 10^{-4}$ (M^{-1} s^{-1}) 15°	25°	35°
trans-Stilbene	37.5	38.2	38.6
cis-Stilbene	1.61	1.77	1.88
Triphenylethylene	1.64	1.69	1.66

responsible for the observed decrease in rate constants.

The effect of temperature on the rate constants has been studied for the ozonolysis of *cis*- and *trans*-stilbene and of triphenylethylene. The results clearly indicate that the rate constants are practically invariant with temperature in the range from 15 to 35 °C. This indicates that the activation energy for this reaction is close to 0. The present results agree with those reported for the ozonolysis of 1-dodecene in the temperature range −40 to 12.5 °C (20).

The activation entropies deduced from the present results for *cis*- and *trans*-stilbene, and triphenylethylene (in CCl_4 solution) are −39, −33, and −39 entropy units respectively. These values are similar to those observed in other cycloadditions (6). The present case is particular in that the activation entropy term represents the major, if not the only, contribution to the activation free energy. Thus, any reduction of the rate constant can be attributed, at least to a major extent, to the fact that a cycloaddition demands a concerted action with well-defined geometric requirements, resulting in very negative $\Delta S^{\ddagger}$ values.

Activation energies close or equal to 0 have been found in the ozonolysis of ethylene (21) and 1-hexene (21) in the gas phase, and of 1-hexene (17) and 1-dodecene (20) in the liquid phase. Contrasting with this situation for the ozone–olefin reaction, the decomposition of the primary ozonides hereby formed exhibits a non-zero activation energy in the limited number of cases which are known, *i.e.*, 1-hexene ($\simeq$7 kcal/mol) (22) and *trans*-3-hexene ($\simeq$8 kcal/mol) (23). These observations suggest that at sufficiently high temperatures and low reactant concentrations the ozone–olefin reaction is the rate determining step, whereas at sufficiently low temperatures the product formation is controlled largely by the decomposition of the primary ozonide.

The financial aid given by the National Research Council of Canada is gratefully acknowledged.

1. J. P. WIBAUT and J. VAN DIJK. Rec. Trav. Chim. Pays-Bas, **65**, 413 (1946); J. VAN DIJK, Rec. Trav. Chim. Pays-Bas, **67**, 945 (1948).
2. J. P. WIBAUT, F. L. J. SIXMA, L. W. KAMPSCHMIDT, and H. BOER. Rec. Trav. Chim. Pays-Bas, **69**, 1355 (1950).
3. F. L. J. SIXMA, H. BOER, and J. P. WIBAUT. Rec. Trav. Chim. Pays-Bas, **70**, 1005 (1951).
4. J. P. WIBAUT and F. L. J. SIXMA. Rec. Trav. Chim. Pays-Bas, **71**, 761 (1952).
5. T. W. NAKAGAWA, L. J. ANDREWS, and R. M. KEEFER. J. Am. Chem. Soc. **82**, 269 (1960).
6. R. HUISGEN. Angew. Chem. Int. Ed. Engl. **2**, 565, 633 (1963).
7. J. J. BUFFALINI and A. P. ALTSHULLER. Can. J. Chem. **43**, 2243 (1965).
8. D. G. WILLIAMSON and R. J. CVETANOVIĆ. J. Am. Chem. Soc. **90**, 3668 (1968).
9. D. G. WILLIAMSON and R. J. CVETANOVIĆ. J. Am. Chem. Soc. **90**, 4248 (1968).
10. T. VRBASKI and R. J. CVETANOVIĆ. Can. J. Chem. **38**, 1053 (1960).
11. Y. K. WEI and R. J. CVETANOVIĆ. Can. J. Chem. **41**, 913 (1963).
12. G. KLUTSCH and S. FLISZÁR. Can. J. Chem. **50**, 2841 (1972).
13. J. CARLES and S. FLISZÁR. Adv. Chem. Ser. **112**, 35 (1972).
14. A. J. WHITWORTH, R. AYOUB, Y. ROUSSEAU, and S. FLISZÁR. J. Am. Chem. Soc. **91**, 7128 (1969).
15. S. FLISZÁR, D. GRAVEL, and E. CAVALIERI. Can. J. Chem. **44**, 1013 (1966); S. FLISZÁR and M. GRANGER. J. Am. Chem. Soc. **91**, 3330 (1969); S. FLISZÁR and J. RENARD. Can. J. Chem. **48**, 3002 (1970); S. FLISZÁR and J. CARLES. J. Am. Chem. Soc. **91**, 2637 (1969); S. FLISZÁR and J. B. CHYLIŃSKA. Can. J. Chem. **46**, 783 (1968).
16. R. CRIEGEE and G. WENNER. Ann. **564**, 9 (1949); R. CRIEGEE. Ann. **583**, 1 (1953); R. CRIEGEE. Rec. Chem. Progr. **18**, 111 (1957); P. S. BAILEY. Chem. Rev. **58**, 926 (1958).
17. S. D. RAZUMOVSKII. Izv. Akad. Nauk SSSR, **2**, 335 (1970).
18. P. S. BAILEY. Chem. Ind. 1148 (1957); P. S. BAILEY and A. G. LANE. J. Am. Chem. Soc. **89**, 4473 (1967).
19. R. W. MURRAY, R. D. YOUSSEFYEH, and P. R. STORY. J. Am. Chem. Soc. **89**, 2429 (1967); **88**, 3143 (1966).
20. G. WAGNER and A. GREINER. Z. Phys. Chem. (Leipzig), **215**, 92 (1960).
21. R. D. CADLE and C. SCHADT. J. Am. Chem. Soc. **74**, 6002 (1952); J. Chem. Phys. **21**, 163 (1953).
22. S. D. RAZUMOVSKII and L. V. BEREZOVA. Izv. Akad. Nauk SSSR, **1**, 207 (1968).
23. F. L. GREENWOOD and L. J. DURHAM. J. Org. Chem. **34**, 3363 (1969).

Can. J. Chem. Downloaded from www.nrcresearchpress.com by 210.87.254.5 on 09/05/12
For personal use only.

Arylsulfanes—Synthesis and Nuclear Magnetic Resonance Spectra

H. J. LANGER[1] AND J. B. HYNE
Alberta Sulphur Research Ltd., University of Calgary, Calgary, Alberta

Received February 15, 1973

The synthesis of a series of variously substituted arylsulfanes of the general formula $RC_6H_4S_xH$ is described. The proton n.m.r. spectra of the members of the series are reported and discussed in terms of intramolecular electronic effects, conformational factors, and hydrogen bonding.

On décrit la synthèse d'une série d'arylsulfanes de formule générale $RC_6H_4S_xH$. Les spectres r.m.n. de ces composés sont décrits et discutés en termes d'effets électroniques intramoléculaires, de facteurs conformationnels et de ponts hydrogène. [Traduit par le journal]

Can. J. Chem., 51, 3403 (1973)

Introduction

The preparation, isolation, and characterization of asymmetrical sulfanes having the general formula ArS_xH has presented a considerable synthetic challenge to many workers. Disproportionation, rearrangement, and the general instability of longer sulfur chains under the preparative reaction conditions have been the major problem areas. Fehér's work (1) on the preparation and isolation of the hydrogen polysulfides or sulfanes (HS_xH) is a classic illustration of such rearrangement and disproportionation. Tsurugi and co-workers (2) have refined the original method of Böhme and Zinner (3) for the preparation of aryldisulfanes using acylchlorosulfanes followed by alcoholysis, thus building up the sulfane chain one atom at a time. In this work an extension of Fehér's original technique using dichloromonosulfane (SCl_2) or dichlorodisulfane (S_2Cl_2) followed by "thiohydrolysis" with liquid hydrogen sulfide has permitted the synthesis of the higher members of the homologous series of substituted arylsulfanes by adding sulfur atoms in steps of two or three at each stage (see Scheme 1).

N.m.r. has been shown to be a useful analytical tool for simultaneously identifying and quantitatively estimating the individual sulfane members in complicated mixtures (4). In a mixture of sulfanes the exchange rate of protons between individual —SH species takes place sufficiently slowly that the n.m.r. spectrum is characterized by separate distinct signals for the sulfhydryl protons. By using the ratios of the respective peak areas a quantitative analysis of the mixture is possible. This analytical method was used successfully to study the formation of sulfanes in the sulfur–H_2S system, and in the kinetic study of the thiol–sulfur reaction (5).

[1]Present address: Ashland Oil, Inc., Columbus, Ohio.

Synthesis

The general procedure for arylsulfane chain lengthening commencing with the appropriate thiol is summarized in Scheme 1. It is important to note that because of the extreme difficulty of separation and purification of higher members of the sulfane series the n.m.r. shift values reported for some tri-, tetra-, and higher homologues are taken from mixtures of the sulfanes. These cases where actual isolation was not performed are clearly identified in the data compilations.

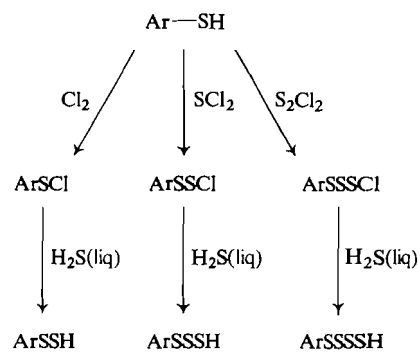

SCHEME 1

Reaction of arylchlorosulfanes (ArS_xCl) with mercaptans rather than H_2S to yield disubstituted sulfanes ($R_1S_xR_2$) has been previously reported (6).

Arylchloromonosulfane, the precursor of the

Can. J. Chem. Downloaded from www.nrcresearchpress.com by 210.87.254.42 on 09/05/12
For personal use only.

TABLE 1. Summary of analytical data for arylsulfanes[a]

Sulfane	Formula	Yield[c] %	Iodometric titration[b] Calcd.	Found	% (by n.m.r.)[c] —S_4H	—S_3H	—S_2H
Phenyldisulfane	C_6H_5SSH	95	17.45	16.96		8	92
p-Methylphenyldisulfane	$CH_3C_6H_4SSH$	98	15.12	14.75		12	88
p-Chlorophenyldisulfane	ClC_6H_4SSH	98	11.49	11.40		1.6	98.4
p-Nitrophenyldisulfane	$NO_2C_6H_4SSH$	94	15.23	15.11			>99
o-Nitrophenyldisulfane	$NO_2C_6H_4SSH$	79	16.36	16.49			>99
Phenyltrisulfane	$C_6H_5S_3H$	90	15.34	15.98		82.2	17.8
p-Methylphenyltrisulfane	$CH_3C_6H_4S_3H$	96	13.84	14.32		84.1	15.9
Phenyltetrasulfane	$C_6H_5S_4H$	73	12.31	13.24	60	40	
p-Methylphenyltetrasulfane	$CH_3C_6H_4S_4H$	80	8.91	9.41	59	41	

[a]See Experimental for details.
[b]Milliliters of 0.1 *N* I_2 solution.
[c]Total yield of sulfane products; distribution indicated by n.m.r.

respective sulfane was synthesized by treatment of an aromatic thiol with chlorine, *i.e.*

$$Ar—SH + Cl_2 \rightarrow Ar—SCl + HCl$$

The arylchlorodisulfane was prepared in good yield and with satisfactory purity by careful, slow addition of the thiol in CS_2 solution to a very large excess of SCl_2 at -70 °C.

$$Ar—SH + SCl_2 \rightarrow Ar—SSCl + HCl$$

The solvent and excess of SCl_2 must be distilled off *in vacuo* at low temperature. Under similar conditions the reaction of excess S_2Cl_2 with ArSH yields ArS_3Cl.

Under rigorous exclusion of moisture an excess of liquid H_2S reacted with the arylchlorosulfanes at -70 °C to yield the corresponding monosubstituted sulfanes according to

$$Ar—S_xCl + H_2S \rightarrow Ar—S_{x+1}H + HCl$$

The reaction proceeds smoothly and it is unnecessary to isolate the intermediate ArS_xCl. The products were obtained in nearly quantitative yields and were yellow viscous liquids at room temperature, soluble in CS_2 and characterized by a less unpleasant odor than the corresponding thiols. They are relatively stable and may be stored for some weeks when kept near 0 °C and under anhydrous conditions. The products were analyzed by iodometric titration and n.m.r. The results are summarized in Table 1.

The absence of sulfur analysis data as a criterion in Table 1 deserves comment. Sulfur analyses, while certainly informative, suffer from the difficulty that with a homologous series such as the sulfanes, a mixture of disproportionated members of the series, *e.g.* penta- and trisulfane can give a sulfur analysis which would correspond to a pure tetrasulfane. Therefore, *in situ* identification by n.m.r., which reflects the specific molecular integrity of the species, was preferred in combination with iodometric titration of the terminal —SH function. Table 1 also shows the percentages of other sulfanes present in the various samples as obtained from n.m.r. analysis.

Following the synthesis of the sulfanes ArS_xH, a number of experiments were carried out mainly in order to support the structure assignments which were initially based on spectroscopic data, by conversion of these compounds into known sulfane derivatives.

Aryldisulfane was oxidized with iodine;

$$2\ ArS_2H + I_2 \rightarrow ArS_4Ar + 2\ HI$$

or was converted to the trisulfane by treatment with ArSCl.

$$ArS_2H + ArSCl \rightarrow ArS_3Ar + HCl$$

Reaction of aryltrisulfane with arylchloromonosulfane yielded diaryltetrasulfane;

$$ArS_3H + ArSCl \rightarrow ArS_4Ar + HCl$$

the end products were characterized (m.p. and mixed m.p.) by comparison with an authentic sample prepared by an independent synthesis.

Several variables must be considered when planning the synthesis of a particular sulfane. These variables are (1) the molar ratio of the thiol to chlorosulfane or of the arylchlorosulfane to hydrogen sulfide, (2) the reaction temperature, and (3) the reaction time, *i.e.* controlled rate of

Can. J. Chem. Downloaded from www.nrcresearchpress.com by 210.87.254.42 on 09/05/12
For personal use only.

TABLE 2. Characteristic chemical shifts[a] of aromatic thiols and of arylsulfanes

	Formula	—SH (τ p.p.m.)	Ring protons[b] (τ p.p.m.)
Thiols			
Benzenethiol	C_6H_5SH	6.71	2.90
p-Methylbenzenethiol	$CH_3C_6H_4SH$	6.79	3.00
p-Chlorobenzenethiol	ClC_6H_4SH	6.63	2.91
p-Nitrobenzenethiol	$NO_2C_6H_4SH$	6.12	2.39
o-Nitrobenzenethiol	$NO_2C_6H_4SH$	5.98	2.34
Sulfanes			
Phenyldisulfane	$C_6H_5S_2H$	6.62	2.68
p-Methylphenyldisulfane	$CH_3C_6H_4S_2H$	6.61	2.83
p-Chlorophenyldisulfane	$ClC_6H_4S_2H$	6.53	2.69
p-Nitrophenyldisulfane	$NO_2C_6H_4S_2H$	6.42	2.02
o-Nitrophenyldisulfane	$NO_2C_6H_4S_2H$	6.81	2.25
Phenyltrisulfane	$C_6H_5S_3H$	6.11	2.74
p-Methylphenyltrisulfane	$CH_3C_6H_4S_3H$	6.18	2.82
p-Chlorophenyltrisulfane	$ClC_6H_4S_3H$	6.05[c]	
Phenyltetrasulfane	$C_6H_5S_4H$	6.02	2.62
p-Methylphenyltetrasulfane	$CH_3C_6H_4S_4H$	6.07	2.85
p-Chlorophenyltetrasulfane	$ClC_6H_4S_4H$	5.86[c]	
Phenylpentasulfane	$C_6H_5S_5H$	5.93[c]	
Phenylhexasulfane	$C_6H_5S_6H$	5.90[c]	
Phenylheptasulfane	$C_6H_5S_7H$	5.88[c]	

[a]TMS internal reference in CS_2 solution, (concentration 1.0 mol l^{-1})
[b]Taken in the center of the multiplet.
[c]The signal positions are estimated and are taken from the sulfane mixture.

addition of reactant. In general, increasing the number of sulfur atoms in the sulfane requires more careful control of these conditions for optimum results.

An interesting observation was made in attempts to catalyze the synthesis of arylsulfanes (ArS_xH) by means of HCl. The reaction was performed both with liquid H_2S saturated with HCl before addition of the arylchlorosulfanes and without addition of HCl. No difference could be observed. This is interesting since Muller and Hyne found (7) in the preparation of HS_3H and HS_4H that satisfactory results were obtained only with H_2S saturated with HCl.

Higher Homologues by Disproportionation and Decomposition

On prolonged standing at room temperature and during distillation, sulfanes were found to decompose into diarylpolysulfanes, thiol, hydrogen sulfide, and sulfur. Attention was focussed in this work on the unsubstituted parent phenylsulfanes. The principal end products of the decomposition of phenyldisulfane, for instance, were sulfur, diphenyldisulfane and tetrasulfane, benzenethiol, and hydrogen sulfide;

$$3ArSSH \rightarrow ArS_xAr + ArSH + H_2S + S$$

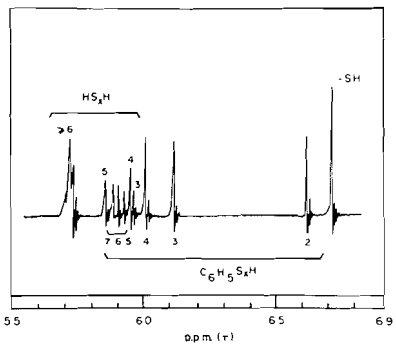

FIG. 1. Expanded n.m.r. spectrum of polysulfane region with assignments. Numbers indicate value of x.

By examining the reaction mixture by n.m.r. during and after distillation it was found that the sulfanes do not decompose directly into the final products Ar—S_xAr, Ar—SH, H_2S, and S but do so through the formation of a number of higher sulfanes of both the ArS_xH and HS_xH type. A typical spectrum of such a polysulfanes mixture showing the presence of the ArS_xH, HS_xH, and parent thiol is shown in Fig. 1. The n.m.r. chemical shifts for the phenylsulfanes are listed in Table 2. In the spectrum the —SH resonance signals are clearly assignable as

Can. J. Chem. Downloaded from www.nrcresearchpress.com by 210.87.254.42 on 09/05/12
For personal use only.

Can. J. Chem. Downloaded from www.nrcresearchpress.com by 210.87.254.42 on 09/05/12
For personal use only.

indicated by the superscript numbers indicating the length of the sulfur chain. The n.m.r. signals resulting from HS_xH species in the spectrum were assigned according to Hyne *et al.* (5). Inspection of Fig. 1 shows that arylsulfanes up to a sulfur chain length of seven may be identified by clearly separated signals. With increasing sulfur chain length chemical shifts of the sulfhydryl protons are shifted downfield. Assignments were made accordingly and confirmed by adding samples of known sulfane composition to the reaction mixture and observing an increase in the area of the appropriate signals.

The reactions involved in the decomposition of arylsulfanes are evidently complex as evidenced by the production of a large number of intermediates and end products. There is a considerable body of results on the thermal decomposition of sulfanes (8–11) and, for the most part, the evidence indicates that a radical mechanism predominates. Analogies between arylsulfane disproportionation and previous studies on the thermal decomposition of HS_xH (11) suggest a primary homolytic dissociation of the S—S bond into free radicals.

$$ArSSH \rightarrow ArS\cdot + \cdot SH$$

Hydrogen abstraction reactions between primary radical products and the parent sulfane must follow the dissociation step above.

$$ArSSH + ArS\cdot \rightarrow ArSH + ArSS\cdot$$

$$ArSSH + HS\cdot \rightarrow H_2S + ArSS\cdot$$

Subsequent reactions may involve radical–radical recombination of the type

$$ArSS\cdot + HS\cdot \rightarrow ArS_3H$$

$$ArSS\cdot + ArSS\cdot \rightarrow ArS_4Ar$$

$$ArS\cdot + ArS\cdot \rightarrow ArS_2Ar$$

Thermal decomposition of the higher sulfanes ArS_3H and ArS_4H would then proceed by a similar initial homolysis;

$$ArS_3H \rightarrow ArS. + .S_2H$$
$$ArS_3H \rightarrow ArS_2. + .SH$$

$$ArS_4H \rightarrow ArS. + .S_3H$$
$$ArS_4H \rightarrow ArS_2. + .S_2H$$
$$ArS_4H \rightarrow ArS_3. + .SH$$

The primary radicals again abstract hydrogen from the parent sulfane which is present in relatively large excess. The occurrence of higher sulfanes of the type ArS_xH and HS_xH with $x \geqslant 6$ indicates that further disproportionation reactions take place and result in chain propagation and chain termination by similar radical–radical recombinations.

While this investigation represents only a cursory examination of the decomposition of arylsulfanes ArS_xH, the results indicate that the decomposition is a complex reaction involving disproportionation into polysulfanes HS_xH and higher and lower members of the series ArS_xH.

Nuclear Magnetic Resonance Spectra

The availability of a range of variously substituted arylsulfanes of the general formula $RC_6H_4S_xH$ has permitted the determination of the proton n.m.r. behavior of the series of compounds and hence the examination of intramolecular electronic transmission effects. Variation of the R substituent through CH_3, H, Cl, and NO_2 provides both electron donating and withdrawing influences on the aromatic ring. Values of x, the sulfur chain length, from 1 to 4 permit examination of the influence of this factor on the transmission of electronic effects from the aromatic ring to the terminal sulfane proton. The pertinent n.m.r. data are reported in Table 2. Marcus and Miller (12) and Tsurugi and co-workers (2) have reported n.m.r. data on substituted thiols ($x = 1$) and disulfanes ($x = 2$) and have commented on the need to extrapolate to zero concentration because of the possibility of intermolecular hydrogen bonding effects. In the substituted arylsulfanes examined in this work the dependence of S—H proton shift on concentration was found to be small in all but the nitro case. All determinations were therefore made at the same dilution (1.0 *M* in CS_2). While these values may differ slightly from infinite dilution values (C_6H_5SSH 6.62 τ, this work; 6.61 τ, ref. 2) the values for the series are internally consistent. Van Wazer and Grant (13) have reported the dependence of methyl proton n.m.r. shift on sulfur chain length for the series of dimethylsulfanes, $CH_3S_xCH_3$. Schmidbaur *et al.* (4) and Muller and Hyne (14) have provided corresponding data for the simple sulfane series, HS_xH. All of these results show a downfield

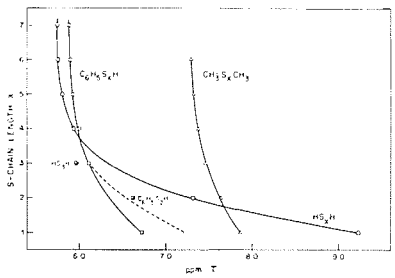

FIG. 2. Dependence of the sulfane proton signal positions on the sulfur chain length. ○ HS_xH: TMS internal reference in CS_2 solution (concentration: 1.0 mol^{-1}); values from reference 14. □ $C_6H_5S_xH$: TMS internal reference in CS_2 solution (concentration: 1.0 mol^{-1}). △ $CH_3S_xCH_3$: TMS internal reference in $(CH_3)_2S$ solution; Values from ref. 13.

shift or deshielding effect on the terminal protons as the sulfane chain length is increased. As illustrated in Fig. 2 the arylsulfanes are no exception to this rule. There is a clear indication, however, that the aryldisulfane is somewhat anomalous as has been noted for the trisulfane in the HS_xH series.

This anomalous behavior in the disulfanes is clearly established by the data for the variously substituted sulfanes plotted in Fig. 3. The *p*-CH_3 and *p*-Cl series both show precisely similar deviations from the smooth curve behavior as is noted for the unsubstituted parent phenylsulfane. Tsurugi and co-workers (2) in their examination of the effect of varying ring substitution on SH proton shift for the RC_6H_4-SSH series concluded that the S—S bond in the disulfane does not transmit conjugation and

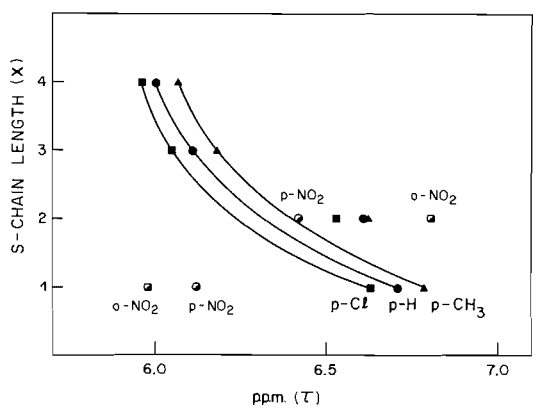

FIG. 3. Sulfhydryl proton signal position of substituted arylsulfanes as a function of sulfur chain length.

permits only very little inductive effect transmission. This might be considered as an explanation for the anomalous behavior of the disulfanes illustrated in Fig. 2 if the phenomenon persisted at higher sulfur chain lengths. Clearly, however, this is not so and it is therefore difficult to accept that by simply extending the sulfur chain the transmission effect is restored.

Downfield shifts from expected values as observed in the case of H_2S_3 are generally attributed to decreased proton shielding resulting from intra- or intermolecular hydrogen bonding. Schmidbaur *et al.* (4) first suggested this explanation for the anomalous n.m.r. signal in H_2S_3 and self association in both thiols and sulfanes has been subsequently demonstrated by i.r. and Raman spectroscopy (31, 32). In the case of phenyldisulfane and the corresponding *p*-methyl and *p*-chloro species, however, the observed anomalous shift of the terminal S—H proton is *upfield* implying increased rather than decreased proton shielding relative to that experienced by other members of the homologous sulfane series. The fact that a change from electron donating to electron withdrawing ring substituents does not significantly affect the anomalous n.m.r. response suggests that the source of the anomaly in the disulfane is not likely inductive or electromeric. While there is a very noticeable concentration effect on n.m.r. shifts in the nitrophenylsulfanes as discussed below the signal position for the other phenylsulfanes is not markedly concentration dependant. This argues against the source of the anomaly being intermolecular association between the —SH proton of one sulfane and the shielding (diamagnetic) basal plane of the aromatic ring of a second phenylsulfane molecule. One possible rationalization of the anomalous shift observation is that the —SH proton in the phenyldisulfane is, by virtue of the C—S—SH bond angle, constrained to move on or close to the "zero effect" surface between the paramagnetic (deshielding) and diamagnetic (shielding) regions associated with the aromatic ring (see Fig. 4). Compared with thiophenol, therefore, the —SH proton in the disulfane would be subject to much less deshielding. In the higher sulfanes the increasing number of rotamer conformations and distance of the terminal SH from the ring will markedly reduce any anomalous shift influence. In a sense, the

Can. J. Chem. Downloaded from www.nrcresearchpress.com by 210.87.254.42 on 09/05/12
For personal use only.

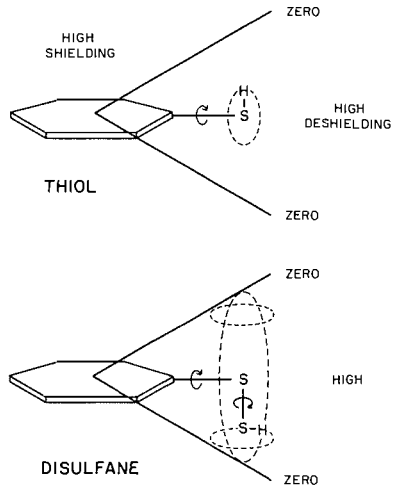

FIG. 4. Anisotropy effects.

apparently anomalous n.m.r. response for the phenyldisulfane is really more a manifestation of "anomalous" deshielding in the parent thiol. The dotted line shown in Fig. 2 represents a graphical interpretation of this suggestion.

In a very recent paper Tsurugi (33) reports the n.m.r. shifts for various benzyl, benzhydryl, and triphenylmethyl sulfanes. The anomalous shift associated with the disulfane is not observed as might be expected due to the insertion of the $-CH_2-$ or $-CH-$ group between the sulfur chain and the ring. The markedly different behavior of the triphenylmethyl sulfane shifts as a function of sulfur chain length is, however, suggested by Tsurugi to be the result of anisotropic factors associated with restricted rotation of the aromatic rings.

The n.m.r. behavior of both the *p*-NO_2 and *o*-NO_2 thiols and sulfanes indicates that these members of the series are significantly different from the other substituted arylsulfanes. The SH proton shift in the *p*-NO_2 case is markedly concentration dependant. The difference between the 1 *M* value and infinite dilution values is 8–10 Hz (0.15 τ). There seems little doubt that intermolecular hydrogen bonding is responsible for this concentration dependence. Confirmation of this conclusion is found in the lack of corresponding proton shift dependence in the *o*-NO_2 case where intramolecular hydrogen bonding would be expected. The added complication of hydrogen bonding, whether intra- or intermolecular, makes it unwise to speculate at this time regarding the relative position of the nitroarylsulfanes in Fig. 3. The anomalous upfield position of the disulfanes relative to the smooth curve prediction noted in the parent, chloro, and methyl substituted series is nonetheless more pronounced in the nitro substituted cases. More extensive examination of the relative roles of hydrogen bonding and conformation effects would be necessary to permit precise analysis of the observed nitro compound shifts but it is unlikely that the upfield shift observed on extending the sulfur chain from one to two atoms is simply an artifact of concentration.

Experimental

Thiols not commercially available were prepared by the standard literature methods indicated below. Each compound was recrystallized or distilled *in vacuo* using a spinning band column just prior to use. All melting points (m.p.) were determined on a Kofler hot stage and are corrected. Boiling points (b.p.) designated by * are converted to pressure used in this work. Some of the thiols were observed to undergo rapid oxidation in the presence of air, particularly in solution. Precautions were therefore taken to minimize contact of the reagent with air.

The work with sulfanes and chlorosulfanes requires special care and cleanliness. All glass apparatus with which these materials come in contact must be thoroughly cleaned with hot chromic acid, carefully dried, and stored in a dust-free atmosphere. All reactions must be protected from moisture and pure starting materials must be used since the intermediates and end products were not purified by distillation due to their very considerable tendency to disproportionate.

Sources of Materials and Reagents

Chlorine (Matheson of Canada Ltd.), was dried and used without further purification. Dichloromonosulfane (sulfenylchloride) (SCl_2) (Hooker Electro Chemical Co.), was stabilized with PCl_3 and redistilled at atmospheric pressure just prior to use. The middle fraction, b.p. 59–60 °C, was employed. Dichlorodisulfane (S_2Cl_2) (Hooker Electro Chemical Co.), was redistilled just prior to use, b.p. 29°C/12 mm. Hydrogen sulfide (Matheson of Canada Ltd.), from a steel cylinder was passed through columns containing $CaCl_2$ and a tube containing P_2O_5, and finally into a container placed in a Dry Ice – acetone bath, where it was condensed and liquefied. The liquefied H_2S was then re-evaporated from this trap into the reaction flask passing through P_2O_5 drying tubes. Carbon disulfide (Fisher Scientific Spectro Grade) was used without further purification. Benzenethiol (Matheson Coleman and Bell) was redistilled before use, b.p. 51–52 °C/12 mm (lit. b.p. 51 °C/12 mm (15)). *p*-Methylbenzenethiol (Aldrich), was recrystallized from ethanol, m.p. 44 °C (lit. m.p. 44 °C (16)). *p*-Chlorobenzenethiol (Matheson Coleman and Bell) was recrystallized from ethanol, m.p. 53–54 °C (lit. m.p. 53–54 °C (17)). *o*-Nitrobenzenethiol was prepared by reduction of the disulfane with glucose and sodium hydroxide following essentially the procedure of Claasz (18). Yield 60% m.p. 57–58° (lit. m.p. 57–58 °C (18)). *p*-Nitrobenzenethiol

Can. J. Chem. Downloaded from www.nrcresearchpress.com by 210.87.254.42 on 09/05/12
For personal use only.

Can. J. Chem. Downloaded from www.nrcresearchpress.com by 210.87.254.42 on 09/05/12
For personal use only.

was prepared in the same manner as the *o*-isomer. Yield 63%, m.p. 77–78 °C (lit. m.p. 77 °C (19)). 2,2′-Dinitrodiphenyldisulfane was prepared by a procedure based on that of R. Möhlau *et al.* (20) from *o*-chloronitrobenzene and sodium disulfide in refluxing ethanol. Yield 64%, m.p. 195 °C (from CH_3CO_2H) (lit. m.p. 195 °C (20)). 4,4′-Dinitro-diphenyldisulfane was prepared from *p*-chloronitrobenzene and sodium disulfide in refluxing ethanol as described by Zinke and Lenhardt (21). Yield 75%, m.p. 181 °C (lit. m.p. 181 °C (21)). Diphenyldisulfane. Benzenethiol in aqueous NH_3 was oxidized with air following the procedure of Steinkopf and Müller (22). Yield 76%, m.p. 61–61.5 °C (lit. m.p. 61.5 °C (22)). Diphenyltrisulfane: the compound was prepared by the method of Chakravarti (23) and recrystallized from ether. Yield 36%, m.p. 28–30 °C (lit. m.p. 30 °C (24)). Diphenyltetrasulfane: following essentially the procedure of Lecher and Holzschneider (25) benzenethiol in dry ether was treated with the calculated amount of S_2Cl_2 to yield the tetrasulfide in 87% yield as crude product. Recrystallization from ether gave pure product, m.p. 33–34 °C (lit. m.p. 34–35 °C (25)). 4,4′-Dimethyl-diphenyltrisulfane was prepared by the same procedure used for diphenyltrisulfane. Recrystallization from acetic acid gave pure product, m.p. 81 °C (lit. m.p. 81–82 °C (16)). 4,4-Dimethyl-diphenyltetrasulfane in the crude form was prepared in the above way (25) in 90% yield and was recrystallized from ethanol, m.p. 75 °C (lit. m.p. 75 °C (26)).

Arylchlorosulfanes

Arylchloromonosulfanes (ArSCl)

The aromatic chloromonosulfanes were synthesized by means of two essentially similar methods involving the interaction of elemental chlorine with the thiols or diaryldisulfanes. The halogenation was conducted at relatively low temperatures under anhydrous conditions in solvents such as CS_2 and CCl_4.

Phenylchloromonosulfane—This was prepared by a slight modification of the method of Lecher and Holzschneider (27). A solution of 5 g freshly distilled thiophenol in 50 ml dry CS_2 was added dropwise under stirring into 150 ml dry CS_2 kept at −5 °C through which a slow current of chlorine dried with sulfuric acid was passed. After evaporating the solvent the product was obtained by fractionating *in vacuo*. Yield 90%, b.p. 78–80 °C/12 mm (lit. b.p. 78–80 °C/12 mm (27)).*

p-Methylphenylchloromonosulfane—This was prepared from *p*-methyl-thiophenol and chlorine at −10 °C as described under the preparation of phenylchloromonosulfane. Yield 80%, b.p. 63–66 °C/1 mm (lit. b.p. 64–66 °C/1 mm (28)).

p-Chlorophenylchloromonosulfane—This compound was prepared from *p*-chlorothiophenol and chlorine as described under the preparation of phenylchloromonosulfane. Yield 82%, b.p. 50–51 °C/0.03 mm (lit. b.p. 50 °C/0.03 mm (29)).

p-Nitrophenylchloromonosulfane—This was prepared from the disulfide and chlorine in CCl_4 at 50–60 °C following the procedure of Zinke and Lenhardt (21). Yield 83%, m.p. 52 °C (lit. m.p. 52 °C (21)).

o-Nitrophenylchloromonosulfane—This was prepared in the same manner as the *p*-isomer above. Yield 70%, m.p. 75 °C (lit. m.p. 75 °C (30)).

Arylchlorodi- and Arylchlorotrisulfanes (ArS_2Cl, ArS_3Cl)

Except for slight variations, each compound was prepared in the same way by reacting an excess of the chloromono- or chlorodisulfane with the corresponding thiol, followed by evaporation of the solvent and of the excess reactant.

General Procedure—A 300 ml, three-necked round-bottomed flask was fitted with a low-temperature thermometer, magnetic stirrer, addition funnel, and condenser. Freshly distilled SCl_2 or S_2Cl_2 was placed in the flask and cooled to −70 °C. Under conditions of careful exclusion of moisture the thiol, dissolved in CS_2, was added dropwise to the chlorosulfane as slowly as was practicable. It was generally found that the more slowly the thiol was added to the chlorosulfane the better the yield. Stirring was continued for 30 min and the mixture then allowed to warm to room temperature. The excess of SCl_2 (or S_2Cl_2) and the solvent were removed by evaporation at reduced pressure and the last traces in high vacuum. The molar ratio of the thiol to chlorosulfane was between 1:20 and 1:30.

Arylchlorodi- and arylchlorotrisulfanes thus prepared were used immediately without further purification.

Arylsulfanes ($Ar—S_xH$)

General Procedure

The reaction was carried out in a 300 ml, two-necked round-bottomed flask, provided with a low-temperature thermometer, addition funnel, Dry Ice condenser, and a magnetic stirrer.

Hydrogen sulfide gas was purified and dried as described above and distilled into the reaction flask, passing through $CaCl_2$ and P_2O_5 tubes. The reaction flask was cooled with a Dry Ice – acetone bath and the gas thus liquefied. The arylchlorosulfane, dissolved in CS_2 was carefully added drop by drop over a period of time under vigorous stirring to the liquefied H_2S, the temperature being maintained at −70 °C. After stirring at −70 °C for 1 h, the excess H_2S was slowly evaporated. The last traces were removed under reduced pressure. The desired product was generally a clear yellow oily liquid. The products were analyzed by n.m.r. and by iodometric titration.

Phenyldisulfane—Following the above method 2.88 g (0.02 mol) of phenylchloromonosulfane and 140 g (4 mol) hydrogen sulfide yielded 2.78 g (95%) product. This was oxidized by iodine and gave diphenyltetrasulfane, m.p. 33–34 °C, mixed m.p. with an authentic sample 33–34 °C. The n.m.r. spectrum showed one sulfhydryl proton at 6.62 τ (—SH) and five aromatic protons at 2.68 τ (center of the multiplet). The product contained also 8% contamination of $C_6H_5S_3H$ as determined by n.m.r. Iodometric titration Calcd. for 0.2482 g substance: 17.45 ml 0.1 *N* I_2. Found: 16.96 ml.

p-Methylphenyldisulfane—In the above way there was obtained 3.10 g (98%) of disulfane from 3.17 g (0.02 mol) of *p*-methylchloromonosulfane and 140 g (4 mol) hydrogen sulfide. The product was oxidized by iodine and gave 4,4′-dimethyldiphenyltetrasulfane, m.p. 75 °C, mixed m.p. with an authentic sample 75 °C. The n.m.r. spectrum showed three methyl protons at 7.70 τ, one sulfhydryl proton at 6.61 τ (—SH), and four aromatic protons at 2.83 τ (center of the multiplet). N.m.r. indi-

Can. J. Chem. Downloaded from www.nrcresearchpress.com by 210.87.254.42 on 09/05/12
For personal use only.

cated that the product contained 12% p-$CH_3C_6H_4S_3H$. Iodometric titration Calcd. for 0.2362 g substance: 15.12 ml 0.1 N I_2. Found: 14.75 ml.

p-Chlorophenyldisulfane—From 3.58 g (0.02 mol) *p*-chlorophenylchlorosulfane and 140 g (4 mol) hydrogen sulfide, 3.46 g (98%) of product was obtained. The n.m.r. spectrum showed one sulfhydryl proton at 6.53 τ (—SH) and four aromatic protons at 2.84 τ (center of the multiplet). Iodometric titration Calcd. for 0.2031 g substance: 11.49 ml 0.1 N I_2. Found: 11.40 ml.

p-Nitrophenyldisulfane—From 3.80 g (0.02 mol) *p*-nitrophenylchlorosulfane and 140 g (4 mol) hydrogen sulfide, 3.50 g (94%) of product was obtained. The n.m.r. spectrum showed one sulfhydryl proton at 6.42 τ (—SH) and four aromatic protons at 2.04 τ (center of the multiplet). N.m.r. indicated that the product was greater than 99% disulfane. Iodometric titration Calcd. for 0.2851 g substance: 15.23 ml 0.1 N I_2. Found: 15.11 ml.

o-Nitrophenyldisulfane—From 2.0 g (0.01 mol) *p*-nitrophenylchlorosulfane was 70 g (2 mol) hydrogen sulfide, 1.56 g (79%) of product was obtained. The n.m.r. spectrum showed one sulfhydryl proton (—SH) at 6.81 τ and four aromatic protons at 2.25 τ (center of the multiplet). N.m.r. indicated that the product was greater than 99% disulfane. Iodometric titration Calcd. for 0.3064 g substance: 16.36 ml 0.1 N I_2. Found: 16.49 ml.

Phenyltrisulfane—From 1.8 g (0.01 mol) phenylchlorodisulfane and 105 g (3 mol) hydrogen sulfide, 1.60 g (90%) of product was obtained. This was allowed to react with phenylchloromonosulfane and gave diphenyltetrasulfane, m.p. 33–34 °C, mixed m.p. with an authentic sample 33–34 °C. The n.m.r. spectrum showed sulfhydryl proton resonance at 6.11 τ (—SH) and aromatic protons at 2.74 τ (center of the multiplet). N.m.r. indicated that the product was 82.2% phenyltrisulfane and 17.8% phenyldisulfane. Iodometric titration Calcd. for 0.2671 g: 15.34 ml 0.1 N I_2. Found: 15.98 ml.

p-Methylphenyltrisulfane—From 2.30 g (0.012 mol) *p*-methylchlorodisulfane and 110 g (3.4 mol) hydrogen sulfide, 2.18 g (96%) of product was obtained. This was allowed to react with *p*-methylchloromonosulfane and gave 4,4′dimethyl-diphenyltetrasulfane, m.p. 75 °C, mixed m.p. with an authentic sample 75 °C. The n.m.r. spectrum showed sulfhydryl proton resonance at 6.18 τ (—SH) and aromatic protons at 2.82 τ (center of the multiplet). N.m.r. indicated that the product was 84.1% *p*-methyltrisulfane and 15.9% *p*-methyldisulfane. Iodometric titration Calcd. for 0.2605 g substance: 13.84 ml 0.1 N I_2. Found: 14.32 ml.

Phenyltetrasulfane—Freshly prepared phenylchlorotrisulfane 2 g (0.01 mol) and 70 g (2 mol) hydrogen sulfide yielded 1.5 g (73%) of product. The n.m.r. spectrum showed sulfhydryl proton resonance at 6.02 τ ($—S_4H$), at 6.11 τ ($—S_3H$), and aromatic protons at 2.62 τ (center of the multiplet). The material contained 60% phenyltetrasulfane and 40% phenyltrisulfane as analyzed by n.m.r. Iodometric titration Calcd. for 0.2541 g substance: 12.31 ml 0.1 N I_2. Found: 9.41 ml.

p-Methylphenyltetrasulfane—From 4.2 g (0.02 mol) *p*-methylphenylchlorotrisulfane and 70 g (2 mol) hydrogen sulfide, 3.2 g (80%) of product was obtained. N.m.r. indicated that the material contined 59% *p*-methylphenyltetrasulfane, sulfhydryl proton resonance at 6.07 τ ($—S_4H$), and 41% *p*-methylphenyltrisulfane, sulfhydryl proton resonance at 6.18 τ (S_3H). The aromatic protons are observed at 2.89 τ (center of the multiplet). Iodometric titration Calcd. for 0.1963 g substance: 8.91 ml 0.1 N I_2. Found 9.41 ml.

Chemical Analysis

For the determination of the arylsulfanes the iodometric method of Böhme and Zinner (3) was employed.

Procedure

The sample 0.10–0.20 g was weighed in a small weighing pipette and dissolved in 20 ml carbon disulfide. An excess of a standard solution of iodine was added and the mixture immediately shaken. Since the titration of the iodine with thiosulfate requires a long time, a back-titration method was adopted, an excess of thiosulfate being first added and the excess then determined by means of a 0.1 N I_2 solution to the starch end point.

Nuclear Magnetic Resonance Analysis

A Varian A-60 high-resolution n.m.r. spectrometer was used to analyze the reaction products. The n.m.r. spectra were determined at 35 °C (probe temperature) using TMS as internal standard. Chemical shifts are given on the τ scale in p.p.m. relative to TMS (τ = 10.00). The chemical shifts for the sulfhydryl and the phenyl protons taken at the center of the multiplet structure are presented in Table 2. Relative areas determined by cutting out tracings of the spectra or counting squares yielded a quantitative measure of relative concentrations of aromatic and sulfhydryl protons of the various sulfanes.

1. F. Fehér and G. Winkhaus, Z. Anorg. Allgem. Chem. **293**, 302 (1958).
2. S. Kawamura, T. Horii, and J. Tsurugi. J. Org. Chem. **36**, 3677 (1971).
3. H. Böhme and G. Zinner. Ann. Chem. **585**, 142 (1954).
4. H. Schmidbaur, M. Schmidt, and W. Siebert. Chem. Ber. **97**, 3374 (1964).
5. (*a*) J. B. Hyne, E. Muller, and T. K. Wiewiorowski. J. Phys. Chem. **70**, 3733 (1966); (*b*) H. J. Langer and J. B. Hyne. Adv. Chem. Ser. **110**, 113 (1972).
6. D. N. Harpp and D. K. Ash. Int. J. Sulfur Chem. A, **1**, 211 (1972) and refs. therein.
7. E. Muller and J. B. Hyne. Can. J. Chem. **46**, 2341 (1968).
8. F. Fehér, W. Laue, and G. Winkhaus. Z. Anorg. Allgem. Chem. **288**, 113 (1956).
9. T. Nakabayashi and J. Tsurugi. J. Org. Chem. **28**, 813 (1963).
10. T. L. Pickering, K. J. Saunders, and A. V. Tobolsky. *In* The chemistry of sulfides. *Edited by* A. V. Tobolsky. Interscience Publishers, New York, N.Y. 1968.
11. E. Muller and J. B. Hyne. J. Am. Chem. Soc. **91**, 1907 (1969).
12. S. H. Marcus and S. I. Miller. J. Phys. Chem. **68**, 331 (1964).
13. J. R. Van Wazer and D. G. Grant. J. Am. Chem. Soc. **86**, 1450 (1964).
14. E. Muller and J. B. Hyne. Can. J. Chem. **46**, 3587 (1968).

15. H. BÖHME and J. WAGNER. Chem. Ber. **75**, 606 (1942).
16. Beilsteins Handbuch der Organischen Chemie, **6**, E 111, 1391 (1966).
17. R. OTTO. Ann. Chem. **143**, 100 (1867).
18. M. CLAASZ. Chem. Ber. **45**, 2424 (1912).
19. L. GATTERMANN. Ann. Chem. **393**, 230 (1912).
20. R. MÖHLAU, H. BEYSCHLAG, and H. KÖHRES. Chem. Ber. **45**, 131 (1912).
21. T. ZINKE and S. LENHARDT. Ann. Chem. **400**, 1 (1913).
22. W. STEINKOPF and S. MÜLLER. Chem. Ber. **56**, 1926 (1923).
23. G. CH. CHAKRAVARTI. J. Chem. Soc. **123**, 964 (1923).
24. Beilsteins Handbuch der Organischen Chemie, **6**, E 111, 1047 (1965).
25. H. LECHER and F. HOLZSCHNEIDER. Chem. Ber. **58**, 417 (1925).
26. P. KLASON. Chem. Ber. **20**, 3413 (1887).
27. H. LECHER and F. HOLZSCHNEIDER. Chem. Ber. **57**, 755 (1924).
28. H. LECHER, F. HOLZSCHNEIDER, K. KÖBERLE, N. SPEER, and P. STOCKLIN. Chem. Ber. **58**, 409 (1925).
29. E. GEBAUER-FÜLNEG. J. Am. Chem. Soc. **49**, 2270 (1927).
30. T. ZINKE. Chem. Ber. **44**, 769 (1911).
31. H. WIESER, P. J. KRUEGER, E. MULLER, and J. B. HYNE. Can. J. Chem. **47**, 1633 (1969).
32. R. BICCA DE ALENCASTRO and C. SANDORFY. Can. J. Chem. **50**, 3594 (1969).
33. J. TSURUGI. Int. J. Sulfur Chem. B **7**, 199 (1972).

Can. J. Chem. Downloaded from www.nrcresearchpress.com by 210.87.254.42 on 09/05/12
For personal use only.

Phosphates d'énols-X. Détermination des isomères géométriques diversement substitués par résonance magnétique nucléaire

EMILE M. GAYDOU

Institut Universitaire de Technologie de Marseille-Nord, Rue des Géraniums, 13337 Marseille Cedex 3, France

Reçu le 28 mars

La configuration des phosphates énoliques *E* et *Z*, substitués sur le premier atome de carbone de la double liaison, a été déterminée dans 27 cas, en utilisant les constantes de couplage $^4J_{POC=C-H}$ et les constantes d'écran selon la méthode de Tobey-Pascual. Les facteurs qui influencent les constantes de couplage $^4J_{POC=C-H}$ et $^5J_{POC=C-CH_3}$ sont discutés.

The *E* and *Z* configuration of enol phosphates substituted on the first carbon of the double bond are determined, in 27 cases, using $^4J_{POC=C-H}$ coupling constants and the Tobey-Pascual substituent shielding constants method. The factors influencing $^4J_{POC=C-H}$ and $^5J_{POC=C-CH_3}$ coupling constants are discussed.

Can. J. Chem., **51**, 3412 (1973)

Introduction

L'étude en r.m.n. de phosphates d'énols substitués sur le carbone 1 a fait l'objet de quelques travaux (1–4). L'absence d'une constante de couplage $^3J_{HH}$ *cis* ou *trans* sur la double liaison de l'enchaînement énolique rendait difficile l'identification des isomères *E* et *Z* résultant de la réaction de Perkow (30) (schéma 1).

Par ailleurs, la valeur absolue de la constante de couplage $^4J_{PH}$ variable suivant la nature de R′, rend l'interprétation des résultats assez délicate. Certains auteurs comme Cohn *et al.* (4) et Stubbe et Kenyon (3) ont utilisé les constantes de couplage $^{13}C^1H$ pour résoudre leurs problèmes. Borowitz *et al.* (2) se heurtent à certaines difficultés en utilisant la méthode de Tobey (5) et Pascual *et al.* (6) pour identifier les isomères *E* et *Z*. Nous avons étudié par r.m.n. du ^1H et du ^{31}P une série de phosphates d'énols substitués sur le carbone 1 (tableau 1). La discussion des constantes de couplages $^4J_{PH}$ nous permettra d'avoir une idée des conformations possibles dans cette série de phosphates. Bothner-By et Trautwein (11) ont montré que la constante de couplage $^3J_{POCH}$ dépend de l'angle dièdre formé par les quatre atomes P, O, C, H. Cette dépendance est similaire à la relation bien connue de Karplus (12). Dans le cas de notre série, nous ne pouvons tenir compte que de la constante $^4J_{POCCH}$.

Avec les hétérocycles contenant un atome de phosphore (10, 13–15, 45), il apparait que la constante $^4J_{POCCH}$ peut prendre des valeurs comprises entre 0 et 6 Hz. Avec les composés en libre rotation, ces constantes sont généralement inférieures à 1 Hz (18 à 22). Dans le cas des phosphates d'énols les constantes $^4J_{POCCH}$ peuvent être de trois types:

(*a*) $^4J_{P-O-\underset{\underset{C}{\diagup\diagdown}}{C}=C-H}$ on notera $^4J_{POCCH\ I}$

(*b*) $^4J_{P-O-\underset{|}{C}=\underset{|}{C}-H}$ on notera $^4J_{POCCH\ II}$ cisoïde

(*c*) $^4J_{P-O-\underset{|}{C}=\underset{|}{C}-H}$ on notera $^4J_{POCCH\ II}$ transoïde

La constante $^4J_{POCCH\ I}$ de type isopropylidénique (7, 17) dépend de deux contributions dues aux électrons π et σ. Peu d'études ont été effectuées dans ce sens à l'exclusion de celles de Stiles *et al.* (1). Les constantes de couplage $^4J_{POCCH\ II}$, de type allylique, peuvent prendre des valeurs positives ou négatives suivant l'importance des contributions π et σ comme nous l'avons montré précédemment (51) et par voie de

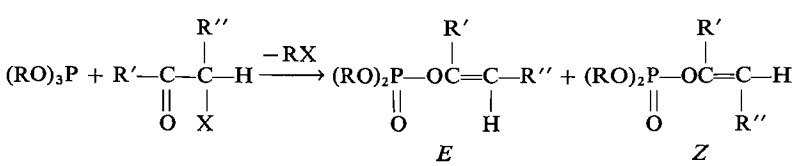

SCHÉMA 1

Can. J. Chem. Downloaded from www.nrcresearchpress.com by 210.87.254.5 on 09/05/12
For personal use only.

TABLEAU 1. Phosphates d'énols étudiés

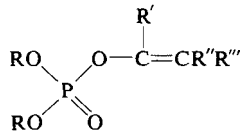

Composé	R	R′	R″	R‴
1	CH_3	CH_3	H	H
2	C_2H_5	CH_3	H	H
3	n-C_4H_9	CH_3	H	H
4	C_6H_5	CH_3	H	H
5	CH_3	CH_3	H	CH_3
6	C_2H_5	CH_3	H	C_6H_5
7	CH_3	CH_3	H	C_6H_5
8	CH_3	CH_3	H	CO_2CH_3
9	CH_3	CH_3	H	Br
10	CH_3	C_6H_5	H	H
11	C_2H_5	C_6H_5	H	H
12	C_6H_5	C_6H_5	H	H
13	C_2H_5	C_6H_5	H	CH_3
14	C_2H_5	C_6H_5	H	Cl
15	CH_3	C_6H_5	H	Br
16	C_2H_5	C_6H_5	H	C_6H_5
17	C_2H_5	C_6H_5	H	$CO_2C_2H_5$
18	H	COOH	H	H
19	CH_3	$COOCH_3$	H	CH_3
20	CH_3	COOH	H	Br
21	CH_3	C_2H_5	H	H
22	CH_3	CH_2—CH_2—CH_2—CH_2		H
23	C_2H_5	CH_2—CH_2—CH_2—CH_2		H
24	C_2H_5	CH_2—CH_2—CH_2—CH_2—CH_2		H
25	C_2H_5	CH_2—CH_2—CH_2		H
26	C_2H_5	OCH_3	Cl	Cl
27	CH_3	CH_2Br	H	H

conséquence, la valeur absolue de ces constantes pourra varier de manière considérable.

Résultats

Les résultats sont presentés en fonction de la nature des substituants sur le carbone 1.

Phosphates d'énols comportant un groupement méthyle sur le carbone 1

Isopropenylphosphates

Nous sommes en présence d'un système du type A_3KLX dans lequel le phosphore (X) intervient comme perturbation du premier ordre. Ce système a été résolu à l'aide d'une version modifiée (9) du programme LAOCOON III (23). L'attribution des différents types de protons peut se faire assez aisément. En effet, le proton en position cisoïde par rapport au groupement phosphate est nettement déblindé car il forme une liaison hydrogène partielle, intramoléculaire, que l'on peut mettre en évidence en élevant la température (fig. 1). Le proton en position transoïde a

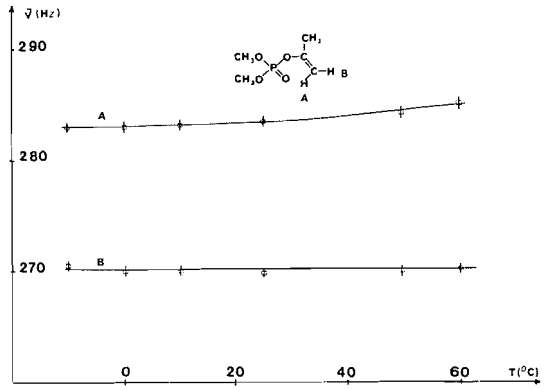

FIG. 1. Influence de la température sur le déplacement chimique des protons vinyliques du composé **1**.

tendance à s'associer pour former des liaisons intermoléculaires que l'on peut atténuer en diminuant la concentration (fig. 2).

L'ensemble des valeurs obtenues est rassemblé dans le tableau 2. On peut remarquer que la

Can. J. Chem. Downloaded from www.nrcresearchpress.com by 210.87.254.5 on 09/05/12
For personal use only.

TABLEAU 2. Caractéristiques r.m.n. de

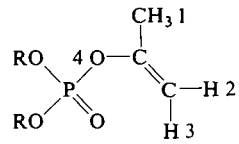

Composé	R	δ10⁶* 1	2	3	δP†	|J| (Hz) 12	13	23	14	24	34
1	CH_3	1.93 ±0.01	4.50 ±0.01	4.90 ±0.01	4.89	1.11 ±0.04	0.01 ±0.03	1.46 ±0.05	0.64 ±0.06	0.07 ±0.08	2.20 ±0.08
2	C_2H_5	1.92 ±0.01	4.48 ±0.01	4.88 ±0.01	6.98	1.22 ±0.04	0.01 ±0.04	1.14 ±0.06	0.48 ±0.08	0.03 ±0.09	2.42 ±0.09
3	*n*-C_4H_9	1.91 ±0.02	4.47 ±0.02	4.87 ±0.02	6.76	1.17 ±0.08	0.07 ±0.06	1.48 ±0.07	0.59 ±0.07	0.03 ±0.08	2.42 ±0.08
4	C_6H_5	1.87 ±0.01	4.51 ±0.01	4.90 ±0.01	18.30	1.15 ±0.03	0.01 ±0.03	1.61 ±0.08	0.65 ±0.06	0.01 ±0.08	2.80 ±0.06

*En p.p.m. par rapport au TMS pris comme référence interne.
†En p.p.m. par rapport à H_3PO_4 à 85% pris comme référence externe (enrigestré à 40.5 MHz).

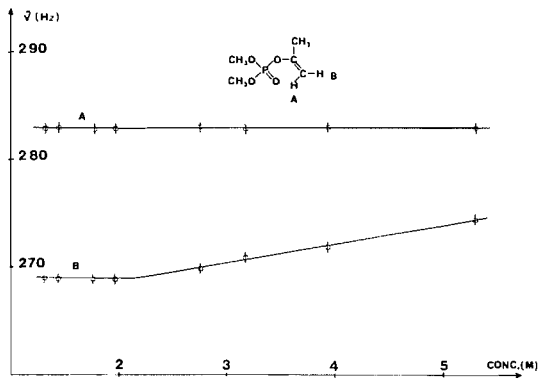

FIG. 2. Influence de la concentration sur le déplacement chimique des protons vinyliques du composé **1**.

constante de couplage allylique cisoïde $^4J_{H_1H_2}$ est systématiquement très supérieure à la constante de couplage allylique transoïde $^4J_{H_1H_3}$. Ce phénomène a d'ailleurs déjà été observé dans le cas du propène (24) des halogéno-2 propènes (25, 26), du phényl-2 propène (27), du méthyl-3 butenyne (28), de l'acrylonitrile (31), etc. Par analogie avec l'étude de Barfield et Chakrabarti (7), on peut penser que ces constantes de couplages sont négatives. En ce qui concerne les constantes $^4J_{POCCH\ I}$ et $^4J_{POCCH\ II}$ cisoïde et transoïde, la nature du groupement R (tableau 2) n'influe pas beaucoup sur les valeurs de ces constantes de couplages. Il est à noter que la présence du groupement méthyle sur le carbone 1a, par contre, une très grosse influence sur la valeur absolue de $^4J_{POCCH\ II}$ cisoïde et transoïde puisque dans le cas du vinylphosphate diméthylique, on a (51)

$$^4J_{POCCH\ II}\ \text{cisoïde} = 1.14 \pm 0.1\ \text{Hz}$$

$$^4J_{POCCH\ II}\ \text{transoïde} = 2.85 \pm 0.1\ \text{Hz}$$

Il n'a pas été possible d'obtenir une variation de la constante de couplage $^4J_{POCCH}$ mesurable dans le cas du composé **1** lorsque l'on fait varier la température de -40 à $+150$ °C dans l'hexachlorobutadiène.

Phosphates d'énols comportant un groupement méthyle sur le carbone 1 et un autre groupement sur le carbone 2

Il est possible d'envisager dans ces conditions deux isomères géométriques *E* et *Z* (29). La

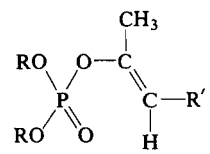

E

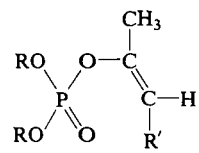

Z

réaction de Perkow (2, 30) n'étant pas absolument stéréospécifique, il était assez difficile d'identifier l'isomère *E* ou *Z*, sans faire une analyse approfondie du spectre r.m.n.

Nous avons rassemblé dans le tableau 3 quelques exemples de phosphates énoliques de ce type, où nous avons fait varier le groupement R′. Les paramètres relatifs au composé **8** sont ceux fournis par Stiles et coll. (1). On peut remarquer que la constante $^4J_{HH}$ allylique cisoïde

Can. J. Chem. Downloaded from www.nrcresearchpress.com by 210.87.254.5 on 09/05/12
For personal use only.

Can. J. Chem. Downloaded from www.nrcresearchpress.com by 210.87.254.5 on 09/05/12
For personal use only.

TABLEAU 3. Caractéristiques r.m.n. de

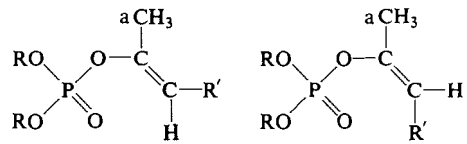

E *Z*

Composé	R	R′	δ10⁶(TMS) P*	a	H_E	H_Z	R	R′	|J| (Hz) $^4J_{POCCH\ I}$	$^4J_{POCCH\ II}$ cisoïde	$^4J_{POCCH\ II}$ transoïde	$^3J_{POCH}$	$^4J_{HCCCH_3}$
1	CH_3	H	4.90	1.93	4.90	4.50	3.78	—	0.65	2.2	0.1	11.5	*trans* ~0 *cis* 1.1
5*E*	CH_3	CH_3	4.24	1.88	5.21	—	3.70	1.60	1.8	2.4		11.5	1.0
5*Z*	CH_3	CH_3	3.94	1.86	—	4.79	3.74	1.60	~0	—	~0.5	11.5	1.1
6*E*	CH_3	C_6H_5		2.07	6.43	—	3.78	7.24	0.5	2.6	—	11.5	1.0
6*Z*	CH_3	C_6H_5		2.15	—	5.65	3.80	7.24	1.5	—	0.7	11.5	1.0
7*E*	C_2H_5	C_6H_5		2.08	6.44	—	4.16(CH_2)	7.26	0.5	2.6		9.0	1.0
7*Z*	C_2H_5	C_6H_5		2.18	—	5.68	4.16(CH_2)	7.26	1.5	—	0.8	9.0	1.0
8*E*†	CH_3	CO_2CH_3	5.90‡	2.36	5.76	—	3.82	3.68	~0	1.8	—	11.4	0.9
8*Z*†	CH_3	CO_2CH_3	5.90‡	2.15	—	5.47	3.88	3.65	1.6	—	0.9	11.4	0.9
9*E*	CH_3	Br	4.57	2.08	6.11	—	3.78	—	1.0	2.4	—	11.3	1.2
9*Z*§	CH_3	Br	4.57	2.07	—	5.62	3.82	—	1.5	—	0.9	11.5	1.5

*Par rapport à H_3PO_4 à 85% pris comme référence externe.
†Référence 1.
‡Référence 49.
§Obtenu par action du NBP (réf. 8).

Can. J. Chem. Downloaded from www.nrcresearchpress.com by 210.87.254.5 on 09/05/12
For personal use only.

TABLEAU 4. Caractéristiques r.m.n. de

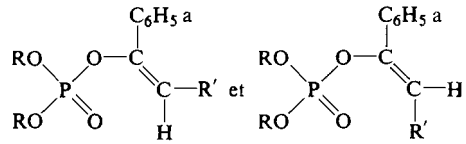

E *Z*

Composé	R	R′	δ10⁶(TMS) P*	a (multiplet)	H_E	H_Z	R		$\lvert J\rvert$ (Hz) $^4J_{POCCH\ II}$ cisoïde	$^4J_{POCCH\ II}$ transoïde	$^3J_{POCH}$
10	CH_3	H	4.22	7.44	5.21		3.75	—	~2.3		11.5
11	C_2H_5	H	10.0	7.40	5.25		4.11(CH_2)	1.25(CH_3)	~2.4		8.0
12	C_6H_5	H	17.8	7.45	5.22		7.20	—	2.4		—
13*E*	C_2H_5	CH_3		7.40	5.77	—	4.15(CH_2)	1.23(CH_3)	2.8	—	8.5
13*Z*	C_2H_5	CH_3		7.40	—	5.60	4.16(CH_2)	1.25(CH_3)	—	2.5	8.5
14*E*	C_2H_5	Cl		7.35	6.45	—	4.14(CH_2)	1.24(CH_3)	2.8	—	9.0
14*Z*	C_2H_5	Cl		7.35	—	6.13	4.14(CH_2)	1.24(CH_3)	—	2.3	9.0
15*E*	CH_3	Br	4.25	7.20	6.45	—	3.65	—	2.8	—	11.5
15*Z*	CH_3	Br	4.75	7.20	—	6.22	3.65	—	—	1.9	11.5
16*E*	C_2H_5	C_6H_5		7.40	6.69	—	4.15(CH_2)	1.25(CH_3)	2.5	—	8.5
16*Z*	C_2H_5	C_6H_5		7.40	—	6.33	4.15(CH_2)	1.25(CH_3)	—	1.0	8.5
17*E*†	C_2H_5	$CO_2C_2H_5$			6.09	—			2.0	—	
17*Z*†	C_2H_5	$CO_2C_2H_5$			—	5.85			—	2.0	

*Par rapport à H_3PO_4 à 85% pris comme référence externe.
†Référence 46.

Can. J. Chem. Downloaded from www.nrcresearchpress.com by 210.87.254.5 on 09/05/12
For personal use only.

est sensiblement égale à $^4J_{HH}$ allylique transoïde, pour R′ ≠ H, dans la plupart des cas. Ce phénomène est analogue à celui observé dans le cas de l'isobutène (26), du méthylvinyléther (32), de l'isoprène (33), etc. Le proton vinylique dans le cas du vinylphosphate *E* est systématiquement plus déblindé que dans le cas du vinylphosphate *Z* correspondant. La constante de couplage $^4J_{POCCH\ I}$ est variable et comprise entre 0 et 1.6 Hz. Nous avons déjà signalé (53), dans le cas du diméthyl-4,5 oxo-2 méthoxy-2 dioxaphosphole-1,3,2 (**28**), que la constante $^4J_{POCCH\ I} \sim 0$. La constante $^4J_{POCCH\ II}$ transoïde est faible et toujours inférieure à 1 Hz. La constante $^4J_{POCCH\ II}$ cisoïde est toujours supérieure à $^4J_{POCCH\ II}$ transoïde et sa valeur oscille entre 1.8 et 2.6 Hz.

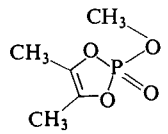

28

Phosphates d'énols comportant un groupement phényle sur le carbone 1

Borowitz *et al.* (2) ont essayé, sans succès, par différentes méthodes, d'obtenir un dérivé phénylé sur le carbone 1 suivant une réaction stéréospécifique. Lorsque l'on est en présence des deux isomères *E* et *Z*, ce sont les spectres les plus difficiles à interpréter car les constantes de couplage sont élevées dans les deux cas. Par exemple avec le bromo-2 phényl-1 vinylphosphate diméthylique (**15**) (tableau 4), la constante

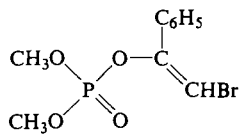

15

de couplage $^4J_{POCCH\ II}$ vaut 1.9 et 2.8 Hz suivant l'isomère considéré.

Il paraît délicat de faire un choix dans ces conditions, compte tenu des résultats précédemment obtenus en ce qui concerne les phosphates d'énols non substitués sur le carbone 1 (9, 51) et substitués par un groupement méthyle. Par contre, dans tous les cas précédemment cités, le proton en position cisoïde par rapport au groupement phosphate, est nettement plus déblindé que le proton en position *trans*. Si l'on se base sur ce phénomène, il est possible de distinguer les deux isomères **15***E* et *Z* et l'on peut faire l'attribution suivante:

$^4J_{POCCH\ II}$ cisoïde = 2.8 Hz

$^4J_{POCCH\ II}$ transoïde = 1.9 Hz

Cette hypothèse est confirmée par les travaux de Stubbe (3). Cet auteur résout le problème de l'identification des composés *E* et *Z* en utilisant les constantes $^{13}C^1H$. En effet, l'action du triméthylphosphite sur l'oxo-2 bromo-3 butanoate (^{13}C-1) de méthyle conduit au mélange des phosphates d'énols **19***E* et *Z* correspondant (schéma 2).

On sait, par ailleurs, que $^3J_{^{13}CCCH}$ *cis* est inférieure à $^3J_{^{13}CCCH}$ *trans* (34). Il est donc possible, dans ces conditions, de discerner sans ambiguité les isomères *E* et *Z* (tableau 5). La variation des constantes de couplage $^4J_{POCCH\ II}$ du composé **19** est du même ordre de grandeur que celle du composé **15**. D'autre part, les travaux de Marecek et Griffith (46) confirment notre hypothèse en ce qui concerne le blindage des protons β vinyliques. En effet, ils arrivent à obtenir sélectivement le diéthyl phosphate énolique **17***Z* ou **17***E* suivant le schéma 3. Le composé **17***Z* pouvait conduire, par ailleurs, au phosphate énolique **29**. Il est à remarquer que, dans le composé **29**, la valeur obtenue par Marecek et Griffith (46) en ce qui concerne la constante de couplage $^4J_{POCCH\ II}$ transoïde est plus faible. Ceci s'explique très bien par le fait que la contribution due aux électrons π est peu importante compte tenu de la géométrie de cette molécule.

Nous avons rassemblé dans le tableau 4, les principaux résultats relatifs aux phosphates

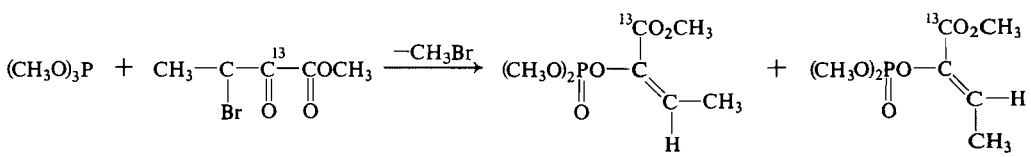

19*E* **19***Z*

SCHÉMA 2

TABLEAU 5. Caractéristiques r.m.n. (3) de

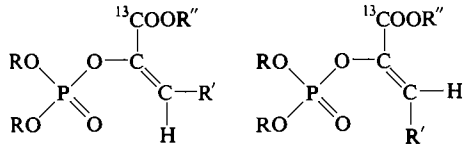

E *Z*

Composé	R	R′	R″	δ10⁶† H_E	δ10⁶† H_Z	|J| (Hz) $^4J_{PH\,II}$ *cis*	|J| (Hz) $^4J_{PH\,II}$ *trans*	|J| (Hz) $^3J\,13C1_H$ *cis*	|J| (Hz) $^3J\,13C1_H$ *trans*
18	H	H	H	5.33	5.15	1.15	1.45	3.1	9.2
19	CH_3	CH_3	CH_3	6.52	6.82	2.8	1.9	2.9	9.5±0.5
20	CH_3	Br	H	7.03	7.27	2.4	1.7		

*Référence 4.
†Par rapport au TMS.

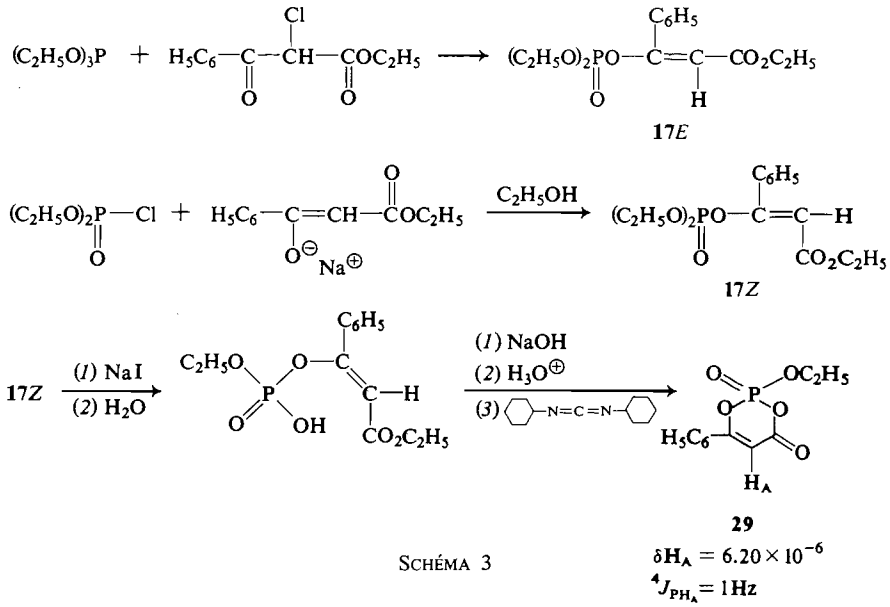

SCHÉMA 3

énoliques comportant un groupement phényle sur le carbone 1. Dans le cas des composés **10** et **11** (R′ = H), il est possible, par élévation de température, de simplifier le système vinylique et d'obtenir un doublet (fig. 3). Dans le cas du composé **12**, le doublet est obtenu à température ambiante. La description et l'étude sommaire en r.m.n. du ^1H effectuée par Tidwell *et al.* (44) montrent que ce phénomène est également observé dans le cas d'une série de α-arylvinylphosphates diéthyliques para et métasubstitués. Une étude approfondie de ce phénomène fera l'objet d'un mémoire ultérieur.

Phosphates d'énols diversement substitués

Nous avons rassemblé dans le tableau 6 quelques résultats relatifs à des phosphates d'énols diversement substitués. La substitution du groupement méthyle par un groupement éthyle ne perturbe que très peu le système (composé **20**). Par contre, si l'on place un groupement bromométhyle sur le carbone 1, on peut constater un phénomène analogue à celui observé dans le cas des dérivés α-phénylés **10**, **11** et **12**, c'est à dire que les deux protons vinyliques ont sensiblement le même déplacement chimique, et la figure de couplage se simplifie par élévation de

Can. J. Chem. Downloaded from www.nrcresearchpress.com by 210.87.254.5 on 09/05/12
For personal use only.

Can. J. Chem. Downloaded from www.nrcresearchpress.com by 210.87.254.5 on 09/05/12
For personal use only.

TABLEAU 6. Caractéristiques r.m.n. de

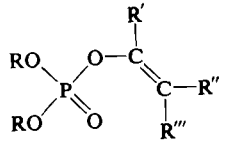

					δ10⁶(TMS)					|J| (Hz)		
Composé	R	R′	R″	R‴	P‡	R	R′	R″	R‴	$^4J_{POCCH\ I}$	$^4J_{POCCH\ II}$ cisoïde	$^4J_{POCCH\ II}$ transoïde
21	CH_3CH_2	CH_3CH_2	H	H	6.10	$\delta CH_2 = 4.09$ $\delta CH_3 = 1.31$	$\delta CH_2 = 2.05$ $\delta CH_3 = 1.31$	4.69	4.92	1	~2.3	~0
22	CH_3	CH_2—CH_2—CH_2—CH_2 a c b	H		4.08	3.78	δa,b = 2.16 (multiplet) δc = 1.69 (multiplet)		5.40		2.0	
23	CH_3CH_2	CH_2—CH_2—CH_2—CH_2 a c b	H		6.25	$\delta CH_2 = 4.12$ $\delta CH_3 = 1.32$	δa,b = 2.15 (multiplet) δc = 1.68 (multiplet)		5.39		2.2	
24*	CH_3CH_2	CH_2—CH_2—CH_2—CH_2—CH_2	H						5.45			
25*	CH_3CH_2	CH_2—CH_2—CH_2	H						5.18			
26	CH_3CH_2	OCH_3	Cl	Cl	7.38	$\delta CH_2 = 4.20$ $\delta CH_3 = 1.30$	3.80	—	—			
27†	CH_3	CH_2Br	H	H	4.82	3.81	4.01	4.98	5.01	~0	~2	~0

*Référence 2.
†À une température de l'ordre de 35°C les deux protons R″ et R‴ deviennent équivalents et l'on ne constate plus que un doublet $J \sim 2.1$ Hz.
‡Par rapport à H_3PO_4 à 85% pris comme référence externe (enregistré à 40.5 MHz).

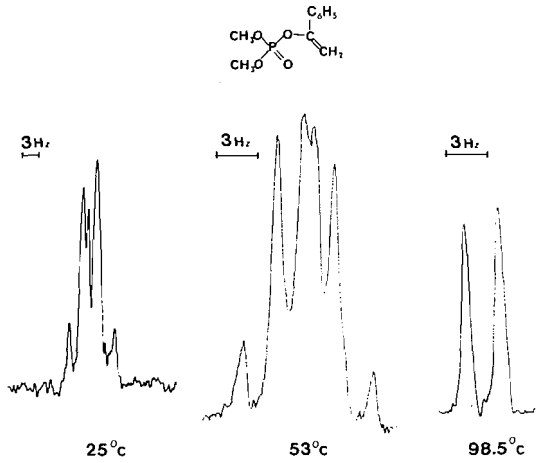

FIG. 3. Simplification du massif des protons vinyliques du composé **10**, par élévation de la température.

température. Le même phénomène est observé avec les dérivés diéthylique et di *n*-butylique. Dans le cas des dérivés cyclaniques **21**, **22**, **23** et **24** on peut constater un fort déblindage du proton vinylique et une constante $^4J_{POCCH\ II}$ cisoïde de l'ordre de 2 Hz.

Discussion des résultats

Il est possible, compte tenu des résultats décrits, d'effectuer une analyse conformationnelle de ces phosphates d'énols. Dans cette étude il faut envisager la rotation autour de la liaison P—O et autour de la liaison O—C (51).

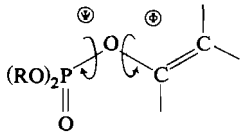

Les deux groupements méthoxy fixés sur l'atome de phosphore sont toujours équivalents dans le domaine de température considéré (−40 à +150 °C). On ne tiendra pas compte, comme nous l'avons fait précédemment (51), de la rotation autour de la liaison P—O.

Nous avons montré, en ce qui concerne l'enchaînement énolique, qu'il est possible d'envisager quatre formes stables pour les phosphates d'énols: deux formes planes où l'angle dièdre ϕ formé par l'intersection des plans P—O—C= et O—C=C prend la valeur 0 ou 180°; deux formes *gauches* où cet angle dièdre peut prendre les valeurs ϕ ou $-\phi$ (fig. 4).

Dans le cas des phosphates d'énols non substitués sur le carbone 1, nous avons montré (51) que la forme la plus stable était celle où l'angle dièdre $\phi = 180°$.

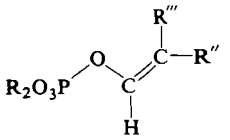

Il paraît logique de supposer que la présence d'un groupement volumineux sur le carbone 1 va augmenter considérablement l'énergie totale de la molécule dans cette conformation, par suite d'une gêne stérique importante entre le groupement R′ et le groupement phosphate.

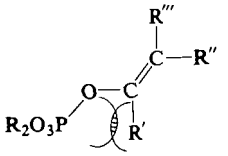

Cas des composés substitués par un méthyle sur le carbone 1

Avec les isopropénylphosphates, on conçoit facilement que la gêne stérique sera du même ordre de grandeur pour $\phi = 0°$ (forme B), et $\phi = 180°$ (forme A) (Fig. 4). Il paraît logique d'envisager comme forme stable une forme *gauche*. La contribution due aux électrons π: $^4J_{PH}{}^{\pi}$ sera donc prépondérante (7, 35–40). Dans le cas d'un fragment isopropénique $CH_3—C=CH_2'$, cette contribution est (7, 35–40)

$$^4J_{HH'}{}^{\pi} = A \sin^2\phi + B \text{ avec (40) } B \sim 0,\ A \sim -3.36$$

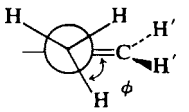

où ϕ est l'angle dièdre représenté ci-dessus. Dans notre cas la constante de couplage $^4J_{P-O-C=C-H\ II}$ sera de la forme

$$\langle {}^4J_{PH}\rangle = x\,{}^4J_{PH}(180°) + y\,{}^4J_{PH}(0°) + 2[1 - (x + y)]{}^4J_{PH}(\phi)$$

x et y étant les populations des formes A et B (fig. 4).

Avec les phosphates isopropéniques, x et y seront très petites compte tenu de la gêne stérique. Par ailleurs, on sait que la contribution due aux électrons σ dans le cas du propane est

Can. J. Chem. Downloaded from www.nrcresearchpress.com by 210.87.254.5 on 09/05/12
For personal use only.

Can. J. Chem. Downloaded from www.nrcresearchpress.com by 210.87.254.5 on 09/05/12
For personal use only.

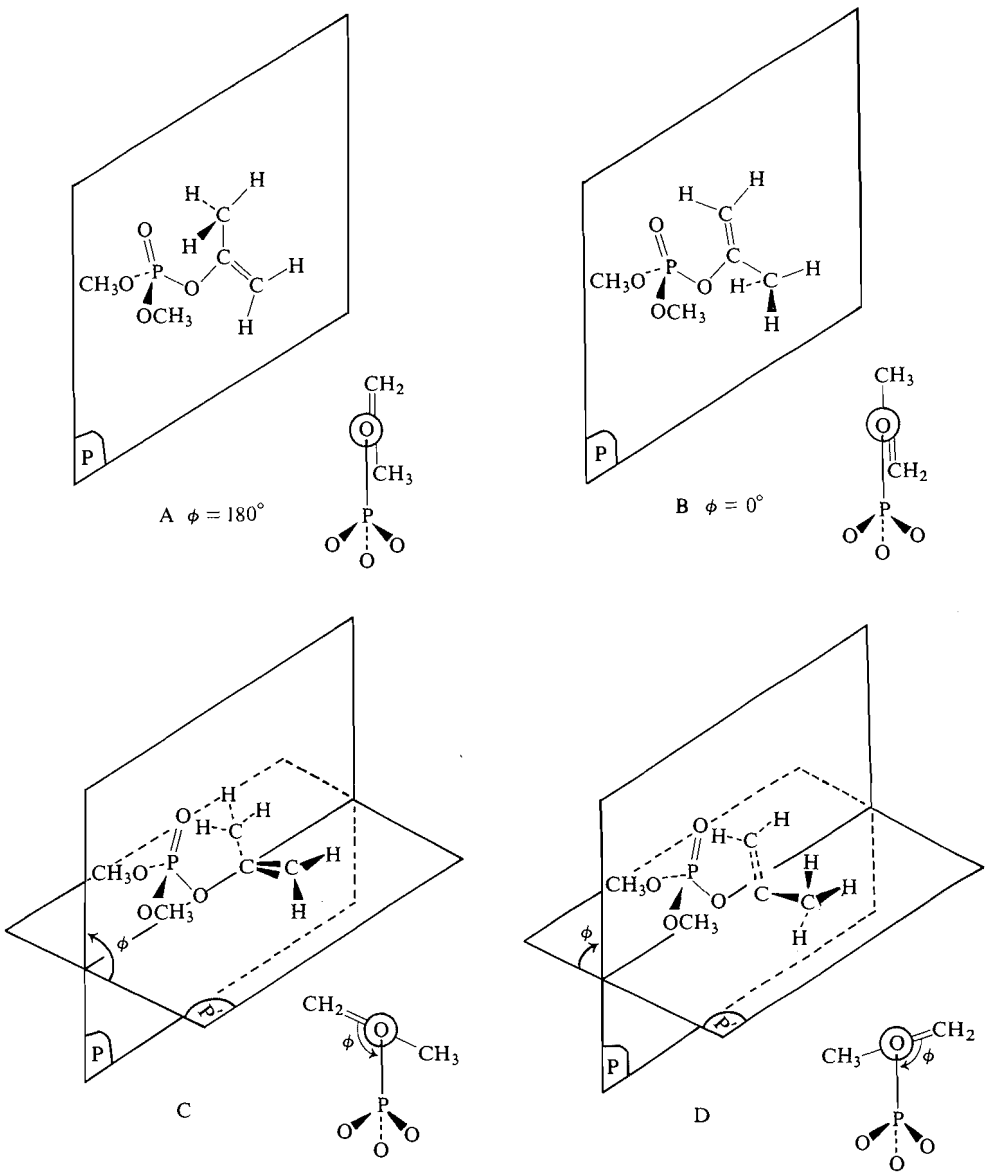

FIG. 4. Conformations stable du méthyl-1 vinylphosphate diméthylique.

positive et telle que (7, 40–43)

$$\langle {}^4J_{HH'}{}^{\sigma}(\text{transoïde})\rangle > \langle {}^4J_{HH'}{}^{\sigma}(\text{cisoïde})\rangle$$

Nous avons montré que le même phénomène se produit dans le cas des phosphates d'énols (51). Dans ces conditions on comprend très bien que pour le composé **1** nous ayons (tableau 7)

$$|{}^4J_{POCCH\ II}\ \text{cisoïde}| > |{}^4J_{POCCH\ II}\ \text{transoïde}|$$

En effet, si la contribution ${}^4J^{\sigma}$ transoïde qui est positive annule la contribution ${}^4J^{\pi}$ transoïde qui est négative, la constante ${}^4J_{POCCH\ II}$ transoïde sera très faible en valeur absolue. La contribution ${}^4J^{\sigma}$ cisoïde étant plus faible que la contribution ${}^4J^{\sigma}$ transoïde, la constante de couplage ${}^4J_{POCCH\ II}$ cisoïde sera supérieure en valeur absolue à la constante de couplage ${}^4J_{POCCH\ II}$ transoïde, les contributions ${}^4J^{\pi}$ transoïde et ${}^4J^{\pi}$ cisoïde étant sensiblement égales (16). En conséquence, on peut penser que ${}^4J_{POCCH\ II}$ cisoïde est négative.

TABLEAU 7. Comparaison des constantes $^4J_{PH\ II}$ dans le cas des vinyl et isopropenylphosphates diméthyliques

	$(MeO)_2P(=O)-O-CH=CH_2$*	$(MeO)_2P(=O)-O-C(CH_3)=CH_2$
$^4J_{POCCH\ II}$† cisoïde	−1.14	−2.20
$^4J_{POCCH\ II}$† transoïde	+2.85	±0.08

*Référence 51.
†En Hz.

TABLEAU 8. Influence de la température sur $^4J_{POCCH\ II}$ cisoïde de **9***E**

Température (°C)	$\lvert^4J_{POCCH\ II}\rvert$† cisoïde
25	2.40
53	2.30
98.5	2.10

*Solvant, hexachlorobutadiene.
†En Hz.

Il n'est pas possible pour l'instant (compte tenu de nos résultats expérimentaux) d'émettre une hypothèse en ce qui concerne le signe de $^4J_{POCCH\ II}$ transoïde dans le cas de **1**. Si l'on augmente la température, on devrait augmenter la population des formes planes *x* et *y* et par voie de conséquence $^4J_{POCCH\ II}$ cisoïde, devrait diminuer en valeur absolue. C'est effectivement ce que l'on observe dans le cas du composé **9***E* comme le montre le tableau 8.

Dans le cas des composés **5***Z*, **6***Z*, **7***Z*, **8***Z* et **9***Z*, $\lvert^4J_{POCCH\ II}\rvert$ transoïde est comprise entre 0.5 et 0.9 Hz. Nous avons vu (51) que la forme B (fig. 4) ne peut exister compte tenu de la gêne stérique provoquée par le substituant placé en position cisoïde par rapport au groupement phosphate. Si la population de la forme plane B est nulle, on constate une augmentation des

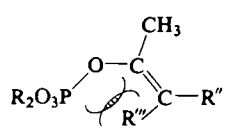

$\phi = 0°$

formes *gauches* et de la forme plane A. Compte tenu du fait que pour les composés **5***Z* à **9***Z*, $\lvert^4J_{POCCH\ II}\rvert$ transoïde est supérieure à celle du composé **1**, cette constante de couplage devrait être négative pour ces cinq composés.

Cas des composés substitués par un groupement autre qu'un méthyle sur le carbone 1

La valeur fortement élevée de $^4J_{POCCH\ II}$ cisoïde autorise l'hypothèse que la forme plane A (ϕ = 180°) ne peut exister dans le cas de cette série substituée par un phényle sur le carbone 1, ou dans la série substituée par un groupement carboxylique sur le carbone 1. Seules les formes planes B (ϕ = 0°) et *gauches* sont susceptibles d'exister dans le cas des composés **10**, **11**, **12**, **13***E*, **14***E*, **15***E*, **16***E*, **17**, **18***E* et **19***E*. La constante $^4J_{POCCH\ II}$ cisoïde doit être négative, par analogie avec les dérivés comportant un méthyle sur le carbone 1. Si l'on augmente la température, la proportion de la forme plane B va augmenter, donc, si la forme *gauche* est la plus stable $^4J_{POCCH\ II}$ cisoïde doit diminuer, c'est ce que l'on observe dans le cas du composé **15***E* comme le montre le tableau 9. Par ailleurs, dans le cas des composés **13***Z*, **14***Z*, **15***Z*, **16***Z*, **18***Z* et **19***Z*, seule la forme *gauche* est susceptible d'exister, ce qui explique, d'une part que $^4J_{POCCH\ II}$ transoïde, dans le cas de **15***Z*, ne varie pas avec la température (tableau 9) et d'autre part une valeur absolue de $^4J_{POCCH\ II}$ transoïde supérieure à celle des dérivés méthylés sur le carbone 1. Dans ces conditions, cette constante de couplage doit être négative car on aura essentiellement une contribution de type π.

Le cas des dérivés diversement substitués et notamment des dérivés cycliques, peut être inclus dans le cadre des dérivés du type méthyl-1 vinylphosphates *E* substitués sur le carbone 2. On peut remarquer, en effet, que $^4J_{POCCH\ II}$ cisoïde est toujours de l'ordre de 2 Hz.

Le déplacement chimique du ^{31}P est d'une manière générale plus positif que pour les dérivés non substitués sur le carbone 1 (51). Ce phénomène pourrait également être en faveur de

Can. J. Chem. Downloaded from www.nrcresearchpress.com by 210.87.254.5 on 09/05/12
For personal use only.

TABLEAU 9. Influence de la température sur $^4J_{POCCH\ II}$ de **15** (dans l'hexachlorobutadiène)

Composé	$\|J\|$ (Hz)	Température (°C) 25	53	98.5
15*E*	$^4J_{POCCH\ II}$ cisoïde	2.80	2.70	2.50
15*Z*	$^4J_{POCCH\ II}$ transoïde	1.90	1.85	1.90

la forme *gauche* en tant que forme prépondérante. On peut penser que, dans ces conditions, l'atome de phosphore se trouve dans le cône d'anisotropie de la double liaison et aura tendance à être plus blindé.

Calcul des déplacements chimiques des protons vinyliques

Nous avons montré qu'il est possible de déterminer le déplacement chimique des protons vinyliques (51*c*) en utilisant la méthode de Tobey (5) et Pascual *et al.* (6). Dans le cas de groupements volumineux, comme les groupements OCH_3 et CO_2CH_3, Tobey (5) montre que σ peut varier de plus de 0.5 p.p.m. Nous avons donc déterminé de nouvelles valeurs de σ *cis* et σ *trans* pour les phosphates d'énols substitués sur le carbone 1, puisque comme le montre la variation des constantes de couplages $^4J_{POCCH\ II}$, il y a une gêne stérique importante entre le substituant sur le carbone 1 et le groupement phosphate. Nous avons choisi pour le calcul de ces constantes σ, 13 phosphates d'énols diversement substitués (**1**, **5**, **6**, **8–10**, **13–17**, **19** et **22**) et l'on trouve

$$\sigma\ cis = -0.08 \text{ p.p.m.}$$
$$\sigma\ trans = +0.36 \text{ p.p.m.}$$

Ces valeurs diffèrent sensiblement de celles déterminées à partir de phosphates d'énols non substitués sur le carbone 1 puisque nous avions trouvé (51*c*)

$$\sigma\ cis = +0.28 \text{ p.p.m.}$$
$$\sigma\ trans = +0.68 \text{ p.p.m.}$$

Les déplacements chimiques calculés à l'aide de ces valeurs sont rassemblés dans le tableau 10. On peut constater une parfaite analogie entre les valeurs calculées et observées, sauf dans le cas de quelques dérivés substitués par un méthyle sur le carbone 1 et dans le cas des composés cyclaniques. Nous avons rassemblé dans le tableau 11 les valeurs observées et calculées en utilisant les contributions aux constantes d'écrans correspondant aux phosphates d'énols substitués ou non sur le carbone 1. Cette méthode nous permet donc, non seulement de déterminer sans ambiguité l'isomère géométrique considéré, mais d'avoir aussi une idée sur la possibilité d'existence de cette molécule suivant une conformation plane. En effet, dans le cas des phosphates non substitués sur le carbone 1, la conformation

TABLEAU 10. Déplacements chimiques (en p.p.m.) calculés et observés pour 37 phosphates d'énols substitués sur le carbone-1. Pour les constantes σ utilisées voir réf. 5*

Composé	δH_E Obs.	δH_E Calc.	δH_Z Obs.	δH_Z Calc.
1	4.90	5.01	4.50	4.59
2	4.88	5.01	4.48	4.59
3	4.87	5.01	4.47	4.59
4	4.90	5.01	4.51	4.59
5*E*	5.21	5.45		
5*Z*			4.79	5.03
6*E*	6.43	6.44		
6*Z*			5.65	5.63
7*E*	6.44	6.44		
7*Z*			5.68	5.63
8*E*‡	5.76	5.85		
8*Z*‡			5.47	5.43
9*E*	6.11	6.03		
9*Z*			5.62	5.61
10	5.21	5.29	5.21	5.13
11	5.25	5.29	5.25	5.13
12	5.22	5.29	5.22	5.13
13*E*	5.77	5.79		
13*Z*			5.60	5.57
14*E*	6.45	6.34		
14*Z*			6.13	6.18
15*E*	6.45	6.31		
15*Z*			6.22	6.15
16*E*†	6.69	6.72		
16*Z*†			6.33	6.22
17*E*‡	6.09	5.97		
17*Z*‡			5.85	5.81
19*E*§	6.52	6.35		
19*Z*§			6.82	6.75
20*E*§	7.03	6.93		
20*Z*§			7.27	7.33
21	4.92	5.01	4.79	4.59
22	5.40	5.76		
23	5.39	5.76		
24	5.45	5.76		
25	5.18	5.76		
27	5.01	5.42	4.98	5.03

*Dans tous les cas des phényles en position 1, nous avons utilisé les constantes de Tobey (5) relatives à un phényle encombré.
†Phényle en position 2, non encombré (5).
‡Référence 6 "solo".
§Références 6 et 48.

Can. J. Chem. Downloaded from www.nrcresearchpress.com by 210.87.254.5 on 09/05/12
For personal use only.

TABLEAU 11. Comparaison entre les déplacements chimiques observés et les déplacements chimiques calculés en utilisant les contributions aux constantes d'écran σ pour les phosphates d'énols substitués ou non sur le carbone 1.

	δH_E			δH_Z		
Composé	Calc. σ *cis* = +0.28	Obs.	Calc. σ *cis* = −0.08	Calc. σ *trans* = +0.68	Obs.	Calc. σ *trans* = +0.36
1	4.65	4.90	5.01	4.27	4.50	4.59
2	4.65	4.88	5.01	4.27	4.48	4.59
3	4.65	4.87	5.01	4.27	4.47	4.59
4	4.65	4.90	5.01	4.27	4.51	4.59
5*E*	5.09	5.21	5.45			
5*Z*				4.71	4.79	5.03
21	4.65	4.92	5.01	4.27	4.69	4.59
22	5.10	5.40	5.76			
23	5.10	5.39	5.76			
24	5.10	5.45	5.76			
25	5.10	5.18	5.76			
27	5.06	5.01	5.42	4.71	4.98	5.03

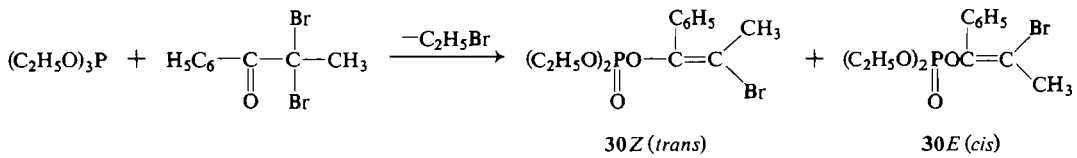

30*Z* (*trans*) **30***E* (*cis*)

SCHÉMA 4

la plus stable est une forme plane. Dans le cas de groupements très volumineux, ces formes planes ne peuvent exister.

Avec les composés **1–5**, **21–27** où les conformations planes peuvent exister, les déplacements chimiques des protons vinyliques observés sont différents de ceux calculés en utilisant les contributions aux constantes d'écrans σ *cis* et σ *trans*. D'une manière générale on peut écrire que l'on a dans tous les cas

$$-0.08 \leqslant \sigma\, cis \leqslant +0.28$$
$$+0.36 \leqslant \sigma\, trans \leqslant +0.68$$

Constantes de couplage $^5J_{POCCCH}$

Lorsque la double liaison de l'enchaînement énolique est totalement substituée, les considérations précédentes ne nous permettent pas de distinguer les différents stéréoisomères susceptibles d'exister. C'est le cas du bromo-2 phényl-1 propenyl phosphate diéthylique (**30**) obtenu par Borowitz *et al.* par action du triéthylphosphite sur la dibromopropiophénone (49) (schéma 4). Il est possible d'identifier les composés **30***Z* et **30***E* en considérant la constante $^5J_{P-O-C=C-C-H}$. Il s'agit d'une constante de type homoallylique qui est relativement importante si la double liaison est fortement substituée. En effet, dans ces conditions, les formes *gauches* seront préférentielles et la valeur absolue de $^5J_{PH}$ sera relativement importante puisque la contribution due aux électrons π, dépend de $\sin^2 \phi$ (7). Par ailleurs, dans le cas des dérivés du butène-2, il a été montré que $^5J_{HH}$ (*trans*) est supérieure à $^5J_{HH}$ (*cis*) d'environ 0.3 Hz (16–50). Nous observons un phénomène analogue dans le cas

TABLEAU 12. Variation de $^5J_{POCCCH}$ dans

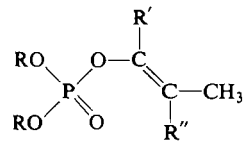

E

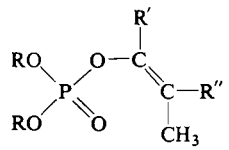

Z

	Phosphate			$^5J_{POCCCH}$	
Composé	R	R′	R″	*E*	*Z*
5	CH_3	CH_3	H	2.4	2.0
13	C_2H_5	C_6H_5	H	3.0	2.5
19*	CH_3	CO_2CH_3	H	3.3	3.0
30	C_2H_5	C_6H_5	Br	3.2†	2.7‡

*Référence 3.
†Z (*trans*).
‡E(*cis*).

Can. J. Chem. Downloaded from www.nrcresearchpress.com by 210.87.254.5 on 09/05/12
For personal use only.

TABLEAU 13.

Composé	Formes supposées	Formes stables	$^4J_{POCCH\ II(Hz)}$ cisoïde	$^4J_{POCCH\ II(Hz)}$ transoïde
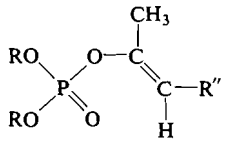	A, B, C, D	C, D	−1.8 à −2.6	—
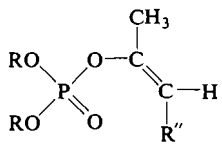	A, C, D	C, D	—	0 à −0.9
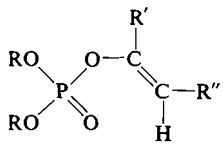 $R' = C_6H_5CO_2R$	B, C, D	C, D	−2.6 à −2.8	—
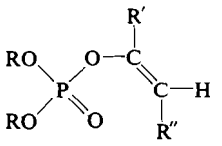 $R' = C_6H_5CO_2R$	C, D	C, D	—	−1.0 à −2.5

de nos dérivés, comme le montre le tableau 12. Le tableau 12 montre bien que le composé **30***Z* est celui où la constante $^5J_{PH} = 3.2$ Hz, ce qui nous permet de dire, compte tenu des résultats obtenus par Borowitz *et al.* (49), que l'action de la dibromopropiophénone conduit à 60% du composé **30***Z* et 40% du couposé **30***E*.

Conclusion

L'analyse r.m.n. des phosphates d'énols *E* et *Z* substitués sur le carbone 1, nous a permis d'identifier ces composés sans ambiguité. Le proton vinylique en position cisoïde sur le carbone 2 est toujours plus déblindé que le proton transoïde sauf dans le cas de **19** et **20**. Une association intramoléculaire se produit et il est possible de la diminuer par élévation de température. Dans le cas où le groupement fixé sur le carbone 1 est un groupement carboxylique, c'est le proton transoïde par rapport au groupement phosphate qui est le plus déblindé (composés **18** et **19**). Les résultats que nous proposons sont en bon accord avec les calculs effectués suivant la méthode de Tobey (5) et Pascual *et al.* (6).

Nous avons pu justifier d'une part, les variations des constantes de couplages $^4J_{POCCH\ II}$ cisoïde et transoïde et d'autre part, déterminer ainsi les conformations susceptibles d'exister et leur stabilité relative par rotation autour de la liaison O—C de l'enchaînement énolique. L'ensemble de ces résultats est résumé dans le tableau 13.

La constante $^5J_{POC=CCH_3}$ est comprise entre 2 et 3.2 Hz suivant la nature des substituants sur la double liaison, mais dans tous les cas envisagés cette constante est supérieure en valeur absolue lorsque le méthyle est en *trans* par rapport au groupement phosphate.

NOTE AJOUTÉE À LA CORRECTION DES ÉPREUVES: L'utilisation de $Eu(DPM)_3$ a permis à Borowitz

Can. J. Chem. Downloaded from www.nrcresearchpress.com by 210.87.254.5 on 09/05/12
For personal use only.

et al. (54) d'étudier les configurations des phosphates énoliques substitués sur le carbone 1. Les résultats qu'il obtient sont en excellent accord avec les nôtres.

Partie expérimentale

La synthèse des produits a été décrite précédemment (52, 53).

Enregistrement des spectres

Les spectres du ^1H ont été enregistrés sur un appareil Varian A 60 ou HA 100, en solution (30% en poids) dans du tétrachlorure de carbone avec du TMS comme référence interne. Les spectres à température variable l'ont été sur un appareil Varian A 60 dans de l'hexachlorobutadiène; quant aux spectres du ^{31}P ils ont été enregistrés sur un appareil HA 100 Varian équipé d'une sonde pour le phosphore à 40.5 MHz.

Calcul des spectres

Les calculs des spectres ont été effectués à l'aide du programme LAOCOON III. Ce programme permet d'optimiser la valeur des glissements chimiques et des constantes de couplage en minimisant l'écart observé entre les raies expérimentales du spectre et les transitions calculées par la méthode des moindres carrés. Ce programme a été adapté sur IBM 360/44, sa capacité a été étendue aux systèmes de sept spins et il lui a été adjoint un programme de tracé de courbes utilisant les fonctions de Lorentz, sur Plotter IBM 1627. A chaque paramètre magnétique optimisé est associée une erreur statistique évaluée sur un intervalle de confiance à 95%.

Nous tenons à exprimer notre reconnaissance à J. R. Llinas pour l'intérêt qu'il a manifesté au cours de ce travail ainsi qu'à Mlle Berger et M. Archavlis pour le grand nombre de spectres qu'ils ont enregistré.

1. A. R. Stiles, C. A. Reilly, G. R. Pollard, C. H. Tieman, L. F. Ward, D. D. Philips, S. B. Soloway et R. R. Whetstone. J. Org. Chem. **26**, 3960 (1961).
2. I. J. Borowitz, S. Firstenberg, E. W. R. Casper et R. K. Crouch. J. Org. Chem. **36**, 3282 (1971).
3. I. A. Stubbe et G. Kenyon. Biochemistry, **10**, 2669 (1971).
4. M. Cohn, J. E. Pearson, E. L. O'Connel et J. A. Rose. J. Am. Chem. Soc. **92**, 4095 (1970).
5. S. W. Tobey. J. Org. Chem. **34**, 1281 (1969).
6. C. Pascual, J. Meier et W. Simon. Helv. Chim. Acta, **49**, 164 (1966).
7. M. Barfield et B. Chakrabarti. Chem. Rev. **69**, 757 (1969).
8. G. Peiffer, A. Guillemonat, J. C. Traynard et E. Gaydou. Bull Soc. Chim. 1304 (1969).
9. E. Gaydou, J. Llinas, G. Peiffer et A. Guillemonat. Ann. Fac. Sci. Marseille, **43**A, 83 (1970).
10. J. P. Albrand, D. Gagnaire et J. B. Robert. Bull. Soc. Chim. 3496 (1969).
11. A. A. Bothner-By et W. P. Trautwein. J. Am. Chem. Soc. **93**, 2189 (1971).
12. M. Karplus. J. Chem. Phys. **30**, 11 (1959).
13. E. J. Boros, K. J. Coskran, R. W. King et J. G. Verkade. J. Am. Chem. Soc. **88**, 1140 (1966).
14. J. P. Majoral et J. Navech. Bull. Soc. Chim. 95 (1971).
15. D. W. White et J. G. Verkade. J. Mag. Res. **3**, 111 (1970).
16. M. Barfield et S. Sternhell. J. Am. Chem. Soc. **94**, 1905 (1972).
17. H. C. Beyerman, D. W. Reinmoudt, A. Sinnema et A. Van. Rec. Trav. Chim. Pays Bas, **85**, 347 (1966).
18. T. H. Sidall et C. A. Prohaska. J. Am. Chem. Soc. **84**, 3967 (1962).
19. R. Burgada, G. Martin et G. Mavel. Bull. Soc. Chim. 2154 (1963).
20. E. Duval, J. Ranft et G. J. Bene. Mol. Phys. **9**, 427 (1965).
21. R. R. Dean et W. McFarlane. Chem. Commun. 840 (1967).
22. M. P. Williamson et C. E. Griffin. J. Phys. Chem. **72**, 4043 (1968).
23. S. Castellano, C. Sun et R. Kostelnik. J. Chem. Phys. **46**, 327 (1967).
24. A. A. Bothner-By et C. Naar-Colin. J. Am. Chem. Soc. **83**, 231 (1961).
25. M. Y. Dewolf et J. D. Baldeschwieler. J. Mol. Spectrosc. **13**, 344 (1964).
26. W. Brugel. Nuclear magnetic resonance spectra and chemical structure. Vol. I. Academic Press, New York. 1967.
27. D. R. Davis et J. D. Roberts. J. Am. Chem. Soc. **84**, 2252 (1962).
28. H. M. Hutton et T. Schaefer. Can. J. Chem. **45**, 1165 (1967).
29. (*a*) J. E. Blackwood, C. L. Gladys, K. L. Loening, A. E. Petrarca et J. E. Rush. J. Am. Chem. Soc. **90**, 509 (1968); (*b*) Nomenclature Section E, Bull. Soc. Chim. n° 15b (1970).
30. F. W. Lichtenthaler. Chem. Rev. **61**, 607 (1961).
31. G. S. Reddy, J. H. Goldstein et L. Mandeil. J. Am. Chem. Soc. **83**, 1300 (1961).
32. R. T. Hobgood, Jr., G. S. Reddy et J. H. Goldstein. J. Phys. Chem. **67**, 110 (1963).
33. D. F. Koster et A. Danti. J. Phys. Chem. **69**, 486 (1965).
34. D. M. Grant et B. V. Cheney. J. Am. Chem. Soc. **89**, 5315 (1967).
35. H. M. McConnell. J. Mol. Spectrosc. **1**, 11 (1957).
36. H. M. McConnell. J. Chem. Phys. **30**, 126 (1959).
37. M. Karplus. J. Chem. Phys. **33**, 1842 (1960).
38. M. Barfield et M. Karplus. J. Am. Chem. Soc. **91**, 1 (1969).
39. Z. Luz. J. Chem. Phys. **48**, 4186 (1968).
40. M. Barfield. J. Chem. Phys. **48**, 4463 (1968).
41. S. Sternhell. Pure Appl. Chem. **14**, 15 (1964).
42. M. Barfield. J. Chem. Phys. **41**, 3825 (1964).
43. E. W. Garbisch. J. Am. Chem. Soc. **86**, 5561 (1964).

Can. J. Chem. Downloaded from www.nrcresearchpress.com by 210.87.254.5 on 09/05/12
For personal use only.

44. R. D. FRAMPTON, T. T. TIDWALL et V. A. YOUNG. J. Am. Chem. Soc. **94**, 1271 (1972).
45. M. KAINOSHO et A. NAKAMURA. Tetrahedron, **25**, 4071 (1969).
46. J. F. MARECEK et D. L. GRIFFITH. J. Am. Chem. Soc. **92**, 917 (1970).
47. E. WINTERFELDT et H. PREUSS. Chem. Ber. **99**, 450 (1966).
48. C. T. ROSS et F. J. BOROS. Anal. Chim. Acta, **52**, 139 (1970).
49. I. J. BOROWITZ, S. FIRSTENBERG, E. W. R. CASPER et R. K. CROUCH. Phosphorus, **1**, 301 (1972).
50. R. R. FRASER. Can. J. Chem. **38**, 549 (1960).
51. (*a*) E. M. GAYDOU. Tetrahedron Lett. 4469 (1972); (*b*) E. M. GAYDOU et J. R. LLINAS. Org. Mag. Res. (à paraître); (*c*) E. M. GAYDOU. Thèse. Marséille, N° CNRS AO 7802 (1972).
52. E. M. GAYDOU. Bull. Soc. Chim. (sous presse).
53. E. M. GAYDOU, R. FREZE et G. BUONO. Bull. Soc. Chim. (sous presse).
54. I. J. BOROWITZ, K. C. YEE et R. K. CROUCH. J. Org. Chem. **38**, 1713 (1973).

Can. J. Chem. Downloaded from www.nrcresearchpress.com by 210.87.254.5 on 09/05/12
For personal use only.

Photoionisation en milieu rigide. Evolution de la fonction de distribution des électrons piégés autour des cations

JACQUES BULLOT, DOMINIQUE CECCALDI, ET ODILE GALLAIS

Laboratoire de Physico-Chimie des Rayonnements, Associé au CNRS, Université de Paris-Sud, centre d'Orsay, 91 Orsay, France

Reçu le 22 mars 1973

Nous proposons un modèle cinétique permettant de décrire la luminescence de recombinaison isotherme (ITL) en milieu rigide. Nous supposons que les cavités piégeantes pré-existent dans le verre et que le champ coulombien du cation crée une distribution continue des profondeurs de piège. La décroissance ITL est une somme infinie de décroissance du 1er ordre résultant de la recombinaison des électrons corrélés. A l'aide de ce modèle, on peut retrouver les décroissances expérimentales avec une précision de $\pm 3\%$. Les solutions numériques sont testées à l'aide d'une fonction de distribution gaussienne pour les électrons piégées (paramètres r_{max} Å et largeur b Å); les paramètres des pièges à électrons sont gardés égaux à $L = 1.70$ Å (demi-largeur) et $\theta\ (r \rightarrow \infty) \simeq 10^3$ s (durée de vie à l'infini). Le modèle est utilisé pour étudier l'évolution de la fonction de distribution des électrons piégés en fonction de plusieurs paramètres expérimentaux. (1) Pendant la relaxation configurationnelle du verre. r_{max} passe de 32.0 à 40.0 Å et b de 6.2 à 9 Å après 24 h de relaxation. Tout au long de l'évolution le nombre d'électrons piégés décroît régulièrement. (2) En fonction de la durée d'irradiation u.v. t_{irrad}. Le maximum de la fonction de distribution s'éloigne du cation quand t_{irrad} augmente. (3) En fonction de l'intensité J de la lumière u.v. Le nombre d'électrons piégés au temps $t = 0$ (arrêt de l'irradiation u.v.) est proportionnel à l'intégrale S de la fonction de distribution à $t = 0$. Quand J varie le modèle indique que S varie comme J^2, c'est-à-dire que l'ionisation est biphotonique—un résultat bien connu. Nous considérons ce résultat comme un test positif de la cohérence interne du modèle.

A kinetic model for describing isothermal recombination luminescence (ITL) of trapped electrons in a rigid medium is proposed. Assuming that cavities in the glass are pre-existing, a continuous trap-depth distribution is generated from the long-range Coulomb field of the cation. ITL decay kinetics simply is the superposition of an infinite sum of first order decays of correlated electrons. This model is able to fit experimental decays within $\pm 3\%$. Numerical solutions are tested by introducing a Gaussian trapped electron distribution function (parameters: r_{max} Å and width b Å) and keeping the formerly found trap parameters: half-width $L = 1.70$ Å and lifetime at infinity $\theta(r \rightarrow \infty) \simeq 10^3$ s. This model is used for studying how the trapped electron distribution function is shifted when experimental conditions are altered. (1) During the glass isothermal relaxation. The initial values $r_{max} = 32.0$ Å, $b = 6.2$ Å found just after cooling are shifted to $r_{max} = 40.0$ Å and $b = 9.0$ Å, 24 h after cooling. The model indicates that the total number of trapped electrons is steadily decreasing as long as the relaxation is proceeding. (2) As a function of the u.v. irradiation period. The trapped electron distribution function is pushed away from the cationic center when t_{irrad} is increasing. Near the saturation plateau the distribution function is no longer shifted; only the total number of trapped electrons is increased. (3) As a function of u.v. light intensity. By integrating as a function of r the trapped electron distribution function at time $t = 0$ when u.v. light is turned off, the resulting area, which is proportional to the total number of trapped electrons, is shown to be proportional to the square of the light intensity. In others words with this model the well-known one-electron two-photon ionization law is recovered. This is to be considered as a test of the model self-consistency.

Can. J. Chem., 51, 3428 (1973)

I. Introduction

Dans un article récent (1), nous avons proposé une interprétation de la cinétique de décroissance de la luminescence isotherme (ou ITL) observée à 77 °K après la photoionisation d'une solution rigide de TMPD[1] dans le 3-MP.[2] Ce modèle nous a permis de retrouver par le calcul la cinétique de décroissance expérimentale et d'étudier sommairement l'influence de la relaxation de la matrice rigide sur celle-ci.

Dans le présent article, nous présentons une étude plus détaillée de l'influence de la relaxation de configuration du verre sur l'évolution de la fonction de distribution des électrons autour des cations, c'est-à-dire en fonction du temps écoulé depuis la trempe du verre. Nous utilisons aussi ce modèle pour étudier comment se déplace la fonction de distribution des électrons

[1]TMPD = *N,N,N-N*-tétraméthylparaphénylènediamine.

[2]3-MP = 3-méthylpentane.

Can. J. Chem. Downloaded from www.nrcresearchpress.com by 210.87.254.6 on 09/05/12
For personal use only.

Can. J. Chem. Downloaded from www.nrcresearchpress.com by 210.87.254.6 on 09/05/12
For personal use only.

piégés quand on fait varier la durée d'irradiation en lumière ultra-violette et l'intensité de celle-ci.

Rappelons tout d'abord que l'irradiation à 77 °K d'une solution rigide de TMPD dans le 3-MP à 313 nm, c'est-à-dire dans la première bande d'absorption du soluté, conduit à l'ionisation de cette molécule par l'absorption consécutive de deux photons (2). Une partie des électrons éjectés dans la matrice rigide est retenue dans des puits de potentiel, ou "pièges", caractéristiques de la matrice considérée. Après la fin de l'irradiation ultra-violette, ces électrons se recombinent avec les cations $TMPD^+$ pour donner une molécule neutre excitée, qui se désexcite partiellement par émission de fluorescence et de phosphorescence (voir par exemple réf. 2). Cette émission (ITL) peut être observée avec une bonne précision à 77 °K pendant un temps très long, de l'ordre de l'heure. Sa cinétique est complexe. Elle dépend des paramètres physiques qui caractérisent les pièges à électron et de la répartition des électrons autour des cations.

Selon nous, les paramètres physiques permettant de décrire les pièges, c'est-à-dire la dimension du piège et sa profondeur, sont caractéristiques d'un solvant donné et restent les mêmes d'un échantillon à l'autre (d'une trempe à l'autre). Par contre, la répartition des électrons piégés autour des cations va varier avec les conditions expérimentales: conditions de préparation du verre (histoire thermique, trempe), évolution isotherme du verre (relaxation de configuration), conditions d'irradiation en lumière ultra-violette (durée de l'irradiation, intensité de la lumière excitatrice, longueur d'onde utilisée, etc.). En abordant ces différents aspects à l'aide du modèle proposé, nous avons pour but à la fois de tester la validité du modèle en retrouvant certains résultats connus et de cerner des paramètres physiques encore mal connus comme ceux qui caractérisent les pièges à électron dans le 3-MP.

II. Modèle cinétique

Le modèle repose sur 5 hypothèses fondamentales.

(1) Il y a dans la matrice rigide un grand nombre de types de cavités $i = 1, 2, \ldots p$, susceptibles de piéger les électrons, auxquelles correspondent des énergies d'activation E_i.

(2) L'éjection de l'électron hors de son piège est activée thermiquement dans le 3-MP. Ceci semble bien démontré (3). Au contraire, dans le cas du méthylcyclohexane, on est tenté de faire l'hypothèse d'un dépiégeage par effet tunnel (4). Cependant, l'un d'entre nous (1*b*) a montré que le modèle thermique pouvait être appliqué dans le cas du méthylcyclohexane à 77 °K.[3]

(3) Nous ne considérons que les électrons piégés qui sont corrélés avec leurs cations-parents, c'est-à-dire ceux qui se recombinent suivant une réaction du premier ordre. Des expériences d'électrophotoluminescence (5) ont montré que ces électrons sont localisés à une distance $r \lesssim 45$–50 Å du cation $TMPD^+$.

(4) Chaque électron corrélé est soumis au champ coulombien du cation-parent. Ce champ à longue portée a pour résultat d'abaisser la barrière de potentiel opposée à l'éjection de l'électron d'une quantité variable en fonction de r et donc de créer une distribution continue des profondeurs de piège, c'est-à-dire une distribution continue des durées de vie des électrons piégés.

(5) Lors de la recombinaison électron–cation, nous négligeons le repiégeage. En effet, on sait que l'électron libre se recombine en un temps $\lesssim 10^{-9}$ s (6).

Dans ces conditions, l'intensité de la luminescence de recombinaison, à un instant t après la fin de l'irradiation, résulte de la superposition de p sommes infinies (il y a p types de pièges) de décroissances du premier ordre, dont les durées de vie ont une distribution continue.

Tel quel le problème reste très complexe. Mais un raisonnement simple va nous montrer que pour un temps d'observation relativement court devant la durée totale de l'émission, on n'observe qu'un seul type de piège et qu'on peut négliger la contribution des pièges profonds (ou très éloignés du cation). En effet, considérons un électron piégé dans l'état lié. Soit L_i une longueur de l'ordre de grandeur de la demi-largeur du piège de type i. Le champ coulombien du cation abaisse la barrière de potentiel opposée au dépiégeage de l'électron d'une quantité $e^2 L_i/\varepsilon r^2$, où ε est la constante diélectrique statique du 3-MP ($\varepsilon \simeq 2$) et e la charge de l'électron. La constante de vitesse de dépiégeage thermique s'écrit

[3]Rappelons que la température de transition vitreuse est $T_g \approx 77$ °K pour le 3-MP, alors que $T_g \approx 90$ °K pour le méthylcyclohexane.

Can. J. Chem. Downloaded from www.nrcresearchpress.com by 210.87.254.6 on 09/05/12
For personal use only.

[1] $k_i(r) = 1/\theta_i(r) = \nu_i \exp\left[-\frac{1}{kT}(E_i - e^2L_i/\varepsilon r^2)\right]$

où ν_i est un facteur de fréquence ($\sim 10^{13}$ s^{-1}) et $\theta_i(r)$ la durée de vie de l'électron dans un piège de type i, à la distance r.

Or, la profondeur de piège $E_i \simeq 0.2$ eV (1*b*) est très grande devant le terme de perturbation $e^2L_i/\varepsilon r^2$. En effet, si on prend $L = 1.70$ Å (1) et $\varepsilon \simeq 2$, ce terme varie de 43×10^{-3} eV à 6×10^{-3} eV quand r passe de 15 Å à 40 Å. Comme par ailleurs à 77 °K, $kT = 6 \times 10^{-3}$ eV, on voit que le rapport $E_i/kT \simeq 0.2/6 \times 10^{-3}$ eV, et donc $k_i(r) = 1/\theta_i(r) \simeq \nu_i \exp -(E_i/kT)$ varient très rapidement avec E_i. Ainsi une faible augmentation de E_i entraîne une très forte augmentation de la durée de vie $\theta_i(r)$ de l'électron piégé. Ceci nous permet de supposer qu'au début de la décroissance de l'ITL, les électrons qui se recombinent sont issus en majorité d'un seul type de piège de profondeur E, la contribution des autres pièges restant négligeable. Ainsi le modèle décrit précédemment (1) avec $i = 1$ reste applicable au début de la décroissance, même si le verre contient plusieurs types de cavités piégeantes. C'est sur cette base que nous allons décrire les résultats expérimentaux et en donner l'interprétation cinétique.

Rappelons que l'intensité de l'ITL à un temps t après la fin de l'irradiation en lumière ultraviolette s'écrit

[2] $I_{ITL}(t) = K \int_0^\infty \frac{D(r, t = 0)}{\theta(r)} \exp[-t/\theta(r)]\, dr$

$D(r,t)$ est la fonction de distribution des électrons au temps t autour des cations, et $\theta(r)$ correspond à l'équation 1 avec $i = 1$ (pour plus de détails voir réf. 1).

L'équation 2 se prête à un calcul numérique à condition qu'on connaisse la longueur L et $\theta(r \to \infty) = \nu \exp(\beta E)$, c'est-à-dire la durée de vie de l'électron piégé dans une cavité de profondeur E située à une très grande distance du cation ($r \gg 50$ Å). De plus, il faut connaître la distribution $D(r,t = 0)$ des électrons à la fin de l'irradiation.

En ce qui concerne L et $\theta(r \to \infty)$, nous considérons que ces paramètres caractérisent le solvant et qu'ils ne doivent pas varier (ou très peu) d'une trempe à l'autre. C'est pourquoi nous leur imposerons dans ce travail les valeurs trouvées avec un échantillon différent (1):

$$L = 1.70 \text{ Å et } \theta(r \to \infty) = 10^3 \text{ s}$$

En ce qui concerne $D(r,t) = 0$, nous ne disposons malheureusement d'aucun renseignement précis sur la distribution réelle des électrons autour des cations. C'est pourquoi nous maintenons une fonction de distribution gaussienne comme dans le travail de la réf. 1:

[3] $D(r,t = 0) = C \exp[-\{(r - r_{max})/b\}^2]$

Nous sommes conscients de l'approximation que représente une telle distribution et pensons qu'en réalité il faudrait choisir une fonction de distribution asymétrique.

III. Partie expérimentale

L'échantillon utilisé est une solution $\sim 10^{-3}$ *M* de TMPD dans le 3-MP. La TMPD est purifiée par sublimation sous vide et le 3-MP par ébullition à reflux sur un mélange de tamis moléculaires ($\frac{1}{3}$ 5A + $\frac{1}{3}$ 10X + $\frac{1}{3}$ 13X) suivie d'une distillation. Dans ces conditions le solvant émet une luminescence parasite environ 10^3 fois plus faible que la luminescence de recombinaison.

L'irradiation en lumière ultra-violette est faite au moyen de la raie 313 nm d'une lampe à vapeur de mercure Osram HBO 200 W/2, isolée à l'aide d'un filtre Jena UG-11. La luminescence émise passe au travers d'un filtre MTO A 365 b, de telle sorte qu'on élimine la phosphorescence et qu'on enregistre seulement la fluorescence de la TMPD. L'échantillon est trempé brutalement à 77 °K au temps $\tau = 0$. On observe ensuite l'évolution de la cinétique de l'ITL en fonction du temps τ qui s'est écoulé entre le moment de la trempe et la fin de l'irradiation. Pour cela on irradie pendant 30 s la solution, enregistre l'ITL pendant environ 30 min et blanchit l'échantillon avec de la lumière visible. Ce cycle est répété un grand nombre de fois jusqu'à ce qu'aucune modification de la cinétique ITL en fonction de τ ne soit plus décelable avec notre dispositif expérimental.

Dans ce qui suit, le temps τ écoulé depuis la trempe de l'échantillon est mesuré en heures et le temps t écoulé depuis la fin d'une irradiation particulière est mesuré en secondes. Nous désignerons par $I^{\tau}_{ITL}(t)$, l'intensité de la luminescence isotherme enregistrée τ h après la trempe de l'échantillon et t s après la fin de l'irradiation à 313 nm. Quand la relaxation de l'échantillon a atteint un palier, nous étudions l'influence de la durée d'irradiation t_{Irrad}, à 313 nm, à flux constant. L'étude en fonction de l'intensité de la lumière excitatrice a été faite dans les mêmes conditions, mais sur un échantillon ayant relaxé pendant 24 h. Les calculs sont effectués à l'aide d'un ordinateur IBM 360.

IV. Relaxation de la matrice de 3-MP

Nous avons suivi l'évolution de la cinétique ITL pendant un temps $\tau \simeq 80$ h. Un palier est atteint à $\tau \simeq 23$ h comme le montre la fig. 1 sur

Can. J. Chem. Downloaded from www.nrcresearchpress.com by 210.87.254.6 on 09/05/12
For personal use only.

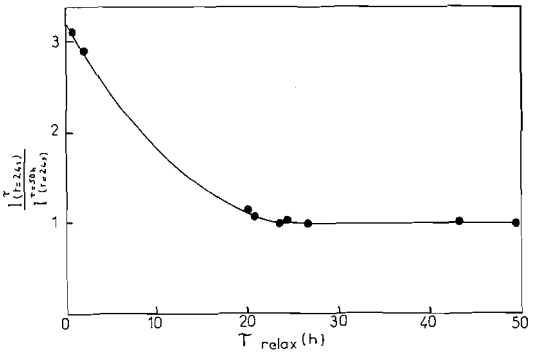

FIG. 1. Variation du rapport $I^{\tau}(t = 24\text{ s})/I^{\tau=50\text{h}}(t = 24\text{ s})$ en fonction du temps écoulé depuis la trempe du verre.

laquelle nous portons le rapport $I^{\tau}_{ITL}(t = 24\text{ s})/I^{\tau\infty}_{ITL}(t = 24\text{ s})$. Quatre cinétiques expérimentales ont été exploitées numériquement pour $\tau = 0.42$ h; 2 h; 20 h et 80 h. Dans chaque cas, un jeu de paramètres r_{max} et b nous permet de retrouver à partir de l'éq. 2 les cinétiques expérimentales avec une bonne précision. La fig. 2 montre que l'accord entre la valeur théorique et la valeur expérimentale est de l'ordre de $\pm 3\%$, pour $t \lesssim 900$ s. Ceci donne une idée de l'erreur introduite par les approximations du modèle cinétique. Pour les temps $t \gtrsim 900$ s, la théorie prévoit une décroissance plus rapide que ne l'indique l'expérience. Ce résultat est compatible avec la remarque du paragraphe II. En effet, il est vraisemblable que pour les temps $t \gtrsim 900$ s, nous observons aussi la recombinaison d'électrons issus de pièges plus profonds que ceux que nous observions pour $t \lesssim 900$ s. Donc l'intensité observée expérimentalement doit être plus grande que l'intensité théorique qui, elle, ne tient compte que des électrons de durées de vie $\theta(r \to \infty) \simeq 10^3$ s.

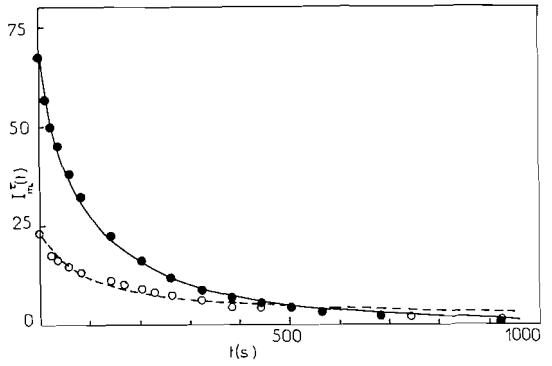

FIG. 2. Cinétique de recombinaison ITL pour des temps de relaxation; $\tau = 0.42$ h (—trait plein) et $\tau = 80$ h (--): ●, points calculés avec $r_{max} = 32$ Å et $b = 6.2$ Å; ○, points calculés avec $r_{max} = 40$ Å et $b = 9$ Å.

Dans le tableau 1, nous avons rassemblé les valeurs choisies pour r_{max} et b qui donnent le meilleur accord avec l'expérience. A titre de comparaison, nous avons consigné les valeurs obtenues dans le travail précédent (1). Celles-ci sont en bon accord avec les notres. Ces résultats peuvent être interprétés à partir de la théorie du volume libre (voir par exemple réf. 7) dans les verres. Selon Kovacs (7*c*) l'évolution isotherme des verres à laquelle correspond une diminution du volume macroscopique[4] est due à la relaxation configurationnelle du milieu amorphe. Le réarrangement moléculaire entraîne la disparition d'un certain nombre de cavités. Dans ces conditions si, comme nous le supposons, les cavités pré-existantes dans le verre sont capables de piéger les électrons, quand τ augmente, les électrons éjectés doivent parcourir en moyenne un trajet de plus en plus long avant d'être piégés. D'où le déplacement de r_{max} et l'élargissement de la fonction de distribution.

Si notre interprétation est correcte, le nombre de cavités disponibles diminuant quand τ augmente, le nombre d'électrons piégés après une irradiation de durée constante (30 s) doit décroître. C'est ce que nous avons vérifié en intégrant la fonction de distribution des électrons piégés à $t = 0$ (éq. 3), soit $S = \int_0^{\infty} D(r,t = 0)dr$.

L'aire S est proportionnelle au nombre d'électrons piégés à un temps τ donné. Les résultats sont consignés dans le tableau 1. S varie d'environ 40% entre $\tau = 0.42$ h et $\tau = 20$ h.

Enfin, nous avons calculé l'évolution de $D(r,t)$ en fonction de t. La fig. 3 montre à $\tau = 0.42$ h l'évolution de $D(r,t)$ entre $t = 36$ s et $t = 600$ s. Le maximum de $D(r,t)$ s'est déplacé d'environ 1.6 Å.

V. Evolution de la fonction de distribution $D(r,t = 0)$ avec la durée d'irradiation en lumière ultra-violette

On sait que, quand on irradie à flux constant une solution rigide de TMPD/3-MP, on observe tout d'abord une augmentation linéaire de l'intensité d'ITL en fonction de la durée

[4]Le verre de glucose, par exemple, trempé à partir de $T = 40$ °C, à 19.8 °C après 100 h de relaxation subitune contraction $(v_{initial} - v_{\infty})/v_{\infty} \simeq 3.6 \times 10^{-3}$ (ref. 7*c*).

TABLEAU 1*

Présent travail				Réf. 1			
τ_{relax} (h)	r_{max} (Å) ±0.2	b (Å) ±0.2	S† (u.a.) ±50	τ_{relax} (h)	r_{max} (Å) ±0.2	b (Å) ±0.2	S† (u.a.) ±50
0.42	32.0	6.2	10 100	1.08	33.5	6.7	22 550
2	33.0	6.5	10 700	2.17	33.9	6.9	20 680
20	40.0	9.0	5 820	8	35.5	7.0	18 850
80	40.0	9.0	5 820				

*L = 1.70 Å; θ ($r \rightarrow \infty$) = 10^3 s pour tous ces calculs.
†$S = \int_0^\infty D(r,t=0)\,dr \propto$ nombre total électrons piégés à $t = 0$.

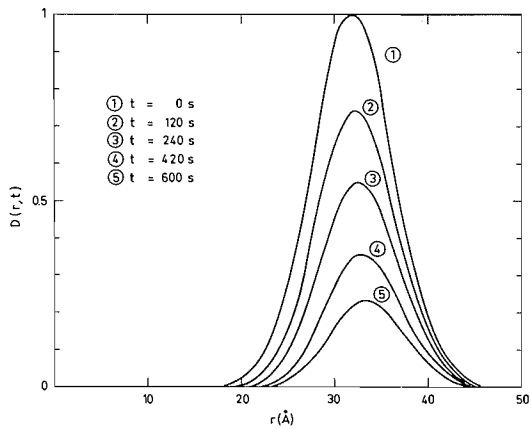

FIG. 3. Evolution de la fonction de distribution des électrons autour du cation, $D(r,t)$ au cours d'une cinétique de décroissance ITL, pour τ_{relax} = 0.42 h. t est le temps écoulé depuis la fin de l'irradiation.

d'irradiation t_{irrad} puis une lente évolution vers un palier.

Parallèlement, la cinétique de décroissance de l'ITL varie rapidement au début et tend vers une cinétique d'équilibre (voir réf. 5, fig. 2). Il est alors intéressant de savoir comment évolue la fonction de distribution des électrons autour des cations quand t_{irrad} augmente. Nous avons donc calculé r_{max}, b et l'aire S pour plusieurs durées d'irradiation. Les observations expérimentales sont faites sur l'échantillon complètement relaxé ($\tau > 80$ h), de telle sorte que nous éliminons toutes les variations de cinétique ITL dues à la relaxation.

Les variations de r_{max}, b et S sont indiquées sur les figs. 4 et 5. r_{max} passe de 35 ± 0.2 Å pour t_{irrad} = 5 s à 40 ± 0.2 Å pour $t_{irrad} \simeq 30$ s; b de 7 ± 0.2 Å à 9 ± 0.2 Å pour les mêmes durées. Pour $t > 30$ s, r_{max} et b restent égaux à 40 et 9 Å. Il est intéressant de noter que pour $t > 30$ s l'aire S continue à augmenter lentement alors que r_{max} et b restent constants. Il est probable qu'on atteint là une des limites du modèle qui s'avère incapable de déterminer avec précision de faibles variations de la fonction de distribution.

La fig. 5 montre que pour $t_{irrad} \lesssim 20$ s, le nombre d'électrons piégés est proportionnel à la durée d'irradiation, un résultat connu qui nous permet de tester la cohérence du modèle.

A la lumière de ces résultats, on voit qu'il y a une expansion de la fonction de distribution autour des cations pendant l'irradiation, mais

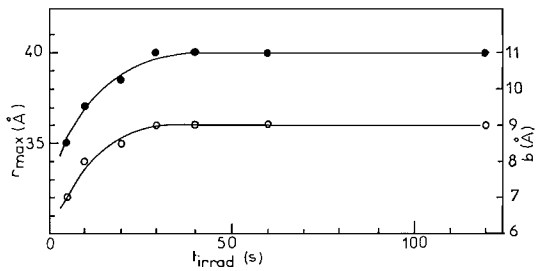

FIG. 4. Variation des paramètres r_{max} et b en fonction de la durée d'irradiation en lumière ultra-violette: ●, r_{max}; ○, b.

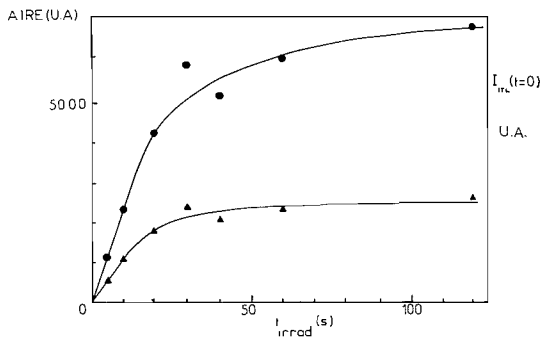

FIG. 5. Variation de l'aire $S = \int_0^\infty D(r,t=0)\,dr$ (○) et de $I_{ITL}(t=0)$ (△) en fonction de la durée d'irradiation en lumière ultra-violette.

Can. J. Chem. Downloaded from www.nrcresearchpress.com by 210.87.254.6 on 09/05/12
For personal use only.

Can. J. Chem. Downloaded from www.nrcresearchpress.com by 210.87.254.6 on 09/05/12
For personal use only.

que, même au voisinage de la saturation, la majorité des électrons restent localisés dans une sphère de rayon ~ 60 Å. De plus, nous pouvons déduire que pendant l'irradiation un certain nombre d'électrons piégés absorbent la lumière excitatrice $\lambda = 313$ nm, et vont se piéger à une plus grande distance du cation. La probabilité d'absorption de cette longueur d'onde est certainement très faible mais non nulle. L'électron dépiégé pourrait alors être promu dans les états excités localisés situés au-dessus de la bande de conduction étudiés par Funabashi et Maruyama (8).

VI. Variation de la fonction de distribution $D(r,t = 0)$ avec l'intensité de la lumière excitatrice

On sait que l'ionisation du système TMPD/3-MP à 77 °K est un mécanisme biphotonique, c'est-à-dire que le nombre d'électrons piégés dans la matrice est proportionnel au carré de l'intensité J de la lumière excitatrice ($\lambda = 313$ nm). Afin de tester la cohérence interne du modèle nous avons voulu vérifier que le nombre d'électrons piégés à $t = 0$ $N \propto S = \int_0^\infty D(r,t = 0)\, dr$ varie comme J^2. Pour cela, nous avons utilisé un échantillon ayant relaxé pendant 15 h et l'irradions avec des intensités J variables, au moyen de filtres appropriés (l'échantillon est donc différent de celui utilisé auparavant paragraphes IV et V). Pour chaque intensité J, nous déterminons r_{max} et b et calculons l'aire S de la fonction de distribution des électrons à $t = 0$. La fig. 6 montre la variation

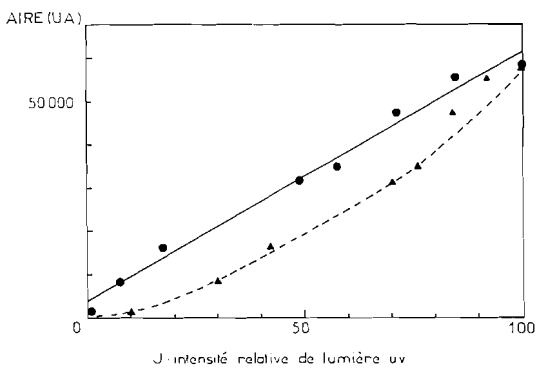

FIG. 6. Vérification à l'aide du modèle que la photoionisation est un phénomène biphotonique. Le nombre d'électrons piégés $N \propto S = \int_0^\infty D(r,t = 0)dr$ est porté en fonction du carré de l'intensité J^2 de la lumière excitatrice (●) et de J (▲). La meilleure droite a pour équation $S = 5.74J^2 + 3886$.

de S en fonction de J^2 et en fonction de J. Il est évident que seuls les points $S = f(J^2)$ s'alignent sur une droite. La meilleure droite qui a été calculée par la méthode des moindres carrés a pour équation: $S = 5.74J^2 + 3886$. Elle passe très près de l'origine (la droite théorique passe évidemment par ce point). Par ailleurs, nous avons porté log S en fonction de log J et obtenu une droite de pente ~ 1.76 au lieu de 2.

TABLEAU 2.*

I (%)	r_{max} (Å)†	b (Å)†	S (u.a.)
100	40.5	9.0	57 800
92.4	40.5	9.0	55 000
84.2	39.0	8.5	47 760
75.8	38.5	8.5	34 860
70	37.5	8.5	31 680
42	36.5	7.5	16 500
27.75	36.5	7.5	8 600
10.9	36	7.5	1 500

*L'échantillon utilisé ici est différent de celui des expériences décrites dans les paragraphes IV et V.
†Comme ci-dessus $L = 1.70$ Å et θ ($r \to \infty$) 10^3 s.

Deux remarques importantes sont à noter.

(1) Les paramètres r_{max} et b varient avec l'intensité de la lumière excitatrice (tableau 2), à condition que le temps d'irradiation soit choisi sur la *partie linéaire* de la courbe de saturation (fig. 6, courbe 1) c'est-à-dire pour $t_{irrad} \lesssim 20$ s.

(2) Si au contraire $t_{irrad} \gtrsim 20$ s, la variation de r_{max} et b est moins rapide et même pour $t = 60$ s, ces paramètres restent constants quelle que soit l'intensité J utilisée.

Parallèlement, et ceci est à souligner, les points $S = f(J^2)$ ne sont plus alignés avec l'origine pour $t_{irrad} \gtrsim 20$ s, c'est-à-dire que sur cette partie de la courbe de saturation, bien que l'ionisation demeure essentiellement biphotonique, des processus de recombinaison et de repiégeage pendant l'irradiation ultra-violette interviennent pour diminuer le rendement de l'ionisation. C'est une conclusion parallèle à celle que nous avons tirée dans le paragraphe V et qui corrobore les études d'électrophotoluminescence. En effet, celles-ci avaient montré qu'on ne pouvait déduire une cinétique perturbée de la cinétique non perturbée que si le temps d'irradiation était choisi sur la partie linéaire de la courbe de saturation (réf. 5, paragraphe IV.C). L'interprétation donnée dans ce travail était qu'au fur et à mesure qu'on

Can. J. Chem. Downloaded from www.nrcresearchpress.com by 210.87.254.6 on 09/05/12
For personal use only.

s'approche de la saturation, les recombinaisons bimoléculaires des électrons avec les cations voisins (et non pas avec les cations-parents) deviennent importantes. Dans la mesure où le présent modèle ne permet de calculer une cinétique expérimentale que s'il y a corrélation entre l'électron et le cation (la cinétique est une somme infinie de décroissances exponentielles), cette conclusion doit être modifiée. Tous les électrons resteraient corrélés et le mauvais accord entre cinétique EPL théorique et EPL expérimentale serait dû aux recombinaisons (corrélées) et au repiégeage des électrons pendant l'irradiation ultra-violette. Quoi qu'il en soit, la fig. 6 montre que le modèle est capable de démontrer que l'ionisation est un processus bi-photonique, et nous considérons ceci comme un test positif pour le modèle.

VII. Conclusion

Le modèle cinétique que nous proposons nous permet:

(1) de décrire la cinétique de décroissance de l'ITL avec une précision $\pm 3\%$, pour des temps d'observation $t \lesssim 900$ s. Au delà de ce temps la cinétique théorique s'écarte de la cinétique expérimentale. Nous interprétons cette différence comme la conséquence de l'existence de plusieurs types de pièges E_i, le modèle ne traitant que le cas simple où il n'existe qu'un piège de profondeur E.

(2) Le piège E est caractérisé par une longueur $L \simeq 1.70$ Å qui est de l'ordre de grandeur de la demi-largeur du piège. L est à rapprocher du paramètre de couplage $d \simeq 1.6$ Å, découvert lors d'études d'électrophotoluminescence (5). L'électron localisé dans un piège E situé à une distance r Å très grande par rapport à 50–60 Å a une durée de vie $\theta(r \to \infty) \sim 10^3$ s. La valeur exacte de E reste indécise puisque dans l'équation $\theta(r \to \infty) = \nu \exp(\beta E) \sim 10^3$ s, le facteur de fréquence ν est inconnu.

(3) La fonction de distribution des électrons autour des cations varie en fonction de nombreux paramètres. Si r_{max} et b caractérisent la fonction de distribution gaussienne que nous avons testée dans ce travail, nous constatons que ces paramètres varient: (*a*) d'une trempe à l'autre; (*b*) pour un même échantillon, avec le temps écoulé depuis la trempe du verre; (*c*) avec la durée d'irradiation en lumière ultra-violette; (*d*) avec l'intensité de la lumière excitatrice à condition que t_{irrad} soit sur la partie linéaire de la courbe de saturation. Bien que la fonction de distribution des électrons piégés que nous avons choisie soit une approximation, il est vraisemblable que les mêmes variations seraient décelées avec une fonction de distribution plus proche de la réalité.

(4) Le fait que le nombre d'électrons piégés diminue quand le temps écoulé depuis la trempe du verre augmente, corrobore la théorie du volume libre qui prévoit qu'au cours de la relaxation isotherme d'un verre certaines cavités disparaissent à la suite de modifications configurationnelles. Les pièges à l'électron seraient ainsi préexistants dans les verres non polaires du type 3-MP. Au contraire, dans les solvants polaires, l'électron libre peut polariser les molécules de solvant voisines et créer ainsi son propre piège.

(5) Enfin, nous constatons que tous les électrons piégés (dépiégeables au cours de l'ITL pour $t < 900$ s) se trouvent situés dans une sphère de rayon $r \sim 50$–60 Å, dont le centre est le cation. Là encore, nous sommes d'accord avec un résultat obtenus par l'étude de l'électrophotoluminescence du même système.

Ces résultats sont encourageants. Toutefois, la description que permet ce modèle simple reste limitée, car il ne tient compte que d'une partie des électrons présents dans le 3-MP après irradiation. Il reste donc à écrire un modèle plus élaboré dans lequel on considère p types de pièges.

1. (*a*) D. Ceccaldi et J. Bullot. Chem. Phys. Lett. **9**, 551 (1971). (*b*) D. Ceccaldi. Thèse de 3° cycle. Orsay, 1971.
2. A. C. Albrecht. Acc. Chem. Res. **3**, 238 (1970).
3. A. C. Albrecht et R. Ott. Communication privée.
4. C. Meyer. Thèse 3° cycle. Orsay; F. Kieffer, M. Magat, C. Meyer, et J. Rigault. Nature, **232**, 130 (1971); F. Kieffer, C. Meyer, et J. Rigault. Chem. Phys. Lett. **11**, 359 (1971).
5. J. Bullot et A. C. Albrecht. J. Chem. Phys. **51**, 2220 (1969).
6. D. S. Kliger, J. D. Laposa, et A. C. Albrecht. J. Chem. Phys. **48**, 4326 (1968).
7. (*a*) M. H. Cohen et D. Turnbull. J. Chem. Phys. **31**, 1164 (1959); (*b*) D. Turnbull et M. H. Cohen. J. Chem. Phys. **34**, 120 (1961); (*c*) A. J. Kovacs. Fortschr. Hochpolym. Forsch. **3**, 394 (1961).
8. K. Funabashi et Y. Maruyama. J. Chem. Phys. **55**, 4494 (1971).

Mean Lifetime of an Embryo in the Homogeneous Nucleation from Solution of the Tetracyanoplatinates(II) of Barium, Calcium, and Magnesium

O. A. BEMPAH AND O. E. HILEMAN, JR.[1]

Department of Chemistry, McMaster University, Hamilton, Ontario

Received August 18, 1972[2]

The mean lifetime of an embryo in the homogeneous nucleation from aqueous solution of the tetracyanoplatinates(II) of barium, calcium, and magnesium has been studied using the droplet technique. Supersaturation in the droplets was generated by selective extraction of the solvent into the surrounding silicone oil. Crystallization in the droplets was followed by photomicrography using plane polarized light.

The data were analyzed using both the classical model and the mean lifetime model of Carlier and Frisch. The experimental results are consistent with the predicted relationship between the logarithm of the nucleation rate or the logarithm of the mean lifetime of an embryo and the inverse of the square of the logarithm of the supersaturation ratio at high supersaturation ratios. The calculated values of the interfacial energy, using both models, are in close enough agreement to justify the assumptions made in the analysis.

La durée de vie moyenne d'un germe lors du processus de nucléation homogène à partir d'une solution aqueuse des tétracyanoplatinates(II) de baryum, de calcium et de magnésium a été étudiée à l'aide de la technique impliquant des gouttelettes de solution. La supersaturation dans les gouttelettes a été obtenue par extraction sélective du solvant dans l'huile de silicone environnante. La cristallisation dans les gouttelettes a été suivie à l'aide de la photomicrographie en utilisant de la lumière polarisée selon un plan.

Les données furent par la suite analysées selon le modèle classique et le modèle impliquant la durée de vie moyenne de Carlier et Frisch. Les résultats expérimentaux sont en accord avec la relation anticipée qui existe entre le logarithme de la vitesse de nucléation ou le logarithme de la durée de vie moyenne d'un germe et l'inverse du carré du logarithme du rapport de supersaturation pour des rapports élevés de supersaturation. Les valeurs calculées de l'énergie interfaciale, en utilisant les deux modèles, sont suffisamment proches pour justifier les hypothèses faites durant l'analyse.

[Traduit par le journal]

Can. J. Chem., **51**, 3435 (1973)

Introduction

The time lapse between the creation of the supersaturated or super-cooled state and the detection of a new phase by some device is known as the induction time or "time lag" (1–3). It is expressed by the equation

$$[1] \qquad t_p = t_i + t_n + t_g$$

where t_i = the time required to attain the steady state embryo distribution; t_n = the time required for nucleation; and t_g = the time required for growth of the nucleus to detectable dimensions.

Attempts at a theoretical evaluation of the induction time "t_p" have been made by several authors, especially Zeldovitch (4), Turnbull (5), and Kantrowitz (6). But for purposes of homogeneous nucleation, none of the factors on the right side of eq. 1 have been evaluated independently until quite recently. Frisch and Carlier (7) have considered the whole question of induction time and found the expression for the mean lifetime of the critical sized embryo to be

$$[2] \quad L_1 = (\pi)^{1/2} \frac{kT\eta^{1/2}d}{\sigma^{1/2}M^{1/2}SC_{A_0}} \times \exp\left[\frac{-(4\pi)^{1/3}(3Md)^{2/3}\sigma}{\eta^{2/3}kT} + \ln S + \frac{16\pi\sigma^3M^2}{3\eta^2d^2(kT)^3 \ln^2 S}\right]$$

where η = Avogadro's number; σ = surface tension in erg/cm^2; d = density in g/cc; M = the g-mol. wt. of solute; S = supersaturation ratio; k = Boltzman's constant; T = the absolute temperature; and C_{A_0} = equilibrium solubility of the solute at the temperature of the experiment.

L_1 may be equated with t_n in eq. 1, since the nucleation time is the time required for a critical-

[1]Author to whom all correspondence should be directed.

[2]Revision received June 13, 1973.

sized embryo to acquire the extra molecule or ion to become a nucleus.

Experimental data on induction time is scarce and as far as can be ascertained, there are no published data on the mean lifetime of an embryo. It was therefore decided that the droplet technique would be used to study this aspect of nucleation from solution.

One major problem associated with the use of the droplet technique in nucleation studies is the creation of sufficient supersaturation within each droplet to ensure crystallization. The reduction of solubility by gradually cooling the droplets limits the usefulness of the method to the study of highly soluble substances because of the narrow temperature range available, *e.g.*, 100 to 0 °C. The technique of generating one of the reaction partners in solution also limits the number of substances which can be studied. The droplet contraction technique is more versatile in that a very high supersaturation can be generated in each of a population of droplets by the selective diffusion of the solvent (water) into the surrounding medium. The latter was the obvious method of choice for our studies on the tetracyanoplatinates.

Experimental

A droplet contraction experiment consists of two parts: (*a*) the dispersion of a saturated aqueous solution of the compound of interest in a suitable silicone oil, and (*b*) photomicrographic recording of the size changes and the crystallization events occurring in the droplet population.

Apparatus

The dispersions were prepared with the aid of a Virtis microhomogenizer (Fisher Scientific Company) and a 7 ml flask which was obtained as an accessory.

The selection of a suitable number of drops within the desired size range was accomplished by centrifugation (International Clinical Centrifuge, Central Scientific Company, Chicago, Illinois). The apparatus was adapted to enable the rotation of Nessler cups.

The Nessler cups (diameter 3.2 cm, height 2.5 cm) were made from Nessler tubes (Fisher Scientific Company). The inside bottom of the thoroughly clean and dry cup was coated with a thin layer of clear silicone fluid (viscosity 60 000 cP). The cup was placed upside down in an oven at 160 °C for about 3 days to drain off excess fluid. On cooling, the inside wall of the cup was wiped clean of fluid. Precautions were taken to exclude dust particles from the cup both immediately before and after its preparation.

The disperisons were examined with a M15 polarizing microscope (Vickers Instruments Inc., Scarborough, Ontario).

Photographs of selected fields of view were taken with an Autowind 35 mm camera and J35 Exposure Unit (Vickers Instruments Inc.). The film used was Ansochrome Color Slide Film – 500 ASA (GAF (Canada) Ltd., Mississauga, Ontario). The photographs were studied with the aid of a Leitz slide projector.

Preparation of the Salts and Their Saturated Solutions

Magnesium Tetracyanoplatinate

A saturated solution of barium tetracyanoplatinate(II) (Alfa Inorganics, Inc., Beverly, Mass.) was prepared by dissolving about 4 g of the salt in 50 ml of deionized water. The solution was warmed to about 60 °C, allowed to cool to room temperature, and then filtered. A saturated magnesium sulfate solution was added to the filtrate. The thick white precipitate of barium sulfate was separated from the solution by centrifugation and then filtration. The filtrate was evaporated until a large amount of precipitate formed. The crude magnesium tetracyanoplatinate was collected and recrystallized twice. The saturated solutions used in the nucleation studies were prepared by dissolving the purified salt in deionized water.

Calcium Tetracyanoplatinate

The preparation of the calcium tetracyanoplatinate was similar in procedure to that used for the magnesium salt except that calcium chromate solution was used to precipitate the barium from solution.

Barium Tetracyanoplatinate

The saturated solutions of the barium salt were prepared from the recrystallized commercial stock.

Procedure

About two drops (0.05 ml) of a freshly filtered saturated solution of the appropriate salt was placed in the microhomogenizer flask containing about 5 ml light mineral oil (viscosity 20 cP). The flask was placed in position on the microhomogenizer stand. The stirrer was lowered to within a few millimeters from the bottom of the flask and the homogenizer turned on for 5 s at a preselected speed of 4000 r.p.m. The resulting dispersion was quickly transferred into a centrifuge tube containing about 5 ml of heavy mineral oil (viscosity 180 cP). The centrifuge tube and contents were rotated for 60 s. By means of a dropping pipette, some of the heavy oil containing droplets of various sizes but no air bubbles was withdrawn and put into the Nessler cup. The Nessler cup was then rotated in the centrifuge for about 90 s. Part of the contents of the cup was decanted off, leaving a layer of droplets anchored in silicone fluid. The side of the cup was wiped clean. Silicone oil (viscosity 100 cP) was added and the whole rotated in the centrifuge for about 5 s. The mineral oil – silicone oil mixture was decanted off and fresh silicone oil (100 cP) added. This operation was usually repeated two or three times, the aim being the exchange of silicone oil for the mineral oil present. Finally a layer of about 2 mm of silicone oil was left on top of the droplet layer. The cup was then placed on the microscope stage, examined, and suitable fields of view selected for observation.

Photographs of these fields were taken at regular intervals varying from 2–4 min depending on the compound.

The photographs were developed and the slides, numbered in sequence, were projected on a calibrated screen. The diameter of each droplet (except the ones of

very small initial diameters, *ca.* 10 μ) was measured on each slide. Also the number of droplets and the time a crystal was first detected in each of them were noted.

Results

Qualitative Observations

One major requirement of the droplet technique experimental system is that the formation of each nucleus must induce the formation of one crystal in one droplet. This implies that the growth rate of the crystallite formed must be fast compared with the nucleation rate so that multiple nucleation in each droplet is avoided. This requirement was met in all the salts described in this study. In the very small droplets with a final diameter range between 8 and 10 μ, the individual droplets solidified completely and suddenly. With the larger droplets (final diameter range of 20 to 30 μ), however, the crystal(s) formed could usually be detected long before the whole droplet soldified completely. Throughout the experiments the contents of a droplet were assumed to have nucleated at the first detection of a crystal.

In the course of observing the droplets under the microscope, each droplet in the population disappeared completely and uniformly and then reappeared before nucleation occurred. This complete and uniform disappearance of the droplets irrespective of size indicates that there is no significant concentration gradient from the center of the droplet to the solution/oil interface. Also, when nucleation occurred, the position of the crystals in the droplets appeared to be random; that is crystals appeared at the edge of some droplets, and in others at the center. (Of course, there was no way to determine the position of crystals which appeared at the solution/oil interface nearest to, or farthest from, the microscope objective; they might appear to lie in the center of the droplet.)

The effect of the dispersion medium (silicone oil and silicone grease) was also studied. Table 1 shows the combinations used and the data found for the calcium salt. The $t_{1/2}$ was taken as the time (in laboratory coordinates) when 50% of the droplets under observation had crystals in them. The data shows that the dispersion medium did not affect the nucleation process. Similar results were found for the other salts.

It has been suspected that in droplet experiments where many droplets in close proximity are observed at the same time, dendrites shoot from crystallized droplets and catalyze the nucleation of neighboring droplets. This "neighborhood effect" if present will generate a nucleation "front"; that is, the photomicrographs will show a field of droplets in which droplets with crystals in them would appear first at one side of the field and progress to the other. This effect was observed in the preliminary studies on ammonium tetracyanoplatinate. Because of this the salt was rejected from any further study. In the case of the remaining compounds studied, the absence of local extraneous effects on particular droplets was indicated by the fact that the spatial distribution in which crystals appeared in the droplets was found to be entirely random.

TABLE 1. Effect of reaction medium on droplet nucleation (for calcium salt)

Silicone oil	Silicone grease	$t_{1/2}$ (min)*
100 cP (used as purchased)	1 000 000 cP	43
100 cP	60 000 cP	56
100 cP (vacuum dried)	1 000 000 cP	56
	60 000 cP	47
200 cP (used as purchased)	1 000 000 cP	61
200 cP (used as purchased)	60 000 cP	45

*Mean $\bar{t}_{1/2}$ = 51.3 min (s.d. = 7.6).

The size range studied for all the compounds was 10 through 60 μ final diameter. It was found that droplets which did not contain a crystal included those of all diameters. Therefore, the probability of a crystal not appearing in a droplet did not depend on its size.

Statistical consistency of the data was also considered, since data from four or five sets of experiments, conducted over a period of time, were necessary to enable a significant number of droplets to be obtained for analysis. The $t_{63\%}$ test showed that the reproducibility of the separate experiments was satiafactory because it was nearly the same for a particular salt. Consequently all the droplets for a particular salt were analyzed together irrespective of the time separating different experimental runs.

Further examination of the photomicrographs revealed that the diameter of each droplet decreased sharply and rapidly at the beginning of the experiment but the decrease tailed off until eventually the diameter remained nearly constant for a time before a crystal appeared in the droplet. It was observed that for some droplets, this near constancy of the diameter

was not attained before nucleation occurred, but these were few in number. The time taken by each droplet to reach this near constant diameter range was found to depend on the initial diameter and on its position in relation to other droplets in the field of view. It must be borne in mind that droplets with different initial diameters could, and did have, the same final diameter. Similarly, droplets of the same initial diameter did not necessarily attain the same final diameter.

Calculation of the Supersaturation Ratio for Each Droplet

The problem is to find the concentration of any component in a droplet located in a medium in which the solvent is transferring from the droplet to the surrounding medium. Physical transfer is assumed, that is, there is no chemical reaction at the droplet/bulk phase interface, and mass transfer corresponds to transfer from a spherical droplet into a stagnant medium. The assumptions in the analysis are:

(1) The concentration of the transferring component in the bulk phase remains constant during the time interval (*i.e.*, small amounts of the transferring phase are actually transferred).

(2) The concentration at the droplet/bulk phase interface corresponds to equilibrium conditions.

(3) The droplet has a uniform concentration.

(4) The equilibrium concentration of the transferring component is independent of the concentration of the nontransferring component in the droplet (this is expected to be realistic for low concentrations).

Using kinetic considerations it has been shown (8) that at the end of time "t" in laboratory coordinates, from the moment when the dispersion was prepared for observation, the concentration of the solute, C_A, is given by

$$[3] \qquad C_A = (C_{A_0} D_0^3)/(D_0^2 - k_2 t)^{3/2}$$

where D_0 = the initial diameter; k_2 = a constant term (8); and $(D_0^2 - k_2 t)^{3/2}$ = the final volume of the droplet.

The supersaturation ratio, C_A/C_{A_0}, then, is given by eq. 4.

$$[4] \qquad S = C_A/C_{A_0} = D_0^3/(D_0^2 - k_2 t)^{3/2}$$

Determination of the Mean Life of an Aggregate of Embryos

The picture that emerges for the rate of change of droplet diameter with time is as illustrated in Fig. 1. Only curves of two droplets which have the same initial diameter are used for clarity of explanation, even though all the droplets used in this study were similarly analyzed. In the figure, $X = 0$ is zero time in laboratory coordinates, and represents the time when the first photomicrograph was taken. $X = t_{B_0}$ and t_{A_0} is the time in laboratory coordinates at which each droplet diameter was just distinguishable from its final diameter. For most droplets the points "M" and "N" represent about 105% of the final diameter, but for droplets of small final diameter (less than 10 μ) they represent about 110% of the final diameter. $X = t_{B_F}$ and $X = t_{A_F}$ are the times in laboratory coordinates when a crystal was detected in droplets B and A respectively. The difference in time between these two identifiable events is given by eqs. 5 and 6.

$$[5] \qquad L_B = t_{B_F} - t_{B_0}$$

$$[6] \qquad L_A = t_{A_F} - t_{A_0}$$

This time interval was determined for each droplet in the population.

For generality, L_A, L_B, etc. were replaced by L_n, where L_n represents the time interval for the nth droplet. Experimentally, L_n varies from zero to infinity. $L_n = 0$ represents those droplets in which crystals appeared before reaching near

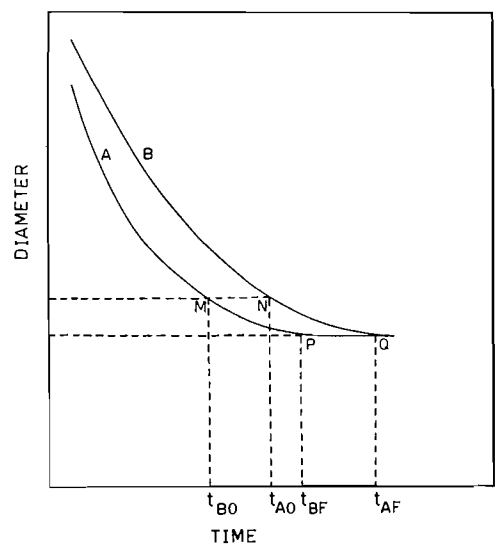

FIG. 1. Schematic diagram of rate of change of droplet diameter *vs.* time.

constancy in diameter, while $L_n = \infty$ represents droplets in which crystals did not appear at all during the duration of the experiment. Observation was normally stopped when more than 98% of the droplets had crystals in them.

The interval, L_n, was identified with the lifetime of an embryo in each droplet. Since nucleation is a probabilistic phenomenon, individual values of L_n are meaningful only when they are viewed as one of an aggregate. To obtain the mean of an aggregate, all the droplets were first grouped according to final diameter ranges at constant supersaturation and the *probability of nucleation vs. time* was plotted on a probability paper. It was found that the time for 63% of the droplets to nucleate, in any size range, was independent of the volume.

The droplets were then grouped according to supersaturation ratios independent of size, and a histogram of the number of droplets nucleating with time was made. The histograms are shown in Figs. 2, 3, and 4. The median time, L_m, for the population of droplets at a particular supersaturation was read from the histogram. This

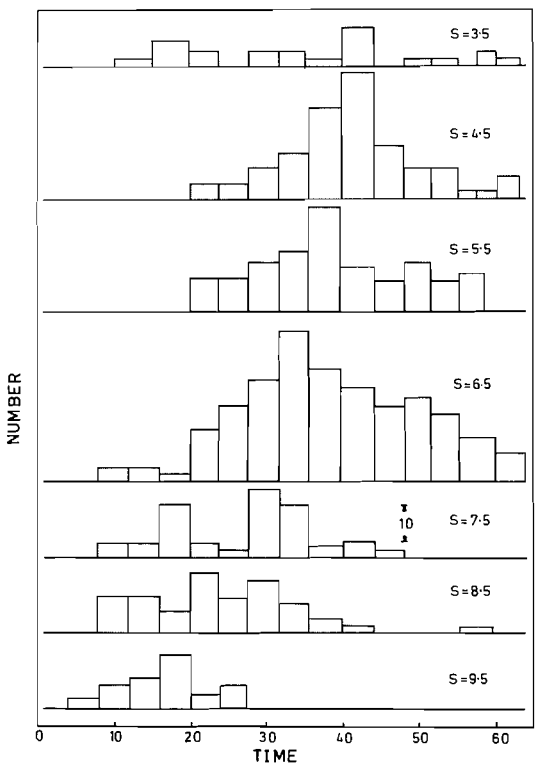

FIG. 2. Histogram of number of droplets nucleating with time for barium tetracyanoplatinate.

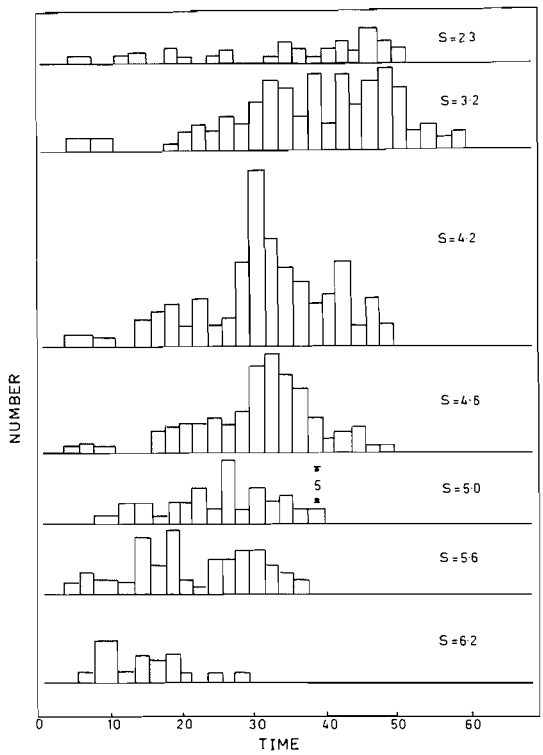

FIG. 3. Histogram of number of droplets nucleating with time for calcium tetracyanoplatinate.

was identified with the L_m of an embryo at any given supersaturation. Rewriting eq. 2 in logarithmic form and writing L_m for L_1 gives eq. 2*a*,

$$[2a] \quad \ln L_m = \ln B - E + (16\pi\sigma^3 v^2)/3(kT)^3 \ln^2 S$$

where B and also E, if σ is assumed constant, are constants and v = the molecular volume in the forming phase.

A plot of $\ln L_m$ *vs.* $(\ln S)^{-2}$ was made for each salt studied (see Fig. 5). The results of the calculation of σ from the slope of each plot are shown in Table 2.

TABLE 2. Summary of parameters obtained using both the classical model and the mean lifetime model of analysis

Compound	σ(erg cm^{-2}) (*a*)*	(*b*)†	n^* (*a*)	r^* (Å) (*a*)	log *A* (*a*)
Barium salt	11.00	9.60	47	13.2	8.70
Calcium salt	9.00	8.70	49	13.7	7.60
Magnesium salt	8.10	6.90	74	14.3	6.80

*(*a*) Calculated using the classical model.
†(*b*) Calculated using the mean lifetime model.

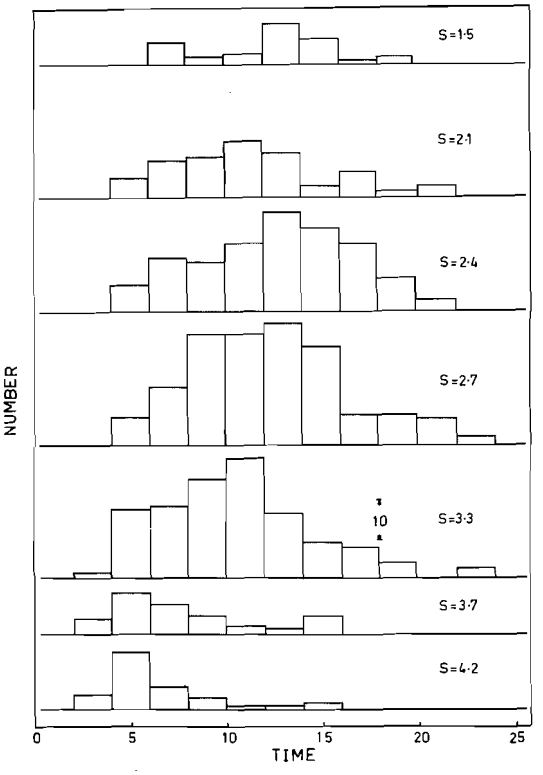

FIG. 4. Histogram of number of droplets nucleating with time for magnesium tetracyanoplatinate.

Calculation of Experimental Rate of Nucleation

The method used here is analogous to that used in reducing experimental observations on freezing water drops to nucleation rates. In such experiments it can be shown (9, 10) that if only N of the original N_0 droplets, each having the same volume V, remain unfrozen after a time interval Δt, then the nucleation rate can be calculated as

$$[7] \qquad J = \frac{1}{V} \cdot \frac{1}{1 - P} \cdot \frac{\Delta P}{\Delta t}$$

where J = the rate of nucleation per second per unit volume (ml) and P = the probability of nucleation.

By means of the histogram of number nucleated *vs.* time for each supersaturation ratio, it was possible to obtain the number N of the total N_0 nucleating at any time. From these data, plots of the probability of nucleation as a function of time were constructed (see Fig. 6). Then the rates of nucleation were calculated with the aid of eq. 7.

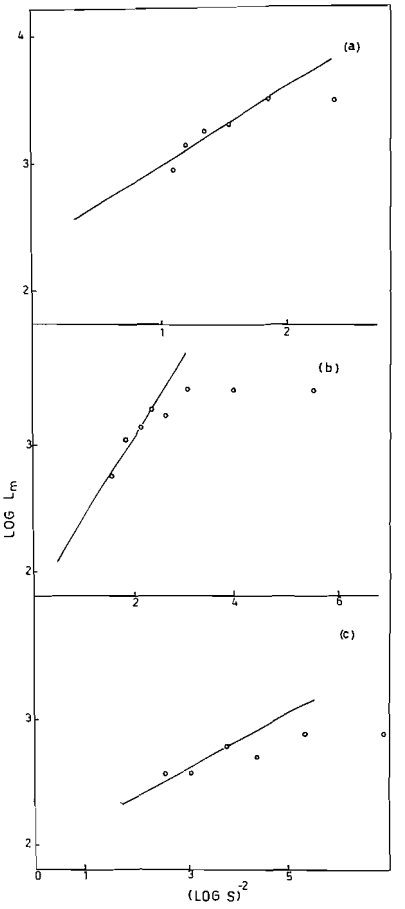

FIG. 5. Logarithm of mean embryo life time *vs.* $(\log S)^{-2}$ for the three salts: (*a*) barium tetracyanoplatinate; (*b*) calcium tetracyanoplatinate; and (*c*) magnesium tetracyanoplatinate.

The J values obtained were plotted against the corresponding supersaturation ratios, as $\log J$ *vs.* $(\log S)^{-2}$, for each of the compounds (see Fig. 7). The values of $\log A$ and σ obtained as intercepts and calculated from the slopes respectively are shown in Table 2.

Other parameters (n^*,r^*) derivable from the classical model were calculated using the values of σ obtained and eqs. 8 and 9.

$$[8] \qquad n^* = 32\pi\sigma^3 v^2/3(kT \ln S^*)^3$$

$$[9] \qquad r^* = 2\sigma v/kT \ln S^*$$

where n^* = number of monomers in the critical nucleus; r^* = radius of the critical nucleus; and S^* = value of S when $J = 1$.

The results of the calculations are shown in Table 2.

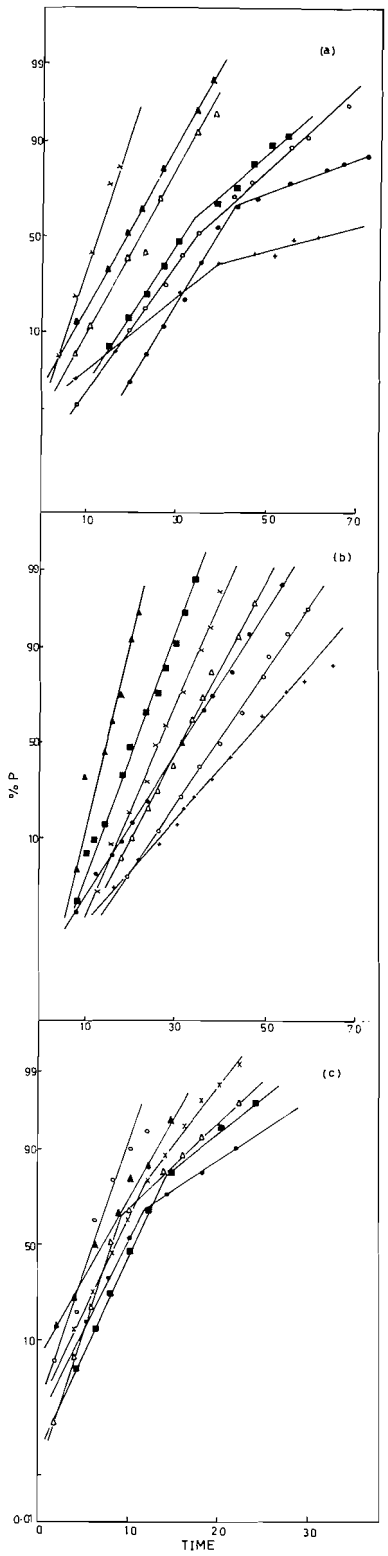

Discussion

In this section, a discussion of the general aspects of the experimental and derived results obtained using both the classical model of analysis and the mean lifetime of embryo model is given.

Close examination of the data shown in Figs. 2–7 reveals that there are two different processes controlling the formation of crystals in the droplet population. This conclusion results from the following collateral observations. Firstly, the value of L_m initially increases to some maximum value then decreases (see Figs. 2–4) as the supersaturation increases. Secondly, the probability *vs.* time plots (Fig. 6) show, at low supersaturation values, two separate droplet populations whose relative frequency distribution curves share a common area. In addition, the first of the two processes tends to overwhelm the second as the supersaturation in the droplet population increases. And thirdly, the anticipated linear relationships expected for the *log* L_m or *log* J *vs.* $(log\ S)^{-2}$ plots were found only for data observed at high supersaturation values. We feel that these observations clearly show that both heterogeneous and homogeneous nucleation processes are taking place in the droplet population.

The values of the rate of nucleation calculated using eq. 7 are limited in accuracy by three major factors. Firstly, the droplet volumes used in this work are not all equivalent as is presumed by the equation; the error involved, however, by using a mean volume is not considerable, especially since the total numbers of the very small and very large droplets in any group of data are less then 10% of the total number of droplets. Since we are dealing with an aggregate of large numbers, this slight deviation is tolerable. Secondly, the probabilistic nature of crystal formation in droplets, which is the basis of eq. 7, must also be considered. The probability of a droplet

FIG. 6. Probability of droplet nucleation *vs.* time at various levels of supersaturation for the three salts. (*a*) Barium tetracyanoplatinate: + = 3.5 ± 0.5; ● = 4.5 ± 0.5; ■ ◐ = 5.5 ± 0.5; ○ = 6.5 ± 0.5; △ = 7.5 ± 0.5; ▲ = 8.5 ± 0.5; × = 9.5 ± 0.5. (*b*) Calcium tetracyanoplatinate: + = 2.8 ± 0.2; ○ = 3.2 ± 0.2; ● = 4.2 ± 0.2; △ = 4.6 ± 0.2; × = 5.0 ± 0.2; ■ ◐ = 5.6 ± 0.2; ▲ = 6.2 ± 0.2. (*c*) Magnesium tetracyanoplatinate: ● = 1.5 ± 0.1; ■ ◐ = 2.1 ± 0.1; △ = 3.0 ± 0.1; × = 3.3 ± 0.1; ▲ = 3.7 ± 0.2; ○ = 4.2 ± 0.2.

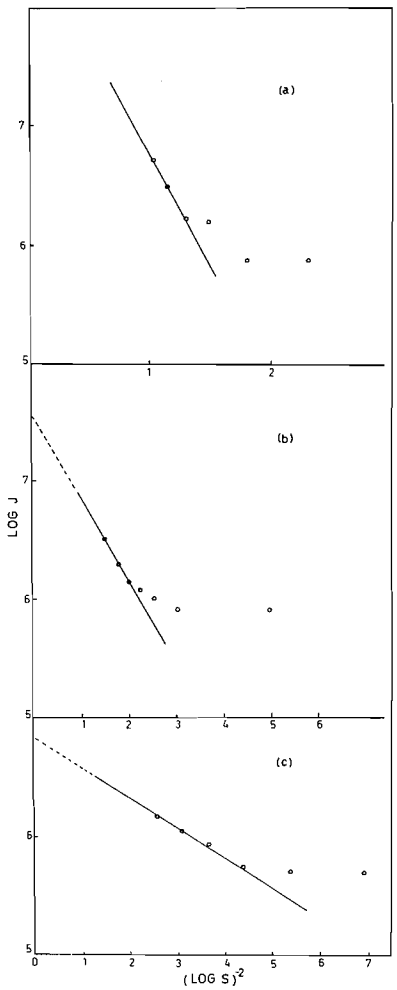

FIG. 7. Logarithm of the rate of nucleation *vs.* $(\log S)^{-2}$ for the three salts. (*a*) Barium tetracyanoplatinate; (*b*) calcium tetracyanoplatinate; and (*c*) magnesium tetracyanoplatinate.

nucleating is determined experimentally by the number of nucleation events (N) occurring in a sample of size (N_0). To make the observed ratio represent reality, a large number of droplets have to be examined. In this work at least 900 droplets were examined for each set of data, thus making it feasible to use the equation for our analysis. Finally, the assumed constant supersaturation over the duration of the "time lag" interval is not strictly realizable. In view of the expected exponential dependence of the nucleation rate on supersaturation ratios, this could lead to a serious error in the calculated rate. The error here may be minimized because an average of a large number of droplets has been used and, in addition, the supersaturation is nearly constant after $S = S^*$.

The experimental values obtained for the pre-exponential or kinetic factor for the barium, calcium and magnesium salts are well below the much debated theoretical value of $10^{25\pm5}$. This is as should be expected. The blocking tendency of ionic charge and water of solvation is not accounted for in the theoretical calculations. These factors will impede and subsequently slow down the rate of addition of monomers to embryos. A slow rate of addition will lower the kinetic factor. In solution it may be necessary to overcome (at least partially) the solvation of the monomers before nucleation can take place. Thus it would be expected that both the energy barrier to desolvation and the large entropy changes coupled with the blocking tendency of escaping solvent molecules will lower the kinetic factor. Also, in highly supersaturated solutions, the viscosity is high, resulting in an increase in the energy barrier to active transport. And finally, the possibility of embryos being charged in ionic solution must be considered. In such a situation the presence of an electrical double layer around the embryo will have a blocking tendency, resulting in a lowered kinetic value. The values obtained in this work are similar, at least in order of magnitude, to values reported in the literature (see Table 7 of ref. 8).

The values of the interfacial energy reported for all the salts were calculated in two different ways. One value was obtained from the mean lifetime model and the other from the classical model. The degree of similarity between these sets of values gives much confidence to the order of magnitude one should expect.

1. H. DAYNES. Proc. Roy. Soc. (Lond.), A, **97**, 286 (1920).
2. W. G. COURTNEY. J. Chem. Phys. **36**, 2009 (1962).
3. H. L. FRISCH. J. Chem. Phys. **27**, 90 (1957).
4. J. B. ZELDOVITCH. Acta Physicochim. URSS, **18**, 1 (1943).
5. D. TURNBULL. Metal. Tech. (June) (1948).
6. A. KANTROWITZ. J. Chem. Phys. **17**, 1097 (1951).
7. H. L. FRISCH and C. C. CARLIER. J. Chem. Phys. **54**, 4326 (1971).
8. O. A. BEMPAH. Ph.D. Thesis. McMaster University, Hamilton, Ontario, 1972.
9. A. E. CARTE. Proc. Phys. Soc. **73**, 324 (1959).
10. J. A. VELAZQUEZ and O. E. HILEMAN, JR. Can. J. Chem. **48**, 2896 (1970).

A Correlation between Critical Volumes and Work Function Data for Electrons in Liquid Hydrocarbons

H. T. DAVIS[1] AND L. D. SCHMIDT[2]

Departments of Chemistry and Chemical Engineering, University of Minnesota, Minneapolis, Minnesota 55455

Received April 2, 1973

Electron-molecule hard-core radii determined with the aid of Springett, Jortner, and Cohen's quasi-free electron theory from electron work function data are shown to correlate with the critical volumes of several hydrocarbons. The radii are approximately equal to the van der Waals radii determined from the critical volumes.

On a montré que les rayons de l'ensemble rigide électron–molécule, déterminés par la théorie de l'électron quasilibre selon Springett, Jortner et Cohen à partir des données fonction travail de l'électron, sont en corrélation avec les volumes critiques de plusieurs hydrocarbures. Les rayons sont pratiquement égaux à ceux de van der Waals déterminés à partir des volumes critiques.

[Traduit par le journal]

Can. J. Chem., 51, 3443 (1973)

Can. J. Chem. Downloaded from www.nrcresearchpress.com by 210.87.254.105 on 09/05/12
For personal use only.

In this article we present a correlation between the critical volumes and the electron–molecule hard-core radii determined from electron work functions in hydrocarbon liquids. The hard-core radii are determined from a theory developed by Springett, Jortner, and Cohen (1) (SJC) for the ground state energy V_0 of quasi-free (conduction) electrons in inert gas liquids. These investigators combine the Wigner–Seitz boundary conditions on an average lattice representation of a liquid with a pseudopotential model in which the electron potential is the sum of the mean-field potential and a hard-core potential representing the repulsive Hartree–Fock pseudopotential. Their final result for the ground state energy of the quasi-free electron is

$$V_0 = T_0 + U_p \quad [1]$$

with

$$U_p = \frac{-3\alpha e^2}{2r_s^4}\left[\frac{8}{7} + \left(1 + \frac{8}{3}\pi\alpha n\right)^{-1}\right] \quad [2]$$

and

$$T_0 = \hbar^2 k_0^2/2m \quad [3]$$

where r_s and k_0 are determined by the relations

$$\tfrac{4}{3}\pi r_s^3 n = 1 \quad [4]$$

and

$$\tan k_0(r_s - a) = k_0 r_s \quad [5]$$

[1]Department of Chemistry and Chemical Engineering.
[2]Department of Chemical Engineering.

α denotes the molecular polarizability, n the number density of the fluid, and a the electron–molecule hard-core cutoff length. Work function measurements provide experimental values of V_0.

According to the SJC theory the ground state energy is the sum of the mean polarization energy U_p and the zero point kinetic energy T_0. The latter is determined essentially by the free volume available to the electron in a Wigner–Seitz cell. If there were no hard-core region, *i.e.* if $a = 0$, then, according to eqs. 5 and 3, k_0 and T_0 would be zero. On the other hand, when $a \neq 0$, the electron in the Wigner–Seitz cell can only move in a concentric sphere of thickness $r_s - a$. This restriction of the motion of the electron gives rise to a finite zero point kinetic energy T_0.

The theoretical values of V_0 compare favorably with the measured work functions of electrons photoinjected into the inert gas liquids (1). In estimating scattering lengths for electrons in hydrocarbons Fueki, Feng, and Kevan (2) and the authors (3) have suggested that the theory is also valid for hydrocarbons if α and a are taken to mean the average (isotropic) molecular polarizability and the average electron–molecule hard-core cutoff. We believe the correlations offered in the present communication represent further evidence that the SJC theory applies to hydrocarbons.

Since both arise from the repulsion between overlapping electron distributions, it seems reasonable to expect the low energy electron–molecule hard-core radius to be proportional to

TABLE 1. Correlation of work function determined electron–molecule hard-core radii, a, with the critical volumes, V_c. The work function data were taken at room temperature (~300 °K) and at the saturated vapor pressure of the fluid being studied

Compound	Observed work functions, V_0(eV)	"Observed" radii a (Å)	$a/V_c^{1/3}$ (Å/(cm^3/mol)$^{1/3}$)
n-Pentane	−0.01[a]	2.03	0.301
Neopentane	−0.43[a]	1.92	0.287
Cyclopentane	−0.28[a]	1.85	0.292
n-Hexane	0.04[a]	2.17	0.304
2,2-Dimethylbutane	−0.15[b]	2.13	0.300
3-Methylpentane	0.01[c]	2.16	0.303
Benzene	−0.14[b]	1.97	0.308
Toluene	−0.22[b]	2.14	0.313
Methyl cyclohexane	0.14[c]	2.23	0.326
2,2,4-Trimethylpentane	−0.18[a]	2.36	0.305
n-Decane	0.22[c]	2.68	0.317

[a]Reference 4.
[b]Reference 5.
[c]Reference 6.

the average molecule-molecule hard-core radius. If these two hard-core radii are proportional to one another, dimensional analysis leads one to expect the ratio of a to the cube root of the critical volume to be the same for nonpolar hydrocarbon fluids. The observed ratios $a/V_c^{1/3}$ are given in Table 1. The ratios are fairly close to the mean value of 0.305 Å/(cm^3/mol)$^{1/3}$. For comparison, we can estimate the molecule–molecule hard-core radius from van der Waals' model, according to which $V_c = 3b_0 = 12[\frac{4}{3}\pi\ a_{vdW}{}^3]$. Thus, we find $a_{vdw}/V_c^{1/3} = 0.271$, a result only about 8% lower than the mean value of $a/V_c^{1/3}$.

We believe the correlation reported here is interesting in itself and lends support to the Springett–Jortner–Cohen model of the work functions of electrons in nonpolar fluids. An important implication of their model is that the work function depends on molecular structure primarily through the packing geometry of the fluid, or, in other words, through the free volume available to the electron as measured by $r_s - a$.

We are grateful to the National Science Foundation and the Petroleum Research Fund for financial support of this work.

1. B. E. SPRINGETT, J. JORTNER, and M. H. COHEN. J. Chem. Phys. **48**, 2720 (1968).
2. K. FUEKI, D. F. FEUG, and L. KEVAN. Chem. Phys. Lett. **13**, 616 (1972).
3. H. T. DAVIS, L. D. SCHMIDT, and R. M. MINDAY. Chem. Phys. Lett. **13**, 413 (1972).
4. R. A. HOLROYD and M. ALLEN. J. Chem. Phys. **54**, 5014 (1971).
5. R. SCHILLER, SZ. VASS, and J. MANDICS. Private communication.
6. R. A. HOLROYD. J. Chem. Phys. **57**, 3007 (1972).

Can. J. Chem. Downloaded from www.nrcresearchpress.com by 210.87.254.105 on 09/05/12
For personal use only.

Spectrométrie de masse des cyclohexanones *gem*-diphénylées. I. Localisation de la charge positive

CLAUDE J. FORTIN, M. FOREST, C. VAZIRI, D. GRAVEL ET YVES ROUSSEAU
Département de chimie, Université de Montréal, C.P. 6128, Montréal, Québec

Reçu le 5 avril

A l'aide de molécules contenant à la fois des groupements *gem*-diphényle et carbonyle, on évalue l'importance relative de ceux-ci en tant que site porteur de charge régissant la fragmentation. L'influence de chaque fonction est reconnue en étudiant des molécules où cette fonction est isolée. Les résultats obtenus démontrent que le carbonyle ne joue pas un rôle important en tant qu'agent directeur de la décomposition des cyclohexanones *gem*-diphénylées par impact électronique. De plus, on trouve que les potentiels d'ionisation des molécules contenant les deux groupes fonctionnels sont très rapprochés de ceux des molécules correspondantes ne contenant que le groupement *gem*-diphénylé.

Using *gem*-diphenyl cyclohexanones as models, the relative importance of *gem*-diphenyl *vs.* carbonyl functions as possible site of localized charge initiating and directing fragmentation has been determined. The influence of each function is recognized by studying molecules where this group has been isolated. The results show that the carbonyl does not play an important role in the *gem*-diphenyl cyclohexanones decomposition under electron impact. Furthermore the ionization potentials of the molecules containing both functions are very close to those of the corresponding molecules comprising the *gem*-diphenyl function exclusively.

Can. J. Chem., **51**, 3445 (1973)

Introduction

Depuis quelques années, un effort considérable a été fait (1–13) dans le but de clarifier le concept de la localisation de la charge positive (ou du centre électrodéficient) dans les processus impliquant la décomposition de molécules par impact électronique. Une des conditions préalables à ces études est liée à la structure des molécules choisies. D'une part, on exige la présence de deux sites favorisés de localisation de charge, sans interférence possible d'autres sites qui gêneraient l'interprétation des résultats. D'autre part, la séparation de ces deux sites doit être assez grande de façon à pouvoir assigner à chacun d'eux son rôle spécifique lors de la fragmentation. Il est évident que la présence de sites adjacents rend difficile le partage des rôles respectifs et que l'on ne saurait alors conclure aux effets de l'un sans parler de l'influence possible des autres fonctions. Il nous a semblé désirable d'étudier les importances relatives des groupes diphényle et carbonyle en tant que sites initiateurs de l'ionisation et de la dégradation en ions fragments. La synthèse des produits étudiés est rapportée ci-dessous et résumée dans le schéma 1.

Partie expérimentale

Les spectres de masse à basse résolution ont été enregistrés à l'aide d'un spectromètre Hitachi RMU-6D par injection directe, la température de la chambre d'ionisation étant 250 °C. Les spectres à haute résolution ont été pris avec un spectromètre AEI MS-902 à double focalisation; la méthode de recouvrement des pics est utilisée pour la mesure précise des masses. L'énergie des électrons ionisants est de 70 eV.

Les spectres r.m.n. ont été déterminés au moyen des appareils JEOL C-60H et 4 H-100 avec référence au tétraméthylsilane; le solvant utilisé est le chloroforme deutérié dans tous les cas. Les spectres i.r. ont été obtenus à l'aide d'un spectrophotomètre Beckman IR-8; les produits sont en solution dans le chloroforme. La chromatographie en phase gazeuse préparative est effectuée sur un chromatographe Varian A90-P3. Les points de fusion sont non corrigés et ont été obtenus avec un appareil Buchi. Les analyses élémentaires ont été confiées à Midwest Microlab Co. Indianapolis.

Diphényl-4,4 cyclohexène-2 one-1 (1)

La méthode utilisée est celle décrite antérieurement par Zimmerman (14): p.f. 92–93° (lit. (14) 88–91.5°).

Diphényl-4,4 cyclohexanone (2)

L'hydrogénation (15) de **1** (6.8 g, 0.0274 mol) en milieu acide acétique glacial (50 ml) contenant 1.09 g de palladium-sur-charbon 10%, fournit après extraction 5.65 g (82%) de diphényl-4,4 cyclohexanone (**2**): p.f. 140–142° (lit. (15) 143–144°); i.r. 1715 cm^{-1} (C=O).

Méthyl-1 diphényl-4,4 cyclohexanol (3)

La méthode utilisée s'inspire des indications rapportées par Houlihan (16). A une suspension de magnésium (1.94 g, 0.08 atome-g) dans 50 ml d'éther anhydre maintenue sous atmosphère d'azote, une solution d'iodure de méthyle (12.5 g, 0.088 mol), dans 20 ml d'éther, est ajoutée goutte à goutte. La solution obtenue est portée à reflux pendant 1 h puis refroidie dans un bain de glace–

Can. J. Chem. Downloaded from www.nrcresearchpress.com by 210.87.254.5 on 09/05/12
For personal use only.

Can. J. Chem. Downloaded from www.nrcresearchpress.com by 210.87.254.5 on 09/05/12
For personal use only.

méthanol. Une solution composée de **2** (10 g, 0.04 mol), dans un mélange de 50 ml de tétrahydrofurane et 25 ml d'éther, est mise en contact avec le réactif de Grignard tout en maintenant la température entre 0 et 5 °C. La température est ensuite ramenée à 25 °C pendant 1 h puis le mélange porté à reflux durant deux heures et enfin refroidi à 5°. Une solution aqueuse et saturée de chlorure d'ammonium est introduite jusqu'à séparation de deux phases. Après extraction à l'éther, lavage, séchage, évaporation du solvant, cristallisation dans le mélange éther – *n*-hexane, la réaction fournit 8.8 g (83%) de **3**: p.f. 110–111°.

Anal. calc. pour $C_{19}H_{22}O$: C, 85.67; H, 8.32. Trouvé: C, 85.51; H, 8.17. Spectre de masse $[M]^+$ à *m/e* 266; i.r. 3620 cm^{-1} (OH libre); r.m.n.: δ 1.1 (s, 3H), 1.97 (s, 1H).

Méthyl-1 diphényl-4,4 cyclohexène (4)

En suivant les indications de Vanderwahl (17), le méthyl-1 diphényl-4,4 cyclohexanol (82.2 g, 0.309 mol) est distillé à 170° sous 0.06 Torr en présence de 50 g de sulfate acide de potassium finement pulvérisé. Après cristallisation (éther–*n*-hexane) 65 g (85%) de **4** sont obtenus: p.f. 49.5–50.5°.

Anal. calc. pour $C_{19}H_{20}$: C, 91.88; H, 8.07. Trouvé: C, 91.47; H, 8.07.

Spectre de masse $[M]^+$ à *m/e* 248; r.m.n. δ 2.34 (t, J = 6 Hz, 2H), 7.2 (s, 10H).

Méthyl-2 diphényl-5,5 cyclohexanone (5)

Une solution de **4** (2.5 g, 0.1 mol) dans 20 ml de diglyme, est additionnée à une solution de borohydrure de sodium (1.77 g, 0.0465 mol) dans 60 ml de diglyme purifié selon la méthode de Brown (18). La température étant maintenue à 25°, 30 ml de diglyme, contenant 4 ml d'éthérate de trifluorure de bore fraîchement distillés, sont introduits goutte à goutte. Après 2 h de contact, 10 ml d'eau sont ajoutés. Le diglyme est alors distillé à 35° sous pression réduite. La pâte collante obtenue est délayée dans 60 ml d'éther anhydre.

Un mélange sulfochromique composé de 22 g de bichromate de sodium, 16.5 ml d'acide sulfurique concentré et complété à 90 ml par de l'eau distillée, est additionné goutte à goutte. Après un reflux de 2 h, la phase aqueuse est décantée et extraite à l'éther selon la méthode usuelle; 24.2 g de produit brut sont obtenus, la purification par chromatographie sur colonne de gel de silice permet d'isoler un produit cristallin: p.f. 72°.

Anal. calc. pour $C_{19}H_{20}O$: C, 86.82; H, 7.63; Trouvé: C, 86.25; H, 7.54.

Spectre de masse $[M]^+$ à *m/e* 264; i.r. 1710 cm^{-1} (C=O); r.m.n. δ 1.00 (d, J = 6 Hz, 3H).

Méthyl-4a oxo-7 diphényl-2,2 octahydro-1,2,3,4,4a,5,6,7 naphtalène (7)

Un mélange de **5** (10.56 g, 0.04 mol), 10 ml d'éthanol et de 10 ml d'une solution obtenue par dissolution de 0.378 g de sodium dans 20 ml d'éthanol absolu est refroidi à −5°. A l'aide d'une seringue, 6.88 ml (0.088 mol) de méthylvinylcétone sont ajoutés lentement. La solution résultante est versée dans une solution aqueuse et glacée de NaCl surmontée d'une phase éthérée. Après extraction et purification sur une colonne de gel de silice, 10.35 g (77%) de méthyl-2(oxo-3 butyl)-2 diphényl-5,5 cyclohexanone (**6**) sont recueillis sous forme d'huile.

Une solution de 45 ml d'hydroxyde de potassium à 5% dans l'eau est ajoutée, sous atmosphère d'azote, à une solution de dicétone **6** (9.131 g, 0.274 mol) dans 15 ml de méthanol. Le mélange réactionnel est porté à reflux et son évolution suivie par c.p.g.; au bout de 4 h la réaction est totale. Après extraction, lavage, séchage et évaporation du solvant, 6.47 g (75%) de **7** sont recueillis: p.f. 101–102°.

Anal. calc. pour $C_{23}H_{24}O$: C, 87.30, H, 7.64. Trouvé: C, 87.47; H, 7.81.

Spectre de masse $[M]^+$ à *m/e* 316; i.r. 1670 cm^{-1} (C=O conjugué); r.m.n. δ 1.3 (s, 3H), 5.95 (s, 1H), 7.22 (s, 10H).

Diphényl-1,1 cyclohexane (8)

La réduction de Wolf–Kishner modifiée par Huang et Minlon (19) effectuée sur la diphényl-4,4 cyclohexanone (**2**) conduit à **8**: p.f. 44–45° (lit. (20) 43–44°). Spectre de masse $[M]^+$ à *m/e* 236.1547, $[M]^+$ calculé pour $C_{18}H_{20}$: 236.1565.

Méthyl-4 diphényl-1,1 cyclohexane (9)

L'hydrogénation catalytique (palladium-sur-charbon, 10%) de **4** (0.3 g, 0.0012 mol) en milieu acide acétique glacial fournit le composé **9**. R.m.n. δ 0.83 (d, J = 5 Hz, 3H); spectre de masse $[M]^+$ à *m/e* 250.1626, $[M]^+$ calculé pour $C_{19}H_{22}$: 250.1676.

Diphényl-3,3 cyclohexène (10)

Le traitement de la cétone **1** (3.0 g, 0.012 mol) par la tosylhydrazine (2.0 g, 0.01 mol) conduit à la tosylhydrazone de la diphényl-4,4 cyclohexène-2 one-1 avec un rendement quantitatif: p.f. 191–193°. La réduction de cette tosylhydrazone (0.9 g, 0.0021 mol) est effectuée en milieu tétrahydrofurane par $LiAlH_4$ (1.2 g, 0.031 mol). Un reflux de 17 h est maintenu; après extraction selon la méthode habituelle, une purification par chromatographie en phase gazeuse préparative (colonne silicone S.E. 30, température 170°) permet l'obtention de l'alcène **10**. R.m.n. δ 1.4 à 2.76 (m, 6H), 5.9 (m, 2H), 7.23 (m, 10H); spectre de masse $[M]^+$ à *m/e* 234.1414, $[M]^+$ calculé pour $C_{18}H_{18}$: 234.1408.

Méthyl-4a diphényl-2,2 octahydro-1,2,3,4,4a,5,6,7 naphtalène (11)

La cétone 7 (0.3 g, 0.0095 mol) est transformée en tosylhydrazone comme précédemment: p.f. 201–202°. La réduction de cette dernière. par $LiAlH_4$ en milieu tétrahydrofurane conduit, après purification par c.p.g. préparative (colonne silicone Q.F.1, température 195°) à l'alcène **11**. Spectre de masse $[M]^+$ à *m/e* 302.2024, $[M]^+$ calculé pour $C_{23}H_{26}$: 302.2034.

Diphényl-2,2 cyclohexanone (13)

Les étapes choisies pour synthétiser la diphényl-2,2 cyclohexanone (**13**) sont celles proposées dans la littérature par Burger et Bennet (21), exception faite pour la dernière.

La cyclopentanone est mise en réaction avec le cyanure de sodium en présence de bisulfite de sodium. Le produit brut est porté à reflux dans l'acide chlorhydrique concentré. Il fournit l'hydroxy-acide correspondant (p.f. 103–104°) qui est estérifié au cours d'un reflux dans le méthanol, en présence d'acide sulfurique. L'addition de 2 mol de bromure de phénylmagnésium sur l'hydroxy ester, ainsi préparé, conduit directement au (diphényl-hydroxy) méthyl-1 cyclopentanol (**12**): p.f. 125–126° (lit. (22) 125°).

Can. J. Chem. Downloaded from www.nrcresearchpress.com by 210.87.254.5 on 09/05/12
For personal use only.

La transposition pinacolique sur le glycol **12** peut être effectuée selon la méthode déjà décrite (23) ou selon la méthode suivante. Une solution de **12** (50 g, 0.187 mol) dans 200 ml d'acide acétique glacial porté à quelques degrés au dessous du point d'ébullition et une solution d'iode (0.3 g) dans 150 ml d'acide acétique glacial chauffé à la même température sont rassemblées rapidement. Le mélange est immédiatement porté à ébullition pendant 5 min puis versé sur 50 g de glace contenant 2 g de thiosulfate de sodium. Le précipité formé est filtré, lavé à l'eau glacée et dissous dans le benzène; la solution résultante est lavée au bicarbonate de sodium, à l'eau, séchée et le solvant chassé. Le résidu est repris dans le méthanol et décoloré par le charbon actif. Après évaporation du solvant et recristallisation dans le méthanol, la réaction fournit 39 g (84%) de diphényl-2,2 cyclohexanone sous forme de paillettes: p.f. 94–95° (lit. (21) 98.5–99°; lit. (24) 99–100°; recristallisation dans l'éthanol dans les deux cas). Une recristallisation dans le *n*-hexane fournit des cristaux en forme de prisme: p.f. 100–101°. Ces deux formes allotropiques de **13** peuvent être converties l'une dans l'autre par changement de solvant de cristallisation, leurs caractéristiques sont parfaitement identiques. Spectre de masse $[M]^+$ à *m/e* 250; i.r. 1710 cm^{-1} (C=O); r.m.n. δ 1.84 (m, 4H), 2.50 (m, 4H), 6.90 et 7.35 (m, 10H).

*n-Butylthiométhylène-2 diphényl-6,6 cyclohexanone (**14**) et Méthyl-2 diphényl-6,6 cyclohexanone (**15**)*

Les tentatives de monoalcoylation directes de la diphényl-2,2 cyclohexanone (**13**) par l'iodure de méthyle en présence d'une base forte (25) (amidure de sodium, *tert*-butylate de potassium) ont conduit invariablement à la diméthyl-2,2 diphényl-6,6 cyclohexanone (**16**). Ainsi le procédé plus long consistant en la réduction du dérivé *n*-butylthiométhylène par le nickel de Raney (26) est mis à profit pour la synthèse de la cétone **15**. Une solution de formiate d'éthyle (30 g, 0.405 mol) fraîchement distillée, dans 40 ml de benzène est additionnée à une suspension de méthylate de sodium (12 g, 0.222 mol) dans 20 ml de benzène anhydre gardé sous atmosphère d'azote à 0° (27). Après refroidissement à −10°, une solution de **13** (20 g, 0.08 mol) dans 40 ml de benzène, est ajoutée goutte à goutte et le milieu réactionnel laissé au repos pendant 16 h, à température ambiante. La masse compacte obtenue est délayée dans 400 ml d'eau glacée puis extraite à l'éther. La phase aqueuse, traitée par l'acide chlorhydrique concentré jusqu'à p*H* neutre, laisse déposer un précipité blanc qui est repris à l'éther; cette fraction éthérée fournit 21.08 g (94.8%) d'hydroxyméthylène-2 diphényl-6,6 cyclohexanone après traitement habituel et recristallisation dans le méthanol: p.f. 88–89°; l'analyse élémentaire et les résultats des méthodes spectroscopiques sont satisfaisants.

Le thioéther énolique **14** est préparé (26) par réaction du *n*-butanethiol fraîchement distillé (12 ml, 0.11 mol) sur de l'hydroxyméthylène-2 diphényl-6,6 cyclohexanone (16 g, 0.0575 mol), en présence de 0.1 g d'acide *p*-toluène sulfonique dans du benzène anhydre (200 ml). L'eau formée est distillée azéotropiquement avec un appareil Dean Stark. Après 1½ h de contact, la réaction est complète (contrôle par chromatographie sur couche mince). Une extraction habituelle suivie d'une distillation du résidu sous 0.2 Torr et d'une cristallisation du distillat dans le mélange éther–méthanol donne 19.13 g (95.2%) de **14**: p.f. 62–63°; spectre de masse $[M]^+$ à *m/e* 350; i.r. 1660 cm^{-1} (C=O conjugué), 1550 cm^{-1} (C=C portant le soufre); r.m.n. δ 7.84 (t, J = 2 Hz, 1H), 7.25 (s, 10H).

Le thioéther **14** (35 g, 0.1 mol) est désulfurisé (26) par introduction dans une suspension préalablement saturée d'hydrogène, composée de 175 ml de nickel de Raney (28) et de 600 ml d'éthanol absolu. Le mélange maintenu vigoureusement agité, est porté à reflux. L'évolution de la réaction est suivie par spectroscopie i.r. Après 1½ h de contact, deux bandes: 1715 cm^{-1} (cétone attendue) et 1665 cm^{-1} sont présentes; cette dernière est due à la méthyl-2 diphényl-6,6 cyclohexène-2 one-1, r.m.n. δ 6.55 (t, J = 4 Hz, 1H) provenant d'une hydrogénolyse de la liaison carbone-soufre et d'une isomérisation subséquente. Le catalyseur est filtré et le mélange brut remis en réaction avec une nouvelle quantité de nickel de Raney saturé d'hydrogène (68 ml). Après 1 h de réaction, dans les conditions citées plus haut, la réduction s'avère complète (disparition de la bande à 1665 cm^{-1}). La séparation du catalyseur et l'évaporation de l'éthanol laissent 17.4 g (66%) de méthyl-2 diphényl-6,6 cyclohexanone (**15**): p.f. 85–86°, (lit. (24) 85–86°).

Anal. calc. pour $C_{19}H_{20}O$: C, 86.32; H, 7.63. Trouvé: C, 86.57; H, 7.85.

Spectre de masse $[M]^+$ à *m/e* 264; i.r. 1710 cm^{-1} (C=O); r.m.n. δ 1.07 (d, 3H).

*Diméthyl-2,2 diphényl-6,6 cyclohexanone (**16**)*

A une solution de *tert*-butylate de potassium (0.08 mol) dans 15 ml de benzène anhydre gardé sous atmosphère d'azote, une solution de **13** (5 g, 0.02 mol) dans 15 ml de benzène anhydre est ajoutée goutte à goutte. Après refroidissement à −10°, un excès d'iodure de méthyle (5.8 g, 0.04 mol) est additionné. Le mélange est porté à reflux pendant 2 h, le solvant distillé et 60 ml d'eau sont ajoutés au résidu blanc obtenu. L'extraction habituelle, suivie d'une distillation sous 0.3 Torr fournit 4.46 g (84.1%) d'un liquide incolore cristallisant dans l'éthanol: p.f. 76–77°.

Anal. calc. pour $C_{20}H_{22}O$: C, 86.29; H, 7.97. Trouvé: C, 86.36; H, 8.05.

Spectre de masse $[M]^+$ à *m/e* 278; i.r. 1710 cm^{-1} (C=O); r.m.n. δ 0.97 (s, 6H), 2.5 (t, J = 6 Hz, 2H).

*Méthyl-2 (chloro-3 butényl-2)-2 diphényl-6,6 cyclohexanone (**17**)*

La méthode utilisée est une modification de celle décrite dans la littérature (29, 30). A une solution de *tert*-butylate de potassium (0.15 mol) dans 150 ml de benzène fraîchement distillé, une solution de cétone **15** (26.4 g, 0.10 mol) dans 50 ml de benzène anhydre est ajouté sous atmosphère d'azote, à 0°. Le mélange réactionnel est ramené à 25° puis porté à reflux pendant 1 h. Après un nouveau refroidissement sur un bain de glace, une solution de dichloro-1,3 butène-2 (24 g, 0.19 mol) dans 100 ml de benzène, est additionnée rapidement. Le mélange est porté à reflux 6 h, laissé à 25° pendant 14 h puis traité à 0 °C par un mélange 1:1 d'acide chlorhydrique concentré – eau. Après extraction à l'éther, le résidu (31.8 g) est analysé par chromatographie sur couche mince et deux produits sont révélés dont un est la cétone de départ (**15**). La séparation est effectuée par chromatographie sur une colonne de gel de silice (benzène) sur une petite quantité de produit. La cétone chlorée (**17**) cristallise dans le *n*-hexane: p.f. 73–74°.

Can. J. Chem. Downloaded from www.nrcresearchpress.com by 210.87.254.5 on 09/05/12
For personal use only.

Anal. calc. pour $C_{23}H_{25}OCl$: C, 78.28; H, 7.14; Cl, 10.05. Trouvé: C, 78.32; H, 7.26; Cl, 10.30.

Spectre de masse $[M]^+$ à *m/e* 352; i.r. 1700 cm^{-1} (C=O), 1665 cm^{-1} (C=C); r.m.n. δ 0.94 (s, 3H), 5.4 (t, J = 7 Hz, 1H), 6.86–7.44 (m, 10H).

*Méthyl-2 (oxo-3 butyl)-2 diphényl-6,6 cyclohexanone (**18**)*

Un courant d'azote est mis à barbotter dans une solution de **17** (1 g, 0.0028 mol) dans 3 ml de dichlorométhane à −20°. Un mélange à 0° d'acide sulfurique concentré et d'eau dans le rapport 9:1 (7 ml) est ajouté rapidement. Le bain de glace–méthanol est maintenu pendant 2 h au cours desquelles l'azote entraîne le gaz chlorhydrique formé, ainsi que le dichlorométhane. La température est ramenée à 25°, le mélange réactionnel précipité sur 20 g de glace et extrait à l'éther. Après lavage, séchage et évaporation, le résidu laisse cristalliser 0.78 g (82%) de dicétone **18** après dilution dans quelques gouttes d'éther: p.f. 96–97°.

Anal. calc. pour $C_{23}H_{26}O_2$: C, 82.60; H, 7.84. Trouvé: C, 82.53; H, 7.90.

Spectre de masse $[M]^+$ à *m/e* 334; i.r. 1705 cm^{-1} (C=O), 1715 cm^{-1} (C=O); r.m.n. δ 0.97 (s, 3H), 2.02 (s, 3H), 7.00 et 7.50 (m, 10H).

*(Méthyl-1 oxo-2 diphényl-3,3 cyclohexyl)-3 propanal (**19**)*

Selon les indications de Hajos et collaborateurs (31), une suspension de 0.4 g d'hydrure de sodium (dispersion dans l'huile à 51%) dans 12 ml de DMSO fraîchement distillé est portée à 60° pendant 1 h. Le tout étant gardé sous atmosphère d'azote, la température est ramenée à 25° et une solution de méthyl-2 diphényl-6,6 cyclohexanone (**15**) (1.1 g, 0.004 mol) dans 12 ml de DMSO est ajoutée goutte à goutte. Après 1½ h de contact à 50° une solution de chloro-3 diéthoxy-1,1 propane (1.3 g, 0.077 mol) dans 6 ml de DMSO est additionnée au mélange. Après extraction, 1.67 g de résidu sont obtenus, contenant outre la cétone de départ (**15**), un nouveau composé; 50 ml de dichlorométhane y sont additionnés. La solution obtenue est hydrolysée (32) par 50 ml d'acide chlorhydrique 2 *N*, agitée pendant 1 h à 25°, portée à reflux pendant 20 min, ce qui provoque la disparition complète du nouveau produit au profit d'un composé plus polaire. Après extraction habituelle, 0.64 g de produit brut est recueilli. Une chromatographie sur colonne de gel de silice (*n*-hexane–éther, 5.3) fournit 0.38 g ce cétone de départ et 0.21 g (16%) de cétoaldéhyde (**19**) cristallisant après dilution dans le *n*-hexane: p.f. 85–86°; spectre de masse $[M]^+$ à *m/e* 320; i.r. 1720 cm^{-1} (C=O), 1695 cm^{-1} (C=O); r.m.n. δ 0.95 (s, 3H), 6.86 et 7.4 (m, 10H), 9.55 (m, 1H).

*Tétradeutério-2,2,5,5 cyclopentanone (**20**)*

Le chauffage sous reflux de la cyclopentanone provoquant une autocondensation, la deutériation est effectuée à température ordinaire (33, 34). La cyclopentanone (20 g, 0.238 mol), 100 ml d'eau lourde et 10 g de carbonate de potassium sont agités vigoureusement (secoueuse) pendant 5 jours. Le taux d'incorporation de deutérium contrôlé par r.m.n. s'avère être supérieur à 90%. L'eau est enlevée avec une seringue et une deuxième deutériation accomplie par addition de 75 ml d'eau lourde et 7.5 g de carbonate de potassium. Une agitation de 6 jours suivie d'une extraction à l'éther et une distillation sous vide donnent 11 g (52%) de **20**. Le spectre r.m.n. (100 Mc, avec découplage de deutérium) révèle un singulet fin centré à 1.975 p.p.m.

*Dideutério-3,3 diphényl-2,2 cyclohexanone (**21**)*

Cette cétone est obtenue à partir de **20** en suivant les méthodes détaillées précédemment (cyclopentanone → **13**) sauf pour l'étape de la transposition pinacolique ou la méthode utilisée est celle de Zaugg (10): p.f. 94–95° (recristallisation dans méthanol); la spectrométrie de masse révèle la composition isotopique suivante: d_3, 5%; d_2, 86%; d_1, 9%; $[M]^+$ à *m/e* 252.1490, $[M]^+$ calculé pour $C_{18}H_{16}O_1D_2$: 252.1482; r.m.n. δ 1.88 (m, 4H), 2.50 (m, 2H), 22 (m, 10H).

*Dideutério-2,2 diphényl cyclohexane (**22**)*

La réduction de Wolf–Kishner (7) effectuée sur la dideutério-3,3 diphényl-2,2 cyclohexanone (**21**) conduit après purification par chromatographie préparative en phase gazeuse (colonne silicone S.E. 30, température 200°), à l'hydrocarbure **22**: p.f. 44–45°; la spectrométrie de masse donne la composition isotopique suivante: d_2, 89%; d_1, 11%; $[M]^+$ à *m/e* 238.1679, $[M]^+$ calculé pour $C_{18}H_{18}O_2$: 238.1690; r.m.n. δ 1.50 (s, élargi 6H), 2.22 (m, 2H), 7.20 (m, 10H).

*Tétradeutério-2,2,6,6 diphényl-4,4 cyclohexanone (**23**)*

Trois deutériations successives de la diphényl-4,4 cyclohexanone (**2**) par de l'eau lourde en milieu basique (carbonate de potassium) contenant des traces de dioxane, fournissent la cétone tétradeutériée (**23**). Spectre de masse: d_4, 95%; r.m.n. δ 2.66 (s, élargi par le couplage $J_{H\text{-}D}$, 4H), 7.30 (s, 10H).

Résultats et discussion

Parmi ceux qui répondent aux critères énoncés, on compte les composés **2**, **3** et **5**. Les produits **7**, **8**, **9** et **11** sont inclus pour fins de comparaison. On doit pouvoir examiner séparément les influences respectives des groupes diphényle et carbonyle en tant que site porteur de charge en favorisant une décomposition amorcée par une des fonctions en l'absence de l'autre. Chaque cyclohexanone *gem*-diphénylée (CGDP) peut ainsi être considérée par rapport à deux analogues, diphénylé (AD) et carbonylé (AC). La première étape de l'étude comporte une mesure des potentiels d'ionisation qui ont été déterminés par la méthode semi-logarithmique (35) en utilisant le xénon comme gaz étalon. Les mesures de potential d'ionisation qui sont rapportées au tableau 1 indiquent que le groupe carbonyle régit l'ionisation pour les analogues carbonylés et que le groupe diphényle joue le même rôle dans le cas des analogues diphénylés. Lorsque les deux fonctions sont en présence, les résultats montrent le rôle prépondérant de la fonction diphényle lors de l'ionisation. On peut ainsi conclure qu'au voisinage de l'énergie minimum requise pour ioniser la molécule, un des électrons est éjecté de la partie de la molécule contenant les deux groupements phényles. Bien qu'il s'agisse d'une extrapolation, il est permis de sup-

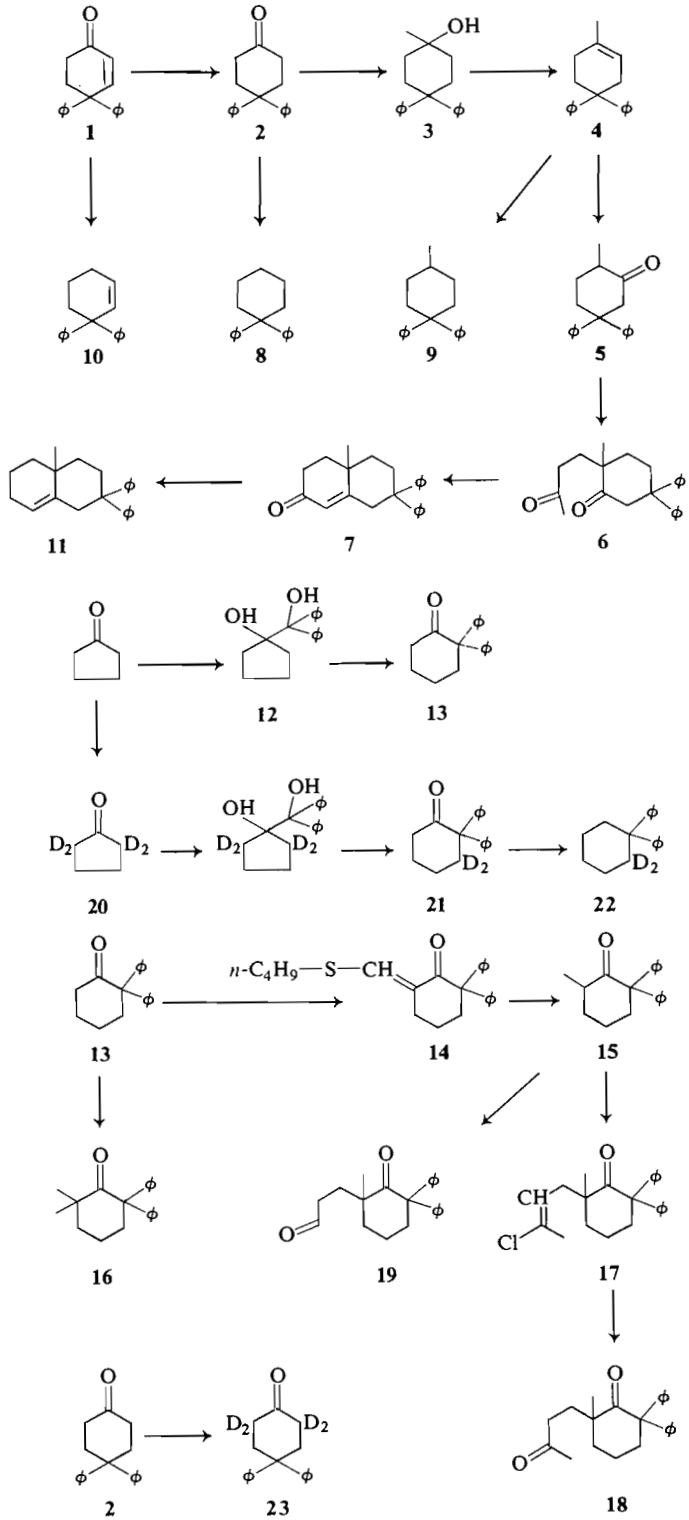

Schéma 1

Can. J. Chem. Downloaded from www.nrcresearchpress.com by 210.87.254.5 on 09/05/12
For personal use only.

TABLEAU 1. Comparaison des potentiels d'ionisation des AC, CDGP et AD (±0.2 eV)

Composé		P.I. (eV)	Composé		P.I. (eV)
AC	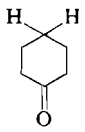		AC	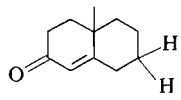	
24		9.5	**26**		9.6
25	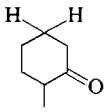	9.5	**28**	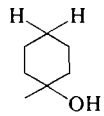	9.8
CGDP	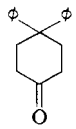		CGDP	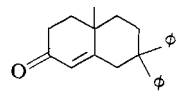	
2		8.8	**7**		8.9
5	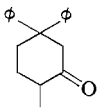	8.8	**3**	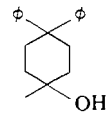	9.2
AD			AD	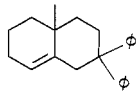	
8		8.9	**11**		8.9
9	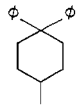	8.8	**9**	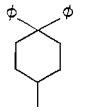	8.8

poser qu'à 70 eV, la fonction diphényle sera celle qui régira la fragmentation (36). On peut vérifier cette assertion en comparant les principaux ions dans les spectres de masse des analogues carbonylés et diphénylés avec ceux issus de la dégradation des produits *gem*-diphénylés carbonylés. Dans chacun des cas, les modes de fragmentation caractéristiques des principaux ions sont établis et comparés. Pour ce faire, on enregistre les spectres à haute résolution et confirme chacune des transitions importantes par la mise en évidence des ions métastables appropriés. De plus, dans les cas critiques, on a marqué certaines positions en remplaçant l'atome d'hydrogène par un deutérium.

Les ions importants provenant de la décomposition des dérivés diphénylés sont rapportés au tableau 2. Il en ressort clairement que tous ces produits donnent effectivement les mêmes ions. De plus, leurs abondances relatives sont comparables. Ceci est compatible avec une fragmentation initiée et dirigée par le groupement diphényle puisque le schéma de fragmentation de ces molécules est indépendant de l'énergie des électrons entre 20 et 70 eV (les ions formés sont les mêmes; seuls leurs % I.R. varient). Les transitions métastables données au tableau 3 indiquent

TABLEAU 2. Intensités relatives des ions principaux des AD (%)

	Composé		
m/e	**8**	**9**	**11**
M^+	68.4	49.8	37.5
193	100.0	100.0	100.0
180	32.1	40.6	11.6
179	10.6	10.6	19.4
178	17.0	14.7	20.8
165	14.4	10.7	20.1
152	2.8	3.5	6.9
128	11.6	1.5	6.2
115	45.5	30.6	45.8
91	39.0	22.5	79.2

Can. J. Chem. Downloaded from www.nrcresearchpress.com by 210.87.254.5 on 09/05/12
For personal use only.

TABLEAU 3. Transitions métastables des principaux ions des AD

M	$\xrightarrow[*]{}$	*m/e* 193 $(C_{15}H_{13})^+$	+ N		
M	$\xrightarrow[*]{}$	*m/e* 180 $(C_{14}H_{12})^+$	+ N_1		
m/e 180	$\xrightarrow[*]{}$	*m/e* 179 $(C_{14}H_{11})^+$	+ H		
m/e 193	$\xrightarrow[*]{}$	*m/e* 178 $(C_{14}H_{10})^+$	+	CH_3	(15)
m/e 180	$\xrightarrow[*]{}$	*m/e* 165 $(C_{13}H_9)^+$	+	CH_3	(15)
m/e 178	$\xrightarrow[*]{}$	*m/e* 152 $(C_{12}H_8)^+$	+	$HC{\equiv}CH$	(26)
m/e 193	$\xrightarrow[*]{}$	*m/e* 115 $(C_9H_7)^+$	+		(78)

la provenance des principaux ions. Le processus primaire donne naissance à deux ions, *m/e* 193 et 180, dont la décomposition produit les autres ions observés. Pour confirmer ces mécanismes de formation ionique, le produit **22** a été synthétisé et ses principaux ions fragments sont énumérés au tableau 4. Les ions à *m/e* 193 et 180 peuvent être expliqués par deux processus bien connus en spectrométrie de masse (37). D'une part le clivage benzylique de la liaison C_1—C_2 suivi d'un transfert spécifique de l'atome d'hydrogène en C-6 avec la perte de C-2, -3 et -4. Ceci conduit à la formation de l'ion à *m/e* 193 dont la charge positive est délocalisée et stabilisée par les deux noyaux phényles. Le produit étant symétrique, il existe une probabilité égale de rupture de la liaison C_1—C_6, accompagnée du transfert de l'un des deutérium en C-2 par un mécanisme identique.

La présence d'un ion à *m/e* 194 dans ce dernier cas confirme le transfert spécifique de l'hydrogène en α du carbone benzylique. Le rapport des intensités relatives *m/e* 193:194 est de 1.3:1.0 (schéma 2).

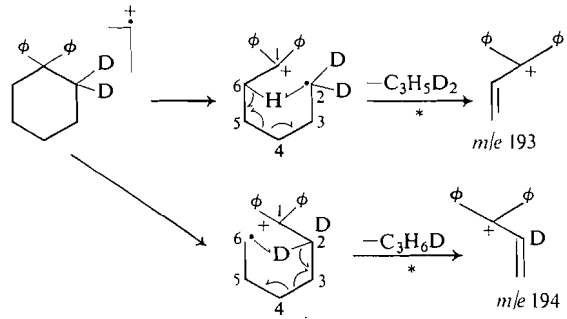

SCHÉMA 2

TABLEAU 4. Intensités relatives des ions principaux du AD et CGDP deutériés (%)

	Composé	
	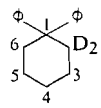	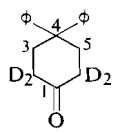
m/e	**22**	**23**
M^+	238 (100.0)	254 (45.8)
193	194 (77.4)	
	193 (98.5)	195 (100.0)
180	182 (10.2)	180 (53.3)
	180 (31.0)*	
179	181 (20.7)	179 (18.7)
	179 (23.4)*	
178	178 (23.8)	178 (13.8)
167	167 (51.0)	167 (3.2)
165	165 (33.3)	165 (24.1)
152	152 (9.5)	152 (3.9)
115	116 (25.8)	117 (19.8)
	115 (47.6)	116 (11.7)
91	93 (9.4)	93 (6.1)
	92 (20.5)	92 (6.7)
	91 (42.8)	91 (5.8)

*Ces pourcentages comprennent les contributions des *m/e* 178 et 179

Ce mécanisme est d'ailleurs analogue à celui proposé pour la formation de l'ion à *m/e* 171 à partir du phényl-10 décaline-*trans* (37). D'autre part, le clivage de la liaison C_1—C_2 (C_1—C_6) peut être concerté avec celui de la liaison C_5—C_6 (C_2—C_3) pour former l'ion à *m/e* 180 (182) (schéma 3).

Le rapport des intensités relatives *m/e* 182:180 est de 1:3. Toutefois il faut noter que l'ion à *m/e* 180 est dû en partie à l'équivalent des ions à *m/e* 178 et 179 contenant respectivement deux et un atome de deutérium. En effet, les ions à *m/e* 193 et 180 sont responsables de la formation des ions à *m/e* 179 et 178 (schéma 4).

Can. J. Chem. Downloaded from www.nrcresearchpress.com by 210.87.254.5 on 09/05/12
For personal use only.

Can. J. Chem. Downloaded from www.nrcresearchpress.com by 210.87.254.5 on 09/05/12
For personal use only.

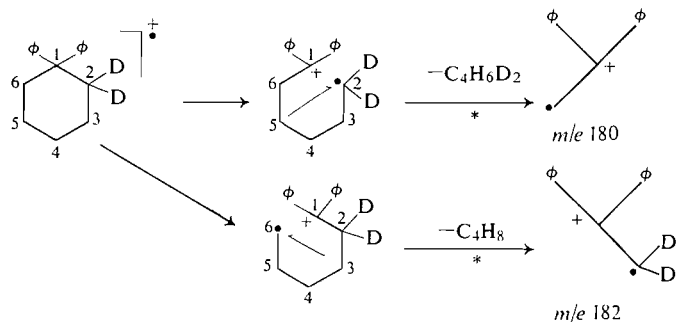

SCHÉMA 3

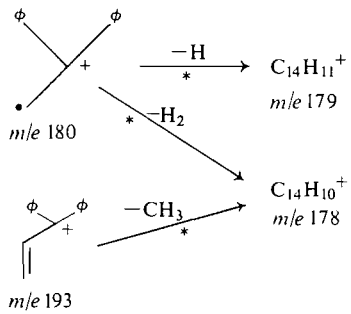

SCHÉMA 4

Une perte de méthyle à partir de l'ion à *m/e* 193, suggérée par un ion métastable à $m^* = 164.20$, mène aussi à la formation du *m/e* 178. Toutefois à cause de la position adjacente de ces deux ions, il n'est pas possible de faire ressortir clairement les résultats obtenus à l'aide de l'analogue deutérié.

La présence d'un métastable à 151.25 confirme la formation du *m/e* 165 à partir de *m/e* 180 par perte de méthyle (schéma 5).

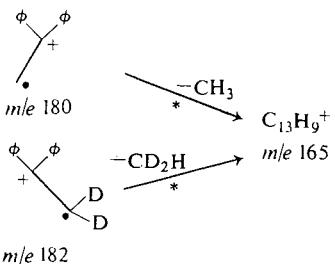

SCHÉMA 5

La perte de CD_2H à partir de l'ion à *m/e* 182 révèle également l'absence de brouillage (scrambling) dans l'ion précurseur précédant la formation de cet ion.

L'observation d'un ion métastable à 68.26 suggère l'ion *m/e* 193 comme précurseur du fragment à *m/e* 115 par perte de benzène (schéma 6).

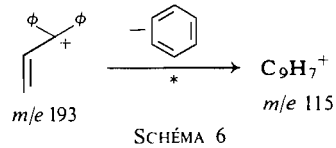

SCHÉMA 6

La deutériation nous indique que l'ion *m/e* 194 mène soit à *m/e* 116, soit *m/e* 115 dans les rapports 1.0:1.0.

L'examen des mécanismes de formation des principaux ions des AC où le carbonyle est le site porteur de charge, est susceptible de nous révéler quels types de fragmentation cette fonction pourrait engendrer dans les produits *gem*-diphénylés carbonylés. Les spectres des composés cyclohexanone, méthyl-2 cyclohexanone, méthyl-1 cyclohexanol et leurs analogues deutériés, étant rapportés dans la littérature (38–40), ne sont pas discutés dans la présente publication.

TABLEAU 5. Intensités relatives des ions principaux des CGDP (%)

	Composé			
m/e	**2**	**5**	**7**	**3**
M^+	42.8	74.0 43.3 (207)	5.9	49.1 21.1 (195) 100.0 (194)
193	100.0	100.0	100.0	24.8
180	87.1	44.7	2.6	49.2
179	49.4	27.9	3.9	26.9
178	51.9	27.7	12.2	18.4
165	68.9	26.6	5.8	26.3
152	12.5	4.9	2.4	4.8
128	11.7	4.3	1.5	4.4
115	78.5	38.7	42.5	18.1
91	50.0	28.8	11.1	34.5

TABLEAU 6. Ions prédits par les mécanismes A et B et intensité relative (I.R.) de ces ions trouvée expérimentalement

Composé		Ions issus du mécanisme (A)	I.R. mesurée (%)	Ions issus du mécanisme (B)	I.R. mesurée (%)
AD	**8**	193	100.0	180	32.1
	9	193	100.0	180	40.6
	11	193	100.0	180	11.8
CGDP	**2**	193	100.0	180	87.1
	5	193	100.0	180	44.7
	7	193	100.0	180	2.6
	3	193	24.8	180	49.2
	2	195	0.0	208	0.0
	5	195	0.0	208	0.0
	3	195	21.1	208	0.0
	7	261	0.0	274	0.0
AC	**24**	55	100.0	42	28.4
	25	69	39.3	56	50.8
	28	71	100.0	58	16.9
	26	55	20.2	122	86.6

Mécanisme (A) (exemples)

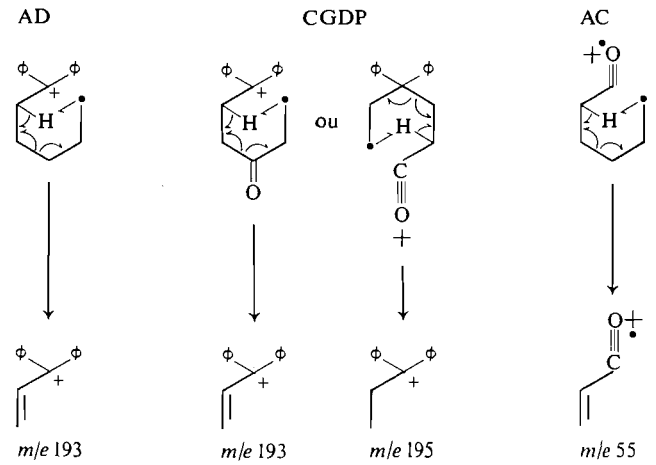

Mécanisme (B) (exemples)

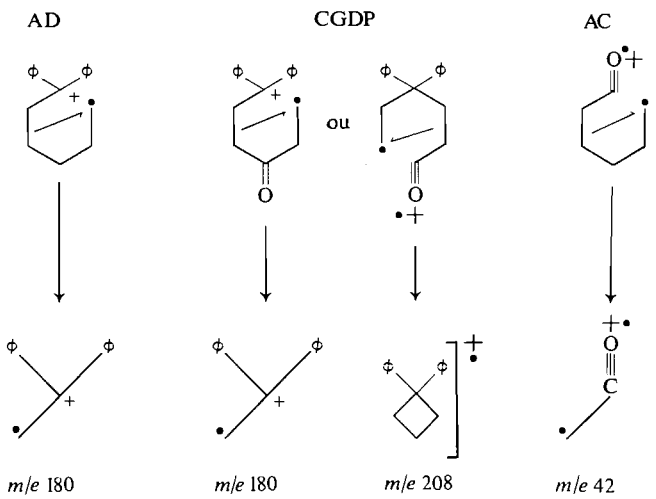

Can. J. Chem. Downloaded from www.nrcresearchpress.com by 210.87.254.5 on 09/05/12
For personal use only.

TABLEAU 7. Potentiels d'ionisation des $CGDP_\alpha$ substitués (± 0.2 eV)

Composé	P.I. (eV)	Composé	P.I. (eV)
13 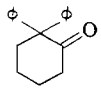	8.8	**14** 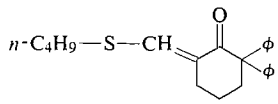	8.9
15 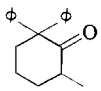	9.0	**17** 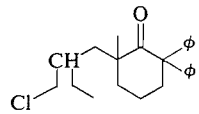	8.7
16 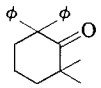	8.7		
18 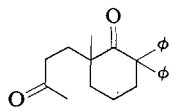	—*	**19** 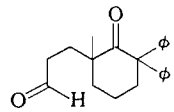	—*

*Par d'ion moléculaire.

Il en est ainsi du méthyl-4a oxo-7 octahydro-1,2,3,4,4a,5,6,7 naphtalène dont les mécanismes de dégradation sont connus, puisqu'il constitue en fait les anneaux A et B d'un squelette stéroide (2).

Le tableau 5 rapporte les intensités relatives des principaux ions fragments pour les composés contenant un groupe diphényle et un groupe carbonyle. On peut constater l'identité de ces ions avec ceux obtenus pour les analogues diphénylés. Ceci confirme que le carbonyle n'est pas le site initiateur de la fragmentation dans ces cas: sa présence n'entraine la formation d'aucun ion important autre que ceux qui se retrouvent dans les analogues diphénylés. L'oxygène est donc expulsé dans chaque cas en tant que constituant du fragment neutre. De plus, les spectres enregistrés à haute résolution, la mesure des ions métastables ainsi que les résultats obtenus pour le produit **23** deutérié (tableau 4) confirment la similitude des mécanismes de formation des ions principaux pour les composés *gem*-diphényles carbonylés et les analogues diphénylés. L'ion à *m/e* 193 se retrouve à *m/e* 195 tel que prévu. Ceci démontre la spécificité de l'abstraction de l'atome d'hydrogène en C-3 et nous amène à suggérer l'absence de brouillage dans l'ion moléculaire. On note aussi qu'il ne peut y avoir de brouillage précédant la formation de l'ion à *m/e* 180 puisque la masse de cet ion demeure inchangée dans le produit deutérié. Des ions métastables à $m^* = 178.0$ et 176.0 indiquent la provenance des *m/e* 179 et 178 à partir de l'ion *m/e* 180. L'ion à *m/e* 178 est aussi formé à partir de *m/e* 193 (195) ainsi que le démontre la présence d'un métastable à 164.2. L'élimination d'un groupe méthyle de l'ion à *m/e* 180 ($m^* = 151.25$) mène à la formation du fragment *m/e* 165. Enfin, l'ion 193 (195) donne aussi naissance à *m/e* 117 et 116 par perte de benzène-d_0 et benzène-d_1 dans les proportions 1.6:1.0 et révèle effectivement la formation de l'ion *m/e* 115 à partir du *m/e* 193. Des transitions métastables à $m^* = 70.20$ et 69.00 le confirment également.

Le tableau comparatif 6 souligne la similitude des mécanismes de formation des ions primaires des AC, CGDP et AD. En considérant ce tableau, on peut attribuer la formation du *m/e* 195 ($C_{15}H_{15}^+$, 21.1%) dans le cas du produit *gem*-diphénylé hydroxylé, au fait que l'oxygène soit dans ce cas particulier le porteur de charge positive. S'il en est ainsi, cet ion constitue alors une exception ce qui n'est pas surprenant, puisque le potentiel d'ionisation de ce produit, par sa valeur plus élevée, indique une influence plus grande du groupement hydroxyle.

D'une façon générale, il ressort de cette étude que les mécanismes menant à la formation des ions 193 et 180 dans le processus primaire des AD, expliquent aussi une grande partie des ions fragments principaux des AC. Mais, lorsque l'on reporte ces mêmes mécanismes de formation sur les CGDP, en assignant à tour de rôle aux deux groupements en présence la fonction de porteur de charge, il en découle qu'aucun ion important n'est engendré lorsque l'oxygène est le site de

Can. J. Chem. Downloaded from www.nrcresearchpress.com by 210.87.254.5 on 09/05/12
For personal use only.

TABLEAU 8. Intensités relatives des ions principaux des $CGDP_\alpha$ (%)

	Composé						
m/e	**13**	**15**	**16**	**18**	**14**	**17**	**19**
M+	30.0	35.9	23.2		18.6	34.1	
		13.1 (236)	19.9 (250)		11.3 (293)	45.9 (233)	16.4 (294)
206	100.0	99.0	89.7	100.0	—	99.5	100.0
193	98.3	100.0	59.4	22.5	100.0	30.9	81.1
180	65.8	83.4	100.0	67.7	3.6	100.0	65.4
179	38.4	32.5	31.0	22.5	4.8	35.4	32.6
178	33.6	35.3	29.7	19.6	12.2	33.1	32.3
167	36.9	43.2	37.9	61.5	5.8	49.7	60.2
165	50.7	48.6	43.7	29.8	9.0	50.0	43.3
152	11.4	8.7	8.0	5.0	3.2	8.3	8.0
129	9.0	6.2	4.5	4.3	4.1	7.2	5.7
128	6.4	6.1	4.4	11.2	3.2	6.1	5.6
115	57.1	48.0	32.1	21.7	33.7	44.1	35.2
103	11.6	11.3	15.0	6.1	4.0	18.5	15.1
91	40.4	30.8	25.4	20.1	19.0	54.7	26.7

localisation de charge (sauf peut-être le cas du *m/e* 195 du composé hydroxylé). De même, l'application aux CGDP des mécanismes menant à la formation d'autres ions importants des AC (38–40) ne donne lieu à la formation d'aucun ion majeur ce qui confirme la conclusion énoncée précédemment.

Effets de la position adjacente des groupements fonctionnels et de la substitution sur le site de localisation de la charge positive

Bien que les produits suivants ne se soumettent pas aux caractéristiques édictées initialement, il est intéressant de voir, à la lumière des résultats obtenus jusqu'ici, si leurs comportements sont affectés soit par la présence du groupement carbonyle en α du carbone benzylique soit par une plus grande substitution, ou si au contraire les conclusions de l'étude précédente s'appliquent intégralement. Leurs potentiels d'ionisation, rapportés au tableau 7, nous indiquent qu'il devrait y avoir peu de changement dans les conclusions générales, puisque l'ionisation, là aussi, est régie entièrement par le groupement diphényle. On remarque, en effet, l'identité des potentiels d'ionisation entre les AD, CGDP et $CGDP_\alpha$. Par ailleurs, le tableau 8 rapportant les % I.R. des ions principaux des $CGDP_\alpha$ suggère une absence complète d'influence du (C=O) ou du substituant. On note effectivement que tous les ions fragments principaux, sauf celui à *m/e* 206, sont exactement les mêmes que dans le cas des AD et CGDP.

L'ion *m/e* 206, qui se retrouve dans la dégradation de six des sept produits, constitue en fait la seule différence par rapport aux AD et CGDP. Dans chacun de ces cas, un ion métastable nous indique qu'il est formé à partir de M^+ et le spectre à haute résolution montre qu'il s'agit de $C_{16}H_{14}^+$. Puisque cet ion ne se retrouve pas dans les spectres des AD et CGDP, on peut en conclure, d'une part, que sa formation dépend de la présence du groupement carbonyle et, d'autre part, que la position adjacente de la fonction cétonique par rapport au carbone benzylique favorise sa formation. Il est aussi intéressant de noter que sa présence peut être expliquée de la même façon que celle de l'ion *m/e* 156 dans le spectre de la phényl-10 décalone-2-*trans* (37) par le transfert de deux atomes d'hydrogène de la partie hydrocarbure et ceci avant la décomposition, tel qu'indiqué au schéma 7.

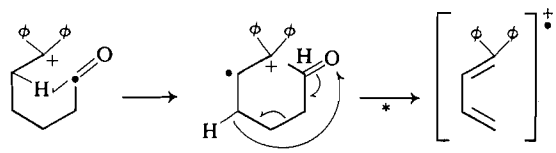

SCHÉMA 7

Conclusions

Il ressort de cette étude que le groupement *gem*-diphényle, dont le potentiel d'ionisation est inférieur à celui du groupe carbonyle, est le principal agent initiateur et directeur de la frag-

Can. J. Chem. Downloaded from www.nrcresearchpress.com by 210.87.254.5 on 09/05/12
For personal use only.

mentation des molécules étudiées. Ceci est confirmé par des mécanismes de dégradation similaires des produits avec et sans fonction carbonyle. L'extrapolation généralement faite que la partie d'une molécule complexe ayant le plus bas potentiel d'ionisation régit la fragmentation principale, semble donc être valide dans le cas présent. Même si les résultats indiquent une fixation de la charge positive sur une partie définie de la molécule, nous ne croyons pas que ceci constitue un argument décisif en faveur de sa localisation lorsque les électrons sont accélérés à un potentiel de 70 V. Suite à une ionisation qui peut se produire n'importe où sur la molécule, il est tout aussi possible de conclure, dans le même sens que Vetter *et al.* (11), à une distribution de charge sur les fonctions carbonyle et diphényle maximisée sur ce dernier groupement. Par ailleurs, la fraction de charge sur le groupe carbonyle ne serait pas suffisante pour induire une redistribution électronique et causer la rupture de liaisons. En effet, le fait de ne pas observer de fragmentation due au carbonyle ne constitue pas en soi une preuve de l'absence de densité de charge positive à cet endroit. Il est évident que ce concept doit être étudié plus à fond.

1. F. W. McLafferty. Determinations of organic structures by physical methods. *Edité par* F. C. Macleod et W. D. Phillips. Academic Press, N.Y. 1962. p. 93; F. W. McLafferty. Mass spectrometry of organic ions. Academic Press, N.Y. 1963. p. 315.
2. H. Budzikiewicz, C. Djerassi et D. Williams. Mass spectrometry of organic compounds. Holden Day. 1967; Structure elucidation of natural products by mass spectrometry. Vol. I et II. Holden Day, San Francisco. 1964; A. M. Duffield, R. T. Aplin, H. Budzikiewicz, C. Djerassi, C. F. Murphy et W. C. Wildman. J. Am. Chem. Soc. **87**, 4902 (1965).
3. J. S. Shannon. Aust. J. Chem. **16**, 683 (1963); S. H. H. Chaston, S. E. Livingston, T. N. Lockyer et J. J. Shannon. Aust. J. Chem. **18**, 1539 (1965).
4. F. W. McLafferty. Chem. Commun. **78** (1965).
5. F. W. McLafferty et T. Wacks. J. Am. Chem. Soc. **89**, 5043 (1967).
6. T. Wacks et F. W. McLafferty. J. Am. Chem. Soc. **89**, 5044 (1967).
7. A. Mandelbaum et K. Biemann. J. Am. Chem. Soc. **90**, 2975 (1968).
8. T. H. Kinstle et W. R. Oliver. J. Am. Chem. Soc. **91**, 1864 (1969).
9. I. Howe et D. H. Williams. J. Am. Chem. Soc. **90**, 5461 (1968).
10. P. J. Wagner. Org. Mass Spectrom. **3**, 1307 (1970).
11. W. Vetter, W. Meister et W. J. Ritchter. Org. Mass Spectrom. **3**, 777 (1970).
12. W. F. A. Grose, T. A. Eggelte et N. M. M. Nibbering. Org. Mass Spectrom. **5**, 833 (1971).
13. G. W. Cable, J. Adelstein, J. Gore et C. Djerassi. Org. Mass Spectrom. **3**, 439 (1970).
14. H. E. Zimmerman et D. I. Schuster. J. Am. Chem. Soc. **84**, 4527 (1962).
15. F. G. Bordwell et K. M. Wellmann. J. Org. Chem. **28**, 2544 (1963).
16. W. J. Houlihan. J. Org. Chem. **27**, 3860 (1962).
17. R. Vanderwahl et H. Schinz. Helv. Chim. Acta, **35**, 2368 (1952).
18. H. C. Brown, K. J. Murray, J. A. Snover et G. Zweifel. J. Am. Chem. Soc. **82**, 4233 (1960).
19. M. Huang et H. Minlon. J. Am. Chem. Soc. **68**, 2487 (1946).
20. F. J. Bajer et H. W. Post. J. Org. Chem. **27**, 1422 (1962).
21. A. Burger et W. B. Bennet. J. Am. Chem. Soc. **72**, 5414 (1950).
22. H. Meerwein. Annalen Der Chemie, 396, 231 (1913).
23. H. E. Zaugg, M. Freifelder et B. W. Horron. J. Org. Chem. **15**, 1191 (1950).
24. F. Salmon-Le Gagneur et Mme. C. Neveu. Bull. Soc. Chim. Fr. 400 (1957).
25. M. A. Haller. Bull. Soc. Chim. Fr. **31**, 1073 (1922).
26. R. E. Ireland et J. A. Marshall. J. Org. Chem. **27**, 1615 (1962).
27. W. S. Johnson et H. Posvic. J. Am. Chem. Soc. **69**, 1361 (1947).
28. R. Mozingo. Org. Synth. Coll. Vol. III, 181 (1955).
29. J. A. Marshall et D. Schaeffer. J. Org. Chem. **30**, 3642 (1965).
30. R. E. Ireland et R. C. Kierstead. J. Org. Chem. **31**, 2543 (1966).
31. Z. G. Hajos, R. A. Micheli, D. R. Parrish et E. P. Oliveto. J. Org. Chem. **32**, 3008 (1967).
32. M. M. Janot, X. Luzinchi et R. Goutarel. Bull. Soc. Chim. Fr. 2109 (1961).
33. Z. Pelah, M. A. Kielczewski, J. M. Wilson, M. Ohashi, H. Budzikiewicz et C. Djerassi. J. Am. Chem. Soc. **85**, 2470 (1963).
34. A. Streitwieser, R. H. Jagow, R. C. Fahey et S. Suzuki. J. Am. Chem. Soc. **80** (1958).
35. F. P. Lossing, A. W. Tickner et W. A. Bryce. J. Chem. Phys. **19**, 1254 (1951).
36. H. J. Svec et G. A. Junk. J. Am. Chem. Soc. **89**, 790 (1967).
37. R. T. Grey et C. Djerassi. Org. Mass Spectrom. **3**, 245 (1970).
38. J. Seibl et T. Gaumann. Helv. Chim. Acta, **46**, 2857 (1963).
39. J. Seibl et T. Gaumann. Z. Anal. Chem. Bd. 197, 33 (1963).
40. A. A. Polyakova, T. I. Popova et M. I. Khotimskaya. Neftekhimiya, **6**, 150 (1966).

Can. J. Chem. Downloaded from www.nrcresearchpress.com by 210.87.254.5 on 09/05/12
For personal use only.

Spectrométrie de masse des cyclohexanones *gem*-diphénylées. II. Chaleurs de formation et structures possibles des principaux ions fragmentaires

CLAUDE J. FORTIN ET YVES ROUSSEAU

Département de Chimie, Université de Montréal, C.P. 6128, Montréal, Québec

Reçu le 19 avril

L'aspect énergétique des processus menant à la formation des principaux ions fragmentaires de cyclohexanones *gem*-diphénylées et de leurs analogues diphénylés est étudié. Plusieurs des ions obtenus de la dégradation de ces produits par impact électronique se retrouvent également dans la décomposition d'un grand nombre de produits aromatiques et font ainsi l'objet de comparaisons. Certaines structures sont proposées pour représenter les ions discutés tandis que certaines autres sont éliminées, en se basant sur leurs chaleurs de formation ioniques.

The energetics of the processes leading to the formation of the major ions of *gem*-diphenyl cyclohexanones and analogues were studied. Many of the ions coming from the electron impact induced decomposition of these products appear in quite a large number of aromatic compounds which can thus be used for comparisons. We are proposing structures to represent these ions while some are eliminated on the basis of their ionic heats of formation.

Can. J. Chem., **51**, 3457 (1973)

Introduction

Un certain nombre de travaux concernant l'étude des structures ioniques communes à partir de différents précurseurs aromatiques ont été rapportés. Ceux-ci se rapportent au benzène (1), à un certain nombre d'alkylbenzène (2), aux isomères du naphtalène et de l'azulène (3), ainsi qu'à un certain nombre de composés diphénylés (4). On propose, dans beaucoup de ces études, la présence d'une structure ionique commune pour expliquer le comportement similaire de certains produits sous impact électronique. Un bon nombre des ions provenant de la dégradation des cyclohexanones *gem*-diphénylées (CGDP) soumises à l'impact électronique se retrouvent aussi lors de la fragmentation de produits tels que le fluorène, le stilbène, le dihydro-9,10 phénanthrène, le phénanthrène, le méthyl-9 fluorène et plusieurs autres. Nous croyons que l'étude de l'aspect énergétique des différents processus de formation des ions peut nous amener à une meilleure compréhension des étapes par lesquelles les ions aromatiques se décomposent. La présente étude a pour but d'une part, d'établir si les ions de même rapport masse/charge provenant des 17 produits *gem*-diphénylés étudiés peuvent être assimilés à une même structure, ou si le fait de varier le substituant peut engendrer la formation de différentes structures ioniques. D'autre part, en se référant à la littérature, il est également possible d'effectuer des corrélations de structures et de tenter d'assigner aux ions fragmentaires principaux une structure probable. A ces fins, les potentiels d'ionisation de tous les produits (5), de même que les potentiels d'apparition de leurs ions fragmentaires principaux, ont été déterminés et les chaleurs de formation des différents ions ont été calculées et comparées. La méthode d'impact électronique étant employée, les conclusions apportées à la possibilité de structures ioniques communes doivent être interprétées sur une base qualitative puisque les ions formés par une telle méthode peuvent

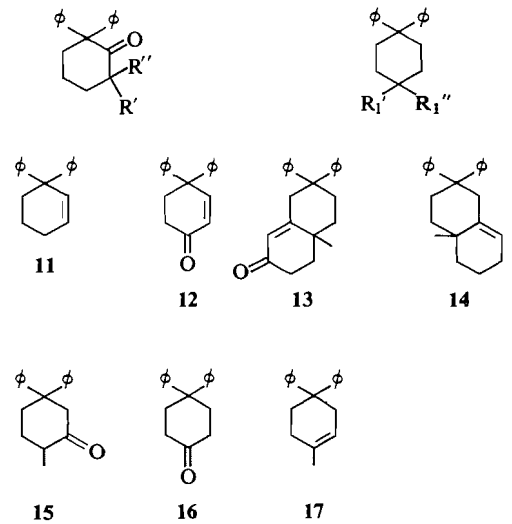

Can. J. Chem. Downloaded from www.nrcresearchpress.com by 210.87.254.105 on 09/05/12
For personal use only.

TABLEAU 1. Liste des produits étudiés

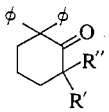

1 R′ = H; R″ = H
2 R′ = H; R″ = CH_3
3 R′ = CH_3; R″ = CH_3

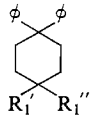

4 R′ = CH_3; R″ = CH_2—CH_2—C(=O)—H
5 R′ = CH_3; R″ = CH_2—CH_2—C(=O)—CH_3
6 R′ = —; R″ = (=CH—S—CH_2—CH_2—CH_2—CH_3)
7 R′ = CH_3; R″ = CH_2—CH=C(Cl)(CH_3)

8 R_1' = H; R_1'' = H
9 R_1' = H; R_1'' = CH_3
10 R_1' = CH_3; R_1'' = OH

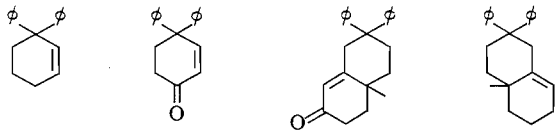

11 **12** **13** **14**

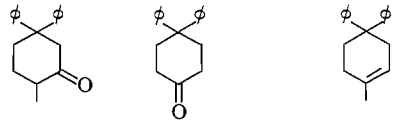

15 **16** **17**

posséder des excès d'énergie interne ou cinétique. Par contre, les conclusions sur le rejet de certaines structures pour représenter les ions discutés sont probablement indépendantes de tels facteurs.

Partie expérimentale

Les potentiels d'apparition sont obtenus à l'aide d'un appareil Hitachi RMU-6D. Le voltage des électrons ionisants est ainsi contrôlé par un potentiomètre, permettant des accroissements successifs de 0.1 V. Les intensités ioniques sont obtenues à l'aide d'un voltmètre digital Weston modèle 240. Le xénon est utilisé comme gaz étalon et la pression xénon–produit est suffisamment basse pour éviter les effets de pression sur le profil de la courbe d'efficacité d'ionisation. La méthode semi-logarithmique (6) a été jugée satisfaisante pour tous les potentiels déterminés. Les valeurs des potentiels d'apparition rapportées sont des moyennes de plusieurs déterminations. La reproductibilité des valeurs de potentiels d'apparition des ions fragments est habituellement de 0.05 à 0.1 eV mais l'incertitude est portée à 0.4 eV. La synthèse des produits utilisés (tableau 1) a été décrite précédemment (5). Les composés de référence méthyl-9 fluorène et dihydro-9,10 phénanthrène ont été obtenus de K et K Laboratories et le fluorène de J. T. Baker Chemical Co.

Résultats et discussion

Il est bien établi maintenant que, sous impact électronique, les alcools engendrent la formation des alcènes correspondants par perte d'une molécule d'eau. Les produits **10** et **17** peuvent donc être utilisés afin de comparer les chaleurs de formation de l'ion $(C_{19}H_{20})^+$ formé par les deux processus suivants:

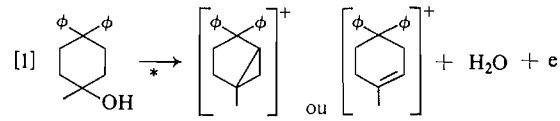

[1] **10** → (*a*) ou (*b*) + H_2O + e

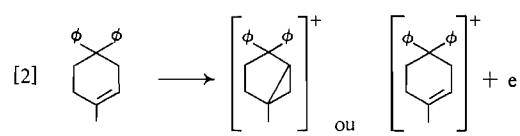

[2] **17** → ou + e

Il semble que dans les cyclohexanols, la perte de H_2O soit attribuable à des éliminations

Can. J. Chem. Downloaded from www.nrcresearchpress.com by 210.87.254.105 on 09/05/12
For personal use only.

TABLEAU 2. Potentiels d'apparition et chaleurs de formation de l'ion *m/e* 248 pour les composés **10** et **17**

Composé	P.A. eV	P.A. kcal/mol	I.R. (%)	ΔH_f(M) (kcal/mol)	$\Delta H_f(248)^+$ (kcal/mol)
10	9.2	214	37.5	−28	240
17	8.7	202	6.0	+41	243

1,4 et 1,3 (7–13). Le premier cas étant géométriquement empêché ici, la formation du *m/e* 248 procéderait alors par perte de l'hydrogène tertiaire (*a*) plutôt que secondaire (*b*). De toute façon, le but proposé n'est pas de déterminer la structure de l'alcène correspondant mais bien de démontrer l'identité ou non de ces structures. Les réactions 1 et 2 nous mènent aux équations suivantes:

$$\Delta H_f{}^1(248)^+ = \text{P.A.}_{248}{}^+ - \Delta H_f(H_2O) + \Delta H_f(\mathbf{10}) - E_1$$

$$\Delta H_f{}^2(248)^+ = \text{P.I.}_{248}{}^+ + \Delta H_f(\mathbf{17}) - E_2$$

Les chaleurs de formation des molécules à l'état fondamental sont calculées théoriquement à l'aide de la méthode de Cox (14, 15) basée sur la contribution de chaque liaison ou groupe de liaisons au ΔH_f. Les termes E_1 et E_2 représentent l'excès d'énergie cinétique libéré durant la formation des ions (16, 17); E_1 est évalué à 0.15 eV à partir de la largeur de l'ion métastable tandis que E_2 peut être négligé (17). Le tableau 2 rapporte les valeurs calculées et mesurées qui mènent au calcul des $\Delta H_f(248)^+$. L'erreur expérimentale sur la détermination des potentiels d'apparition limite la précision des résultats à ± 10 kcal/mol ce qui est suffisant pour conclure à l'identité de structure quelle qu'elle soit, entre ces deux ions, et à vérifier la validité de la méthode employée. Toujours dans cette même optique, il est possible d'étudier l'aspect énergétique de chaque ion important dans les spectres des cyclohexanones *gem*-diphénylées. Les mécanismes de formation de chacun de ces ions sont détaillés à la référence (5).

L'ion à m/e 206

Cet ion est un des plus intenses dans les spectres de six des sept produits (**1**–**5** et **7**) ayant la fonction carbonyle adjacente au carbone benzylique et est absent dans ceux des autres composés. Il semble que ce soit l'influence de cette position adjacente et la présence d'oxygène qui sont responsables de sa formation (5). Dans chaque cas, un ion métastable indique sa provenance à partir de $[M]^{+\cdot}$ et le spectre à haute résolution montre qu'il s'agit de $C_{16}H_{14}{}^+$. Les potentiels d'apparition, présentés au tableau 3 indiquent que la formation de cet ion est favorisée énergétiquement puisque les valeurs sont de quelques dixièmes d'eV seulement au-dessus des potentiels d'ionisation. Les données obtenues pour les chaleurs de formation de cet ion ne permettent pas de conclure à une structure commune quelque soit son précurseur. Toutefois, ces résultats ne sont pas incompatibles avec une telle conclusion, surtout si l'on tient compte du fait qu'il peut être formé avec un excès d'énergie dans certains cas. La valeur du $\Delta H_f(206)^+$ à l'état fondamental se rapproche sans doute plus de celle de **7**.

L'ion à m/e 193

Cet ion est un des plus intenses dans les spectres de 14 des 17 produits. Le fragment expulsé étant radicalaire, la méthode de Franklin (18) est utilisée pour le calcul du ΔH_f(F). Cette méthode assigne au ΔH_f les contributions des différents groupes d'atomes dans une molécule. Une transition métastable indique sa provenance à partir de $[M]^{+\cdot}$ et le spectre à haute résolution montre qu'il s'agit de $C_{15}H_{13}{}^+$. Les données thermodynamiques relatives à cet ion, sont rapportées au tableau 4. Il indique, là aussi, que l'ion à *m/e* 193 est formé avec un excès d'énergie; on peut alors énoncer que le ΔH_f de l'ion $C_{15}H_{13}{}^+$ non-excité se rapproche certainement de la valeur la plus faible soit 231 kcal/mol.

L'ion à m/e 180

Cet ion est important pour la plupart des produits CGDP et AD (analogue diphénylé). Les diverses transitions $M^{+\cdot} \rightarrow 180 + N$ donnent dans chaque cas des ions métastables faibles mais en forme de plateau indiquant que l'ion est formé avec un excès d'énergie cinétique. Celle-ci a été évaluée à 2 kcal/mol. La mesure précise des masses révèle que cet ion est $C_{14}H_{12}{}^+$. Dans chacun des cas, le fragment expulsé peut être sous forme cyclique (dans ce cas, l'énergie

Can. J. Chem. Downloaded from www.nrcresearchpress.com by 210.87.254.105 on 09/05/12
For personal use only.

TABLEAU 3. Potentiels d'apparition et chaleurs de formation de l'ion *m/e* 206

Composé	P.A. eV	P.A. kcal/mol	I.R. (%)	ΔH_f(M) (kcal/mol)	ΔH_f(F) (fragment neutre, kcal/mol)	$\Delta H_f(206)^+$ (kcal/mol)
1	9.6	221	100.0	−5	*a** −27	243
					*b** −38	254
2	9.2	213	99.0	−12	*a* −35	236
					b −43	244
3	9.4	217	89.7	−20	*a* −43	240
					b −50	247
4	9.4	219	100.0	−47	*a* −71	243
					b −77	249
5	9.3	214	100.0	−61	*a* −81	234
					b −90	244
7	9.1	210	99.5	−12	*a* −33	231
					b −43	241
12	9.3	215	100.0	+22	+10	227

**a* sous forme énol; *b* sous forme aldéhyde.

TABLEAU 4. Données thermodynamiques pour l'ion *m/e* 193

Composé	P.A. eV	P.A. kcal/mol	I.R. (%)	ΔH_f(M) (kcal/mol)	ΔH_f(F) (kcal/mol)	$\Delta H_f(193)^+$ (kcal/mol)
1	9.7	224	98.3	−5	−12	231
2	10.3	239	100.0	−12	−23	250
3	10.3	237	59.4	−20	−21	238
4	10.5	244	81.1	−47	−57	254
5	10.6	245	22.5	−61	−63	247
6	10.8	250	100.0	0	+4	246
7	10.6	245	30.9	−12	−16	249
8	10.3	239	100.0	+21	+14	246
9	10.6	245	100.0	+15	+9	251
10	10.1	234	24.8	−29	−34	239
13	9.9	229	100.0	−1	−9	237
14	10.3	239	100.0	+26	+18	247
15	10.8	251	100.0	−12	−18	257
16	10.5	243	100.0	−5	−12	250

reliée à la tension apportée par la cyclisation est incluse) ou sous forme de l'alcène à chaîne ouverte correspondant. Les valeurs rapportées au tableau 5 supposent la forme cyclique, mais dans tous les cas, le ΔH_f de la forme alcène correspondante ne diffère pas de plus de ± 3 kcal/mol de celles rapportées ici. Les résultats indiquent là aussi que la réaction de formation de cet ion se produit avec un excès d'énergie. Dans ce cas, la valeur du ΔH_f(**1**) qui est de 233 kcal/mol, se rapproche probablement le plus de celle de l'ion $C_{14}H_{12}^+$ non-excité. Ces mesures ne sont pas incompatibles avec une identité de structure pour cet ion quelle que soit la substitution du produit précurseur bien qu'elles ne le démontrent pas explicitement.

Un certain nombre de structures ont été proposées pour l'ion à *m/e* 180 à partir de différents précurseurs (19–22); il est souhaitable de savoir si l'une ou l'autre structure peut s'apparenter à celle provenant de la dégradation des CGDP et AD sous impact électronique. Il a été suggéré (19–21) que cet ion puisse être représenté par l'ion radical méthyl-9 fluorène (MF) en se basant sur une étude effectuée à partir de produits deutériés et enrichis en carbone 13. L'énergie requise pour la formation de cet ion à partir du méthyl-9 fluorène révèle effectivement la possibilité d'un tel cas pour l'ion *m/e* 180 de nos produits. Le potentiel d'ionisation de ce produit, n'étant pas rapporté dans la littérature, a été déterminé et se situe à 8.2 eV.

Can. J. Chem. Downloaded from www.nrcresearchpress.com by 210.87.254.105 on 09/05/12
For personal use only.

TABLEAU 5. Données thermodynamiques pour l'ion *m/e* 180

Composé	P.A. eV	P.A. kcal/mol	I.R. (%)	ΔH_f(F) (kcal/mol)	$\Delta H_f(180)^+$ (kcal/mol)
1	9.5	220	65.8	−20	233
2	10.4	240	83.4	−26	253
3	9.9	229	100.0	−35	242
4	10.3	239	65.4	−63	253
5	10.5	241	67.7	−76	253
6	10.1	235	3.6	−10	245
7	10.0	231	100.0	−27	244
8	9.8	228	32.1	+7	242
9	10.1	233	40.6	0	246
10	10.1	234	49.2	−44	248
11	9.8	226	100.0	+34	240
14	9.5	219	11.6	+11	234
15	10.0	231	44.7	−26	244
16	10.0	231	87.1	−20	244
17	9.8	227	100.0	+25	241

NOTE: les ΔH_f(M) sont rapportées au tableau 4. Les valeurs du ΔH_f(11) et ΔH_f(17) sont respectivement de 50 et +40 Kcal/mol.

La chaleur de formation de cette molécule à l'état fondamental, par la méthode de Cox, est de 41 kcal/mol. Ces deux valeurs nous conduisent à un $\Delta H_f{}^{MF}(180)^+$ de 231 kcal/mol ce qui tend à renforcer l'hypothèse d'une structure méthyl-9 fluorène pour l'ion à *m/e* 180 des CGDP et AD. En effet, la comparaison de cette valeur avec celle postulée pour l'ion $C_{14}H_{12}{}^+$ non-excité indique que ces deux ions peuvent être considérés comme isoénergétiques. La possibilité d'autres structures ne doit toutefois pas être exclue ce qui nous incite à effectuer une étude similaire en postulant cette fois l'ion stilbène comme intermédiaire. Bien que sa formation à partir des CGDP et AD exige une migration de phényle, celle-ci ne doit pas être considérée comme un obstacle puisque cet ion assure une stabilisation de la charge positive due à sa conjugaison. D'ailleurs, cette migration de phényle (à partir de carbones adjacents pour former un ion *gem*-diphénylé) est importante pour la formation du *m/e* 165 dans les v-triazoles (23). Les paramètres énergétiques nécessaires ont ainsi été déterminés et mènent aux valeurs suivantes: P.I.(stilbène) = 8.7 eV; ΔH_f(stilbène = 56 kcal/mol (à l'aide de la méthode de Cox). Cette dernière valeur peut d'ailleurs être évaluée expérimentalement de la façon suivante: la chaleur de combustion du stilbène est de −1.765 kcal/mol (24) ce qui nous conduit à un ΔH_{solide} de +39 kcal/mol. La comparaison du $\Delta H_{sublimation}$ de produits aromatiques analogues nous indique que l'ordre de grandeur du $\Delta H_{sublimation}$ (stilbène) $\simeq$ 15–25 kcal/mol. La combinaison des ΔH_{solide} et $\Delta H_{sublimation}$ donne une valeur de ΔH_{gaz}(stilbène), expérimentale comprise entre 54 et 64 kcal/mol ce qui confirme la valeur calculée à l'aide de la méthode de Cox. De ces valeurs, on déduit un ΔH_f de l'ion stilbène compris entre 256–266 kcal/mol. Le tableau 4 nous indique que cette structure ne devrait pas représenter l'ion à *m/e* 180 puisque les énergies calculées pour sa formation, à partir des différents précurseurs, sont plus faibles dans tous les cas que l'énergie minimum requise pour la formation de l'ion stilbène. Enfin, la structure du dihydro-9,10 phénanthrène (DHP) a été proposée (25) également pour représenter l'ion à *m/e* 180. Aucune donnée énergétique n'est rapportée dans la littérature pour cet ion. La méthode de Cox nous mène à une valeur de 37 kcal/mol pour son ΔH de formation à l'état fondamental et son potentiel d'ionisation a été déterminé et se situe à 8.6 eV. A l'aide de ces deux valeurs, sa chaleur de formation ionique est alors calculée comme étant 236 kcal/mol. Cette valeur est très rapprochée de celle du méthyl-9 fluorène et cette proximité nous empêche de discerner entre l'une ou l'autre structure probable pour cet ion même si dans le tableau quelques valeurs du $\Delta H_f{}^{CGDP,AD}(180)^+$ sont inférieures à celle du $\Delta H_f{}^{DHP}(180)^+$. Puisque les deux structures de référence sont isoénergétiques, il est alors possible que l'ion à

Can. J. Chem. Downloaded from www.nrcresearchpress.com by 210.87.254.105 on 09/05/12
For personal use only.

TABLEAU 6. Données thermodynamiques pour l'ion *m/e* 178

Composé	P.A. eV	P.A. kcal/mol	I.R. (%)	$\Delta H_f(178)^+$ (kcal/mol)
1	10.7	248	33.6	263
2	10.3	238	35.3	252
4	10.2	237	32.3	253
5	10.0	232	19.6	247
7	10.5	243	33.1	258
8	10.8	249	17.0	263
9	10.2	237	14.7	252
10	10.5	243	18.4	258
11	10.4	239	14.8	254
14	9.3	215	20.8	230
15	9.6	221	27.7	236
16	10.2	237	51.9	252

m/e 180 dans les CGDP et AD se retrouve sous ces deux formes, la différence d'énergie requise étant fournie par l'excès d'énergie avec lequel l'ion est formé. De cette façon, un équilibre pourrait être établi entre ces deux structures et de là, chacune serait susceptible de se dégrader ultérieurement selon des chemins caractéristiques et différents.

L'ion à m/e 178

La perte de H_2 ou 2H à partir de l'ion à *m/e* 180 conduit à sa formation (haute résolution $C_{14}H_{10}^+$) et ceci est démontré par la présence d'un ion métastable à 176.0. Dans la littérature (26), cet ion est fréquemment associé à la structure du phénanthrène bien qu'une structure du type diphénylacétylène ne soit pas exclue même si cette dernière demande une migration de phényle dans le cas des CGDP et AD. L'énergie de ce processus de formation a été examinée dans chacun des cas et les résultats sont rassemblés au tableau 6. Ceux-ci indiquent une possibilité de structure commune pour cet ion dans le même sens que nous l'avons discuté précédemment. La production de cet ion s'accompagne également d'un excès d'énergie et il est probable que le $\Delta H_f(C_{14}H_{10})^+$ non-excité se rapproche de 230–236 kcal/mol. Ces valeurs supposent notamment la perte de H_2 à partir du *m/e* 180, la perte de 2H conduisant à des valeurs beaucoup trop faibles pour être retenues. Natalis et Franklin (4) rapportent un $\Delta H_f(178)^+$ de 235 kcal/mol pour le phénanthrène. Cette valeur est compatible avec celle rapportée pour le $\Delta H_f^{CGDP,AD}(C_{14}H_{10})^+$ non-excité et supporte l'hypothèse d'une structure phénanthrène pour cet ion. Les mêmes auteurs rapportent également la chaleur de formation ionique du *m/e* 178 à partir du diphénylacétylène comme étant 303 kcal/mol. Cette structure peut alors être éliminée comme possibilité indiquant par là que la migration de phényle nécessaire à sa formation n'est pas favorisée dans les CGDP et AD. Par ailleurs si l'hypothèse des deux structures isoénergétiques pour l'ion *m/e* 180 est valable, l'ion phénanthrène pourrait bien alors provenir de la perte de H_2 à partir de l'intermédiaire dihydro-9,10 phénanthrène.

L'ion à m/e 165

L'ion à *m/e* 165 dans les spectres de méthyl-9 fluorène, diphénylméthane, bromodiphénylméthane, stilbène et dihydro-9,10 phénanthrène correspond au cation fluorényle (27, 28). Cet ion est également présent dans les spectres de 16 des 17 CGDP et AD et est formé par perte d'un radical méthyle à partir de l'ion *m/e* 180 (m^* = 151.25; haute résolution $C_{13}H_9^+$). Les données thermodynamiques pour sa formation sont présentées au tableau 7. On note que la formation de cet ion est plus énergétique que dans le cas des ions discutés précédemment. Une structure commune pour l'ion $C_{13}H_9^+$ peut être supposée pour tous les produits bien qu'elle ne soit pas démontrée rigoureusement. Cet ion est aussi formé avec un excès d'énergie. Par conséquent, le $\Delta H_f^{CGDP,AD}(C_{13}H_9)^+$ non-excité se rapproche probablement de la valeur

TABLEAU 7. Données thermodynamiques pour l'ion *m/e* 165

Composé	P.A. eV	P.A. kcal/mol	I.R. (%)	$\Delta H_f(165)^+$ (kcal/mol)
1	13.8	318	50.7	301
2	14.1	326	48.6	308
3	13.4	311	43.7	293
4	13.6	315	43.3	299
5	13.6	315	29.8	298
6	13.7	318	9.0	296
7	13.3	306	50.0	289
8	13.3	307	14.4	289
9	13.2	305	10.7	288
10	13.9	321	26.3	304
11	13.0	302	33.3	286
12	14.4	332	11.0	314
14	13.4	310	20.1	293
15	14.0	323	26.6	305
16	14.4	334	68.9	317
17	13.4	311	30.0	294

Can. J. Chem. Downloaded from www.nrcresearchpress.com by 210.87.254.105 on 09/05/12
For personal use only.

Can. J. Chem. Downloaded from www.nrcresearchpress.com by 210.87.254.105 on 09/05/12
For personal use only.

minimale qui est de 286 kcal/mol. Afin de vérifier l'hypothèse que l'ion *m/e* 165 puisse être représenté par un cation fluorényle, les potentiels d'apparition du *m/e* 165 des produits fluorène (F) et méthyl-9 fluorène (MF) ont été déterminés comme étant respectivement 12.5 et 11.9 eV. Ces valeurs, combinées avec leurs ΔH de formation à l'état fondamental, nous conduisent aux $\Delta H_f{}^{F}(165)^+ = 282$ kcal/mol et $\Delta H_f{}^{MF}(165)^+ = 284$ kcal/mol. On voit donc, par la comparaison avec la valeur du $\Delta H_f{}^{CGDP,AD}(C_{13}H_9)^+$ non-excité, qu'il est énergétiquement possible d'assigner à l'ion *m/e* 165 une structure fluorényle. Poursuivant l'hypothèse des deux structures isoénergétiques pour représenter le *m/e* 180, le cation fluorényle proviendrait alors de l'intermédiaire méthyl-9 fluorène par perte d'un radical méthyle.

L'ion à m/e 115

La perte de benzène à partir du *m/e* 193 donne naissance à l'ion *m/e* 115, telle que suggérée par la présence d'un ion métastable à 68.26 et le spectre à haute résolution indique qu'il s'agit de $C_9H_7{}^+$. Comme l'ion *m/e* 165, cet ion est formé par un processus requérant plus d'énergie que ceux des autres ions discutés jusqu'ici. Les résultats des calculs thermodynamiques (tableau 8) suggèrent également l'hypothèse de la probabilité d'une structure commune pour cet ion. Natalis et Franklin (4) rapportent la formation de cet ion à partir du biphényl par perte de C_3H_3 et évaluent sa chaleur de formation ionique à 321 kcal/mol. Ces auteurs ne proposent aucune structure pour cet ion fragmentaire mais, les résultats rapportés indiquent qu'elle ne devrait pas s'identifier à celle de l'ion à *m/e* 115 provenant des CGDP et AD. Cet ion est également très intense dans le spectre de l'indène (IN). Pour cette raison, son $\Delta H_f{}^{IN}(115)^+$ a aussi été déterminé. La chaleur de formation de cette molécule à l'état fondamental est de 43 kcal/mol (29) et le potentiel d'apparition de l'ion *m/e* 115 a été mesuré comme étant 12.4 eV ce qui nous conduit à un $\Delta H_f{}^{IN}(115)^+$ de 277 kcal/mol. Bien que la possibilité de la formation d'autres structures ne soit pas exclue, l'ion à *m/e* 115 provenant des CGDP et AD pourrait bien avoir la structure de l'ion indène formé avec un excès d'énergie. Celle-ci est d'ailleurs une des structures proposées pour la formation de l'ion *m/e* 115 à partir de l'ion *m/e* 171 de la phényl-10 décaline-*trans* (30).

TABLEAU 8. Données thermodynamiques pour l'ion *m/e* 115

Composé	P.A. eV	P.A. kcal/mol	I.R. (%)	$\Delta H_f(115)^+$ (kcal/mol)
1	14.1	327	57.1	309
2	13.7	316	48.0	297
3	13.8	319	32.1	300
4	13.4	310	15.1	300
5	14.2	328	21.7	310
6	13.7	316	33.7	306
7	13.7	316	44.1	300
8	13.3	307	45.5	294
9	13.7	316	30.6	302
10	13.7	317	18.1	302
11	13.6	314	9.6	295
13	13.0	301	42.5	290
14	13.2	305	45.8	293
15	13.5	312	38.7	298
16	13.5	312	78.5	299

Conclusion

Les chemins de dégradation des CGDP et AD en ions principaux sont résumés au schéma 1. Les structures rapportées sont celles qui sont corroborées par la mesure des énergies de formation. Le tableau 9 rassemble les structures proposées et rejetées, pour chaque ion traité. Il a été démontré que l'ion à *m/e* 206 est formé à partir du $M^{+\bullet}$ et qu'une structure commune est probable indépendamment de la substitution de l'ion précurseur. Cette conclusion s'applique également à l'ion *m/e* 193. Dans le cas de ces deux ions, et de tous les autres discutés ici, on ne rejette toutefois pas l'idée qu'ils puissent être formés dans des états excités. L'ion à *m/e* 180 est aussi formé avec un excès d'énergie ce qui rend possible un équilibre entre la structure dihydro-9,10 phénanthrène et méthyl-9 fluorène, les chaleurs de formation ioniques de ces deux intermédiaires étant très rapprochées. Chacune de ces deux entités serait alors susceptible de se dégrader selon des chemins différents. Ainsi la perte de H_2 à partir de cet ion pour mener à la formation du *m/e* 178, est compatible avec la forme dihydro-9,10 phénanthrène du *m/e* 180. Il est en effet probable que la structure du *m/e* 178 soit du type phénanthrène tel que montré par les données thermodynamiques. Ces résultats démontrent en outre que cet ion n'est pas assez énergétique pour s'apparenter à une structure diphénylacétylène qui requiert 303 kcal/mol et demande par surcroît une migration de

TABLEAU 9. Synthèse des structures proposées et rejetées en se basant sur les calculs énergétiques

Ions	Structures	Chaleur de formation (kcal/mol) Calculée	Chaleur de formation (kcal/mol) Valeur minimale mesurée
m/e 206	—	—	231
m/e 193	—	—	231
m/e 180	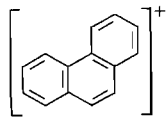	231	233
	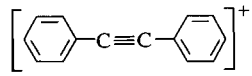	256–266	
	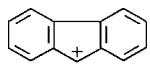	236	
m/e 178	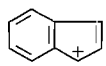	235	230–236
	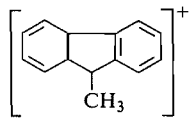	303	
m/e 165	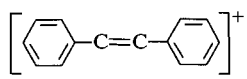	282 284 321	286
	Ion provenant du biphénylène		
m/e 115	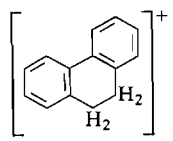	277	290

phényle sur le carbone adjacent. Le cation fluorényle, qui est proposé comme intermédiaire dans la dégradation de plusieurs composés aromatiques, identifie l'ion à *m/e* 165 dans les CGDP et AD et provient de la perte d'un radical méthyle à partir de la structure méthyl-9 fluorène de l'ion à *m/e* 180. Enfin, le fragment à *m/e* 115, provenant de l'ion à *m/e* 193, n'a pas la même structure que celui provenant de la fragmentation du biphényle mais correspond possiblement à l'ion indényle formé avec un excès d'énergie.

Can. J. Chem. Downloaded from www.nrcresearchpress.com by 210.87.254.105 on 09/05/12
For personal use only.

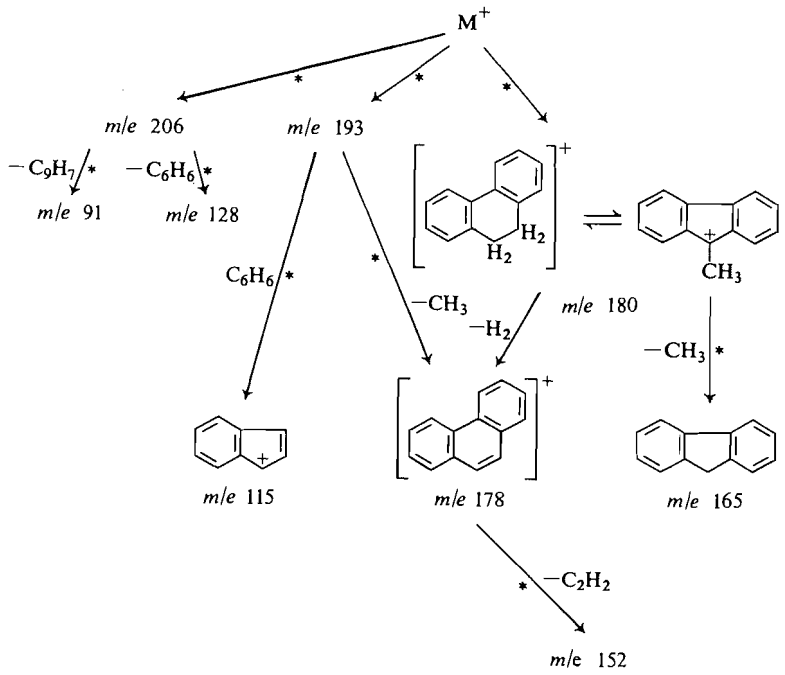

SCHÉMA 1

Le projet fut réalisé grâce à l'assistance financière du Conseil national de recherches du Canada et du Ministère de l'Education du Gouvernement du Québec.

1. J. MOMIGNY, L. BRAKIER et L. D'OR. Bull. Classe Sci. Acad. Roy. Belg. **48**, 1002 (1962).
2. H. M. GRUBB et S. MEYERSON. Mass spectrometry of organic ions. *Edité par* F. W. McLAFFERTY. Academic Press Inc., New York, N.Y. 1963. Chap. 10.
3. R. J. VANBRUNT et M. E. WACKS. J. Chem. Phys. **41**, 3195 (1964).
4. P. NATALIS et J. L. FRANKLIN. J. Phys. Chem. **69**, 2935 (1965).
5. C. J. FORTIN, M. FOREST, C. VAZIRI, D. GRAVEL et Y. ROUSSEAU. Can. J. Chem. This issue.
6. F. P. LOSSING, A. W. TICKNER et W. A. BRYCE. J. Chem. Phys. **19**, 1254 (1951).
7. W. BENZ et K. BIEMANN. J. Am. Chem. Soc. **86**, 2375 (1964); S. MEYERSON et L. C. LEITCH. J. Am. Chem. Soc. **86**, 2555 (1964).
8. A. M. DUFFIELD, S. D. SAMPLE et C. DJERASSI. Chem. Commun. 193 (1966).
9. F. W. McLAFFERTY. Interpretation of mass spectra. W. A. Benjamin Inc., New York, N.Y. 1966. p. 132.
10. M. M. GREEN et J. SCHWAB. Tetrahedron Lett. 2955 (1968).
11. C. G. MACDONALD, J. S. SHANNON et G. SUGOWDZ. Tetrahedron Lett. 807 (1963); H. BUDZIKIEWICZ, Z. PELAH et C. DJERASSI. Monatsh. Chem. **95**, 158 (1964).
12. H. BUDZIKIEWICZ, C. DJERASSI et D. H. WILLIAMS. Mass spectrometry of organic compounds. Holden-Day, San Francisco. Chapt. 2. 1967.
13. C. E. BRION et L. D. HALL. J. Am. Chem. Soc. **88**, 3661 (1966).
14. J. D. COX. Tetrahedron, **18**, 1337 (1962).
15. J. D. COX. Tetrahedron, **19**, 1175 (1963).
16. J. H. BEYNON, R. A. SAUNDERS et A. E. WILLIAMS. Z. Naturforsch. (A) **20**, 180 (1965); (*b*) R. G. COOKS, I. HOWE et D. H. WILLIAMS. Org. Mass Spectrom. **2**, 137 (1969).
17. H. F. GRÜTZMACHER et J. LOHMANN. Liebigs Ann. Chem. **705**, 81 (1967).
18. J. L. FRANKLIN. J. Chem. Phys. **21**, 2029 (1953).
19. R. A. W. JOHNSTONE et B. J. MILLARD. Z. Naturforsch. (A) **21**, 604 (1966).
20. R. A. W. JOHNSTONE et S. D. WARD. J. Chem. Soc. (C) 1805 (1968).
21. R. A. W. JOHNSTONE et S. D. WARD. J. Chem. Soc. (C) 2540 (1968).
22. P. F. DONAGHUE, P. Y. WHITE, J. H. BOWIE, B. D. RONEY et H. J. RODDA. Org. Mass Spectrom. **2**, 1061 (1969).
23. F. COMPERNOLLE et M. DEKEIREL. Org. Mass Spectrom. **5**, 427 (1971).
24. F. D. ROSSINI, D. D. WAGMAN, W. H. EVANS, S. LEVINE et I. JAFFE. Selected values of physical and thermodynamic properties of hydrocarbons and related compounds. Carnegie Press, Pittsburgh, Pa. 1953.
25. A. MAQUESTIAU, Y. VANHAVERBEKE, F. DELALIEU. Bull. Soc. Chim. Belges, **78**, 589 (1969).

Can. J. Chem. Downloaded from www.nrcresearchpress.com by 210.87.254.105 on 09/05/12
For personal use only.

26. J. H. BOWIE, P. F. DONAGHUE, H. J. RODDA et B. K. SIMONS. Tetrahedron, **24**, 3965 (1968).
27. J. H. BOWIE, B. K. SIMONS, P. F. DONAGHUE et R. K. M. KALLURY. Tetrahedron, **25**, 3969 (1969).
28. U. RAPP, H. A. STAAB et C. WUNSCHE. Org. Mass Spectrom. **3**, 45 (1970).
29. J. L. FRANKLIN, J. G. DILLARD, H. M. ROSENSTOCK, J. T. HERRERE, K. DRAXL et F. H. FIELD. Ionization potentials, appearance potentials and heats of formation of gaseous positive ions. U.S. Dep. of Commerce, National Bureau of Standards, NSRDS-NBS 26 (1969).
30. R. T. GRAY et C. DJERASSI. Org. Mass Spectrom. **3**, 245 (1970).

Can. J. Chem. Downloaded from www.nrcresearchpress.com by 210.87.254.105 on 09/05/12
For personal use only.

Effect of Solvents on the Quantum Efficiency of Rubrene Electrogenerated Chemiluminescence

A. PIGHIN
Bell-Northern Research, Ottawa, Canada K1Y 4H7

Received May 3, 1973

A simple and precise method for measuring the efficiency of electrogenerated chemiluminescence (e.g.c.l.) in terms of photons/(Faradaic electron)(Φ_{coul}) is described and applied to rubrene e.g.c.l. A symmetrical square wave potential having a frequency of 20–1000 Hz was employed to produce the e.g.c.l. The electrogenerated ion radicals were shown to be completely stable at these frequencies; consequently, Φ_{coul} was determined in the absence of side reactions. Change of solvent from *N,N*-dimethylformamide (DMF) to equivolume benzene–DMF resulted in an increase in Φ_{coul} from 0.67 to 1.21% at 20 Hz. Φ_{coul} decreased with increasing frequency. Varying the electrolyte (tetra-*n*-butylammonium perchlorate, TBAP) concentration did not affect Φ_{coul}.

Une méthode simple et précise pour mesurer l'efficacité de la chimiluminescence électroengendrée (c.l.e.e.) en termes de photons par électron faradaique (Φ_{coul}) a été décrite et appliquée au rubrène c.l.e.e. Un potentiel d'onde à symétrie carrée ayant une fréquence de 20–1000 Hz a été utilisée pour produire la c.l.e.e. On a montré que les ions radicaux électroengendrés étaient complètement stables à ces fréquences, par conséquent, Φ_{coul} a été déterminé en l'absence de réactions parasites. Le passage de la *N,N*-diméthylformamide (DMF) au mélange équivolume benzène-DMF a pour résultat d'accroître Φ_{coul} de 0.67 à 1.21% à 20 Hz. Φ_{coul} décroît lorsque la fréquence croît. La variation dans la concentration en électrolyte (perchlorate de tétra-*n*-butylammonium, PTBA) n'affecte pas Φ_{coul}.

[Traduit par le journal]

Can. J. Chem., 51, 3467 (1973)

Introduction

The efficiency of electrogenerated chemiluminescence (e.g.c.l.),[1] in this article expressed in photons/(Faradaic electron) and represented by Φ_{coul}, can be a useful parameter in elucidating the e.g.c.l. mechanism. Bard *et al.* (1) have recently reviewed the reported e.g.c.l. efficiencies and discussed the difficulties in these measurements. Rubrene is a popular electrochemiluminescent compound and its reported e.g.c.l. efficiencies range from a low of 0.1% (1) which has been corrected for lost electrogenerated species to a high of 8.7% (2) without any corrections. Bezman and Faulkner (3) obtained intermediate values and recorded greater efficiencies in benzonitrile than in *N,N*-dimethylformamide (DMF). Other e.g.c.l. systems have shown either a solvent composition or electrolyte concentration dependence of their efficiencies (1). In this article, we present evidence of a large solvent effect, a frequency dependence, and no electrolyte concentration effect on the quantum efficiency of stable rubrene e.g.c.l.

[1]Electrogenerated chemiluminescence is abbreviated as ECL in the existing literature. To avoid confusion with Emitter-Coupled Logic we employ e.g.c.l.

Experimental

The rubrene was purchased from the Aldrich Chemical Co. and recrystallized repeatedly from xylene–methanol and then dried by vacuum heating. Tetra-*n*-butylammonium perchlorate (TBAP), polarographic grade from MC&B, was recrystallized repeatedly from ethanol and dried by vacuum heating. The two solvents, Fisher D-133 DMF and Fisher B-414 benzene, were dried with molecular sieves and outgassed. The solutions were prepared and used inside a nitrogen-filled dry box.

The apparatus used to measure Φ_{coul} is illustrated in Fig. 1. The electrolysis cell was formed from a TS 10/30 Pyrex ground glass joint while the electrodes were two parallel 0.020 in. diameter platinum wires rigidly fixed about 1 mm apart by beads of soft glass. A symmetrical square wave potential was employed to electrolyze the solution in the cell. Two identical pulses of light per cycle from each electrode were observed and the overall intensity remained constant for at least several hours of continuous electrolysis. The driving potential was restricted to those values which produced stable e.g.c.l. The bottom of the electrolysis cell rested inside an open box whose walls and floor were made of five 1 cm^2 solar cells connected in parallel. The level of the solution inside the electrolysis cell was kept below the top of the solar cell box. The solar cells were operated in the current mode and their output measured with a picoammeter. The solar cell box was calibrated using a red light-emitting diode of known efficiency (traceable to the National Research Council of Canada). The correction factor was 1.7, *i.e.* (measured current × 1.7) = corrected current. The electrical current through the electrolysis cell was converted

Can. J. Chem. Downloaded from www.nrcresearchpress.com by 210.87.254.40 on 09/05/12
For personal use only.

TABLE 1. Physical properties at 25 °C

	Viscosity (cP)	Diffusion coefficient of rubrene (cm^2/s)	Dielectric constant
0.100 *M* TBAP–DMF	0.89	4.8×10^{-6}	
0.100 *M* TBAP – equivolume benzene–DMF	0.81	5.2×10^{-6}	
Benzene			2.274*
DMF			36.71†

*Reference 4.
†Reference 5.

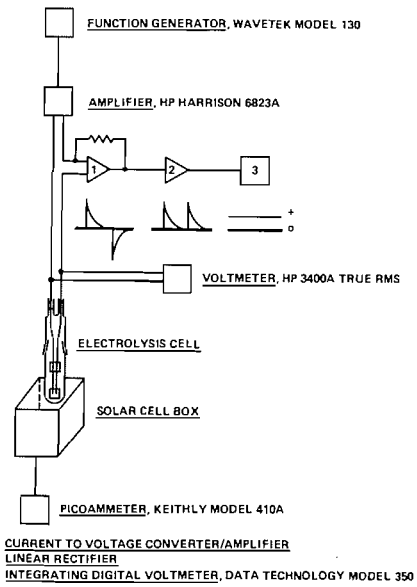

FIG. 1. Experimental apparatus for measuring Φ_{coul}.

and amplified by a factor of 1000 to a voltage, rectified with a fast linear rectifier, and then measured with an integrating digital voltmeter. This signal processing of the electrical current yields the rectified average value of the current. Specifically, 1 V d.c. was equivalent to 1 mA average rectified a.c. The Φ_{coul} experiments were performed at 23 ± 1 °C.

Electrochemical measurements were performed with a Princeton Applied Research Model 170 Electrochemistry System and a three electrode cell. A silver wire immersed in the test solution was used as the reference electrode; it was contained inside a compartment whose Luggin tip extended to within 2 mm of the platinum bead working electrode. The counter electrode consisted of a large platinum wire helix around the working electrode and Luggin tip. *iR* compensation was employed in the recordings.

Results and Discussion

The two solvents employed in this investigation were DMF and equivolume benzene–DMF and were selected for their physical properties (Table 1). The solution viscosities are only slightly different but the dielectric constant of DMF is much greater than that of benzene. It was therefore expected that the bulk dielectric constant of the mixed solvent solution would be significantly less than that of the DMF solution. The viscosities were measured with an Ostwald viscometer that was calibrated with water and the diffusion coefficients of the 1 m*M* rubrene in 0.100 *M* TBAP solutions were determined from chronoamperograms of the reductions at a shielded platinum disk electrode of known area. Note that the products of (viscosity) (diffusion coefficient) are essentially the same in obeyance of the Stokes–Einstein equation (6).

Table 2 contains the potential differences between the half-wave oxidation and reduction potentials of rubrene in both solutions at selected temperatures. These data were derived from cyclic voltammograms of the oxidation and reduction at a scan rate of 100 mV/s with *iR* compensation. The peak potentials were measured from the cyclic voltammogram, $1.109RT/nF$ (7) V were subtracted from their absolute values to obtain the half-wave potentials, and then the

TABLE 2. Variation in the potential difference between the half-wave oxidation and reduction potentials of rubrene with temperature

	$E_{\frac{1}{2},ox} - E_{\frac{1}{2},red}$ (V)	
Temperature (°C)	0.100 *M* TBAP–DMF	0.100 *M* TBAP – equivolume benzene–DMF
0	2.355	2.425
10	2.365	2.435
25	2.365	2.445
35	2.375	2.460
50	2.385	2.470

Can. J. Chem. Downloaded from www.nrcresearchpress.com by 210.87.254.40 on 09/05/12
For personal use only.

TABLE 3. Thermodynamic and spectroscopic data of rubrene

	ΔS° (cal/mol °K)	$-\Delta H_{25\,°C}$ (kcal/mol)	$E_{^1S^*}$ (kcal/mol)	Relative fluorescence efficiency
0.100 *M* TBAP–DMF	13	50.6	52.9	1.0
0.100 *M* TBAP – equivolume benzene–DMF	21	50.0	52.9	1.0

half-wave reduction potential was subtracted from the half-wave oxidation potential. Nemec's (8) equation for calculating *iR* losses for spherical microelectrodes was used to estimate our *iR* losses in the absence of *iR* compensation. The peak currents were about 20 μA in both solutions at 25 °C, the radius of our electrode was about 0.5 mm, and the Luggin tip was positioned about 2 mm from the electrode's surface. The specific conductances of the 0.100 *M* TBAP solutions were measured and were 0.0039 $ohm^{-1}\ cm^{-1}$ for DMF and 0.0023 $ohm^{-1}\ cm^{-1}$ for equivolume benzene–DMF at 25 °C. When all these values are inserted into Nemec's eq. 2, and multiplied by 2 since the *iR* losses occur during both the oxidation and reduction, and are therefore additive, the *iR* losses are calculated to be about 12 mV for the DMF solution and 20 mV for the mixed solvent solution. Assuming that the *iR* compensation is 80% effective, we see that the residual, uncompensated *iR* is only a few mV in both cases. The temperature coefficient of the conductance is negative and greater in magnitude than the positive temperature coefficient of the peak current. Consequently, the amount of residual, uncompensated *iR* tends to decrease with increasing temperature.

From the temperature coefficient of the potential difference between the half-wave oxidation and reduction potentials (Table 2), the standard entropy of the homogeneous electron transfer reaction in each solution was calculated using the following equation in which the symbols have their usual significance:

$$[1] \qquad \Delta S^0 = \frac{nF\Delta(E_{\frac{1}{2},ox} - E_{\frac{1}{2},red})}{\Delta T}$$

The temperature coefficient was assumed to be constant and the slope was calculated using linear regression analysis. The results of these calculations are listed in Table 3 along with other relevant thermodynamic and spectroscopic data of rubrene in both solvents. It should be noted that because the amount of residual, uncompensated *iR* decreases with increasing temperature then the above entropies are slightly *smaller* than the true values.

The change in enthalpies in Table 3 are for the homogeneous electron transfer reaction between the monoanion and monocation radicals of rubrene and were calculated from the equation

$$[2] \qquad -\Delta H_T = nF(E_{\frac{1}{2},ox} - E_{\frac{1}{2},red})_T - T\Delta S^0$$

The energy of the lowest excited singlet ($E_{^1S^*}$) was determined from the crossover point between the absorption and fluorescence spectra of rubrene in each conducting solution. The relative fluorescence efficiencies were obtained by comparing the intensities of the fluorescences of 10^{-5} m*M* rubrene in each conducting solvent. The fluorescences were excited with 4500 Å radiation. Neither solvent absorbs at this wavelength so that the fluorescence intensities did not have to be corrected for differences in absorption but only for the ratio of the squares of the refraction indices of their solutions (9).

An important conclusion can be made from the data in Table 3. The change in enthalpy of the homogeneous electron transfer reaction in both solutions is clearly less than the energy of the emitting species, $E_{^1S^*}$. Residual, uncompensated *iR* in the electrochemical measurements used to calculate the $-\Delta H$'s have made the calculated values of $-\Delta H$ slightly larger (more negative) than the true values. Rubrene e.g.c.l. is therefore "energy deficient" and must proceed in both solutions via the "triplet route" (10). This mechanism is summarized in Table 4. In this scheme, each homogeneous electron transfer reaction produces an average of 3/4 triplets. This fraction is given by spin statistics assuming that the solvent does not preferentially enhance either the formation of triplets or singlets (11). This seems probable considering rubrene is a simple aromatic hydrocarbon (12). Triplet-triplet annihilation can then produce either triplets, singlets, or

Can. J. Chem. Downloaded from www.nrcresearchpress.com by 210.87.254.40 on 09/05/12
For personal use only.

TABLE 4. Rubrene e.g.c.l. mechanism

$R \rightarrow R^+ + e$	Oxidation of rubrene at electrode
$R + e \rightarrow R^-$	Reduction of rubrene at electrode
$R^+ + R^- \rightarrow 3/4\ {}^3R^* + 5/4\ R$	Homogeneous electron transfer reaction/ triplet formation
${}^3R^* + {}^3R^* \rightarrow 1/4\ {}^1R^* + 3/4\ {}^3R^* + R$	Triplet–triplet annihilation/singlet formation
${}^1R^* \rightarrow R + h\nu$	Radiative decay of excited singlet

quintets. If we make the usual assumption that the formation of quintets is energy-forbidden, then spin statistics predict an average yield of 1/4 singlets per triplet-triplet annihilation. The singlets immediately radiate to their ground state with the emission of light. The excited triplets produced by the triplet–triplet annihilation reaction engage in further triplet–triplet encounters, thereby increasing the singlet yield per triplet–triplet annihilation from 1/4 to 2/5. Thus, two electrons (one homogeneous electron transfer reaction) ultimately results in the emission of an average of 3/20 photons. However, about 8 (3) to 17% (2), say 12.5%, of the ion radicals are neutralized by the reversal of the polarity of the electrode potential. The maximum theoretical efficiency of an energy deficient e.g.c.l. system, such as rubrene e.g.c.l., using square wave stimulation is 6.6% photons/electron.

Figure 2 illustrates a typical current–voltage curve of the electrolysis cell. Prior to the appearance of e.g.c.l., the current increases linearly with applied voltage and at constant voltage this current was nearly directly proportional to the frequency. Since these characteristics are peculiar to capacitive currents, then this current must be the current that is needed to polarize the electrode–solution interphase. The abrupt rise in current at about 2.3 V (peak) coincides with the detection of e.g.c.l. Assuming that the Faradaic processes do not alter the double layer capacity and that the double layer capacity remains constant in the potential region for e.g.c.l., then by extrapolating the capacitive current into the region for e.g.c.l. and subtracting it from the total at that potential, the Faradaic current at that voltage is obtained. A plot of the corrected photon current *vs.* the Faradaic current is then made and Φ_{coul} calculated from the slope of this plot. Linear regression analysis was used to obtain the slopes. Figure 3 illustrates one of these plots. The photon current measured with the picoammeter is twice that emitted at one electrode.

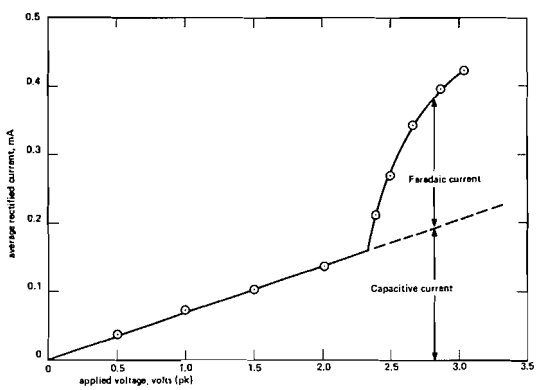

FIG. 2. Typical electrical characteristics of the electrolysis cell. The 1.01 m*M* rubrene in 0.100 *M* TBAP – equivolume benzene–DMF was electrolyzed with 100 Hz square wave potential.

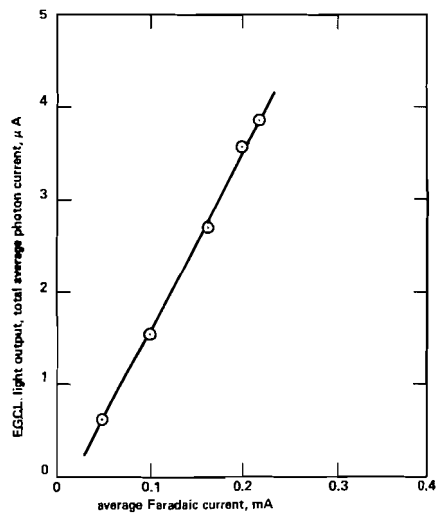

FIG. 3. Typical variation in photon current with Faradaic current. The 1.01 m*M* rubrene in 0.100 *M* TBAP – equivolume benzene–DMF was electrolyzed with 100 Hz square wave potential.

Can. J. Chem. Downloaded from www.nrcresearchpress.com by 210.87.254.40 on 09/05/12
For personal use only.

Can. J. Chem. Downloaded from www.nrcresearchpress.com by 210.87.254.40 on 09/05/12
For personal use only.

Therefore, the Φ_{coul} calculated from this plot must be divided by 2 to obtain the value of Φ_{coul} at each electrode.

The results of our Φ_{coul} measurements are given in Fig. 4. These results, when corrected for the fraction of ion radicals lost by the reversal of the electrode potential (8–17%), are at most 20% of the maximum theoretical value previously calculated.

A frequency dependence of Φ_{coul} is seen in all cases, in contradiction to theory (2). If a quencher were present in the bulk of the solution, the fractional probability of quenching will decrease with increasing frequency because the triplet concentration would increase within a steadily more compact reaction zone. It has been suggested (1) that the triplet state may be quenched by the parent ion radicals and by the electrode. The effectiveness of the former mode is frequency independent because the ratio ion radicals: triplets remains constant with changing frequency whereas the effectiveness of the latter mode increases with increasing frequency because the reaction layer becomes more compact at the electrode. Our frequency dependence of I_{coul} is consistent with quenching of the triplets by the electrode.

Reducing the electrolyte concentration from 0.100 to 0.020 *M* TBAP in DMF did not affect the efficiency of the rubrene e.g.c.l. which is in contrast to the increase reported by Bard *et al.* (1) in the e.g.c.l. efficiency of 9,10-dimethylanthracene-tri-*p*-tolylammonium perchlorate with decreasing electrolyte concentration in TBAP–tetrahydrofuran. In this latter case, ion pairing was suggested as a cause. In our case, TBAP is less dissociated in equivolume benzene–DMF than in DMF (based on conductivity measurements) but the absence of an electrolyte effect on the Φ_{coul} of rubrene in TBAP–DMF renders the degree of electrolyte dissociation unimportant.

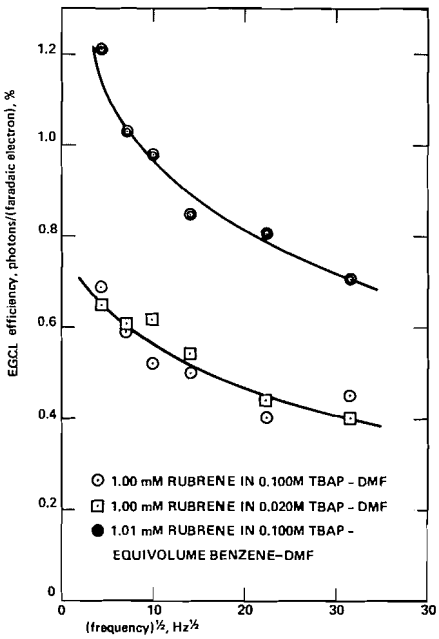

FIG. 4. Variation in Φ_{coul} of rubrene in selected solutions with frequency of driving potential.

Addition of one part of benzene to DMF increased the Φ_{coul} of rubrene from 0.67 to 1.21% at 20 Hz for the same concentration of fluorescor (1 m*M*) and electrolyte (0.100 *M*). The luminescences obtained were spectrally identical and the fluorescence efficiencies are the same in both solutions (Table 3). We established earlier that the e.g.c.l. proceeds in both solutions via the "triplet route".

The greater potential differences between the oxidation and reduction potentials of rubrene in the mixed solvent solution (Table 2) indicates that the rubrene is more strongly solvated in the mixed solvent solution than in the DMF solution. We obtained e.s.r. spectra of the electrogenerated monoanion radicals in both solutions and the spectra were identical: the difference in solvation of the monoanions was either apparently not sufficient to cause a shift in the e.s.r. spectrum or the monoanions were similarly solvated (by DMF) in both solutions. Because of the heteropolar nature of the mixed solvent, *i.e.* one aromatic and one polar component, it is likely that the benzene fraction will preferentially solvate the neutral rubrene, including excited forms, while the DMF fraction will preferentially solvate the ion radicals. If the triplets were quenched by the parent ion radicals and/or electrode, their greater solvation in the mixed solvent system could shield them from the quenching agents thereby accounting for the greater Φ_{coul} in the mixed solvent solution. The common element between our solvent effect on Φ_{coul} and those reported by Bezman and Faulkner (3) and Bard *et al.* (1) is that we all obtained higher efficiencies in the less polar, or more aromatic, solvent.

This work was supported in part by the National Research Council of Canada through its Industrial

Research Assistance Program. The assistance of R. M. van Dyk in the design of the electronic circuitry and of D. P. Malanka in performing the experiments, and the helpful criticism of Dr. M. A. Kabayama are gratefully acknowledged.

1. A. J. BARD, C. P. KESZTHELYI, H. TACHIKAWA, and N. E. TOKEL. *In* Chemiluminescence and bioluminescence. *Edited by* M. J. Cormier, D. M. Hercules, and J. Lee. Plenum Press, New York, N.Y. 1973. p. 193.
2. P. M. SCHWARTZ, R. A. BLEKELEY, and B. B. ROBINSON. J. Phys. Chem. **76**, 1868 (1972).
3. R. BEZMAN and L. R. FAULKNER. J. Am. Chem. Soc. **94**, 6324 (1972); **95**, 3083 (1973).
4. R. C. WEAST. (*Editor*). Handbook of chemistry and physics, 49th ed. The Chemical Rubber Co., Cleveland, Ohio, 1968–1969. p. E58.
5. Du Pont DMF Product Information Bulletin. E. I. Du Pont de Nemours and Co., Wilmington, Delaware. p. 3.
6. C. A. PARKER. Photoluminescence of solutions. Elsevier, London. 1968. p. 76.
7. R. S. NICHOLSON and I. SHAIN. Anal. Chem. **36**, 706 (1964).
8. L. NEMEC. J. Electroanal. Chem. **8**, 166 (1964).
9. J. N. DEMAS and G. A. CROSBY. J. Phys. Chem. **75**, 991 (1971).
10. L. R. FAULKNER, H. TACHIKAWA, and A. J. BARD. J. Am. Chem. Soc. **94**, 691 (1971).
11. G. J. HOYTINK, Discus. Faraday Soc. **45**, 14 (1968).
12. G. J. HOYTINK, *In* Chemiluminescence and bioluminescence. *Edited by* M. J. Cormier, D. M. Hercules, and J. Lee. Plenum Press, New York, N.Y. 1973. p. 147.

Can. J. Chem. Downloaded from www.nrcresearchpress.com by 210.87.254.40 on 09/05/12
For personal use only.

Can. J. Chem. Downloaded from www.nrcresearchpress.com by 210.87.254.6 on 09/05/12
For personal use only.

γ-Deuterium Isotope Effects on Solvolysis of 7-Halonorbornyl Brosylates-6-*d*[1]

NICK H. WERSTIUK, GEORGE TIMMINS, AND FRANK P. CAPPELLI
Department of Chemistry, McMaster University, Hamilton, Ontario

Received June 27, 1973

The γ-deuterium isotope effects for the solvolysis of *anti*- and *syn*-7-chloro-, *anti*- and *syn*-7-bromo-*exo*-2-norbornyl brosylates-6-*endo*-*d* and *syn*-7-chloro-*exo*-2-norbornyl brosylate-5,6-*exo*,*exo*-d_2 in 80:20 EtOH–H_2O, 0.04 *M* NaOAc at 65° are 1.11 ± 0.01, 1.11 ± 0.01, 1.13 ± 0.01, 1.05 ± 0.01, and 1.11 ± 0.01, respectively. The results indicate that the γ-isotope effect observed in the solvolysis of *exo*-norbornyl brosylate likely is not derived via neighboring group (non-vertical) participation of the C_1—C_6 bond.

La solvolyse des brosylates *exo*-2 des chloro-7 *anti* et *syn* et des bromo-7 *anti* et *syn* deutéro-6 *endo* norbornyle ainsi que du brosylate *exo* du chloro-7 *syn* dideutéro-5,6 *exo*,*exo* norbornyle a été effectuée à 65°C, dans un mélange contenant 0.04 *M* de NaOAc dans 80:20 de EtOH–H_2O; les effects isotopiques γ du deutérium ont été évalués respectivement à 1.11 ± 0.01, 1.11 ± 0.01, 1.13 ± 0.01, 1.05 ± 0.01 et 1.11 ± 0.01. Ces résultats indiquent que l'effet isotopique observé dans la solvolyse des brosylates *exo* de norbornyle ne proviennent pas de participation non verticale des liens C_1—C_6.

[Traduit par le journal]

Can. J. Chem., **51**, 3473 (1973)

α-, β-, and γ-deuterium isotope effects have been used extensively to probe the nature of cations generated solvolytically especially in cyclic systems (1–10). We have undertaken solvolysis studies to determine (*a*) the effect of substituents at C-1 and C-7 in the [2.2.1] system on the magnitude of the γ-effect to establish more accurately the origin of the isotope effect (10), (*b*) the stereochemistry of the 1,3-elimination which yields tricyclic product, and (*c*) whether or not the 6-*endo*-C—H bond participates directly in solvolysis especially in "locked"[2] systems (11–14).

In this communication we report (Table 1) the γ-deuterium isotope effects for the solvolysis of the *anti*- and *syn*-7-chloro- (16–19) and bromonorbornyl brosylates in 80:20 EtOH–H_2O containing 0.04 *M* NaOAc.

Surprisingly, the solvolytic γ-isotope effects for the 7-halonorbornyl brosylates are essentially identical and in fact somewhat larger than those observed for *exo*-norbornyl brosylate (3,4). Since 7-halogen certainly retards charge development at C-1 (18) as indicated by the reduced solvolytic reactivity of the halo system, the

TABLE 1. γ-Deuterium isotope effects*†

Substrates	k_H/k_D
1*a* **1***b*	1.11±0.01
2*a* **2***b*	1.05±0.01
3*a* **3***b*	1.11±0.01
4*a* **4***b*	1.13±0.01
1*a* **5**	1.11±0.01

*Mean of four to five runs; the standard deviation of the slope was taken as the error in the slope. For example the data from the computer of one of the runs for 1*a* and *b* were: slope for 1*a* 9.435 × 10^{-3} min^{-1}, standard deviation 3.157 × 10^{-5}; slope for 1*b* 8.525 × 10^{-3}, standard deviation 2.670 × 10^{-5}.

†The 6-*endo*-*d* substrates required for our study were prepared from the halohydrins obtained from the haloacetates prepared by the acid catalyzed (H^+, HOAc; D^+, DOAc) opening of the halonortricyclanes (20). The dideuteriochlorohydrin required for the preparation of 5 was obtained from the addition of HOCl to norbornene-5,6-*endo*,*endo*-d_2 (21). The solvolytic isotope effects were obtained by simultaneously observing the solvolysis of the protiated and deuterated substrates spectrophotometrically (22) in 80:20 EtOH–H_2O, 0.04 *M* in NaOAc at 60–65.00 ± 0.02°.

[1]Presented in part at the 56th Canadian Chemical Conference of the Chemical Institute of Canada, Montreal, Quebec, June, 1973.

[2]A locked [2.2.1] system is one in which non-vertical involvement (15) (a 1,2 Wagner–Meerwein shift) is prohibited by the introduction of the charge destabilizers at C-7 or C-1. For example, a COOMe or C≡N group (11, 13) at C-1 would be a more effective lock than halogen at C-7.

TABLE 2. Relative percent yield and deuterium loss data for halonortricyclanes

	Substrate								
	1*a*	**1***b*	**2***a*	**2***b*	**3***a*	**3***b*	**4***a*	**4***b*	**5**
Relative % yield of tricyclic*†	30±2	20±2	25±2	18±2	21±2	13±2	10±2	7±2	20±2
Fractional % loss of one deuterium‡		79.0		62.0		77.0		69.0	§

*Determined by g.l.p.c. by electronic integration.
†The other products are *syn*- and *anti*-7-halo ethers and alcohols.
‡Determined mass spectrometrically at 12 eV.
§Not determined.

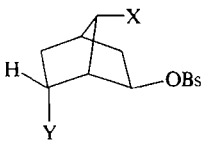

1 X = Cl **2** X = Br
a Y = H
b Y = D

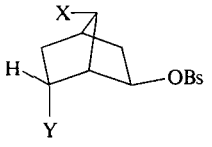

3 X = Cl **4** X = Br
a Y = H
b Y = D

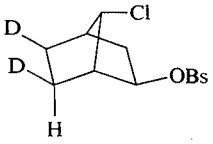

5

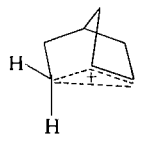

6

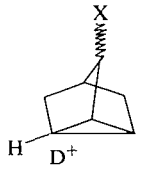

7

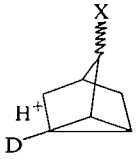

8

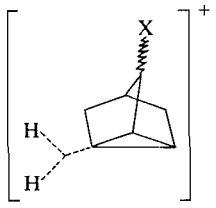

9

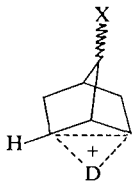

10

degree of norbornonium ion-type (**6**) stabilization in the transition state (neighboring group or non-vertical participation) in the two systems is certainly not the same. Our results therefore cast doubt on the premise that norbornonium ion (**6**) formation is the source of the solvolytic γ-isotope effects observed for the *exo*-2-norbornyl brosylates-6-*d* (3,4).

Direct involvement of the 6-*endo*-C—H(D) bond in the ionization step could account for the isotope effects observed for **1**, **2**, **3**, and **4**. The result for **5** is also accountable on this basis if

Can. J. Chem. Downloaded from www.nrcresearchpress.com by 210.87.254.6 on 09/05/12
For personal use only.

Can. J. Chem. Downloaded from www.nrcresearchpress.com by 210.87.254.6 on 09/05/12
For personal use only.

spatial reorganization of the 6-*exo*-C—H(D) bond is the source of the *exo*-isotope effect. That is, the *exo*-deuterium isotope effect is "α-like", and originates from conversion of a sp^3 C—H bond to a cyclopropyl-like C—H bond (**7** or **10**). Alternatively the solvolytic isotope effect could result from the 1,3-elimination (23) which occurs only *after* ion-pair formation is complete.[3] That the "α-like" effect is important at least in the 1,3-elimination step is supported by the data listed in Table 2. The degree of 1,3-elimination, within experimental error, being the same from **1***b* and **5**, although cleavage of the *endo*-C—H(D) bond is preferred, establishes that the exo "α-like" isotope effect and the isotope effect for cleavage of the *endo*-C—H(D) bond are of comparable magnitude.

A possibility also is that both **7** and **8** contribute to the stabilization of the norbornyl cation so that the 6-*exo*- and 6-*endo*-C—H(D) bonds undergo essentially identical force constant changes during ionization of the brosylate with however no direct involvement of the C_1—C_6 bond. The question then arises as to whether or not the composite of **7** and **8** is the halogen substituted analog (**9**, X = Cl or Br) of H-nortricyclonium ion (**9**, X = H) described by Olah (24).

The endo stereochemical preference (Table 2) established in this study provides additional support for our thesis that loss of a proton occurs via edge-protonated nortricyclane rather than the norbornonium ion and is consistent with previous observations (14) and explains the results obtained by Collins and Benjamin (12) on the solvolysis of deuterated 3-hydroxy-3-phenyl- and 7-hydroxy-7-phenyl-*exo*-2-norbornyl tosylates.

That the γ-effect for the *syn*-7-bromo-brosylate differs from the *anti*-isomer and the chloro systems is of interest. The decreased γ-effect may be due to partial bromonium-3 (Br-3) participation (bonding to C-1) or Br-4 involvement (25,26) in the ion-pair scheme thereby influencing internal return (27,28). A possibility also, as indicated by models, is that the steric interaction of the *syn*-7-bromine and the *exo*-2-brosylate distorts the [2.2.1] system and alters the favorable alignment of the *endo*-C—H(D) bond and developing p orbital.

Financial support by the National Research Council of Canada is gratefully acknowledged.

[3]Steady state treatment of an ion-pair scheme (Scheme 1) which includes the elimination rate constants establishes that the observed γ-isotope effect is a composite of the ionization isotope effect (IIE) and the terms *R* and *S* as described in eq. 1.

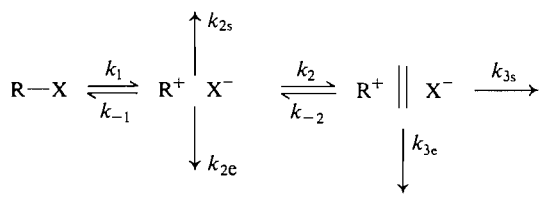

SCHEME 1

$$[1]\quad \left(\frac{k_H}{k_D}\right)_{obs} = \left(\frac{k_{1H}}{k_{1D}}\right)\left(\frac{1+Y_D}{1+Y_H}\right) \times \left(\frac{\frac{k_{2sH}+k_{2eH}}{k_{2H}} + \left(\frac{k_{3eH}}{k_{3sH}}+1\right)\left(\frac{1}{1+Z_H}\right)}{\frac{k_{2sD}+k_{2eD}}{k_{2D}} + \left(\frac{k_{3eD}}{k_{3sD}}+1\right)\left(\frac{1}{1+Z_D}\right)}\right)$$

$$\left(\frac{k_H}{k_D}\right)_{obs} = (IIE)(R)(S)$$

where

$$Y = \frac{k_{-1}+k_{2e}+k_{2s}}{k_2} \quad \text{and} \quad Z = \frac{k_{-2}+k_{3c}}{k_{3s}}$$

That the isotope effects for elimination from ion pairs can control k_H/k_D can be seen from consideration (*S* term) of eq. 1.

1. S. Borčić, V. Belanie-Lipovac, and D. E. Sunko. Croat. Chem. Acta, **33**, 35 (1961).
2. C. C. Lee and E. W. Wong. J. Am. Chem. Soc. **86**, 2753 (1964).
3. B. L. Murr, A. Nickon, T. Swartz, and N. H. Werstiuk. J. Am. Chem. Soc. **89**, 1730 (1967).
4. J. M. Jerkunica, S. Borčić, and D. E. Sunko. J. Am. Chem. Soc. **89**, 1732 (1967).
5. J. M. Jerkunica, S. Borčić, and D. E. Sunko. Chem. Commun. 1302 (1967).
6. J. P. Schaefer, M. J. Dagauri, and D. S. Weinberg. J. Am. Chem. Soc. **89**, 6938 (1967).
7. H. L. Goering and K. Humski. J. Am. Chem. Soc. **91**, 4594 (1969).
8. B. L. Murr and J. A. Conkling, J. Am. Chem. Soc. **92**, 3462 (1970).
9. B. L. Murr and J. A. Conkling. J. Am. Chem. Soc. **92**, 3464 (1970).
10. S. E. Scheppele. Chem. Rev. **72**, 511 (1972).
11. J. W. Wilt and W. J. Wagner. J. Am. Chem. Soc. **90**, 6135 (1968).
12. C. J. Collins and B. M. Benjamin. J. Am. Chem. Soc. **89**, 1652 (1967).
13. R. Muneyuki and T. Yano. J. Am. Chem. Soc. **92**, 746 (1970).

14. N. H. WERSTIUK. Chem. Commun. 1499 (1970).
15. N. A. CLINTON, R. S. BROWN, and T. G. TRAYLOR. J. Am. Chem. Soc. **92**, 5228 (1970).
16. J. D. ROBERTS, F. O. JOHNSON, and R. A. CARBONI. J. Am. Chem. Soc. **76**, 5692 (1954).
17. P. G. GASSMAN and J. M. HORNBACK. J. Am. Chem. Soc. **91**, 4280 (1969).
18. P. G. GASSMAN and J. M. HORNBACK. J. Am. Chem. Soc. **94**, 7010 (1972).
19. H. L. GOERING and M. J. DEGANI, J. Am. Chem. Soc. **91**, 4506 (1969).
20. F. P. CAPPELLI, G. TIMMINS, and N. H. WERSTIUK. Can. J. Chem. **50**, 2163 (1962).
21. N. H. WERSTIUK. Can. J. Chem. **48**, 2310 (1970).
22. N. H. WERSTIUK, R. R. MACDONALD, R. W. OUWEHAND, W. L. CHAN, F. P. CAPPELLI, J. G. BALLARD, R. E. YOUNG, R. E. MASSEY, and G. TIMMINS. Tetrahedron Lett. **49**, 4363 (1970).
23. A. NICKON and N. H. WERSTIUK. J. Am. Chem. Soc. **89**, 3915 (1967).
24. G. A. OLAH. J. Am. Chem. Soc. **94**, 808 (1972).
25. P. E. PETERSON and W. F. BORON. J. Am. Chem. Soc. **93**, 4076 (1971).
26. MARGARET AVRAM, I. POGANY, F. BADEA, I. G. DINULESCU, and C. D. NENITZESCU. Tetrahedron Lett. 3851 (1969).
27. B. L. MURR and M. F. DONNELLY. J. Am. Chem. Soc. **92**, 6686 (1970).
28. B. L. MURR and M. F. DONNELLY. J. Am. Chem. Soc. **92**, 6688 (1970).

Can. J. Chem. Downloaded from www.nrcresearchpress.com by 210.87.254.6 on 09/05/12
For personal use only.

Can. J. Chem. Downloaded from www.nrcresearchpress.com by 210.87.254.40 on 09/05/12
For personal use only.

Canadian Journal of Chemistry

Published by
THE NATIONAL RESEARCH COUNCIL OF CANADA

Journal canadien de chimie

Publié par
LE CONSEIL NATIONAL DE RECHERCHES DU CANADA

Volume 51 Number 21 November 1, 1973 Volume 51 numéro 21 1 novembre 1973

The Crystal and Molecular Structure of *trans*-(Methyl)(but-2-yne)-bis(dimethylphenylphosphine)platinum(II) Hexafluorophosphate $[(CH_3)(H_3CC{\equiv}CCH_3)Pt(P(CH_3)_2C_6H_5)_2]PF_6$

BRIAN W. DAVIES AND NICHOLAS C. PAYNE

Department of Chemistry, University of Western Ontario, London, Ontario, N6A 3K7

Received March 6, 1973

The crystal and molecular structure of *trans*-(methyl)(but-2-yne)bis(dimethylphenylphosphine)-platinum(II) hexafluorophosphate, $[(CH_3)(H_3CC{\equiv}CCH_3)Pt(P(CH_3)_2C_6H_5)_2]PF_6$, has been determined from three dimensional X-ray diffraction data recorded by diffractometric methods. The structure has been refined by full-matrix least-squares methods on F using 1060 unique data to a conventional agreement factor $R = 0.036$. The crystals are orthorhombic, space group $Pnma(D_{2h}^{16})$, with $a = 15.447(5)$, $b = 15.344(4)$, $c = 11.005(3)$ Å, and $Z = 4$. The coordination about the platinum atom is approximately square planar, if the acetylene is considered to be a unidentate ligand. There is crystallographic mirror symmetry imposed on the ions, such that the platinum atom, the methyl carbon atom, and the four carbon atoms of the acetylene ligand all lie on the mirror plane. The acetylene C≡C bond is approximately perpendicular (86.5(1.5)°) to the coordination plane of the platinum atom. The mean platinum–carbon(acetylene) bond length is 2.278(5) Å, and the mean angular departure from linearity of the ligand is 12(4)°. There is a small (156 cm^{-1}) reduction of ν_{str} (C≡C) for the but-2-yne ligand upon coordination, and the acetylenic carbon–carbon bond length, 1.22(3) Å, is not significantly different from the value of 1.21(2) Å observed in the free ligand.

La structure cristalline et moléculaire de l'hexafluorophosphate de platine(II) *trans*-(méthyl)(butyne-2)-bis(diméthylphénylphosphine), $[(CH_3)(H_3CC{\equiv}CCH_3)Pt(P(CH_3)_2C_6H_5)_2]PF_6$ a été élucidée par l'étude des figures de diffraction en trois dimensions des rayons-X enregistrées à l'aide de diverses méthodes de diffractométrie. La structure a été raffinée par la méthode des moindres carrés appliquée sur F à partir de 1060 données et ce, jusqu'à un facteur d'agrément $R = 0.036$. Les cristaux sont du type orthorhombique appartenant au groupe $Pnma(D_{2h}^{16})$; les dimensions de la maille sont $a = 15.447(5)$, $b = 15.344(4)$, $c = 11.005(3)$ Å et $Z = 4$. La coordination autour de l'atome de platine correspond approximativement à une structure plane carrée si l'on considère que le groupe acétylène est un monocoordinat. L'atome de platine, l'atome de carbone du méthyle et les quatre atomes de carbone du coordinat acétylène se situent sur le plan de coordination de l'atome de platine. La longueur moyenne du lien platine–carbone (acétylène) est de 2.278(5) Å et l'écart moyen angulaire par rapport à la linéarité est de 12(4)°. Lors de la coordination, l'on note une légère diminution (156 cm^{-1}) pour le ν_{str} (C≡C) du coordinat butyne-2 alors que la longueur de la liaison carbone–carbone (acétylène), 1.22(3) Å, n'est pas différente, d'une manière significative, de la valeur, 1.21(2), observée dans le coordinat libre.

[Traduit par le journal]

Can. J. Chem., 51, 3477 (1973)

Introduction

Although acetylene complexes of transition metals have been known for many years, there is still considerable interest (1–4) in such complexes, particularly in view of the enhanced reactivity of the coordinated acetylene. To date there have been few structural studies on acetylene complexes. A preliminary communication of the structure of the trigonal Pt(0) complex, bis-(triphenylphosphine)platinum(diphenylacetylene)

Can. J. Chem. Downloaded from www.nrcresearchpress.com by 210.87.254.40 on 09/05/12
For personal use only.

appeared in 1967 (5). A square planar platinum (II) complex, *trans*-dichloro(di-*t*-butylacetylene) (*p*-toluidine) platinum(II), was structurally characterized in 1970 (6). Dickson and Ibers recently described a trigonal Ni(0) complex, bis(*t*-butylisocyanide)(diphenylacetylene)Ni(0) (7). We recently reported a trigonal bipyramidal Pt(II) complex, *trans*-chloromethyl bis(trimethylarsine) platinum(II) hexafluorobut-2-yne, which was postulated as an intermediate in the conversion of an acetylene to a vinyl derivative (8). A second five coordinate acetylene complex of Ir(I) has been described by Kirchner and Ibers (9).

The title compound, **1**, was prepared initially by Chisholm and Clark (10) by the reaction

$$\textit{trans}\text{-}PtClCH_3Q_2 + R{-}C{\equiv}C{-}R' + AgPF_6 \xrightarrow{\text{solvent}} \textit{trans}\text{-}[PtCH_3(R{-}C{\equiv}C{-}R')Q_2]PF_6 + AgCl$$

1

where Q is $P(CH_3)_2C_6H_5$ or $As(CH_3)_3$. The products obtained from the above reaction are dependent on the nature of the acetylene, the ligands Q, the solvent and the reaction conditions. Thus, dialkyl and diaryl acetylenes in methanol generally formed the complexes (**1**), which could be isolated in crystalline form. Monoalkyl acetylenes under similar conditions underwent further reaction to give cationic alkoxycarbene complexes. Disubstituted acetylenes containing electron withdrawing groups produced vinyl complexes. These observations were rationalized by Chisholm and Clark by assuming that formation of the acetylene complex occurred initially, and it was postulated that these acetylene complexes were intermediates that could be regarded as being "metal-stabilized carbonium ions" (11).

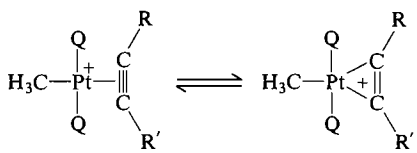

We undertook this structural study of the complex (**1**) both to determine whether the enhanced reactivity of the acetylene was characterized by any particular structural aspects, and also as part of our continuing investigations of acetylene complexes. In addition, it was hoped that further information could be obtained regarding the crystallographic *trans*-influence of the methyl group in these and related complexes.

Experimental

Crystals of *trans*-$[(CH_3)(H_3C{\equiv}CCH_3)Pt(P(CH_3)_2C_6H_5)_2]PF_6$ were supplied by M. H. Chisholm. A preliminary photographic examination of reciprocal lattice layers (0–2)*kl*, *h*(0–2)*l*, and *hk*(0–2) showed the crystals to be orthorhombic, with Laue symmetry *mmm*. Systematic absences of $0kl$ for $k + l \neq 2n$, and of $hk0$ for $h \neq 2n$ are consistent with the centric space group, *Pnma*, (D_{2h}^{16} No. 62), or the acentric space group, $Pna2_1$, (C_{2v}^{9} No. 33), in a non-standard setting (12).

The unit cell dimensions, and their estimated standard deviations at 22 °C were determined from a least-squares refinement of the angular settings of 14 reflections centered on a four circle, computer controlled Picker diffractometer. The density of the crystals was measured by flotation in a mixture of carbon tetrachloride and ethylene dibromide. The value observed, 1.75(2) g cm^{-3}, is in excellent agreement with the calculated value of 1.748 g cm^{-3}, assuming four formula units in the unit cell. There are no crystallographic symmetry constraints imposed on the ion in the acentric space group, $Pna2_1$, but in the centric space group, *Pnma*, each ion must have an internal mirror plane.

Crystal data

$PtP_3F_6C_{21}H_{31}$ f.w. = 685.6

Orthorhombic, $a = 15.447(5)$, $b = 15.344(4)$, $c = 11.005(3)$ Å, $V = 2608$ Å^3, (22 °C, MoKα_1, $\lambda = 0.70926$ Å).

The crystal chosen for data collection was a thin, colorless, diamond shaped plate of approximate dimensions 0.20 × 0.18 × 0.08 mm. An optical examination identified faces of the forms {100} and {011}. The crystal dimensions were determined with a microscope fitted with a micrometer eyepiece in preparation for an absorption correction. The linear absorption coefficient for MoKα radiation is 53.8 cm^{-1} (values for μ/ρ were obtained from the tabulation of Cromer and Liberman (13)). Intensity data were collected using MoKα radiation. The crystal was mounted with b^* offset by approximately 5° from the diffractometer ϕ axis (14). Prior to data collection a number of ω-scans of intense, low angle reflections were performed, using a narrow source and a wide-open counter. A mean width at half height of 0.08° was considered suitable (15). The θ–2θ scan technique was employed, with a scan range of 1°, corrected for dispersion, at a rate of 1/2 deg per min. The incident X-ray beam was filtered through a niobium filter of thickness 0.08 mm situated at the end of the collimator. The diffracted beam was collected after passage through an aperture of dimensions 4 mm × 4 mm situated 32 cm from the crystal. Background counts were made with a stationary crystal, and a stationary counter for 20 s at the limits of each scan. A take-off angle of 1.4° was employed for the source, under which conditions an intensity of 83% of the maximum attainable for a selected reflection was observed. During the collection of data six intense axial reflections (200, $\bar{2}00$, 020, $0\bar{2}0$, 002, $00\bar{2}$) were monitored every 100 reflections. All six standard reflections showed a small linear decay in intensity (approximately 3%) for which no correction was made. All reflections in the range $0 < 2\theta < 45°$ were collected in the octant $hk\bar{l}$, and all reflections in this 2θ range with $-2 \leqslant l < 0$ in the octant hkl were also collected as a test of instrumental and crystal stability. In all the intensities of 2364 reflections were recorded.

Can. J. Chem. Downloaded from www.nrcresearchpress.com by 210.87.254.40 on 09/05/12
For personal use only.

Corrections were applied for background, Lorentz, and polarization factors[1]. Standard deviations were assigned to each observation $(\sigma(I))^2 = \text{COUNT} + \frac{1}{4}(t_c/t_b)^2(b_1 + b_2) + (cI)^2$ where the total count is given by COUNT, measured in a time t_c. b_1 and b_2 are the background counts, each measured in a time t_b. The constant c was chosen as 0.04, and $I = \text{COUNT} - \frac{1}{2}(t_c/t_b)(b_1 + b_2)$. Those reflections with a corrected intensity value greater than three times the estimated standard deviation were considered to be observed. In all there were 1275 such reflections, of which 1060 were unique.

Structure Solution and Refinement

Prior to data collection it had been noticed that the cell dimensions were similar, and the systematic absences identical, to those of an analogous methylmethoxy carbene complex, *trans*-$[(CH_3)(CH_3C(OCH_3))Pt(P(CH_3)_2C_6H_5)_2]PF_6$, the structure of which had previously been determined in this laboratory (16). A comparison of the films of nine reciprocal lattice layers suggested that the two compounds are almost isostructural.

Accordingly, positional parameters for the platinum atom, one phosphorus atom (of the phosphine ligand) and the phosphorus atom of the anion were taken from the carbene study, and the solution attempted in the centric space group assigned to the carbene complex, *Pnma*. Two cycles of full matrix least-squares refinement of F, minimizing the function $\sum w(|F_o| - |F_c|)^2$ led to agreement factors $R_1 = 0.224$ and $R_2 = 0.300$. $|F_o|$ and $|F_c|$ are the observed and calculated structure amplitudes, the weight assigned an observation is defined as $w = 4F_o^2/\sigma^2(F_o^2)$ and $R_1 = \sum(||F_o| - |F_c||)/\sum|F_o|$ and $R_2 = (\sum w(|F_o| - |F_c|)^2/\sum wF_o^2)^{1/2}$. Atomic scattering factors for Pt, P, F, and C were taken from Cromer and Waber's tabulation (17); those for H from Stewart *et al.* (18). The values of $\Delta f'$ and $\Delta f''$ of Cromer and Liberman (13) were included in the calculated structure factors. These agreement factors, and the observed geometry at this stage were considered to justify the model and the choice of space group. A difference Fourier synthesis located the remaining 28 non-hydrogen atoms in the structure. A comparison of the positional parameters obtained with those of the analogous carbene complex showed that the two complexes are, in fact, isomorphous, and almost isostructural. Two further cycles of refinement using only unique *hkl* reflections with all atoms refined with anisotropic thermal parameters (with the exception of the phenyl ring carbon atoms which were refined as a rigid group with D_{6h} symmetry and a carbon–carbon bond length of 1.392 Å (19)) resulted in agreement factors $R_1 = 0.043$ and $R_2 = 0.051$ for 112 variables and 1060 observations. Absorption correction trials showed that the transmission factors varied by as much as 25%. A numerical absorption correction utilizing a 4 × 12 × 8 grid was used (20). The maximum value of the transmission coefficient was 0.697 and the minimum value was 0.519. Two further cycles with all atoms allowed to vibrate anisotropically, and removing the rigid group constraints for the phenyl ring carbon atoms led to agreement factors $R_1 = 0.038$ and $R_2 = 0.043$. Hydrogen atom contributions for the phenyl hydrogen atoms were included in the calculated structure factors at this stage. Idealized positions were assumed with a C—H bond length of 1.05 Å, and a temperature factor of 4.0 Å^2 assigned to each hydrogen atom. A difference Fourier plane was calculated for each of the methyl carbon atoms of the dimethylphenyl phosphine ligand, assuming tetrahedral geometry at each atom (C—H = 1.09 Å, H—C—H = 109° 27′). Positive rings of electron density were seen in each case. The hydrogen atoms for these two methyl groups were best described as spinning rotors and contributions to the calculated structure factors were accordingly calculated (21). No contributions were calculated for the hydrogen atoms of the methyl ligand and of the but-2-yne ligand which lie on the mirror plane. Two further cycles of refinement under these conditions (154 variables and 1060 unique reflections) led to agreement factors $R_1 = 0.036$ and $R_2 = 0.041$.

An examination of the thermal ellipsoids of the acetylene carbon atoms at the conclusion of refinement caused some concern. In particular, C(2) and C(4) showed pronounced anisotropic vibrations. To ascertain whether these vibrations would affect the final geometry of the acetylene ligand, the refinement was also converged with the acetylenic carbon atoms, C(2) and C(3), constrained to vibrate isotropically. No significant change in geometry was observed, the acety-

[1]Computing was performed on the PDP-10 and the CDC Cyber 73/14 at the University of Western Ontario. Fourier syntheses were computed with a version of Zalkin's FORDAP. Statistical studies of intensity distributions were calculated with a version of Dewar's FAME. Least-squares refinements employed WOCLS, a local modification of Ibers' NUCLS, and illustrations were drawn using Johnson's ORTEP. Errors in derived quantities were computed with ORFFE, written by Busing, Martin, and Levy.

Can. J. Chem. Downloaded from www.nrcresearchpress.com by 210.87.254.40 on 09/05/12
For personal use only.

TABLE 2

(*a*) Atomic and group positional and thermal parameters

	x	*y*	*z*	*U*(1,1) or *B**	*U*(2,2)†	*U*(3,3)	*U*(1,2)	*U*(1,3)	*U*(2.3)
Pt	0.23046(5)‡	¼	0.03503(7)	394(4)	337(4)	407(4)	0	−9(6)	0
P(1)	0.2250(2)	0.1001(2)	0.0291(4)	519(20)	367(18)	464(19)	18(19)	−21(27)	−27(20)
P(2)	0.3133(4)	−¼	0.0626(6)	811(44)	456(35)	609(50)	0	30(36)	0
F(1)	0.2487(11)	−¼	0.1673(16)	1442(189)	2475(230)	1190(138)	0	466(123)	0
F(2)	0.3801(11)	−¼	−0.0445(14)	1839(166)	1260(135)	1004(125)	0	567(123)	0
F(3)	0.3701(6)	−0.3225(6)	0.1242(10)	1254(85)	686(61)	1392(92)	138(63)	−357(70)	331(67)
F(4)	0.2609(7)	−0.3230(6)	−0.0044(10)	1388(91)	691(57)	1606(104)	−166(61)	−547(73)	−96(59)
C(11)	0.2054(9)	0.0600(9)	−0.1235(12)	840(124)	549(95)	560(102)	−110(87)	57(83)	−45(85)
C(12)	0.3215(8)	0.0437(8)	0.0734(11)	451(87)	401(85)	635(103)	35(70)	42(72)	49(71)
C(1)	0.4113(15)	¼	−0.1034(23)	930(201)	755(171)	732(172)	0	229(159)	0
C(2)	0.3775(12)	¼	0.0247(23)	4.26(42)					
C(3)	0.3608(13)	¼	0.1329(19)	4.50(47)					
C(4)	0.3668(19)	¼	0.2689(19)	1592(260)	1442(240)	196(137)	0	−370(148)	0
C(5)	0.0995(13)	¼	−0.0191(20)	724(158)	629(139)	657(161)	0	−329(127)	0
1C1	0.1429(8)	0.0532(8)	0.1258(12)	452(91)	282(79)	540(97)	−126(69)	56(74)	−43(74)
1C2	0.1158(10)	0.0971(9)	0.2281(14)	658(110)	356(84)	652(113)	59(79)	46(87)	56(84)
1C3	0.0577(10)	0.0622(11)	0.3091(14)	695(122)	603(112)	702(113)	−165(99)	180(90)	−24(99)
1C4	0.0226(9)	−0.0192(12)	0.2839(16)	355(105)	817(150)	1017(168)	215(99)	209(98)	97(122)
1C5	0.0511(10)	−0.0654(10)	0.1847(17)	647(121)	414(100)	1086(141)	−119(92)	33(108)	61(105)
1C6	0.1097(9)	−0.0299(9)	0.1049(13)	633(107)	439(92)	664(100)	−87(83)	58(85)	95(88)

(*b*) Derived hydrogen atom positional parameters

Atom	*x*	*y*	*z*
H(1)	0.1428	0.1618	0.2439
H(2)	0.0373	0.0981	0.3834
H(3)	−0.0210	−0.0471	0.3441
H(4)	0.0260	−0.1286	0.1653
H(5)	0.1315	−0.0649	0.0258

*Isotropic thermal parameters are given in Å^2.

†The thermal ellipsoid is given by $\exp[-2\pi^2(U_{11}h^2a^{*2} + U_{22}k^2b^{*2} + U_{33}l^2c^{*2} + 2U_{12}hka^*b^*\cos\gamma^* + 2U_{13}hla^*c^*\cos\beta^* + 2U_{23}klb^*c^*\cos\alpha^*)]$ where the U_{ij} are the thermal parameters in terms of mean-square amplitudes of vibration in Angstroms. Values are given as $U \times 10^4$.

‡Numbers in parentheses given here and in other tables are estimated standard deviations in the least significant digits. Values without e.s.d.'s were fixed in the refinements.

Can. J. Chem. Downloaded from www.nrcresearchpress.com by 210.87.254.40 on 09/05/12
For personal use only.

lenic bond length being 1.22(3) Å and the isotropic thermal parameters being 4.3(4) Å^2 and 4.5(5) Å^2 respectively. However, C(4) still showed pronounced anisotropic vibrations. Constraint of the thermal motion of all four acetylenic carbon atoms to be isotropic resulted in an acetylenic bond length of 1.18(3) Å. Of these three models, we prefer that with isotropic thermal parameters for C(2) and C(3), and anisotropic thermal parameters for C(1) and C(4). At convergence, $R_1 = 0.036$ and $R_2 = 0.040$ for 148 variables and 1060 observations. In the final cycle of this refinement, no parameter shift exceeded 0.25 of its estimated standard deviation. The error on an observation of unit weight is 1.14 electrons.

In order to confirm our choice of the centric space group to be correct, the structure was also refined in the acentric group $Pn2_1a$, equipoints (x,y,z), $(\bar{x},\frac{1}{2}+y,\bar{z})$, $(\frac{1}{2}-x,\frac{1}{2}+y,\frac{1}{2}+z)$ and $(\frac{1}{2}+x,y,\frac{1}{2}-z)$. Two cycles of refinement with the carbon atoms assigned isotropic thermal parameters (93 variables, 1275 observations) led to agreement factors $R_1 = 0.050$ and $R_2 = 0.059$. The resulting platinum–phosphorus distances were 2.20 and 2.39 Å, and this model was deemed chemically unfeasible. There also existed the possibility that the chirality of the model was incorrect if the acentric space group is assumed, and two cycles with the *hkl* reflections refined as $h\bar{k}l$ led to agreement factors $R_1 = 0.052$ and $R_2 = 0.061$. Although the platinum–phosphorus distances, 2.27 and 2.31 Å, were comparable, and chemically reasonable, the phosphorus–carbon distances of the phosphine ligands varied from 1.84 to 2.05 Å. Again this model was considered chemically unfeasible. A statistical study of the distribution of the intensities of the absorption corrected data suggested that the centric space group, *Pnma*, best fitted the observed distribution, and the final results presented therefore correspond to the refinement in *Pnma*.

No evidence for extinction was observed. A statistical examination of the structure amplitudes (in terms of F, $\lambda^{-1}\sin\theta$, indices, and diffractometer setting angles (2θ, χ, and Φ)) showed no abnormal trends. We do not feel there is anything systematically at fault with the data; as evidence for this the 358 reflections which were collected in both the *hkl* and $hk\bar{l}$ octants were averaged, and the agreement factor for averaging was 3.3%. In a final difference Fourier synthesis the largest peak of electron density, 0.70(15) e Å^{-3}, at (0.14, 0.26, 0.02) is in the vicinity of the methyl carbon, C(5). In Table 1 a listing of $|F_o|$ and $|F_c|$ is given in electrons together with the weight assigned to each reflection.[2] The final non-group atom positional and thermal parameters are listed in Table 2. In Table 3 the root-mean-square amplitudes of vibration of all the atoms in the asymmetric unit are given.

Description of the Structure

The structure is ionic, with the closest cation–anion interaction being 3.38 Å between F(4) and C(4). A selection of bond distances and bond angles is given in Table 4, together with estimated standard deviations.

The inner coordination sphere of the platinum atom is approximately square planar, if the acetylene is considered to be a unidentate ligand. Figure 1 shows a view of the inner coordination sphere, and some selected bond distances. The atom numbering scheme and an overall view of the cation are shown in Fig. 2.

The four carbon atoms of the acetylene, the platinum atom and the methyl carbon atoms, C(5), all lie on a mirror plane. The phosphine phosphorus atoms, P(1) and P′(1), are related to one another by reflection in this mirror plane.

TABLE 3. Root-mean-square amplitudes of vibration (in Å) × 10^3

Atom	Minimum	Median	Maximum
Pt	184(1)	198(1)	203(1)
P(1)	190(5)	215(6)	230(5)
P(2)	214(8)	246(10)	286(8)
F(1)	289(22)	424(23)	498(23)
F(2)	268(21)	355(19)	461(20)
F(3)	215(14)	339(12)	415(13)
F(4)	242(12)	323(12)	453(13)
C(11)	223(22)	236(21)	299(21)
C(12)	195(21)	212(20)	256(20)
C(1)	241(36)	275(31)	329(33)
C(4)	102(60)	380(32)	410(33)
C(5)	190(34)	251(28)	320(30)
1C1	147(26)	214(22)	245(20)
1C2	182(23)	252(21)	265(21)
1C3	210(26)	250(24)	306(22)
1C4	153(34)	282(24)	340(26)
1C5	189(25)	264(24)	331(22)
1C6	191(24)	257(21)	267(20)

[2]Photocopies of Table 1 of structure amplitudes may be obtained on request, at a nominal charge, from the Depository of Unpublished Data, National Science Library, National Research Council of Canada, Ottawa, K1A 0S2.

TABLE 4. Selected bond distances and bond angles

Atoms	Distance (A)	Atoms	Angle (deg)
Pt—P(1)	2.303(3)	P(1)—Pt—P′(1)	174.7(2)
Pt—C(5)	2.11(2)	P(1)—Pt—C(5)	87.5(1)
Pt—C(2)	2.27(2)	C(2)—Pt—C(3)	31.0(7)
Pt—C(3)	2.28(2)	Pt—P(1)—C(11)	111.8(4)
P(1)—C(11)	1.81(1)	Pt—P(1)—C(12)	116.4(4)
P(1)—C(12)	1.79(1)	Pt—P(1)—1C1	114.0(4)
P(1)—1C1	1.81(1)	C(11)—P(1)—C(12)	103.1(6)
P(2)—F(1)	1.53(2)	C(11)—P(1)—1C1	107.0(6)
P(2)—F(2)	1.57(2)	C(12)—P(1)—1C1	103.4(6)
P(2)—F(3)	1.570(9)	F(1)—P(2)—F(2)	180(1)
P(2)—F(4)	1.567(9)	F(1)—P(2)—F(3)	92.3(6)
C(1)—C(2)	1.50(3)	F(1)—P(2)—F(4)	91.0(7)
C(2)—C(3)	1.22(3)	F(2)—P(2)—F(4)	89.2(7)
C(3)—C(4)	1.50(3)	F(2)—P(2)—F(3)	87.6(7)
		C(1)—C(2)—C(3)	172(2)
		C(2)—C(3)—C(4)	164(2)
		Pt—C(2)—C(3)	75(1)
		Pt—C(3)—C(2)	74(1)
		Pt—C(3)—C(4)	122(2)
		Pt—C(2)—C(1)	113(1)
1C1—1C2	1.38(2)	1C1—1C2—1C3	122(1)
1C2—1C3	1.37(2)	1C2—1C3—1C4	118(1)
1C3—1C4	1.39(2)	1C3—1C4—1C5	120(1)
1C4—1C5	1.37(2)	1C4—1C5—1C6	121(1)
1C5—1C6	1.37(2)	1C5—1C6—1C1	120(1)
1C6—1C1	1.39(2)	1C6—1C1—1C2	118(1)

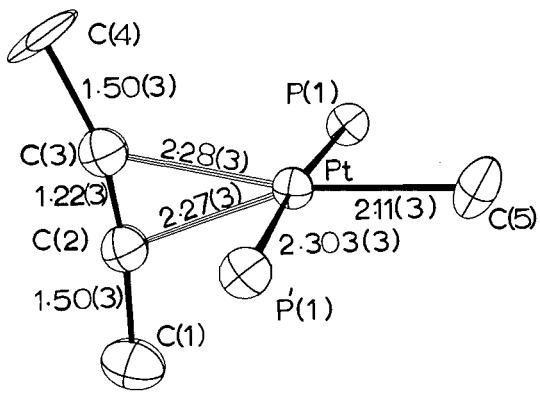

FIG. 1. Inner coordination sphere of the cation. Atoms are plotted as 30% probability thermal ellipsoids.

There is a slight deviation from an ideal square planar geometry, as the P(1)—Pt—P′(1) angle is 174.7(2)° and the P(1)—Pt—C(5) angle is 87.5(1)°. The Pt—C(2) and Pt—C(3) distances are equivalent although the acetylenic carbons C(2) and C(3) are 0.75(3) Å and 0.47(3) Å respectively above and below the plane containing P(1), Pt, and C(5). A weighted least squares plane was calculated through the atoms Pt, P(1), C(5), C(2), and C(3) and the results are shown in Table 5.

TABLE 5. Weighted least squares plane*

Atom	Deviation (Å)
Pt	−0.0019(8)
P(1)	−0.001(4)
C(5)	−0.02(2)
C(2)	0.72(2)
C(3)	−0.49(2)

*Equation of plane: $4.183x + 0.261y - 10.6z = 0.666$.

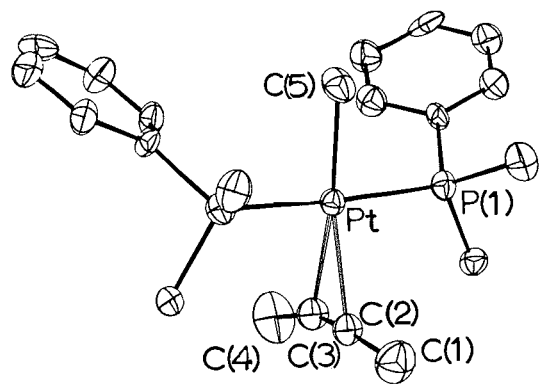

FIG. 2. An overall view of the cation, showing the atom numbering scheme.

Can. J. Chem. Downloaded from www.nrcresearchpress.com by 210.87.254.40 on 09/05/12
For personal use only.

TABLE 6. Comparative details of square planar Pt(II) acetylene complexes

Compound	Mean Pt—C distance (Å)	Mean bend back angle (°)	C≡C bond length	Angle acetylenic bond makes with coordination plane	Reference
trans-$[Cl_2Pt(p\text{-}H_3CC_6H_5NH_2)((t\text{-}C_4H_9)C{\equiv}C(t\text{-}C_4H_9))]$	2.16(2)	16(2)	1.24(2)	85.2	6
trans-$[(CH_3)(H_3CC{\equiv}CCH_3)Pt(P(CH_3)_2C_6H_5)_2]PF_6$	2.278(5)	12(4)	1.22(3)	86.5(1.5)	This work
$CH_3C{\equiv}CCH_3$		0	1.21(2)		30

The platinum–phosphorus distance of 2.303(3) Å is smaller than the sum of the covalent radii, 2.42 A, (22) but comparable to the values of 2.283(3) Å found in *trans*-$[(CH_3)(CH_3C(OCH_3))Pt(P(CH_3)_2C_6H_5)_2]PF_6$ (16), 2.295(4) Å found in *trans*-$[(CH_3)((CH_3)_2NCCH_3)Pt(P(CH_3)_2C_6H_5)_2]PF_6$ (23) and 2.305(3) Å observed in *trans*-$(CH_3)IPt(P(C_6H_5)_3)_2\cdot SO_2$ (24). Other Pt(II)–phosphorus distances determined to date vary considerably, ranging from 2.230(9) Å in $[Cl_4Pt(P(C_3H_7)_3)_2]$ (25) to 2.365(8) Å in $[(CF_3)((CH_3)_4C_4)Pt(P(CH_3)_2C_6H_5)_2]SbF_6$ (26).

The platinum – methyl carbon distance of 2.11(2) Å lies in the range expected for a normal covalent Pt—C σ bond, the sum of the covalent radii being 2.09 Å (22). Thus it appears that the crystallographic *trans*-influence of the but-2-yne ligand is small. It would appear that the lengthening of the Pt—N bond trans to the *t*-butyl acetylene in *trans*-$[Cl_2Pt(p\text{-}H_3C{-}C_6H_4NH_2)((t\text{-}C_4H_9)C{\equiv}C(t\text{-}C_4H_9))]$ may be due to other reasons (6). (The observed Pt—N bond length of 2.10(1) Å, while longer than the radius sum, 2.02 Å, is barely significantly different from the value of 2.05(1) Å observed in *trans*-$[Pt(NH_3)_2Cl_2]$ (27), with $\Delta = 3.5\,\sigma$.) However, the mean platinum – acetylene carbon distance of 2.28(2) Å is longer than any previously reported. In *trans*-$[Cl_2Pt(p\text{-}H_3C{-}C_6H_4NH_2)((t\text{-}C_4H_9)C{\equiv}C(t\text{-}C_4H_9))]$ the mean platinum – acetylene carbon distance is 2.16(2) Å. The difference, 0.12(2) Å, may be attributed to the *trans*-influence of the methyl ligand.

The phosphorus–carbon distances in the dimethylphenylphosphine ligand are 1.81(1), 1.79(1), and 1.81(1) Å. Comparable values of 1.79(1), 1.80(1), and 1.80(1) Å are found in *trans*-$[(CH_3)(CH_3C(OCH_3))Pt(P(CH_3)_2C_6H_5)_2]PF_6$ (16). The mean angle subtended by the carbon atoms at the phosphorus atom is 105(1)°, significantly different from the value (109° 27′) expected for pure sp^3 hybridization.

The mean carbon–carbon bond length in the phenyl ring of the phosphine ligand is 1.380(4) Å, not significantly different from the value of 1.392 Å for free benzene (28). The mean ring angle of the phenyl ring is 120(1)°.

The geometry of the hexafluorophosphate anion is approximately octahedral. The mean P—F distance is 1.55(1) Å. This is shorter than the value observed in $NaPF_6$, 1.58 Å (29), but a difference Fourier synthesis revealed no evidence of disorder in the anion, or residual electron density.

The most interesting feature of the structure, however, is the geometry of the coordinated acetylene. The acetylene adopts the *cis*-bent configuration, the two bend back angles being 16(2) and 8(2)°. These two values are not significantly different from the mean, 12(4)°. The acetylenic carbon–carbon bond length of 1.22(3) is not significantly different from the value observed in the free ligand, 1.21(2) Å. The acetylenic triple bond makes an angle of 86.5(1.5)° with the coordination plane of the platinum atom. A comparable value of 85.2° was observed in *trans*-$[Cl_2Pt(p\text{-}H_3CC_6H_4NH_2)((t\text{-}C_4H_9)C{\equiv}C(t\text{-}C_4H_9))]$. The acetylene – methyl carbon distances of 1.50(3), (C(1)—C(2)), and 1.50(3), (C(3)—C(4)) are not significantly different from the value observed in the free ligand, 1.47(2) Å (30). Table 6 shows some of the values of bond distances and bond angles obtained in this study and in the one previously determined acetylene complex of this type, *trans*-$[Cl_2Pt(p\text{-}H_3CC_6H_4NH_2)((t\text{-}C_4H_9)C{\equiv}C(t\text{-}C_4H_9))]$.

Discussion

Molecular orbital theory best describes the bonding between transition metals and olefins or

Can. J. Chem. Downloaded from www.nrcresearchpress.com by 210.87.254.40 on 09/05/12
For personal use only.

Can. J. Chem. Downloaded from www.nrcresearchpress.com by 210.87.254.40 on 09/05/12
For personal use only.

acetylenes. Maitlis and co-workers (4) proposed a scheme which satisfactorily describes platinum–acetylene bonding in both the trigonal Pt(0) acetylene complexes and the square planar Pt(II) acetylene complexes. In this scheme there are two components to the bonding, *viz.* (*i*) overlap of the acetylene π clouds with empty metal d or dp hybrid orbitals of the appropriate symmetry and energy to form a σ type bond and (*ii*) concomitant donation of electron density from the metal to the vacant π^* orbitals of the acetylene.

The trigonal Pt(0) complexes, which in valence bond theory are considered to contain metallocyclopropene rings, *i.e.* $M\begin{smallmatrix}C\\ \|\\ C\end{smallmatrix}$, in this scheme represent one extreme in a continuum of bond types. The back donation from metal → acetylene is considerable, as evidenced by the large perturbation of the acetylene in these complexes.

The square planar Pt(II) complexes, in which the acetylene perturbation is less, have the σ component as the major contributor to the metal–acetylene bond, and back donation to the acetylene π^* orbitals is less.

The concept of a continuum of bond types can be extended to the trigonal bipyramidal Pt(II) acetylene complexes, which have recently received much attention (31–34). Both the σ and π contributions are important in these complexes.

Blizzard and Santry (35) showed using CNDO calculations that the removal of density from the π_u acetylene orbitals to vacant metal orbitals did not, *per se*, result in a change in the geometry of the coordinated acetylene. However, when it is accompanied by the addition of density to the acetylene π^* orbitals it strongly enhanced the metal–acetylene bonding.

The bonding in **1** corresponds to situation D in the Maitlis scheme (4): in this case the energy of the metal valence shell orbitals is lower than that of the acetylene π orbitals. Thus the bonding orbital has mostly metal character and the antibonding orbital has mostly acetylene character. The large energy difference between the metal orbitals and the acetylene π^* orbitals means that the degree of back bonding is small.

The *trans*-influence of the methyl ligand, as evidenced by the observed bond lengths, has been shown to be large, while that of the but-2-yne ligand is small. This is consistent with the observations that ν_{str} (Pt—CH_3) is approximately 550 cm^{-1}, and the coupling constant J(Pt—CH) for the platinum – methyl carbon bond is 76 Hz (10). Further studies on the structures of platinum–acetylene complexes are in progress.

Note added in proof

Recently in this journal Beauchamp *et al.* (36) reported the structure of $K[Cl_3Pt((C_2H_5)_2C(OH)C{\equiv}CC(OH)(C_2H_5)_2)]$. The C≡C bond length is 1.18(3) Å, and the bend back angles are 21(2)° and 19(2)°, consistent with a weakly perturbed acetylene.

We thank the National Research Council of Canada for support of this work in the form of an operating grant and a bursary (to B.W.D.).

1. F. R. Hartley. Chem. Rev. **69**, 799 (1969).
2. F. R. Hartley. Ang. Chem. Int. Ed. **11**, 596 (1972).
3. J. H. Nelson and H. B. Jonassen. Coord. Chem. Rev. **6**, 27 (1971).
4. E. O. Greaves, C. J. L. Lock, and P. M. Maitlis. Can. J. Chem. **46**, 3879 (1968).
5. J. O. Glanville, J. M. Stewart, and S. O. Grim. J. Organometal. Chem. **7**, P9 (1967).
6. G. R. Davies, W. Hewertson, R. H. B. Mais, P. G. Owston, and C. G. Patel. J. Chem. Soc. A, 1873 (1970).
7. R. S. Dickson and J. A. Ibers. J. Organometal. Chem. **36**, 191 (1972).
8. B. W. Davies, R. J. Puddephatt, and N. C. Payne. Can. J. Chem. **50**, 2276 (1972).
9. R. M. Kirchner and J. A. Ibers. J. Am. Chem. Soc. **95**, 1095 (1973).
10. M. H. Chisholm and H. C. Clark. Inorg. Chem. **10**, 2557 (1971).
11. M. H. Chisholm and H. C. Clark. J. Am. Chem. Soc. **94**, 1532 (1972).
12. International tables for X-ray crystallography. Kynoch Press, Birmingham, England. 1962.
13. D. T. Cromer and D. Liberman. J. Chem. Phys. **53**, 1891 (1970).
14. W. A. Zachariasen. Acta Crystallogr. **18**, 705 (1965).
15. T. C. Furnas. Single crystal orienter instruction manual. General Electric Co., Milwaukee, Wis. 1957.
16. R. F. Stepaniak and N. C. Payne. J. Organometal. Chem. In press.
17. D. T. Cromer and J. A. Waber. Acta Crystallogr. **18**, 104 (1965).
18. R. F. Stewart, E. R. Davidson, and W. T. Simpson. J. Chem. Phys. **42**, 3175 (1965).
19. R. Eisenberg and J. A. Ibers. Inorg. Chem. **4**, 773 (1965).
20. D. Cahen and J. A. Ibers. J. Appl. Cryst. **5**, 298 (1972).
21. J. M. Bijvoet and J. A. A. Ketelaar. J. Am. Chem. Soc. **54**, 625 (1932).
22. L. Pauling. Nature of the chemical bond. 3rd ed. Cornell University Press, Ithaca, New York. 1960.

23. R. F. STEPANIAK and N. C. PAYNE. Inorg. Chem. In press.
24. M. R. SNOW and J. A. IBERS. Inorg. Chem. **12**, 224 (1973).
25. M. BLACK, R. H. B. MAIS, and P. G. OWSTON. Acta Crystallogr. B, **25**, 1760 (1965).
26. D. B. CRUMP and N. C. PAYNE. Inorg. Chem. **12**, 1663 (1973).
27. G. H. W. MILBURN and M. R. TRUTER. J. Chem. Soc. A, 1609 (1966).
28. Interatomic distances. Special Publication No. 11. The Chemical Society, London. M196 (1958).
29. H. BODE and H. CLAUSEN. Z. Anorg. Chem. **265**, 229 (1951); H. BODE and G. TEUFER. Acta Crystallogr. **9**, 825 (1956).
30. E. PIGNATARO and B. POST. Acta Crystallogr. **8**, 672 (1955); L. PAULING, H. D. SPRINGALL, and D. J. PALMER. J. Am. Chem. Soc. **61**, 927 (1939).
31. H. C. CLARK and R. J. PUDDEPHATT. Inorg. Chem. **9**, 2670 (1970).
32. H. C. CLARK and R. J. PUDDEPHATT. Inorg. Chem. **10**, 18 (1971).
33. H. C. CLARK and R. J. PUDDEPHATT. Inorg. Chem. **10**, 416 (1971).
34. H. C. CLARK and L. E. MANZER. J. Am. Chem. Soc. **95**, 3812 (1973).
35. A. C. BLIZZARD and D. P. SANTRY. J. Am. Chem. Soc. **90**, 5749 (1968).
36. A. L. BEAUCHAMP, F. D. ROCHON, and T. THEOPHANIDES. Can. J. Chem. **51**, 126 (1973).

Can. J. Chem. Downloaded from www.nrcresearchpress.com by 210.87.254.40 on 09/05/12
For personal use only.

The Photochemistry of 2-Cyano-1,4-dihydro-1,4-ethenoanthracene

CHRISTOPHER OWEN BENDER AND HELEN DIANA BURGESS[1]
Department of Chemistry, University of Lethbridge, Lethbridge, Alberta

Received May 14, 1973

The direct photolysis of 2-cyano-1,4-dihydro-1,4-ethenoanthracene (**5**) yields 8-cyanocycloocta[*b*]-naphthalene (**8**, $\Phi = 0.02$) and 1- and 6-cyanonaphtho[2,3-*c*]tricyclo-[3.3.0.$0^{2,8}$]octa-3,6-diene (**6**, $\Phi = 0.30$ and **7**, $\Phi = 0.04$). The benzophenone sensitized irradiation of **5** yields **6** ($\Phi = 0.40$) and **7** ($\Phi = 0.04$) only. Deuterium labeling studies reveal that **8** derives from an initial $2\pi + 2\pi$ cycloaddition reaction which proceeds with bonding between the vinyl and vinylcyano bridges.

La photolyse directe du cyano-2 dihydro-1,6 étheno-1,4 anthracène (**5**) conduit au cyano-8 cycloocta-[*b*]naphtalène (**8**, $\Phi = 0.02$) et au cyano-1 et -6 naphto [2,3-*c*] tricyclo [3,3,0,$0^{2,8}$] octadiène-3,6 (**6**, $\Phi = 0.30$ et **7**, $\Phi = 0.04$). L'irradiation sensibilisée par la benzophénone de **5** conduit à **6** ($\Phi = 0.40$) et **7** ($\Phi = 0.04$) seuls. Les études de marquage au deutérium montrent que **8** dérive d'une réaction initiale de cycloaddition $2\pi + 2\pi$ qui procède par liaison entre les ponts vinyle et vinylcyano.
[Traduit par le journal]

Can. J. Chem., **51**, 3486 (1973)

Introduction

Previously we reported that 2,3-naphthobarrelenes seemed to exhibit photoreactivities that were curiously different to those of other mono-fused aromatic barrelenes (1). Principally, 2,3-naphthobarrelenes (*e.g.* **1**) had not been observed to photoisomerize to cyclooctatetraene product (2). Instead, only semibullvalenes (*e.g.* **2**), derived from di-π-methane rearrangement of the triplet excited state species, were found (see Scheme 1).

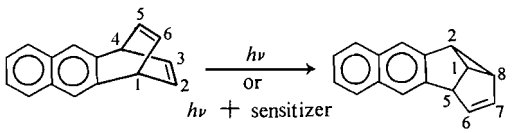

1 **2**

SCHEME 1

In order to examine this behavior further, we have undertaken a study of substituent effects on the photochemistry of the 2,3-naphthobarrelene system. Herein we report our results with 2-cyano-1,4-dihydro-1,4-ethenoanthracene (**5**), the first member thus far to give directly a cyclooctatetraene product, and equally significantly, the first aromatic barrelene to yield a cyclooctatetraene by way of a $2\pi + 2\pi$ cycloaddition mechanism which does not involve initial bridging to the aromatic nucleus.

Results

Although 2-cyanobarrelene (**5**) could be prepared directly by the 1,4-addition of 2,3-naphthyne (**3**) to benzonitrile, the material obtained in this way was difficult to purify. Suitably pure **5** (m.p. 178–180°, $\nu_{CN} = 2220\ cm^{-1}$) could be more conveniently synthesized by cuprous cyanide treatment of 2-bromobarrelene (**4**), isolated from the addition of 2,3-naphthyne (**3**) to bromobenzene (Scheme 2). The structure of **5** follows

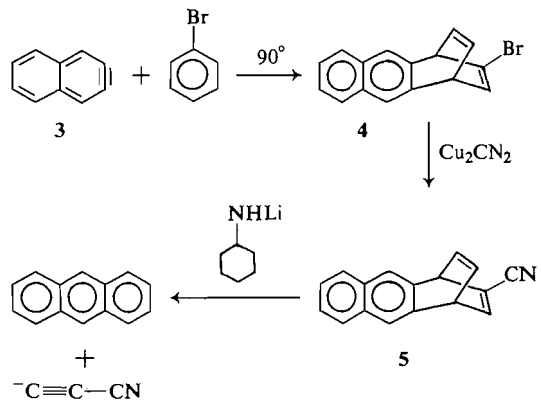

3 **4** **5**

SCHEME 2

from its n.m.r. spectrum which shows a 2H multiplet centered at τ 4.92 (bridgeheads), a 2H multiplet centered at τ 3.12 (ethylene bridge), and a complex 7H absorption region between τ 2.18 and 2.74 (aromatics and vinylcyano proton). Degradative evidence supporting the structure was obtained when anthracene was found to be the main isolable product (41%) from treatment of **5** with lithium cyclohexylamide. The formation of anthracene is rationalized as deriving from initial loss of the acidic vinylcyano

[1]Undergraduate Research Assistant, 1972.

Can. J. Chem. Downloaded from www.nrcresearchpress.com by 210.87.254.105 on 09/05/12
For personal use only.

TABLE 1. The n.m.r. spectra of cyclooctatetraenes[a,f]

Assignment	Description and signal position, τ			
	9[d]	**10**[b]	**11**[c,e]	**8**[b]
Aromatic	2.20–2.88,m	2.24–2.81,m	2.19–3.10,m	2.10–2.60,m
H-6	3.37,*A*B,d	—	3.21,*A*B,d	3.05,*A*B,d
H-7		4.88,*B*M,d	3.86,A*B*M, d of d	3.94,A*B*,d
H-8	4.1,m center	4.15,B*M*N, d of d	4.12,B*M*N, d of d	—
H-9		4.33,M*N*X, d of d	4.28,M*N*X, d of d	3.33,*N*X,d
H-10		3.94,N*X*Y, d of d	4.05,N*X*Y, d of d	3.86,N*X*Y, d of d
H-11	3.37,X*Y*,d	3.23,X*Y*,d	3.42,X*Y*,d	3.05,X*Y*,d

[a]Run on 100 MHz n.m.r. with TMS as internal standard.
[b]$CDCl_3$ solvent.
[c]CCl_4 solvent.
[d]Solvent not stated.
[e]The aliphatic–olefinic region comprises an ABMNXY spin system.
[f]Corresponding coupling constants, where applicable, were within 0.5 Hz; typically $J_{6,7} = J_{8,9} = J_{10,11} = 11.5$ Hz, and $J_{7,8} = J_{9,10} = 3.5$ Hz.

proton of **5**, followed by retro Diels–Alder expulsion of the stabilized cyanoacetylide anion.

The direct irradiation of cyanobarrelene (**5**) led cleanly to the formation of a trace amount of anthracene and three photoproducts isomeric with the starting material (see Scheme 3): 1- and

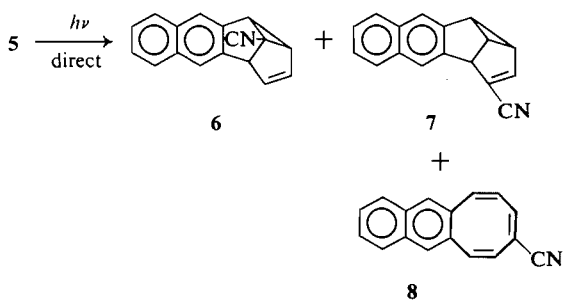

SCHEME 3

6-cyanonaphtho[2,3-*c*]tricyclo[3.3.0.0^{2,8}]octa-3,6-diene (**6** and **7**), and 8-cyanocycloocta[*b*]naphthalene (**8**, CN-COT). The photoproducts were isolated by careful column chromatography on Silicar CC-7. The structures of the semibullvalenes **6** and **7** were deduced from the n.m.r. data (see Experimental), which were characteristic of 2,3-naphthosemibullvalene derivatives (1, 2). In the case of CN-COT (**8**), the proposed structure was assigned on the basis of comparison of its n.m.r. spectral parameters with those of 2,3-naphtho-COT (**9**) (3), 6-methoxy-2,3-naphtho-COT (**10**) (1), and 1,2-naphtho-COT (**11**)[2] (Table 1), and is supported by spin-decoupling experiments: irradiation of H-7 collapsed H-6 to a singlet; irradiation of H-10 collapsed both H-9 and H-11 to singlets; and irradiation of H-9 collapsed H-10 to a doublet ($J_{10,11} = 11.5$ Hz). The deshielding effect of the cyano group on the adjacent coplanar vinyl proton amounts to ~τ 0.9 in both the cyclooctatetraene **8** (H-9) and semibullvalene **7** (H-7), and compares well with the substituent constant of 0.8 for the *cis* proton of acrylonitrile (4). The extent of the deshielding in barrelene **5** could not be ascertained because H-3 was buried in the aromatic region.

To rule out the possibility that cyclooctatetraene **8** is a secondary photoproduct deriving from the further photolysis of **6** or **7**, the individual semibullvalenes were irradiated directly and were found to be essentially unreactive ($\Phi_{dis} < 10^{-4}$). We note, however, that even if **6** or **7** did undergo the well-known phototransformation to COT product via cleavage of the semibullvalene C_2—C_8 and C_1—C_5 bonds (5), this process would, in the first instance, lead to β-cyano COT. This compound was not observed. The direct and sensitized irradiations of CN-COT (**8**) were also examined. Whereas no reaction was detectable upon direct irradiation, the sensitized photolysis of CN-COT (**8**) with benzophenone as sensitizer, did lead to the slow disappearance ($\Phi_{dis} = 0.1$) of starting material, but no identifiable product was obtained.

In contrast to the direct irradiation of barrelene **5**, sensitization with benzophenone led cleanly to the semibullvalenes **6** and **7** only; the

[2]C. O. Bender and H. E. Zimmerman. Unpublished data.

Can. J. Chem. Downloaded from www.nrcresearchpress.com by 210.87.254.105 on 09/05/12
For personal use only.

TABLE 2. Quantum yield data for cyanobarrelene **5**[a]

Run	Reactant concentration (mM)[b]	Sensitizer concentration (mM)[c,d]	% conversion	Products	Quantum yields
1	14.8	—	15	**6**, **7**, and **8**	0.28, 0.035, and 0.02
2	14.8	—	12	**6**, **7**, and **8**	0.30, 0.035, and 0.02
3	12.0	78.3	16	**6** and **7**	0.38 and 0.04
4	13.4	78.8	11	**6** and **7**	0.43 and 0.05

[a]Benzene solvent.
[b]Light of 313 nm was used for direct irradiation.
[c]Light of 343 nm was used for sensitized irradiations.
[d]Benzophenone sensitizer absorbing >95% of incident light.

formation of CN-COT (**8**) was not detected at any conversion level. Thus, it appears that the CN-COT (**8**) formed during the direct irradiation of barrelene **5** derives from the singlet excited state and represents the first example of a $2\pi + 2\pi$ photocycloaddition in the 2,3-naphthobarrelene series.

Quantum yield studies (ferrioxalate actinometry (6)) were carried out with cyanobarrelene **5** to determine the relative efficiencies of the direct and sensitized irradiations and to provide information on the excited state species involved in the transformations; these data are summarized in Table 2.

Mechanistic Considerations

Inspection of the possible modes of $2\pi + 2\pi$ cycloadditions of barrelene **5** shows that CN-COT (**8**) can result from either of two pathways (see Scheme 4): one involving initial vinyl–vinylcyano interaction (pathway *i*), and the other initial naphtho–vinyl interaction (pathway *ii*). Bonding between the naphtho ring and the vinylcyano bridge need not be considered, since this would lead to the unobserved α-CN-COT. To distinguish between the pathways *i* and *ii* the deuterated barrelene **12** was synthesized. This was accomplished by the addition of 2,3-naphthyne to *p*-deuterobromobenzene, followed by treatment of the deuterobromobarrelene product with cuprous cyanide. Labeled material with 94% d_1 content at C-5 was obtained (n.m.r. analysis).

Direct irradiation of deuterobarrelene **12** led to the formation of cyclooctatetraene **15**, containing exclusive β-labeling; the olefinic region of the n.m.r. spectrum of the deuterated COT product showed a doublet centered at τ 3.05 (H-6, J = 11.5 Hz), a broad singlet at τ 3.07 (H-11), a singlet at τ 3.35 (H-9), and a doublet at τ 3.98 (H-7, J = 11.5 Hz). Thus the $2\pi + 2\pi$ cycloaddition proceeds with initial vinyl–vinylcyano bonding.

N.m.r. examination of the labeled semibullvalene product from either direct or sensitized irradiations of barrelene **12** showed the deuterium to be located at C-7 in **6** and C-8 in **7** (*i.e.* **21** and **23**, Scheme 5). However, this label distribution does not permit a unique pathway for the di-π-methane rearrangement to be delineated since although there is only one route that can account for the labeling pattern found in **23** (see Scheme 5, route *i*), there are two which could lead to labeled **21** (route *i* and route *ii*). Thus semibullvalene **21** might arise solely from route *i* or from some combination of routes *i* and *ii*. A means of determining the importance of route *ii* was obtained by examining the fate of the mixture of barrelenes **26**, which was composed of approximately equal amounts of two singly labeled isomers, one incorporating deuterium at C-4 and the other deuterium at C-6 (see Scheme 6). The barrelene mixture **26** was synthesized in essentially the same way as the deuterated barrelene **12** but starting with *m*-deuterobromobenzene; (within experimental error no deuterium isotope effects were discernible in the naphthyne addition stage or in subsequent photoisomerizations).

N.m.r. examination of the 1-cyanosemibullvalene material isolated from either the direct or the benzophenone sensitized irradiations of deuterobarrelene mixture **26** showed the labels to appear exclusively at C-2 and C-6, *i.e.* the semibullvalene mixture **28** was the 1-CN-semibullvalene product. Route *i* is therefore solely utilized in the cyanobarrelene di-π-methane rearrangement.

Can. J. Chem. Downloaded from www.nrcresearchpress.com by 210.87.254.105 on 09/05/12
For personal use only.

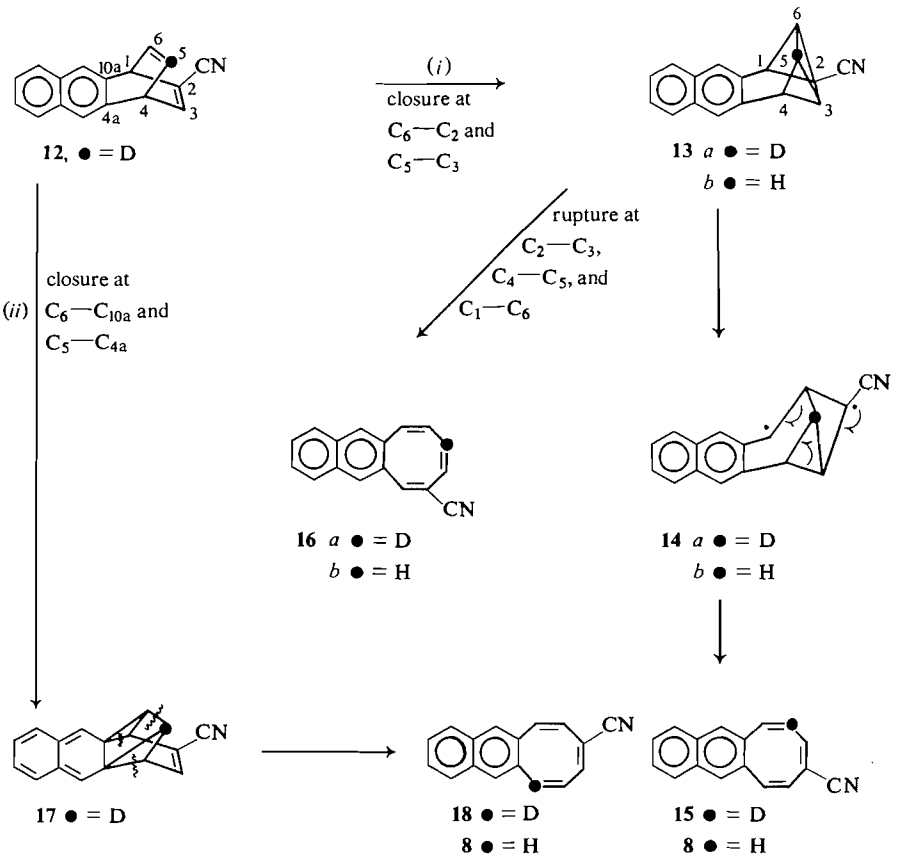

SCHEME 4

Discussion

The formation of the semibullvalenes **6** and **7** in the same ratios (~1:8, within experimental error) and, when the deuterated barrelenes **12** and **26** were used, with the same label locations from direct and sensitized irradiations, suggests that the same triplet excited state species is involved in both excitation processes. The quantum yield data (Table 2) showing the sensitized formation of **6** and **7** to be the slightly more efficient process are also consistent with this view. Thus, although COT product has been obtained from a 2,3-naphthobarrelene, the effect of the cyano group is modest, possibly contributing to a lowering of the transition-state energy of the singlet reaction; the main fate of the barrelene excited singlet state is still a remarkably efficient intersystem crossing to the triplet. The subsequent triplet di-π-methane rearrangement then proceeds by bonding between C-3 and C-5 of the vinylcyano and vinyl bridges. The preference for the formation of **6** over **7** is attributed to the greater stabilization of the radical centers in species **20***b* (naphtho and cyano stabilization) than in **22***b* (naphtho stabilization only).

With respect to the barrelene cycloaddition, the observation that the reaction proceeds without involving bonding to the aromatic nucleus is unique and conflicts with the earlier view that bonding with the aromatic moiety is expected on the basis that this part of the molecule is of lowest singlet excitation energy and therefore concentrated with energy (1, 5). Thus, minimization of energy along the reaction coordinate controls the reaction, not the initial excitation process.

In order to rationalize the vinyl–vinyl bonding preference over the naphtho–vinyl alternatives, it is noted that Zimmerman and his coworkers have developed an excellent method for predicting the favored bridging mode for the

Can. J. Chem. Downloaded from www.nrcresearchpress.com by 210.87.254.105 on 09/05/12
For personal use only.

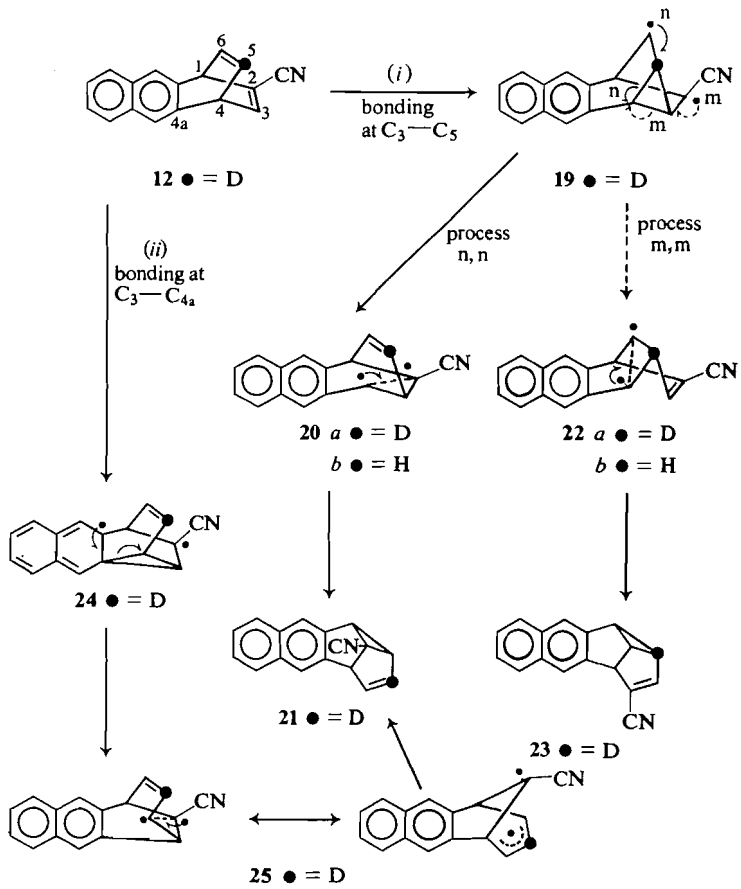

SCHEME 5

di-π-methane rearrangement of excited triplet state aromatic barrelenes (2, 5, 7). Extension of this method to the excited singlet reaction involves considering the initial stages of each possible cycloaddition to be a perturbation of the 2π–2π system into cyclic overlap, wherein a cyclobutadiene-like transition state is approximated prior to formal bonding. The most probable bridging mode is then assigned as that which approximates the cyclobutadiene species of lowest singlet excitation energy. Because of the paucity of information concerning cyclobutadienes, we can presently compare only the u.v. spectra of butadiene itself with that of 1,2-dibromo-3,8-diphenylnaphtho[*b*]cyclobutadiene. Masamune *et al.* (8) have attributed a broad peak at λ_{max} 300–305 nm (ε ~ 100) tailing to 400 nm, to cyclobutadiene, while Cava and Mitchell (9) report that the longest absorption band of 1,2-dibromo-3,8-diphenylnaphtho[*b*]cyclobutadiene (a yellow–orange colored compound) occurs at 270 nm (ε 10 000, shoulder). In the absence of fluorescence spectra for these and model cyano derivatives it is clearly impossible to assign an order for the singlet energies with any certainty but we are nevertheless encouraged that the available evidence indicates that our requirement for a lower singlet energy for cyanocyclobutadiene than for naphtho[*b*]cyclobutadiene or for 1-cyanonaphtho[*b*]cyclobutadiene is not improbable. If this rationale is correct, then it follows that both benzocyclobutadiene and naphtho[*a*]-cyclobutadiene should have singlet excited state energies below that of cyclobutadiene, since aromatic–vinyl bonding is observed for the 2π + 2π cycloaddition in the cases of benzobarrelene (5) and 1,2-naphthobarrelene (2).

Finally, the rearrangement of the proposed cycloaddition intermediate **13***b* to give CN-COT (**8**) but apparently not β-CN-COT (**16***b*), is at-

Can. J. Chem. Downloaded from www.nrcresearchpress.com by 210.87.254.105 on 09/05/12
For personal use only.

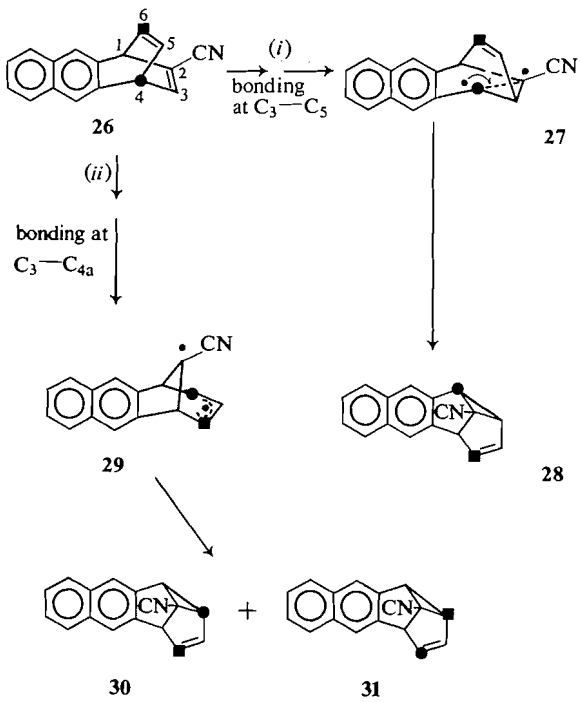

SCHEME 6. Individual structures represent an approximately 50:50 mixture of two component compounds, each singly labeled with deuterium at the positions designated by ● and ■.

tributed to the preferred initial rupture of the C_1—C_2 bond as a consequence of the favorable stabilization afforded the radical centers in the species **14***b* by the cyano and naphtho groups (see Scheme 4).

Experimental

The n.m.r. spectra were run on Varian A-60 and HA-100 instruments with TMS as internal standard. The i.r. spectra were recorded on a Perkin-Elmer Model 337 spectrophotometer, the u.v. spectra on a Cary 15 spectrophotometer, and the mass spectra on an MS 9 (A.E.I.). All m.p. are uncorrected. Elemental analyses were performed by Galbraith Labs. Inc., Knoxville, Tennessee. Benzene solvent for photolyses was shaken three times with acidic potassium permanganate solution, scrubbed with 20% fuming sulfuric acid, washed with 10% aqueous sodium hydroxide, dried ($MgSO_4$), and distilled from calcium hydride. Benzophenone sensitizer was recrystallized twice from ethanol, m.p. 47–49°.

2-Bromo-1,4-dihydro-1,4-ethenoanthracene (4)

A mixture of 6.0 g of 3-diazoniumnaphthalene-2-carboxylate (2) and 1 l of bromobenzene (distilled from calcium hydride) was heated with stirring at 90° for 4 h in a dry nitrogen atmosphere. The mixture was concentrated *in vacuo* and the residue column chromatographed on silicic acid. Elution with cyclohexane gave crude **4** from early fractions and crystallization from ethanol gave 419 mg (5%) m.p. 160–162°: u.v.$_{max}$(hexane) 236 (49 000), 255 sh (9500), 265 (9800), 274 (8300), 284 (4300), 298 (710), 311 (430), 321 (190), and 325 nm (310); n.m.r. (100 MHz, CCl_4) τ 2.40–2.82 (m, 6H, aromatic), 3.28 (m, 3H, vinyl), and 5.28 (m, 2H, bridgehead).

Anal. Calcd. for $C_{16}H_{11}Br$: C, 67.87; H, 3.91; Br, 28.22. Found: C, 67.91; H, 3.91; Br, 27.95.

2-Cyano-1,4-dihydro-1,4-ethenoanthracene (5)

A solution of 288.8 mg (1.02 mmol) of **4** and 231.1 mg (1.29 mmol) of cuprous cyanide in 5 ml of dry DMF was stirred under reflux for 4 h. The mixture was cooled, diluted with 200 ml of benzene, extracted with 5% aqueous HCl (2 × 50 ml), then with 5% aqueous NaOH (2 × 50 ml), and finally with water (50 ml). The benzene solution was dried ($MgSO_4$), concentrated *in vacuo*, and the residue column chromatographed on silicic acid. Elution with 0.5% ether–cyclohexane and crystallization of crude **5** from ethanol gave 183.8 mg (79%) of colorless material, m.p. 178–180°: i.r. (KBr) 2220 cm^{-1}, C≡N; u.v.$_{max}$ (hexane) 232 (55 000), 237 (62 000), 254 (7400), 264 (8100), 273 (7900), 283 (5100), 297 sh (320), 311 (250), 319 (140), and 323 nm (80); n.m.r. (60 MHz, $CDCl_3$) 2.18–2.74 (m, 7H, aromatic and H-3), 3.12 (m, 2H, H-5 and H-6), and 4.92 (m, 2H, bridgeheads).

Anal. Calcd. for $C_{17}H_{11}N$: C, 89.05; H, 4.85; N, 6.10. Found: C, 89.31; H, 4.86; N, 5.83.

Action of Lithium Cyclohexylamide on Cyanobarrelene 5

A solution of 244.8 mg (1.08 mmol) of **5**, 40 ml of cyclohexylamine (CaH_2 dried and distilled), and 4 ml (8.0 mmol) of 2 *M* butyllithium in hexane was stirred at 83° for 45 h in a nitrogen atmosphere. The mixture was cooled, quenched with 50 ml of water, diluted with 250 ml of benzene, and extracted with 10% HCl (2 × 200 ml) and then with water. The benzene solution was dried ($MgSO_4$), concentrated *in vacuo*, and the residue chromatographed on silicic acid with cyclohexane as solvent. Colorless material, 77.6 mg (41%), was obtained, m.p. 200–205°, which was raised to 216–218° by crystallization from ethanol, and was shown by t.l.c., i.r. and mixed m.p. to be identical to anthracene.

Photolysis Apparatus

The same apparatus was used for both preparative runs and quantum yield studies. The apparatus consisted of a "merry-go-round" fitted with a 450 W Hanovia medium-pressure mercury arc and surrounded by a water-cooled quartz immersion well and filter solutions. For direct irradiations, 313 nm light was isolated by a two compartment filter consisting of a 1.5 cm path length of a solution of 28 g of cobaltous sulfate heptahydrate per 100 ml of water, and a 0.6 cm path length of a solution of 0.252 g of potassium carbonate; transmittance was 300–332 nm with a maximum at 313 nm (13%). For benzophenone sensitized irradiations, 343 nm light was isolated by a one compartment filter consisting of a 2.0 cm path length of a solution of 450 g of cobaltous chloride hexahydrate, 60 g of stannous chloride dihydrate, and 150 g of nickel chloride hexahydrate per1.2 l of 20% aqueous HCl; transmittance was 319–382 nm with a maximum at 343 nm (5%). Prior to irradiations, solutions of samples in 35 ml of benzene, contained in 25 × 150 mm Pyrex irradiation tubes, were deoxygenated by nitrogen flushing. The

Can. J. Chem. Downloaded from www.nrcresearchpress.com by 210.87.254.105 on 09/05/12
For personal use only.

Can. J. Chem. Downloaded from www.nrcresearchpress.com by 210.87.254.105 on 09/05/12
For personal use only.

tubes were sealed under a positive pressure of nitrogen, which was maintained throughout the course of photolyses.

Direct Irradiation of Cyanobarrelene **5**

A solution of 260.5 mg (1.14 mmol) of **5** in 35 ml of benzene was photolyzed for 8 h with 313 nm light. The solvent was removed *in vacuo* and the residue was chromatographed on silicic acid and eluted with 0.5% ether–cyclohexane. The first band contained a trace amount of anthracene; (accumulated material from several runs was shown to be identical with an authentic sample). Band two contained 11.0 mg (4%) of **8**, a colorless solid, m.p. 176–178° (from ethanol): i.r. (KBr) 2200 cm^{-1}, C≡N; u.v.$_{max}$ (hexane) 227 (50 500), 247 sh (18 700), 285 (16 000), 292 sh (14 500), 305 sh (6900), and 343 nm sh (1050); n.m.r., see Table 1; Mass spectrum (70 eV, direct inlet) showed molecular ion at *m/e* 229.0899 (93%), $C_{17}H_{11}N$ requires 229.0891.

Band three contained a mixture of **5**, **6**, and **7**. Crystallization of the mixture from ethanol (twice) gave 121.7 mg (45%) of colorless **6**, m.p. 205–207°: i.r. (KBr) 2230 cm^{-1}, C≡N; u.v.$_{max}$ (cyclohexane) 239 (70 000), 267 sh (4600), 275 (5800), 289 (6000), 299 (3800), 314 (610) 317 sh (350), 322 (290), and 327 nm (610); n.m.r. ($CDCl_3$) the aliphatic–olefinic region comprises an ABMXY spin system, τ 2.07–2.76 (m, 6H, aromatic), 4.34 (*A*BM q, 1H, H-6, J_{56} = 2.5 Hz, J_{67} = 5.0 Hz), 4.79 (A*B*X q, 1H, H-7, J_{67} = 5.0 Hz, J_{78} = 3.0 Hz), 5.64 (A*M* d, 1H, H-5, J_{56} = 2.5 Hz), 6.30 (X*Y* d, 1H, H-2, J_{28} = 7.0 Hz), and 6.69 (B*X*Y q, 1H, H-8, J_{28} = 7.0 Hz, J_{78} = 3.0 Hz).

Anal. Found: C, 89.30; H, 4.79.

The mother liquors from the ethanol crystallization of band three were concentrated *in vacuo* to give 119.9 mg of an oil, which upon analysis by n.m.r. was found to contain 26% of **5**, 49% of **6**, and 25% of **7**. The oil was divided into six portions which were rechromatographed separately on a 2 × 200 cm silicic acid column and eluted with 0.5% ether–hexane; 50 ml fractions were collected. In a typical run, fractions 76–88 contained a mixture of **5**, **6**, and **7**; fractions 89–95 contained pure 7. Crystallization of the (ethanol) fractions of **7** from all runs gave 12.1 mg (5%) of colorless material, m.p. 183–185°: i.r. (KBr) 2225 cm^{-1}, C≡N; u.v.$_{max}$ (cyclohexane) 233 (77 600), 262 sh (10 000), 286 (6600), 297 sh (5400), 307 sh (2800), 315 (1750), 322 (980), and 329 nm (1790); n.m.r. (60 MHz, $CDCl_3$) the aliphatic–olefinic region comprises an AMXYZ spin system, τ 2.03–2.81 (m, 6H, aromatic), 3.96 (*A*Z d, 1H, H-7, J_{78} = 3 Hz), 5.79 (*M*X d, 1H, H-5, J_{15} = 6.5 Hz), 6.48 (*X*YZ d of d, 1H, H-1, J_{15} = J_{12} = J_{18} = 6.5 Hz), 6.73 (X*Y*Z t, 1H, H-2, J_{12} = J_{28} = 6.5 Hz), and 7.31 (XY*Z* d of t, 1H, H-8, J_{18} = J_{28} = 6.5 Hz, and J_{78} = 3 Hz). Mass spectrum (70 eV, direct inlet) showed molecular ion at *m/e* 229.0899 (95%).

Sensitized Irradiation of Cyanobarrelene **5**

A solution of 208.1 mg (0.91 mmol) of **5** and 1.0025 g (5.51 mmol) of benzophenone in 35 ml of benzene was photolyzed with 343 nm light for 1.5 h. The solvent was removed *in vacuo* and the residue was chromatographed on silicic acid with 0.5% ether–cyclohexane as eluting agent. The first band contained 931.1 mg of benzophenone, m.p. 47–49°. Band two contained a mixture of **6** and **7**. Recrystallization of the mixture twice from ethanol gave 152.1 mg (73%) of colorless **6**, m.p. 205–207°. Concentration of the mother liquors *in vacuo* gave 54.0 mg of an oil, which upon analysis by n.m.r. was found to contain 69% of **6** and 31% of 7. The oil was divided into three equal portions and each was chromatographed separately on a 2 × 200 cm silicic acid column which was eluted with 0.5% ether–hexane. Compound 7, 8.2 mg (4%), m.p. 182–185°, was obtained from the last fraction of the main band as described in the isolation of **7** from the direct irradiation of **5** (*vide supra*).

Quantum Yield Irradiations

Quantum yield runs were carried out on solutions of samples (*ca.* 0.50 mmol) and benzophenone (*ca.* 2.75 mmol, if any) in 35 ml of benzene solvent, and the lamp output was measured by potassium ferrioxalate actinometry (6). Photolysates were concentrated *in vacuo*, a known amount of *p*-xylene was added as internal standard, and the product composition was determined by n.m.r. analysis; the peak areas were calibrated against authentic mixtures of similar constitution. Quantum yields for the direct and sensitized photolyses of **5** are shown in Table 2.

5-Deuterocyanobarrelene (***12***)

A solution of 140 g (0.59 mol) of *p*-dibromobenzene in 450 ml of ether was added to a stirred mixture of 24.3 g (1.00 g atom) of magnesium turnings, a crystal of iodine, and 50 ml of ether, at a rate that maintained reflux. After all the magnesium had reacted, the cooled solution was treated with 100 ml of 5% DCl in D_2O. The ether layer was separated, dried ($MgSO_4$), concentrated *in vacuo*, and the residue distilled. The fraction of b.p. 151–155° (691 mm), 42 g (45%), was collected.

A mixture of 1.0 g of 3-diazoniumnaphthalene-2-carboxylate and 230 ml of the *p*-deuterated bromobenzene was heated with stirring at 90° for 4 h in a dry nitrogen atmosphere. The mixture was distilled and the distillate was recycled through the decomposition reaction a total of 5 times, in each case using a 1 g portion of the naphthyne precursor. The distillate residues were collected together and after column chromatography, as described for **4** (*vide supra*), 140.0 mg (1.7%) of colorless 4-d_1 was obtained, m.p. 160–162°.

A solution of 125 mg (0.44 mmol) of **4**-d_1 and 93.2 mg (0.52 mmol) of cuprous cyanide in 7 ml of dry DMF was refluxed for 6 h. The reaction was worked-up in the same way as for **5**, to give 59.7 mg (59%) of colorless **12**, m.p. 178–180°: n.m.r. (60 MHz, $CDCl_3$) τ 2.17–2.63 (m, 7.11 ± 0.14 H, aromatic and H-3), 3.08 (d, 1.06 ± 0.02 H, H-6, J_{16} = 5.5 Hz), and 4.92 (m, 2.00 H, bridgeheads), *i.e.*, 94 ± 2% deuteration at C-5 (based on comparison of bridgehead (assumed 0%-d_1) and H-6 proton integrations).

Direct Photolysis of 5-Deuterocyanobarrelene (***12***)

A solution of 187.7 mg (0.82 mmol) of **12** in 35 ml of benzene was photolyzed for 7.2 h with 313 nm light. The products were isolated as described for the direct irradiation of **5** (*vide supra*). Band two contained 5.2 mg (3%) of **15**, m.p. 175–177°: n.m.r. (100 MHz, $CDCl_3$) τ 2.16–2.63 (m, 6.02 ± 0.10 H, aromatic), 3.05 and 3.07 (d, s, 2.00 ± 0.07 H, H-6 and H-11, J_{67} = 11.5 Hz), 3.35 (s, 1.0 H, H-9), and 3.98 (d, 1.08 ± 0.04 H, H-7 and H-10). Hydrogen distribution required for pathway *i* (Scheme 4):

Can. J. Chem. Downloaded from www.nrcresearchpress.com by 210.87.254.105 on 09/05/12
For personal use only.

aromatic, 6.0 H; H-6 and H-11, 2.00 H; H-9, 1.00 H; H-7 and H-10, 1.06 ± 0.02 H.

Recrystallization of band three from ethanol twice gave 107.7 mg (57%) of **21**, m.p. 205–207°: n.m.r. (60 MHz, $CDCl_3$) τ 2.08–2.70 (m, 6.04 ± 0.09 H, aromatic), 4.33 (d, 0.94 ± 0.07 H, H-6, J_{56} = 2.5 Hz), 4.60–5.00 (no discernible signal, 0.07 ± 0.01 H, residual H-7), 5.63 (d, 1.00 H, H-5, J_{56} = 2.5 Hz), 6.32 (d, 1.02 ± 0.07 H, H-2, J_{28} = 7.0 Hz), and 6.73 (d, 1.08 ± 0.09 H, H-8, J_{28} = 7.0 Hz). Hydrogen distribution required for routes *i* or *ii* (Scheme 5): aromatic, 6.00 H; H-6, 1.00 H; H-7, 0.06 ± 0.02 H; H-5, 1.00 H; H-2, 1.00 H; H-8, 1.00 H.

Concentration of the ethanol mother liquors and chromatography of the residue (*vide supra*) gave 5 mg (3%) of **23**, m.p. 181–183°: n.m.r. (100 MHz, $CDCl_3$) τ 2.10–2.77 (m, 6.07 ± 0.11 H, aromatic), 3.96 (s, 0.96 ± 0.08 H, H-7), 5.79 (d, 100 H, H-5, J_{15} = 6.5 Hz), 6.47 (t, 1.02 ± 0.07 H, H-1, J_{12} = J_{15} = 6.5 Hz), 6.75 (d, 1.06 ± 0.08 H, H-2, J_{12} = 6.5 Hz), and 7.00–7.50 (no discernible signal, 0.10 ± 0.05 H, residual H-8). Hydrogen distribution required for route *i* (Scheme 5): aromatic, 6.0 H; H-7, 1.00 H; H-5, 1.00 H; H-1, 1.00 H; H-2, 1.00 H; H-8, 0.06 ± 0.02 H.

*Sensitized Irradiation of 5-Deuterocyanobarrelene (**12**)*

A solution of 172.3 mg (0.75 mmol) of **12** and 771.1 mg (4.23 mmol) of benzophenone in 35 ml of benzene was photolyzed with 343 nm light for 1.2 h. The products were isolated as described for the sensitized irradiation of **5** (*vide supra*). Recrystallization of the contents of band two from ethanol twice gave 111.3 mg (65%) of **21**, m.p. 205–207°: n.m.r. (60 MHz, $CDCl_3$) τ 2.08–2.70 (m, 6.08 ± 0.08 H, aromatic), 4.33 (d, 0.99 ± 0.07 H, H-6, J_{56} = 2.5 Hz), 4.60–5.00 (no discernible signal, 0.05 ± 0.03 H, residual H-7), 5.63 (d, 1.00 H, H-5, J_{56} = 2.5 Hz), 6.32 (d, 1.05 ± 0.09 H, H-2, J_{28} = 7.0 Hz), and 6.73 (d, 1.01 ± 0.12 H, H-8, J_{28} = 7.0 Hz).

Concentration of the ethanol mother liquors and chromatography of the residue (*vide supra*) gave 5 mg (3%) of **23**, m.p. 180–183°: n.m.r. (100 MHz, $CDCl_3$) τ 2.10–2.77 (m, 6.11 ± 0.10 H, aromatic), 3.96 (s, 1.01 ± 0.08 H, H-7), 5.79 (d, 1.00 H, H-5, J_{15} = 6.5 Hz), 6.47 (t, 0.99 ± 0.06 H, H-1, J_{12} = J_{15} = 6.5 Hz), 6.75 (d, 1.09 ± 0.09 H, H-2, J_{12} = 6.5 Hz), and 7.00–7.50 (no discernible signal, 0.06 ± 0.04 H, residual H-8).

*4- and 6-Deuterocyanobarrelene Mixture **26***

Mixture **26**, m.p. 178–180°, was obtained in 1% overall yield (based on naphthyne precursor) using essentially the same method as that used to prepare **12** (*vide supra*), except that *p*-dibromobenzene was replaced by *m*-dibromobenzene in the naphthyne addition stage: n.m.r. (60 MHz, $CDCl_3$) τ 2.13–2.76 (m, 7.00 H, aromatic and H-3), 3.08 (m, 1.53 ± 0.04 H, H-5 and residual H-6), and 4.87 (m, 154 ± 0.03 H, H-1 and residual H-4), *i.e.*, 93 ± 7% d_1 content (assuming 0% d_1 content in aromatics and H-3), distributed at C-4 (46 ± 3%) and C-6 (47 ± 4%).

*Direct Photolysis of 4- and 6-Deuterobarrelene Mixture **26***

A solution of 48.1 mg (0.21 mmol) of **26** in 35 ml of benzene was photolyzed for 3 h with 313 nm light. Chromatography and recrystallization of band three from ethanol (*vide supra*) gave 16.3 mg (34%) of the deuterated 1-cyanosemibullvalene material **28**, m.p. 205–207°: n.m.r. (100 MHz, $CDCl_3$) τ 2.13–2.69 (m, 5.99 ± 0.03 H, aromatic), 4.33 (*A*BM q, 0.53 ± 0.02 H, H-6, J_{56} = 2.5 Hz, J_{67} = 5.0 Hz), 4.78 (m, 1.01 ± 0.01 H, H-7), 5.63 (br s, 1.00 H, H-5), 6.31 (d, 0.55 ± 0.02 H, H-2, J_{28} = 7.0 Hz), and 6.73 (m, 1.00 ± 0.02 H, H-8). Hydrogen distribution required for route *i* (Scheme 6): aromatic, 6.00 H; H-6, 0.53 ± 0.04 H; H-7, 1.00 H; H-5, 1.00 H; H-2, 0.54 ± 0.03 H; H-8, 1.00 H.

*Sensitized Photolysis of 4- and 6-Deuterobarrelene Mixture **26***

A solution of 81.6 mg (0.35 mmol) of **26** and 418.5 mg (2.30 mmol) of benzophenone in 35 ml of benzene was irradiated for 0.5 h with 343 nm light. The deuterated 1-cyanosemibullvalene material (**28**), 26.0 mg (32%), m.p. 205–207°, was isolated from the photolysate via chromatography and ethanol recrystallization (*vide supra*): n.m.r. 100 MHz, $CDCl_3$) τ 2.13–2.69 (m, 6.02 ± 0.04 H, aromatic), 4.33 (*A*BM q, 0.52 ± 0.03 H, H-6, J_{56} = 2.5 Hz, J_{67} = 5.0 Hz), 4.78 (m, 0.99 ± 0.02 H, H-7), 5.63 (br s, 1.00 H, H-5), 6.31 (d, 0.56 ± 0.02 H, H-2, J_{28} = 7.0 Hz), and 6.73 (m, 0.99 ± 0.03 H, H-8).

The authors thank the Spectroscopic Services Laboratory of the University of Alberta for the 100-MHz n.m.r. (Dr. T. Nakashima) and mass spectra (Dr. A. Hogg), and gratefully acknowledge the financial support of the National Research Council of Canada, and the University of Lethbridge Research Committee.

1. C. O. Bender, J. L. M. Elder, A. J. Herbst, and L. E. Miller. Can. J. Chem. **50**, 395 (1972).
2. H. E. Zimmerman and C. O. Bender. J. Am. Chem. Soc. **92**, 4366 (1970).
3. A. Krebs and D. Byrd. Liebigs Ann. Chem. **707**, 66 (1967).
4. C. Pascual, J. Meir, and W. Simon. Helv. Chim. Acta, **49**, 164 (1966).
5. H. E. Zimmerman, R. S. Givens, and R. M. Pagni. J. Am. Chem. Soc. **90**, 6096 (1968).
6. C. G. Hatchard and C. A. Parker. Proc. R. Soc. (London), **A235**, 518 (1956).
7. H. E. Zimmerman and M. Viriot-Villaume. J. Am. Chem. Soc. **95**, 1274 (1973).
8. S. Masamune, M. Suda, H. Ona, and L. M. Seichter. Chem. Commun. 1268 (1972).
9. M. P. Cava and M. J. Mitchell. Cyclobutadiene and related compounds. Academic Press, New York. 1967. p. 246.

Aggregation of *p*-Nitrophenyl Alkanoates in Aqueous Solution. Limitations on Their Use as Substrates in Enzyme Model Studies

J. PETER GUTHRIE

Department of Chemistry, University of Western Ontario, London, Ontario

Received April 18, 1973

p-Nitrophenyl alkanoates are aggregated at extremely low concentrations in aqueous solution. Second-order rate constants for imidazole or hydroxide catalyzed hydrolysis are independent of ester concentration up to a critical concentration of ester, and then decrease with increasing ester concentration. The critical concentrations at 25 °C are: *p*-nitrophenyl hexanoate, 1×10^{-4} *M*; octanoate, 9.6×10^{-6} *M*; decanoate, 1.2×10^{-6} *M*. For the dodecanoate ester, the critical concentration was estimated as *ca.* 10^{-7} *M*. Addition of 10% methanol causes only a modest increase in the critical concentration. The critical concentration probably represents the solubility limit of the ester. The rate constants for the hydrolysis of the longer chain esters evaluated here are significantly larger than those in the literature, suggesting that the earlier work was done using conditions where the esters were aggregated.

Les alcanoates de *p*-nitrophényle donnent lieu à des agrégations en solution aqueuse à des concentrations extrèmement faibles. Les constantes de vitesse du deuxième ordre de l'hydrolyse, catalysée par l'imidazole ou l'hydroxyde, sont indépendantes de la concentration en ester jusqu'à une valeur critique puis décroissent lorsque la concentration en ester croît. Les concentrations critiques à 25 °C sont: pour l'hexanoate de *p*-nitrophényle 1×10^{-4} *M*; octanoate 9.6×10^{-6} *M*, décanoate 1.2×10^{-6} *M*. Pour l'ester dodécanoique la concentration critique a été estimée à *ca.* 10^{-7} *M*. L'addition de 10% de méthanol provoque seulement un accroissement modeste de la concentration critique. Celle-ci représente probablement la solubilité limite de l'ester. Les constantes de vitesse de l'hydrolyse des esters des chaînes plus longues calculées ici sont nettement plus grandes que celles de la littérature laissant penser que les travaux précédents aient été effectués dans des conditions où les esters s'agrégeaient.

[Traduit par le journal]

Can. J. Chem., 51, 3494 (1973)

Can. J. Chem. Downloaded from www.nrcresearchpress.com by 210.87.254.42 on 09/05/12
For personal use only.

Various recent studies (1–4) of enzyme models have used *p*-nitrophenyl alkanoates as substrates in the hope that hydrophobic binding of the alkyl group of the ester to the enzyme model compound would lead to an increased effective concentration of the reactive groups, manifesting itself as a rate enhancement. These substrates appeared attractive because of the ease with which hydrolysis can be followed, their simplicity of structure, and their commercial availability. However, it has not been recognized sufficiently that these compounds have *very* low solubility in water and that a major fraction of a long chain *p*-nitrophenyl alkanoate can be aggregated without observable turbidity. The studies reported in this paper characterize the aqueous solution behavior of the hexanoate, octanoate, and decanoate esters. A preliminary account of this work has been published (5).

Results and Discussion

In Table 1[1] and Fig. 1 are shown the results obtained for the imidazole catalyzed hydrolysis of *p*-nitrophenyl acetate, hexanoate, octanoate, and decanoate at 0.1 *M* ionic strength. For the decanoate ester it is difficult to obtain an accurate value for the limiting rate constant for monomeric ester because of the very small absorbance change at the low concentrations involved. For rates where the small absorbance change is a major source of error, error bounds are shown.

In Table 2[1] and Fig. 2 are shown the results for similar studies of the hydroxide catalyzed hydrolysis. Most of these experiments were done at constant buffer concentration, since the feature of interest was the dependence of the rate constant on the concentration of ester, rather than in the rate constants themselves. After this dependence had been established, sets of experiments at differing buffer concentrations permitted extrapolation to zero buffer, and evaluation of the true rate constant for the hydroxide ion reaction of the monomeric ester.

Buffer catalysis causes increases in the observed rate constants (at 0.03 *M* total carbonate buffer) of 20–25% except for the acetate

[1]Tables 1 and 2 are available, at a nominal charge, from the Depository of Unpublished Data, National Science Library, National Research Council of Canada, Ottawa, Canada K1A 0S2.

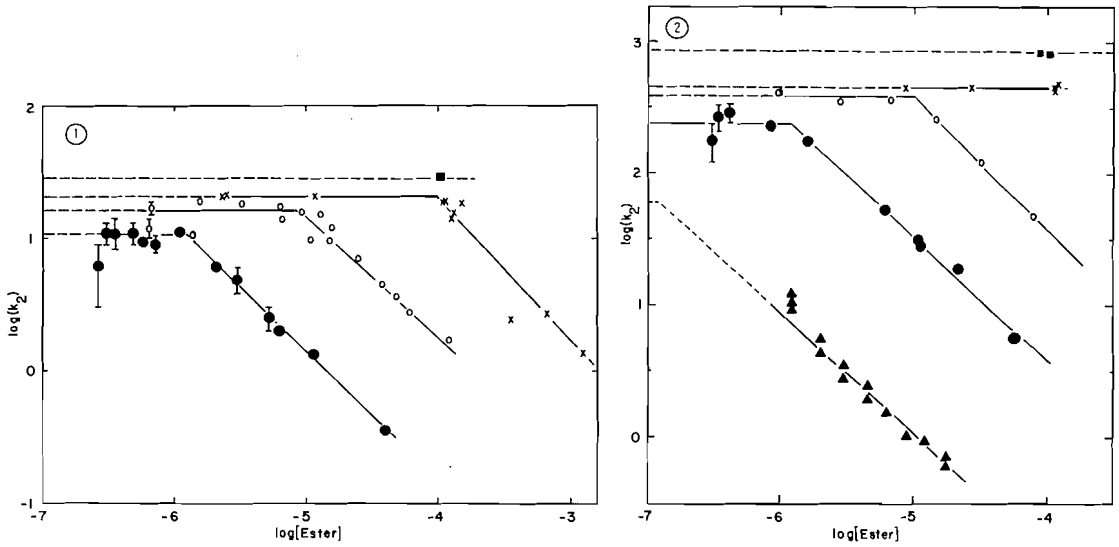

FIG. 1. Reactions of *p*-nitrophenyl acetate (■), hexanoate (X), octanoate (○), and decanoate (●) with imidazole. Dependence of the logarithm of the second-order rate constant on the logarithm of the ester concentration. Critical concentrations are: hexanoate, 1×10^{-4} *M*; octanoate, 9.6×10^{-6} *M*; and decanoate, 1.3×10^{-6} *M*.

FIG. 2. Reactions of *p*-nitrophenyl acetate (■), hexanoate (X), octanoate (○), decanoate (●), and dodecanoate (▲) (data for dodecanoate from ref. 6) with hydroxide ion. Dependence of the logarithms of the second-order rate constant on the logarithm of the ester concentration. Critical concentrations are: octanoate, 1.0×10^{-5} *M*; decanoate, 1.2×10^{-6} *M*; and dodecanoate (estimated, see text), 1.2×10^{-7} *M*.

ester, where the increase is 40%. The rate constants for *p*-nitrophenyl dodecanoate shown on Fig. 2 are from a study by Menger and Portnoy (6) and were measured in 0.1 *N* sodium hydroxide solution. These data show the trend anticipated on the basis of this work and extrapolation (*vide infra*) suggests that the dodecanoate ester will only be monomeric in aqueous solution at concentrations at or below 10^{-7} *M*.

In Fig. 3 are shown plots of log k_2 *vs.* number of carbon atoms in the alkanoate for the reactions of imidazole and hydroxide ion with the monomeric esters. Within experimental error these plots appear linear. This progressive decline in the rate constant seems somewhat surprising since there can be no electrostatic effect on increasing the length of the chain from 6 to 10 carbons and there would be no steric effect if the alkyl chain were in an extended conformation. Bruice and co-workers (7), however, have pointed out that long alkyl chains are expected (8) to be coiled up in aqueous solution and so could have a larger steric bulk. In addition it seems reasonable that for the longer chain esters the alkyl chain could come into contact with the aryl portion of the ester. Examination of space filling models suggests that this is feasible. A molecule coiled back on itself in this manner should have an effective "solvent" near the ester linkage which is much less polar than the bulk solvent and so less favorable to nucleophilic attack on the ester.

Figure 4 shows a plot of the logarithms of the "critical concentrations" for the esters studied here *vs.* $\Sigma\pi$, the Hansch hydrophobicity parameter (9). These points fall on a straight line and furthermore lie close to the empirical line relating *solubility* to $\Sigma\pi$ (10). Extrapolation of the observed correlation permits estimation of the critical concentration for *p*-nitrophenyl dodecanoate; the value so obtained is 1.2×10^{-7} *M* and this value was used in constructing Fig. 2. This concentration falls below the limits imposed by most spectrophotometers, even with 10 cm cells. Thus in aqueous or predominantly aqueous solutions, *p*-nitrophenyl dodecanoate cannot be employed as a monomeric substrate.

The behavior of *p*-nitrophenyl octanoate was studied in 10% methanol – 90% water, since it has been suggested (4) that 10% methanol will abolish aggregation of *p*-nitrophenyl alkanoates. The results (Table 1[1] and Fig. 2 of ref. 5) clearly

Can. J. Chem. Downloaded from www.nrcresearchpress.com by 210.87.254.42 on 09/05/12
For personal use only.

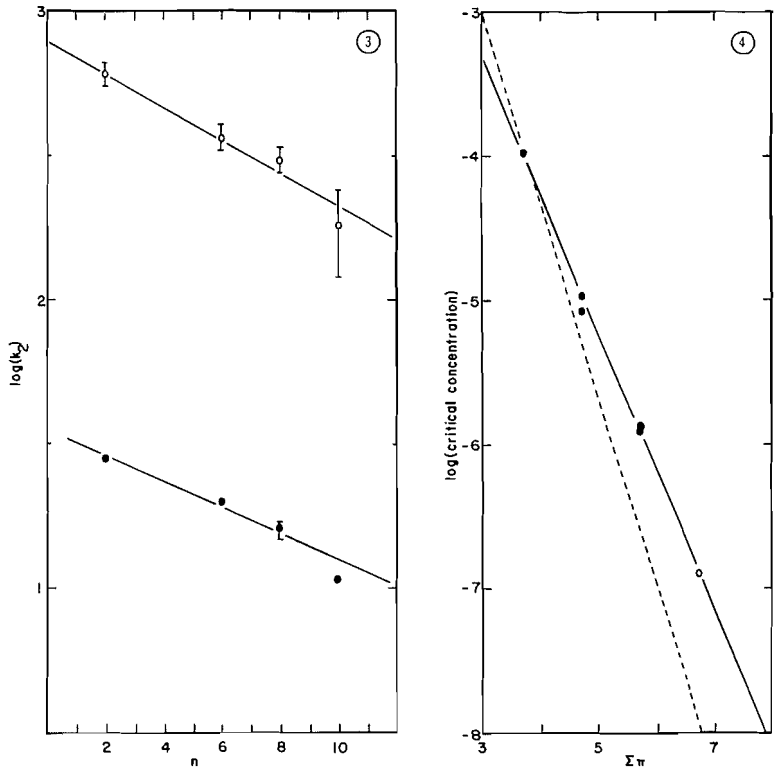

FIG. 3. Relation between rate constants and number of carbons in the alkanoate (n) for reactions of p-nitrophenyl alkanoates with hydroxide (○) and imidazole (●).

FIG. 4. Relation between critical concentration and the Hansch Σπ value. Experimental points (●); point estimated for p-nitrophenyl dodecanoate (○). Σπ values were calculated from values in ref. 9, using log P = 1.49 for C_6H_5OAc, $\pi = 0.24$ for $—NO_2$ (using the value from $O_2N—C_6H_4—OCH_2COOH$, since this is the most nearly analogous compound from the set Hansch has studied), and $\pi = 0.50$ for $—CH_2$. The solid line was drawn through the experimental points; the dashed line was calculated from the empirical equation relating solubility and Σπ (set 11 of ref. 10).

show that although 10% methanol does increase the critical concentration (to 1.6×10^{-5} M) the effect is small and does not alter the qualitative pattern.

Initially it was believed that micelle formation was responsible for the kinetic behavior reported above. However, the low hydrophilicity of the p-nitrophenyl ester moiety is not in accord with this concept, since a stable micelle requires a molecule with both a hydrophobic and a hydrophilic end (11). The nitro group of a p-nitrophenyl ester is probably hydrophobic, judging by the most closely analogous π values which are available (9). The ester group is mildly hydrophilic, but is between the hydrophobic alkyl and aryl groups so that it is not likely that it could be exposed to water while the hydrophobic groups were removed from water. All the behavior of these alkanoates is consistent with the critical concentration being the solubility limit. In particular, the close correspondence between the observed critical concentrations and the solubilities predicted by the empirical correlation of Hansch *et al.* (10) very strongly supports this view. This interpretation is reinforced by phenomena observed when the critical concentration for p-nitrophenyl hexanoate was evaluated. At concentrations above the critical concentration, the solutions were not only turbid but showed visible though minute droplets several minutes after reaction was initiated. Obviously no great significance can be attached to rate constants measured under such disreputable conditions; nevertheless the initial rate constants so obtained gave qualitatively the same behavior when log k_2 was plotted as a function of log [ester] as was shown by the larger esters at lower concentrations. It should be

Can. J. Chem. Downloaded from www.nrcresearchpress.com by 210.87.254.42 on 09/05/12
For personal use only.

TABLE 3. Relative rate constants for reactions of *p*-nitrophenyl alkanoates in aqueous solution at 25°

	This work		Earlier work			
Ester	k_{OH^-} [a,b]	k_{Im} [a,c]	k_{OH^-} [d]	k_{EtIm} [e]	k_{II} [f]	k_{OH^-} [g]
Acetate	1.00	1.00	1.00	1.00	1.00	1.00
Hexanoate	0.61	0.72	0.53	0.81	0.51	0.65
Octanoate	0.50	0.57	0.27	0.11	0.28	0.72
Decanoate	0.30	0.38	0.04	0.03	—	—
Dodecanoate	0.10[h]	—	—	—	0.03	—

[a]Acetonetrile, 0.64 *M*, μ = 0.097 *M* (KCl).
[b]Extrapolated to zero buffer concentration; k_2 for the acetate was 610 M^{-1} min^{-1}.
[c]Tris buffer, 0.00996 *M*, p*H* 7.9, with 0.00996 imidazole; k_2 for the acetate was 28 M^{-1} min^{-1}.
[d]Ref. 3, 0.99% (v/v) acetone; k_2 for the acetate was 724 M^{-1} min^{-1}.
[e]Ref. 3, 0.99% (v/v) acetone; relative rate constants for reaction with *N*-ethyl imidazole; k_2 for the acetate was 24 M^{-1} min^{-1}.
[f]Ref. 4, p*H* 6.80 phosphate buffer, μ = 0.088, with 1.75% acetonitrile, 10.55% methanol. Rate constants for reaction with $(Me_2CHCH_2)_2NCH_2CON(Me)OH$, relative to that for the acetate, 0.693 M^{-1} min^{-1}.
[g]Ref. 12, 1.6% (v/v) acetonitrile; k_2 for the acetate was 620 M^{-1} min^{-1}.
[h]Estimated value; see text.

noted that *p*-nitrophenyl octanoate showed visible turbidity at concentrations well above the critical concentration but not at concentrations just above this limit. *p*-Nitrophenyl decanoate showed no observable turbidity for a wider concentration range above its critical concentration. Thus clear solutions may still have most of the solute present in aggregates if the solute is a large hydrophobic compound.

In Table 3 the results of this investigation are summarized and compared with other work. It is noteworthy that the relative rates for *p*-nitrophenyl octanoate and decanoate reported here are larger than those reported previously. This implies that in the earlier work the conditions were such that these esters were aggregated. Included in Table 3 is an estimated rate constant for *p*-nitrophenyl dodecanoate, obtained using the critical concentration estimated from Fig. 4. Our value for k_{OH^-} for *p*-nitrophenyl octanoate does not agree with that of Marshall and Akgün (12), who were working at concentrations low enough that the ester should have been monomeric; we do not know the reason for this discrepancy.

Jones and Gordon (13, 14) independently developed an analogous kinetic method for determining whether a compound is aggregated and have also found that with very low total concentrations (*ca.* 1×10^{-6} *M*) there can be extensive aggregation without detectable turbidity (13).

In conclusion, the results reported above show that with water as solvent, long chain *p*-nitrophenyl alkanoates are monomeric only at very low concentration. By implication *any* neutral long chain compound will be aggregated at very low concentrations and it is necessary to perform stringent control experiments before any such compounds can be used in studies where 1:1 substrate–catalyst complexes are desired. Furthermore, although we find a decrease in the rate of reaction of the esters with increasing chain length, this decrease is much less than has been reported in various investigations where these compounds have been used as substrates for enzyme models. Accordingly it seems necessary to consider carefully the question of whether 1:1 complexes were being studied in these earlier investigations or whether the phenomenon involved was one of catalyst molecule interacting with a droplet of substrate.

The kinetic method for determining solubility should be of considerable generality and for favorable cases will permit determination of the solubility of *extremely* insoluble compounds where more traditional methods would be very difficult to employ.

Experimental

p-Nitrophenyl alkanoates (Sigma Chemical Co.) were used without further purification and stored in a freezer over desiccant. Purity was checked by measuring initial and final color yield at 400 nm in reaction with *p*H 10 buffer. Imidazole was recrystallized three times (acetone–hexane) and dried *in vacuo* before use. Inorganic reagents were reagent grade. Glass distilled water was used to make up solutions. Acetonitrile (Eastman Spectro grade) was passed through a column of grade 1 acid alumina to remove nucleophilic contaminants.

Can. J. Chem. Downloaded from www.nrcresearchpress.com by 210.87.254.42 on 09/05/12
For personal use only.

Kinetics were measured using a Gilford model 240 spectrophotometer; temperature was regulated (25.0 ± 0.1 °C) with a Braun Thermomix 11 circulator. For dilute solution 10 cm cells were used with a Gilford Model 2470 sample chamber. Stock solutions of esters were prepared in acetonitrile. Reaction was initiated by adding a suitable portion of ester solution (Hamilton Syringe) to thermally equilibrated buffer, containing acetonitrile if needed to maintain constant final acetonitrile concentration. Mixing was accomplished by repeated inversion of the cell. Points were taken at suitable intervals, normally quite frequently for the first half-life, then at least four per half-life for the next 3 or 4 half-lives of reaction. Infinity points were taken after 10 half-lives. For runs at concentrations below the critical concentration, first-order plots were used to evaluate pseudo first-order rate constants. For runs at higher concentration initial rates were used, since marked deviations from first-order behavior were observed. At concentrations well above the critical concentration, first-order plots often showed an initial rather rapid reaction slowing down after a few minutes, then a long nearly linear period extending for 1 or more half-lives, and then an increase in apparent rate of reaction. This is interpreted in terms of an initial metastable state where the aggregation is not completely established, then a period of hydrolysis at a rate dependent on the degree of aggregation, and finally, as the concentration of ester decreased, an increase in the rate of reaction as the aggregate is dispersed. When plots of this type were observed the rate constant was calculated leaving out data from the first 4 min of reaction and using only data from the linear region before the final rate increase occurred. Best lines were fitted by inspection; for runs where the total optical density change was small, error limits were estimated taking the error in absorbance as 0.002, so that the error in $A_\infty - A_0$ is 0.004. These limits were taken account of in drawing the best line and were used to estimate limits of error on the rate constant by drawing the extreme lines which would fit the data. p*H* values were measured at the end of the run (Radiometer p*H* Meter 25SE with a GK301C combined electrode). Second-order rate constants for imidazole reactions were calculated by dividing the observed pseuso first-order rate constant by the total concentration of imidazole. Hydroxide ion activity was calculated from the p*H* measurements and used to calculate the apparent second-order rate constants for the hydroxide ion reactions. For these reactions carbonate buffer was present so that the pseudo first-order rate constant will include a small contribution from buffer catalysis. For each ester a buffer dilution series was done at an ester concentration lower than the critical concentration so that the true hydroxide ion rate constant for monomeric ester could be evaluated.

Financial support from the National Research Council of Canada is gratefully acknowledged.

1. J. R. KNOWLES and C. A. PARSONS. Chem. Commun. 755 (1967).
2. C. A. BLYTH and J. R. KNOWLES. J. Am. Chem. Soc. **93**, 3017 (1971).
3. C. A. BLYTH and J. R. KNOWLES. J. Am. Chem. Soc. **93**, 3021 (1971).
4. R. HERSHFIELD and M. L. BENDER. J. Am. Chem. Soc. **94**, 1376 (1972).
5. J. P. GUTHRIE. Chem. Commun. 897 (1972).
6. F. M. MENGER and C. E. PORTNOY. J. Am. Chem. Soc. **90**, 1875 (1968).
7. T. MAUGH II and T. C. BRUICE. J. Am. Chem. Soc. **93**, 6584 (1971).
8. G. NEMETHY and H. SCHERAGA. J. Chem. Phys. **36**, 3382 (1962).
9. T. FUJITA, J. IWASA, and C. HANSCH. J. Am. Chem. Soc. **86**, 5175 (1964).
10. C. HANSCH, J. E. QUINLAN, and G. L. LAWRENCE. J. Org. Chem. **33**, 347 (1968).
11. E. H. CORDES and R. B. DUNLAP. Acc. Chem. Res. **2**, 329 (1969).
12. T. H. MARSHALL and A. AKGÜN. J. Biol. Chem. **246**, 6019 (1971).
13. J. B. JONES and K. D. GORDON. Steroids, **20**, 449 (1972).
14. J. B. JONES and K. D. GORDON. Biochemistry, **12**, 71 (1973).

Can. J. Chem. Downloaded from www.nrcresearchpress.com by 210.87.254.42 on 09/05/12
For personal use only.

Reaction of an Aryl Thiocyanate with *p*-Nitrothiophenoxide Ion and with Thioacetate Ion; Consequences of Nucleophilic Displacement at Sulfur

MARGARET M. KAYSER AND MARTIN S. GIBSON
Department of Chemistry, Brock University, St. Catharines, Ontario

Received June 1, 1973

Reaction of *p*-acetamidophenyl thiocyanate (Ar_1SCN) with *p*-nitrothiophenol (Ar_2SH) in presence of triethylamine gives the diaryl disulfides Ar_1SSAr_1, Ar_1SSAr_2, and Ar_2SSAr_2. Reaction of Ar_1SCN with potassium thioacetate gives Ar_1SCOMe and Ar_1SSAr_1. The role of cyanide and arylmercaptide ions in equilibration of disulfides is indicated.

La réaction du thiocyanate de *p*-acétamidophényle (Ar_1SCN) avec le *p*-nitrothiophénol (Ar_2SH) en présence de triéthylamine donne les disulfures diarylés Ar_1SSAr_1, Ar_1SSAr_2 et Ar_2SSAr_2. La réaction du Ar_1SCN avec le thioacétate de potassium donne le Ar_1SCOMe et le Ar_1SSAr_1. Le rôle des ions cyanures et arylthiolates en équilibre avec les disulfures est indiqué. [Traduit par le journal]

Can. J. Chem., **51**, 3499 (1973)

Can. J. Chem. Downloaded from www.nrcresearchpress.com by 210.87.254.105 on 09/05/12
For personal use only.

In connection with other work in the 4*H*-1,3,4-benzothiadiazine series (1), we noted that the reactivity of aromatic thiocyanato groups towards sulfur nucleophiles such as thioacetate ion and *p*-nitrothiophenoxide ion was sufficient to vitiate the synthetic work then in hand.[1] We have accordingly examined the corresponding reactions of *p*-acetamidophenyl thiocyanate (**1**) as models for the processes involved.

p-Acetamidophenyl thiocyanate (Ar_1SCN) was treated under nitrogen with *p*-nitrothiophenol (Ar_2SH) in the presence of triethylamine. Some gas evolution was noted (by inference hydrogen cyanide) and a precipitate began to form. This precipitate readily yielded 4,4-dinitrodiphenyl disulfide (**2**),[1] identical with a sample prepared by aerial oxidation of *p*-nitrothiophenol in alkaline solution, raising the question of a similar oxidative origin of **2** from the reaction under investigation. However, this seemed most unlikely in view of the consistency of yields of **2** produced under rigorously anaerobic conditions. Careful examination of the reaction mixture indicated the presence of two other products which were separated with difficulty and identified as the diaryl disulfides **3** and **4** by mass spectrometry and in the case of **4** by correlation with one of the products from the reaction of **1** with thioacetate ion (*vide infra*).

[1]P. D. Callaghan, A. J. Elliott, and M. S. Gibson, unpublished results.

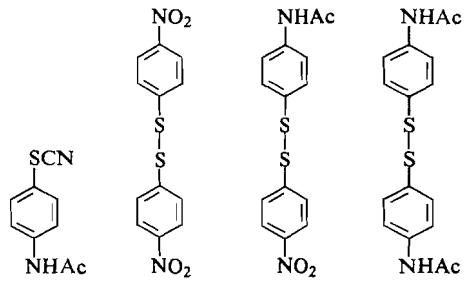

1 **2** **3** **4**

Ar_1 = *p*-$CH_3CONHC_6H_4$; Ar_2 = *p*-$NO_2C_6H_4$

These results may be rationalized in terms of known general reactions (2, 3). *p*-Nitrothiophenoxide ion (Ar_2S^-) displaces cyanide ion from **1** giving the unsymmetrical disulfide **3**. Under alkaline conditions, disulfide **3** may revert by reaction with cyanide ion to starting materials or alternatively proceed to *p*-nitrophenyl thiocyanate (Ar_2SCN) and *p*-acetamidothiophenoxide ion (Ar_1S^-).

[1] $Ar_2S^- + Ar_1S{-}C{\equiv}N \rightleftharpoons Ar_2S{-}SAr_1 + \bar{C}N \rightleftharpoons Ar_2SCN + Ar_1S^-$

The ingredients are now present for the establishment of further equilibria, involving formation of the symmetrical diaryl disulfides **2** and **4** (eqs. 2–5).

[2] $Ar_1S^- + Ar_1SCN \rightleftharpoons Ar_1SSAr_1 + \bar{C}N$

[3] $Ar_2S^- + Ar_2SCN \rightleftharpoons Ar_2SSAr_2 + \bar{C}N$

Can. J. Chem. Downloaded from www.nrcresearchpress.com by 210.87.254.105 on 09/05/12
For personal use only.

[4] $Ar_1S^- + Ar_2SSAr_2 \rightleftharpoons Ar_1SSAr_2 + Ar_2S^-$

[5] $Ar_1S^- + Ar_1SSAr_2 \rightleftharpoons Ar_1SSAr_1 + Ar_2S^-$

The sparing solubility of **2** under the reaction conditions constrains these equilibria such that almost all of the *p*-nitrothiophenol employed is recovered as the symmetrical disulfide **2**. It may be noted that, although nucleophilic displacement at sulfur is clearly implicated in these mechanisms, there is another possible contributing mechanism to the overall equilibrium indicated in [1], namely [6]; process 6 alone, however, is insufficient to provide the observed products.

[6] $Ar_1S{-}C{\equiv}N \quad Ar_1S \quad Ar_1S^- \rightleftharpoons C{=}N^- \rightleftharpoons$; $Ar_2S^- \quad Ar_2S \quad Ar_2{-}S{-}C{\equiv}N$

The reaction of *p*-acetamidophenyl thiocyanate (**1**) with potassium thioacetate in boiling acetonitrile was examined next. This gave *N*,*S*-diacetyl-*p*-aminothiophenol (**5**), with the disulfide **4** as minor product.

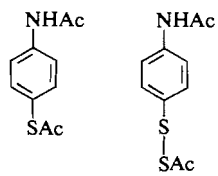

5 **6**

These observations may be accommodated by considerations similar to those above. Nucleophilic displacement of cyanide ion, possibly reversible, by thioacetate ion from **1** would give *p*-acetamidophenyl acetyl disulfide (**6**). Subsequent reaction of **6** with cyanide ion would regenerate the starting materials or, alternatively, lead to acetyl thiocyanate and *p*-acetamidothiophenoxide ion. *p*-Acetamidothiophenoxide ion (Ar_1S^-) may now displace cyanide ion from **1** to give **4** (eq. 2) or thiocyanate ion from the intermediate acetyl thiocyanate to give **5**.

[7] $CH_3COS^- + Ar_1S{-}C{\equiv}N \rightleftharpoons CH_3COS{-}SAr_1 + \bar{C}N$

$\rightleftharpoons CH_3COSCN + Ar_1S^-$

[8] $Ar_1S^- + CH_3COSCN \rightleftharpoons Ar_1SCOCH_3 + \bar{S}CN$

As in the reaction of **1** with *p*-nitrothiophenoxide ion, there is another possible contributing mechanism parallel to that formulated in eq. 6, namely [9].

[9] $Ar_1S{-}C{\equiv}N \quad Ar_1S \quad Ar_1S^- \rightleftharpoons C{=}N^- \rightleftharpoons$; $AcS^- \quad AcS \quad AcS{-}C{\equiv}N$

The possibility that **5** might arise by direct nucleophilic displacement of thiocyanate ion by thioacetate ion is considered unlikely since the *p*-acetamido substituent would contribute little to stabilization of the negative charge on the transition state for such a process.

Experimental

General Methods

General procedures follow those described previously (1). The experiments involving **1** are representative of a number of experiments conducted under slightly differing conditions, but with essentially similar results.

Mass spectra were determined with an AEI-MS30 double-beam double-focusing mass spectrometer.

p-Acetamidophenyl Thiocyanate (1)

Aniline was treated with bromine and potassium thiocyanate to give *p*-aminophenyl thiocyanate (4), which was then acetylated (acetic anhydride – sodium acetate) to give **1**. After crystallization from aqueous methanol, **1** had m.p. 186–187° (lit. (5) m.p. 189°).

Reaction of 1 with p-Nitrothiophenoxide Ion

Compound **1** (1.8 g), *p*-nitrothiophenol (1.4 g), and triethylamine (1 ml) were stirred in ethanol (30 ml) for 2 h. The reaction mixture was flushed continually with nitrogen; some gas evolution was noted (by inference HCN). The yellow solid was collected and combined with further solid material obtained by diluting the filtrate with water. The dried solid (2.7 g) had m.p. 150–155°. The mass spectrum showed peaks at *m/e* 308(M^+, **2**), 320(M^+, **3**) and 332(M^+, **4**). T.l.c. (silica gel) revealed one spot assignable to **2** and a second (elongated) spot assignable to **3** and **4**.

The crude reaction product was chromatographed on Florisil using benzene followed by benzene–ether mixtures as eluants. First eluted was compound **2** (1.3 g) which, after crystallization from ethanol, had m.p. 178–179° (mixed m.p. 178–179°); mass spectrum *m/e* 308(M^+), 292, 278, 276, 262, 232, 215, 171, 155 ($NO_2C_6H_4SH$), 154, 139, 125, and 124.

Later eluates contained residual traces of **2** together with poorly separated mixtures of **3** and **4**. These fractions were combined and evaporated and the resulting material was chromatographed again on Florisil. A small amount of **2** was followed by **3** admixed with **4** and in turn by **4**.

The fractions rich in **3** were combined and evaporated. Three crystallizations from ethanol gave almost pure **3**, m.p. 140°; mass spectrum *m/e* 320(M^+), 303, 290, 288, 278, 267, 246, 236, 192, 167 ($AcNHC_6H_4SH$), 166, 155 ($NO_2C_6H_4SH$), 150, 149, 139, 125, and 124.

The fractions rich in **4** were similarly treated and after three crystallizations from ethanol gave **4**, m.p. 182–183° (lit. (6) for the α-form, m.p. 183°); mass spectrum *m/e* 332(M^+), 300, 290, 198, 167 ($AcNHC_6H_4SH$), 166, 156, 150, 149, 125, and 124.

*Reaction of **1** with Thioacetate Ion*

A mixture of **1** (2.5 g) and potassium thioacetate (1.5 g) in acetonitrile (80 ml) was boiled under reflux for 4 h and then poured into ice-cold water (350 ml) and kept overnight at 0°. The precipitated solid was collected, washed with water, and dried. The dried solid (1.8 g) had m.p. 130–135°. The mass spectrum showed peaks at *m/e* 209(M^+, **5**), 241(M^+, **6**), and 332(M^+, **4**); the peak at *m/e* 241 provides support for the involvement of **6**, although **6** was not isolated in the subsequent procedure.

Crystallization from aqueous ethanol gave a crystalline fraction (A) containing **5** and a small amount of starting material **1** (t.l.c.); concentration of the mother liquor gave a second fraction (B) containing **5** and **4** (t.l.c.). Fraction A, after two crystallizations from aqueous ethanol, gave **5** (1.1 g), m.p. 143–144° (lit. (7) m.p. 143–144°); mass spectrum *m/e* 209(M^+), 167, and 125; n.m.r. ($CDCl_3$), methyl proton signals of equal intensity at δ 2.42 (s) and 2.12 (s).

Fraction B, after two crystallizations from ethanol, gave a few mg of **4**, m.p. and mixed m.p. (with above sample) 182–183°. The mass spectrum was identical with that of the above sample.

We thank the National Research Council of Canada for financial support.

1. I. T. Barnish and M. S. Gibson. J. Chem. Soc. C, 854 (1970); P. D. Callaghan and M. S. Gibson. J. Chem. Soc. C, 2106 (1970).
2. A. J. Parker and N. Kharasch. J. Am. Chem. Soc. **82**, 3071 (1960), and references cited therein.
3. Y. Degani and A. Patchornik. J. Org. Chem. **36**, 2727 (1971).
4. H. P. Kaufmann and W. Oehring. Ber., **59**, 187 (1926).
5. J. W. Dienske. Rec. Trav. Chim. **46**, 154 (1927).
6. O. Hinsberg. Ber., **41**, 626 (1908).
7. O. Hinsberg. Ber., **39**, 2433 (1906).

Can. J. Chem. Downloaded from www.nrcresearchpress.com by 210.87.254.105 on 09/05/12
For personal use only.

Some Reactions of 3β-Mesyloxycholestane-5α,6β-diol and Cholest-2-ene-5α,6β-diol Acetates

P. TSUI AND G. JUST

Department of Chemistry, McGill University, Montreal, Quebec

Received June 22, 1971[1]

Reaction of 3β-mesyloxycholestane-5α,6β-diol 6-monoacetate (**1***e*) with potassium *t*-butoxide gave the 3α,5α-oxycholestan-6β-ol (**4***a*), which rearranged further to 5β,6β-epoxycholestan-3α-ol (**5**). Treatment of **1***c* with triethylamine gave cholest-2-ene-5α,6β-diol diacetate (**7***a*), whereas heating diacetate **1***c* in pyridine–dimethylformamide gave cholestan-3α,5α,6β-triol 3,6-diacetate (**2***a*). Cholest-2-ene-5α,6β-diol diacetate (**7***a*) reacted with *m*-chloroperbenzoic acid to give the α-epoxide **10**. Reaction of **7***a* with aqueous *N*-bromosuccinimide gave 2β-bromo-3α-hydroxy-5α,6β-diacetoxycholestane (**8**). Both epoxide **10** and bromohydrin **8** rearranged in acidic media to the tetrahydrofuran **11**.

La réaction de l'acétate-6 de mésyl-3β cholestane-5α diol-6β (**1***e*) avec le *t*-butylate de potassium, donne l'oxy-5α,3α cholestanol-6β (**4***a*) qui se réarrange ultérieurement en époxy-5β,6β cholestanol-3α (**5**). Le traitement de (**1***c*) avec la triéthylamine, conduit au diacétate de cholestène-2,5α diol-6β (**7***a*), tandis que le chauffage du diacétate (**1***c*) dans un mélange pyridine–diméthylformamide conduit au diacétate-6,3 de cholestanetriol-3α,5α,6β (**2***a*). Le diacétate de cholestène-2,5α diol-6β (**7***a*) réagit avec l'acide *m*-chloroperbenzoique pour donner l'époxyde-α (**10**). La réaction de (**7***a*) avec une solution aqueuse de *N*-bromosuccinimide donne le bromo-2β hydroxy-3α,5α diacétonycholestane-6β (**8**). L'époxyde (**10**) et la bromhydrine (**8**) se réarrangent tous deux en milieu acide en tétrahydrofuranne (**11**).
[Traduit par le journal]

Can. J. Chem., **51**, 3502 (1973)

In connection with some other work, we required a substantial amount of 2β-hydroxy-3α-bromo-5α,6β-diacetoxycholestane. An obvious precursor for such a compound is the readily available cholestane-3β,5α,6β-triol, which can be obtained by oxidation of cholesterol with hydrogen peroxide in formic acid, followed by hydrolysis (1). Acetylation gave the known triacetate **1***a* (2), which was transformed to the mesylate **1***c* via triol diacetate **1***b* (3). This mesylate was heated under reflux in dimethylformamide containing pyridine in order to form the olefin **7***a*. The product obtained, however, was a cholestanetriol diacetate to which we assigned structure **2***a* (Scheme 1). Partial hydrolysis of this diacetate gave triol monoacetate **2***b*. Chromic acid oxidation of both triol monoacetates **2***b* and **1***d* (4) gave the ketone **3**. Since the stereochemistry at position 3 of alcohol **1***d* is known, the stereochemistry of the hydroxy function of **2***b* must be as depicted.

The new compound **2***a* is most likely formed by participation of the 5α-acetate group during the solvolytic reaction. The intermediate acetoxonium ion is then hydrolyzed to give exclusively the 3α-acetate **2***a*.

Since the 5α-acetoxy group seemed to interfere in the desired elimination reaction, we next prepared the 5α-hydroxy-3β-mesylate **1***e*. The compound could be readily obtained by partial hydrolysis of the known cholestan-3β,5α,6β-triol 3,6-diacetate **1***f* (4). Mesylation of the monoacetate **1***d* gave the desired mesylate **1***e* in good yield. Treatment of **1***e* with pyridine in dimethylformamide gave a low yield of the desired olefin **7**. Treatment of **1***e* with potassium *t*-butoxide in *t*-butanol gave two isomeric ethers **4***a* and **5**. Ether **4***a* was an intermediate in the formation of **5**, since it could be converted to **5** by submitting it to the reaction conditions.

Oxetane **4***a* (ν 3420 cm^{-1}, *m/e* 402) exhibited peaks in the n.m.r. at 4.6 p.p.m. (3β-H) and 4.0 p.p.m. (6α-H, $w_{1/2}$ 6 Hz) the latter signal being shifted to 5.17 p.p.m. upon acetylation. The two protons at C-4 appeared as a four-line system centered at 2.65 p.p.m. in both oxetane **4***a* and its acetate **4***b*. Treatment of **4***b* with methanesulfonic acid in ether regenerated the mesylate **1***e*, thereby confirming the structure of oxetane **4***a*.

Epoxide **5** had an i.r. and mass spectrum very similar to that of its 3-epimer **5***a*, which was obtained by treatment of triacetate **1***a* with potassium hydroxide in ethanol (5). Both **5** and **5***a* gave **6** upon Sarett oxidation (6).

[1]Revision received July 16, 1973.

Can. J. Chem. Downloaded from www.nrcresearchpress.com by 210.87.254.40 on 09/05/12
For personal use only.

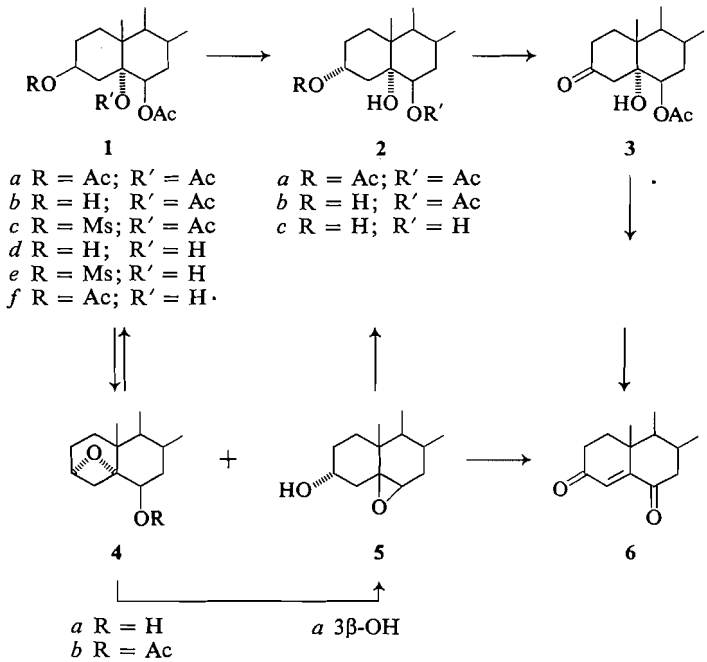

SCHEME 1

The n.m.r. spectra of both **5** and **5***a* were identical except for the position of the 3-hydrogen, which appeared in **5** as a signal at 4.25 p.p.m. ($w_{1/2}$ 10 Hz) and in **5***a* at 3.7 p.p.m. ($w_{1/2} \sim$ 18–20 Hz). This indicated that the hydroxy group in **5** is axial, and its 3-epimer **5***a* equatorial. There is no doubt that the 3-hydroxy group in **5** is α, since treatment of **5** with acid gave the known triol **2***c* (1). Equally, there is no doubt about the stereochemistry of the 3β-hydroxy group in **5***a*, since it was derived from cholesterol by a simple sequence. The 5β,6β-epoxide in **5** and **5***a* must therefore impose on ring B of the steroid molecule a boat-like conformation.

The elimination of methanesulfonic acid was finally achieved upon heating mesylate **1***e* with triethylamine to give **7** (17) in approximately 70% yield. Monoacetate **7** could be converted to diacetate **7***a* by heating **7** with acetyl chloride and *N*,*N*-dimethylaniline (7).

The desired 3α-bromocholestan-2β,5α,6β-triol-5,6-diacetate can in principle be obtained by epoxidation of olefin **7***a*, followed by treatment of the epoxide with hydrobromic acid, if the preferential side of the electrophilic attack is β, or by the action of hypobromous acid on olefin **7***a*, if the preferential side of attack is α (8). At the outset, it was difficult to assess whether the steric hindrance due to the 5α-acetate group would alter the well-known rule of preferential α-side attack in electrophilic reactions on steroids.

Treatment of olefin **7***a* with 1 equiv. of *N*-bromosuccinimide in aqueous dioxane (9) gave bromohydrin **8** as a major product (Scheme 2). The position of the hydroxy group in **8** was established by oxidation of **8** to **9**, which was then dehydrobrominated with lithium carbonate in dimethylformamide (10) to dienone **12**.

The formation of the *trans*-diequatorial bromohydrin bearing the hydroxy group at C-3 could be excluded because of the strong deshielding of the C-19 methyl group in bromohydrin **8**. It therefore seemed that attack of olefin **7***a* by the bromonium ion took place preferentially from the β-side, presumably because of the steric hindrance due to the 5α-acetoxy group.

Since the bromonium ion seemed to have attacked the double bond preferentially from the β-side of the molecule, it was anticipated that epoxidation would lead to the formation of 2β,3β-epoxycholestane-5α,6β-diol diacetate **13**, which could then be converted to the desired bromohydrin by means of hydrobromic acid.

Treatment of olefin **7***a* with *m*-chloroperbenzoic acid gave in good yield the α-epoxide **10**.

Can. J. Chem. Downloaded from www.nrcresearchpress.com by 210.87.254.40 on 09/05/12
For personal use only.

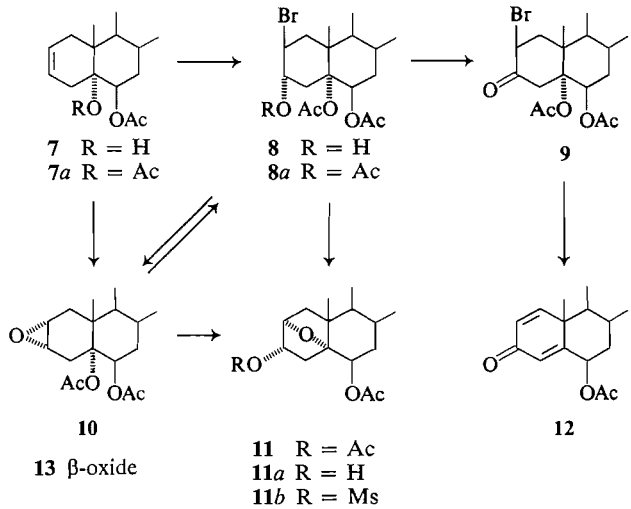

SCHEME 2

The stereochemistry of the epoxide **10** was deduced from the chemical shift of the C-19 methyl group, which remained at the same position as in the starting material. Furthermore, it was identical to the epoxide obtained by base treatment of bromohydrin **8** (11). The reason for a reversal of the preferential side of attack by bromonium ion and by peracid are not clear.

Treatment of the α-epoxide **10** with hydrogen bromide gave, in addition to the expected bromohydrin **8**, a new diacetoxy oxide, to which we assigned structure **11**. The same compound **11** was obtained by treating bromohydrin **8** with *p*-toluenesulfonic acid. The formation of this type of furan has been described recently by H. Tanida and co-workers (12) and by T. Komeno and co-workers (13, 14).[2]

The assignment of structure **11** is supported by its n.m.r. spectrum and decoupling experiments. A peak at 5.32 p.p.m. was assigned to the 6α-H, a double doublet at 4.7 p.p.m. (1H, $J = 7, J = 3$ Hz) to the 3β-H, a doublet at 4.35 p.p.m. (1H, $J = 7$ Hz) to the 2β-H, a four-lines pattern centered at 2.6 p.p.m. (2H, $J = 13$, $J = 7$ Hz) to the methylene protons at C-4, and a sharp signal at 2.0 p.p.m. (6H) was assigned to the acetates at C-3 and -6. The presence of an ABX system was further verified by spin decoupling analysis[3] of the splitting pattern produced by the protons giving rise to signals at 4.7, 4.35, and 2.6 p.p.m.

The formation of **11** may best be rationalized in terms of migration of acetate from 5α to 3α followed by a displacement of the 2β-bromide by the 5α-alcohol. The driving force in this reaction is quite clearly a relief of steric strain between the C-19 methyl group and the β-bromide (14).

The compound **11** was characterized by hydrolysis to the monoacetate **11***a*, ν 3400 and 1760 cm^{-1} and its mesylate **11***b*, ν 1750, 1640, and 1350 cm^{-1}; M^+ 538.

Experimental

All melting points are uncorrected. I.r. spectra were recorded on a Perkin–Elmer 257 grating i.r. spectrophotometer using potassium bromide pellets, unless otherwise stated. Nuclear magnetic resonance spectra were recorded on a Varian T-60 spectrometer using deuterochloroform as solvent and tetramethylsilane as an internal standard. Chemical shifts are reported in p.p.m. Mass spectra were taken on a AEI MS902 spectrometer operating at 75 eV. All t.l.c. was carried out on silica gel HF 254 plates. Analyses were performed by Beller Laboratories, 34 Gottingen, Theaterstrasse 23, Germany.

3β-Mesyloxy-5α,6β-diacetoxycholestane (1c)

Cholestane-3β,5α,6β-triol 5,6-diacetate (**1***b*) (200 mg) in pyridine (3 ml) was cooled to 0°. Mesyl chloride (0.5 ml) was added and the mixture was stirred at 0° for 3 h and poured into ice-water. The precipitate was crystallized from methanol, m.p. 75–78°; ν_{max} 1740, 1380, 1350, 1320, and 1230 cm^{-1}; δ 4.8 (3α-H) and 6.0 p.p.m. (6α-H).

Anal. Calcd. for $C_{32}H_{54}O_7S$: C, 65.95; H, 9.34; S, 5.49. Found: C, 65.82; H, 9.21; S, 5.38.

3β-Mesyloxy-5α-hydroxy-6β-acetoxycholestane (1e)

1*d* (200 mg) in pyridine (3 ml) was cooled to −5°.

[2]We wish to thank the referee for drawing our attention to these papers.

[3]The spin decoupling analysis was performed by Mr. R. Simoneau, the Pulp and Paper Research Institute, McGill University, Montreal, Que.

Can. J. Chem. Downloaded from www.nrcresearchpress.com by 210.87.254.40 on 09/05/12
For personal use only.

Can. J. Chem. Downloaded from www.nrcresearchpress.com by 210.87.254.40 on 09/05/12
For personal use only.

Methanesulfonyl chloride (1 ml) was added and the mixture was stirred at 0° for 5 h. The mixture was poured into ice-water and the precipitate collected was crystallized from chloroform–ether, m.p. 162–166°. Recrystallization from methanol raised the m.p. to 167–168°; ν 3440, 1715, 1370, 1355, and 1330 cm^{-1}.

Anal. Calcd. for $C_{30}H_{52}O_6S$: C, 66.73; H, 9.69; S, 5.92. Found: C, 66.70; H, 9.86; S, 5.99.

Cholestane-3α,5α,6β-triol 3,6-Diacetate (2a)

1*c* (120 mg) was warmed in *N,N*-dimethylformamide (3 ml) and pyridine (1 ml) for 16 h at 102°. The mixture was poured into ice-water and extracted with chloroform (5 × 35 ml). The chloroform solution was washed with 5% hydrochloric acid. The organic layer was dried and evaporated to give a yellow gum. Preparative t.l.c. (ether–hexane 3:1) permitted the isolation of a major band, R_f 0.5, which was extracted with ether. The oil (72 mg) obtained was crystallized from ether–hexane, m.p. 86–88° (lit. (15) 86°); ν_{max} 1730 and 3450 cm^{-1}; δ 4.75 (3α-H), 5.3 (6α-H), and 2.15 p.p.m. (two acetates).

Anal. Calcd. for $C_{31}H_{52}O_5$: C, 73.76; H, 10.38. Found: C, 73.63; H, 10.31.

Partial Hydrolysis of Cholestane-3α,5α,6β-triol 3,6-Diacetate (2a)

A mixture of **2***a* (300 mg), sodium bicarbonate (330 mg), and methanol (30 ml) was stirred at room temperature and the reaction was monitored by t.l.c. After approximately 6 h, the mixture was extracted with ether (5 × 40 ml). The ethereal layer was washed with water (3 × 50 ml) and dried with anhydrous sodium sulfate. Evaporation of solvent gave **2***b* as crystals, m.p. 175–180°; ν_{max} 3480, 3420, and 1720 cm^{-1}, δ 3.8 (3β-H) and 5.3 p.p.m. (6α-H). Recrystallization from methanol twice gave needles, m.p. 181–182°.

Anal. Calcd. for $C_{29}H_{52}O_5.H_2O$: C, 72.45; H, 10.90. Found: C, 72.30; H, 10.37.

Partial Hydrolysis of Cholestane-3β,5α,6β-triol 3,6-Diacetate (1f)

This partial hydrolysis was carried out as described for **2***a*. Two crystallizations from methanol gave needles of **1***d*, m.p. 144–145° (lit. (4) 146°).

Oxidation of Cholestane-3α,5α,6β-triol 6-Acetate (2b) and of 1d

Triol acetate **2***b* (72 mg) was submitted to a Sarett oxidation (6). Crystallization of the reaction product from methanol gave **3**, m.p. 161° (lit. (4) 157–158°). This product was identical to the product of oxidation of **1***d* (mixed m.p., t.l.c., and comparison of i.r. spectra).

Reaction of 3β-Mesyloxy-5α-hydroxy-6β-acetoxycholestane (1e) with Potassium t-Butoxide

1*e* (500 mg) was heated under reflux for 4 h in a nitrogen atmosphere in 50 ml of *t*-butanol containing 300 mg of potassium. The reaction mixture was poured into ice-water. Neutralization with dilute hydrochloric acid and extraction with ether gave an oil (410 mg). Preparative t.l.c. (petroleum ether – ether 1:1) permitted the isolation of two bands.

(*a*) From the band with lowest R_f was obtained 100 mg of **5**, m.p. 120–126°. Recrystallization from methanol gave plates, m.p. 144–146°; ν_{max} 3420, 3320, 1350, and 1240 cm^{-1}; δ 4.2 (1H broad, 3β-H) and 3.1 p.p.m. (1H, J = 3 Hz, 6α-H). The mass spectrum showed a molecular ion at *m/e* 402.

Anal. Calcd. for $C_{27}H_{46}O_2$: C, 80.54; H, 11.52. Found: C, 80.41; H, 11.38.

(*b*) The band with R_f 0.4 gave 210 mg of **4***a*, m.p. 119–123°. Recrystallization from methanol gave 170 mg of **4***a*, m.p. 121–122°; ν_{max} 3450 cm^{-1}; δ 4.05 (1H, triplet 6α-H) and 4.7 p.p.m. (1H, multiplet C_3—H). Mass spectrum provided confirmation of the expected molecular weight of 402.

Anal. Calcd. for $C_{27}H_{46}O_2$: C, 80.54; H, 11.52. Found: C, 80.51; H, 11.32.

3α,5α-Oxycholestan-6β-ol Acetate (4b)

Acetylation of **4***a* (65 mg) in the usual manner gave 82 mg of the acetoxy oxetane **4***b* as an oil. Attempt to crystallize **4***b* failed; ν_{max} 1746 and 1242 cm^{-1}; δ 4.6 (1H, broad C_3—H), 5.15 (1H, multiplet 6α-H), 2.5–2.9 (4H, 2 multiplets), and 2.1 p.p.m. (3H, CH_3CO). The mass spectrum confirmed the expected molecular weight of 444.

Anal. Calcd. for $C_{29}H_{48}O_3$: C, 78.32; H, 10.88. Found: C, 78.12; H, 10.79.

Acid Treatment of 5β,6β-Epoxycholestan-3α-ol (5)

To 35 mg of epoxide **5** in 5 ml of chloroform was added 2 drops of 71% perchloric acid. The mixture was refluxed for 10 min. Anhydrous magnesium sulfate was added and the organic layer was then evaporated to dryness to give a solid. The solid residue was dissolved in 1 ml of pyridine and 0.5 ml of acetic anhydride was added. The mixture was left overnight at room temperature. Removal of solvents *in vacuo* gave crystals of **2***a*, m.p. 85–86°. It was identical with **2***a* obtained from **1***c* (mixed m.p. and comparison of t.l.c. behavior and i.r. spectra).

Reaction of 3α,5α-Oxycholestan-6β-ol Acetate (4b) with Methanesulfonic Acid

To oxetane **4***b* (22 mg) in 5 ml of ether was added 3 drops of methanesulfonic acid and the reaction mixture was stirred at 25° for 4 h. Exactly 4 ml of 10% sodium bicarbonate solution was added to the stirring mixture. The organic layer was separated, dried with 1 g of anhydrous magnesium sulfate, and evaporated giving 19 mg of solid **1***e* which was crystallized from ether, m.p. 169–170°. It was identical with **1***e*, obtained from **1***d* (mixed m.p., comparison of i.r. spectra and t.l.c. mobility).

Reaction of 3α,5α-Oxycholestan-6β-ol Acetate (4b) with Base

A mixture of oxetane **4***b* (22 mg), potassium *t*-butoxide (22 mg), and dry tetrahydrofuran (5 ml) was refluxed for 24 h under a nitrogen atmosphere. The mixture was evaporated to dryness under reduced pressure and the semi-solid was stirred at room temperature with 10 ml of ether. The solid residue was filtered and the filtrate was evaporated to dryness. The gum obtained was shown to contain two compounds, which were identified as hydroxy oxetane **4***a* and epoxide **5** by comparing R_f values and i.r. spectra.

Sarett Oxidation of 5β,6β-Epoxycholestan-3α-ol (5) and of 5β,6β-Epoxycholestan-3β-ol (5a)

A solution of 64 mg of **5** in 1.2 ml of pyridine was mixed with 120 mg of chromium trioxide in 1.2 ml of pyridine and allowed to stand at room temperature

Can. J. Chem. Downloaded from www.nrcresearchpress.com by 210.87.254.40 on 09/05/12
For personal use only.

overnight. The mixture was poured into ice-water and extracted with three portions of benzene–ether 1:1. The extract was passed through celite to break the emulsion. This was dried and evaporated under high vacuum to give a gum. Crystallization from hexane gave leaflets of **6**, m.p. 120–124°; λ_{max} (EtOH) 254 mμ (lit. (4) m.p. 125°, λ_{max} 253 mμ). This product was identical with the product obtained from **3** (t.l.c., mixed m.p.).

Oxidation of the 3β-epimer of **5**, using the same procedure, gave the same dione **6**.

Cholest-4-en-3,6-dione (6)

To **3** (15 mg) dissolved in 3 ml of absolute ethanol, was added 22 mg of solid potassium hydroxide and the mixture was refluxed for 2 h. Evaporation to near dryness and ether extraction gave 11 mg of a solid. The solid was dissolved in 3 ml of acetone, the mixture was cooled to 5° and 1 ml of Jones' reagent (16) was added dropwise. The reaction mixture was allowed to stir at 5° for 1.5 h. Isopropanol (5 ml) was added and the mixture was extracted with ether to give 7 mg of a pale yellow gum. Attempts to crystallize from hexane failed. T.l.c. mobility, i.r. and u.v. spectra of the product proved its identity as **6**.

5α-Hydroxy-6β-acetoxycholest-2-ene (7)

3β-Mesyloxy-5α-hydroxy-6β-acetoxycholestane (**1***e*) (40 g) was refluxed under nitrogen for 38 h with 120 ml of triethylamine. Excess solvent was evaporated completely under reduced pressure. This gave a gum which was chromatographed on alumina (1 kg, activity III). Elution with 1000 ml of petroleum ether gave an impure oil fraction (2.8 g) which was not further characterized. Elution with petroleum ether – benzene 8:1 and 7:1 gave 7 (26.2 g) as an oil, ν_{max} 3500, 3030, 1740, 1660, and 1240 cm^{-1}; δ 5.6 (vinyl protons, 2H), 4.8 (1H, multiplet 6α-H), and 2.0 p.p.m. (CH_3CO, 3H); *m/e* 444, 402, 384, 366.

Anal. Calcd. for $C_{29}H_{48}O_3$: C, 78.32; H, 10.88. Found: C, 78.12; H, 10.81.

5α,6β-Diacetoxycholest-2-ene (7a)

A mixture of 7 (2.3 g), dry chloroform (50 ml), dimethylaniline (20 ml), and acetyl chloride (12 ml) was heated under reflux in a nitrogen atmosphere for 30 h. This was diluted with 500 ml of chloroform and the mixture was washed with 5–10% cold hydrochloric acid solution (5 × 250), with water and dried with anhydrous magnesium sulfate. Evaporation of the organic solvent gave a light blue gum (3.4 g). This was chromatographed on alumina (200 g, activity III). Petroleum ether (400 ml) eluted 1.1 g of dimethylaniline. Elution with petroleum ether – benzene 8:1 (2.4 l) gave 1.4 g of diacetate **7***a* (17) as a solid. Recrystallization from hexane gave needles, m.p. 136–137°; ν_{max} 3030, 1725, 1625, 1250, 1230, and 1210 cm^{-1}; δ 5.95 (multiplet 6α-H), 5.6 (unsymmetric triplet 2 vinyl H), and 2.1 and 2 p.p.m. (2 acetates). The mass spectrum confirmed the expected molecular weight of 486.

Anal. Calcd. for $C_{31}H_{50}O_4$: C, 76.50; H, 10.36. Found: C, 76.55; H, 10.29.

2β-Bromo-3α-hydroxy-5α,6β-diacetoxycholestane (8)

To a mixture of the olefin **7***a* (100 mg) in 2.5 ml of dioxane was added a solution of 60 mg of *N*-bromosuccinimide in 1 ml of water and 1 ml of 5% perchloric acid. The mixture was stirred at room temperature for 2.5 h. Water was added and the product was isolated by filtration. The filtrate was washed with cold water and dried; 112 mg of a fine powder, m.p. 126–129° was obtained. T.l.c. of this compound indicated one spot (chloroform–methanol 95:5 and hexane–ether 1:1). Recrystallization from acetone gave 36 mg of **8** as cubes, m.p. 132–134°; ν_{max} 3480, 1745, 1712, 1245, and 1045; δ 6 (6α-H), 4.43 (multiplet, 2α-H, 3β-H), and 2.1 and 2.2 p.p.m. (singlets, 2 acetates). A second crop of 40 mg of **8**, m.p. 128–131° was further obtained. Evaporation of the solvent from the mother liquor gave 26 mg of a gum. Attempts to recrystallize failed.

Anal. Calcd. for $C_{31}H_{51}O_5Br$: C, 63.80; H, 8.74; Br, 13.70. Found: C, 63.84; H, 8.88; Br, 13.78.

Acetylation of **8** with pyridine – acetic anhydride gave acetate **8** m.p. 173–177°; ν_{max} 2980, 2880, 1750, 1740, 1730, 1265, 1250, 1230, and 1040 cm^{-1}; δ 6 (6α-H), 5.5 (multiplet 3β-H), 4.5 (multiplet 2α-H), and 2.1 p.p.m. (3 acetate peaks).

Anal. Calcd. for $C_{33}H_{53}O_6Br$: Br, 12.81. Found: Br, 12.72.

6β-Acetoxycholesta-1,4-dien-3-one (12)

Bromohydrin **8** (78 mg) in 5 ml of acetic acid was allowed to stand at 25° for 1 day with a mixture of 42 mg of chromic oxide in 2 ml of acetic acid. Excess of chromic acid was destroyed by addition of methanol and the solution was diluted with cold water. Extraction with ether and evaporation gave bromoketone **9** as an oil. Crude **9** was heated at 110° with *N,N*-dimethylformamide (2 ml), lithium carbonate (45 mg), and lithium bromide (17 mg) in a nitrogen atmosphere for 30 h. The reaction mixture was acidified with 5% hydrochloric acid and extracted with chloroform, and the organic solution washed with 5% hydrochloric acid and with water. Evaporation under reduced pressure gave 55 mg of an oil. Preparative t.l.c. (hexane–ether 2:1) permitted the isolation of 45 mg of **12** as a colorless oil, λ_{max} (MeOH) 247 mμ (ε 9800); ν_{max} ($CHCl_3$) 2940, 2860, 1735, 1665, 1620, and 1200 cm^{-1}; δ 7.2 and 6.35 (AB quartet, 1-H, 2-H), 6.42 (singlet, 4-H), 5.6 (multiplet, 6α-H), and 2.18 p.p.m. (6-acetate); *m/e* 440.

Anal. Calcd. for $C_{29}H_{44}O_3$: C, 79.04; H, 10.07. Found: C, 78.69; H, 10.01.

2α,3α-Epoxy-5α,6β-diacetoxycholestane (10)

Olefin **7***a* (300 mg) in 5 ml methylene chloride was stirred at room temperature for 5 h with 200 mg of 85% *m*-chloroperbenzoic acid in 5 ml methylene chloride. After addition of 10% aqueous sodium sulfite solution, the organic layer was washed with 5% aqueous sodium bicarbonate solution and water, and dried. Evaporation gave 340 mg of an oil which solidified upon standing. Recrystallization from methanol gave 195 mg of epoxydiacetate **10**, m.p. 191–193°. Preparative t.l.c. permitted the isolation of 37 mg of **10**, m.p. 188–191° and 12 mg of a solid which was not further characterized. ν_{max} 1740, 1725, 1370, 1250, 1220, 1040, and 1025 cm^{-1}; δ 5.75 (multiplet 6α-H), 3.25 (singlet, 2H), 2.1 and 2 (2 singlets, 2 acetates), and 1.1 p.p.m. (singlet 19-CH_3); *m/e* 502.

Anal. Calcd. for $C_{31}H_{50}O_5$: C, 74.06; H, 10.03. Found: C, 73.80; H, 10.24.

Reaction of 2α,3α-epoxy-5α,6β-diacetoxycholestane (10) with Hydrobromic Acid

Epoxide **10**, m.p. 192–194° (242 mg) in 10 ml of dioxane was stirred with approximately 0.3 ml of 48% hydro-

bromic acid and 0.12 ml of water for 2.5 h at room temperature. The mixture was poured into water and the precipitate (270 mg) was purified by preparative t.l.c. (ethyl acetate – cyclohexane 1:4) (*1*). The band at R_f 0.4 gave 134 mg of bromohydrin **8**, m.p. 139°, which was identical to **8** obtained from the *N*-bromosuccinimide reaction of *7a* (t.l.c., i.r., mixed m.p.) (*2*). The band at R_f 0.55 gave 130 mg of furan **11** which was crystallized from methanol, m.p. 142–145°; ν_{max} 2940, 2860, 1730, 1240, 1210, and 1030 cm^{-1}; δ 5.32 (6α-H), 4.7 (double doublets, collapses upon irradiation at 2.6 p.p.m., 3β-H), 4.38 (doublet, 2β-H), 2.6 (2 doublets, collapse upon irradiation at 4.7 p.p.m., 4α and 4β-H), and 2.0 p.p.m. (3,6-diacetates, 6H); *m/e* 502.

Anal. Calcd. for $C_{31}H_{50}O_5$: C, 74.06; H, 10.03. Found: C, 73.80; H, 9.68.

Reaction of 2β-Bromo-3α-hydroxy-5α,6β-diacetoxycholestane (8) with p-Toluenesulfonic Acid

A mixture of bromohydrin **8** (130 mg) in 8 ml of methylene chloride and a few crystals of *p*-toluenesulfonic acid in 0.25 ml of tetrahydropyran was allowed to stand overnight. The solvent was removed *in vacuo* and the resulting oil reacetylated with acetic anhydride and pyridine. Evaporation and extraction with methylene chloride gave an oil which solidified after some time. The t.l.c. mobility, n.m.r. and i.r. spectra of this oil were identical to those of **11** obtained from epoxide **10**.

Partial Hydrolysis of 2α,5α-Oxy-3α,6β-diacetoxycholestane (11)

3,6-Diacetate **11** (23 mg) was stirred at −4° for 0.5 h with 3 ml of 5% ethanolic potassium hydroxide. Ether extraction gave 18 mg of an oil **11***a*, ν (NaCl) 3400 cm^{-1} (—OH), 1760 cm^{-1} (—OAc); δ 5.4 (m, 1H, 6α-H), 4.38 (d, 1H, J = 6 Hz, 2β-H), 3.9 (m, 1H, 3β-H), and 2.05 p.p.m. (s, 3H, acetate); M^+ 460.

Anal. Calcd. for $C_{29}H_{50}O_5$: C, 72.76; H, 10.53. Found: C, 72.52; H, 10.32.

3α-Mesyloxy-2α,5α-oxy-6β-acetoxycholestane (11b)

Hydroxy-furan **11***a* (45 mg) was stirred at 2° for 4.5 h with a few drops of mesyl chloride in pyridine (3 ml). Work-up as usual gave 62 mg of mesylate **11***b*. Attempts on recrystallization failed. ν 1740 (—OAc), 1370, 1320, and 1260 cm^{-1} (—SO_2—); δ 5.4 (m, 1H, 6α-H), 4.8 (d, 1H, J = 6 Hz, 2β-H), 4.6 (m, 1H, 3β-H), 3.1 (s, 3H, CH_3SO_2—), and 2.1 p.p.m. (s, 3H, CH_3CO—); *m/e* 538, 478, 442, 400, and 382.

Anal. Calcd. for $C_{30}H_{50}O_6S$: C, 66.88; H, 9.36; S, 5.94. Found: C, 66.72; H, 9.40; S, 5.92.

The authors would like to thank Mr. P. Currie for taking the mass spectra, Mr. V. Yu for taking the n.m.r. spectra, and the National Research Council of Canada for financial support.

1. L. Fieser and S. Rajagopalan. J. Am. Chem. Soc. **71**, 3938 (1949).
2. L. Fieser and M. Fieser. Steroids. Reinhold Publishing Corp., N.Y. 1959. p. 198.
3. M. J. Coppen, M. P. Hartshorn, and D. N. Kirk. J. Chem. Soc. 576 (1966).
4. B. Ellis and V. Petrow. J. Chem. Soc. 1078 (1939).
5. A. T. Rowland and H. R. Nace. J. Am. Chem. Soc. **82**, 2833 (1960).
6. G. I. Poos, G. E. Arth, R. E. Beyler, and L. H. Sarett. J. Am. Chem. Soc. **75**, 425 (1953).
7. F. Bladon. J. Chem. Soc. 4883 (1952).
8. I. Roberts and G. E. Kimball. J. Am. Chem. Soc. **59**, 947 (1937).
9. H. L. Slates and N. L. Wendler, J. Am. Chem. Soc. **78**, 3749 (1956).
10. R. Joly, J. Warnant, G. Nomine, and D. Bertin. Bull. Soc. Chim. 366 (1958).
11. C. W. Shoppee, D. N. Jones, and G. H. R. Summers. J. Chem. Soc. 3100 (1957).
12. T. Tsuji, T. Komeno, H. Itani, and H. Tanida. J. Org. Chem. **36**, 1648 (1971).
13. T. Komeno and M. Kishi. Tetrahedron, **27**, 1517 (1971).
14. T. Komeno, H. Itani, H. Iwakura, and K. Nabeyama. Chem. Pharm. Bull. **18**(6), 1145 (1970).
15. Y. Urushibara and K. Mori. Bull. Chem. Soc. Jap. **31**, 1068 (1958).
16. A. Bowers, T. G. Halsall, E. R. H. Jones, and A. J. Lemin. J. Chem. Soc. 2555 (1953).
17. T. Komeno, H. Itani, H. Iwakura, and K. Nabeyama. Chem. Pharm. Bull. (Tokyo), **18**, 1145 (1970).

Can. J. Chem. Downloaded from www.nrcresearchpress.com by 210.87.254.40 on 09/05/12
For personal use only.

Photochemical Studies. XVI.[1] Second Moment Analysis of the Electron Spin Resonance Spectra of Radicals Formed by Ultraviolet Irradiation of 9-Phenylacridine and of Acridine

AZÉLIO CASTELLANO, JEAN-PIERRE CATTEAU, ALAIN LABLACHE-COMBIER

Laboratoire de Chimie Organique Physique, Université des Sciences et Techniques de Lille, B.P. 36, 59650, Villeneuve D'Ascq, France

AND

GUY ALLAN

Laboratoire de Physique des Solides, I.S.E.N., 3, rue F, Baës, 59000, Lille, France

Received March 27, 1973

The irradiation of 9-phenylacridine in methanol, ethanol, or ether leads to the formation of the 9-phenylacridinyl radical. In methanol-d_4, the radical formed is the singly deuterated analog. The structure of these radicals, which exhibit a hyperfine structure in their e.s.r. spectra measured at 233 °K, is supported by simulation of the spectra using calculated spin densities. The agreement between the experimental and theoretical second moment values of the deuterated radical indicates that the parameters previously chosen for the calculation of the theoretical second moments of pyridinyl-type radicals derived from six-membered ring azaaromatics are suitable and that the second moment method can be used in studies of radicals of this type. We conclude that acridine irradiated in methanol-d_4 leads to the formation of the singly deuterated acridinyl radical.

L'irradiation de la phényl-9 acridine dans le méthanol, l'éthanol ou l'éther, a conduit à la formation du radical phényl-9 acridinyle. Dans le méthanol-d_4, le radical formé est l'analogue comportant un seul deutérium. La structure de ces radicaux, dont les spectres r.p.e. montrent une structure hyperfine lorsqu'enregistrés à 233 °K, est en accord avec la reconstitution des spectres à partir des densités de spin calculées. L'accord entre les valeurs expérimentales et théoriques des seconds moments pour les radicaux deutériés montre que les paramètres choisis antérieurement pour le calcul des seconds moments théoriques des radicaux du type pyridinyle obtenus de cycles azaaromatiques à six membres sont cohérents et que la méthode des seconds moments peut être utilisée pour l'étude des radicaux de ce type. On conclut alors que l'acridine irradiée dans le méthanol-d_4 conduit à la formation du radical acridinyle comportant un seul deutérium. [Traduit par le journal]

Can. J. Chem., 51, 3508 (1973)

The second moment method (2) was employed in the characterization of radicals formed by u.v. irradiation of six-membered ring azaaromatics in protic solvents in several of our previous studies. The radicals formed from pyridine (3), quinoline (4), isoquinoline (4), quinoxaline (5), pyrazine (5), pyrimidine (6), phthalazine (7), and cinnoline (7) are stable only in glassy matrices and give no hyperfine splitting in their e.s.r. spectra. On the other hand, the irradiation of 9-phenylacridine in ether, methanol, methanol-d_4, or ethanol leads to radicals stable at room temperature, with hyperfine splittings in the spectra. We have simulated the spectra of these radicals and have found that there is good agreement between the experimental second moment of the radical formed by u.v. irradiation of 9-phenylacridine in methanol-d_4 and its theoretical value calculated from the equation used previously for unstable radicals, with the same parameters (3–7).

The main goal of this paper is to show that, if cautiously used, the second moment method can be an efficient tool in studies of radicals derived from six-membered ring azaaromatic compounds. Zanker and Erhardt (8) have already studied the e.s.r. spectra formed by u.v. irradiation of 9-phenylacridine and of 9-phenylacridane

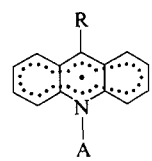

I R = ϕ, A = H III R = H, A = H

II R = ϕ, A = D IV R = H, A = D

[1]For parts XIII, XIV, and XV of this series, see ref. 1 (*a*), (*b*), (*c*) respectively.

Can. J. Chem. Downloaded from www.nrcresearchpress.com by 210.87.254.42 on 09/05/12
For personal use only.

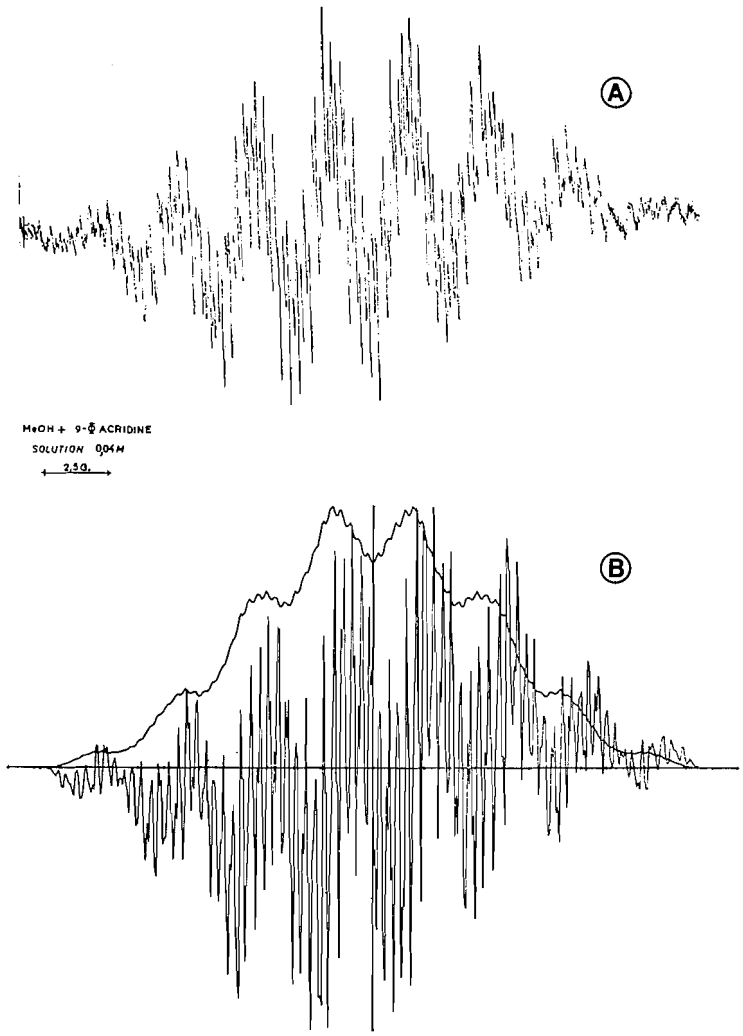

FIG. 1. Experimental (A) and simulated e.s.r. spectra (B) of 9-phenylacridinyl radical II.

in ethanol at 173 °K, but they did not prove the structure of the radicals formed.

The structure which we suggest for the radical derived from 9-phenylacridine is in complete agreement with the structures known from the many previous photochemical studies of the acridine system (for a review on acridine photochemistry, see ref. 9). The π-radicals in the case of 9-phenylacridine are I and II. All these radicals contain sp^2 hybridized N and C-9 atoms.

Results

U.v. irradiation of 9-phenylacridine in 0.2 *M* solution at 233 °K in methanol, ethanol, or ether gives rise to an e.s.r. spectrum containing eight bands with a total width of 23.45 G. When the solvent is methanol-d_4 the spectrum (for the same concentration of 9-phenylacridine) has only seven bands. Its total width is 20.90 G.

If the temperature is lowered following the irradiation, the hyperfine structure disappears rapidly. When the sample becomes glassy, only one band is observed. The width of the band is larger when the solvent is methanol than when it is methanol-d_4. Otherwise, both spectra are identical.

When 9-phenylacridine is irradiated at a lower concentration, the spectrum has a much more complex hyperfine structure which is a function of the concentration and of the temperature. Figures 1*a* and 2*a* show the e.s.r. spectra obtained by irradiation of 0.04 *M* solutions of

Can. J. Chem. Downloaded from www.nrcresearchpress.com by 210.87.254.42 on 09/05/12
For personal use only.

Can. J. Chem. Downloaded from www.nrcresearchpress.com by 210.87.254.42 on 09/05/12
For personal use only.

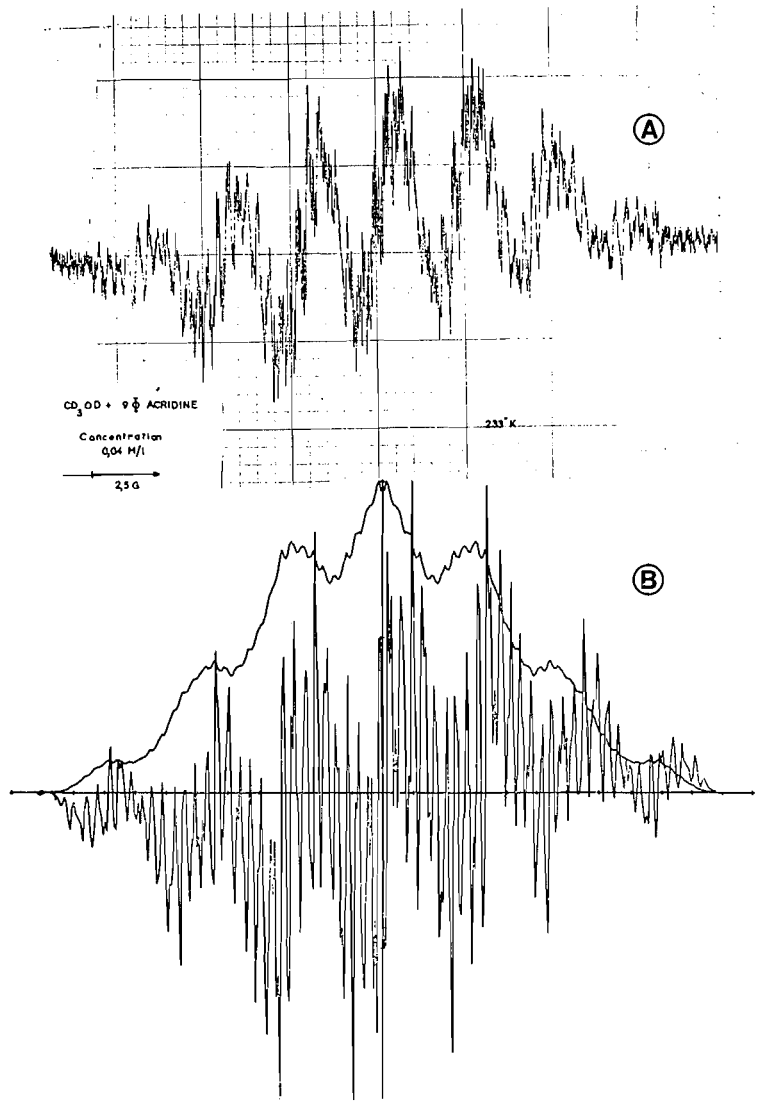

FIG. 2. Experimental (A) and simulated e.s.r. spectra (B) of 9-phenyl-10-deuteroacridinyl radical IV.

9-phenylacridine in methanol and in methanol-d_4, respectively, at 233 °K.

The spectra obtained by irradiation of a 0.2 *M* solution of acridine in methanol or ether are very similar and are observed only at a temperature lower than 173 °K. The signal consists of a broad band with a very poorly resolved hyperfine structure which is different when methanol-d_4 is used as the solvent instead of methanol. It is larger in methanol than in methanol-d_4.

Structure of the Radical Formed by U.V. Irradiation

From our earlier e.s.r. results (3–7) and from the knowledge of acridine photochemistry (9), the observed signals can be identified as those of the π-radicals I and II in the case of 9-phenylacridine and of III and IV in the case of acridine. The C-9 and N atoms in these radicals are sp^2 hybridized. The identification is supported by simulation of the spectra having hyperfine structure and by comparison of the experimental and theoretical second moments. In both cases, calculated spin densities of the radicals were used.

Calculation of Spin Densities

The spin densities were calculated using the McLachlan method (10) as was done in our pre-

Can. J. Chem. Downloaded from www.nrcresearchpress.com by 210.87.254.42 on 09/05/12
For personal use only.

vious studies (4, 5). The parameters were taken in the usual form, *i.e.*

$$\alpha_N = \alpha_C + h\beta_{C-C}$$

(where α_N is the Coulomb integral of the nitrogen, α_C is the Coulomb integral of an electron in the $2p_z$ atomic orbital of carbon and β_{C-C} is the resonance integral of a C—C bond in benzene)

and $$\beta_{C-N} = k\beta_{C-C}$$

β_{C-N} being the resonance integral of the C—N bond.

The numerical values of the coefficients h and k used in our study were: $h = 0.9$, $k = 1$, and $\lambda = 1.2$ where λ is the parameter of the interatomic exchange integral. Its value is that already used by Lunazzi *et al.* in the case of the quinoline and isoquinoline anion radicals (11).

In the case of 9-phenylacridine, the value of the resonance integral between C-9 and C-15 is certainly different from β_0, being a function of the interatomic distance between C-9 and C-15 and of the angle θ between the planes of the phenyl substituent and of the acridine ring. According to Dewar (12), $\beta = \beta_0 \cos\theta$. Wheeler and coworkers (13) have found that the angle of the plane of the phenyl substituent and of the anthracene ring is 68° for the 9,10-diphenylanthracene anion radical and 61° for the corresponding cation radical. They assumed all the interatomic distances between adjacent carbons as equal. In our calculations we have chosen $\beta = 0.3\,\beta_0$ which corresponds to $\theta \simeq 70°$.

Table 1 shows the calculated spin densities for 9-phenylacridinyl radicals, I and II, whereas Table 2 gives the calculated spin densities for acridinyl radicals III and IV.

Simulation of the Spectra with Hyperfine Structure

Spectra obtained from 9-phenylacridine in the liquid phase have been simulated. A series of theoretical coupling constants were calculated from spin densities by varying the Q parameter until the simulated spectra matched the experimental spectrum. The values at which this occurs are: $Q_{C-H} = 25.0$ G; $Q_N = 28.3$ G; $Q_{N-H} = 31.8$ G. These optimized values of Q_N and Q_{CH} are nearly equal to those which were used for the calculation of the theoretical second moment of quinoline (4), isoquinoline (4), and quinoxaline (5) ($Q_N = 28.0$ and $Q_{CH} = 24.5$ G). The value chosen for Q_{N-H} is also very similar to the value (32.0) used by Malrieu and Pullman for a sp^2 hybridized nitrogen (14). Variation of width of the Lorentzian bands can be used to simulate the influence of temperature and of concentration upon the shape of the spectra of the radicals. Figures 1*b* and 2*b* contain the simulated spectra of radicals I and III for a 0.04 *M* solution and a temperature 233 °K. The band width in this case is 0.25 G. The coupling constant of deuterium has been neglected in the simulation of radical II. There is good agreement between the experimental and theoretical total width of the spectrum of radical I: 23.45 and 24.31 G, respectively. The experimental total width of the spectrum of radical II is 20.90 G, the theoretical one 20.75 G. Assuming that $a_{N-D} = 0.15\,a_{N-H}$, we deduce experimentally $a_{N-H} = 3.64$ G. The theoretical value is $a_{N-H} = 3.56$ G.

The agreement between the theoretical and experimental results supports the postulated structure of radicals I and II and indicates that the parameters used in our previous calculations

TABLE 1. 9-Phenylacridinyl radical*

Position	Spin densities calculated for $h = 0.9$; $k = 1$; $\lambda = -1.2$; $\beta = 0.3$
1	0.13770
2	−0.01658
3	0.08423
4	0.03149
5	0.03150
6	0.08422
7	−0.01658
8	0.13770
9	0.42564
10(N)	0.11191
16	0.01049
17	−0.00349
18	0.01088
19	−0.00349
20	0.01050

*Width: experimental 23.95 G; theoretical 24.31 G.

TABLE 2. Acridinyl radical

Position	Spin densities calculated for $h = 0.9$; $k = 1$; $\lambda = -1.2$
1	0.14312
2	−0.01862
3	0.08720
4	0.03167
5	0.03168
6	0.08719
7	−0.01862
8	0.14311
9	0.44065
10(N)	0.11049

TABLE 3. Second moment (G^2)

Solvent	Radical II		Radical IV	
	Experimental	Theoretical	Experimental	Theoretical
Methanol	42		73	
Methanol-d_4	38	31	66	65
Ethanol	41		72	
Ether	45		72	

of spin densities and of coupling constants are consistent with the experimental data.

Second Moments of the Spectra with no Hyperfine Structure

To test the validity of the second moment method, which experimental factors obliged us to use in earlier studies (4, 5), and the values of the parameters used in the calculations of the theoretical second moment, we have determined the experimental and theoretical second moment of the spectra obtained by irradiation of 9-phenylacridine and acridine in a glassy matrix at 113 °K. The experimental second moments have been calculated as about $g = 2.0023$ for solutions in methanol, methanol-d_4, and ether. The results are summarized in Table 3. Note that similar values are obtained for all hydrogenated solvents. When the solvent is methanol-d_4, the second moment is smaller than in methanol, because the N–D coupling constant is lower than the N–H constant although this difference is rather small.

We have calculated the theoretical second moments of radicals II and IV, using the same equations as previously (4, 5). They are deduced from Vincow and Johnson's work (2): the second moment M_2 of radical II is

$$M_2 = M_{2H} + M_{2g} + \frac{\sigma^2}{4} + M_{2N} + M_{2ND}$$

$M_{2H} = \sum_i n_i 174\, \rho_i^2$ contribution of the aromatic hydrogen

$M_{2N} = 914\, \rho_N^2$ contribution of the nitrogen

$M_{2ND} \simeq 0$

For the sum of $M_{2g} + (\sigma^2/4)$, M_{2g} being the contribution of the anisotropy of g and σ the width of the "monocristalline band", we took 10 G^2 as we did previously.

The theoretical value of the second moment calculated from the previous equations is 31 G^2 for radical II, 65 G^2 for radical IV. They agree with the experimental values: 38 and 66 G^2, respectively. Using the second moment method on spectra with unresolved hyperfine structure we conclude that II is the radical formed by u.v. irradiation of 9-phenylacridine in methanol-d_4 and IV is the radical formed under the same conditions from acridine.

Conclusions

The results obtained by simulation of spectra and by calculation of the second moment of the spectra confirm our hypothesis concerning the structure of the radicals formed by u.v. irradiation of 9-phenylacridine in protic solvents.

Radicals I and II are the first to be described of the pyridinyl type, obtained by u.v. irradiation of azaaromatic compounds in a neutral protic solvent, which are stable at room temperature and have a hyperfine structure.

In previous work (3–7) we were unable to obtain radicals in phase other than the glassy one. The spectra so formed had no hyperfine structure and so we were forced to use the second moment method to characterize them and thus were obliged to choose many parameters empirically. The validity of the conclusions made from those calculations was not, therefore, certain.

In this study, we were able to identify a radical with a hyperfine structure and to prove its structure unambiguously by simulation of its spectra. This demonstrates that the parameters chosen for the calculations of the theoretical second moments of the radicals previously studied are reasonable and that the conclusions we made are correct. Thus we are now able to use the second moment method to characterize the structure of pyridinyl type radicals derived from six-membered ring azaaromatic compounds even if their spectra have no hyperfine structure. We conclude from the second moment results that the radical formed by u.v. irradiation of acridine in methanol-d_4 is IV and must be III in methanol and ether.

Can. J. Chem. Downloaded from www.nrcresearchpress.com by 210.87.254.42 on 09/05/12
For personal use only.

Experimental

Products and Solvents

9-Phenylacridine was synthetized by Dr. L. Ivan according to the method of Bernthsen (15). The reaction product was washed with methanol, recrystallized four times from methanol, and dried. Fluka acridine was used without further purification.

Methanol used was Merck methanol for analysis; 100% ethanol and ether were commercial products redistilled four times. Ether was dried over sodium.

Methanol-d_4 was obtained from "Spectrometrie. spin et technique". Its purity was greater than 99%.

Samples and Irradiation

The experimental technique was the same as reported previously (4).

We thank Dr. L. Ivan for the synthesis of a 9-phenylacridine sample.

1. (*a*) P. GRANDCLAUDON, A. LABLACHE-COMBIER, and C. PARKANYI. Tetrahedron, **29**, 651 1973); (*b*) A CASTELLANO, J. P. CATTEAU, and A. LABLACHE-COMBIER. Chem. Commun. 1207 (1972); (*c*) C. CHACHATY, A. LABLACHE-COMBIER, J. C. RONFARD-HARET, and C. LOUCHEUX. C.R. Acad. Sc. Paris, Série C, **276**, 535 (1973).
2. G. VINCOW and P. M. JOHNSON. J. Chem. Phys. **39**, 1143 (1963).
3. S. CAPLAIN, A. CASTELLANO, J. P. CATTEAU, and A. LABLACHE-COMBIER. Tetrahedron, **27**, 3541 (1971).
4. G. ALLAN, A. CASTELLANO, J. P. CATTEAU, and A. LABLACHE-COMBIER. Tetrahedron, **27**, 4687 (1971).
5. G. ALLAN, A. CASTELLANO, J. P. CATTEAU, A. LABLACHE-COMBIER, and B. PLANCKAERT. Tetrahedron, **28**, 3511 (1972).
6. C. CHACHATY and A. E. FORCHIONI, C.R. Acad. Sci. Paris, **264**, 1421 (1967); A. CASTELLANO, J. P. CATTEAU, and A. LABLACHE-COMBIER. Unpublished results.
7. G. ALLAN, A. CASTELLANO, J. P. CATTEAU, A. LABLACHE-COMBIER, and B. PLANCKAERT. Unpublished results.
8. V. ZANKER and E. ERHARDT. B. Bunsenges. Phys. Chem. **72**, 267 (1968).
9. A. LABLACHE-COMBIER. *In* Elements de photochimie avancée. *Edited by* P. Courtot. Hermann, Paris. 1972. p. 289.
10. A. D. MCLACHLAN. Mol. Phys. **3**, 233 (1960).
11. L. LUNAZZI, A. MANGINI, G. F. PÉDULLI, and F. TADDEI. J. Chem. Soc. B, 166 (1970).
12. M. J. S. DEWAR. J. Am. Chem. Soc. **74**, 3345 (1952).
13. L. O. WHEELER, K. S. V. SANTHANAM, and A. J. BARD. J. Phys. Chem. **70**, 404 (1966).
14. J. P. MARLRIEU and B. PULLMAN. Theor. Chim. Acta, **2**, 302 (1964).
15. A. BERNTHSEN. Ann. **224**, 13 (1884).

Can. J. Chem. Downloaded from www.nrcresearchpress.com by 210.87.254.42 on 09/05/12
For personal use only.

Diffusion of Light Hydrocarbons in 5A Zeolite

D. M. RUTHVEN, R. I. DERRAH, AND K. F. LOUGHLIN
Department of Chemical Engineering, University of New Brunswick, Fredericton, New Brunswick

Received March 29, 1973

Experimental diffusivity data are presented for the diffusion of ethane, ethylene, propane, propylene, cyclopropane, *n*-butane, 1-butene, *cis*-2-butene, and *trans*-2-butene in Linde 5A zeolite. It is shown that the concentration dependence of the diffusivity may be accounted for by considering the non-linearity of the equilibrium isotherms. Activation energies for diffusion, derived from the temperature dependence of the limiting diffusivity at zero sorbate concentration, show a clear correlation with the critical diameters of the sorbate molecules. The data are interpreted in terms of the transition state theory of diffusion and it is shown that, for the simpler molecules, this theory gives a quantitatively correct prediction of the pre-exponential factor governing the temperature dependence of the zeolitic diffusivity.

Les données expérimentales de diffusion à travers la zéolite Linde 5A ont été présentées pour l'éthane éthylène, propane, propylène, cyclopropane, *n*-butane, butène-1, *cis* butène-2 et *trans* butène-2. Il a été possible de tenir compte de la dépendance entre la diffusion et la concentration en considérant des équilibres isothermes non linéaires. Les énergies d'activation de diffusion, dérivées à partir de la fonction diffusion limite-température pour une concentration nulle de sorbat, montrent une corrélation claire avec les diamètres critiques des molécules de sorbat. Les données ont été interprétées par rapport à la théorie de l'état de transition de diffusion et on a montré que pour des molécules simples, cette théorie conduit à une bonne prévision quantitative du facteur préexponentiel gouvernant la diffusion zéolitique en fonction de la température. [Traduit par le journal]

Can. J. Chem., **51**, 3514 (1973)

The kinetics of sorption of hydrocarbons in molecular sieve zeolites have been widely studied but there are, as yet, few systems for which the dependence of the zeolitic diffusivity on sorbate concentration, temperature and molecular geometry has been clearly established (1). To obtain such information requires experimental data over a wide range of conditions since, with currently available experimental techniques, the inherent errors can easily conceal the real physical effects. In this laboratory we have used a gravimetric method to measure the diffusivities of several light hydrocarbons in Linde 5A zeolite and the data from these studies (2–4) are analyzed and interpreted in this paper. The diffusivities for each sorbate show regular trends with concentration and temperature and the effect of molecular size is clearly evident. For the simpler molecules, diffusivities predicted theoretically from transition state theory show good agreement with the experimental data.

Experimental

In most of the experiments a Cahn vacuum microbalance system was used to follow the change in weight of a sample of zeolite crystals when subjected to a small differential step change in sorbate pressure. The sorption of *cis*-butene, which is rather slow, was studied in a similar manner using a quartz spring balance in place of the electrobalance (4). Details of the experimental technique and the method by which diffusivities are calculated from the transient sorption curves have been given previously (5, 6). Prior to the experimental measurements the zeolite samples were dehydrated at 375–400 °C, 2×10^{-6} Torr for two days but for regeneration between successive runs a shorter period was sufficient.

Results and Discussion

Concentration Dependence of Diffusivity

Diffusivities calculated from adsorption and desorption curves showed no significant difference provided that the concentration steps over which the sorption curves were measured were sufficiently small. Typical data illustrating the variation of diffusivity with sorbate concentration are shown in Figs. 1 and 2. The data for the other sorbates and at other temperatures showed similar trends and some further curves for the saturated hydrocarbons have been presented elsewhere (6–8).

Within the accuracy of the experimental data the pronounced increase in diffusivity with sorbate concentration may be quantitatively accounted for by considering the non-linearity of the relationship between sorbate activity and concentration, as defined by the equilibrium isotherm. Assuming the driving force for transport within the zeolite lattice to be the gradient

Can. J. Chem. Downloaded from www.nrcresearchpress.com by 210.87.254.6 on 09/05/12
For personal use only.

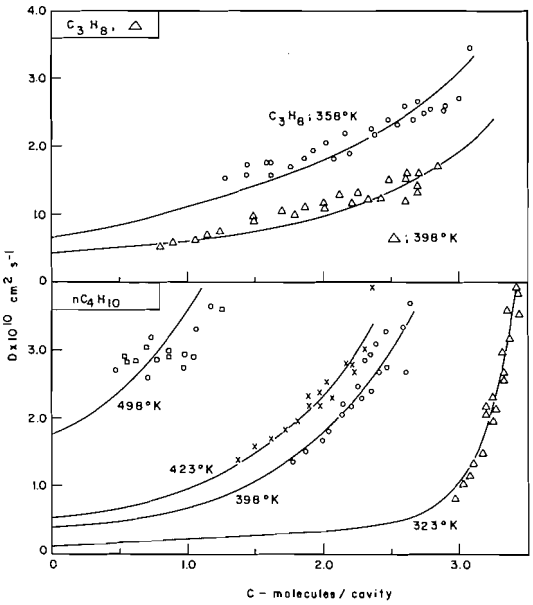

FIG. 1. Variation of zeolitic diffusivity with sorbate concentration (experimental points; theoretical curves from eq. 1).

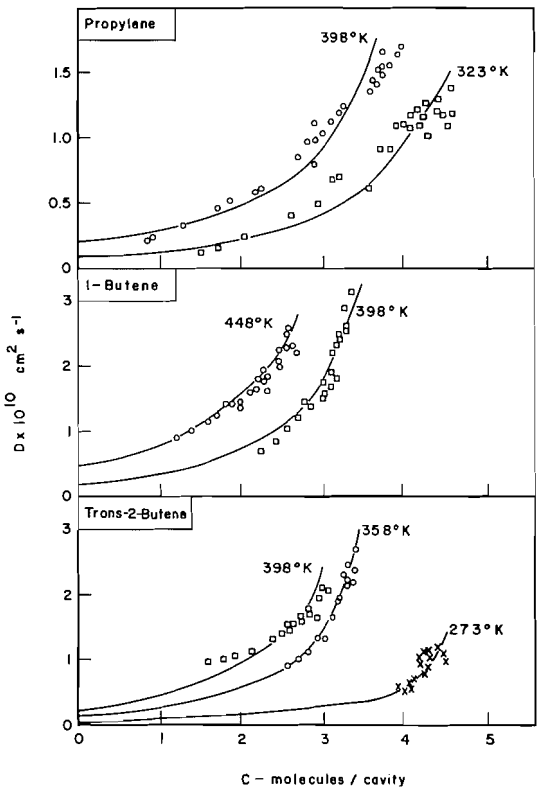

FIG. 2. Variation of zeolitic diffusivity with sorbate concentration (experimental points, theoretical curves from eq. 1).

of chemical potential (1, 7) one may define an intrinsic mobility (B) which is related to the diffusivity by the expression:

$$[1] \quad D = RTB\left(\frac{\partial \ln p}{\partial \ln c}\right)_T = D_0\left(\frac{\partial \ln p}{\partial \ln c}\right)_T$$

where the derivative $(\partial \ln p/\partial \ln c)_T$ represents the gradient of the equilibrium isotherm at temperature T, plotted in logarithmic coordinates.

The equilibrium data obtained from the end points of the sorption curves were fitted, over the range of the experimental measurements, by a polynomial expression from which the derivative $(\partial \ln p/\partial \ln c)_T$ could be readily calculated. This procedure avoids the errors inherent in the use of a model isotherm but the polynomial expression cannot be extrapolated outside the range of the experimental data.

Values of B calculated from the diffusivity data according to eq. 1 showed no significant variation with concentration, suggesting that the concentration dependence of the diffusivity arises entirely from the activity correction term $(\partial \ln p/\partial \ln c)_T$ and that the intrinsic mobility is essentially independent of concentration. The value of $D_0 = RTB$ is thus equal to the limiting diffusivity at low concentrations within the Henry's Law region. Values of D_0, calculated from the average values of the mobility at each temperature, are summarized in Table 1.[1]

In order to obtain theoretical diffusivity–concentration curves over a wider range of concentrations than that covered by the experimental measurements, values of the derivative $(\partial \ln p/\partial \ln c)_T$ were calculated from the best fitting theoretical isotherms (eq. 4 of ref. 9). This theoretical isotherm has been shown to provide a good fit of the experimental equilibrium data for light hydrocarbons in 5A zeolite (9, 10) over the region of low and intermediate sorbate concentrations and it has the correct asymptotic behavior since it reduces, in the low concentration limit, to Henry's Law. Theoretical diffusivity–concentration curves calculated in this way, using the values of D_0 given in Table 1, are

[1]Table 1, which consists of a summary of the values of D_0 calculated from the diffusivity data, is available upon request, at a nominal charge, from the Depository of Unpublished Data, National Science Library, National Research Council of Canada, Ottawa, Canada K1A 0S2.

Can. J. Chem. Downloaded from www.nrcresearchpress.com by 210.87.254.6 on 09/05/12
For personal use only.

TABLE 2. Summary of critical diameters and parameters giving the temperature dependence of Henry constants and limiting diffusivities according to the equations $K = K_0 \exp(q_0/RT)$ and $D_0 = D_* \exp(-E/RT)$

Sorbate	σ' (Å)	$K_0 \times 10^8$ (molecule/cavity Torr)	q_0 (kcal/mol)	$D_* \times 10^8$ ($cm^2\ s^{-1}$)	E (kcal/mol)
CH_4*	1.784	190	4.54	7.2	2.98
C_2H_6	2.063	39.8	6.9	1.28	3.02
C_3H_8	2.80	124	8.1	0.816	3.5
nC_4H_{10}	2.80	86	10.2	0.727	4.0
C_2H_4	1.775	109	8.0	0.198	2.75
C_3H_6	2.65	79	10.0	0.249	3.46
Cyclopropane	2.90	256	8.1	1.06	4.34
1-Butene	2.65	3.12	14.2	0.18	3.44
trans-2-butene	2.65	6.89	13.15	0.255	3.46
cis-2-butene	3.28	—	—	151	9.2

*The values of K_0 and q_0 for the methane are slightly different from those given by Ruthven and Loughlin (9) as a result of the inclusion of additional experimental data (18).

shown in Figs. 1 and 2. The theoretical curves fit the experimental data well, indicating that eq. 1 provides an adequate interpretation of the concentration dependence of the diffusivity. Similar behavior has been recently reported for the diffusion of light paraffins in H-chabazite (11).

The constancy of the mobility should however be regarded as a property of these particular systems rather than as a general property. In all these systems the free diameter of the zeolite window is of the same order as the critical diameter of the sorbate molecules so that the zeolite lattice offers a considerable resistance to diffusion. For the diffusion of small molecules in large port zeolites a concentration dependent mobility is to be expected and has been observed in this laboratory for the diffusion of noble gases in 5A zeolite.

Activation Energies for Diffusion

The temperature dependence of the limiting diffusivity D_0 is illustrated in Fig. 3. Limiting diffusivities for ethane were also measured at several temperatures by an independent technique involving analysis of the breakthrough curves for a molecular sieve column (12). The values so obtained agree well with the gravimetric data, thus providing valuable confirmation of the experimental technique. Apparent activation energies (E) and pre-exponential factors (D_*), defined by the relation $D_0 = D_* e^{-E/RT}$, were calculated from the experimental data by the method of least squares. The theoretical lines are shown in Fig. 3 and the values of the parameters D_* and E are listed in Table 2.

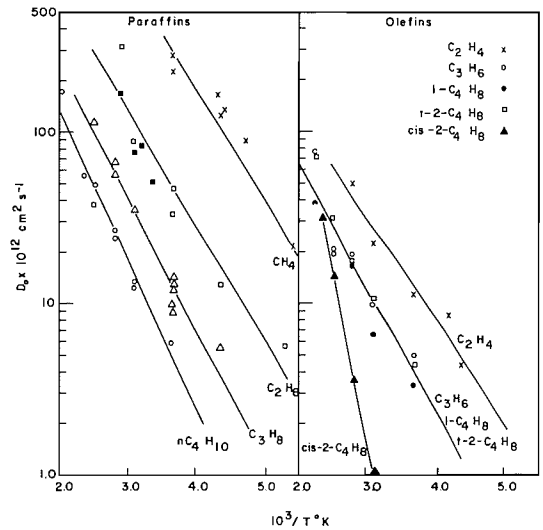

FIG. 3. Temperature dependence of limiting diffusivity for sorption in 5A zeolite (diffusivity data for C_2H_6 calculated from the column studies of Garg (12) are indicated by filled squares).

The increase in activation energy with molecular diameter is illustrated in Fig. 4, which shows the diffusional activation energy plotted against σ'. This dimension, which may be calculated from available bond lengths and angles (13), is defined as the diameter of the smallest cylinder which can be drawn around the molecule, in its most favorable conformation, through the centers of the extreme hydrogen atoms. The values of σ' for the various sorbates are given in Table 2. To obtain the critical diameters of the molecules the effective van der Waals

Can. J. Chem. Downloaded from www.nrcresearchpress.com by 210.87.254.6 on 09/05/12
For personal use only.

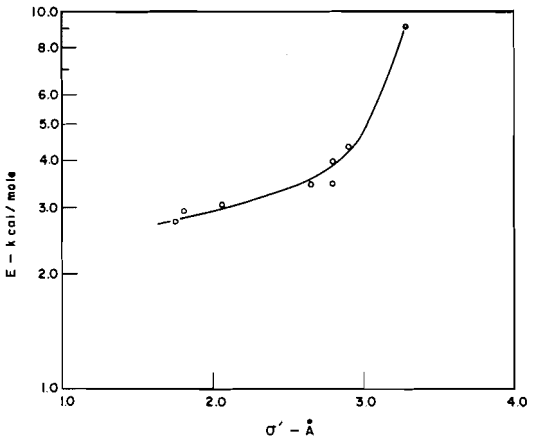

FIG. 4. Variation of diffusional activation energy with critical diameter σ'.

diameter of a hydrogen atom (≃2.3 Å) must be added to σ' (14).

Propylene, 1-butene and *trans*-2-butene all have the same critical diameter and it may be seen that the diffusivities and activation energies for these species are very similar. The critical diameter of *cis*-2-butene is considerably larger, leading to a substantially greater energy of activation. These data provide strong evidence that the activation energy for zeolitic diffusion is determined by the critical diameter of the molecule and that other factors such as molecular weight, chain length or type of bond are of only minor significance.

Correlations of activation energy with molecular diameter have been reported by Barrer and co-workers (15–17) for several gases in natural zeolites. In previous studies of the diffusion of hydrocarbons in type A zeolites, however, the dependence of diffusivity on sorbate concentration has generally not been considered. Such effects may easily conceal the clear correlation which emerges from the present study.

Transition State Theory of Diffusion

A hydrocarbon molecule occluded within a cavity of a type A zeolite crystal is in a region of low potential energy and has considerable freedom of movement within the particular cavity. The diffusion process involves the passage of occluded molecules through the windows between adjacent cavities. In passing through the window the freedom of movement of the sorbate molecule is severely constrained and, depending on the critical diameter, there may also be an appreciable energy barrier due to repulsion forces. The molecule in passage through the window may therefore be identified as the transition state and the following theoretical expression for the limiting diffusivity may be de ved from absolute rate theory (18):

$$[2] \qquad D_0 = \left(\frac{\delta^2}{6h}\right) \frac{1}{K_0} \frac{f_z^*}{f_g'} \exp\left[-(u' + q_0)/kT\right]$$

whence:

$$[3] \qquad D_* = \left(\frac{\delta^2}{6h}\right) \frac{1}{K_0} \frac{f_z^*}{f_g'}$$

$$\frac{E}{R} = \frac{u' + q_0}{k}$$

In these expressions δ is the lattice parameter (12.3×10^{-8} cm for type A zeolites), h and k are respectively Planck's and Boltzmann's constants, u' is the difference in potential energy between a molecule in the window and the same species in the gas phase, q_0 is the limiting heat of sorption at zero sorbate concentration, and K_0 is related to the Henry constant K by the expression $K = K_0 \exp(q_0/kT)$. f_z^* is the partition function for a molecule in the window, for all degrees of freedom except that corresponding to translation through the window, while f_g' represents the partition function per unit volume for a sorbate molecule in the gas phase.

The value of K_0 may be obtained from experimental equilibrium data so that, if the ratio f_z^*/f_g' can be estimated, eq. 3 will give an *a priori* prediction of D_*. The degrees of freedom of the transition state may be represented as a two dimensional oscillation of the center of gravity of the molecule in the plane of the window together with a rotational and/or rocking motion. For molecules with critical diameters equal to or greater than the nominal aperture of the window (~4.2 Å), the vibrational freedom of the center of gravity will be small as a result of repulsion forces, and the principal contribution to the partition function of the transition state will arise from rotation or rocking vibrations. We therefore consider the two limiting cases represented by a freely rotating transition state, having the same rotational freedom as the gaseous molecule at the same temperature, and a transition state having neither rotational nor rocking freedom. Assuming that the internal vibrational degrees of freedom are the same for the transition state as for the gaseous molecule

Can. J. Chem. Downloaded from www.nrcresearchpress.com by 210.87.254.6 on 09/05/12
For personal use only.

TABLE 3. Comparison of experimental and theoretically predicted values of D_* for diffusion in 5A zeolite*

Sorbate	Values of $D_* \times 10^8$ cm^2 s^{-1} Experimental value	Theoretical value for non-rotating transition state	Theoretical value for freely rotating transition state	f_{rot}	Experimental value of f^+ from eq. 6
C_2H_6	1.28	1.01	332	329	1
C_2H_4	0.2	0.24	133	560	1
C_3H_8	0.82	0.014	90	6 500	58
C_3H_6	0.25	0.0077	96	12 500	32
△	1.06	0.015	25	1 700	72
nC_4H_{10}	0.73	0.0021	57	27 000	350
1-C_4H_8	0.18	0.062	1660	27 000	3
trans-2-C_4H_8	0.26	0.028	750	27 000	9

*Theoretical values are calculated for 273 °K. Values of f_{rot} are calculated from data given by Herzberg (23) and Sutton (13). Moments of inertia for the C_4 species are not available, and the value of f_{rot} is based on an approximate estimate.

we have

Free rotation

$$[4] \qquad \frac{f_z^*}{f_g'} = \frac{1}{f_{trans}'}$$

No rotation or rocking

$$[5] \qquad \frac{f_z^*}{f_g'} = \frac{1}{f_{trans}' f_{rot}}$$

where $f_{trans}' = (2\pi mkT/h^2)^{3/2}e$ is the translational partition function per unit volume and $f_{rot} = (8\pi^2 IkT/h^2)^{3/2}(\sqrt{\pi}/s)$ is the rotational partition function for a gaseous molecule of mass m, moment of inertia I, and symmetry number s.

Values of D_* calculated from eqs. 3 and 4 or 5 are compared with the experimental values in Table 3. For the smaller molecules (C_2H_4 and C_2H_6) the assumption of a non-rotating, non-rocking transition state gives a good approximation to the experimental values of D_*. The contribution of rocking vibrations or restricted rotational freedom may be expected to increase with the length of the molecule and the experimental values of D_* for the larger molecules are seen to lie, as expected, between the two theoretical limits.

Also shown in Table 3 are the values of f^+, the partition functions for the transition state calculated directly from the experimental values of D_* according to the relationship:

$$[6] \qquad f^+ = \frac{6hD_*K_0}{\delta^2} f_{trans}' f_{rot}$$

The experimental values of f^+, for all species, are much smaller than the corresponding rotational partition functions suggesting severe inhibition of rotational freedom in the transition state. The rotation of the smaller molecules CH_4 (18), C_2H_6, and C_2H_4 appears to be completely inhibited ($f^+ \simeq 1$) while the numerical values of f^+ for the C_3 and C_4 species are consistent with a weak rocking vibration. However, in view of the inherent uncertainties in the numerical values more detailed analysis is probably not justified.

Comparison of Diffusivities for 4A and 5A Zeolites

The heats of adsorption and the Henry constants for the sorption of light paraffins in the 4A and 5A zeolites have been found to be essentially the same (9) and one may expect that the values of f_z^* will also be similar. Transition state theory (eq. 2) therefore predicts that the values of D_* for the diffusion of a given molecule in the 4A and 5A zeolites should be essentially the same and that the observed difference in diffusivity should be attributable to a difference in the diffusional

TABLE 4. Comparison of experimental diffusivity data for sorption of paraffins in 4A and 5A zeolite

Sorbate	$D_* \times 10^8$ cm^2 s^{-1} 4A	5A	E kcal mol^{-1} 4A	5A
CH_4	5.8*	7.2	7.42*	2.98
	6.24†	1.28	5.66†	3.02
C_2H_6	130‡		7.4‡	
	0.0547§		3.0§	
C_3H_8	1.24§	0.82	8.7§	3.5
n-C_4H_{10}	0.42§	0.73	8.5§	4.0

*Data of Habgood (19).
†Data of Kondis and Dranoff (20).
‡Data of Brandt and Rudloff (21).
§Data of Walker *et al.* (22).

Can. J. Chem. Downloaded from www.nrcresearchpress.com by 210.87.254.6 on 09/05/12
For personal use only.

activation energy which can arise from a difference in the value of u'. This conclusion is supported by the experimental diffusivity data which are summarized in Table 4. It may be seen that the activation energies for diffusion in 4A zeolite are 4–5 kcal greater than for the 5A form and that the values of D_* for methane, propane, and butane are all quite similar. The data for the diffusion of ethane in 4A zeolite however show poor agreement between the results of different studies so no very valid comparison can be made.

Conclusion

For the systems considered in the present paper the variation of zeolitic diffusivity with sorbate concentration may be satisfactorily explained by considering the non-linearity of the relationship between activity and concentration as defined by the equilibrium isotherm. The temperature dependence of the limiting diffusivity at zero concentration may be described by an Arrhenius type of relationship and the activation energies for diffusion show a clear correlation with the critical diameters of the sorbate molecules. Transition state theory provides a satisfactory interpretation of the experimental data and, for the simpler molecules, the theory gives a correct quantitative prediction of the pre-exponential factor D_*.

The continued financial support of the National Research Council of Canada is gratefully acknowledged.

1. R. M. Barrer. Adv. in Chem. **102**, 1 (1971).
2. K. F. Loughlin. Ph. D. Thesis. University of New Brunswick, Fredericton, New Brunswick. 1970.
3. R. I. Derrah. Ph.D. Thesis. University of New Brunswick, Fredericton, New Brunswick. 1973.
4. J. M. McGrath. B.Sc. Thesis. University of New Brunswick, Fredericton, New Brunswick, 1971.
5. K. F. Loughlin, R. I. Derrah, and D. M. Ruthven. Can. J. Chem. Eng. **49**, 66 (1971).
6. D. M. Ruthven and K. F. Loughlin. Chem. Eng. Sci. **26**, 1145 (1971).
7. D. M. Ruthven and K. F. Loughlin. Trans. Faraday Soc. **67**, 1661 (1971).
8. K. F. Loughlin and D. M. Ruthven. Chem. Eng. Sci. **27**, 1401 (1972).
9. D. M. Ruthven and K. F. Loughlin. J. Chem. Soc. Faraday Trans. I, **68**, 696 (1972).
10. R. I. Derrah, K. F. Loughlin, and D. M. Ruthven. J. Chem. Soc. Faraday Trans. I, **68**, 1947 (1972).
11. R. M. Barrer and J. A. Davies. Proc. Roy. Soc. **A322**, 1 (1971).
12. D. R. Garg. Ph.D. Thesis. University of New Brunswick, Fredericton, New Brunswick. 1972.
13. Tables of interatomic distances and configuration. *Edited by* L. E. Sutton. Chem. Soc. London. 1958.
14. L. Pauling. The nature of the chemical bond. Cornell Univ. Press, Ithaca, New York. 1960. p. 257.
15. R. M. Barrer and D. A. Ibbitson. Trans. Faraday Soc. **40**, 207 (1944).
16. R. M. Barrer and D. W. Brook. Trans. Faraday Soc. **49**, 1049 (1953).
17. R. M. Barrer. Trans. Faraday Soc. **45**, 358 (1949).
18. D. M. Ruthven and R. I. Derrah. J. Chem. Soc. Faraday Trans. I, **68**, 2332 (1972).
19. H. W. Habgood. Can. J. Chem. **36**, 1384 (1958).
20. E. F. Kondis and J. S. Dranoff. Adv. in Chem. **102**, 359 (1971).
21. W. W. Brandt and W. Rudloff. J. Phys. Chem. Solids, **26**, 741 (1965).
22. P. L. Walker, L. G. Austin, and S. P. Nandi. Chem. and Phys. of Carbon, **2**, 257 (1966).
23. G. Herzberg. Molecular spectra and molecular structure. Vol. III. Van Nostrand, Princeton, N.J. 1967. p. 581.

Can. J. Chem. Downloaded from www.nrcresearchpress.com by 210.87.254.6 on 09/05/12
For personal use only.

A Kinetic and Surface Study of the Water-Gas Shift Reaction on Manganese(II) Oxide

BORDAN WALTER KRUPAY AND ROBERT ANDERSON ROSS
Department of Chemistry, Lakehead University, Thunder Bay "P", Ontario

Received April 5, 1973

The kinetics of the water-gas shift reaction on a manganese(II) oxide catalyst possessing surface nonstoichiometry has been studied from 300 to 400 °C at atmospheric pressure. The experimental rate expression obtained was $r = k(p_{CO})^{0.75}$ in the carbon monoxide partial pressure range 20 to 80 Torr and $r = k(p_{CO})^{0.5}$ from 100 to 240 Torr. The rate of reaction has been related to the Langmuirian-type adsorption of carbon monoxide and a redox mechanism involving surface oxygen species is proposed. When the reaction rate was determined in increasing 10 °C intervals from 300 °C, two activation energies were observed; 16 ± 0.5 kcal mol^{-1} from 350 to 400 °C and 11 ± 0.5 kcal mol^{-1} from 300 to 340 °C. The temperature at which the change occurs corresponds closely to the Curie temperature of the oxide. The possible use of manganese(II) oxide as a catalyst or catalyst component in a commercial shift process is critically appraised.

La cinétique de la réaction de déplacement eau-gaz sur un catalyseur oxyde de manganèse(II) ayant une surface non stoechiométrique a été étudiée de 300 à 400 °C à la pression atmosphérique. L'expression de vitesse expérimentale obtenue était $r = k(p_{CO})^{0.75}$ dans l'intervalle de pression partielle en monoxyde de carbone de 20 à 80 Torr et $r = k(p_{CO})^{0.5}$ de 100 à 240 Torr. La vitesse de réaction a été reliée à l'adsorption du type Langmuir du monoxyde de carbone et un mécanisme rédox faisant intervenir une espèce oxygène à la surface a été proposé. Lorsque la vitesse de réaction a été déterminée en augmentant la température par des écarts de 10 °C à partir de 300 °C, deux énergies d'activation ont été observées; 16 ± 0.5 kcal mol^{-1} de 350 à 400 °C et 11 ± 0.5 kcal mol^{-1} de 300 à 340 °C. La température à laquelle le changement se produit correspond étroitement à la température de Curie de l'oxyde.

L'utilisation possible de l'oxyde de manganèse(II) comme catalyseur ou constituant d'un catalyseur dans le processus de déplacement a été évaluée de façon critique. [Traduit par le journal]

Can. J. Chem., 51, 3520 (1973)

Introduction

It is well known that the rate of the water-gas shift reaction is a controlling parameter in many established industrial and technological catalytic processes (1). In recent years, new impetus has been given to studies of the reaction over solid catalysts by its importance in hydrocarbon fuel cell operations (2) and in the suppression or removal of gaseous pollutants from the exhausts of internal combustion engines (3).

Although many catalytic studies of the water-gas shift reaction have been reported, these are mainly directed towards the various technological aspects of the reaction and are generally focused on iron oxide-based catalysts (4). In a recent paper (5) the mechanism of the shift reaction on iron(III) oxide was re-examined using an isotope tracer technique and two possible reaction mechanisms were proposed; both of which involve the reaction between adsorbed carbon monoxide and either oxygen or hydroxyl species. Elsewhere, conclusions obtained from rate studies on chromium oxide (6) have been extended to explain the results of catalysis on copper chromite.

No detailed work has been reported on manganese oxides as catalysts for this reaction but their use as a catalyst stabilizer and promoter has received attention for a commercial shift catalyst containing zinc, copper, and chromium components (7). Hence, a kinetic study of the water-gas shift on manganese(II) oxide containing excess lattice oxygen, has been initiated. The general catalytic properties of this oxide are not yet well-defined and were only recently examined specifically in the heterogeneous decompositions of isopropanol (8, 9) and nitrous oxide (10).

Experimental

Apparatus and Procedure

The all-glass flow system and quartz reactor were described previously (11, 12). High-purity helium was used as the carrier gas at atmospheric pressure in the flow system and in the Beckman GC-5 gas chromatograph. Carbon monoxide, water, and carbon dioxide were analyzed by a thermal conductivity bridge at 110 °C using stainless-steel columns, 72 × 0.125 in., o.d., packed with "Poropak Q".

Can. J. Chem. Downloaded from www.nrcresearchpress.com by 210.87.254.6 on 09/05/12
For personal use only.

Can. J. Chem. Downloaded from www.nrcresearchpress.com by 210.87.254.6 on 09/05/12
For personal use only.

Surface areas were determined by low-temperature krypton adsorption (B.E.T.; -196 °C; $\sigma = 21.5$ Å^2).

To establish the experimental conditions for which the reaction rate was not influenced by external or internal diffusion, the influence of space velocity, catalyst mass, and particle size was studied in the usual manner (11). As a result of these preliminary experiments, kinetic measurements were conducted at a total flow rate of 350 ml min^{-1} (N.T.P.) which was equivalent to space velocities from 7.48 to 8.78 (cc gas) (cc. catalyst)$^{-1}$ s^{-1} between 300 and 400 °C.

All reaction rate measurements were made after the steady catalyst activity level was attained and the experimental rates were determined from the rates of carbon dioxide production. The validity of this procedure was established by obtaining a quantitative mass balance for all components at both 320 and 380 °C.

Materials

Manganese(II) oxide. A bulk quantity of α-manganese(III) oxide was prepared as described (9). A calculated amount of this oxide sample was placed in the reactor such that, after reduction, it would yield one gram of manganese(II) oxide. All catalyst samples were pretreated for 5 h at 380°C in the standard water-gas mixture consisting of a 350 ml min^{-1} (N.T.P.) stream of helium containing 40 Torr carbon monoxide and 16 Torr water vapor.

The methods used for the chemical and structural analyses of the catalyst have been described (8, 9).

Carbon monoxide (C.P.; 99.5% minimum), carbon dioxide (Coleman; 99.99%), hydrogen (ultra-high purity; 99.999%), and helium (high purity; 99.995%) were supplied by Matheson of Canada Ltd. and the water in the gas-saturators was de-ionized and boiled prior to use.

Electron transmission micrographs were recorded with a Philips EM 300G electron microscope at 100 kV. Specimens were crushed in an agate mortar and suspended in *n*-butanol. Drops of the suspension were placed on the carbon-support film on 200 mesh copper grids, and the alcohol subsequently removed by evaporation at 10^{-5} Torr.

Results

The Nature of the Catalyst

Analysis of the catalysts after reduction indicated a bulk stoichiometry of $MnO_{1.0}$ but as reported earlier (8) the samples contained enough excess oxygen to retain the black color associated with manganese(III) oxide (13). The colors of the catalyst samples varied slightly with the temperature and time of exposure to the water-gas mixture; catalysts used at 300 °C were darker than those used for periods longer than 24 h at 380 °C. The X-ray powder diffraction patterns of all used catalyst samples showed characteristic lines of manganese(II) oxide only and this together with the chemical analyses of several samples, verified the catalyst composition. Prior to analysis, the pyrophoric catalysts were cooled to room temperature in helium at 100 ml min^{-1} (N.T.P.) before removal from the catalyst reactor in order to prevent spontaneous oxidation.

Rate measurements were recorded after allowing the catalyst to equilibrate in the standard water-gas mixture for 300 min. Constant activity was observed after 100 min exposure time.

Stoichiometric manganese(II) oxide, which was prepared by reducing α-Mn_2O_3 with a surface area 16.5 $\pm$ 0.5 m^2 g^{-1} for 12 h in 600 ml min^{-1} (N.T.P.) of hydrogen at 600 °C (14), yielded catalysts with a surface area 14.5 m^2 g^{-1} and the 12% loss in surface area could not explain the very low activity; less than 1% of that prepared by reduction in the standard water-gas mixture. The stability of the latter catalysts, after continuous exposure to the water-gas mixture for 24 h, showed a decrease of activity per m^2 of less than 10% at 380 °C and a much smaller decrease at 320 °C. Both surface areas and electron transmission micrographs of the catalysts, determined after various periods of exposure, indicated that oxide sintering was an important factor in this loss of activity.

Electron transmission micrographs of the catalyst immediately after the standard pretreatment showed the presence of small crystallites, approximately 700 Å diameter, which were fused into highly irregular macro-structures averaging 0.06 mm in diameter. The irregularity of the fused crystallites diminished with prolonged reaction times at the higher temperatures. Dark-field electron transmission micrographs of sintered samples indicated that large assemblies of crystallites were fused mainly into preferred crystal orientations in contrast to the random distribution expected in the absence of sintering.

Figure 1 shows (*A*) the electron transmission micrograph typical of a freshly prepared catalyst sample; (*B*) the transmission micrograph of a sample exposed at 380 °C for 24 h to the standard water-gas mixture (microscope magnification × 26 000; total magnification × 120 000) and (*C*) the dark-field micrograph of (*B*) (microscope magnification × 26 000; total magnification × 55 000).

These observations were substantiated by surface area measurements which were reproducible on any given sample to within $\pm$0.5 m^2 g^{-1}. Thus, the surface area of a freshly-prepared catalyst sample, 16.5 m^2 g^{-1}, decreased to 16.0 m^2 g^{-1} after 6 h exposure to the standard water-

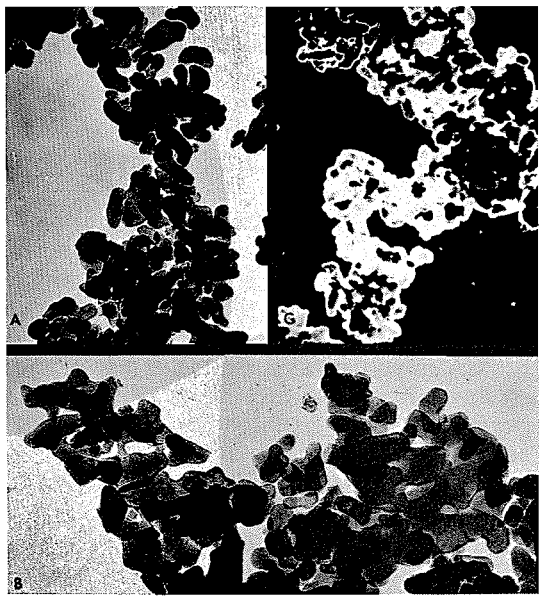

FIG. 1. Electron micrograph (*A*) of a freshly prepared catalyst sample; (*B*), a sample exposed at 380 °C for 24 h to the standard water–gas mixture showing crystallite sintering, (both microscope magnifications × 26 000 and total magnifications × 120 000); and (*C*) the dark-field micrograph of (*B*) (microscope magnification × 26 000 and total magnification × 55 000).

gas mixture at 380 °C, whereas exposures at 320 °C for 7 h did not yield any measurable change in the surface area. After exposure of the catalyst for 48 h at 380 °C the surface area was 14.5 m^2 g^{-1}.

The Relationship between Exposure Time and the Reaction Orders

Reaction orders with respect to carbon monoxide, hydrogen, carbon dioxide, and water vapor were determined at 320 and 380 °C on catalyst samples which had been exposed to the standard water-gas mixture for a maximum of 12 h. Further, reaction orders were re-determined on catalysts which had been exposed to the same mixture for more than 48 h at both these temperatures and no change was observed in the order results.

The Effects of Variations of the Partial Pressures of Carbon Monoxide, Water Vapor, Hydrogen, and Carbon Dioxide on the Reaction Rate

Rate orders were determined at 320 and 380 °C. For carbon dioxide and hydrogen rate-order determinations, the partial pressures of carbon monoxide and water vapor were kept constant at 40 and 16 Torr, respectively. The reaction-rate data are summarized in Table I and the logarithmic plots for the determination of the reaction orders are shown in Fig. 2. Thus, separate variation of the partial pressures of hydrogen from 5.4 to 65.1 Torr, and carbon dioxide from 10.9 to 87.0 Torr showed an overall zero order dependence of the rate of reaction on the partial pressures of both components at each temperature. Similarly, variation of the water vapor pressure from 4 to 56 Torr, while maintaining the carbon monoxide partial pressure at 40 Torr, did not influence the rate of reaction.

The effect of varying the carbon monoxide partial pressure, while maintaining the partial pressure of water vapor at 16 Torr at both temperatures, indicated a reproducible order of 0.75 with respect to carbon monoxide partial pressure in the range 20 to 80 Torr. At 320 °C, this order changed to 0.5 in the partial pressure range 100 to 240 Torr, Fig. 2.

TABLE 1. The effect of variations of the partial pressures of carbon monoxide, water, hydrogen, and carbon dioxide on the rate of the water–gas shift reaction

Component	Partial pressure (Torr)	Rate of reaction × 10^8 (mol m^{-2} s^{-1}) 380 °C	320 °C
Carbon monoxide (p_{H_2O} = 16 Torr)	20	4.84	2.19
	30	—	2.79
	40	8.51	3.39
	60	11.48	4.73
	80	14.79	5.28
	100	18.41	6.76
	120	—	7.50
	174	—	8.59
	240	—	10.47
Water (p_{CO} = 40 Torr)	4	8.22	3.48
	16	8.51	3.68
	32	8.41	3.67
	48	8.32	3.67
	56	8.32	3.68
Hydrogen (p_{CO} = 40 Torr; p_{H_2O} = 16 Torr)	5.4	8.59	—
	21.7	8.71	4.03
	32.6	—	3.98
	54.3	8.67	3.99
	65.1	8.61	3.98
Carbon dioxide (p_{CO} = 40 Torr; p_{H_2O} = 16 Torr)	10.9	8.51	3.85
	43.4	8.13	3.67
	65.0	8.13	3.76
	87.0	8.22	3.80

Can. J. Chem. Downloaded from www.nrcresearchpress.com by 210.87.254.6 on 09/05/12
For personal use only.

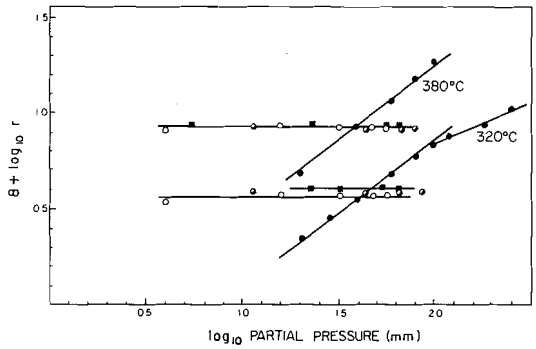

FIG. 2. The effects of variations in the partial pressures of carbon monoxide (●), water vapor (○), carbon dioxide (◑), and hydrogen (■) on the reaction rates at 320 and 380 °C. (for experimental details, see text).

Thus, the rate of reaction r(mol m^{-2} s^{-1}), can be represented as:

[1] $$r = k(p_{CO})^{0.75} \quad (20 \leqslant p_{CO} \leqslant 80 \text{ Torr})$$

and

[2] $$r = k(p_{CO})^{0.5} \quad (100 \leqslant p_{CO} \leqslant 240 \text{ Torr})$$

The Isolated Effects of Components of the Water-Gas Mixture on the Catalyst Surface

A stabilized catalyst sample was exposed to 50 Torr of carbon dioxide in a total gas flow rate of 350 ml min^{-1} (N.T.P.). At 380 °C this resulted in a 98% conversion to carbon monoxide after 7 min exposure. This conversion decreased to zero after 45 min, curve *B*, Fig. 3. When 40 Torr of carbon monoxide was immediately introduced in a separate experiment, an initial 53% conversion to carbon dioxide was measured 6 min later which decreased to zero after 35 min, curve *A*, Fig. 3. Subsequent treatment with 16 Torr of water vapor for 30 min followed by 40 Torr of carbon dioxide did not yield any carbon monoxide. Then, the introduction of the standard water-gas mixture immediately showed a 44% increase in the rate of reaction which returned to the steady level after 30 min; inset Fig. 3, curve *C*.

These results imply that the manganese(II) oxide surface is subject to a reversible redox process with either water vapor or carbon dioxide acting as oxidizing agents and carbon monoxide as a reducing agent for the oxidized surface.

If this enhanced initial activity was associated with the presence of excess surface oxygen, then, an initially lower rate of reaction might be expected to occur on a surface reduced with carbon monoxide. Hence, the stabilized catalyst was

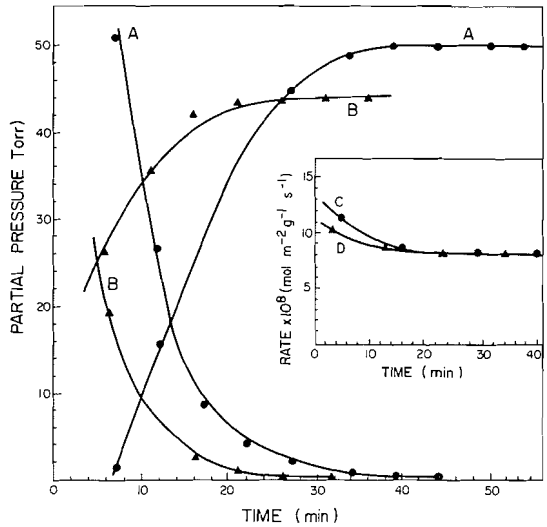

FIG. 3. The isolated effects of carbon monoxide (*A*) and carbon dioxide (*B*) at 380 °C. Inset: the rate of conversion after carbon dioxide (*C*) and carbon monoxide (*D*) treatments.

treated first with 40 Torr of carbon monoxide for 30 min followed immediately by the standard water-gas mixture. Contrary to the expected decrease in reaction rate, a 38% increase was recorded that returned to the original rate of reaction after 20 min; inset Fig. 3, curve *D*.

The Effect of Temperature on the Reaction Rate

The rate of reaction was determined from 300 to 400 °C at progessive 10 °C intervals. After the standard pretreatment, the temperature was lowered to 300 °C and the catalyst left for 9 h in contact with the standard water-gas mixture before determining the rate.

Rate constants were calculated by integration of the rate eq. 1 as a function of concentration rather than partial pressure and the values obtained used in an Arrhenius plot to establish the apparent activation energy, Fig. 4. The plot, curve *A*, shows two distinct regions with activation energies of 16 ± 0.5 kcal mol^{-1} from 350 to 400 °C and 11 ± 0.5 kcal mol^{-1} from 300 to 340 °C. The pre-exponential factors were 1.8×10^9 and 3.7×10^7 molecules$^{0.25}$ $l^{-0.25}$ m^{-2} s^{-1}, respectively. This change in the value of the apparent activation energy was easily reproducible on fresh catalyst samples. When the rates were measured at decreasing 10 °C intervals from 400 to 300 °C using either fresh samples or those previously exhibiting a change in activation energy,

Can. J. Chem. Downloaded from www.nrcresearchpress.com by 210.87.254.6 on 09/05/12
For personal use only.

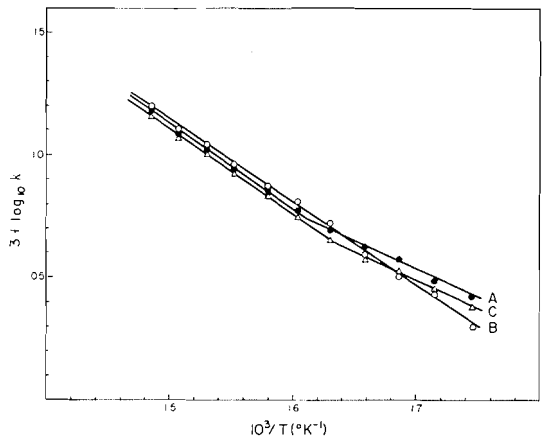

FIG. 4. Arrhenius plots of the reaction rates of the water-gas shift reaction on manganese(II) oxide from 300 to 400 °C. Curves *A* and *C* determined for step-wise temperature increments from 300 to 400 °C; curve *B*, determined from 400 to 300 °C.

a reproducible linear relationship was observed over the entire temperature range with an apparent activation energy of 16 ± 0.5 kcal mol^{-1}, and a pre-exponential factor 1.2 × 10^9 $molecules^{0.25}$ $l^{-0.25}$ m^{-2} s^{-1}, Fig. 4, curve *B*. It is worth noting that the observed change in value of the activation energy corresponds with the Curie temperature of manganese(II) oxide, 337 °C (15).

In order to substantiate these results, the water vapor partial pressure was increased from 16 to 40 Torr while the carbon monoxide partial pressure was maintained at 40 Torr, and the catalyst temperature was again increased in a stepwise fashion. The Arrhenius plot, Fig. 4, curve *C*, showed two distinct regions with activation energies of 16 ± 0.5 kcal mol^{-1} from 350 to 400 °C and 11 ± 0.5 kcal mol^{-1} from 300 to 340 °C with corresponding pre-exponential factors of 1.4 × 10^9 and 2.2 × 10^9 $molecules^{0.25}$ $l^{-0.25}$ m^{-2} s^{-1}, respectively. An activation energy of 18 kcal mol^{-1} has been reported (16) for this catalyst assuming first order kinetics.

Discussion

Previously, the mechanism of the water-gas shift reaction on an iron(III) oxide catalyst promoted with chromium oxide (17) has been interpreted as proceeding via a two-step alternating oxidation–reduction scheme while a concerted redox mechanism has been proposed from results on iron–chromium oxides (18) and copper chromite (19) catalysts. The possibility that rate control is exercised within the surface interactions that take place between adsorbed carbon monoxide and water has been considered to occur on iron(III) oxide based catalysts (4) while an alternative mechanism involving the formation of surface formate species on zinc(II) oxide (20) and magnesium(II) oxide (20, 21) has also been suggested. However, studies of the decomposition of formic acid on manganese(II) oxide (22) have indicated that the formation of formate intermediates is not involved in the water-gas shift reaction on this catalyst from 300 to 400 °C.

Various assumptions were made, in the usual way, with respect to the rate-determining step in the shift reaction and the most satisfactory model was obtained by assuming that rate control was associated with the surface reactions. Thus, if the rate of reaction, r, is determined by the surface coverage, θ, of both carbon monoxide and water absorbed on sites specific to each species, then:

$$[3] \qquad r = k\theta_{CO}\theta_{H_2O}$$

and if θ_{CO} and θ_{H_2O} obey the simple Langmuir relationship, eq. 3 becomes:

$$[4] \qquad r = \frac{k b_{CO} p_{CO} b_{H_2O} p_{H_2O}}{(1 + b_{CO}p_{CO})(1 + b_{H_2O}p_{H_2O})}$$

which is commonly known to describe the Langmuir–Hinshelwood mechanism.

Since it is reasonable to assume from the effect of water-vapor partial pressure on the reaction rate that the amount of water vapor adsorbed is fixed, for example if the water adsorption sites are saturated, then the term $(b_{H_2O}p_{H_2O})$ could be considered constant, so that eq. 3 can be reduced to:

$$[4a] \qquad r = \frac{b_{CO}p_{CO}}{\alpha(1 + b_{CO}p_{CO})}$$

or

$$[5] \qquad \frac{1}{r} = \beta\frac{1}{p_{CO}} + \alpha$$

where $\alpha = (1 + b_{H_2O}p_{H_2O})/(kb_{H_2O}p_{H_2O})$ and $\beta = \alpha/b_{CO}$.

The Langmuir-type plots of $(1/r)$ *vs.* $(1/p_{CO})$ are shown in Fig. 5. Linear plots were obtained over the entire partial pressure range studied from 20 to 240 Torr at 320 °C and 20 to 100 Torr at 380 °C.

The observation that the water-gas conversion can be maintained at the lowest water vapor

Can. J. Chem. Downloaded from www.nrcresearchpress.com by 210.87.254.6 on 09/05/12
For personal use only.

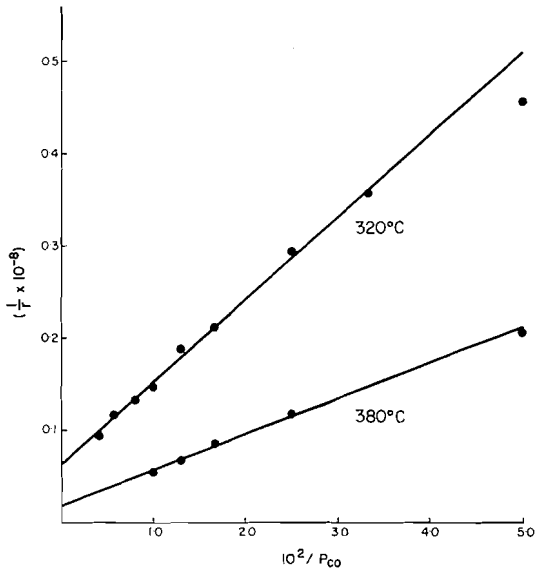

FIG. 5. Langmuir-type plots for the water-gas shift reaction on manganese(II) oxide at 320 and 380 °C.

partial pressure appears to justify the assumption that the amount of adsorbed water vapor is constant. Rapid saturation of adsorption sites specific to water or slow desorption would be expected to result in the observed zero-order correspondence in the experimental rate expression (1).

The derived rate equation (4*a*) also predicts a decrease in the rate of reaction when $\alpha(1 + b_{CO}p_{CO}) > b_{CO}p_{CO}$. This is in agreement with the experimental change detected in the carbon monoxide reaction order from 0.75 in the partial pressure region 20 to 100 Torr, to 0.5 between 120 and 240 Torr. Thus, the 38% increase in the rate of conversion observed after the carbon monoxide pretreatment, curve *D*, Fig. 3, may be associated with an increase in the surface coverage of carbon monoxide as a result of the pretreatment.

A useful indication of the nature of the reaction mechanism can be obtained from the results of the experiments shown in Fig. 3. Thus the surface of the catalyst is susceptible to a reversible oxidation–reduction process since either carbon dioxide or water vapor can act separately as oxidizing agents, as shown, for example, by the 44% increase in the rate of conversion of the water-gas mixture immediately after the pretreatments with water vapor and carbon dioxide. Further, the green manganese oxide with a surface area 14.5 $m^2\ g^{-1}$, prepared by reduction of α-Mn_2O_3 in hydrogen at 600 °C, gave less than 1% of the rate of conversion obtained with the catalyst prepared by reduction in the standard water-gas mixture and a surface area of 16.0 $m^2\ g^{-1}$. Clearly the conversion rate process is sensitive to the stoichiometry of the catalyst studied.

On the basis of the present findings, the mechanism of the surface reaction may be summarized:

$$[6] \qquad CO_{(ads)} + [O] \rightarrow CO_{2(g)} + [\ ]$$

$$[7] \qquad [\ ] + H_2O \rightarrow H_{2(g)} + [O]$$

where [O] and [ ] represent an oxygen atom or ion and an oxide vacancy on the surface of the catalyst, respectively. The rate-determining step is then the reaction between adsorbed carbon monoxide and some surface oxygen species (6).

Studies of the simultaneous dehydrogenation and dehydration of 2–propanol on manganese(II) oxide (9) have shown that the water vapor partial pressure has virtually no effect on the dehydrogenation process but that the dehydration process is inhibited which implies that specific dehydrogenation and dehydration sites exist on the surface of this catalyst. The observed zero order rate dependence on the water vapor partial pressure in the shift reaction suggests that reaction 7 may occur on the dehydrogenation sites since this reaction can be regarded as dehydrogenation. Also the decomposition of N_2O on manganese oxides (10) of variable metal oxidation states has been explained by a redox-type mechanism which is facilitated by the presence of Mn^{III} sites and it was proposed that oxidation reactions should be assisted by conditions that tend to preserve the 3+ oxidation state of the metal. Such a proposal is also consistent with the present results, and the following surface scheme may be suggested here for steady-state catalysis.

The amount of excess surface oxygen would be maintained at a constant level during the course of the conversion. An essentially similar scheme has been proposed to account for catalysis on copper chromite (19).

The results of oxygen-exchange reactions on manganese(IV) oxide indicate that non-uniform oxygen species are present on the oxide surface (23). And while other relevant studies (24) have shown that surface Mn(III)—O bonds are weaker than those formed between manganese(II)

Can. J. Chem. Downloaded from www.nrcresearchpress.com by 210.87.254.6 on 09/05/12
For personal use only.

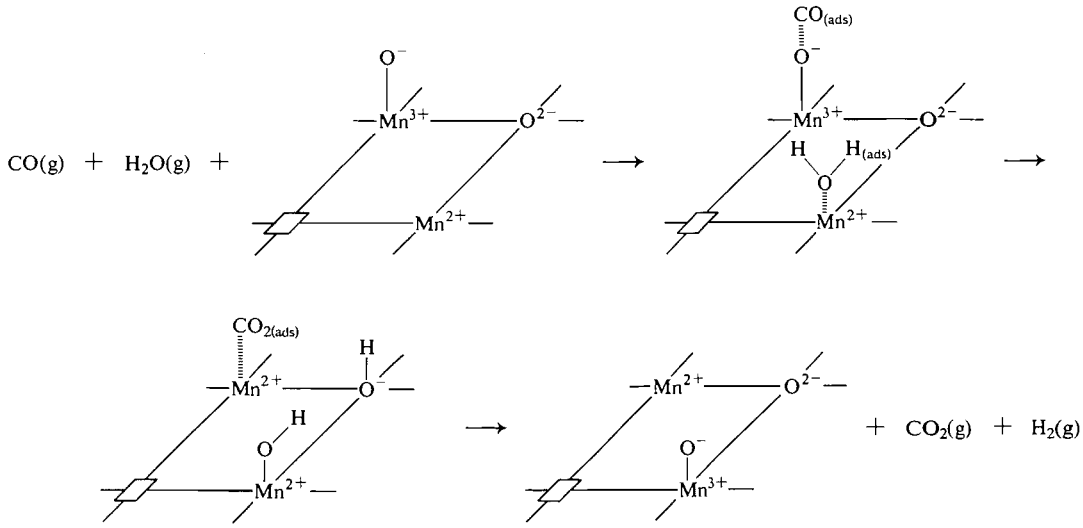

and oxygen, there is also clear evidence that at least two forms of chemisorbed oxygen are present on manganese(II) oxide (10). Hence it is proposed that the change in the value of the apparent activation energy at 340 to 350 °C may be associated with a switch from one type of active surface oxygen species in the reaction to another during the course of the temperature rise. The exact nature of these species is still uncertain (10) but the close correspondence between the temperature at which the apparent activation energy changes and the Curie transition from ferromagnetic to paramagnetic properties of the oxide at 337 °C may be significant. The constant value of the apparent activation energy found from curve *B*, Fig. 4 is believed to be a consequence of the removal or destruction of low-temperature active oxygen sites due to oxide sintering at the higher temperatures before and during the stepwise decrease in temperature from 400 °C. The possibility of characterizing these surface species presents an interesting problem for further study.

It may be concluded that the use of manganese(II) oxide as a major component in commercial shift catalysts would be most favored at temperatures around 300 °C. The major long-term deterioration in the catalytic activity of the oxide would be associated with solid sintering and the loss of excess surface oxygen. It has been observed previously that the conversion efficiency of commercial iron oxide (4) and mixed iron/chromium oxide (25) catalysts is known to fall off as a result of sintering.

We thank Dr. E. F. McCaffrey and Dr. I. M. Hoodless for helpful suggestions and Mr. A. J. MacKenzie and Mr. S. Spivak for expert technical assistance.

1. O. A. Hougen and K. M. Watson. Chemical process principles. Part. III. John Wiley and Sons Inc., New York. 1966. R. M. Stephenson. Introduction to the chemical process industries. Reinhold. 1966. p. 301.
2. K. R. Williams and A. G. Dison. *In* Fuel cell systems. Vol. 2. *Edited by* R. F. Gould. American Chemical Society Publication. 1969.
3. W. C. Gardiner, Jr. Rates and mechanisms of chemical reactions. W. A. Benjamin, Inc., New York. 1969.
4. H. Bohlbro. An investigation on the kinetics of the conversion of carbon monoxide with water vapour over iron oxide based catalysts. Gjellerup, Copenhagen. 1969.
5. S. Oki, J. Happel, M. Hnatow, and Y. Kaneko. Preprint, 5th International Congress on Catalysis, Florida, 1972. North Holland, Amsterdam.
6. G. K. Boreskov, V. Sh. Gruver, and T. M. Yur'eva, Kinet. Katal. **10**, 294 (1969); **10**, 862 (1969).
7. P. Putanov and Z. Jovanovic. Chem. Abstr. **74**, 130840n (1971).
8. E. F. McCaffrey, D. G. Klissurski, and R. A. Ross. J. Catal. **26**, 380 (1972).
9. D. G. Klissurski, E. F. McCaffrey, and R. A. Ross. Can. J. Chem. **49**, 3778 (1971).
10. A. Cimino and V. Indovina. J. Catal. **17**, 54 (1970).
11. R. A. Ross and B. G. Walsh. J. Appl. Chem. **11**, 469 (1961).
12. A. B. Hart, J. McFadyen, and R. A. Ross. Trans. Faraday Soc. **59**, 1458 (1963).
13. M. Ellis, T. E. Moore, and P. W. Selwood. J. Am. Chem. Soc. **72**, 856 (1950).

Can. J. Chem. Downloaded from www.nrcresearchpress.com by 210.87.254.6 on 09/05/12
For personal use only.

14. P. C. RICHARDSON and D. R. ROSSINGTON. J. Catal. **14**, 175 (1969).
15. YA. M. KSENDZOV and V. V. MAKAROV. Sov. Phys. – Solid State, **12**, 2559 (1971).
16. G. K. BORESKOV, V. A. CHIRGINA, L. S. EGOROVA, V. V. POPOVSKII, and T. M. YUR'EVA. Kinet. Katal. **12**, 140 (1971).
17. N. V. KULKOVA and M. I. TEMKIN. Zhur. Fiz. Khim. **23**, 695 (1949).
18. G. V. BORESKOV, A. S. SERGEEVA, and T. M. YUR'EVA. Kinet. Katal. (Engl.), **11**, 1476 (1970).
19. G. K. BORESKOV, V. SH. GRUVER, and T. M. YUR'EVA. Kinet. Katal., **10**, 862 (1969).
20. T. ONISHI, K. TAMARA, A. UENO, and T. YAMAMOTO. Bull. Chem. Soc. Jap. **42**, 3040 (1969).
21. J. J. F. SCHOLTEN, P. MARS, P. G. MENON, and R. VAN HARDEVELD. Proc. 3rd Int. Congr. on Catal. 1965. (Amsterdam, 1964). p. 881.
22. B. W. KRUPAY and R. A. Ross. To be published.
23. G. K. BORESKOV and L. A. KASATKINA. Russ. Chem. Rev. (Engl.), **37**, 613 (1968).
24. G. K. BORESKOV. Advan. Catal. Relat. Subj. **15**, 285 (1964).
25. J. HOOGSCHAGEN and P. ZWIETERING. J. Chem. Phys. **21**, 2224 (1953).

Can. J. Chem. Downloaded from www.nrcresearchpress.com by 210.87.254.6 on 09/05/12
For personal use only.

Solubility Products of Aluminum Hydroxide in Various Ionic Solutions

DAVID T. Y. CHEN

Department of Chemistry, New Asia College, The Chinese University of Hong Kong, Shatin, Hong Kong

Received January 2, 1973

Solubility products of $Al(OH)_3$ were determined in various solutions of NH_4^+, Li^+, Na^+, K^+, and Ca^{2+} ions. Increasing amounts of these hydroxides were added to the respective chloride solutions containing aluminum chloride. The solutions were aged for 3 months. Activities of the OH^- ions were calculated from the p*H* values of the solutions. The total Al concentrations remaining in solutions were determined by Hsu's modified aluminon method. The Al^{3+} ion concentrations were computed using the hydrolysis equilibria of Aveston. The ion product, $a_{Al^{3+}}(a_{OH^-})^3$, was found to vary linearly with the [OH]/[Al] ratio. The solubility product of $Al(OH)_3$ was obtained by extrapolating this ratio to 3. The pK_{sp} values thus obtained were 30.55, 33.15, 30.75, 30.36, and 31.00 in NH_4^+, Li^+, Na^+, K^+, and Ca^{2+} systems respectively. The anomalously low solubility product of $Al(OH)_3$ in the Li^+ system was attributed to the specific "lithium effect".

Les produits de solubilité de $Al(OH)_3$ ont été déterminés dans diverses solutions d'ions NH_4^+, Li^+, Na^+, K^+ et Ca^{2+}. Des quantités croissantes d'hydroxydes ont été ajoutées aux solutions respectives de chlorure contenant du chlorure d'aluminium. Les solutions dataient de 3 mois. Les activités des ions OH^- ont été calculées à partir des valeurs du p*H* des solutions. Les concentrations totales en Al restant en solution ont été déterminées par la méthode modifiée de l'aluminon selon Hsu. Les concentrations en ions Al^{3+} ont été calculées d'après les équilibres d'hydrolyse d'Aveston. Le produit ionique $a_{Al^{3+}}(a_{OH^-})^3$ varie linéairement avec le rapport (OH)/(Al). Le produit de solubilité de $Al(OH)_3$ a été obtenu par extrapolation de ce rapport à 3. Les valeurs pK_{sp} ainsi obtenues ont été de 30.55, 33.15, 30.75, 30.76 et 31.00 pour les systèmes NH_4^+, Li^+, Na^+, K^+ et Ca^{2+} respectivement. Le produit de solubilité anormalement bas de $Al(OH)_3$ dans le système Li^+ a été attribué à l'effet spécifique de lithium.

[Traduit par le journal]

Can. J. Chem., **51**, 3528 (1973)

Introduction

In work described in a previous paper (1) it was found that the thermodynamic solubility product of $Al(OH)_3$ was different when different cations, NH_4^+, Li^+, K^+, were present as counter ions. In that work, bentonite was also present in the system. It might be suspected that the observed difference in the solubility product could be attributed to the presence of clay; $Al(OH)_3$ might form some sort of complex or double salts with different types of clay. It is therefore desirable to investigate the solubility product in the absence of clay and this has been done in the present work.

The solubility product of $Al(OH)_3$ has been investigated by many authors, with considerable discrepancies between the results. Gayer *et al.* (2), for example, obtained a pK_{sp} value of 32.96, Korenman *et al.* (3) one of 29.92. Using a polarographic method, Kovalenko and Nestorovich (4) deduced a pK_{sp} value of 30.32 at 22 °C. Frink and Peech (5) obtained an experimental pK_{sp} value of 33.5, and calculated a pK_{sp} value of 33.8 from thermodynamic data. Recently Turner and Brydon (6) observed that the solubility product of $Al(OH)_3$ in a clay system depends on the amount of $Al(OH)_3$ precipitated; when this amount is large, the pK_{sp} value is 33.0, while when this amount is small, the pK_{sp} value is greater than 33.0. Singh (7) obtained a pK_{sp} value of 33.6 ± 0.1 in the presence of clay. In a later paper (8), the same author reported that the pK_{sp} value of $Al(OH)_3$ in the absence of clay depends on the aluminum ion concentration; the value is 32.1, 32.7, and 33.0 when the latter is 10^{-4}, 10^{-3}, and 10^{-2} *M* respectively.

Experimental

The solubility product of $Al(OH)_3$ in K^+ system was determined by mixing $AlCl_3$ with an equivalent amount of KOH. A solution of 10.0 ml of 0.25 *M* $AlCl_3$ and a solution of 20.0 ml of 1.00 *M* KCl were mixed in a 250 ml Erlenmeyer flask. Then 83.3 ml of 0.090 *M* KOH solution was added slowly with constant shaking, and the mixture was diluted to 200 ml with redistilled water. p*H* measurements were carried out from time to time, using a Metrohm Herisau E388 compensator which can be accurately read to three figures. In the final measurement of p*H*, temperature of the solution was adjusted to 25 °C. After 3 months of aging, the solution was filtered through Whatman No. 42 filter paper and aliquots were taken for analysis. The solubility products of $Al(OH)_3$ in other sys-

Can. J. Chem. Downloaded from www.nrcresearchpress.com by 210.87.254.5 on 09/05/12
For personal use only.

Can. J. Chem. Downloaded from www.nrcresearchpress.com by 210.87.254.5 on 09/05/12
For personal use only.

tems were determined in the following way. A solution of 10.0 ml of 0.25 *M* $AlCl_3$ and 20.0 ml of 1.00 *M* of different alkali chloride solutions were mixed in separate 250 ml Erlenmeyer flasks. Different amounts of approximately 0.1 *M* alkali hydroxide solutions were added to each flask to produce different degrees of turbidity. The mixtures were all diluted to a final volume of 200 ml with redistilled water. The supernatant liquids remained cloudy even after $3\frac{1}{2}$ months of aging. Clear solutions could not be obtained by filtration or high speed centrifugation (10 000 r.p.m. for 1 h). The colloidal suspensions were dialyzed with 0.01 *M* sodium acetate and acetic acid buffer of the same p*H* as that of the sample. Cellulose dialyzing sacs made by the Arthur H. Thomas Company were used, the colloidal suspensions and buffer solutions being shaken overnight to attain equilibrium. In both cases, aluminum contents were determined using Hsu's improved aluminon method (9).

Theoretical

The activities of the OH^- ions were calculated from the p*H* values of the solutions. The activities of the Al^{3+} ions were calculated from their concentrations and their activity coefficients. There are many equations available for computing the activity coefficient of an ionic species; they yield different values. The Debye–Hückel limiting law gives very low values. The Debye–Hückel equation gives slightly higher values than the Davies equation (10). The extended Debye–Hückel equation with the salting out term yields the highest values. The author believes that the large discrepancies among the solubility product data of a certain substance reported by different workers are, at least in part, due to their ways of calculating the activity coefficient. Grunwald and Fong (11) found that the extended Debye–Hückel equation was unsatisfactory and claimed that the value of *a* in the Debye–Hückel equation should be taken as 6 Å. Although different pK_{sp} values were obtained by employing different equations for activity coefficients, the general trend was the same. In the present treatment, the Debye–Hückel equation is used. With $z = 3$, the activity for Al^{3+} ion is

$$[1] \qquad \log \gamma_{Al^{3+}} = \frac{-4.58\sqrt{\mu}}{1 + 1.97\sqrt{\mu}}$$

In computing the ionic strength, the total Al concentration found experimentally was considered as Al^{3+}.

Aluminum exists as several species in aqueous solution. The hydrolysis of Al^{3+} ion has been studied by many workers; different conclusions were obtained. Thus, Brosset and co-workers (12) suggested that aluminum probably exists as a polynuclear complex $Al_6(OH)_{15}^{3+}$ in neutral and weakly acid solutions. Aveston (13) suggested the existence of polynuclear species $Al_2(OH)_2^{4+}$ and $Al_{13}(OH)_{32}^{7+}$. Grunwald and Fong (11) suggested that only the dimer $Al_2(OH)_4(H_2O)_8^{4+}$ was present in solution of an aluminum salt and the existence of this dimer was confirmed by Akitt, Greenwood, and Lester (14) using ^{27}Al n.m.r. technique. The reason that other polynuclear complexes were not found by these authors is certainly due to the high acidity of their system (p$H = 3$). In the present case, the p*H* of the solutions was as high as 5 and even up to 8; therefore the equilibria suggested by Aveston (13) was adopted to calculate the activity of Al^{3+} ion present in the solution. According to Aveston, Al^{3+} ion hydrolyzes in aqueous solution with the existence of the following equilibria:

$$[2] \qquad 2Al^{3+} + 2H_2O \rightleftharpoons Al_2(OH)_2^{4+} + 2H^+$$

$$[3] \quad K_1 = \frac{[Al_2(OH)_2^{4+}]\gamma_{Al_2(OH)_2^{4+}}(a_{H^+})^2}{[Al^{3+}]^2(\gamma_{Al^{3+}})^2} = 10^{-7.07}$$

and

$$[4] \qquad 13Al^{3+} + 32H_2O \rightleftharpoons Al_{13}(OH)_{32}^{7+} + 32H^+$$

$$[5] \quad K_2 = \frac{[Al_{13}(OH)_{32}^{7+}]\gamma_{Al_{13}(OH)_{32}^{7+}}(a_{H^+})^{32}}{[Al^{3+}]^{13}(\gamma_{Al^{3+}})^{13}} = 10^{-104.5}$$

where *a* denotes activities, the square brackets denote concentrations, and γ denotes activity coefficients. From [3] we obtain

$$[6] \quad [Al_2(OH)_2^{4+}] = \frac{10^{-7.07}(\gamma_{Al^{3+}})^2}{\gamma_{Al_2(OH)_2^{4+}}(a_{H^+})^2}[Al^{3+}]^2$$

From [5], we have

$$[7] \quad [Al_{13}(OH)_{32}^{7+}] = \frac{10^{-104.5}(\gamma_{Al^{3+}})^{13}}{\gamma_{Al_{13}(OH)_{32}^{7+}}(a_{H^+})^{32}}[Al^{3+}]^{13}$$

To evaluate the ratio of activity coefficients of two species, the Debye–Hückel's limiting law was simply employed, *i.e.*

$$[8] \qquad \log \gamma_i = -0.509\, z_i^2 \sqrt{u}$$

The following relationships are thus obtained:

$$[9] \qquad \frac{\log \gamma_{Al_2(OH)_2^{4+}}}{\log \gamma_{Al^{3+}}} = 1.78$$

$$[10] \qquad \frac{\log \gamma_{Al_{13}(OH)_{32}^{7+}}}{\log \gamma_{Al^{3+}}} = 5.44$$

or

$$[11] \qquad \gamma_{Al_2(OH)_2^{4+}} = \gamma_{Al^{3+}}^{1.78}$$

$$[12] \qquad \gamma_{Al_{13}(OH)_{32}^{7+}} = \gamma_{Al^{3+}}^{5.44}$$

On the assumption that all other complex species are present to a negligible extent, the following relationship holds,

$$[13] \quad 13[Al_{13}(OH)_{32}^{7+}] + 2[Al_2(OH)_2^{4+}] + [Al^{3+}] = [Al_t]$$

where $[Al_t]$ is the experimentally determined concentration of all the Al species in solution. Substituting eq. 6, 7, 11, and 12 into eq. 13, simplifying, and replacing $\gamma_{Al^{3+}}$ simply by γ, we obtain

$$[14] \quad \frac{13 \times 10^{-104.5}\gamma^{7.56}}{(a_{H^+})^{32}}[Al^{3+}]^{13} + \frac{2 \times 10^{-7.07}\gamma^{0.22}}{(a_{H^+})^2}[Al^{3+}]^2 + [Al^{3+}] - [Al_t] = 0$$

The concentration of the Al^{3+} ion was obtained from a computer solution of the above equation.

Results and Discussion

When alkali hydroxides were added slowly to aluminum salt solutions, the pH increased rapidly at first, then slowly. At the end of titration it again increased rapidly. Figure 1 shows typical titration curves of $AlCl_3$ in different systems. It is interesting to note that the pH of the solution in the NH_4^+ system was the highest when equal amounts of corresponding hydroxides were added to different systems. When all the Al^{3+} ions were precipitated, the pH of the solution in this system was the lowest.

The solubility products of $Al(OH)_3$ in different systems were first determined by the same method as that used in the K^+ system. Equivalent amounts of different alkali hydroxides were added separately to $AlCl_3$ solutions containing the corresponding alkali chlorides. The solutions were cloudy at first, but after standing overnight, white gelatinous precipitates were formed, the supernatant solutions remaining clear. The precipitates in the Na^+ and K^+ systems looked whiter and denser, while those in the Li^+ and NH_4^+ systems looked somewhat translucent.

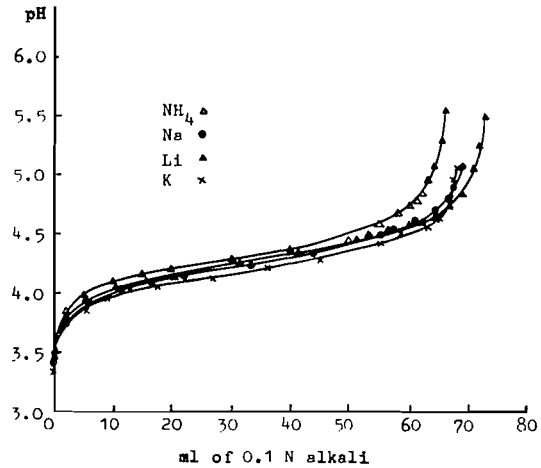

FIG. 1. Titration curves of $AlCl_3$ with hydroxides in different systems.

After aging for 3 months, the pH values of the solutions remained practically constant. The pK_{sp} values were then determined. The results are shown in Table 1. It is seen that only the solubility product of $Al(OH)_3$ in the K^+ system can be determined in this way; the solubilities of $Al(OH)_3$ in the other systems were too small to give determinable amounts of aluminum ions. Slightly different methods were then used to determine the solubility products of $Al(OH)_3$ in other systems, as described in the Experimental section. The results are shown in Tables 2 to 6. If the calculated pK_{sp} values in each system were plotted against the [OH]/[Al] ratio, straight lines were obtained, as shown in Fig. 2.

The solubility product of a crystalline precipitate should be independent of the reagent added, or the amount of precipitate formed.

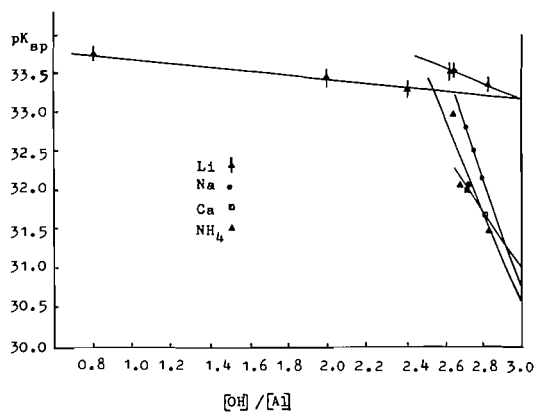

FIG. 2. Variation of pK_{sp} with [OH]/[Al].

Can. J. Chem. Downloaded from www.nrcresearchpress.com by 210.87.254.5 on 09/05/12
For personal use only.

TABLE 1. Solubility product of $Al(OH)_3$ when [OH]/[Al] = 3

	Value			
	NH_4^+	K^+	Na^+	Li^+
Initial pH	8.04	10.39	10.16	6.54
Final pH	7.68	8.27	8.07	5.54
$[Al_t]$ (M)	0	5.43×10^{-5}	Trace	0
μ		0.175		
γ		8.89×10^{-2}		
$[Al^{3+}]$		7.57×10^{-13}		
a_{OH^-}		1.86×10^{-6}		
pK_{sp}		30.36		

TABLE 2. Solubility product of $Al(OH)_3$ in NH_4^+ system

	Value for experiment No.:		
	1	2	3
0.100 M NH_4OH (added) (ml)	66.0	67.0	71.0
Final pH	4.16	4.82	5.88
$[Al_t]$ (M)	3.91×10^{-3}	5.48×10^{-3}	4.70×10^{-3}
μ	0.153	0.160	0.139
γ	9.72×10^{-2}	9.44×10^{-2}	1.04×10^{-1}
$[Al^{3+}]$	3.63×10^{-3}	3.22×10^{-4}	7.46×10^{-7}
a_{OH^-}	1.45×10^{-10}	6.61×10^{-10}	7.59×10^{-9}
[OH]/[Al]	2.64	2.68	2.84
pK_{sp}	32.97	32.06	31.47

TABLE 3. Solubility product of $Al(OH)_3$ in Na^+ system

	Value for experiment No.:		
	4	5	6
0.111 M NaOH (added) (ml)	62.0	61.2	63.0
Final pH	4.27	4.15	4.65
$[Al_t]$ (M)	6.22×10^{-3}	6.40×10^{-3}	6.27×10^{-3}
μ	0.164	0.165	0.164
γ	9.29×10^{-2}	9.25×10^{-2}	9.29×10^{-2}
$[Al^{3+}]$	5.21×10^{-3}	5.74×10^{-3}	8.54×10^{-4}
a_{OH^-}	1.86×10^{-10}	1.41×10^{-10}	4.47×10^{-10}
[OH]/[Al]	2.75	2.71	2.80
pK_{sp}	32.51	32.83	32.15

This is because crystalline precipitates have definite compositions. $Al(OH)_3$ is amorphous; its composition may not be definite. In systems where the [OH]/[Al] ratio is less than 3, there are surplus Al^{3+} ions in the solution. The $Al(OH)_3$ precipitate formed will definitely adsorb some Al^{3+} ions on its surface. Amorphous solids have very large surface area. Since they have no definite structure, there is really no difference between the precipitated Al^{3+} ions and the adsorbed Al^{3+} ions. Surface adsorption is almost a linear function of the concentration of the adsorbable substance when the latter is low. Therefore, we can expect that the composition of the aluminum hydroxide formed, *i.e.* the ratio of [OH]/[Al] in the precipitate, would be a linear function of the added [OH]/[Al] ratio. Since our results show that the pK_{sp} values are linear to the added [OH]/[Al] ratio, it must mean that the pK_{sp} value is also a linear function of the com-

Can. J. Chem. Downloaded from www.nrcresearchpress.com by 210.87.254.5 on 09/05/12
For personal use only.

Can. J. Chem. Downloaded from www.nrcresearchpress.com by 210.87.254.5 on 09/05/12
For personal use only.

TABLE 4. Solubility product of $Al(OH)_3$ in Li^+ system

	Value for experiment No.:		
	7	8	9
0.103 *M* LiOH (added) (ml)	65.2	64.3	69.0
Final p*H*	3.95	3.93	3.99
$[Al_t]$ (*M*)	4.50×10^{-3}	5.63×10^{-3}	5.30×10^{-3}
μ	0.159	0.163	0.160
γ	9.48×10^{-2}	9.32×10^{-2}	9.44×10^{-2}
$[Al^{3+}]$	4.35×10^{-3}	5.42×10^{-3}	5.05×10^{-3}
a_{OH^-}	8.91×10^{-11}	8.51×10^{-11}	9.77×10^{-11}
[OH]/[Al]	2.69	2.65	2.85
pK_{sp}	33.54	33.51	33.35

TABLE 5. Repeat determination of the solubility product of $Al(OH)_3$ in Li^+ system, using less LiOH

	Value for experiment No.:		
	10	11	12
0.100 *M* LiOH (added) (ml)	20.0	60.0	50.0
Final p*H*	3.74	3.94	3.89
$[Al_t]$ (*M*)	1.04×10^{-2}	9.50×10^{-3}	9.10×10^{-3}
μ	0.128	0.174	0.172
γ	1.09×10^{-1}	8.93×10^{-2}	9.00×10^{-2}
$[Al^{3+}]$	1.01×10^{-2}	8.90×10^{-3}	8.65×10^{-3}
a_{OH^-}	5.50×10^{-11}	8.71×10^{-11}	7.76×10^{-11}
[OH]/[Al]	0.80	2.40	2.00
pK_{sp}	33.74	33.28	33.44

TABLE 6. Solubility product of $Al(OH)_3$ in Ca^{2+} system

	Value for experiment No.:		
	13	14	15
0.044 *N* $Ca(OH)_2$ (added) (ml)	154.0	160.0	156.0
Final p*H*	4.88	5.54	4.80
$[Al_t]$ (*M*)	4.45×10^{-3}	8.90×10^{-4}	2.00×10^{-3}
μ	0.122	0.107	0.111
γ	1.13×10^{-1}	1.23×10^{-1}	1.20×10^{-1}
$[Al^{3+}]$	2.04×10^{-4}	4.05×10^{-6}	2.88×10^{-4}
a_{OH^-}	7.59×10^{-10}	3.47×10^{-9}	6.31×10^{-10}
[OH]/[Al]	2.72	2.83	2.75
pK_{sp}	32.00	31.68	32.06

position of the precipitate. If the pK_{sp} values were extrapolated to the added [OH]/[Al] ratio of 3, the value obtained should represent the true pK_{sp} of $Al(OH)_3$. The values thus obtained for the NH^{4+}, Na^+, Ca^{2+}, and Li^+ systems are 30.55, 30.75, 31.00, and 33.15 respectively. For the pK_{sp} values in the Li^+ system two lines with different slopes are shown. Experiments 7, 8, and 9 give a line of steeper slope while experiments 10, 11, and 12 give a line of smaller slope. The reason for this is that the latter experiments were aged for a shorter time, only for about 1 month. Nevertheless, the two lines extrapolate to a common intercept with the [OH]/[Al] = 3 line. This is to be expected, because the common intercept represents the true pK_{sp} of $Al(OH)_3$ in that

Can. J. Chem. Downloaded from www.nrcresearchpress.com by 210.87.254.5 on 09/05/12
For personal use only.

system. Since the composition of the precipitate changes during aging, so will the pK_{sp} value. Therefore the slope of the pK_{sp} *vs.* [OH]/[Al] ratio line is not the same when the aging time is different.

It can therefore be concluded that the solubility of $Al(OH)_3$ in the presence of the Li^+ ion is significantly lower than its solubility in the presence of other metal ions. There is another proof for this fact. When hydroxides were slowly added to the $AlCl_3$ solutions in different systems, the p*H* values increased and the solutions became cloudy. On standing, the cloudiness disappeared and the p*H* of the solutions fell. The behavior was somewhat different in the Li^+ system. The solution may reach a higher p*H* value than in other systems, but with less cloudiness by the addition of a large amount of LiOH. After the solution had been left overnight, considerable precipitate was formed. Much smaller amounts of LiOH than other hydroxides were needed to form small amounts of precipitate. In one experiment (No. 10), the ratio of [OH]/[Al] was only 0.8. On rapid addition of LiOH, the solution showed slight coludiness at first, then cleared up after an hour; however cloudiness returned after standing overnight, small amounts of precipitate being formed on further standing. In the K^+ system, when the ratio of [OH]/[Al] was 0.9, the solution showed slight cloudiness at the end of addition of KOH. Cloudiness disappeared on standing and the solution remained clear afterwards.

It was first thought that $Al(OH)_3$ might form some sort of double or complex salt with LiCl or LiOH. But the precipitate, after it had been freed from chloride by dialysis, was found to contain negligible amounts of Li (0.15%) by atomic absorption analysis. The larger pK_{sp} value of $Al(OH)_3$ in the Li^+ system must, therefore, be attributed to the influence of the Li^+ ions present in the solution. Krishnamurti (15) considered the solubility product of a substance from a dynamic point of view. The rate of dissolution of a precipitate is governed by the coulombic force between the ions in the crystal and the ion–solvent interaction. The rate of recombination of ions to form a crystal is governed by the coulombic force between the ions and their ionic atmosphere as well as the ion–solvent interaction. The last term is less important, because it operates in both directions. The difference in solubility of an ionic substance in aqueous solutions of different compositions is, therefore, due to the coulombic force between its ions and their ionic atmospheres. In the present work the differences among ionic atmospheres in various systems are the cations. The charge density of the bare Ca^{2+} ion is approximately the same as that of the bare Li^+ ion and is greater than those of the other metal ions being investigated, yet the solubility product of $Al(OH)_3$ in the Ca^{2+} system does not differ much from those in other alkali metal systems, but differs markedly from that in the Li^+ system. This rules out the size effect. The abnormal effect of the Li^+ ion as compared to the effect of other metal ions on the solubility product of $Al(OH)_3$ must, therefore, be attributed to a specific effect of the Li^+ ions in solution. This specific "lithium effect" was also observed on the distribution coefficients in their anion exchange separation of the rare earths by Chen and Liao (16).

The author is grateful to Professor J. H. Wang of Yale University for his atomic absorption analysis, and to Mr. L. Li of the computing center of the Chinese University of Hong Kong for solving the higher power equations. He is indebted to professor K. J. Laidler of the University of Ottawa for correcting the manuscript and valuable suggestions.

1. D. CHEN. Can. J. Soil Sci. **45**, 177 (1965).
2. K. H. GAYER, L. C. THOMPSON, and O. T. ZAJIECK. Can. J. Chem. **36**, 1268 (1958).
3. I. M. KORENMAN, F. S. FRAM, and A. I. KUDINOVA. Akad. Nauk. U.S.S.R. **1**, 83 (1953).
4. P. N. KOVALENKO and V. N. NESTOROVICH. Ukrain. Khim. Zh. **18**, 635 (1952).
5. C. R. FRINK and M. PEECH. Soil Sci. Soc. Am. Proc. **26**, 346 (1962).
6. R. C. TURNER and J. E. BRYDON. Soil Sci. **100**, 176 (1965).
7. S. S. SINGH. Soil Sci. **104**, 433 (1967).
8. S. S. SINGH. Can. J. Chem. **47**, 663 (1969).
9. P. H. HSU. Soil Sci. **96**, 230 (1963).
10. C. W. DAVIES. Ion association. Butterworths and Co. Inc., London. 1962. p. 41.
11. E. GRUNWALD and D. W. FONG. J. Phys. Chem. **73**, 650 (1969).
12. C. BROSSET. Acta Chem. Scand. **6**, 910 (1952); C. BROSSET, G. BIEDERMANN, and I. G. SILLEN. Acta Chem. Scand. **8**, 1917 (1954).
13. J. AVESTON. J. Chem. Soc. 4438 (1965).
14. J. W. AKITT, N. N. GREENWOOD, and D. G. LESTER. Chem. Commun. 988 (1969).
15. K. KRISHNAMURTI. Nature. **182**, 1227 (1961); **191**, 1004 (1961).
16. Y. M. CHEN and S. C. LIAO. J. Chin. Chem. Soc. II, **19**, 93 (1972).

On The "Low" *A*-Factors of Alkyl Radical Isomerization

K. J. MINTZ[1] AND D. J. LE ROY

Department of Chemistry, Lash Miller Chemical Laboratories, University of Toronto, Toronto, Ontario M5S 1A1

Received April 5, 1973

Recent chemical activation studies of isomerizations of alkyl and alkenyl radicals involving 5, 6, and 7 member ring complexes are shown to be consistent with earlier thermal studies and support the conclusion that the *A*-factors of these reactions are "low", *i.e.* substantially less than 10^{11} s^{-1}. A possible explanation, consistent with transition state theory, is given in terms of configurational entropy.

Des études récentes d'activation chimique des réactions d'isomérisation de radicaux alkyles et alkényles impliquant des complexes de cycles à 5, 6 et 7 chaînons sont en accord avec des études thermiques antérieures et corroborent la conclusion selon laquelle les facteurs -*A* de ces réactions sont "bas", c'est-à-dire beaucoup moindre que 10^{11} s^{-1}. Une explication possible, en accord avec la théorie des états de transition, est donnée en termes d'entropie configurationnelle. [Traduit par le journal]

Can. J. Chem., **51**, 3534 (1973)

Introduction

Although isomerization of alkyl radicals (by H-shift) had been postulated for some time (1), quantitative kinetic data have been obtained only fairly recently. The first study, by Endrenyi and Le Roy (2) on the isomerization of *n*-pentyl radicals in a thermal system, yielded $k = 1.4 \times 10^7 \exp(-10.8 \times 10^3/RT)$. Somewhat later, Watkins and Ostreko (3), in a similar study on the isomerization of *n*-hexyl radicals, obtained $k = 2.1 \times 10^7 \exp(-8.3 \times 10^3/RT)$. These *A*-factors are difficult to rationalize on the basis of the usual formulation of the transition-state theory since, if reasonable values of entropies of internal rotation are assumed, the predicted *A*-factors are about 10^3 larger. In fact, this discrepancy has led other authors (4) to reject the experimental results. Recently several studies on the isomerization of chemically activated alkyl radicals have been made (5–8) in which the authors have interpreted their results (through the use of activated complex theory) to be consistent only with "normal" *A*-factors, in disagreement with the thermal studies.

The purpose of this paper is to use a recently developed method (9) to obtain approximate *A*-factors directly from experimental data obtained from chemical activation studies, a method which does not require assuming a structure for the activated complex, and to show that they are reasonably consistent with the results of the thermal studies.

[1]Present address: Chemistry Division, National Research Council of Canada, Ottawa, Canada K1A 0R6.

Procedure

Forst (10) has recently derived the following equation for the theoretical rate constant at an energy *E* for a unimolecular reaction, assuming that *A* and E_∞ are temperature independent:

$$[1] \qquad k(E) = A\,N(E - E_\infty)/N(E)$$

where E_∞ is the Arrhenius activation energy for reaction and $N(E)$ is the density of states of the reactant molecule at the energy *E*. Since in many chemical activation studies the energy distribution can be regarded as being monoenergetic, $k(E)$ may be equated to the experimental rate constant, k_a. Hence, eq. 1 allows the calculation of the Arrhenius *A*-factor directly from k_a using only knowledge of the reactant molecule. This method has recently been applied to the decompositions of excited alcohols (9); the results obtained are consistent with decomposition of alkanes in thermal systems.

The densities of states were calculated by a method due to Rabinovitch and Whitten (11) as modified by Forst (12). Knowledge of the vibrational frequencies of the radicals was required. Since they are unknown, they were assumed to be the same as for the corresponding alkanes but with a C—H stretch and two C—H bends eliminated. The frequencies for the *n*-alkanes are available (13); those of the branched alkanes were estimated by analogy with other compounds. It should be stressed that very little uncertainty in *A* is caused by the uncertainty in the frequencies.

The average energies of the activated radicals were calculated by the method previously given (9); the differences between these (shown in Table 1) and those given by the original authors are small and have no significant effect on the results.

Unfortunately, it is impossible to estimate E_∞ with sufficient accuracy to calculate *A* accurately. Almost certainly, E_∞ will not be smaller than the activation energy for intermolecular abstractions (about 8.3 kcal/mol). Therefore, the *A*-factors were calculated for three different values of E_∞, 10, 15, and 20 kcal/mol, covering the range of probable values.

Can. J. Chem. Downloaded from www.nrcresearchpress.com by 210.87.254.105 on 09/05/12
For personal use only.

Can. J. Chem. Downloaded from www.nrcresearchpress.com by 210.87.254.105 on 09/05/12
For personal use only.

The values of k_a in Table 1 are the experimental values reported by the authors cited. According to Hardwidge *et al.* (7), and Larson *et al.* (8), their values are probably accurate to within a factor of two; the others should be rather more accurate.

Discussion

n-Pentyl Radical Isomerization

Watkins and Lawson (5) suggested that chemically activated radicals were involved in the work of Endrenyi and Le Roy (2) and concluded that, since k_a does not have as strong a temperature dependence as $k_{thermal}$, and because both chemical activation and thermal activation contribute to the "apparent" unimolecular rate constant, the observed rate constant would have a smaller temperature dependence than if the reaction were completely thermal. This situation could account for both the "low" A-factor and low activation energy reported by Endrenyi and Le Roy. However, in later experiments (14), Endrenyi and Le Roy added 506 Torr of CO_2 and found no change in the isomerization rate constant of n-pentyl radicals, from which they concluded that there was no evidence for chemical activation in their work. Furthermore, in the study by Watkins and Ostreko (3) on the isomerization of n-hexyl radicals in which a "low" A-factor was also found, addition of excess Xe and also C_3F_8 was found not to change the rate of isomerization and they concluded that "the radicals undergoing isomerization are in thermal equilibrium with the bath".

Very recently, Watkins (15) has suggested that the "low" A-factor in the work of Endrenyi and Le Roy is due to the neglect of the effect of the thermal decomposition of the isomerized radicals. By doing a mass balance on the propene and attributing the "excess" to this decomposition, the Arrhenius parameters were calculated to be: $\log A = 11.7$, $E_\infty = 21$ kcal/mol. However, propene is produced by a large number of reactions in this system; conclusions based on it can be misleading. A careful re-examination of Endrenyi and Le Roy's data shows that the reactions of n- and sec-pentyl radicals with ethylene, acetone, and acetonyl radicals are not negligible as originally assumed. We have therefore made a new analysis of their data; the resultant Arrhenius parameters are: $\log A = 8.5 \pm 0.4$, $E_\infty = 13.0 \pm 0.8$ kcal/mol. (The error limits are standard deviations from the least squares plot.) Although these values are somewhat higher than those originally reported (2), they indicate that no serious error was made in the original analysis and that the A-factor for isomerization determined from the thermal experiments is definitely "low".

Watkins (16) has also studied the isomerization of n-pentyl radicals by a photochemical method and obtained $\log A = 8.3$ and $E_\infty = 15$ kcal/mol. However, these results were considered to be unreliable, supposedly because of experimental complications. The values obtained are remarkably close to the recalculated values of Endrenyi and Le Roy.

In order to interpret their experimental results, Watkins and Lawson postulated a model for the activated complex. From this, they calculated a theoretical rate constant using the R.R.K.M. expression. The latter expression requires knowledge of E_0; since this was not known, they chose a value of E_0 (18–19 kcal/mol) that made the theoretical rate constant equal to the experimental. Obviously, this procedure can not test the chosen model. A value of E_0 of 18–19 kcal/mol implies that the value of E_∞ will be about 19–20 kcal/mol,[2] from which we calculate that A will be about 2×10^{10} s^{-1}, still somewhat less than "normal". On the other hand, if the value of E_∞ is taken to be equal to the activation energy determined by Endrenyi and Le Roy (as revised here), the chemical activation study yields an A-factor of 1.4×10^9 s^{-1}, which is within the error limit of the revised value of Endrenyi and Le Roy.

It should be noted that choosing a model for the complex and assigning frequencies is equivalent to assigning a standard entropy to the model complex and hence, in terms of conventional transition state theory is equivalent to *assigning* an A-factor to the thermal reaction. The value of A corresponding to the model of Watkins and Lawson, calculated from the expression $A = (ekT/h) \exp(\Delta S^*/R)$, is approximately 1×10^{11} s^{-1}.

In a system which involves only chemical activation, a plot of the isomerization:stabilization ratio *vs.* pressure^{-1} should yield a straight line going through the origin. However, Watkins and Lawson found that the intercept of this plot was definitely positive. It is not unreasonable to assume that this was due to the presence of

[2] $E_\infty = E_0 + T\langle\Delta C_v^*\rangle + RT$ (17). Reasonable values of $|T\langle\Delta C_v^*\rangle|$ for the formation of a ring complex are < 1 kcal/mol.

Can. J. Chem. Downloaded from www.nrcresearchpress.com by 210.87.254.105 on 09/05/12
For personal use only.

TABLE 1. Calculated A factors for chemically activated radical isomerization

Reactant*	Product*	k_a‡	E§	A‡ for E_∞ = 10	15	20	A.C.‖	Degeneracy ¶	Reference
P1	P2	3.3×10^{6}	34.1	2.4×10^{8}	2.5×10^{9}	3.2×10^{10}	5	2	5
3M1B1†	3M1B4	4.1×10^{8}	33.8	2.3×10^{10}	2.2×10^{11}	2.5×10^{12}	5	6	6
Hp3	Hp2	9.0×10^{5}	43.2	7.7×10^{7}	8.4×10^{8}	1.0×10^{10}	5	2	7
Hp3	Hp1	$<9\times10^{5}$	43.2	$<7\times10^{7}$	$<8\times10^{8}$	$<1\times10^{10}$	6	3	7
Oc4	Oc2	2.9×10^{4}	44.2	3.1×10^{6}	3.7×10^{7}	5.0×10^{8}	5	2	7
Oc2	Oc4	8×10^{5}	47.4	8×10^{7}	9×10^{8}	1.1×10^{10}	5	2	7
Oc2	Oc3	6.0×10^{7}	47.4	5.7×10^{9}	6.3×10^{10}	8.2×10^{11}	6	2	7
Oc1	Oc4	$>3\times10^{7}$	45.4	$>3\times10^{9}$	$>4\times10^{10}$	$>5\times10^{11}$	6	2	7
N2	N5	1.8×10^{5}	48.4	2.0×10^{7}	2.5×10^{8}	3.4×10^{9}	5	2	7
N2	N4	1.8×10^{7}	48.4	2.0×10^{9}	2.5×10^{10}	3.4×10^{11}	6	2	7
N2	N3	9×10^{5}	48.4	1.0×10^{8}	1.2×10^{9}	1.7×10^{10}	7	2	7
3MP1	2EB1	$<1\times10^{5}$	44.3	$<6\times10^{6}$	$<6\times10^{7}$	$<6\times10^{8}$	5	3	7
3MP1	3MP2	$<1\times10^{6}$	44.3	$<6\times10^{7}$	$<6\times10^{8}$	$<6\times10^{9}$	5	2	7
3MH2	4MH2	1.0×10^{6}	45.3	8.0×10^{7}	8.3×10^{8}	9.7×10^{9}	5	2	7
3MH1	4MH2	$>1\times10^{8}$	43.3	$>9\times10^{9}$	$>9\times10^{10}$	$>1\times10^{12}$	6	2	7
33DMH2	44DMH2	1.6×10^{6}	45.4	1.7×10^{8}	2.0×10^{9}	2.7×10^{10}	5	2	7
33DMH1	44DMH2	$>8\times10^{7}$	43.4	$>9\times10^{9}$	$>1\times10^{11}$	$>2\times10^{12}$	6	2	7
4MH1	3MH3	1×10^{8}	41.0	1.0×10^{10}	1.1×10^{11}	1.5×10^{12}	5	1	8
24DMH1	35DMH3	1.8×10^{7}	42.0	2.1×10^{9}	2.8×10^{10}	4.0×10^{11}	5	1	8
224TMH1	355TMH3	5×10^{6}	43.0	7.3×10^{8}	1.0×10^{10}	1.6×10^{11}	5	1	8
3MH2	4MH1	$>10^{6}$	45.0	$>8\times10^{7}$	$>8\times10^{8}$	$>1\times10^{10}$	6	3	8
35DMH2	24DMH1	$>10^{6}$	46.0	$>1\times10^{8}$	$>1.2\times10^{9}$	$>1.5\times10^{10}$	6	6	8
355TMH2	224TMH1	$>10^{6}$	47.0	$>1.2\times10^{8}$	$>1.6\times10^{9}$	$>2\times10^{10}$	6	9	8

*M = methyl, E = ethyl, H = hexyl, Hp = heptyl, P = pentyl, N = nonyl, Oc = octyl, B = butyl.
†3-Methyl-1-buten-1-yl.
‡In s^{-1}.
§In kcal/mol.
‖Number of atoms in the activated complex.
¶Number of equivalent reaction paths.

Can. J. Chem. Downloaded from www.nrcresearchpress.com by 210.87.254.105 on 09/05/12
For personal use only.

thermal isomerization. An approximate steady-state analysis of their system at the high-pressure limit at 57 °C yields a thermal isomerization rate constant of about 0.2 s^{-1}. This is in good agreement with the extrapolated value of the revised rate constants of Endrenyi and Le Roy, *viz.* 0.3 s^{-1}.

In view of the above discussion, it seems clear that the thermal experiments of Endrenyi and Le Roy and the chemical activation experiments of Watkins and Lawson are mutually consistent. Hence, the experimental evidence seems to favor a "low" A-factor for the isomerization of n-pentyl radicals.

Isomerization of 3-Methyl-1-buten-1-yl Radicals

Applying R.R.K.M. theory to their model[3] of the activated complex, Watkins and O'Deen (6) found that the best agreement with experiment occurred for $E_0 = 17.1$ kcal/mol, slightly smaller than they calculated for the isomerization of n-pentyl radicals. Regardless of the model, one would not expect a large difference in E_0 between these two reactions, both of which involve a five-member ring in the activated complex. Table 1 shows clearly that if E_∞ is about the same, then the A-factor should be about 100 times that for the n-pentyl reaction. Furthermore, if A for the isomerization of 3-methyl-1-buten-1-yl were assumed to be "normal" (10^{11} s^{-1}), then E_∞ would be about 14 kcal/mol which is very close to the recalculated value of the activation energy of n-pentyl isomerization. Hence, this study of the chemically activated isomerization of 3-methyl-1-buten-1-yl gives even more support for the "low" A-factor of n-pentyl radical isomerization.

Other Alkyl Radical Isomerizations

It would seem most likely that all alkyl isomerizations which involve an H atom transfer and a five-member ring in the activated complex have about the same activation energy (within 1–2 kcal/mol). However, it is evident from Table 1 that any choice of a common value of E_∞ leads to the conclusion that the A-factors will range over nearly two orders of magnitude. Furthermore, a reasonable choice of E_∞, *viz.* 15 kcal/mol, yields "low" values of A.

Isomerization involving 6-member rings in the activated complex are generally assumed to have little strain energy, and would therefore be expected to have values of E_∞ similar to that of intermolecular hydrogen abstractions, *viz.* about 8.3 kcal/mol. Again, one can see from Table 1 that whilst there is a large range of values of A, almost all appear to be "low".

Only one isomerization has been studied which involves a 7-member ring in the activated complex (2-nonyl radical). The calculated A-factor for this reaction, which should involve a strain free complex, is significantly smaller than that of the isomerization of the same species via a 6-member ring in the activated complex.

Larson and co-workers (7, 8) have interpreted their results by assuming a certain model of the activated complex (which yields A factors of approximately 10^{11} s^{-1}) and finding the value of E_0 that makes the theoretical (R.R.K.M.) value of k_a equal to the experimental value. This procedure is the same as was used by Watkins and Lawson (5). It seems to us that, at the present time, there is not sufficient experimental evidence to attribute all differences in k_a values solely to differences in E_0, rather than to differences in both A and E_∞.

Estimation of E_∞

Several authors (5–7) have estimated activation energies for these isomerizations by using the value for intermolecular hydrogen abstractions as the base value and then adding in contributions from strain energy estimated by analogy with cyclic carbon compounds. Although this procedure is valid qualitatively and allows one to show, for example, that the activation energy for isomerization of n-pentyl is greater than that of n-hexyl radicals, it is not valid to apply the method quantitatively for the following reasons, derived from the knowledge of the potential-energy surfaces for intermolecular hydrogen atom transfer:

(*1*) The col of the minimum energy path is located at rather larger distances than the equilibrium bond distances.

(*2*) Since a linear reaction path is strongly favored, the use of a symmetric ring for the transition state may not be justified.

(*3*) Tunneling may play an important role in reducing the apparent activation energy.

(*4*) The activation energy of the intramolecular hydrogen abstractions may be slightly higher than that of the intermolecular due to strain caused by eclipsing of H atoms in the activated complex.

[3]This model yields an A-factor of about 1×10^{11} s^{-1}.

Can. J. Chem. Downloaded from www.nrcresearchpress.com by 210.87.254.105 on 09/05/12
For personal use only.

Unfortunately, the experimental data on activation energies of these isomerizations are not yet of sufficient accuracy to allow meaningful comparisons to be made with theory.

Interpretation of the "Low" A-Factors

One possible approach toward an explanation for these effects is contained in the observation of Hardwidge *et al.* (7) that "An H atom transfer occurring internally in a long-chain molecule can be thought of as a 'bimolecular' process between two ends of the molecule with the relative 'translation' being supplied by the excited bending modes". It is evident that one can classify unimolecular reactions of long-chain molecules into two types: (*a*) those involving adjacent centers, and (*b*) those involving non-adjacent centers. Those in the second category could be thought of as involving intramolecular collisions, and possibly requiring a special theoretical treatment.

From the point of view of reaction dynamics, unimolecular reactions of type (*b*) are subject to an additional condition before reaction can take place, namely a unique configuration of the chain. Thus, if a long-chain radical were capable of undergoing reactions of both types, each with the same energy requirement, one would expect the reaction of type (*b*) to be slower.

From the thermodynamic point of view of transition state theory, this difference in rates should be accountable in terms of the differences in entropy of formation of the corresponding complexes, provided that entropies are calculated correctly. In evaluating the molar entropy in the standard state of, say, *n*-pentyl radicals no cognizance is normally taken of the configurational entropy. If this reactant exists in n equally probable different configurations its configurational entropy would be equal to $R \ln n$.

For any chemical reaction in which the "product" also has a configurational entropy of $R \ln n$, for example the formation of a complex for a reaction of type (*a*), the configurational entropy will cancel out (or approximately so) in evaluating the entropy of formation of the complex. In this case, there would be no reason to include the configurational entropy in the evaluation of $\Delta S^{\ddagger}$, for the same reason that one need not include the contribution of nuclear spin in calculating ΔS^0 for chemical reactions. However, if the reaction consists in the formation of a complex for a reaction of type (*b*), the configurational entropy of the reagent will not cancel out completely. The standard entropy of the complex will then be less than that of the reagent, not only by an amount corresponding to the loss of internal rotational degrees of freedom, but also by an amount equal to the loss in configurational entropy. The former is, of course, evaluated in terms of the corresponding partition functions. The latter can only be evaluated by a separate detailed examination of the configurations available to the reagent and the complex.

In summary, it is suggested that in applying transition state theory to unimolecular reactions of type (*b*) the value of $\Delta S^{\ddagger}$ should include the difference in configurational entropy of the reagent and complex.

1. A. Kossiakoff and F. O. Rice. J. Am. Chem. Soc. **65**, 590 (1943); V. B. Sefton and D. J. Le Roy. Can. J. Chem. **34**, 41 (1956).
2. L. Endrenyi and D. J. Le Roy. J. Phys. Chem. **70**, 4081 (1966).
3. K. W. Watkins and L. A. Ostreko. J. Phys. Chem. **73**, 2080 (1969).
4. H. M. Frey and R. Walsh. Chem. Rev. **69**, 103 (1969).
5. K. W. Watkins and D. R. Lawson. J. Phys. Chem. **75**, 1632 (1971).
6. K. W. Watkins and L. A. O'Deen. J. Phys. Chem. **75**, 2665 (1971).
7. E. A. Hardwidge, C. W. Larson, and B. S. Rabinovitch. J. Am. Chem. Soc. **92**, 3278 (1970).
8. C. W. Larson, P. T. Chua, and B. S. Rabinovitch. J. Phys. Chem. **76**, 2507 (1972).
9. K. J. Mintz and R. J. Cvetanović. Can. J. Chem. In press.
10. W. Forst. J. Phys. Chem. **76**, 342 (1972).
11. B. S. Rabinovitch and G. Z. Whitten. J. Chem. Phys. **38**, 2466 (1963).
12. W. Forst. Chem. Rev. **71**, 339 (1971).
13. J. H. Schnachtschneider and R. G. Snyder. Spectrochim. Acta, **19**, 117 (1963).
14. L. Endrenyi. Ph.D. Thesis. University of Toronto, 1967.
15. K. W. Watkins. Can. J. Chem. **50**, 3738 (1972).
16. K. W. Watkins. J. Am. Chem. Soc. **93**, 6355 (1971).
17. S. W. Benson and W. E. O'Neal. Kinetic data on gas-phase unimolecular reactions. NSRDS-NBS 21, Washington, D.C. 1970.

Maleic Anhydride – Triethylamine Complex

MAHMOOD F. MAYAHI AND M. F. EL-BERMANI
Chemistry Department, College of Science, Adhamia, Baghdad, Iraq

Received March 26, 1973

Reaction of triethylamine with maleic anhydride (MA) forms first a yellow solution, which immediately turns into a dark brown product with a large increase in temperature. The addition product is a 1:1 open chain inner salt 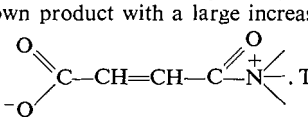 . The spectral properties of this salt are reported.

La réaction de la triéthylamine avec l'anhydride maléique (MA) donne au départ une solution jaune qui devient immédiatement brun foncé avec une augmentation notable de la température. Le produit provient d'une addition 1:1 et correspond à un sel interne en chaîne ouverte 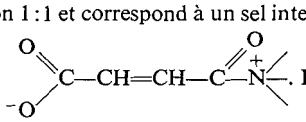 . Les propriétés spectrales de ce sel sont rapportées.

[Traduit par le journal]

Can. J. Chem., **51**, 3539 (1973)

Can. J. Chem. Downloaded from www.nrcresearchpress.com by 210.87.254.5 on 09/05/12
For personal use only.

Introduction

Maleic anhydride enters into many non-photochemical and photochemical reactions both of which may proceed through charge-transfer complexes (1). In this paper we report the reaction of maleic anhydride (MA) with triethylamine (TEA). The MA molecule is planar (2), and it is an acceptor with an electron affinity of 0.11 eV (ref. 1, p. 387), and a dipole moment of 3.95 D (3), while TEA is a strong organic base, with a pK_a of 10.5 (4). Thus the MA–TEA system promises to be an interesting one, in that it shows a two stage reaction, the formation of the expected charge-transfer complex, and the collapse of this complex into a stable product.

Experimental

Maleic anhydride was supplied by British Drug Houses, Poole, England. It was purified by two recrystallizations from chloroform, the solvent being removed under partial vacuum at room temperature. TEA was distilled before use.

The u.v. and visible spectra were recorded on a Unicam SP800, using 1 mm and 10 mm quartz cells. The i.r. spectra were recorded on a Hilger and Watt H 800 NaCl prism spectrophotometer using KBr windows. The n.m.r. spectra were recorded on a Varian 60A at a probe temperature of 37 °C.

The reaction of MA and TEA was done in a 250 ml calorimeter. MA (8.671 g) was added to 10.913 g of TEA (a slight excess of the 1:1 ratio). The temperature was read every 30 s. From a plot of temperature *vs.* time (not shown) it was found that the temperature increased 10° in the first 5 min and increased 50° in the next 4 min, The mixture finally became a dark brown solid after 9 min. Qualitatively MA was added to TEA in a beaker, giving a clear yellow solution which quickly turned into dark brown paste, with evolution of heat. The product was dried in a vacuum desiccator.

Results and Discussion

The formation of the charge-transfer complex, and the collapse of this complex into a dark brown product can be written as follows:

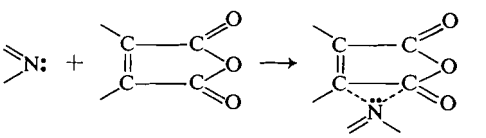

π-complex, yellow

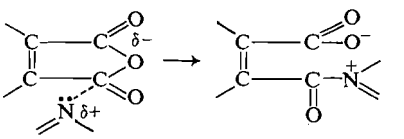

σ-complex dark brown product

The nature of the product was established by u.v., n.m.r., and i.r. studies. Table 1 shows the u.v. and visible spectra of the product. The band in the 210 nm range has a high ε_{max} ($\sim 10^4$), which is of the same order as that of pure MA, indicating the presence of the C=C bond in the product. The bands found in the visible region indicate the presence of the extended conjugated system.

TABLE 1. Ultraviolet and visible spectra of the MA–TEA complex in different solvents*

Solvent	λ_{max} (ε_{max}) (nm)		Pure MA
n-Heptane	206	490, 526	
Ethanol	212 (1.14×10^4)		203 (0.83×10^4)
Methanol	210	350, 407, 510, 540	
Ether	210		
Dioxane	220 (3.75×10^4)		206 (0.77×10^4)
Water	212 (3.4×10^4)	350, 403, 510, 540	210 (2.84×10^4)
TEA	—	490, 537	

*In ethanol, ether, and dioxane, only the u.v. spectra are given because the complex is very slightly soluble in these solvents and no bands in the visible region were observed. The *n*-heptane solution was gently warmed, then cooled before taking the spectrum.

The n.m.r. spectra of the product was obtained in D_2O. The presence of the 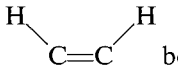 bond is indicated by the band at 6.43δ, compared to that of MA at 6.52δ. The band for the CH_3 group, a triplet, is at 1.026δ in pure TEA, while it is at 1.22δ in the product, a shift of 0.20δ to lower field. The band for the CH_2 group, a quartet, is at 2.56δ in pure TEA, while it is at 3.14δ in the product, a shift of 0.58δ to lower field. The down field shift of both of these bands is due to the electron withdrawing effect of the positive nitrogen $-\overset{+}{N}\equiv$ present in the product.

The i.r. spectrum of a thin film of the product shows bands at 1730 cm^{-1} (a shoulder) and in the 1716 cm^{-1} region, which may be due to the group 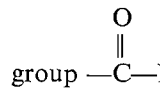 . The loss of resonance in this amide group shifts the $\nu_{C=O}$ from 1680–1650 cm^{-1} in the simple amide to higher wavenumbers. These bands are at lower frequency than that of MA (1853 cm^{-1} and 1784 cm^{-1} in this study) because of loss of ring strain. There is a strong band at 1580 cm^{-1} which may be due to 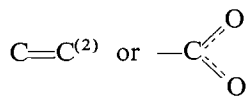 δ–(5). However, the absence of a band in the region 1200–1300 cm^{-1} indicates the disappearance of the C—O bond present in pure MA (ν_{C-O} 1268, 1068 (2), and at 1264 cm^{-1} in this study) thus indicating the opening of the MA ring by TEA in the product.

The participation of π- and σ-complexes in chemical reactions is well known (1). The π-complex involves the interaction between the pair of electrons in TEA and the π-orbitals of both of the C=C and C=O bonds, since the addition of succinic anhydride, with a dipole moment of 3.83 D (3), to TEA does not form a yellow color nor any product.

1. E. FOSTER. (*Editor.*) Organic charge-transfer complexes. Academic Press, London. 1969. pp. 325–326.
2. P. MIRONE and P. CHIORBOLI. Spectrochim. Acta, **18**, 1426 (1962).
3. K. F. WONG and C. A. ECKERT. Chem. Eng. Data, **16**, 56 (1971).
4. J. CLARK and D. D. PERRIN. Q. Rev. **18**, 295 (1964).
5. L. J. BELLAMEY. The infrared spectra of complex molecules. Methuen and Co. Ltd., London. pp. 127–129.

Can. J. Chem. Downloaded from www.nrcresearchpress.com by 210.87.254.5 on 09/05/12
For personal use only.

Theoretical Considerations and Equilibrium Conditions in Analytical Potentiometry. Computer Facilitated Mathematical Analysis of Equilibria in a Multicomponent System

BIHUDHENDRA SARKAR[1] AND THEO P. A. KRUCK

Division of Biochemistry, The Research Institute, The Hospital for Sick Children, Toronto, and Department of Biochemistry, University of Toronto, Toronto, Ontario M5G 1X8

Received June 14, 1972[2]

A method entitled "analytical potentiometry" is described which permits the accurate determination of the stability constants and of the distribution of simultaneously existing complex species in multicomponent systems. A series of computer programs are introduced to facilitate the otherwise tedious mathematical analysis of data. Besides simple binary systems, this method is capable of dealing with mixed ligand coordination complexes and can be adapted to polynuclear systems. For many metal ions, there are no electrodes permitting the accurate determination of those ions over a wide enough concentration range. This method eliminates the need for metal ion specific electrodes. The concentration of free metal ions is determined indirectly by the use of a weak base and the glass electrode. These features bear great significance in resolving complex systems containing multiple species simultaneously which cannot be solved by the commonly known classical methods.

On décrit une méthode appelée "potentiométrie analytique" qui permet une évaluation précise des constantes de stabilité et de distribution de plusieurs espèces de complexes existant simultanément dans des systèmes à plusieurs composantes. On présente aussi une série de programmes de calcul afin de faciliter l'analyse mathématique des résultats qui, autrement, serait laborieuse. En plus des systèmes binaires simples, cette méthode permet d'analyser des mélanges de complexes de coordination et peut être adoptée afin d'étudier des systèmes polynucléaires. Pour plusieurs ions métalliques, il n'existe pas d'électrode permettant une détermination précise de ces ions dans un intervalle de concentration suffisamment large. Cette méthode élimine donc la nécessité de posséder des électrodes spécifiques de ces ions métalliques. La concentration des ions de métal libre est en effet déterminée indirectement en utilisant une base faible et une électrode de verre. Ces qualités sont donc d'une grande utilité lors de l'étude de systèmes complexes contenant plusieurs espèces simultanément qui, autrement, ne pourraient être étudiés par les méthodes classiques que nous connaissons. [Traduit par le journal]

Can. J. Chem., 51, 3541 (1973)

Introduction

The importance of metal ions in biological systems led many bio-inorganic chemists to investigate equilibria between metal ions and biological ligands in aqueous solution. A variety of techniques have been developed to study simple and complex systems (1, 2). Only in recent years, with the introduction of high speed and large memory computers, has it been feasible to study multiple equilibria in solution. The most accurate probes available for measuring concentrations of various ions are ion specific electrodes, especially the glass electrode used to measure p*H*. With proper care, four to five digit accuracy of the e.m.f. can now be obtained between p*H* 2 and 12. Using the glass electrode, Bjerrum (3) demonstrated its usefulness in examining the stepwise equilibrium constants of reactions between metal and ligands, where the ligand was the conjugate base of a weak acid. If proton liberation is involved in the equilibrium reaction, potentiometry will be the method of choice for the study of the stability of the products formed. Using the law of mass action, equilibrium conditions can be analytically defined, which could then describe the whole system.

Several authors (4–13) have elaborated on this subject to follow the fate of an individual constituent in a complex reaction mixture. The purpose of the present study is to determine the stability constants and the quantitative distribution of all reaction products existing simultaneously in the system, and to propose a reasonably noncomplicated technique to study simple or complex equilibria. To facilitate the large amount

[1]To whom correspondence should be addressed.
[2]Revision received May 29, 1973.

Can. J. Chem. Downloaded from www.nrcresearchpress.com by 210.87.254.5 on 09/05/12
For personal use only.

of calculations necessary, we have developed a series of computer programs[3] which can be used individually or serially. The method described has been successfully employed for the study of a number of metal complexes with amino acids and peptides (14–23)[4].

Theoretical Considerations

Derivation of Working Formula from Basic Thermodynamic Concepts (Gibbs–Duhem Equation)

(A) Consider a closed system in equilibrium where any number of reagents A, B, C, D,...react with each other in reversible manner to give the products $A_iB_jC_kD_l$... where, i, j, k, l, ... can be any positive integral number defining the stoichiometric amount of reagents A,B,C, or D integrated into the product molecule $A_iB_jC_kD_l$. For one selected case eq. 1 will describe the system.

$$[1] \qquad iA + jB + kC + lD \leftrightarrows A_iB_jC_kD_l$$

It should be noted that more than one reaction of the type described can occur simultaneously in the system yielding a different product $A_iB_jC_kD_l$.

The Gibbs–Duhem equation describes the relationship between the chemical potential of the reacting species in a closed system. In its differential form the equation reads as shown in eq. 2:

$$[2] \qquad a\mathrm{d}\mu_A + b\mathrm{d}\mu_B + \ldots h\mathrm{d}\mu_H + \ldots z\mathrm{d}\mu_Z + V\mathrm{d}P - S\mathrm{d}T = 0$$

Terms concerning the chemical potential of the solvent are also contained in this statement. Under conditions of constant temperature and pressure eq. 2 reduces to eq. 3:

$$[3] \qquad a\mathrm{d}\mu_A + b\mathrm{d}\mu_B + c\mathrm{d}\mu_C + \ldots h\mathrm{d}\mu_H + \ldots + z\mathrm{d}\mu_Z = 0$$

where $a, b, \ldots, h, z$ are the number of moles of components A, B, ..., H, ..., Z. This holds true for any number of reactants and products in the closed system. It should be noted that this relationship does not contain any assumptions of ideality but states the general condition for equilibrium at constant temperature and pressure. Furthermore, no assumptions have to be made whether the reagents are liquids or solids or whether they are in any other physical form.

For our purposes eq. 3 is not immediately adaptable to experimental design. Utilizing the rule for differentiation of products

$$[4] \qquad \mathrm{d}(uv) = v\mathrm{d}u + u\mathrm{d}v$$

we get

$$[5] \qquad \mathrm{d}(a\mu_A + b\mu_B + \ldots + h\mu_H + \ldots + z\mu_Z) = (a\mathrm{d}\mu_A + b\mathrm{d}\mu_B + \ldots + h\mathrm{d}\mu_H + \ldots + z\mathrm{d}\mu_Z) + (\mu_A\mathrm{d}a + \mu_B\mathrm{d}b + \ldots + \mu_H\mathrm{d}h + \ldots + \mu_Z\mathrm{d}z)$$

Since, at equilibrium, the concentration of all species in the reaction mixture are constant, therefore, $\mathrm{d}a = 0, \mathrm{d}b = 0, \ldots, \mathrm{d}h = 0$. Hence, eq. 5 reduces to eq. 6.

$$[6] \qquad \mathrm{d}(a\mu_A + b\mu_B + \ldots + h\mu_H + \ldots + z\mu_Z) - (a\mathrm{d}\mu_A + b\mathrm{d}\mu_B + \ldots + h\mathrm{d}\mu_H + \ldots + z\mathrm{d}\mu_Z) = 0$$

The chemical potential of a reagent can be expressed as

$$[7] \qquad \mu_A = \mu_A^0 + RT\ln\alpha = \mu_A^0 + RT\ln[\mathrm{A}]$$

where α is the activity of the reagent and under suitable conditions can be approximated by [A], the concentration of A. Also

$$[8] \qquad \mathrm{d}\mu_A = 2.3RT\,\mathrm{d}\log[\mathrm{A}]$$

[3]Computer programs: PLOT, GUESS, and LEASK were written in Fortran IV. The programs have been deposited as document number NAPS-01563 with the ASIS National Auxiliary Publication Service, c/o CCM Information Corp., 866 Third Avenue, New York, N.Y. 10022. A copy may be secured by citing the document number and by remitting $1.00 for microfiche, or $3.00 for photocopies. Advance payment is required. Make cheques or money orders payable to: ASIS-NAPS.

[4]References 20 to 22 are the three consecutive papers following this article.

Can. J. Chem. Downloaded from www.nrcresearchpress.com by 210.87.254.5 on 09/05/12
For personal use only.

Can. J. Chem. Downloaded from www.nrcresearchpress.com by 210.87.254.5 on 09/05/12
For personal use only.

Substituting eq. 8 into eq. 6 and dividing by $2.3RT$ we get

[9] $$\mathrm{d}(a \log [\mathrm{A}] + b \log [\mathrm{B}] + \ldots + h \log [\mathrm{H}] + \ldots + z \log [\mathrm{Z}]) = (a \,\mathrm{d} \log [\mathrm{A}] + b \,\mathrm{d} \log [\mathrm{B}] + \ldots + h \,\mathrm{d} \log [\mathrm{H}] + \ldots + z \,\mathrm{d} \log [\mathrm{Z}])$$

Rearrangement yields eq. 10.

[10] $$(h \,\mathrm{d} \log [\mathrm{H}] + a \,\mathrm{d} \log [\mathrm{A}] + b \,\mathrm{d} \log [\mathrm{B}] + \ldots + z \,\mathrm{d} \log [\mathrm{Z}]) = \mathrm{d}(a \log [\mathrm{A}] + b \log [\mathrm{B}] + \ldots + h \log [\mathrm{H}] + \ldots + z \log [\mathrm{Z}])$$

Integration of eq. 10 yields

[11] $$\int_{\log H_0}^{\log H_1} h \,\mathrm{d} \log [\mathrm{H}] = \int_{\log H_0}^{\log H_1} (\mathrm{d}\, a \log [\mathrm{A}] + \mathrm{d}\, b \log [\mathrm{B}] + \ldots + \mathrm{d}\, m \log [\mathrm{M}] + \ldots + \mathrm{d}\, z \log [\mathrm{Z}]) = [a \log [\mathrm{A}] + b \log [\mathrm{B}] + \ldots + m \log [\mathrm{M}] + \ldots + z \log [\mathrm{Z}]]_{\log H_0}^{\log H_1}$$

Introducing $-\log [\mathrm{H}] = \mathrm{p}H$, $-\log [\mathrm{A}] = \mathrm{p}A$, etc., eq. 11 reads

[12] $$-\int_{\mathrm{p}H_0}^{\mathrm{p}H_1} h \mathrm{d}\mathrm{p}H = -[a\mathrm{p}A + b\mathrm{p}B + \ldots + m\mathrm{p}M + \ldots + z\mathrm{p}Z]_{\mathrm{p}H_0}^{\mathrm{p}H_1}$$

This implies that pA, pB, pM, etc. are a function of pH. Then it can be shown that

[13] $$\int_{\mathrm{p}H_0}^{\mathrm{p}H_1} h \mathrm{d}\mathrm{p}H = a\mathrm{p}\frac{A_i}{A_0} + b\mathrm{p}\frac{B_i}{B_0} + \ldots + m\mathrm{p}\frac{M_i}{M_0} + \ldots + z\mathrm{p}\frac{Z_i}{Z_0}$$

where A_0, B_0, ..., M_0, ..., Z_0 and A_i, B_i, ..., M_i, ..., Z_i are the molar amounts of A, B, ..., M, ..., Z at the beginning and at the end of the event. Now, if we arrange our conditions such that only the concentration of one reactant is varied at any one time, say a change (δm) in the metal concentration takes place, then in order to keep the other terms constant only the addition or removal of extra protons, 'h', to the system will maintain the equilibrium conditions which includes the amount of free protons (pH).

Under these constraints eq. 13 reduces to eq. 14.

[14] $$\delta \int_{\mathrm{p}H_0}^{\mathrm{p}H_1} h \mathrm{d}\mathrm{p}H = \delta\left(m\mathrm{p}\frac{M_i}{M_0}\right)$$

Rearrangement of eq. 14 gives

[15] $$\frac{\delta}{\delta m} \int_{\mathrm{p}H_0}^{\mathrm{p}H_1} h \mathrm{d}\mathrm{p}H = \mathrm{p}M_i - \mathrm{p}M_0$$

or

[16] $$\mathrm{p}M_i = \mathrm{p}M_0 + \int_{\mathrm{p}H_0}^{\mathrm{p}H_1} \frac{\delta h}{\delta m} \mathrm{d}\mathrm{p}H$$

In eq. 16 the term ($\delta h/\delta m$) represents the amount of base δC_{OH} needed to maintain the pH of the system when an amount, δC_{M}, of metal is added to the system. δC_{OH} is representative of (or equal to) the proton liberation δH_1^+ from the ligand or solvent molecules. Therefore, we can rewrite eq. 16 to give

[17] $$\mathrm{p}M_i = \mathrm{p}M_0 + \int_{\mathrm{p}H_0}^{\mathrm{p}H_1} \left(\frac{\delta H_1^+}{\delta C_{\mathrm{M}}}\right)_{A,B,\ldots,P,V,T} \mathrm{d}\mathrm{p}H$$

where H_1^+ is the moles of protons being titrated per liter of solution. Similarly, we can hold constant everything in the system except ligand A, which is varied, and arrive at a similar expression

[18] $$\mathrm{p}A_i = \mathrm{p}A_0 + \int_{\mathrm{p}H_0}^{\mathrm{p}H_1} \left(\frac{\delta H_1^+}{\delta C_{\mathrm{A}}}\right)_{M,B,\ldots,P,V,T} \mathrm{d}\mathrm{p}H$$

Furthermore, our theoretical conditions permit us to derive similar expressions for every component taking part in any one reaction leading to the multispecies equilibrium including binary, ternary, quaternary, polynuclear systems, etc. An expression similar to eq. 18 has been derived in a different manner for a binary (one metal and one ligand) system by Österberg (7) and Sillén (8).

Can. J. Chem. Downloaded from www.nrcresearchpress.com by 210.87.254.5 on 09/05/12
For personal use only.

Their derivations again were based on earlier work by Hedström (4).[5]

Equilibrium Conditions

Consider a reaction mixture which contains, under standard conditions, C_A moles of ligand anion A, C_M moles of metal ion M, and C_H moles of hydrogen ion H, then the mass law will describe the equilibrium situation of the reaction

$$[19] \qquad pM + rA + qH \leftrightarrows M_pH_qA_r$$

and the equilibrium constant for the reaction 19 can be expressed as

$$[20] \qquad \beta_{pqr} = \frac{[M_pH_qA_r]}{m^p h^q a^r}$$

where m, h, a, are the concentrations of free metal ion, hydrogen ion and ligand anions. Then, if four values are known the fifth one may be calculated.

$$[21] \qquad [M_pH_qA_r] = \beta_{pqr} m^p h^q a^r$$

where β_{pqr} is the stoichiometric stability constant of the complex species $M_pH_qA_r$. This holds true for each of the multiple equilibria existing simultaneously in a complex reaction mixture. Since we are dealing with a closed system, all of the reactants can be accounted for in the following manner:

$$[22] \qquad C_M = m + \sum p(\beta_{pqr} m^p h^q a^r)$$

$$[23] \qquad C_H = h + \sum q(\beta_{pqr} m^p h^q a^r)$$

$$[24] \qquad C_A = a + \sum r(\beta_{pqr} m^p h^q a^r)$$

The system can be expanded to the treatment of ternary or quaternary systems by the simple addition of appropriate terms B and C, etc.

Experimental Considerations

In order for the mathematical expressions to hold, we require that the volume and molar concentration of the reactants to remain constant. Also the ionic strength should be kept constant in order to permit the use of molalities instead of activities for the subsequent calculations. At the extremes of the pH scale, the measured pH value does not reflect accurately the hydrogen ion activity. Proper corrections will have to be made in those regions. Experience has shown that in the range between pH 2–11 hydrogen ion concentration can be used to represent the hydrogen ion activity. The proton liberation H_1^+ is only a function of the titrant and is independent of hydrogen ion activity.

Since hydrogen ion activities enter into β value calculations the errors will be propagated accordingly. Hence, the β values of complex species, having maximum concentration in the extreme regions of pH, will also carry the largest bias.

For the evaluation of eq. 18 the integration constant pA_0 has to be obtained first. If the initial conditions can be selected such that no complexation involving proton liberation occurs then pA_0 can be calculated from C_A and the appropriate pK_a of the ligand. In the case of an amino acid–Cu(II) system we would select a starting pH below 2 where little or no complexation takes place. In this case, most of the amino acid molecules will be fully protonated. The concentration of fully protonated amino acid A^+ can be calculated using the Henderson–Hasselbach equation. This calculated concentration will represent the initial condition of the system, hence, the $pA_0{}^+$ is fixed. Calculation of the β values, however, requires values of pA, the completely deprotonated ligand. The conversion of pA^+ to pA is accomplished utilizing the acid dissociation constants for the J-basic ligand

$$[25] \qquad pA_x = pA_x{}^+ + \sum_1^J pK_{a_j} - JpH_x$$

This conversion is performed after eq. 18 has been evaluated. A further illustration of this can be found in the papers following (20, 22).

Evaluation of Stability Constants

Each of the above expressions (eqs. 22–24) represents a system of simultaneous equations of the general form

$$[26] \qquad a_{i,1}x_1 + \ldots a_{i,n}x_n - d_i = 0$$

where $x_1, \ldots, x_n$ may represent a series of unknown stability constants and the elements $a_{i,1} \ldots a_{i,n}$ may represent the corresponding values of $m^p h^q a^r$, *i.e.*

[5]The authors acknowledge the extensive and helpful discussions they have had with Professor W. A. E. McBryde concerning the derivations of equations to describe the equilibria governing complex formation. Unfortunately complete agreement could not be reached and Professor McBryde therefore offers an alternative treatment for the binary system only, which appears in the present issue of the journal immediately following this series of four papers.

Can. J. Chem. Downloaded from www.nrcresearchpress.com by 210.87.254.5 on 09/05/12
For personal use only.

[27] $$a_{i,1} = (m^p h^q a^r)_{i,1}$$

This same situation can be more briefly described in vector notation.

[28] $$A_{ij} \cdot \boldsymbol{x} = \boldsymbol{d}$$

where A_{ij} describes the coefficient matrix with elements a_{ij}, $\boldsymbol{x}$ being a vector which produces the desired result $\boldsymbol{d}$ when $\mathbf{A}_{ij}$ is post-multiplied by $\boldsymbol{x}$. In our case $\mathbf{A}_{ij}$ and $\boldsymbol{d}$ can be calculated from the experimental data, and $\boldsymbol{x}$ becomes the solution vector containing the values $(x_1 \ldots x_n)$ which represent the $\beta_1, \ldots, \beta_n$ values or stability constants.

There are a variety of ways in which equations of this type can be solved. Since observed data have inherent experimental errors associated with them, purely analytical solutions are not very useful. Hence, we decided on solutions which can be obtained by an iterative least squares refinement procedure. The computer program LEASK[3] was designed to find solutions for the unknowns of m sets of equations in n unknowns provided $m \geqslant n$. The operation of this program will be described further on. In order to solve for stability constants, we first must obtain the values for m, a, and h from the experimental data.

Computer Calculations

The programs are described in the order of their use.

Evaluation of Eq. 18 by Program PLOT[3]

All the parameters except pA_0 which are necessary to solve eq. 18 can be calculated from the experimental data which are represented by the titration curves. A value for pA_0 can be calculated from the total concentration of component A. For the ease of processing, the continuous titration curves are converted into digitized tabular form by the operator, preferably, but not essentially, using equal intervals on the pH scale. These data are put on paper tape or cards, which then constitute the input to the program PLOT together with dimension statements and other experimental constants, *i.e.* pK_{a_1}, pK_{a_2}, pK_{a_3} for a tribasic ligand.

Step A: Calculation of the Differential Expressions $\delta H_1^+/\delta C_A$

(1) The input data are read from titration curves such as are represented in Fig. 1. These titration curves, A_1 to A_5, are obtained by titrating metal ligand mixtures of varying composition as prescribed by the particular experimental conditions. These data constitute a three dimensional array (x, y, z) where x stands for the amount of titrant (base) used, y represents the pH, and z stands for the amount of ligand or metal in the system. This array is stored as (x, y) pairs for a series of constant z values. The program first rearranges this array to produce a new array where the (x, z) pairs are stored for a series of constant y values yielding numerical functions $x = f(z)$ at constant y, as shown in Fig. 2.

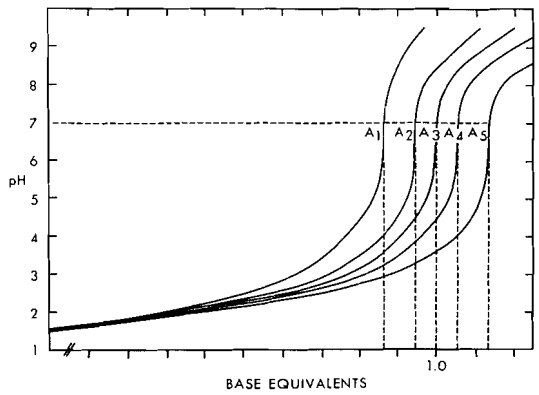

FIG. 1. Typical titration curves for a bidentate amino acid in the presence of Cu(II) with different Cu(II):ligand ratios. Curves A_1 to A_5 represent increasing concentrations of ligand with metal concentration kept constant.

(2) The differential $\delta H_1^+/\delta C_A$ which corresponds to $\delta x/\delta z$ in Fig. 2 at constant pH (constant y) is obtained as the slope of the function $H_1^+ = f(A)$.

(3) Next, the program performs an analytical curve fit to the data $x = f(z)$ using a standard subroutine POLFIT. The series of functions obtained are stored with respect to pH.

(4) A slightly modified version of POLFIT (POLFIT*) is called, and by numerical differentiation, finds the slope of the functions $x = f(z)$ at the midpoint A_i for each pH.

(5) The values found for the slopes $\delta H_1^+/\delta C_A$ are now printed out in tabular form with their respective pH_i values. Fig. 3 graphs an example of this new numerical function

[29] $$\delta H_1^+/\delta C_A = f(\mathrm{p}H)$$

Step B: Evaluation of the integral expression eq. 18

(1) The program again calls the subroutine POLFIT which is now used to fit a curve through the points $(\delta H_1^+/\delta C_A)_i$, pH_i yielding an equation in polynomial form. The integration is accom-

Can. J. Chem. Downloaded from www.nrcresearchpress.com by 210.87.254.5 on 09/05/12
For personal use only.

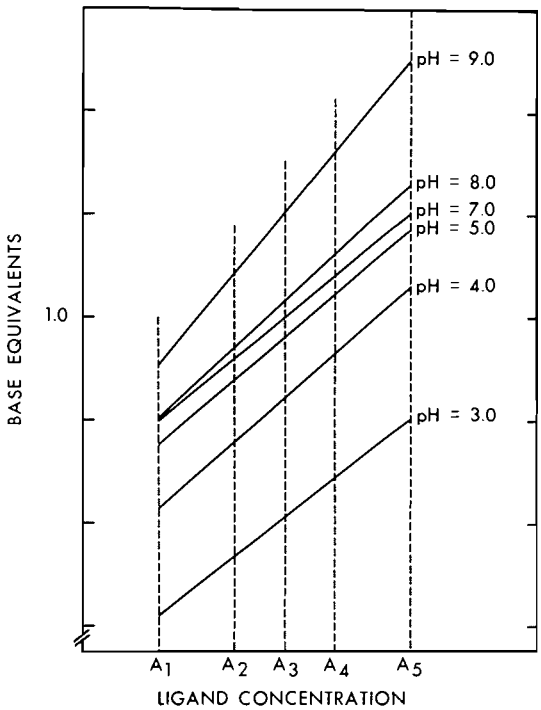

FIG. 2. Base equivalents are graphed as a function of ligand concentration at constant pH values. Solid lines represent the data for the respective pH values and dotted lines represent the ligand concentrations A_1 to A_5.

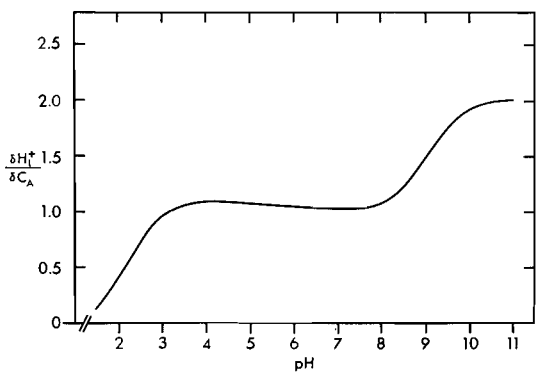

FIG. 3. Proton liberation ($\delta H_1^+/\delta C_A$) is graphed as a function of pH.

plished by appropriate conversion of the terms and subsequent insertion of the limits necessary to evaluate the definite integral.

(2) This transposition is performed by the program and the integral is then evaluated for each upper limit pH_i and added to pA_0 as required by eq. 18. This operation evaluates pA as a function of pH (Fig. 4).

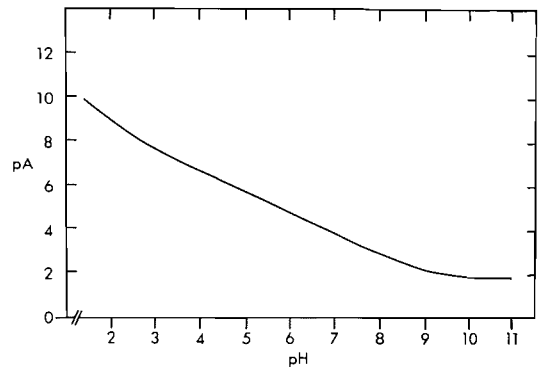

FIG. 4. Unbound ligand concentration (pA) is graphed as a function of pH.

(3) The numerical values of pA_i are printed out in tabular form, which constitutes the final output of the program PLOT. This output is stored under a coded file-name for further usage by subsequent programs.

This same method is followed for any of the constituents whose concentration in the reaction mixture has to be estimated. It should be noted that up to this point pA and pM are obtained as functions of pH only without the need of assuming anything about complexity of the system.

Calculation of the Coefficient Matrix A_{ij} by Program GUESS[3]

(1) The program GUESS reads in the tabular results of $pA = f(pH)$ and $pM = f(pH)$ which were computed by the program PLOT.

(2) For each triplet pA, pM, pH, antilogs are found and then all likely combinations of $m^p h^q a^r$ are performed to give the elements a_{ij} for the matrix $\mathbf{A}_{ij}$ by letting p, q, and r take on values which are likely to represent real complexes.

Assumptions and limitations have to be taken at this point in order to keep the matrix small enough to fit into the computer memory available. It has been found that an upper limit of ten unknowns, representing simultaneously existing complex species, was quite satisfactory. Fewer unknowns of course greatly speed up the processing of the data.

(3) The coefficient matrix $\mathbf{A}_{ij}$ provides the input for the following program LEASK.

Determination of Stability Constants by Program LEASK[3]

The problem at hand is to solve a set of simultaneous equations with n unknowns. Standard techniques of matrix inversion are not usable

Can. J. Chem. Downloaded from www.nrcresearchpress.com by 210.87.254.5 on 09/05/12
For personal use only.

since they operate analytically (no error provisions). They can also produce negative values for the unknowns which, in the case of stability constants, is nonsense. Therefore, we decided to employ an iterative least squares method in our program LEASK which attempts to minimize the error sum $R = \sum_i (d_{i,\text{exptl}} - d_{i,\text{calcd}})^2$ where $d = f(x_1,x_2,...,x_n;a_1,a_2,...,a_n)$ as shown in eq. 26.

Step A

(1) The coefficient matrix $\mathbf{A}_{ij}$ is read into the active part of the computer from an internal file. At the same time, the $\boldsymbol{d}_{\text{exptl}}$, which consists of all the experimental d_i values, is read in and aligned for further processing.

(2) An initial estimate of the elements of the $\boldsymbol{x}$ vector is read in, plus several commands which the program will refer to as it goes through with its execution.

Step B

Minimization of dR/dX. Numerically this is achieved by

(1) Multiplying $\mathbf{A}_{ij}$ with $\boldsymbol{x}$ estimates to give the column vector $\boldsymbol{d}_{\text{calcd}}$. The difference between this and $\boldsymbol{d}_{\text{exptl}}$ is found element by element

$$[30] \qquad (d_{i,\text{exptl}} - d_{i,\text{calcd}}) = F_i$$

and these F_i are squared and summed to give $R = \sum_i F_i^2$ which is stored.

(2) Now the $\boldsymbol{x}$ is operated on element by element, *i.e.*, x_1 is set to $x_1 + x_1 \cdot k$. The computation $\mathbf{A}_{ij} \cdot \boldsymbol{x}' = \boldsymbol{d}'_{\text{calcd}}$ is again executed and the new $\boldsymbol{d}'_{i,\text{calcd}}$ are used to find new $(F''_i)^2$ which sum up to give a new R'. If the test for this trial shows $R > R'$, then this new vector is stored and used as a new first approximation for the next try. If the initial try was bad, as to give $R < R'$, then k will be altered including change of sign until a better minimum is found. If no minimization can be located after a preset number of trials, x_1 is retained and the operation moves on to x_2 and repeats itself.

(3) After $\boldsymbol{x}$ has been scanned completely and a new R' has been found which is smaller than R_i, this new x' will be stored together with R'.

(4) The program loops back to No. 2 above, sets x'_1 equal to $x'_1 + x'_1 \cdot k$, and goes through the logic and arithmetic again to give R''.

(5) If $R'' < R'$, then $\boldsymbol{x}$ will be stored and another iteration will be initiated. However, if $R'' > R'$, then $\boldsymbol{x}$ will be accepted as the solution vector corresponding to the minimum deviation of the calculated from the experimental results and will be printed out in tabular form.

(6) Additional criteria of acceptable convergence are built into the program. Only a predetermined number of oscillations about a constant value for R are allowed. Also, the number of iterations are limited. By the choice of k values the program keeps all x_i's positive or drives them towards the lower limit of computational accuracy. Another criterion of acceptance is provided if all the d_{calcd} come to within a preset percentage of d_{exptl}.

(7) After the minimum $\boldsymbol{x}_{\min}$ is found, the matrix $\mathbf{A}_{ij}$ is multiplied element by element with $\boldsymbol{x}$. These products are printed out in tabular form, they represent the species distribution of all the complexes found in the system analyzed.

Recalling, $[M_pH_qA_r] = \beta_{pqr}a_{ij}$, then each column will represent the concentration of the species at pH_i values and the associated x_j will represent the stability constant for that species.

Discussion

All the classical methods for evaluating stability constants (1) necessitate prior knowledge or assumptions of the species composition before meaningful computations can be performed. The logic contained in the present mathematical treatment of the data and computations for obtaining unbound metal and ligands are rigorous and do not require any assumptions as to the species present in the system. Utilizing eq. 21 and assuming $\log \beta_{pqr} = x$, then inserting values for a, m, and h for different pH values, a pH profile for all the theoretical species $M_pH_qA_r$ can be constructed. If x is set equal to $\log m^p h^q a^r$ then all species will show a maximum concentration of 1.0 (provided $p = 1$) if expressed in terms of bound metal. On the basis of this preliminary species distribution one can judge which species are likely to exist and where on the pH scale they have maximum concentration. If two species show identical shapes, *i.e.* if they overlap all along their pH profile the matrix $\mathbf{A}_{ij}$ cannot be solved because two columns are identical. Then one of the two species must be eliminated before proceeding to program LEASK. If we have proposed a species that does not exist, the program will eliminate it. If we fall short, then the residual error will be large and the species distribution will indicate on the pH scale where it is missing.

The operator will simply come up with a suitable combination of $a_{ij} = f(pH)$ to fill the void.[6]

The batch oriented LETAGROP programs (9) are very versatile in this area of investigation. It requires a large memory computer and the operational expenses are rather high. Whereas our programs are specialized and are aimed at economical operation by using high speed remote terminal time-sharing systems. Even though input data are somewhat different, the output data (β values) are of equivalent precision.

The analytical system proposed here has several features which are desirable and should prove advantageous. Our method in addition to the stability constant values will yield other intermediate data, such as proton liberation data as a function of p*H* and also as a function of metal or ligand concentration. This information is very useful as an aid in structural interpretation (21). Also, while operating these programs in conversational mode, the operator has a constant check on the progress of the computations, which is useful in spotting erroneous input data which would influence the magnitude of the β values and cause large error sum squares. Thus, execution of the program can be terminated prematurely with resulting economy in computer usage. Since this is only possible when operating in conversational mode we have therefore adjusted our programs to run on time-sharing systems accepting FORTRAN IV language.

This work was supported by grants from the John A. Hartford Foundation of New York and the Medical Research Council of Canada.

[6]Our proposed method was verified by Professor W. A. E. McBryde. The well known Cu(II)–glycine system was chosen for the purpose of verification of our method. Using published protonation constants and complex stability constants calculations were performed to produce synthetic data sets equivalent to real titration data (p*H* *vs.* strong base). Also values for p*M* and p*A* for the various p*H* values were calculated. This was done for a variety of C_A and C_M. These synthetic titration data in turn were processed by the Sarkar and Kruck method to produce values for p*A*, p*M*, and the complex stability constants β_{11} and β_{12} for the metal ligand interaction. The values found showed excellent agreement throughout the full range of titration data.

1. F. J. C. Rossotti and H. Rossotti. The determination of stability constants. McGraw Hill Inc., New York, N.Y. 1961.
2. M. T. Beck. Chemistry of complex equilibria. Van Nostrand Reinhold Company, London. 1970.
3. J. Bjerrum. Metal ammine formation in aqueous solution. P. Haase and Son, Copenhagen. 1941.
4. B. Hedström. Acta Chem. Scand. **9**, 613 (1955).
5. J. Lefebvre. J. Chim. Phys. **57**, 553 (1957).
6. J. Lefevbre. J. Chim. Phys. **59**, 581 (1957).
7. R. Österberg. Acta Chem. Scand. **14**, 471 (1960).
8. L. G. Sillén. Acta Chem. Scand. **15**, 1981 (1961).
9. L. G. Sillén and N. Ingri. Acta Chem. Scand. **16**, 173 (1962).
10. L. G. Sillén. Acta Chem. Scand. **18**, 1085 (1964).
11. L. G. Sillén and N. Ingri. Ark. Khem. **23**, 97 (1964).
12. R. Osterberg. Acta Chem. Scand. **19**, 1445 (1965).
13. R.-P. Martin. Rev. Pure Appl. Chem. **19**, 171 (1969).
14. B. Sarkar, Y. Wigfield, M. L. Lee, T. P. A. Kruck, and S. Lau. Proceedings of the XIIth International Conference on Coordination Chemistry. *Edited by* H. C. Freeman. Science Press. Merricville, Sydney, Australia. 1969. p. 126.
15. B. Sarkar, P. E. McLeod, T. P. A. Kruck, S. Lau, and J. Breckenridge. Proceedings of the XIIIth International Conference on Coordination Chemistry. Vol. II. *Edited by* W. Kakolowicz. Polish Academy of Science, Cracow-Zakopane, Poland. 1970. p. 24.
16. B. Sarkar and T. P. A. Kruck. Proceedings of the XIVth International Conference on Coordination Chemistry, Toronto, Canada. 1972. p. 395.
17. B. Sarkar. Proceedings of the IXth International Congress of Biochemistry, Stockholm, Sweden. 1973.
18. B. Sarkar, T. P. A. Kruck, and S. Lau. Proceedings of the XVth International Conference on Coordination Chemistry, Moscow, U.S.S.R. 1973.
19. B. Sarkar, T. P. A. Kruck, and S. Lau. Proceedings of the 56th Canadian Chemical Conference, Montreal, Canada. 1973.
20. T. P. A. Kruck and B. Sarkar. Can. J. Chem. This issue.
21. T. P. A. Kruck and B. Sarkar. Can. J. Chem. This issue.
22. T. P. A. Kruck and B. Sarkar. Can. J. Chem. This issue.
23. D. W. Appleton and B. Sarkar. Proceedings of the Canadian Federation of Biological Societies. Vol. 16. 1973.

Can. J. Chem. Downloaded from www.nrcresearchpress.com by 210.87.254.5 on 09/05/12
For personal use only.

Equilibria of the Simultaneously Existing Multiple Species in the Copper(II)–L-Histidine System

THEO P. A. KRUCK AND BIBUDHENDRA SARKAR[1]

Division of Biochemistry, The Research Institute, The Hospital for Sick Children, Toronto, and Department of Biochemistry, University of Toronto, Toronto, Ontario M5G 1X8

Received June 14, 1972[2]

The complete species distribution and the stability constants of the complex species in the Cu(II)–L-histidine system have been worked out for the p*H* range 2–11. The method of "analytical potentiometry" has been applied successfully to this system having excess ligand with respect to Cu(II) ion. The equilibria of three systems of Cu(II) (M) and L-histidine (H_3A) in molar ratios of 1:2, 1:4, and 1:8 were investigated by this technique in 0.15 *M* NaCl at 25°. The following species were detected in this system: MHA, MA, MH_2A_2, MHA_2, MA_2, $MH_{-1}A_2$, $MH_{-1}A$, and $M_2H_{-2}A_2$. Statistical analysis on the numerical results has been performed and is given as standard deviation together with the individual values for the stability constants.

La distribution complète des espèces et les constantes de stabilité des espèces complexes dans le système Cu(II)–L-histidine ont été étudiés dans le domaine de p*H* de 2 à 11. La méthode de "potentiométrie analytique" a été appliquée avec succès à ce système qui possède un excès de ligand par rapport à l'ion Cu(II). Les équilibres des trois systèmes Cu(II) (M) et L-histidine (H_3A) dans les rapports molaires 1:2, 1:4, et 1:8 ont été étudiés par cette technique dans NaCl 0.1 *M* à 25°. Les espèces suivantes ont été détectées pour ce système: MHA, MA, MH_2A_2, MHA_2, MA_2, $MH_{-1}A_2$, $MH_{-1}A$ et $M_2H_{-2}A_2$. L'analyse statistique du résultat numérique a été faite et donnée comme dérivation standard de même que les valeurs individuelles des constantes de stabilité. [Traduit par le journal]

Can. J. Chem., 51, 3549 (1973)

Introduction

The Cu(II)–L-histidine system has been of interest to many workers in the field of metal complexation because of the many different geometric arrangements that are possible when attempting to coordinate one or two tridentate ligands to Cu(II) ion. The stability constants for Cu(II)–L-histidine complexes of the type MA and MA_2 have been reported by several authors (1). Leberman and Rabin (2) considered the coordination of a water molecule to the 1:1 L-histidine:Cu(II) complex and the subsequent dissociation of a proton from the hydrated complex. However they only reported the stability constants for the species MA and MA_2. Perrin and Sharma (3) later expanded the system to include MHA, MHA_2, MH_2A_2, and all other previously reported species. In addition, they also worked out stability constants for hydroxylated complexes $MH_{-1}A$ and $M_2H_{-2}A_2$. Freeman and Martin (4) had worked out the most exhaustive list of stability constants for this system while studying a mixed complexation reaction involving L-histidine. But, so far, the complete species distribution of all the complexes existing in solution in the p*H* range 2 to 11 has not been worked out in detail.

Our interest in the Cu(II)–L-histidine system dates back to the isolation of the Cu(II)–L-histidine complex from normal human blood serum (5) and the demonstration of the existence of the mixed complex L-histidine – Cu(II) – L-threonine and other mixed complexes (6). Previous work involving Cu(II)–L-histidine complexes (7–10) demonstrated the need for an extensive analysis of the Cu(II)–L-histidine system. This, as well as the need to test our newly proposed analytical technique (11), prompted us to examine the Cu(II)–L-histidine system precisely over as large a p*H* range as possible. The low p*H* and high p*H* cutoff was determined by the need to introduce assumptions beyond these limits relating to the accurate determination of p*H* and activity coefficients.

Experimental Section

Materials

All reagents used were of analytical grade. L-Histidine free base ($[\alpha]_D^{20}$ + 39.9° ± 0.5°) was obtained from Nutritional Biochemicals. The amino acid was tested for its purity by chromatography. It was dried and stored over anhydrous calcium chloride at room temperature

[1]To whom correspondence should be addressed.

[2]Revision received May 29, 1973.

Can. J. Chem. Downloaded from www.nrcresearchpress.com by 210.87.254.6 on 09/05/12
For personal use only.

Can. J. Chem. Downloaded from www.nrcresearchpress.com by 210.87.254.6 on 09/05/12
For personal use only.

under vacuum. The water was first distilled and then deionized by passing it through a commercial ion exchange column ILICO WAY-X research model which had been extensively rinsed with distilled water before use. Prepurified nitrogen was used to maintain a nitrogen atmosphere throughout the titration. The base used for the titration was carbonate free 5.010 *N* NaOH standardized against weighed amounts of dried potassium hydrogen phthalate. It was stored in a dry, CO_2-free atmosphere. A solution of 1.0 *N* HCl was prepared by dilution of constant boiling high purity 6 *N* HCl and subsequently standardized against 5.010 *N* NaOH. The stock solutions of L-histidine, anhydrous $CuCl_2$, and NaCl were prepared from vacuum dried materials. The L-histidine and the $CuCl_2$ solutions were checked titrimetrically.

Titration Apparatus

The potentiometric titrations were performed by a Radiometer automatic titrator. The assembly consisted of the expanded scale p*H* meter pHM26, automatic titrator TTT11B, automatic recorder SBRII, automatic syringe, and the 50 ml thermostated titration assembly set to 25 ± 0.05°.

Electrodes and Calibrations

In order to perform repetitive titrations starting from p*H* 1 through to p*H* 11, it was necessary to select a suitable electrode pair. Both the glass electrode and calomel reference electrode had to be carefully scrutinized. A salt bridge furnished with a porous sintered glass plug was used in conjunction with a radiometer reference electrode K401. The flow rate of the saturated KCl solution was in the order of 50 µl/h. A radiometer glass electrode of the G2222 series was found to be linear over the range of p*H* 1.00 to 11.00 using standard buffer solutions of ±0.02 p*H* unit accuracy. The standard buffer solutions were of p*H* 1.00, 2.00, 3.00, 4.00, 7.00, 9.00, and 11.00. This electrode permitted a maximum of three consecutive titrations before extensive low p*H* incubation became necessary to have stable linear p*H* response. A radiometer glass electrode of the series G202B was found to permit up to five consecutive titrations before instability due to increased impedance set in. Regeneration of this electrode could be obtained by immersing it in 1 *N* HCl for 1 h or else by incubating it overnight in p*H* 7.00 buffer. To calibrate the p*H* scale of the apparatus in terms of hydrogen ion concentration, several solutions of known concentrations of HCl in 0.15 *M* NaCl were titrated before and after every experiment. The solutions were prepared from calibrated standard HCl by exact dilution.

Method

The equilibria of the Cu(II)–L-histidine system can be expressed by the general equation[3]

$$[1] \qquad pM^{2+} + qH^{+} + rA^{-} \leftrightarrows M_pH_qA_r^{(2p+q-r)}$$

The overall equilibrium constant for this system can be defined as

$$[2] \qquad \beta_{pqr} = \frac{[M_pH_qA_r]}{m^p h^q a^r}$$

[3]See preceeding article for definitions of symbols.

Certain experimental conditions must be met in order for the theoretically derived functions (11)[4] to hold. We have presented functions as in eqs. 3 and 4

$$[3] \quad p(H_3A) = p(H_3A)_0 + \int_{pH_0}^{pH_1} \frac{\delta H_1^{+}}{\delta C_A} dpH \Bigg|_{C_M,P,V,T,\mu=\text{constant}}$$

$$[4] \quad pm = pm_0 + \int_{pH_0}^{pH_1} \frac{\delta H_1^{+}}{\delta C_M} dpH \Bigg|_{C_A,P,V,T,\mu=\text{constant}}$$

which permit the calculation of unbound ligand *a* or the unbound metal *m* as a function of p*H* in the presence of other reactants, provided the concentrations of those reactants do not vary. Also, pressure, temperature, and volume must be kept constant. Nitrogen provides an inert atmosphere of constant pressure. A thermostated reaction vessel $T \pm 0.1$ °C is sufficient to provide constant temperature. Constant volume is more difficult to achieve and can only be approximated. It is done by using large volumes of reaction mixtures and keeping the added titrant volume small. The inevitable change of volume, although small, must be taken into account when calculating the hydrogen ion concentration *h* from p*H* values. Furthermore, the activity coefficients of all the reactants must be controlled for eq. 2 to hold. Using a background electrolyte in excess of the concentration of the reacting species permits one to use concentration terms instead of activities of the reactants. In order to relate this system to physiological conditions, 0.15 *M* NaCl was chosen as background electrolyte being fully aware that Cl^- is a ligand for Cu(II) competing to a low degree with L-histidine and OH^- for this metal ion. All titrations were done in duplicate and if they did not agree

Set No.	$C_M \times 10^2$ (*M*)	$C_A \times 10^2$ (*M*)	$C_{HCl} \times 10^2$ (*M*)
M variation			
1	0.0	2.0	14.000
	0.5	2.0	14.005
	1.0	2.0	14.010
2	0.0	4.0	18.000
	1.0	4.0	18.010
	2.0	4.0	18.020
3	0.0	8.0	26.000
	1.0	8.0	26.010
	2.0	8.0	26.020
	3.0	8.0	26.030
	4.0	8.0	26.040
A variation			
4	1.0	2.0	14.010
	1.0	4.0	18.010
	1.0	8.0	26.010
5	2.0	4.0	18.020
	4.0	8.0	26.040

[4]First article in this series.

Can. J. Chem. Downloaded from www.nrcresearchpress.com by 210.87.254.6 on 09/05/12
For personal use only.

within 2 μl on the base scale and 0.05 pH units on the pH scale, then a third titration was performed. Possible zero errors in base delivery were accounted for by comparing inflection points on the titration curves.

"Analytical potentiometry" (11) was used to resolve the Cu(II)–L-histidine system and produce stability constants for all the species detected. Using integrating and differentiating techniques (eqs. 3 and 4) it is possible to deduce from families of titration curves, the free metal m and ligand a concentrations in the system after the initial values m_0 and $[H_3A]_0$ have been determined. At a starting pH of about pH 2 one can calculate the concentration of the fully protonated ligand H_3A species from the known acid dissociation constant pK_a, of the ligand utilizing eq. 5

$$[5] \quad [H_3A] = \frac{C_A}{1 + \text{antilog}\,(pH - pK_a)}$$

At low pH in this system $m_0 = C_M$. Also, during any titration equilibrium must be maintained. None of the total concentrations of reactants excepting h (pH) must change in order for eqs. 3 and 4 to be true. The required change δC_M or δC_A for the mathematical treatment of data was produced by performing different titrations containing systematically varied concentrations of $CuCl_2$ and L-histidine as part of the reaction mixtures. It should be noted that if the pH is low enough that $m_0 = C_M$ then all the titration curves will show a common starting pH as can be seen in Fig. 1. The same is true for the protonated ligand. The method for evaluating the functions given in eqs. 3 and 4 will be discussed later. The resulting data $m = f(pH)$ and $a = f([H_3A]) = f(pH)$ now can be used to evaluate the stability constants of complex species represented by eq. 2.

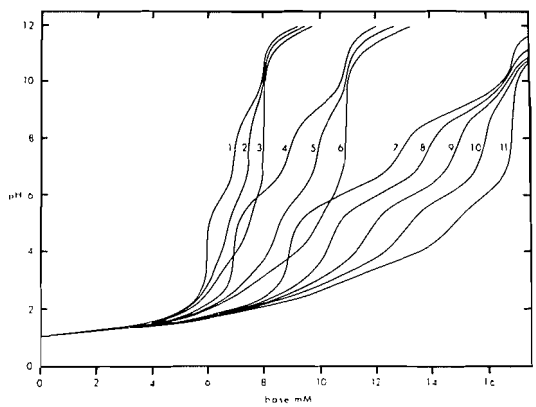

FIG. 1. Titration curves for the system Cu(II)–L-histidine (metal variations). Curve 1, $C_M = 0.0\ M$, $C_A = 20 \times 10^{-3}\ M$; curve 2, $C_M = 5 \times 10^{-3}\ M$, $C_A = 20 \times 10^{-3}\ M$; curve 3, $C_M = 10 \times 10^{-3}\ M$, $C_A = 20 \times 10^{-3}\ M$; curve 4, $C_M = 0.0 \times 10^{-3}\ M$, $C_A = 40 \times 10^{-3}\ M$; curve 5, $C_M = 10 \times 10^{-3}\ M$, $C_A = 40 \times 10^{-3}\ M$; curve 6, $C_M = 20 \times 10^{-3}\ M$, $C_A = 40 \times 10^{-3}\ M$; curve 7, $C_M = 0.0\ M$, $C_A = 80 \times 10^{-3}\ M$; curve 8, $C_M = 10 \times 10^{-3}\ M$, $C_A = 80 \times 10^{-3}\ M$; curve 9, $C_M = 20 \times 10^{-3}\ M$, $C_A = 80 \times 10^{-3}\ M$; curve 10, $C_M = 30 \times 10^{-3}\ M$, $C_A = 80 \times 10^{-3}\ M$; curve 11, $C_M = 40 \times 10^{-3}\ M$, $C_A = 80 \times 10^{-3}\ M$.

Data: C_A, a, C_H *and* h; *System*: A, H

Although good values for the acid dissociation of L-histidine are available from the literature (4) we preferred to check the pK_a values for L-histidine in our system. L-Histidine solutions were titrated in the presence of 0.15 M NaCl with standard acid or base. The values found were in good agreement with literature values (4). Our own values were used in subsequent calculations.

Data: C_M, m, C_A, a, C_H *and* h; *System*: M, A

Potentiometric titrations were carried out on a series of solutions (50 ml volume) of a 0.15 M NaCl, 0.1 N HCl, containing combinations of L-histidine (10, 20, 40, and 80 mM) and $CuCl_2$ (0, 5, 10, 20, 30, and 40 mM).[5]

Calculation of Results

The families of titration curves obtained are presented in Figs. 1 and 2. The data obtained from sets 1–3 were used to obtain the proton liberation $\delta H_1^+/\delta C_M$ at constant pH due to the

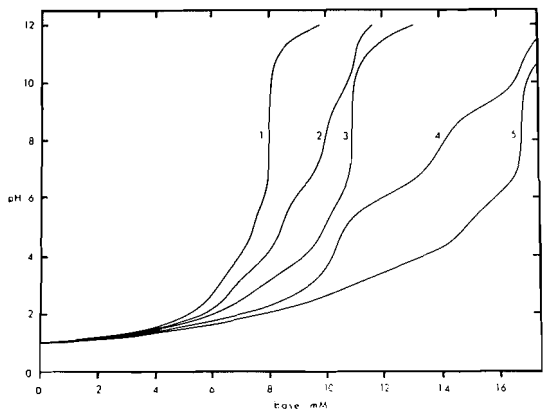

FIG. 2. Titration curves for the system Cu(II)–L-histidine (ligand variations). Curve 1, $C_A = 20 \times 10^{-3}\ M$, $C_M = 10 \times 10^{-3}\ M$; curve 2, $C_A = 40 \times 10^{-3}\ M$, $C_M = 10 \times 10^{-3}\ M$; curve 3, $C_A = 40 \times 10^{-3}\ M$, $C_M = 20 \times 10^{-3}\ M$; curve 4, $C_A = 80 \times 10^{-3}\ M$, $C_M = 10 \times 10^{-3}\ M$; curve 5, $C_A = 80 \times 10^{-3}\ M$, $C_M = 40 \times 10^{-3}\ M$.

[5]The solution of Cu(II)–L-histidine was prepared freshly for each experiment. The maximum time elapsed between the preparation of the Cu(II)–L-histidine solution and the completion of the experiment, was 30 min. This procedure was followed routinely since Cu(II)–L-histidine in aqueous solution is not stable according to the spectral features of the system taken at different time intervals. These spectral features seem to arise from the relatively slow, time-dependent formation of other compounds of undetermined nature. Thus, the experiments with Cu(II)–L-histidine must be completed within a time limit during which formation of no other compounds is assured (17). The titration curves coincided initially at low pH.

Can. J. Chem. Downloaded from www.nrcresearchpress.com by 210.87.254.6 on 09/05/12
For personal use only.

variation of Cu(II) concentration. The data from sets 4 and 5 were processed, yielding the proton displacement $\delta H_1^+/\delta C_A$ at constant pH due to variations of the ligand concentration. The data $\delta H_1^+/\delta C_M$ were further processed according to eq. 4 to obtain pm as a function of pH. Similarly, the data $\delta H_1^+/\delta C_A$ were treated mathematically according to eq. 3 to give p(H_3A) as a function of pH. It should be noted here that

$$[6] \quad pa = p(H_3A) + pK_1 + pK_2 + pK_3 - 3pH$$

A series of computer programs[6] was written for the treatment of these data. The original titration curves were digitized and subsequently the program PLOT was used to normalize and rearrange the raw data. The same program performed operations of curve fitting and differentiation yielding the numerical value of the slopes $\delta H_1^+/\delta C_M$ *vs.* pH in the case of metal variation. Another curve fit was executed on the function $\delta H_1^+/\delta C_M$ and a cumulative integration was performed according to eq. 4 where pH_i was chosen to progress in intervals of 0.5 units starting from pH_0. The resulting output pm *vs.* pH was printed in tabular form. The same program PLOT was employed to evaluate the data for the ligand variation in order to get pa as a function of pH.

The stoichiometric stability constant is expressed in eq. 2. The bound M is represented by the summation of all complex species present.

$$[7] \quad (C_M - m) = \sum p[M_pH_qA_r] = \sum p(\beta_{pqr} m^p h^q a^r)$$

Replacing β_{pqr} and $M^pH^qA^r$ by β_j and C_j respectively eq. 7 becomes

$$[8] \quad (C_M - m) = \sum p\beta_j C_j$$

Equation 8 is of the form

$$[9] \quad y = C_1\beta_1 + C_2\beta_2 + C_n\beta_n$$

Using pH, pm, and pa as input, the program GUESS was employed to calculate the coefficients $(C_1 \ldots C_n)$ and the corresponding y vector. This matrix was solved by the third program LEASK, which is an iterative least squares refinement technique, requiring approximate values for $(\beta_1 \ldots \beta_n)$ to obtain refined values for the stability constants. Repeating this process for the different experimental data from sets 1–5 we obtained the species distributions in 1:2, 1:4, and 1:8 Cu(II)/L-histidine systems in

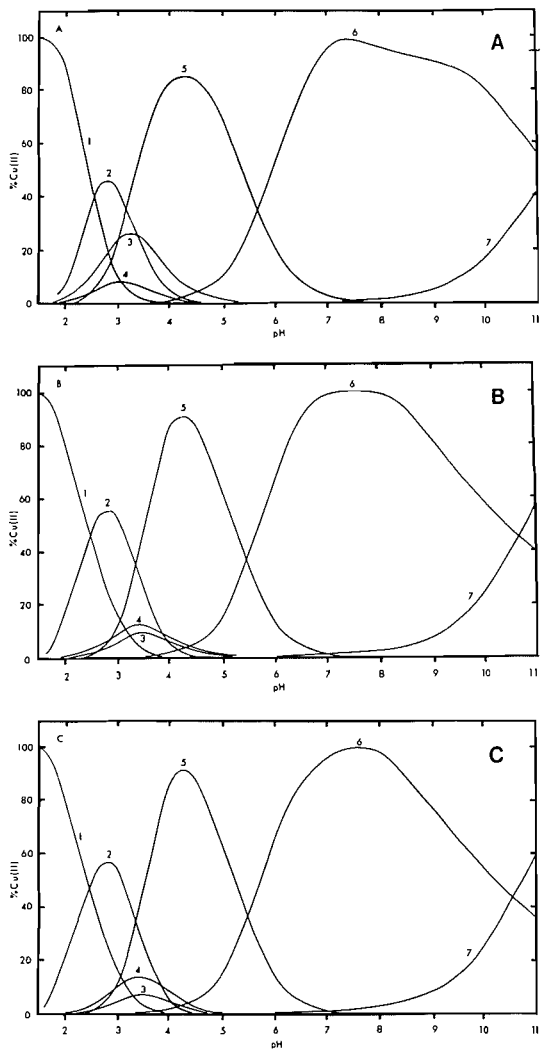

FIG. 3. Species distribution in Cu(II)-L-histidine system as a function of pH. *A*, *B*, and *C* represent the metal to ligand ratios of 1:2, 1:4, and 1:8, respectively. Curve 1, unbound Cu(II); curve 2, MHA; curve 3, MA; curve 4, MH_2A_2; curve 5, MHA_2; curve 6, MA_2; curve 7, $MH_{-1}A_2$.

[6]Three computer programs: PLOT, GUESS, and LEASK were written in Fortran IV. The programs have been deposited as Document No. NAPS-01563 with the ASIS National Auxiliary Publication Service, c/o CCM Information Corp., 866 Third Avenue, New York, N.Y. 10022. A copy may be secured by citing the document number and by remitting $1.00 for microfiche or $3.00 for photocopies. Advance payment is required. Make cheques or money orders payable to: ASIS-NAPS.

TABLE 1. log stability constants (log β_{pqr}) of complex species $M_pH_qA_r$ (M = Cu(II), A = L-histidine in 0.15 *M* NaCl at 25°; standard deviations (s(log β_{pqr})) are shown in parentheses)

			log β_{pqr}					
				Other references				
p	q	r	Present work (0.15 *M* NaCl, 25°)	Ref. 4 (0.1 *M* KNO_3, 25°)	Ref. 3 (0.15 *M* KNO_3, 37°)	Ref. 16 (0.10 *M* KCl, 25°)	Ref. 2 (γ/2 0.01, 25°)	Ref. 15 (0.2 *M* KNO_3, 25°)
0	1	1	9.111 (0.007)	9.117 (0.005)	8.916	9.08	9.16	9.17
0	2	1	15.170 (0.010)	15.158 (0.006)	14.872	15.06	15.16	15.25
0	3	1	16.999 (0.016)	16.92 (0.140)	17.113		16.98	17.02
1	1	1	14.180 (0.009)	14.062 (0.001)	14.03			
1	0	1	10.200 (0.019)	10.13 (0.001)	9.79	10.21	10.56	10.30
1	−1	1	2.000 (0.320)	2.13 (0.010)	2.17			
1	2	2	26.913 (0.090)	26.85 (0.020)				
1	1	2	24.007 (0.057)	23.645 (0.002)	23.05			
1	0	2	18.453 (0.008)	18.10 (0.001)	17.41	18.53	18.81	
2	−2	2	8.043 (0.398)	8.016 (0.004)	6.97			
1	−1	2	7.710 (0.036)					

p*H* range 2–11 (Fig. 3 *A–C*).[7] The respective stability constants of the species are tabulated in Table 1.

All calculations were performed on a General Electric model 440 computer.

Discussion

In the present study the following species were detected and their stability constants have been evaluated: MHA, MA, MHA_2, MH_2A_2, MA_2, $MH_{-1}A$, $M_2H_{-2}A_2$, and $MH_{-1}A_2$. The β values computed are in close agreement with values obtained by other authors (Table 1), excepting the ones obtained for the hydroxylated complex $MH_{-1}A$ and its dimer $M_2H_{-2}A_2$. Our values reported for these complexes tend to come to closer agreement with those reported by Freeman and Martin (4). It should be noted, however, that a slight deviation in these figures may arise from the difficulty of calculating the very small amounts of these complexes being formed when excess ligand is available. Also inspection of the standard deviations reveals very large values casting doubt on the accuracy of the stability constant values presented for these complexes.

In addition, we found that a new species $MH_{-1}A_2$ appears at high p*H* in appreciable amounts reading about 20% of the total bound copper at p*H* 10 and exceeding that amount at higher p*H* values (Fig. 3*A–C*). Comparing the species distributions, apart from the absolute profiles for the individual species, one can see that the relative amounts of MA and MH_2A_2 are varying in accordance with the metal-to-ligand ratio. As the ratio decreases more of the 1:1 complex MA is being formed at the cost of MH_2A_2 while the other complexes MHA and MHA_2 existing in the same p*H* range seem relatively unaffected. This situation would be expected to change drastically once the ratio of Cu(II) to L-histidine is reduced below 1:2. Then the 1:1 complexes predominate as shown by Perrin (12). We are, however, not interested in examining a system which is forced towards favoring certain complexes but rather we wanted to show the influence or lack of it upon the species distribution in the presence of excess ligand. In the range around the physiological p*H* it seems that varying concentrations of excess L-histidine do not change the amount of MA_2 present in the system.

Our method for evaluation of stability constants by program LEASK (11) is sensitive to experimental errors occurring at the extreme values of the p*H* scale. This can be accounted

[7]Although we observed a slow breakdown of L-histidine in the Cu(II)–L-histidine systems at high p*H* which expressed itself in a color change from deep blue to black in the course of several hours, the process did not materially affect our study since the solutions used for potentiometry never spent more than 10 min (usually less) at high p*H* values. At p*H* values beyond 11 the breakdown was noticeable and the data were discarded.

Can. J. Chem. Downloaded from www.nrcresearchpress.com by 210.87.254.6 on 09/05/12
For personal use only.

for by including weighting factors in the simultaneous equation at very low or at very high p*H* values. As an alternative, one can run the titration curves beyond these values, *e.g.* p*H* 1 to 12 and subsequently incorporate only the data between p*H* 2 and p*H* 11 in the calculation of the stability constants. In this manner weighting and biasing the data becomes unnecessary. In these calculations we have taken the latter course, and the resulting values for the stability constants support the applicability of our analytical method. However, if the extreme p*H* regions are of interest weighting factors could be included.

Species distributions are simple enough to be calculated from the experimental data. However, this has never been worked out previously for Cu(II)–L-histidine system covering wide enough p*H* range and in the presence of excess ligand. The knowledge of species distribution is necessary when analyzing structures of complex species in solution in a multispecies system. The delineation of the complete species distribution in this system has helped greatly in the elucidation of structures of the species in the Cu(II)–L-histidine system as well as in the studies of mixed complex equilibria involving L-histidine in the following two papers (13, 14).[8]

This work was supported by grants from the John A. Hartford Foundation of New York and the Medical Research Council of Canada.

[8]References 13 and 14 are the two articles following.

1. L. G. SILLÉN and A. E. MARTELL. Stability constants of metal–ion complexes. Chem. Soc. Special Publ. No. 17. 1964.
2. R. LEBERMAN and B. R. RABIN. Trans. Faraday Soc. **55**, 1660 (1959).
3. D. D. PERRIN and V. S. SHARMA. J. Chem. Soc. A, 727 (1967).
4. H. C. FREEMAN and R.-P. MARTIN. J. Biol. Chem. **244**, 4832 (1969).
5. B. SARKAR and T. P. A. KRUCK. Biochemistry of copper. *Edited by* J. Peisach, P. Aisen, and W. E. Blumberg. Academic Press, New York. 1966.
6. B. SARKAR and T. P. A. KRUCK. Can. J. Biochem. **45**, 2046 (1967).
7. D. I. M. HARRIS and A. SASS-KORTSAK. J. Clin. Invest. **46**, 659 (1967).
8. P. Z. NEUMANN and A. SASS-KORTSAK. J. Clin. Invest. **46**, 646 (1967).
9. B. SARKAR and Y. WIGFIELD. Can. J. Biochem. **46**, 601 (1968).
10. S. LAU and B. SARKAR. J. Biol. Chem. **246**, 5938 (1971).
11. B. SARKAR and T. P. A. KRUCK. Can. J. Chem. This issue.
12. D. D. PERRIN. Nature. **184**, 1868 (1959).
13. T. P. A. KRUCK and B. SARKAR. Can. J. Chem. This issue.
14. T. P. A. KRUCK and B. SARKAR. Can. J. Chem. This issue.
15. A. CHAKRAVORTY and F. A. COTTON. J. Phys. Chem. **67**, 2878 (1963).
16. M. A. DORAN, S. CHABEREK, and A. E. MARTELL. J. Am. Chem. Soc. **86**, 2129 (1964).
17. S. LAU and B. SARKAR. Unpublished results.

Can. J. Chem. Downloaded from www.nrcresearchpress.com by 210.87.254.6 on 09/05/12
For personal use only.

Ternary Coordination Complexes Between Copper(II) and Amino Acids, and an Appraisal of the Enhancement of Ternary Complex Stability

THEO P. A. KRUCK AND BIBUDHENDRA SARKAR[1]

Division of Biochemistry, The Research Institute, The Hospital for Sick Children, Toronto and Department of Biochemistry, University of Toronto, Toronto, Ontario M5G 1X8

Received June 14, 1972[2]

The equilibria involved in the ternary systems Cu(II)–A–B′ and Cu(II)–A–B″ (A = L-histidine, B′ = L-serine, B″ = L-glutamine) have been investigated by potentiometry in aqueous solution (0.15 *M* NaCl, 25°). In the ternary system Cu(II)–A–B′, three mixed complexes (MHAB′, MAB′, and $MH_{-1}AB'$) were detected in addition to the binary complex species (MHA, MA, MH_2A_2, MHA_2, MA_2, $MH_{-1}A_2$, MB′, MB'_2). The results observed in the Cu(II)–A–B″ system were quite similar to the system Cu(II)–A–B′ except that it did not show the presence of the species $MH_{-1}AB''$. The stability constants were refined with a general least squares treatment. In the case of an equimolecular mixture of the constituents, a maximum of about 75% of Cu(II) is present as MAB′ at p*H* 5.5–9 and about 60% of Cu(II) as MAB″ at p*H* 5–10 when the concentration of each constituent is set equal to 10^{-2} *M*. A theoretical analysis and derivations of the expected stability constants of the complexes are presented on the basis of successive formation constants of the individual complexes carrying identical ligands. In each case an enhancement of the stability was observed with the ternary coordination complexes. Attempts have been made to explain the enhanced stability of the ternary coordination complexes.

Les équilibres impliqués dans les systèmes ternaires Cu(II)–A–B′ et Cu(II)–A–B″ (A = L-histidine, B′ = L-sérine, B″ = L-glutamine) ont étudiés par potentiométrie en solution aqueuse (0.15 *M* NaCl, 25°). Dans le système ternaire Cu(II)–A–B′, trois complexes en mélange (MHAB′, MAB′ et $MH_{-1}AB'$) ont été détectés en plus des espèces du complexe binaire (MHA, MA, MH_2A_2, MHA_2, MA_2, $MH_{-1}A_2$, MB′, MB'_2). Les résultats observés pour le système Cu(II)–A–B″ sont très semblables au système Cu(II)–A–B′ à part l'absence des espèces $MH_{-1}AB''$. Les constantes de stabilité ont été raffinées par la méthode générale des moindres carrés. Dans le cas du mélange équimoléculaire de constituants, un maximum d'environ 75% de Cu(II) est présent comme MAB′ à p*H* 5.5–9 et 60% environ de Cu(II) en tant que MAB″ à p*H* 5–10 lorsque la concentration de chaque constituant est de 10^{-2} *M*. Une analyse théorique et les dérivés des constantes de stabilité attendues pour les complexes ont été présentées en se basant sur les constantes de formation successives des complexes individuels portant des ligands identiques. Dans tous les cas, un accroissement de stabilité a été observé pour les complexes ternaires de coordination qu'on a essayé d'expliquer.

[Traduit par le journal]

Can. J. Chem., **51**, 3555 (1973)

Introduction

Ternary coordination complexes are known to play important roles in many biological processes. Many enzymes are known to be activated by metal ions through the formation of enzyme – metal – substrate bridge structures (1). Metal coordination bonds have been suggested to participate in the interaction of polypeptide subunits of multichain enzymes providing the conformational stability of these enzyme molecules (2–5). Ternary coordination also appears to be functional in the mobilization and exchange of trace metals (6–8). It is known that in Cu(II)–amino acid complexes, the Cu(II) ion, with its preferred square planar geometry, binds a maximum of two amino acids. This provides the possibility for mixed Cu(II)–amino acid coordination to occur which has been demonstrated under physiological conditions (9), as well as *in vitro* systems (10–13). As part of a continuing investigation of the biologically important ternary coordination complexes of amino acids, peptides, proteins, and enzymes (6–16), we have made a detailed investigation of the multiple equilibria in two ternary systems: L-histidine–Cu(II)–L-serine and L-histidine–Cu(II)–L-glutamine in 0.15 *M* NaCl at 25°. We also present, in this paper, a theoretical analysis and the derivations of the expected stability constants of the complexes based on the successive formation constants of the individual complexes carrying

[1]To whom correspondence should be addressed.

[2]Revision received May 29, 1973.

Can. J. Chem. Downloaded from www.nrcresearchpress.com by 210.87.254.42 on 09/05/12
For personal use only.

identical ligands. In each case we observed an enhancement of the stability with the ternary coordination complexes.

Experimental Procedure

Materials

All reagents used were of analytical grade. L-Histidine free base ($[\alpha]_D^{20} = 39.9° \pm 0.5°$), L-serine ($[\alpha]_D^{20} = 14.3° \pm 0.2°$), and L-glutamine ($[\alpha]_D^{20} = 31.5° \pm 0.3°$) were obtained from Nutritional Biochemicals, Cleveland, Ohio. The amino acids were tested for purity by chromatography. They were oven-dried at 110° for 1 h and then stored over anhydrous calcium chloride at room temperature under vacuum. Distilled water was deionized by passing it over commercial ion exchange resin (ILICO-WAY-X research model). All titrations were performed under nitrogen atmosphere. Carbonate free base (5.010 *N*) was used, which was standardized against oven-dried potassium hydrogen phthalate. The 1.0 *N* HCl was standardized against the 5.010 *N* base. Stock solutions of the amino acids and $CuCl_2$ were prepared gravimetrically and then standardized titrimetrically.

Titration Apparatus, Electrodes, and Calibrations

The experimental conditions were as mentioned in the previous papers (17, 18) of this series.

Data: *M*, *m*, *A*, *a*, *B'*, *b'*, *B''*, *b''*, *and h*

Potentiometric titrations were carried out on a series of solutions (50 ml total volume) 0.15 *M* in NaCl, and sufficient HCl to bring the starting p*H* close to 1.0.[3] The solutions contained various combinations of concentrations in copper(II) chloride, L-histidine, L-serine, or L-glutamine as outlined under Results section. All titration curves coincided initially at low p*H*. Before each titration the Nernst slope of the glass electrode was checked against standard buffer solutions. The necessary adjustments were performed on the apparatus to ensure linear response throughout the p*H* range 1.0–12.0. The accuracy achieved with repetitive titrations was 0.002 p*H* units and 0.002 ml of base. The duration for the titration of each sample usually was less than 20 min.

Calculation of Results

Computational Methods

Based on the thermodynamic expression for the chemical potential, the following integral expression, eq. 1, can be derived (17)

$$[1] \quad pm = pm_0 + \int_{pH_0}^{pH_1} \frac{\delta H_1^+}{\delta C_M} dpH \Big|_{C_A,\ldots,P,V,T}$$

This permits us to follow the fate of component M which participates in the chemical reaction in the presence of other reactants, provided that the total concentration of these and *P*, *V*, and *T* are kept constant throughout the reaction. The only variation is done on the component M and the resulting proton liberation is observed where m_0 denotes the concentration of the unreacted component M at pH_0.

Calculations were performed to establish the unbound amounts of each reactant taking part in the equilibrium reaction as a function of p*H*. Then the general equilibrium expression, eq. 2

$$[2] \quad \beta_{pqrs} = \frac{[M_pH_qA_rB_s]}{m^p h^q a^r b^s}$$

for the calculation of the stability constants was employed to obtain relationships eqs. 3–5 between the amount of complex formed and the unbound reagents.

$$[3] \quad (C_M - m) = \sum p\,[\beta_{pqrs}\, m^p h^q a^r b^s]$$

$$[4] \quad (C_A - a) = \sum r\,[\beta_{pqrs}\, m^p h^q a^r b^s]$$

$$[5] \quad (C_B - b) = \sum s\,[\beta_{pqrs}\, m^p h^q a^r b^s]$$

Each of these equations could be used to establish the desired relationships. Since we have determined independently *m*, *h*, *a*, and *b*, we can substitute in eq. 3 and get an equation with the stability constants being the only unknowns, its general form being

$$[6] \quad y = C_1\beta_1 + C_2\beta_2 \ldots\ldots C_n\beta_n$$

The *m*, *h*, *a*, and *b* data being functions of p*H* (or *h*) permit us to set up a system of simultaneous equations as in eq. 6 which then can be solved for the stability constants. The evaluation is accomplished by an iterative least squares method which accepts a crude first approximation of the stability constants to be evaluated.

The binary system for the individual amino acid – Cu(II) complexes are worked out separately and the resulting stability constants obtained are used in the calculations of the ternary system amino acid (*A*) – Cu(II) – amino acid (*B*). The excess bound metal not involved in the formation of the homogeneous complexes is assumed to be present in the ternary complexes as bound Cu(II) ion. These ternary complexes and their stability constant β_{pqrs} are evaluated and the total system is refined together to yield a least squares fit with minimized deviations be-

[3]The decision to use 0.15 *M* NaCl was based on the necessity to apply the present results directly to biological systems.

Can. J. Chem. Downloaded from www.nrcresearchpress.com by 210.87.254.42 on 09/05/12
For personal use only.

TABLE 1. log stability constants (log β_{pqrs}) of complex species $M_pH_qA_rB'_{s'}$ or $M_pH_qA_rB''_{s''}$ (M = Cu(II), A = L-histidine, B′ = L-serine, B″ = L-glutamine) in 0.15 *M* NaCl at 25°; standard deviations (s(log β_{pqrs})) are shown in parentheses

							Other references	
p	*q*	*r*	*s′*	*s″*	This investigation (refined values)		(21)(0.15 *M* KNO_3, 37°)	(19)(0.15 *M* KNO_3, 37°)
Cu(II)-L-Serine								
0	2	0	1		11.163	(0.006)		11.019±0.02
0	1	0	1		8.954	(0.009)		8.839±0.02
1	0	0	1		8.010	(0.008)		7.56 ±0.01
1	0	0	2		14.585	(0.010)		14.01 ±0.01
1	−1	0	2		4.772	(0.010)		
1	−2	0	2		−6.18	(0.02)		
L-Histidine–Cu(II)–L-Serine								
1	−1	1	1		6.90	(0.05)		
1	0	1	1		17.540	(0.008)		
1	1	1	1		21.703	(0.010)		
Cu(II)–L-Glutamine								
0	2	0		1	11.360	(0.005)	10.98	
0	1	0		1	8.97	(0.009)	8.83	
1	0	0		1	7.765	(0.004)	7.24	
1	0	0		2	14.613	(0.005)	13.40	
L-Histidine–Cu(II)–L-Glutamine								
1	0	1		1	17.624	(0.009)		
1	1	1		1	21.654	(0.020)		

tween the observed and calculated values of bound reactants.

The vast amount of calculations involved in this analysis were performed on a General Electric 440 computer system. All programs were written in Fortran IV and are deposited with the National Auxiliary Publications Service.[4] Three programs, PLOT, GUESS, and LEASK were employed in this analysis.

Results

Proton – Amino Acid Systems

The H_2B systems were studied by titrating solutions containing H_2B ($C_{B'} = C_{HCl} = 20 \times 10^{-3}$ and $C_{B'} = C_{HCl} = 40 \times 10^{-3}$ *M*; $C_{B''} = C_{HCl} = 20 \times 10^{-3}$ *M* and $C_{B''} = C_{HCl} = 40 \times 10^{-3}$ *M*) in 0.15 *M* NaCl with standard 5.010 *N* NaOH. The results of several titrations were averaged and the resulting values for the dissociation constants with estimated standard deviations are listed in Table 1.

Binary Cu(II) – Amino Acid Systems

Solutions containing various combinations of M and B′ or B″ concentrations in the presence of 0.15 *M* NaCl were titrated through the p*H* range 1.5 – 11.0. The concentrations used to obtain the data are as follows:

System M:B′		
$C_M \times 10^2$ *M*	$C_{B'} \times 10^2$ *M*	$C_{HCl} \times 10^2$ *M*
M variation		
0.0	4.0	14.0
0.5	4.0	14.005
1.0	4.0	14.01
1.5	4.0	14.01
2.0	4.0	14.02
B′ variation		
1.0	2.0	12.01
1.0	3.0	13.01
1.0	4.0	14.01
1.0	5.0	15.01
1.0	6.0	16.01

[4]The programs have been deposited as Document No. NAPS-01563 with the ASIS National Auxiliary Publications Service, c/o CCM Information Corp., 866 Third Avenue, New York, N.Y. 10022. A copy may be secured by citing the document number and by remitting $1.00 for microfiche or $3.00 for photocopies. Advance payment is required. Make cheques or money orders payable to: ASIS-NAPS.

Can. J. Chem. Downloaded from www.nrcresearchpress.com by 210.87.254.42 on 09/05/12
For personal use only.

Can. J. Chem. Downloaded from www.nrcresearchpress.com by 210.87.254.42 on 09/05/12
For personal use only.

System M:B″

$C_M \times 10^2 M$	$C_{B''} \times 10^2 M$	$C_{HCl} \times 10^2 M$
M variation		
0.0	4.0	14.0
0.5	4.0	14.005
1.0	4.0	14.01
1.5	4.0	14.015
2.0	4.0	14.02
B″ variation		
1.0	2.0	12.01
1.0	3.0	13.01
1.0	4.0	14.01
1.0	5.0	15.01
1.0	6.0	16.01

The families of titration curves obtained from these solutions were processed as described and the resulting species distributions were plotted in Figs. 1 and 2, covering the pH range 2–11. The stability constants of the species were calculated and are listed in Table 1. Dimers and polynuclear complexes were looked for but not found in these systems within the mathematical accuracy employed in our calculations. The Cu(II)–L-histidine system is reported separately (18).

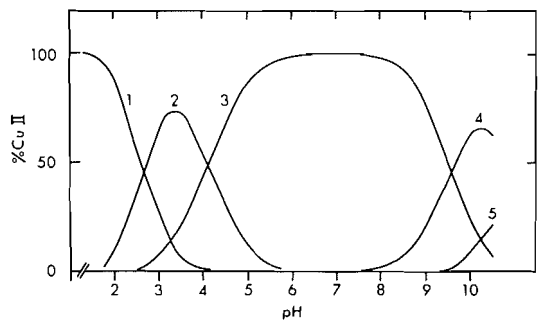

FIG. 1. Variation of complex species concentration with pH in the binary system Cu(II)–L-serine in 0.15 M NaCl at 25°. $C_M = 1 \times 10^{-2} M$, $C_A = C_B = 2 \times 10^{-2} M$. Curve 1, M; curve 2, MB; curve 3, MB_2; curve 4, $MH_{-1}B_2$; curve 5, $MH_{-2}B_2$.

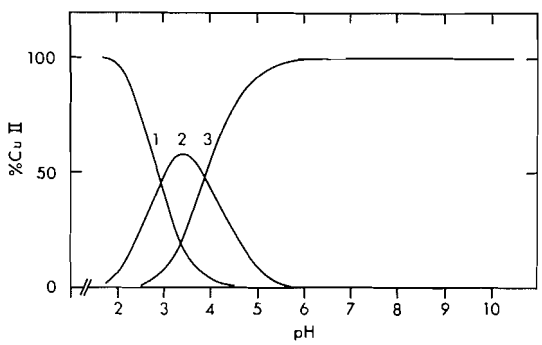

FIG. 2. Variation of complex species concentration with pH in the binary system Cu(II)–L-glutamine in 0.15 M NaCl at 25°. $C_M = 1 \times 10^{-2} M$, $C_A = C_B = 2 \times 10^{-2} M$. Curve 1, M; curve 2, MB′; curve 3, MB'_2.

Ternary Cu(II) – Amino Acid Systems

The experimental data were processed according to the method described. Solutions containing various combinations of M, A, and B′ were titrated from low to high pH. The following two sets of solutions were titrated to obtain the necessary data for the variations of the components under study.

System M:A:B′

$C_M \times 10^2 M$	$C_A \times 10^2 M$	$C_{B'} \times 10^2 M$	$C_{HCl} \times 10^2 M$
M variation			
0.0	2.0	2.0	16.0
0.5	2.0	2.0	16.005
1.0	2.0	2.0	16.01
1.5	2.0	2.0	16.015
2.0	2.0	2.0	16.02
A variation			
1.0	1.0	2.0	14.01
1.0	2.0	2.0	16.01
1.0	3.0	2.0	18.01
B′ variation			
1.0	2.0	1.0	15.01
1.0	2.0	2.0	16.01
1.0	2.0	3.0	17.01

The stability constants were refined together using the program LEASK. The initial estimates of the stability constants were taken from the

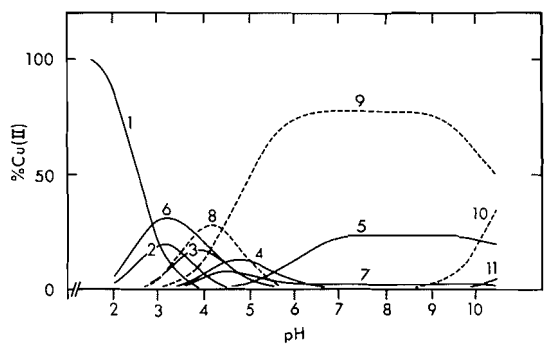

FIG. 3. Variation of complex species concentration with pH in the ternary system L-histidine – Cu(II) – L-serine in 0.15 M NaCl at 25°. $C_M = 1 \times 10^{-2} M$, $C_A = C_B = 2 \times 10^{-2} M$. Solid lines: curve 1, M; curve 2, MHA; curve 3, MA; curve 4, MHA_2; curve 5, MA_2; curve 6, MB; curve 7, MB_2; curve 11, $MH_{-1}B_2$. Broken lines: curve 8, MHAB; curve 9, MAB; curve 10, $MH_{-1}AB$.

Can. J. Chem. Downloaded from www.nrcresearchpress.com by 210.87.254.42 on 09/05/12
For personal use only.

results of the binary Cu(II)–amino acid systems. The first crude estimate for the mixed complexes was obtained by assuming complete formation of the particular species under investigation. The values obtained for the refined stability constants are listed in Table 1. The species distribution is shown in Fig. 3.

System M:A:B″

$C_M \times 10^2 M$	$C_A \times 10^2 M$	$C_{B''} \times 10^2 M$	$C_{HCl} \times 10^2 M$
M variation			
0.0	2.0	2.0	16.0
0.4	2.0	2.0	16.004
0.8	2.0	2.0	16.008
1.0	2.0	2.0	16.01
1.4	2.0	2.0	16.014
2.0	2.0	2.0	16.02
A variation			
1.0	1.0	2.0	14.01
1.0	2.0	2.0	16.01
1.0	3.0	1.0	18.01
B″ variation			
1.0	2.0	1.0	15.01
1.0	2.0	2.0	16.01
1.0	2.0	3.0	17.01

The data were processed as described and the refined values of the stability constants are listed in Table 1. The species distribution of the complexes is shown in Fig. 4.

Discussion

Binary Cu(II) – Amino Acid Complexes

In the Cu(II)–L-serine system investigated by Sharma (19), only two species, MB′ and MB'_2 were reported, having stability constants log $\beta_{101} = 7.56$ and log $\beta_{102} = 14.01$. The system was not examined in a wide enough pH range, and consequently, the formation of the additional species $MH_{-1}B'_2$ and $MH_{-2}B'_2$, which are reported in this paper, were not observed. Our results of the Cu(II)–L-serine system are consistent with those of the Cu(II)–L-threonine system reported earlier by Freeman and Martin (20) as well as by ourselves (15).

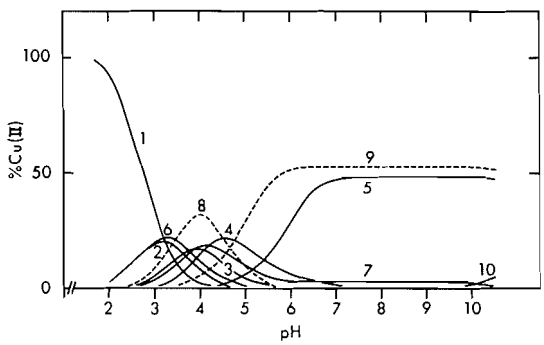

FIG. 4. Variation of complex species concentration with pH in the ternary system L-histidine–Cu(II)–L-glutamine in 0.15 M NaCl at 25°. $C_M = 1 \times 10^{-2} M$, $C_A = C_B = 2 \times 10^{-2} M$. Solid lines: curve 1, M; curve 2, MHA; curve 3, MA; curve 4, MHA_2; curve 5, MA_2; curve 6, MB′; curve 7, MB'_2; curve 10, $MH_{-1}A_2$. Broken lines: curve 8, MHAB′; curve 9, MAB′.

Titration results alone are not good enough to draw any conclusions regarding the structure of a species. However, some pertinent observations must be made. Both pK_1(carboxyl) = 2.21 and pK_2(amino) = 8.95 fell within our titration range. The pK_3(hydroxyl) was not obtained since it was outside the pH range covered in our study. The involvement of the carboxyl and amino groups in both MB′ and MB'_2 is necessary in order to obtain proton balance regarding the titration data. When exceeding pH 8, there is a clear demonstration of extra hydrogen ions being liberated and species such as $MH_{-1}B'_2$ and $MH_{-2}B'_2$ being formed. We do not know at the present time the source of the protons. They can originate from the hydrolysis of water in the formation of these complexes. An alternate source could be the hydroxyl group involvement of L-serine in the above complexes.

In a recent publication, Hallman, Perrin, and Watt (21) reported the β values for the species in the Cu(II)–L-glutamine system at 37° and I = 0.15 M KNO_3 but did not include the species distribution. Since their experimental conditions are markedly different from ours, it is not easy to compare our stability data with those obtained by these authors.

An interesting difference becomes evident if one compares the species distribution of the Cu(II)–L-glutamine system to that of the Cu(II)–L-serine system. The Cu(II)–L-serine system shows the presence of complex species $MH_{-1}B'_2$ and $MH_{-2}B'_2$ while in the Cu(II)–L-glutamine system these species are absent. One way to explain this observation may be that in the Cu(II)–L-serine system the species $MH_{-1}B'_2$ and $MH_{-2}B'_2$ represent hydroxylated complexes where OH^- would originate from H_2O taking up the additional coordination sites. Whereas, in Cu(II)–L-glutamine, the coordination positions are filled and consequently no hydroxyl species were formed. The only likely group is provided by the amide group of glutamine

Can. J. Chem. Downloaded from www.nrcresearchpress.com by 210.87.254.42 on 09/05/12
For personal use only.

which, upon coordination to the central Cu(II) atom, in addition to carboxyl and amino involvement, would then effectively eliminate the hydroxyl group binding. However, until further physicochemical results are obtained on this system, no definitive conclusion can be made on this subject.

Ternary Cu(II) – Amino Acid Complexes

In the L-histidine–Cu(II)–L-serine system, three mixed ligand complexes, MHAB′, MAB′, and $MH_{-1}AB'$ were detected in addition to the binary complexes, MHA, MA, MHA_2, MA_2, $MH_{-1}A_2$, MB′, and MB'_2. Some species which do exist in the binary systems: Cu(II)–L-histidine and Cu(II)–L-serine, have not been detected in appreciable amounts in the ternary system. There was about 35% of Cu(II) present in the protonated mixed ligand complex MHAB′ at p*H* 5. With increasing p*H* the mixed complex MAB′ was formed and accounted for about 75% of Cu(II) in the p*H* range 5.5–9. A closely related mixed ligand complex L-histidine–Cu(II)–L-threonine reported by us earlier (9, 12) showed its unique structure with L-histidine being tridentate involving *N*-amino and *N*-imidazole coordination in a square plane around the Cu(II) ion with the carboxyl oxygen in a very distorted axial position. The amino and carboxyl groups of L-threonine occupied the other positions in the square plane of the Cu(II) coordination square. There was no involvement of the hydroxyl group of L-threonine in Cu(II) coordination. The same results may be expected for MAB′. At p*H* > 9.5 significant amounts of a mixed complex species $MH_{-1}AB'$ was formed. This species may well be an hydroxo complex. However, definite proof of an hydroxyl ion involvement is lacking. The protons could originate either from a water molecule being coordinated or else by dissociation of a proton from the hydroxyl group of serine upon coordination of the alcohol oxygen to the central Cu(II) ion. The same arguments, as raised with the species $MH_{-1}B'_2$ in the binary system, can be applied to this ternary system.

The results observed in the L-histidine–Cu(II)–L-glutamine system were quite similar to the system M:A:B′ discussed earlier, except that there were no species such as $MH_{-1}AB''$. Again, at low p*H* (p*H* < 4) we found that binary Cu(II) complexes predominated and, on raising the p*H* the mixed complexes MHAB″ and MAB″ appeared sequentially with 60% Cu(II) in the form of MAB″ in the p*H* range 5–10. The absence of the species $MH_{-1}AB''$ can be interpreted using arguments similar to those employed in the Cu(II)–L-glutamine system.

An Appraisal of the Enhancement of the Stability Constants of the Ternary Complexes

It was observed in the ternary complex system that the stability constants of the ternary complexes invariably had higher values than those which would be predicted on theoretical grounds based on observations on the isolated binary systems. From successive formation constants of the 1:1 and 1:2 Cu(II):ligand complexes, one could predict on theoretical basis, the stability constant of the mixed complex if one assumes that the addition of the second amino acid is not influenced by the nature of the first amino acid attached to the Cu(II) ion.

For complex MA_2 we have:

$$[7] \qquad M + A \overset{K_1}{\rightleftarrows} MA$$

$$[8] \qquad MA + A \overset{K_2}{\rightleftarrows} MA_2$$

For complex MB_2 we have:

$$[9] \qquad M + B \overset{K'_1}{\rightleftarrows} MB$$

$$[10] \qquad MB + B \overset{K'_2}{\rightleftarrows} MB_2$$

The mixed complex can be arrived at (*i*) by addition of B to MA or, (*ii*) by addition of A to MB to give MAB. Then, if we assume eq. 7 as first step in the "pathway" then, the stability constant of the mixed complex should be arrived at by following "pathway" (*i*).

$$[11] \qquad \beta_{mix(i)} = K_1 K'_2$$

or

$$[12] \qquad \log \beta_{mix(i)} = \log K_1 + \log K'_2$$

where

$$[13] \qquad \log K'_2 = \log \beta'_2 - \log \beta'_1$$

Therefore,

$$[14] \qquad \log \beta_{mix(i)} = \log \beta_1 + \log \beta'_2 - \log \beta'_1$$

If we assume eq. 9 as first step in the "pathway" (*ii*) then we obtain

$$[15] \qquad \log \beta_{mix(ii)} = \log \beta'_1 + \log \beta_2 - \log \beta_1$$

TABLE 2. log stability constants (log β_{pqrs}) of complex species $M_pH_qA_rB_s$; observed and calculated values and their differences ($\Delta \log \beta_{pqrs} = \log \beta_{pqrs(obsvd)} - \log \beta_{pqrs(calcd)}$)

						Calculated values			
p	q	r	s'	s''	Observed values	Pathway (*i*)	$\Delta \log \beta_{pqrs}$	Pathway (*ii*)	$\Delta \log \beta_{pqrs}$
L-*Histidine* – *Cu(II)* – L-*Serine*									
1	0	1	1		17.54	16.67	0.87	16.37	1.17
1	1	1	1		21.70	20.75	0.95	20.73	0.97
L-*Histidine* – *Cu(II)* – L-*Glutamine*									
1	0	1		1	17.62	16.95	0.67	16.12	1.50
1	1	1		1	21.65	21.03	0.62	20.40	1.25

Now, we would expect the log β value of the mixed complex to be somewhere between log $\beta_{mix(i)}$ and log $\beta_{mix(ii)}$. Depending on which "pathway" predominates, one has to incorporate statistical weights (w_i, $i = 1, 2$) which will yield equations of the following type

$$[16] \quad w_1 \log \beta_{mix(i)} = w_1 \log \beta_1 + w_1 \log \beta'_2 - w_1 \log \beta'_1$$

and

$$[17] \quad w_2 \log \beta_{mix(ii)} = w_2 \log \beta'_1 + w_2 \log \beta_2 - w_2 \log \beta_1$$

Then, averaging of these weighted equations should give the expected value as the weighted mean

$$[18] \quad \log \bar{\beta}_{mix(calcd)} = \frac{1}{w_1 + w_2} (w_1 \log \beta_{mix(i)} + w_2 \log \beta_{mix(ii)})$$

or

$$[19] \quad \log \bar{\beta}_{mix(calcd)} = \frac{1}{w_1 + w_2} (w_1 \log \beta_1 + w_1 \log \beta'_2 - w_1 \log \beta'_1 + w_2 \log \beta'_1 + w_2 \log \beta_2 - w_2 \log \beta_1)$$

The weights are generally unknown. If we assume $w_1 = 1$, $w_2 = 0$, Then

$$[20] \quad \log \bar{\beta}_{mix(i)} = \log \beta_1 + \log \beta'_2 - \log \beta'_1$$

And if we assume $w_1 = 0$, $w_2 = 1$, then

$$[21] \quad \log \bar{\beta}_{mix(ii)} = \log \beta'_1 + \log \beta_2 - \log \beta_1$$

For the protonated, hydroxyl, and polynuclear complexes, the arguments and derivations are analogous.

The observed stability constants and the calculated stability constants following either of the "pathways" (*i*) or (*ii*) are presented in Table 2. In these two mixed complex systems we have observed larger values for the mixed complexes than predicted on theoretical grounds. This enhancement phenomenon in the case of heterogeneous ligands represents a striking departure from the theoretical expectations. Explanations at this stage lack precise supporting proof and tend to be highly speculative. In the case of MAB complexes, one can offer the reasonable explanation that the pathway through MA as a first step is preferred, yielding log $\beta_{1011} = 16.67$ which is still 0.87 log units below the observed value for the mixed complex MAB. This is supported by the fact that the stability of MA (log $\beta_{101} = 10.2$) is by two decades higher than the stability constants of MB′ or MB″ (log $\beta_{101} = 8.01$ and $= 7.76$, respectively).

Since even the largest calculated β value, by "pathway" (*i*), is smaller than the observed β value, we must consider other stabilizing influences in the complex molecule. Having two different amino acids linked to the same central Cu(II) ion evidently means additional contribution to the stability of the ternary complex molecule. The electronic structure of the Cu(II) ion must be such that the influences of one ligand can be transmitted through the coordinating bonds to the other remote ligand molecule. This stability enhancement cannot be attributed to the observed pentacoordination of Cu(II) in L-histidine–Cu(II)–L-threonine (12) where L-histidine and L-threonine participate in tridentate and bidentate coordination, respectively. The reasoning that the pentacoordination of Cu(II) would be more stable than either square planar or hexadentate coordination can be ruled out on the evidence that a mixed complex of glycine–Cu(II)–DL-alanine (22) showed a stability constant of log $\beta_{1011} = 15.60$ as compared to a

Can. J. Chem. Downloaded from www.nrcresearchpress.com by 210.87.254.42 on 09/05/12
For personal use only.

calculated value of 15.18. The only explanation can be found in the effects of asymmetry around the central Cu(II) ion. This asymmetry may express itself thermodynamically in the entropy term of the system causing the sizably increased value of the overall stability constant.

This work was supported by the Medical Research Council of Canada and the John A. Hartford Foundation of New York.

1. A. S. MILDVAN and M. COHN. Adv. Enzymol. **33**, 1 (1970).
2. A. AKESON. Biochem. Biophys. Res. Commun. **17**, 211 (1964).
3. H. L. OPPENHEIMER, R. W. GREEN, and R. H. MCKAY. Arch. Biochem. Biophys. **119**, 552 (1967).
4. D. E. DRUM, J. H. HARRISON, T.-K. LI, J. L. BETHUNE, and B. L. VALLEE. Proc. Nat. Acad. Sci. **57**, 1434 (1967).
5. C. N. A. TROTMAN and C. GREENWOOD. Biochem. J. **124**, 25 (1971).
6. B. SARKAR and Y. WIGFIELD. Can. J. Biochem. **46**, 601 (1968).
7. B. SARKAR. Can. J. Biochem. **48**, 1339 (1970).
8. S. LAU and B. SARKAR. J. Biol. Chem. **246**, 5938 (1971).
9. B. SARKAR and T. P. A. KRUCK. Biochemistry of copper. *Edited by* J. Peisach, P. Aisen and W. E. Blumberg. Academic Press, New York. 1966.
10. B. SARKAR and T. P. A. KRUCK. Can. J. Biochem. **45**, 2046 (1967).
11. B. SARKAR, M. BERSOHN, Y. WIGFIELD, and T.-C. CHIANG. Can. J. Biochem. **46**, 595 (1968).
12. H. C. FREEMAN, J. M. GUSS, M. J. HEALY, R.-P. MARTIN, C. E. NOCKHOLDS, and B. SARKAR. Chem. Commun. **225**, (1969).
13. B. SARKAR, M. L. LEE, and R.-P. MARTIN. Proc. Can. Fed. Biol. Soc. **12**, 14 (1969).
14. B. SARKAR, P. E. MCLEOD, T. P. A. KRUCK, S. LAU, and J. BRECKENRIDGE. Proceedings of the XIIIth International Conference on Coordination Chemistry. Vol. II. *Edited by* W. Kakolowicz. Polish Academy of Science, Cracow-Zakopane, Poland. 1970. p. 24.
15. B. SARKAR and T. P. A. KRUCK. Proceedings of the XIVth International Conference on Coordination Chemistry, Toronto, Canada. 1972. p. 395.
16. R.-P. MARTIN, L. MOSONI, and B. SARKAR. J. Biol. Chem. **246**, 5944 (1971).
17. B. SARKAR and T. P. A. KRUCK. Can. J. Chem. This issue.
18. T. P. A. KRUCK and B. SARKAR. Can. J. Chem. This issue.
19. V. S. SHARMA. Biochem. Biophys. Acta **148**, 37 (1967).
20. H. C. FREEMAN and R.-P. MARTIN. J. Biol. Chem. **244**, 4832 (1969).
21. P. S. HALLMAN, D. D. PERRIN, and A. E. WATT. Biochem. J. **121**, 549 (1971).
22. R.-P. MARTIN and R. A. PARIS. Bull. Soc. Chim. 3932 (1963).

Can. J. Chem. Downloaded from www.nrcresearchpress.com by 210.87.254.42 on 09/05/12
For personal use only.

Structure of the Species in the Copper (II)–L-Histidine System

THEO P. A. KRUCK AND BIBUDHENDRA SARKAR[1]

Division of Biochemistry, The Research Institute, The Hospital for Sick Children, Toronto, and Department of Biochemistry, University of Toronto, Toronto, Ontario M5G 1X8

Received June 14, 1972[2]

The presence of simultaneously existing multiple species were taken into account in interpreting the structures of the complex species in the Cu(II)–L-histidine system. A refined proton displacement technique was utilized for structure elucidation of the species in solution. The absorbance and the molar extinction of the individual species were computed from the total absorbance and the species distribution over the p*H* range studied. The i.r. spectra of L-histidine and Cu(II)–L-histidine in D_2O were obtained as a function of p*D*. They were interpreted in view of the species detected in a given p*H* range. The results of the species distribution as a function of p*H*, proton displacement, visible spectra of the individual species, and infrared data, were all combined to make structural interpretations. The following modes of metal coordination were proposed for the major species in the Cu(II)–L-histidine system: MHA, *O*(carboxyl) and *N*(imidazole); MH_2A_2, *O*(carboxyl) and *N*(amino) in both L-histidines; MA, *O*(carboxyl), *N*(imidazole), and *N*(amino); MHA_2 *O*(carboxyl), *N*(imidazole), and *N*(amino) in one L-histidine and *O*(carboxyl) and *N*(amino) in the other; MA_2, *O*(carboxyl). *N*(imidazole), and *N*(amino) in both L-histidines, or *O*(carboxyl), *N*(imidazole), and *N*(amino) in one L-histidine and *N*(amino) and *N*(imidazole) in the other or an equilibrium mixture of both structures.

Lors de l'interprétation des structures des complexes appartenant au système Cu(II)–L-histidine, il a été nécessaire d'envisager la présence de plusieurs espèces pouvant exister simultanément. Une technique raffinée impliquant le déplacement des protons a été utilisée afin d'élucider les structures des espèces en solution. L'absorption ainsi que le coefficient d'extinction molaire de chacune des espèces ont été calculés à partir de l'absorption totale et de la distribution des espèces pour l'intervalle de pHétudié. Les spectres i.r. de la L-histidine et du complexe Cu(II)–L-histidine ont été obtenus dans le D_2O en fonction du p*D*. Ceux-ci furent interprétés en fonction des espèces détectées dans un intervalle de p*H* défini. Les résultats obtenus de la distribution des espèces en fonction du pH, du déplacement des protons, des spectres visibles de chacune des espèces ainsi que des études en i.r., ont été combinés afin d'interpréter les structures. Les différentes méthodes de coordination au métal furent présentées afin d'expliquer les espèces majeures dans le système Cu(II)–L-histidine: MHA, *O*(carbonyle) et *N*(imidazole); MH_2A_2, *O*(carbonyle) et *N*(amino) dans les deux L-histidines; MA, *O*(carbonyle), *N*(imidazole) et *N*(amino); MHA_2, *O*(carbonyle), *N*(imidazole) et *N*(amino) pour un groupe L-histidine et *O*(carbonyle) et *N*(amino) pour l'autre; MA_2, *O*(carbonyle), *N*(imidazole) et *N*(amino) dans les deux L-histidines ou *O*(carbonyle), *N*(imidazole) et *N*(amino) pour un groupe L-histidine et *N*(amino), *N*(imidazole) pour l'autre ou un mélange à l'équilibre des deux structures. [Traduit par le journal]

Can. J. Chem., 51, 3563 (1973)

Introduction

Several proposals have been made for the structures of a number of Cu(II)–L-histidine complexes, based on various physical and chemical studies. Unfortunately, due to the lack of a detailed knowledge of the species distribution throughout the p*H* range of interest, the quantitative implications of multiple species existing simultaneously at the p*H* in question were overlooked in almost all of these investigations. It cannot be overemphasized that the lack of knowledge pertaining to the system concerned can lead to serious errors in making structural interpretation. The physiological implications (1–5) of the Cu(II)–L-histidine complexes make it essential to investigate precisely the structures of the complex species in solution. The species, their stability constants, and their quantitative distribution over a wide p*H* range reported in the preceeding paper (6),[3] provided a suitable platform to study the structure of individual species in solution by physical and chemical means. The combined results of the visible and i.r. spectra, as well as those obtained from the proton displacement studies, were utilized to propose the structures in solution of all the major species in the Cu(II)–L-histidine system.

[1]To whom correspondence should be addressed.

[2]Revision received May 29, 1973.

[3]Preceding article.

Can. J. Chem. Downloaded from www.nrcresearchpress.com by 210.87.254.6 on 09/05/12
For personal use only.

Can. J. Chem. Downloaded from www.nrcresearchpress.com by 210.87.254.6 on 09/05/12
For personal use only.

Experimental Section

Materials

L-Histidine free base ($[\alpha]_D^{20}$ + 39.9° ± 0.5°) was obtained from Nutritional Biochemicals. The purity was tested by chromatography. It was dried at 110° for 24 h and then stored over anhydrous calcium chloride at room temperature under vacuum. The water was first distilled and then deionized by passing it through a commercial ion exchange column (ILICO-WAY-X research model). The base used for p*H* adjustments was carbonate free 5.010 *N* NaOH. The stock solutions of L-histidine and $CuCl_2$ were prepared from vacuum dried materials and subsequently checked titrimetrically. All other reagents were of analytical grade. The deuterated products D_2O, DCl, and NaOD (99% isotopically pure) were obtained from Merck, Sharp and Dohme, Montreal, Canada.

Proton Displacement

Potentiometric titrations were carried out on a series of solutions: 50 ml 0.15 *M* in NaCl, 0.1 *N* in HCl, containing combinations of L-histidine (40 m*M*) and $CuCl_2$ (0, 3, 5, 7, 10, and 20 m*M*). All titration curves coincided initially at low p*H*. Before each titration the calibrations of electrodes and chart recorder were checked. The precision of repetitive titrations was 0.001 p*H* units and 0.002 ml of base. It was necessary to obtain titration curves of samples containing constant amounts of ligand while varying the metal component from sample to sample. A computer program PLOT[4] was used to treat the data. First, the titration curves were digitized and formated for input to this program. Then, a table of $\delta H_1^+/\delta C_M$ was printed out.[5] These results formed the basis for comparison to the theoretical values as done in the proton displacement analysis using the program SELECT.[4]

Spectrophotometric Measurements

A Cary 15 recording spectrophotometer was used to obtain the absorption spectra in the visible region from wavelength 800 to 300 nm. The Cu(II)–L-histidine solutions were measured against L-histidine solutions of the same p*H*, as reference. All experimental conditions regarding the samples measured, were the same as those for the potentiometric titrations. Samples were scanned at a series of p*H* values ranging from p*H* 1.00–11.00 at 25°.

A Beckman IR-20 double beam infrared spectrophotometer was used to obtain the percent transmission spectra in the range 2000 to 800 cm^{-1}. The samples were made up in D_2O taking care to exclude any H_2O contamination. Infrared spectra of 1:2 Cu(II)–L-histidine (0.2 *M*) were obtained using Irtran-2 cells having a lightpath of 0.05 mm. The spectra were obtained at varying p*D* values starting from p*D* 0.8–10.2 at 25°.[6] An even distribution of the sample and exclusion of minute gas bubbles were insured.

Results

Structural Interpretation of Species by Proton Displacement

Information about the specific group involvement in metal–ligand interaction can be obtained if the group in question shows a buffering region in the p*H* range studied or, if the group is fully protonated at that p*H*. In the Cu(II)–L-histidine case, advantage was taken of the well separated buffering regions of carboxyl, imidazole, and amino groups for the above purpose. The proton displacement data shown in Fig. 1 are unbiased.

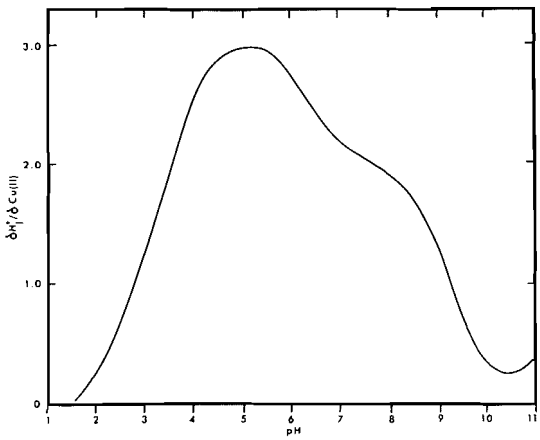

FIG. 1. Proton displacement $\delta H_1^+/\delta C_M$ as a function of p*H* for the 1:4 Cu(II)–L-histidine system.

TABLE 1. Scheme for proton displacement calculations

Coordination pattern*	Number of potential groups involved in coordination†			
	MHA_2		MA_2	
	NH_2	N_{im}	NH_2	N_{im}
A	1	1	2	1
B	2	1	2	0
C	2	0	2	2

*There are several other possible combinations but no reasonable fit could be obtained.
†The numerals indicate the number of protons which will be released upon metal coordination with the particular group listed.

[4]Programs PLOT, SELECT, and LEASK were written in Fortran IV language. The programs have been deposited as Document No. NAPS-01563 with ASIS National Auxiliary Publication Service, c/o CCM Information Corp., 866 Third Avenue, New York, N.Y. 10022. A copy may be secured by citing the document number and by remitting $1.00 for microfiche or $3.00 for photocopies. Advance payment is required. Make cheques or money orders payable to: ASIS-NAPS.

[5]Since in this system it was found that $\delta H_1^+/\delta C_M$ was a linear function of p*H* we can consider $\delta H_1^+/\delta C_M = \Delta C_{OH}/\Delta C_M$.

[6]Differences between p*H* and p*D* values are considered within the tolerances required for meaningful interpretation of the results where p*D* = meter reading + 0.4 (7).

TABLE 2. Differences between the calculated and observed proton displacement data for structure analyses

			$(H_l{}^+_{calcd} - H_l{}^+_{obs})$				
Number	MHA_2	MA_2	p*H* 5.0	p*H* 5.71	p*H* 6.0	p*H* 6.7	p*H* 7.0
1	A	A	−0.91	−0.62	−0.57	−0.16	−0.11
2	A	B	−1.06	−0.94	−0.82	−0.24	−0.16
3	A	C	−0.77	−0.31	−0.32	−0.07	−0.06
4	B	A	−0.11	−0.25	−0.27	−0.10	−0.07
5	B	B	−0.25	−0.56	−0.51	−0.18	−0.12
6	B	C	0.04	0.05	−0.02	−0.01	−0.02
7	C	A	−0.79	−0.44	−0.37	−0.10	−0.07
8	C	B	−0.93	−0.75	−0.62	−0.19	−0.12
9	C	C	−0.64	−0.12	−0.13	−0.02	−0.02

They were obtained without any assumptions concerning probable complex species in solution. In other words, no assumptions had to be made as to the origin of these protons. The total proton liberation, however, must equal the contribution of each species yielding protons when the metal–ligand bonds are formed. In making theoretical calculations of proton displacement at a given p*H*, it is necessary not only to consider all the species in the system, but, also to take into account all possible modes of binding in the metal–ligand complex. The necessary computations were performed with the program SELECT.[4]

The scheme in Table 1 shows the permutations for the possible modes of coordination in the main species MHA_2 and MA_2 existing simultaneously in the p*H* range 5–7. Contributions to the proton displacement data by the small amounts of MA, MH_2A_2, and $MH_{-1}A_2$ in the p*H* range studied were considered to be negligible and therefore were omitted from the calculations. Besides the species considerations, a correction was also made for the lowering of the pK_a of potential groups of the multidentate ligand when previous coordination had occurred through another group. In the p*H* region 5–7, the following transition takes place (6)

[1] $$MHA_2{}^+ \leftrightarrows MA_2 + H^+$$

An estimate of the actual pK_a of the protonated group in MHA_2 can be obtained from the following equations:

[2] $$M + H^+ + 2A \overset{\beta_{112}}{\rightleftharpoons} MHA_2{}^+$$

[3] $$M + 2A \overset{\beta_{102}}{\rightleftharpoons} MA_2$$

Subtracting eq. 3 from eq. 2 yields the desired pK_a of this group

[4] $$pK_a = \log \beta_{112} - \log \beta_{102} = 24.01 - 18.46 = 5.55$$

Utilizing the pK_a values of the potential coordinating groups, sets of theoretical values of proton displacement were obtained on the basis of the various structural assumptions made for multiple species existing simultaneously at a given p*H*. Based upon the goodness of fit between the experimental value of the proton displacement and the theoretical value for an assumed structure, we concluded the possible mode of binding in a given complex species.

The best fit between calculated and observed proton displacement data was obtained in structural combination number (*6*) in Table 2. This combination was consistent with 2 amino, 1 imidazole in MHA_2; 2 amino and 2 imidazole in MA_2. No conclusion can be drawn about the carboxyl involvement from these data since they were obtained in p*H* 5–7, where the carboxyl proton is already titrated.

A previous attempt (8) to employ a similar analysis was not satisfactory because of a lack of knowledge of the species distribution; only average values were obtained. This technique, combined with other supporting methods, should prove very useful in the study of metal–ligand interaction. The resolving power of such an analysis depends largely on the precision of the initial measurements. The chief error in potentiometry arises mainly from the electrodes being used. The only other major source of error arises out of faulty assumptions regarding the system: if a complex species that is present in

Can. J. Chem. Downloaded from www.nrcresearchpress.com by 210.87.254.6 on 09/05/12
For personal use only.

Can. J. Chem. Downloaded from www.nrcresearchpress.com by 210.87.254.6 on 09/05/12
For personal use only.

solution has a potential influence on the analysis and is being ignored, then erroneous results and interpretations are the consequence.

Visible Spectra of the Species

Spectra of solutions containing 1:4 molar ratio of Cu(II) and L-histidine were recorded in the wavelength region 300–800 nm at various pH values. Since a species distribution in 1:4 Cu(II)–L-histidine system had been obtained (ref. 6, Fig. 3*B*) from the potentiometric measurements, we were able to separate the total absorbance into absorptions of the individual species. The only assumptions necessary are, the Beer–Lambert's law is obeyed and, that the total absorbance A_λ is due to the linear summation of the component absorptions. Therefore, for every pH_i value

$$[5] \qquad A_{\lambda,[pH_i]} = \sum_1^n \varepsilon_{\lambda,pqr} C_{pqr}$$

where C_{pqr} is the concentration of the pqrth species and $\varepsilon_{\lambda,pqr}$ is its molar extinction at that wavelength for a 1 cm lightpath. We employed our LEASK[4] program to obtain the absorbance and molar extinction of the species at a given wavelength. The ε_{pqr} values thus obtained were plotted as a function of wavelength λ in Fig. 2.

Results of Infrared Measurements

Infrared spectra for the 1:2 Cu(II)–L-histidine system in D_2O were obtained in the pD range 0.8–10.2. The scans showing the characteristic bands of the antisymmetric carboxyl stretching frequency of L-histidine are presented in Fig. 3. The peaks marked *a* represent the absorption bands due to the antisymmetric stretching of the protonated carboxyl groups ($\nu = 1735$ cm^{-1}), the peaks marked *b* are due to vibrations of the same carboxyl group which has been deprotonated ($\nu = 1622$ cm^{-1}). The pD dependence of these two peaks identifies them as being due to the protonated and deprotonated forms of the carboxyl group. Plotting optical densities of the absorption bands versus pD results in a $pK_{COOH} = 1.8$ at the 50% dissociation point which is in close agreement with our potentiometric results (6).

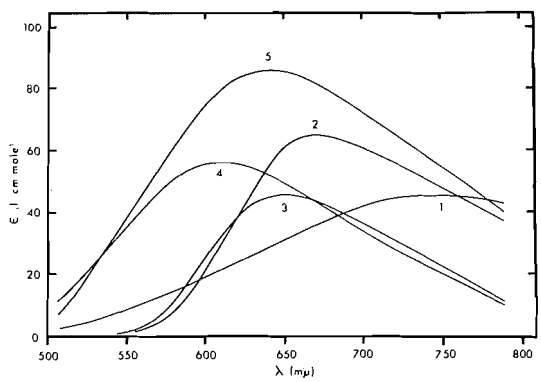

FIG. 2. Computed spectra of the species in the Cu(II)–L-histidine system. Curve 1, MHA; curve 2, MA; curve 3, MHA_2; curve 4, MH_2A_2; curve 5, MA_2.

In Fig. 4, i.r. spectra are shown representing paired systems, where, at selected pD values, the metal-free system is compared to the Cu(II)-containing system. A quantitative presentation of the shifts of the antisymmetric carboxyl stretching frequency is given in Fig. 5, where curve *A* refers to observations on the L-histidine system and curve *B* refers to data obtained from the Cu(II)–L-histidine system. Considering the frequency shift during titration of L-histidine (curve *A*) it is noted that up to pD ~5 the frequency remains constant; however, as the protonated imidazole group releases its proton, this band shifts towards lower frequency. At the end of the imidazole buffering region, we again achieve constant frequency ($\nu = 1612$ cm^{-1}) which persists up to pD ~8.0 with almost constant amplitude. As the pD is raised further, the amplitude decreases rapidly with no further shift in frequency. However, a new band ($\nu = 1578$ cm^{-1}) appears at pD ~8.0, and reaches a maximum amplitude at pD ~10.2 (Fig. 4). This drastic shift in the antisymmetric carboxyl stretching frequency can be attributed to the deprotonation of the carboxyl group plus the inductive effects arising from the deprotonation of both the imidazolium and ammonium groups in L-histidine. Infrared studies of EDTA titration showed similar influence of the deprotonation of the ammonium group in the antisymmetric carboxyl stretching frequency (9).

In Fig. 5, curve *B*, the results of the $\Delta\nu$ *vs.* pD are presented for the 1:2 Cu(II)–L-histidine system, where we selected 1622 cm^{-1} as reference ν. The notable feature of this curve is the stepwise increase in $\Delta\nu$ going from low to high pD. The first inflection occurs at pD ~5.0 where $\Delta\nu = 30$ cm^{-1}. These results are best explained in conjunction with the results obtained by potentiometric analysis. It is shown (ref. 6, Fig. 3*A*) that for the 1:2 Cu(II)–L-histidine system, the species MHA is the major component below

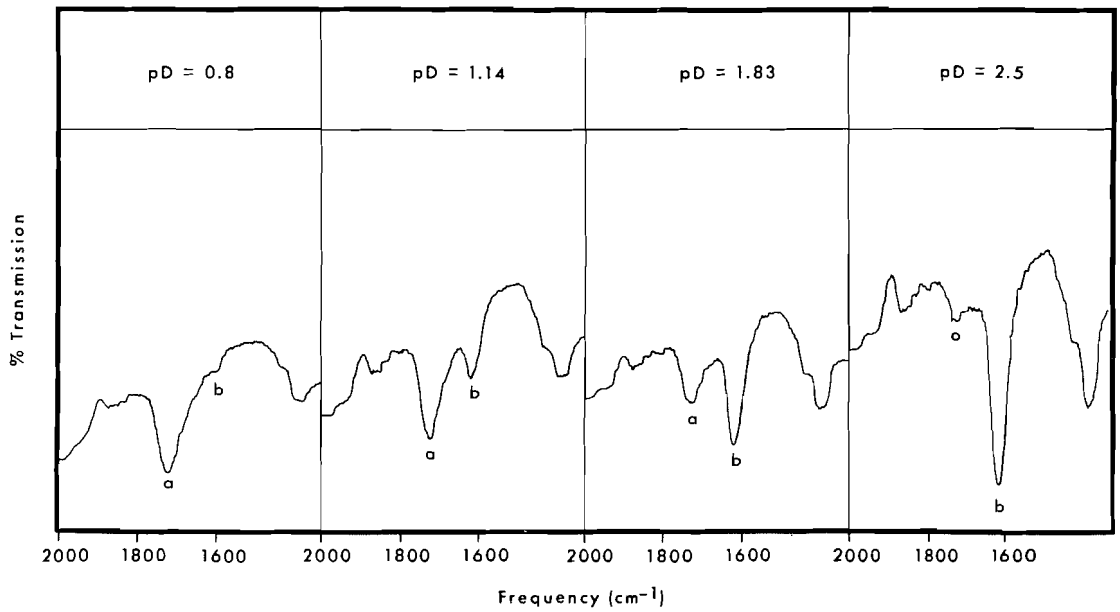

FIG. 3. Infrared spectra showing the antisymmetric carboxyl stretching frequency bands. Peak *a*, protonated carboxyl group; peak *b*, deprotonated carboxyl group.

p*H* 2.5. From infrared observations, we find that at and below p*D* ~2.5 the amplitude of the vibration of the protonated carboxyl group at $\nu = 1735\ cm^{-1}$ decreases upon addition of Cu(II) while the amplitude of the deprotonated carboxyl group increases proportionally to Cu(II) complexation. At the same time a $\Delta\nu$ is observed for the deprotonated carboxyl group due to metal complexation. An example is shown in Fig. 4 (p*D* 2.5). The proton displacement from the carboxyl group due to Cu(II) addition, signifies Cu(II)–carboxyl coordination. As the p*D* is increased, we observe a shift of this absorption band ($\nu = 1612\ cm^{-1}$) towards lower frequency. This tendency continues up to p*D* ~3.0, where a shoulder is formed with an inflection occurring at $\Delta\nu = 11\ cm^{-1}$. The initial part of curve *B* resembles the characteristics of curve *A*. A parallelism can be drawn in curve *B* where a similar shift ($\Delta\nu = 11\ cm^{-1}$) is apparent well below the pK_a of the imidazole group. The p*D* region, where the first plateau in $\Delta\nu$ is reached in curve *B*, coincides with the corresponding p*H* scale where the maximum amount of MHA is formed (ref. 6, Fig. 3*A*). Hence, it is concluded that in MHA, the imidazole group is also coordinated to Cu(II) in conjunction with the carboxyl group. The next species to appear are MA and MH_2A_2. There is a corresponding sharp increase in $\Delta\nu$ indicating carboxyl participation. Complete characterizations of these species are presented in the discussion section in combination with other experimental evidence. Carlson and Brown (10) investigated the 1:1 Cu(II)–L-histidine system and proposed a monodentate complex involving Cu(II)–carboxyl coordination for p*D* < 3.0; but, in their interpretation they appear not to have taken into account that multiple complex species may be present in their system at the p*D* values at which their experimental data were gathered.

The 1:2 Cu(II)–L-histidine complexes rapidly increased in abundance above p*H* 3.0. The species MHA_2 reaches a maximum at p*H* 4.2. Similarly, starting at p*D* 3 (Fig. 5, curve *B*), a sharp increase is seen in the $\Delta\nu$, reaching a plateau ($\Delta\nu = 30\ cm^{-1}$) at p*D* = 5.0 and remaining constant up to p*D* = 10.2. Evidence in support of carboxyl involvement at higher p*D* values is provided by the fact that in the absence of Cu(II) at p*D* 10.2 (Fig. 4) we observe a band at $\nu = 1578\ cm^{-1}$ ($\Delta\nu = 44\ cm^{-1}$) which is due to the deprotonated carboxyl group. However, in the presence of Cu(II) we observe a $\Delta\nu = 30\ cm^{-1}$. Since we do not get comparable shifts in $\Delta\nu$ in the metal-free system, we can ascribe this effect to the carboxyl–Cu(II) interaction of the histidine anion. No observable change

Can. J. Chem. Downloaded from www.nrcresearchpress.com by 210.87.254.6 on 09/05/12
For personal use only.

Can. J. Chem. Downloaded from www.nrcresearchpress.com by 210.87.254.6 on 09/05/12
For personal use only.

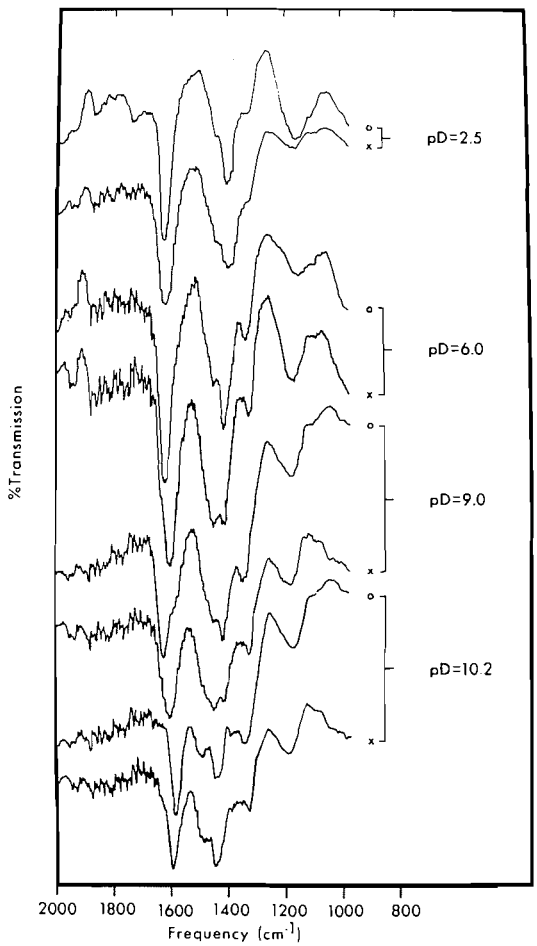

FIG. 4. Infrared spectra of L-histidine and 1:2 Cu(II)–L-histidine in D_2O at different pD values: O, L-histidine; ×, Cu(II)–L-histidine.

occurs in $\Delta\nu$ going from pD 5.0–10.2, where the transition of MHA_2 to MA_2 takes place. The maintaining of the carboxyl binding of both L-histidines in the species MHA_2 and MA_2 is probable since, if one of the carboxyl groups were to leave the coordination sphere of Cu(II), then we would expect a significant absorption peak at $\nu = 1578\ cm^{-1}$. This is not the case. Only one single peak at $\nu = 1592\ cm^{-1}$ is observed.

Discussion

A complete analysis of the equilibria is essential to study the structure of the species in solution in a multispecies system. In the present investigation, the species and their distributions

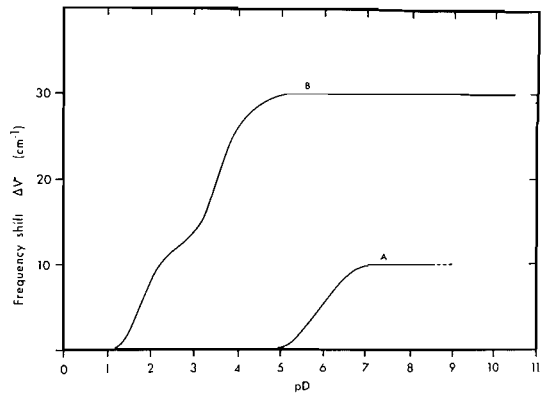

FIG. 5. Shift of the antisymmetric carboxyl stretching frequency ($\Delta\nu$) towards lower frequency from reference $\nu = 1620\ cm^{-1}$. Curve *A*, L-histidine; curve *B*, 1:2 Cu(II)–L-histidine.

over a wide pH range were taken into account to study the structure of individual species in solution by physical and chemical means.[7]

We shall discuss the structure of the species in the 1:2 Cu(II)–L-histidine system as they appear with increasing pH. At pH 2.00, the predominant species is MHA having a structure as shown in Fig. 6*A*, on the basis of the following results. On addition of Cu(II) to L-histidine, an increase in the absorption maximum and a simultaneous shift in the antisymmetric carboxyl stretching frequency of the deprotonated carboxyl group was observed at pD = 2.5 and below (Fig. 5). This observation, in conjunction with potentiometric results, was interpreted as an indication for carboxyl involvement in the species MHA. The imidazole nitrogen binding is also evident from the i.r. results. The location of the λ_{max} of 750 nm of this species (Fig. 2) can be assigned to a carboxyl oxygen and an imidazole nitrogen involvement. Although it has been reported that the introduction of nitrogen in the ligand field surrounding the Cu(II) nucleus causes a shift to a lower wavelength (11), recent

[7]The chemical and physical probes for structural interpretations are not sensitive enough to study the minute amounts of $MH_{-1}A$ and $M_2H_{-2}A_2$. The species $MH_{-1}A_2$ is a high pH species and any structural assignment of this species must be followed with caution, since enough physicochemical data could not be obtained because of the instability of the Cu(II)–L-histidine system in the high pH region. For these reasons, no structures are proposed for the species $MH_{-1}A$, $M_2H_{-2}A_2$, and $MH_{-1}A_2$.

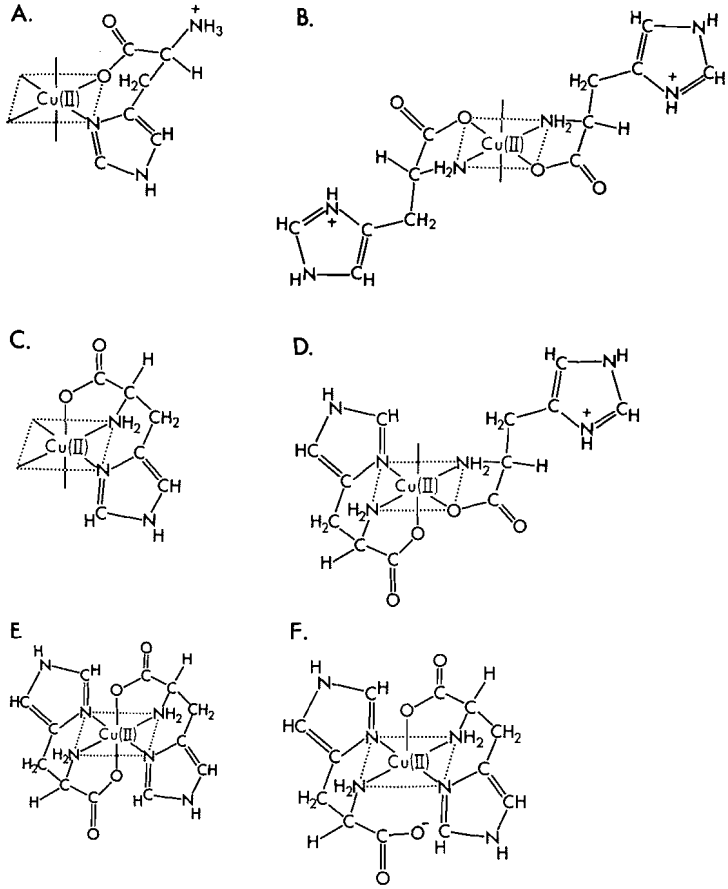

FIG. 6. Proposed structures of the species in the Cu(II)–L-histidine system. *A*, MHA; *B*, MH_2A_2; *C*, MA; *D*, MHA_2; *E* and *F*, MA_2. The diagrams are not to be taken to represent absolute steric configurations.

studies show that all nitrogens do not behave in the same manner. Ligand-field effects of *N*(imidazole) and *O*(carboxyl) appear to be similar (19).

On raising the p*H* the next species to appear are MH_2A_2 and MA which show maximum concentration at almost the same p*H* value (ref. 6, Fig. 3). The infrared data again suggest carboxyl involvement (Fig. 5). The crystal structure of MH_2A_2, which crystallized from a solution of p*H* 3.7 as the dinitrate dihydrate, has been solved (12). In this species two L-histidine molecules coordinate to a central Cu(II) atom, each through the amino nitrogen and carboxyl oxygen as shown in Fig. 6*B*. The observed λ_{max} of 650 nm would indicate carboxyl and amino involvement, hence the structural identity of the species MH_2A_2 in solution and in crystalline state could be demonstrated. The continued shift in carboxyl stretching, as well as deprotonation of 3 hydrogens from the L-histidine molecule in the formation of MA, strongly favor its structure as shown in Fig. 6*C* involving carboxyl, amino, and imidazole groups. The involvement of an amino nitrogen in conjunction with carboxyl and imidazole groups in MA is also consistent with the λ_{max} of 670 nm.

In the p*H* region 4.5–7.5 the major species are MHA_2 and MA_2. The species MHA_2 reaches its maximum concentration at about p*H* 4.5. The i.r. observations suggest carboxyl involvement; the antisymmetric carboxyl stretching frequency reaching a maximum shift of about 30 cm^{-1}. Involvement of the amino nitrogens is also sug-

Can. J. Chem. Downloaded from www.nrcresearchpress.com by 210.87.254.6 on 09/05/12
For personal use only.

Can. J. Chem. Downloaded from www.nrcresearchpress.com by 210.87.254.6 on 09/05/12
For personal use only.

gested by the shift of the λ_{max} towards lower wavelength (λ_{max} = 610 nm). The proton displacement results clearly indicate the involvement of 2 amino and 1 imidazole groups in MHA_2 (Table 2). The complex MHA_2 can be considered a mixed complex similar to the previously reported L-histidine–Cu(II)–L-threonine complex (1). Considering the overall stability constants of these complexes (13), we find a striking similarity in the stepwise addition of the second amino acid. To elaborate this point, the following reactions 6 to 9 are considered:

[6] L-thr + Cu(II) $\overset{\beta_{101}}{\rightleftharpoons}$ Cu(II)–L-thr $\quad \beta_{101} = 8.01$

[7] L-Hhis + Cu(II) $\overset{\beta_{111}}{\rightleftharpoons}$ Cu(II)–L-Hhis $\quad \beta_{111} = 14.18$

[8] Cu(II)–L-thr + L-his $\overset{\beta_{1011}}{\rightleftharpoons}$ L-thr – Cu(II) – L-his $\quad \beta_{1011} = 17.55$

[9] Cu(II)–L-his + L-Hhis $\overset{\beta_{112}}{\rightleftharpoons}$ L-his – Cu(II) – L-Hhis $\quad \beta_{112} = 24.17$

It can be seen that the difference between the overall stability constants of the mixed complexes $\beta_{112} - \beta_{1011} = 6.6$ is close to the difference $\beta_{111} - \beta_{101} = 6.2$ between the first formation constants of the Cu(II)–L-histidine and Cu(II)–L-threonine complexes. It suggests almost equal strength of binding of the second ligand. This thermodynamic evidence points towards a similarity between the structure of MHA_2 and that of L-histidine – Cu(II) – L-threonine (14), where one ligand is tridentate and the second is in bidentate configuration. Thus, for MHA_2 a structure involving 1 imidazole, 2 carboxyl, and 2 amino groups is suggested (Fig. 6*D*).

The greatest controversy had been centered around the structure of MA_2. The investigations by three groups (15–17) using similar experimental techniques resulted in different proposals for the structure of MA_2. The n.m.r. investigation by Sigel and McCormick (18), did not settle the question of all the coordinating groups in MA_2 either. The common shortcomings seem to be a lack of knowledge of the precise concentration of the complex species in their respective systems. Corroborating evidence obtained by a different experimental approach was not presented in order to verify their structural proposals for MA_2. The proton displacement studies definitely indicated quantitative involvement of 2 imidazole and 2 amino groups in MA_2 (Table 2). Since Cu(II) coordination to imidazole nitrogen and carboxyl oxygen appears to show similar ligand field effects (19), the absorption maxima (640 nm) of MA_2 can best be explained by the involvement of amino nitrogens in conjunction with carboxyl and imidazole groups. The involvement of one or two carboxyl groups in MA_2 is evident from the observed frequency shift from 1622 to 1592 cm^{-1} in the region where MA_2 exists almost exclusively. If the carboxyl group was not coordinated, then MA_2 should have shown a major peak at 1578 cm^{-1} for free carboxylate anion. On the contrary, a constant shift of 30 cm^{-1} was observed from p*H* 5–7 (Fig. 5), implicating Cu(II) coordination to the carboxyl oxygen. Thus, in addition to 2 imidazole and 2 amino groups in MA_2, the involvement of at least one, if not both, carboxyl groups, is apparent. This is consistent with our previous suggestion (14) for the structure of MA_2, interpreted on the basis of the crystal structure of the L-histidinato-L-threoninato-aquocopper(II) hydrate. Consequently, MA_2 may either have a structure as shown in Fig. 6*E* or such as shown in Fig. 6*F*. It is also possible that both structures are present in an equilibrium mixture.

This work was supported by grants from the John A. Hartford Foundation of New York, and the Medical Research Council of Canada.

1. B. SARKAR and T. P. A. KRUCK. Biochemistry of copper. *Edited by* J. Peisach, P. Aisen and W. E. Blumberg. Academic Press, New York. 1966.
2. B. SARKAR and Y. WIGFIELD. Can. J. Biochem. **46**, 601 (1968).
3. S. LAU and B. SARKAR. J. Biol. Chem. **246**, 5938 (1971).
4. D. I. M. HARRIS and A. SASS-KORTSAK. J. Clin. Invest. **46**, 659 (1967).
5. P. Z. NEUMANN and A. SASS-KORTSAK. J. Clin. Invest. **46**, 646 (1967).
6. T. P. A. KRUCK and B. SARKAR. Can. J. Chem. This issue.
7. K. MIKKELSEN and S. D. NIELSEN. J. Phys. Chem. **64**, 632 (1960).
8. B. SARKAR and Y. WIGFIELD. J. Biol. Chem. **242**, 5572 (1967).
9. K. NAKAMOTO, Y. MORIMOTO, and A. E. MARTELL. J. Am. Chem. Soc. **85**, 309 (1963).
10. R. N. CARLSON and T. L. BROWN. Inorg. Chem. **5**, 268 (1966).

11. A. S. BRILL, R. B. MARTIN, and R. J. P. WILLIAMS. Electronic aspects of biochemistry. *Edited by* B. Pullman. Academic Press, New York. 1961.
12. B. EVERTSSON. Acta Cryst. **B25**, 30 (1969).
13. B. SARKAR and T. P. A. KRUCK. Proceedings of the XIV International Conference on Coordination Chemistry, Toronto, Canada. 1972.
14. H. C. FREEMAN, J. M. GUSS, M. J. HEALY, R.-P. MARTIN, C. E. NOCKOLDS, and B. SARKAR. Chem. Commun. 225 (1969).
15. K. M. WELLMAN and B. K. WONG. Proc. Nat. Acad. Sci. **64**, 824 (1969).
16. E. W. WILSON, M. KASPERIAN, and R. B. MARTIN. J. Am. Chem. Soc. **92**, 5365 (1970).
17. H. SIGEL, R. E. MACKENZIE, and D. B. MCCORMICK. Biochem. Biophys. Acta, **200**, 411 (1970).
18. H. SIGEL and D. B. MCCORMICK. J. Am. Chem. Soc. **93**, 2041 (1971).
19. H. C. FREEMAN. Private communication.

Can. J. Chem. Downloaded from www.nrcresearchpress.com by 210.87.254.6 on 09/05/12
For personal use only.

On An Extension of the Use of p*H*-Titrations for Determination of Free Metal and Free Ligand Concentrations During Metal Complex Formation

W. A. E. McBryde

Department of Chemistry, University of Waterloo, Waterloo, Ontario N2L 3G1

Received May 30, 1973

A method introduced by R. Osterberg for the measurement of free ligand concentration during the formation of metal complexes has recently been extended by Sarkar and Kruck to include measurement of free metal concentration. The method is based on suitable manipulation of the data from sets of p*H* titrations. This paper gives a new theoretical treatment of the method and its extension, and shows how the functions developed are related to other parameters of complex formation. A special advantage of Osterberg's method as extended is its capability of being applied when protonated or deprotonated complexes form.

La méthode introduite par R. Osterberg pour mesurer la concentration en ligand libre pendant la formation de complexes métalliques a été récemment développée par Sarkar et Kruck pour inclure la mesure de concentration en métal libre. La méthode est basée sur une manipulation convenable des données à partir des tableaux de titration p*H*. Cette communication décrit un nouveau traitement théorique de la méthode et son extension qui montre comment les fonctions développées sont reliées à d'autres paramètres de formation de complexes. Un avantage spécial de la méthode d'Osterberg ainsi étendue est d'être applicable aux formations de complexes protonés et déprotonés.

[Traduit par le journal]

Can. J. Chem., **51**, 3572 (1973)

Introduction

Sarkar and Kruck (1) have recently revived a procedure introduced by Osterberg (2) for the determination of free ligand concentration during the controlled formation of metal–ligand complexes with a view to establishing the stability constants of the latter. These authors have extended Osterberg's procedure to the determination of the free metal concentration, and have improved the practice of the method by introduction of computer-based numerical procedures.

As Beck has pointed out (3), Osterberg's procedure, which is based on a set of p*H* titrations, has the advantage over the earlier Calvin–Bjerrum titrations in that it can be applied even when protonated or deprotonated species are formed. With the addition developed by Sarkar and Kruck it becomes possible to determine in a solution during a p*H*-titration the simultaneous concentrations of free metal ion, free ligand, and free hydrogen ion. The method comprises a powerful tool to analyze complex formation and to assign stability constants, and deserves wider recognition.

It may be inferred from a lack of published applications that the method is either not well known or not well understood. As the writer had the opportunity to examine a pre-publication copy of the papers by Sarkar and Kruck, the occasion was taken to develop the following alternative to Osterberg's derivation of the key relationships. This method of derivation is thought to be based on more chemical and less mathematical intuition than the original, and reveals the relationships among the functions derived and applied in terms of other familiar quantities.

Titration of a Weak Acid in the Absence of Metal Ion

We consider a series of titrations of a weak v-basic acid, each differing in C_L where C_L is the total concentration of ligand in all forms. These titrations may be depicted by a set of titration curves in the form C_H $(= vC_L - C_{OH}$, with suitable allowance being made for any added mineral acid) *vs.* p*H* (C_H = concentration of total ionizable hydrogen free or bound; C_{OH} = concentration of added strong base, adjusted for dilution; pX = $-\log$ [X], thus in this context p*H* refers not to the conventional quantity but to p[H]).

We draw isohydric lines (constant p*H*) at intervals of p*H*, cutting these curves. The points of intersection are displayed as plots of C_H *vs.* C_L, and these comprise a series of straight lines,

Can. J. Chem. Downloaded from www.nrcresearchpress.com by 210.87.254.5 on 09/05/12
For personal use only.

Can. J. Chem. Downloaded from www.nrcresearchpress.com by 210.87.254.5 on 09/05/12
For personal use only.

one for each isohydric pH. The slopes of these give $(\partial C_H/\partial C_L)_H$ for each value of pH. Since the plots of C_H *vs.* C_L are straight lines, the value of $(\partial C_H/\partial C_L)_H$ is independent of C_L. Let us inquire into the nature of this function.

We note the relationships

$$[1] \quad F = 1 + \beta_1^0[H] + \beta_2^0[H]^2 + \beta_3^0[H]^3 + \ldots$$

$$[2] \quad G = \beta_1^0[H] + 2\beta_2^0[H]^2 + 3\beta_3^0[H]^3 + \ldots$$

$$[3] \quad = dF/d \ln [H]$$

$$[4] \quad C_H = [H] - [OH] + G[L]$$

In the above, β_j^0 refers to the cumulative proton association constant for the acid species H_jL ($\beta_j^0 = [H_jL]/[H]^j[L]$).

$$[5] \quad C_L = F[L]$$
$$(\partial C_H/\partial[L])_H = G$$
$$(\partial C_L/\partial[L])_H = F$$

$$[6] \quad (\partial C_H/\partial C_L)_H = G/F = \bar{n}_H$$

where $\bar{n}_H$ is the degree of protonation of ligand L. For a particular titration, *i.e.*, fixed C_L

$$dpL = d \log F$$
$$d \log F/d \log [H] = \bar{n}_H$$
$$dpL = \bar{n}_H \, d \log [H] = -\bar{n}_H \, dpH$$

$$[7] \quad pL - pL_0 = \int_{pH}^{pH_0} \bar{n}_H \, dpH \Big|_{C_L}$$

Equation 7 specifies the relationship between two values of pL and the corresponding values of pH, and indicates that the difference in these values of pL may be expressed by and indeed determined by an integral. From purely experimental quantities, the integrand $\bar{n}_H$ may be taken as values of $(\partial C_H/\partial C_L)_H$, and the integral found as an area under a plot of the latter *vs.* pH. Such a procedure is practically unnecessary since the relationship between pL and pH is already implied by [5]. In this case $(\partial pL/\partial pH)_{C_L} = -\bar{n}_H$, which is independent of the particular value of C_L taken.

Titration of the Same Acid in the Presence of Metal Ion

We next consider a similar series of titrations of the same weak acid, but in the presence of a fixed concentration of metal C_M (C_M = concentration of metal in all forms in solution). The metal is one that reacts with L to form a series of complexes ML, ML_2 ...., which in this case is restricted to mononuclear complexes, not protonated or deprotonated.

In this case, although [4] still applies, [5] must be changed to

$$[8] \quad C_L = F[L] + \bar{n}_L C_M$$

where $\bar{n}_L$ is the degree of metal complex formation (Bjerrum). Then

$$(\partial C_H/\partial[L])_H = G$$
$$(\partial C_L/\partial[L])_H = F + C_M(\partial \bar{n}_L/\partial[L])_H$$

Hence

$$[9] \quad (\partial C_H/\partial C_L)_H = G(F + C_M(\partial \bar{n}_L/\partial[L])_H)^{-1}$$
$$= \bar{n}_H(1 + C_M F^{-1}(\partial \bar{n}_L/\partial[L])_H)^{-1}$$

We may also write

$$(\partial C_L/\partial \ln [L])_H = F[L] + C_M(\partial \bar{n}_L/\partial[L])_H[L]$$
$$(\partial C_L/\partial \ln [H])_L = G[L]$$

Since C_M is held constant C_L is a function of [H] and [L] only. The total differential dC_L may be written

$$dC_L = (\partial C_L/\partial \ln [H])_L \, d \ln [H] + (\partial C_L/\partial \ln [L])_H \, d \ln [L]$$

If we impose the further requirement that C_L is constant, $dC_L = 0$

$$[10] \quad \left(\frac{\partial \ln [L]}{\partial \ln [H]}\right)_{C_L} = \frac{-G}{F + C_M(\partial \bar{n}_L/\partial[L])_H} = -\left(\frac{\partial C_H}{\partial C_L}\right)_H$$

This is the Osterberg relationship, which may also be written

$$[11] \quad pL - pL_0 = \int_{pH}^{pH_0} \left(\frac{\partial C_H}{\partial C_L}\right)_H dpH \Big|_{C_L}$$

This is the same relationship as before, except that $(\partial C_H/\partial C_L)_H$ is no longer $\bar{n}_H$. Two features of the foregoing merit further comment and explanation. Equations 6 and 9 are identical when $C_M = 0$. Equation 9 describes the Osterberg relationship in terms of other parameters of the system of complexes.

To demonstrate the validity of these relationships we have calculated sets of titration data

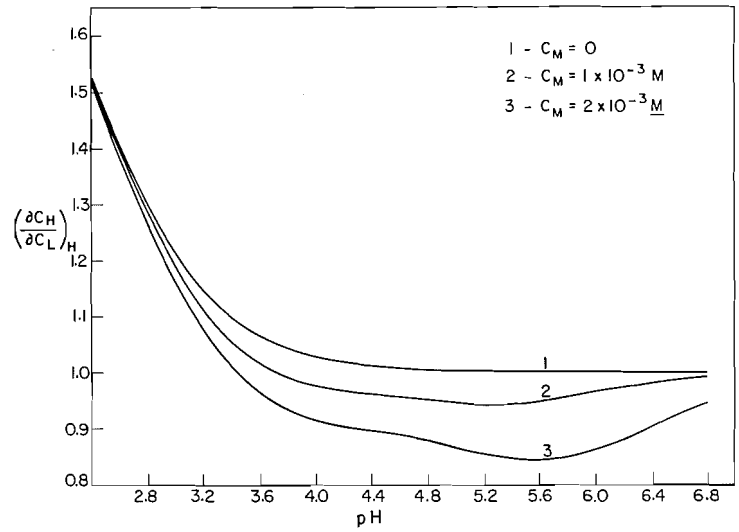

FIG. 1. Values of $(\partial C_H/\partial C_L)_H$ as a function of pH for solutions of glycine with and without copper(II) added. $C_L = 4 \times 10^{-3}$ M.

(pH, C_H) for two model systems, *viz.* copper(II)–glycine and nickel(II)–ethylenediamine, basing these calculations on published values of the appropriate equilibrium constants and selected values of C_M and C_L. We have determined $(\partial C_H/\partial C_L)_H$ in the manner previously described, for a number of pH values, and then also evaluated the function on the right-hand side of eq. 9. The values agreed to within about 1% throughout the full range of the titration data.

Figure 1 shows the calculated values of $(\partial C_H/\partial C_L)_H$ for solutions of glycine with and without copper(II) added. When metal is present the values are smaller than the corresponding values of $\bar{n}_H$ in accord with [9]. In the case of curve 2, Fig. 1, the value of the ordinate is approaching that of curve 1, which is to be expected since at pH 7 in this case $\bar{n}_L \to 2$ and $(\partial \bar{n}_L/\partial[L])_H \to 0$. Also in agreement with [9] curve 3 lies below curve 2 throughout the range shown. At still higher pH when $\bar{n}_H < 1$, all the curves will coincide.

In the absence of metal ion the plots of C_H *vs.* C_L for each chosen [H] take the form of straight lines with slope $\bar{n}_H$. In the account of Osterberg's work with copper(II) complexes of *O*-phosphorylethanolamine (2) these plots again appear as straight lines. From that paper an uncritical reader might infer that values of $(\partial C_H/\partial C_L)_H$ were independent of C_L. However, in evaluating this quantity with the aid of [9] it is apparent that values of $(\partial \bar{n}_L/\partial[L])_H$ are dependent on the value of [L] corresponding to the pH selected. And eq. 8 shows that at a particular pH, [L] depends on C_L.

The point may be illustrated in another way. Equation 11 can be used to evaluate pL once a value of pL_0 has been fixed. It is assumed that the system permits the latter to be done at a pH sufficiently low that $\bar{n}_L \to 0$, in which case $[L]_0 = C_L/[F]_0$. But [11] shows that if $(\partial C_H/\partial C_L)_H$ were independent of C_L, [L] at a particular [H] would always be directly proportional to C_L. Such a proportionality can only be approximated, as [8] shows, if $\bar{n}_L C_M$ is small compared to C_L. Hence plots of C_H *vs.* C_L will only be linear if $C_L \gg C_M$ or if $\bar{n}_L$ remains small. The latter condition will not be suitable if it is desired to study complexes of ligand number greater than unity. Figure 2 shows the curvature in plots of $(\partial C_H/\partial C_L)_H$ for the system nickel(II)–ethylenediamine. The slopes to these curved lines still conform to [9].

Analogous Relationship for Free Metal Concentration

We next consider a series of similar titrations, each differing in C_M but with fixed C_L. The quantity C_H is again plotted against pH to give titration curves, one for each value of C_M. Isohydric lines are again drawn, cutting the titration curves at fixed pH values. The points

Can. J. Chem. Downloaded from www.nrcresearchpress.com by 210.87.254.5 on 09/05/12
For personal use only.

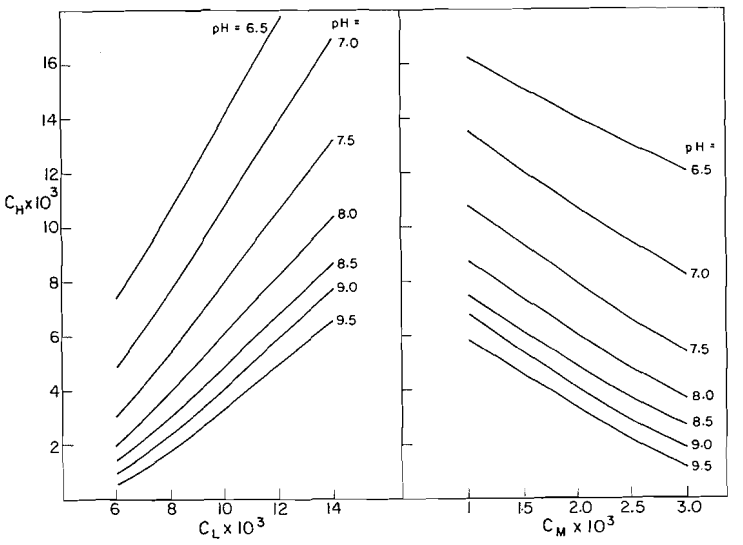

FIG. 2. Typical plots of C_H *vs.* C_L or C_M for the system nickel(II)–ethylenediamine.

of intersection are plotted as C_H *vs.* C_M, one line for each isohydric p*H*. Slopes of these lines are taken at a suitable value of C_M. These slopes comprise a function $(\partial C_H/\partial C_M)_H$ which we proceed to examine.

Equation 4 still applies, and [8] can be rearranged to give

$$C_M = (C_L - F[L])/\bar{n}_L$$

Then

$$(\partial C_H/\partial[L])_H = G$$

$$(\partial C_M/\partial[L])_H = \{-\bar{n}_L F - (C_L - F[L])(\partial\bar{n}_L/\partial[L])_H\}\bar{n}_L^{-2}$$

Whence

$$(\partial C_H/\partial C_M)_H = \frac{-\bar{n}_L^2 G}{\bar{n}_L F + (C_L - F[L])(\partial\bar{n}_L/\partial[L])_H}$$

$$= \frac{-\bar{n}_L G}{F + C_M(\partial\bar{n}_L/\partial[L])_H}$$

$$[12] \qquad = \frac{-\bar{n}_L\bar{n}_H}{1 + C_M F^{-1}(\partial\bar{n}_L/\partial[L])_H}$$

$$[12a] \qquad = -\bar{n}_L\left(\frac{\partial C_H}{\partial C_L}\right)_H$$

This derivation shows that this function can be evaluated for any particular values of C_L and [H]. The function $(\partial C_H/\partial C_L)_H$ will be known for any particular values of C_M and C_L (see above). Again values of the slopes of the plots of C_H *vs.* C_M for a selected value of C_M compared favorably with calculated values of this function for the model systems examined. Figure 3 shows the variation and interrelationship of the quantities $\bar{n}_H$, $\bar{n}_L$, and $(\partial C_H/\partial C_M)_H$ when plotted against p*H* for a solution in the system nickel(II)–ethylenediamine.

The usefulness of this function is shown in the following derivation

$$[13] \quad C_M = [M](1 + \beta_1[L] + \beta_2[L]^2 + \ldots)$$

$$(\partial C_M/\partial \ln [M])_L = C_M$$

$$(\partial C_M/\partial \ln [L])_M = [M](\beta_1[L] + 2\beta_2[L]^2 + \ldots) = \bar{n}_L C_M$$

$$[14] \quad dC_M = C_M\, d\ln [M] + \bar{n}_L\, C_M\, d\ln [L]$$

$$[15] \quad (\partial \ln [M]/\partial \ln [L])_{C_M} = -\bar{n}_L$$

At constant C_M and C_L

$$[16] \quad dpM = -\bar{n}_L\, dpL = \bar{n}_L\left(\frac{\partial C_H}{\partial C_L}\right)_H dpH$$

$$[17] \quad pM - pM_0 = \int_{pH_0}^{pH} \bar{n}_L\left(\frac{\partial C_H}{\partial C_L}\right)_H dpH = \int_{pH}^{pH_0}\left(\frac{\partial C_H}{\partial C_M}\right)_H dpH$$

The foregoing derivation of eqs. 11 and 17 is based on a system of metal complexes which is neither protonated nor deprotonated. However, it is quite simple to reach essentially the same conclusion when allowance is made for addi-

Can. J. Chem. Downloaded from www.nrcresearchpress.com by 210.87.254.5 on 09/05/12
For personal use only.

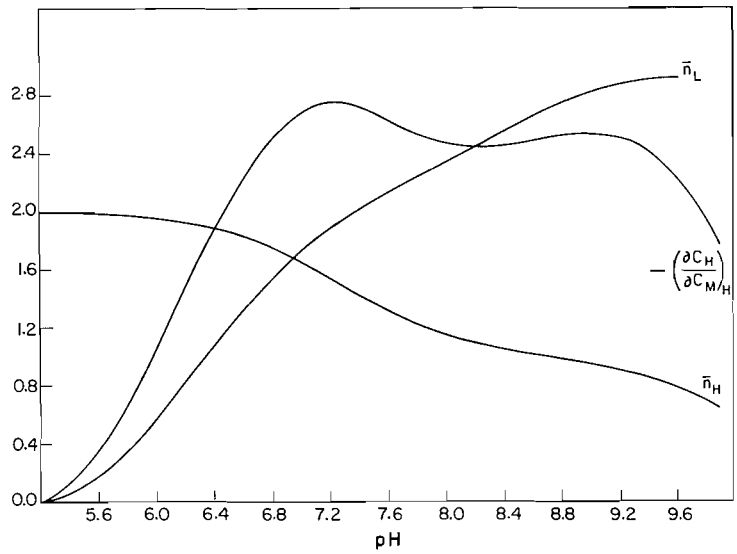

FIG. 3. Function $(\partial C_H/\partial C_M)_H$ and its relationship to $\bar{n}_H$ and $\bar{n}_L$ for the system nickel(II)–ethylenediamine.

tional complexes of this type. The only difference is that eq. 9 defining $(\partial C_H/\partial C_L)_H$ must include in the numerator a term $F^{-1}\sum_{qr}\beta_{qr}[M][H]^q[L]^{r-1}$ (where q may be a positive or negative integer) which arises from the additional complexes. It is also possible to show that these relationships still apply in the presence of a second ligand which forms mixed complexes with the metal and first ligand.

Osterberg (2) showed that $(\partial C_L/\partial \ln [H])_L = (\partial C_H/\partial \ln [L])_H$, and then a transformation previously introduced by Hedström (4) was employed to show that $(\partial \ln [L]/\partial \ln [H])_{C_L} = -(\partial C_H/\partial C_L)_H$ (*cf.* [10]). By entirely similar reasoning Osterberg's equations can be used to show that $(\partial C_M/\partial \ln [H])_M = (\partial C_H/\partial \ln [M])_H$, from which, by Hedström's transformation, one gets $(\partial \ln [M]/\partial \ln [H])_{C_M} = -(\partial C_H/\partial C_M)_H$ (*cf.* [16]). The use in this way of Hedström's transformation, which was derived strictly for a two-component system where no "competitive complex formation with any third reagent C is assumed", at first appeared to the writer as questionable. However, it is evident from [8] and [13] that once values of C_M and C_L are fixed the values of [M], [L], and [H] become interdependent. Thus for any particular value of [H], the values of [M] and [L] become invariant. Hence in evaluating the quantities $(\partial C_H/\partial C_L)_H$ or $(\partial C_H/\partial C_M)_H$ we need not be concerned with the respective variations of the third constituent [M] or [L].

The author is grateful to Janet L. McCourt for working out the computer calculations, and to Dr. B. Sarkar and Mr. T. P. A. Kruck, Hospital for Sick Children, Toronto, for introduction and helpful discussion of the problem. Financial support from the National Research Council of Canada is also gratefully acknowledged.

1. B. SARKAR and T. P. A. KRUCK. Can. J. Chem. This issue.
2. R. OSTERBERG. Acta Chem. Scand. **14**, 471 (1960).
3. M. T. BECK. Chemistry of complex equilibria. Van Nostrand Reinhold Co., London. 1970. p. 152.
4. B. HEDSTRÖM. Acta Chem. Scand. **9**, 613 (1955).

Can. J. Chem. Downloaded from www.nrcresearchpress.com by 210.87.254.5 on 09/05/12
For personal use only.

Etude par Spectroscopie Infrarouge de la Solvatation Préférentielle du Cation Li^+ [1]

ANDRÉ REGIS ET JACQUES CORSET

Laboratoire de Spectrochimie Moléculaire, Université de Paris VI, 75230, Paris Cedex 05 et Laboratoire de Chimie Physique, C.N.R.S., 2, rue Henri Dunant, 94320 Thiais, France

Reçu le 20 février 1973

L'analyse des spectres de vibration de mélanges ternaires $LiClO_4$–S_1–S_2 révèle la solvatation préférentielle du cation Li^+ par l'ammoniac et les amines méthylées (S_2) dans l'acétonitrile ou le tétrahydrofuranne (S_1) et par l'acétonitrile (S_2) dans le nitrométhane (S_1). L'apparition de bandes larges dans la région des vibrations "ion-cage" est liée à la formation de différents édifices $[Li(S_1)_{n-i}(S_2)_i]^+$ dont l'évolution, en fonction du rapport $\rho = [S_2]/[LiClO_4]$, explique les déplacements de fréquence; l'énergie d'interaction ion Li^+ – molécule de solvant diminue quand le nombre de molécules S_2 de la première couche de solvatation augmente. Elle est par contre peu sensible à la constante diélectrique du milieu environnant. La variation de la composition moyenne de cette première couche de solvatation est déterminée par les mesures d'intensités des bandes d'absorption des molécules S_2 non liées au cation; dans les cas favorables ($S_2 = ND_3$, CH_3CN), le nombre de solvatation de cet ion par le solvant pur peut être estimé. Il est montré en outre que le pouvoir solvatant des bases examinées décroit dans l'ordre $NH_3 > CH_3NH_2 > (CH_3)_2NH > (CH_3)_3N > CH_3CN > CH_3NO_2$, en faisant intervenir à la fois les interactions donneur–accepteur et ion–dipole.

The analysis of the infrared spectra of ternary mixtures $LiClO_4$–S_1–S_2 shows a preferential solvation of the Li^+ ion by ammonia and methylamines (S_2) in acetonitrile or tetrahydrofuran (S_1) and by acetonitrile (S_2) in nitromethane (S_1). The appearance of wide bands in the "ion-cage" vibration region is related to the formation of different species $[Li(S_1)_{n-i}(S_2)_i]^+$. The variation of their relative concentration when $\rho = [S_2]/[LiClO_4]$ increases explains the frequency shift of the bands. The interaction energy Li^+ ion – solvent molecule decreases when the number of S_2 molecules in the first solvation shell increases and does not seem to depend on the dielectric constant of the surrounding medium. The mean composition of the first solvation shell is obtained from intensity measurements of absorption bands of the S_2 molecules not bonded to the ions; in favorable cases ($S_2 = ND_3$, CH_3CN) the solvation number of the Li^+ ion in the pure solvent could be estimated. The solvating power of the different bases used is shown to decrease in the order $NH_3 > CH_3NH_2 > (CH_3)_2NH > (CH_3)_3N > CH_3CN > CH_3NO_2$ and involves both donor–acceptor and ion–dipole interactions.

Can. J. Chem., **51**, 3577 (1973)

Introduction

La solvatation des anions X^- par l'acétonitrile (1, 2) et par différents solvants "donneurs de proton" (3–8) a pu être étudiée par spectrométrie de vibration, en milieu ternaire, dans le cas des halogénures de tétraalkylammonium dissous dans un diluant inerte, mais seule la solvatation du cation Na^+ par le tétrahydrofuranne a été analysée à l'aide du tétrabutylaluminate de sodium dans le cyclohexane (9, 10).

Pour des raisons de solubilité, l'étude des sels minéraux nécessite l'emploi de diluants plus actifs, tels que l'acétonitrile ou le nitrométhane (11–15), dont les molécules entrent en compétition avec celles du ligande dans la première couche de solvatation de l'ion. Ces mélanges ternaires comprenant deux solvants S_1 et S_2, S_2 étant plus actifs que S_1, donnent lieu à des équilibres successifs tels que

$$[M(S_1)_{n+1-i}(S_2)_{i-1}]^{z+} + S_2 \overset{K_i}{\rightleftharpoons} [M(S_1)_{n-i}(S_2)_i]^{z+} + S_1$$

n étant le nombre de solvatation de cation M^{z+} dans S_1 pur; $i \geqslant 1$. La composition de la couche de solvatation peut être différente de celle du reste de la solution s'il y a solvatation préférentielle (16, 17).

Notre étude porte sur le cation Li^+. Nous examinerons les vibrations "ion-cage" (2, 18–22) et les vibrations internes des molécules en fonction du rapport $\rho = [S_2]_{total}/[SEL]_{total}$ les mélanges de solvants étant soit l'ammoniac ou les

[1]Ce travail a fait l'objet de communications: Journée de mise au point sur la solvatation des ions, Société de Chimie Physique, Paris, 1970; 54ème Conférence Canadienne de Chimie, Halifax, 1971; Third International Conference on non-aqueous solvents, Michigan State University, 1972.

Can. J. Chem. Downloaded from www.nrcresearchpress.com by 210.87.254.6 on 09/05/12
For personal use only.

amines méthylées dans l'acétonitrile, soit l'acétonitrile dans le nitrométhane.

Résultats expérimentaux[2]

Mélanges perchlorate de lithium – ammoniac, amine-acétonitrile

Les fréquences des vibrations internes des molécules d'ammoniac et d'amines, en solution dans l'acétonitrile pur ou additionné de sel, sont rassemblées dans les tableaux 1–4.

En solution diluée dans une base organique B telle que l'acétonitrile, l'ammoniac et les amines primaires et secondaires forment des complexes (5, 23)

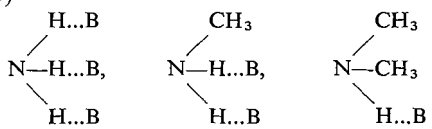

Par suite, leurs vibrations ν(NH) subissent un abaissement de fréquence notable par rapport à celles observées en gaz, sauf pour la diméthylamine;[3] ces vibrations restent fixes en fréquence (figs. 1, 2, 9), leur intensité est proportionnelle aux concentrations (figs. 10 et 11). De même (*cf.* mêmes figures), les bandes d'absorption des vibrations de déformation restent fixes et proportionnelles aux concentrations. Nous admettrons donc que la nature des complexes ne varie pas de façon appréciable dans le domaine étudié ($C \leqslant 2\ M$).

Dans le cas de la triméthylamine, pour les bandes observées (fig. 12, tableau 4) l'intensité varie encore linéairement avec la concentration. L'imprécision des mesures due à la faible solubilité de cette amine explique sans doute la plus grande dispersion des points (fig. 11) (*cf.* cond. expérimentales).

En milieu ternaire, l'addition de faibles quantités ($\rho \sim 1$) d'ammoniac ou d'amine à une solution 0.2 *M* en $LiClO_4$ dans l'acétonitrile, provoque dans la région des vibrations internes de ces molécules l'apparition de bandes d'absorption relativement intense (figs. 1, 2 et 9) que nous attribuons aux molécules engagées dans les complexes.

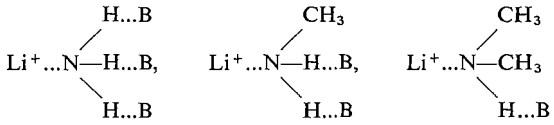

L'interaction par le doublet libre de l'azote (5, 26) perturbe surtout les vibrations de déformation $\nu_2(ND_3)$, $\nu_9(CH_3NH_2)$ et $\nu_{11}(CH_3)_2NH$ (tableaux 1–3); les différences $\Delta\nu = \nu_{ternaire} - \nu_{binaire}$ sont maximales pour les faibles valeurs de ρ; ce sont celles qui ont été relevées dans les tableaux. Les figs. 1, 2, et 9 montrent qu'en outre réapparaissent les absorptions dues aux molécules liées uniquement à l'acétonitrile; elles sont cependant d'intensité moins forte (figs. 1-(2) et 1-(3)), ce qui indique l'existence d'un équilibre entre molécules liées et non liées aux ions Li^+. Pour les vibrations d'élongation ν(NH), cet équilibre ne s'observe nettement que pour la diméthylamine où bandes libres et associées sont suffisamment distinctes (fig. 2). Pour les vibrations de valence de l'ammoniac $\nu(ND)_3$ (fig. 1), il n'apparait qu'un glissement de fréquence avec un élargissement des bandes vers les hautes fréquences quand ρ augmente.

Pour la triméthylamine (fig. 12), les perturbations des bandes observées sont faibles et analogues à celles observées dans les complexes iode–amine (27).

Dans la région des vibrations "ion-cage" (figs. 1, 13, 14, 15) la bande de vibration $\nu(Li^+...N{\equiv}C{-}CH_3)$, relevée à 405 cm^{-1} dans le binaire $LiClO_4$–CH_3CN (1, 2) diminue rapidement d'intensité dès les premières additions d'ammoniac ou d'amine; simultanément apparait, à plus haute fréquence, une bande large dont le maximum se déplace et se stabilise à 545 cm^{-1} pour NH_3 (fig. 13) et 475 cm^{-1} pour ND_3 (fig. 1). La fig. 3 permet de comparer les massifs des vibrations "ion–ligande", des ammoniacates $^7LiNO_3$–$4NH_3$ et $^7LiNO_3$–$4ND_3$ (28) et les bandes observées en solution dans l'acétonitrile pour un rapport ρ = 4: ces dernières correspondent à l'enveloppe des massifs situés vers 450 (ND_3) et 520 cm^{-1} (NH_3) -limités sur la figure par un trait pointillé et attribués aux vibrations de translation cation–ammoniac (28). On peut donc conclure qu'en solution, au moins pour les valeurs élevées de ρ, les bandes sont dues essentiellement aux mouvements de translation des

[2]On peut obtenir les figs. 9–16 à un prix nominal en s'adressant au Dépôt des données non publiées, Bibliothèque scientifique nationale, Conseil national de recherches du Canada, Ottawa, Canada, K1A 0S2.

[3]L'absence anormale de variation de fréquence de cette vibration s'explique peut-être par la variation d'anharmonicité de la liaison N—H, provoquée par la formation de liaison hydrogène (24); à l'état gazeux on a: $\omega_e = 3568\ cm^{-1}$; $\omega_e x_e = 93\ cm^{-1}$ (25).

Can. J. Chem. Downloaded from www.nrcresearchpress.com by 210.87.254.6 on 09/05/12
For personal use only.

Can. J. Chem. Downloaded from www.nrcresearchpress.com by 210.87.254.6 on 09/05/12
For personal use only.

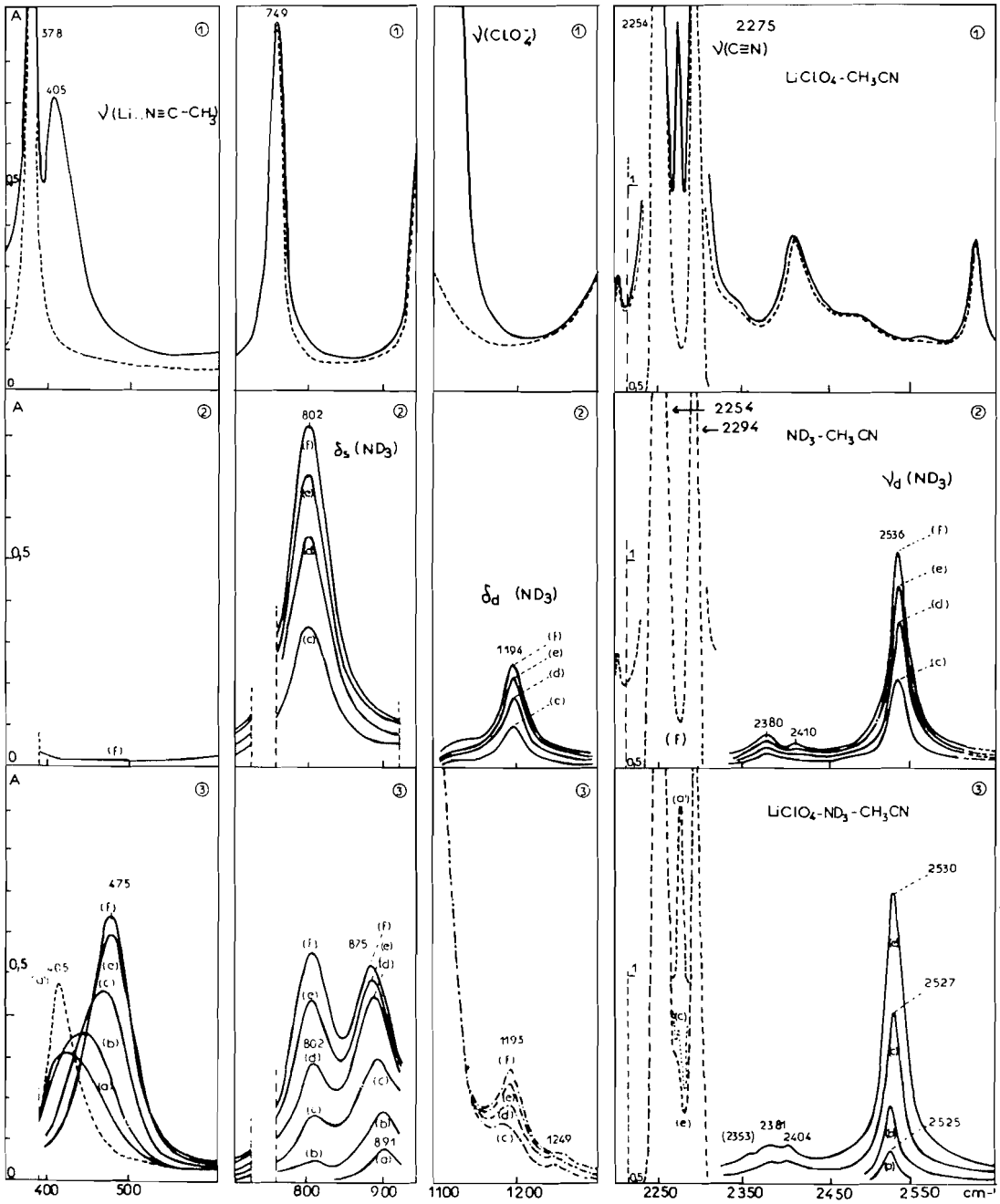

FIG. 1. Spectres d'absorption des mélanges $LiClO_4$–CH_3CN (1), ND_3–CH_3CN (2), $LiClO_4$–ND_3–CH_3CN (3). (1) (—) $LiClO_4$–CH_3CN; $[LiClO_4] = 0.2\,M$; (---) CH_3CN pur. (2) (—) ND_3–CH_3CN; $[ND_3]$ = (c) 0.8; (d) 1.2; (e) 1.6; (f) 2 M; (---) absorption de ND_3 + CH_3CN; $[ND_3] = 2\,M$. (3) $LiClO_4$–ND_3–CH_3CN; $[LiClO_4] \simeq 0.2\,M$; (—) absorptions de ND_3; ρ = (a) 1, (b) 2, (c) 4, (d) 6, (e) 8, (f) 10; (---) absorptions de $LiClO_4$ + ND_3; (---) (a′) $LiClO_4$ + CH_3CN; (c) et (e) absorption du mélange $LiClO_4$–ND_3–CH_3CN; $l = 144\,\mu$ sauf de 350 à 550 cm^{-1} où $l = 117\,\mu$.

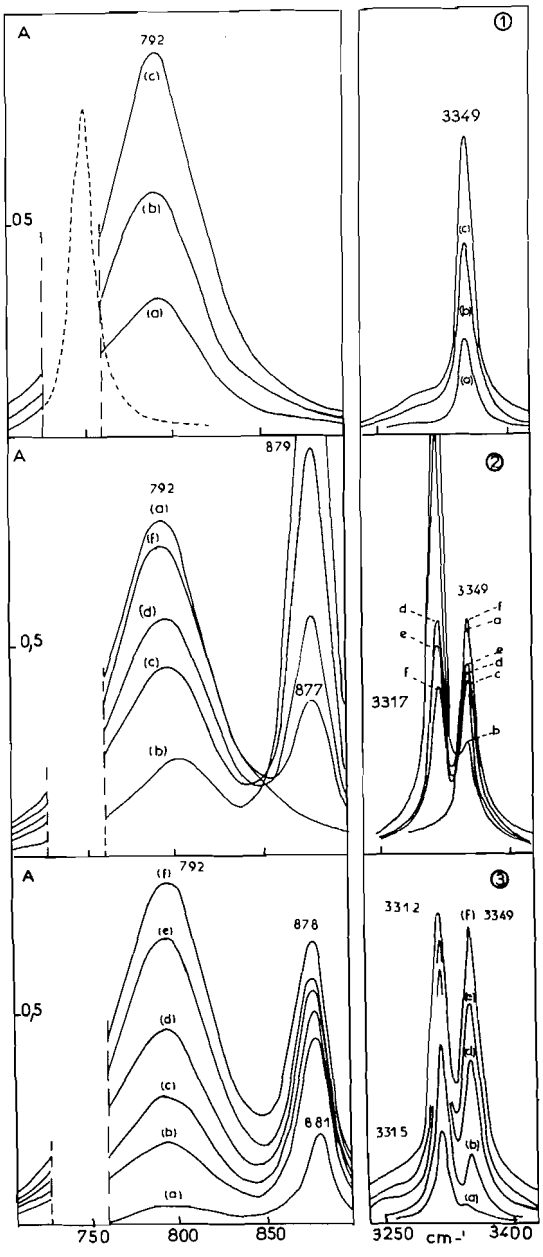

FIG. 2. Spectres d'absorption de mélange $(CH_3)_2NH$–CH_3CN (1) et $LiClO_4$–$(CH_3)_2NH$–CH_3CN à concentration constante en amine (2) et en sel (3). (1) $[(CH_3)_2NH]$ = (a) 0.51, (b) 0.92, (c) 1.44 *M*. (2) $[(CH_3)_2NH]$ = 1.3 *M*, (a) $[LiClO_4] = 0$, ρ = (b) 1.9, (c) 4, (d) 7, (e) 9.3, (f) 14.1. (3) $[LiClO_4] = 0.2$ *M*, ρ = (a) 1, (b) 2.7, (c) 4.2, (d) 5.5, (e) 8, (f) 10. Région 700 à 900 cm^{-1}, $l = 117$ μ et région 3250 à 3400 cm^{-1}, $l = 217$ μ; (---) acétonitrile pur.

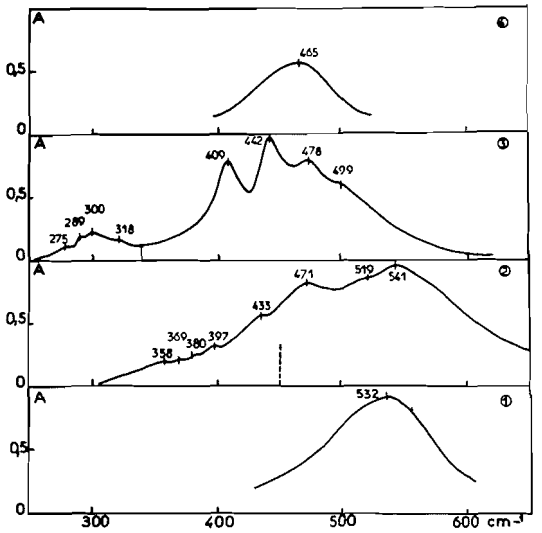

FIG. 3. Comparaison des bandes de vibrations ions–ammoniac d'ammoniacates solides avec celles observées dans les mélanges sel–ammoniac–acétonitrile. (1) Mélange ternaire $LiClO_4$–NH_3–CH_3CN, $[LiClO_4] = 0.25$ *M*, ρ = 4, $l = 108$ μ, $T = 300$ °K. (2) Ammoniacate $^7LiNO_3$, 4 NH_3—dispersion dans le Nujol, $T = 77$ °K. (3) Ammoniacate $^7LiNO_3$, 4 ND_3—dispersion dans le Nujol, $T = 77$ °K. (4) Mélange ternaire $LiClO_4$–ND_3–CH_3CN, $[LiClO_4] = 0.2$ *M*, ρ = 4, $l = 108$ μ, $T = 300$ °K.

molécules d'ammoniac par rapport à l'ion Li^+ dans sa première couche de solvatation.

Pour la monométhylamine, on observe le même phénomène et la bande se stabilise vers 514 cm^{-1} (fig. 14) à une fréquence voisine de celle de l'ammoniac NH_3; cette bande correspond aux mouvements de translation des ions Li^+ par rapport aux molécules d'amine, puisqu'aucune vibration interne n'est attendue dans cette région, la vibration de torsion[4] du groupement NH_2 ayant été située à l'état gazeux à 264 cm^{-1} (29).

Pour les deux autres amines (fig. 15), l'observation est rendue plus difficile par l'apparition de bandes dues probablement à un couplage des vibrations $\nu(Li^+...amine)$ et $\delta(CNC)_{amine}$ pour les molécules d'amines situées dans la première couche de solvatation, couplage déjà observé (2) pour les vibrations $\nu(Li^+...N{\equiv}C{-}CH_3)$ et δ(CCN) de l'acétonitrile; pour la triméthyl-

[4]Cette vibration, élevée en fréquence par complexation de l'amine avec le solvant, est sans doute responsable de l'absorption large dont le maximum est situé vers 350 cm^{-1}.

Can. J. Chem. Downloaded from www.nrcresearchpress.com by 210.87.254.6 on 09/05/12
For personal use only.

TABLEAU 1. Vibrations fondamentales des ammoniacs NH_3 et ND_3 complexés ou non avec les ions Li^+, en solution dans l'acétonitrile et le THF

	NH_3						ND_3		
	CH_3CN	$LiClO_4$–CH_3CN	Δν†	THF	$LiClO_4$–THF	Δν†	CH_3CN	$LiClO_4$–CH_3CN	Δν†
ν_3	3407	3393	−14	3397	3381	−16	2536	2525	−11
ν_1	3312	3305	−7	3307	3294	−13	2410	2404	−6
$2\nu_4$	3252	3260		3243	(3252)		2380	2381	
				(3213)				2353	
ν_4	1632*	1629	+3	1628	1624	+4	1194	1193	+1
ν_2	1035*						802	891	+89

*Référence 47.
†$\Delta\nu = \nu_{\text{ternaire}} - \nu_{\text{binaire}}$.

TABLEAU 2. Vibrations fondamentales de CH_3NH_2 complexé ou non avec les ions Li^+, en solution dans l'acétonitrile

Sym. C_s	*	Gaz*	CH_3CN	$LiClO_4$–CH_3CN	Δν
A''	$\nu_a(NH_2),\nu_{10}$	3427	3393	3369	−24
A'	$\nu_s(NH_2),\nu_1$	3361	3331	3313	−18
A'	$\delta(NH_2),\nu_4$	1623	1592	1607	+15
A'	$W(NH_2),\nu_9$	780	855	965	+110
A'	$W(CH_3),\nu_7$	1130	1146	1182	+36

*Références 29 et 34.

TABLEAU 3. Vibrations fondamentales de $(CH_3)_2NH$ complexé ou non avec les ions Li^+, en solution dans l'acétonitrile

Sym. C_s	*	Gaz*	CH_3CN	$LiClO_4$–CH_3CN	Δν
A'	$\nu(NH),\nu_1$	3351	3349	3312	−37
A'	$r(CH_3),\nu_9$	1145	1150		
A'	$\delta(CNH),\nu_{11}$	735	792	881	+89
A'	$\delta(CNC),\nu_{12}$	383	(390)		

*Références 34, 48, 49.

TABLEAU 4. Vibrations fondamentales de $(CH_3)_3N$ complexé ou non avec les ions Li^+, en solution dans l'acétonitrile

Sym. C_{3v}	*	Gaz*	CH_3CN	$LiClO_4$–CH_3CN	Δν	$(CH_3)_3N$–I_2†	$(CH_3)_3N$, $MgBr_2$‡
E	$r_2(CH_3)$	1272	1270	1260	−10	1256	1251
							1248
							1240.5
A_1	$r_{\parallel}(CH_3)$	1183	1185	1209	+24	1206	1223.5
							1228.5
E	$r_1(CH_3)$	1102	1100			1098	1102.5
							1108.5
							1098
A_1	$\nu_s(NC_3)$	825	826			804	824
							818
E	$\delta_d(NC_3)$	425				465	443
							432
							423
A_1	$\delta_s(NC_3)$	366				435	371

*Références 30, 34, 50.
†Référence 27.
‡Référence 30.

Can. J. Chem. Downloaded from www.nrcresearchpress.com by 210.87.254.6 on 09/05/12
For personal use only.

Can. J. Chem. Downloaded from www.nrcresearchpress.com by 210.87.254.6 on 09/05/12
For personal use only.

amine, on sait en effet que les déformations $\delta(NC_3)$ montent en fréquence par complexation avec l'iode (27) ou le bromure de magnésium (30) (tableau 4); d'autre part, on prévoit que les vibrations $\nu(Li^+...amine)$ correspondent à une bande plus basse en fréquence que celles observées pour l'ammoniac et la monométhylamine. Toutes ces observations dénotent une solvatation préférentielle du cation Li^+ par l'ammoniac ou les amines par rapport à l'acétonitrile, ce qui est en accord avec la diminution d'intensité de la vibration $\nu(CN)_{ass}$ à 2278 cm^{-1} du binaire $LiClO_4$–CH_3CN (1, 2) par addition de ND_3 (fig. 1).

Mélange perchlorate de lithium – acétonitrile – nitrométhane

Les absorptions des vibrations ν(CN) et δ(CCN) de l'acétonitrile (2) en solution dans le nitrométhane apparaissent à 2254 cm^{-1} (fig. 16) et 380 cm^{-1} (fig. 4), la première, très intense, variant proportionnellement avec la concentration. La présence de sel provoque la diminution de leur intensité et fait apparaitre deux autres absorptions, l'une à 2278 cm^{-1}, correspondant aux vibrations des molécules d'acétonitrile liées aux cations, l'autre à 401 cm^{-1} (fig. 4), due à la vibration $\nu(Li^+...N{\equiv}C{-}CH_3)$ couplée avec la déformation de l'angle CCN (2). Il y a superposition avec l'absorption large centrée à 368 cm^{-1}, attribuée aux mouvements de translation relatifs des ions Li^+ et des molécules de nitrométhane de la première couche de solvatation (31). Quand ρ augmente, la bande à 401 cm^{-1} ne varie pratiquement pas en fréquence.

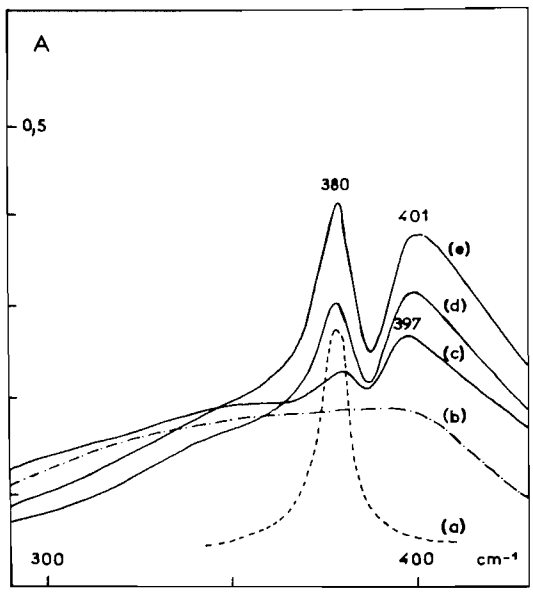

FIG. 4. Spectres dans la région des vibrations ion-cage des mélanges CH_3CN–CH_3NO_2 (---), $LiClO_4$–CH_3NO_2 (-·-) et $LiClO_4$–CH_3CN–CH_3NO_2 (—). (a) $[CH_3CN]$ = 2 *M*, (b) à (e) $[LiClO_4]$ = 0.1 *M*, $[CH_3CN]$ = (b) 0, (c) 0.37, (d) 1.5, (e) 2 *M*. *l* = 200 μ polyéthylène. Toutes les courbes sont obtenues par soustraction de l'absorption du nitrométhane.

Discussion

Déplacement de fréquence—vibration "ion-cage"

La variation de fréquence de la bande due aux vibrations ion-cage en fonction de ρ est représentée sur la fig. 5 pour quelques mélanges ternaires $LiClO_4$–NH_3–CH_3CN, $LiClO_4$–ND_3–CH_3CN et $LiClO_4$–NH_3–THF. Pour les solutions d'ammoniac dans l'acétonitrile, le maximum de la bande se déplace d'abord rapidement, puis se stabilise à 545 cm^{-1} avec NH_3 et à 475 cm^{-1} avec ND_3. Le point d'intersection des deux segments de droite autour desquels se groupent les points figuratifs expérimentaux a une abscisse voisine de ρ = 4; le déplacement progressif de la bande peut s'expliquer par l'existence de différentes espèces $[Li(CH_3CN)_{n-i}(NH_3)_i]^+$ en équilibre dans la solution; à chacun de ces édifices correspond une absorption due aux vibrations ion-cage dont la fréquence est d'autant plus basse que le nombre de molécules

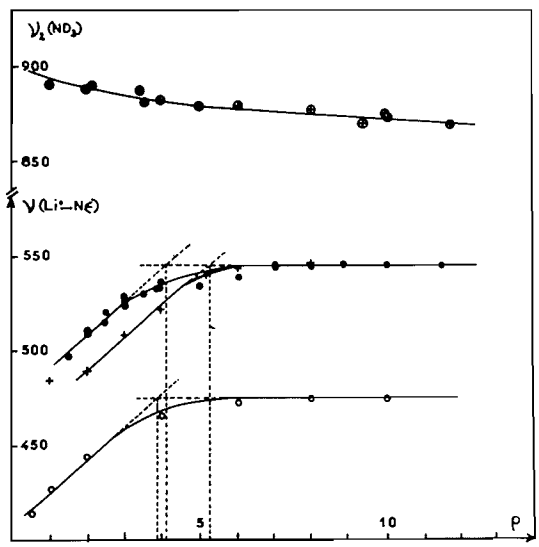

FIG. 5. Déplacement des bandes $\nu_2(ND_3)$, $\nu(Li^+...NH_3)$ et $\nu(Li^+...ND_3)$ en fonction de ρ dans les mélanges ternaires. (●) $LiClO_4$–NH_3–CH_3CN, (+) $LiClO_4$–NH_3–THF, (○ et ●) $LiClO_4$–ND_3–CH_3CN.

Can. J. Chem. Downloaded from www.nrcresearchpress.com by 210.87.254.6 on 09/05/12
For personal use only.

d'acétonitrile, plus lourdes et moins basiques que celles de l'ammoniac, est plus grand. L'absorption large et disymétrique observée serait l'enveloppe de ces différentes bandes. Son déplacement en fréquence serait relié à la variation d'intensité relative des différentes absorptions qui la composent.

Pour le mélange $LiClO_4$–NH_3–THF, c'est à la même fréquence que se stabilise la bande pour des valeurs ρ élevées, mais les deux segments de droite se coupent pour une valeur de ρ voisine de cinq. Le tétrahydrofuranne, plus basique que l'acétonitrile, forme des liaisons "hydrogène" plus fortes avec l'ammoniac et solvate mieux l'ion Li^+; par suite, la compétition des interactions ammoniac–solvant et ammoniac–cation se traduirait par des constantes successives de formation K_1, $K_2 ... K_i$, différentes dans le tétrahydrofuranne et dans l'acétonitrile; cet exemple montre que le nombre déterminé par cette méthode $\nu = f(\rho)$ peut n'être pas significatif de la composition de la première couche de solvatation de l'ion.[5]

Néanmoins, la fréquence limite 545 cm^{-1} étant la même avec le tétrahydrofuranne et l'acétonitrile, on peut penser que pour les valeurs élevées de ρ, la bande observée correspond aux édifices $[Li(NH_3)_4]_{S_1}^+$ où S_1 représente l'acétonitrile ou le tétrahydrofuranne. On constate que la fréquence de vibration ion-cage d'un tel édifice dépend peu de la constante diélectrique du milieu environnant (7.4 pour THF et 36.2 pour CH_3CN); il est d'ailleurs peu probable qu'une constante diélectrique macroscopique ait une signification au niveau du calcul des interactions cation–solvant.

Dans le cas des mélanges $LiClO_4$–CH_3NH_2–CH_3CN, les fréquences des vibrations ion-cage sont relevées sur le graphique de la fig. 6; il n'est plus possible de discerner deux segments de droite. Ce fait est prévisible: on attend des écarts de fréquence plus faibles entre les différents solvates formés et d'autre part, les constantes d'équilibre sont probablement différentes. Il semble donc qu'en plus des restrictions apportées plus haut pour les di- et triméthylamines, ces déplacements de fréquence $\nu = f(\rho)$ ne soient exploitables que si les vibrations ion-cage correspondant aux deux solvants S_I et S_2 sont suffisamment espacées en fréquences.

[5]Wuepper et Popov (12) ont utilisé cette méthode pour des mélanges $LiClO_4$–1-méthyl-2-pyrrolidone-dioxanne.

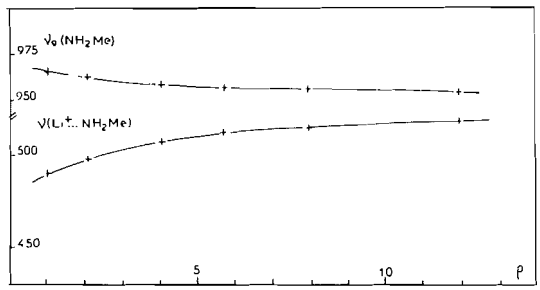

FIG. 6. Déplacement des bandes $\nu_9(NH_2Me)$ et $\nu(Li^+...NH_2Me)$ en fonction de ρ dans les mélanges ternaires $LiClO_4$–NH_2Me–CH_3CN.

Vibrations internes des molécules solvatantes

Pour les vibrations fortement perturbées lors de l'association avec le cation Li^+, telles que les bandes $\nu_2(ND_3)$ et $\nu_9(CH_3NH_2)$ la fréquence de la bande associée varie avec ρ (figs. 5 et 6). En effet si l'on remplace des molécules d'acétonitrile de la première couche de solvatation de l'ion par des molécules d'ammoniac ou d'amines ayant une charge disponible sur l'atome d'azote plus élevée que les molécules d'acétonitrile, l'interaction est maximum pour la première molécule d'ammoniac ou d'amine, et décroit ensuite au fur et à mesure de la substitution des autres molécules d'acétonitrile. Cette interprétation est tout à fait cohérente avec les variations d'enthalpie (32) $\Delta H_{(n-1),n}$ mesurées par spectrométrie de masse pour différents ions à l'état gazeux pour les réactions

$$M^+(S)_{n-1} + S \rightleftharpoons M^+(S)_n$$

n représentant le nombre de molécules de solvant liées au cation.

Quand n augmente, les valeurs de $\Delta H_{(n-1),n}$ diminuent d'autant plus que le cation est moins gros. On sait en effet que la perturbation de la vibration de déformation ν_2 de l'ammoniac lié aux différents cations alcalins ou alcalino-terreux est plus marquée si le cation est petit et chargé (26).

Les perturbations de fréquence des vibrations de valence ν(NH) sont moins importantes (tableaux 1–3): elles augmentent dans l'ordre: ammoniac, monométhylamine, diméthylamine; les écarts moyens étant respectivement de 10, 24 et 37 cm^{-1}. Cette sensibilité accrue des vibrateurs NH à l'interaction avec la paire libre de l'atome d'azote peut être reliée à l'accroissement du pouvoir donneur de proton caractérisé par la valeur des constantes de force de liaison

Can. J. Chem. Downloaded from www.nrcresearchpress.com by 210.87.254.6 on 09/05/12
For personal use only.

K(N—H) mesurées à l'état gazeux (6.4 (33), 6.29 et 5.9 (34) pour l'ammoniac, la monométhylamine et la diméthylamine). Dans le cas de l'ammoniac, la perturbation de fréquence des vibrations de valence, quand on passe du complexe

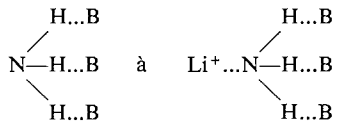

augmente lorsque le tétrahydrofuranne remplace l'acétonitrile (tableau 1). Ce fait s'explique par un effet coopératif déjà signalé à propos de l'ammoniac (26) et de l'eau (13).

Variation d'intensité

Nombre de solvatation

Différentes méthodes de calcul permettent de relier les grandeurs mesurées expérimentalement à la concentration de chaque édifice formé et aux constantes d'équilibre K_i (35, 36). Celle de Bjerrum introduit le nombre moyen $\bar{n}$ caractérisant la composition moyenne de la première couche de solvatation

$$\bar{n} = \frac{\sum [M(S_1)_{n-i}(S_2)_i]^{z+} \times i}{\sum [M(S_1)_{n-i+1}(S_2)_{i-1}]^{z+}} = \frac{[S_2]_{liée} - [S_2]_{libre}}{[Sel]_{total}}$$

Les diminutions d'intensité des bandes correspondant aux vibrations internes des molécules S_2 en interaction avec les molécules S_1 lors de l'addition de sel à un mélange S_2–S_1 permettent de calculer ce nombre moyen. Pour éviter les corrections dues au recouvrement des bandes rendues difficiles par le déplacement en fréquence des bandes associées, nous avons utilisé les vibrations les plus perturbées par le cation. Cependant le peu de précision ne permet pas d'atteindre des valeurs significatives pour les constantes K_i (35–39). C'est pourquoi nous avons préféré suivre l'évolution de $\bar{n}$ en fonction de ρ (figs. 7 et 8). Cette évolution est nette pour les mélanges NH_3–CH_3CN et CH_3CN–CH_3NO_2 bien qu'il ne soit pas possible d'attribuer un sens aux détails des courbes tracées (figs. 7 et 8); cependant, ces courbes tendent vers la valeur 4; valeur généralement attendue pour le nombre de solvatation de l'ion Li^+ dans l'ammoniac liquide (28, 40) ou dans l'acétonitrile pur (2). Ces courbes ne dépendent pas de la concentration en sel, ce qui indique que le perchlorate de lithium est totalement dissocié en ions solvatés dans ces solvants de constante diélectrique relativement élevée ($D_{CH_3CN} = 38$, $D_{CH_3NO_2} = 35.9$), ce qui n'est pas le cas pour les mélanges cyclohexane–tétrahydrofuranne (9, 10).

Pour la diméthylamine, les valeurs de $\bar{n}$ calculées à partir de la vibration ν_1 à 3349 cm^{-1} sont inférieures à celles obtenues à partir de la bande ν_{11} à 792 cm^{-1} pour laquelle nous n'avons pas tenu compte du recouvrement avec sa bande associée (fig. 2). Pour la triméthylamine la vibration r (CH_3) à 1185 cm^{-1}, la plus perturbée est beaucoup moins sensible à la complexation par le cation; il en découle une incertitude sur $\bar{n}$ d'autant plus grande que la courbe d'étalonnage est moins précise (voir conditions expérimentales).

A notre connaissance, deux essais de détermination de n par spectroscopie de vibration ont été effectués avant les nôtres. Wuepper et Popov ont étudié des mélanges $LiClO_4$–CH_3COCH_3–CH_3NO_2 et utilisé la variation d'intensité de la

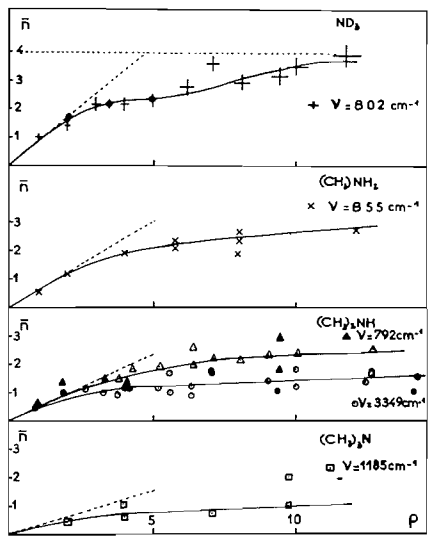

FIG. 7. Nombre de solvatation moyen $\bar{n}$ en fonction de ρ = [Amine]/[$LiClO_4$] en solution dans l'acétonitrile. Les fréquences des bandes utilisées pour les mesures sont indiquées sur les courbes. Les croix, ronds, triangles et carrés clairs indiquent que les mesures ont été effectuées à [$LiClO_4$] = 0.2 M. Les ronds ou triangles foncés indiquent que les mesures ont été effectuées à concentration constante en ammoniac ou amine: [ND_3] = 0.97 M, [CH_3NH_2] = 1.3 M. Pour l'ammoniac ND_3, les dimensions des croix indiquent la précision des points. Une courbe moyenne a été tracée à titre indicatif pour chacun des composés.

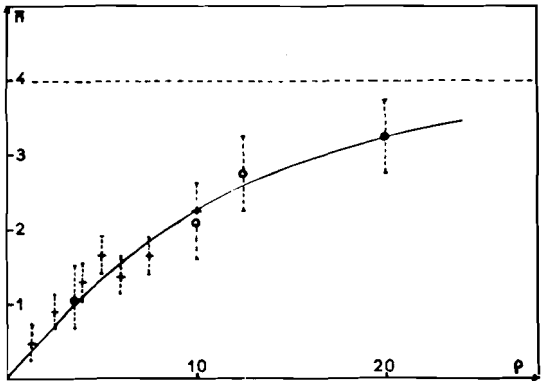

FIG. 8. Nombres moyens de solvatation $\bar{n}$ en fonction de $\rho = [CH_3CN]/[LiClO_4]$ en solution dans le nitrométhane. (+) $[LiClO_4] = 0.2\ M$, (○) $[LiClO_4] = 0.1\ M$. La précision des points est indiquée par un trait pointillé.

bande ion-cage à 425 cm^{-1} (14). Ils ont cru pouvoir mettre en évidence l'apparition de nouvelles espèces. Si l'on trace la courbe "absorption de la bande à 425 cm^{-1}" en fonction de la concentration en sel, la concentration de l'acétone demeurant constante, on observe en effet pour $\rho = 4$ une variation de pente. Mais cette bande étant complexe et englobant l'absorption large due à la solvatation des ions Li^+ par le nitrométhane (31) aucune indication précise ne peut être espérée. Rouvière et coll. (15), pour des mélanges ternaires $LiClO_4$–C_5H_5N–CH_3NO_2, ont utilisé des bandes de vibration interne de la pyridine libre et associée au sel. Le coefficient d'extinction et la fréquence au maximum de la bande associée peuvent varier avec la nature des divers ions complexes formés $[Li(CH_3NO_2)_{n-i}(C_5H_5N)_i]^+$. En outre, dans l'hypothèse où ils seraient les mêmes, la courbe A_{ass} ou $A_{lib} = f(C_{sel})$ renseignerait seulement sur la variation du nombre moyen de solvatation $\bar{n}$, qui ne peut être interprétée de façon simple.

Comparaison du pouvoir solvatant des amines

Malgré l'imprécision des mesures, les courbes de la fig. 7 permettent de comparer valablement les pentes à l'origine. Celles-ci sont respectivement de 0.8; 0.6; 0.45 et 0.30 pour ND_3, CH_3NH_2, $(CH_3)_2NH$, et $(CH_3)_3N$. On constate d'ailleurs que pour une même valeur de ρ les nombres $\bar{n}$ varient dans le même ordre. Ces différences traduisent une décroissance du pouvoir solvatant quand on passe de l'ammoniac aux mono-, di- et triméthylamines.

La comparaison du seul pouvoir donneur d'électron de ces bases, caractérisé soit par leur p*K* (41), soit par l'abaissement de fréquence Δν(OH) du phénol dans les complexes formés avec ces bases, soit par les variations d'enthalpie $\Delta H_{A\ldots D}$ de réaction avec un accepteur d'électrons tel que I_2 ou $B(CH_3)_3$ ou par leur potentiel d'ionisation (*cf.* tableau 3, réf. 42), soit par leur nombre donneur de Guttman (43), ne permet pas d'expliquer un tel comportement. La comparaison de leur moment dipolaire, qui varie de 1.46 à 0.67 D (44) quand on passe de l'ammoniac à la triméthylamine semble par contre indiquer une importante contribution de l'interaction ion-dipole à l'énergie libre de solvatation.

Conditions expérimentales

Produits utilisés—origine et purification

Le perchlorate de lithium $^7LiClO_4$ est un produit K & K Laboratories (anhydre à 99%) que nous avons soumis à un chauffage lent sous vide avant utilisation.

L'acétonitrile (Spectro Prolabo), le tétrahydrofuranne (99% Carlo Erba) et le nitrométhane (Spectro Eastman Kodak) ont été séchés sur tamis moléculaire 4 Å; le nitrométhane contient des traces d'éthylnitrile que nous avons caractérisé par la bande ν(C≡N) à 2252 cm^{-1} (45) et par l'étude du spectre de masse de fragmentation à 70 eV; les points d'ébullition très voisins CH_3NO_2 (101 °C) et CH_3CH_2CN (97.1 °C) n'ont pas permis une purification par distillation. Nous avons vérifié cependant que la concentration de cette impureté était toujours inférieure à 0.05 *M*.

L'ammoniac (Air Liquide) a été purifié par séchage sur sodium puis distillé. L'ammoniac à taux de deutérium supérieur à 98% a été préparé par décomposition du nitrure de magnésium par l'eau lourde (46) puis séché sur sodium.

Les amines CH_3NH_2 et $(CH_3)_2NH$ ont été préparées à partir de leur chlorhydrate, la triméthylamine est un produit Matheson débarassé de traces de monométhylamine par passage sur tamis moléculaire; elles ont toutes été séchées sur sodium et distillées. Leur pureté a été contrôlée par spectroscopie infrarouge.

Préparation des solutions d'ammoniac ou d'amines dans les solvants purs ou contenant un sel. Calcul des concentrations

Pour préparer ces solutions, nous avons piégé à la température de l'azote liquide, une masse connue de gaz dans un volume *V* (5 ou 10 cm^3) de solvant pur ou contenant un sel, préalablement gelé sous vide à cette même température. L'ensemble contenu dans un ballon de 100 cm^3 est progressivement réchauffé jusqu'à la température ambiante, en agitant fortement pour obtenir une dissolution aussi complète que possible du gaz; ce ballon est ouvert en boîte sèche au moment du remplissage des cellules.

Ce mode de préparation doit faire intervenir, dans le calcul des concentrations, l'augmentation de volume Δ*v* du mélange provoquée par la dissolution d'une masse *m* de gaz; ce volume Δ*v* n'étant pas négligeable surtout aux fortes concentrations, celles-ci ont toutes été corrigées en calculant Δ*v* à partir de la densité (*d*) des amines liquides.

Can. J. Chem. Downloaded from www.nrcresearchpress.com by 210.87.254.6 on 09/05/12
For personal use only.

$$\Delta v = \frac{m}{d},\ C_{\text{amine}} = \frac{m/M}{V + m/d} \times 1000\,(M),$$

$$C_{\text{sel}} = \frac{C_0 V}{V + m/d}\,(M)$$

C_0 étant la concentration de la solution de sel avant piégeage du gaz. Au cours d'une série d'expériences réalisées à partir d'une même solution binaire de concentration C_0, la concentration est dite "constante".

La régularité des droites d'étalonnage absorbance = f (concentration) pour les solutions de NH_3, ND_3, CH_3NH_2, et $(CH_3)_2NH$ dans l'acétonitrile prouve que la dissolution des quantités piégées est complète. Cette grande solubilité est due à la formation de liaison hydrogène entre ces molécules et le solvant. Par contre, la plus grande dispersion des points de la droite d'étalonnage obtenue avec la triméthylamine peut provenir d'une dissolution incomplète.

La teneur en eau de tous les solvants et des solutions binaires ou ternaires a été contrôlée par une mesure d'absorption dans la région des vibrations de valence $\nu(OH)_{H_2O}$ sous une épaisseur de 615 μ. Dans le cas de l'utilisation de l'ammoniac ND_3, il a été vérifié de plus, à partir de la vibration ν (NH) des molécules ND_2H, que la quantité de ces molécules qui auraient pu se former en présence de traces d'eau (H_2O) est négligeable. On peut cependant noter (fig. 1) que dans les mélanges ternaires, il s'est formé une faible quantité de ND_2H décelable à partir de la vibration $\nu_4'(ND_2H)$ à 1249 cm^{-1}.

La présence de telles impuretés (H_2O, ND_2H, CH_3CH_2CN) peut conduire à une surestimation de la valeur de $\bar{n}$; en effet, si l'on admet que l'impureté se solvate comme le ligande (ND_2H pour NH_3, CH_3CH_2CN pour CH_3CN) on peut montrer que la valeur mesurée $\bar{n}_{exp}$ est reliée à la valeur réelle n_r par la relation approchée

$$\bar{n}_{\text{exp}} \simeq \bar{n}_r\left(1 + \frac{x}{2C_0}\right)$$

où x est la concentration en impureté et C_0 la concentration en sel.

Enregistrement des spectres

Les spectres sont obtenus avec des cellules à liquide d'épaisseur fixe munies de fenêtres en bromure de potassium (région au dessus de 350 cm^{-1}), en fluorure de calcium (au dessus de 1000 cm^{-1}) et en polyéthylène pour l'étude des solutions dans le nitrométhane, entre 250 et 500 cm^{-1}. Ils ont été enregistrés sur un spectromètre Beckman IR 12, à la température ambiante. La précision des fréquences est de ±1 cm^{-1} pour les bandes fines. Les fréquences estimées pour les épaules sont indiquées entre parenthèses sur les tableaux.

Nous remercions Mademoiselle M. L. Josien, Professeur à l'Université de Paris VI, de l'intérêt qu'elle a porté à ce travail et pour ses conseils lors de la rédaction de ce manuscrit.

1. J. P. Roche et P. V. Huong. J. Chim. Phys. **67**, 211 (1970).
2. J. P. Roche. Thèse Ingénieur Docteur n° 150. Université Bordeaux I. (1971).
3. A. Allerhand et P. V. R. Schleyer. J. Am. Chem. Soc. **85**, 371 (1963); **85**, 1233 (1963).
4. P. Datta et G. M. Barrow. J. Chem. Phys. **43**, 2137 (1965).
5. J. Corset et J. Lascombe. J. Chim. Phys. **64**, 665 (1967).
6. R. D. Green et J. S. Martin. J. Am. Chem. Soc. **90**, 3659 (1968).
7. R. P. Taylor et I. D. Kuntz Jr. J. Phys. Chem. **74**, 4573 (1970).
8. A. Burneau et J. Corset. J. Chim. Phys. **69**, 142 (1972); **69**, 171 (1972).
9. E. G. Höhn, J. A. Olander et M. C. Day. J. Phys. Chem. **73**, 3880 (1969).
10. J. A. Olander et M. C. Day. J. Am. Chem. Soc. **93**, 3584 (1971).
11. I. S. Perelygin et R. N. Stafioulina. Zh. Strukt. Khim. **8**, 205 (1967).
12. J. L. Wuepper et A. I. Popov. J. Am. Chem. Soc. **91**, 4352 (1969).
13. M. H. Baron et C. de Loze. J. Chim. Phys. **68**, 1293 (1971); **68**, 1299 (1971).
14. M. K. Wong, W. J. McKinney et A. I. Popov. J. Phys. Chem. **75**, 56 (1971).
15. J. Rouviere, B. Dimon, B. Brun et J. Salvinien. C.R. Acad. Sci. Ser. C, **274**, 458 (1971).
16. J. Padova. J. Phys. Chem. **72**, 796 (1968).
17. H. Strehlow et H. Schneider. J. Chim. Phys. (spécial), 118 (1969).
18. Z. Kecki et J. Golaszewska. Rocz. Chem. **41**, 1817 (1967).
19. B. W. Maxey et A. I. Popov. J. Am. Chem. Soc. **89**, 2230 (1967).
20. M. J. French et J. L. Wood. J. Chem. Phys. **49**, 2358 (1968).
21. W. F. Edgell, J. Lyford, W. R. Wright, W. Risen Jr. et A. Watts. J. Am. Chem. Soc. **92**, 2240 (1970).
22. B. W. Maxey et A. I. Popov. J. Am. Chem. Soc. **91**, 20 (1969).
23. J. Lauransan. Thèse. Bordeaux. 1967.
24. A. Foldes et C. Sandorfy. J. Mol. Spectr. **20**, 262 (1966).
25. R. A. Russel et H. W. Thompson. Proc. Roy. Soc. Lond. A**234**, 318 (1956).
26. J. Corset, P. V. Huong et J. Lascombe. Spectrochim. Acta, **24A**, 1385 (1968); **24A**, 2045 (1968).
27. K. Yokobayashi, F. Watari et K. Aida. Spectrochim. Acta, **24A**, 1651 (1968).
28. A. Regis et J. Corset. J. Chim. Phys. **69**, 707 (1972).
29. A. P. Gray et R. C. Lord. J. Chem. Phys. **26**, 690 (1957).
30. J. Kress. Thèse Doctorat 3ème cycle. Paris. 1971.
31. A. Regis et J. Corset. J. Chim. Phys. **69**, 1508 (1972).
32. P. Kebarle. Ions, ion-pairs in organic reactions. *Edité par* M. Swarc. J. Wiley and Sons Inc., N.Y. 1972.
33. T. Shimanouchi et I. Suzuki. J. Chem. Phys. **42**, 296 (1965).

Can. J. Chem. Downloaded from www.nrcresearchpress.com by 210.87.254.6 on 09/05/12
For personal use only.

34. G. DELLEPIANE et G. ZERBI. J. Chem. Phys. **48**, 3573 (1968).
35. P. SOUCHAY et J. LEFEBVRE. Equilibres et réactivité des complexes en solution. Masson et Cie, Paris. 1969.
36. A. E. MARTELL et L. G. SILLEN. Stability constants. Chemical Society, London. 1964.
37. J. BJERRUM. Metal ammine formation in aqueous solution. P. Maase and Son, Copenhagen. 1941.
38. L. JOHANSSON. Acta Chem. Scand. **25**, 3569 (1971).
39. H. F. STEGER. Can. J. Chem. **50**, 641 (1972).
40. J. F. HINTON et E. S. AMIS. Chem. Rev. **71**, 627 (1971).
41. G. CHARLOT et B. TREMILLON. Les réactions chimiques dans les solvants et les sels fondus. Gauthier–Villars, Paris. 1963.
42. R. S. DRAGO, D. W. MEEK, R. LONGHI, et M. D. JOESTEN. Inorg. Chem. **2**, 1056 (1963).
43. V. GUTMANN, Coordination chemistry in non-aqueous solutions. Springer Verlag, Wien, New York. 1968.
44. Handbook of chemistry and physics. 44th ed. Chem. Rubber Publishing Co., Cleveland. 1962–63.
45. N. E. DUNCAN et G. J. JANZ. J. Chem. Phys. **23**, 434 (1954).
46. P. BOUCLIER et J. PORTIER. Bull. Soc. Chim. Fr. 738 (1967).
47. J. CORSET, P. V. HUONG et J. LASCOMBE. J. Chim. Phys. **64**, 1707 (1967).
48. A. FINCH, I. J. HYAMS et D. STEELE. J. Mol. Spectr. **16**, 103 (1965).
49. M. J. BUTTLER et D. C. MCKEAN. Spectrochim. Acta, **21**, 465 (1965).
50. J. N. GAYLES. Spectrochim. Acta. **29A**, 1521 (1967).

Can. J. Chem. Downloaded from www.nrcresearchpress.com by 210.87.254.6 on 09/05/12
For personal use only.

The Specific Activity of Silica Supported Platinum for the Catalysis of Hydrogen–Methane Deuterium Exchange[1,2]

NORMAN HENRY SAGERT AND RITA MARY LOUISE POUTEAU

Research Chemistry Branch, Whiteshell Nuclear Research Establishment, Atomic Energy of Canada Limited, Pinawa, Manitoba R0E 1L0

Received March 15, 1973

Rate data are reported as a function of temperature for the exchange of D_2 with CH_4 over a number of platinum–silica catalysts. Two different methods of preparing catalysts, impregnation and ion exchange, were used to get two series of metal particle sizes. Within each series, the particle size was increased by sintering batches in air at temperatures to 800 °C. These methods produced platinum particles ranging from 0.9 to 10 nm diameter. The metal surface areas were measured by hydrogen chemisorption and, where possible, by X-ray diffraction and electron microscopy.

The specific rate coefficients or rate coefficients per unit surface area of platinum varied by a factor of up to 40 within each series and reached a maximum for sintering temperatures of about 500 °C. The maximum specific rate coefficients for CH_4 conversion at 200 °C, and total pressure of 60 kN m^{-2}, were 1.3 and 1.9 × 10^{-6} mol CH_4 m^{-2} s^{-1} for the ion-exchanged and impregnated catalysts respectively. Activation energies were in the range 60 to 100 kJ mol^{-1}. Since a relatively small change in specific rate coefficient was noted between the two series as compared to the changes within each series, no large effect of particle size on the specific rate coefficient was demonstrated. The different specific rate coefficients within the series are ascribed to other effects of sintering, particularly the formation of the lower energy Pt(111) surface. Some evidence was noted for a particle size effect in the distribution of products, with more multiple exchange being observed for the smallest particles.

Les données de vitesse en fonction de la température pour l'échange de D_2 avec CH_4 sur un certain nombre de catalyseurs platine–silice ont été rapportées. Deux méthodes différentes de préparation des catalyseurs (par imprégnation et par échange ionique) ont été utilisées pour obtenir deux types de tailles pour les particules métalliques. Dans chaque type, les dimensions des particules ont été accrues par une opération de frittage dans l'air à des températures allant jusqu'à 800 °C. Ces méthodes conduisent à l'obtention des particules de platine de 0.9 à 10 nm de diamètre. Les aires des surfaces métalliques ont été mesurées par chimisorption de l'hydrogène et par diffraction des rayons X et microscopie électronique quand c'était possible.

Les coefficients de vitesse spécifique ou coefficients de vitesse par unité de surface de platine, varient d'un facteur de 40 à l'intérieur de chaque série et atteignent un maximum pour des températures de frittage d'environ 500 °C. Les coefficients de vitesse spécifique maximale pour la conversion de CH_4 à 200 °C et sous une pression totale de 60 kN m^{-2} ont été de 1.3 et 1.9 × 10^{-6} mol CH_4 m^{-2} s^{-1} pour les catalyseurs obtenus par échange ionique et imprégnation respectivement. Les énergies d'activation varient de 60 à 100 kJ mol^{-1}. Bien qu'un changement relativement faible dans le coefficient de vitesse spécifique ait été noté entre les deux séries comparé aux changements à l'intérieur de chaque série. il n'a pas été possible de démontrer d'effet notable des dimensions des particules sur le coefficient de vitesse spécifique. Les différences dans les coefficients de vitesse spécifique à l'intérieur des séries ont été imputées aux autres effets du frittage, en particulier la formation de surface de Pt(111) de plus basse énergie. Un effet de la taille des particules sur la distribution des produits a été mis en évidence, un échange plus fréquent étant observé pour les particules les plus petites. [Traduit par le journal]

Can. J. Chem., **51**, 3588 (1973)

Introduction

Following a previous study (1) in which we found the specific rate (rate per unit surface area) of the H_2–HDO exchange reaction over silica supported platinum to be essentially independent of particle size, we have examined the D_2–CH_4 exchange over a similar series of supported platinum catalysts. For this geometrically simple exchange reaction, one would not expect any geometric effects on the specific rate in the sense described by Bond (2), Anderson and coworkers (3–5), and Boudart *et al.* (6). However, an electronic effect may exist since, as the size of the particles decreases, the electronic properties of these particles must change from those of bulk metal to those of single atoms (7, 8). Such an

[1]AECL No. 4574.

[2]Presented in part at 56th Chemical Institute of Canada Conference, Montreal, Quebec, June 1973.

Can. J. Chem. Downloaded from www.nrcresearchpress.com by 210.87.254.6 on 09/05/12
For personal use only.

Can. J. Chem. Downloaded from www.nrcresearchpress.com by 210.87.254.6 on 09/05/12
For personal use only.

electronic effect might be more likely with a reaction having a large activation energy than for the H_2–HDO exchange which only has an activation energy of around 40 kJ mol^{-1} (1).

We have examined the D_2–CH_4 exchange over catalysts produced by two common methods for catalyst preparation, impregnation with H_2PtCl_6, and exchange with $Pt(NH_3)_4(OH)_2$, followed by different degrees of sintering to see if activity was more readily correlated with the actual size of the platinum particle, or with the sintering temperature (9).

The mechanism of the methane–deuterium exchange is reasonably well established from the studies of Kemball (10–12) on metal films. Recently Cece and Gonzales (13) noted changes in apparent activation energies for methane–deuterium exchange over supported nickel as a function of particle size.

Experimental

Materials

Reagents

C.P. Grade deuterium (99.5%) was purified by diffusion through a hot palladium–silver thimble. The methane was Research Grade (99.99%). It was admitted to the system through a stainless steel regulator, and was degassed by the freeze–pump–thaw technique at solid nitrogen temperature. Then it was distilled into the storage reservoir, and the final portion was rejected. Standards for the deuterated methanes were obtained commercially.

Catalysts

The preparation of the silica supported catalysts has been described previously (1). For this work, platinum on silica catalysts were prepared by H_2PtCl_6 impregnation and by $Pt(NH_3)_4(OH)_2$ ion exchange. Portions of these catalysts were sintered for 5 h in air at various temperatures to promote crystallite growth. Most catalysts contained 5% (w/w) platinum.

Kinetic Studies

Exchange rates were measured in the Pyrex and Teflon recirculation reactor shown in Fig. 1. The total volume was 8.55×10^{-4} m^3, with about 75% of this volume in the two bulbs and the pump. The pump was a double-acting Teflon-in-glass magnetically actuated pump similar to that described by Chambers *et al.* (14) except that an electronic switching circuit was used. It could circulate up to 7×10^{-5} m^3 s^{-1}, but was usually run at about half speed. The sampling system was arranged so that 10^{-6} m^3 samples could be taken and expanded into pre-evacuated tubes. These sampling tubes contained a small quantity of P_2O_5, added as a precaution against moisture, since the sample tubes were only pumped out during the time between analyses.

Usually about 3×10^{-3} kg of the platinum on silica catalyst were weighed into the reactor and the system evacuated. The catalyst temperature was raised to 150 °C and evacuation continued until about 7×10^{-4} N m^{-2} was obtained. Then trap T was immersed in liquid nitrogen and about 40 kN m^{-2} of D_2 was circulated around the system while the temperature was raised to 300 °C. After 2 h the system was pumped out, and the trap warmed to remove the water which had desorbed from the catalyst. This was a standard pre-treatment.

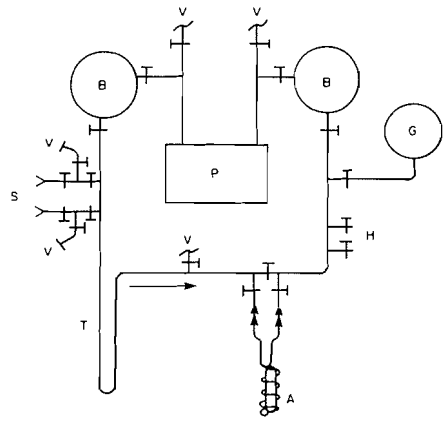

FIG. 1. Schematic diagram of the recirculating system: A, the reactor; B, 2.10×10^{-4} m^3 bulbs; G, pressure gauge; H, to gas purification; P, pump; S, sampling points; T, trap; V, to vacuum.

Before every run the catalyst was reduced at 300 °C for 2 h in 40 kN m^{-2} D_2 and was then evacuated while cooling to the reaction temperature. The catalyst was isolated and D_2 and CH_4 were measured into calibrated portions of the circulating system. Generally a total pressure of 60 kN m^{-2} was used with $D_2/CH_4 = 2$. The circulating system was isolated and gas was circulated for 20 min in order to mix thoroughly. Then, at time zero, the gas flow was diverted through the catalyst and samples were taken at convenient intervals. Analyses were performed on a Consolidated 21-130 mass spectrometer, with H_2, HD, D_2, and isotopic methanes being determined. Spectra were processed by a Varian Data Processing Computer 620i which calculated the gas composition from stored corrected cracking patterns of the standards. The cracking patterns of the standards were additive to within experimental error (±0.1%) showing that there was no exchange among the methanes themselves in the mass spectrometer. Also no exchange was noted between D_2 and CH_4 in the mass spectrometer to within our experimental error (±0.1%), so that deuterium transfer between the "hydrogen" and methane does not occur to a significant extent in our instrument.

Surface Areas and Particle Size Measurements

Surface areas were measured by hydrogen chemisorption at 27 °C and, for most of the impregnated catalysts, by X-ray diffraction and by electron microscopy as previously described (1). For the ion-exchanged catalysts, the particles were too small to be measured by our X-ray diffraction and electron microscopy techniques.

Can. J. Chem. Downloaded from www.nrcresearchpress.com by 210.87.254.6 on 09/05/12
For personal use only.

Results

Rate coefficients for the exchange reactions were calculated from the rates of formation of the deuterated methanes using the first order equations given by Kemball (15). If a deuterium concentration parameter, ϕ, is defined such that

$$[1] \qquad \phi \equiv \sum_i [CH_{4-i}D_i]i$$

with concentrations in mol %, then

$$[2] \qquad \frac{d\phi}{dt} = k_\phi\left(1 - \frac{\phi}{\phi_\infty}\right)$$

if isotope effects are neglected. Here k_ϕ is a rate coefficient equivalent to the number of deuterium atoms entering 100 molecules of methane in unit time, and ϕ_∞ is ϕ at infinite time. On integrating

$$[3] \quad -\log_{10}(\phi_\infty - \phi) = \frac{k_\phi t}{2.303\phi_\infty} - \log_{10}(\phi_\infty - \phi_0)$$

A second similar equation represents the conversion of CH_4:

$$[4] \quad -\log_{10}(X - X_\infty) = \frac{k_x t}{2.303(100 - X_\infty)} - \log_{10}(100 - X_\infty)$$

where X is the percent of CH_4. The ratio M, defined as k_ϕ/k_x, gives the initial average number of hydrogen atoms replaced by deuterium atoms in each methane molecule.

A plot of the results of a typical run according to eqs. 3 and 4 is given in Fig. 2. The equations

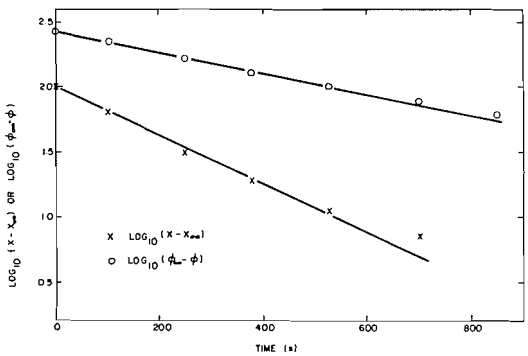

FIG. 2. Logarithmic plots of the conversion of CH_4, and uptake of deuterium as a function of time. Impregnated catalyst sintered at 500 °C. Catalyst temperature 215 °C, CH_4/D_2 = 1/3.6.

fit the data in the initial stages of the reaction, so that k_ϕ,k_x, and M can be determined. Deviations appear at higher conversions. The course of the reaction could be predicted over a longer period using equations developed by Mikovsky and Wei (16). However in this work the simple equations above were adequate.

Values of X_∞ and ϕ_∞ were obtained experimentally at high temperatures, and at lower temperatures ϕ_∞ was calculated from the hydrogen–methane deuterium separation factors given by Varshavskii and Vaisberg (17). Calculated values agreed satisfactorily with experimental values where comparison was possible. X_∞ was calculated using equations described by Apse and Missen (18) which were solved numerically. Calculated X_∞ values also agreed with the experimental values where comparison was possible. Actually, provided the slopes to eqs. 3 and 4 used to evaluate k_x and k_ϕ were taken at short times, the corrections to values of ϕ_∞ and X_∞ used were not critical. Thus between 140 °C and 300 °C the calculated values of ϕ_∞ fell from 230 to 217 compared to the statistical value at infinite temperature of 200. The experimental values were within ± 5 of the calculated values. Similarly between 140 °C and 300 °C the calculated values of X_∞ rose from 2.3 to 4.7 compared to 6.2 at infinite temperature. Experimental values were within ± 0.5.

Reaction parameters should not be affected by pore diffusion. The highest conceivable rate for methane conversion compatible with the speed of the recirculating pump was about $0.2\%\ s^{-1}$. This rate, together with appropriate values of surface area, porosity, and tortuosity factors of the gel (18), led to an estimated value $\Phi_s = 0.1$ for the pore diffusion parameter at the maximum rate (19). This corresponds to an efficiency factor of essentially 1.0 for a thermoneutral reaction with an activation energy of about 80 kJ mol^{-1}.

Typical hydrogen chemisorption isotherms are shown in Fig. 3 for catalysts prepared from H_2PtCl_6 and sintered at various temperatures. The linear portions of these isotherms were extrapolated to low pressure, and the intercepts on the zero pressure axis were taken as the volumes of chemisorbed hydrogen. Surface areas were calculated from these volumes by assuming that the adsorption site for a hydrogen atom covers 8.9×10^{-20} m^2. Particle sizes were then calculated from a knowledge of the surface area

TABLE 1. Particle diameters for H_2PtCl_6 impregnated catalysts

Sintering temperature (°C)	Particle diameter (nm)			
	Hydrogen adsorption (sphere model)	Electron microscopy		X-ray
		$\Sigma n_i d_i^3/\Sigma n_i d_i^2$	$\Sigma n_i d_i^4/\Sigma n_i d_i^3$	
None	2.75	—	—	5.5
300	2.88	3.62	4.08	4.8
400	2.92	4.35	4.90	5.46
500	3.95	5.46	6.26	5.64
600	8.58	7.58	8.82	7.42
700	9.78	7.89	8.95	8.6
800	9.40	9.57	10.94	9.0

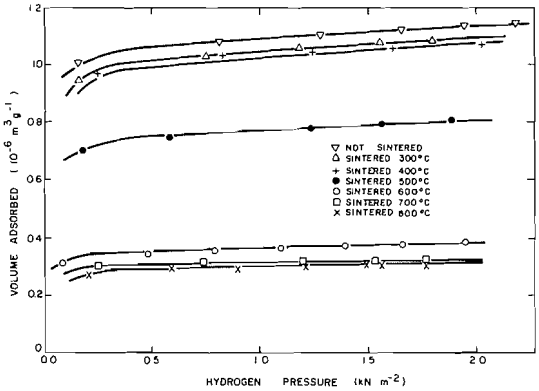

FIG. 3. Hygrogen chemisorption isotherms over impregnated catalysts sintered at indicated temperatures. Adsorption temperature = 27 °C.

and the platinum concentration, assuming the particles to be spherical in shape. Table 1 gives the particle sizes so calculated for the impregnated catalysts, and compares these with sizes obtained from electron microscopic examination, and from X-ray diffraction data using the Debeye–Scherrer line broadening technique. The hydrogen chemisorption gives a surface averaged size, $\Sigma_i n_i d_i^3/\Sigma_i n_i d_i^2$, and the X-ray diffraction gives a volume averaged size, $\Sigma_i n_i d_i^4/\Sigma_i n_i d_i^3$, where n_i and d_i are the number and size of the i'th sized particle. Agreement between these methods is not as good as with the 1% catalysts examined previously (1), although it is still satisfactory. The difference between the two averages is relatively small, indicating a reasonably narrow distribution of particle sizes.

The data in Table 1 imply that the particles are stable in air at temperatures up to 400 °C. At higher temperatures some particles grow by diffusion while the smallest particles disappear. It would appear that at about 700 °C, all the smaller particles have disappeared and a quasi-equilibrium is set up where no particles grow in size at the expense of others. A similar phenomenon was noted by Stolyarenko and Vasev (20) for platinum blacks sintered in air.

From a knowledge of the number of moles of methane and the surface areas of the catalysts, specific rate coefficients (k_x^1 or k_ϕ^1) can be calculated in mol CH_4 (or mol D) m^{-2} s^{-1}. Figure 4 shows k_x^1 data obtained from the impregnated catalysts plotted as a function of temperature in

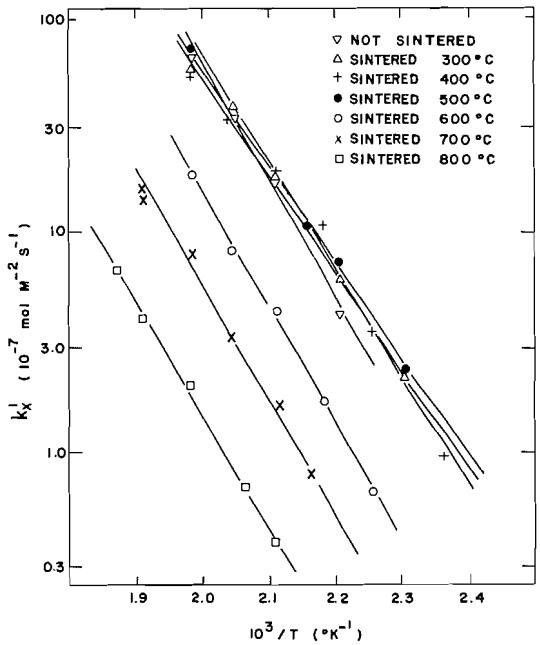

FIG. 4. Specific rates for CH_4 conversion over impregnated catalysts sintered at indicated temperatures. Rates are plotted in the Arrhenius form.

Can. J. Chem. Downloaded from www.nrcresearchpress.com by 210.87.254.6 on 09/05/12
For personal use only.

Can. J. Chem. Downloaded from www.nrcresearchpress.com by 210.87.254.6 on 09/05/12
For personal use only.

the Arrhenius form. The activation energies E_x are reasonably constant at 91 ± 12 kJ mol^{-1}. For the same series of catalysts the activation energies for deuterium appearance, E_ϕ, are 102 ± 16 kJ mol^{-1}. In every case E_ϕ was greater than E_x, implying that multiple exchange has a higher activation energy than single exchange. The value of M was 1.24 ± 0.04, and there was no observable trend with sintering temperature. Similarly, for catalysts prepared by ion exchange E_x was in the range 72 ± 10 kJ mol^{-1} and E_ϕ was 84 ± 12 kJ mol^{-1}. M was significantly higher for this series of catalysts at 1.70 ± 0.15. Thus, interestingly enough, multiple exchange seems to be more important on the smaller particles of the ion exchanged catalyst (Table 1).

Attempts were made to vary the platinum particle size by varying the concentration of platinum in the H_2PtCl_6 impregnating solution. Ideally this technique should give catalysts with the same number of platinum particles, but of varying size (21). In our case, going to a 0.5% platinum on silica catalyst gave a catalyst with a metal surface area of 530 m^2 kg^{-1}, almost exactly 10% that from a 5% catalyst. Hence the particle diameter, 2.6 nm, was almost identical to the 2.8 nm of the 5% catalyst. The rate coefficients were very low, but k_x^1 was about 1×10^{-6} mol CH_4 m^2 s^{-1} at 200 °C. Attempts to make catalysts with greater than 10% platinum gave catalysts with extremely broad size distributions. Since we did not get significantly smaller particles at lower concentrations, and could not make good catalysts with more than 10% platinum, no further effort was devoted to varying particle size by this method. Attempts were made to prepare catalysts by impregnation with $Pt(NH_3)_2(NO_2)_2$ (1). We could not successfully prepare 5% platinum catalysts by this method as electron microscopy indicated that the catalyst produced, even after a multiple evaporation technique, was a mixture of spongy platinum and silica, and was not a true supported catalyst.

To see if carbonaceous poisons were affecting the rate, the exchange was studied at 200 °C over the unsintered ion exchanged catalyst and at 230 °C over the impregnated catalyst sintered at 800 °C, after treating with dry air at 300 °C for 1 h followed by re-reducing. In neither case was the rate changed by more than 10%.

The variation in rate coefficients with varying hydrogen pressure was studied briefly at 215 °C using the H_2PtCl_6 catalyst sintered at 500 °C. The order was 0.7 ± 0.2 in methane and -0.7 ± 0.2 in deuterium.

The specific rate coefficients for CH_4 conversion at 200 °C (k_x^1) are plotted in Fig. 5 as a function of the particle size in a double logarithmic form. Results of McKee and Norton (22) and of Kemball (11) using platinum black and films are included for comparison. The data of McKee and Norton were extrapolated to 200 °C using their kinetic parameters. It is seen that in both our catalyst series the maximum specific rate coefficients are obtained with sintering temperatures of 500 °C. The variations in specific rate coefficients within each series are very much greater than are the variations between each series or between the specific rate coefficients on the much larger platinum black particles. Thus no significant variation in specific rate coefficient with particle size could be demonstrated. The sintering process, however, appears to lead to very large decreases in specific rate coefficients. In fact, the temperature at which the catalyst was sintered seems to be a better indicator of its specific rate coefficient than does the particle size.

Discussion

There is both theoretical and experimental evidence that electronic properties undergo

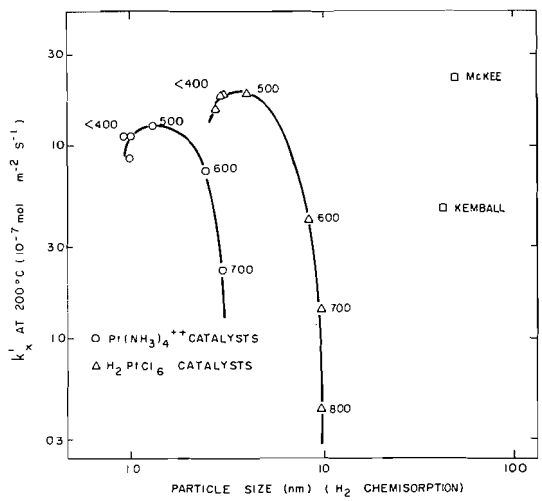

FIG. 5. Specific rates for CH_4 conversion at 200 °C as a function of particle size. Data by Kemball on platinum films (ref. 11) and by McKee and Norton on powders (ref. 22) are included.

Can. J. Chem. Downloaded from www.nrcresearchpress.com by 210.87.254.6 on 09/05/12
For personal use only.

marked changes in going from atomic dispersion to bulk metal (7, 8). The difference between the work function of platinum metal (5.4 eV) and the first ionization potential of the atom (9.0 eV) reflects these electronic changes. Some part of the change between atomic and metallic properties might be expected to occur in the range of particle sizes 1 to 10 nm, as the diameter of the metallic atom is 0.27 nm. However we were not able to demonstrate any clear variation in specific rate coefficient solely with particle size. On examining the data from one set of catalysts (Fig. 5), it seemed that a clear particle size effect had been demonstrated. Unfortunately, when the data from the second set of catalysts was examined, they did not fall on the same curve, and it appeared that the fall in specific rate coefficient at higher sintering temperatures correlated better with the sintering temperature itself, rather than with the particle size produced at that temperature.

There is some indication that the maximum specific rate coefficient is lower for smaller particle sizes if the platinum black of McKee and Norton (22) may be taken as equivalent to a catalyst given only mild sintering. The films of Kemball (11) may be somewhat more ordered and are thus expected to give lower rate coefficients, as discussed below. However, the lower specific rate coefficients with smaller particle sizes may not, in fact, be real. We have previously noted (1) that on chemisorbing H_2 on platinum, the H to Pt ratio is somewhat greater than 1.0 for some very highly dispersed catalysts. In the present case it is about 1.2. The areas given are based on one H atom taken up per surface platinum atom. If more than one is taken up the measured areas will be too large and hence the specific rate coefficients too small. On the other hand, Coenen *et al.* (23) have noted a well defined maximum in the specific rate for hydrogenation of liquid benzene at a particle size of 1.2 nm. Particles smaller than this had a smaller specific rate.

In any case, we were not able to demonstrate any large variation in specific rate coefficients between catalysts receiving the same heat treatment. Thus the D_2–CH_4 exchange, even with activation energies of about 80 kJ mol^{-1}, is probably a "facile" reaction in Boudart's terminology (6). Apparently any electronic changes as the particle size is reduced do not affect the specific rate coefficient. This behavior seems common to a number of reactions such as H_2–D_2 exchange (24), hydrogenations (24–26), dehydrogenations (26), and some simple hydrogenolyses (27). Conversely the isomerization of neopentane (6) is known to be demanding and shows a particle size effect. It is thought that this reaction requires a special triple adsorption site, and thus is demanding for geometric reasons. The same is true for the skeletal reactions of C_6 alkanes studied by Anderson *et al.* (5).

Very large variations in specific rate coefficients with sintering temperature are noted within each series of catalysts. Figure 4 shows that the decrease in specific rate coefficient is associated with the pre-exponential term in the Arrhenius expression, and is not due to a change in activation energy. Possibly the reaction takes place at defects or special adsorption sites which are eliminated by sintering.

A related possibility is that the platinum (111) face, which is a lower energy face and is thus developed on sintering, is ineffective in catalyzing this exchange. Anderson and MacDonald (4) found that the exchange of ethane and propane with D_2 was much slower over (111) nickel than it was over (100) nickel, although, with nickel, the methane–deuterium reaction was not sensitive to surface structure. The platinum (111) face has been shown to adsorb a number of gases, including hydrogen and oxygen, with much more difficulty than does polycrystalline platinum (27). Possibly methane is not easily adsorbed on this face, but is adsorbed on the steps and facets present in the smaller particles (28). Reconstruction of such features could also explain the small increases in specific rate when the catalysts are heated up to 500 °C.

Another possible explanation of the drop in specific rate coefficients with increasing sintering temperature is the diffusion of poisons to the platinum surface. Indeed, Schlatter and Boudart (29) have recently shown that small amounts of carbonaceous material originally adsorbed on the silica gel were able to poison their 0.05% platinum on silica gel catalysts for the hydrogenation of ethylene. However these poisons were removed by giving the catalyst one dose of air at 300 °C. A similar procedure did not affect our specific rate coefficients and it is hard to see how such poisons could survive the sintering procedure. Also our catalysts contain 100 times

Can. J. Chem. Downloaded from www.nrcresearchpress.com by 210.87.254.6 on 09/05/12
For personal use only.

as much platinum as those of Schlatter and Boudart, and therefore should be less susceptible to poisons from the gel. At these reaction temperatures oxygen poisoning should not be apparent. The role of other types of poisons cannot be determined, but it should be recalled that even the least active catalyst has a platinum surface area of 1400 $m^2\ kg^{-1}$, so that about 30 μmol of poison per gram would be required to cover the surface uniformly.

The studies of methane–deuterium exchange over films by Kemball (10–12) showed that CH_3D was formed by step-wise exchange:

[5] $$CH_4 + 2S \rightarrow CH_3—S + H—S$$

[6] $$D_2 + 2S \rightarrow 2D—S$$

[7] $$CH_3—S + D—S \rightarrow CH_3D + 2S$$

[8] $$H—S + D—S \rightarrow HD + 2S$$

where S represents a surface site. Other more highly deuterated products were formed by processes involving methylene radicals, whose hydrogen atoms were easily exchanged. The parameter M is clearly related to the ratio of rates for these two processes. Pure step-wise exchange gives M equal to 1, whereas multiple exchange leads to M values up to 4.

Our results show little variation of M within each series, implying that the relative rates are not affected by sintering but only the number of sites. The ion exchanged catalysts gave M about 1.7 whereas the impregnated catalysts gave M about 1.25. Thus both series of catalysts gave more step-wise than multiple exchange, but the multiple exchange contribution was greater with the smaller particles. On low temperature films at 259 °C, Kemball observed $M = 2.43$ (30). Thus significantly less highly deuterated methanes were produced on our supported catalysts, *i.e.* less CH_2 is initially formed on their surfaces. The activation energy for multiple exchange is higher, and formation of adsorbed methylene requires more energy. Sites with the energy required to form this methylene seem to be less abundant on the supported catalysts than on the film. They are also less abundant on the impregnated catalyst than on the ion exchanged catalyst. This suggests that a true particle size effect may be observable in this respect. The smaller particles should have more special uncoordinated sites (2). It is interesting to note that sintering does not change M significantly even though the particle size changes. This supports our observation that it is the pre-exponential factor and not the activation energy which changes to alter the rate. Sintering seems to remove a portion of the platinum surface, and make it entirely ineffective as a catalyst. It does not seem to modify the energetics of the reaction. Cece and Gonzales (13) noted an increase in M over nickel catalysts as the size increased. However, their smallest particles were about 1.9 nm, which corresponds to the size of particles on our impregnated catalysts.

We were not able to demonstrate any crystallite size effect on the specific rate coefficient for methane–deuterium exchange over supported platinum, but the sintering procedure used to grow platinum particles reduced the specific rate coefficient by other processes. There may be some particle size effect on the relative amount of multiple exchange. This work also provides a further example of the fact that supported catalysts can, under good conditions, yield specific rate data comparable to those obtained on powders and films.

We would like to thank D. Bell, L. M. Carefoot, and G. J. Lobban of the Analytical Science Branch, WNRE, for the mass spectrometric analyses and N. S. McIntyre and M. G. Cook of the same branch for platinum analyses. E. E. Sexton took the electron micrographs and M. Duclos measured the X-ray spectra. We thank our colleagues for useful discussions.

1. N. H. Sagert and R. M. L. Pouteau. Can. J. Chem. **49**, 3411 (1971).
2. G. C. Bond. *In* IV International Congress on Catalysis. *Compiled by* J. W. Hightower. Rice University Printing Department. Houston, Texas. 1969. p. 1217.
3. J. R. Anderson and N. R. Avery. J. Catal. **5**, 446 (1966).
4. J. R. Anderson and R. J. Macdonald. J. Catal. **13**, 345 (1969).
5. J. R. Anderson, R. J. Macdonald, and Y. Shimoyama. J. Catal. **20**, 147 (1971).
6. M. Boudart, A. W. Aldag, L. D. Ptak, and J. E. Benson. J. Catal. **11**, 35 (1968).
7. P. B. Weisz. Ann. Rev. Phys. Chem. **21**, 175 (1970).
8. R. C. Baetzold. J. Catal. **29**, 129 (1973).
9. T. A. Dorling, M. J. Eastlake, and R. L. Moss. J. Catal. **14**, 23 (1969).
10. C. Kemball. Proc. Roy. Soc. Lond. Ser. A, **207**, 539 (1951).
11. C. Kemball. Proc. Roy. Soc. Lond. Ser. A, **217**, 376 (1953).
12. C. Kemball. Catal. Rev. **5**, 33 (1971).

13. J. M. CECE and R. D. GONZALES. J. Catal. **28**, 260 (1973).
14. R. P. CHAMBERS, N. A. DOUGHARTY, and M. BOUDART. J. Catal. **4**, 625 (1965).
15. C. KEMBALL. Adv. Catal. **11**, 223 (1959).
16. R. S. MIKOVSKY and J. WEI. J. Chem. Eng. Sci. **18**, 253 (1963).
17. YA. M. VARSHAVSKII and C. E. VAISBERG. Zh. Fiz. Khim. **29**, 253 (1955).
18. J. I. APSE and R. W. MISSEN. J. Chem. Ed. **44**, 30 (1967).
19. C. N. SATTERFIELD. Mass transfer in heterogeneous catalysis. M.I.T. Press, Cambridge, Mass. 1970.
20. L. I. STOLYARENKO and A. V. VASEV. Electrokhim. **7**, 1380 (1971).
21. T. A. DORLING and R. L. MOSS. J. Catal. **7**, 378 (1967).
22. D. W. MCKEE and F. J. NORTON. J. Phys. Chem. **68**, 481 (1964).
23. J. W. E. COENEN, R. Z. C. VAN MEERTEN, and H. TH RIJNTEN. *In* Catalysis, Proc. V'th International Congress of Catalysis, Vol. 1. *Edited by* S. W. Hightower. North Holland Publishing Co. Amsterdam. 1973. pp. 671–680.
24. O. M. POLTORAK and V. S. BORONIN. Zh. Fiz. Khim. **39**, 2491 (1965).
25. T. A. DORLING and R. L. MOSS. J. Catal. **5**, 111 (1966).
26. M. BOUDART, A. ALDAG, J. E. BENSON, W. A. DOUGHARTY, and C. G. HARKINS. J. Catal. **6**, 92 (1966).
27. O. M. POLTORAK and V. S. BORONIN. Zh. Fiz. Khim. **39**, 1476 (1965).
28. B. LANG, R. W. JOYNER, and G. A. SOMORJAI. Surface Sci. **30**, 454 (1972).
29. J. C. SCHLATTER and M. BOUDART. J. Catal. **24**, 482 (1972).
30. J. R. ANDERSON and B. G. BAKER. *In* Chemisorption and reactions on metallic films. Vol. 2. *Edited by* J. R. Anderson. Academic Press, London. 1971. pp. 100–102.

Can. J. Chem. Downloaded from www.nrcresearchpress.com by 210.87.254.6 on 09/05/12
For personal use only.

Reaction Kinetics of Ground State Fluorine, F(^{2}P), Atoms. I. Measurement of Fluorine Atom Concentrations and the Rates of Reactions F + CHF_3 and F + Cl_2 using Mass Spectrometry

MICHAEL A. A. CLYNE, DONALD J. MCKENNEY,[1] AND (IN PART) RONALD. F. WALKER
Department of Chemistry, Queen Mary College, Mile End Road, London E1 4NS, England

Received May 14, 1973

Reactions of F(^{2}P) atoms generated by a 2.45 GHz discharge in dilute F_2 + He mixtures have been studied mass spectrometrically with a beam inlet system from a fast flow reactor. F atom concentrations have been measured from the consumption of Cl_2 in the simple and extremely rapid bimolecular reaction 1

[1] $$F + Cl_2 \rightarrow FCl + Cl \quad \Delta U^0_{298} = -9 \text{ kJ mol}^{-1}$$

k_1 was determined to be $(1.1 \pm 0.3) \times 10^{-10}$ cm^3 molecule^{-1} s^{-1} at 300 °K.

Rate measurements for the reaction 2, which forms CF_3 radicals, are reported, over the range 301 to 667 °K,

[2] $$F + CHF_3 \rightarrow HF + CF_3 \quad \Delta U^0_{298} = -141 \text{ kJ mol}^{-1}$$

$$\log_{10} k_2 \text{ (cm}^3 \text{ molecule}^{-1} \text{ s}^{-1}) = (-10.98 \pm 0.09) - (522 \pm 164)/T$$

A less detailed survey of the rates at 298 °K of a series of reactions of F with H_2, CH_4, CH_3Cl, CH_2Cl_2, and $CHCl_3$, is also given; in these cases, the source of F was a discharge in CF_4 + Ar, and [F] was measured by titration with ClNO.

Les réactions des atomes F(^{2}P) créés par décharge à 2.45 GHz dans des mélanges dilués de F_2 + He, ont été étudiées par spectrométrie de masse avec un système d'introduction constitué d'un réacteur à flux rapide. Les concentrations en atomes F ont été mesurées à partir de la disparition de Cl_2 selon une réaction bimoléculaire simple et extrêmement rapide 1

[1] $$F + Cl_2 \rightarrow FCl + Cl \quad \Delta U^0_{298} = -9 \text{ kJ mol}^{-1}$$

avec $k_1 = (1.1 \pm 0.3) \times 10^{-10}$ cm^3 molécule^{-1} s^{-1} à 300 °K.

Les mesures de vitesse pour la réaction 2 qui engendre des radicaux CF_3, ont été rapportées dans l'intervalle 301 à 667 °K,

[2] $$F + CHF_3 \rightarrow HF + CF_3 \quad \Delta U^0_{298} = -141 \text{ kJ mol}^{-1}$$

$$\log_{10} k_2 \text{ (cm}^3 \text{ molécule}^{-1} \text{ s}^{-1}) = (-10.98 \pm 0.09) - (522 \pm 164)/T$$

Un survol moins détaillé des vitesses de réactions de F sur H_2, CH_4, CH_3Cl, CH_2Cl_2 et $CHCl_3$ à 298 °K a été également présenté; dans ces cas, la source de F provient d'une décharge de CF_4 + Ar et [F] a été titré par NOCl. [Traduit par le journal]

Can. J. Chem., 51, 3596 (1973)

Introduction

The rates of elementary abstraction reactions involving ground state F(^{2}P) atoms are less satisfactorily known than the rates of corresponding reactions involving Cl atoms. (No distinction is made here between $^2P_{3/2}$ and $^2P_{1/2}$ J-excited atoms having the $2p^5$ ground state electronic configuration; at 300 °K, the equilibrium ratio $[^2P_{1/2}]/[^2P_{3/2}] \simeq 0.08$.) In particular, very few measurements exist of absolute rate constants of reactions suitable for use as primary standards in competitive fluorinations, such as

[3] $$F + H_2 \rightarrow HF + H$$

For this reaction, which seems to be the most fully studied of the series F + RH, the range of recent values of k_3 (cm^{-3} molecule^{-1} s^{-1}) at 298 °K is 1.8×10^{-11} (1) to 6.3×10^{-11} (2), including the intermediate value of 3×10^{-11} (3). Earlier, an indirect value of 1.1×10^{-11} cm^3 molecule^{-1} s^{-1} was suggested (4), but since this value is based on assumed Arrhenius parameters for the F + C_2H_6 reaction, it must be regarded as an estimate.

[1]On sabbatical leave (1971–1972) from Department of Chemistry, University of Windsor, Windsor 11, Ontario.

Can. J. Chem. Downloaded from www.nrcresearchpress.com by 210.87.254.105 on 09/05/12
For personal use only.

Can. J. Chem. Downloaded from www.nrcresearchpress.com by 210.87.254.105 on 09/05/12
For personal use only.

Two of the few direct measurements of the rates of other F atom reactions are the recent studies by Warnatz *et al.* (5) of the reaction

[1] $$F + Cl_2 \rightarrow FCl + Cl$$

and by Kolb and Kaufman (6) of the reaction

$$F + CCl_4 \rightarrow FCl + CCl_3$$

In both cases, mass spectrometric analysis with molecular beam sampling was used.

The scarcity of data on F atom elementary reactions is partially due to the high reactivity of F_2, which often accompanies F atoms, and which thus may complicate the kinetic behavior of F. A second problem is the absence of well-characterized methods for the measurement of F atom concentrations. In addition, most F atom reactions involving abstraction of an H atom are rapid, thus leading to difficulties in the isolation of a single elementary process in studies of F + RH reaction rates. Recently, Homann *et al.* (1) have described the use of a titration based on the reaction

$$F + ClNO \rightarrow FCl + NO$$

however, this method has certain drawbacks such as the difficulty of accurate calibrations with the extremely reactive FCl molecule, and the reaction of NO with F_2 (7) reforming F atoms, in the presence of F_2

$$NO + F_2 \rightarrow FNO + F$$

The use of the $F + H_2$ reaction for the measurement of [F] also entails problems (1) due to the secondary reaction of the H atoms formed with F_2 and by other processes.

The first part of the present work describes a method for the measurement of F atoms (in the presence of F_2) based on the rapid reaction

[1] $$F + Cl_2 \rightarrow FCl + Cl$$

using molecular beam mass spectrometry and a discharge flow system; the consumption of Cl_2 is used to measure [F]. Also, new measurements of k_1 at 298 °K are reported; these confirm the extreme rapidity of the $F + Cl_2$ reaction. The second part of this paper describes the application of this method to the determination of the rate constant from 300 to 667°K for the reaction.

[2] $$F + CHF_3 \rightarrow CF_3 + HF$$

which is a possible clean source of CF_3 radicals. Finally, we briefly describe the results of less extensive measurements of the rates at 298 °K of a variety of F + RH reactions.

Experimental

The mechanisms and rates of reactions of F^2P atoms with compounds RH were investigated by mass spectrometric analysis from a rapid discharge-flow apparatus.

Production of $F(^2P)$ Atoms

In the work on the $F + H_2$, CH_4, CH_3Cl, CH_2Cl_2, and $CHCl_3$ reactions described here, a stream of $F(^2P)$ atoms was produced by means of a 2.45 GHz microwave discharge (25 W) in a mixture of CF_4 (1%) and Ar (6, 8, 9) using a silica discharge tube (10 mm i.d.). The atoms were pumped from the discharge tube through the length of a flow tube of cylindrical cross section (24.1 mm i.d.) provided with a number of reagent inlet jets, beyond which a small sample of gas was continuously sampled from the center of the gas flow to the ion source of a mass spectrometer (see below). As well as $F(^2P)$ atoms, the products of the CF_4 + Ar discharge detected mass spectrometrically included numerous CF^+, CF_2^+, CF_3^+ ions derived from molecular species such as CF_4 and C_2F_6, as well as appreciable SiF_4 and O_2 derived mostly from interaction between the plasma and the silica walls of the discharge tube.

While there was no evidence for any complications in our system due to any unrecombined molecular radicals produced by the discharge, it was felt that the CF_4 + Ar discharge as a source of $F(^2P)$ atoms for quantitative kinetic studies, should be superseded, if possible. Accordingly, a low power microwave discharge (40 W) in a mixture of F_2 ($\simeq$1%) + He ($\simeq$99%) using a F_2 (5%) + He mixture from B.O.C. was investigated as a source of $F(^2P)$ (10, 25).[2] Initially, a discharge tube coated with H_3PO_4, as employed for the production of Cl and Br atoms (11), was used; in this case, low yields of $F(^2P)$ were obtained, with extremely large formation of HF and of species giving PF^+, POF^+ mass peaks. Substitution of a clean silica discharge tube led to formation of large amounts of $F(^2P)$ atoms, containing SiF_4 as the only major impurity (derived mainly from interaction within the discharge zone). Mass spectrometric measurements, using the molecular ion F_2^+ m/e 38 intensities, showed that at least 80% dissociation of F_2 could be achieved when the flow entering the discharge contained $\simeq$0.1% F_2, and at least 60% dissociation from $\simeq$1% F_2. Use of an alumina discharge tube, which eliminates formation of SiF_4 within the discharge (12) was not adopted, since an appreciable formation of SiF_4 occured outside the discharge by interaction of F atoms with the flow tube walls especially at temperatures above 300 °K. This was demonstrated by observation of SiF_4 production when F was removed by reaction with Cl_2 between the discharge tube and the flow tube.

Conventional vacuum techniques were found adequate for handling the diluted F_2 (5%) + He gas mixture; all stopcocks were lubricated with fluorocarbon grease (Voltalef), and fluorocarbon oil (Kel-F) was used for manometers where necessary.

[2]We thank P. B. Davies, R. G. McDonald, and B. A. Thrush for their assistance in introducing us to the F_2 + He gas mixtures.

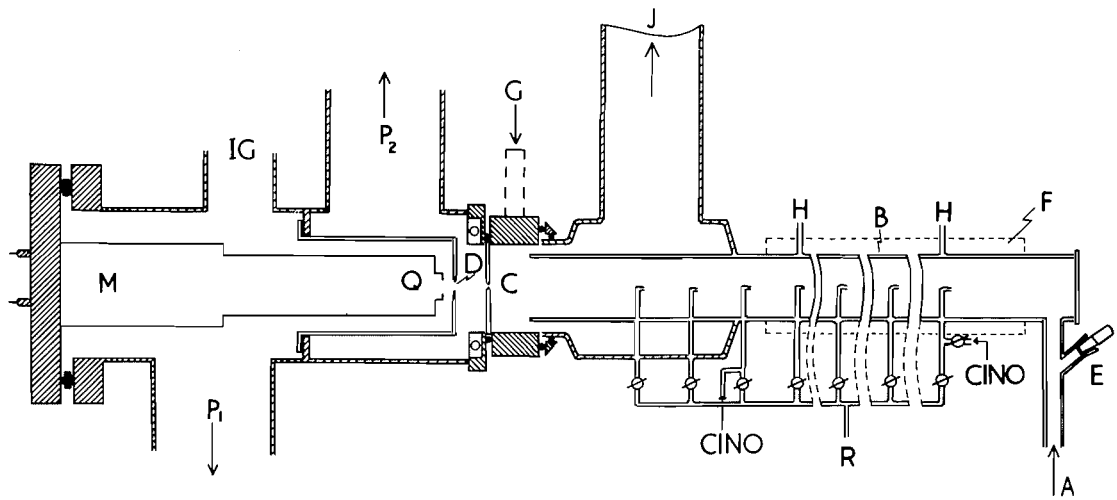

FIG. 1. Schematic arrangement of flow system with on-line mass spectrometric studies of F atom reactions. *A*, flow of F atoms in He carrier from discharge; *B*, silica flow tube; *C*, first pinhole (0.7 mm) separating flow tube from differentially-pumped chamber; *D*, second pinhole (0.7 mm) separating differentially-pumped chamber from quadrupole mass spectrometer *Q* (E.A.I. 150/A); *E*, access to discharge tube; *F*, furnace; *G*, 50 mm gate valve; *H*, connections to total pressure manometer; *IG*, ion gauge; *J*, connection to cold traps and large pump (60 l s^{-1}); *M*, multiplier; P_1, P_2, pumping lines for quadrupole chamber and for differentially-pumped chamber; *R*, reagent inlets.

Flow System for Kinetic Studies

The flow system for kinetic studies of F atom reactions was similar to that described previously (13) except that eight inlet jets were provided at intervals along the flow tube, allowing up to eight different reaction times to be used. In order to obtain the maximum flow velocity for the kinetic studies of the extremely rapid reaction

$$F + Cl_2 \rightarrow ClF + Cl$$

a relatively high flow rate of helium ($\simeq 5 \times 10^{20}$ atom s^{-1}) was employed instead of argon as the carrier gas for the F atom flow. At 300 °K, the maximum linear velocity of flow was then 60 m s^{-1}. Under these conditions, mixing of reactant Cl_2 added to the F atom stream at the inlet closest to the mass spectrometer inlet system was detectably incomplete, as indicated by the constancy of the Cl_2 ion current when the same Cl_2 concentration was added at each inlet jet in the absence of F. Only the remaining seven more distant inlet jets were therefore used for kinetic studies of the F + Cl_2 system. Under these conditions, an appreciable pressure gradient ($\leqslant 25\%$) existed across the reaction zone; the mean pressure was used in all cases for the kinetic analysis. Much lower flow velocities were used for the F + CHF_3 reaction studies, leading to a negligible ($< 5\%$) pressure gradient.

Mass Spectrometer Inlet System

A system of two coaxial pinholes (0.7 mm diameter), separated by a differentially pumped chamber, was used as the interface between the flow tube and the mass spectrometer ion source (Fig. 1). With the flow tube maintained at a pressure of $\simeq 200$ N m^{-2}, the ion source pressure was $\simeq 7 \times 10^{-4}$ N m^{-2}. The inlet system was newly constructed (Fig. 1), and incorporated most of the useful features of the two previous inlet systems (13, 14), without their disadvantages. (*i*) The distance between the first pinhole and ion source was 3 cm, favoring beam formation which is found advantageous for the detection of atoms and radicals, and for maximizing signal-to-background ratios in the mass spectrometer (14). (*ii*) More rapid pumping than previously (13) was provided both in the mass spectrometer chamber, and in the differential chamber separating the two pinholes. The combination of rapid pumping and small separation of the pinholes was achieved using the annular design shown in Fig. 1, based on a 100 mm diameter outer chamber. (*iii*) Although the all-metal mass spectrometer and its vacuum chamber could be baked up to 600 °K, temperature zoning using a water-cooled flange in conjunction with a 50 mm Viton-sealed gate valve allowed isolation of the baked system from the flow tube.

As before, pumping was achieved by means of two identical sets consisting of a double-stage rotary pump, alumina foreline trap, diffusion pump (Edwards, Model EO2, 0.15 m^3 s^{-1} nominal speed, charged with polyphenyl ether), chevron baffle, and liquid N_2 cold trap. Without bakeout the background pressure in the mass spectrometer was routinely 3×10^{-6} N m^{-2} shortly after cessation of sampling from the flow tube, and lower pressures were attainable after continued pumping of the isolated system.

Reagents

Fluoroform was an Air Products (98%) product; the source of F_2 has been described; the remaining reagents were as given previously (13). The fluoroform and chlorine were purified by repeated trap-to-trap distillation under vacuum.

Results and Discussion

Measurement of F(^2P) Atom Concentrations

In one of the few quantitative kinetic studies of F atom reactions, that of Wagner and his co-workers (1, 5), titration of F atoms with nitrosyl

Can. J. Chem. Downloaded from www.nrcresearchpress.com by 210.87.254.105 on 09/05/12
For personal use only.

Can. J. Chem. Downloaded from www.nrcresearchpress.com by 210.87.254.105 on 09/05/12
For personal use only.

chloride has been used to measure absolute F atom concentrations

[4] $$F + ClNO \rightarrow FCl + NO$$

The FCl yield in reaction 4 was measured mass spectrometrically by reference to addition of known concentrations of FCl from a cylinder. This method is closely analogous to the corresponding titration reaction of Cl and Br $^2P_{3/2}$ atoms with ClNO, which have been shown to be very rapid (15) and stoichiometric to form NO (11)

$$Cl + ClNO \rightarrow Cl_2 + NO$$
$$k^{298} = (3.0 \pm 0.5) \times 10^{-11} \text{ cm}^3 \text{ molecule}^{-1} \text{ s}^{-1} \text{ (15)}$$

$$Br + ClNO \rightarrow BrCl + NO$$
$$k^{298} = (1.0 \pm 0.2) \times 10^{-11} \text{ cm}^3 \text{ molecule}^{-1} \text{ s}^{-1} \text{ (15)}$$

The F + ClNO titration must be regarded at the present time as less well-established than the corresponding Cl + ClNO and Br + ClNO titrations (11), since k_4 is not known. Also, FCl is a difficult compound to prepare in a pure state, and it can be expected to react appreciably with glass or silica apparatus (13, 16). Consequently, the calibration of FCl mass spectral ion current may be subject to systematic errors. A variant of the F + ClNO titration, measurement of the concentration of ClNO required to just remove all the F atoms, eliminates the problems of handling FCl, and this method has been used in our preliminary measurements of a number of F + RH rate constants described here. The criterion for consumption of F was taken as no further increase in FCl^+ ion currently on addition of ClNO. Similar limitations of this variant of the ClNO titration method for measurement of [F] to those discussed for measurement of [Cl] and [Br] (11) are expected. At high concentrations of F (and thus of ClNO), the reaction, NO + F_2 → FNO + F, may occur to an appreciable extent, leading to an erroneous value for [F] (7).

The Reaction F + Cl_2 → FCl + Cl as a Titration for [F]

Following preliminary work using the F + ClNO titration (5), we have evaluated the reaction 1

[1] $$F + Cl_2 \rightarrow FCl + Cl \quad \Delta U^0_{298} = -9 \pm 3 \text{ kJ mol}^{-1} \text{ (17)}$$

previously rejected by Wagner *et al.* (5), as a possible titration reaction for the measurement of [F]. The reason for the earlier rejection of this reaction (5) was that the secondary reaction

$$Cl + F_2 \rightarrow FCl + F$$

was expected to be rapid, and consequently F could be partially regenerated by reaction of Cl atoms from reaction 1 with undissociated F_2. This view cannot be sustained, since work in our laboratory (18) and elsewhere (19) shows that the rate of reaction of Cl with F_2 is slow, with a rate constant of $\leqslant 5 \times 10^{-14}$ cm^3 molecule^{-1} s^{-1} at 298 °K (18); the only value previously reported (3.5×10^{-9} cm^3 molecule^{-1} s^{-1}) (20) is an otherwise unfounded estimate based on an analogy with other elementary exothermic reactions. Reaction 1 thus appears to be a promising titration reaction, especially since its rate approaches the hard sphere bimolecular collision frequency at 298 °K (k_1^{298} = 9.1×10^{-11} cm^3 molecule^{-1} s^{-1} according to ref. 5). The equilibrium constant for reaction 1 at 298 °K (using the J.A.N.A.F. thermochemical data (17)[3] is 40. Hence the reverse reaction, FCl + Cl → F + Cl_2 is unlikely to be important below 300 °K, even in the titration of F with Cl_2 to the end point, in which the initial concentrations of F and Cl_2 are approximately equal. With $[Cl_2]_0/[F]_0 > 1$, which leads to a smaller effect of the reaction FCl + Cl, measurement of [F] as $[Cl_2]$ consumed in reaction 1 is straightforward mass spectrometrically, and the calibration of Cl_2^+ ion current with known Cl_2 concentrations is an established technique (11).

Determination of [F] in this manner was verified by comparison of $[Cl_2]$ consumed with relative [FCl] formed in the F + Cl_2 reaction. These experiments verified the absence of detectable Cl atom recombination in the flow tube, or in the sampling system, since Cl_2 consumption, but not FCl formation, would be affected by Cl atom recombination. It was noted that the Cl_2^+ mass peak was completely absent, when Cl_2 was added to excess F under conditions of complete reaction, thus confirming the absence of Cl atom recombination within the sampling system.

Rate constant k_1 for the reaction F + Cl_2 → FCl + Cl

The rate of consumption of Cl_2 at 300 °K was measured mass spectrometrically (m/e 70, $^{35}Cl_2^+$) in the presence of an excess of F atoms; time

[3]These data are based on the lower of two possible values for D_0^0 (FCL). In the (unlikely) event that the higher value for D_0^0 (FCL) is correct, $-\Delta U^0_{298}$, and hence K_{equil}, would be greater than 40.

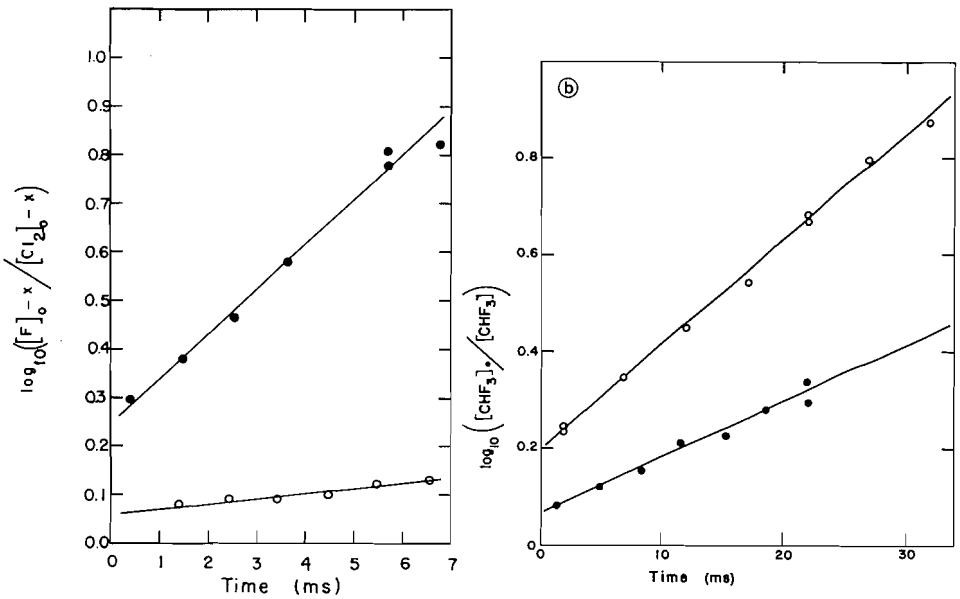

FIG. 2. (*a*) Second order decay plot for the reaction, F + Cl_2 → FCl + Cl (298 °K): ●, $[F]_0 = 5.6 \times 10^{12}$ atom cm^{-3}; ○, $[F]_0 = 3.0 \times 10^{12}$ atom cm^{-3}.
(*b*) Pseudo first-order decay plot for the reaction F + CHF_3 → HF + CF_3 (301 °K): ●, $[F]_0 = 1.3 \times 10^{14}$ atom cm^{-3}; ○, $[F]_0 = 1.9 \times 10^{14}$ atom cm^{-3}. Zero of time scale differs from reaction time = 0.

variation was by addition of the same $[Cl_2]$ at a series of inlets equally spaced at increasing intervals along the flow system from the mass spectrometer inlet system. Kinetic analysis was carried out according to eq. 5,

$$[5] \quad \frac{1}{[F]_0 - [Cl_2]_0} \ln \left\{ \frac{[Cl_2]_0([F]_0 - x)}{[F]_0([Cl_2]_0 - x)} \right\} = kt$$

where x is the concentration of F or Cl_2 that has reacted in time t; $[Cl]_0$ and $[F]_0$ are the initial concentrations. Figure 2 (*a*) shows typical data for the variation of $\log_{10} \{([F]_0 - x)/([Cl_2]_0 - x)\}$ with time.

Since preliminary data showed that the F + Cl_2 reaction was extremely rapid, it was possible to use this reaction for the measurement of [F] as described above. Although the rate of reaction of $\simeq 5 \times 10^{12}$ atom cm^{-3} of F with $\simeq 7 \times 10^{12}$ molecule cm^{-3} of Cl_2 was incomplete within a 5–10 ms time scale, the rate of the same concentration of F with an excess of Cl_2 ($\simeq 25 \times 10^{12}$ molecule cm^{-3}) was complete in this same time scale. The concentration of F under these conditions was taken to be equal to the concentration of Cl_2 consumed, measured mass spectrometrically. The completeness of the F + Cl_2 reaction was verified by noting that, for a constant value of [F], $[Cl_2]$ consumed was independent of time and of $[Cl_2]$ added.

The extreme rapidity of the F + Cl_2 reaction limited the range of conditions accessible for the measurements of the small concentrations of Cl_2 which were required to be measured in the kinetic study, and error limits of ± 25% were estimated for the new value of k_1 given in Table 1*a*.

The value now found for k_1, $(1.1 \pm 0.3) \times 11^{-10}$ cm^3 $molecule^{-1}$ s^{-1} at 300 °K, may be compared with the determination (also using a discharge flow system), using $5[F]_0 = [Cl_2]_0$ with mass spectrometric detection of F removal, FCl formation, and Cl formation by Warnatz *et al.* (5), $\log_{10} k_1$ (cm^3 $molecule^{-1}$ s^{-1}) = $-9.04 - 732/T$, giving $k_1^{298} = 8.6 \times 10^{-11}$. No error limits for k_1 were given by these workers (5).

Rate constant k_2 for the reaction F + CHF_3 → CF_3 + HF

The rate of reaction of fluoroform, CHF_3, with an excess of F atoms was measured using a similar technique to that used for the F + Cl_2 system. In this case pseudo first order kinetic analysis according to eq. 6 was employed.

$$[6] \quad \ln \{[CHF_3]_0/[CHF_3]\} = k_2[F]t$$

Can. J. Chem. Downloaded from www.nrcresearchpress.com by 210.87.254.105 on 09/05/12
For personal use only.

TABLE 1. (*a*) Rate constant k_1 for the reaction $F + Cl_2 \rightarrow FCl + Cl$ at 300 °K

Total pressure (N m^{-2})	$[Cl_2]$ (10^{12} molecule cm^{-3})	[F] (10^{12} atom cm^{-3})	$d \log \left(\frac{[F]_0 - x}{[Cl_2]_0 - x}\right)/dt$ (s^{-1})	$k_1 \times 10^{10}$ (cm^3 molecule^{-1} s^{-1})
118	3.7	5.55	92.8	1.16
130	3.9	5.39	60.0	0.93
132	2.5	2.97	10.8	0.56
130	6.3	6.81	35.3	1.59
				Mean = (1.1 ± 0.3)[a]

[a]Error limits = ±25%.

(*b*) Rate constant k_2 for the reaction $F + CHF_3 \rightarrow HF + CF_3$ from 301 to 667 °K

Total pressure (N m^{-2})	T (°K)	$[CHF_3]_0$ (10^{13} molecule cm^{-3})	[F] (10^{14} atom cm^{-3})	$k_2 \times 10^{13}$ (cm^3 molecule^{-1} s^{-1})
137	301	2.15	1.33	2.0
198	301	5.84	1.87	2.7
134	301	2.96	2.01	2.0
160	301	5.66	0.96	2.2
165	321	6.84	2.19	2.2
156	323	4.50	0.86	2.7
161	357	5.14	1.85	3.2
177	363	3.59	1.58	3.1
138	423	0.84	1.05	5.9
177	434	3.63	1.67	5.0
134	446	2.39	1.05	7.0
156	495	1.27	0.99	9.1
158	515	1.67	1.10	8.0
181	542	1.99	0.34	10.5
150	560	1.48	0.89	20.6
132	563	1.49	0.51	12.8
142	563	1.70	0.59	12.5
170	625	2.17	0.50	17.9
176	628	3.34	0.80	16.8
176	628	2.52	0.33	15.9
110	649	1.16	0.29	15.6
200	667	2.17	0.49	18.6

The relative concentration of CHF_3 was followed mass spectrometrically using the m/e = 51 CHF_2^+ ion peak. (The parent ion peak m/e = 70 CHF_3^+ was not observed.) The initial concentration ratio $[F]/[CHF_3]_0$ was generally around 5; no corrections for F consumption in the $F + CHF_3$ reaction were made, since it was assumed that the F atom concentration would be kept approximately constant by means of the reaction scheme,

$$F + CHF_3 \rightarrow CF_3 + HF,$$

$$CF_3 + F_2 \rightarrow CF_4 + F.$$

Figure 2*b* shows typical data for the pseudo first order decay of $[CHF_3]$ in the presence of excess [F]. A total of 22 sets of measurements were made over the temperature range 301 to 667 °K, and the resulting values for k_2 are given in Table 1*b*. Since k_2 was found to be at least 10^2 less than k_1 up to 500 °K, the effect of wall reaction of F atoms upon the $F + CHF_3$ reaction was marked in comparison with that upon the $F + Cl_2$ reaction. Although negligible at temperatures below 500 °K, the wall reaction of F at high temperatures was found to be as high as 50% attenuation of initial F through the length of the reaction zone. Observations of m/e 38 (F_2^+) suggested that wall recombination was negligible compared with wall reaction (*i.e.* to form $SiF_4 + O_2$). In these cases, the mean value for [F] was used for kinetic analyses in eq. 6.

The least mean squares Arrhenius plot (Fig. 3) gave the following temperature variations for k_2 (301–667 °K), and an activation energy of (10.0 ± 3.1) kJ mol^{-1}

Can. J. Chem. Downloaded from www.nrcresearchpress.com by 210.87.254.105 on 09/05/12
For personal use only.

TABLE 2. Rate constants at 298 °K for F + RH reactions

$$F + RH \xrightarrow{k_{RH}} HF + R;\ k_{RH} = -[F]^{-1}\, d \ln [RH]/dt$$

RH	Number of data	Range of [F] (10^{13} cm^{-3})	k_{RH} (10^{-11} cm^3 molecule^{-1} s^{-1})
CH_4	11	1.5–2.4	6.0 (±100%)
H_2	7	2.1–4.8	2.5 (±50%)
CH_3Cl	8	0.7–1.2	2.4 (±30%)
CH_2Cl_2	10	1.5–3.9	0.96 (±25%)
$CHCl_3$	12	1.7–3.3	0.53 (±25%)

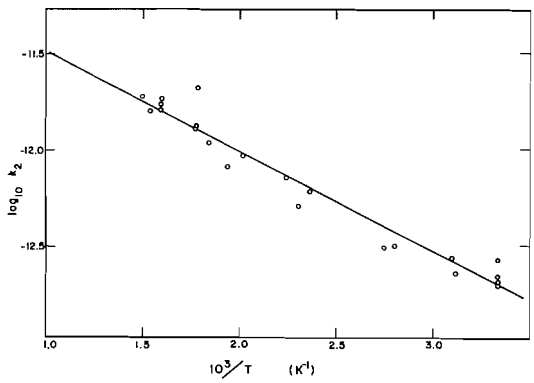

FIG. 3. Arrhenius plot for the reaction F + CHF_3 → HF + CF_3. k_2 in cm^3 molecule^{-1} s^{-1}.

$$\log_{10} k_2\ (\text{cm}^3\ \text{molecule}^{-1}\ \text{s}^{-1}) = (-10.98 \pm 0.09) - (522 \pm 164)/T$$

The stated error is 2σ (σ is the standard error of the estimate).

Rate Constants for the Reaction F + $CHCl_3$, CH_2Cl_2, CH_3Cl, CH_4, and H_2

Rate measurements at 298 °K of a series of F atom reactions which abstract an H atom were carried out using a discharge in CF_4 + Ar mixture as the source of F(^{2}P) atoms. Kinetic analysis was carried out as described above, with [F] ≫ [RH]. These studies were carried out with an earlier mass spectrometric sampling system (13), and absolute F atom concentrations were measured using ClNO titration as described above. The values for the rate constants found here we believed to be less accurate than those for the F + CHF_3 and F + Cl_2 reactions which were determined with improved techniques. However, the existing data on the rate constants for all F atom reactions are sufficiently poor that the present results are thought to represent a considerable improvement in precision. The error limits estimated for the present rate constant measurements widen as the rate constant increases, approaching the lower limit of sensitivity of the apparatus, for the F + CH_4 reaction. Figure 4 shows the data for the F + H_2 reaction; all values for $-d \ln [H_2]/dt$ are plotted as a function of [F]; the gradient of this plot is equated to the second order rate constant k_{H_2}. The scatter of these results is typical of the whole series of rate measurements described in this section. Table 2 summarizes the values obtained for k_{CHCl_3}, $k_{CH_2Cl_2}$, k_{CH_3Cl}, k_{CH_4}, and k_{Cl_2} and their estimated errors.

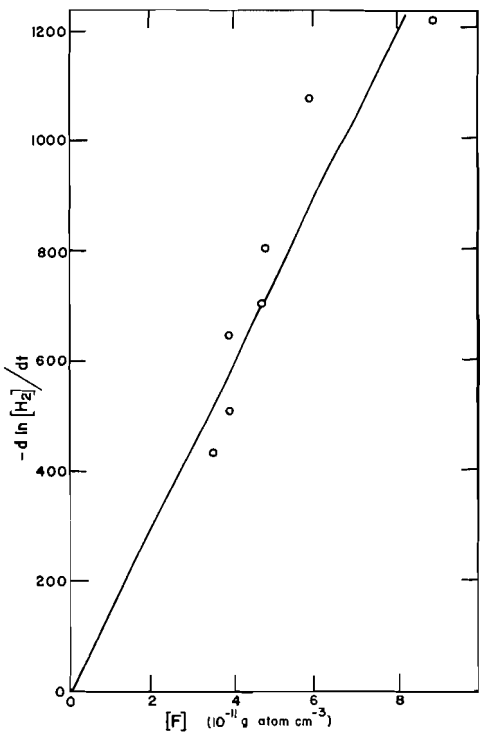

FIG. 4. Kinetics of the F + H_2 reaction. Variation of first order rate constant: d ln $[H_2]/dt$ with [F].

Can. J. Chem. Downloaded from www.nrcresearchpress.com by 210.87.254.105 on 09/05/12
For personal use only.

Can. J. Chem. Downloaded from www.nrcresearchpress.com by 210.87.254.105 on 09/05/12
For personal use only.

TABLE 3. Rate constants for reactions of the type $A + CHB_3 \xrightarrow{k_{A,B}} HA + CB_3$, (A = F, Cl; B = F, Cl)

Reaction	ΔU^0_{298}[a] (kJ mol^{-1})	$\log_{10} k_{A,B}^{298}$ (cm^3 molecule^{-1} s^{-1})[b]	A (cm^3 molecule^{-1} s^{-1})	E (kJ mol^{-1})	Reference
F + CHF_3	−141.0	$(-10.98 \pm 0.09) - (522 \pm 164/T)$	$1.06 \pm 0.24 \times 10^{-11}$	10.0 ± 3.1	This work
F + $CHCl_3$	−190.6	$(-11.29 \pm 0.03) - (144 \pm 11/T)$	$0.51 \pm 0.02 \times 10^{-11}$	2.75 ± 0.20	21
F + $CHCl_3$	−190.6	-11.28 ± 0.11			This work
Cl + CHF_3	−2.3	$-11.55 - (1830 \pm 22/T)$	2.8×10^{-12}	35.1 ± 0.4	23
Cl + $CHCl_3$	−51.9	$-10.94 - (725 \pm 20/T)$	1.15×10^{-11}	14.0 ± 0.4	22

[a]Reference 24.
[b]$\log_{10} k_{A,B} = A - E/2.303\ RT$.

No detailed discussion is given of the present values for these rate constants, k_{RH}, in relation to existing data (1–4, 21) except to note that no anomalies are now apparent, within the admittedly wide range of all the data. The relative values of k_{RH} generally agree satisfactorily with those based upon competitive fluorination studies (4, 22).

Rate Constants for Reaction $A + CHB_3 \xrightarrow{k_{A,B}} HA + CB_3$

Reactions of the type A + CHB_3, where A is F or Cl, and B is a halogen, should be a good source of CB_3 radicals for kinetic studies. Quantitative kinetic data are now available for the following (all exothermic) reactions: F + CHF_3, F + $CHCl_3$, Cl + CHF_3, Cl + $CHCl_3$; Table 3 shows a summary of these data, together with the corresponding values of ΔU^0_{298}.

In fact, none of these reactions is sufficiently rapid at 300 °K with the possible exception of the F + $CHCl_3$ reaction, to be a good source of CB_3 radicals for kinetic studies in flow systems.[4] This is because of the rapid recombination rate of CB_3 radicals, which leads to overlapping of the regions of production and consumption of these radicals.

Further Rate Measurement of F Atom Reactions

The method of measurement of F using the F + Cl_2 reaction, with mass spectrometric analysis of Cl_2 consumption, has been demonstrated for the determination of a rate constant approaching half the bimolecular collision rate at 300 °K (the F + Cl_2 reaction). The use of a more sensitive and noise-free mass spectrometer than the type used here would offer clear advantages for systematic measurements of a range of F atom reaction rate constants, such as F + H_2, over a wide temperature range.

We thank Science Research Council and the Ministry of Defence for partial support of this work.

One of us (D.J.M.) wishes to thank the Queen Mary College for the use of their facilities and Dr. M. A. A. Clyne and his group for generous and stimulating hospitality.

[4]Rapid atom-switching reactions (6) might preclude the use of the F + $CHCl_3$ reaction as a "clean" source of CCl_3 radicals.

1. K. H. Homann, W. C. Solomon, J. Warnatz, H. G. Wagner, and C. Zetzsch. Ber. Phys. Chem. **74**, 585 (1970).
2. K. L. Kompa and J. Wanner. Chem. Phys. Lett. **12**, 560 (1972).
3. V. L. Talrose, A. F. Dodonov, E. B. Gordon, G. K. Lavrovskaya, I. I. Morosov, and A. N. Ponomarev. Int. Symp. Chem. Lasers, Moscow. 1969.
4. G. C. Fettis and J. H. Knox. Progress in reaction kinetics. Vol. 2. Pergamon Press, New York. 1964. p. 1.
5. J. Warnatz, H. G. Wagner, and C. Zetzsch. Ber. Phys. Chem. **75**, 119 (1971).
6. C. E. Kolb and M. Kaufman. J. Phys. Chem. **76**, 947 (1972).
7. D. Rapp and H. S. Johnston. J. Chem. Phys. **33**, 695 (1960).
8. A. Carrington, D. H. Levy, and T. A. Miller. J. Chem. Phys. **45**, 4093 (1966).
9. J. C. Polanyi and D. C. Tardy. J. Chem. Phys. **51**, 5717 (1969).
10. H. G. Wagner, J. Warnatz, and C. Zetzsch. Angew. Chem. Int. Ed. **10**, 564 (1971).
11. M. A. A. Clyne, H. W. Cruse, and R. T. Watson. J. Chem. Soc. Faraday II, **68**, 153 (1972).
12. D. E. Rosner and H. D. Allendorf. J. Phys. Chem. **75**, 308 (1971).
13. Michael A. A. Clyne and Ronald F. Walker. J. Chem. Soc. Faraday I. **69**, 1547 (1973).
14. M. A. A. Clyne and R. T. Watson. Chem. Phys. Lett. **12**, 344 (1971).
15. M. A. A. Clyne and H. W. Cruse. J. Chem. Soc. Faraday II, **68**, 1281 (1972).
16. P. H. Brodersen and J. E. Sicre. Z. Phys. **141**, 515 (1955).
17. J.A.N.A.F. thermochemical tables. 2nd ed. NSRDS-NBS 37, 1971.
18. Michael A. A. Clyne and Robert T. Watson. To be published.
19. G. Schatz and M. Kaufman. J. Phys. Chem. **76**, 3586 (1972).
20. Pyrodynamics, **4**, 371 (1966); from Rate constants of gas phase reactions reference book. Russian version compiled by V. N. Kontratiev, *translated by* L. J. Holtschlag, *edited by* R. M. Fristrom. Nat. Bur. Stand. U.S. Dept. Comm. Washington, D.C. 1972. p. 85.
21. R. Foon and N. A. McAskill. Trans. Faraday Soc. **65**, 3005 (1969).
22. J. H. Knox. Trans. Faraday Soc. **58**, 275 (1962).
23. J. W. Coomber and E. Whittle. Trans. Faraday Soc. **62**, 2183 (1966).
24. J. D. Cox, J. B. Pedley, A. Kirk, S. Seilman, and L. G. Heath. CATCH tables, halogen compounds. School of Molecular Sciences, University of Sussex, Brighton. 1972; Selected values of chemical thermodynamic properties. Nat. Bur. Stand. Tech. Note 270–3. U.S. Government Printing Office, Washington, D.C. 1968.

Can. J. Chem. Downloaded from www.nrcresearchpress.com by 210.87.254.105 on 09/05/12
For personal use only.

Di-imide: Some Physical and Chemical Properties, and the Kinetics and Stoichiometry of the Gas-phase Decomposition[1]

C. WILLIS AND R. A. BACK

Division of Chemistry, National Research Council of Canada, Ottawa, Canada K1A 0R6

Received May 7, 1973

Preparation of di-imide by passing hydrazine vapor through a microwave discharge yields mixtures with NH_3 containing typically about 15% N_2H_2, estimated from the gases evolved on decomposition. The behavior of the mixture (which melts at −65 °C) on warming from −196 to −30 °C suggests a strong interaction between the components. Measurements of magnetic susceptibility and e.p.r. experiments showed that N_2H_2 is not strongly paramagnetic, which with other observations points to a singlet rather than a triplet ground-state.

Di-imide can be vaporized efficiently, together with NH_3, by rapid warming, and the vapor is surprisingly long-lived, with a typical half-life of several minutes at room temperature. The near-u.v. (3200–4400 Å) absorption spectrum of the vapor was photographed; it shows well-defined but diffuse bands, with $\varepsilon_{max} = 6(\pm 3)$ at 3450 Å.

Di-imide decomposes at room temperature in two ways:

$$N_2H_2 \rightarrow N_2 + H_2$$

$$2\ N_2H_2 \rightarrow N_2H_4 + N_2$$

Formation of NH_3 was not observed but cannot be ruled out. The decomposition of the vapor is complicated by a sizeable and variable decomposition that occurs rapidly during the vaporization. The stoichiometry of this and the vapor-phase decomposition depends on total pressure and di-imide concentration. The kinetics of the decomposition of the vapor were studied from 22 to 200 °C by following the disappearance of N_2H_2 by absorption of light at 3450 Å, or the formation of N_2H_4 by absorption at 2400 Å, and by mass spectrometry. The kinetics are complex and can be either first- or second-order, or mixed, depending on surface conditions. The effect of olefin additives on the decomposition was studied, and is also complex.

Mechanisms for the decomposition are discussed, including the possible role of *trans-cis* isomerization. The relatively long lifetime found for di-imide in the gas phase suggests that it may be an important intermediate in many reactions of hydronitrogen systems.

La préparation de la di-imide par passage de vapeur d'hydrazine à travers une décharge microonde conduit à des mélanges de NH_3 contenant environ 15% de N_2H_2, calculés à partir du dégagement gazeux issu de la décomposition. Le comportement de ce mélange (fondant à −65 °C) lors du réchauffement de −196 à −30 °C laisse penser à une interaction forte entre les constituants. Les mesures de susceptibilité magnétique et les expériences de r.p.e. montrent que N_2H_2 n'est pas fortement paramagnétique ce qui, avec d'autres observations, indique un état fondamental singulet plutôt que triplet.

La di-imide avec NH_3 peut être efficacement volatilisée par un chauffage rapide et la vapeur possède une durée de vie longue (ce qui est surprenant) dont la période type est de plusieurs minutes à la température ambiante. Les spectres d'absorption de la vapeur dans le proche u.v. (3200–4400 Å) ont été photographiés et montrent des bandes bien définies quoique diffuses avec $\varepsilon_{max} = 6(\pm 3)$ à 3450 Å.

La di-imide se décompose à la température ambiante de deux façons

$$N_2H_2 \rightarrow N_2 + H_2$$

$$2\ N_2H_2 \rightarrow N_2H_4 + N_2$$

La formation de NH_3 n'a pas été observée mais n'a pas pu être écartée. La décomposition de la vapeur a été compliquée par une autre, notable et variable, qui se produit rapidement lors de la vaporisation. La stoechiométrie de cette dernière et la décomposition en phase vapeur dépendent de la pression totale et de la concentration en di-imide. Les cinétiques de décomposition de la vapeur ont été étudiées de 22 à 200 °C en suivant la disparition de N_2H_2 par absorption de la lumière à 3450 Å et par spectrométrie de masse. Les cinétiques sont complexes et peuvent être soit du premier ou du second ordre, ou un mélange des deux dépendant des conditions de la surface. L'effet de l'addition d'oléfines sur la décomposition a été étudié et est également complexe bien qu'une légère réduction ait été observée.

Les mécanismes de la décomposition ont été discutés incluant le rôle possible d'une isomération *cis-trans*. La durée de vie relativement longue trouvée pour la di-imide en phase gazeuse laisse penser à son importance en tant qu'intermédiaire dans les nombreuses réactions de systèmes hydroazotés.

[Traduit par le journal]

Can. J. Chem., **51**, 3605 (1973)

[1]NRCC 13352.

Can. J. Chem. Downloaded from www.nrcresearchpress.com by 210.87.254.42 on 09/05/12
For personal use only.

Can. J. Chem. Downloaded from www.nrcresearchpress.com by 210.87.254.42 on 09/05/12
For personal use only.

Introduction

Di-imide, HN=NH, the isoelectronic analog of ethylene and O_2, and the first member of the *azo* family of compounds, is of great interest to the chemist. It has generally been thought to be so unstable, however, as to have only a very fleeting existence at room temperature, and our knowledge of it is therefore limited. It appears to be a very active reducing agent in solution in which it can be generated *in situ* by a variety of methods (1), although it has never been detected or isolated in any of these systems. It has been produced and identified spectroscopically in low-temperature matrices (2, 3). It has also been produced and detected in the gas phase in several laboratories. Foner and Hudson (4), in 1958, were the first to detect and identify di-imide, using a mass spectrometer. Di-imide was produced by an electric discharge in hydrazine or hydrazoic acid vapor in a fast-flow system, and was detected downstream from the discharge. They also showed that it could be trapped at −196 °C and regenerated in the gas phase on warming. Blau *et al.* (3) obtained the infrared spectrum of the vapor in a similar system. Trombetti studied the absorption spectrum of the vapor in the ultraviolet and the infrared, using a similar flow system (5). These experiments and those of Foner and Hudson indicated a lifetime of at least a second or two for di-imide vapor at room temperature. There is one other brief report in a Ph.D. thesis by Mock at Harvard (6) which suggests a much longer lifetime. Mock generated di-imide vapor by a microwave discharge through hydrazine and by the thermal decomposition of anthracene di-imine, and observed an apparent half-life of a few *minutes* at low pressure in the inlet manifold of a mass spectrometer, with a measurable signal at $m/e = 30$ persisting for as long as 20 min. Lack of reproducibility and other uncertainties in these experiments led Mock to be understandably cautious in suggesting that di-imide might have a lifetime of this magnitude at room temperature.

With this background, the present work was undertaken to learn more about the chemistry of di-imide vapor, its lifetime, and its mode of decomposition. At an early stage of our experiments it became clear that di-imide was much more stable than generally suspected, and in fact has a lifetime in substantial agreement with Mock's observations. A brief preliminary account of some of this work has already been published (7).

Experimental and Results

Preparation of Di-imide

Di-imide was prepared by a method similar to those of Foner and Hudson (4), Trombetti, (5), and others, with some modifications. Because we appear to have been able to prepare di-imide in larger amounts and higher concentrations than before, this will be described in some detail.

Anhydrous hydrazine (purity >99%) obtained from Matheson, Coleman and Bell was thoroughly degassed by prolonged pumping with stirring. No attempt was made to dry the hydrazine further, although care was taken not to introduce moisture since water appears to catalyze the decomposition of di-imide. Vigorous stirring of the hydrazine, and a water bath around the reservoir held slightly below room temperature, served to maintain a smooth and adequate flow of vapor. A Teflon-and-glass needle valve controlled the flow rate and pressure of hydrazine vapor. Hydrazine vapor flowed through a quartz tube (13 mm o.d.) in which a microwave discharge was excited with an open-reflector antenna powered by a Raytheon 2450 MHz 100-watt therapy unit. The discharge was initiated by a Tesla coil at a fairly low pressure of hydrazine, giving a hot, intense blue–white discharge which yielded no di-imide. Hydrazine pressure was then increased to the point just before the discharge went out (~10 Torr), giving a blueish barely visible discharge with a yellowish core which generated optimum amounts of di-imide. The open-reflector antenna produced more di-imide than did a closed, tuned cavity with better coupling and a more intense discharge. A constriction in the quartz tube just below the discharge improved yields, probably by permitting a higher hydrazine pressure for a given flow rate. Although an apparently feeble, rather cool discharge gave the most di-imide, the yield was nevertheless roughly proportional to the power output of the microwave generator, which was usually set at 100%.

Hydrazine was condensed at −78 °C in a U-trap 30 cm below the discharge. This trap was short and wide to minimize blocking and to give rapid passage of gases. A second U-trap further downstream, made of 15 mm o.d. tubing, was cooled in liquid nitrogen, and di-imide con-

Can. J. Chem. Downloaded from www.nrcresearchpress.com by 210.87.254.42 on 09/05/12
For personal use only.

densed as a bright yellow solid in a ring starting about 5 mm above the surface of the coolant and extending for several cm. Ammonia condensed with the di-imide but was also spread out through the first arm of the U-trap. The intensity of the yellow color in the trap was a convenient indicator of the efficiency of di-imide production. Noncondensible gases, N_2 and H_2, were pumped away continuously. Operation of the discharge for 5 min typically produced an estimated 400 μmol of N_2H_2 and about 10 times as much NH_3 in the trap. Considerable amounts of N_2 and H_2 were formed, and about 90% of the original N_2H_4 was recovered in the first trap, so that the yield of N_2H_2 was less than 1% of the hydrazine passed through the discharge.

To transfer di-imide efficiently from the trap at −196 °C to the gas phase, it was found essential to vaporize it as rapidly as possible. This was done by quickly raising a beaker of warm water (60 to 70 °C) around the trap. Some decomposition always occurred during vaporization, but with this technique di-imide could be vaporized and immediately recondensed in another trap at −196 °C with less than 20% loss. Losses were greater with larger samples, probably because gases evolved hindered the distillation. Large samples were therefore prepared by distilling and collecting smaller batches; as much as 0.5 g of di-imide was collected in this way on several occasions. Attempts to remove some of the tenfold excess of ammonia by pumping as it warmed up, or other fractional distillation, met with limited success despite the apparent higher volatility of ammonia (see Fig. 1 and Table 1).

Finally, it is pleasant to report that in none of our experiments with di-imide in the solid, liquid, or vapor phase, at temperatures up to 200 °C, was there any sign of explosive behavior. The invariable presence of ammonia as a diluent may be a factor in this observation. Di-imide should undoubtedly be treated with some respect despite its apparent docility, as the decomposition to N_2 and H_2 must be highly exothermic (4).

Properties of Solid and Liquid Mixtures of Di-imide with Ammonia

The solid di-imide trapped with ammonia was stable indefinitely at −196 °C, and appeared unchanged on warming to temperatures of about −100 °C. On further warming a visible change occurred at about −81 °C, when the ring of di-imide appeared to wet the glass surface, became whitish-yellow in color, but remained solid, adhering to the walls of the tube. Nothing further happened until −65 °C, when the solid ring melted sharply and ran down to the bottom of the trap as a pale yellow liquid.

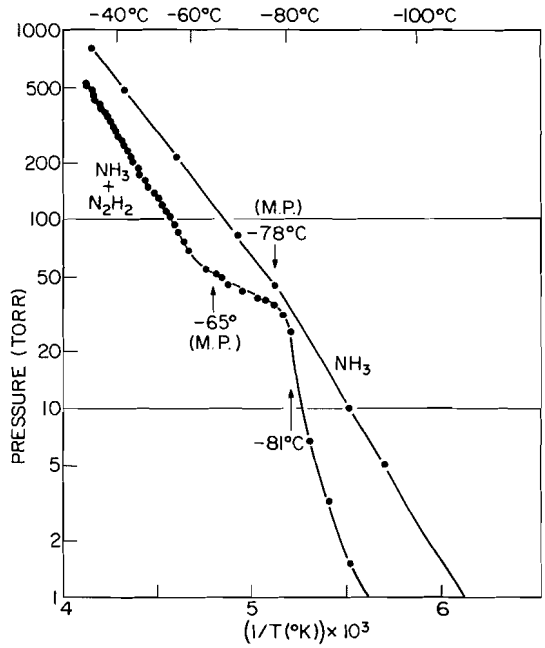

FIG. 1. Van't Hoff plot of ambient pressure over solid and liquid N_2H_2–NH_3 mixture during slow warming.

The behavior on warming was affected considerably by the ambient pressure. If the trap was open to the pumps or attached to a large evacuated volume, and the liquid nitrogen removed, the mixture at first sublimed away, and on melting bubbled vigorously and boiled away. Little or no di-imide could be recovered from the vapor produced from the liquid mixture, even though the latter retained its yellow color as it boiled away; the decomposition appears to occur somehow during the vaporization process itself. In several experiments the trap was immersed in cold liquid isopentane at about −100 °C, and the temperature raised steadily to −30 °C over a period of about 30 min. The volume available for evolved gases was about 200 cc and a manometer was attached. Figure 1 shows the pressure as a function of temperature in a Van't Hoff plot (log p *vs.* $1/T$ (°K)), and for comparison, the known vapor pressure of ammonia. Several points may be noted. No massive evolution of noncondensible gas (N_2 or H_2) accompanied the

TABLE 1. Yields of di-imide estimated from decomposition products*

Discharge time (min)	Remarks	Products (μmol) N_2	H_2	$N_2H_4+NH_3$	N_2H_2	N_2H_2 (%)	Reaction 1 (%)	H_2/N_2
3	One trap-to-trap distillation before vaporization	118	18	1529	218 (168)	13.2 (10.5)	8.3 (10.7)	0.16
3	Vaporized directly from U-trap	140	29	1483	251 (196)	15.5 (12.5)	11.5 (14.8)	0.21
1	Vaporized directly from U-trap	67	22	640	112 (90)	15.8 (13.1)	19.6 (24.4)	0.33
2	Vaporized directly from U-trap	114	29	1117	199 (157)	16.2 (13.2)	14.5 (18.5)	0.25
2	Sample pumped on for 40 s after removing liquid N_2, before vaporizing	71	31	696	111 (91)	14.6 (12.2)	29.0 (34.1)	0.44
10	N_2H_2–NH_3 solid sample, scraped from walls of trap as in magnetic susceptibility experiment.	200	45	1257	355 (278)	24.4 (20.1)	12.7 (16.2)	0.22

*Numbers in columns 6, 7, and 8 not in parentheses are based on the assumption that reaction 3 does not occur; numbers in parentheses are based on the alternate extreme assumption that reaction 2 does not occur. Column 7 shows di-imide yield as a percentage of the total condensable gas (N_2H_2, NH_3 + N_2H_4) present in the trap prior to vaporization.

warming; the pressure was always less than the vapor pressure of ammonia. The solid mixture underwent the changes at −81 and −65 °C described above with no sharp changes in pressure. At temperatures above −65 °C, the liquid was bubbling gently and was probably close to its boiling point from −65 to −30 °C. The heating rate was slow enough that self-cooling of the liquid by evaporation should have been minimal, so that the pressure measured in this region was probably close to the saturation vapor pressure of the NH_3–N_2H_2 mixture. The fact that this was always much less than that of ammonia means both that N_2H_2 is much less volatile and depresses the vapor pressure of the mixture, and that the two compounds interact strongly to form a very nonideal binary mixture. Recent infrared spectra (8) of N_2H_2–NH_3 mixtures in a low-temperature matrix gave evidence for strong hydrogen-bonding, approaching compound formation, on warming from −261 to −240 °C, lending support to our present conclusions.

The physical transitions at −81 and −65 °C are of interest. Pure NH_3 melts at −78 °C, and the first transition might correlate with this melting point, depressed by the N_2H_2 present. Actual melting does not occur, however, and the observed behavior suggests instead formation of a solid solution of NH_3 and N_2H_2 at this point. The ambient pressure falls away from that of pure NH_3 between −81 and −65 °C, perhaps due to a changing composition of the solid solution, while the sharp and invariant melting point at −65 °C suggests a eutectic point. The linear Van't Hoff plot above −65 °C indicates formation of something like an azeotrope at these temperatures.

The slow warming experiment was repeated but with an atmosphere of nitrogen added at the beginning so that no boiling occurred; excess gases evolved were allowed to vent through the manometer. The same transitions occurred at −81 and −65 °C, and there was no visible evolution of gas from the liquid at temperatures up to −25 °C. The latter observation and the persistence of the yellow color suggest that di-imide in ammonia solution is fairly stable in this temperature range.

Magnetic Properties of Di-imide

Trombetti has suggested that the ground state of di-imide is a triplet, ^3B_g, analogous to the $^3\Sigma_g^-$ state of O_2. If this is true, di-imide should, like O_2, be strongly paramagnetic. We therefore examined samples of di-imide, mixed with ammonia as usual, in the solid, liquid, and vapor phases in a Varian E-12 e.p.r. spectrometer.[2] No absorption was observed in any of the samples.

[2]We are grateful to Drs. K. F. Preston and J. R. Morton for their cooperation in these experiments.

Can. J. Chem. Downloaded from www.nrcresearchpress.com by 210.87.254.42 on 09/05/12
For personal use only.

Can. J. Chem. Downloaded from www.nrcresearchpress.com by 210.87.254.42 on 09/05/12
For personal use only.

The solid sample was held at −150 °C and the liquid at −60 °C. The vapor was studied at room temperature in a flow system with a total pressure of several Torr and an estimated partial pressure of N_2H_2 of at least 50 mTorr. A few mTorr of O_2 gave a large signal under similar conditions.

Because a negative result in a spin resonance experiment is perhaps not conclusive, measurements of the magnetic susceptibility of di-imide were undertaken, using a Gouy balance.[3] Two samples were prepared, one by distillation of about 25 mg of the N_2H_2–NH_3 mixture from the U-trap and condensation at −196 °C in the 3 mm o.d. Pyrex tube used in the susceptibility measurements. The other sample (about 60 mg) was prepared by sealing the sample tube to the bottom of the U-tube and scraping the N_2H_2–NH_3 solid from the walls with a magnet sealed in glass, so that it fell into the sample tube as a flaky powder. After filling, both sample tubes were sealed under vacuum and stored at −196 °C. Magnetic susceptibility measurements were made with the samples cooled in liquid oxygen in a special Dewar flask.

Both samples showed a very slight paramagnetism after correction for the diamagnetism of the ammonia and the Pyrex tube. Di-imide content was estimated from the gases evolved on decomposition of samples prepared in a similar way (see below). The slight paramagnetism observed was about 1% of that expected if di-imide had the same magnetic susceptibility as O_2. The source of this weak paramagnetism is not known, and further experiments are planned, but it is clear that solid N_2H_2 at −184 °C is not strongly paramagnetic. This observation and the absence of an e.p.r. absorption appear to weigh strongly against a triplet ground state.

The Absorption Spectrum of Di-imide in the Near-u.v.

In addition to the i.r. and vacuum-u.v. spectra which he studied extensively, Trombetti (5) also reported a very weak, apparently continuous absorption centered around 3500 Å which showed no structure except a slight indication of banding with N_2D_2. We have confirmed the existence of this absorption, and have been able to examine it in much more detail, probably because we attained much higher pressures of di-imide than Trombetti. The spectrum was photographed using a Hilger medium-dispersion quartz spectrograph.[4] A large sample of N_2H_2 and NH_3 was rapidly vaporized into a 7-liter cell, 2 m long, to give a total pressure close to atmospheric and an estimated partial pressure of N_2H_2 of perhaps 50 Torr. Multiple-reflection mirrors gave a light path of 72 m. A strongly banded spectrum was obtained which decayed over a period of a few minutes. Figure 2 shows a densitometer trace from the spectroscopic plate, together with the absorption spectrum of azomethane (9) for comparison. A detailed analysis of the N_2H_2 spectrum will be published elsewhere (10). Spectra taken at higher resolution showed no rotational structure, presumably indicating strong pre-dissociation of the upper state. The absorption by N_2H_2 at 3450 Å proved to be a very convenient way to monitor its concentration during decomposition (see below).

The Electronic Structure of Di-imide in the Ground-state

Di-imide in a sense lies midway between its isoelectronic analogs, O_2 and C_2H_4, so that one might expect either a triplet ground-state, like O_2, or a singlet like C_2H_4. Another isoelectronic species, HNO, which might be regarded as a

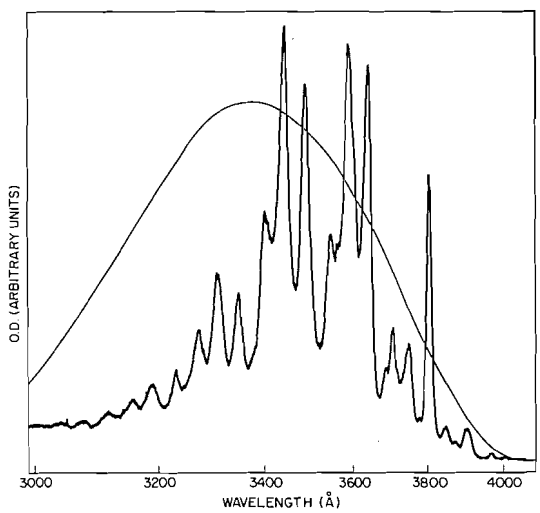

FIG. 2. Densitometer trace from spectrographic plate showing the banded near-u.v. absorption spectrum of N_2H_2 vapor. Also shown is the absorption spectrum of azomethane (8).

[3]We are grateful to Dr. A. D. Westland of the University of Ottawa for performing the magnetic susceptibility measurements.

[4]We wish to thank Dr. D. A. Ramsay, W. Goetz, M. Barnett, and F. Alberti of these Laboratories for their cooperation in these and later spectroscopic experiments.

Can. J. Chem. Downloaded from www.nrcresearchpress.com by 210.87.254.42 on 09/05/12
For personal use only.

"hybrid" of di-imide and O_2, very probably has a singlet ground-state (11). The nature of the ground-state of N_2H_2 has not yet been clearly established. There now appears to be, however, a substantial body of evidence, including some of our present observations, for a singlet rather than a triplet:

(*a*) Di-imide showed no appreciable paramagnetism in the gas phase at room temperature, in the liquid at -60 °C, or in the solid at -184 or -196 °C.

(*b*) All other known azo compounds (*i.e.*, substituted di-imides) have singlet ground-states. The near-u.v. spectra of di-imide and azomethane (Fig. 2) are strikingly similar, if one ignores the vibrational structure in the former. Furthermore, we can estimate a decadic extinction coefficient for di-imide at the maximum (3450 Å) of $6(\pm 3)$ (cm $M)^{-1}$, close to the value of 4.7 at 3380 Å for azomethane (9). All other known azo compounds have singlet ground-states, and the near-u.v. absorption is generally agreed to arise from an $n \rightarrow \pi^*$ transition. If di-imide had a triplet ground-state, the near-u.v. transition would be quite different from that of the azoalkanes, and it would seem highly fortuitous that the spectra should be so similar in respect to both λ_{max} and ε_{max}.

(*c*) If the ground-state of N_2H_2 were a triplet, one might expect a weak triplet–singlet absorption analogous to the $^1\Sigma_g^+ \leftarrow {}^3\Sigma_g^-$ observed in O_2 near 7650 Å. A careful search was conducted for absorption in N_2H_2 between 4500 and 9100 Å, using a 21 ft Eagle spectrograph and path lengths of 80 m, without success. It should be noted that no such absorption at wavelengths longer than that of the near-u.v. $n \rightarrow \pi^*$ transition appears to have been reported for any other azo compound.

(*d*) A molecular orbital calculation of the energies of the electronic states of *trans*-di-imide predicts a singlet ground-state, with the lowest triplet, formed by an $n_+ \rightarrow \pi^*$ transition, lying some 2.8 eV higher (12). It also suggests that the first excited singlet, also an $n_+ \rightarrow \pi^*$ state, is responsible for the near-u.v. absorption, and predicts an energy of 3.92 eV above the ground-state, corresponding to a wavelength of 3160 Å. The treatment also predicts several excited singlet states of about the right energy to account for the strong absorption in the vacuum-u.v.

(*e*) Very recent measurements of the i.r. spectrum of di-imide vapor (13) show an intensity alternation which appears to be unambiguous evidence for a singlet ground-state.

The only evidence for a triplet ground-state is the rotational structure observed by Trombetti (5) in the vacuum-u.v. absorption spectrum, in particular an intensity alternation with the even lines stronger than the odd. This was interpreted as evidence for a ground-state of B_u or B_g electronic symmetry, and from the correlation rules it was concluded that it must be ^3B_g, analogous to the $^3\Sigma_g^-$ ground-state of O_2. There is no obvious alternative to this interpretation. Trombetti's spectrum was obtained using a flow system in which the di-imide passed through the absorption cell within several seconds of its formation in a discharge. This raised the possibility that the spectrum observed was not that of ground-state N_2H_2, but of a short-lived excited triplet state. We have therefore photographed the vacuum-u.v. spectrum again under similar flow conditions; the flow was then stopped, isolating di-imide in the absorption cell, and spectra were taken at intervals as the di-imide decayed. All spectra obtained were essentially identical to Trombetti's, and decayed slowly over a period of several minutes. The intensity alternation in the rotational structure was confirmed, clearer than before because the spectroscopic light source was more uniform, and there seems no doubt that the spectrum observed in the vacuum-u.v. belongs to the same species of di-imide that we have been studying in the present work.

All things considered, the evidence at the present time strongly suggests that di-imide has a singlet ground-state. It is not clear, however, how the vacuum-u.v. spectrum can be reconciled with this conclusion, and until this conflict has been resolved some doubt must remain.

The Decomposition of Di-imide; Products and Stoichiometry

When di-imide decomposes at room temperature, the only products we have observed are N_2, H_2, and N_2H_4. Ammonia may also be produced (see below) but we have no positive evidence for its formation. The only other hydronitrogen compound known to be stable at room temperature is HN_3, which does not appear to be formed. The decomposition may thus be described, formally at least, as the sum of three reactions

[1] $$N_2H_2 \rightarrow N_2 + H_2$$

[2] $$\rightarrow \tfrac{1}{2}(N_2 + N_2H_4)$$

[3] $\rightarrow \frac{2}{3}(N_2 + NH_3)$

In our initial experiments, measurements of the N_2 and H_2 formed in the decomposition was used to assay the amount of di-imide present. The extent of reaction 1 is measured simply by the yield of H_2. Analysis of N_2 and H_2 alone cannot distinguish between reactions 2 and 3. The total di-imide decomposed, however, must lie between $H_2 + 1.5(N_2 - H_2)$ and $H_2 + 2(N_2 - H_2)$, the two limits corresponding to the absence of reactions 2 and 3, respectively. Table 1 shows estimates of the di-imide content of a variety of samples estimated in this way. In each case the sample was isolated in a trap at -196 °C, thoroughly pumped to remove all volatile gases, vaporized into a suitable closed volume by warming, and the di-imide allowed to decompose at room temperature for 20 min, essentially to complete decomposition. N_2 and H_2 were removed through traps at -196 °C by a Toepler pump, measured in a gas burette, and analyzed with a hot Pd thimble. Ammonia present in the traps, together with hydrazine, was vaporized and measured as a gas.

In the first estimate of the rate of decomposition, N_2H_2 was rapidly vaporized, rapidly recondensed at -196 °C after a variable time interval, and the noncondensible gases removed for analysis. The remaining N_2H_2 was then allowed to decompose completely, and the gases measured. Di-imide decomposed and di-imide remaining for each decay time was estimated as before from the measurement of N_2 and H_2. These experiments showed that N_2H_2 vapor decayed with half-life of several minutes. It was also found that even when the di-imide was recondensed within 2 or 3 s of vaporization, a sizeable and variable amount decomposed, never less than about 20%, apparently during the vaporization process itself. It also appeared that the stoichiometry of this decomposition was different from that of the subsequent slow decomposition of the vapor, with relatively more H_2 produced in the latter. To distinguish between the two processes, a sample-splitting technique was required because the decomposition during vaporization was not reproducible. A sample of di-imide was rapidly vaporized simultaneously into two nearly identical 100 ml Pyrex bulbs. Each bulb was then isolated, and in one the di-imide was allowed to decompose completely, while di-imide in the other was rapidly removed and condensed (within 1 or 2 s) at -196 °C. Product gases from the first bulb were those from both the vaporization process and the vapor-phase decomposition, while those from the second were from the vaporization process only. Data obtained in this way are shown in Table 2. The sizeable extent and the irregular variation of the fraction of the N_2H_2 decomposed during vaporization (column 6) may be noted. The ratio of products, H_2/N_2, was found to vary systematically with the amount of N_2H_2 decomposed, and in a different way for each of the two decomposition processes; this is shown in Fig. 3. For the slow decomposition of the vapor the ratio tends towards unity as the amount of N_2H_2 tends towards zero, and towards zero at high concentration of N_2H_2. The H_2/N_2 ratio for the decomposition during vaporization is partially complementary, approaching zero at low N_2H_2 concentrations and levelling out at about 0.31 at high.

Estimation of the relative importance of reactions 2 and 3 proved difficult. Colorimetric determination of N_2H_4 (14) produced in the overall decomposition of N_2H_2 always gave values considerably in excess of $N_2 - H_2$, an impossible result, probably because of extra N_2H_4 coming from stopcock grease and glass surfaces. A direct spectrophotometric measurement of N_2H_4 in the gas phase seemed more promising. The absorption spectrum of hydrazine vapor above 2000 Å was measured[5] and is shown in Fig. 4 together with that of NH_3 (15). Figure 5 shows partial pressure of N_2H_4 measured by light absorption at 2400 Å (where absorption by ammonia was completely negligible) following rapid vaporization of N_2H_2 (with NH_3) from the U-trap into a 10 cm cylindrical quartz cell mounted in a Heath single-beam spectrophotometer. The figure shows clearly the

[5]The only previous information about the absorption spectrum in this region appears to be in the brief accounts by Imanishi in 1931 and Hilgendorff in 1935 (16). Imanishi reported bands with maxima at 2326, 2320, 2276, 2250, and 2225 Å, followed by a continuum below 2200 Å. The only bands we observed, either in the spectrophotometer or in a photographic spectrum taken with a medium-dispersion Hilger spectrograph, correlated with those of NH_3, an impurity which is difficult to remove completely (these were subtracted from the spectrum shown in Fig. 4). It seems probable that Imanishi's bands had a similar origin, although the wavelengths reported seem to be about 100 Å units too high. Hilgendorff reported a highly structured spectrum, undoubtedly that of an impurity.

Can. J. Chem. Downloaded from www.nrcresearchpress.com by 210.87.254.42 on 09/05/12
For personal use only.

TABLE 2. Products of the decomposition of N_2H_2 during vaporization and after vaporization, using sample-splitting technique*

Total N_2H_2 decomposed (μmol)	Products of decomposition (μmol)				% decomposition during vaporization
	During vaporization		After vaporization		
	H_2	N_2	H_2	N_2	
1.67	0.031	0.26	0.80	0.99	29
4.40	0.080	0.89	2.20	2.45	39
8.71	0.22	1.44	3.77	4.91	30
11.0	0.54	2.20	3.89	5.53	35
15.9	0.57	4.38	5.17	6.46	51
22.7	1.47	4.59	6.35	10.67	34
30.4	3.06	9.10	4.21	9.74	50
41.3	3.11	11.40	6.06	13.82	48
43.4	3.23	11.13	6.63	15.50	44
56.1	6.98	21.95	4.54	11.86	66
60.2	7.47	23.90	4.89	12.40	67
69.9	5.74	16.47	7.13	24.90	39
78.5	7.60	23.85	5.41	21.92	51
111.8	10.09	31.80	14.12	36.20	48
179.2	16.95	56.70	2.41	42.60	54

*First and sixth columns are based on assumption that reaction 3 does not occur, *i.e.*, N_2H_2 decomposed $= H_2 + 2(N_2 - H_2)$.

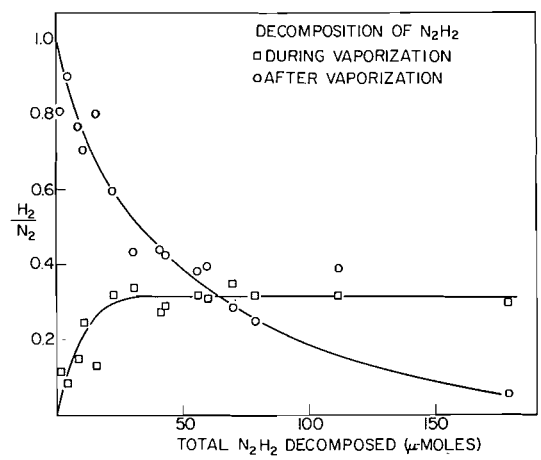

FIG. 3. Product ratios from the decomposition of N_2H_2, using sample-splitting technique.

N_2H_4 initially present, formed during the rapid vaporization, and then the slow increase, over a period of minutes, as the N_2H_2 decomposed. In a series of experiments, di-imide was vaporized into the spectrophotometer cell and isolated. Initial and final pressures of N_2H_4 were measured as in Fig. 5, and after complete decomposition of the N_2H_2, N_2 and H_2 were removed from the cell and measured. Results are shown in Table 3, with all quantities expressed as partial pressures in the reaction cell. Most notable is the large and irregular variation (from 17 to 71%) in the fraction of the total hydrazine present initially, illustrating again the irreproducible character of the decomposition during vaporization. Total product yields were more reproducible; Fig. 6 shows plots of H_2 and N_2H_4 ($\times 2$), which should be equal to the N_2H_2 consumed in reactions 1 and 2, respectively, against total N_2H_2 decomposed. Figure 7 shows a plot of total hydrazine *vs.* $N_2 - H_2$, which should have a slope of one (the straight line in the figure) if reactions 1 and 2 were the only sources of N_2. Yields of N_2H_4 fell well below $N_2 - H_2$ at the higher pressures, which might be attributed to the occurrence of reaction 3. An equally probable cause, however, is a partial fractionation of the sample during the vaporization from the U-trap, as the less-volatile N_2H_4 would tend to be left behind.

To avoid these problems, a sample-splitting technique was used as before to correct for the N_2 and H_2 formed during vaporization. This permitted comparison of yields of N_2 and H_2 from the vapor-phase decomposition alone with the corresponding yields of N_2H_4 built up during the di-imide decay. From such measurements, hydrazine yields were found, within

Can. J. Chem. Downloaded from www.nrcresearchpress.com by 210.87.254.42 on 09/05/12
For personal use only.

TABLE 3. Yields of hydrazine and noncondensible gases from the decomposition of di-imide

Total pressure (Torr)	Total N_2H_4 (Torr)	% of total N_2H_4 present initially	N_2 (Torr)	H_2 (Torr)	Total N_2H_2 decomposed* (Torr)
128	2.27	71	2.56	1.02	4.10
145	1.77	60	2.97	1.15	4.79
216	1.68	36	4.31	1.82	6.80
228	4.34	69	5.52	1.80	9.25
293	4.75	41	9.24	3.75	14.7
301	2.40	39	8.37	4.00	12.7
367	4.23	25	14.2	6.17	22.2
413	3.51	73	5.46	2.61	8.30
471	4.09	54	6.22	2.25	10.2
479	6.17	17	14.4	4.95	23.8
483	7.07	20	22.7	7.90	37.6
522	4.71	48	7.48	2.69	12.3
596	13.27	22	40.9	12.8	68.9
700	9.44	60	23.8	7.49	40.1

*Based on total N_2 and H_2 recovered from reaction vessel after complete decay, assuming $N_2H_2 = H_2 + 2(N_2 - H_2)$. This includes therefore N_2H_2 decomposed during vaporization, the products from which entered the reaction vessel, as well as N_2H_2 which actually entered the reaction vessel as such.

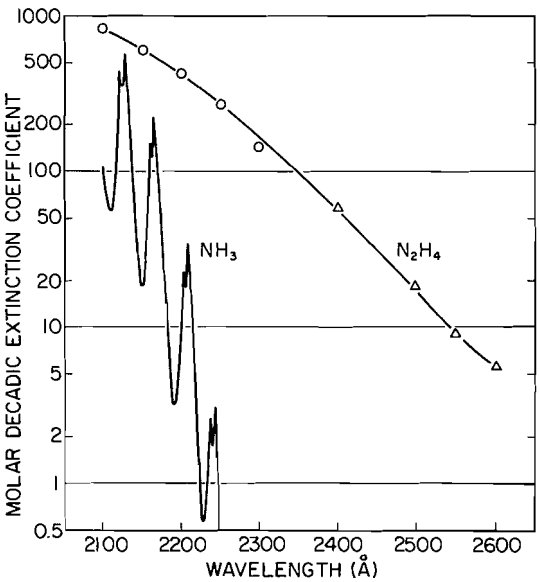

FIG. 4. Absorption spectra of hydrazine and ammonia. ○, single measurements with Cary spectrophotometer; △, from Beer's Law plots, each with several pressures, using Heath spectrophotometer. Spectrum of ammonia taken from Thompson *et al.* (13).

considerable scatter, to be somewhat in excess of the value of $N_2 - H_2$, suggesting that ammonia formation via reaction 3 was not important in the vapor-phase decomposition.

An attempt was also made to detect ammonia production during the decay of N_2H_2 by following the light absorption simultaneously at two wavelengths, 2192 and 2166 Å, the first at a minimum and the second at a maximum in the NH_3 spectrum (Fig. 4). The increase in optical density during the decay was found to be just proportional to the extinction coefficient of N_2H_4 at each wavelength, implying that only N_2H_4 was produced. The strong absorption by NH_3 initially present made this measurement rather insensitive, however, and permitted only

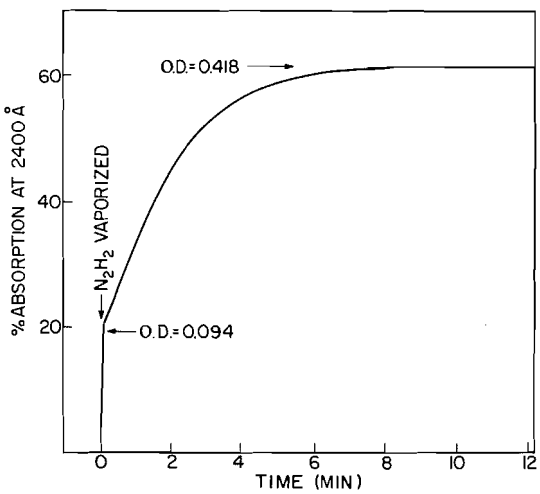

FIG. 5. Absorption at 2400 Å, due to N_2H_4 formed during the decomposition of N_2H_2.

Can. J. Chem. Downloaded from www.nrcresearchpress.com by 210.87.254.42 on 09/05/12
For personal use only.

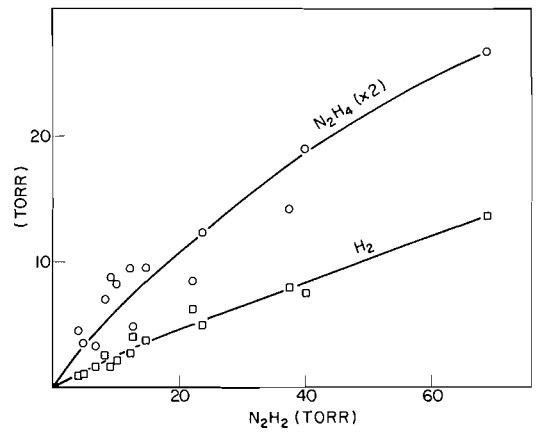

FIG. 6. Yields of H_2 and N_2H_4(× 2) from the decomposition of N_2H_2, corresponding to consumption of N_2H_2 in reactions 1 and 2, respectively.

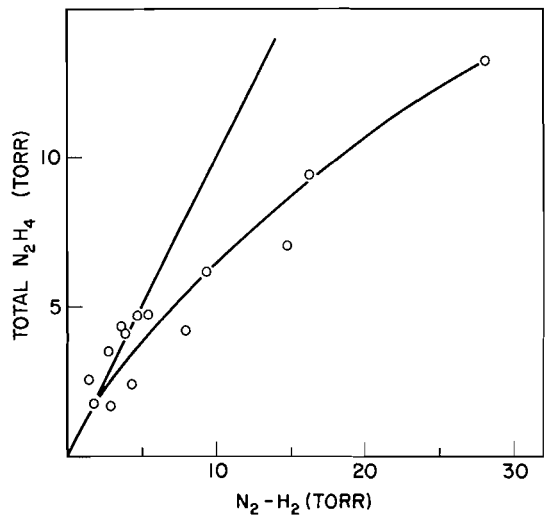

FIG. 7. Yield of N_2H_4 vs. (N_2 − H_2) from the decomposition of N_2H_2. The straight line corresponds to $N_2H_4 = N_2 - H_2$, the stoichiometry expected if reactions 1 and 2 were the only sources of N_2.

a rather large upper limit for reaction 3 of 50% of reaction 2.

To sum up, we have no positive evidence for the occurrence of reaction 3, but the large excess of NH_3 always present and the experimental scatter in the product analysis make it difficult to rule out completely.

The Kinetics of the Decomposition of Di-imide

The kinetics of the vapor-phase decomposition was studied directly by following the absorption of light at 3450 Å in the spectrophotometer cell. A typical decay curve is shown in Fig. 8, and a first-order plot of the same data in Fig. 9. The decay was also followed by observing the increase in N_2H_4 with time by monitoring the absorption at 2400 Å, as in Fig. 5. Essentially identical data were obtained from the disappearance of N_2H_2 and the formation of N_2H_4, indicating a roughly constant stoichiometry throughout the course of the decomposition.

The rate of decomposition appeared to depend on the condition of the surface of the reaction cell. Exposure to air or water vapor always ap-

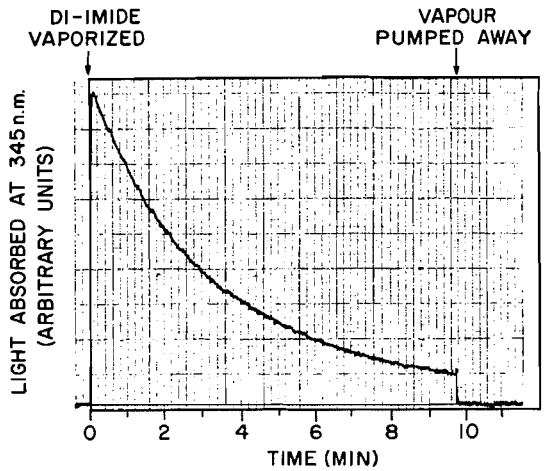

FIG. 8. Disappearance of N_2H_2 in the vapor phase, followed by light absorption at 3450 Å.

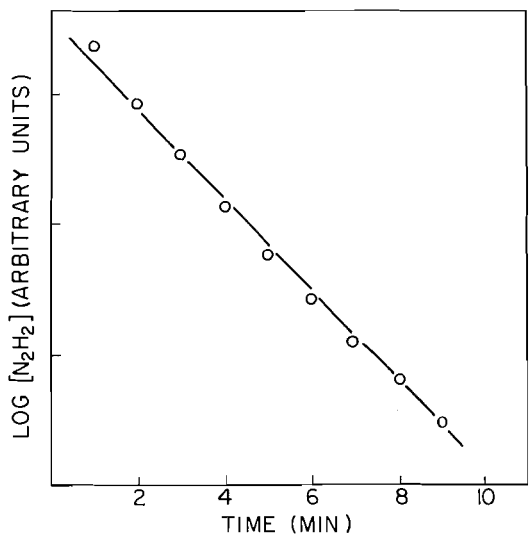

FIG. 9. First-order plot of data from Fig. 8.

Can. J. Chem. Downloaded from www.nrcresearchpress.com by 210.87.254.42 on 09/05/12
For personal use only.

Can. J. Chem. Downloaded from www.nrcresearchpress.com by 210.87.254.42 on 09/05/12
For personal use only.

preciably increased the rate of decomposition, which subsequently returned to its normal value after prolonged pumping (overnight or longer). The cell was given no special surface treatment, and after prolonged pumping and exposure a few times to the N_2H_2–NH_3 mixture and its decomposition products, the rate of decomposition became reproducible to about $\pm 10\%$. A dozen experiments, done intermittently over a period of weeks under roughly similar conditions, gave a first-order rate constant of 3.8 (± 0.5) $\times$ 10^{-3} s^{-1} for the disappearance of di-imide at 22 °C. In another series of experiments the rate of decomposition was measured with varying amounts of di-imide, corresponding roughly to the conditions of the stoichiometric measurements in Fig. 3. The first-order rate constant showed a steady decrease with increasing amounts of N_2H_2, approximately parallel to the decrease in H_2/N_2 from the gas-phase reaction. The cell used in these and most of the other experiments was a quartz cell with Suprasil windows, obtained from Hellma (Canada) Ltd. In a similar cell, 20 cm long, made in our glass shop from commercial quartz tubing and Suprasil windows, rates of decomposition were 2 or 3 times faster, and none of a variety of treatments of the surface had much effect. The decay in a Pyrex vessel was also appreciably faster than in the Hellma cell, which appears to have a surface which is relatively inactive in promoting decomposition of di-imide.

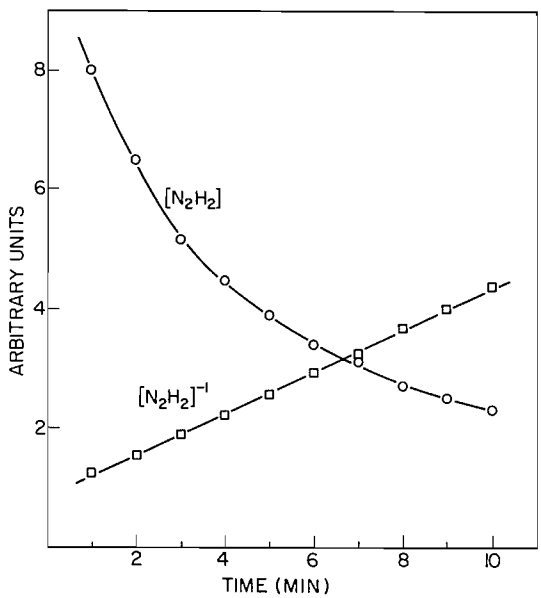

FIG. 10. Plots showing second-order disappearance of N_2H_2 vapor in cell conditioned by butadiene; followed by light absorption at 3450 Å.

A more striking surface effect was observed following some experiments in which the Hellma cell was exposed to butadiene at 200 °C. Subsequently, for several days afterwards, the decomposition of di-imide was markedly slower and showed second-order kinetics. Decay data at 33 °C in the butadiene-conditioned cell are shown in Fig. 10. At higher temperatures, mixed first-and-second-order kinetics were observed, tending towards first-order at longer times. The initial second-order rate constant increased with increasing temperature between 30 and 200 °C, corresponding roughly to an activation energy of about 20 kcal/mol. The half-life at 200 °C, the highest temperature studied, was about 14 s. Over a period of days, with pumping, the cell slowly reverted to its former behavior and di-imide decomposed at about its former rate, generally with simple first-order kinetics. In some experiments an upward curvature was evident in the first-order plot, usually at the beginning of the decay, and examination of earlier data showed that this had occurred in some cases prior to the conditioning by butadiene (Fig. 9, for example, shows distinct curvature). It may be concluded from these experiments that there are (at least) two modes of decomposition of di-imide in the vapor-phase; that the first-order decay in the "normal" cell is surface dependent and was inhibited by conditioning with butadiene at 200 °C, and that the slower, second-order reaction only became evident when the first-order process was inhibited or the N_2H_2 concentration was high.

The decomposition of N_2H_2 was also studied briefly by mass spectrometry.[6] Di-imide (with the usual ammonia) was rapidly vaporized into a tubular Pyrex vessel of about 0.8 l volume to give a total pressure not exceeding a few Torr. A pinhole in a metal disc at one end led to the ionization chamber of an EAI Quad 250A mass spectrometer. Mass spectra were recorded at 10- or 30-s intervals. Signals at m/e = 1, 2, 28, 31, and 32 increased, confirming that H_2, N_2, and N_2H_4 were products of the decomposition, while those at 30 and 29, from N_2H_2, decreased.

[6]Dr. M. R. Dunn collaborated in these experiments.

Can. J. Chem. Downloaded from www.nrcresearchpress.com by 210.87.254.42 on 09/05/12
For personal use only.

Both product formation and di-imide disappearance followed first-order kinetics with a half-life appreciably shorter than that observed in the quartz cell. The faster decay may reflect a more active surface or perhaps the relatively low total pressure and partial pressure of N_2H_2. Once again, the amount of NH_3 initially present was too large to observe with any accuracy whether or not this was a product of the decomposition.

The Effect of Added Gases on the Decomposition of N_2H_2

Figure 11 shows the effect of several added gases on the product ratio, H_2/N_2, for gas-phase decomposition of N_2H_2. The additive was in each case condensed at -196 °C with a roughly constant amount of N_2H_2 and NH_3, and the mixture rapidly vaporized together. Sample splitting was used as before to correct for decomposition during vaporization.

All the additives caused a reduction in the H_2/N_2 ratio. Total product yields were somewhat enhanced, probably because more N_2H_2 was swept into the reaction vessels from the U-trap by the vaporization of the additive. The effect of NH_3 on the H_2/N_2 ratio is significant because NH_3 was present in all our experiments with di-imide. This raises the possibility that the effective variable in Table 2 and Fig. 3 is the pressure of NH_3 rather than the amount of N_2H_2, since the two were roughly proportional. It appears however that the reduction in H_2/N_2 in the experiments shown in Fig. 3, in which the highest pressure of NH_3 was less than 760 Torr, is too large to be explained entirely in this way, although it may be an important factor.

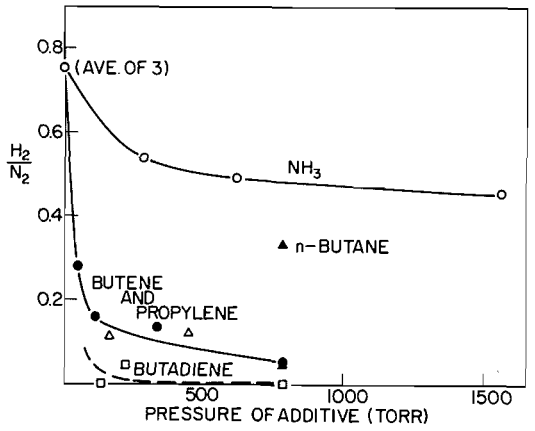

FIG. 11. Effect of additives on the H_2/N_2 ratio from the decomposition of N_2H_2 in the vapor phase.

While *n*-butane was somewhat more effective than NH_3 in reducing the H_2/N_2 ratio, the olefins were very much more effective (Fig. 11). This suggests a reaction of the latter with di-imide, so their effect on the rate of disappearance of di-imide was examined. This was complicated by the surface effects noted earlier, but by alternating experiments with and without olefin present, it was possible to conclude that pressures up to 500 Torr of propylene and *cis*-butene-2 had virtually no effect on the rate of decay, but that butadiene definitely enhanced the rate, perhaps by a factor of 2 with 500 Torr at 33 °C. Pressure of NH_3 in these experiments was typically about 200 Torr. Analysis by gas chromatography showed that butene-1 was formed in the reaction with butadiene, but the amounts were small, less than 5% of the N_2H_2 decomposed. The effect of olefins, and particularly of butadiene, on the decomposition of N_2H_2 thus presents some curious contradictions; a strong suppression of H_2 formation in the gas-phase decomposition (Fig. 11), a much lesser effect on the rate of di-imide disappearance, and relatively little formation of reduction products.

Several other gases were tested for their effect on the rate of disappearance of N_2H_2. Propane, *n*-butane, and nitrogen had no effect at pressures close to atmospheric. Oxygen increased the rate to about the same extent as butadiene.

The Mechanism of the Decomposition of Di-imide

The present study has shown that the decomposition is surprisingly complex, both kinetically and stoichiometrically. The decomposition during vaporization seems most unusual. This is a rapid process, complete in no more than 1 or 2 s. It yields predominately $N_2H_2 + N_2$, but with H_2 becoming important with increasing amount of N_2H_2 (Fig. 3). It does not involve unstable species from the discharge trapped at -196 °C, because it still occurs after one or more trap-to-trap distillations, each new vaporization causing new decomposition. The major part of this decomposition is perhaps most simply explained by a bimolecular reaction

$$[4] \qquad 2\,N_2H_2 \rightarrow N_2 + N_2H_4$$

essentially the same as that occurring more

Can. J. Chem. Downloaded from www.nrcresearchpress.com by 210.87.254.42 on 09/05/12
For personal use only.

slowly in the vapor phase, but greatly enhanced by the much higher concentrations present in the transient liquid phase formed during the rapid vaporization of the NH_3–N_2H_2 mixture. Formation of H_2 and the increase in the H_2/N_2 ratio with increasing sample size is less easily explained.

There appears to be good evidence for at least two concurrent processes in the decomposition of the vapor. It is reasonable to suggest that reaction 1, occurring largely as a surface reaction, can account for the high value of the H_2/N_2 ratio, approaching unity, at low sample size (Fig. 3); a gas-phase component of this reaction cannot be ruled out. The decrease in H_2/N_2 evident in Figs. 3 and 11 can be explained by reaction 4, occurring as a second-order gas-phase reaction which becomes more important as N_2H_2 concentration increases or reaction 1 is suppressed. The kinetic studies, however, showed that disappearance of N_2H_2 could still be purely first-order under conditions where H_2/N_2 was much less than unity and production of N_2 and N_2H_4 must have been important, which requires that reaction 4 proceed in part by first-order kinetics. One interesting possibility, tentatively suggested by Mock (6) and others, is that the rate-controlling step could be the *trans–cis* isomerization of N_2H_2, followed by rapid disappearance of *cis*-N_2H_2 via reaction 4 or reaction 1. *cis*-Di-imide has been observed only in the low-temperature matrix-photolysis of HN_3 in which it was presumably formed by reactions of NH radicals (2). It seems fairly well established that only the *trans* form is present in the vapor phase at room temperature and can be trapped downstream from a discharge in hydrazine vapor (5). This suggests that the *cis* isomer is unstable, and certainly *cis* conformation would seem to be required for reactions 1 and 4. Two theoretical treatments of the *cis–trans* isomerism are inconclusive; one indicated that the *cis* isomer is about 8 kcal/mol more stable (thermodynamically) than the *trans*, with a low activation energy (~12 kcal) for isomerization (17), while the other predicted just the reverse, the *trans* form more stable and a sizeable barrier (~40 kcal) for isomerization (18). *cis*-Di-imide might also be invoked in explaining the decomposition during vaporization. Formation of a certain fraction of *cis* isomer in the liquid phase, followed by rapid decomposition via reactions 1 and 4, could account for some of the unusual features.

In the present discussion of mechanisms, molecular rather than free-radical reactions have been suggested. Plausible free-radical chains can certainly be written, but the low activation energy, the sizeable reaction rate at room temperature, and the lack of inhibition by olefins make these appear rather unlikely. Reactions forming ammonia have also not been discussed because we have no positive evidence for its formation.

Di-imide as an Intermediate in Other systems

Di-imide has been postulated as a transient intermediate in a variety of gas-phase reactions. These include the combination of NH radicals (19, 20), the reaction of NH with HNCO (21) and with HN_3 (22), and in the photolysis (23), pyrolysis (24), and glow discharge decomposition (25) of N_2H_4. It has been detected as an intermediate in the decomposition flame of N_2H_4 (26), and in the reaction of O with N_2H_4 (27). In most of these systems di-imide has been regarded as a very short-lived transient that rapidly decomposed, usually to give simply $N_2 + H_2$. The relatively long lifetime observed in the present study suggests that di-imide could play a much more complex role in the chemistry of these and other hydronitrogen reaction systems. It might well be a major primary product in processes such as photolysis, pyrolysis, or radiolysis, disappearing by a variety of rapid secondary reactions. The mechanisms of such hydronitrogen systems have remained surprisingly obscure and intractable (the precise mode of formation of N_2 in the photolysis of NH_3, for example, is not known) and the possible participation of di-imide as a reactive intermediate in some of these systems should be considered.

Di-imide of course has also been postulated as a transient reactive intermediate in aqueous and other solutions in which it is generated *in situ* (1). There seems little doubt that the active reducing agent in these systems is in fact di-imide, although its behavior (rapid and efficient reduction of olefins, or in their absence "self reduction" (reaction 4), with little or no decomposition to N_2 and H_2 (reaction 1)) seems markedly

Can. J. Chem. Downloaded from www.nrcresearchpress.com by 210.87.254.42 on 09/05/12
For personal use only.

different than that of di-imide in the present study. The difference presumably must be attributed to solvation effects which greatly enhance the rates of the reduction reactions of di-imide. This might involve facilitation of the *trans–cis* isomerization, or preferential formation of the *cis* isomer, since the reduction reactions would seem to require a *cis* configuration. The decomposition of di-imide during vaporization observed in the present work is not unlike the self reduction seen in solution, both in its rapidity and in the preferential decomposition to N_2H_4 and N_2. This tends to support the suggestion that it occurs in a transient liquid ammonia solution formed during the vaporization process, although the apparent stability of di-imide–ammonia mixtures at temperatures up to $-30\,^{\circ}C$ implies a sizeable activation energy if the reaction is to be rapid at the only moderately higher temperatures possible in the vaporizing liquid.

Summary and Conclusions

The present paper describes an investigation of some of the chemistry of "free" di-imide ("free" rather than prepared *in situ* in a reactive medium). The chemistry is obviously complex; more questions have been raised than answered, and much more work is required. Our chief findings may be summarized:

(*1*) It has been established that di-imide is much more stable than was generally supposed, having a lifetime of minutes at room temperature.

(*2*) Preparation, techniques of handling, and analysis of di-imide have been studied and described. Some physical properties of di-imide and di-imide–ammonia mixtures have been measured. Measurements of magnetic susceptibility and e.s.r. experiments showed that di-imide is apparently not strongly paramagnetic.

(*3*) The near-u.v. absorption spectrum of the vapor was measured, and except for a strongly banded structure, was found to be closely similar both in λ_{max} and ε_{max} to that of azomethane and other alkyl azo compounds. This, and the lack of paramagnetism suggest that the ground-state of di-imide is a singlet rather than a triplet.

(*4*) The decomposition of di-imide vapor is complicated by a rapid and sizeable decomposition during vaporization as well as the relatively slow decomposition in the vapor phase. Products of the decomposition are N_2, H_2, N_2H_4, and possibly NH_3. Stoichiometry of the two modes of decomposition was different and was affected by sample size, total pressure and presence of added gases.

(*5*) Kinetics of the decomposition of the vapor was studied spectrophotometrically by following the decrease in light absorption by N_2H_2 at 3450 Å, or the increase in absorption by N_2H_4 at 2400 Å. Kinetics were usually approximately first-order, but the decomposition showed a strong surface dependence, and became second-order in a cell conditioned with butadiene. The kinetics are obviously complex, with at least two concurrent processes involved, a decomposition to $N_2 + H_2$, and a bimolecular reaction yielding $N_2 + N_2H_4$, and with reactions occurring both in the gas phase and on the surface. Mechanisms have been tentatively suggested, and the possible role of *cis*-di-imide discussed.

1. C. E. Miller. J. Chem. Educ. **42**, 254 (1965); S. Hunig, H. R. Muller, and W. Thier. Angew. Chem. **77**, 368 (1965).
2. D. A. Dows, G. C. Pimentel, and E. Whittle. J. Chem. Phys. **23**, 1606 (1955); K. Rosengren and G. C. Pimentel. J. Chem. Phys. **43**, 507 (1965).
3. E. J. Blau, B. F. Hochheimer, and H. J. Unger, J. Chem. Phys. **34**, 1060 (1961); E. J. Blau and B. F. Hochheimer. J. Chem. Phys. **41**, 1174 (1964).
4. S. N. Foner and R. L. Hudson. J. Chem. Phys. **28**, 719 (1958).
5. A. Trombetti. Can. J. Phys. **46**, 1005 (1968); J. Chem. Soc. A, 1086 (1971).
6. W. L. Mock. Ph.D. Thesis. Harvard University. 1964.
7. C. Willis and R. A. Back. Nature, **241**, 43 (1973).
8. V. E. Bondybey and J. W. Nibler. J. Chem. Phys. **58**, 2125 (1973).
9. J. G. Calvert and J. N. Pitts. Photochemistry. Wiley, New York. 1966.
10. C. Willis, D. A. Ramsay, and R. A. Back. To be published.
11. G. Herzberg. Electronic spectra of polyatomic molecules. Van Nostrand, Princeton. 1966.
12. M. B. Robin, R. R. Hart, and N. A. Kuebler. J. Am. Chem. Soc. **89**, 1564 (1967).
13. M. Carlotti, J. W. C. Johns, and A. Trombetti. To be published.
14. G. W. Watt and J. D. Chrisp. Anal. Chem. **24**, 2006 (1952).
15. B. A. Thompson, P. Harteck, and R. R. Reeves, Jr. J. Geophys. Res. **68**, 6431 (1963).

16. S. IMANISHI. Nature, **127**, 782 (1931); Sci. Pap. Inst. Phys. Chem. Res. **15**, 166 (1931); H. J. HILGENDORFF. Z. Phys. **95**, 781 (1935).
17. J. ALSTER and L. A. BURNELLE. J. Am. Chem. Soc. **89**, 1261 (1967).
18. L. J. SCHAAD and H. B. KINSER. J. Phys. Chem. **73**, 1901 (1969).
19. R. A. BACK. J. Chem. Phys. **40**, 3493 (1964).
20. R. W. DIESEN. J. Chem. Phys. **39**, 2121 (1963).
21. W. D. WOOLLEY and R. A. BACK. Can. J. Chem. **46**, 295 (1968).
22. A. O. BECKMAN and R. G. DICKINSON. J. Am. Chem. Soc. **50**, 1870 (1928); **52**, 124 (1930); A. E. MYERS and A. O. BECKMAN. J. Am. Chem. Soc. **57**, 89 (1935).
23. L. J. STIEF and V. J. DECARLO. J. Chem. Phys. **46**, 592 (1967); **49**, 100 (1968); L. J. STIEF. J. Chem. Phys. **52**, 4841 (1970); U. SCHURATH and R. N. SCHINDLER. J. Phys. Chem. **74**, 3188 (1970).
24. L. J. STIEF and V. J. DECARLO. J. Phys. Chem. **71**, 2350 (1967).
25. E. F. LOGAN and J. M. MARCHELLO. J. Chem. Phys. **49**, 3929 (1968); **50**, 2724 (1969).
26. K. H. HOMANN, D. I. MACLEAN, and H. G. WAGNER. Naturwiss, **52**, 12 (1965).
27. S. N. FONER and R. L. HUDSON. J. Chem. Phys. **49**, 3724 (1969).

Can. J. Chem. Downloaded from www.nrcresearchpress.com by 210.87.254.42 on 09/05/12
For personal use only.

Scope and Limitations of a Cyclization Leading to Phenanthrene Derivatives

C. SCHMIDT[1] AND J. THAZHUTHAVEETIL
Department of Chemistry, University of Prince Edward Island, Charlottetown, Prince Edward Island

Received April 30, 1973

The scope and limitations of a modified Bogert–Cook cyclization was investigated. It was found that the sequence is applicable only for the unsubstituted and the meta-substituted series.

La généralité et les limitations d'une réaction de cyclisation de Bogert–Cook modifiée ont été examinées. Il a été trouvé que la séquence est applicable uniquement aux séries de composés non substitués ou substitués en mêta. [Traduit par le journal]

Can. J. Chem., **51**, 3620 (1973)

Can. J. Chem. Downloaded from www.nrcresearchpress.com by 210.87.254.42 on 09/05/12
For personal use only.

Recently we reported on a sequence (1) which could be regarded as a modification of the Bogert–Cook (2) reaction (**1** → **2** → **3**). For obvious reasons this reaction would be more useful if it could be extended to compounds in which the aromatic nuclei are carrying potential functional groups. The present paper gives a full account on the unsubstituted example and reports on all compounds carrying one methoxy group in the aromatic ring. It has been found that the sequence is applicable only to the meta-substituted and the unsubstituted series. Starting with the ortho- and para-substituted Nef adducts **7***a* and *b* led to no useful products.

Results and Discussion

The addition of the appropriately substituted sodium phenylacetylide to 2,6-dimethylcyclohexanone in liquid ammonia led to the acetylene alcohols **1***a* and **1***b* and **7***a* and **7***b*. Apparently only one stereoisomer was formed in these Nef reactions corroborated by the fact that **7***a* and *b* were obtained in crystalline form. Although *o*-methoxyphenylacetylene was previously prepared from benzofurane using a sealed tube (3, 4), we developed a more practical preparation starting with *o*-methoxyacetophenone. The so far neglected traditional method gives a 35% yield after purifying the product as the silver salt.

The Rupe rearrangment of acetylenic alcohols **1***a* and *b* gave unsaturated ketones **2***a* and *b*, respectively, in 60% yield. In both reactions a less polar unidentified polymer was also formed whose formation could not be avoided under various conditions.

Cyclization of unsaturated ketone **2***a* to the tricyclic product **3***a* was carried out in polyphosphoric acid in 90% yield. The appearance of a saturated carbonyl group (i.r. 1710 cm^{-1}) and a three-proton singlet at 8.93 τ corresponding to the angular methyl group are evidence for the tricyclic structure in **3***a*.

From **2***b* the cyclization in polyphosphoric acid led to a crystalline mixture of monoketone **3***b* and diketone **4***b*. The latter compound must have been formed as a result of atmospheric oxidation. Due to the experimental features of the reaction it was impossible to exclude oxygen completely. Since the two compounds could not be separated by re-crystallization or chromatography the entire sample was subjected to SeO_2 oxidation leading to the pure diketone **4***b* in 75% yield.

For diketone **4***b* there is an alternative structural possibility **6**; a similar structure is possible for the corresponding monoketone **3***b*. It is well known from the vast information concerning aromatic substitutions that the formation of a 1,2,3-vicinal trisubstituted isomer is disfavored in comparison to the 1,2,4-trisubstituted compound (5). Since only one isomer was formed in the cyclization, structure **4***b* rather than **6** is assigned to the diketone. This is corroborated by the 220 MHz n.m.r. of diketone **4***b*. The extracted coupling constants in the aromatic region, $J_{6,8}$ = 3.0 Hz, $J_{5,8}$ = 0.1 Hz, and $J_{5,6}$ = 8.8 Hz are in agreement with the accepted meta, para, and ortho values, respectively (6). Structure **6** would have been expected

[1]To whom correspondence should be addressed.

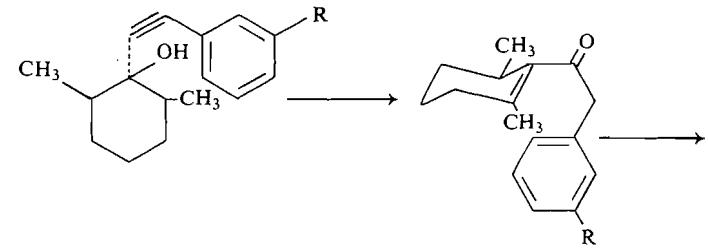

1 2

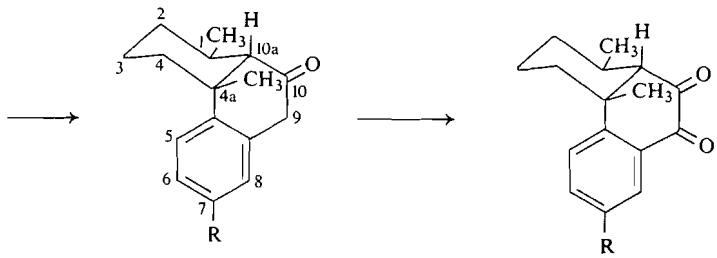

3 4

a R=H
b R=OCH$_3$

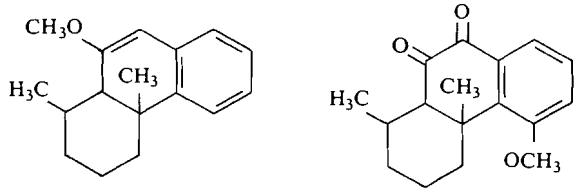

5 6

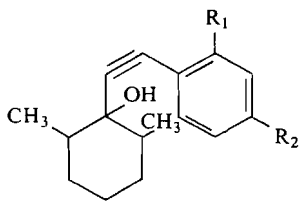

7

a R_1=OCH$_3$; R_2=H
b R_1=H; R_2=CH$_3$O

to have two coupling constants of 8 Hz and another of 3 Hz. The central hydrogen should have appeared as a triplet with two ortho couplings, contrary to the actual splitting pattern: τ 2.73 (m), 2.62 (d), and 2.40 (d).

When the *o*-methoxy substituted phenylacetylene alcohol **7***a* was refluxed with formic acid the product formed contained no carbonyl and its n.m.r. showed the absence of the methoxy group. Consequently it was not investigated any further. The para-substituted isomer **7***b* under the same conditions led to the formation of unidentified polymers only.

The stereochemistry of tricyclic ketone **3***a* was erroneously assigned in our previous publication as *trans* (1). This error should now be corrected.

Can. J. Chem. Downloaded from www.nrcresearchpress.com by 210.87.254.42 on 09/05/12
For personal use only.

Can. J. Chem. Downloaded from www.nrcresearchpress.com by 210.87.254.42 on 09/05/12
For personal use only.

In order to elucidate the stereochemistry of the ring juncture in **3***a* an attempt was made to isomerize it to the thermodynamically more stable product. The alkaline treatment of **3***a* led to complex changes. Refluxing in methyl alcohol containing hydrochloric acid led to the enol ether **5** and diketone **4***a*. In the absence of oxygen under the same conditions only enol ether **5** and monoketone **3***a* were recovered. The fact that enol ether **5** was also formed during the attempted isomerization indicates that enolization indeed took place thus providing suitable conditions for equilibration. This contention could be corroborated by demonstrating that deuterium was incorporated into ketone **3***a* at positions 9 and 10a when the same reaction was carried out in CH_3OD. Therefore, it can be concluded that the thermodynamically more stable isomer was formed during the cyclization, and the necessary conditions were provided for the isomerization.

It is now generally accepted that in angularly methylated hexahydrophenantrene systems the *cis* isomer is more stable than the corresponding *trans*-fused compound (7–9). Therefore, the ring junction in **3***a* is reassigned as *cis*. With SeO_2 the monoketone **3***a* was oxidized to diketone **4***a*. In the n.m.r. of the latter compound a clearly resolved one-proton doublet at $\tau = 7.45, J = 10$ Hz indicates a *trans*-diaxial relationship of the two hydrogens at C-1 and C-10*a*. Consequently, the 4-methyl group in **4***a* is assigned equatorial.

The same stereochemistry is assigned to diketone **4***b* since the angular methyl signal and the one-proton doublet assigned to H_{10a} deviated less than 0.04 p.p.m. in the two diketones. While in the Bogert–Cook reaction a *cis–trans* mixture is formed (8,9), in this cyclization only the *cis* isomer is formed. Naturally the possibility cannot be excluded that the *trans*-fused isomer was also formed in this reaction and then it subsequently isomerized to the thermodynamically more stable *cis*-isomer under the conditions of cyclization. The obtained stereochemical outcome can however be explained more coherently on mechanistic grounds. It is recognized that the unexceptional pathway of *trans*-diaxial addition of a proton and an aryl group on the $\Delta^{1,2}$ double bond of unsaturated ketone **2** should produce the stereochemistry of tricyclic ketone **3**.

Due to its predictable stereochemical outcome, the cyclization discussed here is now used in some synthetic studies in the field of diterpenes.

Experimental

All melting points were taken on a Fisher-Johns melting point apparatus and are uncorrected. The elemental analyses were carried out by Pascher Mikroanalytical Laboratorium, Bonn, West Germany, and Schwarzkopf Mikroanalytical Laboratory, Woodside, N.Y. The i.r. spectra were recorded on a Perkin-Elmer Model 137B infracord spectrophotometer. The u.v. spectrograms were taken on a Coleman-Hitachi Model 124 double-beam grating spectrophotometer. The n.m.r. spectra were recorded on a Varian Associates T60 spectrophotometer. The mass spectra were obtained with a Hitachi Perkin-Elmer Model RMS-4 spectrometer.

1-(Phenylethynyl)-2,6-dimethylcyclohexanol (1a)

To 100 ml of liquid ammonia containing 20 mg of ferric nitrate 240 mg of sodium was added in three portions. The flask was equipped with a magnetic stirrer and a drying tube containing soda lime. After the disappearance of the blue color 1.09 g of phenylacetylene dissolved in 5 ml of dry tetrahydrofuran was added. Stirring was continued for 30 min, then a solution of 1.19 g of 2,6-dimethyl-cyclohexanone in tetrahydrofuran (2 ml) was added in 10 min. The reaction mixture was stirred for 4 h then 2 g of ammonium chloride was added. After the evaporation of ammonia the product was dissolved in water and extracted with ether (4 × 35 ml). The combined ether extracts were washed in succession with saline, diluted sulfuric acid, and sodium bicarbonate solution. After drying ($MgSO_4$) and evaporation 2.0 g (92%) of oily product was obtained. An analytical sample was obtained by microdistillation at 120°/0.5 mm Hg. Mass spectrum (70 eV) *m/e* (relative intensity) 228 (31, parent peak), 210 (13), 171 (80), 129 (38), 102 (100), etc.; i.r. (CCl_4) 3400, 2840, 1600, 1485, 1155 cm^{-1}; u.v.$_{max}$ (95% C_2H_5OH) 252 mμ (ε 17 100), 242 (20 000); n.m.r. (CCl_4) τ 8.85 (d, 6, J = 6 Hz, methyls), 8.60 (cyclohexane protons), 2.80 (m, 5, aromatic protons).

Anal. Calcd. for $C_{16}H_{20}O$: C, 84.16; H, 8.83. Found: C, 84.18; H, 8.85.

1-(2,6-Dimethylcyclohexene-1-yl) Benzyl Ketone (2a)

The acetylenic alcohol **1***a* (1.06 g) was refluxed in 50 ml of 80% formic acid for 2 h. The reaction mixture was diluted with water and extracted with ether (4 × 100 ml). The organic layer was washed with sodium bicarbonate solution and then dried ($MgSO_4$). After evaporation 0.90 g of an oil was obtained. The product consisted of two components which were separated by thick layer chromatography on silica gel plates using benzene for development. The more polar compound **6***a* was isolated in 60% yield (0.605 g). An analytical sample was prepared by microdistillation at 95°/0.3 mm Hg. Mass spectrum (70 eV) *m/e* (relative intensity) M^+ ion (228) absent, 138 (25), 137 (65), 109 (100), 91 (63), etc.; i.r. (CCl_4) 2875, 1685, 1450 cm^{-1}; u.v.$_{max}$ (95% C_2H_5OH), 244 mμ (3800), 211 (8044); n.m.r. (CCl_4) τ 9.18 (d, 3, J = 8 Hz, CH—CH_3), 8.40 (s, 3, =C—CH_3), 6.40 (s, 2, CO—CH_2—Ph), 2.83 (s, 5, aromatic protons).

Anal. Calcd. for $C_{16}H_{20}O$: C, 84.16; H, 8.83. Found: C, 84.13; H, 8.85.

The less polar compound did not contain a carbonyl (i.r.) and it was not characterized any further.

Can. J. Chem. Downloaded from www.nrcresearchpress.com by 210.87.254.42 on 09/05/12
For personal use only.

10(9H)-1,2,3,4,4a,10aα-hexahydro-1α,4aα-dimethylphenanthrone (3a)

(a) Preparation

A sample of 1.046 g of unsaturated ketone **2***a* was heated with polyphosphoric acid (8 g) at 120 °C for 10 min. The cooled reaction mixture was diluted with water and extracted with ether. The organic layer was washed successively with saline and 10% sodium bicarbonate. The ether solution was dried ($MgSO_4$) then evaporated to dryness (1.02 g, 96%). T.l.c. revealed the presence of one component. The solid product was recrystallized from pentane, m.p. 64–65°. Mass spectrum (70 eV) *m/e* (relative intensity) 228 (77, parent), 213 (94), 195 (100), 159 (97); i.r. (CCl_4) 2875, 1710, 1450, 1240 cm^{-1}; u.v.$_{max}$ (95% C_2H_5OH) 282 mμ (ε 1384) and 209 (9300); n.m.r. ($CDCl_3$) τ 9.20 (d, 3, J = 7 Hz, 1-methyl), 8.93 (s, 3, angular methyl), 6.50 (s, 2, CO—CH_2—Ph), 2.80 (m, 5, aromatic).

Anal. Calcd. for $C_{16}H_{20}O$: C, 84.16; H, 8.83. Found: C, 84.14; H, 8.80.

(b) Equilibration of Tricyclic Ketone 3a

The alkaline treatment of **3***a* led to a complicated mixture. Next an acidic treatment was tried.

Ketone **3***a* (276 mg) was refluxed for 3 h in 10 ml of methanol containing 2 drops of concentrated hydrochloric acid. After cooling, the reaction mixture was diluted with water and extracted with ether (4 × 40 ml). The combined ether extracts were washed with saline, sodium bicarbonate solution (5%), and saline in succession. The product consisted of three components which were separated by thick layer chromatography on a silica gel plate using 10:90 ether–benzene for development. The most polar product was isolated in crystalline form (66 mg, 24%). This sample was shown to be identical with diketone **4***a* prepared from monoketone **3***a* with SeO_2 oxidation (*vide infra*).

To the least polar oily product (51 mg, 20%) enol ether structure **5** was assigned; i.r. (CCl_4) 2900, 1647, 1486, 1450, 1370, 1282, 1235, 1193, 1152, 1026 cm^{-1}; u.v.$_{max}$ 277 mμ (11 754), 222 (15 557); n.m.r. ($CDCl_3$) τ 9.1 (d, 3, J = 6 Hz, 1-methyl), 8.87 (s, 3, angular methyl), 6.28 (s, 3, O—CH_3), 4.55 (s, 1, proton at C-9), 2.33 (m, 4, aromatic protons) mass spectrum (70 eV) *m/e* (relative intensity) 242 (38, parent peak), 227 (31), 173 (25), 172 (100), 141 (33), 129 (37), 128 (38). A sample was distilled for analysis at 100°/1 mm Hg.

Anal. Calcd. for $C_{17}H_{22}O$: C, 84.25; H, 9.14. Found: C, 84.23; H, 9.16.

From the middle band of the chromatogram monoketone **3***a* (75 mg) was recovered. When the reaction was carried out under nitrogen only the starting material **3***a* and the enol ether **5** were isolated.

The same isomerization experiment was carried out in the presence of CH_3OD. Ketone **3***a* (200 mg) was refluxed in CH_3OD (2 ml) in the presence of CF_3COOD (0.1 ml) + D_2O (0.2 ml) for 3 h in a nitrogen atmosphere. After evaporation to dryness the entire sample was chromatographed on a silica gel plate (20 × 20). From the least polar band ketone **3***a* (75 mg) was recovered. Its n.m.r. showed that the singlet at 6.50 (CO—CH_2—Ph) decreased to about one fourth its original height. Another slight change was noticeable at 7.9 attributable to position 10*a*. In the aromatic region the signals decreased also by 25%. The position and intensity of the signals at 9.1 (d) and 8.87 (s) have not changed.

1,2,3,4,4a,10aα-Hexahydro-1α,4aα-dimethylphenanthrenequinone (4a)

A solution of monoketone **3***a* (150 mg) in 3 ml of dioxane was mixed with sublimed selenium dioxide (100 mg) and a drop of water. The mixture was stirred and refluxed for 6 h. When the oxidation was complete (t.l.c.) the mixture was filtered. The filtrate was diluted with ether and washed with saline. After drying ($MgSO_4$) and evaporation to dryness, 140 mg (88%) of crystalline diketone was obtained. It was recrystallized from pentane, yellow needles, m.p. 115–117°. Mass spectrum (70 eV) *m/e* (relative intensity) 242 (35, parent), 214 (11), 199 (29), 181 (31), 171 (30), 159 (57), 129 (71), 128 (100); i.r. (CCl_4) 2860, 1730, 1695, 1435, 1370, 1307, 1235 cm^{-1}; u.v.$_{max}$ (95% C_2H_5OH) 283 mμ (ε 8750), 209 (10 454), n.m.r. τ 9.18 (d, 3, J = 6 Hz, 1-methyl), 8.67 (s, 3, angular methyl), 7.45 (d, 1, J = 10 Hz, proton at C-10a), 2.47 (m, 4, aromatic protons).

Anal. Calcd. for $C_{16}H_{18}O_2$: C, 79.31; H, 7.49. Found: C, 79.34; H, 7.51.

1-(m-Methoxyphenylethynyl)-2,6-dimethylcyclohexanol (1b)

The acetylene alcohol **1***b* was prepared as described for **1***a* in a 90% yield using *m*-methoxyphenylacetylene (10). T.l.c. examination showed only one major component and a small amount of polymers. It was purified by thick layer chromatography on silica plates using benzene for development. An analytical sample was distilled at 102°/0.3 mm Hg. Mass spectrum (70 eV) *m/e* (relative intensity) 258 (36), 240 (67), 225 (25), 201 (54), 155 (100); i.r. (CCl_4) 3400, 2890, 1587, 1497, 1157 cm^{-1}; u.v.$_{max}$ (95% C_2H_5OH) 298 mμ (ε 2921), 290 (2900), 252 (15 357), 243.5 (15 357); n.m.r. ($CDCl_3$) τ 8.83 (d, 6, J = 6 Hz, methyls), 8.55 (cyclohexane protons), 6.20 (s, 3, OCH_3), 3.0 (m, 5, aromatic protons).

Anal. Calcd. for $C_{17}H_{22}O_2$: C, 79.03; H, 8.58. Found: C, 79.07; H, 8.53.

1-(2,6-Dimethylcyclohexene-1-yl) m-Methoxybenzyl Ketone (2b)

The acetylenic alcohol **1***b* (9.3 g) was refluxed with 80% formic acid for 2 h and worked-up as described for **2***a*. The two-component mixture was separated by column chromatography on silica gel eluting with benzene. The less polar component contained no carbonyl and had a tendency to polymerize.

The more polar component (5.2 g) was isolated as an oil in 55% yield. Mass spectrum (70 eV) *m/e* (relative intensity) 258 (3, parent), 243 (2), 225 (1), 150 (50), 137 (82), 135 (100); i.r. (CCl_4) 2825, 1675, 1587, 1477, 1443, 1250, 1143, 1042 cm^{-1}; u.v.$_{max}$ (95% C_2H_5OH) 310 mμ (ε 690), 282 (2670), 275 (2987), 208 (15 960); n.m.r. ($CDCl_3$) τ 9.08 (d, 3, J = 6 Hz, CH—CH_3), 8.38 (s, 3, =C—CH_3), 6.23 (s, 5, OCH_3 and CO—CH_2—Ar), 3.20 (m, 4, aromatic). A sample was distilled at 105°/0.3 mm Hg for analysis.

Anal. Calcd. for $C_{17}H_{22}O_2$: C, 79.03; H, 8.58. Found: C, 79.05; H, 8.56.

10(9H)-1,2,3,4,4a,10aα-Hexahydro-1α,4aα-dimethyl-7-methoxyphenanthrone (8b) and 1,2,3,4,4a,10aα-Hexahydro-7-methoxy-1α,4aα-dimethylphenanthrenequinone (4b)

A 1.2 g sample of unsaturated ketone **2***b* was heated with polyphosphoric acid (8 g) at 110° for 10 min. The

Can. J. Chem. Downloaded from www.nrcresearchpress.com by 210.87.254.42 on 09/05/12
For personal use only.

reaction mixture was worked-up as described for **3***a*. The yield of the crystalline product, m.p. 71–75 °C was nearly quantitative. However, even after several recrystallizations from different solvents the pure ketone **3***b* could not be isolated. The contaminant was the corresponding α-diketone, **4***b*, as recognized from the mass and n.m.r. spectra of the samples.

Consequently the mixture was oxidized to pure **4***b*. A solution of **3***b* and **4***b* (142 mg) in dioxane (3 ml) was mixed with sublimed selenium dioxide (80 mg) and a drop of water and heated under reflux for 6 h. When the oxidation was complete (t.l.c.) the product was filtered, diluted with ether, washed with brine, and dried ($MgSO_4$). After evaporation 103 mg (73%) of crystalline diketone was isolated. It was recrystallized from pentane, m.p. 133–135°. Mass spectrum (70 eV) *m/e* (relative intensity) 272 (93, parent), 257 (12), 244 (25), 229 (100), 201 (50); i.r. ($CHCl_3$) 2850, 1724, 1678, 1602, 1493, 1460, 1319, 1285 cm^{-1}; u.v.$_{max}$ (95% C_2H_5OH) 286 mμ (ε 5900), 226 (17 400); n.m.r. at 220 MHz ($CDCl_3$) τ 9.20 (d, 3, J = 6 Hz, CH—CH_3), 8.72 (s, 3, angular methyl), 7.49 (d, 1, J = 10 Hz, proton at C-10a), 6.13 (s, 3, OCH_3), 2.73 (m, 1, $J_{5,6}$ = 8.8 Hz, $J_{6,8}$ = 3.0 Hz, H_6), 2.62 (d, 1, $J_{5,6}$ = 8.8 Hz, $J_{5,8}$ = 0.1 Hz, H_5), 2.40 (d, 1, $J_{6,8}$ = 3.0 Hz, $J_{5,8}$ = 0.1 Hz, H_8).

Anal. Calcd. for $C_{17}H_{20}O_3$: C, 74.97; H, 7.40. Found: C, 74.99; H, 7.42.

o-Methoxyphenylacetylene

To a well-cooled solution of *o*-methoxyacetophenone (35 g) in benzene (100 ml) phosphorous pentachloride (50 g) was added in 45 min while stirring. The product was allowed to stand overnight at room temperature. The yellow solution was poured on ice and extracted with ether (3 × 100 ml). The combined ether extracts were washed with water, dried ($MgSO_4$) and evaporated to dryness. The product was mixed with 95% ethanol (42 ml) and potassium hydroxide (34 g) and refluxed for 24 h. Prior to working-up the mixture was tested for the complete disappearance of the dichloride (t.l.c.). The brown reaction mixture was poured on ice-water and extracted with ether (3 × 100 ml), then the ether was removed by atmospheric distillation. The residue was dissolved in ethyl alcohol (100 ml) and to the magnetically stirred solution 5% $AgNO_3$ solution was dripped until no more precipitate formed. The precipitate was filtered by suction, washed with ethyl alcohol then with ether. After suspending the precipitate in water (200 ml), 35 g of NH_4SCN was added and the mixture was stirred in the presence of ether (200 ml). The AgSCN was removed by filtration on a Buchner funnel and the filtrate was extracted with ether (4 × 100 ml). The combined ether extracts were washed with saline, dried ($MgSO_4$), and the product was distilled at 78–84°/7 mm Hg. Yield: 12 g (35%) colorless oil. Mass spectrum (70 eV) *m/e* (relative intensity) 132 (45, parent), 131 (33), 117 (11), 89 (100); u.v.$_{max}$ (95% C_2H_5OH) 301 mμ (ε 3945), 292 (3945), 250 (11 000), 239 (10 620); i.r. (CCl_4) 3448, 1600, 1274, 1242, 1042 cm^{-1}; n.m.r. ($CDCl_3$) τ 6.70 (s, 1, C≡CH), 6.2 (s, 3, OCH_3), 3.1 (s, 4, aromatic protons). The product was previously characterized (3,4).

1-(o-Methoxyphenylethynyl)-2,6-dimethylcyclohexanol (7a)

Preparation

The Nef addition between 2,6-dimethylcyclohexanone and *o*-methoxyphenylacetylene was carried out as described for **1***a*. A crystalline product was obtained (yield 97%). The analytical sample was prepared by recrystallization from ether, m.p. 84–86°. Mass spectrum (70 eV) *m/e* (relative intensity) 258 (36, parent), 240 (3), 227 (19), 201 (61), 159 (20), 131 (34), 69 (100); i.r. ($CHCl_3$) 3550, 2837, 1595, 1486, 1453, 1282, 1250, 1151, 1117, 1045, 954, 939 cm^{-1}; u.v.$_{max}$ (95% C_2H_5OH) 301 mμ (ε 6161), 292 (6140), 154.5 (20 026), 243 (17 713); n.m.r. ($CDCl_3$) 8.77 (d, 6, J = 6 Hz, methyls), 8.53 (cyclohexane protons), 6.47 (s, 3, OCH_3), 2.90 (m, 4, aromatic protons).

Anal. Calcd. for $C_{17}H_{22}O_2$: C, 79.03; H, 8.58. Found: C, 79.01; H, 8.60.

Formolysis of acetylene alcohol (7a)

A 1.925 g sample of **7***a* was refluxed with 80% formic acid (25 ml) for 3 h. The solution was then diluted with water and extracted with chloroform (3 × 100 ml). The combined chloroform extracts were washed in succession with water, 10% sodium bicarbonate, and water. The dried ($MgSO_4$) solution was evaporated to dryness. A single compound was produced according to t.l.c., which did not contain any carbonyl (i.r.) and lost the methoxy group (n.m.r.). Therefore it was not fully characterized.

1-(p-Methoxyphenylethynyl)-2,6-dimethylcyclohexanol (7b)

Preparation

The Nef addition between 2,6-dimethylcyclohexanone and *p*-methoxyphenylacetylene (11) was carried out as described for **1***a* in 93%. The crystalline product was homogeneous according to t.l.c. It was recrystallized from pentane, m.p. 46–47°. Mass spectrum (70 eV) *m/e* (relative intensity) 258 (24, parent), 244 (21), 243 (100), 225 (31), 201 (33), 135 (98); i.r. (CCl_4) 3500, 2840, 1603, 1500, 1450, 1280, 1260, 1170, 1153, 1035, 960, 940, 833 cm^{-1}; u.v. max (95% C_2H_5OH) 297 mμ (ε 3354), 285.5 (4128), 261 (23 220), 252 (24 940); n.m.r. ($CDCl_3$) τ 8.87 (d, 6, J = 6 Hz, CH—CH_3), 3.0 (g, 4, aromatic).

Anal. Calcd. for $C_{17}H_{22}O_2$: C, 79.03; H, 8.58. Found: C, 79.05; H, 8.56.

The formolysis of **7***b* led to an unidentified polymer.

The financial assistance of the National Research Council of Canada and the Senate Research Committee of University of Prince Edward Island is gratefully acknowledged. The technical assistances of Miss K. Felderhof and Mrs. E. Schmidt are greatly appreciated. The author also wishes to thank Mrs. P. Liu for secretarial work. The administration of the University is thanked for encouragement. Dr. A. A. Grey and the Ontario Research Foundation are thanked for 220 MHz n.m.r. spectra.

1. C. Schmidt and J. Thazhuthaveetil. Tetrahedron Lett. **31**, 2653 (1970).
2. M. T. Bogert. J. Am. Chem. Soc. **57**, 151 (1935).
3. V. Prey and G. Pich. Monatsh. **80**, 790 (1949).
4. A. D. Allen and C. D. Cook. Can. J. Chem. **41**, 1085 (1963).
5. C. R. Noller and R. Adams. J. Am. Soc. **46**, 1892 (1924).
6. L. M. Jackman and S. Sternhell. Applications of nuclear magnetic resonance spectroscopy in

organic chemistry. 2nd Ed. Pergamon Press, New York. 1969. p. 306 and references cited therein.
7. (*a*) M. JULIA and R. LABIA. Bull. Soc. Chim. 4151 (1972); (*b*) Z. G. HAJOS, K. J. DOEBLH, and M. W. GOLDBERG. J. Org. Chem. **29**, 2527 (1964); (*c*) Z. G. HAJOS, D. R. PARRISH, and M. W. GOLDBERG. J. Org. Chem. **30**, 1213 (1965).
8. J. DELOBELLE and M. FETIZON. Bull. Soc. Chim. Fr. 1630 (1961).
9. J. DELOBELLE and M. FETIZON. Bull. Soc. Chim. Fr. 1894 (1961).
10. W. S. JOHNSON, D. K. BANERJEE, W. S. SCHNEIDER, C. D. GUTSCHE, W. E. SHELBERG, and L. J. CHINN. J. Am. Chem. Soc. **74**, 2843 (1952).
11. E. E. SMISSMAN, R. H. JOHNSEN, A. W. CARLSON, and B. F. AYCOCK. J. Am. Chem. Soc. **78**, 3395 (1956).

Can. J. Chem. Downloaded from www.nrcresearchpress.com by 210.87.254.42 on 09/05/12
For personal use only.

A Revision of the Stereochemistry of Lactucin

FRANK WILLIAM BACHELOR
Department of Chemistry, The University of Calgary, Calgary, Alberta T2N 1N4

AND

SHÔ ITÔ
Department of Chemistry, Tohoku University, Sendai, Japan

Received February 5, 1973

On the basis of circular dichroism measurements on lactucin, hydroxyachillin, and acetoxyachillin the stereochemistry of the C-5 hydrogen has been revised to the 5α configuration. The reasons for the former erroneous assignment are reexamined and the structures of several hexahydrolactucin derivatives are reinterpreted.

En se basant sur des mesures de dichroisme circulaire de la lactucine, de l'hydroxyachilline et de l'acétoxyachilline, la stéréochimie de l'hydrogène en C-5 a été révisée et la configuration 5α lui a été attribuée. Les raisons qui ont amenées l'attribution erronée précédente sont réexaminées et les structures de plusieurs dérivés de l'hexahydrolactucine sont réinterprétées.

[Traduit par le journal]

Can. J. Chem., **51**, 3626 (1973)

Lactucin (**1***a*) was the first of a group of sesquiterpenoid lactones to be isolated which contain a carbonyl group at carbon atom 2 of the guaiane carbon skeleton and a unique cross conjugated system (1, 2). Since then, other sesquiterpene lactones have been isolated which have the same chromophore but which vary mainly in their oxygenation pattern and stereochemistry. Among these are matricarin (**2***a*) (3), the achillins (**3***a*, *b*, *c*) (4), and leucodin (**2***c*) (5). The stereochemistry of these latter compounds has been firmly established (6, 7) and lactucin (**1**) appears to be the only member of this group which contains a 5β-hydrogen atom. We have examined the n.m.r. and circular dichroism (c.d.) spectra of lactucin (**1**), hydroxyachillin (**3***b*), and acetoxyachillin (**3***c*) and find that the stereochemistry of the former compound at C-5 must be revised to the α-configuration.

An examination of the n.m.r. of these three compounds shows a great deal of similarity as a whole. Furthermore, all protons have been assigned properly for lactucin and the coupling constants determined by nuclear magnetic double resonance (n.m.d.r.) experiments (Table 1). Thus, coupling constants $J_{5,6}$, $J_{6,7}$, $J_{7,8}$ shown in Table 1 are in good agreement with those in hydroxyachillin and acetoxyachillin. This strongly suggests that these three natural lactones have the same *trans* configurations at C_5—C_6, C_6—C_7, and C_7—C_8.

The identical absolute stereochemistry in these compounds was concluded from their c.d. spectra (*cf.* Table 2). Circular dichroism curves of hydroxyachillin and acetoxyachillin are composed essentially of three maxima, which can be attributed to the n–π* transition of the γ-lactone, π–π* and to the n–π* transition of the dienone. The assignment of the strong positive transition at 252–255 nm to the π–π* transition of the unsaturated system was supported by the strong u.v. absorption at 253 nm (ε 13 200).

The c.d. curve of lactucin contains four transitions. Three transitions at 210!, 248, and 350 nm are in accord with the u.v. maxima, 210! (ε 14 000), 254 (ε 14 200), and 330 (ε 77) and can be assigned to the π–π* transition of the unsaturated lactone, π–π*, and n–π* transition of the dienone system, respectively. The fourth transition at 275 nm is ascribable to the n–π* transition of the unsaturated lactone from the following considerations. A c.d. study of Stöcklin, *et al.* (8) clearly established that (*i*) in spite of a negligible u.v. maximum, the *trans*-α-methylene-γ-lactones incorporated in a guaiane skeleton invariably exhibit a negative Cotton effect due to their n–π* transition at 250–265 nm when the lactones are closed at C-6 and (*ii*) this situation is not altered by the neighboring oxygen functions, unlike the case of *cis* lactones. The 230–300 nm region in the c.d. curve of lactucin is therefore explicable as the result of the overlap of the

Can. J. Chem. Downloaded from www.nrcresearchpress.com by 210.87.254.105 on 09/05/12
For personal use only.

TABLE 1. Proton chemical shifts and coupling constants of lactucin and related compounds[a]

Position	Compound 1	3b	3c
3	6.92 $J_{3,14a} = 2.0$ $J_{3,14b} = 2.0$	6.15	6.17
5	3.65 $J_{5,6} = 10$	3.40 $J_{5,6} = 10$	3.41 $J_{5,6} = 10$
6	3.60 $J_{6,7} = 10$	3.86 $J_{6,7} = 10$	3.90 $J_{6,7} = 10$
7	3.21 $J_{7,8} = 9.9$ $J_{7,13x} = 2.8$	$J_{7,8} = 10$[b]	$J_{7,8} = 10$
8	3.99 $J_{8,9\alpha} = 9.9$	3.74	4.76
9α	2.91 $J_{9\alpha,9\beta} = 13.8$		
9β	2.61		
13		1.29	1.11
13*n*	6.54 $J_{13n,13x} = 2.0$		
13*x*	6.35		
14		2.31	2.30
14α	5.25 $J_{14a,14\beta} = 18.7$		
14β	4.72		
15	2.47	2.44	2.45

[a]All values are in δ relative to internal TMS.
[b]See reference 7.

π–π* transition of the dienone system at ~255 nm and the n–π* transition of the unsaturated lactone at ~265 nm which possess opposite sign. Thus, in all three compounds examined, the π–π* transition of the cross conjugated dienone system has the same positive sign, and therefore, the same chirality. Since the stereochemistry of the C-5 hydrogen atom has been firmly established as α in acetoxyachillin (**3***c*) (7) this must also be the case with lactucin.

The difference in sign of the n–π* transition of the unsaturated ketones is probably caused by the presence of a hydroxymethylene group in lactucin. The reversion of the sign by the presence of hydroxyl or acetoxyl or epoxy groups has precedents (9) and even in these instances the extrema due to the n–π* transition is not affected.[1]

In view of this revision of stereochemistry, it is necessary to reexamine the original proposals to understand why erroneous conclusions were reached. All three of these proposals (1, 2, 10) were based on hexahydrolactucin (**4**). Barton and Narayanan (1) prepared a benzylidene derivative from hexahydrolactucin by isomerizing it first with alcoholic alkali, followed by the reaction with benzaldehyde in acid. They proposed structure **5** for this compound. An adduct of this kind cannot be formed at all if the 8-hydroxyl group and the hydroxymethylene groups are *cis* to each other and also to the 5-hydrogen atom. We propose that the benzylidene compound is in fact the rearranged lactone **6** with the benzylidene bridge across the 6-hydroxyl and hydroxymethylene groups. The conformational analysis of Hendrickson (8) was based on this compound (**5**) and was obviously also incorrect.

Šorm and co-workers (2) based their stereochemistry on the optical rotatory dispersion (o.r.d.) spectrum of hexahydrolactucin and concluded that it had a 1α, 5β hydrogen configuration (**7**). This was based on comparison with the o.r.d. of 15-oxocholestanone (**8**) (11) which contains the *trans*-linked perhydroindanone system. Both showed positive Cotton effects.

However, a survey of the literature revealed that it is not necessarily correct. For example, the compounds **9**–**11**, all containing the *cis*-fused perhydroindanone system, also show positive Cotton effects (12, 13). In addition, compound **12** with the opposite configuration shows a comparable negative Cotton effect (14). The sign of the Cotton effect reveals only the configuration of the hydrogen atom at C-1 but not that at C-5. The smaller amplitude of the Cotton effect ($[\alpha]_{max}$ +1682°) implies a *cis*-perhydroindan-1-one.

[1]K. Kuriyama. Unpublished results.

Can. J. Chem. Downloaded from www.nrcresearchpress.com by 210.87.254.105 on 09/05/12
For personal use only.

Can. J. Chem. Downloaded from www.nrcresearchpress.com by 210.87.254.105 on 09/05/12
For personal use only.

TABLE 2. Circular dichroism maxima of **3***b*, **3***c*, and **1** transitions [θ]

Compounds	π–π* of lactone	π–π* of unsaturated lactone	π–π* of dienone	n–π* of unsaturated lactone	n–π* of dienone
Hydroxyachillin (**3***b*)	−7302 (221 nm)		+6110 (254.5 nm)		+312 (353 nm)
Acetoxyachillin (**3***c*)	−10 970 (210–215 nm)		+7540 (252 nm)		+697 (350 nm) +401 (367 nm sh)
Lactucin (**1**)		+27 900 (210!)	+6565 (248 nm)	−7304 (275.5 nm)	−706 (350 nm)

Can. J. Chem. Downloaded from www.nrcresearchpress.com by 210.87.254.105 on 09/05/12
For personal use only.

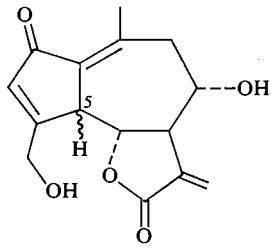

1

a 5β
b 5α

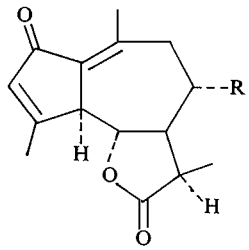

2

a R = H
b R = OH
c R = OAc

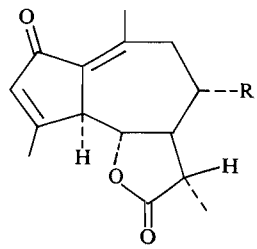

3

a R = H
b R = OH
c R = OAc

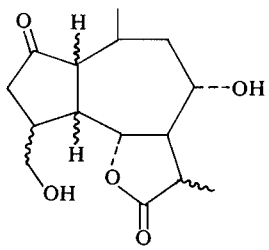

4

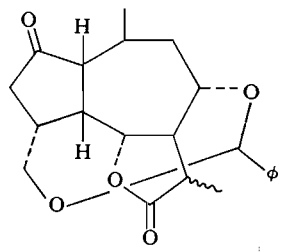

5

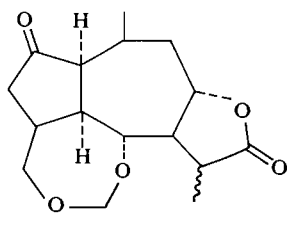

6

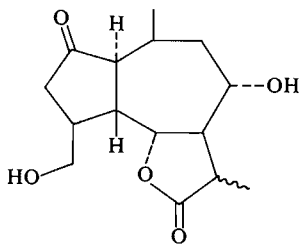

7

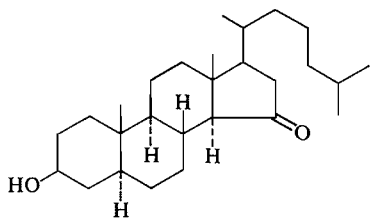

8

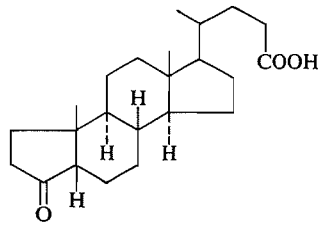

9

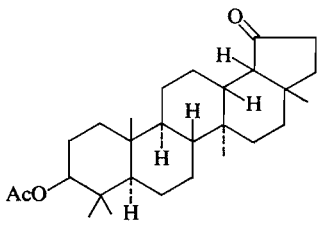

10

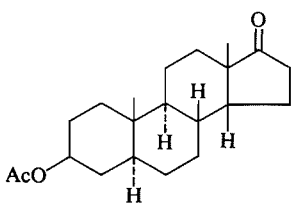

11

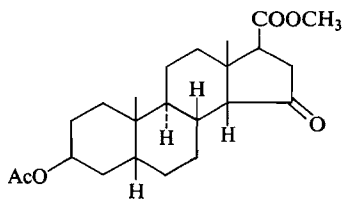

12

On the basis of our studies, the stereochemistry of lactucin must be revised to that as shown in structure **1***b*.

We wish to thank Professor D. H. R. Barton for a generous sample of lactucin. We also thank Dr. K. Kuriyama, Shionogi Research Laboratory, Shionogi & Co., for the information on his unpublished c.d. data.

1. D. H. R. BARTON and C. R. NARAYANAN. J. Chem. Soc. 963 (1958).
2. L. DOBJŠ, M. SOUČEK, M. HORÁK, V. HEROUT, and F. SŐRM. Coll. Czech. Chem. Commun. **23**, 2195 (1958).
3. W. HERZ and K. UEDA. J. Am. Chem. Soc. **83**, 1139 (1961).
4. E. H. WHITE and R. E. K. WINTER. Tetrahedron Lett. **3**, 137 (1963).
5. M. HOLUB and V. HEROUT. Coll. Czech. Chem. Commun. **27**, 2980 (1962).
6. (*a*) E. H. WHITE and J. N. MARX. J. Am. Chem. Soc. **89**, 5511 (1967); (*b*) E. H. WHITE, S. EGUCHI, and J. N. MARX. Tetrahedron, **25**, 2099 (1969); J. N. MARX and E. H. WHITE. Tetrahedron, **25**, 2117 (1969).
7. F. W. BACHELOR, A. B. PARALIKAR, and S. ITÔ. Can. J. Chem. **50**, 333 (1972).
8. W. STÖCKLIN, T. G. WADDELL, and T. A. GEISSMAN. Tetrahedron, **26**, 2397 (1970).
9. G. SNATZKE. *In* Optical rotatory dispersion and circular dichroism in organic chemistry. *Edited by* G. SNATZKE. Heydon & Son Ltd., London. 1967. p. 208; G. SNATZKE. Tetrahedron, **21**, 439 (1965).
10. J. B. HENDRICKSON. Tetrahedron, **19**, 1387 (1963).
11. C. DJERASSI. Optical rotatory dispersion. McGraw-Hill Book Co. Inc., New York. 1960. p. 44.
12. C. DJERASSI, J. OSIECKI, and W. CLOSSON. J. Am. Chem. Soc. **81**, 4587 (1959).
13. C. DJERASSI, R. RINIKER, and B. RINIKER. J. Am. Chem. Soc. **78**, 6362 (1956).
14. A. LARDON, H. P. SIGG, and T. REICHSTEIN. Helv. Chim. Acta, **42**, 1457 (1959).

Can. J. Chem. Downloaded from www.nrcresearchpress.com by 210.87.254.105 on 09/05/12
For personal use only.

A Unique Menschutkin Reaction Involving Fragmentation and Cyclization[1]

RAPHAEL M. OTTENBRITE AND G. RODNEY MYERS
Department of Chemistry and Pharmaceutical Chemistry, Virginia Commonwealth University Richmond, Virginia 23219

Received February 23, 1973

It was found that *N,N,N',N'*-tetramethylmethylenediamine reacted with a number of dihalides to form the corresponding cyclic quaternary ammonium compound and dimethylamine hydrohalide. The process involves a Menschutkin reaction with fragmentation of *N,N*-dimethylmethyleneamine followed by a second Menschutkin reaction to form a cyclic compound. The reaction proceeds best in a polar solvent and the yields are moderate to good.

On a trouvé que la *N,N,N',N'*-tétraméthylméthylènediamine réagit avec un certain nombre de dérivés dihalogénés pour former le sel d'ammonium quaternaire correspondant ainsi que l'halohydrate de la diméthylamine. Ce processus implique une première réaction de Menschutkin provoquant la fragmentation de la *N,N*-diméthylméthylèneamine suivie d'une deuxième réaction de Menschutkin pour former le composé cyclique. La réaction se fait le mieux dans un solvant polaire et les rendements sont de modérés à bons. [Traduit par le journal]

Can. J. Chem., 51, 3631 (1973)

Introduction

The Menschutkin reaction (1) is a well-known process for the formation of quaternary ammonium salts from tertiary amines. It also has been used for the synthesis of quaternary ammonium polyelectrolytes (2) by reacting tertiary diamines with dihalides.

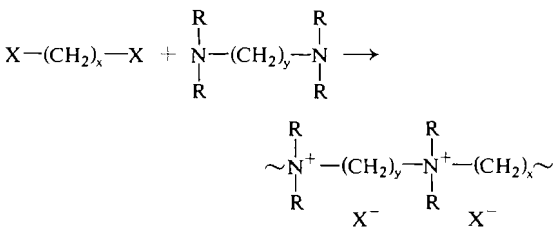

During studies of preparation of new cationic polymers, we observed that *N,N,N',N'*-tetramethylmethylenediamine did not give the expected linear cationic polymer when reacted with dihalides such as 1,4-dibromobutane and 1,5-dibromopentane. It was found that the corresponding cyclic dimethyl quaternary ammonium compounds, 1,1-dimethylpyrrolidinium bromide and 1,1-dimethylpiperidinium bromide, were obtained instead.

This unusual behavior of *N,N,N',N'*-tetramethylmethylenediamine was also observed by

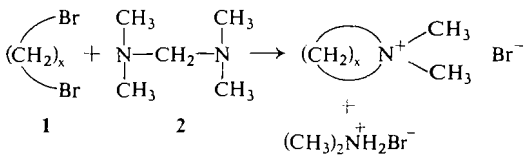

Noguchi and Rembaum (3), who suggested that the reaction product in the case of 1,5-dibromopentane was a 12-membered cyclic diammonium compound. This did not appear feasible from the viewpoint of the initial spectra and thus stimulated our interest in the present work. We, therefore, wish to report the investigation of this reaction and its application to other dihalocompounds.

Results and Discussion

To substantiate that the products that we obtained were in fact the five- and six-membered cyclic quaternary ammonium compounds, these specific compounds were prepared by an independent method (4). Authentic samples of 1,1-dimethylpyrrolidinium bromide and 1,1-dimethylpiperidinium bromide were prepared by reacting dimethylamine with 1,4-dibromobutane and 1,5-dibromopentane, respectively. These compounds were compared spectrometrically with the compounds obtained from *N,N,N',N'*-tetramethylmethylenediamine (2) reacted with the same dibromides.

The i.r. spectrum of the product obtained from dimethylamine and 1,4-dibromobutane was iden-

[1]Presented in part at the 55th Canadian Chemical Conference of the Chemical Institute of Canada, Quebec, June, 1972.

Can. J. Chem. Downloaded from www.nrcresearchpress.com by 210.87.254.6 on 09/05/12
For personal use only.

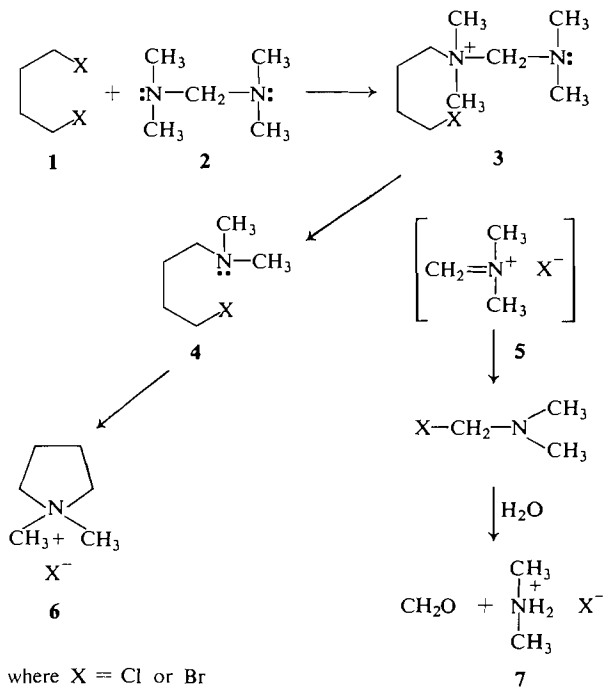

SCHEME 1. Proposed scheme of the cyclization reaction.

tical with the spectrum of the product obtained from dimethylamine and 1,4-dibromobutane. In addition, the n.m.r. spectra were identical. The most convincing evidence was obtained from mass spectra. A very good correlation between the intensities of the individual major peaks was found for both of these compounds; (a similar correlation was found for the minor peaks not listed in the Experimental). It was concluded that the compound obtained from **2** and 1,4-dibromobutane is, in fact, 1,1-dimethylpyrrolidinium bromide.

Similarly, the i.r. and n.m.r. spectra obtained from the products obtained from **2** and from dimethylamine with 1,5-dibromopentane were identical. The mass spectra support the conclusion that the product from **2** and 1,5-dibromopentane is 1,1-dimethylpiperidinium bromide.

It is postulated that compounds **1** and **2** initially undergo a Menschutkin reaction to form a quaternary ammonium intermediate **3**, as illustrated in Scheme 1. This intermediate then appears to undergo cleavage of *N*,*N*-dimethyl(methylene)ammonium halide (**5**) to produce another tertiary amine **4**. This tertiary amine can undergo a second Menschutkin reaction intramolecularly with the remaining halide to form the cyclic quaternary ammonium bromide **6**. We have been unable to isolate intermediate **3** even in nonpolar solvents. Apparently, the energy requirement for this fragmentation step must be low.

The n.m.r. spectrum of the reaction mixture of 1,4-dichlorobut-2-ene and **2** in CCl_3D indicates peaks at δ 3.68 and 8.70 besides those representing the cyclic product. Recently, Schreiber and co-workers (5) have reported the preparation of dimethyl(methylene)ammonium iodide (under anhydrous conditions and N_2 atmosphere) which has n.m.r. peaks at δ 3.67 and 8.18. Thus we feel that **5** is an intermediate in our reaction although its isolation has eluded us. Upon addition of D_2O to the n.m.r. sample tube the peaks at δ 3.68 and 8.70 disappear and a peak at δ 2.73, which is in the region for dimethylammonium chloride (**7**), appears. Further, after quenching a larger scale reaction mixture in H_2O, the 2,4-dinitrophenylhydrazone derivative of formaldehyde was obtained.

The reaction of *N*,*N*,*N*′,*N*′-tetramethylmethylenediamine with 1,4-dibromobutane and with 1,5-dibromopentane was carried out in three

Can. J. Chem. Downloaded from www.nrcresearchpress.com by 210.87.254.6 on 09/05/12
For personal use only.

TABLE 1. The preparation of cyclic ammonium compounds from dihalides and *N,N,N′,N′*-tetramethylmethylenediamine in various solvents

Dihalide	Product	Solvent	% yield[a] (36 h)	% yield[b] (48 h)
1,4-Dibromobutane	1,1-Dimethylpyrrolidinium bromide	DMF	72	79
		CH_3CN	66	74
		$CHCl_3$	27	30[a]
1,5-Dibromopentane	1,1-Dimethylpiperidinium bromide	DMF	74	81
		CH_3CN	68	77
		$CHCl_3$	39	44[a]

[a]Starting material was isolated from the reaction mixture.
[b]Remaining material was an intractable oil and further periods of reaction did not increase yields.

TABLE 2. Products obtained from various dihalides with *N,N,N′,N′*-tetramethylmethylenediamine in acetonitrile

Dihalide	Product	Time (h)	% cyclic yield
Br—$(CH_2)_3$—Br	Polymer	72	—
Br—$(CH_2)_4$—Br	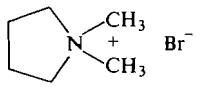	48	74
Br—$(CH_2)_5$—Br	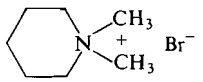	48	77
	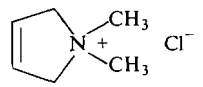	48	78
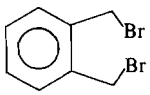	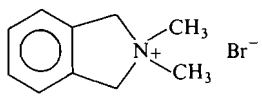	48	73
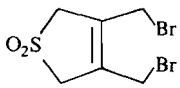	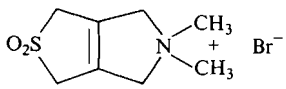	48	70
Br—$(CH_2)_6$—Br	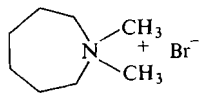	72	11

different solvents: chloroform, acetonitrile, and dimethylformamide. Cyclic products were obtained in each case. The yields were better and rates of reaction appeared to be faster in the more polar solvents, as indicated by the data given in Table 1.

The reaction of **2** was carried out with other dihalides as well. These results are listed in Table 2. Good yields were obtained with halogens in the 1,4- and 1,5-positions. No cyclic product, however, was obtained with the 1,3-dibromopropane. Here the internal strain is too great for easy cyclization, and consequently low molecular weight polymers were obtained instead. The

Can. J. Chem. Downloaded from www.nrcresearchpress.com by 210.87.254.6 on 09/05/12
For personal use only.

1,6-dibromohexane yielded only a small amount (11%) of cyclic product, the low yield being due to the general difficulty in achieving ring formation.

Experimental

The n.m.r. spectra were determined with a Varian A-60, i.r. spectra with a Perkin-Elmer model 257 and the mass spectra with a Dupont model 21-104. The samples were vaporized into the inlet system at 135° and introduced into the source at 250° by heating with a heat gun until enough sample was introduced to obtain the spectrum. Elemental Analyses were obtained on a Perkin-Elmer Analysis Model 240.

Preparation of 1,1-Dimethylpyrrolidinium Bromide with N,N,N′,N′-Tetramethylmethylenediamine

N,N,N′,N′-Tetramethylmethylenediamine (**2**) (2.04 g, 0.02 mol) was added to a solution of 1,4-dibromobutane (4.32 g, 0.02 mol) in 20 ml of acetonitrile. The reaction flask was sealed and the solution stirred by means of a magnetic stirrer. A precipitate appeared within a few hours and the reaction was stirred for 2 days. After this time, precipitation was completed by the addition of 100 ml of 1:1 anhydrous acetone–ether mixture. The product was collected by filtration and washed with dry ether. Recrystallization from isopropanol yielded needle-like crystals that were slightly hygroscopic, 2.2 g, 74%: m.p. (dec.) 340°; ν (KBr) (C—H stretching) 3000–2950, (CH_3 bending) 1465 and 1375, (C—N stretching) 1275, 1250, 1220, and 1000 cm^{-1}; n.m.r. (D_2O, internal standard DSS) δ 2.25 (m, 4), 3.17 (s, 6, N—CH_3), and 3.72 (t, 4, J = Hz, CH_2—N); mass spectrum *m/e* (relative intensity) 28 (43), 42 (100), 57 (85), 84 (84), 85 (48).

Anal. Calcd. for $C_6H_{14}NBr$: C, 40.01; H, 7.78; N, 7.78. Found: C, 39.79; H, 7.83; N, 7.63.

Preparation of 1,1-Dimethylpyrrolidinium Bromide with Dimethylamine

Dimethylamine (4.5 g, 0.1 mol) was added to a solution of 1,4-dibromobutane (4.32 g, 0.02 mol) in 20 ml of methanol. The reaction vessel was sealed with a rubber stopper and the mixture was stirred for 2 days. The mixture was then heated to boiling and Na_2CO_3 was added to decompose the dimethylamine hydrobromide. The mixture was boiled for another 10 min to drive off all the liberated dimethylamine. The hot mixture was filtered and the methanol evaporated. The crude product was obtained quantitatively. Recrystallization was effected from isopropanol: ν (KBr) (C—H stretching) 3000–2940, 1275, 1220, and 1000 cm^{-1}; n.m.r. (D_2O, internal standard DSS) δ 2.25 (m, 4), 3.17 (s, 6, N—CH_3), and 3.72 (t, 4, J = 7 Hz, CH_2—N); mass spectrum *m/e* (relative intensity) 28 (46), 42 (100), 57 (84), 84 (81), 85 (45).

Anal. Calcd. for $C_6H_{14}NBr$: C, 40.01; H, 7.78; N, 7.78. Found: C, 40.43; H, 7.89; N, 7.84.

Preparation of 1,1-Dimethylpiperidinium Bromide with 2

A procedure similar to that described above was followed using **2** (2.04 g, 0.02 mol) with 1,5-dibromopentane in 20 ml of acetonitrile. The product was recrystallized from propanol as hygroscopic needles, (77%): m.p. (dec.) 340°; ν (KBr) (C—H stretching) 3000–2940, (CH_3 bending) 1460 and 1375, (C—N stretching) 1230, and characteristic doublets at 1120, and 1030, 980, 940, and 875 cm^{-1}; n.m.r. (D_2O) δ 1.85 (m, 6), 3.11 (s, 6, N—CH_3), 3.37 (t, 4, J = 5.5 Hz, CH_2—N); mass spectrum *m/e* (relative intensity) 28 (40), 42 (54), 43 (46), 70 (23), 98 (100), 99 (37).

Anal. Calcd. for $C_7H_{16}NBr$: C, 43.31; H, 8.31; N, 7.22. Found: C, 43.43; H, 8.19; N, 7.34.

Preparation of 1,1-Dimethylpiperidinium Bromide with Dimethylamine

A procedure similar to that described above was followed using dimethylamine (4.32 g, 0.02 mol) with 1,5-dibromopentane in 20 ml of methanol. The product was recrystallized from propanol: ν (KBr) (C—H stretching) 3000–2940, (CH_3 bending) 1460 and 1375, (C—N stretching) 1230, and characteristic doublets at 1120 and 1030, 980, 940, and 875 cm^{-1}; n.m.r. (D_2O) δ 1.85 (m, 6), 3.11 (s, 6, N—CH_3), 3.37 (t, 4, J = 5.5 Hz, CH_2—N); mass spectrum *m/e* (relative intensity) 28 (41), 42 (50), 43 (63), 70 (22), 98 (100), 99 (38).

Anal. Calcd. for $C_7H_{16}NBr$: C, 43.31; H, 8.31; N, 7.22. Found: C, 43.39; H, 8.38; N, 7.31.

Procedures for Other Cyclization Reactions with 2.

A general procedure similar to that used in preparing 1,1-dimethylpyrrolidinium bromide was followed in each case. The yields and reaction times are listed in Tables 1 and 2.

The authors wish to thank the National Science Foundation for their financial support through Grant GP 26616. We are also indebted to Dr. Richard Kornfeld of Philip Morris Research Center, Richmond, Virginia, for the mass spectra work and to David Taylor for his assistance in the laboratory.

1. N. MENSCHUTKIN. Z. Physik. Chemie. **5**, 589 (1890).
2. W. KERN and E. BRENNEISEN. J. Prakt. Chem. **159**, 194 (1941).
3. H. NOGUCHI and A. REMBAUM. J. Polym. Sci. B, **7**, 395 (1969).
4. E. R. LITTMANN and C. S. MARVELL. J. Am. Chem. Soc. **52**, 287 (1930).
5. J. SCHREIBER, H. MAAG, N. HASHIMOTO, and A. ESCHENMOSER. Angew. Chem. Int. Eng. Ed. **10**, 330 (1971).

Can. J. Chem. Downloaded from www.nrcresearchpress.com by 210.87.254.6 on 09/05/12
For personal use only.

Restricted Internal Rotation in 1-Arylhydantoins, 3-Arylhydantoins, and 3-Aryl-2-Thiohydantoins: Reversal of the Effective Sizes of Methyl and Chlorine

LAWRENCE D. COLEBROOK, H. GWYNNE GILES, ALESSANDRO GRANATA, AND SIDDIK ICLI
Department of Chemistry, Sir George Williams University, Montreal 107, Quebec

AND

JAMES R. FEHLNER
Department of Chemistry, University of Rochester, Rochester, New York 14627

Received November 14, 1972[1]

In 1-arylhydantoins an *o*-methyl group is effectively larger than an *o*-chloro substituent in restricting rotation about the aryl-C—N bond, whereas in 3-arylhydantoins and 3-aryl-2-thiohydantoins the reverse order of sizes is observed. This difference is attributed to repulsion between the chlorine atom and a carbonyl oxygen atom in the torsional transition state of the 3-aryl compounds.

Dans les aryl-1 hydantoines, un groupe méthyle en ortho est effectivement plus volumineux qu'un substituant chloro en ortho lorsqu'il s'agit d'empêcher la rotation du groupe aryle autour du lien C—N; toutefois dans les aryl-3 hydantoines et les aryl-3 thio-2 hydantoines la grosseur relative des groupes est renversée. Cette différence est attribuée à la répulsion entre l'atome de chlore et l'atome d'oxygène du carbonyle dans l'état de transition de torsion. [Traduit par le journal]

Can. J. Chem., 51, 3635 (1973)

Can. J. Chem. Downloaded from www.nrcresearchpress.com by 210.87.254.42 on 09/05/12
For personal use only.

It has commonly been observed (1, 2) that a methyl group exerts a steric effect greater than that of a chlorine atom, for example, in restricting internal rotation in hindered biphenyls (1). This order is consistent with the relative size of these groups as determined by X-ray crystallographic measurements of van der Waals radii (3).

In an n.m.r. study of restricted rotation about aryl-C—N bonds in 1-arylhydantoins we have found that the same order of relative sizes applies. The free energies of activation for rotation about the C—N bond joining the aryl and heterocyclic moieties are 0.5–1.5 kcal/mol higher for the *o*-methyl compounds than for the *o*-chloro compounds (Table 1).

In contrast, the free energies of activation for rotation of the 3-arylhydantoins and the 3-aryl-2-thiohydantoins (Table 2) indicate a reversal in the relative steric effects of the *o*-methyl and the *o*-chloro substituents on the aryl group. The free energy barriers to rotation about the aryl-C—N bonds are 0.9–2.1 kcal/mol higher for the chloro than for the methyl compounds. This reversal in the relative influences of the *o*-chloro and the *o*-methyl substituents is attributed to the nature of the interactions within the molecules in the transition states for internal rotation.

The rate constants for the internal rotation process in the 1-aryl- and the 3-arylhydantoins were obtained by complete n.m.r. line shape analysis of the temperature dependent 5-methyl or *o*-tolyl-methyl signals over a range of temperatures, using an iterative fitting procedure. The linear least-squares method was used to fit the Arrhenius equation to the data. Except in the cases of **1***a* and *b*, the free energies of activation

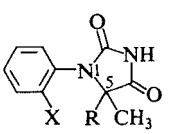

1

a X = CH_3; R = H
b X = Cl; R = H
c X = R = CH_3
d X = Cl; R = CH_3

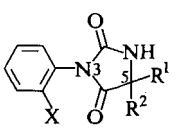

2

a X = R^1 = R^2 = CH_3
b X = Cl; R^1 = R^2 = CH_3
c X = CH_3; R^1 = H; R^2 = C_6H_5
d X = Cl; R^1 = H; R^2 = C_6H_5
e X = CH_3; R^1 = H; R^2 = CH_3
f X = Cl; R^1 = H; R^2 = CH_3

[1]Revision received July 12, 1973.

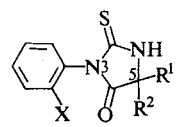

3

a X = CH_3; R^1 = H; R^2 = CH_3
b X = Cl; R^1 = H; R^2 = CH_3

are reported (Tables 1 and 2) for a temperature common to, or falling between, the ranges used for the pair of compounds being compared. For compounds **1***a* and *b*, which could not be studied over an extended temperature range, the rate constants were obtained in the coalescence point region and are reported for the coalescence temperature. Because of the high rotational barriers, the spectra of the thiohydantoins, **3***a* and *b*, do not show collapse at the boiling point of the solvent. Rate constants (at a single temperature) were obtained for **3***a* and *b* by following the equilibration of the thermodynamically less stable diastereomer by repetitively recording the n.m.r. spectrum and measuring the areas under the peaks. The values of $\Delta G^{\ddagger}$ quoted for **1***a* and *b*, **2***c–f*, and **3***a* and *b* correspond to conversion of the less to the more thermodynamically stable rotamer.

Discussion

In their internal rotational ground states, these molecules are expected to adopt conformations with large dihedral angles between the aryl and hetero ring systems because of steric interaction between the *ortho* substituents on the aryl group and the hetero ring. The existence of significant chemical shifts between diastereotopic groups and between protons, located on the hetero ring, of diastereomeric rotational isomers is consistent with anisotropic shielding by the unsymmetrically substituted aryl groups which are constrained to adopt conformations not coplanar with the hetero ring. Since the molecules should have sufficient flexibility in the ground states to minimize steric interactions between the two ring systems it is probable that most of the influence on the values of $\Delta G^{\ddagger}$ in these series of compounds of importance in this study arises from interactions in the transition states.

Ground state effects of substituents are most easily recognized when the rotational isomers are diastereomeric, so that the equilibrium constant is not unity. Comparison of the equilibrium ratios of rotamers of the methyl and the chloro compounds reveals differences consistent with the reversal of the effective sizes of these groups in the 1-aryl and the 3-aryl series. Difficulties in obtaining satisfactory low temperature spectra of **1***a* and *b* precluded accurate measurement of the equilibrium constants, but it is clear that the deviation from unity in the equilibrium ratio is greater for the methyl compound, **1***a*, than for the chloro compound, **1***b*. This is expected if the methyl group is effectively larger than chlorine in the rotational ground states. In contrast, the equilibrium constants at ambient temperature of the 3-aryl-2-thiohydantoins, **3***a* and *b*, are 1.4 ± 0.1 and 1.7 ± 0.1 (90% confidence limits), respectively, the chloro substituent exerting a greater influence than the methyl group in the ground state. Ground state free energy differences between rotamers are, in all cases, smaller than the differences in free energies of activation reported in Tables 1 and 2. The nature of the interactions leading to non-unity equilibrium constants, particularly in the 3-aryl series, is not yet clear and is the subject of further investigation.

TABLE 1. Free energies of activation for 1-arylhydantoins

	Solvent	Temperature (°C)	$\Delta G^{\ddagger}$[a] (kcal/mol)	$\Delta\Delta G^{\ddagger}$[b] (kcal/mol)
1*a*	Acetone-d_6:DMSO-d_6 (4:1)	−32[c]	12.6±0.1	
1*b*	Acetone-d_6:DMSO-d_6 (4:1)	−63[c]	11.1±0.1	1.5
1*c*	DMSO-d_6	60	18.1±0.1	
1*d*	DMSO-d_6	60	17.4±0.1	0.7
1*c*	Pyridine	60	17.6±0.1	
1*d*	Pyridine	60	17.1±0.1	0.5

[a] 90% confidence limits.
[b] $\Delta G^{\ddagger}_{CH_3} - \Delta G^{\ddagger}_{Cl}$.
[c] Coalescence temperatures.

Can. J. Chem. Downloaded from www.nrcresearchpress.com by 210.87.254.42 on 09/05/12
For personal use only.

Can. J. Chem. Downloaded from www.nrcresearchpress.com by 210.87.254.42 on 09/05/12
For personal use only.

TABLE 2. Free energies of activation for 3-arylhydantoins and 3-aryl-2-thiohydantoins

	Solvent	Temperature (°C)	$\Delta G^{\ddagger a}$ (kcal/mol)	$\Delta\Delta G^{\ddagger b}$ (kcal/mol)
2*a*	Pyridine	60	18.3±0.1	
2*b*	Pyridine	60	19.8±0.2	−1.5
2*c*	DMSO-d_6	70	18.7±0.2	
2*d*	DMSO-d_6	70	20.8±0.2	−2.1
2*e*	DMSO-d_6	70	19.3±0.1	
2*f*	Pyridine	70	20.0±0.1	−0.7
3*a*	Pyridine	57.5	24.8±0.1	
3*b*	Pyridine	58.5	25.7±0.1	−0.9

[a] 90% confidence limits.
[b] $\Delta G^{\ddagger}_{CH_3} - \Delta G^{\ddagger}_{Cl}$.

In the 1-arylhydantoins there are two possible transition states for rotation, the *o*-aryl substituent passing either the substituents in the 5-position or the 2-carbonyl group. The significant differences between the rotational barriers of 1-arylhydantoins and 3-arylhydantoins (in which the *o*-aryl substituent must pass a carbonyl group) (Tables 1 and 2), the large increase in $\Delta G^{\ddagger}$ on the introduction of a second methyl group in the 5-position (Table 1), and the failure in this laboratory to observe restricted rotation at temperatures as low as −78 °C in 1-arylhydantoins lacking a substituent in the 5-position, are taken as evidence that the more bulky *ortho* substituent must pass the 5-position in the preferred transition state for rotation in the 1-arylhydantoin series. This conclusion is supported by a study of Dreiding models. In this series, the interaction between the substituents in the 5-position of the heterocyclic moiety and the *o*-chloro or *o*-methyl group should be of a normal steric character.

In the 3-arylhydantoin or 3-aryl-2-thiohydantoin series, the *o*-chloro or *o*-methyl substituent must pass a carbonyl oxygen atom in the transition state for rotation. The preferred pathway in the 2-thiohydantoins must be the one in which the bulky *ortho* substituent passes the carbonyl rather than the more bulky thiocarbonyl group. The two possible transition states in the 3-arylhydantoins appear to be very similar in energy, the *o*-aryl substituent passing either the 2- or the 4-carbonyl oxygen atom. Available evidence does not indicate which of these is the preferred pathway or if there is a significant energy difference between them. It is likely that the increase in the effective size of chlorine relative to methyl results from electrostatic repulsion between the electronegative chlorine and oxygen atoms which increases the energy of the transition state. This influence is lacking in the preferred transition state for rotation in the 1-arylhydantoins.

In addition to its steric effects and through-space electronic effects as an *ortho* substituent, a chlorine substituent on the aryl group may possibly influence the barriers to rotation by through-bond field or mesomeric effects. Mesomeric effects are likely to be significant only in or near the transition state for rotation of the aryl group. In the transition state, the aryl and heterocyclic moieties must be approximately coplanar, allowing maximum or near maximum conjugation between the aryl π-electron system and the lone pair of electrons on the heterocyclic nitrogen atom at the point of attachment. Through-bond field effects may operate in both the transition and the ground states. By influencing the electron distribution in the hetero ring, a chloro substituent might cause sufficient changes in bond lengths and bond angles in the ground and transition states to influence the free energies of activation.

In order to determine the electronic influence of a chlorine substituent on the rotational barriers, the free energies of activation of 3-(2-methyl-4-chlorophenyl)-5-methylhydantoin, **2***g*, and 3-(2-methyl-4-chlorophenyl)-5-phenylhydantoin, **2***h*, both containing a *p*-chloro substituent, were compared (at the same temperature) with those of **2***e* and *c*, respectively. No significant changes in the values of $\Delta G^{\ddagger}$ were observed on the addition of this substituent. Since the through-bond influence of an *o*-chloro substituent should be similar to that of a *p*-chloro substituent, it is concluded that the observed influence of an *o*-chloro substituent is primarily a through-space effect.

Experimental

Proton Magnetic Resonance Measurements

P.m.r. spectra were taken on a Varian HA-100 spectrometer operating in the field sweep mode and employing the standard variable temperature equipment. The temperature dependent portions of the spectra were recorded at maximum convenient scale expansion. Temperatures, believed to be accurate to ± 2 °C, were determined immediately after each spectrum was taken by measuring the peak separation of a standard Varian ethylene glycol or methanol sample.

Data Processing

The spectra of **1***a*-**2***h* were digitized from the charts through the use of a Hewlett-Packard 2114A computer,

Can. J. Chem. Downloaded from www.nrcresearchpress.com by 210.87.254.42 on 09/05/12
For personal use only.

F-3B Line Follower, and 7001AM X-Y recorder. Following transfer from storage on paper tape to magnetic tape, the digitized spectra were subjected to complete line shape analysis by a CDC 3300 or CYBER 70-72 computer using a non-linear regression programme incorporating the appropriate line shape functions.[2] The computer fitted a calculated spectrum to each digitized experimental spectrum, varying the line shape and intensity parameters in an iterative sequence until a best fit was obtained. The natural line width parameters were held constant during fitting at values determined from spectra recorded at sample temperatures where exchange broadening was absent or minimal. This restriction is necessary because the fitting procedure cannot make an adequate distinction between the effects of varying the line width and the lifetime parameters. Possible sources of error associated with temperature dependent chemical shifts (5) were minimized by having the computer find the true chemical shifts for most of the temperature dependent spectra during line shape analysis. Since the fitting process becomes rather insensitive to the chemical shift difference in the coalescence point region and above, the chemical shift parameters were held constant at values extrapolated from lower temperature spectra whenever a plot of chemical shift difference *vs.* temperature revealed significant scattering of points. Such scattering appeared only near the coalescence point, consistent chemical shift values being returned by the computer over most of the temperature range. Extrapolation was limited to the coalescence point region, since chemical shift errors could become significant if extrapolation were continued much beyond this point. Since the lifetime parameters for the two sites were optimized independently, the regression procedure compensated for unequal populations. Computer generated plots of superimposed digitized experimental and best-fit spectra were used for visual checks on the quality of the fitting.

The random error ranges quoted in Tables 1 and 2 are based on linear regression analysis of the fit to the Arrhenius equation in logarithmic form, except for **3***a* and *b*, in which cases the errors are based on non-linear regression analysis of the equilibration data. Systematic errors which are likely to be important in this study may arise from incorrect assignment of the chemical shift and line width parameters in the fitting procedure, and from errors in temperature measurement (5). Experience has shown that the fitting procedure used in this study is sufficiently sensitive to the chemical shift difference (except in the coalescence point region) that errors arising from inaccurate chemical shift differences being employed are likely to be unimportant. A potentially more serious source of systematic error is an incorrect assignment of the natural line width, since the values of the lifetime parameters returned by the computer are very sensitive to the fixed value of the line width parameter employed in the fitting procedure when exchange broadening makes a small contribution to the overall line width (5). In consequence, care must be taken in determining the value of the natural line width to be used in the calculation. Since the measured line widths employed in this study should be reasonably accurate over the sensitive slow exchange region, the systematic line width errors in $\Delta G^{\ddagger}$ are estimated to be less than 0.1 kcal/mol. In general, the error ranges reflect the insensitivity of the $\Delta G^{\ddagger}$ function to both random and systematic errors in the line shape analysis.

The most significant systematic errors in this study are likely to arise from errors in temperature measurement. A systematic temperature calibration error of 2° would produce errors in $\Delta G^{\ddagger}$ of about 0.1 kcal/mol.

Systematic errors must be considered in addition to the random errors quoted in Tables 1 and 2 in evaluating the probable accuracy of the values of $\Delta G^{\ddagger}$ obtained. However, when differences in $\Delta G^{\ddagger}$ values obtained under similar conditions are considered, systematic errors should be less important, provided that these errors are consistently in the same direction. This should be particularly true of systematic temperature errors if results obtained at similar temperatures are being compared. Thus the contribution of systematic errors to the free energy of activation differences in Tables 1 and 2 should be small.

The thermodynamically less stable diastereomeric rotational isomers of **3***a* and *b* were obtained in better than 95% isomeric purity by careful recrystallization from ethanol of the mixture of isomers obtained on synthesis. Equilibration to the thermodynamic mixture of rotamers was followed by repetitively recording the methyl region of the spectra while the sample was maintained at a constant temperature in the n.m.r. spectrometer. The relative proportions of the rotational isomers contributing to the time dependent spectra during equilibration were determined by matching the experimental spectra with a DuPont 310 Curve Resolver, using Lorentzian line shapes. Rate constants were obtained by fitting the experimental ratio *vs.* time curve with the appropriate isomerization function for a reversible first order reaction, using the non-linear regression programme (6).

Materials

The 1-aryl-5-methylhydantoins, **1***a* and *b*, were prepared from *N*-(*o*-tolyl)alanine or *N*-(*o*-chlorophenyl)alanine, respectively, and urea by the method of Wada (7). The 1-aryl-5,5-dimethylhydantoins, **1***c* and *d*, were prepared from *o*-toluidine or *o*-chloroaniline, respectively, and *N*-(2-bromo-2-methylpropionyl)urea (obtained by reaction between 2-bromo-2-methylpropionyl bromide and urea (8)) by the method of Mazover (9).

The 3-arylhydantoins, **2***a–f*, were prepared from *o*-tolyl isocyanate or *o*-chlorophenyl isocyanate and alanine, 2-methylalanine, or α-phenylglycine by the method of Behr and Clarke (10). The 3-aryl-2-thiohydantoins, **3***a* and *b*, were prepared from *o*-tolyl isothiocyanate or *o*-chlorophenyl isothiocyanate (obtained by reaction between *o*-chloroaniline and thiophosgene (11)) and the amino acids, by the method of Pujari and Rout (12). The 2-methyl-4-chlorophenyl isocyanate required for the

[2]In most cases, the line shape equation employed was that formulated by Gutowsky and Holm (4). The six parameters required to specify the line shape and intensity are: the mean lifetimes (not necessarily equal) on each of the two sites, the two chemical shifts, the line width in the absence of exchange broadening (assumed to be identical on each site), and a scaling factor. The Gutowsky and Holm method was extended to simulate the effect of the temperature independent spin coupling between the C-5 methine and methyl protons on the C-5 methyl signal in cases **1***a* and *b*, and **2***f*.

preparation of **2***g* and *h* was prepared from 2-methyl-4-chloroaniline and phosgene using the method of Shriner *et al.* (13).

These compounds were characterized through their p.m.r. and i.r. spectra and elemental analysis or mass spectra.

This work was supported by grants from the National Research Council of Canada.

1. E. L. ELIEL. Stereochemistry of carbon compounds. McGraw-Hill, New York. 1962. pp. 156–164.
2. E. L. ELIEL, N. L. ALLINGER, S. L. ANGYAL, and G. A. MORRISON. Conformational analysis. Interscience, New York. 1965. Chapt. 7.
3. L. PAULING. The nature of the chemical bond. 3rd ed. Cornell University Press, Ithaca, New York. 1960. p. 260.
4. H. S. GUTOWSKY and C. H. HOLM. J. Chem. Phys. **25**, 1228 (1956).
5. R. R. SHOUP, E. D. BECKER, and M. L. MCNEEL. J. Phys. Chem. **76**, 71 (1972).
6. W. E. BENTZ, L. D. COLEBROOK, J. R. FEHLNER, and A. ROSOWSKY. Chem. Commun. 974 (1970).
7. M. WADA. Chem. Ber. **260**, 47 (1933).
8. S. R. SAFIR, H. DALATIAN, W. FANSHAWE, K. CYR, R. LOPRESTI, R. P. WILLIAMS, S. D. UPHAM, L. GOLDMAN, and S. KUSHNER. J. Am. Chem. Soc. **77**, 4840 (1955).
9. Y. G. MAZOVER. J. Gen. Chem. USSR. **22**, 1700 (1952).
10. L. BEHR and H. T. CLARKE. J. Am. Chem. Soc. **54**, 1630 (1932).
11. G. M. DYSON, H. J. GEORGE, and R. F. HUNTER. J. Chem. Soc. 436 (1927).
12. H. K. PUJARI and M. K. ROUT. J. Indian Chem. Soc. **31**, 937 (1954).
13. R. L. SHRINER, W. H. HORNE, and R. F. B. COX. *In* Organic syntheses. Vol. II. *Edited by* A. H. Blatt. John Wiley and Sons, New York. 1943. p. 453.

Can. J. Chem. Downloaded from www.nrcresearchpress.com by 210.87.254.42 on 09/05/12
For personal use only.

A Low Temperature Infrared Study of Hydrogen Bonding in *N*-Alkylacetamides

MARIE-CLAUDE BERNARD-HOUPLAIN AND C. SANDORFY
Département de Chimie, Université de Montréal, Montréal, Québec

Received April 19, 1973

The infrared spectra of *N*-methylacetamide and two other secondary amides were measured in solution at temperatures ranging from 22 to −190 °C in both the fundamental and the overtone regions. At least two hydrogen bonded species are found as association increases with decreasing temperature. The effect of hydrogen bond formation on the anharmonicity of the NH stretching vibration and on the NH stretching – NH bending coupling constant is examined.

Les spectres infrarouges du *N*-methylacetamide et de deux autres amides secondaires ont été mesurés en solution, à des températures allant de 22 à −190 °C, à la fois dans la région de la fondamentale et dans celle des harmoniques. On a établi l'existence d'au moins deux espèces associées par liaison hydrogène en abaissant la température. On a examiné l'effet de la liaison hydrogène sur l'anharmonicité de la vibration de valence NH, et sur la constante de couplage entre les vibrations NH de valence et de déformation.

Can. J. Chem., **51**, 3640 (1973)

Can. J. Chem. Downloaded from www.nrcresearchpress.com by 210.87.254.5 on 09/05/12
For personal use only.

Introduction

In three previous publications (1–3) we reported the results of a low temperature infrared solution study of the self-association of secondary amines. In the present paper we are dealing mainly with *N*-methylacetamide (NMA), although results obtained on *N*-ethylacetamide and *N*-methylpivalamide will also be mentioned.

In a sense, hydrogen bonding in NMA is still a case of self-association, since the same molecule is proton donor and acceptor at the same time. The donor and acceptor sites are different, however, so that the case of amides is intermediate between self-association as it exists in alcohols or amines and association between different molecules. There is general agreement that hydrogen bonding in the case of amides is of the N—H---O type. It is generally admitted too that the CONH group is coplanar because of an appreciable degree of conjugation between the π electrons of the carbonyl group and the nitrogen lone pairs. In *N*-alkyl-amides *cis–trans* isomerism is possible around the C—N bond. The bands due to the fundamental vibrations of dissolved secondary amides were thoroughly studied by several authors (see ref. 4). Attention has also been paid to the overtones of these vibrations (5–8).

We are now presenting the results of a combined low temperature and overtone study, similar to those which were carried out in this laboratory on amines, alcohols (9, 10), and thiols (11).

As in our previous experiments the solvent was a 1:1 mixture of CCl_3F and CF_2Br–CF_2Br (FR) which sets to a glass at low temperatures making it possible to measure solution spectra down to −190 °C. As before we were seeking information on changes in association with decreasing temperature and on the anharmonicity of the vibrations.

The following symbols will be used in connection with the vibrations of an X—H---Y system: ν_1 the X—H stretching vibration; ν_2 the X—H in-plane bending vibration; ν_3 the X---Y bridge stretching vibration.

The fundamentals and overtones will be called ν_i^{01}, ν_i^{02}... where the upper indices stand for the vibrational quantum numbers of the lower and upper levels. Combinations will be referred to as $\nu_1 + \nu_2$, $\nu_1 + 2\nu_2$,... The anharmonicity and coupling constants will be called X_{11}, X_{12},...

There is certain confusion in the literature concerning the signs of anharmonicity constants and our own previous publications are no exception. We shall henceforth take a constant to be negative if its existence diminishes a vibrational frequency and positive if it increases it. Thus anharmonicity constants will be generally negative.

Experimental

The amides were supplied by Eastman Organic Chemicals; *N*-methyl- and *N*-ethylacetamides were distilled and dried under vacuum. *N*-methylpivalamide was used without further purification.

The solvents were 1:1 mixtures of CCl_3F (Freon 11)

Can. J. Chem. Downloaded from www.nrcresearchpress.com by 210.87.254.5 on 09/05/12
For personal use only.

and $C_2Br_2F_4$ (Freon 114B2) (FR) obtained from Dupont de Nemours Co. of Canada. They were distilled and kept over phosphorus pentoxide.

N-methylacetamide-d_6 ($CD_3CONHCD_3$) was purchased from Merck, Sharp and Dohme of Canada Ltd. and was of a minimum isotopic purity of 99%.

N-methylacetamide-N-*d* was prepared by exchange with heavy water (12, 13) and was of a minimum isotopic purity of 95%.

All products were kept and handled in an inert atmosphere to avoid moisture adsorption.The solutions were prepared gravimetrically in volumetric flasks and the concentration was corrected for solvent contraction, admitting a linear dependence of volume with temperature.

The NH fundamentals were measured on a Perkin Elmer 621 spectrometer and the overtones on a Cary 17 instrument.

Other experimental details were given in previous publications from this laboratory (14, 15).

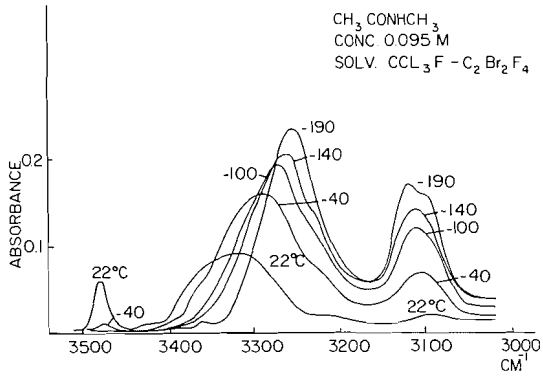

FIG. 1. The infrared spectrum (3500–3000 cm^{-1}) of *N*-methylacetamide at different temperatures in a 1:1 mixture of CCl_3F and CF_2Br–CF_2Br. Concentration at 22 °C: 0.095 *M*; cell length: 0.149 mm.

The Fundamentals

NMA exists practically only in the *trans* form (16). The free NH fundamental is at 3476 cm^{-1} in CCl_4 solution (17). At room temperature, with increasing concentration an associated band appears at 3370 cm^{-1} and moves gradually to lower frequencies. At about 1 *M* the maximum reaches 3300 cm^{-1} and remains there even for the pure liquid. This large shift and the shape of the band indicates that association does not stop at the dimer stage but that higher polymers are successively formed. In sufficiently concentrated solutions a shoulder is observed at 3225 cm^{-1} which has been assigned by Cannon (18) and by Fillaux and De Lozé (19) to a combination of the amide I (mainly C=O stretching) and amide II (mainly NH bending) bands. Another band, at 3100 cm^{-1}, was the target for much discussion (20–23). It has been assigned to the first overtone of amide II in Fermi resonance with the associated NH stretching vibration or to a combination of the NH stretching vibration with a low frequency bridge vibration.

Figure 1 shows the spectra of a 0.095 *M* solution of NMA in FR at different temperatures. The free band is at 3482 cm^{-1} at 22 °C and has a half-width of 18 cm^{-1}. When temperature is decreased, the associated band becomes gradually stronger and moves from 3330 cm^{-1} at 22 °C to 3256 cm^{-1} at −190 °C. The half-width of this band goes from 120 cm^{-1} at 22 °C to 80 cm^{-1} at −190 °C. This is likely to be due to the elimination of certain solute–solvent configurations with unfavorable Boltzmann factors and to the slowdown of thermal motion.

The intensity of the 3100 cm^{-1} band also increases with decreasing temperature. However, this band moves slightly to *higher* frequencies with decreasing temperature. This all but rules out its assignment to an NH *stretching* vibration or to a combination containing that vibration. It disappears upon deuteration, however, showing that it is an NH band. At −190 °C the ratio of the intensities of the NH stretching band and of the 3100 cm^{-1} band is practically independent of concentration between 0.02 and 0.4 *M*. Its intensity increases with decreasing temperature showing that it cannot belong to a difference tone. These facts are all in favor of the assignment of the 3100 cm^{-1} band to the first overtone of the amide II vibration. As temperature decreases the NH stretching band shifts lower, the overtone shifts higher, so that their mutual distance diminishes. Fermi resonance becomes more important and the relative intensity of the overtone with respect to ν_1 increases (Fig. 1).

At the lowest temperature the 3100 cm^{-1} band has two peaks, at 3100 and 3120 cm^{-1}. This could be due to two different associated species as indicated by the existence of two carbonyl bands (see below).

We carried out the same measurements on NMA-d_6 (Fig. 2). The NH stretching region remained the same while the 3100 cm^{-1} band underwent a shift of about 20 cm^{-1} to lower wavenumbers. Since, at the same time, the amide II band shifts by about 10 cm^{-1}, this amounts to an additional argument in favor of the assignment of the 3100 cm^{-1} band to the first overtone of the amide II vibration.

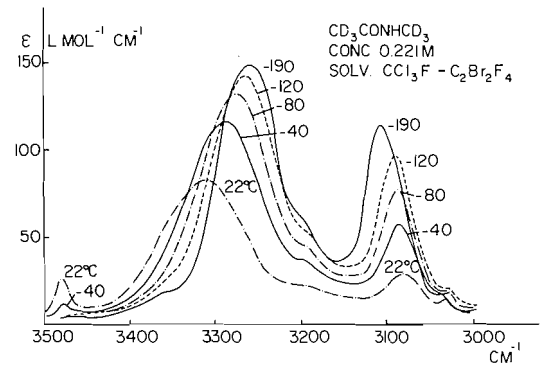

FIG. 2. The infrared spectrum (3500–3000 cm^{-1}) of *N*-methylacetamide-d_6 at different temperatures in a 1:1 mixture of CCl_3F and CF_2Br–CF_2Br. Concentration at 22 °C: 0.221 *M*; cell length: 0.160 mm.

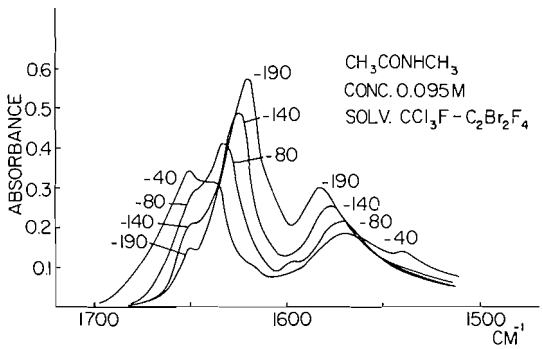

FIG. 3. The infrared spectrum (1700–1500 cm^{-1}) of *N*-methylacetamide at different temperatures in a 1:1 mixture of CCl_3F and CF_2Br–CF_2Br. Concentration at 22 °C: 0.095 *M*; cell length: 0.149 mm.

While the frequency difference between the free NH stretching band measured at 22 °C and the associated band measured at −190 °C is about 230 cm^{-1}, it is only 60 cm^{-1} for the amide II band (1582 cm^{-1} at −190 °C) and, as expected, it is in the opposite sense. The associated amide II band is not very sensitive to temperature changes, it shifts only by about 25 cm^{-1} from 22 to −190 °C toward higher frequencies (Fig. 3).

ν_1^{01} and ν_2^{02} are in Fermi resonance and we shall need their unperturbed values. For computing these we supposed that without Fermi resonance the intensity of ν_2^{02} would be negligible and then used the related equations as given, for example, by Overend (p. 351–352, in ref. 24). The band areas were planimetered out and are, of course, approximate. Table 1 gives the observed and unperturbed values for ν_1^{01} and ν_2^{02} as well as the observed values of ν_2^{01}. ρ stands for the ratio of the observed intensities of ν_1^{01} and ν_2^{02}. From the unperturbed frequencies of ν_2^{02} given in Table 1 we computed the anharmonicity constant for ν_2. It has the low value of about −10 cm^{-1} at −190 °C.

The free amide I (carbonyl) band is found at 1690 cm^{-1} at room temperature. As temperature is lowered two associated bands appear successively (Fig. 3). The one of higher frequencies varies little with temperature while the one of lower frequency shifts rapidly to lower values. At −190 °C the two bands are at 1650 and 1620 cm^{-1} respectively.

Overtones and Combination Tones

In very dilute CCl_4 solutions the free ν_1^{02} band is at 6810 cm^{-1} (half-width 30 cm^{-1}). With increasing concentration three more bands appear; they are at about 6550, 6380, and 6280 cm^{-1} for the pure liquid. In order to interpret these spectra we measured those of NMA-*N*-*d* and NMA-d_6. In alcohols NH + CH type combination bands complicate the respective part of the spectrum (25). This is not the case for amines but the stronger hydrogen bonds present in the amides make them an intermediate case and we wanted to ascertain if such combinations are present in NMA. The result was that the 6280 cm^{-1} band disappeared for both of the deuterated molecules so it must be NH + CH. The two other bands (6550 and 6380 cm^{-1}) remained in NMA-d_6, however.

Figures 4 and 5 show the spectra of NMA (0.095 *M*) and NMA-d_6 (0.221 *M*) in the NH stretching overtone region, at different temperatures in FR. The free band is at 6819 cm^{-1} at room temperature, yielding an anharmonicity constant $(\nu_1^{02}/2) - \nu_1^{01} = -72$ cm^{-1}, a value similar to those found for amines. The free band is still well distinguished at −130 °C while at similar concentrations its fundamental had disappeared at −60 °C. This again underscores the fact that the relative intensity of the free bands is greater at the overtone level than at the level of the fundamental (1, 25).

The comparison of the spectra of NMA and NMA-d_6 shows again that the band at about 6250 cm^{-1} of the former is due to NH + CH combinations. The relative intensity of the two remaining associated bands varies with temperature. Their frequencies shift from 6550 to

Can. J. Chem. Downloaded from www.nrcresearchpress.com by 210.87.254.5 on 09/05/12
For personal use only.

TABLE 1. Observed frequencies, unperturbed frequencies, and experimental intensity ratios (ρ) for *N*-methylacetamide

T (°C)	ν_1^{01} observed	ν_2^{02} observed	ρ	ν_1^{01} unperturbed	ν_2^{02} unperturbed	ν_2^{01} observed
−60	3278	3107	6.84	3256	3129	1570
−100	3271	3110	5.50	3246	3135	1575
−140	3262	3110	4.03	3232	3140	1578
−190	3256	{3110 {3120	3.12	3221	3145	1582

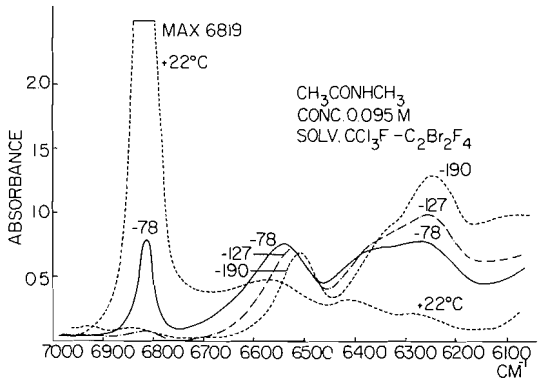

FIG. 4. The infrared spectrum (7000–6100 cm^{-1}) of *N*-methylacetamide at different temperatures in a 1:1 mixture of CCl_3F and CF_2Br–CF_2Br. Concentration at 22 °C: 0.095 *M*; cell length: 8.5 cm.

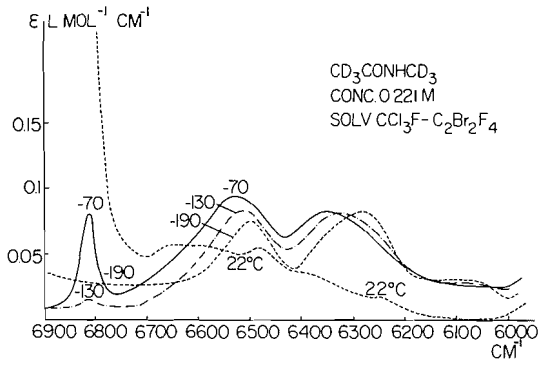

FIG. 5. The infrared spectrum (6900–6000 cm^{-1}) of *N*-methylacetamide-d_6 at different temperatures in a 1:1 mixture of CCl_3F and CF_2Br–CF_2Br. Concentration at 22 °C: 0.221 *M*; cell length: 8.5 cm.

6500 and from 6375 to 6282 cm^{-1} respectively from −20 to −190 °C.

The first associated band (6500 cm^{-1} at −190 °C) might receive contributions from the NH stretching overtone of the less associated species, from N—H---O=C end groups and from the $\nu_1 + 2\nu_2$ combination of the more highly associated species. We assign the second associated band (6282 cm^{-1} at −190 °C) to the first NH stretching overtone of the more highly associated species whose existence has been inferred from observations made in the fundamental region. We shall call these species oligomer and polymer respectively but we shall make no attempt to estimate the number of monomers contained in the adducts.

The higher frequency band (6500 cm^{-1} at −190 °C) cannot be the overtone of the polymer fundamental. This would yield an anharmonicity constant of −6 cm^{-1} with the observed frequencies; if we use the unperturbed value of ν_1 we obtain a positive anharmonicity. Both would contradict all previous observations. Furthermore the very moderate temperature shift of this band (much less than that of the fundamental) also contradicts its assignment to the polymer.

Still another contribution to the apparent intensity of the 6500 cm^{-1} band might be the polymer $\nu_1 + 2\nu_{C=O}$ combination. The $\nu_1 + \nu_{C=O}$ combination, however, was too weak to be observed and the contribution of $\nu_1 + 2\nu_{C=O}$ is therefore not expected to be significant.

For all these reasons we assign the 6282 cm^{-1} band to the first overtone of the polymer NH stretching vibration.

The rapid shift to lower frequencies of the "polymer" band with decreasing temperature is characteristic of stretching overtones (93 cm^{-1} from −20 to −190 °C). The shift of $\nu_1 + \nu_2$, for example, is much slower: only about 30 cm^{-1}. At the same time ν_1 shifts by 50 cm^{-1} to lower frequencies and ν_2 by 24 cm^{-1} to higher frequencies. Asselin and Sandorfy (26) made similar observations for alcohols. Lucazeau and Sandorfy (27) gave examples to the effect that the shifting of combination bands is usually

Can. J. Chem. Downloaded from www.nrcresearchpress.com by 210.87.254.5 on 09/05/12
For personal use only.

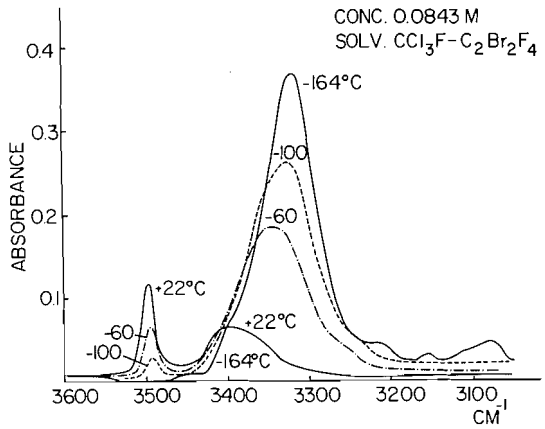

FIG. 6. The infrared spectrum (3600–3100 cm^{-1}) of *N*-methylpivalamide at different temperatures in a 1:1 mixture of CCl_3F and CF_2Br-CF_2Br. Concentration at 22 °C: 0.0843 *M*; cell length: 0.149 mm.

intermediate between that of their constituting fundamentals.

In order to ascertain if there are bands due to simultaneous excitation in the overtone region similar to those which were found for alcohols (15) we carried out an isotopic isolation experiment measuring the spectrum of a 1:9 mixture of NMA and NMA-*N*-*d* from 22 to −190 °C. No significant changes were observed. This eliminates this possibility which was unlikely anyway, since no two N—H bonds are directly linked together in the amide polymers or oligomers.

Measurements similar to those reported for NMA were also carried out on *N*-ethylacetamide. Since the results were practically the same as for NMA we shall not describe them.

N-methylpivalamide yielded one interesting observation. In this sterically hindered molecule ν_1 is at higher frequencies since the hydrogen bonds are weaker, 3340 cm^{-1} at −176 °C (Fig. 6). The ν_2 deformation band is at lower frequencies, 1545 cm^{-1} at −176 °C. Therefore ν_2^{02} is more widely separated from ν_1 and it is much weaker as for NMA. This shows that there is practically no Fermi resonance in this case and, on the other hand it corroborates the assumption that Fermi resonance does take place for NMA between ν_1^{01} and ν_2^{02}.

Discussion

The main purpose of our work has been to examine the effect of hydrogen bond formation on anharmonic coupling constants in the case of secondary amides.

The calculation of the anharmonic coupling constants is hampered by the fact that both the fundamental and the overtone of ν_1 might be influenced by Fermi resonance—with ν_2^{02} and $\nu_1 + 2\nu_2$ respectively—and all we can do is to compute upper and lower limits for X_{11}, X_{22}, and X_{12} using first the observed values of the frequencies and then their unperturbed values.

For the three-atomic model the frequencies are given, to the second order, by the following formulae if ω_1 and ω_2 are the harmonic frequencies of ν_1 and ν_2 and the X_{ij} are the anharmonic coupling constants.

$$[1]\quad \nu_1^{01} = \omega_1 + 2X_{11} + \tfrac{1}{2}X_{12} + \tfrac{1}{2}X_{13}$$

$$[2]\quad \nu_2^{01} = \omega_2 + 2X_{22} + \tfrac{1}{2}X_{12} + \tfrac{1}{2}X_{23}$$

$$[3]\quad \nu_1 + \nu_2 = \omega_1 + \omega_2 + 2X_{11} + 2X_{22} + 2X_{12} + \tfrac{1}{2}X_{13} + \tfrac{1}{2}X_{23}$$

$$[4]\quad \nu_1^{02} = 2\omega_1 + 6X_{11} + X_{12} + X_{13}$$

$$[5]\quad \nu_2^{02} = 2\omega_2 + 6X_{22} + X_{12} + X_{23}$$

$$[6]\quad \nu_1 + 2\nu_2 = \omega_1 + 2\omega_2 + 2X_{11} + 6X_{22} + \tfrac{7}{2}X_{12} + \tfrac{1}{2}X_{13} + X_{23}$$

The observed frequencies are, all for −190 °C and for the polymeric species of NMA,

ν_1^{01}	3256 cm^{-1}
ν_2^{01}	1582 cm^{-1}
ν_2^{02}	3110 cm^{-1}
$\nu_1 + \nu_2$	4882 cm^{-1}
ν_1^{02}	6282 cm^{-1}

From these we obtain

$$X_{11} = \frac{\nu_1^{02}}{2} - \nu_1^{01} = -115\,cm^{-1}$$

$$X_{22} = \frac{\nu_2^{02}}{2} - \nu_2^{01} = -27\,cm^{-1}$$

$$X_{12} = (\nu_1 + \nu_2) - \nu_1^{01} - \nu_2^{01} = +44\,cm^{-1}$$

Using these constants we can estimate the value of $\nu_1 + 2\nu_2$. The sum of the observed ν_1^{01} and twice the observed ν_2^{01} is:

$$\omega_1 + 2\omega_2 + 2X_{11} + 4X_{22} + \tfrac{3}{2}X_{12} + \tfrac{1}{2}X_{13} + X_{23} = 3256 + 2 \times 1582 = 6420\,cm^{-1}$$

Can. J. Chem. Downloaded from www.nrcresearchpress.com by 210.87.254.5 on 09/05/12
For personal use only.

Can. J. Chem. Downloaded from www.nrcresearchpress.com by 210.87.254.5 on 09/05/12
For personal use only.

This is lower than the $\nu_1 + 2\nu_2$ combination [6] by $2X_{22} + 2X_{12}$. Using the above values for X_{22} and X_{12} we have that

$$\nu_1 + 2\nu_2 = 6420 - (2 \times 27) + (2 \times 44) = 6454\ \text{cm}^{-1}$$

while the observed, apparent peak is at 6500 cm^{-1}. If, instead of using the observed frequencies we take the unperturbed values of ν_1^{01} and ν_2^{02} which are 3221 and 3145 cm^{-1} respectively we obtain

$$X_{11} = -80\ \text{cm}^{-1}$$
$$X_{22} = -10\ \text{cm}^{-1}$$
$$X_{12} = +79\ \text{cm}^{-1}$$
$$\nu_1 + 2\nu_2 = 6525\ \text{cm}^{-1}$$

The unperturbed frequencies should not be considered as very accurate. We are dealing with two broad bands whose different parts are affected to different degrees by Fermi resonance. Since the wings facing each other are likely to be affected most the split of the maxima appears to be larger than it is in reality and the unperturbed values lie probably somewhere at halfways between the observed and calculated values. Thus we can give X_{22} an estimated value which is intermediate between -10 and -27. We cannot compare this value to the corresponding value of the free species since ν_2^{02} was not found for the latter.

The coupling constant X_{12} has a value between $+44$ and $+79\ \text{cm}^{-1}$. This is a very significant change from $-7\ \text{cm}^{-1}$ (22 °C) which is the value we obtained for the free species.

The case of X_{11} is more delicate. The mean value of -115 and $-80\ \text{cm}^{-1}$ would be $-98\ \text{cm}^{-1}$ which we believe is close to its real value. The problem is complicated by the possibility of still another Fermi resonance, between ν_1^{02} and $\nu_1 + 2\nu_2$. However, the above calculations show that $\nu_1 + 2\nu_2$ falls into the 6500 cm^{-1} region close to its observed value. Therefore we do not believe that the unperturbed value of ν_1^{02} is greatly different from the observed one. At any rate, our value of X_{11} remains somewhat uncertain. In spite of this it seems to be reasonable to conclude to a moderate increase in X_{12} upon hydrogen bond formation. What causes the uncertainty is essentially the fact that, unlike in the cases of alcohols and amines, $\nu_1 + 2\nu_2$ has a frequency higher, not lower, than ν_1^{02}. Thus while the X_{11} computed with disregard of Fermi resonance are minimum values for alcohols and amines (because the frequency of the overtones was heightened by the resonance) this is not so for amides.

The anharmonicity of ν_2 is weak and still negative but hydrogen bonding increases its value. More important than this is the large increase in the value of the coupling constant X_{12} which becomes positive upon hydrogen bond formation.

Since X_{12} enters the expression of ν_2^{01} [1] it actually raises its frequency by a nonnegligible amount. The usual $\Delta\nu$–ΔH relationships cover probably a number of such anharmonic contributions.

Conclusions

Our low temperature measurements give evidence to the existence of at least two hydrogen bonded adducts for non-sterically hindered amides. The pattern of association is closer to that of alcohols than to that of amines. Contrary to amines the overtones of the associated NH stretching vibration are readily identified.

Associated amides have well defined in-plane deformation bands and there is strong anharmonic coupling between these and the NH stretching vibration. The sizable increase in the value of these coupling constants upon hydrogen bond formation and the Fermi resonance it causes constitute a significant fact for the understanding of the nature of hydrogen bonding.

We acknowledge financial help including a scholarship (M.-C.B.-H.) from the National Research Council of Canada.

1. M-C. Bernard-Houplain and C. Sandorfy. J. Chem. Phys. **56**, 3412 (1972).
2. M-C. Bernard-Houplain, G. Bélanger, and C. Sandorfy. J. Chem. Phys. **57**, 530 (1972).
3. M-C. Bernard-Houplain and C. Sandorfy. Can. J. Chem. **51**, 1075 (1973).
4. L. J. Bellamy. Advances in infrared frequencies. Methuen and Co., Ltd. London. 1968 p. 283.
5. S. Mizushima, T. Simanouti, S. Nagakura, K. Kuratani, M. Tsuboi, H. Baba, and O. Fujioka. J. Am. Chem. Soc. **72**, 3490 (1950).
6. M. Davies, J. C. Evans, and R. L. Jones. Trans. Faraday Soc. **51**, 761 (1955).
7. I. M. Klotz and J. S. Franzen. J. Am. Chem. Soc. **84**, 3461 (1962).
8. Y. H. Shaw and N. C. Li. Can. J. Chem. **48**, 2090 (1970).
9. M. Asselin and C. Sandorfy. J. Mol. Struct. **8**, 145 (1971).

10. C. BOURDÉRON, J.-J. PÉRON, and C. SANDORFY. J. Phys. Chem. **76**, 864 (1972).
11. R. BICCA DE ALENCASTRO and C. SANDORFY. Can. J. Chem. **50**, 3594 (1972).
12. B. SCHNEIDER, A. HORENI, H. PIVCOVA, and J. HONZL. Coll. Czech. Chem. Commun. **30**, 2196 (1965).
13. H. LOWENSTEIN, H. LASSEN, and A. HVIDT. Acta Chem. Scand. **24**, 1687 (1970).
14. G. DUROCHER and C. SANDORFY. J. Mol. Spectry. **20**, 1687 (1966).
15. M. ASSELIN and C. SANDORFY. J. Chem. Phys. **52**, 6130 (1970).
16. H. E. HALLAM and C. M. JONES. J. Mol. Struct. **5**, 1 (1970).
17. M. REY-LAFON, J. LASCOMBE, and M-L. JOSIEN. Ann. Chim. **8**, 493 (1963).
18. C. G. CANNON. Spectrochim. Acta, **16**, 302 (1960).
19. F. FILLAUX and C. DE LOZÉ. J. Chim. Phys. **69**, 36 (1972).
20. T. MIYAZAWA. J. Mol. Spectry. **4**, 168 (1960).
21. D. R. MCLACHLAN and R. A. NYQUIST. Spectrochim. Acta, **20**, 1397 (1964).
22. H. PIVCOVA, B. SCHNEIDER, J. STOKR, and J. JAKES. Coll. Czech. Chem. Commun. **30**, 2215 (1965).
23. E. M. BRADBURY and A. ELLIOTT. Spectrochim. Acta, **19**, 995 (1963).
24. J. OVEREND. Infrared spectroscopy and molecular structure. *Edited by* M. Davies. Elsevier Publishing Co., New York, N.Y. 1963.
25. W. A. P. LUCK and W. DITTER. Ber. Bunsenges. Phys. Chem. **72**, 365 (1968).
26. M. ASSELIN and C. SANDORFY. Can. J. Chem. **49**, 1539 (1971).
27. C. LUCAZEAU and C. SANDORFY. Can. J. Chem. **48**, 3694 (1970).

Can. J. Chem. Downloaded from www.nrcresearchpress.com by 210.87.254.5 on 09/05/12
For personal use only.

Can. J. Chem. Downloaded from www.nrcresearchpress.com by 210.87.254.6 on 09/05/12
For personal use only.

The Racemization of Sulfonium Salts. III. The Racemization of Arylsulfonium Salts

DAVID DARWISH[1] AND CHRISTOPHER E. SCOTT[2]

Department of Chemistry, University of Alberta, Edmonton, Alberta T6G 2G2

Received April 12, 1973

The rate constants for racemization by inversion of a variety of monoaryl- and diarylsulfonium salts are reported. There is a marked steric effect upon the rate of the racemization reaction. An estimate is made of the half-life for racemization of acyclic optically active triarylsulfonium salts.

On rapporte les constantes de vitesses pour la racémisation par inversion d'un certain nombre de sels de mono- et diarylsulfonium. Un effect stérique important influence la vitesse de la réaction de racémisation. Une evaluation est faite de la demi-vie pour la racémisation de sels optiquement actifs de triarylsulfonium acycliques.

Can. J. Chem., 51, 3647 (1973)

In this communication we report on the racemization by inversion (1) of a number of optically active monoaryl- and diarylsulfonium salts, **1** and **2**, respectively. In Table 1 the rate constants for racemization of these salts are compared with one another and with the rate constants for racemization of isopropylethylmethylsulfonium perchlorate, **3**, and benzylethylmethylsulfonium perchlorate, **4** (2). The data provide information on both the electronic and steric effects upon the racemization reaction and allow the estimation of a lower limit for the rate of racemization of acyclic triarylsulfonium salts at 25°.

All the optically active sulfonium salts were prepared by resolution of the corresponding (−)-dibenzoyl hydrogen tartrate salts followed by replacement of the dibenzoyl hydrogen tartrate anion by perchlorate. The salts had the following physical properties[3] [compound, m.p. (°C), $[\alpha]_{365}^{25}$ (°, methanol), concentration (g/100 ml)]: (+)-**1***a*, 74.8–75.8, 10.0,[4] 1.21; (−)-**1***a*, 80.5–82.0, −17.0,[4] 1.10; (+)-**1***b*, 79.6–80.2, 19.5, 0.945; (−)-**1***b*, 34.0–34.5, −69.5, 0.922; (+)-**1***c*, 129.8–130.6, 13.3,[4] 0.926; (−)-**1***c*, 129.8–130.6, −31.2,[4] 0.868; (+)-**1***d*, 27.5–28.5, 32.5,[4] 0.999; (−)-**1***d*, 71.0–71.5, −18.7,[4] 1.21; (+)-**1***e*, 42.0–47.0, 41.3, 1.03; (−)-**1***e*, 50.0–54.0, −19.7, 1.11; (+)-**1***f*, 37.5–39.0, 24.0, 1.20; (−)-**1***f*, 32.5–34.0, −10.8, 1.30; (+)-**2***a*, 56.5–59.5, 21.2, 0.979; (−)-**2***a*, 47.0–50.0, −15.2, 1.17; (+)-**2***b*, 39.0–40, 50.3, 1.05; (−)-**2***b*, 64.0–68.5, −8.1, 1.07; (−)-**3**, 155–160, −10.6, 0.824.

The rate constant for racemization ($k_{rac} = k_\alpha - k_t$) of the active salt is the difference between the polarimetric rate constant, k_α, and the titrimetric rate constant, k_t (2). For all the compounds reported here, except **1***d*, we find $k_\alpha/k_t > 300$, so $k_{rac} = k_\alpha$ within 0.3%.

The rate constants for racemization of **1***a* in solvent methanol are $(2.88 \pm 0.11) \times 10^{-5}\ s^{-1}$ at 50.0° and $(0.074 \pm 0.002) \times 10^{-5}\ s^{-1}$ at 25°.

Two features are clear from the relative rate data. Firstly, aryl groups do not have an appreciable electronic effect upon the rate of racemization of sulfonium salts. A comparison of **1***a* and **3**, where the steric effects of the phenyl and isopropyl groups should be similar, shows that the rate constants for racemization of these salts differ by less than a factor of 2. Similarly a comparison of **1***b*, **1***c*, and **1***d* with **1***a* shows that introduction of a *p*-methoxy, *p*-hydroxy, or *p*-nitro group onto the phenyl group leads to an

[1]Deceased April 15, 1973. Address correspondence to K. R. Kopecky.

[2]National Research Council of Canada Scholarship holder, 1968–1970.

[3]All new compounds gave satisfactory spectral data. All the compounds gave satisfactory analyses except **3**. For **3**, Anal. Calcd. for $C_6H_{15}SClO_4$: C, 32.95; H, 6.91. Found: C, 32.0; H, 6.40.

[4]At 436 nm.

TABLE 1. Relative rates[a] of racemization in solvent methanol of sulfonium salts $R_1R_2R_3S^{\oplus}\ ClO_4^{\ominus}$

Compound	R_1	R_2	R_3	$k_{rel}^{50°}$	$k_{rel}^{25°}$
1*a*	C_6H_5	CH_3	C_2H_5	1.0	1.0
1*b*	p-$CH_3OC_6H_4$	CH_3	C_2H_5	1.61	—
1*c*	p-HOC_6H_4	CH_3	C_2H_5	1.86	—
1*d*	p-$NO_2C_6H_4$	CH_3	C_2H_5	1.19	—
1*e*	C_6H_5	n-C_3H_7	C_2H_5	11.20	14.3
1*f*	C_6H_5	n-C_4H_9	C_2H_5	9.51	11.9
2*a*	p-$CH_3OC_6H_4$	C_6H_5	CH_3	9.82	14.2
2*b*	p-$CH_3OC_6H_4$	C_6H_5	C_2H_5	70.8	112.0
3	i-C_3H_7	CH_3	C_2H_5	1.54	—
4	$C_6H_5CH_2$	CH_3	C_2H_5	0.22	—

[a]Both the (+)- and (−)-enantiomers of each system had identical rates of racemization except for **3** in which only the (−)-enantiomer was obtained.

increase in rate of racemization of less than a factor of 2. Both electron donating and electron withdrawing groups increase the rate of racemization by small amounts. In the presence of 1 equiv. of sodium methoxide in methanol, **1***c* is converted to the corresponding zwitterion (p-O^-) and this material racemizes only 4.3 times faster than **1***a*. This again confirms that any electronic effect associated with substitution on the aromatic ring is very small.

In contrast, there is a marked steric effect upon the racemization rate. In each of the sets of compounds (**4**; **1***a*, **1***b*, **1***c*, or **1***d*), (**4**; **3**), and (**1***a*; **2***a*) a primary alkyl group (not a methyl) has been replaced by an aryl group or an isopropyl group on the sulfonium sulfur atom while maintaining the rest of the substituents constant. Each of these changes results in an increase in the rate constant for racemization by a factor of between 5 and 10. The sets (**1***a* or **3**; **1***e* or **1***f*) and (**2***a*; **2***b*) show that replacement of a methyl group by another primary alkyl group also increases the magnitude of k_{rac} by a factor of *ca.* 10. This result is difficult to rationalize on anything but steric effects. Replacement of a methyl group by an aryl group in set (**1***a*; **2***b*) increases k_{rac} by nearly two powers of 10. These data provide the first strong evidence for steric effects upon the inversion of an acyclic pyramidal system. Steric acceleration of pyramidal inversion has been reported in cyclic systems such as the aziridines, oxaziridines (3), and phosphetanes (4). It has been reported (5) that steric effects are not important in the racemization of acyclic phosphines and sulfoxides.

Using the approximation that replacement of the ethyl group in **2***b* by a substituted phenyl group will increase the rate constant for racemization by a factor of 10, it can be estimated that at 25° in solvent methanol the value of k_{rac} will be $8 \times 10^{-4}\ s^{-1}$ for the racemization of an optically active triarylsulfonium salt, corresponding to a half-life of *ca.* 15 min for the racemization. This estimate is a minimum value for k_{rac} (maximum value for the half-life) since it was made on the assumption that steric effects will be additive in $\log k_{rac}$ whereas one anticipates that at some stage steric effects should cease to be additive and give rise to very large rate accelerations with small structural changes. It is however clear that the previous attempts to prepare optically active triarylsulfonium salts which led to the isolation of racemic sulfonium salts (6, 7[5]) can be accounted for by rapid racemization of the sulfonium salt during the reaction and isolation procedure.

1. D. DARWISH and G. TOURIGNY. J. Am. Chem. Soc. **88**, 4303 (1966).
2. D. DARWISH, S. H. HUI, and R. TOMILSON. J. Am. Chem. Soc. **90**, 5631 (1968).
3. J. M. LEHN. Fortsch. Chem. Forsch. **15**, 311 (1970).
4. S. E. CRAMER, R. J. CHOWAT, C. H. CHANG, and D. W. DAVIS. Tetrahedron Lett. 5799 (1968).
5. R. D. BAECHLER and K. MISLOW. J. Am. Chem. Soc. **92**, 3090 (1970).
6. K. K. ANDERSEN, M. CINQUIMI, and N. E. PAPANIKOLAOU. J. Org. Chem. **35**, 706 (1970).
7. K. K. ANDERSEN. Chem. Commun. 1051 (1971).

[5]Andersen (7) has reported the synthesis of optically active p-tolylethylmethylsulfonium and p-tolylbutylmethylsulfonium salts by treatment of alkoxysulfonium salts with dialkylcadmium compounds.

Can. J. Chem. Downloaded from www.nrcresearchpress.com by 210.87.254.6 on 09/05/12
For personal use only.

A Modified Triester Method for the Synthesis of Deoxyribopolynucleotides

K. ITAKURA, C. P. BAHL, N. KATAGIRI, J. J. MICHNIEWICZ, R. H. WIGHTMAN,[1] AND S. A. NARANG[2]

Division of Biological Sciences, National Research Council of Canada,[3] Ottawa, Canada

Received June 28, 1973

A modified triester method has been developed for the synthesis of oligonucleotides starting from mononucleosides as more economical starting materials. A pentadecanucleotide has been successfully prepared.

Une méthode modifiée faisant appel au triester a été développée pour la synthèse d'oligonucléosides comme produits de départ plus économiques. Un pentadécanucléotide a été préparé avec succès.
[Traduit par le journal]

Can. J. Chem., **51**, 3649 (1973)

Can. J. Chem. Downloaded from www.nrcresearchpress.com by 210.87.254.40 on 09/05/12
For personal use only.

To date, there still remain some crucial methodological problems which must be solved before the chemical synthesis of polynucleotides becomes a reasonably efficacious process. The triester method has recently been examined in various laboratories (1–4) in an attempt to overcome some of the difficulties inherent in the "diester approach", such as low yields with increasing chain length, instability of the internucleotidic phosphodiester bond and cumbersome purification procedures. The essential feature of the "triester approach" involves phosphorylation of the terminal 3′-hydroxyl group of a 5′-protected mononucleoside **1** with a simple monophosphate ester (for example, β-cyanoethyl phosphate, phenyl phosphate, or β,β′,β′-trichloroethyl phosphate) and triisopropylbenzenesulfonylchloride (TPS) followed by subsequent condensation with the primary 5′-hydroxyl group of an incoming suitably 3′-protected nucleoside **6** and additional TPS. Since each internucleotidic bond is present in the desired product as a triester function, purification at each stage by more conventional techniques such as organic solvent extraction followed by a simple chromatography on silica gel columns becomes possible. However, we have observed that the initial phosphorylation reaction of the 3′-hydroxyl group of the starting 5′-protected mononucleoside **1** is incomplete, thus the addition of the incoming 3′-protected mononucleoside **6** leads to a very complicated reaction mixture. These mixtures cannot be completely separated using ordinary silica gel chromatography, hence the advantage of large scale synthesis and high yields is somewhat nullified. However, this difficulty can be overcome by the following simple modification which has also been recently employed by Cramer *et al.* (5). It involves initial phosphorylation of the 5′-protected nucleoside **1** with a suitably substituted phosphate **2** in the presence of TPS, followed by isolation of the phosphorylated product **3** by silica gel column chromatography in 80–85% yield. The phosphodiester group of **3** was further protected with cyanoethanol and TPS to obtain **4** in quantitative yield.

In this communication, we wish to report the effectiveness of compound **4** as the starting material in the synthesis of a pentadecadeoxypolynucleotide (see Scheme 1). Synthesis of dinucleotide was carried out by condensing an anhydrous pyridine solution of 5′-protected nucleoside 3′-phenyl phosphate **3** (20 mmol) with **4** (15 mmol) in the presence of TPS for 20 h at room temperature. After the usual workup, the fully protected dinucleotide was obtained in 70–80% yield by silica gel chromatography. Specific deblocking of the cyanoethyl group with 0.1 *N* aqueous sodium hydroxide in dioxane (4:1 v/v) for 30 seconds at 0° gave **5** which on further condensation with **6** or **4** in the presence of TPS yielded trinucleotides in isolated yields of 65–70%. Employing similar conditions hexanucleotide **11**, nonanucleotide, dodecanucleo-

[1]Guest worker from the Chemistry Department, Carleton University, Ottawa.
[2]Author to whom correspondence should be addressed.
[3]NRCC No. 13460.

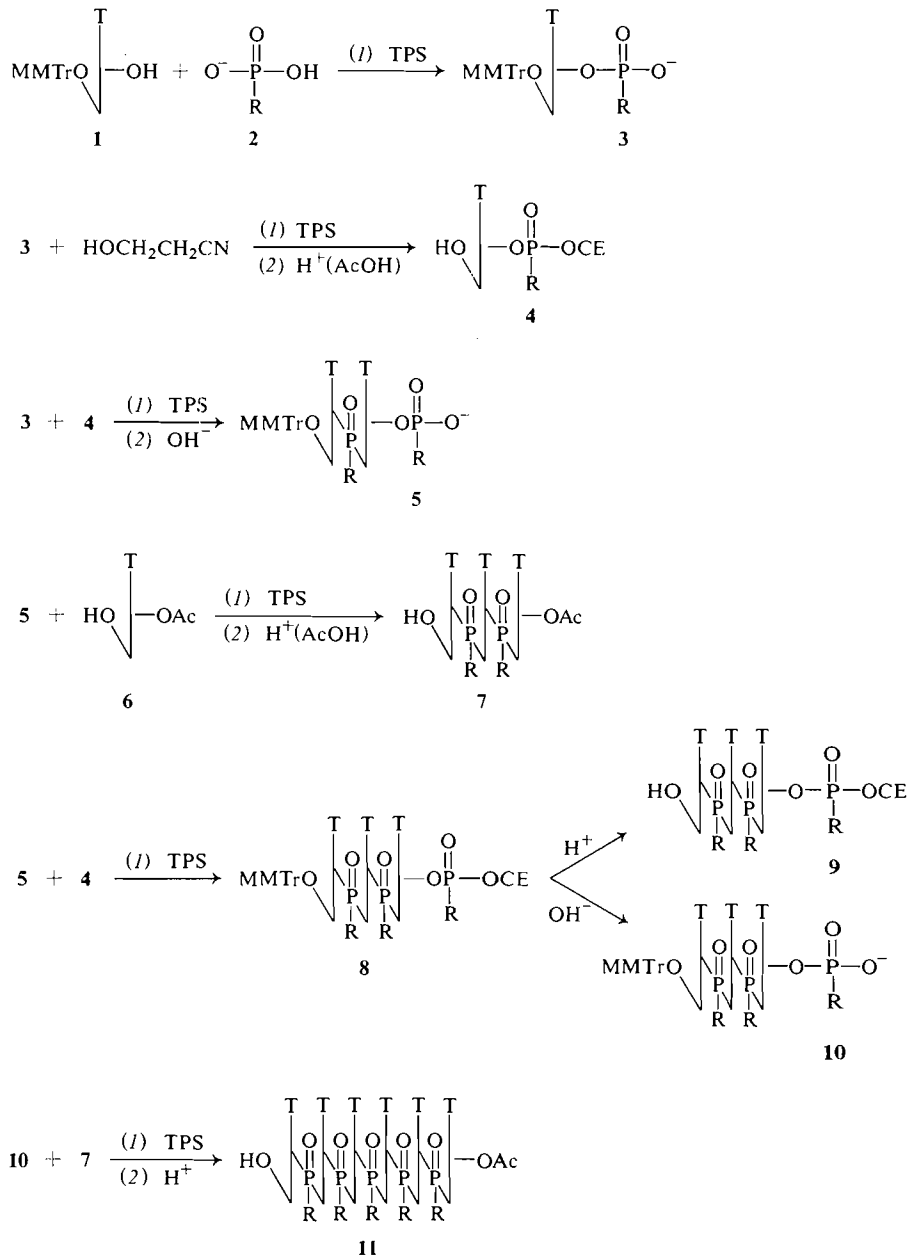

R = *O*—phenyl, *O*—(*o*-chloro)phenyl, *O*—(*p*-methylthio)phenyl

SCHEME 1

tide, and pentadecanucleotide were synthesized in 60, 40, 40, and 20% yields respectively.

The internucleotide phosphate protecting group (phenyl or *o*-chlorophenyl) was removed by treatment with 0.1 *N* sodium hydroxide – dioxane at room temperature. Recovery of the required diester products were 80–90% up to the hexanucleotide but dropped dramatically for the higher chain lengths (*ca.* 20–30%). This difficulty was overcome by using *p*-(methylthio)phenyl as

Can. J. Chem. Downloaded from www.nrcresearchpress.com by 210.87.254.40 on 09/05/12
For personal use only.

a new protecting group for the internucleotide phosphate. This was removed by alkaline treatment after oxidation with *N*-chlorosuccinimide (6) or sodium metaperiodate. The monomethoxytrityl group was removed by acetic acid treatment. Each unprotected intermediate was checked for its purity by t.l.c. on silica gel plates (7) by using aqueous solvent systems such as (i) *n*-propanol – concentrated ammonium hydroxide – water (55:10:35 v/v) and (ii) isobutyric acid – 0.1 *M* ETDA – 1 *M* ammonium hydroxide (100:1.6:60 v/v). Finally these compounds were characterized by their complete degradation with spleen and snake venom phosphodiesterase enzymes.

In conclusion, the modified triester approach for the large scale synthesis of higher polynucleotides seems very promising. Work is in progress for the synthesis of defined sequences and also in the development of more sophisticated protecting groups for the internucleotide phosphate.

One of us (R.H.W.) wishes to acknowledge with thanks Professor C. B. Reese, Cambridge University, for the experience gained in triester work during part of a sabbatical leave (December 1971 to March 1972).

1. R. L. LETSINGER and V. MAHADEVAN. J. Am. Chem. Soc. **87**, 3526 (1965); R. L. LETSINGER and K. K. OGILVIE. J. Am. Chem. Soc. **89**, 4801 (1967).
2. C. B. REESE and R. SAFFHILL. Chem. Commun. 767 (1968); J. H. VAN BOOM, P. M. J. BORGERS, G. R. OWEN, C. B. REESE, and R. SAFFHILL. Chem. Commun. 869 (1971); N. J. CUSACK, C. B. REESE, and J. H. VAN BOOM. Tetrahedron Lett. 2209 (1973).
3. F. ECKSTEIN and I. RIZK. Chem. Ber. **102**, 2326 (1969).
4. T. NEILSON and E. S. WERSTIUK. Can. J. Chem. **49**, 3004 (1971).
5. T. C. CATLIN and F. CRAMER. J. Org. Chem. **38**, 245 (1973).
6. K. L. AGARWAL, F. FRIDKIN, E. JAY, and H. G. KHORANA. J. Am. Chem. Soc. **95**, 2020 (1973).
7. J. J. MICHNIEWICZ, C. P. BAHL, K. ITAKURA, N. KATAGIRI, and S. A. NARANG. J. Chromatgr. In press.

Can. J. Chem. Downloaded from www.nrcresearchpress.com by 210.87.254.40 on 09/05/12
For personal use only.

Can. J. Chem. Downloaded from www.nrcresearchpress.com by 210.87.254.42 on 09/05/12
For personal use only.

Canadian Journal of Chemistry

Published by
THE NATIONAL RESEARCH COUNCIL OF CANADA

Journal canadien de chimie

Publié par
LE CONSEIL NATIONAL DE RECHERCHES DU CANADA

Volume 51 Number 22 November 15, 1973 Volume 51 numéro 22 15 novembre 1973

Pulse Radiolysis of Liquid Deuterated Ammonia[1]

WILLIAM ARTHUR SEDDON, JOHN WALLACE FLETCHER, JOHN JEVCAK, AND FRED CHARLES SOPCHYSHYN

Physical Chemistry Branch, Atomic Energy of Canada Limited, Chalk River Nuclear Laboratories, Chalk River, Ontario

Received May 24, 1973

Pulse radiolysis of solutions of alkali metal amides in deuterated ammonia at −15 °C produces an initial absorption with a maximum at 1500 nm due to the solvated electron, e_{am}^-. This decays on a microsecond time scale giving a residual long lived absorption with a slightly broader spectrum and a maximum displaced to 1640 nm. We suggest the residual absorption is an equilibrium mixture of e_{am}^- and a metal–electron species. The initial decay of e_{am}^- is suppressed by scavenging ND_2 and/or ND^- radicals with dissolved D_2 (1 atm) or $NaBH_4$. Evidence is also obtained for the reaction $ND^- + D_2 \rightarrow e_{am}^-$. It is estimated that $k(e_{am}^- + ND_2)$ and $k(BH_4^- + ND_2) = 2.5 \times 10^{10}$ and 7×10^7 M^{-1} s^{-1}, respectively. Measurements of the initial yield in NH_3 and ND_3 give $G_{e_{am}^-} = 3.3 \pm 0.3$ and 3.6 ± 0.4 molecules/100 eV, respectively.

La radiolyse pulsée de solutions d'amidures de métaux alcalins dans l'ammoniac deuterié à −15 °C provoque une absorption initiale avec un maximum à 1500 nm due à l'électron solvaté e_{am}^-; ce dernier ayant une durée de vie de l'ordre du microseconde conduit à une absorption résiduelle de longue durée avec un spectre plus large et un maximum déplacé à 1640 nm. Nous suggérons que l'absorption résiduelle est un mélange à l'équilibre de e_{am}^- et d'espèce métal–électron. La disparition initiale de e_{am}^- est supprimée par piégeage des radicaux ND_2 et (ou) ND^- par du D_2 dissous (1 atm) ou $NaBH_4$. La réaction $ND^- + D_2 \rightarrow e_{am}^-$ a été également mise en évidence. On a calculé que $k(e_{am}^- + ND_2)$ et $k(BH_4^- + ND_2)$ valaient respectivement 2.5×10^{10} et 7×10^7 M^{-1} s^{-1}. Les mesures de rendement initial en NH_3 et ND_3 ont conduit à $G_{e_{am}^-} = 3.3 \pm 0.3$ et 3.6 ± 0.4 molécules/100 eV respectivement.
[Traduit par le journal]

Can. J. Chem. **51**, 3653 (1973)

Introduction

Extensive investigations on the physical properties of solutions of alkali metals in liquid ammonia have shown that in very dilute solution the predominant species are the solvated electron e_{am}^-, and the metal cation M^+ (1–3). At higher concentrations it is also generally accepted that these species are in equilibrium with an intermediate species of stoichiometry M, probably best described as an ion pair, $(M^+ - e_{am}^-)$. However spin pairing occurs to a considerable extent (4), and magnetic susceptibility studies show that over 90% of the spins are paired in 10^{-1} M solutions of sodium and potassium (5). The nature of this interaction is less obvious and the species e_2^{2-}, M^-, and M_2 have been invoked to explain such results.

Despite this clear evidence of cation–electron interaction the optical spectrum and molar extinction coefficient for e_{am}^- are virtually independent of concentration and the nature of the alkali metal cation (6–8). Nevertheless the peak position is slightly concentration dependent (7, 8). This shift correlates well with the onset and extent of spin pairing (9), and the overall spectrum

[1]AECL No. 4621.

Can. J. Chem. Downloaded from www.nrcresearchpress.com by 210.87.254.42 on 09/05/12
For personal use only.

can be analyzed as a composite of two broadly overlapping absorbances (10).

Pulse radiolysis studies in liquid NH_3 have been reported previously (11–15), while Lok *et al.* (16) have compared the spectrum of solvated electrons as determined by pulse radiolysis and alkali metal solution studies for ammonia and a series of amines and ethers. The agreement between the peak positions in all cases is good. However, in some cases the spectrum attributed to solvated electrons in metal solutions tends to be somewhat broader and the peak positions at slightly higher energies than those found by pulse radiolysis. These observations, taken in conjunction with the concentration effect on the peak position in liquid ammonia, suggested to us that a time dependent shift and broadening of the optical spectrum might be observed in the pulse radiolysis of alkali metal amide solutions.

Using fast infrared detection techniques (17), and ND_3 to minimize solvent absorption (6), we have therefore reinvestigated the solvated electron absorption spectrum in liquid ammonia as a function of time, amide concentration, and temperature. Since measured radiolytic yields for e_{am}^- in liquid ammonia vary considerably we have also attempted to resolve this discrepancy and deduce a more reliable value than the previous determinations which range from $G_{e_{am}^-} =$ 0.35 to 3.0 molecule/100 eV (11, 12, 14, 18, 19).

Experimental

Details of the pulse radiolysis facility and infrared detection techniques have been presented elsewhere (17, 20–22). Briefly, solutions were irradiated with 0.5 to 2.0 μs pulses from a 2.5 MeV Van de Graaff accelerator. Rectangular quartz irradiation cells with an optical path length of 0.5 to 2.0 cm were mounted in a specially designed flow system consisting of an upper reservoir and a lower drainage bulb (22).

For low temperature studies separate jacketed flow systems were constructed in which the reservoir, drain, and float valve were cooled with cold ethanol circulated by a Neslab LT-9 thermostatic circulator. The cell itself was cooled to the same temperature with cold ethanol and N_2 gas in a manner similar to that described by Wardman (23). Temperatures were monitored continuously with a Comark type 1603 electronic thermometer.

Anhydrous liquid ammonia (Matheson Ltd.) was purified by reaction with sodium or potassium followed by fractional distillation into stainless steel storage vessels. Deuterated ammonia obtained from Merck, Sharpe and Dohme Ltd., or synthesized from NaCN and D_2O (24), was purified in a similar manner. $NaBH_4$ (Fisher Chemicals) was used as received.

Potassium (Fisher Chemicals) or sodium (Baker reagent) were stored in a dry box and freshly pressed in the form of 0.1 to 1.0 mm diameter wire of calibrated weight per unit length. Appropriate quantities were placed in a 2–3 mm diameter Pyrex tubing and transferred, either under vacuum or 1 atm D_2 pressure, to the reservoir of the flow system. Metal amide solutions were then obained by distilling ammonia from the lower bulb to the upper reservoir onto the appropriate amount of metal and then bleaching the resulting blue solutions using electrolyzed platinum (25). With this technique fresh solutions of the same or different amide concentrations can be made after each cycle by redistilling the irradiated ammonia from the lower bulb back onto fresh amounts of alkali metal in the reservoir. However it was difficult to obtain solutions completely free of amide since there was always some "carry over" associated with the distillations.

Transient optical absorptions in the region 1000–2000 nm were monitored with a Spectronics SD-8721-2 InSb photovoltaic detector with a rise time (0–100%) $\leqslant$ 200 ns (17). Spectra were obtained using a Bausch and Lomb *f* 3.5 high intensity grating monochromator at a band width $\leqslant$ 40 nm.

For most of the experiments three oscilloscope traces were recorded on a single Polaroid photograph. Examples are given in Figs. 4 and 5 where curve *A* shows the output profile of the analyzing light flash on a time scale of 500 μs/division. Curve *B* shows the transient signal recorded simultaneously with *A*, but at a higher gain, while curve *C* represents the analyzing light baseline on the same amplification and time scale as *B*. The transient signal at lower gain is superimposed on curve *A*.

Results and Discussion

Spectra

The spectrum observed immediately after the pulse in 1.4×10^{-2} *M* potassium deuteroamide solutions in ND_3 is shown in Fig. 1. Using ND_3 permits measurements up to about 2000 nm. As noted previously (11, 13), the transient absorption consists of an initial rapid decay followed by a long lived slow component (inset Fig. 1). At -15 °C the initial absorption (curve 1) has a maximum at 1500 nm while the spectrum of the long lived absorption, observed after 150 μs, has a maximum shifted slightly to 1640 nm. The longer time scale spectrum (curve 2) is normalized to the same relative intensity as spectrum 1. Although small this shift was quite reproducible and comparisons of many experiments indicated the long lived absorption to be somewhat broader.

There seems little doubt that the initial absorption is due to the solvated electron e_{am}^-. Allowing for the isotopic shift in the maximum of 400 cm^{-1} (100 nm) in changing solvent from ND_3 to NH_3 (26), our initial maximum is in good agreement with the peak absorption at 1600 nm obtained for e_{am}^- on the pulse radiolysis of liquid NH_3 at -15 °C (13). Furthermore the maximum

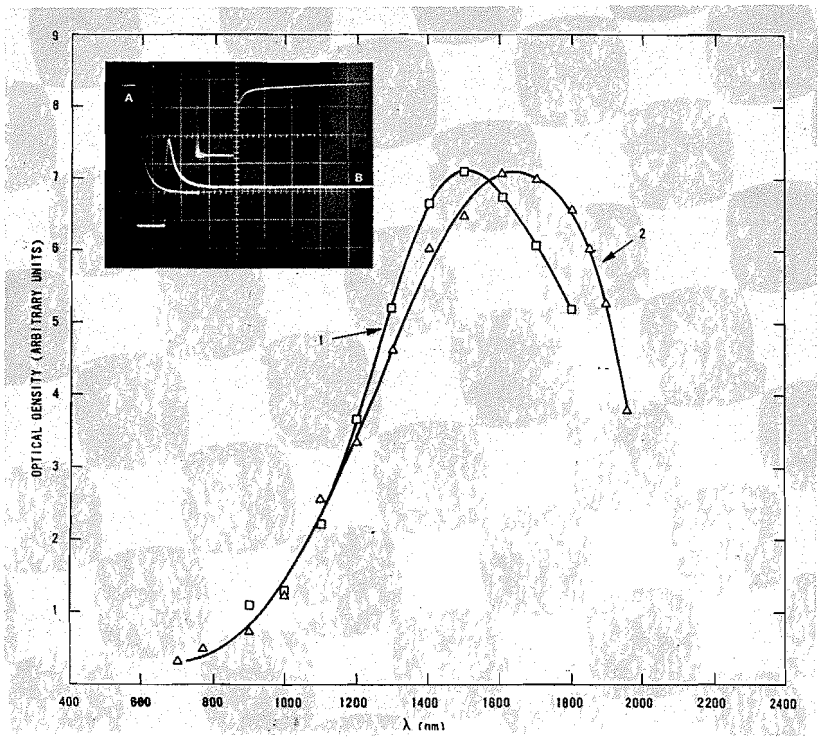

FIG. 1. Optical spectra observed on the pulse radiolysis of solutions containing 1.4×10^{-2} *M* KND_2 in ND_3 at -15 °C. Curve 1, immediately after the pulse; curve 2, 150 μs after the pulse. The inset (trace *B*) shows the transient signal monitored at 1400 nm in a 2.0 cm cell. Ordinate 25% absorption/division, abscissa 5 μs/division, dose/pulse $\sim 3 \times 10^{20}$ eV/l. Trace *A*, see experimental.

observed by pulse radiolysis shifts to higher energies with decreasing temperatures (Fig. 2) with the corresponding blue shift equivalent to a temperature coefficient of ~ 17 cm^{-1}/°C. Comparing this shift with alkali metal ammonia solutions we find values of 14.3 cm^{-1}/°C obtained by Burow and Lagowski (6) using a 2.8×10^{-4} *M* solution of sodium in ND_3 and 21.8 cm^{-1}/°C deduced by Hurley *et al.* (26), for e_{am}^- in sodium/ND_3 solutions extrapolated to infinite dilution (Fig. 3.)

However, in previous pulse radiolysis studies there has been no attempt to compare both the initial and residual absorptions. Although slight, the time dependent shift in peak position we observe is toward longer wavelengths and is consistent with the results observed in alkali metal ammonia solutions (7, 8). For example, in liquid NH_3 at -65 °C the data of Douthit and Dye (7) show a shift in the wavelength of the absorption maximum from 1400 to 1480 nm with increasing concentrations of sodium from $\sim 5 \times 10^{-4}$ to 4×10^{-3} *M* (9). Similarly from optical spectra measured in dilute solutions ($5 \times 10^{-6} - 5 \times 10^{-4}$ *M*) of sodium and potassium in ND_3 (6, 26) it appears that at infinite dilution the absorption maximum lies at shorter wavelengths.

The solid triangles and squares shown in Fig. 3 illustrate the effect of decreasing temperature on the absorption maxima of the initial and long lived species respectively, in 1.4×10^{-2} *M* potassium deuteroamide solutions. The remaining data obtained for sodium solutions in ND_3 were presented by Hurley *et al.* (26) and are shown for comparison. The alkali metal results show a slight shift of the maximum with concentration at the lower temperatures even in 2×10^{-4} *M* solution. On this basis, and from the difference we observed in the short–long time pulse radiolysis spectrum at -15 °C, we expected that such a shift might become more significant at lower temperatures, particularly at the higher concentration used in our experiment.

From Fig. 3 we can see that the maxima of the

Can. J. Chem. Downloaded from www.nrcresearchpress.com by 210.87.254.42 on 09/05/12
For personal use only.

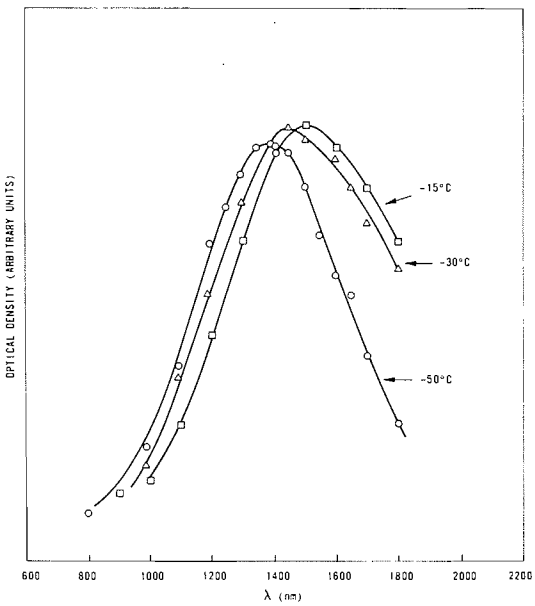

FIG. 2. Effect of temperature on the optical spectra observed immediately after the pulse in solutions containing 1.4×10^{-2} *M* KND_2 in ND_3.

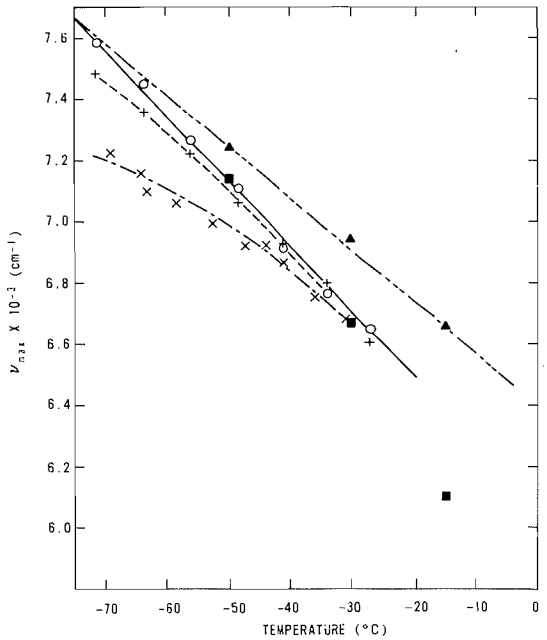

FIG. 3. Effect of temperature on the e_{am}^- maximum in ND_3. Symbols 0, +, and × are data for sodium in ND_3 taken from ref. 26: ○, Hurley infinite dilution; +, Hurley 1.94×10^{-4} *M*; ×, Burow and Lagowski 2.86×10^{-4} *M*. Solid symbols, this work in solutions containing 1.4×10^{-2} *M* KND_2; ▲, immediately after the pulse; ■, 150 μs after the pulse.

initial e_{am}^- absorption (closed triangles) lies at higher energies than the corresponding absorption in alkali metal solutions. The results extrapolate to the infinite dilution value deduced by Hurley *et al.* (26) and support their contention that there is an appreciable shift of the peak position even at low metal concentrations. However, the difference between λ_{max} for the initial and final species did not increase with decreasing temperature in the manner suggested by the alkali metal studies. On the contrary the largest effect was observed at the highest temperature. Considering all the experimental parameters it may simply be that our technique is too imprecise for a definitive answer with respect to the temperature effect. The situation is further complicated in that the existence of ion pairs or spin-paired species probably results in temperature-dependent equilibria among species with slight differences in spectra. Nevertheless the results suggest to us that the residual absorption is best considered as a composite of two, or more, overlapping bands corresponding to e_{am}^- and a metal–electron species.

It is worth noting that our recent results in ethylamine (22, 27), demonstrate that the solvated electron and ion-paired species do have similar, but distinct spectra, with the latter absorbing at higher energies. This is consistent with the observations of Lok *et al.* (16), implying again that the peak positions assigned to solvated electrons in alkali metal solutions correspond to equilibrium mixtures of electron and metal–electron species.

Decay Kinetics of e_{am}^-

In agreement with Dye *et al.* (13), we find the initial rate of e_{am}^- decay in ND_3 follows second order kinetics. This rate of decay is independent of amide concentration. However, the relative proportion of the fast to slow component increases with dose and decreases with amide concentration.

In "pure" and basic ammonia solutions the initial decay of e_{am}^- appears to be due to second order reactions with other radical species produced during the pulse.

[1*a*] $$e_{am}^- + NH_2 \rightarrow NH_2^-$$

[1*b*] $$e_{am}^- + NH \rightarrow NH^-$$

Can. J. Chem. Downloaded from www.nrcresearchpress.com by 210.87.254.42 on 09/05/12
For personal use only.

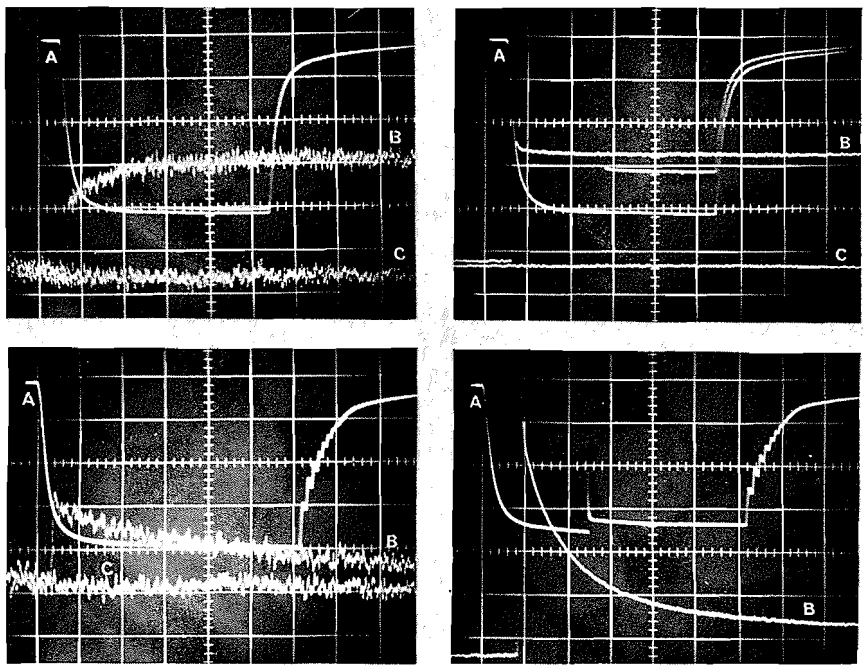

FIG. 4. Oscilloscope traces showing the transient absorptions observed at 1500 nm in a 2.0 cm cell for solutions containing $NaND_2$ in ND_3 in the presence and absence of D_2 (1 atm). Upper left trace *B*, 1.4×10^{-4} *M* $NaND_2/D_2$; ordinate 1.0% absorption/division, abscissa 10 μs/division, dose/pulse $\sim 9 \times 10^{17}$ eV/l. Upper right trace *B*, same solution, ordinate 9.9% absorption/division, abscissa 5 μs/division, dose/pulse 2×10^{19} eV/l. Lower left trace *B*, 1.4×10^{-4} *M* $NaND_2$ (no D_2); ordinate 0.5% absorption/division, abscissa 5.0 μs/division, dose/pulse 9.1×10^{17} eV/l. Lower right trace *B*, same solution, ordinate 11.2% absorption/division, abscissa 5 μs/division, dose/pulse 6.9×10^{19} eV/l. Traces *A* and *C*, see experimental.

[1*c*] $$e_{am}^- + H \rightarrow NH_2^- + H_2$$

Other workers (12, 13, 19) have suggested that reaction 1*a* is the most important. Since the initial decay is independent of base then the dissociation of NH_2, reaction 2*f*, is either quite slow or, by analogy with aqueous solutions (28), $k_{1a} \sim k_3$.

[2] $$NH_2 + NH_2^- \underset{r}{\overset{f}{\rightleftharpoons}} NH^- + NH_3$$

[3] $$e_{am}^- + NH^- \rightarrow 2\,NH_2^-$$

Assuming approximately equal concentrations for e_{am}^- and $NH_2(NH^-)$ and the extinction coefficient $\varepsilon_{e_{am}^-} = 4.9 \times 10^4\ M^{-1}\ cm^{-1}$ for e_{am}^- in metal ammonia solutions (6), then $k_{1a} = 2.5 \times 10^{10}\ M^{-1}\ s^{-1}$. This is in good agreement with the value of $> 10^{10}\ M^{-1}\ s^{-1}$ deduced by Dye *et al.* (13).

It is worth noting here that alkali metal amides are only weakly dissociated in liquid ammonia and that the concentration of NH_2^- is only about 10% in 10^{-2} *M* KNH_2. Values for the dissociation constant range from 2.23×10^{-2} *M* for sodium amide to 1.02×10^{-1} *M* for potassium and cesium amides (29). No distinction is made between reactions involving NH_2^- or KNH_2.

In "pure" ammonia the second order decay of e_{am}^- is complete. The addition of base results in an increasing contribution due to the long lived e_{am}^- species, possibly due to the removal of radiolytically formed NH_4^+,

[4] $$NH_4^+ + NH_2^- \rightarrow 2\,NH_3$$

in competition with

[5] $$e_{am}^- + NH_4^+ \rightarrow NH_3 + H$$

However Dye *et al.* (13) set an upper limit of $k_5 = 6 \pm 2 \times 10^5\ M^{-1}\ s^{-1}$, which suggests reaction 5 is insignificant at low doses. The relative proportion of the long lived component does however increase with amide concentration. In part this may be due to reaction 6, analogous to

Can. J. Chem. Downloaded from www.nrcresearchpress.com by 210.87.254.42 on 09/05/12
For personal use only.

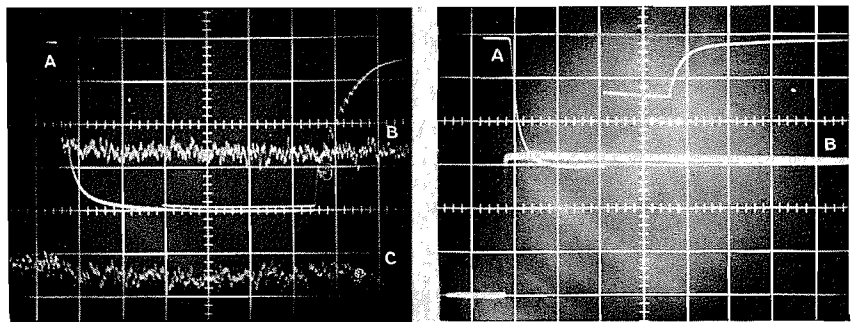

FIG. 5. Oscilloscope traces showing the transient absorptions observed in basic solutions containing $NaBH_4$ in ND_3 and NH_3. Left 1500 nm, 2.0 cm cell, 5×10^{-4} *M* $NaND_2$ and 9×10^{-4} *M* $NaBH_4$ in ND_3; trace *B*, ordinate 1.0% absorption/division, abscissa 5 μs /division, dose/pulse $\sim 2 \times 10^{18}$ eV/l. Right 1400 nm, 1.0 cm cell 3.6×10^{-3} *M* $NaNH_2$ and 1.3×10^{-1} *M* $NaBH_4$ in NH_3; trace *B*, ordinate 16.7% absorption/division, abscissa 50 μs/division, dose/pulse 1.6×10^{20} eV/l. Traces *A* and *C*, see experimental.

the corresponding reaction in aqueous solution (30).

$$[6] \qquad H + NH_2^- \rightarrow e_{am}^-$$

Although our evidence is not conclusive one cannot exclude the rapid formation of a spin-paired species such as M_2 via the neutral ion-pair M

$$[7] \qquad e_{am}^- + M^+ \rightleftharpoons M$$

$$[8] \qquad 2M \rightleftharpoons M_2$$

Species of this nature are clearly formed in alkali metal ammonia solutions (1), and as mentioned above probably contribute to the long lived absorption.

Effect of Added Hydrogen/Deuterium

An increase in the stability of radiolytically produced e_{am}^- has been observed by Belloni *et al.* (19) during the γ-radiolysis of basic solutions of liquid ammonia containing dissolved H_2. Our pulse radiolysis results using both NH_3 and ND_3 show that the initial rapid decay of e_{am}^- can be suppressed in basic solutions containing $\sim 1.7 \times 10^{-3}$ *M* H_2/D_2 (1 atm, −15 °C (31)). Furthermore, at doses $\leqslant \sim 10^{19}$ eV l^{-1} an additional increase in absorption can be seen immediately following the pulse in solutions ranging from 1.4×10^{-5} *M* to 1.4×10^{-3} *M* sodium amide. At higher doses per pulse only a small amount of initial decay is observed, in sharp contrast to the results obtained in the absence of H_2/D_2. These changes are illustrated in the oscilloscope traces reproduced in Fig. 4.

Belloni *et al.* (19) attribute this enhanced stability to the removal of NH_2 radicals, reaction 9 followed by [6],

$$[9] \qquad H_2 + NH_2 \rightarrow H + NH_3$$

$$[6] \qquad H + NH_2^- \rightarrow e_{am}^-$$

Alternatively they suggest the basic entity, NH^-, reacts directly with H_2 to form e_{am}^-

$$[10] \qquad H_2 + NH^- \rightarrow e_{am}^-$$

Reactions 6 and 10 were also proposed much earlier by Dainton *et al.* (18). Our results cannot differentiate between the two possibilities but it is likely that [10] is energetically more favorable. In the gas phase reaction 9 is slow with an estimate for $k_9 \sim 3 \times 10^3\ M^{-1}\ s^{-1}$ (18).

The stationary state concentration of e_{am}^- (32) produced via equilibrium [11] is not a significant factor, relative to the pulse concentrations, in 10^{-3} *M* amide solutions.

$$[11] \qquad \tfrac{1}{2}H_2 + NH_2^- \rightleftharpoons e_{am}^- + NH_3$$

$$K_{-11} = \frac{[NH_2^-]P_{H_2^{1/2}}}{[e_{am}^-]} = 5 \times 10^4\ \text{atm}^{1/2}$$

at low amide concentrations.

Effect of Borohydride Ion

Pulse radiolysis studies in aqueous solution (33) show that the borohydride ion, BH_4^-, reacts with the OH radical with a rate constant $k_{12} = 1.2 \times 10^{10}\ M^{-1}\ s^{-1}$

$$[12] \qquad OH + BH_4^- \rightarrow OH^- + BH_4$$

In liquid ammonia we would expect the corresponding reaction to involve the NH_2 radical

$$[13] \qquad NH_2 + BH_4^- \rightarrow NH_2^- + BH_4$$

Assuming that the rate of decay of e_{am}^- is pre-

Can. J. Chem. Downloaded from www.nrcresearchpress.com by 210.87.254.42 on 09/05/12
For personal use only.

Can. J. Chem. Downloaded from www.nrcresearchpress.com by 210.87.254.42 on 09/05/12
For personal use only.

dominantly affected by competition between reactions 1*a* and 13, then the stability of radiolytically produced e_{am}^- ought to be enhanced in solutions containing BH_4^-. Figure 5 confirms this prediction showing a long lived e_{am}^- absorption in basic solutions of ND_3 and NH_3 containing 9×10^{-4} and 1.3×10^{-1} *M* $NaBH_4$, respectively.

An estimate of k_{13} can be obtained on the basis of a simple competition between reactions 1*a* and 13 where

$$[A] \quad d[NH_2]/d[e_{am}^-] = 1 + k_{13}'/k_{1a}[e_{am}^-]$$

and k_{13}' (the pseudo first order rate constant) = $k_{13}[BH_4^-]$. Assuming at the end of the pulse, time t_0, that the initial concentration $[NH_2]_0 = [e_{am}^-]_0$ and at long times, t_∞, that $[NH_2]_\infty = 0$, then integrating *A* gives

$$[e_{am}^-]_\infty = OD_\infty/\varepsilon_{e_{am}^-} = 2.303k_{13}'/k_{1a} \log \frac{[e_{am}^-]_0}{[e_{am}^-]_\infty}$$

Therefore

$$[B] \quad OD_\infty = 2.303k_{13}'/k_{1a}\varepsilon_{e_{am}^-} \log \frac{OD_0}{OD_\infty}$$

where OD_0 and OD_∞ represent the optical density of e_{am}^- at t_0 and t_∞. In basic solutions containing 9×10^{-4} $NaBH_4$ a plot of OD_∞ against log OD_0/OD_∞ gave a reasonable straight line with a slope 2.303 $\varepsilon_{e_{am}^-} k_{13}'/k_{1a} = 0.29$. Taking $k_{1a} = 2.5 \times 10^{10}\ M^{-1}\ s^{-1}$ and $\varepsilon_{e_{am}^-} = 4.9 \times 10^4\ M^{-1}\ cm^{-1}$ we obtain $k_{13} = 7 \times 10^7\ M^{-1}\ s^{-1}$.

Figure 6 shows a plot of OD_0 and OD_∞ (after 400 μs) as a function of dose per pulse with the curves calculated on the basis of k_{13} and eq. *B*. The overall agreement is quite good but the fit falls off somewhat with increasing dose. This may be due to the second order disappearance of NH_2 radicals assuming relatively greater importance at higher dose rates.

$$[14] \quad NH_2 + NH_2 \rightarrow N_2H_4$$

Separate experiments in 10^{-3} *M* basic solutions containing D_2 (1 atm) and 6×10^{-4} *M* $N_2H_4 \cdot H_2SO_4$ showed no evidence of either a build up or decay following the initial e_{am}^- absorption. This supports Belloni's conclusion that e_{am}^- does not react rapidly with either N_2H_4 or the basic entity $N_2H_3^-$ (19). The slow e_{am}^- decay ($t_{1/2} > 10$ ms) observed in borohydride solutions may be due to

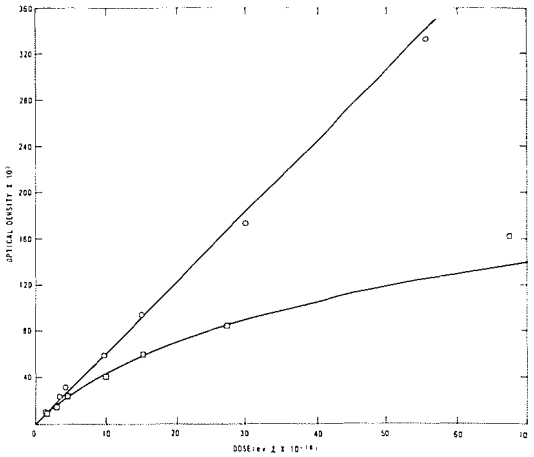

FIG. 6. Optical density of the transient species monitored in a 2.0 cm cell at 1500 nm and −15 °C in solutions containing 5×10^{-4} *M* $NaND_2$ and 9×10^{-4} *M* $NaBH_4$ in ND_3; ○, immediately after the pulse; □, 400 μs after the pulse. Curves are calculated on the basis of equation *B* (see text).

$$[15] \quad e_{am}^- + BH_4 \rightarrow BH_4^-$$

for which we estimate $k_{15} \sim 10^3 \pm 10\ M^{-1}\ s^{-1}$.

Finally the addition of $\sim 2.5 \times 10^{-2}$ *M* $NaBH_4$ to a 1×10^{-3} *M* amide solution containing D_2 (1 atm) produces a signal comparable to Fig. 5 (upper left) and prevents the build up of e_{am}^- such as observed in Fig. 4 (upper left). Since borohydride reacts with NH_2 radicals, reaction 13, this again supports the suggestion that $NH_2(NH^-)$ radicals react with H_2 to produce e_{am}^-.

The results obtained in basic ammonia solutions are quite different to those observed in amines. In amine solutions the addition of dilute concentrations of base completely removes the fast decay and results in the formation of metal–electron species having different spectra (22).

Yield of e_{am}^- in NH_3 and ND_3

Considerable discrepancy exists in the literature concerning the radiolytic yield of e_{am}^-. Values range from $G_{e_{am}^-} \sim 0.35$ (11, 18), 0.75 (19), 1.2 (14) to ~3 mol/100 eV (12). In "pure" ammonia or slightly basic solutions we find the initial absorption is drastically reduced on repetitive pulsing. Therefore measurements were always made using a fresh solution for each pulse. The initial yield was determined immediately after the pulse in basic solutions of NH_3 and ND_3 and in the presence of H_2/D_2 and/or

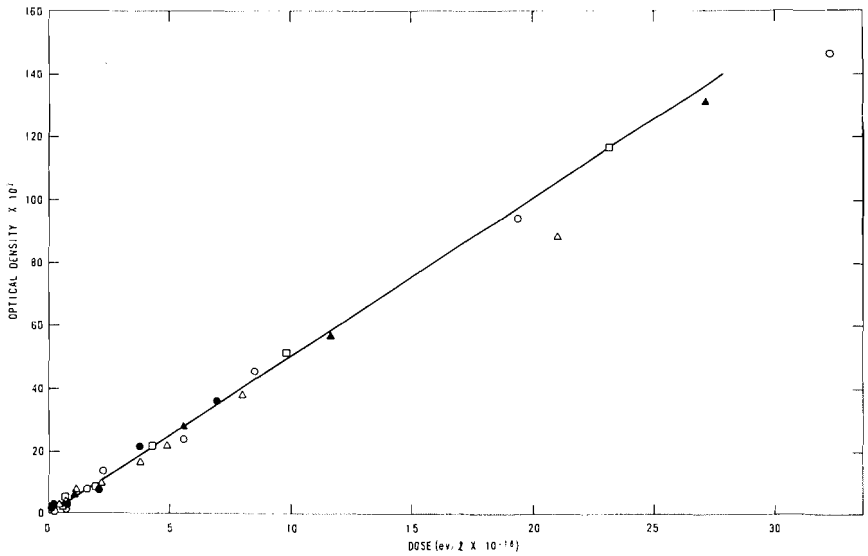

FIG. 7. Optical density of the transient species observed immediately after the pulse in basic solutions of NH_3 containing 1 atm of H_2. Wavelength 1420 nm, path length 2.0 cm; △, 0.01 mM; ○, 0.1 mM; ●, 10 mM; □, 50 mM; and ▲, ~200 mM $NaNH_2$ respectively.

varying concentrations of $NaBH_4$. Yields were deduced by comparison with the thiocyanate dosimeter taking at the peak wavelength $\varepsilon_{e_{am}^-} = 4.9 \times 10^4\ M^{-1}\ cm^{-1}$ and $G\varepsilon$ for $(SCN)_2^- = 2.1 \times 10^4$ (34–36). Dosimetry corrections based on stopping powers per gram for 2.20 MeV electrons in H_2O and ND_3 (37) were within 1% of electron density corrections using $\rho(NH_3) = 0.659\ g\ cm^{-3}$ and the ratio $\rho(ND_3)/\rho(NH_3) = 1.184$ (38).

Figure 7 shows a plot of the optical density, monitored at 1420 nm, as a function of dose for a series of sodium concentrations in NH_3/H_2 solutions. The production of e_{am}^- is linear with dose up to about $2.6 \times 10^{19}\ eV\ l^{-1}$ (~400 rads/pulse). From the slope of this and other similar plots in the absence of H_2 and/or presence of $NaBH_4$ we deduce $G_{e_{am}^-}(NH_3) = 3.3 \pm 0.3$. Similar measurements in ND_3 monitored at 1500 nm were slightly less reproducible giving $G_{e_{am}^-}(ND_3) = 3.6 \pm 0.4$. Although our precision is poor these results suggest a similar trend to the increased yield observed in aqueous solution between H_2O and D_2O (39).

We are unable to explain the low values in the literature unless such results are questionable in terms of dose and/or impurity effects. The high values we obtain certainly merit a re-examination of the mechanism and fate of e_{am}^- in the radiation chemistry of liquid ammonia.

1. J. J. LAGOWSKI and M. J. SIENKO. (*Editors.*) Metal–ammonia solutions. Colloque Weyl. II. Int. Union Pure and Appl. Chem. Butterworth and Co., London. 1970.
2. G. LEPOUTRE and M. J. SIENKO. (*Editors.*) Metal–ammonia solutions. Colloque Weyl. W. A. Benjamin Inc. 1964.
3. R. CATTERALL and N. F. MOTT. Adv. Phys. **18**, 665 (1969).
4. E. C. EVERS and P. W. FRANK, Jr. J. Chem. Phys. **30**, 61 (1959).
5. C. A. HUTCHISON, JR. and R. C. PASTOR. J. Chem. Phys. **21**, 1959 (1953).
6. D. F. BUROW and J. J. LAGOWSKI. Solvated electron. Adv. in Chem. Ser. **50**, 125 (1965).
7. R. C. DOUTHIT and J. L. DYE. J. Am. Chem. Soc. **82**, 4472 (1960).
8. M. GOLD and W. L. JOLLY. Inorg. Chem. **1**, 818 (1962).
9. J. C. THOMPSON. *In* the chemistry of non-aqueous solvents. Vol. II. *Edited by* J. J. Lagowski. Academic Press, New York and London. 1967. p. 265.
10. T. R. TUTTLE, Jr., G. RUBINSTEIN, and S. GOLDEN. J. Phys. Chem. **75**, 3635 (1971).
11. D. M. J. COMPTON, J. F. BRYANT, R. A. CESENA, and B. L. GEHMAN. Pulse radiolysis. Academic Press, New York. 1965. p. 43.
12. B. WARD. Adv. Chem. Ser. **81**, 601 (1968).

Can. J. Chem. Downloaded from www.nrcresearchpress.com by 210.87.254.42 on 09/05/12
For personal use only.

13. J. L. DYE, M. G. DEBACKER, and L. M. DORFMAN. J. Chem. Phys. **52**, 6251 (1970).
14. G. I. KHAIKIN, V. A. ZHIGUNOV, and P. I. DOLIN. High Energy Chem. (Engl. trans.), **5**, 44 (1971).
15. G. I. KHAIKIN, V. A. ZHIGUNOV, and P. I. DOLIN. High Energy Chem. (Engl. trans.), **5**, 72 (1971).
16. M. T. LOK, F. J. TEHAN, and J. L. DYE. J. Phys. Chem. **76**, 2975 (1972).
17. W. A. SEDDON, E. B. SELKIRK, and J. W. FLETCHER. Int. J. Radiat. Phys. Chem. **5**, 323 (1973).
18. F. S. DAINTON, T. SKWARSKI, D. SMITHIES, and E. WEZRANOWSKI. Trans. Faraday Soc. **60**, 1068 (1964).
19. J. BELLONI and J. F. DE LA RENAUDIÈRE. Int. J. Radiat. Phys. Chem. **5**, 22 (1973); **5**, 31 (1973).
20. W. A. SEDDON, C. WILLIS, M. J. YOUNG, and E. B. SELKIRK. Atomic Energy of Canada Limited, Report AECL-3853.
21. W. A. SEDDON, J. W. FLETCHER, and F. C. SOPCHYSHYN. Can. J. Chem. **51**, 1123 (1973).
22. J. W. FLETCHER, W. A. SEDDON, and F. C. SOPCHYSHYN. Can. J. Chem. **51**, 2975 (1973).
23. P. WARDMAN. J. Phys. E, Sci. Instrum. **5**, 17 (1972).
24. U. SCHINDEWOLF. Colloque Weyl II. Int. Union Pure Appl. Chem. *Edited by* J. J. Lagowski and M. J. Sienko. Butterworth and Co., London. 1970. p. 495.
25. M. OTTOLENGHI and H. LINSCHITZ. Solvated electron. Adv. Chem. Ser. **50**, 149 (1965).
26. I. HURLEY, T. R. TUTTLE, JR., and S. GOLDEN. Colloque Weyl II. Int. Union Pure Appl. Chem. *Edited by* J. J. Lagowski and M. J. Sienko. Butterworth and Co., London. 1970. p. 503.
27. J. W. FLETCHER, W. A. SEDDON, J. JEVCAK, and F. C. SOPCHYSHYN. Chem. Phys. Lett. **18**, 592 (1973).
28. G. V. BUXTON. Trans. Faraday Soc. **65**, 2150 (1969).
29. R. DELMAS, P. COURVOISIER, and J. RAVOIRE. Adv. Chem. Ser. **89**, 25 (1969).
30. M. S. MATHESON and J. RABANI. J. Phys. Chem. **69**, 1324 (1965).
31. R. G. MOORE and F. D. OTTO. Can. J. Chem. Eng. **50**, 313 (1972).
32. E. J. KIRSCHKE and W. L. JOLLY. Inorg. Chem. **6**, 855 (1967).
33. J. H. BAXENDALE, A. BRECCIA, and M. D. WARD. Int. J. Radiat. Phys. Chem. **2**, 167 (1970).
34. G. E. ADAMS, J. W. BOAG, and B. D. MICHAEL. Pulse radiolysis. Academic Press, London. 1965. p. 117.
35. J. H. BAXENDALE, P. L. T. BEVAN, and D. A. STOTT. Trans. Faraday Soc. **64**, 2389 (1968).
36. E. M. FIELDEN and N. W. HOLM. Manual on radiation dosimetry. *Edited by* N. W. Holm and R. J. Berry. Marcel Dekker, Inc., New York. 1970. p. 288.
37. M. J. BERGER and S. M. SELTZER. Tables of energy losses and ranges of electrons and positrons. NASA Report SP-3012. 1964.
38. C. A. HUTCHISON, JR. and D. E. O'REILLY. J. Chem. Phys. **34**, 163 (1961).
39. E. J. HART and M. ANBAR. The hydrated electron. Wiley–Interscience, New York. 1970. p. 76.

Can. J. Chem. Downloaded from www.nrcresearchpress.com by 210.87.254.42 on 09/05/12
For personal use only.

Determination of the Heat of Formation of Octafluorotoluene and Calculation of $D[C_6F_5—F] - D[C_6F_5—CF_3]$

MICHAEL J. KRECH
Chemistry Department, Wilfred Laurier University, Waterloo, Ontario

AND

STANLEY JAMES W. PRICE[1] AND WAYNE F. YARED
Chemistry Department, University of Windsor, Windsor, Ontario N9B 3P4

Received April 24, 1973

The heat of formation of octafluorotoluene has been determined using the direct combustion method previously developed for hexafluorobenzene. As in the hexafluorobenzene case the combustion of octafluorotoluene in oxygen yields CO_2, CF_4, and F_2. With a ten-fold excess of oxygen the CO_2 to CF_4 ratio is 3.85 ± 0.06. A full material balance was obtained. The value of $\Delta H_{f298}^0(C_6F_5CF_{3,g}) = -303.2 \pm 1.8$ kcal mol^{-1} may be combined with the enthalpies of formation of C_6F_6, CF_3, and F to give $D[C_6F_5—F] - D[C_6F_5—CF_3] = 55.7 \pm 4.0$ kcal mol^{-1}.

La chaleur de formation de l'octafluorotoluène a été déterminée en faisant appel à la méthode de combustion directe mise au point antérieurement. Comme dans le cas de l'hexafluorobenzène, la combustion de l'octafluorotoluène dans l'oxygène fournit du CO_2, du CF_4 et du F_2. Avec de l'oxygène en excès (10 fois la quantité nécessaire), le rapport de CO_2 sur CF_4 est de 3.85 ± 0.06. Une balance complète de tous les réactifs a été obtenue. La valeur de $\Delta H_{f298}^0(C_6F_5CF_{3,g}) = -303.2 \pm 1.8$ kcal/mol peut être combinée avec les enthalpies de formation de C_6F_6, CF_3 et F pour donner $D[C_6F_5—F] - D[C_6F_5—CF_3] = 55.7 \pm 4.0$ kcal/mol. [Traduit par le journal]

Can. J. Chem. 51, 3662 (1973)

Introduction

Enthalpies of formation have previously been reported for C_6F_6 (1–3), C_6F_5H (2), C_6F_5Cl (2), C_6F_5OH (2), and $C_6F_5CH_3$ (2). With the exception of the study of C_6F_6 done in this laboratory (3) all determinations involved combustion using an auxiliary material to ensure complete combustion and minimize CF_4 formation, containment of the sample in either polyester bags of polyethylene capsules and the use of water in the bomb to convert fluorine containing products other than CF_4 into aqueous HF. In the case of C_6F_5Cl a solution of As_2O_3 was used to reduce all chlorine to the chloride.

The present paper describes the measurement of the heat of combustion of octafluorotoluene in a platinum lined rotating bomb using the method previously developed for hexafluorobenzene (3). No water or other auxiliary materials are employed. The compound is contained in an open platinum crucible. With approximately a tenfold excess of oxygen complete combustion is easily obtained and the only products are CO_2, CF_4, and F_2.

[1]To whom correspondence should be addressed.

Experimental

Octafluorotoluene

The octafluorotoluene used was obtained from the Imperial Smelting Corporation. Three bulb-to-bulb distillations were carried out with head and tail fractions being discarded each time. The final product had the following physical properties (values in parentheses are those reported by the manufacturer (4)]: b.p. = 103.8 °C (104.0), $n_D^{25} = 1.3649$ (1.3656), s.g. at 20 °C = 1.762 (1.766). Analysis by gas chromatography (t.c. detector, 6 ft × 1/4 in o.d. polypropylene glycol column, isothermal operation at 110 °C, He carrier, 60 cc/min) showed one minor impurity which was estimated to represent about 0.01% of the sample. The impurity had a corrected relative retention with respect to the octafluorotoluene of 1.57. Further identification or purification was not attempted.

A modified Ramsay–Young system was used to measure the vapor pressure of C_7F_8 over the range 12–61 °C. Approximately 40 vapor pressure measurements were made over two separate runs. As in the case of C_6F_6 (3) the conventional $\log p$ *vs.* $10^3/T$ plot was very slightly curved. The data may be represented by

$$[1] \quad \log_{10} P\,(\text{cm}) = 29.098 - \frac{3122.2}{T} - 7.348 \log_{10} T$$

The resulting heat of vaporization and average heat capacity differences (vapor–liquid) are $\Delta H_{298}^0 = 9.95 \pm 0.05$ kcal mol^{-1} and $\langle \Delta C_p \rangle$ 12–61 °C $= -14.6$ cal deg^{-1} mol^{-1}. The error limits on ΔH are representative of the uncertainty in the precision only.

Can. J. Chem. Downloaded from www.nrcresearchpress.com by 210.87.254.6 on 09/05/12
For personal use only.

TABLE 1. Combustion data and calculated enthalpy of formation for octafluorotoluene

Mass C_7F_8 (g)	ΔT_{cor} (°C)	CO_2/CF_4* (by g.c.)	CO_2 collected (g)	F_2 collected (g)	$\Delta H_{f298}^0(C_6F_5CF_{3,g})$ (kcal/mol)
1.438	0.7636	3.90	1.439 (97)†	0.266 (103)†	−302.9
1.450	0.7692	3.85	1.506 (100)	0.259 (100)	−303.5
1.409	0.7506	3.79	1.429 (98)	0.239 (95)	−301.3
1.397	0.7409		1.440 (100)	0.243 (97)	−303.9
1.451	0.7702	3.88	1.510 (100)	0.271 (103)	−303.2
1.424	0.7534	3.89	1.472 (100)	0.259 (100)	−304.8
1.407	0.7474	3.82			−302.9
1.400	0.7438	3.82			−302.8
1.374	0.7297				−304.1

* = molar ratio. Additional typical data (see ref. 9 for notation): ΔE, ign/cal = 2.41, ε(cal)(−Δt_c)/cal = −3188.3, $\Delta E_c^0/M$(compound)/cal g^{-1} = −2250.

†% theoretical yield (to nearest whole %) based on the average CO_2/CF_4 molar ratio, 3.85, and on the assumption that the only products are CF_4, CO_2, and F_2.

As previously noted (3) the boiling points and $\langle \Delta C_p \rangle$ values for C_6H_6 and C_6F_6 are very similar. The boiling point of C_7F_8 is approximately 7° lower than that of C_7H_8 but the $\langle \Delta C_p \rangle$ values are again very close ($\langle \Delta C_p \rangle$ 25 °C for toluene −12.8 cal deg^{-1} mol^{-1} (5)).

Full fluorination of C_6H_6 or $C_6H_5CH_3$ has only a small effect of $\Delta H^0_{vaporization}$ *e.g.* $\Delta H_{vap}^0(C_6F_6) - \Delta H_{vap}^0(C_6H_6) = 0.5$ kcal mol^{-1}, $\Delta H_{vap}^0(C_7F_8) - \Delta H_{vap}^0(C_7H_8) = 0.87$ kcal mol^{-1}. Obviously, however, the values per gram differ by more than a factor of two. It is perhaps interesting to note that at least in the case of benzene and toluene full fluorination produces almost identical decreases in the heat of vaporization per gram (58.3 and 57.8 cal g^{-1}, respectively).

Apparatus and Calorimetric Procedure

The apparatus and all procedures were identical to those previously used for C_6F_6 (3).

The rate of loss of $C_6F_5CF_3$ from the platinum crucible in which it was weighed was determined to be 0.11 mg s^{-1}. The time between weighing the crucible containing the octafluorotoluene and sealing the bomb was such that less than 0.3% of the total sample was lost by evaporation. The correction for weight loss based on the time from weighing to sealing and on the rate of evaporation is estimated to be accurate to better than ±3%. The error in sample weight generated by the open dish procedure should therefore be less than 0.01%.

Analysis of Reaction Products

All analytical procedures were essentially the same as those used for hexafluorobenzene (3). Using a 6 ft. × 1/4 in. o.d. silica gel column at 25 °C with a helium carrier flow rate of 15 cc/min, uncorrected retention times for O_2, CF_4, and CO_2 are 1 min 30 s, 3 min 12 s, and 12 min 36 s, respectively.

Results and Discussion

The results of the $C_6F_5CF_3$ combustion studies are given in Table 1. The average CO_2/CF_4 ratio is 3.85 with a *probable error* (6) of ±0.011. It should be noted that a change of 0.01 in this ratio leads to a change of approximately 0.38 kcal mol^{-1} in ΔH_{f298}^0 ($C_6F_5CF_{3,g}$). As previously reported (3) gas chromatographic calibration for CO_2 may be done with the pure gas. However, under conditions used in the present work calibration for CF_4 must be done with CF_4–O_2 mixtures similar to those in the bomb after combustion. Calibration with pure CF_4 leads to an error in the CO_2/CF_4 ratio that results in an error of about 7–8 kcal mol^{-1} in ΔH_{f298}^0 ($C_6F_5CF_{3,g}$).

The only detectable products are CO_2, CF_4, and F_2. The material balance for carbon shown in Table 1 indicates that formation of other carbon containing products is unlikely. A similar observation may be made with respect to fluorine compounds. However, the handling and analysis of fluorine is subject to greater uncertainty and this is reflected in the greater scatter in per cent of the theoretical fluorine obtained.

To determine if small quantities of F_2O are produced the contents of the bomb were analyzed by gas chromatography using a 6 ft × 1/4 in. o.d. silica gel column at −60 °C with a helium flow rate of 15 cc/min. Under these conditions the relative retention of F_2O to O_2 is 3.75 so that any peak for F_2O is well separated from the massive O_2 peak. No F_2O could be detected. Mass spectrometric tests for F_2O (based on m/e = 54 and 35) were also negative.

Based on the observed products and the average CO_2/CF_4 ratio of 3.85 the combustion reaction may be written,

$$[2]\quad C_6F_5CF_3 + 5.556O_2 \rightarrow 5.556CO_2 + 1.444CF_4 + 1.112F_2$$

With the exception of $C_6F_5CF_3$ all reactants and products are in the gaseous state. The

Can. J. Chem. Downloaded from www.nrcresearchpress.com by 210.87.254.6 on 09/05/12
For personal use only.

Can. J. Chem. Downloaded from www.nrcresearchpress.com by 210.87.254.6 on 09/05/12
For personal use only.

octafluorotoluene is present largely as a liquid but under the initial conditions used (23.5 °C, 450 p.s.i. O_2, 320 cc bomb) 0.125 g will be in the vapor state at the time of combustion.

For calculation of ΔH_{f298}^0 ($C_6F_5CF_{3,g}$) the standard heats of formation of the combustion products were taken as ΔH_{f298}^0 ($CO_{2,g}$) = −94.0517 kcal mol^{-1} (7); ΔH_{f298}^0 ($CF_{4,g}$) = −223.0 kcal mol^{-1} (8). The required correction for the $C_6F_5CF_3$ in the liquid state, $[(w - 0.125)/w]\Delta H_{298}^0$ (vaporization) where w = weight of the $C_6F_5CF_3$ sample in grams, was based on the heat of vaporization determined in the present work, 9.95 kcal mol^{-1}. The average value of ΔH_{f298}^0 ($C_6F_5CF_{3,g}$) is −303.2 ± 1.8 kcal mol^{-1}. The statistical probable error of the mean (6) is ±0.55 kcal mol^{-1}. Based on factors other than possible errors in the heats of formation of CO_2 and CF_4 an overall error of ±2.0 kcal mol^{-1} is estimated.

The value for ΔH_{f298}^0 ($CO_{2,g}$) is well established. However an alternate value for ΔH_{f298}^0 ($CF_{4,g}$) is available, −221 kcal mol^{-1} (7). This leads to ΔH_{f298}^0 ($C_6F_5CF_{3,g}$) = −300.3 kcal mol^{-1}.

Based on ΔH_{f298}^0 (F,g) = 18.9 kcal mol^{-1} (7), ΔH_{f298}^0 ($CF_{3,g}$) = −114 kcal mol^{-1} (7), ΔH_{f298}^0 ($C_6F_{6,g}$) = −226.0 kcal mol^{-1} (3), and ΔH_{f298}^0 ($C_6F_5CF_{3,g}$) = −303.2 kcal mol^{-1} $D[C_6F_5—F] - D[C_6F_5—CF_3]$ = 55.7 ± 4.0 kcal mol^{-1}. Use of ΔH_{f298}^0 ($C_6F_{6,g}$) and ΔH_{f298}^0 ($C_6F_5CF_{3,g}$) based on ΔH_{f298}^0 (CF_4) = −221 kcal mol^{-1} (−224.0 kcal mol^{-1} and −300.3 kcal mol^{-1} respectively) leads to only a slight increase in the bond energy difference (56.6 *vs.* 55.7 kcal mol^{-1}). In any case the bond energy difference calculation should be based on ΔH_{f0}^0 values. However for two such similar molecules the integrated ΔC_p correction should approximately cancel, making the error due to the use of 298 °K values negligible.

A comparison may be made of $D[C_6H_5—H] - D[C_6H_5—CH_3]$ with the corresponding difference in the perfluoro compounds. From high temperature studies of the reaction of CF_3 with benzene (10) $D[C_6H_5—H]$ = 110.2 kcal mol^{-1}. Benson and O'Neal (11) have estimated $D[C_6H_5—CH_3]$ as 102 kcal mol^{-1}. Using the more recent value of $\Delta H_{f298}^0(C_6H_{5,g})$ = 77.9 kcal mol^{-1} (10) leads to $D[C_6H_5—CH_3]$ = 99.9 kcal mol^{-1}. The difference $D[C_6H_5—H] - D[C_6H_5—CH_3]$ = 10.3 kcal mol^{-1} is obviously much less than in the perfluoro case, 55.8 kcal mol^{-1}. Since independent values of $D[C_6F_5—F]$ and $D[C_6F_5—CF_3]$ are not available individual comparisons cannot be made. In the simple aliphatics $D[CH_3—CH_3]$ = 88 kcal mol^{-1} (11), $D[CF_3—CF_3]$ = 92 kcal mol^{-1} (11), $D[CH_3—H]$ = 104 kcal mol^{-1} (10) and from thermochemistry (7) $D[CF_3—F]$ = 126 kcal mol^{-1}. It is tempting to say on this basis that $D[C_6F_5—CF_3]$ may be approximately equal to $D[C_6H_5—CH_3]$ so that $D[C_6F_5—F] \gg D[C_6H_5—H]$. However this ignores the implications of full fluorination of the aromatic ring which might in fact lead to $D[C_6F_5—CF_3] < D[C_6H_5—CH_3]$. An independent determination of either $D[C_6F_5—CF_3]$ or $D[C_6F_5—F]$ is obviously needed.

This work has been supported by an operating grant from the National Research Council of Canada.

1. J. D. Cox, H. A. Gundry, and A. J. Head. Trans. Faraday Soc. **60**, 653 (1964).
2. J. D. Cox, H. A. Gundry, D. Harrup, and A. J. Head. J. Chem. Thermodyn. **1**, 77 (1969).
3. M. Krech, S. J. W. Price, and W. F. Yared. Can. J. Chem. **50**, 2935 (1972).
4. Highly fluorinated aromatic and alicyclic compounds. Imperial Smelting Company, St. Andrews Road, Avonmouth, Bristol BS11 9HP, England.
5. D. W. Scott, G. B. Guthrie, J. F. Messerly, S. S. Todd, W. T. Berg, I. A. Hossenlopp, and J. P. McCullough. J. Phys. Chem. **66**, 911 (1962).
6. Handbook of tables for mathematics. 3rd ed. The Chemical Rubber Co., Cleveland, Ohio. 1967. p. 876.
7. Selected values of chemical thermodynamic properties. National Bureau of Standards. U.S. Tech. Notes No. 270–3 1968.
8. E. Greenberg and W. N. Hubbard. J. Phys. Chem. **72** (1), 222 (1968).
9. J. Coops, R. S. Jessup, and K. Van Nes. *In* Experimental thermochemistry. Vol. 1. *Edited by* F. D. Rossini. Interscience, New York. 1956.
10. G. A. Chamberlain and E. Whittle. Trans. Faraday Soc. **67**, 2077 (1971).
11. S. W. Benson and H. E. O'Neal. Kinetic data on gas phase unimolecular reactions. NSRDS-NBS 21. Washington, D.C. 1970.

Photodecomposition of Fe(III) Aminopolycarboxylates

JOHN H. CAREY AND COOPER H. LANGFORD[1]
Department of Chemistry, Carleton University, Ottawa, Canada K1S 5B6

Received May 22, 1973

Aminopolycarboxylate complexes of Fe(III) and Cu(II) may have an interesting natural water photochemistry. As a convenient model system, the photodecarboxylation of ferric–EDTA complexes was studied at 30.0 °C using 3500 Å light. The hydrolytic forms present at p*H* of 8.00 and 9.00 were observed to have quantum yields below 0.10 and varying from species to species. The oxo-bridged dimer was unreactive. This is discussed from the viewpoint of the changed spin selection rules and changed spectral states of the dimer as compared to monomer. The reaction products in the ferric–EDTA system were seen to parallel those of the previously studied ferric–NTA system; the primary products of the reaction being CO_2, CH_2O, Fe(II), and ethylenediaminetriacetic acid.

Les complexes du type aminopolycarboxylate de Fe(III) et de Cu(II) semblent posséder une photochimie intéressante dans l'eau naturelle. La photodécarboxylation de complexes EDTA–Fe(III) a été étudiée, comme système modèle, à 30.0 °C en utilisant une source lumineuse irradiant à 3500 Å. Les formes hydrolytiques présentes à p*H* 8.00 et 9.00 possèdent, comme il a été observé, des rendements quantiques inférieurs à 0.10 variant selon les espèces. Le dimère oxo-ponté n'est pas réactif. Ce fait est discuté en ce qui a trait aux règles de sélections de spin et aux états d'excitation qui, pour le dimère, sont différents de ceux du monomère. Les produits de réaction dans le système EDTA–Fe(III) se sont révélés être en accord avec ceux obtenus antérieurement dans le cas du système NTA–Fe(III); les principaux produits de la réaction sont CO_2, CH_2O, Fe(II) et acide éthylènediaminetriacétique.
[Traduit par le journal]

Can. J. Chem. **51**, 3665 (1973)

Can. J. Chem. Downloaded from www.nrcresearchpress.com by 210.87.254.6 on 09/05/12
For personal use only.

Introduction

The decomposition reactions of aminopolycarboxylates have assumed importance in recent years due to their proposed use as detergent builders, their accumulation in waste waters (1, 2), and other reasons. The chemistry of nitrilotriacetic acid (NTA) and similar aminopolycarboxylates in natural waters consists mainly of the reactions of their metal complexes; significantly those formed with iron and copper (2). The photochemical degradation of ferric nitrilotriacetate complexes has been studied and the decomposition pathway shown to be

$$2[Fe^{III}(NTA)] \rightarrow [Fe^{II}(NTA)]^- + [Fe^{II}(IDA)] + CH_2O + CO_2$$

$$[Fe^{II}(IDA)] \xrightarrow{O_2} [Fe^{III}(IDA)]$$

The quantum efficiency of this decomposition decreases with increasing p*H* (2).

The charge transfer region of the cupric complex has also been shown to be active in photodecarboxylation along a similar pathway and the variation of formaldehyde quantum yields with p*H* resembled that obtained in the FeNTA system (3). Since it is known that ferric complexes of aminopolycarboxylates form dimeric structures in basic solutions (4) the possibility that the dimer may be responsible for this p*H* dependence of quantum efficiency has been raised (2).

Although the ferric ethylenediaminetetraacetate (EDTA) complex has been known for some time to undergo photodecarboxylation, the products other than CO_2 have not been determined (5). There has, however, been extensive work done on monomer–dimer equilibria as well as studies on the electronic and crystal structures of the dimer (5–10). The dimer is a strongly colored species exhibiting a much more intense ligand field spectrum than the monomer. This is interpreted to indicate that the transition from the $^6A_1$ ground state to quartet excited states has been made more allowed by dimerization (9). (This may reflect relaxation of the spin selection rule due to spin–spin interaction across the oxo-bridge. Spin–spin coupling is thought to be responsible for the lowering of the magnetic moment of iron complexes upon dimerization (9).)

It is plausible to suggest that the increase in allowed character of the ligand field transitions makes ligand field states more efficient for relaxation of a charge transfer excited state and

[1]To whom correspondence should be addressed.

thus leads to a lower quantum efficiency of reaction in the dimer (2).

In order to investigate the effect of dimer concentration on quantum yield and also to determine whether the proposed pathway for Fe(III)-NTA decarboxylation may be extended to other aminopolycarboxylate complexes, we have conducted a study of the photochemistry of Fe(III)–EDTA in basic solutions.

Experimental

The NaFe(III)EDTA·$3H_2O$ was prepared according to standard procedures (11) and recrystallized twice from distilled water. Solutions to be irradiated were made up from a 0.1 *M* FeEDTA stock solution and were buffered in 1.15×10^{-2} *M* Na_2EDTA. The p*H* was adjusted to p*H* 8.00 and 9.00 using a Fisher "accumet" p*H* meter. It was found that when 0.1 *M* NaOH was added to the more concentrated iron solutions (> 0.02 *M*) precipitation of some of the iron occurred, even when vigorously stirred with a magnetic stirrer. This problem was eliminated by changing the order of the additions. The amount of 0.1 *M* NaOH needed was estimated with the aid of a trial run. The Na_2EDTA buffer (5 ml, 6.25×10^{-2} *M*) was added to the required amount of base and the solution diluted to 15 or 20 ml. The appropriate amount of FeEDTA stock solution was then added and the solution was further diluted to 24 ml. The p*H* of this solution was adjusted to 8.00 or 9.00 using 0.1 *M* NaOH and then was diluted to 25 ml. With suitably pure FeEDTA, no precipitate occurred at concentrations below 0.040 *M*. All preparations were made under red safelights and solutions were stored in foil-wrapped flasks until use.

Irradiations were performed in a jacketed Pyrex cell of 2 cm diameter which was thermostated to 30.0 ± 0.1 °C. The cell was sealed with a serum cap and nitrogen was bubbled for 20 min to deaerate the solution. After deaeration, solutions were immediately irradiated at 3500 Å in a Rayonnet photoreactor to 1–5% reaction. The photolytes were analyzed for Fe(II) with buffered *o*-phenanthroline solution (12) which had also been deaerated. Light intensities were determined using ferrioxalate actinometry (12).

Several solutions of 0.1 *M* FeEDTA were deaerated and irradiated until decolorization was obtained. The iron(II) was re-oxidized by bubbling air through the solutions for 12 h and then iron was completely precipitated by addition of NaOH. The precipitate was removed by centrifugation and the supernatant was concentrated on a rotary evaporator. Addition of ethanol precipitated a gummy white solid. The precipitate was washed with ethanol and ether and air dried. This material was assumed to contain product aminopolycarboxylate ligands and EDTA. Cobalt complexes of these ligands were synthesized following published procedures and separated by ion exchange (13). Nuclear magnetic resonance spectra were recorded in D_2O on a Varian T-60 spectrophotometer and visible–u.v. measurements were made in either a Cary 14 or a Gilford 240 spectrophotometer.

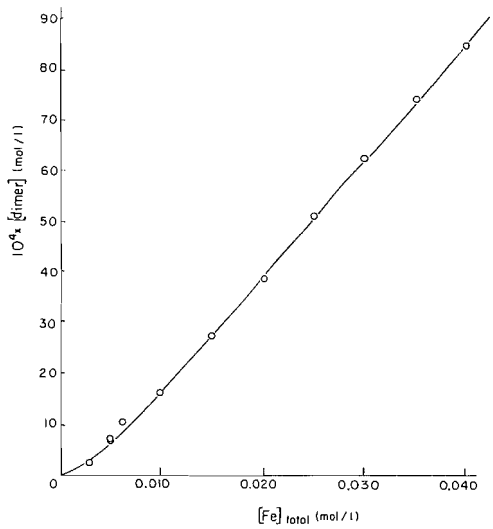

FIG. 1. The dimer concentration at p*H* = 9.00 as a function of total iron concentration.

Results and Discussion

Effect of Dimer on Quantum Yield

The effects of the various hydrolytic forms of FeEDTA upon the quantum efficiency of photoreduction were studied by irradiation of solutions of FeEDTA buffered to p*H* 8.00 and 9.00. One coordination position in FeEDTA complexes is occupied by a solvent derived ligand. In addition to oxo-bridged dimer, hydroxo monomer is present at these p*H* values. At p*H* of 8.00, both hydroxo and aquo monomers are present with an hydroxo/aquo monomer ratio of 3.6 (4). When the p*H* is increased to 9.00, however, 97% of the monomer is present as hydroxo monomer and for this reason, the aquo monomer was not considered a significant absorber at the higher p*H* and was omitted from calculations. The dimer/monomer ratio was adjusted by varying the total iron concentration. The variation of dimer concentration with total iron at p*H* 9.00 is shown in Fig. 1.

The quantum efficiencies for photoreduction, based on production of iron(II), for various total iron concentrations are given in Table 1. After an initial decrease in yield as total iron increased, a plateau value was reached for each p*H* as shown in Fig. 2(*a*) and (*b*). A comparison of Fig. 1 and Fig. 2(*b*) reveals that the limiting value for quantum yield was reached at nearly the same total iron concentration as the curve in Fig. 1

Can. J. Chem. Downloaded from www.nrcresearchpress.com by 210.87.254.6 on 09/05/12
For personal use only.

TABLE 1. Fe(II) quantum yields as a function of total iron concentration, $T = 30°$

$pH = 8.00$		$pH = 9.00$	
$[Fe]_{tot}(M)$	Φ_{obs}	$[Fe]_{tot}(M)$	Φ_{obs}
0.00500	0.059±0.002	0.00300	0.042±0.002
0.00800	0.056	0.00500	0.037
0.0100	0.055	0.00500	0.035
0.0100	0.054	0.00700	0.034
0.0110	0.047	0.0100	0.025
0.0130	0.047	0.0150	0.026
0.0150	0.038	0.0200	0.024
0.0150	0.039	0.0250	0.021
0.0160	0.031	0.0300	0.022
0.0200	0.029	0.0350	0.025
0.0280	0.026	0.0400	0.024
0.0320	0.026		
0.0360	0.026		

became linear. Thus, when the dimer/hydroxo monomer ratio became constant, as shown by linearity in Fig. 1, the quantum yield also became constant.

If the quantum yields of the hydroxo-monomer and the dimer are different, then the observed quantum yield will depend on the fraction of light absorbed by each species. Thus, at pH of 9.00 we have eq. 1.

$$[1] \qquad \Phi_{obs} = A_d\Phi_d + A_{mOH}\Phi_{mOH}$$

In eq. 1, A_d = fraction of light absorbed by dimer, A_{mOH} = fraction of light absorbed by hydroxo monomer, Φ_d = quantum yield of dimer, Φ_m = quantum yield of hydroxo monomer and, finally, Φ_{obs} = observed quantum yield. The fraction of light absorbed by each species can be calculated if both the concentrations and molar absorptivities are known. In dilute solution, at pH = 11.00, only hydroxo monomer is present and a molar absorptivity at 350 nm of 770 was estimated. Using this value and the absorption spectra recorded at pH = 9.00 in short (0.1 mm) path length cells, a dimer absorptivity of 5100 at 350 nm was estimated. (The dimer concentrations could be obtained from the absorbance at 540 nm (11) using a molar absorptivity of 121.)

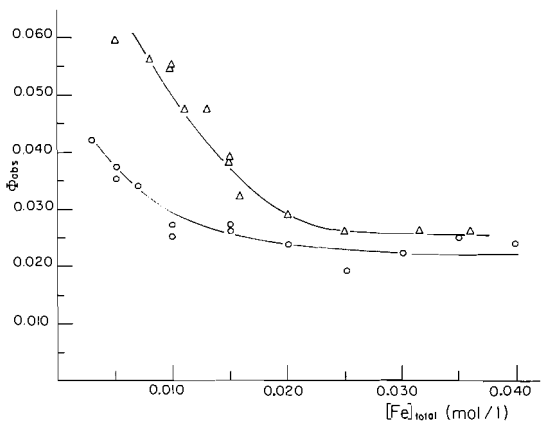

FIG. 2. The quantum yield for photoreduction based on Fe(II) production as a function of total iron concentration: (*a*) pH = 8.00 (△) (*b*) pH = 9.00 (○).

The correlation between the fraction of light absorbed by dimer and observed quantum yield is shown in Fig. 3. This analysis was not performed on the data for pH = 8.00 since there were three absorbing species.

From the intercepts of Fig. 3, quantum yields of hydroxo-monomer and dimer can be estimated, as Φ(monomer) = 0.065, and Φ(dimer) ≃ 0. These values confirm the earlier speculation that the reduction of quantum yield in basic solution is predominantly due to dimer formation. This indicates the existence of an efficient pathway for radiationless relaxation which doesn't exist in the monomers. The possibility that this pathway may involve relaxation through ligand field states transitions to which have been made more allowed in the dimer has already been mentioned. The ligand field bands of the dimer are claimed to be a factor of 10 more intense than the corresponding bands in the monomers, pre-

Can. J. Chem. Downloaded from www.nrcresearchpress.com by 210.87.254.6 on 09/05/12
For personal use only.

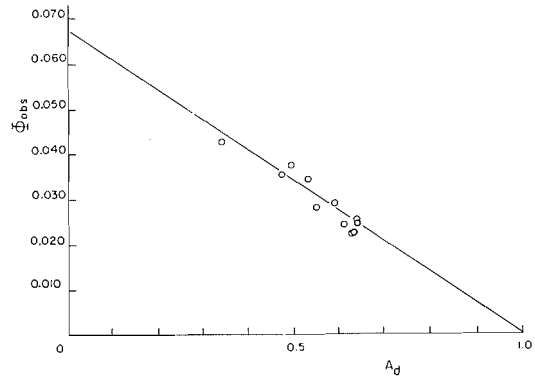

FIG. 3. The variation of quantum yield for photoreduction based on Fe(II) production as a function of the fraction of light absorbed by the dimer (A_d), based on the relationship $\Phi_{obs} = \Phi_m - A_d\ (\Phi_m - \Phi_d)$ which is easily derived from eq. 1.

sumably due to relaxation of the spin selection rules through spin–spin coupling across the Fe—O—Fe bridge. Thus, a pathway for radiationless relaxation which involved coupling of the charge transfer excited state with these ligand field states may be more efficient in the dimer.

In the u.v. spectrum of the dimer, however, there are several absorption maxima which have been termed simultaneous-pair electronic (s.p.e.) bands (8). These correspond to simultaneous excitation to ligand field states on both iron centers by absorption of one photon. It is claimed that pair transitions in which spin does not change on excitation are fully allowed. Thus, these s.p.e. bands may be very intense and the possibility arises that the 350 nm light absorbed by the dimer may not excite the molecule predominantly to a charge transfer excited state but to excited ligand field states on both iron atoms. The ligand field band of the dimer was irradiated at 540 nm, a wavelength where only dimer absorbs. No photoreduction could be observed. Thus a very low quantum yield for the photoredox process would not be unexpected if excitation led to ligand field excited states. Unfortunately, no assignment can be made as to the degree to which charge transfer or s.p.e. states is excited. This distinction may not be necessary, however, since the existence of the s.p.e. bands iso-energetic with the charge transfer bands probably would allow strong coupling to occur between these states. Thus, an efficient pathway could be provided for the deactivation of charge transfer excited states through energy transfer to ligand field states with which they are strongly coupled. That this happens may be indicated from the assignment of Φ_d since some measurable degree of photoreduction should occur if charge transfer states are populated and do not relax efficiently. From Fig. 3, it is apparent that a conservative upper limit of 0.010 can be assigned to Φ_d and the actual value is probably much nearer zero. Thus, since significant reduction is not observed in the dimer, it seems that the charge transfer state is strongly coupled to some other states which are inactive to photoreduction.

Stoichiometry

The Fe–NTA system has as primary products of the photoreduction, carbon dioxide, formaldehyde, and the iron(II) complexes of NTA and IDA. In the Fe–EDTA system, the presence of formaldehyde was confirmed by the formation of a 2,4-dinitrophenylhydrazone derivative (m.p. 163–165 °C) upon the addition of 2,4-dinitrophenylhydrazine reagent (14). Formaldehyde quantum yields were determined using the method of Lappin and Clark (15) on samples irradiated to less than 5% conversion and are given in Table 2. They confirm, within the limits of experimental uncertainty, the 2:1 ratio of iron(II) to formaldehyde in the products. In order to determine the other product of the ligand oxidation, a "decolorized" solution was reoxidized and the iron precipitated. The ligand mixture, which was expected to be 50% EDTA and 50% oxidized product, was reacted with cobalt(II) in air to produce the cobalt(III) complexes. After separation of these complexes by ion exchange, according to established procedure (13), the two aquo complexes obtained were converted to chloro complexes (13) and the n.m.r. spectra recorded in mixtures of HCl with D_2O to limit solvent ^1H concentrations. The two spectra are shown in Fig. 4. The spectrum of Co(EDTA)Cl shown resembles that reported by Day and Reilley (16) for the same complex, while that of the oxidized ligand is very similar to the spectrum of $Co(ED3A)NO_2$ (ED3A = ethylenediaminetriacetic acid) reported by Blackmer, Hamm, and Legg (13). In particular, both the oxidized ligand complex and $Co(ED3A)NO_2$ exhibit a broad band at 6.5 p.p.m. indicative of an amine proton. Both spectra have doublets at 3.2 and 3.5 p.p.m. and a singlet at 4.7 p.p.m. The

Can. J. Chem. Downloaded from www.nrcresearchpress.com by 210.87.254.6 on 09/05/12
For personal use only.

TABLE 2. Quantum yields for CH_2O production at pH = 9.00

[Fe]	Φ_{CH_2O}	$\Phi_{Fe(II)}$	Φ_{Fe}/Φ_{CH_2O}
0.00600	0.021 ± 0.002	0.035 ± 0.002	1.8
0.00800	0.019	0.032	1.7

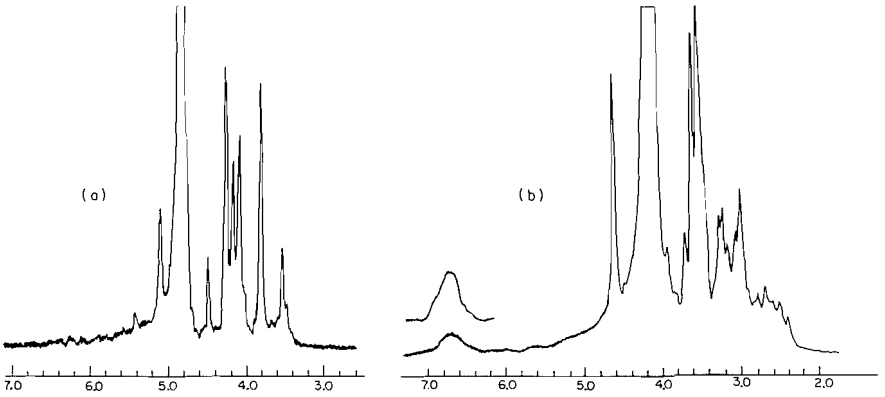

FIG. 4. The n.m.r. spectra of the cobalt complexes prepared by treating cobalt(II) with the ligand mixture obtained by precipitation of the iron from a photolyzed sample of FeEDTA. The complexes were separated by ion exchange since species (*a*) was neutral at pH = 5.00, while species (*b*) was anionic at pH = 5.00.

several peaks seen by Blackmer *et al.* in the 4.0 p.p.m. region were an unresolved peak in our spectrum. The assignment of an amine function to the oxidized ligand was confirmed by a ninhydrin test performed on the ligand mixture and on pure EDTA. The test was positive only for the oxidized ligand mixture. (Although the alternative of the $=N—CH_2\cdot$ radical to abstracting a hydrogen to produce $=N—CH_3$ was considered, the n.m.r. spectrum shows this is not the case since the spectrum of $Co(MeEDTA)NO_2^-$ is known and has a methyl proton singlet at 2.0–2.5 p.p.m. (17).)

In another experiment, two identical samples of 0.1 *M* FeEDTA were taken. One was decolorized as before and the other left in the dark. The iron was precipitated from both and upon precipitation of the ligands with ethanol, n.m.r. spectra in D_2O were recorded. These are shown in Fig. 5. That obtained for an unirradiated sample was identical to a bench sample of Na_2EDTA. The irradiated sample exhibited a splitting of both original peaks. The peak due to $N—CH_2—$ protons was split into two approximately equal broadened peaks which indicates that one end of the EDTA is now different from the other. The peak due to the $N—CH_2—COO^-$ protons also is split but in appropriately a 2:1 ratio. Both these observations are consistent with removal of one acetate group and substitution of a proton which would exchange rapidly in D_2O. There was no peak at low δ which might be expected if an $—N—CH_2\cdot$ radical formed by initial loss of CO_2 could pick up a hydrogen to give $—N—CH_3$.

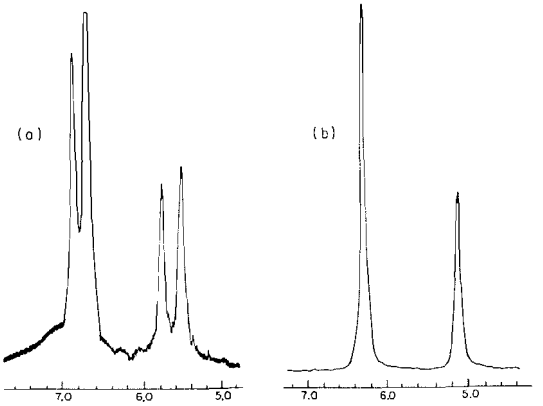

FIG. 5. The n.m.r. spectra of the ligands obtained after precipitation of the iron from two solutions of FeEDTA; (*a*) a sample irradiated to decolorization and reoxidized and (*b*) an unirradiated sample.

Can. J. Chem. Downloaded from www.nrcresearchpress.com by 210.87.254.6 on 09/05/12
For personal use only.

[2a] 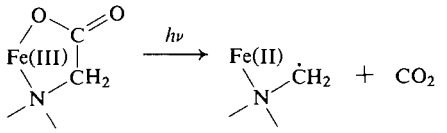

[2b] 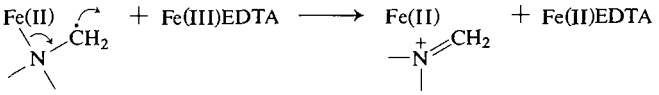

[2c] 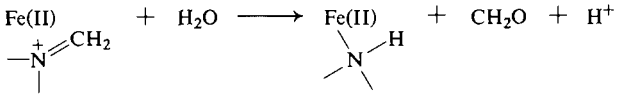

From these results, we propose that a plausible pathway for photodecarboxylation of ferric aminopolycarboxylates can be represented by eq. 2.

Since formaldehyde has been observed in the cupric–NTA photoreaction this pathway may be general. It is worth noting that non-biological decomposition of amino acids by natural waters is slow (18) and that a parallel photochemical path for amino acids may well be significant.

We thank the National Research Council of Canada and Environment Canada for support of this work.

1. M. E. BENDER, W. R. MATSON, and R. A. JORDAN. Environ. Sci. Tech. **4**, 520 (1971).
2. T. TROTT, R. W. HENWOOD, and C. H. LANGFORD. Environ. Sci. Tech. **6**, 367 (1972).
3. C. H. LANGFORD, M. WINGHAM, and V. S. SASTRI. Environ. Sci. Tech. In press.
4. R. L. GUSTAFSON and A. E. MARTELL. J. Phys. Chem. **67**, 576 (1963).
5. L. H. HALL and J. L. LAMBERT. J. Am. Chem. Soc. **90**, 2036 (1968); D. G. HILL-COTTINGHAM. Nature, 347 (1955).
6. H. SCHUGAR, C. WALLING, R. B. JONES, and H. B. GRAY. J. Am. Chem. Soc. **89**, 3712 (1967).
7. S. J. LIPPARD, H. SCHUGAR, and C. WALLING. Inorg. Chem. **6**, 1825 (1967).
8. H. SCHUGAR, G. R. ROSSMAN, J. THIBEAULT, and H. B. GRAY. Chem. Phys. Lett. **6**, 26 (1970).
9. H. SCHUGAR, G. R. ROSSMAN, C. G. BARRACLOUGH, and H. B. GRAY. J. Am. Chem. Soc. **94**, 2683 (1972).
10. A. D. GILMOUR and A. MCAULEY. Inorg. Chim. Acta, **4**, 158 (1970).
11. H. SCHUGAR, A. T. HUBBARD, F. C. ANSON, and H. B. GRAY. J. Am. Chem. Soc. **90**, 71 (1969).
12. C. G. HATCHARD and C. A. PARKER. Proc. R. Soc. (Lond.), A, **235**, 518 (1956).
13. G. L. BLACKMER, R. E. HAMM, and J. I. LEGG. J. Am. Chem. Soc. **91**, 6632 (1969).
14. A. I. VOGEL. Practical organic chemistry. 3rd ed. Longmans, Green and Co. Ltd., London. 1957. p. 1061.
15. G. R. LAPPIN and L. C. CLARK. Anal. Chem. **23**, 541 (1951).
16. R. J. DAY and C. N. REILLEY. Anal. Chem. **36**, 1070 (1964).
17. G. L. BLACKMER and J. L. SUDMEIER. Inorg. Chem. **10**, 2019 (1971).
18. J. L. BADA. Adv. Chem. Ser. **106**, 309 (1971).

Can. J. Chem. Downloaded from www.nrcresearchpress.com by 210.87.254.6 on 09/05/12
For personal use only.

The Reactions of Active Nitrogen with Simple Alcohols[1]

JOHN M. ROSCOE AND SHARON G. ROSCOE
Department of Chemistry, Acadia University, Wolfville, Nova Scotia

Received April 19, 1973

The reactions of active nitrogen with CH_3OH, C_2H_5OH, n-C_3H_7OH and iso-C_3H_7OH have been studied as a function of temperature. The rate constants for these reactions fit the following expressions:

N + CH_3OH	$\log k = 11.38 \pm 0.08 - (36 \pm 4)/RT$
N + C_2H_5OH	$\log k = 11.30 \pm 0.04 - (35 \pm 2)/RT$
N + n-C_3H_7OH	$\log k = 9.44 \pm 0.04 - (30 \pm 2)/RT$
N + iso-C_3H_7OH	$\log k = 11.93 \pm 0.05 - (39 \pm 2)/RT$

(Activation energies are in kJ/mol. Rate constants are in l mol^{-1} s^{-1}.)

Experiments with CH_3OH, CH_3OD, and CD_3OD indicate a small primary isotope effect for OH and a secondary isotope effect for CH. This, with other data, implies that abstraction of a H atom from the alcohol is not an important initial step.

Consumption of N atoms ranged from 4.7 to 7.1 times the alcohol consumed. With the exception of the reaction of active nitrogen with iso-C_3H_7OH, the only detectable stable reaction product was HCN. Intervention of O atoms as intermediates appears to be important in all the reactions. In the reaction of active nitrogen with iso-C_3H_7OH, acetone, and acetonitrile were also found as products in amounts of about 26% and 14% respectively of the HCN yield. These products appear to arise through O atom intervention.

Mechanisms for the reactions and the nature of the activated state in the initial step are discussed.

Les réactions de l'azote actif avec le CH_3OH, le C_2H_5OH, le n-C_3H_7OH et l'iso-C_3H_7OH ont été étudiées en fonction de la température. Les constantes de vitesse de ces réactions peuvent être exprimées par les expressions suivantes:

N + CH_3OH	$\log k = 11.38 \pm 0.008 - (36 \pm 4)/RT$
N + C_2H_5OH	$\log k = 11.30 \pm 0.04 - (35 \pm 2)/RT$
N + n-C_3H_7OH	$\log k = 9.44 \pm 0.04 - (30 \pm 2)/RT$
N + iso-C_3H_7OH	$\log k = 11.93 \pm 0.05 - (39 \pm 2)/RT$

(les énergies d'activation sont exprimées en kJ/mol. Les constantes de vitesse sont exprimées en l mol^{-1} s^{-1}.)

Les expériences avec le CH_3OH, CH_3OD et CD_3OD ont révélées la présence d'un faible effet isotopique primaire pour OH et d'un effet isotopique secondaire pour CH. Ce fait, combiné avec d'autres résultats, implique que la perte d'un atome H appartenant à l'alcool n'est une étape initiale importante.

La consommation des atomes d'azote est de 4.7 à 7.1 fois plus grande que celle de l'alcool. A l'exception de la réaction de l'azote actif avec l'iso-C_3H_7OH, les seul produit stable qui fut détecté était le HCN. L'intervention des atomes d'oxygène comme intermédiaires semble être importante pour toutes les réactions. Dans la réaction de l'azote actif avec l'iso-C_3H_7OH, on a trouvé comme produits de réaction, l'acétone et l'acétonitrile dans des quantités égales à 26 et 14% respectivement du rendement en HCN. Ces produits semblent provenir de l'intervention de l'atome d'oxygène lors de la réaction.

On discute des mécanismes réactionnels et de la nature de l'état activé lors de l'étape initiale.

[Traduit par le journal]

Can. J. Chem. 51, 3671 (1973)

The only previous work on the reactions of active nitrogen with alcohols is that on the reactions of CH_3OH (1) and of C_2H_5OH and iso-C_3H_7OH (2). These reactions were reported to give HCN and H_2O as the main condensable products, together with lesser amounts (less than 2%) of C_2H_6, CH_3CN, C_2H_4, C_2N_2, and CO. The activation energies of the reactions were estimated to range from 13 to 15 kJ/mol. Our interest in these reactions stemmed from their rather small activation energies which implied somewhat faster reactions than those of active nitrogen with other saturated organic compounds.

[1]Presented in part at the 55th Canadian Chemical Conference of the Chemical Institute of Canada, Quebec, June, 1972.

Can. J. Chem. Downloaded from www.nrcresearchpress.com by 210.87.254.6 on 09/05/12
For personal use only.

Since the earlier work did not clearly establish either the initial steps in these reactions or their mechanisms, we decided to investigate them in more detail.

Experimental

The reactions were studied in a conventional flow system similar to that described by Westenberg and deHaas (3). The apparatus differed from theirs in that the moveable reactant inlet entered at the end of the reaction vessel downstream from the discharge and either a high voltage d.c. discharge or a microwave discharge could be used to produce the active nitrogen. The reaction vessel was coated with boric acid for most of the experiments, and no difference was found between the results obtained in a clean reactor and the coated reactor. The results obtained with the high voltage discharge were the same as those obtained with the microwave discharge, the latter being preferred because of its greater convenience. Nitrogen (Linde 99.99%) was purified by passing it through a furnace packed with copper turnings and heated to 400 °C, a furnace packed with oxidized copper turnings and heated to 400 °C, and a trap cooled in liquid nitrogen.[2] The entire purification train operated at atmospheric pressure and the purified N_2 was metered from it through a needle valve and a calibrated capillary. All alcohols were purified by repeated fractional distillation until no impurities could be detected by gas chromatography. Their purity was estimated to be better than 99.999%. In addition, CH_3OH and C_2H_5OH were refluxed with a small quantity of magnesium turnings and iodine before fractional distillation.

Nitrogen atoms were measured by the NO titration method (4, 5) using photometric end point detection. Spectroscopic examination of the gas stream immediately downstream from the titration point showed no emission other than that from NO or NO_2 near the titration end point. The NO used in these titrations was purified by passing it through silica gel at −80 °C followed by bulb-to-bulb distillation.

Reaction products, with the exception of HCN, were analyzed by gas chromatography on a 10-foot Porapak Q column using either a flame ionization or a thermal conductivity detector as required. The reaction products could be sampled directly with a Toepler pump for analysis by gas chromatography, or they could be collected in traps cooled in liquid nitrogen, dissolved in a suitable solvent, and then analyzed. The identity of the reaction products was confirmed by separating them by gas chromatography on an 8-foot column of 10% Carbowax on Chromosorb W and comparing their infrared and n.m.r. spectra with those of authentic samples. Infrared spectra were recorded on a Perkin–Elmer model 457 spectrometer and n.m.r. spectra were obtained with a Perkin–Elmer model R24 60 MHz spectrometer.

HCN was determined by trapping it for a known time and titrating it with $AgNO_3$ (6).

[2]Unpublished results by A. A. Westenberg, J. M. Roscoe, and N. deHaas show that this purification procedure is necessary even with nitrogen of 99.997% purity.

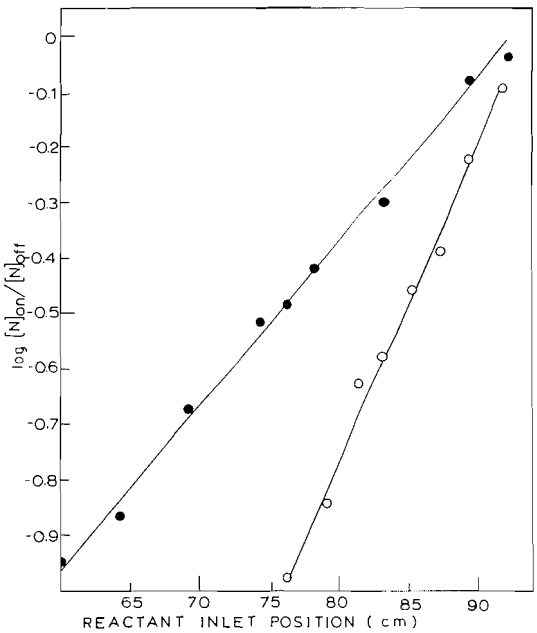

FIG. 1. Typical pseudo-first order kinetic plot. ○, $T = 449$ °K, [iso-C_3H_7OH] = 7.53×10^{-7} M, [N] = 4.35×10^{-8} M; ●, $T = 391$ °K, [iso-C_3H_7OH] = 1.17×10^{-6} M, [N] = 1.10×10^{-7} M.

Rate constants were measured in the presence of at least a 10-fold excess of alcohol to ensure pseudo-first order kinetics. Typical results are shown in Fig. 1. The N atom concentrations were measured with the reactant "on" and "off" at each reaction time to cancel first order atom loss at the walls (3).

Results and Discussion

Kinetics

Preliminary experiments on the reaction of CH_3OH with active nitrogen gave an activation energy of 13 kJ/mol, in excellent agreement with the results of the earlier work (1). The alcohol used in these experiments contained about 0.1% of an impurity as indicated by gas chromatography. When the CH_3OH was purified as outlined in the experimental section, it reacted with active nitrogen with an activation energy of 36 ± 4 kJ/mol. It was concluded that the reaction of CH_3OH and presumably the reactions of the other alcohols are sensitive to very small amounts of impurities and that rigorous purification was necessary.

The only exothermic reaction that can be written for the attack of a N atom on CH_3OH is

[1] $N + CH_3OH \rightarrow HNO + CH_3$ ($\Delta H = -38$ kJ/mol)

Can. J. Chem. Downloaded from www.nrcresearchpress.com by 210.87.254.6 on 09/05/12
For personal use only.

TABLE 1. Isotope effects on the reaction of active nitrogen with CH_3OH

Reaction	Temperature (°K)	Pressure (Torr)	Velocity (m/s)	[ROD] (mol/l)	k (l/mol s)	k_{CH_3OH}/k
$N + CH_3OD$	302	1.08	3.91	2.49×10^{-6}	5.7×10^{4}	3.4
	299	1.09	3.90	3.34	4.3	3.5
	303	1.92	2.28	7.54	4.1	4.2
	306	1.15	3.79	3.92	6.5	3.1
						Average = 3.6 ± 0.4
$N + CD_3OD$	340	1.08	4.44	2.53	14	5.9
	344	1.09	4.52	3.50	11	8.6
	346	1.12	4.46	3.72	11	9.1
						Average = 8 ± 1

Since HNO has the ground state term $^1\Delta$ (7), this reaction might not conserve spin and could have a relatively large activation energy. However, there is also a $^3\Sigma^-$ term which is thought to lie very close to the $^1\Delta$ term (7). If the HNO were formed in the $^3\Sigma^-$ state, it is likely that the reaction would still be exothermic and spin would then be conserved.

Although it is generally felt that N (^4S) atoms are the main reactive species in active nitrogen, significant concentrations of N_2 $A(^3\Sigma_u^+)$ may also be present (8) and these species have been implicated in some of the slower reactions of active nitrogen (ref. 8, p. 505). Meyer and coworkers have found that N_2 $A(^3\Sigma_u^+)$ is quenched by CH_3OH possibly producing CH_3 and OH radicals (9), and it is therefore necessary to examine the possibility that the reactions studied here might be initiated in this way.

In experiments such as ours, N_2 $A(^3\Sigma_u^+)$ formed in the discharge is efficiently quenched at the walls well upstream from the reactant inlet (10) so the only significant source of these excited molecules is homogeneous recombination of N atoms. This would have given second order consumption of N atoms rather than the observed first order behavior. Furthermore, the rate constants would then have varied with the N atom concentration. Such variation was not observed in spite of a ten-fold variation in the N atom concentration.

If the reactions studied here were initiated by quenching of N_2 $A(^3\Sigma_u^+)$, both the initial step and the subsequent reactions of the resultant free radicals with N atoms would have relatively small activation energies. Our experiments, on the other hand, indicate rather large activation energies for the reactions of the alcohols with active nitrogen.

The concentration of N_2 $A(^3\Sigma_u^+)$ in active nitrogen has been estimated to be about 10^{-3} times the N atom concentration (11). It is unlikely that such a small concentration of these excited species could cause the observed rate of consumption of N atoms. Furthermore, since the concentration of these excited molecules depends on the square of the N atom concentration, the importance of quenching in the overall reaction should decrease rapidly with increasing reaction time and consequent rapid consumption of N atoms.

As will be seen later, the suggestion that N atoms are responsible for initiating the reactions of active nitrogen with the alcohols allows us to postulate a mechanism which is consistent and general for all the reactions studied and which quantitatively accounts for the observed stoichiometries of the reactions. The assumption of initiation by N_2 $A(^3\Sigma_u^+)$ does not yield such a mechanism.

In view of the above discussion, we are led to reject quenching of N_2 $A(^3\Sigma_u^+)$ as an important initial step in the reactions of active nitrogen with the alcohols, although it may possibly intervene to a very small extent.

In an effort to obtain more definitive information about the initial step in the reaction of CH_3OH with active nitrogen, the deuterium isotope effect was measured for this reaction. The results are summarized in Table 1.

In experiments with CH_3OH and CH_3OD, the isotope effect ratio was 3.6 ± 0.4 which is greater than the value for a secondary effect (2.0 for O—D (12)) but less than the maximum value for a primary effect (18 for D (12)). This implies that the O—H bond is weakened but not entirely broken in the activated state. In experiments with CH_3OD and CD_3OD, the isotope

Can. J. Chem. Downloaded from www.nrcresearchpress.com by 210.87.254.6 on 09/05/12
For personal use only.

effect ratio was 2.2 ± 0.6 which compares favorably with the maximum value of 1.74 for a secondary isotope effect for C—D (ref. 12, p. 98). This implies that abstraction of a H atom from the CH_3 group is unimportant. A plausible activated state might be

$$N + CH_3OH \rightarrow \left[CH_3\text{---}O\overset{N}{\cdots\cdots}H \right]^{\ddagger} \rightarrow CH_3 + HNO$$

A general initiation step for the reactions of N atoms with the alcohols would then be

[2] $$N + ROH \rightarrow R + HNO$$

The kinetic data are summarized in Table 2 and Fig. 2. The preexponential factor for the reaction of n-C_3H_7OH with active nitrogen is significantly smaller than those for the other reactions. Assuming that the [CNOH] part of the activated state makes the main contribution to the entropy of activation, the entropy of this group may be estimated from the measured entropy of activation and tables of partial bond entropies (13). The pertinent data are presented in Table 3. The results for CH_3OH, C_2H_5OH, and iso-C_3H_7OH give a remarkably constant value of 178 ± 2 J mol^{-1} deg^{-1} for the partial group entropy of [CNOH]. The value obtained for the reaction of active nitrogen with n-C_3H_7OH is 38 J mol^{-1} deg^{-1} less than this.

The only structural difference between n-C_3H_7OH and the other alcohols is the presence of a β-CH_3 group. This can produce two effects. First, rotation of the C_2H_5 group about the C_2H_5—CH_2OH bond may be hindered in the activated state by the [NOH] group, while this rotation should not be hindered to the same extent in n-C_3H_7OH itself. Thus, the relatively free rotation of the C_2H_5 group would be replaced, in the activated state, by a torsional mode. Since the other alcohols studied do not have β-CH_3 groups, this hindered rotation would not be important. Secondly, rotation of [NOH] about the C---O bond in the activated state may be hindered by the C_2H_5 group. In the reactions of the other alcohols, rotation of [NOH] about the C---O bond should not be greatly hindered. This means that only in n-C_3H_7OH would rotation of [NOH] be effectively a torsional mode. These two torsional modes would make the entropy of activation and hence the entropy of the [CNOH] group in the reaction of n-C_3H_7OH smaller than for the reactions of the other alcohols. These conclusions are borne out by examination of space-filling models of the alcohols.

With the exception of n-C_3H_7OH, the activation energies of the reactions of active nitrogen with the alcohols increase with increasing C—O bond strength (14) within experimental error. This is reasonable if the C—O bond is broken in the rate determining step. Since a smaller activation energy was found for the n-C_3H_7OH reaction, an additional factor must be considered here. The small entropy of activation for this reaction relative to the values obtained for the reactions of the other alcohols implies that a smaller proportion of collisions are reactive. The rotation of the C_2H_5 group in n-C_3H_7OH effectively hinders attack by the N atom at the end of the O—H bond nearest the O atom. In terms of the postulated initiation step, steric hindrance to N atom attack in the reaction of n-C_3H_7OH hinders collisions that would tend to increase the activation energy since they occur at one end of the O—H bond and require more than the average energy to form the cyclic activated state. Collisions occurring between the O and H atoms require less energy since they orient the N atom favorably for formation of the cyclic complex. It seems possible, then, that the lower activation energy for the reaction of n-C_3H_7OH might simply reflect an average over a larger proportion of lower energy reactive collisions than was true for the reactions of the other alcohols.

Reaction Mechanisms

Since the products of the reactions of iso-C_3H_7OH with active nitrogen differed from those of the reactions of the other alcohols, the results for the reactions of the other alcohols will be discussed first.

The only stable product detected in the reactions of CH_3OH, C_2H_5OH, and n-C_3H_7OH with active nitrogen was HCN. The yields of HCN are plotted against the relative alcohol concentration in Fig. 3. The stoichiometries of these reactions are given in Table 4. The average values of $\Delta[ROH]/\Delta[N]$ were used to convert the measured (effective) rate constants to the absolute rate constants reported in Tables 1 and 2. In all cases, a relatively small proportion of the N atoms consumed are found as HCN.

The failure to detect measureable amounts of H_2O in the reactions of the alcohols with active

Can. J. Chem. Downloaded from www.nrcresearchpress.com by 210.87.254.6 on 09/05/12
For personal use only.

TABLE 2. Rate constants for the reactions of active nitrogen with the alcohols*

Reaction	Temperature (°K)	Pressure (Torr)	Velocity (m/s)	$[ROH] \times 10^6$ (mol/l)	$k \times 10^{-5}$ (l/mol s)
$N + CH_3OH$	309	1.07	4.14	4.63	2.4
	322	1.70	2.42	3.46	2.3
	329	1.38	3.42	5.39	6.7
	332	1.39	3.67	7.91	7.8
	344	1.39	3.66	6.88	7.6
	360	1.39	3.83	5.86	16
	371	1.40	3.89	5.73	24
	409	1.56	3.97	2.84	63
	409	1.56	3.94	2.41	68
	$\log k = 11.38 \pm 0.08 - (36 \pm 4)/RT$				
$N + C_2H_5OH$	312	1.12	3.96	3.87	2.4
	326	1.12	4.11	2.80	5.5
	336	1.12	4.23	2.84	7.3
	340	1.12	4.25	2.87	8.8
	351	1.12	4.42	2.60	12
	361	1.10	4.44	1.18	19
	378	1.63	3.80	1.57	26
	397	1.27	4.66	1.65	56
	404	1.62	3.89	1.67	49
	425	1.61	4.12	1.38	104
	$\log k = 11.30 \pm 0.04 - (35 \pm 2)/RT$				
$N + n\text{-}C_3H_7OH$	354	1.39	4.20	2.95	0.76
	354	1.39	4.20	2.95	1.1
	365	1.48	4.63	4.38	1.6
	384	1.34	4.96	6.19	1.7
	384	1.34	4.96	6.19	2.5
	395	1.35	4.73	2.14	3.2
	395	1.33	4.66	1.76	3.5
	407	1.41	4.96	2.15	4.9
	417	1.41	4.75	1.48	4.3
	420	1.39	5.30	4.38	4.9
	422	1.36	5.15	3.86	6.2
	428	1.29	5.32	6.31	5.9
	430	1.38	5.46	1.55	6.2
	443	1.37	5.70	5.63	7.9
	466	1.40	5.64	2.17	13
	482	1.37	5.89	2.30	16
	494	1.37	5.99	2.10	20
	$\log k = 9.44 \pm 0.04 - (30 \pm 2)/RT$				
$N + iso\text{-}C_3H_7OH$	304	1.28	3.30	2.03	2.2
	321	1.73	3.00	1.58	3.0
	321	1.22	3.50	0.860	3.5
	330	1.37	3.92	0.871	5.4
	339	1.25	3.64	1.98	6.3
	349	1.16	3.66	1.74	12
	384	0.857	7.34	0.674	36
	391	1.24	4.20	1.32	46
	403	0.832	7.94	0.632	67
	418	0.882	7.50	0.838	103
	449	0.865	8.21	0.651	304
	$\log k = 11.93 \pm 0.05 - (39 \pm 2)/RT$				

*Activation energies are reported in kJ/mol.

nitrogen differs from the results of the earlier work (1, 2) in which substantial amounts of H_2O were found. The present experiments used gas chromatography on Porapak Q to determine H_2O, while the earlier experiments used the Karl Fischer titration. The limit of detection of

Can. J. Chem. Downloaded from www.nrcresearchpress.com by 210.87.254.6 on 09/05/12
For personal use only.

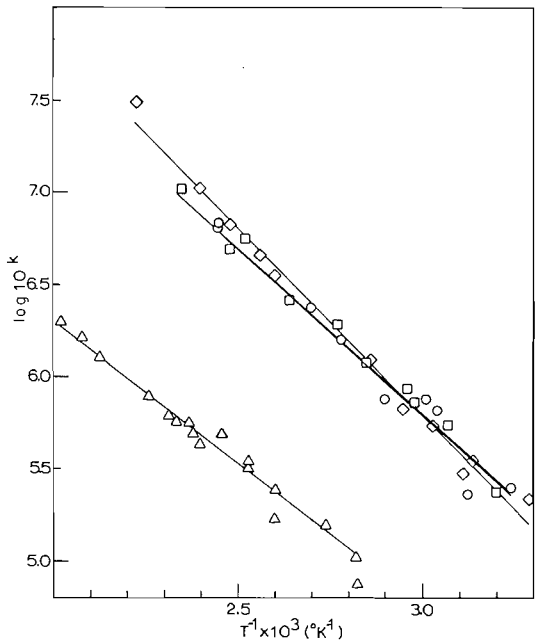

FIG. 2. Arrhenius plots for the reactions of active nitrogen with the alcohols. ○, CH_3OH; □, C_2H_5OH; △, n-C_3H_7OH; ◇, iso-C_3H_7OH.

H_2O by gas chromatography was about 10^{-10} M or $[H_2O]/\Delta[N] = 10^{-3}$ compared with about 10^{-5} M using Karl Fischer reagent. Our experiments should therefore have been more sensitive for the determination of H_2O than the method used in the earlier work. Furthermore, blank determinations showed that Karl Fischer reagent titrates HCN and iso-C_3H_7OH making it useless for accurate H_2O determinations. This may well have been a source of error in the earlier work.

The following general mechanism quantitatively accounts for the observed stoichiometries of the reactions of the normal alcohols with active nitrogen.

[1a] $C_nH_{2n+1}OH + N \rightarrow HNO + C_nH_{2n+1}$

[3] $C_nH_{2n+1} + nN \rightarrow nHCN + \frac{n+1}{2} H_2$

[4] $HNO + N \rightarrow NH + NO$

[5] $NH + N \rightarrow N_2 + H$

[6] $NO + N \rightarrow N_2 + O$

An alternative to reaction 3 might be

[7] $C_nH_{2n+1} + N \rightarrow C_mH_{2m+2} + HCN$ $(m = n - 1)$

Since the saturated hydrocarbons C_mH_{2m+2} are unreactive with active nitrogen (15), reaction 7 would reduce the stoichiometric ratios far below those measured. The strongest reason for rejecting reaction 7, however, is that saturated hydrocarbons were not detected among the reaction products.

Reaction 3 is intended to give the ultimate fate of the organic free radicals. The details of the elementary steps involved are still a matter of controversy. Inclusion of reaction 3 does, however, give the experimentally observed stoichiometries.

The reactions postulated so far produce both H atoms and O atoms. Wagner and co-workers have recently reported an activation energy of 22 kJ/mol for the reaction of H atoms with CH_3OH (16), and it seems reasonable to expect similar activation energies for the reactions of H atoms with the other alcohols. This relatively large activation energy should effectively prevent H atoms from intervening efficiently in the reactions of the alcohols with active nitrogen. In particular, such intervention in the reaction of CH_3OH with active nitrogen would have produced H_2O and CH_4 (16). The apparent absence of these species among the reaction products suggests that H atom intervention is indeed negligible.

Cvetanović and co-workers have investigated the reactions of several alcohols with O atoms (17, 18). From their data, it appears that these reactions are some 100 times faster than the corresponding N atom reactions at room temperature. As a result, intervention of the O atoms from reaction 6 must be considered in interpreting the results of the N atom reactions with the alcohols.

Cvetanović has shown that the reaction of O atoms with CH_3OH is initiated by (18)

[8] $O + CH_3OH \rightarrow CH_2OH + OH$

followed by

[9] $CH_2OH \rightarrow H_2C{:}O + H$

[10] $2\,CH_2OH \rightarrow HOCH_2CH_2OH$

of which reaction 9 seems to be the more important. Formaldehyde formed in [9] would react with active nitrogen to produce CO (19). However, neither CO nor ethylene glycol were found in the reaction products from the reaction of CH_3OH with active nitrogen suggesting either

Can. J. Chem. Downloaded from www.nrcresearchpress.com by 210.87.254.6 on 09/05/12
For personal use only.

TABLE 3. Entropy data for the reactions of active nitrogen with the alcohols

Species	ΔS_0 (J/mol deg)	ΔS_0(R—) (J/mol deg)	$\Delta S_0{}^{\ddagger}$ (J/mol deg)	ΔS_0(C---O---H) (J/mol deg)
N Atom	133	—	—	—
CH_3OH	236	162	−27	180
C_2H_5OH	310	235	−29	179
iso-C_3H_7OH	500	308	−17	176
n-C_3H_7OH	592	384	−64	139

TABLE 4. Stoichiometric data for the reactions of active nitrogen with the primary alcohols

Reaction	[HCN]/Δ[N]		Δ[ROH]/Δ[N]	
	Measured	Calculated	Measured	Calculated
N + CH_3OH	0.21±0.01	0.200	0.21±0.01	0.200
N + C_2H_5OH	0.330±0.005	0.333	0.16±0.01	0.167
N + n-C_3H_7OH	0.41±0.02	0.429	0.14±0.02	0.143

TABLE 5. Stoichiometric data for the reaction of active nitrogen with isopropanol

$\frac{[\text{iso-}C_3H_7OH]}{[N]_0}$	$\frac{\Delta[\text{iso-}C_3H_7OH]}{\Delta[N]}$	$\frac{[(CH_3)_2C{:}O]}{\Delta[N]}$	$\frac{[CH_3CN]}{\Delta[N]}$
5.04	0.21	0.082	0.045
5.04	0.22	0.086	0.048
5.04	0.19	0.066	0.037
5.04	0.21	0.079	0.043
5.04	0.22	0.087	0.044
2.89	0.23	0.094	0.052
3.72	0.19	0.069	0.038
3.72	0.22	0.073	0.041
Average =	0.21±0.01	0.079±0.008	0.043±0.008

that O atom intervention is unimportant or that the products of reaction 8 react very rapidly with active nitrogen. Thrush has shown that OH radicals react very rapidly with N atoms (20). It will also be seen that the reaction of iso-C_3H_7OH with active nitrogen cannot be easily explained without including O atom intervention. The following general mechanism may therefore be suggested to account for the intervention of O atoms in the reactions of the alcohols with active nitrogen.

[8a] $\quad O + C_nH_{2n+1}OH \rightarrow C_nH_{2n}OH + OH$

[11] $\quad N + OH \rightarrow NO + H$

[6] $\quad N + NO \rightarrow N_2 + O$

[12] $\quad nN + C_nH_{2n}OH \rightarrow nHCN + \frac{n}{2}H_2 + OH$

The stoichiometries with respect to HCN production and alcohol consumption are identical to those from the reactions initiated by N atom attack on the alcohol (reactions 1a, 3–6) and intervention in this way by O atoms is therefore consistent with the observed stoichiometries for the reactions of the primary alcohols.

An alternative to reaction 12 is

[13] $\quad N + C_nH_{2n}OH \rightarrow HCN + C_mH_{2m+1}OH \; (m = n - 1)$

This reaction does not conserve spin and is therefore likely to be slow. Furthermore, it produces H_2O in the CH_3OH reaction and lower alcohols in the other reactions. The failure to detect these species among the reaction products suggests that reaction 13 is relatively

Can. J. Chem. Downloaded from www.nrcresearchpress.com by 210.87.254.6 on 09/05/12
For personal use only.

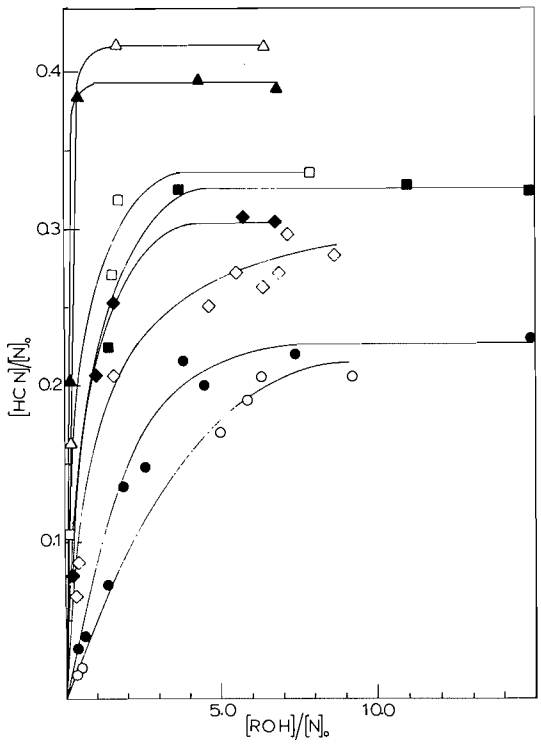

FIG. 3. Yields of HCN in the reactions of active nitrogen with the alcohols. ○, CH_3OH at 301 °K; ●, CH_3OH at 350 °K; □, C_2H_5OH at 300 °K; ■, C_2H_5OH at 460 °K; △, n-C_3H_7OH at 342 °K; ▲, n-C_3H_7OH at 467 °K; ◇, iso-C_3H_7OH at 327 °K; ◆, iso-C_3H_7OH at 460 °K.

unimportant. The occurrence of reaction 13 to any significant extent would alter the predicted stoichiometries so that the mechanism would no longer be consistent with experiment. It is therefore concluded that reaction 13 is relatively unimportant.

The reactions postulated so far produce aliphatic free radicals (R) and OH radicals. Further complication of the reactions by R would produce saturated hydrocarbons which do not react readily with active nitrogen (15). The absence of such substances among the reaction products suggests that intervention by R is relatively unimportant. Similarly, intervention by OH would produce H_2O by attack on the parent alcohol and the absence of H_2O from the reaction products indicates that OH intervention is also unimportant.

It seems reasonable to assume that N atoms attack iso-C_3H_7OH in the same way as the other alcohols and that the general mechanism postulated earlier applies. The predicted stoichiometries would then be the same as for n-C_3H_7OH. The measured stoichiometries differ greatly from those for n-C_3H_7OH (Fig. 3, Tables 4 and 5). In addition, both acetone and acetonitrile were found among the reaction products and the general mechanism without O atom intervention gives no means of producing these species. A satisfactory explanation of these discrepancies can, however, be found in the O atom intervention in this reaction. Reaction 8*a* would produce a $(CH_3)_2COH$ radical which differs from the radicals formed from the primary alcohols in having no α-H atom. Attack by a N atom might thus not produce HCN directly, but could result in the reaction

[14] $N + (CH_3)_2COH \rightarrow CH_3CN + CH_3 + OH$

In addition, acetone could be formed in the reaction

[9*a*] $(CH_3)_2COH \rightarrow (CH_3)_2C{:}O + H$

The appearance of both acetone and acetonitrile suggests that $(CH_3)_2COH$ radicals may react less readily with N atoms than RCHOH radicals since reaction 9 was apparently unimportant in the reactions of the primary alcohols. The apparent absence of pinacol from the reaction products confirms Cventanović's observation that dimerization is less important than disproportion of the alkoxyl radicals via [9] (18).

The ratio $[(CH_3)_2C{:}O]/[CH_3CN]$ was 1.8 ± 0.2 from the results of eight runs in which the iso-C_3H_7OH concentration was large enough to ensure that this is a limiting value. This result may be combined with the HCN limiting yield to estimate the relative lengths of the reaction sequences initiated by O atoms and N atoms respectively, according to the mechanisms postulated above. Such a calculation indicates that the O atom initiated reaction takes place 1.2 times for each occurrence of the N atom initiated sequence. From this, the remaining stoichiometric ratios may be calculated and compared with the experimental values as shown below.

Stoichiometric ratios

Ratio	Calculated	Found
$\Delta[C_3H_7OH]/\Delta[N]$	0.20	0.21 ± 0.01
$[CH_3CN]/\Delta[N]$	0.039	0.043 ± 0.008
$[(CH_3)_2C{:}O]/\Delta[N]$	0.071	0.079 ± 0.008

Can. J. Chem. Downloaded from www.nrcresearchpress.com by 210.87.254.6 on 09/05/12
For personal use only.

The results are in good agreement with the calculated values and suggest that the postulated mechanism is essentially correct.

We wish to thank Dr. P. W. Rasmussen for helpful discussions and the National Research Council of Canada for financial support.

1. M. J. SOLE and P. A. GARTAGANIS. Can. J. Chem. **41**, 1097 (1963).
2. P. A. GARTAGANIS Can. J. Chem. **43**, 935 (1965).
3. A. A. WESTENBERG and N. DEHAAS. J. Chem. Phys. **46**, 490 (1967).
4. G. B. KISTIAKOWSKY and G. G. VOLPI. J. Chem. Phys. **27**, 1141 (1957).
5. F. KAUFMAN and J. R. KELSO. J. Chem. Phys. **27**, 1209 (1957).
6. I. M. KOLTHOFF and E. B. SANDELL. Textbook of quantitative inorganic analysis. 3rd ed., MacMillan Co., New York, N.Y. 1963. p. 546.
7. G. HERZBERG. Electronic spectra of polyatomic molecules. D. van Nostrand Co. Inc., Princeton, N.J. 1966. p. 496.
8. A. N. WRIGHT and C. A. WINKLER. Active nitrogen. Academic Press, New York, N.Y. 1968. Chapt. 3.
9. J. A. MEYER, D. W. SETSER, and W. G. CLARK. J. Phys. Chem. **76**, 1 (1972).
10. W. L. STARR and T. M. SHAW. J. Chem. Phys. **44**, 4181 (1966).
11. I. M. CAMPBELL and B. A. THRUSH. Trans. Faraday Soc. **64**, 1275 (1968).
12. K. J. LAIDLER. Chemical kinetics. 2nd ed. McGraw-Hill Co., New York, N.Y. 1965. p. 97.
13. S. W. BENSON. The foundations of chemical kinetics. McGraw-Hill Co., New York, N.Y. 1960. p. 665.
14. C. T. MORTIMER. Reaction heats and bond strengths. Pergamon Press, New York, N.Y. 1962. p. 136.
15. G. R. BROWN and C. A. WINKLER. Angew. Chem. Int. Ed. **9**, 181 (1970).
16. W.-K. ADERS and H. GG. WAGNER. Zeit. Phys. Chem. **74**, 224 (1971).
17. A. KATO and R. J. CVETANOVIĆ. Can. J. Chem. **45**, 1845 (1967).
18. A. KATO and R. J. CVETANOVIĆ. Can. J. Chem. **46**, 235 (1968).
19. L. V. WHITING. Ph.D. Thesis. McGill University, Montreal, Quebec. 1971.
20. I. M. CAMPBELL and B. A. THRUSH. Trans. Faraday Soc. **64**, 1265 (1968).

Can. J. Chem. Downloaded from www.nrcresearchpress.com by 210.87.254.6 on 09/05/12
For personal use only.

Reaction of Active Nitrogen with Tetrachloroethylene

WILLIAM ERNEST JONES AND MANIT RUJIMETHABHAS[1]
Department of Chemistry, Dalhousie University, Halifax, Nova Scotia

Received January 2, 1973

The reaction of active nitrogen with tetrachloroethylene yielded cyanogen chloride, trichloroacetonitrile, cyanogen, chlorine, and carbon tetrachloride. In addition, a yellow–brown polymer was found on the glass wall. A brief discussion of a possible mechanism is given.

La réaction de l'azote actif avec le tétrachlorure d'éthylène conduit à un mélange de chlorure de cyanogène, de trichloroacétonitrile, de cyanogène, de chlore et de tétrachlorure de carbone. De plus un polymère jaune–brun se retrouve sur la paroi du verre. Une brève discussion du mécanisme possible est présentée. [Traduit par le journal]

Can. J. Chem. **51**, 3680 (1973)

Introduction

The reaction of active nitrogen with tetrachloroethylene (TCE) at room temperature gives a bright peach-colored flame. However, the flame boundary is not as well defined as it is in the reaction of active nitrogen with perfluorocarbons. It is therefore impossible to study the kinetics by the diffusion flame method as has been done with the perfluorocarbons (1). At a high reactant flow rate, the flame is quenched only a few centimeters from the reactant nozzle. As the flow rate of TCE decreases, the flame extends farther down stream from the reaction vessel. For example, at a very small TCE flow rate and in a well-darkened room, the flame emission can be seen to extend to the product trap. The gaseous products are: cyanogen chloride (CNCl), trichloroacetonitrile (CCl_3CN), cyanogen ($(CN)_2$), chlorine (Cl_2), carbon tetrachloride (CCl_4), and unreacted TCE. A yellow–brown solid "polymer" forms as a deposit on the glass wall of the reaction vessel and on the reactant inlet.

Jennings and Linnett (2, 3) investigated the emission from the reaction flame of active nitrogen with TCE and found the CN violet and red systems and C—Cl bands. However, no bands corresponding to the C_2 swan bands or to the then unknown N—Cl molecule were detected. Kiess and Broida (4) studied the reaction flame by using active nitrogen generated by electrodeless discharge and reported that the CN(0,0) violet emission was much more intense than the CN(10,4) red emission. The authors could not indicate any specific mechanism leading to the CN emission.

Previous workers have not investigated the products of the reaction. In this paper, we report the determination of the reaction products.

Experimental

Apparatus

The reaction was studied in a conventional fast flow system with a Pyrex reaction vessel of 40 cm length and 6 cm o.d. Purified nitrogen from Canadian Liquid Air Corporation was further purified by passing it through (*a*) a liquid nitrogen trap packed with copper turnings, (*b*) a column of heated copper at 425 °C, and (*c*) another liquid nitrogen trap. The purified nitrogen passed through a capillary flow meter and was activated by a condensed electric discharge. The nitrogen atom concentration was obtained by the NO gas titration technique (5, 6). The nitrogen atom flow rate was found to be 3.2 μmol s^{-1} at 1.75 Torr. The reaction products were studied by gas chromatography using a 10 ft column packed with chromosorb P coated with 30% tricresyl phosphate. The separation was most effective when the column oven was subjected to a non-linear temperature program. After introduction of the sample, the column remained at room temperature for 7 min, and then was heated to 370 °K where it remained until the last compound appeared. The products were identified by comparison of retention times and the identification was checked by infrared and mass spectroscopy.

A reaction vessel 60 cm long and 2.5 cm in diameter was used to study the emission from the reaction. Both ends of this reaction vessel were equipped with quartz windows. The flame was monitored by viewing the reaction vessel end-on with a Heath EU-700 monochromator at a slit width of 350 μ. The emission bands were recorded from 2000–7500 Å. For these reactions, the active nitrogen was generated by a 200 W microwave unit operating at 2450 MHz and at a power output of 75–80%. The reaction was studied at 1.2 Torr.

[1]Holder of a Colombo Plan Scholarship.

Can. J. Chem. Downloaded from www.nrcresearchpress.com by 210.87.254.42 on 09/05/12
For personal use only.

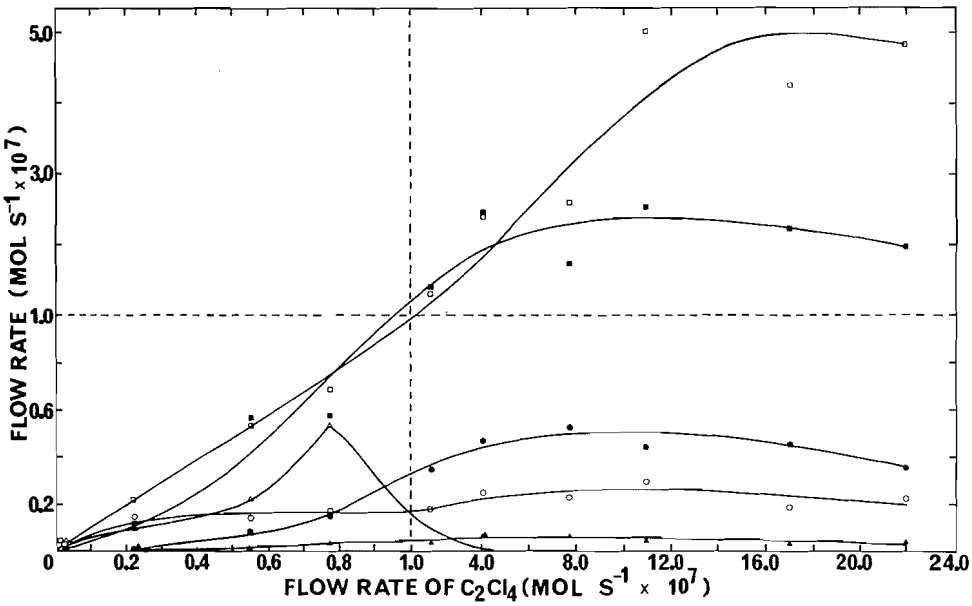

FIG. 1. Reaction of active nitrogen with tetrachloroethylene at 25 ± 5 °C. □ = C_2Cl_4 reacted; product flow rates are: ○ = $(CN)_2$; △ = Cl_2; ■ = CNCl; ▲ = CCl_4; ● = CCl_3CN. The dashed lines indicate change of scale.

Materials

TCE and CCl_3CN were obtained from Eastman Kodak Company. The TCE was purified by double distillation and stored away from light. $(CN)_2$ and Cl_2 were obtained from Matheson of Canada Ltd. The $(CN)_2$ was purified by bulb-to-bulb distillation. CCl_4 was obtained from Fisher Scientific Co. The CNCl was prepared by a standard method (7) and purified by bulb-to-bulb distillation. TCE, CCl_3CN, $(CN)_2$, CCl_4, and CNCl were all degassed at Dry Ice – acetone temperature while Cl_2 was degassed at liquid nitrogen temperature.

NO was obtained from Matheson of Canada Limited and purified by condensation in and evaporation from ascarite (8–20 mesh). It was condensed at liquid nitrogen temperature and degassed.

Results and Discussion

The reaction of active nitrogen with TCE yields CNCl, CCl_3CN, $(CN)_2$, Cl_2, and CCl_4. It also yields a yellow-brown polymer on the glass wall of the reaction vessel. The yield of these products at various flow rates of TCE is given in Table 1,[2] and shown graphically in Fig. 1. From Fig. 1, it can be seen that at very low TCE flow rates, the only detectable products are $(CN)_2$, Cl_2, and CNCl. At low flow rates, the flame emission was found to extend downstream from the TCE nozzle to the product trap. As the ratio [TCE]/[N] was increased by increasing the TCE flow rate, the flame "tail" was shortened until, at high TCE flow rates, the flame was completely quenched within a few centimeters of the TCE nozzle. The product flow rate of CNCl increased as CCl_4 and CCl_3CN began to appear. The product flow rates reached maximum values at about 1.1 μmol s^{-1} of TCE (Fig. 1).

Carbon balances have been found to be better than 95% at very low TCE flow rates and as poor as 50% at high TCE flow rates. The poor carbon balances at high TCE flow rates are probably due to increasing formation of polymer since the polymer appeared to build up on the wall much more rapidly at high flow rates than at low flow rates. Unfortunately, it was not possible to make quantitative measurements of the polymer yield.

Elemental analysis of the polymer showed it to have the composition C : N : Cl = 1.6 : 1.0 : 1.6. A sample of the polymer, which collected on the reaction vessel walls during a number of runs, was decomposed under vacuum over the temperature range 298–523 °K. The major product was Cl_2 with relatively small amounts of C_2Cl_4,

[2]Table 1 is available, at a nominal charge, from the Depository of Unpublished Data, National Science Library, National Research Council of Canada, Ottawa, Canada K1A 0S2.

Can. J. Chem. Downloaded from www.nrcresearchpress.com by 210.87.254.42 on 09/05/12
For personal use only.

Can. J. Chem. Downloaded from www.nrcresearchpress.com by 210.87.254.42 on 09/05/12
For personal use only.

CCl_4, CNCl, and N_2 also being formed. After several hours of decomposition, the residue had turned very dark in color.

Up to a TCE flow rate of 0.4 μmol s^{-1}, approximately 50% of the chlorine originally present could be accounted for. Above this flow rate, the amount of chlorine which could be accounted for by the products decreased drastically. The polymer contained a certain amount of chlorine. However, this amount was not sufficient to account for the chlorine loss at high flow rates. It was noted that, even at very low temperatures (80 °C), small amounts of Cl_2 evolved from the polymer. It is possible that Cl_2 was physically adsorbed by the polymer. If physical adsorption did not occur, the reported elemental analysis for chlorine must be low. It was also possible that Cl_2 was adsorbed by stopcock grease present in the system. This was found to occur in the reaction of active nitrogen with $COCl_2$ (8).

The reaction flame consisted of an intense emission composed of the CN red ($A^2\Pi$–$X^2\Sigma^+$) and CN violet ($B^2\Sigma^+$–$X^2\Sigma^+$) systems (9). Since the work of Jennings and Linett (2, 3), a spectrum of the NCl molecule has been observed in the region 615–703 nm (10). Although this region was studied carefully, no spectrum of the NCl radical was observed. However, as noted by Colin and Jones (10), the NCl spectrum is extremely weak and difficult to observe against the CN emission background.

When the flow rate of TCE was adjusted properly, the flame emission near the nozzle was very intense while, farther down stream, the emission appeared to oscillate with an extremely bright pink–white flame. Such an oscillatory phenomenon suggested that the flame involved chain reactions (11). This flame oscillation was clearly visible in the system in which the active nitrogen was generated by the microwave discharge. However, it was barely observed in the system where the condensed electric discharge was used to activate the nitrogen. This was probably due to the oscillation of the discharge itself.

Because of the formation of polymer and the resulting significant loss of carbon and chlorine, it was difficult to determine the kinetics and, with the present information, it is only possible to discuss several general reactions which are important in the overall mechanism.

The primary step may involve attack by $N(^4S)$ as in reaction 1 or energy transfer from the excited molecule $N_2(A^3\Sigma_u^+)$ as in reaction 2.

[1] $N(^4S) + C_2Cl_4 \rightarrow [C_2Cl_4N]_{complex} \rightarrow$ products

[2] $N_2(A^3\Sigma_u^+) + C_2Cl_4 \rightarrow N_2(X^1\Sigma_g^+) + C_2Cl_4^*$

Both reactions 1 and 2 would yield chlorocarbon radicals and Cl while reaction 1 would also yield CNCl.

The chlorocarbon radicals would subsequently react with nitrogen atoms as in the following reactions:

[3] $RCl + N \rightarrow CNCl + R'$

[4] $RCl + N \rightarrow CNCl + R'' + Cl$

Reactions 3 and 4 as well as reaction 1 would account for the major product CNCl.

In addition to the chlorocarbon radicals formed in reactions 1 and 2, the radical C_2Cl_5 would be formed by adding chlorine atoms to C_2Cl_4 as in reaction 5.

[5] $C_2Cl_4 + Cl \rightarrow C_2Cl_5$

This reaction is known to occur readily (12–14).

Cyanogen results from the recombination of CN radicals formed when CNCl is excited by $N_2(A^3\Sigma_u^+)$ as in reactions 6 and 7.

[6] $N_2(A^3\Sigma_u^+) + CNCl \rightarrow N_2(X^1\Sigma_g^+) + CNCl^*$

[7] $CNCl^* \rightarrow CN + Cl$

These reactions have been proposed by Bayes (15) from studies of the reaction of active nitrogen with CNCl.

The CN radicals, formed as in reaction 7, may also attack CNCl to form $(CN)_2$ and Cl. They might also attack CCl_3 to yield the second major product of the reaction CCl_3CN as in the following reaction:

[8] $CCl_3 + CN \rightarrow CCl_3CN$

The product CCl_4, which is formed in relatively smaller amounts, probably results from the addition of Cl atoms to CCl_3.

Despite the fact that no spectra of NCl were observed in the emission flame, it is impossible to eliminate it as an intermediate species. NCl would be expected to form as in the following reaction:

[9] $Cl_2(^1\Sigma) + N(^4S) \rightarrow NCl(^3\Sigma) + Cl(^2P)$

This reaction has been proposed by Phillips and

co-workers (16, 17) in their study of the reaction of active nitrogen with Cl_2. If NCl formed, it would react rapidly (18) with $N(^4S)$ as in reaction 10.

[10] $$NCl + N(^4S) \rightarrow N_2 + Cl$$

Thus, the formation of NCl and its subsequent reaction with $N(^4S)$ could explain the significant loss of N atoms during the active nitrogen–TCE reaction. A maximum 23% of the original concentration of N atoms appears in the products (Table 1).

M.R. wishes to acknowledge his scholarship from the Canadian International Development Agency. We also acknowledge financial assistance from the National Research Council of Canada.

1. M. RUJIMETHABHAS and W. E. JONES. Can. J. Chem. **50**, 346 (1972).
2. K. R. JENNINGS and J. W. LINNETT. Nature, **180**, 1272 (1957).
3. K. R. JENNINGS and J. W. LINNETT. Trans. Faraday Soc. **56**, 1737 (1960).
4. N. H. KIESS and H. P. BROIDA. Proc. 7th Symp. (Int.) Combust. 1958. (Pub. 1959). p. 207.
5. (*a*) A. A. WESTENBERG and N. DE HAAS. J. Chem. Phys. **40**, 3087 (1964); (*b*) L. ELIAS. J. Chem. Phys. **42**, 4311 (1965).
6. J. T. HERRON. J. Phys. Chem. **69**, 2736 (1965).
7. G. BRAUER. (*Editor*). Handbook of preparative inorganic chemistry. Vol. 1. 2nd ed. Academic Press. New York, N.Y. 1963. Method I. p. 662.
8. R. R. BAKER and C. A. WINKLER. Can. J. Chem. **49**, 3846 (1971).
9. R. W. B. PEARSE and A. G. GAYDON. The identification of molecular spectra. 3rd ed., Chapman and Hall, London. 1963.
10. R. COLIN and W. E. JONES. Can. J. Phys. **45**, 301 (1967).
11. D. A. FRANK-KAMENETSKII. Diffusion and heat transfer in chemical kinetics. Plenum Press, New York. 1969.
12. J. A. FRANKLIN, G. HUYBRECHTS, and C. CILLIEN. Trans. Faraday Soc. **65**, 2094 (1969).
13. J. KNOX and K. D. WAUGH. Trans. Faraday Soc. **65**, 1585 (1969).
14. D. D. DAVIS, W. BRAUN, and A. M. BASS. Inter. J. Chem. Kinet. **2**, 101 (1970).
15. K. D. BAYES. Can. J. Chem. **39**, 1074 (1961).
16. K. S. RAXWORTHY and L. F. PHILLIPS. Can. J. Chem. **42**, 2928 (1964).
17. M. R. GRIGOR and L. F. PHILLIPS. Proc. 11th Symp. (Int.) Combust. 1966. (Pub. 1967). p. 1171.
18. C. G. FREEMAN and L. F. PHILLIPS. J. Phys. Chem. **72**, 3028 (1968).

Can. J. Chem. Downloaded from www.nrcresearchpress.com by 210.87.254.42 on 09/05/12
For personal use only.

Structure cristalline et moléculaire du cyclopentadiényle dicarbonyle dioxyde de soufre manganèse $MnC_5H_5(CO)_2SO_2$

CLAUDE BARBEAU ET RAM JANAM DUBEY
Département de Chimie, Université Laval, Québec, Québec

Reçu le 1 mai 1973

Le composé $MnC_5H_5(CO)_2SO_2$ cristallise dans le système monoclinique, groupe d'espace $P2_1/c$, dans une maille de dimensions $a = 10.98(2)$ Å, $b = 10.63(2)$ Å, $c = 7.43(2)$ Å. $\beta = 100.75(8)°$ avec $Z = 4$. La structure a été déterminée à partir de 1512 réflexions recueillies sur films de chambre de précession. Le facteur résiduel R se situe à 0.093 après affinement par moindres carrés (matrice complète). La liaison Mn—S (2.037(5) Å) paraît très forte en présentant une distance inférieure de 0.3 Å à la somme des rayons covalents. La distance moyenne Mn—$C_{C_5H_5}$ (2.09(2) Å) est inférieure à celle généralement observée dans les complexes cyclopentadiényle-manganèse. Les deux groupements CO sont distincts. Un encombrement au niveau des ligands SO_2 et CO pourrait expliquer en partie l'instabilité du complexe.

The compound $MnC_5H_5(CO)_2SO_2$ crystallizes in the monoclinic system, space group $P2_1/c$, in a unit cell of dimensions $a = 10.98(2)$ Å, $b = 10.63(2)$ Å, $c = 7.43(2)$ Å, $\beta = 100.75(8)°$ with $Z = 4$. The structure was determined from 1512 reflections obtained on films from a precession camera; the residual factor, R, was 0.093 after a full matrix least-squares refinement. The Mn—S bond seems very strong having a length (2.037(5) Å) which is smaller than the sum of the covalent radii by 0.3 Å. The average distance Mn—$C_{C_5H_5}$ (2.09(2) Å) is less than that usually observed in manganese-cyclopentadienyl complexes. The two CO groups are distinct. The instability of the complex might be explained, in part, by the crowding of the SO_2 and CO ligands. [Journal translation]

Can. J. Chem. **51**, 3684 (1973)

Introduction

Dans notre étude sur l'influence d'un groupe donneur D sur les paramètres atomiques du métal carbonyle $MnC_5H_5(CO)_{3-x}D_x$, nous avons déjà montré (1) que la triphénylphosphine n'affectait que les liaisons Mn—C—O. A l'opposé de $P(C_6H_5)_3$, le groupe SO_2 remplace difficilement une molécule de monoxyde de carbone de $MnC_5H_5(CO)_3$ en formant un composé (*a*) beaucoup moins stable (*b*) dont le moment dipolaire est plus faible (2) et (*c*) qui présente des fréquences de vibration de valence CO beaucoup plus élevées que le composé $MnC_5H_5(CO)_2P(C_6H_5)_3$ (2).

L'étude de ce composé a été entreprise dans le but de connaître les conséquences structurales sur le reste de la molécule du remplacement d'un groupe CO par un ligand qui possède les qualités à la fois d'un acide et d'une base de Lewis.

Partie expérimentale

Le remplacement d'un groupe CO par le dioxyde de soufre s'effectue par voie indirecte en utilisant le complexe $MnC_5H_5(CO)_2CH_3OH$ comme intermédiaire.

Une solution de 300 mg de $MnC_5H_5(CO)_3$ dans 50 ml de méthanol est soumise à l'irradiation d'une lampe à vapeur de mercure de type General Electric H-100 A4/T. Le monoxyde de carbone est chassé de la solution par le passage continu d'un courant d'azote. Lorsque le complexe rouge vif $MnC_5H_5(CO)_2CH_3OH$ est formé, on introduit graduellement du dioxyde de soufre en faisant barboter alternativement de l'azote et un mélange N_2–SO_2. La solution passe alors lentement du rouge à l'orangé, coloration caractéristique de $MnC_5H_5(CO)_2SO_2$. Puisque un excès de SO_2 conduit à la décomposition du complexe, le passage du mélange N_2–SO_2 est interrompu dès que la coloration orangée s'atténue ou qu'une teinte verte apparaît. Après l'évaporation sous vide de la solution, on retire du résidu la quantité de $MnC_5H_5(CO)_3$ qui n'a pas réagi, en sublimant sous vide à 40 °C. $MnC_5H_5(CO)_2SO_2$ est obtenu pur (~100 mg) par sublimation subséquente sous vide à 70 °C.

L'évaporation lente, sous atmosphère d'azote, d'une solution saturée de $MnC_5H_5(CO)_2SO_2$ dans l'éthanol, donne des cristaux orangés tabulaires de dimensions moyennes 0.5 × 0.3 × 1.0 mm.

Données cristallines

$C_7H_5MnO_4S$ m.m. 240.1

Monoclinique $P2_1/c$, $a = 10.98(2)$, $b = 10.63(2)$, $c = 7.43(2)$ Å, $\beta = 100.75(8)°$, $V = 851$ Å^3, $\rho_o = 1.85(2)$, $Z = 4$, $\rho_c = 1.87$ (20 °C, Mo K$\bar{\alpha}$, $\lambda = 0.71069$ Å).

La mesure de la densité a été effectuée selon la méthode de flottaison dans une solution aqueuse de bromure de zinc et de chlorure de césium.

Les paramètres cristallins ont été obtenus à partir de clichés de chambre à précession de Buerger en utilisant des réflexions de haut indice sur les niveaux zéro, après calibrage avec un cristal de chlorure de sodium.

Le groupe spatial $P2_1/c$ est déduit de l'extinction systé-

Can. J. Chem. Downloaded from www.nrcresearchpress.com by 210.87.254.42 on 09/05/12
For personal use only.

TABLEAU 1. Coordonnées atomiques ($\times 10^4$) et coefficients d'agitation thermique ($\times 10^3$)[a,b]

Atome	x	y	z	U_{11}	U_{22}	U_{33}	U_{12}	U_{13}	U_{23}
Mn	2464(2)	0170(2)	1389(3)	29(1)	17(1)	33(1)	−1(1)	6(1)	1(1)
S	3934(4)	1123(3)	0745(7)	42(2)	28(2)	98(3)	−3(2)	29(2)	10(2)
O(1)	1346(13)	−0423(12)	−2351(14)	105(9)	81(9)	28(5)	19(8)	−0(6)	−7(6)
O(2)	0985(12)	2482(10)	1191(20)	74(8)	42(6)	116(11)	33(6)	26(8)	−12(7)
O(4)	5163(10)	0939(12)	1669(20)	40(6)	68(7)	123(11)	−21(6)	15(6)	−18(8)
O(5)	3838(13)	2046(15)	−0618(23)	85(9)	89(10)	146(15)	−15(8)	44(10)	68(10)
C(1)	1802(14)	−0154(12)	−0837(18)	61(8)	30(6)	35(7)	10(6)	1(6)	12(6)
C(2)	1586(13)	1593(14)	1307(20)	45(8)	42(7)	49(8)	−16(7)	18(7)	−15(7)
C(4)	2675(24)	−1750(12)	2122(22)	143(18)	15(6)	44(8)	10(9)	33(11)	11(6)
C(5)	1551(24)	−1317(25)	2442(30)	98(18)	111(18)	53(12)	−57(15)	−35(13)	30(12)
C(6)	1741(20)	−0458(29)	3653(36)	65(12)	166(26)	97(17)	11(15)	37(12)	99(18)
C(7)	2971(24)	−0215(18)	4155(25)	123(18)	58(10)	47(9)	12(12)	−19(11)	1(8)
C(8)	3604(15)	−1026(20)	3173(32)	34(8)	78(13)	122(17)	8(8)	−3(10)	59(13)

[a]Le facteur de température de chaque atome est de la forme $\exp\{-2\pi^2(a^{*2}h^2U_{11} + b^{*2}k^2U_{22} + c^{*2}l^2U_{33} + 2a^*b^*hkU_{12} + 2a^*c^*hlU_{13} + 2b^*c^*klU_{23})\}$.
[b]Les écarts-types sont indiqués entre parenthèses.

matique des réflexions $0k0$ pour $k \neq 2n$ et de celle des réflexions $h0l$ pour $l \neq 2n$.

La chambre à précession de Buerger a été utilisée pour obtenir les intensités de 12 strates (3 le long de chaque axe cristallin et 3 le long de $[0\bar{1}1]$). Quarante clichés avec des temps d'exposition se situant entre 10 min et 16 h ont servi à recueillir les intensités de plus de 2000 réflexions. L'instabilité du composé sous les rayons X a nécessité l'utilisation de cinq cristaux dont les dimensions se situaient autour de 0.2 × 0.3 × 0.2 mm. Les intensités ont été mesurées à l'aide d'un microdensitomètre de type Wooster Mark IV. Toute réflexion visuellement absente a été considérée non-observée; l'intensité attribuée à chacune de ces réflexions correspond à la moitié de l'intensité minimale. La mise sur échelle commune de toutes les données photographiques a été faite selon la méthode de Hamilton, Rollet, et Sparks (3). Le coefficient d'absorption linéaire ayant comme valeur $\mu = 18.1\ cm^{-1}$, seules les corrections de Lorentz et celles de polarisation ont été apportées sur les intensités. 1512 réflexions indépendantes ont servi aux calculs effectués sur ordinateur IBM 360/50 à l'aide des programmes du système X-RAY-70 de Stewart (4).

Détermination de la structure

Les coordonnées de l'atome Mn ont été obtenues à partir de la fonction de Patterson tridimensionnelle. Deux synthèses de Fourier ont permis de localiser les autres atomes. Le facteur de désaccord

$$R = \sum(|\,|F_o| - |F_c|\,|)/\sum|F_o|$$

se situait alors à 0.33.

L'affinement des paramètres atomiques et des coefficients d'agitation thermique a été réalisé par la méthode des moindres carrés (matrice complète) en minimisant la quantité $S = \Sigma w(|F_o| - |F_c|)^2$.

Quatre cycles d'affinement en isotropie thermique et avec des poids w unitaires ont amené l'indice R à 0.15. Trois itérations en anisotropie thermique amènent un abaissement de R jusqu'à 0.094. A ce stade, la pondération utilisée $w(=1/\sigma^2)$ a été exprimée en termes de $\sigma = 0.062F_o + 1.199 + 4.616/F_o$, les coefficients étant choisis pour minimiser l'écart entre les facteurs de structure observés et calculés. Deux cycles d'affinement en anisotropie ont donné un R final de 0.092 pour les 1056 réflexions observées. L'indice résiduel pour l'ensemble des 1512 réflexions est 0.093.

Une série différence-Fourier n'a montré aucun pic significatif, la valeur maximale étant inférieure à 0.9 e/Å^3. Au cours des deux derniers cycles les paramètres n'ont subi aucun changement supérieur à 0.06σ tandis que le changement moyen était 0.01 fois l'écart-type.

Les facteurs de forme atomique utilisés sont ceux de Cromer et Mann (5). La liste des facteurs de structure observés et calculés a été versée au dépôt des données non publiées.[1] Les valeurs finales des paramètres apparaissent dans le tableau 1.

Description de la structure

La fig. 1 représente une vue de la maille élémentaire projetée sur le plan 010 alors que la fig. 2 montre une des quatre molécules avec quelques-uns des paramètres moléculaires présentés au tableau 2.

Les deux composés $MnC_5H_5(CO)_3$ (**1**) (6) et $MnC_5H_5(CO)_2SO_2$ (**2**), présentés en projection orthogonale à la fig. 3, cristallisent dans le même système selon des paramètres cristallins assez semblables (819 et 851 Å^3). L'empilement est cependant réalisé de façon plus dégagée avec **2** puisque la distance intermoléculaire minimale (sans tenir compte des atomes H) est de 4.2 Å alors qu'elle n'est que de 3.4 Å dans **1**. Les atomes Mn sont distants de 7.4 Å. Comme le montrent la fig. 3 et le tableau 4, aucune rotation

[1]On peut obtenir la liste des facteurs à un prix nominal, en s'adressant au Dépôt des données non publiées, Bibliothèque scientifique nationale, Conseil national de recherches du Canada, Ottawa, Canada, K1A 0S2.

Can. J. Chem. Downloaded from www.nrcresearchpress.com by 210.87.254.42 on 09/05/12
For personal use only.

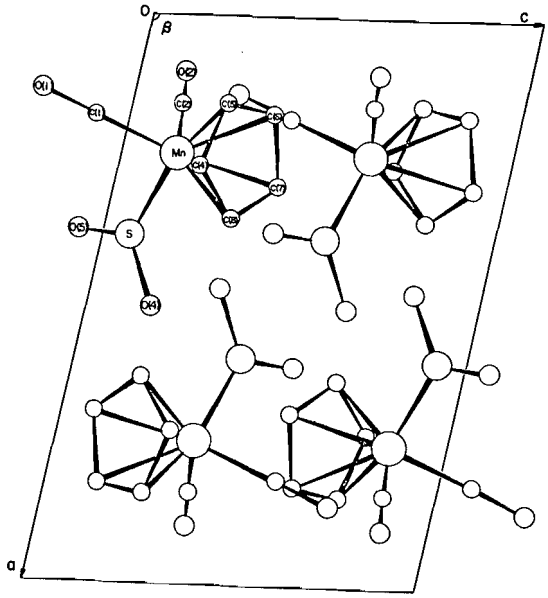

FIG. 1. Disposition des molécules dans la maille selon une projection parallèle à l'axe *b*.

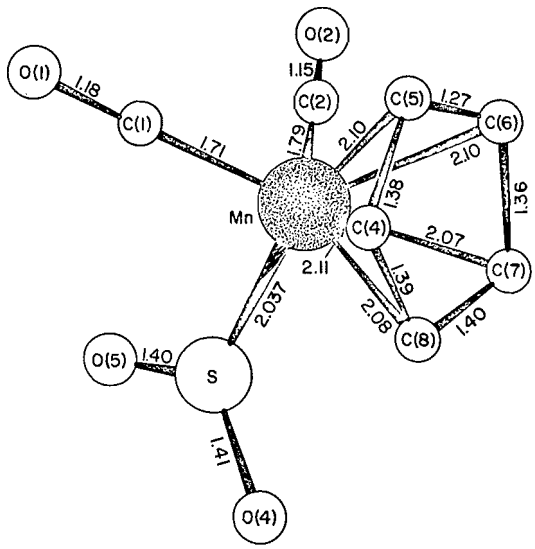

FIG. 2. Vue perspective de $MnC_5H_5(CO)_2SO_2$.

du cycle autour de l'axe perpendiculaire au plan du cylopentadiényle et aucune déformation angulaire importante du groupe Mn—C—O ne sont apparues à la suite du remplacement d'un groupe CO par SO_2.

Le tableau 3 présente les paramètres des plans constitués par le cycle C_5H_5 et l'ensemble

TABLEAU 2. Distances interatomiques et angles de valence[a]

Liaison	Distance (Å)	Liaison	Angle (deg)
Mn—C(1)	1.710(14)	C(1)—Mn—C(2)	90.55(62)
Mn—C(2)	1.788(16)	C(1)—Mn—S	94.85(53)
Mn—S	2.037(5)	C(2)—Mn—S	90.96(46)
		O(1)—Mn—O(2)	90.22(38)
C(1)—O(1)	1.177(16)	O(1)—Mn—S	95.45(35)
C(2)—O(2)	1.147(17)	O(2)—Mn—S	91.51(31)
		O(1)—Mn—C(2)	90.58(48)
Mn—C(4)	2.113(13)	O(2)—Mn—C(1)	90.22(38)
Mn—C(5)	2.100(21)	S—Mn—O(4)	22.05(24)
Mn—C(6)	2.098(18)	S—Mn—O(5)	22.76(25)
Mn—C(7)	2.066(19)		
Mn—C(8)	2.077(16)	Mn—C(1)—O(1)	178 (1)
		Mn—C(2)—O(2)	177 (1)
C(4)—C(5)	1.378(32)	Mn—S—O(4)	123.06(61)
C(5)—C(6)	1.271(36)	Mn—S—O(5)	124.30(64)
C(6)—C(7)	1.355(30)		
C(7)—C(8)	1.396(29)	C(4)—C(5)—C(6)	109 (2)
C(8)—C(4)	1.394(26)	C(5)—C(6)—C(7)	111 (2)
		C(6)—C(7)—C(8)	108 (2)
S—O(4)	1.408(12)	C(7)—C(8)—C(4)	104 (2)
S—O(5)	1.400(13)	C(8)—C(4)—C(5)	108 (2)
		O(4)—S—O(5)	112.62(83)

[a]Les écarts-types sont indiqués entre parenthèses.

Mn—SO_2. Ce dernier plan se présente quasi-perpendiculaire (89°) à celui du cyclopentadiényle. Cette orientation place O(5) à mi-distance des carbones carbonyle C(1) (3.22(3) Å) et C(2) (3.12(3) Å). L'atome O(4) se situe alors voisin du carbone C(8) (3.03(5) Å) du cyclopentadiényle. Ces distances C---O sont très voisines de la somme des rayons van der Waals (7) de l'oxygène (1.50 Å) et du carbone (1.70 Å). Contrairement à beaucoup de composés (8), où l'angle entre la normale au plan de SO_2 et l'axe de liaison Mn—S se situe autour de 20°, nous observons un angle de 90°, angle attendu si l'hybridation au niveau du soufre est de type sp^2. Cet angle de 90° est également observé dans $[Ru(NH_3)_4(SO_2)Cl]Cl$ (**3**) (9). Dans **2** et **3** l'indice de coordination du métal est 6 tandis que dans les composés où l'angle est voisin de 20° l'indice était égal ou inférieur à 5. Sans rejeter l'hypothèse de l'hybridation sp^2, on doit cependant remarquer que l'arrangement de SO_2 dans **2** et **3** présente le minimum d'interactions avec les autres ligands.

Les plus fortes interactions intramoléculaires ont apparemment lieu entre C(1) et S (2.77(2) Å) et entre C(2) et S (2.73(2) Å). Ces distances sont

Can. J. Chem. Downloaded from www.nrcresearchpress.com by 210.87.254.42 on 09/05/12
For personal use only.

Can. J. Chem. Downloaded from www.nrcresearchpress.com by 210.87.254.42 on 09/05/12
For personal use only.

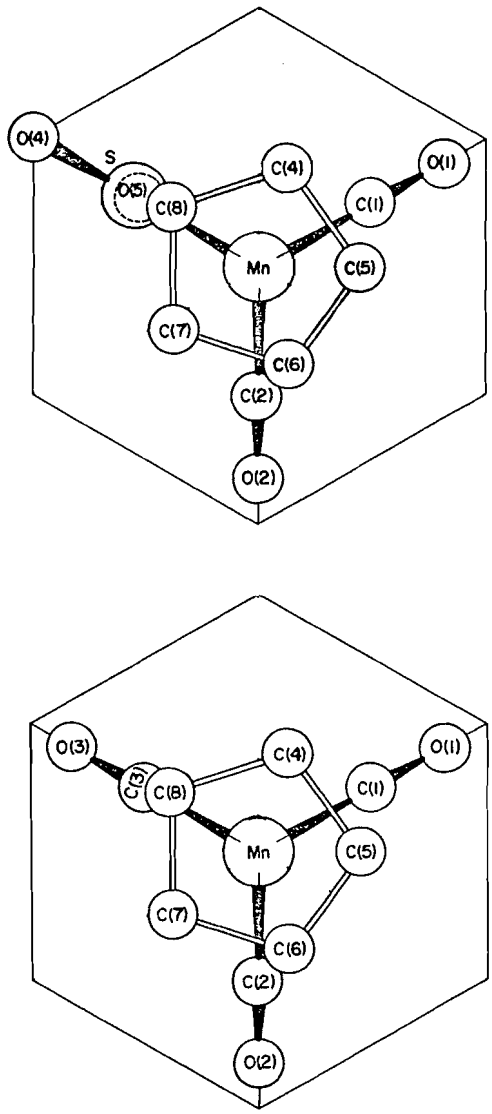

FIG. 3. Projection orthogonale des composés $MnC_5H_5(CO)_3$ et $MnC_5H_5(CO)_2SO_2$ dans un plan parallèle à celui du cycle cyclopentadiényle.

inférieures de 0.7 Å à la somme des rayons de van der Waals du carbone (1.70 Å) et du soufre (1.80 Å). Des répulsions de charge se manifestant à si courte distance pourraient expliquer la faible stabilité du composé **2** et l'impossibilité apparente à préparer et à isoler le composé disubstitué $MnC_5H_5(CO)(SO_2)_2$.

Alors que les distances M—S, observées dans la plupart des composés contenant M—SO_2 (8), sont très voisines (±0.1 Å) de la somme des rayons covalents du soufre (1.04 Å) et du métal M, la distance Mn—S (2.037(5) Å) est inférieure par plus de 0.3 Å à la somme des rayons covalents de S et de Mn (1.39 Å) (10). De nouveau le dioxyde de soufre se comporte de façon analogue dans les composés **2** et **3** (Ru—S = 2.072(3) Å). Dans ces deux composés d'arrangement octaédrique, la liaison M—S présente fort probablement un caractère élevé de double liaison résultant d'un retour de charges M → SO_2, ce qui serait conforme aux propriétés d'acide de Lewis du dioxyde de soufre. La liaison S—O du SO_2 présente une distance (1.40(1) Å) et une ouverture angulaire O—S—O (112.6(8)°) semblables aux valeurs observées dans les complexes métalliques (8), et assez voisines de celles obtenues pour le dioxyde de soufre cristallin, (1.43(2) Å) et (120(2)°) (11). L'écart minime ($-30\ cm^{-1}$) dans les fréquences de vibration de valence de SO_2 en passant de SO_2 cristallin (1140 et 1303 cm^{-1}) (12) à $MnC_5H_5(CO)_2SO_2$ (1110 et 1270 cm^{-1} (Nujol)), la similitude des fréquences S—O dans les complexes métalliques (8) ainsi que l'invariance statistique des distances S—O tendent à indiquer que la liaison Mn—S est formée sans que la liaison S—O en soit affectée.

Toute liaison π de retour (M→S) s'effectuerait donc par voie de recouvrement d'orbitales atomiques vides du soufre avec les orbitales remplies du métal.

Au niveau du cycle cyclopentadiényle, peu de changements statistiquement significatifs sont apparus à la suite du remplacement d'un groupement CO par SO_2. La distance moyenne Mn—$C_{C_5H_5}$ (2.09(2) Å) dans **2** est "inférieure" à la moyenne de 2.15(2) Å, observée dans tous les composés du cyclopentadiényle manganèse. La distance moyenne C—C est cependant semblable à celle observée dans $MnC_5H_5(CO)_3$ (6) (tableau 4). Le coordinat SO_2 provoque, à l'intérieur des liaisons Mn—C—O, des changements moins importants que le coordinat $P(C_6H_5)_3$. En effet, les fréquences de vibration de valence C—O dans **2** (2000–1956 cm^{-1}) sont plus voisines de celles de $MnC_5H_5(CO)_3$ (2028–1940 cm^{-1}) que ne le sont les fréquences C—O dans $MnC_5H_5(CO)_2P(C_6H_5)_3$ (1930–1861 cm^{-1}). D'autre part, le groupement C(2)—O(2) présente une distance Mn—C (1.788(16) Å) et une distance C—O (1.147(17) Å) égales à celles observées dans $MnC_5H_5(CO)_3$ (1.79(2)–1.14(2) Å) alors que dans $MnC_5H_5(CO)_2P(C_6H_5)_3$ les distances Mn—C (1.766(12)–1.740(10) Å) et

TABLEAU 3. Plans moyens

(*a*) Coefficients des équations des plans: $lX + mY + nZ - p = 0$[a]

Plan	*l*	*m*	*n*	*p*	χ^2
A	0.0806	0.6726	−0.7356	2.1632	2.0
B	0.2416	−0.7095	−0.6620	0.1619	1.8

[a]Le système orthonormé des axes de référence comprend *X* le long de *a*, *Y* dans le plan *ab* et *Z* le long de *c**.

(*b*) Distances (Å) de chacun des atomes à leur plan

Plan A		Plan B	
C(4)	−0.0133	Mn	−0.0001
C(5)	0.0210	S	0.0028
C(6)	−0.0109	O(4)	−0.0096
C(7)	−0.0038	O(5)	−0.0147
C(8)	0.0112		

TABLEAU 4. Comparaison des distances interatomiques moyennes et des angles de valence dans les composés $MnC_5H_5(CO)_2X$ (X = SO_2, $P(C_6H_5)_3$, CO)[a]

Liaison	SO_2	$P(C_6H_5)_3$	CO[b]
Mn—C_{CO}	1.75(2)[c]	1.75(2)[d]	1.79(2)
Mn—$C_{C_5H_5}$	2.09(2)	2.15(1)	2.15(2)
C—O	1.16(2)	1.17(2)	1.14(2)
$C_{C_5H_5}$—$C_{C_5H_5}$	1.36(3)	1.42(2)	1.39(2)
OC—Mn—CO	90.5(6)	92.4(4)	91[e]
X—Mn—CO	92.9(5)	91.6(3)	92[e]
Mn—C—O	178(1)	178(1)	179[e]

[a]Distances en Angströms et angles de valence en degrés.
[b]C(3)—O(3), groupement qui occupe la même position relative que SO_2 ou $P(C_6H_5)_3$.
[c]Les deux distances ne sont pas statistiquement indentiques.
[d]L'écart indiqué est la moyenne des écarts-types estimés.
[e]Aucun écart-type n'est fourni.

C—O (1.168(12)–1.173(11) Å) (1) montrent que la liaison Mn—C—O a été affectée par un retour π plus important que dans $MnC_5H_5(CO)_3$. Les paramètres associés au groupement C(1)—O(1) pouraient expliquer en partie certaines observations faites sur d'autres régions de la molécule **2**. Sans rejeter la possibilité que les paramètres structuraux de C(1) soient légèrement erronés, on doit cependant noter que C(1)—O(1) est le coordinat situé le plus près d'une position trans au carbone du cycle qui forme la plus courte liaison Mn—C dans **2** (2.07(2) Å) et la plus longue dans $MnC_5H_5(CO)_2P(C_6H_5)_3$ (2.16(2) Å). En outre on observe un angle S—Mn—C(1) voisin de 95°, valeur semblable à celle de l'angle C(3)—Mn—C(1) observée dans $MnC_5H_5(CO)_3$ mais différente de celle de 90° pour l'angle P—Mn—C(1) dans $MnC_5H_5(CO)_2P(C_6H_5)_3$ et les angles C(1)—Mn—C(2) et C(2)—Mn—X(C(3),S,P) dans les trois composés. La forte interaction S----C(1) pourrait causer, par répulsion coulombique, l'ouverture angulaire observée.

Conclusion

Le remplacement d'un groupement CO par SO_2 introduit des changements au niveau de la liaison Mn—$C_{C_5H_5}$ en favorisant une courte liaison Mn—S par voie de liaison dative Mn→S importante. La disposition de SO_2 relative aux autres ligands, l'encombrement autour du manganèse et la présence de dipoles peuvent être considérés comme facteurs importants de l'instabilité du composé $MnC_5H_5(CO)_2SO_2$.

Nous remercions le Ministère de l'Education du Québec pour son aide financière ainsi que le Conseil national de recherches du Canada pour un apport matériel.

1. C. BARBEAU, K. S. DICHMANN et L. RICARD. Can. J. Chem. **51**, 3027 (1973).
2. W. STROHMEIER et H. HELLMANN. Ber. Bunsenges. Phys. Chem. **68**, 482 (1964).
3. W. C. HAMILTON, J. S. ROLLETT et R. A. SPARKS. Acta Cryst. **18**, 129 (1965).
4. J. M. STEWART, F. A. KUNDELL et J. C. BALDWIN. The X-RAY-70 system. Univ. of Maryland. 1970.
5. D. T. CROMER et J. B. MANN. Acta Cryst. A, **24**, 321 (1968).
6. A. F. BERNDT et R. E. MARSH. Acta Cryst. **16**, 118 (1963).

Can. J. Chem. Downloaded from www.nrcresearchpress.com by 210.87.254.42 on 09/05/12
For personal use only.

7. A. DONDI. J. Phys. Chem. **68**, 441 (1964).
8. M. R. SNOW et J. A. IBERS. Inorg. Chem. **12**, 224 (1973); D. VAN DER HELM, J. D. CHILDS, et S. D. CHRISTIAN. Chem. Commun. 887 (1969); J. D. DUNITZ. Acta Cryst. **9**, 579 (1956); K. W. MUIR et J. A. IBERS. Inorg. Chem. **5**, 405 (1966).
9. L. H. VOGT JR., J. L. KATZ et S. E. WIBERLEY. Inorg. Chem. **4**, 1157 (1965).
10. F. A. COTTON et D. C. RICHARDSON. Inorg. Chem. **5**, 1851 (1966).
11. B. POST, R. S. SCHWARTZ et I. FANKUCHEN. Acta Cryst. **5**, 372 (1952).
12. P. A. GIGUÈRE et M. FALK. Can. J. Chem. **34**, 1833 (1956).

Can. J. Chem. Downloaded from www.nrcresearchpress.com by 210.87.254.42 on 09/05/12
For personal use only.

Erratum: The Electronic Spectra of Tetragonal Chromium(III) Complexes

M. KEETON, B. FA-CHUN CHOU, AND A. B. P. LEVER
The Department of Chemistry, York University, Downsview, Ontario

Received August 24, 1973

(Ref.: Can. J. Chem. **49**, 192 (1971))

Can. J. Chem. **51**, 3690 (1973)

In Table 3, the parameter set for $Cren_2(OH)_2^+$ was incorrectly calculated. The correct values are: *Ds*, −1183; *Dt*, 150; Δ_1, −4302; Δ_3, −3987; $e_{\pi L}'$, 0*; $e_{\sigma L}'$, 6640; $e_{\pi Z}'$, 2151; $e_{\sigma Z}'$, 8633; $d\pi$, 2151; $d\sigma$, 1495; *B*, 789; Dq_L, 1992; Dq_Z, 1730 cm^{-1}; Assignment, II.

The correction does not materially alter the discussion except that the hydroxyl ion is seen to be as good a π donor as fluorine towards chromium(III) and to be a substantially better σ donor than fluorine.

Can. J. Chem. Downloaded from www.nrcresearchpress.com by 210.87.254.42 on 09/05/12
For personal use only.

Crystal and Molecular Structure of Benzylidenimine Tetrasulfide, $(C_6H_5CHN)_2S_4$

JAMES C. BARRICK, CRISPIN CALVO, AND FREDRIC P. OLSEN
Department of Chemistry, McMaster University, Hamilton, Ontario L8S 4M1

Received April 18, 1973

The structure of the title compound has been determined. Crystals are monoclinic with space group $P2_1/a$, $Z = 4$, $a = 13.83(1)$, $b = 19.66(2)$, $c = 5.983(5)$ Å, $\beta = 101.4(1)°$, $d_{calcd} = 1.404$, $d_{obs} = 1.40(1)$. A full-matrix least-squares refinement on 1085 unique reflections of positive intensity measure produced a conventional R of 0.066. The spiral arrangement of the S_4 chains (nearly generating a 3_1 axis) is such that the two aromatic rings are eclipsed. Alternation in bond length along the sulfur chain was observed, the long inner bond being 2.083(4) Å and the shorter outer bonds averaging 2.026(3) Å in length. No intermolecular non-bonding interactions involving sulfur were found.

La structure du composé en titre a été déterminée. Les cristaux sont monocliniques, de groupe d'espace $P2_1/a$, avec $Z = 4$, $a = 13.83(1)$, $b = 19.66(2)$, $c = 5.983(5)$ Å, $\beta = 101.4(1)°$, $d_{calcd} = 1.404$, $d_{obs} = 1.40(1)$. Un raffinement par les matrices des moindres carrés appliqué aux 1085 réflexions uniques d'intensité positive mesurée conduit à un R conventionnel de 0.066. L'arrangement en spirale des chaînes S_4 (créant presque un axe 3_1) est tel que les deux cycles aromatiques sont éclipsés. Une alternance dans les longueurs de liaison le long de la chaîne sulfurée a été observée, les grandes liaisons vers l'intérieur étant de 2.083(4) Å et les liaisons courtes vers l'extérieur de 2.026(3) Å en moyenne. Des interactions non liantes mettant en jeu le soufre ont été trouvées. [Traduit par le journal]

Can. J. Chem., 51, 3691 (1973)

Can. J. Chem. Downloaded from www.nrcresearchpress.com by 210.87.254.105 on 09/05/12
For personal use only.

The reaction of tetrasulfur tetranitride with benzylamine leads to a product (1) formulated (2) as benzylidenimine tetrasulfide. This material appears to be a rather common product from reactions of species containing sulfur and benzyl groups; it has also been isolated from the reaction of benzylamine with sulfur in the presence of lead oxide (2, 3), from the decomposition of *N*-benzylheptasulfurimide (4), from the reaction of sulfur monochloride (5, 6), or disulfur trichloride (5) with benzylamine and from the decomposition of benzylamine disulfide (6). At least four alternate structures have been suggested although the combined evidence of elemental analysis, molecular weight, i.r., and n.m.r. would seem to eliminate most of them.

Recently, the structures of several tetrasulfides have been determined. These include tetraethoxy-2,3,4,5,10,11,12,13-octathiatricyclo-[12,2,2,2$^{(6,9)}$]eicose-6,8,14,16,17,19-hexaene (**2**) (7), 1,2,3,4-tetrathiadecaline (**3**) (8), *N*,*N*′-dimethyl-3,6-epitetrathio-2,5-piperazinedione (**4**) (9, 10) and bis(cyclopentadienyl)tungsten tetrasulfide (**5**) (11). In **3**, the 3 sulfur–sulfur bond lengths were of equal length while in **2** and **4** alternation of sulfur–sulfur bond lengths in the order short-long-short was observed and in **5** alternation in the order long-short-long was found. Possible similar alternation of bond lengths has been reported previously (12–14) in inorganic sulfur chains but with a lack of consistency or conviction. Only in the recent cases are differences in sulfur–sulfur bond lengths clearly outside the experimental errors in the measurements.

In view of the interest in bond length alternation in organotetrasulfides and to resolve any residual uncertainty in the structure of **1**, we have determined the crystal and molecular structure of this material.

Experimental

Crystal Data

Benzylidenimine tetrasulfide, $(C_6H_5CHN)_2S_4$, was obtained from the reaction of sulfur with benzylamine in the presence of lead oxide as previously described (6). Recrystallization from hot methanol gave yellow needles of m.p. 100.5–102 °C. Crystals suitable for X-ray analysis were subsequently grown from benzene solution.

Weissenberg photographs (hkn, $n = 0$–5) showed systematic absences of type $k = 2n + 1$ on the $0k0$ axis and $h = 2n + 1$ in the $h0l$ layer establishing the space group $P2_1/a$. Accurate unit cell parameters were determined by least squares adjustment of a, b, c, and β to 2θ, ω, and χ angles for 15 well-centered reflections collected at room temperature on a Syntex P$\bar{1}$ Automatic Diffractometer and were $a = 13.83(1)$, $b = 19.66(2)$, $c = 5.983(5)$ Å, and $\beta = 101.4(1)°$. The density, measured by

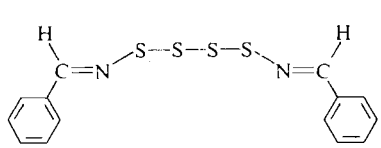

1

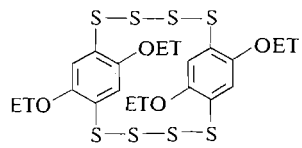

2

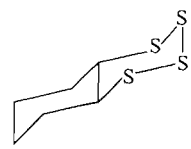

3

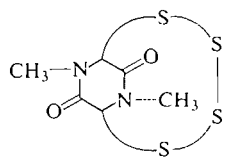

4

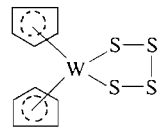

5

flotation in *n*-heptane/carbon tetrachloride, was 1.40(1) g/cm^3; calcd. for $Z = 4$, 1.404 g/cm^3.

Collection of Data and Solution of the Structure

The preliminary (15) solution of the structure was carried out on intensity data obtained from *hkn*(n = 0–5) CuK$_\alpha$ Weissenberg and *skl*(s = 0–4) MoK$_\alpha$ Precession film data. Following data reduction, the application of direct methods in the X-Ray 67 system of programs to the 1038 observed symmetry independent reflections determined enough phases to allow the positions of the four sulfur atoms to be discerned in a Fourier synthesis (E-map). Alternating electron density and difference syntheses with least squares refinement of atomic positions led gradually to the location of the remaining non-hydrogen atoms. Introduction of anisotropic thermal parameters decreased the discrepancy index from 0.15 to 0.075. Although the structure refined readily, up to 4σ variations in carbon–carbon lengths were observed in the aromatic rings. Possible explanations including libration and disorder were considered, but the quality of the data was judged insufficient to allow an unequivocal conclusion.

Subsequently, a new set of intensity data was collected to $2\theta = 40°$ on a Syntex $P\bar{1}$ Automatic Diffractometer using carbon monochromatized MoKα radiation (λ = 0.71069 Å) with a monochromator setting of 12°. The linear absorption coefficient was 5.6 cm^{-1}, and the crystal dimensions were 0.15 × 0.18 × 0.35 mm (the long axis being parallel to the ϕ axis). Maximum variations in transmission factors were ± 1%, consequently, no absorption corrections were made. Intensities were measured using a variable scan time in the θ–2θ technique with stationary counts on each side of the peak for 1/2 of the scan time to establish background. Thus, the peak intensity, $N_{Pk} = N_T - N_{Bg1} - N_{Bg2}$ where N_T is the total peak count and N_{Bg1} and N_{Bg2} are background counts. σ_I's were derived from

$$\sqrt{\sigma_{Pk}^2 + (0.02|F_o|^2)^2}$$

where the second term allows for machine instability and

$$\sigma_{Pk} = \sqrt{N_T + N_{Bg1} + N_{Bg2}}$$

After averaging equivalent reflections, 1085 unique reflections of positive intensity measure remained of which 737 had $I > 3\sigma$ and were considered as "observed". After correction for Lorentz and Polarization effects using the XRAY-67 Program DATRDN, these gave the structure factors used for comparison with those calculated from the model structure.[1]

Refinement of the 182 positional and anisotropic thermal parameters, including a parameter for extinction corrections (17, 18), by full-matrix least squares methods using the program CUDLS[2] led to an unweighted discrepancy index of 0.066 for all reflections and a weighted value of 0.038 where

$$R = \frac{\sum ||F_o| - |F_c||}{\sum |F_o|}$$

and

$$R_W = \sqrt{\frac{\sum w(|F_o| - |F_c|)^2}{\sum w|F_o|^2}}$$

The function minimized in the least squares refinement was $\Sigma w(F_o - F_c)^2$. Unobserved reflections ($I < 3\sigma$), measuring more than their calculated values, were given zero weight and did not affect the refinement while those measuring less than their calculated value did. In the last cycle, 240 reflections with $I < 3\sigma$ supplemented the 737 with $I > 3\sigma$ in this manner. The weighting scheme used took the form

$$W = 1/[0.011|F_o| + 0.0027|F_o|^2 + 364\sigma^2/|F_o|^2]$$

where the σ's were derived from counting statistics. The maximum shift/error in the final cycle was 0.16. The hydrogen atoms were included in their expected positions with $U_{iso} = 0.06$ Å^2, but were not refined.

Table 1 lists observed and calculated structure factors[3] and Table 2 gives atomic positions and temperature

[1]Atomic scattering factors used were those quoted in the International Tables (16).

[2]CUDLS was written by J. Stephens.

[3]Table 1 is available at a nominal charge, upon request, from the Depository of Unpublished Data, National Science Library, National Research Council of Canada, Ottawa, Canada K1A 0S2.

Can. J. Chem. Downloaded from www.nrcresearchpress.com by 210.87.254.105 on 09/05/12
For personal use only.

TABLE 2. Positional and thermal*† parameters for benzylidenimine tetrasulfide

Atom	x/a	y/b	z/c	U_{11}	U_{22}	U_{33}	U_{12}	U_{13}	U_{23}
S1	0.5696(1)	0.3786(1)	0.5505(3)	95(2)	80(2)	70(1)	5(1)	3(1)	−14(1)
S2	0.5431(1)	0.4419(1)	0.2793(4)	79(2)	56(1)	102(2)	−13(1)	18(1)	0(1)
S3	0.3903(1)	0.4499(1)	0.1828(3)	86(2)	50(1)	97(2)	8(1)	14(1)	− 4(1)
S4	0.3520(1)	0.3951(1)	0.8906(3)	96(2)	67(1)	77(2)	− 5(1)	2(1)	14(1)
N1	0.5849(4)	0.2992(3)	0.4748(11)	74(5)	65(4)	50(4)	7(3)	3(4)	− 1(4)
N2	0.3299(4)	0.3146(3)	0.9470(11)	73(4)	52(4)	65(5)	− 2(3)	− 5(4)	3(4)
C1	0.5765(4)	0.2794(4)	0.2687(15)	39(5)	55(6)	61(6)	1(3)	1(4)	8(5)
C2	0.5895(5)	0.2076(4)	0.2160(16)	52(5)	64(7)	55(7)	− 6(4)	3(5)	1(7)
C3	0.5610(6)	0.1851(4)	0.9956(18)	88(7)	52(7)	87(8)	7(4)	7(5)	− 1(5)
C4	0.5688(6)	0.1171(6)	0.9403(14)	101(7)	107(9)	70(7)	8(6)	9(5)	− 6(7)
C5	0.6083(7)	0.0717(4)	0.1051(24)	111(8)	81(7)	119(9)	9(6)	39(7)	−20(9)
C6	0.6402(7)	0.0941(5)	0.3233(21)	158(10)	61(8)	113(9)	35(6)	32(7)	29(7)
C7	0.6310(6)	0.1603(5)	0.3787(13)	108(7)	75(7)	62(7)	22(5)	0(5)	16(6)
C8	0.3411(5)	0.2904(4)	0.1465(15)	49(5)	48(5)	75(7)	− 1(4)	3(5)	8(5)
C9	0.3228(5)	0.2193(4)	0.1896(16)	47(5)	61(6)	35(6)	2(4)	10(4)	2(6)
C10	0.3493(5)	0.1941(4)	0.4074(16)	77(6)	69(6)	61(7)	−18(4)	6(5)	− 1(5)
C11	0.3380(6)	0.1258(5)	0.4516(14)	95(6)	87(7)	61(6)	− 9(5)	3(5)	23(6)
C12	0.2972(6)	0.0828(4)	0.2776(19)	83(6)	63(6)	87(7)	− 6(5)	8(5)	11(7)
C13	0.2694(5)	0.1077(5)	0.0626(15)	79(6)	64(6)	66(7)	−15(5)	1(5)	− 7(5)
C14	0.2825(5)	0.1751(4)	0.0171(12)	80(6)	52(6)	51(6)	− 2(4)	4(5)	− 2(6)

Atom	x/a	y/b	z/c	Atom	x/a	y/b	z/c
H1	0.5495	0.3117	0.1500	H8	0.3693	0.3205	0.2719
H3	0.5328	0.2171	0.8771	H10	0.3776	0.2247	0.5301
H4	0.5469	0.1011	0.7855	H11	0.3539	0.1084	0.6057
H5	0.6151	0.0242	0.0688	H12	0.2883	0.0350	0.3084
H6	0.6687	0.0621	0.4416	H13	0.2412	0.0771	0.9400
H7	0.6531	0.1763	0.5345	H14	0.2666	0.1925	0.8628

*U_{ij} in Å² × 10³.
†U_{iso} for H held invariant at 0.06 Å².

factors[4] along with their estimated standard deviations. Table 3 gives bond lengths and angles and their estimated standard deviations.

Results and Discussion

Figure 1 shows a stereoscopic view of the molecule looking down the *a* axis. The structure is clearly monomeric with an S_4 chain terminated by benzylidenimine fragments. The two aromatic rings are approximately superimposed since the sulfur chain folds back upon itself nearly generating a non-crystallographic 3_1 axis extending over the four sulfur atoms as shown in Fig. 2.

Phenyl Rings

The average C—C distance within the rings is 1.372 Å with maximum and average deviations of 0.018 and 0.008 Å. The maximum deviation from the average is 1.2σ, and the average value is in good agreement with the accepted (19) value of 1.392(4) Å considering that corrections for translational and librational effects have not been applied. The average bond angle within the rings is 120.2° with maximum and average deviations of 2.9° and 1.0°, respectively. Both rings are quite planar with maximum and average deviations of 0.015 Å (C_2,C_3) and 0.009 Å. The least squares plane defined by $C_2 \ldots C_7$ (Ring A) makes an angle of 21.9° with that defined by $C_9 \ldots C_{14}$ (Ring B) so as to tilt C_5 and C_{12} apart (4.62 Å) and C_2 and C_9 together (3.67 Å). The planes of rings A and B intersect the 3_1 axis at angles of 83° and 81.5°, respectively.

C–Phenyl and C–N Bonds

The aliphatic C—C bonds, averaging 1.460(8) Å, are short as expected for conjugation of the aromatic ring with the C—N double bond. C_1 and C_8 lie within 0.05 and 0.07 Å, respectively,

[4]Thermal factors are in Å² and were obtained from $U_{ij} = \beta_{ij}/2\pi^2 a_i^* a_j^*$ where the β_{ij}'s appear as the effect of temperature through $\exp[-\beta_{11}h^2 + 2\beta_{12}hk \ldots)]$ in the structure factor expression and the a_i^*'s are the reciprocal lattice vectors. These units were chosen so that U = mean square thermal displacement directly.

Can. J. Chem. Downloaded from www.nrcresearchpress.com by 210.87.254.105 on 09/05/12
For personal use only.

TABLE 3. Bond lengths and angles in benzylidenimine tetrasulfide*

Bond	Distance (Å)	Bond	Distance (Å)	Bond	Distance (Å)
S_1—S_2	2.020(4)	C_1—C_2	1.466(11)	C_8—C_9	1.453(11)
S_2—S_3	2.083(4)	C_2—C_3	1.373(14)	C_9—C_{10}	1.374(13)
S_3—S_4	2.033(4)	C_3—C_4	1.386(15)	C_{10}—C_{11}	1.384(13)
S_1—N_1	1.651(6)	C_4—C_5	1.362(15)	C_{11}—C_{12}	1.372(13)
S_4—N_2	1.658(6)	C_5—C_6	1.366(18)	C_{12}—C_{13}	1.359(14)
N_1—C_1	1.276(11)	C_6—C_7	1.354(15)	C_{13}—C_{14}	1.372(13)
N_2—C_8	1.266(11)	C_7—C_2	1.386(12)	C_{14}—C_9	1.380(11)

Bonds	Angle (deg)	Bonds	Angle (deg)
S_1—S_2—S_3	106.4(3)	C_6—C_7—C_2	121.2(11)
S_2—S_3—S_4	106.0(2)	C_7—C_2—C_3	117.3(13)
N_1—S_1—S_2	112.0(3)	C_7—C_2—C_1	123.2(10)
N_2—S_4—S_3	111.0(3)	N_2—C_8—C_9	122.4(9)
S_1—N_1—C_1	124.2(5)	C_8—C_9—C_{10}	119.5(10)
S_4—N_2—C_8	123.9(5)	C_9—C_{10}—C_{11}	120.8(11)
N_1—C_1—C_2	120.7(9)	C_{10}—C_{11}—C_{12}	119.9(11)
C_1—C_2—C_3	119.5(10)	C_{11}—C_{12}—C_{13}	119.5(11)
C_2—C_3—C_4	121.3(12)	C_{12}—C_{13}—C_{14}	120.9(13)
C_3—C_4—C_5	119.9(12)	C_{14}—C_9—C_{10}	118.3(12)
C_4—C_5—C_6	119.2(12)	C_{14}—C_9—C_8	122.2(12)
C_5—C_6—C_7	121.0(16)	C_9—C_{14}—C_{13}	120.6(10)

*Estimated standard deviations (in parentheses) include both positional uncertainty in refinement and also that arising from errors in the cell parameters.

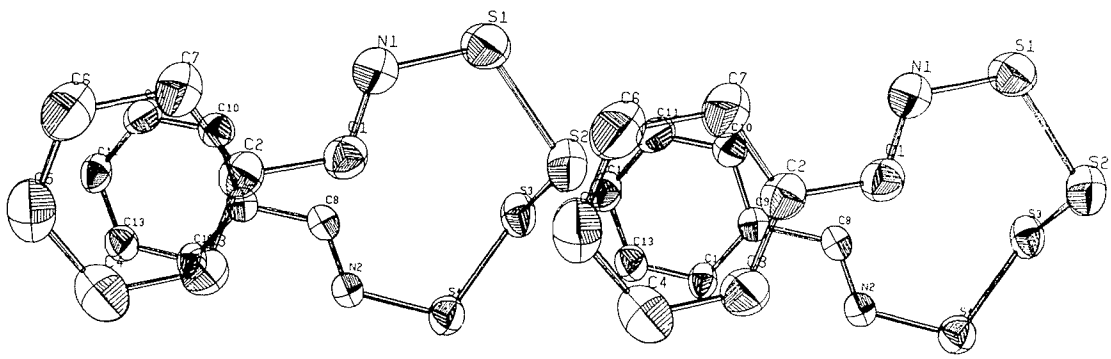

FIG. 1. Stereoscopic view of benzylidenimine tetrasulfide looking down the *a* axis.

of the planes of the rings while N_1 and N_2 lie 0.32 and 0.25 Å, respectively, from these planes. The C—C—N angles average 121.6(7)°. The C—N double bonds average 1.271(8) Å. All these bond lengths and angles are reasonable and in good agreement with those previously found in benzylidenimine fragments (20). The C—N—S angles average 124.0(4)° and the C—C—N—S dihedral angles are 1.1° and 3.0°, respectively, for C_1—N_1 and C_8—N_2. The tilt of the planes of the aromatic rings leads to a C_1—C_8 distance of 3.20 Å. The nitrogens are in a "*trans*" rather than a "*cis*" arrangement, however, and are quite far apart.

Sulfur–Nitrogen Bonds

The average N—S distance at 1.655(5) Å is short in comparison to the value of 1.76 Å found in sulfamic acid (21) or the sum of the single bond covalent radii (22) of 1.74 Å but is not unusual when compared to other typical sulfur nitrogen

Can. J. Chem. Downloaded from www.nrcresearchpress.com by 210.87.254.105 on 09/05/12
For personal use only.

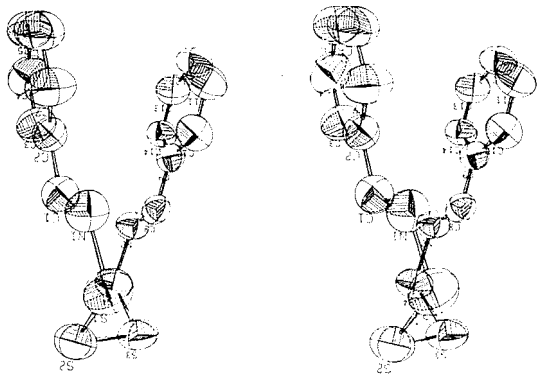

FIG. 2. Stereoscopic view of benzylidenimine tetrasulfide looking down the pseudo-3_1 axis of the sulfur chain.

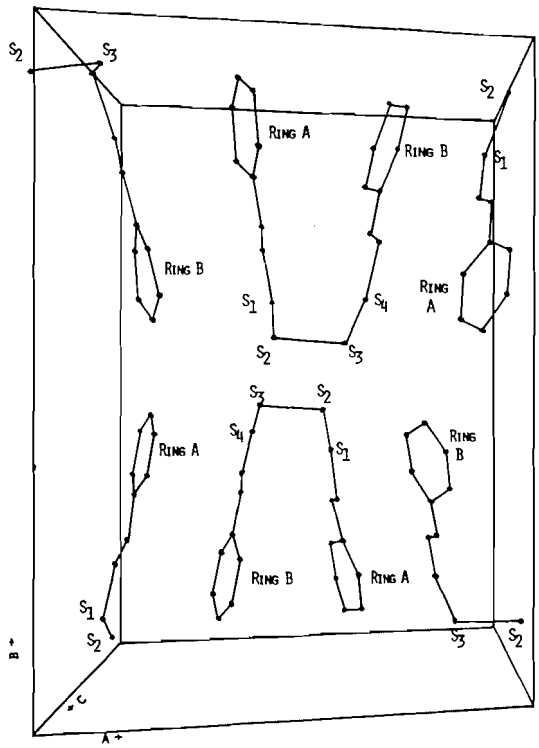

FIG. 3. Packing of benzylidenimine tetrasulfide.

"single" bonds where a lone pair resides on nitrogen and some $d\pi$–$p\pi$ overlap is likely to occur. Examples for comparison include 1.66 Å in (23) (*p*-chlorophenyl)$_2S_3N_2$, 1.66 Å in (24) $S_4N_4F_4$, 1.628 Å in (25) 1,2,5-thiadiazole and 1.672 Å in (26) 1,3-$S_6N_2H_2$. Normal "double" bonds between S and N are generally shorter with typical lengths of 1.54 Å in (24) $S_4N_4F_4$, 1.55 Å in (23) (*p*-chlorophenyl)$_2S_3N_2$, 1.53 and 1.56 Å in (27) di-*p*-tolylsulfurdiimide, and 1.533 Å in (28) $(CH_3)_2S(NH)_2$. The N—S—S angles average 111.5(3)°. The C—N—S—S dihedral angles are surprisingly small at 3.0 and 3.3°, respectively, for N_1—S_1 and N_2—S_4.

The Sulfur–Sulfur Bonds

As a consequence of the small dihedral angles around both the N—S and C—N bonds, each C—N—S—S unit lies quite near to the plane of the aromatic ring to which it is bound. For ring B, S_3 and S_4 lie 0.03 and 0.36 Å out of the plane while for ring A, S_1 and S_2 lie 0.41 and 0.07 Å from the plane defined by the ring carbon atoms. Thus, the molecule might be considered as two approximately coplanar units (see Fig. 3) joined by the S_2—S_3 bond. Planes fit to the two halves of the molecule have maximum and average deviations of 0.18 and 0.07 Å and make an angle of 22.5°, *i.e.*, only 0.6° greater than the planes generated by the ring carbons alone. The outer two ("in plane") sulfur–sulfur bond lengths differ by 0.013 Å with a σ_Δ of 0.006 Å where $\sigma_\Delta^2 = \sigma_1^2 + \sigma_2^2$ and are therefore judged "equivalent". The best value is 2.026(3) Å where $\sigma^2 = 1/\sum(1/\sigma_i^2)$. The bond angles $S_1S_2S_3$ and $S_2S_3S_4$ differ by 0.4(4)° with an average value of 106.2(2)°. In comparing the inner ("between planes") and outer ("in plane") sulfur bond lengths, correlation must be considered, and $\sigma_\Delta^2 = \sigma_{AB}^2 + \sigma_{AC}^2 + \sigma_A^2 \cos\theta$ where σ_{AA} and σ_{AC} are the e.s.d.'s on the two bonds, σ_A is the isotropic positional error on the shared atom and θ is the angle between the bonds. The "between plane" S—S bond length is 2.083(4) Å. The difference between the inner and outer S—S bonds is then 0.057 Å with a σ_Δ of 0.006 Å. This difference of between 9 and 10 pooled standard deviations cannot be explained away as random experimental error. Since no systematic errors of this magnitude appear likely, the "between planes" S—S bond is judged significantly longer than the "in plane" S—S bonds. Therefore, alternation of S—S bond length of type short-long-short, occurs in the tetrasulfide chain.

This situation is directly analogous to that observed in **2** and **4**. There is excellent agreement in the lengths of the outer (short) bonds between the three structures, 2.026(3) Å in benzylidenimine tetrasulfide, 2.028(2) in **2** and 2.0244(9) in **4**.

Can. J. Chem. Downloaded from www.nrcresearchpress.com by 210.87.254.105 on 09/05/12
For personal use only.

The longer internal S—S bonds are less obviously equivalent. In **2**, the internal bond is 2.066(2) Å while in benzylidenimine it is 2.083(4) Å and in **4** it is 2.076(1). These lengths compare to a S—S bond length of 2.048(2) Å in (29, 30) elemental S_8.

The benzylidenimine tetrasulfide molecular geometry is such that the two organic parts of the molecule are on one side of the spiral of sulfur atoms. Within the unit cell two spirals pack back to back (Fig. 3). These pairs extend throughout the crystal in the *c* direction.

The closest intermolecular contact distance (ignoring hydrogen atoms) is 3.54 Å (C_1—C_9), a distance in good agreement with the effective thickness of the aromatic ring. The closest intermolecular contact distance involving sulfur is 3.56 Å (C_{12}—S_2) where the sum of van der Waals radii is 3.55 Å.

The van der Waals radius of sulfur is generally taken as 1.85 Å; the closest S—S intermolecular contact is 3.73 Å (S_1—S_3) with others at 3.74 (S_2—S_4), 3.75 (S_2—S_3) and 3.82 Å (S_2—S_3). The intramolecular $C_1 \ldots S_2$ and $C_8 \ldots S_3$ distances are however rather short at 3.23 and 3.21 Å. This point is of interest in relation to the structure (7) of **2** where quite substantial non-bonding interactions between oxygen and the outer S atoms of the tetrasulfide chain offered a possible explanation for the S—S bond length alternation observed in that compound.

This work was carried out under a grant from the National Research Council of Canada.

1. R. SCHENCK. Ann. **290**, 171 (1896).
2. Y. SASAKI and F. P. OLSEN. Can. J. Chem. **49**, 271 (1971).
3. T. G. LEVI. Gazzetta, **61**, 294 (1931).
4. B. A. OLSEN and F. P. OLSEN. Inorg. Chem. **8**, 1736 (1969).
5. J. S. POND. Ph.D. Thesis. Univ. of Minn., Minneapolis, Minn., 1964.
6. Y. SASAKI and F. P. OLSEN. Can. J. Chem. **49**, 283 (1971).
7. J. C. RICCI, JR. and I. BERNAL. J. Chem. Soc. B, 1928 (1971).
8. F. FEHER, A. KLAEREN, and K. H. LINKE. Angew. Chem. Int. Ed. **9**, 895 (1970).
9. B. R. DAVIS and I. BERNAL. Proc. Nat. Acad. Sci. USA, **70**, 279 (1973).
10. B. R. DAVIS, I. BERNAL, A. U. SCHMIDT. Angew. Chem. Int. Ed. **11**, 632 (1972).
11. B. R. DAVIS and I. BERNAL. J. Cryst. Mol. Struct. **2**, 135 (1972).
12. O. FOSS and O. T. JOMSLAND. Acta Chem. Scand. **10**, 424 (1956); **12**, 44 (1958).
13. S. C. ABRAHAMS. Acta Cryst. **7**, 423 (1954).
14. S. C. ABRAHAMS and J. L. BERNSTEIN. Acta Cryst. **B25**, 2365 (1969).
15. J. C. BARRICK, C. CALVO, and F. P. OLSEN. Chem. Commun. 1043 (1971).
16. International tables for X-ray crystallographers. Vol. 3. Kynoch Press, Birmingham, England. 1962. p. 202.
17. J. S. STEPHENS and D. W. J. CRUICKSHANK. Acta Cryst. **B26**, 223 (1970).
18. W. H. ZACHARIASEN. Acta Cryst. **16**, 1142 (1963).
19. E. G. COX, D. W. J. CRUICKSHANK, and J. A. S. SMITH. Proc. R. Soc. **A247**, 1 (1958).
20. U. C. SINHA. Acta Cryst. **B26**, 889 (1970).
21. R. L. SASS. Acta Cryst. **13**, 320 (1960).
22. L. PAULING. The nature of the chemical bond. 3rd ed. Cornell University Press, Ithaca, New York. 1960.
23. F. P. OLSEN and J. C. BARRICK. Inorg. Chem. **11**, 1353 (1973).
24. G. A. WIEGERS and A. VOS. Acta Cryst. **16**, 152 (1963).
25. R. A. BONHAM and F. A. MOMANY. J. Am. Chem. Soc. **83**, 4475 (1961).
26. H. J. POSTMA, F. VAN BOLHUIS, and A. VOS. Acta Cryst. **B27**, 2480 (1971).
27. G. LEANDRI, V. BUSETTI, G. VALLE, and M. MAMMI. Chem. Comm. 413 (1970).
28. H. OBERHAMMER and W. ZEIL. Z. Naturforsch **24A**, 1612 (1970).
29. G. A. SLACK. Phys. Revs. **139A**, 511 (1965).
30. A. SUGAWARA. J. Appl. Chem. **36**, 2375 (1965).

Can. J. Chem. Downloaded from www.nrcresearchpress.com by 210.87.254.105 on 09/05/12
For personal use only.

Crystal and Molecular Structure of Benzylidenimine Trisulfide

JAMES C. BARRICK, CRISPIN CALVO, AND FREDRIC P. OLSEN
The Department of Chemistry, McMaster University, Hamilton, Ontario L8S 4M1

Received April 18, 1973

The crystal and molecular structure of benzylidenimine trisulfide has been determined. Crystals are orthorhombic with $a = 16.610(2)$, $b = 9.984(6)$, $c = 4.386(4)$, $Z = 2$ and space group $P2_12_12$. 773 unique reflections of positive measured intensity, recorded with a Syntex P$\bar{1}$ Automatic Diffractometer, were refined by full-matrix least-square methods to a conventional R value of 0.023. The molecule has a crystallographic two-fold axis and S—S bond lengths of 2.051(1) Å. These are intermediate in length between the long inner and short outer S—S bonds of the chemically analogous tetrasulfide. The S—N and N—C bond lengths are 1.661(3) and 1.269(3), respectively. The crystal packing is determined by S—S van der Waals interaction between adjacent molecules along the c axis.

La structure cristalline et moléculaire du trisulfure de benzylidénimine a été déterminée. Les cristaux sont orthorhombiques avec $a = 16.610(2)$, $b = 9.984(6)$, $c = 4.386(4)$, $Z = 2$ et le groupe d'espace est $P2_12_12$. 773 réflexions uniques d'intensité mesurée positive et enregistrées sur un diffractomètre automatique Syntex P$\bar{1}$, ont été raffinées par la méthode des matrices des moindres carrés jusqu'à une valeur conventionnelle pour R de 0.023. La molécule a un axe cristallographique d'ordre 2 et les longueurs des liaisons S—S sont de 2.051(1) Å. Celles-ci sont intermédiaires entre les longues liaisons internes et les courtes liaisons externes S—S des analogues chimiques tétrasulfurés. Les longueurs des liaisons S—N et N—C sont de 1.661(3) et 1.269(3), respectivement. Le remplissage du cristal est déterminé par les interactions S—S de Van der Waals entre les molécules adjacentes le long de l'axe c.

[Traduit par le journal]

Can. J. Chem. 51, 3697 (1973)

Can. J. Chem. Downloaded from www.nrcresearchpress.com by 210.87.254.6 on 09/05/12
For personal use only.

Alternation of sulfur–sulfur bond lengths has been observed in benzylidenimine tetrasulfide (1), **1***a*, as well as in 7,15,17,19-tetraethoxy-2,3,4,5,10,11,12,13-octathiatricyclo[12,2,2,$2^{6,9}$]-eicosa-6,8,14,16,17,19-hexaene (2), **2**, *N*,*N*′-dimethyl-3,6-epitetrathio-2,5-piperazinedione (3, 4), **3**, and bis(cyclopentadienyl)tungsten tetrasulfide (5), **4**, but not in 1,2,3,4-tetrathiadecalin, **5**, (6). Possible explanations might include such factors as "butadiene-like" conjugation across the S_4 chain (2), inductive effects leading to shortening of the outer S—S bonds in **1***a*–**4**, resonance forms involving dπ–pπ overlap at the terminal sulfur in **1***a*–**4** leading to redistribution of electron density along the sulfur chain, hyperconjugation (7), and internal redistribution of electron density within the tetrasulfide chain. A choice between these explanations cannot reasonably be made based only on the observed tetrasulfide bond length alternation since there is no well established "normal" sulfur–sulfur single bond length. (The value in elemental sulfur may well contain contributions from dπ–pπ double bonding, and thus this is not an acceptable reference.) Accurate structural data providing both bond lengths and angles on a series of closely related compounds with varying number of atoms in the sulfur chain would be invaluable.

This paper reports the crystal and molecular structure of benzylidenimine trisulfide, (**1***b*), with a view to providing data which can be compared with that of benzylidenimine tetrasulfide (**1***a*) and benzylidenimine disulfide, (**1***c*), reported in a paper to follow.

Experimental

Preparation of Compound

Benzylidenimine trisulfide was obtained from the reaction of sulfur with benzylamine (in presence of lead oxide) at the 3:1 molar ratio calculated (8) to maximize the yield of this product. The crude material was taken up in ether and filtered to remove lead sulfide. The ether was removed under vacuum and the product recrystallized from an amount of refluxing methanol sufficient to dissolve approximately half the product. Upon cooling to room temperature, the bulk of the tetrasulfide was precipitated and removed. The solution was then refrigerated for several hours whereupon a crop of fairly pure disulfide precipitated. The remaining solution was concentrated to a small volume and chilled to precipitate a mixture of about equal parts of benzylidenimine tri- and tetrasulfides. This material was taken up in a hot benzene–hexane solution and upon cooling gave the desired trisulfide in 90–95% purity. A subsequent recrystallization of the latter from benzene–hexane gave white needles of m.p. 125–126 °C, lit. (8) 125–126°. Using

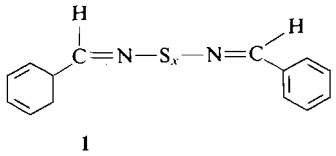

1

a $x = 4$
b $x = 3$
c $x = 2$

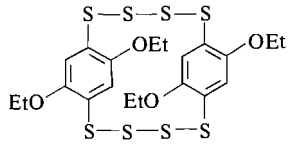

2

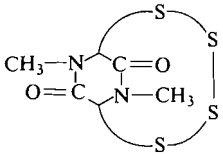

3

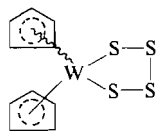

4

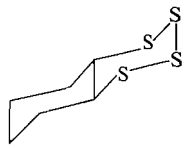

5

this method approximately 0.5 g of high purity trisulfide could be obtained from 10 g of benzylamine.

Crystal Data

$C_{14}H_{12}N_2S_3$

Orthorhombic, $a = 16.610(2)$, $b = 9.984(6)$, $c = 4.386(4)$ Å, $V = 727.3$ Å^3, $D_m = 1.4$, $Z = 2$, $D_c = 1.390$, space group $P2_12_12$.

Weissenberg photographs established the crystal system as orthorhombic and showed systematic absences of the type $h00$ for h odd and $0k0$ for k odd. Accurate unit cell parameters were obtained by least-squares adjustment of the lattice parameters to the experimental values of 2θ, ω, and χ using 13 well centered reflections measured on a Syntex P$\bar{1}$ Automatic Diffractometer with graphite monochromatized (take off angle of 12°) MoK$_\alpha$ radiation ($\lambda = 0.71069$ Å).

Intensity data to $2\theta = 40°$ were recorded on the above diffractometer in the θ–2θ technique. Stationary counts on each side of the peak for one half the scan time established background. Thus, the peak intensity, $N_{Pk} = N_T - N_{Bg1} - N_{Bg2}$ where N_T is the total peak count and N_{Bg1} and N_{Bg2} are background counts. σ_I's were derived from $\sqrt{\sigma_{Pk}^2 + (0.02|F_o|^2)^2}$ where $\sigma_{Pk}^2 = N_T + N_{Bg1} + N_{Bg2}$. The linear absorption coefficient was 4.9 cm^{-1} and the crystal used had dimensions of 0.27 mm × 0.39 mm × 0.59 mm (with the long axis parallel to the spindle axis). After averaging of equivalent reflections, 773 symmetry independent reflections of positive intensity measure remained of which 715 had $I > 3\sigma$ and were treated as "observed". After correction for Lorentz and polarization effects using the XRAY-67 Program DATRDN these gave the structure factors used to calculate Patterson functions and for comparison with those calculated from model structures.[1]

Solution of the Structure

The central sulfur was placed on the two-fold axis as required by the number of formulae units per cell ($Z = 2$). The $hk0$ and $0kl$ Patterson projections yielded the coordinates of the S and N atoms. Carbon positions were then gradually located from successive electron density and difference Fourier syntheses (SYMFOU)[2] and least-squares refinement (CUDLS)[2]. Hydrogen atom positions with isotropic temperature factors were refined from the positions corresponding to sp^2 hybridization at carbon and a C—H bond length of 0.97 Å. The function minimized in the full-matrix least squares refinement was $\Sigma w(F_o - F_c)^2$. Unobserved reflections measuring more than their calculated values did not effect the refinement while those measuring less than their calculated value did. In the final cycle there were 58 such reflections which supplemented the 715 observed reflections. When anisotropic temperature factors were refined for all non hydrogen atoms, a total of 112 parameters were varied including those for scale and extinction (10, 11) corrections. The weighting scheme used in the final cycle of refinement took the form

$$w = 1/[0.007 + 0.007|F_o| + 0.00012|F_o|^2 + 12\sigma^2/|F_o|^2]$$

where the σ's were derived from counting statistics. The maximum shift/error was 0.054 in the final cycle of refinement. The final unweighted R was 0.023 for the observed reflections and 0.026 for all reflections; the weighted R for both cases was 0.031 where

$$R = \frac{\sum ||F_o| - |F_c||}{|F_o|}$$

and

$$R_w = \sqrt{\frac{\sum w(|F_o| - |F_c|)^2}{\sum w|F_o|^2}}$$

The calculated and observed structure factors are listed[3] in Table 1 and the final values of the positional

[1]Atomic scattering factors used were those quoted in the International tables (9).

[2]Computer programs CUDLS and SYMFOU were written locally by J. Stephens and J. Rutherford, respectively.

[3]Table 1 is available, at a nominal charge, from the Depository of Unpublished Data, National Science Library, National Research Council of Canada, Ottawa, Canada K1A 0S2.

Can. J. Chem. Downloaded from www.nrcresearchpress.com by 210.87.254.6 on 09/05/12
For personal use only.

TABLE 2. Final parameters for benzylidenimine trisulfide

	Positions			$10^3 \times$ Temperature parameters[4]					
Atom	x/a	y/b	z/c	U_{11}	U_{22}	U_{33}	U_{12}	U_{13}	U_{23}
S_1	0.0000	0.0000	0.3034(2)	52.9(5)	77.4(6)	43.4(4)	−1.5(5)	0.0	0.0
S_2	0.0168(1)	0.1626(1)	0.0250(2)	47.7(3)	50.2(4)	71.9(4)	3.9(3)	−4.8(3)	−5.9(4)
N	0.1097(1)	0.1663(2)	0.8847(5)	50(1)	48(1)	60(1)	−2(1)	−6(1)	−4(1)
C_1	0.1637(2)	0.0780(2)	0.9260(6)	52(1)	44(1)	46(1)	−4(1)	−6(1)	−5(1)
C_2	0.2434(1)	0.0887(2)	0.7864(6)	48(1)	42(1)	45(1)	−4(1)	−6(1)	−6(1)
C_3	0.2639(2)	0.1962(2)	0.6024(7)	56(1)	45(1)	55(1)	1(1)	−4(1)	5(1)
C_4	0.3398(2)	0.2052(3)	0.4765(8)	65(2)	59(2)	62(2)	−11(1)	3(2)	7(2)
C_5	0.3959(2)	0.1053(3)	0.5307(8)	47(1)	67(2)	70(2)	−5(1)	0(2)	6(2)
C_6	0.3763(2)	0.9992(3)	0.7127(7)	53(1)	62(2)	79(2)	7(1)	−6(2)	1(2)
C_7	0.3006(2)	0.9898(3)	0.8396(7)	58(2)	45(1)	65(2)	−2(1)	−5(1)	7(2)
				U_{iso}					
H_1	0.154(2)	0.005(3)	0.042(6)	33(7)					
H_3	0.224(1)	0.257(3)	0.562(7)	25(7)					
H_4	0.352(2)	0.277(3)	0.562(7)	41(9)					
H_5	0.446(2)	0.115(3)	0.452(8)	43(9)					
H_6	0.481(2)	0.928(3)	0.765(8)	50(9)					
H_7	0.288(2)	0.919(3)	0.946(9)	44(9)					

TABLE 3. Bond lengths and angles in benzylidenimine trisulfide*

Bond	Distance (Å)	Bond	Distance (Å)	Bond	Distance (Å)
S_1—S_2	2.051(1)	C_3—C_4	1.379(4)	C_1—H_1	0.91(3)
S_2—N	1.661(3)	C_4—C_5	1.385(4)	C_3—H_3	0.91(3)
N—C_1	1.269(3)	C_5—C_6	1.366(4)	C_4—H_4	0.89(3)
C_1—C_2	1.464(4)	C_6—C_7	1.378(4)	C_5—H_5	0.90(3)
C_2—C_3	1.385(3)	C_7—C_2	1.390(4)	C_6—H_6	1.01(3)
				C_7—H_7	0.88(3)

Bonds	Angle (deg)	Bonds	Angle (deg)
$S_2S_1S_2'$	106.9(2)	$C_3C_2C_7$	118.7(3)
S_1S_2N	111.4(2)	$C_2C_3C_4$	120.6(4)
S_2NC_1	126.0(2)	$C_3C_4C_5$	119.9(4)
NC_1C_2	121.9(4)	$C_4C_5C_6$	119.9(4)
$C_1C_2C_3$	121.5(3)	$C_5C_6C_7$	120.4(4)
$C_1C_2C_7$	119.8(4)	$C_6C_7C_2$	120.5(4)

*Estimated standard deviations include errors in both positions and cell dimensions.

and thermal[4] parameters of all atoms are given in Table 2. Table 3 lists bond lengths and angles of interest.

Results and Discussion

Figure 1 shows the molecule looking down the b axis. The molecule contains a crystallographic two-fold axis which lies along the c axis. The overall structure is clearly that of benzylidenimine trisulfide with a molecular conformation in which the two aromatic rings are well separated from each other as opposed to benzylidenimine tetrasulfide where the two rings were nearly eclipsed (1).

The Phenyl Ring

The phenyl ring carbons are quite planar with maximum and average deviations of 0.004 (C_5) and 0.002 Å, respectively. The average carbon–carbon bond length (in the ring) of 1.381 Å,

[4]All temperature factors reported herein are in Å^2 and were obtained from $U_{iso} = B_{iso}/8\pi^2$ and $U_{ij} = \beta_{ij}/2\pi^2 a_i^* a_j^*$ where the β_{ij}'s appear as the effect of temperature through $\exp[-\beta_{11}h^2 + 2\beta_{12}hk...]$ in the structure factor expression and the a_i^*'s are the reciprocal lattice vectors. These units are chosen so that U = mean square thermal displacements directly.

Can. J. Chem. Downloaded from www.nrcresearchpress.com by 210.87.254.6 on 09/05/12
For personal use only.

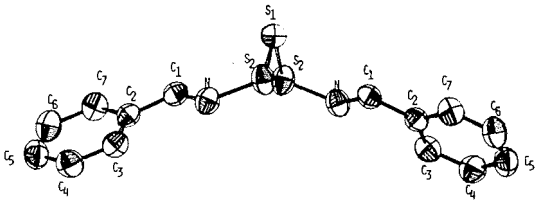

FIG. 1. View of benzylidenimine trisulfide looking down the *b* axis.

with maximum and average deviations of 0.015 (C_5—C_6) and 0.006 Å, is in good agreement with values of 1.372 in the tetrasulfide (**1***a*) and 1.380 in **2** (2). Considering that translational and librational corrections have not been applied, it agrees well with the accepted (12) value of 1.392(4) Å. The average C—C—C angle for the ring is 120.0° with maximum and average deviations of 1.3° (C_2) and 0.5°. The average carbon–hydrogen bond distance refined to 0.92 Å with maximum and average deviations of 0.09 and 0.03 Å. Riding corrections (13), if applied, would lead to an average value of 0.94 Å. The maximum deviations of a ring hydrogen from the plane defined by C_2—C_7 is 0.05 Å (H_6) and the average deviation for the five is 0.04 Å.

The C-Phenyl and C–N Bonds

The aliphatic C—C bond at 1.464(4) Å and the C—N double bond at 1.269(3) Å are both in excellent agreement with the corresponding values of 1.460(8) and 1.271(8) Å observed in benzylidenimine tetrasulfide (**1***a*). As expected for conjugation of the C—N double bond with the aromatic ring, C_1 and N lie just 0.013 and 0.020 Å from the plane defined by the ring carbon atoms. The C—C—N and C—N—S angles at 121.9(4)° and 126.0(2)° compare well with values of 121.6(4)° and 124.0(4)° in the tetrasulfide. The C—C—N—S dihedral angle at 1.5° is also in good agreement with the corresponding values of 1.1° and 3.0° found in the tetrasulfide.

The Sulfur–Nitrogen Bond

As in the tetrasulfide, the N—S distance is short compared to sulfamic acid but is typical of more ordinary "single bond" lengths where some dπ–pπ overlap is likely. The value of 1.661(3) Å found here compares very well with the value of 1.655(5) Å found in the tetrasulfide. The N—S—S angle at 111.4(2)° and also the quite small C—N—S—S dihedral angle of 3.5° are indistinguishable from the values of 111.5(3)° for the former and 3.0 and 3.3° for the latter angles in the tetrasulfide. Thus, all structural aspects including bond lengths, angles, and dihedral angles at the C—C, C—N, and N—S bonds are effectively identical in benzylidenimine tri- and tetrasulfides.

The Sulfur–Sulfur Bond

In benzylidenimine tetrasulfide, the molecular geometry could be described as two nearly coplanar units each containing a fairly short S—S bond and being joined by a fairly long S—S bond. These "in plane" bonds and "between plane" bonds in the tetrasulfide were 2.026(3) and 2.083(4) Å in length, respectively. The nearly identical molecular geometry in benzylidenimine trisulfide, including the comparable small C—N—S—S dihedral angle, requires that the whole unique half molecule be very nearly coplanar. Indeed, a single plane can be fit to the whole asymmetric unit in the trisulfide with maximum and average deviations (excluding hydrogen) of 0.031 (S_1) and 0.012 Å Thus, while the tetrasulfide was composed of two planes joined by an S—S bond, the full trisulfide molecule is composed of two planes sharing a common sulfur atom (S_1). Since the S—S bond in the trisulfide lies in the molecular plane, one might perhaps expect it to be comparable to the "in plane" S—S bonds in the tetrasulfide. The sulfur–sulfur bond length in the trisulfide is 2.051(1) Å. It therefore differs from the "in plane" tetrasulfide bonds by 0.025 Å with a σ_Δ of 0.003 Å where $\sigma_\Delta^2 = \sigma_1^2 + \sigma_2^2$. This difference of 8 pooled e.s.d.'s is taken as a "significant" difference especially considering the excellent agreement between all other aspects of the two structures. Comparing the trisulfide S—S bond with the longer "between planes" S—S bond in the tetrasulfide gives a difference of 0.032 Å with a σ_Δ of 0.004 Å, again 8 pooled e.s.d.'s, an amount taken as "significant". Thus, the S—S bond in benzylidenimine trisulfide is intermediate in length and unique from either the long or short S—S bonds in benzylidenimine tetrasulfide. Its length of 2.051(1) Å is in excellent agreement with those of 2.048(4) and 2.050(4) recently reported (14) in 1,2,3-trithio-3-ferrocenophene **6** and is somewhat shorter than the 2.083 Å found (15) in **7**.

Like the N—S—S angles, the S—S—S angles

Can. J. Chem. Downloaded from www.nrcresearchpress.com by 210.87.254.6 on 09/05/12
For personal use only.

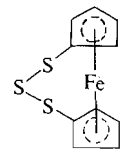

6

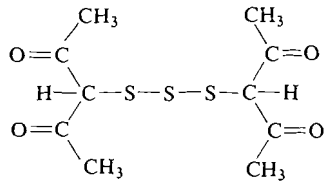

7

are very nearly identical in the tri- and tetrasulfide. The S—S—S angle is 106.9(2) in the trisulfide compared to 106.2(2)° in the tetrasulfide. The N—S—S—S dihedral angle in benzylidenimine trisulfide at 101.8° is, however, about 10° greater than that in the tetrasulfide where the comparable values were 90.6° and 94.3°. It is, however, less than the 106.5° found for the S—S—S—S dihedral angle in the tetrasulfide. Thus, the [C_6H_5CHNSS—] unit has nearly identical geometry in the two compounds save for a slight shortening of the S—S bonds in the tetrasulfide. There are slight differences in the dihedral angles at the sulfur–sulfur bond and the "extra" S—S bond in the tetrasulfide is quite long.

Within the crystal lattice, the three sulfur atoms form a vee pointing up the *c* axis. The two nitrogen atoms lie on opposite sides of the plane formed by these 3 sulfur atoms in contrast to **6** where the two adjoining atoms (carbon) lie on the same side of this plane. The sulfur vee's stack closely on top of one another to give an arrow effect pointing up the *c* axis. In the *b* direction, these arrows alternate side by side with screw related arrows pointing down through the structure. The cell is one molecule thick in *c*. The S_1—S_2 intermolecular non-bonding distance of 3.568 Å is just slightly less than the sum of van der Waal's radii (3.70 Å) and might indicate some possible weak interaction. Possible support for such an interaction comes from the observed decomposition of the crystal. On standing over a period of several months, a yellow streak develops down the middle of the crystal in the *c* direction. Eventually, the whole crystal becomes covered with a powdery yellow excrescence. This decomposition, which leads to major amounts of benzylidenimine di- and tetrasulfides (the latter yellow), could proceed by sulfur chain growth in the direction of the non-bonding interactions. It should be noted, however, that the intermolecular contact distance in elemental S_6 is (16) only 3.50 Å. It seems unlikely that interaction of this limited extent would result in any substantial effect on S—S bond lengths although this possibility cannot be fully excluded. As in the tetrasulfide, the $C_1 \ldots S_1$ intramolecular distance at 3.28 Å is rather short.

This work was supported under a grant from the National Research Council of Canada.

1. J. C. Barrick, C. Calvo, and F. P. Olsen. Chem. Commun. 1043 (1971); Can. J. Chem. This issue.
2. J. C. Ricci, Jr. and I. Bernal. J. Chem. Soc. B, 1928 (1971).
3. B. R. Davis and I. Bernal. Proc. Nat. Acad. Sci. U.S.A. **70**, 279 (1973).
4. B. R. Davis, I. Bernal, and U. Schmidt. Angew. Chem. Int. Ed. **11**, 632 (1972).
5. B. R. Davis and I. Bernal. J. Cryst. Mol. Struct. **2**, 135 (1972).
6. F. Feher, A. Klaeren, and K. H. Linke. Angew. Chem. Int. Ed. **9**, 895 (1970).
7. G. Winnewisser, M. Winnewisser, and W. Gordy. J. Chem. Phys. **49**, 3465 (1968).
8. Y. Sasaki and F. P. Olsen. Can. J. Chem. **49**, 283 (1971).
9. International tables for X-ray crystallographers. Vol. 3. Kynoch Press, Birmingham, England. 1962. p. 202.
10. J. S. Stephens and D. W. J. Cruickshank. Acta Cryst. **B26**, 223 (1970).
11. W. H. Zachariasen. Acta. Cryst. **16**, 1142 (1963).
12. E. G. Cox, D. W. J. Cruickshank, and J. A. S. Smith. Proc. R. Soc. A**247**, 1 (1958).
13. W. R. Busing and H. A. Levy. Acta Cryst. **17**, 142 (1964).
14. B. R. Davis and I. Bernal. J. Cryst. Mol. Struct. **2**, 107 (1972).
15. L. F. Power. Acta Cryst. **B27**, 181 (1971).
16. J. Donohue, A. Caron, and E. Goldisch. J. Am. Chem. Soc. **83**, 3748 (1961).

Can. J. Chem. Downloaded from www.nrcresearchpress.com by 210.87.254.6 on 09/05/12
For personal use only.

The Synthesis, Mössbauer and Infrared Spectra of some Dialkyltin Salts of Phosphorus Oxy-acids

T. CHIVERS AND J. H. G. VAN ROODE
Department of Chemistry, The University of Calgary, Calgary, Alberta T2N 1N4

AND

J. N. R. RUDDICK AND J. R. SAMS
Department of Chemistry, The University of British Columbia, Vancouver 8, British Columbia

Received April 11, 1973

A number of dialkyltin(IV) salts of phosphorus oxy-acids $R_2Sn(PO_2H_2)_2$ (R = CH_3, C_2H_5, *n*-C_4H_9), R_2SnPO_3X (R = CH_3, C_2H_5, *n*-C_4H_9, X = H; R = CH_3, X = F, OH), and $[(CH_3)_2Sn]_3(PO_4)_2$ have been prepared in aqueous solution from the appropriate dialkyltin(IV) dichloride and the sodium salts of phosphorus oxy-acids.

Infrared and ^{119}Sn Mössbauer spectra of the dialkyltin dihypophosphites, $R_2Sn(PO_2H_2)_2$, are consistent with hexacoordination for tin with the alkyl groups in *trans*-octahedral positions and bidentate bridging hypophosphite groups coordinated through oxygens. For the dialkyltin phosphites, R_2SnPO_3X, polymeric structures with a non-linear R_2Sn arrangement are involved, and the magnetic hyperfine Mössbauer spectrum (X = F) is consistent with either distorted *trans*-octahedral or distorted trigonal bipyramidal structures (with both apical or both equatorial methyl groups). In $[(CH_3)_2Sn]_3(PO_4)_2$ the three tin environments are indistinguishable by Mössbauer spectroscopy, but the high value of the asymmetry parameter $\eta \simeq 0.8$ suggests penta- rather than hexacoordination about tin, for which at least one three-coordinate oxygen per formula unit must be invoked.

Un nombre de sels de dialkylstannates d'oxy-acides de phosphore $R_2Sn(PO_2H_2)_2$ (R = CH_3, C_2H_5, *n*-C_4H_9), R_2SnPO_3X (R = CH_3, C_2H_5, *n*-C_4H_9, X = H; R = CH_3, X = F, OH) et $[(CH_3)_2Sn]_3(PO_4)_2$ ont été préparé en solution aqueuse à partir du dichlorure de dialkylstannate adéquat et des sels de sodium des oxy-acides de phosphore. L'infrarouge et le spectre de Mössbauer de ^{119}Sn des dihypophosphites de dialkylstannate, $R_2Sn(PO_2H_2)_2$, sont consistants avec l'hexacoordination de l'étain avec les groupes alkyles dans des positions octahédrique-*trans* avec les groupes hypophosphites bidentates formant des ponts par coordination avec les oxygènes. En ce qui concerne les phosphites de dialkylstannate, R_2SnPO_3X, des structures polymériques avec une non-linéarité pour les arrangements du R_2Sn sont impliquées, et le spectre magnétique hyperfin de Mössbauer (X = F), est consistant soit avec une forme octahédrique-*trans* distordue, ou une forme bipyramidale trigonale distordue (avec les deux groupes méthyles apicaux, ou équatoriaux). Dans $[(CH_3)_2Sn]_3(PO_4)_2$, les trois étains environnants sont indistinguables par la spectroscopie de Mössbauer, mais la grande valeur du paramètre assymétrique $\eta \simeq 0.8$ suggère une pentacoordination plutôt qu'une hexacoordination par rapport à l'étain, pour conclure enfin que l'un des trois oxygènes coordinants par unité de formule doit être invoqué.

[Traduit par le journal]

Can. J. Chem. **51**, 3702 (1973)

Introduction

There has been considerable recent interest in organotin(IV) derivatives of inorganic acids but studies of such derivatives of phosphorus oxy-acids are few. Aqueous solutions of dimethyltin dichloride are known to react in a simple manner with $Na_2HPO_4 \cdot 12H_2O$ and $NaH_2PO_2 \cdot H_2O$ to give $(CH_3)_2SnHPO_4$ and $(CH_3)_2Sn(H_2PO_2)_2 \cdot 2H_2O$, respectively (1). Anhydrous triorganotin(IV) phosphates $(R_3Sn)_3PO_4$ (R = C_6H_5 (2), *n*-C_4H_9 (3)) have also been reported, but structural information is lacking. The recently described dialkyltin(IV) bis(difluorophosphates) $R_2Sn(PO_2F_2)_2$ (4), prepared by solvolysis of dialkyltin(IV) chlorides in an excess of difluorophosphoric acid, have been assigned a structure in which the tin atom is hexacoordinate with the alkyl groups in *trans*-octahedral positions and bidentate bridging difluorophosphate groups coordinated through oxygens, on the basis of ^{119}Sn Mössbauer and vibrational spectra. In view of the biological activity of organotin(IV) derivatives (5) and their use as pesticides and fungicides (5, 6), the products of reactions between organotin(IV) compounds and phosphates or phosphites appeared to be worthy of more detailed study.

In this investigation aqueous solutions of

Can. J. Chem. Downloaded from www.nrcresearchpress.com by 210.87.254.105 on 09/05/12
For personal use only.

TABLE 1. Analytical data for $R_2Sn(PO_2H_2)_2$ (R = CH_3, C_2H_5, n-C_4H_9), R_2SnPO_3X (R = CH_3, C_2H_5, n-C_4H_9, X = H; R = CH_3, X = OH, F), and $[(CH_3)_2Sn]_3(PO_4)_2$

Compound	Melting point* (°C)	Analysis (%) C Calcd	C Found	H Calcd	H Found
$(CH_3)_2Sn(PO_2H_2)_2$	217	8.62	8.66	3.62	3.48
$(C_2H_5)_2Sn(PO_2H_2)_2$	214	15.66	15.63	4.60	4.46
$(n\text{-}C_4H_9)_2Sn(PO_2H_2)_2$	183	26.48	26.22	6.11	5.90
$(CH_3)_2SnPO_3H$	312	10.50	10.52	3.08	2.79
$(C_2H_5)_2SnPO_3H$	305	18.71	18.97	4.32	4.01
$(n\text{-}C_4H_9)_2SnPO_3H$	285	30.71	31.08	6.12	6.11
$(CH_3)_2SnPO_4H$	>350(d)	9.81	9.98	2.88	3.02
$[(CH_3)_2Sn]_3(PO_4)_2$	>350(d)	11.33	11.32	2.85	2.48
$(CH_3)_2SnPO_3F$†	>350(d)	9.74	9.64	2.45	2.53

*(d) denotes decomposition.
†Calcd: P, 12.55; F, 7.70%; Found: P, 12.23; F, 7.49%.

dialkyltin(IV) chlorides were allowed to react with aqueous solutions of $NaH_2PO_2 \cdot H_2O$, $Na_2HPO_3 \cdot 5H_2O$, $Na_2HPO_4 \cdot 2H_2O$, $NaH_2PO_4 \cdot H_2O$, $Na_3PO_4 \cdot 12H_2O$, and K_2PO_3F to give the dialkyltin(IV) salts of the corresponding phosphorus oxy-acids as insoluble white precipitates. Since the phosphorus oxy-anions studied are derived from either mono-, di-, or tri-basic acids a variety of structures is possible for the dialkyltin(IV) derivatives. We have investigated these structures using infrared and conventional Mössbauer spectroscopy. In three cases, $(CH_3)_2Sn(PO_2H_2)_2$, $(CH_3)_2SnPO_3F$, and $[(CH_3)_2Sn]_3(PO_4)_2$, the Mössbauer spectra were measured in the presence of a large magnetic field in order to determine the sign of the electric field gradient (e.f.g.) at the ^{119}Sn nucleus and magnitude of the asymmetry parameter, η, in an attempt to distinguish between various geometrical arrangements of groups around tin.

Experimental

I. Chemicals

The sources of chemicals are indicated below: $NaH_2PO_2 \cdot H_2O$, $Na_2HPO_3 \cdot 5H_2O$, and $NaH_2PO_4 \cdot H_2O$ (Fisher), $Na_2HPO_4 \cdot 2H_2O$ (Baker), $Na_3PO_4 \cdot 12H_2O$ (British Drug Houses), K_2PO_3F (Research Organic/Inorganic Chemical Corp.). These were reagent grade chemicals used without further purification. $(CH_3)_2SnCl_2$ and $(n\text{-}C_4H_9)_2SnCl_2$ were kindly donated by M and T Chemicals Inc.; $(C_2H_5)_2SnCl_2$ was prepared from $(C_2H_5)_4Sn$ by the redistribution procedure (7). Purification of organotin(IV) chlorides was carried out by vacuum sublimation where necessary.

II. Instrumentation

Infrared spectra were obtained using a Perkin–Elmer 337 spectrometer. The Mössbauer spectrometer has been described previously (8).

III. Preparations

(a) In Aqueous Solution

The preparations were carried out according to the previously described procedure (1). Aqueous solutions of the dialkyltin(IV) dichlorides (for $(n\text{-}C_4H_9)_2SnCl_2$ ether was used as solvent) were added to aqueous solutions of the sodium or potassium salts of the phosphorus oxy-acid in a stoichiometric ratio appropriate for the complete replacement of chlorines on tin by the phosphorus oxy-anion. White precipitates of alkyltin(IV) phosphates or phosphites were produced either immediately, on shaking for a few minutes, or on standing for a few days. The products were filtered off, washed with water then methanol, and dried in an Aberhalden pistol (80°/0.1 mm) before being submitted for analysis.

IV. Analytical Results

All compounds were identified by C and H microanalysis, performed by Chemalytics Inc., Arizona, U.S.A. P and F analysis were carried out by Alfred Bernhardt, Microanalytical Laboratory, Elbach, W. Germany. The results together with the melting or decomposition points are listed in Table 1.

V. Infrared Spectra

Infrared spectra were obtained as mulls (Nujol) using KBr plates (International Crystal Labs.). The major absorption bands, together with assignments, for the dialkyltin(IV) bishypophosphites and the dialkyltin(IV) phosphites are summarized in Tables 2 and 3, respectively. Infrared spectra for other compounds are shown below (cm^{-1}). $(CH_3)_2SnPO_3F$: 1211s, 1170s,b, 1050s, 920w, 880w,sh, 855s, 807s, 590s, 544m, 517m; $(CH_3)_2SnPO_4H$: 3300b, 1200w, 1132s, 1104s, 1065s, 1030s, 888s, 800s, 630w, 590m, 550m, 519m; $[(CH_3)_2Sn]_3(PO_4)_2$: 1194w, 1112s, 1070s,b, 1000s, 975s, 950m, 790s, 645w, 604w, 572w–m, 536w–m, 450m.

Results and Discussion

I. Synthesis

Aqueous solutions of dialkyltin(IV) dichlorides react rapidly with aqueous solutions of

Can. J. Chem. Downloaded from www.nrcresearchpress.com by 210.87.254.105 on 09/05/12
For personal use only.

TABLE 2. Infrared spectra of dialkyltin(IV) bishypophosphites $R_2Sn(H_2PO_2)_2$ and $NaH_2PO_2 \cdot H_2O$ (cm^{-1})*†

		$R_2Sn(H_2PO_2)_2$, R =		
$NaH_2PO_2 \cdot H_2O$	Assignment	CH_3	C_2H_5	n-C_4H_9
2360s	$\nu_s PH_2(A_1)$	2420s	2370sh	2380sh
2295s	$\nu_{as} PH_2(B_1)$	2370s	2360s	2370s
1230s	$\nu_{as} PO_2(B_2)$	1145s	1145s	1145s
1160s	PH_2bend(A_1)	1155s	1156s	1160s
1090s	PH_2wagging(B_2)	1082s	1085s	1082s
1060s	$\nu_s PO_2(A_1)$	1046s	1054s	1058s
820s	PH_2rocking(B_1)	808s	809s	812s
	Sn—C rocking	800s	688m	690m
	ν_{as}Sn—C	582m	552m	645m
472s	PO_2 bend(A_1)	450m	472m	480m

*s = strong, m = medium, sh = shoulder; ν_s = symmetric stretch, ν_{as} = asymmetric stretch.
†Internal modes of the R groups are not included.

TABLE 3. Infrared spectra of R_2SnPO_3H (R = CH_3, C_2H_5, n-C_4H_9), K_2PO_3H (aq. soln.) and $BaPO_3H$

K_2PO_3H*	$BaPO_3H$*	Assignment	$(CH_3)_2SnPO_3H$	$(C_2H_5)_2SnPO_3H$†	$(n$-$C_4H_9)_2SnPO_3H$†
2315m,sh	2410m,sh	$\nu PH(A_1)$	2410s	2360m	2360m
			2375m,sh	2340w,sh	2340w,sh
			1200m	1180s	
			1150s,b		1150m,sh
	1110vs,b		1115s,sh	1120s,b	
1085vs,b	1083vs,b	$\nu_{as} PO_3(E)$	1088s	1070s,b	1070s,b
			1055s,sh		
	1021w,sh				
1027vs,b	1006w,sh	PH def(E)			
979m,sh	977m,sh	$\nu_s PO_3(A_1)$	1015s	1022s	1005s
				1000s	
				942s	950w,sh
		SnC_2rocking	790s,b	680s	672m
			610s,sh		
			600s		
567m	591m	PO_3sym.def(A)	585m	585m,sh	588m
		$\nu_{as} SnC_2$	575m,sh	572m,b	580m,b
			548w		540w,sh
		$\nu_s SnC_2$	528w	528w,b	515w,b
465m,b	498m	PO_3asym.def(E)	482m	482m	
	471m		433m	410m	420w

*Reference 9.
†Internal modes of the R group overlap the 1000–1200 cm^{-1} and are not included. Assignment of $\nu_{as}SnC_2$ and $\nu_s SnC_2$ is not possible due to overlap with PO_3 deformation modes.

$NaH_2PO_2 \cdot H_2O$, $Na_2HPO_3 \cdot 5H_2O$, $Na_2HPO_4 \cdot 2H_2O$, $Na_3PO_4 \cdot 12H_2O$, or K_2PO_3F to give high yields of the dialkyltin(IV) salts of the corresponding phosphorus oxy-acid. Analytical data and infrared spectra showed that these derivatives, after drying, were anhydrous. When aqueous solutions of dimethyltin dichloride and $NaH_2PO_4 \cdot H_2O$ were mixed a high yield of $(CH_3)_2SnPO_4H$, identified by analysis, infrared and ^{119}Sn Mössbauer spectra, was obtained. At pH 7, $[HPO_4^{2-}]/[H_2PO_4^-] \simeq 1$, and this ratio increases with increase in pH so that reaction with the doubly charged anion is perhaps not unexpected.

II. Infrared Spectra

The infrared spectra of the dialkyltin(IV) bishypophosphites are shown in Table 2. For the $H_2PO_2^-$ ion, assuming C_{2v} symmetry, there should be nine normal vibrations (9). All of these except one (the PH_2 twisting mode which belongs to the group A_2 and should

Can. J. Chem. Downloaded from www.nrcresearchpress.com by 210.87.254.105 on 09/05/12
For personal use only.

Can. J. Chem. Downloaded from www.nrcresearchpress.com by 210.87.254.105 on 09/05/12
For personal use only.

occur only in the Raman spectrum) are observed in the infrared spectra of alkali metal hypophosphites and of dialkyltin(IV) bishypophosphites. This observation suggests that C_{2v} symmetry is conserved in the dialkyltin(IV) compounds as expected for a bidentate bridging $H_2PO_2^-$ group with bridging through oxygens. Table 2 shows the assignments of the remaining eight fundamentals for all $R_2Sn(PO_2H_2)_2$. The following features are interesting: (*a*) only one type of PO_2H_2 group appears to be present in the dialkyltin(IV) bishypophosphites; (*b*) increasing the size of the alkyl group has little effect on the frequencies of the eight fundamental vibrations; (*c*) positional changes have occurred when compared to the ionic $H_2PO_2^-$ in $NaH_2PO_2 \cdot H_2O$. Of the P—O stretching modes, the asymmetric one is lowered by about 85 cm^{-1} whereas the symmetric mode is lowered by <15 cm^{-1}. If coordination occurs through oxygen the net lowering of $\nu PO_{average}$ can be explained partly by charge withdrawal from the P—O into the Sn—O bond region as observed for dialkyltin(IV) bis(difluorophosphates) (4). The average P—H stretching mode is found at higher frequencies (35–65 cm^{-1}) compared to $H_2PO_2^-$, indicating an overall strengthening of the P—H bonds in the dialkyltin(IV) derivatives.

Further structural information is obtained from the tin–carbon stretching modes for dialkyltin(IV) bishypophosphites. In the infrared spectra only $\nu_{as}Sn—C_2$ and not $\nu_sSn—C_2$ is observed for all compounds, suggesting that the carbon–tin–carbon group is in a linear or nearly linear arrangement. The structural model most consistent with these observations is identical to the one suggested for other dimethyltin(IV) derivatives, $(CH_3)_2SnX_2$ (X = PO_2F_2 (4), sulfonate (10–12), F (13)): hexacoordination for tin with the methyl groups in *trans*-octahedral positions and the PO_2H_2 groups acting as bridging, bidentate ligands resulting in sheet-like polymers (see Fig. 1).

The infrared spectra of the dialkyltin(IV) phosphites R_2SnPO_3H are compared with the spectrum of K_2PO_3H in Table 3. The vibrational spectra of the HPO_3^{2-} ion have been analyzed assuming C_{3v} symmetry (9). As expected, three bands due to totally symmetric vibrations and three bands due to doubly degenerate vibrations are observed. The PO_3 symmetric and asymmetric stretching modes

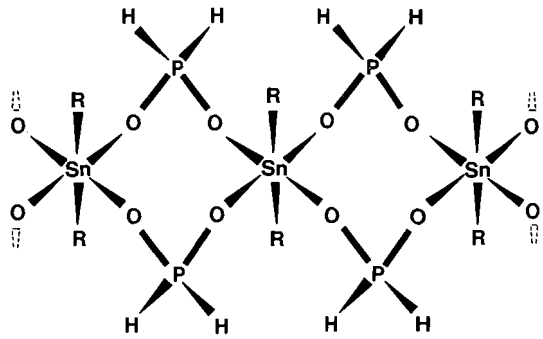

FIG. 1. Suggested structure for $R_2Sn(PO_2H_2)_2$ compounds.

were assigned to a sharp band at 980 cm^{-1} and a broad band at 1100 cm^{-1}, respectively (9). In $(CH_3)_2SnPO_3H$ these bands are shifted to 1015 cm^{-1} and *ca.* 1140 cm^{-1}, and the number of bands observed in the 1000–1200 cm^{-1} region indicates that there is a considerable lowering of the C_{3v} symmetry of the HPO_3^{2-} group. In the other two dialkyltin(IV) phosphites (R = C_2H_5, n-C_4H_9) this region of the spectrum is somewhat obscured by the bands due to the internal modes of the R groups. However, a small shift to higher frequency of ν_sPO_3 is observed. In $(CH_3)_2SnPO_3H$ both asymmetric and symmetric Sn—C_2 stretching frequencies are observed, suggesting a non-linear C—Sn—C arrangement. The high melting points and insolubility in nonpolar solvents of these compounds together with the infrared data suggest polymeric structures involving penta- or hexa-coordinate tin (see Section III).

Support for a polymeric structure for R_2SnPO_3X types comes from a comparison of the infrared spectrum of $(CH_3)_2SnPO_3F$ with that of K_2PO_3F. The following features in the spectrum of the dimethyltin(IV) derivative are significant: (*a*) $\nu_{as}PO_3$ is shifted *ca.* 30 cm^{-1} to lower frequency while ν_sPO_3 is shifted 45 cm^{-1} to higher frequency, (*b*) both $\nu_{as}SnC_2$ and ν_sSnC_2 are observed at 590 and 517 cm^{-1}, respectively, (*c*) νPF is shifted 140 cm^{-1} to higher frequency. Similar, but smaller, shifts in the PF_2 stretching frequencies have previously been observed for dialkyltin(IV) bisdifluorophosphates (4) and are explained in terms of back donation from lone pairs on fluorine into the empty 3d orbitals on phosphorus. The shift in νPF observed for $(CH_3)_2SnPO_3F$ clearly rules

TABLE 4. ^{119}Sn Mössbauer parameters at liquid nitrogen temperature

Compound	δ*†	ΔE_Q*	Γ_1*	Γ_2*	R‡
$(CH_3)_2Sn(PO_2H_2)_2$	1.26	+4.36	1.07	1.05	0.15
$(C_2H_5)_2Sn(PO_2H_2)_2$	1.46	4.47	1.09	1.08	Small
$(n\text{-}C_4H_9)_2Sn(PO_2H_2)_2$	1.42	4.47	1.09	1.10	Small
$(CH_3)_2Sn(PO_2F_2)_2$§	1.53	5.13	0.90	0.92	0.05
$(CH_3)_2Sn(SO_3F)_2$‖	1.82	5.54			
$(CH_3)_2SnPO_3F$	1.38	+4.16	1.20	1.24	0.16
$(CH_3)_2SnPO_3H$	1.28	3.99	1.23	1.19	0.28
$(C_2H_5)_2SnPO_3H$	1.40	3.81	1.03	1.05	Small
$(n\text{-}C_4H_9)_2SnPO_3H$	1.41	3.87	1.13	1.23	Nil
$(CH_3)_2SnPO_4H$	1.19	3.62	1.17	1.15	0.41
$[(CH_3)_2Sn]_3(PO_4)_2$	1.11	+3.10	1.31	1.29	0.15

*In mm s^{-1}, ± 0.05 mm s^{-1}.
†Relative to $BaSnO_3$.
‡Ratio of % absorption at room temperature to that at liquid nitrogen temperature.
§Reference 4.
‖Reference 11.

out any F—Sn bonding and the possibility of a tetradentate PO_3F group. Hexacoordination about tin can, therefore, only be achieved if there is one trivalent oxygen per formula unit.

We consider next dimethyltin(IV) orthophosphate, $[(CH_3)_2Sn]_3(PO_4)_2$. The free anion has T_d symmetry and two strong bands corresponding to the anti-symmetrical (ν_3) stretching vibration (*ca.* 1080 cm^{-1}) and the ν_4 anti-symmetrical deformation (*ca.* 500 cm^{-1}) are expected in the infrared spectrum (14). In $[(CH_3)_2Sn]_3PO_4$ the symmetry of the PO_4 group is clearly considerably lowered since at least five bands can be resolved in the 950–1150 cm^{-1} region and three bands are observed in the 500–650 cm^{-1} region. In addition, both ν_sSnC_2 and $\nu_{as}SnC_2$ are observed in the infrared spectrum indicating a non-linear C—Sn—C structure. The infrared spectrum, and the high melting point and insolubility of this compound are consistent with a polymeric structure (see Section III).

III. ^{119}Sn Mössbauer Spectra

The splitting of the $I = 3/2$ excited state of the ^{119}Sn nucleus by an electric field gradient (e.f.g.) is given by

$$\Delta E_Q = \tfrac{1}{2}e^2qQ\,(1 + \eta^2/3)^{1/2}$$

where $eq = V_{zz} = -$(e.f.g.), eQ is the nuclear quadrupole moment, and the asymmetry parameter η is defined as

$$\eta = |V_{xx} - V_{yy}|/V_{zz}$$

The $V_{\alpha\alpha}$ are the diagonal elements of the e.f.g. tensor, chosen such that $|V_{zz}| \geqslant |V_{yy}| \geqslant |V_{xx}|$. A conventional Mössbauer measurement suffices to determine only $|\Delta E_Q|$. However, the application of a large magnetic field (e.g. 15–50 kG) lifts the degeneracy of the m_I substates and the resulting spectral pattern enables one to determine the sign of the quadrupole coupling constant e^2qQ and the magnitude of η. We adopt the usual sign convention for ^{119}Sn that e^2qQ is positive for a prolate charge distribution at the nucleus. Note that since eQ is negative for ^{119}Sn, e^2qQ and V_{zz} carry opposite signs.

Mössbauer isomer shifts (δ, relative to barium stannate), quadrupole splittings, and line widths (Γ, full-width at half-maximum) are given in Table 4, along with data for some related oxyacid derivatives. Two general comments can be made concerning these data. First, ΔE_Q values greater than 3 mm s^{-1} are observed for all the compounds, a fact which strongly suggests penta- or hexacoordination about tin. Second, in every case but one ($(n\text{-}C_4H_9)_2SnPO_3H$) resonant γ-ray absorption at room temperature is seen, indicative of bridged, polymeric structures. Since no special precautions were taken to control carefully the absorber thickness, the R values in Table 4 are only of semi-quantitative significance for inter-sample comparison.

Previously reported (4) infrared, Raman, and Mössbauer data for $(CH_3)_2Sn(PO_2F_2)_2$, and Mössbauer data for $(CH_3)_2Sn(PO_2H_2)_2$ and $(CH_3)_2Sn(HPhPO_2)_2$ are fully consistent with *trans*-octahedral structures in which linear $(CH_3)_2Sn$ groups are bridged by bidentate PO_2XX' moieties, analogous to the structure of $(CH_3)_2Sn(SO_3F)_2$ (10–12).

Can. J. Chem. Downloaded from www.nrcresearchpress.com by 210.87.254.105 on 09/05/12
For personal use only.

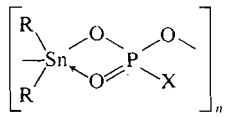

FIG. 2. Pentacoordinate structure for R_2SnPO_3X compounds.

We have now measured the Mössbauer spectrum of $(CH_3)_2Sn(PO_2H_2)_2$ at 4.2 °K in an applied longitudinal magnetic field of 50 kG. The quadrupole coupling constant e^2qQ is positive, confirming the prolate charge distribution expected for a *trans*-octahedral structure. Moreover, $\eta \simeq 0$, consistent with a (nearly) linear C—Sn—C arrangement and the absence of $\nu_s Sn—C_2$ in the infrared spectrum. The similar δ and ΔE_Q values observed for the diethyl- and dibutyltin(IV) hypophosphites leaves little doubt that these derivatives also have *trans*-octahedral structures.

On the other hand the infrared spectra of the $(CH_3)_2SnPO_3X$ compounds (X = F, H, OH) all show a band attributable to $\nu_s Sn—C_2$, and the Mössbauer quadrupole splittings are also somewhat lower than one might expect for oxy-acid derivatives having *trans*-octahedral symmetry. These results suggest that if the tin atom is hexacoordinate in these derivatives there is a fairly strong distortion of the C—Sn—C angle from 180°. Since such a structure also requires one trivalent oxygen per formula unit, it seemed wise to consider the possibility that the $(CH_3)_2SnPO_3X$ derivatives might have pentacoordinate structures (Fig. 2), similar to that proposed for poly(dibutyltin *n*-octylphosphonate) (15). If we assume a regular trigonal bipyramidal arrangement of the groups bonded to tin (distortions will be considered explicitly below), there are three possible configurations of the methyl groups: (*a*) apical–apical; (*b*) apical–equatorial; (*c*) equatorial–equatorial. On the basis of isovalent hybridization ideas one would expect structure (*c*) to be preferred and (*a*) to be highly unlikely. (It should be noted that in the $(CH_3)_2SnCl_3^-$ anion, both methyl groups are in the equatorial plane (16).) Since these various possibilities should lead to differences in η and the sign of e^2qQ, it was hoped that magnetically perturbed Mössbauer spectra together with the other data might allow a choice to be made.

In order to predict the sign of e^2qQ and magnitude of η expected for each of the possible structures we have used the point-charge formalism, in which the e.f.g. is taken to be a sum of contributions from the various ligands L:

$$eq = \sum_L [L](3\cos^2\theta_L - 1).$$

The [L] values are usually referred to as partial quadrupole splittings (p.q.s.). For each of the structures we consider here the e.f.g. tensor can be diagonalized for arbitrary [L] values (17). To observe general trends it is most convenient to calculate η and ΔE_Q as a function of the ratio [X]/[R], where X refers to the more electronegative substituent. It is well established for organotin(IV) compounds that the organic groups make the major contribution to the e.f.g. at tin, so that we need only consider the range $-1 \leqslant [X]/[R] \leqslant 1$. (In principle all p.q.s. values should have the same (negative) sign. However, a recently suggested empirical scale (18) arbitrarily sets $[Cl]^6 = 0$, where the superscript denotes the coordination number of tin in a given compound. On this scale, p.q.s. values for a number of oxy-acid anions have positive values, and for this reason we have included negative values of the ratio [X]/[R] in our calculations.)

In Fig. 3 are plotted calculated values of ΔE_Q (in units of $\frac{1}{2}eQ[R]$) and η for structures (*b*) and (*c*) as a function of [X]/[R]. Since eQ is negative for ^{119}Sn, we have assumed [R] is also negative in order to obtain the correct positive coupling constant for a *trans*-R_2SnX_4 species. For structure (*a*), $\eta = 0$ everywhere and ΔE_Q^{calcd} is a linear function of [X]/[R] ranging in value from $\frac{7}{2}eQ[R]$ to $+\frac{1}{2}eQ[R]$ as [X]/[R] increases from -1 to $+1$. For a *trans*-octahedral structure the corresponding ΔE_Q^{calcd} values range linearly from $+4eQ[R]$ to 0. Because the appearance of $\nu_s Sn—C_2$ in the i.r. spectra of these molecules argues against a linear C—Sn—C arrangement, we have also calculated the effect of distorting the latter two structures by lowering the C—Sn—C angle to 150°. In both cases there is only a small change in ΔE_Q^{calcd} over most of the range of [X]/[R], and for values of this ratio less than 2/3, η does not exceed about 0.4 in either case.

Since the e.f.g. tensor is traceless it is clear that η will be unity whenever one of the diagonal elements vanishes. For structures (*b*) and (*c*), V_{yy} is the first element to vanish as [X]/[R] increases from -1, and in both cases this occurs at [X]/[R] = 2/3. Values of the p.q.s. ratio greater than this are physically unreasonable

Can. J. Chem. Downloaded from www.nrcresearchpress.com by 210.87.254.105 on 09/05/12
For personal use only.

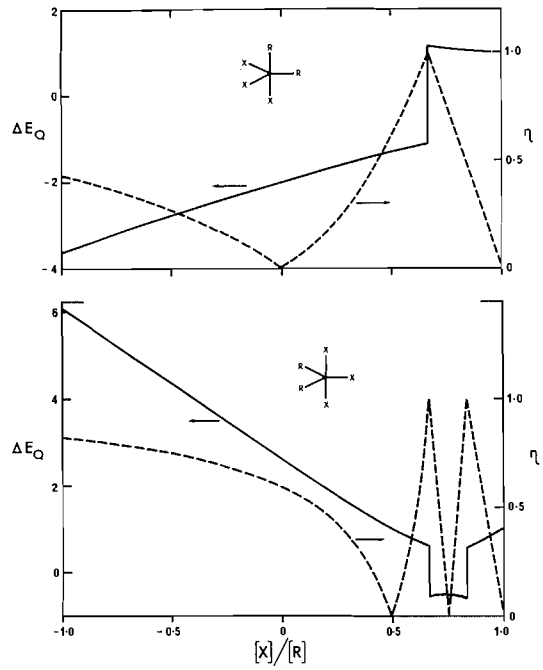

FIG. 3. Calculated values of ΔE_Q (in units of $\frac{1}{2}eQ[R]$) and η as a function of the partial quadrupole splitting ratio of the ligands for two different assumed R_2SnX_3 geometries.

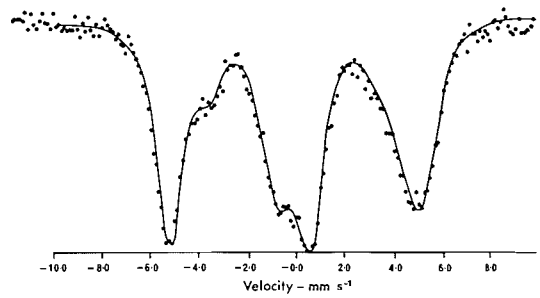

FIG. 4. Mössbauer spectrum of $(CH_3)_2SnPO_3F$ at 4.2 °K in an applied longitudinal magnetic field of 50 kG. The solid curve is the theoretically computed spectrum assuming $\Delta E_Q = +4.16$ mm s^{-1}, $\eta = 0.10$, $\Gamma = 1.20$ mm s^{-1}, $H'' = 50$ kG.

since they would imply that the σ-bonding characteristics of a methyl group and a PO_3X group are nearly the same; thus we need only be concerned with those portions of the curves lying to the left of this point. It should be noted that for structure (*b*) $\Delta E_Q^{\text{calcd}} < 0$ everywhere in this domain of [X]/[R] values while for structure (*c*) $\Delta E_Q^{\text{calcd}} > 0$.

The Mössbauer spectrum of $(CH_3)_2SnPO_3F$ at 4.2 °K in a longitudinal magnetic field of 50 kG is shown in Fig. 4, from which it is clear that e^2qQ is positive and η close to zero. This spectrum has been compared with theoretically computed spectra for a number of different η values, and best agreement is obtained for $\eta = 0.1$. The fit is nearly as good for $\eta = 0$, but noticeably poorer for $\eta = 0.2$, so that the value 0.1 is probably close to an upper limit for η.

While the positive sign of e^2qQ appears to rule out structure (*b*), it is worth considering the effects of distortions from regular trigonal bipyramidal bond angles. For all values of the R—Sn—R angle between the tetrahedral angle and its supplement (keeping all X—Sn—X angles fixed) the sign of e^2qQ remains negative for this structure. Distortions of the equatorial X—Sn—X bond angle between 109.5 and 180° (maintaining R—Sn—R at 90°) also fail to yield a positive e^2qQ for physically acceptable p.q.s. ratios. We, therefore, conclude that $(CH_3)_2SnPO_3F$ does not have structure (*b*).

It is somewhat more difficult to rule out structure (*c*) since the predicted sign of e^2qQ is correct. However, from Fig. 3 it will be seen that for $\eta < 0.1$ the only acceptable [X]/[R] values are those within the narrow range $0.46 < [X]/[R] < 0.52$. To compare the corresponding range of $\Delta E_Q^{\text{calcd}}$ values with the measured quadrupole splitting one would have to assign a p.q.s. value to the methyl group; unfortunately, there is no unique or even unambiguous way of doing this in the present case. What we *can* say is that the very small range of [X]/[R] values consistent with the measured η, and indeed the magnitude of [X]/[R] of about 0.5, make it appear exceedingly unlikely that $(CH_3)_2SnPO_3F$ has a regular structure of type (*c*).

It now remains to investigate the effects of distortions from strict trigonal bipyramidal bond angles for such a pentacoordinate structure. Throughout the region $-1 \leqslant [X]/[R] \leqslant 2/3$ the *z*-axis of the e.f.g. tensor is normal to both Sn—X bond axes (in the undistorted structure (*c*)), from which it follows that very large distortions of the X—Sn—X angles are required in order to cause an appreciable change in either η or $\Delta E_Q^{\text{calcd}}$. On the other hand, distortions of the R—Sn—R angle will have a much more

Can. J. Chem. Downloaded from www.nrcresearchpress.com by 210.87.254.105 on 09/05/12
For personal use only.

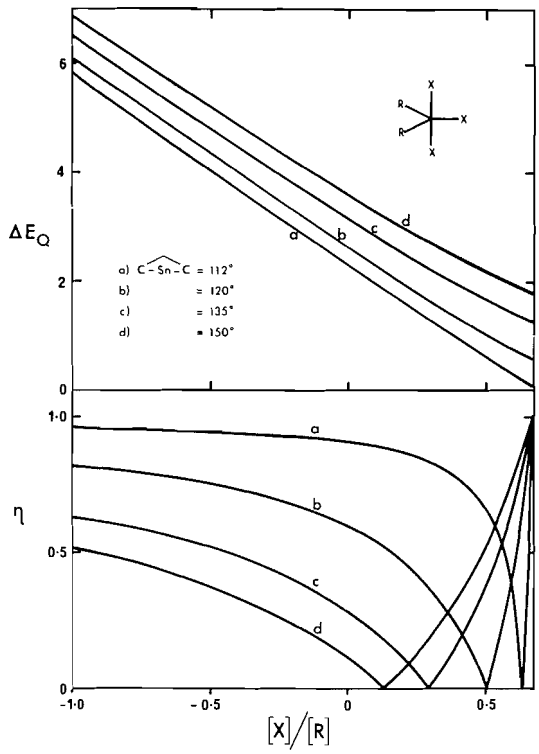

FIG. 5. Calculated values of ΔE_Q (in units of $\frac{1}{2}eQ[R]$) and η for a trigonal bipyramidal R_2SnX_3 compound with equatorial R groups as a function of the R—Sn—R angle. Other angles at tin are assumed to be undistorted.

pronounced influence since the R groups lie in the *yz* plane. We have, therefore, computed η and $\Delta E_Q^{\text{calcd}}$ for a number of R—Sn—R angles with the X—Sn—X angles undistorted. Some of the results are shown in Fig. 5. For an R—Sn—R angle of 109.5°, $V_{xx} = 0$, $V_{zz} = -V_{yy}$ and $\eta = 1$ independent of [X]/[R]; further closing of the angle leads to a negative sign for e^2qQ and results which are qualitatively similar to those for structure (*b*). For R—Sn—R angles greater than 120°, $\Delta E_Q^{\text{calcd}}$ increases monotonically with the bond angle for any value of the p.q.s. ratio $\leqslant 2/3$. At the same time the range of [X]/[R] consistent with $\eta \leqslant 0.1$ widens slightly and shifts towards smaller positive, and eventually negative, values. The net result of increasing the R—Sn—R angle is thus to make such a pentacoordinate structure somewhat more probable. It is appropriate to note, however, that on the p.q.s. scale of Clark *et al.* (18) the PO_3F^{2-} group would be expected (by comparison with data for other oxy-acid anions) to have a p.q.s. value such that the ratio $[PO_3F]/[CH_3]$ would be in the range 0.0 to −0.1. According to our calculations, consistency of this ratio with the observed η value would require a C—Sn—C angle of at least 150°.

We, therefore, appear to be left with three possible structures for $(CH_3)_2SnPO_3F$, none of which is inconsistent with the i.r. and Mössbauer data: distorted *trans*-octahedral, distorted trigonal bipyramidal with apical methyl groups, and trigonal bipyramidal with equatorial methyl groups and a C—Sn—C angle considerably larger than 120°. Of these, we consider the *trans*-octahedral structure to be the most likely, but there seems to be no way of making a definite choice from the available data.

Whatever the actual structure of $(CH_3)_2SnPO_3F$, it is not unreasonable to surmise that the other R_2SnPO_3X compounds reported here have similar structures. Thus in the methyltin derivatives both isomer shift and quadrupole splitting decrease as X is changed from F to H to OH, *i.e.*, as the strength of the parent acid decreases. Such a trend is not unexpected for essentially isostructural compounds (11, 19, 20) and the explanation parallels that given elsewhere (11).

The trends observed in isomer shifts and quadrupole splittings in the two series R_2SnPO_3H and $R_2Sn(PO_2H_2)_2$ (R = CH_3, C_2H_5, *n*-C_4H_9) also merit some comment. In each series δ increases from CH_3 to C_2H_5 and remains essentially constant for C_2H_5 and *n*-C_4H_9. Analogous trends have been observed (4) for dialkyltin(IV) difluorides, bis(difluorophosphates), bis(fluorosulfates), and bis(trifluoromethylsulfonates), as well as for some other isostructural pairs of CH_3 and C_2H_5 organotin compounds (21). In the absence of a significant structural change with change in R, these trends imply a greater electronegativity for CH_3 than for C_2H_5 or *n*-C_4H_9. This is consistent with the group electronegativities reported by Hinze (22) for CH_3 and C_2H_5, although we are not aware of a numerical value for *n*-C_4H_9. In terms of the bonding model we have proposed elsewhere (4, 11) for dialkyltin(IV) salts of oxyacids, the increase in δ from CH_3 to C_2H_5 and *n*-C_4H_9 for a given anion should be accompanied by an increase in ΔE_Q. While this is in fact the case for the $H_2PO_2^-$ salts, the opposite is observed for the HPO_3^{2-} derivatives. All four series of compounds (4)

Can. J. Chem. Downloaded from www.nrcresearchpress.com by 210.87.254.105 on 09/05/12
For personal use only.

Can. J. Chem. Downloaded from www.nrcresearchpress.com by 210.87.254.105 on 09/05/12
For personal use only.

R_2SnY_2 (R = CH_3, C_2H_5, n-C_3H_7, n-C_4H_9; Y = F, PO_2F_2, SO_3CF_3, SO_3F) show behavior similar to that in R_2SnPO_3H, but the explanation of these trends is not obvious. Conceivably, steric factors could be of importance.

In their Mössbauer spectra at liquid nitrogen temperature, none of the $(CH_3)_2SnPO_2X$ compounds (X = F, H, OH) shows any appreciable difference in width, intensity, or area of the two lines of the quadrupole doublet. However, at room temperature a pronounced integral asymmetry is observed for X = F and H, where the area ratios of high-energy to low-energy lines (A_h/A_l) are 0.74 and 0.83, respectively; there is also some indication of a slight asymmetry in the spectrum of $(CH_3)_2SnHPO_4$ (A_h/A_l = 0.93). This asymmetry is illustrated in Fig. 6 for $(CH_3)_2SnHPO_3$. Since for a given compound spectra at the two temperatures were always recorded on the identical absorber with identical orientation relative to the γ-ray beam, and since no asymmetry is observed at low temperature, these effects cannot be attributed to preferential orientation of the crystallites in the absorbers. The temperature dependence of the quadrupolar asymmetry in these compounds is characteristic of the Gol'danskii–Karyagin effect arising from an anisotropy of the lattice phonon modes, and we surmise this is the effect being observed. It is interesting that similar asymmetry is observed for $(CH_3)_2Sn(H_2PO_2)_2$ but not apparently for $(CH_3)_2Sn(PO_2F_2)_2$ (4) or $(CH_3)_2Sn(SO_3F)_2$ (11).

The remaining derivative, $[(CH_3)_2Sn]_3(PO_4)_2$ gives the lowest δ and ΔE_Q values of all the compounds reported here. Since there are only two phosphoryl groups per three tin atoms in a formula unit, one might expect to find two distinctly different environments for tin in this compound, *e.g.* one tetracoordinate and two pentacoordinate tin atoms. Although the line widths observed for this compound are somewhat broader than those found for the other derivatives they are not sufficiently broad to be interpreted in terms of two different coordination numbers for tin in the compound. In an external magnetic field of 50 kG the Mössbauer spectrum is essentially "first order"; *i.e.*, it does not appear to consist of two overlapping hyperfine-split patterns. Thus any difference in environments of the tin atoms in this compound is not detectable via Mössbauer spectroscopy. The quadrupole coupling constant e^2qQ for

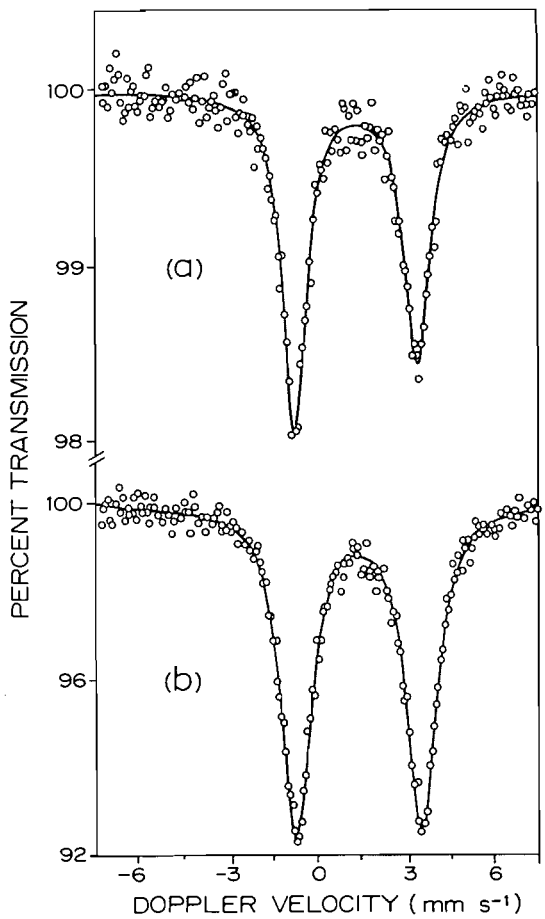

FIG. 6. Mössbauer spectra of $(CH_3)_2SnHPO_3$ at (*a*) room temperature, and (*b*) liquid nitrogen temperature.

$[(CH_3)_2Sn]_3(PO_4)_2$ is positive, as for the other dimethyltin derivatives studied here, but in this case η is large (η ≃ 0.8). This fact argues against a distorted *trans*-octahedral structure, and the ΔE_Q value is considerably larger than expected for a *cis*-octahedral compound. In view of the room-temperature Mössbauer resonance observed we are led to propose a bridged polymeric structure in which all the tin atoms are most probably pentacoordinate. For three five-coordinate tin atoms per formula unit, a total of fifteen bonds to tin are required. Six of these bonds are to CH_3 groups; the remaining nine must be supplied by the two PO_4^{3-} groups. Such a structure must, therefore, necessarily invoke at least one three-coordinate oxygen.

Financial support from the National Research Council of Canada and generous gifts of organotin chlorides from M & T Chemicals Inc., Rahway, New Jersey, are gratefully acknowledged.

1. D. SEYFERTH and F. G. A. STONE. J. Am. Chem. Soc. **79**, 515 (1959).
2. T. N. SRIVASTAVA and S. K. TANDON. Indian J. Appl. Chem. **26**, 171 (1963).
3. J. M. CHURCH. Chem. Abstr. **48**, 1420e (1954).
4. T. H. TAN, J. R. DALZIEL, P. A. YEATS, J. R. SAMS, R. C. THOMPSON, and F. AUBKE. Can. J. Chem. **50**, 1843 (1972).
5. W. P. NEUMANN. The organic chemistry of tin. (Engl. Transl.) John Wiley, New York, 1970.
6. R. C. POLLER. The chemistry of organotin compounds. Logos, London, 1970.
7. R. J. ANGELICI. Synthesis and technique in inorganic chemistry. W. B. Saunders, Toronto. 1969. p. 159.
8. P. A. YEATS, B. L. POH, B. F. E. FORD, J. R. SAMS, and F. AUBKE. J. Chem. Soc. A, 2188 (1970).
9. M. TSUBOI. J. Am. Chem. Soc. **79**, 1351 (1957).
10. P. A. YEATS, B. F. E. FORD, J. R. SAMS, and F. AUBKE. Chem. Commun. 791 (1969).
11. P. A. YEATS, J. R. SAMS, and F. AUBKE. Inorg. Chem. **11**, 2634 (1972).
12. F. A. ALLEN, J. LERBSCHER, and J. TROTTER. J. Chem. Soc. A, 2507 (1971).
13. E. O. SCHLEMPER and W. C. HAMILTON. Inorg. Chem. **5**, 995 (1966).
14. D. E. C. CORBRIDGE. *In* topics in phosphorus chemistry. Vol 6. *Edited by* M. Grayson and E. J. Griffith. Wiley, New York. 1969. p. 269.
15. R. E. RIDENOUR and E. E. FLAGG. J. Organomet. Chem. **16**, 393 (1969).
16. F. W. B. EINSTEIN and B. R. PENFOLD. J. Chem. Soc. A, 3019 (1968).
17. J. R. SAMS. *In* MTP international review of science. Phys. Chem. Ser. 1. Vol. 4. *Edited by* A. D. Buckingham. 1972. Chapt. 3.
18. M. G. CLARK, A. G. MADDOCK, and R. H. PLATT. J. Chem. Soc. A, 281 (1972).
19. C. PODER and J. R. SAMS. J. Organomet. Chem. **19**, 67 (1969).
20. B. F. E. FORD and J. R. SAMS. J. Organomet. Chem. **31**, 47 (1971).
21. P. J. SMITH. Organomet. Chem. Rev. A, **5**, 373 (1970).
22. J. HINZE. Fortschr. Chem. **9**, 448 (1968).

Can. J. Chem. Downloaded from www.nrcresearchpress.com by 210.87.254.105 on 09/05/12
For personal use only.

The Reduction of Acetamidopentaamminecobalt(III) by Chromium(II)

ROBERT J. BALAHURA AND LYNDA HUTLEY
Department of Chemistry, University of Guelph, Guelph, Ontario

Received May 25, 1973

The reduction of nitrogen bonded acetamidopentaamminecobalt(III) by chromium(II) has been studied. The acetamido complex is a reasonably strong acid attributed to the equilibrium

$$(NH_3)_5CoNH_2CO(CH_3)^{3+} \rightleftharpoons (NH_3)_5CoNHCO(CH_3)^{2+} + H^+$$

which has a pK_a of 2.16 ± 0.08 at 25.0° and μ = 0.01 *M*. The reduction process has the rate law

$$-\mathrm{d}\ \ln [(NH_3)_5CoNH_2CO(CH_3)]/\mathrm{d}t = k\ [Cr^{2+}]/[H^+]$$

For reduction of the conjugate base $k = k_{NH}K_a$ and $k_{NH} = 5.23 \times 10^{-2}\ M^{-1}\ s^{-1}$ at 25.1°, with ΔH = 14.5 ± 2 kcal mol^{-1} and ΔS = 16 ± 6 e.u. respectively. The rate law is indicative of an inner-sphere process. The orientation of the ligand is thought to be important for the reduction of the acetamido and the related carboxylato complexes, and this is discussed.

On a étudié la réduction par le chrome(II) du complexe acétamidopentaamine cobalt(III) lié à l'azote. Le complexe acétamido est un acide relativement fort obéissant à l'équilibre suivant:

$$(NH_3)_5CoNH_2CO(CH_3)^{3+} \rightleftharpoons (NH_3)_5CoNHCO(CH_3)^{2+} + H^+$$

et dont le pK_a est égal à 2.16 ± 0.08 à 25 °C (μ = 0.01 *M*). Le processus de réduction obéit à l'expression de vitesse suivante:

$$-\mathrm{d}\ \ln [(NH_3)_5CoNH_2CO(CH_3)]/\mathrm{d}t = k\ [Cr^{2+}]/[H^+]$$

Pour la réduction de la base conjuguée, la constante k est égale à $k_{NH}K_a$ ou $k_{NH} = 5.23 \times 10^{-2}\ M^{-1}\ s^{-1}$ à 25.1°; de même les valeurs de ΔH et de ΔS sont respectivement de 14.5 ± 2 kcal mol^{-1} et de 16 ± 6 u.e. L'expression de vitesse est caractéristique d'un processus du type sphère interne. L'orientation du coordinat est, semble-t-il, importante pour ce qui est de la réduction du groupe acétamido et des complexes carboxylate semblables; cette dernière relation est d'ailleurs discutée.

[Traduit par le journal]

Can. J. Chem. **51**, 3712 (1973)

The reduction of formatopentaamminecobalt(III) by chromium(II) is approximately twenty times faster than the reduction of the corresponding acetato complex (1). The small variation in rates for the reduction of $(NH_3)_5CoO_2C{-}R^{2+}$ for R = CH_3, C_6H_5, $ClCH_2$, Cl_2CH, and CF_3 can satisfactorily be explained by considering changes in steric requirements due to the R groups. Inductive effects appear to have a negligible effect on the rate of reduction. The rather large rate difference between the formato and the remaining carboxylato complexes may be a result of a different orientation of the bound formate with respect to the other carboxylates. The two possible configurations are shown below.

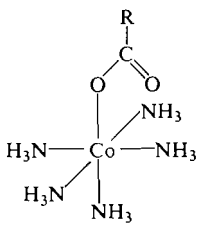

Ia

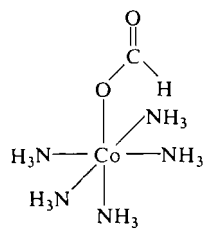

IIa

If configuration **I***a* is adopted by all the carboxylates except formate then regardless of whether the reductant attacks at the carbonyl or bound oxygen only small variations in rate due to steric effects would be expected. Based on models, one would predict that configuration **II***a* is only possible for the formato complex and would result in complete exposure of the carbonyl oxygen to attack by the reductant. Thus a much faster reduction rate might be anticipated.

The same argument can be applied to the reduction of the analogous formamido and acetamidopentaamminecobalt(III) complexes given below.

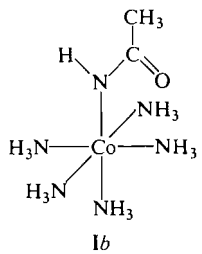

Ib

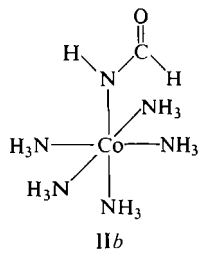

IIb

The chromium(II) reduction of formamido-

Can. J. Chem. Downloaded from www.nrcresearchpress.com by 210.87.254.6 on 09/05/12
For personal use only.

Can. J. Chem. Downloaded from www.nrcresearchpress.com by 210.87.254.6 on 09/05/12
For personal use only.

pentaamminecobalt(III) proceeds by attack of the reductant at the carbonyl oxygen producing $(OH_2)_5CrOC(H)NH_2^{3+}$ as product (2). It was of interest to study the reduction of the acetamidopentaamminecobalt(III) complex, **I***b*, in order to test the previous arguments.

Experimental Section

Reagents

Standard solutions of perchloric acid, lithium perchlorate, and chromous perchlorate were prepared as described previously (2).

All solutions for kinetic runs were handled using standard syringe techniques under an argon atmosphere.

Preparation of $[Co(NH_3)_5NHCO(CH_3)](ClO_4)_2$

Twenty grams of aquopentaamminecobalt(III) perchlorate were dissolved in approximately 100 ml of trimethylphosphate (or triethylphosphate) containing molecular sieves. To this solution 40 g of acetamide were added and the mixture heated on a steam bath for 4 h. After cooling. the mixture was filtered and the filtrate added to a solution of 500 ml of *s*-butyl alcohol and 500 ml diethyl ether in order to precipitate the complex. The complex so obtained was recrystallized from warm water and submitted to cation exchange chromatography on Rexyn 102(H) in the sodium ion form. The required complex was moved down the column with 0.3 *M* NaCl leaving behind higher charged species. The former was eluted from the column with 0.6 *M* NaCl and solid $NaClO_4$ added to precipitate the complex. This complex was recrystallized once from a dilute solution of $NaClO_4$.

Anal. Calcd. for $[(NH_3)_5CoNHCO(CH_3)](ClO_4)_2$: C, 6.00; H, 4.74; N, 21.0. Found: C, 6.08; H, 4.75; N, 20.9.

The visible absorption spectrum in water shows maxima at 251 nm (ε, 2.4 × 10^3), 351 nm (ε, 83.5), and 486 nm (ε, 71.1). In 1.0 *M* perchloric acid the protonated species $(NH_3)_5CoNH_2CO(CH_3)^{3+}$ predominates and has maxima at 341 nm (ε, 57.5) and 477 nm (ε, 61.5), with no maximum in the ultraviolet.

Solid $[(NH_3)_5CoNH_2CO(CH_3)](ClO_4)_3$ can be obtained by dissolving the basic form in water and adding concentrated perchloric acid until precipitation begins. This solid should not be washed with EtOH or ether since this causes removal of a proton and yields a mixture of the acidic and basic forms. Titration of a 5.8 × 10^{-3} *M* solution of $[(NH_3)_5CoNH_2CO(CH_3)](ClO_4)_3$ with 0.1 *M* KOH gave an equivalent weight of 496 as compared to the theroretical value of 502.

Determination of Ionization Constants

The equilibrium constant for the reaction

$$(NH_3)_5CoNH_2CO(CH_3)^{3+} \rightleftharpoons (NH_3)_5CoNHCO(CH_3)^{2+} + H^+$$

was determined potentiometrically by titrating 0.01 *M* solutions of the acid form of the complex with 0.1 *M* KOH at 25.0, 35.0, and 45.0 °C. An apparent pK_a was also evaluated spectrophotometrically at 265 nm at a constant ionic strength of 1.0 *M* using $LiClO_4$. The pK_a values were evaluated using the procedures outlined by Albert and Serjeant (3).

Kinetic Measurements

All reactions were carried out in cylindrical cells sealed with rubber serum caps in the absence of oxygen.

The reactions were run under pseudo first order conditions (reductant in a 15–20 fold excess over oxidant). The observed rate constant was determined from the slope of a plot of log $(A_t - A_\infty)$ *vs.* time, where A_t and A_∞ are the absorbances at time t and after the reaction is complete. The rate constant was also determined using the Guggenheim method (4). The latter method was found to be, in general, more reliable because the long reaction times made A_∞ difficult to determine due to air oxidation.

All reactions were followed by observing the decrease in absorbance of the cobalt(III) complex at 485 nm. Absorbance *vs.* time data was acquired using a Beckman Acta C111 Spectrophotometer. The temperature of the solution in the spectrophotometer cell was controlled by pumping water from a Colora constant temperature bath through special blocks which housed the cells. The temperature of the bath was regulated with a Thermistemp controller, with the thermistor probe inserted in the block which housed the cell.

Product analysis was carried out by ion exchange on Dowex 50W-X8 cation exchange resin at 0 °C using standard methods. The products were characterized spectrophotometrically. The extinction coefficients were determined using the chromium concentration which was determined spectrophotometrically as chromate. The stoichiometry of the reaction was shown to be 1:1 by collecting total chromium for a reaction where Co(III) and Cr(II) were the same.

Physical Measurements

p*H* measurements were made with a Radiometer model 26, p*H* meter.

Proton magnetic resonance spectra were obtained with a Varian A60 spectrometer.

Infrared spectra were recorded on a Beckman IR 12 Spectrophotometer.

Results

The analytical results are consistent with formulation of the complex as $(NH_3)_5CoNHC(=O^{2+})CH_3$.

It is important to establish the bonding atom unambiguously since there is a possibility of acetamide being bonded via the carbonyl oxygen as well as via the nitrogen of the NH_2 group.

Qualitatively, the complex is orange in color as expected for nitrogen coordination, as opposed to pink for oxygen coordination. The visible spectrum is also consistent with nitrogen bonding and is almost identical to that found for $(NH_3)_5CoNHC(=O^{2+})H$ (2).

The proton magnetic resonance spectrum shows the expected resonances due to the coordinated ligand $-CH_3$ at 8.03 τ and H—*H* at 6.27 τ. Also, the resonance due to the four *cis*-NH_3

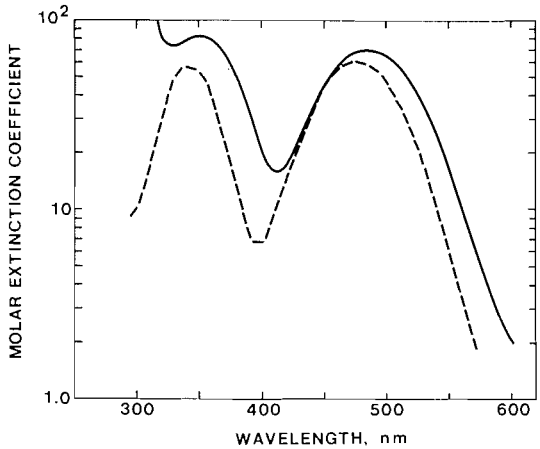

FIG. 1. Visible spectra of $[(NH_3)_5CoNHC(O)CH_3](ClO_4)_2$ in H_2O (—), and 1.0 *M* $HClO_4$ (---).

and the *trans*-NH_3 protons occurs at 6.77 τ. The latter observation is also indicative of nitrogen bonding as discussed previously (2).

The fact that the complex undergoes an acid–base reaction in the p*H* region 1–6 is the best evidence that the nitrogen is coordinated to cobalt. Since acetamide has a pK_a of approximately 14, a large enhancement of acidity would only be expected for protons which are bonded to the atom adjacent to $(NH_3)_5Co^{3+}$.

The large differences in the u.v. and visible spectra of the acetamido complex in H_2O and 1.0 *M* $HClO_4$ are then especially indicative of nitrogen coordination. The differences in the spectra are shown in Fig. 1. These changes are identical to those observed for the formamido (2) and sulfamato (5) complexes. The difference in the spectra in acidic and neutral solution can be understood in terms of the following acid–base equilibrium.

$$(NH_3)_5CoNH_2C(=O)CH_3^{3+} \underset{}{\overset{K_a}{\rightleftharpoons}} (NH_3)_5CoNHC(=O)CH_3^{2+} + H^+$$

The equilibrium constant for the above reaction was determined potentiometrically by titration of the acidic form with 0.1 *M* KOH. The pK_a's at 25.0, 35.0, and 45.0 °C are 2.16 ± 0.08, 2.04 ± 0.10, and 1.95 ± 0.10 respectively. These values give $\Delta H^0 = 4.8 \pm 3$ kcal mol^{-1} and $\Delta S^0 = 6 \pm 8$ cal mol^{-1} deg^{-1}.[1] At 25.0 °C the apparent pK_a determined spectrophotometrically at $\mu = 1.0$ ($LiClO_4$) is 2.94 ± 0.20. The increase in pK_a upon increase in the ionic strength results from stabilization of the higher charged species in the higher ionic strength medium. These values are consistent with those obtained previously for the formamide complex: 1.63 at low ionic strength and 2.16 at $\mu = 1.0$ $(LiClO)_4$. We have obtained a pK_a of 1.59 ± 0.08 for the formamide complex by potentiometric titration at 0.02 *M* in good agreement with the previously quoted value which was obtained spectrally.

A consideration of simple inductive effects would predict that the acetamide complex should be a weaker acid than the formamide complex due to the electron releasing effect of the methyl group in agreement with the experimentally determined values.

The infrared spectra of the acidic and basic forms of the complex are indicative of a delocalized system as shown.

$$(NH_3)_5CoN(H)=C(-O)CH_3^{2+}$$

The carbonyl stretching frequencies of the acid and base forms of the complex appear at 1695 cm^{-1} and 1560 cm^{-1} as opposed to 1714 cm^{-1} for the free ligand (6). One would expect the ν(C=O) for the acidic form to be very near the free ligand value since delocalization is not possible for this complex. The crystal structure of the basic form also indicates that the O=C=N system is delocalized (7).

The reduction of the acetamido complex was found to obey the following rate law:

$$[1] \quad \frac{-d \ln [(NH_3)_5CoNH_2CO(CH_3)]}{dt} = \frac{k[Cr^{2+}]}{[H^+]} = k_{obs}[Cr^{2+}]$$

[1]The errors assigned to the pK_a's were determined by taking the scatter from the mean of a set of results as defined in ref. 3. The rather large errors in ΔH^0 and ΔS^0 result from the overlap between data obtained at successive temperatures. The reproducibility of the results from determination to determination is ±0.02 pK_a unit which suggests a smaller deviation than is the case.

Can. J. Chem. Downloaded from www.nrcresearchpress.com by 210.87.254.6 on 09/05/12
For personal use only.

TABLE 1. Kinetic data for the reduction of acetamidopentaamminecobalt(III) by Cr(II)*†

T (°C)	[Co(III)] × 10^3 (M)	[Cr(II)] × 10^2 (M)	[H^+] (M)	k_{obs} × 10^4‡ (M^{-1} s^{-1})
25.1	6.05	12.8	0.100	5.89
	5.76	12.8	0.158	3.63
	5.52	12.8	0.208	2.76
	5.84	12.8	0.208	2.78
35.1	1.94	9.28	0.102	19.0
	5.22	9.82	0.121	16.6
	5.13	9.82	0.181	10.9
	5.10	9.82	0.181	10.7
	5.07	9.28	0.242	8.84
	4.73	9.28	0.303	7.49
	5.22	9.82	0.303	7.20
	5.16	9.82	0.422	6.10
45.0	5.95	6.18	0.100	50.0
	6.07	6.18	0.100	49.7
	6.01	6.18	0.100	49.8
	6.10	6.18	0.100	48.4
	5.98	6.18	0.100	50.4
	1.82	9.28	0.121	42.0
	3.10	9.28	0.181	28.9
	5.07	9.28	0.455	15.5

*μ = 1.0 ($LiClO_4$).
†Concentrations are initial values in molar units.
‡It is estimated that the individual rate constants are accurate to within 4%.

The data are given in Table 1. Figure 2 shows a plot of k_{obs} *vs.* $[H^+]^{-1}$ which is linear as predicted by the rate law. This rate law is consistent with the mechanism

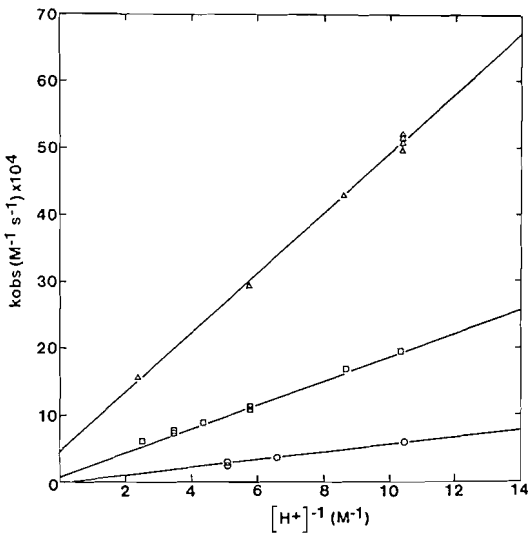

FIG. 2. Dependence of the reduction rate of acetamidopentaamminecobalt(III) by chromium(II) on [H^+], μ = 1.0 M ($LiClO_4$), ○, 25.1; □, 35.1; △, 45.0 °C.

$$(NH_3)_5CoNH_2CO(CH_3)^{3+} \underset{}{\overset{K_a}{\rightleftharpoons}} (NH_3)_5CoNHCO(CH_3)^{2+} + H^+$$

$$(NH_3)_5CoNHCO(CH_3)^{2+} + Cr^{2+} \xrightarrow{k_{NH}} \text{Products}$$

This mechanism gives the rate law

$$[2] \quad \frac{-d \ln [(NH_3)_5CoNH_2CO(CH_3)]}{dt} = \frac{k_{NH}K_a}{K_a + [H^+]} [Cr^{2+}]$$

Since $[H^+] \gg K_a$ for all the runs, $k = K_a k_{NH}$. The specific rate constant k_{NH} can be determined from the slope of the lines in Fig. 2 divided by the K_a at the appropriate temperature. Table 2 gives a summary of the kinetic parameters.

The intercept corresponding to the plots in Fig. 2 could represent the reduction of $(NH_3)_5CoNH_2CO(CH_3)^{3+}$. The values of the intercepts obtained from the least-squares treatment gave -1.4×10^{-5}, $+1.4 \times 10^{-4}$, and 5.3×10^{-4} M^{-1} s^{-1} at 25, 35, and 45 °C respectively. These values are approximately 500 times smaller than those for k_{NH} and could not be reliably estab-

Can. J. Chem. Downloaded from www.nrcresearchpress.com by 210.87.254.6 on 09/05/12
For personal use only.

TABLE 2. Summary of equilibrium and kinetic parameters for the Cr^{2+} reduction of acetamidopentaamminecobalt(III)*

T (°C)	Slope (s^{-1})†	K_a (M)	$k_{NH} = \frac{\text{slope}}{K_a}$ ($M^{-1}s^{-1}$)	$\Delta H^{\ddagger}$ (kcal mol^{-1})	$\Delta S^{\ddagger}$ (e.u.)
25.1	6.01×10^{-5}	1.15×10^{-3}	5.23×10^{-2}	14.5 ± 2	−16 ± 6
35.1	17.8×10^{-5}	1.51×10^{-3}	11.8×10^{-2}		
45.0	44.3×10^{-5}	1.86×10^{-3}	23.8×10^{-2}		

*μ = 1.0 ($LiClO_4$).
†Obtained by a least squares fit to the equation $k_{obs} = C$ + slope $[H^+]^{-1}$.

lished due to the difficulty in obtaining accurate data at high hydrogen ion concentrations.

The nature of the "products" in the proposed mechanism were investigated by cation exchange chromatography of reaction mixtures. In all cases only $Cr(OH_2)_6^{3+}$ was isolated when an oxygen bonded acetamide complex of $(OH_2)_5Cr^{3+}$ might be expected. However, due to the long times (10–30 h) involved for the reactions this initial product would probably be hydrolyzed to $Cr(OH_2)_6^{3+}$. In one analysis with [Co(III)] = 0.01, [Cr(II)] = 0.01 and $[H^+]$ = 0.07 the extinction coefficients of the Cr(III) product were higher than those of $Cr(OH_2)_6^{3+}$ and indicate that at least some acetamide complex remains after the long work up time. It was not possible to isolate this complex by further chromatography.

Discussion

The product analysis indicates that the final chromium(III) complex formed in the reaction is the hexaaquo ion. This would imply that an outer-sphere mechanism is the preferred mode of reaction. However, an outer-sphere reaction would not be expected to be sensitive to hydrogen ion concentration and the strong inverse hydrogen ion dependence indicated in the rate law favors the inner-sphere path. Following the arguments put forth regarding the reduction of the formamido complex the reaction of the acetamido complex probably also proceeds via attack at the carbonyl oxygen with initial transfer of the ligand as shown below:

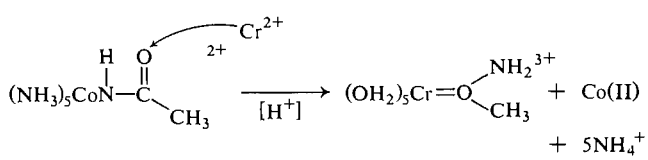

The delocalized O=C=N bond system which is possible only in the basic form of the complex seems to provide the most favorable electron transfer path.

A comparison of the rate of reduction of the acetamido and formamido complexes at 25.0 °C shows that the latter is reduced about 34 times faster than the former. This could be due to the steric requirements of the acetamido complex. In this case, the methyl group would be forced up and away from the *cis*-ammines in the cobalt complex while the carbonyl oxygen is pointing down between two of the *cis*-ammines, **I***b*. This arrangement would sterically hinder attack at the carbonyl oxygen by the reductant. In the formamido complex the smaller hydrogen atom can point down between the two *cis*-ammines thus leaving the carbonyl oxygen pointing away from the plane of the *cis*-ammines and completely exposed to attack by the reductant, **II***b*. The same arguments can be applied to the reduction of the formato and acetato complexes. The similarity in the rate differences between the formato–acetato and formamido–acetamido systems supports the above arguments.

The crystal structures of the acetato (8) and acetamido (7) complexes indicate that, at least in the solid state, configuration **I** is adopted. More pertinent to solution studies is the fact that the formato complex has been shown to exist in configuration **II** by the observation of a nuclear Overhauser effect (9).

The authors wish to thank the National Research Council of Canada for an operating grant to R.J.B. (A6642) and also the referees for helpful criticism.

Can. J. Chem. Downloaded from www.nrcresearchpress.com by 210.87.254.6 on 09/05/12
For personal use only.

1. M. BARRETT, J. SWINEHART, and H. TAUBE. Inorg. Chem. **10**, 1983 (1971).
2. R. J. BALAHURA and R. B. JORDAN. J. Am. Chem. Soc. **92**, 1533 (1970).
3. A. ALBERT and E. SERJEANT. The determination of ionization constants. Chapman and Hall Ltd., London, England. 1971. pp. 9–22.
4. A. A. FROST and R. G. PEARSON. Kinetics and mechanism. 2nd ed. John Wiley and Sons, New York, N.Y. 1961. p. 49.
5. L. L. PO and R. B. JORDAN. Inorg. Chem. **7**, 526 (1968).
6. L. J. BELLAMY. *In* Advances in infrared group frequencies. Methuen and Co., Great Britain. 1968. p. 155.
7. M. L. SCHNEIDER, G. FERGUSON, and R. J. BALAHURA. Can. J. Chem. **51**, 2180 (1973).
8. E. B. FLEISCHER and R. FROST. J. Am. Chem. Soc. **87**, 3998 (1965).
9. R. J. BALAHURA and R. B. JORDAN. Inorg. Chem. **12**, 1438 (1973).

Can. J. Chem. Downloaded from www.nrcresearchpress.com by 210.87.254.6 on 09/05/12
For personal use only.

Kinetics of the Gas Phase Reactions of (+)-*trans*-2,3-Divinyloxirane

ROBERT J. CRAWFORD, VESNA VUKOV, AND HIROKAZU TOKUNAGA
Department of Chemistry, University of Alberta, Edmonton, Alberta T6G 2G2

Received July 20, 1973

The racemization of (+)-2,3-divinyloxirane is facile at 150°, $\log (k_1/s^{-1}) = (11.3 \pm 0.5) - (30.1 \pm 0.4)/\theta$ where $\theta = 2.303RT$ in kcal mol^{-1}. A slower but competitive rearrangement yields racemic 2-vinyl-2,3-dihydrofuran. The mechanisms of these reactions are discussed in terms of electrocyclic processes.

La racémisation du (+) divinyl-2,3 oxiranne est facile à 150°, $\log (k_1/s^{-1}) = (11.3 \pm 0.5) - (30.1 \pm 0.4)/\theta$ où $\theta = 2.303RT$ exprimé en kcal/mol. Un réarrangement beaucoup plus lent mais compétitif conduit au vinyl-2 dihydro-2,3 furanne racémique. Les mécanismes de ces réactions sont discutés en termes de processus électrocycliques. [Traduit par le journal]

Can. J. Chem. **51**, 3718 (1973)

Introduction

Thermally induced isomerizations of strained cyclic systems offer an excellent means of studying bond cleavage processes, thus cyclopropanes have been extensively studied (1). Oxiranes provide a similar vehicle with which to study both carbon–carbon and carbon–oxygen cleavage. Although such studies have been plagued by surface catalysis, recently there have been reported several studies which have minimized this drawback (2). The racemization of oxiranes offers a unique probe in examining the reaction in greater detail since it provides the most sensitive method of detecting the reversible electrocyclic process of carbonyl ylide formation (eq. 1) (3). We have previously examined, in

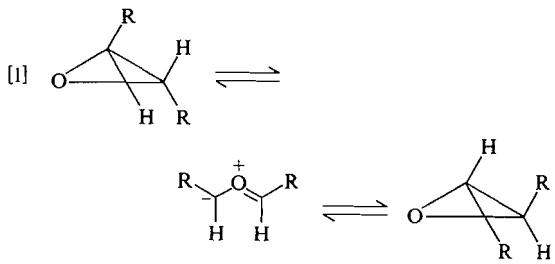

solution, the racemization and the *cis–trans* isomerization of 2,3-diaryloxiranes (3). The oxirane **1***a* racemizes, at 207°, 220 times more rapidly than it undergoes *trans* to *cis* isomerization. This observation was explained in terms of the carbonyl ylide intermediate for the racemization process. However it is not clear as to how the geometrical isomerization occurred. One possibility involves the intervention of a zwitterion species, *e.g.* **3**, produced by a carbon–oxygen heterolytic cleavage of **1***a*. Analogous intermediates have been implicated by Yankee and Cram (4) for the reactions of substituted cyclopropanes in solution.

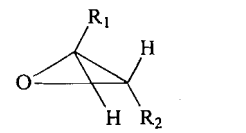

1

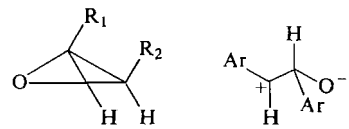

2 **3**

a R_1 = phenyl; R_2 = *p*-tolyl
b $R_1 = R_2$ = vinyl

In order to minimize the complication of zwitterion formation, we have chosen an oxirane system that is readily isomerized in the gas phase. Both *cis*- and *trans*-2,3-divinyloxirane (**1***b* and **2***b*) have been synthesized and their conversions to vinyldihydrofuran (**4**) and 4,5-dihydrooxepin (**5**) have been observed (5, 6).

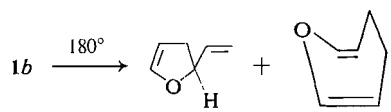

4 **5**

Can. J. Chem. Downloaded from www.nrcresearchpress.com by 210.87.254.5 on 09/05/12
For personal use only.

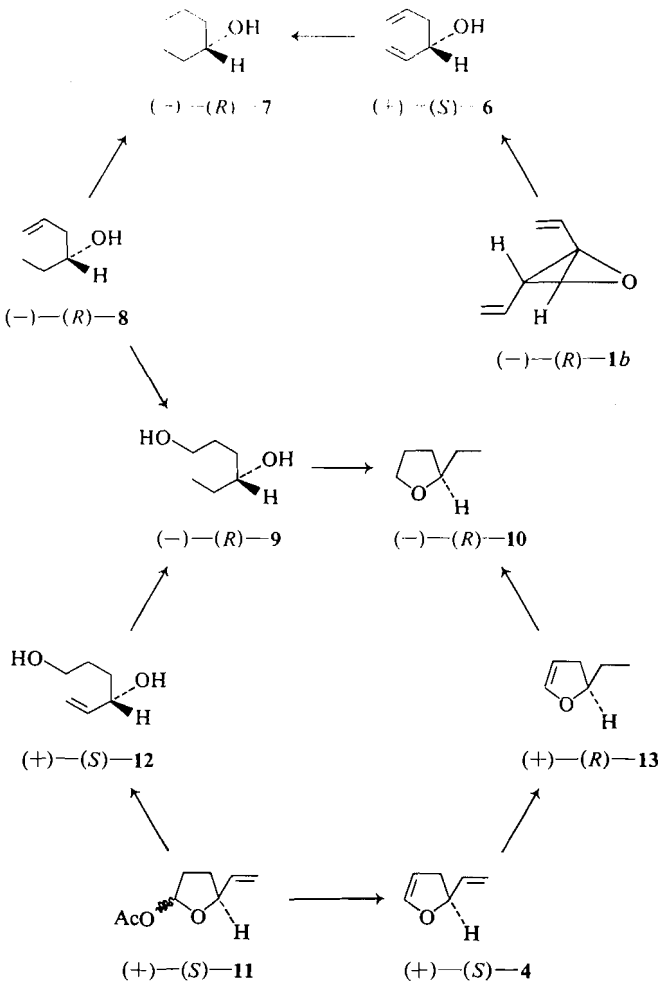

SCHEME 1

Results

(a) Synthesis and Stereochemistry

Chiral **1***b* was prepared in two ways. When samples prepared by the partial asymmetric destruction of **1***b* using di-3-pinanylborane (7) were studied, a significant infinity rotation was observed. Subsequently we prepared and resolved, via the brucine salt of the phthalate half-ester, samples of *threo*-4-chloro-1,5-hexadien-3-ol. The infinity rotations observed in the racemization studies of the oxirane prepared in this latter manner were essentially equal to zero. The absolute configuration and optical purity of **1***b* has been correlated with **4** and with (+)-3-hexanol (8) (Scheme 1). The rotational data for each of the compounds used are listed in Table 1.

(b) Kinetics of the Conversion of 1b to 4 and 5

Vogel and Gunther (5) have referred, in a footnote, to an earlier study carried out in Cologne and report $\Delta H^{\ddagger} = 36.0$ kcal mol^{-1} and $\Delta S^{\ddagger} = -0.4$ e.u. The product proportions (**4** and **5**) were said to be "practically independent of temperature", and thus it was concluded that **4** and **5** likely arise from a common intermediate. It was necessary for our purposes to define more exactly the kinetics and any temperature dependence of the product ratio. Table 2 gives the rate data and the product proportions observed from samples of **1***b* at 700 Torr. The samples were analyzed by gas chromatographic (g.c.) techniques using 1,2-dimethoxyethane as an internal standard and a Hewlett Packard

Can. J. Chem. Downloaded from www.nrcresearchpress.com by 210.87.254.5 on 09/05/12
For personal use only.

TABLE 1. Optical purity and absolute configuration of compounds in Scheme 1[a]

Compound	Concentration (g/100 ml)	α_{obs} (temperature, °)	Optical purity (%)	Configuration	Maximum rotation
1*b*	4.41	−0.374 (22)	81.3	*R*	−10.42
1*b**	4.41	−3.852 (22)	81.3	*R*	−107.4
6	7.04	+0.956 (20)	44.5	*S*	+30.5
7	Neat	−2.593 (20)	44.5	*R*	−5.83[b]
7	5.26	−0.175 (20)	44.5	*R*	−7.46
8	Neat	−0.057 (22)	8.57	*R*	−0.665
9	9.95	−0.111 (22)	8.57	*R*	−13.01
10	12.2	−0.099 (22)	8.57	*R*	−9.46
11	2.00	+0.089 (25)	12.9	*S*	+34.5
12*	2.12	+0.105 (25)	5.69	*S*	+87.0
13	1.92	+0.106 (25)	12.9	*R*	+43.0
4	2.38	+0.096 (25)	12.9	*S*	+31.3
4*	2.38	+0.269 (25)	12.9	*S*	+87.6

[a]Rotations in 2-propanol; $l = 1.00$ dm; $\lambda = 589$ nm, asterisk indicates $\lambda = 365$ nm.
[b]$[\alpha]_D$ −7.13 using density of 0.819 g/ml^{-1}, see ref. 8.

TABLE 2. Rate constants and product composition for the reactions of **1***b*

Temperature (±0.04°)	$10^6(k_2+k_3)$ (s^{-1})	% **4**	% **5**
160.08	5.48±0.09	73.4±0.1[a]	26.6±0.1
179.97	34.2 ±0.3	71.1±0.2	28.9±0.2
190.30	88.0 ±0.8	70.4±0.2	29.6±0.2
200.05	194±2	69.8±0.2	30.2±0.2
220.02	—	68.4±0.2	31.6±0.2

[a]The error quoted is the standard deviation of five analyses.

TABLE 3. Activation parameters for the reactions at 150° of **1***b* and (+)-(*S*)-**1***b* as in Scheme 2

	log *A*	E_a (kcal mol^{-1})	$\Delta H^{\ddagger}$ (kcal mol^{-1})	$\Delta S^{\ddagger}$ (cal deg^{-1} mol^{-1})
k_1	11.34	30.8±0.5	29.9±0.5	−9±1
k_2	12.74	36.0±0.4	35.1±0.4	−3±1
k_3	13.17	37.7±0.4	36.8±0.4	−1±1

3370A electronic integrator. A typical rate study is given in the Experimental section. Partitioning the data into separate rate constants gives the activation parameters indicated in Table 3. The rate constants correspond to those indicated in Scheme 2.

(c) Racemization of 1b

Samples of **1***b* were degassed in Pyrex break-seals and the amount was adjusted to give 1 atm at 150°. The samples were heated for the appropriate length of time in a well thermostated oil bath. After quenching the reaction in an ice-water bath the break-seals were attached to the vacuum line, opened, and the contents transferred to a tared 1-ml volumetric flask. The contents of the flask were allowed to come to room temperature and the flask was removed from the vacuum line and weighed. In each case the vapor transfer was quantitative. 2-Propanol was then added to a volume of 1 ml and the weight of the solution measured accurately. The concentration of **1***b* in 2-propanol was calculated on a percentage weight basis to avoid volumetric errors. The rotations of the solutions, at 25°, were then measured at four wavelengths and the appropriate

Can. J. Chem. Downloaded from www.nrcresearchpress.com by 210.87.254.5 on 09/05/12
For personal use only.

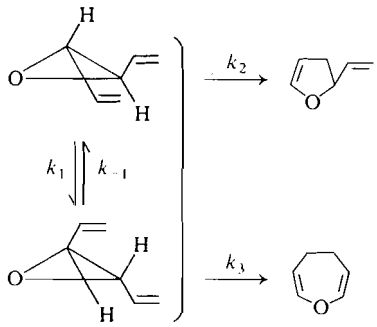

SCHEME 2

cell corrections were made. A typical run is given in the Experimental section. Using data obtained at 365 nm, rate constants could be duplicated to within $\pm 1\%$. The rate data for the racemization is listed in Table 4. The observed rate of loss of optical activity is given by k_α and the value for k_1 was obtained from the relationship $2k_1 = k_\alpha - (k_2 + k_3)$. The values of k_2 and k_3 were obtained by extrapolation from the rates at higher temperatures. The activation parameters for the rate k_1 are listed in Table 3 along with those for the other processes measured.

(d) Stereochemistry of the Formation of **4**

The formation of **4** may occur via a sigmatropic $\sigma^2a + \pi^2s$ process (9) in which case (−)-(*R*)-**1***b* would produce (−)-(*R*)-**4** by inversion of the migrating center. Upon inspection of molecular models it would seem that a $\sigma^2s + \pi^2a$ process is not a probable pathway. It is possible that **4** is produced from **1***b* via a carbonyl ylide, in which case the **4** produced directly from chiral **1***b* would be racemic. Chuche and collaborators (10) have invoked carbonyl ylides to explain the stereochemistry of the dihydrofurans produced from vinyloxiranes. Control samples of **4** did not racemize at temperatures less than 250°. A sample of (−)-(*R*)-**1***b* of 81.3% optical purity was heated to 200.01 ± 0.02° for 10.5 h and the vinyldihydrofuran (**4**) was separated and purified by preparative gas chromatography. The 2-vinyl-2,3-dihydrofuran produced was greater than 99.6% racemic. Taking into account the competitive racemization of **1***b* the **4** produced would have displayed a $[\alpha]^{25}_{365}$ −4.70°.[1] The value observed, +0.285°, is indicative of a small excess of retention over inversion. The size of the measured rotation, +0.068°, at 365 nm, could be due to trace impurities even though care was taken to prevent such possibilities.

[1]From optically pure **1***b* we would expect to find **4** of $k_2/0.698k_\alpha$ enantiomeric purity. At 200° this ratio is 0.0659. The factor 0.698 comes from the percentage of **4** in the final mixture of **4** and **5**.

Experimental

The i.r. spectra were obtained on a Perkin-Elmer 421 Spectrophotometer and the n.m.r. spectra were obtained using a Varian A-60. All rotations were measured in a thermostated cell on a Perkin-Elmer Model 141 Polarimeter. Preparative gas chromatography (g.c.) was carried out using a Nester Faust Model 850 Prepkromatic.

Resolution of trans-2,3-Divinyloxirane (1b) by Di-3-pinanylborane

A mixture of racemic **1***b* (5.10 g, 20 mmol) and diglyme (5 ml) was placed in a 50-ml three-necked flask equipped with a condenser, magnetic stirrer, and a rubber septum. The mixture was cooled to −20° and kept under an atmosphere of nitrogen. Di-3-pinanylborane (20 mmol) in diglyme was introduced, using a syringe, in a dropwise manner through the rubber septum. The reaction mixture was maintained at −20° for 1 h and then allowed to warm to 0°. Water (5 ml) was added and the mixture distilled at 10 Torr. The distillate consisted of unreacted **1***b*, some (+)-α-pinene, water, and diglyme. After drying over anhydrous sodium sulfate the unreacted **1***b* was isolated by preparative g.c. (10 ft, 15% β,β′-oxydipropionitrile on firebrick, 60°). The presence of about 1% of **5** was indicated as the only impurity by analytical g.c. The recovered **1***b* (2.0 g) was optically active $[\alpha]^{24}_{365}$ −8.74° (5.33 g/100 ml, 2-propanol), calculated optical purity of 8.14%.

Preparation of (+)-(S)-1,5-Hexadien-3-ol (6) from (−)-(R)-1b

The epoxide (−)-(*R*)-**1***b* (300 mg, 3.1 mmol, optical purity 8.14%) in dry ether (2 ml) was added dropwise to a solution of lithium aluminum hydride (0.114 g, 3.1 mmol) in dry ether (6 ml). After the addition, the mixture was stirred at room temperature for 3 h. The excess hydride was then destroyed by the addition of moist ether at 0°. The aluminate complex was decomposed by the addition of 3 *M* sodium hydroxide and the solution extracted three times with ether. After drying over anhydrous sodium sulfate the ether layer was concentrated by fractional distillation and the product (+)-(*S*)-**6** was isolated by preparative g.c. (15% carbowax on chromosorb B, 70°), $[\alpha]^{25}_{365}$ +9.15° (2.12 g/100 ml, 2-propanol). The n.m.r. and i.r. spectra of the product were identical with an authentic sample (11).

Diimide Reduction of (+)-(S)-6 to (−)-(R)-3-Hexanol (7)

A sample of (+)-(*S*)-**6** (2.7 g, 27 mmol), $[\alpha]^{25}_{365}$ +49.73° (10.2 g/100 ml, 2-propanol) obtained by resolution of the brucine salt of 1,5-hexadien-3-yl hydrogen phthalate, was placed in a 500-ml flask along with sodium azodicarboxylate (17.8 g, 137 mmol) in methanol (220 ml). The suspension was stirred and acetic acid (13.2 g, 220 mmol) in methanol (137 ml) was added dropwise. After stirring for an additional 30 min water was added

Can. J. Chem. Downloaded from www.nrcresearchpress.com by 210.87.254.5 on 09/05/12
For personal use only.

TABLE 4. Rate constants for the loss of optical activity from (+)-**1***b*

Temperature ±0.04°	$10^5 k_\alpha$ (s^{-1})	$10^5(k_2+k_3)$ (s^{-1})	$10^5 k_1$ (s^{-1})
150.04	5.79±0.10 5.77±0.17	0.19	2.90±0.05 2.79±0.09
160.09	14.2 ±0.2	0.52	6.84±0.10
170.02	30.1 ±0.3	1.35	14.4 ±0.2

until the yellow color disappeared. The mixture was extracted several times with pentane and the combined extracts were dried over anhydrous sodium sulfate. The drying agent was then removed and the solution distilled through a Vigreux column. Yield, 2.1 g (80%); b.p. 129°/700 Torr; $[\alpha]^{22}_D$ −2.593° (neat, l = 1 dm, density 0.819 g ml^{-1}); $[\alpha]^{22}_{365}$ −4.950° (neat, l = 1 dm, density 0.819 g ml^{-1}); $[\alpha]^{22}_D$ −3.314° (5.26 g/100 ml, 2-propanol). Kenyon and Poplett (8) give $[\alpha]^{22}_D$ −7.13° for optically pure (−)-(*R*)-3-hexanol. The n.m.r. and i.r. spectra were identical with those of an authentic sample of 3-hexanol.

*Resolution of 5-Hexen-3-ol (**8**)*

The alcohol, **8**, was prepared by the procedure of Gaudemar (13) using activated zinc, allyl bromide, and propionaldehyde in tetrahydrofuran (THF). The alcohol was partially resolved through its phthalate half-ester following the procedure of Levine and Haller (12). See Table 1 for the rotational data.

*Preparation of (−)-(R)-1,4-Hexanediol (**9**) from (−)-(R)-**8***

A solution of diborane in THF (23 ml, 15 mmol) at 0° was added dropwise to (−)-(*R*)-**8** (3.0 g, 25 mmol) in dry THF (75 ml). The mixture was stirred 30 min before the excess diborane was decomposed with moist THF at 0°. Sodium hydroxide (45 ml, 3 *M*) was added followed by hydrogen peroxide (15 ml, 30%) while the temperature was maintained at 30–50°. After 1 h solid potassium carbonate (40 g) was added and the THF layer separated. The aqueous layer was extracted twice with THF and the THF portions combined and dried over anhydrous magnesium sulfate. The drying agent was removed by filtration and fractional distillation gave the product **9** (3.2 g, 90%), b.p. 128–131°/16 Torr (lit. (14) 134–135°/19 Torr). Analysis by g.c. indicated the presence of 3% of 2,4-hexanediol as the only impurity. The rotational data is given in Table 1.

*Preparation of (−)-(R)-2-Ethyltetrahydrofuran (**10**) from (−)-(R)-**9***

The procedure used was essentially that of Coates and Melvin (15). *p*-Toluenesulfonyl chloride (5.2 g, 27 mmol) was added slowly to a solution of (−)-(*S*)-**9** (3.6 g, 25 mmol) in dry pyridine (36 ml) maintained at 0°. The reaction mixture was allowed to warm to room temperature and stirring continued for 30 min. Cold water was then added and the reaction mixture was extracted six times with pentane. The pentane extracts were combined and washed with 2 *N* hydrochloric acid then dried over anhydrous magnesium sulfate. Careful fractionation through a spinning band column gave (−)-10 (0.97 g, 30%) of greater than 99% purity by g.c., b.p. 106°/700 Torr (lit. (16) 108°/758 Torr).

*Resolution of 2-Acetoxy-5-vinyltetrahydrofuran (**11**)*

A solution of **11** (65.4 g, 420 mmol) (17) in dry THF (50 ml) was added over a period of 1 h to a suspension of di-3-pinanylborane (7) (160 mmol) in ether and diglyme at −15 to −20°. The reaction mixture was stirred for 4 h at 0° and then water (6 ml) was added to destroy the excess borohydride. All of the volatile components were then distilled at 0.1 Torr and 50°. The crude distillate contained diglyme, α-pinene, ether, and (+)-(*S*)-**11**. Fractional distillation gave 20.4 g (63%) of **11**, b.p. 68–71°/4.5 Torr (17). See Table 1 for rotational data.

While the method of synthesis of **11** (17) does not preclude an isomeric pair, the reactant was primarily of one isomer, as judged by n.m.r., and after the resolution process consisted of a ratio of 20:1. No attempt was made to identify these isomers.

*Preparation of (+)-(S)-3-Vinyl-2,3-dihydrofuran (**4**) from (+)-(S)-**11***

A solution of (+)-(*S*)-**11** (20 g, 138 mmol) in ether (160 ml) was passed slowly, in a stream of nitrogen, through a column of glass beads heated to 245°. The condensate from the Dry-Ice – acetone trap was then washed three times with a saturated sodium carbonate solution and dried over anhydrous sodium sulfate. After filtration the solution was concentrated to 10 ml and then subjected to preparative g.c. (column 6 ft, β,β′-oxydipropionitrile, 60°). Yield 3.6 g (30%) of (+)-**4**. See Table 1 for rotational data. The n.m.r. and i.r. spectra were identical to those obtained from an authentic sample.

*Diimide Reduction of (+)-(S)-**4** to (+)-(R)-**13***

The technique used to reduce **4** to **13** was essentially that described above for the reduction of **6** to 7. Some reduction (approximately 10%) to **10** did occur, but the major product isolated by preparative g.c. (6 ft, β,β′-oxydipropionitrile, 60°) was (+)-(*R*)-**13** (68%). The n.m.r. spectrum δ_{TMS} ($CDCl_3$): 0.96 (t, 3H, CH_3); 1.59 (*q*, 2H, —CH_2—); 7.5 (m, 2H, ring CH_2); 4.5 (m, 1H, 3° ring H); 4.86 (*q*, 1H, *J* = 2.8 Hz, vinyl H); 6.26 (*q*, 1H, *J* = 2.5 Hz, vinyl H).

*Reduction of (+)-(R)-**13** to (−)-(R)-2-Ethylfuran (**10**)*

A solution of sodium borohydride (170 mg, 4.47 mmol) in methanol (4 ml) was added dropwise to a solution of rhodium trichloride trihydrate (342 mg) in methanol (90 ml). Charcoal (2 g) was then added to the solution under an atmosphere of nitrogen. The flask was then immersed

Can. J. Chem. Downloaded from www.nrcresearchpress.com by 210.87.254.5 on 09/05/12
For personal use only.

Can. J. Chem. Downloaded from www.nrcresearchpress.com by 210.87.254.5 on 09/05/12
For personal use only.

in a Dry-Ice – acetone bath and (+)-(*R*)-**13** (1.7 g, 17 mmol) was added. Hydrogen was then passed through the flask for 4 h at −78°, 2 h at −30°, and 2 h at 0°. The reaction mixture was filtered and 200 ml of water was added. The solution was extracted with pentane and the pentane layer, after drying over anhydrous sodium sulfate, was concentrated to 10 ml. Preparative g.c. (6 ft, β,β′-oxydipropionitrile, 65°) gave 1.23 g (73%) of (−)-**10**. See Table 1 for rotational data. The n.m.r. and i.r. spectra were identical with those of an authentic sample (16).

*Reduction of (+)-(S)-**11** to (+)-(S)-5-Hexene-1,4-diol (**12**)*

A solution of lithium aluminum hydride (20 g, 520 mmol) dissolved in dry ether (250 ml) was placed in a 1-l three-necked flask fitted with a dropping funnel, reflux condenser, and a gas inlet tube. Upon cooling to 0° a solution of (+)-**11** (13 g, 87 mmol) was added dropwise over a period of 2 h. The reaction mixture was then allowed to stand overnight at room temperature and ethyl acetate was added to destroy the excess hydride. Water was then added carefully followed by Celite (40 g). The ether solution was filtered and the Celite residue was washed six times with ether. The combined ether portions were concentrated to 100 ml and dried over anhydrous sodium sulfate. The ether was then removed and distillation gave 9.04 g (94%) of (+)-**12**, b.p. 65–67°/0.01 Torr (lit. (18) 98–100°/1.8 Torr). See Table 1 for rotational data.

*Reduction of (+)-(S)-**12** to (−)-(R)-1,4-Hexanediol (**9**)*

The procedure used was the same as that for the reduction of **6** to **7**. From 63 mmol of **12** there was obtained 6.97 g (74%) of **9**. The i.r. n.m.r., and g.c. retention time were identical with those of the sample obtained by the hydration of **7**, except that there was no trace of 2,4-hexanediol as an impurity.

Preparation of threo-4-Chloro-1,5-hexadiene-3-ol

A 2:1 mixture of **1***b* and **5** (38 g, 390 mmol) was added simultaneously with dry hydrogen chloride to anhydrous ether (400 ml) containing a small amount of thymol blue maintained at −50°. The red color indicated the presence of excess hydrogen chloride. Upon completion of addition the reaction mixture was washed with cold aqueous sodium bicarbonate, then with a saturated sodium chloride solution. The ether layer was dried over anhydrous sodium sulfate, filtered, and concentrated. Distillation caused darkening and isomerization so the crude alcohol was used directly in preparing the half-ester.

Preparation of threo-4-Chloro-1,5-hexadien-3-yl Hydrogen Phthalate

The crude *threo*-4-chloro-1,5-hexadien-3-ol (35 g, 260 mmol) was added to dry pyridine (48 ml) and phthalic anhydride (38.6 g, 280 mmol). The mixture was stirred overnight at room temperature and then warmed to 85° for 1 h before ice, ether, and concentrated hydrochloric acid (72.5 ml) were added. The ether layer was separated and the aqueous layer extracted several times with ether. The combined ether layers were dried over anhydrous sodium sulfate and after filtration the solvent was removed. The remaining syrup (63 g) was poured into a solution of sodium carbonate (22 g) in water (24 ml). The solution was extracted with ether and the extracts discarded. Concentrated hydrochloric acid (60 ml) was added to the aqueous layer and the phthalate extracted with chloroform. After drying the chloroform was removed and there remained 50.2 g (67% based on crude chlorohydrin) of the phthalate ester which after being recrystallized from a benzene – Skelly B mixture gave m.p. 72–72.5°.

Anal. Calcd. for $C_{14}H_{13}ClO_4$: C, 59.89; H, 4.63; Cl, 12.65. Found: C, 59.68; H, 4.84; Cl, 12.42.

Resolution of threo-4-Chloro-1,5-hexadien-3-yl Hydrogen Phthalate and its Conversion to (−)-1b

threo-4-Chloro-1,5-hexadien-3-yl hydrogen phthalate (38.7 g, 140 mmol) was added to dry acetone (100 ml) and the solution heated to boiling. Brucine (37.8 g, 82 mmol) was added and the clear solution allowed to cool slowly to 0°. The solid was collected and repeatedly crystallized from acetone until the m.p. raised to 150–151°. The half-ester was isolated by extraction with ether from an acidified solution of the salt. After removal of the ether there remained 7.5 g of the phthalate $[\alpha]^{21}_{D}$ +13.20, (2.84 g/100 ml, 2-propanol).

The resolved half-ester (7.5 g, 26 mmol) was dissolved in aqueous sodium carbonate and the solution added dropwise to a hot solution of sodium hydroxide (10-fold excess) such that water and the divinyloxirane distilled out. The oxirane layer was separated and dried over 4A molecular sieves. Yield 2 g, 78%. G.c. analysis indicated a purity of greater than 98%. The impurities were identified by mass spectrograph – g.c. to be acetone, ether, and allylmethyl ketone. $[\alpha]^{21}_{589}$ −8.48; $[\alpha]^{21}_{365}$ −87.35, (4.41 g/100 ml, 2-propanol).

Racemization Kinetics

In a typical run a sample of (−)-(*R*)-**1***b* (about 1 mmol) was weighed and degassed on a vacuum line. It was then vapor transferred to a 30 ml break-seal. The tube was sealed off and removed from the vacuum line to a constant temperature bath. At the appropriate time the tube was removed and quenched in an ice-water bath. It was then attached to the vacuum line and after a pressure of 10 microns was achieved the break-seal was opened and the contents vapor transferred to weighed 1-ml volumetric flask cooled in liquid nitrogen. The contents of the volumetric flask were then allowed to come to room temperature and after careful removal of any grease from the joint the flask was weighed. Isopropyl alcohol was added up to a volume of 1 ml and the weight of the solution obtained. Concentrations of **1***b* in the solution were calculated in percentage weight to avoid any volumetric error. A tube corresponding to zero time and an infinity tube were put through the same manipulations for each run.

The solution was then transferred to a thermostated polarimeter tube (1-ml volume, 1.001 dm long) and the rotation was measured. Precision of the measurement was ±0.002°. All samples were analyzed by g.c. after the rotation was measured. A sample run at 160.09° consists of the following data: 10^5 s, $[\alpha_t]/[\alpha_0]$; 0.180, 0.846; 0.540, 0.479; 0.900, 0.302; 1.14, 0.213; 1.50, 0.126; 1.80, 0.0843; infinity tube 3 days, 0.000. These results give $k_\alpha = (14.2 \pm 0.2) \times 10^{-5}\ s^{-1}$.

Can. J. Chem. Downloaded from www.nrcresearchpress.com by 210.87.254.5 on 09/05/12
For personal use only.

Kinetics of the Rearrangement of 1b to 4 and 5

A sample of **1***b* (25–30 mg) was placed in a 10 ml ampoule, degassed by three freeze–thaw cycles, sealed, and placed in a constant temperature oil bath. The tubes were removed from the bath at the appropriate time and the reaction was quenched. After opening, each tube was analyzed, in pentuplicate, on a Perkin-Elmer Model 900 Gas Chromatograph equipped with a Hewlett Packard 3370A Integrator. Some runs were conducted using 1,2-dimethoxyethane as a reference and some without a reference. A 150 ft, β,β′-oxydipropionitrile wall-coated column was used at 60° with a flame detector. A sample run at 190.30 ± 0.05° for the rate of disappearance of **1***b* is: 10^3 s $[\mathbf{1}b]^t/[\mathbf{1}b]^0$; 1.80, 0.863; 6.60, 0.582; 9.00, 0.464; 12.0, 0.369; 14.4, 0.289; 16.8, 0.236; 19.2, 0.185; these results give $k_2 + k_3 = (8.80 \pm 0.12) \times 10^{-5}$ s^{-1}.

Product Studies

(*a*) Sealed ampoules of **1***b* were heated for approximately two half-lives at temperatures from 160 to 220°. Each sample was then analyzed and the final kinetic results, along with the probable error as calculated from the standard deviation, are shown in Table 3.

(*b*) A sample of *trans*-2,3-divinyloxirane (1.5 g, 16 mmol) $[\alpha]^{25}_{365}$ −87.35, 81.3% optical purity was degassed and sealed into tubes such as to render a pressure of 1 atm at 200°. The tubes were then placed in a thermostated oil bath at 200.0 ± 0.1° for 10.5 h (10 half-lives for $k_2 + k_3$). The vinyldihydrofuran produced was separated from the 4,5-dihydrooxepine by preparative g.c. and its rotation measured $[\alpha]^{22}_{365}$ +0.058° (neat, 1 cm), $[\alpha]^{22}_{365}$ +0.285° (23.8 g/100 ml, 2-propanol). Thus, the product **4** was found to be greater than 99.6% racemic.

Discussion

(*a*) *The Mechanism of the Racemization Process*

The most facile reaction of the oxirane, **1***b*, is the racemization process. Since this is formally a simultaneous inversion of two chiral centers the reversible conrotatory opening of the oxirane to produce a carbonyl ylide best fits the requirements (see eq. 1) (3, 19). It is of interest to note that a negative entropy of activation ($\Delta S^{\ddagger}$ −9 e.u.) occurs during this bond cleavage reaction. This is consistent with the loss of the rotational degrees of freedom associated with the two vinyl groups.

(*b*) *The Mechanism of Vinyldihydrofuran Foundation*

The oxirane **1***b* may open to carbonyl ylides of 10 different configurations (see Fig. 1); of these *a–f* are produced by a conrotatory ring opening. The vinyldihydrofuran, **4**, is produced by the formation of the carbon–carbon bond between positions 2 and 3. Since the major part of the vinyldihydrofuran produced is racemic, even for that which has not racemized at the

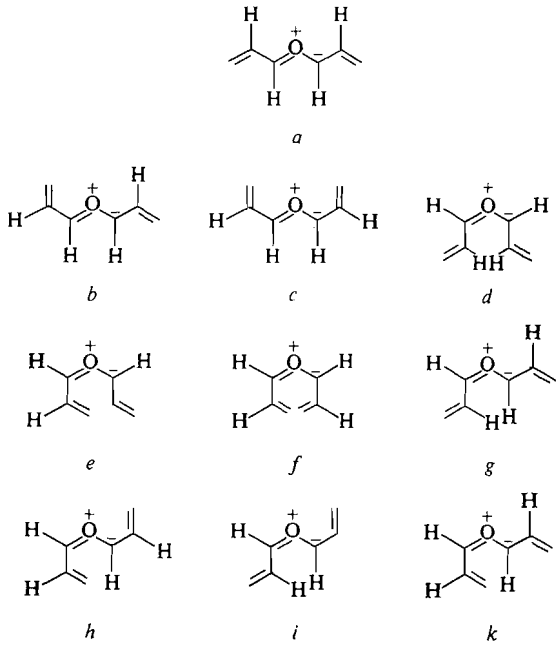

FIG. 1. Configurations of carbonyl ylide **13**.

epoxide stage, then a planar intermediate such as the carbonyl ylide is a reasonable candidate as an intermediate. The opening of a ring such as **4** is disrotatory and could produce carbonyl ylide **13***e*, *f*, *h*, or *k*. While *e* and *f* are common

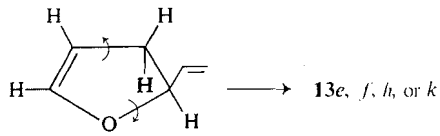

to both sets, *i.e.* those arising from **1***b* and **4**, they are also sterically very crowded. The stereochemical studies of Chuche and co-workers (10) indicate that an isomerization about the carbon–oxygen bond of the carbonyl ylide must occur, the *cis*-oxirane being ruled out since it gives rise to the dihydrooxepine exclusively (6). Isomerization at the carbonyl ylide stage is similarly capable of explaining the *trans–cis* isomerization of oxirane (resulting in the formation of **5**). Thus a scheme such as

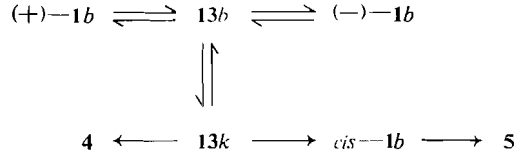

is capable of fitting all of the stereochemical and kinetic data. Schemes using carbonyl ylide **13***c* and its isomerization to **13***h* are equally valid. For the conversion of (+)-**1***b* to **4** the data require that we have at least one planar intermediate and it is most readily reconciled with an isomerization from one of the members of the set **13***a*–**13***b* to the set **13***g*–**13***k*.

(c) The Zwitterion Intermediate **3**

This study was initially undertaken to minimize the role of the zwitterion intermediate **3**. In the 2,3-divinyloxirane system if any of the *cis* isomer is produced then it will be immediately converted to 4,5-dihydrooxepine (**5**) (6), and thus the rate of *trans* to *cis* isomerization in this system cannot exceed the value of k_3. The ratio k_1/k_3 at 200° for **1***b* is 22.6 while for **1***a* the same rate ratio at 200° is 212 (3). If the geometrical isomerization, as manifested by dihydrooxepine formation, is a feasible gas phase process proceeding via the cleavage of the carbon–carbon bond then it is not unlikely that the *trans–cis* isomerization occurs via a carbonyl ylide isomerization. While the carbonyl ylide as written looks like a very polar structure it would appear that solvation is not critical to the formation of such a species. We are now attempting to elucidate whether there are any significant solvent effects upon carbonyl–ylide ring openings.

The authors wish to acknowledge the financial assistance of the National Research Council of Canada. They also wish to thank Mrs. Fay Podruzny for measuring product proportions. We wish to acknowledge fruitful discussions with Prof. Josselin Chuche of Reims, France.

1. (*a*) H. M. FREY. Adv. in physical organic chemistry. Vol. 4. Academic Press, New York. 1966. p. 147; (*b*) R. G. BERGMAN and W. L. CARTER. J. Am. Chem. Soc. **91**, 7411 (1969); (c) M. ARAI and R. J. CRAWFORD. Can. J. Chem. **50**, 2158 (1972).
2. M. C. FLOWERS and R. M. PARKER. J. Chem. Soc. (B), 1980 (1971).
3. H. H. J. MACDONALD and R. J. CRAWFORD. Can. J. Chem. **50**, 428 (1972).
4. E. W. YANKEE and D. J. CRAM. J. Am. Chem. Soc. **92**, 6328, 6329, 6331 (1970).
5. E. VOGEL and H. GUNTHER. Ang. Chem. Int. Ed. **6**, 395 (1967).
6. E. L. STOGRYN, M. H. GIANNI, and A. J. PASSANNANTE. J. Org. Chem. **29**, 1275 (1964).
7. H. C. BROWN and G. ZWEIFEL. J. Am. Chem. Soc. **83**, 486 (1961).
8. H. C. BROWN, N. R. AYYANGAR, and G. ZWEIFEL. J. Am. Chem. Soc. **86**, 397 (1964); J. KENYON and R. POPLETT. J. Chem. Soc. 273 (1945).
9. R. B. WOODWARD and R. HOFFMANN. The conservation of orbital symmetry. Academic Press, New York. 1969.
10. (*a*) J. C. POMMELET, N. MANISSE, and J. CHUCHE. Tetrahedron, **28**, 3929; (*b*) J. C. PALADINI and J. CHUCHE. Tetrahedron Lett. 4383 (1971).
11. L. W. BUTZ, E. W. J. BUTZ, and A. M. GADDIS. J. Org. Chem. **5**, 171 (1940).
12. P. L. LEVINE and H. L. HALLER. J. Biol. Chem. **83**, 185 (1929).
13. M. GAUDEMAR. Bull. Soc. Chim. **175**, 974 (1962).
14. C. GLACET. C. R. **218**, 283 (1944).
15. R. M. COATES and L. S. MELVIN, JR. J. Org. Chem. **35**, 865 (1970).
16. R. PAUL. Bull. Soc. Chim. **5**, 1053 (1938).
17. C. GLACET. Ann. Chim. [**12**] **2**, 293 (1947).
18. S. F. BIRCH, R. A. DEAN, and N. J. HUNTER. J. Org. Chem. **23**, 1390 (1952).
19. H. HAMBERGER and R. HUISGEN. Chem. Commun. 1190 (1971); A. DAHMEN, H. HAMBERGER, R. HUISGEN, and V. MARKOWSKI. Chem. Commun. 1192 (1971).

Can. J. Chem. Downloaded from www.nrcresearchpress.com by 210.87.254.5 on 09/05/12
For personal use only.

Lanthanide Induced Enhancement of Enantiomeric Shifts in Chiral Solvents and its Use in the Determination of Optical Purity

C. P. R. JENNISON[1] AND DONALD MACKAY
Department of Chemistry, University of Waterloo, Waterloo, Ontario

Received May 22, 1973

The chemical shift difference (Δv) between corresponding groups in enantiomers in the presence of both a chiral solvent ((−)-2,2,2-trifluorophenylethanol or (+)-1-phenylethylamine) and an achiral lanthanide shift reagent ($Eu(dpm)_3$ or $Eu(fod)_3$) is much greater than in the chiral solvent alone. In general, for simple molecules having one coordination site the Δv was smaller than that obtained with the chiral shift reagent $Eu(HFC)_3$. Comparable values of Δv, however, were obtained with the 1,3,4-oxadiazine derivatives **4***a* and *b*, and **5**, suggesting that the "chiral solvate shift system" is best suited to differentiating more complex enantiomers having several coordination sites.

The shift system was used to determine the optical purity of two partially resolved substances. One of these was the (+)-oxadiazine **4***a*, produced in the asymmetric isomerization of the bridged pyridazine **3***a* by (+)-camphor-10-sulfonic acid, and optically enriched by only one fractional crystallization. The enantiomeric enrichment in the isomerization was 4.21 ± 0.08%.

La différence de déplacement chimique (Δv) entre groupes correspondants dans des énantiomères en présence à la fois d'un solvant chiral ((−)-trifluoro-2,2,2 phényléthanol ou (+)-phényl-l éthylamine) et d'un réactif "shift" achiral ($Eu(dpm)_3$ ou $Eu(fod)_3$) est beaucoup plus grande que dans le cas du solvant chiral seul. En général, pour des molécules simples ayant un site de coordination, Δv est plus petit que la valeur obtenue avec le réactif chiral $Eu(HFC)_3$. Cependant, des valeurs comparables de Δv ont été obtenues avec les dérivés d'oxadiazine-1,3,4, **4***a* et *b*, et **5**, laissant penser que le système solvaté par un solvant chiral est plus adapté à la différenciation des énantiomères plus complexes possédant plusieurs sites de coordination.

Ce système a été utilisé pour déterminer la pureté optique de deux substances partiellement résolues. L'une d'elles était la (+)-oxadiazine **4***a* produite par isomération asymétrique de la pyridazine pontée **3***a* par l'acide (+)-camphosulfonique-10 puis enrichie optiquement par une seule cristallisation fractionnée. L'enrichissement optique de l'isomération a été de 4.21 ± 0.08%.

[Traduit par le journal]

Can. J. Chem. **51**, 3726 (1973)

Introduction

The rendering of enantiomeric groups anisochronous in the presence of a chiral solvent (1, 2, 8, 9) or more recently of lanthanide derived chiral shift reagents (3–9) has now been thoroughly documented. Determinations of absolute configuration (1, 2, 10–13), optical purity (1, 6), and geminal coupling constants (7, 8) have been made possible without the necessity of first making the groups diastereomeric by suitable chemical transformations.

We have recently reported (14) the successful asymmetric isomerization of the Diels–Alder adduct **1** to the optically active 1,3,4-oxadiazine derivative **2** under the influence of (+)-camphor-10-sulfonic acid as catalyst. The product was optically enriched by fractional crystallization and its optical purity then determined both by the isotopic dilution method (15) and by converting the sample into a mixture of diastereomeric methoxymandelyl derivatives which was analyzed by n.m.r. spectroscopy (16). The value obtained corresponded to an enantiomeric enrichment of 1.34% in the original isomerization of the adduct.

We reasoned that the highly substituted derivative of **1**, the adduct **3***a*, would be more stereoselective in its isomerization to **4***a* with the same catalyst. We became interested in methods for the direct determination of the optical purity of structures like **2** and **4** without resorting to their conversion into diastereomers.[2] The

[1]On leave of absence from the Department of Chemical and Metallurgical Technology, Ryerson Polytechnical Institute, Toronto, Ontario, Canada.

[2]An objection to this approach, apart from the extra steps involved. is that conversion may not occur equally efficiently with each enantiomer and that there may be some induced loss of configurational purity at the original optically active centers. Either effect would cause the diastereomeric ratio to differ from the enantiomeric one. In any event attempts to make diastereomers from **4***a* by the methods successfully used for **2** caused extensive decomposition.

Can. J. Chem. Downloaded from www.nrcresearchpress.com by 210.87.254.5 on 09/05/12
For personal use only.

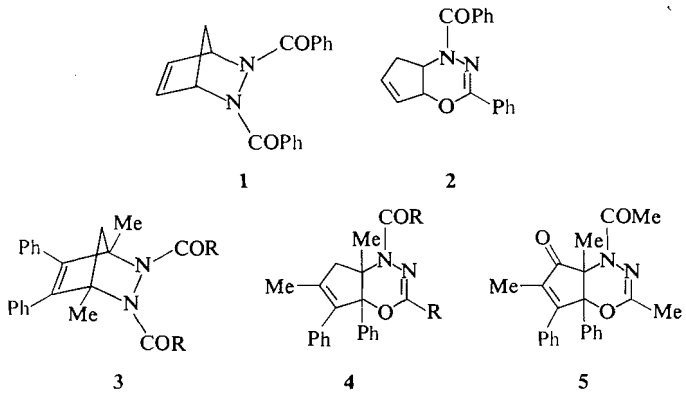

1 2

3 4 5

a R = Ph
b R = Me

presence of functional groups in **2** and **4** which should be responsive both to solvation by a hygrogen-bonding chiral solvent and to coordination by a lanthanide suggested to us a use for a combination of these reagent types. We thought such a combination, for which we propose the term "chiral solvate shift system" would prove superior in separating enantiomeric hydrogens than a chiral solvent alone and might be comparable or superior in effectiveness to a chiral lanthanide. The shift between enantiomeric hydrogens generated by the chiral solvent could be enhanced by coordination of the lanthanide with the substrate, the chiral solvent, or both. An advantage of the chiral solvate shift system lies in the ready availability, commercially or by synthesis, of a range both of suitable optically pure solvents and of lanthanide derivatives, which provides the potentially large choice of combinations which might be needed for a broad spectrum of substrate types.

We now report advantages and limitations of chiral solvate shift systems obtained from *R*-(+)-1-phenylethylamine (PEA) and *R*-(−)-1-phenyl-2,2,2-trifluoroethanol (TFPE) as solvents, and $Eu(dpm)_3$ and $Eu(fod)_3$ as shift reagents. As substrates we have used not only the oxadiazines **4***a* and *b*, and the related derivative **5** from 2,5-dimethyl-3,4-diphenylcyclopentadienone, but also the simpler models, the racemic compounds 1-phenylethylamine (**6**), amphetamine (1-methyl-2-phenylethylamine) (**7**), methyl alanate (**8**), and methyl phenyl sulfoxide (**9**), which were examined in some detail. For comparison purposes results for most of the latter compounds with chiral solvents alone or with chiral lanthanides were obtained from the literature or were determined by us under conditions similar to those used for our chiral solvate shift systems.

PEA TFPE

Experimental

R-(+)-1-Phenylethylamine, $[\alpha]_D^{20}$ 36° minimum (neat) was supplied by Baker Chemical Co., $Eu(dpm)_3$ and $Eu(fod)_3$ by Pierce Chemical Co., and $Eu(HFC)_3$ (tris(3-heptafluoropropylhydroxymethylene-(+)-camphorato)europium) by Stohler Isotope Chemicals. *R*-(−)-1-Phenyl-2,2,2-trifluoroethanol was synthesized as described by Pirkle *et al.* (17) and had $[\alpha]_D^{20}$ −39.8° (97% optical purity).

(±)-Amphetamine was made by admixture of the enantiomeric forms purchased from Aldrich Chemical Co. (±)-Methyl phenyl sulfoxide was prepared by oxidation of the sulfide (Eastman) (18). (±)-Methyl alanate was stored as the hydrochloride from which it was liberated as needed by passing dry ammonia into a suspension in the n.m.r. solvent and filtering. Excess of dissolved ammonia was removed by addition of sufficient ester hydrochloride and re-filtering.

The synthesis and properties of 3*a* and *b*, **4***a* and *b*, and **5** will be discussed fully in forthcoming publications as part of a general study of isomerization reactions of adducts of azodiaroyl compounds; their structures have been unambiguously assigned.

N.m.r. spectra were obtained on a Varian T-60 or HA-100 spectrometer. The r.f. level was at all times optimized and the spectra recorded at sweep rates of 1 or 2 Hz s^{-1}. Values for chemical shift separations are accurate to within ± 0.002 p.p.m.

Solutions for Tables 1 and 2 were made by weighing out the calculated quantities of substrate, chiral solvent, and achiral solvent in the molar ratios indicated. The lanthanide was then added in the required amounts to give

Can. J. Chem. Downloaded from www.nrcresearchpress.com by 210.87.254.5 on 09/05/12
For personal use only.

Can. J. Chem. Downloaded from www.nrcresearchpress.com by 210.87.254.5 on 09/05/12
For personal use only.

TABLE 1. Comparison of chiral solvate shift system with chiral solvents alone and with a chiral lanthanide shift reagent in the separation of enantiomeric methyls

S	CS	AS	L	S:CS:AS:L (mol ratio)	Methyl position	$\Delta\nu_{Me}$*	($\Delta\nu_{Me}$†, $\Delta\nu_{Me}$‡)
Oxadiazine **4***a*	TFPE	C_6H_6	$Eu(fod)_3$	1:6:6:0.20	Vinyl Me	0.01	(<0.01, 0.00)
	TFPE	C_6H_6	$Eu(fod)_3$	1:6:6:0.20	Quaternary Me	0.10	(0.02, 0.05)
	TFPE	C_6H_6	$Eu(fod)_3$	1:15:5:0.20	Vinyl Me	0.02	
	TFPE	C_6H_6	$Eu(fod)_3$	1:15:5:0.20	Quaternary Me	0.14	
Oxadiazine **4***b*	TFPE	C_6H_6	$Eu(fod)_3$	1:15:5:0.30	Vinyl Me	0.01	
	TFPE	C_6H_6	$Eu(fod)_3$	1:15:5:0.30	Quaternary Me	0.08	
	TFPE	C_6H_6	$Eu(fod)_3$	1:15:5:0.30	Amide or imidoyl Me	0.06§	
	PEA	C_6H_6	$Eu(fod)_3$	1:15:5:0.30	Quaternary Me	0.03§	
Oxadiazine **5**	TFPE	C_6H_6	$Eu(fod)_3$	1:6:6:0.20	Vinyl Me	0.00	(0.00, 0.00)
	TFPE	C_6H_6	$Eu(fod)_3$	1:6:6:0.20	Quaternary Me	0.11	(0.04, 0.09)
	TFPE	C_6H_6	$Eu(fod)_3$	1:6:6:0.20	Amide Me	0.09	(0.00, 0.07)
	TFPE	C_6H_6	$Eu(fod)_3$	1:6:6:0.20	Imidoyl Me	0.12	(0.06, 0.15)
	PEA	C_6H_6	$Eu(fod)_3$	1:6:6:0.20	Vinyl Me	0.00	
	PEA	C_6H_6	$Eu(fod)_3$	1:6:6:0.20	Quaternary Me	0.05	
	PEA	C_6H_6	$Eu(fod)_3$	1:6:6:0.20	Amide Me	0.04	
	PEA	C_6H_6	$Eu(fod)_3$	1:6:6:0.20	Imidoyl Me	0.08	
1-Phenylethylamine (**6**)	TFPE	$CDCl_3$	$Eu(dpm)_3$	1:2:3:0.20		0.04	(0.00, 0.13)
	TFPE	$CDCl_3$	$Eu(dpm)_3$	1:3:2:0.30		0.05	
Amphetamine (**7**)	TFPE	$CDCl_3$	$Eu(dpm)_3$	1:2:3:0.20		0.00‖	
	PEA	C_6H_6	$Eu(dpm)_3$	1:3:3:0.20		0.05	(0.00, 0.10)
	PEA	C_6H_6	$Eu(dpm)_3$	1:3:2:0.65		0.14	
Methyl alanate (**8**)	TFPE	$CDCl_3$	$Eu(dpm)_3$	1:3:3:0.20	Tertiary Me	0.04	(0.03, 0.05)
	PEA	$CDCl_3$	$Eu(dpm)_3$	1:4:3:0.20		0.04¶	
	PEA	$CDCl_3$	$Eu(dpm)_3$	1:3:3:0.30		0.05	
Methyl phenyl sulfoxide (**9**)	TFPE	$CDCl_3$	$Eu(dpm)_3$	1:2:3:0.20		0.00‖	
	PEA	C_6H_6	$Eu(dpm)_3$	1:3:3:0.20		0.015	(0.00, 0.06)
	PEA	$CDCl_3$	$Eu(dpm)_3$	1:2:3:0.60		0.03	

*Differentail enantiomeric shift in p.p.m. of the specified "chiral solvate shift system". [S] ≃ 0.5–1.5, [L] ≃ 0.1–0.6.
†Differential enantiomeric shift in p.p.m. in the chiral solvate system before addition of lanthanide shift reagent.
‡Differential enantiomeric shift in p.p.m. of S in AS with $Eu(HFC)_3$ of mole ratio 1:12:0.20 where [S] ≃ 1.0.
§Assignment uncertain.
‖Extensive broadening.
¶Aminolysis by the chiral solvent to give diastereomeric amides is ruled out by the absence of a methanol peak in the spectrum.

TABLE 2. Effects of L:S and CS:S ratios on the shift between enantiomeric methyl groups of (±)-1-phenylethlyamine in $CDCl_3$ containing TFPE and $Eu(dpm)_3$

S:CS:AS:L (mol ratio)				L:S	CS:S	$\Delta\nu_{Me}$ (p.p.m.)
1	2	3	0.1	0.1	2	0.020
1	0.25	4.75	0.2	0.2	0.25	0.000
1	0.50	4.50	0.2	0.2	0.50	0.020
1	0.75	4.25	0.2	0.2	0.75	0.033
1	1	4	0.2	0.2	1	0.042
1	2	3	0.2	0.2	2	0.040
1	3	2	0.2	0.2	3	0.033
1	2	3	0.3	0.3	2	0.048
1	3	2	0.3	0.3	3	0.044

successive runs at increasing lanthanide concentrations. Solutions for Table 3 were made by weighing out all four components for the initial solution and then diluting with known weights of achiral solvent. The total volumes were obtained using the densities of the solvents and the substrate, the volume of the lanthanide being ignored. Volume changes on mixing were shown to be negligible.

Asymmetric Isomerization of 3a

To a solution of the adduct **3***a* (6.5 g, 13.4 mmol) in dry benzene (800 ml) was added (+)-camphor-10-sulfonic acid (0.325 g, 10.0 mol%) and the resulting solution was shaken for 2 min. It was then immediately extracted with 2 × 50 ml portions of 2% sodium hydrogen carbonate, washed with water (50 ml), dried ($MgSO_4$), and evaporated to give the oxadiazine **4***a* (6.0 g, 92%) of $[\alpha]_{578}^{20}$ 8.80° (benzene, 0.160 g in 13.0 ml). A Zeiss photoelectric precision polarimeter was used for the determination of optical rotations.

Fractional crystallization from methanol gave little optical enrichment, though it was the solvent of choice in the work-up of optically active **2** (14). Benzene – petroleum ether (b.p. 35–60°) was successful, a 4.0 g sample giving almost racemic oxadiazine as a crystalline precipitate, m.p. 161.5–163° and from the mother liquor 0.24 g of oxadiazine of $[\alpha]_{578}^{20}$ 44.8° (benzene, 0.240 g in 3.0 ml).

Determination of Optical Purity

Amphetamine

A mixture of the enantiomers with the (−)-form in excess to give an optical purity of 22.6% was prepared and analyzed at 60 MHz and 35° in PEA–benzene in the presence of $Eu(dpm)_3$ (molar ratio 1:3:3:0.2). The two enantiomeric methyl doublets are shown in Fig. 1, J = 6.4 Hz, $\Delta\nu_{Me}$ = 2.8 Hz, and $w_{\frac{1}{2}} < 2$ Hz. The optical purity was found to be readily measurable as the average of the peak heights for each doublet, which were in the ratio of 1.60 ± 0.09:1, corresponding to an optical purity of 23.0 ± 1.2%. Direct area determination was not attempted in view of the difficulties arising from peak overlap.

Oxadiazine (4a)

The optically enriched sample of $[\alpha]_{578}^{20}$ 44.8° (benzene), described above, was analyzed at 100 MHz in TPFE–benzene in the presence of $Eu(fod)_3$. At 35° $\Delta\nu_{Me}$ was 14 Hz, but the peak resolution was rather poor, $w_{\frac{1}{2}}$ being 5–6 Hz. At 70°, for a molar composition of 1:15:5:0.20,[3] much sharper methyl lines were obtained, with a value of $w_{\frac{1}{2}}$ = 2.2 Hz for the more intense one, and even though $\Delta\nu_{Me}$ was reduced to 8.0 Hz, separation was nearly complete[4] (Fig. 2). Area ratios were determined by

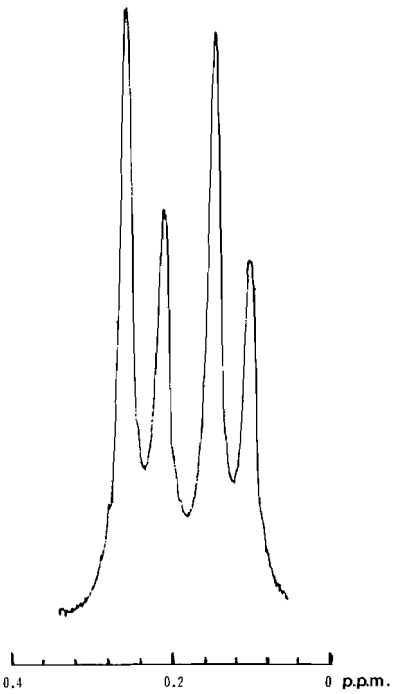

FIG. 1. 60 MHz spectrum of the Me doublets of amphetamine of 22.6% optical purity at 35° in PEA–benzene in the presence of $Eu(dpm)_3$ (mol ratio 1:3:3:0.2).

[3]The higher temperature allowed a large proportion of the rather viscous TFPE to be used.

[4]The decrease of ligand induced shifts with increasing temperature has been noted by others (19). We have found it to be quite general for enantiomeric shifts as well.

Can. J. Chem. Downloaded from www.nrcresearchpress.com by 210.87.254.5 on 09/05/12
For personal use only.

Can. J. Chem. Downloaded from www.nrcresearchpress.com by 210.87.254.5 on 09/05/12
For personal use only.

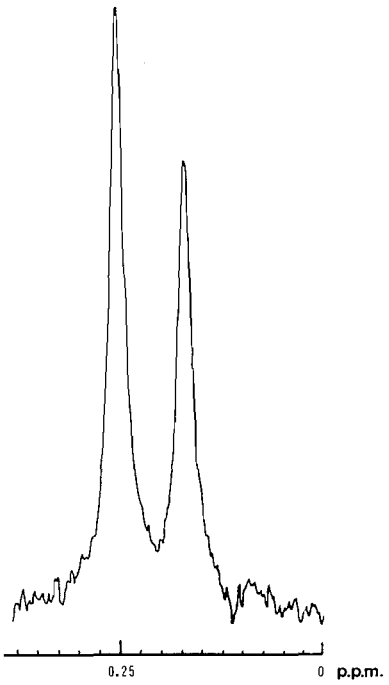

FIG. 2. 100 MHz spectrum of enriched (±)-oxadiazine **4***a* at 70° showing the quaternary Me in TFPE–benzene in the presence of $Eu(fod)_3$ (mol ratio 1:15:5:0.2).

photocopying (10 times), cutting out, and weighing, and showed the optical purity to be 21.4 ± 0.4%. This value leads to an enantiomeric enrichment of 4.21 ± 0.08% in the original isomerization and a rotation of $[\alpha]_{578}^{20}$ 209 ± 4° (benzene) for optically pure **4***a*.

Results and Discussion

Table 1 shows the effect on the shift ($\Delta\nu_{Me}$) between the methyl groups in the enantiomers of the substrates S (**4**–**9**) caused by variation in the nature of the chiral solvent CS, the achiral solvent AS (benzene or chloroform-*d*), and the lanthanide L. The enantiomeric shifts, under otherwise comparable conditions, are shown in brackets for CS only and for the chiral lanthanide $Eu(HFC)_3$.

Consecutive entries for the same system show the effect of variations in the molar ratios of S:CS:AS:L.

The chiral solvate systems are clearly in general superior to CS alone.[5] They are inferior to $Eu(HFC)_3$ in the case of the simple models **6**–**9** with one coordination site, but are comparable or in some instances superior for the structurally more complex oxadiazines **4** and **5** which contain a number of coordination sites.

For **6**–**9** $Eu(fod)_3$ was in all cases ineffective, molecules like these clearly requiring the more sterically demanding $Eu(dpm)_3$. Both lanthanides gave enantiomeric shifts with the oxadiazines but $Eu(fod)_3$ gave larger shifts, probably due to its greater Lewis acidity, since the oxadiazines are only weakly basic.

Both chiral solvents were successful in general (two exceptions in the case of TFPE with **7** and **9** are noted) but for the oxadiazines the alcohol was the solvent of choice. Its greater hydrogen-bonding power is evidently utilized to full advantage with the large number of potential hydrogen bonding sites in the substrates.

The effect of variation in concentration within a given system is shown in Table 2 for the methyl groups in (±)-1-phenylethylamine at nine different compositions of the amine in $CDCl_3$–TFPE in the presence of $Eu(dpm)_3$; the ratio of S:(CS + AS) is held constant. The $\Delta\nu_{Me}$ values are strongly tied to the L:S ratio for constant CS:S ratio (runs 1, 6, and 8, and runs 7 and 9), though not quite in a linear fashion. The shift is very sensitive to the CS:S ratio below a value of about unity (runs 2–5), at which it reaches a maximum and then decreases rather slowly as the ratio rises (runs 5–7), till the point where viscosity reduces the resolution and line separation is obscured.

Solvation by TFPE may be presumed to occur preferentially at the amine and it is probable that at low TFPE concentrations the mechanism is one in which unsolvated lanthanide enhances the methyl shift difference between diastereomeric assemblies of solvated amine. At a solvation level of 1:1 or less, one "side" of the amine is still exposed for direct coordination with the lanthanide. Further addition of TFPE works adversely, either because it solvates the amine further and inhibits coordination action, or because it starts to solvate the lanthanide, in preference to the monosolvated amine, and by thus competing for the lanthanide reduces the bound time of the latter with the amine, and hence the enantiomeric shift.

The optimum solvation level of 1:1 found for 1-phenylethylamine may of course not be general for other substrates. However, our

[5]The measurements of $\Delta\nu_{Me}$ in CS alone were all made at 60 MHz. Though most of them show zero value, it is likely that separations of up to 0.01 p.p.m. might have been detected for some of them at 100 MHz.

TABLE 3. Effect of [L] on the shift between enantiomeric methyl groups of (±)-1-phenylethylamine in benzene containing (*a*) TFPE and $Eu(dpm)_3$ and (*b*) $Eu(HFC)_3$

	S:CS:AS:L (mol ratio)				[L] × $10^2(M)$	$\Delta\nu_{Me}$ (p.p.m.)
(*a*)	1	2	3	0.2	29	0.050
	1	2	12	0.2	13	0.048
	1	2	48	0.2	4.0	0.041
	1	2	84	0.2	2.3	0.039
(*b*)	1		5	0.1	16	0.117
	1		11	0.1	9.3	0.117
	1		17	0.1	6.0	0.117
	1		23	0.1	4.4	0.117
	1		100	0.1	1.1	0.083
	1		550	0.1	0.2	0.048
	1		1100	0.1	0.1	0.015

experiments suggest that for simple molecules no advantage is to be gained with CS:S ratios higher than 2 or 3, but that for substrates like the oxadiazines, with a large number of sites capable of hydrogen bonding, improvements can be expected for CS:S ratios up to about 10.

For strongly coordinating substrates at least the enantiomeric shift is rather insensitive to the absolute [L] over a wide concentration range provided an appropriate [L]/[S] is maintained. This is illustrated in Table 3*a* which shows the effect of dilution with AS, again on the 1-phenylethylamine–TFPE–$Eu(dpm)_3$ system at a fixed molar ratio of 1:2:0.2. A 10-fold drop in [L] causes only a slight decrease in $\Delta\nu_{Me}$. The chiral shift reagent $Eu(HFC)_3$ likewise gives shift values which remain almost unchanged till a very low [L] is reached[6] (Table 3*b*).

Despite the success of the chiral solvate shift systems in generating enantiomeric shifts for a range of racemic substrates[7] we failed to obtain any enantiotopic shifts between the protons of prochiral methylene (*e.g.* benzyl alcohol, benzylamine, or benzyl cyanide) or methyl (*e.g.* dimethyl sulfoxide) groups, or between the methyl groups in *meso* compounds (*e.g. meso*-dimethyl tartrate). In this respect our shift system is quite inferior to chiral lanthanides like $Eu(HFC)_3$ with which impressive results have been reported, especially with benzylic protons (7).

The utilization of enantiomeric shifts in the determination of optical purity requires the shift to be great enough to provide complete or nearly complete peak separation, in order that peak area determinations can be made.

Many of the examples of Table 1 did not show sufficient separation to be useful in this sense but two examples are given in Figs. 1 and 2 which illustrate the potential of the method. Figure 1 shows the methyl doublet portion of the 60 MHz spectrum of a prepared sample of (−)-amphetamine of 22.6% optical purity. Good agreement with this value was obtained simply from peak height measurements (see Experimental Section). The peaks in Fig. 2 are those of the quaternary methyl groups in the 100 MHz spectrum of the oxadiazine **4***a*, and represent the fulfilment of our objective stated earlier, namely the direct determination of the optical purity of the product of an asymmetric reaction.

The isomerization of the adduct **3***a* in the presence of (+)-camphor-10-sulfonic acid was carried out under conditions identical to those used for **1** (14). The oxadiazine **4***a*, formed essentially quantitatively, had $[\alpha]_{578}^{20}$ + 8.80 (benzene). Fractional crystallization from benzene – petroleum ether (b.p. 35–60°) gave a nearly racemic crystalline precipitate and evaporation of the mother liquor gave crystalline material of $[\alpha]_{578}^{20}$ + 44.8° (benzene). The optical purity of this partially resolved sample was determined directly by 100 MHz n.m.r. analysis of TFPE–benzene in the presence of $Eu(fod)_3$ at 70° (Fig. 2). Area determination led to an optical purity of 21.4 ± 0.4%, corresponding to an enantiomeric enrichment of 4.21 ± 0.08% in the original asymmetric isomerization and a rotation of $[\alpha]_{578}^{20}$ 209 ± 4° for optically pure **4***a*. The stereoselectivity is thus much greater in the isomerization of **3***a* than of **1**, as expected.

We thank the National Research Council of Canada and the University of Waterloo for financial support of this work.

1. W. H. PIRKLE and S. D. BEARE. J. Am. Chem. Soc. **91**, 5150, 5475 (1969) and references therein.
2. W. H. PIRKLE, R. L. MUNTZ, and I. C. PAUL. J. Am. Chem. Soc. **93**, 2817 (1971).

[6]A concentration of [L] = 1×10^{-2} *M* represents the use of about 6 mg each of $Eu(HFC)_3$ and the amine in the n.m.r. sample tube. Indeed for both shift systems the lower limit of observation of the enantiomeric shift in this particular substrate was set by the capabilities of the spectrometer.

[7]We had failures here too, notably dimethyl tartrate, 2-butanol, 2-octanol, benzoin, and 1-phenylethanol.

Can. J. Chem. Downloaded from www.nrcresearchpress.com by 210.87.254.5 on 09/05/12
For personal use only.

3. G. M. WHITESIDES and D. W. LEWIS. J. Am. Chem. Soc. **93**, 5914 (1971).
4. G. M. WHITESIDES and D. W. LEWIS. J. Am. Chem. Soc. **92**, 6979 (1970).
5. H. L. GOERING, J. N. EIKENBERRY, and G. S. KOERMER. J. Am. Chem. Soc. **93**, 5913 (1971).
6. R. R. FRASER, M. A. PETIT, and J. K. SAUNDERS. Chem. Commun. 1450 (1971) and references therein.
7. R. R. FRASER, M. A. PETIT, and M. MISKOW. J. Am. Chem. Soc. **94**, 3253 (1972).
8. W. H. PIRKLE, S. D. BEARE, M. KAINOSHO, and K. AJISAKA. J. Am. Chem. Soc. **94**, 5924 (1972).
9. R. v. AMMON and R. D. FISCHER. Angew. Chem. Int. Ed. **11**, 675 (1972).
10. W. H. PIRKLE and S. D. BEARE. J. Am. Chem. Soc. **89**, 5485 (1967).
11. W. H. PIRKLE and S. D. BEARE. Tetrahedron Lett. 2579 (1968).
12. W. H. PIRKLE, T. G. BURLINGAME, and S. D. BEARE. Tetrahedron Lett. 5849 (1968).
13. W. H. PIRKLE and S. D. BEARE. J. Am. Chem. Soc. **90**, 6250 (1968).
14. C. P. R. JENNISON and D. MACKAY. Tetrahedron. **29**, 1255 (1973).
15. J. A. BERSON and D. A. BEN-EFRAIM. J. Am. Chem. Soc. **81**, 4083 (1959).
16. M. RABAN. The stereochemistry of groups in molecules: applications to NMR spectroscopy, asymmetric synthesis and the determination of optical purity. Ph.D. Thesis, Princeton University, Princeton, N.J. 1967.
17. W. H. PIRKLE, S. D. BEARE, and T. G. BURLINGAME. J. Org. Chem. **34**, 470 (1969).
18. *In* Organic syntheses. Vol. 46, *Edited by* E. J. Corey. John Wiley and Sons, Inc., New York. 1966. p. 78.
19. C. BEAUTE, S. CORNEL, D. LELANDAIS, N. THOAI, and Z. W. WOLKOWSKI. Tetrahedron Lett. 1099 (1972) and references therein.

Can. J. Chem. Downloaded from www.nrcresearchpress.com by 210.87.254.5 on 09/05/12
For personal use only.

Estimation of Phenols by the 4-Aminoantipyrine Method. II. Products from *para*-Substituted Alkylphenols

PETER F. JONES AND K. E. JOHNSON

Regina Water Research Institute, University of Saskatchewan, Regina, Saskatchewan S4S 0A2

Received May 17, 1973

4-Aminoantipyrine reacts with *p*-alkylphenols on oxidation with potassium ferricyanide to give yellow *ortho*-quinoneimides. These undergo a thermal and base-catalyzed rearrangement to benzodihydrooxazepines.

L'amino-4 antipyrine réagit avec les *p*-alkylphénols oxydés par le ferricyanure de potassium pour donner des *ortho*-quinonimides jaunes. Ces dernières se transforment sous l'influence de la chaleur ou des bases pour fournir des benzodihydrooxazépines. [Traduit par le journal]

Can. J. Chem. **51**, 3733 (1973)

We have recently confirmed (1) that the colorimetric estimation, using 4-aminoantipyrine (**1**), of phenols which are either unsubstituted, or have a readily eliminated substituent at the *para* position, involves oxidative *para* coupling to form red *p*-quinoneimide dyes **2** (see Scheme 1).

We now report the results of a study where the *para* position of the phenol is blocked by an alkyl group. Emerson (2) found that phenols having an alkyl, aryl, nitro, nitroso, benzoyl, ester, or aldehyde group in the *para* position did not show a color response to the 4-aminoantipyrine test. From this he correctly concluded that a positive color reaction involved oxidative *para* coupling. However, Czech workers (3) have recently reported that when the Emerson reaction is carried out with *p*-alkylphenols using higher concentrations of reagents, a turbidity is produced. The precipitate was isolated from *p*-cresol. Although initially yellow, on purification it gave a white, photochromic solid, m.p. 225–227°. On the sole basis of a molecular formula, itself incorrectly computed from elemental analyses, it was concluded that the latter compound arose from *ortho* coupling.

The lack of conclusive evidence for this, the first reported example of oxidative *ortho* coupling in this system, has led us to reinvestigate the reaction. The oxidation of a mixture of *p*-cresol and 4-aminoantipyrine by potassium ferricyanide did indeed result in the formation of a yellow precipitate (Scheme 2). Recrystallization from ethanol gave a cream solid, m.p. 224–227°, which appears to be the same product as that previously reported. However, the p.m.r.

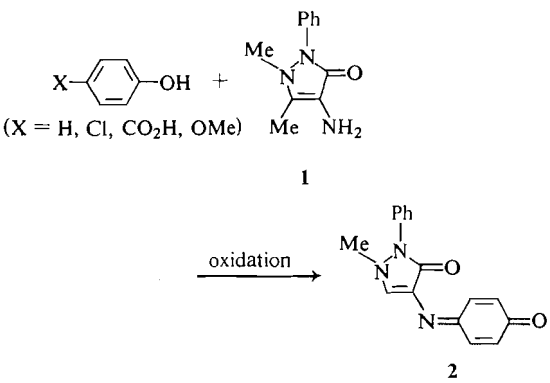

SCHEME 1

spectrum of this compound revealed that it could not be the *o*-quinoneimide adduct **3***a*, since it displayed only two methyl singlets, whereas **3***a* should have three such signals.

Comparison of the p.m.r. spectrum of the crude original product with that of the purified sample showed that the latter was not present to

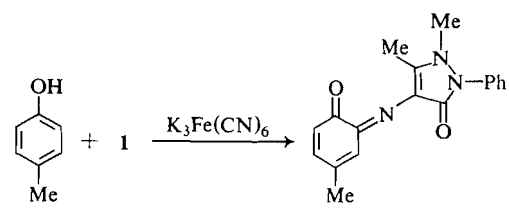

SCHEME 2

Can. J. Chem. Downloaded from www.nrcresearchpress.com by 210.87.254.105 on 09/05/12
For personal use only.

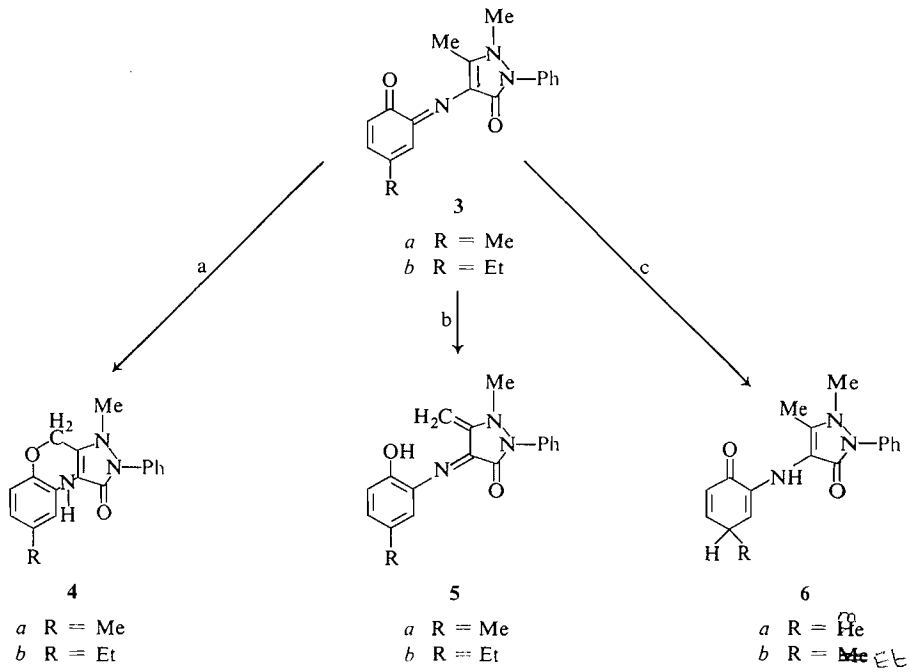

SCHEME 3

any extent initially. This suggests that recrystallization must have resulted in decomposition of the initial adduct. Accordingly, conditions were sought where the initial yellow adduct could be purified without decomposition. This was simply achieved by using non-hydroxylic solvents in the recrystallization step. A bright yellow solid was obtained, whose p.m.r. spectrum displayed the three methyl singlets required for **3***a*.

The p.m.r. spectra of the two compounds differ notably in the removal of a C—Me singlet at δ 1.52 originally present in **3***a*, and its replacement by a two proton singlet at δ 5.00 in the rearranged product. The position of the latter signal is suggestive of the formation from a methyl group of either an exocyclic methylene group or the allylic protons of an allyl ether. In the i.r. spectrum of the rearranged product, bands at 2.95 and 3.05 μ, absent in starting **3***a*, indicate the formation of an —OH or —NH group. Further evidence for this is seen in the p.m.r. spectrum of the rearranged compound by the presence of a broad, one proton singlet at δ 6.12, which is removed on deuteration. From these observations, two different reactions appear possible, either the loss of the antipyryl *C*-methyl group to form a phenol **5***a* (path *b*) or the heterocycle **4***a* (path *a*),[1] or the removal of the methyl group of the original phenol to give a *para*-quinonemethide, **6***a* (path *c*) (see Scheme 3).

The above evidence is insufficient to allow a decision between these possibilities. Accordingly, to find which of the two *C*-methyl groups was involved in the above rearrangements, the reaction was carried out with *p*-ethylphenol under conditions where the rearranged product would be expected. In this case, it should be simple to distinguish the formation of **4***b* or **5***b* from that of the *p*-quinonemethide **6***b*.

In fact, the p.m.r. spectrum of the reaction product clearly reveals that path *c* cannot be the operative reaction, since the retention of the ethyl group, and also the formation of the methylene group as a two proton singlet at an identical position to that of the rearrangement product from *p*-cresol can be seen. On the basis of the spectroscopic evidence alone, it is difficult to distinguish between the formation of the phenols **5***a* and *b* or their ring closed counterparts, the substituted dihydro-oxazepines **4***a* and *b*. The observation that the methylene protons appear as a singlet might seem to favor **4***a* and *b*,

[1]We thank a referee for pointing out this possibility.

Can. J. Chem. Downloaded from www.nrcresearchpress.com by 210.87.254.105 on 09/05/12
For personal use only.

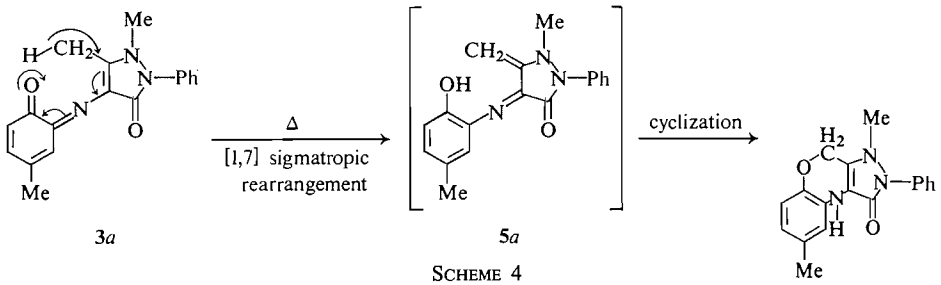

SCHEME 4

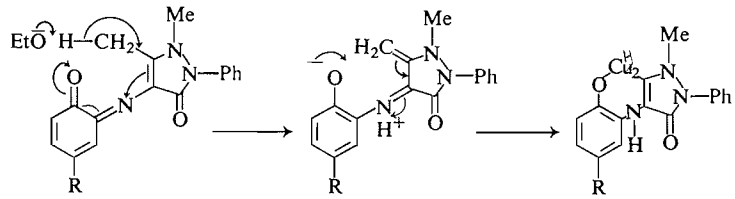

SCHEME 5

whose allylic protons are equivalent, whereas the methylene protons of **5***a* and *b* should be non-equivalent. However, it is frequently found that non-equivalent exocyclic methylene protons do not show geminal coupling (4*a*), therefore the phenol structures cannot be ruled out on this basis. They may be rejected on chemical evidence, however, since the *p*-cresol rearrangement product is completely insoluble in 5% aqueous sodium hydroxide and gives no color with ferric chloride, both reactions which are used to characterize phenols (5).

Unusual behavior on melting of the *o*-quinoneimide adduct **3***a* suggested that the above rearrangement might also occur thermally. The yellow compound melted at 148–150°. With increase in temperature, the melt decolorized and partially crystallized. Final remelting occurred at 210–220°, suspiciously similar to the m.p. of rearranged **4***a*. The thermolysis could be conveniently followed by p.m.r. spectroscopy in bromobenzene solvent, in which **3***a* showed methyl singlets at δ 1.00, 1.90, and 2.21 p.p.m. On heating the sample at 139°, these signals diminished in intensity, and the build-up of new signals at δ 1.75, 2.11, and 4.44 p.p.m. was seen. After 20 min the starting signals had been completely removed, and the new signals, in the ratio 3:3:2, were the only ones present. They were found to be identical to those of an authentic sample of **4***a* in bromobenzene. Rearranged **4***a* was recovered in good yield from the thermolysis mixture.

The thermal reaction may proceed through an intramolecular cyclization mechanism, possibly with an initial [1,7] sigmatropic rearrangement to the isomeric phenol **5***a*, which then undergoes cyclization (see Scheme 4). This would presuppose that the *o*-quinoneimide must be in a suitable configuration for interaction, namely with the antipyryl ring *syn* to the carbonyl group. The unusually high field position of the antipyryl *C*-methyl signal of **3***a* at δ 1.52 p.p.m., being shielded by approximately 1 p.p.m. compared with the corresponding group in *para*-quinoneimides, where the signal appears in the range δ 2.49–2.60 p.p.m. (1), would indicate that **3***a* does exist in the ground state configuration shown. Shielding of a proton located above the plane of the carbonyl group is well documented (4*b*).

The proposed initial [1,7] sigmatropic shift is allowed thermally as an antarafacial process by the Woodward–Hoffmann rules (6).

The ease of rearrangement of the *o*-quinoneimides in hydroxylic solvent at or below room temperature suggests the operation of an alternative mechanism, possibly involving a base-catalyzed reaction with an external nucleophile, presumably ethoxide ion (Scheme 5). Some evidence to support a base-catalyzed rearrangement has been obtained. Thus **3***a* appeared to be stable

Can. J. Chem. Downloaded from www.nrcresearchpress.com by 210.87.254.105 on 09/05/12
For personal use only.

in deuterochloroform solvent, only 8% rearrangement being observed after 3 days at room temperature. However, addition of pyridine to the reaction mixture accelerated the rearrangement since 78% isomerization occurred after a further 3 days. After rearrangement was seen to be complete, **4***a* was isolated in 56% yield.

Experimental

4-Aminoantipyrine (Aldrich) and the starting phenols were purchased from commercial suppliers and were used without further purification. Buffer solution of p*H* 10.4 was prepared by dissolving dry buffer salt (Fisher) in distilled water.

Melting points were taken on a hot stage apparatus and are uncorrected. Microanalyses were performed by Galbraith Laboratories Inc., Knoxville, Tennessee. P.m.r. spectra were recorded on a Varian A-60 spectrometer in deuterochloroform solvent and with tetramethylsilane as an internal standard. I.r. spectra were obtained on a Beckman IR 8 instrument with polystyrene calibration.

Reaction of 4-Aminoantipyrine with p-Cresol

(*a*) To a stirred mixture of 0.35 g (0.0032 mol) of *p*-cresol and 1.1 g (0.0054 mol) of 4-aminoantipyrine in 250 ml of buffer solution was added, in one portion, 21 g (0.064 mol) of potassium ferricyanide. A yellow precipitate immediately formed. The reaction mixture was stirred for 30 min and the solid was filtered off, washed with water, and was allowed to dry in air in the dark. The crude yellow product, 1.16 g, m.p. 29–120°, was recrystallized from 95% ethanol to give 0.25 g of **4***a* as gleaming cream flakes, m.p. 218–222°. Addition of water to the filtrate gave, on standing, further solid, m.p. 210–220°. Both crops had identical spectra and the total yield of **4***a* was 0.38 g (38%). Further recrystallization from ethanol gave the analytical sample, m.p. 224–227°. P.m.r. δ 7.7–6.7 (m, 8H, aromatic), 6.12 (broad s, 1H, removed on addition of D_2O, N*H*), 5.00 (s, 2H, CH_2), 2.81 (s, 3H, NMe), 2.25 (s, 3H, CMe); i.r. ($CHCl_3$) 2.95, 3.05 (NH), 6.02 (C=O).

Anal. Calcd. for $C_{18}H_{17}N_3O_2$: C, 70.34; H, 5.58; N, 13.67. Found: C, 70.44; H, 5.61; N, 13.62.

The product was completely insoluble in 5% aqueous sodium hydroxide, even on heating, and an ethanolic solution showed no noticeable color change on addition of ferric chloride solution.

(*b*) The dried yellow precipitate, prepared as above from 0.31 g (0.0029 mol) of *p*-cresol, 1.1 g (0.0054 mol) of 4-aminoantipyrine, and 20 g (0.061 mol) of potassium ferricyanide in 250 ml of buffer solution, was dissolved in methylene chloride. Addition of petroleum ether (b.p. 100–115°) precipitated 0.17 g of amorphous solid, m.p. 115–140°, whose p.m.r. spectrum was similar to that of unidentified impurities obtained during the preparation of some *p*-quinoneimides (1). The clear yellow filtrate was evaporated and the resulting solid was recrystallized from pentane to give 0.39 g (44%) of yellow **3***a*, m.p. 145–155°. The p.m.r. spectrum indicated the product was an 87:13 mixture of **3***a* and **4***a*. Several recrystallizations from pentane gave pure **3***a*, m.p. 148–150° (resolidifies and remelts 210–220°). P.m.r. δ 8.22–8.00 (m, 2H, vinyl), 7.70–6.85 (m, 6H, aromatic + vinyl), 2.74 (s, 3H, NMe), 2.37 (s, 3H, CMe), 1.52 (s, 3H, antipyryl CMe); i.r. ($CHCl_3$) 5.89, 6.06 μ (C=O).

Anal. Calcd. for $C_{18}H_{17}N_3O_2$: C, 70.34; H, 5.58; N, 13.67. Found: C, 70.40; H, 5.67; N, 13.70.

Reaction of 4-Aminoantipyrine with p-Ethylphenol

To a stirred mixture of 0.35 g (0.0029 mol) of *p*-ethylphenol and 1.2 g (0.0059 mol) of 4-aminoantipyrine in 250 ml of buffer solution was added, in one portion, 20 g (0.061 mol) of potassium ferricyanide. A yellow precipitate immediately formed. The reaction mixture was filtered after 30 min and the yellow solid obtained was dissolved in 95% ethanol. The solution on cooling deposited 0.24 g of **4***b*, m.p. 199–201°. Addition of water to the filtrate gave, on standing, further solid, m.p. 198–200°. The total yield of **4***b* was 0.39 g (42%). Further recrystallization from ethanol gave the analytical sample, m.p. 199–201°. P.m.r. δ 7.7–6.6 (m, 8H, aromatic), 6.35 (broad s, 1H, NH), 5.00 (s, 2H, CH_2), 2.81 (s, 3H, NMe), 2.53 (q, J = 8 Hz, 2H, CH_2CH_3), 1.16 (t, J = 8 Hz, 3H, CH_2CH_3); i.r. ($CHCl_3$), 2.95, 3.05 (NH), 6.02 μ (C=O).

Anal. Calcd. for $C_{19}H_{19}N_3O_2$: C, 71.01; H, 5.96; N, 13.08. Found: C, 71.27; H, 6.10; N, 13.08.

Thermal Rearrangement of **3***a*

A 60 mg (0.0002 mol) sample of **3***a* was dissolved in approximately 0.5 ml of bromobenzene. A p.m.r. spectrum of the solution showed three singlets at δ 1.00, 1.90, and 2.21 p.p.m. (external TMS). The n.m.r. sample tube was placed in a preheated oil bath at 139°. The sample was withdrawn after 10 min and the p.m.r. spectrum was examined. It showed a diminution of the intensities of the above three singlets and the formation of new singlets at δ 1.75, 2.11, and 4.45 p.p.m. These new signals were in the ratio 3:3:2 and subsequent examination of an authentic sample of **4***a* in bromobenzene revealed peaks at identical positions. The ratio of **3***a*:**4***a* was 24:76, as estimated from peak heights. After a further 10 min at 139°, the signals of starting **3***a* were completely removed and **4***a* appeared to be the sole product. Addition of petroleum ether (b.p. 100–115°) to the sample precipitated 48 mg (80%) of crude **4***a*, m.p. 200–214°. A solution of this product in deuterochloroform showed a p.m.r. spectrum identical to that of authentic **4***a*. Further purification by recrystallization from 95% ethanol gave 25 mg (42%) of pure **4***a*, m.p. 217–221°.

Base-catalyzed Rearrangement of **3***a*

A 50 mg (0.00016 mol) sample of **3***a* was dissolved in approximately 0.5 ml of deuterochloroform. The solution was stored in the dark at room temperature. After 3 days, the p.m.r. spectrum showed 8% rearrangement to **4***a*. Pyridine, approximately 0.26 g (0.0032 mol), was added by dropper to the solution. The mixture was stored in the dark and its p.m.r. spectrum was examined at intervals. The observed extent of rearrangement to **4***a* was 14 (3h), 36 (24 h), 60 (44 h), and 78% (70 h). Examination after 6 days showed complete rearrangement to **4***a*. Addition of petroleum ether (b.p. 100–115°) precipitated 28 mg (56%) of **4***a*, m.p. 215–222°.

Grateful acknowledgement is made to the National Research Council of Canada for its generous support of this work.

Can. J. Chem. Downloaded from www.nrcresearchpress.com by 210.87.254.105 on 09/05/12
For personal use only.

1. PETER F. JONES and K. E. JOHNSON. Can. J. Chem. In press.
2. E. EMERSON. J. Org. Chem. **8**, 417 (1943).
3. D. SVOBODOVA and J. GASPARIC. Coll. Czech. Chem. Commun. **35**, 1567 (1970).
4. R. K. NORRIS and S. STERNHELL. Applications of nuclear magnetic resonance spectroscopy in organic chemistry. 2nd Ed. Pergamon Press, London. 1969. (*a*) p. 278; (*b*) p. 91.
5. A. I. VOGEL. Elementary practical organic analysis. Part 2. 2nd Ed. Longman, London. 1971. p. 202.
6. R. B. WOODWARD and R. HOFFMANN. The conservation of orbital symmetry. Verlag Chemie, Weinheim. 1971. Chapt. 7.

Can. J. Chem. Downloaded from www.nrcresearchpress.com by 210.87.254.105 on 09/05/12
For personal use only.

Arrhenius Parameters for Reaction of *tert*-Butylperoxy Radicals with some Hindered Phenols and Aromatic Amines[1]

JAMES ANTHONY HOWARD AND EDWARD FURIMSKY
Division of Chemistry, National Research Council of Canada, Ottawa, Canada K1A 0R9

Received May 14, 1973

The reaction of *tert*-butylperoxy radicals with some 2,6-di-*tert*-butyl-4-substituted phenols, α-naphthol, α-naphthylamine, and *N*-phenyl-α-naphthylamine has been studied by following the change in radical concentration with time using an e.p.r. spectrometer. Rates of radical decay were first-order in both reactants and were not influenced by the presence of *tert*-butyl hydroperoxide.

Absolute values of the second-order rate constants were measured from −35 to −100° and the preexponential factors and activation energies fell in the range 10^4–10^5 M^{-1} s^{-1} and 0.5–1.0 kcal mol^{-1}. Rate constants for deuterated phenols (OD) and aromatic amines (ND) were an order of magnitude lower than for the corresponding light compounds.

There was no evidence for quantum mechanical tunneling in these hydrogen atom transfer reactions and it would appear that the activation parameters are low because reaction initially involves the formation of a hydrogen bonded peroxy radical – phenol (or aromatic amine) complex, followed by the transfer of a hydrogen atom within the complex.

Les réactions des radicaux peroxy-*tert*-butyliques avec quelques di-*tert*-butyl-2,6 phénols substitués en position 4, α-naphtol, α-naphthylamine et la *N*-phényl-α-naphthylamine ont été étudiées en suivant la variation de la concentration en radicaux avec le temps en utilisant un spectromètre de résonance paraélectronique. Les vitesses de disparition des radicaux sont du premier ordre pour les deux réactifs et ne sont pas influencées par la présence d'hydroperoxyde de *tert*-butyle. Les valeurs absolues des constantes de vitesse de second ordre sont mesurées de −35 à −100°, et les facteurs préexponentiels ainsi que les énergies d'activation sont compris dans l'écart de 10^4–10^5 M^{-1} s^{-1} et 0.5–1.0 kcal mol^{-1}. Les constantes de vitesses pour les phénols deutériés (OD) et les amines aromatiques (ND) sont dans un ordre de grandeur plus faible que pour les composés légers correspondants. Il n'y a pas d'évidence pour un effet tunnel de mécanique quantique dans ces réactions de transfert d'atomes d'hydrogène, et il apparaît que les paramètres d'activation sont bas parce que la réaction initiale implique la formation d'un complexe hydrogène lié à un radical peroxyphénol (ou amine aromatique), suivie par le transfert d'un atome d'hydrogène à l'intérieur du complexe. [Traduit par le journal]

Can. J. Chem. **51**, 3738 (1973)

Can. J. Chem. Downloaded from www.nrcresearchpress.com by 210.87.254.42 on 09/05/12
For personal use only.

Introduction

Hindered phenols and aromatic amines (AH) are widely used for the protection of organic materials against atmospheric autoxidation (1–4). These compounds function as antioxidants because they undergo a rapid bimolecular hydrogen atom transfer reaction with a chain propagating alkylperoxy radical (ROO·) to produce a free radical A· which is unable to propagate the chain.

$$\text{[1]} \qquad \mathrm{ROO\cdot} + \mathrm{AH} \underset{k_{-1}}{\overset{k_1}{\rightleftharpoons}} \mathrm{ROOH} + \mathrm{A\cdot}$$

There have been several kinetic studies of reaction 1 in solution but they have generally been confined to one temperature (2). In the few cases where absolute values of k_1 were determined over a temperature range, the Arrhenius parameters obtained were unreliable (2). This is because to determine an absolute value for k_1, it is necessary to carry out complete kinetic analyses of the uninhibited and inhibited autoxidations of the substrate (RH) from which ROO· was derived.[2]

In this paper we report the results of a *direct* kinetic e.s.r. study of the reaction of *tert*-butylperoxy radicals with a variety of 2,6-di-*tert*-butyl-4-substituted phenols, aromatic amines, and α-naphthol. Since this work was carried out over a substantial temperature range we are able to report accurate Arrhenius parameters for these reactions.

[1]Issued as NRCC No. 13373.

[2]This means that absolute values of the rate constants for the mutual reaction of ROO· ($2k_t$) and for the reaction of ROO· with RH (k_p) have to be determined in addition to the rate constant ratios $k_p/(2k_t)^{1/2}$ and k_p/k_1.

[2] 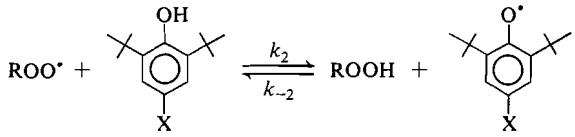

[3] 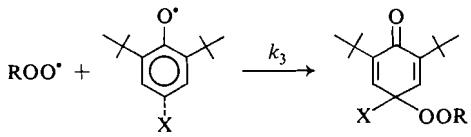

Experimental

The apparatus and experimental procedure used to determine bimolecular rate constants for reactions of *tert*-butylperoxy radicals have been described previously (5).

The 2,6-di-*tert*-butyl-4-substituted phenols, α-naphthol, and the aromatic amines were either commercial products or samples which had been prepared previously in our laboratory (6, 7). They were purified before use by recrystallization, sublimation or zone refining. Deuteration of phenolic and amino hydrogens was accomplished by adding a drop of D_2O to a standard solution (*ca.* 0.3 cc) of the undeuterated compound in an e.s.r. tube. The tube was then shaken for periods of time from 1–24 h. Deuteration of phenolic and amino hydrogens is rapid by this technique (8, 9).

Azoisobutane (Merck, Sharpe and Dohme of Canada Ltd), isopentane (Phillips Research Grade), and trichlorofluoromethane (Matheson) were used without further purification. Toluene (Phillips Research Grade) was passed through basic alumina before use.

Results and Discussion

2,6-Di-tert-butyl-4-substituted Phenols

Conventional kinetic studies have shown that overall rates of hydrocarbon autoxidation inhibited by 2,6-di-*tert*-butyl-4-substituted phenols are proportional to the rate of chain initiation and inversely proportional to the phenol concentration (8, 10–14). This implies that reaction of a chain carrying alkylperoxy radical and a phenol is bimolecular. Induction period studies have demonstrated that most of these phenols react with 2 equiv. of peroxy radicals (14, 15). The only exception was 2,6-di-*tert*-butyl-4-chlorophenol (BClP) which, at 65°, scavenged one peroxy radical (15). At the high ratios of peroxy radical to phenol used in the present work and the lower reaction temperatures this phenol behaved like the other phenols and reacted with 2 equiv. of peroxy radicals.

This was demonstrated by following the build-up of the concentration of *tert*-butylperoxy radicals during continuous photolysis of azoisobutane in oxygenated isopentane in the presence of BClP at −100°. The rate of radical production (R_i) was determined in the absence of the phenol and the time taken to reach this rate in the presence of a known concentration of BClP (τ) gave the number of radicals scavenged by each molecule of phenol from $R_i = n[AH]/\tau$. Both 2,6-di-*tert*-butyl-4-methylphenol (BMP) and BClP gave values of n equal to two by this technique.

The overall reaction of a 2,6-di-*tert*-butyl-4-substituted phenol with an alkylperoxy radical can, therefore, be described by eqs. 2 and 3.

The reverse of reaction 3 can be neglected at low temperatures because 4-alkylperoxy-2,6-di-*tert*-butylcyclohexadienones are quite stable at room temperature (15).

Reactions 2 and 3 (assuming a steady state concentration of phenoxy radicals) give the following expression for the rate of disappearance of ROO·

$$\text{I} \qquad \frac{-\mathrm{d}[\mathrm{ROO}\cdot]}{\mathrm{d}t} = \frac{2k_2k_3[\mathrm{ROO}\cdot][\mathrm{AH}]}{k_3 + k_{-2}\dfrac{[\mathrm{ROOH}]}{[\mathrm{ROO}\cdot]}}$$

In the case where $k_3 \gg k_{-2}$ [ROOH]/[ROO·] this rate expression reduces to

$$\text{II} \qquad \frac{-\mathrm{d}[\mathrm{ROO}\cdot]}{\mathrm{d}t} = 2k_2[\mathrm{ROO}\cdot][\mathrm{AH}]$$

Rates of decay of *tert*-butylperoxy radicals (from −37 to −100°) in the presence of a large excess of a 2,6-di-*tert*-butyl-4-substituted phenol (where the 4-substituent was methoxy (BMeOP), *tert*-butyl (BBP), methyl (BMP), chloro (BClP), cyano (BCNP), formyl (BCHOP), carboxy (BCOOHP), or carbo-*tert*-butoxy (BC(O)OP) and the unsubstituted phenol (BP)) in either isopentane, trichlorofluoromethane, or toluene were exactly first-order

Can. J. Chem. Downloaded from www.nrcresearchpress.com by 210.87.254.42 on 09/05/12
For personal use only.

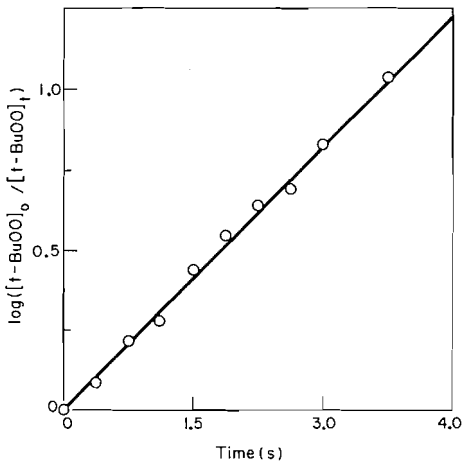

FIG. 1. A first-order plot of log (relative radical concentration) *vs.* time for the disappearance of *tert*-butylperoxy radicals in the presence of 2,6-di-*tert*-butyl-4-methylphenol (1.1×10^{-4} *M*) in isopentane at $-100°$.

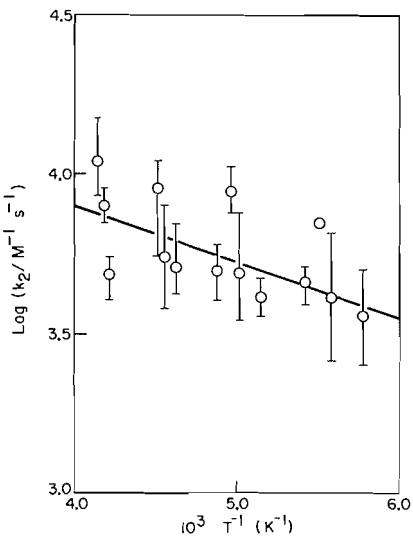

FIG. 2. A plot of log (k_2/M^{-1} s^{-1}) for 2,6-di-*tert*-butyl-4-methylphenol *vs.* the reciprocal of the absolute temperature.

(see *e.g.* Fig. 1). The pseudo first-order rate constants were proportional to the phenol concentration to the first power. The kinetic expression II was, therefore, strictly obeyed for these reactions.

Rates of radical decay were not influenced by the presence of *tert*-butyl hydroperoxide (0.1 *M*) and consequently the reverse of reaction 2 was unimportant.

Average absolute values of k_2, at the highest and lowest temperatures used in this work, are given in Table 1.[3] Plots of log (k_2/M^{-1} s^{-1}) against the reciprocal of the absolute temperature (see *e.g.*, Fig. 2) yielded the Arrhenius parameters listed in Table 1.

TABLE 1. Rate constants and Arrhenius parameters for reaction of *tert*-butylperoxy radicals with 2,6-di-*tert*-butyl-4-substituted phenols

Phenol	10^{-4} (k_2/M^{-1} s^{-1})		log (A_2/M^{-1} s^{-1})	E_2/kcal mol^{-1}
	−37 °C	−98 °C		
BMeOP	2.3	2.1	4.7±0.2	0.4±0.2
BBP	0.70	0.45	4.2±0.2	0.5±0.2
BMP	0.50	0.40	4.6±0.2	0.8±0.2
BP	0.34	0.15	4.3±0.2	1.0±0.15
BClP	0.50	0.40	4.3±0.2	0.5±0.2
BCNP	0.10	0.05	4.0±0.3	1.0±0.3
BCHOP	0.085	0.046	3.7±0.2	0.8±0.2
BCOOHP	0.07	0.025	3.8±0.3	1.0±0.2
BC(O)OBP	0.09	0.035	3.8±0.2	1.0±0.2

Extrapolation of the Arrhenius equation for BMP to 40 and 60° gave k_2 values of 1.1×10^4 and 1.2×10^4 M^{-1} s^{-1}. These values are in good agreement with those estimated for reaction of this phenol with cumylperoxy ($k^{40°} = 1.2 \times 10^4$ M^{-1} s^{-1} (16)), tetralylperoxy ($k^{40°} = 2.75 \times 10^4$ M^{-1} s^{-1} (16); $k^{40°} = 2.8 \times 10^4$ M^{-1} s^{-1} (17); $k^{65°} = 3.6 \times 10^4$ M^{-1} s^{-1} (11)), 9,10-dihydroanthracyl-9-peroxy ($k^{30°} = 1.1 \times 10^4$ M^{-1} s^{-1} (17)), and poly(peroxystyryl)peroxy radicals ($k^{65°} = 2.7 \times 10^4$ M^{-1} s^{-1} (11)). It has been suggested (17) that the rate constant for the reaction of BMP with peroxy radicals decreases in a regular manner with increasing size of the hydrocarbon moiety of the peroxy radical. The similarity between the reactivities of *tert*-butylperoxy and poly(peroxystyryl)peroxy to this phenol suggest that if there is a difference in reactivity between alkylperoxy radicals it is within the limits of error involved in the determination of absolute rate constants.

[3]Only the average rate constants for reaction of *tert*-butylperoxy radicals with 2,6-di-*tert*-butyl-4-substituted phenols, α-naphthol, and the aromatic amines at the highest and lowest temperatures are quoted in this paper. A complete compilation of the values of k_2 and k_7 is available, at nominal charge, from the Depository of Unpublished Data, National Science Library, National Research Council of Canada, Ottawa, Canada K1A 0S2. Copies of these tables can be obtained by writing to this address.

Can. J. Chem. Downloaded from www.nrcresearchpress.com by 210.87.254.42 on 09/05/12
For personal use only.

Can. J. Chem. Downloaded from www.nrcresearchpress.com by 210.87.254.42 on 09/05/12
For personal use only.

Arrhenius parameters for reaction of most of the phenols with alkylperoxy radicals have not been determined previously. Preexponential factors of $10^{5.6}$–$10^{8.3}$ M^{-1} s^{-1} and activation energies of 3.0–5.6 kcal mol^{-1} have, however, been reported for reaction of BMP with several alkylperoxy radicals (2). More recently Mahoney and DaRooge (17) have calculated an A-factor of $10^{4.46}$ M^{-1} s^{-1} and an activation energy of 0 kcal mol^{-1} for reaction of tetralylperoxy radicals with 2,4,6-tri-*tert*-butylphenol. The A-factors and activation energies that we found for reaction of all the hindered phenols with *tert*-butylperoxy radicals are in good agreement with Mahoney and DaRooge's values. Rate constants for the transfer of a hydrogen atom from a hindered phenol to an alkylperoxy radical are, therefore, characterized by activation parameters that are significantly lower than those usually found for metathesis reactions involving a hydrogen atom (18).

Low activation parameters have been found for other hydrogen atom transfer reactions between oxy radicals (19–22) although the exchange reaction between di-*tert*-butyliminoxyl and di-*tert*-butylhydroxylamine has a substantial activation energy (7 ± 2 kcal mol^{-1}) (23).

It has been suggested that the low activation energies for transfer of a hydrogen atom between two oxy radicals is due to the formation of a hydrogen bonded free radical – molecule complex (24). Reaction of *tert*-butylperoxy radicals with hindered phenols would be represented by reactions 4, 5, and 6.

[4] *tert*-BuOO + 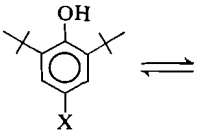 ⇌ *tert*-BuOO····H—O 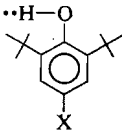

1

[5] **1** ⇌ *tert*-BuOO—H····O 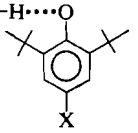

2

[6] **2** ⇌ *tert*-BuOOH + 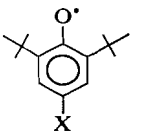

If k_{-4} and $k_{-6} \gg k_5$ the rate controlling step is the transfer of a hydrogen atom within the activated complex and

$$2k_2 = 2k_5k_4/k_{-4}$$

The overall activation energy (E_2) will be lower than for a normal hydrogen atom transfer reaction because of the negative heat of formation of the hydrogen bonded complex (24).

It is conceivable that the hydrogen atom in the hydrogen bonded complex **1** can tunnel through the potential energy barrier between the reactants and the products. Tunneling is possible because the formation of a hydrogen bonded complex between the reactants would be expected to narrow the barrier to reaction. The low activation energy associated with a reaction which involves tunneling would produce a lower than normal preexponential factor.

Linear plots of log k for the reaction of poly(peroxystyryl)peroxy and tetralylperoxy radicals with 2,6-di-*tert*-butyl-4-substituted phenols at 65° against Brown's σ^+ substituent constants (10, 13) have been presented as evidence in support of a dipolar contribution (**3**) to the activated complex for this hydrogen atom transfer reaction.

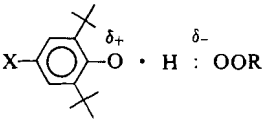

3

When the values of log $(k_2/M^{-1}\,s^{-1})$ at −37 and −98° were plotted against σ^+ the following correlations were obtained

$$\log (k_2^{-37°}/M^{-1}\,s^{-1}) = 3.5 - 1.00 \times \sigma^+ \quad (r = 0.94) \quad \text{and}$$

$$\log (k_2^{-98°}/M^{-1}\,s^{-1}) = 3.3 - 1.23 \times \sigma^+ \quad (r = 0.91)$$

Since the variations in k_2 with the nature of the 4-substituent are almost certainly due to differences in activation energies it is not surprising

TABLE 2. Rate constants for reaction of *tert*-butylperoxy radicals with some hindered phenols in solvents of different polarity

Phenol	$10^{-4}(k_2/M^{-1}\,s^{-1})$ −36 °C	−55 °C	−76 °C	−95 °C
BCNP				
A[a]	0.1	0.075	0.055	0.05
B	0.05	0.02	0.012	0.011
BP				
A	0.25	0.18	0.15	—
B	0.12	0.11	0.1	—
BMeOP				
A	2.3	2.0	2.0	1.5
B	1.25	1.2	1.1	1.15

[a]A, Trichlorofluoromethane; B, Trichlorofluoromethane and acetonitrate (3.8 *M*).

TABLE 3. Rate constants and Arrhenius parameters for reaction of *tert*-butylperoxy radicals with some deuterated 2,6-di-*tert*-butyl-4-substituted phenols (OD)[a]

Phenol	$10^{-4}(k_2/M^{-1}\,s^{-1})$ −34 °C	−97 °C	log $(A_2/M^{-1}\,s^{-1})$	E_2/kcal mol^{-1}
BMeOP	0.19(11)	0.14(14)	3.7±0.2	0.5±0.2
BMP	0.06(11.0)	0.04(24)	4.2±0.3	1.4±0.3
BP	0.015(11)	0.006(20)	3.3±0.2	1.2±0.2
BClP	0.2(4.4)	0.042(10)	5.1±0.5	2.0±0.4
BCNP	0.01(11)	0.003(26)	—	—

[a]The numbers in parentheses give the rate constant ratios k_2^H/k_2^D. Values of k_2^H were determined in the presence of H_2O and may not correspond exactly to the rate constants that can be calculated from the appropriate activation parameters

that the slopes of these correlations (*i.e.*, the ρ^+ values) decrease with an increase in temperature.

Extrapolation of the ρ^+ values to 65° yielded a value of ~ -0.8, lower than experimental values of ρ^+ for poly(peroxystyryl)peroxy (−1.12) and tetralylperoxy (−1.36). The lower ρ^+ value for *tert*-butylperoxy may reflect the lower electronegativity of this radical compared with the secondary alkylperoxy radicals.

Rate constants for hydrogen atom abstraction reactions, which involve a dipolar transition state, should increase when the polarity of the reaction medium is increased (25). However, rate constants for a number of hydrogen atom transfer reactions between oxyl radicals actually *decrease* as the solvent polarity is increased (24, 26). We found that the values of k_2 for BCNP, BP, and BMeOP are lower in trichlorofluoromethane containing acetonitrile (3.8 *M*) than they are in undiluted trichlorofluoromethane (Table 2).

It is well known that hindered phenols can hydrogen bond to acetonitrile (25). It would, therefore, appear that for some hydrogen atom transfer reactions between oxy radicals (especially those which have low activation energies) reactant–solvent interactions overshadow transition state – solvent interactions and the rate constant is decreased rather than enhanced by an increase in the polarity of the medium.

Deuterated 2,6-Di-tert-butyl-4-substituted Phenols

Rates of decay of *tert*-butylperoxy radicals in the presence of deuterated (OD) BMeOP, BMP, BP, BCNP, and BClP in either isopentane or trichlorofluoromethane were also found to obey the kinetic expression II.

Values of k_2 for the undeuterated phenols were identical in the absence and presence of a drop of H_2O which indicated that the only influence D_2O had on the reaction was to deuterate the phenolic hydrogen.

Rate constants[3] and activation parameters for the deuterated phenols are given in Table 3. The numbers in parentheses give the rate constant ratios k_2^H/k_2^D obtained at the highest and lowest temperatures. In all cases a substantial deuterium isotope effect was obtained, the magnitude of which decreased as the temperature was increased. Large primary deuterium isotope effects (~ 10) have been reported for reaction of poly(peroxystyryl)peroxy (8) and tetralylperoxy radicals (11) with BMP at 65°. Several other hydrogen atom transfer reactions between oxy radicals also exhibit substantial isotope effects (26, 27).

Extrapolation of k_2^H/k_2^D ratios for BMP to 65° gave a value of $k_2^H/k_2^D = 5$–6, somewhat lower than experimental values of 10–11 for the secondary alkylperoxy radicals. This difference probably reflects the errors involved in the two methods of determining absolute rate constants rather than to curvature of the Arrhenius plots.

For most of the phenols there was very little difference between A_2^H and A_2^D, and E_2^H and E_2^D. Consequently it was not possible to decide which activation parameter was reponsible for the large isotope effects. Enough kinetic data were, however, accumulated for BMP and BMP(OD) to calculate that $\log(A_2^D/A_2^H) = 0.92$ and $E_2^D - E_2^H = 0.6$ kcal mol^{-1}. The similarity between preexponential factors for BMP and

Can. J. Chem. Downloaded from www.nrcresearchpress.com by 210.87.254.42 on 09/05/12
For personal use only.

Can. J. Chem. Downloaded from www.nrcresearchpress.com by 210.87.254.42 on 09/05/12
For personal use only.

BMP(OD), in conjunction with the apparent linearity of the Arrhenius plot for BMP (*vide supra*), implies that tunneling does not have an important effect on the activation parameters for transfer of a hydrogen atom between a peroxy radical and a hindered phenol. The difference in the activation energies of 0.6 kcal mol^{-1} is less than would be expected on the basis of a simple zero-point energy effect on the height of the barrier to reaction (8).

α-Naphthol

A kinetic study of the influence of α-naphthol on the 2,2,3,3-tetraphenylbutane initiated autoxidation of 9,10-dihydroanthracene (14) has demonstrated that this phenol behaves like a hindered phenol, *i.e.*, all the α-naphthoxy radicals produced by a reaction analogous to [2] are consumed by reaction with a second peroxy radical [3].

Decays of *tert*-butylperoxy radicals in the presence of α-naphthol and α-naphthol(OD) in isopentane or trichlorofluoromethane accurately obeyed the kinetic expression II and *tert*-butyl hydroperoxide (0.1 M) had no effect on rates of radical decay. Absolute values of k_2 for these two compounds were determined over a temperature range[3] *e.g.*, $k_2^{H}(-74°) = 3.5 \times 10^4\ M^{-1}\ s^{-1}$ and $k_2^{H}(-105°) = 1.5 \times 10^4\ M^{-1}\ s^{-1}$, and $k_2^{D}(-74°) = 0.3 \times 10^4\ M^{-1}\ s^{-1}$ and $k_2^{D}(-105°) = 0.08 \times 10^4\ M^{-1}\ s^{-1}$ and gave the Arrhenius equations

$$\log (k_2/M^{-1}\ s^{-1}) = (6.4 \pm 0.8) - (1.7 \pm 0.6)/\theta$$

and

$$\log (k_2/M^{-1}\ s^{-1}) = (6.4 \pm 0.7) - (2.7 \pm 0.6)/\theta$$

for α-naphthol and α-naphthol(OD), respectively, where $\theta = 2.303RT$ kcal mol^{-1}.

α-Naphthol has approximately the same reactivity to *tert*-butylperoxy radicals at low temperatures as the most efficient hindered phenol studied in this work, BMeOP. The value of A_2 for α-naphthol is about 2 log units larger than for the hindered phenols with a correspondingly larger activation energy. This implies that the entropy of activation is about 10 e.u. less negative for α-naphthol than it is for a hindered phenol.

From Mahoney's work (14) it is possible to calculate a value of $2.0 \times 10^5\ M^{-1}\ s^{-1}$ at 60° for the rate constant for reaction of 9,10-dihydroanthracyl-9-peroxy radicals with α-naphthol[4] which is in satisfactory agreement with the value of $1.9 \times 10^5\ M^{-1}\ s^{-1}$ obtained by extrapolation of the values of k_2 to this temperature.

Replacement of the phenolic hydrogen of α-naphthol with deuterium produced a substantial isotope effect on k_2, *e.g.*, at $-74°$ $k_2^{H}/k_2^{D} = 11$ and at $-105°$ $k_2^{H}/k_2^{D} = 18$. Again it would appear that tunneling has no influence on this hydrogen atom transfer reaction since $\log (A_2^{H}/A_2^{D}) = 1.0$ and $E_2^{D} - E_2^{H} \sim 1.0$ kcal mol^{-1}.

Aromatic Amines

Kinetic studies of the influence of aromatic amines on hydrocarbon autoxidation at ambient temperatures have established that these compounds can undergo a chain termination reaction by donating a hydrogen atom to a chain propagating peroxy radical (9, 28).

$$[7] \qquad \mathrm{ROO\cdot} + \rangle\mathrm{NH} \xrightarrow{k_7} \mathrm{ROOH} + \rangle\mathrm{N\cdot}$$

The amino radical formed in reaction 7 may react with a peroxy radical to give nonradical products or undergo an oxygen atom transfer reaction to give an alkoxy radical (RO·) and a nitroxide ($\rangle$NO·).

$$[10] \qquad \mathrm{ROO\cdot} + \rangle\mathrm{N\cdot} \rightarrow \text{Non-radical products}$$

$$[11] \qquad \mathrm{ROO\cdot} + \rangle\mathrm{N\cdot} \rightarrow \mathrm{RO\cdot} + \rangle\mathrm{NO\cdot}$$

If all the amino radicals are destroyed by reaction 10 the stoichiometric factor n for the aromatic amine – peroxy radical reaction will be two. However, if a significant fraction of the amino radicals undergo reaction 11 or the self reaction 12

$$[12] \qquad \rangle\mathrm{N\cdot} + \rangle\mathrm{N\cdot} \rightarrow \text{Non-radical products}$$

the value of n could be less than 2. Using the induction period method described above n was found to be 2 for α-naphthylamine (AN), *N*-phenyl-α-naphthylamine (PAN), and *N*-phenyl-β-naphthylamine (PBN).

Rates of disappearance of *tert*-butylperoxy radicals were followed from −40 to −110° in the presence of a large excess of AN, β-naphthylamine (BN), PAN, PBN, diphenylamine, and

[4]Using a propagation rate constant of $3.3 \times 10^2\ M^{-1}\ s^{-1}$ at 30° for 9,10-dihydroanthracene and an activation energy of 8.3 kcal mol^{-1} (2).

TABLE 4. Rate constants and Arrhenius parameters[a] for reaction of *tert*-butylperoxy radicals with deuterated and normal α-naphthylamine and *N*-phenyl-α-naphthylamine

Amine	$10^{-4}(k_7/M^{-1}\,s^{-1})$			$\log(A_7/M^{-1}\,s^{-1})$	E_7/kcal mol^{-1}
	−35 °C	−84 °C	−97 °C		
AN	0.15	0.10	—	3.9±0.5	1.0±0.5
AN(ND_2)	0.0065	0.0045	—	2.7±0.5	1.0±0.5
PAN	1.25	—	1.0	5.1±0.5	1.0±0.4
PAN(ND)	0.31	—	0.12	3.8±0.4	0.7±0.4

[a]Per reactive hydrogen.

N,*N*′-diphenyl-*p*-phenylenediamine in either isopentane or trichlorofluoromethane.

Reliable values of k_7 could not be determined for PBN, diphenylamine, and *N*,*N*′-diphenyl-*p*-phenylenediamine. This was because a nitroxide was produced immediately a reaction mixture was photolyzed and the low field line of the nitroxide triplet overlapped the *tert*-butylperoxy signal.

Values of $-d[tert\text{-}BuOO\cdot]/dt$ for AN, PAN, and BN, and the deuterated analogs were accurately first-order in both reactants. Rates of radical decay in the presence of AN and PAN were not influenced by the addition of *tert*-butyl hydroperoxide (0.1 *M*). This implies that α-naphthylamino and *N*-phenyl-α-naphthylamino radicals do not abstract a hydroperoxidic hydrogen at the low temperatures used in this work. *tert*-Butyl hydroperoxide did, however, slow down the rate of disappearance of *tert*-butylperoxy radicals in the presence of BN. This compound must react with peroxy radicals by a mechanism analogous to non-hindered phenols and consequently will not be considered further in this paper.

Absolute values of k_7[3] and Arrhenius parameters per active hydrogen for AN, AN(ND_2), PAN, and PAN(ND) are given in Table 4.

N-phenyl-α-naphthylamine is about 10 times more reactive than α-naphthylamine to *tert*-butylperoxy radicals and has about the same reactivity as BMeOP to this radical. The difference in reactivity between PAN and AN would appear to be because of a difference in entropy of activation rather than to a difference in enthalpy of activation. It is interesting to note that there was no measurable difference between A_7 and A_2, and E_7 and E_2 for PAN and BMeOP.

Rates of disappearance of *tert*-butylperoxy radicals in the presence of AN(ND_2) and PAN(ND) were much slower than they were in the presence of the same concentrations of AN and PBN. The rate constant ratio k_7^H/k_7^D was approximately 20 for AN and 5–6 for PBN.

Experimentally determined values of $\log A_7^D$ were about one log unit less than values of $\log A_7^H$ for both AN and PBN. This difference in preexponential factors is probably the result of experimental error rather than to a larger entropy of activation for the deuterated compound.

Conclusions

The hydrogen atom transfer reaction between the *tert*-butylperoxy radical and 2,6-*tert*-butyl-4-substituted phenols, α-naphthol, α-naphthylamine, and *N*-phenyl-α-naphthylamine is characterized by low Arrhenius parameters (10^4–10^5 $M^{-1}\,s^{-1}$ and 0.5–1.0 kcal mol^{-1}) and moderately large deuterium isotope effects (k^H/k^D = 10–20). In most cases the logarithm of the ratio of the preexponential factors for a deuterated and light compound was ~1.0 with the difference in rate constant being the result of a larger activation energy for the deuterated compound. Arrhenius plots for this reaction would appear to be linear from −100° to +65° which implies that quantum mechanical tunneling does not have an important influence on these reactions. The low activation parameters would appear to be because the reaction involves the formation of a hydrogen bonded free radical – reactant complex followed by the transfer of a hydrogen atom within the complex.

We thank the Chevron Research Company for financial support in the form of a Fellowship to one of us (E.F.) and Dr. K. U. Ingold for his continuing interest and advice throughout the course of this work.

Can. J. Chem. Downloaded from www.nrcresearchpress.com by 210.87.254.42 on 09/05/12
For personal use only.

1. L. R. MAHONEY. Angew. Chem. Int. Ed. Engl. **8**, 547 (1969).
2. J. A. HOWARD. Adv. Free Rad. Chem. **4**, 49 (1972).
3. K. U. INGOLD. Chem. Soc. Spec. Publ. No. 24, 285 (1970).
4. K. ADAMIC, D. F. BOWMAN, and K. U. INGOLD. J. Am. Oil Chem. Soc. **47**, 109 (1970).
5. E. FURIMSKY and J. A. HOWARD. J. Am. Chem. Soc. **95**, 369 (1973).
6. K. U. INGOLD. J. Phys. Chem. **64**, 1636 (1960).
7. K. U. INGOLD. Can. J. Chem. **38**, 1092 (1960).
8. J. A. HOWARD and K. U. INGOLD. Can. J. Chem. **40**, 1851 (1962).
9. I. T. BROWNLIE and K. U. INGOLD. Can. J. Chem. **44**, 861 (1966).
10. J. A. HOWARD and K. U. INGOLD. Can. J. Chem. **41**, 2800 (1963).
11. J. A. HOWARD and K. U. INGOLD. Can. J. Chem. **42**, 2324 (1964).
12. D. V. GARDNER, J. A. HOWARD, and K. U. INGOLD. Can. J. Chem. **42**, 2847 (1964).
13. J. A. HOWARD and K. U. INGOLD. Can. J. Chem. **43**, 2724 (1965).
14. L. R. MAHONEY. J. Am. Chem. Soc. **88**, 3035 (1966).
15. E. C. HORSWILL, J. A. HOWARD, and K. U. INGOLD. Can. J. Chem. **44**, 985 (1966).
16. H. BERGER, A. M. W. BLAAUW, M. M. AL, and P. SMAEL. Adv. Chem. Ser. No. 75, 346 (1968).
17. L. R. MAHONEY and M. A. DAROOGE. J. Am. Chem. Soc. **92**, 4063 (1970).
18. S. W. BENSON. Thermochemical kinetics. John Wiley and Sons, Inc., New York, N.Y. 1968.
19. R. W. KREILICK and S. I. WEISSMAN. J. Am. Chem. Soc. **84**, 306 (1962).
20. R. W. KREILICK and S. I. WEISSMAN. J. Am. Chem. Soc. **88**, 2645 (1966).
21. M. R. ARICK and S. I. WEISSMAN. J. Am. Chem. Soc. **90**, 1654 (1968).
22. L. R. MAHONEY and M. A. DAROOGE. J. Am. Chem. Soc. **92**, 890 (1970).
23. G. D. MENDENHALL and K. U. INGOLD. J. Am. Chem. Soc. **95**, 627 (1973).
24. L. R. MAHONEY and M. A. DAROOGE. J. Am. Chem. Soc. **94**, 7002 (1972).
25. J. A. HOWARD and K. U. INGOLD. Can. J. Chem. **42**, 1044 (1964).
26. M. A. DAROOGE and L. R. MAHONEY. J. Org. Chem. **32**, 1 (1967).
27. J. A. HOWARD, W. J. SCHWALM, and K. U. INGOLD. Adv. Chem. Ser. No. 75, 6 (1968).
28. I. T. BROWNLIE and K. U. INGOLD. Can. J. Chem. **45**, 2419 (1967).

Can. J. Chem. Downloaded from www.nrcresearchpress.com by 210.87.254.42 on 09/05/12
For personal use only.

Application of Carbon-13 Nuclear Magnetic Resonance to Conformational Analysis of Trimethylene Sulfites

GERALD W. BUCHANAN[1]
Department of Chemistry, Carleton University, Ottawa, Canada K1S 5B6

J. B. STOTHERS[2]
Department of Chemistry, University of Western Ontario, London 72, Ontario

AND

GORDON WOOD
Department of Chemistry, University of Windsor, Windsor 11, Ontario

Carbon-13 n.m.r. chemical shifts are reported for trimethylene sulfite, 10 alkyl derivatives, and a related 1,3,2-dioxathiane. Data are discussed in terms of possible chair and twist conformations and in some cases the data permit definitive conformational assignments. Results are compared with previous conclusions based on proton n.m.r. and dipole moment measurements. The orientation of the S=O group is shown to have a very pronounced influence on the C-4 and -6 ring carbon shieldings.

On rapporte les déplacements chimiques en r.m.n. ^{13}C du sulfite de triméthylène, de 10 dérivés alkylés et d'une dioxathiane-1,3,2 qui leur est relié. Les donnés sont discutées en termes de conformations chaise et croisée possibles; dans quelques cas les résultats permettent de faire des attributions conformationnelles définitives. Les résultats sont comparés avec des conclusions antérieures basées sur la r.m.n. du proton et sur des mesures de moments dipolaires. On montre que l'orientation du groupe S=O a une profonde influence sur le blindage des C-4 et -6 du cycle. [Traduit par le journal]

Can. J. Chem. 51, 3746 (1973)

Introduction

In recent years considerable effort has been directed towards elucidating the conformations of substituted trimethylene sulfites. The picture appears to be clear for the parent compound in which a chair conformation with an axial S=O group dominates (1, 2). Also a strong preference for the axial orientation ($-\Delta G^\circ_{S=O}$ = 2.1 kcal/mol) has been demonstrated (3). The situation remains doubtful, however, regarding predominant conformations in alkyl substituted materials. From dipole moment (3) and ^1H n.m.r. studies the existence of non-chair conformations for several derivatives has been suggested, particularly for compounds containing *syn*-axial methyl groups at the C-4 and -6 ring positions (4, 5).

It is now well established that ^{13}C n.m.r. chemical shifts are an order of magnitude more sensitive to steric factors than ^1H shifts in favorable cases (6, 7). Thus in an attempt to gain further insight into the geometries of trimethylene sulfites in solution we have obtained the ^{13}C n.m.r. shieldings of 10 alkylated derivatives. To delineate some of the factors affecting the shieldings a related 1,3,2-dioxathiane has been studied. Results are compared with published findings for 1,3-dioxanes (8) and 1,3,2-dioxaphosphorinanes (9).

Results and Discussion

^{13}C n.m.r. shieldings for trimethylene sulfite and 10 alkyl derivatives are presented in Table 1 while data for related systems are collected in Table 2.

Assignments for **1** are apparent from observed integrated intensity ratios. Differences in nuclear Overhauser enhancements for methylene carbons of this type will be minimal. For alkylated materials ring carbon assignments follow directly from empirically established trends of alkyl substitution on carbon resonances (10). In **2**, for example, the downfield shift of 7 p.p.m. for C-4 on replacement of a hydrogen by a methyl is reminiscent of the 9 p.p.m. deshielding effect observed in hydrocarbons (10). The β-deshielding effect on C-5 of similar magnitude is again consistent with the early hydrocarbon findings.

[1]To whom correspondence should be addressed
[2]Part 36 in series "^{13}C n.m.r. Studies"; for part 35 see ref. 18.

Can. J. Chem. Downloaded from www.nrcresearchpress.com by 210.87.254.42 on 09/05/12
For personal use only.

Can. J. Chem. Downloaded from www.nrcresearchpress.com by 210.87.254.42 on 09/05/12
For personal use only.

TABLE 1. ^{13}C n.m.r. chemical shifts for trimethylene sulfites

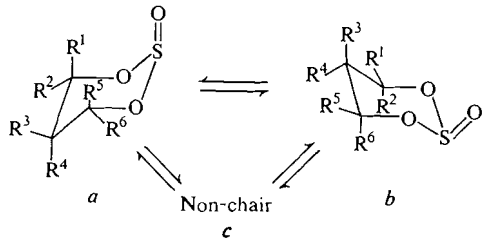

Compound	Substituent	Conformation†	δ_C (±0.1 p.p.m. from TMS)*										
			C-4	C-5	C-6	R^1	R^2	R^3	R^4	R^5	R^6	$(CH_3)_3C$	$(CH_3)_3C$
1		*a*	57.1	26.0	57.1								
2	$R^2 = CH_3$	*a*	64.1	33.3	57.4		21.2						
3	$R^1 = CH_3$	*b,c*	63.0	31.1	57.4	21.6							
4	$R^2 = R^6 = CH_3$	*a*	64.6	40.7	64.6		21.1				21.1		
5	$R^2 = R^5 = CH_3$	*a,c*	62.2	37.9	71.5		21.0			22.4			
6	$R^1 = R^5 = CH_3$	*b*	73.7	38.7	73.7	21.3				21.3			
7	$R^1 = R^2 = R^6 = CH_3$	*a,c*	80.6	44.0	60.5	28.8	32.2				21.2		
8	$R^1 = R^2 = R^5 = CH_3$	*b,c*	81.7	41.9	70.3	31.5	26.4			22.0			
9	$R^1 = R^2 = R^5 = R^6 = CH_3$	*c*	79.0	44.9	79.0	32.9	30.4			32.9	30.4		
10	$R^3 = t$-Bu	*a*	59.1	44.0	59.1							27.0	31.4
11	$R^4 = t$-Bu	*a,c*	61.5	44.2	61.5							28.1	32.0

*Solution 0.1–0.3 *M* in $CDCl_3$.
†As previously assigned (ref. 4).

TABLE 2. ^{13}C n.m.r. chemical shifts for related compounds*

Compound	
12*	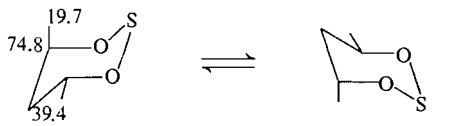
13†	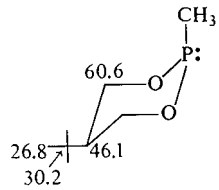
14†	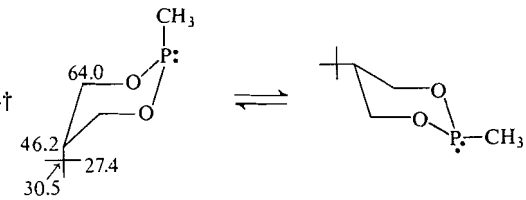
	2 : 1

*Solution 0.1 *M* in $CDCl_3$; δ C (± 0.1 p.p.m. from TMS).
†From ref. 9 (75% v:v solutions in C_6D_6).

For methyl carbons in **5**, **7**, and **8**, assignments were verified by specific ^1H decoupling experiments, since it is known (4) that protons of axial methyl groups in trimethylene sulfites are deshielded relative to their equatorial counterparts. From dipole moments and ^1H n.m.r. (4), compounds **2** and **4** are deemed to be in chair conformations with axial S=O functions. The equatorial methyl carbon shieldings are identical (21.1 ± 0.1 p.p.m.) for these materials. It is interesting to note the similarity with the equatorial methyls in **6**, a compound judged to be entirely in a chair conformation with an *equatorial* S=O grouping. Apparently an equatorial methyl carbon at C-4 or -6 will resonate near 21.1 p.p.m. regardless of the orientation of the S=O moiety.

In striking contrast, employing **4** and **6** as model compounds, it is clear that the orientation of the S=O has a very large influence on the C-4 and -6 ring carbon shieldings. In **4**, where the axial hydrogens on C-4 and -6 are *syn*-axial to the exocyclic oxygen, C-4 and -6 are shielded by *ca.* 9 p.p.m. relative to their counterparts in **6**. Presumably this is another example of the upfield γ steric shift (6, 7, 11, 12, 16).

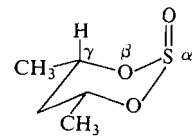

4

In **4** the axial S=O bond is *gauche* with respect to the O—C-4 (O—C-6) bond but in **6** the equatorial S=O will be *anti*. Nonbonded interactions between the axial oxygen in **4** and the axial hydrogens at C-4 and -6 are probably sufficient to perturb the electron distribution about C-4 and -6 and increase their shielding. A theoretical model for the γ effect based on charge polarization has been proposed (12). It is interesting that the magnitude of the upfield shift in the epimeric sulfites is nearly twice that observed in epimeric 4-*t*-butylcyclohexanols (6, 13). For the *cis* isomer of the cyclohexanols the C-3 and -5 ring carbons are shielded by 4.7 p.p.m. relative to the corresponding carbons of the *trans* form. In 1,3 dioxanes (8), where the interatomic distances are somewhat decreased, the steric interactions between an axial CH_3 at C-2 and the axial hydrogens at C-4 and -6 induce an upfield shift of 6.5 p.p.m. in the latter carbon resonances.

Supporting evidence for a predominantly steric origin of the upfield γ shift in **4** is gained from the results for the dioxathiane **12**, which lacks the exocyclic oxygen and is a mixture of rapidly inverting chair forms at room temperature (14). In **12**, C-4 and -6 appear at 74.8 p.p.m. which is reasonably close to those in **6** (73.7 p.p.m.) but 10 p.p.m. less shielded than C-4 and -6 of **4**.

The remaining 4,6-dimethyl trimethylene sulfite **5** is thought to exist as a mixture of a chair form with axial S=O and a non-chair form (4). The 21.0 shielding for the methyl on C-4 indicates an equatorial orientation for this group but the methyl on C-6 appears at measurably lower field at 22.4 p.p.m. If the methyl were

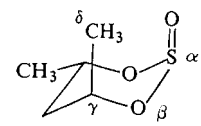

5

Can. J. Chem. Downloaded from www.nrcresearchpress.com by 210.87.254.42 on 09/05/12
For personal use only.

Can. J. Chem. Downloaded from www.nrcresearchpress.com by 210.87.254.42 on 09/05/12
For personal use only.

axial it would be *syn*-axial to the exocyclic oxygen and an appreciable steric interaction is expected. For sterically interacting "δ" methyl groups it has recently been found that appreciable deshielding effects are operative (15). A primary example is 1,8-dimethylnaphthalene in which the methyls are deshielded by 6.6 p.p.m. relative to those in the 1,4-dimethyl derivative. Apparently a related deshielding δ effect is responsible for the low field shift of the axial methyl on C-6 of **5**, although in sulfites with an axial S=O group, the possibility of local anisotropic contributions to the shieldings cannot be disregarded.

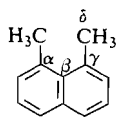

It is notable that the C-4 methine carbon of **5** is *ca.* 2 p.p.m. upfield from that in **4**. Steric interactions between the axial methyl on C-6 and the axial H on C-4 (γ effect) are likely to be causing this shielding. The magnitude of the effect, however, is only about half of that (3.97 p.p.m.) seen for the axial conformer of methylcyclohexane (10, 16). This may imply some contribution from a form other than a chair in agreement with conclusions based on dipole moment and ^{1}H n.m.r. data.

The monomethyl sulfite **3** is judged from ^{1}H n.m.r. and dipole moments to be a mixture of a chair with equatorial S=O (*b*) and some non-chair form (*c*). If (*b*) were the only contributing conformation then the methyl signal should appear near 21.1 p.p.m. as expected for a pure equatorial substituent. The observed shift of 21.6 p.p.m. implies some contribution from an axial or quasi-axial methyl, since a deshielding δ effect appears to be operative. Notably the C-4 shift of **3** (63.0) is rather similar to that of **2** (64.1) and **4** (64.6). If **3** exists to an appreciable extent in a chair with axial S=O, there will be strong nonbonded interactions between the exocyclic oxygen and the *syn*-axial methyl group. This would be expected to lead to increased shielding at C-4, as observed. Thus, in contrast to earlier interpretations (4), ^{13}C shifts suggest that a chair form (*a*) of **3** is extensively populated. Distinction between (*b*) and (*c*) as minor contributors, however, cannot be made.

In the trimethyl sulfites **7** and **8**, replacement of both hydrogens on C-4 by methyl groups shifts the C-4 resonance substantially downfield as expected from the established trends of alkyl substitution (10). The most striking difference between these isomers, however, is the 10 p.p.m. upfield shift for C-6 of **7** relative to C-6 in **8**. If a chair form with an axial S=O predominates for **7**, then this observation can be explained on the basis of the upfield γ-steric shifts noted earlier. The axial methine proton at C-6 will experience non-bonded interactions with the axial methyl at C-4 and the axial exocyclic oxygen atom. It is interesting to note that relative to **4**, C-6 of **7** is shielded by 4.1 p.p.m. This upfield shift is nearly identical to that observed in an axial methyl substituted cyclohexane (16) and suggests that for **7** a chair conformation with an axial methyl at C-4 is highly populated. In support of this is the 21.2 p.p.m. shift for the methyl at C-6 indicating an essentially pure equatorial disposition. Thus for **7** ^{13}C n.m.r. results suggest that conformation (*a*) predominates and little evidence for a non-chair form (*c*) exists in contrast to conclusions based on ^{1}H n.m.r. and dipole moments.

Compound **8** shows similar dipole moment behavior to **3** and is judged to be a mixture of mostly a chair with equatorial S=O (*b*) and some non-chair form (*c*). The 22.0 p.p.m. shift for the methyl at C-6 of **8** indicates that this function cannot be solely equatorial and therefore some form other than (*b*) must be appreciably populated. Further insight is gained by comparing the C-6 shift of **8** with that of **6**. In **8** C-6 is shielded by 3.4 p.p.m. relative to **6** and accordingly a large contribution from a chair with an axial methyl at C-4 appears likely. The upfield shift, however, is less than that seen for axial methylcyclohexane (10, 16) suggesting minor contributions from either (*a*) or (*c*).

Assuming that **7** exists almost exclusively in conformation (*a*) and **8** is mainly in form (*b*) the shifts of the axial methyls at C-4 can be rationalized on the basis of the previously described deshielding δ effect. In **7** there will be a δ interaction between the axial exocyclic oxygen and the axial methyl at C-4 whereas in the major form of **8** no such interaction will exist. As a result the axial methyl at C-4 of **7** is appreciably deshielded (by 2.4 p.p.m.) relative to its counterpart in **8**.

The tetramethyl substituted sulfite **9** has been assigned a non-chair geometry on basis of ^{1}H

Can. J. Chem. Downloaded from www.nrcresearchpress.com by 210.87.254.42 on 09/05/12
For personal use only.

n.m.r. and dipole moments (3, 4). Carbon shieldings for the *gem*-dimethyl groups are distinctly different from those in the predominantly chair forms **7** and **8**. On these grounds ^{13}C n.m.r. results lend support to the earlier conclusions.

The C-4 and -6 shifts of the *t*-butyl sulfites **10** and **11** provide a clue as to their predominant conformations. For **10** the dominant form is no doubt a chair with an equatorial *t*-butyl group and an axial S=O (3, 4). Compound **11**, however, is deemed to be a mixture of *trans*-diaxial chair (*a*) and a twist form (*c*). If **11** had a large component of a *trans*-diequatorial chair (*b*), a considerable deshielding effect relative to **10** should be observed at the C-4 and -6 carbons due to a removal of the *gauche* interaction of the S=O bond with the O—C-4 and O—C-6 bonds. Employing compound **4** as a model for pure axial S=O and **6** for pure equatorial S=O, a difference of near 9 p.p.m. might be expected between **10** and **11**. The observed deshielding in **11**, however, amounts to only 2.4 p.p.m. at C-4 and -6 ruling out extensive contributions from a *trans*-diequatorial chair.

It is interesting to note that the quaternary *t*-butyl carbon and the methyl carbons of **11** are deshielded by *ca.* 1 p.p.m. relative to their counterparts in **10**. By comparison, in *cis*-2-methyl-5-*t*-butyl-1,3-dioxane (**15**), the corresponding carbons are deshielded by 2 p.p.m. relative to those in the *trans*-isomer **16** (8, 17). The epimeric 2-methyl-5-*t*-butyl-1,3,2-dioxaphosphorinanes **13** and **14** (Table 2) show a similar,

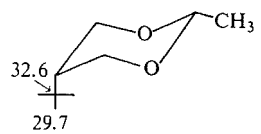

15

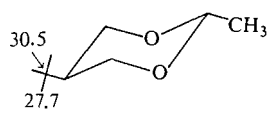

16

albeit smaller effect which is attributed to the presence of an equilibrium mixture in the *trans*-isomer (9). For an axial substituent at the 5-position of these three classes of compounds no *syn*-axial hydrogens are present, and it appears that the ring oxygen atoms preferentially deshield an axial moiety. If (*a*) were the only contributor to the structure of **11**, a larger deshielding trend close to that of the 1,3-dioxanes would be expected. We conclude therefore that **11** is an equilibrium mixture of about 70% (*a*) with the remaining forms being (*b*) and/or (*c*).

Conclusions

It is clear that ^{13}C n.m.r. constitutes a useful addition to the available methods for examining geometries of trimethylene sulfites. Shieldings at the C-4 and -6 ring carbons combined with those for substituent methyl and *t*-butyl groups give valuable insight into trimethylene sulfite conformation. For C-5 ring carbons no trends consistent with conformational changes are evident. Shieldings at this position reflect the previous observation (4) that association phenomena in any form most strongly perturb the electronic environment about this carbon. The present paper includes additional evidence for an important deshielding δ effect on carbon resonances.

Experimental

Materials

Syntheses for all compounds have been described previously (3, 14).

Spectra

Compounds were examined as 0.1–0.3 *M* solutions in $CDCl_3$ containing TMS as an internal standard. No significant dilution effects on the shieldings were observed over this concentration range. All spectra were obtained at 25.2 MHz most commonly under conditions of complete proton noise decoupling. Except for **11**, a Varian XL-100-15 spectrometer operating in the Fourier Transform mode was employed using 5 mm spinning sample tubes. Compound **11** was examined using a Varian XL-100-12 spectrometer, with spectral accumulations accomplished by a C-1024 time averaging computer on an 8-mm sample tube.

We thank the National Research Council of Canada for financial support.

1. D. G. Hellier, J. G. Tillet, H. F. van Woerden, and R. F. M. White. Chem. Ind. (London), 1956 (1963).
2. P. Albriktsen Acta Chem. Scand. **25**, 478 (1971).
3. G. Wood, J. M. McIntosh, and M. H. Miskow. Can. J. Chem. **49**, 1202 (1971).
4. G. Wood, G. W. Buchanan, and M. H. Miskow. Can. J. Chem. **50**, 521 (1972) and references therein.
5. P. Albriktsen. Acta Chem. Scand. **26**, 3678 (1972).

6. G. W. BUCHANAN, D. A. ROSS, and J. B. STOTHERS. J. Am. Chem. Soc. **88**, 4301 (1966).
7. J. B. STOTHERS. Carbon-13 NMR spectroscopy. Academic Press, New York, N.Y. 1972; N. K. WILSON and J. B. STOTHERS. Topics in stereochemistry. Vol. 8. *Edited by* E. L. Eliel and N. L. Allinger. Interscience, New York, N.Y. 1973.
8. A. J. JONES, E. L. ELIEL, D. M. GRANT, M. C. KNOEBER, and W. F. BAILEY. J. Am. Chem. Soc. **93**, 4772 (1971).
9. W. G. BENTRUDE, K. C. YEE, R. D. BERTRAND, and D. M. GRANT. J. Am. Chem. Soc. **93**, 797 (1971).
10. D. M. GRANT and E. G. PAUL. J. Am. Chem. Soc. **86**, 2984 (1964); D. K. DALLING and D. M. GRANT. J. Am. Chem. Soc. **89**, 6612 (1967), **94**, 5318 (1972).
11. W. R. WOOLFENDEN and D. M. GRANT. J. Am. Chem. Soc. **88**, 1496 (1966).
12. D. M. GRANT and B. V. CHENEY. J. Am. Chem. Soc. **89**, 5315 (1967).
13. J. D. ROBERTS, F. J. WEIGERT, J. I. KROSCHWITZ, and H. J. REICH. J. Am. Chem. Soc. **92**, 1338 (1970).
14. G. WOOD and R. M. SRIVASTAVA. Tetrahedron Lett. 2937 (1971); G. WOOD, R. M. SRIVASTAVA, and B. ADLAM. Can. J. Chem. **51**, 1200 (1973).
15. S. H. GROVER, J. P. GUTHRIE, J. B. STOTHERS, and C. T. TAN. J. Mag. Res. **10**, 227 (1973).
16. F. A. L. ANET, C. H. BRADLEY, and G. W. BUCHANAN. J. Am. Chem. Soc. **93**, 258 (1971).
17. E. L. ELIEL and M. C. KNOEBER. J. Am. Chem. Soc. **88**, 5347 (1966).
18. M. H. CHISHOLM, H. C. CLARK, L. E. MANZER, and J. B. STOTHERS. J. Am. Chem. Soc. In press.

Can. J. Chem. Downloaded from www.nrcresearchpress.com by 210.87.254.42 on 09/05/12
For personal use only.

The Isomeric Enol Acetates of Acetylacetone. Evidence for an Unusual Stabilizing Interaction between *cis* Acetyl and Acetoxy Groups

DENNIS V. C. AWANG
Department of National Health and Welfare, Tunney's Pasture, Ottawa, Canada K1A OL2

Received July 23, 1973

The configuration and conformation of the isomeric enol acetates of acetylacetone have been elucidated. P.m.r. shift data obtained by the use of tris(1,1,1,2,2,3,3-heptafluoro-7,7-dimethyl-4,6-octanedionato)-europium(III) ($Eu(fod)_3$) allow assignment of the (*S*)-*cis* conformation to both isomers. The remarkable stability of the isomer having acetyl *cis* to acetoxy is attributed to neighboring group interaction, a rationale consistent with p.m.r. spectroscopic data.

La configuration et la conformation des deux acétates énoliques de l'acétylacétone ont été élucidées. Les déplacements chimiques paramagnétiques de r.m.p. obtenus par l'emploi du tris(1,1,1,2,2,3,3-heptafluoro-7,7-dimethyl-4,6-octanedionato)europium(III) ($Eu(fod)_3$) démontre une conformation (*S*)-*cis* pour les deux isomères. La stabilité remarquable de l'isomère ayant le groupement acétyl en position *cis* par rapport au groupement acétoxy est attribuée à l'interaction des groupements environnants et sa rationalisation est supportée par des données spectroscopiques obtenues par r.m.p.

Can. J. Chem. **51**, 3752 (1973

Can. J. Chem. Downloaded from www.nrcresearchpress.com by 210.87.254.105 on 09/05/12
For personal use only.

It has been reported (1) that acetylacetone is converted to an enol acetate in good yield when refluxed with isopropenyl acetate in the presence of an acid catalyst. We have repeated this preparation several times and it has been observed to give rise consistently to *two* isomeric monoacetates, hitherto unreported, in close to a 1:1 ratio.[1]

The physical properties of these enol acetates are too similar to permit separation by fractional distillation but the pure liquid isomers can readily be obtained by preparative t.l.c.

The configuration and conformation of the two isomeric methyl enol ethers of acetylacetone have recently been assessed by observation of nuclear Overhauser effects and p.m.r. solvent shift techniques (3); conclusions based on analysis of data collected in the latter study were supported by $Eu(thd)_3$-induced shift data (4).[2] The less stable isomer, having acetyl *cis* to methoxyl adopts the (*S*)-*trans* conformation (**1***a*) and suffers remarkably facile acid-catalyzed isomerization to the other isomer in which the acetyl group is *trans* to methoxyl in an (*S*)-*cis* conformation (**2**). Compound **1** also undergoes ready thermal isomerization to **2**.

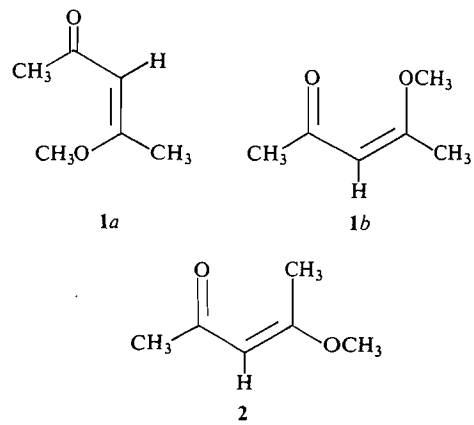

1*a* **1***b*

2

Adoption of the (*S*)-*trans* conformation, generally disfavored by β-disubstituted-α,β-unsaturated acyclic ketones, was attributed to a strong repulsive interaction between *cis* methoxyl and carbonyl in the (*S*)-*cis* conformation (**1***b*) of the less stable enol ether. An analogous situation was expected to exist in the case of the enol acetates of acetylacetone. However, no hope of isolating the acetate corresponding to **1** was seriously entertained, since no mild and relatively neutral method for preparation of enol acetates

[1]Taylor *et al.* (2) have reported a 90% yield of *O*-acetyl derivative from treatment of the thallium(I) salt of acetylacetone with acetylchloride at −78°. However, no spectral data were cited in support of structure.

[2]Tris(2,2,6,6-tetramethyl-3,5-heptanedionato)europium (III), also referred to as tris(dipivalomethanato)europium (III) ($Eu(DPM)_3$).

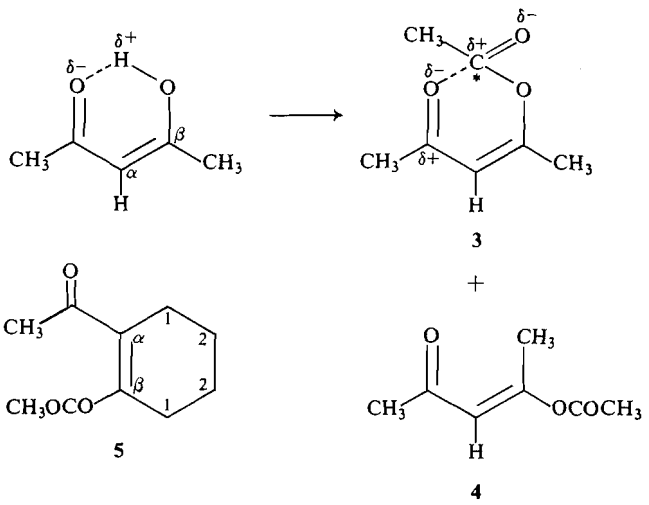

SCHEME 1

(comparable with the diazomethane method which yields **1**) is yet available.

The configuration and conformation of the isomeric enol acetates were revealed by examination of their p.m.r. spectra utilizing the superior paramagnetic shift reagent, tris(1,1,1,2,2,3,3-heptafluoro - 7,7 - dimethyl - 4,6 - octanedionato)-europium(III) ($Eu(fod)_3$) (5); $Eu(thd)_3$, which was successfully employed in the case of the analogous methyl enol ethers, was of no assistance, presumably because of the reduced Lewis basicity of the enol acetates, allied with a low inherent solubility of the reagent in organic solvents.

As illustrated in Scheme 1, the preferred conformation for both enol acetates of acetylacetone is the (*S*)-*cis*. The increased stability of acetate **3** compared with the analogous enol ether **1** is attributed to a stabilizing attractive interaction between acetyl oxygen and the carbonyl carbon atom of the *cis* acetate group. Table 1 lists Δ_{Eu} values (6), which represent the slopes of the straight lines obtained from plots of δ *vs.* $Eu(fod)_3$/substrate mol ratio; the larger the Δ_{Eu} value the greater the particular proton or set of protons is shifted downfield by the shift reagent.

The assignments made on the basis of $Eu(fod)_3$-induced shifts observed for enol acetate **4** are reinforced by observations of its benzene-induced shifts (3) (Table 2), complexation occurring predominantly at acetyl carbonyl.

The shifts induced by solvent benzene in the proton signals of **3**, however, are not so readily rationalized, being of the same sense and of almost identical value for all protons in the molecule. These enigmatic benzene-induced shifts, the identical Δ_{Eu} values for acetate and acetyl protons,[3] and the fact that the latter two groups of protons exhibit a smaller Δ_{Eu} value than does the vinylic proton, can be explained on the basis of competitive complexation. Involvement of a lone pair of electrons of acetyl oxygen in an electrostatic interaction[4] with the carbonyl carbon of the acetoxy group (as illustrated in Scheme 1) would be expected to reduce the ability of acetyl oxygen to complex with the shift reagent. It is not yet possible to separate electronic from purely steric components. Also the relative values for Δ_{Eu} indicate that when europium is coordinated with either doubly bonded oxygen atom, the methyl protons alpha to the other must be rather less influenced by the ligand than is the vinylic proton.

The fact that the enol acetate (**5**) of 2-acetylcyclohexanone, a cyclic analog of acetate **3**, exists predominantly in the (*S*)-*trans* conforma-

[3]The p.m.r. signal for these protons, under the influence of the shift reagent, is markedly broadened compared with all other signals.

[4]A ^{13}C spectroscopic study bearing upon the nature of this interaction and on conformational variation among some enol derivatives of labile 1,3-diketones will be the subject of a forthcoming publication.

Can. J. Chem. Downloaded from www.nrcresearchpress.com by 210.87.254.105 on 09/05/12
For personal use only.

TABLE 1. Δ_{Eu} values for protons of enol acetates of acetylacetone and 2-acetylcyclohexanone

Compound	=CH	$=CCH_3$	$OCOCH_3$	$CCOCH_3$
3	11.6	5.6	7.5	7.5
4	12.0	14.7	5.0	17.5
5[a]	—	—	4.8	12.9

[a]Under the influence of the shift reagent the ring proton pattern is resolved into three broad resonances of relative intensity 1:1:2, corresponding to Δ_{Eu} values of 11.1, 5.6, and 2.8, respectively. Since complexation occurs predominantly at the oxygen atom of the acetyl group, the former resonances are assigned to the methylene protons attached to α-C-1 and -2 carbon atoms; the latter resonance would then be due to the paired β-C-1 and -2 protons.

TABLE 2. Chemical shift displacement[a] of the p.m.r. signals of the enol acetates of acetylacetone and 2-acetylcyclohexanone, induced by benzene solvent

Compound	=CH	$=CCH_3$	$OCOCH_3$	$CCOCH_3$
3	+0.23	+0.25	+0.25	+0.25
4	+0.12	−0.02	+0.40	+0.10
5[b]	—	—	+0.42	+0.01

[a]$\delta_{CCl_4} - \delta_{benzene}$ in p.p.m.
[b]The α-C-1 and -2 protons undergo a positive shift of 0.01 p.p.m. while the β-C-1 and -2 protons are displaced by 0.42 p.p.m. in the same sense.

tion may be explained on the basis of ring constraint in the cyclic compound, preventing rotation about the olefinic bond; such rotation may be necessary for an attractive interaction sufficiently great to counteract the serious 1,3 O–O repulsion that would normally disfavor the (*S*)-*cis* conformation for such molecules.

Experimental

The p.m.r. spectra were recorded using a Varian A-60A spectrometer; spectral grade solvents containing tetramethylsilane (TMS) as internal reference were employed in all cases. The i.r. spectra were obtained with a Perkin-Elmer Model 621 spectrophotometer and u.v. spectra on a Beckman DB spectrophotometer.

Enol acetates **3**, **4**, and **5** were prepared by the method of Hagemeyer and Hull (1) employing commercially available isopropenyl acetate, acetylacetone, and 2-acetylcyclohexanone. The latter two compounds were distilled prior to use.

Enol Acetates 3 and 4

Fractional distillation of the product of reaction of acetylacetone with isopropenylacetate yielded a mixture of isomers **3** and **4**, b.p. 88–90°/6 mm, in a ratio of 9:11, as estimated by integration of the p.m.r. signals of their respective vinylic protons. (No evidence of *C*-acetylation was found.)

The isomers were isolated by preparative t.l.c. on 20 × 20 cm glass plates, precoated with silica gel GF of thickness 1 mm (Fisher), using benzene–ether (9:1). Isomer **4** gives a higher R_f value under these conditions.

Spectral characteristics for **3** are: p.m.r. (CCl_4) δ 5.72 (s, 1H), 2.13 (s, 3H, $=CCH_3$), and 2.00 p.p.m. (s, 6H, $CCOCH_3$; $OCOCH_3$); i.r. ($CHCl_3$) ν 1755 (C=O, ester), 1690 (C=O, ketone), 1655 (?), and 1625 cm^{-1} (C=C); u.v. (95% EtOH) λ_{max} 230 nm (ε 9350). Spectral characteristics for **4** are: p.m.r. (CCl_4) δ 5.98 (s, 1H),[5] 2.25 (d, 3H, $C=CH_3$, $J_{1,3}$ = 1.3 Hz), 2.11 (s, 3H, $OCOCH_3$), and 2.08 p.p.m. (s, 3H, $CCOCH_3$);[6] i.r. ($CHCl_3$) ν 1755 (C=O, ester), 1695 (C=O, ketone), and 1615 cm^{-1} (C=C); u.v. (95% EtOH) λ_{max} 229 nm (ε 6480).

Enol Acetate 5

Enol acetate **5** was obtained pure in 75% yield by fractional distillation of the neutralized reaction product. It had b.p. 95–96°/4.5 mm.

[5]This signal is considerably broadened compared with that of the vinylic proton signal for acetate 3, whose allylic methyl protons are much less strongly coupled and give rise to a sharp singlet under all conditions of observation employed in this study. Its appearance 0.26 p.p.m. downfield from the vinylic proton signal for acetate 3 is probably not significantly due to any deshielding anisotropic effect of the *cis* acetoxy group, since the p.m.r. (60 MHz, CCl_4) signals for the vinylic protons of isopropenyl acetate are coincident. This latter observation prompted Jackman and Wiley (7) to conclude that the acetoxy substituent "prefers those conformations in which the carbonyl group is well removed from *cis*-β-olefinic proton".

[6]These assignments were arrived at by observation of the relative movement of the two signals when very small quantities of the shift reagent were added to the sample solution. No crossover of signals was noted.

Can. J. Chem. Downloaded from www.nrcresearchpress.com by 210.87.254.105 on 09/05/12
For personal use only.

Spectral characteristics for **5** are: p.m.r. (CCl_4) δ 2.17 (s, 3H, $CCOCH_3$)[6], 2.13 (s, 3H, $OCOCH_3$),[6] and 2.25 and 1.70 p.p.m. (centers of multiplets, corresponding to 4H each, of α-C-1 and -2, and β-C-1 and -2, respectively); i.r. ($CHCl_3$) ν 1755 (C=O, ester), 1710 (C=O, ketone), 1690 (?), and 1650 cm^{-1} (C=C); u.v. (95% EtOH) λ_{max} 239 nm (ε 7360).

The author acknowledges the excellent technical assistance of Mr. A. Vincent and is grateful to Mr. H. W. Avdovich for recording the p.m.r. spectra.

1. H. J. Hagemeyer, Jr. and D. C. Hull. Ind. and Eng. Chem. **41**, 2920 (1949).
2. E. C. Taylor, G. H. Hawks, III, and A. McKillop. J. Am. Chem. Soc. **90**, 2421 (1968).
3. D. V. C. Awang. Can. J. Chem. **49**, 2672 (1971).
4. D. V. C. Awang and A. Vincent. J. Org. Chem. **37**, 2625 (1972).
5. R. E. Rondeau and R. E. Sievers. J. Am. Chem. Soc. **93**, 1522 (1971).
6. P. V. DeMarco, T. K. Elzey, R. B. Lewis, and E. Wenkert. J. Am. Chem. Soc. **92**, 5734, 5737 (1970).
7. L. M. Jackman and R. H. Wiley. J. Chem. Soc. 2881 (1960).

Can. J. Chem. Downloaded from www.nrcresearchpress.com by 210.87.254.105 on 09/05/12
For personal use only.

The Use of Polymer Supports in Organic Synthesis. III.[1] Selective Chemical Reactions on One Aldehyde Group of Symmetrical Dialdehydes

CLIFFORD C. LEZNOFF AND JACK Y. WONG
Department of Chemistry, York University, Downsview, Ontario

Received June 11, 1973

An insoluble polymer support system incorporating a diol functional group was prepared. The symmetrical dialdehydes, terephthalaldehyde and isophthalaldehyde, were attached to the polymer through acetal formation, constituting a unique method of blocking one aldehyde group of symmetrical dialdehydes. The free aldehyde group was reacted with hydroxylamine to give the mono-oximes of the terephthalaldehyde and isophthalaldehyde upon acid cleavage from the polymer. Similarly, the polymer bound aldehydes were reacted with Wittig reagents to give *p*- and *m*-formylstilbenes and 1-*p*- and -*m*-formylphenyl-4-phenyl-1,3-butadienes. The crossed aldol condensation of acetophenone with the symmetrical dialdehydes gave the 3-*p*- and -*m*-formylphenyl-1-phenyl-2-propene-1-ones (formylchalcones) in high yield. The Grignard reaction of phenylmagnesium bromide on the polymer bound aldehyde gave (*p*- and *m*-formylphenyl)phenylcarbinol in quantitative yield. Reduction of the polymer bound free aldehydes with sodium bis(2-methoxyethoxy)-aluminum hydride gave *p*- and *m*-hydroxymethylbenzaldehydes. Similarly the mixed benzoin condensation of polymer bound terephthalaldehyde and isophthalaldehyde gave *p*- and *m*-formylbenzils.

Un support insoluble, à base de polymère possédant un groupe fonctionnel diol, a été préparé. Les dialdéhydes symétriques, téréphthalaldéhyde et isophthalaldéhyde, ont été fixés au polymère sous forme d'acétal constituant ainsi une méthode unique de blocage d'un seul groupe aldéhyde dans les dialdéhydes symétriques. Le groupe aldéhyde libre a été mis en réaction avec l'hydroxylamine pour conduire aux mono-oximes de téréphthalaldéhyde et isophthalaldéhyde, après clivage acide. De la même façon, les aldéhydes fixés au polymère réagissent sur les réactifs de Wittig pour conduire aux *p*- et *m*-formylstilbènes et aux *p*- et *m*-formylphényl-1 phényl-4 butadiènes-1,3. La condensation aldol croisée entre l'acétophénone et les dialdéhydes symétriques conduit aux *p*- et *m*-formylphényl-3 phényl-1 propène-2 ones-1 (formyl chalcones) avec un rendement élevé. La réaction de Grignard entre le bromure de phénylmagnésium et l'aldéhyde fixé au polymère conduit aux (*p*- et *m*-formylphényl)phénylcarbinol avec un rendement quantitatif. La réduction des groupes aldéhydes libres par l'hydrure de sodium bis(méthoxy-2 éthoxy)-aluminium conduit aux *p*- et *m*-hydroxyméthylbenzaldéhydes. De façon semblable, la condensation benzoine mixte du téréphthalaldéhyde et isophthalaldéhyde fixés au polymère conduit aux *p*- et *m*-formylbenzyles. [Traduit par le journal]

Can. J. Chem. **51**, 3756 (1973)

The use of insoluble polymer supports in the synthesis of polypeptides (1), polynucleotides (2), and polysaccharides (3) has been well documented. The general application of insoluble polymer supports to organic synthetic problems has only recently received scattered attention (4). We have previously shown how an insoluble polymer support, containing acid chloride groups (5) can be used as a selective blocking group for completely symmetrical diols and hence the preparation of monotrityl and monotetrahydropyranyl derivatives of symmetrical diols were facilitated (6, 7).

We now describe a procedure in which symmetrical dialdehydes are attached to a modified insoluble Merrifield polymer (**1**) through an acetal linkage of only one aldehyde group, leaving the other aldehyde group available for reaction. This procedure constitutes a unique method of blocking one aldehyde group of a symmetrical dialdehyde.

A suitable modified Merrifield polymer was prepared by reacting a commercially available Merrifield polymer (**1**) (2% cross-linked polystyrene beads with 1.7 mmol of $-CH_2Cl$ groups per gram of resin, obtained from Schwarz/Mann), with the sodium salt of 2,2-dimethyl-1,3-dioxolane-4-methanol in excess 2,2-dimethyl-1,3-dioxolane-4-methanol[2] as solvent to give resin **2**, as shown in Scheme 1. Acid hydrolysis of **2** with dilute HCl in aqueous dioxane (1:1) gave resin **3** containing a vicinal diol functional group

[1]For Part II see ref. 7.

[2]Purchased from Aldrich Chemical Co.

Can. J. Chem. Downloaded from www.nrcresearchpress.com by 210.87.254.42 on 09/05/12
For personal use only.

Can. J. Chem. Downloaded from www.nrcresearchpress.com by 210.87.254.42 on 09/05/12
For personal use only.

available for acetal formation. The i.r. spectrum of **3** exhibited O—H absorption at 3415 cm^{-1} and C—O absorption at 1058 cm^{-1}.

Resin **3** reacted with excess terephthalaldehyde (**4**) or isophthalaldehyde (**5**) in anhydrous dioxane, containing *m*-benzenedisulfonic acid as a catalyst and magnesium sulfate to absorb the liberated water, to yield resins **6** or **7** containing aldehydes **4** or **5** respectively. The i.r. spectra of resins **6** and **7** exhibited typical aldehyde absorption at 1700 cm^{-1} showing that one aldehyde function did not form an acetal. The use of excess aldehyde ensured that only monoacetal formation would predominate. The amount of aldehyde attached to the polymer was determined by acid hydrolysis of **6** and **7** in aqueous dioxane (1:1) with dilute HCl to yield **4** and **5** respectively. It was thus shown that resin **6** contained 0.34 mmol of **4** per gram and resin **7** contained 0.35 mmol of **5** per gram. Thus the capacities of resins **6** and **7** are very high compared to resins described in earlier publications (1–7).

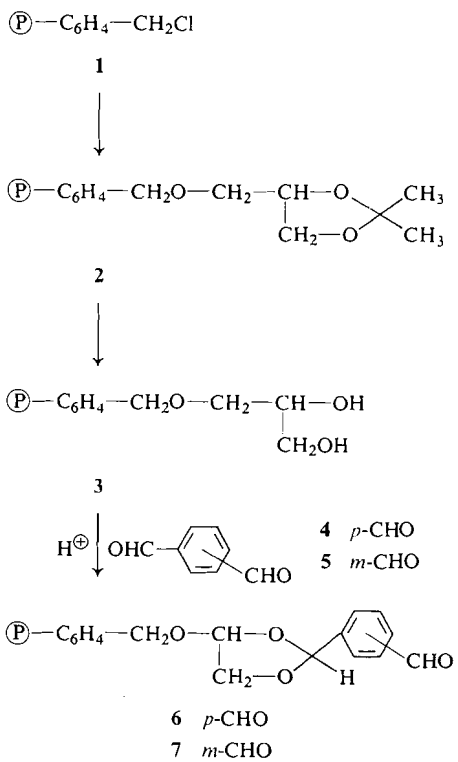

SCHEME 1

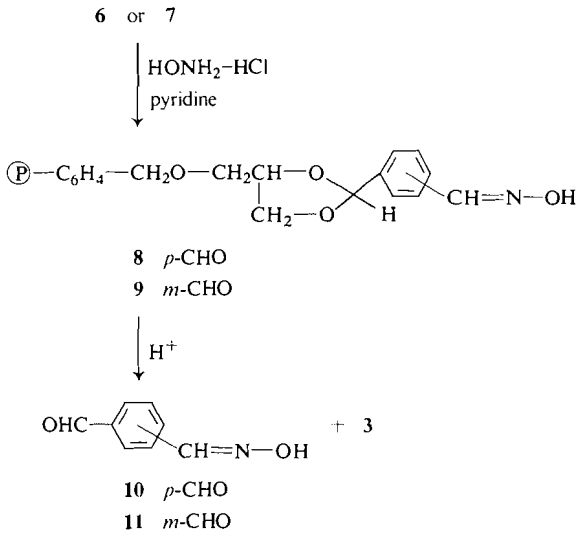

SCHEME 2

Chemical syntheses designed to react with only one aldehyde group of symmetrical dialdehydes are quite rare and have met with success in only a few instances under special conditions (8) and even then difficulties of separation of reagents and products were apparent.

The following chemical reaction types illustrate how resin aldehydes **6** and **7** can be used to prepare largely unknown and poorly accessible compounds containing free formyl groups.

Oxime Formation

For example, the simple mono-oximes of terephthalaldehyde (**4**) and isophthalaldehyde (**5**) are unreported but these derivatives are readily synthesized using resins **6** and **7**.

In a typical reaction sequence as outlined in Scheme 2, resin **6** or **7** and an excess of hydroxylamine hydrochloride in pyridine gave after 24 h the resin oximes **8** or **9**. Acid hydrolysis of **8** or **9** as before gave terephthalaldehyde mono-oxime (**10**) and isophthalaldehyde mono-oxime (**11**) in 86 and 71% yield, respectively.[3] Elemental analysis and mass spectral data were consistent with structures **10** and **11**. Both oximes **10** and **11** exhibited strong parent ions in their mass spectra and a peak at *m/e* 120 indicating the expected loss of a formyl group by α-cleavage. The i.r. spectra

[3]All yields are based on the amount of **4** (or **5**) released from resin **6** (or **7**) upon acid hydrolysis.

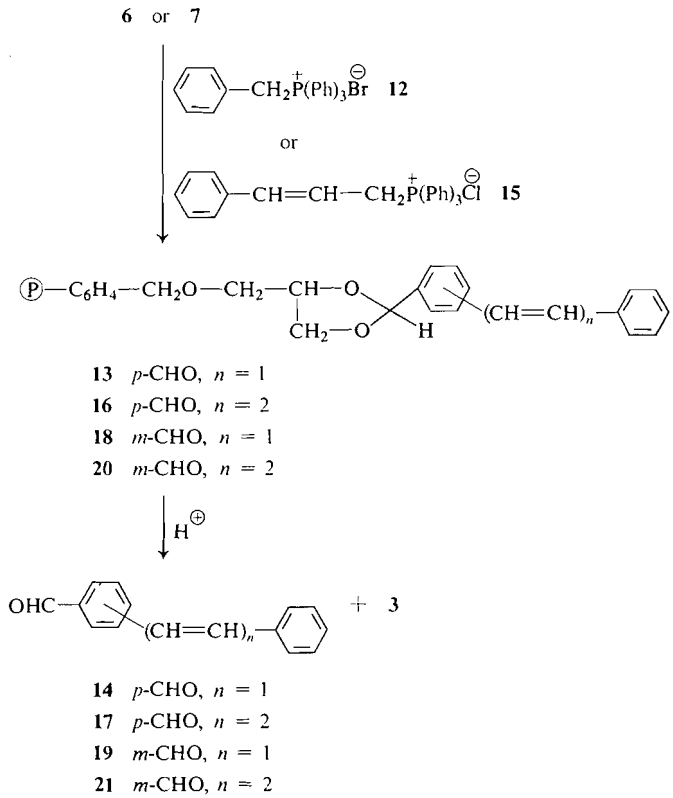

SCHEME 3

of **10** and **11** showed characteristic C=O and O—H absorption.[4]

The Wittig Reaction

It was decided to examine the Wittig reaction with the monoprotected dialdehydes **6** and **7** with benzyltriphenylphosphonium bromide and cinnamyltriphenylphosphonium chloride as the products of these reactions, formylstilbenes and 1-formylphenyl-4-phenyl-1,3-butadienes were unknown compounds, difficult to prepare by other methods, and were essential in other studies in this laboratory, involving the photochemistry of diarylpolyenes (9).

Thus reaction of the resin aldehyde **6** and benzyltriphenylphosphonium bromide (**12**) in anhydrous dimethylformamide and sodium methoxide gave resin **13**, as shown in Scheme 3. The i.r. spectrum of resin **13** showed some residual aldehyde absorption at 1692 cm^{-1}. Acid hydrolysis of resin **13** as before gave used resin **3** and crude *p*-formylstilbene (**14**) which on further purification by t.l.c. gave pale yellow needles of **14** in 76% yield. Similarly, the resin aldehyde **6** and cinnamyltriphenylphosphonium chloride (**15**) gave resin **16** which on treatment with acid yielded 1-*p*-formylphenyl-4-phenyl-1,3-butadiene (**17**) in 59% yield.

Likewise, the Wittig reaction of resin aldehyde **7** with **12** gave resin **18** which on acid treatment yielded *m*-formylstilbene (**19**) in 50% yield. Reaction of resin **7** with **15** gave resin **20** which on acid treatment gave 1-*m*-formylphenyl-4-phenyl-1,3-butadiene (**21**) in 27% yield.

The mass spectra of **14**, **17**, **19**, and **21** exhibited parent ions and (M − 29) peaks due to the loss of the formyl group by α-cleavage. The i.r. spectra of **14**, **17**, **19**, and **21** showed absorption for the formyl and olefin moieties. The u.v. spectra of these products showed the characteristic stilbene and 1,4-diphenyl-1,3-butadiene absorption (9).

[4]Full spectral data are described in the Experimental section.

Can. J. Chem. Downloaded from www.nrcresearchpress.com by 210.87.254.42 on 09/05/12
For personal use only.

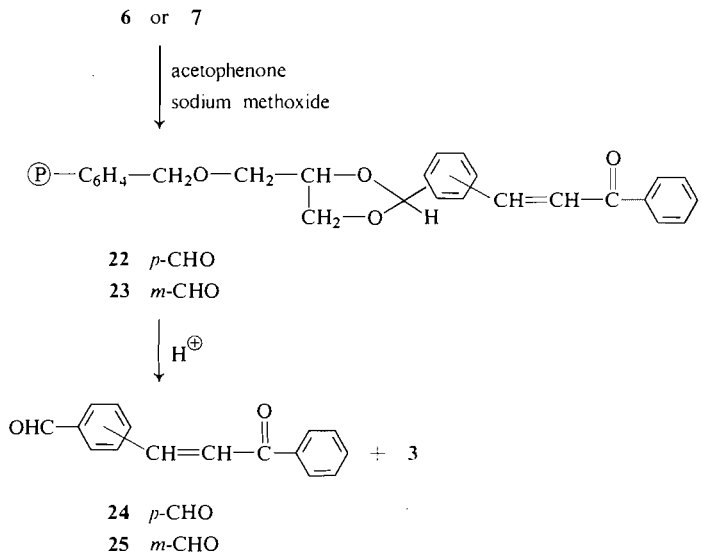

SCHEME 4

The Crossed Aldol Condensation

In experiments designed to test the feasibility of conducting mixed condensation reactions involving the mono-protected symmetrical aldehydes **4** and **5**, the cross aldol condensations of resin aldehydes **6** and **7** with acetophenone were attempted.

Resin aldehydes **6** and **7** were condensed with acetophenone and sodium methoxide in absolute ethanol to yield resin chalcones **22** and **23** respectively. Cleavage of the chalcones from resins **22** and **23** gave the chalcones 3-*p*-formylphenyl-1-phenyl-2-propen-1-one (**24**) (10) and 3-*m*-formylphenyl-1-phenyl-2-propen-1-one (**25**) in 100 and 96% yields respectively[5] as shown in Scheme 4.

The mass spectra of **24** and **25** exhibited parent ions and (M − 29) peaks due to the loss of the formyl group by α-cleavage. The i.r. spectra of **24** and **25** showed typical carbonyl and olefin absorption. The u.v. spectra were typical of chalcones.

The Benzoin Condensation

Attempts at conducting mixed benzoin condensations invariably lead to intractable mixtures of symmetrical benzoins and mixed or crossed benzoins.

It was envisoned that a polymer supported aldehyde could react with excess benzaldehyde under the conditions of the benzoin condensation. The insoluble polymer supported aromatic aldehydes could then react with benzaldehyde to give mixed or crossed benzoins exclusively. All symmetrical benzoin and excess reagents would simply be filtered from the insoluble resin containing the crossed benzoin.

To this end resin aldehyde **6** was treated with benzaldehyde and sodium cyanide in absolute ethanol to give resin **26**, as shown in Scheme 5. Acid cleavage of **26** gave a complex mixture of products which were chromatographed on preparative t.l.c. The major fraction, obtained in only 6% yield, consisted of *p*-formylbenzil (**27**). Similarly, reaction of aldehyde resin **7** with benzaldehyde in a benzoin condensation led to resin **28** which on acid cleavage gave *m*-formylbenzil (**29**) in 4% yield.

The mass spectra of **27** and **29** were very characteristic of benzils and not benzoins and exhibited parent ions and symmetrical cleavage of the α-diketones to give fragment ions at *m/e* 105 and 134 characteristic of the benzoyl group and the formylbenzoyl groups respectively. Furthermore, the i.r. spectra of **27** and **29** exhibited strong carbonyl absorption but a noted absence of O—H absorption. Thus it appears that the crossed benzils **27** and **29** are formed by oxidation of preformed benzoins.

[5]The chalcone **24** was previously obtained in only 30% yield (10).

Can. J. Chem. Downloaded from www.nrcresearchpress.com by 210.87.254.42 on 09/05/12
For personal use only.

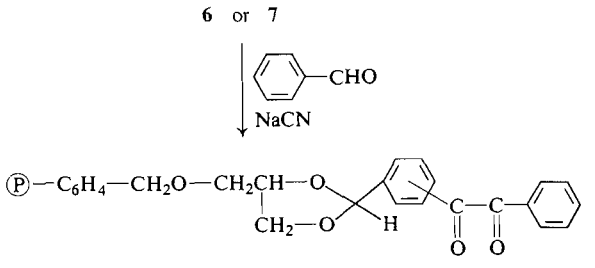

26 *p*-CHO
28 *m*-CHO

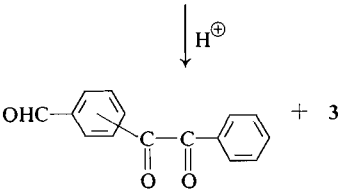

27 *p*-CHO
29 *m*-CHO

SCHEME 5

The Grignard Reaction

The reaction of Grignard reagents with symmetrical dialdehydes would inevitably lead to poorly separable mixtures containing the di-adduct, the mono-addition product, and unreacted starting material. The selective formation of the mono-addition product can be achieved using insoluble polymer supports as outlined in Scheme 6.

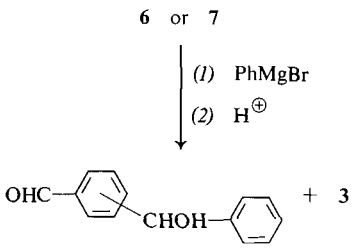

30 *p*-CHO
31 *m*-CHO

SCHEME 6

The resin aldehyde **6** was reacted with phenylmagnesium bromide in tetrahydrofuran to yield a resin alcohol which was not isolated, but directly treated with acid to give resin **3** and (*p*-formylphenyl)phenylcarbinol (**30**) (*p*-formylbenzhydrol) in 99% yield. Similarly resin aldehyde **7** was treated with phenylmagnesium bromide to give (*m*-formylphenyl)phenylcarbinol (**31**) (*m*-formylbenzhydrol) in 100% yield.

The mass spectra of **30** and **31** exhibited parent ions and peaks at 105 indicative of the formylphenyl group. The i.r. spectra of **30** and **31** showed C=O and O—H absorption.

Reductions with Metal Hydrides

As shown above, the synthesis of secondary alcohols containing free formyl groups was achieved through the use of the Grignard reaction. An attempt was made to synthesize primary alcohols containing formyl groups by metal hydride reduction of appropriate symmetrical dialdehydes mono-protected by the insoluble resin.

A suspension of resin aldehyde **6** with sodium bis(2-methoxyethoxy)-aluminum hydride in benzene gave a suspension of resin alcohol. The suspension was treated directly with dilute acid to effect cleavage from the polymer of the reaction product and gave *p*-hydroxymethylbenzaldehyde (**32**) (11) in 17% yield[6] as shown in Scheme 7.

[6]The reaction of **6** with lithium aluminum hydride in tetrahydrofuran or sodium borohydride in methanol and subsequent acid cleavage gave no **32** or **33**.

Can. J. Chem. Downloaded from www.nrcresearchpress.com by 210.87.254.42 on 09/05/12
For personal use only.

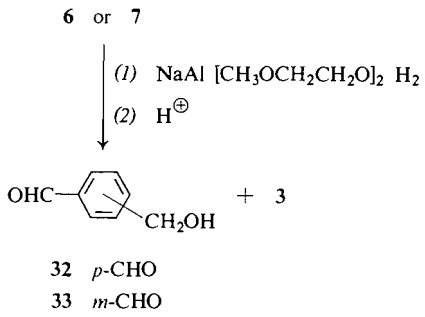

SCHEME 7

Similarly, reaction of resin aldehyde **7** with sodium bis(2-methoxyethoxy)-aluminum hydride gave *m*-hydroxymethylbenzaldehyde (**33**) in 8% yield. The poor yields of **32** and **33** are probably due to ready polymerization of these compounds. The susceptibility of these compounds to polymerization probably accounts for the fact that **33** was previously unrecorded and **32** recorded rarely (11).

The mass spectra of **32** and **33** exhibited parent ions and also showed peaks at *m/e* 107 resulting from loss of the formyl group by α-cleavage. The i.r. spectra of **32** and **33** showed C=O and O—H absorption. The n.m.r. spectra of **32** and **33** were consistent with the assigned structures.

Advantages and Limitations of Organic Synthesis Using Resin 3

The primary advantage of using resin **3** in organic synthesis was shown in the selective high yield formation of the unreported mono-oximes **10** and **11**, the formylstilbenes **14** and **19**, the formylphenyl butadienes **17** and **21**, the formylchalcones **24** and **25**, and the formylbenzhydrols **30** and **31**, from the commercially available symmetrical dialdehydes **4** and **5**. Classical preparations of some of these products from **4** and **5** would invariably lead to poorly separable mixtures of di-adducts, mono-adducts, and starting material (10, 11).[7]

It should be noted that the yields of all products obtained from isophthalaldehyde via resin **7** were slightly but consistently lower than the products from terephthalaldehyde via resin **6**. Thus it appears that steric hindrance of the less accessible meta formyl group in resin **7** plays a role in determining the yields of products derived from this resin.

In an experiment designed to test the quality of the *used* resin **3**, this resin was subjected to the reaction sequence outlined in Scheme 2 using aldehyde **4** and phosphonium salt **12**. Product **14** was obtained once again in 73% yield showing that resin **3** had not deteriorated during the reaction sequence and hence was completely regenerable. The used polymer obtained in the sequence leading to the preparation of monotrityl ethers of symmetrical diols suffered considerable deterioration (6, 7). The recovery in this instance of a completely regenerable polymer constitutes a major step in the *practical* use of polymer supports in organic synthesis.

One limitation to using an acetal linkage to attach molecules to insoluble polymer supports lies in the fact that only reactions conducted under basic conditions can be employed, as are all of the reactions described in this paper. A further limitation results from this same condition, namely that the procedures used for washing the polymer free of excess reactants and reagents cannot employ acid conditions. The Grignard reaction and the metal hydride reductions of resin aldehydes **6** and **7** result in metal salts of resin alcohols. These salts are gelatinous which creates filtering problems. The gelatinous precipitates can be solubilized by acid but of course this procedure causes cleavage of the products from the resin. Thus the Grignard products **30** and **31** were obtained by direct cleavage of the adducts obtained from the Grignard reagent with resin aldehydes **6** and **7**. For this example, this procedure was not a disadvantage as the products were still obtained in high yield but if one wanted the benzhydrol products to remain attached to the polymer for a possible sequential synthesis, the limitation against the use of acid would become serious. The limitation against using acid was more apparent in the syntheses of the hydroxymethylbenzaldehydes **32** and **33** resulting in low yields of these compounds.

The role of solvent in planning organic syntheses on insoluble polymer supports is very important but at times unpredictable. Generally, one likes to do reactions on insoluble resins in solvents that swell the polymer such as pyridine and dimethylformamide. The syntheses of the mono-oximes **10** and **11** in pyridine, and the stilbenes **14** and **19** and the butadienes **17** and **21**

[7]The mono-oxime of *o*-phthalaldehyde is known (12) and was obtained as an oil in 70% yield.

Can. J. Chem. Downloaded from www.nrcresearchpress.com by 210.87.254.42 on 09/05/12
For personal use only.

Can. J. Chem. Downloaded from www.nrcresearchpress.com by 210.87.254.42 on 09/05/12
For personal use only.

in dimethylformamide in high yields emphasize the importance of a *good* solvent. The formylbenzhydrols **30** and **31**, however, were synthesized in high yield in an only partially acceptable solvent, tetrahydrofuran, while the formylchalcones **24** and **25** were prepared in very high yield in absolute ethanol, a poor solvent for swelling the polymer. Thus, the poor yields of the hydroxymethylbenzaldehydes **32** and **33** obtained from reaction in benzene, a *good* solvent, were probably due to other reasons, although it should be noted that the metal hydride reductions of **6** and **7** in tetrahydrofuran and in methanol, poorer solvents, gave no product and thus the change in solvent (or metal hydride) allowed at least some product to be realized. The poor yields obtained in the benzoin condensation could be due to solvent effects but an attempt to accomplish the benzoin condensation in dimethylformamide, a *good* solvent, resulted in yields of benzils **27** and **29** identical to that in absolute ethanol, a *poor* solvent. Thus the role of solvent is important in organic synthesis on insoluble resins but should not be an inhibiting factor in attempting an organic synthesis.

It has thus been demonstrated that general organic syntheses can be accomplished in high yield on insoluble polymer supports, with recovery of a completely regenerable polymer. Most important of all, because of the high capacity of the insoluble polymer it becomes feasible to react only one aldehyde group of symmetrical dialdehydes with a series of organic reagents in a standard practical procedure, yielding reasonable quantities of products.

The development of further organic synthetic methods using insoluble polymer supports is in progress.

Experimental

All melting points were determined on a Kofler hot stage and are uncorrected. The i.r. spectra were recorded on a Unicam SP1000 i.r. spectrophotometer using KBr discs unless otherwise stated. The u.v. spectra were measured using a Unicam SP800A u.v. spectrometer and benzene as solvent. The n.m.r. spectra were measured on a Varian A60 spectrometer using tetramethylsilane as an internal standard ($\delta = 0$ p.p.m.) and deuterochloroform as solvent. Mass spectra were recorded on a Hitachi-Perkin-Elmer RMU-6 mass spectrometer. The number in brackets after the indicated ion shows the % of the base peak represented by that ion. Silica gel was used for thin- and thick-layer chromatography. Microanalyses were performed by Dr. C. Daesslé of Montreal. Filtering procedures were done under vacuum using a sinter-glass funnel. All the stirring described below was performed using a Fisher magnetic stirrer.

Preparation of Polymer 2

Sodium (2 g) was added to 60 ml of 2,2-dimethyl-1,3-dioxolane-4-methanol (Aldrich Chemical Co.) in a 250 ml round-bottom flask. The mixture was stirred until all the sodium had dissolved. The Merrifield resin (4.87 g) (**1**) (2% cross-linked polystyrene beads with 1.7 mmol of $-CH_2Cl$ groups per gram of resin, obtained from Schwarz/Mann) was then added. The mixture was stirred at room temperature overnight and at 80 °C for 24 h. The resin was collected by filtration and washed three times with dioxane, six times with water, three times with ethanol–water (1:1), three times with ethanol, and three times with dry ether to give 5.88 g of polymer, ν_{max} 1128–1058 cm^{-1} (C—O—C).

Preparation of Polymer 3

Polymer **2** (5.88 g) was suspended in a mixture of dioxane and 1 *M* hydrochloric acid (1:1, 60 ml). The mixture was stirred for 48 h at room temperature. The resin was filtered and washed six times with water, once with acetone, three times with ethanol, and three times with dry ether to give 5.82 g of polymer diol **3**. The i.r. spectrum showed a vicinal diol functional group at ν_{max} 3415 cm^{-1} (OH), 1058 cm^{-1} (C—O—C).

Preparation of Polymer Aldehydes 6 and 7

In a typical procedure, 4.25 g of polymer **3** was suspended in 60 ml of anhydrous dioxane. Excess terephthalaldehyde (**4**) or isophthalaldehyde (**5**) (2 g) and 0.10 g of *m*-benzenedisulfonic acid as catalyst were added. To the mixture was added 2.00 g of anhydrous sodium sulfate to absorb liberated water and the reaction was stirred at room temperature for 48 h under exclusion of moisture ($CaCl_2$, drying tube). The resin was filtered, neutralized with anhydrous pyridine (to prevent cleavage of the aldehyde from the polymer by hydrolysis of the acetal linkage), and filtered twice. Then the resin was washed twice with pyridine–water (1:1), ten times with water (to remove sodium sulfate), three times with ethanol, and at least three times with dry ether. The i.r. spectra of **6** and **7** exhibited typical aldehyde absorption at 1700 cm^{-1}; resin **6**, ν_{max} 1700 cm^{-1}; resin **7**, ν_{max} 1698 cm^{-1}.

Preparation of Mono-oximes 10 and 11

Resin **6** (3.27 g) was suspended in 50 ml of anhydrous pyridine. Excess hydroxylamine hydrochloride (2.50 g) was added. The mixture was stirred at room temperature for 48 h. The resin was filtered and washed three times with pyridine, three times with pyridine–water (1:1), three times with water, three times with ethanol, and three times with dry ether to give the resin **8** (3.43 g). A suspension of 3.43 g of resin **8** and 40 ml of a 1:1 mixture of dioxane and dilute hydrochloric acid was stirred for 48 h at room temperature. The resin was filtered and washed six times with water, once with acetone, three times with ethanol, and three times with ether. The aqueous filtrate was extracted with three aliquots of ether. The combined ether extracts were washed six times with water, dried over Na_2SO_4, and evaporated to give a slightly impure solid which was purified by preparative t.l.c. on silica gel (eluant $CHCl_3$) to give 0.1421 g (86%) of analytically pure terephthalaldehyde mono-oxime (**10**) m.p. 122–127°. No starting terephthalaldehyde **4** was

Can. J. Chem. Downloaded from www.nrcresearchpress.com by 210.87.254.42 on 09/05/12
For personal use only.

detected. I.r. spectrum, ν_{max} (Nujol) 3415 cm^{-1} (OH), 1680 cm^{-1} (C=O); mass spectrum, *m/e* 149 (19) (M^+), 120 (5) ($M^+ - CHO$), 105 (10) ($M^+ - CH{=}NOH$), 131 (100) ($M^+ - H_2O$).

Anal. Calcd. for $C_8H_7NO_2$: C, 64.43; H, 4.69; N, 9.39. Found: C, 64.45; H, 4.89; N, 9.60.

Similarly, treatment of resin 7 (3.31 g) as described above gave the resin **9**. Acid hydrolysis of **9** and identical work-up as before yielded 0.1201 g (71%) of analytically pure isophthalaldehyde mono-oxime, as an oil, (**11**) and 0.0105 g of starting aldehyde **5**. I.r. spectrum, ν_{max} (neat) 3360 cm^{-1} (OH), 1685 cm^{-1} (C=O); mass spectrum *m/e* 149 (30) (M^+), 120 (100) ($M^+ - CHO$), 105 (10) ($M^+ - CH{=}N{-}OH$).

Anal. Calcd. for $C_8H_7NO_2$: C, 64.43; H, 4.69; N, 9.39. Found: C, 64.23; H, 4.80; N, 9.25.

*Preparation of p-Formylstilbene (**14**) and 1-p-Formylphenyl-4-phenyl-1,3-butadiene (**17**)*

To a solution of benzyltriphenylphosphonium bromide (**12**) (4.00 g) in anhydrous dimethylformamide (60 ml) was added powdered sodium methoxide (2.50 g). After stirring for 5 min, when the solution turned orange, resin **6** (5.77 g) was added to give, after stirring 24 h at room temperature, the resin **13**. Resin **13** was separated by filtration, washed three times with DMF, three times with DMF–water (1:1), three times with water, three times with methanol, and three times with ether. Acid hydrolysis of resin **13** as before and using an identical work-up gave used resin **3** and crude *p*-formylstilbene (**14**). Further purification by preparative t.l.c. on silica gel (eluant 10% $CHCl_3$ – 90% C_6H_6) gave 0.310 g of analytically pure **14**, m.p. 101–105°, in 76% yield and 0.057 g of starting terephthalaldehyde (**4**). I.r. spectrum, ν_{max} (Nujol) 1699, 972 cm^{-1}; mass spectrum, *m/e* 208 (100) (M^+), 179 (30) ($M^+ - CHO$); u.v. spectrum, λ_{max} 335 mμ (ε 33 300).

Similarly, the addition of resin **6** (6.15 g) to the Wittig reagent, cinnamyltriphenylphosphonium chloride (**18**) as described above gave the resin **16**. Acid hydrolysis of **16** and using an identical work-up as before yielded 0.299 g (59%) of analytically pure 1-*p*-formylphenyl-4-phenyl-1,3-butadiene (**17**), m.p. 128, and also 0.088 g of starting aldehyde **4**. I.r. spectrum, ν_{max} (Nujol), 1691, 996 cm^{-1}, mass spectrum, *m/e* 234 (100) (M^+), 205 (100) ($M^+ - CHO$); u.v. spectrum, λ_{max} 347, 362, 379 mμ (ε 39 800, 49 100, 35 100).

Anal. Calcd. for $C_{17}H_{14}O$: C, 87.18; H, 5.98. Found: C, 87.13; H, 5.66.

*Preparation of 1-m-Formylstilbene (**19**) and 1-m-Formylphenyl-4-phenyl-1,3-butadiene (**21**)*

To a solution of benzyltriphenylphosphonium bromide (**12**) (4.00 g) in anhydrous dimethylformamide (60 ml) was added powdered sodium methoxide (2.50 g). After stirring for 5 min, when the solution turned orange, resin **7** (6.07 g) was added to give, after stirring 24 h at room temperature, the resin **18**. Resin **18** was separated by filtration and washed three times with DMF, three times with DMF–water (1:1), three times with water, three times with methanol, and three times with ether. Acid hydrolysis of resin **18** as before and using an identical work-up gave used resin **3** and crude *m*-formylstilbene (**19**). Further purification by preparative t.l.c. on silica gel (eluant 10% $CHCl_3$: 90% C_6H_6) gave 0.239 g of analytically pure **19**, m.p. 104–107°, in 50% yield and 0.100 g of starting aldehyde **5**. I.r. spectrum, ν_{max} (Nujol) 1692, 970 cm^{-1}; mass spectrum, *m/e* 208 (100) (M^+), 179 (100) ($M^+ - CHO$); u.v. spectrum, λ_{max} 300 mμ (ε 26 600).

Anal. Calcd. for $C_{15}H_{12}O$: C, 86.54; H, 5.77. Found: C, 86.86; H, 5.56.

Similarly, the addition of resin 7 (6.49 g) to the Wittig reagent, cinnamyltriphenylphosphonium chloride (**15**), as described above gave the resin **20**. Acid hydrolysis of **20** and using an identical work-up as before yielded 0.147 g (27%) of analytically pure 1-*m*-formylphenyl-4-phenyl-1,3-butadiene (**21**), m.p. 132–136°, and 0.188 g of starting aldehyde **5**. I.r. spectrum, ν_{max} (Nujol) 1690, 990 cm^{-1}; mass spectrum, *m/e* 234 (100) (M^+), 205 (100) ($M^+ - CHO$); u.v. spectrum, λ_{max} 325, 335, 354 mμ (ε 42 100, 45 000, 29 300).

Anal. Calcd. for $C_{17}H_{14}O$: C, 87.18; H, 5.98. Found: C, 87.05; H, 5.56.

*Preparation of Formylchalcones **24** and **25***

Resin **6** (4.31 g) was suspended in 60 ml of absolute ethanol. Excess acetophenone (4.00 g) and sodium methoxide powder (3.50 g) were added. The mixture was stirred at room temperature for 48 h with exclusion of moisture ($CaCl_2$ drying tube). The resin **22** was filtered off and washed three times with ethanol, three times with ethanol–water, three times with water, three times with methanol, and three times with dry ether. Acid hydrolysis of resin **22** as described previously and using an identical work-up gave used resin **3** and crude 3-*p*-formylphenyl-1-phenyl-2-propen-1-one (**24**). Further purification by preparative t.l.c. on silica gel (eluant $CHCl_3$) gave 0.369 g of analytically pure **24**, m.p. 121° (lit. (10) m.p. 125°), in 100% yield. I.r. spectrum, ν_{max} (Nujol) 1600, 1675, 1687 cm^{-1}; mass spectrum, *m/e* 236 (10) (M^+), 207 (8) ($M^+ - CHO$), 105 (90) (benzoyl); u.v. spectrum, λ_{max} 280 mμ (ε 3300).

Similarly, treatment of resin **7** as described above gave the resin **23**. Acid hydrolysis of resin **23** and using an identical work-up as before yielded 0.341 g (96%) of analytically pure 3-*m*-formylphenyl-1-phenyl-2-propen-1-one (**25**). I.r. spectrum, ν_{max} (neat) 1600, 1680, 1690 cm^{-1}; mass spectrum, *m/e* 236 (46) (M^+), 207 (30) ($M^+ - CHO$); u.v. spectrum, λ_{max} 292 mμ (ε 6780).

Anal. Calcd. for $C_{16}H_{12}O_2$: C, 81.36; H, 5.09. Found: C, 81.35; H, 5.38.

*Preparation of Formylbenzils **27** and **29***

The aldehyde resin **6** (4.33 g) was suspended in a mixture of ethyl alcohol, dioxane, and water (1:1:1, 120 ml). To this was added sodium cyanide (2.50 g) in 30 ml of water. The mixture was stirred overnight at 80 °C. Then excess benzaldehyde (4.00 g) was added and the mixture was stirred at 80 °C for another 24 h to give resin **26**. Resin **26** was collected by filtration and washed three times with dioxane–water (1:1), three times with water, three times with ethanol–water (1:1), three times with ethanol, and three times with ether. Acid cleavage of resin **26** as described previously and using an identical work-up gave used resin **3** and a complex mixture of products which were chromatographed on preparative t.l.c. (eluant 5% ether – 95% $CHCl_3$). The yield of 1-*p*-formylbenzil (**27**), as an oil, was 0.0195 g (6%). I.r. spectrum, ν_{max} (neat) 1670–1710 cm^{-1}, broad, (C=O); mass spectrum, *m/e* 238 (3) (M^+), 209 (0.3) ($M^+ - CHO$), 105 (100) (benzoyl), 134 (33) (formylbenzoyl).

Can. J. Chem. Downloaded from www.nrcresearchpress.com by 210.87.254.42 on 09/05/12
For personal use only.

Anal. Calcd. for $C_{15}H_{10}O_3$: C, 75.63; H, 4.20. Found: C, 75.71; H, 4.38.

Similarly, reaction of aldehyde resin **7** (5.33 g) with benzaldehyde in a benzoin condensation described above led to resin **28** which on acid cleavage and using an identical work-up gave used resin **3** and a complex mixture of products. Purification by preparative t.l.c. on silica gel (eluant 5% ether – 95% $CHCl_3$) yielded 0.0165 g (4%) of *m*-formylbenzil (**29**), as an oil. I.r. spectrum, ν_{max} (neat) 1670–1705 cm^{-1} (broad) (C=O); mass spectrum, *m/e* 238 (0.6) (M^+), 209 (0.3) ($M^+ - CHO$), 105 (100) (benzoyl), 134 (33) (formylbenzoyl).

Anal. Calcd. for $C_{15}H_{10}O_3$: C, 75.63; H, 4.20. Found: C, 75.57; H, 4.32.

Preparation of Formylbenzhydrols 30 and 31

Phenylmagnesium bromide was prepared as follows. To a solution of magnesium (2 g) and iodine (0.010 g) in 125 ml of anhydrous tetrahydrofuran was added dropwise with stirring bromobenzene (13.2 g) in 20 ml of tetrahydrofuran. The mixture was refluxed for 1 h until all the magnesium had dissolved.

The resin aldehyde **6** (5.57 g) was then reacted with the phenylmagnesium bromide in anhydrous tetrahydrofuran at room temperature for 48 h to give a resin alcohol which was not isolated but directly treated with acid and using an identical work-up as before yielded resin **3** and (*p*-formylphenyl)phenylcarbinol (**30**). Purification by preparative t.l.c. on silica gel (eluant $CHCl_3$) yielded 0.397 g (99%) of analytically pure **30**. I.r. spectrum, ν_{max} (neat) 1695 cm^{-1} (C=O), 3440 cm^{-1} (OH); mass spectrum, *m/e* 212 (23) (M^+), 183 (16) ($M^+ - CHO$), 105 (100) (formylphenyl); u.v. spectrum, λ_{max} (ethanol) 213, 259 mμ (ε 16 900, 16 400).

Anal. Calcd. for $C_{14}H_{12}O_2$: C, 79.24; H, 5.66. Found: C, 78.99; H, 5.47.

Similarly, reacting aldehyde resin **7** (4.63 g) with phenylmagnesium bromide in accordance with the method described above gave a resin alcohol which was directly treated with acid, and using an identical work-up as before yielded resin **3** and (*m*-formylphenyl)phenylcarbinol (**31**). Purification by preparative t.l.c. on silica gel (eluant $CHCl_3$) yielded 0.342 g (100%) of analytically pure (**31**), as an oil. I.r. spectrum, ν_{max} (neat) 1688 cm^{-1} (C=O), 3400 cm^{-1} (OH); mass spectrum, *m/e* 212 (11) (M^+), 183 (0.3) ($M^+ - CHO$), 105 (100) (formylphenyl); u.v. spectrum, λ_{max} (ethanol) 213, 251, 291 mμ (ε 25 100, 12 300; 2620).

Anal. Calcd. for $C_{14}H_{12}O_2$: C, 79.24; H, 5.66. Found: C, 79.23; H, 5.61.

Preparation of p- and m-Hydroxymethylbenzaldehydes (32) and (33)

The aldehyde resin **6** (5.08 g) was suspended in 60 ml of anhydrous benzene. Addition of 20 ml of a 70% solution of sodium bis(2-methoxyethoxy)-aluminum hydride in benzene to the above mixture gave, after stirring for 48 h at room temperature with exclusion of moisture ($CaCl_2$ drying tube), a suspension of a resin alcohol. The suspension was treated directly with dilute acid in a manner described previously to effect cleavage from the polymer of the reaction product. Similar work-up as before and purification by preparative t.l.c. on silica gel (eluant 5% ether – 95% $CHCl_3$) yielded 0.039 g (17%) of analytically pure *p*-hydroxymethylbenzaldehyde (**32**) (11). I.r. spectrum ν_{max} (neat) 1690 (C=O), 3400 cm^{-1} (OH); mass spectrum, *m/e* 136 (4) (M^+), 134 (100) ($M^+ - 2H$), 105 (10) ($M^+ - CH_2OH$); n.m.r. spectrum, 2.42 p.p.m. (1H, OH proton), 4.81 p.p.m. (2H, CH_2 singlet), 8.18–7.35 p.p.m. (4H, four aromatic protons, AB pattern), 10.10 p.p.m. (1H, aldehyde proton, singlet).

Similarly, treatment of aldehyde resin **7** (7.07 g) with sodium bis(2-methoxyethoxy)-aluminum hydride in anhydrous benzene, in a manner identical to that of aldehyde resin **6** as described above, gave a suspension of a resin alcohol. This suspension was treated directly with dilute acid followed by work-up as before. Purification by preparative t.l.c. on silica gel (eluant 5% ether – 95% $CHCl_3$) yielded 0.026 g (8%) of analytically pure *m*-hydroxymethylbenzaldehyde (**33**). I.r. spectrum, ν_{max} (neat) 1695 (C=O), 3440 cm^{-1} (OH); mass spectrum, *m/e* 136 (3) (M^+), 134 (3) ($M^+ - 2H$), 105 (10) ($M^+ - CH_2OH$); n.m.r. spectrum, 3.08 p.p.m. (1H, OH proton), 4.80 p.p.m. (2H, CH_2 protons), 7.88–7.19 p.p.m. (4H, aromatic protons), 10.05 p.p.m. (1H, aldehyde proton, singlet).

Anal. Calcd. for $C_8H_8O_2$: C, 70.59; H, 5.88. Found: C, 70.61; H, 5.90.

The authors wish to thank the National Research Council of Canada for a grant in aid of this research.

1. R. B. Merrifield. J. Am. Chem. Soc. **85**, 2149 (1963); R. B. Merrifield. Science, **150**, 178 (1965).
2. R. L. Letsinger and V. Mahadevan. J. Am. Chem. Soc. **88**, 5319 (1966).
3. J. M. Frechet and C. Schuerch. J. Am. Chem. Soc. **93**, 492 (1971).
4. I. T. Harrison and S. Harrison. J. Am. Chem. Soc. **89**, 5723 (1967); R. H. Grubbs and L. C. Kroll. J. Am. Chem. Soc. **93**, 3062 (1971); R. L. Lazcanot and J. E. Germain. Bull. Chim. Soc. Fr. 1869 (1971); F. Camps, J. Castells, J. Font, and F. Vela. Tetrahedron Lett. 1715 (1971); S. V. McKinley and J. W. Rakshys, Jr. Chem. Commun. 134 (1972); M. A. Kraus and A. Patchornik. J. Am. Chem. Soc. **93**, 7325 (1971); J. I. Crowley and H. Rapoport. J. Am. Chem. Soc. **92**, 6363 (1970).
5. T. Kusama and H. Hayatsu. Chem. Pharm. Bull. **18**, 319 (1970).
6. C. C. Leznoff and J. Y. Wong. Can. J. Chem. **50**, 2892 (1972).
7. J. Y. Wong and C. C. Leznoff. Can. J. Chem. **51**, 2452 (1973).
8. A. A. Baum. J. Am. Chem. Soc. **94**, 6866 (1972).
9. C. C. Leznoff and R. J. Hayward. Can. J. Chem. **48**, 1842 (1970); R. J. Hayward, A. C. Hopkinson, and C. C. Leznoff. Tetrahedron, **28**, 439 (1972).
10. H. V. Lendenfeld. Monatsch. Chem. **27**, 969 (1906).
11. W. Löw. Ann. Chem. **231**, 361 (1885).
12. J. P. Griffiths and C. K. Ingold. J. Chem. Soc. **125**, 1700 (1925).

A Novel Synthesis of *N*-Styryl Heterocycles

J. ROKACH, Y. GIRARD, AND J. G. ATKINSON
Merck Frosst Laboratories, Kirkland, Quebec

Received March 30, 1973

Reaction of the anions of a variety of 2-carboethoxy *N*-heterocycles with styrene oxide yields directly the *N*-(*trans*-2-styryl)-2-carboxylic acids. The reaction has been shown to proceed through a lactone intermediate which undergoes rapid elimination to form the unsaturated acid. The reaction has been used to alkylate 2-carboethoxy pyrrole, diethyl pyrazole-3,5-dicarboxylate, ethyl indole-2-carboxylate, ethyl benzimidazole-2-carboxylate, and ethyl 2-pyrrolidone-5-carboxylate. Yields were 82, 88, 93.5, 57, and 5% respectively.

1-(*trans*-2-Styryl)benzimidazole-2-carboxylic acid of m.p. 75–77 °C undergoes an interesting, reversible solid-state transformation to a high melting (255–260 °C), presumably zwitterionic, form.

La réaction d'anions d'une variété de carboéthoxy-2 *N*-hétérocycles avec l'époxide de styrène donne directement les acides *N*-(*trans*-styryl-2) hétérocycles-2 carboxyliques. Le mécanisme de la réaction passe par une lactone intermédiaire qui subit une élimination rapide pour donner ainsi l'acide insaturé. Ont été alkylés par ce procédé le carboéthoxy-2-pyrrole, le dicarboéthoxy-3,5-pyrazole, le carboéthoxy-2-indole, le carboéthoxy-2-benzimidazole et le carboéthoxy-5-pyrrolidone-2 avec des rendements respectifs de 82, 88, 93.5, 57 et 5%.

Il est intéressant de noter que l'acide (*trans*-styryl-2)-1-benzimidazole-2-carboxylique de p.f. 75–77 °C, se transforme réversiblement à l'état solide en un produit de p.f. 255–260 °C, vraisemblablement le zwitterion.

Can. J. Chem. **51**, 3765 (1973)

As part of a synthetic program in our laboratories we required an efficient general synthesis of 2-carboxy *N*-heterocycles substituted on nitrogen with β-styryl and β-phenethyl groups (*e.g.* **1**). Accordingly, we investigated the alkylation of a series of 2-carboethoxy *N*-heterocycles and are reporting the discovery of a novel and efficient synthesis of the desired compounds.

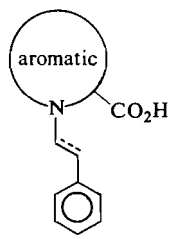

1

Results

Reaction of the ethyl pyrrole-2-carboxylate anion **2** in DMF with 2-phenethyl bromide gave a low yield (<5%) of the desired *N*-alkylation product, **3** (eq. 1). The main course of the reaction probably involved β-elimination to form styrene. A number of experiments served to confirm the initial result and no conditions were found which gave good yields of the desired product. Omote and co-workers (1) have also reported a similar type of reaction between indole and β-phenethyl bromide (or iodide), and obtained trace amounts of *N*-phenethyl indole. Alkylation of the anion **2** with styrene oxide in DMF was then investigated. It was anticipated that the initially formed alkoxide **4** would ring close to form the lactone **5**. Hydrogenolysis of the lactone was expected to lead to the desired phenethyl carboxylic acid **6** (eq. 2). Alkylation did occur, but surprisingly the product directly isolated was found to be 1-(*trans*-2-styryl)-pyrrole-2-carboxylic acid (**7**) (eq. 3).

Using NaH or potassium *t*-butoxide as the base and running the reaction in DMF at 110° for 1–2 h gave rise to an excellent yield (82%) of the product **7**. The elevated temperature was found to be very advantageous as at room temperature the yield was only about 25% after 24 h, and longer reaction times did not substantially improve the yield.

Further investigation with a series of 2-carboethoxy *N*-heterocycles showed that the reaction was of general applicability and that excellent yields of the *N*-(*trans*-2-styryl)-2-

Can. J. Chem. Downloaded from www.nrcresearchpress.com by 210.87.254.5 on 09/05/12
For personal use only.

[1]

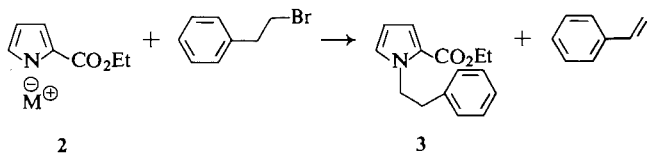

2 3

[2]

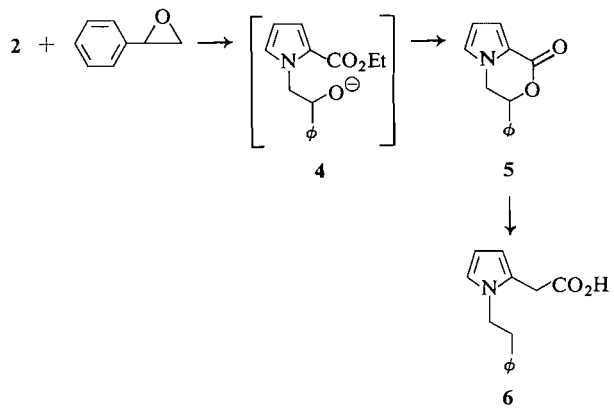

4 5 6

[3]

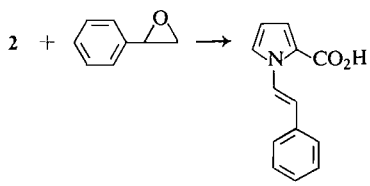

7

carboxylic acids could be readily obtained by this procedure (Table 1). Entry 5 of Table 1 (ethyl 2-pyrrolidone-5-carboxylate) indicates that the reaction is applicable to aliphatic as well as aromatic systems, although in lower yield. As can be seen in the Experimental, a particularly pleasing aspect of the reaction is the purity of the products as isolated directly from the reaction mixture. In all cases, there was no indication of impurities in the crude products as judged by the n.m.r. spectra and t.l.c., and there was little or no improvement in the m.p. upon recrystallization. The *N*-(2-styryl)carboxylic acids thus obtained could be hydrogenated quantitatively to *N*-(2-phenethyl)carboxylic acids (thus completing the original aim of the work in high overall yields).

At the time that our work was nearing completion, a publication by Irwin and Wheeler (2) appeared describing the reaction of the anion of ethyl pyrrole-2-carboxylate with a series of epoxides, and our work confirms and extends the results of these authors. Our assignments agree with those of Irwin and Wheeler (2), and in all cases the *trans* configuration is assigned to the styryl double bond on the basis of the large (~15 Hz) coupling constant between the two protons of the vinyl moiety.

A careful search was made in order to isolate the proposed lactone intermediates of type **5**. In the cases of the indole and benzimidazole compounds (entries 3 and 4, Table 1), it was possible to isolate low yields (~2%) of the lactones directly from the reaction mixture. The major product in each case was still the *N*-(*trans*-2-styryl)-2-carboxylic acid. The lactones were highly crystalline compounds and their structures could be unambiguously assigned on the basis of the i.r. and n.m.r. spectra, the details of which are given in Table 1. The assignment of shifts to the protons H_A and H_B in the lactones is based on the assumption that the *trans* hydrogens will have the larger of the two coupling constants with the tertiary proton H_C. The fact that there is a significant difference in the vicinal coupling constants indicates that

Can. J. Chem. Downloaded from www.nrcresearchpress.com by 210.87.254.5 on 09/05/12
For personal use only.

TABLE 1. Synthesis of *N*-styryl derivatives from styrene oxide

Entry	Starting material	Product	Yield (%)	M.p. (°C)	Spectral data
1	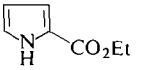	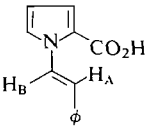	82	183–185*	J_{AB} 15 Hz
2	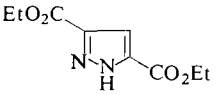	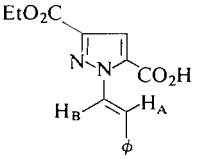	88	165–167	J_{AB} 15 Hz
3	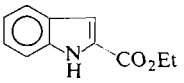	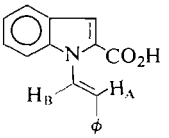	93.5	222–224	J_{AB} 15 Hz
		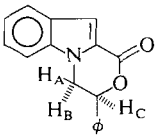		180–182	(CDCl$_3$) δ_A 4.20 J_{AB} 13 Hz δ_B 4.58 J_{AC} 10.5 Hz δ_C 5.80 J_{BC} 4 Hz ν(C=O) 1735 cm^{-1} (KBr)
4	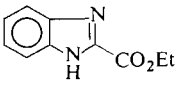	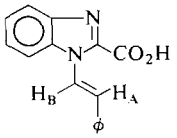	57	75–77 (dec.)	J_{AB} 15 Hz (Na salt)
		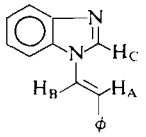	quantitatively from acid	93–95	(CDCl$_3$) δ_C 8.84 J_{AB} 15 Hz
		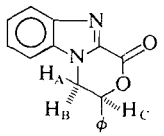		215–217	(DMSO-d_6) δ_A 4.63 J_{AB} 13.5 Hz δ_B 5.05 J_{AC} 10.5 Hz δ_C 6.25 J_{BC} 4 Hz ν(C=O) 1740 cm^{-1} (KBr)
5	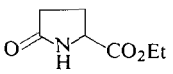	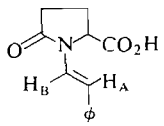	5	165	J_{AB} 14.5 Hz

*Literature (1) m.p. 178–179 °C.

H_C is in fact in a pseudoaxial configuration. Figure 1 shows a photograph of the n.m.r. spectrum of the indole lactone with a proposed configuration for the molecule.

Discussion

The results of Irwin and Wheeler (2) taken with those presently reported show that the reaction of 2-carboethoxy *N*-heterocycles is a

Can. J. Chem. Downloaded from www.nrcresearchpress.com by 210.87.254.5 on 09/05/12
For personal use only.

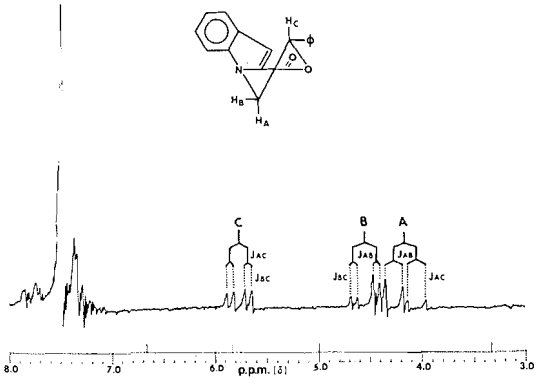

FIG. 1. N.m.r. spectrum of the lactone from the reaction of ethyl indole-2-carboxylate with styrene oxide (60 MHz, $CDCl_3$ solvent).

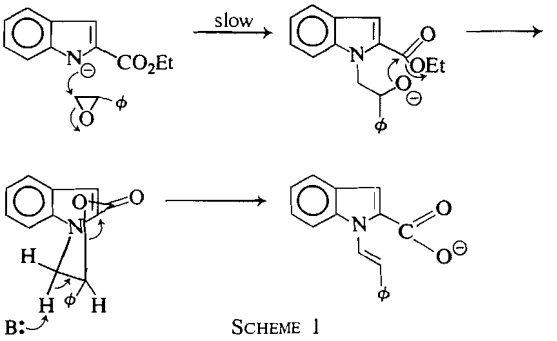

SCHEME 1

generally applicable reaction for the synthesis of 2-carboxy *N*-(β-styryl) compounds. The previous workers employed mainly ethyl pyrrole-2-carboxylate with a variety of epoxides and we have demonstrated, using styrene oxide, that the heterocyclic molecule can be varied considerably.

Irwin and Wheeler had reasonably proposed that the formation of the styryl carboxylic acids must go through a lactone intermediate which then undergoes β-elimination under the basic conditions of the reaction. They were able to isolate a lactone from the reaction with cyclohexene oxide, but this lactone did not undergo the elimination reaction because, as the authors point out, the stereochemistry of the material does not permit a transoid transition state.

We have been able to complete the mechanistic picture by isolation of the lactones from the reaction of styrene oxide with ethyl indole-2-carboxylate and ethyl benzimidazole-2-carboxylate. Both of these lactones, when treated under the conditions of the original reaction, were converted rapidly and in high yields to the styryl carboxylic acids. The ease of the conversion of the lactones to the final product indicates why they are normally isolated in very low yields or not at all.

The mechanistic picture thus derived is shown in Scheme 1 using styrene oxide and ethyl indole-2-carboxylate and is essentially identical to that proposed by Irwin and Wheeler.

Given the demonstrated rapidity of the last step of the scheme and the fact that starting material can be seen by t.l.c. until near the end of the reaction, one can also reasonably propose that the slow step is the initial alkylation by the the epoxide.

The properties of the product derived from ethyl benzimidazole-2-carboxylate and styrene oxide were found to be somewhat unusual and merit some discussion.

The product undergoes decarboxylation with extreme ease and if the work-up is done as usual with HCl, only the decarboxylated product is isolated (Table 1, entry 4). If acetic acid is used, the product can be isolated in good yield. Upon dissolving in organic solvents at room temperature, the acid decarboxylates neatly and quantitatively to 1-(2-styryl)benzimidazole in the time required to run the n.m.r. spectrum. The sodium salt, in contrast, is quite stable, and a satisfactory n.m.r. spectrum could be obtained in DMSO-d_6.

The solid acid of m.p. 75–77°, upon standing for several days at room temperature, undergoes a transformation to a high melting, very insoluble form. There is a concomitant change of the carboxyl band in the i.r. spectrum (KBr) from 1685 (sharp) to 1640 cm^{-1} (broad). Careful treatment with acetic acid regenerates the original form. This indicates that on standing the material is changing from a free acid to a zwitterionic form as shown in Scheme 2.

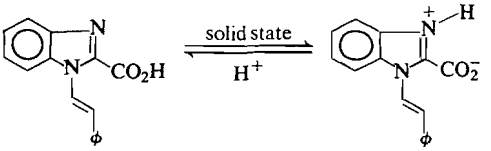

m.p. 75–77°
$\nu_{(KBr)}$ 1685 cm^{-1}

m.p. 255–260°
$\nu_{(KBr)}$ 1640 cm^{-1}

SCHEME 2

Can. J. Chem. Downloaded from www.nrcresearchpress.com by 210.87.254.5 on 09/05/12
For personal use only.

TABLE 2. Ultraviolet spectra of *N*-styryl heterocycle (EtOH)

Structure		λ max (nm)	log Σ
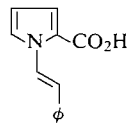		208	4.12
		221	4.14
		243	4.02
		305	4.24
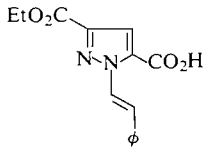		209	4.25
		226 sh	4.17
		317	4.23
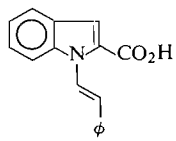		211 sh	4.30
		225	4.40
		284	4.30
		327	3.98
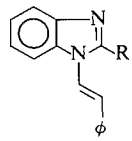	R = CO_2Na	213	4 37
		275*	4.19
	R = CO_2H†	211	4 30
		271	4 25
		302	4 13
	R = H	212	4 32
		270	4.37
		303	4.30

*Tailed out to 340 nm.
†The acid has undoubtedly largely decarboxylated during the spectrum.

Experimental

Melting points are uncorrected.

Ethyl benzimidazole-2-carboxylate was prepared according to Copeland and Ray (3). Ethyl 2-pyrrolidone-5-carboxylate and ethyl pyrrole-2-carboxylate were prepared by esterification of the corresponding acids. All the remaining starting materials were commercially available. All new compounds gave correct elemental analysis. The u.v. spectra are collected in Table 2.

N-(trans-Styryl)pyrrole-2-carboxylic Acid

Ethyl pyrrole-2-carboxylate (11.7 g, 0.084 mol) was dissolved in 50 cc dry DMF and sodium hydride powder (2 g, 0.084 mol) added to the stirred solution. When hydrogen evolution had ceased (2–3 h), styrene oxide (14 g, 0.115 mol) was added and the solution warmed at 110–120 °C for 1 h. (Reaction followed by t.l.c. for disappearance of starting material.) The reaction mixture was cooled, ice-water added (~300 cc), the resulting solution extracted with ether, and the water layer cooled and acidified with dilute HCl. The precipitated white solid was filtered, washed with water, and dried, yielding 14.6 g of pure product (82% yield), m.p. 183–184 °C. A sample recrystallized from methanol had m.p. 183–185 °C.

1-(trans-Styryl)pyrazole-3-carboethoxy-5-carboxylic Acid

Diethyl pyrazole-3,5-dicarboxylate (24 g, 0.113 mol) was dissolved in 300 cc dry DMF and potassium *t*-butoxide (13.2 g, 0.116 mol) added to the stirred solution. After 15 min, styrene oxide (18 g, 0.150 mol) was added and the mixture heated at 120 °C for 1–2 h (reaction followed by t.l.c. for disappearance of starting material). The cooled reaction mixture was diluted with ice-water (1000 ml), extracted with ether, and the water layer cooled and acidified with dilute HCl. The precipitated white solid was filtered, washed with water, and dried, yielding 28.4 g of pure product (88% yield), m.p. 165–167 °C, unchanged by recrystallization from methanol.

N-Styrylindole-2-carboxylic Acid

Sodium hydride powder (3.5 g, 0.146 mol) was added to a stirred solution of ethyl indole-2-carboxylate (25 g, 0.132 mol) in 250 ml dry DMF. After the hydrogen evolution had stopped, styrene oxide (30 g, 0.250 mol) was added and the mixture heated at 110 °C for 1½ h. The mixture was cooled, water added, and the solution extracted with ether. The water layer was acidified with excess dilute HCl. The precipitated solid was filtered, washed with water, and dried, yielding 32.5 g (93.5% yield), m.p. 222–224 °C, unchanged on recrystallization from methanol.

In a separate run ethyl indole-2-carboxylate (1.89 g, 10 mmol) and sodium hydride (260 mg, 11 mmol) were heated at 110° with styrene oxide (2.4 g, 20 mmol) and

Can. J. Chem. Downloaded from www.nrcresearchpress.com by 210.87.254.5 on 09/05/12
For personal use only.

the reaction stopped before completion. The reaction was worked-up as above and the ether extracts dried and evaporated to dryness. The residue (1.6 g) was triturated with ether – petroleum ether. The precipitated crystals (50 mg) were filtered to yield the lactone, m.p. 180–182 °C. Recrystallization from methanol did not improve the melting point.

The lactone (45 mg) was dissolved in ½ cc DMF and 19 mg potassium *t*-butoxide (1 equiv.) added and the mixture stirred at room temperature for 15 min. The reaction was diluted with water, acidified, and extracted with ether. The ether solution yielded 40 mg of a yellowish solid, identical by t.l.c. to the acid isolated above. This was recrystallized from methanol, m.p. 218–222 °C, mixed melting point 220–222 °C, with an i.r. spectrum identical to that of the authentic acid.

1-Styrylbenzimidazole-2-carboxylic Acid

To a stirred solution of ethyl benzimidazole-2-carboxylate (3.8 g, 0.020 mol) in 60 ml dry DMF, was added sodium hydride powder (520 mg, 0.022 mol). After 1 h styrene oxide (4.8 g, 0.040 mol) was added and the mixture heated at 110 °C for 2 h. The mixture was cooled, ice-water added, and the mixture extracted with ether. A suspended solid was filtered (30 mg) and proved to be the lactone, m.p. 215–217 °C. The ether extracts were dried and evaporated to dryness and the oily residue (2.6 g) treated with some ether and filtered to yield a further 30 mg of lactone.

The water layer was carefully acidified with acetic acid and the precipitated white solid was dried under vacuum at room temperature to yield the acid (3 g, 57% yield), m.p. 75–77 °C (dec.).

If the acidification is done with HCl, decarboxylation occurs and 1-styrylbenzimidazole is obtained, m.p. 93–94 °C. A sample of the acid recrystallized from cyclohexane similarly yielded the decarboxylated material, m.p. 93–94 °C.

When the acid is stored for a few days the m.p. increases to 255–260 °C and the i.r. spectrum shows a shift in the C=O absorption from 1685 to 1640 cm^{-1}. This compound, treated with AcOH in the cold, regenerates the original form of the acid, m.p. 74–76 °C, and the C=O band is restored to its original position and sharpness.

1-Styryl-2-pyrrolidone-5-carboxylic Acid

Ethyl 2-pyrrolidone-5-carboxylate (1.57 g, 10 mmol) was dissolved in DMF (20 cc) and sodium hydride (260 mg) added. After 1 h a two-fold excess of styrene oxide (2.4 g) was added and the mixture heated at 180 °C for ½ h. Ice-water was added to the cooled reaction mixture which was then extracted with ether. The water layer was acidified with dilute HCl, extracted with ether, and the ether dried and evaporated. The oily residue (350 mg) solidified on standing, m.p. 165 °C ($CHCl_3$).

1. Y. Omote, T. Nakamura, K.-T. Kuo, and N. Sugiyama. Chem. Abstr. **65**, 16928b (1966).
2. W. J. Irwin and D. L. Wheeler. Tetrahedron, **28**, 1113 (1972).
3. R. A. B. Copeland and A. R. Ray. J. Am. Chem. Soc. **65**, 1072 (1943).

Can. J. Chem. Downloaded from www.nrcresearchpress.com by 210.87.254.5 on 09/05/12
For personal use only.

The Rate of Recombination of H Atoms in the Presence of NH_3

L. TENG[1] AND C. A. WINKLER
Department of Chemistry, McGill University, Montreal, Quebec

Received June 11, 1973

The rate constant for the homogeneous recombination of H atoms in the presence of NH_3, with He as carrier gas, has been determined at 298 °K in a fast flow system, over the pressure range 1.50 to 4.55 Torr, using e.s.r. technique. A value of either 4.00×10^{16} or 5.14×10^{16} $cm^6\ mol^{-2}\ s^{-1}$ was calculated, depending upon the rate constant taken, or estimated, from the literature for the recombination in the presence of helium.

A l'aide d'un système à débit rapide, on a déterminé la constante de vitesse pour la recombinaison homogène d'atomes d'hydrogène en présence de NH_3 en utilisant l'He comme gaz porteur à 298 °K pour des pressions allant de 1.50 à 4.55 Torr. A l'aide de la technique r.p.e., la valeur de cette constante s'est révélée être soit 4.00×10^{16} ou soit 5.14×10^{16} $cm^6\ mol^{-2}\ s^{-1}$ selon la valeur choisie ou estimée, à partir de la littérature, de la constante de vitesse se rattachant à la recombinaison en présence d'hélium.
[Traduit par le journal]

Can. J. Chem. **51**, 3771 (1973)

Can. J. Chem. Downloaded from www.nrcresearchpress.com by 210.87.254.6 on 09/05/12
For personal use only.

The recombination of hydrogen atoms has been extensively studied with one of H_2, He, or Ar as the third body, both at room temperature (in flow system) and higher temperatures (in flames or shock tubes) (1). Values of the rate constants were found in the range 3 to 6×10^{15} $cm^6\ mol^{-2}\ s^{-1}$. A few recent investigations have been made in the presence of other inert gases. Measurements at room temperature with N_2 and CO_2 (2), and with H_2O (3), as third bodies yielded values of 3×10^{15} to 9×10^{16} $cm^6\ mol^{-2}\ s^{-1}$ while measurements at higher temperatures (approximately 1550–1900 °K) gave values of 6×10^{14} to 5×10^{15} $cm^6\ mol^{-2}\ s^{-1}$ with the third bodies N_2, $CO + CO_2$, and H_2O (4, 5).

In the present investigation, the recombination of H atoms in the presence of NH_3 has been studied at room temperature using electron spin resonance to determine the H atom concentration. No consumption of NH_3 was observed, in agreement with observations by Kurylo *et al.* (6).

Experimental and Results

Hydrogen atoms were generated by electrode or microwave discharge through a H_2 + He mixture in which the H_2 content was varied in the range 0 to 5%. Hydrogen (99.99%) was passed through a "Deoxo" unit followed by a liquid N_2 trap, then mixed with He (99.995%) which had also been passed through a liquid N_2 trap. From the discharge, the gas mixture passed through a Pyrex tube 26 mm i.d. and 83 cm long, fitted with a movable jet through which NH_3 (99.99%) was added. The inner wall of the Pyrex tube was coated with boric acid to reduce the heterogeneous recombination of H atoms. Pressures were measured at the mid-point of the tube with a McLeod gauge.

The change in H atom concentration was measured with a Varian Model V-4502-12 e.s.r. spectrometer, 100 Kc/s modulation, with a 9 in. magnet, and a Model 4531 multipurpose cavity. The cavity operated in a TE_{012} mode and accepted a sample tube of 11 mm o.d. It was connected to the low-power arm of the microwave bridge. The signal of the e.s.r. was calibrated by determining the maximum extents to which the H atoms reacted with excess HI and HBr (7).

Calculation of Rate Constants

The reactions to be considered are

$$[1] \qquad H + H + NH_3 \xrightarrow{k_1} H_2 + NH_3$$

$$[2] \qquad H + H + He \xrightarrow{k_2} H_2 + He$$

$$[3] \qquad H + \text{Wall} \xrightarrow{k_3} \tfrac{1}{2}H_2 + \text{Wall}$$

The decay of H atoms may be represented by[2]

$$[4] \qquad \frac{-d[H]}{dt} = k_1[NH_3][H]^2 + k_2[He][H]^2 + k_3[H]$$

[1]Postdoctoral Fellow.

[2]It may be assumed that H and H_2, at their low concentrations in these experiments, contribute negligibly as third bodies to atom recombination.

TABLE 1. Measurements of the rate constant k_1 for $H + H + NH_3 \rightarrow H_2 + NH_3$

Pressure (Torr)	Linear velocity (cm/s)	$[NH_3](\times 10^8)$ (mol/cm^3)	$[H]_0(\times 10^{10})$ (mol/cm^3)	$[He](\times 10^7)$ (mol/cm^3)	k_3 (s^{-1})	$k_1(\times 10^{16})$ ($cm^6\ mol^{-2}\ s^{-1}$)
1.50	181	0.80	3.51	0.78	3.95	4.16
1.55	187	1.36	5.16	0.76	3.97	3.95
1.61	187	1.81	3.29	0.76	3.80	4.05
1.62	185	1.82	5.19	0.76	3.95	4.23
2.45	210	0.71	4.18	1.34	3.25	3.84
2.45	210	0.71	1.39	1.34	3.22	4.02
2.50	214	1.58	1.39	1.31	3.32	3.91
2.50	214	1.58	4.18	1.31	3.27	4.05
3.45	272	0.55	2.10	1.95	2.92	3.86
3.45	272	0.55	0.75	1.95	2.85	3.95
3.50	274	1.23	0.75	1.93	2.90	3.99
3.50	274	1.23	2.10	1.93	2.89	3.80
4.50	361	0.41	2.24	2.52	2.69	4.02
4.50	361	0.41	0.84	2.52	2.75	4.15
4.55	364	0.93	0.84	2.50	2.70	4.06
4.55	364	0.93	2.24	2.50	2.77	3.97
					Av.	4.00 ± 0.09

On integration

$$[5]\quad \ln\frac{[H]_0}{[H]_t} - \ln\frac{k_1[NH_3][H]_0 + k_2[He][H]_0 + k_3}{k_1[NH_3][H]_t + k_2[He][H]_t + k_3} = k_3 t$$

In the absence of NH_3, with known reaction times t_1 and t_2, for which $[H]_{t_1}$ and $[H]_{t_2}$ are determined for given [He]

$$[6]\quad \ln\frac{[H]_{t_2}}{[H]_{t_1}} + \ln\frac{k_2[He][H]_{t_1} + k_3}{k_2[He][H]_{t_2} + k_3} = k_3(t_1 - t_2)$$

or

$$[7]\quad \frac{[H]_{t_2}}{[H]_{t_1}}\left(\frac{k_2[He][H]_{t_1} + k_3}{k_2[He][H]_{t_2} + k_3}\right) = e^{k_3(t_1 - t_2)}$$

For $k_3(t_1 - t_2)$ not in excess of about 0.4

$$[8]\quad \frac{[H]_{t_2}}{[H]_{t_1}}\left(\frac{k_2[He][H]_{t_1} + k_3}{k_2[He][H]_{t_2} + k_3}\right) = k_3(t_1 - t_2) + 1$$

Insertion of the appropriate experimental data into this relation, together with the recently determined value of k_2 (2), permitted the value of k_3 applicable to the present system to be estimated.

When NH_3 was added between the H inlet and the e.s.r. cavity the rate of recombination of H atoms was increased for given values of the pressure and of [He], although the increased flow rate through the tube reduced the extent to which the H atom signal was decreased at the e.s.r. cavity. Several calibration curves were made of the e.s.r. signal against the H atom concentration, determined with the HI or HBr procedure, corresponding to several positions at which NH_3 was added between the H atom inlet and cavity. This allowed values of $[H]_t$ to be calculated in the presence of NH_3 from the change of e.s.r. signal. From the known values of k_2, k_3, $[NH_3]$, [He], and measured values of $[H]_{t_1}$ and $[H]_{t_2}$ for reaction times t_1 and t_2, respectively, the value of k_1 was then calculable from

$$[9]\quad \left(\frac{[H]_{t_2}k_1[NH_3][H]_{t_1} + k_2[He][H]_{t_1} + k_3}{[H]_{t_1}k_1[NH_3][H]_{t_2} + k_2[He][H]_{t_2} + k_3}\right) = 1 + k_3(t_1 - t_2)$$

Rate constants for the recombination of H atoms in the presence of NH_3 are given in Table 1 for a range of pressures from 1.50–4.55 Torr, with various NH_3, He, and H concentrations. The values are corrected for longitudinal diffusion of the hydrogen atoms (8, 9).

The value of k_2 used in the above calculations (2) is approximately one-half that estimated from the results of Kaufman and co-workers (10) for $H + H + H_2$ in conjunction with the ratio of 1.3

Can. J. Chem. Downloaded from www.nrcresearchpress.com by 210.87.254.6 on 09/05/12
For personal use only.

for the effectiveness of He relative to H_2 (2). If the latter value is used in eqs. 8 and 9, k_3 is changed by less than 5% and the value of k_1 becomes 5.14×10^{16} cm^6 mol^{-2} s^{-1}. From either calculation, it appears that NH_3 has roughly one-half the efficiency of H_2O as a third body for recombination of H atoms.

The authors are grateful to the Department of Chemistry of Sir George Williams University, Montreal, for unrestricted use of its electron spin resonance equipment, and to the National Research Council of Canada for financial assistance.

1. L. TENG, S. D. MACKNIGHT, and W. E. JONES. Chem. Rev. To be published.
2. J. E. BENNETT and D. R. BLACKMORE. 13th Symp. Combust. 51 (1971).
3. V. H. EBERIUS, K. HOYLSMANN, and H. GG. WAGNER. Ber. Bunsen. Phys. Chem. **73**, 962 (1969).
4. C. R. HALSTEND and D. R. JENKINS. 12th Symp. Combust. 979 (1968).
5. R. W. GETZINGER and L. S. BLAIR. Combust. Flame, **13**, 271 (1969).
6. M. J. KURYLO, G. A. HOLLINDEN, H. F. LEFEVRE, and R. B. TIMMONS. J. Chem. Phys. **51**, 4497 (1969).
7. D. M. WILES and C. A. WINKLER. J. Phys. Chem. **61**, 620 (1957).
8. F. KAUFMAN. Prog. React. Kinet. **1**, 12 (1961).
9. A. A. WESTENBERG. Adv. Heat Transfer, **3**, 253 (1966).
10. D. O. HAM, D. W. TRAINER, and F. KAUFMAN. J. Chem. Phys. **53**, 4395 (1970).

Can. J. Chem. Downloaded from www.nrcresearchpress.com by 210.87.254.6 on 09/05/12
For personal use only.

Molecular Motion in Azulene and the Azulene–(*s*)-Trinitrobenzene Molecular Complex in the Solid State

C. A. FYFE AND G. J. KUPFERSCHMIDT
Department of Chemistry, University of Guelph, Guelph, Ontario

Received December 15, 1972[1]

Molecular motion of azulene in its own molecular crystal and in its complex with trinitrobenzene has been shown from wide-line n.m.r. and spin–lattice relaxation time measurements to occur in the solid state. Calculations of the n.m.r. spectral parameters based on a model where the azulene molecules are reorienting in their molecular planes by 180° jumps give satisfactory agreement with experimental values. The results are discussed with respect to the available X-ray data.

On a montré à l'aide de la r.m.n. large bande et de mesures des temps de relaxation spin–réseau que le mouvement moléculaire de l'azulène dans sa propre structure cristalline ainsi que dans celle de son complexe avec la trinitrobenzène se produit à l'état solide. Les calculs des paramètres spectraux en r.m.n. basés sur un modèle où les molécules d'azulène se réorientent dans les plans moléculaires par des changements de 180° sont en proche accord avec les valeurs expérimentales. On discute des résultats en fonction des données disponibles à l'aide des expériences en rayons-X.

[Traduit par le journal]

Can. J. Chem. 51, 3774 (1973)

Introduction

Several attempts have been made to determine the crystal structure of azulene (1–6). The first investigation was by Günthard and co-workers (1), who suggested the centrosymmetric space group $P2_1/a$ with two molecules in the unit cell. Since azulene is not itself centrosymmetric, a disordered structure was implied. However, subsequent independent investigations by Robertson and Shearer (2) and by Takeuchi and Pepinsky (3) suggested an ordered structure based on the non-centric space group *Pa*. Support for an ordered structure was also claimed from an examination of the external morphology of the crystal (4). However, further work by Robertson and co-workers showed that the structure based on the non-centric space group *Pa* could not be successfully refined, whereas that based on the centric $P2_1/a$ could (5, 6). The occupancy of a single site was the statistical distribution of molecules over two possible sites as shown in Fig. 1, the 'average' occupancy being centrosymmetric. No unusual intermolecular contacts were introduced by the disorder, but the molecular structure was not accurately determined since, because of the overlapping of the three pairs of atoms indicated in Fig. 1, seven other slightly different molecules are possible. Although the molecule drawn in Fig. 1 was considered the most reasonable, there was still a severe limitation to the accuracy of the determination.

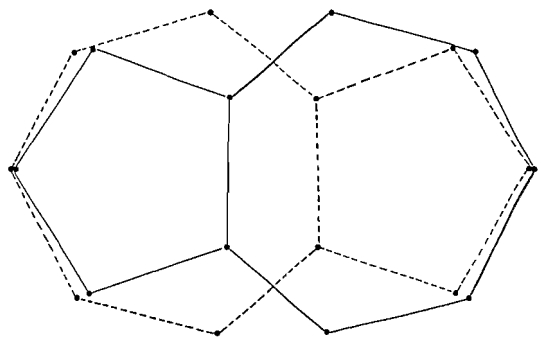

FIG. 1. Schematic representation of the statistical occupancy of a single site in the room temperature azulene crystal as found by Robertson *et al.* (6).

Brown and Wallwork (7) attempted to determine the room temperature structure of the azulene–trinitrobenzene complex but found that 'disorder' in the azulene portion of the molecule prevented refinement, although a structure is given in their paper showing a single orientation of azulene molecules.

The determination of the crystal structure of the complex of azulene with trinitrobenzene was undertaken independently by Hanson (8) as a further attempt to determine the molecular geometry of azulene. In an elegant piece of work,

[1]Revision received July 31, 1973.

Can. J. Chem. Downloaded from www.nrcresearchpress.com by 210.87.254.5 on 09/05/12
For personal use only.

Can. J. Chem. Downloaded from www.nrcresearchpress.com by 210.87.254.5 on 09/05/12
For personal use only.

he chose a temperature of −95 °C, and was able to successfully refine the structure at this temperature. The suggested structure involved 93% of the azulene molecules adopting one orientation, and only 7% adopting the alternative orientation by 180° rotation in their molecular planes as shown in Fig. 1.

Several aromatic molecules are known to possess considerable motional freedom in the solid state (9–11) and solid state n.m.r. has proven to be a powerful tool for its investigation. Although the aromatic compounds investigated often show no disorder due to their reorientation because of their high symmetry, there is no *a priori* reason why this must be so.

The purpose of the present work was to determine whether the disorder shown in the case of azulene was of a static or dynamic nature, whether there was any reorientation in the case of the complex, and the relationship of any motional processes to the results of the X-ray structure determinations.

Experimental

Azulene was supplied by the Aldrich Chemical Company and was used without further purification. The complex was prepared by mixing hot equimolar solutions of trinitrobenzene and azulene in toluene. The cooled solution yielded blue-black crystals, m.p. 165–166 °C (lit. (12) 167 °C), which analyzed correctly for a 1:1 complex.

Slow passage n.m.r. spectra were recorded on a Varian H.A. 100A spectrometer with a 15″ magnet. Signal modulation and detection were achieved using a P.A.R. H.R. 8 lock-in amplifier and an H.P. 465A amplifier. Samples were sealed in thin-walled 12 mm o.d. tubes. Temperature variation was achieved using a standard variable temperature accessory, and temperatures were recorded directly using a copper/constantan thermocouple fused into the top of the sample. Several spectra were recorded at each temperature and the average parameters taken.

T_1 measurements on azulene were made with a 30 MHz pulsed spectrometer built from commercial units using a saturation method with a 90° pulse of approximately 2.5 μs. T_1 measurements on the complex were made on a Bruker pulsed spectrometer at 30 MHz using a 90°–τ–90° pulse sequence and a pulse length of 1.5 ms (see acknowledgments).

D.s.c. measurements were made on a Perkin Elmer Differential Scanning Calorimeter, Model 1B (see acknowledgments).

All calculations were performed on the University of Guelph's I.B.M. 360-50 computer using Fortran IV programs.

Results and Discussion

Slow Passage Measurements

The ^{1}H n.m.r. spectrum of solid azulene was found to be temperature dependent (Fig. 2, inset) indicative of some reorientation process. The linewidth and second moment parameters both show a transition, centered at ~310 °K. The anomalous change in the second moment parameters may be an artifact due to saturation, as T_1 in this region is extremely long (see later). The results of calculations of the theoretical second moments for a rigid lattice (13), and for motion (14) between the two alternate sites by 180° jumps, are shown in Table 1 compared with the experimentally observed values, and will be discussed in detail. The second moment ΔH^2 in a rigid lattice can be calculated from the formulation of Van Vleck (13), eq. 1,

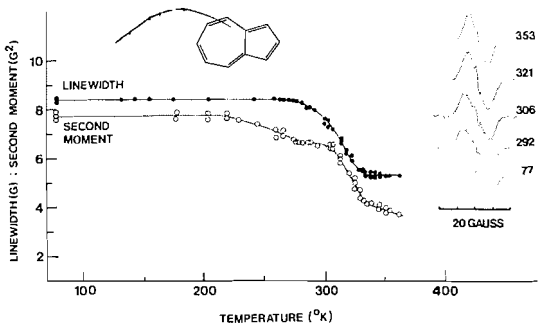

FIG. 2. The temperature dependence of the linewidth (filled circles) and second moment (open circles) parameters of the proton resonance of azulene in the solid state with (inset) representative spectra recorded at the temperatures indicated by the vertical arrows.

$$[1] \quad \Delta H^2 = \frac{9}{16}\gamma^2 h^2 \sum_{i,j} \left(\frac{3\cos^2\theta_{ij} - 1}{r_{ij}^3} \right)^2$$

where r_{ij} is the internuclear distance between atoms i, j and θ is the angle between their internuclear vector and the applied magnetic field. The summation is carried out for all pairs of interactions i, j.

For a polycrystalline sample, the term $(3\cos^2\theta_{ij} - 1)^2$ must be averaged over all the positions of the crystallites becoming 4/5 and yielding [2].

$$[2] \quad \Delta H^2 = \frac{9}{16}\gamma^2 h^2 \sum_{i,j} r_{ij}^{-6}$$

In practice, this interaction is often divided further into an intramolecular contribution from the atoms within a single molecule and an intermolecular contribution from the interactions between the atoms of different molecules. It is possible to calculate the former at least approxi-

Can. J. Chem. Downloaded from www.nrcresearchpress.com by 210.87.254.5 on 09/05/12
For personal use only.

mately from the molecular structure, whereas the latter may only be calculated from a knowledge of the crystal structure or else estimated.

In the case of azulene the molecular structure taken was that considered most probable by Robertson *et al.* (6); hydrogen atoms were generated at a C—H bond length of 1.08 Å by bisecting the ccc angle whose apex was the carbon to which the hydrogen was attached. Calculation of the rigid lattice second moment as described above by the formulation of Van Vleck (13) gives an intramolecular second moment of 4.24 G^2 and an intermolecular second moment of 4.42 G^2, giving a total second moment of 8.66 G^2 compared to the limiting low-temperature second moment of 7.8 G^2. The difference is attributed to the intramolecular second moment being too high. Intramolecular second moments found for polycyclic aromatics are in the range 3.0 ± 0.5 G^2 (21, 22, 24), and the value for the azulene molecule itself in the complex where the coordinates are much better defined is 2.8 G^2. It is thought that the difference in the present case is due to the inherent inaccuracies introduced by the disorder, as discussed in the introduction, and the value found for azulene in the complex was used. There may also be inaccuracies in the intermolecular second moment, but these are liable to be much smaller, as the internuclear distances involved are larger.

In the presence of motion, the term

$$\left(\frac{3\cos^2\theta_{jk} - 1}{r_{jk}^3}\right)^2$$

in eq. 1 must be averaged over the motion. The intramolecular contribution is simplest, since the term r_{jk} remains constant throughout the motion for a rigid molecule such as azulene (not all cases need have this simplification). Gutowsky and Pake (26) have shown that averaging over the motion and then over the powder reduces this term to $(3\cos^2\alpha_{ij} - 1)^2/r_{ij}^6$ where α_{jk} is the angle between the rotation axis and the internuclear vector. The average obtains only for axes of order $\geqslant 3$. In the case of a twofold axis, the term is unchanged as the motion exactly reverses the direction of the internuclear vectors.

For the intramolecular contribution, the term

$$\left(\frac{3\cos^2\theta_{ij} - 1}{r_{ij}^3}\right)^2$$

must again be averaged. In this case, however, the vector r_{ij} changes not only in direction, but also in length. Averaging the above term firstly over all the positions occupied by the two atoms in the reorientation, and then averaging over the powder yields [3].

$$[3]\quad \left\langle\left\langle \frac{3\cos^2\theta_{ij} - 1}{r_{ij}^3}\right\rangle^2\right\rangle = \frac{1}{p^2q^2}\sum_{i=1}^{p}\sum_{j=1}^{q}\frac{1}{r_{ij}^6}\left[\frac{4}{5}\frac{(3\cos^2\theta_{ij} - 1)^2}{2} + \frac{4}{15}(3\cos\theta_{ij}\sin\theta_{ij}\sin\Psi_{ij})^2 + \frac{4}{15}(3\cos\theta_{ij}\sin\theta_{ij}\cos\Psi_{ij})^2 + \frac{1}{15}(3\sin^2\theta_{ij}\cos 2\Psi_{ij})^2 + \frac{1}{15}(3\sin^2\theta_{ij}\sin 2\Psi_{ij})^2\right]$$

Where the summations are made over the N positions occupied by the internuclear vector determined by the p sites occupied by atom i and the q sites occupied by atom j and θ_{ij} and ϕ_{ij} are the polar angles made by the vector ***ij*** with an arbitrary origin. These equations are identical to those deduced by Michel and co-workers (14) and may be used directly in calculations. The averaging for the intramolecular case for a rigid molecule is, in fact, a special case of the more general eq. 3 where the distance r_{ij} does not change. In the present work Van Vleck's formula was modified using [3] for the calculation of both inter- and intramolecular interactions.

Calculation of the theoretical second moment for motion between the two alternate sites leaves the intramolecular second moment unchanged, but causes a drop in the intermolecular contribution to 1.14 G^2, giving a total second moment in reasonable agreement with that experimentally observed.

Although the disorder found crystallographically could theoretically be obtained by rotating the azulene molecule by 180° around an axis in its plane passing through the center of gravity of the molecule (end over end rotation), this possibility is ruled out by the infinitely large repulsive interactions it introduces between the molecule being rotated and the other molecules in the lattice, and in-plane rotation by 180° is thought to be the only reasonable motion.

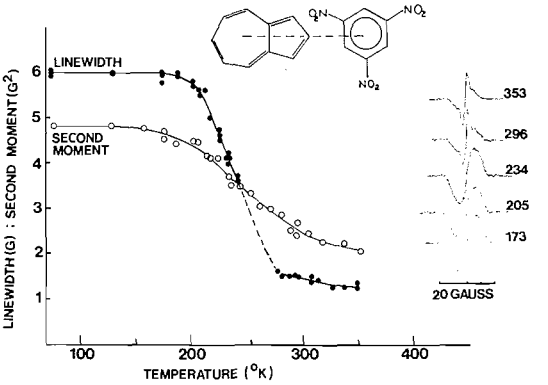

FIG. 3. The temperature dependence of the linewidth (filled circles) and second moment (open circles) parameters of the proton resonance of the azulene–trinitrobenzene molecular complex with (inset) representative spectra recorded at the temperatures indicated by the vertical arrows.

The proton resonance of the complex is similarly temperature dependent (Fig. 3) showing linewidth and second moment changes centered about 250 °K. The discontinuous linewidth change shown in Fig. 3 is due to a change in signal shape. The narrow component in the high-temperature spectra is thought due to the three protons on the trinitrobenzene molecule which will be broadened only slightly as there are no protons 'ortho' to them in the molecule.

The limiting low- and high-temperature second moments are again compared with calculated theoretical values in Table 1. The basic molecular unit taken for the calculation of the intramolecular contribution was a molecule of complex, *i.e.* one azulene and one trinitrobenzene molecule. There is good agreement (Table 1) between the observed low-temperature value and calculated rigid lattice second moment, and tolerable agreement between the limiting high-temperature second moment and the theoretical value calculated for motion of the azulene molecule between two sites related by 180° while the trinitrobenzene molecules are still rigid. There is very little change in the total intramolecular contribution for the complex, since only the interactions between the two rings average.

Calculation of the theoretical second moment based on a model where both the azulene and the trinitrobenzene molecules are moving, the latter round its threefold axis, also yields a value which agrees reasonably well with the observed high-temperature second moment (Table 1). It is not thought possible to distinguish between these two cases from the calculations but it is possible that both molecules could be moving.[2]

The slow passage experiments thus suggest that there is motion of the azulene molecules in both cases. Because discrete positions are shown by the X-ray measurements, the motions must be by 180° 'flips'. The onset of motion occurs at a much lower temperature in the complex.

T_1 Measurements

The spin-lattice relaxation times of azulene and the complex are shown plotted as their logarithms against the reciprocal of absolute temperature in Fig. 4. Both sets are very temperature dependent, indicative of the presence of some reorientation process, in agreement with the results from the slow passage experiments. In the case of the complex, the expected minimum in the curve is found, but azulene itself melts before its minimum is reached. In the case of azulene, T_1 measurements could not be performed below 290 °K due to the very long values of T_1. As indicated above, those large values of T_1 may have caused anomalous values of the second moment parameters because of distortion of the signal shape due to saturation.

Activation Energies

Activation energies calculated from a least-square fit to the linear portions of the T_1 curves are given in Table 2. Also given are the value for azulene from a fit of the modified B.P.P. equation (15, 16) to the linewidth transition, and values for both the azulene and the complex from the Waugh estimate (17) of $37T$, where T is the temperature of the linewidth transition. The overall agreement between all the results is probably fortuitous, as the second methods are considerably more empirical than the T_1 measurements.

That the azulene molecule in complex has a lower activation energy for reorientation than it does in its own molecular crystal suggests certain critical intermolecular contacts have been broken by the layer structure of the complex, and is consistent with results of other systems (11). The reorientation of the azulene molecule in the complex also shows directly that although

[2]The authors are grateful to a referee who suggested this possibility.

Can. J. Chem. Downloaded from www.nrcresearchpress.com by 210.87.254.5 on 09/05/12
For personal use only.

TABLE 1. Observed and calculated second moment parameters (in G^2) for azulene and the azulene-trinitrobenzene molecular complex for the various motions indicated for the azulene moieties[a]

Molecule	State	Calculated			Observed	T(°K)
		Intra	Inter	Total		
Azulene	R[b]	3.0±0.5[c]	4.42	7.4 ±0.5	7.8±0.3	<270
	M[b]	3.0±0.5[c]	1.14	4.14±0.5	3.8±0.3	>350
Azulene-trinitrobenzene complex	R[b]	2.46[c]	2.15	4.61±0.5	4.2±0.3	<200
Azulene moving	M[b]	2.45[c]	0.89	3.34±0.5		
Azulene and trinitrobenzene both moving	M[b,d]	2.45[c]	0.54	2.99±0.5	2.2±0.3	>320

[a]For details of the calculations see the text.
[b]R = rigid, M = moving.
[c]In the case of azulene itself, there is no change in the intramolecular contribution to the second moment as the motion is one of 180° flips. In the case of the complex, the intramolecular drops vary slightly because the basic unit considered consists of both components. The contributions from these other interactions are, however, very small.
[d]The author would like to acknowledge the assistance of one of the referees in pointing out this possibility.

the molecule is unsymmetrical, there is no strong localization of the charge transfer interaction at any point in the molecule.

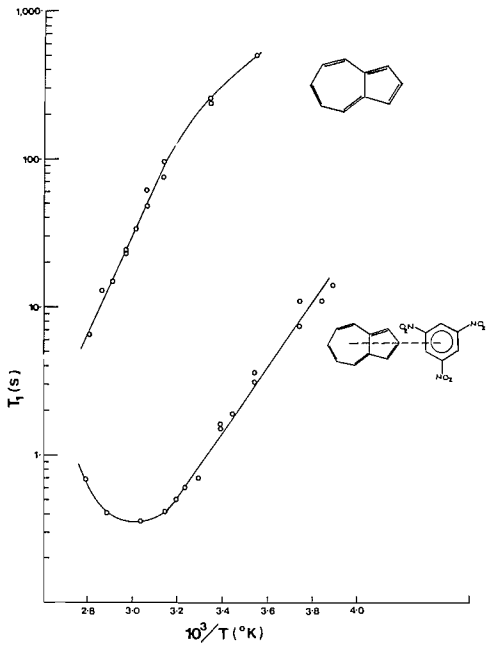

FIG. 4. Spin-lattice relaxation time (T_1, s) of the proton resonance of azulene (upper curve) and the azulene-trinitrobenzene molecular complex (lower curve) plotted as their logarithms against the reciprocal of absolute temperature.

Thermodynamic Results

If there is reorientation of the azulene molecules at room temperature, and if there is no disordered low-temperature phase with an associated zero point entropy, then there should be an order-disorder transition at, or below, the temperature of the n.m.r. linewidth transition, since the latter is the result of a kinetic process.

Accordingly, d.s.c. measurements were made in the appropriate temperature range. These, however, failed to reveal any such transitions although the melting transition was clearly identified. This is thought to be due to the relatively small value of the entropy change involved (R ln 2, in the case of azulene, and half this value for the complex), the relative insensitivity of the apparatus, and the large number of degrees over which transitions of this type typically occur (18). A proper thermodynamic investigation using an adiabatic calorimeter to resolve this point would be of interest.[3]

Conclusions

The azulene molecules in both azulene and its complex with trinitrobenzene are considered to be in dynamic equilibrium between the two alternate sites rotated by 180° as suggested by the

[3]Personal communication from Prof. E. F. Westrum Jr. indicates that his group has recently completed such a study.

Can. J. Chem. Downloaded from www.nrcresearchpress.com by 210.87.254.5 on 09/05/12
For personal use only.

TABLE 2. The activation energies (kcal mol^{-1}) for the reorientation processes in azulene and the azulene–trinitrobenzene molecular complex as determined by the methods indicated

	T_1 measurements	B.P.P. approximation	Waugh estimate
Azulene	15.4±0.4	16.2±0.5	11.4
Azulene–trinitrobenzene complex	9.7±0.3	—[a]	9.3

[a]Not applicable due to changes in spectral shape.

X-ray investigation of azulene (6). If a structure determination is found possible for the azulene–trinitrobenzene complex at room temperature, it should show the same type of disorder in the azulene moiety. The low-temperature structure determination of the complex by Hanson (8) is thought to have been done at the low-temperature end of an order–disorder transition involving the azulene molecules. A lower temperature still would perhaps remove the residual 7% of the alternate orientation. Similarly, a structure determination of azulene at some temperature below 270 °K should show only a single occupancy of the sites. The exact temperatures of the transitions will be best determined calorimetrically.

The conclusions from the results here may perhaps be extended to other compounds involving the azulene moiety whose structures have recently been determined (19, 20). Thus, in the case of the organometallic molecule azulene – dimolybdenum hexacarbonyl, the azulene moiety is disordered (19). From the present work, the disorder is thought to be of a dynamic nature, and the bonding between the metal atoms and the azulene weaker and much less localized than in other similar compounds, for example azulene – diiron pentacarbonyl (20) where an ordered azulene structure is found.

Several polycyclic aromatic molecules have now been shown to possess a dynamic, rather than static, structure in the solid state (21–24). A theoretical interpretation of why this should be so, as well as a prediction of the activation energies involved, is currently in progress (25).

The authors would like to acknowledge the financial assistance of the National Research Council of Canada for a grant in aid of research (to C.A.F.) and for a major equipment grant for the purchase of the spectrometer, and also the Research Advisory Board of the University of Guelph. They would also like to thank Dr. J. Stevens for the use of his d.s.c. apparatus and Dr. Pintar and Dr. R. Knispel, University of Waterloo, for the use of their pulse spectrometers and for their assistance in making the T_1 measurements.

1. H. H. GÜNTHARD, P. A. PLATTNER, and E. BRANDENBERGER. Experientia, **4**, 425 (1948).
2. J. M. ROBERTSON and H. M. M. SHEARER. Nature, **177**, 885 (1956).
3. Y. TAKEUCHI and R. PEPINSKY. Science, **124**, 126 (1956).
4. J. D. BERNAL. Nature, **178**, 40 (1956).
5. J. M. ROBERTSON, H. M. M. SHEARER, G. A. SIM, and D. G. WATSON. Nature, **182**, 177 (1958).
6. J. M. ROBERTSON, H. M. M. SHEARER, G. A. SIM, and D. G. WATSON. Acta Cryst. **15**, 1 (1962).
7. D. S. BROWN and S. C. WALLWORK. Acta Cryst. **19**, 149 (1965).
8. A. W. HANSON. Acta. Cryst. **19**, 19 (1965).
9. (*a*) E. R. ANDREW. J. Phys. Chem. Solids, **18**, 9 (1961). (*b*) E. R. ANDREW and P. S. ALLEN. J. Chim. Phys. **63**, 85 (1966). (*c*) E. R. ANDREW. Ber. Bunsenges. Phys. Chem. **67**, 295 (1963).
10. J. G. POWLES. Arch. Sci. (Geneva), **12**, 87 (1959).
11. C. A. FYFE. Molecular motion in complexes, adducts and related species in the solid state. *In* Molecular complexes. Vol. 1. *Edited by* R. Foster. Logos Press, London. 1973.
12. Dictionary of organic compounds. Vol. 1. Eyre and Spottiswoode Publishers Ltd., London. 1965.
13. J. H. VAN VLECK. Phys. Rev. **74**, 1168 (1948).
14. J. MICHEL, M. DRIFFORD, and P. RIGNY. J. Chim. Phys. **67**, 31 (1970).
15. N. BLOEMBERGEN, E. M. PURCELL, and R. POUND. Phys. Rev. **73**, 679 (1948).
16. G. W. SMITH. J. Chem. Phys. **50**, 3595 (1969).
17. J. S. WAUGH and E. I. FEDIN. Sov. Phys. Solid State. **4**, 1633 (1963).
18. E. F. WESTRUM JR. and J. P. MCCULLOCH. *In* Physics and chemistry of the organic solid state. Vol. 1, *Edited by* D. Fox, M. M. Labes, and A. Weissberger. Interscience, N.Y. 1963.
19. M. R. CHURCHILL and P. H. BIRD. Chem. Commun. 746 (1967). J. S. MCKECHNIE and I. C. PAUL. Chem. Commun. 747 (1967).
20. M. R. CHURCHILL. Inorg. Chem. **6**, 190 (1967).
21. (*a*) E. R. ANDREW. J. Chem. Phys. **18**, 607

Can. J. Chem. Downloaded from www.nrcresearchpress.com by 210.87.254.5 on 09/05/12
For personal use only.

(1950). (*b*) E. R. ANDREW and R. G. EADES. Proc. Roy. Soc. Lond. A, **218**, 537 (1953).
22. C. A. FYFE, D. F. R. GILSON, and K. H. THOMPSON. Chem. Phys. Lett. **5**, 215 (1970).
23. C. A. FYFE and G. J. KUPFERSCHMIDT. Unpublished results.
24. C. A. FYFE, B. A. DUNELL, and J. RIPMEESTER. Can. J. Chem. **49**, 3332 (1971).
25. R. K. BOYD, C. A. FYFE, and D. A. WRIGHT. Unpublished results.
26. H. S. GUTOWSKY and G. E. PAKE. J. Chem. Phys. **18**, 162 (1950).

Can. J. Chem. Downloaded from www.nrcresearchpress.com by 210.87.254.5 on 09/05/12
For personal use only.

On the Aggregation of Bovine Serum Albumin in 0.1 *M* Salt Solutions

NANETTE O. DEL ROSARIO AND SIAO FANG SUN
Department of Chemistry, St. John's University, Jamaica, New York 11439

Received March 29, 1973

The molecular weight of bovine serum albumin at neutral p*H* in 0.1 *M* salt solutions was determined with light scattering measurements. Simultaneously, preferential binding of a salt to the protein was calculated. It was found that the protein aggregates in KI and KSCN, but not in KCl, LiCl, and LiBr solutions. Analysis of the sedimentation behavior has confirmed aggregation as a molecular phenomenon, not an artifact.

Le poids moléculaire de sérum d'albumine de boeuf a été déterminé par diffusion de la lumière à pH neutre dans des solutions contenant 0.1 *M* de sel. Simultanément on a calculé l'attachement préférentiel d'un sel à la protéine. On a trouvé que la protéine forme des aggrégats dans le KI et e KSCN mais pas des solutions de KCl, LiCl et LiBr. L'analyse des patrons de sédimentation a confirmé que l'aggrégation est un phénomène moléculaire et non un artéfact. [Traduit par le journal]

Can. J. Chem. **51**, 3781 (1973)

Can. J. Chem. Downloaded from www.nrcresearchpress.com by 210.87.254.40 on 09/05/12
For personal use only.

Bovine serum albumin aggregates in 0.1 M NaCl solution below p*H* 4.0 (1–3). It is generally agreed that aggregation is related to molecular expansion. Since at p*H* values above the N → F transition, albumin exists in a compact form, albumin has been assumed to be a non-associating protein. For example, the studies of the binding of Cl^-, I^-, and SCN^- to albumin (4–6) all ignored the aggregation. In this paper we shall demonstrate that at neutral p*H* (*ca.* 5.2) albumin also forms aggregates in the presence of some though not all salts. The molecular weight of albumin at neutral p*H*, ionic strength 0.10 and room temperature was determined and the preferential binding of each salt to the protein was compared, using the technique of light scattering. Supplementary information about aggregation was obtained with sedimentation measurements.

Experimental

Materials

Armour crystalline bovine serum albumin, Lot Nos. A 69908, F 71601, and D 71209, was deionized by Dintzis' method (7). The dimer content varied from 1% to 5% depending upon the lot as judged from sedimentation velocity analyses. No significant differences were detected in light scattering experiments whichever lot was used.

The salts used, KCl, KI, and KSCN were Baker analyzed reagents, while LiCl and LiBr were Matheson, Coleman and Bell reagent grade. Glass-distilled water was used in all the experiments.

Light Scattering

Advantage was taken on the theory of light scattering in multi-component systems that if the light scattering and the refractive index increments are measured on solutions which are at constant chemical potential with the solvent, then the light scattering equation for a multicomponent system may be reduced to an equation similar to a 2-component system (8–10). Thus in a three component system (water-1, protein-2, and salt-3), the plot of $HC_2/\Delta\tau$ *vs.* C_2 would give the true molecular weight M_2, H being the Debye parameter, C_2 the concentration in g/ml and $\Delta\tau$ the excess turbidity of the solution over the solvent. If the solutions are not at constant chemical potential but at constant concentration of the solvent system, then the plot of $HC_2/\Delta\tau$ *vs.* C_2 can only give M_2', the apparent molecular weight of component 2 (protein), not the true molecular weight. Nevertheless the relation between M_2 and M_2' enables one to calculate a quantity $(\partial g_3/\partial g_2)_{T,\mu_1,\mu_3}$ which is the preferential binding of the number of grams of the salt to one gram of the protein on molar or molal basis, g being the number of grams, T the temperature, and μ the chemical potential (8, 10). In order to make use of the multicomponent theory, which we shall discuss in greater detail in latter sections, to analyze data, experiments were carried out with the protein solutions under constant chemical potential of component 3 as well as under constant concentration of component 3. To achieve the condition of constant chemical potential of component 3, the protein solution was dialyzed in equilibrium with the solvent which contained the same concentration of the salt as the protein solution. To achieve the condition of constant concentration of component 3, the solution was not dialyzed, but the concentration of the salt was the same as that of the dialyzed solution and was kept constant for both the solution and the solvent.

Light scattering measurements were made at 546 nm and room temperature using a Brice-Phoenix Dual Photomultiplier Photometer, Model 2000-D. All the solutions were freshly prepared prior to use. In the experiments without dialysis, the solution with the concentration of protein 6.0×10^{-3} g/ml was ultracentrifuged for 30 min at 64 000 r.p.m. with a Spinco L preparative ultracentrifuge and filtered several times using a Millipore filter of porosity 0.22 μ. Turbidity measurements were

TABLE 1. Light scattering data of bovine serum albumin in 0.1 *M* salt solutions

Salt (0.1 *M*)	p*H**		dn/dC_2		Slope × 10^4		*y*-intercept × 10^5	
	Undial.	Dial.	Undial.	Dial.	Undial.	Dial.	Undial.	Dial.
KCl	5.33	5.42	0.193	0.193	1.22	−6.28	1.41	1.43
LiCl	5.11	5.33	0.183	0.184	−1.71	−0.88	1.44	1.38
LiBr	5.25	5.43	0.188	0.190	2.80	1.06	1.51	1.41
KI	5.51	5.53	0.183	0.168	4.86	1.44	0.68	1.06
KSCN	5.49	5.75	0.173	0.182	4.15	1.11	0.94	1.25

*Of most concentrated protein solution.

first made on this solution and then on the solutions which were diluted by adding the solvent directly into the cell. Mixing was accomplished by swerving, partial inversion and, in some runs, by a micromagnetic stirrer. In the experiments with dialysis, five solutions of different protein concentrations in the range of 1.0×10^{-3} to 6.0×10^{-3} g/ml without ultracentrifugation were filtered several times using the same Millipore filter of same porosity, 0.22 μ. Turbidity measurement was taken with each solution as an independent experiment. The light scattering cell used was D-101 of the semi-octagonal type. The minimum amount of solution required for this cell is 30 ml.

The concentration of filtered bovine serum albumin stock solution was determined by the measurement of optical density in a Cary 14 spectrophotometer using $E_{1cm}^{1\%} = 6.67$ at 279 nm (11). It was also determined by drying the sample in a vacuum oven at 107°. The agreement was good.

Refractive Index Increments

The same solutions used for the light scattering measurements were used for the refractive index increment measurements. The experiments were performed in a Brice-Phoenix differential refractometer, Model BP-2000V at 546 nm, equipped with a Forma temperature control unit to keep the temperature at 25°. The instrument was calibrated with KCl solutions which were prepared from samples, reagent grade, dried in a vacuum oven at 110° over Drierite. The calibration constant was determined using the data of Kruis (12). For the measurements of $(\partial n/\partial C_2)_{T,\mu_1,\mu_3}$, (in which n is the refractive index and C is the concentration in g/ml), one compartment of the differential cell was filled with the dialyzed protein solution and the other compartment with its dialyzate. For the measurements of $(\partial n/\partial C_2)_{T,p,m_3}$, where p is the pressure and m is the concentration in molal, one compartment was filled with the undialyzed protein solution and the other with the solvent (a salt solution).

Measurements of $(\partial n/\partial C_3)_{m_2}$ were taken with a Bausch and Lomb refractometer of Abbe type. The refractive index reading at sodium line was converted to 546 nm using the equation

$$n_x = A + \frac{B}{\lambda_x^2}$$

where

$$A = n_D - 2.8796 \times 10^{-6} B$$

and

$$B = 0.52364 \times 10^{-6}(n_F - n_C)$$

The values of $(n_F - n_C)$ were calculated using the table provided by the manufacturer of the refractometer. The partial specific volume of the protein, $\bar{v}_2$, which was 0.734 ml/g, was taken to be constant for all the solutions, whether for a dialyzed or undialyzed protein (13, 14). The value of $\bar{v}_3$ was determined from the density (15) using graphic methods (16).

Sedimentation Velocity

Sedimentation velocity experiments were carried out with a Spinco Model E analytical ultracentrifuge, equipped with a phase plate and rotor temperature indicator and control (r.t.i.c.) unit. The r.t.i.c. was calibrated according to the method suggested in the manufacturer's manual. The temperature was set at 20° and kept constant. The rotor speed was set at 60 000 r.p.m. for each run and was checked regularly. Photographs were taken at 16 min intervals. The plates were measured with a Nikon comparator Mod 6C. Protein concentrations were about 0.90 g/100 ml.

Results

The differential refractive index and light scattering measurements of this study were undertaken for more than three years. Almost all possible kinds of techniques have been tried. The results reported in this paper were selected from six to twelve determinations of each solution.

Refractive Index Increments

The values of dn/dC_2 for dialyzed as well as undialyzed albumin in salt solutions are listed in Table 1. They are all independent of the protein concentration. A probable error in dn/dC_2 values is in the range of 0.001–0.003 as determined by the least-squares method.

The refractive index increment varies from salt to salt both for dialyzed and undialyzed solutions, but it tends to be invariant between dialyzed and undialyzed solutions for KCl, LiCl, and LiBr. An appreciable change in value was observed between dialyzed and undialyzed proteins for KI and KSCN. We have paid special attention to these two salt solutions, particularly

Can. J. Chem. Downloaded from www.nrcresearchpress.com by 210.87.254.40 on 09/05/12
For personal use only.

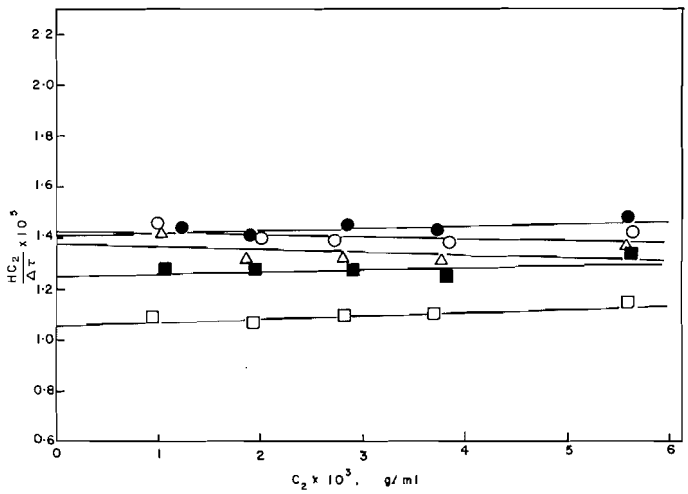

FIG. 1. Turbidity of dialyzed bovine serum albumin in aqueous 0.1 *M* salt solutions: ○, KCl; △, LiCl; ●, LiBr; □, KI; ■, KSCN.

to KI. Among the five salt solutions, KI is supposed to be the least stable. Iodide is easily oxidized to iodine upon standing. For example, color develops for 1 *M* KI solution within 2 h. However, for 0.1 *M* KI solution which we used in this study, the solution was stable for about a week. Our measurements were usually taken on freshly prepared solutions for undialyzed protein and within 24 h for dialyzed protein. Only for the test of reversibility, measurements were taken in 5 days after the solution was prepared. We have checked the amount of iodide in the solvent (0.1 *M* KI) by a conventional method: the solvent was oxidized quantitatively to iodine and the iodine was titrated with thiosulfate. We did not find any loss of iodide in the solvent and we believed that no impurity was developed in KI solution. Since KSCN solution is very stable, we did not perform any analysis on the change of property of this solution.

Dialyzed Bovine Serum Albumin Solutions

Light scattering data for dialyzed bovine serum albumin solutions are plotted in the form of $HC_2/\Delta\tau$ *vs.* C_2 according to Debye equation

$$[1] \qquad \frac{HC_2}{\Delta\tau} = \frac{1}{M_2} + 2BC_2$$

where

$$H = \frac{32\pi^3 n^2 (\partial n/\partial C_2)^2}{3N\lambda^4}$$

In this expression λ is the wavelength *in vacuo* of the light used, in cm, and N is the Avogadro's number. The results are shown in Fig. 1. Although bovine serum albumin is known for its intrinsic anisotropy, depolarization of light scattering by the protein was found to be very small (17). No correction for depolarization was made for $\Delta\tau$.

The slopes, the extrapolated intercepts, and the resulting data are listed in Table 1. The straight lines were determined by the least-squares method. Almost all the experimental points for each solution fall on a straight line. The slopes of most straight lines were expected to be close to zero, since for an isoionic protein or for a protein solution at ionic strength 0.15, the slope is usually found to be near zero (18). Although the slopes were not exactly zero as shown in Fig. 1, the numerical values that we have obtained were not as reliable as those of intercepts. Also the signs of the slopes were not as meaningful as in the case of salt-free protein solutions. The slopes for KI and KSCN were expected to be negative, but they were positive; whereas, negative slopes were obtained with KCl and LiCl which were expected to be positive. In the light scattering study of β-lactoglobulin A in water–methanol mixtures, the slopes were positive with concentration of methanol in volume %: 0, 20, 30, and 40; negative with concentration of methanol 50, 60, and 80, even though no aggregation was found in these solvent mixtures (10). It is for this reason we did not calculate the β factors (*i.e.* β_{22} and β_{23}) from

Can. J. Chem. Downloaded from www.nrcresearchpress.com by 210.87.254.40 on 09/05/12
For personal use only.

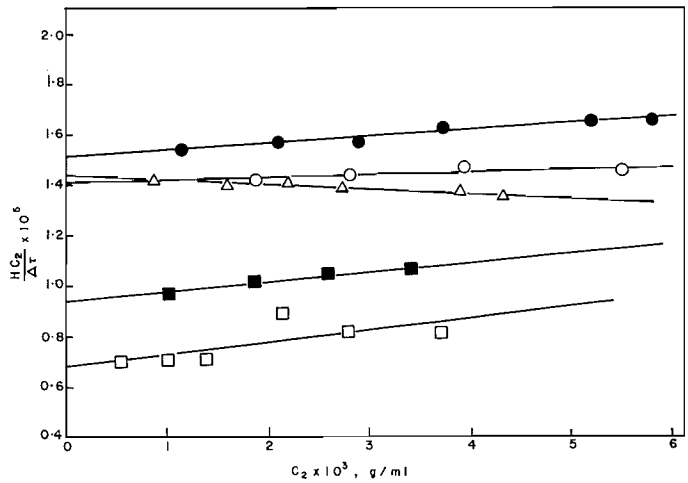

FIG. 2. Turbidity of undialyzed bovine serum albumin in aqueous 0.1 *M* salt solutions: ○, KCl; △, LiCl; ●, LiBr; □, KI; ■, KSCN.

the values of slopes where β's are non-ideality parameters.

Undialyzed Bovine Serum Albumin Solutions

Plots of $HC_2/\Delta\tau$ *vs.* C_2 for undialyzed bovine serum albumin in the same series of salt solutions are illustrated in Fig. 2 and the resulting data are listed in Table 1. The lines in Fig. 2 are similar to those in Fig. 1, but the numerical values of the slopes and intercepts are different. Again the least-squares method was used to determine the slopes and intercepts.

Calculated Data

As we mentioned before, from the plot of $HC_2/\Delta\tau$ *vs.* C_2 for the undialyzed solutions, we obtain the value of $1/M_2'$ (the intercept at $C_2 = 0$), whereas from the plot for the dialyzed solutions, we obtain the value of $1/M_2$. The value of M_2' is the apparent molecular weight of the protein and that of M_2 its true molecular weight. The two quantities, M_2 and M_2', are related in the form (9, 10),

$$[2a] \qquad M_2' = M_2(1 + D)^2$$

where (8)

$$[2b] \qquad D = \frac{(\partial n/\partial g_3)_{T,p,g_2}}{(\partial n/\partial g_2)_{T,p,g_3}} \left(\frac{\partial g_3}{\partial g_2}\right)_{T,\mu_1,\mu_3}$$

or (10)

$$[2c] \qquad D = \frac{(1 - C_3\bar{v}_3)(\partial n/\partial C_3)_{m_2}}{(1 - C_2\bar{v}_2)(\partial n/\partial C_2)_{m_3}} \times \frac{M_3}{M_2}\left(\frac{\partial m_3}{\partial m_2}\right)_{T,\mu_1,\mu_3}$$

The quantity $(\partial g_3/\partial g_2)_{T,\mu_1,\mu_3}$ in eq. 2*b* is the preferential binding of the number of grams of the salt to one gram of the protein on molar basis, whereas the quantity $(\partial m_3/\partial m_2)_{T,\mu_1,\mu_3}$ is the number of moles of the salt bound to a mole of protein on molal basis. The latter quantity can also be converted into $(\partial g_3/\partial g_2)_{T,\mu_1,\mu_3}$, the number of grams of the salt bound per gram of protein on molal basis, using the equation (10)

$$[3] \qquad (\partial g_3/\partial g_2)_{T,\mu_1,\mu_3} = M_3/M_2(\partial m_3/\partial m_2)_{T,\mu_1,\mu_3}$$

Equation 3 is based upon the assumption that

$$(\partial m_3/\partial m_2)_{T,p,\mu_3} \cong (\partial m_3/\partial m_2)_{T,\mu_1,\mu_3}$$

The molal scale is preferred for the reason that the protein volume is not included (19).

Table 2 gives the molecular data for light scattering calculations. In Table 3 are listed all the calculated values: molecular weight, $(\partial m_3/\partial m_2)_{T,\mu_1,\mu_3}$ and $(\partial g_3/\partial g_2)_{T,\mu_1,\mu_3}$.

Time Dependency and Reproducibility

Light scattering and differential refractive index measurements were taken on the protein in 0.1 *M* salt solution after dialysis for 1 night, 2 nights, 4 nights, and 6 nights respectively. It was found that there is virtually no change in the values of $(\partial n/\partial C_2)_{T,\mu_1,\mu_3}$, $\Delta\tau$ and molecular weight for the protein after dialysis for 1 night or 2 nights. This indicates that equilibrium has most likely been reached after dialysis overnight. If, however, dialysis was carried out longer than 2 nights, there was some change in the measured

Can. J. Chem. Downloaded from www.nrcresearchpress.com by 210.87.254.40 on 09/05/12
For personal use only.

Can. J. Chem. Downloaded from www.nrcresearchpress.com by 210.87.254.40 on 09/05/12
For personal use only.

TABLE 2. Molecular data for light scattering calculations

Salt (0.1 M)	$\bar{v}_3$	$\left(\frac{\partial n}{\partial C_3}\right)_{m_2}$
KCl	0.298	0.122
LiCl	0.500	0.200
LiBr	0.300	0.141
KI	0.298	0.127
KSCN	0.528	0.229

TABLE 3. Molecular weights and preferential bindings

Salt (0.1 M)	Mol. wt.	$\left(\frac{\partial m_3}{\partial m_2}\right)_{T,\mu_1,\mu_3}$	$\left(\frac{\partial g_3}{\partial g_2}\right)_{T,\mu_1,\mu_3}$
KCl	69 900	12.1	0.013
LiCl	72 500	−31.2	−0.018
LiBr	71 000	−37.2	−0.045
KI	94 300	204	0.358
KSCN	80 000	99	0.120

values. The change followed this pattern: $(\partial n/\partial C_2)_{T,\mu_1,\mu_3}$ decreased, $\Delta\tau$ increased and the overall molecular weight increased. The magnitude of the change depended on the salt. For example, at 0.1 M KCl solution the values of $(\partial n/\partial C_2)_{T,\mu_1,\mu_3}$ were 0.193 (1 day old) and 0.188 (6 days old); the values of $\Delta\tau$ for the protein concentration 0.001 g/ml were 3.206 (1 day old) and 3.251 (6 days old); and the molecular weight as determined from the intercept of the plot $HC_2/\Delta\tau$ *vs.* C_2 was 5% higher for the 6 day-old protein than for the 1 day-old protein. At 0.1 M KI solution, the values of $(\partial n/\partial C_2)_{T,\mu_1,\mu_3}$ were 0.168 (1 day old) and 0.152 (5 days old); $\Delta\tau$ for the protein concentration 0.001 g/ml were 3.424 (1 day old) and 4.037 (5 days old); and the molecular weight increased about 40%.

The reproducibility of light scattering data often poses a problem. There are three major sources of error: C_2, dn/dC_2, and $\Delta\tau$. The error in C_2 is usually due to uncertainty in the dilution. This error is generally not serious, particularly in the determination of molecular weight in our dialyzed solution. (We did not use the dilution technique for the dialyzed solution.) Furthermore, due to the large quantity of solution prepared for the measurements, experimental error in the determination of concentration was minimized. Errors in the determination of dn/dC_2 and $\Delta\tau$ seem to be more serious and they may or may not be in the same direction. If the errors are in the same direction, they may cancel each other or be minimized; for the error of dn/dC_2 was incorporated in the numerator and that of $\Delta\tau$ in the denominator in the term of $HC_2/\Delta\tau$. If the errors are in opposite directions, the overall error increases, and the uncertainty in the determination of molecular weight and preferential binding becomes large.

Molecular weight was more reproducible in some salt solutions than in others. Unexpectedly, the reproducibility of molecular weight determination of bovine serum albumin in 0.1 M LiCl solution was much better than in 0.1 M KCl solution which we used as the reference. The accuracy of the molecular weight in each salt solution was about $\pm 1\,000$ g/mole. The value was estimated from the results of the best two or three runs.

Reversibility

To test the reversibility of changes in molecular weight, light scattering, and differential refractive index measurements were carried out on bovine serum albumin in 0.1 M salt solutions which were dialyzed twice, first against the solvent and then against pure water. Each dialysis was performed in the cold room overnight to make sure that osmotic equilibrium was reached. In the dialysis of the dialyzed protein solution against pure water, the water was changed several times. Figure 3 shows the results of a representative experiment, the reversibility test on bovine serum albumin in 0.1 M KI solution. The molecular weight of bovine serum albumin in water at very low ionic strength is known to be 70 000, almost the same as that in 0.1 M KCl solution. At 0.1 M KI solution, the molecular weight increased to 94 300 (from the y-intercept of line 1, Fig. 3). After the small ions I^- were diffused away from the same salt solution, the molecular weight of the protein came back to 70 000 (from line 2, Fig. 3). This indicates that the effect of KI on the molecular weight of the protein is a reversible process, in agreement with the general behavior of bovine serum albumin in aqueous solutions as observed in other measurements, *e.g.* viscosity (20) and titration (21). This is also in agreement with the current thinking that neutral salts perturb macromolecular structures in a cooperative transition of the order ⇄ disorder type (22).

Sedimentation Velocity

The values of the sedimentation coefficients were corrected to the reference state (water at

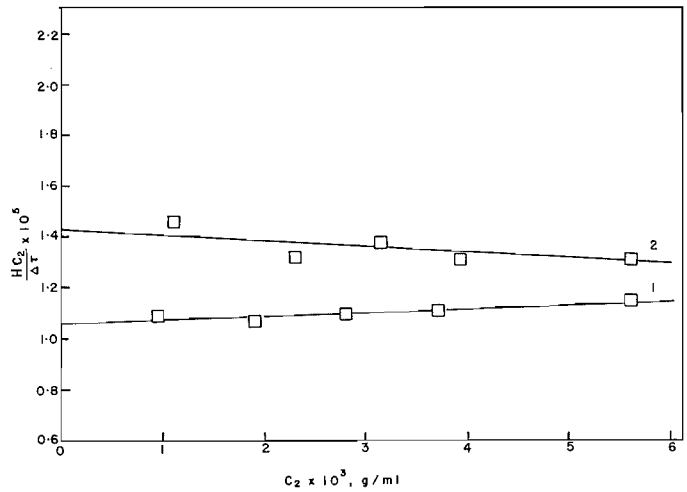

FIG. 3. Test for the reversibility of aggregation of bovine serum albumin in 0.1 *M* KI solution. Line 1, dialyzed solution; line 2, reversed from the dialyzed solution.

20°) according to the following equation

$$S_{20,w} = S_{20,m}\frac{\eta_{20,m}}{\eta_{20,w}}\frac{(1 - \bar{v}\rho)_{20,w}}{(1 - \bar{v}\rho)_{20,m}}$$

where η is the viscosity, ρ the density, and the subscripts m and w refer to the solvent mixture and water, respectively.

The density data were calculated by the equation

$$\rho = \rho_0 + \frac{1 - \bar{v}\rho_0}{100} C$$

where ρ_0 is the density of the solvent and C is the concentration of the protein in g/100 ml. The density of solvent data ρ_0 was obtained from the International Critical Tables and the value of $\eta_{20,m}/\eta_{20,w}$ was determined experimentally.

Assuming that the aggregates are dimers, the percentage of dimer was estimated by dividing the area of the fast component by the total area (14). The Johnson–Ogston effect being small (2), no correction was made for the estimation of the observed areas.

The values of sedimentation coefficient and the percentage of dimer are listed in Table 4. The sedimentation coefficient of albumin is almost identical for KCl, LiCl, LiBr, and KSCN, but is significantly different for KI. The percentage of dimer is the same for KCl, LiCl, and LiBr, higher for KI and KSCN.

TABLE 4. Sedimentation coefficient and percentage of dimer

Salt (0.1 *M*)	$S_{20,w} \times 10^{13}$	% dimer
KCl	4.19	4
LiCl	4.18	4
LiBr	4.19	4
KI	4.31	18
KSCN	4.22	8

Discussion

Several different values of molecular weight of bovine serum albumin have been reported in literature: 69 000 from osmotic pressure measurements (4), 66 500 from ultracentrifuge sedimentation measurements (23) and 66 000 by summing up the individual molecular weights of amino acids that constitute the protein (24). The molecular weight we obtained for the albumin in 0.1 *M* KCl solution which we used as a reference for comparison with other salts is 69 900, within the range of literature values.

Reichmann and Charlwood (1), who also carried out light scattering measurements, reported the molecular weight for the unaggregated bovine serum albumin (at neutral p*H* in 0.10 *M* NaCl solution or at p*H* 1.9 in the presence of 0.10 *M* NaCl) to be 77 000 – 79 000 and for aggregated protein (at p*H* 1.9 in the absence of salt) to be 120 000. Their value of the unaggre-

Can. J. Chem. Downloaded from www.nrcresearchpress.com by 210.87.254.40 on 09/05/12
For personal use only.

Can. J. Chem. Downloaded from www.nrcresearchpress.com by 210.87.254.40 on 09/05/12
For personal use only.

gated protein is much higher than ours. It seems that light scattering measurements tend to yield higher values; for example, 77 000 (18) and 72 000 (25).

The values of preferential salt binding for bovine serum albumin are in the order of LiBr < LiCl < KCl < KSCN < KI. The negative values for LiCl and LiBr indicate a deficiency in binding, *i.e.* the Li^+ is not favored over water for interaction in the vicinity of the protein. Scatchard *et al.* (26) have shown that the intrinsic binding constant k_1 and the affinity constant k_2 are both much larger for SCN^- than Cl^- in binding to bovine serum albumin. Using the k values reported by Scatchard *et al.*, Edsall *et al.* (18) have calculated the values of $\bar{\nu}$, the number of these two anions bound per mole of protein. Their value for serum albumin in NaCl solution at ionic strength 0.183 is 10.1, in comparison with our preferential binding in KCl solution at ionic strength 0.1, 12.1. In NaSCN solution at ionic strength 0.183, their value is 24.0, in comparison with ours in KSCN solution at ionic strength 0.1, 99.0. In view of the fact that preferential binding is not binding *per se*, the agreement of the two sets of values is satisfactory.

Preferential binding of salt seems to be related to the weight average molecular weight of the protein. The binding values being relatively low in KCl, LiCl, and LiBr solutions, the protein does not aggregate. The binding values being high in KSCN and KI solutions, the protein does aggregate.

Since the increase in molecular weight of albumin in KI and KSCN solutions is not large, especially in KSCN solution, one might wonder if the aggregations that we believe to be from the light scattering study could be artifacts due to a small quantity of colloidal impurity. Upon examining the sedimentation behavior of the protein in salt solutions, this does not seem to be the case. The percentage of dimer is larger in KI and KSCN than in other salt solutions. It is true that commercially available serum albumin may contain dimers as high as 10% (14), depending upon the lot of preparations, but our comparison was made on the same lot of protein which contained only 4% of dimer. The increase in dimers to 8% in KSCN solution and to 18% in KI solution could not be considered as an artifact.

If we assume the molecular weight of the monomer to be 70 000 and the weight average molecular weight of the mixture of monomer and dimer to be 94 400, then the weight fraction of dimer is 34%. This 34% will be in excess of the 4% dimer already in the monomer. However, the ultracentrifuge data indicate only 14% dimer in excess. Thus there is no quantitative agreement between the two types of experiments. Nevertheless, the qualitative agreement suggests that aggregation behavior in KI and KSCN solutions is most likely a true indication of the protein's behavior.

On the basis of our observations we are led to the following two conclusions: (1) Since, at the same pH (*ca.* 5.4) and same ionic strength (0.1), bovine serum albumin aggregates in KSCN and KI solutions, but not in KCl, LiCl, and LiBr solutions, the ionic strength is not a contributing factor to the aggregation. The usual interpretation that the aggregation of the protein at low pH is a result of electrostatic interaction of residues carrying the same charge seems to be inapplicable here; (2) In view of the reversibility in light scattering measurements, the process of aggregation of bovine serum albumin in salt solutions is equilibrium controlled and not rate controlled.

The assistance of Dr. Tiang Shing Chang in this work is gratefully acknowledged.

1. M. E. Reichmann and P. A. Charlwood. Can. J. Chem **32**, 1092 (1954).
2. P. Bro, S. J. Singer, and J. M. Sturtevant. J. Am. Chem. Soc. **80**, 389 (1958).
3. E. J. Williams and J. F. Foster. J. Am. Chem. Soc. **82**, 3741 (1960).
4. G. Scatchard, A. C. Batchelder, and A. Brown. J. Am. Chem. Soc. **68**, 2320 (1946).
5. R. H. McMenamy, M. I. Madeja, and F. Watson. J. Biol. Chem. **243**, 2328 (1968).
6. C. S. Pande and R. H. McMenamy. Arch. Biochem. Biophys. **136**, 260 (1970).
7. H. M. Dintzis. Ph.D. Thesis. Harvard University, 1952.
8. A. Vrij and J. Th. G. Overbeek. J. Colloid Sci. **17**, 570 (1962).
9. E. F. Casassa and H. Eisenberg. Advan. Protein Chem. **19**, 287 (1964).
10. H. Inoue and S. N. Timasheff. J. Am. Chem. Soc. **90**, 1890 (1968).
11. J. F. Foster and M. D. Sterman. J. Am. Chem. Soc. **78**, 3656 (1956).
12. A. Kruis. Z. Phys. Chem. (Leipzig), **34B**, 13 (1936).
13. M. O. Dayhoff, G. E. Perlmann, and D. A. MacInnes. J. Am. Chem. Soc. **74**, 2515 (1952).
14. K. E. van Holde and S. F. Sun. J. Am. Chem. Soc. **84**, 66 (1962).

15. International critical tables. Vol. 3. McGraw-Hill Book Co., Inc., New York. 1930. p. 77.
16. G. N. LEWIS and M. RANDALL. Thermodynamics. 2nd ed. *Revised by* K. S. Pitzer and L. Brewer. McGraw-Hill Book Co., Inc., New York. 1961. p. 207.
17. E. P. GEIDUSCHEK. J. Polym. Sci. **13**, 408 (1954).
18. J. T. EDSALL, H. EDELHOCH, R. LONTRIE, and P. R. MORRISON. J. Am. Chem. Soc. **72**, 4641 (1950).
19. M. E. NOELKEN. Biochemistry, **9**, 4122 (1970).
20. S. F. SUN. Arch. Biochem. Biophys. **129**, 411 (1969).
21. S. F. SUN. Biochim. Biophys. Acta, **200**, 433 (1970).
22. P. H. VON HIPPEL and T. SCHLEICH. *In* Structure and stability of biological macromolecules. *Edited by* Timasheff and Fasman. Marcel Dekker, Inc., New York. 1969. pp. 417–574.
23. R. L. BALDWIN. Biochem. J. **65**, 503 (1957).
24. P. E. SPAHR and J. T. EDSALL. J. Biol. Chem. **239**, 850 (1964).
25. W. P. HARRINGTON, P. JOHNSON, and R. H. OTTEWILL. Biochem. J. **62**, 569 (1956).
26. G. SCATCHARD, I. H. SCHEINBERG, and S. H. ARMSTRONG. J. Am. Chem. Soc. **72**, 535, 540 (1950).

Can. J. Chem. Downloaded from www.nrcresearchpress.com by 210.87.254.40 on 09/05/12
For personal use only.

Erratum: Acid Ionizations of Nitroalkanes in Aqueous Solution

TAKEKI MATSUI AND LOREN G. HEPLER
Department of Chemistry, University of Lethbridge, Lethbridge, Alberta
Received September 7, 1973
(Ref.: Can. J. Chem. **51**, 1941 (1973))

Can. J. Chem. **51**, 3789 (1973)

The nitropropanes in Table 3 are listed in reverse order. The third entry should be 1-Nitropropane (pK = 8.98, etc.) and the fourth should be 2-Nitropropane (pK = 7.7, etc.).

Can. J. Chem. Downloaded from www.nrcresearchpress.com by 210.87.254.5 on 09/05/12
For personal use only.

Cleavage of the Sulfur–Sulfur Bond in 2,4-Dinitrophenyl-4-substituted-phenyl Disulfides by *trans*-[IrCl(CO) (PPh_3)$_2$]. A Kinetic Study

CHIU T. LAM[1] AND CAESAR V. SENOFF[2]

Departn.ent of Chemistry, University of Guelph, Guelph, Ontario N1G 2W1

Received May 25, 1973

The kinetics of the reaction between *trans*-[IrCl(CO)(PPh_3)$_2$] and a series of 2,4-dinitrophenyl-4-substituted-phenyl disulfides, $YC_6H_4SSC_6H_3(NO_2)_2$ (Y = Br, F, H, CH_3, or CH_3O) have been investigated in toluene between 70 and 90°. These reactions were found to follow simple second order kinetics, rate = k_2[IrCl(CO)(PPh_3)$_2$][$YC_6H_4SSC_6H_3(NO_2)_2$]. The rates of reaction were also found to be insensitive to the nature of the para substituent, Y. This fact together with the observed activation parameters, $\Delta H^{\ddagger} \sim 17$ kcal mol^{-1} and $\Delta S^{\ddagger} \sim -19$ cal mol^{-1} deg^{-1}, have been interpreted as indicating that the initial step in these reactions involves a nucleophilic attack by the iridium atom at the sulfur atom bonded to the 2,4-dinitrophenyl group, followed by the formation of a three-centered transition state. An overall mechanism for these reactions is presented and discussed.

La cinétique des réactions entre le [IrCl(CO)(PPh_3)$_2$]-*trans* et une série de disulfures de dinitro-2,4 phényle et de phényle substitué en position-4 $YC_6H_4SSC_6H_3(NO_2)_2$ (Y = Br, F, H, CH_3 ou CH_3O) a été étudiée dans le toluène entre 70 et 90°. On a montré que ces réactions suivent une cinétique du second ordre où l'équation de vitesse peut s'exprimer ainsi: vitesse = k_2[IrCl(CO)(PPh_3)$_2$][$YC_6H_4SSC_6H_3(NO_2)_2$]. De même, on a montré que la vitesse des réactions était indepéndante de la nature du substituant Y en position para. Ce fait combiné avec les paramètres d'activation observés, $\Delta H^{\ddagger} \sim 17$ kcal mol^{-1} et $\Delta S^{\ddagger} \sim -19$ cal mol^{-1} deg^{-1}, nous ont amenés à considérer que l'étape initiale de ces réactions implique une attaque nucléophile par l'atome d'iridium sur l'atome de soufre relié au groupe dinitro-2,4 phényle, suivie par la formation d'un état de transition à trois centres. On présente et on discute le mécanisme global de ces réactions. [Traduit par le journal]

Can. J. Chem. **51**, 3790 (1973)

Can. J. Chem. Downloaded from www.nrcresearchpress.com by 210.87.254.42 on 09/05/12
For personal use only.

In recent years the detailed mechanistic aspects of oxidative-addition reactions have been the subject of several reports in the literature (1–9). Particular attention has been focused on the reactions of *trans*-[IrX(CO)(PPh_3)$_2$] (X = Cl, Br, or I) which are capable of undergoing oxidative-addition with a wide variety of addenda (10–15). The results of several investigations related to the reactivity of arenethiols towards low valent transition metal complexes have been reported from this laboratory (3, 16–18) and recently we have extended this work to include a series of 2,4-dinitrodiphenyl-4-substituted-phenyl disulfides (19). These particular organic disulfides were shown to react with *trans*-[IrX(CO)(PPh_3)$_2$] according to eq. 1.

$$[1]\quad 2[IrX(CO)(PPh_3)_2] + 2ArSSAr' \rightarrow [IrX(SAr)(SAr')(CO)(PPh_3)]_2 + 2PPh_3$$

where X = Cl, Br, or I, Ar = a para-substituted benzene ring, and Ar′ = 2,4-dinitrophenyl. We now wish to report the results of a kinetic study of reaction 1 when X = Cl.

Results and Discussion

The preparation and characterization of the products of reaction 1 have been previously reported (19). Representative kinetic data for the reactions studied are shown in Table 1. Kinetic data at various temperatures are summarized in Table 2. These data indicate that the rates of reaction are dependent on the concentration of the substrate, [IrCl(CO)(PPh_3)$_2$], and the concentration of the reacting disulfide. Plots of the pseudo first-order rate constant, k_{obs}, *vs.* [$YC_6H_4SSC_6H_3(NO_2)_2$] were linear with zero intercepts. These plots are shown in Fig 1. and indicate that reaction 1 obeys a simple second-order rate law, equation 2.

$$[2]\quad \frac{-d[IrCl(CO)(PPh_3)_2]}{dt} = k_2[IrCl(CO)(PPh_3)_2][YC_6H_4SSC_6H_3(NO_2)_2]$$

[1]Present address: Department of Chemistry, Columbia University, New York, N.Y.

[2]Address all correspondence to this author.

Can. J. Chem. Downloaded from www.nrcresearchpress.com by 210.87.254.42 on 09/05/12
For personal use only.

TABLE 1. Kinetic data for the reaction 2 *trans*-$[IrCl(CO)(PPh_3)_2]$ + 2ArSSAr′ → $[IrCl(SAr)(SAr')(CO)(PPh_3)]_2$ + $2PPh_3$ in toluene at 70°

ArSSAr′*	[ArSSAr′] (M)	$10^4 k_{obs}$ (s^{-1})	$10^3 k_2$ ($M^{-1} s^{-1}$)
Br†	0.078	2.3	2.9
	0.106	3.2	3.0
	0.138	4.4	3.2
	0.226	7.5	3.3
F†	0.062	2.1	3.4
	0.116	4.3	3.7
	0.137	4.6	3.4
	0.149	5.5	3.7
H†	0.089	1.9	2.1
	0.124	2.3	1.9
	0.153	3.2	2.1
	0.199	3.8	1.9
CH_3†	0.115	3.8	3.3
	0.151	4.5	3.0
	0.181	5.9	3.3
	0.219	7.5	3.4
CH_3O†	0.100	4.5	4.5
	0.134	6.4	4.8
	0.168	8.0	4.8
	0.204	9.8	4.8

*Ar′ = 2,4-$(O_2N)_2C_6H_3$; Ar = 4-YC_6H_4.
†Para substituent, Y.

TABLE 2. Second-order rate constants for the reaction 2 *trans*-$[IrCl(CO)(PPh_3)_2]$ + 2ArSSAr′ → $[IrCl(SAr)(SAr')(CO)(PPh_3)]_2$ + $2PPh_3$ in toluene

T (°C)	ArSSAr′*	$10^3 k_2$ ($M^{-1} s^{-1}$)
70	Br†	3.3
75		4.2
80		6.4
90		13.4
70	F†	3.6
75		6.1
80		8.2
90		16.8
70	H†	1.9
75		3.2
80		4.9
90		8.8
70	CH_3†	3.3
75		4.1
80		7.0
90		14.1
70	CH_3O†	4.8
75		5.4
80		7.7
90		19.6

*Ar = 2,4-$(O_2N)_2C_6H_3$; Ar = 4-YC_6H_4.
†Para substituent, Y.

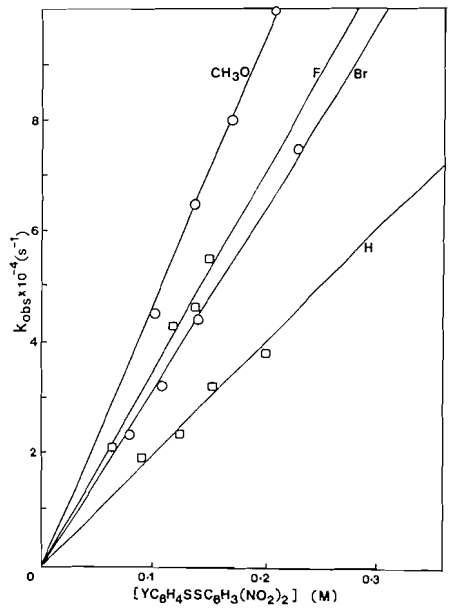

FIG. 1. Plot of k_{obs} *vs.* $[YC_6H_4SSC_6H_3(NO_2)_2]$.

This rate law is similar to that commonly found for oxidative-addition reactions of *trans*-$[IrCl(CO)(PPh_3)_2]$ (13).

Examination of the second-order rate constants given in Table 2 indicates that the rate of reaction 1 is not significantly sensitive to a change in the nature of the para substituent, Y, located on one of the phenyl rings of the incoming disulfide. This behavior is somewhat different from the substituent effect noted for other incoming reactants such as $YC_6H_4CH_2Cl$ (1) and YC_6H_4SH (3) where Y = an electron withdrawing or an electron releasing substituent in the para position.

Assuming a second-order rate, the rates of reaction were also determined at three other temperatures and the activation parameters for reaction 1 were calculated using the Eyring equation, [3]. These parameters are presented in Table 3.

$$[3] \qquad k_2 = \frac{kT}{h} \exp\left(\frac{-\Delta G^{\ddagger}}{RT}\right)$$

It may be noted that the enthalpies and entropies of activation for reaction 1 are insensitive to the nature of the incoming disulfide. Also, $\Delta H^{\ddagger}$ is ~ 8 kcal greater than the corresponding $\Delta H^{\ddagger}$ for the reaction of *trans*-$[IrCl(CO)(PPh_3)_2]$ with

TABLE 3. Activation parameters*

Y†	$\Delta H^{\ddagger}$ (kcal mol^{-1})	$\Delta S^{\ddagger}$ (cal mol^{-1} deg^{-1})
Br	17.0	−20.6
F	17.7	−18.2
H	17.8	−19.0
CH_3	18.0	−18.0
CH_3O	17.3	−19.2

*Estimated uncertainties are ± 1 kcal mol^{-1} for $\Delta H^{\ddagger}$ and ± 3 cal mol^{-1} deg^{-1} for $\Delta S^{\ddagger}$.
†Y = para substituent in $YC_6H_4SSC_6H_3(NO_2)_2$.

YC_6H_4SH (3) which is a reflection of the greater difficulty to cleave a sulfur–sulfur bond than a sulfur–hydrogen bond by this particular iridium(I) substrate. The enthalpies of activation for reaction 1 also strongly suggest that dissociation of the sulfur–sulfur bond does not occur as a distinguishable step during the course of the reaction. Although the values of $\Delta S^{\ddagger}$ for reaction 1 are somewhat less negative than those reported for the addition of an arenethiol to this iridium(I) substrate (3), they are not inconsistent with the presence of a three-centered transition state.

A mechanism which is consistent with the aforementioned kinetic data may now be proposed, *i.e.*,

$$[4]\quad \textit{trans}\text{-}[IrCl(CO)(PPh_3)_2] + ArSSAr' \xrightarrow[\text{slow}]{k_2} [IrCl(SAr)(SAr')(CO)(PPh_3)_2]$$

$$[5]\quad [IrCl(SAr)(SAr')(CO)(PPh_3)_2] \xrightarrow{\text{fast}} [IrCl(SAr)(SAr')(CO)(PPh_3)] + PPh_3$$

$$[6]\quad [IrCl(SAr)(SAr')(CO)(PPh_3)] \xrightarrow{\text{fast}} \tfrac{1}{2}\,[IrCl(SAr)(SAr')(CO)(PPh_3)]_2$$

In the rate determining step, [4], the initial process leading to the activated complex may be regarded as a nucleophilic attack by the iridium atom at one of the sulfur atoms of the disulfide. Since the rate of reaction is independent of the nature of the substituent, Y, the iridium presumably attacks at the sulfur atom which is bonded to the 2,4-dinitrophenyl group. In the ground state this particular sulfur atom would be expected to be slightly positive relative to the other sulfur atom in the disulfide by virtue of the two NO_2 substituents. Consequently, the initial process leading to the activated complex may also be regarded as an electrophilic attack by this positive sulfur atom at the iridium atom, since iridium formally loses two electrons during the course of the reaction. If the preferred stereochemistry about the sulfur–sulfur bond is taken into account (20) the iridium complex acting as a nucleophile must initially attack the sulfur–sulfur bond from the "back-side" as shown below.

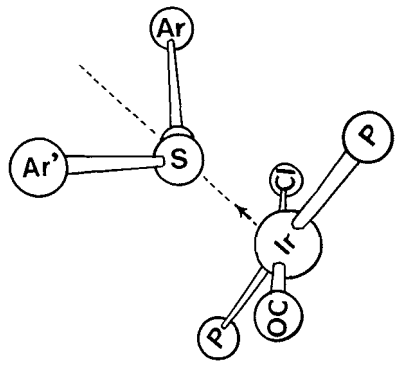

This will give rise to a three-centered activated complex in which there is formation of two iridium sulfur bonds with concomitant weakening of the sulfur–sulfur bond. This activated complex is shown below and is consistent with

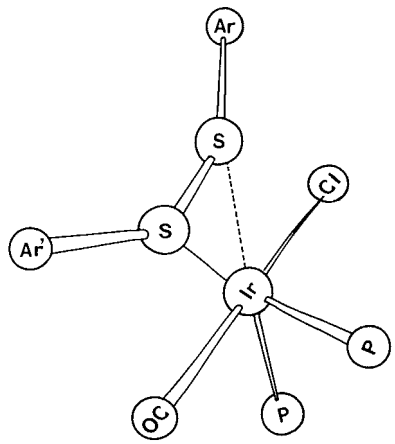

the negative entropies of activation obtained for reaction 1. It is also similar to that previously proposed for other oxidative addition reactions of *trans*-$[IrCl(CO)(PPh_3)_2]$ (1, 3, 4). However, the absence of any substituent effect also suggests that the amount of bond formation between iridium and the SC_6H_4Y portion of the incoming disulfide is significantly less than that

Can. J. Chem. Downloaded from www.nrcresearchpress.com by 210.87.254.42 on 09/05/12
For personal use only.

TABLE 4. k_{obs} values for the reaction of *trans*-[IrCl(CO)(PPh_3)$_2$] with ArSSAr′ in the presence of added triphenylphosphine obtained in toluene at 70°*

ArSSAr′† (*M*)	10^4[PPh_3] (*M*)	k_{obs} (s^{-1})
Br‡	—	2.3
	3.8	4.0
	6.0	6.0
	8.3	8.3
	9.0	9.7
CH_3§	—	3.8
	5.4	4.2
	10.9	6.4
	13.9	6.8
	18.7	9.9

*[IrCl(CO)(PPh_3)$_2$] = 2.5×10^{-3} *M*.
†Ar = 2,4-$(O_2N)_2C_6H_3$; Ar = 4-BrC_6H_4 or 4-$CH_3C_6H_4$.
‡[ArSSAr′] = 0.078 *M*.
§[ArSSAr′] = 0.115 *M*.

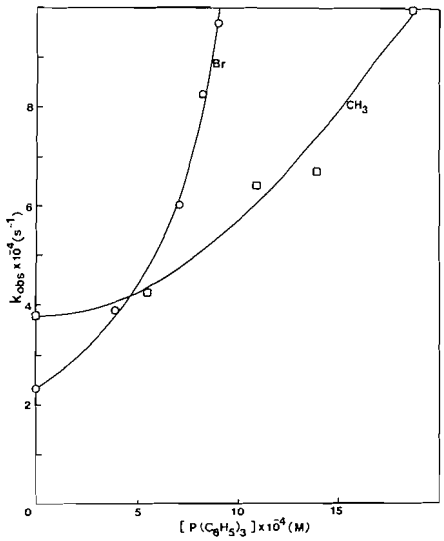

FIG. 2. Plot of k_{obs} *vs.* [$P(C_6H_5)_3$].

between iridium and the $SC_6H_3(NO_2)_2$ portion of the disulfide in the transition state. This could partially account for the slight increase in entropy in going from an arenethiol to a 2,4-dinitrophenyl-4-substituted-phenyl disulfide as the incoming addendum.

It is interesting to note that the rate determining step in the proposed mechanism ([4]–[6]) is formally an oxidative-addition even though the overall reaction may be regarded as an oxidative-elimination reaction. The inherent tendency of a thiolato ligand to act as a bridging group appears to be the "driving force" leading to the observed dimeric product. The initial oxidative addition product rapidly loses a molecule of triphenylphosphine to form a coordinatively unsaturated five-coordinated species which then rapidly dimerizes to the observed product. At present it is not possible to *unambiguously* assign the stereochemistry associated with those species intervening between the substrate, *trans*-[IrCl(CO)(PPh_3)$_2$], and the product, [IrCl(SAr)(SAr′)(CO)(PPh_3)]$_2$.

Since triphenylphosphine is liberated in reaction 1, the dependence of the rate of reaction on the concentration of added triphenylphosphine was also examined. Kinetic data pertaining to this are given in Table 4 and a plot of k_{obs} *vs.* the concentration of added triphenylphosphine is shown in Fig. 2. These data clearly show that the rate of reaction *increases* with increasing concentration of triphenylphosphine. Consequently, any mechanism which invokes a dissociative step involving triphenylphosphine may be discounted for reaction 1. In addition, the product isolated from the reaction in the presence of added triphenylphosphine is not the same as that isolated from the reaction in the absence of added triphenylphosphine. These particular products exhibit a single ν_{CO} band at about 2055 cm^{-1} (Nujol) which is ~ 10 cm^{-1} lower than that observed for the corresponding [IrCl(SAr)(SAr′)(CO)(PPh_3)]$_2$ complexes. The precise nature of these complexes has not yet been elucidated.

It is noteworthy that the kinetic data presented herein indicate that the iridium(I) substrate acting as a nucleophile initially attacks the sulfur atom bonded to the 2,4-dinitrophenyl group. As a consequence of this interpretation, the previously proposed (3) initial step leading to the activated complex in the reaction between *trans*-IrX(CO)(PPh_3)$_2$ (X = Cl, Br, or I) and HSC_6H_4Y must now be amended to one in which the iridium(I) substrate attacks the *hydrogen atom* of the arenethiol (or an electrophilic attack by hydrogen at iridium). This is not unreasonable in view of the fact that a number of transition metal complexes are capable of being protonated to form well defined hydride derivatives (21).

Can. J. Chem. Downloaded from www.nrcresearchpress.com by 210.87.254.42 on 09/05/12
For personal use only.

Experimental

Materials Used and Isolation of Reaction Products

These have been described elsewhere (19).

Kinetic Measurements

The kinetics of reaction 1 were followed spectrophotometrically with a Beckman IR-12 double beam recording spectrophotometer by monitoring the disappearance of the carbonyl peak at 1959 cm^{-1} in the infrared spectrum of the iridium(I) substrate. The kinetic data were obtained under pseudo first-order kinetic conditions using at least a 30-fold excess of the organic disulfide. The initial concentration of the iridium(I) complex was 2.5×10^{-3} *M* while the concentration of disulfide was varied between 0.06–0.2 *M*. Although the product of the reaction between *trans*-$[IrCl(CO)(PPh_3)_2]$ and 4-$O_2NC_6H_4SSC_6H_3(NO_2)_2$ has been isolated and characterized (19), we were not able to measure the rate of this reaction because of the poor solubility of this particular disulfide in toluene.

All kinetic runs were carried out in toluene which had been dried over sodium, degassed, and then saturated with nitrogen. Individual solutions of the iridium(I) complex and the appropriate disulfide used in a given kinetic run were thermostatted for approximately 1 h prior to mixing. The solution containing the disulfide was added to the solution containing the iridium(I) substrate by means of a hypodermic syringe in order to ensure rapid and complete mixing. Aliquots (*ca.*, 0.5 ml) were then withdrawn at fixed intervals of time and the transmittance at 1959 cm^{-1} recorded. Pseudo first-order rate constants were calculated from the slopes of plots of ln A_t *vs.* time where A_t = the absorbance at time, *t*. These plots were found to be linear for at least 60% reaction and the k_{obs} values were reproducible to $\pm 10\%$ or better. Second-order rate constants were calculated from the slopes of plots of k_{obs} *vs.* the concentration of incoming disulfide.

The continued financial support to one of us (C.V.S.) in the form of an operating grant from the National Research Council of Canada is gratefully acknowledged.

1. R. Ugo, A. Pasani, A. Fusi, and S. Cenini. J. Am. Chem. Soc. **94**, 7374 (1972).
2. J. F. Harrod, C. A. Smith, and K. A. Than. J. Am. Chem. Soc. **94**, 8321 (1972).
3. J. R. Gaylor and C. V. Senoff. Can. J. Chem. **50**, 1868 (1972).
4. L. Vaska and M. F. Werneke. N.Y. Acad. Sci. **33**, 70 (1971).
5. L. Vaska, L. S. Chen, and C. V. Senoff. Science. **174**, 587 (1971).
6. L. Vaska and L. S. Chen. Chem. Commun. 1080 (1971).
7. J. A. Smith, M. Green, and D. C. Wood. J. Chem. Soc. A, 1847 (1970).
8. J. F. Harrod and C. A. Smith. J. Am. Chem. Soc. **92**, 2699 (1970).
9. J. Halpern and P. B. Chock. J. Am. Chem. Soc. **88**, 3511 (1966).
10. T. A. George and D. D. Watkins. Inorg. Chem. **12**, 398 (1973).
11. Y. S. Sohn and A. L. Balch. J. Am. Chem. Soc. **95**, 1144 (1972).
12. D. N. Cash and R. O. Harris. Can. J. Chem. **49**, 867 (1971).
13. J. Halpern. Acc. Chem. Res. **3**, 386 (1970).
14. L. Vaska. Acc. Chem. Res. **1**, 335 (1968).
15. J. P. Collman and W. R. Roper. Adv. Organomet. Chem. **7**, 63 (1968).
16. J. L. Herdé and C. V. Senoff. Can. J. Chem. **51**, 1016 (1973).
17. A. E. Keskinen and C. V. Senoff. J. Organomet. Chem. **37**, 201 (1972).
18. C. V. Senoff. Can. J. Chem. **48**, 2444 (1970).
19. C. T. Lam and C. V. Senoff. J. Organomet. Chem. In press.
20. J. L. Kice. *In* Sulfur in organic and inorganic chemistry. *Edited by* A. Senning. Marcel Dekker, Inc., N.Y. 1971. p. 153.
21. R. A. Schunn. *In* Transition metal hydrides. Vol. 1. *Edited by* E. L. Muetterties Marcel Dekker, Inc., N.Y. 1971.

Can. J. Chem. Downloaded from www.nrcresearchpress.com by 210.87.254.42 on 09/05/12
For personal use only.

Kinetics of Exchange of Dimethylsulfoxide between Hexakis-(dimethylsulfoxide)chromium(III) and Solvent: Pressure Effect and Mechanism

DEBRA LYNN CARLE AND THOMAS WILSON SWADDLE
Department of Chemistry, The University of Calgary, Calgary, Alberta T2N 1N4

Received June 22, 1973

For the exchange of *all six* dimethylsulfoxide (DMSO) ligands in $Cr(DMSO)_6^{3+}$ with perdeuterated DMSO solvent, the first-order rate constant (75°) = 5.5×10^{-5} s^{-1}, while $\Delta H^* = 23.1$ kcal mol^{-1}, $\Delta S^* = -11.8$ cal deg^{-1} mol^{-1}, and $\Delta V^* = -11.3$ cm^3 mol^{-1}. These and other data are indicative of an associative interchange mechanism for substitution in Cr(III) DMSO complexes in DMSO.

Pour l'échange *des six* groupes diméthylsulfoxyde (DMSO) agissant comme ligands dans $Cr(DMSO)_6^{3+}$ par du DMSO prédeutéré agissant comme solvant, la constante de vitesse du premier ordre à 75° est de 5.5×10^{-5} s^{-1} alors que le $\Delta H^* = 23.1$ kcal/mol, le $\Delta S^* = -11.8$ cal deg^{-1} mol^{-1} et le $\Delta V^* = -11.3$ cm^3 mol^{-1}. Ces données et d'autres auraient tendance à montrer que le mécanisme de la substitution du DMSO dans les complexes Cr(III) DMSO est du type d'interchangement associatif.
[Traduit par le journal]

Can. J. Chem. **51**, 3795 (1973)

Introduction

We have recently presented data concerning the effects of pressure on the rates of substitution reactions of some simple cationic chromium(III) (1–3), rhodium(III) (2), and cobalt(III) (4) complexes in aqueous solution, and have argued that the results imply a dissociative interchange (I_d) mechanism in the Co(III) series but an associative interchange (I_a) mechanism for the Rh(III) and Cr(III) reactions. In particular, the effect of pressure on the rate of exchange of $H_2{}^{18}O$ between $Cr(H_2O)_6^{3+}$ and solvent water is characterized by a volume of activation ΔV^* of -9.3 cm^3 mol^{-1}, which, because this reaction involves no development or dissipation of ionic charges and is "symmetrical", constitutes strong evidence for extensive bond-making by the incoming H_2O on going to the transition state.

This leads to the question of whether the proposed associative mechanism for the solvent exchange is peculiar to water as solvent, or whether the mechanism is characteristic of the Cr(III) center and can operate in other solvents having moderate donor properties. The DMSO/$Cr(DMSO)_6^{3+}$ exchange reaction (DMSO = dimethylsulfoxide) provides an appropriate system to examine in the context of this question, since the reaction is conveniently followed by proton magnetic resonance (p.m.r.) techniques using DMSO-d_6 as solvent and $Cr(DMSO\text{-}h_6)_6^{3+}$ as solute (5–7), and also because the molar volume of the DMSO (71.0 cm^3 mol^{-1} for the pure liquid at 20°) is large compared with that of water, so that ΔV^* should be even more sensitive as a mechanistic criterion for solvent exchange in DMSO as compared to water. Furthermore, DMSO is attractive because it differs substantially from water in its solvent properties, being non-protonic and having a dielectric constant of 46.6 at 25° as compared with 78.3 for water.

Experimental

Materials

Dimethylsulfoxide-d_6 (99.5% d_6; Stohler Isotope Co.) was dried over a 4A molecular sieve (Guild Corp.) before use. *P*-Dimethoxybenzene (Matheson, Coleman and Bell) and *p*-dichlorobenzene (Eastman Organic Chemicals) were recrystallized from absolute ethanol before use and dried under vacuum.

Preparation of Hexakis(dimethylsulfoxide)chromium(III) Perchlorate

Chromium(III) nitrate nonahydrate (Fisher Scientific; 4.0 g) in 1.5 ml water was added to 6.0 ml DMSO (Fisher Scientific) and heated at ~65° on the steambath for 2 h. On cooling, a green solid separated, and this was filtered and redissolved in 10.0 ml DMSO on the steambath. Addition of 50 ml 1.0 *M* aqueous $HClO_4$ (*N.B.* concentrated $HClO_4$ solutions must *not* be added to DMSO—explosion hazard!) precipitated a green solid which was redissolved in DMSO and reprecipitated in the same way. The product was recrystallized from about 4 ml hot DMSO and dried under vacuum (0.8 g).

Anal. Calcd. for $[Cr(DMSO)_6](ClO_4)_3$: Cr, 6.34; C, 17.6; H, 4.4; N, 0.0. Found: Cr, 6.31; C, 17.6; H, 4.9; N, 0.0.

Can. J. Chem. Downloaded from www.nrcresearchpress.com by 210.87.254.105 on 09/05/12
For personal use only.

TABLE 1. Kinetics of exchange of all six dimethylsulfoxide ligands in $Cr(DMSO)_6(ClO_4)_3$ with DMSO-d_6 solvent

Temp., °C	Pressure, kbar	[Cr(III)], *m*	[Standard], *m*	10^5k, s^{-1}
55.0	0.001	0.0240	0.133	0.7±0.1
75.0		0.0212	0.082*	6.3±0.3
		0.0304	0.347	5.4±0.2
		0.0608	0.318	5.9±0.2
		0.0304	0.163	5.3±0.2
85.0		0.0209	0.165	15.4±0.5
95.0		0.0251	0.149	36.0±2.0
75.0	0.032	0.0271	0.160	5.9±0.2
	1.023	0.0280	0.168	9.6±0.8
	1.52	0.0282	0.170	10.3±0.2
	2.25	0.0299	0.195	12.7±0.5
	3.04	0.0399	0.234	18.9±0.3

*Standard was *p*-dimethoxybenzene; in all other cases, standard was *p*-dichlorobenzene.

This compound is potentially explosive, and was therefore prepared only in small batches and kept in the dark.

Kinetics

Solutions of $[Cr(DMSO)_6](ClO_4)_3$ and a p.m.r. reference compound (*p*-dimethoxybenzene or *p*-dichlorobenzene) in DMSO-d_6 were prepared by weight. The progress of the reaction at atmospheric pressure was followed by removing samples at appropriate intervals from the solution contained in a closed light-proof vessel in a thermostat (±0.1°), and freezing them until required; the p.m.r. spectra of the thawed samples were then measured with a Varian A-60 spectrometer at 21°, first in chronological order, then in reverse order, and then at random, so as to average out any variations in the spectrometer response with time. The concentration of the freed DMSO-h_6 in each sample was determined by measuring the area or (equally satisfactorily) the height of the DMSO-h_6 resonance (R_t) relative to that of the ring protons in the aromatic standard substance; the equilibrium value R_∞ was obtained from samples which had been thermostatted for at least eight half-lives of the reaction.

Alternatively, the reaction mixture was thermostatted in a p.m.r. tube, which was removed periodically, chilled to 21°, and replaced in the thermostat after its p.m.r. spectrum had been measured; this procedure was less satisfactory than the above (though more economical) because of the significant time-dependence of the response of the spectrometer on some occasions.

The pressure dependence of the reaction rate was measured by removing samples from a pressurized syringe as described previously (4, 8), except that a Hastelloy-B capillary outlet tube was used instead of a tantalum tube. Because DMSO is relatively high-melting, it was necessary to immerse the assembly in the thermostat (75.0 ± 0.1°) as far as the sample valve stem seating to prevent the solution freezing under pressure.

Results

Plots of $\ln(R_\infty - R_t)$ *vs.* time were linear, within the experimental uncertainty, and the first-order rate coefficients k (for the exchange of *all six* DMSO ligands) and their standard deviations are listed in Table 1; the reproducibility of the k values from one run to another was somewhat poorer than suggested by these standard deviations, which might be increased by about 50% accordingly. Rate coefficients k' for the exchange of *single* DMSO ligands are given by $k/6$, *e.g.*, $k' = 0.9_2 \times 10^{-5}\ s^{-1}$ at 75.0° and 1 bar. The nature of the reference solute and the concentration of the complex perchlorate did not affect the values of k seriously. Values of k obtained using the pressure assembly at low pressures corresponded satisfactorily with those obtained at atmospheric pressure, while the value of k listed for 85° (1 bar) agrees well with that obtained in Langford's laboratory (5–7).

An Eyring plot of the data obtained at atmospheric pressure was linear, and gave an enthalpy of activation $\Delta H^* = 23.1 \pm 0.5$ kcal mol^{-1} and an entropy of activation ΔS^* of -11.8 ± 1.5 cal deg^{-1} mol^{-1} for the exchange of *all six* DMSO ligands (or -15.4 ± 1.5 for the exchange of *one* of the six). A plot of $\ln k$ *vs.* pressure was also linear, within the experimental uncertainty, and the corresponding value of ΔV^* was $-11.3 \pm 1.0\ cm^3\ mol^{-1}$.

Discussion

The values of k listed in Table 1 for 75.0°, 1 bar, and various concentrations of $[Cr(DMSO)_6](ClO_4)_3$ are sufficiently close to the weighted mean of $5.5 \times 10^{-5}\ s^{-1}$ to indicate that $Cr(DMSO)_6^{3+}$–ClO_4^- ion pairing is either insignificant or else does not affect the solvent exchange rate appreciably. Ion pairing may indeed be negligible in this system in the concentration range of interest, since Palmer and Watts

Can. J. Chem. Downloaded from www.nrcresearchpress.com by 210.87.254.105 on 09/05/12
For personal use only.

Can. J. Chem. Downloaded from www.nrcresearchpress.com by 210.87.254.105 on 09/05/12
For personal use only.

(9) found no evidence for ion pairing between $Cr(en)_2Cl_2^+$ and perchlorate in DMSO; it is true that we are concerned here with a tripositive rather than a monopositive cation, but Bott *et al.* (10) have pointed out that the magnitude of the charge on large complex cations is not necessarily a major factor governing their tendency to form ion pairs.

The value of ΔV^* (-11 cm^3 mol^{-1}) indicates a substantial contraction on going from the ground state to the transition state, and, since electrostrictive effects are not involved and the entering and leaving groups are identical, this implies that the mechanism is associative (1–4). This ΔV^* value is somewhat more negative than that (-9.3 cm^3 mol^{-1}) recorded for the $Cr(H_2O)_6^{3+}$–$H_2{}^{18}O$ exchange reaction (1), which is to be expected if the mechanisms are similar because of the larger molecular size of DMSO relative to water—this factor being partially offset by the hydrogen-bonded open structure believed to be present in the solvation sheath in water (2) but necessarily absent in the non-protonic solvent DMSO.

Langford *et al.* (6) have shown that the rate of DMSO–$Cr(DMSO)_6^{3+}$ exchange in DMSO–nitromethane mixtures is virtually independent of the DMSO content of the solvent down to the point where DMSO occupies not more than 0.4 mol fraction of the sites of the solvation sheath, although further increases in the occupancy of the solvation sheath by nitromethane lead to reduced DMSO exchange rates. This is interpreted (6) in terms of the presence of a uniquely firmly bound DMSO molecule in the solvation sheath, this singular DMSO being responsible for the exchange process by an associative mechanism.

This hypothesis is clearly consistent with our mechanistic conclusions based on the volume of activation, and indeed consideration of the non-planar geometry and relatively great bulk of the DMSO ligands of the first coordination sphere leads us to the conclusion that the close approach of the solvating DMSO molecules is impossible except in one specific location. Let us imagine the $Cr(DMSO)_6^{3+}$ ion, arranged so that one C_3 axis of the CrO_6 octahedron is vertical, and suppose that a solvating DMSO molecule moves towards the Cr center down this axis (the faces of the octahedron being the obvious places for closest approach). In order to permit the closest approach of this molecule, the three bulky, O-bonded DMSO ligands associated with this uppermost face must rotate away from the incoming molecule, so directing their methyl groups downward; this in turn will force the other three DMSO ligands to reorient in the same direction (giving an appearance reminiscent of the leaves of a palm-tree). Thus, the side and bottom faces of the octahedron become blocked by the methyl groups, so that the close approach of the solvent molecule down the vertical axis has prevented close approach of any of the other solvating DMSO molecules.

The high degree of ordering inherent in such a process, especially as it proceeds onwards to effect ligand substitution, provides an explanation for the surprisingly strongly negative ΔS^* value for DMSO exchange at the Cr(III) center (-15 cal deg^{-1} mol^{-1} for the exchange of one ligand, *cf.* 0 for water exchange (1)), since the rotational freedom of the DMSO ligands will be severely reduced as the reaction proceeds to the seven-coordinate transition state. This very low entropy of activation is responsible for the slowness of DMSO exchange relative to water exchange (by a factor of 30 at 75° or 14 at 25°, on the basis of the activation parameters (1)), despite the fact that ΔH^* is only 23 kcal mol^{-1} for the DMSO system as compared with 26 for water. The DMSO exchange reaction is about 2×10^3 times slower than the exchange between hexaamminechromium(III) ion and liquid ammonia solvent at 25° (11, 12), but the comparison is not very illuminating since the latter reaction shows a marked dependence of rate upon ammonium and perchlorate ion concentrations, and evidently proceeds *via* the ion pair $\{Cr(NH_3)_5NH_2^{2+}, ClO_4^-\}$.

Lo (13) and Watts (14) have found that the anation of $Cr(DMSO)_6^{3+}$ by various anions X^- (X = Cl, NCS, and N_3) proceeds by an interchange mechanism involving an ion pair:

$$[1]\quad Cr(DMSO)_6^{3+} + X^- \underset{\text{fast}}{\overset{K}{\rightleftharpoons}} \{Cr(DMSO)_6^{3+}, X^-\}$$

$$[2]\quad \{Cr(DMSO)_6^{3+}, X^-\} \underset{\text{slow}}{\overset{k_i}{\longrightarrow}} Cr(DMSO)_5X^{2+} + DMSO$$

The values of k_i at 75° for $X^- = Cl^-$, NCS^-, and N_3^- are about 2×10^{-5}, 2×10^{-4}, and $(5 \text{ to } 6) \times 10^{-3}$ s^{-1} respectively, as compared with our value $k = 5.5 \times 10^{-5}$ s^{-1} for the exchange of all six DMSO ligands with the solvent. Thus, it seems that NCS^- can enter the first

coordination sphere of Cr(III) about 4 times faster, and azide ion some 100 times faster, than the spontaneous exchange of DMSO. This is incompatible with a dissociative interchange (I_d) mechanism, which would require that Cr–DMSO bond-breaking be rate determining in the formation of $Cr(DMSO)_5X^{2+}$. Thus, we have once again an associative interchange (I_a) mechanism, with the various X^- displaying their relative nucleophilic powers towards Cr(III), $Cl^- < NCS^- \ll N_3^-$; this marked dependence of k_i on the nature of X^- is, in any event, contrary to experience with systems which evidently do react by an I_d process (15). The foregoing assumes that the rate of solvent exchange in the ion pair $\{Cr(DMSO)_6^{3+}, X^-\}$ is the same as in the free ion $Cr(DMSO)_6^{3+}$, but this is in accordance with the observations of Duffy and Earley (16) and Monacelli and Viel (17) for aquo-exchange involving ion-paired complex cations in water.

We thank Dr. C. H. Langford for suggesting this topic and for much helpful discussion and advice, Drs. D. W. Watts and D. Lo Siaw-Teck for discussions and exchange of data, and the President's General Research Fund of the University of Calgary for financial assistance.

1. D. R. Stranks and T. W. Swaddle. J. Am. Chem. Soc. **93**, 2783 (1971).
2. T. W. Swaddle and D. R. Stranks. J. Am. Chem. Soc. **94**, 8357 (1972).
3. G. Guastalla and T. W. Swaddle. Can. J. Chem. **51**, 821 (1973).
4. W. E. Jones, L. R. Carey, and T. W. Swaddle. Can. J. Chem. **50**, 2739 (1972).
5. H. F. M. Chung. Ph.D Thesis, Carleton University, Ottawa, Ontario. 1971.
6. C. H. Langford, R. Scharfe, and R. Jackson. Inorg. Nucl. Chem. Lett. In press.
7. C. H. Langford. Personal communication.
8. L. R. Carey, W. E. Jones, and T. W. Swaddle. Inorg. Chem. **10**, 1566 (1971).
9. D. A. Palmer and D. W. Watts. Inorg. Chem. **10**, 281 (1971).
10. H. L. Bott, A. J. Poë, and K. Shaw. J. Chem. Soc. A, 1745 (1970).
11. T. W. Swaddle, L. F. Coleman, and J. P. Hunt. Inorg. Chem. **2**, 950 (1963).
12. H. H. Glaeser and J. P. Hunt. Inorg. Chem. **3**, 1245 (1964).
13. D. Lo Siaw-Teck. Ph.D. Thesis, University of Western Australia, Nedlands, W.A., 1972, and personal communication.
14. D. W. Watts. Personal communication.
15. C. H. Langford and W. R. Muir. J. Am. Chem. Soc. **89**, 3144 (1967).
16. N. V. Duffy and J. E. Earley. J. Am. Chem. Soc. **89**, 272 (1967).
17. F. Monacelli and E. Viel. Inorg. Chim. Acta, **1**, 467 (1967).

Can. J. Chem. Downloaded from www.nrcresearchpress.com by 210.87.254.105 on 09/05/12
For personal use only.

The *tert*-Butyldimethylsilyl Group as a Protecting Group in Deoxynucleosides

KELVIN K. OGILVIE
Department of Chemistry, University of Manitoba, Winnipeg, Manitoba R3T 2N2

Received June 12, 1973

tert-Butyldimethylsilyl chloride reacts selectively with hydroxyl groups in nucleosides and preferentially with the 5′-hydroxyl of deoxynucleosides. The *tert*-butyldimethylsilyl group can be removed under conditions which do not affect other commonly used acid or base labile protecting groups, yet it is stable to phosphorylation conditions. This allows for the synthesis of a variety of protected deoxynucleosides in good yields and introduces a versatile new protecting group to the nucleoside and nucleotide field.

Le chlorure de *tert*-butyldiméthylsilyle réagit sélectivement avec les groupes hydroxyles des nucléosides et préférentiellement avec les hydroxyl-5′ des désoxynucléosides. Tout en étant stable dans les conditions de phosphorylation, le groupe *tert*-butyldiméthylsilyle peut être enlevé dans des conditions qui n'affectent pas d'autres groupes protecteurs utilisés couramment et qui sont labiles en milieux acide ou basique. Ceci permet d'effectuer, avec de bons rendements, la synthèse d'un grande nombre de déoxynucléosides protégés et d'introduire un nouveau groupement protecteur versatile au domaine des nucléosides et des nucléotides. [Traduit par le journal]

Can. J. Chem. **51**, 3799 (1973)

Can. J. Chem. Downloaded from www.nrcresearchpress.com by 210.87.254.6 on 09/05/12
For personal use only.

During our investigations into the synthesis and indentification of nucleosides and nucleotides (1, 2) we have been seeking versatile hydroxyl-protecting groups. We describe in this report the use of the *tert*-butyldimethylsilyl (TBDMS) group for protecting hydroxyl functions in deoxynucleosides (3) and the subsequent synthesis of a number of nucleoside derivatives which have not previously been easy to prepare.

tert-Butyldimethylsilyl chloride (TBDMSCL) is prepared by the reaction of *tert*-butyllithium with dichlorodimethylsilane (4). Corey and Venkateswarlu have described the use of TBDMSCL (in DMF at 35 °C in the presence of imidazole) for protecting the hydroxyl groups of a number of alcohols of interest in the synthesis of prostaglandins (5). We have applied these same conditions to the deoxynucleosides and find that: (*a*) TBDMSCL reacts preferentially with the 5′-hydroxyl group; (*b*) the reaction is rapid even at room temperature and the extent of the reaction and distribution of products depends on the amount of imidazole present; (*c*) even in the presence of excess TBDMSCL reaction occurs preferentially with hydroxyl groups and not with amino groups; (*d*) the TBDMS group is stable to phosphorylation conditions; and (*e*) the TBDMS group can be removed with $(n\text{-butyl})_4NF$ in tetrahydrofuran (THF) as described by Corey and Venkateswarlu (5) without affecting other acid or base labile protecting groups on the nucleoside. This has facilitated the preparation of a number of protected nucleosides.

The preparation of the silyl derivatives (Scheme 1) simply requires dissolving the nucleoside, TBDMSCL and imidazole in *N*,*N*-dimethylformamide (DMF). Our initial experiments were carried out at 37 °C. However, we find the reactions are over very quickly (within 30 min) at room temperature with no significant change in yields (Table 1). Further there appears to be little change in product composition for reactions times of 1–24 h.

The amount of imidazole present is important in terms of total yield and also ratio of products (Table 1). We find that for thymidine and *N*-protected nucleosides a ratio of nucleoside: TBDMSCL:imidazole near 1:1.1:2.2 gives the highest yields of 5′-isomers **2**. Reducing the amount of imidazole decreases the total yield of products and increases the ratio of **3**:**2**. Imidazole or other catalyst is essential to the reaction since the absence of imidazole in DMF gives ~5% total yield. However if pyridine is used as solvent in place of DMF, the pyridine also effectively replaces imidazole as catalyst (Table 1). For nucleosides possessing a free amino group the above ratio of reagents generally changes to 1:2.2:4:4 for optimum yields of **2**. However, even under conditions where we obtain di-*O*-silylated nucleosides in

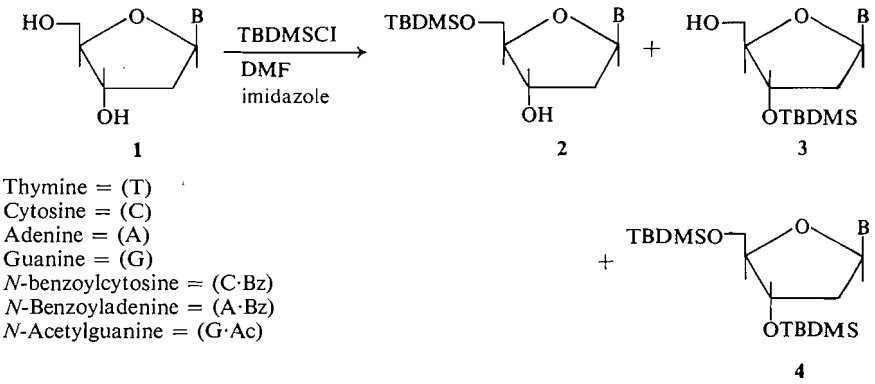

SCHEME 1

TABLE 1. Reactions of deoxynucleosides with TBDMSCL

Starting material (1 mmol)	Ratio 1:TBDMSCL:imidazole	Solvent (1 ml)	Temperature (°C)	Time (h)	Products (% yields)* 1	2	3	4	Other† (mg)
1*a*	1:1.1:1.1	DMF	37	24	14	33	20	28	
1*a*	1:1.1:2.2	DMF	37	24	3	75	4	15	
1*a*	1:1.1:2.2	DMF	37	1	10	75	2	14	
1*a*	1:1.1:2.2	DMF	22	1	10	73	1	15	
1*a*	1:1.5:3.0	DMF	37	15	5	48	3	43	
1*a*	1:1.1:4.4	DMF	37	24	4	76	5	14	
1*a*	1:1.1:0	DMF	37	24	94	1.4	3.1	1	
1*a*	1:1.1:0	Pyridine	37	24	15	64	1.5	13	
1*b*·HCl	1:1.1:2.2	DMF	22	15	32	55	6	3	
1*b*·HCl	1:2.2:4.4	DMF	22	15	<1	88	3	10	
1*b*·HCl	1:4.4:8.8	DMF	22	15	—	—	—	93	8
1*c*	1:1.1:1.1	DMF	22	15	80	15	1.4	<1	
1*c*	1:2.2:4.4	DMF	22	15	<1	80	1.6	17	
1*c*	1:4.4:8.8	DMF	22	15	—	19	<1	71	57
1*d*	1:1.1:2.2	DMF	22	15	45	32	12	5	
1*d*	1:2.2:4.4	DMF	22	15	2	76	4	16	
1*d*	1:3.3:6.6	DMF	22	15	—	—	—	97	
1*e*	1:1.1:2.2	DMF	37	20	22	59	1	16	
1*e*	1:1.1:2.2	DMF	22	15	10	62	8	18	
1*e*	1:2.2:4.4	DMF	22	15	—	2	2	96	
1*f*	1:1.5:3.0	DMF	22	2	14	68	6	8	
1*g*	1:1.1:2.2	DMF	22	15	23	58	5	12	

*Actual experimental yields. Products isolated by t.l.c.
†In both cases where polysilyated products were isolated the mass spectrum indicated three silyl groups on the nucleoside.

90% yields we seldom isolated trisilylated nucleosides (*N*-substitution). This preference of TBDMSCL for reaction with the hydroxyl groups of nucleosides adds considerable versatility to nucleoside protecting groups and allows easy manipulation of a variety of protecting groups.

We have generally found that nucleosides substituted on the 3′-hydroxyl group move more rapidly on t.l.c. than the 5′-isomers. In our reactions to produce the 5′-TBDMS derivatives we expected, because of the bulk of the silylating agent, that the 5′-isomer would predominate. In six out of the seven cases where we observed two monosilylated products from the reaction of TBDMSCL with a nucleoside (Scheme 1) the slower moving (5′) isomer predominated over the faster moving (3′) isomer (see Tables 1, 2). The exception was deoxycytidine where **3***b* moved slightly slower on t.l.c. than **2***b* in the 8:2 solvent (see Experimental).

Can. J. Chem. Downloaded from www.nrcresearchpress.com by 210.87.254.6 on 09/05/12
For personal use only.

Can. J. Chem. Downloaded from www.nrcresearchpress.com by 210.87.254.6 on 09/05/12
For personal use only.

TABLE 2. Physical properties of silylated nucleosides

Compound	M.p. (°C)	Crystallized from	λ_{max} (EtOH) (nm)	Analysis: Calculated C	Calculated H	Calculated N	Found C	Found H	Found N	R_f values† Ethyl acetate	R_f values† THF	R_f values† 8:2‡
2*a*	198–199	ethanol–water	267	53.91	7.92	7.86	54.05	8.03	7.81	0.50	0.80	0.74
3*a*	83–84	ethanol–water	267	53.91	7.92	7.86	53.81	8.16	7.72	0.58	0.84	0.79
4*a*	144–145	hexane	267	53.13	8.99	5.95	56.06	9.09	5.86	0.73	0.90	0.84
2*b*	240–242	ethanol–water	274,240sh	52.76	7.96	12.31	52.64	8.04	12.18	0.00	0.22	0.46
3*b*	163–165	ethanol–water	273,238sh	52.76	7.96	12.31	52.60	8.10	12.22	0.00	0.22	0.40
4*b*	188–189	ether	274,240sh	55.34	9.07	9.22	55.26	9.09	9.16	0.12	0.35	0.64
2*c*	165–166	ether–hexane	260	52.58	7.51	19.01	52.58	7.51	19.01	0.23	0.71	0.70
3*c*	216–217	ether–hexane	260	52.58	7.51	19.01	52.45	7.50	19.22	0.36	0.77	0.76
4*c*	132.5–133	hexane	260	55.07	8.61	14.60	54.97	8.64	14.51	0.55	0.80	0.77
2*d*	dec. > 230	ethanol–water	255,275sh	50.37	7.13	18.36	50.09	7.05	18.08	0.00	0.08	0.30
3*d*	82–84	ethanol–water	255,273sh	50.37	7.13	18.36	50.45	7.08	18.12	0.00	0.08	0.50
4*d*	dec. > 265	ethanol	255,275sh	53.30	8.34	14.13	53.25	8.41	14.01	0.07	0.25	0.56
2*e*	130–132	THF–hexane	305,260	59.30	7.01	9.43	59.50	7.20	9.26	0.22	0.70	0.70
3*e*	*	*	305,260	59.30	7.01	9.43	59.43	6.93	9.33	0.45	0.80	0.80
4*e*	138–139	*	305,260,236sh	60.07	8.10	7.51	60.22	8.18	7.65	0.55	0.91	0.84
2*f*	98–99	water	280,260sh,253sh	58.82	6.65	14.91	59.12	6.78	14.76	0.26	0.79	0.86
3*f*	128–131	ethanol	280,260sh,253sh	58.82	6.65	14.91	59.08	6.85	15.08	0.46	0.83	0.90
4*f*	67–68	*	280,260sh,253sh	59.65	7.77	11.99	59.60	7.71	12.12	0.80	0.82	0.90
2*g*	123–125	ethanol–water	280,260,255	51.05	6.90	16.54	50.75	6.82	16.65	0.05	streak	0.50
3*g*	191–192	ethanol	280,260,255	51.05	6.90	16.54	50.82	6.73	16.55	0.05	streak	0.58
4*g*	105–107	ethanol	280,260,255	53.60	8.06	13.02	53.47	8.02	13.12	0.16	streak	0.83

*Samples obtained as dry solids and/or in small quantities and usually did not show sharp melting points. Mass spectrum, t.l.c., and elemental analysis indicated compounds were pure.

†Eastman chromatogram sheets 6060, silica gel with indicator.

‡8:2 refers to a solvent composed of chloroform:ethanol (8:2, v/v).

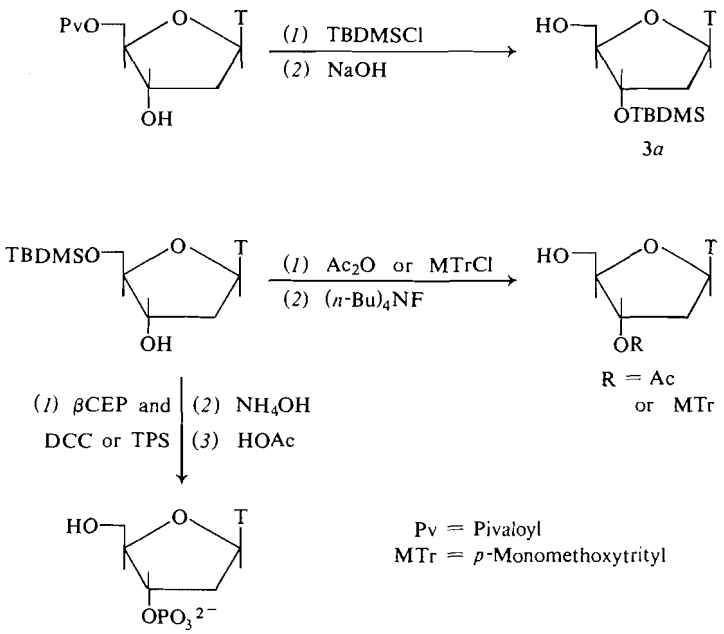

SCHEME 2

To confirm the identity of the isomers **2***b* and **3***b*, we prepared **3***b* by an alternate route. $O^{5'}$-Acetyl-*N*-benzoyldeoxycytidine was treated with TBDMSCL followed by removal of the acetyl group with NH_4OH and the benzoyl group with hydrazine hydrate. This produced **3***b* identical to the slower moving product from the reaction of **1***b* with TBDMSCL.

To confirm the identity of the isomers **2***a* and **3***a* of thymidine we treated $O^{5'}$-pivaloylthymidine with TBDMSCL and hydrolyzed the intermediate with 0.5 *N* NaOH. The product was isolated by t.l.c. and found to be identical to the faster moving monosilylated thymidine which is **3***a*. We have detected no isomerization of **2***a* and **3***a* under these conditions. Furthermore **2***a* was reacted in separate experiments with acetic anhydride and monomethoxytrityl chloride (Scheme 2). Removal of the silyl group with $(n\text{-Bu})_4NF$ in THF produced the known compounds $O^{3'}$-acetylthymidine (6) and $O^{3'}$-monomethoxytritylthymidine (1*b*) in 95 and 94% isolated yields respectively.

Further proof of the identities of **2***a* and **3***a* was obtained by phosphorylation and enzymatic analysis of the products. Compound **2***a* was phosphorylated using β-cyanoethylphosphate (βCEP) and either *N*,*N'*-dicyclohexylcarbodiimide (DCC) or triisopropylbenzenesulfonyl chloride (TPS) as condensing agents. Following condensation the protecting groups were removed with 9 *M* NH_4OH at 60 °C for 1 h (βCEP) and 80% acetic acid on a steam bath for 15 min (TBDMS). The yields of thymidine-3′ phosphate (Tp) from the two reactions were 100 and 98% respectively. The product Tp was unaffected by 5′-nucleotidase but was converted to thymidine with alkaline phosphatase. Compound **3***a* was similarly converted to thymidine-5′ phosphate (p.T.) which was hydrolized to thymidine with 5′-nucleotidase. These results not only confirm the identity of **2***a* and **3***a* but demonstrate the stability of the TBDMS group to phosphorylating conditions.

A major advantage of the TBDMS group is its compatibility with other commonly used protecting groups. This has greatly facilitated the preparation of nucleoside derivatives which are otherwise more difficult to obtain. For example the silyl group can be removed (see Table 3) with $(n\text{-Bu})_4NF$ in THF at room temperature for 30 min (5). These conditions do not affect acid labile groups (*e.g.* trityl) base labile protecting groups in general (*O*- or *N*-derivatives) and the β-benzoylpropionyl group in particular. On the other hand the hydrazine hydrate solution which removes *N*-acyl groups and the β-benzoylpropionyl group (7) has no

Can. J. Chem. Downloaded from www.nrcresearchpress.com by 210.87.254.6 on 09/05/12
For personal use only.

Can. J. Chem. Downloaded from www.nrcresearchpress.com by 210.87.254.6 on 09/05/12
For personal use only.

TABLE 3. Hydrolysis of the TBDMS group from **2***a*

Reagent used	Temperature (°C)	Time	% hydrolysis
$(n\text{-Bu})_4NF$ in THF	22	30 min	100
80% HOAC	Steam bath	15 min	100
0.5 *N* NaOH EtOH:H_2O (1:1)	22	24 h	80
9 *M* NH_4OH	60	1 h	6
15% NH_4OH in EtOH	22	2 h	0
H_2NNH_2: HOAc: Pyridine (1:6:24, (v/v/v)	22	24 h	0

affect on the TBDMS group. Thus treatment of **4***b* and **4***c* with benzoic anhydride and **4***d* with acetic anhydride followed by reaction with $(n\text{-Bu})_4NF$ leads to high yields of *N*-benzoyldeoxycytidine (**5***e*), *N*-benzoyldeoxyadenosine (**5***f*), and *N*-acetyldeoxyguanosine (**5***g*).

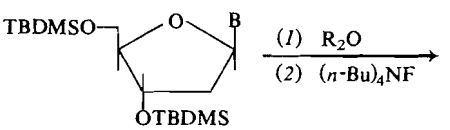

4*b–d* R = Benzoyl or Acetyl

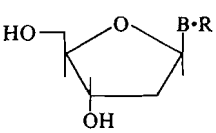

5

e; B = C; R = Bz
f; B = A; R = Bz
g; B = G; R = Ac

A very useful set of derivatives can easily be obtained as outlined in Scheme 3. Treatment of **2***b* with benzoyl chloride or by heating with benzoic anhydride followed by removal of the silyl group gives **7***e* in 80 and 82% yields respectively. **7***f* and *g* were obtained in a similar fashion in 93 and 86% respectively. We have found that **2***b* reacts with benzoic anhydride in pyridine at room temperature to produce 5′-TBDMS-*N*-benzoyldeoxycytidine (**2***c*) in good yield. This contrasts with **2***c* and *d* which react with benzoic anhydride and acetic anhydride respectively to give preferential *O*-acylation (**6***c* and *d*). The use of excess reagent and gentle heating causes *N*-acylation in these cases as well. Treatment of compounds **7** with hydrazine hydrate solution produces the 3′-acylated derivatives **8** in 90% yields.

Derivatives such as **7** are thus available from the starting nucleosides in two–three steps, two of the steps being ½ h reactions and overall yields being in the 50% range. Existing routes to these compounds usually require more and longer steps and lower overall yields. For example an existing route to **7***e* involves (8) tritylating deoxycytidine (62% yield) followed by benzoylation (71%) and removal of the trityl group (42%) to produce **7***e* in 18.5% overall yield. The acid hydrolsysis of the trityl group also causes hydrolysis of the *N*-glycoside bond in *N*-acylated nucleosides, a problem of particular importance with deoxyadenosine derivatives (9).

One of our goals in the nucleotide area is the development of methods which allow for the rapid identification of isomeric nucleoside and nucleotide derivatives even in very small amounts or from reaction mixtures. To this end we have been employing mass spectrometry (2). We have previously observed different fragmentation patterns from acyl groups of isomeric substituted nucleosides. We had hoped that the TBDMS group would increase the volatility of nucleoside derivatives and give clearly discernable fragmentation patterns from 3′- and 5′-isomeric derivatives. Most importantly, in addition to its use as an identification handle, the TBDMS group is a chemically useful protecting group. Table 4 shows some diagnostically important fragments from the mass spectra of the isomeric compounds **2** and **3**. Clearly fragmentation is significantly different between isomers. The ratio of peaks varies with temperature and with instrument conditions. A full analysis of the spectra of these silylated nucleosides will be presented shortly (10).

A possibility existed that the methyl groups on the TBDMS group of 3′- and 5′-isomers might show different resonances in the n.m.r. However, in the isomeric thymidines no useful distinction could be made with **2***a* having singlets δ ($CDCl_3$) of 0.14 ($(CH_3)_2Si$), 0.92 ($(CH_3)_3CSi$), and 1.91 p.p.m. (5-CH_3) and **3***a* showing singlets at 0.094 ($(CH_3)_2Si$), 0.89 ($(CH_3)_3CSi$), and 1.87 p.p.m. (5-CH_3). These differences are very slight and not considered by us to be of immediate practical use.

We have found most of the silylated nucleo-

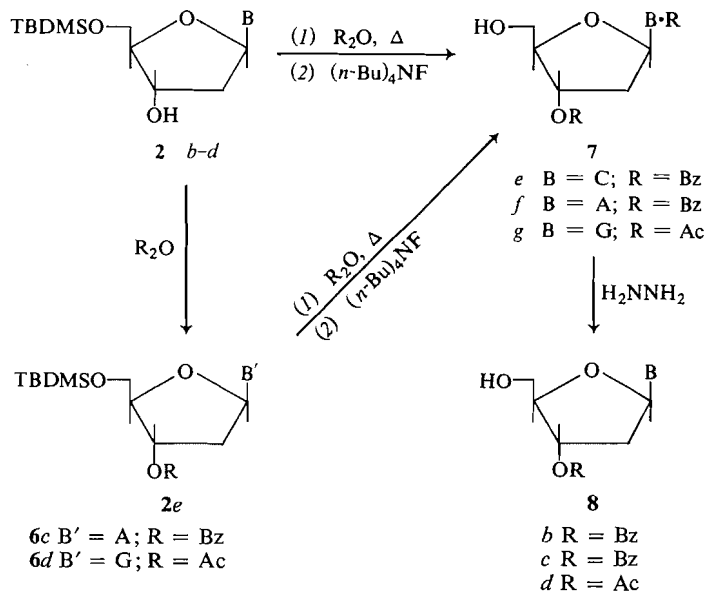

SCHEME 3

TABLE 4. Some diagnostically important fragments from the mass spectra* of **2** and **3**

Compound	Temperature (°C)	Fragment, relative intensities M − 57	M − 75	M − 93	M − 155
2*a*	120	100	428	117	31
3*a*	120	100	0	0	455
2*b*	250	100	714	4	142
3*b*	200	100	83	0	800
2*c*	170	100	36	1	5.2
3*c*	100	100	0	0	224
2*d*	280	100	675	147	0
3*d*	280	100	12	0	112

*Spectra recorded on a Finnigan 1015 mass spectrometer.

sides to be crystalline compounds with sharp melting points. In a few cases initial attempts to induce crystallization have failed and the compounds were obtained as dry solids usually without clear melting points. As crystalline solids the silylated derivatives are stable for at least 10 months but we have detected loss of the protecting group on long standing in aqueous or alcohol solution. Gummy samples in which solvent has been incompletely removed also show deterioration on standing.

In conclusion we have found that TBDMSCL reacts selectively with the hydroxyl groups of nucleosides and preferentially with the 5′-hydroxyl group. Because of the compatibility of the TBDMS group with other acid and base labile protecting groups almost complete manipulation of protecting groups is now possible. The TBDMS group is stable to phosphorylation. The use of the TBDMS group is characterizing isomeric nucleosides and its use in synthesizing oligonucleotides in the ribose series will be described shortly.

Experimental

General Procedures

A detailed description of all our general procedures including solvent purification, chromatography techniques and reagents, phosphorylation procedures, enzyme assays, and analytical and instrumental methods and instruments has been given in detail in ref. 1*a* with the

Can. J. Chem. Downloaded from www.nrcresearchpress.com by 210.87.254.6 on 09/05/12
For personal use only.

Can. J. Chem. Downloaded from www.nrcresearchpress.com by 210.87.254.6 on 09/05/12
For personal use only.

following exceptions. Thin layer chromatography solvent 8:2 is used in this paper as an abbreviation for a solvent composed of chloroform: ethanol (8:2, v/v). Mass spectra were recorded on a Finnigan 1015 mass spectrometer. *tert*-Butyldimethylsilyl chloride, m.p. 121–125 °C, was prepared according to the method of Sommer and Taylor (4); it is also commercially available from Willow Brook Labs Inc. $(n\text{-Bu})_4NF$ solution was prepared by neutralizing $(n\text{-Bu})_4NOH$ with HF in methanol. After removal of the solvent, benzene–acetonitrile was evaporated from the residue several times. The residue was dried over P_2O_5 and made up to volume in THF (0.5 *M*). After treating a nucleoside derivative with the $(n\text{-Bu})_4NF$ reagent, the solution was usually passed through a short column of Monday DSF-5 silica gel previously prepared on a t.l.c. plate. This procedure removed salts and greatly enhanced subsequent t.l.c. separations of products.

Synthesis of Compounds 2, 3, and 4 from 1

In all cases the nucleoside **1** (1 mmol) TBDMSCL and imidazole were added to 1 ml of DMF and the solution stirred at the desired temperature. At the end of the reaction the solution was applied to three t.l.c. plates developed first in ether and then in chloroform–ethanol (8:2). The separated bands were eluted with ethanol which on concentration yielded the products. Results are listed in Tables 1 and 2. Larger scale reactions were also carried out in a direct scale-up of this procedure. Specific changes for certain nucleosides are as follows.

Thymidine. T.l.c. plates were developed only in ether.

Deoxycytidine. T.l.c. plates were developed in THF. The starting nucleoside was deoxycytidine·HCl.

Deoxyguanosine. During the reactions most of the compound **4***d* precipitates and can be collected by filtration prior to chromatography.

N-Benzoyldeoxycytidine. T.l.c. plates developed only in ether.

N-Benzoyldeoxyadenosine. T.l.c. plates developed twice in ether.

$O^{5'}$-Pivaloyl-$O^{3'}$-TBDMS-thymidine

5′-Pivaloylthymidine (163 mg, 0.5 mmol), TBDMSCL (100 mg, 0.67 mmol), and imidazole (85 mg, 1.25 mol) were dissolved in DMF (0.5 ml) and stirred at 37 °C for 16 h. The solution was applied to two t.l.c. plates developed in ether. The single product band was eluted with ether, solvent was removed at reduced pressure and the residue was crystallized from ethanol to yield 200 mg (91%) of $O^{5'}$-pivaloyl-$O^{3'}$-TBDMS thymidine; m.p. 150–151 °C; $R_f^1(Et_2O)$ 0.53; λ_{max} (EtOH) 208 and 266 nm; parent ion in mass spectrum at *m/e* 440.

Anal. Calcd. for $C_{21}H_{32}N_2O_6Si$: C, 57.24; H, 8.23; N, 6.36. Found: C, 57.11; H, 8.16; N, 6.42.

$O^{3'}$-TBDMS-thymidine (3a)

The above product (100 mg) was dissolved in 1 ml of THF and ethanol (1 ml) and 2*N* NaOH (1 ml) were added. The solution was stirred at room temperature for 6 h. The solution was neutralized with Dowex 50 W-X8 (pyridinium form), concentrated to a small volume and applied to a t.l.c. plate which was developed in ether. The product band and a thymidine band (at the origin) were eluted with ether and ethanol respectively. Thymidine was obtained in a 20% yield. The product **3***a* crystallized from ethanol–water, 55 mg (68%), m.p. 83–85 °C (see Table 2 for properties and analysis).

$O^{5'}$-Acetyl-N-benzoyldeoxycytidine, $O^{3'}$-Acetyl-N-benzoyldeoxycytidine, and $O^{3'}$,$O^{5'}$-Diacetyl-N-benzoyldeoxycytidine

Compound **1***e* (331 mg, 1 mmol) was dissolved in pyridine (5 ml) and acetic anhydride (0.1 ml) was added dropwise to the solution. After 1 h an additional 0.05 ml of acetic anhydride was added and the solution was stirred for a further 3 h. Ethanol (10 ml) was added and the solvents were removed at reduced pressure. The residue was applied to five t.l.c. plates which were developed three times in ethyl acetate. Beautiful separation occurred between the four bands which were eluted with ethanol. On concentration of each of the ethanol solutions the products crystallized from solution and were collected as follows.

The fastest moving material on t.l.c. was $O^{3'}$,$O^{5'}$-diacetyl-*N*-benzoyldeoxycytidine (54 mg, 13%): m.p. 193–194 °C; R_f (EtOAc) 0.36; *m/e* 415; λ_{max} (EtOH) 305 and 260 nm.

Anal. Calcd. for $C_{20}H_{21}N_3O_7$: C, 57.83; H, 5.09; N, 10.12. Found: C, 57.65; H, 5.01; N 10.05.

The next slowest product was $O^{3'}$-acetyl-*N*-benzoyldeoxycytidine (30 mg, 8%): m.p. 180–182 °C; R_f (EtOAc) 0.25; *m/e* 373; λ_{max} (EtOH) 305 and 260 nm.

Anal. Calcd. for $C_{18}H_{19}N_3O_6$: C, 57.90; H, 5.13; N, 11.25. Found: C, 57.85; H, 5.10; N, 11.28.

The second slowest product was $O^{5'}$-acetyl-*N*-benzoyldeoxycytidine (160 mg, 43%): m.p. 165–166 °C; R_f (EtOAc) 0.16; *m/e* 373; λ_{max} (EtOH) 305 and 260 nm.

Anal. Calcd. for $C_{18}H_{19}N_3O_6$: C, 57.90; H, 5.13; N, 11.25. Found: C, 57.82; H, 5.06; N, 11.32.

The slowest moving product on t.l.c. was **1***e* of which 83 mg (25%) was recovered.

$O^{3'}$-TBDMS-deoxycytidine (3b)

$O^{5'}$-Acetyl-*N*-benzoyldeoxycytidine (94 mg, 0.25 mmol), TBDMSCL (75 mg, 0.5 mmol), and imidazole (68 mg, 1 mmol) were added to DMF (0.5 ml) and the solution was stirred for 2 h. Thin layer chromatography showed complete conversion of starting material to a new product R_f (EtOAc) 0.65. The produce was separated from other reactants by passing it through a short column of silica gel (3 × 3.5 cm) with ether. The ether was evaporated and the residue was stirred with 50% NH_4OH in ethanol (4 ml) for 8 h. The solvents were removed at reduced pressure and the residue was dissolved in a solution containing pyridine (2.4 ml), acetic acid (0.6 ml), and hydrazine hydrate (0.1 ml). After 15 h the solvents were removed at reduced pressure and the residue was applied to a t.l.c. plate which was developed first in ether and then in 8:2. The product band was eluted with ethanol which on concentration yielded **3***b* (60%), see Table 2.

A second faster moving nucleoside band was obtained from the t.l.c. plate and was identified as $O^{5'}$-acetyl-$O^{3'}$-TBDMS-deoxycytidine: m.p. 120–122 °C (21%); $R_f^{8:2}$ 0.60; λ_{max} (EtOH) 274, 238 sh.

Anal. Calcd. for $C_{18}H_{29}N_5O_4Si$: C, 53.24; H, 7.62; N, 10.96. Found: C, 52.87; H, 7.55; N, 10.82.

Phosphorylations

Compounds **2***a* and **3***a* (50 mg in each experiment) were phosphorylated with β-cyanoethylphosphate using

Can. J. Chem. Downloaded from www.nrcresearchpress.com by 210.87.254.6 on 09/05/12
For personal use only.

either dicyclohexylcarbodiimide or triisopropylbenzenesulfonyl chloride as condensing agents using established procedures (1, 11, 12). The β-cyanoethyl group was removed using 9 *M* NH_4OH at 60 °C for 1 h. After removal of solvents the residue was heated on a steam bath for 15 min with 2 ml of 80% acetic acid. The solution was then concentrated at reduced pressure and applied to Whatman 3 mm paper developed in solvent A. Yields are described in the text.

Enzyme Studies

The procedures used for the 5′-nucleotidase and alkaline phosphatase have been described (1*a*). For each analysis 10 $O.D._{.267}$ units of nucleoside monophosphate were used and the product isolated by paper chromatography in solvent A (1*a*). The nucleoside monophosphate (Tp) obtained from **2***a* was resistant to 5′-nucleotidase but yielded thymidine when treated with alkaline phosphatase. From **3***a*, the nucleoside monophosphate (pT) gave thymidine when treated with either 5′-nucleotidase or alkaline phosphatase.

General Procedure for the Synthesis of **5***e–g*

Compound **4** (1 mmol) was dissolved in 5 ml of pyridine and an excess (5 mmol) of the anhydride (benzoic for **4***b* and **4***c* and acetic for **4***d*) was added. The solution was then stirred at room temperature for 24 h for **4***b*, heated on the steam bath for 3 h for **4***c*, and stirred at room temperature for 20 h followed by heating on a steam bath for 1 h for **4***d*. Solvents were removed at reduced pressure and by repeated evaporation of ethanol. $(n\text{-Bu})_4NF$ (2 ml) in THF was added and the solution stirred at room temperature for 30 min. The THF was evaporated and the residue dissolved in ethanol and applied to two t.l.c. plates developed in 8:2. The product band was eluted with ethanol and on concentration of the solvent compounds **5***e–g* were obtained in 94, 92, and 86% yields respectively. The products were identified by comparison to authentic samples prepared by the procedures of Khorana and co-workers (9). The compounds prepared by our procedure were identical (m.p., u.v., chromatography, and mass spectrometry) to those prepared by the Khorana procedure.

$O^{5'}$-TBDMS-$O^{3'}$,N-dibenzoyldeoxycytidine

Procedure (a)

Compound **2***b* (250 mg, 0.73 mmol) was dissolved in 5 ml of pyridine and 1 ml of benzoyl chloride was added. The solution was stirred at room temperature for 3 h, ethanol was added, and the solvents were removed at reduced pressure. The residue was dissolved in ethanol and applied to two t.l.c. plates developed in ether. The major product was eluted with ether and on evaporation of the solvent 350 mg (87%) of a white solid, m.p. 166–167 °C, were obtained: λ_{max} (EtOH) 305, 260, and 231 nm; *m/e* 549; R_f (Et_2O) 0.33, R_f (EtOAc) 0.41.

Anal. Calcd. for $C_{29}H_{35}N_3O_6Si$: C, 63.37; H, 6.41; N, 7.64. Found: C, 63.25; H, 6.40; N, 7.72.

Procedure (b)

Compound **2***b* (341 mg, 1 mmol) and benzoic anhydride (1.35 g, 6 mmol) were dissolved in pyridine (10 ml) and heated on a steam bath for 3 h. The solution was poured into ice and water (400 ml) and allowed to stand overnight. The solid was collected by filtration, dissolved in ethanol, and applied to two t.l.c. plates developed with ether. The product was eluted with ether, which on evaporation yielded 500 mg (91%) of 5′-TBDMS-3′,N-dibenzoyldeoxycytidine.

Procedure (c)

Compound **2***e* (100 mg) was heated with 1 mmol of benzoic anhydride in pyridine (2 ml) for 2 h on a steam bath and worked-up as in (*a*) above to give the desired product in 95% yield.

*$O^{5'}$-TBDMS-N-benzoyldeoxycytidine (**2***e*)*

Compound **2***b* (220 mg, 0.64 mmol) and benzoic anhydride (226 mg, 1 mol) were dissolved in pyridine (2 ml) and stirred at room temperature for 3 h. The solution was applied directly to two t.l.c. plates which were developed first in ether and then in ethyl acetate. Three nucleoside bands were eluted and were identified as **2***b* (40 mg, 14%), **2***e* (160 mg, 56%), and 5′-TBDMS-$O^{3'}$-N-dibenzoyldeoxycytidine (50 mg, 14%).

*$O^{3'}$,N-Dibenzoyldeoxycytidine (**7***e*)*

$O^{5'}$-TBDMS-$O^{3'}$,N-dibenzoyldeoxycytidine (550 mg, 1 mmol) was added to $(n\text{-Bu})_4NF$ in THF (4 ml) and the solution was stirred for 30 min. The solution was passed through a short (2 × 3 cm) column of silica gel which was thoroughly washed with THF. The THF solution was concentrated at reduced pressure and applied to four t.l.c. plates which were developed in ether. The product was eluted with ethanol and, on concentration of the solution, crystallized to give **7***e* (400 mg, 92%): m.p. 218–220 °C; λ_{max} (EtOH) 304, 260, and 232 nm; R_f (Et_2O) 0.20, R_f (EtOAc); *m/e* 435 (8).

*$O^{3'}$-Benzoyldeoxycytidine (**8***b*)*

Compound **7***e* (305 mg, 0.7 mmol) was added to a solution containing pyridine (2.4 ml), acetic acid (0.6 ml), and hydrazine hydrate (0.1 ml) and the resulting solution was stirred for 20 h. Ethanol was added and the solvents were concentrated at reduced pressure and applied to two t.l.c. plates developed first in THF and then in ethanol. The product was eluted with ethanol which on complete evaporation left a white solid (**8***b*, 210 mg, 91%): m.p. dec. > 185 °C; λ_{max} EtOH 273 and 232 nm; R_f (THF) 0.07, R_f (8:2) 0.47; and *m/e* 331.

Anal. Calcd. for $C_{16}H_{17}N_3O_5$: C, 58.07; H, 5.16; N, 12.66. Found: C, 58.01; H, 5.02; N, 12.75.

*$O^{5'}$-TBDMS-$O^{3'}$-benzoyldeoxyadenosine (**6***c*)*

Compound **2***c* (300 mg, 0.82 mmol) and benzoic anhydride (560 mg, 2.47 mmol) were added to pyridine (4 ml) and the solution was stirred at room temperature for 2.5 days. The solution was concentrated at reduced pressure and applied to three t.l.c. plates which were developed in ether yielding three nucleoside bands. These were eluted separately with ethanol and on concentration gave **2***c* (104 mg, 35%) and **6***c* (195 mg, 50%); m.p. 75–76 °C; λ_{max} (EtOH) 260 and 231 nm; R_f (Et_2O) 0.20, R_f (8:2) 0.80; *m/e* 469. Compound **6***c* will crystallize on slow evaporation of an ethanol – water solution.

Anal. Calcd. for $C_{23}H_{31}N_5O_4Si$: C, 58.82; H, 6.65; N, 14.91. Found: C, 59.01; H, 6.62; N, 14.83.

From the above reaction 48 mg of a material R_f (Et_2O) 0.25 was obtained and tentatively identified as $O^{5'}$-TBDMS-$O^{3'}$,N-dibenzoyldeoxyadenosine (λ_{max} (EtOH) 280 and 231 nm; *m/e* 516 (M − 57)).

*$O^{3'}$-N-Dibenzoyldeoxyadenosine (**7***f*)*

(*a*) Compound **2***c* (730 mg, 2 mmol) and benzoic anhydride (1.8 g, 8 mmol) were dissolved in pyridine (10 ml)

Can. J. Chem. Downloaded from www.nrcresearchpress.com by 210.87.254.6 on 09/05/12
For personal use only.

and heated on a steam bath for 2 h. The solution was allowed to stir at room temperature for an additional 12 h whereupon ethanol (10 ml) was added and the solvents were removed at reduced pressure. The dry residue was dissolved in 5 ml of the $(n\text{-Bu})_4$NF solution and stirred for 30 min. The solution was filtered through a short (2 × 3 cm) column of silica gel which was washed with THF. The THF solution was concentrated at reduced pressure and applied to four t.l.c. plates which were developed twice in ethyl acetate. The product was eluted with ethanol and on concentration of the ethanol solution, **7***f* crystallized (850 mg, 93%): m.p. 112–114 °C; λ_{max} (EtOH) 280 and 233 nm; R_f (EtOAc) 0.26, R_f (THF) 0.77, R_f (8:2) 0.84; *m/e* 459.

Anal. Calcd. for $C_{24}H_{21}N_5O_5$: C, 62.74; H, 4.61; N, 15.24. Found: C, 62.66; H, 4.70; N, 15.15.

(*b*) The same general procedure as in (*a*) above gave a 92% yield of **7***f* starting from **6***c*.

*$O^{3'}$-Benzoyldeoxyadenosine (**8***c*)*

(*a*) Compound **7***f* (300 mg, 0.65 mmol) was treated with hydrazine in pyridine – acetic acid as above for **8***b*. The product crystallized from the reaction mixture and was collected by filtration, washed with ether, and dried to give **8***c* (220 mg, 96%). Compound **8***c* crystallized from ethanol: m.p. 264–265 °C; λ_{max}(EtOH) 259 and 232 nm; R_f (EtOAc) 0.12, R_f (THF) 0.63, R_f (8:2) 0.72; *m/e* 355.

Anal. Calcd. for $C_{17}H_{17}N_5O_4$: C, 57.46; H, 4.82; N, 19.71. Found: C, 57.40; H, 4.85; N, 19.65.

(*b*) Compound **8***c* was also obtained from **6***c* in 95% yield by treating **6***c* with $(n\text{-Bu})_4$NF solution in the usual manner.

*$O^{5'}$-TBDMS-$O^{3'}$-Acetyldeoxyguanosine (**6***d*)*

Compound **2***d* (285 mg, 0.75 mmol) and acetic anhydride (1 ml) were added to pyridine (5 ml) and stirred at room temperature for 2 days. The solution had become very viscous and a large amount of precipitate had formed which was collected by filtration and washed successively with pyridine, ether, and hexane. This solid material (190 mg) was pure **6***d*: m.p. dec. > 280 °C; λ_{max} (EtOH) 255 nm; R_f (THF) 0.10, R_f (8:2) 0.55; *m/e* 423. The filtrate and washings were applied to a t.l.c. plate developed in 8:2. An additional 87 mg of **6***d* was obtained.

Anal. Calcd. for $C_{18}H_{29}N_5O_5Si$: C, 51.04; H, 6.90; N, 16.53. Found: C, 49.88; H, 6.86; N, 16.45.

From the above t.l.c. plate 20 mg of a material having R_f (8:2) 0.71; λ_{max} (EtOH) 281, 261, and 255 nm; m.p. 188–189 °C; *m/e* 465, and without further characterization was assumed to be $O^{5'}$-TBDMS-$O^{3'}$,*N*-diacetyldeoxyguanosine.

*$O^{3'}$-N-Diacetyldeoxyguanosine (**7***g*)*

(*a*) The above experiment was repeated except that the solution was heated on a steam bath for 2 h, followed by the addition of ethanol (10 ml), and evaporation of the solvents. The residue was treated with 2 ml of the $(n\text{-Bu})_4$NF solution and following work-up as described for **7***f* (except that t.l.c. plates were developed in 8:2), the product **7***g* was obtained in 86% yield: m.p. 130–132 °C; λ_{max} (EtOH) 280, 260, and 255 nm; R_f (THF) 0.10, R_f (8:2) 0.50; and *m/e* 351.

Anal. Calcd. for $C_{14}H_{17}N_5O_6$: C, 47.86; H, 4.88; N, 19.94. Found: C, 47.80; H, 4.82; N, 19.98.

(*b*) **7***g* was obtained in 90% yield by treating **2***g* with acetic anhydride in pyridine at room temperature and work-up as in (*a*) above.

*$O^{3'}$-Acetyldeoxyguanosine (**8***d*)*

(*a*) Compound **6***d* (85 mg, 0.2 mmol) was treated with 1 ml of the $(n\text{-Bu})_4$NF reagent in the usual manner. The product **8***d* was isolated by t.l.c. in 8:2 in 89% yield: m.p. slow dec. > 225 °C; λ_{max} (EtOH) 255 nm; R_f (THF) 0.00, R_f (8:2) 0.40; and *m/e* 309. This compound has been previously reported in the literature (13), m.p. dec. > 240 °C.

(*b*) Compound **8***d* was also obtained from **7***g* in 92% yield by treating **7***g* with the hydrazine in pyridine – acetic acid reagent.

Financial assistance from the National Research Council of Canada is gratefully acknowledged.

1. (*a*) K. K. Ogilvie and L. A. Slotin. Can. J. Chem. **51**, 2397 (1973); (*b*) K. K. Ogilvie and R. L. Letsinger. J. Org. Chem. **32**, 2365 (1967).
2. J. B. Westmore, D. C. K. Lin, and K. K. Ogilvie. Org. Mass Spectrom. **7**, 317 (1973).
3. K. K. Ogilvie and D. J. Iwacha. Tetrahedron Lett. 317 (1973).
4. L. H. Sommer and L. J. Taylor. J. Am. Chem. Soc. **76**, 1030 (1954).
5. E. J. Corey and A. Venkateswarlu. J. Am. Chem. Soc. **94**, 6190 (1972).
6. A. M. Michelson and A. R. Todd. J. Chem. Soc. 951 (1953).
7. R. L. Letsinger, P. S. Miller, and G. W. Grams. Tetrahedron Lett. 2621 (1968).
8. E. Benz, N. F. Elmore, and L. Goldman. J. Org. Chem. **30**, 3067 (1965).
9. H. Schaller, G. Weimann, B. Lerch, and H. G. Khorana. J. Am. Chem. Soc. **85**, 3821 (1963).
10. K. K. Ogilvie and J. B. Westmore. In preparation.
11. R. Lohrmann and H. G. Khorana. J. Am. Chem. Soc. **88**, 829 (1966).
12. G. M. Tener. J. Am. Chem. Soc. **83**, 159 (1961), G. Weimann and H. G. Khorana. J. Am. Chem. Soc. **84**, 419 (1962).
13. D. H. Hayes, A. M. Michelson, and A. R. Todd. J. Chem. Soc. 808 (1955).

Irradiation Studies. III. The Products from 4-Phenylterephthalophenone and Their Syntheses[1]

DOUGLAS PAUL THIEMANN,[2,3] DONALD E. PEARSON, AND DAVID JAMES THOENNES[2]
Department of Chemistry, Vanderbilt University, Nashville, Tennessee 37235

Received May 2, 1973

The photoreduction products of the irradiation of 4-phenylterephthalophenone in pyridine – isopropyl alcohol were 4-(4-phenylbenzoyl)benzhydrol (**2**) and the unexpected product, 4-benzoyl-4′-phenylbenzhydrol (**3**). The structures have been confirmed by an independent synthesis of each. A possible mechanism is discussed.

Les produits de la photoréduction obtenus par irradiation de la phényl-4 téréphtalophénone dans un mélange pyridine – propanol-2 sont le (phényl-4 benzoyl)-4 benzydrol (**2**) et le benzoyl-4 phényl-4′ benzydrol (**3**) qui est inattendu. Les structures de ces produits ont été confirmées par des synthèses indépendantes. Un mécanisme possible est discuté. [Traduit par le journal]

Can. J. Chem. **51**, 3808 (1973)

Can. J. Chem. Downloaded from www.nrcresearchpress.com by 210.87.254.40 on 09/05/12
For personal use only.

The photoreduction of terephthalophenone and a variety of other aromatic ketones has been studied by Pearson and Thiemann (2) and by other workers (3, 4, 7, 8). Our work on the photochemistry of aromatic ketones included a study of the photoreduction of 4-phenylterephthalophenone (**1**). It was expected that the carbonyl group adjacent to the biphenyl linkage would not undergo photopinacolization, but that the other carbonyl group might be photoreduced in the presence of isopropyl alcohol. For example, 4-phenylbenzophenone does not photoreduce to the pinacol under similar conditions (5).

The stoichiometry of the photoreduction of 4-phenylterephthalophenone (from the amount of acetone produced) indicated that each molecule of diketone **1** had abstracted two hydrogen atoms. Thus, it was thought that the diketone **1** was completely reduced to a polymer similar to that obtained in the case of terephthalophenone (2). However, examination of the i.r. spectrum of the product indicated that approximately 50% of the carbonyl functions still remained. The n.m.r. spectrum at this point indicated the presence of a methinyl hydrogen and hence a CHOH type linkage. The photoreduction product of **1** was tentatively identified as 4-(4-phenylbenzoyl)-benzhydrol (**2**) but the possibility of the isomer, 4-benzoyl-4′-phenylbenzhydrol (**3**) could not be ignored. To confirm the structure of the product, an independent synthesis of both isomers was carried out.

The ketoalcohol **2** was prepared by two slightly different methods. In one case, an excess of the Grignard reagent of 4-bromobiphenyl was allowed to react with 4-cyanobenzhydrol. In the other case, 4-biphenyllithium was prepared from 4-bromobiphenyl and butyllithium and allowed to react with 4-cyanobenzhydrol. These reactions are illustrated in reaction 1.

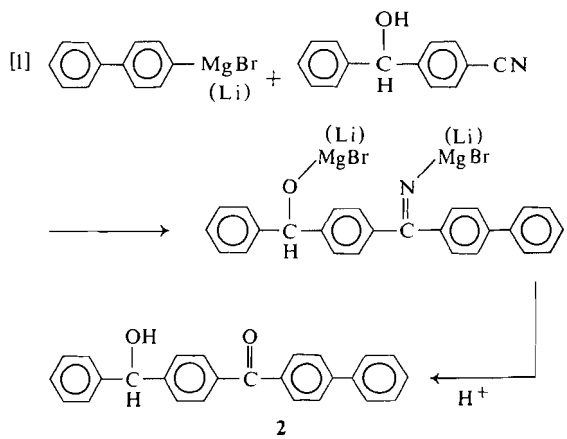

2

The yield of the lithium reaction was poor. The nitrile appears to be quite resistant to attack by the biphenyllithium, perhaps because the actual species being attacked is the lithium salt of 4-cyanobenzhydrol.

The Grignard method for preparing 4-(4-phenylbenzoyl)benzhydrol is the preferred method because of the superior yield and because the product obtained is considerably purer.

[1]For Parts I and II see refs. 1 and 2.
[2]Abstracted from the Ph.D. theses of D.P.T. and D.J.T.
[3]Present address: Sherwin-Williams Co. of Canada Ltd., Montreal, Quebec.

Can. J. Chem. Downloaded from www.nrcresearchpress.com by 210.87.254.40 on 09/05/12
For personal use only.

To obtain the isomeric ketoalcohol **3**, two methods were again developed, the second one a rather elegant and straightforward method avoiding the ketalization of the first method in reaction 2.

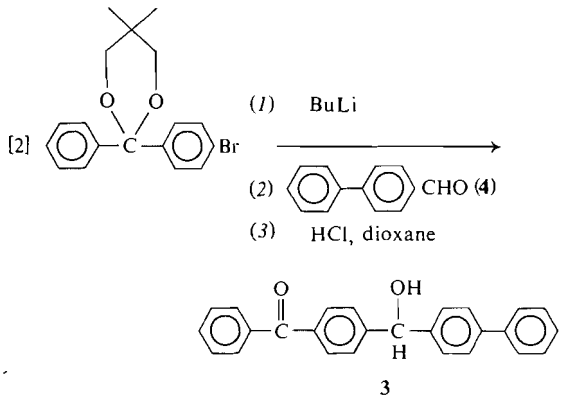

The two methyl groups of the protecting ketal in 4-bromobenzophenone neopentylene ketal, above, are chemically nonequivalent and are seen as two distinct singlets, δ 0.86 and 0.97, in the n.m.r.

The second method involved the addition of the biphenylyl-copper(I) directly to the ketoaldehyde **5** in reaction 3.

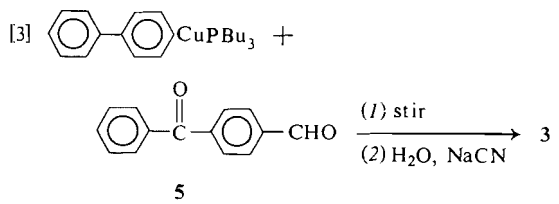

The melting points of the products from both methods were identical, 145–146°, and the yield of the second method, the arylcopper procedure, was 60%.

Results and Discussion

A comparison of the properties of the two isomers, **2** and **3**, and the product obtained on column chromatography of the irradiation mixture of 4-phenylterephthalophenone is given in Table 1.

The mass spectral data and u.v. spectra in Table 1 indicated that a mixture of the two isomers was at hand, an indication supported also by its wide melting point but good analysis. But the 100 MHz n.m.r. spectra truly confirmed the presence of a mixture whereby the two methinyl hydrogen signals, one for each of the isomers, were separate and distinct. From the comparative heights of these two signals obtained from the original crude mixture, the ratio of 4-benzoyl-4′-phenylbenzhydrol (**3**), to 4-(4-phenylbenzoyl)benzhydrol (**2**), was 2:1.

The isolation of the least probable isomer, **3**, in the largest amount is surprising. One possible mechanism is given in reaction 4.

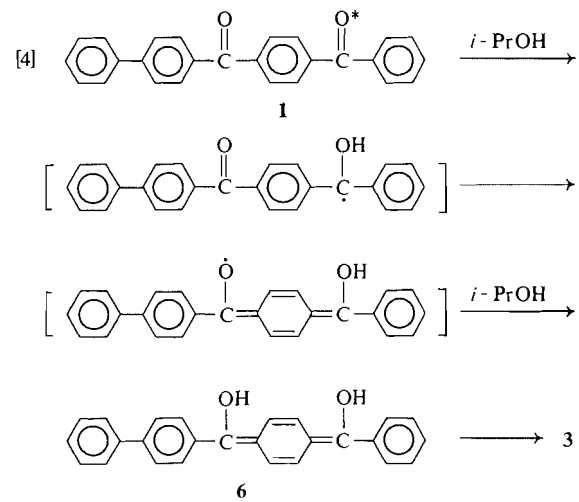

This mechanism is unlikely for several reasons. The intermediate **6** would be expected to give a bright yellow color similar to that of terephthalophenone (2). No color was observed during irradiation. The reduction is slow, and the product is the alcohol, not the pinacol.

The u.v. spectrum of 4-phenylterephthalophenone shows one absorption band at 298 mμ (ε 24 000) and another at 266 mμ (ε 30 000). Both of these are strong and appear to be π–π* bands. No n–π* band was observed. It is suggested that the photoreduction of 4-phenylterephthalophenone proceeds through a π–π* triplet. This is in agreement with the fact that the rate of photoreduction is quite slow. It is thought that the carbonyl next to the biphenyl group is the one which is excited in the π–π* band of lower energy and this accounts for the predominance of photoreduction at this carbonyl. The hydrogen abstracting power of the π–π* triplet is quite low and the rate of photoreduction is slow. Hence, the steady state concentration of ketyl radicals is very low and coupling to give the pinacol would be rare. Instead, the ketyl

TABLE 1. Comparison of product of irradiation of 4-phenylterephthalophenone and the independently prepared isomers

Compound	M.p.	N.m.r. (100 MHz) (p.p.m.)	Mass spectrum (70 eV)		U.v. (95% alcohol) ν_{max}	U.v. (95% alcohol) ε
4-(4-Phenylbenzoyl)benzhydrol	145.2–145.9	Methinyl 5.86 Aromatic 7.3–7.8	77(68) 155(2) 183(19) 364(96)	105(100) 181(88) 259(98)	291	24 800
4-Benzoyl-4′-phenylbenzhydrol	145.0–146.0	Methinyl 5.92 Aromatic 7.2–7.9	77(88) 155(75) 183(68) 364(94)	105(100) 181(50) 259(5)	257	34 700
Product of irradiation of 4-phenylterephthalophenone	136–138 softens at 132	Methinyl 5.92, 5.86 Aromatic 7.2–7.9	77(70) 155(47) 183(45) 364(100)	105(98) 181(61) 259(39)	261	26 600

radical would abstract a hydrogen atom from the solvent to form the secondary alcohol.

Experimental[4]

Irradiation of 4-Phenylterephthalophenone

4-Phenylterephthalophenone (0.205 g) was weighed into a 10-ml ampoule and 5.00 ml of a standard 80:20 pyridine – isopropyl alcohol solution added. The solution was then degassed with nitrogen, sealed with a serum cap, and irradiated as a stirred solution in a water bath at 25°. The irradiation was carried out using a Sylvania 400 W (H33-1CP), medium-pressure mercury lamp. The outer jacket of this lamp was made of borosilicate glass which cuts out all irradiation below 300 nm. The diketone **1** was not completely soluble in the pyridine solution but was soluble after 50 h of irradiation, the solution becoming a light yellow color. This color was not due to an oxygen-sensitive intermediate such as the one observed in the case of terephthalophenone (2).

After an irradiation period of 350 h, the yellow solution was allowed to stand for several days. During this time, 0.015 g of white platelets which proved to be starting diketone were deposited: m.p. 193–196°; m.p. of diketone **1** is 195°. The solvent was then removed from the irradiated solution and 0.19 g of a yellow crystalline solid was obtained. Chromatography on silica gel using hexane–chloroform gave 0.03 g of diketone **1** and 0.14 g of a white solid which was recrystallized from ethanol and from hexane. The spectral and physical data as compared to those of isomers **2** and **3** indicated that this compound was mainly 4-benzoyl-4′-phenylbenzhydrol (**3**): m.p. 136–138° (softens at 131°); i.r. (KBr) 3430, 1650, 1600, 1310, 1275, 755, 745, and 690 cm^{-1}; n.m.r. ($CDCl_3$) δ 2.9 (s (broad), 1, CHO*H* exchangeable with D_2O), 5.92 (s, 1, C*H*OH), 7.2–7.9 (m, 18, aromatic *H*); the u.v. and mass spectra are given in Table 1.

Anal. Calcd. for $C_{26}H_{20}O_2$: C, 85.69; H, 5.53. Found: C, 85.87; H, 5.54.

Preparation of 4-Cyanobenzhydrol

4-Cyanobenzhydrol was prepared by the reduction of the corresponding ketone with sodium borohydride at room temperature in isopropyl alcohol. After recrystallization from petroleum ether, a 90% yield of 4-cyanobenzhydrol was obtained: m.p. 67.8–69.3; i.r. (Nujol) 3460 (b), 2220, 1045, and 690 cm^{-1}; n.m.r. ($CDCl_3$) δ 3.90 (s (broad), 1, CHO*H*), 5.67 (s, 1, C*H*OH), 7.25–7.40 (d, 9, aromatic *H*).

Anal. Calcd. for $C_{14}H_{11}NO$: C, 80.36; H, 5.30. Found: C, 80.15; H, 5.18.

Preparation of 4-(4-Phenylbenzoyl)benzhydrol (2)

4-Cyanobenzhydrol (3.6 g, 0.017 mol) was treated with a three-fold excess of 4-biphenylmagnesium bromide in dry refluxing ether for 8–10 h. The magnesium complex precipitated and was removed by filtration. This was hydrolyzed with 10% hydrochloric acid and after work-up gave 3.0 g (44%) of 4-(4-phenylbenzoyl)benzhydrol. This was recrystallized from butyl chloride and isopropyl alcohol to give white platelets of **2**: m.p. 145.2–145.9°; i.r. (KBr) 3500 (broad), 1650, 930, 740, and 690 cm^{-1}; n.m.r. ($CDCl_3$) δ 2.8 (s, (broad), 1, CHO*H*), 5.86 (s, 1, C*H*OH), 7.3–7.8 (m, 18, aromatic *H*).

Anal. Calcd. for $C_{26}H_{20}O_2$: C, 85.69; H, 5.53. Found: C, 85.82; H, 5.49.

Preparation of 4-Phenylbenzaldehyde (4)

4-Bromobiphenyl (11.5 g, 0.05 mol) in 75 ml of dry ether was treated with 0.075 mol of butyllithium and the

[4]All melting points are uncorrected and were taken with a Thomas Capillary Melting Point Apparatus. N.m.r. spectra were taken with a Varian A-60 instrument. We are indebted to the National Science Foundation for aid (Grant 1683) in purchasing this instrument. Mass spectra were obtained with a LKB-9000 spectrometer and we are indebted to the National Science Foundation for aid (Grant GU-2057) in purchasing this instrument. I.r. spectra were obtained with a Beckman IR-10. U.v. spectra were obtained with a Cary 14 recording spectrophotometer. Analyses were by Galbraith Laboratories, Knoxville, Tenn.

Can. J. Chem. Downloaded from www.nrcresearchpress.com by 210.87.254.40 on 09/05/12
For personal use only.

Can. J. Chem. Downloaded from www.nrcresearchpress.com by 210.87.254.40 on 09/05/12
For personal use only.

exchange allowed to proceed at room temperature for 45 min. *N,N*-Dimethylformamide (19 g, 0.26 mol) was added cautiously at 0°. After addition, the solution was maintained at room temperature for 90 min prior to hydrolysis. After normal work-up and recrystallization from cyclohexane, 7.0 g (77%) of 4-phenylbenzaldehyde was obtained as white platelets: m.p. 58–59.5° (ref. 6 p. 401 m.p. 60°); i.r. (neat) 1700, 1600, 830, 750, and 690 cm^{-1}; n.m.r. (CCl_4) δ 7.2–7.9 (m, 9, aromatic *H*), 9.94 (s, 1, C*H*O).

Preparation of 4-Benzoyl-4′-phenylbenzhydrol Neopentylene Ketal (5)

4-Bromobenzophenone was treated with a slight excess of neopentyl glycol and a catalytic amount of *p*-toluenesulfonic acid in refluxing benzene to give a 91% yield of 4-bromobenzophenone neopentylene ketal. Recrystallization from ethanol gave white needles: m.p. 85.8–86.3; n.m.r. (CCl_4) δ 0.86 (s, 3, CH_3), 0.97 (s, 3, CH_3), 3.50 (s, 4, CH_2), 7.1–7.5 (m, 9, aromatic *H*).

Treatment of the above bromo ketal with an equivalent amount of butyllithium gave the corresponding 4-lithio compound which was then allowed to react with 4-phenylbenzaldehyde to give 4-benzoyl-4′-phenylbenzhydrol neopentylene ketal (**5**). Recrystallization from ethanol gave an 82% yield of **5**: m.p. 157.5–158.5; n.m.r. ($CDCl_3$) δ 0.92 (s, 3, CH_3), 0.97 (s, 3, CH_3), 2.33 (s (broad), 1, CHO*H*), 3.59 (s, 4, CH_2), 5.76 (s, 1, CHO*H*), 7.2–7.6 (m, 14, aromatic *H*).

Anal. Calcd. for $C_{31}H_{30}O_3$: C, 82.64; H, 6.71. Found: C, 82.50; H, 6.72.

Preparation of 4-Benzoyl-4′-phenylbenzhydrol (3)

The above ketal was hydrolyzed at room temperature for 48 h in 150 ml of dioxane and 50 ml of 10% hydrochloric acid. Recrystallization from benzene–hexane, from butyl chloride, and from isopropyl alcohol gave white platelets of 4-benzoyl-4′-phenylbenzhydrol: m.p. 145.0–146.0°; n.m.r. ($CDCl_3$) δ 3.0 (s (broad), 1, CHO*H*), 5.92 (s, 1, C*H*OH), 7.2–7.9 (m, 18, aromatic *H*); $u.v._{max}$ (95% ethanol) 257 nm (ε 34 700).

Anal. Calcd. for $C_{26}H_{20}O_2$: C, 85.69; H, 5.53. Found: C, 85.85; H, 5.52.

Alternate Method for Preparation of 4-Benzoyl-4-phenylbenzhydrol (3)

A solution of 4.8 g, 20.6 mmol, of 4-bromobiphenyl in 20 ml of ether was added to a solution of 8.5 ml of 2.45 *M* butyllithium (20.8 mmol) in 50 ml of dry THF and 40 ml of ether at −70° over a period of 2 min. After stirring at −70° for 2 min, the pasty, white slurry was warmed to 0° whereupon the solution cleared. At 0°, tributylphosphine (4.2 g, 20.8 mmol) was added followed by cuprous iodide (4.1 g, 20.8 mmol) giving a green, cloudy solution. To this solution, 4-benzoylbenzaldehyde (2.1 g, 10 mmol) was added in one lot and the mixture stirred at 0° for 1.5 h and at 25° for 1.5 h. *In a hood*, the dark green mixture was treated with water turning it brown and then with 40 ml of 10% aqueous sodium cyanide giving two yellow layers with a film of metallic copper at the interface. The ether phase was separated, washed with more sodium cyanide solution, water, and then dilute hydrochloric acid, water, and then dried with magnesium sulfate. After evaporation, the pale yellow solid, 5.3 g, was triturated with boiling hexane twice to yield 2.6 g of white solid, m.p. 125–139°. Recrystallization from 20 ml of benzene and 30 ml of hexane gave 2.2 g (61%) of white crystals, m.p. 143.5–145.5°. An analytical sample melted at 145–146°.

Anal. Calcd. for $C_{26}H_{20}O_2$: C, 85.69; H, 5.53. Found: C, 85.94; H, 5.74.

The n.m.r. was identical to that of **3** prepared via the lithium exchange reaction.

The authors are indebted to the Stenographic Services of the Richard B. Russell Research Center, Athens, Georgia and Mrs. I. B. Reid of the Technical Dept., Sherwin-Williams Co. of Canada Ltd., Montreal, Quebec, for aid in preparation of this manuscript.

1. D. E. Pearson and M. Y. Moss. Tetrahedron Lett. 3791 (1967).
2. D. E. Pearson and D. P. Thiemann. J. Polym. Sci. Part A-1. **8**, 2103 (1970).
3. J. Higgins and D. A. McCombs. Chem. Tech. 176 (1972).
4. F. C. Deschryer, T. Tran Van, and G. Smets. J. Polym. Sci. Part B. **9**, 425 (1971).
5. W. D. Cohen. Rec. Trav. Chim. **39**, 243 (1920).
6. I. Heilbron. Dictionary of organic compounds. Oxford University Press, 1965.
7. J. Higgins, A. H. Johannes, J. F. Jones, R. Schulta, D. A. McCombs, and C. S. Menon. J. Polym. Sci. Part A-1, **8**, 1987 (1970).
8. D. A. McCombs, C. S. Menon, and J. Higgins. J. Polym. Sci. Part A-1, **9**, 1261 (1971).

The Carbon-13 Nuclear Magnetic Resonance Spectra of 2-Acetamido-2-deoxy-D-hexoses and some Specifically Deuteriated, *O*-Acetylated, and Phosphorylated Derivatives[1]

D. R. BUNDLE,[2] H. J. JENNINGS, AND IAN C. P. SMITH

Division of Biological Sciences, National Research Council of Canada, Ottawa, Canada K1A 0R6

Received June 7, 1973

The ^{13}C n.m.r. spectra of the 2-acetamido-2-deoxy-D-hexoses and some 3-*O*-acetyl and 1-phosphate derivatives are assigned and discussed. To facilitate the interpretation of the spectra, an initial assignment of the resonances in the spectrum of 2-acetamido-2-deoxy-D-glucose was required. For this purpose, both the 3-^2H and 4-^2H derivatives of this acetamido-hexose were synthesized. These syntheses are reported together with those of 2-acetamido-3-*O*-acetyl-2-deoxy-D-glucose and 2-acetamido-2-deoxy α- and β-D-glucose-1-phosphate. These model compounds were used to study substituent effects related to the 2-acetamido-2-deoxy-D-hexose-containing polysaccharide antigens of *N. meningitidis*.

On explique et on discute des spectres r.m.n. du ^{13}C d'acétamido-2 déoxy-2 D-hexoses et de quelques dérivés *O*-acétyle-3 et phosphate-1. Afin de faciliter l'interprétation des spectres, une attribution initiale des résonances dans le spectre de l'acétamido-2 deoxy-2 D-glucose a dû être effectuée. Dans ce but les dérivés ^2H-3 et ^2H-3 de cet acetamido hexose ont tous deux été synthétisés. Ces synthèses sont rapportées ainsi que celles de l'acétamido-2 *O*-acétyle-3 déoxy-2 D-glucose et de l'acétamido-2 déoxy-2 α- et β-D-glucose phosphate-1. Ces composés modèles ont été utilisés afin d'étudier les effets des substituants reliés au polysaccharide antigène de la *N. meningitidis* contenant l'acétamido-2 déoxy-2 D-hexose.

[Traduit par le journal]

Can. J. Chem. 51, 3812 (1973)

Introduction

To assist in our structural studies on the hexosamine-containing meningococcal polysaccharide antigens using ^{13}C n.m.r. (1), we required chemical shift data on a number of their monomeric units. Although the ^{13}C spectra of the hexoses have been well documented (2–5), only a preliminary investigation of one of the hexosamines (D-glucosamine hydrochloride) has been reported (6). The two hexosamine-containing meningococcal polysaccharides under investigation were those from Serogroup A and X. The former has been shown to be a partially *O*-acetylated 2-acetamido-2-deoxy-mannose phosphate homopolymer (7) and the latter a 2-acetamido-2-deoxy-glucose phosphate homopolymer (8). Therefore, in addition to the assignment of the resonances in the ^{13}C spectra of the hexosamines, the effects of 3-*O*-acetylation and anomeric phosphorylation of 2-acetamido-2-deoxy-D-glucose were studied. These model compounds and the 3-^2H and 4-^2H derivatives of 2-acetamido-2-deoxy-D-glucose were synthesized. The ^{13}C data for the latter compounds formed the basis of the assignments made in the spectra of the other 2-acetamido-2-deoxy-hexoses and the 3-*O*-acetyl and 1-phosphorylated derivatives of 2-acetamido-2-deoxy-D-glucose. Published data (9) on the equilibrated mixtures of the 2-acetamido-2-deoxy-D-hexoses were also correlated with peak intensities in the spectra to corroborate the assignments.

Results and Discussion

Synthesis

The synthesis of the 3-^2H, 4-^2H, and 3-*O*-acetyl derivatives of 2-acetamido-2-deoxy-D-glucose was accomplished by the initial synthesis of benzyl 2-acetamido-2-deoxy-β-D-glucopyranoside (**1**). This derivative was chosen in order that the reducing sugar could be generated under the mild conditions of hydrogenolysis. Previous methods employed for the synthesis of benzyl glycosides involving acid-catalyzed glycosidation have resulted in either low yields (10) or the formation of an anomeric mixture of glycosides (11) depending on the temperature used. The method described herein involves the Königs-Knorr condensation of 2-acetamido-3,4,6-tri-*O*-acetyl-2-deoxy-α-D-glucopyranosyl chloride with benzyl alcohol; it gave benzyl 2-acetamido-3,4,6-tri-*O*-acetyl-2-deoxy-β-D-glucopyranoside (**2**) in good

[1]Issued as NRCC No. 13416.

[2]NRCC Postdoctorate Fellow 1971–1973.

Can. J. Chem. Downloaded from www.nrcresearchpress.com by 210.87.254.42 on 09/05/12
For personal use only.

Can. J. Chem. Downloaded from www.nrcresearchpress.com by 210.87.254.42 on 09/05/12
For personal use only.

yields (85%) from which **1** could be produced in quantitative yields by catalytic deacetylation.

The 3-^{2}H derivative of 2-acetamido-2-deoxy-D-glucose was prepared by the initial oxidation of benzyl 2-acetamido-4,6-*O*-benzylidene-2-deoxy-β-D-glucopyranoside (**5**) using dimethylsulfoxide and acetic anhydride (12). This oxidation gave almost quantitative yields of benzyl 2-acetamido-4,6-*O*-benzylidene-2-deoxy-β-D-*ribo*-hexopyranosid-3-ulose (**8**). Following the

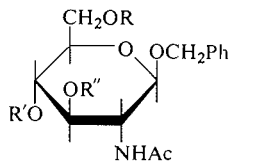

1 R = R′ = R″ = H
2 R = R′ = R″ = Ac
3 R = R′ = H; R″ = Ac
4 R = Tr; R′ = H; R″ = Ac

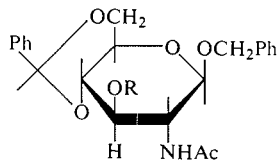

5 R = H
6 R = CH_2Ph

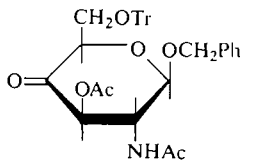

7

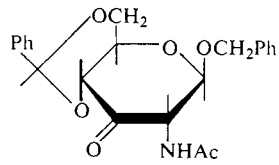

8

reduction of **8** with sodium borodeuteride and subsequent deacetylation; the benzyl glycosides of the D-*gluco* and D-*allo* epimers were separated by the method of Austin and co-workers (13). Catalytic hydrogenation of the separated benzyl glycosides yielded 3-^{2}H-2-acetamido-2-deoxy-D-glucose and its D-*allo* epimer in the ratio of 2.4:1.0 respectively.

The synthesis of 4-^{2}H-2-acetamido-2-deoxy-D-glucose was performed in a similar manner but the synthesis of the initial 4-ketone proved to be more difficult. Oxidation experiments involving ester blocking groups (14) on C-6 and -3 of **1** resulted in extensive degradation and poor yields of the 4-ketone using both dimethylsulfoxide – acetic anhydride and ruthenium tetroxide (15). The desirability of ether protecting groups was indicated and an attempt to prepare the initial 3-*O*-benzyl ether was made. The benzylation of **5** was attempted using benzyl chloride, but the reaction produced extremely low yields of **6** (10–15%) presumably due to *N*-benzylation (16). Therefore, this route was abandoned. It was discovered eventually that the introduction of an ether group at C-6 was the critical factor involved in obtaining good yields of the oxidation product, presumably avoiding the problem of β-elimination, which is probably promoted by an ester group at C-6. Compound **5** was acetylated at C-3 and the benzylidene group was removed by selective acidic hydrolysis to give crystalline **3**. Compound **3** was tritylated at C-6 to yield crystalline benzyl 2-acetamido-3-*O*-acetyl-6-*O*-trityl-2-deoxy-β-D-glucopyranoside (**4**) which was oxidized using dimethylsulfoxide – acetic anhydride (12) to give excellent yields of benzyl 2-acetamido-3-*O*-acetyl-6-*O*-trityl-2-deoxy-β-D-*xylo*-hexopyranosid-4-ulose (**7**). The 4-ketone (**7**) was reduced with sodium borodeuteride, deacetylated, and detritylated. The benzyl group was removed from the epimeric mixture of glycosides by an identical procedure to that used previously. The resultant 4-^{2}H-2-acetamido-2-deoxy-D-glucose and its D-*galacto* epimer were separated by preparative paper chromatography.

2-Acetamido-3-*O*-acetyl-2-deoxy-D-glucose was prepared by the catalytic hydrogenolysis of **3**, and the α- and β-1-phosphate derivatives were prepared by the method previously reported to yield the crystalline α-1-phosphate derivative (17). Using this method we obtained a mixture of both the α- and β-anomers which were used as an unresolved mixture in the n.m.r. determinations.

^{13}C *Nuclear Magnetic Resonance*

The carbon-13 chemical shifts of the 2-acetamido-2-deoxy-α- and -β-D-hexoses are shown in Table 1. In general the chemical shifts of the individual carbons of each acetamido-hexose can be correlated with the observed chemical shifts of its analogous hexose (4, 5) except for some characteristic differences associated with the introduction of an acetamido group at C-2 of the pyranose ring. Thus the lowest field signals (175.7–176.1 p.p.m.) and the highest field signals (23.2–23.5 p.p.m.) are assigned to the carbonyl and methyl moieties of the 2-acetamido groups. In addition the 2-acetamido group resulted in a substantial upfield shift of the C-2 signal relative to that of their analogous hexoses and enabled C-2 to be assigned quite readily. This displacement of the C-2 resonance was found to be 17.6 p.p.m. for 2-acetamido-2-deoxy-D-glucose; a displacement of considerable magnitude has also been reported for 2-amino-2-deoxy-D-glucose hydrochloride (6). The resonances at 92.1–

Can. J. Chem. Downloaded from www.nrcresearchpress.com by 210.87.254.42 on 09/05/12
For personal use only.

TABLE 1. Carbon-13 chemical shifts[a] for 2-acetamido-2-deoxy-hexoses and some *O*-acetylated and phosphorylated derivatives

Compound	C-1	C-2	C-3	C-4	C-5	C-6	CH_3 (—$NHCOCH_3$)	C=O (—$NHCOCH_3$)	Σ ^{13}C chemical shifts[b]
α-D-GlcNAc	92.1	55.3	72.0[c]	71.4[c]	72.8	61.9	23.3	175.7	425.6
β-D-GlcNAc	96.2	58.0	75.2[c]	71.2[c]	77.2	62.0	23.5	175.9	439.6
α-D-ManNAc	94.3	54.4	70.1	68.0	73.2	61.7	23.2	175.9	421.7
β-D-ManNAc	94.3	55.3	73.2	67.8	77.5	61.7	23.2	176.8	429.7
α-D-GalNAc	92.2	51.4	68.6	69.7[c]	71.6	62.4	23.2	176.1	415.9
β-D-GalNAc	96.5	54.9	72.3	69.0[c]	76.3	62.2	23.4	175.8	431.1
α-D-GlcNAc-1-phosphate	93.9[d]	55.3[e]	72.6	71.2	73.2	61.9	23.2	175.8	—
β-D-GlcNAc-1-phosphate	96.7[f]	57.7[g]	75.3	71.2	77.4	62.3	23.6	176.2	—
3-*O*-acetyl-α-D-GlcNAc	92.2	53.4	75.1	69.1	72.6	61.7	23.2 21.5[h]	175.5 175.1[h]	—
3-*O*-acetyl-β-D-GlcNAc	95.6	56.3	77.0	69.1	77.0	61.8	23.0 21.5[h]	175.7 175.1[h]	—

[a]In p.p.m. from external tetramethylsilane.
[b]Sum of chemical shifts of carbons 1–6.
[c]Resonances assigned by deuterium labelling.
[d]$^2J_{^{31}P-^{13}C} = 5.0$ Hz.
[e]$^3J_{^{31}P-^{13}C} = 6.9$ Hz.
[f]$^2J_{^{31}P-^{13}C} = 4.3$ Hz.
[g]$^3J_{^{31}P-^{13}C} = 7.2$ Hz.
[h]Resonances assigned to the *O*-acetyl group.

Can. J. Chem. Downloaded from www.nrcresearchpress.com by 210.87.254.42 on 09/05/12
For personal use only.

96.5 p.p.m. were attributed to the anomeric carbons (C-1) by comparison with the equivalent downfield position of the C-1 resonance in the hexose series (4, 5). The resonances at 62.0 and 61.9 p.p.m. in the spectrum of 2-acetamido-2-deoxy-D-glucose were assigned to C-6 of the β- and α-anomers, respectively, by the appearance of triplets of relative intensity 1:2:1 in the undecoupled spectrum and by their relative intensities. Unequivocal assignment of the remaining resonances (C-3, -4, and -5) in the spectrum of 2-acetamido-2-deoxy-D-glucose were accomplished by utilizing the loss in intensity due to lack of nuclear Overhauser enhancement and the presence of spin coupling to ^2H caused by deuteration (18, 19). A comparison of the spectra of 2-acetamido-2-deoxy-D-glucose and its 3-^2H and 4-^2H derivatives is shown in Fig. 1. These spectra illustrate quite clearly that substitution of deuterium for hydrogen caused the complete collapse of resonances attributable to C-3 and -4 of the α- and β-anomers of 2-acetamido-2-deoxy-D-glucose. Similar disappearances of these signals have been obtained using deuteriated glucose (20). Except for C-4 of 2-acetamido-2-deoxy-D-galactose, which was also assigned by deuterium labelling, all the other assignments in Table 1 were made tentatively by correlation with those assigned for 2-acetamido-2-deoxy-D-glucose and corroborated by comparison with the published data on the hexoses (4, 5).

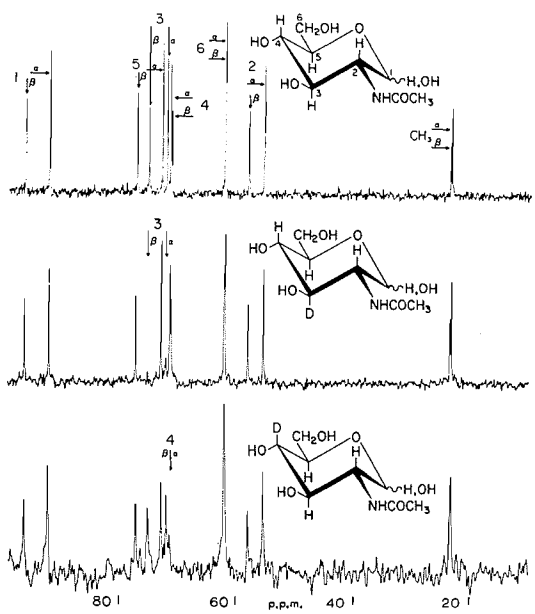

FIG. 1. Comparison of the ^{13}C n.m.r. spectrum of 2-acetamido-2-deoxy-α- and -β-D-glucose with the spectra of its 3-^2H and 4-^2H derivatives.

The dependence of all carbon resonances (with the exception of C-4 for the 1-phosphate and 3-*O*-acetyl derivatives) on the anomeric configuration of the compounds in Table 1 is striking. Similar behavior for C-2 to C-5 has been detected for glucose, galactose, and mannose (4) but the higher resolution available with second generation spectrometers allows observation of a small effect on C-6 (21). It is also noteworthy that the methyl and carbonyl groups of the acetamido moiety on C-2 are sensitive to the anomeric configuration. Thus, all the ^{13}C resonances allow estimates of the dominant anomers at equilibrium which are in qualitative agreement with values determined by more conventional means (9).

Most of the empirical relationships that can be obtained from the chemical shift data on the 2-acetamido-2-deoxy-D-hexoses were found to be similar to those previously found for the analogous hexoses (4). This is not surprising in view of their close structural and conformational relationships. Chemical shift differences due to the change in orientation at the anomeric center, obtained from Table 1, are only marginally different from those obtained from the equivalent hexose data (4), C-1, -2, -3, and -5 being the most affected. It is interesting to note, however, that, although the C-1 anomeric shift difference was the smallest for D-mannose in the hexose series (4), in the case of 2-acetamido-2-deoxy-D-mannose the C-1 signals of the α- and β-anomers are coincident.

Another similarity with the hexose data is the comparison of the overall shielding of the ring carbons as measured by the sum of the observed chemical shifts in each sugar (4). These are recorded in Table 1 and indicate that the α- and β-2-acetamido-2-deoxy-D-hexoses can be placed in the same order as their analogous hexoses. This order has been shown to reflect broadly the differences in conformational stability of the hexoses (4).

The influences of axial groups on the other ring carbons have been studied in derivatives of cyclohexane (22–24), the inositols (25), and the aldohexoses (4, 5). The axial group has been shown to result in changes in chemical shift on the α-carbon to which it is attached, the adjacent β-carbon, and the γ-carbon, but only slightly the

TABLE 2. Carbon-13 shielding differences (p.p.m.)[a] between epimeric 2-acetamido-2-deoxy-hexoses

Epimers	C-1	C-2	C-3	C-4	C-5	C-6
α-D-*gluco* – α-D-*manno*	−2.2	+0.9	+1.9	+3.4	−0.4	+0.2
β-D-*gluco* – β-D-*manno*	+1.9	+2.7	+2.0	+3.4	−0.3	+0.3
α-D-*gluco* – α-D-*galacto*	−0.1	+3.9	+3.4	+1.7	+1.2	−0.5
β-D-*gluco* – β-D-*galacto*	−0.3	+3.1	+2.9	+2.2	+0.9	−0.2

[a]Obtained from data in Table 1.

TABLE 3. Carbon-13 shielding differences (p.p.m.)[a] between 2-acetamido-2-deoxy-D-glucose and its substituted derivatives

Substituent	C-1	C-2	C-3	C-4	C-5	C-6
3-*O*-Acetyl (α-D)	+0.1	−1.9	+3.1	−2.3	−0.2	−0.2
3-*O*-Acetyl (β-D)	−0.6	−1.7	+1.8	−2.1	−0.2	−0.2
1-Phosphate (α-D)	+1.8	0.0	+0.6	−0.2	+0.4	0.0
1-Phosphate (β-D)	+0.5	−0.3	+0.1	0.0	+0.2	+0.3

[a]Obtained from data in Table 1; a positive difference indicates that the resonance in the substituted compound occurs at lower magnetic field.

δ-carbon. Table 2 illustrates the effect of the introduction of axial groups to the 2-acetamido-2-deoxy-α- and -β-D-hexoses using the α- and β-D-*gluco* epimers as the reference molecules. The axial acetamido group at C-2 of 2-acetamido-2-deoxy-α- and -β-D-mannose gave shieldings very similar to those found for the axial hydroxyl group on C-2 of mannose (4) except for a significant enhancement in the magnitude of the shielding effect on C-4 (γ-carbon). This enhancement which was approximately 1.0–1.3 p.p.m. could be attributed to the increase in axial shielding of the γ-carbon (4, 25) due to the larger size of the acetamido group when compared to the smaller hydroxyl group at C-2 of D-mannose. However, this enhancement persisted in the opposite situation found in 2-acetamido-2-deoxy-α- and -β-D-galactose, where an axial hydroxyl group at C-4 is situated γ to an equatorial acetamido group on C-2. Obviously in this case the enhancement (1.3 p.p.m.) over the effect found in D-galactose cannot be due to steric factors involving the larger size of the acetamido group and other factors must be invoked.

Substituent effects on the chemical shifts of the ring carbons of 2-acetamido-2-deoxy-D-glucose are listed in Table 3. The differences were obtained by comparison of the spectra of the α- and β-anomers of the substituted and unsubstituted compounds. The introduction of a 3-*O*-acetyl group had a profound effect on the α-carbon (C-3) and also the β-carbons (C-2 and -4); the effect diminishes at the γ-carbons (C-1 and -5). The substituent effect on the α-carbon is well documented for the methyl hexopyranosides (4), 3-*O*-methyl-D-glucose (4, 5) and some *O*-methylated inositols (25). In all cases the α-carbon was considerably deshielded, resulting in a downfield shift of its resonance by 7–10 p.p.m. By comparison, a considerably smaller downfield shift was caused by the 3-*O*-acetyl substitution of 2-acetamido-2-deoxy-D-glucose (3.1 and 1.8 p.p.m. for the α- and β-anomers respectively). However, of considerable interest was the increased shielding of the β-carbons by the *O*-acetyl group when compared to that caused by an *O*-methyl group in aldopyranose molecules. This shift in 2-acetamido-3-*O*-acetyl-2-deoxy-D-glucose of approximately 2.0 p.p.m. is of much greater magnitude than that reported (5) for the equivalent 3-*O*-methyl shift in D-glucose (0.5–1.0 p.p.m.). This could be due to the conformation adopted by the *O*-acetyl group on the pyranose ring (26).

Addition of a phosphate group at C-1 of 2-acetamido-2-deoxy-D-glucose resulted in downfield shifts of the C-1 resonances (0.5 and 1.8 p.p.m. for the β- and α-anomers, respectively) which were smaller than those observed (~2.5 p.p.m.) for substitution at C-2′, -3′, or -5′ of the ribose moiety of nucleosides (27–31). This reflects the special properties of the anomeric center. The deshielding effects of the phosphate group are also considerably smaller than those obtained by the introduction of an anomeric methyl group in the hexoses (4). Unlike the introduction

Can. J. Chem. Downloaded from www.nrcresearchpress.com by 210.87.254.42 on 09/05/12
For personal use only.

Can. J. Chem. Downloaded from www.nrcresearchpress.com by 210.87.254.42 on 09/05/12
For personal use only.

of an *O*-acetyl group on C-3 of 2-acetamido-2-deoxy-D-glucose the substituent effect of the anomeric phosphate group was not relayed to the adjacent β-carbon (C-2) to any extent, as observed in the ribose series (27–31). This has also been found to be the case with the methyl glycopyranosides (4) where the large substituent effect on C-1 is only relayed to a minimum extent to C-2.

Couplings between ^{31}P and ^{13}C are also manifest in the spectra of the phosphates, Table 1. In the nucleotides the couplings through two bonds ($^2J_{^{31}P-^{13}C}$) were found to be 5 ± 1 Hz (27–31). The two bond couplings for the anomeric 2-acetamido-2-deoxy-D-glucose phosphates also fall within this range. The three bond couplings between ^{31}P and ^{13}C ($^3J_{^{31}P-^{13}C}$) have been shown previously to depend on the dihedral angle between the ^{31}POC and $OC^{13}C$ planes, allowing an estimation of the populations of the possible rotational isomers (27–31). The data in Table 1 ($^3J_{P,C-2} \approx 7$ Hz) indicate that the monomeric phosphates have a strong preference for the extended conformation, C_2-*trans*, as has been found for the corresponding polysaccharides (1).

Experimental

Melting points were determined on a Fisher-Johns apparatus and are uncorrected, and optical rotations were measured at 21 ± 3°. Preparative paper chromatography was carried out on Whatman 3MM paper impregnated with sodium tetraborate using the solvent system (v/v), butan-1-ol – pyridine – water (4 : 6 : 3) (32). T.l.c. was performed on silica gel coated plates with the following solvent systems (v/v): (A) benzene – propan-1-ol (4 : 1) and (B) benzene–acetone (4 : 1). An F and M (model 420) chromatograph was used for g.l.c. analysis using a 10% Neopentylglycol sebacate column at 240°. ^{13}C n.m.r. spectra were recorded in 12 mm tubes at 37° on a Varian XL-100-15 spectrometer operating at 25.16 MHz in the pulsed Fourier transform mode with complete proton decoupling. The computers used in these studies (Varian 620-i and Varian 620-L) allowed aquisition of 4096 and 8192 output data points, respectively, in the transformed spectra. Chemical shifts are reported in parts per million (p.p.m.) downfield from external tetramethylsilane, and deuterium oxide was used as the source of the lock signal. All the 2-acetamido-2-deoxy-hexoses and derivatives were run in deuterium oxide, at concentrations of 100 mg/ml, after having attained their mutarotational equilibria.

Benzyl 2-Acetamido-3,4,6-tri-O-acetyl-2-deoxy-β-D-*glucopyranoside (2)*

Benzyl alcohol (300 ml, 3 mol), previously dried over 3A molecular sieve, was stirred with Drierite (100 g) and mercuric cyanide (84 g) for 1 h in anhydrous benzene before the addition of 2-acetamido-3,4,6-tri-*O*-acetyl-α-D-glucopyranosyl chloride (33) (63 g, 0.17 mol). The suspension was stirred vigorously for 48 h and then poured into chloroform (1 l). The chloroform solution was filtered, extracted with 10% sodium chloride, washed (×3) with water, and dried over anhydrous sodium sulfate. Concentration of the solution, initially at 12 mm Hg and then at 1 mm Hg to remove excess benzyl alcohol gave a syrup that crystallized after dissolution in hot ethanol. Concentration of the mother liquors yielded further product. Recrystallization from ethanol gave crystals (64 g, 85%) of m.p. 168–169° and $[\alpha]_D$ −41° (*c*, 1.0 in methanol). These constants are in close agreement with those quoted in the literature (33).

Benzyl 2-Acetamido-2-deoxy-β-D-*glucopyranoside (1)*

Sodium (20 mg) in methanol (4 ml) was added to a solution of **2** (43.2 g) in methanol (600 ml) and the solution kept for 16 h at 4°. Long colorless needles (21 g, 94%) of **1** were formed having m.p. 206–207° and $[\alpha]_D$ −48.5° (*c*, 1.0 in water). Lit. (11) reports m.p. 207–208° and $[\alpha]_D$ −48.0 (in water for **1**).

Benzyl 2-Acetamido-4,6-O-benzylidene-2-deoxy-β-D-*ribo-hexopyranosid-3-ulose (8)*

Benzyl 2-acetamido-4,6-*O*-benzylidene-2-deoxy-β-D-glucopyranoside (**5**) (11) (10 mmol) in dimethylsulfoxide (70 ml) and acetic anhydride (25 ml) was stirred and allowed to stand at room temperature for 48 h. The reaction mixture was poured into saturated sodium bicarbonate solution (1 l) which caused the precipitation of crude **8**. The precipitate was filtered, washed extensively with cold water, and dried in a vacuum over phosphorus pentoxide. Recrystallization of the residue (3.7 g) from chloroform–acetone gave crystalline **8** (2.7 g, 67%) of m.p. 262–265° (dec.) and $[\alpha]_D$ −65.5° (*c*, 1.0 in dioxane). ν_{max} 1740 (C=O) and 1655 cm^{-1} (—$NHCOCH_3$).

Anal. Calcd. for $C_{22}H_{23}O_6N$: C, 66.49; H, 5.83; N, 3.52. Found: C, 65.93; H, 5.59; N, 3.31.

Benzyl 2-Acetamido-3-^{2}H-2-deoxy-β-D-*gluco- and* -D-*allo-pyranosides*

Crystalline **8** (2.5 g) was stirred in methanol (800 ml) with sodium borodeuteride (800 mg) for 16 h at room temperature. During the reduction the insoluble ketone (**8**) dissolved and then some of the epimeric products began to precipitate. The solution was concentrated to a solid residue, the residue was dissolved in chloroform, and the chloroform solution was washed with dilute acetic acid, water (×3), and dried over anhydrous sodium sulfate. Removal of the sodium sulfate by filtration and concentration of the chloroform solution gave a solid residue (2.3 g) containing the 3-^{2}H derivative of **5** and its D-*allo* epimer. Removal of the benzylidene group was accomplished by heating the residue at 100° in 75% acetic acid until solution was complete (15 mm). The resulting solution was evaporated to dryness and co-evaporated a number of times with water and toluene. The white solid (1.5 g) was dissolved in the minimum amount of water containing several drops of ethanol (total volume 5 ml) which was applied to a column 2.5 × 30 cm of ion-exchange resin (Dowex 1-X2, 200–400 mesh) (OH^- form) which was eluted with water. Fractions (5 ml) were monitored for u.v. absorption (280 mμ). Two peaks were obtained and the corresponding fractions were concentrated to dryness and recrystallized from ethanol. The D-*gluco*

Can. J. Chem. Downloaded from www.nrcresearchpress.com by 210.87.254.42 on 09/05/12
For personal use only.

isomer (500 mg) had m.p. 208–209° and $[\alpha]_D$ −47° (*c*, 1.0 in water). Lit. reports (11) m.p. 207–208° and $[\alpha]_D$ −48 (H_2O). The D-*allo* isomer (300 mg) had m.p. 165–168° and $[\alpha]_D$ −119 (*c*, 1.0 in pyridine). Lit. reports (34) m.p. 156–158° and $[\alpha]_D$ −114° (pyridine).

2-Acetamido-3-^{2}H-2-deoxy-D-*glucose and* -D-*allose*

The epimeric benzyl glycosides above (250 mg) were dissolved separately in ethanol–water (50 ml) and hydrogenated over palladium black (50 mg) for 4 h at room temperature. The solutions were then filtered and concentrated to dryness. The homogeneity of each product was determined by g.l.c. analysis of a small sample of its reduced peracetate (35) using authentic samples of 2-acetamido-2-deoxy-D-glucitol and its D-allitol epimer prepared as described by Gross and Jeanloz (11). Both homogeneous epimers were used without recrystallization for the n.m.r. determinations.

Benzyl 2-Acetamido-3-O-acetyl-2-deoxy-β-D-*glucopyranoside (3)*

Crystalline **5** (7 g) was treated in pyridine (150 ml) with acetic anhydride (10 ml) and the reaction left to stand for 16 h. The solution was poured into ice–water (1.5 l) and a highly crystalline product was filtered off after 30 min. Benzyl 2-acetamido-3-*O*-acetyl-4,6-*O*-benzylidine-2-deoxy-β-D-glucopyranoside (7.6 g, 98%) was obtained directly in an analytically pure state, the physical constants being identical to those reported in the literature (11). Removal of the 4,6-benzylidene group was achieved by heating it with 75% aqueous acetic acid at 100° for 40 min. Concentration of the solution to dryness and co-evaporation with water and toluene left a solid residue which was recrystallized from ethanol–water to give crystals (4.25 g, 70% based on **5**) of m.p. 184–185° and $[\alpha]_D$ −78° (*c*, 2.0 in methanol).

Anal. Calcd. for $C_{17}H_{23}O_7N$: C, 57.76; H, 6.56; N, 3.96. Found: C, 57.68; H, 6.66: N, 3.86.

Benzyl 2-Acetamido-3-O-acetyl-6-O-trityl-2-deoxy-β-D-*glucopyranoside (4)*

A solution of **3** (6 g) in pyridine (100 ml) was stirred with triphenylchloromethane (4.35 g) and left for 3 days at room temperature. T.l.c. analysis in solvent A indicated that the reaction was complete after 2.5 days. The reaction mixture was poured into ice–water and the solid product was allowed to settle after which the supernatant was decanted. The solid was dissolved in chloroform (500 ml) and the chloroform solution was washed (×3) with water and dried over anhydrous sodium sulfate. Concentration of the solution to 30 ml and the addition of light petroleum (b.p. 30–60°) gave crystals of **4** (4.5 g). A further 3 g of **4** was obtained from the mother liquors by an identical procedure. Total yield of **4** was 7.5 g (74%). It had m.p. 122–124° and $[\alpha]_D$ −58° (*c*, 2.0 in chloroform).

Anal. Calcd. for $C_{36}H_{37}O_7N$: C, 72.60; H, 6.22; N, 2.35. Found: C, 72.98; H, 6.36; N, 2.15.

Benzyl 2-Acetamido-3-O-acetyl-6-O-trityl-2-deoxy-β-D-*hexopyranosid-4-ulose (7)*

Crystalline **4** (3 g) was dissolved in dimethylsulfoxide (20 ml) and to this solution was added acetic anhydride (10 ml). The oxidation was left at room temperature and monitored by t.l.c. analysis in solvent B. After 48 h no trace of **4** was detectable and the reaction mixture was poured into ice–water (400 ml). After 10 min the aqueous phase was decanted from an oil which had separated at the bottom of the beaker. The oil was dissolved in chloroform and the chloroform solution was washed with water, dried over anhydrous sodium sulfate, filtered, and concentrated to a syrup (2.7 g). Trituration of the syrup with ether caused it to crystallize and recrystallization from di-isopropyl ether containing a few drops of ethanol gave crystalline **7** of m.p. 165–167° and $[\alpha]_D$ −33.5° (*c*, 2.4 in chloroform). ν_{max} 1760 (C=O), 1740 ($OCOCH_3$), and 1670 cm^{-1} ($NHCOCH_3$).

Anal. Calcd. for $C_{36}H_{35}O_7N$: C, 72.85; H, 5.90; N, 2.36. Found: C, 72.15; H, 6.11; N, 2.18.

2-Acetamido-4-^{2}H-2-deoxy-D-*gluco- and* -D-*galactopyranose*

Crystalline **7** (1.6 g) was dissolved in methanol (50 ml) and sodium borodeuteride (400 mg) was added. The solution was allowed to stand for 16 h and was then concentrated to a solid residue. The residue was dissolved in 80% acetic acid containing a trace of ethanol and the solution was heated at 100° for 30 min. The solution was once more evaporated to a solid residue and the borate was removed by co-distillation with methanol. The solid residue (750 mg) was dissolved in ethanol–water containing a trace of acetic acid and hydrogenated over palladium black (100 mg). Filtration and concentration of the solution followed by g.l.c. analysis of the products as described previously (35) indicated that 2-acetamido-2-deoxy-D-glucose and its D-*galacto* epimer were the sole products of the reduction of **7**. The epimeric mixture of 4-^{2}H-2-acetamido-2-deoxy-hexoses were separated by preparative paper chromatography in solvent C (32). Borate was removed from each fraction by co-distillation with methanol and the syrupy products, shown to be pure by g.l.c. analysis (35), were used in the n.m.r. determinations without crystallization.

2-Acetamido-3-O-acetyl-2-deoxy-D-*glucose*

Crystalline **3** (400 mg) was dissolved in aqueous ethanol and hydrogenated over palladium black catalyst (50 mg). After 16 h the uptake of hydrogen had ceased and the catalyst was removed by filtration. Concentration of the clear filtrate gave a mobile syrup which crystallized on standing. Recrystallization from ethanol–ether (1:2) gave crystals (200 mg, 67%) of m.p. 157–160° having $[\alpha]_D$ +19° (*c*, 1.0 in ethanol; equilibrium).

Anal. Calcd. for $C_{10}H_{17}O_7N$: C, 45.63; H, 6.46; N, 5.32. Found: C, 45.47; H, 6.59; N, 5.38.

Benzyl 2-Acetamido-3-O-benzyl-4,6-O-benzylidene-2-deoxy-β-D-*glucopyranoside (6)*

The benzyl ether was prepared essentially by the method of Croon and co-workers (36) using 2 g of **5** and a reaction time of 8 h. The reaction mixture was filtered, concentrated to small volume, and the 3-*O*-benzyl ether (**6**) was precipitated almost quantitatively by pouring the concentrated solution into ethanol. This was determined by t.l.c. analysis (solvent B) of the mother liquors, which were shown to contain at least one major component having a greater mobility than the 3-*O*-benzyl ether or **5**. The precipitated 3-*O*-benzyl ether (**6**) was recrystallized from pyridine–ethanol (1:1) to give needles (300 mg, 12.3%) of m.p. 283° and $[\alpha]_D$ −97.5° (*c*, 1.0 in pyridine).

Anal. Calcd. for $C_{29}H_{31}O_6N$: C, 71.16; H, 6.33; N, 2.86. Found: C, 70.70; H, 6.48; N, 2.89.

Yields of up to 16% could be obtained by shorter reaction times (4 h).

1. D. R. BUNDLE, H. J. JENNINGS, and I. C. P. SMITH. J. Biol. Chem. In press.
2. A. S. PERLIN, B. CASU, and H. J. KOCH. Tetrahedron Lett. 2921 (1969).
3. L. D. HALL and L. F. JOHNSON. Chem. Commun. 509 (1969).
4. A. S. PERLIN, B. CASU, and H. J. KOCH. Can. J. Chem. **48**, 2596 (1970).
5. D. E. DORMAN and J. D. ROBERTS. J. Am. Chem. Soc. **92**, 1355 (1970).
6. A. S. PERLIN, N. M. K. MG YING KIN, S. S. BHATACHARGEE, and L. F. JOHNSON. Can. J. Chem. **50**, 2437 (1972).
7. T.-Y. LIU, E. C. GOTSCHLICH, E. K. JONSSEN, and J. R. WYSOCK. J. Biol. Chem. **246**, 2849 (1971).
8. D. R. BUNDLE, H. J. JENNINGS, and C. P. KENNY. Carbohydr. Res. **26**, 268 (1973).
9. D. HORTON, J. S. JEWELL, and K. D. PHILIPS. J. Org. Chem. **31**, 4022 (1966).
10. R. KUHN, H. H. BAER, and A. I. SEELIGER. Ann. Chem. **236**, 611 (1958).
11. P. H. GROSS and R. JEANLOZ. J. Org. Chem. **32**, 2759 (1967).
12. J. D. ALBRIGHT and L. GOLDMAN. J. Am. Chem. Soc. **87**, 4214 (1965).
13. P. W. AUSTIN, F. E. HARDY, J. G. BUCHANAN, and J. BADDILEY. J. Chem. Soc. 5350 (1963).
14. D. R. BUNDLE and H. J. JENNINGS. To be published.
15. C. L. STEVENS and C. P. BRYANT. Meth. Carbohydr. Chem. **6**, 337 (1972).
16. D. HORTON. The Amino Sugars. Vol. 1A. *Edited by* R. W. JEANLOZ. Academic Press, New York. 1969.
17. A. YA. KHORLIN, S. E. ZURABYAN, and T. S. ANTONENKO. Tetrahedron Lett. 4803 (1970).
18. H. SPIESECKE and W. G. SCHNEIDER. J. Chem. Phys. **35**, 722 (1961).
19. F. J. WEIGERT and J. D. ROBERTS. J. Am. Chem. Soc. **89**, 2967 (1967).
20. H. J. KOCH and A. S. PERLIN. Carbohydr. Res. **15**, 403 (1970).
21. H. J. JENNINGS and I. C. P. SMITH. J. Am. Chem. Soc. **95**, 606 (1973).
22. D. M. GRANT and E. G. PAUL. J. Am. Chem. Soc. **86**, 2984 (1964).
23. D. K. DALLING and D. M. GRANT. J. Am. Chem. Soc. **89**, 6612 (1967).
24. G. W. BUCHANAN, D. A. ROSS, and J. D. ROBERTS. J. Am. Chem. Soc. **88**, 4301 (1966).
25. D. E. DORMAN, S. J. ANGYAL, and J. D. ROBERTS. J. Am. Chem. Soc. **92**, 1351 (1970).
26. D. E. DORMAN and J. D. ROBERTS. J. Am. Chem. Soc. **93**, 4463 (1971).
27. H. H. MANTSCH and I. C. P. SMITH. Biochem. Biophys. Res. Commun. **46**, 808 (1972).
28. R. D. LAPPER, H. H. MANTSCH, and I. C. P. SMITH. J. Am. Chem. Soc. **94**, 6243 (1972).
29. I. C. P. SMITH, H. H. MANTSCH, R. D. LAPPER, R. DESLAURIERS, and T. SCHLEICH. *In* Conformations of biological molecules and polymers. *Edited by* E. Bergmann and B. Pullman. Academic Press, New York. 1973. p. 381.
30. B. J. BLACKBURN, R. D. LAPPER, and I. C. P. SMITH. J. Am. Chem. Soc. **95**, 2873 (1973).
31. R. D. LAPPER, H. H. MANTSCH, and I. C. P. SMITH. J. Am. Chem. Soc. **95**, 2878 (1973).
32. S. OHKUMA. Proc. Jap. Acad. **38**, 562 (1962).
33. D. HORTON. Org. syntheses. Vol. 1. John Wiley and Son, Inc., New York. 1966. p. 46.
34. K. MIYAI, H. K. ZIMMERMAN, and P. H. GROSS. J. Org. Chem. **34**, 1635 (1969).
35. M. B. PERRY and A. C. WEBB. Can. J. Biochem. **46**, 1163 (1968).
36. I. CROON and B. LINDBERG. Acta Chem. Scand. **13**, 593 (1959).

Can. J. Chem. Downloaded from www.nrcresearchpress.com by 210.87.254.42 on 09/05/12
For personal use only.

Hydrolysis of Substituted Diphenylacetaldehyde Ethylene Glycol Cyclic Acetals in Aqueous Hydrochloric Acid[1]

BRUCE L. JENSEN[2] AND RAYMOND E. COUNSELL

Laboratory of Medicinal Chemistry, College of Pharmacy, The University of Michigan, Ann Arbor, Michigan 48104

Received May 24, 1973

The chemistry of DDT and DDD derivatives was explored by studying the steric and electronic effects on the hydrolysis of a variety of substituted diphenylacetaldehyde ethylene glycol cyclic acetals. This investigation demonstrated that *ortho* substituents, *p*-nitro, and *p*-methoxy groups affect the product distribution in different ways. The mechanistic details of this work are discussed.

La chimie des dérivés du DDT et du DDD a été examinée en étudiant les effets électroniques et stériques sur l'hydrolyse d'une variété d'acétals cycliques formés entre l'éthylène glycol et des diphénylacétaldéhydes substitués. Cette étude a démontré que les substituants *ortho* et les groupes *p*-nitro et *p*-méthoxy affectent la distribution des produits de différentes manières. Les détails mécanistiques de ce travail sont discutés. [Traduit par le journal]

Can. J. Chem., **51**, 3820 (1973)

The widespread use of 2,2-di(*p*-chlorophenyl)-1,1,1-trichloroethane (DDT) as a pesticide as well as the more limited use of 2-(*o*-chlorophenyl)-2-(*p*-chlorophenyl)-1,1-dichloroethane (*o,p'*-DDD) as the only clinically approved agent for the treatment of adrenocortical carcinoma has prompted numerous chemical investigations in these classes of compounds (1–12).

Because of the immense biological importance of these compounds, the hydrolysis of cyclic acetals **1** related to DDT and DDD has recently been studied (5, 7, 8, 10, 11). This particularly interesting reaction affords the corresponding benzophenone **2**, diphenylacetaldehyde **3**, and deoxybenzoin **4** in varying proportions. The formation of benzophenones from this reaction has received additional attention and only recently McKinney and co-workers (12) have shown that this conversion probably proceeds via the enol ether **6** and the α-hydroxy aldehyde **7**. Furthermore, the ratio of diphenylacetaldehyde **3** to benzophenone **2** was shown by this group (12) and others (7) to vary considerably depending on the hydrolysis conditions and it was suggested that steric inhibition also influenced this reaction.

The steric dependence of this reaction was explained on the basis by which the benzhydryl carbon can undergo oxidation. By comparing the *p,p'*-, *o,p'*-, and *o,o'*-dichloro systems, McKinney *et al.* demonstrated that steric hindrance to removal of the benzhydryl proton by the *o*-chlorine atom and subsequent steric inhibition of resonance stabilization would influence the progress of this reaction. However, this group made no further attempt to substantiate their

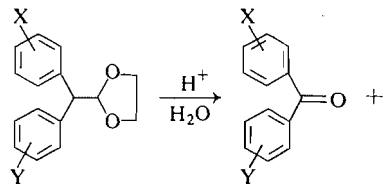

1 2

a X = Y = H
b X = H; Y = *p*-Cl
c X = Y = *o*-Cl
d X = *o*-Cl; Y = *p*-Cl
e X = Y = *p*-Cl
f X = Y = *p*-F
g X = Y = *p*-NO_2
h X = Y = *p*-CH_3O

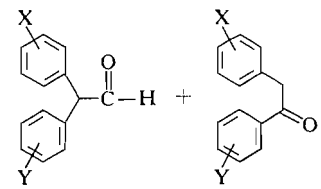

3 4

[1]This investigation was supported by the U.S. Public Health Service under Research Grants No. CA-49340 and CA-08349.

[2]National Institutes of Health Postdoctoral Fellow, 1970–1972; present address: Department of Chemistry, University of Maine, Orono, Maine 04473.

Can. J. Chem. Downloaded from www.nrcresearchpress.com by 210.87.254.42 on 09/05/12
For personal use only.

Can. J. Chem. Downloaded from www.nrcresearchpress.com by 210.87.254.42 on 09/05/12
For personal use only.

predictions nor were the electronic influences on this reaction explored.

As part of a continuing interest in DDD and DDT compounds, we have investigated the electronic and steric effects on the product distribution when a variety of substituted diphenylacetaldehyde ethylene glycol cyclic acetals **1** were hydrolyzed in boiling 20% aqueous hydrochloric acid. The diphenylacetaldehydes **3***a–h* were obtained commercially or were synthesized from the appropriate benzophenone via Darzen's glycidic ester synthesis. The cyclic acetals **1***a–h* were prepared by treating the diphenylacetaldehydes with ethylene glycol in refluxing benzene containing *p*-toluenesulfonic acid as a catalyst. Aqueous 20% hydrochloric acid was chosen as the hydrolysis medium because of its non-oxidative properties and its inability to form esters with intermediates in the hydrolysis reaction.

G.l.c., i.r., and n.m.r. spectroscopy were employed for characterization of the products and their relative amounts.

Results

G.l.c. analyses for the hydrolysis of the cyclic acetals **1***a–h* in 20% aqueous hydrochloric acid for 6 h are tabulated in Table 1.

TABLE 1. Product distribution and percentages from the hydrolysis of cyclic acetals **1***a–h*

Cyclic acetal **1**	Hydrolysis product (%)		
	Aldehyde **3**	Benzophenone **2**	Deoxybenzoin **4**
a	89	11	0
b	69	31	0
c	100	0	0
d	100	0	0
e	89	11	0
f	88	12	0
g	100	0	0
h	77	4	19

Discussion

From the product distribution shown above, three mechanistic pathways seem to be operative during the hydrolysis of the cyclic acetals **1***a–h* (Scheme 1). Furthermore, the central intermediate structure **6** in this sequence can be used to account for the results obtained. Protonation of an acetal oxygen would give rise to **5**. At this point both steric and electronic factors may influence the course of the reaction.

In cases **1***c–d*, where *ortho* substituents were present, no benzophenones were formed. These results are consistent with McKinney *et al.* findings that steric hindrance to the removal of the benzhydryl proton is probably prevented by *ortho* substituents. Subsequent steric inhibition of resonance stabilization after proton removal would also preclude path *a*. This factor is demonstrated further when *p*-fluoro, -chloro, and -hydrogen substituents are present. These substituents are not capable of steric effects and the small electronic influences of such groups would not be expected to influence the course of the reaction. Thus, in these cases, both pathways *a* and *b* are operative.

In the cases of **1***g–h*, strongly electron releasing and electron withdrawing groups clearly influence the product distribution. Path *c*, which involves an aryl migration, would be favored for **1***h* because of the high migratory aptitude of the *p*-anisyl group (13). The finding that 19% of the hydrolysis products is *p,p'*-dimethoxydeoxybenzoin supported this prediction. As would be expected, no aryl migration product was detected from the hydrolysis of **1***g* since the *p*-nitrophenyl group is a poor migrating group in this carbonium ion rearrangement. Furthermore, only *p,p'*-dinitrodiphenylacetaldehyde (**3***g*), resulting from path *b*, was formed. This result can be explained by the facility by which either **5** or **6** can react with water. The powerful withdrawing effects of the nitro groups would favor the formation of the carbonium ion **5** as opposed to a benzhydryl carbonium ion. Furthermore, the loss of a proton from **5** to give the enol ether **6** would also be favored by the strongly electron withdrawing groups. In either case, the rapid addition of water would afford **8**. An analogous process is the rapidity by which aldehydes and ketones form stable hydrates when electron withdrawing groups are in close proximity to the carbonyl group (14). This mode of addition has been demonstrated further by Tadros *et al.* (11) who have shown that **6** can readily be converted to the corresponding cyclic acetal in concentrated hydrochloric acid.

An additional indication of the substituent effects on the benzhydryl proton in this reaction is also evident from a comparison of the chemical shifts of the benzhydryl proton in the cyclic acetals **1***a–h*. An *o*-chloro substituent shows a strong deshielding effect on the benzhydryl proton when compared with the corresponding

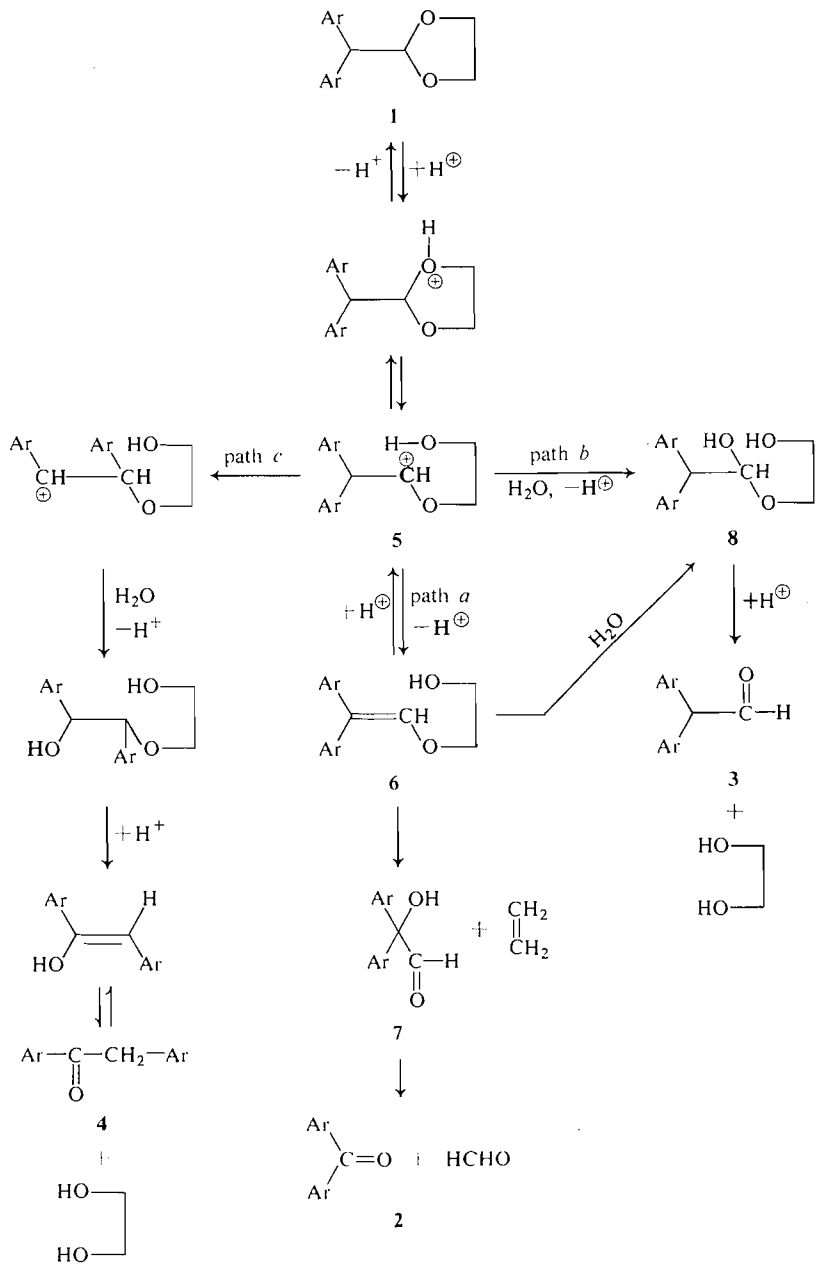

SCHEME 1

para substituents (6). In general, the benzhydryl proton doublet appeared at τ 5.88–5.80 for the acetals having *para* substituents. The one exception was **1***g* whose *p,p'*-dinitro substituents inductively deshield the benzhydryl proton and it appeared at τ 5.52. The most notable deshielding effects by substituents occurred in **1***d* and *c*, whose benzhydryl protons appeared at τ 5.28 and 4.78, respectively. The proton on the adjacent carbon, on the other hand, was virtually unaffected by the substituents. These data correlate well with recent reports (15, 16); a summary of the n.m.r. data for the cyclic acetals **1***a–h* is presented in Table 4.

Can. J. Chem. Downloaded from www.nrcresearchpress.com by 210.87.254.42 on 09/05/12
For personal use only.

TABLE 2. Physical and analytical data for substituted diphenylacetaldehydes *3a–h*

	3		2,4-DNP derivative				
			% C		% H		
	M.p. (°C)	B.p. (°C) (mm)	Calcd.	Found	Calcd.	Found	M.p. (°C)
*a**	—	315 (dec.)					
b	—	135 (0.05)	58.47	58.65	3.68		152–155
*c**	86–87	—					
d†	—	172 (0.2)					
e	—	160 (0.35)	53.95	53.92	3.16	3.25	178–180
f	—	127 (0.25)	58.25	58.11	3.42	3.33	185–186
g‡	§	—	51.50	51.37	3.02	2.94	190–193
h	104–105	—					

*Aldrich chemicals.
†Reference 3.
‡Reference 17.
§Hydration of aldehyde very rapid, no melting point recorded.

Experimental

General

Melting points were obtained with a Fisher-Johns melting point apparatus and are uncorrected. Boiling points are uncorrected. The n.m.r. spectra were recorded on a Varian A-60A spectrometer in CCl_4 or $CDCl_3$ with tetramethylsilane as an internal standard. I.r. spectra were determined on a Perkin-Elmer Model 337 spectrophotometer. G.l.c. analyses were performed on a Varian Aerograph Model 90 P (thermal conductivity) gas chromatograph using a 5 ft × 0.25 in. stainless steel column packed with 10% SE 30 on 100/120 mesh Var A port 30 or on a Loenco Model 160 (flame ionization) gas chromatograph using a 6 ft × 0.125 in. stainless steel column packed with 3% OV-17 on 100/120 mesh Chromosorb G. Microanalyses were performed by Spang Microanalytical Laboratories, Ann Arbor, Michigan.

Materials

Preparation of Substituted Diphenylacetaldehydes 3a–h

Diphenylacetaldehyde (*3a*) and *o,o'*-dichlorodiphenylacetaldehyde (*3c*) were commercially available (Aldrich Chemical Company).

Preparation of p,p'-Dimethoxydiphenylacetaldehyde (3h) This compound was prepared according to the method of Tiffeneau and Orekhoff (17).

Preparation of Diphenylacetaldehydes 3b,d–g These aldehydes were obtained from the appropriate benzophenones via Darzen's glycidic ester synthesis according to procedures developed by Horton and co-workers (3) and Counsell *et al.* (8). The general method is illustrated by the preparation of *p,p'*-dinitrodiphenylacetaldehyde (*3g*).

Under an atmosphere of dry nitrogen gas, 57% sodium hydride dispersion (8.0 g, 0.173 mol) was added to a slurry of *p,p'*-dinitrobenzophenone (18) (21.8 g, 0.08 mol) in ethyl chloroacetate (150 ml) over a period of 4 h. The slow addition was accompanied by a gradual increase in temperature. About half way through the addition, gentle boiling was accompanied by a darkening of the color of the solution. After the exothermic reaction subsided, the remaining sodium hydride was added slowly. After the addition, the dark solution was heated for 16 h at 45° and then at 100° for 1 h. The cool reaction mixture was poured into ice-cold 15% aqueous hydrochloric acid (1 l). Ether (500 ml) was added to the mixture and this was stirred thoroughly. The solid which separated was collected by filtration, washed with cold ether and water, and air dried. Recrystallization of this solid from acetone–water (Norit) afforded 12.2 g (42%) of ethyl β,β-di(*p*-nitrophenyl)glycidate as light yellow crystals: m.p. 120–122° (analytical sample m.p. 125–126°); n.m.r. ($CDCl_3$) τ 2.06 (m, 8, Ar*H*), 5.94 (s, 1, C*H*), 5.95 (q, 2, CH_2, J = 7.0 Hz), and 8.94 (t, 3, CH_3, J = 7.0 Hz).

Anal. Calcd. for $C_{17}H_{14}N_2O_7$: C, 56.98; H, 3.93. Found: C, 56.94; H, 3.84.

Ethyl β,β-di(*p*-nitrophenyl)glycidate (6.0 g, 0.016 mol) and sodium carbonate (4.5 g, 0.043 mol) were stirred and refluxed in water (500 ml) for 30 min. The mixture was cooled and filtered. The filtrate was acidified with dilute hydrochloric acid and the resulting precipitate collected by filtration. After washing with water and 95% ethanol and drying, di(*p*-nitrophenyl)glycidic acid (3.0 g, 50%) melted with loss of carbon dioxide at 200–210°.

Under aspirator pressure, di(*p*-nitrophenyl)glycidic acid (2.0 g, 0.006 mol) was heated at 190–210° for 15 min. As the acid melted, evolution of carbon dioxide was vigorous and gradually subsided. The dark oil soon hardened and melted at 65–75°. Extraction of the oil into ether afforded 1.2 g (70%) of *p,p'*-dinitrodiphenylacetaldehyde as orange crystals after drying and evaporation of the ethereal extract. This compound formed hydration products very rapidly and, consequently, had to be used as such for subsequent reactions. Its 2,4-dinitrophenylhydrazone derivative was prepared in ethanol and recrystallized from ethyl acetate – petroleum ether (b.p. 30–60°) and melted at 190–193°.

Physical and analytical data for the substituted diphenylacetaldehydes *3a–h* and their 2,4-dinitrophenylhydrazone (2,4-DNP) derivatives are summarized in Table 2.

Can. J. Chem. Downloaded from www.nrcresearchpress.com by 210.87.254.42 on 09/05/12
For personal use only.

TABLE 3. Physical and analytical data for substituted diphenylacetaldehyde ethylene glycol cyclic acetals **1***a–h*

1	M.p. (°C)	% yield	Recrystallization media	% C		% H	
				Calcd.	Found	Calcd.	Found
*a**	77–80	87	Acetone–water				
b	47–49	88	Methanol–water	69.94	70.01	5.50	5.53
c	88–89	82	Acetone–water	62.15	62.13	4.56	4.66
d	79–80	65	Ethanol–water	62.15	62.07	4.56	4.45
e†	94–95	21*	Hexane				
f	76–78	43	Methanol	69.55	69.60	5.10	5.03
g	151–152	62	Benzene – petroleum ether	58.18	58.26	4.27	4.24
h	107–108	86	Ethanol	71.98	72.25	6.71	6.69

*Reference 19.
†Prepared by the method of Riemschneider *et al.* (5).

TABLE 4. Nuclear magnetic resonance data for cyclic acetals **1***a–h*

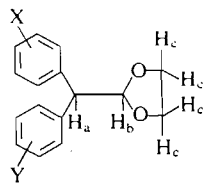

1

	Substituents		N.m.r. data τ					
	X	Y	H_a	H_b	H_c	Ar*H*	X,Y	Solvent
a	H	H	5.82	4.56	6.42	2.76	—	CCl_4
b	H	*p*-Cl	5.80	4.50	6.22	2.68	—	$CDCl_3$
c	*o*-Cl	*o*-Cl	4.78	4.52	6.32	2.70	—	CCl_4
d	*p*-Cl	*o*-Cl	5.28	4.56	6.32	2.74	—	CCl_4
e	*p*-Cl	*p*-Cl	5.83	4.56	6.24	2.75	—	$CDCl_3$
f	*p*-F	*p*-F	5.77	4.53	6.22	2.83	—	$CDCl_3$
g	*p*-NO_2	*p*-NO_2	5.52	4.46	6.20	2.12	—	$CDCl_3$
h	*p*-CH_3O	*p*-CH_3O	5.88	4.54	6.24	2.92	6.20 (2 CH_3O)	$CDCl_3$

Preparation of Substituted Diphenylacetaldehyde Ethylene Glycol Cyclic Acetals **1***a–h*

The general procedure is exemplified by the synthesis of *p,p'*-difluorodiphenylacetaldehyde ethylene glycol cyclic acetal. *p,p'*-Difluorodiphenylacetaldehyde (2.3 g, 0.01 mol), dry ethylene glycol (4 ml), and *p*-toluenesulfonic acid (0.5 g) were refluxed in benzene (100 ml) using a Dean-Stark water trap for 8 h. The solvent was removed *in vacuo* and ice-water (100 ml) was added to the residue. The resulting precipitate was collected by filtration, washed with water, and air dried. Recrystallization of this solid from methanol furnished 1.2 g (43%) of **1***f* as colorless crystals, m.p. 76–78°.

Physical and analytical data for the substituted diphenylacetaldehyde ethylene glycol cyclic acetals **1***a–h* are shown in Table 3. The n.m.r. data for these compounds are tabulated in Table 4.

Product Study

The following general procedure was used for the hydrolysis of **1***a–h* in 20% aqueous hydrochloric acid. Aqueous 20% hydrochloric acid was prepared from 40 ml concentrated hydrochloric acid and 30 ml water. The acetal (1.0 g) was refluxed in 20% aqueous hydrochloric acid (50 ml) for 6 h. The cooled mixture was extracted with chloroform (3 × 35 ml) and the combined extracts were washed with water before drying over sodium sulfate. Filtration and evaporation of the extract left oils which were subjected to g.l.c. analyses. Retention times were compared with authentic samples as well as comparisons of their i.r. and n.m.r. spectras. G.l.c. analyses data are presented in Table 1.

The authors wish to thank Dr. G. Wellman for his assistance on this problem.

Can. J. Chem. Downloaded from www.nrcresearchpress.com by 210.87.254.42 on 09/05/12
For personal use only.

1. H. L. HALLER, P. D. BARTLETT, N. L. DRAKE, M. S. NEWMAN, S. J. CRISTOL, C. M. EAKER, R. A. HAYES, G. W. KILMER, B. MAGERLEIN, G. P. MUELLER, A. SCHNEIDER, and W. WHEATLEY. J. Am. Chem. Soc. **67**, 1591 (1945).
2. S. J. CRISTOL and H. L. HALLER. J. Am. Chem. Soc. **70**, 1323 (1948).
3. T. INOI, P. GERICKE, and W. J. HORTON. J. Org. Chem. **27**, 4597 (1962).
4. K. Y. ZEE-CHENG and C. C. CHENG. J. Med. Pharm. Chem. **5**, 1008 (1962).
5. R. RIEMSCHNEIDER, I. AHRLÉ, W. COHNEN, and E. HEILMANN. Chem. Ber. **92**, 900 (1959).
6. R. E. COUNSELL and R. E. WILLETTE. J. Pharm. Sci. **55**, 1012 (1966).
7. W. TADROS, A. B. SAKLA, and M. K. KHALIL. J. Chem. Soc. (C), 373 (1966).
8. R. E. COUNSELL, V. V. RANADE, L. K. LALA, and B. H. HONG. J. Med. Chem. **11**, 380 (1968).
9. R. E. COUNSELL, V. V. RANADE, P. POCHA, R. E. WILLETTE, and W. DIGUILO. J. Pharm. Sci. **57**, 1657 (1968).
10. A. B. SAKLA, W. TADROS, and A. A. A. HELMY. J. Chem. Soc. (C), 1044 (1969).
11. A. B. SAKLA, W. TADROS, and M. K. KHALIEL. J. Chem. Soc. (C), 409 (1970).
12. J. D. MCKINNEY, R. E. HAWK, E. L. BOOZER, and J. E. SUGGS. Can. J. Chem. **49**, 3877 (1971).
13. J. HINE. Physical organic chemistry. McGraw-Hill, New York, N.Y. 1962. p. 328.
14. R. BRESLOW. Organic reaction mechanisms. Benjamin, New York, N.Y. 1969. p. 184.
15. L. M. JACKMAN and S. STERNHELL. Applications of nuclear magnetic resonance spectroscopy in organic chemistry. Pergamon Press, Elmsford, N.Y. 1969. pp. 170–175.
16. L. H. KEITH, A. L. ALFORD, and A. W. GARRISON. J. Assoc. Offic. Aar. Chemistr, **52**, 1074. (1969).
17. A. TIFFENEAU and A. ORÉKHOFF. Bull. Soc. Chim. Fr. **33**, 1832 (1823).
18. L. HASKELBERG and D. LAVIE. J. Am. Chem. Soc. **71**, 2580 (1949).
19. E. F. RIENER, W. E. GRAIG, and T. J. DURKIN. Chem. Abstr. **52**, 20209h (1958).

Can. J. Chem. Downloaded from www.nrcresearchpress.com by 210.87.254.42 on 09/05/12
For personal use only.

Can. J. Chem. Downloaded from www.nrcresearchpress.com by 210.87.254.42 on 09/05/12
For personal use only.

Canadian Journal of Chemistry

Published by
THE NATIONAL RESEARCH COUNCIL OF CANADA

Journal canadien de chimie

Publié par
LE CONSEIL NATIONAL DE RECHERCHES DU CANADA

Volume 51 Number 23 December 1, 1973 Volume 51 numéro 23 1 decembre 1973

Evidence Against a Hydrogen Abstraction Mechanism in the Photorearrangement of Azoxybenzene to 2-Hydroxyazobenzene[1]

DAVID J. W. GOON, N. G. MURRAY, JEAN-PIERRE SCHOCH, AND N. J. BUNCE[2]
Department of Chemistry, University of Guelph, Guelph, Ontario

Received January 22, 1973

In an attempt to distinguish between ionic and free radical mechanisms for the photorearrangement of azoxybenzene to 2-hydroxyazobenzene, aromatic azoxycompounds carrying C—H functions *ortho* to the azoxy linkage have been prepared and irradiated. The failure of these weaker C—H bonds to divert the reaction from its normal course argues against a hydrogen abstraction – hydroxyl transfer mechanism. This conclusion is supported by the observation of a 30-fold increase in quantum yield for 2-hydroxyazobenzene formation on changing from a non-polar to a polar solvent and by the kinetic deuterium isotope effect, which is too small for the primary isotope effect required by the abstraction mechanism. It is concluded that the experimental observations to date may most easily be accommodated in the route originally proposed by Badger and Buttery, where the rearrangement is seen as a substitution by oxygen at the *ortho* ring carbon.

Afin de distinguer entre un mécanisme à caractère ionique et un mécanisme impliquant des radicaux libres lors du photoréarrangement de l'azoxybenzène en hydroxy-2 azobenzène, on a préparé et irradié des composés "azoxy" aromatiques comportant des fonctions C—H en position *ortho* du lien azoxy. Ces liens C—H plus faibles s'étant révélés incapables de dévier la réaction de son cours normal, on en conclut alors qu'un mécanisme impliquant l'enlèvement d'un hydrogène puis transfert du groupe OH ne saurait être considéré. Cette conclusion est d'ailleurs en accord avec l'observation selon laquelle une augmentation (par un facteur de 30) du rendement quantique est enregistrée lors de la formation de l'hydroxy-2 azobenzène lorsque l'on passe d'un solvant non-polaire à un solvant polaire, de même qu'elle est en accord avec l'effet isotopique causé par le deutérium trop faible pour être un effet isotopique primaire qui serait normal pour le mécanisme impliquant l'enlèvement d'un hydrogène. On en conclut alors que les données expérimentales, jusqu'à présent, conduisent au mécanisme proposé à l'origine par Badger et Buttery selon lequel le réarrangement est le résultat d'une substitution par l'oxygène au carbone du cycle en position *ortho*. [Traduit par le journal]

Can. J. Chem., 51, 3827 (1973)

The instability of aromatic azoxy compounds to light has long been recognized as being due to to their transformation into *o*-hydroxyazo compounds (1). The rearrangement apparently proceeds from the $^1\pi,\pi^*$ excited state of the azoxy compound, since Tanikaga *et al.* have shown (2) that no n,π^* band appears in the absorption spectrum of azoxybenzene and that deliberate excitation of the triplet state by photosensitization causes photoreduction as well as oxygen migration. Previously, Badger and Buttery (3) had found that unsymmetrical azoxybenzenes such as **1** rearrange exclusively

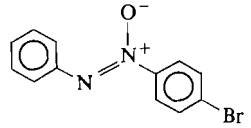

1

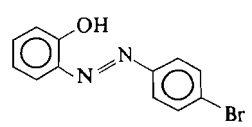

2

[1]Presented in part at the 54th and 56th Canadian Chemical Conferences of the Chemical Institute of Canada, Halifax, Nova Scotia, May 1971 and Montreal, Quebec, June 1973.

[2]To whom correspondence should be addressed.

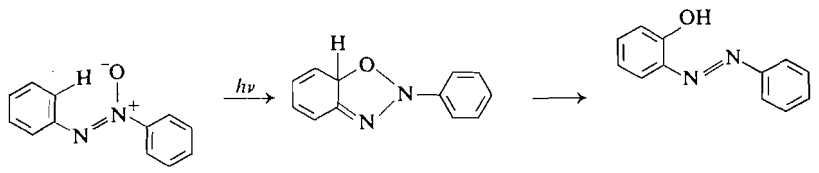

SCHEME 1

to **2**, where the azoxy oxygen migrates to the aromatic ring farther from its point of departure. They proposed the intramolecular mechanism of Scheme 1, in which the rearrangement is initiated by nucleophilic attack of the azoxy oxygen on the appropriate ring carbon, giving the cyclic intermediate **A**. The intramolecular character of the reaction and the direction of oxygen migration have both been confirmed by ^{18}O (4) and ^{15}N (5) isotopic labelling experiments. All of this work has been reviewed recently (6).

Although the Badger and Buttery mechanism has been widely accepted, to date no other experiments have been carried out to support it and in one study (7), Oae *et al.* have argued that a radical mechanism for the photorearrangement better explains the experimental facts. One possibility for such a mechanism is a radical analog of Scheme 1, although it is questionable whether any distinction can be drawn between an ionic and a radical Scheme 1, since an excited state of azoxybenzene inevitably carries unpaired electrons. Another is the hydrogen abstraction pathway of Scheme 2, in which

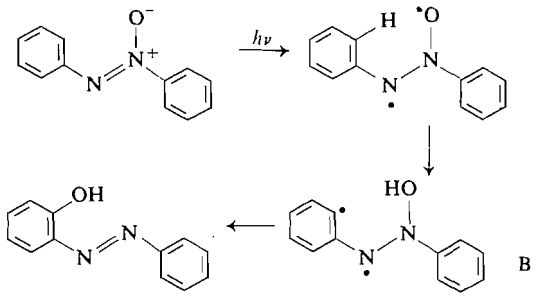

SCHEME 2

homolytic hydrogen abstraction from the conveniently situated *ortho* position of the distant aromatic ring is followed by hydroxyl transfer. This route is similar to the mechanism widely accepted (8) for oxygen migration in the photorearrangement of *o*-nitrobenzaldehyde to *o*-nitrosobenzoic acid and is attractive in view of the electronic similarities between the azoxy-

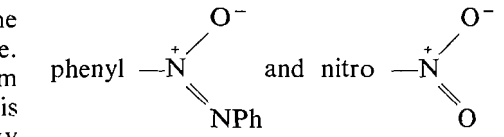

phenyl and nitro groups.

In addition, the crystal structure of an azoxybenzene derivative, 4,4′-azoxyanisole, shows that at least in the solid state, the azoxy group and the distant benzene ring are essentially coplanar, with the oxygen and *o*-hydrogen separated by only 2.3 Å (9). Assuming a comparable excited state geometry, this should facilitate a hydrogen abstraction mechanism.

The purpose of the present study has been to choose between these alternative modes of rearrangement on experimental grounds. We believe that the results presented here allow us to exclude the abstraction mechanism, but we are unable on the present evidence to confirm all the details of the Badger and Buttery mechanism (Scheme 1).

Results and Discussion

In the mechanism of Scheme 2, oxygen migration is preceded by homolytic hydrogen abstraction by oxygen. The ease of reaction should thus parallel the weakness of the C—H bond to be broken, as in typical hydrogen abstractions by free radicals (10), in the photochemical Norrish type II elimination of alkyl ketones (11), and in the intermolecular photoreduction of benzophenone by hydrogen-donating solvents (12). We therefore postulated that if there were available with comparable geometry a C—H bond weaker than the bonds to the distant *ortho* hydrogens, then the more weakly bound hydrogen should be abstracted preferentially. This would divert the arrangement from its usual course. We sought to study systems with the features of **3**, where both the distant *ortho* hydrogen and the benzylic hydrogen are separated from the azoxy oxygen by four intervening atoms. Abstraction of the *ortho* hydrogen gives **4**, the normal product, whereas abstraction of the

Can. J. Chem. Downloaded from www.nrcresearchpress.com by 210.87.254.42 on 09/05/12
For personal use only.

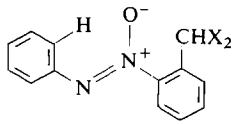

3

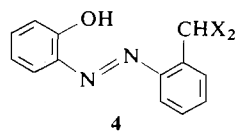

4

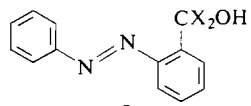

5

benzylic hydrogen should lead to oxygen insertion at the benzylic site, *viz.* **5**.

Azoxybenzenes with Benzylic Hydrogens: Synthesis

The compounds selected for study were **6**–**11**, all of which were potentially able to undergo both normal and abnormal modes of rearrangement, and **12** and **13** in which the normal rearrangement pathway was blocked.

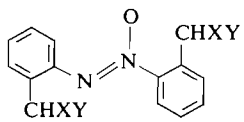

6 X = Y = H
7 X = Y = CH_3
8 X = H; Y = C_6H_5
9 X = Y = OCH_3
10 X = Y = OC_2H_5
11 XY = O
15 XY = —OCH_2CH_2O—

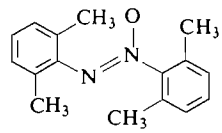

12

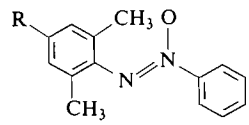

13 R = H
14 R = CH_3

With the exception of the unsymmetrical **13**, which was obtained by oxidation[3] of the condensation product of nitrosobenzene and 2,6-dimethylaniline, all the azoxy compounds were obtained by reduction of appropriate nitro compounds. Most of the nitro compounds were reduced using CH_3OH–NaOH (14), CH_3OH–Na (15), or by metallic thallium (16) giving the azoxy compound directly. For the tetramethyl compound **12**, hitherto difficult to prepare (17), lithium aluminum hydride reduction to the azo compound was followed by peracid oxidation.[4] An attempt to use this route to prepare **9** from *o*-nitrobenzaldehyde dimethylacetal failed because the metal hydride cleaved the acetal function, giving a variety of products including 2,2′-azotoluene but very little of the desired azo compound **16**.

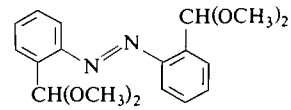

16

A major synthetic problem was the liberation of the azoxybenzaldehyde **11** from its acetals. Carefully controlled hydrolysis of **10** gave the best yield of **11**, but even this was modest (25%); too-vigorous hydrolysis led to destruction of **11** and formation of colorless condensation products as noted previously (19). Very mild conditions gave incompletely hydrolyzed products identified as 2,2′-azoxybenzaldehyde 2-dialkyl acetals; there is still some doubt as to whether these should be represented as **17** or **18**, although we favor **17** slightly. No conclusions

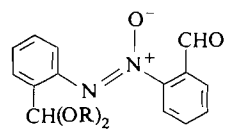

17

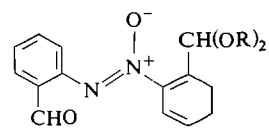

18

could be drawn about the position of the azoxy oxygen by comparing the chemical shifts (recorded in the experimental section) of —CHO and —$CH(OCH_3)_2$ in **17** or **18** (R = CH_3) with those of model compounds **9**, **11**, **16**, and 3-hydroxy-2,2′-azobenzaldehyde bisdimethyl acetal (**27**). Mass spectrometry has been used to differentiate between the isomers of simple unsymmetrical azoxy compounds (20), since C—N cleavage occurs more abundantly on the side adjacent to the azoxy oxygen. Although our azoxybenzaldehyde derivatives undergo much more complex fragmentation than the compounds previously studied, the greater abundance of $[C_6H_4CHO]^+$ over $[C_6H_4CH(OR)_2]^+$ lends some support to structure **17** over **18**. In addition, photolysis of small quantities of **17** (R = CH_3 and C_2H_5) did not give hydroxyazo

[3]Oxidation of the 2,6-disubstituted azobenzene gives almost exclusively 2,6-dimethyl-*NNO*-azoxybenzene (**13**) because of steric hindrance (13).

[4]Since completion of this work, the preparation of **12** by oxidation of 2,6-dimethylaniline with AgO has been reported (18).

Can. J. Chem. Downloaded from www.nrcresearchpress.com by 210.87.254.42 on 09/05/12
For personal use only.

Can. J. Chem. Downloaded from www.nrcresearchpress.com by 210.87.254.42 on 09/05/12
For personal use only.

compounds, nor indeed any tractable products; as shown below, this behavior is similar to that of **11**, rather than of **9** and **10** which photorearrange normally. This also favors structure **17** rather than **18**, since **17**, like **11**, has the CHO and N—O functions on adjacent carbon atoms.

Azoxybenzenes with Benzylic Hydrogens: Photolysis

In the first series of experiments, compounds **6–11** were irradiated in benzene solution using Pyrex equipment ($\lambda > 300$ nm). From compounds **6–10** no abnormal products of structure **5** were obtained; instead the expected 2-hydroxyazobenzene was the sole or major product. 2,2′-Azoxybenzaldehyde (**11**) behaved differently; it photolyzed more rapidly and gave a derivative of the abnormal rearrangement product but no hydroxyazo compound. The behavior of compounds **6–10** seems to be inconsistent with a rearrangement pathway initiated by hydrogen abstraction since the alternate C—H bonds available were in all cases weaker than an aromatic C—H bond. In contrast, typical free radical hydrogen abstractors are very unreactive towards aromatic hydrogens (21) but abstract readily from the appropriate positions of toluenes (21), cumenes (21), diphenylmethanes (21), acetals (22), and aldehydes (23). In the following paragraphs the results of the photolyses are examined in more detail.

Photolysis of the dimethyl compound **6** gave a different product mixture according to the conditions. Direct photolysis in dilute benzene solution gave the normal product **19**; using a more concentrated solution, **19** was accompanied by a new photoproduct, a deep red

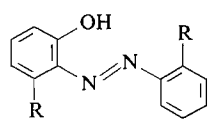

19 R = CH_3
23 R = $CH(CH_3)_2$
24 R = $CH_2C_6H_5$
27 R = $CH(OCH_3)_2$
28 R = $CH(OC_2H_5)_2$

compound whose mass spectrum (M^+ 344) and n.m.r. spectrum indicated a structure with three tolyl rings, one of them hydroxyl substituted. An identical substance was obtained by the action of *o*-toluenediazonium chloride on **19**; since diazonium couplings invariably take place at a free *para* position (24), this suggests **20** as the structure of the new compound.

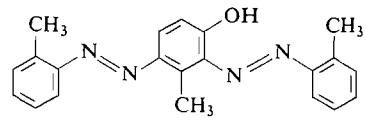

20

An irradiation of **6** was carried out in the presence of benzophenone to determine whether oxygen migration into the side chain could be induced under conditions known (2) to favor hydrogen abstraction. Under these conditions the reaction was much slower but no insertion into the side chain was observed. Instead, the normal product **19** was accompanied by the isomer **21**, previously obtained by Lewis and Reiss (25) as a by-product of the rearrangement of **6** in ethanol. Lewis and Reiss also obtained another isomeric photoproduct, **22**, but we did not observe this in our reactions in benzene.

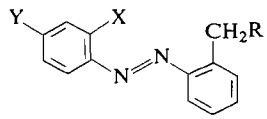

21 R = H; X = OH; Y = CH_3
22 R = H; X = CH_3; Y = OH
25 R = C_6H_5; X = OH; Y = $CH_2C_6H_5$
26 R = C_6H_5; X = $CH_2C_6H_5$; Y = OH

These abnormal products **20–22** look as though they might arise through the coupling of an *o*-toluenediazonium cation with an appropriate phenol. Lewis and Reiss (25) considered the possibility of fragmentation of **19** on photolysis giving the by-products by the mechanism of Scheme 3 but had to reject this proposal on the grounds that **19** is photostable, an observation which we confirm. In addition, photolysis of azobenzene in a mixture of benzene and phenol gives neither *p*-hydroxyazobenzene (from attack of a benzenediazonium radical or ion on phenol) nor biphenyl (from the action of a phenyl radical on benzene), indicating that C—N bond fission did not occur; indeed, the available evidence (26) suggests that aromatic azo compounds cleave at the N—N rather than the C—N bonds upon irradiation. We currently believe that diazonium ion intermediates are involved as intermediates in the formation of these side products **20–22** but that they are the result of fragmentation of a precursor of **19**

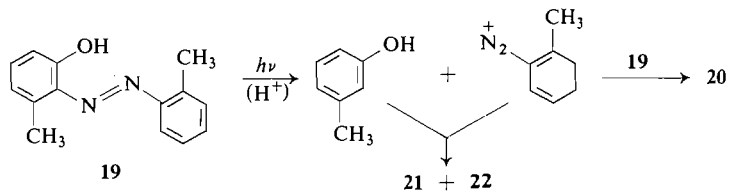

SCHEME 3

rather than of **19** itself. This work is still in progress and will be published elsewhere.

Azoxytoluene **6** has also been photolyzed in quartz equipment in the presence of benzophenone using 2-propanol as the solvent. Under these conditions photoreduction to 2,2′-azotoluene accompanied the photorearrangement, thereby demonstrating that hydrogen abstraction was occurring. Even so, no migration of oxygen into the side chain was observed, implying that hydrogen abstraction was wholly intermolecular (from the solvent).

It was thus concluded that oxygen migration to a side chain methyl group is less facile than insertion into the benzylic bond, despite the higher bond dissociation energy of the latter (27). This conclusion is confirmed by the results of photolysis of **12** and **13**, where the normal rearrangement cannot occur. These compounds do not undergo benzylic insertion; instead they are very photostable, being slowly converted to tar but not to tractable products. A parallel observation has been made previously (25) regarding **14** which suffers no change in electronic spectrum on irradiation. We observed reaction only in **13**, which underwent *cis–trans* photoisomerization.

Photolysis of **7** proceeded normally, giving only the expected rearrangement product **23** and a compound believed to be the *cis* isomer of **7** because it reverted to **7** on work-up. A variety of low yield photoproducts was obtained on illumination of azoxydiphenylmethane **8**; of these, three were isolated in quantities sufficient to permit a partial characterization. They are believed to be **24–26**, the analogs of **19**, **21**, and **22** formed on irradiation of **6**.

Irradiation of the acetals **9** and **10** gave the *o*-hydroxyazo compounds, **27** and **28** respectively, together with numerous other low yield products which were incompletely characterized. The products from **9**, which we were unable to purify, had n.m.r. spectra with resonances typical of —CHO and —CO_2CH_3 groups as well as OCH_3, OH, and aromatic C—H linkages, suggesting the possibility of photofragmentation of the acetal group (CHO) and oxygen insertion into the benzylic side chain (CO_2CH_3). In the presence of benzophenone, none of the usual product **27** could be obtained from **9**, but compounds with CHO and CO_2CH_3 groups in their n.m.r. spectra were still observed.

2,2′-Azoxybenzaldehyde photolyzed faster than the other compounds but gave no *o*-hydroxyazo compound. Instead, there was obtained the lactone **29**, a known (19, 28) transformation product of 2′-formylphenylazo-2-benzoic acid (**30**), the expected result of oxygen migration into the benzaldehyde group. While **11** thus

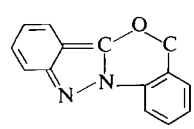

29

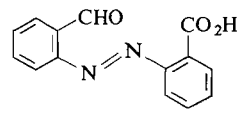

30

undergoes the abnormal rather than the normal mode of oxygen migration on photolysis, the greater rapidity of reaction of **11** than of **6–10** and the structural similarity between **11** and *o*-nitrobenzaldehyde, which also photorearranges efficiently (8), suggests the possibility of a change of mechanism in this case.

From this series of experiments we may conclude that while oxygen migration to a benzylic site is possible, as in **11**, or cannot be excluded, as in **9** and **10**, it does not take place as readily as would be predicted on the basis of the hydrogen abstraction mechanism of Scheme 2. Direct competition between abstraction of an aromatic hydrogen and a more weakly bound benzylic hydrogen should have resulted in preferential abstraction at the benzylic site. Scheme 1 is thus more consistent with these observations than Scheme 2, although we must add this reservation: steric factors might make attainment of the transition state for benzylic abstraction less facile than that for aromatic C—H removal, causing the weak benzylic bonds

Can. J. Chem. Downloaded from www.nrcresearchpress.com by 210.87.254.42 on 09/05/12
For personal use only.

TABLE 1. Variation with solvent in the quantum yield and deuterium isotope effect for 2-hydroxyazobenzene formation on photolysis of azoxybenzene and its d_{10} analog

Solvent	Φ		k_2[e]	Φ^H/Φ^D
	Relative	Absolute		
95% ethanol	1.00[a]	0.22[c]	1.00[a]	1.26±0.07(6)
100% ethanol	0.875±0.03(8)[b]	0.19	0.84	1.27±0.10(8)[d]
Methanol	0.761±0.04(9)	0.16	0.71	0.98±0.05(4)
Acetic acid	0.998±0.08(7)	0.22	0.99	—
Acetonitrile	0.509±0.03(7)	0.11	0.45	—
10% aqueous acetonitrile	0.764±0.02(7)	0.17	0.72	—
Benzene	0.170±0.01(8)	0.037	0.14	1.25±0.15(6)
Cyclohexane	0.038±0.004(4)	0.008	0.03	—

[a]Assumed; data are for appearance of 2-hydroxyazobenzene.
[b]Number of determinations in parentheses; ± values are statistical deviations (58).
[c]Measured directly; other values calculated from relative Φ.
[d]Data for disappearance of azoxybenzene were 1.37 ± 0.15 (2).
[e]Refers only to mechanism of Scheme 2; see text.

of **6**–**10** and of **12** to be immune towards attack. This kind of argument has been made by Gore and Wheeler (29), who have interpreted anomalies in the electronic spectra of 2,2′-disubstituted azoxybenzenes in terms of steric hindrance to coplanarity. On the other hand, Tanikaga (30) in his study of the *normal* azoxybenzene photorearrangement has presented evidence that steric factors are unimportant in his systems. To try to gain information about the possible influence of steric factors in the azoxybenzene photorearrangement, we carried out a number of experiments using azoxybenzene itself, where steric factors should be unimportant.

Solvent Effects

In the first series of these experiments, the rate of photorearrangement of azoxybenzene was compared in eight solvents of differing polarity. Relative and absolute quantum yields for 2-hydroxyazobenzene formation are given in Table 1. To try to interpret the results obtained, the following analysis was used. Schemes 1 and 2 may both be abbreviated as in eq. 1 in terms of an excited state of azoxybenzene A* and an intermediate I which yields product. Assuming

[1] $$A_0 \underset{k_1}{\overset{h\nu}{\rightleftharpoons}} A^* \xrightarrow{k_2} I \begin{cases} \xrightarrow{k_3} \text{Product} \\ \xrightarrow{k_4} A_0 \end{cases}$$

steady states of A* and I, the quantum yield Φ for product formation is given in eq. 2.

[2] $$\Phi = k_2k_3/(k_3 + k_4)(k_1 + k_2)$$

This expression only simplifies significantly if $k_3 \gg k_4$ when

[2a] $$\Phi \simeq k_2/(k_1 + k_2) \text{ or } k_2 = k_1\Phi/(1 - \Phi)$$

If the abstraction mechanism, Scheme 2, were to represent the reaction pathway, it could be shown that k_3 would indeed be greater than k_4 by the following argument. Since proton transfer reactions are very rapid, it is likely that intermediate B of Scheme 2 would have a long enough lifetime to exchange its proton with the medium; if it now returns to azoxybenzene, the hydrogen atoms of the medium should be incorporated into the starting material. Photolyses of azoxybenzene in CH_3CN–D_2O and of azoxybenzene-d_{10} in ethanol gave no incorporation of the alternate hydrogen isotope into the starting azoxy compound when the irradiations were carried out to partial conversion and the starting material recovered. Thus if Scheme 2 is the mechanism, $k_3 \gg k_4$, and the rates of the abstraction steps (k_2) are proportional to $\Phi/(1 - \Phi)$, assuming that the fluorescence lifetime of azoxybenzene ($1/k_1$) is independent of solvent; this is probably true within the approximations of the above argument (31).

The relative quantum yields of Table 1 thus approximate to relative rate constants (k_2) as applied to Scheme 2. They cannot be applied to Scheme 1, since we have no knowledge of the relative magnitude of k_3 and k_4 if this mechanism is operating. However, the data of Table 1 make it unlikely that Scheme 2 is the proper mechanism, in that a factor of about 30 separates the

Can. J. Chem. Downloaded from www.nrcresearchpress.com by 210.87.254.42 on 09/05/12
For personal use only.

Can. J. Chem. Downloaded from www.nrcresearchpress.com by 210.87.254.42 on 09/05/12
For personal use only.

quantum yields for cyclohexane and 95% ethanol. This is suggestive of a polar mechanism. Polar media may either increase the rate of formation of the intermediate, or they must promote the breakdown of the intermediate to product rather than to A_0.

Deuterium Isotope Effect

The hydrogen abstraction pathway of Scheme 2 ought to show a moderately large primary deuterium isotope effect for the rate-limiting removal of the strongly bound aromatic hydrogen. Relative quantum yields Φ^H/Φ^D for the rearrangement of azoxybenzene-d_0 and -d_{10} were determined in four different solvents and are reported in Table 1; in each case the isotope effect was very small.

The problem in interpreting this isotope effect is that we may not in this case simply assume that the fluorescent lifetimes of the d_0 and d_{10} compounds will be equal, since the *triplet* excited state lifetimes of aromatic molecules are now well known to be increased by up to a power of 10 by perdeuteration (32). Several theories have been advanced to account for this effect (32), which is known to be due to changes in the rates of radiationless return to the ground state in the protio and deuterio molecules. One possibility (33) is a decrease in the Franck–Condon factor for the deuterio molecule, since T_1 has to overlap with a higher vibrational level of S_0 in the deuterio than in the protio molecule, due to C—D vibrational quanta being smaller than those of C—H. This reduces the probability of radiationless transition and increases the triplet lifetime. Similar considerations should apply to radiationless decay from singlet excited states but less is known about the magnitude of the effect for lack of experimental data. Ideally one would like to measure the fluorescence lifetimes of azoxybenzene-d_0 and -d_{10} experimentally. An attempt to do this was made in collaboration with Dr. W. R. Ware and Mr. T. Nemzek of the University of Western Ontario, using the single photon counting technique, but unfortunately, azoxybenzene was found to be non-fluorescent, an upper limit on Φ_F being about 10^{-4}.

Studies on the aromatic hydrocarbons pyrene and coronene and their perdeuterated analogs have indicated that deuteration has very little effect on the fluorescence lifetimes of these molecules either at 77 °K or at room temperature (34). In private correspondence, Dr. J. L. Kropp of TRW Inc. has suggested that the change in lifetime would not normally exceed ±20% on deuteration. This may not be true of our system however, where almost 80% of all excited singlet molecules are disappearing by non-radiative and non-photochemical processes.

To the extent that we can assume that there is no large deuterium isotope effect on the rate constants for radiationless processes, we believe that the observed small isotope effect is not the result of superimposing a large kinetic isotope effect upon a longer singlet lifetime in the d_{10} system. Taking the mean value from Table 1 of $\Phi^H/\Phi^D = 1.22$, a 20% spread in either direction gives us a likely range of $k^H/k^D = 0.98$–1.46, which is smaller than would have been expected for a primary effect for abstraction from the strong aryl C—H bond. For example, abstraction by oxygen from saturated sites in the type II reaction of aralkyl ketones displays $k^H/k^D = 4.8$ (35), comparable with the isotope effects observed in wholly aliphatic ketones (36) and comparable also with hydrogen abstraction by oxygen in the *t*-butoxy radical (37). For the isotope effect exhibited in the azoxybenzene photorearrangement to be primary, the azoxy oxygen would have to be at least as reactive a hydrogen abstractor as the chlorine atom and far more so than typical oxyradicals (37). Taken together with the evidence already presented, this small isotope effect excludes Scheme 2 as a likely mechanism.[5]

Scheme 1 could accommodate the observed isotope effect in one of two ways: first, if the removal of hydrogen from the Badger and Buttery intermediate A rather than the formation of the intermediate is the slow step in the reaction; second, if the formation of the intermediate is the slow step but the isotope effect being observed is secondary rather than primary. This latter explanation seems less likely in that conversion of sp^2 centers to sp^3 is usually accompanied by an inverse isotope effect $k^H < k^D$ (38), although both normal and inverse secondary deuterium isotope effects have been

[5]The small isotope effect cannot be the result of hydrogen abstraction being either non-rate-determining or reversible ($k_4 > k_3$) from the lack of isotopic exchange in the experiments of the previous section.

observed in electrophilic aromatic substitution (39). At present, we cannot distinguish these possibilities.

Conclusions

Taken together, we believe that the experiments described constitute strong evidence against a hydrogen abstraction mechanism for the azoxybenzene photorearrangement. First, the benzylic C—H bonds of the 2,2′-disubstituted azoxybenzenes are unreactive despite the lower bond dissociation energies of benzylic *vs.* aryl C—H bonds. Second, the rate of reaction increases in polar solvents, suggestive of a polar rather than a radical pathway. Third, the deuterium isotope effect is far too small to be associated with a primary isotope effect for abstraction of the strongly bound aryl hydrogen.

In addition, a $^1\pi,\pi^*$ state is responsible for the azoxybenzene photorearrangement (2), whereas most photochemical hydrogen abstractions *e.g.* of ketones (40) or nitrocompounds (41) proceed from n,π^* states. Although exceptions are known (42, 43), this behavior is suggestive of a mechanism not involving hydrogen abstraction. Lastly, we have found that the photorearrangement of azoxybenzene in styrene solution does not cause polymerization of the styrene, indicating that free radical intermediates are not present.

On all these grounds, we believe that a mechanism involving aromatic substitution, as proposed by Badger and Buttery (3) better accommodates our experimental data than a hydrogen abstraction pathway. A remaining problem is whether the azoxy oxygen attacking the aromatic ring is electron rich, as originally proposed by Badger and Buttery, or electron poor, since the azo linkage is known (44) to be able to stabilize the charge of the intermediates for either nucleophilic or electrophilic substitution at the *ortho* and *para* positions. The literature is unhelpful on the effect of polar substituents on the rate of photorearrangement; Tanikaga (30) found that electron donating or withdrawing substituents at the 4,4′-positions of azoxybenzene alike reduced the efficiency of oxygen migration. We are currently investigating this aspect of the problem and hope to report our findings in a later paper.

Experimental

Irradiations were carried out in an immersion well apparatus, using a Hanovia Model 679A 450 W mercury arc and a cooling well constructed of Pyrex glass to filter out short wave ($\lambda < 300$ nm) radiation. The outer jacket, which was equipped with a reflux condenser, had a volume of 300 ml with the cooling well in place and was constructed with a flat base to permit agitation of the solution by means of a magnetic stirrer. For irradiations carried out in the absence of oxygen, a similar outer vessel was used except that agitation was provided by means of a nitrogen flush through a porosity C sintered glass disc which was positioned near the base of the apparatus, an inlet tube for the nitrogen being sealed into the outer wall of the jacket. Relative rate and quantum yield experiments used the same source and cooling jacket, and were run in corked Pyrex ampoules in batches of eight using a Rayonet "Merry-go-round" apparatus.

Chromatographic separations on columns were run using standard alumina and silica gel adsorbents; preparative t.l.c. was run on 20 × 40 cm plates using a Brinkmann "sandwich" style apparatus or on 20 cm × 1 m plates using a Shandon preparative layer apparatus. The adsorbent was E. Merck Type 7747 silica gel PF_{254} incorporating a fluorescing agent to locate the bands; the developing solvent is indicated in parentheses in the individual procedures. Analytical t.l.c. plates were prepared using the same silica gel adsorbent and occasionally also using J. T. Baker Type 9F alumina. After separation of the reaction mixtures by preparative t.l.c., the bands were scraped off and extracted using a Soxhlet extractor for further purification. For identification of the 2-hydroxyazo compounds, use was made of the characteristic (45) mass spectral fragmentation pattern of azo compounds ($ArN{=}NAr' \rightarrow Ar^+, ArN_2^+, Ar'^+, Ar'N_2^+$) and the well-known (46) low field n.m.r. resonance exhibited by a hydroxyl group situated *ortho* to an azo linkage. Microanalyses on purified samples were carried out either by Mr. H. S. McKinnon of this department or by Dr. C. Daesslé, Montreal.

Solvents were reagent grade materials and were dried and distilled before use. Petroleum ether, b.p. 30–60°, was fractionally distilled to remove high boiling residues. Melting points were run on a Mel-Temp apparatus and are uncorrected. Spectroscopic instruments used included a Pye Unicam SP800 u.v.-visible, Beckman IR5A i.r., Varian Associates A60-A n.m.r., and Varian MAT model CH7 mass spectrometer, which was operated at 70 eV ionizing voltage.

*2,2′-Azoxytoluene (**6**)*

2-Nitrotoluene (British Drug Houses, 0.5 mol) was added over a period of 40 min to a mixture of sodium hydroxide (1 mol) and methanol (100 ml) at reflux. The mixture was heated to reflux for 1 h, cooled, and poured into water (250 ml). The solids were collected by suction, dissolved in benzene, and passed through a 2.5 × 16 cm column of alumina, using benzene as the eluent. Recrystallization from methanol of the material obtained gave 2,2′-azoxytoluene (18 g, 32%): m.p. 57.5–58° (lit. (47) 59°); n.m.r. (CCl_4) δ 2.28, 2.42 (2 singlets, 2 CH_3 groups), 7.0–8.1 (multiplet, 8 ArH).

*Irradiation of **6***

(*a*) A solution of **6** (0.149 g) in benzene (300 ml) was irradiated for 35 min. Evaporation of the solvent and resolution of the residue by preparative t.l.c. (40% benzene in petroleum ether) gave 0.031 g of red solid:

Can. J. Chem. Downloaded from www.nrcresearchpress.com by 210.87.254.42 on 09/05/12
For personal use only.

Can. J. Chem. Downloaded from www.nrcresearchpress.com by 210.87.254.42 on 09/05/12
For personal use only.

m.p. 70–80°; m.p. after recrystallization from ethanol 92–93.5° (lit. (25) for 2-hydroxy-6,2′-dimethylazobenzene 97°); n.m.r. ($CDCl_3$) δ 2.7 and 2.8 (2 singlets, 2 CH_3 groups), 6.8–8.2 (multiplet, 7 ArH), 14.0 (singlet, OH).

(*b*) A solution of **6** (0.20 g) in benzene (200 ml) was irradiated for 30 min. Evaporation of the solvent and resolution by preparative t.l.c. gave two bands. The more mobile band (97 mg) was **19**, red needles from methanol: m.p. 95–96°; u.v. (EtOH) λ_{max} 395 (sh) (ε 10 000), 335 (21 000), and 240 nm (8500).

Anal. Calcd. for $C_{14}H_{14}N_2O$: N, 12.4. Found: N, 12.4.

The less mobile band (12 mg), a dark brown solid, m.p. 167–169°, was identified as 3-methyl-2,4-bis(*o*-tolylazo)phenol (**20**), having i.r., n.m.r., and mass spectra identical to authentic **20**, prepared in 48% yield by the action of excess *o*-toluenedizaonium chloride on **19** (0.04 g). Data obtained for authentic sample of **20**: m.p. 168–171°; n.m.r. ($CDCl_3$) δ 2.61, 2.70, 3.12 (3 singlets, 3 CH_3 groups), 6.6–8.0 (multiplet, 10 ArH), 14.65 (singlet, OH); u.v. (EtOH) λ_{max} 420 (sh) (ε 5900), 350 (32 000), and 235 nm (11 000); mass spectrum M^+ 344, other prominent peaks at *m/e* 243, 215, 119, 91.

Anal. Calcd. for $C_{21}H_{20}N_4O$: N, 16.3. Found: N, 16.7.

(*c*) Sensitized irradiation: a solution **6** (0.998 g) and benzophenone (4.3 g) in benzene (260 ml) was degassed under reflux using oxygen-free nitrogen,[6] then irradiated for 35 min under nitrogen. The solvent was removed, the residue taken up in ethanol, and a solution of 2,4-dinitrophenylhydrazine (4.7 g) in H_2SO_4–H_2O–EtOH was added. Filtration of the cooled solution afforded benzophenone 2,4-dinitrophenylhydrazone (9.0 g), m.p. 229–230° (lit. (48) 231°). Neutralization of the excess acid, drying, and evaporation afforded a residue which was resolved by preparative t.l.c. (20% benzene in petroleum ether) to give four bands.

Band 1 (13 mg) would not crystallize and was discarded. Band 2 (87 mg), a mixture, was red crystals, m.p. 100–102°, and was further resolved by preparative t.l.c. (petroleum ether) to give two major bands, 2A and 2B. Band 2A (21 mg) had m.p. 86–88°, and on recrystallization from ethanol was identified as **19**: m.p. 94.5–95°; n.m.r. (CCl_4) δ 2.66 and 2.70 (2 singlets, 2 CH_3 groups), 6.7–8.0 (multiplet, 7 ArH), 13.5 (singlet, OH); mass spectrum *m/e* (relative intensity) 226 (M^+) (37), 135 (24), 107 (69), 91 (100). Band 2B (30 mg) was obtained as fine orange needles from ethanol: m.p. 123–124° (lit. (25) for 2-hydroxy-4,2′-dimethylazobenzene (**21**), 126°); n.m.r. (CCl_4) δ 2.36 and 2.60 (2 singlets, 2 CH_3 groups), 6.7–8.0 (multiplet, 7 ArH), 11.1 (singlet, OH); mass spectrum *m/e* (relative intensity) 226 (M^+) (47), 135 (31), 107 (100), 91 (91).

Band 3 (10 mg) was a brown semi-solid. Recrystallization from ethanol gave 1 mg, m.p. 184–185°. This compound is possibly **20**; the mass spectrum showed a probable molecular ion near *m/e* 340.

Band 4 (538 mg) was an orange solid, m.p. 39–43°, and had the n.m.r. spectrum of the starting material. Recrystallization from ethanol gave recovered **6**, 480 mg, m.p. 56–57.5°.

(*d*) Sensitized irradiation using an unfiltered mercury arc: a solution of **6** (0.50 g), and benzophenone (1.0 g) in 2-propanol (300 ml) was degassed and irradiated for 20 min. Resolution of the evaporated reaction mixture by t.l.c. gave 2,2′-azotoluene (107 mg), m.p. 52–54° (lit. (49) 55°); M^+ 210, azoxytoluene (30 mg, estimated by u.v., λ_{max} 312 nm, ε 11 000); and the hydroxyazo compound **19** (34 mg, estimated by u.v.).

Photolysis of ***19***

A solution of **19** (26 mg) in benzene (2.0 ml) was irradiated for 6 h in a 5 ml Pyrex flask equipped with reflux condenser, using an external source. Analytical t.l.c. showed only one spot in the reaction mixture, and passage of the reaction mixture through a short column of silica gel, eluting with benzene, allowed recovery of **19** (22 mg), m.p. 94–96°.

Irradiation of Azobenzene

(*a*) A solution of azobenzene (0.75 g) in benzene (200 ml) was irradiated for 13 h. Evaporation of the solvent and chromatography on alumina (60 g), eluting with benzene, gave *trans*-azobenzene (0.53 g), m.p. 67–68° and *cis*-azobenzene (0.14 g), which changed to *trans* by heating in benzene. No biphenyl could be detected (t.l.c., v.p.c.).

(*b*) A mixture of azobenzene (0.1 g), phenol (2.0 g), and benzene (200 ml) was irradiated for 3 h. After evaporation of the solvent, neutral and acidic extracts were made. The neutral extract contained *cis*- and *trans*-azobenzene (0.09 g) but not biphenyl (t.l.c. analysis, alumina plates), and the colorless acidic material contained only phenol (1.95 g).

*2,2′,6,6′-Tetramethylazoxybenzene (****12****)*

To a solution of lithium aluminum hydride (5.0 g) in dry ether (500 ml) was added in small portions a solution of 2,6-dimethylnitrobenzene (Eastman Kodak, 20 g) in ether (30 ml) and the mixture was heated to reflux for 17 h. After quenching the excess lithium aluminum hydride with ethyl acetate, the organic phase was washed with 2 *M* sulfuric acid, dried, and evaporated. The residue was chromatographed on silica gel (120 g) when 5% benzene in petroleum ether (b.p. 60–80°) eluted 2,2′,6,6′-tetramethylazobenzene (2.0 g), m.p. 46–47° (lit. (50) 47°). Later fractions gave recovered starting material (3.1 g).

The azocompound (1.65 g) was oxidized with 30% H_2O_2 (10 ml) in acetic acid (100 ml) at 60° affording 2,2′,6,6′-tetramethylazoxybenzene in quantitative yield. After recrystallization from methanol, the product was yellow rods, m.p. 89.5–90° (lit. (17) 91°).

Anal. Calcd. for $C_{16}H_{18}N_2O$: C, 75.5; H, 7.1; N, 11.0. Found: C, 75.8; H, 6.8; N, 11.2.

Irradiation of ***12***

A solution of **12** (0.495 g) in benzene was irradiated for 5 h. Evaporation of the solvent and preparative t.l.c. (20% benzene in petroleum) gave the starting material (0.386 g), m.p. 90–91°, as the only isolable material. An irradiation in the presence of benzophenone gave similar results.

[6]Prepared by passing commercial high purity nitrogen through a chromous chloride solution (made from $HgCl_2$ (15 g), zinc dust (5 g), and $CrCl_3$ (5 g) in 200 ml water), then dried by passage through concentrated H_2SO_4 and a tower of granular $CaCl_2$, and finally saturated with benzene to minimize loss of the solvent.

Can. J. Chem. Downloaded from www.nrcresearchpress.com by 210.87.254.42 on 09/05/12
For personal use only.

*2,6-Dimethyl-NNO-azoxybenzene (**13**)*

To a solution of nitrosobenzene (1.6 g), prepared by the method of Vogel (51), in ethanol (15 ml), was added a solution of 2,6-dimethylaniline (3.0 ml) in acetic acid (5 ml). The mixture was heated to 80° for 15 min, cooled, washed with base, taken up into ether, dried, and evaporated. The residue was chromatographed on silica gel (60 g) when 30% benzene in petroleum ether, b.p. 60–80°, eluted 2,6-dimethylazobenzene (1.07 g) as a red oil (52), pure by t.l.c.

Anal. Calcd. for $C_{14}H_{14}N_2$: N, 13.3. Found: N, 13.5.

Oxidation of the azo compound (1.03 g) using 30% H_2O_2 (2.0 ml) in acetic acid (15 ml) at 60° for 6 h gave 2,6-dimethyl-*NNO*-azoxybenzene (1.09 g) as a pale yellow oil.

Anal. Calcd. for $C_{14}H_{14}N_2O$: N, 12.6. Found: N, 12.5.

N.m.r. (CCl_4) δ 2.07, 2.27 (2 singlets, ratio 78:22, CH_3 groups), 6.8-8.5 (multiplet, 8 ArH).

*Irradiation of **13***

A solution of **13** (107 mg) in benzene (75 ml) was irradiated with an external source for 1 h. Evaporation of the solvent and chromatography of the residue on alumina (50 g), eluting with benzene, gave the starting material (98 mg); the n.m.r. spectrum was unchanged from that of the starting material except that the ratio of the two CH_3 resonances was now 91:9.

*2,2′-Azoxycumene (**7**)*

2-Nitrocumene (K and K) was found by n.m.r. to be a mixture of approximately 70% *ortho*, 25% *para*, and 5% *meta* isomers. Resolution was effected on 1.5 g samples using alumina columns (350 g), eluting with benzene–petroleum (15:80), when the first fractions to elute were pure by t.l.c. From two such resolutions a total of 1.65 g of material was obtained[7], n_D^{20} 1.5200 (lit. (53) for *o*-nitrocumene 1.5248; for *m*- 1.5303; for *p*- 1.5369). This material was reduced at reflux for 2 h using thallium[8] (6.1 g) and ethanol (55 ml) (16). After the addition of potassium iodide (6 g) the mixture was stirred for 1 h, filtered and evaporated. The residue, dissolved in benzene, was chromatographed over alumina (30 g) when benzene–petroleum (4:6) eluted the azoxy compound (0.63 g, 44%), an oil which was purified by crystallization from ethanol at −80° and dried *in vacuo* for several hours. N.m.r. (CCl_4) δ 1.22, 1.29 (two doublets, J = 7 Hz, 12H, CH_3), 3.35, 3.45 (two superimposed septets, J = 7 Hz, 2 CH), 7.10–8.30 (multiplet, 8 ArH); mass spectrum (relative intensity) *m/e* 282 (M^+) (<1), and prominent ions at *m/e* 266, 250, 240, 149, 133, 131, 121, 119, 118, 116, 107, 106, 105, 104, 103, 91 (100).

Anal. Calcd. for $C_{18}H_{22}N_2O$: C, 76.55; H, 7.86; N, 9.93. Found: C, 76.43; H, 7.59; N, 10.11.

*Irradiation of **7***

A solution of **7** (0.630 g) in benzene (300 ml) was irradiated under nitrogen for 1 h, during which time the starting material completely reacted (t.l.c.) and was replaced by two major components. Evaporation of solvent and resolution by preparative t.l.c. (20% benzene in petroleum) gave four bands. The most mobile, band 1 (123 mg), a red oil, was a mixture containing one major component, which was isolated pure by running a second preparative plate. Subsequent precipitation from methanol at −80° followed by drying *in vacuo* gave 2-hydroxy-6,2′-diisopropylazobenzene, **23** (60 mg): n.m.r. (CCl_4) δ 1.25, 1.35 (two doublets, J = 7 Hz, 12H, CH_3), 2.91, 3.73 (two septets, J = 7 Hz, 2 CH), 6.75–7.90 (multiplet, 7 ArH), 12.70 (singlet 1H, OH); u.v. (ethanol) λ_{max} 337 (ε 18 500), 248 (8200), and 243 nm (8000); mass spectrum *m/e* (relative intensity) 282 (M^+) (61), 267 (94), 135 (39), 133 (100), 132 (55), 91 (84).

Anal. Calcd. for $C_{18}H_{22}N_2O$: C, 76.55; H, 7.86; N, 9.93. Found: C, 77.21; H, 7.53; N, 10.10.

Band 2 from the t.l.c. resolution (16 mg) was a mixture and could not be resolved further. Band 3 (290 mg) on isolation had the n.m.r. and R_f of the starting material and was presumed to be the *cis* isomer of 7 which on work-up reverted to starting material; band 4 (32 mg) was shown by t.l.c. to be a mixture of at least four compounds and was discarded.

*2,2′-Dibenzylazoxybenzene (**8**)*

2-Nitrodiphenylmethane was prepared from *o*-nitrobenzyl chloride (Aldrich) and benzene–$AlCl_3$ by the method of Geigy and Königs (54). The procedure was modified in that the crude product was partly purified by passage through a 30 g column of alumina before steam distillation. From 6.5 g of benzyl chloride was obtained 6.5 g of partly purified material, 3 g of which was steam distilled to give 1.7 g of 2-nitrodiphenylmethane (pure by t.l.c.). Thallium reduction (16) of this material overnight and the usual work-up gave an oil; this crystallized on standing and was further purified by preparative t.l.c. (benzene–petroleum, 1:1) affording the product (0.60 g), which crystallized from ethanol, 0.48 g: m.p. 53–56°; mass spectrum *m/e* 378 (M^+), see Table 2; n.m.r. (CCl_4) δ 3.99, 4.17 (singlets, two CH_2 groups), 7.0–8.2 (multiplet 18 ArH).

Anal. Calcd. for $C_{26}H_{22}N_2O$: C, 82.50; H, 5.86; N, 7.41. Found: C, 82.56; H, 6.16; N, 7.65.

*Irradiation of **8***

A solution of **8** (0.45 g) in benzene (300 ml) was irradiated for 2 h, after which the solvent was evaporated and the residue resolved by preparative t.l.c. (benzene–petroleum, 1:1). Three major bands were obtained. The most mobile band comprised 50 mg red solid, m.p. 95–105°, not improved by repeated recrystallization from ethanol, and was found to be a mixture by t.l.c. on alumina. Chromatography of band 1 on alumina (20 g), eluting with petroleum containing increasing amounts of benzene (up to 25% v/v), gave three fractions. The most mobile, band 1A (2 mg), red crystals, had m.p. 168–170°; band 1B, red crystals (2 mg), had m.p. 102–105°; band 1C, red crystals (8 mg), had m.p. 130–131°, softened at 121°. The mass spectra of these three compounds, recorded in Table 2, showed that they were all isomers of **8**, consistent with structures **24**–**26**. Too little material was obtained to run n.m.r. spectra, but using the reported (25) method, it was shown that 1C was compound **26** by u.v., since it alone had a pronounced red shift when the spectrum was run in the presence of 10^{-2} *M* potassium

[7]The purified *o*-nitrocumene discolored rapidly upon exposure to air, so it and the subsequent cumyl derivatives were handled and stored under nitrogen.

[8]Molten commercial thallium (British Drug Houses) was poured into water and washed with ethanol.

TABLE 2. Mass spectral fragmentation patterns of compounds **8**, **24**, **25**, and **26**

	Relative abundance of ion			
m/e	**8**	Band 1A	Band 1B	Band 1C (**26**)
379	31	30	19	29
378(M^+)	100	93	61	100
377	25	47	23	17
363	4	—	—	—
362	5	4	—	—
302	24	18	24	20
301	100	100	100	84
287	10	13	14	4
223	3	9	—	—
211	13	—	—	8
199	4	—	9	5
196	8	11	14	—
195	7	—	—	—
183	28	10	34	27
182	19	19	24	13
181	19	10	10	15
180	46	25	7	35
168	11	4	11	9
167	41	12	21	28
166	20	11	16	16
165	59	37	49	43
155	6	—	—	—
154	5	—	—	—
153	16	—	13	13
152	31	6	22	24
151	5	14	7	4
150	9	3	8	7

hydroxide (see Table 3). Hence 1A and 1B were **24** and **25**, though not necessarily respectively. Attempts to find free (compound **26**) and chelated (**24** and **25**) hydroxyl stretching frequencies in the i.r. were unsuccessful due to lack of material, though there was some indication of a free hydroxyl group in 1C (ν_{max} (CS_2) 3550 cm^{-1}).

Band 2 from the preparative t.l.c. plate was starting material (200 mg), while band 3 (red oil 80 mg) was a mixture by t.l.c. Attempts to obtain pure materials from this fraction were unsuccessful.

2-Nitrobenzaldehyde Dimethyl Acetal (34)

2-Nitrobenzaldehyde (Aldrich, 0.1 mol) was dissolved in a mixture of methanol (100 ml) and concentrated hydrochloric acid (1.5 ml). After 17 h at room temperature, the solution was basified with sodium methoxide, evaporated down, and water added. Extraction with ether, followed by evaporation of the organic phase gave the acetal (94%) as a colorless or yellow oil: n.m.r. (neat liquid) δ 3.33 (singlet, 6H, OCH_3), 5.95 (singlet, 1 CH), 7.31–7.95 (multiplet, 4 ArH).

2,2′-Azoxybenzaldehyde Bisdimethyl Acetal (9)

The acetal **34** was reduced by the method of Bamberger (15) using sodium and methanol. The crude azoxy compound was recrystallized from ethanol giving **9** (65%), m.p. 52–56° (lit. (15) 59°). When the reaction time was prolonged in order to improve the conversion, further reduction occurred. Fractional crystallization gave **9** (20%), together with 2,2′-azobenzaldehyde bisdimethylacetal (**16**) (13%): m.p. 142–143° (lit. (55) 144°); n.m.r. (CCl_4) δ 3.25 (singlet, 12H, OCH_3), 6.27 (singlet, 2CH), 7.25–7.85 (multiplet, 8 ArH).

Anal. Calcd. for $C_{18}H_{22}N_2O_4$: C, 65.43; H, 6.71; N, 8.48. Found: C, 65.48; H, 6.90; N, 8.44.

An attempt to prepare **9** by lithium aluminum hydride reduction of **34** to **16** followed by oxidation was unsuccessful. A reaction using **34** (0.06 mol) gave a crude reduction product (6.9 g) which was partly resolved by chromatography on silica gel. The least polar material, a red solid (0.25 g), eluted with 20% benzene in petroleum, n.m.r. (CCl_4) δ 2.16 (singlet), 7.2 (multiplet), area ratio 3:4. Oxidation with hydrogen peroxide in acetic acid gave a pale solid (0.24 g), m.p. 56–57.5°, undepressed by admixture with authentic 2,2′azoxytoluene (**6**), and with an identical n.m.r. Intermediate fractions from the column were red and had n.m.r. resonances characteristic of CHO, aromatic, OCH_3, and CH_3 protons, but were all mixtures. These were followed by unreacted **34** (2.5 g). The last fraction, removed from the column with methanol crystallized from methanol as orange plates (0.10 g), m.p. 139–141° with n.m.r. identical to **16** described above.

Anal. for $C_{18}H_{22}N_2O_4$: Found: C, 65.42; H, 6.64; N, 8.50.

Mass spectrum *m/e* 330 (M^+ absent), prominent peaks at *m/e* 282, 268, 267, 251, 237, 236, 235, 221, 194, 159, 130.

The best route to **9** was thallium reduction of **34**.

Can. J. Chem. Downloaded from www.nrcresearchpress.com by 210.87.254.42 on 09/05/12
For personal use only.

TABLE 3. Ultraviolet absorptions in ethanol of the products of irradiation of **8**

Compound	Neutral solution		10^{-2} *M* KOH	
	λ_{max} (nm)	log ε	λ_{max} (nm)	log ε
Band 1A	340	4.22	338	4.12
	243	3.80	243	3.84
	237	3.76	236	3.80
Band 1B	342	4.33	338	4.21
	245	3.84	246	3.89
	240	3.84	240	3.89
Band 1C (**26**)	376 sh	4.19	441	4.01
	334	4.31	325	4.11
	245	3.99	242	4.05
	240	3.93		

After the usual work-up, **9** was obtained as orange crystals from ethanol (64%): m.p. 54–56° (lit. (15) 59°); n.m.r. (CCl_4) δ 3.22, 3.24 (two singlets, 12H, OCH_3), 5.60, 5.90 (two singlets, 2 CH), 7.08–7.84 (multiplet, 8 ArH); u.v. (ethanol) λ_{max} 232 (log ε 4.0) and 307 nm (3.9).

Anal. Calcd. for $C_{18}H_{22}N_2O_5$: C, 62.41; H, 6.40; N, 8.09. Found: C, 62.79; H, 6.52; N, 8.07.

Irradiation of ***9***

A solution of **9** (1.00 g) in benzene (300 ml) was irradiated for 8 h. After removal of solvent, the residue was resolved by preparative t.l.c. (chloroform) to give three bands.

The most mobile band, band 1, was orange (439 mg), m.p. 82–84° after several recrystallizations from ethanol, and was identified as 3-hydroxy-2,2′-azobenzaldehyde bisdimethylacetal (27): n.m.r. (CCl_4) δ 3.50, 3.52 (two singlets, 12H, OCH_3), 6.07, 6.48 (two singlets, 2 CH), 7.00–8.14 (multiplet, 7 ArH), 12.76 (singlet, OH).

Anal. Calcd. for $C_{18}H_{22}N_2O_5$: C, 62.48; H, 6.39; N, 8.07. Found: C, 62.65; H, 6.48; N, 8.08.

Bands 2 and 3 were incompletely resolved and were further separated by t.l.c. Band 2 (54 mg) was starting material. Band 3 (34 mg) was an oil: n.m.r. (CCl_4) δ 3.30, 3.40, 3.50 (singlets OCH_3?), 3.80, 3.87 (singlets, $COOCH_3$?), 5.57, 5.62, 5.74, 6.23 (singlets CH), 6.7–7.7 (multiplet ArH). This substance was a mixture and could not be resolved further.

A second irradiation gave, in addition to **27**, various other poorly resolved and incompletely characterized materials whose n.m.r. spectra showed resonances typical of aromatic, —CHO, $\diagdown\!\!\diagup$CH, —$COOCH_3$, —OCH_3 and hydrogen bonded —OH groups. When the irradiation was carried out under nitrogen and in the presence of benzophenone, three products were obtained, but none could be obtained pure. Their n.m.r. spectra all showed the presence of —CHO protons, but low field resonances characteristic of hydrogen-bonded OH groups were absent.

*2,2′-Azoxybenzaldehyde Bisdiethyl Acetal (**10**)*

2-Nitrobenzaldehyde was converted to its diethylacetal in 91% yield: n.m.r. (neat) δ 1.10 (triplet, J = 7 Hz, 6H, CH_3), 3.50 (quartet, J = 7 Hz, 4H, CH_2), 5.84 (singlet, 1 CH), 7.16–7.74 (multiplet, 4 ArH). Thallium reduction (16) of the acetal gave the azoxycompound **10** (42%), m.p. 70–72°. A better yield was obtained by reduction of the acetal with sodium and methanol (15); after recrystallization of the crude product from ethanol the yield of **10** was 65%: m.p. 73–75° (lit. (15) 76°); n.m.r. (CCl_4) δ 1.13 (triplet, J = 7 Hz, 12 H, CH_3), 3.4 (two close quartets, J = 7 Hz, 8H, CH_2), 5.90, 6.17 (two singlets, CH), 7.2–8.0 (multiplet, 8 ArH). The mass spectrum showed a very small M^+ (*m/e* 402), first major peak *m/e* 384.

Anal. Calcd. for $C_{22}H_{30}N_2O_5$: C, 65.65, H, 7.51; N, 6.96. Found: C, 65.81; H, 7.57; N, 6.92.

Irradiation of ***10***

A solution of **10** (1.00 g) in benzene (300 ml) was irradiated for 1 h. Evaporation of solvent and resolution of the residue by t.l.c. (chloroform) gave four bands. Band 1 (131 mg) was a mixture: n.m.r. (CCl_4) δ 1.20 (two triplets, area 103, CH_3), 3.6 (two quartets, area 63, CH_2), 5.86, 6.00, 6.15, 6.43 (singlets areas 5:3:5:2, CH), 7.15–8.06 (multiplet, area 59, ArH), 12.36, 12.74 (two singlets, areas 1:4, OH). Recrystallization from petroleum ether, b.p. 30–60°, then from ethanol gave the major component; m.p. 85–86°; mass spectrum *m/e* (relative intensity) 402 (M^+ absent), 356 (2), 328 (20), 327 (100), 312 (20), 311 (31), 284, (47), 253 (80), 237 (71), 151 (31), 120 (7).

Anal. Calcd. for **28**, $C_{22}H_{30}N_2O_5$: C, 65.65; H, 7.51; N, 6.96. Found: C, 65.38; H, 7.83; N, 6.98.

Band 2 from the t.l.c. plate (646 mg) was starting material, m.p. 72.5–74°, after crystallization from petroleum. Band 3 (156 mg), an oil, appeared to be the *cis* isomer of the starting material, since on recrystallization it was converted to **10**, m.p. 71–73°. Band 4, a red oil (32 mg), was unidentified; its n.m.r. spectrum was similar to that of **10** and had no low field resonances typical of hydrogen-bonded OH protons.

*2,2′-Azoxybenzaldehyde Bisethylene Acetal (**15**)*

2-Nitrobenzaldehyde was converted to its ethyleneacetal (90%), n.m.r. (neat): δ 3.90 (singlet, 4H, CH_2), 6.47 (singlet, 1 CH), 7.3–8.0 (multiplet, 4 ArH). The acetal was reduced by the thallium and ethanol method

Can. J. Chem. Downloaded from www.nrcresearchpress.com by 210.87.254.42 on 09/05/12
For personal use only.

Can. J. Chem. Downloaded from www.nrcresearchpress.com by 210.87.254.42 on 09/05/12
For personal use only.

(16) to give the azoxy compound **15** as yellow needles from ethanol (66%): m.p. 103.5–104.5°; n.m.r. ($CDCl_3$) δ 3.95 (close multiplet, 8H, CH_2), 6.30, 6.48 (two singlets 2H, CH), 7.24–8.30 (multiplet, 8 ArH). The mass spectrum showed M^+ (*m/e* 342) and other prominent ions at *m/e* 296, 253, 234, 192, 177, 163.

Anal. Calcd. for $C_{18}H_{18}N_2O_5$: C, 63.13; H, 5.30; N, 8.19. Found: C, 62.61; H, 5.37; N, 8.00.

*2'-Formylphenyl-ONN-2-azoxybenzaldehyde Dimethyl Acetal (**17**), R = CH_3*

The bisdimethylacetal **9** (1.95 g) was dissolved in warm methanol (50 ml), then water (20 ml) and concentrated hydrochloric acid (1 ml) were added with stirring. After 2 min, the solution was diluted with water (50 ml) and extracted with chloroform. The organic phase was washed ($NaHCO_3$), dried ($MgSO_4$), and evaporated, and the residue recrystallized from ethanol to give the compound (0.52 g) as tan crystals: m.p. 59–60°; n.m.r. ($CDCl_3$) δ 3.30 (singlet, 6H, OCH_3), 5.95 (singlet, 1 CH), 7.26–8.10 (multiplet, 8 ArH), 10.44 (singlet, 1 CHO); u.v. (EtOH); λ_{max} 308, 248, and 214 nm (ε undetermined but smaller for the 308 nm band); mass spectrum *m/e* (relative intensity) 300 (M^+ absent), 246 (26), 233 (52), 220 (38), 193 (28), 180 (100), 151 (6), 150 (12), 149 (44), 119 (32), 105 (48), 91 (72), 77 (86).

Anal. Calcd. for $C_{16}H_{16}N_2O_4$: C, 63.99; H, 5.37; N, 9.33. Found: C, 64.00; H, 5.45; N, 9.23.

From a 1 h irradiation of this substance (0.255 g) in benzene, only starting material (94 mg) could be recovered.

*2'-Formylphenyl-ONN-2-azoxybenzaldehyde Diethyl Acetal (**17**), R = C_2H_5*

To a solution of **10** (1.0 g) in glacial acetic acid (3 ml) and acetonitrile (2 ml) cooled in an ice-bath was added water (0.75 ml) and 0.2 *M* hydrochloric acid (0.7 ml). After 2 min, water (10 ml) was added dropwise. Extraction into chloroform and treatment of the organic phase as above gave an oil (0.61 g) which was purified by preparative t.l.c. (benzene) to give the azoxy compound as a yellow oil (0.54 g) which crystallized at −80° from petroleum: m.p. 37–38.5°; n.m.r. (CCl_4) δ 1.12 (triplet, J = 7 Hz, 6H, CH_3), 3.53 (quartet, J = 7 Hz, 4H, CH_2), 6.13 (singlet, 1 CH), 7.17–8.23 (multiplet, 8 ArH), 10.48 (singlet, 1 CHO); mass spectrum *m/e* 328 (M^+ absent), major peaks at *m/e* 311, 237, 211, 208, 134, 105. Only very minor peaks were present at *m/e* 179, 180.

Anal. Calcd. for $C_{18}H_{20}N_2O_4$: C, 65.84; H, 6.14; N, 8.53. Found: C, 65.66; H, 6.13; N, 8.65.

*2,2'-Azoxybenzaldehyde (**11**)*

After several unsuccessful attempts to hydrolyze the acetals **9**, **10**, and **15**, the most successful procedure was the following modification of Bamberger's method (19).

The bisdiethylacetal **10** (2.0 g) was dissolved in glacial acetic acid (7 ml) with the minimum amount of heating. The yellow solution was cooled in ice, and water (1.5 ml) and 2 *M* hydrochloric acid (1.4 ml) were added. A white emulsion formed; this clarified on shaking, and after < 30 s, the solution began to turn brown. After a further 2.5 min, water (9 ml) was added dropwise with shaking (a white precipitate formed after 6 ml had been added), and the mixture was kept at 0° for 15 min more before suction filtration. The crude solid was taken into chloroform, washed ($NaHCO_3$), dried ($MgSO_4$), and the solution concentrated to < 10 ml for purification by t.l.c. (chloroform). The one major band afforded 1.8 g of crude solid, yellow needles (0.31 g) from ethanol[9]: m.p. 113–114° (lit. (19) 118°); n.m.r. ($CDCl_3$) δ 6.97–8.33 (multiplet, 8 ArH), 10.45 (singlet, 2 CHO); mass spectrum M^+ (*m/e* 254).

Anal. Calcd. for $C_{14}H_{10}N_2O_3$: C, 66.13; H, 3.96; N, 11.02. Found: C, 65.30; H, 3.92; N, 10.88.

The poor analysis is probably because **11** decomposes to a considerable extent in a few days at the ambient temperature.

*Irradiation of **11***

(*a*) In benzene: a solution of **11** (0.769 g) in benzene (300 ml) was irradiated for 20 min by which time a yellow solid was present. The solvent was removed and the residue (including the yellow substance) was resolved by preparative t.l.c. (chloroform) to give two major bands, neither of them red. Band 1 (225 mg) crystallized from ethanol as tan needles, m.p. 109–110°, and had the same n.m.r. spectrum as **11**. Band 2 (26 mg) was **29**, colorless crystals from chloroform–ether: m.p. 288–290° (lit (19) 294°); i.r. ($CHCl_3$) ν_{max} 1690 cm^{-1}; mass spectrum *m/e* (relative intensity) 236 (M^+) (100), 208 (38), 179 (33), 76 (37).

(*b*) In isopropanol: a solution of **11** (0.296 g) in isopropanol (300 ml) was irradiated for 1 h. Evaporation and t.l.c. resolution as above gave two colorless bands. Band 1 (6 mg) was unidentified; band 2 (36 mg) was starting material, tan needles from ethanol, m.p. 105–110°.

Quantum Yield Determinations

Azoxybenzene, m.p. 35–36°, was prepared by the method of Lachman (14): u.v. (ethanol) λ_{max} 231 (ε 9560), 267 (7990), and 323 nm (15 800), ε < 140. Irradiation in benzene and resolution by preparative t.l.c. (benzene–petroleum, 1:1) gave 2-hydroxyazobenzene, red needles from ethanol: m.p. 79–80° (lit. (56) 81°); u.v. (ethanol) λ_{max} 244 (ε 8110), 325 (16 800), 375 nm (8250), ε_{410} = 4480. For the quantum yield measurements, solutions of azoxybenzene in 95% ethanol and of the modified ferrioxalate actinometer described by Kurien (57) were irradiated simultaneously using a Rayonet "Merry-go-round". A filter solution (5 cm) of $NiSO_4 \cdot 6H_2O$ (90 g/l) and $CoSO_4 \cdot 7H_2O$ (48 g/l) was used to restrict the absorption of light to the region 300–330 nm where both azoxybenzene and the actinometer absorb strongly. Samples were withdrawn during the irradiation and analyzed by u.v. (Bausch and Lomb, Spectronic 70); ferrous phenanthroline formation was monitored at 510 nm (ε 11 000) and 2-hydroxyazobenzene formation at 410 nm. Knowing the quantum yield (1.10) for ferrous ion formation in the actionometer, the ratio of the initial slopes of the plots of ferrous phenanthroline and 2-hydroxyazobenzene formation with time gave the quantum yield for 2-hydroxyazobenzene formation as 0.217 ± 0.015 (11 runs).[10] Deviations were calculated by the usual method (58).

[9]It is important not to heat solutions of **11** any more than necessary, or decomposition results.

[10]NOTE ADDED IN PROOF: The quantum yield for this reaction has been determined (61) as ~0.008 in 95% ethanol. At present, we see no cause for discrepancy between our results and theirs. We wish to thank Dr. Jaffé for sending us a copy of his paper before publication.

Solvent Effect on Photoreactivity of Azoxybenzene

Solutions (about 7×10^{-5} *M*) of azoxybenzene in various solvents were irradiated simultaneously using the "Merry-go-round". Aliquots of the reaction mixture were withdrawn at intervals, and the formation of 2-hydroxyazobenzene was followed by monitoring the absorbance at 410 nm. First-order rate constants were evaluated by plotting log $(A_\infty - A_0)/(A_0 - A_t)$ against time, first-order kinetics being followed for better than one half-life. From the results obtained were calculated the data of Table 1.

Azoxybenzene-d_{10}

Thallium reduction (16) of nitrobenzene-d_5 (Stohler Isotope Chemicals) gave the azoxycompound as yellow needles from ethanol (36% after two recrystallizations): m.p. 34.5–36°; mass spectrum *m/e* (relative intensity) 208 (M^+) (37), 192 (5), 157 (6), 110 (11), 98 (8), 96 (24), 83 (100), 70 (18), 68 (16), 54 (30).

Anal. Calcd. for $C_{12}D_{10}N_2O$: N, 13.45. Found: N, 13.41.

Deuterium Isotope Effect for Azoxybenzene Photorearrangement

Solutions of azoxybenzene and azoxybenzene-d_{10} were irradiated simultaneously and first-order rate constants for 2-hydroxyazobenzene formation at 410 nm (in one experiment for azoxybenzene disappearance, monitored at 265 nm) were obtained as described above. The data are summarized in Table 1.

Irradiation of Azoxybenzene-d_{10} in Ethanol

A solution of azoxybenzene-d_{10} (302 mg) in 95% ethanol (300 ml) was irradiated for 1.5 h. The solvent was evaporated and the residue resolved by preparative t.l.c. (20% benzene in petroleum). Azoxybenzene-d_{10} (187 mg), m.p. 34.5–35°, and 2-hydroxyazobenzene-d_9 (89 mg), m.p. 79–80°, were obtained. After reservation of a sample of azoxybenzene-d_{10} for mass spectrometry, 185 mg was dissolved in fresh 95% ethanol (300 ml), and irradiated for a further 1.5 h. Azoxybenzene-d_{10} (57 mg) and 2-hydroxyazobenzene-d_9 (85 mg) were recovered. Several mass spectra were run on the starting sample of azoxybenzene-d_{10} and on each of the recovered samples, and the ratios of the peaks at *m/e* 206, 207, 208 were compared: starting material, $(4.9 \pm 0.2):(6.9 \pm 0.2):100$; first recovered sample, $(4.9 \pm 0.4):(6.1 \pm 0.3):100$; second recovered sample, $(4.5 \pm 0.1):(6.9 \pm 0.2):100$.

Irradiation of Azoxybenzene in CH_3CN–D_2O

A solution of azoxybenzene (305 mg) in dry (59) acetonitrile (300 ml) and deuterium oxide (20 ml) was irradiated for 1 h. Work-up as above gave azoxybenzene (60 mg) and 2-hydroxyazobenzene (77 mg). Several mass spectra were run to compare the ratio of the peaks at *m/e* 198 and 199 in the starting and recovered azoxybenzene samples: starting material, $100:(14.5 \pm 0.3)$; recovered sample, $100:(14.3 \pm 0.3)$.

Fluorescence Measurements

Using a Farrand Mark I fluorometer no fluorescence could be observed from azoxybenzene (10^{-3}–10^{-5} *M*) or azoxybenzene-d_{10} in purified ethanol, methanol, or hexane solutions. Ethanol and hexane solutions were also examined by Dr. W. R. Ware and Mr. T. Nemzek of the University of Western Ontario using the single photon counting technique (60), but again, no emission was observed.

Irradiation of Azoxybenzene in Styrene

Solutions of azoxybenzene (0.10 g) in styrene (30 ml) from which the stabilizer had been removed were irradiated in corked ampoules for 6 h using the Merry-go-round. The solutions were poured into methanol and the weight of polystyrene determined. From two experiments the weight of polymer was 0.01 and 0.01 g; in control experiments where the azoxybenzene was omitted the weight was 0.50 and 0.55 g.

We wish to thank the National Research Council of Canada for their generous financial support of this work. We also express thanks to Dr. J. L. Kropp of the Systems Group of TRW Inc. for a helpful correspondence concerning the effects of deuteration on the singlet lifetimes of aromatic hydrocarbons, to Dr. R. D. McAlpine formerly of this department for discussions on the same subject, to Dr. W. R. Ware and Mr. T. Nemzek of the University of Western Ontario for their kindness in making fluorescence measurements on azoxybenzene, and to Dr. A. McKillop of the University of East Anglia for correspondence on the proper method of purifying the thallium metal for reducing aromatic nitrocompounds.

1. H. M. KNIPSCHEER. Rec. Trav. Chim. **22**, 1 (1903).
2. (*a*) R. TANIKAGA, K. MARUYAMA, R. GOTO, and A. KAJI. Tetrahedron Lett. 5925 (1966); (*b*) R. TANIKAGA. Bull. Chem. Soc. Jap. **41**, 1664 (1968).
3. G. M. BADGER and R. G. BUTTERY. J. Chem. Soc. 2243 (1954).
4. (*a*) M. M. SHEMYAKIN, T. E. AGADZHANYAN, V. I. MAIMIND, R. V. KUDRYAVTSEV, and D. N. KURSANOV. Dokl. Akad. Nauk SSSR, **135**, 346 (1960); Chem. Abstr., **55**, 11337d (1961); (*b*) S. OAE, T. FUKUMOTO, and M. YAMAGAMI. Bull. Chem. Soc. Jap. **34**, 1873 (1961).
5. M. M. SHEMYAKIN, V. I. MAIMIND, and B. K. VAICHUNAITE. Chem. Ind. 755 (1958); Zh. Obshch. Khim. **28**, 1708 (1958); Chem. Abstr., **53**, 1201f (1959).
6. G. G. SPENCE, E. C. TAYLOR, and O. BUCHARDT. Chem. Rev. **70**, 231 (1970); E. BUNCEL. *In* Mechanisms of molecular migrations. Vol. 1. *Edited by* B. S. Thyagarajan. Interscience, London. 1969. pp. 104–110.
7. S. OAE, T. FUKOMOTO, and M. YAMAGAMI. Bull. Chem. Soc. Jap. **36**, 601 (1963).
8. (*a*) D. C. NECKERS. Mechanistic organic photochemistry. Reinhold, New York. 1967. p. 207; (*b*) H. A. MORRISON. Chemistry of the nitro and nitroso groups. *Edited by* H. Feuer. Wiley-Interscience, London. 1969. p. 166.
9. W. R. KRIGBAUM, Y. CHATANI, and P. G. BARBER. Acta Cryst. **26**B, 97 (1970).
10. C. WALLING. Free radicals in solution. John Wiley and Sons Inc., New York. 1957. Chapt. 8.
11. P. J. WAGNER. Acc. Chem. Res. **4**, 168 (1971); Tetrahedron Lett. 5385 (1968).
12. C. WALLING and M. J. GIBIAN. J. Am. Chem.

Can. J. Chem. Downloaded from www.nrcresearchpress.com by 210.87.254.42 on 09/05/12
For personal use only.

Can. J. Chem. Downloaded from www.nrcresearchpress.com by 210.87.254.42 on 09/05/12
For personal use only.

Soc. **86**, 3902 (1964); **87**, 3361 (1965); reference 8a p. 167.
13. M. A. BERWICK and R. E. RONDEAU. J. Org. Chem. **37**, 2409 (1972).
14. A. LACHMAN. J. Am. Chem. Soc. **24**, 1178 (1902).
15. E. BAMBERGER. Ber. **44**, 1970 (1911).
16. A. MCKILLOP, R. A. RAPHAEL, and E. C. TAYLOR. J. Org. Chem. **35**, 1670 (1970).
17. E. BAMBERGER. Ber. **59**, 430 (1926).
18. B. ORTIZ, P. VILLANUEVA, and F. WALLS. J. Org. Chem. **37**, 2748 (1972).
19. E. BAMBERGER. Ber. **44**, 1975 (1911); P. CARRÉ. Ann. Chim. (Paris), **19**, 210 (1910) and references cited therein.
20. J. H. BOWIE, R. G. COOKS, and G. E. LEWIS. Aust. J. Chem. **20**, 1601 (1967).
21. W. A. PRYOR. Free radicals. McGraw-Hill Book Co., New York. 1966. Chapt. 12; W. A. THALER. *In* Methods in free radical chemistry. *Edited by* E. S. Huyser. Marcel Dekker, New York. 1969. p. 158; K. H. LEE. Tetrahedron, **25**, 4363 (1969).
22. E. N. MARVELL and M. J. JONCICH. J. Am. Chem. Soc. **73**, 973 (1951).
23. (*a*) G. A. RAZUVAEV, I. F. SPASSKAYA, and V. S. ETLIS. Zh. Obsch. Khim. **29**, 2978 (1959); Chem. Abstr. **54**, 11978 h (1960); (*b*) K. H. LEE. Tetrahedron, **24**, 4793 (1968); **26**, 2041 (1970).
24. H. ZOLLINGER. Azo and diazo chemistry. Interscience, London. 1961. p. 253.
25. G. E. LEWIS and J. A. REISS. Aust. J. Chem. **19**, 1887 (1966).
26. (*a*) J. K. S. WAN, L. D. HESS, and J. N. PITTS. J. Am. Chem. Soc. **86**, 2069 (1964); J. A. BARLTROP and N. J. BUNCE. J. Chem. Soc. (C), 1467 (1968).
27. J. A. KERR. Chem. Rev. **66**, 465 (1966).
28. E. BAMBERGER. Ber. **39**, 4266 (1906); E. BAMBERGER and J. LUBIN. Ber. **42**, 1706 (1909); G. HELLER. Ber. **49**, 527, 545 (1916).
29. P. H. GORE and O. H. WHEELER. J. Am. Chem. Soc. **78**, 2160 (1956).
30. R. TANIKAGA. Bull. Chem. Soc. Jap. **41**, 2151 (1968).
31. A. N. FLETCHER. J. Phys. Chem. **72**, 2742 (1968); W. R. DAWSON and M. W. WINDSOR. J. Phys. Chem. **72**, 3251 (1968).
32. D. PHILLIPS. Photochemistry I. Specialist Periodical Report. The Chemical Society (London). 1970. Chapt. 1.
33. G. W. ROBINSON and R. P. FROSCH. J. Chem. Phys. **37**, 1962 (1962), **38**, 1187 (1963); G. W. ROBINSON. J. Chem. Phys. **47**, 1967 (1967).
34. W. R. DAWSON and J. L. KROPP. J. Phys. Chem. **73**, 693 (1969); P. F. JONES and S. SIEGEL. Chem. Phys. Lett. **2**, 486 (1968); J. Chem. Phys. **50**, 1134 (1969); J. L. KROPP, W. R. DAWSON, and M. W. WINDSOR. J. Phys. Chem. **73**, 1747 (1969).
35. P. J. WAGNER, P. A. KELSO, and R. G. ZEPP. J. Am. Chem. Soc. **94**, 7480 (1972).
36. D. R. COULSON and N. C. YANG. J. Am. Chem. Soc. **88**, 4511 (1966); A. PADWA and W. BERGMARK. Tetrahedron Lett. 5795 (1968).
37. N. J. BUNCE. Can. J. Chem. **50**, 3109 (1972).
38. E. A. HALEVI. Progr. Phys. Org. Chem. **1**, 109 (1963).
39. H. ZOLLINGER. Adv. Phys. Org. Chem. **2**, 163 (1964).
40. W. M. MOORE, G. S. HAMMOND, and R. P. FOSS. J. Am. Chem. Soc. **83**, 2789 (1961); G. S. HAMMOND, W. P. BAKER, and W. M. MOORE. J. Am. Chem. Soc. **83**, 2795 (1961); G. PORTER and P. SUPPAN. Proc. Chem. Soc. 191 (1964).
41. R. HURLEY and A. C. TESTA. J. Am. Chem. Soc. **90**, 1949 (1968).
42. W. TROTTER and A. C. TESTA. J. Am. Chem. Soc. **90**, 7044 (1968).
43. M. P. SERVÉ and A. W. BRYANT. Tetrahedron Lett. 2663 (1972) and references cited therein.
44. J. MILLER. Aromatic nucleophilic substitution. Elsevier, Amsterdam. 1968. pp. 77, 127; C. D. HOUGHTON and W. A. WATERS. J. Chem. Soc. 1018 (1950); J. BURNS, H. MCCOMBIE, and H. A. SCARBOROUGH. J. Chem. Soc. 2928 (1928).
45. J. H. BOWIE, G. E. LEWIS, and R. G. COOKS. J. Chem. Soc. (B), 621 (1967).
46. L. W. REEVES. Can. J. Chem. **38**, 748 (1960).
47. E. MÜLLER and W. KREUTZMANN. Ann. **495**, 132 (1932).
48. M. BUSCH and H. KUNDER. Ber. **49**, 317 (1916).
49. D. VORLÄNDER and F. MEYER. Ann. **320**, 127 (1902).
50. J. T. EDWARDS. J. Chem. Soc. 222 (1956).
51. A. I. VOGEL. A textbook of practical organic chemistry. Longmans, London. 1948. p. 603.
52. P. GRAMMATICAKIS. C. R. **245**, 1145 (1957).
53. H. C. BROWN and W. H. BONNER. J. Am. Chem. Soc. **76**, 605 (1954).
54. E. GEIGY and W. KÖNIGS. Ber. **18**, 2400 (1885).
55. P. FREUNDLER. Bull. Soc. Chim. Fr. **31**, 450 (1904).
56. E. BAMBERGER. Ber. **33**, 1950 (1900).
57. K. C. KURIEN. J. Chem. Soc. (B), 2081 (1971).
58. Handbook of chemistry and physics. *Edited by* R. C. Weast. 49th ed. Chemical Rubber Co., Cleveland, Ohio. 1968.
59. G. A. FORCIER and J. W. OLVER. Anal. Chem. **37**, 1447 (1965).
60. W. R. WARE and C. LEWIS. J. Chem. Phys. **57**, 3546 (1972) and references cited therein.
61. R. H. SQUIRE and H. H. JAFFÉ. J. Am. Chem. Soc. In press.

Metabolites of *Cyathus helenae*. A New Class of Diterpenoids

WILLIAM A. AYER AND HUBERT TAUBE
Chemistry Department, University of Alberta, Edmonton, Alberta T6G 2E1

Received June 4, 1973

Allocyathin B_3 and cyathin A_3, metabolites of the bird's nest fungus *Cyathus helenae* Brodie are shown to possess structures **2***a* ⇄ **3***a* and **5***a* ⇄ **6***a*, respectively. In the solid state allocyathin B_3 exists in the hydroxyketone form **2***a*, while cyathin A_3 is in the hemiketal form **6***a*. In each case acetylation gives the diacetyl derivative of the hydroxyketone form whereas treatment with methanolic HCl gives an internal ketal. Allocyathin B_3 and cyathin A_3 have been correlated by hydrogenation to the common product **13***a*, and by transformation of each to the aldehyde **12***a*. These compounds are representatives of a new class of diterpenoids. Their biogenesis from geranylgeranyl pyrophosphate is discussed.

On a montré que l'allocyathine B_3 et la cyathine A_3, deux métabolites du champignon *Cyathus helenae* Brodie ("nid d'oiseaux") possèdent respectivement les structures **2***a* ⇋ **3***a* et **5***a* ⇋ **6***a*. A l'état solide, l'allocyathine B_3 existe sous la forme hydroxycétone **2***a* alors que la cyathine A_3 existe sous la forme d'un hémiacétal **6***a*. Dans chacun des cas, l'acétylation a conduit au dérivé diacétylé de la forme hydroxycétone alors que le traitement par HCl dans le méthanol a conduit à un acétal interne. L'allocyathine B_3 et la cyathine A_3 ont conduit toutes deux par hydrogénation au seul produit **13***a* et par transformation à l'aldéhyde **12***a*. Ces composés sont les membres d'une nouvelle classe de diterpénoïdes. On discute de leur biogénèse à partir du pyrophosphate de géranylgéranyle.

[Traduit par le journal]

Can. J. Chem., **51**, 3842 (1973)

In 1965 H. J. Brodie discovered a new bird's nest fungus of the genus *Cyathus* growing in the Rocky Mountains of Alberta. The species was given the designation *Cyathus helenae* (1). Subsequently, Brodie and co-workers succeeded in growing the fungus in liquid culture and showed that the metabolites possessed antibiotic activity (2). At the same time we reported on the isolation and preliminary characterization of some of the metabolites (2). We now wish to present a detailed account[1] of the studies leading to the elucidation of the structure of two of the diterpenoid components of the "cyathin complex".

The isolation procedure previously reported (2) was based mainly on a combination of column and thin-layer chromatography (t.l.c.) on the ethyl acetate extract obtained from the culture broth. A material with R_f 0.4 (silica gel G, chloroform–methanol 9:1) which appeared chromatographically pure was obtained and called cyathin A_3. However, careful inspection of the n.m.r. spectrum of the acetyl derivative indicated that this material consisted of two components: a compound A and its dihydro derivative B.[2]

Chromatography on silica gel impregnated with silver nitrate, a standard technique (4) for separating compounds with differing degrees of unsaturation, proved to be successful in separating A from B. The R_f values for the system 10% silver nitrate – silica gel, Skellysolve B – acetone (2:3), are 0.51 for A and 0.60 for B. This difference allows easy separation of the two components by preparative t.l.c. (p.t.l.c.). The molecular formula of A is $C_{20}H_{28}O_3$, that of B, $C_{20}H_{30}O_3$; the name cyathin A_3 has been retained for compound B and compound A is called allocyathin B_3 conforming to the system of nomenclature devised earlier (2).

The chemistry of allocyathin B_3 will be discussed first, since an exhaustive study of spectra of this compound and two key derivatives, *O*,*O*-diacetylallocyathin B_3 and "allocyathin B_3 methyl ketal", allowed an unambiguous solution of the structural problem.

Allocyathin B_3 has the composition $C_{20}H_{28}O_3$ as determined by high resolution mass spectrometry (h.r.m.s.).[3] The i.r. spectrum in chloroform displays hydroxyl absorption and a broad band of medium intensity at 1650 cm^{-1}. This absorption band, which is assigned to an α,β-unsatu-

[1]A preliminary report of some of these findings has appeared (3).

[2]In most preparations, B was the major component; in a few instances, however, A predominated.

[3]Because of the small quantities of pure material available, most of the molecular formulas in this series have been determined by high resolution mass spectrometry.

Can. J. Chem. Downloaded from www.nrcresearchpress.com by 210.87.254.5 on 09/05/12
For personal use only.

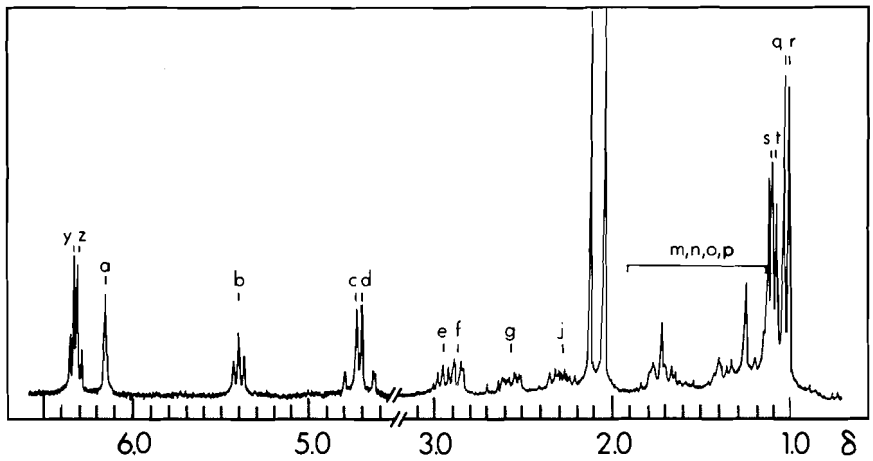

FIG. 1. Nuclear magnetic resonance spectrum (220 MHz) of *O,O*-diacetylallocyathin B_3 in $CDCl_3$.

rated carbonyl group, appears in the same position in the solid-phase spectrum in which it is much stronger and sharper. The decreased intensity in solution indicates that the carbonyl group is partially in a hemiketal form as will be discussed later. A weak but sharp band at 3060 cm^{-1} indicates olefinic hydrogen(s). The u.v. spectrum has a somewhat unsymmetrical maximum at 235 nm with ε 5000 (shown to result from two overlapping chromophores). The c.d. spectrum displays a positive maximum at 327 nm with a dichroic absorption (Δε) of +1.6, assigned to the n–π* transition of an α,β-unsaturated carbonyl group. The n.m.r. spectrum of allocyathin B_3 (100 MHz) has but one readily analyzable (5) feature: an AB quartet centered at δ 6.26 with $\Delta\nu = 7$ Hz and $J = 5$ Hz; the remainder of the spectrum is poorly defined (tautomerism?) and was of limited value in the structural study.

Acetylation of allocyathin B_3 gave an *O,O*-diacetyl derivative as indicated by a molecular weight increase of 84 a.m.u. ($C_{20}H_{28}O_3 \rightarrow C_{24}H_{32}O_5$), 3-proton singlets in the n.m.r. at δ 2.05 and 2.12, and i.r. absorption at 1745 cm^{-1}. The i.r. spectrum also shows absorption at 1685 and 1655(sh) attributed to an α,β-unsaturated carbonyl system. The u.v. spectrum (isooctane) shows maxima at 325 (ε 140), 254 (ε 4800), and 225 nm (ε 9000). The maxima at 325 and 225 nm are assigned to the n–π* and π–π* transitions of the α,β-unsaturated carbonyl; the 254 nm absorption, as shown below, is due to a cyclopentadiene moiety. A strong c.d. maximum at 330 nm (Δε +4.1) further confirms the presence of an α,β-unsaturated carbonyl. Nuclear magnetic resonance spectra determined at 100 and 220 MHz (Fig. 1 and Table 1) using both $CDCl_3$ and C_6D_6 as solvents proved to be extremely revealing. Part structures **A**, **B**, **C**, and **D**, where (C) indicates a carbon atom bearing no hydrogen, were apparent.

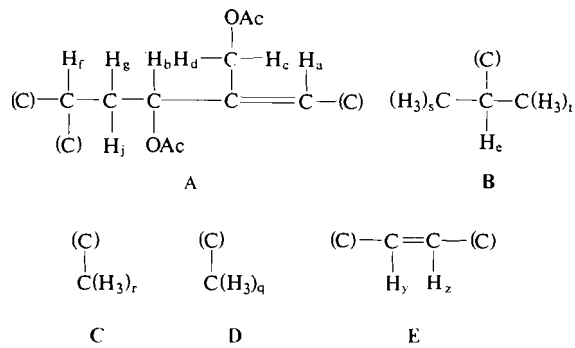

Proton f at δ 2.87 ($CDCl_3$) has two vicinal couplings, an equatorial–axial type coupling of 3 Hz with proton g and an axial–axial like coupling of 10.5 Hz with j. Protons g (δ 2.56) and j (δ 2.27) show, besides the above mentioned coupling, a mutual geminal coupling of 14 Hz and each a vicinal coupling of 6.5 Hz with proton b. Besides these, proton b (δ 5.39) has only weak couplings (~0.5 Hz), better observed in the case of cyathin A_3, with protons a, c, and d. The nonequivalent protons c (δ 4.75) and d (δ 4.68) are geminally coupled (14.5 Hz) and are each further split by an allylic coupling of 1.5 Hz with proton a. Proton a, which must be olefinic since it resonates at low field (δ 6.15), displays

Can. J. Chem. Downloaded from www.nrcresearchpress.com by 210.87.254.5 on 09/05/12
For personal use only.

Can. J. Chem. Downloaded from www.nrcresearchpress.com by 210.87.254.5 on 09/05/12
For personal use only.

only the above-mentioned small couplings and consequently is located at the other end of the isolated spin system **A**. Protons b, c, and d must be located on carbon atoms bearing acetoxyl groups since the nonacetylated compound does not show signals at these shift values.

Proton e (δ 2.96) gives rise to a septet (the outer two lines are not always apparent) which has typical acyclic vicinal coupling (7 Hz) (5). Nuclear magnetic double resonance (n.m.d.r.) experiments show that e is coupled to a pair of doublets, s and t, at δ 1.12 and 0.99. Only part structure **B**, an isolated isopropyl group, is consistent with this pattern.

Three-proton singlets at δ 1.04 and 1.00 are due to quaternary methyl groups **C** and **D**. Part structure **E** is revealed by the isolated AB quartet at δ 6.34 and 6.31. The coupling constant of 5.5 Hz is in the range expected for olefinic coupling in a five-membered ring (6). The observed chemical shifts indicate the presence of a cyclopentadiene rather than a cyclopentene moiety (ref. 5*a*, p. 188: δ 6.42 and 5.60, respectively). The remaining four protons give rise to a very complex signal pattern in the region δ 1.9–1.1. Since all spin systems mentioned above appear to be isolated systems, this pattern suggests an isolated ABCD-system of two adjacent methylene groups.

When allocyathin B_3 is treated with methanolic HCl at room temperature it is transformed into a compound $C_{21}H_{30}O_3$. The transformation is accompanied by loss of the n–π* c.d. band at 326 nm and is conveniently monitored in this way. The net reaction is one of methylation and corresponds to the transformation of a hydroxy ketone (or hemiketal) to an internal half methyl ketal. The i.r. spectrum (CCl_4) of this derivative is considerably better defined than that of the diacetyl derivative or the parent compound, possibly a reflection of the more rigid conformation. The i.r. spectrum shows hydroxyl absorption (3620, 3470 cm^{-1}), olefinic C—H stretching (3100, 3050 cm^{-1}), and lacks carbonyl absorption. Ultraviolet and c.d. spectra confirm the absence of carbonyl absorption although both spectra display an absorption band centered at *ca.* 255 nm: the c.d. spectrum has a minimum at 252 (Δε −3.6), the u.v. spectrum a maximum at 256 nm (ε 4200). The u.v. spectrum is in good agreement with that expected for a 5,5-dialkylcyclopentadiene bearing two alkyl substituents.[4] Consequently we may expand part structure **E** to **F**.

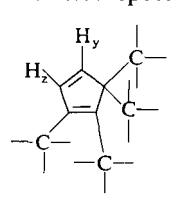

F

This part structure is compatible with the n.m.r. spectra, since protons y and z are coupled only to each other and the additional olefinic proton is accounted for in **A**. The mass spectrum of the ketal, unlike that of the parent compound, is completely dominated by an intense peak at *m/e* 141 corresponding to the ion $C_7H_9O_3$ (h.r.m.s.) which contains *all three oxygen atoms of the ketal.* This shows that the three oxygens in allocyathin B_3 are located on six contiguous carbon atoms. Since two oxygens are accounted for in part structure **A** and the third is incorporated into an α,β-unsaturated ketone, the carbonyl group must be attached to the carbon carrying proton a. Part structure **A** may thus be expanded to **G**. Since it is the secondary hydroxyl

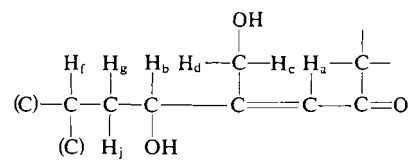

G

which is involved in ketal formation (see below), part structure **H** follows for the methyl ketal.

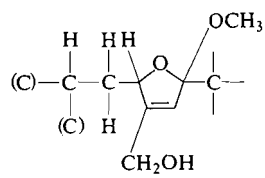

H

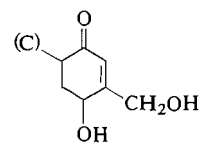

I

It seemed unlikely that the unsaturated carbonyl system **G** was part of a six-membered ring (as in **I**) since much higher extinction coefficients would then be expected for the π–π* transition than are observed. It is also difficult to rationalize

[4]Published examples (7) indicate that 5,5-dialkylcyclopentadienes absorb at about 250 nm and that each further alkyl substituent contributes an increment of 3–4 nm. Extinction coefficients are in the range 3000–4500.

Can. J. Chem. Downloaded from www.nrcresearchpress.com by 210.87.254.5 on 09/05/12
For personal use only.

TABLE 2. Characterization of cyanthin A_3 and allocyathin B_3 and derivatives[a]

Compound	Formula	Exact mass		Strong mass peaks	T.l.c.[b]		M.p. (°C)	Optical rotation			U.v.		C.d.				I.r.	
		Calcd.	Found		Solvent	R_f		Solvent	Conc.	$[\alpha]_D$	Solvent	λ_{max} (ε)	Solvent	Conc.	λ_{ext}	($\Delta\varepsilon$)	Solvent	ν_{max}
2*a* ⇄ **3***a*	$C_{20}H_{28}O_3$	316.2039	316.2031	316	A	0.40	143–144	m	0.26	−250	m	235 (5100)	m	0.26	327	(+1.6)	c	3580, 3400, 1650 (m)
					A*	0.28											k	3050 (w), 1650 (s)
2*b*	$C_{24}H_{32}O_5$	400.2250	400.2244	201, 187	B	0.40	—	i	0.10	−110	i	325 (140), 254 (4800) 225 (9000)	i	0.10	330	(+4.0)	t	3060 (w), 1745 (s) 1685 (m), 1655 (sh)
3*b*	$C_{21}H_{30}O_3$	330.2195	330.2190	141	B	0.34	—	i	0.18	−230	i	256 (4200)	i	0.07	252	(−3.6)	t	3610, 3470, 3100 (w), 3050 (w)
3*c*	$C_{23}H_{32}O_4$	372.2301	372.2305	183	B	0.55	—	i	0.1	−230	i	255 (5600)	i	0.1	243	(−2.2)		3100 (w), 3050 (w) 1740 (s)
4	$C_{28}H_{34}O_8$	498.2265	498.2254	357, 400	B	0.24	185–187	d	0.12	−72	d	319 (110), 230 sh (5200)	d	0.12	327	(+1.8)	c	1848 (w), 1776 (s) 1741 (s), 1683 (m)
5*a* ⇄ **6***a*	$C_{20}H_{30}O_3$	318.2195	318.2195	303, 191	A	0.40	148–150	m	0.26	−155	d	324 (43)	d	0.260	332	(+0.73)	c	3600, 3400, 1650 (m)
					A*	0.38					m	315 (51), 230 sh (2300)	m	0.244	325	(+0.95)	n	3320
5*b*	$C_{24}H_{34}O_5$	402.2406	402.2404	282, 189	B	0.40	—	i	0.13	−64	i	323 (126), 230 sh (7300)	i	0.13	330	(+2.7)	t	1750 (s), 1690 (m) 1660 (sh)
6*b*	$C_{21}H_{32}O_3$	332.2352	332.2356	141	B	0.36	—	m	0.24	−154	m	End absorption only	m	0.24	—		t	3600
6*c*	$C_{23}H_{34}O_4$	374.2457	374.2450	183	B	0.57	59–60		—		i	End absorption only	i	0.18	—		t	1740 (s)
7*a*	$C_{21}H_{34}O_4$	350.2457	350.2463	190, 175	A	0.45	60–65	m	0.5	−22	m	End absorption only	m	0.5	290	(−0.05)	c	3570, 3400 1690 (w)
7*b*	$C_{21}H_{34}O_4$	350.2457	350.2459	190, 175	A	0.38	—		—			—			—		c	3570, 3400
8	$(C_{23}H_{36}O_5)$	—		—	B	0.19	—		—			—			—		c	3580, 3380 1743 (s)
9	$C_{25}H_{38}O_6$	434.2668	434.2679	173	B	0.42		i	0.1	−96	i	282 (150)	i	0.1	298	(−1.9)	c	1738 (s), 1696 (s)
10	$C_{21}H_{34}O_3$	334.2508	334.2503	190, 175	B	0.37	—		—			—			—		t	3630
11	$C_{21}H_{34}O_2$	318.2559	318.2550	190, 175	B	0.70	—		—			—			—		t	—
12*a*	$C_{21}H_{32}O_3$	332.2352	332.2343	190, 175	B	0.54	115–130	i	0.22	−39	i	282 (122)	i	0.22	290	(+1.2)	t	2710 (w), 1725 (s)
12*b*	$(C_{21}H_{32}O_3)$	—		—	B	0.51	—		—			—			—		t	2710 (w), 1725 (s)
13*a*	$C_{20}H_{32}O_3$	320.2352	320.2347	190, 175	A	0.40	157–159	m	0.11	−45	m	295 (15)	m	0.11	289	(−0.11)	c	3600, 1685 (m)
					A*	0.48											k	3380
13*b*	$C_{24}H_{36}O_5$	404.2563	404.2575	284, 241	B	0.50	126–128	i	0.10	−120	i	290 (58)	i	0.10	295	(−0.43)	k	1730 (s), 1688 (s)
14	$(C_{20}H_{30}O_3)$	—		—	A	0.43	—		—		m	253 (1800)			—			—
15*a*	$C_{20}H_{32}O_3$	320.2352	320.2359	190, 175	A	0.45	—		—			—			—		c	3590, 3410 1685 (s)
					A*	0.48												
15*b*	$C_{24}H_{36}O_5$	404.2563	404.2568	284, 189	B	0.50	—		—			—			—		k	3050 (w), 1740 (s) 1691 (s)

[a]Abbreviations: c = chloroform, d = dioxane, i = isooctane, k = KBr, m = methanol, n = Nujol, t = carbon tetrachloride. Units for λ, nm; ν, cm^{-1}.
[b]T.l.c. on silica gel; 10% $AgNO_3$ – silica gel when * after solvent system; A = chloroform–methanol 9:1; B = Skellysolve B – acetone 3:1.

Can. J. Chem. Downloaded from www.nrcresearchpress.com by 210.87.254.5 on 09/05/12
For personal use only.

TABLE 1. Nuclear magnetic resonance data for allocyathin B_3 derivatives [a,b]

Compound		y[c]	z[c]	a	b	c	d	e	f	g	j	m, n, o, p	q, r	s, t	u, v	w		
		H-1	H-2	H-13	H-11	H-15a	H-15b	H-18	H-5	H-10a	H-10b	H-7, H-8	H-16, H-17	H-19, H-20	OAc at C-11 and/or C-15	OMe at C-14	H-1′	H-2′
	δ ($CDCl_3$)	6.34	6.31	6.15	5.39	4.75	4.68	2.96	2.87	2.56	2.27	1.9–1.1	1.04; 1.00	1.12; 1.10	2.12; 2.05	—	—	—
	δ (C_6D_6)	—	—	—	5.41	4.75	4.64	3.06	3.06	2.63	2.41	1.9–1.2	1.22; 1.02	1.20; 1.14	1.74; 1.72	—	—	—
2*b*	Multiplicity	d	d	ddd	ddd	dd	dd	qq	qq	ddd	ddd	u	s; s	d; d	s; s	—	—	—
	Coupling constants (Hz)	5.5	5.5	1.5, 1.5, 0.5	6.5, 6.5, 0.5	14.5, 1.5	14.5, 1.5	7, 7	10.5, 3	14, 6.5, 3	14, 10.5, 6.5	—	—; —	7; 7	—; —	—	—	—
	Coupling partner	z	y	c, d, b	g, j, a	d, a	c, a	s, t	j, g	j, b, f	g, f, b	—	—; —	e; e	—; —	—	—	—
	δ ($CDCl_3$)	6.30	6.22	6.11	4.82	4.35	4.35	3.00	?	?	?	1.8–1.1	0.97; 0.83	1.13; 1.07	—	3.36	—	—
	δ (C_6D_6)	—	—	—	4.72	3.86	3.86	3.05	2.68	1.4?	2.48	1.8–1.1	1.18; 1.02	1.16; 1.12	—	3.41	—	—
3*b*[d]	Multiplicity	d	d	dd	(dm)	dd	dd	qq	dd	(dd)	ddd	u	s; s	d; d	—	s	—	—
	Coupling constants (Hz)	5.5	5.5	1.5, 1.5	(3, —)	14, 1.5	14, 1.5	7.7	12.5, 3.5	(12.5, 3.5)	12.5, 12.5, 3	—	—; —	7; 7	—	—	—	—
	Coupling partner	z	y	c, d	(j, —)	d, a	c, a	s, t	j, g	(j, f)	g, f, b	—	—; —	e; e	—	—	—	—
3*c*	δ (C_6D_6)	6.36	6.23	5.93	4.55	4.44	4.30	2.95	2.60	1.3?	2.30	1.8–1.1	1.14; 1.03	1.12; 1.08	1.59	3.27	—	—
	δ ($CDCl_3$)	2.95	6.04	6.04	5.32	4.77		2.73	?	2.5?	2.5?	1.8–1.0	1.41; 1.02	1.22; 1.01	2.15; 1.98	—	3.86	3.27
	Multiplicity	dd	(d)	(t)	m	d		qq	?	?	?	u	s; s	d; d	s; s	—	dd	d
4	Coupling constants (Hz)	4.5, 3	(3)	(1.5)	$w_{\frac{1}{2}} = 10$	1.5		7, 7	?	?	?	—	—; —	7; 7	—; —	—	8, 4.5	8
	Coupling partner	H-1′, H-2	H-1	(H-15)	—	H-13		H-19, H-20	?	?	?	—	—; —	e; e	—; —	—	H-2′, H-1	H-1′

[a]s = singlet, d = doublet, t = triplet, q = quartet, m = multiplet, u = unresolved, ( ) = implied or indirect, ? = tentative or not analyzable.
[b]Coupling partners in same order as coupling constants.
[c]Differentiation between H-1 and H-2 not possible for **2***b*, **3***b*, and **3***c*.
[d]Coupling pattern derived from analysis of **3***b* and **3***c*.

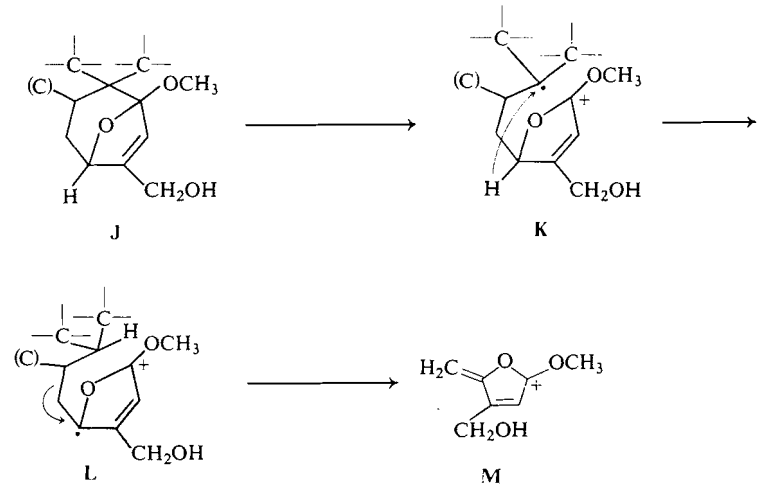

SCHEME 1

the formation of the *m/e* 141 ion on the basis of a ketal derived from a system such as **I**. Such an ion may, however, readily be accounted for (Scheme 1) if the original carbocyclic ring is (at least) seven-membered. α-Cleavage (**J** → **K**) followed by hydrogen shift (five-membered transition state **K**) and cleavage (**L**) yields the highly resonance-stabilized ion **M**.

The n.m.r. spectrum of the ketal (Table 2) is similar to that of the diacetyl derivative. Noteworthy is the fact that the splitting pattern for proton b (δ 4.72) has changed considerably. Nuclear magnetic double resonance experiments show that the couplings with j and g are now only 3 Hz and <1 Hz, respectively. This coupling pattern is reminiscent of that displayed by protons attached to the bridgehead carbon in bicyclo[2.2.1] systems (*5a*).

The acetyl derivative of allocyathin B_3 methyl ketal was prepared in order to provide unequivocal evidence that it is indeed the secondary hydroxyl group which is involved in ketal formation. The n.m.r. spectrum (C_6D_6) shows a single three proton singlet at δ 1.59 confirming monoacetylation; the methylene protons, c and d, of the primary alcohol underwent a downfield shift of 0.4 p.p.m., a typical "acylation shift" (ref. *5b*, p. 122) for primary alcohols, whereas signal b was not shifted.

The low chemical shifts of protons e and f in the various n.m.r. spectra suggest that part structures **B** and **G** are attached to **F** as in **N** or **O**.[5] Twenty-four of the 28 protons and 17 of the 20 carbon atoms are accounted for in the expanded part structures **C**, **D**, and **O** (or the alternative **N**). The functionality defined dictates a tricyclic system. The remaining three carbons must be attached to the carbonyl carbon, to the carbon bearing proton f, and, possibly, to the saturated carbon of the cyclopentadiene moiety. The only structural possibilities remaining at this point are shown in Scheme 2.

Structures **P**, **Q**, and **R** have a double bond at a bridgehead carbon and thus contradict Bredt's rule. Attempts to build molecular models strengthened the view that these structures could be excluded. Structures **S** and **T** (in each case two positional isomers possible on cyclopentadiene ring) may be disregarded since the n.m.r. spectra lack signals in the region typical of cyclopropyl protons, *i.e.*, between δ 1.0 and 0.0, and because of the stability of allocyathin B_3 to acid conditions (ketal formation). Structure **U** has a methylene group α to the carbonyl. The corresponding protons should give rise to signals between δ 3.0 and 2.0. Since this is not observed,

[5]Attachment of either of the carbons bearing proton e or f to the carbonyl group in **G** could also account for such shifts. However, if the carbon carrying proton f were attached to the carbonyl carbon a six-membered ring would result and this has been shown to be unlikely. The fact that the chemical shifts of protons e and f remain essentially unchanged after ketalization also serves to exclude the possibility that they are α to the carbonyl.

Can. J. Chem. Downloaded from www.nrcresearchpress.com by 210.87.254.5 on 09/05/12
For personal use only.

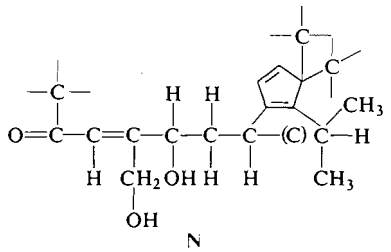

N

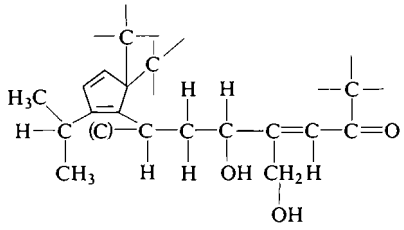

O

this structure is ruled out. The same reasoning applies to **V**. Moreover, **V** contains two isolated methylene groups which should give rise to two discernible AB quartets. Such is not the case. Structure **W** then remains as a unique solution to the structural problem. At this stage it was not possible to completely define the relative stereochemistry of allocyathin B_3. At the same time that the studies described here were in progress, we had initiated with others in these laboratories an X-ray crystallographic study of cyathin A_3. Shortly after structure **W** (= **2***a* without stereochemical implication) had been deduced for allocyathin B_3 and consequently structure **5***a* (without stereochemical implication) for cyathin A_3 (see below) the X-ray structure determination was completed (8) and revealed that crystalline cyathin A_3 exists in the internal hemiketal form **1** (=**6***a*) with the relative stereochemistry shown in **1**. We have arbitrarily selected H-5 (H_f in the discussion above) to be situated on the β-face of the molecule and shall adhere to that convention throughout the paper. Recent work (8) has shown that **1** also represents the absolute configuration of cyathin A_3. Since allocyathin B_3 has been correlated with cyathin

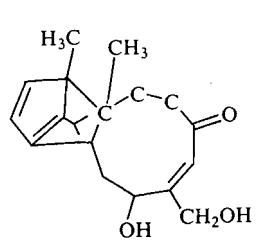

P

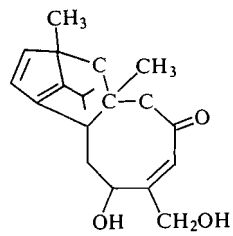

Q

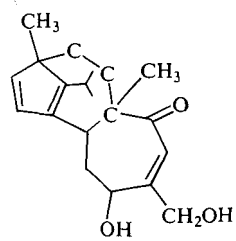

R

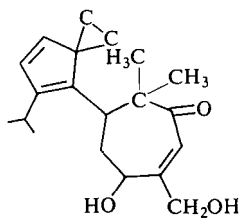

S

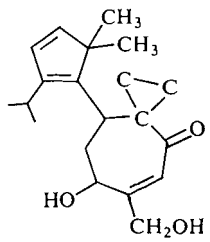

T

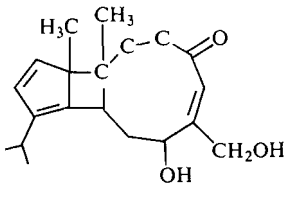

U

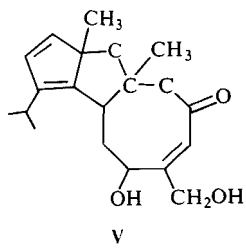

V

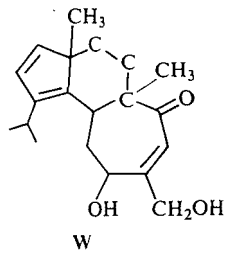

W

SCHEME 2

Can. J. Chem. Downloaded from www.nrcresearchpress.com by 210.87.254.5 on 09/05/12
For personal use only.

Can. J. Chem. Downloaded from www.nrcresearchpress.com by 210.87.254.5 on 09/05/12
For personal use only.

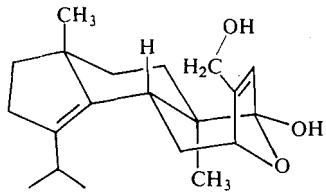

1

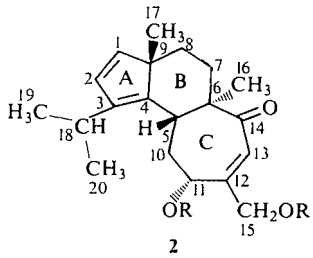

2

a R = H
b R = Ac

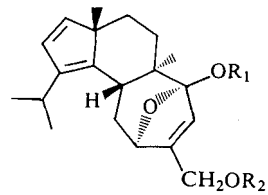

3

a $R_1 = R_2 = H$
b $R_1 = CH_3; R_2 = H$
c $R_1 = CH_3; R_2 = Ac$

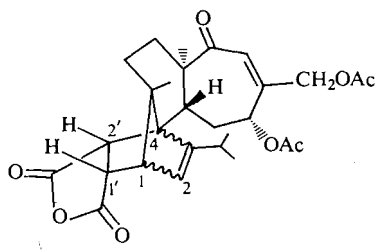

4

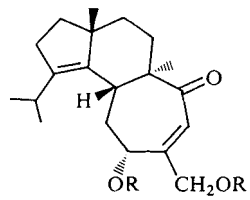

5

a R = H
b R = Ac

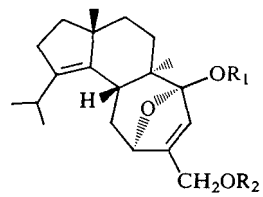

6

a $R_1 = R_2 = H$
b $R_1 = CH_3; R_2 = H$
c $R_1 = CH_3; R_2 = Ac$

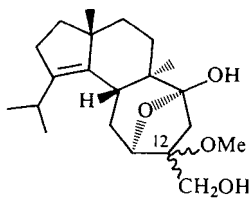

7

a Major epimer
b Minor epimer

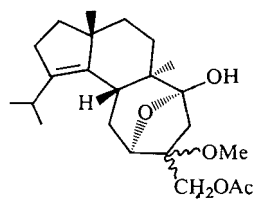

8

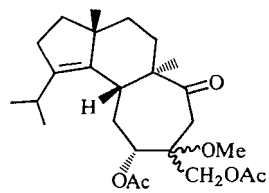

9

A_3 (see below), **2***a* ⇄ **3***a* represents the absolute stereochemistry of allocyathin B_3. The keto form (**2***a*) of allocyathin B_3 possesses four chiral centers and has the 5*R*, 6*R*, 9*S*, 11*R* configuration according to the Cahn, Ingold, Prelog notation (9). In cyathin A_3 the configuration is 5*R*, 6*R*, 9*R*, 11*R* (8).

We may now assign structure **2***b* to the diacetyl derivative of allocyathin B_3 (*O*,*O*-diacetylallocyathin B_3), **3***b* to allocyathin B_3 methyl ketal, and **3***c* to *O*-acetylallocyathin B_3 methyl ketal.

The presence of the cyclopentadiene moiety in allocyathin B_3 was further confirmed by formation of a Diels–Alder adduct. When a benzene solution of **2***b* and maleic anhydride was heated to 70° the crystalline adduct **4** was formed in good yield. The n.m.r. spectrum shows the typical coupling pattern expected for a bicyclo-[2.2.1]heptene system; in particular, H-1 is coupled to H-1′ by 4.5 Hz (*exo* coupling) proving that the adduct has the expected *endo* configuration (ref. 5*a*, p. 289). We are unable to determine

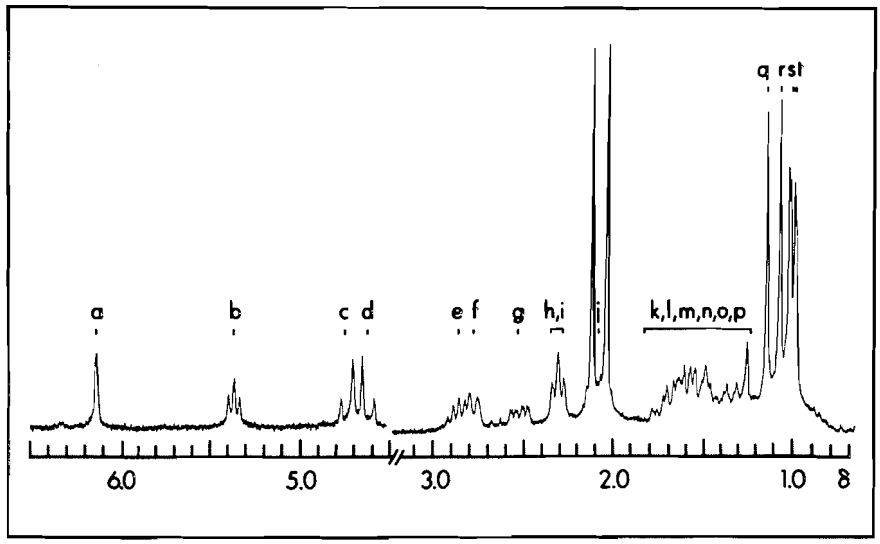

FIG. 2. Nuclear magnetic resonance spectrum (220 MHz) of *O,O*-diacetylcyathin A_3 in $CDCl_3$.

the configuration at C-1 and -4 (*i.e.*, whether addition has occurred to the α or the β face).

In contrast to allocyathin B_3, cyathin A_3 crystallizes in the hemiketal form as is evidenced by the solid phase i.r. spectrum which lacks absorption in the 1750–1650 cm^{-1} region. The i.r., u.v., and c.d. spectra taken in solution display absorption bands which are assigned to an α,β-unsaturated carbonyl group; however the 1650 cm^{-1} band is, as in allocyathin B_3, only of medium intensity and consequently cyathin A_3 appears to exist in solution as an equilibrium mixture of the tautomeric forms **5***a* and **6***a*.

O,O-Diacetylcyathin A_3 (**5***b*) was prepared in the same way as *O,O*-diacetylallocyathin B_3 (**2***b*). No rearrangement occurred during acetylation, since under mild alkaline hydrolysis conditions (K_2CO_3 – aqueous CH_3OH) **5***b* could be converted back to **5***a*. In fact we have noticed that simple storage of **5***b* in methanol will effect the same conversion. The spectroscopic data obtained with **5***b* are similar to those obtained for **2***b*, except for those features which are associated with the cyclopentadiene chromophore. The more characteristic features are: i.r. maximum at 1690 cm^{-1} with a shoulder at 1670 cm^{-1}; u.v. maximum (isooctane) at 323 nm (ε 130), shoulder at 225 nm (ε 8700), assigned to n–π* and π–π* transitions of the α,β-unsaturated carbonyl system, respectively; c.d. maximum at 330 nm (Δε +2.73). The n.m.r. spectra (Fig. 2 and Table 3) lack the AB quartet in the δ 6.0–6.5 region; instead, they display two additional unresolved signals in the δ 1.2–1.8 region for the two protons on C-1 and signals for another two protons at ~δ 2.3 attributable to the allylic protons at C-2 (the coupling pattern for this multiplet could not be analyzed). The remaining protons give chemical shifts and coupling patterns similar to those of **2***b*, with the exception that the signal for H-10α (axial proton j) is obscured by that of the allylic methylene at C-2.

The methyl ketal **6***b* formed almost instantaneously when cyathin A_3 was treated with dilute methanolic hydrochloric acid. Ketal formation is reversible since cyathin A_3 can be recovered after mild acid hydrolysis. The spectroscopic data for **6***b* is in complete agreement with the assigned structure (see Tables 2 and 3). The most characteristic feature of the n.m.r. spectrum is the narrow multiplet at δ 4.79 ($CDCl_3$) for the bridgehead proton H-11 (proton b) shown to be coupled to H-10α (3 Hz) and H-10β (~0.5 Hz) by n.m.d.r. experiments. The acetyl derivative **6***c* was formed in the usual manner and displayed the expected properties (see Tables 2 and 3).

During the investigation of these compounds we frequently encountered complications when reactions were conducted under alkaline conditions (*e.g.*, attempted hydrolysis of *O*-acetyl derivatives with hydroxide catalysis). When this observation was followed up by control experiments it was found that the epimeric conjugate

Can. J. Chem. Downloaded from www.nrcresearchpress.com by 210.87.254.5 on 09/05/12
For personal use only.

TABLE 3. Nuclear magnetic resonance data for cyathin A_3 derivatives[a]

	H-1, H-7 and H-8	H-2	H-5β	H-10α	H-10β	H-11β	H-12	H-13a	H-13b	H-15a	H-15b	H-16 and H-17	H-18	H-19 and H-20	OAc at C-11 and/or C-15	OMe at C-12	OMe at C-14
	1.9–1.1	2.3	2.78	2.05	2.53	5.36	—	6.13		4.75	4.63	1.15; 1.06	2.85	1.00; 0.99	2.12; 2.04	—	—
	1.9–1.1	2.3	2.94	2.21	2.64	5.37	—	—		4.71	4.52	1.36; 1.07	2.94	1.08; 1.03	1.74; 1.72	—	—
	u	u	dd	ddd	ddd	ddddd	—	ddd		ddd	ddd	s; s	qq	d; d	s; s	—	—
	—	—	10, 2.5	14, 10, 7	14, 6, 2.5	7, 6, 0.5, 0.5, 0.5	—	1.5, 0.5, 0.5		14, 1.5, 0.5	14, 1.5, 0.5	—; —	7, 7	H-18, H-18	—; —	—	—
	—	—	H-10α, H-10β	H-10β, H-5β H-11β	H-10α, H-11β H-5β	H-10α, H-10β H-3, H-15a, H-15b	—	H-15a, H-15b, H-11β		H-15b, H-13 H-11β	H-15a, H-13 H-11β	—; —	H-19, H-20	7; 7	—; —	—	—
	1.8–1.2	2.2	2.4	2.25	1.4	4.79	—	6.06		4.34	4.34	1.01; 0.97	2.95	1.03; 0.93	—	—	3.31
	1.9–1.2	2.2	2.44	2.19	1.35	4.60	—	5.86		3.76	3.76	1.31; 1.01	2.96	1.04; 0.93	—	—	3.34
	u	u	dm	ddd	(dd)	dm	—	dd		dd	dd	s; s	qq	d; d	—	—	s
	—	—	12, —	12, 12, 3	(12, ?)	3, —	—	1.5, 1.5		16, 1.5	16, 1.5	—; —	6.5, 6.5	6.5 ; 6.5	—	—	—
	—	—	H-10α, —	H-10β, H-5β H-11β	H-10α, H-5β	H-10α, —	—	H-15a, H-15b		H-15b, H-13	H-15a, H-13	—; —	H-19, H-20	H-18; H-18	—	—	—
	1.9–1.2	2.2	2.43	2.20	1.4	4.56	—	5.88		4.49	4.32	1.28; 1.02	2.94	1.03; 0.91	1.63	—	3.28
	1.7–1.3	~2.3	~2.3	~2.3	~1.9	4.27	—	~2.3	~2.3	3.81	3.65	1.03; 1.00	2.88	0.99; 0.91	—	3.36	—
	1.7–1.3	~2.3	~2.3	~2.3	~1.9	4.21	—	~2.3	~2.3	3.76	3.56	1.00; 0.98	2.93	0.96; 0.88	—	3.30	—
	1.7–1.3	~2.3	~2.3	~2.3	1.85 (?)	4.27	—	~2.3	~2.3	4.57	4.04	1.01; 0.99	2.84	0.97; 0.89	2.09	3.28	—
	?	?	?	?	(dd)	m	—	?	?	d	d	s	qq	d; d	s	s	—
	?	?	?	?	15, 2	$w_{\frac{1}{2}} = 7$	—	?	?	13	13	s	7, 7	7; 7	—	—	—
	?	?	?	?	(H-10α, H-11β)	(H-10α, H-10β)	—	?	?	H-15b	H-15a	—	H-19, H-20	H-18; H-18	—	—	—
	1.8–1.2	2.3	2.8	2.3?	2.0 (?)	5.02	—	3.07	2.81	4.27	4.13	1.14; 1.06	2.84	0.96; 0.95	2.10: 2.09	3.39	—
	u	u	u	u	u	dd	—	d	d	d	d	s; s	dd	d; d	s; s	s	—
	—	—	—	—	—	11, 4	—	13	13	11	11	—; —	7, 7	7; 7	—; —	—	—
	—	—	—	—	—	(H-10α, H-10β)	—	H-13b	H-13a	H-15b	H-15a	—; —	H-19, H-20	H-18; H-18	—; —	—	—
	1.7–1.1	2.2	2.3	2.2	2.2	4.42	2.53	?	?	9.64		0.87; 0.77	2.78	0.88; 0.78	—	—	3.10
	u	u	u	u	u	m	ddd	—	—	d		s; s	qq	d; d	—	—	s
	—	—	—	—	—	$w_{\frac{1}{2}} = 5$	9, 4, 2	—	—	2		—; —	7, 7	7; 7	—	—	—
	—	—	—	—	—	—	H-13β, H-13α H-11β	—	—	H-12β		—; —	H-19, H-20	H-18; H-18	—	—	—
	1.8–1.1	2.3	2.86	?	2.40	4.77	2.0	3.01	?	4.08	3.99	1.16; 1.02	2.69	0.95; 0.95	2.08; 2.05	—	—
	1.6–1.0	2.2	2.85	1.5?	2.57	4.86	1.9	2.83	2.31	4.10	3.91	1.10; 0.97	2.69	0.97; 0.98	1.68; 1.68	—	—
	u	u	d(d)	(ddd)	dd(d)	ddd	(ddddd)	dd	dd	dd	dd	s; s	qq	d; d	s; s	—	—
	—	—	10, (1)	(14, 11, 10)	14, 4, (1)	11, 11, 4	(12, 11, 6, 3, 2)	12, 12	12, 2	11, 6	11, 3	—; —	7, 7	7; 7	—; —	—	—
	—	—	H-10α, H-10β	H-10β, H-11β H-5β	H-10α, H-11β H-5β	H-10α, H-12 H-10β	H-13a, H-11β H-15a, H-15b H-13b	H-13b, H-12	H-13a, H-12	H-15b, H-12	H-15a, H-12	—; —	H-19, H-20	H-18; H-18	—; —	—	—

[a] Same as in Table 1.
[b] 6b.
[c] that of 8.

Can. J. Chem. Downloaded from www.nrcresearchpress.com by 210.87.254.5 on 09/05/12
For personal use only.

Can. J. Chem. Downloaded from www.nrcresearchpress.com by 210.87.254.5 on 09/05/12
For personal use only.

addition products **7***a* and *b* were formed in a ratio of about 4:1 when cyathin A_3 was allowed to stand overnight in dilute methanolic potassium hydroxide. The R_f values of the two products differed sufficiently to allow separation by p.t.l.c. The predominant isomer was obtained in pure form, the minor one in a purity of only ~70% (estimated by n.m.r. spectroscopy). The major epimer **7***a* has the molecular composition $C_{21}H_{34}O_4$ (h.r.m.s.); the u.v. (no maxima near either 290 or 230 nm), c.d. (weak negative minimum at 290 nm, $\Delta\varepsilon$ −0.05), and i.r. spectra (extremely weak carbonyl absorption at 1690 cm^{-1}) all indicate that the adduct exists almost exclusively in the hemiketal form. The n.m.r. spectrum ($CDCl_3$) shows a three-proton singlet at δ 3.36 for the methoxyl group and a relatively narrow multiplet at δ 4.27 for H-11. No assignments can be made with respect to coupling patterns and chemical shifts of H-2, -5, -10, and -13 as together they give rise to a complex signal in the region δ 2.4–2.1. The minor epimer **7***b* was characterized only by its i.r. spectrum (no carbonyl absorption) and n.m.r. spectrum (see Table 3) which exhibits a pattern similar to that of **7***a* (on which it is superimposed, since **7***a* is the impurity in the sample of **7***b*).

Acetylation of **7***a* at 50° for 1.5 h gave the monoacetyl derivative **8**. The i.r. spectrum of **8** shows hydroxyl absorption at 3380 and 3580 cm^{-1}, and acetoxyl absorption at 1743 cm^{-1} with a very weak shoulder at ~1690 cm^{-1} (keto tautomer). The n.m.r. spectrum shows an acetyl methyl signal at δ 2.09; protons H-15a and H-15*b* are shifted downfield by about 0.6 p.p.m. relative to **7***a*. These data establish that **8** exists mainly in the hemiketal form and that it is the primary hydroxyl group which is acetylated.

The diacetyl derivative **9** was prepared by heating **8** with acetic anhydride – pyridine – benzene under reflux for several hours. The presence of the keto group was revealed by the u.v. (maximum at 282 nm, ε 150), c.d. (298 nm, $\Delta\varepsilon$ −1.9), and i.r. spectra (strong absorption at 1696 cm^{-1}). The n.m.r. spectrum ($CDCl_3$) displays two acetyl signals (δ 2.10 and 2.09). The signals for the protons at C-13 appear at somewhat lower field than those of **7***a* and **8** and give rise to an AB quartet centered at δ 2.94 with $\Delta\nu = 26$ Hz and $J = 13$ Hz. The signal for H-11 is shifted downfield by 0.75 p.p.m. (δ 5.02) when compared with the corresponding signal in **7***a* or **8** and appears as a clean doublet of doublets with coupling constants of 11 Hz (presumably due to axial–axial type coupling with H-10α) and 4 Hz (axial–equatorial type coupling with H-10β). The configuration at C-12 has not been established.

All attempts to hydrogenate allocyathin B_3 (or one of its derivatives) selectively to cyathin A_3 (or one of its derivatives) met with failure. It was therefore necessary to correlate the two series via a common hydrogenation product. Under various hydrogenation conditions (10) cyathin A_3 methyl ketal (**6***b*) was transformed,

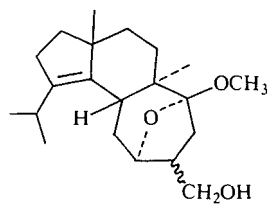

10

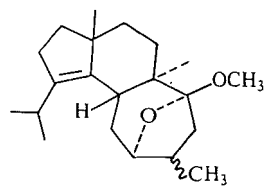

11

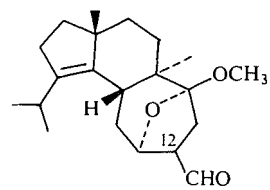

12

a α-CHO(*exo*)
b β-CHO(*endo*)

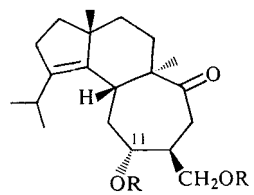

13

a R = H
b R = Ac

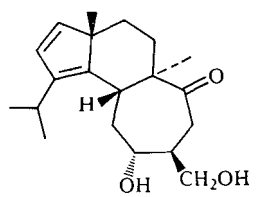

14

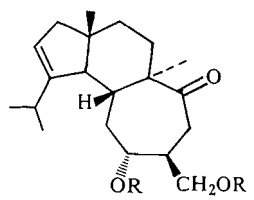

15

a R = H
b R = Ac

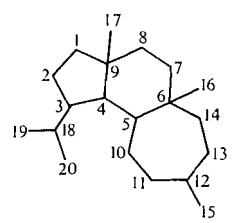

16

Can. J. Chem. Downloaded from www.nrcresearchpress.com by 210.87.254.5 on 09/05/12
For personal use only.

in varying degree, to three different products (each possibly consisting of a pair of C-12 epimers). These are assigned structures **10** (product of normal hydrogenation), **11** (hydrogenolysis and hydrogenation), and **12** (allylic rearrangement). Assignments **10** and **11** must be considered tentative as they were arrived at only on the basis of mass and i.r. spectroscopy. When 5% Pd–C was used as catalyst aldehyde **12***a* was the predominant product. As shown by h.r.m.s., it is isomeric with the starting material; the aldehyde function is apparent from the i.r. (2710 and 1725 cm^{-1}) and n.m.r. spectra (δ 9.64, $J = 2$ Hz). The assignment of configuration at C-12 is based on the coupling pattern of H-12 (δ 2.53), revealed by decoupling experiments: $J_{12,13a} = 9$, $J_{12,13b} = 4$, $J_{12,15} = 2$, and $J_{12,11} < 0.5$ Hz. The latter value allows us to assign the *endo* configuration (β) to H-12 and *exo* configuration (α) to the aldehyde function. When allocyathin B_3 methyl ketal (**3***b*) was subjected to hydrogenation using 5% Pd–C as catalyst the products were **10**, **11**, and the *endo* aldehyde **12***b*. The *endo* aldehyde **12***b* differed in R_f value and i.r. spectrum from the epimeric **12***a*. When **12***b* was allowed to stand in methanol containing sodium carbonate it isomerized to **12***a*, identical (t.l.c. behavior, i.r. spectrum) with that obtained from cyathin A_3. The different product distribution (**12***a* *vs.* **12***b*) is attributed to slight variations in p*H* during the different hydrogenations.

In another series of experiments, cyathin A_3 and allocyathin B_3 were subjected to hydrogenation. Reproducible results were obtained using ethyl acetate as solvent, 5% Pt–C as catalyst, and traces of sodium bicarbonate as a buffer. Under these conditions crystalline dihydrocyathin A_3 (**13***a*) is formed in good yield from cyathin A_3. Crystalline **13***a* exists in the hemiketal form as shown by the solid-phase i.r. spectrum (no carbonyl absorption); in solution both hemiketal and keto forms are present in equilibrium since fairly substantial carbonyl absorption bands are observed in the i.r., u.v., and c.d. spectra. Due presumably to this equilibrium the n.m.r. spectrum is poorly defined. The diacetyl derivative **13***b* also crystallizes readily. The ketonic absorption is much stronger in the various spectra (see Table 2) and the n.m.r. spectrum (C_6D_6) is well defined. Proton H-11 resonating at δ 4.86 shows couplings of 11, 11, and 4 Hz assigned to interactions with H-10α, H-12, and H-10β, respectively. The large coupling indicates a *trans*-coplanar relationship between H-11 and H-12. If we assume that ring C occupies a twist chair conformation (11) with the axis carbon at C-6 (this being the only carbon that carries two substituents) and further assume that the chiral center C-11 was not inverted during the hydrogenation we conclude that H-12 must be *trans* to H-11 and consequently occupies the α position. This conformation places all substituents in energetically favorable positions (11), those at C-6 into isoclinal and those at C-5, -11, and -12 into equatorial positions. The remaining n.m.r. data are summarized in Table 3 and indicate that hydrogenation has occurred stereoselectively from the α side to produce only one epimer. This may be due to the fact that it is the hemiketal form of cyathin A_3 which actually undergoes hydrogenation. The α side is the more freely accessible *exo* side of the bicyclo-[3.2.1] system. When allocyathin B_3 is subjected to the same hydrogenation conditions as cyathin A_3 it appears that the Δ^{12} bond is hydrogenated selectively. Assignment of structure **14** to this intermediate product remains tentative as it was characterized only by its u.v. spectrum which displays a typical cyclopentadiene chromophore at 253 nm. Under somewhat more vigorous conditions the cyclopentadiene moiety is also reduced. A major product (the desired **13***a*) and a minor one (presumably **15***a*, due to 1,4 addition) were formed in a ratio of ~3:1 along with traces of unidentified compounds. Separation of the two isomers was effected by p.t.l.c., although in one instance this was not necessary since the major product crystallized selectively.

The usual spectroscopic characteristics of the major product and its diacetyl derivative were obtained and compared with those of dihydrocyathin A_3; they are identical within the limits of experimental error. In particular, m.p.'s were the same, mixture m.p.'s were undepressed, solid-phase i.r. spectra were identical for both the parent compound and the diacetyl derivative and the richly detailed n.m.r. spectra and the o.r.d. and c.d. spectra of the diacetyl derivatives were superimposable.

The hydrogenation experiments serve to confirm the relationship between cyathin A_3 and allocyathin B_3 and thus establish structure **1** (without stereochemical implications) for cyathin A_3. Since, on the other hand, the full structure of cyathin A_3 (including absolute stereochemistry) has been established by X-ray crystallog-

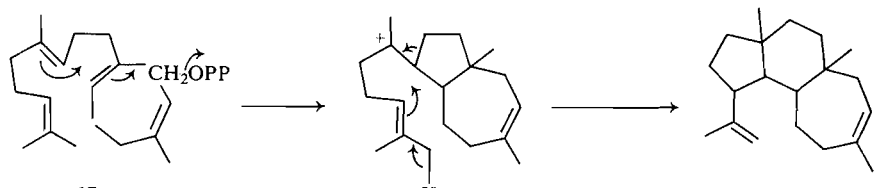

SCHEME 3

raphy, these experiments also serve to establish the complete structure of allocyathin B_3 as **2***a*, provided we make the reasonable assumption that the chiral centers C-5, -6, -9, and -11 are not altered during the hydrogenation.[6]

The molecular formulas of the cyathins together with the fact that they contain five *C*-methyl group equivalents suggested at an early stage that they belong to the diterpenoid group of natural products (12). The carbon skeleton **16**, for which we suggest the name cyathane, does not appear to have been encountered previously among the diterpenes (13). It may also be noted that allocyathin B_3 is one of the very few cyclopentadienes that have been isolated from natural sources. Geranylgeranyl pyrophosphate (**17**) is regarded as the biogenetic precursor of the cyclic dieterpenoids (14). The carbon skeleton of the cyathins may be derived from geranylgeranyl pyrophosphate as illustrated in Scheme 3, or by variations on this theme. Various oxidative and reductive processes lead to the individual cyathins. Recent work has led to the elucidation of the structures of two additional members of this family of compounds (15) and to their correlation with cyathin A_3 and allocyathin B_3.

Experimental

High resolution mass spectra were recorded on an A.E.I. model MS-9 mass spectrometer, i.r. spectra on a Perkin-Elmer model 421 dual grating spectrometer, u.v. spectra on a Cary model 14M spectrophotometer, c.d. and o.r.d. spectra (only the $[\alpha]_D$ values are reported here) on a Jasco model 5 spectropolarimeter, and 100 MHz n.m.r. spectra on a Varian HA-100 spectrometer. A Varian HR-220 spectrometer at the Ontario Research Foundation, Sheridan Park, Ontario, was used to measure the 220 MHz n.m.r. spectra of **2***b* and **5***b*. Melting points were determined on a Leitz-Wetzlar hot-stage or a Fisher-Johns melting point apparatus. The various data obtained with these instruments are reported in Tables 1, 2, and 3.

Plates for t.l.c. were prepared with equipment available from DESAGA Heidelberg. Ordinary t.l.c. plates were prepared with Silica Gel G (E. Merck, Darmstadt) to which 1% Electronic Phosphor (General Electric, Cleveland) was added. Argentated silica gel was prepared by mixing Silica Gel G (45 g) with $AgNO_3$ (5 g in 100 ml water). For analytical t.l.c., the thickness of the layers varied from 0.3–0.5 mm, for p.t.l.c. from 0.5–0.7 mm. In p.t.l.c. compounds were detected by viewing under shortwave (254 nm) u.v. light (ordinary t.l.c.) or longwave (325 nm) u.v. light after the plates were sprayed with 0.2% solution of ethanolic 2′,7′-dichlorofluorescein in 95% ethanol. In the case of analytical t.l.c. spraying with 30% H_2SO_4 and heat charring served as an alternative method. The chromatograms were developed with $CHCl_3$–MeOH 9:1 (system A, to separate polar substances) or Skellysolve B – acetone 3:1 (system B, to separate less polar substances) unless otherwise specified.

Unless otherwise noted, acetylations were carried out by using an "acetylation solution" prepared from 0.16 ml pyridine and 0.08 ml acetic anhydride made up to 1 ml with benzene. When acetylation was complete (as indicated by t.l.c.) excess reagents were usually removed by "purging" with benzene, *i.e.*, evaporating the mixture at reduced pressure, dissolving the residue in benzene, evaporating, and repeating the process 2–3 times. Solvents were usually evaporated under reduced pressure (water aspirator) with the aid of a rotary evaporator at a bath temperature of 40–50°. Skellysolve B refers to Skelly Oil Company light petroleum, b.p. 62–70°.

Separation of Allocyathin B_3 (A) and Cyathin A_3 (B)

Cyathin A_3 – mixture (240 mg), isolated as reported previously (2), was applied to two t.l.c. plates each supporting a layer of 0.05 × 20 × 100 cm of 10% $AgNO_3$ – silica gel. The plates were developed with Skellysolve B – acetone 2:3, sprayed with a 0.2% solution of 2′,7′-dichlorofluorescein in ethanol, and viewed under longwave u.v. light to locate the zones containing allocyathin B_3 and cyathin A_3. The zones were scraped off and eluted with ether (250 ml). After evaporation, 79 mg allocyathin B_3 and 117 mg cyathin A_3 were obtained. Cyathin A_3 crystallized after trituration with acetone and could be further purified by recrystallization from benzene or benzene–cyclohexane mixtures.

Anal. Calcd. for $C_{20}H_{30}O_3$: C, 75.43; H, 9.50. Found:

[6]The hydrogens on the two centers which could conceivably be inverted (double bond migration on the catalyst surface) during hydrogenation, C-5 and -11, both give rise to well-defined n.m.r. signals. Since these signals are very similar in both series, it is considered unlikely that cyathin A_3 and allocyathin B_3 differ at either or both of these chiral centers.

Can. J. Chem. Downloaded from www.nrcresearchpress.com by 210.87.254.5 on 09/05/12
For personal use only.

C, 75.37, 75.46; H, 9.59, 9.68%. Further characterization is described in Tables 2 and 3.

Allocyathin B_3 could only be crystallized after it had been subjected to an acetylation–deacetylation procedure, as described below, with further purification by p.t.l.c. at each stage. Allocyathin B_3 was then recrystallized from Skellysolve B – benzene. Characterization of allocyathin B_3 and its derivatives is described in Tables 1 and 2.

Preparation of O,O-Diacetylallocyathin B_3 (2b)

Allocyathin B_3 (19 mg) was treated with acetylation solution (1 ml) for 4.5 h at 45°. The usual work-up followed by p.t.l.c. (system B) yielded *O,O*-diacetylallocyathin B_3 (13 mg). When the reaction mixture was worked-up after 1 h, the monoacetyl derivative (C-15 hydroxyl acetylated) was the major product.

Methanolysis of O,O-Diacetylallocyathin B_3

O,O-Diacetylallocyathin B_3 (102 mg) was dissolved in methanol (10 ml) and K_2CO_3 (6.5 mg) was added. As judged by t.l.c., deacetylation occurred immediately. This material yielded crystalline allocyathin B_3 after evaporation, removal of salts, and p.t.l.c.

Preparation of Allocyathin B_3 Methyl Ketal (3b)

To a solution of allocyathin B_3 (31 mg) in methanol (20 ml) was added a saturated solution of HCl in methanol (1 ml). After 0.5 h the solution was neutralized with Na_2CO_3 (800 mg), insoluble material removed by filtration, and the solvent evaporated. The residue was dissolved in ether, filtered, and evaporated to give crude product (28 mg). Purification by p.t.l.c. (system B) yielded pure allocyathin B_3 methyl ketal (20 mg) which could not be obtained in crystalline form.

Preparation of O-Acetylallocyathin B_3 Methyl Ketal (3c)

Allocyathin B_3 methyl ketal (20 mg) was treated with a solution of pyridine (0.16 ml) and acetic anhydride (0.08 ml) in dichloromethane (1 ml) for 1 h at 30° and then for 0.5 h at 40°. The crude product was purified by p.t.l.c. (system B) to give *O*-acetylallocyathin B_3 methyl ketal which could not be crystallized but was used directly for spectroscopic measurements.

Preparation of Diels–Alder Adduct 4

A solution of maleic anhydride (3.25 mg, 0.033 mmol) in benzene (0.13 ml) was added to *O,O*-diacetylallocyathin B_3 (13 mg, 0.033 mmol) in a 5-ml conical flask. The flask was heated to ~70° for 19 h. Evaporation of the solvent left crude adduct (18 mg), which was purified by p.t.l.c. (solvent system Skellysolve B – acetone, 2:1) to yield crystalline **4** (6 mg).

Preparation of O,O-Diacetylcyathin A_3 (5b)

Crystalline cyathin A_3 (20 mg) was treated with a solution of pyridine (0.16 ml) and acetic anhydride (0.08 ml) in dichloromethane (1.0 ml) for 0.5 h at 26° (monoacetylation), and for 10 h at 35° (diacetylation, as judged by t.l.c.). The usual work-up yielded crude product (20 mg) as a nearly colorless gum. Purification by p.t.l.c. (system B), followed by molecular distillation at 105–120°/0.02–0.2 mm gave pure *O,O*-diacetylcyathin A_3 (15 mg) which could not be induced to crystallize.

Hydrolysis of O,O-Diacetylcyathin A_3

O,O-Diacetylcyathin A_3 (23 mg) was treated at room temperature with a solution of 2% K_2CO_3 in 80% aqueous methanol (1.5 ml) for 0.5 h. The reaction mixture was then diluted with water (2 ml), extracted with ether (25 ml), and washed with water until neutral. Evaporation of the dried ($MgSO_4$) extract yielded a product which was identical with cyathin A_3 according to t.l.c., mass, and i.r. spectra.

Preparation of Cyathin A_3 Methyl Ketal (6b)

Crystalline cyathin A_3 (20 mg), dissolved in methanol (10 ml), was treated with a saturated solution of HCl in methanol (10 drops) for 0.5 h. The solution was then neutralized with Na_2CO_3 (120 mg) and the solvent evaporated. The residue was taken up in ether, the suspension filtered, and the ether evaporated to yield cyathin A_3 methyl ketal (22 mg) which showed a single spot on t.l.c.

Hydrolysis of Cyathin A_3 Methyl Ketal

Cyathin A_3 methyl ketal (40 mg) was dissolved in acetone – water – concentrated HCl (20:2:1) (23 ml) and kept for 18 h at 32°. The solution was neutralized with Na_2CO_3, filtered, and most of the acetone evaporated. The resulting aqueous suspension was extracted with ether, dried ($MgSO_4$), filtered, and evaporated to give crude product (36 mg). Purification by p.t.l.c. (system A) gave cyathin A_3 (11 mg) which crystallized upon trituration with acetone. Identity was established by t.l.c. and i.r. spectrum (KBr pellet).

Preparation of O-Acetylcyathin A_3 Methyl Ketal (6c)

Cyathin A_3 methyl ketal (20 mg) was treated with a solution of pyridine (0.16 ml) and acetic anhydride (0.08 ml) in dichloromethane (1 ml) for 1.25 h at 26° and for 1 h at 40°. The usual work-up yielded *O*-acetylcyathin A_3 methyl ketal which crystallized upon storage in the refrigerator.

Preparation of Methanol Adducts 7a and 7b

Cyathin A_3 (20 mg) was dissolved in a solution of 2% KOH in methanol (1.0 ml) and allowed to stand for 17 h at room temperature. The solution was concentrated under a nitrogen stream and subjected to p.t.l.c. (system A) to yield crude **7a** (17.5 mg) and crude **7b** (3.7 mg). Crude **7a** was subjected once more to purification by p.t.l.c. and obtained in pure form as judged by t.l.c. and n.m.r. Crude **7b** was chromatographed (p.t.l.c.) twice more but could only be obtained in a purity of *ca.* 70% (as judged by n.m.r., the remaining 30% being **7a**).

Preparation of 8

The major adduct **7a** (17 mg) was treated with acetylation solution (1 ml) for 1.5 h at 40° and 1.5 h at 50°. The usual work-up yielded crude **8** (20 mg) with which the data listed in Table 2 were obtained.

Preparation of 9

The monoacetyl derivative **8** (20 mg) was dissolved in acetylation solution (1 ml) and heated under reflux for 24 h. The usual work-up yielded crude product (18 mg). Purification by p.t.l.c. (system B) yielded **9** (11 mg), which could not be crystallized.

Hydrogenation of Cyathin A_3 Methyl Ketal

Crystalline cyathin A_3 (30 mg) dissolved in methanol (60 ml) was treated with a saturated solution of HCl in methanol (1 ml) for 0.5 h. Dry Na_2CO_3 (1 g) was added, the mixture stirred until the solution was neutral, and the insoluble material filtered off. Palladium–charcoal (5%,

Can. J. Chem. Downloaded from www.nrcresearchpress.com by 210.87.254.5 on 09/05/12
For personal use only.

Can. J. Chem. Downloaded from www.nrcresearchpress.com by 210.87.254.5 on 09/05/12
For personal use only.

50 mg) was added to the filtrate and the mixture stirred in an atmosphere of hydrogen for 0.5 h at room temperature. The catalyst was removed by filtration and the solvent evaporated. The residue was taken up in ether, filtered, and the solvent evaporated. The crude product (28 mg) consisted mainly of two components, alcohol **10** and aldehyde **12***a*, along with trace amounts of **11** (the latter identified by t.l.c.). The aldehyde (12 mg) and the alcohol (7 mg) were separated by p.t.l.c. (system B). No attempt was made to isolate **11**. Alcohol **10** could not be crystallized. Aldehyde **12***a* crystallized spontaneously after evaporation of the solvent from the appropriate chromatographic fraction and was recrystallized from Skellysolve B.

Hydrogenation of Allocyathin B_3 Methyl Ketal

Allocyathin B_3 methyl ketal (purified by p.t.l.c., 10 mg), dissolved in methanol (20 ml), was hydrogenated over 5% Pd–C (20 mg) at atmospheric pressure and room temperature for 17 min. The catalyst was filtered off and the solvent evaporated. The crude product (9 mg) was separated by p.t.l.c. (system B) and found to be a mixture of **10** (1 mg), **11** (3 mg), and **12***b* (1 mg).

Aldehyde **12***b* isomerized to **12***a* when allowed to stand in a saturated solution of Na_2CO_3 in methanol (1 ml) for 28 h at room temperature. The solvent was evaporated, the residue taken up in ether, filtered, and evaporated. The i.r. spectrum and t.l.c. characteristics of the product were indistinguishable from those of aldehyde **12***a* obtained from cyathin A_3. The small amount (~0.5 mg), however, precluded attempts at recrystallization.

Hydrogenation of Cyathin A_3

Cyathin A_3 (30 mg), 5% Pt–C (15 mg), and $NaHCO_3$ (30 mg) in ethyl acetate (30 ml) were hydrogenated at room temperature and atmosphere pressure for 10 min. Catalyst and undissolved $NaHCO_3$ were removed by filtration and the solvent was evaporated to give a crude hydrogenation product (35 mg). Crystallization from benzene yielded 12,13-dihydrocyathin A_3 (**13***a*) (10 mg). The mother liquors contained mainly **13***a* and this material was used for acetylation (see below).

Hydrogen of Allocyathin B_3

(a) "Incomplete" Hydrogenation

In an exploratory experiment, allocyathin B_3 (4 mg), 5% Pt–C (5 mg), and $NaHCO_3$ (4 mg) were suspended in ethyl acetate (4 ml) and hydrogenated at room temperature and atmospheric pressure for 5 min. Catalyst, $NaHCO_3$, and solvent were removed and the crude product investigated by u.v. and mass spectroscopy which indicated that 11,12-dihydroallocyathin B_3 (**14**) had formed.

(b) "Complete" Hydrogenation

Crystalline allocyathin B_3 (10.4 mg), 5% Pt–C (10 mg), and $NaHCO_3$ (10 mg) were suspended in ethyl acetate (10 ml) and hydrogenated at room temperature and atmospheric pressure for 30 min. Filtration and evaporation yielded crude product (11.2 mg) which consisted mainly of **13***a* and **15***a*. This material was subjected to p.t.l.c. (system A) and **13***a* (6.7 mg) and **15***a* (2.6 mg), both slightly impure, were obtained. In a separate hydrogenation experiment involving allocyathin B_3, 1,2,12,13-tetrahydroallocyathin B_3 (12,13-dihydrocyathin A_3, **13***a*) crystallized directly from the hydrogenation product. Identity of this product with that obtained from cyathin A_3 was established by means of t.l.c., m.p., mixed m.p., and i.r. spectroscopy.

Preparation of 13b

(a) From Cyathin A_3

Crude **13***a* (residue from the crystallization, 20 mg) was treated with acetylation solution (1 ml) at 50° for 10 h. The usual work-up gave a crude product (24 mg) which was combined with material of similar purity obtained in a separate experiment (7 mg) and subjected to p.t.l.c. (system B). In this way the diacetyl derivative **13***b* (12.7 mg) was obtained. It crystallized from ether and could be recrystallized from Skellysolve B.

(b) From Allocyathin B_3

1,2,12,13-Tetrahydroallocyathin B_3 (the material described under the heading "Hydrogenation of Allocyathin B_3", 6.7 mg) was treated with acetylation solution (0.7 ml) at 50° for 17 h. The usual work-up followed by p.t.l.c. (system B) gave the diacetyl derivative **13***b* (6.2 mg) which crystallized from ether. Identity between this material and material derived from cyathin A_3 was established by t.l.c., m.p., mixed m.p., and u.v., o.r.d., c.d., i.r., and n.m.r. spectroscopy.

Preparation of 15b

15*a* (2.6 mg) was treated with acetylation solution (0.3 ml) at 50° for 17 h. The usual work-up yielded crude product (2.6 mg) which was purified by p.t.l.c. (system B) to give **15***b* (0.8 mg). This material crystallized when triturated with ether.

We wish to thank Professor Harold J. Brodie, Department of Botany, University of Alberta, for drawing this problem to our attention and for the help and instruction in microbiological techniques that he and Dr. B. N. Johri provided. We also wish to acknowledge the contributions of our colleague, the late Dr. A. D. Allbutt, to the early stages of this work. The financial support provided by the National Research Council of Canada is gratefully acknowledged.

1. H. J. Brodie. Can. J. Bot. **44**, 1235 (1966).
2. A. D. Allbutt, W. A. Ayer, H. J. Brodie, B. N. Johri, and H. Taube. Can. J. Microbiol. **17**, 1401 (1971).
3. W. A. Ayer and H. Taube. Tetrahedron Lett. 1917 (1972).
4. (*a*) A. S. Gupta and S. Dev. J. Chromatogr. **12**, 189 (1963). (*b*) H. Rönsch and K. Schreiber. J. Chromatogr. **30**, 149 (1967).
5. (*a*) L. M. Jackman and S. Sternhell. Applications of nuclear magnetic resonance spectroscopy in organic chemistry. 2nd ed. Pergamon Press, Oxford. 1969. (*b*) R. M. Silverstein and G. C. Bassler. Spectrometric identification of organic compounds. 2nd ed. John Wiley, New York. 1968.
6. O. L. Chapman. J. Am. Chem. Soc. **85**, 2014 (1963).
7. (*a*) C. F. Wilcox, Jr. and M. Mesirov. J. Org. Chem. **25**, 1841 (1960). (*b*) R. S. Rouse

and W. E. TYLER. J. Org. Chem. **26**, 3525 (1961). (*c*) S. MCLEAN and P. HAYNES. Tetrahedron, **21**, 2313, 2343 (1965).
8. M. J. BENNETT and R. M. TUGGLE. Submitted for publication.
9. R. S. CAHN, C. K. INGOLD, and V. PRELOG. Experientia, **12**, 81 (1956).
10. (*a*) R. L. AUGUSTINE. Catalytic hydrogenation. Dekker, New York. 1965. (*b*) M. FREIFELDER. Practical catalytic hydrogenation. Wiley-Interscience, New York. 1971. (*c*) P. N. RYLANDER. Catalytic hydrogenation over platinum metals. Academic Press, New York. 1967.
11. (*a*) J. B. HENDRICKSON. J. Am. Chem. Soc. **89**, 7047 (1967). (*b*)E. S. GLAZER, R. KNORR, C. GANTER, and J. D. ROBERTS. J. Am. Chem. Soc. **94**, 6026 (1972).
12. W. TEMPLETON. An introduction to the chemistry of terpenoids and steroids. Butterworths, London. 1969. p. 104.
13. T. K. DEVON and A. I. SCOTT. Handbook of naturally occurring compounds. Vol. II. Academic Press, New York. 1972. pp. 185–274.
14. D. V. BANTHORPE and B. V. CHARLWOOD. *In* Chemistry of terpenes and terpenoids. *Edited by* A. A. Newman. Academic Press, New York. 1972. p. 375.
15. W. A. AYER and L. L. CARSTENS. Can. J. Chem. **51**, 3157 (1973).

Can. J. Chem. Downloaded from www.nrcresearchpress.com by 210.87.254.5 on 09/05/12
For personal use only.

Reactivity of the Thallium(I) Salts of 3-Hydroxy-1,3,5(10)-estratrien-17-one and 1,3,5(10)-Estratriene-3,17β-diol. Preparation of 17-Oxoestra-1,3,5(10)-trien-3-yl 2′-Acetamido-3′,4′,6′-tri-*O*-acetyl-2′-deoxy-β-D-glucopyranoside[1]

ALENKA PAQUET AND DONALD S. LAYNE
Department of Biochemistry, University of Ottawa, Ottawa, Canada K1N 6N5

Received April 12, 1973

Thallium(I) salts of estrone and 17β-estradiol were prepared in high yields by the reaction of estrone or 17β-estradiol with thallium(I) ethoxide. Both compounds were found to be reactive intermediates for alkylation and acylation of the steroid. The preparation and characterization of 17-oxoestra-1,3,5(10)-trien-3-yl 2′-acetamido-2′-deoxy-β-D-glucopyranoside by reaction of the thallium(I) salt of estrone with 2-trifluoroacetamido-3,4,6-tri-*O*-acetyl-2-deoxy-β-D-glucopyranosyl bromide is described.

Les sels de thallium(I) de l'estrone et de l'estradiol-17β ont été préparés avec de bons rendements par réaction de l'estrone ou de l'estradiol-17β avec l'éthylate de thallium(I). On a trouvé que les deux composés sont des intermédiaires réactifs pour l'alkylation et l'acylation du stéroide. On décrit la préparation et la caractérisation de l'acétamido-2′ déoxy-2′ β-D-glucopyranoside de l'oxo-17 estratriène-1,3,5(10)yle par réaction du sel de thallium(I) de l'estrone avec le bromure du trifluoroacétamido-2 tri-*O*-acétyl-3,4,6 déoxy-2 β-D-glucopyranosyle. [Traduit par le journal]

Can. J. Chem., **51**, 3855 (1973)

Since the initial recognition (1) that steroid glucuronides were present in human and animal excreta, many syntheses of these compounds have been reported (2). In the past 10 years evidence has accumulated that steroid glucuronides may be important in determining the transport as well as the rate and route of excretion of hormonally active steroids (2). In addition, glucosides, galactosides, and *N*-acetylglucosaminides of the estrogens have been found in tissues of the human and other animals (3, 4). These findings have focused attention on the physiological importance of steroid glycosides and on improved methods for their preparation. These latter have almost exclusively been concerned with increasing the yields obtained in the standard Koenigs–Knorr synthesis, and Bernstein and his collaborators (5, 6) have achieved yields of up to 70% of extrogen glucuronides and *N*-acetylglucosaminides by the use of cadmium carbonate as a catalyst in this reaction.

We have been interested in the development of syntheses which might be adaptable to the preparation, for use in physiological studies, of glycosides of radioactive steroids of high specific activity. Both the Koenigs–Knorr and the modified Helferich synthesis (7) are cumbersome for this purpose, and furthermore, in our hands, the yields obtained by Bernstein's procedure (5, 6) were highly variable, being extremely dependent on the source, purity, and crystalline state of the cadmium carbonate used. We therefore explored the use of thallium(I) salts of the phenolic steroid estrogens as intermediates in glycoside synthesis, using the procedures which have been described by Taylor, McKillop, and their coworkers (8, 9) for the preparation of derivatives of several other classes of compounds.

The thallium(I) salts of estrone and the 3-monothallium(I) salt of 17β-estradiol were prepared in practically quantitative yields by the reaction of the respective steroids with thallium(I) ethoxide. In initial experiments to explore the reactivity of these salts, it was found that their reaction with acyl or alkyl halides led to the facile formation of the corresponding acyl or alkyl derivatives of the steroids. The 3-acetates and 3-benzoates of both estrone and 17β-estradiol, as well as the 3-methyl and 3-benzyl ethers of these steroids, were obtained in yields of the order of 90%. The convenience and effectiveness of the procedure might well make it preferable in some instances to the usual methods of preparing these steroid derivatives, in similar yields, by the use of the appropriate anhydride or halide in pyridine (ref. 10 p. 30 and ref. 11).

The thallium(I) salt of estrone **1** was converted

[1]Supported by grant MA-3287 from the Medical Research Council of Canada.

Can. J. Chem. Downloaded from www.nrcresearchpress.com by 210.87.254.40 on 09/05/12
For personal use only.

Can. J. Chem. Downloaded from www.nrcresearchpress.com by 210.87.254.40 on 09/05/12
For personal use only.

into various glycosides in several solvent systems. The reaction gave low yields when chlorinated solvents (chloroform, dichloromethane) were used. High yields, which were reproducible, were obtained in benzene. Only a limited number of relatively easily available sugar derivatives were investigated in the present work. The reaction of the thallium(I) salt of estrone **1** with 2,3,4,6-tetra-*O*-acetyl-α-D-glucopyranosyl bromide produced only a 16% yield of the glycoside **6**, while the analogous reaction with 2,3,4,6-tetra-*O*-acetyl-α-D-galactopyranosyl bromide failed, as did the reaction with methyl 2,3,4-tri-*O*-acetyl-1-bromo-1-deoxy-α-D-glucopyranuronate. However, when the highly reactive 2-trifluoracetamido-3,4,6-tri-*O*-acetyl-2-deoxy-αD-glucopyranosyl bromide (**12**) was used (12), the reaction proceeded rapidly at room temperature and yielded 86% of pure 17-oxoestra-1,3,5(10)-trien-3-yl 2′-trifluoroacetamido-3,4,6-tri-*O*-acetyl-2-deoxy-β-D-glucopyranoside (**7**). Removal of acetyl groups from this product yielded the free amine **8** in crude form which was then either submitted to selective *N*-acetylation (13) by acetic anhydride in ethanolic solution or was fully acetylated with acetic anhydride in pyridine. The glycoside **9** obtained by the latter procedure was de-*O*-acetylated by treatment overnight at 0° with dry ammonia in chloroform–methanol (14). The 17-oxoestra-1,3,5(10)-trien-3-yl 2′-acetamido-2′-deoxy-β-D-glucopyranoside (**10**) obtained was compared with that synthesized by a conventional Koenigs–Knorr synthesis from estrone and 2-acetamido-3,4,6-tri-*O*-acetyl-α-D-glucopyranosyl chloride in acetone in the presence of 1 *M* NaOH and cadmium chloride. The two compounds had identical i.r. spectra and there was no depression of the melting point on mixing of the two.

The fact that, in a 30 min reaction time at room temperature with the thallium(I) salt of estrone an 86% yield of glycoside was obtained, whereas the less reactive sodium salt of estrone gave a much lower yield of 26% under the same conditions, indicates that 2-trifluoroacetamido-3,4,6-tri-*O*-acetyl-2-deoxy-α-D-glucopyranosyl bromide (**12**) is a very reactive glycosylating agent for the phenolic hydroxyl group of the steroid. The trifluoracetyl group can be easily introduced or removed under mild conditions, and it has therefore often been used (12, 15, 16) in nucleoside and glycoside syntheses involving 2-deoxy-2-amino sugars. The use of the trifluoracetyl as a non-participating group to avoid the formation of an oxazoline ring has been described by Strachan *et al.* (17) and discussed by Meyer zu Reckendorf *et al.* (18).

The β-D-anomeric linkage of the steroid glycosides synthesized in this work was established by the application of Klyne's rule (19).

The formation, by way of the thallium(I) salts, of ethers, esters, and glycosides of the phenolic hydroxyl group of the estrogens proceeds rapidly at room temperature under neutral conditions. The easy removal by filtration of precipitated thallium(I) halide makes the work-up simple and convenient as compared to previously reported methods (ref. 10 p. 204 and refs. 11 and 24).

Experimental

The following procedures were used unless otherwise stated. Melting points were determined on a Thomas-Hoover Capillary melting point apparatus and i.r. spectra on a Unicam SP200 spectrometer in chloroform solution or Nujol. Nuclear magnetic resonance spectra were determined on a Varian HA-100 or a Varian T-60 spectrometer in deuterochloroform or in dimethylsulfoxide solution, with tetramethylsilane as internal standard. Specific rotations were measured on a Perkin-Elmer 141 polarimeter in chloroform or methanol. T.l.c. was carried out on plates of Silica gel H and column chromatography on Silica gel 60 (70–230 mesh, ASTM). Both adsorbents were obtained from Merck, Darmstadt.

Thallium(I) Salt of Estrone ***1***

(i) Method using Benzene–ethanol as Solvent

Thallium(I) ethoxide (20) (250 mg) was added slowly with stirring to a suspension of 267 mg of estrone in a mixture of 4 ml of benzene and 2.5 ml of ethanol. Within a few minutes estrone was dissolved and another white crystalline precipitate appeared. The reaction mixture was left overnight at 4° and was then filtered to yield 426 mg (91%) of **1**.

(ii) Method using Ethanol as Solvent

Thallium(I) ethoxide (270 mg) was added with stirring to a solution of 270 mg of estrone in hot ethanol. A white crystalline product was separated by filtration. A further 150 mg of thallium(I) ethoxide in ethanol was added to the mother liquor and the crystalline product was again removed by filtration. The total yield was 368 mg (78%) of the thallium(I) salt of estrone **1**, m.p. 188–195° (dec.).

Anal. Calcd. for $C_{18}H_{21}O_2Tl.2H_2O$: C, 42.41; H, 4.15. Found: C, 42.65; H, 4.40.

3-Monothallium(I) Salt of 17β-Estradiol ***1′***

Thallium(I) ethoxide 925 mg was added to a suspension of 1 g of 17β-estradiol in a mixture of 15 ml of benzene and 10 ml of ethanol. The mixture was stirred at room temperature overnight and was then evaporated under vacuum to one quarter of its original volume. On the

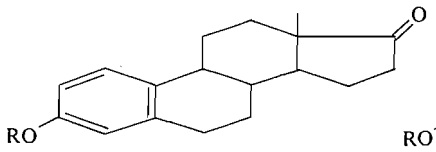

1 R = Tl
2 R = $COCH_3$

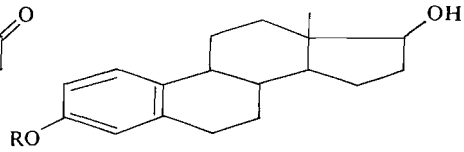

1′ R = Tl
2′ R = $COCH_3$

3 R = CO 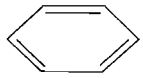

3′ R = CO 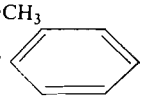

4 R = CH_3
5 R = CH_2 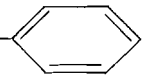

4′ R = CH_3
5′ R = CH_2

6 R = H_3COCO 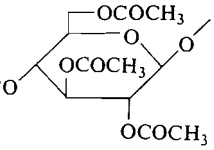

7 R = H_3COCO 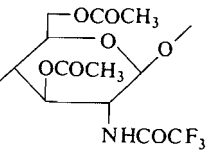

11 R = H_3COCO 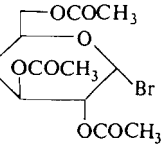

8 R = HO 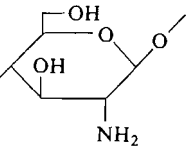

9 R = H_3COCO 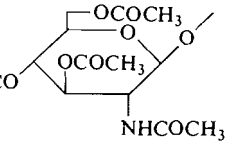

12 R = H_3COCO 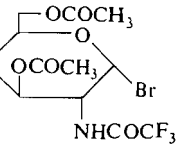

10 R = HO 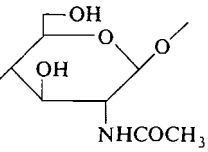

Can. J. Chem. Downloaded from www.nrcresearchpress.com by 210.87.254.40 on 09/05/12
For personal use only.

addition of 10 ml of ether a white crystalline solid was separated by filtration. A yield of 1.734 g (98%) of **1′** was obtained: m.p. (dec.) 180–200°; $[\alpha]_D^{25}$ +27.4° (*c*, 1.66 in pyridine). Analysis: drying under elevated temperature to remove solvent resulted in decomposition, precluding valid elemental analysis.

3-Acetoxyestra-1,3,5(10)-trien-17-one (2) and 3-Benzoyloxyestra-1,3,5(10)-trien-17-one (3). 3-Acetoxy-17β-hydroxyestra-1,3,5(10)-triene (2′) and 3-Benzoyloxy-17β-hydroxyestra-1,3,5(10)-triene (3′)

The thallium(I) salt of the steroid was suspended in benzene and a slight excess of acetylchloride or of benzoyl chloride in benzene solution was added slowly with stirring. The reaction vessel was kept in cold water during the addition. The inorganic precipitate was filtered off, washed with benzene, and the washings were added to the filtrate which was washed with a 10% (w/v) aqueous solution of sodium carbonate and then with 5% hydrochloric acid and with water. The organic layer was dried over sodium sulfate and concentrated. The following esters were obtained in crystalline form (>90%) by this procedure: **2**, m.p. 124° (lit. (21) 125°); **3**, m.p. 216° (lit. (21) m.p. 218°); **2′**, m.p. 134–136° (lit. (22) 136–138°); **3′**, m.p. 193° (methanol–water) (lit. (23) 192–193°) (methanol–water). The i.r. spectra of chloroform solutions were in accord with these structures.

3-Methoxyestra-1,3,5(10)-trien-17-one (4) and 3-Benzyloxyestra-1,3,5(10)-trien-17-one (5). 3-Methoxy-17β-hydroxyestra-1,3,5(10)-triene (4′) and 3-Benzyloxy-17β-hydroxyestra-1,3,5(10)-triene (5′)

The 3-monothallium(I) salt of steroid (100 mg) was dissolved in 2 ml of dimethylsulfoxide and a slight excess of methyl iodide or benzyl bromide was added. After 10 min 5 ml of chloroform and a small amount of Celite were added. The inorganic precipitate was filtered off and washed with chloroform. The filtrate and washings were combined and concentrated by evaporation, aqueous methanol was added, and the crystalline precipitate was separated by filtration and recrystallized from methanol–water. The following ethers were obtained: **4** (92%), m.p. 165° (lit. (24) m.p. 161–162°); **5** (80%), m.p. 134° (lit. (21) m.p. 136°); **4′** (94%), m.p. 96–98° (fuse), 118–120° (melting) (lit. (23) m.p. 97–98°); **5′** (94%), m.p. 83° (lit. (23) m.p. 82–84°). Infrared spectra in chloroform were in accord with these structures.

Etherifications in Dimethylformamide

The thallium(I) salt of estrone (100–110 mg) was dissolved in dimethylformamide and a slight excess of methyl iodide or of benzyl bromide was added. The reaction mixture was heated with stirring at 70° for 3 h in the methylation reaction and at 55° for 4 h in the benzylation reaction. The inorganic precipitate was removed by filtration through a pad of Celite and was washed with chloroform. The washings were added to the filtrate, which was concentrated by evaporation. Crystalline products **4** and **5** were obtained in the yields over 90%.

17-Oxoestra-1,3,5(10)-trien-3-yl 2′,3′,4′,6′-Tetra-O-acetyl-β-D-glucopyranoside (6)

2,3,4,6-Tetra-*O*-acetyl-α-D-glucopyranosyl bromide (**11**) (411 mg) was added in two portions to a suspension of 470 mg of the thallium(I) salt of estrone **1** in 10 ml of benzene. The reaction mixture was stirred at room temperature for 3 days. The inorganic precipitate was removed by filtration. After evaporation and separation of a small amount of unreacted steroid, 97 mg of glycoside **6** was obtained (16%), m.p. 139–141° (lit. (5, 7) m.p. 140–142°).

17-Oxoestra-1,3,5(10)-trien-3-yl 2-Trifluoroacetamido-3′,4′,6′-tri-O-acetyl-2-deoxy-β-D-glucopyranoside (7)

(i) From the Thallium(I) Salt of Estrone

The thallium(I) salt of estrone (650 mg) was added in small portions to a solution of 634 mg of 2-trifluoroacetamido-3,4,6-tri-*O*-acetyl-2-deoxy-α-D-glucopyranosyl bromide (**12**) in 10 ml of dry benzene. The reaction mixture was stirred at room temperature for 30 min. The inorganic product was removed by filtration through a Celite pad and washed with benzene. The filtrate and washings were combined and washed with a small amount of water, dried over sodium sulfate, and evaporated to dryness. On crystallization from dichloromethane–ether–hexane 865 mg of crude material yielded 765 mg (86%) of **7**: m.p. 203–205°; $[\alpha]_D^{27}$ +51° (*c*, 0.5 in chloroform). These constants remained unchanged on further crystallization. Infrared (chloroform) ν_{max} 1720–1745, 1545, 1510, 1200–1250, and 1180 cm^{-1}; n.m.r. (Varian HA-100, $CDCl_3$) 7.22 (H-1 and N—H; 2 protons, spacing 20 Hz), 6.75 (H-2, -4; 2 protons, m, 12 Hz), broad signal from 5.4 to 5.02 (H-1′, -3′, -4′, 3 protons), 4.2 (Hs-6′ and H-2′; 3 protons; m, spacing 16 Hz), 2.06, 2.0 and 1.99 (3 acetates, 9 protons, 3 singlets) and 0.84 δ (C-18 methyl group; 3 protons, singlet).

Anal. Calcd. for $C_{32}H_{38}F_3NO_{10}$: C, 58.80; H, 5.86; N, 2.14. Found: C, 58.57; H, 6.03; N, 2.08.

(ii) From the Sodium Salt of Estrone

To a solution of 296 mg of the sodium salt of estrone (prepared from sodium methoxide and estrone in methanol) in benzene 471 mg of bromide **12** was added in three portions. The reaction mixture was stirred at room temperature for 3 days and the inorganic material was then removed by filtration. The filtrate and washings were washed with a small amount of water, dried over sodium sulfate, and evaporated to dryness. During the evaporation 88 mg of unreacted steroid was separated. The residue was chromatographed on a column containing 10 times its weight of silica gel. Benzene eluates gave 172.6 mg (26%) of crystalline **7** (m.p. 200–203°). Further eluates contained a mixture of unreacted steroid and of a partly decomposed sugar component and were not further investigated.

17-Oxoestra-1-3-5(10)-trien-3-yl 2′-Amino-2′-deoxy-β-D-glucopyranoside (8)

A solution of 200 mg of glycoside **7** in 15 ml of chloroform and 30 ml of methanol was saturated with dry ammonia at 0° and allowed to stand at room temperature for 7 days. The solution was evaporated under reduced pressure to an oily residue. Water was added and the product was isolated by extraction into chloroform – isopropyl alcohol (3 : 2). Evaporation gave 100 mg (76%) of amorphous material **8**: $[\alpha]_D^{24}$ +59° (*c*, 0.2 in methanol); i.r. ν_{max} 3500–2800, 1720, and 1497 cm^{-1}.

Can. J. Chem. Downloaded from www.nrcresearchpress.com by 210.87.254.40 on 09/05/12
For personal use only.

Can. J. Chem. Downloaded from www.nrcresearchpress.com by 210.87.254.40 on 09/05/12
For personal use only.

17-Oxoestra-1,3,5(10)-trien-3-yl 2′-Acetamido-3′,4′,6′-tri-O-acetyl-2′-deoxy-β-D-glucopyranoside (9)

Compound **7** (100 mg) was converted into 17-oxoestra-1,3,5(10)-trien-3-yl 2′-amino-3′4′6′-trihydroxy-2′-deoxy-β-D-glucopyranoside (**8**) by means of ammonia as described above, and the crude product was dissolved in pyridine and acetylated by the addition of 3 ml of acetic anhydride. The reaction mixture was allowed to stand overnight at room temperature. After work-up 88 mg of *O,N*-acetate **9** was obtained (96%). The product was chromatographed on a column containing 50 times its weight of silica gel. Chloroform eluates contained 80 mg (87%) of **9** as a white amorphous solid: $[\alpha]_D^{24}$ +70° (*c*, 0.129 in chloroform) $[M]_D$ +419°, $[M]_D$ calcd. +351° for β-D-glycosidic linkage ($[M]_D$ of methyl 3,4,6-tri-*O*-acetyl-*N*-acetyl-glucosaminide −75.8°, $[M]_D$ of estrone +427°); i.r. ν_{max} 1720–1760, 1545–1510, 1200–1250, 1180 cm^{-1}; n.m.r. (Varian HA-100) 7.1 (1 proton; d; $J_{1,2}$ = 8 Hz), 6.8 (H-2, -4; 2 protons, m, spacing 10 Hz), 5.7 (N—H; 1 proton; d, J = 9 Hz), broad signal from 5.53 to 5.02 (H-1′, -3′, -4′; 3 protons), 4.2 (H-2′, Hs-6′; 3 protons; m, spacing 13 Hz), 3.89 (H-5′, 1 proton; m over 14 Hz), 2.86 (H-6; 2 protons, m, spacing 12 Hz), 2.06, 2.03, 2.01 (3 acetates, 9 protons, 3 singlets), 1.93 (*N*-acetate; 3 protons; singlet), and 0.89 δ (C-18 methyl; 3 protons; singlet).

17-Oxoestra-1,3,5(10)-trien-3-yl 2′-Acetamido-2′-deoxy-β-D-glucopyranoside (10)

(i) By Selective Acetylation of the Free Amine 8

A solution of 90 mg of **8** in 2 ml of absolute ethanol was treated with 0.02 ml of acetic anhydride. After 2 h at room temperature the solvents were removed under vacuum, the residue was dissolved in a 5% (v/v) solution of ethanol in benzene, and filtered through twice its weight of silica gel. The crude product was crystallized from aqueous methanol to yield 45 mg (45%) of **10**: m.p. 225° (softening), 228–230°; $[\alpha]_D^{25}$ +130° (*c*, 0.1 in methanol); i.r. (Nujol) ν_{max} 3500–2800, 1728, 1680, 1510 cm^{-1}.

Anal. Calcd. for $C_{26}H_{35}NO_7$ $1\frac{1}{2}$ CH_3OH: C, 63.32; H, 7.92; N, 2.68. Found: C, 63.05; H, 7.63; N, 2.82.

(ii) By Selective De-O-acetylation of the Fully Acetylated Glycoside 9

A solution of 60 mg of 17-oxoestra-1,3,5(10)-trien-3-yl 2′-acetamidoacetyl-2′-deoxy-β-D-glucopyranoside (**9**) in 3 ml of chloroform and 10 ml of methanol was saturated with dry ammonia at 0° and allowed to stand at 0° overnight. The product was extracted into chloroform – isopropyl alcohol (3:2). After the addition of water to the reaction mixture 43 mg of crude material was obtained. Crystallization from ethanol–water yielded 40 mg (85%) of **10**.

1. S. L. Cohen and G. F. Marrian. Biochem. J. **30**, 57 (1936).
2. S. Bernstein, J. P. Dusza, and J. P. Joseph. *In* Chemical and biological aspects of steroid conjugation. *Edited by* S. Bernstein and S. Solomon. Academic Press Inc., New York. 1970. p. 1.
3. D. S. Layne. *In* Metabolic conjugation and metabolic hydrolysis. *Edited by* W. H. Fishman. Academic Press Inc., New York. 1970. p. 21.
4. D. G. Williamson, D. C. Collins, and D. S. Layne. J. Biol. Chem. **247**, 3286 (1972).
5. R. B. Conrow and S. Bernstein. J. Org. Chem. **36**, 863 (1971).
6. J. P. Joseph, J. P. Dusza, and S. Bernstein. Biochemistry, **10**, 2941 (1971).
7. A. Polakova-Paquet and D. S. Layne. Steroids, **18**, 4, 477 (1971).
8. E. C. Taylor, Y. Maki, and A. McKillop. J. Org. Chem. **34**, 1170 (1969).
9. E. C. Taylor and G. W. McLay. J. Am. Chem. Soc. **90**, 2422 (1968).
10. C. J. W. Brooks. *In* Rodd's Chemistry of carbon compounds. Vol. II^D. Elsevier, Amsterdam. 1970.
11. H. J. E. Loewenthal. Tetrahedron, **6**, 269 (1959).
12. M. L. Wolfrom and P. J. Conigliaro. Carbohydr. Res. **11**, 63 (1969).
13. A. C. Richardson and K. A. McLauchlan. J. Chem. Soc. 2499 (1962).
14. L. Hough and A. C. Richardson. *In* Rodd's Chemistry of carbon compounds. Vol. 1^F. Elsevier, Amsterdam. 1967. p. 470.
15. M. L. Wolfrom and H. B. Bhatt. J. Org. Chem. **32**, 1821 (1967).
16. H. Newman. J. Org. Chem. **30**, 1287 (1965).
17. R. G. Strachan, W. V. Rugle, T. Y. Shen, and R. Hirschmann. J. Org. Chem. **31**, 507 (1966).
18. W. Meyer zu Reckendorf and N. Wassiliadu-Micheli. Chem. Ber. **103**, 1792 (1970).
19. W. Klyne. Biochem. J. **47**, (1950). xli.
20. M. Fieser and L. F. Fieser. Reagents for organic chemistry. Vol. 2. Wiley, New York. 1969. p. 407.
21. Elsevier's Encyclopedia of organic chemistry. Vol. 14S, F. Radt, Springer-Verlag, Berlin. 1959. pp. 2555–2557.
22. H. Fex, K. E. Lundwall, and A. Olsson. Acta Chem. Scand. **22**, 254 (1968).
23. Elsevier's Encyclopedia of organic chemistry. Vol. 14S. Elsevier, New York. 1956. pp. 1972–1975.
24. J. S. Elce, J. G. D. Carpenter, and A. E. Kellie. J. Chem. Soc. (C), 542 (1967).

Investigation of the Polymers Formed in Reactor Irradiated Aniline and Pyridine

MAHMOUD F. BARAKAT[1] AND FAWZI M. ABDELKERIM[2]
Nuclear Chemistry Department, Atomic Energy Authority, Cairo, Egypt

Received February 27, 1973

In reactor irradiated aniline or pyridine most of the radiocarbon generated by the $^{14}N(n,p)^{14}C$ reaction was found preferentially localized in a polymer-like material, brown in color, frequently lustrous and constituting 15–30% of the initial amount of the irradiated material. This stimulated us to try to obtain an idea about the chemical groupings existing in these highly radioactive materials and thereafter to deduce their possible formation pathways.

By comparing the i.r. spectra of these polymers with those of the corresponding pure compounds it was possible to detect some changes in the spectra on polymerization and consequently it was possible to identify some basic structural groups existing. Based on these findings some polymerization reaction mechanisms have been suggested. In general, polymer formation was assumed to take place through the formation of polymerization centers produced by the rupture of the aromatic rings to give highly unsaturated fragments and radicals. These are capable of adding different radicals and fragments formed in the irradiated material by radiolysis or by the action of energetic recoil atoms. Cross linking between individual polymer chains was observed. The preferential localisation of ^{14}C in the polymer fraction could be attributed to the great capacity of the recoil atoms to form reactive secondary species such as $^{14}CH_3^{\cdot}$, $^{14}CH_2^{\cdot\cdot}$, or $^{14}CH^{\cdot\cdot\cdot}$ which participate in polymer formation.

L'aniline ou la pyridine irradiée dans un réacteur où la majorité des radiocarbones produits provient de la réaction $^{14}N(n,p)^{14}C$, se retrouve préférentiellement, comme il a été trouvé, sous forme d'un produit du type polymère, de couleur brunâtre souvent reluisant et comportant 15–30% de la quantité initiale du matériel irradié. Cette constatation nous a alors amené à rechercher les différents groupements chimiques présent dans ces produits hautement radioactifs et par suite à en déduire les différentes voies possibles de formation.

En comparant les spectres i.r. de ces polymères avec ceux des espèces pures correspondantes, il fut possible de déceler certains changements dans les spectres à la suite de la polymérisation et par suite il fut possible d'identifier quelques groupes structuraux présents. En se basant sur ces données, quelques mécanismes de réactions de polymérisation furent entrevues. En général, la formation des polymères semble se produire à la suite de la formation de centres de polymérisation découlant de la rupture des cycles aromatiques pour donner des fragments hautement insaturés ainsi que des radicaux. Ceux-ci sont capables d'additionner différents radicaux et différents fragments formés dans le matériel irradié par radiolyse ou à la suite de l'action d'atomes très énergétiques. On a aussi observé la formation de ponts entre différentes chaînes polymériques individuelles. On a attribué la localisation préférentielle du ^{14}C dans la fraction contenant le polymère à la grande facilité des atomes énergétiques à former des espèces réactives secondaires telles $^{14}CH_3^{\cdot}$, $^{14}CH_2^{\cdot\cdot}$ ou $^{14}CH^{\cdot\cdot\cdot}$ qui participent à la formation des polymères.
[Traduit par le journal]

Can. J. Chem., **51**, 3860 (1973)

Introduction

Reactor irradiation of systems containing organic nitrogen frequently leads to the transformation of a relatively small fraction of the irradiated material into a lustrous polymer-like material, brown in color, and containing the greater fraction of the induced carbon-14 activity (1–5). The non-polymeric fraction produced consists essentially of the labelled parent material together with some other ^{14}C-labelled synthetic products. Although numerous publications have appeared dealing with the mechanism of formation of the different radioactive chemical species present in the non-polymeric fraction resulting from the reactions of the newly born carbon recoils with the molecules of the irradiated materials (6–13), not much is known about the nature, properties, and structures of the highly radioactive polymeric products obtained. This stimulated us to study some of these polymers in order to get an idea about the chemical groups

[1]Present address: Chemistry Department, Faculty of Science, University of Libya, Tripoli P.O. Box 656, Libya.

[2]Permanent address: Optical Spectroscopy Unit, National Research Center, Dokki, Cairo, Egypt.

Can. J. Chem. Downloaded from www.nrcresearchpress.com by 210.87.254.105 on 09/05/12
For personal use only.

TABLE 1. Irradiation conditions and results of analyses of reactor irradiated aniline and pyridine samples

	Aniline		Pyridine	
	I	II	I	II
Irradiation time, (h)	48	48	48	170
Thermal neutron flux $\times 10^{-13}$ (n/cm^2 s)	0.7	0.3	0.7	1.1
Accompanying fast neutron flux $\times 10^{-13}$ (n/cm^2 s)	0.26	0.11	0.26	0.39
Specific activity of the irradiated samples $\times 10^{-6}$ (c.p.m.)	2.95/ml	1.25/ml	3.7/ml	21.69/g
Polymer yield (%)	35	15	25	100
Polymer radiochemical yield (%)*	93	90.5	93	100
No. of molecules polymerized per each ^{14}C atom in polymer $\times 10^{-5}$	1.9	2.0	1.2	0.8

*The complementary part was found in the non-polymeric fraction.

existing in them and then attempt to deduce the possible mechanisms of their formation.

In a previous publication (14) it was shown by the use of i.r. spectroscopy that the polymers formed in reactor irradiated benzene or toluene in the presence of AlN, used as a source of nitrogen for carbon recoils generation, have a polystyrene-like structure. Further clarification of the nature of the polymerization processes, particularly those in which recoil carbons participate, requires a systematic study of the polymers formed in different irradiated media.

In the present work the polymers formed in reactor irradiated aniline and pyridine have been isolated, purified, and investigated by i.r. absorption spectroscopy. The i.r. spectra of the polymers were compared with those of the corresponding pure compounds in order to identify and interpret the changes in the different absorption bands which occur on polymerization. Based on these findings some mechanisms have been proposed for the formation of these polymers.

Experimental

Chemicals

All chemicals used were obtained from British Drug Houses and were of AnalaR grade. Aniline was twice distilled under reduced pressure, dried for several days over KOH pellets, and then repeatedly purified by fractional distillation. The fraction collected at 184 °C was used. Pyridine was also dried over KOH pellets and then repeatedly distilled using a fractionating column. The fraction collected at 115.5 °C was used. Purity of the target materials was tested by the refractive indices and also by analytical g.l.c. of microliter samples at elevated equipment sensitivity.

Preparation of Targets and Irradiation

Quartz ampoules, half filled with the organic materials to be irradiated, were attached to a high vacuum line and were sealed under vacuum as described in a previous publication (13). Irradiations were carried out in the 2 MW research reactor of the Atomic Energy Authority (Egypt). The irradiation conditions are given in Table 1. The maximum sample temperature during irradiation did not exceed 80 °C. After irradiation the samples were kept for several months before being opened and used.

Separation and Analysis of the Polymeric Products

The non-polymeric fraction consisting of all volatile components in the aniline samples, irradiated using either of the two different thermal neutron fluxes, was distilled off after the addition of the following carriers: diethylamine, benzene, toluene, *p*-xylene, *N*-methylaniline, *o*-toluidine, and *N*-ethylaniline as described before (12). The dark brown solid polymer remaining in the distilling flask was taken up in ethanol or chloroform and analyzed by t.l.c. using silica gel G uniformly spread on glass plates. Before use the plates were activated by heating at 150 °C for 2 h. Pure benzene was used as a solvent and iodine vapor was used to detect the spots on the chromatograms. It was found that a well defined dark brown polymer spot remained at the starting point, while some other faintly colored spots were found with R_f values consistent with those of some of the carriers added before separating the polymer by distillation. Consequently, the polymeric fraction in irradiated aniline was purified by t.l.c. using several plates. After developing the plates the pure polymer was collected by scraping followed by elution from the support material by carbon tetrachloride. After evaporation of the solvent the specific activity of the polymer was determined. The solution of the polymer in chloroform was used for the i.r. spectrophotometric analysis.

In the case of pyridine it was found that sample II, irradiated with the higher thermal neutron flux, had been completely transformed into a brown solid polymeric material. When pulverized, this was transformed into a pale yellow powder soluble in chloroform. Using a 14% solution of methanol in benzene as a solvent in the analysis of the polymer sample by t.l.c., it was found that in addition to the main polymer spot remaining at the starting point of the chromatogram, three other very faint

Can. J. Chem. Downloaded from www.nrcresearchpress.com by 210.87.254.105 on 09/05/12
For personal use only.

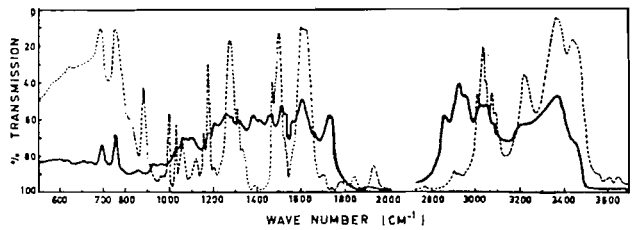

FIG. 1. The i.r. spectrum of the ^{14}C-labelled polymer separated from reactor irradiated aniline (solid line) and that of pure liquid aniline (dotted line).

spots were obtained with R_f values 0.54, 0.69, and 0.88 respectively. The polymer in the other pyridine sample (I) was taken up in pyridine, after the removal of the non-polymeric volatile fraction by distillation, and analyzed by t.l.c. In addition to the main polymer spot remaining at the starting point, a very faint spot was found on the chromatogram with R_f 0.52. As in the case of aniline, the purified pyridine polymer was used for radioactivity measurements and also for obtaining the i.r. spectra.

The i.r. spectra were measured using a fully automatic double beam i.r. spectrophotometer (UR10) Carl Zeis, Jena, with KBr prism (600–700 cm^{-1}), NaCl prism (700–2000 cm^{-1}), and a LiF prism for the region 2700–3800 cm^{-1}. Slit program 4 was used in the measurements. The polymer spectra were measured using thin polymer films deposited on KBr plates by evaporation of small amounts of the chloroform solution of the polymers. The reference spectra of pure liquid aniline or pyridine were recorded using liquid cells with 0.03 mm thickness.

Radioactivity measurements were made by ignition of samples using a dry combustion apparatus followed by measuring the activity of radioactive carbon dioxide formed using the internal flow-monitoring gas counter (15).

Results and Discussion

Table 1 shows that the extent of polymer formation increased with increasing the neutron flux; it is also seen that about 10^5 molecules of the irradiated liquids were transformed into the polymer for each carbon-14 recoil atom formation event. This shows that polymer formation in the strong reactor irradiation field occurs mainly as a radiation effect, probably through free radical or ion-molecule reactions (16). In these reactions carbon recoils preferentially participate. This is explained by their interaction with molecules or molecular fragments which initiate or participate in these reactions finally leading to polymer formation.

Examination of the i.r. spectra of the polymers separated from the two irradiated aniline samples revealed their remarkable identity. This indicates that increasing the irradiation time or neutron flux affects only the quantity of the polymer, as deduced from the observed increase of the polymer yield, and not its composition. Comparing the i.r. spectrum of the polymer formed in the irradiated aniline sample I with that of pure liquid aniline (Fig. 1), one observes the characteristic bands of the phenyl ring of aniline in both spectra, *i.e.* at 1508 and 1610 cm^{-1} due to the aromatic C—C stretching vibrations and also at 3030 and 3060 cm^{-1} due to aromatic C—H stretching vibrations. Moreover, the bands due to the C—H out of plane deformation vibrations of the monosubstituted aromatic ring appeared nearly at the same positions in both spectra, *i.e.* at 695 and 750 cm^{-1} in the polymer spectrum and at 692 and 755 cm^{-1} in the pure liquid aniline spectrum (17, 18). This indicates that additional substitution in the phenyl ring of aniline did not play an important part in the polymerization. On the other hand, remarkable changes were found to occur in the characteristic bands of the amino group of aniline. Thus, the $—NH_2$ deformation vibration band at 1630 cm^{-1} (19, 20) completely disappeared while the phenyl—NH_2 stretching vibration band at 1280 cm^{-1} (19, 21) were found to decrease in intensity. A similar decrease was also observed in the symmetric and antisymmetric $—NH_2$ stretching vibration bands appearing at 3355 and 3435 cm^{-1} (19). At the same time, a new band appeared at 1530 cm^{-1} which could be assigned to the —NH bending vibrations of a secondary aromatic amine (22). In addition, a new weak band appeared at 1250 cm^{-1} which could be due to the —NH group of a secondary aromatic amine (19, 21, 22). From all these changes it seems reasonable to conclude that the primary aromatic amino group in aniline transformed into a secondary one on polymerization.

In the spectrum of the polymer separated from irradiated aniline, two new bands appeared at 1390 and 1465 cm^{-1} due to the symmetric and antisymmetric bending vibrations of CH_3 groups,

Can. J. Chem. Downloaded from www.nrcresearchpress.com by 210.87.254.105 on 09/05/12
For personal use only.

Can. J. Chem. Downloaded from www.nrcresearchpress.com by 210.87.254.105 on 09/05/12
For personal use only.

in addition to the new band appearing at 1450 cm^{-1} due to the bending vibrations of CH_2 groups (23, 24). The presence of CH_2 and CH_3 groups could be further confirmed by the presence of the two new bands at 2920 and 2955 cm^{-1}, which are due to the antisymmetric stretching vibrations of CH_2 and CH_3 groups respectively (23, 24). Moreover, a new band appeared at 2845 cm^{-1} due to the CH_2 and/or CH_3 symmetric stretching vibrations. The very small shoulder at 740 cm^{-1} could be assigned to the rocking vibrations of CH_2 groups present in a long chain consisting of more than four carbon atoms (23). It is worth mentioning that the weak, but well defined, band observed at 850 cm^{-1} and normally assigned to the wagging vibrations of trisubstituted olefinic groups (25), probably indicates the presence of unsaturated branched aliphatic chains in the polymer. Moreover, the shoulder appearing at 1660 cm^{-1} indicates the possible presence of aliphatic C=C bonds (23) while the band appearing at 1200 cm^{-1} indicates the presence of tertiary branching in the polymer (23, 26).

The band appearing at 1730 cm^{-1} due to the carbonyl group stretching vibrations is probably an indication of the occurrence of some oxidation in the polymer during the chemical treatment that followed reactor irradiation (27, 28).

From the above mentioned interpretations of spectral data it is evident that the polymer contains anilide groups attached to aliphatic carbon chains which contain some double bonds and are possibly branched. Some residual $-NH_2$ groups could still be present in the polymer. In fact, a probable structure of an individual polymer chain could be represented by the following empirical formula:

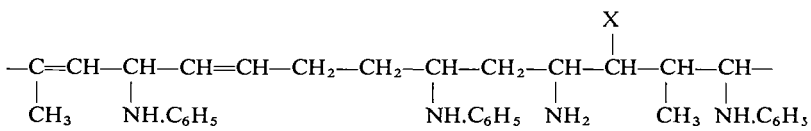

The end groups are likely to be CH_2=CH— or CH_3— groups. Cross linking between individual polymer chains could be through the point X.

The foregoing discussions lead to the assumption that polymer formation occurs in two successive steps. In the first step, rupture of the phenyl rings takes place with the formation of highly reactive unsaturated radicals shown in eq. 1 and/or smaller fragments of similar composition.

[1] 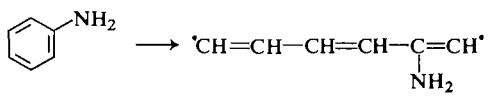

This need not be due entirely to the strong irradiation field in the reactor but also could occur as a result of the collisions occurring between energetic recoil carbons and the phenyl ring carbons without stabilization of the formed intermediates (2, 14). All products formed in this way could be considered as good centers for initiating and promoting polymer formation. In the second step, "building up" of the polymer takes place through the addition to the above-mentioned unsaturated fragments of different radicals, such as $H^{\cdot}$, $CH^{\cdot\cdot\cdot}$, $CH_2^{\cdot\cdot}$, $CH_3^{\cdot}$, $C_6H_5^{\cdot}$, and $C_6H_5NH^{\cdot}$, formed as a result of the fragmentation processes occurring in the molecules of the irradiated material. It is possible to assume that the latter radicals are formed with greater probability due to the ease with which the lone pair of electrons on nitrogen are displaced towards the phenyl ring leaving the nitrogen atom positively charged (29) and thus facilitating hydrogen removal from the amino group of aniline. The absence of absorption bands at 790 cm^{-1}, normally attributed to the presence of disubstitution in the benzene nucleus, probably indicates that anilide and/or phenyl radicals are the only aromatic radicals involved in polymer formation. Further building up of the polymer could occur both by addition to end groups and by cross linking of individual straight polymer chains, either directly or through $-CH_2$ linkages.

The preferential localization of carbon-14 in the polymer may be explained by the fact that the energetic recoil carbons, present as atoms, ions, or free radicals such as $^{14}CH^{\cdot\cdot\cdot}$, $^{14}CH_2^{\cdot\cdot}$, or $^{14}CH_3^{\cdot}$, readily participate in or act as initiators of the addition reactions leading to the formation of polymer chains as indicated above. The absence of disubstituted benzene in the polymer indicates that the well-known insertion reaction of carbon recoils in C—H bonds probably leads

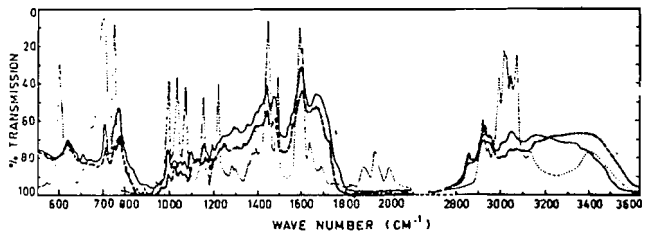

FIG. 2. The i.r. spectra of the ^{14}C-labelled polymer separated from irradiated pyridine sample I (dashed line), pyridine sample II (solid line), together with the i.r. spectrum of pure liquid pyridine (dotted line).

to intermediates that abstract hydrogen more readily to form different labelled toluidines (12) rather than interacting with different fragments to form a polymeric product. The reason for this somewhat unexpected behavior could not be explained on the basis of the present data.

Considering the i.r. spectra of pure liquid pyridine and of the polymer separated from reactor irradiated pyridine, both shown in Fig. 2, it is possible to observe the bands at 710 and 775 cm^{-1} which can be assigned to the C—H out of plane deformation vibrations of 3-substituted pyridine (30, 31). The shoulder appearing at 750 cm^{-1} may be attributed to the C—H out of plane deformation vibrations of 2-substituted pyridine (30, 31) present in small amounts relative to 3-substituted pyridine. The presence of 3- and 2-substituted pyridyl groups in the polymer could be further confirmed by observing the bands appearing at 1475 and 1595 cm^{-1} normally assigned to the ring stretching vibrations of 3- and 2-substituted pyridine (30, 32). The characteristic C—H stretching vibrations of the aromatic ring were observed at 3010 and 3050 cm^{-1}. The combination and overtone bands appearing in the regions 1800–2000 and 2900–2950 cm^{-1}, in the pure pyridine spectrum, completely disappeared in the polymer spectrum. Instead of the latter bands, two new bands appeared at 2925 and 2955 cm^{-1} which are normally assigned to the antisymmetric stretching vibrations of CH_2 and CH_3 groups respectively. The presence of these groups could be further confirmed by observing the bands at 2850 cm^{-1} due to the symmetric stretching vibrations of CH_2 and CH_3 groups. At the same time, the shoulder at 1390 cm^{-1} could be due to CH_3 symmetric bending vibrations while the band at 1440 cm^{-1} may be assigned to the antisymmetric bending vibrations of CH_2 or CH_3 groups.

In the polymer spectrum, shown in Fig. 2, a new band appeared at 1670 cm^{-1}. This could be assigned, most likely, to —C=N— group (33). The same band could also indicate the presence of a carbonyl group in a straight carbon chain containing double bonds (34, 35). The band appearing at 1197 cm^{-1} probably indicates the presence of aliphatic branched chains (23).

From the foregoing interpretation of spectral data it seems possible to conclude that the polymer formed in irradiated pyridine consists mainly of pyridyl groups attached in the 3- or 2-positions to aliphatic carbon chains, that are probably branched, represented as follows:

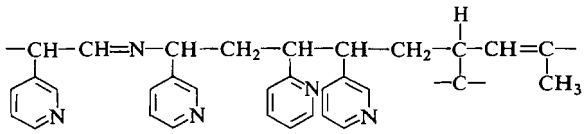

Similar to the case of the polymer formed in irradiated aniline, the formation of the polymer in irradiated pyridine probably took place in two steps. The first involves the pyridine ring rupture, more likely through the breaking of a C—N bond, which is less stable than the C—C bond (29), according to the reaction shown in eq. 2.

[2] 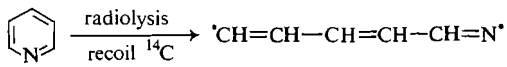

This is followed by the "building up" step in which the different radicals formed in the irradiated matrix, such as H', C_5H_4N', CH_2'', etc., add to the double bonds of the highly unsaturated radicals or fragments formed in the first step.

It is important to note that, in the spectrum of the polymer formed in pyridine sample I, the intensity of the band appearing at 2925 cm^{-1}, due to the aliphatic CH_2 stretching vibrations, is greater than the intensity of the band appearing at 3050 cm^{-1}, due to the aromatic CH stretching vibrations, whereas in the spectrum of the polymer separated from the other pyridine

Can. J. Chem. Downloaded from www.nrcresearchpress.com by 210.87.254.105 on 09/05/12
For personal use only.

sample (II) the contrary could be observed. This should indicate that the aliphatic/aromatic ratio is greater in the first product than in the second one, *i.e.* aromatization of the aliphatic straight chain takes place gradually as the irradiation time increases. Furthermore it is possible to observe that the shoulder at 1660 cm^{-1}, normally attributed to aliphatic C=C bond stretching vibrations (23), apparent in the spectrum of the polymer separated from pyridine sample I, disappeared completely in the spectrum of the polymer separated from sample II. These findings are in reasonable agreement with the abovementioned polymer formation mechanism and indicate that saturation of the double bonds in the primarily formed straight carbon atom chains occurs as the irradiation time increases. The observed preferential addition of pyridyl radicals in the β position could be explained on the basis of the well-known fact that positions 3 and 5 are points of high electron density in the pyridine nucleus (29), and consequently reaction is easiest with the π electrons of the double bonds through these positions.

The preferential localization of ^{14}C in the polymers formed in pyridine could be explained on the same basis as in the case of aniline.

Finally, it should be clear that it is practically very difficult to put forward a definite structure for the polymers formed in reactor irradiated organic systems. In the present study, it was only possible to suggest some empirical formulae and some probable mechanisms leading to the formation of such high specific activity products.

1. M. F. BARAKAT. Atompraxis, **13**, 112 (1967).
2. A. SCHRODT and W. F. LIBBY. J. Am. Chem. Soc. **78**, 1267 (1956).
3. M. F. BARAKAT and A. H. ZAHRAN. Radiochim. Acta, **17**, 65 (1972).
4. T. W. LAPP and R. W. KISER. J. Phys. Chem. **67**, 612 (1963).
5. T. W. LAPP and R. W. KISER. J. Phys. Chem. **66**, 153 (1962).
6. A. P. WOLF. Ann. Rev. Nucl. Sci. **10**, 259 (1960).
7. A. P. WOLF. Chemical effects of nuclear transformations. Vol. 2. IAEA, Vienna. 1961. p. 3.
8. A. P. WOLF. Advances in physical organic chemistry. Vol. 2. *Edited by* V. Gold. Academic Press, New York. 1964. p. 201.
9. R. WOLFGANG. Progress in reaction kinetics. Vol. 3. Pergamon Press, Oxford. 1965. p. 97.
10. M. F. BARAKAT, L. P. FIRSOVA, and AN. N. NESMEYANOF. Radiokhimia (USSR), **6**, 605 (1964).
11. M. F. BARAKAT, L. P. FIRSOVA, and AN. N. NESMEYANOF. Radiokhimia (USSR), **6**, 626 (1964).
12. M. F. BARAKAT and A. H. ZAHRAN. Isotopenpraxis, **6**, 95 (1970).
13. M. F. BARAKAT and A. H. ZAHRAN. Radiochim. Acta, **13**, 152 (1970).
14. M. F. BARAKAT and F. M. ABDELKERIM. J. Inorg. Nucl. Chem. **33**, 2301 (1971).
15. M. F. BARAKAT. Indian J. Chem. **5**, 200 (1967).
16. S. E. EATON. Nucleonics, **18**, 134 (1960).
17. N. B. CALTHUP. J. Opt. Soc. Am. **40**, 397 (1956).
18. A. R. KATRITZKY. Q. Rev. **13**, 353 (1959).
19. L. J. BELLAMY and R. L. WILLIAMS. Spectrochim. Acta, **9**, 341 (1957).
20. J. E. STEWART. J. Chem. Phys. **30**, 1259 (1959).
21. A. R. KATRITZKY and R. A. JONES. J. Chem. Soc. 3674 (1959).
22. D. HADZI and M. SKRHLJAK. J. Chem. Soc. 843 (1957).
23. H. L. MCMURRY and V. THORNTON. Anal. Chem. **24**, 318 (1952).
24. S. E. WIBERLEY, S. C. BUNCE, and W. H. BAUER. Anal. Chem. **32**, 217 (1960).
25. W. J. POTTS and R. A. NYQUIST. Spectrochim. Acta, **15**, 679 (1959).
26. N. SHEPPARD and D. S. SIMPSON. Q. Rev. **7**, 19 (1953).
27. D. S. BALLANTINE, G. J. DIENES, and B. MONOWITZ. Brookhaven National Laboratory rep. No. 1677 (1953).
28. F. M. ABDEL KERIM, A. M. ELAGRAMY, and K. A. MAHMOUD. Egypt. J. Phys. **3**, 81 (1972).
29. P. H. HERMANS. Introduction to theoretical organic chemistry. Elsevier Publishing Company, Amsterdam. 1954.
30. H. SHINDO. Pharm. Bull. (Tokyo), **5**, 472 (1957).
31. H. E. PODALL. Anal. Chem. **29**, 1423 (1957).
32. G. L. COOK and F. A. CHURCH. J. Phys. Chem. **61**, 548 (1957).
33. J. FABIAN, M. LEGRAND, and P. POIRER. Bull. Soc. Chim. Fr. **23**, 1499 (1956).
34. N. H. CROMWELL, F. A. MILLER, A. R. JOHNSON, R. L. FRANK, and D. J. WALLACE. J. Am. Chem. Soc. **71**, 3337 (1949).
35. J. F. GROVE and H. A. WILLIS. J. Chem. Soc. 877 (1951).

Can. J. Chem. Downloaded from www.nrcresearchpress.com by 210.87.254.105 on 09/05/12
For personal use only.

Internal Substitution of 5α-Lanostane on C-5, C-6, and C-8[1]

O. E. EDWARDS AND Z. PARYZEK[2]

Division of Biological Sciences, National Research Council of Canada, Ottawa, Canada K1A 0R6

Received January 5, 1973[3]

Thermolysis of 3β-acetoxy-11-oxolanostan-7α-yl azidoformate gave the cyclic carbamate of 3β-acetoxy-5α-amino-11-oxolanostan-7α-ol (9%) and the corresponding 6α-amino (52%) derivative. 3β-Acetoxy-11-oxolanostan-7β-yl azidoformate gave the cyclic carbamate of 3β-acetoxy-6α-amino-11-oxolanostan-7β-ol (52%) and the corresponding 6β-amino (26%) and 8β-amino (7%) derivatives. Some features of the ^{13}C.m.r. and c.d. spectra of the above compounds and related steroids are described.

La thermolyse de l'azidoformate-7α, d'acétoxy-3β-oxo-11 lanostanyle conduit au carbamate cyclique de l'acétoxy-3β amino-5α-oxo-11 lanostanol-7α (9%) et au dérivé amino-6α (52%) correspondant. L'azidoformate-7β de l'acétoxy-3β oxo-11 lanostanyle fournit le carbamate cyclique de l'acétoxy-3β amino-6α-oxo-11-lanostanol-7β (52%) et les dérivés amino-6β (26%) et amino-8β (7) correspondants. On décrit aussi quelques caractéristiques des spectres ^{13}C.m.r. et c.d. des composés mentionnés plus haut ainsi que d'autres stéroides qui leur sont reliés. [Traduit par le journal]

Can. J. Chem., **51**, 3866 (1973)

Two skeletons related to lanostane which are of exceptional interest are those of the cucurbitacins (**1**) (1) and of the fusidanes (protostanes) **2** related to probable intermediates in the biosynthesis of lanosterol (2). We attempted to produce good yields of substituted lanostanes which might be converted to compounds with these skeletons.

Attempts to produce compounds with the cucurbitane skeleton have been made by ApSimon and Rosenfeld (3), Guest and Marples (4), and Levy and Lavie (5), by the action of Lewis acids on 9α,11α-oxidolanostane derivatives. No migration of the 10-methyl group was observed. However, since we had obtained efficient migration of the 10-methyl group to C-9 during deamination of a 9α-amino-11-keto steroid (6) we hoped to extend this to deamination of 9α-amino-3β-acetoxylanostan-11-one (**3**) and 8β-amino-3β-acetoxylanostan-7-one (**4**).

Attempts to prepare a 9β,11β-oxidolanostane derivative from which the 9α-amino-11-ketone might be prepared (6) have so far failed in this laboratory (7) and in that of Marples (4).

Since approach of external reagents to the α-face of a 9,11 double bond in lanostane derivatives is somewhat impeded by the 14α-methyl group, an approach using intramolecular cyclization appeared to be one of the most promising alternatives for substituting C-9. Curran and Angier (8) had obtained a 45% yield of the oxazolidinone **5** by pyrolysis of 1-adamantanyl azidoformate, and Kreher and Kühling (9) had shown that thermal decomposition of hexahydrobenzyl azidoformate gave a 3:1 ratio of the oxazolidinone **6** and the tetrahydro-1,3-oxazin-2-one (**7**). Breslow and coworkers (10) and Lwowski (11) found that the insertion factor for different types of CH bonds was in the ratio tertiary–secondary–primary = 30:10:1. Hence we had reason to hope that the nitrene produced from the 7α-azidoformate **8**

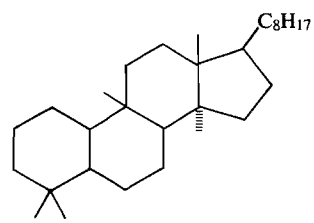

1

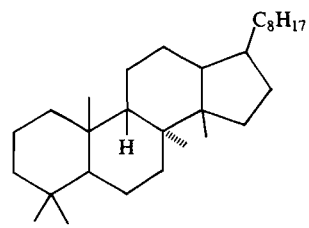

2

[1]Issued as NRCC No. 13442. Presented in part at the Symposium on Heterocyclic Chemistry, Poznan, July 24–26, 1972.

[2]NRCC Postdoctorate Fellow 1971–1972.

[3]Revision received July 26, 1973.

Can. J. Chem. Downloaded from www.nrcresearchpress.com by 210.87.254.6 on 09/05/12
For personal use only.

Can. J. Chem. Downloaded from www.nrcresearchpress.com by 210.87.254.6 on 09/05/12
For personal use only.

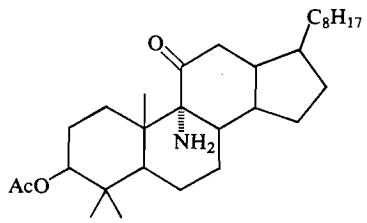

3

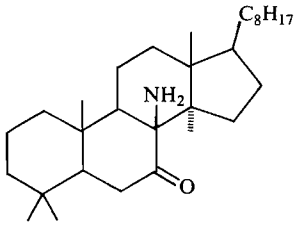

4

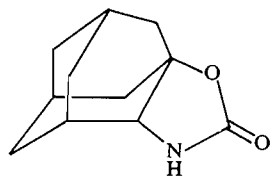

5

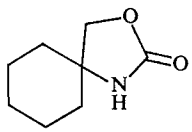

6

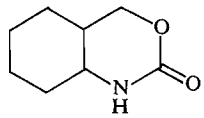

7

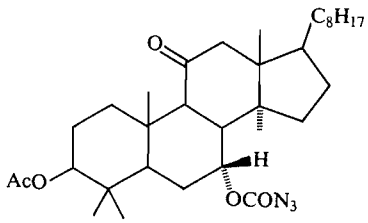

8

would preferentially attack the 5α- and 9α-CH bonds.[4]

Dihydrolanosterol was converted via 3β-acetoxy-7,11-dioxolanost-8-ene to a mixture of 3β-acetoxy-11-oxolanostan-7α-ol (**9**, R = H) and the corresponding 7β-alcohol (12*a*, 13). Phosgene converted the alcohols to the chloroformates, then sodium azide in dimethyl formamide transformed these to the desired azidoformates.

A solution of the 7α-azidoformate **8** in carbon tetrachloride in a sealed tube was maintained at 140–142° for 2 h. By this time the azide group had disappeared (i.r.) and a mixture of at least five products had formed. These were separated by column chromatography and preparative t.l.c., and the four major components characterized. The main product (52%) clearly arose from insertion into the 6α-CH bond. Its i.r. spectrum (ν_{max} ($CHCl_3$) 1760 cm^{-1}) was characteristic of an oxazolidinone. In addition a new low-field hydrogen (δ 3.83; triplet, $J_{5,6}$ = 10.6 Hz; $J_{6,7}$ = 5 Hz) was present in its p.m.r. spectrum and the coupling constants were as expected for a 6α orientation. Hence we assign it structure **10**. Its ^{13}C.m.r. spectrum is described below.

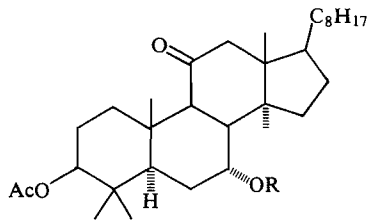

9

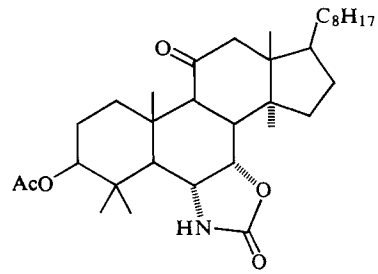

10

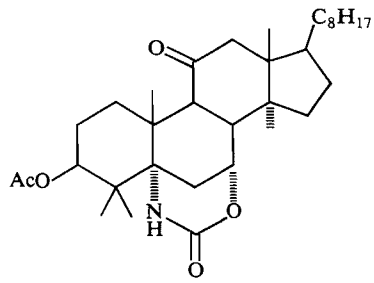

11

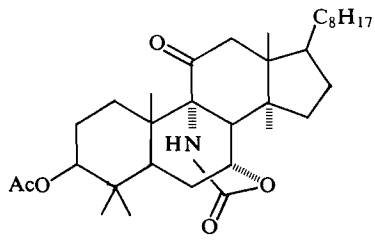

12

[4]The only related work for lanostane skeleton seems to be functionalization of C-32 (14α-methyl) by photolysis of the 7α-nitrite or action of lead tetraacetate–iodine on the 7α-alcohol (12).

TABLE 1.

Compound	ν_{max}*	ε	c.d. (Δε)	δ† C-11	δ† C-3
23 (R = $NHCOCH_3$)	295	46	+0.80	204.8	73
23 (R = $NHCOOCH_3$)	296	44	+0.86	205.4	73
23 (R = H)	301	25	+0.18	210.9	73
11	296	30	+1.33	211.0	74.9
9 (R = $CONH_2$)	295	39	+0.60	208.6	80.5
9 (R = H)	302	27	+0.43		
3β-Acetoxy-11-keto lanostane	301	25	+0.43		

*In dioxane.
†In $CDCl_3$; ^{13}C.m.r. signal relative to TMS = 0.

The next most abundant nitrogen-containing product was a tetrahydro-1,3-oxazinone (ν_{max} ($CHCl_3$) near 1690 cm^{-1}). It gave no low-field p.m.r. signals other than the ones for the 3- and 7-hydrogens, since it was the product of attack on C-5 or C-9. We had anticipated that the u.v. spectrum would distinguish these, since the nπ* transition for ketone carbonyls with axial electronegative substituents such as methoxyl, halogen, and azide (6, 14) groups is at wavelength longer and of higher intensity than that of the unsubstituted ketone. Since the unknown product and 3β-acetoxy-11-ketolanostane had very similar absorption (Table 1) it appeared that the compound has structure **11**. On the other hand c.d. evidence appeared to demand the alternate structure **12** with a 9α substituent (see below). However its ^{13}C.m.r. (see below) was consistent with the 5-substituted structure, and chemical transformations confirmed that it was indeed **11**.

The compound was very resistant to acid or alkaline hydrolysis. Meerwein's reagent converted it to an imino ether. Treatment of this ether with base only hydrolyzed the 3-acetoxy group, while acid hydrolysis gave back the tetrahydrooxazinone. The tetrahydrooxazinone was inert to nitrosyl chloride or dinitrogen tetroxide, so direct deamination was not possible. Hence an indirect proof of structure was used.

Sodium borohydride reduced the ketone carbonyl and hydrolyzed the 3-acetoxy group. The resulting diol was transformed by pivaloyl chloride into a monopivaloyloxy derivative. Dehydration of this with thionyl chloride – pyridine gave a trisubstituted olefin without disturbing the cyclic urethane group. It must therefore have structure **14**, proving the intermediates to be **13** (R = H or pivaloyl) and the original tetrahydrooxazinone to be **11**.

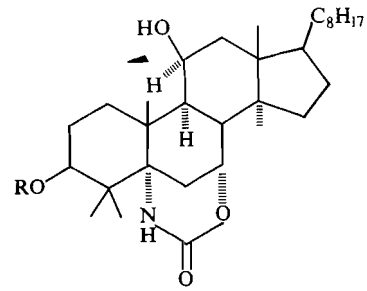

13

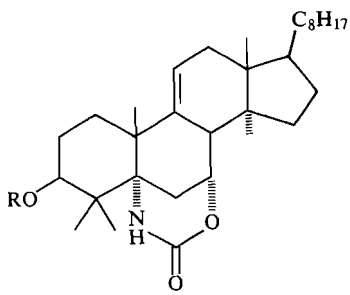

14

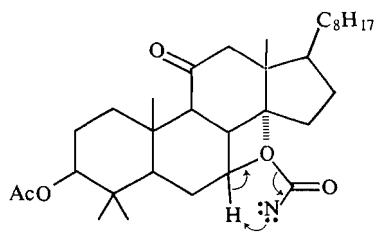

15

The third product characterized was the simple urethane of the 7α-alcohol, presumably formed by abstraction of hydrogen from other molecules by the *triplet* state of the nitrene. The fourth product was 3β-acetoxylanosta-7,11-

Can. J. Chem. Downloaded from www.nrcresearchpress.com by 210.87.254.6 on 09/05/12
For personal use only.

Can. J. Chem. Downloaded from www.nrcresearchpress.com by 210.87.254.6 on 09/05/12
For personal use only.

dione. It seems likely that this arose by thermal fragmentation of the nitrene as illustrated in **15**.

The yield of **11** was roughly 9%. Hence other factors were overriding the discrimination factor mentioned earlier. It seems certain that the azide decomposition to nitrene and the insertion of the nitrene into saturated CH bonds are independent events. Hence the observations of Breslow and co-workers (10) regarding the reaction of ethyl azidoformate with 2-methylbutane imply that ethoxycarbonyl nitrene survives numerous collisions with primary CH bonds before it reacts. Thus in the lanostane cases the *nitrene* rotamer ratios are large factors in determining which CH bonds will be attacked. A family of rotamers roughly represented by **16** must be the most highly populated one. This would account for the relatively high yield of 6α-substituted product. This also has the potential of giving insertion into the 5-CH bond, but the low yield of **11** despite the tertiary nature of the hydrogen, indicates that approach to the CH bond is impeded by the 4α-methyl group and the 6α-hydrogen.

A second family of rotamers represented by **17** does not participate to any extent, since it would permit insertion into the 5- and 9-CH bonds with equal facility.

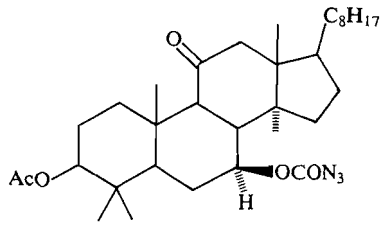

18

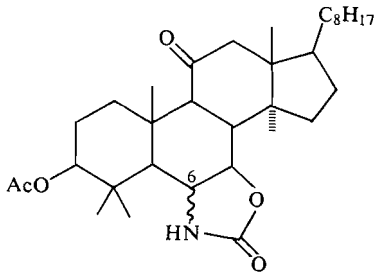

19

a 6α-amino

b 6β-amino

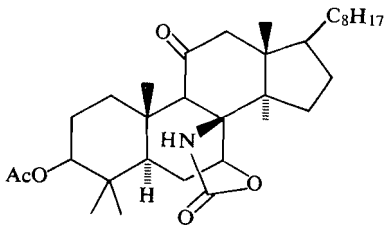

20

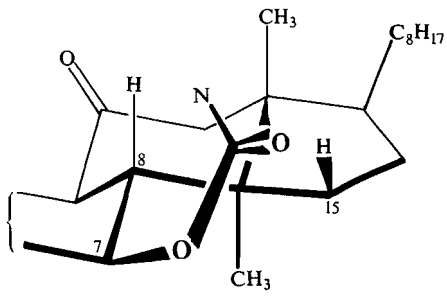

21

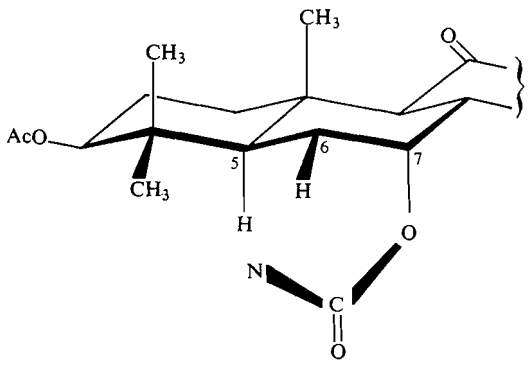

16

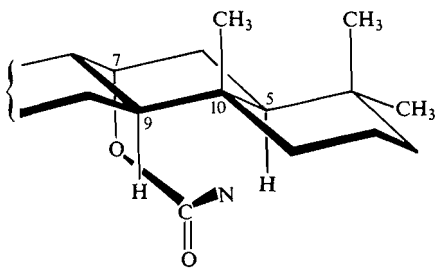

17

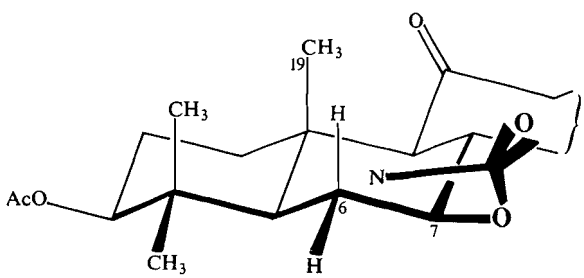

22

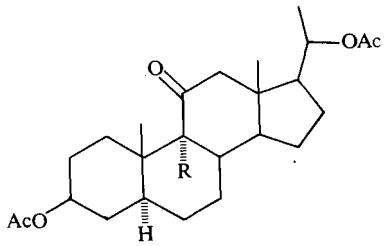

23

Photolysis of the 7α-azidoformate in methylene chloride appeared to give a more complex mixture than the thermolysis, hence this was not pursued further.

In a manner analogous to that for the 7α isomer, 3β-acetoxy-11-oxolanostan-7β-ol was converted to the azidoformate **18**. Thermolysis at 140° converted this to a mixture of at least three compounds. Again, products of insertion into the C-6 hydrogen bonds (**19**) predominated (78%) with the ratio of 6α to 6β insertion being at least 2:1. The 6α isomer was identified by the fact that the axial 6β-hydrogen and the 7α-hydrogen gave rise to two triplets with $J = 10$ centered at δ 3.65 and 3.99 in its p.m.r. spectrum. The product of insertion into the C-8–hydrogen bond (**20**) was only formed in 7% yield.

The product ratios are again accounted for on the basis of nitrene rotamers and non-bonded repulsion in the transition state. Examination of models showed that only rotamer **21** enables formation of a three-center cyclic transition state for insertion into the C-8—H bond. Because of repulsive interaction with the 15β hydrogen this rotamer is unfavorable, hence the low yield of **20**. Rotamer **22** appears to be the only one permitting close-enough approach to the 6-hydrogens for insertion. To account for the higher percentage of insertion into the 6α-CH bond we suggest that repulsive interaction of the β-hydrogen with C-19, as the transition state for insertion develops, raises its energy relative to that of the 6α case.

The proton-decoupled ^{13}C.m.r. spectrum of **11**, in comparison with those of 9-substituted steroidal molecules (**23**, R = $NHCOCH_3$ or $NHCOOCH_3$) supported the 5-substituted structure. In the models an upfield shift of *ca.* 5 p.p.m. was noted for the carbonyl carbon, relative to the corresponding 11-ketone with no substituent on C-9 (Table 1) (see ref. 15). In contrast the carbonyl of **11** had no such displacement (Table 1). A 5 p.p.m. upfield shift of C-3 in the spectrum of **11** was observed. This too is more consistent with substitution on C-5 rather than on the more remote C-9.

As mentioned above, the c.d. spectrum of **11** corresponded well with that of the 9α-amido-11-ketopregnane models **23** (Table 1). However we now must conclude that the presence of the acylamino group on C-5 in a positive octant is the source of the sizeable positive ΔΔε for **11**.

The failure to obtain the 9-substituted derivative and the low yield of the 8-substituted one, discourages this approach to cucurbitanes and protostanes. However substitution of C-9 from an 11α-azidoformate remains an interesting possibility.

Experimental

Infrared spectra were taken on a Perkin-Elmer model 257 grating spectrophotometer, with chloroform as solvent; p.m.r. spectra were determined using a Varian A-60-A spectrometer using deuteriochloroform as solvent and TMS as internal reference; ^{13}C.m.r. spectra were obtained using a Varian XL-100 Fourier transform spectrometer using external TMS in deuteriochloroform as reference; u.v. spectra were recorded using a Cary model 11 spectrophotometer and o.r.d–c.d. spectra on a Durrum-Jasco model ORD-5 spectropolarimeter, all in 95% ethanol. Thin-layer chromatography was done using silica gel. Rotations were for solutions in chloroform with concentrations near 10 g/l.

Materials

Crude lanosterol (Sigma Chemical Co.) was converted into 3β-acetoxylanostan-7,11-dione, which was reduced catalytically to 3β-acetoxy-11-oxolanostan-7α-ol (12) or with sodium borohydride, to 3β-acetoxy-11-oxolanostan-7β-ol (12).

3β-Acetoxy-11-oxolanostan-7α-yl Chloroformate

3β-Acetoxy-11-oxolanostan-7α-ol (153 mg) was dissolved in 15 ml of benzene. To this was added 108 mg of phosgene–pyridine complex (16) and the mixture stirred at room temperature for 25 min. The benzene solution was washed three times with cold water, dried with sodium sulfate, and evaporated. The 167 mg of oily residue crystallized in the presence of *n*-pentane. Two recrystallizations from *n*-hexane gave 130 mg of the chloroformate: m.p. 128–132°; ν_{max} 1770, 1726, and 1700 cm^{-1}; $[\alpha]_D$ +21°.

Anal. Calcd. for $C_{33}H_{53}O_5Cl$: C, 70.12; H, 9.45; Cl, 6.30. Found: C, 70.29; H, 9.60; Cl, 6.13.

3β-Acetoxy-11-oxolanostan-7α-yl Azidoformate (8)

To a solution of 472 mg of 3β-acetoxy-11-oxolanostan-7α-yl chloroformate in 30 ml of dimethylformamide was added 800 mg of sodium azide. The mixture was stirred for 3 h at 50 °C, 5 ml of water was then added and the product extracted into benzene. The benzene layer was washed three times with water, dried over magnesium sulfate and evaporated. The 474 mg of residue was recrystallized from methanol. The azidoformate had m.p. 123–125°; ν_{max} 2185, 2135, 1720, and 1700 cm^{-1}; $[\alpha]_D$ +2°.

Can. J. Chem. Downloaded from www.nrcresearchpress.com by 210.87.254.6 on 09/05/12
For personal use only.

Can. J. Chem. Downloaded from www.nrcresearchpress.com by 210.87.254.6 on 09/05/12
For personal use only.

Anal. Calcd. for $C_{33}H_{53}O_5N_3$: C, 69.32; H, 9.34; N, 7.35. Found: C, 69.45; H, 9.70; N, 7.07.

*Thermolysis of 3β-Acetoxy-11-oxolanostan-7α-yl Azidoformate (**8**)*

A solution of 905 mg of **8** in 50 ml of carbon tetrachloride in a sealed tube was maintained at 140–142° for 1 h, 45 min. The cooled solution was washed with sodium bicarbonate solution, dried over magnesium sulfate, and distilled. The residual oil was adsorbed onto a column of 120 g of neutral alumina, grade III. The column was eluted with benzene, benzene–ether mixtures, ether, and ether–methanol mixtures. The main products are listed in the order of their emergence:

3β-Acetoxylanostan-7,11-dione

The crude fraction (47 mg) after purification by t.l.c. gave 40 mg m.p. 216–218° (lit. (12) 223–224°). Its i.r. and n.m.r. spectra were identical with those of authentic 3β-acetoxylanostan-7,11-dione.

*Carbamate of 3β-Acetoxy-11-oxolanostan-7α-ol (**9**, R = $CONH_2$)*

Crude weight 58 mg. T.l.c. purification followed by recrystallization from methanol gave a product with m.p. 235–240°. It had ν_{max} 3540, 3430, 1725, 1700, and 1585 cm^{-1}; ν_{max} 293 nm (ε 51); p.m.r. signals at δ 5.29 (broad singlet, 7β-H), 5.07 (s, NH), 4.69 (t, 3α-H); ^{13}C.m.r. signals at 208.6 (C-11), 171.1 (3β-O*C*OCH$_3$), 155.9 (O*C*ONH), 80.5 (C-3), and 72.0 (C-7) p.p.m.; $[\alpha]_D$ +18°.

Anal. Calcd. for $C_{33}H_{55}NO_5$: C, 72.62; H, 10.16; N, 2.57. Found: C, 72.78; H, 9.97; N, 2.50.

*Cyclic Carbamate of 3β-Acetoxy-6α-amino-11-oxolanostan-7α-ol (**10**)*

The 478 mg needed only recrystallization from ethanol – methylene chloride to give **9** m.p. 258–262°. It had ν_{max} 3500, 3300, 1760, 1735, and 1702 cm^{-1}; p.m.r. signals at δ 6.76 (s, NH), 4.60 (d, J = 5 Hz, 7β-H), 4.44 (t, J = 7 Hz, 3α-H), 3.83 (broad q, J_1 = 10 Hz, J_2 = 5 Hz, 6β-H); ^{13}C.m.r. signals at 210.6 (C-11), 170.7 (3β-OCOCH$_3$), 158.9 (OCONH), 79.4 (C-7), and 55.8 (C-6); $[\alpha]_D$ +27°.

Anal. Calcd. for $C_{33}H_{53}O_5N$: C, 72.89; H, 9.82; N, 2.58. Found: C, 72.73; H, 10.00; N, 2.53.

*Cyclic Carbamate of 3β-Acetoxy-5α-amino-11-oxolanostan-7α-ol (**11**)*

The crude product (119 mg) was purified by preparative t.l.c. followed by recrystallizations from acetone and ethanol – methylene chloride. It then gave a single spot on t.l.c. and gave sharp spectra. However its m.p. still had the range 278–292° unaltered on further recrystallization. It had ν_{max} 3340, 1725, and 1690 cm^{-1}; λ_{max} 296 nm (ε 34); and p.m.r. signals at δ 5.87 (s, NH), 5.10 (broad, 3α-H), 4.67 (broad singlet, 7β-H); $[\alpha]_D$ +18°. It gave ^{13}C.m.r. signals at 211.0 (C-11), 170.6 (3β-O*C*OCH$_3$), 153.6 (O*C*ONH), 74.9 (C-3), 74.4 (C-7), and 64.2 (C-5) p.p.m.

Anal. Calcd. for $C_{33}H_{53}O_5N$: C, 72.84; H, 9.82; N, 2.58. Found: C, 72.69; H, 9.98; N, 2.49.

In a larger run the yields were: **9**, 7%; **10**, 50%; **11**, 9%.

*3β-Acetoxy-11-oxolanostan-7β-yl Azidoformate (**18**)*

Phosgene was bubbled into a solution of 1.34 g of 3β-acetoxy-11-oxolanostan-7β-ol and 0.8 ml of pyridine in 70 ml of benzene for 1.5 h. The reaction mixture was washed three times with water, dried over magnesium sulfate, then the solvent removed under reduced pressure. The crude chloroformate was dissolved in 6 ml of dry dimethylformamide. After addition of 1.3 g of sodium azide the mixture was heated at 55–60° for 4 h. Water was added to the cooled solution, the product extracted into benzene, and the benzene washed three times with water. The benzene layers gave 1.53 g of crude crystalline azidoformate. After recrystallization from acetone–methanol it had m.p. 141–146°; ν_{max} 2185, 2135, 1725, and 1705 cm^{-1}; $[\alpha]_D$ +34°.

Anal. Calcd. for $C_{35}H_{53}O_5N_3$: C, 69.32; H, 9.34; N, 7.35. Found: C, 69.14; H, 9.51; N, 7.32.

*Thermolysis of **18***

A solution of 720 mg of **18** in 50 ml of carbon tetrachloride in a sealed tube was kept at 140–142° for 70 min. It was then washed with sodium bicarbonate solution, dried, and distilled. The residue was given a preliminary purification by chromatography on alumina (activity III), then separated into two main fractions by preparative t.l.c. The one with higher R_f was rich in oxazolidinone **20** while the more polar one contained a mixture of the two epimeric oxazolidinones **19**. These were separated by fractional crystallization from methanol – methylene chloride and ethanol–chloroform mixtures.

*Cyclic Carbamate of 3β-Acetoxy-6α-amino-11-oxolanostan-7β-ol (**19a**)*

This had m.p. 268–276°; ν_{max} 3440, 1758, 1730, and 1705 cm^{-1}; p.m.r. signals at δ 6.58 (s, NH), 4.40 (t, J = 8 Hz, 3α-H), 3.99 (t, J = 10 Hz, 7α-H), 3.65 (t, J = 10 Hz, 6β-H); $[\alpha]_D$ +54°.

Anal. Calcd. for $C_{35}H_{53}O_5N$: C, 72.89; H, 9.82; N, 2.58. Found: C, 72.88; H, 10.02; N, 2.51.

*Cyclic Carbamate of 3β-Acetoxy-6β-amino-11-oxolanostan-7β-ol (**16b**)*

This had m.p. 307–313°; ν_{max} 3460, 1755, 1730, and 1705 cm^{-1}; p.m.r. signals at δ 5.78 (s, NH), 4.60 (t, J = 8 Hz, 3α-H), 4.32 (multiplet, 6α- and 7α-H); $[\alpha]_D$ +90°.

Anal. Calcd. for $C_{35}H_{53}O_5N$: C, 72.89; H, 9.82; N, 2.58. Found: C, 72.74; H, 9.99; N, 2.50.

*Cyclic Carbamate of 3β-Acetoxy-8β-amino-11-oxolanostan-7β-ol (**20**)*

The 45 mg of product was recrystallized from methanol – methylene chloride to give **17**, m.p. 315–320°. It had ν_{max} 3490, 1755, 1730, and 1715 cm^{-1}; p.m.r. signals at δ 5.34 (s, NH), 4.67 (t, J = 7 Hz, 3α-H), 4.42 (t, J = 8 Hz, 7α-H); $[\alpha]_D$ +46°.

Anal. Calcd. for $C_{33}H_{53}O_5N$: C, 72.89; H, 9.82; N, 2.58. Found: C, 72.67; H, 9.68; N, 2.37.

*Partial Hydrolysis of **11***

A solution of 203 mg of carbamate **11** and 115 mg of potassium hydroxide in 5 ml of ethanol and 0.5 ml of dioxane was refluxed for 15 min. After dilution with water, the mixture was extracted with chloroform. The 190 mg of crystalline product melted at 245–248° and gave n.m.r. signals at δ 6.70 (NH), 4.58 (7β-H), 3.86 (3α-H); ν_{max} 3600–3100, 3450, 1705, 1685 cm^{-1}. This is consistent with the 3β-hydroxy-11-keto carbamate.

*11β-Hydroxy-3β-pivalate (**13**) (R = pivaloyl)*

A solution of 100 mg of the 3β-hydroxy-11-keto car-

Can. J. Chem. Downloaded from www.nrcresearchpress.com by 210.87.254.6 on 09/05/12
For personal use only.

bamate in 2 ml of methanol was refluxed gently while 95 mg of sodium borohydride was added in 15-mg portions over a period of 16 h.

The reaction mixture was diluted with water then extracted with chloroform. The dried ($MgSO_4$) chloroform layers gave 96 mg of product giving one spot on a t.l.c. plate (chloroform–ethanol, 10:1). This was dissolved in 2 ml of pyridine, 0.2 ml of pivaloyl chloride added then the mixture left for 18 h at room temperature. After addition of ice water, the product was extracted into benzene. The benzene solution was washed with dilute hydrochloric acid, sodium bicarbonate solution, then with water, dried ($MgSO_4$), and distilled. The residue was purified by preparative t.l.c. (10:1 chloroform–ethanol) giving 70 mg of crystalline solid. After recrystallization from methanol – methylene chloride it had m.p. 302–312° and gave one spot on a t.l.c. plate (10:1 $CHCl_3$—EtOH). It had ν_{max} 3605, 3440, 1725, and 1690 cm^{-1} and gave n.m.r. signals at δ 5.40 (NH), 4.85 (3α-H), 4.56 (7α-H), and 4.29 (11α-H).

Anal. Calcd. for $C_{36}H_{61}NO_5$: C, 73.55; H, 10.46; N, 2.38. Found: C, 73.51; H, 10.74; N, 2.33.

*3β-Pivaloyloxy-5α-lanost-9(11)-ene-5α(N),7α(O)-carbamate (**14**)*

The 3β-pivaloyloxy-11β-hydroxy carbamate (**13**) (R = pivaloyl) (65 mg) was dissolved in 0.5 ml of pyridine and the solution cooled to 5 °C. After addition of 0.03 ml of thionyl chloride the mixture was left at 5 °C for 15 min. After dilution with ice water the product was extracted into benzene, the benzene layers washed with water, dilute acid, sodium bicarbonate solution, and water, dried and distilled. The 64 mg of crystalline product after one recrystallization from ethanol had m.p. 282–288°; $[\alpha]_D$ +25°; and ν_{max} 3440, 3040, 1725, and 1700 cm^{-1}. It gave n.m.r. signals at δ 5.48 (NH), 5.42 (11-H), 4.83 (3α-H), 4.65 (7β-H).

Anal. Calcd. for $C_{36}H_{59}NO_4$: C, 75.88; H, 10.44; N, 2.46. Found: C, 75.76; H, 10.51; N, 2.39.

*3β,20β-Diacetoxy-9α-methoxycarbon-amido-5α-pregnan-11-one (**23**, R = $NHCOOCH_3$)*

A mixture of 126 mg of 3β,20β-diacetoxy-9α-aminopregnane-11-one (6), 1 ml of methyl chloroformate, and 3 ml of pure chloroform was refluxed gently for 5 days. The solution was taken to dryness under reduced pressure, the residue dissolved in methylene chloride, and the solution filtered through a short column of neutral alumina (Activity I). The 160 mg of crystalline product was recrystallized repeatedly to give a m.p. 228–230°; $[\alpha]_D$ +71°; ν_{max} 3450, 1730, and 1505 cm^{-1}. It gave p.m.r. signals at δ 5.38 (NH), 4.90 (broad, 2H, C*H*OAc), 3.83 (OCH_3), 2.1 (6H, OAc); and ^{13}C.m.r. signals at 205.4 (C-11); 170.8 and 170.5 (3β- and 20β-O*C*OCH_3); 156.2 (N-*C*OCH_3); 72.9 and 72.4 (C-3 and C-20); and 66.8 (C-9) p.p.m.

Anal. Calcd. for $C_{27}H_{41}NO_7$: C, 65.96; H, 8.41; N, 2.85. Found: C, 65.89; H, 8.51; N, 2.56.

*3β,20β-Diacetoxy-9α-acetamido-5α-pregnane-11-one (**23**, R = $NHCOCH_3$)*

A solution of 86 mg of 3β,20β-diacetoxy-9α-aminopregnan-11-one (6) in 1.3 ml of acetic anhydride was heated at 130° for 2h. The product crystallized from the hot solution. After cooling, 83 mg of crystals were collected by filtration. These were recrystallized from ethanol – methylene chloride to give the *N*-acetyl derivative, m.p. 324–332°; $[\alpha]_D$ +67°; ν_{max} 3450, 1725, 1682, and 1505 cm^{-1}. It gave p.m.r. signals at δ 6.02 (NH), 4.76 broad (3α- and 20α-H), 2.13 ($NCOCH_3$), 2.05 ($OCOCH_3$), 1.20 (C-19), and 0.61 (C-18); and ^{13}C.m.r. signals at 204.8 (C-11); 170.9, 170.0, 169.7 (3β- and 20β-O*C*OCH_3 and *N*-*C*OCH_3); 73.1 and 72.4 (C-3 and C-20); 67.0 (C-9) p.p.m.

Anal. Calcd. for $C_{27}H_{41}NO_6$: C, 68.18; H, 8.69; N, 2.94. Found: C, 68.06; H, 8.82; N, 3.01.

*3β-Acetoxy-11-oxolanostan-7α-yl Carbamate (**9**, R = $CONH_2$)*

Aqueous ammonia (28%, 0.5 ml) was added to a stirred ice-cold solution of 3β-acetoxy-11-oxolanostan-7α-yl chloroformate in 1 ml of tetrahydrofuran. After 3 h at 0° water was added and the product extracted into chloroform. The 99 mg of crystalline product was recrystallized from methanol giving the carbamate with m.p. 237–240° and ν_{max} 3540, 3435, 1725, 1700, 1585, and 1400 cm^{-1}. It gave n.m.r. signals at δ 5.17 (7β-H), 5.04 (NH_2), and 4.58 (3α-H).

Anal. Calcd. for $C_{33}H_{55}NO_5$: C, 72.62; H, 10.16; N, 2.57. Found: C, 72.69; H, 10.22; N, 2.61.

We thank Dr. W. A. Ayer for valuable criticism, Mr. R. Kolt for technical assistance, Mr. H. Seguin for microanalyses, Drs. R. Deslauriers, R. Lapper, and I. C. P. Smith for the ^{13}C.m.r. spectra, and Dr. P. Morand for the o.r.d.–c.d. spectra.

1. S. M. Kupchan, C. W. Sigal, L. J. Guttman, R. J. Restivo, and R. F. Bryan. J. Am Chem. Soc. **94**, 1353 (1972); S. M. Kupchan, R. M. Smith, Y. Aynechi, and M. Maruyama. J. Org. Chem. **35**, 2891 (1970); R. W. Doskotch and C. D. Hufford. Can. J. Chem. **48**, 1787 (1970).
2. A. Eschenmoser. Helv. Chim. Acta, **38**, 1850 (1955); C. J. W. Brooks. *In* Rodd, Chemistry of carbon compounds. Elsevier, Amsterdam. 1970. pp. 162–163; J. D. Connolly. *In* Terpenoids and steroids. Vol. 2. Chemical Society Specialist Periodical Reports, 1972. p. 159.
3. J. M. Rosenfeld. Ph.D. Thesis. Carleton University, Ottawa, Canada. 1970.
4. I. G. Guest and B. A. Marples. J. Chem. Soc. (C), 1468 (1971).
5. E. C. Levy and D. Lavie. Israel J. Chem. **8**, 677 (1970).
6. O. E. Edwards and T. Sano. Can. J. Chem. **47**, 3489 (1969).
7. J. P. Devlin. Unpublished work.
8. W. V. Curran and R. B. Angier. Chem. Commun. 563 (1967).
9. R. Kreher and D. Kühling. Angew. Chem. Int. Ed. **4**, 69 (1965).
10. D. S. Breslow, J. J. Prosser, A. F. Marcantonio, and C. A. Genge. J. Am. Chem. Soc. **89**, 2384 (1967).
11. W. Lwowski. *In* Nitrenes. *Edited by* W. Lwowski. Interscience Publishers, New York. 1970. p. 201.

12. (*a*) C. W. SHOPPEE, N. W. HUGHES, and R. E. LACK. J. Chem. Soc. (C), 2359 (1966); (*b*) P. L. BATTEN, T. J. BENTLEY, R. B. BOAR, R. W. DRAPER, J. F. MCGHIE, and D. H. R. BARTON. J. Chem. Soc. Perkin I, 739 (1972); (*c*) J. FRIED, J. W. BROWN, and L. BORKENHAGEN. Proc. Int. Congr. Horm. Ster. 2nd. Milan. 1966 (Publ. 1967), p. 336. C.A. **69**, 5240*e*.
13. D. H. R. BARTON, A. HAMEED, and J. F. MCGHIE. Tetrahedron Lett. 4343 (1965).
14. R. C. COOKSON and S. H. DANDEGAONKER. J. Chem. Soc. 352 (1955).
15. J. B. STOTHERS, I. S. Y. WANG, D. OUCHI, and E. W. WARNHOFF. J. Am. Chem. Soc. **93**, 6702 (1971).
16. C. SCHOLTISSEK. Chem. Ber. **89**, 2562 (1956).

Can. J. Chem. Downloaded from www.nrcresearchpress.com by 210.87.254.6 on 09/05/12
For personal use only.

Lanthanide Shift Reagents in ^{13}C Nuclear Magnetic Resonance: Quantitative Determination of Pseudocontact Shifts and Assignment of ^{13}C Chemical Shifts of Steroids

JOHN W. APSIMON
Department of Chemistry, Carleton University, Ottawa, Canada K1S 5B6

AND

HELMUT BEIERBECK AND JOHN K. SAUNDERS
Département de chimie, Université de Sherbrooke, Sherbrooke, Québec

Received May 14, 1973

The ^{13}C n.m.r. chemical shifts of some monofunctional keto- and hydroxy-steroids were monitored as a function of the concentration of added shift reagent, $Pr(fod)_3$ or $Eu(fod)_3$, and the observed induced shifts were fitted to the geometric quantities in the one-term pseudocontact shielding equation. The correlation between experimental and calculated shifts was quantitative for all carbons except those closest to the complexing site, where contact interactions are most noticeable. With $Pr(fod)_3$ the carbonyl and hydroxyl carbons and the alpha carbons usually had to be excluded from the calculations in order to optimize the correlation between predicted and observed induced shifts for the remaining nuclei and to derive reasonable adduct geometries. With $Eu(fod)_3$, contact shifts were also noticeable at the beta carbons and the europium shift reagents are therefore less useful in ^{13}C n.m.r. spectroscopy. It is shown that the application of shift reagents, in conjunction with off-resonance decoupling, permits the assignment of practically all carbon chemical shifts of the steroids studied.

Les spectres r.m.n. du carbone-13 des céto et hydroxy stéroides monofunctionnels sont étudiés en fonction de la concentration des réactifs paramagnétiques de déplacement chimique, $Pr(fod)_3$ et $Eu(fod)_3$. Les déplacements induits observés sont ajustès aux quantités géométriques de l'équation pseudocontact. Si on néglige les 3 carbones les plus proches du métal pour $Pr(fod)_3$ et les 5 carbones les plus proches pour $Eu(fod)_3$, la correlation entre les déplacements expérimentaux et les déplacements calculés sont excellents. On peut interpréter l'observation de correlation dans le cas des carbones proche du métal en terme d'une interaction contact entre ces carbones et le metal. Nous suggérons que pour ces systèmes $Pr(fod)_3$ est le meilleur reactif pour l'observation des déplacements pseudocontact. Nous montrons comment on peut utiliser le réactif paramagnétique avec le couplage liens-résonance pour alterner les déplacements chimiques de tous les carbones des stériodes etudiés.

Can. J. Chem., **51**, 3874 (1973)

It is now well established (1–8) that lanthanide induced shifts are quantitatively reproduced by the one-term pseudocontact shielding eq. 1 for axially symmetric complexes.

$$[1] \qquad \Delta_i = C(1-3\cos^2\theta_i)/R_i^3$$

However, the success of eq. 1 in the lanthanide series is more likely the result of conformational averaging in solution (9) than due to the formation of axially symmetric shift reagent – substrate adducts, since there is no evidence of axial symmetry in the solid state (10–12). In addition to the dipolar shifts there is, however, evidence of contact interactions at the nuclei closest to the complexing site (2, 7, 8, 13).

The value of quantitative applications of eq. 1 in ^{13}C n.m.r. spectroscopy has already been demonstrated with the complete assignment of the carbon resonances of borneol (2, 7) and isoborneol (7). In order to assess the utility of the lanthanide shift reagents for spectral assignments of larger molecules we studied the effects of $Pr(fod)_3$ and $Eu(fod)_3$ on the ^{13}C n.m.r. chemical shifts of a series of monofunctional keto and hydroxy steroids.

Results and Discussion

The ^{13}C chemical shifts for the hydroxy and keto steroids are given in Table 1. Most signals could be assigned by comparison with c.m.r. spectra of steroids reported by Roberts and coworkers (18). The remaining assignments are based on the shift reagent studies described below. We return to these assignments after a discussion of the shift reagent results.

The $Pr(fod)_3$ induced shifts are given in Table

Can. J. Chem. Downloaded from www.nrcresearchpress.com by 210.87.254.105 on 09/05/12
For personal use only.

TABLE 1. ^{13}C chemical shifts for some keto- and hydroxyandrostanes and for the cholesterol nucleus, in p.p.m. downfield from TMS

Carbon No.	3-CO	4-CO	15-CO	16-CO	17-CO	3α-OH	3β-OH	Chol.*	17α-OH	17β-OH
1	38.7	37.7	38.7	38.4	38.7	32.4	37.2	37.4	38.9	38.8
2	38.2	22.7	22.2	22.2	22.2	29.1	31.7	31.8	22.3	22.2
3	211.8	41.3	26.7	26.8	26.8	66.7	71.4	71.9	26.8	26.8
4	44.8	213.3	28.9	28.9	28.8	35.9	38.3	42.5	29.1	29.1
5	46.9	59.3	47.2	47.0	47.1	39.2	45.0	130.9	47.1	47.2
6	29.1	20.5	28.6	29.0	29.0	28.7	28.9	121.8	29.1	29.1
7	32.2	30.8	30.7	32.5	31.0	32.4	32.6	32.1	32.6	31.8
8	35.9	35.4	32.5	35.1	35.2	35.9	36.0	32.1	35.9	35.7
9	54.2	54.8	55.0	54.8	54.9	54.7	54.8	50.3	54.9	55.1
10	35.9	42.7	36.5	36.5	36.5	36.3	35.7	36.6	36.4	36.4
11	21.6	21.7	20.4	20.4	20.1	20.9	21.4	21.2	20.3	20.5
12	38.7	38.9	39.4	38.4	31.7	39.0	39.1	39.9	31.6	36.9
13	40.9	40.8	39.2	39.2	47.8	40.9	40.9	42.5	45.4	43.0
14	54.5	54.4	63.5	51.9	51.6	54.7	54.8	56.9	48.9	51.3
15	25.6	25.4	216.9	39.3	21.8	25.5	25.6	24.4	24.6	23.4
16	20.6	20.5	35.1	218.7	35.9	20.5	20.5	28.2	32.4	30.6
17	40.5	40.4	35.2	56.0	221.2	40.5	40.6	56.4	80.1	82.1
18	17.6	17.6	18.3	18.1	13.8	17.8	17.7	12.0	17.2	11.3
19	11.5	13.8	12.2	12.3	12.2	11.2	12.5	19.5	12.2	12.4

*Cholesterol.

2, together with the differences between observed and calculated induced shifts. The results in Table 2 fully justify the use of eq. 1 in the lanthanide series. The correlation between observed shifts and the geometric quantities $(1-3\cos^2\theta)/R_i^3$ is essentially quantitative for all carbons outside the C—(C—OH)—C and C—(C=O)—C moieties, if these closest carbons are omitted from the calculations, and the corresponding metal–oxygen distances are found to be of the order of magnitude (*ca.* 2.5 Å) expected from X-ray crystallographic studies of shift reagent – substrate adducts (10, 12). The lack of agreement between calculation and experiment for the carbons closest to the lanthanide metal is most likely due to contact interactions. If the induced shifts for the C—(C—OH)—C and C—(C=O)—C fragments were excluded from the calculations the predicted upfield shifts for the carbonyl carbons were far too small, whereas the predicted shifts for the hydroxyl carbons were somewhat too large, with the exception of 3β-hydroxyandrostane (Table 2). If the shifts for the C—(C—OH)—C, and C—(C=O)—C fragments were included in the calculations excellent agreement with experiment was achieved for the carbonyl, as well as the hydroxyl carbons (Table 3). However, the fit for the remaining carbons deteriorated and the Pr—O distances became unrealistically long for the ketones and too short for the hydroxides. Not surprisingly optimization of the fit of eq. 1 to the observed shifts leads to geometries which best reproduce the experimental values for the carbons which experience the largest shifts. Because of their $1/R^3$ dependence the induced shifts for carbons close to the functional group decrease more rapidly than those for more remote carbons. Contact interactions reinforcing the pseudocontact shifts, as for the hydroxyl carbons, will increase this difference and result in an apparent decrease of the Pr—O bond lengths. Contact shifts opposing the pseudocontact shifts, as for the carbonyl carbons, decrease this difference and cause an apparent increase of the Pr—O distances.

Contact interactions are also noticeable at the alpha carbons, especially if they are tertiary or quaternary. The observed induced shifts for the quaternary carbons alpha to the hydroxyl carbons are lower than the induced shifts for secondary alpha carbons and lower than the calculated pseudocontact shifts. Similarly with the ketosteroids the induced shifts for tertiary and quaternary alpha carbons are significantly smaller than those of the secondary alpha carbons and smaller than the predicted values (Tables 2 and 3).

It was considerably more difficult to correlate $Eu(fod)_3$ induced carbon chemical shifts with the geometric quantities in eq. 1. With this shift reagent contact interactions seem to extend to the beta carbons and it was usually necessary to

Can. J. Chem. Downloaded from www.nrcresearchpress.com by 210.87.254.105 on 09/05/12
For personal use only.

Can. J. Chem. Downloaded from www.nrcresearchpress.com by 210.87.254.105 on 09/05/12
For personal use only.

TABLE 2. $Pr(fod)_3$ induced shifts Δ_{obs} and differences $\Delta\Delta = (\Delta_{obs} - \Delta_{calcd})$ between observed and calculated induced shifts

Carbon No.	3-CO		4-CO		15-CO		16-CO		17-CO		3α-OH		3β-OH		Chol.		17α-OH		17β-OH	
	Δ_{obs}	ΔΔ	Δ_{obs}	ΔΔ	Δ_{obs}	ΔΔ	Δ_{obs}	ΔΔ	Δ_{obs}	ΔΔ	Δ_{obs}	ΔΔ	Δ_{obs}	ΔΔ	Δ_{obs}	ΔΔ	Δ_{obs}	ΔΔ	Δ_{obs}	ΔΔ
1	5.45	0.03	3.73	−0.22	1.11	0.02	0.57	−0.02	0.80	0.08	9.87	0.17	5.60	0.00	4.69	0.01	1.27	0.09	0.70	−0.08
2	9.19	−1.93*	4.80	0.07	0.66	0.01	0.32	−0.08	0.48	0.04	14.82	0.82*	13.43	−0.15*	11.01	−0.13	0.65	−0.03	0.47	−0.02
3	15.87	−11.20*	9.95	−0.29*	—†	—†	0.31	−0.02	0.44	0.07	32.88	5.09*	31.95	−0.47*	24.94	0.53*	0.78	0.13	0.39	−0.05
4	9.71	−1.62*	12.65	−13.14*	0.70	0.08	0.32	−0.09	0.53	0.03	13.42	−0.79*	14.37	−0.33*	11.00	0.06	0.86	−0.08	0.49	−0.01
5	5.54	0.15	7.20	−3.04*	1.40	−0.03	0.66	0.01	0.88	0.09	9.65	−0.19	5.68	−0.08	5.12	0.57	1.48	−0.12	0.73	−0.07
6	2.40	−0.11	7.80	0.40	2.16	0.18	0.83	0.06	0.95	0.05	4.72	0.12	3.05	0.12	1.97	−0.51	2.00	0.14	0.90	0.10
7	1.44	0.09	3.07	−0.04	5.27	−0.20	1.40	0.04	1.44	0.03	2.81	0.00	1.66	−0.07	1.34	−0.02	2.92	−0.15	1.32	0.02
8	1.31	−0.04	2.20	−0.14	5.95	0.05	1.97	−0.11	2.42	−0.09	2.59	−0.03	1.66	−0.04	1.34	0.03	4.51	−0.10	2.23	0.05
9	2.10	0.09	2.51	−0.36	2.66	−0.24	1.31	−0.07	1.97	−0.06	3.99	−0.04	2.29	−0.06	1.91	0.07	3.74	−0.06	1.81	−0.05
10	3.84	−0.21	4.96	−0.30	1.58	−0.11	0.89	0.06	1.01	−0.10	7.14	0.12	4.82	0.16	3.81	0.30	1.93	−0.02	1.05	0.05
11	1.31	−0.05	1.70	0.02	2.38	0.07	1.45	0.03	2.62	−0.10	2.55	0.02	1.59	−0.04	1.31	0.02	4.35	0.17	2.45	0.08
12	0.83	0.10	1.28	0.18	2.69	0.00	2.18	0.04	6.40	0.11	1.41	0.02	1.07	0.08	0.78	−0.02	9.61	−0.08	5.25	0.12
13	0.65	0.02	0.74	−0.23	4.86	0.09	4.18	−0.02	6.11	−3.27*	1.01	−0.16	0.95	0.08	0.62	−0.06	11.19	−1.17*	7.60	−1.21*
14	0.74	0.01	1.32	−0.01	5.40	−2.69*	4.25	0.05	4.81	−0.09	1.41	−0.05	0.92	−0.12	0.78	−0.01	8.81	−0.15	4.17	−0.14
15	0.45	−0.01	0.66	−0.16	16.65	−3.04*	7.56	−0.53*	4.20	0.05	0.89	0.01	0.77	0.06	0.56	0.01	7.80	0.41	3.94	0.09
16	0.25	−0.05	0.45	−0.13	10.13	1.64*	15.12	−6.49*	8.76	0.14*	0.63	0.08	0.49	−0.03	0.35	−0.05	13.29	0.78*	8.95	0.52*
17	0.22	−0.13	0.50	−0.16	4.60	0.21	7.31	−0.96*	13.56	−10.63*	0.80	0.15	0.56	−0.02	0.44	−0.01	28.95	3.85*	19.73	1.57*
18	0.62	−0.01	0.80	0.06	3.86	−0.08	3.29	−0.01	6.51	0.77	0.93	−0.14	0.89	0.08	0.66	0.00	5.83	−0.08	6.70	−0.07
19	2.83	−0.29	4.30	0.27	1.35	0.05	0.84	0.08	1.01	−0.03	4.28	−0.16	3.91	−0.08	2.90	−0.07	1.56	−0.02	0.79	0.10
R‡	0.016		0.038		0.020		0.011		0.013		0.011		0.008		0.027		0.015		0.012	
Pr—O	2.33		2.26		2.78		2.14		2.22		2.65		1.81		2.20		2.77		2.32	

*Excluded from calculations.
†Signals hidden under shift reagent peak.
‡$R = \Sigma(\Delta_{obs} - \Delta_{calcd})^2 / \Sigma\Delta_{obs}^2$.

Can. J. Chem. Downloaded from www.nrcresearchpress.com by 210.87.254.105 on 09/05/12
For personal use only.

TABLE 3. Relative differences $(\Delta_{obs}-\Delta_{calcd})/\Delta_{obs}$ between observed and calculated $Pr(fod)_3$ induced shifts, with the C—(C—OH)—C and C—(C=O)—C carbons excluded and included in the calculations

	C_α	C=O	C_α'	R	Pr—O		C_α	C—OH	C_α'	R	Pr—O
3-CO	C-2	C-3	C-4			3α-OH	C-2	C-3	C-4		
Excl.	−0.21	−0.71	−0.17	0.016	2.33	Excl.	0.06	0.15	−0.06	0.011	2.65
Incl.	0.04	−0.01	0.02	0.031	4.25	Incl.	0.04	0.00	−0.06	0.031	2.15
4-CO	C-3	C-4	C-5			3β-OH	C-2	C-3	C-4		
Excl.	−0.03	−1.04	−0.42	0.038	2.26	Excl.	−0.01	−0.01	0.03	0.008	1.81
Incl.	0.13	−0.05	−0.03	0.099	4.77	Incl.	0.00	0.00	0.02	0.012	1.88
15-CO	C-16	C-15	C-14			Chol.	C-2	C-3	C-4		
Excl.	0.16	−0.18	−0.55	0.020	2.78	Excl.	−0.01	0.02	0.01	0.027	2.20
Incl.	0.01	0.03	−0.31	0.104	4.05	Incl.	−0.02	0.00	0.00	0.027	2.08
16-CO	C-15	C-16	C-17			17α-OH	C-16	C-17	C-13		
Excl.	−0.07	−0.43	−0.13	0.011	2.14	Excl.	0.06	0.13	−0.11	0.015	2.77
Incl.	0.01	0.00	−0.01	0.017	3.50	Incl.	0.02	0.00	−0.18	0.023	2.39
17-CO	C-16	C-17	C-13			17β-OH	C-16	C-17	C-13		
Excl.	0.16	−0.78	−0.53	0.013	2.22	Excl.	0.06	0.08	−0.16	0.012	2.32
Incl.	0.00	0.01	−0.13	0.055	4.49	Incl.	0.01	0.00	−0.23	0.017	2.21

TABLE 4. Observed $Eu(fod)_3$ induced shifts Δ_{obs} and differences $\Delta\Delta = (\Delta_{calcd} - \Delta_{obs})$ between calculated and observed shifts‡

Carbon No.	3-CO		17-CO		3β-OH		17β-OH	
	Δ_{obs}	$\Delta\Delta$	Δ_{obs}	$\Delta\Delta$	Δ_{obs}	$\Delta\Delta$	Δ_{obs}	$\Delta\Delta$
1	3.00	−0.01	0.38	0.01	3.31	1.28*	0.73	0.17
2	3.33	2.62*	0.26	−0.03	8.94	1.09*	0.38	0.20
3	14.40	−0.01	0.26	−0.08	36.10	−14.89*	0.36	0.13
4	4.25	1.71*	—†	—†	10.25	0.05	0.79	−0.26
5	3.13	−0.46	0.55	−0.13	4.14	0.11	0.90	−0.19
6	0.78	0.25	—†	—†	2.04	0.02	0.79	0.00
7	0.54	−0.03	0.94	0.01	1.12	0.06	1.14	0.08
8	0.70	−0.08	1.72	0.07	1.50	−0.22	2.23	−0.07
9	0.95	0.09	1.43	−0.08	1.56	0.31	1.91	0.02
10	1.90	0.22	0.91	−0.20	4.17	−0.54	1.13	−0.03
11	0.66	0.09	1.79	0.09	1.47	−0.05	2.26	0.32
12	0.42	−0.02	4.69	−0.07	0.74	0.11	5.63	−0.51
13	0.32	−0.01	1.41	5.72*	0.68	0.03	4.83	3.52*
14	0.31	0.01	3.17	0.45	0.71	0.06	3.35	0.73
15	0.20	−0.03	3.50	−0.33	0.63	−0.13	3.65	−0.26
16	0.14	−0.03	7.97	−1.22*	0.48	−0.11	9.33	−1.51*
17	0.17	0.00	18.35	−0.01	0.43	0.02	30.13	−12.79
18	0.29	0.03	6.00	−1.54*	0.75	−0.06	7.10	−0.06
19	1.36	0.27	1.03	−0.31*	−3.31	−0.05	1.02	−0.15
R	0.040		0.028		0.018		0.032	
Eu—O	2.39		2.31		2.64		2.46	

*Excluded from calculations.
†Signals hidden by shift reagent peak.
‡Positive residuals ΔΔ, if significant, denote upfield contact shifts.

exclude at least one of the beta carbon shifts from the calculations to assure convergence and to find reasonable adduct geometries (Table 4). The induced shifts for tertiary and quaternary alpha carbons contain particularly large contact contributions. For instance, the signal of C-14 in 15-ketoandrostane was shifted upfield by $Eu(fod)_3$, *i.e.* the contact shift exceeded the pseudocontact shift in this case. Sample results with $Eu(fod)_3$ are found in Table 4. Figure 1 shows a comparison of optimized Pr and Eu metal coordinates relative to four of the steroids. In view of the sensitivity of the lanthanide metal locations to contact shifts the Pr and Eu coordinates are considered as satisfactorily close.

$Pr(fod)_3$ and $Eu(fod)_3$ induce contact shifts of opposite sign. With $Pr(fod)_3$ upfield contact shifts are observed for hydroxyl carbons, downfield shifts for the carbonyl carbons and also for tertiary and quaternary alpha carbons in both types of steroids. $Eu(fod)_3$ caused downfield contact shifts for hydroxyl carbons and upfield shifts for all tertiary and quaternary alpha carbons. The predicted pseudocontact shifts for the carbonyl carbons agreed well with the observed induced shifts, which is undoubtedly due to a

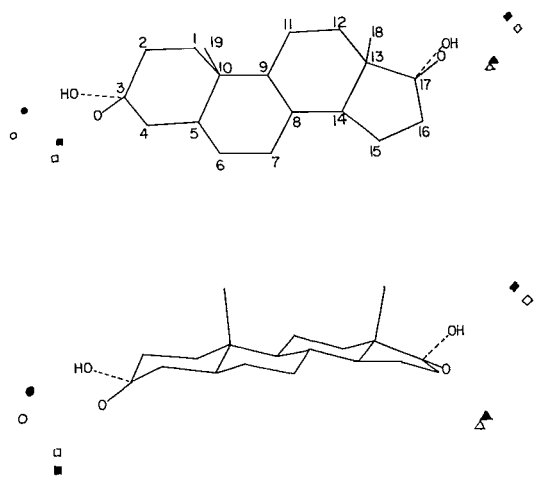

FIG. 1. Europium and praseodymium metal positions, relative to the steroid molecule, for several androstane derivatives: ○, 3β-hydroxide; □, 3 ketone; ◇, 17β-hydroxide; △, 17 ketone; all open symbols, $Pr(fod)_3$; all closed symbols, $Eu(fod)_3$.

fortuitous cancellation of upfield and downfield contact shifts. A change of sign of the contact shifts on going from Pr to Eu has also been observed in shift reagent studies of borneol and isoborneol (8), of quinoline (13) and studies of

Can. J. Chem. Downloaded from www.nrcresearchpress.com by 210.87.254.105 on 09/05/12
For personal use only.

Can. J. Chem. Downloaded from www.nrcresearchpress.com by 210.87.254.105 on 09/05/12
For personal use only.

isotropic shifts induced by the tripositive ions Pr^{3+} and Eu^{3+} (19).

As mentioned at the beginning most signals could be assigned by comparison with related steroids studied by Roberts and co-workers (18). Their assignments are supported by the present shift reagent results, with the exception of the chemical shifts for carbons 12 and 16 of cholesterol which have to be interchanged (*vide infra*). It is shown in this section that the combined application of lanthanide shift reagents and off-resonance decoupling permits an independent assignment of practically all ^{13}C chemical shifts of any of the steroids. 3-Ketoandrostane may serve as an example of the A-ring-substituted steroids. The off-resonance decoupled spectrum, before or after addition of shift reagent, allows one to distinguish primary, secondary, tertiary, and quaternary carbons. Qualitatively the lanthanide induced shifts are expected to decrease in the order

$$3 > 2 \sim 4 > 1 \sim 5 > 6 \sim 10 \sim 19 > 7 \sim 8 \sim 9 \sim 11 > 12 \sim 13 \sim 14 \sim 18 > 15 \sim 16 \sim 17$$

Combined with the results of off-resonance decoupling experiments this leads to the series

CH_3 $19 > 18$

CH_2 $2 \sim 4 > 1 > 6 > 7 \sim 11 > 15 \sim 16 \sim 17$

CH $5 > 8 \sim 9 > 14$

C $10 > 13$

and to reasonably certain assignments for carbons 1, 3, 5, 6, 10, 12, 13, 14, 18, and 19. A least-squares fit of the pseudocontact equation to the induced shifts for these carbons confirmed these assignments and distinguished carbons 8 and 9 (Table 5). Carbons 15, 16, and 17 cannot be assigned from the shift reagent results alone. However, by comparison with the chemical shifts of C-1 and C-12 the lowfield signal has to be due to C-17 and carbons 15 and 16 can then be distinguished on the basis of the predicted induced shifts. The induced shifts for C-15 and C-16 are close, but these assignments are supported by the results for the other A-ring-substituted steroids (Table 2). The signals of C-2 and C-4, and those of C-7 and C-11 cannot be distinguished on the basis of the lanthanide induced shifts and have been assigned according to Roberts (18).

The assignment of the carbon chemical shifts in D-ring-substituted steroids is exemplified by 17-ketoandrostane. Qualitatively the induced shifts are expected to decrease in the order

CH_3 $18 > 19$

CH_2 $16 > 15 \sim 12 > 11 > 7 > 6 > 1 \sim 4 > 2 \sim 3$

CH $14 > 8 \sim 9 > 5$

C $13 > 10$

leading to rather unambiguous assignments for carbons 5, 6, 7, 10, 11, 13, 14, 16, 17, 18, and 19. The resonances for the pairs of carbons 1/4, 2/3, 8/9, and 12/15 remain to be distinguished. The chemical shift of C-4 has to be close to that of C-6, and C-1 and C-4 are assigned accordingly. A least-squares fit of eq. 1 to the induced shifts for these carbons led to the unequivocal assignment of C-12 and C-15, and of C-8 and C-9 (Table 5); C-2 and C-3 cannot be assigned unambiguously from the induced shifts and were assigned according to Roberts (18).

With the exception of C-12 and C-16 in cholesterol the c.m.r. chemical shifts assigned on the basis of lanthanide induced shifts agree with the assignments made by Roberts and co-workers (18) for related steroids. The induced shifts for carbons 12 and 16 in cholesterol as well as the other A-ring-substituted steroids are unambiguous evidence (Table 2) that the downfield signal is due to C-12 and the upfield peak due to C-16. This is not unreasonable since the C-12 chemical shift is expected to be close to that of C-1 due to the structural similarities about the two sites. In addition, the C-12 resonance now moves upfield on going from the A-ring ketones and hydroxides to the 17-ketone similar to the upfield shift of C-6 upon introducing a keto group into position 4. Thus the assignments of C-12 and C-16 for all cholestane derivatives in reference 18 have to be reversed.

Conclusions

The quantitative correlation between the pseudocontact eq. 1 and the observed chemical shifts induced in the ^{13}C n.m.r. spectra of the keto and hydroxy steroids is further evidence for the $(1-3\cos^2\theta_i)/R_i^3$ dependence of the dipolar shifts induced by the lanthanide shift reagents. However, the unrealistic adduct geometries required to reproduce the observed induced shifts for the

Can. J. Chem. Downloaded from www.nrcresearchpress.com by 210.87.254.105 on 09/05/12
For personal use only.

TABLE 5. Stepwise assignment of the $Pr(fod)_3$ induced ^{13}C chemical shifts in 3-keto- and 17-ketoandrostane

Carbon No.	3-Ketoandrostane					17-Ketoandrostane				
	Δ_{obs}	$\Delta_{calcd} \rightarrow \Delta_{obs}$		$\Delta_{calcd} \rightarrow \Delta_{obs}$		Δ_{obs}	$\Delta_{calcd} \rightarrow \Delta_{obs}$		$\Delta_{calcd} \rightarrow \Delta_{obs}$	
1	5.45	5.36	5.45	5.41	5.45	0.80	0.76	0.80	0.72	0.80
2	9.19/9.71*†	11.14	9.19*§	11.36	9.19*	0.44/0.48†	0.48	0.44/0.48†	0.44	0.48§
3	15.87*	41.13	15.87*	29.25	15.87*	0.44/0.48†	0.42	0.44/0.48†	0.37	0.44§
4	9.19/9.71*†	11.67	9.71*§	11.58	9.71	0.53	0.53	0.53	0.50	0.53
5	5.54	5.52	5.54	5.41	5.54	0.88	0.84	0.88	0.79	0.88
6	2.40	2.32	2.40	2.49	2.40	0.95	0.93	0.95	0.90	0.95
7	1.31/1.44†	1.44	1.44§	1.36	1.44	1.44	1.45	1.44	1.41	1.44
8	1.31/2.10†	1.39	1.31‡	1.35	1.31	1.97/2.42†	2.47	2.42	2.51	2.42
9	1.31/2.10†	2.09	2.10‡	2.01	2.10	1.97/2.42†	2.04	1.97	2.03	1.97
10	3.84	3.99	3.84	4.06	3.84	1.01	1.12	1.01	1.11	1.01
11	1.31/1.44†	1.34	1.31§	1.35	1.31	2.62	2.61	2.62	2.72	2.62
12	0.83	0.81	0.83	0.73	0.83	4.20/6.40†	6.04	6.40	6.29	6.40
13	0.65	0.69	0.65	0.63	0.65	6.11*	9.16	6.11	9.38*	6.11
14	0.74	0.85	0.74	0.74	0.74	4.81	4.81	4.81	4.90	4.81
15	0.22/0.25/0.45†	0.55	0.25/0.45†	0.47	0.45‡	4.20/6.40†	3.96	4.20	4.15	4.20
16	0.22/0.25/0.45†	0.40	0.25/0.45†	0.31	0.25‡	8.76*	8.00	8.76	8.62*	8.76
17	0.22/0.25/0.45†	0.46	0.22§	0.37	0.22	13.56*	24.61	13.56	24.23*	13.56
18	0.62	0.59	0.62	0.63	0.62	6.51	5.25	6.51	5.74	6.51
19	2.83	2.55	2.83	3.10	2.83	1.01	0.98	1.01	1.04	1.01

*Observed induced shifts excluded from calculations because of contact interactions.
†Observed induced shifts unassigned at this stage.
‡Observed induced shifts assigned by comparison to predicted pseudocontact shifts (preceding column).
§Observed induced shifts assigned on the basis of chemical shifts.

Can. J. Chem. Downloaded from www.nrcresearchpress.com by 210.87.254.105 on 09/05/12
For personal use only.

closest carbons, and the lack of agreement between observation and predictions based on acceptable metal–oxygen bond lengths, are clear evidence of contact interaction at the carbons closest to the complexing site. The $Eu(fod)_3$ induced contact shifts are larger and noticeably further along the carbon chain than the $Pr(fod)_3$ induced contact shifts. For this reason $Pr(fod)_3$ is the more useful shift reagent in ^{13}C n.m.r. spectroscopy. Finally, it was demonstrated that the combined application of off-resonance decoupling and lanthanide shift reagents permits the assignment of practically all carbon chemical shifts of the steroids studied.

Experimental and Calculations

The hydroxy and keto steroids were available in the laboratory. $Pr(fod)_3$ and $Eu(fod)_3$ were purchased from Norell Chemical Co. and used without further purification. The ^{13}C n.m.r. spectra of the steroids were recorded as 0.2 *M* solutions in $CDCl_3$. For every substrate 0.5 *M* shift reagent solutions in $CDCl_3$ were freshly prepared. All manipulations of shift reagents were carried out as quickly as possible but no special precautions were taken to exclude moisture. Five aliquots of the shift reagent solutions were added to the steroids to reach a maximum shift reagent – substrate concentration ratio of 0.5. All ^{13}C n.m.r. spectra were recorded on a Bruker HX 90 n.m.r. spectrometer equipped with a Nicolet 1083 instrument computer for Fourier transform spectroscopy. The probe temperature was 37 °C.

The chemical shifts before and after addition of shift reagent were plotted against the sums of the shifts in each spectrum, which were scaled from zero to unity. The "observed induced shifts Δ_{obs}" reported in Tables 2 and 4 are the slopes in these plots (14, 15). The root-mean-squares deviations of the experimental points from the lines were of the order of 0.05 p.p.m. The steroidal carbon coordinates used in the calculations were those for androsterone (16) and 3β-chloro-5-androsten-17β-ol (17), as determined by X-ray crystallography. The oxygen coordinates were calculated assuming standard bond lengths and angles. The lanthanide metal position relative to the substrate and the fit between observed and calculated induced shifts were optimized as described previously (6). Briefly, the method consists of expanding the pseudo-contact eq. 1 in a Taylor series in the proportionality constant *C* and three Cartesian coordinates for the lanthanide atom. The sum of the squares of the deviations is then minimized iteratively by a linear least-squares fit of the expanded equation to the observed induced shifts. The minimum was usually located after five or six iterations, depending on the starting parameters. The calculations were performed on the IBM 360 computer at the Université de Sherbrooke, with programs written in Fortran IV language.

We wish to acknowledge generous financial assistance from the National Research Council of Canada and the Ministre de l'Education du Québec.

1. J. Briggs, F. A. Hart, and G. P. Moss. Chem. Commun. 1506 (1970).
2. J. Briggs, F. A. Hart, G. P. Moss, and E. W. Randall. Chem. Commun. 364 (1971).
3. S. Farid, A. Ateya, and M. Maggio. Chem. Commun. 1285 (1971).
4. M. R. Willcott III, R. E. Lenkinski, and R. E. Davis. J. Am. Chem. Soc. **94**, 1742 (1972).
5. P. V. DeMarco, B. J. Cerimele, R. W. Crane, and A. L. Thakkar. Tetrahedron Lett. 3539 (1972).
6. J. W. ApSimon and H. Beierbeck. Tetrahedron Lett. 581 (1973).
7. G. E. Hawkes, D. Leibfritz, D. W. Roberts, and J. D. Roberts. J. Am. Chem. Soc. **95**, 1659 (1973).
8. G. E. Hawkes, C. Marzin, S. R. Johns, and J. D. Roberts. J. Am. Chem. Soc. **95**, 1661 (1973).
9. J. M. Briggs, G. P. Moss, E. W. Randall, and K. D. Sales. Chem. Commun. 1180 (1972).
10. W. DeW. Horrocks Jr., J. P. Sipe III, and J. R. Luber. J. Am. Chem. Soc. **93**, 5258 (1971).
11. W. DeW. Horrocks Jr. and J. P. Sipe III. Science, **177**, 994 (1972).
12. R. E. Cramer and K. Seff. Chem. Commun. 400 (1972).
13. A. A. Chalmers and K. G. R. Pachler. Tetrahedron Lett. 4033 (1972).
14. J. W. ApSimon and H. Beierbeck. Chem. Commun. 172 (1972).
15. J. W. ApSimon, H. Beierbeck, and A. Fruchier. Can. J. Chem. **50**, 2725 (1972).
16. D. F. High and J. Kraut. Acta Cryst. **21**, 88 (1966).
17. C. M. Weeks, A. Cooper, and D. A. Norton. Acta Cryst. B**27**, 531 (1971).
18. H. J. Reich, M. Jautelat, M. T. Messe, F. J. Weigert, and J. D. Roberts. J. Am. Chem. Soc. **91**, 7445 (1969).
19. W. B. Lewis, J. A. Jackson, J. F. Lemons, and H. Taube. J. Chem. Phys. **36**, 694 (1962).

Studies on Metal Hydroxy Compounds. XIV. Thermal Analyses, Calorimetry, and Decomposition Kinetics of Heterocationic Hydroxy Chloride Compounds

AH-DONG LEU,[1] PALEPU RAMAMURTHY,[2] AND ETALO A. SECCO[3]
Chemistry Department, St. Francis Xavier University, Antigonish, Nova Scotia

Received June 25, 1973

Studies were carried out on two series of mixed metal hydroxy chloride compounds of the type $x\text{Me(OH)}_2.y\text{MCl}_2$ where Me = Cd, Cu and M = Mn, Co, Ni, Cu, Zn, Cd, Mg, or Ca.

Thermal analyses for the Cd–M series reveal that the initial mode of decomposition involves a dehydroxylation step with a concomitant metathetical reaction between MCl_2 and CdO. The compound $CdCl_2.2CdO$ is formed and decomposes at higher temperature leading to the eventual volatilization of $CdCl_2$. The kinetics of thermal decomposition follow a simple first-order rate equation. The sole exception to this general pattern of behavior is the Cd–Zn compound.

The initial mode of thermal decomposition of the Cu–M series compounds follows a parallel pattern described for the Cd–M series. The kinetic data for the Cu–M series are fitted into three groups: (*i*) phase boundary control embracing the contracting sphere and contracting plate model equations, (*ii*) A-E type equation with $n = 2$, and (*iii*) first-order rate equation.

On a étudié deux séries de hydroxychlorures métalliques du type mixte $x\text{Me(OH)}_2.y\text{MCl}_2$ où Me = Cd, Cu et M = Mn, Co, Ni, Cu, Zn, Cd, Mg ou Ca.

Des analyses thermiques pour la série Cd–M ont montré que le mode initial de décomposition implique une déshydroxylation avec une réaction de double décomposition concomitante entre MCl_2 et CdO. Le composé $CdCl_2.2CdO$ est formé et se décompose à des températures plus élevées en entraînant la volatilisation éventuelle du $CdCl_2$. La cinétique de la décomposition thermique obéit à une équation de vitesse du premier ordre. La seule exception à ce type général de comportement est le composé Cd–Zn.

Le mode initial de décomposition thermique de la série Cu–M suit un processus parallèle à celui décrit pour la série Cd–M. Les données cinétiques pour la série Cu–M sont résumées en trois groupes: (*i*) contrôle topochimique quand la réaction commence à la surface extérieure du solide et progresse en trois dimensions (modèle d'une sphère contractante) ou quand la réaction progresse en deux dimensions (modèle d'une lame contractante); (*ii*) équation du type A-E avec $n = 2$ et (*iii*) équation de vitesse du premier ordre. [Traduit par le journal]

Can. J. Chem., **51**, 3882 (1973)

Introduction

An earlier study on metal basic halides involving the cadmium derivative (1) showed that the reaction between CdO and $CdCl_2$ in aqueous solution gave a solid compound of composition CdOHCl, *viz.*

$$[1]\quad CdO_{(s)} + CdCl_{2(s)} + H_2O_{(l)} \xrightarrow{\sim 80\,^\circ C} 2\,CdOHCl_{(s)}$$

When NaCl was used instead of $CdCl_2$ under similar conditions a white precipitate (2) was again obtained whose composition was found to be $Na_2Cd(OH)_2Cl_2$, *i.e.*,

$$[2]\quad CdO_{(s)} + 2\,NaCl_{(s)} + H_2O_{(l)} \xrightarrow{\sim 80\,^\circ C} Na_2Cd(OH)_2Cl_{2(s)}$$

The existence of such mixed metal hydroxychloride compounds prompted us to extend the previous studies reported on bivalent metal hydroxyhalides (1, 3, 4) and mixed metal hydroxides (5) to assess the effect of a different metal halide presence on the thermal stability and decomposition kinetics of a given hydroxide.

This paper contains results on thermal analyses, calorimetry, and decomposition kinetics on two series of mixed metal hydroxychloride compounds of the type $x\text{Me(OH)}_2.y\text{MCl}_2$ where Me = Cd or Cu and M = Mn, Co, Ni, Cu, Zn, Cd, Mg, or Ca.

Experimental

Preparation

All compounds used in this study were prepared in this laboratory. The mixed-Cu compounds were obtained by following the known procedure of Feitknecht and Maget (6) whereas the mixed-Cd compounds were prepared by digesting CdO in an aqueous solution of metal chloride,

[1]Taken from M.Sc. thesis of A.-D.L.

[2]Present address: Chemistry Department, University of Ottawa, Ottawa, Canada.

[3]To whom correspondence should be addressed.

Can. J. Chem. Downloaded from www.nrcresearchpress.com by 210.87.254.5 on 09/05/12
For personal use only.

TABLE 1. Elemental quantitative analysis of the mixed metal hydroxy chlorides (Cd series)

Compound	Mole ratio Cd	Mole ratio M	%Cl Obs.	%Cl Theor.	%OH Obs.	%OH Theor.	%Cd Obs.	%Cd Theor.	%M Obs.	%M Theor.	Empirical formula
Cd–Cu	1	2	18.31	18.75	18.74	17.96	30.18	29.70	33.61	33.58	$CdCu_2(OH)_4Cl_2$
Cd–Zn	1	4	12.55	12.33	23.40	22.23					$CdZn_4(OH)_8Cl_2$
Cd–Ni	9	4	11.66	11.78	19.86	18.89	56.12	56.23	13.09	13.05	$Cd_9Ni_4(OH)_{20}Cl_6$
Cd–Co	3	1	12.62	12.59	18.62	17.90	59.32	59.24	10.63	10.35	$Cd_3Co(OH)_6Cl_2$
Cd_7Mg_2	7	2	12.01	11.70	19.19	19.50	64.18	64.72	4.15	4.00	$Cd_3Mg_2(OH)_{14}Cl_4$
Cd–Mn	4	1	14.41	14.58	16.72	16.29	61.63	61.58	7.43	7.52	$Cd_4Mn(OH)_7Cl_3$

MCl_2, at 75–80 °C for 2–4 days. Two-fold excess of MCl_2 over CdO ensured complete consumption of the oxide.

All chemicals used, except CdO, were commercially supplied reagent grade material. The CdO was obtained from the decomposition of cadmium basic oxalate (7) which had the desired property of higher reactivity compared to the commercially available reagent grade oxide (1).

The precipitates were filtered and washed thoroughly with distilled water and then dried at 110 °C overnight.

The identities of the Cu–M compounds were confirmed by the available X-ray diffraction patterns (6) and in an indirect manner by correlating the thermogravimetric analysis with the X-ray patterns of the solid residues. All compounds were determined to be in the constant atomic relationship $MCl_2.3Cu(OH)_2$ except for Ca which was $CaCl_2.4Cu(OH)_2$.

The new Cd–M compounds were identified by elemental quantitative analysis.

Elemental Quantitative Analysis

All chemicals used were at least of reagent grade. Aqueous solutions were prepared with water distilled in a Pyrex distillation apparatus. The glassware was cleaned with acidic cleaning solution followed by thorough rinsing; the volumetric glassware was also soaked in hot alkaline disodium ethylenediamine tetra-acetate (EDTA) solution and then rinsed thoroughly.

The mole ratio of the two cations, x and y in the compound, $xCd(OH)_2.yMCl_2$, was determined by EDTA titration (8–10) initially for a known or standard solution in two steps: (*a*) masking and demasking agents present (8, 9); (*b*) masking and demasking agents absent. The volume V_a consumed in step (*a*) corresponded to the presence of one cation while V_b concerned in (*b*) corresponded to both cations. V_a and V_b represented the measured mole ratio of the cations which was then compared to the known value of the standard solution. The method giving a discrepancy of $< 2\%$ was deemed satisfactory for analysis of the unknown solution containing the prepared compound.

The Cl content of each compound was determined by the Volhard method (11) and the OH content was obtained from the weight loss due to the dehydroxylation in TG.

Instrumental Analysis

The heating and cooling curves, calorimetric measurements, and isothermal kinetic traces were obtained as previously described (4). The heating rate used was usually 20 °C/min and an ambient atmosphere of dry N_2 (Matheson Prepurified Grade with a stated impurity of 0.003% O_2) at a flow rate of 2 SCFH was maintained during all experiments.

The X-ray diffraction traces of the samples were recorded on a Norelco X-ray diffractometer unit using CuK_α or MoK_α radiation (12); the identities of the residues were confirmed by the available X-ray diffraction patterns (13).

Results and Discussion

Elemental Quantitative Analysis

The cation mole ratio results of the standard solutions as determined in our analytical procedure incorporated errors ranging from 0.24% to 1.53%. Using the nearest integer ratio ($x:y$) along with the Cl analysis and the OH content from TG weight loss, the empirical formula for each compound of the type $Cd_kM_l(OH)_mCl_n$ was found and is presented in Table 1.

The k and l values in $Cd_kZn_l(OH)_mCl_n$ could not be determined quantitatively because of the difficulty in the separation of Cd and Zn. With prior knowledge of the compound $Zn_5(OH)_8Cl_2$ (14) the mixed compound was assumed to be $Cd_kZn_l(OH)_8Cl_2$ where $k + l = 5$. All evidence from thermal analysis and X-ray diffraction of intermediate products supports the assignment of $k = 1$ and $l = 4$, *i.e.* $CdZn_4(OH)_8Cl_2$.

Thermogravimetry

The results of TG are presented in Table 2; the proposed over-all decomposition reaction and steps are those which best fit the observed weight loss. The intermediate and final products were further confirmed by X-ray diffraction and correlated with DTA curves.

Cd–M Compounds

The first step in the decomposition reaction occurs, as expected, via dehydroxylation which can be represented by the general overall equation

Can. J. Chem. Downloaded from www.nrcresearchpress.com by 210.87.254.5 on 09/05/12
For personal use only.

TABLE 2. Thermogravimetric analysis

Compound	Step No.	*Temperature range (°C)	% Total weight lost Obs.	% Total weight lost Theor.	Reaction†
$CdCu_2(OH)_4Cl_2$	1	130–370	9.59	9.53	A
	2	400–735	46.50	45.30	C
$CdZn_4(OH)_8Cl_2$	1	150–400	12.14	12.02	A
	2	450–720	43.32	43.95	D
$Cd_9Ni_4(OH)_{20}Cl_6$	1	250–460	10.45	10.00	A
	2	480–740	40.64	40.57	D
$Cd_3Co(OH)_6Cl_2$	1	140–380	9.60	9.49	A
	2	480–735	42.44	41.69	D
$Cd_7Mg_2(OH)_{14}Cl_4$	1	310–440	10.10	10.38	A
	2	460–720	41.10	40.55	D
$Cd_4Mn(OH)_7Cl_3$	1	130–380	8.80	8.62	A
	2	410–730	46.52	46.29	D
$ZnCl_2.3Cu(OH)_2$	1	270–350	12.50	12.60	A
	2	350–450	15.60	20.84	B
	3	450–710	55.60	44.10	C
$NiCl_2.3Cu(OH)_2$	1	270–410	13.20	12.80	A
	2	410–485	18.98	21.20	B
	3	485–770	56.20	43.60	C
$CoCl_2.3Cu(OH)_2$	1	250–380	13.10	12.70	A
	2	380–460	15.56	21.70	B
	3	460–755	57.20	44.70	C
$CdCl_2.3Cu(OH)_2$	1	260–450	11.30	11.30	A
	2	500–770	48.20	47.60	D
$MgCl_2.3Cu(OH)_2$	1	325–530	18.80	18.50	F
	2	530–780	60.20	48.60	C
$CaCl_2.4Cu(OH)_2$	1	300–420	14.30	14.30	A
	2	420–			E

*Onset and terminal temperatures.
†A, dehydroxylation; B, disproportionation of $CuCl_2$; C, volatilization of Cu_2Cl_2 and partial chlorination of oxide; D, E, volatilization of $CdCl_2$, $CaCl_2$, respectively; F, dehydroxylation and dechlorination.

[3] $$Cd_kM_l(OH)_mCl_{n(s)} \rightarrow aCdO_{(s)} + bMO_{(s)} + cCdCl_{2(s)} + dH_2O_{(g)}$$

where M = Cu, Co, Mg, Mn, Ni, and Zn. The coefficients are related as follows, $a + c = k$; $b = l$; $m = 2d = a + b + d$; $2c = n$. The second weight loss process for all compounds, excepting Cd–Cu, is assigned to the volatilization of $CdCl_2$; the Cd–Cu compound weight loss is best fitted to Cu_2Cl_2 volatilization.

Cu–M Compounds

The first step in the decomposition of the Zn, Ni, and Co compounds involves dehydroxylation to yield CuO, metal chloride, and water, *i.e.*

[4*a*] $$MCl_2.3Cu(OH)_{2(s)} \rightarrow MCl_{2(s)} + 3CuO_{(s)} + 3H_2O_{(g)}$$

This reaction is followed immediately by the metathetical reactions of the chloride with CuO where no weight loss is involved, *i.e.*

[4*b*] $$MCl_{2(s)} + CuO_{(s)} \rightarrow CuCl_{2(s)} + MO_{(s)}$$

The second and third steps in the heating curve are due to disproportionation of $CuCl_2$ and subsequent volatilization of Cu_2Cl_2 (15). The higher observed weight loss for the volatilization of Cu_2Cl_2 shown in Table 2 is due to partial chlorination of CuO as previously reported (15).

The Cd and Ca compounds undergo simple dehydroxylation with no ensuing metathetical reaction, *i.e. viz.* [4*a*]. The second step is the volatilization of the chloride which in the case of $CaCl_2$ was incomplete up to 900 °C.

$MgCl_2.3Cu(OH)_2$ decomposed via simultaneous dehydroxylation and dechlorination, *i.e.*

Can. J. Chem. Downloaded from www.nrcresearchpress.com by 210.87.254.5 on 09/05/12
For personal use only.

TABLE 3. Differential thermal analyses

Compound	Peak* No.	Peak temperature (°C)	Reaction†
$CdCu_2(OH)_4Cl_2$	1	295	A
	2	555	C
	3	665	D
$CdZn_4(OH)_8Cl_2$	1	265	A
	2	575	C
$Cd_9Ni_4(OH)_{20}Cl_6$	1	390	A
	2	680	D
$Cd_3Co(OH)_6Cl_2$	1	380	A
	2	565	C
	3	665	D
$Cd_7Mg_2(OH)_{14}Cl_4$	1	425	A
	2	695	D
$Cd_4Mn(OH)_7Cl_3$	1	395	A
	2	565	C
	3	670	D
$ZnCl_2.3Cu(OH)_2$	1 (doublet)	330	A, G
	2	455	B
$NiCl_2.3Cu(OH)_2$	1	430	A
	2	530	E
$CoCl_2.3Cu(OH)_2$	1	350	A
	2	515	E
$CdCl_2.3Cu(OH)_2$	1	290	A
	2	565	C
$MgCl_2.3Cu(OH)_2$	1	500	F
$CaCl_2.4Cu(OH)_2$	1	360	A

*All endotherms.
†A, dehydroxylation; B, disproportionation of $CuCl_2$ and fusion of Cu_2Cl_2; C, fusion of $CdCl_2$; D, decomposition of $CdCl_2.2CdO$; E, disproportionation of $CuCl_2$ and partial chlorination of oxide; F, dehydroxylation and dechlorination; G, fusion of $ZnCl_2$ and metathesis of $ZnCl_2$ + CuO.

[5] $MgCl_2.3Cu(OH)_{2(s)} \rightarrow MgO_{(s)} + 2CuO_{(s)} + \frac{1}{2}Cu_2Cl_{2(l)} + \frac{1}{2}Cl_2 + 3H_2O_{(g)}$

which is followed by volatilization of Cu_2Cl_2.

Differential Thermal Analysis

The DTA results are presented in Table 3 and these thermal effects are interpreted in terms of processes consistent with the TG data.

Cd–M Compounds

Two or three endotherms were observed in the heating curves of this series. The first endotherm is dehydroxylation according to [3] which is followed by the $CdCl_2$ melting endotherm between 555–575 °C if the amount of $CdCl_2$ exceeded CdO by the mole ratio 1:2 (16). The final endotherm 665–695 °C observed in all compounds, excepting Cd–Zn, originates in the decomposition of $CdCl_2.2\,CdO$ (16). The absence of this latter endotherm in $CdZn_4(OH)_8Cl_2$ implies the absence of CdO in the product, *i.e.* $CdCl_2.4Zn(OH)_2$, confirming the earlier interpretation that $Zn_5(OH)_8Cl_2$ is more properly represented by $ZnCl_2.4\,Zn(OH)_2$.

The cooling curve for the residue from each decomposed compound, from 800 °C to room temperature, exhibited exotherms characteristic of $CdCl_2$–CdO presence with two exceptions, Cd–Zn and Cd–Cu compounds. $CdZn_4(OH)_8Cl_2$ showed the $CdCl_2$ fusion exotherm only. On the other hand $CdCu_2(OH)_4Cl_2$ showed two exotherms, 480 °C and 440 °C, associated with the Cu_2Cl_2–$CdCl_2$ binary system of solid solution with minimum melting point (24). Although the latter two exotherm temperature peaks could be mistaken for the temperatures normally observed for Cu_2Cl_2 solidification and the $\gamma \rightarrow \beta$ transi-

Can. J. Chem. Downloaded from www.nrcresearchpress.com by 210.87.254.5 on 09/05/12
For personal use only.

TABLE 4. Results of decomposition of kinetics

Compound	Temperature range (°C)	Number of temperatures	Rate expression	Activation energy E_a (kcal/mol)	log A
$CdZn_4(OH)_8Cl_2$	220–260	5	second order	29.3±0.4	11.6
$CdCu_2(OH)_4Cl_2$	280–320	5	first order	25.3±0.3	9.1
$Cd_9Ni_4(OH)_{20}Cl_6$	320–360	5	first order	32.6±0.1	11.1
$Cd_3Co(OH)_6Cl_2$	300–340	5	first order	27.5±0.2	9.4
$Cd_7Mg_2(OH)_{14}Cl_4$	350–390	4	first order	30.1±0.5	9.5
$Cd_4Mn(OH)_7Cl_3$	280–320	5	first order	28.7±0.3	9.3
$CdCl_2.3Cu(OH)_2$	280–315	5		48±3	17.7
$ZnCl_2.3Cu(OH)_2$	300–350	6	$-\ln(1-\alpha) = (kt)^2$	34±1	11.8
$NiCl_2.3Cu(OH)_2$	340–380	6	$1-(1-\alpha)^{\frac{1}{2}} = kt$	36±1	12.1
$CoCl_2.3Cu(OH)_2$	320–355	6	$1-(1-\alpha)^{\frac{1}{2}} = kt$	34±1	11.2
$MgCl_2.3Cu(OH)_2$	400–430	6	$1-(1-\alpha)^{\frac{1}{2}} = kt$	74±2	22.6
$CaCl_2.4Cu(OH)_2$	335–360	6	$1-(1-\alpha)^{1/3} = kt$	66±4	22.2

tion, the exotherm profiles differed significantly in both instances.

Cu–M Compounds

The heating trace up to 700 °C for Cu–Ni and Cu–Co compounds revealed two endotherms corresponding to simultaneous dehydroxylation and metathetical reactions according to [4*a*] and [4*b*] followed by disproportionation of $CuCl_2$. On cooling, two exotherms at 460 °C and 420 °C are identified with fusion and structural transition in Cu_2Cl_2, respectively (15).

Two endotherms appeared on heating $ZnCl_2.3Cu(OH)_2$. The first endotherm consisted of a doublet described by [4*a*] and followed by $ZnCl_2$ melting and the metathetical reaction 4*b*. Cooling the residue revealed two exotherms at 440 and 420 °C involving Cu_2Cl_2 transitions.

$CdCl_2.3Cu(OH)_2$ showed two endotherms on heating; these endotherms correspond to dehydroxylation via [4*a*] and melting of $CdCl_2$. The solidification exotherm of $CdCl_2$ was confirmed on cooling.

Only one endotherm was observed on heating $MgCl_2.3Cu(OH)_2$ described by reaction 5, involving simultaneous dehydroxylation and $CuCl_2$ disproportionation. The cooling curve of the residue revealed the two exotherms characteristic of Cu_2Cl_2.

The heating trace of $CaCl_2.4Cu(OH)_2$ displayed one endotherm due to dehydroxylation analogous to [4*a*].

Reaction Kinetics Data

The recorded weight loss *vs.* time trace was converted to decomposition fraction, α, *vs.* time plot according to the overall reactions 3, 4*a*, or 5. The experimental α, t, data were processed through all the known solid state kinetic rate equations. The best linear fit between the data and the rate expressions over the maximum reaction fraction $\alpha \sim 0.90$ and over the temperature range studied are presented in Table 4. The fitting of the data to a particular rate expression was straightforward and clear-cut in each case.

Cd–M Compounds

The kinetic data for all compounds, except Cd–Zn, were fitted to simple first-order kinetics; $CdZn_4(OH)_8Cl_2$ rate data fit the second-order rate law presented in its integrated form (17) by

$$1/(1-\alpha) = 1 + kt \qquad [6]$$

The activation energy, E_a, values of all Cd–M compounds fall within the range 25–32 kcal/mol which compare with 26.3 kcal/mol for $Cd(OH)_2$. The striking similarity in E_a values suggests a fundamentally similar decomposition mechanism and activated complex state. The fundamental step for a first-order dehydroxylation rate is visualized as an OH abstraction by a highly mobile H species.

The E_a value for the dehydroxylation reaction in the Ni, Mg, and Mn compounds is lower than its respective ΔH value. The observation that $E_a < \Delta H$ is at variance with current rate theory (18) and the literature of endothermic decomposition reactions (19). Recently, Fichte and Flanagan (20) reported a similar result, *i.e.* $E_a < \Delta H$, and have cited Somorjai and Lester's discussion on evaporation processes (21) to illustrate that the condition $E_a > \Delta H$ is not a necessary condition for solid-state dehydration reactions. However we are inclined to assign our result of $E_a < \Delta H$ to concomitant secondary

Can. J. Chem. Downloaded from www.nrcresearchpress.com by 210.87.254.5 on 09/05/12
For personal use only.

TABLE 5. Heats of decomposition and values of ΔH_f^0

Compound	Temperature range (°C)*	Heat of Decomposition ΔH_w	Heat of Decomposition ΔH_c†	$-\Delta H_f^0$ (kcal/mol)
Cd $Cu_2(OH)_4Cl_2$	220–315	11.8	23.6±1.7	‡
Cd $Zn_4(OH)_8Cl_2$	195–270	6.8	27.4±0.7	668
$Cd_9Ni_4(OH)_{20}Cl_6$	265–400	‡	101±1	‡
$Cd_3Co(OH)_6Cl_2$	270–385	6.3	18.8±0.4	464
$Cd_7Mg_2(OH)_{14}Cl_4$	300–415	‡	48.3±1.9	‡
$Cd_4Mn(OH)_7Cl_3$	310–430	‡	35.0±1.8	‡
Zn $Cl_2.3Cu(OH)_2$	255–350	12.1	36.3±0.3	405
Ni $Cl_2.3Cu(OH)_2$	300–415	11.7	35.0±0.5	395
Cd $Cl_2.3Cu(OH)_2$	240–355	11.7	35.0±0.2	413
Co $Cl_2.3Cu(OH)_2$	280–370	12.0	36.0±1.0	398
Mg $Cl_2.3Cu(OH)_2$	400–530	14.7	44.0±1.0	482
Ca $Cl_2.4Cu(OH)_2$	270–370	13.0	42.0±0.4	612

*Onset and terminal temperatures.
†All determinations were done in triplicate; ΔH_c values are given with their average deviation; ΔH_w, heat of decomposition in kcal/mole of H_2O formed; ΔH_c, heat of decomposition in kcal/mole of compound decomposed; ΔH_f, heat of formation of the hydroxychloride compound.
‡Unable to calculate because of unknown secondary effects.

endothermic solid-state effects, such as metathetical reactions, etc.

The Arrhenius pre-exponential term, A, values are less than 10^{13}. Since $A = [10^{13}Q^*/Q]$ where Q^* and Q from absolute rate theory represent the complete partition functions of the activated complex, excluding the reaction coordinate, and of the reactant, respectively then $Q^* < Q$ implies that the complex is more restricted in its modes of freedom relative to the reactant. Cordes' analysis (22) for a bimolecular first-order reaction yields a predicted A range 10^9–10^{11} which spans the interval of A values cited in Table 4.

Cu–M Compounds

The compounds can be classified on the basis of their reaction kinetics into three groups.

(*i*) Phase boundary control with the kinetic data for $CaCl_2.4Cu(OH)_2$ fitting the contracting sphere model, *viz.*

$$[7] \qquad 1 - (1 - \alpha)^{1/3} = kt$$

and the kinetic data for $NiCl_2.3Cu(OH)_2$, $CoCl_2.3Cu(OH)_2$, and $MgCl_2.3Cu(OH)_2$ fitting the contracting plate model, *viz.*

$$[8] \qquad 1 - (1 - \alpha)^{\frac{1}{2}} = kt$$

(*ii*) The Avrami–Erofeyev (A–E) type equation with $n = 2$, *viz.*

$$[9] \qquad -\ln(1 - \alpha) = kt^2$$

as found for $ZnCl_2.3Cu(OH)_2$.

(*iii*) First order rate kinetics as observed for $CdCl_2.3Cu(OH)_2$.

The activation energy E_a values range from 34 to 74 kcal/mol. This wide range of values and compared to 18 kcal/mol for $Cu(OH)_2$, strongly suggests different mechanisms and activated complex configurations for $Cu(OH)_2$ dehydroxylation. This feature is a striking contrast to the apparently similar mechanism of dehydroxylation in the $Cd(OH)_2$ compounds.

The interpretation of the Arrhenius pre-exponential term A values parallels the analysis given above in an earlier report (23).

Calorimetric Measurements

The calorimetric results are presented in Table 5 according to the overall eqs. 3 and [4] for Cd–M and Cu–M compounds, respectively for the temperature range cited; the heat of formation of each compound is included.

The values of ΔH per mole of H_2O formed are lower for all the heterocationic Cd hydroxychlorides relative to the analogous value for $Cd(OH)_2$. On the other hand, the heterocationic Cu compounds exhibited slightly higher values for ΔH per mole of H_2O formed relative to that for $Cu(OH)_2$. The thermal stability of each heterocationic compound is greater than its parent hydroxide as evidenced by the higher decomposition temperature. It also can be concluded that the presence of the bivalent metal chloride MCl_2 has had a positive effect on strengthening the Cu—OH bond whereas the presence of MCl_2 in $Cd(OH)_2$ has significantly weakened the Cd—OH bond.

Can. J. Chem. Downloaded from www.nrcresearchpress.com by 210.87.254.5 on 09/05/12
For personal use only.

This study emphasizes the dependence of thermal stability of hydroxy-compounds on two distinct parameters: (*i*) a kinetic factor, related to the separation of OH groups and identified by the decomposition temperature range, and (*ii*) a thermodynamic factor, intimately linked to OH bond strength as indicated by the value of ΔH per mole of H_2O formed.

Grateful acknowledgment is made to the National Research Council of Canada for financial support of this research program.

1. O. K. SRIVASTAVA and E. A. SECCO. Can. J. Chem. **45**, 1375 (1967).
2. P. RAMAMURTHY and E. A. SECCO. Unpublished results.
3. P. RAMAMURTHY and E. A. SECCO. Can. J. Chem. **46**, 3605 (1968).
4. P. RAMAMURTHY and E. A. SECCO. Can. J. Chem. **48**, 2656 (1970).
5. P. RAMAMURTHY and E. A. SECCO. Can. J. Chem. **49**, 2813 (1971).
6. W. FEITKNECHT and K. MAGET. Helv. Chem. Acta, **32**, 1653 (1949).
7. G. DENK and J. ALT. Z. Anorg. Allg. Chem. **285**, 134 (1956).
8. T. S. WEST. Complexometry with EDTA and related reagents. 3rd ed. BDH Chemical Ltd., England Broglia Press. Bournemouth 1969. Chapt. 5, 8.
9. G. SCHWARZENBACH. Complexometric titrations. *Translated by* H. Irving. Methuen and Co. Ltd., London, 1957. Chapt. 6. pp. 51, 59.
10. R. B. FISHER and D. G. PETERS. Basic theory and practice of quantitative chemical analysis. 3rd ed. W. B. Saunders Co., Philadelphia. 1968. p. 439.
11. A. I. VOGEL. Textbook of quantitative inorganic analysis. 3rd ed. John Wiley and Sons Inc., New York. 1966. p. 266.
12. E. A. SECCO. Can. J. Chem. **42**, 2143 (1964).
13. A.S.T.M. File Index.
14. O. K. SRIVASTAVA and E. A. SECCO. Can. J. Chem. **45**, 579, 585 (1967).
15. P. RAMAMURTHY and E. A. SECCO. Can. J. Chem. **47**, 2185 (1969).
16. P. RAMAMURTHY and E. A. SECCO. Can. J. Chem. **47**, 1045 (1969).
17. T. BANSAGI, E. A. SECCO, O. K. SRIVASTAVA, and R. R. MARTIN. Can. J. Chem. **46**, 2881 (1968).
18. S. GLASSTONE, K. LAIDLER, and H. EYRING. Theory of rate processes. McGraw-Hill, New York. 1941. p. 100.
19. W. E. GARNER. Chemistry of the solid state. Butterworths, London. 1955. Chapt. 8.
20. P. M. FICHTE and T. B. FLANAGAN. Trans. Faraday Soc. **67**, 1467 (1971).
21. G. A. SOMORJAI and J. LESTER. Progress in solid state chemistry. Vol. 4. *Edited by* H. Reiss. 1967. p. 1.
22. H. F. CORDES. J. Phys. Chem. **72**, 2185 (1968).
23. P. RAMAMURTHY and E. A. SECCO. Can. J. Chem. **47**, 2181 (1969).
24. ERNEST M. LEVIN, CARL R. ROBBINS, and HOWARD F. MCMURDIE. Phase diagrams for ceramists. The American Ceramic Society, Inc. Columbus, Ohio. 1964. p. 375 No. 1250.

Can. J. Chem. Downloaded from www.nrcresearchpress.com by 210.87.254.5 on 09/05/12
For personal use only.

Etude par resonance magnetique des mouvements moléculaires dans l'acrylonitrile solide

BUU BAN
Laboratoire de Photophysique Moléculaire, Faculté des Sciences, 91, Orsay

ET

C. CHACHATY
Service de Chimie-Physique, C.E.N. de Saclay, B.P. N°2, 91, Gif sur Yvette

Reçu le 12 mars 1973

Les transitions de phase et les mouvements moléculaires de l'acrylonitrile solide et de son homologue deutérié CH_2=CDCN ont été étudiés entre 100 °K et le point de fusion (191 °K) par r.m.n. large bande et par des mesures du temps de relaxation T_1. La phase I (164° < T < 191 °K) est piégée sous forme métastable par refroidissement rapide de l'acrylonitrile à 77 °K. Elle donne la phase II stable entre 113 °K et 164 °K par recuit prolongé à 155–160 °K. Le passage de la phase II à la phase III, stable aux plus basses températures, s'effectue à 113 °K. La phase III peut être considérée comme rigide au-dessous de 105 °K. La phase II est caractérisée par un mouvement de libration des molécules autour d'un axe passant par l'azote et le milieu de la double liaison vinylique. En phase I, l'acrylonitrile effectue un mouvement de réorientation d'ordre deux autour de cet axe avec une énergie d'activation de 4.2 kcal mol^{-1}.

On a étudié également, par r.p.e., les mouvements moléculaires des radicaux péroxyles produits par addition d'oxygène sur les radicaux préalablement formés par irradiation γ à 77 °K. La variation de l'anisotropie de g avec la température ne présente aucune discontinuité aux transitions de phases et l'énergie d'activation de réorientation est seulement de 0.65 kcal mol^{-1} ce qui suggère qu'il s'agit de radicaux macromoléculaires dont on n'observe que la rotation interne.

Phase transitions and molecular motions in solid acrylonitrile and its deuterated homologue CH_2=CDCN, have been studied between 100 and 191 °K (m.p.) by wide line n.m.r. and by T_1 relaxation time measurements. Phase I (164 °K < T < 191 °K) is trapped and becomes metastable by quick cooling of acrylonitrile at 77 °K. It changes into the phase II, stable between 113 °K and 164 °K by a long duration annealing at 155–160 °K. The phase II → phase III transition occurs at 113 °K. It may be assumed that phase III, stable below this temperature, is rigid at T < 105 °K. Phase II may be characterized by a rotational oscillation of molecules around an axis defined by the N atom and the middle of the vinyl double bond. In phase I, acrylonitrile molecules undergo a binary reorientation motion around this axis with an activation energy of 4.2 kcal mol^{-1}. The motion of peroxy radicals, trapped in acrylonitrile has been also studied by e.s.r. These radicals were produced by oxygen addition to free radicals previously formed by γ irradiation of acrylonitrile at 77 °K. The g anisotropy variation with temperature, shows no discontinuities at phase transitions, the activation of reorientation of peroxy radicals being 0.65 kcal mol^{-1}. This result suggests that we are dealing in fact with macroradicals, the internal rotation of which is only observable in a solid matrix.

Can. J. Chem., **51**, 3889 (1973)

Introduction

L'acrylonitrile est le premier monomère vinylique dont la polymérisation amorcée par irradiation γ en phase solide, à basses températures, a été observée (1, 2). Tout de suite la question s'est posée de savoir si cette réaction n'a lieu qu'au point de fusion à 191 °K, où si elle se produit réellement en phase solide.

La calorimétrie (3) a permis une mise en évidence directe de la polymérisation en phase solide. Des mesures effectuées par cette méthode sur le monomère non irradié ont en outre montré l'existence d'une transition de phase à 160 °K. La diffraction de rayons X (4) indique que l'acrylonitrile possède en fait trois phases stables entre 77 °K et 191 °K: phase I entre 164 et 191 °K, phase II entre 113 °K et 164 °K, phase III en dessous de 113 °K.

Nous nous sommes donc proposés d'étudier par r.m.n. large bande et par relaxation nucléaire les mouvements moléculaires qui se produisent dans ces trois phases. Des mesures complémentaires de résonance paramagnétique électronique ont été effectuées pour étudier les mouvements de réorientation des radicaux libres formés par irradiation γ de ce monomère.

Can. J. Chem. Downloaded from www.nrcresearchpress.com by 210.87.254.40 on 09/05/12
For personal use only.

Can. J. Chem. Downloaded from www.nrcresearchpress.com by 210.87.254.40 on 09/05/12
For personal use only.

Conditions experimentales

L'acrylonitrile a été purifié par distillation en atmosphère d'azote, après séchage sur tamis moléculaire, puis dégazé et scellé sous vide. Nous avons utilisé également des échantillons d'acrylonitrile monodeutérié $CH_2{=}CD{-}CN$, le taux de deutériation en α du groupe CN étant d'environ 95%.

Les mesures de r.m.n. large bande ont été effectuées sur un spectromètre JEOL JNM W40 fonctionnant à 40 MHz. La température de l'échantillon était régulée à $\pm 1°$, au-dessus de 100 °K, par un jet d'azote gazeux refroidi. Quelques mesures à $T \leqslant 100$ °K ont été faites à 16 MHz à l'aide d'un spectromètre VARIAN V 4502 utilisable aussi bien en r.p.e. qu'en r.m.n. large bande grâce à l'adjonction d'une unité radiofréquence V 4210 A. Pour les expériences de r.p.e., les mesures du facteur g ont été effectuées par rapport à un échantillon de référence, en utilisant une cavité double V 4532 et en déterminant la valeur du champ magnétique à l'aide d'une sonde à résonance protonique Varian F8.

Le temps de relaxation T_1 des protons a été mesuré par écho de spin, à l'aide d'un spectromètre fonctionnant à 25 MHz, réalisé à l'Institut d'Electronique de la Faculté des Sciences d'Orsay. Nous avons utilisé la méthode des séquences 90°, τ, 90° pour $T_1 > 7$ s et la méthode de Carr et Purcell (5) pour $T_1 < 7$ s. Le système de variation thermique permettait de contrôler la température à ± 0.1 °K.

Resultats et interpretation

(1) Identification des phases

La variation de la largeur totale et du second moment de l'acrylonitrile normal en fonction de la température sont données sur la Fig. 1.

(*i*) Les portions (*a*) représentent les variations à température décroissante. Le prolongement du palier de la phase I vers les basses températures ($T < 164$ °K) indique que cette phase est "piégée" à basse température.

(*ii*) Les portions (*b*), celles à température croissante de 103 °K à 153 °K. Vers 153 °K on assiste à des variations irréversibles, le second moment varie brusquement de 5.5 G^2 à 7.5 G^2. Ceci indique le dépiégeage de la phase I métastable et l'apparition de la phase II, stable entre 115 et 164 °K.

(*iii*) Après ce recuit à 153 °K, les variations de la largeur de raie et du second moment en fonction de la température croissant de 103 °K à la température de fusion, sont représentées sur les portions (*c*).

La fig. 5 donne les variations de la largeur de raie et du second moment de l'A.N. monodeutérié, après recuit à 150–160 °K, en fonction de la température croissante.

La Fig. 6 représente la variation du temps de relaxation spin réseau T_1, pour un échantillon

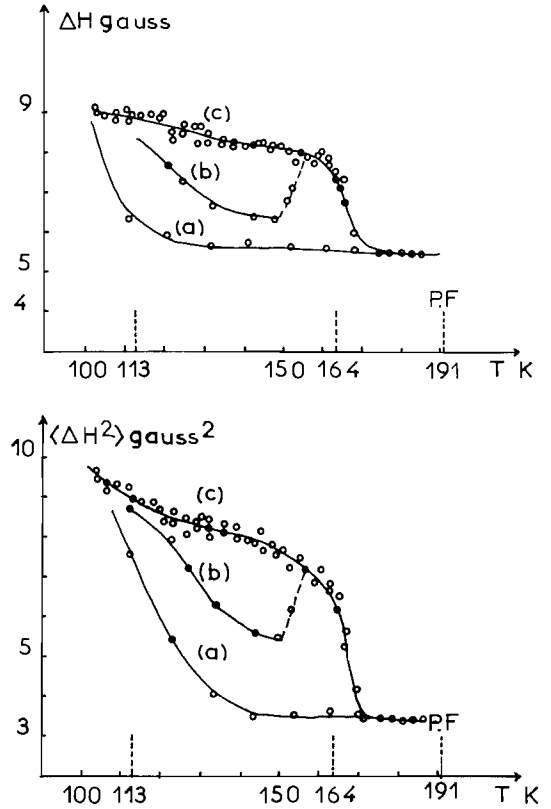

FIG. 1. Variation de la largeur (ΔH) et du second moment ($\langle \Delta H^2 \rangle$) du spectre de l'acrylonitrile normal en fonction de la température: (*a*) refroidissement progressif; (*b*) réchauffement jusqu'à 153 °K; (*c*) variation réversible avec la température jusqu'à 160 °K puis réchauffement jusqu'à 191 °K (P.F.).

après recuit à 153 °K en fonction de l'inverse de la température.

Les courbes $T_1 = f(T^{-1})$ présentent des variations nettes au voisinage de 113 °K et 164 °K confirmant ainsi l'existence des transitions de phases solide–solide à ces températures trouvées par d'autres techniques (3, 4): la phase III est située dans le domaine de températures inférieures à 113 °K; la phase II, obtenue après recuit à 153 °K est comprise entre 113 °K et 164 °K, et la phase I, comprise entre 164 °K et le point de fusion. La diminution du second moment vers 113 °K est moins brusque que celle vers 164 °K indiquant ainsi pour le premier cas une transition ordre–désordre libérant progressivement les mouvements moléculaires, et pour le deuxième cas une transition thermodynamique libérant brusquement les mouvements moléculaires (transition du 1er ordre).

Can. J. Chem. Downloaded from www.nrcresearchpress.com by 210.87.254.40 on 09/05/12
For personal use only.

(2) Etude par R.M.N. des mouvements moléculaires

(a) Acrylonitrile normal

Pour préciser les mouvements moléculaires se produisant dans chaque phase, nous devons connaître les données cristallographiques correspondantes. Or seules sont connues celles de la phase I (4). En supposant cette phase rigide la formule de Van Vleck (6) permet de calculer le second moment théorique:

$$[1]\quad \langle \Delta H^2 \rangle^{\text{rig}} = \frac{6}{5} I(I+1) g^2 \beta^2 N^{-1} \sum_{i<j} r_{ij}^{-6}$$
$$= 6.856\,\text{G}^2(\text{intra}) + 2.628(\text{inter})$$
$$= 9.48\,\text{G}^2$$

les distances interprotons étant calculées sur ordinateur IBM 360/91 d'après les données de Renaud (4) et de Reddy *et al.* (7). Pour la contribution intermoléculaire la sommation $\sum_{i<j} r_{ij}^{-6}$ s'effectue sur toutes les distances des protons situés à l'intérieur d'une sphère de 10 Å de rayon. A l'extérieur de cette sphère la sommation est remplacée par une intégrale dont la contribution est d'ailleurs négligeable (10^{-4} G^2).

En passant de la phase I à la phase III, on peut admettre que la géométrie de la molécule demeure invariante. Seule change alors la contribution intermoléculaire qui passe d'une valeur théorique de 2.63 G^2 à 3.2 G^2 si l'on admet une contraction volumique de l'ordre de 10%, ce qui nous donne un second moment total de 10 G^2. Le second moment experimental à 105 °K est de 9.5 G^2, donc très proche de la valeur théorique, ce qui indique que la phase III est rigide à cette température. A la transition III → II, $\langle \Delta H^2 \rangle$ n'est plus que de 9 G^2 et continue à décroître à mesure que l'on élève la température, sans atteindre de palier jusqu'à la transition II → I.

La décroissance du second moment dans les phases III et II peut être attribuée à des mouvements de libration d'amplitude de plus en plus grande. Etant donné la géométrie de la molécule, nous envisageons comme axe de libration, l'axe Δ passant par l'azote et par le milieu de la double liaison C=C (fig. 2). Ce choix est dicté par un "libre volume de rotation" maximum autour de cet axe ainsi que par un mouvement d'inertie plus faible ($I = 1.89 \times 10^{-39}$ g cm^2) que celui relatif aux axes N≡C ($I = 3.72 \times 10^{-39}$ g cm^2) et C=C ($I = 12 \times 10^{-39}$ g cm^2).

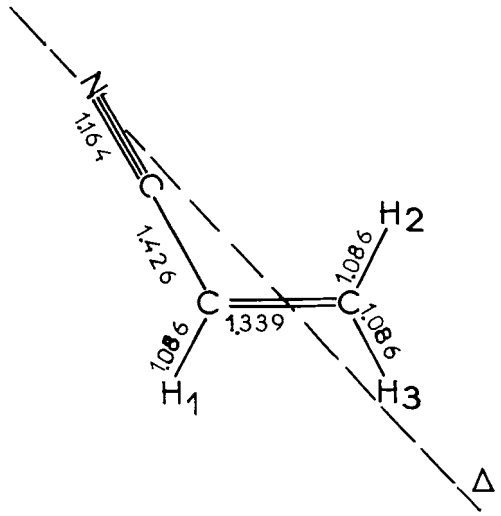

FIG. 2. Structure de la molécule d'acrylonitrile.

En outre l'axe Δ est pratiquement parallèle au vecteur moment dipolaire de la molécule (8) et à l'arête C de la maille cristalline de la phase I.

Le second moment intramoléculaire dans le cas d'une libration d'amplitude α est donné par la relation (9):

$$[2]\quad \langle \Delta H^2 \rangle^{\text{lib}} = \frac{3}{2} I(I+1) g^2 \beta^2 N^{-1} \sum_{i<j} B_{ij}$$

avec

$$B_{ij} = \frac{4}{5}\left[1 - \frac{3}{4}(1 - J_0^2(\alpha)) \sin^2 2\gamma_{ij} - \frac{3}{4}(1 - J_0^2(2\alpha)) \sin^4 \gamma_{ij}\right] r_{ij}^{-6}$$

γ_{ij} étant l'angle que fait la droite joignant les noyaux i, j avec l'axe de libration et α l'amplitude de libration. L'angle γ_{23} que fait l'axe Δ avec le vecteur interatomique $\overrightarrow{r_{23}}$, calculé à partir des données de Reddy (7) est de 41° 41′ (Fig. 2).

La fig. 3 donne la variation du second moment avec l'amplitude de libration α, calculée en admettant que le terme intermoléculaire se réduit dans la même proportion que le terme intramoléculaire donné par la relation 2. On constate ainsi que la décroissance de $\langle \Delta H^2 \rangle$ de 9 à 6 G^2 en phase II correspond à une variation d'amplitude de libration de 15° à 45° autour de l'axe Δ.

Pour préciser le mouvement de la phase I, nous avons envisagé des mouvements de réorientation d'ordre deux autour des liaisons N≡C, C=C et de l'axe Δ. La contribution intramolé-

Can. J. Chem. Downloaded from www.nrcresearchpress.com by 210.87.254.40 on 09/05/12
For personal use only.

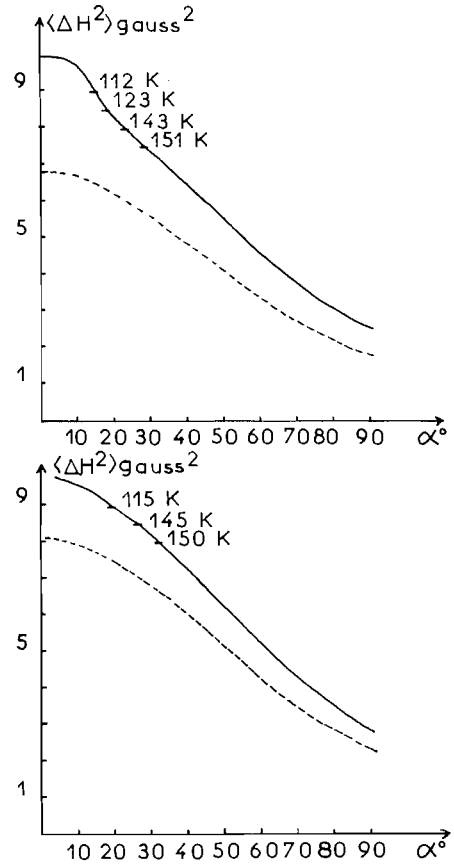

FIG. 3. Variation du second moment (---, intra, — total) en fonction de l'amplitude de libration de l'acrylonitrile normal (diagramme supérieur) et de l'acrylonitrile α deutérié (diagramme inférieur).

culaire au second moment se calcule alors d'après la formule de Eades (10):

$$[3]\quad \langle \Delta H^2 \rangle_{\text{intra}}^{\text{réor}} = \frac{6}{5} I(I+1) g^2 \beta^2 N^{-1} \times \sum_{i<j} (1 - 3\cos^2 \gamma_{ij} \sin^2 \gamma_{ij}) r_{ij}^{-6}$$

tandis que la contribution intermoléculaire se calcule en "projetant" les noyaux sur l'axe de réorientation. Nous obtenons ainsi pour les axes:

$$\text{N}\equiv\text{C},\ \langle \Delta H^2 \rangle_{\text{réor}} = 3.031\ \text{G}^2(\text{intra}) + 1.320\ \text{G}^2(\text{inter}) = 4.35\ \text{G}^2$$

$$\text{C}=\text{C},\ \langle \Delta H^2 \rangle_{\text{réor}} = 6.646\ \text{G}^2(\text{intra}) + 1.87\ \text{G}^2(\text{inter}) = 8.52\ \text{G}^2$$

$$\Delta,\ \langle \Delta H^2 \rangle_{\text{réor}} = 1.986\ \text{G}^2(\text{intra}) + 1.329\ \text{G}^2(\text{inter}) = 3.31\ \text{G}^2$$

La valeur 4.35 G^2 ne correspond à aucune valeur expérimentale; remarquons que la valeur 8.52 G^2 est égale à celle trouvée expérimentalement vers 125 °K (phase II), il serait alors tentant de caractériser la phase II par un mouvement de réorientation d'ordre deux autour de la liaison C=C, mais nous avons précédemment exclu cette éventualité à cause de l'encombrement stérique du réseau. D'autre part l'absence de palier du second moment dans la phase II rend difficile l'attribution d'un mouvement de réorientation (11) à cette phase.

Le second moment calculé pour la rotation de la molécule autour de l'axe Δ est par contre en excellent accord avec la valeur de 3.3 ± 0.1 G^2 obtenue pour la phase I. Renaud (4) pense qu'il y a diffusion des molécules en phase I, mais un tel mouvement, s'il existe n'affecterait qu'une très faible proportion des molécules puisqu'il ne parait pas influer sur le second moment.

(b) Acrylonitrile α deutérié

Dans tout le domaine de température étudié, le spectre r.m.n. de l'acrylonitrile ordinaire est un triplet (fig. 4). Une telle structure est difficilement interprétable à partir des données que l'on a sur l'interaction dipolaire entre les protons de cette molécule. On sait en effet que l'on peut observer un triplet dans le cas de trois protons équidistants (12) mais dans celui de l'acrylonitrile, la distance entre les protons géminaux H_2

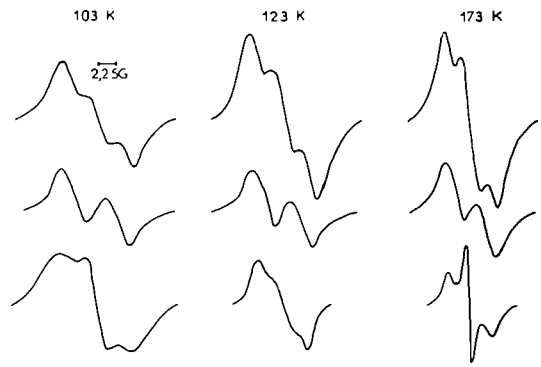

FIG. 4. Spectres r.m.n. de l'acrylonitrile: 1ère ligne, acrylonitrile normal, 2ème ligne, acrylonitrile deutérié, 3ème ligne, acrylonitrile normal irradié à 77 °K (dose 2 Mrads).

Can. J. Chem. Downloaded from www.nrcresearchpress.com by 210.87.254.40 on 09/05/12
For personal use only.

et H_3 (1.88 Å) est nettement plus faible que $d(H_1H_2) = 3.069$ Å et $d(H_1H_3) = 2.425$ Å. On pourrait éventuellement attribuer l'existence de la bande centrale à une certaine proportion de molécules en réorientation rapide, mais cela n'est en général observé qu'au voisinage des points de transition ou dans le cas de phases métastables.

Ceci nous a amenés à effectuer les mêmes expériences sur le produit monodeutérié CH_2CD—CN. Les spectres présentent une structure de doublet comme l'on s'y attend (voir fig. 4). Cette structure persiste pratiquement jusqu'au point de fusion. La variation de la largeur ΔH du doublet et du second moment en fonction de la température est représentée sur la fig. 5. Nous allons d'abord étudier la variation de ΔH en fonction des mouvements moléculaires envisagés pour l'A.N. normal.

Pour un réseau rigide, la largeur du doublet relatif aux protons géminaux H_2 H_3 sera (13):

$$[4] \qquad \Delta H_{rig} = \frac{3}{2} g\beta r^{-3} = 6.3\ \text{G}$$

La largeur expérimentale à 103 °K est de 4.5 G, la différence de 1.8 G avec la valeur théorique pour un réseau rigide correspond sans doute en grande partie à l'élargissement dipolaire des raies qui tend à rapprocher les sommets du doublet.

La diminution de la largeur du doublet devient sensible à partir de 115 °K. Dans le cas d'une paire de noyaux qui se réorientent rapidement entre deux directions extrêmes faisant entre elles un angle 2β, cette réduction est donnée par la relation (14):

$$[5] \qquad \rho = |1 - 3\sin^2\beta|$$

l'angle β étant lié aux angles α et γ définis plus haut par la relation

$$[6] \qquad \sin\beta = \sin\alpha \sin\gamma$$

prenons par exemple, $\alpha = 30°$, γ étant égal à 41°, 41′ on a $\beta = 19°$, 30′, $\rho = 0.67$ et donc $\Delta H = 4.2$ G. L'examen des figs. 1, 3, et 5 indique que cette valeur de α correspond à $T \sim 150$ °K. La valeur expérimentale de ΔH est de 3.8 G pour CH_2=CD—CN à cette température (fig. 5), donc en assez bon accord avec la valeur calculée plus haut si l'on considère l'élargissement des raies.

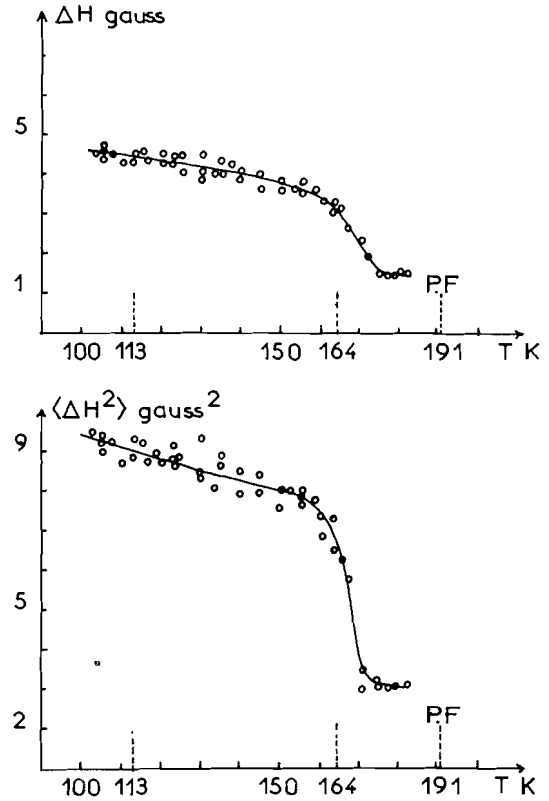

FIG. 5. Variation de ΔH et de $\langle \Delta H^2 \rangle$ en fonction de la température, pour l'acrylonitrile α deutérié.

La largeur du doublet diminue rapidement au voisinage de la transition II → I, à 164 °K, pour atteindre une valeur de 1.5 G en phase I. Dans l'hypothèse d'une réorientation de l'acrylonitrile autour de l'axe binaire Δ, en phase I, la largeur du doublet peut être encore calculée par la relation (5) dans laquelle β devient égal à γ puisque $\alpha = 90°$, et l'on obtient $\Delta H_{réor} = 2.07$ G comparable à la valeur expérimentale de 1.5 G.

Comme pour l'A.N. normal, nous avons calculé sur l'IBM 360/91 les seconds moments suivant la formule de Van Vleck (6) pour un échantillon polycristallin:

$$[7] \quad \langle \Delta H^2 \rangle = \frac{6}{5} I(I+1) g^2\beta^2 N^{-1} \sum_{i<j} r_{ij}^{-6} + \frac{8}{15} S(S+1) g_D{}^2\beta^2 N^{-1} \sum_{i<k}{}' r_{ik}^{-6}$$

La sommation $\sum_{i<j}$ s'effectue sur les protons i et j, $\sum'_{i<k}$ sur les protons i et les deuterons k dont $S = 1$ et $g_D = 0.8573$.

Can. J. Chem. Downloaded from www.nrcresearchpress.com by 210.87.254.40 on 09/05/12
For personal use only.

Pour la phase I supposée rigide

$$\langle \Delta H^2 \rangle_{rig} = 8.114\ G^2(\text{intra}) + 1.401\ G^2(\text{inter}) = 9.52\ G^2$$

Il est à remarquer que dans le second moment intramoléculaire, la contribution des protons géminaux est de loin la plus importante (8.08 G^2).

En admettant, comme précédemment, une contraction volumique de 10% lorsqu'on passe de la phase I à la phase III, nous trouvons un second moment intermoléculaire de 1.7 G^2 et donc un second moment global de 9.8 G^2, en bon accord avec la valeur de 9.4 G^2 obtenue à 103 °K.

Pour un mouvement de réorientation du vecteur r_{23} entre deux positions extrêmes faisant un angle 2β, le second moment devient (14):

$$[8] \quad \langle \Delta H^2 \rangle = \left| 1 - \frac{3}{4} \sin^2 2\beta \right| \langle \Delta H^2 \rangle_{rig}$$

ce qui nous donne pour l'angle $\beta = 19°30'$ envisagé précédemment pour $T = 150$ °K, $\langle \Delta H^2 \rangle = 7.96\ G^2$.

La fig. 3 donne la variation de $\langle \Delta H^2 \rangle_{lib.}$ en fonction de l'amplitude de libration α, calculée à partir de la relation (2) avec un terme supplémentaire relatif au deutéron, en supposant comme précédemment que les contributions intra et intermoléculaires varient dans la même proportion. Pour $\alpha = 30°$ on obtient ainsi $\langle \Delta H^2 \rangle_{lib.} = 6.79\ G^2$ (intra) + 1.42 G^2 (inter) = 8.21 G^2. Les relations 8 et 3 donnent donc des résultats très voisins, proches de la valeur expérimentale de $8 \pm 0.2\ G^2$, obtenue vers 150 °K.

Quand la molécule de $CH_2{=}CD{-}CN$ se réoriente autour de l'axe binaire Δ, en phase I, la relation de Eades (10) s'écrit:

$$[9] \quad \langle \Delta H^2 \rangle_{intra}^{réor} = \frac{6}{5} I(I+1) g_H{}^2 \beta^2 \times \frac{1}{2}(1 - 3\cos^2 \gamma_{23} \sin^2 \gamma_{23}) r_{23}{}^{-6} + \frac{8}{15} S(S+1) g_D{}^2 \beta^2 \times \frac{1}{3} \sum_{i=2,3} (1 - 3\cos^2 \gamma_{1i} \sin^2 \gamma_{1i}) r_{1i}{}^{-6}$$

La contribution intermoléculaire étant calculée en projetant les vecteurs intermoléculaires sur l'axe Δ, le second moment global devient:

$$\langle \Delta H^2 \rangle_{réor} = 2.11\ G^2(\text{inter}) + 0.887\ G^2(\text{inter}) = 3.0\ G^2$$

en excellent accord avec le résultat expérimental (fig. 5).

Les résultats relatifs à l'acrylonitrile deutérié recoupent donc bien ceux obtenus pour l'acrylonitrile normal et confirment l'hypothèse d'une libration (phase II) puis d'une rotation (phase I) de cette molécule autour de l'axe Δ.

(3) Temps de relaxation spin réseau

La variation du temps de relaxation spin–réseau T_1 en fonction de l'inverse de la température ($T^{-1} \times 10^3$) indique que dans les phases I et II (fig. 6), les mouvements moléculaires contribuent efficacement à la relaxation spin–réseau.

Pour un mouvement moléculaire pas trop lent, comme c'est le cas ici, et caractérisé par un temps de corrélation unique à une température donnée, la théorie de Bloembergen, Purcell, et Pound (15) revue par Kubo et Tomita (16) donne:

$$[10a] \quad T_1{}^{-1} = C\left\{\frac{\tau_c}{1 + \omega_0{}^2\tau_c{}^2} + \frac{4\tau_c}{1 + 4\omega_0{}^2\tau_c{}^2}\right\}$$

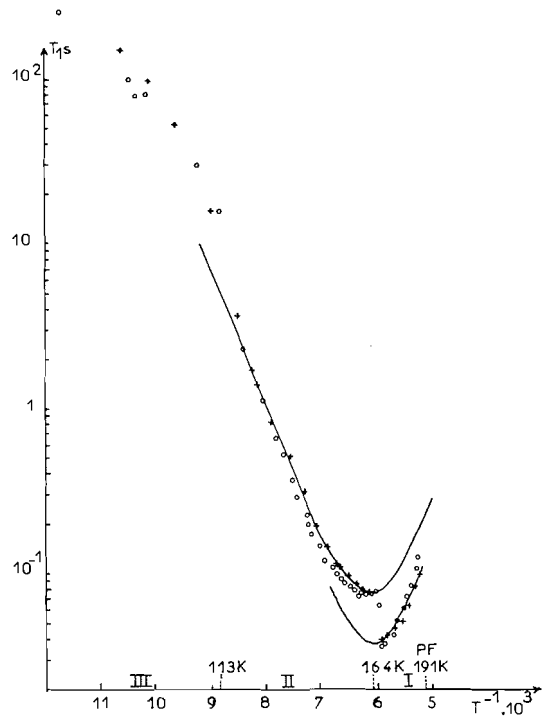

FIG. 6. Temps de relaxation spin réseau en fonction de la température: (+ + +) acrylonitrile normal, (○○○) acrylonitrile α deutérié. Le tracé continu correspond aux valeurs théoriques de T_1 calculées d'après les formules 10*a* et 11 (voir texte).

Can. J. Chem. Downloaded from www.nrcresearchpress.com by 210.87.254.40 on 09/05/12
For personal use only.

Si d'autre part τ_c suit la loi d'Arrhenius

[11] $$\tau_c = \tau_0 e^{E/kT}$$

les parties linéaires de la courbe $T_1 = f(T^{-1})$ permettent de calculer les énergies d'activation des mouvements moléculaires.

Pour l'A.N. normal, ces énergies sont de 4.2 et 3.7 kcal mol^{-1} respectivement pour les phases I et II.

La phase II possède un temps de relaxation minimum $T^{II}{}_{1\ min} = 78$ ms vers 163 K, le temps de corrélation correspondant est $\tau_c = 0.6158/\omega_o = 3.9 \times 10^{-9}$ s, le coefficient C de la formule 10*a* étant égal à $(\omega_0/1.425\ T^{II}{}_{1\ min}) = 1.4 \times 10^9\ s^{-2}$.

La variation brusque de T_1 vers 164 °K (fig. 6) s'explique bien par la transition de phase II → I qui libère le mouvement de réorientation de la molécule autour de l'axe binaire Δ comme nous avons vu dans la section 2.

Dans la phase I le temps de relaxation possède un minimum $T^{I}{}_{1\ min} = 38$ ms vers 164 °K.

Pour un mouvement de réorientation autour d'un axe binaire, le temps de relaxation spin réseau peut être décrit par la formule approchée (voir l'appendice pour les détails de calcul):

[10*b*] $$T_1^{-1} = \frac{3}{5}\gamma^4\hbar^2 I(I+1)N^{-1} \times \sum_{i<j}^{N} r_{ij}^{-6} \sin^2 2\gamma_{ij} \times \left\{\frac{\tau_c}{1+\omega_0^2\tau_c^2} + \frac{4\tau_c}{1+4\omega_0^2\tau_c^2}\right\}$$

Dans ce calcul de T_1 nous avons négligé la corrélation entre les mouvements des vecteurs internucléaires r_{12}, r_{13}, et r_{23}, c'est-à-dire supposé que la relaxation longitudinale est régie par une seule exponentielle.

Nous avons effectivement observé pour $T_1 > 7$ s que l'aimantation nucléaire décroit exponentiellement, par contre la méthode du "τ null" de Carr et Purcell (5), utilisée pour $T_1 < 7$ s ne permet pas de savoir si la décroissance est exponentielle ou non. Cependant, nous pensons que notre approximation n'est pas trop mauvaise, car la contribution essentielle à la relaxation provient du mouvement de r_{23}, $r_{23}{}^{-6}$ étant beaucoup plus grand que $r_{12}{}^{-6}$ et $r_{13}{}^{-6}$.

En ne considérant que la contribution intramoléculaire, nous trouvons d'après la relation 10*b* un T_1 théorique de:

$$T^{I}{}_{1\ min} = \frac{\omega_o}{1.425C} = 47\ \text{ms}$$

Cette valeur est supérieure à la valeur expérimentale 38 ms, ceci est dû sans doute à ce que nous avons négligé la relaxation croisée et la contribution intermoléculaire. Pour tenir compte de cette dernière contribution nous employons la relation (15):

[12] $$T_{1\ min} = \frac{\omega_0}{1.425C} = \frac{\omega_0}{1.425\gamma^2\langle\Delta H^2\rangle_{mod}}$$

où $\langle\Delta H^2\rangle_{mod}$ est le second moment modulé par le mouvement:

$$\langle\Delta H^2\rangle_{mod} = \langle\Delta H^2\rangle_{rig} - \langle\Delta H^2\rangle_{réor} = 10\ G^2 - 3.3\ G^2 = 6.7\ G^2$$

la formule 12 donne alors $T^{I}{}_{1\ min} = 35$ ms en bon accord avec la valeur expérimentale. Les courbes continues des fig. 6 et 7 sont calculeés à partir des relations 10*a* et 11, avec les valeurs

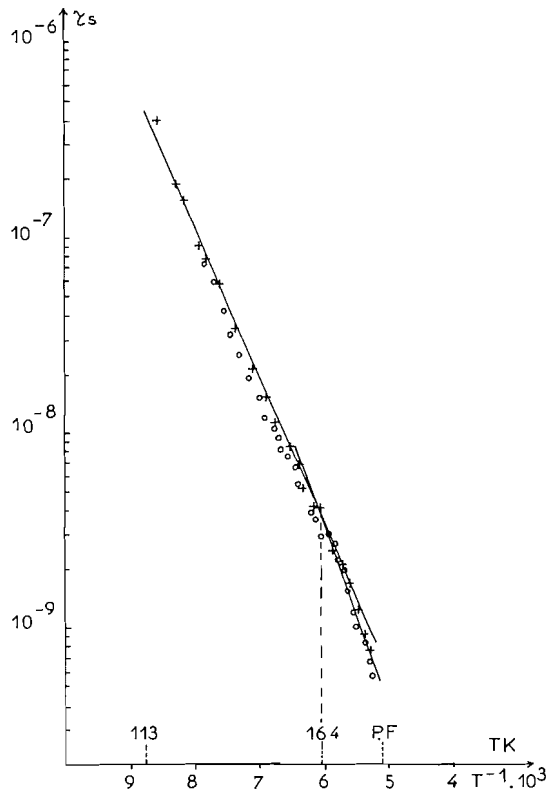

FIG. 7. Temps de corrélation de réorientation de l'acrylonitrile normal (+++) et de l'acrylonitrile deutérié (○○○).

Can. J. Chem. Downloaded from www.nrcresearchpress.com by 210.87.254.40 on 09/05/12
For personal use only.

experimentales de C et E relatives à l'A.N. normal.

L'allure générale des courbes $T_1 = f(T^{-1})$ et $\tau_c = f(T^{-1})$ (figs. 6 et 7), relative à l'A.N. α-deutérie est analogue à celle relative à l'A.N. normal. Ceci est prévisible quand on se rappelle que $\gamma_H/\gamma_D = 6.5$ et que les quantités $r_{DH_2}{}^{-6}$ et $r_{DH_3}{}^{-6}$ sont négligeables devant $r_{H_2H_3}{}^{-6}$.

Pour l'A.N. α-deutérié les énergies d'activation sont légèrement plus grandes que celles pour l'A.N. normal, respectivement de 4 kcal mol^{-1} et de 5 kcal mol^{-1} dans les phases II et I; et les T_1 minima sont légèrement plus petits (respectivement 72 ms et 35 ms dans les phases II et I).

Dans la phase I le $T_{1\,min}$ calculé d'après (10*b*) sera de

$$T^{I}{}_{1\,min} = \frac{\omega_0}{1.425C} = 39 \text{ ms}$$

tandis que la formule 12 avec:

$$\langle \Delta H^2 \rangle_{mod} = 9.8\ G^2 - 3.0\ G^2 = 6.8\ G^2$$

nous donne $T^{I}{}_{1\,min} = 34$ ms en bon accord avec la valeur expérimentale.

Remarquons cependant que l'hypothèse d'un τ_c unique à chaque température n'est pas tout à fait réaliste. L'étude par l'absorption diélectrique (17) en phase I montre en effet l'existence d'une distribution des temps de corrélation. Malheureusement l'absence des mesures du temps de relaxation spin réseau suivant le champs tournant $T_{1\rho}$ et des mesures de T_1 avec différentes fréquence ν_0 ne nous permet pas d'aller plus loin dans notre analyse.

(4) R.M.N. de l'acrylonitrile irradié

Les mesures à basses températures sont rendues difficiles par la longueur du temps de relaxation T_1 qui devient non négligeable par rapport à la durée normale d'enregistrement d'un spectre. Le procédé le plus efficace pour réduire T_1 consiste à irradier le composé étudié pour y former des radicaux libres (18). Nous avons tenté d'appliquer cette méthode à l'acrylonitrile en supposant que la polymérisation ne progresse rapidement qu'au voisinage du point de fusion, en phase I. Pour un échantillon refroidi rapidement à 77 °K et irradié à des doses de 1 à 2 Mrads, nous avons constaté que la phase I piégée ne donne pas la phase II par recuit à 150 °K, ce qui suggère que le polymère déjà présent dans la matrice inhibe la transition phase métastable → phase stable.

Si l'on recuit préalablement à l'irradiation le monomère de façon à obtenir la phase II puis au refroidissement la phase III, on constate que le second moment relatif à la phase II varie de 7 G^2 à 3 G^2 entre 113 et 164 °K (fig. 8) alors qu'il est compris entre 9 G^2 et 6.5 G^2 pour le monomère non irradié. Cela confirme l'existence d'un polymérisation à ces basses températures, qui contribue à désorganiser le réseau.

En outre, on observe à la transition II → I (fig. 4) la croissance quasi instantanée d'une raie étroite ($\Delta H = 0.3$ G), superposée au spectre normal, et caractéristique de certaines polymérisations en phase solide (19) attribuable à la réorientation rapide des molécules dans les défauts du réseau créés par les chaînes croissantes de polymère (19). L'amplitude de cette raie atteint une valeur limite en quelques minutes. Ce

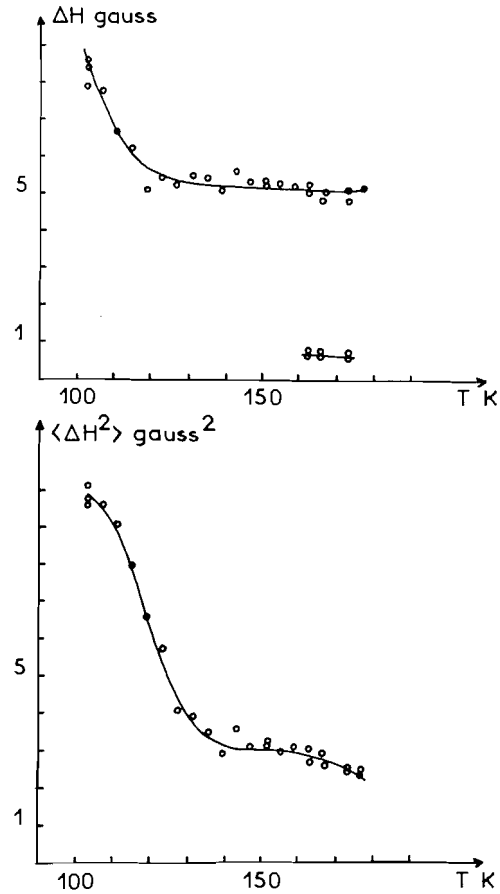

FIG. 8. Variation de ΔH et de $\langle \Delta H^2 \rangle$ avec la température pour l'anylonitrile normal irradié à 77 °K (dose 2 Mrads) après recuit à 153 °K.

Can. J. Chem. Downloaded from www.nrcresearchpress.com by 210.87.254.40 on 09/05/12
For personal use only.

fait est à rapprocher des résultats de mesures calorimétriques de Tal'Roze et coll. (20) qui ont mis en évidence une durée de croissance des chaînes de l'ordre de 30 s à la transition II → I (qu'ils situent à 157 °K et non à 164 °K).

(5) Résonance paramagnétique électronique

La résonance paramagnétique électronique des radicaux provenant de l'irradiation γ de l'acrylonitrile a fait l'objet de plusieurs travaux (21–24). Selon Bensasson et coll. (21, 22) le radical $CH_3\dot{C}H$—CN est initialement formé à 77 °K. Il disparaît au réchauffement par addition sur le monomère et formation du radical macromoléculaire ~~CH_2—$\dot{C}H$—CN (21, 22). Bol'shakov et coll. (24) ont proposé une interprétation différente du spectre de R.P.E. qu'ils attribuent à la présence des radicaux CH_3—$\dot{C}H$—CN et CH_2=$\dot{C}$—CN, ne participant pas à la polymérisation, qui serait donc exclusivement ionique. La réduction du second moment des spectres de ces radicaux leur a permis de mesurer une énergie d'activation de réorientation qu'ils supposent égale à celle des molécules de la matrice. Cette méthode nous paraît contestable car la contribution relative des différents radicaux au second moment peut varier avec la température du fait de leur vitesse différente de recombinaison. En outre le terme prédominant du second moment provient du couplage isotrope des protons, invariant avec la réorientation globale d'un radical.

Pour éviter ces difficultés, nous avons irradié l'acrylonitrile en présence d'oxygène et réchauffé les échantillons jusqu'à peroxydation complète des radicaux.

L'échantillon était alors trempé à 77 °K et subissait par la suite un traitement analogue à celui effectué par les expériences de r.m.n.

La structure des spectres r.p.e. des radicaux peroxyles ne dépend que de l'anisotropie du tenseur g, approximativement axial selon la liaison O—O·. En matrice rigide à 77 °K, la position des singularités correspondant aux valeurs principales de g (fig. 9) nous donne $g_{\parallel} = 2.0360$, $g_{\perp} = 2.00285$ et $g_{iso} = 2.0139$. La réduction progressive de l'anisotropie de g avec la température permet de mesurer le temps de corrélation de réorientation d'un radical (25). Cette méthode a été précédemment appliquée au cas de radicaux peroxyles (26, 27). et nous allons brièvement en rappeler le principe.

Pour un mouvement de réorientation isotrope,

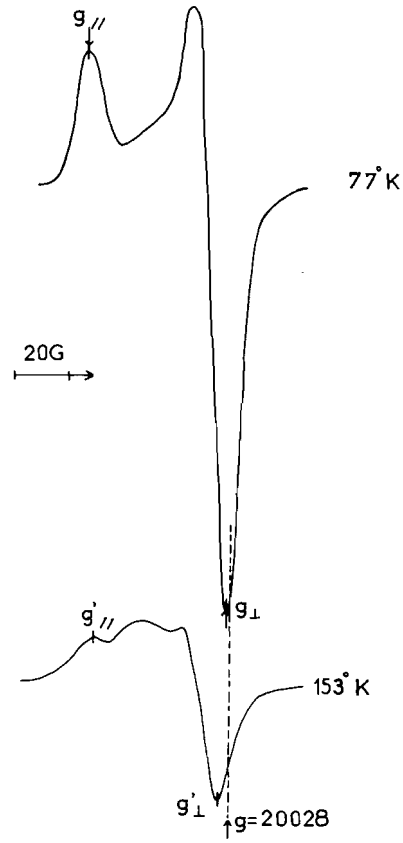

FIG. 9. Spectres r.p.e. des radicaux peroxyles piégés dans l'acrylonitrile.

les singularités $g_{\parallel}$ et $g_{\perp}$ convergent progressivement vers la position correspondant à $g_i = 1/3\,(g_{\parallel} + 2\,g_{\perp})$ le déplacement de la singularité $g_{\parallel}$ étant le plus facilement mesurable. En présence d'un mouvement de réorientation, de temps de corrélation τ_c, la position de cette singularité est donnée par la relation (25, 26):

$$[13]\quad g_{\parallel}'^2 = S + (g_{\parallel}^2 - S)\frac{2}{\pi}\arctan\frac{\tau_c}{T_2}$$

avec

$$S = \frac{1}{3}(g_{\parallel}^2 + 2g_{\perp}^2)_{rig}$$

T_2 étant le temps de relaxation dipolaire électronique que l'on peut déduire de la largeur homogène des raies, déterminée à partir de leur largeur réelle par des expériences de saturation progressive. Cette méthode n'étant pas applicable puisque les signaux ne se saturent pas pour le champ radiofréquence maximum dont nous disposons ($H_1 \sim 1$ G), nous avons évalué T_2 à

5×10^{-8} s d'après des études analogues effectuées sur d'autres monomères vinyliques (28).

On peut également déterminer τ_c à partir de la relation (13), en mesurant le second moment des spectres dont la valeur théorique est (29):

$$[14] \quad \langle \Delta H^2 \rangle = \frac{{H_0}^2}{5}\left(\varepsilon_{\parallel}'^2 + \frac{8}{3}\varepsilon_{\perp}'^2 + \frac{4}{3}\varepsilon_{\parallel}'\varepsilon_{\perp}'\right) + \frac{\lambda^2}{4}$$

avec

$$\varepsilon_{\parallel}' = \frac{g_{\parallel}'}{g_0} - 1 \qquad \varepsilon_{\perp}' = \frac{g_{\perp}'}{g_0} - 1 = \frac{1}{2}(3\varepsilon_i - \varepsilon_{\parallel})$$

H_0 étant le champ de résonance de l'échantillon de référence, correspondant dans le cas présent à $g_0 = 2.0028$. λ est la largeur gaussienne des raies égale en moyenne à 6 G dans le domaine de température étudié. A 77 °K en matrice rigide, la valeur théorique de $\langle \Delta H^2 \rangle$ pour $H_0 = 3280$ G est de 599 G^2. Entre 77 et 180 °K, le second moment expérimental décroît d'une manière continue de 610 G^2 à 500 G^2.

La variation de τ_c avec la température permet de mesurer l'énergie d'activation de réorientation. La comparaison des résultats obtenus par mesure du déplacement du pic $g_{\parallel}'$ et par mesure du second moment, permet d'évaluer la largeur de la distribution des énergies d'activation (27). Dans le cas présent les résultats obtenus par les deux méthodes coïncident ce qui indique une distribution étroite des temps de corrélation. On a obtenu ainsi $E = 0.65 \pm 0.05$ kcal mol^{-1} avec un terme préexponentiel $\tau_0 = (2.3 \pm 0.4)\ 10^{-2}$ $T_2 \sim 10^{-9}$ s (fig. 10).

L'énergie d'activation est donc très inférieure à celle trouvée par écho de spin pour la réorientation des molécules de la matrice en phase II ($E = 3.7$ kcal mol^{-1}) et correspond plus vraisemblablement à la rotation du groupement peroxyle qu'à la réorientation globale du radical. Ce résultat, joint au fait que la variation de l'anisotropie de g et celle de $\langle \Delta H^2 \rangle$, ne présentent aucune discontinuité au voisinage des transitions de phase suggère que les radicaux dont on a observé la peroxydation sont en fait des macroradicaux conformément à l'interprétation de Bensasson et coll. (21, 22) et non des radicaux monomères tels que CH_3 $\dot{C}H$—CN ou $CH_2{=}\dot{C}$—CN comme le proposent Bolshakov et coll. (24), ce qui n'exclut pas d'ailleurs la prédominance d'un mécanisme ionique de polymérisation (24).

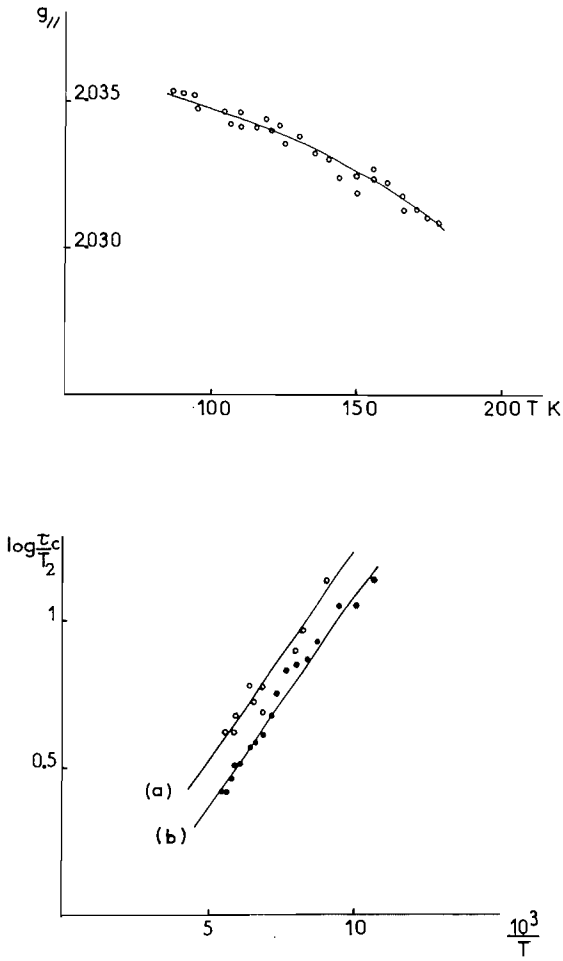

FIG. 10. Diagramme supérieur: variation de $g_{\parallel}'$ avec la température; Diagramme inférieur: temps de corrélation de réorientation des radicaux peroxyles en fonction de $1/T$: (*a*) calculés à partir de $\langle \Delta H^2 \rangle$ (relations 13 et 14); (*b*) calculés à partir de $g_{\parallel}'$ déterminé directement sur les spectres.

Les auteurs remercient vivement M. Guibé, Maître de Recherche à l'Institut d'Electronique de la Faculté des Sciences d'Orsay, qui a eu l'obligeance de mettre à leur disposition un spectromètre à écho de spin, ainsi que M. Truong, Ingénieur au C.N.R.S., pour son aimable coopération expérimentale. Ils remercient également M. Herbert, Ingénieur au C.E.A., qui a bien voulu synthétiser l'acrylonitrile deutérié, ainsi que l'un des rapporteurs de cet article, pour ses remarques et suggestions, qui nous ont été très utiles.

Appendice

Nous partons de la relation, pour une paire de noyaux (11):

Can. J. Chem. Downloaded from www.nrcresearchpress.com by 210.87.254.40 on 09/05/12
For personal use only.

Can. J. Chem. Downloaded from www.nrcresearchpress.com by 210.87.254.40 on 09/05/12
For personal use only.

$$[1]\quad T_1^{-1} = \frac{3}{2}\gamma^4\hbar^2 I(I+1)\{J^{(1)}(\omega_0) + J^{(2)}(2\omega_0)\}r^{-6}$$

Les fonctions densité spectrale $J^{(k)}$ étant des transformées de Fourier des fonctions d'auto corrélation

$$[2]\quad J^{(k)}(\omega_k) = \int_{-\infty}^{\infty} \langle F^{(k)}(t)F^{(k)}(t+\tau)\rangle\, e^{-i\omega_0\tau}\, d\tau$$

avec les fonctions aléatoires (30)

$$[3]\quad F^{(1)}(t) = (1 + im)n \qquad F^{(2)}(t) = (1 + im)^2$$

l,m,n étant des cosinus directeurs du vecteur internucléaire $\boldsymbol{r}$ par rapport à un système d'axes fixes $S(\boldsymbol{X},\boldsymbol{Y},\boldsymbol{Z})$ avec $\boldsymbol{Z}||\boldsymbol{H}_0$. Nous repérons $\boldsymbol{r}$ dans un système $S'(\boldsymbol{X}',\boldsymbol{Y}',\boldsymbol{Z}')$ lié à la molécule par $\boldsymbol{r} = r(\sin\gamma\boldsymbol{X}' + \cos\gamma\boldsymbol{Z}')$, avec $\boldsymbol{Z}'$ pris parallèle à l'axe de réorientation Δ. Le système S'est relié au système S par des angles d'Eluler θ,φ,ψ et le passage de S' à S se fait par la matrice

$$[4]\quad M = \begin{vmatrix} \cos\varphi\cos\psi - \sin\varphi\sin\psi\cos\theta & -\cos\varphi\sin\psi - \sin\varphi\cos\psi\cos\theta & \sin\varphi\sin\theta \\ \sin\varphi\cos\psi + \cos\varphi\sin\psi\cos\theta & -\sin\varphi\sin\psi + \cos\varphi\cos\psi\cos\theta & -\cos\varphi\sin\theta \\ \sin\psi\sin\theta & \cos\psi\sin\theta & \cos\theta \end{vmatrix}$$

Compte tenu de (4), (3) s'écrit:

$$[5]\quad \begin{aligned} F^{(1)}(t) &= \{\sin^2\gamma\sin\theta\sin 2\psi + \sin 2\gamma\cos\theta\cos\psi \\ &\quad + i[\sin^2\gamma\sin 2\theta\sin^2\psi - \cos^2\gamma\sin 2\theta + \sin 2\gamma\cos 2\theta\sin\psi]\}e^{i\varphi}/2 \\ F^{(2)}(t) &= \{\sin^2\gamma\cos^2\psi - \sin^2\gamma\sin^2\psi\cos^2\theta - \cos^2\gamma\sin^2\theta + \tfrac{1}{2}\sin 2\gamma\sin 2\theta\sin\psi \\ &\quad + i[\sin^2\gamma\cos\theta\sin 2\psi - \sin 2\gamma\sin\theta\cos\psi]\}e^{i2\varphi} \end{aligned}$$

Soit $p(\psi,t)$ la probabilité de trouver $\boldsymbol{r}$ dans l'orientation ψ à l'instant t et $p(\psi',t)$ la probabilité de trouver $\boldsymbol{r}$ dans l'orientation ψ' à l'instant t. Supposons qu'il y a équiprobabilité pour que $\boldsymbol{r}$ passe de ψ' à ψ et de ψ à ψ'

$$W_{\psi\to\psi'} = W_{\psi'\to\psi} = W$$

nous aurons les équations d'évolution suivantes

$$[6]\quad \frac{dp(\psi,t)}{dt} = -Wp(\psi,t) + Wp(\psi',t) \qquad \frac{dp(\psi',t)}{dt} = Wp(\psi,t) - Wp(\psi',t)$$

A un instant quelconque t il est évident que

$$p(\psi,t) + p(\psi',t) = 1$$

par suite (6) a comme solution

$$[7]\quad p(\psi,t) = \frac{1}{2}(1 + Ce^{-t/\tau_c}) \qquad p(\psi',t) = \frac{1}{2}(1 - Ce^{-t/\tau_c})$$

$\tau_c = (2W)^{-1}$ étant défini comme temps de corrélation.

Nous définissons les probabilités conditionnelles suivantes: $P(f,i,\tau)$: probabilité de trouver $\boldsymbol{r}$ dans une orientation f à l'instant $t+\tau$, sachant qu'à l'instant t $\boldsymbol{r}$ se trouve dans l'orientation i. Comme il y a quatre combinaisons possibles pour le couple (f,i)

$$P(\psi,\psi,\tau) = p(\psi,\tau) \text{ avec } p(\psi,0) = 1 \text{ en prenant } t = 0$$

$$[8]\quad \begin{aligned} P(\psi',\psi',\tau) &= p(\psi',\tau) \text{ avec } p(\psi',0) = 1 \\ P(\psi',\psi,\tau) &= p(\psi',\tau) \text{ avec } p(\psi',0) = 0 \\ P(\psi,\psi',\tau) &= p(\psi,\tau) \text{ avec } p(\psi,0) = 0 \end{aligned}$$

compte tenu de (7), (8) devient alors

$$P(\psi,\psi,\tau) = P(\psi',\psi',\tau) = \frac{1}{2}(1 + e^{-\tau/\tau_c})$$

$$P(\psi',\psi,\tau) = P(\psi,\psi',\tau) = \frac{1}{2}(1 - e^{-\tau/\tau_c})$$

Dans le calcul des fonctions d'auto corrélation nous devons tenir compte de ces quatre possibilités

$$\langle F^{(k)}(0)F^{(k)}(\tau)\rangle = \sum_{(f,i)=\psi,\psi'} F^{(k)}(0)p(i,0)F^{(k)}(f,i,\tau)P(f,i,\tau)$$

et les fonctions de densité spectrale deviennent

$$J^{(1)}(\omega_0) = A\frac{\tau_c}{1 + \omega_0{}^2\tau_0{}^2}$$

$$J^{(2)}(2\omega_0) = B\frac{\tau_c}{1 + 4\omega_0{}^2\tau_c{}^2}$$

avec

$$A = \frac{1}{16}\{\sin^2\gamma\sin\theta(\sin 2\psi' - \sin 2\psi) + \sin 2\gamma\cos\theta(\cos\psi' - \cos\psi)^2 + \sin^2\gamma\sin 2\theta(\sin^2\psi' - \sin^2\psi) + \sin 2\gamma\cos 2\theta(\sin\psi' - \sin\psi)^2\}$$

$$B = \frac{1}{4}\sin^2\gamma(\cos^2\psi' - \cos^2\psi) - \sin^2\gamma\cos^2\theta(\sin^2\psi' - \sin^2\psi) + \frac{1}{2}\sin 2\gamma\sin 2\theta(\sin\psi' - \sin\psi)^2 + \sin^2\gamma\cos\theta(\sin 2\psi' - \sin 2\psi) - \sin 2\gamma\sin\theta(\cos\psi - \cos\psi')^2\}$$

Pour un échantillon polycristallin nous devons moyenner A et B dans tout l'espace, et en posant $\psi' - \psi = \alpha$ nous obtenons

$$T_1{}^{-1} = \frac{3}{20}\gamma^4\hbar^2 I(I+1)[\sin^4\gamma(1 - \cos 2\alpha) + \sin^2 2\gamma(1 - \cos\alpha)] \times \left\{\frac{\tau_c}{1 + \omega_0{}^2\tau_c{}^2} + \frac{4\tau_c}{1 + 4\omega_0{}^2\tau_c{}^2}\right\} r^{-6}$$

rappelons que γ étant l'angle que fait $\boldsymbol{r}$ avec l'axe de réorientation Δ.

Dans le cas où Δ est un axe binaire

$$T_1{}^{-1} = \frac{3}{10}\gamma^4\hbar^2 I(I+1)\sin^2 2\gamma \times \left\{\frac{\tau_c}{1 + \omega_0{}^2\tau_c{}^2} + \frac{4\tau_c}{1 + 4\omega_0{}^2\tau_c{}^2}\right\} r^{-6}$$

En supposant qu'il n'y a pas de relation de phase entre les mouvements des divers $\boldsymbol{r}_{ij}$, nous pouvons écrire

$$T_1{}^{-1} = \frac{3}{5}\gamma^4\hbar^2 I(I+1)N^{-1}\sum_{i<j}\sin^2 2\gamma_{ij} r_{ij}{}^{-6} \times \left\{\frac{\tau_c}{1 + \omega_0{}^2\tau_c{}^2} + \frac{4\tau_c}{1 + 4\omega_0{}^2\tau_c{}^2}\right\}$$

1. R. Bensasson et R. Marx. J. Polym. Sci. **48**, 53 (1961).
2. N. Sobue et Y. Tabata. J. Polym. Sci. **43**, 459 (1960).
3. R. Bensasson, A. Dworkin, et R. Marx. J. Polym. Sci. C. **4**, 881 (1963).
4. M. Renaud. Thèse Doctorat d'Etat. Paris, 1968.
5. H. Y. Carr et E. M. Purcell. Phys. Rev. **94**, 630 (1954).
6. J. H. Van Vleck. Phys. Rev. **74**, 1168 (1948).
7. R. H. Reddy, J. H. Goldstein, et L. Mandell. J. Am. Chem. Soc. **83**, 1300 (1961).
8. C. C. Costaing et B. P. Stoicheff. J. Chem. Phys. **30**, 777 (1959).
9. E. R. Andrew. J. Chem. Phys. **18**, 607 (1950).
10. R. G. Eades. Thèse de Ph.D. Université de St. Andrews, 1952.
11. A. Abragam. Les principes du magnétisme nucléaire. Presses Universitaires de France. 1968.
12. E. R. Andrew et R. Bersohn. J. Chem. Phys. **18**, 159 (1950).
13. G. E. Pake. J. Chem. Phys. **16**, 327 (1948).
14. E. R. Andrew et J. R. Brookeman. J. Magn. Res. **2**, 259 (1970).
15. N. Bloembergen, E. M. Purcell, et R. V. Pound. Phys. Rev. **73**, 679 (1948).
16. R. Kubo et K. Tomita. J. Phys. Soc. Jap. **9**, 888 (1954).
17. B. Bechet-Patte. Thèse 3e cycle. Faculté des Sciences d'Orsay, 1967.
18. C. Brot. Comptes rendus du Xe colloque Ampère. Leipzig. 1961. North Holland Publ., Amsterdam. 1962. p. 318.
19. C. Chachaty, A. Forchioni, et Buu Ban. J. Polym. Sci. Part B, **9**, 483 (1971).
20. D. A. Kritskaya, A. N. Ponomarev et V. L. Tal'roze. Khim. Vyz. Energ. **4**, 332 (1970).
21. R. Marx et R. Bensasson. J. Chim. Phys. **56**, 673 (1960).
22. R. Bensasson, A. Bernas, M. Bodard, et R. Marx. J. Chim. Phys. **60**, 950 (1963).
23. Yoon Jin Chung, Keiji Takeda, et Ffrancon Williams. Macromolecules, **3**, 264 (1970).
24. A. I. Bol'shakov, V. P. Mel'nikov, A. I. Mikhailov, I. M. Barkalov, et V. I. Goldanskii. Khim. Vys. Energ. **5**, 57 (1971).
25. F. K. Kneubühl. J. Chem. Phys. **33**, 1074 (1960).
26. S. Moriuchi, N. Nakamura, S. Shimada, H. Kashiwabara, et J. Sohma. Polym. **11**, 630 (1970).
27. Buu Ban, C. Chachaty, M. Renaud, et R. Fourme. Can. J. Chem. **49**, 2953 (1971).
28. C. Chachaty et A. Forchioni. J. Polym. Sci. Part A1, **10**, 1905, 1923 (1972).
29. R. Lefebvre et J. Maruani. J. Chem. Phys. **42**, 1480 (1965).
30. D. E. Woessner. J. Chem. Phys. **36**, 1 (1962).

Can. J. Chem. Downloaded from www.nrcresearchpress.com by 210.87.254.40 on 09/05/12
For personal use only.

Chain Length Determination of Fatty Acids by Raman Spectroscopy

CHARLES H. WARREN AND DONALD L. HOOPER
Department of Chemistry, Dalhousie University, Halifax, Nova Scotia

Received June 15, 1973

For saturated long chain fatty acids, as for hydrocarbons, the odd order "accordion mode" vibrations are Raman active. These "accordion mode" vibrations have been used to provide qualitative and quantitative analysis of mixtures of acids in the range C_{12}–C_{24}.

Pour les acides gras à longue chaîne de même que pour les hydrocarbures, les vibrations d'ordre impaire du "type accordéon" sont actives en Raman. Ces vibrations ont été utilisées pour analyser qualitativement et quantitativement des mélanges d'acides de C_{12} à C_{24}.

[Traduit par le journal]

Can. J. Chem., **51**, 3901 (1973)

The room temperature infrared spectrum of a long chain fatty acid in the solid phase exhibits in the region 1180–1350 cm^{-1} a characteristic "progression" of bands spaced about 20 cm^{-1} apart. The number of bands in such a progression, assigned to the —CH_2— wagging motion, has been correlated with the number of $-CH_2-$ units in the hydrocarbon chain of the fatty acid. This correlation has been used (1) as the basis of an infrared method of chain length determination, although this region of the spectrum is partially obscured by the 1307 cm^{-1} peak attributed to the C—O—H linkage of free acids. This peak is, of course, not present in the spectrum of the alkali metal salt of a fatty acid, and in general more reliable results are obtained (2) by conversion of the fatty acid to the soap. Even if this is done, it is difficult to identify the components of a mixture of acids having different chain lengths, as there are many absorption peaks for each chain length, some of which may overlap the peaks of other chain lengths. Quantitative analysis of chain length distribution of such a mixture is almost impossible.

Schaufele *et al.* (3) have reported that the Raman scattering spectra of short chain polymethylenes show a series of bands below 600 cm^{-1} whose frequency varies inversely with chain length. These Raman active transitions arise from the longitudinal acoustical vibration (l.a.) of the carbon skeleton and the overtones of l.a. They are represented as the symmetric longitudinal accordion-like motion of an extended zig-zag carbon chain (Fig. 1). The Raman wavenumber shifts $\Delta\tilde{\nu}$ for these vibrations are approximately linear in (m/n) where m is the order of the vibration and n is the number of carbon atoms in the chain. The fundamental l.a. vibration ($m = 1$) is the most intense of the series observed for a particular chain length, with the intensities of the overtones approximately proportional to $(1/m)$. Only overtones corresponding to odd values of m are observed, as to a first approximation, even values of m correspond to vibrations that give no change in the molecular polarizability.[1] For each chain length, n, there are only a limited number of frequencies intense enough for observation and these frequencies are different from the frequencies observed for other chain lengths. For very long chain hydrocarbons the frequency differences are sufficiently great to allow identification of different hydrocarbons in a mixture.

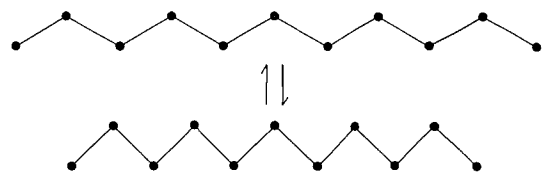

FIG. 1. The l.a. accordion mode of an extended normal hydrocarbon molecule.

As the carboxyl group of a fatty acid should act as only a small perturbation on the accordion-like motion of the hydrocarbon chain, a Raman investigation of fatty acids should give a simple relation between the wavenumber shifts of l.a. modes and the chain length with the possibility of using this correlation in the identification of acids. We wish to report such an investigation for the fatty acids in the range of chain lengths

[1]This selection rule will be relaxed slightly for fatty acids since the replacement of one methyl group of the polymethylenes by a carboxyl group reduces the symmetry of the molecule.

Can. J. Chem. Downloaded from www.nrcresearchpress.com by 210.87.254.105 on 09/05/12
For personal use only.

Can. J. Chem. Downloaded from www.nrcresearchpress.com by 210.87.254.105 on 09/05/12
For personal use only.

(C_{12}–C_{24}) of the acids derived from natural oils. The results indicate the possibility of using the l.a. modes for both qualitative and quantitative analysis of fatty acid mixtures.

Experimental

The fatty acids used in this investigation were commercial samples used without further purification after a g.l.c. check of the purity. Raman spectra were recorded for each acid in the solid state at room temperature. The polycrystalline powder, pressed into a small pellet, was placed on a Spex 180° viewing platform. The 4880 Å line (*ca.* 800 mW) of a Carson Model 101 Argon-ion laser was used as the incident light source, and light scattered at 180° to the incident radiation was collected and focussed on the entrance slit (*ca.* 3 cm^{-1}) of a Spex 1401 double monochromator containing two 1200 lines/mm gratings blazed at 5000 Å. A photon counting detection system consisting of a Bendex Channeltron Photon counter tube and an SSR amplifier–discriminator and ratemeter was used to provide the output to the recorder. Some of the spectra were also recorded in digital form through the use of an interface which couples the monochromator and the associated photon detection system to a Wang 700C programmable calculator. The interface and capability of the resulting system have been previously described (4). The spectral data in digital form were stored on a Wang 710 Disc Drive. The advantages of this latter method are that background and frequency correction, digital smoothing and peak location can be performed automatically.

Raman spectra were also recorded for mixtures of fatty acids. These mixtures were prepared by weighing out the individual components, melting them together, and then pressing the cooled mixture into a pellet.

A high background scattering is frequently encountered in the Raman spectra of polymeric samples (5, 6). The background intensity decays with time and does not reappear when the laser is temporarily extinguished provided the sample is kept in the same position. This phenomenon was observed with a number of our samples. Although the decay rate varies from sample to sample it was found that satisfactory spectra could be obtained after the samples were illuminated with the incident laser light for approximately 30 min. There was no evidence of any sample deterioration by the laser and the spectra were reproducible.

Results and Discussion

Figure 2 shows the 0–600 cm^{-1} portion of the Raman spectrum of a typical saturated straight chain fatty acid. Although there is a sloping baseline resulting from background scattering, the l.a. frequencies corresponding to $m = 1, 3, 5$ are observed.[2] The wavenumber shifts measured from such spectra are accurate to ± 2 cm^{-1} and in each case the frequency observed for a fatty acid is similar to, but slightly shifted from, the corresponding frequency in the hydrocarbon of the same chain length.

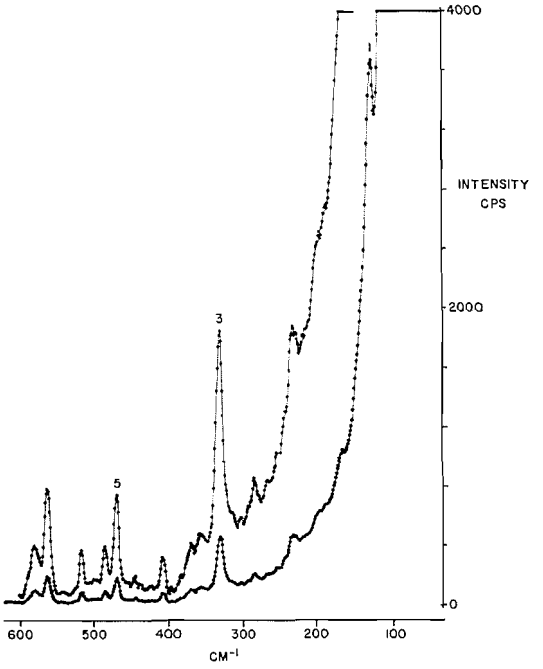

FIG. 2. Raman scattering by crystalline $C_{20}H_{40}O_2$.

Schaufele *et al.* showed that the frequencies of the accordion modes for finite polymethylene chains could be fitted to a polynomial in (m/n) of the form

$$[1] \quad \Delta\tilde{\nu} = A_1 + A_2(m/n) + A_3(m/n)^2 + ... + A_7(m/n)^6$$

For small values of m/n the linear term is sufficient, but for $m/n > \sim 0.08$ the higher order terms in m/n must be included. The observed l.a. modes for the fatty acids were also found to obey an equation of the form [1] with values of the parameters A_1–A_7 determined from a least squares treatment of the experimental frequencies. Figure 3 shows the dependence of frequency on the ratio (m/n) for the l.a. modes of fatty acids. The least squares treatment of the data enabled us to verify the assignment of some of the less intense overtones. Table 1 compares the observed frequencies for the C_{12}–C_{24} acids with those calculated from eq. 1. The simplest application of both Fig. 3 and Table 1 would be in the identification of a single fatty acid. Since the fundamental and the overtones ($m = 3, 5$) are generally observed, the presence of all three

[2]In a number of the longer chain acids, overtones corresponding to $m = 2, 4, 6$ were observed, but with an intensity much less than that of the odd overtones.

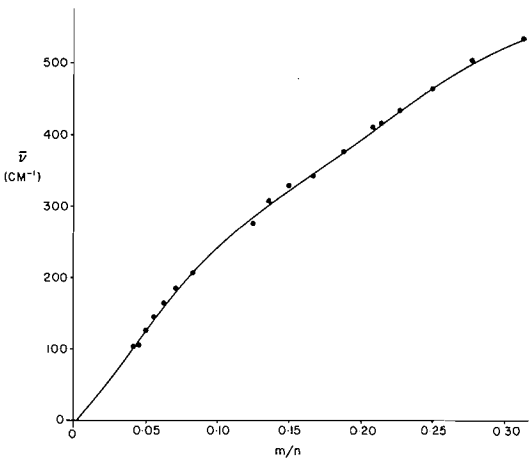

FIG. 3. Low frequency Raman bands plotted as a function of m/n.

TABLE 1. Longitudinal acoustical accordion mode frequencies of straight chain fatty acids

		$\Delta\bar{\nu}$(cm^{-1})	
n	m	Observed	Calculated
12	1	206	208
	3	465	468
14	1	184	181
	3	417	416
16	1	164	159
	3	377	377
	5	535	536
18	1	145	141
	3	343	347
	5	505	502
20	1	126	126
	3	329	323
	5	465	468
22	1	105	113
	3	307	303
	5	435	436
24	1	103	103
	3	276	286
	5	411	408

bands could be used to confirm the estimate of chain length, even in the presence of impurities.

Figure 4 shows part of the Raman spectrum observed for a mixture of myristic, palmitic, and stearic acids. The labelled peaks in this figure correspond to the $m = 3$ transition of each fatty acid. For detection of the components of a mixture of chain lengths, the fundamental l.a. frequencies could be used, but their relatively greater intensity is obscured by the very strong Rayleigh line. The overtones corresponding to $m = 5$ transitions are so much weaker that for a multicomponent mixture these peaks are almost lost in background noise.

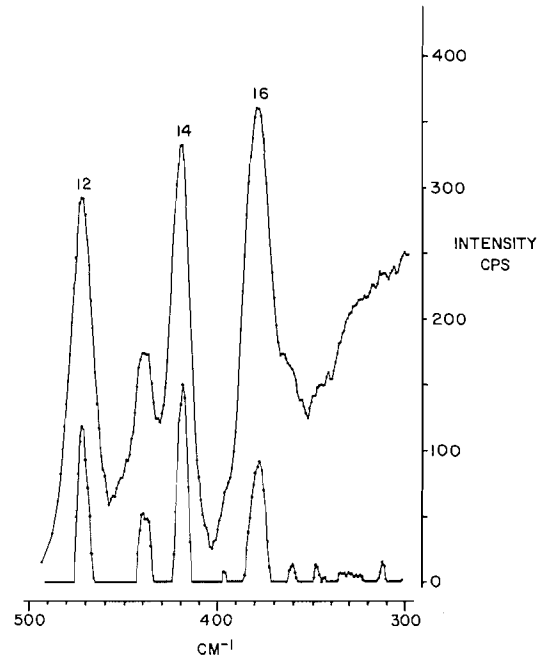

FIG. 4. Observed $m = 3$ overtones (upper curve) for a mixture of $C_{12}H_{24}O_2$, $C_{14}H_{28}O_2$, and $C_{16}H_{32}O_2$. The lower curve represents the negative of the second derivative of the upper curve.

Comparison of the ratio of peak heights in the spectra of mixtures of palmitic and stearic acid with the ratio of mole fractions of the two acids showed an approximate linear relation between the two ratios, but the difficulty of measuring accurate peak heights above a sloping baseline introduces considerable error if this method were to be used for the quantitative analysis of mixtures. The problem of the sloping base line was minimized by measuring the negative portion of the 2nd derivative spectrum, which is also illustrated in Fig. 4. The second derivative spectrum is obtained from the original digitized spectrum (4) by using the procedure of Savitsky and Golay (7, 8). Although the second derivatives of peaks wouldn't be expected to be strictly proportional to the peak height, a much better linear relation was found between the ratios of the second derivatives of the palmitic and stearic $m = 3$ peaks and the mole fraction ratios in our mixtures of

Can. J. Chem. Downloaded from www.nrcresearchpress.com by 210.87.254.105 on 09/05/12
For personal use only.

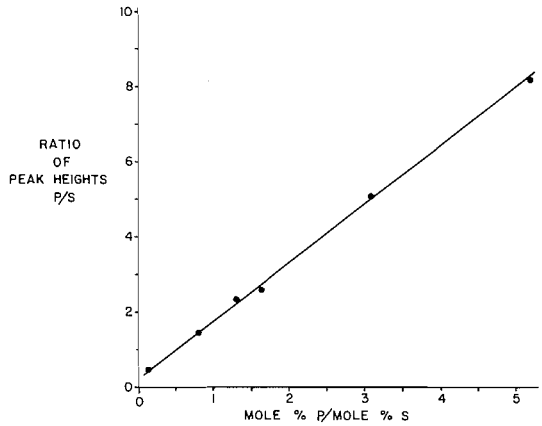

FIG. 5. Ratio of the 2nd derivative peak heights of the $m = 3$ overtones *vs.* the ratio of their mole percentages for mixtures of palmitic and stearic acids.

the two acids. Figure 5 illustrates this relation, which is linear to within experimental error. If second derivative spectra are used, quantitative analysis by the Raman method is both accurate and straightforward.

The superiority of the Raman over infrared methods of chain length determination has been demonstrated. No derivative formation is required, mixtures may be analyzed as well as single acids, and the percentage of each acid in a mixture is easily determined. This should be of interest to those interested in the chain length determination of acids derived from naturally occurring oils, most probably as an adjunct to the different chromatographic methods of analysis.

This work was supported by the National Research Council of Canada.

1. R. N. JONES, A. F. MCKAY, and R. G. SINCLAIR. J. Am. Chem. Soc. **74**, 2575 (1952).
2. R. A. MEIKELJOHN, R. J. MEYER, S. M. ARONOVIC, H. A. SCHNETTE, and V. W. MELOCH. Anal. Chem. **29**, 329 (1953).
3. R. F. SCHAUFELE and T. SHIMANOUCHI. J. Chem. Phys. **47**, 3605 (1967).
4. C. H. WARREN and L. RAMALEY. Appl. Opt. **12**, 1976 (1973).
5. M. J. GALL, P. J. HENDRA, D. S. WATSON, and C. J. PEACOCK. Appl. Spectrosc. **24**, 423 (1971).
6. J. E. D. DAVIES, P. HODGE, J. A. BARVE, F. D. GUNSTONE, and I. A. ISMAIL. J. Chem. Soc. Perkin II, 1557 (1972).
7. A. SAVITZKY and M. J. E. GOLAY. Anal. Chem. **36**, 1627 (1964).
8. J. STEINIER, Y. TERMONIA, and J. DELTOUR. Anal. Chem. **44**, 1909 (1972).

Can. J. Chem. Downloaded from www.nrcresearchpress.com by 210.87.254.105 on 09/05/12
For personal use only.

Spectrum, Kinetics, and Radiation Chemical Yield of Solvated Electrons in Hexamethylphosphoric Triamide

ERIC A. SHAEDE AND LEON M. DORFMAN
Department of Chemistry, The Ohio State University, Columbus, Ohio 43210

AND

GARRY J. FLYNN AND DAVID C. WALKER
Department of Chemistry, The University of British Columbia, Vancouver 8, British Columbia

Received June 29, 1973

The spectrum, yield, and kinetics of solvated electrons in hexamethylphosphoric triamide were investigated by the pulse radiolysis method. The optical absorption band is in the infrared with a maximum at 2200 ± 100 nm. The molar absorptivity at this maximum is (3.2 ± 0.5) × 10^4 M^{-1} cm^{-1}, and the oscillator strength for the transition is estimated to be $f = 0.7 \pm 0.2$. A free ion yield of $G(e_s^-) = 2.3 \pm 0.4$ solvated electrons/100 eV was determined from the observed yields of anthracene and pyrene radical anions formed by electron attachment.

Kinetic studies provided values of the rate constants for the reaction of solvated electrons with anthracene and N_2O. The decay mechanism of the solvated electrons in the absence of added solutes was found to be complex, and the half-life (in the range of 2 to 50 μs) was dependent on experimental conditions. A second transient species, absorbing at wavelengths below 500 nm, was observed but not identified. In solutions containing bromide ion the species Br_2^- was observed. The pulse radiolysis of stable solutions of e_s^-, formed by dissolving sodium metal in HMPA, is also reported.

On a étudié le spectre, le rendement ainsi que la cinétique d'électrons solvatés dans le triamidure d'hexaméthyl phosphore (HMPA) à l'aide de la méthode de radiolyse par pulsations. La bande d'absorption optique se situe dans l'infrarouge avec un maximum se trouvant à 2200 ± 100 nm. La capacité d'absorption molaire à ce maximum est de (3.2 ± 0.5) × 10^4 M^{-1} cm^{-1} et la force de l'oscillateur pour la transition est évaluée à $f = 0.7 \pm 0.2$. Un rendement en ion libre de $G(e_s^-) = 2.3 \pm 0.4$ électrons solvatés/100 eV a été déterminé à partir des rendements observés pour la formation, par fixation d'un électron, d'anions radicalaires de l'anthracène et du pyrène.

Des études cinétiques ont permis d'obtenir les constantes de vitesse pour la réaction d'électrons solvatés avec l'anthracène et le N_2O. Le mécanisme de disparition des électrons solvatés en absence de solutés ajoutés s'est révélé complexe et le temps de demi-vie (variant de 2 à 50 μs) est dépendant des conditions expérimentales. Une seconde espèce transitoire, absorbant à des longueurs d'onde inférieures à 500 nm, a été observée mais n'a pu être identifiée. Dans des solutions contenant l'ion bromure, on a observé la présence de l'espèce Br_2^-. On discute aussi de la radiolyse par pulsations des solutions stables de e_s^-, formées par dissolution de sodium métallique dans du HMPA.

[Traduit par le journal]

Can. J. Chem., **51**, 3905 (1973)

Introduction

Information about the physical characteristics of solvated electrons, with particular attention to the optical properties in solvents (1–4) of widely differing molecular structure and dielectric behavior, is useful in assessing the validity of theoretical models (5) which have been postulated to describe these species. Hexamethylphosphoric triamide (HMPA) is a particularly interesting solvent since it is a liquid of moderately high dielectric constant which solvates negative ions extremely weakly and positive ions very strongly (6). Studies of the chemical behavior of solvated electrons by pulse radiolysis of pure liquids may have general implications in many areas of chemistry because of the possible role of these species as intermediates in reactions such as the Birch reduction, in electrochemical processes, and in electron transfer reactions. Information about the ability of a solvent to stabilize electrons, and about the reactivity of these species toward other materials, is thus of interest.

HMPA, $[(CH_3)_2N]_3PO$, is an aprotic solvent with a macroscopic dielectric constant of 30 at 20 °C and a large dipole moment (5.3 D at 25 °C). Alkali metals dissolve in HMPA to form relatively stable solutions of solvated electrons that are characterized by an optical absorption band in the infrared (7, 8) and by narrow e.s.r.

Can. J. Chem. Downloaded from www.nrcresearchpress.com by 210.87.254.40 on 09/05/12
For personal use only.

Can. J. Chem. Downloaded from www.nrcresearchpress.com by 210.87.254.40 on 09/05/12
For personal use only.

lines (9, 10). There is evidence that solvated electrons may be produced in HMPA at the surface of a noble metal cathode by electrolysis of LiCl solutions (11).

There have been two recent studies on various aspects of solvated electrons formed by pulse radiolysis of HMPA (12, 13) which suggest the absorption band occurs at $\lambda > 1500$ nm. We report here a pulse radiolysis investigation of the physical and chemical properties of solvated electrons in which the wavelength range studied covers the region of the absorption band maximum. Some of the results are in general qualitative agreement but are substantially different in certain important respects from those already published (12, 13).

Experimental

Pulse radiolysis experiments utilized 4 MeV electrons from a Varian V7715A electron linear accelerator. The details of the apparatus have been described earlier (14). Pulse widths ranged from 10 to 1200 ns with a dose rate of about 10^{19} rad s^{-1}. Transient optical absorption measurements involved the use of one of several photomultiplier tubes (RCA 7200, 7102, 1P28) for wavelengths below 1200 nm, and an indium antimonide photodiode with fast response circuitry (4) for wavelengths between 800 and 2300 nm. The 10–90% risetime of the fast infrared detector was about 100 ns with a somewhat longer 1% settling time. For some experiments where time resolution of about 5 ns was required, a photomultiplier system (RCA 1P28 or HTV 196) with a 2 ns risetime was used with a Fairchild 777V dual beam oscilloscope. A Tektronix 545 dual beam oscilloscope was also used. A 500W xenon arc which could be flashed in synchronization with the electron pulse was used as light source. In the majority of the experiments Suprasil quartz cells with a 20 mm optical path contained the samples; sometimes with two light passes were used. Thin Vitrosil cells (3 mm) allowed for measurements in the infrared region to nearly 2300 nm where the solvent absorption was great. Bausch and Lomb high intensity grating monochromators were utilized for wavelength selection over the entire spectral region. Appropriate Corning glass filters were placed in the optical path before the cell to prevent photolysis of the solutions and in front of the monochromator to eliminate second order and scattered light. A 0.1 M aqueous KSCN solution saturated with nitrous oxide was used for dosimetry. The transient species absorbing at 500 nm was monitored and the value (15) of $G\varepsilon^{500} = 4.2 \times 10^4\ M^{-1}\ cm^{-1}$ molecule $(100\ eV)^{-1}$ was used to calculate the absorbed dose in water. As a secondary dosimeter, hydrated electrons were observed in pure water samples at 715 nm where $G\varepsilon^{715}$ was taken (ref. 16, p. 42) to be $5.0 \times 10^4\ M^{-1}\ cm^{-1}$ molecule $(100\ eV)^{-1}$. The dose absorbed by the HMPA samples was obtained by correcting for the relative electron densities of water and HMPA. Pulse to pulse reproducibility of the accelerator was generally better than $\pm 5\%$ of the mean. The two dosimetry methods gave results within 10% of each other and an average of the values was used in the calculations.

Purification of HMPA involved stirring Dow Chemical Company "Dorcol" brand HMPA with metallic sodium under vacuum until a dark blue solution of solvated electrons had been formed. The sodium solution was then fractionally distilled under vacuum, vacuum fractionated and the middle portion collected in an evacuated flask equipped with a Teflon stopcock. Samples were then prepared by re-distilling the HMPA from the storage flask directly into the radiolysis cells under vacuum. The samples were finally subjected to a multiple freeze–thaw procedure to remove residual traces of dissolved oxygen.

All chemicals used as scavengers were analytical reagent grade or better. Pyrene and anthracene were Aldrich "Gold Label" zone refined grade rated at 99.9+% purity. Nitrous oxide was purified by trap-to-trap distillation on a vacuum line and solutions were prepared by freezing measured quantities into the radiolysis cells. The concentration of dissolved N_2O was then calculated from an empirical solubility relationship (17).

Results and Discussion

Transient Absorption Spectra

Figure 1 shows the spectrum obtained from measurements of the optical absorption at the end of 400 or 500 ns electron pulses in pure HMPA over the wavelength range 300–2300 nm. The data represent the results of several series of experiments using both the 3 mm and 20 mm optical pathlengths with appropriate normalization. The inset of Fig. 1 is a representative example of the quality of the transient signals used in the spectral mapping. It was obtained at 2150 nm with a 3 mm optical path using a 500 ns pulse. 2300 nm represents the long wavelength limit of our detection capability as a result of solvent absorption and decrease in emission intensity of the light source.

A single species contributed the absorbance over the wavelength range from 500 to 2300 nm as is evident from the fact that the decay characteristics of the transient absorptions were identical over this wavelength range. This infrared absorption band may be assigned fairly confidently to the solvated electron because of the following observations. The lifetime of the absorption was drastically reduced by even trace amounts of oxygen, nitrous oxide, pyrene, and anthracene, all of which are good electron scavengers. Radical anions of the aromatic compounds were formed in the scavenging process. The spectrum of Fig. 1 is furthermore very similar to that reported for solvated electrons in sodium solutions in HMPA over the

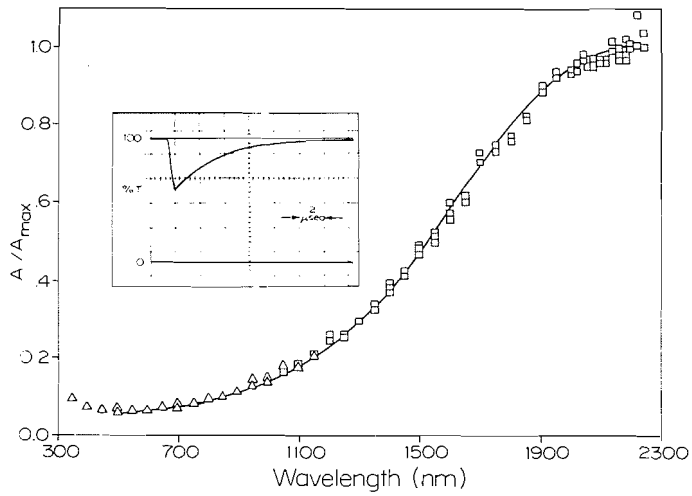

FIG. 1. Absorption spectrum of e_s^- in HMPA produced by pulse radiolysis. □, 3 mm cell, 500 ns pulse and InSb diode detector; △, 40 mm path length, 400 ns pulse and photomultiplier detector (normalized over the region 900–1150 nm). A_{max} represents the absorbance at 2200 nm. At $\lambda < 500$ nm another species, in addition to e_s^-, also contributes to the absorption. Inset: typical oscilloscope trace at 2150 nm using InSb detector.

wavelength range 1000–2300 nm (8) when these two spectra are normalized at 1500 nm.

We conclude that the maximum of the absorption is at 2200 ± 100 nm. The data shown in Fig. 1 strongly suggest that the maximum is at 2200 nm or at a slightly longer wavelength. The maximum is so near our long wavelength detection limit (2300 nm) as to preclude an unequivocal determination of λ_{max} directly. A confirmation of the value of λ_{max} may, however, be obtained independently by an extrapolation of data for the binary solution HMPA–ethylenediamine, as had been done with various ethers (4). λ_{max} for the binary solutions changes monotonically between the maxima for the pure liquids. Extrapolation to pure HMPA, as in Fig. 2, gives $\lambda_{max} = 2150 \pm 100$ nm in agreement with the value from Fig. 1.

Below 500 nm at least one other species contributes to the absorbance. By using nitrous oxide to remove the electron absorption, the contribution of e_s^- below 500 nm was shown to decrease over the wavelength range 500 to 300 nm.

Despite its substantial dielectric constant, HMPA apparently solvates electrons only very weakly as is evident from the transition energy of only 0.57 eV at the absorption band maximum. In this regard, HMPA seems similar to dimethylsulfoxide, another strongly polar, aprotic solvent, which solvates electrons very weakly, giving rise to a near-infrared absorption band

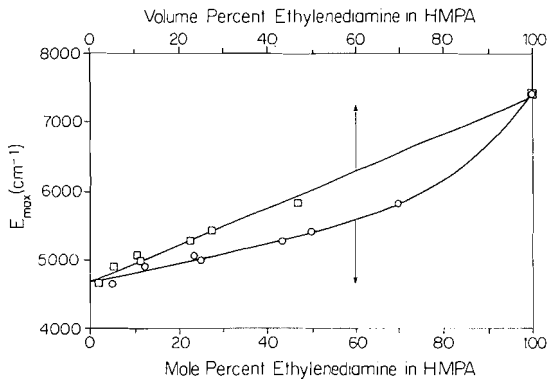

FIG. 2. Absorption maximum of the solvated electron in the binary liquid system ethylenediamine–HMPA. The energy of the band maximum (units of cm^{-1}) is plotted against (*i*) mol % ethylenediamine, ○; and (*ii*) vol % ethylenediamine, □. The extrapolation to pure HMPA gives $\lambda_{max}^{HMPA} = 2150$ nm.

(18). The absorption band shape in HMPA also closely resembles that observed for solvated electrons produced by pulse radiolysis in several weakly polar aprotic ethers (4) and low temperature glassy hydrocarbons (19). Very weak solvation of electrons in HMPA may be rationalized by considering the fact that the positive end of the P=O dipole is diffused over the three dimethylamine groups. Furthermore, the molecule is so bulky that cavities already present in the liquid, or induced by the excess electrons, will necessarily be quite large, thereby con-

Can. J. Chem. Downloaded from www.nrcresearchpress.com by 210.87.254.40 on 09/05/12
For personal use only.

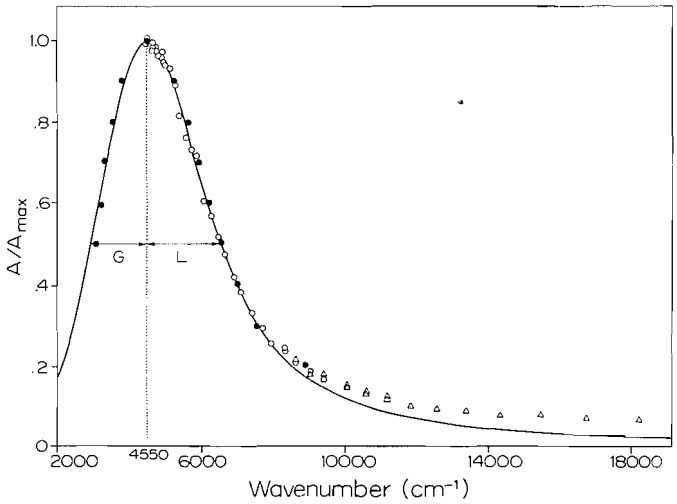

FIG. 3. Combined Gaussian-Lorentzian fit to the observed absorption spectrum plotted on an energy scale. Data same as Fig. 1 plus the published data for Na solution in HMPA (8) represented by ●, the filled circles. G and L represent half of the independently variable "half-widths" for the functions described in the text and give the half-width for the total absorption band of only 3600 cm^{-1} (0.45 eV).

ferring an extended charge distribution commensurate with the infrared absorption band. If a calculation of the vacancy size in the liquid is made for a tetrahedral configuration of four dipole-oriented HMPA molecules, it is found to be a hole of radius 5 Å. Indeed, any fit of a continuum-cavity model requires a cavity radius of about 4 Å for this band. This large cavity size may be contrasted with calculated radii between 1–2 Å for solvated electrons in water and alcohols.

It has been shown (20) that a Gaussian–Lorentzian shape function may be used to curve-fit solvated electron absorption band data. In Fig. 3 the function

$$y(\bar{\nu}) = \exp\left\{-\frac{\ln 2(\bar{\nu}_m - \bar{\nu}_i)^2}{(H_{1/2}{}^G)^2}\right\} \quad \text{for } \bar{\nu}_i < \bar{\nu}_m$$

$$y(\bar{\nu}) = \frac{(H_{1/2}{}^L)^2}{(H_{1/2}{}^L)^2 + (\bar{\nu}_i - \bar{\nu}_m)^2} \quad \text{for } \bar{\nu}_i > \bar{\nu}_m$$

is shown fitted to the data from Fig. 1 plotted on an energy scale taking $\bar{\nu}_m = 4550\ cm^{-1}$ corresponding to $\lambda_{max} = 2200$ nm as reference point. $H_{1/2}{}^G$ and $H_{1/2}{}^L$ are the independently variable "half-widths" for the Gaussian and Lorentzian functions shown as *G* and *L* in Fig. 3. Also included in Fig. 3 is the spectrum obtained by Brooks and Dewald (8) for the sodium solution in HMPA over the wavelength range 1000–3200 nm. The data indicate that the presence of sodium does not perturb the spectrum either with respect to shape on the high energy side or to the position of λ_{max}. Below 1000 nm other species besides e_s^- contribute to the absorption in sodium solutions. The deviation of the solvated electron spectrum from the Lorentzian function in the high energy region has recently been noticed in several amines and ethers (4).

The half-width of the absorption band in HMPA is 3600 cm^{-1} (0.45 eV) as is evident from Fig. 3. This value is similar to that in tetrahydrofuran (4), but smaller than that observed for many other solvated electron bands. Half-widths in the range from 0.7 to 1.5 eV are generally found for e_s^- in alcohols, water, and amines. The electron band in ammonia is narrower at half-height, with $W_{1/2} = 3100\ cm^{-1}$ (0.39 eV) (20).

Mal'tsev *et al.* (12) and Nauta and van Huis (13) have both observed the tail of the absorption band over the spectral range 500 to 1500 nm which they attributed to e_s^-. When their data are compared with that of Fig. 1 the shape coincides quite well for ref. 13 (but rather poorly for ref. 12) when normalized at 1500 nm; but the absolute intensities differ considerably.

The other species which contributed to the transient absorption in pulse-irradiated HMPA at wavelengths below 500 nm was not identified. It was substantially longer lived than the absorption of the solvated electron, as noted previously (13), but its decay was complex and kinetic data

Can. J. Chem. Downloaded from www.nrcresearchpress.com by 210.87.254.40 on 09/05/12
For personal use only.

Can. J. Chem. Downloaded from www.nrcresearchpress.com by 210.87.254.40 on 09/05/12
For personal use only.

suggested it may have been involved in the decay mechanism of the solvated electron. Low concentrations of hydrogen, water, or methanol had no observable effect on this transient absorption, nor on that due to e_s^-. Addition of bromide ion led to the formation of Br_2^- which masked the absorption below 500 nm. Addition of N_2O or O_2 to remove the electron absorption did not lead to a sufficiently simplified system to permit a spectral assignment.

Molar Absorptivity and Oscillator Strength of e_s^- Band

When pyrene (Py) or anthracene (An) were present in pulse irradiated HMPA the corresponding radical anion absorption bands shown in Fig. 4 were produced. These bands are very similar to those published for the mononegative ions in tetrahydrofuran (21) with peaks at 495 and 740 nm for Py^- and An^- respectively. The maximum molar absorptivities of the anions were taken to be the same as measured in tetrahydrofuran, assuming no solvent dependence, namely $5.0 \times 10^4\ M^{-1}\ cm^{-1}$ for pyrene and $1.0 \times 10^4\ M^{-1}\ cm^{-1}$ for anthracene. Direct comparison of the e_s^- absorption at 1000 nm in pure HMPA with the radical anion absorption in the same sample, after the addition in vacuo of small amounts of An or Py, established $\varepsilon = (4.75 \pm 0.4) \times 10^3\ M^{-1}\ cm^{-1}$ for e_s^- in HMPA at 1000 nm. Using the measured ratio of 6.7 ± 0.4 for the absorbance at 2200 nm to that at 1000 nm the molar absorptivity at the band maximum was calculated to be $\varepsilon = (3.2 \pm 0.5) \times 10^4\ M^{-1}\ cm^{-1}$.

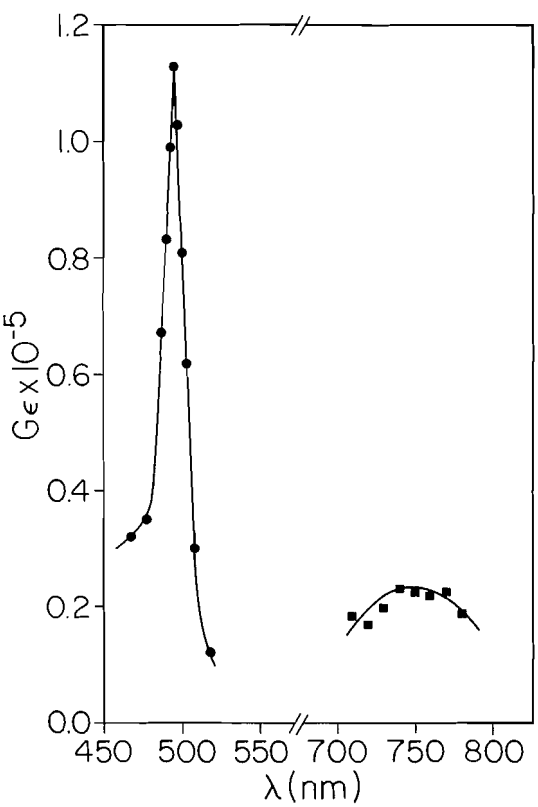

FIG. 4. Radiation produced transients observed at (*i*) 470–520 nm for $(2.6 \pm 0.1) \times 10^{-3}\ M$ pyrene and (*ii*) 710–780 nm for $6.3 \pm 0.5) \times 10^{-4}\ M$ anthracene in HMPA. The species are attributed to the aromatic negative ions.

Integration of the area under the total absorption band, as simulated by the Gaussian–Lorentzian function in Fig. 3, using the relationship

$$f = 4.3 \times 10^{-9} \int_{\bar{\nu}=0}^{\bar{\nu}=\infty} \varepsilon(\bar{\nu})\, d\bar{\nu}$$

(this does not take into account corrections for the refractive index of the liquid (22)), gives a value for the oscillator strength $f = 0.7 \pm 0.2$ for e_s^- in HMPA. This large oscillator strength is in accord with similar determinations for other solvated electrons (ref. 16, p. 40, ref. 23).

Yield of Solvated Electrons

No fast geminate decay of the solvated electron absorption could be observed with the fastest available time resolution of 5 ns. This is probably to be expected for a liquid of such high dielectric constant in which the Onsager escape radius is quite small resulting in a short lifetime for geminate ion-pairs. Since the electron decay half-life is several microseconds it can be assumed that the absorption observable after 5 ns corresponds almost entirely to the free ion yield.

For various scavenger concentrations the radiation yields presented in the Table were obtained. At these concentrations the electron absorption band was completely eliminated. Since the yield is nearly independent of concentration when this was $> 10^{-4}\ M$ it can be accepted that quantitative conversion of the free electrons to anions was occurring at these concentrations. (Py^- formed by scavenging geminate electrons at 0.1 M could have undergone charge neutralization in lieu of e_s^- in the spurs. No fast decay of Py^- was observed on a 5 ns

Can. J. Chem. Downloaded from www.nrcresearchpress.com by 210.87.254.40 on 09/05/12
For personal use only.

TABLE 1. Radiation yield of aromatic anions from anthracene (An) and pyrene (Py) at various concentrations for ~1 krad pulses

	Solute	Yield
Anthracene	$(6\pm2)\times10^{-5}$ *M*	$G(An^-)$ 1.9±0.4
	$(6.3\pm0.5)\times10^{-4}$ *M*	2.3±0.4
Pyrene	$(3.2\pm0.3)\times10^{-4}$ *M*	$G(Py^-)$ 2.1±0.4
	$(2.6\pm0.1)\times10^{-3}$ *M*	2.3±0.4
	$(1.2\pm0.1)\times10^{-1}$ *M*	2.4±0.4

time scale.) Addition of ~0.1 *M* N_2O to samples containing $<10^{-3}$ *M* Py or An resulted in reduction to ~5% in initial yield of the aromatic anions observed. This suggests that the aromatic cations Py^+ or An^+ do not contribute to the absorption at 495 nm or 740 nm in this system. Based on the data given in Table 1 we conclude that for the free ion yield $G(e_s^-) = 2.3 \pm 0.4$ in HMPA.

This yield is in good agreement with the value of 2.4 ± 0.3 measured by Nauta and van Huis (13) but twice as large as $G(e_s^-) = 1.2$ reported by Mal'tsev *et al.* (12). A yield of 2.3 is somewhat higher than would be expected simply on the basis of previously demonstrated empirical correlations between the free ion yield and a liquid's static dielectric constant (24). This probably stems from a rather high mobility of the solvated electrons in HMPA due to its nearly spherical shape (25) which could lead to a higher than normal escape probability. In addition, steric screening of the positive counter-ion and the strongly aprotic nature of the liquid may cause relatively inefficient charge neutralization processes in HMPA. However, this free-ion yield is substantially lower than $G(N_2)$ from γ-irradiated N_2O solutions of HMPA (26).

Our $G\varepsilon$ values are about twice as large as those estimated by Nauta and van Huis (13) and more than ten times those reported at 1600 nm by Mal'tsev *et al.* (12). One possible explanation for the low $G\varepsilon$ values found in the latter studies is the fact that they used comparatively long radiation pulses during which a significant fraction of their solvated electrons would have decayed. This explanation is supported by their four-fold increase in $G(e_s^-)$ on addition of ~0.2 *M* Br^- (12).

Kinetic Studies

(i) Decay of e_s^-

The lifetime of the solvated electron in pure irradiated HMPA was found to increase with decreasing dose per pulse and to be sensitive to sample purification and preparation techniques. Using low dose pulses (~300 rad) in a carefully deoxygenated sample first half-lives approaching 50 μs could be achieved. Analysis of the e_s^- decays (for various doses) showed them to arise from mixed first- and second-order processes with the second-order components always having $k \sim 2 \times 10^{10}\ M^{-1}\ s^{-1}$. This is consistent with the anticipated reactions involved

$$[1] \qquad e_s^- + X \xrightarrow{k_1} [X^-]$$

$$[2] \qquad e_s^- + e_s^- \xrightarrow{2k_2} [e_2^{2-}]$$

$$[3] \qquad e_s^- + S^+ \xrightarrow{k_3} [S]$$

where X represents species contributing to all decays which are not second-order in e_s^- including impurities and other radiation products, and S^+ is the solvent counter-ion or its decomposition product.

In an attempt to decide if radiation-produced species contributed to [1], some experiments were performed on the pulse radiolysis of blue solutions of Na metal dissolved in HMPA which already contained substantial (but unknown) concentrations of solvated electrons (presumably in equilibrium with Na^-). Typical oscilloscope traces are shown in Fig. 5 from which it is clear that the radiation pulse creates additional solvated electrons but that the overall processes lead to a net loss in the concentration of e_s^-. Furthermore, the net loss is comparable in magnitude to the radiation yield of solvated elec-

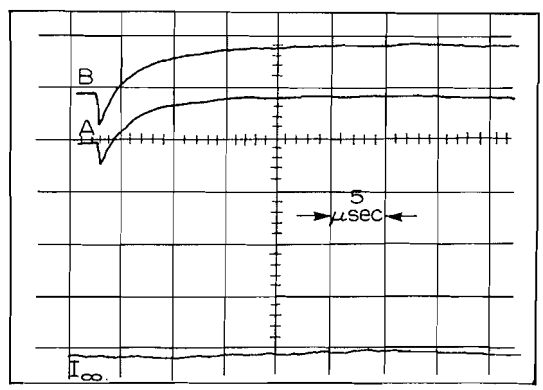

FIG. 5. Effect of electron pulses on a solution of Na in HMPA at 750 nm. The second pulse, B, followed 10 s after the first and showed that the pulses give an initial increase in e_s^- concentration, but a net permanent loss of the species. Similar results were found at 1550 nm.

Can. J. Chem. Downloaded from www.nrcresearchpress.com by 210.87.254.40 on 09/05/12
For personal use only.

trons. If only reactions 2 and 3 were involved the initial and final concentrations of e_s^- would have been the same. The Na solutions obviously do not contain impurities with which e_s^- reacts, so that one must conclude that other radiation-produced species, such as free radicals, contribute significantly to e_s^- decay according to reaction 1.

(ii) Kinetic Studies with Anthracene and Nitrous Oxide

For solutions containing anthracene at 6×10^{-5} M the rate of electron decay, observed at 1000 nm, corresponded almost exactly to the rate of build-up of absorption due to An^- at 740 nm. Representative traces for a solution containing $(6 \pm 2) \times 10^{-5}$ M anthracene are shown in Fig. 6*a* and *b*. The absorption at 740 nm (Fig. 6*b*) includes a contribution from e_s^- (equal to that shown in Fig. 6*a* multiplied by the ratio of extinction coefficients of e_s^- at 740 and 1000 nm obtained from Fig. 1). On applying this correction the rate constant for formation of An^- was evaluated to be $(1.7 \pm 0.2) \times 10^6$ s^{-1} from the linear plot of log $(A_{2.5} - A_t)$ against time, where $A_{2.5}$ is the absorbance 2.5 μs after the pulse (plateau value) and A_t the absorbance at time t. The data of Fig. 6*a* were shown to correspond to a first-order decay with $k = (1.5 \pm 0.2) \times 10^6$ s^{-1}. From these one calculates the rate constant for reaction 4;

$$[4] \qquad e_s^- + An \xrightarrow{k_4} An^-$$

to be $k_4 = (3 \pm 1) \times 10^{10}$ M^{-1} s^{-1}.

A solution of 8×10^{-4} M N_2O in HMPA was made by condensing into the cell a known quantity of N_2O (the solubility of N_2O in HMPA having been measured (17) to be 1.85×10^{-4} M mm^{-1}). For this solution the rate of reaction 5.

$$[5] \qquad e_s^- + N_2O \xrightarrow{k_5} [N_2O^-]$$

was evaluated in two ways. Firstly, by measuring the steady state absorbance of e_s^- at 1000 nm during a constant dose-rate 700 ns pulse, which gave a pseudo first-order rate constant of $(1.2 \pm 0.3) \times 10^7$ s^{-1}. Secondly, by analysis of the pseudo first-order decay following the pulse, the value $(1.1 \pm 0.3) \times 10^7$ s^{-1} was obtained. These correspond to $k_5 = (1.4 \pm 0.4) \times 10^{10}$ M^{-1} s^{-1}. It may be noted that this is about three-fold larger than the analogous reaction in water (27) and thus seems contrary to the reported lower mobility of e_s^- in HMPA (12).

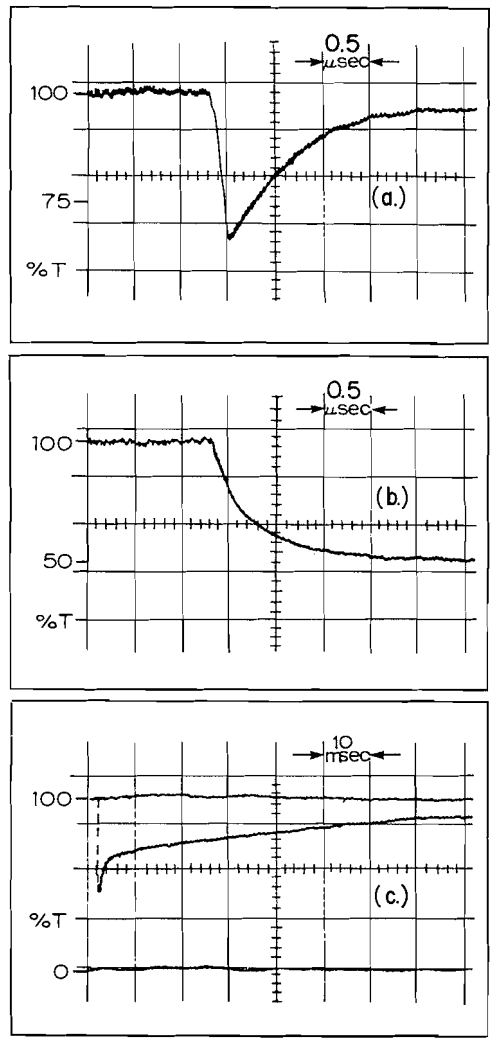

FIG. 6. (*a*) Decay of absorption due to e_s^- at 1000 nm in a solution containing $(6 \pm 2) \times 10^{-5}$ M anthracene in HMPA following a 200 ns pulse. (*b*) Build-up of the absorption due to An^- at 740 nm for the same solution as in (*a*). (*c*) Decay of absorption due to An^- at 750 nm in a solution containing $(6.3 \pm 0.5) \times 10^{-4}$ M anthracene in HMPA.

In dilute solutions of anthracene (or pyrene) to which small concentrations of N_2O were also added, the initial yields of the aromatic anions were substantially smaller than in the absence of N_2O; but the decay rate of An^- (or Py^-) was essentially unchanged. This is consistent with a competition between reactions 4 and 5 for e_s^-, and it also means that there is no charge exchange between An^- and N_2O or between N_2O^- and An. By contrast, in the presence of some oxygen the Py^- decay rate was greatly

Can. J. Chem. Downloaded from www.nrcresearchpress.com by 210.87.254.40 on 09/05/12
For personal use only.

enhanced implying that an interaction between the aromatic anions and O_2 does occur.

The decay processes of the aromatic anions in the absence of a second solute were not investigated in detail but showed two distinct decay regions, as can be seen for An^- in Fig. 6*c*. The faster decay step occurs over microseconds and probably results from neutralization with the radiation-produced counter-ions; but a substantial second portion of the decay is very slow, extending over tens of milliseconds.

Solutions Containing Bromide Ions

The presence of 0.14 *M* LiBr, or 0.17 *M* NaBr, in pulse irradiated HMPA resulted in a 35% increase in the yield of solvated electrons, to $G(e_s^-) = 3.1 \pm 0.4$. Bromide ions also increased the electron's lifetime significantly, thereby corroborating the probable involvement of reaction 3 in electron decay. In these solutions a new absorption band with $\lambda_{max} \sim 360$ nm was observed, which is similar to that found in aqueous Br^- solutions and attributed to Br_2^- (28). The yield of Br_2^- from a 10^{-2} *M* Br^- solution was about half that from the 0.14 *M* solution but the absorbance found at 360 nm all grew-in during the radiation pulse and was certainly complete in $< 10^{-6}$ s. Evidently the species scavenged have alternative fates involving fast reactions.

For the NaBr solutions, the spectrum was carefully studied over the region 700 to 1000 nm in search of contributions from species such as Na^- which have been observed at ~750 nm in sodium solutions in HMPA (8) and which were reported in pulse radiolysis (12). At the end of the pulse the absorption spectrum for a 0.17 *M* NaBr solution was identical to that shown in Fig. 1 for pure HMPA in this wavelength region. However, some 30 μs after the radiation pulse, when ~97% of the solvated electrons had decayed, there was some evidence of an absorption band with a maximum near 750 nm. The intensity of this new band was very small and probably amounted to less than 5% of the initial electron absorption in this region.

Br_2^- is believed to be formed in water when Br^- scavenges the oxidizing species which result from positive ion decay, and by analogy we assume this happens in HMPA also. From the measured absorbance at 360 nm for the 0.14 *M* solution of LiBr in HMPA, one calculates $G\varepsilon = 21\,000\ M^{-1}\ cm^{-1}$ molecule $(100\ eV)^{-1}$. This value reduces to a value for Br_2^- of 15 000 when appropriate correction is made for the absorbance of e_s^- at 360 nm. It would be reduced further (to ~12 000) if the second transient species shown in Fig. 1 to absorb at 360 nm was also present in the irradiated Br^- solutions. There is controversy regarding the magnitude of $\varepsilon_{Br_2^-}^{360}$ with values of either 8 200 or 12 000 $M^{-1}\ cm^{-1}$ reported for aqueous solutions (29). Thus $G(Br_2^-)$ may have a value of 1.2 or 1.8 for 0.14 *M* Br^- in HMPA. These values are much lower than the corresponding $G(e_s^-) = 3.1 \pm 0.4$ in the same solution but are significantly larger than the increased yield of electrons caused by the presence of Br^-. It is possible that even at the highest Br^- concentration all the available oxidizing species were not scavenged. Perhaps the low yield of Br_2^- and the very slow decay of part of the An^- absorption together suggest that there are rapid alternative decay paths available to the primary HMPA positive ions, only some of which give rise to reaction with Br^- and An^-.

We are grateful for support of this research by the U.S. Atomic Energy Commission (at the Ohio State University) and the National Research Council of Canada (at the University of British Columbia and for a Graduate Scholarship to G.J.F.). We are also most grateful to Mr. John Richter for the continued maintenance and improvement of the pulse radiolysis apparatus, and are indebted to Dr. F. Y. Jou for obtaining the absorption data in HMPA–EDA which helped to determine λ_{max} for HMPA.

1. E. J. Hart and J. W. Boag. J. Am. Chem. Soc. **84**, 4090 (1962).
2. R. R. Dewald and J. L. Dye. J. Phys. Chem. **68**, 121 (1964).
3. M. C. Sauer, Jr., S. Arai, and L. M. Dorfman. J. Chem. Phys. **42**, 708 (1965).
4. (*a*) L. M. Dorfman, F. Y. Jou, and R. Wageman. Ber. Bunsen-Gesell. Phys. Chem. **75**, 681 (1971). (*b*) F. Y. Jou and L. M. Dorfman. J. Chem. Phys. **58**, 4715 (1973).
5. (*a*) J. Jortner. *In* Radiation chemistry of aqueous systems. *Edited by* G. Stein. Interscience. 1968. p. 91. (*b*) P. Delahay. J. Chem. Phys. **55**, 4188 (1971). (*c*) D. A. Copeland, N. R. Kestner, and J. Jortner. J. Chem. Phys. **53**, 1189 (1970). (*d*) K. Fueki, D-F Feng, and L. Kevan. J. Am. Chem. Soc. **95**, 1398 (1973).
6. H. Normant. Angew. Chem. Int. Ed. **6**, 1046 (1967).
7. G. Fraenkel, S. H. Ellis, and D. T. Dix. J. Am. Chem. Soc. **87**, 1406 (1965).
8. J. M. Brooks and R. R. Dewald. J. Phys. Chem. **72**, 2655 (1968).

9. R. CATTERALL, L. P. STODULSKI, and M. C. R. SYMONS. J. Chem. Soc. A, 437 (1968).
10. K. V. S. RAO and M. C. R. SYMONS. J. Chem. Soc. Faraday II, **68**, 2081 (1972).
11. H. W. STERNBERG, R. E. MARKBY, I. WENDER, and D. M. MOHILNER. J. Am. Chem. Soc. **89**, 186 (1967).
12. (*a*) E. I. MAL'TSEV, A. V. VANNIKOV, and N. A. BACH. Radiat. Effects, **11**, 79 (1971). (*b*) E. I. MAL'TSEV and A. V. VANNIKOV. Dokl. Akad, Nauk SSSR, **200**, 379 (1971).
13. E. NAUTA and C. VAN HUIS. J. Chem. Soc. Faraday I, 647 (1972).
14. W. D. FELIX, B. L. GALL, and L. M. DORFMAN. J. Phys. Chem. **71**, 384 (1967).
15. G. E. ADAMS, J. W. BOAG, J. CURRANT, and B. D. MICHAEL. *In* Pulse radiolysis. *Edited by* M. Ebert *et al.* Academic Press, London. 1965. p. 117.
16. E. J. HART and M. ANBAR. *In* The hydrated electron. Wiley, N.Y. 1970.
17. G. J. FLYNN. Unpublished data.
18. (*a*) D. C. WALKER, N. V. KLASSEN, and H. A. GILLIS. Chem. Phys. Lett. **10**, 636 (1971). (*b*) T. K. COOPER, D. C. WALKER, H. A. GILLIS, and N. V. KLASSEN. Can. J. Chem. **51**, 2195 (1973).
19. J. LIN, K. TSUJI, and FF. WILLIAMS. J. Am. Chem. Soc. **90**, 2766 (1968).
20. J. L. DYE, M. G. DEBACKER, and L. M. DORFMAN. J. Chem. Phys. **52**, 6251 (1970).
21. D. GILL, J. JAGUR-GRODZINSKI, and M. SZWARZ. Trans. Faraday Soc. **60**, 1424 (1964).
22. R. BENSASSON and E. J. LAND. Trans. Faraday Soc. **67**, 1904 (1971).
23. R. K. QUINN and J. J. LAGOWSKI. J. Phys. Chem. **73**, 2326 (1969).
24. (*a*) G. R. FREEMAN and J. M. FAYADH. J. Chem. Phys. **43**, 86 (1965). (*b*) E. HAYON. J. Chem. Phys. **53**, 2353 (1970).
25. P. H. TEWARI and G. R. FREEMAN. J. Chem. Phys. **49**, 4394 (1968).
26. (*a*) G. J. FLYNN. B.Sc. Thesis. University of British Columbia, Vancouver, British Columbia. 1969. (*b*) G. J. FLYNN and D. C. WALKER. To be published.
27. M. ANBAR and P. NETA. Int. J. Appl. Radiat. Isot. **18**, 493 (1967).
28. L. I. GROSSWEINER and M. S. MATHESON. J. Chem. Phys. **23**, 2443 (1955).
29. (*a*) H. C. SUTTON, G. E. ADAMS, J. W. BOAG, and B. D. MICHAEL. *In* Pulse radiolysis. *Edited by* M. Ebert *et al.* Academic Press. 1965. p. 61. (*b*) B. CERCEK. Int. J. Radiat. Phys. Chem. **4**, 25 (1972). (*c*) D. ZEHARI and J. RABANI. J. Phys. Chem. **76**, 312 (1972).

Can. J. Chem. Downloaded from www.nrcresearchpress.com by 210.87.254.40 on 09/05/12
For personal use only.

Organic Sulfur Mechanisms. 14. Kinetic Resolution in the Reaction of a Sulfene with an Amine

JAMES FREDERICK KING, SOO-KHOON SIM, AND SHIU-KANG LAURENCE LI

Department of Chemistry, University of Western Ontario, London, Ontario N6A 3K7

Received May 30, 1973

The reaction of camphor-10-sulfonyl chloride (**1**) with menthylamine (**2**) is shown by deuterium exchange experiments to proceed principally via the sulfene and the kinetic resolution first observed by Read and Storey (1) demonstrated to arise in the sulfene trapping step. This work constitutes the first authenticated kinetic resolution by a sulfene and also provides new kinetic evidence complementary to earlier work for the existence of a sulfene in the reaction of an alkanesulfonyl chloride with an amine. Evidence is also presented that a small but clearly detectable amount of "unexchanged" product in the deuterium exchange reactions arises via a direct displacement of the amine on the sulfonyl chloride; no kinetic resolution in this latter process was detectable.

Des expériences d'échange du deutérium ont permis de montrer que la réaction du chlorure de camphre-10 sulfonyle (**1**) avec la méthylamine (**2**) passe principalement par l'intermédiaire du sulfène et que la résolution cinétique observée la première fois par Read et Storey (1) se produit lors de l'étape de captage du sulfène. Ce travail fait état de la première résolution cinétique authentique par un sulfène et apporte une preuve cinétique supplémentaire aux travaux antérieurs de l'existence d'un sulfène lors de la réaction d'un chlorure d'alcane sulfonyle avec une amine. La preuve est également faite qu'une faible mais aisément détectable quantité de produit "non échangé" lors des réactions d'échange du deutérium provient d'un déplacement direct de l'amine sur le chlorure de sulfonyle; aucune résolution cinétique pour ce dernier processus n'a pu être mise en évidence. [Traduit par le journal]

Can. J. Chem., **51**, 3914 (1973)

Introduction

In 1930 Read and Storey (1) reported that (+)-camphor-10-sulfonyl chloride (**1**) effected a measure of kinetic resolution with racemic menthylamine (**2**) and with its stereoisomers isomenthylamine and neomenthylamine. With equimolar amounts of $\mathbf{1}_+$ and $\mathbf{2}_\pm$, for example, the recovered menthylamine hydrochloride contained about twice as much of the (+)-isomer as the (−)-isomer.[1] In 1968, Okamoto *et al.* (2) extended this work to include six more primary amines (with which relatively little resolution was observed) and carried out rate studies designed to yield the activation parameters for the reactions of the enantiomeric menthylamines. To this end these authors measured the rate of reaction of $\mathbf{2}_-$ with $\mathbf{1}_+$ and then estimated the rate of the reaction of the dextrorotatory amine, $\mathbf{2}_+$, with $\mathbf{1}_+$ from the measured rate of $\mathbf{2}_-$ with $\mathbf{1}_+$ taken with the extent of the kinetic resolution of the racemic menthylamine with the (+)-sulfonyl chloride. Such a method of estimation is justified only if the product ratios and rate ratios are both determined in the same stage of the reaction. This would be the case if, as seemed reasonable to the Japanese authors, the reaction of **1** were to take place by a mechanism involving direct attack of the amine on the sulfur of the sulfonyl group, as has been proposed for the reaction of *arenesulfonyl* chlorides. *Alkanesulfonyl* halides, at least those with α-hydrogens, have been found in our experience to react with amines with the formation of a sulfene as a short-lived intermediate; furthermore, in the cases examined the rate-determining and product-forming steps were *different* (3) and hence the work of Okamoto *et al.* (2) would probably require correction. We were reinforced in our expectation that a sulfene might be an intermediate in these reactions by the knowledge that the reaction of **1** with triethylamine gives a chlorosulfine ("camphorchlorosulfoxide") by a process believed to involve a sulfene (4, 5).

It appeared to us worthwhile to perform a

[1]Throughout this paper we designate the signs of the rotation of enantiomeric reagents by a subscript sign, *e.g.* $\mathbf{2}_-$ refers to (−)-menthylamine, $\mathbf{1}_+$ to (+)-camphor-10-sulfonyl chloride, and $\mathbf{2}_\pm$ to (±)-menthylamine, etc. For the diastereomeric products in this paper two consecutive subscript signs suffice to indicate each diastereomer unambiguously. The first sign refers to the sign of the parent camphor-10-sulfonic acid (or sulfonyl chloride) and the second gives the sign of the parent menthylamine. Hence for the four diastereomers symbolized by **3** ($\mathbf{3}_{+-}$, $\mathbf{3}_{-+}$, $\mathbf{3}_{++}$, $\mathbf{3}_{--}$), the first refers to that obtained from $\mathbf{1}_+$ and $\mathbf{2}_-$, the second to that from $\mathbf{1}_-$ and $\mathbf{2}_+$, and so on.

Can. J. Chem. Downloaded from www.nrcresearchpress.com by 210.87.254.5 on 09/05/12
For personal use only.

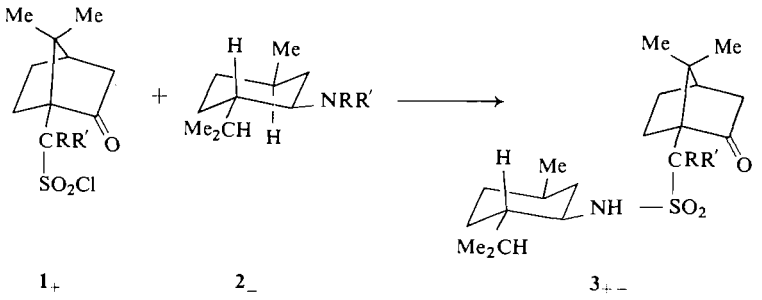

$\mathbf{1}_+$ $\mathbf{2}_-$ $\mathbf{3}_{+-}$

a R=R′=H
b R=H; R′=D
c R=R′=D

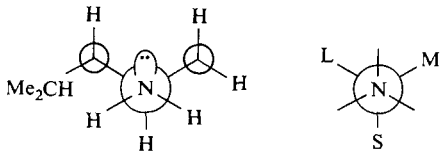

4 **5**

simple test for the intermediacy of a sulfene, since this could provide the first example of an authenticated kinetic resolution via a sulfene and might perhaps also provide a way of gaining further insight into the difficultly accessible problem of the detailed mechanism of the reaction of sulfenes with amines and related sulfene traps. On the other hand, if the major part of the reaction should prove to be a direct displacement on the sulfur, it would be the first such reaction of a basic amine with an alkanesulfonyl chloride bearing a α-hydrogen and could provide new information about the direct displacement *vs.* sulfene processes.

Results and Discussion

Evidence for the Sulfene Reaction

(+)-Camphor-10-sulfonyl-10,10-d_2 chloride ($\mathbf{1}c_+$) was prepared by repeated reactions of (+)-camphor-10-sulfonyl chloride with triethylamine and D_2O followed by regeneration of the chloride with PCl_5. The first of these reactions gives the monodeuteriated product, $\mathbf{1}b_+$, showing that sulfene was generated from **1** with triethylamine and D_2O. Reaction of the dideuteriated sulfonyl chloride, $\mathbf{1}c_+$ with a 10-fold molar quantity of (−)-menthylamine ($\mathbf{2}a_-$) gave the appropriate sulfonamide (**3**) in which the ratio of the mono- to dideuteriated compounds was about 83:14. Using the protiated sulfonyl chloride $\mathbf{1}a_+$ and (−)-menthylamine-d_2 ($\mathbf{2}c_-$) the sample of **3** contained mono- and undeuteriated amides in the ratio 92:8. Though it is evident that more than 80% of the product (and hence at least some of the kinetic resolution) arises in the sulfene reaction, the presence of "unexchanged"[2] sulfonamide would allow the possibility that some of the product (and hence, again, part of the kinetic resolution) comes from a direct displacement on sulfur by the amino nitrogen. As is shown in the subsection entitled *The Direct Displacement Reaction*, however, we have found that, in fact, there is little or no kinetic resolution in the direct displacement process in this case.

The Stereoselectivity of the Separate Steps of the Sulfene Process

Since it would appear that essentially all of the kinetic resolution arises via the elimination–addition (*i.e.* sulfene) mechanism, we turn to the question of how much of the kinetic resolution arises in the formation of the sulfene and how

[2]"Unexchanged" amide refers to the CD_2-amide (3*c*) obtained from the CD_2-sulfonyl chloride (1*c*) and to the CH_2-amide (3*a*) from the CH_2-chloride (1*a*). It is almost certain that at least part of the "unexchanged" product arises by reaction of the sulfene with the amine with uptake of a hydrogen isotope of the same kind as was lost in the sulfene formation, *i.e.*, some of the "unexchanged" amide is formed in a sulfene reaction with an unobservable hydrogen exchange.

Can. J. Chem. Downloaded from www.nrcresearchpress.com by 210.87.254.5 on 09/05/12
For personal use only.

Can. J. Chem. Downloaded from www.nrcresearchpress.com by 210.87.254.5 on 09/05/12
For personal use only.

much in the trapping step. Intuitively it would seem that the sulfene trapping step would be the one giving most of the resolution but the possibility of some resolution occurring in the first stage, which gives sulfene and menthylamine hydrochloride, cannot be dismissed without evidence. If the (+)-amine, for example, were to react faster than the (−)-amine and *if* the excess (+)-amine hydrochloride so formed were relatively slow to donate a hydrogen to the (−)-amine, then the concentration of the free (−)-amine would exceed that of the free (+)-amine and kinetic resolution could ensue even if the rate constants for trapping of the sulfene by the two amines were the same. The slow hydrogen transfer required by this supposition might conceivably arise if there were either (*a*) very rapid precipitation of the amine hydrochloride or perhaps (*b*) tight aggregation of the hydrochloride. The former is excluded in the present instance, however, by the fact that in this case the amine hydrochloride, uniquely in our experience, does not precipitate from benzene or toluene solution.

In the absence of information about how readily the proton is transferred from the (+)-hydrochloride to the (−)-amine under these conditions, we answered the question of how much kinetic resolution arises in each of the two steps of the reaction simply by measuring each directly, *i.e.*, by (*a*) determining the rate constants for the reaction of $\mathbf{1}a_+$ with $\mathbf{2}a_+$ and $\mathbf{2}a_-$, respectively, and (*b*) measuring the stereoselectivity of the second step under conditions in which the sulfene is generated by an achiral base and hence without any possibility of kinetic resolution in that step.

For the reaction of $\mathbf{1}a_+$ with $\mathbf{2}a_+$ and $\mathbf{2}a_-$ in toluene at −10° we obtained good second-order plots for >60% reaction, from which we calculated the rate constants, 2.49×10^{-2} and 2.41×10^{-2} M^{-1} s^{-1} for $\mathbf{2}a_+$ and $\mathbf{2}a_-$, respectively. These results clearly show that virtually no kinetic resolution could arise in the sulfene forming step, even in the unlikely circumstance of a complete absence of any kind of proton exchange between the amines and their hydrochlorides. Okamoto *et al.* (2) measured the rate of the reaction of $\mathbf{1}a_+$ and $\mathbf{2}a_-$ in toluene at somewhat lower temperatures and higher concentration and obtained slightly curved rate plots; extrapolation of their data to −10° gives a rate constant of 2.8×10^{-2} M^{-1} s^{-1} in fair agreement with our value. It is evident from the above results (which confirm the reasoning given in the Introduction) that there is no relationship between the ratio of the above rate constants (for the reactions of $\mathbf{2}a_+$ and $\mathbf{2}a_-$) and the product ratios, and that the procedure of Okamoto *et al.* for estimating the rate constant for the reaction of $\mathbf{2}a_+$ on the assumption of such a relation is therefore incorrect.

In order to measure the stereoselectivity in the second step without any complications arising in the first step, it was necessary to find an achiral base which reacts at a sufficiently fast rate to be the principal reagent effecting dehydrohalogenation of **1**. 1,4-Diazabicyclo[2.2.2]octane (DABCO) was found to react with $\mathbf{1}a_+$ in toluene at −10° using 2-propanol as the sulfene trap, with a rate constant of 2.26×10^{-1} M^{-1} s^{-1}, *i.e.* almost 10 times that for either of the menthylamines. In a reaction of $\mathbf{1}a_+$ with DABCO and $\mathbf{2}a_\pm$ (molar ratio 1:4:2) in toluene at −10°, in which virtually all of the sulfene would be formed by reaction of $\mathbf{1}a_+$ with DABCO, we observed a product ratio $\mathbf{3}a_{+-}/\mathbf{3}a_{++}$ of 1.9. In the absence of DABCO, using the same conditions and quantities, exactly the same product ratio was obtained.

It is clear that the kinetic resolution discussed here arises more or less entirely in the reaction of the chiral sulfene with chiral traps; this work constitutes the first demonstration that sulfenes show sufficient discrimination in their reaction with enantiomers to be able to lead to significant kinetic resolution. As has been noted already by Okamoto *et al.* (2), there is a measure of consistency in the stereochemistry of the amine which reacts faster with the sulfene derived from $\mathbf{1}a_+$; in each case the faster reacting enantiomer of menthylamine, neomenthylamine, and isomenthylamine has the configuration shown in **4**. Okamoto *et al.* point out that this is the *R* configuration and that the faster reacting enantiomer had the *R* configuration in three of their four other cases which showed any resolution at all and in which the absolute configuration was known. In our view the use of the Cahn–Ingold–Prelog descriptors (which are not based on, and only approximately correlated with, effective steric bulk) is less appropriate than merely ordering the groups attached to the carbon bearing the amino group as large, medium, and small (L, M, and S). Assuming that the methine bearing the isopropyl group is "larger" in the present sense than the methylene, this leads to the representation **5** for the faster reacting enantiomer of each

Can. J. Chem. Downloaded from www.nrcresearchpress.com by 210.87.254.5 on 09/05/12
For personal use only.

of the menthylamines. The other amines studied by Okamoto *et al.* all show such low stereoselectivities[3] (3% or less) that it is doubtful if their results with these compounds can be of much value in determining the geometry of the sulfene trapping reaction. The consistency shown in the reactions of the three diastereomeric menthylamines suggests that the observed kinetic resolution ought to be explicable in simple conformational terms, but in our view the mechanism of the addition of amines to sulfenes is not sufficiently well understood to warrant such an explication at present.

The Rate–Product Discrepancy, Nonreciprocal Kinetic Resolution, and the Intermediacy of a Sulfene

In the above subsection it is noted that the ratio of the measured rate constants differs from the ratio of the products. It was pointed out a number of years ago by Ingold and co-workers (7, 8) that such a rate–product discrepancy *requires* the presence of an intermediate (see also refs. 9 and 10); in the present instance this intermediate may be identified as the sulfene. Although evidence from deuteration experiments for the involvement of sulfene has already been presented, corroboration is not unwelcome.

It is of interest that although we have presented kinetic evidence for the intermediacy of sulfene before (3), our previous method is inapplicable in the present case. We had previously shown that the rate of the reaction of methanesulfonyl chloride, triethylamine and 2-propanol (which leads to isopropyl methanesulfonate) was independent of the 2-propanol concentration, thereby requiring the presence of an intermediate which reacts with the alcohol in a fast second step. With the reaction of **1***a* and **2***a*, **2***a* is the sulfene generating base as well as the trap and the reaction is first order in **2***a*; this circumstance no longer allows the sulfene mechanism and, for example, the direct displacement process to be differentiated by the kinetic order of the reaction. The observation of the rate–product discrepancy, however, does allow such a distinction, and hence is complementary to our earlier study (3).

Very closely related to the rate–product discrepancy is the phenomenon that we have named "nonreciprocal kinetic resolution" which, as we have recently pointed out (11), arises in the reaction of **1***a* and **2***a*. The defining feature of nonreciprocal kinetic resolution is that the stereoselectivity[3] of the reaction of, say, $\mathbf{A}_{\pm}$ with $\mathbf{B}_{+}$ is *different* from that of $\mathbf{B}_{\pm}$ with $\mathbf{A}_{+}$. In the present case we found a stereoselectivity of about 30% in the reaction of $\mathbf{1}_{+}$ with $\mathbf{2}_{\pm}$ (in ageement with previous reports (1, 2)), whereas with $\mathbf{1}_{\pm}$ and $\mathbf{2}_{-}$ there was little or no stereoselectivity ($1 \pm 1\%$) (11). It can be shown that under pseudo first-order conditions the product ratio from the reaction of $\mathbf{1}_{\pm}$ with $\mathbf{2}_{-}$ gives the ratio of the measured rate constants (11) and hence, that as means of demonstrating the presence of an intermediate, the rate–product discrepancy and nonreciprocal kinetic resolution are identical in their essential argument but are quite different experimentally: the former requires kinetic measurements but can be used with achiral reagents; the latter requires that a chiral intermediate react with a chiral reagent but dispenses with measurement of rates. The use of kinetic resolution promises to be of considerable value in a number of ways in the study of reaction mechanisms, but the topic is sufficiently extensive that we shall defer further discussion to a later account.

Practical Synthetic Application of Kinetic Resolution via Sulfenes

The purpose of the present study was primarily, of course, mechanistic and only peripherally concerned with the practical problem of resolution of racemic modifications. Except for enzymic processes, kinetic asymmetric transformations (of which kinetic resolution is an example) have found relatively little practical application in the resolution of racemic materials. In the course of this work we required a sample of (+)-menthylamine, the "unnatural" enantiomer, and in fact to obtain our first sample we used the partially resolved mixture as our starting material for the resolution via the tartrates (12). The resolution was completed without difficulty but there was no clear evidence that this route is any more efficient than starting with $\mathbf{2}_{\pm}$. Cursory examination of the mixture of diastereomeric sulfonamides (**3**) obtained by reaction with $\mathbf{1}_{+}$ did not lead to any easy method for separating the components; recrystallization gradually leads to enrichment in the originally less abundant isomer (derived from $\mathbf{2}_{+}$) but the process in our hands was slow.

A spectacular illustration of the practical use-

[3]Percent stereoselectivity is defined (6) as $100(D_1 - D_2)/(D_1 + D_2)$, where D_1 and D_2 refer to the yields of the diastereomers produced in the greater and lesser amounts, respectively.

Can. J. Chem. Downloaded from www.nrcresearchpress.com by 210.87.254.5 on 09/05/12
For personal use only.

fulness of kinetic resolution was recently described by Wiesner *et al.* (13), who found that one enantiomer of their synthetic relay for the total synthesis of the alkaloid delphinine reacted more or less *quantitatively* with $\mathbf{1}a_-$ and pyridine leaving the desired "natural" enantiomer essentially uncontaminated with the enantiomer of the unnatural configuration. Since **1***a* reacts with a mixture of pyridine and piperidine-*d* (which like the delphinine relay is a cyclic secondary amine) to give the monodeuteriated sulfonamide, it seems highly likely that the remarkable resolution achieved by Wiesner *et al.* occurred via the sulfene.

The Direct Displacement Reaction

Although, as is noted above, the deuterium labelling experiments indicate that at least 80% of the product is formed by the sulfene mechanism, there is some "unexchanged" product generated; from $\mathbf{1}a_+$ and $\mathbf{2}c_-$ this amounts to about 8% of the total and with $\mathbf{1}c_+$ and $\mathbf{2}a_-$ there is 13 to 14% "unexchanged" sulfonamide (**3***c*). This raises the question of whether there is another, concurrent mechanism and if there is, what is its stereoselectivity?

One straightforward explanation for these data is that there is simply a non-sulfene mechanism, presumably a direct displacement on sulfur, which contributes to a small but significant extent. Such a mechanism has been accepted for a long time as the mechanism of reaction of arenesulfonyl chlorides (see ref. 14 and the earlier work cited therein) and presumably operates with other sulfonyl chlorides lacking α-hydrogens. Though the possibility has been raised (15, 16), clear evidence for its incursion in the reaction of amines with those alkanesulfonyl chlorides that bear α-hydrogens has been lacking. We wish to show here that our data for the reaction of **1** and **2** are *not* consistent with any mechanism that we have been able to devise in which all of the product is formed via the sulfene but are in good agreement with a sulfene process together with a small contribution by a direct displacement mechanism. Deuterium labelling experiments (some of which have been mentioned above) and a determination of the rate constant for the reaction of $\mathbf{1}c_+$ with $\mathbf{2}a_-$ ($7.36 \times 10^{-3}\ M^{-1}\ s^{-1}$) are consistent with the following approximate values relating the parameters in Scheme 1: $k_{1H}/k_S = 30$, $k_{1H}/k_{1D} = 3.3$, $k_{2H}/k_{2D} = 1.15$, and $k_{1D}/k_S = 9$; *i.e.* with menthylamine about 3% of the reaction of $\mathbf{1}a_+$

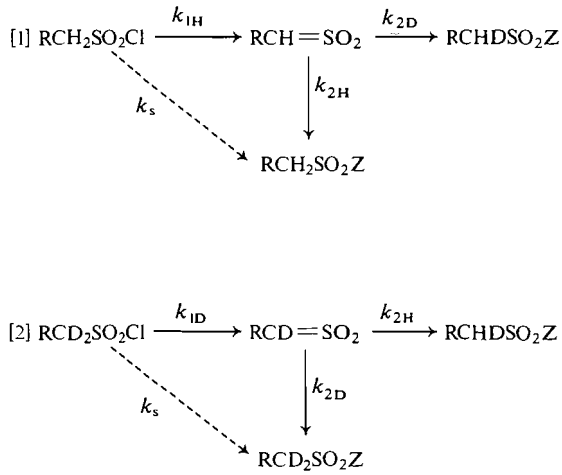

SCHEME 1

and 10% of the reaction of $\mathbf{1}c_+$ proceed via the direct displacement process.

In contrast to the ease with which our experiments may be accommodated by assuming a small amount of direct displacement, a number of difficulties arise if we attempt to account for the data exclusively on the basis of the sulfene processes (indicated by the solid arrows in Scheme 1). A portion of the "unexchanged" product can, and indeed must, arise by uptake during the trapping step of some of the hydrogen isotope released into the medium by the formation of the sulfene from the sulfonyl chloride. In the present experiments there were 10 mol of amine (each with two hydrogens) for each mol of sulfonyl chloride (each releasing one hydrogen) and hence, if there were no kinetic isotope effect in the trapping step, 5% of the product would be "unexchanged" product formed by such a process. But we have observed that starting with *either* $\mathbf{1}a_+$ or $\mathbf{1}c_+$ the amount of "unexchanged" product is greater than 5%, and hence this mechanism is not sufficient to account for all of the "unexchanged" material. Further, a kinetic isotope effect in the trapping step would not help matters since to the extent that it would allow a proportion of unexchanged product greater than 5% for one reaction, it would require a corresponding amount less than 5% for the other.

A variation in the above mechanism has been discussed earlier (16) but for the reasons which follow it seems to us unlikely to be of significance in the present system. This mechanism

Can. J. Chem. Downloaded from www.nrcresearchpress.com by 210.87.254.5 on 09/05/12
For personal use only.

postulates that the sulfene trapping step is sufficiently fast that the hydrogen recently abstracted from the sulfonyl chloride has not had sufficient time to diffuse very far from the reaction site and hence there is a higher *local* concentration of the isotope originally on the sulfonyl chloride in the vicinity of the sulfene trapping reaction than in the body of the reaction as a whole. In such a scheme the factor deciding the ratio of "unexchanged" product to exchanged in, say, reaction 1 is not the overall ratio of active hydrogen to active deuterium as determined by the ratios of the starting materials but rather the average effective ratio of available protons to deuterons while the sulfene trapping process is taking place. We shall designate this "effective ratio of H to D" by x and hence the ratio of "unexchanged" to exchanged product in [1] is $(RCH_2SO_2Z/RCHDSO_2Z)_1 = k_{2H}x/k_{2D}$.

Similarly, if we designate the corresponding "effective ratio of D to H" in reaction 2 as x', then $(RCD_2SO_2Z/RCHDSO_2Z)_2 = k_{2D}x'/k_{2H}$.

It seems likely that in the reaction medium used for these experiments (methylene chloride) simple diffusion is the principal mechanism by which the hydrogen recently abstracted from the sulfonyl chloride departs from the site of sulfene formation. Further, the diffusion rates for the amine or ammonium salt will be much the same whether protiated or deuteriated, and therefore it seems likely that x and x' would be approximately equal. This leads to the approximation $(RCD_2SO_2Z/RCHDSO_2Z)_2 \approx k_{2D}x/k_{2H}$ and hence to eq. 3.

$$[3]\quad \frac{(RCH_2SO_2Z/RCHDSO_2Z)_1}{(RCD_2SO_2Z/RCHDSO_2Z)_2} \approx \left(\frac{k_{2H}}{k_{2D}}\right)^2$$

From the data already presented above, in the reactions of $\mathbf{1}c_+$ and $\mathbf{2}a_-$, and $\mathbf{1}a_+$ and $\mathbf{2}c_-$, the left side of eq. 3 is numerically equal to $8/90 \div 14/83 = 0.53$ or $k_{2H}/k_{2D} = 0.73$. In other words, in order to account for the amounts of "unexchanged" product from $\mathbf{1}a_+$ and $\mathbf{1}c_+$ on the basis of the "local concentration effect", there must be a distinct inverse isotope effect in the sulfene trapping step.

Such an isotope effect, however, does not show up in the reaction of this sulfene with menthylamine. This was shown by treating $\mathbf{1}a_+$ and $\mathbf{1}c_+$ each with a mixture obtained by combining equal quantities of $\mathbf{2}a_-$ and $\mathbf{2}c_-$ (*i.e.* an equilibrium mixture of $\mathbf{2}a_-$, $\mathbf{2}c_-$, and $\mathbf{2}b_-$ with the last predominating). The respective amounts of RCH_2SO_2Z and $RCHDSO_2Z$ from $\mathbf{1}a_+$ were 56 and 41%, and of RCD_2SO_2Z and $RCHDSO_2Z$ from $\mathbf{1}c_+$ were 50 and 47%. It is clear simply from inspection of these results that there is no inverse isotope effect in the addition of menthylamine to the sulfene. (Alternatively, referring to eq. 3, these data yield a different value for k_{2H}/k_{2D} which, in effect, means that eq. 3 is not valid and hence that the "local concentration effect" does not account for the "unexchanged" products in the reactions of $\mathbf{1}a_+$ and $\mathbf{1}c_+$ with menthylamine.) Participation of the "local concentration effect" to some extent is not excluded by these results but as is mentioned above the data can be satisfactorily rationalized without using the hypothesis at all.

This leads us to return to the conclusion that the "unexchanged" product comes partly from a direct displacement process, and thereby raises a further question: is there any stereoselectivity in the direct displacement reaction of **1** and **2**? It would appear, in fact, that within the precision of our method, there is no significant kinetic resolution in this reaction. This conclusion is derived as follows. In the reaction of $\mathbf{1}c_+$ with the "other" enantiomer of menthylamine, *i.e.* $\mathbf{2}a_+$, the "unexchanged" material constituted 13% of the total; this, within experimental uncertainty, is the same as that found with $\mathbf{2}a_-$. This implies that k_1/k_S in the reaction with $\mathbf{1}_+$ is the same for $\mathbf{2}a_+$ and $\mathbf{2}a_-$. As has been mentioned in an earlier subsection, k_1, the rate of sulfene formation, is (except, of course, for the 3% direct displacement) given by the measured rate of chloride ion formation, and this was found to be virtually the same for $\mathbf{2}a_-$ and $\mathbf{2}a_+$ with $\mathbf{1}a_+$. It follows that the values of k_S for the reactions of $\mathbf{2}a_-$ and $\mathbf{2}a_+$ with $\mathbf{1}_+$ must also be about the same, *i.e.* there is no kinetic resolution detectable (by this means) in the direct displacement reaction path.

The conclusions drawn above led us to wonder if the low levels of stereoselectivity observed by Okamoto *et al.* (2) might arise because these bases were reacting by a direct displacement mechanism rather than a sulfene process. Reaction of one of these amines, (±)-1-phenylethylamine, with $\mathbf{1}c_+$, however, led to incorporation of roughly 80% of one protium equivalent at C-10 (as judged by n.m.r.), indicating that the sulfene reaction is also the major process with this amine, and hence that the low stereoselectivity observed does not arise because of a completely different

mechanism from that which operates with menthylamine.

Experimental

I.r. spectra were recorded in carbon tetrachloride or chloroform solution on a Beckman IR-10 or IR-20A instrument. The n.m.r. spectra were run in deuteriochloroform on a Varian HA-100, A-60, or T-60 spectrometer with tetramethylsilane as internal standard. Mass spectra were obtained with a Varian M-66 mass spectrometer. The methylene chloride, toluene, and dioxane used as reaction solvents were stored over molecular sieves and found by analysis with an Aquatest Automatic Karl Fischer titrator to contain < 50 p.p.m. of water. Melting points were determined on a Gallenkamp melting point apparatus and are uncorrected. Ether and toluene extracts were dried over anhydrous magnesium sulfate. Methylene chloride extracts were dried by washing with saturated sodium chloride solution then passing through a small plug of cotton wool. Solvents were removed from solutions with a rotary evaporator in conjunction with a water aspirator.

Camphor-10-sulfonyl Chlorides $\mathbf{1}a_+$ *and* $\mathbf{1}a_\pm$

These compounds were prepared according to the method of Smiles and Hilditch (17). Treatment of (+)-camphor-10-sulfonic acid (Aldrich Chemical Co.) (20 g, 86 mmol) with thionyl chloride (43 g, 360 mmol) gave 19 g (76 mmol, 88%) of (+)-camphor-10-sulfonyl chloride. Recrystallization from cyclohexane yielded colorless plates, m.p. 66–67°; lit. (17) m.p. 67–68°.

In a similar manner, $\mathbf{1}a_\pm$ was prepared from (±)-camphor-10-sulfonic acid (18) in 80% yield, m.p. 83–84.5°; lit. (17) m.p. 81–83°.

The n.m.r. spectrum ($CDCl_3$) showed bands at δ 2.70–1.50 (m, 7H), 1.15 (s, 3H), 0.95 (s, 3H), and the C-10 methylene protons appeared as an AB quartet (δ_A 4.33 1H, δ_B 3.80 p.p.m. 1H, J = 14 Hz).

(+)-Camphor-10-sulfonyl-10-d_2 Chloride $\mathbf{1}c_+$

To a solution of (+)-camphor-10-sulfonyl chloride ($\mathbf{1}a_+$) (5.0 g, 20 mmol) in dioxane (20 ml) was added slowly by means of a dropping funnel a solution of triethylamine (15 ml), D_2O (15 ml), and dioxane (10 ml). The resulting solution was stirred for ½ h and then evaporated to dryness. The residue was taken up with CH_2Cl_2 and then treated with excess of phosphorus pentachloride (15 g, 72 mmol). The solution was washed with water until the washing was neutral. Solvent removal gave 4.5 g (18 mmol, 90%) of crude sulfonyl chloride $\mathbf{1}b_+$.

The n.m.r. spectrum showed partial deuteration at C-10 (δ 4.33, 0.74H; 3.80, 0.36H).

Further treatment of $\mathbf{1}b_+$ with triethylamine and D_2O followed by regeneration of the sulfonyl chloride with PCl_5 (four more cycles) gave 1.55 g (6.2 mmol, 31%) of product, $\mathbf{1}c_+$; the n.m.r. spectrum $(CDCl)_3$ showed almost complete absence of the absorption at δ4.33 and 3.80, corresponding to a maximum amount of about 10% of the monodeuteriated sulfonyl chloride ($\mathbf{1}b_+$).

Menthylamines $\mathbf{2}a_\pm$ *and* $\mathbf{2}a_-$

(±)-Menthylamine ($\mathbf{2}a_\pm$) (b.p. 120/155 mm) and (−)-menthylamine ($\mathbf{2}a_-$) (b.p. 100/14 mm) were prepared from the corresponding form of menthol following the method of Sandborn (19) and Andres and Andreef (20). Oxidation of (−)-menthol with sodium dichromate gave 79% yield of menthone, b.p. 142° 110 mm, lit. (19) b.p. 209°. Treatment of (−)-menthone with hydroxylamine acetate yielded menthone oxime in 64% yield. (−)-Menthylamine ($\mathbf{2}a_-$) was obtained in 95% yield by reducing the menthone oxime with sodium in ethanol. The hydrochloride of (−)-menthylamine had $[\alpha]_D$ −36.4° (H_2O); lit. (12) $[\alpha]_D$ −36.6° (H_2O).

(−)-Menthylamine-d_2 ($\mathbf{2}c_-$*)*

(−)-Menthylamine ($\mathbf{2}a_-$) (3.8 g, 25 mmol) dissolved in ether was shaken for ½ min or more with four batches of D_2O (5 ml each) in a separatory funnel. The solvent was then evaporated and the menthylamine distilled under reduced pressure (b.p. 120/150 mm). The deuterium content of the deuterated amine was determined by n.m.r. to be > 1.96 atom D/mol.

(+)-Camphor-10-sulfonyl-(−)-menthylamide ($\mathbf{3}a_{+-}$*)*

To a solution of (−)-menthylamine ($\mathbf{2}a_-$) (380 mg, 2.5 mmol) in CH_2Cl_2 was added a solution of (+)-camphor-10-sulfonyl chloride ($\mathbf{1}a_+$) (132 mg, 0.53 mmol) in CH_2Cl_2. The solution was kept at room temperature for 4 h. It was then washed twice with 1 *N* HCl solution and then with H_2O. After solvent removal, 180 mg (0.48 mmol, 90% yield) of crude sulfonamide $\mathbf{3}a_{+-}$ was obtained. Recrystallization from ether–pentane gave colorless needles, m.p. 137–138°, $[\alpha]_D$ −27.8° (benzene); lit. (1) m.p. 139° $[\alpha]_D$ −28.0 (benzene).

The n.m.r. spectrum ($CDCl_3$) showed the amine proton as a doublet at δ 5.15 (1H); the methylene protons at C-10 appeared as an AB quartet: δ_A 3.40 (1H), δ_B 3.04 (1H), J_{AB} = 14 Hz. The remaining protons appeared as complex multiplets at 2.40–0.80 p.p.m. (m, 32H).

The i.r. spectrum ($CHCl_3$) showed absorption at 3280 (NH), 1738 (C=O), 1310, and 1130 cm^{-1} (SO_2). The mass spectrum gave a molecular ion peak at *m/e* 369.

(+)-Camphor-10-sulfonyl-(+)-menthylamide ($\mathbf{3}a_{++}$*)*

Following the procedure described for the preparation of $\mathbf{3}a_{+-}$, the title compound was obtained from $\mathbf{1}a_+$ (126 mg, 0.5 mmol) and $\mathbf{2}a_+$ (115 mg, 1 mmol) in 78% yield. Recrystallization from 1:1 ether–pentane gave colorless needles, m.p. 142–143° $[\alpha]_D$ +61° (benzene). The enantiomer (−)-camphor-10-sulfonyl-(−)-menthylamide ($\mathbf{3}a_{--}$) is reported (1) to have m.p. 143° and $[\alpha]_D$ −60.1° (benzene).

The n.m.r. spectrum ($CDCl_3$) showed the amine proton as a doublet at δ 5.15 (1H); the two hydrogens on C-10 appeared as an AB quartet: δ_A 3.50 (1H), δ_B 3.00 (1H), J_{AB} = 14 Hz. The remaining protons appeared as a complex multiplet at 2.40–0.80 (32 H). The i.r. spectrum ($CHCl_3$) showed absorption at 3260 (NH), 1730 (C=O), 1310 and 1130 cm^{-1} (SO_2). The mass spectrum showed a parent ion peak at *m/e* 369.

Deuterium Exchange in the Reaction of Camphor-10-sulfonyl Chloride with Menthylamine

These reactions were carried out as described above for the preparation of (+)-camphor-10-sulfonyl-(−)-menthylamide ($\mathbf{3}a_{+-}$).

(a) $\mathbf{1}a_+$ *with* $\mathbf{2}c$

(+)-Camphor-10-sulfonyl chloride ($\mathbf{1}a_+$) (110 mg, 0.44 mmol) and (−)-menthylamine-d_2 ($\mathbf{2}c_-$) (665 mg, 4.2 mmol) in CH_2Cl_2 (6 ml) gave 152 mg (0.42 mmol, 93% yield) of (+)-camphor-10-sulfonyl-(−)-menthylamide-10-

Can. J. Chem. Downloaded from www.nrcresearchpress.com by 210.87.254.5 on 09/05/12
For personal use only.

Can. J. Chem. Downloaded from www.nrcresearchpress.com by 210.87.254.5 on 09/05/12
For personal use only.

d ($3b_{+-}$). The n.m.r. spectrum ($CDCl_3$) showed partial deuteriation at C-10. The mass spectrum showed peaks at *m/e* 369 and 370, corresponding to 8% $3c_{+-}$ and 92% $3b_{+-}$. Control spectra of natural abundance sulfonamide ($3a_{+-}$) and of the same deuteriated sulfonamide sample at different times indicated that the error in these percentage compositions (and those which follow) is about ± 1 or slightly less. Intensity contributions from natural isotopes were calculated as described by Hamming and Foster (21).

(b) $1c_+$ *with* $2a_-$

(+)-Camphor-10-sulfonyl-10-d_2 chloride ($1c_+$) (69 mg, 0.3 mmol) with (−)-menthylamine ($2a_-$) (418 mg, 3 mmol) gave 78 mg (0.21 mmol, 78% yield) of the sulfonamide (3_{+-}). The n.m.r. spectrum showed protium incorporation at C-10 corresponding to roughly one hydrogen per molecule. The mass spectrum showed peaks at *m/e* 369, 370, and 371 corresponding to 3% $3a_{+-}$, 83% $3b_{+-}$, and 14% $3c_{+-}$.

A sample of partial deuteriated sulfonamide (containing mostly $3b_{+-}$) was allowed to stand with $2a_-$ in CH_2Cl_2 solution for 20 h at room temperature. The mass spectrum of the recovered material was identical within experimental error to that obtained prior to treatment with $2a_-$.

(c) $1c_+$ *with* $2a_+$

(+)-Camphor-10-sulfonyl-*10*-d_2 ($1c_+$) (30.4 mg, 0.12 mmol) and (+)-menthylamine (2_+) (187 mg, 1.2 mmol), obtained as described below, gave 30 mg (0.08 mmol, 67% yield) of the sulfonamide (3_{++}). The n.m.r. spectrum showed protium incorporation corresponding to uptake of roughly one protium atom at C-10 per molecule. The mass spectrum showed peaks at *m/e* 369, 370, and 371 corresponding to 4% $3a_{++}$, 83% $3b_{++}$, and 13% $3c_{++}$.

(d) $1a_+$ *with an Equimolar Mixture of* $2a_-$ *and* $2c_-$

(+)-Camphor-10-sulfonyl chloride ($1a_+$) (125 mg, 0.5 mmol) and 775 mg (5 mmol) of a mixture obtained by mixing equimolar amounts of (−)-menthylamine ($2a_-$) and (−)-menthylamine-d_2 ($2c_-$) gave 207 mg of sulfonamide (3_{+-}). The mass spectrum showed peaks at *m/e* 369 and 370 corresponding to 58% $3a_{+-}$ and 42% $3b_{+-}$.

(e) $1c_+$ *with an Equimolar Mixture of* $2a_-$ *and* $2c_-$

(+)-Camphor-10-sulfonyl-*10*-*d* chloride ($1c_+$) (127 mg, 0.5 mmol) and 805 mg (5.2 mmol) of the same equimolar mixture of $2a_-$ and $2c_-$ as used above gave 258 mg of sulfonamide (3_{+-}). The mass spectrum showed peaks at 369, 370, and 371 corresponding to 3% $3a_{+-}$, 47% $3b_{+-}$, and 50% $3c_{+-}$.

Kinetic Resolution Experiments

(a) (+)-Camphor-10-sulfonyl Chloride ($1a_+$*) with (±)-Menthylamine (*$2a$*)*

In a typical experiment, a solution of $1a_+$ (130 mg, 0.5 mmol) in toluene (10 ml) was mixed with a solution of $2a_\pm$ (156 mg, 1.0 mmol) in toluene (15 ml) at −10°. The homogeneous solution was kept at −10 ± 0.2° for 2 h and then allowed to warm up. It was then extracted twice with 1 *N* HCl solution, washed with water and dried. Solvent removal gave 149 mg (0.40 mmol, 81% yield) of a mixture of (+)-camphor-10-sulfonyl-(−)-menthylamide ($3a_{+-}$) and (+)-camphor-10-sulfonyl-(+)-menthylamide ($3a_{++}$). In the n.m.r. spectrum, the C-10 methylene proton signals as well as the amide proton signals of the two diastereomers were sufficiently separated to allow integration which showed the mixture to contain 65% of **3** and 35% of **4** corresponding to 30% stereoselectivity. The specific rotation ($[\alpha]_D$ +2.9° (benzene)) of the sulfonamide mixture showed a stereoselectivity of 30.8%.

The aqueous solution from the acid extraction was made basic with 6 *N* NaOH solution. The menthylamine liberated was extracted twice with CH_2Cl_2. The organic layer was then dried and solvent removed. The menthylamine obtained was treated with concentrated HCl giving 93 mg (0.49 mmol, 97%) of menthylamine hydrochloride. Its specific rotation $[\alpha]_D$ +10.6° (water) corresponded to a stereoselectivity of 30%.

(b) (±)-Camphor-10-sulfonyl Chloride ($1a_\pm$*) with (−)-Menthylamine (*$2a_-$*)*

A solution of $1a_\pm$ (252 mg, 1 mmol) in toluene (10 ml) was mixed with a solution of $2a_-$ (154 mg, 1 mmol) in toluene (5 ml) at −10°. After being kept at −10 ± 0.2° for 2 h, the solution was worked-up following the procedure described previously. The crude toluene extract after washing with HCl solution and evaporation of solvent was a mixture of $1a_\pm$ (50%), $3a_{+-}$ (25%), and $3a_{--}$ (25%) as shown by n.m.r. spectroscopy.

This mixture was then dissolved in 1,2-dimethoxyethane. The unreacted sulfonyl chloride was hydrolyzed with 6 *N* NaOH solution. After acidification, the solvent was evaporated and the residue taken up with CH_2Cl_2. After washing with H_2O, drying, and solvent removal, 160 mg (0.43 mol, 86%) of a mixture (as shown by n.m.r.) of $3a_{+-}$ (50%) and $3a_{--}$ (50%) was obtained. The optical rotation of the sulfonamide mixture ($[\alpha]_D$ −44.2° (benzene)) corresponded to stereoselectivity of 1%.

(c) (+)-Camphor-10-sulfonyl Chloride ($1a_+$*) with DABCO and (±)-Menthylamine (*$2a_\pm$*)*

A solution of $1a_+$ (124 mg, 0.5 mmol) in toluene (10 ml) was mixed with a solution of $2a_\pm$ (156 mg, 1 mmol) and 1,4-diaza[2.2.2]bicyclooctane (DABCO) (230 mg, 2 mmol) in toluene (5 ml) at −10°. The solution was kept at −10 ± 0.2° for 2 h and then allowed to warm to room temperature. It was extracted twice with 1 *N* HCl solution, then with H_2O and dried. Removal of solvent left 140 mg (0.38 mmol, 76%) of crude sulfonamide mixture estimated by n.m.r. to contain 65% $3a_{+-}$ and 35% $3a_{++}$, corresponding to a stereoselectivity of 30%.

Resolution of (±)-Menthylamine ($2a_\pm$*)*

The partially resolved menthylamine (0.37 g, 214 mmol) recovered from a reaction of $1a_+$ with excess $2a_\pm$ was treated with an equimolar quantity of (+)-tartaric acid in warm alcohol. After solvent removal, the crude menthylamine hydrogen tartrate was recrystallized (five times) from water to give 64 mg (0.2 mmol, 8.3%) of (+)-menthylamine-(+)-hydrogen tartrate, m.p. 166–167°, $[\alpha]_D$ + 37.6° (H_2O), lit. (12) m.p. 168°, $[\alpha]_D$ + 37.1° (H_2O)). This provided a sample of seeds for future fractional recrystallizations of material obtained by reaction of (+)-tartaric acid with (±)-methylamine (not partially resolved). The free $2a_+$ was obtained by extraction of a basified aqueous solution of the tartrate with CH_2Cl_2, followed by removal of the solvent and distillation under reduced pressure.

Kinetic Measurements

A stock solution of $1a_+$ (or $1c_+$) in toluene was prepared by dissolving a known weight of 1_+ in toluene. The

Can. J. Chem. Downloaded from www.nrcresearchpress.com by 210.87.254.5 on 09/05/12
For personal use only.

initial concentration of the solution was determined by titration of chloride with silver nitrate solution (0.025 *N*) after the solution was allowed to react with the base solution for an interval of at least 10 half-lives.

A stock solution of base about ten times as concentrated as the substrate solution was also prepared by dissolving the calculated amount of base in toluene. The concentration of the base was determined by titration with standard HCl solution (0.1 *N*).

For rate measurement, 5 ml of the substrate solution and 5 ml of base solution kept in separate flasks were immersed into the constant temperature (±0.2°) compartment of the "Kryothermat KT-62" as described previously (3). After ½ h, when both solutions reached the desired temperature (−10° the two solutions were mixed as quickly as possible. Timing was started at the beginning of the mixing. After the appropriate time interval, the reaction was quenched with 2 ml of cold saturated formic acid in toluene. The resulting solution was then extracted twice with 20 ml of water and the combined aqueous solution was titrated with silver nitrate solution (0.025 *N*).

The rate constants were obtained from the slope of a plot of $\log [b - 2x)/(a - x)$ *vs.* t, where b is the initial concentration of base, a the initial concentration of $\mathbf{1}_+$ and x the amount of reaction after time t. At least five points in the range from 10% to at least 60% reaction were measured to construct the plots. For the reaction of $\mathbf{1}_+$ with DABCO and 2-propanol, the procedure was the same except that the 2-propanol was mixed with the base, and $\log [(b - x)/(a - x)$ vs. t was plotted to obtain the rate constant.

Reaction of (+)-Camphor-10-Sulfonyl-10-d_2 Chloride ($\mathbf{1}c_+$) with (±)-1-Phenylethylamine

(+)-Camphor-10-sulfonyl-*10-d_2* chloride ($\mathbf{1}c_+$) (160 mg, 0.63 mmol) was added to a solution of (±)-1-phenylethylamine (766 mg, 6.3 mmol) in CH_2Cl_2 (13 ml) and the mixture left for 4½ h. It was then washed with 1 *N* HCl and water, and dried. Removal of the solvent left an essentially quantitative yield of the sulfonamide (mixture of diastereomers). The n.m.r. spectrum showed peaks at the appropriate positions in the range 2.5–3.5 p.p.m. corresponding in intensity to roughly 80% of one protium in C-10. The positions of the C-10 methylenes in the fully protiated diastereomeric sulfonamides were obtained by examining the n.m.r. spectra of the crude product obtained similarly from $\mathbf{1}a_+$. The intensities of these two C-10 AB quartets were approximately the same, indicating that under these conditions there is little or no kinetic resolution in the reaction, *i.e.* the result is much the same as that observed by Okamoto *et al.* (2) for the reaction in benzene at 27–30°.

Reaction of (+)-Camphor-10-Sulfonyl Chloride ($\mathbf{1}a_+$) with Piperidine-d and Pyridine

Piperidine (4 ml) was dissolved in D_2O (5 ml) and then extracted with CH_2Cl_2 (10 ml). The CH_2Cl_2 layer was shaken for ½ min with four more batches of D_2O (5 ml) and then passed through a plug of cotton wool into a 50-ml flask. Fractional distillation gave piperidine-*d* (1.2 ml).

To a solution of piperidine-*d* (1 ml, 860 mg, 10 mmol) in pyridine (2 ml) was added (+)-camphor-10-sulfonyl chloride (125 mg, 0.5 mmol). After 3½ h at room temperature, the mixture was taken up in ether, washed twice with 3 *N* HCl and once with water, and dried. Removal of the solvent gave 118 mg of product which except for the region 2.5–3.5 p.p.m. was identical with that obtained by similar treatment of ordinary (protiated) piperidine. The 2.5–3.5 p.p.m. region in the spectrum of the amide from the ordinary piperidine shows an AB quartet δ_A 2.72, δ_B 3.28, J = 14 Hz with a large unresolved peak at 3.22 p.p.m. (due to the nitrogen-bearing methylenes of the piperidine) superimposed. The product from the reaction with piperidine-*d* showed only a small residue of the AB quartet and a new peak at 2.75 p.p.m. appropriate to a CHD replacing a CH_2 group; the corresponding peak expected at ~3.25 p.p.m. was obscured by the large peak at 3.22 p.p.m. A control experiment with piperidine-*d* and the natural-abundance sulfonpiperidide showed that no significant deuterium uptake occurs after formation of the amide.

We thank the National Research Council of Canada for financial support of this work.

1. J. Read and R. A. Storey. J. Chem. Soc. 2761 (1930).
2. K. Okamoto, E. Minami, and H. Shingu. Bull. Chem. Soc. Jap. **41**, 1426 (1968).
3. J. F. King and T. W. S. Lee. J. Am. Chem. Soc. **91**, 6524 (1969); T. W. S. Lee. Ph.D. Thesis, University of Western Ontario, London, Ontario, 1969.
4. E. Wedekind, D. Schenk, and R. Stüsser. Ber. **56**, 633 (1923).
5. J. F. King and T. Durst. Can. J. Chem. **44**, 819 (1966).
6. K. Mislow. Introduction to stereochemistry. W. A. Benjamin, New York, N.Y. 1966. p. 128.
7. L. C. Bateman, E. D. Hughes, and C. K. Ingold. J. Chem. Soc. 881 (1938).
8. L. C. Bateman, M. G. Church, E. D. Hughes, C. K. Ingold, and N. A. Taher. J. Chem. Soc. 979 (1940).
9. M. L. Bender. *In* Investigation of rates and mechanisms of reactions. *Edited by* S. L. Friess, E. S. Lewis, and A. Weissberger. Technique of organic chemistry. Vol. VIII. Part II. *Edited by* A. Weissberger. Interscience, New York, N.Y. 1963. p. 1480.
10. R. Huisgen. Angew. Chem. Int. Ed. **9**, 751 (1970).
11. J. F. King and S. K. Sim. J. Am. Chem. Soc. **95**, 4448 (1973).
12. J. Read, C. C. Steele, and P. G. Carter. J. Chem. Soc. 23 (1929).
13. K. Wiesner, E. W. K. Jay, T. Y. R. Tsai, C. Demerson, L. Jay, T. Kanno, J. Křepinský, A. Vilím, and C. S. Wu. Can. J. Chem. **50**, 1925 (1972).
14. O. Rogne. J. Chem. Soc. (B), 1294 (1968) and later papers in this series.
15. W. E. Truce and R. W. Campbell. J. Am. Chem. Soc. **88**, 3599 (1966).
16. J. F. King and T. Durst. J. Am. Chem. Soc. **87**, 5684 (1965).
17. S. Smiles and T. P. Hilditch. J. Chem. Soc. **91**, 519 (1907).
18. P. D. Bartlett and L. H. Knox. Org. Synth. **45**, 12 (1945).
19. L. T. Sandborn. Org. Synth. Coll. Vol. I, 340.
20. G. Andres and A. Andreef. Ber. **25**, 609 (1892).
21. M. C. Hamming and N. G. Foster. Interpretation of mass spectra of organic compounds. Academic Press, New York, N.Y. 1972. p. 646.

Reduction of 5α-Cholestan-3-one with Water as a Hydrogen Donor in the Presence of Precipitated Metals[1]

MASAYOSHI ISHIGE, MICHIO SHIOTA, AND YUKIKO IDENO
Chemical Laboratory, Ochanomizu University, Otsuka, Bunkyo-ku, Tokyo, Japan

Received April 26, 1973

Reduction of 5α-cholestan-3-one with various precipitated metals using water as a hydrogen donor was investigated. Precipitated cobalt in *t*-BuOH and nickel in dioxane afforded 5α-cholestan-3α-ol favorably. Some multi-component precipitated metals were found to show high activity.

On a examiné la réduction de la 5α-cholestanone-3 par divers métaux précipités et utilisant de l'eau comme donneur d'hydrogène. Du cobalt précipité dans le *t*-BuOH et du nickel dans la dioxanne mènent favorablement au 5α-cholestanol-3α. On a trouvé que quelques métaux précipités contenant plusieurs composants possèdent une grande activité. [Traduit par le journal]

Can. J. Chem., **51**, 3923 (1973)

Can. J. Chem. Downloaded from www.nrcresearchpress.com by 210.87.254.40 on 09/05/12
For personal use only.

Introduction

Some information has been given on the features of the reduction catalyzed by precipitated nickel (1–4), which is performed by heating organic substrates with water in the presence of precipitated nickel (ppt-Ni in abbreviation).[2] One of the unique characteristics of this reaction is the fact that water is used as a hydrogen donor. In comparison with the studies on the utility and mechanism of the reaction, the stereochemistry has been examined to a lesser extent. Furthermore, the slowness of the reaction often presents difficulties, especially when the dioxane–water mixed solvent is used.

With the purpose of studying this reduction method further, we investigated the reactivity and stereochemistry in the reduction of 5α-cholestan-3-one using various ppt-metals. The condition under which the formation of 5α-cholestan-3α-ol was favored was also examined.

Experimental

A. Precipitated Metals

1. Ppt-Ni[3]

A mixture of zinc dust (10 g) and distilled water (*ca.* 3 ml) in an Erlenmeyer flask was heated to 80 °C. An aqueous solution (10 ml) containing 4.04 g of nickel chloride (hexahydrate), pre-heated at 80 °C, was added to the hot zinc dust mud at once with vigorous shaking. A violent ion-exchange reaction was stopped by cooling with water after about 2 min. The deposited solid was collected on a filter paper by suction, washed successively with water, ethanol, and ether, and then dried on a filter paper. The ppt-Ni thus obtained contains about 1 g of nickel, supported on zinc metal and zinc compounds.

2. Ppt-Co and Ppt-Cu[3]

Instead of nickel chloride, 4.04 g of cobalt(II) chloride (hexahydrate) and 2.86 g of copper(II) chloride (dihydrate) were used with 10 g of zinc for the preparation of ppt-Co and ppt-Cu respectively, by the procedure described above.

3. Ppt-metals of Multi-component System

Ppt-Ni–Co (2:1) and ppt-Ni–Cu (2:1)[4] were prepared by using a mixture of 2.69 g of nickel chloride and either 1.34 g of cobalt(II) chloride or 0.95 g of copper(II) chloride. Ppt-Ni–Co–Cu (2:1:1) was prepared from a mixture of 2.02 g of nickel chloride, 1.01 g of cobalt(II) chloride, and 0.72 g of copper(II) chloride.

Other ppt-metals were also prepared from the mixture of the corresponding metal chlorides as follows: ppt-Ni–Co (10:1), 3.67 g of nickel chloride and 0.37 g of cobalt(II) chloride; ppt-Ni–Cu (10:1), 3.67 g of nickel chloride and 0.26 g of copper(II) chloride; ppt-Ni–Mn (10:1), 3.67 g of nickel chloride and 0.31 g of manganese(II) chloride (tetrahydrate); ppt-Ni–Co–Cu (20:2:1), 3.51 g of nickel chloride, 0.35 g of cobalt(II) chloride, and 0.12 g of copper(II) chloride; ppt-Ni–Co–Mn (20:2:1), 3.51 g of nickel chloride, 0.35 g of cobalt(II) chloride, and 0.15 g of manganese(II) chloride; ppt-Ni – Co – Cr (20:2:1), 3.51 g of nickel chloride, 0.35 g

[1]Presented in part at the 28th Annual Meeting of the Chemical Society of Japan in Tokyo, Japan, April 1973.

[2]The ppt-Ni itself possesses no ability to catalyze the ordinary hydrogenation with hydrogen gas. However, the acid or alkali treatment of ppt-Ni leads to Urushibara nickel catalysts; *cf.* ref. 5.

[3]It has been shown that various kinds of ppt-metals are obtainable as the result of the different combinations of the source materials used and the procedures employed. In this work, we adopted the ordinary types of ppt-Ni, -Co, and -Cu prepared by the simplified procedure; see footnote 2, pp. 29–60.

[4]The numerals in parentheses denote the ratio of atom numbers of the metals based on the metal chlorides used as source materials of each ppt-metal. The representation of zinc ratio is ignored.

Can. J. Chem. Downloaded from www.nrcresearchpress.com by 210.87.254.40 on 09/05/12
For personal use only.

of cobalt(II) chloride, and 0.20 g of chromium(III) chloride (hexahydrate).

B. Reduction

1. Reduction with Ppt-metals (Tables 1 and 2)

A mixture of 18 mg of 5α-cholestan-3-one, 3 ml of an organic solvent, 0.1 ml of water, and 0.20 g of each ppt-metal was kept at 80–83 °C for 20 h in a sealed tube.

2. Reduction with Ppt-metals of Higher Activity (Table 3)

Each sealed tube containing 0.200 g of ppt-metal and 1.00 ml portion of the solution prepared from 5α-cholestan-3-one (180 mg), *t*-BuOH (10 ml), and H_2O (1.00 ml) was kept at 80 ± 0.1 °C for 65 min.

C. Analysis

The reaction mixture was analyzed by gas chromatography after trimethylsilylation of the resulting sterols with *N,O*-bis(trimethylsilyl)acetamide. The gas chromatograms were taken on Shimadzu GC-4APF instrument by using a glass column packed with 1.5% Silicone OV-17 on silanized Shimalite W (80–100 mesh, 4 mm ϕ × 3 m) under the following conditions: column temperature, *ca.* 250 °C; carrier gas, nitrogen; flow rate, *ca.* 0.91 ml/s; detector, HFID.

Results and Discussion

Effect of Organic Solvents on the Reaction

Effect of organic solvents on the reactivity and stereoselectivity on the reduction of 5α-cholestan-3-one with ppt-Ni is shown in Table 1. It was found that the ketone was much more readily reduced to corresponding sterols in a protic solvent than in an aprotic solvent. The effect of the alcohols used on the relative reactivity was found to be in the following order; *n*-BuOH > *i*-PrOH > *t*-BuOH. Methanol and ethanol as solvents were undesirable because of low solubility of the substrate in these solvent–water systems. The alcohols probably play a dual role, serving both as a solvent and as a hydrogen donor, since the steroid ketone was hydrogenated in anhydrous *t*-BuOH to some extent. However, from the fact that the reduction occurred much faster in *t*-BuOH–H_2O than in *t*-BuOH alone, it may be concluded that coexistence of water and the alcohol is greatly responsible for the acceleration of the reaction.

TABLE 1. Solvent effect on the reduction of 5α-cholestan-3-one with ppt-Ni*

Solvent†	Ketone reacted (%)	Composition of the products (%) 3α-ol	3β-ol
Isopropyl alcohol	89	42	58
n-Butyl alcohol	95	48	52
t-Butyl alcohol	82	39	61
Dioxane	15	59	41
Tetrahydrofuran	5	38	62

*The results in Tables 1–3 were reproducible within 3% error with respect to the ketone reacted and within 2% error with respect to the composition of the products.

†Each organic solvent is used by mixing it with a given amount of water required for the reduction.

In aprotic solvents, such as dioxane and tetrahydrofuran, the reaction proceeded very slowly.

With regard to stereoselectivity of the products, the results were not so different in *i*-PrOH, *t*-BuOH, and tetrahydrofuran (39–42% with respect to 3α-ol). *n*-Butyl alcohol was, however, slightly favorable for the formation of 3α-ol. It was observed that dioxane characteristically favored the formation of 3α-ol rather than 3β-ol.

General Aspects of the Activities of Ppt-metals

It was previously suggested that ppt-metal with higher activity would be obtainable by a proper combination of metals (2, 3). Thus, we have prepared ppt-metals of multi-component systems and applied them to the reduction of 5α-cholestan-3-one. The results of representative experiments in *t*-BuOH–H_2O (listed in Table 2) show the relative activities of ppt-metals in the following order: Ni – Co – Cu (2:1:1) > Ni–Co (2:1) ≃ Ni–Cu (2:1) ≃ Ni > Co > Cu. The result indicates that coexistence of cobalt and copper with nickel may effectively promote the activity of nickel catalyst, though cobalt or copper itself contributes slightly to the change in activity of nickel.

However, it must be pointed out that the activity of each ppt-metal depends on the reaction conditions. In dioxane–H_2O, the order of relative activities alters as follows: Cu > Ni – Co – Cu (2:1:1) ≃ Ni–Cu (2:1) ≃ Ni ≃ Ni–Co (2:1) > Co. From the facts, it is inferred that some metals are sensitively deactivated by dioxane and others are not;[5] for instance, cobalt is strongly poisoned by dioxane, whereas copper is hardly deactivated by it. As for the dependence of activity on solvents, nickel seems to rank between the two.

Preparation of Ppt-metals of Higher Activity

A suitable combination of metals with nickel

[5]Generally, the reduction was markedly retarded by a trace of chromium as a contaminant in 5α-cholestan-3-one; cobalt was the most strongly deactivated of all the metals used, while the activity of copper was hardly influenced.

TABLE 2. Activities and stereoselectivities of various ppt-metals in the reduction of 5α-cholestan-3-one in the mixed solvents of *t*-BuOH–H_2O and dioxane–H_2O

Solvent	Ppt-metal	Ketone reacted (%)	Composition of the products (%) 3α-ol	3β-ol
t-BuOH–H_2O	Ni	82	39	61
	Co	53	68	32
	Cu	47	28	72
	Ni–Co (2:1)	85	38	62
	Ni–Cu (2:1)	83	39	61
	Ni–Co–Cu (2:1:1)	90	36	64
Dioxane–H_2O	Ni	15	59	41
	Co	3	51	49
	Cu	43	39	61
	Ni–Co (2:1)	12	58	42
	Ni–Cu (2:1)	15	49	51
	Ni–Co–Cu (2:1:1)	15	62	38

was extensively explored to increase the catalytic activity of ppt-metal.

The data in Table 3 show the promotion in relative activity of ppt-Ni – Cu and Ni – Co – Cu, and, especially, of ppt-Ni–Mn and Ni–Co–Mn.

Though the precipitation of manganese by the ion-exchange reaction with zinc would not be expected, it is inferred that the inclusion of some manganese in precipitates may occur during the course of the preparation of ppt-Ni–Mn and ppt-Ni–Co–Mn, because manganese clearly contributes to the promotion of activity of both ppt-Ni–Co–Mn and Urushibara-Ni, Co,Mn-A which is prepared by the removal of zinc and zinc compounds from ppt-Ni–Co–Mn with acetic acid. This result also suggests that the catalytic activity of ppt-metal is largely dependent on the nature of the crystallite of nickel but not on zinc.

The addition of chromium was unfavorable for the increase of the catalytic activity of nickel.

TABLE 3. The results of the reduction of 5α-cholestan-3-one using various ppt-metals with higher activity

Ppt-metal	Ketone reacted (%)	Composition of the products (%) 3α-ol	3β-ol
Co	Trace	—	—
Ni	Trace	—	—
Ni–Co (10:1)	12	35	65
Ni–Cu (10:1)	32	33	67
Ni–Mn (10:1)	56	35	65
Ni–Co–Cu (2:1:1)	32	36	64
Ni–Co–Cu (20:2:1)	31	29	71
Ni–Co–Mn (20:2:1)	60	33	67
Ni–Co–Cr (20:2:1)	7	36	64

Relation between Metal and Stereoselectivity

It should be noted that the 3α-ol was favorably produced in *t*-BuOH–H_2O in the presence of ppt-Co (68%) (Table 2). On the other hand, ppt-Cu was the least selective for the formation of 3α-ol under the same reaction condition. In the *t*-BuOH–H_2O system, little difference in selectivity between other ppt-metals was observed in the formation of 3α-ol.

The intrinsic nature of cobalt to give favorably the 3α-ol proved to be invariable even in the conversion of ppt-Co to Urushibara-Co-A by acid treatment; for example, the hydrogenation of 5α-cholestan-3-one with Urushibara-Co-A in *t*-BuOH at 35 °C for 4 h under the hydrogen pressure of 100 kg/cm^2 gave 5α-cholestan-3α-ol (61% yield, m.p. 188–189 °C) and 5α-cholestan-3β-ol (39% yield, m.p. 140–141.5 °C). This result provides an example of the favorable formation of 3α-ol in 5α-steroid by the catalytic hydrogenation under the practically neutral condition.[6]

[6]The catalytic hydrogenation of 5α-cholestan-3-one with Urushibara-Ni-A in dioxane at 72–75 °C afforded 3α-ol in 62% yield. In *t*-BuOH, the formation of 3α-ol was not favored (38%) (6). These results were similar to those obtained with ppt-Ni.

Can. J. Chem. Downloaded from www.nrcresearchpress.com by 210.87.254.40 on 09/05/12
For personal use only.

TABLE 4. Reduction by refluxing 5α- and 5β-cholestan-3-one with water in the presence of ppt-Ni*

Substrate	Solvent	Ketone reacted (%)	Composition of the products (%)	
			3α-ol	3β-ol
5α-Cholestan-3-one	*t*-BuOH–H_2O	100	40	60
	Dioxane–H_2O	68	48	52
5β-Cholestan-3-one	*t*-BuOH–H_2O	80	*ca.* 100	—
	Dioxane–H_2O	44	99	1

*Reaction condition: substrate, 90 mg; ppt-Ni, 1.0 g; organic solvent, 5 ml; water, 0.5 ml; reaction time, 7 h.

As compared with the reactions in *t*-BuOH–H_2O, a general tendency to increase the selectivity of 3α-ol was observed in dioxane–H_2O in the presence of various ppt-metals (Table 2). However, in the cases with ppt-Cu and ppt-Ni–Cu (2:1), the trend was not so conspicuous as in other cases. When ppt-Co was used in dioxane–H_2O, the proportion of 3α-ol was decreased markedly.

Reduction of 5α- and 5β-Cholestan-3-one by Refluxing with Water in the Presence of Ppt-Ni

5α- and 5β-Cholestan-3-one were hydrogenated to the corresponding sterols by refluxing in *t*-BuOH–H_2O or dioxane–H_2O in the presence of ppt-Ni. The results are summarized in Table 4.

The composition of the products from 5α-cholestan-3-one in refluxing *t*-BuOH–H_2O was similar to that described in Table 2. 5β-Cholestan-3-one gave exclusively the 3α-ol.

In refluxing, a long reaction time was required for the completion of the reaction as compared with the case in a sealed tube. The reasons may be attributable mainly to the loss of generated hydrogen gas and to the deactivation of nickel by oxygen in the air.

The reduction with ppt-Co under reflux was not conducted effectively. This result may also be attributed to the fact that ppt-Co is sensitive to catalyst poisons.

It was observed that 3β-acetoxy-5α-cholestan-6-one was not reduced by this method. This fact may indicate that reduction by this method may be influenced by the steric environment at C-6.

1. K. SAKAI and K. WATANABE. Bull. Chem. Soc. Jap. **40**, 1548 (1967).
2. K. SAKAI, M. ISHIGE, H. KONO, I. MOTOYAMA, K. WATANABE, and K. HATA. Bull. Chem. Soc. Jap. **41**, 1902 (1968).
3. K. SAKAI, M. ISHIGE, K. WATANABE, and K. HATA. Bull. Chem. Soc. Jap. **43**, 1172 (1970).
4. H. KONO, M. ISHIGE, K. SAKAI, M. SHIGA, I. MOTOYAMA, and K. HATA. Bull. Chem. Soc. Jap. **43**, 867 (1970).
5. K. HATA. Urushibara catalysts. University of Tokyo Press, Tokyo. 1971.
6. M. ISHIGE and M. SHIOTA. Synthesis, 171, 1973.

Can. J. Chem. Downloaded from www.nrcresearchpress.com by 210.87.254.40 on 09/05/12
For personal use only.

The Interaction of Sulfite Ion with 2,4,6-Trinitrobenzaldehyde: Kinetic, Equilibrium, and Proton Magnetic Resonance Studies

NEVEN MARENDIC AND ALBERT RICHARD NORRIS
Department of Chemistry, Queen's University, Kingston, Ontario

Received June 4, 1973

Sulfite ion reacts with 2,4,6-trinitrobenzaldehyde in aqueous solution of ionic strength 0.14 *M* to yield a 1:1 σ-complex at low sulfite concentrations and a 2:1 σ-complex at high sulfite concentrations. The visible absorption characteristics of these two σ-complexes as well as equilibrium constants and relevant thermodynamic parameters for their formation have been determined. P.m.r. studies demonstrate that two isomeric forms of the 1:1 σ-complex occur in aqueous dimethylsulfoxide solution and two isomeric forms of the 2:1 σ-complex occur in water. In both the 1:1 and the 2:1 complexes isomers are found which contain sulfite ion attached to the C-1 carbon and one of the isomeric 2:1 σ-complexes is postulated to exist in *cis* and *trans* forms. Observations are presented concerning the kinetics of the very rapid formation of the 1:1 σ-complex in water.

L'ion sulfite réagit avec la trinitro-2,4,6 benzaldehyde en solution aqueuse de force ionique 0.14 *M* pour donner un complexe 1:1 à des concentrations faibles de sulfite et un complexe 2:1 à des concentrations élevées de sulfite. On a déterminé les caractéristiques d'absorption de ces deux complexes ainsi que les constantes d'équilibres et les paramètres thermodynamiques se rapportant à leur formation. Des études en r.m.p. ont montré que deux formes isomériques du complexe 1:1 se forment en solution aqueuse de sulfoxyde de diméthyle et que deux formes isomériques du complexe 2:1 se forment dans l'eau. On a trouvé dans les deux complexes 1:1 et 2:1 des isomères qui contiennent l'ion sulfite relié au carbone C-1. De même on admet que l'un des complexes 2:1 isomériques existe sous des formes *cis* et *trans*. On présente aussi des observations se rattachant à la cinétique de formation très rapide du complexe 1:1 dans l'eau. [Traduit par le journal]

Can. J. Chem., **51**, 3927 (1973)

Introduction

In an earlier paper describing our observations concerning the reaction of sulfite ion with 1,3,5-trinitrobenzene (1) we reported the visible absorption characteristics of the 1:1 σ-complexes of sulfite ion with 2,4,6-trinitrotoluene and 2,4,6-trinitrobenzaldehyde. Since that time information has become available concerning the visible absorption characteristics and p.m.r. spectra of a number of 1:1 and 2:1 sulfite ion – 1-X-2,4,6-trinitrobenzene σ-complexes (X = H, HO, CH_3O, NH_2, $NHCH_3$, $NH(C_6H_5)$, $N(CH_3)_2$, and $N(CH_3)(C_6H_5)$) (2–4), but no further data have been published concerning the sulfite ion – 2,4,6-trinitrobenzaldehyde reaction. In connection with kinetic studies of 1:1 complex formation in the reactions of sulfite ion with a number of 1-X-2,4,6-trinitrobenzenes (X = H, NH_2, $NHCH_3$, and $N(CH_3)_2$), and as part of a study involving the σ-complex formation reactions of 2,4,6-trinitrobenzaldehyde (5) we have investigated in more detail the sulfite ion – 2,4,6-trinitrobenzaldehyde reaction. The visible absorption characteristics of the 1:1 and 2:1 σ-complexes, equilibrium constants, and relevant thermodynamic parameters for the formation of the 1:1 and 2:1 σ-complexes, the p.m.r. spectra of the 1:1 and 2:1 σ-complexes, and observations regarding the kinetics of formation of the 1:1 σ-complex in aqueous solution are now reported.

Experimental

(1) Reagents

Sodium sulfite and potassium nitrate were both A. R. grade reagents (Fisher Scientific) and were used as received. 2,4,6-Trinitrobenzaldehyde (Aldrich Chemical Co.) was purified by carbon black treatment in benzene–ethanol solution, recrystallized several times from ethanol, and dried *in vacuo* over phosphorus(V) pentoxide, m.p. 119.0–119.5 °C. All other reagents used were A.R. grade or better.

Doubly distilled and deionized water was boiled for approximately 30 min to remove dissolved gases then allowed to cool to room temperature and stored under a nitrogen atmosphere. Absolute ethanol was purified by distillation from magnesium turnings in an atmosphere of nitrogen.

A 2,4,6-trinitrobenzaldehyde stock solution ($\sim 2 \times 10^{-3}$ *M*) was prepared by dissolving a weighed amount of dried compound in a known volume of ethanol. Solutions of 2,4,6-trinitrobenzaldehyde used in the kinetic and equilibrium studies were freshly prepared prior to use by appropriate dilution (usually 1–100 ml) of an aliquot of

Can. J. Chem. Downloaded from www.nrcresearchpress.com by 210.87.254.6 on 09/05/12
For personal use only.

Can. J. Chem. Downloaded from www.nrcresearchpress.com by 210.87.254.6 on 09/05/12
For personal use only.

the stock solution with 0.14 M aqueous potassium nitrate solution.

Sodium sulfite and potassium nitrate stock solutions were always prepared immediately before use. The composition of the stock sodium sulfite solution was determined each time by iodimetric titration (6). Sodium sulfite solutions used in the kinetic and equilibrium studies were prepared by dilution of aliquots of the stock solution with 0.14 M aqueous potassium nitrate solution. The pH's of the stock solutions and the solutions used in the equilibrium and kinetic studies were checked with a pH meter and, if required, adjusted to a particular pH value by the addition of small amounts of 2×10^{-3} M sodium hydroxide or hydrochloric acid. The amount of added acid or base was generally so small that neither the concentration nor ionic strength of the solutions was affected by this procedure.

(2) Procedures

(a) Equilibrium Studies

In most instances a 1.0-cm cell containing 1.50 ml of 2,4,6-trinitrobenzaldehyde test solution (approximately 2×10^{-5} M) at an ionic strength of 0.14 M (KNO_3), a second cell containing 2–3 ml of sodium sulphite solution of desired concentration and ionic strength 0.14 M (KNO_3), and a syringe were placed in the thermostatted cell holder of the spectrophotometer and allowed to stand for 20 min in order to reach thermal equilibrium. A 1.50-ml sample of the sodium sulphite solution was then quickly transferred by syringe to the cell containing the 2,4,6-trinitrobenzaldehyde solution; the solution was thoroughly mixed, allowed to stand for approximately 2 min, and its spectrum recorded. When solutions of low sulfite ion concentration were required 10.0 ml of aqueous potassium nitrate solution was placed in a 5.0-cm cell and the cell and contents allowed to come to thermal equilibrium with the thermostatted cell compartment. Small volumes of the sodium sulfite and 2,4,6-trinitrobenzaldehyde stock solutions were then added by means of microliter syringes, the solution was mixed thoroughly and its spectrum recorded. Changes in the concentrations of sodium sulfite and 2,4,6-trinitrobenzaldehyde as a result of dilution were taken into account where necessary.

(b) Stopped-flow Kinetic Studies

Solutions containing 2,4,6-trinitrobenzaldehyde (at approximately 2×10^{-5} M) and sodium sulfite were prepared immediately prior to the kinetic run by dilution of known volumes of the corresponding stock solutions with 0.14 M aqueous potassium nitrate solution. Before each run the drive syringes were rinsed three times with the appropriate solution, filled to capacity, and allowed 20 min to reach thermal equilibrium with the bath. In the course of the kinetic measurements the concentration of 2,4,6-trinitrobenzaldehyde was generally kept constant and therefore, only the sodium sulfite solutions were changed. Each time this was done the drive syringe was flushed thoroughly with the new sodium sulfite solution before being filled for the kinetic run.

For the most part the kinetic runs were monitored by following the change in absorbance at 460 nm. In some runs absorbance changes at 500 and 580 nm were also recorded. Traces on the storage oscilloscope of absorbance *vs.* time were recorded photographically when at least two consecutive runs gave identical traces. The kinetic curves were then transferred from the photographs to cm-graph paper and the values of absorbance as a function of time read from the graph paper used to construct plots of $\ln (A_\infty - A_t)$ *vs.* time; (A_∞ and A_t refer to absorbances at times infinity and t, respectively). The slopes of the $\ln (A_\infty - A_t)$ *vs.* time plots yielded pseudo first-order rate constants k_{obs}. As a check on this procedure values of k_{obs} were also calculated using absorbance values read directly from the photographs. Values of k_{obs} obtained by using the two methods were, within experimental error, generally the same. Although more time-consuming the first method had the advantage of yielding accurate absorbance values at a larger number of times. As a result, the k_{obs} values calculated using this method generally had lower error limits associated with them.

(c) Proton Magnetic Resonance Studies

Solutions in aqueous dimethylsulfoxide (30% v/v water) were prepared by dissolving 2,4,6-trinitrobenzaldehyde in dimethylsulfoxide and mixing this solution with the required amount of aqueous sodium sulfite solution. The concentration of 2,4,6-trinitrobenzaldehyde was kept constant (0.10–0.15 M) while the concentration of sodium sulfite was varied over the range 0.10–2.0 M.

Solutions in water were prepared either by dissolving solid 2,4,6-trinitrobenzaldehyde directly in an aqueous sodium sulfite solution or by dissolving 2,4,6-trinitrobenzaldehyde in carbon tetrachloride and shaking this solution with a concentrated aqueous solution of sodium sulfite. The recorded spectra were independent of the method of preparation of the solutions. The concentration of 2,4,6-trinitrobenzaldehyde was kept constant (0.10–0.12 M) and the sodium sulfite concentration varied over the range 0.10–1.2 M.

All chemical shifts are quoted relative to internal tetramethylsilane (TMS).

(3) Instruments

Optical measurements in the equilibrium studies were carried out on a Cary 14 recording spectrophotometer using matched silica cells of 1.0- and 5.0-cm path lengths. Temperature in the cells was maintained constant to ± 0.1 °C by circulating water from a constant temperature bath through a specially designed cell holder in the spectrophotometer.

Proton magnetic resonance spectra were recorded on a Bruker HX-60 spectrometer employing the HDO peak in aqueous solution and the TMS peak in aqueous dimethylsulfoxide solution as the "internal lock". The probe temperature was generally about 20 °C.

Kinetic measurements were carried out on a Durrum-Gibson stopped-flow spectrophotometer. A closed circuit temperature control system utilizing an Ultra Kryomat TK30D constant temperature bath kept the temperature in the valve-block, drive syringes, and observation cell constant to within ± 0.1 °C. Temperature-jump or conventional stopped-flow cells of 2.0-cm path length were used. Minimum "dead times" of the two cells were 10 and 2 ms, respectively. For most of the kinetic runs the normal mode of operations of the stopped-flow spectrophotometer was modified so as to yield an oscilloscope trace of absorbance as a function of time rather than percent transmission as a function of time.

TABLE 1. Proton magnetic resonance data for 2,4,6-trinitrobenzaldehyde and the sulfite ion – 2,4,6-trinitrobenzaldehyde complexes formed in aqueous dimethylsulfoxide and water. Relative intensities of the resonances are in parentheses

Compound	Solvent[a]	Chemical shifts (p.p.m.) H_a	H_α	H_β
2,4,6-Trinitrobenzaldehyde	A	−0.52 (1)	0.83 (2)	—
2,4,6-Trinitrobenzaldehyde	B	−0.62 (1)	0.73 (2)	—
1	A	−0.18 (1)	1.72 (2)	—
2	A	−0.38 (1)	1.82 (1) $J_{H_\alpha-H_\beta} \simeq 1.5$ Hz	4.08 (1)
3	B	−0.18 (1)	—	4.13 (2)
4	B			
cis		−0.05 (1)	1.45 (1)	3.95 (1)
trans		0.17 (1)	1.27 (1)	4.05 (1)

[a]Solvent designations: A, aqueous dimethylsulfoxide 30% (v/v water); B, water.

Measurements of p*H* were carried out with an EIL Model 23A p*H* meter which is capable of measuring the p*H* with an accuracy of ±0.02 p*H* units. Calibration of the p*H* meter with standard buffer solutions of p*H* 7.40 ± 0.02 and p*H* 10.00 ± 0.02 at 25 °C was performed prior to each measurement.

Results and Discussion

In aqueous dimethylsulfoxide (30% v/v water) 2,4,6-trinitrobenzaldehyde shows resonance absorbances at τ −0.52 and 0.83 (both singlets, ratio 1:2). The resonance absorbances characteristic of the complexes generated in this medium were found at τ −0.38 (singlet), −0.18 (singlet), 1.72 (singlet), 1.82 (doublet), and 4.08 p.p.m. (doublet). No changes were observed in the number of resonance absorbances or in the relative intensities of the absorbances over a period of at least a day at room temperature.

The observed spectra are consistent with the solutions containing, in addition to free 2,4,6-trinitrobenzaldehyde, only the two isomeric 1:1 σ-complexes **1** and **2**. Assignments of the reso-

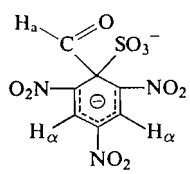

1

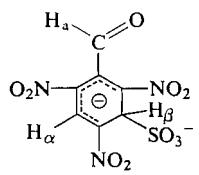

2

nance absorbances of the hydrogens in these two complexes, as given in Table 1, are based by analogy with the chemical shifts observed in other related 1:1 σ-complexes. The assignment of the ring H_α and H_β protons in **2** is consistent with the observed chemical shifts in the 1:1 sulfite ion complexes of 1,3,5-trinitrobenzene, 2,4,6-trinitroanisole, picramide, and *N*-methyl- and *N*,*N*-dimethylpicramide (2). The smaller upfield shift of the H_α resonance in complex **1** as compared to the upfield shift of the H_α resonance in complex **2** has previously been observed in the corresponding complexes of 2,4,6-trinitroanisole with both cyanide ion and methoxide ion (7–12). The observation that the aldehyde proton in **1** is upfield from the aldehyde proton in **2** is also consistent with the chemical shifts observed for the hydrogens of the methoxyl groups in the corresponding complexes (the C-1 and -3 complexes) of cyanide ion and methoxide ion with 2,4,6-trinitroanisole (7–12).

Over the range of sodium sulfite concentrations employed in the experiments the two 1:1 σ-complexes **1** and **2** were present at approximately equal concentrations and no evidence could be found for the formation of any 2:1 σ-complexes. The increased stability of 1:1 as compared to 2:1 sulfite ion – 1-X-2,4,6-trinitrobenzene σ-complexes in aqueous solutions of high dimethylsulfoxide content has been attributed to better solvation by dimethylsulfoxide than by water of the charge-delocalized 1:1 σ-complex (4, 13).

Complex **1** is the first 1:1 σ-complex of sulfite ion with a 1-X-2,4,6-trinitrobenzene (X other than H) in which addition has been shown to occur at the C-1 position. In all previous adducts investigated only addition at C-3 (or -5) was observed.

In aqueous solutions at low sulfite ion concentrations p.m.r. spectra recorded immediately on mixing show, in addition to resonances attrib-

Can. J. Chem. Downloaded from www.nrcresearchpress.com by 210.87.254.6 on 09/05/12
For personal use only.

Can. J. Chem. Downloaded from www.nrcresearchpress.com by 210.87.254.6 on 09/05/12
For personal use only.

uted to the parent 2,4,6-trinitrobenzaldehyde, eight resonance absorbances located at τ −0.18, −0.05, 0.17, 1.27, 1.45, 3.95, 4.05, and 4.13 p.p.m. All the resonance absorbances appear to be singlets. In marked contrast to what is observed in the case of aqueous dimethylsulfoxide solutions the pattern of resonance absorbances observed in water undergoes fairly rapid changes with time. These changes are always more rapid at higher temperatures and/or higher sulfite ion concentrations. Intermediate spectra show absorbances at τ 0.35 (often, but not invariably) and at τ 1.58 while the final spectra showed in all cases only a single resonance absorbance at τ 1.58.

The number and the positions of the initial resonance absorbances observed could be consistent with solutions containing either a mixture of the complexes **2**, **3**, and **4** or a solution consisting of complex **3** and the *cis* and *trans* isomers of **4**. In view of the large excess of sulfite ion to

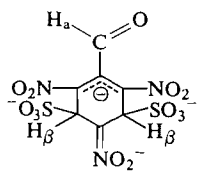

3 **4**

2,4,6-trinitrobenzaldehyde normally present in solution, the large equilibrium constant associated with 2:1 σ-complex formation in aqueous solution (*vide infra*) and the apparent insensitivity of the relative intensities of the various resonances attributable to the complexes to changes in sulfite ion concentration over the range 0.10–1.20 *M*, the experimental data seem more in accord with the latter possibility, *i.e.* under all conditions the solutions are thought to contain only 2:1 σ-complexes.

Assignments of the resonance absorbances of the hydrogens in complex **3** and the *cis* and *trans* isomers of **4** are given in Table 1.

For complex **3** the chemical shifts of the H_β protons are comparable to those found for the sulfite-containing 2:1 complexes of 1,3,5-trinitrobenzene, 2,4,6-trinitroanisole, picramide, and *N*-substituted picramides (2). No covalency change occurs at the C-1 position in complex **3** so the small upfield shift ($\Delta\tau = 0.44$) of the aldehyde hydrogen in the complex relative to the aldehyde hydrogen in the parent 2,4,6-trinitrobenzaldehyde must reflect primarily the increase in negative charge density in the C-1 position of complex **3**.

All the protons attributed to the *cis* and *trans* isomers of **4** show upfield shifts relative to the resonance absorbances of the parent compound. The shifts are largest ($\Delta\tau = 3.32$ and 3.22) for the H_β protons and smallest for the H_α protons ($\Delta\tau = 0.54$ and 0.72). The positions of the resonance absorbances of the H_β protons of **4** in water are very close to those observed for the H_β protons of **2** in aqueous dimethylsulfoxide. The aldehyde hydrogens of the two isomers show larger upfield shifts ($\Delta\tau = 0.57$ and 0.79) than that observed for the aldehyde hydrogen in complex **3** consistent with the fact that a covalency change occurs at the C-1 position of both the *cis* and *trans* forms of **4** but not at the C-1 position of **3**. Though coupling between H_α and H_β protons was observed for complex **2**, coupling between the H_α and H_β protons in the *cis* and *trans* forms of **4** could not be observed.[1] As a result definite assignments of the H_a, H_α, and H_β protons to the *cis* and *trans* forms of **4** is not possible, nor is it possible at this stage to say whether the *cis* or the *trans* isomer is the preferred species at equilibrium. In any event the preference of the *cis* form over the *trans* form (or *vice versa*) under the reaction conditions necessary to obtain the p.m.r. spectra is slight.

Even at the lowest concentrations of sulfite ion that could be used in order to obtain the p.m.r. spectra of the complexes formed in aqueous solution (~0.09 *M*) there was no evidence for the existence of 1:1 σ-complexes such as **1** or **2**. Crampton (2) has previously reported on the increased stability, relative to the 1:1 complexes, of 2:1 complexes of sulfite ion with 1,3,5-trinitrobenzene, 2,4,6-trinitroanisole, and picramide in aqueous solution. The presence of 2:1 but not 1:1 complexes suggests that the 2:1 complexes, which have far more localized charges than the 1:1 complexes, are considerably more strongly solvated by water than are the 1:1 complexes.

Complex **4** is the first 2:1 σ-complex of sulfite ion with a 1-X-2,4,6-trinitrobenzene for which addition has been shown to occur at both the

[1]Coupling between H_α and H_β protons can be resolved in the 1:1 sulfite ion – 1,3,5-trinitrobenzene complex but not in the 2:1 sulfite ion – 1,3,5-trinitrobenzene complex (2).

Can. J. Chem. Downloaded from www.nrcresearchpress.com by 210.87.254.6 on 09/05/12
For personal use only.

C-1 and the -3 (or -5) position. Previously reported 2:1 σ-complexes between sulfite ion and a variety of 1-X-2,4,6-trinitrobenzenes all possessed structures similar to that observed for complex **3** *i.e.* addition had occurred only at the C-3 and -5 positions (4, 13).

The failure to detect addition of sulfite ion at an X-substituted carbon in other 1-X-2,4,6-trinitrobenzene 1:1 and 2:1 σ-complexes has been ascribed to two causes. One is steric strain effect associated with the addition of a sulfite ion at a carbon already bearing a large substituent X; the other is a specific solvation effect which arises because the sulfite ion in the complex still carries a formal negative charge and consequently must still be extensively solvated. Neither steric strain effects nor the solvation requirements of the 1:1 σ-complexes would be expected to be much different in complexes in which X = CHO as compared to those in which X = O^-, OCH_3, $NHCH_3$, and $N(CH_3)_2$. Other factors must also be important then in determining the point of addition of the sulfite ion. The electron withdrawing effect of the aldehyde group may be one such factor. Thus cyanide ion, which would be expected to have less stringent solvation requirements and give rise to much smaller steric strain effects than sulfite, reacts with 2,4,6-trinitrobenzaldehyde to yield only the C-1 complex even at low temperatures (5). It might be argued that, in the special case for which X = COH and the anion is sulfite ion, the electron withdrawing effect of the aldehyde group together with better solvation and coplanarity with the ring of the para nitro group and the possible release of steric compression (4, 13) in the C-1 complex (**1**) relative to the parent compound might partially offset the more favorable steric and solvation requirements of the C-3 complex (**2**). As a result both isomeric complexes are observed.

If this argument is correct the relative proportions of the two isomeric 1:1 σ-complexes **1** and **2** present in the system should be strongly solvent dependent and the existence of 1:1 C-1 complexes should occur only in those cases in which X is strongly electron withdrawing and the anion is small. These ideas are currently being tested.

The nature of the species formed as a result of the decomposition of complexes **3** and **4** is not known. The resonance absorbances at τ 1.58 could possibly be assigned to ring hydrogens in a compound such as **5**, but no effort was made to isolate such a species from the final reaction mixtures.

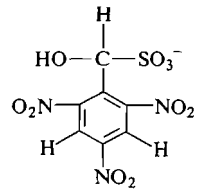

5

Aqueous solutions containing both 2,4,6-trinitrobenzaldehyde ($\sim 2 \times 10^{-5}$ *M*) and sodium sulfite (10^{-4}–10^{-2} *M*) in the p*H* range 7.50–10.0 are red in color though neither component alone absorbs in the region 370–700 nm under these conditions.

Studies of the visible absorption spectra of solutions containing a fixed concentration of 2,4,6-trinitrobenzaldehyde (typically $\sim 2 \times 10^{-5}$ *M*) and a variable concentration of sodium sulfite indicate the existence of two equilibria involving 2,4,6-trinitrobenzaldehyde and sulfite ion. The first is dominant at sulfite concentrations below 1.3×10^{-3} *M* while the second becomes apparent at sulfite concentrations above 1.3×10^{-3} *M* and is complete in solutions containing from 0.60–0.80 *M* sodium sulfite. Further changes in the visible absorption spectra are not observed as the concentration of sodium sulfite is increased above 0.80 *M*. Typical absorption curves are shown in Fig. 1. Sharp isosbestic points are observed at 480 and 527 nm at all temperatures over the range 0–50 °C.

The absorption characteristics of the species formed at sulfite concentrations $< 1.3 \times 10^{-3}$ *M* (λ_{max} 458 nm, shoulder mid point at 540 nm) are similar to those reported for the 1:1 σ-complexes of sulfite ion with 1,3,5-trinitrobenzene, 2,4,6-trinitrotoluene, 2,4,6-trinitroanisole, and picramide (1, 2, 14). The absorption characteristics of the species formed at high sulfite ion concentrations (λ_{max} 500 nm) are similar to those reported for a number of 2:1 sulfite ion complexes of 1-X-2,4,6-trinitrobenzenes, X = H, CH_3O, NH_2, $NHCH_3$, and $N(CH_3)_2$ (2). The positions of the absorption maxima are independent of temperature over the range 0–50 °C.

The above observations suggest that the two equilibria in solution are associated with the reversible formation of 1:1 and 2:1 sulfite

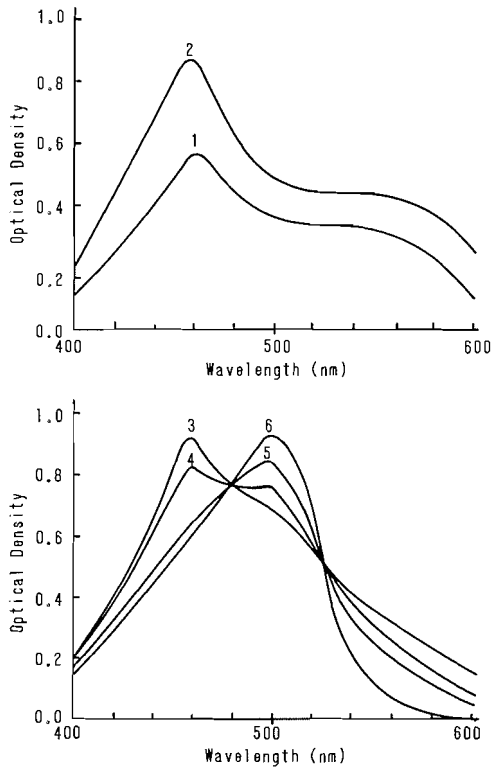

FIG. 1. Absorption spectra of 2,4,6-trinitrobenzaldehyde (1.0×10^{-5} *M*) in water containing the following molarities of sodium sulfite: (*1*) 0.0001; (*2*) 0.003; (*3*) 0.025; (*4*) 0.05; (*5*) 0.10; (*6*) 0.60. *T*, 24.0 °C. Ionic strength for all solutions but (*6*) 0.14 *M* (KNO_3).

ion – 2,4,6-trinitrobenzaldehyde σ-complexes. Schematically the processes can be formulated as

[1] 2,4,6-Trinitrobenzaldehyde + $SO_3^{2-} \rightleftharpoons C_1$

and

[2] $C_1 + SO_3^{2-} \rightleftharpoons C_2$

where K_1 and K_2 are the equilibrium constants associated with the formation of the 1:1 and 2:1 complexes, respectively.

The 1:1 stoichiometry of the 2,4,6-trinitrobenzaldehyde – sulfite ion complex formed at fixed 2,4,6-trinitrobenzaldehyde concentrations ($\sim 1 \times 10^{-5}$ *M*) and concentrations of sulfite ion in the range 1.0×10^{-4} to 1.3×10^{-2} *M* was established through the use of the graphical test method reported by Coleman, Varga, and Mastin (15) and by the use of the method of continuous variations (16).

Absorbance data for solutions of fixed initial concentrations of 2,4,6-trinitrobenzaldehyde ($[A_0]$) and sodium sulfite ion concentrations 1.0×10^{-3} to 1.30×10^{-4} *M*, when plotted in the form $[A_0]$/absorbance *vs.* $1/[B_0]$ (where $[B_0]$ is the initial sodium sulfite concentration), gave excellent straight lines from whose slopes and intercept values of the equilibrium constant for 1:1 σ-complex formation (K_1) and molar extinction coefficients (ε_1) of the complex at the wavelength at which absorbances were recorded were calculated (Benesi-Hildebrand (B–H) method (17)). Values of K_1 and ε_1 determined at a number of different temperatures and wavelengths are tabulated in Table 2. The excellent linearity of the B–H plots, the non-dependence of K_1 on wavelength, and the constancy of ε_1 as a function of temperature offer further evidence that only a single 1:1 σ-complex is being studied under the quoted reaction conditions. The results of the p.m.r. studies suggest that the 1:1 complex could be either **1** or **2**. Unfortunately, the visible absorption data cannot be used to differentiate between these two possibilities (4, 13, 14).

At any wavelength the molar extinction coefficient of the 2:1 σ-complex formed between 2,4,6-trinitrobenzaldehyde and sulfite ion could be found directly since conversion of 2,4,6-trinitrobenzaldehyde to the 2:1 complex was complete at high sulfite concentrations. Employing molar extinction coefficients (ε_2) found in this manner and known K_1 and ε_1 values the concentration of the 2:1 complex and the equilibrium constant for formation of the 2:1 complex could be calculated for solutions of different initial concentrations of sodium sulfite and 2,4,6-trinitrobenzaldehyde. Values of ε_2 and K_2 obtained in this way are tabulated in Table 3. The K_2 values are independent of the wavelength at which absorbance data are recorded while the values of ε_2, like the values of ε_1, are, within experimental error, temperature independent.

Mean values of the equilibrium constants K_1 and K_2 and mean molar extinction coefficients ε_1 and ε_2 at the wavelengths of maximum absorption (458 and 500 nm, respectively) at different temperatures are given in Table 4.

Enthalpies of formation ($\Delta H°$) and entropies of formation ($\Delta S°$) associated with both 1:1 and 2:1 σ-complex formation were obtained from plots of log K_1 and log K_2 *vs.* $1/T$. Relevant values are -2.41 ± 0.16 kcal mol^{-1} and 11.36 ± 1.05 cal deg^{-1} mol^{-1} and -8.53 ± 0.10 kcal mol^{-1} and -21.80 ± 2.36 cal deg^{-1} mol^{-1} for

Can. J. Chem. Downloaded from www.nrcresearchpress.com by 210.87.254.6 on 09/05/12
For personal use only.

TABLE 2. Equilibrium constants for 1:1 complex formation and molar extinction coefficients of the 1:1 complex determined at different temperatures and wavelengths. Ionic strength 0.14 M (KNO_3)

	$K_1 \times 10^{-4}$ (M^{-1}) at wavelength (nm)[a]			$\varepsilon_1 \times 10^{-4}$ (M^{-1} cm^{-1}) at wavelength (nm)[a]		
T (°C)	458	500	580	458	500	580
4.0	2.52±0.12	2.50±0.12	2.46±0.14	2.18±0.03	1.13±0.02	0.86±0.02
10.0	2.31±0.10	2.25±0.12	2.22±0.13	2.17±0.02	1.13±0.02	0.84±0.01
16.7	2.12±0.10	1.98±0.12	1.99±0.12	2.19±0.03	1.14±0.02	0.86±0.01
24.0	1.84±0.09	1.82±0.11	1.85±0.15	2.20±0.02	1.16±0.01	0.87±0.02

[a]Error limits on K and ε are based on the error limits associated with the "least squares" slopes and intercepts of the Benesi–Hildebrand plots.

TABLE 3. Equilibrium constants for 2:1 complex formation and molar extinction coefficients of the 2:1 complex determined at different temperatures and wavelengths. Ionic strength 0.14 M

	K_2 (M^{-1}) at wavelength (nm)		$\varepsilon_2 \times 10^{-4}$ (M^{-1} cm^{-1}) at wavelength (nm)	
T (°C)	458	500	458	500
4.0	95.1±4.4	96.4±6.0	1.39±0.01	1.80±0.02
10.0	62.6±2.0	65.2±1.7	1.40±0.01	1.82±0.03
16.6	49.6±2.5	52.0±2.2	1.39±0.01	1.84±0.02
24.0	31.4±1.5	31.8±1.4	1.38±0.02	1.85±0.02

TABLE 4. Mean equilibrium constants (K_1, K_2) and molar extinction coefficients (ε_1, ε_2) at different temperatures for the TNBA – sulphite ion system in water. Ionic strength 0.14 M (KNO_3)

T (°C)	$K_1 \times 10^{-4}$ (M^{-1})	$\varepsilon_1 \times 10^{-4}$ (M^{-1} cm^{-1}) 458 nm	K_2 (M^{-1})	$\varepsilon_2 \times 10^{-4}$ (M^{-1} cm^{-1}) 500 nm
4.0	2.49±0.14	2.18±0.03	95.7±4.3	1.80±0.01
10.0	2.26±0.13	2.17±0.02	64.2±2.2	1.82±0.02
16.7	2.03±0.14	2.19±0.03	50.8±2.3	1.84±0.01
24.0	1.84±0.13	2.20±0.02	31.7±1.1	1.85±0.02

the $\Delta H°$ and $\Delta S°$ of formation of the 1:1 and 2:1 complexes respectively. The errors in $\Delta H°$ and $\Delta S°$ are based on a "least squares" treatment of the data in the log K *vs.* $1/T$ plots.

The values of $\Delta H°$ and $\Delta S°$ for formation of the 1:1 sulfite ion – 2,4,6-trinitrobenzaldehyde σ-complex differ from the $\Delta H°$ and $\Delta S°$ values reported for formation of the 1:1 sulfite ion – 1,3,5-trinitrobenzene σ-complex. The lack of published thermodynamic data for the formation of other 1:1 and 2:1 sulfite ion – 1-X-2,4,6-trinitrobenzene complexes precludes any detailed analysis of the thermodynamic parameters at this time.[2] The large values of $\Delta H°$ and $\Delta S°$ associated with the formation of the 2:1 σ-complex may reflect the better solvation by water of the charge-localized 2:1 complex than the charge-delocalized 1:1 complex.

Stopped-flow techniques were employed to study the kinetics of the sulfite ion – 2,4,6-trinitrobenzaldehyde. These studies, which were

[2]Kinetic and thermodynamic studies of the formation of the 1:1 sulfite ion complexes of picramide, *N*-methylpicramide, and *N*,*N*-dimethylpicramide have been completed . The results of these studies have been submitted for publication (A.R. Norris and P. J. Sheridan).

Can. J. Chem. Downloaded from www.nrcresearchpress.com by 210.87.254.6 on 09/05/12
For personal use only.

Can. J. Chem. Downloaded from www.nrcresearchpress.com by 210.87.254.6 on 09/05/12
For personal use only.

carried out over a range of sodium sulfite (2.6×10^{-5} to 1.12×10^{-3} M) and 2,4,6-trinitrobenzaldehyde (9.7×10^{-6} to 2.0×10^{-5} M) concentrations, at different temperatures (10.0 to 35.0 °C) and in solutions of varying pH (7.50–10.00), indicated there were always two reactions taking place in solution. The first was a very fast reaction ($t_{1/2} < 5$ ms) which, under all the experimental conditions we were able to employ, was complete in too short a time to allow for any detailed study of its rate dependence on various reaction parameters. The absorption spectrum of the species formed at the completion of this first reaction could be recorded however, and was identical in all respects to that of a 1:1 sulfite ion – 2,4,6-trinitrobenzaldehyde complex. The second reaction which was characterized by values of $t_{\frac{1}{2}}$ in the range 50–100 ms could be more extensively studied. At all reaction temperatures the rate of this reaction was found to be independent of the initial concentration of 2,4,6-trinitrobenzaldehyde, independent of pH over the range 7.5–10.0[3] and linearly dependent on the initial concentration of sulfite ion at low concentrations of sodium sulfite, but independent of sulfite concentration at high sodium sulfite concentrations. The absorption spectrum of the species present at the termination of this reaction was also characteristic of 1:1 sulfite ion – 2,4,6-trinitrobenzaldehyde complex.

The kinetic observations seem compatible with the following scheme

$$\text{TNBA} + \text{SO}_3^{2-} \underset{k_{-1}}{\overset{k_1}{\rightleftharpoons}} \text{A} \qquad [3]$$

$$\text{TNBA} + \text{SO}_3^{2-} \underset{k_{-2}}{\overset{k_2}{\rightleftharpoons}} \text{B} \qquad [4]$$

where the first equilibrium is established much more rapidly than the second, but in which $k_1/k_{-1} \ll k_2/k_{-2}$. A and B are formulated as isomeric 1:1 σ-complexes differing only in the position of addition of the sulfite ion. The formation of 1:1 σ-complexes of methoxide ion with 2,4,6-trinitroanisole has been shown to follow the above reaction scheme with the C-3 adduct being the kinetically favored species and the C-1 adduct being the thermodynamically favored species (18). While p.m.r. studies of the sulfite ion – 2,4,6-trinitrobenzaldehyde reaction in aqueous solution have to be carried out under conditions such that only the isomeric 2:1 σ-complexes are formed, the isomeric 1:1 σ-complexes **1** and **2** were observed as stable entities in aqueous dimethylsulfoxide solution and may be presumed to exist as well in aqueous solution under appropriate conditions.

The lack of accurate rate constants for the second reaction over a wide range of low sulfite ion concentrations renders a detailed analysis of kinetic data in terms of the proposed scheme unwarranted at this time. The data that are available suggest k_2 has a value (at 25°) in the range 9×10^4 M^{-1} s^{-1}. This rate constant is very close to that reported by Bernasconi and Bergstrom (19) for the formation of the 1:1 sulfite ion – 1,3,5-trinitrobenzene complex and is in the range of the specific rate constants observed for 1:1 σ-complex formation between sulfite ion and picramide, *N*-methylpicramide, and *N*,*N*-dimethylpicramide.[4] For each of these four reactions sulfite ion attacks at a hydrogen-bearing ring carbon. Studies using the T-jump technique are in progress in an attempt to obtain more extensive and more reliable kinetic data for both the fast and very fast reactions.

Financial support by the National Research Council of Canada is gratefully acknowledged.

[3]Separate studies were carried out to ensure that under the experimental conditions used in the kinetic and equilibrium experiments there were no complications due to the interaction of hydroxide ion and 2,4,6-trinitrobenzaldehyde. These studies indicated that over the temperature range 0–50 °C the formation of the hydroxide ion – 2,4,6-trinitrobenzaldehyde complex was only important at pH values greater than 10. Relevant thermodynamic, spectroscopic, and kinetic data associated with the 1:1 hydroxide ion – 2,4,6-trinitrobenzaldehyde σ-complex are $K = 5.0 \times 10^3$ M^{-1} at 25.0 °C (based on equilibrium studies), $\varepsilon_{430} = 2.0 \pm 0.1 \times 10^4$ M^{-1} cm^{-1}, $\varepsilon_{530} = 1.3 \pm 0.1 \times 10^4$ M^{-1} cm^{-1}, $k_1 = 5.2 \times 10^2$ M^{-1} s^{-1} and $k_{-1} = 0.1$ s^{-1}. All values are quoted for solutions of ionic strength 0.14 M (KNO_3).

1. A. R. Norris. Can. J. Chem. **45**, 175 (1967).
2. M. R. Crampton. J. Chem. Soc. (B), 1341 (1967).
3. M. R. Crampton and M. El Gharini. J. Chem. Soc. (B), 330 (1969).
4. M. J. Strauss. Chem. Rev. **70**, 667 (1970).
5. E. Buncel, A. R. Norris, and W. Proudlock. Can. J. Chem. **46**, 2759 (1968).
6. A. I. Vogel. A textbook of quantitative inorganic analysis. Longmans, London. 1968. p. 343.
7. A. R. Norris. Can. J. Chem. **47**, 2895 (1969).
8. M. R. Crampton and V. Gold. J. Chem. Soc. 3293 (1964).

[4]A. R. Norris and P. Sheridan. To be published.

9. J. H. FENDLER, E. J. FENDLER, and C. E. GRIFFIN. J. Org. Chem. **34**, 689 (1969).
10. M. R. CRAMPTON and V. GOLD. J. Chem. Soc. (B), 893 (1966).
11. K. C. SERVIS. J. Am. Chem. Soc. **89**, 1508 (1967).
12. R. FOSTER and C. A. FYFE. Tetrahedron, **21**, 3363 (1965).
13. M. R. CRAMPTON. Adv. Phys. Org. Chem. **7**, 211 (1969).
14. E. BUNCEL, A. R. NORRIS, and K. E. RUSSELL. Quart. Rev. London, **22**, 123 (1968).
15. J. S. COLEMAN, L. P. VARGA, and H. MASTIN. Inorg. Chem. **9**, 1015 (1970).
16. P. JOB. C.R. **180**, 928 (1925).
17. H. BENESI and J. HILDEBRAND. J. Am. Chem. Soc. **71**, 2703 (1949).
18. C. F. BERNASCONI. J. Am. Chem. Soc. **93**, 6975 (1971).
19. C. F. BERNASCONI and R. G. BERGSTROM. J. Am. Chem. Soc. **95**, 3603 (1973).

Can. J. Chem. Downloaded from www.nrcresearchpress.com by 210.87.254.6 on 09/05/12
For personal use only.

Water Soluble Steroids with Catalytic Substituents II. Synthesis of 3β-(4(5)-Imidazolyl)-5α-androstane-11β,17β,-diamine and Comparison of its Catalytic Properties with Those of 17β-(4(5)-Imidazolyl)-5α-androstane-3β,11β-diamine

J. Peter Guthrie and Yasutsugu Ueda

Department of Chemistry, University of Western Ontario, London, Ontario

Received May 7, 1973

3β-(4(5)-Imidazolyl)-5α-androstane-11β,17β-diamine, **15**, has been synthesized in a multistep process from adrenosterone, **2**, starting with lithium ammonia reduction to give 11α,17β-dihydroxy-5α-androstan-3-one, **3**, which was converted to its diacetate, **4**. Ethynylation at the 3 keto group gave the ethynyl triol **5**, purified as its 11,17-diacetate **6**. Acid catalyzed rearrangement of **6** gave 3-acetyl-5α-androst-2-ene-11α,17β-diol diacetate, 7. This was hydrogenated, and then subjected to base catalyzed hydrolysis and equilibration to give crystalline 3β-acetyl-5α-androstane-11α,17β-diol, **9**, which was converted to 3β-acetoxyacetyl-5α-androstane-11α,17β-diol, **10**, using lead tetraacetate. After hydrolysis to the triol, **11**, the Weidenhagen reaction led to formation of 3β-imidazolyl-5α-androstane-11α,17β-diol, **12**. Finally oxidation to the dione, **13**, formation of the dioxime, **14**, and hydrogenation give **15**. As expected **15** is a better catalyst than 17β-(4(5)-imidazolyl-5α-androstane-3β,11β-diamine, **1**, for the hydrolysis of aryl esters of acids with hydrophobic substituents, but the effect is small. With **1** there is a marked electrostatic rate enhancement or retardation when charged groups are present on the aryl esters; this effect is much smaller for **15**.

La synthèse de l'(imidazolyl-4(5))-3β androstane-5α diamine-11β,17β, **15**, a été réalisée en plusieurs étapes à partir de l'adrénostérone, **2**, qui, soumis à une réduction avec du lithium dans l'ammoniaque, a donné le dihydroxy-11α,17β androstan-5α one-3, **3**, lequel a été converti en diacétate, **4**. L'éthynylation du groupe céto-3 a conduit à l'éthylnyl triol **5**, que l'on purifie en formant de diacétate-11,17 **6**. Le réarrangement catalysé par l'acide de **6** a conduit à l'acétyl-3 androst-5α ène-2 diol diacétate-11α,17β, **7**. Ce dernier composé fut hydrogéné, puis soumis à une hydrolyse basique et à une équilibration pour donner l'acétyl-3β androstane-5α diol-11α,17β, **9**, cristallin qui a été transformé en acétoxyacétyl-3β androstane-5α diol-11α,17β, **10**, en utilisant du tétraacétate de plomb. Après hydrolyse pour obtenir le triol, **11**, la réaction de Weidenhagen a conduit à la formation d'imidazolyl-3β androstane-5α diol-1α,17β, **12**. Finalement le produit **15** fut obtenu par oxydation de **12** en dione **13** suivie par la formation du dioxime **14** et par hydrogénation de ce dernier composé. Comme prévu, **15** est un meilleur catalyseur que l'(imidazolyl-4(5))-17β androstane-5α diamine-3β,11β, **1**, pour l'hydrolyse des esters aryles d'acides possédant des substituants hydrophobes, mais l'effet est faible. Avec le composé **1**, on a noté une augmentation ou une diminution electrostatique dans la vitesse lorsque des groupes chargés sont présents dans les esters aryles; cet effet est beaucoup plus faible pour **15**. [Traduit par le journal]

Can. J. Chem., **51**, 3936 (1973)

Recently (1) we reported the synthesis of 17β-imidazolyl-5α-androstane-3β,11β-diamine, **1**, a water soluble steroid with a potentially catalytic substituent. We have investigated the kinetics of the reactions of this steroid with several aryl esters of acids which contain hydrophobic substituents, and found a rate enhancement attributable to hydrophobic binding between substrate and catalyst (2). Koshland and co-workers have proposed (3–6) a theory of "orbital steering" as a source of a large fraction of enzymic rate enhancements; this theory states that a reaction is greatly accelerated if the reactant atoms are held in close proximity and in the optimum relative orientation for reaction. Koshland and co-workers estimate (3, 5) that for lactonization the orientation effect is at least 10^4 in rate. There has been considerable controversy over the concept of orbital steering (7–9). Nevertheless it is clear that some reactions at least are much faster when they are intramolecular and the reactant atoms are held close together. Examination of space filling models convinced us that although the 17β-imidazolyl group in **1** is quasi-equatorial and can act as a catalyst for the hydrolysis of its substrates, the imidazole nitrogen-3 is not optimally oriented, being too high above the plane of the molecule. A 17α-imidazole would be much worse since the nitrogen lone pair would be directed almost parallel to the plane of the molecule and would not readily react with any hydrophobically bound substrate.

Can. J. Chem. Downloaded from www.nrcresearchpress.com by 210.87.254.5 on 09/05/12
For personal use only.

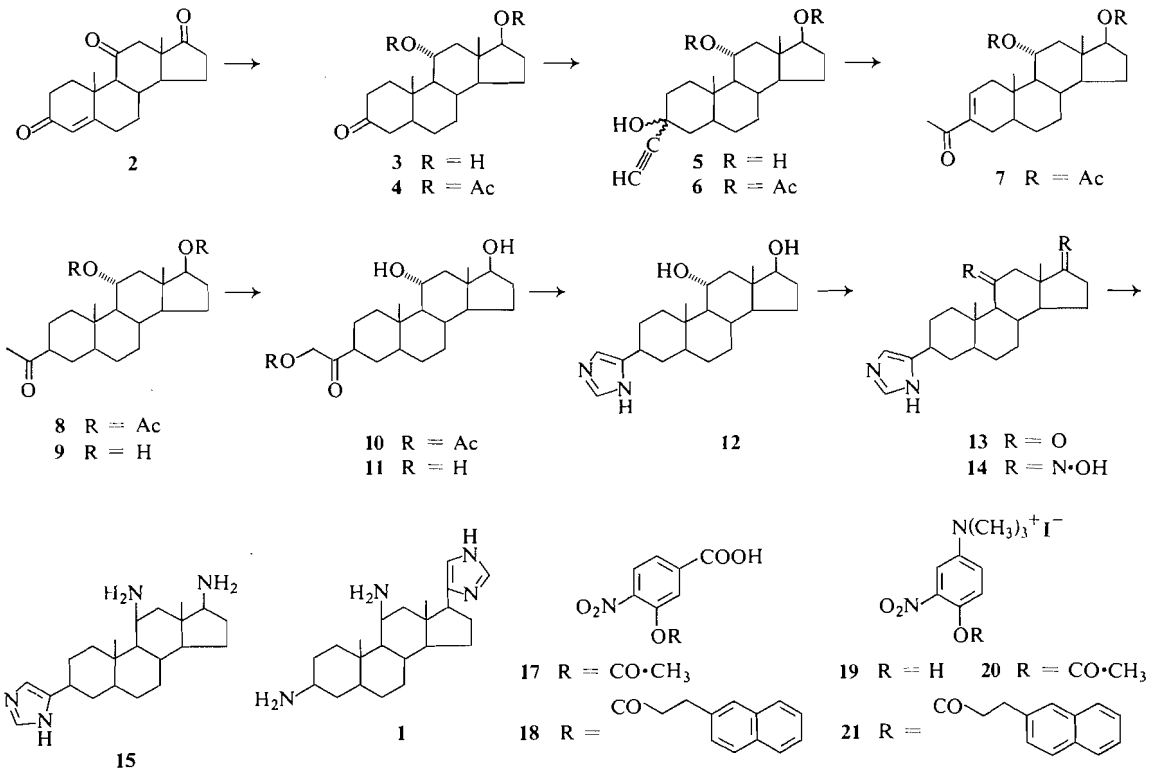

SCHEME 1

A 3β-imidazole would however be truly equatorial and better positioned to react with a substrate which was also in contact with the lower surface of the steroid.

It seemed to us of considerable interest to determine how sensitive the imidazole catalyzed ester hydrolysis was to the orientation of the imidazole group. Accordingly we have prepared 3β-(4(5)-imidazolyl)-5α-androstane-11β,17β-diamine, **15**. We wish to report the synthesis of this compound, and some investigations of its catalytic properties, relative to **1**.

Results and Discussion

Synthesis

The approach used is outlined in Scheme 1. Adrenosterone, **2**, could be reduced with lithium in liquid ammonia to the desired 3-oxo-5α-androstane-11α,17β-diol, **3**, albeit in modest yield. Major by-products were the triol and 3,17-dioxo-5α-androstane-11α-ol which presumably results from formation of the 17-enolate. At best only 45% yield of **3** was obtainable. Compound **3** was converted to the diacetate **4**, for which the stereochemistry at C-5 could be established unambiguously by ^{13}C n.m.r. spectroscopy. The chemical shift of the C-19 signal differs by 10 p.p.m. depending on whether the A–B ring junction is *cis* or *trans* (10) and can be predicted for either stereochemistry on the basis of previous studies of the ^{13}C spectra of steroids (10, 11). The diacetate **4** was then treated with the lithium acetylide – ethylenediamine complex in 1:1 benzene – dimethylacetamide. The crude product, mostly **5**, was acetylated to give the diacetate **6**; the acetylation was monitored by t.l.c. and stopped before significant amounts of triacetate formed. Compound **6** was purified and then converted to **7** by heating with strongly acidic ion exchange resin; hydrogenation of **7** led to **8**. Basic hydrolysis of **8** gave **9** and will[1] also lead to equilibration at C_3; the preferred orientation of an acetyl group has been shown to be equatorial (12). Lead tetraacetate oxidation of **9** produced **10** in good yield. Unfortunately **10** could not be used directly for production of

[1]Equilibrium is established in 49 h at 56° with 0.1 *M* sodium methoxide (12); the conditions used in this work (11 h at reflux with 0.35 *M* sodium methoxide) should also give complete equilibration.

Can. J. Chem. Downloaded from www.nrcresearchpress.com by 210.87.254.5 on 09/05/12
For personal use only.

TABLE 1. Rate constants for hydrolysis of esters[a]

Ester	Background rate (no catalyst) k_{obs} (min^{-1})	Catalyzed rate k_2[b] (M^{-1} min^{-1}) Imidazole	**15**	**1**	Hydrophobic effect **15**	**1**	Electrostatic effect **15**	**1**	k_{rel}[c] **15**	**1**	k_{rel}^{15}/k_{rel}^{1}
16	0.000854	26.0	24.3	25.5	—	—			0.935	0.980	0.954
17	0.000716	56.9	58.7	305			1.10[f]	5.47[f]	1.03	5.36	0.192
18	0.000666	55.7	180	700	3.14[d]	2.34[d]			3.23	12.6	0.256
20	0.00469	247	123	90.0			0.532[g]	0.372[g]	0.497	0.365	1.40
21	0.00428	316	370	234	2.4[e]	2.1[e]			1.2	0.740	1.62

[a]In aqueous solution, 0.62 M acetonitrile, ionic strength = 0.097 M (KCl), 0.00996 M Tris buffer, pH 7.9; temperature = 25.0 ± 0.1 °C.
[b]Observed pseudo first-order rate constant, corrected for the background rate, divided by the total concentration of catalyst.
[c]k_2 for the steroidal imidazole divided by k_2 for imidazole.
[d]k_{rel} for **18** divided by k_{rel} for **17**.
[e]k_{rel} for **21** divided by k_{rel} for **20**.
[f]k_{rel} for **17** divided by k_{rel} for **16**.
[g]k_{rel} for **20** divided by k_{rel} for **16**.

the imidazole compound **12** but had to be hydrolyzed to **11** with some attendant loss of material. Then conversion of **11** to **12** went in essentially quantitative yield, using the modified conditions for the Weidenhagen (13, 14) synthesis devised (1) for the preparation of **1**. Overall yields for the introduction of the imidazole group were 12% (yield of **11** from **4**). The worst losses were suffered in the oxidation–hydrolysis sequence from **8** to **11**. The diol **12** could be transformed first to the dione **13** and then to the dioxime **14** almost quantitatively. Unfortunately the hydrogenation to give **15** proceeded with difficulty and in mediocre yield. The n.m.r. spectrum of **15** showed that the desired stereochemistry had been obtained, since the methyne proton on C-11 had $\Delta\nu_{\frac{1}{2}} = 10$ Hz, as expected for an equatorial hydrogen, and the methyne proton on C-17 had $\Delta\nu_{\frac{1}{2}} = 8.5$ Hz, as expected for a 17α proton.[2]

Kinetics

p-Nitrophenyl acetate, **16**, and substrates **17**–**21** were used with both **1** and **15** in order to compare the catalytic efficiencies of the two steroidal imidazoles with the results shown in the Table 1. In order to compare the various reactions, it is desirable to correct for differences in inherent reactivity of the substrates and catalysts. For each substrate, calculating k_{rel}, the relative rate constant for a steroidal imidazole with imidazole as standard, corrects for any differences in intrinsic reactivity of the substrates. Since *p*-nitrophenyl acetate, **16**, shows a relative rate of 0.94 with **15** and 0.98 with **1**, we conclude that the intrinsic reactivity of the steroidal imidazoles is virtually identical to that of imidazole. Imidazole is well known (16) to act as a nucleophilic catalyst for the hydrolysis of aryl esters; we assume that the steroidal imidazoles are also acting as nucleophilic catalysts. Any deviations of k_{rel} from unity must represent a stabilizing or destabilizing influence present in the transition state for these more complicated substrates but absent for **16**. The ratio of k_{rel} values for **18** to **17** or **21** to **20** should cancel the effects of the charged leaving group and give a measure of the magnitude of the hydrophobic interaction between the naphthyl ring and the α surface of the steroid. This treatment shows that there is a rate enhancement of about two-fold on adding a naphthyl group as hydrophobic binding moiety. Furthermore the rate enhancements are in both cases slightly larger for **15** than for **1** indicating that indeed the 3β-imidazole is more accessible than the 17β imidazole. Figure 1 shows the geometry of the intermediate formed after attack of the imidazole on the ester carbonyl and before expulsion of phenoxide. This drawing is based on CPK space filling models which show the steroid and aromatic rings in

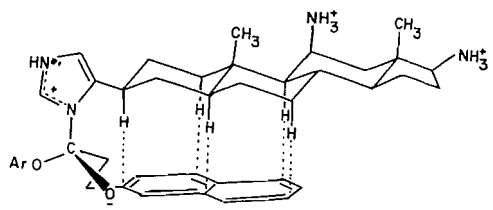

FIG. 1. Geometry of intermediate formed after attack of the imidazole on the ester carbonyl and before expulsion of phenoxide.

[2]Using the empirical relations (15) $\nu_{\frac{1}{2}} = J_{AX}+J_{BX}$ and observed values of J or $\Delta\nu_{\frac{1}{2}}$ (15, 18).

Can. J. Chem. Downloaded from www.nrcresearchpress.com by 210.87.254.5 on 09/05/12
For personal use only.

Can. J. Chem. Downloaded from www.nrcresearchpress.com by 210.87.254.5 on 09/05/12
For personal use only.

van der Waals' contact. However for the substrates tested so far the effect is very small. The ratio of k_{rel} values for **17** to **16** or **20** to **16** should provide an estimate of the effect of the charged substituent on the leaving group. These electrostatic effects are small for **15** but considerably larger for **1**. Inspection of space filling models shows that for **1** the charged substituents are closer to the 11β-ammonium group than they are in **15**, and that in fact very close contact between the carboxylate of **17** or **18** and the 11β-ammonium is quite possible and requires no obvious crowding or distortion.

This small orientational effect may result from the flexibility of the substrates **18** and **21**, a flexibility introduced so that the carbonyl carbon can become covalently bonded to the imidazole nitrogen while the hydrophobic side chain is in contact with the α surface of the steroid; examination of molecular models showed that two methylene groups was the minimum required (see Fig. 1). However this flexibility will doubtless decrease the sensitivity of the catalytic effect to small changes in orientation. For less flexible substrates we may hope to see a greater effect and experiments in this direction are now under way.

Experimental

Melting points were determined on a Thomas Hoover capillary melting point apparatus and are uncorrected. Infrared spectra were recorded with a Beckman IR-20A spectrometer. Nuclear magnetic resonance spectra were obtained with Varian T-60 or HA-100 spectrometers. Chemical shifts were recorded in p.p.m. downfield from internal tetramethylsilane for the neutral compounds in organic solvents and from internal sodium 2,2-dimethyl-2-silapentane-5-sulfonate for the water soluble compounds in D_2O. Mallinckrodt Silicic Acid (100 mesh) No. 2847 and neutral silica, silicAR CC-7 (100–200 mesh) No. 7083 were used for column chromatography. E. Merck Silica Gel G.F.-254 No. 7730 was used for t.l.c. and Silica Gel P.F.-254, No. 7747 was used for preparative layer chromatography. Imidazole containing compounds were detected using the Pauly reagent (17). Dowex 50 W (50–100 mesh) was washed thoroughly, cycled several times from sodium form to acid form, and finally converted to the acid form and dried *in vacuo* over $CaCl_2$. Linde 4A molecular sieves were used for solvent drying. During work-up, organic extracts normally were washed with saturated aqueous sodium chloride solution, dried over anhydrous sodium sulfate, and evaporated to dryness *in vacuo*.

11α,17β-Dihydroxy-5α-androstan-3-one (3)

A solution of adrenosterone, **2** (Upjohn Company, m.p. 218–220°, 10.0 g) in dioxane (500 ml, dried over molecular sieves) was added to a solution of lithium (3.0 g) in anhydrous liquid ammonia (3 l) over a period of 20 min with good stirring. After stirring another 20 min, the blue color was discharged by the addition of solid ammonium chloride and the ammonia was allowed to evaporate under a nitrogen atmosphere. Water was added to the residue; the product was extracted with methylene chloride three times, and the organic extracts were dried and evaporated. Crystallization of the residue from methanol gave 11α,17β-dihydroxy-5α-androstan-3-one, **3** (2.0 g). The crystallization mother liquor was subjected to column chromatography on silicic acid; elution with chloroform methanol (98:2) gave another 2.5 g of **3**. Total yield of **3** was 4.5 g (45%): m.p. 183–185 °C; n.m.r. ($CDCl_3$) δ 0.78 (3H, s, C_{18}-Me), 1.15 (3H, s, C_{19}-Me), 3.3 ~ 4.2 p.p.m. (2H, overlapping signals from $C_{11\beta}$-H, and $C_{17\alpha}$-H) (lit. (18) δ 0.78 (C_{18}-Me), 1.14 (C_{19}-Me), 3.96 (C_{11}-βH), 3.66 (C_{17}-αH)); i.r. (KBr disc) 3230 (OH), 1715 cm^{-1} (ketone). Major byproducts were isolated by column chromatography (mentioned above) and identified as 11α-hydroxy-5α-androstane-3,17-dione: m.p. 193–195 °C, (lit. (19) 194–195 °C); i.r. ($CHCl_3$) 3450 (—OH), 1730 (5-membered cyclic ketone), 1700 cm^{-1} (ketone); n.m.r. ($CDCl_3$) δ 0.93 (3H, s, C_{18}-Me), 1.17 (3H, s, C_{19}-Me), 4.0 p.p.m. (1H, br s $\Delta\nu_{\frac{1}{2}}$ = 12 Hz, $C_{11\beta}$-H) and 5α-androstane-3β,11α,17β-triol: m.p. 241–243 °C; n.m.r. ($CDCl_3$) δ 0.73 (3H, s, C_{18}-Me) 0.95 (3H, s, C_{19}-Me), 3.4–4.2 p.p.m. (3H, overlapping signals from $C_{3\alpha}$-H, $C_{11\beta}$-H, and $C_{17\alpha}$-H). Calculated δ, using Zürcher's (20) values: 0.76 (C_{18}-Me) and 0.94 (C_{19}-Me).

11α-17β-Dihydroxy-5α-androstan-3-one Diacetate (4)

Compound **3** (7.9 g) in anhydrous pyridine (30 ml) was acetylated using acetic anhydride (15 ml) at room temperature overnight. Crystallization of the product from ethanol gave 7.7 g of **4**: m.p. 192–193 °C; i.r. ($CHCl_3$) 1710 (ketone and ester), 1240 cm^{-1} (acetate); n.m.r. ($CDCl_3$) δ 0.86 (3H, s, C_{18}-Me), 1.10 (3H, s, C_{19}-Me), 1.96 (3H, s, —OAc), 2.01 (3H, s, —OAc), 4.66 (1H, br t, J = 7 Hz, $C_{17\alpha}$-H), 5.2 p.p.m. (1H, m, $C_{11\beta}$-H) (lit. (18) δ 0.86 (C_{18}-Me), 1.11 (C_{19}-Me), 4.62 (C_{17}-αH), 5.17 (C_{11}-βH)), ^{13}C n.m.r. ($CDCl_3$) δ 11.90 (C-19), 12.70 (C-18).

3ξ-Ethynyl-5α-androstane-3ξ,11α,17β-triol 11,17-Diacetate (6)

Lithium acetylide ethylenediamine (55 g, 0.55 mol; Foote Mineral Company) was placed in a nitrogen-flushed flask, followed by 385 ml of 1:1 benzene – *N,N*-dimethylacetamide (21). To it a solution of diacetate, **4** (21.4 g, 55 mmol) in 150 ml of the same solvent mixture was added dropwise over a period of 15 min at room temperature with stirring. After stirring 2 h under a nitrogen atmosphere, cold water (200 ml) was added slowly under ice-cooling with vigorous stirring and organic materials were extracted with ethyl acetate (3 × 200 ml). The organic layer was washed with 6 *N* HCl (4 × 200 ml), dried and evaporated, yielding 17.7 g of crude **5**, which was acetylated in anhydrous pyridine (100 ml) – acetic anhydride (18 ml) at room temperature. The acetylation was followed by t.l.c. ($CHCl_3$–CH_3OH 98:2) and stopped by pouring the reaction mixture slowly with stirring into cold 2 *N* H_2SO_4 (720 ml) before appreciable amounts of the triacetate formed. T.l.c. analysis of the crude product ($CHCl_3$–CH_3OH 98:2) showed, in addition to **6** as major component, *ca.* 10% of triacetate and *ca.* 20% of **4**. Crystallization from ethanol gave 8.7 g of **6**, containing a

Can. J. Chem. Downloaded from www.nrcresearchpress.com by 210.87.254.5 on 09/05/12
For personal use only.

small amount of impurity (t.l.c. analysis) which was presumed to be the C-3 epimer. Column chromatography of the mother liquors on silicic acid (200 g) with chloroform as eluant gave triacetate and 4.5 g of **6**. Total yield of **6** was 13.2 g (31.8 mmol, 58% based on **4**). An analytical sample, recrystallized from ethanol showed a single spot on t.l.c.: m.p. 218–218.5°; i.r. (KBr) 3480 (OH), 3250 (C≡C—H), 2120 (C≡C), 1740, 1715 cm^{-1} (ester); n.m.r ($CDCl_3$) δ 0.83 (3H, s, C_{18}-Me), 0.90 (3H, s, C_{19}-Me), 1.97 (3H, s, OAc), 2.00 (3H, s, OAc), 2.48 (1H, s, ethynyl-H), 4.67 (1H, br t, J = 8 Hz, $C_{17\alpha}$-H), 5.19 p.p.m. (1H, m, $C_{11\beta}$-H).

Anal. Calcd. for $C_{25}H_{30}O_5$: C, 72.08; H, 8.71. Found: C, 71.99; H, 8.82.

3α-Ethynyl-5α-androstane-3β,11α,17β-triol triacetate, isolated as a by-product of the preparation of **6**, was identified on the basis of its n.m.r. spectrum: n.m.r. ($CDCl_3$) δ 0.84 (3H, s, C_{18}-Me), 0.93 (3H, s, C_{19}-Me), 1.99 (3H, s, OAc), 2.02 (6H, s, 2 OAc), 2.61 (1H, s, ethynyl-H) 4.65 (1H, br t, J = 8 Hz, $C_{17\alpha}$-H) 5.2 p.p.m. (1H, m, $C_{11\beta}$-H).

3-Acetyl-5α-androst-2-ene-11α,17β-diol Diacetate (7)

A stirred mixture of **6** (12.9 g, 31 mmol), glacial acetic acid (12.4 ml), and Dowex 50W (23.5 g) was heated at reflux under a nitrogen atmosphere for 12 h (22). After cooling the reaction mixture, the resin was filtered off and washed with methanol until the filtrates were clear. The combined filtrates and washings were evaporated to dryness. Crystallization of the residue from ethanol gave 4.7 g of 7. The mother liquor was acetylated in pyridine (20 ml) – acetic anhydride (10 ml) at room temperature overnight. Crystallization from ethanol of the residue after work-up gave 1.8 g of **7**. The mother liquor was purified by column chromatography on silicic acid (100 g), eluting with benzene – diethyl ether (97:3) to give another 3.4 g of 7 as a white solid. Total yield of **8** was 9.9 g (77% based on **6**). An analytical sample was obtained by recrystallization from methanol: m.p. 172–173 °C; i.r. ($CHCl_3$) 1730 (ester), 1660 cm^{-1} (C=C—C=O); n.m.r. ($CDCl_3$) δ 0.80 (3H, s, C_{18}-Me), 0.85 (3H, s, C_{19}-Me), 2.00 (1H, s, two —OAc), 2.25 (3H, s, C_3-acetyl-Me), 4.63 (1H, br t, J = 7 Hz, $C_{17\alpha}$-H), 5.2 (1H, m, $C_{11\beta}$-H), 6.7 p.p.m. (1H, br, C_2-H); u.v. λ_{max} (CH_3OH) 233 (ε 1.1 × 10^4), 300 nm (ε ≃ 70).

Anal. Calcd. for $C_{25}H_{36}O_5$: C, 72.08; H, 8.71. Found: C, 72.44; H, 8.77.

3β-Acetyl-5α-androstane-11α,17β-diol (9)

A suspension of **7** (9.5 g, 22.6 mmol) and 5% palladium–carbon catalyst (1.9 g) in ethanol (500 ml) containing 0.5 ml of pyridine (23) was hydrogenated at 1 atm and 25 °C until t.l.c. showed no u.v. absorbing spot. The catalyst was filtered off, washed with ethanol and the filtrate was evaporated to dryness, yielding 9.3 g of **8** as a pale yellow syrup: n.m.r. ($CDCl_3$) δ 0.83 (3H, s, C_{18}-Me), 0.90 (3H, s, C_{19}-Me), 1.98 (3H, s, —OAc), 2.03 (3H, s, —OAc), 2.13 (3H, s, acetyl-Me), 4.67 (1H, br t, J = 7 Hz, $C_{17\alpha}$-H), 5.2 p.p.m. (1H, m, $C_{11\beta}$-H). Without any purification crude **8** (9.3 g) in methanol (200 ml) containing 15 ml of 5 *N* sodium methoxide in methanol was heated at reflux under a nitrogen atmosphere for 11 h. The reaction mixture was extracted with ethyl acetate after addition of saturated sodium chloride and the organic phase was dried and evaporated. Crystallization from ethyl acetate gave 4.65 g of **9**. Another 1.23 g of crystalline **9** was obtained from the crystallization mother liquor by repeating the above procedure (hydrolysis–crystallization). Total yield of crystalline **9** 5.88 g (17.6 mmol, 78% based on 7). An analytical sample was obtained by crystallization from 95% ethanol: m.p. 186.5–187.5 °C; i.r. ($CHCl_3$) 3600 (—OH), 1690 cm^{-1} (ketone); n.m.r. ($CDCl_3$) δ 0.74 (3H, s, C_{18}-Me), 0.93 (3H, s, C_{19}-Me), 2.12 (3H, s, acetyl-Me), 3.5 (1H, m, $C_{17\alpha}$-H), 4.0 p.p.m. (1H, m, $C_{11\beta}$-H).

Anal. Calcd. for $C_{21}H_{34}O_3$: C, 75.40; H, 10.25. Found: C, 75.32; H, 10.18.

3β-Acetoxyacetyl-5α-androstane-11α,17β-diol (10)

To a mixture of crystalline **9** (5.01 g, 15 mmol) and lead tetraacetate (9.31 g, 21 mmol, British Drug Houses Ltd.) in benzene–methanol (95:5) (210 ml) boron trifluoride – diethyl ether complex (27.9 ml) was added dropwise over a period of 5 min with stirring under ice-cooling and a nitrogen atmosphere (24). After stirring at room temperature for 4 h, the starch iodide test for lead tetraacetate was negative. Water was added to the reaction mixture; the products were extracted with ethyl acetate. The organic phase was washed with saturated aqueous sodium chloride, saturated aqueous sodium bicarbonate, and then dried and evaporated.

The residue was rinsed with diethyl ether to yield 3.43 g of **10** as a white powder. The filtrate was evaporated to dryness and purified by column chromatography on neutral silica (50 g) eluted with chloroform-methanol (98:2) giving another 1.33 g of **10**. Total yield of **10** (powder) was 4.76 g (12.1 mmol, 81% based on **9**). The n.m.r. spectrum showed the presence of a small amount of an impurity of unknown constitution, which was more conveniently removed after the next step. An analytical sample was obtained by recrystallizing 10 times from 95% ethanol: m.p. 183–183.5 °C; i.r. ($CHCl_3$) 3600 (—OH), 1735, 1715 cm^{-1}; n.m.r. ($CDCl_3$) δ 0.70 (3H, s, C_{18}-Me), 0.93 (3H, s, C_{19}-Me), 2.15 (3H, s, OAc), 4.71 (2H, s, —CH_2-in the acetoxyketone), 3.5–4.2 (2H, m, overlapping signals from $C_{11\beta}$-H and $C_{17\alpha}$-H).

Anal. Calcd. for $C_{23}H_{36}O_5$: C, 70.37; H, 9.25. Found: C, 70.08; H, 9.23.

3β-Glycolyl-5α-androstane-11α,17β-diol (11)

A mixture of 2 *N* methanolic potassium hydroxide (12 ml) and water (4 ml) was slowly added to **10** (4.60 g) in methanol (240 ml) under ice-cooling and a nitrogen atmosphere. The solution was allowed to attain room temperature and let stand for 2.5 h. The excess of base was neutralized with acetic acid, most of the solvent was removed *in vacuo*, water was added to the residue, the products were extracted with ethyl acetate and the organic phase was dried and evaporated, yielding 3.95 g of crude **11** as a white solid which showed two spots on t.l.c. Column chromatography on 90 g of silica gel (neutral) with chloroform–methanol (98:2) as eluant yielded **11** (1.90 g) as a white solid and 1.50 g of a mixture of **12** and an unknown material which was not identical with either **10** or **9**, but identical with the unknown impurity in crude **10** based on n.m.r. data (in $CDCl_3$ δ 3.40 (s), 4.07 p.p.m. (s)). An analytical sample of **10** was obtained by recrystallization from acetone: m.p. 180–181°; n.m.r. ($CDCl_3$) δ 0.75 (3H, s, C_{18}-Me), 0.97 (3H, s, C_{19}-Me), 3.5–4.2 (2H, m, overlapping signals from $C_{11\beta}$-H and $C_{17\alpha}$-H),

Can. J. Chem. Downloaded from www.nrcresearchpress.com by 210.87.254.5 on 09/05/12
For personal use only.

4.30 p.p.m. (2H, s, methylene proton in α-hydroxy ketone).

Anal. Calcd. for $C_{21}H_{34}O_4$: C, 71.96; H, 9.78. Found: C, 71.42; H, 9.75.

3β-Imidazolyl-5α-androstane-11α,17β-diol (12)

To a solution of **10** (1.86 g, 5.3 mmol) in 95% ethanol (145 ml) was added formalin (Shawinigan 37% formaldehyde) (9.1 ml) and a solution of cupric acetate monohydrate (2.18 g), water (5.5 ml), and concentrated ammonia (31.5 ml). The solution was refluxed for 4 h, at which time t.l.c. ($CHCl_3$–CH_3OH 80:20) showed that the reaction was over. The reaction mixture was allowed to cool and after addition of saturated aqueous sodium chloride, the product was extracted with ethyl acetate until the extracts were Pauly negative (17). The combined extracts were washed with 1 *M* aqueous ammonium hydroxide, dried and evaporated, yielding 1.9 g of **12** as a white powder. An analytical sample was obtained by recrystallization from methanol–water: m.p. 272° (dec.); n.m.r. (pyridine) δ 1.02 (3H, s, C_{18}-Me), 1.08 (3H, s, C_{19}-Me), 3.55 (3/2H, s, $\frac{1}{2}CH_3OH$), 3.8–4.6 p.p.m. (2H, m, overlapping peaks from $C_{11\beta}$-H and $C_{17\alpha}$-H).

Anal. Calcd. for $C_{22}H_{34}O_2N_2 \cdot \frac{1}{2}CH_3OH$: C, 72.15; H, 9.69; N, 7.48. Found: C, 72.59; H, 9.78; N, 7.30.

3β-Imidazolyl-5α-androstane-11,17-dione (13)

Crude **12** (1.83 g, 5.1 mmol) was dissolved in a mixture of 2 *N* aqueous sulfuric acid (25.5 ml) and acetone (51 ml), to which was added 10 ml of Jones' reagent (2 *M* in chromium trioxide, 3.3 *M* in sulfuric acid) dropwise with stirring. The reaction mixture was allowed to stir at room temperature for 2 h, at which time t.l.c. ($CHCl_3$–CH_3OH 80:20 showed that there was no remaining starting material. Concentrated ammonia was added to basify the reaction mixture and the product was extracted with ethyl acetate. The ethyl acetate extracts were dried and evaporated, yielding 1.78 g (5.03 mmol, 98.5%) of crude **13** as a pale yellow solid, which was crystallized from methanol: m.p. 278 °C (dec.); i.r. (KBr) 1725 (C_{17}-ketone), 1690 cm^{-1} (C_{11}-ketone); n.m.r. ($CDCl_3$) δ 0.80 (3H, s, C_{18}-Me), 1.03 p.p.m. (3H, s, C_{19}-Me); n.m.r. (D_2O using the monohydrochloride of **14**), δ 0.73 (3H, s, C_{18}-Me), 0.95 (3H, s, C_{19}-Me), 7.1 (1H, s, 5 (4) H of imidazolium ring), 8.5 p.p.m. (1H, s, 2H of imidazolium ring).

3β-Imidazolyl-11,17-bisoximido-5α-androstane (14)

A mixture of crude **13** (1.5 g) and hydroxylamine hydrochloride (3.0 g) in 90% aqueous pyridine (30 ml) was heated at reflux for 12 h. After cooling the reaction mixture, the pyridine was removed *in vacuo* thoroughly, 1 *N* aqueous sodium hydroxide (50 ml) was added to the residue and the product was extracted with ethyl acetate until the extracts were Pauly negative. The ethyl acetate extracts were dried and evaporated, giving quantitative recovery of crude **14** as a pale yellow powder. Crystallization from methanol–water gave colorless crystalline **14**. An analytical sample was obtained by recrystallization from methanol–water: m.p. 300 °C (dec.); i.r. (KBr) 3600, 3400, 1630 cm^{-1} (C=N in oxime); n.m.r. (CD_3CO_2D) δ 0.90 (3H, s, C_{18}-Me), 1.15 p.p.m. (3H, s, C_{19}-Me).

Anal. Calcd. for $C_{22}H_{32}O_2N_4$: C, 68.72; H, 8.39; N, 14.57. Found: C, 68.81; H, 8.39; N, 14.23.

3β-Imidazolyl-5α-androstane-11β,17β-diamine (15)

Crystalline **14**, (576 mg, 1.5 mmol) was dissolved in methanol (6 ml) and 1 *N* aqueous hydrochloric acid (1.5 ml) was added: evaporation gave the monohydrochloride of **14** as a white powder. This monohydrochloride was dissolved in glacial acetic acid (15 ml) and hydrogenated over PtO_2 (200 mg) at 450 p.s.i. and room temperature for 48 h. The hydrogenation was interrupted and PtO_2 (200 mg) and 3 *N* HCl (0.33 ml) were added. The hydrogenation was continued under the same conditions for 70 h. The hydrogenation was interrupted again and PtO_2 (200 mg) and 3 *N* HCl (0.25 ml) were added; hydrogenation was continued under the same conditions for 70 hours. After filtering off the catalyst and washing thoroughly with glacial acetic acid, the filtrates and washings were combined and evaporated to dryness. The residue was chromatographed on neutral silica (20 g), eluting first with 10% 1 *M* ammonia in methanol – 90% chloroform, then with 15% 1 *M* ammonia in methanol – 85% chloroform. Pooling appropriate fractions gave 161 mg of **15**. A second column chromatography of this material on neutral silica (5 g) eluting with 10% 1 *M* ammonia in methanol – 90% $CHCl_3$ gave 105 mg of **15** as a pale yellow syrup. This material dissolved in methanol – *n*-propanol was treated with 3 *N* HCl (0.295 ml) and evaporated to dryness yielding 132 mg of the trihydrochloride of **15**, a white powder. This trihydrochloride of **15** was dissolved in the minimum amount of boiling methanol, *n*-propanol was added to the boiling methanol solution and methanol was driven off at the boiling point until an abundant precipitate had formed. This operation was repeated several times for an analytical sample and a sample for kinetic studies: m.p. > 350 °C; n.m.r. (D_2O) 100 MHz, δ 1.04 (6H, s, C_{18} and C_{19}-Me), 3.24 (1H, br t, J = 8.5 Hz, $C_{17\alpha}$-H), 3.55 (1H, t, J = 7.0 Hz, $\frac{1}{2}CH_3CH_2$-CH_2OH), 4.05 (1H, br s, $\Delta\nu\frac{1}{2}$ = 10 Hz, $C_{11\alpha}$-H), 7.23 (1H, s, 5 (4) H of imidazolium ring), 8.60 p.p.m. (1H, s, 2H of imidazolium ring).

Anal. Calcd. for $C_{22}H_{39}N_4Cl_3 \cdot \frac{1}{2}C_3H_7OH.3/2H_2O$: C, 53.96; H, 8.87; N, 10.71. Found: C, 54.09; H, 8.87; N, 10.40.

Substrates for Kinetics

p-Nitrophenyl acetate (Eastman, m.p. 75–77°) was used without further purification. 4-Hydroxy-3-nitrophenyl trimethylammonium iodide, **19**, was prepared according to the procedure of Bruice *et al.* (25), m.p. 220–221° (lit. (25) m.p. 220°).

3-Acetoxy-4-nitrobenzoic Acid

To a stirred solution of 3-hydroxy-4-nitrobenzoic acid (Aldrich, m.p. 231–237°, 0.915 g) and triethylamine (1.01 g) in DMF (5 ml) was added acetic anhydride (0.51 g). After stirring 1 h at room temperature, 1 *N* HCl (30 ml) was added, and the mixture was extracted with diethyl ether (3 × 30 ml). The combined extracts were washed with water (twice), dried (Na_2SO_4), and evaporated. The residue (1.02 g) was crystallized from 95% ethanol, m.p. 187–188°.

Anal. Calcd. for $C_9H_7NO_6$: C, 48.01; H, 3.09. Found: C, 47.97; H, 3.09.

3-(3-(2-Naphthyl)propanoyloxy)-4-nitrobenzoic Acid (18)

3-(2-Naphthyl)propionic acid (prepared from 2-naph-

thaldehyde (26)) (1.0 g) in dry DMF (5 ml), was cooled in an ice bath, treated with triethylamine (0.48 ml) and then ethyl chloroformate (0.53 ml), and stirred 5 min. To this stirred mixture was added a solution of 3-hydroxy-4-nitrobenzoic acid (0.92 g) and triethylamine (0.96 ml) in dry DMF (4 ml). The ice bath was removed and the mixture was stirred 30 min, then poured into 1 *N* HCl (30 ml) and extracted into ethyl acetate (30 ml). The organic layer was washed with water (three times) and saturated aqueous sodium chloride (once), dried (Na_2SO_4), and evaporated. The residue was purified by preparative layer chromatography (Merck Silica Gel PF 254) using 95:5:1 benzene – ethanol – acetic acid as solvent and crystallized from benzene–cyclohexane, m.p. 186–188°.

Anal. Calcd. for $C_{20}H_{15}NO_6$: C, 65.75; H, 4.15. Found: C, 66.24; H, 4.21.

4-Acetoxy-3-nitrophenyltrimethylammonium Iodide (20)

To a suspension of **19** (0.972 g) in DMF (6 ml) was added triethylamine (0.303 g). After 30 min stirring, acetic anhydride (0.306 g) was added and the mixture was stirred 1 h, and then evaporated to dryness. Crystallization from 1:1 ethanol–water gave 0.745 g **20**, m.p. 152–157° (dec.). Recrystallization gave material of m.p. 154–156.5° (dec.) (lit. (25) m.p. 151–155°).

4-(3-(2-Naphthyl)propanoyloxy)-3-nitrophenyltrimethylammonium Iodide (21)

To a suspension of **19** (0.324 g) in DMF (1 ml) was added triethylamine (0.202 g) and the mixture was stirred 30 min at room temperature. Then to this stirred solution was added the mixed anhydride formed by stirring 3-(2-naphthyl)propanoic acid (0.200 g) in trifluoracetic anhydride (0.210 g) for 30 min at room temperature. The combined reaction mixture was stirred 20 min at room temperature and evaporated to dryness *in vacuo*. The residue was crystallized from 95% ethanol to give 0.385 g of **21**. After three recrystallizations, it had m.p. 158–160°.

Anal. Calcd. for $C_{22}H_{23}N_2O_4I$: C, 52.18; H, 4.58. Found: C, 52.20; H, 4.50.

Kinetics

Esters were added as solutions in acetonitrile from a microliter syringe to buffer containing imidazole or steroid in 1-cm cuvettes of 3 ml or 1 ml capacity and the solutions mixed by inverting the stoppered cuvettes. Appearance of phenolate ion was followed at 400 nm for **16**, **20**, and **21** and at 420 nm for **17** and **18**. Solutions were brought to the desired calculated ionic strength with KCl. p*H* was determined at the end of each run. Pseudo first-order rate constants were calculated from first order plots which were linear to at least 3 half-lives.

We gratefully acknowledge financial support from the National Research Council of Canada, and a generous gift of adrenosterone from the Upjohn Company, Kalamazoo, Mich. We wish to thank Dr. J. B. Stothers of this department for the ^{13}C n.m.r. spectra.

1. J. P. GUTHRIE. Can. J. Chem. **50**, 3993 (1972).
2. J. P. GUTHRIE and Y. UEDA. Fed. Proc. Fed. Am. Soc. Exp. Biol. **32**, 628 (1973).
3. D. R. STORM and D. E. KOSHLAND, JR. Proc. Natl. Acad. Sci. U.S. **66**, 445 (1970).
4. A. DAFFORN and D. E. KOSHLAND, JR. Proc. Natl. Acad. Sci. U.S. **68**, 2463 (1971).
5. D. R. STORM and D. E. KOSHLAND, JR. J. Am. Chem. Soc. **94**, 5805 (1972).
6. D. R. STORM and D. E. KOSHLAND, JR. J. Am. Chem. Soc. **94**, 5815 (1972).
7. M. I. PAGE and W. P. JENCKS. Proc. Natl. Acad. Sci. U.S. **68**, 1678 (1971).
8. T. C. BRUICE, A. BROWN, and D. O. HARRIS. Proc. Natl. Acad. Sci. U.S. **68**, 658 (1971).
9. B. CAPON. J. Chem. Soc. B, 1207 (1971).
10. (*a*) J. L. GOUGH, J. P. GUTHRIE, and J. B. STOTHERS. Chem. Commun. 979 (1972). (*b*) B. BALOGH, D. M. WILSON, and A. L. BARLINGAME. Nature, **233**, 261 (1971).
11. H. J. REICH, M. JAUTELAT, M. T. MESSE, F. J. WEIGERT, and J. D. ROBERTS. J. Am. Chem. Soc. **91**, 7445 (1969).
12. E. L. ELIEL and M. C. REESE. J. Am. Chem. Soc. **90**, 1560 (1968).
13. R. WEIDENHAGEN and R. HERRMANN. Ber. **68**, 1953 (1935).
14. R. WEIDENHAGEN, R. HERRMANN, and H. WEGNER. Ber. **70**, 570 (1937).
15. G. GLASER and E. J. GABBAY. J. Org. Chem. **35**, 2907 (1970).
16. T. C. BRUICE and S. J. BENKOVIC. Bioorganic mechanisms. Vol. 1. W. A. Benjamin Inc., New York. 1966. pp. 46–66, and references contained therein.
17. H. PAULY. Z. Physiol. Chem. **42**, 508 (1904).
18. J. E. BRIDGEMAN, P. C. CHERRY, A. S. CLEGG, J. M. EVANS, E. R. H. JONES, A. KASAL, V. KUMAR, G. D. MEAKINS, Y. MORISAWA, E. E. RICHARDS, and P. D. WOODGATE. J. Chem. Soc. (C), 250 (1970).
19. C. MEYSTRE, J. KALVODA, G. ANNER, and A. WETTSTEIN. Helv. Chim. Acta, **46**, 2844 (1963).
20. R. F. ZÜRCHER. Helv. Chim. Acta, **46**, 2054 (1963).
21. O. F. BEUMEL, JR. and R. F. HARRIS. J. Org. Chem. **29**, 1872 (1964).
22. M. S. NEWMAN. J. Am. Chem. Soc. **75**, 4740 (1953).
23. H. J. RINGOLD. J. Am. Chem. Soc. **82**, 961 (1960).
24. J. D. COCKER, H. B. HENBEST, G. H. PHILLIPPS, G. D. SLATER, and D. A. THOMAS. J. Chem. Soc. 6 (1965).
25. T. C. BRUICE, J. KATZHENDLER, and L. R. FEDOR. J. Am. Chem. Soc. **90**, 1333 (1968).
26. J. N. CHATTERJEA and K. PRASAD. J. Ind. Chem. Soc. **37**, 359 (1960).

Can. J. Chem. Downloaded from www.nrcresearchpress.com by 210.87.254.5 on 09/05/12
For personal use only.

Biosynthesis of Lycomarasmin

C. R. POPPLESTONE AND A. M. UNRAU
Department of Chemistry, Simon Fraser University, Burnaby 2, British Columbia

Received April 2, 1973

Cultures of *Fusarium oxysporum Schl. emend. Sny. et Hans. f. lycopersici (Sacc.) Sny. et Hans.* grown on a liquid medium with glucose as the principal carbon source produce, among other products, the phytotoxin lycomarasmin. Acid hydrolysis of lycomarasmin results in the formation of aspartic acid, glycine, and pyruvic acid. Tracer studies showed that glycine-U-^{14}C, L-serine-U-^{14}C, DL-aspartic acid-4-^{14}C, DL-alanine-1-^{14}C, and glucose-U-^{14}C served as relatively efficient precursors of the lycomarasmin molecule. DL-Aspartic acid-4-^{14}C was incorporated into the 4-carbon fragment without label scrambling. Glycine was found to be the most efficient precursor of the 2-carbon fragment while glucose afforded the most efficient and direct route for the 3-carbon fragment.

Des cultures de *Fusarium oxysporum Schl. emend. Syn. et Hans. f. lycopersici (Sacc.) Syn. et Hans.* se développant sur un médium liquide avec comme source principale de carbone, le glucose, ont produit plusieurs composés dont la phytotoxine, lycomarasmine. L'hydrolyse acide de la lycomarasmine a conduit à la formation d'acide aspartique, de glycine et d'acide pyruvique. Des études avec des éléments marqueurs ont montré que la glycine-U^{14}C, la L-serine-U^{14}C, l'acide DL-aspartique-4-^{14}C, la DL-alanine-1-^{14}C et le glucose-U-^{14}C sont des précurseurs relativement efficaces de la molécule de lycomarasmine. L'acide DL-aspartique-4-^{14}C a été incorporé dans le fragment du carbone-4 sans aucun mélange du marqueur. La glycine s'est révélée être le précurseur le plus efficace du fragment carbone-2 alors que la glucose représente le chemin le plus efficace et le plus direct pour l'obtention du fragment carbone-3.
[Traduit par le journal]

Can. J. Chem., **51**, 3943 (1973)

Introduction

Lycomarasmin, the structure of which was determined in 1962 (1), is a phytotoxin produced by various strains of *Fusarium*. At least two other wilt toxins are produced by *Fusarium oxysporum, f. lycopersici*, one of which is fusaric acid (2). The biosynthesis of this pyridine alkaloid has been established (3, 4). Topical application of fusaric acid and lycomarasmin results in rapid wilting and necrosis of leaves. Whether the wilting symptoms exhibited by infected plants, particularly during high transpiration stress, is directly due to the systemic presence of these alkaloids or due to tylosis is not entirely clear. It is known that high concentrations of these wilt toxins are only produced in still cultures (5). Time course studies have shown that lycomarasmin made its first appearance in 40-day-old culture filtrates, after which the amount of lycomarasmin rose steadily at least until the 85th day (5).

The structure of lycomarasmin (**1**) indicates that at least some parts of the molecule could well be derived from simple amino acids or their deaminated keto analogs. A subdivision of the molecule into its apparent structural units gives rise to a series of well-known metabolic intermediates all of which could conceivably serve as immediate biogenetic precursors. Thus, acid hydrolysis of lycomarasmin gives rise to aspartic acid, pyruvic acid, and glycine (1), some or all of which might serve as building units. We now wish to describe labelling experiments which would either unequivocally determine the actual precursors or at least significantly narrow down the possible alternatives.

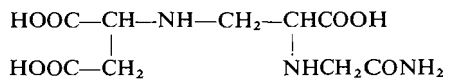

1

Experimental

Growth Conditions of Fungus

Fusarium oxysporum Schl. emend. Sny. et Hans. f. lycopersici (Sacc.) Sny. et Hans., Strain n. 5414, kindly supplied by Dr. S. Naef-Roth, Institut fur Spezielle Botanik der Eidgenossischen Technischen Hochschule, Zurich, was used in all experiments. Stock cultures were maintained on potato dextrose agar slants.

Culture media was inoculated by transferring the mycelium to 2-l Erlenmeyer flasks containing 500 ml modified Richards' medium (6) and maintained (still culture) at 25 °C in the dark. Lycomarasmin was isolated, after requisite growth intervals, from the culture filtrates according to the procedure described by Hardegger *et al.* (1), m.p. 225–228° (dec.)(lit. (1) 227–229°), $[\alpha]_D^{25}$ −48° (6).

Can. J. Chem. Downloaded from www.nrcresearchpress.com by 210.87.254.5 on 09/05/12
For personal use only.

Can. J. Chem. Downloaded from www.nrcresearchpress.com by 210.87.254.5 on 09/05/12
For personal use only.

Radioisotopic Techniques

(a) Radioactive Materials and Adminstration

DL-Aspartic acid-1-^{14}C, DL-alanine-1-^{14}C, L-serine-U-^{14}C, glycine-U-^{14}C, glycine-2-^{14}C, D-glucose-U-^{14}C, D-glucose-6-^{3}H, and L-aspartic acid-2,3-^{3}H were obtained from the International Chemical and Nuclear Corporation, California, and New England Nuclear, Massachusetts.

An aqueous solution of each radioactive tracer was prepared in a standard volumetric flask and sterilized for 30 min at 130 °C. Aliquots of the appropriate solution were administered to cultures which had been growing for 2–4 months using a sterilized hypodermic syringe fitted with a 12 in. needle. The solution containing the radioactive compound was injected into the culture medium below the mycelial pad.

(b) Assay of Radioactivity

Aqueous solutions of amino acids were counted in a scintillator solution consisting of naphthalene (100 g) and 2,5-diphenyloxazole (PPO) (5 g) dissolved in dioxane (1 l).

Toluene solutions of the 2,4-dinitrophenylhydrazone derivative of pyruvic acid were counted in a scintillator solution consisting of PPO (4 g) and POPOP (50 mg) per liter of toluene.

Lycomarasmin, crystallized to constant activity, was dissolved in 0.02 *N* sodium hydroxide and counted as previously described for amino acids.

Radioactivity of $^{14}CO_2$ was assayed using the procedure described by Jaffray and Alvarez (7). The radioactivity in the samples was assayed in a Beckman LS 200B automatic liquid-scintillation counter under the specified conditions. Background corrections were made and the observed counting rate was converted to an absolute value.

Acid Hydrolysis of Lycomarasmin

Lycomarasmin (100 mg) dissolved in 6 *N* hydrochloric acid (5 ml) was heated in a sealed tube for 7 h at 140–150 °C. After cooling, the solution was transferred to a 50-ml flask and connected to the vacuum pump via a Dry Ice – acetone cold trap (−78 °C). The flask was warmed carefully to completely remove the solvent (the remaining residue contained amino acids) and the condensate in the trap added to a solution of 2,4-dinitrophenylhydrazine (50 mg) in hot 6 *N* hydrochloric acid (5 ml). The resulting solution was heated on a water bath for 5 min and then stored at 4 °C for 15 h during which time the 2,4-DNPH derivative of pyruvic acid crystallized. The derivative was collected (centrifugation), dissolved in a solution (5 ml) of 2 *N* sodium carbonate, and filtered to remove unreacted reagent. The filtrate was carefully acidified with 50% hydrochloric acid and the resulting precipitate collected. The 2,4-DNPH derivative was washed with 1–2 ml of water and dried under vacuum (27 mg, 28%), m.p. 215–217 °C, mixture m.p. 214–216 °C.

The residue of amino acids was, after addition of water (10 ml), again concentrated to dryness *in vacuo* to effect removal of residual HCl. The mixture of amino acids was dissolved in water (2–3 ml) and separated using a Dowex 1 (×8) acetate column (1 × 10 cm). Glycine was eluted with water (35 ml) and aspartic acid with 0.5 *N* acetic acid (60 ml).

Each fraction was evaporated to dryness. The residues were dissolved in water (2–3 ml) and, after addition of charcoal, filtered through a 2-mm layer of Celite 535. The filtrate was concentrated to a small volume (1–3 ml) upon which the amino acid crystallized by the addition of ethanol (1–5 ml). For aspartic acid, glacial acetic acid (0.5 ml) was also added. Each amino acid was crystallized to constant activity and counted as described.

Aqueous Hydrolysis of Lycomarasmin

Lycomarasmin (200 mg), suspended in water (7 ml), was heated in a sealed tube for 2½ h at 200 °C. After cooling, the solution was removed and transferred to a 50 ml-flask and evaporated to dryness under vacuum. An aqueous solution of the residue was decolorized with charcoal. After filtering through a pad of Celite, the mixture of amino acids was partially separated on a Dowex 1 (×8) acetate column (1 × 10 cm). Glycine and alanine were eluted with water (35 ml) and aspartic acid with 0.5 *N* acetic acid (60 ml). Aspartic acid was crystallized as described previously.

The mixture of alanine and glycine was resolved on a Dowex 50 (×8) (H^+) column (8). The amino acids were eluted with 1 *N* hydrochloric acid at a rate of 8 ml/h and collected in 10-ml fractions in which glycine was eluted first followed by alanine. The fractions containing the individual amino acids, as detected by paper chromatography, were combined and evaporated to dryness *in vacuo*. Residual HCl was removed from the samples by elution with water through a Dowex 1 (×8) (acetate) column and the amino acids crystallized from aqueous ethanol to constant activity.

Paper Chromatography

Amino acids were identified by paper chromatography (Whatman No. 1) using the following three different solvent systems: (*i*) pyridine – acetic acid – water 50:35:15, (*ii*) pyridine–water 65:35, and (*iii*) phenol–water (1).

Skeletal Degradation of Amino Acids and Malic Acid

The chemical degradation of amino acids and malic acids for localization of radioactivity was carried out according to published procedures (9).

Results and Discussion

As a first approach toward determining the biogenetic origin of the lycomarasmin molecule, cultures of *F. lycopersici* were inoculated with ^{14}C-labelled amino acids and the specific activity of the toxin determined. This was followed by hydrolytic cleavage of the alkaloid and comparison of specific activities of the hydrolysis products.

As a regular procedure, the still cultures were maintained at 25° in the dark for 7 weeks after which 50 μCi of ^{14}C-labelled amino acid was distributed between six cultures. Two series of experiments were performed in which the cultures were harvested after 5- and 24-h contact with the labelled compounds. Crystalline lycomarasmin was isolated using a published isola-

TABLE 1. Specific activity of lycomarasmin

Precursor administered	Specific activity of precursor $\times 10^{-9}$ (d.p.m./mmol)	Specific activity of lycomarasmin $\times 10^{-4}$ (d.p.m./mmol)		Dilution $\times 10^{6}$	
		5 h	24 h	5 h	24 h
Glycine-U-^{14}C	242	0.22	3.34	110	7.3
L-serine-U-^{14}C	278	0.64	3.25	43	8.6
DL-Aspartic acid-4-^{14}C	4.66	0.17	1.67	2.7	0.3
DL-Alanine-1-^{14}C	7.24	0.10	2.01	7.2	0.4

tion procedure (1). The specific activities of the toxin and hydrolysis products of labelled toxin are shown in Tables 1, 2, and 3.

The results in Table 1 indicate that the administered ^{14}C-labelled amino acids can serve as relatively efficient precursors. The label distribution observed in Tables 2 and 3 can be explained in terms of known enzymatic interconversions of the respective amino acids, and will be considered in some detail in the succeeding sections concerned with the incorporation of specific precursors.

TABLE 2. Specific activity of hydrolysis products of 5 h ^{14}C-labelled lycomarasmin

Precursor	Specific activity $\times 10^{-3}$ (d.p.m./mmol)		
	Glycine	Aspartic acid	Pyruvic acid (as 2,4-DNPH)
Glycine-U-^{14}C	0.54	0.31	1.52
L-Serine-U-^{14}C	2.20	0.74	3.78
DL-Aspartic acid-4-^{14}C	<0.1	0.61	1.05
DL-Alanine-1-^{14}C	<0.1	0.10	1.12

TABLE 3. Specific activities of hydrolysis products of 24 h ^{14}C-labelled lycomarasmin

Precursor	Specific activity $\times 10^{-4}$ (d.p.m./mmol)		
	Glycine	Aspartic acid	Pyruvic acid (as 2,4-DNPH)
Glycine-U-^{14}C	1.04	0.37	1.54
L-Serine-U-^{14}C	0.97	0.44	1.44
DL-Aspartic acid-4-C^{14}	0.07	1.12	0.41
DL-Alanine-1-^{14}C	0.05	0.99	0.97

TABLE 4. Specific activities of hydrolysis products of lycomarasmin from cultures inoculated with glycine-2-^{14}C

Hydrolysis product	Specific activity $\times 10^{-4}$ (d.p.m./mmol)
Glycine	7.75
Aspartic acid	1.83
Pyruvic acid	4.04

Glycine-U-^{14}C, Glycine-2-^{14}C, and Serine-U-^{14}C Labelling Experiments

In the case of the 2-carbon and 3-carbon fragments, label distribution might be expected on the basis of the glycine–serine interconversion via the biological aldol–retro–aldol reaction. Glycine may be incorporated as such or may be deaminated and the generated glyoxylate in turn condensed with a suitable 3-carbon fragment.

Incorporation of glycine and serine-U-^{14}C into the 4-carbon fragment (aspartic acid) can occur via the pathway glycine → serine → pyruvate $\xrightarrow{CO_2}$ oxaloacetate → aspartate.

A labelling experiment with specifically labelled glycine-2-^{14}C was designed to establish the origin of the 2-carbon fragment. Six cultures, 10 weeks old, were labelled for 48 h with 100 μCi glycine-2-^{14}C. The isolated lycomarasmin had a specific activity of 1.67×10^{5} d.p.m./mmol and the specific activities of the hydrolysis products are shown in Table 4.

The glycine was degraded by oxidation with ninhydrin and carbon 1, counted as CO_2, was found to contain 28% of the label and carbon 2, counted as the dimedone derivative of formaldehyde, contained 72% of the label. This distribution of label can be rationalized on the basis of randomization of label in the TCA cycle and regeneration of glycine by transamination of glyoxylate from the glyoxylate cycle. Despite

Can. J. Chem. Downloaded from www.nrcresearchpress.com by 210.87.254.5 on 09/05/12
For personal use only.

Can. J. Chem. Downloaded from www.nrcresearchpress.com by 210.87.254.5 on 09/05/12
For personal use only.

this randomization of label, glycine-2-^{14}C was incorporated with relatively high efficiency into the 2-carbon fragment.

In view of the results of the labelling experiments with uniformly labelled glycine and serine and also with specifically labelled glycine, it is reasonable to propose that glycine is a prime precursor to the 2-carbon fragment. These experiments do not however yield unequivocal information as to whether glycine participates as such or is first deaminated to glyoxylate before condensation with the 3-carbon fragment.

Aspartic Acid-4-^{14}C, Aspartic Acid-2,3-^{3}H, and Alanine-1-^{14}C Labelling Experiments

The experimental results (Tables 1 and 3) indicate that aspartate can serve as the 4-carbon source and may also contribute to the 3-carbon fragment. The reason for the relatively low specific activity of the lycomarasmin from the aspartic acid-4-^{14}C labelling experiment may be attributed to the generally accepted high biological lability of this amino acid. It is significant to note that almost 70% of the label which is incorporated into lycomarasmin enters the 4-carbon fragment and 25% into the 3-carbon fragment while very little activity ($\sim$5%) enters the 2-carbon fragment. The observed incorporation of label into the 3-carbon fragment could readily occur via fumarate ($C_4 \equiv C_1$) → malate → oxaloacetate → phosphoenolpyruvate(PEP) → 3-hydroxypyruvate → serine.

Both D- and L-isomers of alanine can be used as the sole carbon source for several species of *Fusaria* (10). Incorporation of label from alanine-1-^{14}C into aspartate (the 4-carbon fragment) could occur via pyruvate → oxaloacetate → fumarate. Oxaloacetate thus derived by carboxylation may give rise to PEP which can eventually give rise to 3-hydroxypyruvate via a similar pathway as indicated for aspartic acid and so enter the 3-carbon fragment.

The low distribution (2.5%) of label from alanine-1-^{14}C into the 2-carbon fragment is of the same magnitude as that observed for aspartic acid-4-^{14}C (5%). Based on the assumption that the label from both these compounds enters the 3-carbon fragment by a similar pathway, these results suggest that their conversion into a suitable 3-carbon source does not proceed past 3-hydroxypyruvate to any significant extent since conversion of this compound into serine would, as has been shown, lead to incorporation of label into C-1 of glycine. The low level of ^{14}C that was incorporated in glycine indicates that the glyoxylate cycle is operative at an accordingly low level.

In order to differentiate between the two possibilities of the 4-carbon fragment being derived directly from either fumarate or aspartate, aspartic acid isolated from lycomarasmin was first degraded by deamination to malic acid followed by decarboxylation to acetaldehyde.

The total carboxyl activity of malic acid and also the activity at C-1 were determined in separate experiments, and the activity at C-4 obtained by difference.

Table 5 shows the distribution of ^{14}C in the carbon atoms of aspartic acid (specific activity = 1.12×10^4 d.p.m./mmol) obtained from lycomarasmin isolated from cultures which had been labelled 24 h with DL-aspartic acid-4-^{14}C. The distribution is expressed as a percentage of the total activity detected.

The overall pattern therefore strongly suggested that the entry of C-1, -2, -3, and -4 of aspartic acid occurs mainly as an intact (or at least isotopically identically reconstituted) carbon chain into the 4-carbon component of lycomarasmin.

The relatively specific incorporation of aspartic acid-4-^{14}C therefore eliminates the possibility of direct participation of fumarate and suggests that aspartate may be incorporated directly or as oxaloacetate. With a view to differentiating between these two possible precursors, a feeding

TABLE 5. Distribution of label in aspartic acid

HOOC—CH(NH_2)—CH_2—COOH Carbon No.	% distribution of recovered radioactivity
1	6
2	< 5
3	< 5
4	94

TABLE 6. Specific activities from L-aspartic acid-2,3-^{3}H experiment

	Specific activity (d.p.m./mmol)
Lycomarasmin	3.14×10^5
Glycine	6.0×10^3
Aspartic acid	7.92×10^3

Can. J. Chem. Downloaded from www.nrcresearchpress.com by 210.87.254.5 on 09/05/12
For personal use only.

experiment with L-aspartic acid-2,3-^{3}H was performed.

L-Aspartic acid-2,3-^{3}H (1000 μCi) was distributed equally between six cultures. It was found necessary to extend the feeding period to 14 days in order to increase the incorporation of ^{3}H to a measurable quantity for subsequent degradation experiments. Lycomarasmin (200 mg) was added as carrier during the work-up procedure to give a final yield of 250 mg which on acid hydrolysis gave 114 mg of aspartic acid and 60 mg glycine. The results of this feeding experiment are summarized in Table 6. It was not found possible to determine the specific activity of the 2,4-DNPH derivative of pyruvic acid due to severe color quenching in the tritium channel.

Aspartic acid isolated from lycomarasmin was degraded in a similar way as in the previous experiment, with the exception that acetaldehyde was further degraded by the iodoform reaction to give C-2 as formate. Degradation of the isolated aspartic acid by the sequence described resulted in only 1.5% of the label of malate being detected in the formic acid derived from C-2 of aspartate. It was not possible to determine the activity of the iodo-form because of quenching in the tritium channel. This low level of activity at C-2 is most probably the result of this amino acid undergoing transamination at a faster rate than its direct incorporation into lycomarasmin and the experiment does not, therefore, conclusively differentiate the participation of aspartate from that of oxaloacetate.

The tritium from aspartic acid-2,3-^{3}H can be incorporated into the 2-carbon fragment (glycine) via a slow but sufficiently operative glyoxylate cycle particularly over the necessary extended feeding period. This observation is in accord with the slow ^{14}C incorporation from aspartate and alanine described above. The somewhat higher incorporation of tritium is attributable to the longer feeding period employed in this experiment.

The biogenetic reaction sequence involved, followed by the requisite chemical degradations are summarized in Scheme 1.

D-*Glucose-U-*^{14}*C and* D-*Glucose-6-*^{3}*H Labelling Experiments*

Based on our previous findings that aspartic acid and glycine furnish the carbon atoms for the 4- and 2-carbon fragments respectively, possibilities for the origin of the 3-carbon fragment are a 3-carbon amino acid such as serine, or 3-carbon compounds derived from glucose such as 3-hydroxypyruvate, phosphoenolpyruvate or pyruvate. With a view to determining the participation of the latter three compounds a labelling experiment with glucose-U-^{14}C was carried out.

D-Glucose-U-^{14}C (180 mCi/mmol, 500 μCi) was distributed between six 10-week-old cultures and the lycomarasmin isolated after a 24 h labelling period. The specific activities of lycomarasmin and the hydrolysis products have been divided by 10 before entry into Table 7 for comparison purposes with those from the amino acid labelling experiments, in which 50 μCi of each amino acid was fed.

The results in Table 7 suggest that either glucose is a more immediate precursor of the 3-carbon fragment than the amino acids or that it penetrates to the site of synthesis more easily. However, previous analytical studies of the culture medium have shown that the organism is depleted in glucose after 30 days growth (11) thus largely eliminating the possibility that glucose serves as an immediate precursor at such a time. External application of ^{14}C-labelled amino acids results in their dilution by the relatively large pool of unlabelled amino acids in the medium (11) prior to their transport to the site of synthesis resulting in relatively low specific activity of lycomarasmin. Glucose, on the other hand, will undergo rapid catabolism inside the cells resulting in production of numerous 2- and 3-carbon compounds and provided they undergo transamination near the site of synthesis, the specific activity of lycomarasmin will be relatively high. Unless this transamination process occurs near the site of synthesis, the release of the freshly derived amino acids into the general amino acid pool would consequently give specific activities not

TABLE 7. Specific activities from D-glucose-U-^{14}C labelling experiment

	Specific activity (d.p.m./mmol)
Lycomarasmin	12.6
Glycine	3.16
Aspartic acid	2.47
Pyruvic acid	5.00

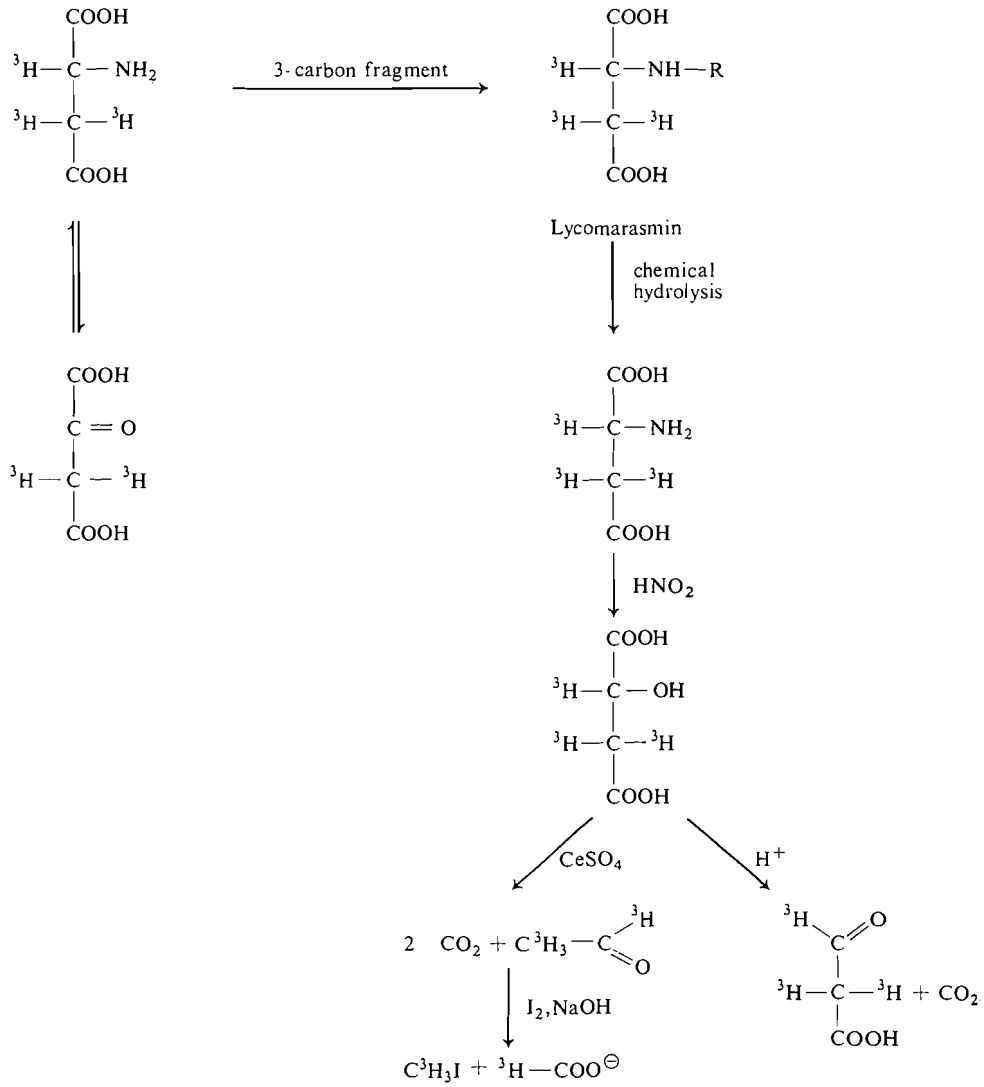

SCHEME 1

too different from direct administration of labelled amino acids.

Cochrane *et al.* (12) supplied *F. oxysporum* with glucose-U-^{14}C and subsequently demonstrated that less than 5% of the glucose label remains in the medium. The present finding of a relatively higher incorporation of glucose into lycomarasmin as compared with the amino acids may therefore simply indicate that permeability barriers exist.

Nevertheless, the relatively high incorporation of activity in the 3-carbon fragment (pyruvate) suggests that this part of the molecule is relatively efficiently derived from glucose.

It was reasoned that the information gained from a dual labelling experiment with D-glucose-U-^{14}C-6^{3}H would elucidate the mechanism by which the 4-carbon fragment condenses with the 3-carbon fragment.

For the detection of tritium in the 3-carbon fragment, it was found necessary to count this fragment as alanine rather than pyruvic acid because of the intense color quenching caused by the 2,4-DNPH derivative. For this reason, the lycomarasmin was subjected to aqueous hydrolysis giving glycine, alanine, and aspartic acid. It was also necessary to extend the feeding period to 40 h in order to increase the incorpora-

Can. J. Chem. Downloaded from www.nrcresearchpress.com by 210.87.254.5 on 09/05/12
For personal use only.

TABLE 8. Hydrolysis products of lycomarasmin from dual labelling experiment

	^{14}C (d.p.m./mg)	^{3}H (d.p.m./mg)	$^{14}C/^{3}H$
Glycine	5650	1105	10.2:1
Aspartic acid	2501	1175	4.3:1
Alanine	6350	1340	9.5:1

tion of ^{14}C and ^{3}H to a measurable quantity for the calculation of the $^{3}H/^{14}C$ ratio.

The results of this dual labelling experiment in which 500 μCi of D-glucose-U-^{14}C and 1000 μCi of D-glucose-6-^{3}H were distributed between six cultures are summarized in Table 8. During the work-up procedure 50 mg carrier lycomarasmin were added to give a final yield of 330 mg. Each $^{14}C/^{3}H$ ratio was divided by the $^{14}C/^{3}H$ ratio of the original glucose to give the ratio that would have been obtained if the $^{14}C/^{3}H$ ratio in the glucose had been 1:1 before entry into Table 8.

Consideration of the pathway by which the 3-carbon fragment is derived from glucose leads to the prediction that retention of ^{3}H at C-3 will result in a $^{14}C/^{3}H$ ratio comparable to the initial value, *i.e.*, 1:1 corrected. Similarly, loss of one tritium atom at C-3 will result in a ratio of about 2:1, corrected. The observed value of $^{14}C/^{3}H$ in alanine derived from pyruvic acid is 9.5:1 corrected, showing a substantial loss of tritium which cannot be explained by the loss of one tritium atom. This loss of tritium can, however, be rationalized on the basis of the tritium atoms (at C-6 in the original glucose) undergoing relatively rapid chemical or biological exchange before incorporation into lycomarasmin. This could occur by the pathway PEP → pyruvate → oxaloacetate → PEP → 3-carbon fragment of lycomarasmin.

Summary

The experimental results described herein indicate that metabolites occupying rather key positions in well established metabolic cycles serve as efficient precursors of the different parts of the wilt toxin. The administered glycine-2-^{14}C was primarily incorporated without extensive label randomization; however, the results do not unequivocally distinguish between the participation of either glycine or glyocylate, or both. Feeding of aspartic acid-4-^{14}C showed that the entry of C-1, -2, -3, and -4 of aspartate occurs mainly as an intact carbon chain into the 4-carbon fragment of lycomarasmin, although experiments with aspartic acid-2,3-^{3}H were inconclusive in differentiating between the participation of oxaloacetate from that of aspartate.

The labels from alanine-1-^{14}C and aspartic acid-4-^{14}C were incorporated to only a small extent into the 2-carbon fragment of lycomarasmin indicating the conversion of these compounds does not proceed past 3-hydroxypyruvate. Taken in conjunction with results from a glucose-U-^{14}C feeding experiment, the above experiments indicate that the probable precursor of the 3-carbon fragment is a compound readily derived from glucose such as phosphoenolpyruvate. From a mechanistic approach, the condensation of aspartate, phosphoenolpyruvate and glycine could directly lead to the formation of the wilt toxin.

1. E. HARDEGGER, P. LIECHTI, L. M. JACKMAN, A. BOLLER, and P. A. PLATTNER. Helv. Chem. Acta, **46**, 60 (1963).
2. T. YABUTA. J. Agric. Chem. Soc. Jap. **10**, 1059 (1934).
3. R. D. HILL, A. M. UNRAU, and D. T. CANVIN. Can. J. Chem. **44**, 2077 (1966).
4. D. DESATY, A. G. MCINNES, D. G. SMITH, and L. C. VINING. Can. J. Biochem. **46**, 1293 (1968).
5. A. E. DIMOND and P. E. WAGGONER. Phytopathology, **43**, 195 (1953).
6. PL. A. PLATTNER and N. CLAUSON-KAAS. Helv. Chem. Acta, **28**, 188 (1945).
7. H. JAFFRAY and J. ALVAREZ. Anal. Chem. **33**, 612 (1961).
8. C. H. W. HIRS, S. MOORE, and W. H. STEIN. J. Am. Chem. Soc. **76**, 6063 (1954).
9. S. ARONOFF. Techniques of radiochemistry. Hafner Publ. Co. Inc. N.Y.
10. J. C. WIRTH and F. F. NORD. Arch. Biochem. **2**, 463 (1943).
11. B. D. SANWALL. Phytopathol. Z. **25**, 333 (1956).
12. V. W. COCKRANE, S. J. BERRY, F. G. SIMON, J. C. COCKRANE, C. B. COLLINS, J. A. LEVY, and P. K. HOLMES. Plant Physiol. **38**, 533 (1963).

Can. J. Chem. Downloaded from www.nrcresearchpress.com by 210.87.254.5 on 09/05/12
For personal use only.

A Rapid Route to Hex-1-enopyran-3-uloses[1]

BERT FRASER-REID, D. L. WALKER,[2] S. Y-K TAM,[3] AND N. L. HOLDER[4]

Chemistry Department, University of Waterloo, Waterloo, Ontario

Received June 18, 1973

Whereas the pseudo-axial 3-hydroxyl group of allal derivatives is known to be inert to manganese dioxide oxidation, the equatorial counterpart in glucal derivatives is shown to be readily oxidized. Thus glucal is converted to the 6-*O*-triphenylmethyl ether or 6-*O*-benzoyl ester to promote solubility in chloroform, and the derivatives are oxidized in that solvent in 12 h or less.

Acetonation of glucal is readily accomplished in 45 min using 2,2-dimethoxypropane and *p*-toluenesulfonic acid in dimethylformamide; the product may be oxidized directly either with manganese dioxide or dipyridine chromium oxide. Thus it is possible to obtain 1–3-g quantities of the crystalline acetonated enone from triacetyl glucal (via deacetylation, acetonation, and oxidation) in 3–4 h.

If the acetonation medium stands for 2 h methyl 2,3-dideoxy-4,6-*O*-isopropylidene-α-D-*erythro*-hex-2-enopyranoside is obtained. The mechanism of its formation in the reaction medium is discussed.

Alors que le groupe hydroxy-3 pseudo-axial des dérivés allal est reconnu inerte vis-à-vis de l'oxydation par le bioxyde de manganèse, on montre que le groupe équatorial des dérivés glucal est rapidement oxydé. Ainsi, le glucal est transformé en dérivé triphénylméthoxy-6 ou benzoxy-6 afin d'augmenter sa solubilité dans le chloroforme et les dérivés sont oxydés dans ce solvant en douze heures ou moins.

L'acétonation du glucal est aisément réalisé en 45 min à l'aide du diméthoxy-2,2 propane et l'acide *p*-toluènesulfonique dans la diméthyl formamide; le produit peut être directement oxydé avec du bioxyde de manganèse ou avec le complexe dipyridine oxyde de chrome. Il est possible à partir du glucal triacétylé d'obtenir en 3–4 heures des quantités de 1–3 g de l'énone acétoné sous forme cristalline (par l'intermédiaire de la déacétylation, de l'acétonation et de l'oxydation).

Si le milieu réactionnel de l'acétonation est maintenu durant 2 h, on obtient le didéoxy-2,3 *O*-isopropylidène-4,6 α-D-érythro hexèno-2 pyrannoside de méthyle. On discute le mécanisme de sa formation.

[Traduit par le journal]

Can. J. Chem., **51**, 3950 (1973)

In pursuing our interest in the chemistry of carbohydrate conjugated enones (1) we need to have an assortment of dihydro γ-pyrone type molecules such as **1** which (*a*) are obtainable from readily available materials and, in addition, may be equipped with either (*b*) acid- or (*c*) base-labile protecting groups, the choice being dictated by our ultimate designs for the molecule. Existing routes (2) do not fill requirements (*a*) and (*c*). The parent substance **7***d* has been synthesized recently (3) but the sensitivity of this substance to acid (*vide infra*) indicates that it would not likely survive conditions for preparing derivatives such as **1***a*.

Glucal (**2***a*) seemed to be a precursor via which all three requirements could be met but we were mindful of Collins' experience (2*b*) that the allylic alcohol in compound **3** was not oxidized by manganese dioxide. Having ourselves encountered anomalies in the oxidation of epimeric allylic alcohols (4) we were interested to see

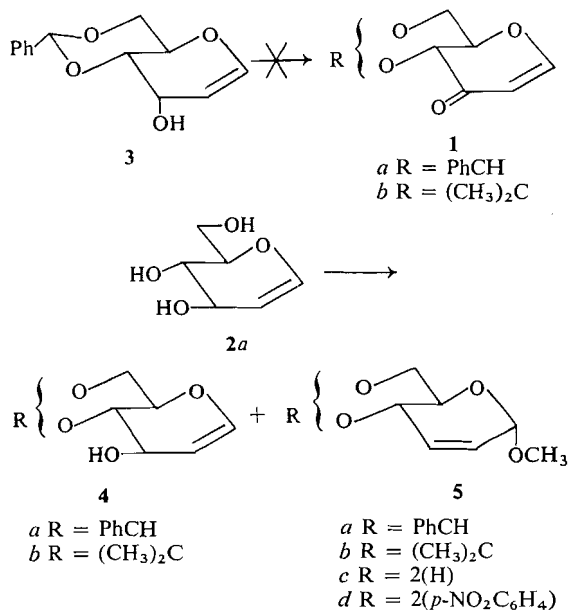

3

1
a R = PhCH
b R = $(CH_3)_2C$

2*a*

4
a R = PhCH
b R = $(CH_3)_2C$

5
a R = PhCH
b R = $(CH_3)_2C$
c R = 2(H)
d R = 2(*p*-$NO_2C_6H_4$)

[1]Pyranosiduloses Part VIII. For Part VII see ref. 14.

[2]Year III, Undergraduate Summer Research Participant, 1972.

[3]Recipient of a University of Waterloo Bursary 1972–1973.

[4]Taken in part from the Ph.D. Thesis of N.L.H., University of Waterloo, 1973. Present address: Gillette Research Institute, Rockville, Maryland, U.S.A.

Can. J. Chem. Downloaded from www.nrcresearchpress.com by 210.87.254.105 on 09/05/12
For personal use only.

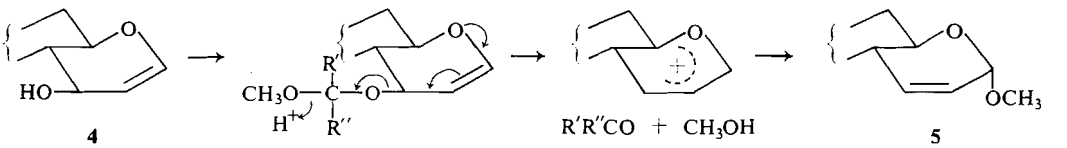

$R' = R'' = CH_3$
or $R' = H$; $R'' = Ph$

SCHEME I

whether the equatorial alcohol in **4** would respond differently from its axial counterpart in **3**. We report herein the results of this study.

Given the failure of **3** to be oxidized by manganese dioxide, the appropriate candidate for testing was the equatorial isomer **4***a*. However attempts to prepare this substance from glucal (**2***a*) in the usual way with benzaldehyde and zinc chloride (5) did not give useful amounts of the material. Therefore the method of Evans *et al.* (6) was tried.

Glucal (**2***a*) was treated with α,α-dimethoxytoluene in the presence of *p*-toluenesulfonic acid at room temperature. A plethora of products was given, one of which was recognizable from t.l.c. and subsequently by isolation as olefin **5***a*. The conversion must be a highly efficient process, since **5***a* was formed in appreciable amounts (t.l.c.) very early in the reaction, even though considerable starting material remained unreacted.

The conversion of **4***a* → **5***a* is reminiscent of the well-known process in which acetylated glycals are transformed into hex-2-enopyranosides by acidified alcohols (7). Unfortunately we were unable to develop conditions that would provide for a viable synthetic process, **2***a* → **5***a*. Prolonged standing at room temperature and/or heating of the reaction mixture caused extensive decomposition.

For the rearrangement of the acetylated glycals, the favored mechanism invokes anchimeric assistance by the acetyl groups and therefore would be inoperable for the conversion of **4***a* → **5***a*. Conceivably, the process could be facilitated by formation of the mixed hemiacetal **6**, as outlined in Scheme 1.[5] Interestingly, the only other case, to our knowledge, in which a glycal with a free hydroxyl group at carbon-3 has been successfully rearranged to an hex-2-enopyranoside also involved ketal-type solvent. Ferrier and Prasad, upon treating D-glucal with boron trifluoride in dimethoxymethane also obtained **5***c* (8).

Acetonation of glucal proved to be more controllable than the foregoing benzylidination. Thus glucal (**2***a*) obtained from triacetyl glucal **2***b* (9) was treated with 2,2-dimethoxypropane in dimethylformamide, acidified to p*H* 3 with *p*-toluenesulfonic acid. After 45 min a mixture was obtained from which **4***b* could be separated chromatographically as an oil in 44% yield (from **2***b*). When the reaction was allowed to go for 2 h, two other substances, R_f 0.62 and 0.27, had formed in addition to **4***b* (R_f 0.43). The fastest running substance was isolated as a syrup and was assigned structure **5***b* because of the similarity of its n.m.r. spectrum to that of well-known **5***a*. The syrupy material (**5***b*) and **5***a* were deblocked separately by treatment with *p*-toluenesulfonic acid in dry methanol to afford the same diol **5***c*, which was converted to the known di-*O*-*p*-nitrobenzoate **5***d* (8).

Compound **4***b* underwent manganese dioxide oxidation smoothly in 2–3 days to give the crystalline ketone **1***b* in 73% yield. Alternatively the oxidation could be accomplished in 15 min (77% yield) using dipyridine chromium oxide in methylene chloride (10).

It could be estimated from the n.m.r. spectrum that the 45 min acetonation product contained >90% of **4***b*. Therefore in practice the crude acetonation product was oxidized directly. Furthermore, if **2***b* was deacetylated by the methanol–water–triethylamine method and the oxidation done with the chromium oxide complex (10), it was possible to obtain 1–3 g (~20%) quantities of crystalline **1***b* from **2***b* in 3–4 h, without purification of intermediates.

The foregoing success meant that the equatorial alcohol in glucal derivatives, unlike the axial alcohol in the previously reported allal derivatives (2), would respond to manganese dioxide treatment. An obvious limitation is that the derivative must be soluble in chloroform.

[5]We are indebted to a referee for this suggestion.

Can. J. Chem. Downloaded from www.nrcresearchpress.com by 210.87.254.105 on 09/05/12
For personal use only.

This can readily be arranged by taking advantage of the high reactivity of the primary alcohol as has been done in the preparation of 6-*O*-*p*-toluenesulfonyl-D-glucal (11). Thus glucal **2***a* was furnished with either the base-labile benzoyl group (**2***c*) or the acid-labile triphenylmethyl group (**2***d*), and the material in each case was oxidized to the enones **7***a* and *b*, respectively. The former is a crystalline material, the latter is crystallized as the acetate **7***c*.

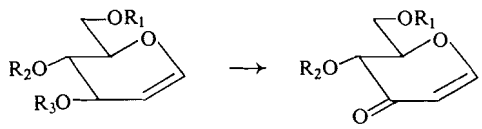

2 **7**

a $R_1 = R_2 = R_3 = H$ *a* $R_1 = PhCO$; $R_2 = H$
b $R_1 = R_2 = R_3 = Ac$ *b* $R_1 = Ph_3C$; $R_2 = H$
c $R_1 = PhCO$; $R_2 = R_3 = H$ *c* $R_1 = Ph_3C$; $R_2 = Ac$
d $R_1 = Ph_3C$; $R_2 = R_3 = H$ *d* $R_1 = R_2 = H$

In practice crystalline triacetal glucal (**2***b*) was deacetylated, and the crude glucal was treated with a 10% deficiency of the reagent. The unreacted glucal was extracted from the chloroform solution with water and the chloroform-soluble material was usually oxidized directly (particularly when preparing a small amount (1–2 g) of the enone), thereby postponing chromatographic separation until the final step.

Unfortunately attempts to remove the blocking group from **7***a* (with dilute base) or **7***b* (with dilute acid) to obtain the free parent enone **7***d* were unsuccessful. In both cases the enone was destroyed, judging from the n.m.r. spectrum. Deep-seated degradation of **7***b* by acid was indicated by the formation of formaldehyde.

The spectral data of these enones compare well with those of its congeners reported previously (2). In **1***b* for example, H-1 and H-2 are doublets ($J_{12} = 6$ Hz) at δ 7.26 and 5.43, respectively. The former signal in **1***a* and **7***a–c* is of course obscured by the aromatic protons. It is interesting to note that the u.v. absorption of **1***b* occurs at very much longer wavelength than that of other enones (2*c*). In the hex-2-enopyranosid-4-uloses (1*b*) and hex-3-enopyranosid-2-uloses (1*c*) the absorption in ethanol has λ_{max} at ~220 nm (ε ~9000). In **1***b* however, the absorption shows λ_{max} at 260 nm (ε 8048) which corresponds favorably with the maximum (263 nm) reported for related 2,3-dihydro-2,6-dihydro-4-pyrones (12).

We verified that compound **3** was inert to the conditions under which the glucal derivatives (**4**, **2***c* and *d*) reacted with manganese dioxide. Nickon and co-workers reported some time ago, that in some steroidal allylic alcohols, the axial epimer was less readily oxidized than the equatorial (13). In the present case the difference is more dramatic, since **3** was still unchanged after 2 weeks while **4** and **2***c* and *d* were oxidized in 0.5–3 days. A similar anomaly was noted by us in the resistance of an axially-disposed allylic alcohol in the anomers of some pent-2-enopyranosides (3). An attempt is being made by us to determine the reason for the absolute resistance of these axial alcohols. However, *the phenomenon is not general for axial allylic alcohols in carbohydrate molecules*, since 5*c* and its carbon-4 epimer were oxidized with equal readiness. Similarly hex-3-enopyranosides are oxidized to the same 2-ketone regardless of the orientation of the carbon-2 hydroxyl group.

Experimental

Melting points were determined on a Fisher-Johns heating stage and are uncorrected. Elemental analyses were performed by Chemalytics Inc., Tempe, Arizona 85281 and Microanalyses Laboratory, Toronto, Ontario. The n.m.r. spectra ($CDCl_3$, TMS) were determined on a Varian T-60 spectrometer, the *J* values quoted being the spacing measured directly from the spectra. Infrared spectra were determined on a Beckman model I.R.-10 spectrometer using 0.1-mm sodium chloride solution cells (chloroform as solvent). Ultraviolet spectra were obtained from a Beckman DBG Grating Spectrophotometer and a Cary Recording Spectrophotometer Model 14 (methanol as solvent). Mass spectra were measured with a CEC model 21-110B double focusing instrument at an i.p. of 70 eV. Optical rotations were determined on a Carl Zeiss model LEP nür 370740 Lichtelektusches Praizisionpolarimeter at 23 °C.

Thin-layer chromatography was performed on glass plates coated with silica gel (HF-254, E. Merck) to a thickness of 0.3 mm. Unless otherwise stated the chromatograms were developed in petroleum ether (30–60°) – ethyl acetate (1:1), dried, viewed under u.v. light, and then sprayed with concentrated sulfuric acid. For column chromatography E. Merck Silica Gel (0.063–0.20 mm 70–230 mesh, A.S.T.M.) was used.

The procedure for manganese dioxide oxidation was as described previously (1).

The glucal **2***a* used for the preparations below was usually the crude non-crystalline material obtained by deacetylation of triacetyl glucal (9) **2***b* by one of the following methods: (*A*) Triacetyl glucal **2***b* (25 g) was dissolved in absolute methanol (400 ml) and stirred for 3 h with anhydrous sodium carbonate (25 g). The solids were removed by filtration and the filtrate was evaporated leaving a thick syrup. (*B*) Triacetyl glucal **2***b* was dissolved in a minimum amount of methanol–water–triethylamine

Can. J. Chem. Downloaded from www.nrcresearchpress.com by 210.87.254.105 on 09/05/12
For personal use only.

Can. J. Chem. Downloaded from www.nrcresearchpress.com by 210.87.254.105 on 09/05/12
For personal use only.

mixture (5:4:1) and when t.l.c. showed the reaction to be complete (1–1½ h) the solution was poured into excess chloroform. The aqueous layer was isolated and washed twice with chloroform and then evaporated. Persistent traces of triethylamine could be removed by dissolving the residue in water and stirring with a small amount of acidic ion-exchange resin.

*1,2-Dideoxy-4,6-O-isopropylidene-*D*-arabino-hex-1-enopyranose*, **4***b*

To a solution of crystalline glucal (**2***a*) (2.0 g; 13.7 mmol) in dry dimethylformamide (50 ml) was added 2,2-dimethoxypropane (8 ml, 5 mol equiv.). The mixture was acidified to p*H* 3 (test paper) with *p*-toluenesulfonic acid and allowed to stand at room temperature for 45 min when t.l.c. visualized with iodine vapor showed appreciable amounts of a new substance **4***b*, R_f 0.43. The reaction was quenched with saturated sodium bicarbonate solution and extracted with chloroform (3 × 50 ml). The dried (Na_2SO_4) chloroform layer upon evaporation yielded an oily residue (1.7 g). N.m.r. analysis indicated that **4***b* constituted ~90% of this residue. A faster running substance **5***b*, R_f 0.62 (*vide infra*), was also detected by t.l.c. Compound **4***b* was isolated by silica column chromatography using petroleum ether – ethyl acetate (1:1) as eluant. Pure **4***b* (1.1 g, 44% yield) was isolated as an oil. Significant n.m.r. features were: δ 1.50 and 1.55 (pair of singlets, 6, $(CH_3)_2C$); 4.80 (q, 1, J_{12} = 6.0, J_{23} = 2.0 Hz, H-2); 6.37 (q, 1, J_{12} = 6, J_{13} = 2.0 Hz, H-1). The oil was characterized as its *p*-nitrobenzoate m.p. 111.5–112°; $[\alpha]_D^{23}$ −131.9° (*c*, 1.23 in chloroform).

Anal. Calcd. for $C_{16}H_{17}O_7N$: C, 57.31; H, 5.11; N, 4.18. Found: C, 57.35; H, 5.16; N, 4.26.

*1,2-Dideoxy-4,6-O-isopropylidene-*D*-erythro-hex-1-enopyran-3-ulose*, **1***b*

(*i*) The oily product (0.6 g) from 45-min acetonation of glucal was dissolved in 300 ml of chloroform and stirred with 9 g of activated manganese dioxide for 3 days. Removal of the manganese dioxide by filtration and evaporation of the filtrate afforded only an oily residue which crystallized on standing yielding 0.44 g of **1***b* (73% yield) after recrystallization from ether.

(*ii*) A portion (0.28 g) of the crude acetonation product and 2.4 g of dipyridine chromium(VI) oxide (10) in methylene chloride (10 ml) were stirred at room temperature for 15 min. The solution was filtered and the filter cake was washed with ether. The filtrate was evaporated to dryness and traces of pyridine removed by codistillation with toluene. Crystallization of the residue as in (*i*) afforded 0.22 g (77% yield) of **1***b*.

(*iii*) Glucal **2***a* (crude oil from deacetylation of 20 g of triacetyl glucal **2***b*) was dissolved in 180 ml of dried dimethylformamide and treated with dimethoxypropane (30 ml) and *p*-toluenesulfonic acid (~3.3 g) to achieve p*H* ~3. The reaction was quenched after 45 min with saturated sodium bicarbonate and worked up as described above. The oil from the dried chloroform extract (8.5 g) was dissolved in 320 ml of dried methylene chloride and freshly prepared dipyridine chromium oxide (70 g) was added in one lot while maintaining vigorous stirring with a mechanical stirrer. After 15 min the solution was filtered through celite and the filtrate was evaporated to a small volume and then diluted with ether and washed successively with 10% sulfuric acid (to remove pyridine), sodium bicarbonate, and water. The ether layer afforded an oil which crystallized readily from ether, to give **1***b* (2.9 g, 21% from **2***b*): R_f 0.4; m.p. 104–105°; $[\alpha]_D^{23}$ +206.57° (*c*, 5.0 in $CHCl_3$); I.r. ($CHCl_3$) ν_{max} 1700, 1600 (α,β-unsaturated ketone) 1250, 1060 (C═C—O—C), 1195 cm^{-1} ($(CH_3)_2C$); u.v. (ethanol) λ_{max} 260 nm (ε 8048); n.m.r.: δ 1.5 (s, 6, $(CH_3)_2C$), 3.8–4.3 (m, 4, H-4, H-5, H-6, H-6′), 5.43 (d, 1, J_{12} = 6.0 Hz, H-2), and 7.26 (d, 1, J_{12} = 6.0 Hz, H-1).

Anal. Calcd. for $C_9H_{12}O_4$: C, 58.69; H, 6.57. Found: C, 58.64; H, 6.40.

*Methyl 2,3-Dideoxy-4,6-O-isopropylidene-*α*-*D*-erythro-hex-2-enopyranoside*, **5***b*

The oily acetonation product of crude glucal (3.6 g) was oxidized by manganese dioxide as described above to give a solid residue (2.6 g). T.l.c. showed ketone **1***b* (R_f 0.40), and faster (R_f 0.62) and slower (R_f 0.27) running substances, the latter being in trace amounts. The mixture was chromatographed on a silica column and eluted with petroleum ether – ethyl acetate (1:1), whereby the material of R_f 0.62 was recovered as a mobile oil (0.280 g) $[\alpha]_D^{23}$ +54.6° (*c*, 2.20 in chloroform); n.m.r. H-1, H-2, H-3 at δ 4.90, 5.70, and 6.07, respectively; J_{12} = 10.0 Hz. For the known analog **5***a*, the corresponding values are 5.0, 5.84, and 6.1, respectively.

A portion of the oil (0.140 g) was dissolved in dry methanol (5 ml) and *p*-toluenesulfonic acid (0.025 g) was added. T.l.c. indicated the disappearance of **5***b* after 5 min. The solution was diluted with dry methanol (20 ml) and neutralized with barium carbonate. The solids were removed by filtration, and the filtrate poured into water and extracted with ether. The aqueous layer was evaporated to dryness and the residue converted to the di-*O*-*p*-nitrobenzoate **5***d* for comparison with an authentic specimen,[6] m.p. and mixture m.p., 170–171°.

*1,2-Dideoxy-4-O-acetyl-6-O-triphenylmethyl-*D*-erythro-hex-1-enopyran-3-ulose*, **7***c*

The syrupy glucal **2***a* from 25 g (0.092 mol) of **2***b* (method *A*) was dissolved in a mixture of pyridine (300 ml) and methylene chloride (100 ml), and trityl chloride (30 g, 0.108 mol) was added to the stirred solution at room temperature. After 2 days, the mixture was poured into ice water, extracted with chloroform, and the organic layer was washed with sulfuric acid, sodium bicarbonate, and then dried with sodium sulfate. Evaporation of the solvent yielded a thick oil which, after chromatography on a silica column, afforded 30 g (84% from **2***b*) of **2***c*. (The need for chromatography at this stage could be obviated by working on 2–5-g quantities of **2***b* and by using a deficiency of trityl chloride.) Crude **2***c* (15 g) was dissolved in chloroform (1500 ml) and stirred with manganese dioxide (60 g). The reaction was finished in 8 h and the solids were removed by filtration. The filtrate afforded **7***b* (13 g 85% from **2***c*) as an oil, which was acetylated with pyridine (120 ml) and acetic acid anhydride (20 ml). Customary work-up afforded **7***c* which crystallized from ether, m.p. 143.5–144.5°; $[\alpha]_D^{23}$ +230.9° (*c*, 1.55 in $CHCl_3$).

[6]We are indebted to Professor R. J. Ferrier for an authentic sample of **5***d*.

Anal. Calcd. for $C_{27}H_{24}O_5$: C, 75.68; H, 5.65. Found: C, 75.47; H, 5.67.

*6-O-Benzoyl-1,2-dideoxy-*D*-erythro-hex-1-enopyran-3-ulose*, *7a*

Crystalline glucal **2***a* (2.0 g, 1.37 mmol) was dissolved in pyridine (100 ml) and methylene chloride (50 ml). The solution was cooled in a Dry Ice – acetone bath to −76° and benzoyl chloride (1.7 ml, 1.47 mmol) in 20 ml methylene chloride was added dropwise over 1 h. At this time the solution was poured into ice water and the product extracted into methylene chloride and processed in the usual way. The resulting oil (3 g) was treated with manganese dioxide (14 g) in chloroform (200 ml). After 12 h the solution was filtered, the filtrate was evaporated, and the product was chromatographed eluting with petroleum ether – ethyl acetate (1:1). Compound **7***a* (0.95 g, 26%) was obtained by crystallization from cold ethanol, m.p. 94–95°; $[\alpha]_D^{23}+207.2°$ (*c*,1.16 in chloroform).

Anal. Calcd. for $C_{13}H_{12}O_5$: C, 62.90; H, 4.87. Found: C, 62.73; H, 5.10.

We express our gratitude to the National Research Council of Canada, Bristol Laboratories, and the University of Waterloo for the financial support that made this work possible.

1. (*a*) B. Fraser-Reid, A. McLean, and E. W. Usherwood. J. Am. Chem. Soc. **91**, 5292 (1969). (*b*) B. Fraser-Reid, A. McLean, E. W. Usherwood, and M. Yunker. Can. J. Chem. **98**, 2877 (1970). (*c*) B. Fraser-Reid and N. L. Holder. Chem. Commun. 31 (1972).
2. (*a*) P. M. Collins, P. Gupta, and R. Iyer. J. Chem. Soc. **C**, 1670 (1972). (*b*) P. M. Collins. Carbohydr. Res. **11**, 125 (1969). (*c*) P. J. Benyon, P. M. Collins, P. T. Doganges, and W. G. Overend. J. Chem. Soc. **C**, 1131 (1966).
3. J. M. J. Tronchet, J. Tronchet, and A. Birkhauser. Helv. Chim. Acta, **53**, 1489 (1970).
4. B. Fraser-Reid, B. J. Carthy, N. L. Holder, and M. Yunker. Can. J. Chem. **49**, 3039 (1971).
5. M. Sharma and R. K. Brown. Can. J. Chem. **44**, 2825 (1966).
6. M. E. Evans. Carbohydr. Res. **21**, 473 (1972); M. E. Evans, F. W. Parrish, and L. Long. Carbohydr. Res. **3**, 453 (1967).
7. B. Helferich. Adv. Carbohydr. Chem. 7, 209 (1952).
8. R. J. Ferrier and N. Prasad. J. Chem. Soc. **C**, 570 (1969).
9. W. Roth and W. Pigman. Meth. Carbohydr. Chem. **2**, 405 (1963).
10. J. C. Collins. Tetrahedron Lett. 3363 (1969).
11. T. Maki and S. Tejima. Chem. Pharm. Bull. (Jap.), **15**, 1367 (1967).
12. P. Yates and D. T. MacGregor. Can. J. Chem. **51**, 1267 (1973).
13. A. Nickon and J. F. Bagli. J. Am. Chem. Soc. **83**, 1498 (1961); A. Nickon. N. Schwartz, J. B. Di Giorgio, and D. A. Widdowson. **30**, 1711 (1965).
14. S. Y-K Tam, D. E. Iley, N. L. Holder, D. R. Hicks, and B. Fraser-Reid. Can. J. Chem. In Press.

Can. J. Chem. Downloaded from www.nrcresearchpress.com by 210.87.254.105 on 09/05/12
For personal use only.

The Question of Conformational Restriction in the *trans*-Cyclononene Ring of Caryophyllene[1]

E. W. WARNHOFF AND V. SRINIVASAN
Department of Chemistry, University of Western Ontario, London, Ontario
Received September 18, 1972[2]

The possibility that the barrier to rotation of the *trans* double bond within the nine-membered ring of caryophyllene might be high enough to prevent the interconversion of conformers **2** and **3** near room temperature has been examined. Contrary to earlier reports, it has been found that two *trans* epoxides are formed on peracid epoxidation of caryophyllene and hence both conformers are present. Attempts to determine whether **2** and **3** are interconverting near room temperature were inconclusive.

On a étudié la possibilité selon laquelle la barrière à la rotation de la double liaison *trans* à l'intérieur du cycle à neuf membres du caryophyllène puisse être suffisamment élevée pour empêcher l'interconversion des conformères **2** et **3** à température ambiante. Contrairement aux rapports antérieurs, on a trouvé que deux époxydes *trans* sont formés lors de l'époxydation du caryophyllène par un peracide, confirmant ainsi la présence des deux conformères. Les essais afin de déterminer si **2** et **3** peuvent s'interconvertir à température ambiante n'ont pas permis d'en venir à une conclusion.
[Traduit par le journal]

Can. J. Chem., **51**, 3955 (1973)

Introduction

There has been considerable interest in the existence of stable conformational isomers due to restricted rotation in medium ring cycloalkenes and in this regard our attention was drawn some time ago to the sesquiterpene caryophyllene. In the voluminous chemical literature on this molecule (1), certain observations suggested the possibility of severe restriction to rotation of its *trans*-cyclononene double bond about the attached single bonds to carbon. This possibility acquired increased interest when it was found by Cope *et al.* that both *trans*-cycloöctene and *trans*-cyclononene could be resolved (2, 3). Although racemization of these resolved cycloalkenes merely requires rotation about the single bonds of these molecules, in particular 180° rotation of the *trans* double bond, optically active *trans*-cycloöctene was only slowly racemized at 132° ($t_{1/2}$ = 122 h) (4). On the other hand, *trans*-cyclononene was not optically stable at room temperature and had a half life of about four minutes at 0° (3). However, the barrier to rotation of the *trans* double bond of caryophyllene (**2** ⇌ **3**) about the single bonds *a* could be higher than that of *trans*-cyclononene.[3]

Among the earlier recorded observations possibly indicative of restricted rotation is the formation of two nitrosochlorides from isocaryophyllene (**13**) with the *cis* endocyclic double bond, whereas caryophyllene gave a single nitrosochloride (5). All three nitrosochlorides were formed by addition to the trisubstituted double bond since each gave the same compound on reaction with benzylamine. A second and more significant finding was that the reaction of isocaryophyllene (**13**) with monoperphthalic acid gave approximately equal amounts of two isomeric oxides, **16** and **17**, of the *cis* endocyclic double bond, while caryophyllene afforded a

[1]Presented in part at the Symposium on the Chemistry of Natural Products, Vancouver, B.C., June 1968.
[2]Revision received August 23, 1973.

[3]The *trans*-fused cyclobutane ring and its attached exocyclic methylene group remove some of the freedom of rotation in the cyclononene ring of caryophyllene, but on the other hand the H—H repulsive non-bonded interactions during rotation might be less serious for caryophyllene than for *trans*-cycloöctene. The balance of angle and torsional strain and non-bonded interactions for the two molecules is not obvious. Since interconversion of **2** and **3** must occur by movement of one substituent on the double bond through the "hole" in the nine-membered ring, the probability of 180° rotation about bonds *a* in **2** or **3** relative to the same rotation in *trans*-cyclononene will be halved by the presence of the allylic methyl group which cannot pass through the "hole".

Can. J. Chem. Downloaded from www.nrcresearchpress.com by 210.87.254.5 on 09/05/12
For personal use only.

Can. J. Chem. Downloaded from www.nrcresearchpress.com by 210.87.254.5 on 09/05/12
For personal use only.

single pure oxide, **4**,[4] of the *trans* endocyclic double bond in 82% yield after recrystallization. "Careful examination of the product from caryophyllene showed no indication of a second oxide" (7). The *cis* endocyclic double bond of the less rigid isocaryophyllene not only has greater freedom to change from one extreme conformation to the other (**14** ⇌ **15**), but in **14** and **15** and each intermediate conformation both sides of the double bond are exposed. However, as pointed out by Barton and co-workers (6), that arrangement of the nine-membered ring of caryophyllene with the least angle and torsional strain and fewest repulsive non-bonded interactions has the plane of the endocyclic double bond perpendicular to the plane of the cyclobutane ring. There are two such conformers, **2** and **3**, in each of which only one face of the π-bond is exposed to attack, the other side being *completely* shielded by the rest of the molecule. Consequently, each conformer can only give rise to a single endocyclic 1,2-epoxide. While the above observations might merely have been reflections of the less sensitive analytical techniques available at the time, the possibility of restricted rotation merited investigation.

If, as suggested by the foregoing discussion, only a single oxide (**4**) were formed from caryophyllene, there would be, *a priori*, three possible explanations: (*a*) Conformers **2** and **3** are interconvertible by rotation about bonds *a* and appreciable amounts of each are present at room temperature. One (**2**) reacts faster with peracid (*ca.* 10–50 times) than the other but slower than the **2** ⇌ **3** interconversion. (*b*) Conformers **2** and **3** are interconvertible by rotation about bonds *a*, but conformer **2** is present in great excess (*ca.* 50:1 or greater) and rates of epoxidation of both conformers are nearly the same. (*c*) Conformers **2** and **3** are not interconvertible by rotation and caryophyllene is actually only conformer **2**. The first two conceivable explanations for the reported formation of only one oxide seemed unreasonable after examination of Stuart–Briegleb and Dreiding models of **2** and **3**. Hence, explanation (*c*) was implicated. At the time the work described herein was done, the chemistry of caryophyllene did not raise any serious obstacle to this interpretation since, in any acid-catalyzed reaction of the molecule, there was always the possibility of prior isomerization to isocaryophyllene (a known reaction; also *trans*-cyclononene is easily isomerized to *cis*-cyclononene by acid (8)) from which products could arise.[5] Nor was explanation (*c*) excluded by the total synthesis of *dl*-caryophyllene (9) since the relative stereochemistry of the boldface methyl and C_1-hydrogen in the key intermediate **18** was unknown.

However, since this work was completed, Nickon *et al.* (10) have described a mechanistic study which *requires* the presence of both conformers **2** and **3** in caryophyllene and hence excludes the possibility of caryophyllene existing *only* in conformation **2**. When **1** was cyclized in D_2SO_4 to caryolan-1-ol-9-d_1 (**19**) and clov-2-ene-9-d_1 (**20**), the deuterium atom in **19** was entirely β and that in **20** was entirely α. This result is only consistent with stereospecific anti addition of D^+ and $=CH_2$ to the *trans* endocyclic double bond (**2** → **20** and **3** → **19**) (10). Control experiments showed that isocaryophyllene, although formed, did not give caryolanol or clovene under the conditions used. Although yields of **19** and **20** were not given, this study in conjunction with the previous discussion implies, but does not prove, that conformers **2** and **3** are interconvertible near room temperature.

Results and Discussion

After initial attempts to observe changes in the n.m.r. spectrum of caryophyllene at higher and lower temperatures were inconclusive (see Experimental), our investigation of restricted rotation centered on the determination of whether only one epoxide was indeed produced in the reaction of this sesquiterpene with peracid. For this purpose a sample of caryophyllene was carefully purified to a minimum of 97% caryophyllene (see Experimental).[6] When equimolar

[4]The determination of the stereochemistry of this monoepoxide is described in ref. 6.

[5]For example, the observation that oxidation of caryophyllene with hydrogen peroxide plus vanadium pentoxide gave in addition to **4** about 10% of caryolan-1,9β-diol (**19**, OH for D), a cyclization product expected from **5**, was ambiguous since (*a*) the purity of the caryophyllene was not established, (*b*) there was no proof that the caryolan-1,9β-diol originated from an epoxide, (*c*) the presence of some *cis* oxide **16** was not excluded, (*d*) the product was subjected to an acid treatment, and (*e*) the course of the acid-catalyzed cyclization of **16**, which might lead to caryolan-1,9β-diol if not concerted, has not been investigated.

[6]The remaining ~3% consisted of traces of at least five other compounds.

Can. J. Chem. Downloaded from www.nrcresearchpress.com by 210.87.254.5 on 09/05/12
For personal use only.

quantities of this caryophyllene and monoperphthalic acid were allowed to react at 4° in ethereal solution, the crude product obtained in 98.5% yield gave four spots on t.l.c. corresponding in increasing order of polarity to ~0.5% isocaryophyllene, 2% of recovered caryophyllene, 94% of monoepoxide, and 2–3% of bisepoxide.[7] Direct crystallization of a portion of the crude product from methanol gave the well known monoepoxide **4**, m.p. 63.5–64°, $[\alpha]_D$ −79.4°, in 65–72% yield. However, the i.r. and n.m.r. spectra and the optical rotation ($[\alpha]_D$ −46°) of the crude product revealed the presence in the monoepoxide fraction of another unidentified component amounting to about 20% of the crude oxidation product.

The unknown compound was concentrated in the crystallization mother liquors from removal of successive crops of **4**. Material of m.p. 29–31° (single t.l.c. spot) containing approximately equal amounts of **4** and its companion was obtained. Further attempts to separate these compounds by low temperature crystallization and g.l.p.c. were unsuccessful[8] and therefore the mixture was used for further experiments. The most obvious differences in the n.m.r. spectra (Fig. 1) of pure monoepoxide **4** and the mixture are the additional singlet methyl peak at δ 1.23, the additional olefinic absorption at δ 5.09, and the extra *gem*-dimethyl peaks at δ 0.95 and 0.97.

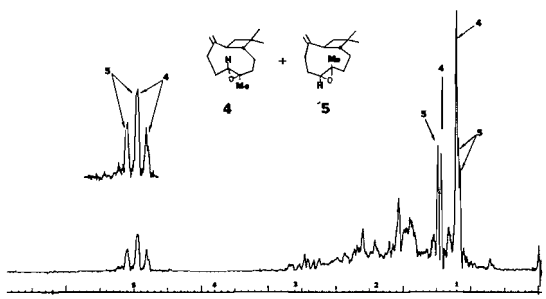

FIG. 1. Nuclear magnetic resonance spectrum of caryophyllene oxide mixture (**4** + **5**) in $CDCl_3$ solution at 60 MHz.

[7]Caryophyllene monoxide reacts much slower than caryophyllene with peracid. A sample of monoxide oxidized under the same conditions gave only about 40% of bisepoxide after 24 h at 4°.

[8]In metal g.l.p.c. columns caryophyllene oxide undergoes a variety of reactions (11). In an all glass apparatus the mixture apparently survived unchanged but no separation was obtained with the silicone SE-30 and neopentyl glycol succinate columns used.

The i.r. spectrum of the mixture did not contain carbonyl or hydroxyl absorption. That the unknown component is not either of the two *cis* epoxides **16** ($[\alpha]_D$ −7°) or **17** ($[\alpha]_D$ +23°) (7) can be seen from the distinguishing n.m.r. peaks listed in Table 1 and from the calculated optical rotation ($[\alpha]_D$ +80°) of the unknown. Nor has epoxidation occurred at the exocyclic methylene group of caryophyllene since the n.m.r. spectrum of the mixture lacks allylic methyl absorption and the ratio of olefinic protons to the rest is 2:22. Therefore, the unknown component was an oxide, most likely the missing *trans* monoepoxide **5**, and proof of this was provided in the following manner.

In the hope of obtaining separable derivatives, the exocyclic methylene group of the mixture of two epoxides was oxidized with permanganate, but the two keto epoxides formed were likewise inseparable in our hands. However, in the n.m.r. spectrum of the mixture the peaks which did not correspond to those of the known keto epoxide (**4** with =O in place of $=CH_2$) were different from the peaks of the two isocaryophyllene keto epoxides (**16** and **17** with =O in place of $=CH_2$) (see Table 1). The calculated optical rotation ($[\alpha]_D$ +187° in MeOH) was also different from that of the isocaryophyllene keto epoxides ($[\alpha]_D$ −72° and −13° in MeOH) (7).

Finally, the OsO_4-catalyzed hydroxylation of the epoxide mixture was resorted to because it was known that the only significant product of this reagent with the known caryophyllene oxide **4** was Treibs' 119° glycol **8***a* (12), and therefore any other products from the hydroxylation of the oxide mixture must have arisen from the other oxide. To facilitate separation the crude mixture of glycols obtained was subjected to mild acetylation with acetic anhydride – pyridine at room temperature. The crude acetylation product which had two major t.l.c. spots, R_f 0.55 and 0.40, and a minor spot at 0.15, was separated into components by preparative t.l.c. The least polar product, R_f 0.55, was found to be the diacetate of Treibs' 119° diol (**8***b*).

The other major component (R_f 0.40), a beautifully crystalline diol monoacetate of m.p. 159°, therefore, had come from the other unknown oxide. Saponification gave a diol, m.p. 136°, which was not identical with the diols (m.p. 130 and 196°) obtained from either of the isocaryophyllene oxides **16** and **17** (13). The diol contained a secondary hydroxyl group (ready

TABLE 1. Distinguishing n.m.r. data (δ) for the *cis*- and *trans*-caryophyllene oxides and keto oxides in $CDCl_3$ solution at 60 MHz

Isomer	Nuclear magnetic resonance data (δ)		
	gem-diMe	C_4-Me	$=CH_2$
trans-Oxide **4**	1.00 (2Me)	1.19	4.87, 4.97
trans-Oxide **5**	0.95, 0.97	1.23	4.97, 5.09
cis-Oxide **16**	1.00 (2Me)	1.27	4.67, 4.80
cis-Oxide **17**	1.00, 1.06	1.25	4.91 (2H)
trans-Keto oxide **4** (=O for $=CH_2$)	1.03 (2Me)	1.30	—
trans-Keto oxide **5** (=O for CH_2)	1.03 (2Me)	1.18	—
cis-Keto oxide **16** (=O for $=CH_2$)	1.02, 1.07	1.41	—
cis-Keto oxide **17** (=O for $=CH_2$)	1.01, 1.11	1.24	—

acetylation at room temperature, $\Delta\delta \sim 1.2$ p.p.m. for C*H*OH → C*H*OAc, oxidation to ketone) and a tertiary hydroxyl group (not acetylated at room temperature; 159° monoacetate not oxidized by chromic acid – pyridine). The hydroxyl groups were not vicinal since the diol did not react with $NaIO_4$. In addition the diol contained a methylene group attached to an ethereal oxygen (δ 3.87 (2H), not shifted on acetylation). The only structure that will account for the features without carbon skeleton rearrangement is **11***a*, resulting from intramolecular attack of the initial 1,2-diol **7** on the epoxide ring. This structure was confirmed in the following way. Oxidation of the diol with chromic acid – pyridine gave the hydroxy ketone **10**. On Wolff–Kishner reduction the α-alkoxy ketone **10** underwent

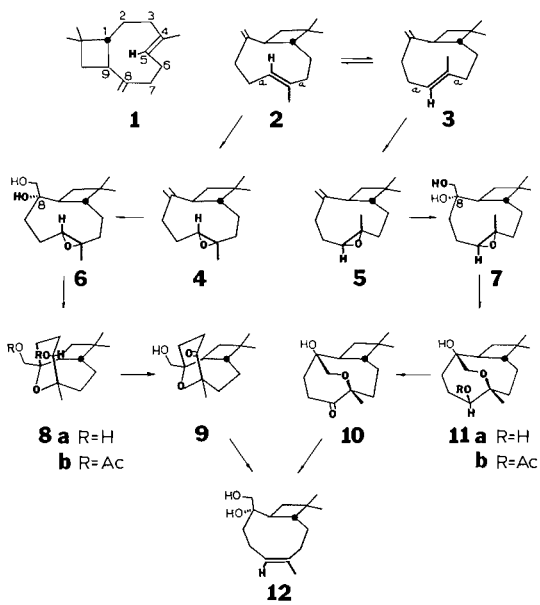

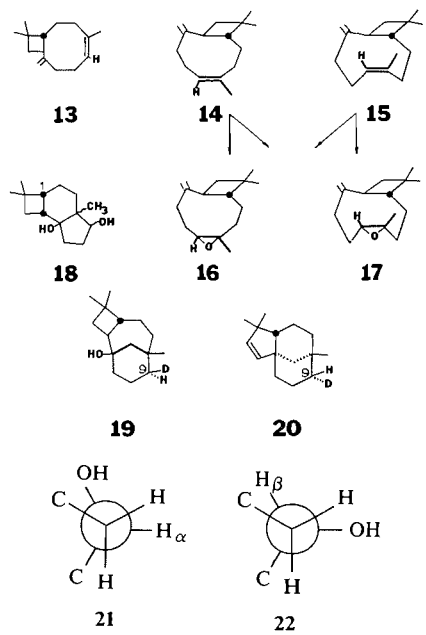

reductive elimination to the unsaturated 1,2-diol **12**, m.p. 92°, which proved to be identical with that obtained from Treibs' 119° glycol by the same sequence of reactions (12). Therefore, there has been no carbon skeleton rearrangement either in the formation of the unknown oxide or its reaction with OsO_4. Because of this identity the configuration of C-8 is the same in both the 119 and 136° glycols. This stereochemistry has been convincingly shown to be that resulting from α-attack of OsO_4 on the exocyclic methylene group (12). Consequently the stereochemistry of the 136° glycol must be that shown in **11***a*. Closure of the oxide ring by attack of the primary hydroxyl group on the epoxide ring with inversion can only lead to a relatively strain-free *cis*-

Can. J. Chem. Downloaded from www.nrcresearchpress.com by 210.87.254.5 on 09/05/12
For personal use only.

Can. J. Chem. Downloaded from www.nrcresearchpress.com by 210.87.254.5 on 09/05/12
For personal use only.

[4.3.2] system if the methyl configuration at the epoxide ring is β[9] (same side as the reference H at C-1) as in **5** and **7**. In what is apparently the most stable conformation of **11***a* and *b* the configuration of the secondary oxygen function must be β to account for the small width at half-height (7–8 Hz) of the n.m.r. signal due to the α-hydrogen (see **21**) on the carbon atom bearing the acetate; if this hydrogen were β as in (**22**), there would be an ~anti vicinal CH_2 coupling and a larger half-width (~15–25 Hz). Since the *cis* oxide **16** has been proved to be absent from our caryophyllene epoxidation product, the stereostructure of **11***a* for the 136° glycol could only result from the other *trans* epoxide **5** and therefore the presence of **11***a* constitutes proof of the formation of **5** during the epoxidation of caryophyllene and likewise proof of the existence of conformer **3** in caryophyllene.

The further question of whether the two conformers **2** and **3** are interconvertible near room temperature was probed by examining the dependence of the ratio of the two epoxides **4** and **5** on solvent, temperature, and peracid when monoepoxidation was carried to completion under conditions not affecting the oxides. The ratios of monoepoxides **5**:**4** (calculated by integration of the olefinic n.m.r. absorption) from the following sets of conditions: perbenzoic acid – benzene, 25° (15:85); perbenzoic acid – chloroform – tetraethylammonium benzoate buffer, 5° (17:83);[9] monoperphthalic acid – ether, −30° (22:78); and hydrogen peroxide – benzonitrile – potassium bicarbonate – methanol, 25° (hetrogeneous) (21:79) were not sufficiently different for any conclusions to be drawn regarding conformational interconversion. At present the best, although weak, evidence for interconversion at room temperature is the variable temperature n.m.r. study (see Experimental).

Experimental

For instruments and general procedures see ref. 12.

Purification of Caryophyllene (1)

Crude clove oil (*Eugenia caryophyllata*) terpene residue (~1.5 l) obtained from Fritsche Bros., Toronto, from which the phenol esters had been removed by saponification was fractionally distilled through a 60-cm vacuum-jacketed spinning band column at 10 Torr, and fractions of 10–15 ml were collected. The fractions having b.p. 109–110° (10 Torr) and $[\alpha]_D$ −9.46° to −9.04° (neat) were combined (250 ml) and refractionated. Each 10-ml fraction was examined by t.l.c. developed in petroleum ether (b.p. 60–80°). Typical R_f values were isocaryophyllene 0.96, caryophyllene 0.82, and humulene 0.70.[10] Later distillation fractions (56 g) containing only caryophyllene and humulene by t.l.c. analysis were combined in 100 ml of petroleum ether (b.p. 30–60°). The colorless solution was washed 10 times with 10-ml portions of aqueous $AgNO_3$ (60 g dissolved in 100 ml). This treatment removed all of the humulene (15) together with some of the caryophyllene. The petroleum ether solution of **1** was washed with water, dried over $MgSO_4$ and then percolated first through a column of 120 g of silica gel (B.D.H. for chromatography) and finally through a column of 100 g of neutral alumina (Woelm) with the aid of additional petroleum ether to remove any traces of oxygenated impurities.[11] Distillation gave a total of 39.1 g of **1**, b.p. 136–136.5° (15 mm), $[\alpha]_D^{21}$ −15.0° (*c*, 2.60 in chloroform) with only a very faint odor. T.l.c. showed less than ~0.5% of an impurity corresponding in R_f to isocaryophyllene **13**. G.l.p.c. analysis of the caryophyllene indicated it be 97% pure, the remaining impurities being small amounts of at least five compounds. To determine whether these trace compounds were being formed from **1** in the g.l.p.c. apparatus, another carefully fractionated sample of caryophyllene, $[\alpha]_D^{23}$ −15.2° (*c*, 5.03 in chloroform) from a different source, *Strobilanthopsis linifolia*,[12] was also analyzed on the same g.l.p.c. column and apparatus. From the fact that the two samples give different amounts of partly different g.l.p.c. peaks (Table 2),[13] at least most of the peaks are not due to artifacts but correspond to impurities in the samples. Furthermore the proportion of compounds in the *Eugenia* caryophyllene showed no change when the injection block temperature was varied from 207 to 240°. Even at an injection block temperature of 290°, there was still 96.5% caryophyllene and only traces (totalling 0.16%) of three new g.l.p.c. peaks appearing together with very slight variations in the other peaks.

Variable Temperature N.m.r. Study

The p.m.r. spectrum of caryophyllene in both CS_2 and $CDCl_3$ solution was examined at 100 MHz from +50° down to −90°. The 100 MHz spectra at −20°, −40°, −60°, −70°, and −90° were similar but differed slightly from that taken at +30° in that there was (*i*) a slight bulge on the high field side of the overlapping *gem*-dimethyl

[9]Chloroform solutions of perbenzoic acid on standing apparently generate enough strong acid (HCl?) to catalyze further reactions of the epoxides **4** and **5** to more polar (t.l.c.) products. These side reactions, which are responsible for the incorrect result reported on p. 82 of ref. 13, are suppressed by the addition of benzoate anion buffer to the epoxidation mixture.

[10]Miller and Kirchner (14) first noted that these sesquiterpenes could be readily separated by t.l.c. After partial charring caryophyllene gave a beautiful deep indigo color.

[11]On standing in air pure **1** develops traces of oxygenated impurities which remain at the application point on t.l.c. in petroleum ether.

[12]Kindly provided by Y. Hikino, Dr. R. E. Williams, and Professor P. de Mayo.

[13]We would like to thank Drs. J. B. DiGiorgio, T. Swartz, and A. Nickon for these g.l.p.c. analyses.

TABLE 2. G.l.p.c. analyses of caryophyllene samples[a]

Peak	% from *Eugenia*	% from *Strobilanthopsis*	E:S	Relative retention time
A	0.03	0.03	1:1	0.77
B	0.52	0.23	2.3:1	0.83
C	Absent	0.72	—	0.88
D	0.29	0.16	1.8:1	0.92
Caryophyllene	97.07	98.69		1.00
E	0.30	Absent	—	1.90
F	1.79	0.16	11.2:1	2.30

[a]Golay Castorwax column at 150°, injection block 240°, 20 p.s.i. He pressure.

peaks, (*ii*) a slight bulge on the high field side of the narrow absorption at δ 1.60, (*iii*) the highfield peak of the exocyclic methylene group was better resolved, and (*iv*) two new broad peaks appeared adjacent to the two exocyclic methylene peaks (see Fig. 2). While these changes can be interpreted in terms of the two conformers **2** and **3** being "frozen out" on the n.m.r. time scale and having small chemical shift differences for certain protons, the lack of better separation makes such an interpretation ambiguous.

*Epoxidation of Caryophyllene (**1**)*

To a solution of 7.420 g (36.4 mmol) of 97% pure caryophyllene in 5 ml of ether chilled in an ice bath was added 100 ml of an ice cold ethereal solution of monoperphthalic acid (16) containing 36.3 mmol of peracid. The reaction was kept at ~5° for 9 h when no peracid remained. The decanted ethereal solution was washed twice with water, twice with aqueous Na_2CO_3 solution, and dried over $MgSO_4$. Removal of solvent left 7.860 g (98.5%) of colorless viscous oil, $[\alpha]_D^{20}$ −46.0° (*c*, 2.15 in chloroform). Quantitative t.l.c. with petroleum ether (b.p. 60–80°) gave three spots with R_f 0.95 (<0.5% of **13**), 0.78 (~2% of **1**), and 0.00 (oxygenated products). T.l.c. with the more polar system ethyl acetate – petroleum ether (15:85) gave three spots with R_f 1.00 (**1** + **13**), 0.77 (94% of monoepoxides), and 0.25 (~3% of bis-epoxides).

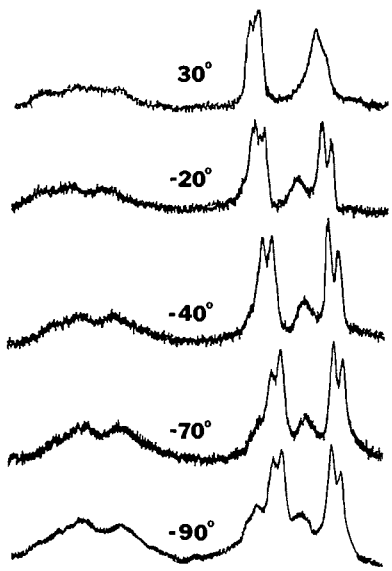

FIG. 2. Variable temperature n.m.r. spectra of the olefinic proton absorption of caryophyllene in $CDCl_3$ solution at 100 MHz.

Recrystallization of the crude product from 12 ml of methanol yielded 5.167 g (68.5%) of large colorless crystals of **4**, $[\alpha]_D^{20}$ −72.1° (*c*, 2.18 in chloroform) and mother liquor *A* (see below). Further recrystallization from methanol raised the melting point to 63.5–64°, $[\alpha]_D^{20}$ −79.4° (*c*, 2.32 in chloroform) (lit. (17) m.p. 64°, $[\alpha]_D$ −68°).[14]

From recrystallization mother liquor *A* above, a second crop of 1.345 g of less pure **4** was removed. The 1.34 g of colorless oil $[\alpha]_D^{20}$ 0° (*c*, 2.26 in chloroform) remaining in the mother liquors of the second crop was recrystallized twice from methanol and once from petroleum ether (b.p. 30–60°) without appreciable change in composition (n.m.r., $[\alpha]_D$). The thrice recrystallized material (775 mg) had m.p. 29–31° with a few small crystals not melting until 48°, $[\alpha]_D$ 0° (*c*, 2.46 in chloroform). Comparison of the integrated n.m.r. peaks at δ 4.87 (from **4**) and 5.09 (from **5**) (Fig. 1) gave a ratio of 4:5 of 50:50. The *calculated* optical rotation of **5** from these data is $[\alpha]_D^{19}$ +80° (chloroform). Attempted zone refinement in a narrow tube did not change the composition. I.r. peaks at 1280 and 1070 cm^{-1} are moderately intense in the spectrum of **5** but weak or missing from that of **4**.

Integration of the δ 4.85 and 5.10 n.m.r. peaks in the crude epoxidation product from various reactions (ether, monoperphthalic acid, ~5°) gave the amount of **5** formed as 16–20%.

*Permanganate Oxidation of Epoxides **4** + **5***

To a solution of 2.075 g (9.43 mmol) of a mixture of epoxides **4** + **5** (~1:1) in 25 ml of acetone and 1 ml of water was added with stirring (magnetic bar) 4.08 g of powdered $KMnO_4$ in small portions during 1.5 h. Extraction with ether after dissolution of the MnO_2 in H_2SO_4

[14]That **4** was stable to phthalic acid under the epoxidation conditions was proved by allowing a mixture of 300 mg of **4**, 50 mg of phthalic acid, and 20 ml of ether to stand at 4° for 25 h. Work up gave 286 mg (95%) of pure **4** (i.r. and t.l.c.).

Can. J. Chem. Downloaded from www.nrcresearchpress.com by 210.87.254.5 on 09/05/12
For personal use only.

Can. J. Chem. Downloaded from www.nrcresearchpress.com by 210.87.254.5 on 09/05/12
For personal use only.

gave 1.315 g (~63%) of colorless oil. Chromatography on alumina (Woelm basic, activity II) gave a total of 765 mg (36% from **4** + **5**) of almost pure liquid keto oxide mixture, $[\alpha]^{25}$ −71° (*c*, 1.96 in chloroform). The n.m.r. spectrum of a sample of the keto oxide mixture not containing any **4** or **5** had two peaks corresponding to the methyl group on the epoxide ring at δ 1.18 and 1.30. Integration gave 23–36% of keto epoxide **5** (=O for $=CH_2$) in various fractions. Calculation of the optical rotation of keto epoxide **5** (=O for $=CH_2$) from the n.m.r. integrations and the $[\alpha]_D$ −148° (*c*, 1.95 in chloroform) of pure keto epoxide **4** (=O for $=CH_2$) gave $[\alpha]_D^{25}$ +187° (chloroform or methanol).[15] Attempts to separate the two keto epoxides by chromatography were unsuccessful.

*OsO_4 Hydroxylation of Epoxides **4** + **5***

A solution of 867 mg (3.94 mmol) of the 1:1 mixture of **4** + **5** in 4 ml of ether was added to an ice cold solution of 989 mg (3.90 mmol) of OsO_4 in 2 ml of ether plus 2 ml of pyridine. After 127 h the reaction mixture was worked up by evaporation of solvent, reflux with ethanol – mannitol – sodium hydroxide, and extraction with ether after aqueous dilution. The partially crystalline product (809 mg, 81%) was acetylated at room temperature with 2 ml of acetic anhydride and 5 ml of pyridine for 23 h. Work-up gave 895 mg of partially crystalline product whose t.l.c. (ethyl acetate – petroleum ether (b.p. 60–80°), 50:50) had three spots R_f 0.55, 0.40, and 0.15.[16] This acetylation product was combined with another 786 mg from a similar reaction. Recrystallization from ether – petroleum ether gave 560 mg of felted needles of **11***b* (R_f 0.40) contaminated with the diol of R_f 0.15. The material (1.13 g) from the mother liquor was chromatographed on four preparative t.l.c. plates developed in ethyl acetate – petroleum ether (b.p. 60–80°), 15:85.

Extraction of the least polar zone gave 631 mg (37% based on OsO_4 product) of pure oily Treibs' glycol diacetate **8***b*, R_f 0.55. Saponification of the acetate with methanolic KOH produced 471 mg (99%) of Treibs' glycol **8***a*, which after one recrystallization from chloroform – petroleum ether had m.p. 116–119° (lit. (17) m.p. 119°) undepressed by an authentic specimen.

From the middle thick layer zone and the 560 mg of impure **11***b* from recrystallization of the crude acetylation mixture above, there was obtained by further t.l.c. and recrystallization from ether – petroleum ether (b.p. 60–80°) 685 mg (40% based on OsO_4 product) of colorless needles of pure monoacetate **11***b*, m.p. 158–159°; $[\alpha]_D^{19}$ +18.0° (*c*, 1.90 in chloroform); ν_{max} 3598 and 3420 (OH), and 1725 cm^{-1} (ester C=O).

Anal. Calcd. for $C_{17}H_{28}O_4$ (296.4): C, 68.89; H, 9.52. Found: C, 69.06; H, 9.96.

When a mixture of 26 mg of monoacetate **11***b*, 30 mg of CrO_3 and 1 ml of pyridine was allowed to stand for 39 h, the **11***b* was recovered quantitatively on passage of the reaction mixture through alumina in methylene chloride.

[15]The optical rotations of the keto epoxides are the same within 1–2% in methanol and chloroform.

[16]In one reaction there was a faint fourth spot, R_f 0.25, perhaps due to **7** because it was removed by $NaIO_4$ treatment.

*136° Glycol **11***a*

Saponification of 165 mg (0.56 mmol) of monoacetate **11***b* in 10 ml of methanol containing 200 mg of NaOH gave 130 mg (92%) of solid diol **11***a* (single t.l.c. spot). Three recrystallizations from ether – petroleum ether gave colorless felted needles which rearranged above 120° to short hexagonal prisms melting at 135–136°, $[\alpha]_D$ 0.0° (*c*, 0.91 in chloroform), ν_{max} 3448 cm^{-1} (OH).

Anal. Calcd. for $C_{15}H_{26}O_3$ (254.3): C, 70.82; H, 10.29. Found: C, 70.94; H, 10.34.

Glycol **11***a* (20 mg) was unchanged on standing with 40 mg of $NaIO_4$ in 2 ml of methanol and 0.5 ml of water at room temperature for 6.5 h.

*Hydroxy Ketone **10***

A solution of 162 mg (0.64 mmol) of 136° diol **11***a* in 2.3 ml of pyridine was added at room temperature to the orange complex of 107 mg (1.07 mmol) of CrO_3 in 1 ml of pyridine. After 20 h at room temperature, the reaction mixture was diluted with methylene chloride and passed through a short column of alumina (Woelm neutral, activity IV) to yield 159 mg of crude ketone containing ~20% of **11***a*. Preparative t.l.c. and recrystallization from ether – petroleum ether (b.p. 60–80°) gave colorless needle-like prisms of **10**, m.p. 82–83°; $[\alpha]_D$ +2° (*c*, 0.45 in chloroform); ν_{max} 3570 and 3448 (OH), and 1701 cm^{-1} (seven-ring ketone C=O).

Anal. Calcd. for $C_{15}H_{24}O_3$ (252.3): C, 71.39; H, 9.57. Found: C, 71.11; H, 9.55.

*Wolff–Kishner Reduction of Hydroxy Ketone **10***

To a solution of 37 mg (0.14 mmol) of hydroxy ketone **10** in 3 ml of triethylene glycol were added 1.5 ml of hydrazine hydrate (85%) and six KOH pellets. The mixture was refluxed (oil bath 145°) for 2 h, after which the excess hydrazine hydrate was distilled. The temperature of the oil bath was raised to 200° and maintained there for 4.5 h. Dilution with water and extraction with ether gave 20 mg (60%) of colorless oil, which on t.l.c. in ethyl acetate gave a single spot of the same R_f 0.70 as **12** obtained from Wolff–Kishner reduction of **9** (12). The oil crystallized on chilling and was recrystallized once from petroleum ether (b.p. 30–60°) to give small crystals, m.p. 87–90° undepressed on admixture with **12**, m.p. 91–92°, from **9**.

1. (*a*) J. L. SIMONSEN and D. H. R. BARTON. The Terpenes. Vol. III. Cambridge University Press. 1952. pp. 39–71; (*b*) A. NICKON. Perfum. Essent. Oil Rec. **45**, 149 (1954).
2. A. C. COPE, C. R. GANELLIN, H. W. JOHNSON, T. V. VAN AUKEN, and H. J. S. WINKLER. J. Am. Chem. Soc. **85**, 3276 (1963).
3. A. C. COPE, K. BANHOLZER, H. KELLER, B. A. PAWSON, J. J. WHANG, and H. J. S. WINKLER. J. Am. Chem. Soc. **87**, 3644 (1965).
4. A. C. COPE and B. A. PAWSON. J. Am. Chem. Soc. **87**, 3649 (1965).
5. O. WALLACH and W. WALKER. Ann. **271**, 288 (1892); O. SCHREINER and E. KREMERS. Pharm. Arch. **2**, 293 (1899).
6. A. AEBI, D. H. R. BARTON, A. W. BURGSTAHLER, and A. S. LINDSAY. J. Chem. Soc. 4659 (1954).
7. G. R. RAMAGE and R. WHITEHEAD. J. Chem. Soc. 4336 (1954).

8. K. ZIEGLER and H. WILMS. Ann. **567**, 1 (1950).
9. E. J. COREY, R. B. MITRA, and H. UDA. J. Am. Chem. Soc. **85**, 362 (1963).
10. (*a*) A. NICKON, F. Y. EDAMURA, T. IWADARE, K. MATSUO, F. J. MCGUIRE, and J. S. ROBERTS. J. Am. Chem. Soc. **90**, 4196 (1968); (*b*) F. Y. EDAMURA and A. NICKON. J. Org. Chem. **35**, 1509 (1970).
11. I. C. NIGAM and L. LEVI. J. Org. Chem. **30**, 653 (1965).
12. E. W. WARNHOFF and V. SRINIVASAN. Can. J. Chem. **44**, 2259 (1966).
13. V. SRINIVASAN. Ph.D. Thesis, University of Western Ontario, London, Ontario, 1968.
14. J. M. MILLER and J. G. KIRCHNER. Anal. Chem. **25**, 1107 (1953).
15. R. P. HILDEBRAND, M. D. SUTHERLAND, and O. J. WATERS. Chem. Ind. 489 (1959).
16. G. B. PAYNE. J. Org. Chem. **24**, 1354 (1959).
17. W. TREIBS. Chem. Ber. **80**, 56 (1947).

Can. J. Chem. Downloaded from www.nrcresearchpress.com by 210.87.254.5 on 09/05/12
For personal use only.

Alkyl Inductive Effects on Molecular Ionization Potentials. XVI. Esters

LEONARD S. LEVITT, HARRY F. WIDING, AND BARBARA W. LEVITT
Department of Chemistry, College of Science, University of Texas, El Paso, Texas 79968

Received June 25, 1973

Correlation of molecular ionization potentials, E_I, with Taft's alkyl inductive substituent constants, $\sigma_{I(R)}$, has now been extended to include the esters. It is found that three series of esters, the formates, acetates, and methyl alkanoates, fall on three separate straight lines in accord with the general equation $E_I = E_0 + a_I\sigma_{I(R)}$, where E_0 is the intercept and a_I the slope. The average standard error for the three lines is 0.024 eV with an average correlation coefficient of 0.992, showing that the alkyl substituent exerts an inductive influence on the electron density at the site suffering the electron loss: a lone pair on either the carbonyl or alkoxy oxygen atom. Evidence is deduced for the site of electron expulsion and a prediction is made concerning the site of vapor phase protonation of esters and carboxylic acids. E_I values presently not available experimentally are predicted for several esters.

La corrélation entre les potentiels d'ionisation moléculaire, E_I, et les constantes de Taft traitant de l'effet inductif de substituants alcoyles, $\sigma_{I(R)}$, a maintenant été étendue aux esters. On a trouvé que trois séries d'esters, les formates, les acétates et les méthyl alcanoates, se retrouvent sur trois lignes droites séparées, ce qui est en accord avec l'équation générale $E_I = E_0 + a_I\sigma_{I(R)}$ où E_0 est l'ordonnée à l'origine et a_I la pente. L'erreur standard moyenne pour les trois lignes est égale à 0.024 eV et le coefficient moyen de corrélation à 0.992, montrant que le substituant alcoyle exerce un effet inductif sur la densité électronique au site subissant la perte d'électrons: une paire libre soit sur l'atome oxygène carbonyle ou soit sur l'oxygène du groupe alcoxy. On présente des preuves en faveur du site où se produit l'expulsion d'électrons; de même on fait une prédiction concernant le site de protonation en phase vapeur d'esters et d'acides carboxyliques. Les valeurs de E_I qui ne sont pas encore expérimentalement accesibles, sont prédites pour plusieurs esters. [Traduit par le journal]

Can. J. Chem., **51**, 3963 (1973)

We demonstrate in this paper that the ionization potentials of various series of carboxylate esters are linearly correlated with Taft's alkyl inductive substituent constants, σ_I (1).

A huge body of data relating to many physical properties of organic molecules has been correlated with different sets of substituent constants, such as σ_I, σ^* (2), and Hammett's original (3) σ and its offshoots. The ionization energies of the alcohols (4*a*), ethers (4*b*), thiols (4*c*), thioethers (4*d*), alkyl halides (4*e*), ketones (4*f*), carboxylic acids (4*g*), copper acetylacetonates (4*h*), amines (4*i*), nitriles (5), nitroalkanes (5), *n*-alkanes (6), alkenes (7), alkynes (8), and disulfides (9) have recently been shown to be linear functions of both the inductive and polar substituent constants.

Assuming the validity of Koopmans' theorem (10) which identifies the first adiabatic ionization energy with the energy of the highest occupied molecular orbital, the electron must be lost from a non-bonding lone pair on one of the oxygens of the carboxyl group (11). This may be represented by the following equation

$$R{-}CO_2{-}R' \xrightarrow{E_I} R{-}\overset{+}{C}O_2{-}R' + e^-$$

Evidence will be given later in this paper pertaining to *which* oxygen is the probable site of electron loss. It is quite apparent that electron-releasing alkyl groups should increase the electron density at the relatively electronegative carboxyl group and consequently facilitate ionization of the molecule. A similar effect should manifest itself in a greater basicity, the greater the electron density at the carboxyl group, as in the case of alcohols (12).

The $\sigma_{I(R)}$ values and the experimentally determined (13) photoionization potentials of three series of esters, HCOOR, MeCOOR, and RCOOMe are given in Table 1.

Good correlations are obtained when the E_I values are plotted *vs.* σ_I for the corresponding R groups of the three series of esters. The equations for the regression lines are given by the following

$$E_{HCO_2R} = E_0 + a_I\sigma_{I(R)}$$

$$E_{MeCO_2R} = E_0' + a_I\sigma_{I(R)}$$

$$E_{RCO_2Me} = E_{HCO_2Me} + a_I\sigma_{I(R)}$$

The slopes, a_I, are found to be 20.79, 15.99, and 12.84 eV, respectively, for the formates, acetates, and methyl alkanoates. It should be pointed out that only the methyl alkanoate line (RCO_2Me),

Can. J. Chem. Downloaded from www.nrcresearchpress.com by 210.87.254.42 on 09/05/12
For personal use only.

Can. J. Chem. Downloaded from www.nrcresearchpress.com by 210.87.254.42 on 09/05/12
For personal use only.

TABLE 1. Experimental photoionization potentials of three series of esters, with the corresponding σ_I values and calculated first ionization potentials

Esters	σ_I[a]	E_I(eV) Exp.[b]	E_I(eV) Calcd.
Formates			
HCO_2Me	−0.046	10.82	10.80
HCO_2Et	−0.055	10.61	10.62
HCO_2n-Pr	−0.058	10.54	10.55
HCO_2n-Bu	−0.060[c]	10.50	10.51
HCO_2i-Bu	−0.064[d]	10.46	10.43
HCO_2t-Bu	−0.074	—[e]	10.22
Acetates			
$MeCO_2Me$	−0.046	10.27	10.25
$MeCO_2Et$	−0.055	10.11	10.11
$MeCO_2n$-Pr	−0.058	10.04	10.06
$MeCO_2i$-Pr	−0.064	9.99	9.97
$MeCO_2n$-Bu	−0.060[c]	10.01	10.03
$MeCO_2i$-Bu	−0.064[d]	9.97	9.97
$MeCO_2s$-Bu	−0.068[d]	9.91	9.90
$MeCO_2t$-Bu	−0.074	—[e]	9.81
Methyl alkanoates			
HCO_2Me	0.000	10.82	10.83
$MeCO_2Me$	−0.046	10.27	10.24
$EtCO_2Me$	−0.055	10.15	10.12
n-$PrCO_2Me$	−0.058	10.07	10.08
i-$PrCO_2Me$	−0.064	9.98	10.01
t-$BuCO_2Me$	−0.074	—[e]	9.88

[a]From ref. 1.
[b]From ref. 13.
[c]From ref. 4*a*.
[d]From ref. 4*e*.
[e]Experimental value unavailable.

has its intercept essentially at the E_I value of the hydrogen-substituted ester (methyl formate, 10.82 eV). The intercepts for the other two lines, E_0 and E_0', on the other hand, do not correspond to their hydrogen-substituted analogs because these would be carboxylic acids (not esters) and this effect will be discussed later in this paper. The three intercepts are, respectively, 11.76, 10.99, and 10.83 eV, and therefore we can write:

$$E_{HCO_2R} = 11.76 + 20.8\sigma_{I(R)} \pm 0.02 \text{ eV}$$

$$E_{MeCO_2R} = 10.99 + 16.0\sigma_{I(R)} \pm 0.02 \text{ eV}$$

$$E_{RCO_2Me} = 10.83 + 12.8\sigma_{I(R)} \pm 0.03 \text{ eV}$$

the corresponding correlation coefficients being 0.990, 0.989, and 0.997. These correlations once again demonstrate that the effect of alkyl substituents on the electron density of the atom which loses the electron, is essentially an inductive effect. Comparing the last two columns of Table 1 it is readily seen that the calculated and experimental E_I values are in excellent agreement. Calculated estimates are also given in the Table for HCO_2t-Bu, $MeCO_2t$-Bu, and t-$BuCO_2Me$, for which PI or PES values have not yet been obtained. Although the a_I constants have eV units, they are analogous to the reaction constants, ρ_I, and constitute measures of the susceptibility of the reaction sites to substituent effects. The a_I values observed here may be compared to those observed in the correlations of the E_I values of alcohols (4*a*) (37.5), ethers (4*b*) (28.0), ketones (4*f*) (14.0), and carboxylic acids (4*g*) (15.4).

The carboxylic acids, upon vapor phase ionization, lose an electron from the non-bonding lone pair of the carbonyl oxygen (4*g*). In the case of the esters, however, the electron loss, evidently, is from the non-bonding lone pair of the alkoxy oxygen. This can be seen by comparing the a_I value of the alkyl acetates (16.0) with that of the methyl alkanoates (12.8), which shows that a change in the alkyl substituent on the alkoxy oxygen has a larger inductive effect than a corresponding change of the alkyl group on the carbonyl group. It is for this reason, the non-equivalence of the inductive effects of the R groups in the two different positions, that a plot of $\sum\sigma_{I(R)}$ *vs.* E_I does *not* give a straight line for the esters in general; instead three separate lines are obtained for the three classes of esters discussed here. Thus we can rewrite the ionization equation, shown above, as

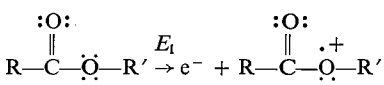

Since we have stressed throughout this entire series of papers that ionization occurs at the atom with the highest electron density (presumably due to interelectron repulsions), this implies, in our present case, that the gas phase protonation of esters should occur at the alkoxy oxygen (the most basic site) (12*a*, *b*), whereas carboxylic acids should be protonated on the carbonyl oxygen (4*g*). In a very recent study (12*c*) of gas phase proton affinities of esters and acids, this question could not be resolved; but both esters and acids are protonated on the carbonyl oxygen atom in solution (14). It seems quite possible, in view of the apparent near-equivalence of electron density at the two oxygens, that the protonation site varies for different esters depending on the magnitude of σ_I for R and R′. Furthermore, the a_I

value for the formates is closer to that for ethers than are those for the other esters, and this may indicate that *only* the formates, with no polarizable alkyl group nearby to increase the electron density at the carbonyl oxygen, suffer the electron loss and vapor phase protonation at the alkoxy oxygen. In accord with this view is the fact that the a_I values of the other two series of esters are very close in value to those of the ketones and carboxylic acids.

The site of protonation in solution may or may not correspond to the gas-phase protonation due to solvation energies and entropies, etc. For example, a study (15) of the gas phase proton affinities of NH_3 and methylamines indicated a different order of basicity than that which is observed in solution.

1. R. W. TAFT, JR. and I. C. LEWIS. Tetrahedron, **5**, 210 (1959).
2. R. W. TAFT, JR. *In* Steric effects in organic chemistry. *Edited by* M. S. Newman. Wiley, New York. 1956. p. 619.
3. L. P. HAMMETT. Chem. Rev. **17**, 125 (1935).
4. B. W. LEVITT and L. S. LEVITT. (*a*) Chem. Ind. 990 (1970); (*b*) Experientia, **26**, 1183 (1970); (*c*) J. Org. Chem. **37**, 332 (1972); (*d*) Israel J. Chem. **9**, 711 (1971); (*e*) Tetrahedron, **29**, 941 (1973); (*f*) Chem. Ind. 724 (1972); (*g*) Chem. Ind. 185 (1973); (*h*) J. Coord. Chem. In press; (*i*) Israel J. Chem. **9**, 71 (1971).
5. B. W. LEVITT, H. F. WIDING, and L. S. LEVITT. Chem. Ind. 793 (1973).
6. H. F. WIDING and L. S. LEVITT. Tetrahedron. In press.
7. L. S. LEVITT, B. W. LEVITT, and C. PÁRKÁNYI. Tetrahedron, **28**, 3369 (1972).
8. L. S. LEVITT. Chem. Ind. 638 (1973).
9. L. S. LEVITT and B. W. LEVITT. Chem. Ind. 132 (1973); L. S. LEVITT and C. PÁRKÁNYI. Int. J. Sulf. Chem. In press.
10. T. KOOPMANS. Physica, **1**, 104 (1933); R. S. MULLIKEN. J. Chem. Phys. **3**, 564 (1935); Phys. Rev. **74**, 736 (1948); J. C. LORQUET. Rev. Mod. Phys. **32**, 312 (1960).
11. M. SIMONETTA and S. CARRÀ. *In* The chemistry of the carboxylic acids and esters. *Edited by* S. Patai. Interscience, London. 1971. p. 1.
12. L. S. LEVITT and B. W. LEVITT. (*a*) J. Phys. Chem. **74**, 1812 (1970); (b) Tetrahedron, **27**, 3777 (1971); (*c*) J. L. LONG and B. MUNSON. J. Am. Chem. Soc. **95**, 2427 (1973).
13. K. WATANABE, T. NAKAYAMA, and J. MOTTL. J. Quant. Spectrosc. Radiat. Transf. **2**, 369 (1962).
14. (*a*) G. FRAENKEL. J. Chem. Phys. **55**, 5480 (1971); (b) G. A. OLAH and A. M. WHITE. J. Am. Chem. Soc. **89**, 3591 (1967) and G. A. OLAH, D. H. O'BRIEN, and A. M. WHITE. J. Am. Chem. Soc. **89**, 5694 (1967).
15. (*a*) M. S. B. MUNSON. J. Am. Chem. Soc. **87**, 2332 (1965); (b) W. G. HENDERSON, M. TAAGERPERA, D. HOLTZ, R. T. MCIVER, JR., J. L. BEAUCHAMP, and R. W. TAFT. J. Am. Chem. Soc. **94**, 4727 (1972).

Can. J. Chem. Downloaded from www.nrcresearchpress.com by 210.87.254.42 on 09/05/12
For personal use only.

Effect of Electron Scavenger on the γ-Radiolysis of Gaseous Propane at High Densities

MASARU NISHIKAWA, YOH-ICHI YAMAGUCHI, KAZUO FUJITA, KAZUNORI KON, AND TETSURO OKAMOTO

Department of Pure and Applied Sciences, University of Tokyo, 3-8-1, Komaba, Meguro, Tokyo, Japan

Received December 28, 1972[1]

Hydrogen formation from γ-radiolysis of gaseous propane at 120 ± 1 °C was studied as the function of density in the range from 0.1 to 0.5 g/ml. $G(H_2)$ gradually decreased with density from 8.0 at 0.12 g/ml towards the liquid-phase value of 6.4 at room temperature. $G(H_2)$ in the presence of SF_6 showed similar decrease from 3.9 to 3.0. The decrease was discussed in comparison to the abrupt drop in G-values from the radiolysis of ammonia at high density (11). The separation distances of ion–electron pairs were estimated from the analysis of the electron scavenging reaction.

Les rendements en hydrogène ont été mesurés par γ-radiolyse du propane à 120 ± 1 °C à des densité allant de 0.1 a 0.5 g/ml avec et sans SF_6. La diminution des rendements dans les deux cas avec la densité est plus faible que dans le cas de la radiolyse d'ammoniac gazeux. Les reactions d'électrons avec SF_6 sont analysés selon un modèle théorique, et les distances séparant les paires ion–électron sont estimés.

Can. J. Chem., **51**, 3966 (1973)

Although radiation chemistry of propane has been studied repeatedly both in liquid and gas phase (1), much less attention has been paid to the intermediate phase of high density gas. For example, it appears that the yields of hydrogen in this region, with and without electron scavengers, have not yet been reported. The difference in the yield in the presence and absence of electron scavengers is usually considered to represent the contribution of dissociative neutralization to the product formation. It is of some interest to see how the importance of such a process changes with density. Furthermore, the kinetic analysis of electron scavenging reactions in this region is expected to yield information related to the electron thermalization distances. Thus the study of gaseous propane radiolysis at high densities appears appropriate. We wish to report here the results of such a study with both ends in view, using SF_6 as the scavenger.

Experimental

Takachiho Research Grade propane was purified by storing with hydrogen over platinum on alumina catalyst for several days in order to eliminate olefinic impurities, and then by bulb-to-bulb distillation. Matheson Research Grade propane (99.98% min) was used without further purification for some of the runs; the results agreed within experimental errors. SF_6 used was Matheson Research Grade as received except for bulb-to-bulb distillation. The method of sample preparation in general, irradiation and dosimetry were described previously (2). However, a metal valve (Hoke Packless Valve) was used at the inlet of sample gases into the irradiation cells in order to avoid adsorption and/or contamination of gases by the stopcock grease for low-concentration runs.

Doses were approximately 7×10^{18} eV/g (^{60}Co-γ) for most samples except where dose *vs.* yield relationship was tested. The dose rate was 2.39×10^{18} eV/g h at the start of the study. The yield of hydrogen was determined by combustion over cupric oxide furnace at about 350 °C.

Results and Discussion

Figure 1 shows the variation of $G(H_2)$ from propane radiolysis at 120 ± 1 °C (T_{cr} of propane = 95.6 °C) upon addition of SF_6 at different densities. The values at $d = 0.50$ g/ml were for liquid propane at 20 ± 2 °C. The shape of the curves clearly indicates the density dependence of the efficiency of electron scavenging reactions.

It has been a well known fact that the yield of a product produced in a charge scavenging reaction increases linearly with the square root of the scavenger concentration in the lower concentration range (3, 4). Hummel has treated this problem theoretically and obtained an equation which shows such a square root dependence (5):

$$G(P) = f\{G_{fi} + G_{gi}(A[S])^{1/2}\}$$

where $G(P)$, G_{fi}, and G_{gi} represent the yields of a product, free and geminate ions, respectively,

[1]Revision received July 30, 1973.

Can. J. Chem. Downloaded from www.nrcresearchpress.com by 210.87.254.40 on 09/05/12
For personal use only.

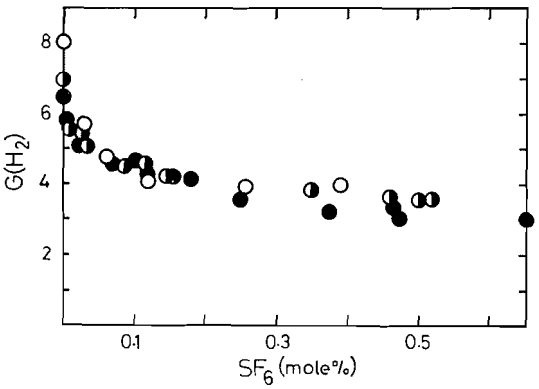

FIG. 1. Dependence of hydrogen yields on the concentration of SF_6 in the radiolysis of propane at 120 °C at different densities; ○, 0.12 ± 0.01 g/ml; ◑, 0.35 ± 0.01 g/ml; ●, 0.50 g/ml (iquid phase, 20 ± 2 °C).

[S] is the concentration of the scavenger, A is a scavenging efficiency parameter, and f is the efficiency of formation of the product from charge scavenging.

The depression of hydrogen yields $\Delta G(H_2)$ upon addition of SF_6 when plotted against the square root of SF_6 concentration was shown to conform to such an expression except at the lowest density studied, 0.12 g/ml (Fig. 2). The failure of the square root model at this density may be because the behavior of thermalizing electrons in that density region deviates seriously from that in the condensed medium, *i.e.*, the diffusive motion. The intercepts $(\Delta G(H_2)_0)$ obtained in Fig. 2 are identified with $f \cdot G_{fi}$. Then, by assuming the maximum depression of hydrogen yield observed in Fig. 1 as $f(G_{fi} + G_{gi})$,[2] one can calculate the ratio G_{fi}/G_{tot}. Assuming further a Gaussian distribution of the separation distances of ion–electron pairs (r), and with the use of the equation (6):

$$G_{fi}/G_{tot} = \int_0^\infty (4r^2/\pi^{1/2} \cdot b^3) \exp(-r^2/b^2 - r_c/r)dr$$

[2]A referee suggested to use the empirical equation found by Schuler's group (16) in order to obtain $f \cdot G_{gi}$. However, the validity of the equation is not proved in the present system, nor did the plot according to the equation yield meaningful figures even in the liquid propane at room temperature. High mobility of electrons expected in the present system might be related to the failure. The assumption $f(G_{fi} + G_{gi}) = \Delta G(H_2)_{max}$ has been used by Fujisaki *et al.* (1*a*). Further, the shape of the curves in Fig. 1 and the fact that $\Delta G(H_2)_{max}$ of the present study is the largest so far found may justify the use of the assumption at least as the zeroth order approximation.

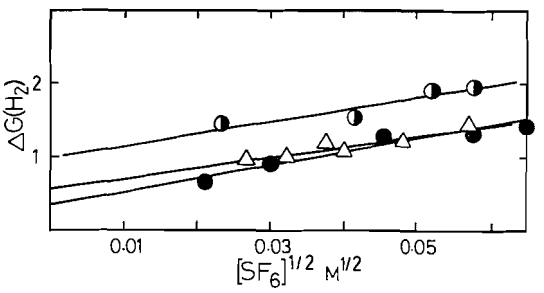

FIG. 2. Decrease of hydrogen yields in the radiolysis of propane at various densities as functions of the square root of the molar concentration of SF_6; ◑, 0.35 ± 0.01 g/ml; △, 0.42 ± 0.01 g/ml; ●, 0.50 g/ml (liquid phase, 20 ± 2 °C).

one obtains the value of b which is the most probable value of r. Values of b thus calculated, and the product of b and the gas density d are listed in Table 1 together with the values of other parameters. These b and $b \cdot d$ values agree reasonably well to those determined in a similar experiment using N_2O as the electron scavenger (8)[3]. Further, the $b \cdot d$ values are in fair agreement with that obtained from the electrical measurement in the liquid at 183 °K, 59×10^{-8} g/cm^2 (7). A gradual increase in $b \cdot d$ with density confirms a previous observation (8). The agreement of $b \cdot d$ values obtained with different electron scavengers, if not fortuitous, is significant, since $b \cdot d$ is considered to be the most meaningful parameter related to the efficiency of the electron energy loss process in a medium (6). At the present time we do not intend to explain the observation except a speculative argument given elsewhere (8).

The slopes of the square-root plot (Fig. 2) together with $\Delta G(H_2)_{max} - \Delta G(H_2)_0$ $(= f \cdot G_{gi})$ at a given density give the A values listed in Table 1. A values decrease with the increase in density. The trend is somewhat different from that observed with N_2O as the scavenger. The reason for this discrepancy is not obvious at present.

The variation with density of $G(H_2)$ from pure propane and from C_3H_8–SF_6 (*ca.* 0.7 mol %) are shown in Fig. 3. The values for the liquid phase obtained in this work were 6.4 and 3.0 in the absence and presence of SF_6, which are higher than the corresponding values, 4.8 and 2.5 (0 °C), of Fujisaki *et al.* (1*a*). Lower values of the latter may be due to the higher total dose used in

[3]Preliminary results indicated otherwise when we quoted the present work in ref. 8.

Can. J. Chem. Downloaded from www.nrcresearchpress.com by 210.87.254.40 on 09/05/12
For personal use only.

TABLE 1. Electron ranges and kinetic parameter values

Density (g/ml)	$\Delta G(H_2)_0$	$\Delta G(H_2)_{max}$	G_{fi}/G_{tot}	ε*	r_c† (Å)	b (Å)	$b.d$‡	A (M^{-1})
0.36±0.01	0.98	3.3	0.80	1.45	293	233 (208)§	84 (73)	49
0.43±0.01	0.57	2.9	0.20	1.55	274	155 (176)	66 (74)	35
0.50 (20 °C)	0.36	3.4	0.11	1.66	343	135 (116)	65 (58)	30

*Calculated by the Debye equation using the values of parameters quoted in ref. 7.
†Onsager distance, $e^2/\varepsilon kt$.
‡In 10^{-8} g/cm².
§Figures in parentheses are those obtained with N_2O (ref. 8).

their work. Robinson and Freeman reported still lower values of 4.6 and 1.8 at 183 °K using N_2O (9). Our maximum $\Delta G(H_2)$ in the liquid phase is larger than either of them.

$G(H_2)$ from pure propane is seen to decrease gradually with density. This is in contrast to the abrupt drop in $G(H_2)$ from ammonia radiolysis that takes place at lower densities than those studied in this work (10). However, a similar gradual change was observed in the case of ethane (11) and butanes (12). The difference can be explained in terms of differences in the neutralization process at high densities in ammonia and in hydrocarbons. We proposed that in gaseous ammonia at high densities ion–ion neutralization ($NH_4^+ + NH_2^-$) prevails, which does not lead to hydrogen formation, over that between ion–electron ($NH_4^+ + e^-$) (10). Formation of solvated electrons in supercritical ammonia was recently observed with approximately constant yield above $d \simeq 0.2$ g/ml (13). Ward observed that they rapidly react with NH_2 forming NH_2^- which in turn reacts rapidly with NH_4^+ in liquid ammonia (14). The fact that sharp decrease in $G(H_2)$ begins in the density region where solvation of electrons becomes important is an indirect evidence for the proposed mechanism. Then, in hydrocarbons where solvated electrons are not produced except at very low temperatures (15), it seems obvious that the neutralization remains between ions and electrons throughout the density range and that such a sharp change in the yield cannot occur.

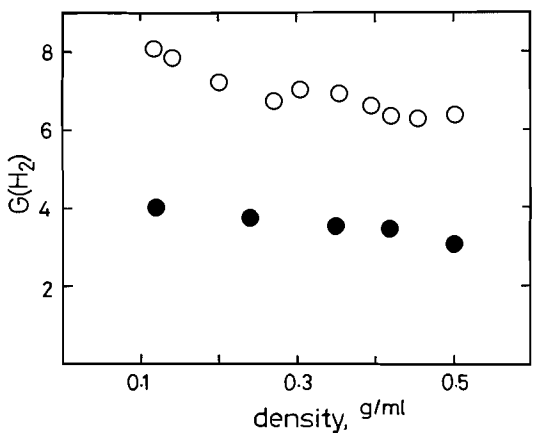

FIG. 3. Dependence of hydrogen yields from propane radiolysis on the gas density; ○, no additive; ●, ≃ 0.7% SF_6.

The gradual decrease in the contribution of the neutralization process to H_2 formation with density might be ascribed to the cage effect and to the deactivation of excited states formed upon neutralization in view of the results of isotopic analysis of hydrogen (1*a*). However, this analysis also shows that the change in the composition of hydrogen from gas to liquid phase radiolysis is rather complicated. Therefore it is not warranted in this work to speculate further the relative importance of the conceivable causes for the over-all decrease of $G(H_2)$ such as deactivation of excited ions and molecules, and the cage effect.

1. (*a*) N. FUJISAKI, S. SHIDA, and Y. HATANO. J. Chem. Phys. **52**, 556 (1970); (*b*) References prior to 1968 are reviewed by G. G. Meisels. Fundamental processes in radiation chemistry. *Edited by* P. Ausloos. Interscience Publ., New York. 1968. Chapt. 6.
2. M. YOSHIMURA, M. CHOSA, Y. SOMA, and M. NISHIKAWA. J. Chem. Phys. **57**, 1626 (1972).
3. P. A. SCALA, S. G. LIAS, and P. AUSLOOS. J. Am. Chem. Soc. **88**, 5701 (1966).
4. FF. WILLIAMS. J. Am. Chem. Soc. **86**, 3954 (1968).

Can. J. Chem. Downloaded from www.nrcresearchpress.com by 210.87.254.40 on 09/05/12
For personal use only.

5. A. HUMMEL. J. Chem. Phys. **48**, 3268 (1968).
6. W. F. SCHMIDT and A. O. ALLEN. J. Phys. Chem. **72**, 3730 (1968).
7. M. G. ROBINSON, P. G. FUOCHI, G. R. FREEMAN. Can. J. Chem. **49**, 3657 (1971).
8. Y. YAMAGUCHI and M. NISHIKAWA. J. Chem. Phys. In press.
9. M. G. ROBINSON and G. R. FREEMAN. J. Chem. Phys. **55**, 5644 (1971).
10. M. NISHIKAWA, K. KURODA, and N. MATSUURA. Bull. Chem. Soc. Jap. **42**, 116 (1969).
11. C. M. WODETZKI, P. A. MCCUSKER, and D. B. PETERSON. J. Phys. Chem. **69**, 1045 (1965).
12. T. MIYAZAKI and S. SHIDA. Bull. Chem. Soc. Jap. **38**, 716 (1965); **39**, 2344 (1966).
13. R. OLINGER, U. SCHINDEWOLF, A. GAATHON, and J. JORTNER. Ber. Bunsenges. **75**, 690 (1971).
14. B. WARD. Advan. Chem. Ser. **81**, 601 (1968).
15. H. A. GILLIS, N. V. KLASSEN, G. G. TEATHER, and K. H. LOKAN. Chem. Phys. Lett. **10**, 481 (1971).
16. J. M. WARMAN, K.-D. ASMUS, and R. H. SCHULER. Adv. Chem. Ser. **82**, 25 (1968).

Can. J. Chem. Downloaded from www.nrcresearchpress.com by 210.87.254.40 on 09/05/12
For personal use only.

Mercury(II) Complexes of L-Cysteine Methyl Ester

GEORGE A. NEVILLE[1] AND MATHS BERLIN
The Institute of Hygiene, University of Lund, Magle Stora Kyrkogata 12, S-223 50 Lund, Sweden
and
Organic Chemistry 2, Chemical Center, Box 740, University of Lund, S-220 07 Lund 7, Sweden

Received May 30, 1973

The mercurial complexation of L-cysteine methyl ester hydrochloride with mercury(II) nitrate, chloride, and acetate has been investigated at low p*H*. Bis(methyl L-cysteineato)mercury(II) hydrochloride hydronitrate monohydrate, following isolation and extensive characterization, was shown to be the substance reported in the literature as the dihydrochloride sesquihydrate complex. The preparation and properties of bis(methyl L-cysteineato)mercury(II) dihydrochloride monohydrate are reported for the first time. The properties and structural features of the complexes are discussed mainly in the context of investigations utilizing infrared, ^{1}H- and ^{13}C-n.m.r. spectroscopy.

La complexation du chlorhydrate de l'ester méthylique de la L-cysteine par le nitrate, le chlorure et l'acétate de mercure(II) a été étudiée en fonction de bas p*H*. On a montré après isolement et caractérisation que le chlorhydrate hydronitrate monohydraté de bis(méthyl L-cysteineato) de mercure(II) est en réalité le produit rapporté dans la littérature comme étant le complexe dichlorhydrate sesquihydraté. La synthèse ainsi que les propriétés du dichlorhydrate monohydraté de bis(méthyl L-cysteineato) de mercure(II) sont rapportées pour la première fois. Les propriétés ainsi que les caractéristiques structurales des complexes sont décrites surtout en fonction des études effectuées à l'aide de la spectroscopie i.r. et de la r.m.n. ^{1}H et ^{13}C. [Traduit par le journal]

Can. J. Chem., **51**, 3970 (1973)

Introduction

Few mercury complexes of amino acids have been isolated and subjected to structural characterization in spite of the long known affinity of this element for such substrates and its use in analytical biochemistry. In the course of work undertaken to investigate the nature of some mercurial complexes of interest for toxicological investigations of biotransport and biotransformation, mercury(II) complexes of L-cysteine methyl ester were obtained whose properties were found to be at variance with those reported in the literature. During potentiometric study of the interaction of cysteine methyl ester hydrochloride with various metal ions, Porter, Perrin, and Hay (1) isolated a complex by the use of mercury(II) nitrate which they reported to be bis-(methyl L-cysteineato)mercury(II) dihydrochloride sesquihydrate. Reinvestigation and extension of this work has revealed that the reported complex contains both nitrate and chloride ions and that it differs in the solid state from the dihydrochloride complex prepared separately and now authenticated. This paper describes the preparation of the 2:1 complexes of cysteine methyl ester hydrochloride from mercury(II) nitrate, chloride, and acetate and an investigation of their properties by infrared, ^{1}H- and ^{13}C-n.m.r. spectroscopy and X-ray diffraction.

Results and Discussion

X-Ray diffraction confirmed the crystalline nature of the products and served admirably to differentiate between the closely related *bis*-(methyl L-cysteineato)mercury(II) hydrochloride, hydronitrate monohydrate, and the dihydrochloride monohydrate. The complexes were obtained as thin needles, approx. 0.5 × 0.02 mm for the chloride–nitrate complex and less than half this size in the case of the dichloride complex. Because better crystals could not be grown for crystallographic analysis, the $\sin^2\phi$ values from X-ray diffraction have been submitted to the Depository of Unpublished Data.[2]

[1]1972 Centennial Fellow of the Medical Research Council of Canada. Present address: Health and Welfare Canada, Tunney's Pasture, Ottawa, Canada K1A 0L2.

[2]$\sin^2\phi$ data for the X-ray powder diffraction patterns and band frequencies for the infrared spectra of bis-(methyl L-cysteineato)mercury(II) hydrochloride, hydronitrate monohydrate, and of the corresponding dihydrochloride monohydrate are available upon request, at a nominal charge, from the Depository of Unpublished Data, National Science Library, National Research Council of Canada, Ottawa, Canada K1A 0S2.

Can. J. Chem. Downloaded from www.nrcresearchpress.com by 210.87.254.40 on 09/05/12
For personal use only.

Can. J. Chem. Downloaded from www.nrcresearchpress.com by 210.87.254.40 on 09/05/12
For personal use only.

The presence of an infrared band at 1365 cm^{-1} which occurs in the range 1380–1350 cm^{-1} usually associated with asymmetric NO_3 stretching (2), suggested the presence of inorganic nitrate in the complex prepared according to the conditions reported by Porter *et al.* (1). This band is absent in the complex prepared from L-cysteine methyl ester hydrochloride and mercury(II) chloride. Attempts to verify the presence of nitrate ion by laser Raman spectroscopy and obtain complementary information of ν(SH), ν(C—S), and other modes failed due to rapid degradation of the sample in the laser beam. Complete microanalysis established the stoichiometry of the complex prepared with mercury(II) nitrate and showed it to have the composition $(C_4H_9NO_2S)_2ClHgNO_3 \cdot H_2O$ consistent with the presence of one nitrate ion. Porter's reported composition, $C_8H_{18}Cl_2HgN_2O_4S_2$ 1.5 H_2O appears to have been based solely on analysis for C and H, and no other infrared bands were reported for the complex apart from ν(H_2O) 3450, 3650, ν(NH) 3000, δ(NH) 1576, and ν(CO) 1745.

The infrared spectra obtained for the chloride–nitrate and dichloride complexes may be compared in Fig. 1. Although each complex is hydrated it appears from band contours and observed frequencies for ν(OH) that water is less strongly hydrogen bonded in the chloride–nitrate complex than in the dichloride complex. Neither complex shows the combination band of medium strength near 2000 cm^{-1} which is so striking in the parent substance, but each complex shows a broad ν(N—H) band centered near 2900 cm^{-1} characteristic of substituted ammonium ion interaction with simple anions (3). The dihydrochloride complex shows typical fine structure[2] for substituted ammonium chloride salts on the low frequency side (2650–2200 cm^{-1}) of the ν(N—H) band. In contrast, the hydrochloride hydronitrate complex shows evidence of both chloride interaction by weak shoulder development at 2300 cm^{-1} and nitrate interaction resulting in the ν(N—H) band being less broad and more highly shouldered near 2900 cm^{-1}. Little data is available on ν(Hg—S), but from values reported for this mode in $Hg(SCN)_2$ (278 cm^{-1}) and $Hg(SCN)_4^{2-}$ (239 cm^{-1}) (4) and in CH_3SHgCH_3 (333 cm^{-1}) (5), it would appear that the broad band near 365 cm^{-1} in both the hydrochloride hydronitrate complex and the dihydrochloride complex may be due to ν(Hg—S).

The results of n.m.r. spectroscopic study of the complexes and parent substance in D_2O solution are summarized in Tables 1 and 2. Horsley and Sternlicht (6) have investigated the dependence of methylene ^{13}C and proton chemical shifts on p*D* of various amino acids. Horsley *et al.* (7) have also examined natural abundance ^{13}C spectra of amino acids. In the range p*D* 0–2, the very small variation in chemical shift can be ignored in relation to the very much larger shifts induced by the presence of a paramagnetic element like mercury. Because ^{13}C chemical shifts reflect primarily the local charge density, the large downfield shift (~4 p.p.m.) for the methylene carbon atoms in the mercury complexes of cysteine methyl ester (Table 2) indicates that sulfur is bonded to mercury. The relatively smaller ^{13}C downfield shifts for the methine and carboxyl carbons relative to the parent substance appear to arise solely from the operation of the inductive effect. In solution, therefore, these complexes do not appear to have other possible ligands, amino or carboxy, engaged in mercurial complexation as might be found in chelated structures.

The proton n.m.r. spectral results (Table 2), obtained from the same solutions used for ^{13}C study, are consistent with the ^{13}C results in showing the same relative order for chemical shift, $CH > CH_3 > CH_2$, and a marked downfield shift for the methylene protons of the mercury complexes relative to the parent compound. The practically invariant ^{13}C and ^{1}H frequencies for the methyl ester afford an internal check on the relative frequencies for other groups within the complexes and parent compound. The observed equivalence for the methylene protons in both the parent substance and the complexes precludes the measurement of separate vicinal coupling constants and the determination of relative rotameter populations.

Attempts were made to study bonding in the solid state of these complexes by means of electron spectroscopy for chemical analysis (ESCA), but decomposition of the samples on platinum foil even at −100 °C prevented this. Degradation of the samples was indicated during scanning by deterioration of the mercury signal and by the development of multiple mercury bands indicating the formation of mercury in other oxidation states.

The degree of hydration of the complexes was established from the microanalyses for H and O. For these complexes, in which the hydrogen

Can. J. Chem. Downloaded from www.nrcresearchpress.com by 210.87.254.40 on 09/05/12
For personal use only.

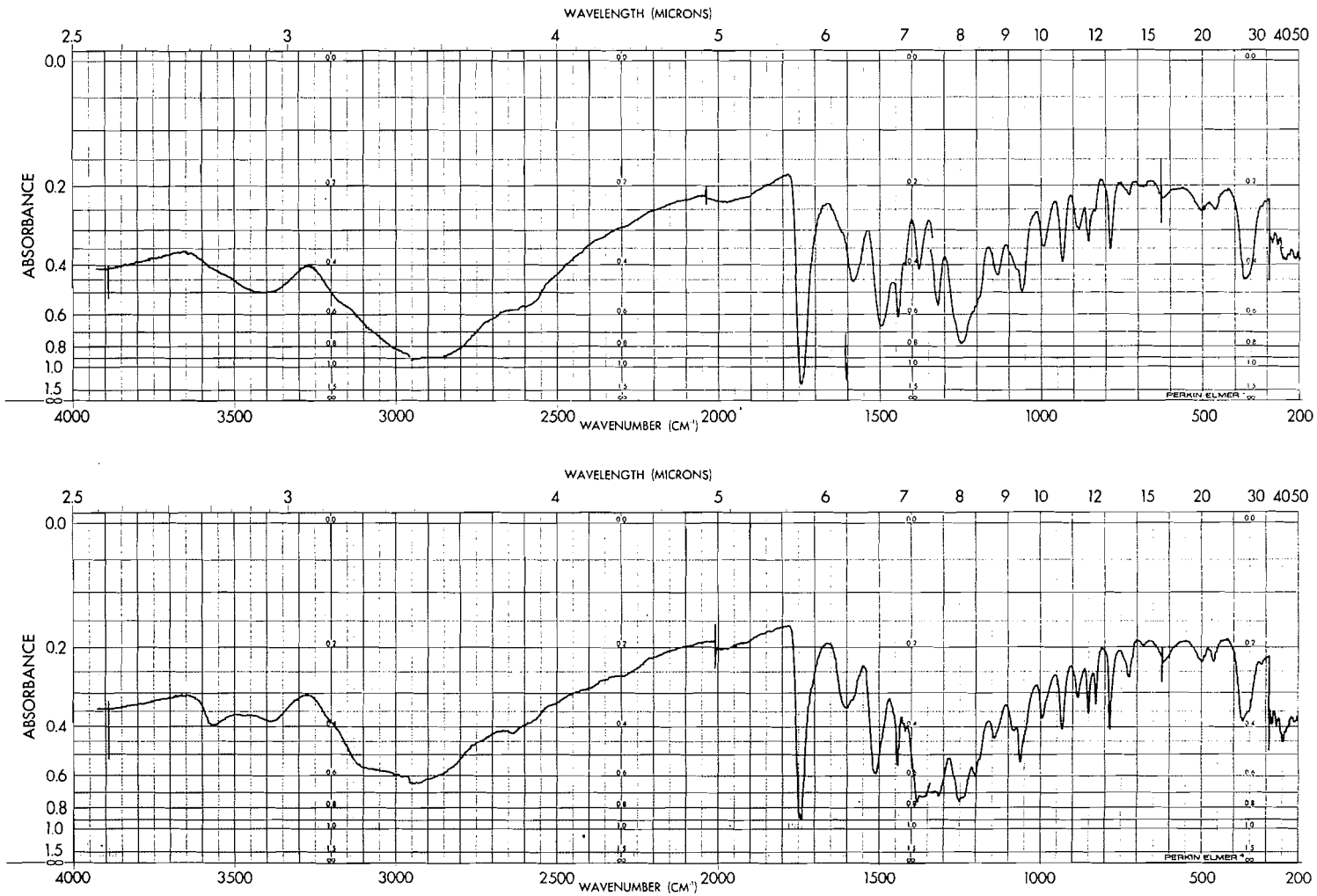

FIG. 1. Infrared spectra of bis(methyl L-cysteineato)mercury(II) complexes: the hydrochloride hydronitrate monohydrate (lower) and the dihydrochloride monohydrate (upper).

TABLE 1. ^{13}C-n.m.r. chemical shifts for D_2O solutions (pD = 1.3) of L-cysteine methyl ester, bis(methyl L-cysteineato)mercury(II) hydrochloride hydronitrate monohydrate and the dihydrochloride monohydrate

Compound	Concentration (M)	Shift (p.p.m. relative to TMS)			
		CH_2	CH_3	CH	CO_2Me
$HSCH_2CH(NH_3Cl)CO_2CH_3$	0.50	24.8	54.8	55.3	169.6
$(C_4H_9NO_2S)_2ClHgNO_3 \cdot H_2O$	2.9	29.0	55.3	56.8	169.8
$(C_4H_9NO_2S)_2HgCl_2 \cdot H_2O$	3.0	29.0	54.9	56.1	169.7

TABLE 2. Proton n.m.r. Data for D_2O Solutions (pD = 1.3) of L-cysteine methyl ester hydrochloride, bis(methyl L-cysteineato)mercury(II) hydrochloride hydronitrate monohydrate and the dihydrochloride monohydrate

Compound	Concentration (M)	δ_{CH_3}*	δ_{CH}	δ_{CH_2}	$J_{\alpha\beta}$ (Hz)
$HSCH_2CH(NH_3Cl)CO_2CH_3$	0.50	4.30	4.85	3.60	5.1
$(C_4H_9NO_2S)_2ClHgNO_3 \cdot H_2O$	2.9	4.35	4.90	4.05	5.4
$(C_4H_9NO_2S)_2HgCl_2 \cdot H_2O$	3.0	4.35	4.95	4.10	5.4

*δ measured in p.p.m. downfield from external TMS.

content is low, the oxygen analysis is the best determinant. The percent drying loss (50°/HV) does not appear to be a satisfactory means for determining extent of hydration in these mercurial complexes. Attempts were made to determine the degree of hydration by means of differential scanning calorimetry, using nylon capsule liners. The complexes were found to be thermally labile, the thermal degradation being unreproducible and seemingly dependent on both starting temperature and rate of heating. Substances containing both mercury and sulfur are usually notorious for study by thermometric techniques (8).

Experimental

Instrumentation

X-ray diffraction powder patterns were obtained using Guinier-Hägg cameras from samples mixed with KCl (BDH, Analar).

Infrared spectra were measured with a Perkin–Elmer Model 621 spectrometer using fluorolube mulls and NaCl windows from 4000–1340 cm^{-1} and Nujol mulls with caesium iodide windows from 1340–200 cm^{-1}.

^{13}C-n.m.r. spectra were obtained with a Varian XL-100 spectrometer following accumulation and Fourier transformation of signals in both proton decoupled and coupled modes. Proton spectra were obtained with a Varian A-60A spectrometer. The parent substance and dihydrochloride complex dissolved readily in D_2O (5 ml) giving solutions at pD 2.6 and 2.1, respectively. The hydrochloride hydronitrate complex required the addition of two drops of trifluoroacetic acid for dissolution resulting in pD of 1.3. The pD of the other solutions was adjusted to 1.3 by addition of TFA, but no spectral changes were observed on charge of pD. The pH of D_2O solutions was measured with a glass electrode and pH meter, and the measurements were converted to pD values as directed by Gutfreund (9).

Microanalyses

Microanalyses were performed by Alfred Bernhardt, Mikroanalytische Laboratorium, 5251 Elbach über Engelskirchen, Fritz-Pregl-Strasse 14–16, W. Germany. Appropriate separatory processes were employed to eliminate the interference of mercury with the C, H, and Cl determinations. Sulfur was analyzed by a reductive process.

Preparations of Complexes

Bis(methyl L-cysteineato)mercury(II) Hydrochloride Hydronitrate Monohydrate

To L-cysteine methyl ester hydrochloride (0.350 g, 0.002 mol, Sigma 98%) in water (10 ml) was added dropwise with magnetic stirring, a solution of mercury(II) nitrate monohydrate (0.343 g, 0.001 mol, BDH Analar) in water (20 ml). (Two drops of conc. HNO_3 were added to the mercury(II) nitrate to dissolve the salt.) No turbidity or crystallization occurred upon addition of the $Hg(NO_3)_2$ contrary to the observations of Porter *et al.* (1). The mixture (p$H \sim 1.0$) was subjected to rotary evaporation (20 mm Hg, 60°) to obtain a fluffy white solid. The solid was recrystallized from a minimum volume of hot 95% ethanol. On cooling, the solution produced a mass of extremely fine needles which required the addition of more ethanol for collection by filtration. The solid was washed with acetone and dried over NaOH pellets *in vacuo*. The yield was 0.46 g or 38%.

To a solution of L-cysteine methyl ester hydrochloride (0.875 g, 0.005 mol, Sigma 98%) in warm (50–60°) 95% ethanol (30 ml), a solution of mercury(II) nitrate monohydrate (0.855 g, 0.0025 mol, BDH Analar) in warm water (10 ml), containing a few drops of conc. HNO_3,

Can. J. Chem. Downloaded from www.nrcresearchpress.com by 210.87.254.40 on 09/05/12
For personal use only.

Can. J. Chem. Downloaded from www.nrcresearchpress.com by 210.87.254.40 on 09/05/12
For personal use only.

was added dropwise with magnetic stirring. Immediate precipitation was followed by fairly rapid dissolution. On cooling, the solution gave a voluminous, semi-immobilized fibrous product. More ethanol was added to facilitate collection of the solid which was washed with acetone and dried over NaOH pellets *in vacuo* (20 mm Hg, 25°). The yield of product was 1.40 g or 47%.

X-ray diffraction showed the solid to be identical with the product obtained under aqueous conditions. The product gave a positive chloride test after dissolution in dilute nitric acid. Mass spectra featured mercurial cluster peaks at *m/e* 461, 372, 357, 327, 313, and 202 based on the 202 Hg isotope.

Anal. Calcd. for $(C_4H_9NO_2S)_2ClHgNO_3 \cdot H_2O$ (m.w. 586.46): C, 16.38; H, 3.44; O, 21.83; N, 7.17; Cl, 6.05; Hg, 34.21; S, 10.93. Found: C, 16.26; H, 3.15; O, 21.85 and 21.63; N, 7.09; Cl, 5.89; Hg, 34.04; S, 10.77.

Bis(methyl L-cysteineato)mercury(II) Dihydrochloride Monohydrate

(a) Using Mercury(II) Chloride

To a warm solution (50–60°) of L-cysteine methyl ester hydrochloride (0.875 g, 0.005 mol, Sigma 98%) in 95% ethanol (30 ml) was added dropwise with magnetic stirring a warm solution of mercury(II) chloride (0.678 g, 0.0025 mol, BDH Analar) in 95% ethanol (10 ml). The instantly formed precipitate dissolves fairly rapidly to give a solution from which massive crystallization of white, feathery solid is obtained within a half hour of the addition. Additional ethanol was used to loosen and transfer the solid during collection. The solid was washed with acetone and dried several hours over NaOH pellets *in vacuo* (20 mm Hg, 25°). The yield was 1.16 g or 41%.

The product gave a positive chloride test after dissolution in dilute nitric acid. X-Ray diffraction patterns and infrared spectra showed the product to be different from that prepared with mercury(II) nitrate. Mass spectra showed mercurial cluster peaks at *m/e* 371, 313, and 202 (reported for ^{202}Hg isotope) and base peak at *m/e* 160.

Anal. Calcd. for $(C_4H_9NO_2S)_2HgCl_2 \cdot H_2O$ (m.w. 559.91): C, 17.16; H, 3.60; O, 14.29; N, 5.00; Cl, 12.67; Hg, 35.83; S, 11.45; H_2O, 3.22. Found: C, 17.21; H, 3.67; O, 14.34; N, 5.14; Cl, 12.37; Hg, 35.75; S, 11.26, and % drying loss (50°/HV), 3.18.

(b) Using Mercury(II) Acetate

To a warm solution (50–60°) of L-cysteine methyl ester hydrochloride (0.875 g, 0.005 mol, Sigma 98%) in 95% ethanol (30 ml) was added dropwise with magnetic stirring a solution (25–30°) of mercury(II) acetate (0.798 g, 0.0025 mol, BDH Analar) in methanol (10 ml). (The use of ethanol and higher alcohols and methanolic solutions at higher temperature results in the rapid formation of a yellow precipitate identified by X-ray diffraction as mercury(II) oxide.) Precipitation occurred instantly on mixing but dissolved fairly quickly except towards the end of the addition when very finely divided solid began to accumulate. No further crystallization occurred at room temperature, but a massive, immobilized solid was obtained with ordinary refrigeration consisting of very thin, glistening needles.

During filtration of the cold mixture, most of the solid redissolved, however; a small portion (Fr. A) was collected, washed with 95% ethanol and set to dry. The mother liquor was treated with diethyl ether until just turbid (no turbidity produced with acetone) and returned to the refrigerator. Within 15 min, the mixture was immobilized by a mass of feathery, silk-like solid. The solid (Fr. B) was collected, washed with ether – 95% ethanol (1:1 and dried over NaOH pellets *in vacuo*. X-ray diffraction patterns showed fractions A and B were identical and that the product of this reaction was identical to that obtained using mercury(II) chloride. The overall yield was 41%.

We are indebted to Prof. Börje Wickberg (Organic Chemistry, Lund Institute of Technology) for provision of laboratory space. The stimulus and advice of Prof. Bengt Aurivillius and of Dr. Karin Aurivillius (Inorganic Chemistry, Lund Institute of Technology) in matters related to crystal growing and crystallography is much appreciated as well as the determination of numerous powder diffraction patterns by Christer Hansson. We are grateful to Dr. Ragnar Larsson (Inorganic Chemistry, University of Lund) for infrared and ESCA instrumentation, for stimulating discussions related to their application and to Börje Folkesson for his careful ESCA investigations. We are particularly indebted to Prof. Sture Forsén (Physical Chemistry, University of Lund) for the availability of n.m.r. instrumentation and to Dr. Torbjörn Drakenberg for determining n.m.r. spectra. It is a pleasure to recognize Prof. Stig Sunner (Thermochemistry, University of Lund) as a major advocate of the Lund Chemical Center as an interdisciplinary center for chemical research and to acknowledge his interest and discussions of thermometric investigations performed by Bengt Falk. The Medical Research Council of Canada is generously thanked for the award of a Centennial Fellowship to G.A.N.

1. L. J. PORTER, D. D. PERRIN, and R. W. HAY. J. Chem. Soc. (A), 118 (1969).
2. F. A. MILLER and C. H. WILKINS. Anal. Chem. **24**, 1253 (1952).
3. G. A. NEVILLE and Z. R. REGNIER. Can. J. Chem. **41**, 4229 (1969).
4. R. P. J. COONEY and J. R. HALL. Aust. J. Chem. **22**, 2117 (1969).
5. R. A. NYQUIST and J. R. MANN. Spectrochim. Acta, **28A**, 511 (1972).
6. W. J. HORSLEY and H. STERNLICHT. J. Am. Chem. Soc. **90**, 3738 (1968).
7. W. HORSLEY, H. STERNLICHT, and J. S. COHEN. J. Am. Chem. Soc. **92**, 680 (1970).
8. STIG SUNNER. Personal communication.
9. H. GUTFREUND. Enzymes: physical principles. Wiley–Interscience, New York. 1972. p. 173.

Kinetics of the Reaction of Nickel(II) and 2,2′-Bipyridine in Ethanol

M. L. SANDUJA AND W. MACF. SMITH
Department of Chemistry, Queen's University, Kingston, Ontario

Received June 15, 1973

The kinetics of formation of the monobipyridine complex of nickel(II) in ethanol has been studied with stopped-flow methods over the temperature range 7 to 35 °C. The value of the second order rate constant k_f at 25 °C of 6.6×10^{-3} M^{-1} s^{-1} and the values of $\Delta H^{\ddagger}$ (10.1 ± 1.0 kcal mol^{-1}) and of $\Delta S^{\ddagger}$ (-7.3 ± 3.4 cal deg^{-1} mol^{-1}) are close to the corresponding values for ethanol exchange on nickel(II) and suggest that the mechanism is dissociative interchange. However the difference in the values of the kinetic parameters of this reaction and those previously reported for the reactions involving the chemically similar phenanthroline imply a degree of ligand specificity for the reactions in ethanol which is considerably larger than is the case for reactions in water and methanol and that a common I_d mechanism with monodentate formation being rate controlling is not applicable to both reactions.

La cinétique de formation du complexe monobipyridine de nickel(II) dans l'éthanol a été étudiée à l'aide de méthodes à débit interrompue dans l'intervalle de températures allant de 7 à 35 °C. La valeur de la constante de vitesse du second ordre k_f à 25 °C (6.6×10^{-3} M^{-1} s^{-1}) et les valeurs de $\Delta H^{\ddagger}$ (10.1 ± 1.0 kcal mol^{-1}) et de $\Delta S^{\ddagger}$ (-7.3 ± 3.4 cal deg^{-1} mol^{-1}) sont proches des valeurs correspondantes pour l'échange de l'éthanol sur le nickel(II) et suggèrent que le mécanisme est du type échange mutuel dissociatif. Cependant la différence dans les valeurs des paramètres cinétiques de cette réaction et celles précédemment rapportées pour des réactions avec la phénanthroline (qui est chimiquement similaire) implique un degré de spécificité du coordinat pour les réactions dans l'éthanol beaucoup plus élevé que pour les réactions dans l'eau et dans le méthanol. De plus cette différence implique qu'un mécanisme I_d commun, où la formation d'un monocoordinat serait l'étape déterminant la vitesse, n'est pas applicable aux deux réactions. [Traduit par le journal]

Can. J. Chem., **51**, 3975 (1973)

To expand information about the kinetic behavior of nickel(II) in non-aqueous solvents we have investigated the reactions of nickel(II) with several ligands in ethanol. Our results for the reactions involving 1,10-phenanthroline have been reported (1). We considered that our data were consistent with a mechanism which was dissociative interchange (I_d) (2) although the kinetic parameters deviated significantly from those reported by Breivogel (3) for ethanol exchange on nickel(II) and the rate constant for the reaction was somewhat higher than would be anticipated on the basis of a simple I_d mechanism and a magnitude for the association constant for the encounter pair based on the Fuoss–Eigen relation (4) for an uncharged ligand and a solvated nickel(II) ion. We report here on the reaction of nickel(II) with 2,2′-bipyridine, a ligand which is analogous to phenanthroline in its bidentate nature, its coordinating atoms, and high association constant involving nickel(II), but differing in the decreased rigidity of its structure which has been considered to be a possible source of difference in kinetic behavior.

Experimental

Experimental procedures including treatment of ethanol and preparation and handling of solutions of nickel perchlorate and perchloric acid were as previously reported (1). The 2,2′-bipyridine (Fisher reagent) was used without further purification. Lithium perchlorate (K and K laboratories) and lithium nitrate (Fisher reagent) apart from drying over silica gel and Drierite were used without further purification. Kinetic measurements were made with a model D-150 Durrum-Gibson stopped-flow spectrophotometer and spectrophotometric measurements relating to equilibria with a Beckman DK1 spectrophotometer.

The majority of kinetic runs involved solutions in which the concentration of nickel(II) perchlorate was 2.0×10^{-3} M and that of bipyridine 2.0×10^{-5} M, but for some runs the concentration of nickel(II) was 4.0×10^{-3} or 6.0×10^{-3} M and that of bipyridine 4.0×10^{-5} M. As in the previous work a trace of perchloric acid ($\sim 4 \times 10^{-7}$ M) was added to the solution used in the kinetic runs to avoid possible complications associated with solvolysis of nickel(II). The spectrophotometric properties of the slightly acidified solutions of bipyridine were identical with those of solutions to which no acid was added. At higher acidities at λ 300 and 310 nm there is a marked increase in absorbance to a value which remained substantially constant over concentrations of perchloric acid ranging from 2.2×10^{-3} to 7.9×10^{-3} M (the highest concentration investigated) over which range the monoprotonated form is presumably

Can. J. Chem. Downloaded from www.nrcresearchpress.com by 210.87.254.40 on 09/05/12
For personal use only.

TABLE 1. Values for the rate constant k_f for the formation of $Ni(bipy)^{2+}$ in ethanol

Temperature (°C)	Added electrolyte	I (M)	[Ni(II)] $M\times10^3$	[Bipy] $M\times10^5$	$k_f\times10^{-3}$ (M^{-1} s^{-1})
7.1	None	0.006	2.0	2.0	2.0±0.14
15	None	0.006	2.0	2.0	4.2±0.03
25	None	0.006	2.0	2.0	6.6±0.5
		0.012	4.0	2.0	6.6±0.2
		0.018	6.0	2.0	6.8±0.8
		0.006	2.0	4.0	6.8±0.4
	TBA ClO_4	0.050	2.0	2.0	5.9±0.2
	$NaClO_4$	0.050	2.0	2.0	6.0±0.2
	$LiClO_4$	0.050	2.0	2.0	6.2±0.3
	$LiNO_3$	0.050	7.0	2.0	10.5±0.3
35	None	0.006	2.0	2.0	11.8±0.1

the dominant species. At λ 300 nm, the wavelength used to monitor the course of the reaction, the extinction coefficient of the complex is approximately 3.6-fold greater than that of bipyridine. That complexing was complete under the conditions of the kinetic runs was confirmed by the fact that an increase of 3.6-fold in the concentration of nickel(II) over 2.0×10^{-3} M at constant concentration of bipyridine of 2.0×10^{-5} M yielded no significant increase in absorbance. In the majority of kinetic runs the only electrolyte present was the reactant nickel perchlorate and the trace of perchloric acid. Some runs were made with addition of one of sodium perchlorate, tetrabutyl ammonium perchlorate, lithium perchlorate, and lithium nitrate which if present in completely dissociated form would have yielded an ionic strength of 0.050.

The data were interpreted as previously described (1) on the assumption, which is supported by the data given below, that the reaction

$$[1]\qquad Ni^{2+} + bipy \xrightarrow{k_f} Ni(bipy)^{2+}$$

is second order overall. Since the initial concentration of nickel(II) was in substantial excess over that of bipyridine (100-fold in most runs) the reaction is pseudo first order and the slope of the line of regression for the plot of log $(A - A_\infty)$ against time was identified with $-k_f[Ni]_0/2.303$ where $[Ni]_0$ represents the initial concentration of nickel(II). The absorbance A was obtained from a photographic record of oscilloscope traces of absorbance against time.

Results and Discussion

Values for the rate constant (k_f) with 95% confidence limits and a summary of the conditions for the kinetic runs are given in Table 1. The values under I represent the ionic strength corresponding to complete dissociation of the nickel perchlorate and any other added electrolyte. The data for 25 °C imply no significant dependence of k_f on the concentration of reactant. It also appears that the rate is not sensitively dependent on the concentration of perchlorate, sodium, lithium, or tetrabutyl ammonium ions or on the concentration of nickel(II). Runs were carried out at 25 °C with addition of 1 and 2 wt. % of water and these indicated a significant increase in rate constant to the values 8.6 ± 0.47 and 7.6 ± 0.64 M^{-1} s^{-1}. Values for the parameters implied by the data from runs with no added electrolyte are $\Delta H^{\ddagger} = 10.1 \pm 1.0$ kcal mol^{-1} and $\Delta S^{\ddagger} = -7.3 \pm 3.4$ cal deg^{-1} mol^{-1}.

The values of the kinetic parameters for the reaction of bipyridine with nickel(II) are significantly different from those for the reaction involving phenanthroline (1) which are $\Delta H^{\ddagger} = 15.9 \pm 1.0$ kcal mol^{-1} and $\Delta S^{\ddagger} = 15.4 \pm 3.2$ cal mol^{-1} deg^{-1} whereas they approach those obtained by Breivogel for solvent exchange on nickel(II) in ethanol (3) which are $\Delta H^{\ddagger} = 10.8 \pm 1.5$ kcal mol^{-1} and $\Delta S^{\ddagger} = -4 \pm 5$ cal mol^{-1} deg^{-1}. Also the value of k_f at 25 °C of 6.6×10^3 M^{-1} s^{-1} for the reaction of bipyridine with nickel(II) may be contrasted with the value of 31×10^3 M^{-1} s^{-1} for the reaction of phenanthroline in ethanol. At lower temperatures the values of k_f for the two reactions approach and at higher temperatures they diverge; k_f (phen)/k_f (bipy) is ~2.2 at 7 °C and ~5.7 at 35 °C.

The interchange mechanism involving a bidentate ligand may be summarized as

$$[2]\qquad \begin{aligned} NiS_6^{2+} + L &\overset{K_0}{\rightleftharpoons} NiS_6^{2+}\cdot L \\ NiS_6^{2+}\cdot L &\underset{k_{-1}}{\overset{k_1}{\rightleftharpoons}} NiS_5\cdot L^{2+} + S \\ NiS_5L^{2+} &\xrightarrow{k_2} NiS_4L^{2+} + S \end{aligned}$$

where $NiS_6^{2+}\cdot L$ represents the encounter pair (outer complex) between solvated nickel(II) and the entering ligand L and $NiS_5\cdot L^{2+}$ represents

Can. J. Chem. Downloaded from www.nrcresearchpress.com by 210.87.254.40 on 09/05/12
For personal use only.

Can. J. Chem. Downloaded from www.nrcresearchpress.com by 210.87.254.40 on 09/05/12
For personal use only.

an intermediate monodentate (inner) complex. On the basis of this mechanism

$$[3] \qquad k_f = K_0 k_1 \frac{k_2}{k_{-1} + k_2}$$

For reactions involving nickel(II) and uncharged ligands in water k_f is approximately the same for mono- and bidentate ligands (5) which is consistent with the assumption that $k_2 \gg k_{-1}$, that k_1 is rate controlling, and that $k_f = k_1 K_0$. Using estimates for K_0 based on the Eigen–Fuoss relation, the value implied for k_1 is of the same order as that of the rate constant for solvent exchange. The ratio $R = (4/3)\, k_f/K_0 k_s$ has been proposed (6) as a convenient measure of whether the mechanism is of such simple dissociative interchange character where k_s is the rate constant for solvent exchange on the nickel(II) ion. For reactions of nickel(II) in water, R ranges in value from 0.2 to 0.6 for mono- and bidentate ligands when a value for the separation of centers, a, in the encounter complex is assigned a value of 5 Å. Assuming a value of 9 Å for a for the reactions of nickel(II) in ethanol the value for K_0 implied by the Eigen–Fuoss relation is 1.8 M^{-1}. Using this value for K_0 and Breivogel's value of 11×10^3 s^{-1} for k_s, the rate constant for ethanol exchange on nickel, yields values for R of 0.33 for the reaction involving bipyridine and 1.6 for the reaction involving phenanthroline. In view of the uncertainty in the value adopted for K_0, the somewhat high value for the reaction involving phenanthroline should not be considered as definitely ruling out an essentially dissociative interchange mechanism, but the value of k_f for the reaction of bipyridine is sufficiently smaller than that of phenanthroline to imply real differences in the details of the two reactions.

Considering the similarity of the ligands it is unlikely that the difference in the value of k_f is a reflection of differences in K_0. The closeness of the values of the kinetic parameters for the reaction involving bipyridine and those involving ethanol exchange, along with appreciation that the temperature coefficient for K_0 must be small, tempts one to consider that the reaction involving bipyridine is "normal", *i.e.* of simple I_d character with $k_f = K_0 k_1$, and that the reaction involving phenanthroline is "abnormal". The high values of k_f and its temperature coefficient (and so for $\Delta H^{\ddagger}$ and $\Delta S^{\ddagger}$) for the reaction involving phenanthroline relative to those for the reaction involving bipyridine might be the consequence of phenanthroline reacting via both an I_d pathway and one involving relatively large values for the energy and entropy of activation. In view of the correspondence in values of the thermodynamic parameters for the reactions of solvated nickel(II) with solvent and with bipyridine, the difference in values of the parameters for the reactions involving phenanthroline and bipyridine, and the relatively high value of k_f (phenanthroline) relative to k_s (solvent exchange), such a hypothesis seems preferable to one which considers k_{-1}/k_2 larger for the bipyridine reaction than for the phenanthroline reaction, as has been suggested by Chattopadhyay and Coetzee (6) for the corresponding reactions in dimethyl sulfoxide.

Admittedly, however, the uncertainty in the values of K_0 and the possibility of competition between the steps with rate constants k_{-1} and k_2 where bidentate ligands are involved do complicate the interpretation of our data. Information about the reactions of uncharged unidentate ligands would be free of the second complication and would assist assessment of the nature of ligand specificity in the various reactions of nickel(II) in ethanol.

1. M. L. Sanduja and W. MacF. Smith. Can. J. Chem. **50**, 3861 (1972).
2. C. H. Langford and H. B. Gray. Ligand substitution processes. W. A. Benjamin, New York. 1966.
3. F. W. Breivogel. J. Phys. Chem. **73**, 4205 (1969).
4. (*a*) R. M. Fuoss. J. Am. Chem. Soc. **80**, 5059 (1958). (*b*) M. Eigen. Z. Phys. Chem. NFI 176 (1954).
5. R. Wilkins. Acc. Chem. Res. **3**, 408 (1970).
6. P. K. Chattopadhyay and J. F. Coetzee. Inorg. Chem. **12**, 113 (1973).

The Synthesis of Songorine: A Simplified Synthesis of the Aromatic Intermediate

KAREL WIESNER, PAK-TSUN HO, DING CHANG, YIU KUEN LAM, CONNIE SHII JEOU PAN, AND WU YUN REN

Natural Products Research Center, University of New Brunswick, Fredericton, New Brunswick

Received June 21, 1973

A simple conversion of the previously described (1) tricyclic ester **1** into the pentacyclic songorine intermediate **21** is described. The process is stereospecific and it operates in an overall yield of 7.8%.

On présente une méthode simple pour transformer l'ester tricyclique **1** décrit précédemment en intermédiaire pentacyclique **21** de la songorine. Le procédé est stéréospécifique et effectué avec un rendement global de 7.8%. [Traduit par le journal]

Can. J. Chem., **51**, 3978 (1973)

Can. J. Chem. Downloaded from www.nrcresearchpress.com by 210.87.254.105 on 09/05/12
For personal use only.

We have described recently (1) a simple synthesis of the tricyclic ester **1** via the sequence **i** → **ii** → **iii** → **iv** → **1**. Compound **1** was then converted to the benzene sulfonyl aziridine **v** which selectively rearranged on acetolysis to compound **vi**.

The conversion of the tricyclic ester **vi** to the desired songorine intermediate **21** was also published in a preliminary report (1*b*, 2). Since large amounts of the intermediate **21** were required we wished to develop the synthetic process to a maximum of simplicity and efficiency. It turned out that the section of the synthesis between **vi** and **21** is the only one which could be fundamentally improved. The differential manipulation of the functions in compound **vi** required some five steps which might be eliminated by a suitable modification of the process.

Such a modification was indeed found, but it was necessary to abandon compound **vi** and to go back to the tricyclic ester **1** as starting material. Consequently we wish to describe in the present paper in detail the preferred and simplified route to the intermediate **21**. The overall yield in this new stereospecific conversion of **1** to **21** is 7.8% and thus this process provides a reliable platform for the continuation of the synthesis.

The tricyclic ester **1** was reduced with lithium aluminum hydride to the primary alcohol **2** and this compound was oxidized with *N*,*N*′-dicyclohexylcarbodiimide, dimethylsulfoxide, and pyridine in anhydrous benzene (3) to the aldehyde **3** in excellent yield.[1] The side chain destined to form ring A of songorine with its substituent was attached next. The aldehyde **3** was treated with an excess of the Grignard reagent prepared from 1-bromo-3-benzyloxybutane (4) in ether. A mixture of diastereoisomers represented by the formula **4** was obtained in a quantitative yield.

The oily mixture **4** was now converted to the *exo* benzenesulfonyl aziridine by treatment with an excess of benzenesulfonyl azide in benzene. The aziridine was quite unstable and it was consequently immediately subjected to acetolysis. Acetic acid and sodium acetate were added to the reaction mixture and stirring was continued at room temperature for several days. The crystalline mixture of diastereoisomers represented by the formula **5** was obtained in a yield of 84%. The mixture appeared to consist mainly of two components which differed in the configuration of the hydroxyl marked by the asterisk in formula **5**. For characterization the two components were separated by preparative t.l.c. and recrystallized for analysis. They were obtained in approximately equal quantities.

The aziridine rearrangement was completely regiospecific and the desired "compound" **5** was the only product detected in the reaction mixture. This clearly is due to the powerful influence of the aromatic methoxyl which increases the migratory aptitude of the bond in the *para* position.[2]

At this stage it was necessary to perform a reductive cleavage of the sulfonamide group and to replace it by an *N*-acetyl group. One of the subsequent steps in the synthesis involves the

[1] All spectral data for all compounds are recorded in the Experimental. They are mentioned in the Discussion only when specially relevant.

[2] For a full discussion of the influence of substituents on aziridine rearrangements see ref. 1*a*.

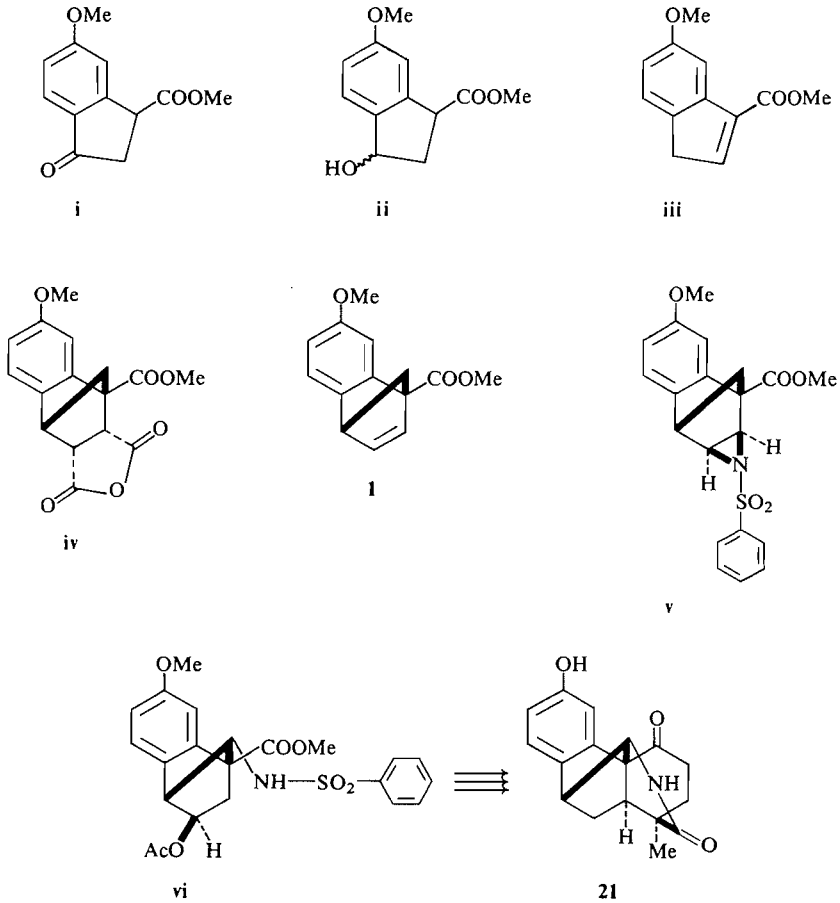

SCHEME 1

closure of ring A by an aldol condensation and the yield of this reaction is excellent if the nitrogen is blocked by acetylation but poor in the presence of the acidic sulfonamide group. The mixture of diastereoisomers **5** was reduced with an excess of $LiAlH_4$ in refluxing dioxane and the product was immediately acetylated with acetic anhydride and pyridine. The diastereoisomeric mixture **6** was obtained in a yield of 85%. The two major components of the mixture epimeric on the carbon marked by the asterisk in formula **6** were again isolated for characterization by preparative t.l.c.

The next task was to prepare the material for the closure of ring A by converting it into the diketone **9**. Fortunately, it turned out that the required partial hydrolysis of **6** to **7** proceeded with complete selectivity and practically quantitatively. The diastereoisomeric mixture **7** was converted into the diols **8** by hydrogenolysis and further into the mixture of the two epimeric diketones **9** by oxidation with chromium trioxide in pyridine. Both epimers **9** were crystalline and they were obtained in approximately equal quantities. They both showed in the i.r. spectrum a five-membered ketone at 1750 cm^{-1} and in the n.m.r. spectrum four methyl singlets. (β-epimer: τ 6.17 (—OCH_3), 7.84 (—$\overset{\overset{O}{\|}}{C}$—$CH_3$), 7.87 ($O$—$\overset{\overset{O}{\|}}{C}$—$CH_3$), and 7.94 p.p.m. ($N$—$\overset{\overset{O}{\|}}{C}$—$CH_3$)).

The mixture of the two diketones **9** was subjected to an aldol condensation in refluxing methanolic potassium carbonate. The two epimers **10** were obtained as a crystalline mixture in a yield of 88% and they were separated for

Can. J. Chem. Downloaded from www.nrcresearchpress.com by 210.87.254.105 on 09/05/12
For personal use only.

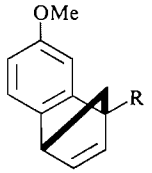

1 R = COOMe
2 R = CH_2OH
3 R = CHO

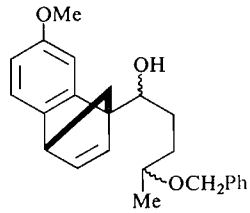

4

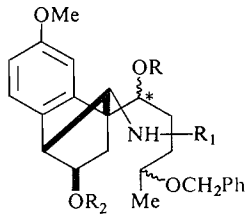

5 R = H; R_1 = SO_2Ph; R_2 = $-\overset{\overset{O}{\|}}{C}-Me$

6 R = R_1 = R_2 = $-\overset{\overset{O}{\|}}{C}-Me$

7 R = R_1 = $-\overset{\overset{O}{\|}}{C}-Me$; R_2 = H

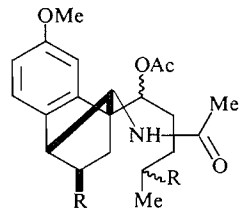

8 R = OH
9 R = =O

SCHEME 2

characterization by preparative t.l.c. The configuration of the hydroxyl in the two epimers **10** was assigned by n.m.r. spectroscopy. The aromatic hydrogen marked by the asterisk in formula **10** produces a narrow doublet at τ 3.24 p.p.m. in the β- and τ 2.87 p.p.m. in the α-epimer. This is due to the close proximity of this hydrogen and the ring A substituent in the α-epimer.[3]

[3]In the case of the epimeric pair **10** the assignment of configuration was corroborated by a complete X-ray structure analysis performed by Dr. J. F. Blount (Hoffmann-La Roche, Nutley, New Jersey) on a heavy atom derivative of the β-epimer of compound **16**. A chemical proof of this configuration was the observation of an $N \rightarrow O$ acetyl migration in the course of the preparation of this derivative (*cf.* ref. 2).

The operation which faced us now was the stereospecific addition of a one carbon element in the β position of the α,β-unsaturated ketone system of **10** and the ring closure of this new function with the nitrogen. The method which we have developed for related systems, *i.e.*, the addition of cyanide (5), turned out to be useless in the present case since the cyanide ion added selectively *anti* to the nitrogen.

The problem was finally solved as follows. Photoaddition of vinyl acetate to the mixture of the two epimers **10** gave two epimers of compound **11**. For characterization they were separated by preparative t.l.c. and the α-epimer was crystalline. The configuration of the acetoxy group in both epimers **11** is tentative and there is no evidence for it apart from *a priori* considerations of more favorable geometry and orbital overlap. On the other hand the peculiar regiospecificity of the photoaddition and the stereochemistry of the cyclobutane ring are certain from subsequent transformations and n.m.r. spectroscopy. The most remarkable feature in the n.m.r. spectra of both epimers **11** is the extremely high field position of the carbon–methyl group singlet. (β-Epimer, τ 9.70 p.p.m.;

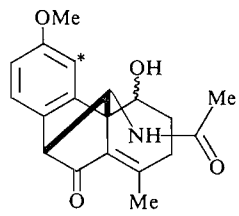

10

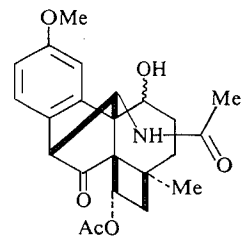

11

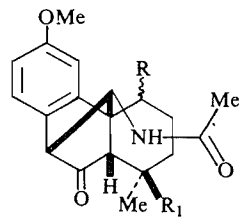

12 R = OH; R_1 = CH_2CHO
13 R = OAc; R_1 = CH=CHOAc
14 R = OAc; R_1 = CHO
15 R = OAc; R_1 = COOMe
16 R = OH; R_1 = COOMe
17 R = =O; R_1 = COOMe
18 R = ; R_1 = COOMe

SCHEME 3

Can. J. Chem. Downloaded from www.nrcresearchpress.com by 210.87.254.105 on 09/05/12
For personal use only.

Can. J. Chem. Downloaded from www.nrcresearchpress.com by 210.87.254.105 on 09/05/12
For personal use only.

α-epimer, τ 9.66 p.p.m.). This is due to the shielding effect of the anisole ring on the methyl group and is only possible if the stereochemistry of the entire skeleton is as indicated in the formula **11**.

Saponification of "compound" **11** with methanolic potassium hydroxide gave a quantitative yield of the two epimers represented by formula **12**. They were oily and were separated for characterization by preparative t.l.c. The n.m.r. spectra of both compounds showed an aldehydic proton (β-epimer, τ −0.17 p.p.m.; α-epimer, τ −0.24 p.p.m.) and it was thus clear that after the hydrolysis of the acetoxy group the resulting alcohol opened by a reverse aldol reaction. Inspection of the n.m.r. spectra allowed also an unambiguous configurational assignment to the skeleton. Both epimers still showed a singlet for the carbon–methyl group at an abnormally high field (β-epimer, τ 9.54 p.p.m.; α-epimer, τ 9.50 p.p.m.). Consequently the AB *cis* stereochemistry of the photoadduct was preserved after the base catalyzed ring opening with simultaneous equilibration of the AB ring junction. We must therefore assume that this steric arrangement is more stable than the desired AB *trans* configuration. The operations which had to be executed at this point involved the shortening of the group R_1 in formula **12** by one carbon, epimerization of the AB ring junction and ring closure of the group R_1 with the nitrogen. The two epimers **12** were converted by enol acetylation to the two epimeric acetates **13**. These compounds were oxidized by osmic acid – periodate (6) to the noraldehydes **14** and oxidized further by the Jones method, followed by esterification with diazomethane to the acetoxy esters **15**. All these transformations were executed in excellent yields and the oily products were separated for characterization into the individual epimers by preparative t.l.c. The high-field methyl singlets in the n.m.r. spectra of these intermediates indicated that all of them had the same AB *cis* configuration. The structure and configuration of the β-epimer of compound **16** was furthermore rigorously confirmed when Dr. J. F. Blount, Hoffmann La Roche, Nutley, New Jersey, performed an X-ray analysis on a heavy atom derivative of this material (*cf.* ref. 2).

Mild alkaline hydrolysis of the epimers **15** yielded the hydroxy esters **16** and these were finally oxidized by the Jones method to the single crystalline diketo ester **17**, the synthesis of which was thus fully stereospecific.[4]

Ketalization of the diketone **17** with ethylene glycol and *p*-toluenesulfonic acid in benzene gave a quantitative yield of the crystalline ketal **18** which still showed the carbonyl maximum of the five-membered ring B ketone (1750 cm^{-1}) in the i.r. spectrum.

Finally the stage was set for the closure of the nitrogen ring. In compound **18**, of course, ring formation between the ester group and the nitrogen is sterically impossible because of the *cis* fusion of the rings A and B. However, we believed that in a solution sufficiently basic to enolize to a small extent the hydrogen next to the ring B ketone a certain amount of the AB *trans* isomer will be formed by reprotonation of the enolate ion. This material will then have opportunity to cyclize by lactam formation. Once cyclization occurs the system will be locked permanently and will be unable to go back to a *cisoid* derivative. This in fact turned out to be correct. The ketal ester **18** was heated under reflux with methanolic sodium methoxide and the beautifully crystalline lactam **19** was obtained in a yield of 80%. The i.r. spectrum of compound **19** showed carbonyl maxima at 1750 and 1675 cm^{-1} for the ketone and lactam and very significantly the carbon–methyl group singlet in the n.m.r. spectrum showed a normal expected chemical shift (τ 8.66 p.p.m.). In the *cisoid* ketal ester **18** the same carbon–methyl group singlet is located at τ 9.43 p.p.m.

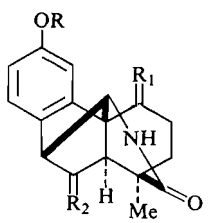

19 R = Me; R_1 = 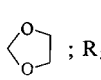 ; R_2 = =O

20 R = Me; R_1 = 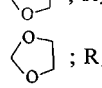 ; R_2 = H_2

21 R = H; R_1 = =O; R_2 = H_2

SCHEME 4

[4]Since $LiAlH_4$ reductions of the ring A keto group in the songorine skeleton are known to yield stereospecifically "natural" β-hydroxy derivatives it is clear that the configuration of the ring A hydroxyl will also present no problems in the future. The ketone **17** was obtained not only from the mixture of the two epimers **15** but also from each epimer separately.

Can. J. Chem. Downloaded from www.nrcresearchpress.com by 210.87.254.105 on 09/05/12
For personal use only.

Wolff–Kishner reduction of compound **19** proceeded with no difficulty and yielded 89% of the highly crystalline ketal **20**.[5] Finally heating of the ketal **20** under reflux in a mixture of hydrobromic and acetic acid gave the high melting crystalline phenol **21** in an 86% yield. The process described in the present communication can supply very simply and efficiently the aromatic intermediate not only for songorine, but also if suitable modifications are introduced for a variety of other diterpene alkaloids. The chief advantage of the method is that it automatically provides the typical substitution pattern in rings A and B of delphinine type alkaloids simultaneously with the construction of the skeleton. This is an advantage which obviously is not fully utilized in the case of songorine.

The question remains whether the process described is the simplest and most efficient one possible. We do not believe this to be the case. It will probably turn out to be feasible to find a one carbon anionic reagent which will add to the α,β-unsaturated ketone **10** with the correct stereochemistry. Thus it should be possible to proceed from compound **10** directly to products of the type **16**. However, while we plan to return to these experiments in the future the present form of the synthesis is already highly satisfactory for our present purposes.

Experimental

*Reduction of the Ester **1** to the Alcohol **2***

To a cold stirred mixture of $LiAlH_4$ (3 g) in anhydrous ether (120 ml), a solution of the ester **1** (9.96 g) in anhydrous ether (110 ml) was added dropwise. The reaction mixture was stirred for 1 h at room temperature, and worked up by careful addition of wet ether (1000 ml) and then of 10% aqueous sodium hydroxide (2 ml). The white precipitate was filtered and the filtrate was evaporated to give 8.56 g of the pure alcohol **2** as an oil homogeneous in t.l.c.

Mol. Wt. Calcd. for $C_{13}H_{14}O_2$: 202. Found (mass spectroscopy): 202.

I.r. ($CHCl_3$): 3625 cm^{-1} (hydroxyl); n.m.r. ($CDCl_3$): τ 3.18 (m, 2H, vinylic protons), 5.71 (s, 2H, methylene of primary alcohol), 6.26 (s, 3H, aromatic methoxyl), 7.73 p.p.m. (q, 2H, apex protons).

*Oxidation of **2** to the Aldehyde **3***

Trifluoroacetic acid (1.76 ml) was added to a solution of the primary alcohol **2** (8.46 g), *N,N'*-dicyclohexylcarbodiimide (26 g), anhydrous dimethylsulfoxide (70 ml) and pyridine (3.54 ml) in benzene (80 ml). The solution was stirred for 12 h at room temperature and diluted with ether (300 ml) and *n*-hexane (700 ml). A solution of oxalic acid (7.96 g) in methanol (53 ml) was added slowly with stirring in order to destroy the excess of diimide and the white precipitate was removed by filtration. The filtrate was washed several times with a saturated sodium chloride solution, dried over anhydrous magnesium sulfate and evaporated to dryness. Chromatography of the yellow residue on silica gel and elution with benzene yielded 7.12 g (85%) of the oily aldehyde **3** homogeneous in t.l.c.

Mol. Wt. Calcd. for $C_{13}H_{12}O_2$: 200. Found (mass spectroscopy): 200.

I.r. ($CHCl_3$): 2950, 2848, 2740, 1725 cm^{-1} (aldehyde); n.m.r. ($CDCl_3$): τ −1.28 (s, 1H, aldehyde), 3.10 (m, 2H, vinylic protons), 6.02 (m, 1H, benzylic bridgehead proton), 6.23 (s, 3H, aromatic methoxyl), 7.25 p.p.m. (d, 2H, apex protons).

*Preparation of the Alcohol **4***

A solution of 1-bromo-3-benzyloxybutane (4) (14.6 g, two-fold excess) in absolute ether (200 ml) was added dropwise to a warm stirred mixture of magnesium turnings (1.5 g) in absolute ether (20 ml) in a nitrogen atmosphere. When the addition of the bromide solution was complete, reflux was maintained for about ½ h.

A solution of the aldehyde **3** (6 g) in absolute ether (120 ml) was added dropwise under reflux to the well-stirred Grignard solution. When the addition was completed, the reaction mixture was heated under reflux in a nitrogen atmosphere for 12 h. After cooling, ether (500 ml) was added and the unreacted magnesium metal was removed. A 10% aqueous ammonium chloride solution (200 ml) was added to the reaction mixture under stirring. After removal of the aqueous layer, the ether solution was washed with water, dried, and evaporated to dryness. The residue was chromatographed on silica gel, using ether–benzene (v/v 1:9) as eluant. The yield of the oily alcohol **4** was quantitative (10.6 g).

Mol. Wt. Calcd. for $C_{24}H_{28}O_3$: 364.2031. Found (high resolution mass spectroscopy): 364.2039.

I.r. ($CHCl_3$): 3615, 3415 cm^{-1} (hydroxyl); n.m.r. ($CDCl_3$): τ 3.06 (m, 2H, vinylic protons), 5.45 (q, 2H, benzylic protons), 5.60 (unresolved m, 1H, hydrogen unshielded by secondary hydroxyl), 6.27 (s, 3H, aromatic methoxyl), 8.75 p.p.m. (d, 3H, methyl protons).

*Preparation of the Rearranged Compound **5***

A solution of the unsaturated compound **4** (10 g) and an excess of benzenesulfonyl azide (20 g) in anhydrous benzene (50 ml) was stirred for 6 days at room temperature. Sodium acetate (6 g) and glacial acetic acid (70 ml) were added in one portion and the mixture was stirred for 5 days at room temperature. The reaction mixture was diluted with chloroform (1000 ml) and washed with saturated aqueous sodium bicarbonate (2 × 200 ml), followed by saturated aqueous sodium chloride. The organic layer was dried over anhydrous magnesium sulfate. Evaporation of the solvent gave a yellow residue which was subjected to chromatography on silica gel. Elution with benzene–ether (8:2) gave 13.6 g (84%) of the crystalline product **5**.

This material was a mixture (1:1) of two epimers, when analyzed by t.l.c. on silica gel using benzene–ether (7:4)

[5]In a derivative similar to **19** (R_1 = —OH, R_2 = =O) desulfurization of a thioketal and Wolff–Kishner reduction yielded the same ring B desoxy compound in both cases in a high yield.

Can. J. Chem. Downloaded from www.nrcresearchpress.com by 210.87.254.105 on 09/05/12
For personal use only.

as solvent. A small portion (100 mg) was separated by preparative t.l.c. and two epimeric alcohols were obtained in equal amount: the β-epimer (50 mg) with a larger R_F value and the α-epimer (50 mg) with a smaller R_F value. Both epimers were recrystallized from ether and they were homogeneous in t.l.c.

(*i*) β-Epimer, m.p. 146–147 °C.

Anal. Calcd. for $C_{32}H_{37}O_7NS$ (mol. wt. 579): C, 66.29; H, 6.43; N, 2.42. Found (mass spectroscopy 579): C, 66.30; H, 6.42; N, 2.52.

I.r. ($CHCl_3$): 3565 (hydroxyl), 3385 (NH), 1735 cm^{-1} (acetate); n.m.r. ($CDCl_3$): τ 2.86 (d, J = 8 Hz, 1H, hydrogen *meta* to aromatic methoxyl), 3.23 (d, J = 2.5 Hz, 1H, hydrogen *ortho* to aromatic methoxyl), 3.41 (q, J = 8 Hz, J = 2.5 Hz, 1H, hydrogen *ortho* to aromatic methoxyl), 4.08 (d, 1H, —N(H)—), 5.30 (m, 1H, proton unshielded by acetoxyl), 5.81 (m, 1H, proton unshielded by hydroxyl), 6.82 (broad s, 1H, benzylic bridgehead proton), 7.88 p.p.m. (s, 3H, acetoxy methyl).

(*ii*) α-Epimer, m.p. 167.5–168 °C.

Anal. Calcd. for $C_{32}H_{37}O_7NS$ (mol. wt. 579): C, 66.29; H, 6.43; N, 2.42. Found (mass spectroscopy 579): C, 66.14; H, 6.42; N, 2.54. The mass spectra of both epimers were identical.

I.r. ($CHCl_3$): 3455 (hydroxyl), 3375 (NH), 1740 cm^{-1} (acetate); n.m.r. ($CDCl_3$): τ 2.91 (d, J = 8 Hz, 1H, hydrogen *meta* to aromatic methoxyl), 2.99 (d, J = 2.5 Hz, 1H, hydrogen *ortho* to aromatic methoxyl), 3.37 (q, J = 8 Hz, J = 2.5 Hz, 1H, hydrogen *ortho* to aromatic methoxyl), 4.11 (d, 1H, —N(H)—), 5.33 (m, 1H, proton unshielded by acetoxyl), 5.85 (m, 1H, proton unshielded by hydroxyl), 6.98 (broad s, 1H, benzylic bridgehead proton), 7.89 p.p.m. (s, 3H, acetoxy methyl).

Conversion of Compound **5** *to the N-Acetyl Amide* **6**

To a stirred solution of compound **5** (13 g) in anhydrous dioxane (400 ml), an excess of $LiAlH_4$ (15 g) was added in one portion. The mixture was refluxed under nitrogen for 27 h. After cooling, the excess of hydride was decomposed by careful addition of wet ether (600 ml) and of 10% aqueous sodium hydroxide (6 ml). The white precipitate was removed by filtration and washed with tetrahydrofuran (8 × 100 ml). The combined filtrates were evaporated under reduced pressure to give 8.84 g of material which was immediately acetylated with acetic anhydride (20 ml) and anhydrous pyridine (80 ml) for 24 h at room temperature. Most of the solvent was evaporated *in vacuo* and the residue was dissolved in chloroform (1500 ml). The chloroform solution was washed with dilute hydrochloric acid, dilute aqueous sodium bicarbonate, and water. After drying over magnesium sulfate, evaporation gave a yellow residue which was chromatographed on silica gel. Elution with ether–benzene (3:7) yielded 9.98 g (85%) of the *N*-acetyl amide **6** as a thick oil. For analysis, the two epimers were separated by preparative t.l.c.

(*i*) β-Epimer (larger R_F value).

Mol. Wt. Calcd. for $C_{30}H_{37}O_7N$: 523.2570. Found (high resolution mass spectroscopy): 523.2566.

I.r. ($CHCl_3$): 3461 (NH), 1738 (acetate), 1678 cm^{-1} (amide); n.m.r. ($CDCl_3$): τ 4.63 (m, 1H, proton deshielded by acetoxyl), 5.26 (m, 1H, proton deshielded by acetoxyl), 6.25 (s, 3H, aromatic methoxyl), 6.68 (broad s, 1H, benzylic bridgehead proton), 7.91 (s, 3H, acetoxy methyl), 7.94 (s, 3H, acetoxy methyl), 7.99 (s, 3H, —N(C=O)—CH_3), 8.84 p.p.m. (d, 3H, methyl).

(*ii*) α-Epimer (smaller R_F value).

Mol. Wt. Calcd. for $C_{30}H_{37}O_7N$: 523.2570. Found (high resolution mass spectroscopy): 523.2557. The mass spectrum was identical with the mass spectrum of the β-epimer.

I.r. ($CHCl_3$): 3462 (NH), 1737 (acetate), 1678 cm^{-1} (amide); n.m.r. ($CDCl_3$): τ 4.45 (m, 1H, proton deshielded by acetoxyl), 5.21 (m, 1H, proton deshielded by acetoxyl), 6.26 (s, 3H, aromatic methoxyl), 6.59 (broad s, 1H, benzylic bridgehead proton), 7.90 (s, 6H, two acetoxy methyl), 7.99 (s, 3H, —N(C=O)—CH_3), 8.81 p.p.m. (d, 3H, methyl).

Selective Hydrolysis of the Diacetate **6** *to the Hydroxyacetate* **7**

The diacetate **6** (9 g) was dissolved in methanolic potassium carbonate (400 ml, p*H* 8.5) and the reaction mixture was stirred at room temperature. The course of the reaction was followed by t.l.c. In this case the reaction was allowed to proceed for 16 h, after which time the reaction mixture was neutralized with 5% hydrochloric acid (2 ml) and poured into saturated aqueous sodium chloride (600 ml). It was extracted with chloroform (5 × 200 ml) and the combined extracts were washed with saturated sodium chloride, dried, and evaporated to dryness. The hydroxyacetate **7** (8.16 g) was isolated as the sole product and the yield was quantitative. A small portion (100 mg) of the material was taken out and the two epimers separated by preparative t.l.c. (methanol–ether 4:96) as colorless foam homogeneous in t.l.c. Ratio of the epimers was 1:1.

(*i*) β-Isomer (larger R_F value).

Mol. Wt. Calcd. for $C_{28}H_{35}O_6N$: 481.2464. Found (high resolution mass spectroscopy): 481.2472.

I.r. ($CHCl_3$): 3625 (hydroxyl), 3410 (NH), 1730 (acetate), 1675 cm^{-1} (amide); n.m.r. ($CDCl_3$): τ 4.63 (m, 1H, proton unshielded by acetoxyl), 6.21 (s, 3H, aromatic methoxyl), 6.89 (broad s, 1H, benzylic bridgehead proton), 7.92 (s, 3H, acetoxy methyl), 8.03 (s, 3H, —N(C=O)—CH_3), 8.81 p.p.m. (d, 3H, methyl).

(*ii*) α-Epimer (smaller R_F value).

Mol. Wt. Calcd. for $C_{28}H_{35}O_6N$: 481.2464. Found (high resolution mass spectroscopy): 481.2472. The mass spectra of both epimers were identical.

I.r. ($CHCl_3$): 3610 (hydroxyl), 3425 (NH), 1730 (acetate), 1675 cm^{-1} (amide); n.m.r. ($CDCl_3$): τ 4.70 (m, 1H, proton unshielded by acetoxyl), 6.25 (s, 3H, aromatic methoxyl), 6.90 (broad s, 1H, benzylic bridgehead proton), 7.94 (s, 3H, acetoxy methyl), 8.04 (s, 3H, —N(C=O)—CH_3), 8.80 p.p.m. (d, 3H, methyl).

Can. J. Chem. Downloaded from www.nrcresearchpress.com by 210.87.254.105 on 09/05/12
For personal use only.

Preparation of the Acetoxy Diol 8

To a solution of the benzyloxy ether **7** (8 g) in methanol (200 ml), 10% palladium on charcoal (1 g) was added. The mixture was hydrogenated at atmospheric pressure and room temperature overnight. The catalyst was filtered off and washed with methanol. The methanolic solution was evaporated under reduced pressure and the diol **8** (6.4 g) was obtained as a colorless foam in a quantitative yield. For analysis, the two epimers were separated by preparative t.l.c.

(*i*) β-Epimer (larger R_F value).

Mol. Wt. Calcd. for $C_{21}H_{29}O_6N$: 391.1995. Found (mass spectroscopy): 391.2001.

I.r. ($CHCl_3$): 3610, 3460 (hydroxyl), 3400 (NH), 1731 (acetate), 1670 cm^{-1} (amide); n.m.r. ($CDCl_3$): τ 2.16 (d, J = 9 Hz, 1H, —N—H), 4.62 (m, 1H, proton unshielded by acetoxyl), 5.75 (d, J = 9 Hz, 1H, apex proton), 6.20 (s, 3H, aromatic methoxyl), 6.85 (broad s, 1H, benzylic bridgehead proton), 7.91 (s, 3H, acetoxy methyl), 7.98 (s, 3H, —N—C(=O)—CH_3), 8.82 p.p.m. (d, 3H, methyl).

(*ii*) α-Epimer (smaller R_F value).

Mol. Wt. Calcd. for $C_{21}H_{29}O_6N$: 391.1995. Found (mass spectroscopy): 391.2001. The mass spectra of both epimers were identical.

I.r. ($CHCl_3$): 3610 (hydroxyl), 3408 (NH), 1733 (acetate), 1670 cm^{-1} (amide); n.m.r. ($CDCl_3$): τ 2.49 (d, J = 9 Hz, 1H, —NH), 4.46 (m, 1H, proton unshielded by acetoxyl), 5.71 (d, J = 9 Hz, 1H, apex proton), 6.23 (s, 3H, aromatic methoxyl), 6.90 (broad s, 1H, benzylic bridgehead proton), 7.93 (s, 3H, acetoxy methyl), 8.05 (s, 3H, —N—C(=O)—CH_3), 8.84 p.p.m. (d, 3H, methyl).

Preparation of the Diketone 9

A solution of the diol **8** (6.4 g) in pyridine (40 ml) was added slowly at room temperature to a stirred solution of chromium trioxide (7 g) in pyridine (50 ml). The mixture was stirred for 2 days at room temperature after which time it was diluted with ether (400 ml) and chloroform (100 ml). The brown precipitate was filtered and washed with ether. The combined filtrates were washed with dilute hydrochloric acid, 10% aqueous sodium bicarbonate and finally with water. Evaporation of the solvent and removal of the yellow color by filtration through a short neutral alumina column (100 g, activity grade II) gave 5.1 g (80%) of the diketone **9** as white crystals. The two epimers were separated by preparative t.l.c. (ether–methanol 9:1) and recrystallized for analysis. The ratio of the epimers was 1:1.

(*i*) β-Epimer (larger R_F value), m.p. 115°.

Anal. Calcd. for $C_{20}H_{23}O_6N$ (mol. wt. 387): C, 65.10; H, 6.50; N, 3.61. Found (mass spectroscopy, 387): C, 64.98; H, 6.52; N, 3.60.

I.r. ($CHCl_3$): 3430 (NH), 1750 (five-membered ketone), 1720 (ketone), 1680 cm^{-1} (amide); n.m.r. ($CDCl_3$): τ 4.64 (m, 1H, proton deshielded by acetoxyl), 6.17 (s, 3H, aromatic methoxyl), 6.40 (broad s, 1H, benzylic bridgehead proton), 7.84 (s, 3H, —C(=O)—CH_3), 7.87 (s, 3H, acetoxy methyl), 7.97 p.p.m. (s, 3H, —N—C(=O)—CH_3).

(*ii*) α-Epimer (smaller R_F value), m.p. 175°.

Anal. Calcd. for $C_{20}H_{23}O_6N$ (mol. wt. 387): C, 65.10; H, 6.50; N, 3.61. Found (mass spectroscopy 387): C, 64.99; H, 6.47; N, 3.58. The mass spectra of both epimers were identical.

I.r. ($CHCl_3$): 3450 (NH), 1750 (five-membered ketone), 1720 (ketone), 1680 cm^{-1} (amide); n.m.r. ($CDCl_3$): τ 4.30 (m, 1H, proton deshielded by acetoxyl), 6.07 (s, 3H, aromatic methoxyl), 6.30 (broad s, 1H, benzylic bridgehead proton), 7.80 (s, 3H, —C(=O)—CH_3), 7.84 (s, 3H, acetoxy methyl), 8.00 p.p.m. (s, 3H, —N—C(=O)—CH_3).

Preparation of the α,β-Unsaturated Ketone 10

A solution of the diketone **9** (8.8 g) in saturated methanolic potassium carbonate (200 ml) was refluxed for 10 h in a nitrogen atmosphere. The mixture was neutralized by careful addition of dilute hydrochloric acid. Most of the solvent was removed *in vacuo* and the residue was suspended in saturated aqueous sodium chloride (300 ml). The aqueous phase was extracted with methylene dichloride (4 × 200 ml) and the combined extracts were washed with saturated sodium chloride and dried over anhydrous magnesium sulfate. After evaporation of the solvent, the ketone **10** was obtained by crystallization from ether–chloroform. The yield was 6.62 g (88%). This crystalline material was a mixture (1:1) of two epimers when examined by t.l.c. on silica gel using chloroform–ether–methanol (70:30:6) as developing solvent. For analysis, samples of the two epimers were obtained by preparative t.l.c. and crystallized from ether.

(*i*) β-Epimer (larger R_F value), m.p. 205°.

Anal. Calcd. for $C_{19}H_{21}O_4N$ (mol. wt. 327): C, 69.69; H, 6.40; N, 4.20. Found (mass spectroscopy 327): C, 69.71; H, 6.39; N, 4.18.

I.r. ($CHCl_3$): 3550 (hydroxyl), 3400 (NH), 1725 (conjugated five-membered ketone), 1660 cm^{-1} (conjugated double bond and amide); u.v. (EtOH): λ_{max} 241[6] nm (log ε 4.01); n.m.r. ($CDCl_3$): τ 2.81 (d, J = 8 Hz, 1H, —N—H), 2.87 (d, J = 10 Hz, 1H, hydrogen-*meta* to methoxyl), 3.24 (d, J = 3 Hz, 1H, hydrogen-*ortho* to methoxyl), 3.32 (q, J = 10 Hz, J = 3 Hz, hydrogen-*ortho* to methoxyl), 5.60 (d, J = 8 Hz, 1H, apex proton), 6.24 (s, 3H, aromatic methoxyl), 6.30 (broad s, 1H, benzylic bridgehead proton), 7.87 (s, 3H, >C=C(—CH_3)—), 8.04 p.p.m. (s, 3H, —N—C(=O)—CH_3).

(*ii*) α-Epimer (smaller R_F value), m.p. 242°.

Mol. Wt. Calcd. for $C_{19}H_{21}O_4N$: 327.1471. Found

[6]These values were in error in the preliminary communication, *cf.* (2).

Can. J. Chem. Downloaded from www.nrcresearchpress.com by 210.87.254.105 on 09/05/12
For personal use only.

(high resolution mass spectroscopy): 327.1465. The mass spectra of both epimers were identical.

I.r. ($CHCl_3$): 3500 (hydroxyl), 3400 (NH), 1725 (conjugated five-membered ketone), 1660 cm^{-1} (conjugated double bond and amide); u.v. (EtOH): λ_{max} 239[6] nm (log ε 4.02); n.m.r. ($CDCl_3$): τ 2.81 (d, J = 10 Hz, 1H, hydrogen-*meta* to methoxyl), 2.87 (d, J = 3 Hz, 1H, hydrogen-*ortho* to methoxyl), 3.20 (d, J = 9 Hz, 1H, —N—H), 3.40 (q, J = 10 Hz, J = 3 Hz, 1H, hydrogen-*ortho* to methoxyl), 5.40 (d, J = 9 Hz, 1H, apex proton), 6.20 (s, 3H, aromatic methoxyl), 6.50 (broad s, 1H, benzylic bridgehead proton), 7.90 (s, 3H, —C=C—CH_3), 7.97 p.p.m. (s, 3H, —N—C(=O)—CH_3).

Preparation of the Photoadduct ***11***

To a solution of the α,β-unsaturated ketone **10** (15 g) in freshly distilled tetrahydrofuran (2000 ml), a great excess of distilled vinyl acetate (1000 ml) was added. The solution was irradiated continuously with a 400 W Hanovia Mercury lamp (Pyrex was used as filter) at −20° for 12 h under nitrogen. After evaporation of the solvent, the photoadduct **11** was purified by crystallization from ether. 7.4 g of the crystalline photoadduct was obtained and chromatography of the mother liquor on silica gel gave another 9.52 g. The yield was thus 16.92 g (89%). For analysis, the two epimers were separated by preparative t.l.c. on silica gel. The α-epimer crystallized from ether (m.p. 254–256°) while the β-epimer when pure remained a white foam. Both epimers were homogeneous in t.l.c.

(*i*) β-Epimer.

Mol. Wt. Calcd. for $C_{23}H_{27}O_6N$: 413. Found (mass spectroscopy): 413. The mass spectra of both epimers were completely identical.

I.r. ($CHCl_3$): 3500 (hydroxyl), 3420 (NH), 1750 (five-membered ketone), 1740 (acetate), 1670 cm^{-1} (amide); n.m.r. ($CDCl_3$): τ 3.00 (d, 1H, —N—H), 4.56 (q, 1H, proton unshielded by acetoxyl), 5.07 (t, 1H, proton unshielded by hydroxyl), 5.80 (d, 1H, apex proton), 6.11 (broad s, 1H, benzylic bridgehead proton), 6.17 (s, 3H, aromatic methoxyl, 7.84 (s, 3H, acetoxy methyl), 8.10 (s, 3H, —N—C(=O)—CH_3), 9.70 p.p.m. (s, 3H, methyl shielded by benzene ring).

(*ii*) α-Epimer.

Anal. Calcd. for $C_{23}H_{27}O_6N$ (mol. wt. 413): C, 66.81; H, 6.58; N, 3.39. Found (mass spectroscopy, 413): C, 66.80; H, 6.59; N, 3.37.

I.r. ($CHCl_3$): 3500 (hydroxyl), 3440 (NH), 1750 (five-membered ketone), 1738 (acetate), 1670 cm^{-1} (amide); n.m.r. ($CDCl_3$): τ 3.13 (d, 1H, —N—H), 4.54 (q, 1H, proton unshielded by acetoxyl), 5.10 (t, 1H, proton unshielded by hydroxyl), 5.74 (d, 1H, apex proton), 6.20 (s, 3H, aromatic methoxyl), 6.37 (broad s, 1H, benzylic bridgehead proton), 7.87 (s, 3H, acetoxy methyl), 8.07 (s, 3H, —N—C(=O)—CH_3), 9.66 p.p.m. (s, 3H, methyl shielded by benzene ring).

Hydrolysis of the Photoadduct ***11*** *to the Aldehyde* ***12***

The photoadduct **11** (16 g) was hydrolyzed in 1% methanolic potassium hydroxide (120 ml) for ½ h at room temperature. The mixture was poured into water and extracted with chloroform (5 × 200 ml). The combined extracts were washed with water and dried over magnesium sulfate. Evaporation of the solvent gave 14.1 g of the aldehyde **12** as a foam. The yield was quantitative. The material consisted of two epimers (1:1) and a small portion was separated by preparative t.l.c. Both epimers were foams homogeneous in t.l.c.

(*i*) β-Epimer.

Mol. Wt. Calcd. for $C_{21}H_{25}O_5N$: 371.1674. Found (high resolution mass spectroscopy): 371.1679.

I.r. ($CHCl_3$): 3450–3300 (hydroxyl and NH), 2710 (aldehyde C—H), 1740 (five-membered ketone), 1715 (aldehyde), 1670 cm^{-1} (amide); n.m.r. ($CDCl_3$): τ −0.17 (t, 1H, aldehydic proton), 2.40 (d, J = 3 Hz, —N—H), 5.34 (broad s, 1H, proton unshielded by hydroxyl), 5.97 (d, J = 3 Hz, apex proton), 6.20 (s, 3H, aromatic methoxyl), 7.30 (q, 2H, —C—CH_2—CHO), 8.00 (s, 3H, —N—C(=O)—CH_3), 9.54 p.p.m. (s, 3H, tertiary methyl shielded by benzene ring).

(*ii*) α-Epimer.

Mol. Wt. Calcd. for $C_{21}H_{25}O_5N$: 371.1674. Found (high resolution mass spectroscopy): 371.1677. The mass spectra of both epimers were identical.

I.r. ($CHCl_3$): 3450–3300 (hydroxyl and NH), 2710 (aldehyde C—H), 1740 (five-membered ketone), 1715 (aldehyde), 1670 cm^{-1} (amide); n.m.r. ($CDCl_3$): τ −0.24 (t, 1H, aldehydic proton), 2.37 (d, J = 7 Hz, 1H, —N—H), 5.70 (d, J = 7 Hz, 1H, apex proton), 6.03 (broad s, 1H, proton unshielded by hydroxyl), 6.20 (s, 3H, aromatic methoxyl), 7.40 (broad s, 2H, —C—CH_2—CHO), 7.94 (s, 3H, —N—C(=O)—CH_3), 9.50 p.p.m. (s, 3H, tertiary methyl shielded by benzene ring).

Preparation of the Enol Acetate ***13***

A mixture of the aldehyde **12** (14 g), freshly fused sodium acetate (9 g) and distilled acetic anhydride (600 ml) was heated under reflux for 8 h under nitrogen. After removing the solvent *in vacuo* below 100°, a large amount of ether (1000 ml) and water (500 ml) was added to the residue. The organic layer was collected and dried over anhydrous magnesium sulfate. Evaporation of the solvent gave a yellow residue which was chromatographed on silica gel. Elution with chloroform–methanol (98:2) gave

13.2 g of the product **13**. For analysis, the two epimers were isolated by preparative t.l.c.; both were thick oils homogeneous in t.l.c.

(*i*) β-Epimer.

Mol. Wt. Calcd. for $C_{25}H_{29}O_7N$: 455. Found (mass spectroscopy): 455.

I.r. ($CHCl_3$): 3400 (NH), 1750 (ketone and acetate), 1680 cm^{-1} (amide); n.m.r. ($CDCl_3$): τ 2.75 (d, J = 12 Hz, 1H, vinylic proton), 4.00 (d, J = 12 Hz, 1H, vinylic proton), 4.23 (broad s, 1H, proton unshielded by acetoxyl), 6.20 (s, 3H, aromatic methoxyl), 6.34 (broad s, 1H, benzylic bridgehead proton), 7.90 (s, 6H, acetoxy methyl), 8.04 (s, 3H, —N(—C(=O)—CH_3)—), 9.54 p.p.m. (s, 3H. tertiary methyl shielded by benzene ring).

(*ii*) α-Epimer.

Mol. Wt. Calcd. for $C_{25}H_{29}O_7N$: 455. Found (mass spectroscopy): 455. The mass spectra of both epimers were completely identical.

I.r. ($CHCl_3$): 3400 (NH), 1750 (ketone and acetate), 1680 cm^{-1} (amide); n.m.r. ($CDCl_3$): τ 2.89 (d, J = 12 Hz, 1H, vinylic proton), 4.14 (d, J = 12 Hz, 1H, vinylic proton), 5.07 (t, 1H, proton unshielded by acetoxyl), 6.14 (aromatic methoxyl), 6.37 (broad s, 1H, benzylic bridgehead proton), 7.87 (s, 6H, acetoxy methyl), 8.04 (s, 3H, —N(—C(=O)—CH_3)—), 9.47 p.p.m. (s, 3H, tertiary methyl shielded by benzene ring).

*Cleavage of Compound **13** to the Nor-aldehyde **14***

A mixture of the enol acetate **13** (13.2 g), osmium tetroxide (1.2 g) and acetic acid (5 ml) in tetrahydrofuran (600 ml) was stirred for 3½ h at room temperature. During this process the mixture turned dark, and sodium metaperiodate powder (12 g) in water (50 ml) was added to the dark solution. The mixture was stirred for an additional 4 h at room temperature. The precipitate was filtered off and washed thoroughly with tetrahydrofuran (200 ml). The filtrate was partially evaporated *in vacuo* and the residue was dissolved in chloroform (1000 ml). The chloroform solution was washed with water (3 × 400 ml), dried and evaporated to dryness. Column chromatography of the residue on silica gel yielded 8 g (70%) of the product **14** as a waxy material. A small portion was separated by preparative t.l.c. Both epimers were thick oils homogeneous in t.l.c. in several solvent systems.

(*i*) β-Epimer.

Mol. Wt. Calcd. for $C_{22}H_{25}O_6N$: 399.1704. Found (high resolution mass spectroscopy): 399.1709.

I.r. ($CHCl_3$): 3450 (NH), 2820, 2710 (aldehyde C—H), 1740 (ketone and acetate), 1730 (aldehyde), 1680 cm^{-1} (amide); n.m.r. ($CDCl_3$): τ −0.40 (s, 1H, aldehyde), 4.27 (m, 1H, proton unshielded by acetoxyl), 6.20 (s, 3H, aromatic methoxyl), 6.37 (broad s, 1H, benzylic bridgehead proton), 7.94 (s, 3H, acetoxy methyl), 8.04 (s, 3H, —N(—C(=O)—CH_3)—), 9.70 p.p.m. (s, 3H, tertiary methyl shielded by benzene ring).

(*ii*) α-Epimer.

Mol. Wt. Calcd. for $C_{22}H_{25}O_6N$: 399. Found (mass spectroscopy): 399. The mass spectra of both epimers were entirely identical.

I.r. ($CHCl_3$): 3450, 3400 (NH), 2820, 2710 (aldehyde C—H), 1740 (ketone and acetate), 1735 (aldehyde), 1685 cm^{-1} (amide); n.m.r. $CDCl_3$): τ −0.40 (s, 1H, aldehyde), 5.00 (t, 1H, proton unshielded by acetoxyl), 6.17 (s, 3H, aromatic methoxyl), 6.30 (broad s, 1H, benzylic bridgehead proton), 7.87 (s, 3H, acetoxy methyl), 8.00 (s, 3H, —N(—C(=O)—CH_3)—), 9.40 p.p.m. (s, 3H, tertiary methyl shielded by benzene ring).

*Conversion of the Aldehyde **14** to the Keto Ester **15***

Jones' reagent (5 ml) was added dropwise to a stirred solution of the aldehyde **14** (8.56 g) in 10% aqueous sulfuric acid (5 ml) and acetone (50 ml). The mixture was stirred at room temperature for 1 h. Saturated aqueous sodium chloride was added and the solution was extracted exhaustively with methylene dichloride. The combined extracts were dried over anhydrous sodium sulfate and evaporated to give 8.61 g of the crude acid which was converted to the methyl ester by treatment with an excess of diazomethane in methanol–ether at room temperature. Removal of the solvent and chromatography of the crude product on silica gel gave 7.43 g (80%) of the keto ester **15** as a thick oil. For analysis, the two epimers were separated by preparative t.l.c. Both epimers were thick oils, homogeneous in t.l.c.

(*i*) β-Epimer.

Mol. Wt. Calcd. for $C_{23}H_{27}O_7N$: 429.1816. Found (high resolution mass spectroscopy): 429.1819.

I.r. ($CHCl_3$): 3350 (NH), 1750 (ketone), 1728, 1720 (acetate, ester), 1680 cm^{-1} (amide); n.m.r. ($CDCl_3$): τ 4.20 (m, 1H, proton unshielded by acetoxyl), 6.17 (s, 3H, aromatic methoxyl), 6.24 (s, 3H, —C(=O)—OCH_3), 6.34 (broad s, 1H, benzylic bridgehead proton), 7.84 (s, 3H, acetoxy methyl), 7.94 (s, 3H, —N(—C(=O)—CH_3)—), 9.44 p.p.m. (s, 3H, tertiary methyl shielded by benzene ring).

(*ii*) α-Epimer.

Mol. Wt. Calcd. for $C_{23}H_{27}O_7N$: 429.1816. Found (high resolution mass spectroscopy): 429.1818. The mass spectra of both epimers were identical.

I.r. ($CHCl_3$): 3420 (NH), 1750 (ketone), 1735, 1730 (acetate, ester), 1690 cm^{-1} (amide); n.m.r. ($CDCl_3$): τ 4.96 (t, 1H, proton unshielded by acetoxyl), 6.15 (s, 3H, aromatic methoxyl), 6.26 (s, 3H, —C(=O)—OCH_3), 7.90 (s, 3H, acetoxy methyl), 7.97 (s, 3H, —N(—C(=O)—CH_3)—), 9.37 p.p.m. (s, 3H, tertiary methyl shielded by benzene ring).

Can. J. Chem. Downloaded from www.nrcresearchpress.com by 210.87.254.105 on 09/05/12
For personal use only.

Can. J. Chem. Downloaded from www.nrcresearchpress.com by 210.87.254.105 on 09/05/12
For personal use only.

Preparation of the Hydroxy Ester ***16***

The acetoxy ester **15** (7.2 g) was dissolved in methanol (30 ml) and 1% aqueous potassium hydroxide (10 ml) was added. The solution was stirred for 3 h at room temperature. After work-up in the usual manner, 6.24 g (96%) of the hydroxy ester **16** was obtained as a colorless oil. The analytical samples of the two epimers were obtained by preparative t.l.c. and both were oils homogeneous in t.l.c.

(*i*) β-Epimer.

Mol. Wt. Calcd. for $C_{21}H_{25}O_6N$: 387.1682. Found (high resolution mass spectroscopy): 387.1684.

I.r. ($CHCl_3$): 3500 (hydroxyl), 3440 (NH), 1750 (ketone), 1725 (ester), 1670 cm^{-1} (amide); n.m.r. ($CDCl_3$): τ 2.34 (d, J = 8 Hz, 1H, —N(H)—), 5.34 (broad s, 1H, proton unshielded by hydroxyl), 5.87 (d, J = 8 Hz, 1H, apex proton), 6.20 (s, 3H, aromatic methoxyl), 6.30 (s, 3H, —C(=O)—OCH_3), 7.97 (s, 3H, —N(—C(=O)—CH_3)—), 9.44 p.p.m. (s, 3H, tertiary methyl shielded by benzene ring).

(*ii*) α-Epimer.

Mol. Wt. Calcd. for $C_{21}H_{25}O_6N$: 387.1682. Found (high resolution mass spectroscopy): 387.1685. The mass spectra of both epimers were completely identical.

I.r. ($CHCl_3$): 3500 (hydroxyl), 3440 (NH), 1750 (ketone), 1725 (ester), 1670 cm^{-1} (amide); n.m.r. ($CDCl_3$) τ 2.33 (d, J = 7 Hz, 1H, —NH), 5.69 (d, J = 7 Hz, 1H, apex proton), 6.11 (t, 1H, proton unshielded by hydroxyl), 6.19 (s, 3H, aromatic methoxyl), 6.30 (s, 3H, —C(=O)—OCH_3), 7.90 (s, 3H, —N(—C(=O)—CH_3)—), 9.41 p.p.m. (s, 3H, tertiary methyl shielded by benzene ring).

Oxidation of ***16*** *to the Diketone* ***17***

Compound **16** (6.24 g) dissolved in acetone (80 ml) was oxidized at 0° with a slight excess of Jones' reagent for 2 h. The reaction mixture was poured into water and the product was extracted with chloroform. The chloroform solution was washed with water and dried over anhydrous magnesium sulfate. Evaporation of the solvent gave 5.18 g (83%) of the diketone **17** which was crystallized from ether–chloroform as white crystals homogeneous in t.l.c. in several solvent systems. An analytical sample was prepared by recrystallization from ether, and melted at 109°.

Anal. Calcd. for $C_{21}H_{23}O_6N$ (mol. wt. 385): C, 65.45; H, 6.02; N, 3.64. Found (mass spectroscopy, 385): C, 65.41; H, 6.09; N, 3.63.

I.r. ($CHCl_3$): 3450 (NH), 1750 (five-membered ketone), 1725 (ester), 1710 (six-membered ketone), 1680 cm^{-1} (amide); n.m.r. ($CDCl_3$): τ 2.98 (d, J = 7 Hz, 1H, —N(H)—), 5.33 (d, J = 7 Hz, 1H, apex proton), 4.03 (broad s, 1H, benzylic bridgehead proton), 6.20 (s, 3H, aromatic methoxyl), 6.23 (s, 3H, —C(=O)—OCH_3), 8.03 (s, 3H, —N(—C(=O)—CH_3)—), 9.40 p.p.m. (s, 3H, tertiary methyl shielded by benzene ring).

Preparation of the Keto Ketal ***18***

The diketone **17** (5.18 g) was dissolved in anhydrous benzene (300 ml) to which ethylene glycol (2 ml) and *p*-toluenesulfonic acid (850 mg) were added. The solution was heated under reflux for 1½ h with a water separator. The cooled reaction mixture was worked up by the usual procedure. The ketal **18** was crystallized from ether and melted at 245°. The yield was quantitative.

Anal. Calcd. for $C_{23}H_{27}O_7N$: C, 64.32; H, 6.33; N, 3.26. Found: C, 64.29; H, 6.32; N, 3.29.

I.r. ($CHCl_3$): 3410 (NH), 1750 (five-membered ketone), 1720 (ester), 1670 cm^{-1} (amide); n.m.r. ($CDCl_3$): τ 5.93 (m, 4H, dioxolane hydrogen), 6.20 (s, 3H, aromatic methoxyl), 6.25 (s, 3H, —C(=O)—OCH_3), 8.00 (s, 3H, —N(—C(=O)—CH_3)—), 9.43 p.p.m. (s, 3H, tertiary methyl shielded by benzene ring).

Cyclization of Compound ***18*** *to the Keto Lactam* ***19***

A solution of the keto ester **18** (5.71 g) in absolute methanol (50 ml) was added to a solution of sodium methoxide prepared by dissolving sodium metal (2 g) in absolute methanol (50 ml). The mixture was heated under reflux for 26 h in a nitrogen atmosphere. Most of the methanol was removed *in vacuo* and the residue was dissolved in ice water (200 ml). The solution was extracted with chloroform (4 × 150 ml) and the combined extracts were washed with water, dried, and evaporated to dryness. Crystallization of the solid residue from chloroform–ether gave the pure lactam **19**, m.p. 264°. The yield was 3.75 g (80%).

Anal. Calcd. for $C_{20}H_{21}O_5N$: C, 67.59; H, 5.96; N, 3.94. Found: C, 67.55; H, 5.87; N, 3.97.

I.r. ($CHCl_3$): 3400 (NH), 1750 (ketone), 1675 cm^{-1} (lactam); n.m.r. ($CDCl_3$): τ 5.80 (m, 4H, dioxolane hydrogen), 6.23 (s, 3H, aromatic methoxyl), 8.66 (s, 3H, tertiary methyl).

Wolff–Kishner Reduction of the Keto Lactam ***19***

A mixture of the lactam **19** (3.6 g), 95% hydrazine (48 g), hydrazine dihydrochloride (9.6 g) and triethylene glycol (150 ml) was heated at 130° (oil bath temperature) for 4 h with stirring. Potassium hydroxide pellets (13 g) were added in portions with stirring and the temperature was gradually raised to 190° (oil bath). The solution was stirred at that temperature for 5 h. The whole process was operated in a nitrogen atmosphere. After cooling, saturated aqueous sodium chloride (200 ml) was added and the mixture was extracted with chloroform (4 × 200 ml). The chloroform extracts were washed with water, dried, and evaporated to dryness. The pure reduction product **20** (3.1 g, 89%) was obtained by crystallization from ether and it melted at 233°.

Anal. Calcd. for $C_{20}H_{23}O_4N$ (mol. wt. 341): C, 70.36;

H, 6.79; N, 4.10. Found (mass spectroscopy, 341): C, 70.49; H, 6.80; N, 4.06.

I.r. ($CHCl_3$): 3400 (NH), 1665 cm^{-1} (lactam); n.m.r. ($CDCl_3$): τ 3.63 (broad s, 1H, —NH), 5.80 (m, 4H, dioxolane hydrogen), 6.20 (s, 3H, aromatic methoxyl), 6.46 (broad s, 1H, apex proton), 6.83 (m, 1H, benzylic bridgehead proton), 8.76 p.p.m. (s, 3H, tertiary methyl).

Preparation of the Phenol ***21***

A solution of compound **20** (2.6 g) in 48% hydrobromic acid (50 ml) and glacial acetic acid (35 ml) was refluxed for 4 h under nitrogen. After cooling, water was added and the product was extracted with methylene dichloride. Evaporation of the solvent yielded 1.82 g (86%) of the highly crystalline phenol **21**. The analytical sample was prepared by recrystallization from chloroform–methanol to a constant melting point of 301° (dec.).

Mol. Wt. Calcd. for $C_{17}H_{17}O_3N$: 283.1214. Found (high resolution mass spectroscopy): 283.1208.

I.r. ($CHCl_3$): 3500–3300 (OH and NH), 1718 (ketone in six-membered ring), 1655 cm^{-1} (lactam); n.m.r. ($CDCl_3$—CD_3OD): τ 3.12 (d, J = 8 Hz, 1H, aromatic hydrogen), 3.13 (d, J = 3 Hz, 1H, aromatic hydrogen), 3.52 (q, J = 8 Hz, J = 3 Hz, 1H, aromatic hydrogen), 6.43 (broad s, 1H, apex proton), 6.67 (m, 1H, benzylic bridgehead proton), 8.82 p.p.m. (s, 3H, tertiary methyl).

The generous support of the National Research Council of Canada, Ottawa, and the Hoffmann-La Roche Company, Nutley, New Jersey and Dorval, Quebec, is gratefully acknowledged.

1. (*a*) K. Wiesner, Pak-Tsun Ho, R. C. Jain, S. F. Lee, S. Oida, and A. Philipp. Can. J. Chem. **51**, 1448 (1973). (*b*) Pak-Tsun Ho, S. Oida, and K. Wiesner. Chem. Commun. 883 (1972).
2. K. Wiesner, Pak-Tsun Ho, D. Chang, and J. F. Blount. Experientia, **28**, 766 (1972).
3. K. E. Pfitzner and J. G. Moffatt. J. Am. Chem. Soc. **87**, 5661 (1965).
4. G. Stork. Pure Appl. Chem. **9**, 131 (1964).
5. (*a*) K. Wiesner and J. Santroch. Tetrahedron Lett. 5939 (1966). (*b*) K. Wiesner, W. L. Kao, and J. Santroch. Can. J. Chem. **47**, 2431 (1969). (*c*) K. Wiesner, E. W. K. Jay, T. Y. R. Tsai, C. Demerson, Lizzie Jay, T. Kanno, J. Křepinský, A. Vilím, and C. S. Wu. Can. J. Chem. **50**, 1925 (1972).
6. R. Pappo, D. S. Allen, R. U. Lemieux, and W. J. Johnson. J. Org. Chem. **21**, 478 (1956).

Can. J. Chem. Downloaded from www.nrcresearchpress.com by 210.87.254.105 on 09/05/12
For personal use only.

Unusual Reactivity Differences in the Decalone Series

CIRILL SCHMIDT

Department of Chemistry, University of Prince Edward Island, Charlottetown, Prince Edward Island

Received May 17, 1973

It was found that an 8α-axial substituent in a 2α,5α,9β-trimethyl-1,4-decaldione system exercises an extraordinary steric hindrance in the reduction of the 1-keto group. Therefore the 4-keto group was reduced in the three compounds **7***b*, **13**, and **22** with complete selectivity. In the absence of such a substituent the 1-keto group is reduced in preference to the 4-keto group (1, 5) with almost complete selectivity. An interplay of 1,3-diaxial and 1,3-*peri*-diequatorial interactions is involved to explain the unusual stereochemical behavior in these compounds. The blocking effect of the 8α-axial group was found to be independent of its own polarity. The steric preference of the reductions does not seem to be influenced by variously located double bonds in the decaline system.

On a trouvé qu'un substituant axial en position 8α de la triméthyl-2α,5α,9β décaldione-1,4 excerce un effet stérique extraordinaire sur la réduction du groupe cétonique en position 1. Une sélectivité complète en faveur de la réduction du groupe cétonique en position 4 a donc été observée lors de la réduction des composés **7***b*, **13** et **22**. En l'absence d'un tel substituant, le groupe cétonique en position 1 est réduit de préférence à celui en 4 (1, 5) avec une sélectivité presque complète. Une combinaison d'interactions diaxiales-1,3 et *péri*-diéquatoriales-1,3 est invoquée pour expliquer la stéréochimie inhabituelle de ces réductions. L'influence du groupe axial en 8α est indépendant de sa polarité. Il apparait que la préférence stérique des réductions ne serait pas influencée par la présence de doubles liaisons dans le système décalinique. [Traduit par le journal]

Can. J. Chem., **51**, 3989 (1973)

In the course of our synthetic studies toward decanortriterpenes we encountered a number of unprecedented selective reductions in the decalin series. The results of these reactions revealed an interesting interplay of several 1,3-interactions leading to a peculiar stereochemical behavior which might be relevant to the field of terpene synthesis.

The reduction of *trans*-diketone **1** (1) with $LiAlOC(CH_3)_3H$ in tetrahydrofuran led to the formation of ketone alcohol **2** in 80% yield, as evidenced by a one proton doublet at $\tau = 6.07$, $J = 8$ Hz. In retrospective this result can be readily rationalized.

An axial approach of the hydride ion to C-4 is impeded by a 1,3-diaxial interaction in the transition state as in the reduction of 6-keto steroids (2). In addition to that interference, the 4-keto group in **1** is also shielded by a 1,3-*peri*-diequatorial interaction. The seriousness of the latter stereochemical effect could be compared to an $A^{(1,3)}$ strain (3*b*) pertinently documented by the fact that the 6-β-hydroxy isomer **4** is favored relative to the 6-α-hydroxy derivative **3** (3*a*).

As a result of these two 1,3 interactions at the 4-keto group in diketone **1** the reduction takes place preferentially at the 1-keto group by an uninhibited axial attack from the α side.

It could be assumed that the special steric hindrance at C-4 in diketone **1** might be attributed at least partially to a particular conformation imposed on the structure by the $\Delta^{(7,8)}$ double bond. Such a conformational distortion (4, 5) must however be of small importance in this instance since the saturated diketone **5** was also reduced preferentially at C-1 leading to ketone alcohol **6**.

Since we wished to retain the keto group at C-1 we decided to increase the steric hindrance in its immediate vicinity. Therefore the acetate **7***b* was prepared from the corresponding alcohol **7***a* (1).

According to the well-known stereochemistry of the Diels–Alder transition state (6) the 8-hydroxyl and the 8-acetoxy groups in compounds **7***a* and **7***b* respectively are axial since the ring junction could be assigned as *trans* on the basis of previous chemical evidence (1, 7).

To our satisfaction and surprise we found that the 1-keto group was completely inert in acetate **7***b* when it was reduced with a large excess of sodium borohydride in methanol at room temperature in 24 h. Thus ketone alcohol **8** was formed in virtually quantitative yield by the reduction of the 4-keto group. A comparison of the chemical behavior of compounds **1**, **5**, and **7***b* suggests that the apparent cause of this remark-

Can. J. Chem. Downloaded from www.nrcresearchpress.com by 210.87.254.42 on 09/05/12
For personal use only.

able reversal of steric preference must be the axial acetoxy group at C-8 in acetate **7***b*.

In order to study the influence of the size of the 8-axial substituent on the reactivity of the 1-keto group we prepared the diol ketone **9** by methanolysis of acetate **8**. It is to be mentioned that during the methanolysis of acetate **8** to diol ketone **9** the 8-axial OH might have been converted to the corresponding equatorial isomer via a reversible retroaldol condensation. However, this possibility can be excluded by recognizing that the coupling constants of the triplet corresponding to H_8 in compounds **7***b*, **8**, **9**, and **10** remain unchanged ($J_{AX} = J_{BX} = 2.5$ Hz). An equatorial OH at the same position would require an axial hydrogen at C-8 giving rise to a coupling constant of approximately 10 Hz.

It was found that compound **9** was reduced in 1 h with $NaBH_4$ in methanol at room temperature to the triol **10**. This oily compound was characterized in terms of crystalline triketone **11** to which it was oxidized with Jones' reagent. However, it would be unjustified to attribute this large increase in reactivity entirely to the difference in size of OH relative to the acetoxy group in compounds **9** and **8** respectively. It is believed that complexing between the borohydride and the 8-hydroxy group might have preceded the attack of a hydride ion on the 1-keto group in ketone diol **9**. Such an intramolecular reduction might have been responsible for the fast reduction of the 1-keto group in compound **9**.

The assumption that in the transition state of these reductions a crucial 1,3-diaxial interaction is involved can be supported by one of our compounds in which positions 1 and 8 were actually linked together. When the diol ketone **9** was treated in liquid ammonia with sodium *o*-methoxyphenylacetylide the cyclic vinyl ether **12***a* was formed as evidenced by appropriate n.m.r. data and the presence of only one acetylable hydroxyl (**12***a* → **12***b*). Such a cyclic compound is possible only if the relative position of substituents at C-1 and C-8 is *cis* in the decalin system. This finding corroborates the assumption that the nucleophile encounters a critical 1,3-diaxial interaction when it attacks the 1-keto group from an α-axial direction. For the addition of alcohols to acetylenes in alkaline conditions numerous examples can be cited (8).

The triketone **11** was most conveniently obtained by the oxidation of diketone alcohol **7***a* with Jones' reagent. It is noteworthy that compound **11** exhibited a double carbonyl peak (1740, 1725 cm^{-1}) attributable to a *cisoid* 1,3-diketone (9) in addition to the normal peak at 1703 assigned to the 4-keto group.

Since we wished to investigate the reactivity of the 1-keto group in this system further, triketone **11** was reacted with a large excess of ethylene glycol in the presence of boronfluoride ethereate and methylene chloride at room temperature. As suspected from the previous results a monoketal, **13**, was obtained in almost quantitative yield.

The fact that in compound **13** the 4-keto group was not ketalized can be understood in terms of a 1,3-diaxial and a 1,3-*peri*-diequatorial interaction already invoked in connection with the reduction previously discussed **1** → **2**. Since in the i.r. of **13** the double carbonyl band characteristic of 1,3-dicarbonyls disappeared, either the 1-keto group or 8-keto group is ketalized. Rigorous proof of structure **13** will be presented after derivatives **14**, **15**, and **16** are discussed.

The reduction of diketone ketal **13** in methanol with sodium borohydride at room temperature in 8 h led to a quantitative yield of alcohol **14**. A one proton multiplet at $\tau = 5.50$, $J = 4.5$, 9.5, and 6 Hz, showed that the 4-keto group was reduced in compound **13**. These coupling constants corroborate the equatorial assignment of H_4, since an axial hydrogen at C-4 should have been indicated by two coupling constants of approximately 10 Hz. A similar argument can be used for the stereochemical assignment of the same hydrogen in compound **8** thus confirming the β-axial position of the 4-hydroxyl group in both compounds.

The ring juncture in triketone **11** and diketone ketal **13** was assigned with the help of double irradiation experiments in their 220 MHz n.m.r. Irradiating at the position of the 5-methyl group located the hydrogen on C-5. When the latter proton was irradiated the low field doublet corresponding to the hydrogen on C-10 was affected. The coupling constant in both cases was found to be 10.6 Hz corresponding to a *trans*-diaxial arrangement.

As far as the ring junction in compounds **11** and **13** is concerned a *trans* isomer and two *cis* conformations should be considered. The relative stereochemistry of the methyls at C-5 and C-9 is *trans*, since the precursor of these compounds originated from a Diels–Alder reaction (1, 7). The well established transition state of the latter reac-

Can. J. Chem. Downloaded from www.nrcresearchpress.com by 210.87.254.42 on 09/05/12
For personal use only.

Can. J. Chem. Downloaded from www.nrcresearchpress.com by 210.87.254.42 on 09/05/12
For personal use only.

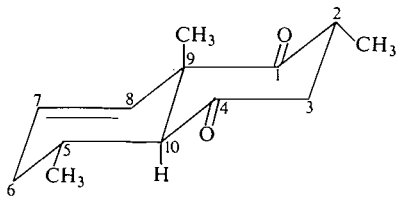

1

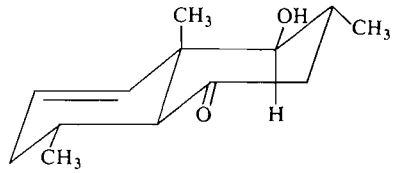

2

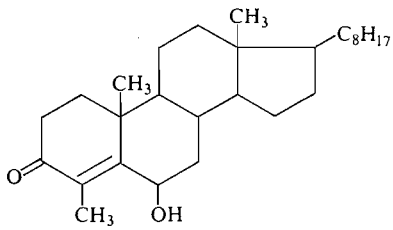

3 α-OH
4 β-OH

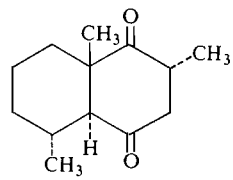

5

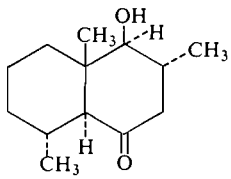

6

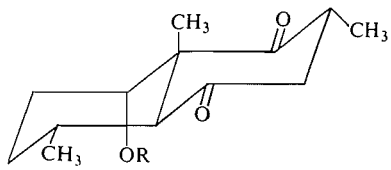

7
a R = H
b R = $COCH_3$

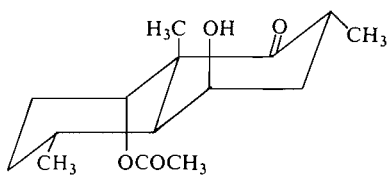

8

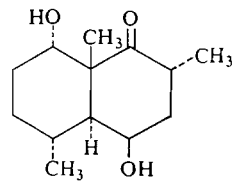

9

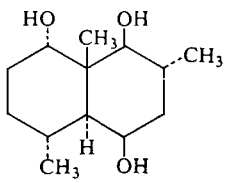

10

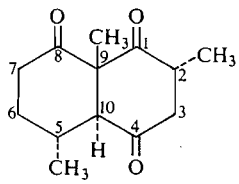

11

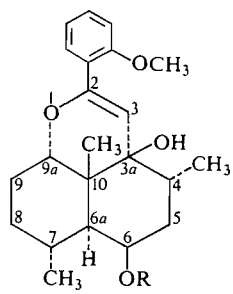

12
a R = H
b R = $COCH_3$

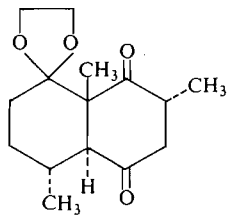

13

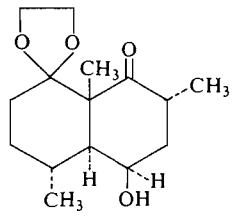

14

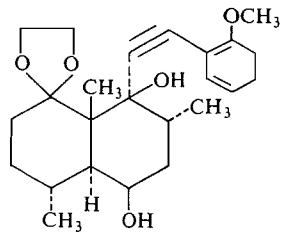

15

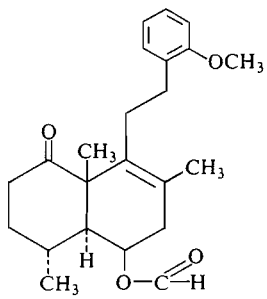

16

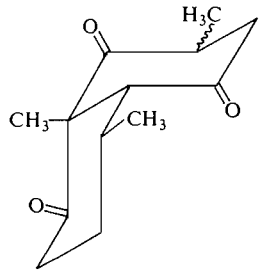

17

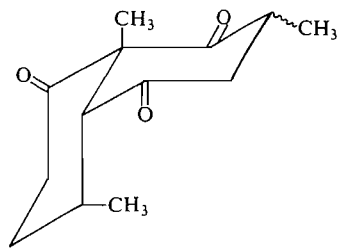

18

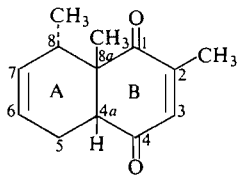

19

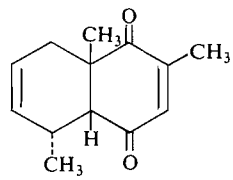

20

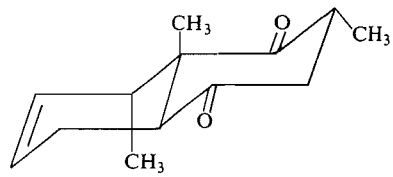

22 = 33

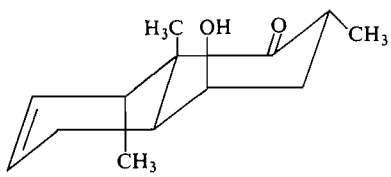

34

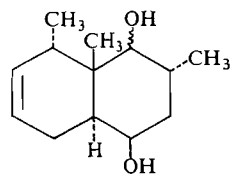

35

tion is known to place the substituents at these positions in a *trans* relative position (6). The two *cis* conformations for triketone **11** are depicted as formulae **17** and **18**.[1] A *trans*-diaxial arrangement of H_5 and H_{10} is compatible only with structure **11** but not with **17** or **18**. The 1-keto group in compound **14** could be reacted only under vigorous conditions. Refluxing of **14** in tetrahydrofuran for 8 h with an excess of bromomagnesium *o*-methoxyphenylacetylide led to adduct **15**. After hydrogenation of **15** and refluxing in 85% formic acid the olefin **16** was formed. In the n.m.r. of **16** a three proton singlet at $\tau = 8.2$ clearly indicates the presence of a methyl group situated on a double bond. The structure of **16** clarifies the location of the dioxolane group in compound **13** at C-8 since an olefinic methyl

[1]The stereochemistry at C-2 in formulae **17** and **18** was drawn undefined since it is irrelevant for this argument.

Can. J. Chem. Downloaded from www.nrcresearchpress.com by 210.87.254.42 on 09/05/12
For personal use only.

Can. J. Chem. Downloaded from www.nrcresearchpress.com by 210.87.254.42 on 09/05/12
For personal use only.

could not have formed in this sequence if the 8-keto group had been unprotected.

The stereochemical assignment for **13**, **14**, and **15** is completely certain since the structure of **16** was also elucidated by X-ray crystallography and will be published in connection with some other work (10). The stereochemical assignment of the 4-β-hydroxyl in compounds **14** and **15** is also firmly established by the crystallographic structure determination. Since the energy difference between *trans*- and *cis*-9-methyldecalones is quite small (11) we had to corroborate our stereochemical assignments by the most reliable methods available.

Although in compound **14** the 8-axial substituent was incorporated in a dioxolane ring the deceleration of reactivity at C-1 was just as pronounced as in the case of acetate **7***b*. It can be summarized therefore, that all compounds presented here which carry an oxygenated 8-axial substituent exhibit this remarkable blocking effect with the exception of ketone diol **11** which contains an axial OH only.

It was thought to be desirable to replace the oxygenated group by a neutral methyl substituent in position 8 and examine the question whether this phenomenon is due to electronic effects or to steric hindrance only. Thus, the Diels–Alder adduct **19** was prepared in a yield of 85% from piperylene and 2,6-dimethylbenzoquinone. *A priori* two products, **19** and **20**, could have formed. As in numerous other Diels–Alder additions only one of the possible adducts, **19**, could be isolated (6). The structural proof for the location of the methyl group in ring A of adduct **19** is outlined in Scheme 1[2] and it is self-explanatory.

A clearly resolved one proton doublet in the n.m.r. of keto alcohol **25** at $\tau = 5.76$ ($J = 8$ Hz) indicates that the less hindered 4-keto group was ketalized in dioxolane **23**. Baeyer–Villiger oxidation led to the ε-lactone **28**, which was converted without isolation to the more stable γ-lactone **29** after methanolysis. Bromination of ketone lactone **30** with 1 mol of bromine in acetic acid led to the bromoketone **31**. The elimination of HBr in dimethylformamide in the presence of LiBr and Li_2CO_3 gave the α,β-unsaturated ketone **32** which contained two olefinic hydrogens but no n.m.r. signal corresponding to a methyl group situated on a double bond. Therefore it was shown that the methyl group in ring A of adduct **19** was not attached to C-5, thus excluding compound **20** while proving structure **19** for the Diels–Alder adduct formed.

The stereochemistry of diketone **22** is represented as **33**. Because of the isomerization **21** → **22** = **33** the ring juncture can be assigned *trans* in the latter compound. The chemical shift of the angular methyl and one of the methyl doublets change by 0.39 and −0.22 p.p.m. respectively as a result of isomerization from the *cis* diketone **21** to its *trans* isomer **22**. The second methyl doublet is not affected and it is assigned to the 2-methyl group. It follows from the stereochemistry of the Diels–Alder transition state that the 8-methyl group must be *trans* to the angular methyl (6). Consequently the 8-methyl group is axial in compound **22** = **33** and can be used in this study.

With an excess of sodium borohydride in methanol the diketone **22** = **33** was reduced at room temperature in 18 h to the ketone alcohol **34**. Further reduction to the diol **35** could be achieved only by refluxing in THF with $LiAlH_4$ for 15 h producing a two component mixture. It should be mentioned that compounds **8**, **14**, and **34** were all treated with a large excess of sodium borohydride under the same conditions as described previously but they were recovered unchanged. Therefore, it was concluded that the low reactivity of the 1-keto group in **7***b*, **13**, and **22** = **33** is due to steric hindrance rather than to electric effects and it is caused by the 8-axial group which transmits its effect by a 1,3-diaxial interaction arising in the transition state.

In relation to our data we should mention that the rate of saponification of *trans*-1α-decalyl acid succinate was found to be 14 times slower than that of the *trans*-2β isomer (12). The ester group is present in both compounds in an axial position but the *trans*-1α-isomer contains an extra 1,3-diaxial interaction to which the rate decrease was attributed.

The influence of the decalin system on these saponification rates is impressive in spite of the fact that the site of reaction ($^-OH + RCOOR \rightarrow RCO^-(OH)OR$) (13) is removed from the decalin ring by two atoms.

In the reduction of our 1-decalones by sodium borohydride the stereochemical influence of the

[2]It should be mentioned that prior to undertaking the rather elaborate degradation, diol **35** was subjected to dehydrogenation. The product was, however, an unidentified trimethylnaphthaline indicating that a rearrangement interfered with the structure elucidation.

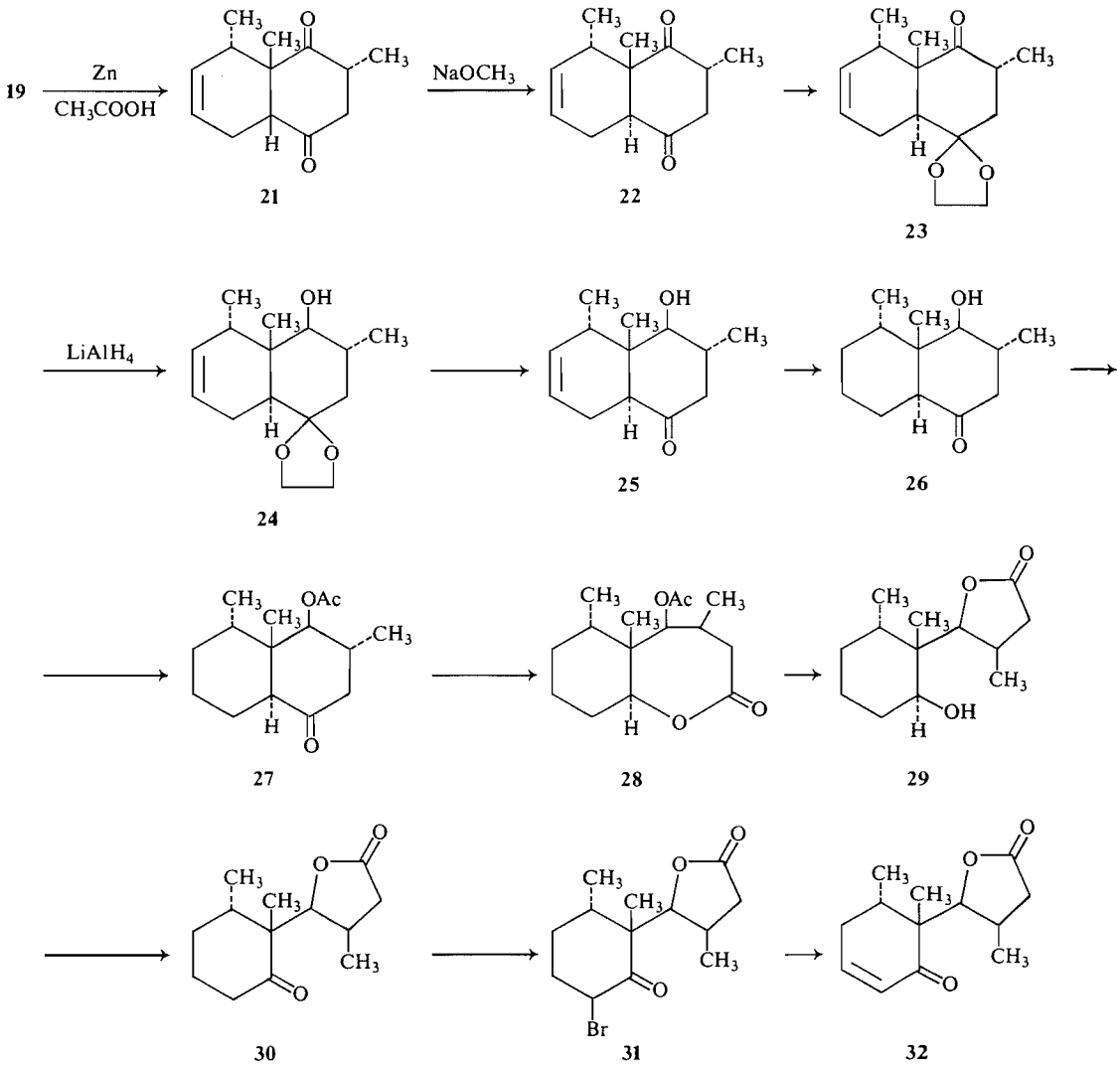

SCHEME 1

decaline ring must be two atoms closer to the site of reaction than in the cases of saponification cited (11*a*, p. 236 and 12).

Due to this and to the larger size of the 8-axial substituent involved in the 1,3-diaxial interaction of the transition state, the 1-keto group in compounds 7*b*, **13**, and **33** is inert at room temperature with sodium borohydride in methanol. It is pertinent to mention that *trans*-2α,9β-dimethyl-1-decalone (15) and a similarly substituted decalone (16) lacking an 8-α-substituent exhibited facile reactivity at the 1-keto group.

It is unlikely that the $\Delta^{(6,7)}$ double bond would exert a pronounced decelerative effect on the 1-keto group, by conformational transmission (4, 5), since all three compounds 7*b*, **13**, and **33** showed qualitatively the same steric hindrance at the 1-keto group, although a double bond was present only in compound **33**.

From the data presented here it appears that the 8-α-axial-decalin effect is a special case of 1,3-diaxial interaction which could be utilized to protect the 1-keto group of the *trans*-decalin system under the conditions described.

In summary the compounds discussed here add further examples of the decalin type to the interesting cases discussed by Sandris and Ourisson (14) in which 1,3-interactions drasti-

Can. J. Chem. Downloaded from www.nrcresearchpress.com by 210.87.254.42 on 09/05/12
For personal use only.

Can. J. Chem. Downloaded from www.nrcresearchpress.com by 210.87.254.42 on 09/05/12
For personal use only.

cally change the stereochemical behavior of cyclohexanes and terpenes.

Experimental[3]

trans-1β-Hydroxy-2α,5α,9β-trimethyl-7-octal-4-one (2)

To a solution of 7.32 g of diketone 1 in dry tetrahydrofuran (200 ml) 10.27 g of $LiAlOC(CH_3)_3H$ was added in 2 h. The reaction mixture was stirred magnetically at room temperature for 12 h, then it was poured on ice. The solution was extracted with ether (4 × 300 ml). After washing with water and drying ($MgSO_4$) the solution concentrated to dryness. The crystalline residue was recrystallized from benzene–chloroform giving 6.10 g of pure ketone alcohol **2** (yield 83%, m.p. 108–112°). The mother liquor contained some diol, it was therefore freed from all solvents and oxidized with Jones' reagent in acetone (25 ml) furnishing 0.50 g of diketone **1**. An analytical sample of the ketone alcohol **2** was prepared by recrystallizing from benzene–chloroform: m.p. 115°; mass spectrum (70 eV) *m/e* (relative intensity) 208 (30, parent peak), 193 (10), 175 (8), 150 (20), 135 (100); i.r. ($CHCl_3$) 3650, 2950, 1710, 1460, 1360, 1240, 1050, 990, 980, 840 cm^{-1}; u.v.$_{max}$ (96% C_2H_5OH) 215 mμ (ε 350); n.m.r. at 60 MHz ($CDCl_3$) τ 9.1 (s, 3, angular methyl), 9.00 (d, 3, J = 6 Hz, CH—CH_3), 8.93 (d, 3, J = 6 Hz, CH—CH_3), 6.07 (d, 1, J = 8 Hz, C*H*OH), 4.43 (m, 2, olefinic protons).

Anal. Calcd. for $C_{13}H_{20}O_2$: C, 74.96; H, 9.68. Found: C, 74.98; H, 9.65.

trans-2α,5α,9β-Trimethyl-1,4-decaldione (5)

A solution of diketone **1** (250 mg) in methanol (30 ml) was hydrogenated for 18 h at a pressure of 30 p.s.i. in the presence of 30 mg of PtO_2. After filtration and evaporation a t.l.c. homogeneous crystalline product was obtained (250 mg, yield quantitative). An analytical sample was obtained by recrystallizing from benzene–pentane: m.p. 99–101°; i.r.($CHCl_3$) 2980, 1720, 1475, 1380, 1160, 1100, 1020 cm^{-1}; u.v. end absorption; n.m.r. at 60 MHz ($CDCl_3$) τ 9.14 (s, 3, angular methyl), 9.03 (d, 3, J = 6 Hz, CH—CH_3), 8.90 (d, 3, J = 6 Hz, CH—CH_3); mass spectrum (70 eV) *m/e* (relative intensity) 208 (100, parent), 193 (50), 180 (20), 137 (80).

Anal. Calcd. for $C_{13}H_{20}O_2$: C, 74.96; H, 9.68. Found C, 75.11; H, 9.70.

trans-1β-Hydroxy-2α,5α,9β-trimethyl-4-decalone (6)

To a solution of diketone **5** (380 mg) in dry THF (30 ml) $LiAlOC(CH_3)_3H$ (620 mg) was added in 1 h while stirring magnetically at room temperature. The reaction mixture was stirred for 18 h at room temperature. Then the solution was poured on ice and the product was extracted with ether (4 × 100 ml). After washing with water, drying ($MgSO_4$) and evaporation an oily product (350 mg, yield 90%) was obtained which crystallized on rubbing. The t.l.c. homogeneous product was recrystallized from benzene–pentane for analysis: m.p. 104–106°; i.r. ($CHCl_3$) 3650, 2900, 1710, 1450, 1370, 1050, 990, 970 cm^{-1}; u.v. end absorption; n.m.r. at 60 MHz ($CDCl_3$) τ 9.17 (s, 3, angular methyl), 9.10 (d, 3, J = 6 Hz, CH—CH_3), 8.87 (d, 3, J = 6 Hz, CH—CH_3), 6.13 (d, 1, J = 8 Hz, C*H*OH); mass spectrum (70 eV) *m/e* (relative intensity) 210 (30, parent), 195 (15), 137 (100), 123 (45).

Anal. Calcd. for $C_{13}H_{22}O_2$: C, 74.24; H, 10.54. Found: C, 74.10; H, 10.49.

trans-8α-Acetoxy-2α,5α,9β-trimethyl-1,4-decaldione (7b)

A solution of 600 mg of diketone alcohol **7a** (1) in pyridine (6 ml) and acetic anhydride (6 ml) was allowed to stand overnight. The reaction mixture was poured on ice and extracted with ether (4 × 30 ml). The combined ether extracts were washed in the presence of ice with 10% sulfuric acid, then with 5% sodium bicarbonate solution. After drying ($MgSO_4$) and evaporation 650 mg of t.l.c. homogeneous crystalline product was obtained, m.p. 145° (yield 94%). An analytical sample was prepared by recrystallizing from benzene–pentane m.p. 149°; mass spectrum (70 eV) *m/e* (relative intensity) 266 (40, parent peak), 224 (20), 206 (100), 195 (10), 191 (10); i.r. ($CHCl_3$) 2915, 1740, 1720, 1455, 1370, 1240, 1115, 1020, 990, 910 cm^{-1}; u.v.$_{max}$ (96% C_2H_5OH) 210 mμ (ε 450); n.m.r. at 60 MHz ($CDCl_3$) ε 9.17 (s, 3, angular methyl), 9.00 (d, 3, J = 6 Hz, CH—CH_3), 8.9 (d, 3, J = 6 Hz, CH—CH_3), 8.07 (s, 3, CH_3OCO), 4.97 (t, 1, $J_{AX} = J_{BX}$ = 2.5 Hz, C*H*OCOCH$_3$).

Anal. Calcd. for $C_{15}H_{22}O_4$: C, 67.65; H, 8.33. Found: C, 67.63; H, 8.37.

trans-4β-Hydroxy-8α-acetoxy-2α,5α,9β-trimethyl-1-decalone (8)

To a solution of 16 g of **7b** in methanol (200 ml) 7.70 g of $NaBH_4$ was added in 1 h while cooling with ice water and stirring magnetically. The solution was stirred at room temperature for 16 h. Then the reaction mixture was poured on ice and acetic acid (20 ml) and extracted with chloroform (4 × 400 ml). The combined extracts were washed with 5% $NaHCO_3$ solution and water in succession. After drying ($MgSO_4$) and evaporation 14.5 g of the homogeneous, crystalline material was obtained, m.p. 110° (yield 91%). An analytical sample was prepared by recrystallizing from benzene–pentane: m.p. 118–119°; mass spectrum (70 eV) *m/e* (relative intensity) 268 (5, parent peak), 225 (10), 208 (100), 163 (20), 152 (20), 141 (70); i.r. ($CHCl_3$) 3500, 2950, 1720, 1450, 1370, 1240, 1120, 1080, 1020, 980, 910 cm^{-1}; u.v.$_{max}$ (96% C_2H_5OH) 210 mμ (ε 300); n.m.r. at 60 MHz ($CDCl_3$) τ 9.03 (d, 3, J = 6 Hz, CH—CH_3), 9.00 (d, 3, J = 6 Hz, CH—CH_3), 8.83 (s, 3, angular methyl), 8.10 (s, 3, $OCOCH_3$), 5.50 (m, 1, J = 5, 9, 6 Hz, C*H*OH), 4.97 (t, 1, $J_{AX} = J_{BX}$ = 2.5 Hz, C*H*—$OCOCH_3$).

Anal. Calcd. for $C_{15}H_{24}O_4$: C, 67.14; H, 9.01. Found: C, 67.17; H, 9.03.

An attempt was made to ascertain that the product was not reduced under the same conditions any further in the following manner.

The hydroxy ketone **8** (160 mg) was treated with sodium borohydride (770 mg) in 30 ml of methanol for 18 h. After

[3]All melting points were taken on a Fisher–Johns melting point apparatus and are uncorrected. The elemental analyses were carried out by Pascher Mikroanalytical Laboratorium, Bonn, West Germany, and Schwarzkopf Mikroanalytical Laboratory, Woodside, N.Y. The i.r. spectra were recorded on a Perkin–Elmer Model 137 B infracord spectrophotometer. The u.v. spectrograms were taken on a Coleman–Hitachi Model 124 double-beam grating spectrophotometer. The n.m.r. spectra were recorded on a Varian Associates T60 spectrophotometer. The mass spectra were obtained with a Hitachi Perkin–Elmer Model RMS-4 spectrometer.

Can. J. Chem. Downloaded from www.nrcresearchpress.com by 210.87.254.42 on 09/05/12
For personal use only.

the same work-up it was recognized that only the starting material **8** was recovered.

*trans-4β,8α-Dihydroxy-2α,5α,9β-trimethyl-1-decalone (**9**)*

A solution of 5 g of ketone acetate **8** was dissolved in methanol (25 ml) and allowed to stand overnight in the presence of sodium methylate (prepared from 0.3 g of sodium and 5 ml of methanol). The reaction mixture was poured on water (150 ml) and extracted with chloroform (4 × 100 ml). The combined chloroform extracts were washed with water and dried ($MgSO_4$). After evaporation the residue crystallized on rubbing with pentane giving 4.2 g (yield quantitative) of t.l.c. homogeneous product. An analytical sample was prepared by recrystallizing from benzene: m.p. 118–120°; mass spectrum (70 eV) *m/e* (relative intensity) 226 (7, parent peak), 208 (3), 190 (3), 184 (6), 141 (100); i.r. ($CHCl_3$) 3600, 2950, 1710, 1450, 1380, 1240, 1065, 1020, 1000, 990, 920 cm^{-1}; u.v.$_{max}$ (96% C_2H_5OH) 210 mμ (ε 296); n.m.r. at 60 MHz ($CDCl_3$) τ 9.02 (d, 6, J = 6 Hz, 2-methyl and 5-methyl), 8.63 (s, 3, angular methyl), 6.00 (t, 1, $J_{AX} = J_{BX}$ = 2.5 Hz, C*H*OH), 5.6 (m, 1, C*H*OH).

Anal. Calcd. for $C_{13}H_{22}O_3$: C, 68.99; H, 9.80. Found: C, 68.96; H, 9.78.

*trans-1β,4β,8α-Trihydroxy-2α,5α,9β-trimethyldecalin (**10**)*

A solution of 300 mg of ketone diol **9** in methanol (10 ml) was stirred at room temperature for 1 h with 150 mg of $NaBH_4$. The reaction mixture was poured on water (50 ml) and extracted with chloroform (4 × 50 ml). After washing the extracts with water, the dried ($MgSO_4$) solution was evaporated to dryness. The oily material (280 mg, 90%) resisted all attempts to crystallize it but appeared homogeneous in t.l.c., mass spectrum (70 eV) *m/e* (relative intensity) 228 (10, parent peak), 210 (20), 192 (15), 174 (5), 159 (100); i.r. ($CHCl_3$) 3450, 2950, 1450, 1400, 1300, 1170, 1020, 970, 915, 870 cm^{-1}; u.v. end absorption; n.m.r. at 60 MHz ($CDCl_3$) τ 9.00 (d, 6, J = 6 Hz, 2-methyl and 5-methyl), 8.83 (s, 3, angular methyl), 6.00 (t, 1, $J_{AX} = J_{BX}$ = 2.5 Hz, C*H*OH), 5.6 (m, 2, two C*H*OC).

The triol **10** (270 mg) was dissolved in acetone (5 ml) and titrated with Jones' reagent. The reaction mixture was poured on water (30 ml) and extracted with chloroform (4 × 30 ml). After drying ($MgSO_4$) and evaporation the crystalline material (230 mg) was identified as the already characterized triketone **11**.

*trans-2α,5α,9β-Trimethyldecal-1,4,8-trione (**11**)*

To a solution of 65 g of diketone alcohol **7***a* in acetone (600 ml) 120 ml of Jones' reagent (17) was dripped in 1 h while cooling with ice water and stirring with a mechanical stirrer. The permanently brown solution was stirred at room temperature for 1 h. Then the reaction mixture was poured on ice water and extracted with ether (4 × 1 l). The combined ether extracts were washed in succession with water, diluted $NaHCO_3$ solution, and water again. The dried ($MgSO_4$) solution was evaporated to dryness *in vacuo* giving 60 g (92%) of t.l.c. homogeneous crystalline triketone. An analytical sample was prepared by recrystallization from benzene–pentane: m.p. 115–117°C mass spectrum (70 eV) *m/e* (relative intensity) 222 (100, parent peak), 207 (10), 194 (50); i.r. ($CHCl_3$) 2950, 1740, 1725, 1703, and 1454 cm^{-1}; u.v.$_{max}$ (96% C_2H_2OH) 218 mμ (ε 678), 290 (113); n.m.r. at 220 MHz ($CDCl_3$) τ 8.90 (d, 3, J = 6 Hz, CH*C*H_3), 8.87 (d, 3, J = 6 Hz, CH*C*H_3), 8.71 (s, 3, angular methyl), 8.50 (m, 1), 8.11 (m, 2), 7.87 (m, 1), 7.68 (m, 1), 7.21 (m, 2), 6.75 (d, 1, J = 10.6 Hz, H_{10}, superimposed on a one proton multiplet). Irradiation of the CH_3—CH at 8.90 showed that H_5 was buried at 8.11. When the latter position was irradiated the doublet at 6.75 was affected. The coupling constant J = 10.6 Hz is compatible with a *trans* diaxial relationship between H_5 and H_{10}.

Anal. Calcd. for $C_{13}H_{18}O_3$: C, 70.24; H, 8.16. Found: C, 70.21; H, 8.14.

*3aβ,4,5,6,6aα,7,8,9,9a,10β-Decahydro-2-o-methoxyphenyl-3aβ,6β-dihydroxy-4α,7α,10β-trimethylnaptho-1,8-bc Pyran (**12***a*)

In 1 l of magnetically stirred liquid ammonia sodium amide was prepared from 5.97 g of sodium catalyzed with $Fe(NO_3)_3$. After the complete disappearance of the blue color a solution of 16 g of *o*-methoxyphenylacetylene in dry tetrahydrofuran (30 ml) was dripped to the solution in 10 min. Then the reaction mixture was stirred magnetically for 1 h. The dihydroxyketone **9** (11.70 g) dissolved in dry tetrahydrofuran (30 ml) was dripped to it in ½ h. The liquid ammonia solution was stirred for 6 h. After the addition of NH_4Cl (10 g) the ammonia was allowed to evaporate. To the residue ether (0.5 l) was added and while stirring and cooling with ice, water (100 ml) was dripped in. After separation the water layer was extracted with ether (4 × 0.5 l).

The ether solution was evaporated to dryness. Next the excess *o*-methoxyphenylacetylene was precipitated. The residue was dissolved in 96% C_2H_5OH (50 ml) then 5% $Ag(NH_3)_2OH$ was dripped in to it until no more precipitate was formed (a sample of filtrate was checked). After filtering and washing the precipitate with alcohol and ether the filtrate was diluted with water (100 ml) and extracted with ether (4 × 100 ml). The ether extracts were washed with saline and dried ($MgSO_4$). After evaporation the t.l.c. homogeneous material crystallized (14.8 g, yield 80%) m.p. 208–215°. An analytical sample was prepared by recrystallizing from benzene–pentane: m.p. 218–220°, mass spectrum (70 eV) *m/e* (relative intensity) 358 (80), 340 (15), 325 (50), 307 (20), 298 (15), 279 (10), 210 (100); i.r. ($CHCl_3$) 3600, 2950, 1650, 1600, 1480, 1450, 1340, 1280, 1240, 1120, 1020, 980, 900 cm^{-1}; u.v.$_{max}$ (96% C_2H_5OH) 213 mμ (ε 14 850), 230 (11 130), 265 (18 550), 275 (18 550), 300 (11 130), 311 (10 000); n.m.r. at 60 MHz ($CDCl_3$) τ 9.1 (d, 3, J = 6 Hz, CH—CH_3), 8.77 (s, 3, angular methyl), 8.63 (d, 3, J = 6 Hz, CH—CH_3), 6.13 (s, 3, CH_3O), 5.83 (m, 1, C*H*OH), 5.67 (t, 1, $J_{AX} = J_{BX}$ = 2.5 Hz H_{9a}), 3.87 (s, 1, olefinic proton), 3.00 (m, 3, aromatic), 1.8 (d, 1, aromatic).

Anal. Calcd. for $C_{22}H_{30}O_4$: C, 73.71; H, 8.44. Found: C, 73.74; H, 8.43.

*3aβ,4,5,6,6aα,7,8,9,9a,10β-Decahydro-2-o-methoxyphenyl-3aβ-hydroxy-6β-acetoxy-4α,7α,10β-trimethylnaphtho-1,8-bc Pyran (**12***b*)

A solution of 500 mg of compound **12***a* in pyridine (3 ml) and acetic anhydride (3 ml) was heated at 70° for 3 h. The reaction mixture was poured on ice and extracted with ether (4 × 50 ml). The combined ether extracts were washed in the presence of ice with diluted sulfuric acid then with sodium bicarbonate solution until the water

Can. J. Chem. Downloaded from www.nrcresearchpress.com by 210.87.254.42 on 09/05/12
For personal use only.

phase remained slightly alkaline. After drying ($MgSO_4$) and evaporation the crystalline material (510 mg, yield 95%, m.p. 125–130°) appeared to be homogeneous in t.l.c. An analytical sample was prepared by recrystallizing from benzene–pentane: m.p. 134–135°, mass spectrum (70 eV) *m/e* (relative intensity) 400 (70, parent peak), 384 (10), 352 (5), 340 (10), 322 (100), 307 (70); i.r. ($CHCl_3$) 2950, 1725, 1650, 1480, 1460, 1350, 1240, 1120, 1080, 1030, 980, 950, 760 cm^{-1}; u.v.$_{max}$ (96% C_2H_5OH) 213 mμ (ε 12 800), 230 (11 500), 265 (19 200), 275 (19 200), 300 (10 750), 311 (8 980); n.m.r. at 60 MHz τ 9.23 (d, 3, J = 6 Hz, CH—CH_3), 8.83 (s, 3, angular methyl), 8.70 (d, 3, J = 6 Hz, CH—CH_3), 7.93 (s, 3, CH_3COO), 6.17 (s, 3, CH_3O), 5.67 (t, 1, $J_{AX} = J_{BX}$ = 2.5 Hz, CHORCHOH), 4.83 (m, 1, CHOCOCH$_3$), 3.83 (s, 1, olefinic proton), 3.00 (m, 3, aromatic protons), 1.83 (m, 1, aromatic proton).

Anal. Calcd. for $C_{24}H_{32}O_5$: C, 71.97; H, 8.05. Found: C, 71.93; H, 8.07.

*trans-8,8-Ethylenedioxy-2α,5α,9β-trimethyl-1,4-decaldione (**13**)*

To an ice cold stirred mixture of 40 g of triketone **11** dissolved in 100 ml of ethylene glycol and 600 ml of methylene chloride 40 ml of boronfluoride ethereate was dripped in 10–15 min. Then the two-phase system was stirred overnight at room temperature. The flask was protected with a $CaCl_2$ tube. Next morning the reaction mixture was poured on crushed ice (500 g) and K_2CO_3 (100 g). The solution was extracted with CH_2Cl_2 (0.5 l) four times. The combined extracts were washed twice with water, dried ($MgSO_4$), then evaporated to dryness yielding 38.5 g (80% of crystalline t.l.c. homogeneous product). An analytical sample was prepared by recrystallizing from benzene-pentane: m.p. 108° C; mass spectrum (70 eV) *m/e* (relative intensity) 266 (20, parent peak), 251 (5), 126 (100); i.r. ($CHCl_3$) 2950, 1712, 1460, 1070, 975, 945, 910 cm^{-1}; u.v.$_{max}$ (96% C_2H_5OH) 214 mμ (ε 395); n.m.r. at 220 MHz τ 8.97 (d, 3, J = 6 Hz, CH—CH_3), 8.94 (s, 3, angular methyl), 8.93 (d, 3, J = 6 Hz, CH—CH_3), 8.61 (m, 1), 8.49 (m, 1), 8.32 (m, 2), 7.61 (m, 2), 7.23 (g, 1), 6.64 (d, 1, J = 10.8 Hz, H_{10}, superimposed on a one proton multiplet), 6.09 (m, 4, O—CH_2—CH_2—O). The doublet at 6.64 was suspected to be due to H_{10}. Double irradiation at the latter position affected a part of the multiplet at 7.61. Decoupling the latter resonance collapsed the lowfield methyl doublet. The reverse decoupling experiments were also carried out. The doublet at 6.64 collapses when the buried multiplet at 7.61 is irradiated. But the other multiplet underneath H_{10} at 6.64 is not affected. The coupling constant of 10.8 Hz at 6.64 is compatible with a *trans* diaxial relationship between H_5 and H_{10}.

Anal. Calcd. for $C_{15}H_{22}O_4$: C, 67.65; H, 8.33. Found: C, 67.61; H, 8.31.

*trans-4β-Hydroxy-8,8-ethylenedioxy-2α,5α,9β-trimethyl-4-decalone (**14**)*

To a stirred ice cold solution of 42 g of diketoneketal **13** in methanol (400 ml) 30 g of $NaBH_4$ was added in 1 h while maintaining the temperature below 15 °C. The solution was then stirred for 4 h at room temperature. The reaction mixture was poured on ice and water and extracted with $CHCl_3$ (4 × 0.5 l). The dried ($MgSO_4$) solution was evaporated to dryness furnishing 41 g of t.l.c. homogeneous, crystalline product (yield 97%). An analytical sample was prepared by recrystallizing from benzene–pentane: m.p. 120°; mass spectrum (70 eV) *m/e* (relative intensity) 268 (100, parent peak), 239 (20), 225 (20), 205 (30); i.r. ($CHCl_3$) 3620, 3500, 2940, 1720, 1640, 1375 cm^{-1}; u.v.$_{max}$ (96% C_2H_5OH) 210 mμ (ε 418); n.m.r. at 60 MHz ($CDCl_3$) τ 9.07 (d, 3, J = 6 Hz, CHCH_3) 8.97 (d, 3, J = 6 Hz, CHCH_3), 8.77 (s, 3, angular methyl), 6.10 (m, 4, O—CH_2CH_2—O), 5.50 (m, 1, J = 4.5, 9.5, 6 Hz, CHOH).

Anal. Calcd. for $C_{15}H_{24}O_4$: C, 67.14; H, 9.01. Found: C, 67.11; H, 8.99.

An attempt was made to reduce the product **14** further under the same conditions as described for compound **8**. However only the unchanged **14** was recovered.

*trans-1α-(o-Methoxyphenylethynyl)-1β,4β-dihydroxy-8,8-ethylenedioxy-2α,5α,9β-trimethyldecalin (**15**)*

203 ml of 2.95 M CH_3MgBr solution (Arapahoe) was dripped into a solution of 82.3 g of *o*-methoxy-phenylacetylene in dry tetrahydrofuran (1 l). The addition was carried out in ½ h with ice cooling in an atmosphere of dry N_2 while stirring. The 2-l, three-neck flask was equipped with a mechanical stirrer, reflux condenser ($CaCl_2$ drying tube), dripping funnel, and an opening for the continuous introduction of dry N_2. The reaction mixture was allowed to stir for 20 min at room temperature then it was refluxed for 10 min. Then it was cooled down to 5° and a solution of 42 g of compound **14** in dry THF was added in ½ h. The reaction mixture was then refluxed for 8 h under a stream of anhydrous nitrogen. The reaction mixture was poured on ice then it was diluted with 1 l of chloroform and the emulsion was filtered on celite. The clear filtrate was extracted with chloroform (3 × 0.5 l). The combined chloroform extracts were washed with water then dried ($MgSO_4$). After evaporation the residue was examined by t.l.c. indicating the complete disappearance of starting material and the presence of the acetylene and the product only. The residue was then dissolved in 300 ml of ethanol and while stirring 0.4 g mol of Ag-$(NH_3)_2OH$ (prepared in ½ l of distilled water) was dripped into it in 20 min. The yellow acetylene precipitate was filtered on a Buchner funnel. The precipitate was washed with ½ l of ether. The filtrate was extracted with ether (4 × 0.5 l). After drying ($MgSO_4$) and evaporation the residue was dissolved in 1 l of $CHCl_3$ and dried again ($MgSO_4$). After evaporation the oily residue was dissolved in 100 ml of benzene and allowed to crystallize and 38 g of crystalline **15** was collected (yield 65%), m.p. 95°. An analytical sample was prepared by recrystallizing from benzene–pentane, m.p. 100°; mass spectrum (70 eV) *m/e* (relative intensity) 400 (5, parent peak), 382 (100), 364 (100), 349 (80), i.r. ($CHCl_3$) 3300, 2850, 1580, 1470, 1440, 1240, 1100, 1010, 980, 940, 900 cm^{-1}; u.v.$_{max}$ (96% C_2H_5OH) 209 mμ (ε 20 600), 219 (18 000), 247 (12 000), 257 (12 850), 291 (5150), 301 (6000): n.m.r. at 60 MHz ($CDCl_3$) τ 9 (d, 3, J = 6 Hz, CH—CH_3), 6.17 (s, 3, CH_3O), 6 (m, 5, O—CH_2—CH_2—O and CHOH), 3.0 (m, 4, aromatic protons).

Anal. Calcd. for $C_{24}H_{32}O_5$: C, 71.97; H, 8.05. Found: C, 71.93; H, 8.03.

*trans-1-(2-o-Methoxyphenylethyl)-4β-formoxy-2,5α,9β-trimethyl-1-octal-8-one (**16**)*

Twenty grams of Nef adduct **15** was hydrogenated for 24 h in methanol (300 ml) in the presence of 300 mg of 5% Pd–charcoal. After filtration the methanol was com-

Can. J. Chem. Downloaded from www.nrcresearchpress.com by 210.87.254.42 on 09/05/12
For personal use only.

pletely removed. Spectroscopic examination by n.m.r. and u.v. indicated the complete disappearance of the starting material. According to t.l.c. only one product was present, which was refluxed in 85% formic acid (100 ml) for 8 h. The reaction mixture was poured into water (500 ml) and extracted with ether (4 × 500 ml). The ether extracts were washed successively with saline, 5% sodium bicarbonate, and saline. The dried ($MgSO_4$) ether extracts were evaporated to dryness. T.l.c. showed the presence of one major product and a minor product in such minute quantities that we were unable to characterize it. The major compound was obtained by crystallizing from benzene–pentane (16 g, yield 87%, m.p. 120°). An analytical sample was prepared by recrystallizing from benzene–pentane: m.p. 130°; mass spectrum (70 eV) *m/e* (relative intensity) 370 (4, parent peak), 352 (2), 324 (30), 306 (70), 291 (100), 249 (55); i.r. ($CHCl_3$) 2950, 1720 (broad), 1600, 1480, 1450, 1230, 1160, 1040, 830 cm^{-1}; u.v.$_{max}$ (96% C_2H_5OH) 224 mμ (ε 7850), 273 (1990), 279 (1850): n.m.r. at 60 MHz ($CDCl_3$) τ 9.03 (d, 3, J = 6 Hz, CH—CH_3), 8.37 (s, 3, angular methyl), 8.20 (s, 3, =C—CH_3), 6.17 (s, 3, CH_3O) 4.50 (m, 1, C*H*OCOH), 3.00 (m, 4, aromatic protons), 1.9 (s, 1, OCO*H*).

Anal. Calcd. for $C_{23}H_{30}O_4$: C, 74.56; H, 8.16. Found: C, 74.58; H, 8.14.

*cis-1,4,4a,5,8,8a-Hexahydro-2,8α,8aβ-trimethyl-1,4-dioxonaphthalene (**19**)*

2,6-Dimethylbenzoquinone (20 g) and piperylene (100 g, 95:5 *trans–cis* mixture) were refluxed for 24 h in benzene (500 ml). After evaporating the excessive piperylene and benzene the reaction mixture was distilled *in vacuo* at 0.7 mm Hg using a short Vigreux column. The first fraction boiling at 20–100°/0.7 mm Hg contained a few per cent of quinone which crystallized in the column. After its complete evaporation the distillation was interrupted and the crystalline material was removed. The product distilled at 100–105°/0.7 mm Hg, giving 26 g (85%) of product whose gas chromatographic purity was found to be better than 95%; i.r. ($CHCl_3$) 3050, 2950, 1685, 1610, 1450, 1360, 1350, 1200, 1050, 900 cm^{-1}; u.v.$_{max}$ (96% C_2H_5OH) 242 mμ (ε 11 500); n.m.r. ($CDCl_3$) τ 9.26 (d, 3, J = 6 Hz, 8-methyl), 8.66 (s, 3, 8a-methyl), 8.08 (s, 3, 2-methyl), 4.52 (m, 2, olefinic), 3.45 (m, 1, H_3). Characterized as its monosemicarbazone, m.p. 196–200°.

Anal. Calcd. for $C_{14}H_{19}ON_3$: C, 64.35; H, 7.33; N, 16.08. Found: C, 64.33; H, 7.35; N, 1610.

*cis-2α,8α,9β-Trimethyl-6-octal-1,4-dione (**21**)*

A solution of adduct **19** (60 g) in acetic acid (200 ml) and water (200 ml) was heated at 55° with zinc dust (40 g) while stirring for 12 h. Acetone (500 ml) was poured into the cool solution and after filtration the solution was concentrated *in vacuo*. The residue was dissolved in ether, extracted with diluted sodium bicarbonate solution, then with water. The dry solution ($MgSO_4$) was concentrated to dryness. This oily product (58 g, 95%) crystallized after two days. An analytical sample was obtained by recrystallizing from benzene–hexane: m.p. 43°; i.r. ($CHCl_3$) 2950, 1710, 1455, 1000 cm^{-1}; u.v. end absorption; n.m.r. ($CDCl_3$) τ 9.27 (d, 3, J = 6 Hz, 8-methyl), 8.83 (d, 3, J = 6 Hz, 2-methyl), 8.67 (s, 3, angular methyl), 4.44 (m, 2, olefinic protons).

Anal. Calcd. for $C_{13}H_{18}O_2$: C, 75.69; H, 8.80. Found: C, 75.71; H, 8.78.

*trans-2α,8α,9β-Trimethyl-6-octal-1,4-dione (**22**)*

Five g of *cis*-diketone **21** dissolved in methanol (50 ml) was refluxed for 3 h in the presence of a catalytic amount of sodium methylate. After the addition of acetic acid (0.2 ml) the methyl alcohol was removed *in vacuo*. The residue was dissolved in chloroform (100 ml) and washed with diluted sodium bicarbonate solution. Then the solution was dried ($MgSO_4$) and evaporated to dryness. The crystalline product (5 g) was homogeneous according to t.l.c. An analytical sample was prepared by recrystallizing from benzene–hexane: m.p. 95 °C; i.r. ($CHCl_3$) 2950, 1710, 1460, 1050, 850 cm^{-1}; u.v. end absorption; n.m.r. ($CDCl_3$) τ 9.09 (d, 3, J = 6 Hz, 8-methyl), 9.06 (s, 3, angular methyl), 8.86 (d, 3, J = 6 Hz, 2-methyl), 4.36 (m, 2, olefinic protons).

Anal. Calcd. for $C_{13}H_{18}O_2$: C, 75.69; H, 8.80. Found: C, 75.67; H, 8.79.

*trans-4,4-Ethylenedioxy-2α,8α,9β-trimethyl-6-octal-1-one (**23**)*

Diketone **22** (10 g), ethylene glycol (7 ml), and *p*-toluene sulfonic acid (80 mg) were refluxed for 24 h in benzene using a Dean–Stark head for the removal of water. The benzene solution was washed with diluted $NaHCO_3$ solution then with saline twice. After the removal of benzene a colorless, t.l.c. homogeneous oil (10.7 g, 88%) was obtained: i.r. ($CHCl_3$) 2950, 1715, 1460, 1299, 1176, 1156, 1111, 1053, 1003 cm^{-1}; u.v. end absorption; n.m.r. ($CDCl_3$) τ 9.25 (d, 3, J = 6 Hz, CH—CH_3), 8.89 (d, 3, J = 6 Hz, CH—CH_3), 8.73 (s, 3, angular methyl), 6.02 (m, 4, O—CH_2—CH_2—O), 4.42 (m, 2, olefinic protons). Characterized in terms of alcohol **7**.

*trans-1β-Hydroxy-4,4-ethylenedioxy-2α,8α,9β-trimethyl-6-octalin (**24**)*

A solution of monoketal ketone **23** (10 g) in dry tetrahydrofuran (25 ml) was added dropwise to a stirred suspension of $LiAlH_4$ (10 g) in dry tetrahydrofuran (100 ml) at room temperature. It was then refluxed for 24 h under anhydrous conditions. The reaction mixture was decomposed with cold water. After filtration and washing the inorganic material was washed with ether. The filtrate was extracted with ether (3 × 10 ml) then the combined extracts were washed with saline and dried ($MgSO_4$). A crystalline residue was obtained on evaporation of the ether (9.1 g, 90%). An analytical sample was prepared by recrystallizing from benzene–pentane: m.p. 106–107°; i.r. ($CHCl_3$) 3660, 2950, 2900, 1460, 1120, 1050, 980 cm^{-1}; u.v. end absorption: n.m.r. ($CDCl_3$) τ 8.75–9.08 (m, 9, methyls), 6.04–6.3 (m, 5, C*H*OH and O—CH_2—CH_2—O), 4.41 (m, 2, olefinic protons).

Anal. Calcd. for $C_{15}H_{24}O_3$: C, 71.39; H, 9.59. Found: C, 71.37; H, 9.62.

*trans-1β-Hydroxy-2α,8α,9β-trimethyl-6-octal-4-one (**25**)*

A solution of ketalalcohol **24** (7.5 g) in methanol (50 ml) was hydrolyzed at room temperature with 10% sulfuric acid (20 ml) while stirring for 5 h. With sodium bicarbonate the solution was neutralized, then the solution was diluted with water (150 ml) and extracted with ether (4 × 80 ml). The combined ether extracts were washed with saline and dried ($MgSO_4$). After the evaporation of ether the residue crystallized on rubbir g (4.9 g, 90%). An analytical sample was obtained by recrystallizing from benzene – petroleum ether: m.p. 111–112°; i.r. ($CHCl_3$) 3650, 3550,

Can. J. Chem. Downloaded from www.nrcresearchpress.com by 210.87.254.42 on 09/05/12
For personal use only.

2950, 2900, 1710, 1290, 1042 cm^{-1}; u.v. end absorption; n.m.r. ($CDCl_3$) τ 9.1 (s, 3, angular methyl), 8.93 (d, 3, J = 6 Hz, CH—CH_3), 8.86 (d, 3, J = 6 Hz, CHCH_3), 5.76 (d, 1, J = 8 Hz, CHOH), 4.4 (m, 2, olefinic protons).

Anal. Calcd. for $C_{13}H_{20}O_2$: C, 74.96; H, 9.68. Found: C, 74.99; H, 9.70.

*trans-1β-Hydroxy-2α,8α,9β-trimethyl-decal-4-one (**26**)*

The unsaturated keto alcohol **25** (5 g) was hydrogenated in methanol (75 ml) using 10% Pd-on-charcoal (200 mg) at 20 p.s.i. for 20 h at room temperature. After filtering the catalyst and evaporation a crystalline, t.l.c. homogeneous product (4.8 g, 96%) was obtained. An analytical sample was obtained by recrystallizing from benzene – petroleum ether: m.p. 129–131°; i.r. ($CHCl_3$) 3600, 3480, 2950, 1710, 1460, 1200 cm^{-1}; u.v. end absorption; n.m.r. ($CDCl_3$) τ 9.05 (s, 3, angular methyl), 8.95 (d, 3, J = 6 Hz, CHCH_3), 8.84 (d, 3, J = 6 Hz, CHCH_3), 5.82 (d, 1, J = 8 Hz, CH—OH).

Anal. Calcd. for $C_{13}H_{22}O_2$: C, 74.24; H, 10.54. Found: C, 74.27; H, 10.55.

*trans-1β-Acetoxy-2α,8α,9β-trimethyl-decal-4-one (**27**)*

A solution of the saturated keto alcohol **26** (1 g) in 7 ml of acetyl chloride was refluxed for 3 h. (Acetic anhydride and pyridine at room temperature failed to esterify keto alcohol **26**.) After evaporating the excess acetyl chloride *in vacuo* a colorless oil was obtained which was dissolved in ether (20 ml) and was successively washed with sodium bicarbonate and saline. The combined extracts were dried ($MgSO_4$) and concentrated *in vacuo*. The colorless oil (1.1 g, 94%) appeared to completely homogeneous in t.l.c.; i.r. ($CHCl_3$) 2950, 1739, 1710, 1460, 1200, 950 cm^{-1}; u.v. end absorption; n.m.r. ($CDCl_3$) τ 9.00 (s, 3, angular methyl), 8.90 (d, 3, J = 6 Hz, two CH—CH_3), 7.87 (s, 3, $OCOCH_3$), 4.46 (d, 1, J = 8 Hz, CH—$OCOCH_3$). The acetoxy ketone **27** was characterized in terms of crystalline γ-lactone **29**.

*3-Methyl-4-hydroxy-4-(1-6β-hydroxy-1β,2α-dimethylcyclohexyl)-1-butanoic Acid γ-Lactone (**29**). Baeyer–Villiger Oxidation Followed by Methanolysis **27** → **28** → **29***

Trifluoroacetic anhydride (20 ml) was stirred in a round-bottomed flask at 0–5 °C and then 98% hydrogen peroxide (2.7 ml) was added dropwise in 10 min. The reagent was stirred for 2 h then a solution of keto acetate **27** (900 mg) in trifluoroacetic acid (5 ml) was added to it dropwise in 30 min at 0–5°. The reaction mixture was allowed to react at the same temperature for 2 h then it was poured on ice and the product was extracted with ether (4 × 100 ml). After washing the combined ether extracts with saline the solution was dried ($MgSO_4$) and concentrated *in vacuo*. The crude ε-lactone (**28**) was saponified without isolation in 20 ml of methanol containing sodium methylate (380 mg) at room temperature in 18 h. After neutralizing with 10% H_2SO_4 the product was extracted with ether (4 × 70 ml). With saline the combined extract was washed, then it was dried ($MgSO_4$). On evaporation *in vacuo* the residue crystallized. After recrystallization from benzene – petroleum ether 460 mg of γ-lactone **29** (64% based on keto acetate **27**) was obtained: m.p. 123–124°; i.r. ($CHCl_3$) 3580, 3450, 2950, 1770, 1460, 1180 cm^{-1}; u.v. end absorption; n.m.r. ($CDCl_3$) τ 9.02 (s, 3, angular methyl), 8.90 (d, 3, J = 6 Hz, CHCH_3); 8.77 (d, 3, J = 6 Hz, CHCH_3), 6.17 (m, 1, CH—OH), 5.69 (d, 1, J = 5 Hz, CHOCO).

Anal. Calcd. for $C_{13}H_{22}O_3$: C, 68.99; H, 9.80. Found: C, 69.01; H, 9.78.

*3-Methyl-4-hydroxy-4-(1-1β,2α-dimethyl-6-oxocyclohexyl)butanoic Acid γ-Lactone (**30**)*

A solution of hydroxy-γ-lactone **29** (400 mg) dissolved in acetone (10 ml) was oxidized with Jones' reagent. The reaction mixture was then poured on water (50 ml) and extracted with ether (4 × 50 ml). The combined ether extracts were washed with 5% $NaHCO_3$ then with saline. After drying ($MgSO_4$) and evaporation a crystalline residue was obtained. Recrystallizing from benzene – petroleum ether gave 310 mg (77%) of ketone **30**: m.p. 99–100°; i.r. ($CHCl_3$) 2950, 1780, 1710, 1450, 1180, 1000 cm^{-1}; u.v. end absorption; n.m.r. ($CDCl_3$) τ 8.96 (d, 6, J = 6 Hz, two CH—CH_3), 8.78 (s, 3, angular methyl), 5.45 (d, 1, J = 3 Hz, CHOCO).

Anal. Calcd. for $C_{13}H_{20}O_3$: C, 69.61; H, 8.99. Found: C, 69.63; H, 8.97.

*3-Methyl-4-hydroxy-4-(1-1β,2α-dimethyl-6-oxocyclohex-4-enyl)butanoic Acid γ-Lactone (**32**)*

The keto lactone **30** (500 mg) dissolved in acetic acid (5 ml) was brominated with 1 equiv bromine (357 mg) dissolved in 8 ml of acetic acid. The bromine solution was added at 0–5° in 20 min and the reaction mixture was allowed to stand for 2 h at room temperature. After diluting with water (100 ml) the product was extracted with ether (4 × 50 ml). The combined extracts were washed in succession with saline, 5% sodium bicarbonate, and saline. Drying ($MgSO_4$) was followed by evaporation *in vacuo*. The light brown oil (600 mg) appeared to be homogeneous in t.l.c.; i.r. ($CHCl_3$) 2950, 1780, 1725, 1460 cm^{-1}. Without further isolation the bromoketone lactone **31** was subjected to elimination.

Lithium bromide (480 mg) and lithium carbonate (800 mg) were stirred in dry dimethylformamide under a nitrogen atmosphere at 120–125° for 30 min. The bromo compound 31 (600 mg) dissolved in dimethylformamide (20 ml) was added to above reagent after cooling, then the reaction mixture was stirred for 2 h at 120–125°. After pouring the solution on ice and acetic acid the product was extracted with methylene chloride (4 × 70 ml). The organic phase was washed with sodium bicarbonate and saline in succession. After drying ($MgSO_4$) and evaporation an oily product was obtained which was purified by preparative thick layer chromatography on silica gel developing with benzene. Then the sample was microdistilled at approximately 105°/0.3 mm Hg (310 mg, 62%): mass spectrum (70 eV) *m/e* (relative intensity) 222 (15 parent peak), 207 (25), 182 (100), 140 (70); i.r. ($CHCl_3$) 2950, 1780, 1680, 1455, 1200, 1000 cm^{-1}; $u.v._{max}$ (96% C_2H_5OH) 228 mμ (ε 11 100), n.m.r. ($CDCl_3$) τ 8.87 (d, 6, J = 6 Hz, two CHCH_3), 8.83 (s, 3, angular methyl), 5.6 (d, 1, J = 4 Hz, CHOCO), 4.02 (d, 1, J = 11 Hz, HC=CH—C=O), 3.08 (m, 1, CH=CH—C=O).

Anal. Calcd. for $C_{13}H_{18}O_3$: C, 70.24; H, 8.16. Found: C, 70.36; H, 8.22.

*trans-4β-Hydroxy-2α,8α,9β-trimethyl-6-octal-1-one (**34**)*

To a solution of diketone **22** = **33** (4.5) in methanol (100 ml) and water (6 ml) sodium borohydride (750 mg) was added while stirring at 5–10° in 1 h. The reaction mix-

ture was then stirred overnight at room temperature. After pouring the solution on ice and water (200 ml) extraction was carried out with ether (4 × 150 ml). The combined ether extracts were washed with saline then dried ($MgSO_4$) and evaporated to dryness. On standing overnight the residue crystallized (4.3 g, 95%). An analytical sample was obtained by recrystallizing from benzene – petroleum ether; m.p. 95°; i.r. ($CDCl_3$) 3630, 3540, 2950, 1710, 1640, 1460, 1350, 1000, 970 cm^{-1}; u.v. end absorption; n.m.r. ($CDCl_3$) τ 9.08 (d, 3, J = 5 Hz, $CHCH_3$), 8.95 (d, 3, J = 6 Hz, $CHCH_3$), 8.73 (s, 3, angular methyl), 6.03 (m, 1, $CHOH$), 4.46 (m, 2, olefinic protons).

Anal. Calcd. for $C_{13}H_{20}O_2$: C, 74.96; H, 9.68. Found: C, 74.98; H, 9.68.

An attempt was made to reduce ketone alcohol **34** further under the same conditions as described for compound **8**. However only the starting material **34** was recovered.

trans-1,4-Dihydroxy-2α,8α,9β-trimethyl-6-octalin (35)

A solution of ketone alcohol **34** (1 g) in dry tetrahydrofuran (35 ml) was refluxed and stirred with $LiAlH_4$ (0.8 g). Samples withdrawn every 3 h showed that the CO i.r. band disappeared only after 15 h. The reaction mixture was then decomposed by the addition of water. After filtering on a Büchner funnel and washing with ether the product was extracted with ether (4 × 100 ml). The combined ether extracts were washed with water, dried ($MgSO_4$) and evaporated to dryness (0.85 g, 84%). According to t.l.c. the oily product consists of two closely related isomers which could not be separated. Mass spectrum (70 eV) *m/e* (relative intensity) 210 (20, parent peak), 192 (35), 177 (100), 159 (15); i.r. ($CHCl_3$) 3640, 3530, 2960, 1460, 1250, 1200, 1150 cm^{-1}; u.v. end absorption; n.m.r. ($CDCl_3$) τ 9.1–8.6 (methyl signals), 6.0–6.1 (CH—OH) signals).

The diol mixture was oxidized with Jones' reagent to the crystalline diketone **22** = **33** in terms of which it was characterized.

For financial assistance the National Research Council of Canada and the Research Corporation are acknowledged. The technical assistances of Mrs. E. Schmidt and Mr. C. Dube are greatly appreciated. Mr. S. Sabnis is thanked for carrying out the last reactions of Scheme 1. The University of Prince Edward Island is thanked for financial support also. Special thanks are due to Professor Z. Valenta for helpful discussion.

1. C. SCHMIDT. J. Org. Chem. **35**, 1324 (1970).
2. C. W. SHOPPEE and G. H. R. SUMMERS. J. Chem. Soc. 3361 (1952).
3. (*a*) C. W. SHOPPEE, F. P. JOHNSON, R. E. LACK, R. J. RAWSON, and S. STERNHELL. J. Chem. Soc. 2476 (1965). (*b*) F. JOHNSON. Chem. Rev. **68**, 389 (1968).
4. D. H. R. BARTON, A. J. HEAD, and P. J. MAY. J. Chem. Soc. 935 (1957).
5. D. H. R. BARTON, F. MCCAPRA, P. J. MAY, and F. THUDIUM. J. Chem. Soc. 1297 (1960).
6. (*a*) J. SAUER. Angew. Chem. Int. Ed. Engl. **6**, 16 (1967). (*b*) A. WASSERMANN. Diels–Alder reactions. Elsevier Publishing Corp., New York, N.Y. 1965. (*c*) A. S. ONISHCHENKO, Diene synthesis. Israel Program for Scientific Translations, Jerusalem. 1964.
7. M. T. H. LIU and C. SCHMIDT. Tetrahedron, **27**, 5289 (1971).
8. H. G. VIEHE. Chemistry of acetylenes. Marcel Dekker, New York. 1969.
9. S. N. ANANCENKO, J. J. BEREZIN, and I. V. TORGOV. Bull. Acad. Sci. U.S.S.R. 1644 (1960).
10. F. BRISSE and C. SCHMIDT. Unpublished results.
11. (*a*) E. L. ELIEL, N. L. ALLINGER, S. J. ANGYAL, and G. A. MORRISON. Conformational analysis. Interscience Publishers, New York. 1966. (*b*) M. HANACK. Conformation theory. Academic Press, New York. 1965.
12. (*a*) W. HUCKEL. Ber. **67A**, 129 (1934). (*b*) W. HUCKEL, H. HAVELOSS, K. K. KUMETAT, D. ULLMANN, and W. DOLL. Ann. **533**, 128 (1937).
13. M. L. BENDER. J. Am. Chem. Soc. **73**, 1626 (1951).
14. C. SANDRIS and G. OURISSON. Bull. Soc. Chim. Fr. 1524 (1958).
15. W. S. JOHNSON, S. L. GRAY, J. K. CRANDALL, and D. M. BAILEY. J. Am. Chem. Soc. **86**, 1968 (1964).
16. F. SONDHEIMER and E. ELAD. J. Am. Chem. Soc. 1967 (1958).
17. M. FIESER and L. FIESER. Reagents for organic synthesis. Wiley-Interscience, New York. 1969. p. 142.

Can. J. Chem. Downloaded from www.nrcresearchpress.com by 210.87.254.42 on 09/05/12
For personal use only.

Can. J. Chem. Downloaded from www.nrcresearchpress.com by 210.87.254.40 on 09/05/12
For personal use only.

Methyl Isocyanide as a Key Molecule in Thermal Explosion Theory

HUW O. PRITCHARD

Centre for Research in Experimental Space Science, York University, Downsview, Ontario M3J 1P3

AND

BRIAN J. TYLER

Chemistry Department, U.M.I.S.T., Manchester 1, England

Thermal explosion limits have been measured in the temperature range 285–351 °C for methyl isocyanide and at 351 °C for mixtures of methyl isocyanide and methyl cyanide. We suggest that the methyl isocyanide isomerization is potentially the best reaction system against which to test thermal explosion theories, but at the present time certain kinetic, thermochemical, and thermodynamic data are not available with sufficient accuracy.

Les limites d'explosion thermique ont été évaluées dans l'intervalle de température allant de 285–351 °C pour l'isocyanure de méthyle et à 351 °C pour des mélanges isocyanure de méthyle et cyanure de méthyle. Le système réactionnel impliquant l'isomérisation de l'isocyanure de méthyle est, comme nous le suggérons, possiblement le meilleur système pour la vérification des théories d'explosion thermique; cependant, certaines données cinétiques, thermochimiques et thermodynamiques ne peuvent être présentement obtenues avec une précision suffisante. [Traduit par le journal]

Can. J. Chem., **51**, 4001 (1973)

Precise experimental tests of thermal explosion theory (1) require an exothermic reaction for which the mechanism and Arrhenius parameters are sufficiently well established to give accurate estimates of rates under explosive conditions. Typically the rates required will be at least an order of magnitude greater than those determined in kinetic investigations; in addition, the thermal conductivity of each gas mixture used, the heat of reaction, and the effect of diluents must be known. Few reactions meet these demanding requirements; those used recently have been either complex reactions (2) or of uncertain mechanism (3, 4). We suggest that the thermal isomerization of methyl isocyanide would be an ideal reaction for testing thermal explosion theory, including the effects of convection and reactant consumption, and now report some exploratory experiments designed to test this proposal.

The thermal isomerization of methyl isocyanide to methyl cyanide is exothermic to about 14.7 kcal mol^{-1} (5) and has been the subject of extensive kinetic studies because of its importance as a reaction against which to test theories of unimolecular reaction. The reaction is exceptionally clean and is almost entirely free of side reactions (6–8); in addition, the stability of the product and its thermodynamic similarity to the reactant molecule make it useful as a diluent and as a model molecule for admission studies.

Explosion limits were found by conventional techniques (2, 9) using a 1170-cc spherical Pyrex vessel equipped with a 0.0025-cm diameter thermocouple positioned in the center to monitor the temperature rise, and a rapid-response pressure transducer at the entry tube to measure the pressure in the vessel. In the subcritical region, the reaction was clean in the sense that the products were completely condensable, although we found one small side product (<1%) having the same retention time as ethyl cyanide; in the critical region, however, noncondensables were formed, except in the 3:1 dilution case described below. Since the observed explosion pressures were well into the fall-off region for the isomerization, the rate-constant data for 1–100 Torr at 230 °C (6) were represented as

$$[1] \quad \log_{10} k = -4.4266 + 0.7820 \log_{10} p - 0.09861 (\log_{10} p)^2$$

with p in Torr and the rate constant k_T at the experimental temperature and pressure was esti-

TABLE 1. Thermal explosion limits for methyl isocyanide

T (°C)	p_c (Torr)	ΔT_{max} (°C)	B*	λ_0†$\times 10^6$ cal(cm °C s)$^{-1}$	Rayleigh‡ No.	k_T§ (s^{-1})	δ_c*
284.6	42.5±0.5	28.8	55.6	86.0	1825	1.33×10^{-2}	6.94
292.2	28.7±0.2	31.3	53.7	88.8	770	1.72×10^{-2}	5.64
299.1	22.2±0.2	42.0	52.0	91.5	430	2.23×10^{-2}	5.29
311.9	14.70±0.07	37.6	49.2	96.5	165	3.62×10^{-2}	5.04
322.8	10.80±0.10	40.8	46.9	101.0	80	5.40×10^{-2}	5.00
334.7	7.75±0.10	41.4	44.6	105.5	35	8.10×10^{-2}	4.86
343.6	6.20±0.10	42.4	42.9	109.7	20	1.09×10^{-1}	4.81
350.7	5.25±0.05	38.5	41.6	112.7	15	1.38×10^{-1}	4.85

*For definitions of B and δ_c, see ref. 10; heat capacity data required for calculation of B taken from ref. 11.
†These are values for CH_3CN, estimated by extrapolating viscosity data of Craven and Lambert (12) and f_{obs} values of Vines and Bennett (13), and it is assumed that the thermal conductivity of CH_3NC is the same (*cf.* also ref. 6); our own measurements at 25 °C for CH_3CN and CH_3NC, respectively, give λ_0 values of 21.8 × 10^{-6} and 22.5 × 10^{-6} cal cm^{-1} °C^{-1} s^{-1}, with β values of 120 and 30% atm^{-1}, supporting this assumption reasonably well.
‡Calculated for a temperature rise ΔT = 40 °C, and using thermodynamic constants for CH_3CN.
§Calculated by substituting p_c into eq. 1 to get the rate constant at 230 °C, and then assuming an activation energy of 36500 cal mol^{-1}.

mated using the low-pressure activation energy of 36.5 ± 0.2 kcal mol^{-1} (6); this uncertainty in E introduces a shift of ±(0.15–0.20) in the calculated values of the critical initial rate parameter δ_c (10) at the test temperatures.

Table 1 presents explosion limit data for methyl isocyanide. The predicted values of δ_c and of ΔT_{max}, allowing for reactant consumption but ignoring convection and diffusion, are 4.1–4.3 and 40–50 °C, respectively (10); above 300 °C, the agreement is excellent, considering the nature of the extrapolation for k_T. At 300 °C and below, the large values of δ_c appear to be associated with convective processes. Figure 1 shows three just-critical temperature and pressure recordings for different cases. In Fig. 1*a*, the observed temperature at the center rises discontinuously, implying that explosion commenced elsewhere in the vessel; this effect is just discernible at 300 °C, but at higher temperatures there is no discontinuity in the temperature trace *cf.* Fig. 1*b*. The onset of these convective effects seems to be associated with Rayleigh numbers >400 and causes the maximum observed temperature rises (ΔT_{max}) to be rather low, as would be expected (4, 9).

The model calculations (10) also predict that if B (the dimensionless adiabatic temperature rise) is less than 14, an explosion proper will not occur because of excessive reactant consumption during the induction period. This is clearly shown in Fig. 1*c* where an inflection occurs, but the temperature rise dies because of reactant consumption, in this case at a value of $\Delta T \approx 225$ °C; there is also no sudden rise in the transducer plot, unlike the normal explosion cases. These

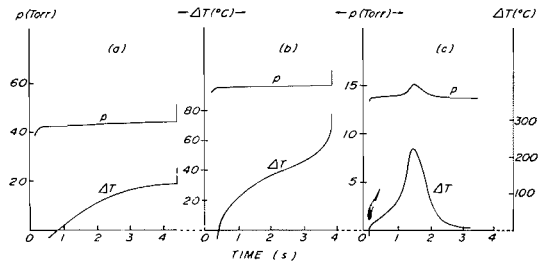

FIG. 1. Temperature and pressure traces in three just-critical experiments: (*a*) pure CH_3NC, T = 284.6 °C, initial pressure = 43.0 Torr; (*b*) pure CH_3NC, T = 311.9 °C, initial pressure = 14.8 Torr; and (*c*) mixture, CH_3NC + $3CH_3CN$, T = 350.7 °C, initial pressure = 13.8 Torr.

traces were obtained with a 3:1 CH_3CN–CH_3NC mixture, giving a B value of about 10 on the assumption that the two molecules have identical heat capacities; the data for this and for a 1:1 mixture are presented in Table 2, where it is seen that although Fig. 1*c* shows the expected behavior at low B, agreement with predicted critical parameters is poor. Reexamination of the model calculations (10) reveals that under these conditions, severe concentration gradients would also occur near threshold (10*b*) and therefore the simple theory without diffusion is inadequate in this regime.

We conclude therefore that this reaction shows considerable promise of being the best one against which to make precise tests of thermal explosion theory, once the following improved experimental data have been provided: (*i*) heats of formation of CH_3NC and CH_3CN; (*ii*) kinetic rate data, in the absence of self-heating, at much

Can. J. Chem. Downloaded from www.nrcresearchpress.com by 210.87.254.40 on 09/05/12
For personal use only.

TABLE 2. Thermal explosion limits for methyl isocyanide – methyl cyanide mixtures at 350.7 °C*

Reaction mixture	p_c (Torr)	ΔT_{max} (°C)	B	$k_T\ddagger \times 10$ (s^{-1})	δ_c Observed§	δ_c Theoretical‖
CH_3NC	5.25 ± 0.05	38.5	41.6	1.38	4.85	4.4
$CH_3NC + CH_3CN$	8.35 ± 0.05	76.1	20.8	1.79	5.01	5.1
$CH_3NC + 3CH_3CN$	13.64 ± 0.10	86.7†	10.4	2.35	5.37	~7

*See footnotes to Table 1 for additional information.
†Highest value obtaned for a temperature trace not showing an inflection.
‡Calculated as explained in footnote § of Table 1 on the assumption that the collision efficiency for CH_3CN is 0.91 of that for CH_3NC (14).
§Assuming both molecules have identical thermal conductivities.
‖From ref. 10*b*.

higher temperatures, together with a definitive characterisation of side reactions (if any); and (*iii*) thermal conductivity data up to at least 400 °C for CH_3CN (in anticipation of extension of the temperature range of these experiments) and for CH_3NC up to as high a temperature as is feasible. The authors of this paper hope to undertake task *ii* above and the further development of the model calculations to include diffusion, and hope that others may be persuaded to undertake experiments *i* and *iii*.

This work was performed while one of the authors (H.O.P.) was Visiting Professor at U.M.I.S.T., and travel assistance from the National Research Council of Canada and from the Nuffield Foundation is gratefully acknowledged. We would also like to thank Dr. C. K. Yip for providing a pure sample of methyl isocyanide.

1. D. A. FRANK-KAMENETSKII. Diffusion and heat exchange in chemical kinetics. Princeton University Press, 1955.
2. D. H. FINE, P. GRAY, and R. MACKINVEN. Proc. R. Soc. (London), A**316**, 255 (1970).
3. N. J. GERRI and F. KAUFMAN. Tenth Symposium (International) on Combustion. The Combustion Institute, 1965. p. 227.
4. P. G. ASHMORE, B. J. TYLER, and T. A. B. WESLEY. Eleventh Symposium (International) on Combustion. The Combustion Institute, 1967. p. 1133.
5. National Bureau of Standards, Washington, D.C. Technical Note 270–3.
6. F. W. SCHNEIDER and B. S. RABINOVITCH. J. Am. Chem. Soc. **84**, 4215 (1962).
7. C. K. YIP and H. O. PRITCHARD. Can. J. Chem. **48**, 2942 (1970).
8. T. FUJIMOTO, F. M. WANG, and B. S. RABINOVITCH. Can. J. Chem. **50**, 3251 (1972).
9. B. J. TYLER and W. H. ARCHER. To be published.
10. B. J. TYLER and T. A. B. WESLEY. (*a*) Eleventh Symposium (International) on Combustion. The Combustion Institute, 1967. p. 1115; (*b*) unpublished results.
11. S. W. BENSON. Thermochemical kinetics. John Wiley & Sons, New York. 1968.
12. P. M. CRAVEN and J. D. LAMBERT. Proc. R. Soc. (London), A**205**, 439 (1951).
13. R. G. VINES and L. A. BENNETT. J. Chem. Phys. **22**, 360 (1954).
14. S. P. PAVLOU and B. S. RABINOVITCH. J. Phys. Chem. **75**, 3037 (1971).

Can. J. Chem. Downloaded from www.nrcresearchpress.com by 210.87.254.40 on 09/05/12
For personal use only.

Can. J. Chem. Downloaded from www.nrcresearchpress.com by 210.87.254.6 on 09/05/12
For personal use only.

Canadian Journal of Chemistry

Published by
THE NATIONAL RESEARCH COUNCIL OF CANADA

Journal canadien de chimie

Publié par
LE CONSEIL NATIONAL DE RECHERCHES DU CANADA

Volume 51 Number 24 December 15, 1973 Volume 51 numéro 24 15 décembre 1973

The Densities, Viscosities, and Diffusion Coefficients of Solutions of Mono-, Di-, and Triethylamine in Water

A. N. CAMPBELL AND S. Y. LAM

Department of Chemistry, University of Manitoba, Winnipeg, Manitoba R3T 2N2

Received January 18, 1973[1]

The densities, relative viscosities, and diffusion coefficients of the binary systems, monoethylamine–water, diethylamine–water, both at 25 °C, and triethylamine–water at 17 °C, slightly below its lower critical solution temperature, were investigated experimentally.

Densities were determined with Ostwald–Sprengel type pycnometers and viscosities by means of Cannon and Fenske viscometer. The diffusion coefficients of the amines in aqueous solution were obtained by the Stokes diaphragm cell method. Monoethylamine has the highest diffusion rate. Plotting D *vs.* c and extrapolating to $c = 0$ gives an apparent D^0 which, for all three amines, is notably smaller than the value given by the Nernst model.

Les densités, les viscosités relatives et les coefficients de diffusion des systèmes binaires, monoéthylamine–eau et diéthylamine-eau à 25 °C et du système triethylamine–eau à 17 °C, légèrement en dessous de sa plus basse température de solution cinétique ont été étudiés expérimentalement.

Les densités ont été déterminées à l'aide d'un pycnomètre de type Ostwald–Sprengel, les viscosités à l'aide d'un viscosimètre de Cannon et Fenske. Les coefficients de diffusion des amines en solutions aqueuses ont été obtenus par la méthode de la cellule à diaphragme de Stokes.

La monoéthylamine a la plus haute vitesse de diffusion. En reportant D en fonction de c et en extrapolant pour la valeur $c = 0$ on obtient pour les trois amines une valeur de D^0 nettement plus faible que la valeur donnée par le modèle de Nernst. [Traduit par le journal]

Can. J. Chem., **51**, 4005 (1973)

Introduction

This work deals principally with the determination of the diffusion coefficients, in water, of mono-, di-, and triethylamine. Viscosities of binary mixtures of the amines and water were also measured, since viscosity is necessary in the study of diffusion. The temperature chosen for the investigation of the completely miscible systems monoethylamine–water and diethylamine–water was 25 °C. Since we found that mixtures of monoethylamine and water containing more than about 70 mol% amine boiled at 25 °C, measurements were not extended beyond this upper limit of concentration. For the system triethylamine–water, the temperature of investigation was 17 °C, since the two components are completely miscible at this temperature. Both triethylamine–water and diethylamine–water have lower critical solution temperatures, *i.e.* the mutual solubility decreases with rising temperature. This common behavior is presumably determined by the same pattern of molecular interaction in solution.

Experimental

Water of specific conductance of the order of 1×10^{-6} ohm^{-1} cm^{-1} was obtained by passing ordinary distilled water through an ion exchange column with a mixed bed of ion-exchange resins. The amines were the best com-

[1]Revision received August 22, 1973.

Can. J. Chem. Downloaded from www.nrcresearchpress.com by 210.87.254.6 on 09/05/12
For personal use only.

mercial products. Triethylamine and diethylamine were refluxed with sodium and with sodium hydroxide pellets and distilled. The fractions used distilled at 88.8 ± 0.5 and 55.7 ± 0.5 °C for triethylamine and diethylamine, respectively. Weighed samples of the distilled amines neutralized the theoretical quantities of hydrochloric acid within ±0.2%, using methyl red as indicator. Monoethylamine was used without further purification.

Preparation and Analysis of Solutions

Aqueous stock solutions of known concentrations of triethylamine and of diethylamine were prepared by mixing conductivity water and amine in known masses. The densities were determined and hence the compositions of the stock solutions were known in weight percent, mole percent, molality, and molarity. A stock solution of approximately 70 mol% monoethylamine was prepared in the same way. Because of the volatility of monoethylamine, however, the concentrations of the dilute solutions prepared by diluting this stock solution were obtained volumetrically, by adding excess of standard HCl and back titrating with standard NaOH, using methyl red as indicator. The densities of these diluted solutions were also determined.

Density Measurements

Densities were determined with Ostwald-Sprengel type pycnometers, of approximately 25 ml capacity.

Viscosity Measurements

Viscosities were measured with a Cannon and Fenske (1) type viscometer, with a run time of about 400 s. It was calibrated with water at 17 and 25 °C. The run times were reproducible within 0.05%.

Diffusion Measurements

Diffusion coefficients were measured by the Stokes magnetically stirred diaphragm cell method (2). A slight modification of the Stokes cell was made. Instead of the rubber stoppers used by Stokes, the necks of the cell were closed with a capillary bore stopcock at the bottom and with a fine capillary plug at the top.

In order to keep the diaphragm in the degassed condition, in all subsequent transfers of solution or solvent to and from the cell compartments, special side-hole pipettes recommended by Janz and Mayer (3) were used. Since the amine solutions had smaller densities than that of water, the former were placed in the upper compartment. The duration of the pre-diffusion run was determined by the Gordon criterion (4), $t = 1.2l^2/D$, where D is the diffusion coefficient and l the thickness of the frit.

The stirring rate within the cell was 60 r.p.m., sufficiently rapid to prevent the formation of layers of stagnant solution in the vicinity of the cell diaphragm, since Stokes (2) reported that any rate between 25 and 80 r.p.m. was sufficient. The diaphragm cell constant was obtained at 25 °C by using approximately 1 M potassium chloride solution in the lower compartment and pure water in the upper. The cell constant was redetermined after every three runs and the cell constant for each experimental run obtained by interpolation.

With an analytical error less than 0.2%, a precision of about ±0.5% is to be expected in the integral diffusion coefficient. The concentrations of the solutions were kept above 0.05 M, because, as pointed out by Stokes (2), surface transport in the diaphragm could lead to considerable errors below this concentration.

Results

Densities and Relative Viscosities

The experimental results are to be found in the Depository of Unpublished Results.[2] From the densities, the partial molar volumes have been obtained by the method of intercepts and these are reproduced graphically in Figs. 1 and 2. The viscosities are expressed graphically as functions of mole fraction and of volume fraction of amine in Fig. 3.

Diffusion Coefficients

The experimental results are to be found in Depository, or, in full detail, in the Ph.D. thesis of S. Y. Lam. (5).

Figure 4 gives graphical representation of differential diffusion coefficients as functions of concentration.

We also attempted to fit the experimental diffusion coefficients to the Hartley–Crank equation (6–8) but, as one of the referees has pointed out, there is some doubt whether the Hartley–Crank equation is really applicable to these hydrophobic solutes, we have relegated the cal-

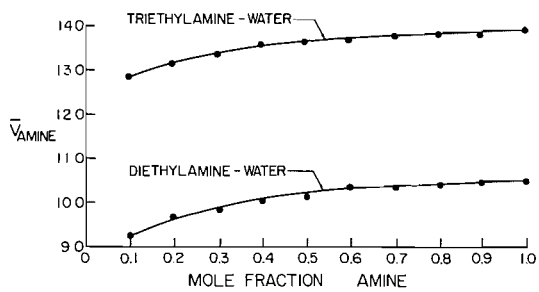

FIG. 1. Partial molar volumes of amines.

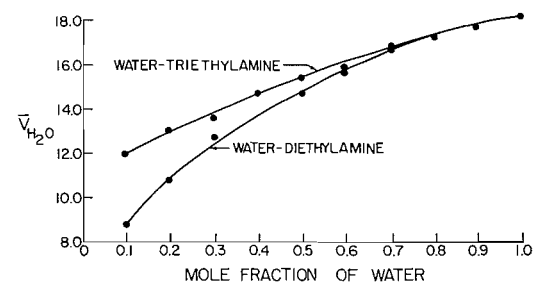

FIG. 2. Partial molar volumes of water.

[2]Complete set of tabular data is available, at a nominal charge, from the Depository of Unpublished Data, National Science Library, National Research Council of Canada, Ottawa, Canada K1A 0S2.

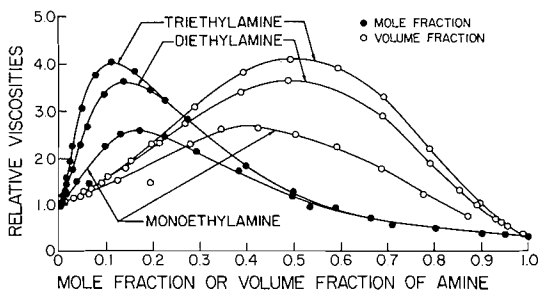

FIG. 3. Relative viscosity *vs.* composition.

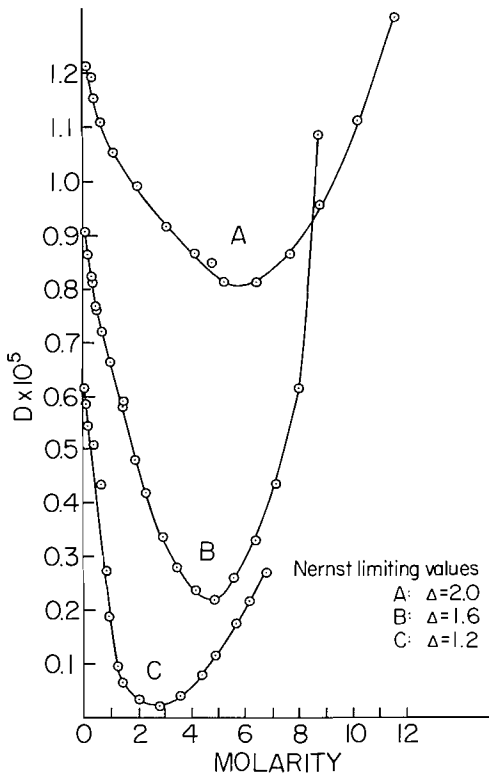

FIG. 4. *D vs. c* for monoethylamine and diethylamine in aqueous solutions at 25 °C, and for triethylamine at 17 °C. (*A* = monoethylamine; *B* = diethylamine; *C* = triethylamine; Nernst limiting value = Δ.)

culations and graphs to the Depository of Unpublished Data.

Summary

Of the ethylamines, monoethylamine has the highest derived diffusion coefficient at infinite dilution. Examination of diffusion data in the literature indicates an increase of about 25% in numerical value when the temperature increases by 10°. Even allowing for this, however, the derived diffusion coefficient of triethylamine is still the smallest. The Nernst limiting values are higher than the corresponding derived values and this is not surprising, since the Nernst values are calculated by regarding the diffusing entities as "aminium" and hydroxyl ions; the mobility of the hydroxyl ion is exceptionally high.

While the viscosities of all three systems are practically the same in the regions dilute with respect to water and to amine (the viscosities of all three pure amines are practically the same), a pronounced maximum viscosity occurs at volume fraction 0.5 for di- and triethylamine (the two systems which are known to exhibit partial miscibility under appropriate conditions). A similar maximum occurs at volume fraction 0.4, for monoethylamine.

The values of D, the integral diffusion coefficient, were plotted against c, the concentration of amine. The calculated Nernst limiting values are: $D° = 2.002 \times 10^{-5}$ for monoethylamine at 25 °C; 1.640×10^{-5} for diethylamine at 25 °C; and 1.192×10^{-5} for triethylamine at 17 °C.

To calculate these limiting values, it is necessary that the limiting ionic conductances should be known and these we have recently determined (9). It is not surprising that the curves do not extrapolate to the values of D^0, since the calculation assumes complete ionization and this is never attained with weak electrolytes like the ethylamines, except perhaps at a theoretically infinite dilution.

The shapes of the curves of Fig. 4, despite the fact that the temperatures are not all the same, show considerable similarity. They all show a distinct minimum. Though this minimum does not occur exactly at the composition corresponding to the maximum in viscosity, there is an obvious connection; other things being equal, the more viscous the medium, the more slowly the particle will diffuse.

In general, the diffusion coefficients decrease from monoethylamine to triethylamine. At the minimum, the magnitudes of the diffusion coefficients rounded off to powers of ten, diminish from about 1×10^{-5} cm^2/s for monoethylamine, to 0.1×10^{-5} cm^2/s for diethylamine, to 0.01×10^{-5} cm^2/s for triethylamine, and this is low in comparison with the values found for most substances, which are of the order of 1×10^{-5} cm^2/s.

Krichevskii and Tsekhanskaya (10) also found the diffusion rate of triethylamine to be low.

Can. J. Chem. Downloaded from www.nrcresearchpress.com by 210.87.254.6 on 09/05/12
For personal use only.

1. M. J. CANNON and M. R. FENSKE. Ind. Eng. Chem. Anal. Ed. **10**, 299 (1938).
2. R. H. STOKES. J. Am. Chem. Soc. **72**, 763 (1950).
3. G. J. JANZ and G. E. MAYER. Office of Saline Walter, U.S. Department of the Interior, Research and Development Progress Report No. 196 (1966).
4. A. R. GORDON. Ann. N.Y. Acad. Sci. **46**, 285 (1945).
5. S. Y. LAM. Ph.D. Thesis. University of Manitoba. Winnipeg, Manitoba. 1972.
6. G. S. HARTLEY and J. CRANK. Trans. Faraday Soc. **45**, 801 (1949).
7. B. F. WISHAW and R. H. STOKES. J. Am. Chem. Soc. **76**, 2065 (1954).
8. R. A. ROBINSON and R. H. STOKES. Electrolyte solutions. 2nd ed. Butterworth Scientific Publications, London. 1959. p. 325.
9. A. N. CAMPBELL and S. Y. LAM. Can. J. Chem. **51**, 551 (1973).
10. I. R. KRICHEVSKII and YU. V. TSEKHANSKAYA. Zh. Fiz. Khim. **30**, 2315 (1956).

Can. J. Chem. Downloaded from www.nrcresearchpress.com by 210.87.254.6 on 09/05/12
For personal use only.

Electron Spin Resonance Studies in Aqueous Solution: Fragmentation of Radical Intermediates Derived from β-Amino Alcohols

TERRY FOSTER AND PAUL RONALD WEST

Department of Chemistry, University of Victoria, Victoria, British Columbia

Received June 18, 1973

In acidic aqueous solution, oxidation of the β-amino alcohols $R_3\overset{+}{N}CH_2CH_2OH$, I, and $R_3\overset{+}{N}CH_2CHOHCH_3$, II, (R = H, alkyl) using the Ti(III)–H_2O_2 flow technique gave the radicals $R_3\overset{+}{N}CH_2\dot{C}HOH$, and $R_3\overset{+}{N}CH_2\dot{C}OHCH_3$. The spectrum of $(CH_3)_2\overset{+}{N}HCH_2\dot{C}OHCH_3$ shows restricted rotation about the C_1—C_2 bond assigned to intramolecular hydrogen bonding.

Under neutral conditions, oxidation of I gave the spectrum of $\cdot CH_2CHO$, and of II the acetonyl radical $\cdot CH_2COCH_3$. It is proposed that elimination occurs by deprotonation of the abstraction radical in a hydrogen-bonded conformation, followed by rapid fragmentation to yield the α-carbonyl radical.

En solution aqueuse acidique, l'oxydation des β-amino alcools $R_3\overset{+}{N}CH_2CH_2OH$, **1**, et $R_3\overset{+}{N}CH_2CHOHCH_3$, **II** (R = H, alcoyle) en utilisant le système Ti(III)–H_2O_2 a conduit aux radicaux $R_3\overset{+}{N}CH_2\dot{C}HOH$ et $R_3\overset{+}{N}CH_2\dot{C}OHCH_3$. Le spectre de $(CH_3)_2\overset{+}{N}HCH_2\dot{C}OHCH_3$ a révélé une rotation limitée autour du lien C_1—C_2 attribuable à un enchaînement par liaison hydrogène intramoléculaire.

Dans des conditions neutres, l'oxydation de **I** a conduit au $\cdot CH_2CHO$ alors que l'oxydation de **II** a conduit au radical acétonyle, $\cdot CH_2COCH_3$. On suggère que l'élimination s'effectue par déprotonation du radical d'abstraction dans une conformation comportant une liaison hydrogène, puis par fragmentation rapide pour donner le radical α-carbonyle. [Traduit par le journal]

Can. J. Chem., **51**, 4009 (1973)

Introduction

In reaction with the hydroxyl radical, many alcohols **1** undergo preferential hydrogen atom abstraction at the α (carbinol) carbon (eq. 1).

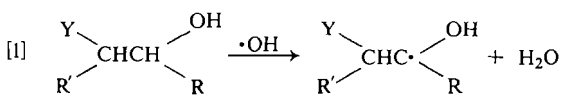

[1]

R, R′ = H, alkyl

1 **2**

The secondary radicals **2** have been detected by e.s.r. spectroscopy during radiolysis of aqueous solutions (1), photolysis of alcohols containing hydrogen peroxide (2), and by use of the Ti(III)–H_2O_2 reaction in a rapid flow system (3). When the alcohol bears certain β substituents (notably Cl, Br, and OH), radical **2** may undergo a polar elimination process generating an α-carbonyl radical **3** and losing the substituent Y^- (eq. 2) (4, 5).

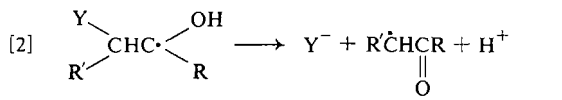

[2]

2 **3**

Acid-catalysis of the elimination of hydroxide ion during oxidation of 1,2-ethanediol (**1** R, R′ = H, Y = OH) was demonstrated in photolysis studies (2), and in the Ti(III)–H_2O_2 experiments (4) by e.s.r. observation of radical **5** (eq. 3).

[3]

4 **5**

By way of confirmation, a recent pulse radiolysis study indicated this elimination was complete at p*H* 1.0 immediately following a 5 μs pulse (6).

In the p*H* 4.0–7.0 range, however, only the abstraction radical **4** was detected in the e.p.r. and pulse radiolysis work. It has been suggested that the rate of the uncatalyzed elimination (eq. 2), was too slow at high steady-state radical concentrations to compete with bimolecular termination (7). Indeed, continuous γ irradiation of neutral aqueous solutions of 1,2-ethanediol containing added H_2O_2 (7) or N_2O (8) revealed a chain reaction that produced acetaldehyde. It was proposed that at these lower radical concentrations, elimination did occur and that radical **5** propagated the chain. Furthermore, e.s.r. spectra of α-carbonyl radicals **3** were recorded at p*H* 4.6 for 1,2-propanediol oxidation (**1** R = H, R′ = CH_3, Y = OH) and under neutral conditions for 2,3-butanediol (**1** R, R′ = CH_3,

Can. J. Chem. Downloaded from www.nrcresearchpress.com by 210.87.254.42 on 09/05/12
For personal use only.

Can. J. Chem. Downloaded from www.nrcresearchpress.com by 210.87.254.42 on 09/05/12
For personal use only.

Y = OH) (5). The observation of deoxy sugars as products of the photolysis (9) and radiolysis (10) of neutral aqueous solutions of carbohydrates was also rationalized by the same reaction sequence (reactions 1, 2).

An apparent change in this established mechanism of elimination has been reported in the case of quaternary *N*-methyl derivatives of 2-aminoethanol. Electron spin resonance studies on the γ irradiation of crystalline choline chloride (**1** R, R′ = H, Y = $(CH_3)_3\overset{+}{N}$—) (11), and on the oxidation of its aqueous solutions in the Ti(III)–H_2O_2 systems (5) both assigned $(CH_3)_3\overset{+}{N}\cdot$ as the only observed fragmentation or elimination radical. Homolysis of the β C—N bond was proposed to account for cation radical formation (eq. 4). Interest in the solid state radiolysis arose from the efficient chain production of acetaldehyde and trimethylamine hydrochloride (G = 55 000) (12, 13).

$$[4]\quad (CH_3)_3\overset{+}{N}CH_2\dot{C}HOH \rightarrow (CH_3)_3\overset{+}{N}\cdot + CH_2{=}CHOH \rightleftharpoons CH_3CHO$$

In solution at pH 1.0, 2-hydroxyethyltriethylammonium chloride (**1** R, R′ = H, Y = $(CH_3CH_2)_3\overset{+}{N}$—) also gave the cation radical spectrum (5). However, under the same conditions other 2-aminoethanol derivatives (Y = $\overset{+}{N}H_3$, $CH_3\overset{+}{N}H_2$, $(CH_3)_3\overset{+}{N}H$) gave only the abstraction radicals **2**. The results are unexpected in view of the usual tendency of a quaternary nitrogen substituent to be eliminated as the amine moiety, just as predicted on the basis of the previously observed elimination reactions (reaction 2).

In this paper we report an e.s.r. study on the oxidation of both 2-aminoethanol (**1** R, R′ = H, Y = $\overset{+}{N}H_3$) and 1-amino-2-propanol (**1** R = CH_3, R′ = H, Y = $\overset{+}{N}H_3$) and related *N*-alkyl derivatives, in both acidic and neutral solution. Conditions are established under which the established polar radical elimination pathway (reaction 2) is operative for these substrates.

Experimental

General

For the aqueous flow experiments, a Varian E-6S X-band e.s.r. spectrometer was equipped with a commercial all-quartz two-entry T-mixing chamber (Varian model E-249) having a specified mixing volume of 2.5×10^{-3} ml. The flat sample cell is an integral part of the device, providing a total reacting volume to the view point of 0.080 ml. Flow rates for the two reactant solutions of 150 ml per min were generated by gravity feed, and controlled by a water aspirator applied to the exit tubing. A Gilmont #13 "Compact" flowmeter was inserted in each stream. Hyperfine splitting constants (h.f.s.) were measured to ±0.1 G, and g values to ±0.0002 employing Fremy's salt (a_N = 13.0 G, g = 2.0055) as a standard (14). Alternatively, direct comparison was made to the $\cdot CH_2OH$ radical (a_{CH_2} = 17.57 G, g = 2.0032) generated during the flow experiment by addition of a large excess of methanol as co-substrate (15).

pH measurements (to ±0.1 units) were made on all reactant and effluant solutions. Water from the building supply was routinely used after determining that its substitution for distilled water made no detectable change in the nature or quality of the spectra that were obtained. Commercially available aminoalcohols and inorganic reagents were of Fisher Certified Reagent or Aldrich reagent grade unless otherwise specified. In the amine syntheses, n.m.r. spectra were recorded on a Perkin–Elmer R12A instrument employing CCl_4 solvent and TMS as internal standard, or D_2O with TMS external.

Flow Experiments

(a) Acidic Conditions

In the oxidation of the aminoalcohols at pH 2.0, one reactant stream contained 0.02 M titanium(III) chloride (Fisher Reagent, 20% solution) adjusted to pH 2.0 with concentrated sulfuric acid; and the other stream contained 0.1 M hydrogen peroxide (Fisher Certified, 30% solution), and 0.5 M alcohol substrate, acidified to pH 2.0 with concentrated sulfuric acid. All solutions were deaerated with oxygen-free nitrogen gas for at least 15 min prior to reaction. Titanium(III) stock solution was not added until after degassing to minimize oxidation of the metal ion.

(b) Neutral Conditions

After deaerating a 0.02 M solution of disodium ethylenediaminetetraacetate, titanium(III) chloride was added to a final concentration of 0.02 M; and the pH adjusted to 7.5 with concentrated NH_4OH (d = 0.880). The second solution was made 0.5 M in organic substrate, 0.1 M in hydrogen peroxide, and adjusted to pH 7.5 with concentrated sulfuric acid. It should be noted that a reduction in the pH of the effluant solution to pH 6.5–7.0 is observed. (In this work we have ensured that the results reported at pH 2.0 for the abstraction radicals do not qualitatively change in the range 1.5–2.5 unless specified. Similarly eliminations reported at pH 7.0 have been verified in the range 6.0–8.0.)

(c) Reduction with the Formic Acid Radical ·COOH

The reduction of chloroacetone $ClCH_2COCH_3$ and the aminoketone $(CH_3)_2NCH_2COCH_3$ via the oxidation of formic acid was carried out using an all-glass mixing device that allows the simultaneous mixing of three reactant streams. The design has been previously described by Norman and co-worker (16). In these experiments, one stream contained 0.02 M titanium(III) chloride and 0.5 M formic acid, the second 0.1 M hydrogen peroxide, and the third 0.5 M organic substrate. All solutions were adjusted to pH 2.0 prior to reaction.

TABLE 1. Hyperfine splitting constants for the radicals $R_3\overset{+}{N}CH_2\dot{C}HOH$;* R = H, CH_3, $HOCH_2CH_2$

	Aminoalcohol	a_{CH_α}	$a_{CH_2\beta}$	a_N	a_{OH}	a_{NH^+}
6	$\overset{+}{N}H_3CH_2CH_2OH$	18.0	11.6	10.5	1.0	—†
7	$CH_3\overset{+}{N}H_2CH_2CH_2OH$	18.6	11.0	11.0	1.0	0.8(2H)
8	$(CH_3)_2\overset{+}{N}HCH_2CH_2OH$	19.0	9.9	12.0	1.4	1.4(1H)
9	$(CH_3)_3\overset{+}{N}CH_2CH_2OH$	19.7	8.5	13.6	1.8	—
10	$\overset{+}{N}H_2(CH_2CH_2OH)_2$	18.5	10.9	11.0	1.1	1.1(2H)
11	$\overset{+}{N}H(CH_2CH_2OH)_3$	19.1	9.7	11.9	1.2	1.2(1H)

*g-Values of all radicals were 2.0032 ± 0.0002.
†No further resolved splitting, line width 0.5 G.

(d) Spectral Simulation

A program (QCPE 160) was used that allowed simulation of two or more radicals with different g-value and line width.[1]

Preparation of Aminoalcohols

(i) 2-Hydroxyethyltriethylammonium Chloride

2-Chloroethanol (40.0 g, 0.5 mol) and triethylamine (25.0 g, 0.25 mol) were heated under reflux for 7 h. On cooling, two layers formed. The lower layer, containing the desired quaternary salt and excess 2-chloroethanol, was washed repeatedly with ether, and the resulting syrup recrystallized from ethanol–ether to yield 30 g (0.18 mol; n.m.r. (D_2O): 8.76 (9H, t, J = 7.5 Hz), 5.67 (6H, q, J = 7.5 Hz), 5.77 (2H, m), and 5.10 (2H, m).

(ii) 2-Hydroxypropyltrimethylammonium Chloride

A solution of *N,N*-dimethylamino-2-propanol (50.0 g, 0.49 mol) in 500 ml of absolute ethanol was heated under reflux (Dry Ice – acetone condenser) while chloromethane was bubbled through the mixture until an aliquot no longer showed $(CH_3)_2N$–n.m.r. absorption. After cooling the reaction mixture (Dry Ice – acetone), anhydrous ether was added until precipitation ceased. Recrystallization (ethanol–ether) and vacuum desiccation (10 h) gave the hygroscopic salt (69 g, 0.45 mol), m.p. 163–165° (lit. (17) 165°); n.m.r. (D_2O): 6.90 (9H, s), 8.86 (3H, d, J = 7.0 Hz), 6.59 (s) and 6.78 (d, J = 0.5 Hz) total 2H, and 5.65 (1H, m).

(iii) 1-(N-methylamino)-2-propanol and 1-(N-methyl,N-(2-hydroxypropyl)-amino)-2-propanol

Both amines were isolated from the reaction of propylene oxide and methylamine. Propylene oxide (40 g, 0.7 mol) and methylamine (28 g, 0.33 mol), the latter added as the 40% aqueous solution, were heated under reflux for 30 min. On distillation (1 atm) 1-(*N*-methylamino)-2-propanol was collected at 148–150° (10 g, 0.11 mol); n.m.r. (D_2O): 7.83 (3H, s), 8.97 (2H, d, J = 7.0 Hz), 7.62 (2H, d, J = 7.0 Hz), and 6.23 (1H, sextet, J = 7.0 Hz). 1-(*N*-methyl,*N*-(2-hydroxypropyl)amino)-2-propanol was collected at 225 °C (28 g, 0.19 mol); n.m.r. (D_2O): 8.41 (6H, d, J = 7.0 Hz), 5.57 (2H, sextet, J = 7.0 Hz), and 7.17 (7H, m, CH_3—N and CH_2). Prolonged reflux led to increased yields of *tertiary* amine, but no attempt to optimize the yields of the respective amines has been made.

(iv) N,N-Dimethylamino-2-propanone

The reaction of bromoacetone with aqueous dimethylamine by the method of Craig *et al.* (18) gave *N,N*-dimethylamino-2-propanone in 40% yield, b.p. 115° (lit. (18) 114°); n.m.r. (CCl_4): 7.79 (6H, s), 7.07 (2H, s), and 7.94 (3H, s).

Results

2-Aminoethanol and Related Compounds

(i) Hydrogen Abstraction Radicals

In acidic aqueous solution, all the aminoalcohols under consideration are in the protonated form. The deactivating effect of a $-\overset{+}{N}(R)_3$ substituent (R = alkyl or H) on hydrogen abstraction by the electrophilic OH radical is consistent with the exclusive observation of the radicals $R_3\overset{+}{N}CH_2\dot{C}HOH$ at pH 2.0. In Table 1, the hyperfine splitting constants (h.f.s.) for a series of these abstraction radicals show a pattern of low β hydrogen h.f.s. constants (10–13 G) and relatively large β nitrogen splitting (10–12 G).[2] In the case of the radical $CH_3\overset{+}{N}H_2CH_2\dot{C}HOH$, we report for the first time the resolution of the NH and OH h.f.s. constants for radicals of this type. The fine structure consists of a doublet (a_{OH}(1H) = 1.0 G) of triplets ($a_{NH_2^+}$ (2H) = 0.8 G) recorded in a spectrum with line width <0.1 G. In the pH range indi-

[1]By B. S. Snowden Jr. and E. T. Strom of Mobile Research and Development Corporation, Dallas.

[2]Agreement to within experimental error is noted with values published after the completion of this work by Norman and co-workers for compounds (**6–9**) (5).

Can. J. Chem. Downloaded from www.nrcresearchpress.com by 210.87.254.42 on 09/05/12
For personal use only.

Can. J. Chem. Downloaded from www.nrcresearchpress.com by 210.87.254.42 on 09/05/12
For personal use only.

cated no other resonances are observed for these compounds, while signal intensity is near the maximum observed using the flow technique. In particular repeated attempts to observe the radical $(CH_3)_3\overset{+}{N}\cdot$ from choline chloride oxidation ($R_3\overset{+}{N}$— = $(CH_3)_3\overset{+}{N}$—) were unsuccessful.[3]

(ii) Secondary Elimination Radicals

(a) Acetaldehyde Radical $\cdot CH_2CHO$

Oxidation of the aminoalcohols **6–8** and **10** (Table 1) at p*H* 6.5–7.5 (effluant) provided spectra dominated by the $\cdot CH_2CHO$ radical. Previously unreported in neutral aqueous solution, this species has spectral parameters unchanged from those at p*H* 1.0 (4), namely $a_{CH_2}(2H) = 19.0$ G, $g = 2.0045$, and a line width of 1.0 G. In addition, one detects weaker resonances from the radicals **12–14** associated with generation of $\cdot CH_2CHO$ in aqueous solution (5).[4]

$\cdot CH_2CH(OH)_2$ $HOCH_2\dot{C}HOH$ $O{=}CHCH_2CH_2\dot{C}HOH$

12 **13** **14**

At p*H* 6.5–7.5, spectra of sufficient intensity to interpret have not yet been observed for triethanolamine **11** and the quaternary ion $(CH_3)_3\overset{+}{N}CH_2CH_2OH$, **9**. However, for all of the compounds **6–11**, the abstraction radical spectrum (*e.g.* $R_3\overset{+}{N}CH_2\dot{C}HOH$) does *not* persist under conditions where $\cdot CH_2CHO$ and related species are detected (p*H* > 5.0).

(b) Fragmentation of $(CH_3CH_2)_3\overset{+}{N}CH_2\dot{C}HOH$

At p*H* 1.6, the triethyl quaternary ion $(CH_3CH_2)_3\overset{+}{N}CH_2CH_2OH$ gave an intense spectrum attributed to $(CH_3CH_2)_3\overset{+}{N}\cdot$ ($a_N(1) = 20.2$ G, $a_{CH_2}(6H) = 22.1$ G) as previously reported (5).[5] At p*H* 2.5–4.0, a complex spectrum appeared dominated by the radical $\cdot CH_2CH(OH)_2$ **12** ($a_{CH_2}(2H) = 22.4$ G, $a_{CH}(1H) = 18.7$ G, $g = 2.0025$); with weaker lines clearly assigned to the species $HOCH_2\dot{C}HOH$ **13** ($a_{CH_2}(2H) = 9.4$ G, $a_{CH}(1H) = 18.0$ G, $a_{OH}(1H) = 1.0$ G, $g = 2.0032$) and $O{=}CHCH_2CH_2\dot{C}HOH$ **14** ($a_{CH}(1H) = 15.2$ G, $a_{CH_2}(2H) = 20.2$, γCH_2 splitting unresolved, $g = 2.0032$). In striking contrast to choline, no spectra of simple abstraction radicals are identified at p*H* 1.5–2.5.

1-Amino-2-Propanol and Related Compounds

(i) Hydrogen Abstraction Radicals

In Table 2, h.f.s. constants are given for the radicals $R_3\overset{+}{N}CH_2\dot{C}OHCH_3$ (R = H, alkyl) observed during the oxidation of the corresponding alcohols at p*H* 2.0–4.5. In the spectra from **16–18**, the N—H hydrogen splittings are again resolved, but no splitting due to the OH group can be detected. However, at p*H* 2.0 in water, no splitting due to hydroxyl hydrogen is detected for the radical $(CH_3)_2\dot{C}OH$ a good model for **16–18**. In the spectra of **17** and **18** severe broadening of the central lines of the β-hydrogen triplet creates the impression of a single (doublet) splitting. Indeed this apparent anomaly in the spectrum from **17** led us to examine the oxidation of **18**. Computer simulation shows the spectra to be compatible with splitting from two β-hydrogens only if the central lines of each triplet are assigned a higher line width (0.8 G) than the remaining resonances. The phenomenon is analyzed in terms of hindered rotation (see Discussion).

(ii) Secondary Elimination Radicals

At p*H* 6.5–7.5, the dominant signal from **15–18** was the acetonyl radical $\cdot CH_2COCH_3$ ($a_{CH_2}(2H) = 19.7$ G, $a_{CH_3}(3H) = 1.1$ G, $g = 2.0042$). The central quartet is resolved, but has a line width twice as great as the wing multiplets. The drastic simplification of the spectrum makes evident in each case a weaker spectrum of radicals of the type $\cdot CH_2CHOHCH_2\overset{+}{N}R_3$ ($g = 2.0025$), mostly appearing as an unresolved quartet with broadened center lines ($a(3H) = 22.7 \pm 0.5$ G). Only in the case of $\overset{+}{N}H_3CH_2CHOH\dot{C}H_2$ was further resolution possible ($a_{CH_2}(2H) = 22.4$ G, $a_{CH}(1H) = 24.0$ G). The line width of the wing resonances was still 1.3 G, evidently due to an unresolved γ hydrogen splitting (compare $\cdot CH_2CHOHCH_3$, $a_{CH_3}(3H) = 0.8$ G) (19). However, referring to $\cdot CH_2$-

[3]Simulated spectra of the $(CH_3)_3\overset{+}{N}CH_2\dot{C}HOH$ species with low percentage intensities of the resonances from $(CH_3)_3\overset{+}{N}\cdot$ ($a_{CH_3}(9H) = 28.6$ G, $a_N(1) = 20.3$ G) were used to evaluate the experiments.

[4]In neutral solution, we suggest ·OH addition to $CH_2{=}CHOH$ in the continuing secular equilibrium is the likely source of **12** and **13** with **14** arising from $\cdot CH_2CHO$ addition to the enol as previously suggested (5).

[5]The lack of observation of $(CH_3)_3\overset{+}{N}\cdot$ from choline oxidation in this work must then be attributed to not achieving the exact conditions of the earlier study (5).

TABLE 2. Hyperfine splitting constants for the radicals $R_3\overset{+}{N}CH_2\dot{C}OHCH_3$;* R = H, CH_3, $CH_2CH(CH_3)OH$

	Aminoalcohol	$a_{\beta CH_3}$	$a_{\beta CH_2}$	a_N	a_{N-H^+}
15	$\overset{+}{N}H_3CH_2CHOHCH_3$	21.3	11.6	9.7	—†
16	$CH_3\overset{+}{N}H_2CH_2CHOHCH_3$	21.9	11.0	11.0	1.0(2H)
17	$(CH_3)_2\overset{+}{N}HCH_2CHOHCH_3$	21.7	9.9‡	12.5	1.4(1H)
18	$(CH_3CHOHCH_2)(CH_3)\overset{+}{N}HCH_2CHOHCH_3$	21.5	9.8‡	12.5	1.4(1H)

*g-Values were 2.0032 ± 0.0002.
†No further splitting was resolved.
‡The center lines of the triplet splitting are broadened and detected only in the outer multiplets.

$CHOHCH_2OH$ as a model ($a_{CH_2}(2H)$ = 22.3 G, $a_{CHOH}(1H)$ = 24.6 G) (5), the above assignment seems appropriate.

Both at p*H* 2.0 and at p*H* 7.0, oxidation of the quaternary cation $(CH_3)_3\overset{+}{N}CH_2CHOHCH_3$ gives the same spectrum, assigned as $(CH_3)_3\overset{+}{N}CH_2CHOH\dot{C}H_2$ (a(3H) = 22.7 ± 0.5, g = 2.0025).

Reduction of α-Substituted Ketones

The oxidation of formic acid (0.5 *M*) in the presence of the aminoketone cation, $(CH_3)_2\overset{+}{N}HCH_2COCH_3$ was undertaken as a route to the anomalous abstraction radical from alcohol **17** via one-electron reduction of the carbonyl group by $\cdot CO_2H$. At p*H* 2.0, reduction did occur to give a weak spectrum of the desired abstraction radical, but also an equal intensity of the acetonyl radical. At p*H* 4.0 only the radical $\cdot CH_2COCH_3$ was observed. When chloroacetone replaced the aminoketone as substrate, acetonyl radical was again the sole species observed at p*H* 4.0. Evidently the intermediate anion radical eliminates the β substituent in a process closely akin to the eliminations from alcohol abstraction radicals (see Discussion).

Discussion

The anomalously low β h.f.s. constants that are observed for organic π radicals of the type $YCH_2\dot{C}HX$ have been analyzed by Norman and co-workers (20) in a wide-ranging general treatment. Observing that the phenomenon was restricted to cases where Y was an electron acceptor and X had an available electron pair, he proposed a preferred conformation of the radical that gained stabilization as a result of this substitution pattern. Employing the radical $\overset{+}{N}H_3CH_2\dot{C}HOH$ from 2-aminoethanol as an example, the conformation **19** with dihedral angle θ = 60° is consistent with the observed value of $a_{\beta CH_2}(2H)$ = 11.6 G. In some instances, even lower

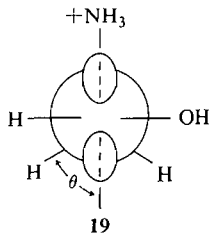

19

βCH_2 h.f.s. constants are observed; for example $a_{CH_2}(2H)$ = 8.5 G for the choline derived radical $(CH_3)_3\overset{+}{N}CH_2\dot{C}HOH$. Further lowering beyond that predicted by **19** is attributed to the electron delocalization shown in structures **20** and **21**, a model that suggests planarity

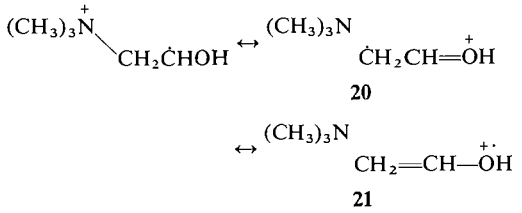

20 **21**

at the α-carbon and a distortion from tetrahedral geometry at the β-carbon (20). Furthermore, the relatively large β-nitrogen h.f.s. constants are accommodated. Such stabilization would make **19** a preferred conformation.

In the present work, further examples of low β-hydrogen and large β-nitrogen h.f.s. values are noted in the radicals $CH_3\dot{C}OHCH_2\overset{+}{N}H_3$ and $CH_3\dot{C}OHCH_2\overset{+}{N}H_2CH_3$ (Table 2, **15**, **16**). More-

Can. J. Chem. Downloaded from www.nrcresearchpress.com by 210.87.254.42 on 09/05/12
For personal use only.

Can. J. Chem. Downloaded from www.nrcresearchpress.com by 210.87.254.42 on 09/05/12
For personal use only.

over radicals of the type $R_2NHCH_2\dot{C}OHCH_3$ (Table 2, **17**, **18**) have marked broadening of the center lines of β-hydrogen triplets. In consequence we suggest an additional factor that plays a role in determining radical conformation where intramolecular hydrogen-bonding is possible.

Consider $\overset{+}{N}H_3CH_2CHOHCH_3$, having as one preferred conformation the hydrogen bonded form **22** prior to hydrogen abstraction. One predicts then conformers **23** and **24** will result if intramolecular hydrogen bonding continues as a significant factor in the radical. By focussing

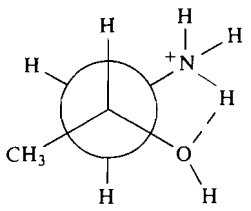

22

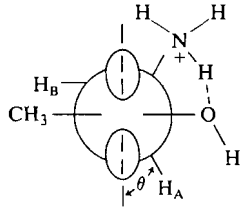

23

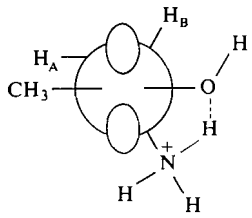

24

attention on one of the β hydrogens, H_A, we can project a value of $a_{\beta CH_2}$ for conformation **23**. Applying the McConnell relationship (eq. 5),

$$[5] \qquad a_H = B_0 + B\cos^2\theta$$

we set $B_0 \simeq 0$ and $B = 42.6$ following the basic approach taken by Norman and co-workers (20).[6] Then with $\theta = 30°$, $a_{H_A} = 31.95$. In conformation **24**, we assume $\theta = 0$ for H_A yielding $a_{H_A} = 0$ in the approximation. For equal but preferred population of just these two conformations, one predicts $a_{CH_2}(2H) = 15.98$ G. Clearly, the observed value ($a_{CH_2}(2H) = 11.6$) is somewhat lower, just as often noted for the alternative hypothesis based on conformation **19** (20). In the hydrogen-bonded model, the further depression in $a_{\beta CH_2}$ is ascribed to distortion of the β carbon tetrahedral geometry towards planarity by net displacement of the amino group toward C-α, energetically compensated for by retention of the optimum hydrogen-bonding between $\overset{+}{N}H_3$ and OH.

The hypothesis accommodates the observation of a selective line broadening in the 1-(*N*,*N*-dimethylamino)-2-propanol abstraction radical.[7] We propose **25** as the stable conformation of the substrate leading to **26** as one conformation of the radical.[8] First, the n.m.r. spectrum of the cation **25** in aqueous hydrochloric acid (p*H* 2.0)

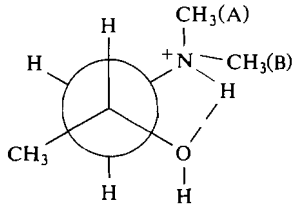

25

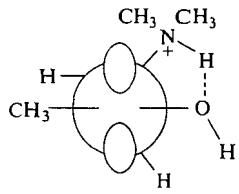

26

shows two distinct *N*-methyl resonances at 6.47 (CH_3(A)) and 6.37 (CH_3(B)), each split by a single proton ($\overset{+}{N}$—H, $J = 2$ Hz). Secondly, the magnitude of the $\overset{+}{N}$—H splitting (e.s.r.) for **26** ($a_{NH}^{+} = 1.4$ G) is compatible with direct interaction of the hydrogen with the oxygen atom bonded to the alpha carbon. For example, in the maleic acid reduction radical **27**, the bridging hydrogen has $a_H(1) = 1.1$ G, and is not exchange broadened at p*H* 1.0 (21).

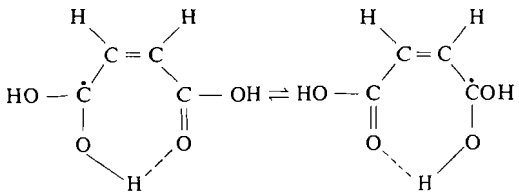

27

Indeed, both the observation of large β-nitrogen h.f.s. and $\overset{+}{N}H$ splitting throughout the series of radicals from the aminoalcohols is consistent with population of hydrogen-bonded conformations. Broadening of the center line of the triplets is compatible with slow interconversion

[6]Calculated from $a_{CH_3} = 21.3$ G in $CH_3\dot{C}OHCH_2\overset{+}{N}H_3$ with $\langle\cos^2\theta = 1/2\rangle$ for a freely rotating methyl group.

[7]The authors acknowledge a referee's suggestions in interpretation of this phenomenon.

[8]In analogy to **23** and **24**, an equivalent enantiomeric conformation exists.

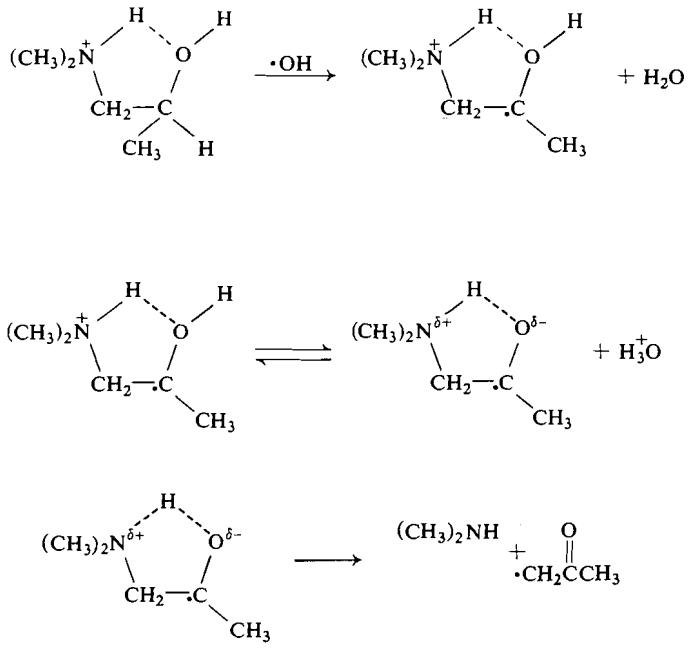

SCHEME I

of the equivalent conformers on the e.s.r. time scale.

In support of the interpretation we note that the phenomenon is observed for two distinct substrates and that one of the radicals $(CH_3)_2\overset{+}{N}HCH_2\dot{C}OHCH_3$ has been generated by an independent route (reduction of *N,N*-dimethylamino-2-propanone).

Clearly for radicals such as $CH_3OCH_2\dot{C}HOCH_3$, only the Norman analysis in terms of conformations of the type **19** is appropriate (20). We propose that *in addition* conformations of the type **23** and **24** are populated in the aminoalcohols and contribute to lowered β-hydrogen h.f.s. values. For highly hindered cases, restricted rotation in the radical can be observed as a line broadening effect.

Elimination Processes in β-Aminoalcohol Abstraction Radicals

The observation of α carbonyl radical spectra in the p*H* range 6.5–7.5 is compatible with deprotonation of an abstraction radical, followed by rapid fragmentation of its conjugate base. The sequence is outlined in Scheme I for $(CH_3)_2\overset{+}{N}HCH_2\dot{C}OHCH_3$ adopting the proposed intramolecularly hydrogen-bonded conformation.

For the mechanism to be operative, it is clearly necessary that the pK_a of the abstraction radical be markedly lower than that of the amine precursor. Presently available data from e.s.r. studies during irradiation of alcohols indicate that the pK_a of an α-alcohol radical is lower by from 4–8 units in comparison with that of the alcohol substrate (22). For instance, 2-propanol has pK_a = 17.1, while $(CH_3)_2\dot{C}OH$ has pK_a 12.03. Even more striking is the acidity of $(CF_3)_2\dot{C}OH$, pK_a = 1.7. Similarly, chloral hydrate and

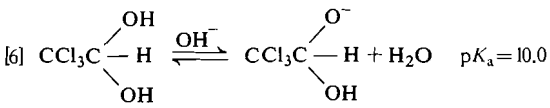

[6] $CCl_3C(OH)_2H \rightleftharpoons CCl_3C(O^-)(OH)H + H_2O$ pK_a = 10.0

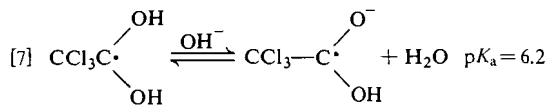

[7] $CCl_3C(OH)_2\cdot \rightleftharpoons CCl_3C(O^-)(OH)\cdot + H_2O$ pK_a = 6.2

its abstraction radical show the same trend (reactions 6, 7) (23). Moreover, the effect of an electron-withdrawing $R_3{}^+N$-group on alcohol radical acidity should be comparable to that of the CCl_3 group. For example, betaine, $(CH_3)_3\overset{+}{N}—CH_2COOH$ (pK_a = 1.83) is a stronger acid

Can. J. Chem. Downloaded from www.nrcresearchpress.com by 210.87.254.42 on 09/05/12
For personal use only.

Can. J. Chem. Downloaded from www.nrcresearchpress.com by 210.87.254.42 on 09/05/12
For personal use only.

than acetic acid, CH_3COOH ($pK_a = 4.75$). By analogy, then, the abstraction radical from $(CH_3)_2\overset{+}{N}HCH_2CHOHCH_3$ ($pK_a = 9.3$) will have a pK_a value at least as low as 6.0. Elimination is clearly in evidence in solutions $pH \geqslant 6.0$.[9]

Using pulse radiolysis Henglein and co-workers have observed the conversion of the 1,2-dihydroxyethyl radical $CH_2OH\dot{C}HOH$ to acetaldehyde radical $\cdot CH_2CHO$ at pH 8.5 (reaction 8) (6).

$$[8]\quad HOCH_2\dot{C}HOH \overset{OH^-}{\rightleftharpoons} HOCH_2\dot{C}HO^- \rightarrow \cdot CH_2CHO + OH^-$$

We consider the β-aminoalcohol radical elimination to be an analogous reaction via the conjugate base of the initial abstraction radical. In summary, e.s.r. observation of a significant steady state population of the α-carbonyl radicals at pH 7.0 probably reflects a significantly faster rate of elimination of the deprotonated radical than of the acid form at pH 2.0. If such is the case then under *in vivo* conditions (*e.g.* pH 7.3), radicals from biologically important 2-aminoethanol derivatives (serine, choline) may eliminate in competition with repair even by efficient hydrogen transfer agents.

The observation of the acetonyl radical from reduction of *N*,*N*-dimethylamino-2-propanone is fully consistent with the proposed elimination. First, Fessenden and co-worker have demonstrated that the reducing radical $\cdot CO_2H$ is not active in direct deamination reactions that would yield the α-carbonyl radical directly (*e.g.* reaction 9) (24).

$$[9]\quad \cdot CO_2H + (CH_3)_2\overset{+}{N}HCH_2COCH_3 \not\rightarrow \cdot CH_2COCH_3 + (CH_3)_2NH + CO_2 + H^+$$

Observation of the $\cdot CH_2COCH_3$ species at higher acidity than in aminoalcohol oxidation can be understood in terms of direct formation of the deprotonated intermediate **28** by electron transfer to the carbonyl group (21). Fragmentation is then assumed to occur before the protonation equilibrium can be established (eq. 10).

[10]

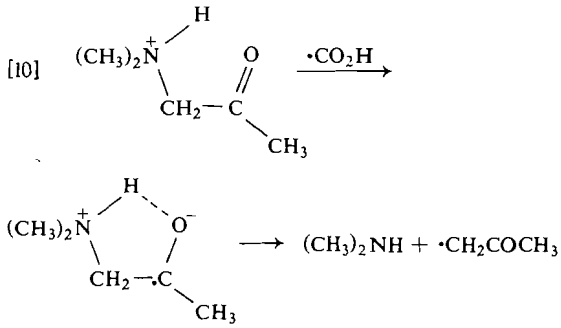

Spectra of $R_3N\cdot^+$ in Quaternary Cation Oxidation

Spectra of sufficient intensity to analyze were not achieved for $(CH_3)_3\overset{+}{N}CH_2CHOHCH_3$ oxidation at pH 1.0 and 7.0 or for choline cation oxidation at pH 7.0. At pH 1.0 only the radical $(CH_3)_3\overset{+}{N}CH_2\dot{C}HOH$ was observed from choline. However, for both cations at pH 1.0 and 7.0 we have observed that trimethylamine hydrochloride and acetone or acetaldehyde, respectively, are the major products of photolysis of their aqueous solutions containing H_2O_2 (25). Accordingly, further efforts to identify the elimination radicals by e.s.r. particularly at pH 7.0 are being made prior to speculation on the mechanism in these instances.

In the case of $(CH_3CH_2)_3\overset{+}{N}CH_2CH_2OH$, the radical $(CH_3CH_2)_3\overset{+}{N}\cdot$ was observed at pH 1.6. However, at pH 2.5–4.0 the spectra of $\dot{C}H_2$-$CH(OH)_2$ and associated species were recorded, with no trace of cation radical remaining. By analogy to previous considerations (5) we postulate the usual heterolysis (reaction 11). In order to accommodate

$$[11]\quad (CH_3CH_2)_3\overset{+}{N}CH_2\dot{C}HOH \rightarrow [(CH_3CH_2)_3\dot{N}\ \ \dot{C}H_2CH{=}\overset{+}{O}H] \rightarrow (CH_3CH_2)_3\overset{+}{N}H + \dot{C}H_2CHO$$

the appearance of the cation radical at pH 1.6, either a change in mechanism (homolysis of the C—N bond) (reaction 4) or electron-transfer from the amine to the radical in a cage reaction is required (reaction 12).

$$[12]\quad (CH_3CH_2)_3N: + \dot{C}H_2CH{=}\overset{+}{O}H \rightarrow (CH_3CH_2)_3\overset{+}{N}\cdot + CH_2{=}CHOH$$

[9]Clearly if elimination from the deprotonated form were highly favored kinetically, reaction could be observed at a pH one or two units lower than the actual pK_a.

Can. J. Chem. Downloaded from www.nrcresearchpress.com by 210.87.254.42 on 09/05/12
For personal use only.

Clearly the protonated amine is not an oxidizable species, so only transfer from the amine is viable. *Tertiary* amines are readily oxidized, *e.g.* tri-*n*-propylamine in acetonitrile at $E_p = -0.87$ V (26). Henglein has recently measured the reducing potential of the *neutral* acetaldehyde radical $\dot{C}H_2CHO$ as -0.75 V by polarographic current measurements during pulse irradiation (6). If one admits only a modest increase in reducing potential for the protonated form $\dot{C}H_2\overset{+}{C}HOH$ in close proximity to the amine, an electron transfer is clearly possible. Walling and El-Taliawi (27) have demonstrated reduction of $\dot{C}H_2COCH_3$ by ferrous ion in the Fenton reagent oxidation of acetone (reaction 13), another example of reduction of α-carbonyl radicals.

[13] $\cdot CH_2COCH_3 + Fe^{II} \rightarrow \bar{C}H_2COCH_3 + Fe^{III}$

We favor the electron-transfer as preferable to postulating a complete change in mechanism over such a narrow range of p*H*, but clearly more examples of such cation radical generation would be desirable.

The authors acknowledge the generous support of the University of Victoria Committee on Research Leave and Travel and the National Research Council of Canada in operating grants. An N.R.C.C. equipment grant made possible the e.s.r. spectrometer installation. The assistance of Dr. A. Tweedale (University of Victoria Computing Center) with the spectral simulation program was much appreciated.

The authors appreciate the helpful comments of Professor R. O. C. Norman who read the manuscript.

1. K. Eiben and R. W. Fessenden. J. Phys. Chem. **75**, 1186 (1971).
2. R. Livingston and H. Zeldes. J. Am. Chem. Soc. **88**, 4333 (1966).
3. W. T. Dixon and R. O. C. Norman. J. Chem. Soc. 3119 (1963).
4. (*a*) A. L. Buley, R. O. C. Norman, and R. J. Pritchett. J. Chem. Soc. B, 849 (1966). (*b*) R. J. Pritchett and R. O. C. Norman. J. Chem. Soc. B, 1329 (1967).
5. B. C. Gilbert, J. P. Larkin, and R. O. C. Norman. J. Chem. Soc. Perkin II, 794 (1972).
6. K. M. Bansal, M. Grätzel, A. Henglein, and E. Janata. J. Phys. Chem. **77**, 16 (1973).
7. C. E. Burchill and K. M. Perron. Can. J. Chem. **49**, 2382 (1971).
8. C. Von Sonntag and E. Thoms. Z. Naturforsch. **25**B, 1405 (1970).
9. H. Scherz. Carbohydr. Res. **14**, 417 (1970).
10. H. Scherz. Radiat. Res. **43**, 12 (1970).
11. M. C. R. Symons. J. Chem. Soc. Faraday Transaction II. **68**, 216 (1972).
12. R. O. Lindblom, R. M. Lemmon, and M. Calvin. J. Am. Chem. Soc. **83**, 2484 (1961).
13. M. A. Smith and R. M. Lemmon. J. Phys. Chem. **69**, 3370 (1965).
14. J. Q. Adams, S. W. Nicksic, and J. R. Thomas. J. Chem. Phys. **45**, 654 (1966).
15. G. P. Laroff and R. W. Fessenden. J. Chem. Phys. **57**, 5614 (1972).
16. D. J. Edge and R. O. C. Norman. J. Chem. Soc. B, 182 (1969).
17. R. T. Major and J. K. Cline. J. Am. Chem. Soc. **54**, 242 (1932).
18. J. C. Graig, D. M. Temple, and B. Moore. Aust. J. Chem. **14**, 84 (1960).
19. R. O. C. Norman and P. R. West. J. Chem. Soc. B, 389 (1969).
20. A. J. Dobbs, B. C. Gilbert, and R. O. C. Norman. J. Chem. Soc. Perkin II, 786 (1972).
21. N. H. Anderson, A. J. Dobbs, D. J. Edge, R. O. C. Norman, and P. R. West. J. Chem. Soc. B, 1004 (1971).
22. G. P. Laroff and R. W. Fessenden. J. Phys. Chem. **77**, 1283 (1973).
23. T. Eriksen, A. Henglein, and K. Stockhausen. J. Chem. Soc. Faraday Trans. **1**, 337 (1973).
24. P. Neta and R. W. Fessenden. J. Phys. Chem. **74**, 2263 (1970).
25. T. Foster and P. R. West. Unpublished results.
26. C. K. Mann. Anal. Chem. **36**, 2424 (1964).
27. C. Walling and G. M. El-Taliawi. J. Am. Chem. Soc. **95**, 844 (1973).

Mutual Solubilities of Hydrocarbons and Water at 0 and 25 °C

JIRI POLAK AND BENJAMIN C.-Y. LU

Department of Chemical Engineering, University of Ottawa, Ottawa, Canada K1N 6N5

Received July 23, 1973

Mutual solubilities of 14 paraffinic and 6 aromatic hydrocarbons and water were determined experimentally at 0 and 25 °C. The solubilities are generally smaller at 0 than at 25 °C except the solubilities of paraffins in water which are larger at 0 than at 25 °C. The coefficients of the Redlich–Kister equation were evaluated from the experimental data and correlated as a function of molar volume of liquid hydrocarbons and group contributions. The correlation allows calculation of the mutual solubilities of paraffinic and aromatic hydrocarbons and water at 0 and 25 °C from the knowledge of the molar volume of liquid and the contribution of their component groups.

On a déterminé expérimentalement à 0 et à 25 °C la solubilité mutuelle de l'eau et de 14 hydrocarbures paraffiniques et de 6 hydrocarbures aromatiques. La solubilité est généralement plus faible à 0 qu'à 25 °C à l'exception de la solubilité des paraffines dans l'eau qui est plus grande à 0 qu'à 25 °C. Les coefficients de l'équation Redlich–Kister ont été évalués à partir de données expérimentales et reliés en termes d'une fonction du volume molaire des hydrocarbures liquides et des contributions des groupes. Cette relation permet le calcul de la solubilité respective des hydrocarbures paraffiniques et aromatiques et de l'eau à 0 et à 25 °C à partir de la connaissance du volume molaire du liquide et de la contribution des groupes qui les composent. [Traduit par le journal]

Can. J. Chem., **51**, 4018 (1973)

Can. J. Chem. Downloaded from www.nrcresearchpress.com by 210.87.254.40 on 09/05/12
For personal use only.

Introduction

The mutual solubilities of liquid hydrocarbons and water are quite low, generally in the order of parts per million by weight. Nevertheless, hydrocarbons and water are not completely insoluble and even the minute amounts dissolved are of interest and importance.

From the practical point of view, a knowledge of the solubilities of hydrocarbons in water is necessary for evaluating the impact of oil spills, as hydrocarbons are the main constituents of the crude oil and oil products. The data on the solubilities of water in hydrocarbons are useful in the evaluation of the amount of water dissolved in oil and oil products.

The experimental data on the mutual solubilities of hydrocarbons and water obtained from simultaneous determinations at different temperatures are useful to the understanding of the solution behavior of these compounds.

Experimental

Materials

Most of the liquid hydrocarbons used in this investigation were pure grade reagents (99%+), with the exception of 3-methylhexane which was technical grade (95%+), and were supplied by Phillips Petroleum Co. Toluene was spectroquality reagent grade and was obtained from Matheson, Coleman and Bell, *o*- and *p*-xylenes were pure grade and supplied by Eastman Organics. All hydrocarbons were purified by shaking three times with distilled water, in the amount of 5 parts of water per part of hydrocarbon, in a separatory funnel to remove trace amounts of soluble components and emulsifiers which might be present.

Dodecane was olefin-free (99% pure) and was obtained from Matheson, Coleman and Bell. It was distilled under vacuum to remove traces of low boiling components which might interfere with the gas chromatographic analysis. Distilled water was used throughout this work.

Apparatus and Technique

Approximately 50 ml of hydrocarbon together with 50 ml of distilled water were placed in a 125 ml Hypo-vial, which was closed with a Teflon coated rubber septum and placed in a constant-temperature water bath. In this investigation, the bath was maintained at 0 ± 0.02 °C and at 25 ± 0.01 °C. Two methods were used to equilibrate water with hydrocarbons. Initially, the system under consideration was stirred using a magnetic stirrer for 24 h. The vial was then left in the bath for at least 3 days to ensure the separation of the layers. However, it was subsequently found that when the components were allowed to remain in contact for a sufficiently long period of time (2–4 days) without stirring, the solubility also reached a constant value. For the majority of the experimental determinations, the vials were therefore kept in the thermostat without stirring for at least 7 days before samples were taken for analysis. An excellent agreement was obtained between the results of the two methods.

Determination of the Solubility of Hydrocarbons in Water

In this case, the sample of the bottom (water rich) layer must be taken for analysis. For this reason, the vials were placed in the bath with their necks down. To collect the sample, the vial was taken out of the bath, and dried with tissue; then the septum was pierced with the hypodermic needle of a 30 ml syringe. A second needle, connected to

Can. J. Chem. Downloaded from www.nrcresearchpress.com by 210.87.254.40 on 09/05/12
For personal use only.

a compressed air source, was then introduced to push the liquid into the syringe. A sample about 15 ml was taken for each analysis, with the exact amount determined by weighing. The sample was placed in a 15 ml Hypo-vial, which was filled beforehand with approximately 2 ml of dodecane solution containing a known amount of benzene or toluene (whenever benzene interfered with the hydrocarbon during the analysis, toluene was used instead). The Hypo-vial was then closed with a Teflon coated rubber septum.

The vial was closed and hand shaken for 5 min and then, after the water and hydrocarbon layers had separated, 0.1 to 2 μl (depending on the solubility) of the dodecane layer was injected into a Hewlett–Packard model 5750B chromatograph equipped with a flame ionization detector and a model 3373B integrator. The samples were analyzed using a 6 ft long, 1/4 in. diameter stainless steel column packed with 3% Carbowax 20M on Chromosorb T, 30/60 mesh.

The temperature of the chromatographic oven was initially maintained at 80 °C. After the peaks of hydrocarbon and benzene or toluene had been integrated, the oven temperature was increased to 220 °C and kept there for about 8 min to remove all of the relatively high boiling dodecane. The temperature was then lowered to 80 °C and after stabilization the next sample was analyzed. Each analysis took about 20–30 min. The temperature of the injection port and the detector was kept at 220 °C. Between repeated analyses of unknown samples prepared as described above, the known-composition standard solutions of dodecane with hydrocarbon and benzene (toluene) at approximately the same concentrations, and treated the same way as the unknown samples (*i.e.* shaken with the same amount of water), were analyzed. In this manner, the ratio of the response factors of hydrocarbon and benzene (toluene) was determined and the amount of hydrocarbon could be calculated.

Determination of the Solubility of Water in Hydrocarbons

The water–hydrocarbon mixture was equilibrated in a similar manner but with the vial opening at the top during the equilibration. After equilibrating for at least 7 days, the vial was lifted partially from the bath and the septum was thoroughly washed with methanol and dried. Approximately 15 ml of the hydrocarbon layer was taken into a syringe after pressurizing the vial with dry air and injected into a titrimeter vessel (with the exact amount determined by weighing of the syringe), and titrated. A Metrohm model E452 Karl Fischer titrator equipped with a 10 ml buret was used. Commercial stabilized Karl Fischer reagent (Fisher Scientific Co.) was diluted to a titer of about 0.15 mg H_2O/ml. The reagent was frequently standardized with sodium tartrate.

An excess amount of the Karl Fischer reagent was always added to ensure the fast reaction of the small amount of water. The standardized methanol was then added in such an amount so that the titration was always completed by the Karl Fischer reagent.

For measurements at 0 °C ethylene glycol was added to the water bath. Precautions were taken to prevent contamination of the samples with glycol. In some cases after the measurements were made at 0 °C the same vials were again thermostated at 25 °C; subsequently measured solubilities agreed within experimental error with those obtained for the fresh samples.

All measurements of the solubility of hydrocarbons in water were repeated at least twice, some, such as *n*-hexane, as many as 10 times. The determinations of the solubility of water in hydrocarbons were repeated at least three times.

The precision of the measurements of the solubility of hydrocarbons in water is in the mean ±1.7%; for solubilities which are under 5 p.p.m., it is ±4%. The precision of the solubilities of water in hydrocarbons is ±3.1% at 25 °C and ±4.7% at 0 °C.

Results and Discussion

The experimentally determined solubilities are listed in Table 1 along with some experimental values available in the literature for 25 °C. Hardly any definitive conclusions can be drawn from this comparison. The experimental data reported from different sources are usually quite different, with the discrepancy in values being much larger than the quoted precision.

For the solubilities of hydrocarbons in water, for example, for *n*-hexane, which is only slightly soluble, the three most recently reported values (1–3) vary from 9.5–18.3 p.p.m. Probably because of the magnitude of their solubilities, the agreement for aromatics is generally better. The results from this investigation for paraffinic hydrocarbons are in most cases larger than those obtained by McAuliffe (2). For the solubilities of water in hydrocarbons the values obtained in this investigation are generally lower than those published for paraffins and close to the values listed for aromatics.

In the literature, most of the solubility data are reported at 25 °C. Little is known about the temperature dependence of the solubility of hydrocarbons in water. The work of Nelson and de Ligny (3) partially confirms our findings of higher solubilities of paraffins in water at 0 °C than at 25 °C. Their experimentally determined values indicated an increase in the solubility with a decrease in temperature for *n*-pentane from 25 to 4 °C and for *n*-octane from 25 to 5 °C. On the other hand, their results for *n*-hexane and *n*-heptane indicated a decrease in the solubility from 25 to about 4 °C. Although in some cases, such as *n*-hexane, the change of solubility with temperature is within experimental error, in other cases, such as heptane and octane, the difference seems to be definite.

The available data in the literature on the solubility of water in hydrocarbons show a decline with a decrease in temperature (4–6) which is in agreement with the findings of this investigation.

Can. J. Chem. Downloaded from www.nrcresearchpress.com by 210.87.254.40 on 09/05/12
For personal use only.

TABLE 1. Mutual solubilities of hydrocarbons and water at 0 and 25 °C

Compound	Solubility of hydrocarbon in water (p.p.m.)*			Solubility of water in hydrocarbon (p.p.m.)*		
	Experimental		Literature	Experimental		Literature†
	0 °C	25 °C	25 °C	0 °C	25 °C	25 °C
n-Pentane	65.7	47.6	38.5(2), 40.4(3)	26	101	120(6)
n-Hexane	16.5	12.4	12.3(1), 9.5(2), 18.3(3)	28	90	140(4)
n-Heptane	4.39	3.37	2.93(2), 2.66(3)	26	82	134(4), 91(5), 151(6)
n-Octane	1.35	0.85	0.66(2), 0.88(3)	23	79	132(4)
2-Methylbutane	72.4	49.6	47.8(2)	28	96	138(4), 112(6)
2-Methylpentane	19.45	15.7	14.2(1), 13.8(2)	29	90	
3-Methylpentane	21.5	17.9	12.8(2)	23	94	
3-Methylhexane	5.24	4.95		25	74	
2,2-Dimethylbutane	39.4	23.8	18.4(2)	32	84	
2,3-Dimethylbutane	32.9	22.5		30	90	151(4)
2,4-Dimethylpentane	6.50	5.50	4.06(2)	31	81	
2,2,4-Trimethylpentane	2.46	2.05	2.44(2)	23	80	158(4)
2,3,4-Trimethylpentane	2.34	2.30		20	74	
2,2,5-Trimethylhexane	0.79	0.54	1.15(2)	25	75	
Benzene	1678‡	1755	1770(1), 1780(2), 1795(15)	302§	691	666(4), 522(6), 694(14)
Toluene	724	573	515(2), 629(15)	228	543	538(4)
Ethylbenzene	197	177	152(2), 209(15)	178	442	438(4)
o-Xylene	142	213	175(2)	185	456	
m-Xylene	196	162	197(15)	188	432	469(4)
p-Xylene	164‡	185	199(15)	—‖	440	

*Grams in 10^6 grams of solution (p.p.m. by weight).
†Including interpolated and extrapolated values.
‡Hydrocarbons were at supercooled liquid state.
§Solubility in supercooled liquid.
‖Not possible to determine the solubility because the supercooled liquid always froze during the sample collection. However, in the correlation, value of 190 p.p.m. was used.

Can. J. Chem. Downloaded from www.nrcresearchpress.com by 210.87.254.40 on 09/05/12
For personal use only.

Correlation of the Solubilities

The mixture of hydrocarbon (HC) and water (w) represents a typical binary system with partially miscible components. The condition for equilibrium between two liquid phases may be expressed in terms of the fugacities

$$[1] \qquad f_{HC} = \bar{f}_{HC}$$

$$[2] \qquad f_w = \bar{f}_w$$

where the bar denotes the hydrocarbon rich phase. Because $f_i = x_i\gamma_i f_i^0$

$$[3] \qquad x_{HC}\gamma_{HC} = \bar{x}_{HC}\bar{\gamma}_{HC}$$

$$[4] \qquad x_w\gamma_w = \bar{x}_w\bar{\gamma}_w$$

In these equations, x is the liquid mole fraction, γ is the Raoult's law activity coefficient and f^0 is the standard state fugacity. The subscripts HC, w, and i refer to hydrocarbon, water, and component i, respectively.

It has been shown by Leinonen *et al.* (7) that the coefficient K in the Redlich–Kister equation,

$$[5] \qquad g^E = x_{HC}(1 - x_{HC})\,K$$

can be correlated with the molar volumes and other structural parameters of the dissolved hydrocarbon molecule. In eq. 5, g^E is the molar excess Gibbs free energy. Equation 5, which allows the calculation of K from only one experimental value for solubility of each component, implies that the g^E curve is symmetrical. Unfortunately this does not hold for the hydrocarbon–water systems.

A further expansion of eq. 5 yields

$$[6] \quad g^E = RTx_{HC}(1 - x_{HC})[A + B(1 - 2x_{HC})]$$

To determine the parameters A and B, a pair of points such as the mutual solubilities is needed. From eq. 6 together with eqs. 3 and 4 the following expressions are derived:

$$[7] \quad A[(1 - x_{HC})^2 - \bar{x}_w{}^2] + B[-6x_{HC} + 9x_{HC}{}^2 - 4x_{HC}{}^3 + 6(1 - \bar{x}_w) - 9(1 - \bar{x}_w)^2 + 4(1 - \bar{x}_w)^3] = \ln\left(\frac{1 - \bar{x}_w}{x_{HC}}\right)$$

and

$$[8] \quad A[x_{HC}{}^2 - (1 - \bar{x}_w)^2] + B[3x_{HC}{}^2 - 4x_{HC}{}^3 - 3(1 - \bar{x}_w)^2 + 4(1 - \bar{x}_w)^3] = \ln\left(\frac{\bar{x}_w}{1 - x_{HC}}\right)$$

in which x_{HC} and $\bar{x}_w$ are, respectively, the solubilities of hydrocarbon in water and water in hydrocarbon, expressed in mole fractions. The parameters A and B were calculated by solving eqs. 7 and 8 simultaneously.

The calculated A and B values, like the parameter K of eq. 5 (1), display a dependence on the hydrocarbon liquid molar volume and other molecular parameters as shown in Figs. 1 and 2. To correlate coefficients A and B, and therefore the solubilities, the following equations were used:

$$[9] \qquad A = C_{A_1}V_i + \sum_{i=2}^{7} C_{A_i}n_i$$

$$[10] \qquad B = C_{B_1}V_i + \sum_{i=2}^{7} C_{B_i}n_i$$

In these equations V_i is the liquid molar volume, expressed in terms of $cm^3\ g\ mol^{-1}$, and n_i is the

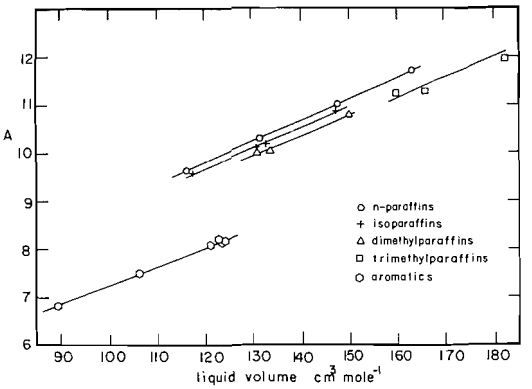

FIG. 1. Plot of parameter A *vs.* liquid molar volumes of hydrocarbons.

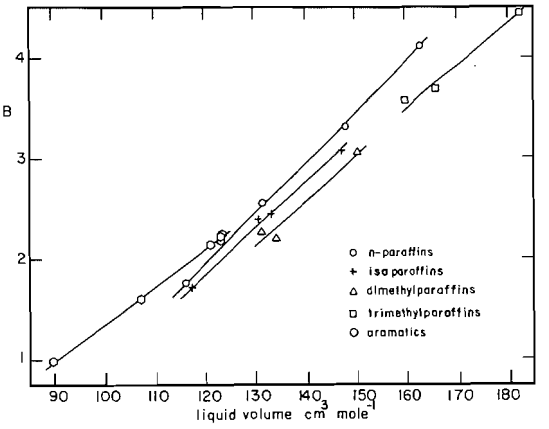

FIG. 2. Plot of parameter B *vs.* liquid molar volumes of hydrocarbons.

TABLE 2. Coefficients of eqs. 9 and 10

		25 °C		0 °C	
i	Group or property	C_{A_i}	C_{B_i}	C_{A_i}	C_{B_i}
1	Volume	0.02306	0.02058	−0.02040	0.01779
2	CH_3—	2.97571	−0.95356	4.63484	−1.21691
3	—CH_2—	0.32934	0.43558	1.02098	0.48634
4	—CH—	−2.44926	1.68675	−2.70958	2.09649
5	—C—	−5.31870	2.87305	−6.55307	3.56926
6	=CH—(in benzene ring)	0.79215	−0.14996	1.49667	−0.18018
7	=C—(in benzene ring)	−1.89802	1.08183	−2.08991	1.40298

number of the groups i present in the molecule. Values of the coefficients C_{A_i} and C_{B_i} are given in Table 2. The groups were chosen in such a way as to express the molecules concerned in terms of a minimum number of groups. The contributions attributed to the individual groups are listed in Table 2 as C_{A_i} and C_{B_i} for $i = 2$ to 7. In this table, all the bonds shown as free are connected to atoms other than hydrogen. As an example, the value of A for 2,2,4-trimethylpentane at 25 °C ($V_i = 166.07$ cm^3 g-mol^{-1}) is obtained as follows

$$A = 0.02306 \times 166.07 + 5 \times 2.97571 + 0.32934 + (-2.44926) + (-5.31870) = 11.2695$$

Similarly, $B = 3.6453$. Based on these values, the solubility of 2,2,4-trimethylpentane in water is calculated to be 2.11 p.p.m. and the solubility of water in 2,2,4-trimethylpentane to be 77.0 p.p.m.

In the calculation at 25 °C, the molar volumes were calculated from the densities ($d_{25°}$) listed in ref. 8. At 0 °C, the method of ref. 9 was adopted using $d_{25°}$ as the reference density.

From the coefficients (group contributions) given in Table 2, and a knowledge of the molar volume and molecular groups, the values of A and B can be obtained. Thus, the mutual solubilities of hydrocarbons and water can be calculated by means of eqs. 7 and 8. Because of the very low values of the solubilities, $x_{HC} \approx 1/\gamma_{HC}$, and at the limiting condition, where $x_{HC} \to 0$, $\ln \gamma_{HC} = A + B$. Therefore

$$[11] \qquad x_{HC} = \frac{1}{e^{(A+B)}}$$

Similarly

$$[12] \qquad \bar{x}_w = \frac{1}{e^{(A-B)}}$$

The calculated results obtained from these equations were compared with those obtained from eqs. 7 and 8 and the difference was found to be very small. For this reason, eqs. 11 and 12 are recommended for calculating solubilities from the known A and B values for their simplicity.

A comparison of the experimental and calculated solubilities at 25 °C is given in Table 3. A similar comparison has been done for 0 °C. The average deviations are 10.88% for the solubilities of hydrocarbons in water and 7.59% for the solubilities of water in the hydrocarbons.

It should be mentioned that eq. 6 was arbitrarily chosen to express the dependence of the excess Gibbs free energy on the liquid phase composition. Other expressions, such as the van Laar equation, may be used in a similar manner. The van Laar equation was actually tried in this investigation. Apart from the fact that the calculation of the van Laar parameters is more difficult due to the nonlinear nature of the equation there appears to be practically no difference between the correlation based on the parameters of eq. 6 and the van Laar equation. This is a consequence of the low solubility values and the nature of the limiting γ values.

Since γ's are expressed in terms of A and B, which are functions of the group contributions, our correlation is thus linked with two other works.

It has been shown by Deal, Derr, and coworkers (10–12) that the limiting values of the

Can. J. Chem. Downloaded from www.nrcresearchpress.com by 210.87.254.40 on 09/05/12
For personal use only.

TABLE 3. Comparison of the experimental and calculated solubilities at 25 °C

Compound	Solubility of hydrocarbon in water (p.p.m.)			Solubility of water in hydrocarbon (p.p.m.)		
	Experimental	Calculated	Deviation (%)*	Experimental	Calculated	Deviation (%)*
n-Pentane	47.6	44.6	6.35	101	99	1.71
n-Hexane	12.4	12.6	−1.67	90	89	0.98
n-Heptane	3.37	3.41	−1.28	82	82	0.08
n-Octane	0.85	0.92	−7.67	79	77	2.50
2-Methylbutane	49.6	55.2	−11.35	96	99	−2.59
2-Methylpentane	15.7	15.6	0.53	90	88	2.30
3-Methylpentane	17.9	17.2	3.70	94	89	5.31
3-Methylhexane	4.95	4.62	6.69	74	82	−9.56
2,2-Dimethylbutane	23.8	23.0	3.15	84	90	−7.07
2,3-Dimethylbutane	22.5	22.0	1.99	90	88	2.43
2,4-Dimethylpentane	5.50	5.26	4.34	81	80	0.73
2,2,4-Trimethylpentane	2.05	2.11	−3.05	80	77	4.00
2,3,4-Trimethylpentane	2.30	2.38	−3.57	74	76	−2.57
2,2,5-Trimethylhexane	0.54	0.54	0.00	75	73	2.87
Benzene	1755	1857	−5.79	691	649	6.03
Toluene	573	583	−1.67	543	523	3.64
Ethylbenzene	177	154	12.85	442	485	−9.77
o-Xylene	213	204	4.17	456	435	4.60
m-Xylene	162	185	−13.97	432	433	−0.13
p-Xylene	185	181	2.16	440	432	1.80
Average deviation			4.80			3.53

*Deviations were determined before the calculated values were rounded off.

activity coefficients for a homologous series of solutes in a fixed or homologous series of solvents are, with a good approximation, a function of the group of the molecules involved.

Similarly Irmann (13) has shown that for a wide variety of hydrocarbons and their halogen derivatives, the logarithm of $1/S$, where S is the solubility of the organic material, can be calculated as the sum of atomic and structural parameters. The fact that $1/S$ is related to $1/x$ links his correlation with the one presented in this work.

The authors are indebted to the National Research Council of Canada for financial support. Technical assistance of Mr. G. Gasperetti is also acknowledged.

1. P. J. LEINONEN and D. MACKAY. Can. J. Chem. Eng. **51**, 230 (1973).
2. C. MCAULIFFE. J. Phys. Chem. **70**, 1267 (1966).
3. H. D. NELSON and C. L. DE LIGNY. Rec. Trav. Chim. Pays-Bas, **87**, 528 (1968).
4. B. A. ENGLIN, A. F. PLATE, V. M. TUGOLUKOV, and M. A. PRYANISHNIKOVA. Chim. Technol. Topl. Masel, No. 9, 42 (1965).
5. P. SCHATZBERG. J. Phys. Chem. **67**, 776 (1963).
6. C. BLACK, G. G. JORIS, and H. S. TAYLOR. J. Chem. Phys. **16**, 537 (1948).
7. P. J. LEINONEN, D. MACKAY, and C. R. PHILLIPS. Can. J. Chem. Eng. **49**, 288 (1971).
8. R. R. DREISBACH. Physical properties of chemical compounds. Adv. Chem. Ser. Vol. 15 (1955), 22 (1959), Am. Chem. Soc., Publ. Washington.
9. B. C.-Y. LU, J. A. RUETHER, C. HSI, and C.-H. CHIU. J. Chem. Eng. Data, **18**, 241 (1973).
10. G. J. PIEROTTI, C. H. DEAL, and E. L. DERR. Ind. Eng. Chem. **51**, 95 (1959).
11. C. H. DEAL, E. L. DERR, and M. N. PAPADOPOULOS. Ind. Eng. Chem. Fundam. **1**, 17 (1962).
12. C. H. DEAL and E. L. DERR. Ind. Eng. Chem. **60**, 28 (1968).
13. F. IRMANN. Chem.-Ing.-Tech. **37**, 789 (1965).
14. L. A. K. STAVELEY, J. H. E. JEFFES, and J. A. E. MOY. Trans. Faraday Soc. **39**, 5 (1943).
15. R. L. BOHON and W. F. CLAUSSEN. J. Am. Chem. Soc. **73**, 1571 (1951).

Can. J. Chem. Downloaded from www.nrcresearchpress.com by 210.87.254.40 on 09/05/12
For personal use only.

A ^{19}F Nuclear Magnetic Resonance Study of Polymeric Fluoroanions of Tin(IV) and Titanium(IV)

P. A. W. DEAN

Department of Chemistry, University of Western Ontario, London, Ontario

Received July 16, 1973

Fluorine n.m.r. has been used to demonstrate the existence of fluorine-bridged polymeric fluoroanions of tin(IV) and titanium(IV) in liquid sulfur dioxide solution. In the system TiF_4–$(Pr_2^nNH_2)_2TiF_6$ the species formed are: $Ti_2F_{11}^{3-}$; a species $(TiF_5)_n^{n-}$, which has a structure consisting of *cis* fluorine-bridged TiF_6 octahedra and is most probably $Ti_2F_{10}^{2-}$; $Ti_2F_9^-$; other fluorine-bridged polymers. The spectra of $(TiF_5)_n^{n-}$ and $Ti_2F_9^-$ are complex due to the effects of magnetic nonequivalence; the spectrum of $(TiF_5)_n^{n-}$ has been analyzed in detail. Both $Sn_2F_{11}^{3-}$ and $(SnF_5)_n^{n-}$, which has a structure like $(TiF_5)_n^{n-}$, are formed in SnF_4–$(Pr_2^nNH_2)_2SnF_6$.

La r.m.n. du fluor a été utilisée pour démontrer en solution liquide d'anhydride sulfureux l'existence de fluoroanions de l'étain(IV) et du titanium(IV) polymériques comportant des ponts fluor. Dans le système TiF_4–$(Pr_2^nNH_2)_2TiF_6$ les espèces présentes sont: $Ti_2F_{11}^{3-}$; une espèce $(TiF_5)_n^{n-}$ qui possède une structure composée d'octaèdres TiF_6 pontés de manière *cis* au fluor et qui est probablement $Ti_2F_{10}^{2-}$; $Ti_2F_9^-$; d'autres polymères comportant des ponts fluor. Les spectres de $(TiF_5)_n^{n-}$ et de $Ti_2F_9^-$ sont complexes principalement à cause des effets de nonéquivalence magnétique; le spectre de $(TiF_5)_n^{n-}$ est décrit en détail. Les deux espèces $Sn_2F_{11}^{3-}$ et $(SnF_5)_n^{n-}$, qui possède une structure identique à $(TiF_5)_n^{n-}$, sont formées dans le système SnF_4–$(Pr_2^nNH_2)_2SnF_6$.

[Traduit par le journal]

Can. J. Chem., **51**, 4024 (1973)

Introduction

Fluorine-bridging occurs in crystalline stannic fluoride (1) and in some organotin fluorides in the solid state (2). The structure of solid titanium tetrafluoride is presently unknown, but it is also thought to involve fluorine-bridging (3). The occurrence of discrete fluorine-bridged polymeric fluoroanions of tin(IV) and titanium(IV) would therefore seem possible also. However, no such anions have been reported for tin(IV) and the situation for titanium(IV) is unclear. A continuous variation study (4) of the binary system TiF_4–TiF_6^{2-} in acetone provided evidence for the existence of species of empirical formula $Ti_2F_9^-$ and TiF_5^-, and could not rule out the possibility that complexes of the type $[(TiF_4)_xF]_n^{n-}$ occur, but the extent of polymerization and solvation of these anions and hence their structures could not be determined (5). Similarly an anion of the empirical formula $Ti_2F_9^-$, but of unknown structure, was thought to be formed in the system arene – TiF_4 – HF (6).

We now report ^{19}F spectroscopic data for the systems TiF_4–TiF_6^{2-} and SnF_4–SnF_6^{2-} in liquid sulfur dioxide. These data provide evidence for the occurrence and structures of polymeric fluoroanions of tin(IV) and titanium(IV).

Results and Discussion

The System TiF_4–$(Pr_2^nNH_2)_2TiF_6$ in SO_2

Titanium tetrafluoride itself is insoluble in SO_2, but solutions of TiF_6^{2-} dissolve TiF_4 up to $TiF_4/TiF_6^{2-} = 3$. In the region where $TiF_4/TiF_6^{2-} \lesssim 1$ this reaction is noticeably exothermic at room temperature, the solvent boiling; larger amounts of TiF_4 dissolve less vigorously. When $TiF_4/TiF_6^{2-} \gtrsim 1$ initial complete dissolution is followed, in a period of *ca.* 10 min, by formation of small amounts of insoluble crystalline material. In all cases the solutions are colorless.

The ^{19}F n.m.r. spectra of the TiF_4–TiF_6^{2-} solutions show broad lines at room temperature, presumably due to relatively rapid fluorine exchange. At low temperatures, however, fine structure is observed. Figure 1*a* shows the spectrum of a solution with $TiF_4/TiF_6^{2-}/SO_2 = 1/3.2/36$, measured at $-80°$. In addition to the singlet -89.6 p.p.m. below $CFCl_3$, which is due to TiF_6^{2-}, there is also observed a doublet of quintets, *1*, a doublet of doublets, *2*, and a multiplet, *3*, of at least 11 lines, the relative intensities of resonances *1*, *2*, and *3* being 2:8:1. By analogy with the ^{19}F n.m.r. spectrum of $Ta_2F_{11}^-$ (7), resonances *1*, *2*, and *3* may be assigned to the $Ti_2F_{11}^{3-}$ anion **1**.

Can. J. Chem. Downloaded from www.nrcresearchpress.com by 210.87.254.105 on 09/05/12
For personal use only.

Can. J. Chem. Downloaded from www.nrcresearchpress.com by 210.87.254.105 on 09/05/12
For personal use only.

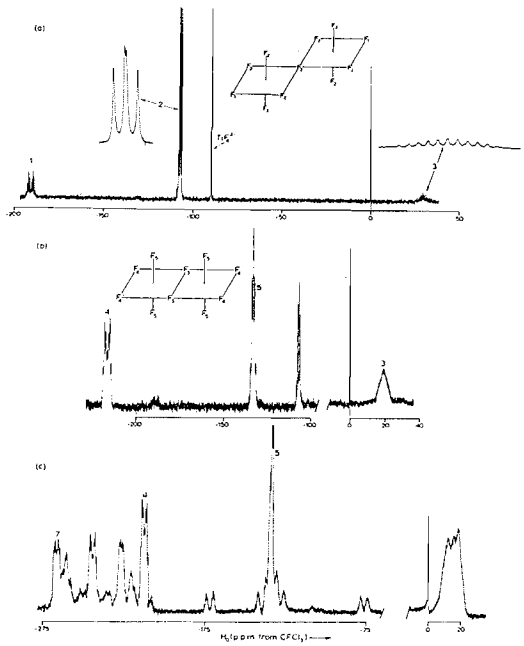

FIG. 1. (*a*) The 56.4 MHz ^{19}F n.m.r. spectrum of a solution with $TiF_4/TiF_6^{2-}/SO_2 = 1.0/3.2/36$, measured at $-80°$. (*b*) The 56.4 MHz ^{19}F n.m.r. spectrum of a solution with $TiF_4/TiF_6^{2-}/SO_2 = 1.0/1.1/12$, at $-80°$. (*c*) The 58.3 MHz ^{19}F n.m.r. spectrum of the supernatant liquor in a mixture with $TiF_4/TiF_6^{2-}/SO_2 = 1.6/1.0/14$, at $-70°$.

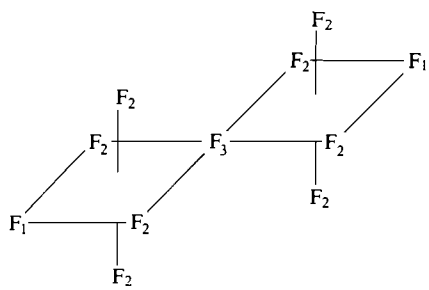

1

The chemical shifts and coupling constants for this ion are given in Table 1. Since $J_{13} \approx J_{23}$, the signal due to F_3, which should be a triplet (by coupling to the two fluorines F_1) of nonets (by coupling to the eight fluorines F_2) will appear theoretically as a 15 line multiplet with intensities 1:8:28:48:86:102:121:156:121:102:86:48:28:8:1. Eleven of these lines are observed experimentally, with approximately the correct relative intensities. The $Ti_2F_{11}^{3-}$ anion must be formed according to the overall equation

$$3TiF_6^{2-} + TiF_4 \rightarrow 2Ti_2F_{11}^{3-}$$

As the relative amount of TiF_4 is increased towards $TiF_4/TiF_6^{2-} = 1$, new signals appear in the spectrum, and the amounts of $Ti_2F_{11}^{3-}$ and TiF_6^{2-} in solution diminish. The new resonances, labelled *3*, *4*, and *5* in Fig. 1*b*, are, respectively, a broad line, a complex symmetrical multiplet, and an apparent quintet. The intensities 3:4:5 are in the constant ratio 1:2:2, and the total intensity *3* + *4* + *5* is at a maximum, relative to the rest of the spectrum, at $TiF_4/TiF_6^{2-} = 1$. In at least some of the region between $\frac{1}{3} < TiF_4/TiF_6^{2-} < 1$, *e.g.* when $TiF_4/TiF_6^{2-} = \frac{1}{2}$, the signals *3*, *4*, and *5* are observed at the same time as the resonances of TiF_6^{2-} and $Ti_2F_{11}^{3-}$.

Since the species responsible for *3*, *4*, and *5* reaches its maximum relative concentration when $TiF_4/TiF_6^{2-} = 1$, it must be of the form $(TiF_5)_n^{n-}$. As is the case for SbF_5 (8), the 1:2:2 intensities of *3*, *4*, and *5* are explicable only in terms of dimers or higher polymers consisting of MF_6 octahedra linked via *cis* fluorine-bridges. For the exact formulation $(TiF_5)_n^{n-}$ the fluorine-bridged ions must be cyclic as in the case of $Ti_2F_{10}^{2-}$, **2**, the $(TiF_5)_n^{n-}$ anion is favored on the basis of further evidence (*vide infra*).

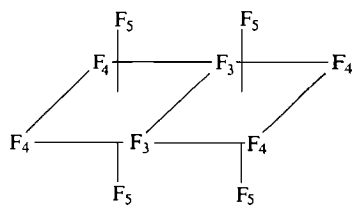

2

The position and relative intensity of resonance *3* show that it is due to the bridging fluorine F_3. The spectrum of the $Ti_2F_{11}^{3-}$ ion (*vide supra*) suggests that those fluorines giving rise to signals at lowest field are *trans* to a bridging fluorine. Resonance 4 is therefore assigned to F_4; this assignment is borne out by a detailed analysis of the spectrum (*vide infra*). Thus the signal labelled *5* must be from F_5.

We have analyzed the spectrum of $(TiF_5)_n^{n-}$ using the approximation,[1] previously employed

[1]Thus must be recognized as an approximation since a small coupling *between* linked octahedra is a distinct possibility; a coupling of 1.5 Hz has been observed (18) between the terminal fluorines on the two octahedra in $[F_4O\,^{183}WFWOF_4]^-$.

TABLE 1. ^{19}F n.m.r. spectral parameters for polymeric fluoroanions of titanium(IV)

Ion	Fluorine assignment[a]	Chemical shift[bc] (p.p.m.)	Fluorine–fluorine coupling constants (Hz)
$Ti_2F_{11}^{3-}$	*1*	−191	$J_{12} = 38 \pm 1$
	2	−107	$J_{13} = 135 \pm 2$
	3	29	$J_{23} = 44 \pm 1$
$Ti_2F_{10}^{2-}$	3	19	$J_{33'} = 10$[d]; $J_{34} = \pm 45$[d];
	4	−214	$J_{34'} = \pm 135$[d]; $J_{35} = 44 \pm 1$;
	5	−133	$J_{44'} = 25$[d]; $J_{45} = 41 \pm 1$
$Ti_2F_9^-$	6	18	
	7	−266	—[e]

[a]For numbering scheme and method of assignment see text.
[b]Relative to internal $CFCl_3$; at −60° $(Pr_2^nNH_2)_2TiF_6$ in resonates at: −89.7 (11% solution); −87.9 (38% solution).
[c]Concentration and temperature dependent: mid-range values are quoted.
[d]Calculated values (see text).
[e]Analogous coupling constants probably have values similar to $Ti_2F_{10}^{2-}$ (see text).

for a detailed analysis of the spectrum of SbF_5 (9), that the resonances of F_4 and F_5 can be simulated by considering the coupling between fluorines in a single octahedral MF_6 unit. Within this unit, the spectrum depends on six coupling constants, $J_{33'}$, J_{34}, $J_{34'}$, J_{35}, $J_{44'}$, and J_{45}; J_{55} does not affect the spectrum. As in the case of SbF_5 (9), analysis of the spectrum was achieved by generating theoretical spectra using the general n.m.r. spectral program LAOCN3 of Bothner-By and Castellano (10), calculating a line shape as the sum of the Lorenzian curves for the individual theoretical transitions, and comparing the plotted theoretical spectrum with the observed spectrum. The observed chemical shifts are widely separated so that the spin system can be described as $AA'M_2XX'$, any second order effects in the spectrum arising almost entirely from the presence of magnetic nonequivalence in the TiF_6 unit.

The resonance due to F_5 is expected to be a triplet (by a coupling of J_{45} to the two fluorines F_4) of triplets (by coupling of J_{35} to the two fluorines F_3). The resonance *5* (Fig. 1*b*) appears to be a quintet with a splitting of 42 Hz, indicating $J_{45} \approx J_{35} \approx 42$ Hz. The resonance from F_4 is shown in Fig. 2*a*. The theoretical treatment indicates that the splitting between the two largest lines of the F_4 multiplet is $|J_{34} + J_{34'}|$. This splitting is found to be 180 Hz. It is highly unlikely that this, by coincidence, is equal to the sum of the two analogous coupling constants in $Ti_2F_{11}^{3-}$ ($J_{23} = 44$ Hz; $J_{13} = 135$ Hz), so J_{34} and $J_{34'}$ were set at 45 and 135 Hz (both

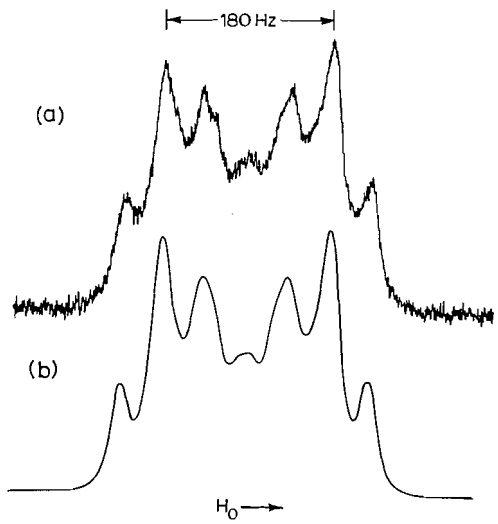

FIG. 2. (*a*) The resonance due to F_4 of $(TiF_5)_n^{n-}$ in the −80° 56.4 MHz ^{19}F n.m.r. spectrum of a solution with $TiF_4/TiF_6^{2-}/SO_2 = 1.0/1.1/12$. (*b*) The calculated spectrum for F_4 of $(TiF_5)_n^{n-}$.

with the same sign) as trial values. Since we find that the frequency between the two outermost lines is $\{|J_{34} + J_{34'}| + 2|J_{45}|\}$, J_{45} can be determined as 41 Hz and, hence, from the "quintet" of F_5, $J_{35} = 44$ Hz. With the values J_{34}, $J_{34'}$, J_{45}, and $J_{34} = \pm 45$, ± 135, 41, and 44 Hz, $J_{33'}$ and $J_{44'}$ were varied over the range 0–300 Hz and 0–80 Hz, respectively,[2] and the

[2]*cis* couplings between terminal fluorines in titanium fluoro-complexes have been reported in the range 31–52 Hz.

Can. J. Chem. Downloaded from www.nrcresearchpress.com by 210.87.254.105 on 09/05/12
For personal use only.

Can. J. Chem. Downloaded from www.nrcresearchpress.com by 210.87.254.105 on 09/05/12
For personal use only.

linewidth was also varied, until the shapes of the center of the multiplet and of the shoulders on the lines closest the center were best reproduced. Only a small range of values for $J_{33'}$, $J_{44'}$ and the linewidth produced *both* the central resonance *and* the shoulders. Having the best values for $J_{33'}$ and $J_{44'}$ for fixed values of the other four coupling constants, J_{34} (and thus $J_{34'}$), $J_{33'}$, and $J_{44'}$ were allowed to vary over ± 5 Hz until the closest fit was found. At this point a charge of ± 2Hz in any one coupling constant produced a noticeably poorer fit. In Fig. 2 the best theoretical spectrum, having a line width of 23 Hz, is compared with the experimental spectrum. The best values of the coupling constants are given in Table 1, which also lists the chemical shift data for $(TiF_5)_n^{n-}$ (as $Ti_2F_{10}^{2-}$). Of particular interest among the coupling constants calculated are the small sizes of $J_{33'}$ and $J_{44'}$. For transition metal species no couplings of the same type as $J_{33'}$ have been reported. However, the magnitude of $J_{44'}$, the smallest coupling reported between *cis* terminal fluorines bound to Ti(IV),[2] is consistent with the argument of Dyer and Ragsdale (11) that *cis*- coupling between terminal fluorines depends on the angle between these. In the present case the angle F_4—Ti—F_4 should be greater than 90°, as is the angle between the corresponding halogen atoms in $Ti_2Cl_{10}^{2-}$ (12), VF_5 (13), NbF_5 (14), and TaF_5 (14), whereas in other complexes which have been investigated, the F—Ti—F angles were probably 90° or less (see, for example, ref. 11).

The ^{19}F n.m.r. spectra of the supernatant liquor above mixtures with $1 < TiF_4/TiF_6^{2-} < 3$ are exceedingly complicated (we noted earlier that small amounts of insoluble material are formed in this range). A typical example, the −70° spectrum of a mixture where $TiF_4/TiF_6^{2-}/SO_2 = 1.6/1.0/14$, is shown in Fig. 1*c*. We are unable, at present, to assign many of the resonances in these spectra, though we can determine the types of species giving rise to them (*vide infra*). As TiF_4/TiF_6^{2-} approaches 3, the resonances in the region from 0 to 250 p.p.m. below $CFCl_3$ diminish in intensity, the signals *4* and *5* of $(TiF_5)_n^{n-}$ disappearing first. Concurrently, the resonance labelled *7* in Fig. 1*c*, and a broadened quintet-like resonance at ϕ 18.1, increase in intensity, until, at $TiF_4/TiF_6^{2-} \sim 3$ or in the supernatant liquor of a mixture with $TiF_4/TiF_6^{2-} > 3$, these two resonances comprise the bulk of the spectrum as is shown in Fig. 3.

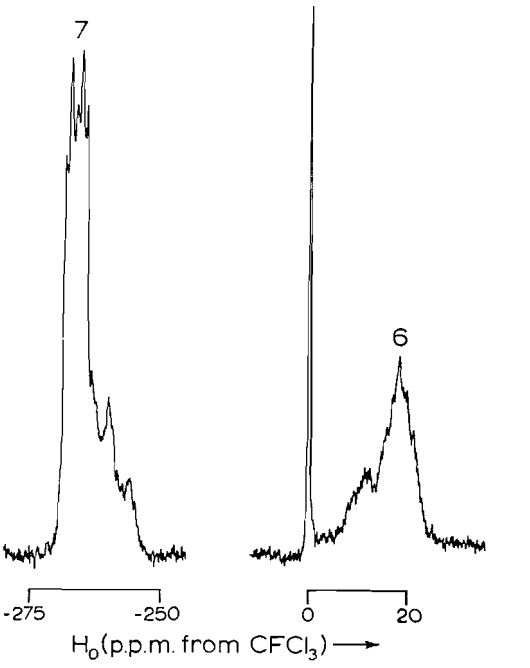

FIG. 3. The 58.3 MHz ^{19}F n.m.r. spectrum of the supernatant liquor in a mixture with $TiF_4/TiF_6^{2-}/SO_2 = 5.0/1.0/36$, at −60°.

By a consideration of the spectra of $Ti_2F_{11}^{3-}$ and $(TiF_5)_n^{n-}$ (see above), the symmetrical downfield multiplet *7* can reliably be assigned to terminal fluorines, and the "quintet", *6*, to bridging fluorines. The relative intensities of *6* and *7* are 1:2 and the intensities of these signals relative to others in the spectrum is not constant, so that *6* and *7* alone must arise from one species. Assuming that the titanium will remain six-coordinate, as in $Ti_2F_{11}^{3-}$ and $(TiF_n)^{n-}$ (*vide supra*), a single formulation is possible for a species where the number of terminal fluorines is twice the number of bridging fluorines, *i.e.* it is $Ti_2F_9^-$, having a face-joined bioctahedral structure, represented by **3**.

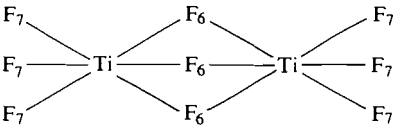

3

This formulation is consistent with resonances *6* and *7* reaching their maximum intensity at $TiF_4/TiF_6^{2-} = 3$, as $Ti_2F_9^-$ would be formed according to the overall equation

$$3\ TiF_4 + TiF_6^{2-} \rightarrow 2\ Ti_2F_9^-$$

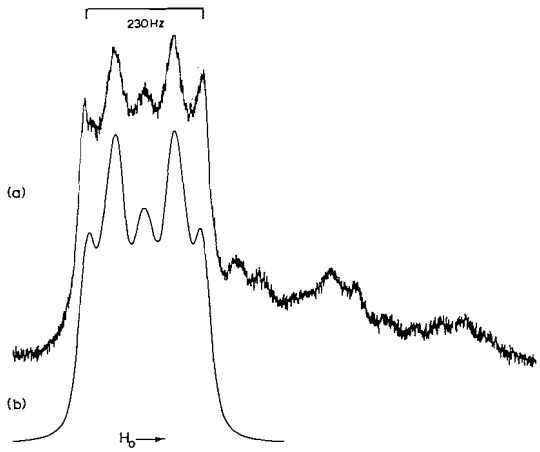

FIG. 4. (*a*) The resonance due to F_7 of $Ti_2F_9^-$ in the $-60°$ 58.3 MHz ^{19}F n.m.r. spectrum of the supernatant liquor in a mixture with $TiF_4/TiF_6^{2-}/SO_2 = 5.0/1.0/36$. (*b*) Theoretical spectrum for F_7 of $Ti_2F_9^-$ generated using $J_{66'} = 10, J_{67} = \pm 47, J_{67'} = \pm 132, J_{77'} = 25$ Hz, and a linewidth of 40 Hz.

The unusually-shaped multiplet[3] due to F_7 is shown in greater detail in Fig. 4*a*. Since this signal appears as five broadish resonances it is not sensible to attempt an analysis of the spectrum by the method used for $(TiF_5)_n^{n-}$ (*vide supra*) which would require values for four coupling constants, $J_{66'}$, J_{67}, $J_{67'}$, and $J_{77'}$. However, we have values of the analogous coupling constants for $(TiF_5)_n^{n-}$, *i.e.* for $J_{33'}$, J_{34}, $J_{34'}$, and J_{44}, and, using values close to these, the essential features of the resonance 7 can be reproduced, as shown in Fig. 4*b*. The fit of experimental is not perfect but is certainly good enough to confirm that the signal 7 is due to F_7 of $Ti_2F_9^-$ and to suggest that corresponding couplings in $(TiF_5)_n^{n-}$ and $Ti_2F_9^-$ have similar values. The chemical shifts of $Ti_2F_9^-$ are given in Table 1.

Since a four-membered 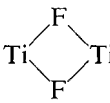 ring exists in $Ti_2F_9^-$, it could clearly exist in $Ti_2F_{10}^{2-}$ and on this basis we suggest that the species $(TiF_5)_n^{n-}$ is most probably the dimer **2**. If so, the series $Ti_2F_{11}^{3-}$, $Ti_2F_{10}^{2-}$, and $Ti_2F_9^-$ is the only one reported in which corner-, edge-, and face-bound bioctahedra are known for the same metal, oxidation state and halogen. In any event the complex resonances appearing in the spectra of mixtures with $1 < TiF_4/TiF_6^{2-} < 3$, *e.g.* Fig. 1*c*, can now be assigned to trimers or higher polymers as (*i*) they are not due to the 1:1 species, (*ii*) they do not arise from the dimeric $Ti_2F_9^-$ ion.

The chemical shifts in Table 1 deserve further comment. The spectra of all three dimeric species have in common relatively low field resonances for terminal fluorines and surprisingly high field shifts for the bridging fluorines. The latter phenomenon has also been noted by other workers (7) for $Ta_2F_{11}^-$, $Nb_2F_{11}^-$, and some related ions. This situation resembles that found in the ^{17}O n.m.r. spectrum of the dichromate ion (15) where the signal of the bridging oxygen occurs 784 p.p.m. above that of the terminal oxygens. For $Cr_2O_7^-$ the chemical shift difference has been interpreted (16) in terms of different double-bond characters in the two types of Cr—O bonds: the terminal oxygens can readily double-bond to the chromium, whereas the bridging oxygen, due to a bent Cr—O—Cr linkage, cannot. Presumably the same explanation applies in the present case: there is convincing evidence for partial double-bonding between titanium(IV) and terminal fluorides (ref. 17 and references cited therein), and the formation of bent Ti—F—Ti linkages in

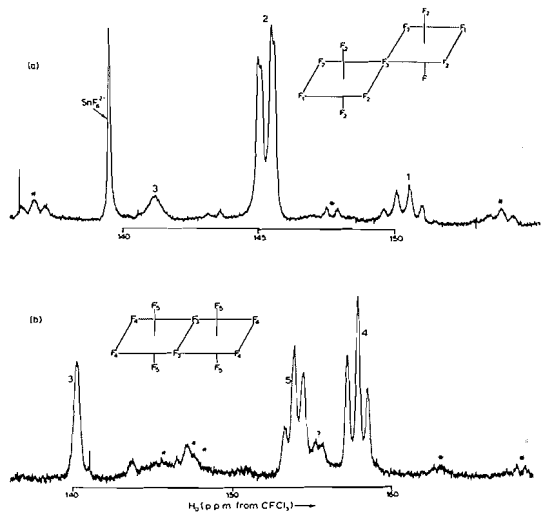

FIG. 5. (*a*) The 94.1 MHz ^{19}F n.m.r. spectrum of a solution with $SnF_4/SnF_6^{2-}/SO_2 = 1.0/3.0/26$, measured at $-60°$. (*b*) The 94.1 MHz ^{19}F n.m.r. spectrum of a solution with $SnF_4/SnF_6^{2-}/SO_2 = 1.0/1.0/11$, at $-60°$. (The starred resonances are $^{117/119}Sn$ satellites.)

[3]We were unable to prepare a sample free of the resonances overlapping and on the high field side of that due to F_7.

Can. J. Chem. Downloaded from www.nrcresearchpress.com by 210.87.254.105 on 09/05/12
For personal use only.

TABLE 2. ^{19}F n.m.r. spectral parameters for polymeric fluoroanions of tin(IV)

Ion	Fluorine assignment[a]	Chemical shift[b] (p.p.m.)	Average[c] tin–fluorine coupling constant (Hz)	Fluorine–fluorine coupling constants (Hz)
$Sn_2F_{11}^{3-}$	1	150.6	?	$J_{12} = 46 \pm 1$
	2	145.1	1638 ± 10	$J_{13} < 10$
	3	141.2[d]	?	$J_{23} = 11 \pm 1$
$Sn_2F_{10}^{2-}$	3	140.4[e]	~1340	J_{34} small
	4	158.1[f]	1950 ± 20	$J_{34'}$ small
	5	154.2[g]	~1690	$J_{45} = 58 \pm 1$

[a]For numbering scheme and method of assignment see text.
[b]Relative to internal $CFCl_3$; at $-60°$, $(Pr^n_2NH_2)_2SnF_6$ in SO_2 resonates at: 137.8 (11% solution); 139.8 (38% solution).
[c]Average of $J(^{119}Sn—F)$ and $J(^{117}Sn—F)$; for SnF_6^{2-} at $-60°$, $J(^{119}Sn—F) = 1604 \pm 4$ Hz.
[d]Width at half height ~55 Hz.
[e]Width at half height ~48 Hz.
[f]Width of components at half height ~25 Hz.
[g]Width of components at half height ~36 Hz.

$Ti_2F_9^-$, $Ti_2F_{10}^{2-}$, and probably $Ti_2F_{11}^{3-}$ also, is expected to restrict multiple-bonding between Ti(IV) and the bridging fluorines considerably.

The System SnF_4–$(Pr^n_2NH_2)_2SnF_6$ in SO_2

Stannic fluoride will dissolve in SO_2 solutions of SnF_6^{2-} only up to $SnF_4/SnF_6^{2-} = 1$. The dissolution of the insoluble SnF_4 is slower than that of TiF_4 in TiF_6^{2-} solutions and not noticeably exothermic.

Fine structure can be observed in the low temperature ^{19}F n.m.r. spectra of the SnF_4–SnF_6^{2-} solutions. Figure 5*a* shows the $-60°$ spectrum of a solution with $SnF_4/SnF_6^{2-}/SO_2 = 1.0/3.0/26$. In addition to a signal from SnF_6^{2-} with its appropriate $^{117/119}Sn$ satellites, the spectrum also shows three resonances, labelled *1*, *2*, and *3* in Fig. 5*a*, having relative intensities 2:8:1. In addition, the $^{117/119}Sn$ satellites of resonance *2* are observed, but those of resonances *1* and *3* are not seen, presumably due to their weakness and/or broadness. The resonances *1*, *2*, and *3* are attributed to the $Sn_2F_{11}^{3-}$ anion with structure **1**. The most intense absorption is a distorted doublet of doublets, which may be assigned to the fluorines F_2 coupled to the neighboring terminal fluorine F_1 and the bridging fluorine F_3. The fluorines F_1 are coupled to four nearest fluorines F_2, and their resonance appears as a quintet distorted towards *2*; evidently J_{13} is small (< 10 Hz) as no further splitting of the quintet is observed. The resonance *3* should be a nonet by coupling to the eight equivalent fluorines F_2, but no fine structure is observed in *3*. The n.m.r. parameters for $Sn_2F_{11}^{3-}$ are given in Table 2. The order of the chemical shifts of F_1, F_2, and F_3 is the same as found in $As_2F_{11}^-$ (19) and $Sb_2F_{11}^-$ (20), but the spread of the spectrum (9.4 p.p.m.) is smaller than that for either $As_2F_{11}^-$ (64 p.p.m. (19)) or $Sb_2F_{11}^-$ (42–49 p.p.m. (9, 20)). Thus even though J_{12} and J_{23} for $Sn_2F_{11}^{3-}$ are smaller than for the analogous Group V dimers, the spectrum of the tin(IV) ion shows greater second-order distortions than do the spectra of either of the other two at the same frequency.

The low-temperature n.m.r. spectrum of a solution with $SnF_4/SnF_6^{2-} = 1$ consists essentially of three resonances, labelled *3*, *4*, and *5* in Fig. 5*b*, together with their $^{117/119}Sn$ satellites. Resonance *3* is a broad singlet, *4* a relatively sharp triplet (slightly distorted towards 5 by second order effects) and *5* a broad distorted triplet; *3*, *4*, and *5* have intensities 1:2:2. As in the case of $Ti_2F_{10}^{2-}$ (see earlier) this spectrum must be interpreted in terms of an $(MF_5)_n^{n-}$ ion with a cyclic structure of *cis* linked MF_6 octahedra. The simplest such ion would be $Sn_2F_{10}^{2-}$ with structure **2**. The types of species occurring in the TiF_4–TiF_6^{2-} system (see above), coupled with the well-known (21) similarity between the chemistries of tin(IV) and titanium(IV), would suggest that $(SnF_5)_n^{n-}$ is, in fact, $Sn_2F_{10}^{2-}$, and it will be referred to as such for further discussion.

By comparison with the spectrum of SbF_5 (9), the resonances *3*, *4*, and *5* may be assigned to fluorines F_3, F_4, and F_5 of **2**. Like the spectra of $Ti_2F_{10}^{2-}$ and SbF_5 (9), the spectrum of $Sn_2F_{10}^{2-}$ should show the effects of magnetic

Can. J. Chem. Downloaded from www.nrcresearchpress.com by 210.87.254.105 on 09/05/12
For personal use only.

nonequivalence. The only obvious manifestation of these effects is the broadness of triplet 5 compared with triplet 4. Presumably the simplicity of the spectrum in Fig. 5*b* is a result of J_{45} being much larger than either J_{34} or $J_{34'}$.

The n.m.r. spectral parameters for $Sn_2F_{10}^{2-}$ are given in Table 2. Of particular interest is the sizeable $^{117/119}Sn$ coupling to the bridging fluorines F_3. This coupling, apparently the first of its type unambiguously identified for a non-transitional element, is of comparable size to many tin–terminal fluorine couplings (see, for example, ref. 22).

Experimental

Reagents

Di-*n*-propylammonium hexafluoro-stannate(IV) and -titanate(IV) were prepared as previously reported (23). Titanium tetrafluoride (Ozark–Mahoning Co.) was purified by sublimation at ~150° in an all-quartz apparatus and used as soon as possible after purification. Sulfur dioxide (Matheson of Canada Ltd., anhydrous grade) was dried by standing over 3A Molecular Sieves in the gas phase. Stannic fluoride (Ozark–Mahoning Co.) was used as received.

^{19}F Nuclear Magnetic Resonance Spectra

The n.m.r. spectra were obtained using Varian DA-60 or HA-100 spectrometers modified as reported earlier (24).

Sample Preparation

Samples were made up in well-dried all-glass vessels consisting of a mixing chamber which was open at the top via $\frac{1}{4}$ in. o.d. tubing and had a sidearm leading via a fine sinter to an n.m.r. tube. In a drybox, appropriate amounts of solid reactants were weighed into the mixing chamber, and the apparatus was closed by a detachable top. The apparatus was attached to a calibrated all-glass vacuum line and evacuated. Appropriate amounts of SO_2 and $CFCl_3$ were condensed into the mixing vessel. The apparatus was then sealed off at the $\frac{1}{4}$ in. tubing and allowed to warm to room temperature. Reaction of TiF_4–TiF_6^{2-} mixtures was rapid (a few minutes for complete dissolution) but that of SnF_4–SnF_6^{2-} mixtures was slower. In the case of $SnF_4/SnF_6^{2-} = 1$, warming to 40° for several hours was necessary to obtain complete dissolution of the SnF_4. The solution was now transferred via the sinter to the n.m.r. tube, and the mixing vessel and sidearm washed with SO_2 to ensure as complete a transfer of material as possible to the n.m.r. tube. The sample in the n.m.r. tube was frozen in liquid nitrogen and the tube sealed, thus separating it from the rest of the apparatus. Samples prepared in this manner were stable for long periods at room temperature. The ^1H n.m.r. spectra showed no evidence for decomposition of the cation.

We thank the National Research Council of Canada for generous financial assistance. We are also grateful to Mrs. H. Schroeder of the University of Western Ontario and Mr. J. I. A. Thompson of McMaster University for expert technical assistance in obtaining the n.m.r. spectra, and to Dr. S. Castellano, of the Mellon Institute, Pittsburgh, for providing a copy of his n.m.r. spectra plot program NMRPLOT.

1. R. Hoppe and W. Dähne. Naturwiss. **49**. 254 (1962).
2. H. C. Clark, R. J. O'Brien, and J. Trotter. J. Chem. Soc. 2332 (1964); E. O. Schlemper and W. C. Hamilton. Inorg. Chem. **5**, 995 (1966).
3. R. D. Euler and E. F. Westrum. J. Phys. Chem. **65**, 132 (1961).
4. P. Job. Ann. Chim. **9**, 113 (1928); F. Woldbye. Acta Chem. Scand. **9**, 299 (1955); M. M. Jones. J. Am. Chem. Soc. **81**, 4485 (1959).
5. J. A. Chandler, J. E. Waller, and R. S. Drago. Inorg. Chem. **1**, 65 (1962).
6. D. A. McCaulay, W. S. Higley, and A. P. Lien. J. Am. Chem. Soc. **78**, 3009 (1956).
7. S. Brownstein. Inorg. Chem. **12**, 584 (1973).
8. C. J. Hoffman, B. E. Holder, and W. L. Jolly. J. Phys. Chem. **62**, 364 (1958).
9. J. Bacon, P. A. W. Dean, and R. J. Gillespie. Can. J. Chem. **48**, 3413 (1970).
10. A. A. Bothner-By and S. M. Castellano. LAOCN3. The Mellon Institute, Pittsburgh.
11. D. S. Dyer and R. O. Ragsdale. J. Phys. Chem. **71**, 2308 (1967).
12. T. J. Kistenmacher and G. D. Stucky. Inorg. Chem. **10**, 122 (1971).
13. A. J. Edwards and G. R. Jones. J. Chem. Soc. A, 1651 (1969).
14. A. J. Edwards. J. Chem. Soc. 3714 (1964).
15. B. N. Figgis, R. G. Kidd, and R. S. Nyholm. Can. J. Chem. **43**, 145 (1965).
16. R. G. Kidd. Can. J. Chem. **45**, 605 (1967).
17. C. E. Michelson, D. S. Dyer, and R. O. Ragsdale. J. Chem. Soc. A, 2296 (1970).
18. W. McFarlane, A. M. Noble, and J. M. Winfield. J. Chem. Soc. A, 948 (1971).
19. P. A. W. Dean, R. J. Gillespie, R. Hulme, and D. A. Humphreys. J. Chem. Soc. A, 341 (1971).
20. R. J. Gillespie and K. C. Moss. J. Chem. Soc. A, 1170 (1966).
21. F. A. Cotton and G. Wilkinson. Advanced inorganic chemistry. 3rd ed. Interscience Publishers. New York. p. 807.
22. P. A. W. Dean and D. F. Evans. J. Chem. Soc. A, 1154 (1968).
23. P. A. W. Dean and D. F. Evans. J. Chem. Soc. A, 698 (1967).
24. P. A. W. Dean and R. J. Gillespie. J. Am. Chem. Soc. **91**, 7260 (1970).

Can. J. Chem. Downloaded from www.nrcresearchpress.com by 210.87.254.105 on 09/05/12
For personal use only.

Hydrogen–Water Deuterium Exchange over Graphon Supported Group VIII Noble Metals[1]

NORMAN HENRY SAGERT AND RITA MARY LOUISE POUTEAU

Research Chemistry Branch, Atomic Energy of Canada Limited, Whiteshell Nuclear Research Establishment, Pinawa, Manitoba R0E 1L0

Received June 25, 1973

Specific activities of Group VIII noble metals supported on Graphon have been determined for hydrogen–water deuterium exchange. Metal surface areas, which are required to calculate specific activities, were measured by hydrogen chemisorption, and by reaction of hydrogen with chemisorbed oxygen. For the second triad metals, ruthenium, rhodium, and palladium, and in the temperature range 140 to 225 °C, the variation of activity was Ru < Rh > Pd. For the third triad metals, osmium, iridium, and platinum, the variation of activities was Os < Ir < Pt in the same range of temperature. Apparent activation energies were measured over this temperature range, and orders of reaction with respect to hydrogen and water were measured at 160 °C (200 °C for Pt). From these data, activation energies for the surface exchange reaction were calculated. In the second triad the activation energies decrease slightly with increasing atomic number, but in the third triad they decrease quite markedly with increasing atomic number. A good correlation was obtained between the activation energy for surface exchange and the thermionic work function of the metal. This supports our earlier suggestion that Graphon is able to donate electrons to the metal and thus lower the activation energy for the surface exchange.

L'activité spécifique de métaux nobles du groupe VIII fixés sur Graphon a été déterminée pour l'échange de deutérium H_2–HDO. La superficie de la surface métallique, qui est nécessaire lors du calcul des activités spécifiques, a été évaluée à l'aide de la chemisorption de l'hydrogène ainsi qu'à l'aide de la réaction de l'hydrogène avec de l'oxygène chemisorbé. Pour la seconde triade de métaux, ruthénium, rhodium et palladium, et dans l'intervalle de températures allant de 140 à 225 °C, la variation d'activité a été dans l'ordre Ru < Rh > Pd. Pour la troisième triade de métaux, osmium, iridium et platine, la variation d'activité a été dans l'ordre Os < Ir < Pt dans le même intervalle de températures. Les énergies apparentes d'activation ont été mesurées pour cet intervalle de températures alors que l'ordre des réactions par rapport à l'hydrogène et à l'eau a été déterminé à 160 °C (200 °C pour le Pt). A partir de ces données, on a calculé pour les réactions d'échange se faisant en surface les énergies d'activation. Dans la seconde triade, les énergies d'activation diminuent légèrement selon l'ordre croissant des numéros atomiques, alors que dans la troisième triade elles diminuent selon l'ordre croissant des numéros atomiques d'une façon assez marquée. Une bonne corrélation a été obtenue entre l'énergie d'activation pour l'échange en surface et la fonction du travail thermionique du métal. Ce fait est en accord avec nos suggestions antérieurs voulant que le Graphon est capable de donner des électrons au métal et ainsi diminuer l'énergie d'activation nécessaire à l'échange en surface. [Traduit par le journal]

Can. J. Chem., **51**, 4031 (1973)

Introduction

Group VIII metals have been shown to be good catalysts for most hydrogenation, dehydrogenation, and hydrogenolysis reactions. This is partly, if not entirely, because they are able to adsorb hydrogen in its atomic form (1). However, it has not been easy to compare activities over a number of these metals because the results are complicated by varying heats of reaction, varying selectivities, and self poisoning. Isotopic exchange reactions offer a partial solution to this problem as there is a very small heat of reaction, and no large chemical difference between reactants and products. However, isotopic exchange reactions involving hydrocarbons can still be affected by self poisoning from side reactions, or indeed, from the main reaction if many hydrogen atoms are stripped from a single carbon atom (2).

Hydrogen–water deuterium isotope exchange is a reaction which does not involve such complications (3, 4). Moreover it is a sterically simple or "facile" reaction (5), so that in studying it over a series of metals the electronic, or chemical, effects should predominate over geometric effects. The reaction is very slow over unpromoted metals of the first triad, iron, cobalt, and nickel (6), but was found to take place with acceptable rates over metals of the second and third triads of Group VIII, the

[1]AECL No. 4632.

Can. J. Chem. Downloaded from www.nrcresearchpress.com by 210.87.254.42 on 09/05/12
For personal use only.

TABLE 1. Properties of the graphon supported catalysts

Metal	Impregnating solution	Calculated site area (10^{-20} m^2)	Metal surface area (m^2 kg^{-1})	Metal dispersion (%)
1% Pd	$(NH_4)_2PdCl_6$	8.8	890	53
1% Rh	$RhCl_3$	8.4	890	48
1% Ru	$RuCl_3 \cdot 1$–$3H_2O$	11.0	260	18
0.5% Pt	H_2PtCl_6	8.9	240	52
1% Ir	H_2IrCl_6	8.6	820	84
1% Os	H_2OsCl_6	11.7	(800)	(85)

so-called noble metals. Therefore the reaction was studied over these six metals, ruthenium, rhodium, palladium, osmium, iridium, and platinum. To compare activities in a meaningful way, rates should be compared per unit surface area of exposed metal. In recent years methods have been developed for measuring surface areas of noble metals by selective chemisorption (7, 8) and by surface titrations (9). These methods may not be accurate to better than $\pm 30\%$, but they are generally reproducible to $\pm 10\%$.

Earlier work (4) indicated that support effects could be important. In this work the support chosen was Graphon, a highly graphitized carbon black. We previously suggested (4) that, for metals with work functions higher than 4.6 eV, some donation of electrons to the metal from the Graphon occurs. We have tested this hypothesis by using metals of varying work function.

Experimental

Apparatus and Procedure

Rates were measured in a flow system at atmospheric pressure, as previously described (4, 5). The HD concentrations were measured either by gas chromatography or with a Consolidated 21-621 mass spectrometer fitted with a continuous inlet. The mass spectrometer was calibrated for HD by equilibrating hydrogen with water of known deuterium content. In addition, the correction for H_3^+ was measured by passing deuterium-free H_2 through the mass spectrometer. This hydrogen was generated from the action of finely divided calcium on water containing only 1.6 p.p.m. deuterium. Argon was used as a diluent to reduce the partial pressure of hydrogen (4). Catalysts were reduced *in situ* with hydrogen at 300 °C for 18 h, and thereafter were kept overnight at 180 °C in flowing hydrogen. Generally several hours of conditioning in a hydrogen–water flow were necessary before reproducible results could be obtained after the initial reduction. If catalysts were kept in flowing hydrogen at 180 °C overnight their activity remained stable.

The total surface area of the Graphon support has been reported previously (4). Metal surface areas were measured by Boudart's hydrogen titration technique (9), by electron microscopy (5) and, for Pt, Ir, and Ru, by hydrogen chemisorption. For area measurements, catalysts were reduced under the same conditions used in the catalytic studies. They were then evacuated for 16 h to 2×10^{-4} Nm^{-2} and either a hydrogen chemisorption isotherm was measured, or a titration was done. Water isotherms were measured volumetrically at 27 °C. Corrections were made for the adsorption of water vapor in an empty cell.

Materials

Sources and methods of purifying water, D_2O, hydrogen, and argon have been described (4, 5). The preparation of the 0.5% platinum on Graphon catalysts was described previously (4). Because of their lower activities, the other catalysts were prepared as 1% metal on Graphon by impregnation with an appropriate compound (Table 1). Graphon was wetted with a solution containing the required amount of metal and the slurry was evaporated to dryness. The catalysts were then dried overnight at 100 °C.

Results

Metal surface areas of the catalysts are given in Table 1. These were calculated from the amount of hydrogen taken up using the stoichiometry proposed by Benson and Boudart (10).

[1] $$PtO + \tfrac{3}{2}H_2 \rightarrow PtH + H_2O$$

The number of sites measured in this way agreed with the number estimated from hydrogen chemisorption to within 20%, which was considered adequate for our purposes. From the number of sites, surface areas were calculated using the site areas listed. Relative site areas were estimated by averaging the site areas of crystal faces with high densities of atoms (28). The absolute site area of platinum was taken as 8.9×10^{-20} m^2 (11). The titration gave more reproducible results for the number of sites so this number was used. However, for osmium the Boudart titration did not seem to work and hydrogen chemisorption gave very low amounts adsorbed. Therefore, the surface area of osmium was estimated from the electron micrographs,

Can. J. Chem. Downloaded from www.nrcresearchpress.com by 210.87.254.42 on 09/05/12
For personal use only.

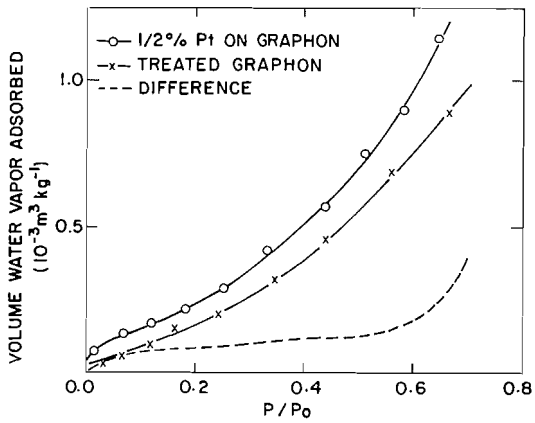

FIG. 1. Water adsorption isotherms for ½% Pt on Graphon catalyst and HCl treated Graphon measured at 27° C.

and the value in Table 1 is bracketed because it is considerably less accurate. Electron micrographs of other catalysts yielded surface areas agreeing with those obtained chemically to within ±50%, assuming spherical particles. In fact the particles were usually somewhat elongated.

Water vapor isotherms were measured at 27 °C for all catalysts, and Fig. 1 shows the results obtained with the platinum catalyst. We attempted to estimate the amount of water adsorbed on the platinum by measuring a water isotherm over Graphon which had been treated as the catalysts, apart from substituting HCl for the equivalent amount of chlorine in the impregnating compound. Untreated Graphon took up no water at all at relative pressures (P/P_0) smaller than 0.5. As a crude approximation, the difference between the water adsorbed on the treated Graphon and the water adsorbed on the catalyst was taken as that adsorbed on the platinum. A type II isotherm was observed which did not turn up until P/P_0 was greater than 0.5. Although the adsorption is primarily physical, the flat portion of the isotherm was well enough defined so that the Langmuir isotherm is obeyed for $P/P_0 < 0.5$. If the area of the water molecule is 1.06×10^{-19} m^2 (12), the metal surface areas, measured by hydrogen titration, imply a full water monolayer on the metal at 1.25×10^{-4} m^3 kg^{-1}, so that the plateau corresponds to $\theta_{H_2O} = 1.0$. However, low water coverages for the catalyst as a whole were calculated previously from kinetic data (4). This suggests that most of the water adsorbed on the support takes part in the reaction. In the present work, the reaction orders were measured in a region of intermediate water coverage at 160 °C or at 200 °C where P/P_0 equals 0.03_7 or 0.015, respectively.

The reaction rate coefficient, k, in moles of HD per kilogram of catalyst per second is given by eq. 2 (3–6) for water containing less than 5% deuterium.

$$[2] \qquad k = \frac{F}{(\alpha+\gamma)W} \ln \frac{n_e - n_0}{n_e - n}$$

F is the hydrogen flow rate in mol^{-1}, W is the catalyst weight in kg, α is the reciprocal of the equilibrium constant for reaction 3 and γ is the ratio of hydrogen pressure to water pressure.

$$[3] \qquad HDO + H_2 \rightleftarrows H_2O + HD$$

The n's represent HD concentrations, respectively at equilibrium (n_e), before reaction (n_0), and after reaction (n). The rate coefficient, k, would be the initial rate of reaction 3 in the forward direction if experiments could be done with pure HDO and H_2 (3, 4). Equation 2 is analogous to equations developed by Harris (13), and used by Kemball (14) in studies of the exchange of D_2 with hydrocarbons. Further consideration of the derivation of eq. 2 makes it clear that the rate is in moles of HD produced, not D_2 as earlier stated (4, 5). References in our earlier papers to D_2 should be taken as referring to HD. Previously we have shown that, with this type of catalyst, the rate is not controlled by internal or external diffusion (4).

Specific rates, or activities, were obtained by dividing the rate coefficient, k, by the surface area of the metal per kg of catalyst as given in Table 1. These specific rates are shown in Fig. 2 as a function of temperature, plotted in the Arrhenius form. All the data shown were obtained with a hydrogen pressure of 78.0 kN m^{-2} and a water pressure of 23.7 kN m^{-2}, and were calculated from plots of $\ln(n_e - n_0)/(n_e - n)$ against W/F. Table 2 summarizes the specific rates at 160 °C, the apparent activation energies, E_{app}, defined as $\partial \ln k/\partial(1/T)$ at constant pressure, and the reaction orders with respect to water and hydrogen. Reaction orders were defined as $(\partial \ln k/\partial \ln P_{H_2})_{T,P_{H_2O}}$ and were obtained from double logarithmic plots of k against pressure, where the pressure was usually varied over about one order of magni-

Can. J. Chem. Downloaded from www.nrcresearchpress.com by 210.87.254.42 on 09/05/12
For personal use only.

TABLE 2. Kinetic parameters for the H_2–HDO deuterium exchange over Graphon supported group VIII noble metals

Catalyst	Specific rate at 160 °C (10^{-4} mol m^{-2} s^{-1})	Order in water† "a" ±0.1	Order in hydrogen† "b" ±0.1	Temperature where orders measured (°C)	E_{app}* (kJ mol^{-1})	E_0 (kJ mol^{-1})
1%Pd	0.13_5	0.0	0.0	160	75	80
1% Rh	1.0_2	0.9	0.0	160	$43._5$	89
1% Ru	0.68	0.4	0.2	160	62	103
0.5% Pt	9.15	0.5_5	0.0	200	8.0	36
1% Ir	1.46	0.3	0.0	160	42	57
1% Os	(0.4_5)	0.4	0.4	160	40	102

*Measured in high temperature range.
†$a = 1 - \theta_{H_2O}$, $b = \frac{1}{2}(1 - \theta_H)$.

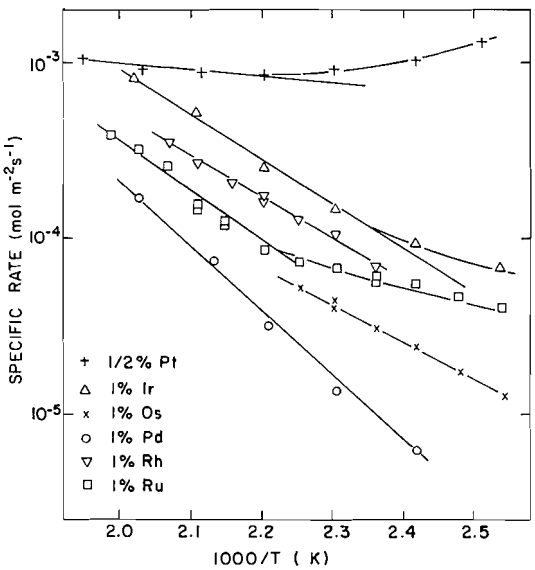

FIG. 2. Arrhenius plots of specific rates, measured with $P_{H_2} = 78.0$ kN m^{-2} and $P_{H_2O} = 23.7$ kN m^{-2}.

tude. Over this relatively small range of pressure, straight lines were obtained so that the rate expression could be written as

$$[4] \qquad k = k^1 P_{H_2O}{}^a P_{H_2}{}^b$$

Sandler (15) has shown that for the ortho–para hydrogen conversion, which follows a rate law in which the rate is proportional to the hydrogen pressure to the nth power, the apparent activation energy (E_{app}) is related to the true activation energy (E_0) by eq. *5a*

$$[5a] \qquad E_0 = E_{app} + n\lambda_{H_2}$$

where λ_{H_2} is the heat of desorption of H_2. Eley (16) later confirmed this and showed that n equaled $(1 - \theta)$ where θ is the surface coverage. Following these authors, it is easily shown that, for the rate expression in eq. 4, the true surface activation energy, E_0, and the apparent activation energy, E_{app}, are related by eq. *5b*

$$[5b] \qquad E_0 = E_{app} + b\lambda_{H_2} + a\lambda_{H_2O}$$

where λ_{H_2} and λ_{H_2O} are the heats of desorption of hydrogen and water respectively. Furthermore a equals $(1 - \theta_{H_2O})$ and $2b$ equals $(1 - \theta_H)$. Heats of desorption of hydrogen from ruthenium and osmium were required and these were taken as 105 kJ mol^{-1} (ref. 1, pp. 74–86). The heat of desorption of water was taken as 50 kJ mol^{-1}, about 10% greater than the heat of vaporization, in accordance with the results of Cole (17). It is easily shown that the form of hydrogen dependence used in eq. *5b* is correct even if a dissociative mechanism is involved in hydrogen adsorption. This also follows from Sandler's general derivation using the Freundlich isotherm. Considering the approximations involved the values of E_0 may not be valid to better than ±10 kJ mol^{-1}.

Figure 3 shows specific rates at 160 °C and E_0's plotted against periodic group number. Specific rates rise steadily for the third triad metals of group VIII, but peak at Rh for the second triad metals. This pattern would be the same at any of the temperatures investigated, although the shape of the curves would be different. A number of correlations of E_0 with various metallic properties were attempted. The best, shown in Fig. 4, was the correlation with the thermionic work functions selected by Bouwman and Sachtler (18). More scatter is noted when E_0 is plotted against the photoelectric work functions of the same authors.

Can. J. Chem. Downloaded from www.nrcresearchpress.com by 210.87.254.42 on 09/05/12
For personal use only.

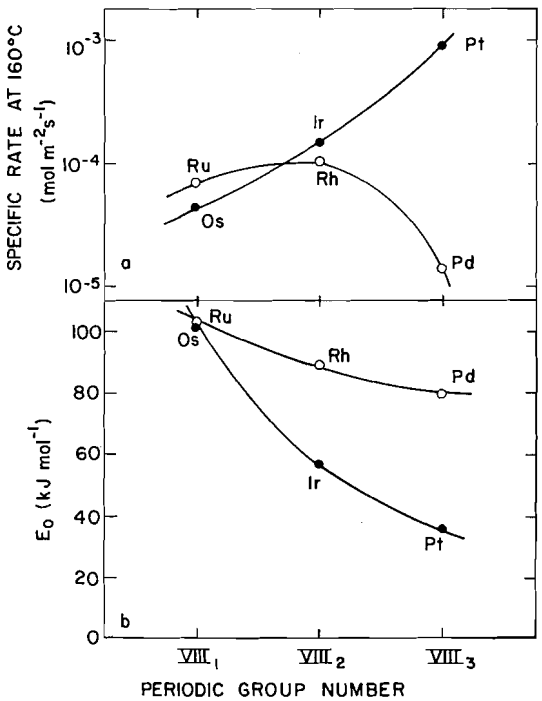

FIG. 3. Correlation of specific rate at 160 °C (*a*) and chemical activation energy, E_0 (*b*) with periodic group number.

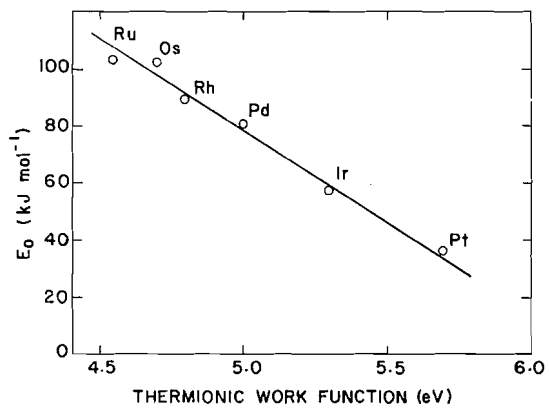

FIG. 4. Correlation of chemical activation energy with the thermionic work functions selected by Bouwman and Sachtler (ref. 18).

Discussion

The mechanism previously proposed for hydrogen–water exchange over platinum supported on alumina (3) and Graphon (6) is summarized below. It involves the adsorption of hydrogen and water vapor at different sites, I and II respectively.

[6] $H_2(g) + 2\,(I) \rightleftarrows 2H_{ads}$

[7] $HDO(v) + (II) \rightleftarrows HDO_{ads}$

[8] $H_{ads} + HDO_{ads} \rightleftarrows H_2O_{ads} + D_{ads}$

[9] $H_{ads} + D_{ads} \rightleftarrows HD\,(g) + 2(I)$

[10] $H_2O_{ads} \rightleftarrows H_2O\,(v) + (II)$

Reaction 8 is taken to be rate limiting, and this leads (3, 4) to the rate expression:

[11] $$k = k_8K_7K_{10}\theta_{H_2O}\theta_H$$

where k_i is the forward rate constant for reaction i and K_i is the equilibrium constant for equilibrium i. If equilibria are maintained between the gas and the surface, the product K_7K_{10} will be a constant corresponding to the isotope effect for adsorption of HDO relative to H_2O. Thus the ratio will be close to unity. Therefore

[12] $$k = k_8\theta_{H_2O}\theta_H$$

Reaction 8 may consist of a number of steps. Hallaba and Abdel-Wahab (19) have adopted the original suggestion of Farkas (20) that reaction 8 consists of the fast formation of a hydroxide film, followed by slow reduction of that film. However, if the adsorption of water does not affect adsorption of hydrogen, it is impossible to distinguish such a sequence kinetically from a single step reaction.

Taking reaction 9 as rate determining leads (4) to eq. 13

[13] $$k = k_9K_7K_8K_{10}\theta_H^2$$

As the reaction over all the metals showed some dependence on water pressure and a dependence on hydrogen pressure less than 0.5, it is unlikely that reaction 9 is rate determining. Conversely, if the rate of water adsorption were rate limiting, then

[14] $$k = k_7K_{10}\theta_{H_2O}$$

This case is not clearly excluded, because the high hydrogen pressures result in a weak dependence of rate on hydrogen pressure, *i.e.* a full hydrogen coverage is usually maintained. However for osmium and ruthenium a measurable dependence of rate on hydrogen pressure was observed. For these catalysts water adsorption–desorption is clearly not the rate determining step, and by implication it is unlikely for the other metals as well. Therefore the rate equation is taken as eq. 12 with chemical exchange rate-determining.

Can. J. Chem. Downloaded from www.nrcresearchpress.com by 210.87.254.42 on 09/05/12
For personal use only.

Can. J. Chem. Downloaded from www.nrcresearchpress.com by 210.87.254.42 on 09/05/12
For personal use only.

Our previous study (4) on platinum at lower temperatures indicated that exchange took place with water which was weakly bonded to the platinum, and that, kinetically, the water coverage was low. This work suggests that the water coverage on the metal is fairly high. The apparent contradiction may be resolved if we postulate that much of the water adsorbed on the support is kinetically equivalent to water adsorbed on the metal. Since Graphon untreated with chloride adsorbs little water, it would seem that the chloride forms the hydrophilic sites on the surface. The chloride is formed from decomposing particles of chloroplatinic acid, so it is reasonable to assume that most of the hydrophilic sites are formed close to the metal particles. The water adsorbed on these sites then participates in the reaction in a manner similar to that suggested by Rolston for alumina supported platinum (3).

From the experimental orders, obtained by fitting data to the empirical eq. 4, and the apparent activation energies, we can use eq. 5*b* to calculate and compare the true activation energies (E_0). These are taken to be activation energies for the surface exchange, reaction 8, although it is recognized that with different metals, reaction 8 may be broken down into a number of different steps, which may vary with the different metals.

We are now in a position to make some comparisons of activity patterns for this reaction as a function of the position of the metal in the periodic table (Fig. 3*a*). For the third triad metals, osmium, iridium, and platinum, specific activity rises steadily as the atomic number increases. For the second triad metals, ruthenium, rhodium, and palladium, the specific activity passes through a small maximum at rhodium in position 2 of group VIII. This pattern is remarkably similar to that observed by Dalla Betta *et al.* (21) for the hydrogenation of cyclopropane, a reaction termed facile by Boudart *et al.* (22). The activity pattern is very different for reactions such as the hydrogenolysis of ethane, where activities fall steeply in each triad with increasing atomic number (21). It is interesting to note that the hydrogenation of cyclopropane and of many olefins does not require dissociative chemisorption and may well proceed through π-bonded intermediates (21, 23). These reactions are usually facile as well. Thus the activity pattern observed suggests that hydrogen–water exchange is a facile reaction and that water may be not dissociatively bonded to the surface. The bonding may be by electron donation from p orbitals of the oxygen to the unfilled d bands of the metal (ref. 1, p. 219).

The chemical activation energies, E_0, fall as the atomic number rises in each triad, although the fall is much more noticeable in the third triad, (Fig. 3*b*). If our suggestions about the mechanism are correct, then E_0 corresponds to E_8, (eq. 12) and thus E_8 is lowered on the more noble metals of higher atomic number. Correlations of E_0 with various properties such as percentage d-band character, and metallic radius were attempted, but these only gave correlations within each triad. However, all the E_0's were well correlated with the thermionic work functions (Fig. 4). The slope of the line in Fig. 4 indicates that for each kJ mol^{-1} that the work function is raised, E_0 is lowered by 0.67 kJ mol^{-1}. The validity of this correlation is somewhat tentative, largely because of the great variations in reported work functions. However, we have taken a set of thermionic work functions collected by Bouwman and Sachtler (18). If the set of photoelectric work functions at 373 °A collected by the same authors (18) is used, in conjunction with their own recent value for palladium of 5.1 eV (24), a good correlation is obtained with a slope of -0.8. However, work functions are notoriously sensitive to variations in purity and surface structure. Thus the quantitative nature of the correlation is extremely tentative. It seems reasonably well established however that platinum has a higher work function than the other metals. As a point of reference, it should be noted that a recent determination of the gas phase equivalent to reaction 8 gives an activation energy of about 85 kJ mol^{-1} (25). The presence of a surface would alter this value, but nevertheless it is quite close to that observed over metals of low work function.

We have suggested (4) that the high work function of platinum and iridium relative to Graphon (4.5 eV) leads to significant negative charging of the metal, and consequently to a metal–hydrogen bond more polarized in the sense $M^{\delta+}$–$H^{\delta-}$. Such polarization should lower E_8. Similar electron donation has recently been postulated for the alkali metal promotion of supported ruthenium ammonia synthesis catalysts (26). This is our preferred interpretation in the light of our earlier work on carbon sup-

Can. J. Chem. Downloaded from www.nrcresearchpress.com by 210.87.254.42 on 09/05/12
For personal use only.

ported Graphon, in which the activation energies for surface exchange fell with increased graphitizing temperature of the support. However, it is possible that the lower E_0's on iridium and platinum are due to properties of the metal alone, rather than to a metal–support interaction. Further work on unsupported metals, presently in progress, should show whether or not this is the case. Another alternative interpretation is that over the catalysts with the highest rates, the mechanism is changing to one where the adsorption–desorption of water is rate determining. In this case eq. 14 shows that we would be measuring E_7. The value of E_7, corrected for the order of the reaction and heat of adsorption, would be the activation energy for water adsorption which should be small. However, for reaction 7 to be rate determining, reaction 8 would have to be in equilibrium. Thus E_8 should have fallen to a value even lower than that quoted. Therefore this interpretation would not invalidate our conclusions about E_8.

No correlation was established between the reaction orders with respect to water and either the specific activity or the activation energy for surface exchange. On the other hand, some correlation was noted in the order with respect to hydrogen. For dissociative hydrogen adsorption Eley's approach equates b with $\frac{1}{2}(1 - \theta_H)$. Thus the hydrogen atom coverages are all unity with exception of the two least noble metals ruthenium ($\theta_H = 0.6 \pm 0.2$) and osmium ($\theta_H = 0.2 \pm 0.2$). For these two Graphon supported metals, the calculated hydrogen coverages are definitely lower than unity. This would account for the difficulty we encountered in measuring osmium surface areas by the usual techniques. No such difficulty has been noted by Sinfelt and co-workers using silica supported ruthenium and osmium (8, 27). Possibly this low hydrogen coverage results from an interaction between Graphon and the metal.

In summary, we have shown that the pattern of specific activities for hydrogen–water deuterium exchange is very similar to that for cyclopropane hydrogenation. Thus our hydrogen–water exchange is probably a "facile" reaction and shows much less variation in specific rate than does a demanding reaction such as ethane hydrogenolysis. In contrast to cyclopropane hydrogenation, however, surface activation energies fall for metals of higher work function. This may be truly a property of the metal, or it may result from a support effect whereby electrons are donated to the metal.

We thank W. M. Thurston, General Chemistry Branch, CRNL, for preparation and analysis of the deuterium-free water. E. E. Sexton of the Materials Science Branch, WNRE, took the electron micrographs. We also thank G. G. Strathdee, J. H. Rolston, and H. C. Chen for useful discussions.

1. G. C. Bond. Catalysis by metals. Academic Press, London, 1962.
2. C. Kemball. Catal. Rev. **5**, 33 (1971).
3. J. H. Rolston and J. W. Goodale. Can. J. Chem. **50**, 1900 (1972).
4. N. H. Sagert and R. M. L. Pouteau. Can. J. Chem. **50**, 3686 (1972).
5. N. H. Sagert and R. M. L. Pouteau. Can. J. Chem. **49**, 3411 (1971).
6. P. Margineanu and A. Olariu. J. Catal. **8**, 359 (1967).
7. J. H. Sinfelt and D. J. C. Yates. J. Catal. **8**, 82 (1967).
8. J. H. Sinfelt. Catal. Rev. **3**, 175 (1969).
9. M. Boudart. Adv. Catal. Rel. Subj. **20**, 153 (1969).
10. J. E. Benson and M. Boudart. J. Catal. **4**, 704 (1965).
11. T. A. Dorling, C. J. Burlace, and R. L. Moss. J. Catal. **12**, 207 (1968).
12. S. J. Gregg and K. S. W. Sing. Adsorption, surface area, and porosity. Academic Press, London. 1967 p. 82.
13. G. M. Harris. Trans. Faraday Soc. **47**, 716 (1951).
14. C. Kemball. Adv. Catal. Rel. Subj. **11**, 223 (1959).
15. Y. L. Sandler. J. Chem. Phys. **21**, 2243 (1953).
16. D. D. Eley. Nature, **194**, 1076 (1962).
17. H. D. F. Cole. Ph.D. Thesis. The University of Texas, Austin, Texas, 1964.
18. R. Bouwman and W. M. H. Sachtler. Surface Sci. **24**, 140 (1971).
19. E. Hallaba and E. M. Abdel-Wahab. Zeit. Anorg. Alleg. Chem. **388**, 169 (1972).
20. A. Farkas. Trans. Faraday Soc. **32**, 922 (1936).
21. R. A. Dalla Betta, J. A. Cusumano, and J. H. Sinfelt. J. Catal. **19**, 343 (1970).
22. M. Boudart, A. W. Aldag, J. E. Benson, N. A. Dougharty, and C. G. Harkins. J. Catal. **6**, 92 (1966).
23. J. J. Rooney and G. Webb. J. Catal. **3**, 488 (1964).
24. R. Bouwman, G. J. M. Lippits, and W. M. H. Sachtler. J. Catal. **25**, 350 (1972).
25. N. E. Bibler and R. F. Firestone. J. Phys. Chem. **76**, 621 (1972); J. Phys. Chem. **76**, 4041 (1972).
26. K. I. Aika, H. Hori, and A. Ozaki. J. Catal. **27**, 424 (1972).
27. J. H. Sinfelt and D. J. C. Yates. J. Catal. **10**, 362 (1968).
28. J. H. Rolston. Private communication.

Dielectric Loss of Adsorbed Polar Molecules[1]

T. McMULLEN

Department of Chemistry, St. Francis Xavier University, Antigonish, Nova Scotia

Received February 27, 1973

A theory of the dielectric susceptibility of polar gases adsorbed on ionic solids is presented. The rotational oscillator model of an adsorbed polar molecule is used, and dielectric loss is assumed to occur by phonon emission and absorption. For linear coupling of the rotational oscillator to the lattice vibrations, an exact solution is found using diagrammatic perturbation theory at finite temperature. In this model, appreciable loss is only found if the density of phonon states near the classical oscillator frequency is reasonably large, and it is suggested that this is to be expected in situations where the rotational oscillator model is valid. The method can be extended to more complex adsorbate–lattice interactions.

On présente une théorie traitant de la susceptibilité diélectrique de gaz polaires adsorbés sur des solides ioniques. On utilise le modèle d'oscillateur de rotation d'une molécule polaire adsorbée. De même, on suppose que la perte diélectrique se produit par émission et par absorption d'un phonon. En ce qui a trait au couplage linéaire de l'oscillateur de rotation avec les vibrations du réseau, on a trouvé une solution exacte en utilisant la théorie de perturbation graphique à température fixée. Dans ce modèle, on a trouvé une perte appréciable seulement lorsque la densité des états du phonon proches de la fréquence de l'oscillateur classique est suffisament grande; on propose que cet état doit prévaloir dans les situations où le modèle d'oscillateur de rotation est valide. La méthode peut être appliquée à des interactions réseauproduit adsorbé plus complexes. [Traduit par le journal]

Can. J. Chem., **51**, 4038 (1973)

Introduction

The interpretation of measurements of the dielectric behavior of adsorbed species (1) is a difficult task, and only the simplest of adsorbate–adsorbent systems as yet permit any sort of detailed description. Small polar molecules physically adsorbed on the surface of an ionic crystal form such a system, and have been investigated both experimentally (1, 2) and theoretically (1, 3). Often, it is assumed that a frequency dependent dielectric constant can be assigned separately to the adsorbed phase. This fundamental idealization permits one to ignore the effect of the field due to polarization induced in the solid when calculating the susceptibility of the adsorbed phase. The adsorbed molecules can be regarded simply as moving in a potential due to the surface in response to the applied field.

We will make this idealization here, and consider the dielectric susceptibility of an isolated small polar molecule adsorbed on the surface of an ionic crystal, such as hydrogen chloride on sodium chloride. The problem of assigning a dielectric constant to the adsorbed phase has been discussed previously (3), and we suppose that a reasonable "experimental" value of this susceptibility is available.

The rotational oscillator model of a small polar adsorbed molecule was introduced by Kurbatov (4), and its development has been reviewed by McIntosh (1). The most recent treatment is that of McMullen and McIntosh (3) who use a correlation function approach to determine the frequency dependent susceptibility. These authors introduce dielectric loss by proposing a "strong collision" type of approximation with a phenomonological mean free time. This mechanism, as the authors point out, does not seem to be a particularly realistic model of the physical system, and there seems to be no way of determining their relaxation time from first principles. It is this defect we wish to rectify in the present article by constructing a more detailed model of the interaction between the rotational oscillator and the vibrating crystal lattice of the adsorbent.

Dielectric loss is due to energy dissipation to the lattice vibrations. The oscillating electric field causes the adsorbed polar molecule to oscillate. The polar molecule is bound to the ions of the substrate, and thus exerts a force on these ions as it moves. This causes the adsorbate lattice itself to vibrate, and the phonons generated

[1]Research supported by the National Research Council of Canada and by the St. Francis Xavier University Council for Research.

Can. J. Chem. Downloaded from www.nrcresearchpress.com by 210.87.254.6 on 09/05/12
For personal use only.

Can. J. Chem. Downloaded from www.nrcresearchpress.com by 210.87.254.6 on 09/05/12
For personal use only.

carry energy away from the adsorbed molecule, and so indirectly from the oscillating electric field. Creation of additional phonons can, of course, be regarded as heating the lattice.

To describe this process we use the language of Green functions at non-zero temperature (5). This formalism provides a convenient and general approach, and allows us to include temperature effects. An approximation to the coupling of the adsorbed molecule to the lattice will be introduced in Section 3 which makes the problem exactly soluble, but corresponds to ignoring the temperature dependence of the susceptibility. Nevertheless, this approximation describes a tightly bound "true" rotational oscillator which makes only small excursions from equilibrium, and is applicable to rotational oscillators at low temperatures. Also, the main purpose of the present article is to outline an approach to the problem, and an exactly soluble model best serves this purpose.

Dielectric Susceptibility

Previous treatments of the rotational oscillator model of an isolated rotational oscillator on a surface have assumed a classical oscillator. In order to treat the interaction with the quantized lattice vibrations we use a quantized oscillator. The assumptions used in constructing the quantized oscillator model are essentially identical with those used in the classical model, and need no comment here. The quantum mechanical analog of the classical correlation function expression for the susceptibility (ref. 3, p. 1009) is needed and will be derived in this section.

The Hamiltonian of the crystal and N point dipoles in an electric field may be written as

$$H - \sum_{i=1}^{N} \boldsymbol{\mu}_i \cdot \boldsymbol{E}$$

where $\boldsymbol{\mu}_i$ is the dipole moment operator of the ith dipole, and the field is

$$\boldsymbol{E}(t) = \frac{1}{\sqrt{2\pi}} \int_{-\infty}^{\infty} d\omega e^{-i\omega t} \boldsymbol{E}(\omega)$$

The dipole moment of the N oscillators is

$$[1] \qquad \boldsymbol{M}(t) = \left\langle \sum_i \boldsymbol{\mu}_i(t) \right\rangle$$

where $\langle\rangle$ indicates the trace over the canonical density matrix $\rho_0 = \exp\{\beta(\Omega - H)\}$ (the chemical potential of oscillators is zero, and $\beta = 1/kT$) characterizing the system at $t = -\infty$ before the field is switched on adiabatically.

Equation 1 is written in the Heisenberg picture. Changing to the interaction picture defined by the perturbation due to the field, and retaining only the terms

$$1 - i \int_{-\infty}^{t} dt' \sum_{i=1}^{N} \boldsymbol{\mu}_i(t') \cdot \boldsymbol{E}(t')$$

in the expansion of the time development operator, we find, to lowest order in $\boldsymbol{E}$

$$[2] \quad \boldsymbol{M}(t) = i \int_{-\infty}^{t} dt' \sum_{ij} \langle [\boldsymbol{\mu}_j(t') \cdot \boldsymbol{E}(t'), \boldsymbol{\mu}_i(t)] \rangle$$

([,] indicates the commutator of the two operators) if we take $\sum_i \langle \boldsymbol{\mu}_i \rangle = 0$. Writing M^E and μ_i^E for the components of $\boldsymbol{M}$ and $\boldsymbol{\mu}_i$ in the field direction, the frequency-dependent susceptibility of the dipoles is

$$[3] \qquad \chi(\omega) \equiv \frac{M^E(\omega)}{E(\omega)} = -i \sum_{ij} \int_0^{\infty} dt e^{i\omega t} \langle [\mu_i^E, \mu_j^E(t)] \rangle$$

This equation is the quantum analog of the classical expression for the susceptibility; the classical correlation function is replaced by the retarded commutator $-i\langle[\mu_i^E, \mu_j^E(t)]\rangle\theta(t)$ where $\theta(t)$ is the unit step function. The relation between the susceptibility and the dielectric constant is given in ref. 3.

If the dipole moments of the dipoles are permanent and of identical magnitude μ, the operator μ_i^E is μ times the operator giving the angle between the dipole orientation and the field direction, and can be expressed in terms of the angular displacement of the ith dipole from equilibrium. It is convenient to rewrite [3] as

$$[4] \quad \chi(\omega) = -2 \sum_{ij} \int_0^{\infty} dt e^{i\omega t} \operatorname{Im} \langle \mu_i^E(t) \mu_j^E \rangle$$

Since we do not know the actual adsorption sites, let us consider the dipoles to be adsorbed on a NaCl lattice as shown in Fig. 1. They are located along the lines joining positive and negative ions so that there are four equilibrium orientations, all equally populated. If a coordinate system is chosen so that the x and y axes lie along the equilibrium directions, if θ, ϕ indicate the field direction, and if $\phi_i = 0, \pi/2, \pi, 3\pi/2$ gives the equilibrium orientation of the ith dipole while x_i measures the angular devia-

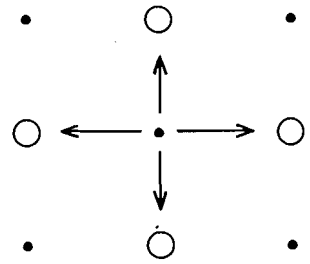

FIG. 1. The equilibrium positions of dipoles adsorbed on the (100) surface of a NaCl lattice.

tion from this position, we have

$$[5]\quad \mu_i^E = \mu \sin\theta\,[\cos(\phi - \phi_i)\cos x_i + \sin(\phi - \phi_i)\sin x_i]$$

The adsorbent consists of very many surfaces oriented at random to the field direction, however, and we must average over all angles θ,ϕ to obtain

$$[6]\quad \langle \mu_i^E(t)\mu_j^E\rangle = \frac{\mu^2}{3}[\cos\Delta_{ij}\langle\cos x_i(t)\cos x_j\rangle - \sin\Delta_{ij}\langle\sin x_i(t)\cos x_j\rangle + \sin\Delta_{ij}\langle\cos x_i(t)\sin x_j\rangle + \cos\Delta_{ij}\langle\sin x_i(t)\sin x_j\rangle]$$

where

$$\Delta_{ij} \equiv \phi_i - \phi_j$$

Trigonometric functions of operators are defined by their power series. Recognizing that equal time correlation functions are real, [4] and [6] give

$$[7]\quad \chi(\omega) = -\tfrac{2}{3}\mu^2 \sum_{ij}\int_0^\infty dt e^{i\omega t} \times \mathrm{Im}\{\cos\Delta_{ij}[\langle x_i(t)x_j\rangle + \tfrac{1}{4}\langle x_i^2(t)x_j^2\rangle + \ldots] + \tfrac{1}{2}\sin\Delta_{ij}[\langle x_i^2(t)x_j\rangle - \langle x_i(t)x_j^2\rangle + \ldots]\}$$

This is an expansion in increasing order correlation functions, and presumably for small displacements from equilibrium the higher order correlations can be neglected. If the oscillator is assumed to be tightly bound

$$[8]\quad \chi(\omega) \simeq -\tfrac{2}{3}\mu^2 \sum_{ij}\int_0^\infty dt e^{i\omega t} \times \mathrm{Im}\{\cos\Delta_{ij}\langle x_i(t)x_j\rangle\}$$

an approximation which is essentially that used to obtain equation 36 of ref. 3.

All dipoles are equivalent to the one at, say, $j = 0$, and ϕ_j can be arbitrarily chosen as zero so that [8] becomes

$$[9]\quad \chi(\omega) = -\tfrac{2}{3}N\mu^2 \sum_i \cos\phi_i \int_0^\infty dt e^{i\omega t} \times \mathrm{Im}\langle x_i(t)x_0\rangle$$

If surface coverage is so low that the dipoles do not interact with each other, then $\langle x_i(t)x_0\rangle = 0$ for $i \neq 0$, and we have the simple result

$$[10]\quad \chi(\omega) = -\tfrac{2}{3}N\mu^2 \int_0^\infty dt e^{i\omega t}\,\mathrm{Re}\{-i\langle x(t)x\rangle\}$$

where the subscript zero has been suppressed.

Oscillator on a Rigid Lattice

An isolated oscillator on a rigid lattice should give the $1/\tau_0 \to 0$ limit of the result given on p. 1009 of ref. 3. The Hamiltonian of an isolated rotational oscillator which does not interact with the adsorbate lattice vibrations:

$$[11]\quad H_{osc}^0 = p^2/2I + \tfrac{1}{2}k_0x^2$$

may, with the aid of the annihilation operator

$$[12]\quad c \equiv \frac{1}{\sqrt{2I\omega_c}}(I\omega_c x + ip)$$

where $\omega_c = \sqrt{k_0/I}$ is the classical oscillator frequency, be rewritten as

$$[13]\quad H_{osc}^0 = \omega_c(c^\dagger c + \tfrac{1}{2}),\quad \hbar = 1$$

On defining the "field" operator

$$[14]\quad \theta \equiv c + c^\dagger$$

for this oscillator, we have as well

$$[15]\quad x = \frac{1}{\sqrt{2I\omega_c}}\theta$$

Let us define the free time ordered Green function for the oscillator as

$$[16]\quad G_0(t) \equiv -i\langle(\theta(t)\theta^\dagger)_+\rangle$$

where $(\ )_+$ indicates the usual time ordering operator: that is

$$[17]\quad (A(t_1)B(t_2))_+ \equiv \begin{cases} A(t_1)B(t_2) & t_1 > t_2 \\ B(t_2)A(t_1) & t_1 < t_2 \end{cases}$$

if A and B are boson creation or annihilation operators (there is a sign change on reversing if A and B are fermion operators). The Green function is introduced as a time ordered product simply because it is easier to evaluate ground state expectation values of time ordered operator

Can. J. Chem. Downloaded from www.nrcresearchpress.com by 210.87.254.6 on 09/05/12
For personal use only.

Can. J. Chem. Downloaded from www.nrcresearchpress.com by 210.87.254.6 on 09/05/12
For personal use only.

products than, say, ordinary products. Since in [10] $t > 0$ it can be rewritten

$$[18]\quad \chi(\omega) = -\frac{N\mu^2}{3I\omega_c}\int_0^\infty dt e^{i\omega t}\,\mathrm{Re}\,G_0(t)$$

Using [14], G_0 is simple to evaluate, since

$$\langle (c(t)c)_+\rangle = \langle (c^\dagger(t)c^\dagger)_+\rangle = 0$$

and, with the aid of

$$c^\dagger(t) = \exp\{iH_{osc}{}^0 t\}\, c^\dagger \exp\{-iH_{osc}{}^0 t\}$$

$$[19]\quad \langle (c^\dagger(t)c)_+\rangle = \begin{cases}\langle c^\dagger c\rangle e^{i\omega_c t} & t > 0\\ \langle cc^\dagger\rangle e^{i\omega_c t} & t < 0\end{cases}$$

Similarly

$$[20]\quad \langle (c(t)c^\dagger)_+\rangle = \begin{cases}\langle cc^\dagger\rangle e^{-i\omega_c t} & t > 0\\ \langle c^\dagger c\rangle e^{-i\omega_c t} & t < 0\end{cases}$$

The creation and annihilation operators satisfy the commutation law $[c,c\dagger] = 1$, and $\langle c\dagger c\rangle$ is just the expectation value of the number of quanta present at the appropriate temperature

$$[21]\quad \langle c^\dagger c\rangle = \frac{\mathrm{Tr}\, e^{-\beta H^0_{osc}} c^\dagger c}{\mathrm{Tr}\, e^{-\beta H^0_{osc}}} = \frac{1}{e^{\beta\omega_c} - 1}$$

Thus

$$[22]\quad G_0(t) = -i\{e^{-i\omega_c t} f^{\pm}(\omega_c) + e^{i\omega_c t} f^{\mp}(\omega_c)\} \qquad t \gtrless 0$$

where

$$[23]\quad f^{\pm}(\omega) \equiv \pm\,[1 - e^{\mp\beta\omega}]^{-1}$$

so that after performing the time integral in [18]

$$[24]\quad \chi(\omega) = \frac{N\mu^2}{3I}\frac{1}{\omega_c{}^2 - \omega^2}$$

in agreement with ref. 3 as $1/\tau_0 \to 0$. The classical and quantum results are identical, as expected, since the possibility of tunneling has been ignored.

Oscillator–Phonon Coupling

The preceding treatment gives no loss; the susceptibility given by [24] is purely real. This happens, of course, because there is no means of dissipating energy from the field. If the oscillator is coupled to a deformable, rather than rigid, adsorbent lattice, energy from the field can be dissipated. The field causes the oscillator to oscillate, and its motion in turn sets the lattice vibrating, and the phonons so created carry away energy, essentially in the form of heat. Thus, our model must be supplemented in two ways; we must know how the oscillator is coupled to the phonons, and we must know something about the phonons themselves.

The lattice modes required are those of a crystal with a surface. Surface phonons can occur, and have been investigated (6 and references therein), and certainly an adsorbed molecule samples the vibrational modes at the surface. As we will see shortly, these modes should be determined, not for a clean surface, but for a surface plus an adsorbed molecule at its equilibrium orientation. These modes can be found and used in the following calculations. However, surface mode frequencies typically differ from bulk mode frequencies by a factor of only about $\frac{1}{2}$, and the translational symmetry of the bulk crystal leads to particularly simple expressions for ion displacements. Consequently, we make here the simplifying, although unnecessary, assumption that the lattice vibrations are those of the bulk lattice, and take for the Hamiltonian of the lattice

$$[25]\quad H^0{}_{latt} = \sum_{q\lambda}\omega_{q\lambda}(a_{q\lambda}{}^\dagger a_{q\lambda} + \tfrac{1}{2})$$

where $a_{q\lambda}$ annihilates a phonon of the λth mode and wavevector $\boldsymbol{q}$, and $\omega_{q\lambda}$ is the corresponding phonon frequency (7). A correct treatment would replace the quantum numbers $q\lambda$ with ones describing the true normal modes, although the form of $H^0{}_{latt}$ would remain unaltered.

The displacement from equilibrium of the bth ion in the lth unit cell is given by

$$[26]\quad \boldsymbol{\eta}_{l,b} = \sum_{q\lambda}(2\omega_{q\lambda}N_c M_b)^{-1/2}\, e^{i\boldsymbol{q}\cdot\boldsymbol{R}_l{}^0}\boldsymbol{\varepsilon}_{qb\lambda}\phi_{q\lambda}$$

where N_c is the number of unit cells, M_b the mass of the bth ion, $\boldsymbol{R}_l{}^0$ the position vector locating the lth cell, and

$$[27]\quad \phi_{q\lambda} = a_{q\lambda} + a^\dagger{}_{-q\lambda}$$

the phonon field operator. Sums over $\boldsymbol{q}$ are restricted to the first Brillouin zone throughout.

When the polar molecule is placed on the clean surface of the crystal at orientation x, there is an energy of interaction $u(x,\boldsymbol{\eta}_{l,b})$, which can be expanded as

$$u(x,\boldsymbol{\eta}_{l,b}) = u(0,0) + x\frac{\partial u}{\partial x} + \sum_{l,b}\boldsymbol{\eta}_{l,b}\cdot\frac{\partial u}{\partial \boldsymbol{\eta}_{l,b}} + \tfrac{1}{2}x^2\frac{\partial^2 u}{\partial x^2} + \tfrac{1}{2}\sum_{\substack{l,b\\ l',b'}}\boldsymbol{\eta}_{l,b}\cdot\frac{\partial^2 u}{\partial\boldsymbol{\eta}_{l,b}\,\partial\boldsymbol{\eta}_{l',b'}}\cdot\boldsymbol{\eta}_{l',b'} + \tfrac{1}{2}\sum_{l,b}x\cdot\frac{\partial^2 u}{\partial x\,\partial\boldsymbol{\eta}_{l,b}}\cdot\boldsymbol{\eta}_{l,b} + \cdots$$

Can. J. Chem. Downloaded from www.nrcresearchpress.com by 210.87.254.6 on 09/05/12
For personal use only.

where all derivatives are evaluated for x and all $\eta_{l,b}$ zero. The second term is zero, since $x = 0$ is the equilibrium orientation. The third describes the change induced in the equilibrium ion positions, and the fifth the change in the ion frequencies. We suppose that these two terms are included when determining the phonons. The fourth term is the harmonic potential $\frac{1}{2}k_0x^2$ of the dipole on the rigid lattice, and the sixth the interaction term of interest to us. Higher terms will be neglected.

In order to construct an explicit expression for this sixth term, the interaction of the oscillator with the phonons, the adsorption site and orientation of the adsorbed molecule must be known. Let us suppose that the oscillator is a point dipole located at the mid-point of the line joining a positive adsorbent ion to a negative one (Fig. 2). When the ions are at their equilibrium positions ($\eta_{l,b} = 0$), the potential acting on the rotational oscillator is $V(x) = \frac{1}{2}k_0x^2$. If the ions move, this is altered. The dipole's equilibrium orientation is different, and the force constant likely changes. That is, the potential is now $\frac{1}{2}k(\eta_{l,b})[x - \xi(\eta_{l,b})]^2$ where $k(\eta_{l,b} = 0) = k_0, \xi(0) = 0$. Presumably k and ξ depend only on the positions of the neighboring ions, which we call 1 and 2, and we may expand

$$[28] \quad k(\eta_{l,b}) = k_0 + \boldsymbol{\eta}_1 \cdot \boldsymbol{k}_1 + \boldsymbol{\eta}_2 \cdot \boldsymbol{k}_2 + \ldots$$

with

$$\boldsymbol{k}_1 \equiv \frac{\partial k}{\partial \boldsymbol{\eta}_1} \qquad \boldsymbol{k}_2 = \frac{\partial k}{\partial \boldsymbol{\eta}_2}$$

and

$$[29] \quad \xi(\eta_{l,b}) = \boldsymbol{\eta}_1 \cdot \boldsymbol{\xi}_1 + \boldsymbol{\eta}_2 \cdot \boldsymbol{\xi}_2 + \ldots$$

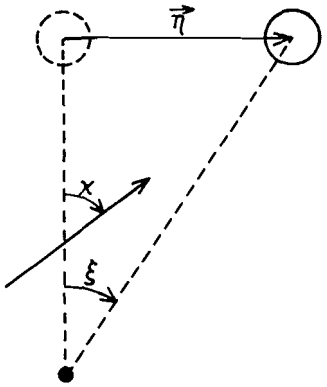

FIG. 2. Dipole on a deformed lattice.

where

$$\boldsymbol{\xi}_1 = \frac{\partial \xi}{\partial \boldsymbol{\eta}_1} \qquad \boldsymbol{\xi}_2 = \frac{\partial \xi}{\partial \boldsymbol{\eta}_2}$$

This gives for the change in potential seen by the oscillator on moving the ions from their equilibrium positions

$$[30] \quad \Delta V \equiv \tfrac{1}{2}k(\eta_{l,b})[x - \xi(\eta_{l,b})]^2 - \tfrac{1}{2}k_0x^2 = -k_0\boldsymbol{\xi}_1 \cdot x\boldsymbol{\eta}_1 - k_0\boldsymbol{\xi}_2 \cdot x\boldsymbol{\eta}_2 + \tfrac{1}{2}\boldsymbol{k}_1 \cdot x^2\boldsymbol{\eta}_1 + \tfrac{1}{2}\boldsymbol{k}_2 \cdot x^2\boldsymbol{\eta}_2 + \ldots$$

For small displacements of the ions (that is, low temperatures and weak coupling to the oscillators) the higher powers of ionic displacements can be neglected. In addition, let us suppose that the oscillator only makes small angular excursions from equilibrium as well, and retain only the first order terms in x. It is easy to formally include more $\boldsymbol{\eta}_{l,b}$'s, and write the interaction between a single rotational oscillator and the lattice as

$$[31] \quad H' = \sum_{l,b} \boldsymbol{g}_{l,b} \cdot \boldsymbol{\eta}_{l,b} x$$

where $\boldsymbol{g}_{l,b} = -k_0\,\boldsymbol{\xi}_{l,b}$. Using [15] and [26],

$$[32] \quad H' = \sum_{q\lambda} g_{q\lambda}\phi_{q\lambda}\theta$$

with

$$[33] \quad g_{q\lambda} \equiv \sum_{l,b} \frac{1}{\sqrt{4I\omega_c\omega_{q\lambda}N_cM_b}}\, e^{i\boldsymbol{q}\cdot\boldsymbol{R}_l^0}\boldsymbol{\varepsilon}_{qb\lambda} \cdot \boldsymbol{g}_{l,b}$$

The quantity $g_{q\lambda}$ measures the strength of the coupling between the rotational oscillator and the phonon of wavevector $\boldsymbol{q}$ and mode λ. The strongest coupling is to the optic modes, in which the positive and negative ions vibrate 180° out of phase, rather than to the acoustic modes, where they move in phase. We will see later, however, that this is not the only factor that determines which phonons are important in causing dielectric loss. Energy is also important, for the rotational oscillator tends to resonate with phonons of the same frequency.

Oscillator on a Vibrating Lattice

A single rotational oscillator interacting with an adsorbate lattice is described by the Hamiltonian

$$[34] \quad H = H^0 + H'$$

where the non-interacting part is

Can. J. Chem. Downloaded from www.nrcresearchpress.com by 210.87.254.6 on 09/05/12
For personal use only.

[35] $$H^0 = H^0_{\text{osc}} + H^0_{\text{latt}}$$

In this situation, the susceptibility given by [10] becomes

[36] $$\chi(\omega) = -\frac{N\mu^2}{3I\omega_c}\int_0^\infty dt e^{i\omega t}\,\text{Re}\,G(t)$$

where

[37] $$G(t) = -i\langle(\theta(t)\theta^\dagger)_+\rangle$$

in contrast to [18] and [16]. The difference between [37] and [16] is the Hamiltonian; the operators are in a Heisenberg picture, and develop in time according to $\theta(t) = \exp\{iHt\}\theta \exp\{-iHt\}$ where in [37] H is given by [34], whereas in [16] H is just the H^0_{osc} of [13]. G_0 is the free Green function of the oscillator, and G is the true Green function.

The techniques for evaluation of thermodynamic Green functions such as [37] are by now well known, and are given in the books by Fetter and Walecka (5) or Abrikosov *et al.* (8). The methods have their origin in quantum field theory, although the extension to non-zero temperature (the thermodynamic Green function) was developed for the solid state many-body problem. They provide a very convenient way of handling the interactions of many particles, such as the large number of phonons in the present problem.

G is evaluated by exploiting the formal similarity of the time development operator exp $\{-iHt\}$ and the canonical density operator exp $\{-\beta H\}$ which, with $\tau = -i\beta$, may be written exp $\{iH\tau\}$. Let us generalize the definition [37] to imaginary time arguments in the interval $(-\tau,\tau)$ of the imaginary t-axis by specifying $-\tau$ as the "earliest time" and τ as the "latest time". This defines the ordering operation $(\ )_+$ for imaginary times in this interval. It is just a generalization, for it can be shown that $G(t)$ for real times is given by analytic continuation from $(0,\tau)$ for positive times and from $(-\tau,0)$ for negative times. There is a branch cut in the complex t-plane along the real axis. It turns out that $G(t)$ is periodic in the interval $(-\tau,\tau)$ and can be expanded as a Fourier series

[38] $$G(t) = \frac{1}{\tau}\sum_n G(\omega_n)e^{-i\omega_n t} \qquad \omega_n = \frac{2\pi n}{\tau}$$

where the sum runs over $n = 0, \pm1, \pm2, \ldots$. The existence of this series enables us to conveniently evaluate the required $G(t)$, continue to real time, and find the susceptibility from [36]. Rather than do this directly, however, it is easier to proceed somewhat differently.

The real part of $G(t)$ is, for $t > 0$

[39] $$\begin{aligned}\text{Re}\{-i\langle\theta(t)\theta^\dagger\rangle\} &= \tfrac{1}{2}\{-i\langle\theta(t)\theta^\dagger\rangle \\ &\quad + i\langle\theta\theta^\dagger(t)\rangle\} \\ &= -\frac{i}{2}\langle[\theta(t),\theta^\dagger]\rangle\end{aligned}$$

since θ is hermitian, and [36] may be rewritten as

[40] $$\chi(\omega) = -\frac{N\mu^2}{6I\omega_c}G^R(\omega)$$

using the expansion

[41] $$G^R(t) = \frac{1}{2\pi}\int_{-\infty}^{\infty} d\omega e^{-i\omega t}G^R(\omega)$$

where

[42] $$G^R(t) = -i\langle[\theta(t),\theta^\dagger]\rangle\theta(t)$$

That is, we have returned to [3] in order to find a concise and convenient expression for $\chi(\omega)$. The new function $G^R(t)$ is called the retarded Green function, as opposed to the time-ordered function [37]. We have pointed out that it is $G(t)$ which is convenient to evaluate, or more precisely the Fourier transform $G(\omega_n)$. The convenience of [40] is simply this: $G^R(\omega)$ is just the analytic continuation of $G(\omega_n)$ from the points ω_n to just above the real ω-axis; the appropriate continuation has been shown to be unique (9). This is the same thing as saying that $G(t)$ for positive times is the analytic continuation of $G(t)$ from $(0,\tau)$ so that using [40] instead of [36] merely saves Fourier transforming to the t-variable and then back again.

The procedure we now use for finding $G(\omega_n)$ is well known, and will only be outlined briefly. The t variable is considered to be in $(0,\tau)$ throughout. We change states and operators from the Heisenberg picture to the interaction picture defined by H', and so can write

[43] $$\begin{aligned}e^{-iHt} &\equiv e^{-iH^0t}U(t,0) \\ e^{-\beta H} &= e^{-iH^0\tau}U(\tau,0)\end{aligned}$$

where

[44] $$U(t,0) = \exp\left(-i\int_0^t dt'H'(t')\right)_+$$

Then

[45] $$G(t) = -i\langle(\theta(t)\theta^\dagger U(\tau,0))_+\rangle_0/\langle U(\tau,0)\rangle_0$$

where $\langle\rangle_0$ indicates the trace over the unper-

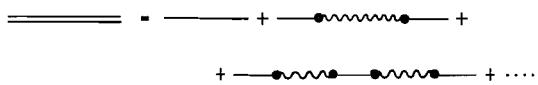

FIG. 3. The expansion of $G(t)$. G_0 is represented by a straight line, D_0 by a wiggley line, and $g_{q\lambda}$ by a dot. The double line represents G.

turbed density operator $e^{-\beta H^0}$. $U(\tau,0)$ is next expanded in powers of H', and the generalized (to non-zero temperatures) Wick's theorem (5) applied. The various terms in the expansion of numerator and denominator of [45] are most easily represented pictorially (*e.g.* Fig. 3); terms of odd order in H' vanish, unlinked diagrams cancel, and in order $2m$ there are precisely $(2m)!$ topologically equivalent diagrams. Hence, since $g_{-q\lambda} = g_{q\lambda}{}^*$:

$$[46]\quad G(t) = \sum_{m=0}^{\infty} \sum_{q_1\lambda_1} \cdots \sum_{q_m\lambda_m} |g_{q_1\lambda_1}|^2 \times |g_{q_2\lambda_2}|^2 \cdots |g_{q_m\lambda_m}|^2 \times \int_0^\tau dt_1 \cdots \int_0^\tau dt_{2m} G_0(t - t_{2m}) \times D^0{}_{q_m\lambda_m}(t_{2m} - t_{2m-1}) \times \cdots \times G_0(t_3 - t_2) D^0{}_{q_1\lambda_1}(t_2 - t_1) G_0(t_1)$$

where G_0 is as defined in [16], but with an imaginary time argument, and

$$[47]\quad D^0{}_{q\lambda}(t) = -i\langle \phi_{-q\lambda}(t) \phi^\dagger{}_{-q\lambda} \rangle_0$$

is the propagator for phonons of wavevector q and mode λ. $G_0(t)$ and $D^0{}_{q\lambda}(t)$ can be expanded in Fourier series as was $G(t)$ in [38]. Inserting these expansions in [46] we find

$$[48]\quad G(\omega_n) = \sum_{m=0}^{\infty} \sum_{q_1\lambda_1} |g_{q_1\lambda_1}|^2 \cdots \sum_{q_m\lambda_m} |g_{q_m\lambda_m}|^2 \times [G_0(\omega_n)]^{m+1} D^0{}_{q_1\lambda_1}(\omega_n) \cdots D^0{}_{q_m\lambda_m}(\omega_n)$$

The series sums to

$$[49]\quad G(\omega_n) = \frac{G_0(\omega_n)}{1 - G_0(\omega_n)\Pi(\omega_n)}$$

where

$$[50]\quad \Pi(\omega_n) = \sum_{q\lambda} |g_{q\lambda}|^2 D^0{}_{q\lambda}(\omega_n)$$

is the self energy of the rotational oscillator in this model.

$G_0(t)$ and $D^0{}_{q\lambda}(t)$ are easily found by the arguments following [20], since the operators involved now develop in time under the unperturbed Hamiltonian H^0, and

$$[51]\quad G_0(\omega_n) = \frac{2\omega_c}{\omega_n{}^2 - \omega_c{}^2}$$

$$[52]\quad D^0{}_{q\lambda}(\omega_n) = \frac{2\omega_{q\lambda}}{\omega_n{}^2 - \omega_{q\lambda}{}^2}$$

Thus, we have found $G(\omega_n)$, and since $G^R(\omega)$ is its analytic continuation to just above the real axis

$$[53]\quad G^R(\omega) = G(\omega + i\eta) = \frac{2\omega_c}{\omega^2 - \omega_c{}^2\left[1 + \frac{2}{\omega_c}\Pi(\omega + i\eta)\right]}$$

where η is a positive infinitesimal. $\Pi(\omega)$, and hence $G(\omega)$, has a branch cut along the real axis.

If ω_c, $g_{q\lambda}$, and $\omega_{q\lambda}$ are known, the susceptibility is given by combining [40], [53], [50], and [52]. The form of the result [53] is a general one, irrespective of the coupling between the oscillator and the phonons. Even if the coupling is nonlinear (or if there is phonon–phonon scattering), a self-energy $\Pi(\omega)$ can still be defined, although only for linear coupling is it given by [50]. The self-energy has both a real and an imaginary part, making $\chi(\omega)$ complex, and giving dielectric loss.

It is convenient to introduce the dimensionless weighted density of states

$$[54]\quad \alpha^2(\omega)F(\omega) \equiv \sum_{q\lambda} \frac{|g_{q\lambda}|^2}{\omega_{q\lambda}} \delta(\omega - \omega_{q\lambda})$$

where $F(\omega)$ is the usual phonon frequency distribution

$$[55]\quad F(\omega) \equiv \frac{1}{N_c} \sum_{q\lambda} \delta(\omega - \omega_{q\lambda})$$

and $\alpha(\omega)$ an "averaged" oscillator–phonon coupling. (This trick has been used elsewhere; a rather similar example is found in ref. 10.) The self energy may, using this, be written

$$[56]\quad \Pi(\omega) = \int_{-\infty}^{\infty} d\omega' \alpha^2 F(\omega') \frac{2\omega'}{\omega^2 - \omega'^2}$$

where to shorten the notation $\alpha^2(\omega)F(\omega)$ has been written $\alpha^2 F(\omega)$. $\alpha^2 F$ is zero except along a finite portion of the positive real axis, and $\Pi(\omega)$ has a cut extending along this portion. In addition, the denominator of [53] may have a zero on the real axis outside this cut, but elsewhere on the physical sheet $G(\omega)$ is analytic.

On separating the real and imaginary parts of the self-energy, [53] can be written

Can. J. Chem. Downloaded from www.nrcresearchpress.com by 210.87.254.6 on 09/05/12
For personal use only.

Can. J. Chem. Downloaded from www.nrcresearchpress.com by 210.87.254.6 on 09/05/12
For personal use only.

$$[57] \qquad G^R(\omega) = 2\omega_c \frac{\omega^2 - \omega_c^2 - 2\omega_c \operatorname{Re}\Pi(\omega) + 2i\omega_c \operatorname{Im}\Pi(\omega + i\eta)}{[\omega^2 - \omega_c^2 - 2\omega_c \operatorname{Re}\Pi(\omega)]^2 + [2\omega_c \operatorname{Im}\Pi(\omega + i\eta)]^2}$$

where, from [56]

$$[58] \quad \operatorname{Re}\Pi(\omega) = -\int_{-\infty}^{\infty} \omega' d\omega' \alpha^2 F(\omega') \left[\frac{1}{\omega' + \omega} + \frac{1}{\omega' - \omega}\right]$$

$$[59] \quad \operatorname{Im}\Pi(\omega + i\eta) = -\pi\omega[\alpha^2 F(\omega) + \alpha^2 F(-\omega)]$$

(In [58] $\int$ indicates that the principle value is to be taken). If an appropriate form for $\alpha^2 F$ is available (see, *e.g.*, ref. 10), that is, if the coupling and the lattice phonon spectrum are known, [58] and [59] can easily be evaluated, numerically if necessary. If we now set

$$[60] \qquad \Delta(\omega) \equiv \frac{2}{\omega_c} \operatorname{Re}\Pi(\omega)$$

$$[61] \qquad \Gamma(\omega) \equiv 2\omega_c \operatorname{Im}\Pi(\omega + i\eta)$$

then

$$[62] \quad \chi(\omega) = -\frac{N\mu^2}{3I} \frac{\omega^2 - \omega_c^2[1 + \Delta(\omega)] + i\Gamma(\omega)}{\{\omega^2 - \omega_c^2[1 + \Delta(\omega)]\}^2 + \{\Gamma(\omega)\}^2}$$

It is $\Gamma(\omega)$, that is, the imaginary part of Π, that determines the energy dissipation. The real part Δ merely shifts the frequency from that of the isolated oscillator ω_c, and $\omega_c\sqrt{1 + \Delta(\omega)}$ can be regarded as the effective classical oscillator frequency seen by an applied field of frequency ω. Δ is normally negative at lower frequencies, for the effective moment of inertia of the oscillator increases as it starts to drag part of the lattice along. If $G^R(t)$ is calculated, Γ acts as a damping factor governing the time rate of decay of a quantum of energy added to the oscillator.

Simple Phonon Model

In this section we attempt to gain some insight into the formula [62] by choosing the simplest possible model for $\alpha^2 F$, a model which is certainly only qualitatively valid. In a crystal with two atoms per unit cell, there are six phonon modes, three optic modes in which the two different ions move in opposite directions (*i.e.* 180° out of phase) and three acoustic modes in which the two ions move in phase near $q = 0$. Each group of three consists of a longitudinal and two transverse branches. (The phonon spectrum of sodium chloride has recently been measured by inelastic neutron scattering (11).)

The measuring frequencies used experimentally have been much lower than the typically THz frequencies of the optic modes, so that although the dipole is likely coupled most strongly to the optic modes, they do not, from [59], contribute to Γ in the frequency range of interest. They can provide a more or less frequency independent contribution to Δ, but it is the loss that is of interest here. Consequently, we include only the acoustic modes. Even assuming that the dipole is only coupled to the two ions in the unit cell at the origin, the resulting

$$[63] \quad g_{q\lambda} = \frac{1}{\sqrt{4I\omega_c\omega_{q\lambda}}} \left(\frac{\boldsymbol{\varepsilon}_{q1\lambda} \cdot \boldsymbol{g}_{01}}{\sqrt{M_1}} + \frac{\boldsymbol{\varepsilon}_{q2\lambda} \cdot \boldsymbol{g}_{02}}{\sqrt{M_2}}\right)$$

requires the polarization vectors in addition to the phonon dispersion curve. This author is unaware of any simple model that can be used to evaluate [63] directly, and it probably requires a calculation for the specific material of interest, as in the approach of Bergersen *et al.* (10). The detailed structure of $\alpha^2 F$ is likely not important, however. It would be very optimistic to suppose that dielectric measurements are a *sensitive* probe of surface phonons. Thus, let us assume that $\alpha^2 F$ is proportional to a constant effective coupling to acoustic phonons α_a^2 times the density of acoustic phonon states as given by the Debye model (*e.g.* Ziman 1964)

$$[64] \qquad \alpha^2 F(\omega) = 9\,\alpha_a^2 \omega^2/\omega_D^3$$

where ω_D is the Debye frequency for (all) the acoustic modes. This gives

$$[65] \qquad \Gamma(\omega) = -18\pi\alpha_a^2\omega_c(\omega/\omega_D)^3$$

and

$$[66] \quad \Delta(\omega) = -24\frac{\alpha_a^2}{\omega_c}\left[1 + 3(\omega/\omega_D)^2 + \tfrac{3}{2}(\omega/\omega_D)^3 \ln\left|\frac{\omega_D - \omega}{\omega_D + \omega}\right|\right]$$

Using these in [62], we find an explicit expression for $\chi(\omega)$ in this simple model, and this appears very different in form from the result of McMullen and McIntosh (3). However, as illustrated in Figs. 4 and 5, the resulting plots of

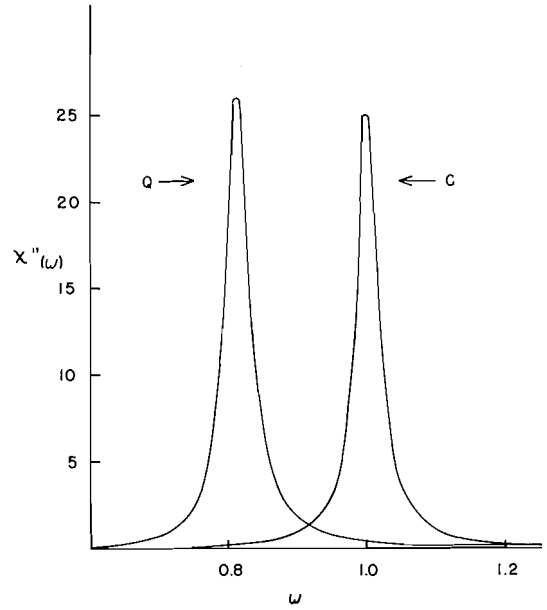

FIG. 4. The real part of the susceptibility as a function of frequency. Curve Q is the present result with $\alpha_a = 0.1$ and $\omega_D = 2\omega_c$. Curve C is the classical result of ref. 3 with $\tau_0 = 50$. Frequency is expressed in units of ω_c, and susceptibility in units of $N\mu^2/3I\omega_c^2$.

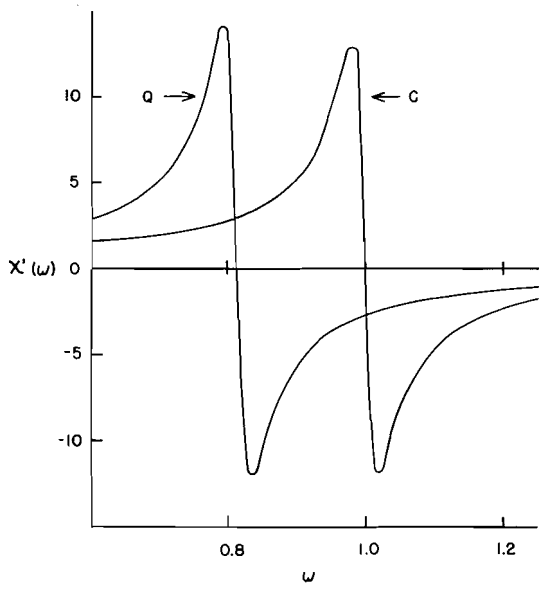

FIG. 5. The imaginary part of the susceptibility. Labels and units are as in Fig. 4.

the susceptibility are quite similar except for the frequency shift caused by $\Delta(\omega)$. In these figures, no serious attempt has been made to adjust the parameters to match peak height and width, and $\alpha_a = 0.1$ is likely an upper limit for any imaginable physical system.

Γ, due to its $(\omega/\omega_D)^3$ dependence, is almost vanishingly small in the frequencies (up to GHz, see *e.g.* ref. 1) usually employed experimentally in dielectric measurements. If ω_c is very much less than $\omega_D \sim 10^{12}$ s^{-1} the loss peak looks very much like a δ-function, and experimental loss peaks at MHz or GHz frequencies, of course, don't. This indicates that anharmonic terms in the oscillator–phonon coupling are very important, and that higher powers of x should be retained in [30] in order to properly describe the system if loss occurs at these frequencies. That is, the conditions for validity of the true rotational oscillator model are not very well satisfied. It is easy to demonstrate that this is to be expected, for if a dipole is a rotational oscillator at temperature T, $\frac{1}{2}k_0x^2 \gtrsim \beta^{-1}$ for x about 1 radian. Using a reasonable estimate of the moment of inertia of hydrogen chloride, we find

$$\beta\omega_c \gtrsim \sqrt{\frac{100\ ^\circ\mathrm{K}}{T}} \qquad [67]$$

as a necessary condition for rotational oscillations. Unless ω_c is high, that is, of the order of thermal energies, the adsorbed molecule is something between a free Debye rotator and a rotational oscillator.

Discussion

The dielectric susceptibility of a tightly bound rotational oscillator (one which makes only small excursions from its equilibrium orientation) has been calculated. It has not been necessary to introduce a phenomenological relaxation time as was done previously (3). Instead, a self energy appears naturally in the theory, and can be evaluated exactly in the simple model used. This self energy depends on the coupling of the adsorbed molecule to the substrate lattice and on the properties of the lattice phonons. The latter can be presumed known, for they can be independently measured by inelastic neutron scattering (11). The coupling must be derived from knowledge (or assumption) about the nature of the adsorption site and the

Can. J. Chem. Downloaded from www.nrcresearchpress.com by 210.87.254.6 on 09/05/12
For personal use only.

forces between adsorbate and adsorbent. Thus, dielectric loss experiments are best regarded as measuring these forces, and the intention of this article has been to take a step toward making this measurement quantitative.

In addition, we have found that a "pure" rotational oscillator shows very little dielectric loss at frequencies much below typical phonon frequencies. It seems unlikely that an isolated adsorbed molecule will exhibit true resonance absorption at low frequencies. It should be emphasized, however, that in some systems the experimental results cannot be explained on the basis of a Debye rotator model, but show resonance behavior (1). It will be interesting to extend the present theory to non-linear couplings to find temperature dependent self energies, for even if the "pure" rotational oscillator model of this paper does not occur, the improved theory may realistically describe adsorbate–adsorbent systems in a microscopic way.

Discussions with B. Bergersen, R. L. McIntosh, D. A. Pink, and especially J. P. Carbotte were very helpful in clarifying the ideas presented here.

1. R. L. McIntosh. Dielectric behavior of physically adsorbed gases. Marcel Dekker, Inc., New York. 1966.
2. T. McMullen, E. D. Crozier, and R. McIntosh. Can. J. Chem. **46**, 2945 (1968).
3. T. McMullen and R. McIntosh. Can. J. Chem. **47**, 1001 (1969).
4. L. N. Kurbatov. J. Phys. Chem. Acad. Sci. USSR, **24**, 899 (1950).
5. A. L. Fetter and J. D. Walecka. Quantum theory of many-particle systems. McGraw–Hill Book Co., New York. 1971.
6. T. S. Chen, G. P. Alldredge, F. W. de Wette, and R. E. Allen. Phys. Rev. B **6**, 627 (1972).
7. J. M. Ziman. Principles of the theory of solids. Cambridge University Press, London. 1964.
8. A. A. Abrikosov, L. P. Gorkov, and I. E. Dzyaloshinski. Methods of quantum field theory in statistical physics. Prentice–Hall, Inc. Englewood Cliffs, N.J. 1963.
9. G. Baym and N. D. Mermin. J. Math. Phys. **2**, 232 (1961).
10. B. Bergersen, T. McMullen, and J. P. Carbotte. Can. J. Phys. **49**, 3155 (1971).
11. R. E. Schmunk and D. R. Winder. J. Phys. Chem. Solids, **31**, 131 (1970).

Can. J. Chem. Downloaded from www.nrcresearchpress.com by 210.87.254.6 on 09/05/12
For personal use only.

The Radiolysis of Water Vapor at Very High Dose Rates. I. Hydrogen Yields from H_2O, H_2O–HCl, and H_2O–HBr Mixtures[1]

A. W. Boyd, C. Willis,[2] and O. A. Miller

Physical Chemistry Branch, Chalk River Nuclear Laboratories, Atomic Energy of Canada Limited, Chalk River, Ontario

Received June 22, 1973

The plateau yields of hydrogen from the Febetron radiolysis of mixtures of water vapor with up to 8 mol% of HCl or HBr are $G(H_2) = 7.9 \pm 0.2$ and $G(H_2) = 4.6 \pm 0.2$ with 1 mol% SF_6. These yields are consistent with $G(H) = 7.45$ in pure water vapor and $G(H) = 4.15$ in water vapor with SF_6. In the Febetron radiolysis of pure water vapor at 2×10^{27} eV g^{-1} s^{-1} and densities of $\sim$1 mg ml^{-1} $G(H_2) = 1.65 \pm 0.05$ from 164 to 190 °C. This yield is reduced to $G(H_2) = 0.90 \pm 0.05$ on the addition of 1 mol% SF_6. Using a second order equivalent rate constant for the disappearance of the OH radicals in water vapor at 1 mg ml^{-1} of 2×10^{10} M^{-1} s^{-1} these yields are consistent with rate constant values for the reactions $H + OH (+H_2O) \rightarrow H_2O$, $OH + OH (+H_2O) \rightarrow H_2O_2$, and $H + H (+H_2O) \rightarrow H_2$, of $1.7 \pm 0.1 \times 10^{10}$ M^{-1} s^{-1}, $1.5 \pm 0.5 \times 10^9$ M^{-1} s^{-1}, and $3 \pm 1 \times 10^8$ M^{-1} s^{-1}, respectively.

Le rendement au palier en hydrogène lors de la radiolyse avec une Febetron de vapeur d'eau mélangée à des quantités allant jusqu'a 8 mol % de HCl ou HBr est $G(H_2) = 7.9 \pm 0.2$. Il devient $G(H_2) = 4.6 \pm 0.2$ lors de la présence supplémentaire de 1 mol % de SF_6. Ces rendements sont cohérents avec ceux obtenus pour la vapeur d'eau pure, $G(H) = 7.45$ et $G(H) = 4.15$ en présence de SF_6. Dans la radiolyse avec un Febetron de la vapeur d'eau pure à 2×10^{27} eV g^{-1} s^{-1} et aux densités 1 mg ml^{-1} $G(H_2) = 1.65 \pm 0.05$ entre 164 et 190 °C. Ce rendement est ramené à $G(H_2) = 0.90 \pm 0.05$ lors de l'addition de 1 mol % de SF_6. En utilisant une constante de vitesse équivalente au second ordre de 2×10^{10} M^{-1} s^{-1} pour la disparition des radicaux OH dans la vapeur d'eau à une densité de 1 mg ml^{-1}, ces rendements sont cohérents avec ceux des réactions $H + OH (+H_2O) \rightarrow H_2O$; $OH + OH (+H_2O) \rightarrow H_2O_2$; $H + H (+ H_2O) \rightarrow H_2$ en prenant pour constantes de vitesse respectivement les valeurs $1{,}7 \pm 0.1 \times 10^{10}$ M^{-1} s^{-1}; $1.5 \pm 0.5 \times 10^9$ M^{-1} s^{-1} et $3 \pm 1 \times 10^8$ M^{-1} s^{-1}.

[Traduit par le journal]

Can. J. Chem., **51**, 4048 (1973)

Introduction

This paper gives the results of yield measurements from the Febetron radiolysis of pure water vapor and mixtures of water vapor with HCl and with HBr. The following paper (1) gives the results of both yield and isotope effect measurements from the Febetron radiolysis of H_2O–D_2O vapor mixtures.

This work was undertaken for two main reasons. The first of these is the difference in the radiolytic H atom yields derived from different low dose rate irradiations of water vapor. The total hydrogen yields from the radiolysis of water vapor with a few mole percent of alkanes or alcohols vary by little more than a G unit and have a maximum value of $G(H_2) = 9$ (ref. 2, Table 13 and references contained therein). Since the unimolecular decomposition of water vapor to hydrogen has a yield of $G(H_2) = 0.45$ (2) the H atom yield is not more than $G(H) = 8.5$. The exchange yield observed in the radiolysis of D_2–H_2O and H_2–D_2O mixtures is $G(HD) = 13.1 \pm 0.3$ (3) and this has been interpreted as a measure of the H atom yield. An obvious source of uncertainty in these systems is the neutralization reaction. We can specify neither the positive nor the negative ion involved and moreover they may well be different in the different mixtures. These uncertainties arise from the relative slowness of ion-neutralization reactions in low intensity experiments. Many ion–molecule reactions can occur before neutralization and only extremely low concentrations of products or impurities are required to change the identities of the ions which finally are neutralized (4). At Febetron intensities however because of high ion concentrations the ion neutralization reactions are very rapid and we can often specify with considerable certainty the identities of the ions in the neutralization process.

It is obviously of interest then to determine

[1]AECL No. 4641.

[2]Present address: Division of Chemistry, National Research Council of Canada, Ottawa, Canada K1A 0R6.

Can. J. Chem. Downloaded from www.nrcresearchpress.com by 210.87.254.6 on 09/05/12
For personal use only.

Can. J. Chem. Downloaded from www.nrcresearchpress.com by 210.87.254.6 on 09/05/12
For personal use only.

the hydrogen yield from the Febetron radiolysis of water vapor. Ideally we should use the same systems as those used at low dose rates but interpretation of these systems is very complex at Febetron dose rates. For example at low dose rates in H_2O–c–C_6H_{12} mixtures the H atoms act simply as in reaction 1. At Febetron intensities the high radical concentrations reduce the yield by reactions 2–6 and make it difficult to obtain a precise H atom yield (5). We require then a scavenger which leads to H_2 yields that are unambiguous. Hydrogen chloride and hydrogen bromide react rapidly with both H atoms and OH radicals and the radical product of these reactions (Cl or Br atoms) react relatively slowly with H atoms. Also the radiolytic behavior of HCl and HBr at high dose rates is well established (6).

[1] $$H + C_6H_{12} \rightarrow H_2 + C_6H_{11}$$

[2] $$H + H + M \rightarrow H_2 + M$$

[3] $$H + OH + M \rightarrow H_2O + M$$

[4] $$OH + C_6H_{12} \rightarrow H_2O + C_6H_{11}$$

[5] $$H + C_6H_{11} + M \rightarrow C_6H_{12} + M$$

[6] $$H + C_6H_{11} \rightarrow H_2 + C_6H_{10}$$

The second reason for our present work is the possibility of establishing rate constants for reactions 3 and 7 in water vapor.

[7] $$OH + OH + M \rightarrow H_2O_2 + M$$

The rate constant for the second order disappearance of OH radicals in water vapor at 1 atm has been determined by Gordon and Mulac (7). Their value, which is largely the sum of $k_3 + 2k_7$ is $2 \times 10^{10}\ M^{-1}\ s^{-1}$. We could expect the hydrogen yield from H atom reactions in pure water vapor at Febetron intensities will be controlled mainly by reactions 2, 3, and 7. Reaction 2 is known to be slow relative to reactions 3 and 7 (8) therefore the observed hydrogen yield should be a function of the ratio of reactions 3 and 7.

Experimental

Irradiations and Dosimetry

The irradiations were done with a Febetron 705.[3] The samples were contained in quartz cells heated in a furnace as described in ref. 9. The mean absorbed dose in the cells using nitrous oxide dosimetry with $G(N_2) = 12.4$ (6, 10, 11) was 1×10^{20} eV g^{-1} per pulse. This dose is independent of density over the range of densities in these irradiations. The mean dose rate was $\sim 2 \times 10^{27}$ eV g^{-1} s^{-1}. The stopping power corrections in going from N_2O to H_2O, HCl, and HBr are 1.143, 0.925, and 0.76, respectively (6).

Materials and Analyses

The water was pre-irradiated and triply distilled. To free the water of dissolved gases it was injected from a micro-pipette into a liquid nitrogen cooled evacuated bulb through a rubber septum and then subjected to several freeze–pump–thaw cycles. The hydrogen bromide and hydrogen chloride were purified as described in ref. 6. The sulfur hexafluoride was purified by freeze–pump–thaw cycles.

The volume of radiolytic gas noncondensible at 77 °K was measured with a McLeod gauge and its composition was determined by mass spectrometry.

Results

H_2O–HCl, H_2O–HBr

The hydrogen yields from H_2O–HCl mixtures with and without 1 mol% SF_6 are shown in Fig. 1. These yields were calculated using the total energy absorbed in the mixture by both the H_2O and HCl but not by SF_6. The hydrogen yield from pure HCl is $G(H_2) = 8.0 \pm 0.2$ (6). Therefore the plateau yield of $G(H_2) = 7.9 \pm 0.2$ in Fig. 1 corresponds to the sum of the unimolecular hydrogen yield plus the hydrogen atom yield from pure water assuming all the hydrogen atoms react with HCl to give hydrogen.

The hydrogen yields from H_2O–HBr mixtures with and without 1 mol% SF_6 are shown in Fig. 2. These were calculated in the same way as in the H_2O–HCl mixtures. As the yield of hydrogen from pure HBr is $G(H_2) = 9.8 \pm 0.2$ (6) the plateau yield from H_2O–HBr mixtures $G(H_2) = 8.0 \pm 0.2$ must be decreased by 1 to 2%.

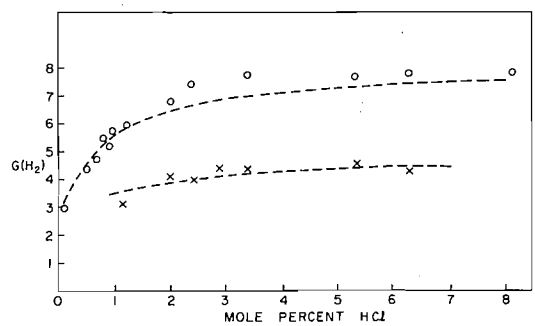

FIG. 1. Hydrogen yields from the Febetron radiolysis of water vapor – HCl mixtures. 2×10^{27} eV g^{-1} s^{-1}, 1×10^{20} eV g^{-1}, 160 °C, 1000 Torr. ○, H_2O–HCl; ×, H_2O – HCl – 9 mol% SF_6; ---, calculated; see discussion.

[3]Manufactured by Field Emission Corporation, McMinnville, Oregon, U.S.A.

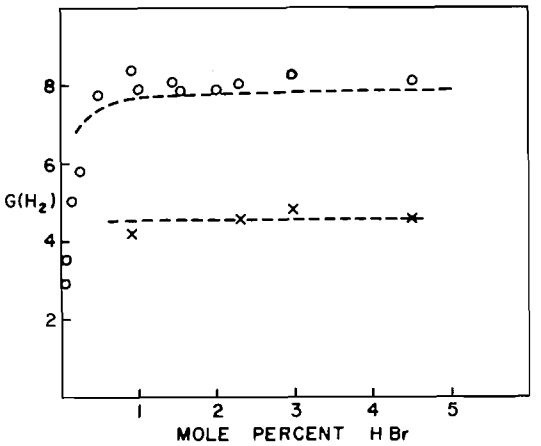

FIG. 2. Hydrogen yields from the Febetron radiolysis of water vapor – HBr mixtures. 2×10^{27} eV g^{-1} s^{-1}, 1×10^{20} eV g^{-1}, 160 °C, 1000 Torr. ○, H_2O–HBr; ×, H_2O – HBr – 1 mol% SF_6; ---, calculated; see discussion.

H_2O, H_2O–SF_6

The yields of hydrogen from the radiolysis of pure water vapor at temperatures from 164 to 400 °C and at doses in the range 1×10^{20} to 3×10^{20} eV g^{-1} are listed in Table 1. The yield in mixtures of water vapor with 1 mol% SF_6 at 164 °C, 1 mg ml^{-1}, 2×10^{27} eV g^{-1} s^{-1}, 1×10^{20} eV g^{-1} is $G(H_2) = 0.91 \pm 0.02$ based on three determinations. This yield was calculated using only the energy deposited in the water.

Discussion

H_2O–HCl, H_2O–HBr

The best values of the total hydrogen yields extrapolated to zero concentration of the additives from Figs. 1 and 2 appear to $G(H_2) = 7.9 \pm 0.2$ and $G(H_2) = 4.6 \pm 0.2$ in the presence of an electron scavenger. Taking the unimolecular yield of hydrogen from reaction 8 to be 0.45 (2) the yields of H atoms from water

[8] $$H_2O \rightsquigarrow H_2 + O$$

vapor are $G(H) = 7.45$ and $G(H) = 4.15$ in the presence of SF_6. The decrease with the addition of SF_6 $\Delta G(H_2) = 3.3$ is in very good agreement with the ion pair yield in water vapor as $W = 30 \pm 0.1$ eV (12–14).

We shall assume that the relative primary ion yields under our conditions are the same as the ion abundances determined by low pressure mass spectrometry. Combining these abundances with the above experimental yields and ion molecule reaction rates (ref. 2, Tables 2 and 9 and references contained therein) gives the following principal reactions for radical formation in water vapor.

[9] $$H_2O \rightsquigarrow H_2O^+ + e \qquad G = 2.7$$

[10] $$H_2O \rightsquigarrow H + OH^+ + e \qquad G = 0.6$$

[11] $$H_2O^+ + H_2O \rightarrow H_3O^+ + OH$$

[12] $$OH^+ + H_2O \rightarrow H_3O^+ + O$$

[13] $$H_3O^+ + nH_2O \rightarrow [H(H_2O)_{n+1}]^+$$

[14] $$[H(H_2O)_{n+1}]^+ + e \rightarrow H + (n+1)H_2O$$

[15] $$H_2O \rightsquigarrow H + OH \qquad G = 3.55$$

[8] $$H_2O \rightsquigarrow H_2 + O \qquad G = 0.45$$

The total yields then are $G(H) = 7.45$, $G(OH) = 6.25$, $G(O) = 1.05$, and $G_{H_2} = 0.45$. It would appear that no hydrogen atoms result from neutralization in the presence of SF_6. It might be argued that there are two H atoms per neutralization in H_2O–HCl or H_2O–HBr mixtures and that this yield is reduced to one on the addition of SF_6. This would mean, then, a dissociative excitation yield of less than one. Moreover, at low dose rates the energy available for neutralization does not appear to be sufficient to give 2 H atoms (3). Thus with SF_6, reaction 13 should be replaced by a reaction such as [16].

[16] $$[H(H_2O)_{n+1}]^+ + SF_6^- \rightarrow HF + SF_5 + (n+1)H_2O$$

The yields in this system are then $G(H) = 4.15$, $G(OH) = 6.25$, $G(O) = 1.05$, and $G_{H_2} = 0.45$.

It is clear that our values for the hydrogen produced by abstraction from the hydrogen halides support the low dose rate radiolysis values for hydrogen obtained by abstraction

TABLE 1. Hydrogen yields from the Febetron radiolysis of water vapor; dose rate, 2×10^{27} eV g^{-1} s^{-1}; vapor densities in the range 0.5–1.0 mg/ml

Temperature (°C)	Dose ($\times 10^{20}$ eV g^{-1})	$G(H_2)$
164	1	1.64
164	2	1.69
164	3	1.44
190	1	1.66
285	1	1.79
295	1	1.81
335	1	2.77
400	1	3.12

Can. J. Chem. Downloaded from www.nrcresearchpress.com by 210.87.254.6 on 09/05/12
For personal use only.

TABLE 2. Atom and radical reactions in the Febetron radiolysis of water vapor

	Reaction	Rate constant (M^{-1} s^{-1})* at 160 °C	Reference
[2]	$H + H + H_2O \rightarrow H_2 + H_2O$	1 to 8 × 10^8†	15, 16, 8
[3]	$H + OH + H_2O \rightarrow 2H_2O$	2 × 10^{10} ($2k_7$)	7
[7]	$OH + OH + H_2O \rightarrow H_2O_2 + H_2O$	2 × 10^{10} (k_3)	7
[19]	$O + OH \rightarrow O_2 + H$	2.6 × 10^{10}	17
[20]	$H + O_2 + H_2O \rightarrow HO_2 + H_2O$	1 × 10^9‡	18, 8
[21]	$H + HO_2 \rightarrow H_2 + O_2$	6.2 × 10^9†	19
[22]	$H + HO_2 \rightarrow OH + OH$	2.1 × 10^9†	19
[23]	$H + HO_2 \rightarrow H_2O + O$	1.1 × 10^9†	19
[24]	$HO_2 + HO_2 \rightarrow H_2O_2 + O_2$	2.2 × 10^9	20
[25]	$H + O + H_2O \rightarrow OH + H_2O$	4 × 10^8	21
[26]	$H + H_2O_2 \rightarrow H_2O + OH$	6 × 10^7	22
[27]	$OH + H_2O_2 \rightarrow H_2O + HO_2$	1.3 × 10^9	23
[28]	$OH + H_2 \rightarrow H_2O + H$	5.4 × 10^7§	24
[29]	$OH + OH \rightarrow H_2O + O$	5.1 × 10^8	24
[30]	$O + O + H_2O \rightarrow O_2 + H_2O$	4 × 10^7	25, 26
[31]	$O + H_2 \rightarrow H + OH$	2.1 × 10^5	27, 28

*For 3 body reactions these are the equivalent second order rate constants in water vapor at 1 mg ml^{-1}.
†See discussion in text.
‡Assuming H_2O as a third body is 10 times more effective than H_2.
§Using E_a = 5.2 kcal mol^{-1}.

from organic additives in water vapor. The yield of hydrogen or H atoms from dissociative excitation should be independent of dose rate. Even at Febetron dose rates neutralization of H_2O^+ or OH^+ reactions 17 and 18 will not

[17] $$H_2O^+ + e \rightarrow H + OH$$

[18] $$OH^+ + e \rightarrow O + H$$

compete with reactions 11 or 12 due to the high values of k_{11} and k_{12} (ref. 2, Tables 2 and 9) and the high concentration of H_2O. As discussed in the Introduction the identities of the ions in reaction 13 are expected to be dependent on dose rate and the nature of the additive. Certainly more extensive clustering of the positive ion will occur at the low dose rates as well as electron attachment to O_2. Despite these changes it appears that the H atom yield formed by ionic processes is close to the ion pair yield in both our hydrogen halide mixture and the low dose rate organic mixtures. We shall show in the following section that the reduction in the H_2 yield from the Febetron radiolysis of pure water vapor on the addition of SF_6 is also consistent with one H atom per neutralization.

We shall also discuss later the dependence of the H_2 yield on the concentrations of HCl and HBr.

H_2O, H_2O–SF_6

The observed yields of hydrogen in pure water vapor and water vapor – SF_6 mixtures are made up of the unimolecular hydrogen yield $G(H_2)$ = 0.45 and the net result of all the reactions of H atoms, OH radicals, and O atoms during and following the Febetron pulse. The yields of these species resulting from reactions 8–16 have been given in the preceding section.

The rate constants at 160 °C for the reactions of radicals and molecules that appear to be relevant at our conditions are listed in Table 2. It obviously cannot be assumed that the observed H_2 yields are a function of the primary yields and the rate constants of reactions 3 and 7 only. To determine the contributions of all these reactions to the hydrogen yield we have used the computer program of Schmidt (29). The input data are the primary yields and concentrations, the rate constants of the reactions, the total dose, and the length and shape of the electron pulse. The resulting calculated values include the concentration and yield of each species as a function of time and the contribution of each reaction. By using a range of values for each of k_2, k_3, and k_7 we were able to obtain calculated H_2 yields which agreed with the observed yields in both pure H_2O and H_2O containing SF_6. These values and the contributions of the other reactions are listed in Table 3. A measure of the uncertainty in the derived values of k_2, k_3, and k_7 rate constants is given by the results listed in Table 4. It can be seen that the observed hydrogen yields in both water vapor and water vapor – SF_6 mixtures can be

Can. J. Chem. Downloaded from www.nrcresearchpress.com by 210.87.254.6 on 09/05/12
For personal use only.

TABLE 3. Contributions of reactions in the Febetron radiolysis of water: 2×10^{27} eV g^{-1} s^{-1}, 1×10^{20} eV g^{-1}, 1 mg/ml^{-1}, 160 °C

	Reaction	Rate constant (M^{-1} s^{-1}) at 160 °C*	G ($G(H_2) = 1.69$)
[2]	$H + H + H_2O \rightarrow H_2 + H_2O$	4×10^8	0.77
[3]	$H + OH + H_2O \rightarrow 2H_2O$	1.8×10^{10}	5.12
[7]	$OH + OH + H_2O \rightarrow H_2O_2 + H_2O$	2×10^9	0.27
[19]	$O + OH \rightarrow O_2 + H$	2.6×10^{10}	0.97
[20]	$H + O_2 + H_2O \rightarrow HO_2 + H_2O$	1×10^9	0.84
[21]	$H + HO_2 \rightarrow H_2 + O_2$	6.2×10^9	0.47
[22]	$H + HO_2 \rightarrow OH + OH$	2.7×10^9	0.20
[23]	$H + HO_2 \rightarrow H_2O + O$	1.1×10^9	0.08
[24]	$HO_2 + HO_2 \rightarrow H_2O_2 + O_2$	2.2×10^9	0.03
[25]	$H + O + H_2O \rightarrow OH + H_2O$	4×10^8	0.12
[26]	$H + H_2O_2 \rightarrow H_2O + OH$	6×10^7	0.02
[27]	$OH + H_2O_2 \rightarrow H_2O + HO_2$	1.3×10^9	0.02
[28]	$OH + H_2 \rightarrow H_2O + H$	5.4×10^7	0.004
[29]	$OH + OH \rightarrow H_2O + O$	5.1×10^8	0.07
[30]	$O + O + H_2O \rightarrow O_2 + H_2O$	4×10^7	0.004
[31]	$O + H_2 \rightarrow H + OH$	2.1×10^5	0.0002

*For 3 body reactions these are the equivalent 2nd order rate constants in H_2O vapor at 1 mg/ml.

TABLE 4. Dependence of calculated hydrogen yields from the Febetron radiolysis of water vapor on rate constant values (units of k in M^{-1} s^{-1})

Values of k_3 and k_7	$G(H_2)$									
	$k_2 = 1 \times 10^8$		$k_2 = 2 \times 10^8$		$k_2 = 4 \times 10^8$		$k_2 = 6 \times 10^8$		$k_2 = 8 \times 10^8$	
	Pure	SF_6	Pure	SF_6	Pure	SF_6	Pure	SF_6	Pure	SF_6
$k_3 = 1.9 \times 10^{10}$ $2k_7 = 1 \times 10^9$	1.36	0.67	1.46	0.69	1.60	0.72	1.69	0.74	1.75	0.77
$k_3 = 1.8 \times 10^{10}$ $2k_7 = 2 \times 10^9$	1.43	0.75	1.54	0.78	1.69	0.81	1.79	0.85	1.86	0.88
$k_3 = 1.7 \times 10^{10}$ $2k_7 = 3 \times 10^9$	1.50	0.83	1.62	0.86	1.79	0.91	1.89	0.94	1.97	0.98
$k_3 = 1.6 \times 10^{10}$ $2k_7 = 4 \times 10^9$	1.57	0.90	1.70	0.94	1.88	1.00	1.99	1.04	2.07	1.08
$k_3 = 1.5 \times 10^{10}$ $2k_7 = 5 \times 10^9$	1.64	0.97	1.78	1.01	1.97	1.07	2.09	1.12	2.16	1.16
$k_3 = 1.4 \times 10^{10}$ $2k_7 = 6 \times 10^9$	1.71	1.03	1.87	1.07	2.08	1.15	2.18	1.20	2.26	1.25
$k_3 = 1.3 \times 10^{10}$ $2k_7 = 7 \times 10^9$	1.78	1.09	1.95	1.14	2.15	1.23	2.28	1.28	2.46	1.34

fitted by the following range of values: $k_2 = 3 \pm 1 \times 10^8$ M^{-1} s^{-1}, $k_3 = 1.7 \pm 0.1 \times 10^{10}$ M^{-1} s^{-1}, and $2k_7 = 3 \pm 1 \times 10^9$ M^{-1} s^{-1}.

These values of k_3 and k_7 are of course based on $k_3 + 2k_7 = 2 \times 10^{10}$ M^{-1} s^{-1} (7). There is no value reported for k_2 under our conditions but the above range of values is consistent with what is known. Ham *et al.* (15) have determined the rate constant for H atom recombination with H_2 as the third body over the temperature range 77 to 300 °K and obtain a rate constant of $8.3 \pm 0.4 \times 10^{-33}$ cm^6 molecule^{-2} s^{-1} at 298 °K. This value and the calculated values of Shui and Appleton (16) together indicate a rate constant of 6×10^{-33} cm^6 molecule^{-2} s^{-1} at 160 °C (1×10^8 M^{-1} s^{-1} in H_2 at 1 atm). Thrush (8) puts an upper limit of 10 on the ratio k_{H+H+H_2O}/k_{H+H+H_2} at 300 °K.

The other major reactions occurring are [19]–[22]. The uncertainties in the first two of these are believed to be within ±50% and changes of this order in k_{19} and k_{20} do not change the calculated value of $G(H_2)$ by more than the experimental uncertainties in the

Can. J. Chem. Downloaded from www.nrcresearchpress.com by 210.87.254.6 on 09/05/12
For personal use only.

TABLE 5. Reactions in the Febetron radiolysis of mixtures of water vapor with HCl or HBr (in addition to those in Table 2)

	Reaction	Rate constant* (M^{-1} s^{-1}) at 160 °C	Reference
[32]	$H + HCl \rightarrow H_2 + Cl$	3.8×10^8	31
[33]	$OH + HCl \rightarrow H_2O + Cl$	1.2×10^9†	32
[34]	$Cl + Cl + H_2O \rightarrow Cl_2 + H_2O$	1×10^9‡	33
[35]	$H_2 + Cl \rightarrow H + HCl$	8×10^7	31
[36]	$H + Cl + H_2O \rightarrow HCl + H_2O$	1×10^9	Assumed
[37]	$H + Cl_2 \rightarrow HCl + Cl$	4.6×10^{10}	34
[38]	$H + HBr \rightarrow H_2 + Br$	4.5×10^9	35–37
[39]	$OH + HBr \rightarrow H_2O + Br$	5×10^9§	37
[40]	$Br + Br + H_2O \rightarrow Br_2 + H_2O$	4×10^8‖	38
[41]	$H + Br_2 \rightarrow HBr + Br$	8.5×10^{10}	39
[42]	$H + Br + H_2O \rightarrow HBr + H_2O$	1×10^9	Assumed

*For three body reactions these are the equivalent 2nd order rate constants in H_2O vapor at 1 mg ml^{-1}.
†Using $E_a = 2$ kcal mol^{-1}.
‡Assuming third body efficiency of H_2O is the same as that of Cl_2.
§Using $E_a = 1$ kcal mol^{-1}.
‖Assuming third body efficiency of H_2O is the same as that of CF_3Br.

observed yields. There is no reported value of k_{21}, k_{22}, or k_{23} though their ratios are known (19) and Baulch *et al.* (30) recommend a value of 1×10^{10} M^{-1} s^{-1} for k_{21}. However changing k_{21} or k_{22} by a factor of four changes the calculated value of $G(H_2)$ by less than 5%.

The increase in $G(H_2)$ with temperature is most probably due to the temperature dependence of reaction 3, the major reaction of H atoms. The activation energies of reactions 19–22 should be small. We are now in a position to calculate the concentration dependence of the hydrogen yields from the radiolysis of the water vapor – hydrogen halide mixtures. The rate constants for the reactions occurring in these mixtures, in addition to those in Table 2, are listed in Table 5.

The hydrogen yields calculated using the computer program are shown by the broken lines in Figs. 1 and 2. The agreement between the calculated and observed values is in general within the experimental errors. We have discussed the relation of the uncertainties in the rate constants in Table 2 to the calculated $G(H_2)$ values for water vapor. There are also uncertainties in the rate constants for the atom recombination reactions in Table 5, *i.e.* [34], [36], [40], and [42].

To determine if limits can be set on these rate constants or those previously discussed *e.g.* k_2, k_3, the contributions of each reaction to the hydrogen yield in the water vapor – hydrogen halide mixtures have been calculated for different concentrations. The results are shown in Table 6.

At low concentrations *i.e.* 0.2 and 1 mol% HCl and 0.2 mol% HBr the calculated hydrogen yield can be seen to be dependent on a large number of rate constants. There are large uncertainties in k_{34}, k_{36}, k_{40}, and k_{42} and in k_2 and k_7. It is thus very difficult to set limits on these uncertainties by comparison of the calculated and observed yield at these concentrations.

At 6 mol% HBr the contributions of reactions 41 and 42 are so small that even a factor of 10 increase in k_{41} and k_{42} would not affect the calculated hydrogen yield. This shows that practically all the H atoms react as in [38] and that the observed hydrogen yield is a true measure of the H atom yield from water vapor. In 6 mol% HCl the calculated yield is slightly lower than the observed yield. This difference cannot be accounted for by any reasonable changes in k_{34} or k_{37}. The results can however be used to set an upper limit on k_{36}. Assuming that its contribution cannot be more than 0.3 G units $k_{36} \leqslant 3 \times 10^9$ M^{-1} s^{-1}.

Conclusions

The yields of hydrogen from the Febetron radiolysis of water vapor – HCl and water vapor – HBr mixtures $G(H_2) = 7.9 \pm 0.2$ are in agreement with those from the low dose rate radiolysis of water vapor – alkane mixtures. In both systems the hydrogen yields are reduced by approximately 3 G units on the addition of an electron scavenger. Since the ion pair yield in water vapor is 3.3 there is a yield of an H atom per neutralization.

Can. J. Chem. Downloaded from www.nrcresearchpress.com by 210.87.254.6 on 09/05/12
For personal use only.

TABLE 6. Contributions of reactions in the Febetron radiolysis of H_2O–HCl and H_2O–HBr mixtures; (2×10^{27} eV g^{-1} s^{-1}, 1×10^{20} eV g^{-1}, 1 mg ml^{-1}, 160 °C)

		G					
		0.2 mol%		1 mol%		6 mol%	
	Reaction	HCl	HBr	HCl	HBr	HCl	HBr
	$G(H_2)$ =	3.61	6.79	5.56	7.67	7.34	7.87
[2]	$H + H + H_2O \rightarrow H_2 + H_2O$	0.20	0.04	0.07	0.008	0.02	0.001
[3]	$H + OH + H_2O \rightarrow 2H_2O$	3.01	1.17	1.26	0.28	0.27	0.04
[7]	$OH + OH + H_2O \rightarrow H_2O_2 + H_2O$	0.18	0.10	0.07	0.02	0.02	0.004
[19]	$O + OH \rightarrow H + O_2$	0.61	0.37	0.30	0.10	0.08	0.02
[20]	$H + O_2 + H_2O \rightarrow HO_2 + H_2O$	0.08	0.006	0.01	$<10^{-4}$	0.001	$<10^{-5}$
[21]	$H + HO_2 \rightarrow H_2 + O_2$	0.02	$<10^{-3}$	0.002	$<10^{-5}$	$<10^{-5}$	$<10^{-7}$
[22]	$H + HO_2 \rightarrow 2OH$	0.01	$<10^{-3}$	0.001	$<10^{-5}$	$<10^{-5}$	$<10^{-7}$
[24]	$HO_2 + HO_2 \rightarrow H_2O_2 + O_2$	0.01	$<10^{-3}$	0.001	$<10^{-5}$	$<10^{-5}$	$<10^{-7}$
[32]	$H + HCl \rightarrow H_2 + Cl$	3.53		6.05		7.81	
[33]	$OH + HCl \rightarrow H_2O + Cl$	2.23		4.49		5.86	
[34]	$Cl + Cl + H_2O \rightarrow Cl_2 + H_2O$	1.69		4.03		5.91	
[35]	$H_2 + Cl \rightarrow H + HCl$	0.58		1.01		0.94	
[36]	$H + Cl + H_2O \rightarrow HCl + H_2O$	0.47		0.30		0.09	
[37]	$H + Cl_2 \rightarrow HCl + Cl$	1.13		0.99		0.26	
[38]	$H + HBr \rightarrow H_2 + Br$		6.30		7.21		7.42
[39]	$OH + HBr \rightarrow H_2O + Br$		4.51		5.82		6.0
[40]	$Br + Br + H_2O \rightarrow Br_2 + H_2O$		5.27		5.93		6.80
[41]	$H + Br_2 \rightarrow HBr + Br$		0.12		0.009		$<10^{-3}$
[42]	$H + Br + H_2O \rightarrow HBr + H_2O$		0.15		0.04		0.007

The yields of hydrogen from pure water vapor and water vapor with an electron scavenger are $G(H_2) = 1.65$ and $G(H_2) = 0.90$. Taking the unimolecular yield of hydrogen to be $G_{H_2} = 0.45$ the yields of hydrogen resulting from the reactions of hydrogen atoms are $G(H_2) = 1.2$ in pure water vapor and $G(H_2) = 0.45$ in the presence of an electron scavenger. These yields are consistent with one H atom per neutralization. From these yields a set of rate constants for the reactions for the recombination of H atoms and OH radicals can be derived, *i.e.*

$$H + OH + (H_2O) \rightarrow H_2O$$
$$k = 1.7 \pm 0.1 \times 10^{10}\ M^{-1}\ s^{-1}$$

$$OH + OH + (H_2O) \rightarrow H_2O_2$$
$$2k = 3 \pm 1 \times 10^{9}\ M^{-1}\ s^{-1}$$

$$H + H + (H_2O) \rightarrow H_2$$
$$k = 3 \pm 1 \times 10^{8}\ M^{-1}\ s^{-1}$$

Comparison of the observed hydrogen yields in water vapor – HCl mixtures with those calculated from the H atom yields and the reaction rate constants leads to an upper limit of $3 \times 10^{9}\ M^{-1}\ s^{-1}$ for the reaction

$$H + Cl\ (+H_2O) \rightarrow HCl$$

1. A. W. BOYD, C. WILLIS, and O. A. MILLER. Can. J. Chem. This issue.
2. R. S. DIXON. Radiat. Res. Rev. **2**, 237 (1970).
3. N. E. BIBLER and R. F. FIRESTONE. J. Phys. Chem. **76**, 621 (1972).
4. C. WILLIS, A. W. BOYD, and M. J. YOUNG. Can. J. Chem. **48**, 1515 (1970).
5. A. W. BOYD, C. WILLIS, and O. A. MILLER. Unpublished results.
6. C. WILLIS, A. W. BOYD, and D. A. ARMSTRONG. Can. J. Chem. **47**, 3783 (1969).
7. S. GORDON and W. MULAC. Private communication.
8. B. A. THRUSH. Prog. React. Kinet. **3**, 63 (1965).
9. C. WILLIS, A. W. BOYD, and O. A. MILLER. Can. J. Chem. **47**, 3007 (1969).
10. C. WILLIS, O. A. MILLER, A. E. ROTHWELL, and A. W. BOYD. Adv. Chem. Ser. **81**, 539 (1968).
11. C. WILLIS, A. W. BOYD, and O. A. MILLER. Radiat. Res. **46**, 428 (1971).
12. C. WINGATE, W. GROSS, and G. FAILLA. Radiat. Res. **8**, 411 (1958).
13. J. BOOZ and H. G. EBERT. Strahlentherapie, **7**, 120 (1963).
14. P. ALDER and H. K. BOTHE. Z. Naturforsch. **20***a*, 1700 (1965).
15. D. O. HAM, D. W. TRAINOR, and F. KAUFMAN. J. Chem. Phys. **53**, 4395 (1970).
16. V. H. SHUI and J. P. APPLETON. J. Chem. Phys. **55**, 3126 (1971).
17. J. E. BREEN and G. P. GLASS. J. Chem. Phys. **52**, 1082 (1970).
18. J. J. AHUMADA, J. V. MICHAEL, and D. T. OSBORNE. J. Chem. Phys. **57**, 3736 (1972).

Can. J. Chem. Downloaded from www.nrcresearchpress.com by 210.87.254.6 on 09/05/12
For personal use only.

19. A. A. WESTENBERG and N. DE HAAS. J. Phys. Chem. **76**, 1586 (1972).
20. T. T. PAUKERT and H. S. JOHNSTON. J. Chem. Phys. **56**, 2824 (1972).
21. G. L. SCHOTT. J. Chem. Phys. **32**, 710 (1960).
22. S. N. FONER and R. L. HUDSON. J. Chem. Phys. **36**, 2681 (1962).
23. N. R. GREINER. J. Phys. Chem. **72**, 406 (1968).
24. G. DIXON-LEWIS, W. F. WILSON, and A. A. WESTENBERG. J. Chem. Phys. **44**, 2877 (1966).
25. F. KAUFMAN. Prog. React. Kinet. **1**, 1 (1961).
26. H. I. SCHIFF. Can. J. Chem. **47**, 1903 (1969).
27. A. A. WESTENBERG and N. DE HAAS. J. Chem. Phys. **47**, 4241 (1967).
28. A. A. WESTENBERG and N. DE HAAS. J. Chem. Phys. **50**, 2512 (1969).
29. K. H. SCHMIDT. USAEC Res. and Dev. Rep. ANL-7693 (1970).
30. P. L. BAULCH, D. D. DRYSDALE, D. G. HORNE, and A. C. LLOYD. Evaluated kinetic data for high temperature reactions. Vol. I. Homogeneous gas phase reactions of the H_2–O_2 System. Butterworths, London. 1972.
31. A. A. WESTENBERG and N. DE HAAS. J. Chem. Phys. **48**, 4405 (1968).
32. G. A. TAKACS and G. P. GLASS. Private communication.
33. E. HUTTON. Nature, **203**, 835 (1964).
34. R. G. ALBRIGHT, A. F. DODONO, G. K. LABRONSKAYA, I. I. MOROSOV, and V. L. TAL'ROZE. J. Chem. Phys. **50**, 3632 (1969).
35. H. STEINER. Proc. R. Soc. **173**A, 531 (1939).
36. G. B. STEINER and G. H. RINGROSE. J. Chem. Phys. **43**, 4129 (1965).
37. G. A. TAKACS and G. P. GLASS. J. Phys. Chem. **77**, 1060 (1973).
38. B. A. DE GRAAFF and K. J. LANG. J. Phys. Chem. **74**, 4181 (1970).
39. R. A. FASS. J. Phys. Chem. **74**, 984 (1970).

Can. J. Chem. Downloaded from www.nrcresearchpress.com by 210.87.254.6 on 09/05/12
For personal use only.

The Radiolysis of Water Vapor at Very High Dose Rates. II. Isotope Effects in the Hydrogen Yield from H_2O–D_2O Mixtures[1]

A. W. Boyd, C. Willis,[2] and O. A. Miller

Physical Chemistry Branch, Chalk River Nuclear Laboratories, Atomic Energy of Canada Limited, Chalk River, Ontario

Received June 22, 1973

The isotope effect in the formation of hydrogen has been measured for H_2O–D_2O mixtures (10–90% H_2O, 0.5–1.0 mg ml^{-1}, 412–138 °C) with and without 1 mol% SF_6 at 2×10^{27} eV g^{-1} s^{-1}. The values of α ((H/D) radiolytic hydrogen/(H/D) H_2O–D_2O) for the reactions of hydrogen atoms are in the range 3–6 varying with H/D ratio of the substrate. Consideration of possible mechanisms for these large α values leads to the conclusions that reaction of the hydrogen atoms to form hydrogen involves the substrate and that the species H_3O may be formed as an intermediate.

L'effet isotopique dans la formation d'hydrogène a été mesuré pour des mélanges H_2O–D_2O (10–90% H_2O. 0.5–1.0 mg ml^{-1}, 412–138 °C) en présence et en absence d'une mol % de SF_6 à 2×10^{27} eV g^{-1} s^{-1}. Les valeurs de α ((H/D) hydrogène radiolytique /(H/D) H_2O–D_2O) pour les réactions des atomes d'hydrogène varient de 3 à 6 en fonction du rapport H/D du substrat. L'étude des mécanismes possibles pour ces grandes valeurs de α amène à conclure que la réaction des atomes d'hydrogène pour former l'hydrogène fait intervenir le substrat et que les espèces H_3O peuvent se former comme intermédiaires.
[Traduit par le journal]

Can. J. Chem., **51**, 4056 (1973)

Introduction

The results in the preceding paper (1) are consistent with a total H atom yield of $G(H) = 7.45$ and a yield of one H atom per neutralization both in irradiated pure water vapor and water vapor – hydrogen halide mixtures. They support the H atom yields derived from the low dose rate irradiations of water vapor – alkane mixtures (2) but provide no explanation for the high yields of $G(HD) = 13.1$ obtained in low dose rate irradiations of H_2O–D_2 and D_2O–H_2 mixtures (3).

However the results in ref. 1 do show that there is a measurable, consistent hydrogen yield from the Febetron radiolysis of water vapor that does not change over a considerable range of absorbed dose and temperature (at least below 250 °C). We have carried out a study of the isotope effects in this hydrogen yield both as a further study of radiolytic isotope effects in water (4) and in the hope that the results might resolve the high exchange yields.

Experimental

The methods of sample preparation, irradiation, dosimetry, and measurements of the total hydrogen formed were the same as those described in ref. 1.

The H_2, HD, and D_2 contents of the hydrogen were determined with a calibrated CEC-21-610 mass spectrometer. The calibration was done with mixtures of H_2 and D_2 equilibrated on a platinum filament at 900–950 °C (see ref. 4 for details).

Both the H_2O (isotopic D content 150 p.p.m.) and D_2O (isotopic purity 99.58%) were preirradiated and triply distilled.

Results

The values of α as a function of H_2O concentration[3] at a dose rate of 2×10^{27} eV g^{-1} s^{-1}, 160 °C, and a vapor density of 1 mg ml^{-1} are shown in Fig. 1 for H_2O–D_2O vapor mixtures with and without 1 mol% SF_6. It can be seen that there is a large isotope effect in both the pure system and that containing the electron scavenger.

The total hydrogen yields for the same mixtures and conditions are shown in Fig. 2. The yields are constant and can be taken to be G (total hydrogen) $= 1.65 \pm 0.15$ in H_2O–D_2O and G(total hydrogen) $= 0.90 \pm 0.15$ in H_2O–D_2O, 1 mol% SF_6 over the whole range of H_2O concentration.

The α values and total hydrogen yields from the irradiation of 66.6 mol% H_2O – 33.3 mol% D_2O mixtures at temperatures from 138–412 °C are listed in Table 1.

[1] AECL No. 4642.

[2] Present address: Division of Chemistry, National Research Council of Canada, Ottawa, Canada K1A OR6.

[3] α = (H/D) radiolytic hydrogen/(H/D) H_2O–D_2O mixture.

Can. J. Chem. Downloaded from www.nrcresearchpress.com by 84.22.46.98 on 09/08/12
For personal use only.

TABLE 1. Temperature dependence of isotope effects and total hydrogen yields in the Febetron radiolysis of a mixture of 66.7% H_2O–33.3% D_2O vapor; vapor densities in the range 1–0.5 mg ml^{-1}

Temperature °C	α		$G(H_2 + HD + D_2)$
	Observed	Corrected*	
138	2.23	3.60	1.64
163	2.35	3.84	1.63
180	2.01	2.96	1.68
225	2.16	3.24	1.61
320	2.18	2.74	2.50
412	2.26	2.53	3.16

*Corrected for the contribution of unimolecular hydrogen as described in the text.

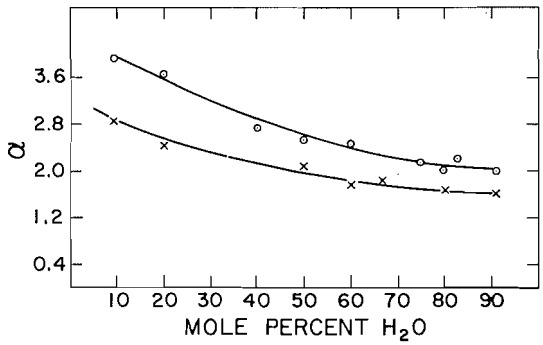

FIG. 1. Measured isotope effects in the total yield of hydrogen from H_2O–D_2O vapor irradiations. Dose 1×10^{20} eV g^{-1}; average dose rate 2×10^{27} eV g^{-1} s^{-1}, 1000 Torr, 160 °C, (vapor density 1 mg/ml). ○, H_2O–D_2O; ×, H_2O–D_2O + 1 mol% SF_6.

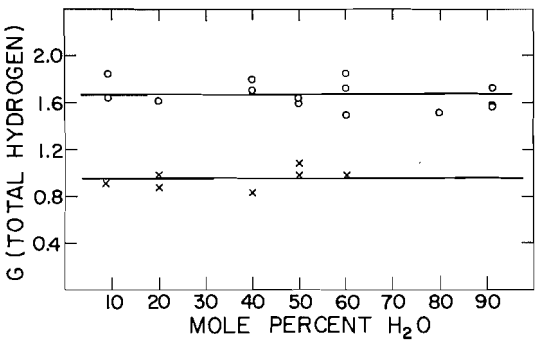

FIG. 2. Hydrogen yields from H_2O–D_2O vapor irradiations. Dose 1×10^{20} eV g^{-1}; average dose rate 2×10^{27} eV g^{-1} s^{-1}; 1000 Torr, 160 °C. ○, H_2O–D_2O; ×, H_2O–D_2O + 1 mol% SF_6.

Correction for Unimolecular H_2 Yield

The observed hydrogen yields in Fig. 2 are made up of the unimolecular yield of hydrogen and the hydrogen resulting from the reactions of hydrogen atoms. The value of the former which is assumed to be due to reaction 1 is the same in both H_2O and D_2O and has the value $G_{H_2} = G_{D_2} = 0.45$ (2).

[1] $$H_2O \rightsquigarrow H_2 + O$$

If this molecular yield is correctly represented by reaction 1 then approximately one-third of the hydrogen in pure water and one-half the hydrogen in water vapor containing 1 mol% SF_6 must be produced with no isotope effect. The observed α values in Fig. 1 were corrected to obtain the isotope effect in the reactions of H atoms as follows. The amounts of radiolytic H_2, HD, and D_2 from reaction 1 were calculated from the isotopic content of the H_2O–D_2O mixture. This isotopic content was calculated assuming that $K = (HDO)^2/(H_2O)(D_2O) = 4$. This is the maximum value that K can have and the minimum must be greater than 3.74, the value at 25 °C (5). Both values give the same concentrations of H_2O, HDO, and D_2O within 2% in our mixtures. These amounts of H_2, HD, and D_2 from [1] were subtracted from the total amounts of H_2, HD, and D_2 formed. Corrected α values were then calculated using the remaining concentrations of H_2, HD, and D_2. These corrected α values are shown in Fig. 3. As can be seen the corrected α values vary from $\alpha \approx 3$ for high H_2O to $\alpha \gtrsim 6$ for high D_2O and are practically the same in the presence and absence of SF_6.

Discussion

Isotope Effects in the Formation of H Atoms

The inference to be drawn from the identity of the corrected α values with and without SF_6, that is with and without ionic contributions, is that the separation factors for atom production by ionic and non-ionic processes are equal. At first sight this would appear to be in conflict with low dose rate observations. Johnson and

Can. J. Chem. Downloaded from www.nrcresearchpress.com by 84.22.46.98 on 09/08/12
For personal use only.

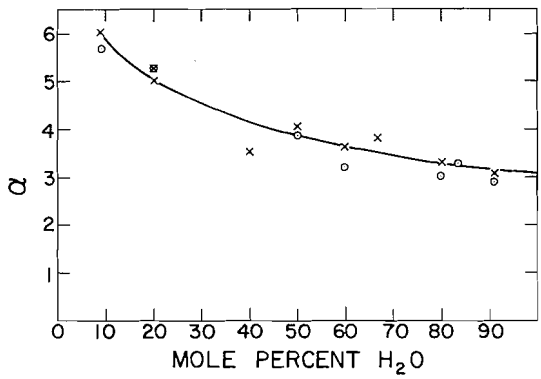

FIG. 3. Isotope effects in the reactions of hydrogen atoms from H_2O–D_2O vapor irradiations. Dose 1×10^{20} eV g^{-1}; average dose rate 2×10^{27} eV g^{-1} s^{-1}, 1000 Torr, 160 °C. ○, H_2O–D_2O; ×, H_2O–D_2O + 1 mol% SF_6.

Simic (6) irradiated H_2O–D_2O vapor mixtures at 140 °C in the presence of 1.5 mol% propane at 10^{16} eV g^{-1} s^{-1}. Under these conditions all the H and D atoms from the water vapor abstract a H atom from the propane and any isotope effect in their formation is reflected in the yields of H_2 and HD. They used mixtures with and without SF_6 and corrected for the unimolecular contribution to the yields by the same method as we have used above. They obtained $\alpha = 1.1 \pm 0.1$ for the formation of hydrogen atoms by dissociative excitation and $\alpha = 2.1 \pm 0.4$ for the formation of hydrogen atoms by neutralization reactions.

The results in ref. 1 indicate that the yield of H atoms from dissociative excitation of H_2O is independent of dose rate over the range 10^{16} to 10^{28} eV g^{-1} s^{-1}. We would expect therefore that there should be no effect of dose rate on any isotope effect in the dissociative excitation of HOD. Indeed, it is difficult to envisage an intensity effect if dissociative excitation is a simple Franck–Condon controlled, "vertical" excitation process. Thus Johnson and Simic's value of $\alpha = 1.1 \pm 0.1$ should be valid at Febetron dose rates. However as discussed in ref. 1 the ionic processes which lead to the formation of H atoms will be different at the two dose rates. The probable reaction sequences are:

10^{27} eV g^{-1} s^{-1}

[2] $H_2O \rightarrow H_2O^+ + e$

[3] $H_2O^+ + H_2O \rightarrow H_3O^+ + OH$

[4] $H_3O^+ + nH_2O \rightarrow [H(H_2O)_{n+1}]^+$

[5] $[H(H_2O)_{n+1}]^+ + e \rightarrow H + (n+1)H_2O$

10^{16} eV g^{-1} s^{-1}

[2] $H_2O \rightarrow H_2O^+ + e$

[6] $e + O_2 + H_2O \rightarrow O_2^- + H_2O$

[3] $H_2O^+ + H_2O \rightarrow H_3O^+ + OH$

[7] $H_3O^+ + \begin{pmatrix} H_2O \\ C_3H_8 \end{pmatrix} \rightarrow [?]$

[8] $[?]^+ + O_2^- \rightarrow H + [?]$

Although reactions 5 and 8 both give one H atom there may be different isotope effects in these reactions.

As discussed above within our experimental error we do not see any difference in the α values with or without 1 mol% SF_6 and it therefore seems most reasonable to assume that there is no isotope effect in the formation of H atoms either by dissociative excitation or ionic processes in the Febetron irradiations, in other words α is close to unity for both processes.

Mechanism of the Isotope Effect

From the above discussions and the results of the calculations described in ref. 1 the isotope effect observed appears to arise from radical reactions, essentially reactions 9–14. The contributions of the other reactions to the hydrogen yield are so small that it is unlikely that they can produce any sizeable effect.

[9] $H + H + H_2O \rightarrow H_2 + H_2O$

[10] $H + OH + H_2O \rightarrow 2\,H_2O$

[11] $O + OH \rightarrow O_2 + H$

[12] $H + O_2 + H_2O \rightarrow HO_2 + H_2O$

[13] $H + HO_2 \rightarrow H_2 + O_2$

[14] $H + HO_2 \rightarrow 2\,OH$

Measurements of the isotope effect for reactions 9 and 12 have been reported but with third bodies other than H_2O. The ratio of k_{H+H+H_2}/k_{D+D+D_2} given by Ham *et al.* is 1.4 (7). This is in agreement with the calculations of Roberts and Bernstein (8). Bennett and Blackmore (9) however, report a value of 0.8 for this ratio. For the ratio k_{H+O_2+M}/k_{D+O_2+M} in reaction 12 Baldwin *et al.* (10) obtain 0.86 at 500 °C, M = H_2, and Clyne and Thrush (11) obtained 0.7 ± 0.2 at 293 °K and 0.9 ± 0.2 at 244 and 225°K, M = Ar, and 0.6 ± 0.2 at 293°K, M = He.

Reaction 9 is significantly slower than the other reactions. This means that hydrogen atoms will only react to form hydrogen by reaction

Can. J. Chem. Downloaded from www.nrcresearchpress.com by 84.22.46.98 on 09/08/12
For personal use only.

Can. J. Chem. Downloaded from www.nrcresearchpress.com by 84.22.46.98 on 09/08/12
For personal use only.

9 when few OH radicals remain unreacted and therefore these H atoms have a single reaction channel. No isotope effect due to the rate of this reaction then will be reflected in the hydrogen produced. This, coupled with the small α values observed for this reaction with other third bodies, suggests that there should be little preference for a change in the H/D ratio due to reaction 9. From the previous work discussed above, the isotope effect due to reaction 12 is expected to be small and if anything in the opposite direction to our overall observed α values.

Thus, if the observed isotope effect is to be explained by reactions 9–14, the explanation must reside in reactions 10, 11, 13, and 14. Reactions 11, 13, and 14 are very fast and consequently must have very small activation energies and a small isotopic dependence of their rate constants. For reaction 10 to account for the observed α values it is required that $k_{10H} < 3k_{10D}$. This seems very unlikely in view of the observed isotope effects in reactions 9 and 12. More significantly this inequality would result in a markedly lower total hydrogen yield with increasing D_2O concentration, in direct contrast to the observed consistency of that yield over the entire composition range studied. Furthermore, the yields as a function of temperature for 66.6% H_2O – 33.3% D_2O agree very well with those for 100% H_2O (1).

We have made extensive calculations, of the type described in ref. 1, to try and fit the radical mechanism to explain the observed α values and at the same time the constant total hydrogen yield. We varied each of the significant rate constants by a factor of four about the best value given in the tables. Although it was possible to obtain an α value ≈ 3, approximately constant over the concentration range, this gave a decrease in the total hydrogen yield as the concentration of D_2O was increased. We were unable to fit a mechanism to an increasing α value from 3–6 with a constant total hydrogen yield.

It seems, therefore, that the observed α values cannot be explained by primary processes nor by the simple radical mechanism discussed above.

An alternative mechanism which can possibly account for the α values is isotopic exchange with the substrate during the formation of hydrogen by reaction 9, and possibly reaction 13. This can schematically be envisaged as, for example

[9′] $$H + H + D_2O \rightarrow HD + HDO$$

Immediately this would explain the independence of the total hydrogen yield on the H_2O–D_2O ratio.

For a reaction of the type [9′] we must postulate a first step of the form of reaction 15

[15] $$H + H_2O \rightarrow H_3O$$
$$D + H_2O \rightarrow H_2DO$$
$$H + HDO \rightarrow H_2DO$$
$$\text{etc.}$$

This could be followed either by reaction 16 or reaction 17

[16] $$H + H_2DO \rightarrow H_2 + HDO$$
$$D + H_2DO \rightarrow H_2 + D_2O$$
$$\text{etc.}$$

[17] $$H_3O + H_2DO \rightarrow H_2 + H_2O + HDO$$
$$D_3O + HD_2O \rightarrow HD + 2\,D_2O$$
$$\text{etc.}$$

What we mean these reactions to imply is association of the H atom or D atom with the substrate, for example H···HDO, and that when the associated atom reacts by [16] or [17] the molecules of association are intimately involved in the complex which decomposes to give hydrogen with preferential elimination of H_2 (or HD) rather than HD (or D_2). We do not necessarily mean to imply a complete equivalence of the three hydrogen atoms in the associated atom system, H_3O, etc.

The existence of an H_3O species is not a new suggestion. From mass spectroscopic measurements it has been suggested that H_3O can be formed with an appreciable lifetime (12). Also on the basis of simple thermodynamic cycles both $H(H_2O)$ and $H(NH_3)$ have predicted stabilities of at least 5–10 kcal mol^{-1} (13). More generally, chaperone mechanisms for three body reactions of the type

$$A + B \rightarrow AB$$
$$AB + A \rightarrow A_2 + B$$

implicitly require an associated atom of the type H_3O, etc.

Any significant involvement of reactions 18 or 19

[18] $$H + D_2O \rightarrow HDO + D$$

[19] $$H + D_2O \rightarrow HD + OD$$

Can. J. Chem. Downloaded from www.nrcresearchpress.com by 84.22.46.98 on 09/08/12
For personal use only.

or isotope variations of these reactions appears to be ruled out by their high activation energies, 19–22 kcal (3), and the small temperature dependence of our observed α values.

We cannot distinguish between reactions 16 and 17 on the basis of the increase from $\alpha \approx 3$ to $\alpha \approx 6$ on going from high to low H_2O/D_2O ratios. At high H_2O concentrations the α value is dependent on k_{16}/k_{16a} or k_{17}/k_{17a}, at high D_2O concentrations α is largely dependent on k_{16b}/k_{16c} or k_{17b}/k_{17c}. We would expect that if $k_{16b}/k_{16c} > k_{16}/k_{16a}$ then $k_{17b}/k_{17c} > k_{17}/k_{17a}$.

[16a] $H + H_2DO \rightarrow HD + H_2O$

[17a] $H_3O + H_2DO \rightarrow HD + 2H_2O$

[16b] $D + HD_2O \rightarrow HD + D_2O$

[16c] $D + HD_2O \rightarrow D_2 + HDO$

[17b] $D_3O + HD_2O \rightarrow HD + 2D_2O$

[17c] $D_3O + HD_2O \rightarrow D_2 + HDO + D_2O$

This mechanism provides a possible explanation of the high exchange yields of Bibler and Firestone (3), *i.e.*, $G(HD) = 13.1 \pm 0.3$ in the radiolysis of both D_2–H_2O and H_2–D_2O mixtures. This high HD yield could be due to the contributions of reactions 15 and 20 in D_2–H_2O mixtures and of reactions 15 and 21 in H_2–D_2O mixtures.

[15] $D + H_2O \rightarrow H_2DO$

[20] $D_2 + H_2DO \rightarrow HD + D + HDO$

[20a] $D_2 + H_2DO \rightarrow D_2 + D + H_2O$

[15] $H + D_2O \rightarrow HD_2O$

[21] $H_2 + HD_2O \rightarrow HD + H + HDO$

[21a] $H_2 + HD_2O \rightarrow H_2 + H + D_2O$

This mechanism requires that the stability of H_3O be great enough to survive several thousand encounters with H_2O before reacting with H_2. This could be possible if only vibrational de-excitation of the initially formed associated atom occurred in the collisions with H_2O. There will also be D atoms in D_2–H_2O mixtures and H atoms in H_2–D_2O mixtures from reactions 22 and 22a.

[22] $D_2 + OH \rightarrow HDO + D$

[22a] $H_2 + OD \rightarrow HDO + H$

To account for the observed increase of $G(HD) \approx 6.7$ by this mechanism requires then the ratios k_{20}/k_{20a} and k_{21}/k_{21a} be approximately equal and less than unity. Their values are of course dependent on the chain length. It would appear that these requirements are possible but we cannot say more on the basis of our present knowledge.

Conclusions

It is difficult to explain the observed α values of 3–6 for the hydrogen found in the Febetron radiolysis of H_2O–D_2O vapor mixtures without assuming H atoms react with involvement of the substrate and presumably the formation of a hydrogen atom water molecule complex. That this complex should be H_3O is supported by mass spectrometric evidence (12) and thermodynamic considerations (13).

Isotope effects in the reactions of H_3O may explain the high exchange yields in H_2O–D_2O or D_2O–H_2O radiolysis as well as the α values reported in this paper.

It is of interest that there are also kinetic data supporting the formation of the analogous radical NH_4 in H atom – ammonia mixtures. Back and Terao (14) have obtained a value for the rate constant for the recombination of NH_2 radicals of $4 \times 10^{10}\ M^{-1}\ s^{-1}$. We have shown (15) that in 1 atm of NH_3 the rate constant for the reaction between NH_2 and H atoms to form NH_3 is $\approx 10 k_{NH_2+NH_2}$. We have also shown (15) that in 1 atm of NH_3 the rate constant for the removal of H atoms by propene is $\approx 0.5 k_{H+NH_2}$. The resulting values of k_{H+NH_2} and $k_{H+C_3H_6}$ are $\sim 4 \times 10^{11}$ and $1 \times 10^{10}\ M^{-1}\ s^{-1}$, respectively. The former is much larger than could be reasonably expected and the latter is almost certainly less than $10^9\ M^{-1}\ s^{-1}$ (16, 17). A possible explanation of both these anomalies is that the rate constants obtained are for the reactions of NH_4 with NH_2 and C_3H_6.

1. A. W. Boyd, C. Willis, and O. A. Miller. Can. J. Chem. This issue.
2. R. S. Dixon. Radiat. Res. Rev. **2**, 237 (1970).
3. N. E. Bibler and R. F. Firestone. J. Phys. Chem. **76**, 621 (1972).
4. A. W. Boyd, C. Willis, and G. C. Lalor. Can. J. Chem. **50**, 83 (1972).
5. W. A. Van Hook. J. Phys. Chem. **76**, 3040 (1972).
6. G. R. A. Johnson and M. Simic. *In* The chemistry of ionization and excitation. *Edited by* G. R. A. Johnson and G. Scholes. Taylor and Francis. London. 1967. p. 211.
7. D. O. Ham, D. W. Trainor, and F. Kaufman. J. Chem. Phys. **53**, 4395 (1970).

8. R. E. ROBERTS and R. B. BERNSTEIN. Chem. Phys. Lett. **6**, 282 (1970).
9. J. E. BENNETT and D. R. BLACKMORE. J. Chem. Phys. **53**, 4400 (1970).
10. R. R. BALDWIN, B. N. ROSSITER, and R. W. WALKER. Trans. Faraday Soc. **66**, 2004 (1970).
11. M. A. A. CLYNE and B. A. THRUSH. Proc. R. Soc. A**275**, 559 (1963).
12. C. E. MELTON and H. W. JOY. J. Chem. Phys. **46**, 4275 (1967).
13. H. J. BERNSTEIN. J. Am. Chem. Soc. **85**, 484 (1963).
14. R. A. BACK and T. TERAO. Private communication.
15. A. W. BOYD, C. WILLIS, and O. A. MILLER. Can. J. Chem. **49**, 2283 (1971).
16. J. A. EYRE, T. HIKIDA, and L. M. DORFMAN. J. Chem. Phys. **53**, 1281 (1970).
17. R. J. CVETANOVIĆ and L. C. DOYLE. J. Chem. Phys. **50**, 4705 (1969).

Can. J. Chem. Downloaded from www.nrcresearchpress.com by 84.22.46.98 on 09/08/12
For personal use only.

The Rotational Oscillations of Tetrahydrofuran in Tetrahydrofuran Clathrate Hydrate[1]

D. D. KLUG AND E. WHALLEY

Division of Chemistry, National Research Council of Canada, Ottawa, Canada

Received June 8, 1973

The absorptivity of tetrahydrofuran clathrate hydrate in the range 70–7 cm^{-1} has been measured at several temperatures in the range 17–80 K. There are two broad bands with maxima at 25 and 38 cm^{-1} which are due to the rotational oscillations of tetrahydrofuran molecules in their cages. The integrated absorptivity yields an effective dipole moment for the oscillation of 1.63 D, which is close to the gas-phase value. The negative second moment of the absorptivity yields the contribution 0.105 $\pm$ ~0.007 to the low-frequency refractive index, in good agreement with a less accurate value from dielectric measurements. The orientational disorder of the water molecules causes a distribution of potentials hindering the rotational oscillations of the guest molecules, and a detailed analysis of the shapes of the bands yields directly the distribution of force constants for the oscillations.

La capacité d'absorption du clathrate hydraté de tétrahydrofuranne entre 70 et 7 cm^{-1} a été mesurée pour des températures variant de 17 à 80 K. Il y a deux bandes larges avec des maxima à 25 et 38 cm^{-1} qui sont causées par les oscillations de rotation des molécules de tétrahydrofuranne dans leur environnement. La valeur de la capacité d'absorption a permis d'évaluer le moment dipolaire effectif à 1.63 D ce qui est une valeur proche de celle de la phase gazeuse. La valeur du second moment négatif de la capacité d'absorption a apporté une contribution de 0.105 $\pm$ 0.007 à l'indice de réfraction à base fréquence, ce qui est en accord avec la valeur moins précise obtenue par mesures diélectriques. Le désordre d'orientation des molécules d'eau provoque une distribution de potentiels perturbant les oscillations de rotation des molécules-hôtes. Une analyse détaillée de la forme des bandes a permis d'obtenir directement la distribution des constantes de force pour les oscillations.

[Traduit par le journal]

Can. J. Chem., **51**, 4062 (1973)

Introduction

The intensity of absorption by the intermolecular translational and rotational motions of molecules in molecular crystals is not well understood in detail, in contrast with the intensity of absorption due to the translational motion of ions, which is understood in reasonable detail in simple salts (1). The dipole absorption arises, of course, from rotational motions of permanent dipole moments and from induction of dipole moments due to intermolecular interaction.

The only reasonably accurate intensities due to rotational vibrations so far reported appear to be on carbonyl sulfide (2), chlorine and bromine cyanide (3), ice (4, 5), hydrogen chloride and bromide (6) (the translational vibrations were included in these measurements), and hydrogen cyanide (7). The three studies on hydrogen-bonded systems concluded that the librating dipole was appreciably less than that in the vapor, presumably because of incompletely understood polarization occurring in the crystals, whereas those on chlorine and bromine cyanides and on carbonyl sulfide gave good agreement with the calculated intensities based on gas-phase dipole moments. Thus, although non-hydrogen-bonded crystals appear to be reasonably well understood, only three examples have been studied.

Absorption by induced moments is well understood in crystalline hydrogen (8), which has been studied in great detail from many points of view. The sum of the intensities of the two translational vibrations in solid carbon dioxide (9) agrees well with that expected for quadrupole – induced dipole moments (10) but the ratio of intensities is 1.5 instead of 5.4 as calculated, perhaps because of uncertainties in the normal coordinates used in the theory. The integrated intensity of the translational vibrations in α-nitrogen (11) is only one fourth of that expected for quadrupole-induced moments. The integrated absorption due to the translational vibrations of ice is about 1/16 of that expected for dipole- and quadrupole-induced dipole moments (12), and that of crystalline chlorine is about 1/35 of that calculated for quadrupole-induced dipole moments (13). It must be

[1]NRCC No. 13456.

Can. J. Chem. Downloaded from www.nrcresearchpress.com by 210.87.254.6 on 09/05/12
For personal use only.

Can. J. Chem. Downloaded from www.nrcresearchpress.com by 210.87.254.6 on 09/05/12
For personal use only.

concluded that absorption due to induced moments is not well understood at all except in the simplest molecules.

The main purpose of this paper is to further our understanding of the intensities of intermolecular vibrations by reporting the absorptivity of the rotational vibrations of the guest molecule in a solid in which there is little coupling of the rotational vibrations. The rotational vibrations of tetrahydrofuran in its clathrate hydrate have been studied mainly for the following reason. Tetrahydrofuran clathrate hydrate, which has structure II and is ideally $C_4H_8O \cdot 17H_2O$ (14), has an infrared polarizability derived from dielectric measurements (15) that corresponds to a contribution of 0.11 ± 0.05 to the low-frequency refractive index and that is not due to the water molecules. This has been attributed by Davidson (15) to the rotational oscillations of the tetrahydrofuran molecules in their cages, and a frequency of about 20 cm^{-1} was deduced from an approximate treatment. One of the purposes of the present measurements was to verify this absorption and determine from it the infrared contribution to the low-frequency refractive index.

Because the tetrahydrofuran molecules are far enough apart that coupling between the rotational oscillations of neighbors is small (see Section 3 of Results), the restoring force is due almost entirely to the interaction between the guest and the water molecules in the cage wall and so something can be learned about these from the frequencies. In addition, since the water molecules in the clathrate are orientationally disordered, the forces between the guest and the cage may vary from cage to cage, and the breadth of the bands extrapolated to 0 K should be a measure of the effect of the orientational disorder on these forces. Rotational oscillations of some molecules in clathrates have been observed previously (16–19), but none in clathrate hydrates, except one report of the detection of low-frequency absorption in ethylene oxide clathrate hydrate (20), and no integrated intensities have been reported except an approximate estimate of the intensity of hydrogen chloride in β-quinol clathrate (16).

Experimental methods

Eastman Kodak tetrahydrofuran was refluxed over and distilled from calcium hydride, and was supplied by Dr. S. R. Gough.

Tetrahydrofuran clathrate hydrate was prepared by freezing in a shallow Teflon cup solutions that had about 1% more tetrahydrofuran than in the ideal stoichiometric composition, to guard against possible loss by evaporation. It was held, along with a few drops of tetrahydrofuran that was not in contact with the sample to ensure a saturated atmosphere, for at least 24 h at 0 C in an ice bath to allow complete conversion (21), and was then cooled to ~100 K in the cold gas from rapidly boiling liquid nitrogen. The surface of the hydrate was scraped level with the rim of the cup using a cooled razor blade, and the thickness of the sample plus the base of the cup was measured to ±25 μm by a cooled micrometer. The sample thickness was obtained from this measurement and the thickness of the base of the cup measured at the same temperature. The sample thicknesses were uniform to ±25 μm and covered the range 0.58 to 1.32 mm.

The sample was covered with a cap that was wedged to prevent interference fringes and was mounted, using silicone grease to improve thermal contact, in the cold finger of a Sulfrian Cryogenics liquid-helium-cooled optical Dewar fitted with wedged polyethylene windows. The sample was cooled to the required temperature in the range 17–80 K by pumping liquid helium from the reservoir through a tube in the cold finger. The temperature of the cup was measured by a chromel–constantan thermocouple attached to it by a screwed copper ring, using silicone grease to increase thermal contact, and was kept to ±1 K of the required temperature. The thermocouple e.m.f. was measured to ±0.1 μV by a Cambridge Vernier potentiometer and was calibrated at the temperature of boiling liquid nitrogen, hydrogen, and helium.

Sulfur hexafluoride hydrate (22) containing more than 90% hydrate and less than 10% ice was supplied to us by Dr. S. R. Gough and Dr. D. W. Davidson. The fine powder that was supplied was pressed into discs of the required thickness in the range 1–2 mm at 195 K under a pressure of about 300 bar, and these were placed in the Teflon cups.

The spectrometer was an R.I.I.C. lamellar grating LR-100 interferometer operating in the range 70–4 cm^{-1} using vitreous silica (23) or the crossed-transmission-grating low-pass filters supplied with the instrument. The spectra at temperatures >17 K were taken with a Unicam SP-50 Golay cell, and the 17-K spectra were taken with a Texas Instruments doped-germanium bolometer fitted with cold wedged crystal quartz and cold black polyethylene filters. The spectrometer was evacuated to about 50 μm Hg except for the sample chamber which was isolated from the optical chamber by a wedged polyethylene window and was purged with dry air. A resolution of 0.9 cm^{-1} was used for all samples at 17 K and 0.45 cm^{-1} for all other samples, with scan times of 35 or 70 min. The background run for each sample was taken at the sample temperature with the cap placed on the base of the empty Teflon cup. Triangular apodization was used in processing the spectra.

In calculating the absorptivity, the reflection loss from the various surfaces was allowed for. The background spectra were obtained with the base of the wedged cap in contact with the base of the cup in an attempt to remove interference fringes. But intereference fringes due to the base of the cup were obtained except at the lowest frequencies, showing that complete optical contact

between the base of the cup and the cap was not obtained. In the sample configuration, it was assumed that the sample was in good contact with the base of the cup, but, by analogy with the observations of the preceding sentence, not with the cap. Above about 20 cm^{-1}, the effect of errors in these assumptions, such as uncertain gaps and differences between the refractive index of the sample and the cup, might cause an error in the absorptivity of $\sim$1 cm^{-1}, compared with the standard deviation of duplicate runs (see below) of $\sim$1 cm^{-1}. The reflection error falls below $\sim$20 cm^{-1} because the effect of the gap decreases with increasing wavelength.

Results and Discussion

The absorptivity of tetrahydrofuran clathrate hydrate at various temperatures is shown in Fig. 1. The 17-K spectrum was obtained from the average of four spectra and four backgrounds on each of two samples 0.635 and 0.584 mm thick and three spectra and three backgrounds on a sample 1.32 mm thick. The spectrum consists of two broad absorption bands centered at 25 and 38 cm^{-1}. The standard deviation of the absorptivity for duplicate runs on the sample averaged at several frequencies was $\sim$0.5 cm^{-1}, and the standard deviation for the three sets of spectra averaged at several frequencies in the region of overlap was $\sim$0.6 cm^{-1}. The spectra at temperatures higher than 17 K were the average of two or more spectra on samples of different thicknesses.

The apparent absorptivity of the compressed powder of sulfur hexafluoride clathrate hydrate, which also has structure II (22), is largely due to scattering from the interfaces of the particles it was made from, and it is not clear that any absorption was detected. It has, however, no absorption comparable to that of the two strong bands in tetrahydrofuran hydrate. These two bands are therefore due to the rotational oscillations of tetrahydrofuran.

The tetrahydrofuran molecule appears to be nearly planar in the equilibrium configuration but with a small barrier to pseudorotation, and the polar axis appears to be a principal axis of inertia (24). The equilibrium configuration appears to be of C_2 symmetry, but is not far from the planar C_{2v}. It is enclosed in cages which on the average have the symmetry T_d but which depart from the average symmetry due to the disorder of the orientations of the water molecules. A tetrahydrofuran molecule in an average cage will by symmetry oscillate about the principal axes if its symmetry is taken as C_{2v}. However, in a real disordered cage it will not in general oscillate about its principal axes and the normal coordinates of the oscillations are not known. This is of no consequence for the treatment of Sections 1 and 2 of Results. In Section 3 of Results, the average interaction constants for rotations about the principal axes, which is zero by the average symmetry if the molecule is C_{2v}, will be assumed to hold for all cages.

(1) Integrated Absorptivity

There are three degrees of rotational freedom per molecule, and these can be characterized by small rotational displacements θ_x, θ_y, θ_z about the three principal axes of inertia. In general, a normal vibration will consist of the coupled oscillations of neighboring molecules. The tetrahydrofuran molecules are contained in the hexakaidecahedral cages whose centers are 7.40 Å apart (25). The main mechanism for the coupling of the rotational vibrations of molecules in neighboring cages is the dipole–dipole interaction. Maximum coupling occurs when the dipoles are in line, and the coupling constant is then

$$[1] \qquad \frac{\partial^2 V}{\partial\theta_1\partial\theta_2} = \pm\frac{2\mu^2}{r^3}$$

where θ_1 and θ_2 are the displacements in the same plane of the dipolar axes of the molecules from the line of the cage centers, and the polarization of the intervening water molecules is neglected. Since the centers of the cages are 7.40 Å apart the coupling constant from eq. 1 is $\pm$13 ferg rad^{-2}.[2] This value is an upper limit because the dipoles will usually be less favorably oriented and because the intervening water molecules will be polarized. It is therefore much smaller than the rotational force constants due to interaction with the cage, which are 600 and 450 ferg rad^{-2} for rotation about the two nonpolar axes (see below), and so coupling between neighboring molecules can be neglected.

The normal coordinates Q_1, Q_2, and Q_3 for the rotational vibrations of a molecule are related to the moment-of-inertia-reduced rotational displacements ϕ_x, ϕ_y, ϕ_z about the principal axes by the matrix relation

$$[2] \qquad \mathbf{Q} = \mathbf{L}\boldsymbol{\phi}$$

where $\mathbf{Q}$ and $\boldsymbol{\phi}$ are the vectors representing the normal and reduced rotational coordinates and

[2] 1 ferg = 10^{-15} erg.

Can. J. Chem. Downloaded from www.nrcresearchpress.com by 210.87.254.6 on 09/05/12
For personal use only.

Can. J. Chem. Downloaded from www.nrcresearchpress.com by 210.87.254.6 on 09/05/12
For personal use only.

L is the transformation matrix. Because the kinetic energy T can be written

$$[3] \qquad 2T = \tilde{\dot{Q}}\dot{Q} = \tilde{\dot{\phi}}\dot{\phi}$$

where $\tilde{Q}$ is the transpose of Q, the matrix **L** is orthonormal. The integrated intensity of absorption of normal vibration i of a polycrystal is (26)

$$[4] \qquad A_i = \frac{(n^2 + 2)^2}{9n}\frac{N\pi}{3c^2}\left(\frac{\partial\mu}{\partial Q_i}\right)^2$$

where n is the refractive index excluding the effects of the band being considered, N the number density of molecules, c the speed of light, and μ the dipole moment of the crystal.

If the refractive index is the same for all bands to a sufficient approximation, the sum of the integrated intensities is proportional to $\tilde{\boldsymbol{\mu}}_Q\,\boldsymbol{\mu}_Q$ where $\boldsymbol{\mu}_Q$ is the vector with components $|\partial\boldsymbol{\mu}/\partial Q_1|$, etc. But

$$[5] \qquad \boldsymbol{\mu}_Q = \boldsymbol{L}^{-1}\,\boldsymbol{\mu}_\phi$$

where $\boldsymbol{\mu}_\phi$ is the vector with components $\partial\boldsymbol{\mu}/\partial\phi_{\alpha i}$, etc., $\alpha = x, y,$ or z, and i denotes the particular molecule so that

$$[6] \qquad \tilde{\boldsymbol{\mu}}_Q\boldsymbol{\mu}_Q = \tilde{\boldsymbol{\mu}}_\phi\,\tilde{\boldsymbol{L}}\boldsymbol{L}\boldsymbol{\mu}_\phi$$

Since **L** is orthonormal, eq. 6 implies that

$$[7] \qquad \tilde{\boldsymbol{\mu}}_Q\boldsymbol{\mu}_Q = \tilde{\boldsymbol{\mu}}_\phi\boldsymbol{\mu}_\phi$$

and so

$$\tilde{\boldsymbol{\mu}}_Q\boldsymbol{\mu}_Q = \sum_{\substack{\alpha=x,y,z\\ i}}\left(\frac{\partial\mu}{\partial\phi_{\alpha i}}\right)^2 = N\sum_{\alpha=x,y,z}\frac{{\mu_\alpha}^2}{I_\alpha}$$

where $\boldsymbol{\mu}_\alpha$ is the dipole moment of the ith molecule perpendicular to the α principal axis, I_α the moment of inertia about that axis. The integrated intensity of absorption is therefore independent of the coupling of the motions about the principal axes. This is a special case of a more general sum rule due to Gordon (27).

The translational vibrations, which are active because of induced moments, can be included in this treatment. The measured absorption includes them, but the spectrum of sulfur hexafluoride hydrate suggests that they are much weaker than those due to the permanent moment, and for present purposes they can be neglected. The reason for this can be seen qualitatively from the following crude arguments. For rotational vibrations $(\partial\mu/\partial Q)^2$ is of the magnitude μ^2/mr^2 where μ is the dipole moment, m the mass of an atom, and r an intramolecular distance. Since μ is of the magnitude er where e is the electronic charge, the intensity is proportional to a quantity like e^2/m. For the translational vibrations in which the activity is due to induction of a dipole in neighboring molecules,

$$[8] \qquad \left(\frac{\partial\mu}{\partial Q}\right)^2 = \frac{\alpha^2}{M}\left(\frac{\partial E}{\partial a}\right)^2$$

where α is the polarizability of a molecule, E is the electric field of the permanent dipole, a is a typical intermolecular distance, and M is a molecular weight. α is of the magnitude r^3 and $(\partial E/\partial a)^2$ is of the magnitude e^2r^2/Ma^8.

It follows that $(\partial\mu/\partial Q)^2$ is of the magnitude $e^2(r/a)^8/M$. The ratio of intensities of permanent and dipole-induced moments is therefore of the magnitude $(r/a)^8\ m/M$. Since r/a is the ratio of typical intra- and intermolecular distances, it is about 1/2, and m/M is 1/2 or less, so the ratio of intensities is of the magnitude $(1/2)^9$. The induced intensity is therefore of the magnitude of 0.002 of the intensity due to the rotation of the permanent dipole, and it can be neglected.

For tetrahydrofuran, one of the principal axes is, according to the pure rotational microwave absorption of the vapor (24), within experimental error coincident with the polar axis. Rotation about this axis will therefore not be observed in the infrared. If the polar axis is the z axis, it follows that the total integrated absorption A is

$$[9] \qquad A = \frac{(n^2 + 2)^2}{9n}\frac{N\pi}{3c^2}\mu^2\left(\frac{1}{I_x} + \frac{1}{I_y}\right)$$

independent of the actual form of the normal vibrations, if n can be taken as independent of wave number. The limiting low- and high-frequency refractive indexes of the clathrate on either side of the absorption band differ by 0.105 (see below). Since the limiting low- and high-frequency refractive indexes are about 1.76 and 1.87, the limiting low- and high-frequency values of $(n^2 + 2)^2/9n$ are 1.795 and 1.64, and to a sufficient accuracy the actual values can be replaced by the mean.

Since the water molecules in the clathrates are orientationally disordered, there are no selection rules governing their infrared activity, and the water molecules in the clathrate should absorb in a manner similar to that of ice I (28). Un-

Can. J. Chem. Downloaded from www.nrcresearchpress.com by 210.87.254.6 on 09/05/12
For personal use only.

fortunately, the absorption in the sulfur hexafluoride clathrate is obscured by scattering. However, the absorption is relatively small and can be allowed for accurately enough as follows.

The absorption of ice in this region is due to the acoustic vibrations, and if the correlation of the orientations of the molecules is neglected, the absorption is predicted to follow the formula (28)

$$[10] \quad K(\nu) = 3\pi^2(\varepsilon_0 - \varepsilon_\infty)\{(\varepsilon_0 + 2)/(\varepsilon_\infty + 2)\} \times \varepsilon_0^{-1/2}\nu_D^{-3}\nu^4$$

where ε_0 and ε_∞ are the limiting low- and high-frequency permittivities of the translational band and ν_D is the Debye frequency expressed in wave numbers. This formula is not well obeyed by ice Ih for two main reasons. The first is that inadequate account was taken of the effect of the local correlation of the molecular orientations (29), leading to an error of a factor of about 5 in the absorptivity (30), and the Debye distribution of frequencies, which was assumed in deriving eq. 10, is not exactly obeyed, and this causes an absorptivity at the higher frequencies that is not exactly proportional to the fourth power of the frequency. The formula has not, therefore, been used directly, but has been used to scale the absorptivity of ice to that of the clathrate by adjusting ε_0 and ε_∞ using the Clausius–Mossotti relation and the densities of ice and the empty clathrate, and adjusting the Debye frequency according to the relation

$$\nu_D \propto \rho v^3$$

where ρ is the density and v the speed of sound, and

$$v \propto \rho^{-1/2}$$

According to this treatment, using 0.809 g cm^{-3} for the density of the empty clathrate from the unit cell parameters (14), the absorptivity of the empty clathrate is 0.76 of that of ice I. The absorptivity so obtained using absorptivities of ice I reported by Whalley and Labbé (28) and some unpublished values of Klug's, is plotted in Fig. 1 as curve I.

The difference between the absorptivity due to ice and the total absorptivity is that due to the tetrahydrofuran, and this is plotted in Fig. 2 for the 17-K spectrum. The absorption below 7 cm^{-1} was obtained by extrapolating a graph of log K *vs* log ν and is shown as a broken line

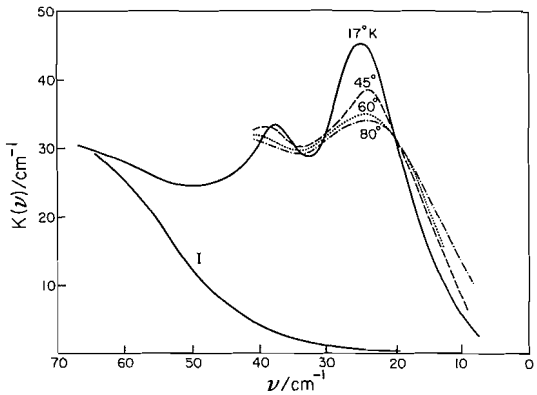

FIG. 1. Absorptivity of tetrahydrofuran clathrate hydrate at several temperatures. The curve labelled I is the presumed absorptivity due to the translational lattice vibrations of the ice framework as calculated in Section 1 of Results section.

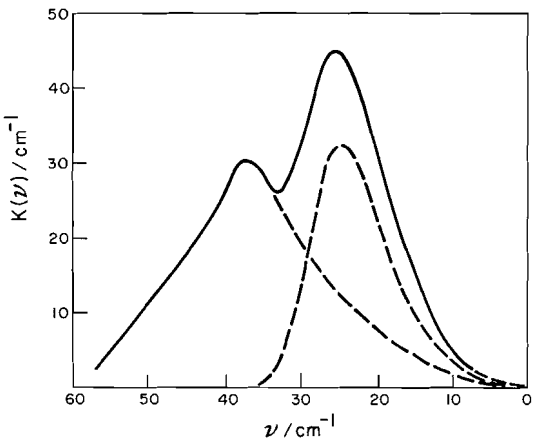

FIG. 2. Absorptivity due to the tetrahydrofuran in tetrahydrofuran clathrate hydrate at 17 K, obtained from the 17-K spectrum in Fig. 1 and the presumed absorptivity of the ice framework. The broken line indicates the resolution into the bands illustrated in Figs. 4 and 5.

in Fig. 2. The integrated absorptivity of the 17-K spectrum obtained using the trapezoidal rule is 420 $\pm$ ~40 cm mmol^{-1}. About half the quoted uncertainty is due to the uncertainty of the absorptivity of the empty clathrate and was obtained by assuming that the adsorptivity of the empty clathrate could be the arithmetic mean of the absorptivity as calculated above and the actual absorptivity of ice I. The other half of the quoted uncertainty is due to the uncertainty in the sample thickness and the reflection losses, and the reproducibility of the spectrometer.

The effective dipole moment μ_{eff} calculated from eq. 9 and the integrated absorptivity, as-

Can. J. Chem. Downloaded from www.nrcresearchpress.com by 210.87.254.6 on 09/05/12
For personal use only.

suming that

$$I_x = 209.2 \times 10^{-40} \text{ g cm}^2$$

$$I_y = 118.1 \times 10^{-40} \text{ g cm}^2 \quad (24)$$

where the x axis is perpendicular to the "plane" of the ring, and the y axis is in the "plane",

$$N = 1.62 \times 10^{21} \text{ cm}^{-3} \quad (14)$$

$$n = 1.82 \quad (15)$$

is

$$\mu_{\text{eff}} = 1.63 \pm \sim 0.08 \text{ D}$$

In the gas phase, the tetrahydrofuran molecule undergoes pseudorotation, and its dipole moment depends strongly on its pseudorotation quantum number. In the zero level it is 1.75 D, and in the second and third levels it falls to the value 1.52 D (24). The pseudorotation is either quenched or greatly damped in the clathrate (see Section 6 of Results), and so the appropriate gas-phase dipole moment to compare with the measured transition moment is not obvious. Dipole moments measured in solution range from 1.63 to 1.84 D (31), and it is not clear which is the most appropriate. The agreement, nevertheless, between the effective and directly measured moments is reasonably close.

(2) Contribution to the Low-frequency Refractive Index

The contribution Δn to the low-frequency refractive index due to these bands is given by the Kramers–Kronig relation

$$[11] \qquad \Delta n = (2\pi)^{-2} \int_{\text{band}} K\nu^{-2} \, d\nu$$

The integral for the spectrum of Fig. 2, which is corrected for ice absorption, was evaluated using the trapezoidal rule, and yielded

$$\Delta n = 0.105 \pm \sim 0.007$$

where the error is an estimated standard error from the uncertainty of the ice absorption as described in Section 1 (contribution ± 0.002) and the remaining causes of the uncertainty of the absorptivity (contribution $\pm \sim 0.006$). The value agrees much better than expected with the 0.11 ± 0.05 from dielectric measurements (15).

(3) Detailed Analysis of the Band

The spectrum appears to consist of two broad bands centered at about 25 and 38 cm^{-1} having a ratio of frequencies of 1.52. They are presumably due to the oscillation of the tetrahydrofuran molecules about two axes perpendicular to the polar axis. If the oscillations were about the principal axes with equal force constants, the ratio of frequencies, which is 1.52, would be equal to the square root of the inverse ratio of the principal moments of inertia, which is 1.33. As was argued at the beginning of this section the oscillations in the average cage are about principal axes, and since the most probable cage is the average one, the ratio of frequencies must depart from the expected value due to the unequal force constants for rotation about the two active axes. The axis perpendicular to the plane will be labelled x and that in the plane will be labelled y. The effect of the moments of inertia is to make the oscillations about the axis of higher moment (x) have the lower frequency and lower integrated area. It appears from Fig. 2 that this could be true only if the high-frequency band is much broader than the low-frequency band. It will be shown later that this is probably so. If this conclusion is accepted, then the force constants for rotation about the x and y axes are 465 and 606 ferg rad^{-2} from the peak frequencies. A more detailed analysis of the bands as described below changes these force constants slightly.

The source of the potential energy restricting rotation can be investigated by means of these frequencies. The barrier arises of course from the interaction of the tetrahydrofuran with the water molecules in the cage. The main sources of the interaction are the dispersion, repulsive, and electrostatic forces.

The electrostatic forces can be shown to be unimportant as follows. If an electric field E making an angle θ to the equilibrium dipole direction of the tetrahydrofuran molecule is present, it contributes a term $\mu E \cos\theta$ to the force constant. According to Davidson (32), the average dipolar field in a large cage in the structure II hydrate is about 15 kesV cm^{-1}. If θ is zero, this contributes a term 24 ferg rad^{-2} which is $<5\%$ of the force constants, and contributes only about $2\frac{1}{2}\%$ to the frequency. Even a field that is several times larger than the average field would contribute a force constant much smaller than that observed. It follows that the main barrier to reorientation is not the electrostatic field of the water molecules. It must be due therefore to their repulsive and van der Waals attractive forces.

Since the molecule is in a tetrahedral (symmetry of the average cage T_d) cage and has, at

Can. J. Chem. Downloaded from www.nrcresearchpress.com by 210.87.254.6 on 09/05/12
For personal use only.

least approximately, C_{2v} symmetry, it is in a stationary potential with respect to small rotational displacements about axes perpendicular to the polar axis when it is aligned either way along the four 3-fold or the three 2-fold axes. There are therefore at least 14 orientations of the polar axis at which the potential energy of the molecule is in a minimum with respect to rotations of the polar axis. Since tetrahydrofuran has at most a 2-fold axis, when the tetrahydrofuran molecule is aligned along a 3-fold (C_{3v}) axis there are at least 3 orientations about the polar axis at which the potential energy is a minimum. Likewise, when it is aligned along a 2-fold axis of the tetrahedron, there must be at least 2 orientations at which the potential energy is a minimum. In addition, the molecule has a pentagonal ring, and there are at least 5 possible orientations of this ring about the axis perpendicular to it. It is clear that an accurate analysis of the potential minima of tetrahydrofuran in the cage would be a formidable task, and cannot be attempted with the data we have.

Something about the periodicity of the potential function of the polar axis can, however, be learned from a simple model. The tetrahydrofuran molecule is replaced by an axially symmetric molecule which imitates it in an appropriate way, and considered to be in a potential of the form

$$V = V_0(1-\cos n\theta) \qquad [12]$$

where n is the periodicity of the potential. Small oscillations in this potential have a frequency ν in wave numbers given by

$$\nu = (n/2\pi c)(V_0/I)^{1/2} \qquad [13]$$

where I is the appropriate moment of inertia. When the geometric mean frequency and moment of inertia are inserted into eq. 13, the value

$$n^2V_0 = 7.7 \text{ kcal mol}^{-1} \qquad [14]$$

is obtained.

The temperature dependence of the dielectric relaxation time suggests that a suitably weighted average barrier height $2V_0$ is 0.92 kcal mol^{-1} (15). From this value and eq. 14

$$n = 4.1$$

This suggests that the potential energy is a minimum when the polar axis coincides with the crystallographic trigonal axes. The dipole moment then points into the center of a hexagonal ring (or alternatively in the opposite direction).

(4) Breadth of the Bands

The bands are very broad even at 17 K. To determine if they appear to be approaching zero width at 0 K, the absorptivity at several frequencies at the lower end of the bands is plotted against temperature in Fig. 3. It is clear that unless a major change occurs below 17 K, the bands are very broad at 0 K. The breadth is therefore due largely to a variation in the force constant from cage to cage.

This variation can arise from several factors as follows:

(*i*) The tetrahydrofuran molecule occupies a number of nonequivalent minima in the cage.

(*ii*) The van der Waals, repulsive, and other nonelectrostatic forces vary from cage to cage because of the orientational disorder of the water molecules.

(*iii*) The electrostatic field in the cages varies from cage to cage because of the disorder of the water molecules.

(*iv*) The coupling between neighboring tetrahydrofuran molecules produces a band of vibrations, each member of which will be active because of the disorder.

(*v*) Anharmonicity.

The contributions *ii–iv* cause an essentially temperature-independent width, while the first and last cause a temperature-dependent width. The intermolecular coupling and electrostatic contribution can be immediately eliminated as the discussion in Sections 1 and 3 shows them to

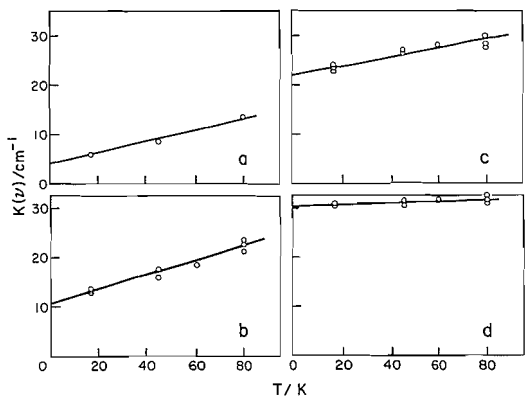

FIG. 3. Absorptivity at several temperatures at several frequencies in the low-frequency part of the band. The frequencies of the four plots are *a*, 10 cm^{-1}; *b*, 14 cm^{-1}; *c*, 18 cm^{-1}; *d*, 20 cm^{-1}.

Can. J. Chem. Downloaded from www.nrcresearchpress.com by 210.87.254.6 on 09/05/12
For personal use only.

be too small unless the fields are much bigger than those Davidson calculated.

The tetrahydrofuran molecule almost certainly occupies several minima and if some of them do not become unoccupied until well below 17 K, the breadth can be understood. There is, however, no independent evidence of this effect.

Little is known about the effect of orientations on the van der Waals and repulsive forces of a water molecule with other molecules. The van der Waals forces depend upon the polarizabilities of the molecules in a simple model, and since the polarizability of a water molecule is almost independent of orientation (33, 34), the van der Waals forces should be nearly independent of the orientation. On the other hand, the hydrogen atoms in the wall of the cage which encloses a tetrahydrofuran molecule, which take part in hydrogen bonds O—H---O, can be attached to either oxygen atom subject only to the requirements of the ice rules. The hydrogen atoms therefore occupy one of two positions about 0.7 Å apart. The repulsive potential due to the interactions of these hydrogen atoms with the hydrogen atoms of tetrahydrofuran, which is likely to be approximately of the form $Ae^{-\rho r}$, where A and ρ are constants and r the hydrogen–hydrogen distance, will depend on the hydrogen atom positions, and it seems likely that the width of the band is dominated by this effect. The anharmonicity of the potential of tetrahydrofuran as a function of orientation and of the interaction of the tetrahydrofuran with the water molecules cannot explain the temperature-independent width at 0 K.

It seems clear that the main source of the breadth of the bands is the distribution of the repulsive forces, although other forces may contribute. If this is true, then information about the distribution of potential constants can be obtained from the spectrum.

Let us assume that each oscillator has its characteristic force constant k and effective moment of inertia I, so that its wave number is given by

$$\nu^2 = k/4\pi^2c^2I$$

If each oscillator has the same integrated absorption intensity, as it should since the same dipole moment is oscillating in all vibrations, then a plot of K against ν^2, as given in Fig. 4 which is derived directly from Fig. 2, is a plot of the distribution $g(k/4\pi^2c^2I)$ of the values of

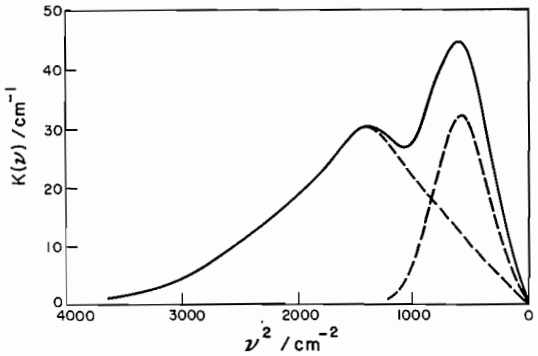

FIG. 4. Absorptivity of tetrahydrofuran in tetrahydrofuran clathrate hydrate, as shown in Fig. 2, replotted against the square of the wave number. The broken line shows the spectrum resolved into two bands assuming that they are related to one another by a multiplicative constant.

$k/4\pi^2c^2I$ against $k/4\pi^2c^2I$. If we further assume that the distribution of k/I in one of the bands that compose the spectrum is the same as the distribution of $\alpha k/I$ in the other, where α is a constant that allows for the differences in force constants and moments of inertia, then the two bands can be resolved as shown in Fig. 4. This resolution yields the superposed curves of $g(\alpha k/I)$ against $\alpha k/I$ for the two bands in Fig. 5, where $\alpha = 4\pi^2c^2$ for the 25 cm^{-1} band and $0.43 \times 4\pi^2c^2$ for the 38 cm^{-1} band. This

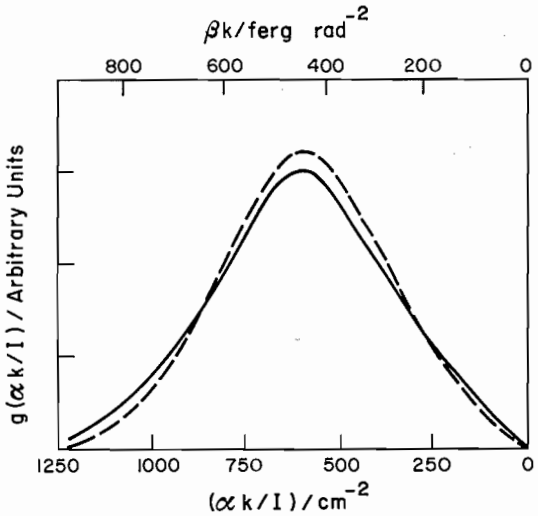

FIG. 5. The density of the quantity $\alpha k/I$ or βk for the two bands of Fig. 4. The scale of the abscissa at the bottom represents $\alpha k/I$ where α is $4\pi^2c^2$ for the 25 cm^{-1} band and $0.43 \times 4\pi^2c^2$ for the 39 cm^{-1} band. The scale of the abscissa at the top represents βk where β is 1 for the 25 cm^{-1} band and 1.34 for the 38 cm^{-1} band.

Can. J. Chem. Downloaded from www.nrcresearchpress.com by 210.87.254.6 on 09/05/12
For personal use only.

particular fit is, of course, not unique but is consistent with the assumption that $g(\alpha k/I)$ is the same for the two bands. The mean force constants for the high- and low-frequency bands respectively are 600 and 450 ferg rad^{-2} and the widths at half height are about 580 and 400 ferg rad^{-2}. The distribution of force constants is indicated by the upper abscissa of Fig. 5, where β is 1 for the 25 cm^{-1} band and 1.34 for the 38 cm^{-1} band.

This resolution of the two bands can be translated into a resolution of the two bands in the spectrum of $K(\nu)$ against ν, and the resolved bands are shown in Fig. 2. The ratio of areas of the two bands is 1.69, compared with the expected value of 1.77 if the oscillations occur about principal axes. Within the limitations of the (partly arbitrary) analysis therefore, the oscillations occur about principal axes.

The two bands can be assigned in the reverse order, when the ratio of force constants for rotation about the x and y axes would be about 4. The curve of Fig. 2 would then be resolved so that the low-frequency band had the higher area, and the distribution of force constants in the two bands would be less simply related. Although this assignment cannot be rigorously eliminated, it seems less probable.

(5) Effect of Temperature on the Breadth of the Bands

The bands broaden greatly as the temperature is increased. This could be due to

(*i*) limited life-time of the excited vibrational states due to transitions to lower states, and interaction with lattice vibrations,

(*ii*) limited life-time due to reorientation of the molecules,

(*iii*) increasing occupancy of the higher potential minima which would have different force constants.

The reorientation time at 88 K is ~11 ps (35), which corresponds to a half width of ~0.5 cm^{-1}, and so this reorientation does not contribute appreciably to the width even at 80 K. The relaxation does, however, contribute appreciably to the absorptivity at low frequencies. From the dielectric data at 88 K (35), the absorptivity at 5 cm^{-1} due to the relaxation would be about 3.5 cm^{-1} if the (important) effects of inertia were neglected. The actual absorptivity would be less than this, but nevertheless it contributes an important part of the observed absorptivity at low frequencies and 80 K.

Some of the broadening is undoubtedly due to the life-time of the states due to interaction with the lattice vibrations, and no doubt increasing occupancy of higher potential minima contributes also.

(6) Pseudorotation in the Clathrate

The tetrahydrofuran molecule undergoes pseudorotation in the gas phase, and the energy levels have been obtained from spectra taken at room temperature (36). At 17 K, the tetrahydrofuran molecules are mainly in the lowest few pseudorotational levels, and transitions below ~20 cm^{-1} might be observable in the clathrate if pseudorotation occurs. The number of tetrahydrofuran molecules per unit area of the sample is similar in the clathrate samples used in this work and the samples (36) used for the gas spectra. Unfortunately, there appears to be no way of reliably predicting the intensities. No features attributable to pseudorotation were observed in the clathrate spectra. It follows that either the pseudorotation is quenched or the bands are too weak to be observed, because either they are intrinsically weak or they are broadened by the interaction with the cage.

Summary

(*1*) The far-infrared spectrum of polycrystalline tetrahydrofuran clathrate hydrate contains two broad bands centered at 25 and 38 cm^{-1}, that are due to the rotational oscillations of the tetrahydrofuran molecule.

(*2*) The integrated absorptivity of the bands yields a value for the oscillating dipole moment of 1.63 $\pm$ 0.08 D, which is close to the gas-phase and solution values.

(*3*) The negative second moment of the band about zero frequency yields the contribution to the low-frequency refractive index of 0.105 $\pm$ ~0.007, which agrees with the less accurate value from the dielectric properties.

(*4*) The bands are due to rotations about the principal axes perpendicular to the polar axis, and yield force constants for rotation about the axes perpendicular to the plane of the ring and in the plane of 600 and 450 ferg rad^{-2}, respectively.

(*5*) The great breadths of the bands at low temperatures is due mainly to a variation of force constants from cage to cage. This occurs mainly because the orientational disorder of the water molecules results in a variation of the

hydrogen(water)–hydrogen(tetrahydrofuran) interaction.

(*6*) If the distribution of force constants for rotation about the two principal axes is assumed to be similar, an internally consistent resolution of the two bands can be obtained.

(*7*) The pseudorotation of tetrahydrofuran, which occurs in the isolated molecule, is either quenched in the clathrate hydrate due to the interaction with the cage wall or is too weak to be observed.

1. M. BORN and K. HUANG. Dynamical theory of crystal lattices. Oxford University Press, London. 1954.
2. H. B. FRIEDRICH. J. Chem. Phys. **47**, 4269 (1967).
3. H. B. FRIEDRICH. J. Chem. Phys. **52**, 3005 (1970).
4. S. IKAWA and S. MAEDA. Spectrochim. Acta, **24A**, 655 (1968).
5. J. E. BERTIE, H. J. LABBÉ, and E. WHALLEY. J. Chem. Phys. **50**, 4501 (1969).
6. R. E. CARLSON and H. B. FRIEDRICH. J. Chem. Phys. **54**, 2794 (1971).
7. P. F. KRAUSS and H. B. FRIEDRICH. J. Chem. Phys. **76**, 1140 (1972).
8. J. VAN KRANENDONK and G. KARL. Rev. Mod. Phys. **40**, 531 (1968).
9. K. G. BROWN and W. T. KING. J. Chem. Phys. **52**, 4433 (1970).
10. O. SCHNEPP. J. Chem. Phys. **46**, 3983 (1967).
11. R. V. ST. LOUIS and O. SCHNEPP. J. Chem. Phys. **50**, 5177 (1969).
12. E. WHALLEY. Can. J. Chem. **50**, 310 (1972).
13. P. T. T. WONG and E. WHALLEY. Can. J. Phys. **50**, 1856 (1972).
14. D. F. SARGENT and L. D. CALVERT. J. Phys. Chem. **70**, 2689 (1966).
15. D. W. DAVIDSON. Clathrate hydrates. *In* Water and crystalline hydrates. *Edited by* F. Franks. Plenum Press, New York. 1973.
16. S. J. ALLEN, JR. J. Chem. Phys. **44**, 394 (1966).
17. J. C. BURGIEL, H. MEYER, and P. L. RICHARDS. J. Chem. Phys. **43**, 4291 (1965).
18. P. R. DAVIES. Discuss. Faraday Soc. **48**, 181 (1969).
19. T. MATSUO, H. SUGA, and S. SEKI. J. Phys. Soc. Jap. **30**, 785 (1971).
20. J. E. BERTIE and D. A. OTHEN. Can. J. Chem. **50**, 3443 (1972).
21. S. R. GOUGH and D. W. DAVIDSON. Can. J. Chem. **49**, 2691 (1971).
22. M. VON STACKELBERG and W. JAHNS. Z. Electrochem. **58**, 163 (1954).
23. P. T. T. WONG, D. D. KLUG, and E. WHALLEY. J. Opt. Soc. Am. **62**, 533 (1972).
24. G. G. ENGERHOLM, A. C. LUNTZ, W. D. GWINN, and D. O. HARRIS. J. Chem. Phys. **50**, 2446 (1969).
25. T. C. W. MAK and R. K. MCMULLAN. J. Chem. Phys. **42**, 2732 (1965).
26. E. B. WILSON, J. C. DECIUS, and P. C. CROSS. Molecular vibrations. McGraw–Hill, New York. 1955.
27. R. G. GORDON. J. Chem. Phys. **38**, 1724 (1963).
28. E. WHALLEY and H. J. LABBÉ. J. Chem. Phys. **51**, 3120 (1969).
29. D. D. KLUG and E. WHALLEY. J. Chem. Phys. **56**, 553 (1972).
30. D. D. KLUG and E. WHALLEY. *In* Physics and chemistry of ice. *Edited by* E. Whalley, S. J. Jones, and L. W. Gold. Royal Society of Canada. 1973.
31. A. L. MCCLELLAN. Tables of experimental dipole moments. W. H. Freeman, San Francisco. 1963.
32. D. W. DAVIDSON. Can. J. Chem. **49**, 1224 (1971).
33. W. H. ORTTUNG and J. A. MEYERS. J. Phys. Chem. **67**, 1905 (1963).
34. P. T. T. WONG and E. WHALLEY. To be published.
35. M. DAVIES and K. WILLIAMS. Trans. Faraday Soc. **64**, 529 (1968).
36. J. A. GREENHOUSE and H. L. STRAUSS. J. Chem. Phys. **50**, 124 (1969).

Can. J. Chem. Downloaded from www.nrcresearchpress.com by 210.87.254.6 on 09/05/12
For personal use only.

An Electron Spin Resonance Study of the Reaction of Nitrogen Dioxide with Metal Acetylacetonates

WILLIAM H. WOLODARSKY, JOSHUA FANIRAN,[1] AND JEFFREY K. S. WAN
Department of Chemistry, Queen's University, Kingston, Ontario

Received June 18, 1973

The reaction of nitrogen dioxide with several metal acetylacetonates was studied by electron spin resonance. Those metal complexes that have stable lower oxidation state (*i.e.* Cu(II), Fe(III), Co(III), and VO(II)) react to form iminoxy radicals, while those metals not readily reduced (*i.e.* Zn(II), Cr(III), and Ce(III)) do not give iminoxy radicals. On the basis of the e.s.r. results, a simple mechanism was proposed to account for the formation of iminoxyacetylacetone radicals. A low temperature study of the e.s.r. spectra of the iminoxy-Cu(II)hexafluoroacetylacetonate suggested that a π-complex is formed between the organic radical and the Cu(II) compound.

La réaction du bioxyde d'azote avec plusieurs acétylacétonates de métaux a été étudiée à l'aide de la résonnance de spin électronique. Les complexes métalliques qui possèdent les plus bas états d'oxydation stables (*i.e.* Cu(II), Fe(III), Co(III) et VO(II)) réagissent pour former des radicaux iminoxy alors que les métaux qui ne sont pas facilement réduits (*i.e.* Zn(II), Cr(III) et Ce(III)) ne donnent pas ces radicaux iminoxy. En se basant sur les résultats r.s.e., on propose un mécanisme simple tenant compte de la formation des radicaux iminoxyacétylacétone. Une étude des spectres r.s.e. à basse température de l'iminoxy-Cu(II) hexafluoroacétylacétonate a suggéré qu'un complexe-π se forme entre le radical organique et le composé du Cu(II). [Traduit par le journal]

Can. J. Chem., **51**, 4072 (1973)

Introduction

Metal acetylacetonates are complexes with a partially covalent metal–oxygen bond (1). As such their reactions are often described as analogous to aromatic systems; the central hydrogen atom of the chelate ring can be replaced by a variety of groups under apparently electrophilic conditions (2). The reaction of nitrogen dioxide or its dimer with metal acetylacetonates has been studied with a view toward isolating and identifying products (3). Thus, in an excess of nitrogen dioxide, the acetylacetonates of Cu(II), Ni(II), Pt(II), and Al(III) yield the corresponding 3-nitro derivatives. Although it has been established (4) that the reaction of nitrogen dioxide with the acetylacetone ligands alone leads to the formation of stable iminoxy radicals such as

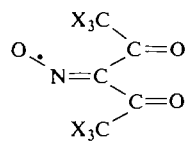

few e.s.r. studies had been reported on the system with metal acetylacetonates. In addition, there is a possibility that the organic iminoxy radical may form a molecular complex with the metal acetylacetonates. For example, the Cu(II)-hexafluoroacetylacetonate has recently been the subject of some interest, concerning its electron-acceptor properties. Zelonka and Baird (5) have reported the preparation of the molecular complex between Cu(II)hexafluoroacetylacetonate and di-*tert*-butyl nitroxide radical. The structure of the complex, however, was not studied in detail by e.s.r. spectroscopy.

In this paper we wish to report an e.s.r. investigation of the reaction of nitrogen dioxide with several metal acetylacetonates at room temperature. A detailed e.s.r. analysis of the low temperature spectra obtained in the Cu(II)hexafluoroacetylacetonate system reveals the molecular association in the form of a π-bonding between the organic iminoxy radical and the Cu(II) complex.

Experimental

Electron spin resonance spectra were recorded with an X-band Varian V4502 spectrometer using 100 kHz modulation and auxiliary equipment. The g values were measured relative to DPPH ($g = 2.0036$) as the standard.

Nitrogen dioxide (Matheson) was purified by bubbling oxygen through the liquid at 0 °C. This was repeated until the frozen nitrogen dioxide was pure white. Phosphorus pentoxide was added as a drying agent and the sample was refrigerated at −10 °C in a darkened vessel.

[1]Permanent address: Department of Chemistry, University of Ibadan, Nigeria.

Can. J. Chem. Downloaded from www.nrcresearchpress.com by 210.87.254.6 on 09/05/12
For personal use only.

TABLE 1. Electron spin resonance parameters of iminoxy radicals formed from the reaction of nitrogen dioxide with metal acetylacetonates in chloroform

Metal complex	A_N (G)	$A_X^{(CX_3)}$ (G)	Metal splitting (G)	g value	Line width (G)
$Cu(acac)_2$	27.5 ± 0.1*		$A_{Cu} = 78 \pm 2$	2.0044 ± 0.0002*	2.0
$Cu(trifluoroacac)_2$	27.5	5.0(F)	$A_{Cu} = 70 \pm 2$	2.0039	2.0
$Cu(hexafluoroacac)_2$	30.0	5.3(F)	$A_{Cu} = 52 \pm 2$	2.0038	0.7
$VO(acac)_2$	27.5	—	$A_V = 105 \pm 5$	—	2.0
$Co(acac)_3$	27.5	0.4(H)	—	2.0044	0.05
$Fe(acac)_3$	27.5	—	—	—	2.0

*The errors reported here are the standard deviation among separate measurements. The overall accuracy of these values is limited by the accuracy of the field-dial in the spectrometer.

All solvents used were purified by conventional methods. Oximinoacetylacetone was prepared by the method of Wolff and co-workers (6), and recrystallized twice from cyclohexane and identified by i.r. All metal acetylacetonates were supplied by PCR, Inc. or by Alpha Inorganic, and were used after recrystallization purification. Bis-(3-nitroacetylacetonate)Cu(II) was prepared by the method of Djordjeric and co-workers (3).

Solutions of metal acetylacetonates were normally prepared at a concentration less than 0.01 M. In a typical experiment nitrogen dioxide in the amount of about 8×10^{-7} mol was distilled into a previously degassed solution contained in a 3 mm tubing. The sample tube was then sealed off under a vacuum of 10^{-5} Torr for e.s.r. study. Low temperature studies at 77 °K were carried out to obtain further information from the anisotropy of the g and hyperfine coupling values.

Results and Discussion

The reaction of nitrogen dioxide at room temperature with Cu(II), VO(II), Fe(III), and Co(III) acetylacetonates yielded organic radicals whose hyperfine splittings and g values are consistent with the iminoxy acetylacetone radical (4). The e.s.r. parameters of these observed radicals are given in Table 1.

The cupric and vanadium complexes are paramagnetic and therefore their e.s.r. spectra are superimposed on the organic free radical spectra. Ferric complexes, although paramagnetic, have very broad lines at room temperature and thus the spectrum of the ferric complex could not be observed. One interesting feature of the iminoxy radical spectra derived from the metal complexes is that the hyperfine splitting of the methyl protons is not observed due to line-broadening. This effect may arise from the interaction of the metal with the organic radical since addition of Cu(II) complex to the iminoxy radical derived alone from the ligand causes the immediate disappearance of the proton splittings with simultaneous broadening of the ^{14}N lines. The nature of this interaction will be shown later as due to molecular association in the form of a π-complex.

An oxidation-reduction mechanism was proposed to account for the formation of the iminoxy radicals

$$[1] \quad M(acac)_n + (NO_2)_2 \rightarrow M(acac)_{n-1} + NO(acac) + \dot{N}O_3$$

The reactive species could be $NO^+NO_3^-$ with NO^+ attacking the central carbon atom. In each case the nitroso derivative (NO(acac)) rearranges to the oxime which is then further oxidized to the iminoxy radical by nitrogen dioxide. Evidence for the metal reduction in reaction 1 was provided by the fact that those metal complexes (Cu(II), Fe(III), Co(III), and VO(II)) having stable lower oxidation states react to give the iminoxy radicals, while those metal complexes, such as Zn(II), Cr(III), and Ce(III), which are not readily reduced do not lead to iminoxy radical formation.

That substitution occurring at the central hydrogen atom of the chelate ring is proved by the fact that Cu(3-nitroacac)$_2$ does not yield an iminoxy radical. Evidence has also been presented (4) that the precursor of these iminoxy radicals is probably the corresponding oxime formed by rearrangements of the intermediate nitroso compounds. For example, experiments have been carried out to show that oxidation of oximinoacetylacetone by nitrogen dioxide gives the iminoxy acetylacetone radical. Wolodarsky and Wan (7) have demonstrated that iminoxy radicals derived from tri- or hexafluoroacetylacetone may have two conformations depending upon the solvent. However, in the present metal complex systems, the conformers are not observed as the lines are broadened beyond resolution of the isomer fine structures.

Further experiments were carried out to investigate the possibility of molecular association

Can. J. Chem. Downloaded from www.nrcresearchpress.com by 210.87.254.6 on 09/05/12
For personal use only.

Can. J. Chem. Downloaded from www.nrcresearchpress.com by 210.87.254.6 on 09/05/12
For personal use only.

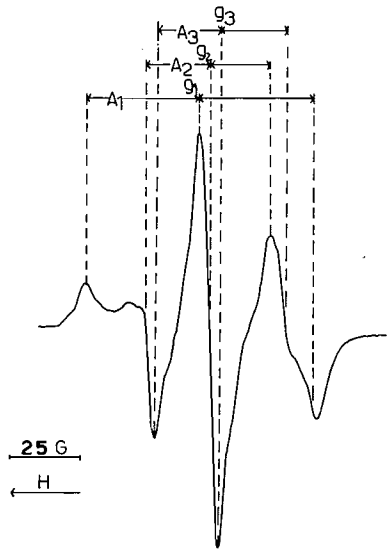

FIG. 1. The low temperature (77 °K) e.s.r. spectrum of the iminoxyacetylacetone radical in chloroform.

between the metal complexes and the organic iminoxy radicals. The low temperature (77 °K) spectrum of the iminoxy radical in the absence of metal complexes is presented in Fig. 1. The analysis of this powder spectrum gives the following results: $g_1 = 2.0023 \pm 0.0002$, $g_2 = 2.0043$, $g_3 = 2.0063$, $a_1 = 39.1 \pm 0.08$ G; $a_2 = 21.9$ G; $a_3 = 21.9$ G. Taking the $a_{iso} = 27.6$ G from the room temperature isotropic spectrum, it is apparent that $a_{\parallel} = 11.5$ G and $a_{\perp} = -5.7$ G. Fortunately the principle values of the hyperfine and g tensors of the iminoxy radical derived from γ irradiated single crystal of dimethylglyoxime have been analyzed in details by Miyagawa and Gordy (8). It is possible to relate the principle axes of the dimethylglyoxime radical to the powder spectrum of the iminoxyacetylacetone radical: $g_z = 2.0023 \pm 0.0002$, $g_y = 2.0043$, $g_x = 2.0063$, $a_z = 11.5 \pm 0.08$ G; $a_y = -5.7$ G; $a_x = -5.7$ G; where the x, y, z axes are defined similar to that in the dimethyl glyoxime radical (8) and for our purpose the z-axis is taken approximately 120° from the C=N and —N—O bonds, *i.e.* along a sp^2 lobe, and the x-axis is perpendicular to the molecular framework. Since the hyperfine tensor is axially symmetric with the maximum value along the z-axis, it appears that the electron density is concentrated in the sp^2 orbital of the nitrogen. Taking the average values of $B_0 = 18.4$ G and $A_0 = 595$ G for nitrogen (9), $c_{2p}{}^2 = 0.312$ and $c_{2s}{}^2 = 0.046$. The total spin density on the nitrogen is therefore equal to 0.358 in the uncomplexed iminoxyacetylacetone radical.

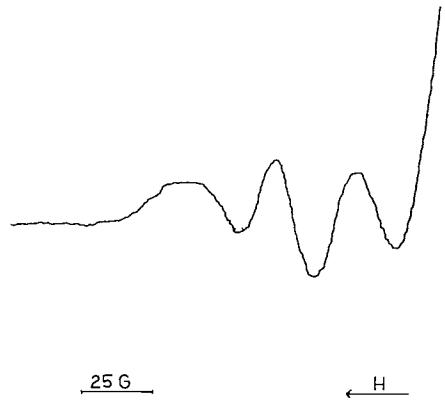

FIG. 2. The low temperature (77 °K) e.s.r. spectrum of the iminoxyacetylacetone radical in chloroform with the presence of Cu(II)hexafluoroacetylacetonate. The Cu(II) spectrum is not shown here.

The low temperature (77 °K) spectrum of the same iminoxyacetylacetone radicals in the presence of Cu(II)hexafluoroacetylacetonate is given in Fig. 2. Several other metal complexes were used but only the Cu(II)hexafluoroacetylacetonate afforded the least overlap between the metal lines and the nitrogen triplet splittings. It was established that the Cu(II) spectrum was not changed significantly in the presence or absence of the iminoxy radicals. However, in the presence of the Cu(II) complex, the iminoxy radical yielded the following spectral parameters: $g_z = 2.0015 \pm 0.0002$, $g_y = 2.0050$, $g_x = 2.0097$, $a_z = 9.8 \pm 0.08$ G; $a_y = -7.2$ G; $a_x = -2.7$ G. The hyperfine tensor is not axially symmetric but can be broken into two tensors

$$\begin{vmatrix} 9.8 & & \\ & -7.2 & \\ & & -2.7 \end{vmatrix} = \begin{vmatrix} 11.4 & & \\ & -5.7 & \\ & & -5.7 \end{vmatrix} + \begin{vmatrix} -1.6 & & \\ & -1.5 & \\ & & 3.0 \end{vmatrix}$$

one of which is symmetric about the z-axis and the other being symmetric about the x-axis. These can be taken as indicative of electron density in the sp^2 and p_x orbitals, respectively. Using the same average values of B_0 and A_0 (9), the iminoxy radical in the presence of the Cu(II) complex gives the following spin density on the nitrogen: $c_{2p_z}{}^2 = 0.310$, $c_{2p_x}{}^2 = 0.082$, and $c_{2s}{}^2 = 0.050$. In comparing these data with those

for the uncomplexed iminoxy radicals given above, it is apparent that the electron spin has penetrated the $2p_x$ orbital, which is perpendicular to the molecular framework, presumably as a result of some interaction with the Cu(II) complex. The same conclusions can be drawn when different solvent such as dichloromethane was used instead of chloroform.

It should be pointed out that the value of $c_{2p_z}{}^2$ is less certain since the z-component of the anisotropic tensor was determined from a section of the radical spectrum (Fig. 2) that overlapped to a small extent with the Cu(II) spectrum. The value for the $c_{2p_x}{}^2$, however, is more reliable since it was derived from A_x and A_y which were obtained from the section of spectrum where overlap was minimal.

On the basis of the e.s.r. results, the nature of the interaction between the organic iminoxy radical and the Cu(II) complex is most likely the formation of the π-complex:

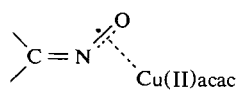

The increase in the value of g_z for the complexed iminoxy radical from 2.0063 to 2.0097 suggests that there is some degree of orbital mixing between the organic radical and the metal. It is not known at the present time why this π-bonding is preferred over the structure involving the mixing of the σ-orbital of the iminoxy radical with the $d_z{}^2$ orbital of the Cu(II).

The research is supported by the National Research Council of Canada.

1. H. R. GERSMANN and J. D. SWALEN. J. Chem. Phys. **36**, 3221 (1962).
2. J. P. COLLMAN. Angew. Chem. Int. Ed. **4**, 132 (1965).
3. C. DJORDJEVIC, J. LEWIS, and R. S. NYHOLM. J. Chem. Soc. 4778 (1962).
4. W. H. WOLODARSKY. Ph.D. Thesis. Queen's University, Kingston, Ontario. 1973; A. HUDSON. Aust. J. Chem. **19**, 1971 (1966).
5. R. ZELONKA and M. C. BAIRD. J. Am. Chem. Soc. **93**, 6066 (1971).
6. L. WOLFF, P. BOCK, G. LORENTZ, and P. TRAPPE. Ann. Chem. **129**, 325 (1902).
7. W. H. WOLODARSKY and J. K. S. WAN. Spectrosc. Lett. **6**, 429 (1973).
8. I. MIYAGAWA and W. GORDY. J. Chem. Phys. **30**, 1590 (1959).
9. P. B. AYSCOUGH. Electron spin resonance in chemistry. Methuen Co. 1967. p. 438.

Can. J. Chem. Downloaded from www.nrcresearchpress.com by 210.87.254.6 on 09/05/12
For personal use only.

Unusual Long-Range Spin–Spin Coupling in Norbornane-2,3-diones. Proton Magnetic Resonance Spectrum and X-Ray Structure Analysis of 6-*endo*-Bromo-1,5,5-trimethylnorbornane-2,3-dione

G. F. Hambly, Jeanette Leitch, Peter Yates, and S. C. Nyburg

Lash Miller Chemical Laboratories, University of Toronto, Toronto, Ontario M5S 1A1

Received June 29, 1973

Several norbornane-2,3-diones show in their proton magnetic resonance spectra an unusual long-range spin–spin coupling, $^4J_{46x} = 1.0$–1.5 Hz. An X-ray structure analysis of 6-*endo*-bromo-1,5,5-trimethylnorbornane-2,3-dione shows that the norbornane framework deviates only slightly from mirror symmetry. This makes it unlikely that the unusual coupling in the norbornane-2,3-diones is due to distortion of the norbornane framework and lends credence to the view that it is due to substituent effects.

Plusieurs norbornanedione-2,3 possèdent dans leur spectre r.m.n. du proton un couplage spin–spin à longue distance qui est inusité $^4J_{46x} = 1.0$–1.5 Hz. Une analyse par rayons-X de la structure de l'endo-bromo-6 triméthyl-1,5,5 norbornanedione-2,3 montre que le squelette du norbornane devie très peu de la symétrie par rapport à un miroir. Ce résultat implique qu'il est peu probable que le couplage inusité soit dû à une distortion du squelette du norbornane et amène à croire qu'il est dû à des effets de substituants.
[Traduit par le journal]

Can. J. Chem., **51**, 4076 (1973)

Three types of long-range proton couplings (^4J) have been generally recognized in the p.m.r. spectra of norbornane derivatives (**1**), *viz.* J_{14} (1.0–1.6 Hz), J_{2x6x} (1.0–1.8 Hz), and J_{2n7a} (1.7–4 Hz) (1). Each of these is associated with an approximately planar W geometry of the two

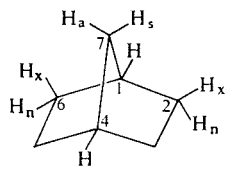

1

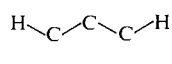

2

protons and a three carbon atom chain (**2**) (2). Theoretical arguments have been advanced to account for the occurrence of significant long-range proton coupling in systems with this geometry (1). Although long-range coupling has been observed in four-bond systems involving three sp^3 carbon atoms with other geometries, the coupling constants are usually appreciably smaller (≤ 0.5 Hz) (1, 3, 4).[1]

It is therefore of considerable interest that Gagnaire and Rassat and their co-workers (5, 6) have observed a fourth type of significant long-range coupling (J_{13x}) in the case of the two norbornane-2,3-diones **3** ($J_{46x} > 1$ Hz) and **4** ($J_{46x} = +1.1$ Hz),[2] where the four-bond systems corresponding with those referred to above might be expected to show gross deviation from the coplanar W geometry **2**. We ourselves (7) have made similar observations in the case of the norbornane-2,3-diones **5**–**9**, whose spectra all show significant coupling of the H_1–H_{3x} type (Table 1).

In considering the origin of this unusual long-range coupling, which has not been detected in the spectra of simple norbornanes or norborn-

TABLE 1. H_4–H_{6x} coupling constants for norbornane-2,3-diones and related compounds

Compound	Solvent	J_{46x}	Reference
3	C_6H_6/C_5H_5N	≥ 1	5
5	$CDCl_3$	1.1	This work
6	$CDCl_3$	1.0	This work
7	$CDCl_3$	1.2	This work
8	$CDCl_3$	1.25	This work
4	C_6D_6	1.2	6
9	$CDCl_3$	1.5	This work
11	$CDCl_3$	2.0	11
12	C_5H_5N	1.2 (J_{46x}) 2.2 (J_{42x})	12
13	C_6D_6	1.0	13

[1]We follow Sternhell (4) in arbitrarily attaching significance to coupling constants > 1 Hz because of our prime concern with the application of spin–spin coupling to structural problems.

[2]These and subsequent structural formulas do not imply designations of absolute configurations.

Can. J. Chem. Downloaded from www.nrcresearchpress.com by 210.87.254.5 on 09/05/12
For personal use only.

Can. J. Chem. Downloaded from www.nrcresearchpress.com by 210.87.254.5 on 09/05/12
For personal use only.

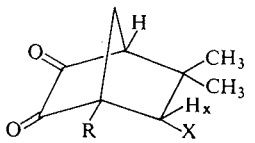

3 R = CH_3, X = $OCOC_6H_5$
5 R = H, X = $OCOCH_3$
6 R = H, X = OCH_3
7 R = CH_3, X = Cl
8 R = CH_3, X = Br

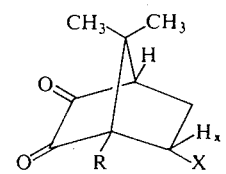

4 R = CH_3, X = $OCOC_6H_5$
9 R = H, X = Br
10 R = CH_3, X = H

anones, it occurred to us that it might arise because of appreciable skewing of the α-diketone groups as a result of dipole–dipole interaction (8).[3] Such skewing could result in a conformation in which H_4 and H_{6x} much more closely approach the planar W geometry **2** than they do in simple norbornanes and norbornanones, where distortion of the norbornane framework is expected to be small (10).

We were encouraged in this view by the circumstance that the spectra of the 2-diazo 3-ones (7) corresponding to the 2,3-diones **5**–**8** gave no evidence of analogous H_4–H_{6x} coupling, which could be attributable to replacement of a skewed α-diketone function by a planar α-diazo ketone function. Further, significant long-range coupling constants have been reported for analogous proton pairs in the more complex norbornane derivatives **11**–**13** (11–13) (Table 1), and it could be postulated that the additional ring in each of these compounds distorts the geometry in such fashion as to favor a closer than usual approach to the planar W arrangement for the coupled protons.[5]

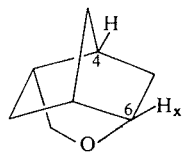

11

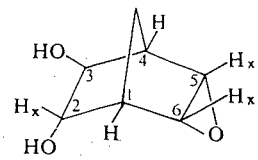

12

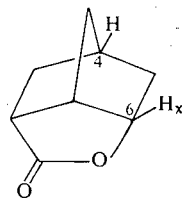

13

An X-ray crystallographic examination of compound **8** was therefore undertaken to determine whether evidence could be obtained for a skewed dicarbonyl system in the crystalline state. The structure and dimensions of **8** are shown in Figs. 1 and 2.

A quantitative estimate of the distortion of the norbornane framework can be obtained by checking this for mirror symmetry. An undistorted skeleton will have a mirror plane through C(7) and the mid-points of the bonds C(2)—C(3) and C(5)—C(6). This can be checked by a best molecular fit routine (14) in which the best fit is found between the molecule itself and its mirror image, the atoms matched being the mirror image of C(1) with the original C(4), etc. In this way we can place the molecules of reasonably accurately known structure containing the norbornane framework (but without additional distortion due to further bridging) in order of deviation from mirror symmetry.

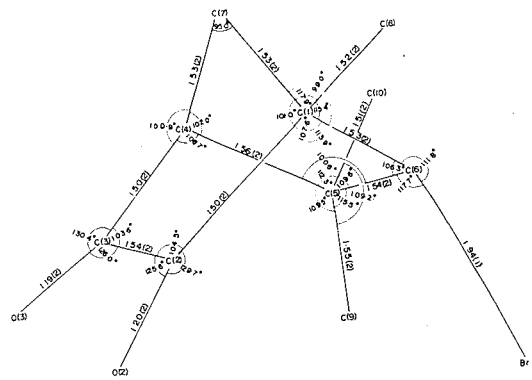

FIG. 1. Dimensions of molecule.

[3]Such a skewing has been invoked to interpret the electronic spectrum and circular dichroism of camphorquinone (**10**) (9), whose crystal structure has recently been determined by Silverton and Bright (9*b*) (see footnote 4).

[4]We thank Dr. L. Tsai, U.S. National Institutes of Health, for informing us of these results before publication.

[5]It is recognized that additional factors would have to be involved in the case of **12**, since no significant J_{15x} was observed.

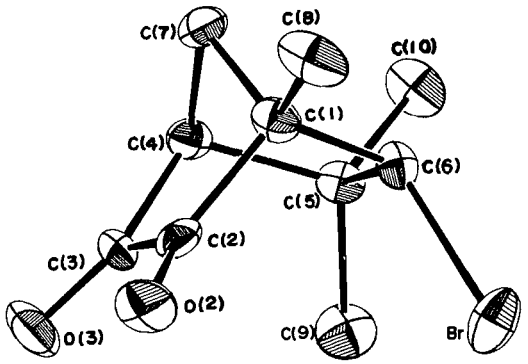

FIG. 2. ORTEP plot of molecule showing 15% probability ellipsoids.

The quantitative estimate we use is the sum of the squares of the distances between the atoms in their best fitting positions. Amongst known structures we find the most closely symmetric ($\sum d^2 = 0.0079$ Å^2) is the hydrobromide salt of

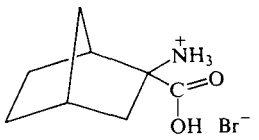

14

(−)-2-*exo*-aminonorbornane-2-carboxylic acid, **14** (15), and the most distorted ($\sum d^2 = 0.0703$ Å^2) is 3-*exo*-(*N*-benzyl-*N*-methylaminomethyl)-2-*endo*-norbornanol, **15** (16). Altona and Sundaralingam (10) also give the latter as the most distorted norbornane nucleus in a known structure.

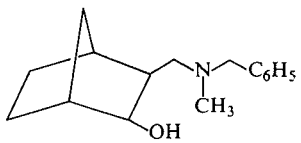

15

The present molecule lies between these extremes ($\sum d^2 = 0.0107$ Å^2) but clearly nearer the undistorted end of the range. Further evidence of lack of distortion is provided by the close planarity of that part of the molecule containing the α-diketo-group, namely C(1), C(2), C(3), C(4), O(2), and O(3). This system is closely coplanar, the maximum deviation from the plane being that of atom C(2), $d = 0.027$ Å. The only other structure analysis known to us of a molecule containing the α-diketo group is that of camphorquinone (**10**) (9*b*). In this molecule there is also remarkably little skewing of the α-diketo group. Thus in the present structure the dihedral angle C(2)C(3)C(4)/C(1)C(2)C(3) is 1.73° and in the two crystallographically independent molecules of camphorquinone it is 0.1° and 2.9°. The α-diketo groups in these molecules have therefore closely similar conformations.

Amongst molecules of norbornane type of known structure we find that the bond lengths at C(7) are inversely correlated with the C(1)—C(7)—C(4) bond angle and the present molecule fits in well with this trend. A similarly good fit is found for C(1)—C(2), C(3)—C(4), C(4)—C(5), and C(6)—C(1) lengths which are inversely correlated with the sum of the bond angles at C(1) and C(4).

A virtually undistorted molecule such as the present one has a three carbon atom chain (**2**) (C(4)—C(6)) in which the hydrogen atoms at C(4) and C(6) are not at all coplanar with the carbon atoms ($d = 0.96$ and 0.35 Å, respectively). Although it is possible that the molecule is more distorted in solution, the crystal structure makes it unlikely that there is a large angle of skew and suggests that this is not a major factor in the occurrence of the unusual long-range couplings in **3**–**9**. It is more probable that the major factor is a substituent effect (1), as previously suggested (5), arising from the presence of electronegative substituents at each of the carbon atoms bearing the coupled protons.[6] In each case one of these is the strongly electron-withdrawing α-dicarbonyl functions; the absence of significant H_4–H_{6x} coupling in the case of the 2-diazo 3-ones corresponding to the 2,3-diones **5**–**8** may be attributable to the reduced electronegativity of this substituent.

Experimental

Compound **5** was prepared by the method of Meinwald, Gassman, and Hurst (17). Compounds **6**–**9** were prepared and purified by standard methods (7, 18). For X-ray analysis of **8** the crystal data are:
Orthorhombic, $a = 11.40(1)$, $b = 11.58(2)$, $c = 8.39(1)$ Å, $V = 1073$ Å^3; space group $P2_12_12_1$, $\rho_o = 1.48$, $Z = 4$, $\rho_c = 1.51$ (20 °C; CuKα, $\lambda = 1.542$ Å).

Intensity data were collected in 2θ-scan mode by a Canberra-automated Picker diffractometer using filtered CuKα radiation. Out of 1055 measured intensities 754 were observed on the basis $I > \sqrt{2}\sigma(I)$ where $\sigma(I) =$

[6]It must be noted, however, that Barfield and Chakrabarti (1) have suggested on a tentative basis that introduction of electronegative substituents at the terminal carbon atoms of a planar W system (**2**) gives rise to a negative shift of the corresponding $^4J_{HH}$. Since it has been shown in the case of **4** that J_{46x} is positive (6), the present proposal requires a substituent effect in the opposite sense.

Can. J. Chem. Downloaded from www.nrcresearchpress.com by 210.87.254.5 on 09/05/12
For personal use only.

TABLE 2. Final positional and thermal atomic parameters × 10^4 (e.s.d.'s in parenthesis), temperature factor = exp $-(h^2\beta_{11} + k^2\beta_{22} + l^2\beta_{33} + 2hk\beta_{12} + 2hl\beta_{13} + 2kl\beta_{23})$

Atom	x	y	z	β_{11}	β_{22}	β_{33}	β_{12}	β_{13}	β_{23}
Br	6890(1)	5319(2)	6016(3)	93(11)	210(3)	310(4)	40(2)	−9(2)	16(3)
O(2)	4396(2)	4313(9)	8391(14)	224(16)	93(10)	271(24)	20(10)	45(17)	91(13)
O(3)	2704(10)	4229(9)	5704(19)	150(12)	93(9)	516(37)	−51(9)	−29(18)	2(17)
C(1)	4718(13)	6275(12)	7415(18)	134(16)	81(13)	159(24)	−3(12)	1(18)	23(16)
C(2)	4223(13)	5072(12)	7453(19)	115(14)	91(14)	180(26)	25(11)	65(17)	−12(17)
C(3)	3326(11)	5028(10)	6056(22)	95(12)	55(11)	357(36)	−13(9)	39(21)	11(20)
C(4)	3425(11)	6204(12)	5328(17)	81(11)	75(12)	209(25)	10(10)	−35(13)	−13(15)
C(5)	4676(12)	6306(12)	4483(12)	114(13)	82(12)	71(17)	−1(11)	−28(12)	−13(12)
C(6)	5526(10)	6380(10)	5933(16)	90(10)	95(12)	127(19)	−17(9)	−5(14)	−1(16)
C(7)	3614(13)	6950(12)	6817(17)	119(13)	84(13)	182(26)	29(11)	40(16)	13(16)
C(8)	5295(20)	6654(13)	8970(20)	331(31)	105(14)	123(21)	−40(18)	40(31)	16(18)
C(9)	4871(15)	5244(16)	3382(17)	171(18)	152(18)	169(25)	3(18)	−39(18)	−46(19)
C(10)	4782(15)	7399(14)	3505(15)	202(20)	127(16)	95(21)	−28(16)	−18(17)	25(16)

TABLE 3. Fractional atomic coordinates of hydrogen atoms (× 10^3) used in F_c

Atom	x	y	z
H(4)	266	644	461
H(6)	590	724	591
H(7)	286	694	764
H(7A)	380	785	653
H(8)	622	697	872
H(8A)	480	739	944
H(8B)	540	620	980
H(9)	493	448	413
H(9A)	572	536	279
H(9B)	440	500	260
H(10)	406	743	259
H(10A)	580	740	280
H(10B)	475	818	419

(peak + background)$^{1/2}$. No absorption corrections were made.

Phases were first assigned from the Br positions and subsequent analysis was uneventful. Full matrix anisotropic least squares refinement was carried out taking e.s.d.s in F_o as $\sigma(F) = ((\sigma(I)/(\mathrm{Lp}))^2 + 0.02F_o^4)^{1/2}/2F_o$ where Lp is the Lorentz polarization correction and using scattering factors of Cromer and Mann (19). After all non-hydrogen parameters had been refined four (non-methyl) hydrogen atoms were located on the final electron density difference map but those associated with the methyl groups were more diffuse. The positions chosen for these were those giving the highest electron density difference compatible with tetrahedral stereochemistry and a C—H bond length of 1.08 Å. These hydrogens were included in the final calculation of F_c giving them the same anisotropic temperature factors as the carbon atoms to which they were attached. The final residual for observed reflections was 0.072.[7]

Positional and thermal parameters are given in Tables 2 and 3 and a dimensioned molecule and an ORTEP plot in Figs. 1 and 2.

[7]Table of F_o and F_c values is available at a nominal charge from the Depository of Unpublished Data, National Science Library, National Research Council of Canada, Ottawa, Canada K1A 0S2.

We thank the National Research Council of Canada for support of this work.

1. M. BARFIELD and B. CHAKRABARTI. Chem. Rev. **69**, 757 (1969).
2. A. RASSAT, C. W. JEFFORD, J. M. LEHN, and B. WAEGELL. Tetrahedron Lett. 233 (1964).
3. L. M. JACKMAN and S. STERNHELL. Applications of nuclear magnetic spectroscopy in organic chemistry. 2nd ed. Pergamon Press, Oxford. 1968. p. 335.
4. S. STERNHELL. Q. Rev. **23**, 236 (1969).
5. G. CHALIER, A. RASSAT, and A. ROUSSEAU. Bull. Chem. Soc. Fr. 428 (1966).
6. G. CHALIER, D. GAGNAIRE, and A. RASSAT. Bull. Chem. Soc. Fr. 387 (1969).
7. G. F. HAMBLY. Ph.D. Thesis. University of Toronto, Toronto, Ontario. 1970.
8. N. J. LEONARD and P. M. MADER. J. Am. Chem. Soc. **72**, 5388 (1950).
9. (*a*) E. CHARNEY and L. TSAI. J. Am. Chem. Soc. **93**, 7123 (1971). (*b*) L. TSAI, E. CHARNEY, J. V. SILVERTON, and W. M. BRIGHT. To be published.
10. C. ALTONA and M. SUNDARALINGAM. J. Am. Chem. Soc. **92**, 1995 (1970).
11. P. J. KROPP and H. J. KRAUSS. J. Am. Chem. Soc. **91**, 7466 (1969).
12. J. PAASIVIRTA and P. ÄYRÄS. Suomen Kemi. B**41**, 281 (1970).
13. K. C. RAMEY, R. M. MORIARTY, H. GOPAL, and T. ADAMS. Org. Mag. Res. **1**, 101 (1969); *cf.* K. C. RAMEY, D. C. LINI, R. M. MORIARTY, H. GOPAL, and H. G. WELSH. J. Am. Chem. Soc. **89**, 2401 (1967).
14. S. C. NYBURG. To be published.
15. P. A. APGAR and M. L. LUDWIG. J. Am. Chem. Soc. **94**, 964 (1972).
16. A. V. FRATINI, K. BRITTS, and I. L. KARLE. J. Phys. Chem. **71**, 2482 (1967).
17. J. MEINWALD, P. G. GASSMAN, and J. J. HURST. J. Am. Chem. Soc. **84**, 3722 (1962).
18. P. YATES and G. F. HAMBLY. To be published.
19. D. T. CROMER and J. B. MANN. Acta Cryst. A**24**, 321 (1968).

Can. J. Chem. Downloaded from www.nrcresearchpress.com by 210.87.254.5 on 09/05/12
For personal use only.

Lanthanide Induced Shifts in the Proton Magnetic Resonance Spectra of Cyclic Amines

DONALD L. HOOPER AND ALZBETA KARDOS
Chemistry Department, Dalhousie University, Halifax, Nova Scotia

Received June 11, 1973

Complex formation between europium tris(dipivalatomethane), $Eu(DPM)_3$, and cyclic amines is not accompanied by inversion of the amine configuration, even for 2-alkyl and 2,6-dialkylpiperidines, where inversion of the amine configuration accompanies formation of the usual amine derivatives. There is, however, a steric effect of C-2 or C-6 substitution, in that the magnitude of the lanthanide induced shifts is sharply reduced.

Lors de la formation de complexes entre l'europium tris(dipivalatométhane), $Eu(DPM)_3$, et des amines cycliques, aucune inversion de la configuration de l'amine ne fut observée même dans le cas d'alcoyl-2 ou de dialcoyl-2,6 pipéridines où l'inversion de la configuration de l'amine accompagne la formation des dérivés usuels de l'amine. Cependant, un effet stérique provenant de la substitution en C-2 ou C-6, fut observé et se traduit par une légère réduction de l'ampleur des déplacements chimiques induits par la lanthanide. [Traduit par le journal]

Can. J. Chem., **51**, 4080 (1973)

Determination of the configuration of cyclic amines from analysis of p.m.r. spectra is often complicated by the small chemical shift differences between a number of closely coupled protons. The magnitude of these chemical shift differences can be increased in the spectra of *N*-acetyl and *N*-nitroso derivatives; however, unless the cyclic amine is symmetrically substituted, hindered rotation about the N—CO or N—NO bonds can lead to even more complex spectra. In the case of the simple 2-alkyl and 2,6-dialkylpiperidines, where the alkyl groups are known to be equatorial, formation of the *N*-acetyl derivative forces inversion of the configuration with the alkyl groups becoming axial (1). Similarly, formation of the *N*-carbothionic acid derivatives by reaction with carbon disulfide is accompanied by inversion of configuration (2).

The power of lanthanide "shift reagents" (3) in the simplification of complex spectra has been well established and the assignment of configuration to substituted piperidines should be straightforward. The magnitude of a lanthanide induced chemical shift (l.i.s.) is a function of both the distance to a particular proton from the lanthanide atom at the center of the complex and of the angle between the principal magnetic axis of the complex and a line drawn joining the lanthanide atom to the proton, with the result that for a cyclic system such as a cyclohexanol addition of a "shift reagent" separates the signals of axial and equatorial protons at a particular carbon as well as those of protons at different carbon atoms (4). There remains, however, the possibility of a steric effect when the complex is formed between a piperidine with bulky substituents close to the nitrogen atom and the already bulky lanthanide complex which acts as the "shift reagent". Steric effects on complex formation have been postulated for other substrates, *e.g.* to explain the much greater l.i.s. observed (5) for the *trans* conformation compared with the *cis* conformation of *O*-dimethyl and *O*-diisobutyl esters of methylthiocarbamic acid.

We have measured lanthanide induced shifts for 2% solutions in $CDCl_3$–TMS of the substituted piperidines listed in Table 1, with the molar ratio of europium tris(dipivalatomethane), $Eu(DPM)_3$, to amine varying from 0.00 to 0.30. The $Eu(DPM)_3$ was a single fresh sample stored over P_2O_5 in a desiccator before use. A steric effect is observed, but it is not inversion of the ring configuration. At low values of the ratio, $[Eu(DPM)_3]/[amine]$, the p.m.r. signals corresponding to the C-2 and C-6 protons are somewhat broadened and the chemical shift differences increased, however, the characteristic spin coupling constants are still observed, indicating that the configuration has not changed. With increasing relative concentration of $Eu(DPM)_3$ the broadening of signals obscures all the fine structure, nevertheless graphs of the magnitude of the lanthanide induced shift versus molar ratio $[Eu(DPM)_3]/[amine]$ are linear over the range studied. Thus inversion of configura-

Can. J. Chem. Downloaded from www.nrcresearchpress.com by 210.87.254.6 on 09/05/12
For personal use only.

TABLE 1. Slopes of graphs of lanthanide induced chemical shifts for some substituted piperidines *vs.* molar ratio of $Eu(DPM)_3$ to amine in $CDCl_3$–TMS solution

Compound	Slope (p.p.m.)			
	NH	C_6-H(eq)	C_6-H(ax)	CH_3
3-Methylpiperidine	55	18.0	17.0	5.0
2-Methylpiperidine	51	15.0	9.6	7.8
2-Ethylpiperidine	35	12.3	—*	2.5†
2-Propylpiperidine	36	11.5	—*	0.6†
2,6-Dimethylpiperidine	29.5	—	2.8	3.3

*Obscured by alkyl signals.
†Terminal CH_3 of the alkyl group.

tion has not occurred even at high $Eu(DPM)_3$ concentrations.

Table 1 lists the slopes of some of these l.i.s. *vs.* molar ratio graphs. As the slope of such a graph is the magnitude of the lanthanide induced shift which would be observed for a 1/1 molar ratio of "shift reagent" and substrate, a comparison of the slopes for corresponding protons in a series of similar molecules measures any steric effect on complex formation. The observed reduction in the l.i.s. with increasing substitution at C-2 and C-6 could mean either a change in the geometry of the complex, for example, an increase in the separation of the europium and nitrogen atoms bonded in the complex, or a reduction in the equilibrium constant for complex formation. Calculation of the geometry, using the McConnell equation is not likely to be meaningful, as the broadening observed for the signals of C-2 and C-6 protons quite probably is caused by a contact contribution to the l.i.s., as well as the pseudo-contact term for which the McConnell equation applies.

For the range of $Eu(DPM)_3$/amine concentrations used in this work, the p.m.r. signals of the other piperidine ring protons were to a large extent, complex multiplets, or were observed by alkyl signals. However, it would be expected that any effect reducing the value of the equilibrium constant for complex formation would reduce the observed l.i.s. for all protons in the substrate molecule.

The use of lanthanide induced shift measurements will lead to a proper assignment of the configuration of cyclic amines, but only if due consideration is paid to the number and size of substituents close to the nitrogen atom and their effect on the value of lanthanide induced shifts.

The authors acknowledge financial support by the National Research Council of Canada and thank Dr. T. P. Forrest for the gift of samples of the cyclic amines used in this work.

1. Y. L. CHOW, C. J. COLON and J. N. S. TOM. Can. J. Chem. **46**, 2821 (1968).
2. T. P. FORREST and S. RAY. Chem. Commun. 1537 (1970).
3. C. C. HINCKLEY. J. Am. Chem. Soc. **91**, 5160 (1969).
4. P. V. DEMARCO, T. K. ELZEY, R. B. LEWIS, and E. WENKERT. J. Am. Chem. Soc. **92**, 5734 (1970).
5. R. A. BAUMAN. Tetrahedron Lett. 419 (1971).

Can. J. Chem. Downloaded from www.nrcresearchpress.com by 210.87.254.6 on 09/05/12
For personal use only.

Organic Sulfur Mechanisms. 15. The Stereochemistry of α-Hydrogen Exchange in the Simple Cyclic Sulfoxide 1,3 Dihydrobenzo[*c*]thiophene 2-Oxide

JAMES FREDERICK KING AND JOHN RICHARD DU MANOIR

Department of Chemistry, University of Western Ontario, London, Ontario

Received July 25, 1973

In NaOD–D_2O at 5.0° the α-hydrogens *trans* to the oxygen in 1,3-dihydrobenzo[*c*]thiophene 2-oxide (**1**) exchange 67 times faster than the *cis*. The *cis* hydrogens in turn exchange slightly faster than the *faster* of the α-hydrogens of the methylene group in benzyl methyl sulfoxide. Treatment of **1** with methyllithium followed by rapid quenching with DCl leads to a predominantly *cis*-monodeuterated product. It is also shown that the hydrogen removal in the lithiation step involves loss of the *cis* hydrogen and that the lithiation of **1** is much faster than that of benzyl methyl sulfoxide. Comparison of these results with the Rauk–Wolfe–Csizmadia nonempirical calculations on α-sulfinyl carbanions indicates that current theoretical understanding is as yet incomplete.

Dans le NaOD–D_2O à 5.0°, les hydrogènes-α *trans* par rapport à l'oxygène dans l'oxyde-2 de dihydro-1,3 benzo[*c*]thiophène (**1**) s'échangent 67 fois plus rapidement que les hydrogènes *cis*. Les hydrogènes *cis*, à leur tour, s'échangent légèrement plus vite que le plus rapide des hydrogènes-α du groupe méthelène dans le sulfoxyde de benzyle et de méthyle. La réaction de **1** avec du méthyllithium arrêtée brusquement par du DCl à conduit majoritairement à un composé *cis* monodeutérié. On montre aussi que l'enlèvement d'un hydrogène lors de l'étape de lithiation implique la perte de l'hydrogène *cis*, et que la lithiation de **1** est beaucoup plus rapide que celle du sulfoxyde de benzyle et de méthyle. La comparaison de ces résultats avec les calculs non-empiriques de Rauk–Wolfe–Csizmadia sur les carbanions α-sulfinyles montre que l'interprétation théorique courante est encore à ce stade-ci incomplète.

[Traduit par le journal]

Can. J. Chem., **51**, 4082 (1973)

Asymmetric induction in reactions involving α-sulfinyl carbanions and related species has been much studied in recent years (1–18), though a truly predictive theoretical description of these reactions for practical use has not as yet been elaborated. In the hope of contributing to the development of such a rationale we describe our observations with 1,3-dihydrobenzo[*c*]thiophene 2-oxide (**1**), a simple cyclic sulfoxide in which the asymmetric induction derives entirely from one prochiral sulfur atom and in which a number of the steric features of these reactions can be seen very easily.

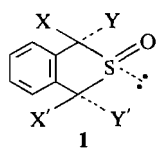

1

a X = Y = X′ = Y′ = H
b X = X′ = H; Y = Y′ = D
c X = X′ = D; Y = Y′ = H
d X (or X′) = D; Y = Y′ = X′ (or X) = H
e X (or X′) = H; Y = Y′ = X′ (or X) = D
f X = Y = X′ = Y′ = D

The n.m.r. spectrum of **1***a* in $CDCl_3$ shows an AB quartet, δ_A 4.13, δ_B 4.28 p.p.m., J = 16 Hz, due to the diastereotopic hydrogens of the mutually enantiotopic methylene groups. When **1***a* is treated with NaOD in D_2O, the quartet is first quickly replaced by a 1:1:1 triplet at δ 4.12 (J = 2.2 Hz) which after increasing in area to become close to half of that of the original AB quartet subsequently gradually disappears entirely; these results signify a rapid exchange of the lower field protons followed by much slower exchange of the epimeric hydrogens. The stereochemistry of the α-hydrogens is assigned by "shift reagent" experiments, which have been shown by recent studies (19) to provide an apparently reliable method for determining the configuration of hydrogens in cyclic sulfoxides. Addition of $Eu(dpm)_3$ to the solution of **1***a* gave a very strong downfield shift of the higher field signal and a smaller shift of the lower field component of the AB quartet. The higher field proton (which is the slower exchanging one in D_2O) is therefore *cis* (*syn*-periplanar (18)) to the oxygen[1]

[1]The geometry of **1** is not known precisely. A fully planar skeleton (in which the dihedral angle of the *cis* and *trans* hydrogens with the oxygen would be 0° and 120°, respectively) would have the least angle strain but eclipsing interactions along the C—S bonds could distort the system from full planarity, though not beyond the ±30° limits of the Klyne–Prelog descriptors.

Can. J. Chem. Downloaded from www.nrcresearchpress.com by 210.87.254.5 on 09/05/12
For personal use only.

TABLE 1. Hydrogen–deuterium exchange in the lithiation–acidification of sulfoxide **1**

Starting material			Isotopic composition of product (%)	Change in deuterium content (at. % excess deuterium)			Stereochemistry of exchange (from n.m.r.)
Major component	Isotopic composition (%)	Quenching acid*		From mass spectrum	From D analysis	From n.m.r.	
1*a*	d_0 100	DCl	d_0 14.7 d_1 71.7 d_2 12.8 d_3 0.2 d_4 0.5	12.5 increase	12.3 increase	13.7 increase	*cis* (88%) *trans* (12%)
1*b*	d_0 0 d_1 6.0 d_2 79.0 d_3 12.6 d_4 2.4	DCl	d_0 0 d_1 3.1 d_2 11.3 d_3 62.2 d_4 23.3	11.7 increase	10.6 increase	11.9 increase	*cis*†
1*c*	d_0 0 d_1 10.6 d_2 71.6 d_3 12.6 d_4 5.1	HCl	d_0 11.9 d_1 63.6 d_2 20.8 d_3 2.8 d_4 0.8	12.0 decrease	11.3 decrease	10.7 decrease	*cis*†
1*f*	d_0 0 d_1 0 d_2 0 d_3 5.3 d_4 94.6	HCl	d_0 0 d_1 0 d_2 17.9 d_3 77.0 d_4 5.1	12.7 decrease	13.4 decrease	13.9 decrease	*cis* (93%) *trans* (7%)

*The lithio derivatives of **1***a* and *b* were also quenched with HCl, and those of **1***c* and *f* with DCl. The product was in each case indistinguishable from starting material except with **1***c* (and DCl), which showed a slight increase (2.5% by n.m.r. 1.5% by deuterium analysis) in the amount of deuterium; the apparently exceptional behaviour of **1***c* probably arises from the presence of a significant proportion of *cis* hydrogens in the starting material (note particularly the relatively high proportion of d_1 sulfoxide).

†The n.m.r. spectra show the *cis* exchange to be much the more important, but do not appear to warrant a more quantitative interpretation.

and the low-field, more rapidly exchanged proton (in D_2O), *trans* (*anti*-clinal) to the oxygen. Quantitative n.m.r. studies gave the following pseudo-first-order rate constants for the exchange in 0.1 *M* NaOD in D_2O at 5°: $k'_{trans} = 2.2 \times 10^{-3}\ s^{-1}$, $k'_{cis} = 3.3 \times 10^{-5}\ s^{-1}$, $k'_{trans}/k'_{cis} = 67$. Under the same conditions with benzyl methyl sulfoxide, we found for the faster hydrogen of the methylene group $k' = 3.1 \times 10^{-5}\ s^{-1}$, slightly less than that of the slower hydrogens in **1***a*.

Durst and Fraser and their co-workers (7) have shown that the relative rates of exchange of the two diastereotopic methylene hydrogens in benzyl methyl sulfoxide are altered by changing base or solvent. We have obtained a similar result with **1**; with an equimolar amount of methyllithium in tetrahydrofuran at 0° followed by rapid quenching with DCl in D_2O, **1***a* gave principally the *cis*-monodeuterated sulfoxide **1***d*.

For the reactions with NaOD in D_2O, both the principle of microscopic reversibility and the fact that one may readily isolate a fairly pure sample (>70%) of **1***b* by simple exchange of **1***a*, require that the proton abstraction and deuteron addition proceed with the same stereochemistry, *i.e.* that a *trans* hydrogen be removed and the deuteron enter *trans* (to the oxygen). With the methyllithium reaction the disposition of the deuterium in the product gives information about the stereochemistry (preferentially *cis*) of the *quenching* step only; the experiments summarized in Table 1 show the proton *removal* step to be preferentially *cis* as well. For example, compound **1***b* (in which the deuterium atoms are *trans* to the oxygen) on lithiation followed by quenching with DCl gave chiefly the trideuterated product (**1***e*), thereby showing that the lithiation abstracted one of the protium atoms (which are *cis* to the oxygen). In addition, quenching of the lithio derivative of **1***b* with HCl gave back essentially unchanged **1***b*, as expected. That the above results did not derive from a deuterium isotope effect was shown by the corresponding experiments starting with **1***c*, which has the deuterium atoms *cis* to the oxygen. With **1***c* lithiation proceeds with abstraction of a deuteron as shown by trapping with (*i*) HCl to give principally the monodeuterated product

Can. J. Chem. Downloaded from www.nrcresearchpress.com by 210.87.254.5 on 09/05/12
For personal use only.

Can. J. Chem. Downloaded from www.nrcresearchpress.com by 210.87.254.5 on 09/05/12
For personal use only.

(**1***d*) and (*ii*) with DCl to give back **1***c*; it is evident that the preference for removal of a *cis* hydrogen is more than sufficient to outweigh completely any favouring of the *trans* hydrogens arising from a primary kinetic isotope effect.

The process of lithiation and quenching of **1** thus proceeds with overall retention of configuration at the α-carbon. Very recently Viau and Durst (16) have found similar retention of configuration in the exchange of the benzylic hydrogen of benzyl *t*-butyl sulfoxide by reaction with methyllithium followed by quenching with water. The analogous reaction of benzyl methyl sulfoxide, however, is not as clearcut. It has been reported that the reaction of butyllithium followed by water proceeds with overall inversion of configuration (17, 18) but the work of Viau and Durst (16) implies that retention is the major process; the reported stereoselectivities for the deprotonation step, however, are apparently not large (16, 17) even if there is disagreement as to their magnitude. It seems likely that the comparatively low stereoselectivity observed in the deprotonation of benzyl methyl sulfoxide derives from the high conformational mobility of that molecule (relative to **1** or benzyl *t*-butyl sulfoxide), which allows either of the diastereotopic hydrogens to become easily oriented in a conformation favorable for deprotonation.

Inspection of the data in Table 1 shows that in addition to the principal results discussed above, there are formed in these reactions significant amounts of multiexchanged products. The origin of these materials is not established but it seems likely that they arise at least in part from reaction of more than one molecule of alkyllithium. When 2 equiv. of methyllithium were used instead of 1.1 (as in the experiments in Table 1), **1***a* gave a product in which about 1.5 hydrogens per molecule were exchanged. It is also conceivable that some of the anomalous products could have arisen by base-catalyzed exchange in the aqueous medium during quenching but experiments using different rates of addition of acid or different stirring speeds during quenching gave no support for this notion.

With **1***b* and *c*, which contain both α-protium and α-deuterium atoms, there is a possibility of intermolecular hydrogen scrambling prior to quenching. When **1***a* was treated with methyllithium and then with **1***f* and the mixture allowed to stand for 10 min before quenching with HCl, the n.m.r. spectrum of the recovered sulfoxide showed CH_2 and CHD peaks of roughly equal intensity, indicating extensive exchange of the hydrogens. When the addition of **1***f* was followed by immediate quenching, however, the scrambling was almost completely suppressed; since the latter conditions more closely approximate those used to obtain the data in Table 1, it is unlikely that intermolecular hydrogen exchange prior to quenching is of any importance in those experiments. With **1***a* and *f*, of course, such exchange is impossible; it was found that the composition of the product was essentially the same with either a rapid quench or a 10 min wait before quenching but the recovered material in the former case was less discoloured and more readily obtained crystalline.

It has been noted above that the reaction of **1** in aqueous medium is faster than that of benzyl methyl sulfoxide. The cyclic sulfoxide (**1**) is also more reactive to methyllithium than benzyl methyl sulfoxide, as was shown by a competition experiment in which methyllithium, **1***a*, and benzyl methyl sulfoxide in the molar ratio 2:1:2 were mixed and quenched with DCl as before; the n.m.r. spectrum of the product showed that **1** was extensively exchanged whereas the benzyl methyl sulfoxide was apparently unaltered.

Rauk, Wolfe, and Csizmadia (4) have reported nonempirical calculations on the dependence on geometry of the energy of formation of an α-sulfinyl carbanion. Their calculations indicate that in the planar conformation of **1** the *anti*-clinal anion (which is close to the lower energy maximum) would be formed more readily than the *syn*-periplanar anion (which lies about halfway up the higher energy maximum). This corresponds to our observations in aqueous medium, but because the *syn*-periplanar species corresponds to a region of maximum slope, any prediction on this basis is highly suspect without precise knowledge of the geometry of the molecule. The results with methyllithium, of course, since they are opposite to those found with NaOD in D_2O cannot be similarly explained. It is perhaps conceivable that the conformation of **1** is altered from that in D_2O to give an "envelope" conformation with the oxygen quasi-axial; this could give dihedral angles appropriate (according to the m.o. calculations) to the faster exchange of the hydrogens *cis* to the oxygen, but this hypothetical alteration of conformation is not readily accounted for and certainly would not have been predicted.

Can. J. Chem. Downloaded from www.nrcresearchpress.com by 210.87.254.5 on 09/05/12
For personal use only.

Much more disquieting, however, is the fact that the m.o. calculations do not appear to be consistent with the comparatively slow rate of reaction of benzyl methyl sulfoxide in *either* reaction medium, even though conformations calculated to be much more favorable than those accessible to **1** (and its anion) would appear to be readily available.

The Rauk–Wolfe–Csizmadia calculations specifically omit solvation and other "external" effects, except insofar as these can be accounted for on the basis of conformational changes; it is highly unlikely that all of the medium effects observed to date, especially those found with comparatively rigid systems such as that used in the present study, can be thus explained. It would appear then that the theoretical calculations are not in themselves sufficient to enable prediction of the ease of formation of α-sulfinyl carbanions under the varying conditions commonly employed and that further work, both experimental and theoretical, seems in order.

Experimental

Melting points were determined on a Kofler hot stage and are uncorrected. The i.r. spectra were obtained with a Beckman IR-20A spectrophotometer using chloroform as solvent and sodium chloride cells. Unless otherwise stated, the n.m.r. spectra were determined on a Varian HA-100 spectrometer with $CDCl_3$ as solvent. The mass spectra (m.s.) were obtained on a Varian M-66 instrument; the correction tables of Hamming and Foster (21) were used when estimating isotopic composition from the mass spectrum. Deuterium analyses were performed by Josef Nemeth, Urbana, Ill. Magnesium sulfate (anhydrous) was used as the drying agent for organic solutions.

1,3-Dihydrobenzo[c]thiophene 2-Oxide (1a)

To a rapidly stirred solution of sodium metaperiodate (25.7g, 0.12 mol) in water (230 ml) was added dropwise molten 1,3-dihydrobenzo[c]thiophene (14.8 g, 0.11 mol) (22). The mixture was stirred at room temperature for 1 h, then cooled to 0° for 3 h. The white precipitate (sodium iodate) was removed by filtration and washed with cold water. The filtrate and washings were extracted three times with methylene chloride. The extracts were dried and the solvent evaporated to give yellow crystals (16.4 g). The crude product was dissolved in ether and filtered through neutral alumina to remove the coloured impurities. The ether was evaporated and the crystalline residue recrystallized from benzene–pentane to give colourless plates, m.p. 89–91° (15.6 g, 93.5%); i.r.: 1040(s) and 1485, 1210, and 1125 cm^{-1} (all weak); n.m.r.: AB quartet (4H), δ_A 4.13 and δ_B 4.28 (J = 16 Hz), singlet 7.35 p.p.m. (4H); with $Eu(dpm)_3$ shift reagent 0.3 equiv AB quartet δ_A 6.92 and δ_B 5.73 p.p.m.

Anal. Calcd. for C_8H_8OS: C, 63.13; H, 5.30; S, 21.06. Found: C, 63.35; H, 5.49; S, 21.18.

trans-1,2-cis-1,3-1,3-Dihydrobenzo[c]thiophene-1,3-d_2 2-Oxide (1b)

To a stirred, ice-cooled solution of NaOD in D_2O (10 ml, 0.1 *N*) was added 5 mmol of sulfoxide **1***a* (0.76 g). This solution was stirred at 0° for 60 min, then quenched with 0.1 *N* HCl (12 ml). The aqueous solution was extracted twice with methylene chloride. The extracts were dried and solvent removed to give a quantitative yield of crystalline sulfoxide. Recrystallization from benzene–pentane gave colourless plates, m.p. 89–90°; n.m.r.: triplet 4.12 p.p.m. (1:1:1, J = 2.2 Hz, 2H), singlet 7.35 p.p.m. (4H). With 0.3 equiv $Eu(dpm)_3$ shift reagent, the triplet is shifted to 6.87 p.p.m. The isotopic composition was estimated from the peaks at *m/e* 152 to 156: d_0, 0; d_1, 6.0; d_2, 79.0; d_3, 12.6; d_4, 2.4%, average 26.4 at. % excess deuterium.

Anal. Calcd. for $C_8H_6D_2OS$: 25.00 at. % excess deuterium. Found: 25.50 at. %.

1,3-Dihydrobenzo[c]thiophene-1,1,3,3-d_4 2-Oxide (1f)

A solution of the sulfoxide **1***a* (1 g) in 0.1 *N* NaOD (25 ml) was warmed to 50° for 1 h. The reaction was quenched with 0.5 *N* HCl (10 ml) and extracted with methylene chloride. The extracts were dried and solvent evaporated to give crystalline product (1.0 g, 98%). Recrystallization from benzene–pentane gave colourless plates, m.p. 90–91°. The n.m.r. indicated quantitative exchange of the methylene protons; the m.s. showed: d_3, 5.3; d_4, 94.6%; average 49.3 at. % excess D.

Anal. Calcd. for $C_8H_4D_4OS$: 50.00 at. % excess deuterium. Found: 47.85 at. %.

cis-1,2-cis-1,3-1,3-Dihydrobenzo[c]thiophene-1,3-d_2 2-Oxide (1c)

The tetradeuterated sulfoxide **1***f* (400 mg) was dissolved in aqueous sodium hydroxide (10 ml, 0.1 *N*) at 0° and allowed to react for 3 h. Upon quenching with 0.5 *N* HCl (4 ml), the solution was extracted with methylene chloride and the extracts were dried and solvent evaporated to give crystalline sulfoxide (391 mg, 99%). Recrystallization from benzene–pentane gave colourless plates (340 mg, 86%), m.p. 89–90.5°; n.m.r. triplet 4.25 p.p.m. (1:1:1, J = 2.2 Hz, 2H), singlet 7.31 p.p.m. (4H). With 0.3 equiv $Eu(dpm)_3$ shift reagent, the triplet is shifted to 5.81 p.p.m.; m.s.: d_0, 0; d_1, 10.6; d_2, 71.6; d_3, 12.6; d_4, 5.1%; average, 26.5 at. % excess deuterium.

Anal. Calcd. for $C_8H_6D_2OS$: 25.00 at. % excess deuterium. Found: 24.90 at. %.

Measurement of Deuterium Exchange Rates in Aqueous Medium

1,3-Dihydrobenzo[c]thiophene 2-Oxide (1a)

The rate of exchange of the hydrogens *trans* to the oxygen was much faster than the exchange rate of the *cis* hydrogens, so that the exchange of either set could be studied separately. In both cases, a solution of sulfoxide (10.00 mmol, 0.40 *N*) in 0.10 *N* NaOD–D_2O (25.00 ml) was prepared at 5.0° and 2-ml aliquots were withdrawn at appropriate intervals (2 min for the *trans* hydrogens or 60 min for the *cis* hydrogens). The samples were quenched in HCl (1 ml, 0.5 *N*) and the partially exchanged sulfoxide recovered by extraction with methylene chloride. The crude samples were recrystallized from benzene–pentane. The n.m.r. of each was then recorded on a Varian T-60 instrument equipped with a signal-lock device. The

Can. J. Chem. Downloaded from www.nrcresearchpress.com by 210.87.254.5 on 09/05/12
For personal use only.

samples were run in $CDCl_3$–TMS with an equal weight of Eu(fod)$_3$ shift reagent. Percent exchange for the *trans* hydrogens was determined by comparing the integral for the *trans* hydrogens with that of the aromatic hydrogens. The slope (obtained by the method of least squares) of a plot of log (100 − % exchange) *vs.* t was divided by 2.303, thereby giving directly the rate constant for the exchange of each *trans* hydrogen. The corresponding rate constant for the *cis* hydrogens was obtained similarly from the integral of the signal due to the *cis* hydrogens. The pseudo-first-order rate constants so obtained were $k_{trans} = 2.2 \times 10^{-3}$ s^{-1}, $k_{cis} = 3.3 \times 10^{-5}$ s^{-1}, and $k_{trans}/k_{cis} = 67$.

Benzyl Methyl Sulfoxide

The rate difference between the diastereotopic benzylic hydrogens of benzyl methyl sulfoxide was not sufficiently large to allow determination of the individual rates in the same way as had been used with **1** and a modified procedure was required. A solution (20 ml) of benzyl methyl sulfoxide (8.00 mmol, 0.40 *N*) in 0.10 *N* NaOD–D_2O at 5.0° was prepared. Aliquots (2 ml) were withdrawn and quenched at suitable intervals (2 h for the fast exchange or 12 h for the slow exchange) and the sulfoxide isolated and recrystallized from petroleum ether (b.p. 30–60°). The n.m.r. spectra were recorded on a Varian T-60 spectrometer and the total amount of exchange determined from the integration. The rates of exchange of the two hydrogens were calculated from a plot of log [100 − % exchange] as a function of time. The slower exchange rate was determined directly from the linear part of the graph and the best slope extrapolated back to $t = 0$. The differences between this line and the curve for the faster exchanging proton were plotted as a function of time to give a linear slope from which the faster rate was calculated. The pseudo-first-order rates thus determined were $k_1 = 3.1 \times 10^{-5}$ s^{-1}, $k_2 = 1.4 \times 10^{-6}$ s^{-1}, and $k_1/k_2 = 22$.

α-Exchange of 1,3-Dihydrobenzo[c]thiophene 2-Oxide by the Lithiation and Quenching Procedure

Typically, the sulfoxide (1 mmol) was dissolved in 30 ml tetrahydrofuran (freshly distilled from calcium hydride) under nitrogen and the solution cooled to 0°. Methyllithium (1.1 mmol, in ether) was then added to the rapidly stirred solution through a serum cap, using a hypodermic syringe. The resulting yellow solution was rapidly quenched (within 10 s) with DCl–D_2O (1 ml, *ca.* 4 *N*) or aqueous HCl (5 ml, 0.5 *N*). This mixture was quickly worked up by diluting with water and extracting twice with methylene chloride. The extracts were dried and solvent evaporated. The residue was transferred immediately to a thick layer silica gel plate and developed with ethyl acetate. The first band above the baseline was isolated, treated with decolourizing carbon, and crystallized from benzene–pentane. Recrystallization gave colourless plates with sharp melting points with about 50% recovery or better. The product analyses are shown in Table 1.

The following experiments were carried out to determine the effect of varying some of the reaction conditions. (*i*) When the sulfoxide (**1***a*) was treated under conditions identical to those given above except that the DCl was added 10 min after addition of the methyllithium, the recovered product after recrystallization (~30%) showed the presence of 12 at. % excess deuterium by n.m.r.; m.s.: d_0, 19.2; d_1, 68.0; d_2, 11.9; d_3, 0.5; d_4, 0.4%; average 11.9 at. % excess deuterium. (*ii*) With **1***a* and 2 mmol of methyllithium (1.34 ml, 1.5 *M*) and otherwise identical conditions as those used to obtain the data in Table 1 the n.m.r. spectrum of the product (24 mg, 15%) showed the presence of 19 at. % excess deuterium (*i.e.* about 1.5 deuterium atoms per molecule); m.s. showed d_0, 4.0; d_1, 60.2; d_2, 31.5; d_3, 3.9; d_4, 0.4%; average 17.1 at. % excess deuterium. (*iii*) Sulfoxide **1***a* (76 mg, 0.5 mmol) in tetrahydrofuran (40 ml) was treated at 0° with methyllithium (0.5 mmol) and the mixture allowed to stand for 10 min. Then **1***f* (78 mg, 0.5 mmol) dissolved in tetrahydrofuran (5 ml) was added and the mixture allowed to stand for 10 min. Work-up as above yielded an oily product (127 mg, 83%) which was purified by t.l.c. (developing with methylene chloride). The n.m.r. spectrum showed considerable exchange manifest by a decrease in the AB quartet pattern of the methylene group and a sizeable CHD signal (roughly the same area as the CH_2 signal). When the above experiment was repeated except that the addition of **1***f* was followed immediately (3 or 4 sec later) by acid quenching, the n.m.r. spectrum of the product (137 mg, 87%) indicated much diminished (< 5%) formation of the CHD products.

Competition of Sulfoxide 1a and Benzyl Methyl Sulfoxide for Methyllithium

Sulfoxide **1***a* (152 mg, 1 mmol) and benzyl methyl sulfoxide (308 mg, 2 mmol) were dissolved in 40 ml tetrahydrofuran (freshly distilled from calcium hydride) under nitrogen. (This ratio of the two sulfoxides gives a 1:1 ratio of benzylic hydrogens α to the sulfinyl groups). This solution was cooled to −78° and 1 mmol of methyllithium (0.67 ml, 1.5 *M*) in ether was added through a serum cap (hypodermic syringe). The resulting yellow solution was quenched within 10 s with DCl–D_2O (1 ml, *ca.* 4 *N*). This was quickly worked up by diluting with water and extracting twice with methylene chloride. The extracts were dried, treated with decolourizing carbon, and the solvent evaporated to give a yellow oil (417 mg, 90%). The n.m.r. of the crude product showed no detectable impurities. From the integration, it was deduced that the ratio of deuterium incorporation for **1***a* *vs.* benzyl methyl sulfoxide was 11 to 1.

We thank Dr. M. C. Woods for aid and advice on the "shift reagent" experiments, Professors R. R. Fraser and T. Durst (University of Ottawa) for helpful discussions and unpublished information, and the National Research Council of Canada for financial support.

1. D. J. Cram and S. H. Pine. J. Am. Chem. Soc. **85**, 1096 (1963).
2. A. Rauk, E. Buncel, R. Y. Moir, and S. Wolfe. J. Am. Chem. Soc. **87**, 5498 (1965).
3. S. Wolfe and A. Rauk. Chem. Commun. 778 (1966).
4. A. Rauk, S. Wolfe, and I. G. Csizmadia. Can. J. Chem. **47**, 113 (1969).
5. M. Nishio. Chem. Commun. 562 (1968).
6. R. R. Fraser and F. J. Schuber. Chem. Commun. 397 (1969); Can. J. Chem. **48**, 633 (1970).
7. T. Durst, R. R. Fraser, M. R. McClory, R. B. Swingle, R. Viau, and Y. Y. Wigfield. Can. J. Chem. **48**, 2148 (1970).

8. T. DURST, R. VIAU, and M. R. MCCLORY. J. Am. Chem. Soc. **93**, 3077 (1971).
9. R. R. FRASER, F. J. SCHUBER, and Y. Y. WIGFIELD. Abstracts V Symposium on Organic Sulphur Chemistry, Lund, Sweden. IB.2 (1972).
10. T. DURST and R. VIAU. Abstracts V Symposium on Organic Sulphur Chemistry, Lund, Sweden, IB.3 (1972).
11. B. J. HUTCHINSON, K. K. ANDERSEN, and A. R. KATRITZKY. J. Am. Chem. Soc. **91**, 3839 (1969).
12. J. E. BALDWIN, R. E. HACKLER, and R. M. SCOTT. Chem. Commun. 1415 (1969).
13. M. CINQUINI, S. COLONNA, U. FOLLI, and F. MONTANARI. Bøll. Sci. Fac. Chim. Ind. Bologna, **27**, 203 (1969).
14. R. LETT, S. BORY, B. MOREAU, and A. MARQUET. Tetrahedron Lett. 3255 (1971).
15. K. NISHIHATA and M. NISHIO. Tetrahedron Lett. 4839 (1972).
16. R. VIAU and T. DURST. J. Am. Chem. Soc. **95**, 1346 (1973).
17. K. NISHIHATA and M. NISHIO. J. Chem. Soc. Perkin II, 1730 (1972).
18. M. B. D'AMORE and J. I. BRAUMAN. Chem. Commun. 398 (1973).
19. R. R. FRASER and Y. Y. WIGFIELD. Chem. Commun. 1471 (1970); R. R. FRASER, T. DURST, M. R. MCCLORY, R. VIAU, and Y. Y. WIGFIELD. Inter. J. Sulfur Chem. **A1**, 133 (1971).
20. W. KLYNE and V. PRELOG. Experientia, **16**, 521 (1960).
21. M. C. HAMMING and N. G. FOSTER. Interpretation of mass spectra of organic compounds, Academic Press, New York, N.Y. 1972, p. 646.
22. J. F. KING, A. HAWSON, B. L. HUSTON, L. J. DANKS, and J. KOMERY. Can. J. Chem. **49**, 943 (1971).

Can. J. Chem. Downloaded from www.nrcresearchpress.com by 210.87.254.5 on 09/05/12
For personal use only.

An Electron Spin Resonance Method for Monitoring the Progressive Replacement of Fluorine by Alkoxy Groups in Perfluorobenzophenone[1]

FREDERICK PETER SARGENT AND MARSHALL GRANT BAILEY

Research Chemistry Branch, Atomic Energy of Canada Limited, Whiteshell Nuclear Research Establishment, Pinawa, Manitoba R0E 1L0

Received July 6, 1973

The use of electron spin resonance (e.s.r.) to follow the course of a chemical reaction which does not involve paramagnetic intermediates is reported. The principle of the method is the conversion of the reaction product into a paramagnetic species which may be characterized by e.s.r. In the present example, photoconversion of ketones into radical anions is used to follow the successive displacement of fluorine from perfluorobenzophenone.

On rapporte l'utilisation de la résonnance paramagnétique électronique (r.p.e.) pour établir la nature du chemin suivi par une réaction chimique qui n'implique pas d'intermédiaires paramagnétiques. Le principe de la méthode est de transformer le produit de la réaction en une espèce paramagnétique caractérisable par r.p.e. A titre d'exemple, on utilise la photoconversion de cétones en radicaux anions pour examiner les déplacements successifs du fluor en perfluorobenzophénone.

[Traduit par le journal]

Can. J. Chem., 51, 4088 (1973)

Introduction

Displacement of fluorine from highly fluorinated aromatic compounds is well known and is an important synthesis route for many partly fluorinated compounds (1). During our studies (2) of the photochemistry of perfluorobenzophenone, $(C_6F_5)_2CO$, henceforth referred to as PFB, a simple method for demonstrating and monitoring the successive replacement of fluorine by methoxide groups in basic methanol solutions was discovered. This replacement process is generalized in eqs. 1 and 2.

[1] $$C_nF_m + CH_3O^- \rightarrow C_nF_{m-1}OCH_3 + F^-$$

[2] $$C_nF_p(OCH_3)_q + CH_3O^- \rightarrow C_nF_{p-1}(OCH_3)_{q+1} + F^-$$

The method involves photoconversion of the ketone into its radical anion (3, 4). The number of fluorines replaced may be deduced from the changes in the e.s.r. spectra.

Experimental

The e.s.r. spectra were obtained with a Varian V-4500 spectrometer. The magnetic field sweep was calibrated with aqueous solutions of Fremy's salt assuming a_N to be 13.0 G. All chemicals were reagent grade and were used as received. Solutions of methoxide were prepared by dissolving freshly cut pieces of sodium in methanol. The photolyses were performed in the sample cavity of the e.s.r. spectrometer with a 100-W, compact-arc, medium-pressure, mercury lamp.

Results and Discussion

A methanolic solution containing 0.1 mol/kg PFB and 1 mol/kg methoxide was prepared by mixing. Aliquots of this were taken at various times after mixing and photolyzed *in situ* in the e.s.r. spectrometer. The spectrum shown in Fig. 1 was observed immediately after mixing. This closely resembles that reported by Brown and Williams (5), the interpretation being given in Table 1. We also assign this spectrum to the radical anion of 4,4'-dimethoxyoctofluorobenzophenone, $(C_6F_4OMe)_2CO$. The presence of this ketone shows that the two *para* fluorines of PFB which have a hyperfine splitting of 8.36 G (2), have been replaced by methoxy groups which do not give a resolvable hyperfine splitting, in the e.s.r. spectrum of the anion.

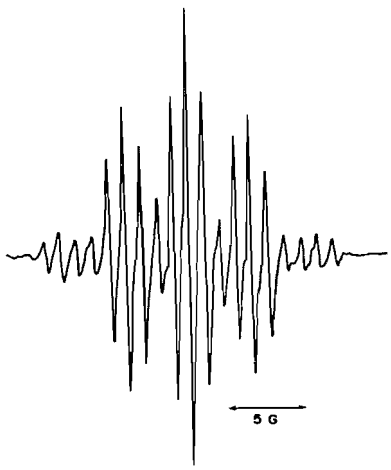

FIG. 1. The e.s.r. spectrum observed during the photolysis of solutions of methoxide and perfluorobenzophenone immediately after mixing.

[1]AECL No. 4637.

Can. J. Chem. Downloaded from www.nrcresearchpress.com by 210.87.254.105 on 09/05/12
For personal use only.

Can. J. Chem. Downloaded from www.nrcresearchpress.com by 210.87.254.105 on 09/05/12
For personal use only.

TABLE 1. The e.s.r. hyperfine splitting (G) for the observed spectra. The numbers in parentheses are the number of equivalent fluorine nuclei

	Position	
Spectrum	*ortho*	*meta*
Fig. 1	4.57 (4)	1.14 (4)
Fig. 2	4.65 (2)	0.87 (4)
Fig. 3	5.90 (1)	1.6 (2)

Photolysis of an aliquot of the mixture 1 h after mixing gave the spectrum shown in Fig. 2 and described in Table 1. The prominent features of the spectrum are a triplet of quintets. These originate from an anion containing only six fluorine atoms. The four fluorines of 0.87 G were assigned to the *meta* positions. The remaining two fluorine nuclei are clearly at *ortho* positions but the spectra do not indicate which positions. From steric considerations, this radical was assigned to the ketyl of 2,2′,4,4′-tetramethoxyhexafluorobenzophenone. The presence of this ketone shows that after the two *para* fluorines are substituted, two *ortho* fluorines are replaced by methoxide.

Photolysis of an aliquot of the mixture 1 week after mixing gave the spectrum shown in Fig. 3 and Table 1. The major features of this are a doublet of triplets which would arise from three fluorine nuclei, two of which are equivalent. The latter have a hyperfine splitting of 1.58 G and undoubtedly occupy *meta* positions. The remaining fluorine with splitting of 5.9 G must originate from an *ortho* position. Therefore this spectrum shows the presence of a heptamethoxytrifluorobenzophenone. The sharp central features of the spectrum in Fig. 3 arise from residual tetramethoxyhexafluorobenzophenone.

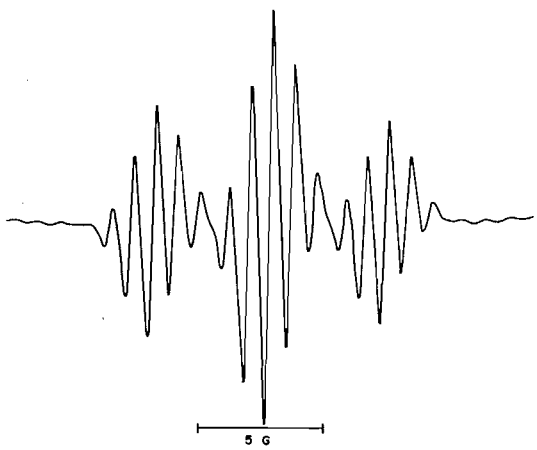

FIG. 2. The e.s.r. spectrum observed during the photolysis of solutions of methoxide and perfluorobenzophenone 1 h after mixing.

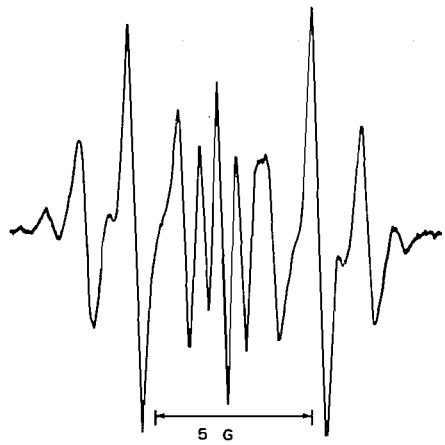

FIG. 3. The e.s.r. spectrum observed during the photolysis of solutions of methoxide and perfluorobenzophenone one week after mixing.

When solutions of PFB and methoxide were mixed and continuously photolyzed, similar changes are observed. Therefore the successive nucleophilic replacement of fluorine by methoxy groups are not affected by the photolysis. The latter merely serves as a probe to determine the progress of the reaction.

Summary

The observations reported demonstrate the use of e.s.r. to follow the successive replacements of fluorine in perfluorobenzophenone by methoxy groups. The principle of the method is the conversion of the products of a chemical reaction into a paramagnetic species which may be characterized by e.s.r. This conversion may be made by any means suitable to the system under study. In the present example, the well-known photoconversion of ketones to radical anions (3, 4) was used. Other methods could involve radiolysis, thermolysis, electrolysis, the reaction with alkali metals, or oxidation–reduction reactions.

1. J. C. TATLOW. Endeavour, **22**, 89 (1963).
2. F. P. SARGENT and M. G. BAILEY. Can. J. Chem. **49**, 2350 (1971).
3. G. A. RUSSELL and E. J. GELLS. Tetrahedron Lett. **20**, 1333 (1963).
4. P. B. AYSCOUGH and F. P. SARGENT. Chem. Commun. 94 (1963).
5. J. K. BROWN and W. G. WILLIAMS. Trans. Faraday Soc. **64**, 298 (1968).

Carbonium Ion Rearrangement with Retention at the Migration Terminus

FERRERS R. S. CLARK AND JOHN WARKENTIN
Department of Chemistry, McMaster University, Hamilton, Ontario

Received July 13, 1973

The isomeric 7-*t*-butylbicyclo[2.2.1]hept-2-en-7-ols afford isomeric dienes (7-methyl-7-(2′-propenyl)-bicyclo[2.2.1]hept-2-enes) by Wagner–Meerwein rearrangement on treatment with thionyl bromide or acid. Methyl migration in the nonclassical 7-*t*-butylbicyclo[2.2.1]hept-2-en-7-yl cation intermediate occurs with a substantial *syn* preference, in sharp contrast to the *anti* preference exhibited in capture of similar cations by external nucleophiles. The result is interpreted in terms of a steric factor.

Les *t*-butyl-7 bicyclo[2.2.1]heptène-2 ols-7 isomériques conduisent aux dienes isomériques (méthyl-7 (propènyl-2′)-7 bicyclo[2.2.1.]heptène-2) à l'aide d'un réarrangement Wagner-Meerwein lorsque l'on traite les alcools avec du bromure de thionyle ou de l'acide. La migration du méthyl dans le cation intermédiaire non-classique *t*-butyl-7 bicyclo[2.2.1.]heptène-2 yle-7 se produit préférentiellement de manière *syn*, ce qui est en désaccord avec la préférence *anti* manifestée lors de la fixation de cations similaires par des nucléophiles externes. On explique ce résultat par l'intervention d'un facteur stérique.

Can. J. Chem., 51, 4090 (1973)

Rearrangements involving migration of an atom or a group from one quaternary carbon atom to another through a carbocation intermediate generally proceed with net inversion of the migration terminus. There are exceptions to this generalization, notably cases in which geometric constraints are such as to effectively rule out migration to one face of the cation center. A 6,2-hydride shift in a bicyclo[2.2.1]-hept-2-yl cation (eq. 1) probably involves the *endo* face of the cationic center,[1] regardless of

[1] 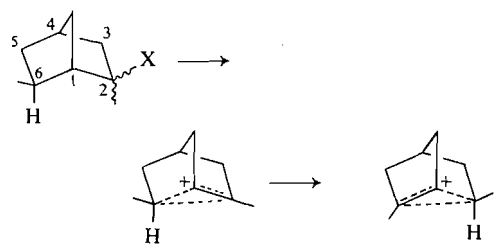

whether the cation originated from *exo* or *endo* precursor. For stepwise reaction (eq. 1) the stereochemical course of migration, with respect to C-2, should be defined without reference to the identity of the starting isomer, since such identity is lost prior to rearrangement. In rearrangement of the cation, the substituent "leaving" C-2 is C-1; the bond order between C-1 and C-2 decreasing as a consequence of 6,2-hydride transfer. The stereochemical outcome at the migration terminus is therefore retention of configuration (2). The stereochemical outcome of 6,2-migration concerted with C—X heterolysis would be defined in terms of precursor structure in the usual way, *exo* and *endo* precursors having rearranged with inversion and retention, respectively.

The mechanistic similarity between intramolecular rearrangement and nucleophilic substitution at saturated carbon is generally recognized. This similarity extends to nonclassical cation systems in which either reaction involves a nominal leaving group consisting of part of the molecular framework, held to the migration terminus (or the site of substitution) of the ion by a partial bond. Bicyclo[2.2.1]hept-2-yl cations are captured with a strong *exo* preference, even if *exo* approach is hindered by a 7-methyl substituent (3–5). Rearrangement of such cations, by 2,3-hydride transfer (6) or alkyl migration (7, 8), is also highly *exo* selective. Similarly, all 7-norbornenyl cations studied to date react faster with nucleophiles at the *anti*-C_7 face than at the *syn* face. The preference for inversion, which is very high in the 7-unsubstituted (9–11) and the 7-ethyl cations (12), becomes less pronounced in cases where the 7-substituent is a good electron donor, such as *p*-anisyl (13) or alkoxy (14, 15). Intramolecular attacks at C-7 of such ions, by migration of a group from a 7-substituent to C-7, should show analogous preferences. In a case of hydride transfer (eq. 2) migration was, in fact, highly

[1]Although *endo–endo* migration has not been established in the unsubstituted system, it has been demonstrated in the 2-carboxy-3-methyl-5-norbornyl cation (1).

Can. J. Chem. Downloaded from www.nrcresearchpress.com by 210.87.254.6 on 09/05/12
For personal use only.

TABLE 1. Reactions of norbornenols (**1**) and (**2**)

Reactant(s) and ratios	Conditions	Products (relative %) 3	4	5	Yield(%)
1:**2** = 1:1.8	$SOBr_2$, CCl_4, reflux[a]	94	6	0[b]	84
1	HOAc, 83°, 3h	No reaction			
2	HOAc, 83°, 3h	17	0	0	17[c]
1	HOAc, 108°, 2h	No reaction			
1	HOAc, 108°, 4 days	92	8	0	20[c]
1	HOAc, 108°, 13 days	83	17	0	60
2	HOAc, 108°, 2 h	97	3	0	>95
2	HOAc, 108°, 13 days	86	14	0	>95
1 or **2**[d]	HOAc, 2% H_2SO_4, 22.5°, 6 h	28	31	33	101[e]
1:**2** = 1:1	HOAc, 10% H_2SO_4, 22.5°, 3 h	4.9	4.9	74	13[f]

[a]A mixture of the two alcohols gave only one bromide on treatment with $SOBr_2$ in Et_3N. The (*E*)-configuration was assigned, on the basis of its n.m.r. spectrum.
[b]A zero means that the material in question was not detectable by g.l.p.c.; *i.e.*, $< \sim 2\%$.
[c]Plus starting material.
[d]Each isomer separately gave the results shown.
[e]An unidentified material (**8**, 27%) was present. The total yield is based on the assumption that **8** is an isomer of the dienes.
[f]The mixture contained **8** (11%), another unidentified product **9** (5%), and materials, probably polymeric, which were not extracted into petroleum ether. The yield was estimated assuming that **9** is also an isomer of the dienes.

[2] 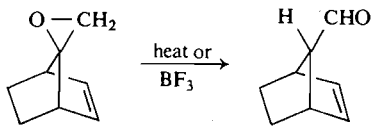

anti selective (16) and the authors concluded that a nonclassical ion must be an intermediate.[2] Although there are no reported cases of alkyl migrations to C-7 of 7-norbornenyl cations, one would predict the analogous preference for inversion at C-7; that is, for *anti* migration. Therefore it came as a surprise to us when we found a marked *syn* preference in such a process.

Results and Discussion

Treatment of the isomeric (*Z*)- and (*E*)-7-*t*-butylnorbornen-7-ols (**1** and **2**, respectively) with thionyl bromide in refluxing CCl_4, with acetic acid, and with acetic acid containing sulfuric acid gave the results listed in Table 1. Gross structures of the isomeric dienes, (*E*)- and (*Z*)-7-methyl-7-(2′-propenyl)bicyclo[2.2.1]hept-2-enes (**3** and **4**, respectively) followed from elemental analysis, from their characteristic norbornene-like p.m.r. spectra, and from their interconversion in acid with concurrent formation of ether (**5**). Assignment of stereochemistry to **3** and **4** rests on the 8% nuclear Overhauser effect (n.O.e.) found on irradiation of the 7-methyl signal of **3** while observing the vinyl signal.[3] Diene **4** did not show a corresponding, measurable n.O.e. The analogous n.O.e. value in a model for **3**, (*E*)-7-acetoxy-7-methylnorbornene, was 5%.

The results in Table 1 are consistent only with reaction mechanisms involving the nonclassical 7-*t*-butylbicyclo[2.2.1]hept-2-en-7-yl cation as intermediate. A common intermediate is indicated in the fact that **1** and **2** give the same mixture of **3**, **4**, and **5**.[4] That the intermediate is a nonclassical ion is suggested by much analogy (18), for all known norborn-2-en-7-yl cations, with the possible exception of the 7-*p*-anisyl (13), the 7-*p*-dimethylaminophenyl (13), and some 7-alkoxy analogs (14, 15), all of which derive

[2]If a nonclassical ion mechanism is correct, then either isomer of the substrate would give the same product and the stereochemistry of the migration step is correctly described as inversion at the migration terminus. The authors (16) called their stereochemistry retention; which focuses attention on the substrate rather than on the immediate precursor of the rearranged ion.

[3]Average of six measurements. The separation between methyl and C-2,3 vinyl hydrogens that corresponds to a n.O.e. value of 8% is about 3 Å (17).

[4]Rows 4 and 6, 5 and 7, or 8 of Table 1.

Can. J. Chem. Downloaded from www.nrcresearchpress.com by 210.87.254.6 on 09/05/12
For personal use only.

[3] 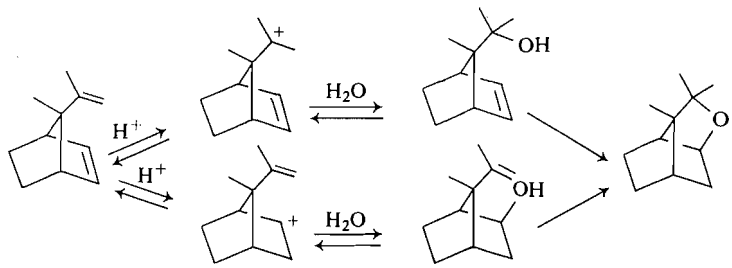

conjugative stabilization from the 7-substituent which the *t*-butyl group cannot provide, are best described as nonclassical ions. The greater reactivity of **2**, relative to that of **1**, is in keeping with anchimeric assistance to rate-determining formation of the nonclassical 7-*t*-butylbicyclo-[2.2.1]hept-2-en-7-yl cation. Since the formal leaving group in subsequent rearrangement of that ion is the bridging etheno group, the stereochemistry at the migration terminus is retention of configuration. A rationale for this preference is discussed below.

Equilibration of dienes **3** and **4**, which must occur by the reverse of the Wagner–Meerwein rearrangements which formed them, is slow in acetic acid. This means that the initial diene ratio is determined largely by kinetics. The thermodynamic diene ratio appears to be close to 1:1, as expected on the basis of the small difference between the steric requirements at the *syn* and *anti* faces (15). Formation of ether (**5**) in the more acidic media is readily accounted for by either or both of the pathways of eq. 3.

We now turn to discussion of the stereochemistry of methyl migration. Electronic interaction energies, from simple LCAO calculations (6), favor the inversion mode for similar migrations. The facts that external nucleophiles prefer *anti* approach and that hydride transfer (eq. 2) shows the same selectivity suggest that the reversal in the present case is not stereoelectronically determined. It is also unlikely that thermodynamics favors *syn* migration, for both steric and electronic effects in the product cations should favor the cation resulting from *anti* migration. The reasons for this prediction are the above-mentioned lesser hindrance at the *syn* face and the fact that stabilization by π-electron bridging, although quite small in ions of the type resulting from *anti* migration (19), must be absent altogether in the ion from *syn* migration.

We suggest that a steric factor, operating at the transition state for *anti* migration, opposes and dominates over a favorable electronic factor for that process. Electronically favorable geometries for the cation intermediate must be those which permit delocalization into neighboring π and σ bonds. Two such geometries, differing in the way conjugation is achieved between C—C bonds of the *t*-butyl group and the electron deficient orbital at C-7, are illustrated below.

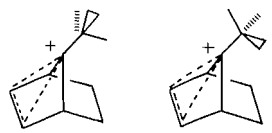

6 **7**

These conformations are also those necessary for migration to C-7 with good overlap; **6** leading to the transition state for *anti* migration and **7** leading to that for *syn* migration. Geometry **6**, in which a methyl group is placed directly over the ethano bridge, probably involves substantial non-bonded interactions which must increase in magnitude as the transition state for *anti* migration is reached; first, because CH_3 moves toward C-7 and second, because C-7 moves closer to C-5,6 as the homoallylic conjugation is destroyed. On the other hand, migration from conformation **7** involves the migrating CH_3 group in a relatively open area; C-7 swinging away from C-2,3 as migration progresses. Concurrent flattening of the developing isopropyl substituent probably prevents the development of strong nonbonded repulsions on the other side. A similar steric factor, preventing the ready attainment of certain conformations, has been invoked to account for reactions of norbornen-7-one and norbornan-7-one with diazomethane (20) or dimethylsulfoxonium methylide (21) and for the ratio of hydrogen migration to ring enlargement in acetolysis of 7-arylsulfonyloxymethylbicyclo[2.2.1] systems (22).

Whatever the reasons for the surprising

Can. J. Chem. Downloaded from www.nrcresearchpress.com by 210.87.254.6 on 09/05/12
For personal use only.

TABLE 2. Analyses and p.m.r. spectra

			p.m.r. (δ, CCl_4, TMS)[b]				
Compound	% C[a]	% H[a]	C-2,3	$=CH_2$	C-1,4	C_7—CH_3	$=\!\!<^{CH_3}$
3	89.12 89.31	10.88 10.93	5.48	4.56	2.56	0.92	1.56
4	89.12 88.74	10.88 10.80	5.95	4.64	2.60	1.00	1.68
5	79.46 79.61	10.91 10.89	See text				

[a]Calculated in upper rows, analytical results in lower rows.
[b]Varian HA-100 instrument. The C-5,6 proton signals are very similar in the two diene isomers and are not useful for distinguishing between them.

stereochemistry discussed above, it is clear that the very useful general rules for the stereochemistries of nucleophilic and electrophilic substitutions at saturated carbon do allow for exceptions. Brown and Lane (23) recently published an example of electrophilic substitution with inversion. Our example can be considered a case of nucleophilic substitution with retention.

Experimental

Product Analyses

Crude products were analyzed by g.l.p.c. using a Carbowax 20M column (15% on 60–80 mesh Chromosorb W, 10 ft × 1/4 in.) in a Varian Aerograph A90-P3 instrument equipped with thermal conductivity detector, with helium as the carrier gas. The thermal conductivities of products **3**, **4**, and **5** were assumed to be identical and ratios of products were obtained by triangulation of peaks in the g.l.p.c. traces. Pure samples of **3** and **4** collected from the column were neither interconverted nor hydrated to **5** on reinjection. Similarly, **5** passed through the column unchanged.

(E)- and (Z)-7-t-Butylbicyclo[2.2.1]hept-2-en-7-ol (1 and 2)

Synthesis, separation and spectra of these compounds have been published (24).

Reaction with Thionyl Bromide

A solution of **1** and **2** (**1**:**2** = 1:1.8, 0.470 g, 3.01 mmol) in carbon tetrachloride (2 ml) was added to a stirring solution of thionyl bromide (1.35 g, 6.50 mmol) in 15 ml of carbon tetrachloride. The resulting solution, protected against moisture, was refluxed in the dark for 2.5 h before it was cooled and poured into water (150 ml). The CCl_4 layer, after washing with water, drying, and evaporation of the solvent gave a yellow oil (0.357 g, 84%) which was found (g.l.p.c.) to contain, in addition to a trace of solvent, only dienes **3** and **4** in the ratio **4**:**3** = 15.8:1. At 118° and 52 ml min^{-1}, **3** and **4** were eluted in 6.5 and 8.0 min, respectively.

Reactions in Acetic Acid

A solution of **1** and **2** (1:1 ratio, 200 mg) in acetic acid (10 ml) was unchanged (p.m.r.) after 20 h at room temperature.

Alcohol **1** (11.5 mg) in acetic acid (0.50 ml) was heated in a sealed tube for 3 h at 83°. The solution was poured into water and the resulting mixture was extracted with petroleum ether (b.p. 30–42°). Washing of the hydrocarbon extract with dilute aqueous bicarbonate, drying and concentration gave a colorless oil (11.2 mg) which contained (g.l.p.c.) only **1**, the starting material.

Alcohol **2** (7.2 mg) in acetic acid (0.50 ml) was treated as described above for **1**. The same work-up gave a colorless oil (7.4 mg) which contained solvent, starting material (83%) and **3** (17%), but not **4**.

A solution of **1** and **2** (1:1 ratio, 200 mg) in 10 ml of acetic acid was sealed under vacuum into a heavy-walled tube. After 2 h at 140 ± 5°, the mixture was cooled and worked-up as described above. Both alcohols were absent and the ratio of dienes was **3**:**4** = 3.6:1.

Data pertaining to reactions in acetic acid at 108° (Table 1) were obtained by procedures analogous to that described above.

Reactions in Acetic Acid Containing Sulfuric Acid

A solution of **2** (117.8 mg, 0.795 mmol) in acetic acid containing 2% by volume of concentrated (95.5% minimum) sulfuric acid (50 ml), at 22.5°, turned orange about 1 min after mixing. After 6 h at that temperature the solution was added to water (75 ml) and the resulting solution was extracted with low-boiling petroleum ether (20 ml). The water layer was neutralized with sodium bicarbonate before reextraction with petroleum ether. The combined extract was washed with dilute bicarbonate and with water before it was dried and concentrated to give a sweet-smelling yellow oil (92.7 mg).

The exactly analogous procedure with alcohol **1** (58.6 mg) gave the same yellow oil (52.1 mg). Analysis by g.l.p.c. gave identical traces for the two samples; their composition is shown in Table 1. Relative retention times were: unknown **8**, 0.25; **3**, 0.31; **4**, 0.38; unknown **9**, 0.51 and **5**, 1.0. Proton magnetic resonance of **5** (Varian T-60, δ, CCl_4, TMS): 3.86 (t, 1, H—C_2—O); 1.14 (s, 3, $C(CH_3)_2$), 1.04 (s, 3, $C(CH_3)_2$), individual methyl groups of the *gem* dimethyl component not assigned; 0.96 (s, 3, C_7-CH_3); 0.7–2.25 (overlapping multiplets, 8, CH_2 and bridgehead).

In a similar experiment, a mixture of **1** and **2** (**1**:**2** =

Can. J. Chem. Downloaded from www.nrcresearchpress.com by 210.87.254.6 on 09/05/12
For personal use only.

1:1, 0.660 g, 1.08 mmol) was dissolved in acetic acid containing 10% by volume of sulfuric acid (10 ml). The solution, which turned black in 5 min, was worked up as described above after 3 h at 22.5°. An oil (77 mg) was obtained which was gas chromatographed on SE30 (20% on Chromosorb W, 60–80 mesh, 5 ft × 1/4 in., 125°, 42 ml min^{-1}). This column did not separate **3** from **4** but gave their combined percentage as 9.8. Three other components were separated from the dienes, as indicated in Table 1. The carbowax column described above separated **3** and **4** clearly to give small peaks of roughly equal area. The numbers 4.9% in Table 1 were obtained by dividing 9.8% by two rather than by triangulating the small, resolved diene peaks. Spectra and analyses pertaining to **3** and **4** are in Table 2.

Nuclear Overhauser Effects

Samples for n.O.e. studies were prepared as follows. A solution of the compound in carbon tetrachloride, containing TMS to serve as internal lock, was filtered through fine sintered glass into a carefully cleaned n.m.r. tube sealed to a ground joint. The tube was then transferred to a vacuum line and put through five degassing cycles, with the pressure below 5 μ in each cycle, before it was sealed.

(*E*)-7-Methylbicyclo[2.2.1]hept-2-en-7-yl acetate, the reference compound for the n.O.e. studies, was made by acetylating the known (22) (*E*)-7-methylbicyclo[2.2.1]-hept-2-en-7-ol with acetyl chloride in tetrahydrofuran containing pyridine. Spectra of the product agreed with those reported by Erman (22).

This work was supported by the National Research Council of Canada. We are indebted to Mr. Brian Sayer, Dr. R. A. Bell, and Dr. J. K. Saunders for the n.O.e. measurements.

1. J. A. Berson and P. W. Grubb. J. Am. Chem. Soc. **87**, 4016 (1965).
2. H. M. Bell and H. C. Brown. J. Am. Chem. Soc. **86**, 5007 (1964), footnote 3.
3. J. A. Berson. Molecular rearrangements. *Edited by* P. de Mayo. Interscience Publishers, New York, N.Y. 1963. Chapt. 3.
4. A. Colter, E. F. Friedrich, N. J. Holness, and S. Winstein. J. Am. Chem. Soc. **87**, 378 (1965).
5. R. Howe, E. C. Friedrich, and S. Winstein. J. Am. Chem. Soc. **87**, 379 (1965).
6. J. A. Berson, J. H. Hammons, A. W. McRowe, R. G. Bergman, A. Remanick, and D. Houston. J. Am. Chem. Soc. **89**, 2590 (1967).
7. P. D. Bartlett, E. R. Webster, C. E. Dills, and H. G. Richey, Jr. Ann. **623**, 217 (1959).
8. P. D. Bartlett, C. E. Dills, and H. G. Richey, Jr. J. Am. Chem. Soc. **82**, 5414 (1960).
9. S. Winstein, M. Shatavsky, C. Norton, and R. B. Woodward. J. Am. Chem. Soc. **77**, 4183 (1955).
10. S. Winstein and E. T. Stafford. J. Am. Chem. Soc. **79**, 505 (1957).
11. H. Tanida, T. Tsuji, and T. Irie. J. Org. Chem. **31**, 3941 (1966).
12. J. A. Berson, D. S. Donald, and W. J. Libbey. J. Am. Chem. Soc. **91**, 5580 (1969).
13. P. G. Gassman and A. F. Fentiman. J. Am. Chem. Soc. **92**, 2549 (1970).
14. H. A. Davis and R. K. Brown. Can. J. Chem. **51**, 361 (1973).
15. S. R. Korn and J. Warkentin. Manuscript submitted.
16. R. K. Bly and R. S. Bly. J. Org. Chem. **28**, 3165 (1963).
17. (*a*) R. A. Bell and J. K. Saunders. Can. J. Chem. **48**, 1114 (1970); (*b*) P. D. Kennewell. J. Chem. Ed. **47**, 278 (1970).
18. P. D. Bartlett. Nonclassical ions, reprints and commentary. Benjamin, Inc. 1965.
19. R. K. Bly and R. S. Bly. J. Org. Chem. **31**, 1577 (1966).
20. R. S. Bly, F. B. Culp, Jr., and R. K. Bly. J. Org. Chem. **35**, 2235 (1970).
21. R. K. Bly and R. S. Bly. J. Org. Chem. **34**, 304 (1969).
22. J. A. Berson, J. W. Foley, J. M. McKenna, H. Junge, D. S. Donald, R. T. Luibrand, N. G. Kundu, W. J. Libbey, M. S. Poonian, J. J. Gajewski, and J. B. E. Allen. J. Am. Chem. Soc. **93**, 1299 (1971) and references therein.
23. H. C. Brown and C. F. Lane. J. Chem. Soc. (D), 521 (1971).
24. F. R. S. Clark and J. Warkentin. Can. J. Chem. **49**, 2223 (1971).
25. W. F. Erman. J. Org. Chem. **32**, 765 (1967).

Can. J. Chem. Downloaded from www.nrcresearchpress.com by 210.87.254.6 on 09/05/12
For personal use only.

Electron Spin Resonance Study of the Cation Radicals of 1,5-Dihydronaphthyridine and Di-*N*-methyl-1,5-Naphthyridine

PAUL D. SULLIVAN AND WILLIAM W. PAUDLER[1]

Department of Chemistry, Ohio University, Athens, Ohio 45701

Received June 5, 1973

The e.s.r. spectra of the cation radicals 1,5-di-*N*-methylnaphthyridine (**1**) and 1,5-dihydronaphthyridine (**2**) in trifluoroacetic acid have been reported and analyzed. The splitting constants of **2** are unequivocally assigned by comparison of the spectra of several partially deuterated derivatives. The methyl proton splitting constant of **1** is thought to be low in comparison with other similar radicals and possible reasons for this anomaly are discussed.

On rapporte et analyse les spectres r.p.e. des cations radicaux di-*N*-méthyl-1,5 naphtyridine (**1**) et dihydro-1,5 naphtyridine (**2**) dans l'acide trifluoroacétique. Les constantes de couplages de **2** sont attribuées sans équivoque par comparaison avec les spectres de plusieurs dérivés partiellement deutériés. On croit que la constante de couplage du proton du groupe méthyle de **1** est faible par comparaison avec d'autres radicaux similaires et les raisons possibles pour cette anomalie sont discutées.

[Traduit par le journal]

Can. J. Chem., **51**, 4095 (1973)

Introduction

Recent studies have described the synthesis of the diquaternary di-*N*-alkylated naphthyridine salts (1, 2). It was also observed (2) that the zinc reduction of an aqueous solution of di-*N*-methyl-1,5-naphthyridine difluorosulfonate gave a green solution which was attributed to the formation of the cation radical **1**. The e.s.r. spectrum of the

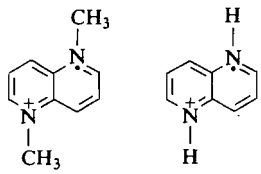

1 **2**

radical was not obtained, nor have the resolved spectra of any cation radicals derived from naphthyridines previously been observed to the best of our knowledge. It is the purpose of this paper to report the analysis of the e.s.r. spectra of the cation radicals of 1,5-dihydronaphthyridine (**2**) and of di-*N*-methyl-1,5-naphthyridine (**1**) and to describe some attempts to prepare cation radicals from other naphthyridines.

Experimental

The naphthyridines studied were synthesized as previously described (1). The cation radicals were prepared by reduction of the naphthyridines with zinc dust in trifluoroacetic acid (TFA) (3, 4). The reaction was carried out under vacuum in an inverted U-tube and the radical concentration was varied by dilution until the best e.s.r. spectrum was obtained. The e.s.r. spectra were measured on a Varian E-15 spectrometer in a dual cavity using a sample of the perylene radical anion as a secondary standard. Computer simulations of the experimental spectra were carried out as previously described (5).

Results and Discussion

Intense, well resolved e.s.r. spectra (line width 50 mG) attributed to the radical cation **1** were obtained when the diquaternary salt was reduced with zinc dust in TFA. The parent 1,5-naphthyridine, under the same reducing conditions, also gave a well resolved e.s.r. spectrum of the dihydronaphthyridine cation radical (**2**). The intensity was, however, considerably decreased over that of **1** and the radical decayed slowly (half-life 15 min) at room temperature. The analysis of the spectrum was considerably simplified due to the availability of some selectively deuterated 1,5-naphthyridines (6). Thus, the e.s.r. spectra of the cation radicals of 4,8-dideuterio-1,5-dihydronaphthyridine and 2,6-dideuterio-1,5-dihydronaphthyridine together with 1,5-dideuterionaphthyridine (formed in deuterated trifluoroacetic acid) served to unequivocally analyze the spectra in terms of the splitting constants shown in Table 1. Computer simulations of the spectra showed excellent agreement with the experimental results. By analogy with the results for **2** the spectrum of **1** was readily

[1]Present address: Department of Chemistry, University of Alabama, University, Alabama 35486.

Can. J. Chem. Downloaded from www.nrcresearchpress.com by 210.87.254.40 on 09/05/12
For personal use only.

Can. J. Chem. Downloaded from www.nrcresearchpress.com by 210.87.254.40 on 09/05/12
For personal use only.

TABLE 1. E.s.r. splitting constants (experimental and calculated) for the 1,5-dihydro- and 1,5-dimethylnaphthyridine cation radicals

			Splitting constant (G)[a]		
			a^H		
Substituent	a^N	$a_{NH}{}^H$	2,6	3,7	4,8
None	2.86	3.37	4.64	1.08	6.25
2,6-Dideuterio	2.87	3.39	0.72[b]	1.08	6.27
4,8-Dideuterio	2.86	3.36	4.65	1.08	0.96[b]
Di-*N*-deuterio	2.81	0.52[b]	4.82	1.06	6.10
Di-*N*-methyl	3.40	2.21[c]	4.34	1.30	6.02
Anion radical[d]	3.36		3.01	1.72	5.80
Calculated[e]	2.51		4.47	0.32	6.36

[a]All splitting constants ± 0.01 G.
[b]Deuterium splitting, *ca.* 0.1538 times proton splitting.
[c]Methyl group proton splittings.
[d]Obtained from refs. 7 and 8.
[e]Calculated from McLachlan-HMO method with $h_N = 1.30$ $k_{CN} = 0.95$, the splitting constants obtained from $a_{CH}{}^H = \rho_C{}^\pi Q_{CH}{}^H$ and $a^N = \rho_N{}^\pi Q_{N(CH)}{}^N$ where $Q_{CH}{}^H = 27$ G, $Q_N{}^N = 25$ G.

analyzed and the splitting constants are also shown in Table 1. For comparison purpose Table 1 also includes the e.s.r. spectral parameters for the 1,5-naphthyridine anion radicals (7–8) and also the calculated parameters obtained from a McLachlan-HMO calculation using previously suggested parameters for the nitrogen atom and carbon–nitrogen bond (9). The calculated values are in reasonable agreement with the experimental parameters.

It is instructive to compare the results for **1** and **2** with those for similar compounds which can be found in the literature (see Table 2). The quantities of interest are the change in the nitrogen splitting constant on methyl substitution, the ratio of the nitrogen splitting to the NH proton splitting ($a^N/a_{NH}{}^H$) in the protonated compounds, and the ratio of the nitrogen splitting to the methyl splitting ($a^N/a_{NCH_3}{}^H$) in the *N*-methyl compounds. As can be seen in Table 2 the nitrogen splitting constant usually increases by 15 to 30% upon methyl substitution, and in this regard radicals **1** and **2** behave normally. For the protonated compounds the $a^N/a_{NH}{}^H$ ratio is usually slightly less than one (except for the hydrazine cation radical) and again **2** is normal in this regard. For the *N*-methyl compounds the ratio $a^N/a_{NCH_3}{}^H$ is usually slightly greater than one and clearly **1** is anomalous in this respect. The only other reported cation radical which shows an anomalous ratio of this magnitude is the tetrakis(dimethylamino)ethylene cation radical, but in this compound there is considerable steric hindrance to rotation about the C—N bond and the molecule is presumably able to relieve this strain by adopting a non-planar configuration. In radical **1**, there will be a steric interaction between the methyl group and the peri protons but it seems unlikely that such an interaction could cause such a large deviation. The lack of any temperature dependence of the splitting constants also argues against a steric effect. A better explanation might perhaps lie in the effect of charge and charge distributions on the methyl group splitting constant and clearly further investigation is called for on this point.

Several other di-*N*-alkylated naphthyridine salts (1,6-, 1,7-, and 1,8-) were reacted with zinc in TFA in an effort to produce their corresponding cation radicals. However, no e.s.r. signals were detected. This is not unexpected in the case of the 1,6- and 1,8-derivatives since these compounds do not belong to the class of radicals known as violenes (11) as do the 1,5- and 1,7-derivatives. It is, therefore not possible to write favorable valence bond structures which allow the unpaired electron to be localized onto both nitrogen atoms for the 1,6- and 1,8-derivatives. The 1,7-compound does however belong to the violene class and should show an extra stability towards the formation of a cation

TABLE 2. Comparison of results for various cation radicals

	Splitting constant (G)		
Cation radical	a^N	$a^N/a_{NH}{}^H$	$a^N/a_{NCH_3}{}^H$
1	3.40		1.54
2	2.86	0.85	
$CH_3NC_4H_4NCH_3$[a]	8.36		1.05
HNC_4H_4NH[b]	7.40	0.93	
$CH_3N{\cdot}C_{10}H_8{\cdot}NCH_3$[c]	4.23		1.06
$HN{\cdot}C_{10}H_8NH$[c]	3.54	0.88	
$(CH_3)_2N{\cdot}C_6H_4{\cdot}N(CH_3)_2$[d]	6.99		1.03
$H_2N{\cdot}C_6H_4{\cdot}NH_2$[d]	5.29	0.90	
$(CH_3)_2N{\cdot}C_{12}H_8{\cdot}N(CH_3)_2$[d]	4.88		1.04
$H_2N{\cdot}C_{12}H_8{\cdot}NH_2$[d]	3.60	0.91	
$(CH_3)_2N{\cdot}N(CH_3)_2$[e]	13.4		1.06
$H_2N{\cdot}NH_2$[f]	11.0	1.05	
$((CH_3)_2N)_2C_2(N(CH_3)_2)_2$[g]	4.90		1.60

[a]Di-*N*-methylpyrazine (12).
[b]Dihydropyrazine, (13).
[c]Methylviologen and 4 4′-dihydrodipyridyl, (14).
[d]Wurster's Blue, *p*-phenylenediamine, 4,4′-bis(dimethylamino)biphenyl, 4 4′-diaminobiphenyl (15).
[e]Reference 16.
[f]References 17 and 18.
[g]Tetrakis(dimethylamino)ethylene, ref. 10.

radical. The chemical reduction method used may not, however, be the method of choice for this compound. Of the other naphthyridines which were not available to us the 2,8- and 2,6-derivatives belong to the violene class and may be chemically reducible to stable cation radicals.

Acknowledgement is made to the Research Corporation for partial support of this research.

1. D. J. POKORNY and W. W. PAUDLER. Can. J. Chem. **51**, 476 (1973).
2. L. A. SUMMERS and J. E. DICKESON. Chem. Commun. 1183 (1967).
3. J. R. BOLTON, A. CARRINGTON, and J. DOS SANTOS VEIGA. Mol. Phys. **5**, 466 (1962).
4. T. J. CURPHY. J. Am. Chem. Soc. **87**, 2063 (1965).
5. P. D. SULLIVAN. J. Phys. Chem. **74**, 2563 (1970).
6. D. J. POKORNY. Ph.D. Thesis, Ohio University, Athens, Ohio. 1972.
7. P. CAVALIERI D'ORO, R. DANIELI, G. MACCAGNANI, G. F. PEDULLI, and P. PALMIERI. Mol. Phys. **20**, 365 (1971).
8. D. M. W. VAN DEM HAM, J. J. DU SART, and D. VAN DER MEER. Mol. Phys. **21**, 989 (1971).
9. P. D. SULLIVAN and J. R. BOLTON. J. Mag. Res. **1**, 357 (1969).
10. K. KUTAWA and D. H. GESKE. J. Am. Chem. Soc. **86**, 2101 (1964).
11. S. HUNIG. Pure Appl. Chem. **15**, 109 (1967).
12. M. K. AHN and C. S. JOHNSON. J. Chem. Phys. **50**, 632 (1969).
13. B. L. BARTON and G. K. FRAENKEL. J. Chem. Phys. **41**, 1455 (1964).
14. C. S. JOHNSON and H. S. GUTOWSKY. J. Chem. Phys. **39**, 58 (1963).
15. G. HORSMAN. *In* Magnetic resonance and relaxation. *Edited by* R. Blinc. North Holland Publishing Co., Amsterdam. 1967. p. 578.
16. S. F. NELSON. J. Am. Chem. Soc. **88**, 1930 (1966).
17. T. V. ATKINSON and A. J. BARD. J. Phys. Chem. **75**, 2043 (1971).
18. P. SMITH, R. D. STEVENS, and R. A. KABA. J. Phys. Chem. **75**, 2048 (1971).

Can. J. Chem. Downloaded from www.nrcresearchpress.com by 210.87.254.40 on 09/05/12
For personal use only.

The Addition of Hypobromous Acid to Δ^4-Steroids

PETER MORAND AND ALENKA POLAKOVA-PAQUET
Department of Chemistry, University of Ottawa, Ottawa, Canada K1N 6N5

Received July 12, 1973

The addition of hypobromous acid to 4-cholesten-3β-yl acetate (**1**) has been found to result in the formation of a significant amount of 4β-bromo-5α-cholestane-3β,5-diol 3-acetate (**3**) as well as of 5-bromo-5α-cholestane-3β,4β-diol 4-acetate (**2***a*). Evidence is presented in support of the structure proposed for the former and confirmation of the structure of the latter, about which there is disagreement, is adduced. The conversion of **2***a* to 4-cholestene-3β,19-diol 3-acetate (**9**) by treatment with lead tetraacetate and subsequent opening of the 4β,19-oxide ring is described.

L'addition de l'acide hypobromeux à l'acétate de cholestène-4 yl-3β (**1**) a conduit à la formation d'une quantité significative d'acétate-3 du bromo-4β cholestane-5α diol-3β,5 (**3**) et d'acétate-4 du bromo-5 cholestane-5α diol-3β,4β (**2***a*). On apporte des preuves en faveur de la structure proposée pour le premier et pour confirmer la structure du dernier, autour de laquelle il existe un désaccord. On décrit la transformation de **2***a* en acétate-3 de cholestène-4 diol-3β,19 (**9**) par traitement avec du tétraacétate de plomb ainsi que l'ouverture subséquente du cycle oxyde-4β,19. [Traduit par le journal]

Can. J. Chem., **51**, 4098 (1973)

Can. J. Chem. Downloaded from www.nrcresearchpress.com by 210.87.254.105 on 09/05/12
For personal use only.

Introduction

As part of our investigation of approaches to the synthesis of the A/B-ring system of strophanthidin (1) we were interested in the conversion of readily available 3-oxo-Δ^4-steroids into 19-oxygenated derivatives. A key transformation in this sequence involves the addition of hypobromous acid to the 4,5-double bond after reduction of the C-3 ketone group and subsequent acetylation to the 3β-acetoxy derivative. This reaction was first reported by Collins (2) on 4-cholesten-3β-yl acetate (**1**) and the product isolated was identified as 4α-bromo-5β-cholestane-3β,5-diol 3-acetate (**4**, see Scheme 2). In a subsequent paper (3) evidence is presented to exclude the known bromohydrin **2***b*, with similar physical constants, as an alternative structure. However, Julia and Fürer (4) have concluded that the compound obtained must be 5-bromo-5α-cholestane-3β,4β-diol 4-acetate (**2***a*). Their proposed structure easily accounts for the isolation of the ketone **7** and of the 4β,5β-epoxide **6***a* by oxidation of **2***a* followed by treatment with base. The same compounds are reported by Collins (3) who invokes the rearrangement of the bromohydrin **4** during the course of oxidation. Although Collins reported an alternative synthesis of the bromohydrin **4** by treatment of 5β-cholest-3-en-5β-ol with acetyl hypobromite, Julia and Fürer have argued that, under the reaction conditions, allylic rearrangement is likely to occur, resulting in the formation of 5-bromo-5α-cholestane-3β,4β-diol 4-acetate (**2***a*). Recent work in our laboratory on the allylic rearrangement of Δ^6-5α-hydroxy steroids under mild acidic conditions (5) supports this assumption.

The formation of a compound with an acetoxy group at C-4 instead of the bromohydrin **2***b* by the addition of hypobromous acid to 4-cholesten-3β-yl acetate (**1**) has been rationalized (4) by considering the participation of the 3β-acetoxy group in the α-side addition of the bromonium ion to the double bond (see scheme 1). This is consistent

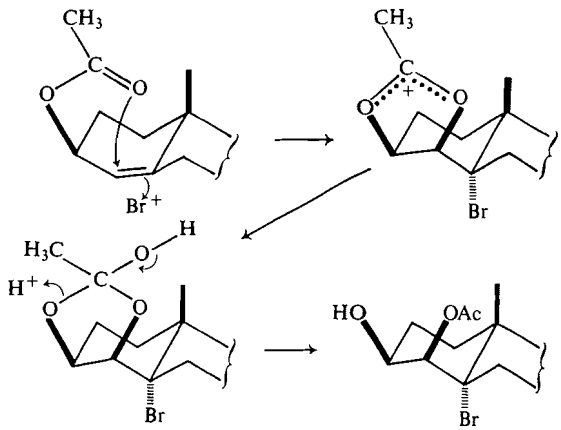

SCHEME 1

with the observed (6) neighboring group participation of the C-3 acetoxy group in the opening of a 4α,5α-epoxide and the preference for the 4β- over the 3β-position by an acetoxy group (7).

Can. J. Chem. Downloaded from www.nrcresearchpress.com by 210.87.254.105 on 09/05/12
For personal use only.

The results reported here confirm the structure proposed by Julia and Fürer for the disputed compound. Furthermore, we have found that a second substance, formed during the reaction, can be isolated and its structure has been elucidated. The synthesis of 4-cholestene-3β,19-diol 3-acetate (**9**) from 5-bromo-5α-cholestane-3β,4β-diol 4-acetate (**2***a*) is also described.

Results and Discussion

When 4-cholesten-3β-yl acetate (**1**) was treated with *N*-bromosuccinimide and perchloric acid, two compounds were isolated in yields of 46 and 14%, respectively. The major product had a higher melting point (156–157°) than reported by either Collins (2) (147°) or Julia and Fürer (4) (148°). Its n.m.r. spectrum, which was not reported by these authors, indicated (8) a *trans* A/B-ring junction (half-band width of 11 Hz for the 3α-proton signal) and an equatorial proton at C-4 (τ 4.40, J_{ae} = 2.0 Hz). Treatment of this compound with potassium hydroxide in aqueous methanol and subsequent oxidation gave a substance identified as 4β,5-oxido-5β-cholestan-3-one (**6***a*) on the basis of its melting point (9) and the expected optical rotatory dispersion (o.r.d.) curve (10). There seems to be little doubt, therefore, that the compound isolated by Collins (2, 3) and by Julia and Fürer (4) is 5-bromo-5α-cholestane-3β,4β-diol 4-acetate (**2***b*).

The second product isolated from the reaction mixture was identified as 4β-bromo-5α-cholestane-3β,5-diol 3-acetate (**3**) on the basis of its elemental analysis, spectral properties and chemical reactions. The i.r. spectrum indicated the presence of acetoxy and hydroxy groups. In the n.m.r. spectrum, a broad signal at τ 4.60 (half-band width of 12 Hz) and a doublet centered at τ 5.6 (J_{ae} = 2.0 Hz) were observed. The former could be attributed to an axial proton at C-3 and the latter to an equatorial proton (8) at C-4.

Whereas the major product **2***a* was converted into the diacetate **2***c* on treatment with acetic anhydride in pyridine at room temperature, the second product was unchanged under these conditions. Similarly, while **2***a* was easily oxidized with Jones' reagent (11) to the ketone **7**, the lower yield product was recovered unchanged when subjected to these reaction conditions. However, when the latter was treated with base, the product isolated was identified as 4α,5-oxido-5α-cholestan-3β-ol (**5***b*) on the basis of its n.m.r. spectrum which exhibited a broad signal centered at τ 6.15 (3α-proton) and a singlet (12) at τ 7.20 (4β-proton in a 4α,5α-epoxide). Oxidation of this alcohol **5***b* gave 4α,5-oxido-5α-cholestan-3-one (**6***b*) whose structure was confirmed by the "reversed Cotton effect" observed in its o.r.d. curve (10).

The formation of 4β-bromo-5α-cholestane-3β,5-diol 3-acetate (**3**) implies β-side attack of bromonium ion on the 4,5-double bond with subsequent diaxial opening of the cyclic intermediate by hydroxide ion to give the bromohydrin **3**. In this reaction sequence the participation of the 3β-acetoxy group is excluded and this substituent therefore remains unchanged in the product isolated. It appears that the addition of hypobromous acid is less stereospecific in Δ^4-steroids than in Δ^5-steroids where formation of the analogous 6β-bromo-5α-hydroxy derivatives has never been detected (13). The increased accessibility of the β-side of the molecule in Δ^4-steroids has been observed (14) in other types of reactions involving the double bond.

Treatment of 5-bromo-5α-cholestane-3β,4β-diol 4-acetate (**2***a*) with lead tetraacetate under the conditions reported by Julia and Lorne (15) gave a mixture of many products which could not be separated. By modifying the reaction conditions (see Experimental) it was possible to isolate two products in yields of 25 and 17%, respectively.

The substance obtained in lower yield was identified as 4β,5-oxido-5β-cholestan-3β-ol acetate (**5***a*, acetate) on the basis of the n.m.r. spectrum which showed a singlet at τ 7.82 (acetate group), a doublet (12) centered at τ 6.80 (4α-proton of 4β,5β-epoxide), and a multiplet at τ 4.80 (C-3 proton). The formation of an analogous epoxide has also been observed (16) in the reaction of 5α-bromo-6β-hydroxy steroids with lead tetraacetate but it is not clear what mechanism is involved in its formation.

The structure of the major product is considered to be 5-bromo-4β,19-oxido-5α-cholestan-3β-ol acetate (**8**) on the basis of its elemental analysis, spectral properties, and the fact that it was easily converted to 4-cholestene-3β,19-diol 3-acetate (**9**) by treatment with zinc dust in dimethylformamide. The i.r. spectrum showed a low intensity band at 1490 cm^{-1} assigned (17) to the C—H scissoring of the protons in the methylene group of the oxide ring. Similarly, the n.m.r. spectrum indicated the presence of a methylene

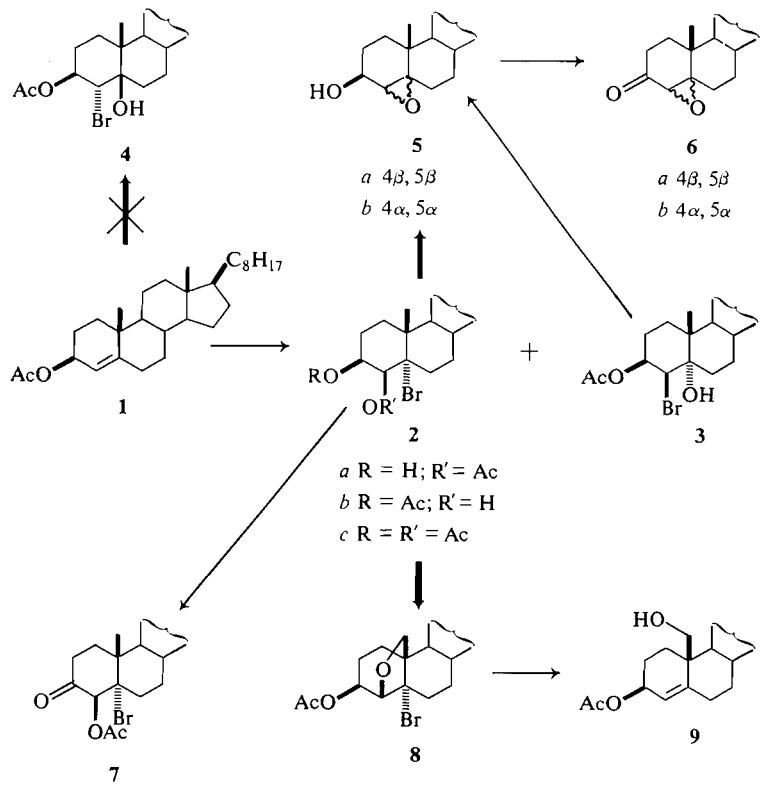

SCHEME 2

group adjacent to an ether linkage (quartets at τ 5.80, 5.82, 6.19, 6.35) as well as of an equatorial acetoxy group.

Julia and Lorne (15) have postulated a cyclic intermediate involving the *cis* hydroxy and acetoxy groups at C-3 and C-4, respectively (as shown earlier) to rationalize the formation of the 4β,19-oxide. The direct participation of an adjacent methoxy group has also been reported (16) in the reaction of steroidal alcohols with lead tetraacetate.

Experimental

Melting points were determined on a Hoover Uni-Melt apparatus and are uncorrected. Infrared and n.m.r. spectra were recorded on a Beckman IR-8 i.r. spectrophotometer and on a Varian V-4302 60 Mc spectrometer, respectively. A Durrum-Jasco automatic spectropolarimeter, Model ORD-5, and a Perkin-Elmer 141 recording polarimeter were used to determine optical rotatory dispersion curves and optical rotations, respectively. Microanalyses were performed by G. Daesslé, Organic Microanalyses, Montreal. SilicaR (200–300 mesh) was used as an adsorbant for column chromatography. Silica gel G (according to Stahl) was used as adsorbant for t.l.c. and sulfuric acid was used as spraying agent. In working up the products of reactions the organic extracts were washed with dilute HCl solution and/or $NaHCO_3$ solution, dried over anhydrous $MgSO_4$, and evaporated to dryness under reduced pressure.

Addition of Hypobromous Acid to 4-Cholesten-3β-yl Acetate (1)

To a solution of 4-cholesten-3β-yl acetate (**1**) (18) (m.p. 82–84°, $[\alpha]_D$ +9.5°, 6.30 g, 1.48 mmol) in dioxane (120 ml), *N*-bromosuccinimide (4.2 g) and 0.2 *N* $HClO_4$ (23 ml) were added with stirring at a temperature of 10°. After maintaining these conditions for 1.5 h, water (100 ml) was added and the solid (7.45 g) which precipitated was collected by filtration. Crystallization from acetone gave two crops (3.21 and 0.50 g, 46%) of *5-bromo-5α-cholestane-3β,4β-diol 4-acetate* (**2***a*): m.p. 156–157° (lit. (2, 4) m.p. 147 and 148°); $[\alpha]_D$ +27° (*c*, 0.4 in $CHCl_3$); n.m.r. ($CDCl_3$) τ 7.88 (singlet, 4β-OAc), 5.15 (multiplet, 3α-H, $w_{\frac{1}{2}}$ = 11 Hz), 4.40 (doublet, 4α-H, J_{ae} = 2.0 Hz); i.r. ($CHCl_3$) 3590 (—OH), 1735 (—$OCOCH_3$) cm^{-1}.

The mother liquors from the above crystallization were taken to dryness and an aliquot (200 mg) was chromatographed using benzene as eluant. In this manner a crystalline substance (52 mg), identified as 4β-*bromo*-5α-*cholestane-3β,5-diol 3-acetate* (**3**), was isolated. Crystallization from acetone gave an analytical sample (50 mg) which exhibited m.p. 152–154°; $[\alpha]_D$ −10° (*c*, 0.2 in $CHCl_3$); n.m.r. ($CDCl_3$) τ 7.80 (singlet, 3β-OAc), 5.60 (doublet, 4α-H, J_{ae} = 2.0 Hz), 4.60 (multiplet, 3α-H, $w_{\frac{1}{2}}$ = 12 Hz); i.r. ($CHCl_3$) 3420–3500 (—OH), 1735 (—$OCOCH_3$) cm^{-1}. In a subsequent experiment, the yield of **3** increased to 28% when it crystallized directly from the mother liquors.

Can. J. Chem. Downloaded from www.nrcresearchpress.com by 210.87.254.105 on 09/05/12
For personal use only.

Can. J. Chem. Downloaded from www.nrcresearchpress.com by 210.87.254.105 on 09/05/12
For personal use only.

Anal. Calcd. for $C_{29}H_{49}O_3Br$: C, 66.26; H, 9.39; Br, 15.25. Found: C, 66.24; H, 8.93; Br, 15.51.

Reactions of 5-Bromo-5α-cholestane-3β,4β-diol 4-Acetate (2a) and of 4β-Bromo-5α-cholestane-3β,5-diol 3-Acetate (3)

(*i*) *Acetylation*

Treatment of 5-bromo-5α-cholestane-3β,4β-diol 4-acetate (**2a**) (31 mg) with acetic anhydride (0.2 ml) and pyridine (0.4 ml) and working up in the usual way gave pure *5-bromo-5α-cholestane-3β,4β-diol diacetate* (**2c**) (16 mg) after crystallization from ether. It had m.p. 149.5–151°; $[\alpha]_D$ +24° (*c*, 0.21 in $CHCl_3$) (lit. (4) m.p. 149.5–150.5°, $[\alpha]_D$ +25°).

When 4β-bromo-5α-cholestane-3β,5-diol 3-acetate (**3**) was treated under the same acetylating conditions, it was recovered unchanged.

(*ii*) *Oxidation*

5-Bromo-5α-cholestane-3β,4β-diol 4-acetate (**2a**) (11.4 mg) in acetone (0.4 ml) was treated with Jones' reagent (0.05 ml) and left standing at room temperature for 2 h. Excess isopropyl alcohol was then added and, after working up in the usual way, pure *5-bromo-4β-hydroxy-5α-cholestan-3-one acetate* (7) (8.0 mg) was obtained with m.p. 128–129°; $[\alpha]_D$ +100° (lit. (3) m.p. 117–122° (capillary), 126–127° (dec.); $[\alpha]_D$ +99° and (4) m.p. 124–125°; $[\alpha]_D$ +91°).

4β-Bromo-5α-cholestane-3β,5-diol 3-acetate (**3**) (10.0 mg) was recovered unchanged when an attempt was made to oxidize this compound under the conditions described above.

(*iii*) *Epoxidation and Oxidation*

To a suspension of **2a** (40.5 mg) in methanol (2.0 ml) was added 1.0 ml of KOH solution (1.2 g of KOH in 1.5 ml of H_2O and 12 ml of CH_3OH) and the reaction mixture was refluxed for 0.5 h. Water (2.0 ml) was then added, the methanol removed under reduced pressure, and the organic material extracted with chloroform. Working up in the usual way gave *4β,5-oxido-5β-cholestan-3β-ol* (**5a**) as a foamy solid (30.8 mg). The i.r. spectrum indicated the absence of acetate and the presence of an hydroxy group (3600–3500 cm^{-1}); n.m.r. ($CDCl_3$) τ 6.82 (doublet, 4α-H, J_{ae} = 2.0 Hz), 5.90 (multiplet, 3α-H, $w_{\frac{1}{2}}$ = 10 Hz). Oxidation of this alcohol in acetone (2.0 ml) with Jones' reagent (0.03 ml) at 0° and then allowing to stand at room temperature for 0.3 h gave, after usual work-up, a crude product which was purified by chromatography. Elution with benzene gave a solid which, on crystallization from ether, yielded pure *4β,5-oxido-5β-cholestan-3-one* (**6a**): m.p. 115–117° (lit. (4) m.p. 113–114°); o.r.d. (dioxane) $[\Phi]_{450}$ +750°, $[\Phi]_{338}$ +6750°, $[\Phi]_{332}$ +6500°, $[\Phi]_{327}$ +6670°, $[\Phi]_{285}$ −6410°.

Treatment of **3** (48.0 mg) with base under the conditions described above gave *4α,5-oxido-5α-cholestan-3β-ol* (**5b**) as a foamy solid (39.6 mg). No acetate absorption was observed in the i.r. spectrum but the presence of an hydroxyl group (3600–3500 cm^{-1}) was indicated; n.m.r. ($CDCl_3$) τ 7.20 (singlet, 4β-H), 6.15 (multiplet, 3α-H, $w_{\frac{1}{2}}$ = 11 Hz). Oxidation of this alcohol (10.0 mg) in the manner already described gave crude *4α,5-oxido-5α-cholestan-3-one* (**6b**) (7.6 mg) which could be purified by crystallization from ether. It had m.p. 118–121° (lit. (2) m.p. 123–124.5°); $[\Phi]_{450}$ −360°, $[\Phi]_{337}$ −6550°, $[\Phi]_{331}$ −6450°, $[\Phi]_{327}$ −6800°, $[\Phi]_{282}$ +9150°.

5-Bromo-4β,19-oxido-5α-cholestan-3β-ol Acetate (8)

Lead tetraacetate (8.0 g, previously dried over P_2O_5) and $BaCO_3$ (1.0 g) were added to cyclohexane (180 ml) and this mixture was heated under reflux for 0.3 h. 5-Bromo-5α-cholestane-3β,4β-diol 4-acetate (**2a**) (0.50 g, 9.5 mmol) was then added and refluxing continued for an additional 18 h. After cooling the reaction mixture, the insoluble material was removed by filtration through celite and the filtrate was worked up in the usual way. The oily product (0.48 g) was chromatographed on silica gel using benzene as eluant. The first fraction (102 mg) could be crystallized from ether (80 mg, 17%) and this substance was identified as *4β,5-oxido-5β-cholestan-3β-ol acetate*: m.p. 85–90°; $[\alpha]_D$ −18° (*c*, 0.1 in $CHCl_3$) (lit. (9) m.p. 89–90°, $[\alpha]_D$ −21 ± 1°); n.m.r. ($CDCl_3$): τ 7.82 (singlet, 3β-OAc), 6.80 (doublet, 4α-H, J_{ae} = 4.0 Hz), 4.80 (multiplet 3α-H, $w_{\frac{1}{2}}$ = 16 Hz).

Further elution with benzene gave 5-bromo-4β,19-oxido-5α-cholestan-3β-ol acetate (**8**) (127 mg, 25%). An analytical sample, obtained by crystallization from benzene–methanol exhibited m.p. 154–156°; $[\alpha]_D$ −2° (*c*, 0.13 in $CHCl_3$); n.m.r. ($CDCl_3$) τ 7.90 (singlet, 3β-OAc), 6.35, 6.19, 5.82, 5.80 (quartet, —OCH_2—, J_{AB} = 3.0 Hz), 4.30 (multiplet, 3α-H, $w_{\frac{1}{2}}$ = 11 Hz); i.r. ($CHCl_3$) 1490 (—OCH_2—) cm^{-1}.

Anal. Calcd. for $C_{29}H_{47}O_3Br$: C, 66.52; H, 9.05; Br, 15.26. Found: C, 66.30; H, 8.73; Br, 15.05.

Further fractions were obtained in non-crystalline form, mostly as mixtures (t.l.c.), and these were not submitted to further separation and identification.

4-Cholestene-3β,19-diol 3-Acetate (9)

Zinc dust (325 mg) was added in small portions over a period of 0.3 h to a stirred solution of 5-bromo-4β,19-oxido-5α-cholestan-3β-ol acetate (**8**) (32 mg, 0.06 mmol) in DMF (3.2 ml) at 50°. These conditions were maintained for another 4.0 h and the reaction mixture was then cooled and the zinc removed by filtration through celite. Working up in the usual way gave a crude product (27 mg) which crystallized from methanol as 4-cholestene-3β,19-diol 3-acetate (**9**) (15 mg): m.p. 116°; $[\alpha]_D$ +20° (*c*, 0.1 in $CHCl_3$); n.m.r. ($CDCl_3$): τ 8.0 (singlet, 3β-OAc), 6.45, 6.35, 6.15, 5.90 (quartet, —OCH_2—, J_{AB} = 5.0 Hz), 4.75 (multiplet, 3α-OAc, $w_{\frac{1}{2}}$ = 8.0 Hz), 4.35 (singlet, 4-H).

The authors gratefully acknowledge the financial support of the National Research Council of Canada.

1. P. MORAND and M. KAUFMAN. Can. J. Chem. **49**, 3185 (1971).
2. D. J. COLLINS. J. Chem. Soc. 3919 (1959).
3. D. J. COLLINS. Aust. J. Chem. **16**, 658 (1963).
4. S. JULIA and B. FÜRER. C. R. **257**, 710 (1963); Bull. Soc. Chim. Fr. 1114 (1966).
5. P. MORAND and A. VAN TONGERLOO. Chem. Commun. 7 (1972); Steroids **21**, 47 (1973).
6. S. JULIA and J. P. LAVAUX. Bull. Soc. Chim. Fr. 1238 (1963).
7. S. M. KUPCHAN, P. SLADE, R. J. YOUNG, and G. W. A. MILNE. Tetrahedron, **18**, 499 (1962).
8. N. S. BHACCA and D. H. WILLIAMS. Applications of NMR spectroscopy in organic chemistry. Holden-Day Inc., San Francisco, 1966. pp. 51 and 79.

9. PL. A. PLATTNER, H. HEUSSER, and A. B. KULKARNI. Helv. Chim. Acta **31**, 1822 (1948).
10. C. DJERASSI, W. KLYNE, T. NORIN, G. OHLOFF, and E. KLEIN. Tetrahedron, **21**, 163 (1965).
11. K. BOWDEN, I. M. HEILBRON, E. R. H. JONES, and B. C. L. WEEDON. J. Chem. Soc. 79 (1946).
12. D. J. COLLINS, J. J. HOBBS, and S. STERNHELL. Tetrahedron Lett. 623 (1963).
13. V. GRENVILLE, D. K. PATEL, V. PETROW, I. A. STUART-WEBB, and D. M. WILLIAMSON. J. Chem. Soc. 4105 (1957); M. AKHTAR and D. H. R. BARTON. J. Am. Chem. Soc. **84**, 1496 (1962).
14. L. F. FIESER and M. FIESER. Steroids. Reinhold Publishing Corporation, New York, 1959. p. 271.
15. S. JULIA and R. LORNE. C. R. **268**, 1617 (1969).
16. P. MORAND and M. KAUFMAN. J. Org. Chem. **34**, 2175 (1969).
17. J. F. BAGLI, P. MORAND, and R. GAUDRY. J. Org. Chem. **28**, 1207 (1963).
18. H. MCKENNIS and G. W. GAFFNEY. J. Biol. Chem. **175**, 217 (1948).

Can. J. Chem. Downloaded from www.nrcresearchpress.com by 210.87.254.105 on 09/05/12
For personal use only.

Ring C Functionalized Diterpenoids. Part I. The Hypoiodite Reaction as a Route to Ring C Functionalized Kauranes and Phyllocladanes

ALAN JAMES MCALEES AND ROBERT MCCRINDLE[1]

Chemistry Department, University of Guelph, Guelph, Ontario N1G 2W1

Received July 26, 1973

16β-*ent*-17-Kauranol (**1***a*), the corresponding C-19 ester (**1***b*), and 16β,17-phyllocladanol (**2**), on reaction with lead tetraacetate – iodine in refluxing cyclohexane, suffered intramolecular attack mainly at C-11. Thus **1***a* gave as major products the 11-en-17-ol (**3***a*) and the 11β-iodo-12β,17-ether (**4***a*), along with minor amounts of the 9,11-en-12β,17-ether (**5**), the 11β,17-ether (**6***a*), and, resulting from attack at C-12, the 12β,17-ether (**7**). The phyllocladanol **2** gave the 11β,17-ether (**8**) and the 9,11-en-12β,17-ether (**9**). The assignment of structures **6***a*, **7**, and **8** to the ethers rests on their conversion with ruthenium tetroxide into the corresponding lactones, **10**, **11**, and **12**.

L'*ent*-16β Kauranol-17 (**1***a*), l'ester C-19 correspondant (**1***b*) et le phyllocladanol-16β,17 (**2**), subissent une attaque intramoléculaire principalement au site C-11 lorsqu'ils sont reflués dans le cyclohexane en présence de tétraacétate de plomb–iode. Ainsi, **1***a* a donné, comme produits majeurs, l'ène-11 ol-17 (**3***a*) et l'éther-12β,17 iodo-11β (**4***a*), en même temps que des petites quantités d'éther-12β,17 ène-9,11 (**5**), d'éther-11β,17 (**6***a*) ainsi que d'éther-12β,17 (**7**) résultant de l'attaque en C-12. Le phyllocladanol **2** a conduit à l'éther-11β,17 (**8**) et à l'éther-12β,17 ène-9,11 (**9**). L'attribution des structures **6***a*, **7** et **8** aux éthers est basée sur leur transformation à l'aide du tétroxyde de ruthénium en lactones correspondantes, **10**, **11** et **12**. [Traduit par le journal]

Can. J. Chem., **51**, 4103 (1973)

In connection with work on carbonium ion rearrangements in the tetracyclic diterpenoid field, we have been exploring routes to 13-substituted atisiranes and 12-substituted kauranes and beyeranes. An additional incentive for these studies has been the discovery of a wide range of natural products with ring C functionality. Compounds of this type include alkaloids derived from atisirene (1–4) and rearranged atisirenes (aconitine) (5), kaurenes (6–9) and modified kauranes (10,11) (including gibberellins (12,13) and alkaloids (14–16)), and beyeranes (17). No synthetic approaches to such systems have been reported apart from that of Coates and Bertram (18) for the beyerane type. The present paper deals with the introduction of substituents into ring C of kauranes and phyllocladanes. In subsequent papers, routes to analogously substituted atisanes and beyeranes will be described.

The considerable synthetic utility of the hypoiodite reaction of alcohols, which usually results in attack at a δ-carbon atom, has been reviewed (19). We have now applied this reaction to the *ent*-kauranols **1***a* and *b*, and to the phyllocladanol **2**, in which the *endo* carbinol functions are ideally situated for intramolecular attack on ring C. Since *ent*-kauren-19-oic acid (**13***a*), accompanied by trachylobanic acid, is readily obtainable from the common sunflower (20), our first experiments were carried out using the kauranol ester **1***b*, which was prepared by hydroboration–oxidation of methyl *ent*-kauren-19-oate (**13***b*).

[1]To whom correspondence should be addressed.

Results

A mixture of ester **1***b*, 1 g-equiv. of iodine, excess lead tetraacetate, and calcium carbonate in refluxing cyclohexane was irradiated with a tungsten lamp, the reaction being allowed to proceed for 1.5 h although the color of the iodine had disappeared after 35–40 min. Thin layer chromatography of the reaction mixture after work-up indicated the presence of at least four products, the most polar pair of which had very similar R_f values. On standing in solution or on warming on the water bath during the removal of solvent under vacuum, the color of iodine appeared, suggesting that HI was being eliminated from a reaction product and subsequently undergoing air oxidation. Accordingly, the mixture was treated with pyridine and then reexamined by t.l.c., which showed the disappearance of the most polar product and an increase in the intensity of the neighbouring spot. The three main products in this later mixture were then

Can. J. Chem. Downloaded from www.nrcresearchpress.com by 210.87.254.6 on 09/05/12
For personal use only.

Can. J. Chem. Downloaded from www.nrcresearchpress.com by 210.87.254.6 on 09/05/12
For personal use only.

separated by column chromatography over alumina and then preparative t.l.c.

The most polar "product" in fact proved to be a mixture of methyl 17-hydroxy-*ent*-kaur-11-en-19-oate (**3***b*) and starting material with the former predominating. Pure **3***b* (*vide infra*) had m.p. 105–107.5° and $\nu_{OH}(CCl_4)$ 3637 cm^{-1}, the primary nature of the alcohol function being confirmed by the n.m.r. spectrum (τ 6.47, 2 H-17, d, $J \sim 7$ Hz) which also revealed the presence of the 11,12 double bond, H-11 appearing at τ 4.43 (dd, J = 10 and 3.4 Hz) and H-12 at τ 4.08 (apparent dd with additional broadening, J_{obs} = 10 and 5.5 Hz) (*cf.* ref. 9.).

The principal product of intermediate polarity **4***b*, m.p. 107–109°, lacks hydroxyl absorption in the i.r. and is rather unstable, the color of iodine appearing on storage at room temperature, either in the solid state or in solution. The resulting inference that **4***b* is an iodoether is supported by its n.m.r. spectrum, which shows multiplets at τ 5.63 (dd, H-12, J = 8 and 4.5 Hz) and 5.95–6.35 (complex m, H-11 + 2 H-17), and by its reaction with zinc and acetic acid in diethyl ether to give **3***b*. The stereochemistry at C-11 and ring size of the ether in **4***b* are assigned by analogy with the corresponding product (**4***a*) obtained from **1***a* and discussed below.

The n.m.r. spectrum of the least polar principal product (**6***b*, m.p. 153–155°) has resonances at τ 6.07 (narrow m, H-11), 6.22, and 6.66 (each broadened d, 2 H-17, J_{obs} = 10 Hz), indicating that it is an ether. The assignment of structure **6***b* is based on the finding that oxidation of the related compound **6***a* with ruthenium tetroxide gives a δ-lactone (*vide infra*).

In subsequent investigations, we turned to 16β-*ent*-17-kauranol (**1***a*)[2] since the minor products of the hypoiodite reaction of this compound are more tractable than those from **1***b* and since important peaks in the n.m.r. spectra of products from the latter are partly obscured by the carbomethoxy resonance. The reaction of **1***a* was carried out as indicated above for **1***b* except that the reaction was stopped soon after

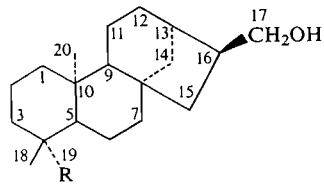

1

a R = CH_3
b R = CO_2CH_3

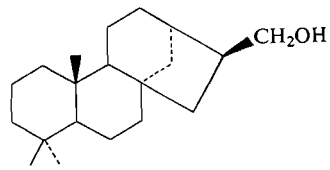

2

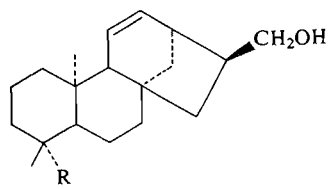

3

a R = CH_3
b R = CO_2CH_3

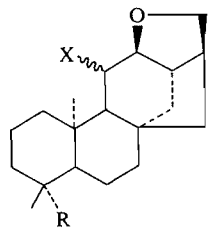

4

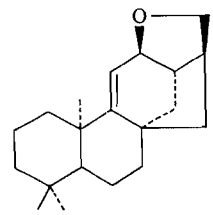

5

a R = CH_3; X = βI
b R = CO_2CH_3; X = βI
c R = CO_2CH_3; X = αOAc
d R = CO_2CH_3; X = αOH
e R = CH_3; X = βOH

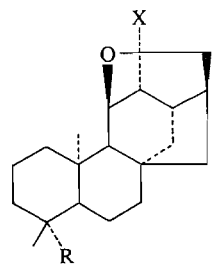

6

a R = CH_3; X = H
b R = CO_2CH_3; X = H
c R = CO_2CH_3; X = OAc
d R = CO_2CH_3; X = OH

[2]When the hypoiodite reaction of **1***b* was repeated using excess iodine to ensure complete consumption of starting material and conversion of any **3***b* formed to **4***b* (see Discussion), the resulting mixture contained two new products, the acetates **4***c* and **6***c*. As these had very similar R_f values on t.l.c., they were separated by hydrolysis to the corresponding alcohols, **4***d* and **6***d*, respectively, followed by preparative t.l.c. Acetylation of **4***d* and **6***d* with acetic anhydride – pyridine regenerated **4***c* and **6***c*.

Can. J. Chem. Downloaded from www.nrcresearchpress.com by 210.87.254.6 on 09/05/12
For personal use only.

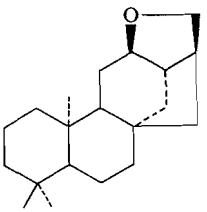

7

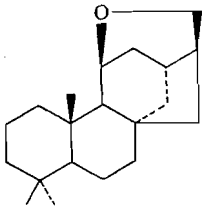

8

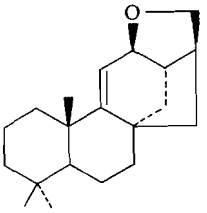

9

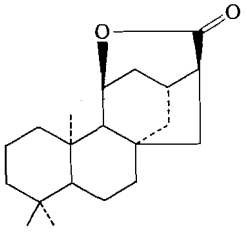

10

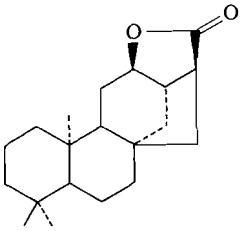

11

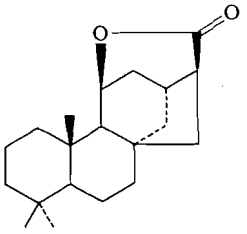

12

(10 min) the color of the iodine had disappeared. Thin-layer chromatography of the reaction mixture indicated the presence of three major products, the more polar pair having very similar R_f values. As before, the color of iodine appeared when the mixture was allowed to stand at room temperature and treatment with pyridine led to the disappearance of the most polar major product with concommitant buildup of the product with similar R_f value. Column chromatography over alumina of the mixture remaining after pyridine treatment led to separation of the two major products and to partial resolution of the minor products, which were further purified by t.l.c.

The more polar major "product" proved to be a mixture of **3***a*: m.p. 162–163°; $\nu_{OH}(CCl_4)$ 3639 cm^{-1}; τ 9.20, 9.13, 9.08 (all s, quaternary C—CH_3's), 6.43 (d, 2 H-17, J = 7.2 Hz), 4.41 (dd, H-11, J = 9.5 and 3.5 Hz), and 4.07 (apparent dd with additional broadening, H-12, J_{obs} = 10 and ~6 Hz); and starting material (**1***a*) in which the former predominated.

The less polar major product, **4***a*, m.p. 110–110.5°; τ 9.19, 9.14, 9.01 (all s, quaternary C—CH_3's), 6.33–5.95 (complex m, 2 H-17 + H-11), and 5.62 (dd, H-12, $J_{12,11}$ = 8 Hz, $J_{12,13}$ = 4.8 Hz), decomposes slowly in the solid state or in solution with the appearance of the color of iodine and reacts with zinc and acetic acid in ether to give **3***a* in high yield. Reaction of **4***a* with lithium aluminum hydride gives an ether (**7**) in high yield plus a little **3***a*. The ether (**7**) was identical with one of the minor products of the hypoiodite reaction of **1***a* and the elucidation of its structure is discussed below. The iodine atom in **4***a* is assigned the 11β-configuration rather than 11α on the basis of the observed coupling constants and on the finding that the C-10 methyl resonance position is not markedly altered on going from **4***a* to **7** (9.01 and 9.10, *cf.* C-10 methyl resonance in **6***a* at τ 9.03).

By careful preparative t.l.c. two minor products,[3] which were slightly less polar than **4***a* and did not show clearly on the original analytical plate, were isolated. The assignment of structure **5** to the more polar of these, m.p. 86–89°, is based on the n.m.r. spectrum which shows peaks at τ 6.73 (dd, βH-17, J_{obs} ~3.5 and ~9 Hz), 6.05 (t, αH-17, J_{obs} ~8.5 Hz), 5.42 (apparent dd, H-12, J_{obs} ~3.5 and ~7 Hz), and 4.85 (d, H-11, J_{obs} ~3.5 Hz). Examination of models of **5** shows that βH-17 lies in the shielding zone of the 9,11-double bond and hence should resonate at higher field than αH-17. The second minor product was obtained as an oil which ran as a single spot on analytical t.l.c. but failed to crystallize. The n.m.r. spectrum of this impure material showed it to be essentially identical with the main product (**7**) of reaction of iodoether **4***a* with lithium aluminum hydride. The compound (**7**) thus obtained could be crystallized, although with some difficulty, and had m.p. 41.5–43.5°, its formulation as an ether being sustained by peaks at τ 6.1–6.5 (complex m, 2 H-17) and 5.6–5.9 (complex m, H-12) in its n.m.r. spectrum. This resonance pattern differs markedly from that observed for the ether **6***b* previously obtained from the kauranol ester **1***b*. Examination of models of 16β-*ent*-17-kauranol (**1***a*) and of the 11β,17-(**6**) and 12β,17-(**7**) ethers in the light of the suggested mechanism of the hypoiodite reaction (19) indicated that both five- and six-membered ring ethers might be

[3]A further minor product, **4***e*, was isolated from the mixture obtained in a subsequent hypoiodite reaction of **1***a* under the same conditions as before.

Can. J. Chem. Downloaded from www.nrcresearchpress.com by 210.87.254.6 on 09/05/12
For personal use only.

formed from **1**. This examination also suggests that the lone proton α to the ether function should have larger coupling constants with neighbouring protons in the tetrahydrofuran (**7**) than in the tetrahydropyran (**6**). This is consistent with the observation of a relatively narrow multiplet for H-11 in **6***b* and a much broader multiplet for H-12 in **7**. However, as it was desirable to have more conclusive evidence for the nature of the cyclic ether functions in these compounds, we decided to attempt the oxidation of the ethers to the corresponding lactones using ruthenium tetroxide (21, 22). Thus, a catalytic quantity of a solution of RuO_4 in carbon tetrachloride was added to the impure ether (**7**), isolated from the hypoiodite reaction of **1***a*, in the same solvent and the resulting mixture was stirred vigorously at room temperature with excess of an aqueous solution of sodium periodate. The progress of the reaction was followed by t.l.c. When all the starting material had disappeared (10 days), t.l.c. indicated the presence of two products and a trace of polar material. After separation by preparative t.l.c., the major and less polar product, the γ-lactone **11**, had m.p. 170–171°; $\nu_{C=O}(CCl_4)$ 1778 cm^{-1}; τ 6.82–7.33 (m, H-13 + H-16) and 5.00–5.28 (m, H-12). The minor product had m.p. 175–176°; τ 6.97–7.55 (m, H-13 + H-16), 5.52 (narrow m, H-11); and $\nu_{C=O}(CCl_4)$ 1749 cm^{-1}, which suggests that it is the δ-lactone **10** and that the impurity in the tetrahydrofuran (**7**) obtained by the hypoiodite reaction of **1***a* is 11β,17-oxido-16β-*ent*-kaurane (**6***a*). This was confirmed by the preparation of **6***a* from **1***a* and the subsequent oxidation of the former with ruthenium tetroxide – sodium periodate to **10** (*vide infra*).

The hypoiodite reaction of 16β,17-phyllocladanol (**2**), obtained by hydroboration–oxidation of phyllocladene, under the same conditions as those used for **1***a* gave a mixture which again liberated iodine on standing. Treatment with pyridine as before gave a mixture which appeared to contain three principal components (t.l.c.), all appreciably less polar than starting material. These were readily separated by preparative t.l.c.

The least polar and main product had m.p. 71.5–73° and lacked hydroxyl absorption in the infrared. The n.m.r. spectrum showed peaks at τ 6.60 and 6.27 (each broadened d, 2 H-17, $J_{obs} = 10$ Hz) and 5.65 (m, H-11). The close similarity of this portion of the n.m.r. spectrum to the same region in the spectra of **6***a* and *b* suggested the formulation of this product as 11β,17-oxido-16β-phyllocladane (**8**). This was confirmed by the oxidation of **8** to **12**, which had m.p. 188–189°; $\nu_{C=O}(CCl_4)$ 1754 and 1745 cm^{-1}; and τ 5.10 (m, H-11).

The "product" of intermediate polarity was obtained as an oil which appeared uniform on analytical t.l.c. but the complexity of the methyl region of the n.m.r. spectrum showed it to be a mixture. Absorption in the low-field region of the n.m.r. spectrum suggested the presence of ether(s), accordingly, the mixture was oxidized with ruthenium tetroxide – sodium periodate. The resulting mixture appeared to contain at least four components (t.l.c.) which we have not attempted to separate due to shortage of material.

The most polar product isolated from the hypoiodite reaction of **2** is the ene-ether **9**, m.p. 82–87°. The n.m.r. spectrum of the latter, from which its structure was deduced, is very similar to that of **5**, showing peaks at τ 6.77 (dd, βH-17, $J_{obs} \sim 9$ and ~ 4 Hz), 6.05 (t, αH-17, $J_{obs} \sim 9$ Hz), 5.44 (broadened dd, H-12, $J_{obs} \sim 3.5$ and ~ 6 Hz), and 4.83 (d, H-11, $J_{obs} \sim 3.5$ Hz).

Discussion

The hypoiodite reaction of an alcohol can be envisaged as involving the formation of an oxygen radical (Scheme 1; **i** → **ii**) which may subsequently abstract a suitably disposed hydrogen atom, usually from a δ-carbon atom via a six-membered ring transition state, to give a carbon radical (Scheme 1; **iii**) (19). The carbon radical can then react with an iodine atom to give an iodohydrin (**iii** → **iv**). If the carbon atom originally attacked is a methylene carbon, the resulting iodohydrin (**iv**) may react further by the pathways outlined in Scheme 1.

Examination of models of 16β-*ent*-17-kauranol (**1***a*) and 16β,17-phyllocladanol (**2**) indicates that the derived oxygen radicals should be able to abstract a β-hydrogen from either C-12 (δ-carbon) or C-11 (ε-carbon). It has been suggested (19) that reaction is most favoured if the distance between the centers of the oxygen atom and the carbon atom from which hydrogen is abstracted lies in the range 2.5–2.7 Å, and if a linear transition state (—O · · · H · · · C—) is possible. On this basis, it would appear that attack at C-11 should occur more readily than attack at C-12 (*cf.* **14**–**17**). This conclusion is confirmed by the

Can. J. Chem. Downloaded from www.nrcresearchpress.com by 210.87.254.6 on 09/05/12
For personal use only.

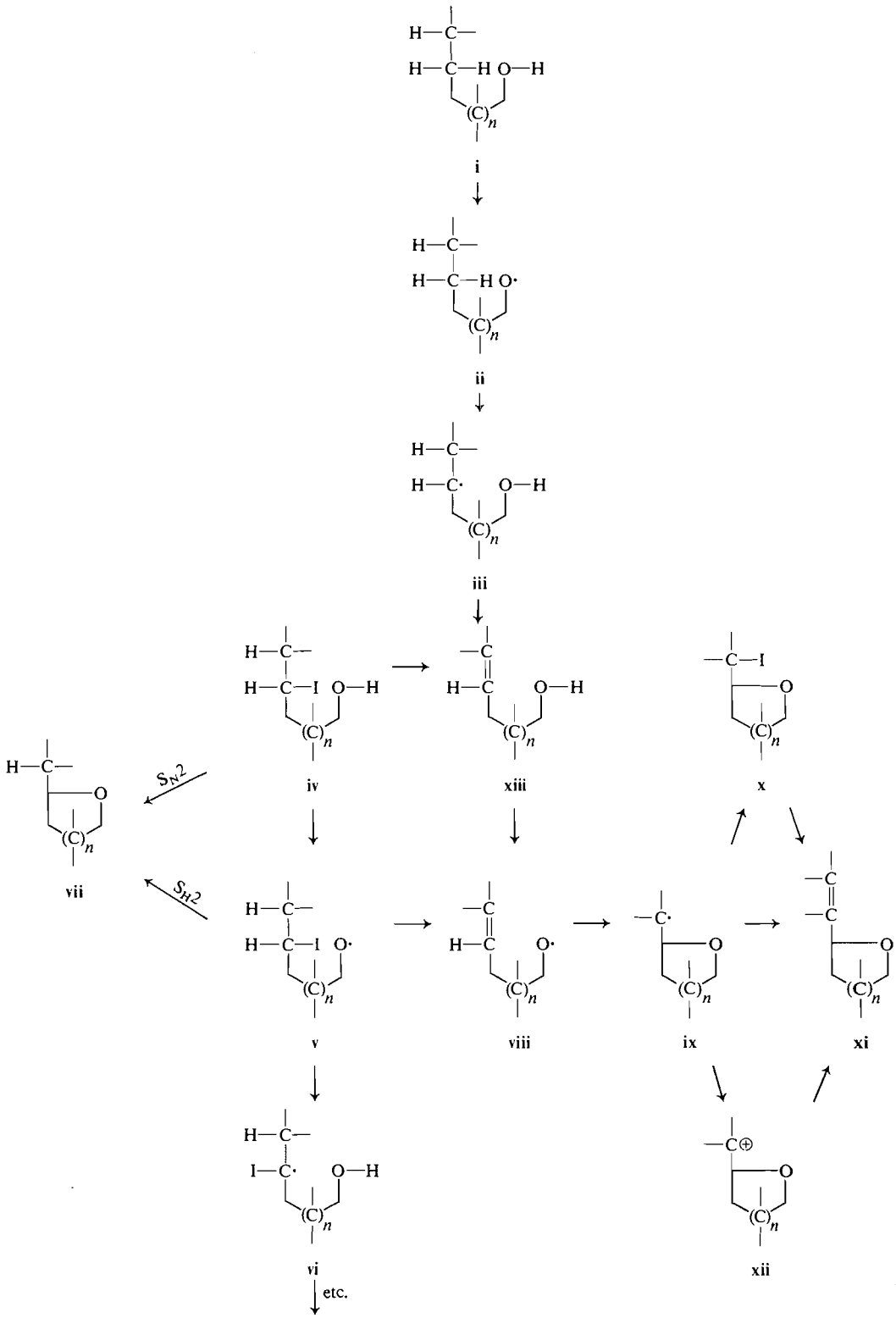

SCHEME 1

Can. J. Chem. Downloaded from www.nrcresearchpress.com by 210.87.254.6 on 09/05/12
For personal use only.

nature of the products isolated from **1***a* (or *b*) and **2**.

The C-12 radical from **1***a* should suffer attack by an iodine atom to give the 12α-iodide preferentially (*cf.* **15**).[4] This iodine atom would then be suitably disposed to undergo intramolecular displacement in an S_N2 or S_H2 process (Scheme 1; **iv** → **v**, **vii**; $n = 1$) with formation of the tetrahydrofuran **7** (**15**). Alternatively, the 12α-iodide from **1***a* might lose HI with the formation of an 11,12 double bond (Scheme 1; **iv** → **viii** etc.; $n = 1$), leading eventually to **3***a*, **4***a*, and **5**. However, the low yield of **7** from **1***a* suggests that initial abstraction of a hydrogen atom from C-12 is not of major importance.

The C-11 radical from **1***a* should undergo attack by iodine from the β face (*cf.* **14**) to give the 11β-iodide (**18***a*) in which the iodine is not suitably disposed to undergo an S_N2 or S_H2 displacement with formation of the tetrahydropyran, **6***a* (Scheme 1; **iv** → **v**, **vii**; $n = 2$). However, this axial iodide (**18***a*) should suffer ready elimination of HI to give **3***a*. Elimination to give a 9,11 double bond is not favourable since H-9 is *cis* to the 11β-iodine (*cf.* elimination of 11β-tosylate in ref. 9). It would thus appear likely that the unstable products of the hypoiodite reaction of **1***a* and *b*, which disappear on treatment with pyridine, are the 11β-iodides, **18***a* and *b*, respectively. However, we still have to explain the formation of the tetrahydropyrans **6***a* and *b*, the latter having been obtained in fair yield from a prolonged reaction, while only traces of the former were present in a reaction which was stopped soon after the color of iodine had disappeared. From this it was inferred that these ethers are probably formed by reaction of **1***a* or *b* with lead tetraacetate alone (23), a pathway which will gain in importance after consumption of all or most of the available iodine. This was confirmed by repeating the hypoiodite reaction of **1***a* and continuing the reflux for 3h. Thin-layer chromatography of the product after work-up now showed a distinct spot of somewhat greater R_f than the iodoether (**4***a*). This product proved to be **6***a*, m.p. 123–125°; τ 6.22 and 6.61 (each d, 2 H-17, J_{obs} = 10.5 Hz) and 6.07 (narrow m,

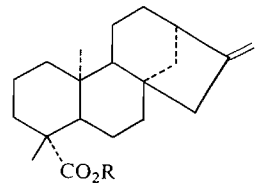

13
a R = H
b R = CH_3

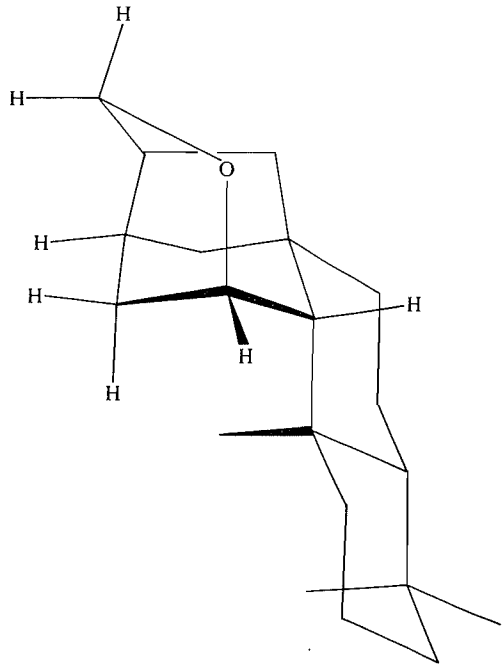

14

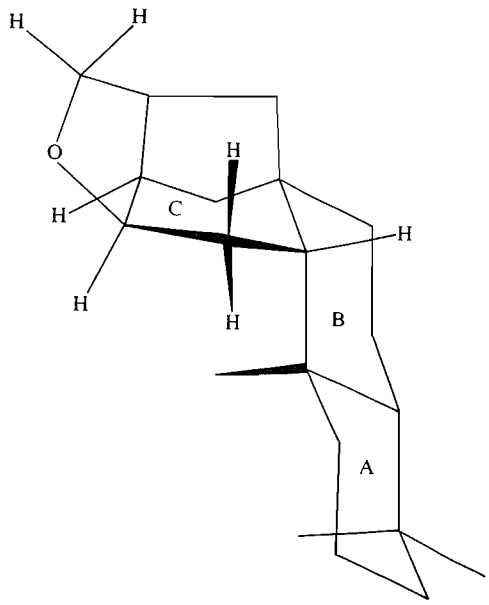

15

[4]We have considered various conformations for this compound, including the possibility of a full boat ring C, but that drawn, with this ring flattened, appears preferable. The presence of an 11α- or 11β-iodo substituent (see later) should enhance the preference for this conformation.

Can. J. Chem. Downloaded from www.nrcresearchpress.com by 210.87.254.6 on 09/05/12
For personal use only.

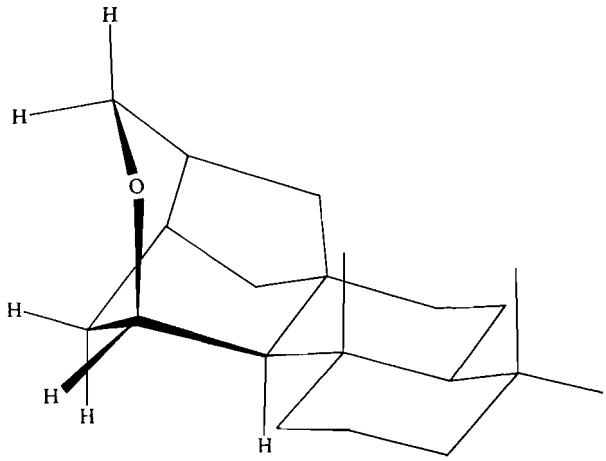

16

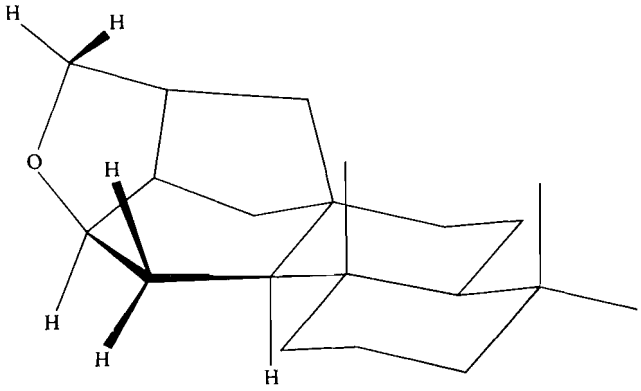

17

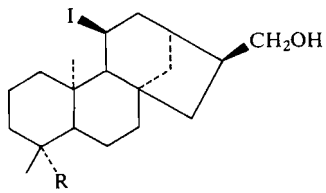

18

8*a* R = CH_3
8*b* R = CO_2CH_3

H-11), which, on oxidation with ruthenium tetroxide – sodium periodate, gave the lactone **10**. Further, reaction of **1***a* with lead tetraacetate alone (23) in refluxing cyclohexane for 24 h gave almost pure **6***a*, supporting the contention that the hypoiodite reaction of the former proceeds mainly via hydrogen abstraction from C-11.

The remaining products from **1***a* may arise via the oxygen radical derivable from **3***a* (Scheme 1; **viii** → **x**, **xi**; $n = 1$). Indeed, **3***a*, under the same reaction conditions as **1***a*, gives a high yield of **4***a*. This iodoether (**4***a*) does not appear to be a precursor of **5** since the former was recovered from attempts to eliminate HI with base (pyridine at room temperature or sodium methoxide in refluxing methanol–THF). This would suggest that H-9 is *cis* to the iodine at C-11, supporting the assignment of the 11β configuration to the latter. The ene-ether (**5**) may therefore arise via oxidation of the C-11 radical to a carbonium ion followed by proton elimination (Scheme 1; **ix** → **xii** → **xi**; $n = 1$). This con-

Can. J. Chem. Downloaded from www.nrcresearchpress.com by 210.87.254.6 on 09/05/12
For personal use only.

clusion is reinforced by the observation of an increased yield of **5** in the prolonged hypoiodite reaction of **1***a*. It should therefore be possible to prepare **5** from **3***a* by reaction with lead tetraacetate alone.

Similar arguments to those presented above may be applied to explain the products of the hypoiodite reaction of 16β,17-phyllocladanol (**2**). Thus the C-11 radical derived from **2** would be expected to give the 11α-iodide (*cf.* **16**), which, in contrast to the case above, is suitably oriented to undergo S_N2 or S_H2 displacement with formation of **8** (**16**) which is in fact the principal product. Elimination of HI is probably less favourable in this case than for **18***a* (*b*) since the 11α-iodine is equatorial in the most stable (chair) conformation of ring C. As before, H-9 is *cis* to the iodine so that elimination of HI should give a $\Delta^{11,12}$ intermediate from which the ene-ether **9** may subsequently be derived as outlined for **5** above. It is perhaps surprising that no iodo-ether (**17** with I in place of 11α-H) was isolated, since this product would be expected to resist HI elimination by analogy with **4***a*.

The C-12 radical derived from **2** could probably attach iodine on either the α or the β side (*cf.* **17**), the former intermediate being expected to give an ether (**17**) via an S_N2 or S_H2 process, while the latter could be a precursor of **9** and other products. Unfortunately, the quantity of starting material available has precluded a study of the minor products of the hypoiodite reaction of **2**.

Experimental

Melting points were determined on a Kofler hot-stage apparatus and are uncorrected. For analytical and preparative t.l.c. chromatoplates were spread with Kieselgel G. (Merck). Alumina (Fisher) and silica gel (Baker) used for column chromatography were 80–200 and 40–140 mesh, respectively. Lead tetraacetate (British Drug Houses) was dried for several hours at 0.02 mm Hg and cyclohexane was distilled from calcium hydride immediately before use. Light petroleum was of b.p. 60–80°. Microanalyses were by Mr. S. McKinnon, Guelph. Infrared solution spectra were recorded in carbon tetrachloride on a Beckmann I.R. 12 spectrophotometer, and p.m.r. spectra on a Varian Associates A-60A spectrometer, in carbon tetrachloride unless otherwise stated.

Methyl ent-Kauren-19-oate and Methyl ent-Trachyloban-19-oate from Helianthus annuus

The literature method (20) was modified to the following. Mature, dried sunflower heads were ground after removal of the seeds (courtesy of the local bird population) and the resulting powder (5 kg) was packed into a large chromatography column. Elution with ether until no further material was extracted afforded an oil (300 g) containing *ent*-kaurenoic and *ent*-trachylobanic acids. A considerable proportion of unwanted material in this mixture was conveniently separated from the acids by dry column chromatography over silica gel (900 g) using light petroleum (1500 ml) as the developing solvent. The acid-enriched fraction thus obtained (35 g) was then subjected to column chromatography over silica gel (600 g). Elution with ethyl acetate – light petroleum (1:99; 500 ml) gave most of the material less polar than the desired acids; ethyl acetate – light petroleum (1:49; 500 ml) gave initially a mixture of acids and some less polar material, and subsequently, the acids plus more polar material; and finally ethyl acetate – light petroleum (3:97 → 1:19; 1500 ml) eluted the remainder of the acids along with more polar material. The last two sets of fractions were combined (28 g) and esterified with diazomethane, and the esters were chromatographed over 12% silver nitrate – silica gel in batches of 7 g of mixture to 250 g of adsorbent. Elution with ethyl acetate – light petroleum mixtures of gradually increasing polarity (0 → 1:49) gave methyl *ent*-trachyloban-19-oate (8 g) and methyl *ent*-kauren-19-oate (14 g).

Hydroboration–Oxidation of Methyl ent-Kauren-19-oate

Boron trifluoride etherate (1.80 g) in diglyme (5 ml) was added dropwise with stirring to a mixture of methyl *ent*-kauren-19-oate (2.00 g) and sodium borohydride (0.36 g) in diglyme (35 ml) under nitrogen at room temperature. The mixture was stirred under nitrogen for a further 2 h, then water (2 ml) was added, followed by 3 *N* sodium hydroxide solution (4 ml) and 30% hydrogen peroxide (8 ml). After stirring overnight, the mixture was poured into water (300 ml) and extracted with ether (3 × 75 ml). The combined ether extracts were dried (Na_2SO_4) and evaporated to give an oil which was chromatographed on alumina (45 g), elution with ethyl acetate – light petroleum (1:9) giving pure methyl 17-hydroxy-16β-*ent*-kauran-19-oate (1.47 g); m.p. 120–122°; ν_{OH} 3638 cm^{-1}, after crystallization from hexane.

Anal. Calcd. for $C_{21}H_{34}O_3$: C, 75.41; H, 10.25. Found: C, 75.28; H, 10.51.

The Hypoiodite Reaction of Methyl 17-Hydroxy-16β-ent-kauran-19-oate

A mixture of lead tetraacetate (5.75 g) and calcium carbonate (3.0 g) was stirred for 10 min in refluxing cyclohexane (200 ml), then the kauranol (**1***b*, 1.47 g) and iodine (0.60 g) were added and refluxing was continued while the mixture was irradiated with a 150 W tungsten lamp. After 40 min the color of the iodine had virtually disappeared. The reaction was allowed to proceed for a total of 1.5 h then the mixture was cooled, filtered, and the insoluble material washed with ether, the ether washings being combined with the filtrate. The filtrate was washed successively with sodium thiosulfate solution, water, and brine, and dried over Na_2SO_4. On standing, the initially clear, colorless solution turned light brown due to the liberation of iodine. Filtration and evaporation *in vacuo* on the water bath gave a dark residue (2.01 g), t.l.c. of which (ethyl acetate – light petroleum, 1:9) indicated the presence of four principal components. The dark product was dissolved in pyridine (10 ml) and left overnight at room temperature, after which it was poured into

Can. J. Chem. Downloaded from www.nrcresearchpress.com by 210.87.254.6 on 09/05/12
For personal use only.

ether and the ether solution washed successively with water, sodium thiosulphate solution, water, and brine, then dried over Na_2SO_4. Filtration and evaporation of the ether gave an oil (1.80 g) which liberated iodine very slowly and which showed the presence of only three of the original four main spots on t.l.c., the most polar component in the original mixture having disappeared. The oil was chromatographed on alumina (45 g) and eluted with ethyl acetate – light petroleum mixtures ($0 \rightarrow 1:9$) and finally with ethyl acetate alone. This separated the principal components, which were further purified by preparative t.l.c. using 1:9 ethyl acetate – light petroleum for the ether (**6***b*) and iodoether (**4***b*) and 1:3 ethyl acetate – light petroleum for the kaurenol (**3***b*). The least polar principal product (**6***b*; 0.195 g, 13.3%), on crystallization from methanol, had m.p. 153–155°; τ 9.27 (s, 3 H-20), 8.85 (s, 3 H-18), 6.42 (s, O—CH_3), 6.60 and 6.22 (each broadened d, 2 H-17, J_{obs} = 10 Hz), and 6.07 (narrow m, H-11).

Anal. Calcd. for $C_{21}H_{32}O_3$: C, 75.86; H, 9.70. Found: C, 75.90; H, 9.82.

The iodoether (**4***b*; 0.410 g, 20.3%), after crystallization from hexane, had m.p. 107–109°; τ 9.21 (s, 3 H-20), 8.88 (s, 3 H-18), 6.41 (s, O—CH_3), 5.95–6.35 (complex m partly obscured by O—CH_3 resonance, 2 H-17 + H-11) and 5.63 (dd, H-12, J = 4.5 and 8 Hz). Since this product decomposed slowly in the solid state and the color of iodine appeared in the solvent in the course of attempted crystallization, it was not analysed.

On crystallization from hexane, the kaurenol (**3***b*; 0.400 g, 27.4%) isolated above had m.p. 103–105.5°. Comparison with pure material (*vide infra*), m.p. 105–107.5°, ν_{OH} 3637 cm^{-1}, suggested that the former contained a little of the starting alcohol (**1***b*). The n.m.r. spectrum of pure **3***b* shows peaks at τ ($CDCl_3$) 9.26 (s, 3 H-20), 8.83 (s, 3 H-18), 6.47 (d, 2 H-17, $J \sim 7$ Hz), 6.39 (s, O—CH_3), 4.43 (dd, H-11, J = 10 and 3.4 Hz), and 4.08 (broadened dd, H-12, J_{obs} = 10 and ~5.5 Hz).

Anal. Calcd. for $C_{21}H_{32}O_3$: C, 75.86; H, 9.70. Found: C, 75.75; H, 9.61.

Reaction of Methyl 11β-Iodo-12β,17-oxido-16β-ent-kauran-19-oate with Zinc and Acetic Acid

The iodoether (**4***b*; 0.218 g) was dissolved in dry ether (10 ml), acetic acid (1 ml) and zinc dust (0.20 g) were added and the mixture was stirred overnight at room temperature. Thin-layer chromatography (ethyl acetate – light petroleum, 3:17) showed the presence of a single product with the same R_f as methyl 17-hydroxy-16β-*ent*-kaur-11-en-19-oate (**3***b*). The reaction mixture was filtered, shaken with excess potassium hydroxide solution, and dried over Na_2SO_4. Filtration and evaporation of the solvent left a solid residue (0.159 g) which gave pure **3***b* on crystallization from hexane.

The Hypoiodite Reaction of 1b using Excess Iodine

When the hypoiodite reaction of **1***b* was carried out as above but using double the amount of iodine, t.l.c. showed that all of the starting material had been consumed and a new spot of lower R_f than **4***b* was clearly evident. After work-up as outlined above, followed by column chromatography over alumina, this new "product" was isolated as a viscous oil whose n.m.r. spectrum showed it to be a mixture, peaks at τ ~8 and ~5 suggesting the presence of secondary acetate(s). The oil was subjected to mild hydrolysis (2 h reflux in dilute 1:1 aqueous methanolic NaOH and the mixture of two alcohols thus obtained was readily separated by preparative t.l.c. (ethyl acetate – light petroleum, 3:17).

The more polar alcohol (**6***d*), on crystallization from hexane had m.p. 169–171°; ν_{OH} 3628 cm^{-1} (free; concentration, 2 mg/ml. Contrast **4***e*); τ ($CDCl_3$) 9.06 (s, 3 H-20), 8.82 (s, 3 H-18), 6.47 and 6.05 (each broadened d, 2 H-17, J_{obs} = 10 Hz), 6.37 (s, O-CH_3), 6.07 (narrow m, H-11), and 5.78 (m, H-12); *cf.* n.m.r. spectrum of **6***b*.

Anal. Calcd. for $C_{21}H_{32}O_4$: C, 72.38; H, 9.26. Found: C, 72.29; H, 9.25.

On crystallization from hexane, the less polar alcohol (**4***d*) had m.p. 162–165°; ν_{OH} 3624 cm^{-1} (free; concentration, 2.0 mg/ml. Contrast **4***e*); τ ($CDCl_3$) 8.88 and 8.82 (both s, quaternary C—CH_3's), 6.33 (s, O—CH_3), 6.18 (main peak of m; minor peaks to higher and lower fields obscured; 2 H-17), and 5.77–6.0 (m, H-11 + H-12); *cf.* n.m.r. spectrum of **4***b*.

Anal. Calcd. for $C_{21}H_{32}O_4$: C, 72.38; H, 9.26. Found: C, 72.12; H, 9.26.

Treatment of the alcohols **6***d* and **4***d* with acetic anhydride – pyridine (3 h on steam bath followed by 18 h at room temperature) gave the corresponding acetates, **6***c* and **4***c*.

The former, on crystallization from hexane, had m.p. 103–104°; τ 9.20 (s, 3 H-20), 8.83 (s, 3 H-18), 8.02 (s, OCOCH_3), 6.52 and 6.02 (each broadened d, 2 H-17, J_{obs} = 10.5 Hz), 6.37 (s, O—CH_3), 6.12 (narrow m, H-11), and 4.92 (m, H-12).

Anal. Calcd. for $C_{23}H_{34}O_5$: C, 70.74; H, 8.78. Found: C, 70.64; H, 9.05.

On crystallization from hexane, **4***c* had m.p. 137.5–140°; τ 9.10 (s, 3 H-20), 8.87 (s, 3 H-18), 8.03 (s, OCOCH_3), 6.37 (s, O—CH_3), 5.83 to ~6.33 (m, H-12 + 2 H-17), and 4.87 (dd, H-12, J = 4.5 and 2.7 Hz). (Contrast last with low-field dd observed for **4***a*, *b*, and *e*).

Anal. Calcd. for $C_{23}H_{34}O_5$: C, 70.74; H, 8.78. Found: C, 70.82; H, 8.91.

The Hypoiodite Reaction of 16β-ent-17-Kauranol (24)

A mixture of lead tetraacetate (11.68 g) and calcium carbonate (6.0 g) was stirred in refluxing cyclohexane (250 ml) for 10 min and **1***a* (2.50 g) and iodine (1.13 g) were then added, stirring and heating being continued while the mixture was irradiated as before. After about 40 min, most of the iodine color had disappeared, and when, during a further 10 min, no visible change in the faint pink color of the solution occurred, the mixture was allowed to cool and the solution was filtered. The solid residue was washed with ether, and the combined filtrate and washings were shaken in succession with sodium thiosulfate solution, water, and brine, and dried over Na_2SO_4. The initially clear, colorless solution thus obtained darkened on standing due to the liberation of iodine. Filtration and evaporation of the solvents gave a dark oil which appeared to contain three major components (t.l.c.). The oil was dissolved in pyridine (10 ml) and left overnight at room temperature. The resulting mixture was taken up in ether, and this solution washed successively with sodium thiosulfate solution, water, and brine, and dried over Na_2SO_4. Thin-layer chromatography of the material remaining after filtration and evaporation of solvent showed that the most polar major spot had disappeared. This mixture (2.56 g) was now

Can. J. Chem. Downloaded from www.nrcresearchpress.com by 210.87.254.6 on 09/05/12
For personal use only.

subjected to column chromatography over alumina (60 g), elution being performed with ethyl acetate – light petroleum mixtures, and the resulting fractions were further purified by preparative t.l.c. as follows.

Elution of the column with light petroleum and with ethyl acetate – light petroleum (1:199) gave a complex mixture (0.235 g) containing eight or nine components (t.l.c.). This mixture was not examined further.

Elution with ethyl acetate – light petroleum (1:99) gave a mixture containing **7**, **5**, and **4*a***. Preparative t.l.c. of this mixture was carried out with ethyl acetate – light petroleum (3:97; run four times). The sample of **7** (106 mg, 4.3%) thus obtained was an oil which appeared as a uniform, single spot on t.l.c. but which would only solidify partly on attempted crystallization from methanol, or on sublimation at 80–90°/0.02 mm Hg. Pure **7** was obtained by reduction of **4*a*** with lithium aluminum hydride (*vide infra*).

On crystallization from methanol–water, **5** (101 mg, 4.1%) had m.p. 86–89°; τ 9.15, 9.07, 8.91 (all s, quaternary C—CH_3's), 6.73 (dd, βH-17, J_{obs} ~3.5 and ~9 Hz), 6.05 (t, αH-17, J_{obs} ~8.5 Hz), 5.42 (broadened dd, H-12, J_{obs} ~3.5 and 7 Hz), and 4.85 (d, H-11, J_{obs} ~3.5 Hz).

Anal. Calcd. for $C_{20}H_{30}O$: C, 83.86; H, 10.56. Found: C, 83.99; H, 10.88.

Pure iodoether (**4*a***) was obtained on elution of the column with ethyl acetate – light petroleum (3:197) and combined with material purified by preparative t.l.c. of preceding and subsequent column fractions to give a total of 0.717 g (20.1%), m.p. 110–110.5° on crystallization from methanol. The n.m.r. spectrum of **4*a*** shows peaks at τ 9.19, 9.14, 9.01 (all s, quaternary C—CH_3's), 6.33–5.95 (complex m, 2 H-17 + H-11), and 5.62 (well resolved dd, H-12, J = 8 and 4.8 Hz; relative peak heights, high field → low field, 21:20:14.5:14).

Anal. Calcd. for $C_{20}H_{31}IO$: C, 57.97; H, 7.54. Found: C, 57.96; H, 7.65.

Fractions eluted with ethyl acetate – light petroleum (3:97 → 9:191) contained a mixture of at least seven components (0.201 g) according to analytical t.l.c. and were not examined further on this occasion (*vide infra*).

Elution with ethyl acetate – light petroleum (1:19) then more polar mixtures gave **3*a*** plus a small amount of more polar material. Most of the **3*a*** was isolated by direct crystallization from hexane and the remainder recovered from the mother liquors by preparative t.l.c. using ethyl acetate – light petroleum (1:9). This product (0.904 g, 36.4%) had m.p. 160–161.5°. Comparison of its n.m.r. spectrum with that of **3*a*** prepared from **4*a*** (*vide infra*) suggested that it contained a little **1*a***.

As indicated above, column fractions of polarity between those containing **4*a*** and **3*a*** contained a complex mixture of compounds. On one occasion, when the hypoiodite reaction of **1*a*** was repeated using the same conditions as before, a fraction which contained a component slightly less polar than **3*a*** was obtained. Preparative t.l.c. (ethyl acetate – light petroleum, 1:19; run five times) and crystallization from hexane gave **4*e***, which had m.p. 103.5–104.5; ν_{OH} 3566 cm^{-1} (intramolecular hydrogen bond; concentration, 1.5 mg/ml. Contrast **4*d*** and **6*d***); τ 9.14 (6H), 8.98 (both s, quaternary C—CH_3's), ~6.35–6.78 (broad m, H-12 + O*H*), 6.00 to ~6.4 (complex m, 2 H-17), and 5.76 (dd, H-11, J = 9 and 6 Hz) (*cf.* n.m.r. spectrum of **4*a***); and sublimes readily at 80°/0.01 mm Hg.

Anal. Calcd. for $C_{20}H_{32}O_2$: C, 78.90; H, 10.59. Found: C, 79.27; H, 10.49.

Reaction of 11β-Iodo-12β,17-oxido-16β-ent-kaurane (4a) with Zinc and Acetic Acid

Zinc dust (2.0 g) and glacial acetic acid (2 ml) were added to a solution of **4*a*** (0.547 g) in dry ether (30 ml) and the resulting mixture was stirred for 24 h at room temperature. The mixture was filtered and the filtrate washed with excess potassium hydroxide solution, dried over Na_2SO_4, filtered, and evaporated to leave a white solid (0.388 g) which ran as a single spot on t.l.c. (ethyl acetate – light petroleum, 1:9). Crystallization from hexane gave pure **3*a***, m.p. 162–163°; ν_{OH} 3639 cm^{-1}; τ 9.20, 9.13, 9.08 (all s, quaternary C—CH_3's), 6.43 (d, 2 H-17, J = 7.2 Hz), 4.41 (dd, H-11, J = 9.5 and 3.5 Hz), and 4.07 (broadened dd, H-12, J ~10 and ~6 Hz).

Anal. Calcd. for $C_{20}H_{32}O$: C, 83.27; H, 11.18. Found: C, 82.98; H, 11.25.

Reduction of 4a with Lithium Aluminum Hydride

The iodoether **4*a*** (200 mg) in ether (100 ml) was refluxed overnight with lithium aluminum hydride (100 mg). Fresh lithium aluminum hydride (100 mg) was then added and heating continued for a further 20 h. The mixture was cooled and ethyl acetate (5 ml) added, followed by water (0.2 ml), 15% NaOH (0.2 ml), and water (0.6 ml) with continuous stirring. The resulting granular precipitate and the solvent were removed to give an oil. Thin-layer chromatography of this oil (ethyl acetate – light petroleum, 1:9) indicated the presence of two products which were separated by preparative t.l.c. (same solvent) and identified as **3*a*** (0.022 g) and **7** (0.107 g). The latter crystallized from methanol only on cooling to 0–5° and had m.p. 41.5–43.5° (with some softening around 36°); τ 9.17, 9.10 (6H) (both s, quaternary C—CH_3's), 6.1–6.5 (complex m, 2 H-17), and 5.6–5.9 (complex m, H-12).

Anal. Calcd. for $C_{20}H_{32}O$: C, 83.27; H, 11.18. Found: C, 83.48; H, 11.18.

Ruthenium Tetroxide Solution in Carbon Tetrachloride

This solution was prepared according to a literature method (22) by oxidation of RuO_2 with aqueous sodium periodate and extraction of the RuO_4 formed into CCl_4. The resulting solution contained ~1.5 mg RuO_4/ml.

Oxidation of Impure 12β,17-Oxido-16β-ent-kaurane (7) with Ruthenium Tetroxide – Sodium Periodate.

Impure ether **7** [0.156 g; from $Pb(OAc)_4$–I_2 reaction of **1*a***] in carbon tetrachloride (10 ml) was stirred vigorously with sodium periodate (1.0 g) and water (10 ml), and ruthenium tetroxide solution (2 ml) added. The light yellow RuO_4 solution turned brown-black immediately on mixing with the substrate. After 2 days' stirring at room temperature, t.l.c. (ethyl acetate – light petroleum, 1:9) indicated that **7** was reacting rather slowly so more RuO_4 solution (3 ml) and sodium periodate (1.0 g) in water (10 ml) were added. Fresh sodium periodate (1.0 g) was added after 5 and 8 days of reaction. After 10 days, t.l.c. indicated that all of the starting material had been consumed and that two more polar products had been formed. The aqueous and carbon tetrachloride layers were separated and ethanol (1 ml) was added to the latter to destroy any RuO_4 present. Evaporation of the solvent gave a product darkened by ruthenium residues. This was

Can. J. Chem. Downloaded from www.nrcresearchpress.com by 210.87.254.6 on 09/05/12
For personal use only.

taken up in ethyl acetate and passed through a short alumina column to give a colorless solution which on evaporation yielded a mixture (0.107 g) of **10** and **11**. These were separated by preparative t.l.c. in ethyl acetate – light petroleum (1:19, run eight times). The major, less polar product, **11**, on crystallization from hexane, had m.p. 170–171°; $\nu_{C=O}$ 1778 cm^{-1}; τ 9.17, 9.08 (6H) (both s, quaternary C—CH_3's), 6.82–7.33 (m, H-13 + H-16), 5.00–5.28 (m, H-12).

Anal. Calcd. for $C_{20}H_{30}O_2$: C, 79.42; H, 10.00. Found: C, 79.71; H, 10.32.

The minor, more polar product (**10**) had m.p. 175.5–176° on crystallization from hexane and $\nu_{C=O}$ 1749 cm^{-1}; τ 9.14, 9.10, 8.98 (all s, quaternary C—CH_3's), 6.97–7.55 (m, H-13 + H-16), 5.52 (narrow m, H-11).

Anal. Calcd. for $C_{20}H_{30}O_2$: C, 79.42; H, 10.00. Found: C, 79.50; H, 10.30.

Hydroboration–Oxidation of Phyllocladene

The procedure was analogous to that used in the hydroboration–oxidation of *ent*-kaurene (24). On crystallization from hexane, the product (**2**) had m.p. 136–146°; τ ($CDCl_3$) 9.18, 9.14, 9.09 (all s, quaternary C—CH_3's), 6.28 (d, 2 H-17, J = 7 Hz).

Anal. Calcd. for $C_{20}H_{34}O$: C, 82.69; H, 11.80. Found: C, 82.63; H, 11.49.

The Hypoiodite Reaction of 16β-Phyllocladan-17-ol (2)

The phyllocladanol (**2**; 0.476 g) and iodine (0.214 g) were added to a mixture of lead tetraacetate (3.0 g) and calcium carbonate (1.5 g) in cyclohexane (50 ml) which had been refluxing and stirring for 10 min. After about 30 min irradiation with a 150 W tungsten lamp, the color of the iodine had disappeared. The mixture was cooled and worked up as outlined for **1***a* and *b*. Thin-layer chromatography of the product (0.70 g) which liberated iodine on standing, showed the presence of three principal components with similar polarities and several minor ones. Treatment with pyridine (3 ml) and work-up as before gave an oil (0.591 g), t.l.c. of which (ethyl acetate – light petroleum, 1:19) indicated that the three major products had survived but that two minor products (one slightly more polar than the most polar major component and one slightly less polar than the least polar major component) had disappeared. The mixture was then separated into five fractions by preparative t.l.c. (ethyl acetate – light petroleum, 1:19).

The least polar fraction (0.056 g) contained a mixture of products less polar than **8** and has not been examined further.

The second fraction (**8**; 0.183 g, 38.7%), on crystallization from methanol had m.p. 71.5–73°; τ 9.16 (6H), 8.67 (both s, quaternary C—CH_3's), 6.60 and 6.27 (each broadened d, 2 H-17, J = 10 Hz), and 5.65 (m, H-11).

Anal. Calcd. for $C_{20}H_{32}O$: C, 83.27; H, 11.18. Found: C, 83.50; H, 11.23.

The third fraction was obtained as an oil which could not be induced to crystallize although it appeared as a single spot on t.l.c. The n.m.r. spectrum showed it to be a mixture, at least five individual peaks being detectable in the methyl region. The lower field portion of the n.m.r. spectrum showed a multiplet similar to that due to 2 H-17 in **8**, but including additional peaks which partly obscured the lower field doublet, and a multiplet at τ 5.6–5.95. The last two features resemble the H-12 multiplet of **7** and the H-12 and H-11 multiplets of **4***a* (or *b*). Finally, a weak multiplet was discernible at τ 4.4–4.65. The ruthenium tetroxide oxidation of this mixture resulted in complete consumption of the substrate but a poor yield of a complex mixture was obtained. It has not been investigated further.

The fourth fraction (**9**; 0.065 g, 13.8%) could not be persuaded to solidify in the presence of solvent but had m.p. 82–87° after sublimation at 80°/0.01 mm Hg. The n.m.r. spectrum shows peaks at τ 9.16, 9.12, 8.86 (all s, quaternary C—CH_3's), 6.77 (dd, βH-17, J_{obs} ~9 and ~4 Hz), 6.05 (t, αH-17, J_{obs} ~9 Hz), 5.44 (broadened dd, H-12, J_{obs} ~3.5 and ~6 Hz), and 4.83 (d, H-11, J ~3.5 Hz).

Anal. Calcd. for $C_{20}H_{30}O$: C, 83.86; H, 10.56. Found: C, 83.73; H, 10.87.

Oxidation of 11β,17-Oxido-16β-phyllocladane (8) with Ruthenium Tetroxide – Sodium Periodate

Ruthenium tetroxide solution (2 ml) was added to a mixture of **8** (0.141 g) in carbon tetrachloride (10 ml), sodium metaperiodate (1.0 g), and water (10 ml), and the mixture stirred rapidly at room temperature. Fresh sodium periodate (1.0 g) and water (10 ml) were added on the third and eighth day. After a total of 10 days, all the starting material had disappeared (t.l.c.; ethyl acetate – light petroleum, 1:9) and a single, more polar product had formed. Work-up as for **7** gave a solid (**12**; 0.132 g) which had m.p. 188–189° on crystallization from hexane; $\nu_{C=O}$ 1754 and 1745 cm^{-1}; τ ($CDCl_3$) 9.15 (6H), 8.80 (both s, quaternary C—CH_3's), 5.10 (m, H-11).

Anal. Calcd. for $C_{20}H_{30}O_2$: C, 79.42; H, 10.00. Found: C, 79.47; H, 9.90.

The Prolonged Hypoiodite Reaction of 16β-ent-Kauran-17-ol (1a)

The hypoiodite reaction of **1***a* (1.31 g) was conducted as before [0.60 g I_2, 4.00 g $Pb(OAc)_4$, 2.00 g $CaCO_3$] except that irradiation with stirring and heating were continued for 3 h. Work-up and column chromatography of the mixture were carried out as already described to give, in addition to the previously isolated products (**3***a*, **4***a*, **5**) the ether **6***a* (0.233 g, 17.9%) which, on crystallization from methanol, had m.p. 123–125°; τ 9.17, 9.13, 9.03 (all s, quaternary C—CH_3's), 6.61 and 6.22 (each d, 2 H-17, J = 10.5 Hz), 6.07 (narrow m, H-11).

Anal. Calcd. for $C_{20}H_{32}O$: C, 83.27; H, 11.18. Found: C, 83.15; H, 11.30.

The yield of **5** obtained in this instance (0.180 g, 13.9%) was markedly greater than that obtained in the previous run on **1***a* (4.1%).

Oxidation of 11β,17-Oxido-16β-ent-kaurane (6a) with Ruthenium Tetroxide – Sodium Periodate

The mother liquors from successive crystallizations of **6***a* were collected (0.113 g) and oxidized with ruthenium tetroxide solution (2 ml) and aqueous sodium periodate as before. Work-up gave a mixture (0.083 g) which contained one major component, one slightly less polar minor component and a trace of polar material. Separation was accomplished by preparative t.l.c. (ethyl acetate – light petroleum, 1:19; run eight times) when the major component proved to be **10** and the minor one **11**.

Reaction of 16β-ent-Kauran-17-ol (1a) with Lead Tetraacetate

A mixture of **1***a* (0.062 g) and lead tetraacetate (0.500 g)

in cyclohexane (50 ml) was refluxed for 24 h. The resulting mixture was cooled and filtered and the solvent evaporated to give an oil (0.066 g) which crystallized readily on standing. Thin-layer chromatography suggested the presence of a single product less polar than the starting material, and the n.m.r. spectrum showed it to be essentially pure **6***a*.

The Hypoiodite Reaction of 16β-ent-Kaur-11-en-17-ol (3a)

The hypoiodite reaction of **3***a* (0.100 g), iodine (0.045 g), lead tetraacetate (0.50 g), and calcium carbonate (0.50 g) in cyclohexane (50 ml) was complete (t.l.c.) in about 30 min. Work-up as described earlier gave an oil (0.145 g) which solidified on standing. Analytical t.l.c. (ethyl acetate – light petroleum, 3:97; run four times) showed the presence of one major product, one less polar minor product, and traces of polar material. Preparative t.l.c. (same solvent) and crystallization from methanol gave the major component, **4***a* (0.107 g).

We thank the National Research Council of Canada for an operating grant.

1. M. Przybylska. Can. J. Chem. **40**, 566 (1962).
2. S. W. Pelletier, K. N. Iyer, V. K. Bhalla, M. G. Newton, and R. Aneja. Chem. Commun. 393 (1970).
3. S. W. Pelletier, K. N. Iyer, L. H. Wright, M. G. Newton, and N. Singh. J. Am. Chem. Soc. **93**, 5942 (1971).
4. Y. Ichinohe and M. Yamaguchi. Tetrahedron Lett. 2323 (1970).
5. J. R. Hanson. The tetracyclic diterpenes. Pergamon Press, Oxford. 1968. pp. 82–98.
6. P. R. Jefferies and R. W. Retallack. Aust. J. Chem. **21**, 2085 (1968).
7. C. H. Brieskorn and E. Pöhlmann. Ber. **102**, 2621 (1969).
8. L. A. Cuevas, F. G. Jimenez, and A. R. de Vivar. Rev. Latinoam. Quim. **3**, 22 (1972).
9. J. D. Connolly and I. M. S. Thornton. J. Chem. Soc. Perkin Trans. **1**, 736 (1973).
10. T. Kubota and I. Kubo. Bull. Chem. Soc. Japan, **42**, 1778 (1969).
11. E. Fujita, T. Fujita, M. Taoka, H. Katayama, and M. Shibuya. Tetrahedron Lett. 421 (1970).
12. Y. Yamaguchi, T. Yokota, N. Murofushi, Y. Ogawa, and N. Takahashi. Agr. Biol. Chem. Japan, **34**, 1439 (1970).
13. T. Yokota, N. Murofushi, N. Takahashi, and S. Tamura. Agr. Biol. Chem. Japan, **35**, 441, 573 (1971).
14. K. Wiesner, S. Ito, and Z. Valenta, Experientia, **14**, 167 (1958).
15. T. Okamoto, M. Natsume, Y. Iitaka, A. Yoshino, and T. Amiya. Chem. Pharm. Bull. Tokyo, **13**, 1270 (1965).
16. W. A. Denne, S. R. Johns, J. A. Lamberton, A. M. Mathieson, and H. Suares. Tetrahedron Lett. 2727 (1972).
17. K. H. Pegel, L. P. L. Piacenza, L. Phillips, and E. S. Waight. Chem. Commun. 1346 (1971).
18. R. M. Coates and E. F. Bertram. J. Org. Chem. **36**, 2625 (1971).
19. J. Kalvoda and K. Heusler. Synthesis, 501 (1971).
20. J. St. Pyrek. Tetrahedron, **26**, 5029 (1970).
21. L. M. Berkowitz and P. N. Rylander. J. Am. Chem. Soc. **80**, 6682 (1958).
22. H. Nakata. Tetrahedron, **19**, 1959 (1963).
23. M. Lj. Mihailovic and Z. Cekovic. Synthesis, 209 (1970).
24. J. R. Hanson. Tetrahedron, **23**, 801 (1967).

Can. J. Chem. Downloaded from www.nrcresearchpress.com by 210.87.254.6 on 09/05/12
For personal use only.

Smiles Rearrangement in Hydrazonyl Systems: Extension of a Recent 4*H*-1,3,4-Benzoxadiazine Synthesis

ARTHUR J. ELLIOTT

Department of Chemistry, McMaster University, Hamilton, Ontario

AND

MARTIN S. GIBSON, MARGARET M. KAYSER, AND GORDON A. PAWELCHAK

Department of Chemistry, Brock University, St. Catharines, Ontario[1]

Received July 13, 1973

Hydrazonyl aryl ethers derived from hydrazonyl halides $Ar_1CBr{=}NNHC_6H_3XY$ (2, 4) and (*a*) *o*- and *p*-nitrophenols or (*b*) pentachlorophenol undergo a facile base-catalyzed Smiles rearrangement to *N*-aroyl-*N'*,*N'*-diarylhydrazines typified by:

$$Ar_1C(OAr_2){=}NNHC_6H_3XY \rightarrow Ar_1CONHNAr_2C_6H_3XY$$

e.g. **6** → **7**, **8** → **9**, **10** → **11**.

If the 2-substituent X is Br or F and the 4-substituent Y is electron attracting, the *N*-aroyl-*N'*,*N'*-diarylhydrazines can be cyclized under basic conditions to 4-aryl-4*H*-1,3,4-benzoxadiazines by displacement of X, *i.e.* **7** → **13**, **9** → **14**. However, in the analogous cyclization of *N*-benzoyl-*N'*-(2,4-dibromophenyl)-*N'*-pentachlorophenylhydrazine (**11**), chlorine rather than bromine is displaced and the migrating ring ($Ar_2 = C_6Cl_5$) in **10** → **11** becomes the benzene ring of the benzoxadiazine, *i.e.* **11** → **15**.

Independent syntheses of two 4-aryl-4*H*-1,3,4-benzoxadiazines (**13***a* and **14**), from 7-bromo-2-phenyl-4*H*-1,3,4-benzoxadiazine (**5***a*) and *o*- and *p*-fluoronitrobenzene respectively, are reported.

Les ethers hydrazonyl aryle dérivés des halides hydrazonyl $Ar_1CBr{=}NNHC_6H_3XY$ (2, 4) et (*a*) *o*-, *p*-nitrophénol ou (*b*) pentachlorophénol subissent une simple réarrangement de Smiles à catalisation alkaline pour donner *N*-aroyle-*N'*,*N'*-diarylhydrazines tels que:

$$Ar_1C(OAr_2){=}NNHC_6H_3XY \rightarrow Ar_1CONHNAr_2C_6H_3XY$$

e.g. **6** → **7**, **8** → **9**, **10** → **11**.

Si le 2-substituant X est du Br ou du F et le 4-substituant Y est un groupe attirant les electrons, les *N*-aroyle-*N'*,*N'*-diarylhydrazines peuvent cycliser dans des conditions alkalines de façon pour donner 4-aryle-4*H*-1,3,4-benzoxadiazines par le déplacement du X, *i.e.* **7** → **13**, **9** → **14**. Cependant, dans le cyclisation analogue de *N*-benzoyl-*N'*-(2,4-dibromophényle)-*N'*-pentachlorophényl hydrazine (**11**), le chlore plûtot que le brome est déplacé et l'anneau migrateur ($Ar_2 = C_6Cl_5$) en **10** → **11** devient l'anneau benzoic de la benzoxadiazine, *i.e.* **11** → **15**.

On présente aussi les deux synthèses indépendantes de **13***a* et **14**, les 4-aryle-4*H*-1,3,4-benzoxadiazines à partir de 7-bromo-2-phényle-4*H*-1,3,4-benzoxadiazine (**5***a*) et *o*-, *p*-fluoronitrobénzene respectivements.

Can. J. Chem., **51**, 4115 (1973)

A recent synthesis of 4*H*-1,3,4-benzoxadiazines employs various hydrazonyl bromides (**1**), where X = Br or F and Y = Br or NO_2, as starting materials (1). These are converted by reaction with sodium acetate to the corresponding *N*-acetyl-*N'*-aroyl-*N*-arylhydrazines (**3**), presumably by way of hydrazonyl acetates (**2**) though the latter are not isolated. Compounds **3**, on base treatment, give **4** by nucleophilic displacement of the substituent X; in some cases, a subsequent deacetylation (**4** → **5**) is observed under the reaction conditions (Scheme 1). This synthesis supplements the alternative synthesis due to Huisgen and Fleischmann (2).

In order to examine reactions of the type **2** → **3**, a less labile migrating group is required. To this end a number of phenoxy derivatives have been synthesized in which the electron deficiency of the phenoxy ring is controlled by choice of substituents. It was anticipated that if base-catalyzed rearrangement of these compounds were possible, it would lead to *N*-aryl derivatives analogous to **3**. Such an *O* → *N* aryl transfer would provide analogy for the *O* → *N* acyl transfer proposed in **2** → **3** and would represent a Smiles rearrangement (3) on a hydrazonyl skeleton as template. It was hoped further that some of these *N*-aryl derivatives

[1]Address for correspondence.

Can. J. Chem. Downloaded from www.nrcresearchpress.com by 210.87.254.5 on 09/05/12
For personal use only.

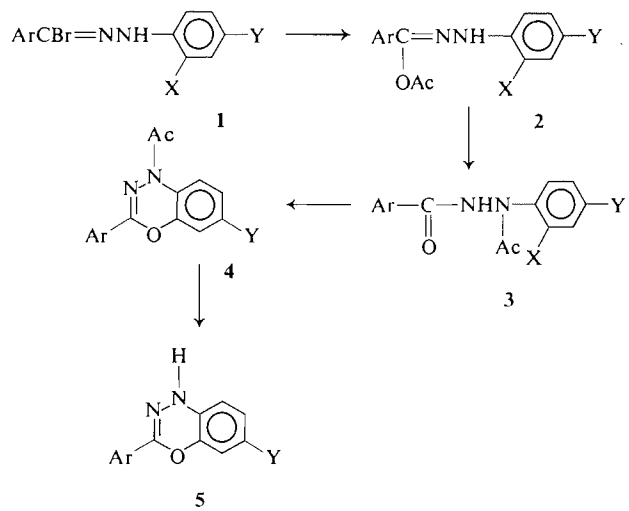

SCHEME 1

would be useful intermediates for syntheses of 4-aryl-4*H*-1,3,4-benzoxadiazines and so permit generalization (1) of the recent benzoxadiazine synthesis typified by **3** → **4**.

Certain of our observations, noted below, are germane to the thermal isomerisation (Chapman rearrangement) of aryl hydrazonyl ethers (aryl hydrazonates), which has recently been the subject of communications from other laboratories (4).

For convenience, the readily available nitrophenols have been principally used in this study. First, equivalent amounts of hydrazonyl bromide **1***a* and *p*-nitrophenol were stirred together in ethanol with added triethylamine at room temperature to give hydrazonyl *p*-nitrophenyl ether **6***a*. The latter rearranged smoothly in boiling ethanol–triethylamine to the corresponding hydrazide **7***a*. The mass spectra of **6***a* and **7***a* proved interesting. Only **6***a* lost the elements of *p*-nitrophenol on electron impact, an observation in agreement with structure **6***a* (*m/e* 350 for ^{79}Br isotope, 12% of base peak). Further examination of the mass spectrum of **6***a*, and correlation with that of **7***a*, permitted assignment of peaks at *m/e* 384 and 370 to the rearranged compound **7***a*, *i.e.* assignment after allowing for $O \rightarrow N$ aryl transfer. There was no evidence for reverse aryl migration in the mass spectrum of **7***a*.

Other hydrazonyl halides (**1***b–h*), similarly treated with *p*-nitrophenol and triethylamine, gave the corresponding hydrazonyl *p*-nitrophenyl ethers (**6***b–h*). Each of these ethers rearranged to the corresponding hydrazide **7** in refluxing ethanol–triethylamine, generally within a few minutes. Compounds (**6***d* and *f*) which contained electron-attracting groups in the *N*-aryl ring, required longer reaction times for complete rearrangement, reflecting the decreased nucleophilicity of the appropriate nitrogen atom in such compounds (Scheme 2).

Studies were then extended to *o*- and *m*- nitrophenols. It was found that *o*-nitrophenol and hydrazonyl halides (**1***a* and *g*) gave the corresponding hydrazonyl *o*-nitrophenyl ethers (**8***a* and *g*) and that these rearranged smoothly to the corresponding hydrazides (**9***a* and *g*) in boiling ethanol–triethylamine. Under similar conditions, the hydrazonyl aryl ether from **1***a* and *m*-nitrophenol was recovered, and more forcing conditions resulted in decomposition. The last compound examined was hydrazonyl aryl ether **10** from **1***a* and pentachlorophenol; this compound rearranged in boiling ethanol–triethylamine to give hydrazide **11**, though the latter compound was not obtained in an analytically pure condition (Scheme 3).

At this stage, in order to obtain some indication that the base-catalyzed rearrangement was intramolecular, the hydrazonyl ethers **6***g* and **8***a* were rearranged in admixture. Intramolecular rearrangement would give **7***g* and **9***a* respectively, whilst an intermolecular rearrangement, for example resulting from dissociation and recombination, would provide in addition **7***a* and **9***g*. The choice of compounds **6***g* and **8***a* was based

Can. J. Chem. Downloaded from www.nrcresearchpress.com by 210.87.254.5 on 09/05/12
For personal use only.

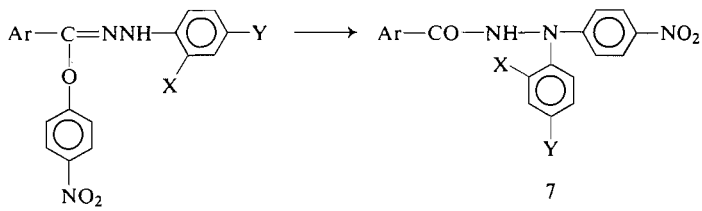

6 7

a Ar = C_6H_5; X = Y = Br
b Ar = *p*-$CH_3OC_6H_4$; X = Y = Br
c Ar = *p*-ClC_6H_4; X = Y = Br
d Ar = C_6H_5; X = Br; Y = CO_2Et
e Ar = C_6H_5; X = F; Y = Br
f Ar = C_6H_5; X = Br; Y = NO_2
g Ar = C_6H_5; X = Y = H (Cl instead of Br in **1**)
h Ar = $C_6H_5CH{:}CH{-}$; X = Y = H (Cl instead of Br in **1**)

SCHEME 2

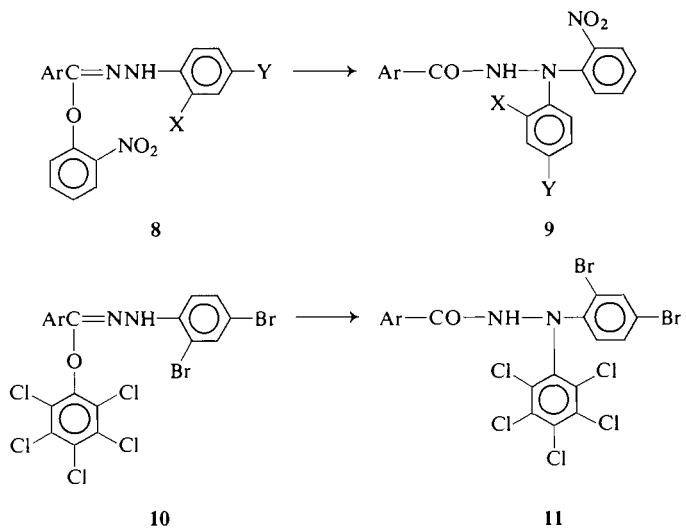

8 9 10 11

SCHEME 3

on similar reactivity, good yields on rearrangement, and ease of separation and identification of the possible products. The mixture produced by rearranging **6***g* and **8***a* in admixture under these conditions contained, within the limits of detection chromatographically, only **7***g* and **9***a*.

Our view is that these rearrangements are intramolecular and proceed through a five-membered cyclic transition state, *e.g.* **12** (Scheme 4). In the cases where the migrating group is *o*- or *p*-nitrophenyl, the transition state is stabilized by delocalisation involving the NO_2 group. No such delocalisation is possible in the case of *m*-nitrophenyl and, under the reaction conditions employed, no rearrangement occurs. In the case of pentachlorophenyl, the ring is sufficiently electron deficient for inductive stabilization of

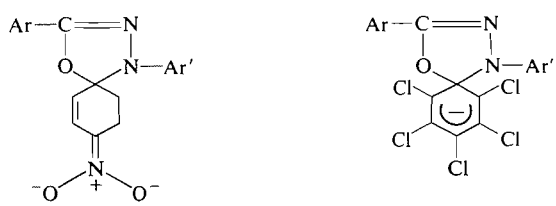

12

SCHEME 4

Can. J. Chem. Downloaded from www.nrcresearchpress.com by 210.87.254.5 on 09/05/12
For personal use only.

the minus charge on the migrating ring to allow rearrangement to proceed.

The thermally-induced or Chapman rearrangement of hydrazonyl aryl ethers to *N*-aroyl-*N'*,*N'*-diarylhydrazines, rather than the isomeric *N*-aroyl-*N*,*N'*-diarylhydrazines, is of some current interest (4).

[1] $Ar_1C(OAr_2) = NNHAr_3 \rightarrow Ar_1CONHNAr_2Ar_3$

Rearrangement occurs readily at 200°. Our investigations have not encompassed these conditions but we have noted that no detectable rearrangement (t.l.c.) occurs, *e.g.*, during m.p. determination of **6***a* (118°). Part of the evidence for structural assignment to the products from thermal rearrangement of hydrazonyl aryl ethers comes from hydrolysis to the corresponding *N*,*N*-diarylhydrazines and it has been pointed out that this would provide a useful route to such hydrazines. Whilst this is undoubtedly true, it may be difficult to achieve hydrolysis successfully with more heavily substituted compounds (5). In particular, no success attended our efforts with **9***a* under normal conditions.

Extension of the previously reported 4*H*-1,3,4-benzoxadiazine synthesis (1) was the next objective. The cyclization of a series of the foregoing hydrazides (**7***a–f*) was effected by boiling with an equivalent amount of sodium hydroxide in dimethylformamide–triethylamine mixture for several hours. In most cases, the desired product (**13***a–f*) was isolated chromatographically, the yields ranging from 25–96%.

The presence of electron-withdrawing groups in the *N*-aryl rings and of electron-releasing groups in the *C*-aryl ring would be expected to aid the cyclization. This appears to be so, except for the case of **7***d*. However, in this case, competitive hydrolysis by sodium hydroxide of the ester function would replace an electron withdrawing ethoxycarbonyl group by carboxylate anion and cyclization would then be expected to take place reluctantly, if at all; the benzoxadiazine isolated (**13***d*, 25%) is that derived from the unhydrolyzed hydrazide **7***d* (Scheme 5).

Comparison of **7***a* with **7***e* shows that changing the leaving group from bromine to fluorine results in smoother cyclization and increased yield of the benzoxadiazine **13***a*. In fact **7***e* is converted entirely to benzoxadiazine **13***a* and the yield (96%) represents the material obtained after work-up. In view of this, the mechanism favored for the reaction **7** → **13** is analogous to

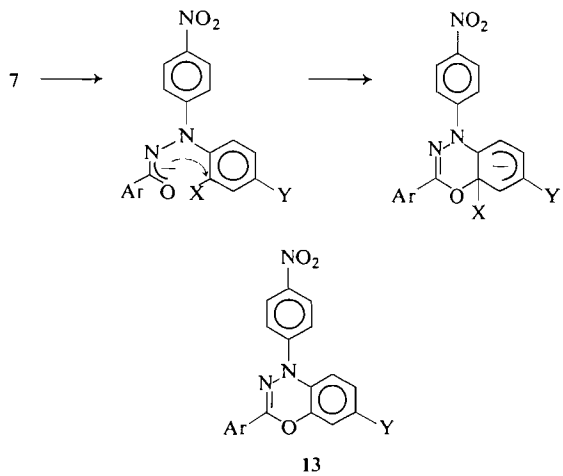

SCHEME 5

that proposed earlier for the cyclization **3** → **4**, except that the *p*-nitrophenyl substituent is not as labile as an acetyl group and is not removed under the reaction conditions, *i.e.* the reaction corresponding to **4** → **5** is not observed (1). The anionic species derived from **7**, or possibly the zwitterionic conjugate acid, is thought to attack the 2-position of the appropriate *N*-aryl ring to form the heterocyclic ring by nucleophilic displacement of halogen.

The structure of **13***a* was confirmed by an alternative synthesis. When **5***a* and *p*-fluoronitrobenzene were boiled together in acetonitrile–triethylamine for 4 h, **13***a* was obtained in 66% yield.

The cyclization of *N*-benzoyl-*N'*-(2,4-dibromophenyl)-*N'*-*o*-nitrophenylhydrazine (**9***a*) posed the alternatives of cyclization by displacement of bromine or by displacement of nitro group. When **9***a* was treated as for the foregoing hydrazides, only **14** was obtained; there was no evidence of other cyclized product (t.l.c.). This oxadiazine was also synthesized from **5***a* and *o*-fluoronitrobenzene.

The cyclization of *N*-benzoyl-*N'*-(2,4-dibromophenyl)-*N'*-pentachlorophenylhydrazine (**11**) posed similar alternatives. In earlier work on synthesis of 4*H*-1,3,4-benzothiadiazines (**6**) it had been noted that no benzothiadiazine formation occurred when compounds (**1**, X = Cl) were treated with potassium thioacetate, though reaction was successful when X = F, Br, or I. However, more heavily chlorinated aromatic rings do undergo nucleophilic displacement of chlorine, and the reactions are synthetically

Can. J. Chem. Downloaded from www.nrcresearchpress.com by 210.87.254.5 on 09/05/12
For personal use only.

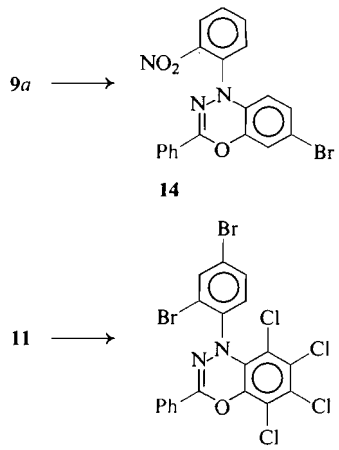

SCHEME 6

useful (7). In the event, **11**, was cyclized to **15** by displacement of chlorine, with no evidence of other cyclized product (t.l.c.) (Scheme 6).

The present work establishes that aryl hydrazonyl ethers substituted such that the *O*-aryl ring is sufficiently electron deficient, undergo a facile base-catalyzed Smiles rearrangement to give the corresponding *N*-arylhydrazide, *e.g.* **6** → **7**, **8** → **9**, **10** → **11**. The *N*-arylhydrazides thus available are, for given substituents X and Y, eminently suitable intermediates for synthesis of 4-aryl-4*H*-1,3,4-benzoxadiazines. In many cases, the aryl group migrating in the Smiles rearrangement becomes the 4-aryl substituent in the benzoxadiazine finally produced, *e.g.* **6** → **7** → **13**, **8** → **9** → **14**. However, this is not necessarily so, as shown by the conversion **10** → **11** → **15** in which the aryl group migrating in the Smiles rearrangement is finally incorporated as the benzene ring of the benzoxadiazine ring system.

Experimental

General procedures follow those described previously (1). Mass spectra were determined with an AEI-MS30 double beam double focussing mass spectrometer, unless otherwise stated.

Hydrazonyl Halides: Preparation of **1***h* (*8*)

A mixture of *N*-cinnamoyl-*N'*-phenylhydrazine (12.0 g, 0.05 mol), phosphorus pentachloride (11.9 g, 0.055 mol) and dry ether (100 ml) was boiled under reflux for 78 h. The brown solution was cooled and treated with an ethereal solution of phenol until no further reaction was observed. Ethanol was then added and ether was removed by concentration *in vacuo*. The solid was filtered off and crystallized from ethanol to give *N*-α-*chlorocinnamylidene-N'-phenylhydrazine* (**1***h*) as plates (5.8 g, 45%), m.p. 150–151°.

Anal. Calcd. for $C_{15}H_{13}ClN_2$: C, 70.18; H, 5.07; N, 10.92. Found: C, 70.06; H, 5.08; N, 10.74.

Compound **1***h* gave an intense red coloration when heated with phenylhydrazine in ethanol.

Preparation of Hydrazonyl Aryl Ethers

As general procedure, the hydrazonyl halide (0.01 mol) and the phenol (0.01 mol) were stirred in ethanol (EtOH) or acetonitrile (MeCN) containing triethylamine (NEt_3, 0.02 mol) at room temperature, usually for 2 h. The product was collected by (*a*) filtration or (*b*) dilution of the reaction mixture with water followed by filtration, and then washed, dried and purified by crystallization.

Hydrazonyl Aryl Ethers from **1***a*

Compound **1***a* (9) (4.33 g), *p*-nitrophenol (1.39 g), EtOH (30 ml), and NEt_3 (2 ml) gave *N*-α-(*p-nitrophenoxy*)-*benzylidene-N'-(2,4-dibromophenyl)hydrazine* (**6***a*) (3.44 g, 70%) as yellow prisms, m.p. 100–101° or yellow needles, m.p. 117–118° (from ethanol); n.m.r. (CCl_4) δ 8.25 (s, NH), 8.3 (A) and 7.2 (B) (A_2B_2q, J = 8 Hz), and 7.9–7.35 (m, 8H); mass spectrum *m/e* 493/491/489 (M^+), 477/475/473, 463/461/459, 412/410, 411/409, 400/398/396, 354/352/350 ($M^+ - HOC_6H_4NO_2$), 344/342/340, 274/272, 252/250/248 ($Br_2C_6H_3NH$), 225/223/221, 171/169, 139 ($HOC_6H_4NO_2$), 105, 103, and 77. Low intensity peaks at *m/e* 388/386/384, 374/372/370, and 372/370/368 are attributable to rearranged material. A mass spectrum obtained using an AEI-MS902 spectrometer (200–300°) showed some differences, notably reduced intensity of peak *m/e* 354/352/350 and increased intensities of peaks due to rearranged material.

The compound did not undergo detectable rearrangement (t.l.c.) during m.p. determination.

Anal. Calcd. for $C_{19}H_{13}Br_2N_3O_3$: C, 46.44; H, 2.65; Br, 32.59; N, 8.55. Found: C, 46.5; H, 2.7; N, 8.6.

Compound **1***a* (2.0 g), *m*-nitrophenol (0.64 g), EtOH (25 ml) and NEt_3 (1 ml) gave the corresponding *hydrazonyl aryl ether* (1.24 g, 55%) as yellow prisms, m.p. 117–118° (from ethanol).

Anal. Found: C, 46.5; H, 2.9; Br, 32.5; N, 8.5.

Similarly, **1***a* (4.33 g), *o*-nitrophenol (1.39 g), EtOH (25 ml) and NEt_3 (2 ml) gave **8***a* (3.97 g, 81%) as yellow prisms, m.p. 106° or yellow needles, m.p. 122–124° (from ethanol).

Anal. Found: C, 46.6; H, 2.6; Br, 32.8; N, 8.6

Compound **1***a* (4.33 g), pentachlorophenol (2.66 g), EtOH (30 ml), and NEt_3 (1 ml) gave **10** (5.2 g, 84%) as colorless needles, m.p. 165° (from ethanol).

Anal. Calcd. for $C_{19}H_9Br_2Cl_5N_2O$: C, 36.86; H, 1.46; N, 4.53. Found: C, 37.1; H, 1.7; N, 4.7.

Hydrazonyl Aryl Ethers from **1**, *b–h*

Compound **1***b* (10) (4.64 g), *p*-nitrophenol (1.39 g), EtOH (25 ml), and NEt_3 (2 ml) gave **6***b* (4.73 g, 90%) as yellow needles, m.p. 143–144° (from ethanol – ethyl acetate).

Anal. Calcd. for $C_{20}H_{15}Br_2N_3O_4$; C, 46.06; H, 2.88; N, 8.06. Found: C, 45.99; H, 2.88; N. 8.03.

Compound **1***c* (1) (4.67 g), *p*-nitrophenol (1.39 g), EtOH (30 ml), and NEt_3 (2ml) gave **6***c* (4.4 g, 84%) as yellow needles, m.p. 151° (from *t*-amyl alcohol – benzene).

Anal. Calcd. for $C_{19}H_{12}Br_2ClN_3O_3$: C, 43.39; H, 2.28; N, 7.99. Found: C, 43.8; H, 2.5; N. 7.9.

Can. J. Chem. Downloaded from www.nrcresearchpress.com by 210.87.254.5 on 09/05/12
For personal use only.

Can. J. Chem. Downloaded from www.nrcresearchpress.com by 210.87.254.5 on 09/05/12
For personal use only.

Compound **1***d* (1) (2.13 g), *p*-nitrophenol (0.69 g), EtOH (20 ml), and NEt_3 (0.5 ml) gave **6***d* (1.49 g, 62%) as needles, m.p. 145° (from ethanol).

Anal. Calcd. for $C_{22}H_{18}BrN_3O_5$: C, 54.55; H, 3.72; Br, 16.53; N, 8.68. Found: C, 54.5; H, 3.7; Br. 16.7; N, 8.7.

Compound **1***e* (6) (3.72 g), *p*-nitrophenol (1.39 g), MeCN (30 ml), and NEt_3 (1ml) gave **6***e* (3.85 g. 90%) as yellow needles. m.p. 115° (from benzene–hexane).

Anal. Calcd. for $C_{19}H_{13}BrFN_3O_3$: C, 53.02; H, 3.02; N, 9.77. Found: C, 53.22; H, 3.14; N, 9.68.

Compound **1***f* (11) (3.99 g), *p*-nitrophenol (1.39 g), EtOH (30 ml), and NEt_3 (1 ml) gave **6***f* (3.8 g, 83%) as yellow plates, m.p. 192° (from toluene).

Anal. Calcd. for $C_{19}H_{13}BrN_4O_5$: C, 49.89; H, 2.84; Br, 17.51; N, 12.25. Found: C, 50.0; H, 3.0; Br, 17.3; N, 12.4.

Compound **1***g* (8) (2.3 g), *p*-nitrophenol (1.39 g), EtOH (60 ml), and NEt_3 (2 ml) gave, after 3 h, **6***g* (1.2 g, 36%) as yellow needles, m.p. 138–139° (from ethanol) (lit. (4*c*) m.p. 134°).

Anal. Calcd. for $C_{19}H_{15}N_3O_3$: C, 68.47; H, 4.50; N, 12.61. Found: C, 68.68; H, 4.59; N, 12.43.

Similarly, **1***g* (2.3 g), *o*-nitrophenol (1.39 g), EtOH (60 ml), and NEt_3 (2 ml) gave, after 3 h, **8***g* (1.5 g, 45%) as yellow needles, m.p. 122–123° (from ethanol).

Anal. Found: C, 68.12; H, 4.44; N, 12.65.

Compound **1***h* (1.4 g), *p*-nitrophenol (0.75 g), EtOH (25 ml) and NEt_3 (1 ml), stirred overnight, gave **6***h* (0.5 g, 25%) as pale orange needles, m.p. 182–183° (from ethanol).

Anal. Calcd. for $C_{21}H_{17}N_3O_3$: C, 70.19; H, 4.74; N, 11.70. Found: C, 70.06; H, 4.85; N, 11.52.

N-Aroyl-N′,N′-diarylhydrazines by Smiles Rearrangement of Hydrazonyl Aryl Ethers

As general procedure, the hydrazonyl aryl ether in 1:1 EtOH–NEt_3 mixture was boiled under reflux for 15 min. In some cases, the product separated on cooling; otherwise solvents were removed *in vacuo* and the product was crystallized.

Compound **6***a* (0.5 g, 0.001 mol) in EtOH (5 ml) and NEt_3 (5 ml) gave *N-benzoyl-N′-(2,4-dibromophenyl)-N′-p-nitrophenylhydrazine* (7*a*) (0.34 g, 68%) as prisms, m.p. 215–216° (from benzene); i.r. (KBr) 1645 cm^{-1} (C=O); n.m.r. (DMSO-d_6) δ 11.4 (s, NH), 8.0 (A) and 6.65 (B) (A_2B_2q, J = 9Hz), and 7.9–7.3 (m, 8H); mass spectrum *m/e* 493/491/489 (M^+), 477/475/473, 463/461/459, 412/410, 411/409, 395/393, 388/386/384 (M^+ – PhCO), 374/372/370 (M^+ – PhCON), 372/370/368 (M^+ – $PhCONH_2$), 344/342/340, 342/340/338, 309/307, 263/261/259, 246/244, 199, 166, 121, 106, 105, 104, 103 and 77.

Anal. Calcd. for $C_{19}H_{13}Br_2N_3O_3$: C, 46.44; H, 2.65; Br, 32.59; N, 8.55. Found: C, 46.3; H, 2.6; N, 8.4.

Similarly, **8***a* (0.5 g) in EtOH (5 ml) and NEt_3 (5 ml) gave **9***a* (0.32 g, 64%) as yellow needles, m.p. 200–201° (from benzene–hexane).

Anal. Found: C, 46.4; H, 2.9; Br, 32.8; N, 8.8.

The isomeric hydrazonyl *m*-nitrophenyl ether did not rearrange under these conditions, even after 2 h, nor when boiled under reflux in 2,6-lutidine for 1 h. Under more vigorous conditions (DMF–NEt_3) decomposition ensued.

Compound **6***b* (3 g) in EtOH (15 ml) and NEt_3 (15 ml) gave **7***b* (2.5 g, 83%) as cream needles, m.p. 235° (from ethanol – ethyl acetate).

Anal. Calcd. for $C_{20}H_{15}Br_2N_3O_4$: C, 46.07; H, 2.88; Br, 30.71. Found: C, 46.04; H, 3.01; Br, 30.89.

Compound **6***c* (0.5 g) in EtOH (5 ml) and NEt_3 (5 ml) gave **7***c* (0.32 g, 64%) as cream needles, m.p. 235° (from reaction mixture).

Anal. Calcd. for $C_{19}H_{12}Br_2ClN_3O_3$: C, 43.39; H, 2.28; N, 7.99. Found: C, 43.4; H, 2.4; N, 8.0.

Compound **6***d* (0.5 g) in EtOH (5 ml) and NEt_3 (5 ml) gave, after 2 h, **7***d* (0.31 g, 62%) as pale yellow prisms, m.p. 119° (from benzene–hexane).

Anal. Calcd. for $C_{22}H_{18}BrN_3O_5$: C, 54.55; H, 3.72; Br, 16.53; N, 8.68. Found: C, 54.7; H, 3.9; Br. 16.5; N, 8.6.

Compound **6***e* (2.15 g) in MeCN (15 ml) and NEt_3 (15 ml) gave **7***e* (1.9 g, 88%) as needles, m.p. 214–216° (from benzene).

Anal. Calcd. for $C_{19}H_{13}BrFN_3O_3$: C, 53.02; H, 3.02. Found: C, 53.15; H, 3.10.

Compound **6***f* (0.5 g) in EtOH (5ml) and NEt_3 (5 ml) gave, after 2 h. **7***f* (0.41 g, 82%) as yellow prisms, m.p. 286° (trituration with boiling hexane–toluene).

Anal. Calcd. for $C_{19}H_{13}BrN_4O_5$: C, 49.89; H, 2.84; Br, 17.51; N, 12.25. Found: C, 50.2; H, 2.8; Br, 17.7; N, 12.35.

Compound **6***g* (0.5 g) in EtOH (10 ml) and NEt_3 (5 ml) gave, after 1 h, **7***g* (0.3g, 60%) as cream needles, m.p. 173–174° (from benzene) (lit. (4*c*) m.p. 178–180°).

Anal. Calcd. for $C_{19}H_{15}N_3O_3$: C, 68.47; H, 4.50; N, 12.61. Found: C, 68.85; H, 4.45; N, 12.61.

Similarly, **8***g* (0.5 g) in EtOH (10 ml) and NEt_3 (5 ml) gave, after 1 h, **9***g* (0.3 g, 60%) as yellow needles, m.p. 171–172° (from benzene).

Anal. Found: C, 68.24; H, 4.38; N, 12.60.

Compound **6***h* (0.3 g) in EtOH (15 ml) and NEt_3 (5 ml) gave, after 2 h. **7***h* (0.17 g, 57%) as yellow needles, m.p. 155–156° (from benzene, then from ethanol).

Anal. Calcd. for $C_{21}H_{17}N_3O_3$; C, 70.19; H, 4.74; N, 11.70. Found: C, 70.38; H, 4.89; N, 11.79.

Compound **10** (0.5 g) in EtOH (5 ml) and NEt_3 (5 ml) gave, after 1 h, **11** (0.4 g, 80%) as needles, m.p. 248–249° (from hexane).

Anal. Calcd. for $C_{19}H_9Br_2Cl_5N_2O$ (mol. wt. 618.5): C, 36.86; H, 1.46; N, 4.53. Found (620, vapor pressure, acetone): C, 39.2; H, 1.9; N, 4.5.

Rearrangement of 6g and 8a in Admixture

T.l.c. (silica gel, $CHCl_3$) of reference mixtures of **7***g* (R_f 0.33), **7***a* (R_f 0.39), **9***g* (R_f 0.51), and **9***a* (R_f 0.60) showed that **7***a* and **9***g* were each detectable in mixtures containing **7***g* (49.5% w/w), **7***a* (0.5%), **9***g* (0.5%), and **9***a* (49.5%).

A mixture of **6***g* (0.3 g) and **8***a* (0.3 g) in EtOH (15 ml) and NEt_3 (5 ml) was boiled under reflux for 1 h and the mixture of rearranged products was isolated by evaporation of solvents *in vacuo*. T.l.c. showed that **7***g* and **9***a*, but not **7***a* and **9***g*, were present. The mixture was chromatographed to yield **9***a* and **7***g*; these compounds were identified after crystallization by correlation (i.r., t.l.c., mixture m.p.) with reference samples. The eluates collected between **9***a* and **7***g* were evaporated and examined by t.l.c.; there was no indication of the presence of **7***a* or **9***g*.

Attempted Debenzoylation of 9a

Attempts to debenzoylate **9***a* by hydrolysis (24 h

Can. J. Chem. Downloaded from www.nrcresearchpress.com by 210.87.254.5 on 09/05/12
For personal use only.

reflux with 1:1 ethanol – concentrated HCl) or by ethanolysis (12 h reflux with 5–6% ethanolic sodium ethoxide) were unsuccessful; **9***a* was recovered.

Preparation of Substituted 4H-1,3,4-Benzoxadiazines from N-Aroyl-N′,N′-diarylhydrazines

As general procedure, equivalent amounts of the *N*-aroyl-*N*′,*N*′-diarylhydrazine and sodium hydroxide were dissolved in a mixture of dimethylformamide (DMF) and NEt_3 and boiled under reflux for 6 h. The solution was cooled, poured into excess 5% acetic acid, and the solid was collected, washed with water, and dried. Except where directly crystallized, the crude products were chromatographed on Florisil (toluene as eluant) and the fraction containing the fluorescent product was collected.

Compound **7***a* (4.91 g, 0.01 mol), sodium hydroxide (0.4 g, 0.01 mol), DMF (25 ml), and NEt_3 (5 ml) yielded *7-bromo-4-p-nitrophenyl-2-phenyl-4H-1,3,4-benzoxadiazine* (**13***a*) (1.2 g, 29%) as yellow-orange needles, m.p. 221–222° (from benzene). The yield was improved in a subsequent experiment (79%, 10 h).

Anal. Calcd. for $C_{19}H_{12}BrN_3O_3$: C, 55.61; H, 2.93; N, 10.24. Found: C, 54.97; H, 2.90; N, 10.09.

Compound **7***e* (2.15 g), sodium hydroxide (0.2 g), DMF (25 ml), and NEt_3 (5 ml) also gave **13***a* (2.0 g, 97%) as needles, m.p. 221–222° (direct crystallization from benzene); mixture m.p. (with above sample) 221–222°.

Compound **7***b* (1.3 g), sodium hydroxide (0.1 g), DMF (15 ml) and NEt_3 (5 ml) gave **13***b* (0.8 g, 73%) as orange needles, m.p. 179–180° (from ethanol – ethyl acetate).

Anal. Calcd. for $C_{20}H_{14}BrN_3O_4$: C, 54.55; H, 3.18; Br, 18.18. Found: C, 54.26; H, 3.35; Br, 18.48.

Compound **7***c* (2.6 g), sodium hydroxide (0.2 g), DMF (25 ml), and NEt_3 (5 ml) gave **13***c* (0.8 g, 36%) as yellow needles, m.p. 267–268° (from benzene).

Anal. Calcd. for $C_{19}H_{11}BrClN_3O_3$: C, 51.29; H, 2.47; N, 9.45. Found: C, 51.29; H, 2.54; N, 9.80.

Compound **7***d* (1.21 g), sodium hydroxide (0.1 g), DMF (15 ml), and NEt_3 (2 ml) gave **13***d* (0.26 g, 25%) as yellow-orange prisms, m.p. 217° (from toluene).

Anal. Calcd. for $C_{22}H_{17}N_3O_5$: C, 65.51; H, 4.22; N, 10.42. Found: C, 65.66; H, 4.14; N, 10.31.

Compound **7***f* (4.57 g), sodium hydroxide (0.4 g), DMF (25 ml), and NEt_3 (5 ml) gave **13***f* (2.3 g, 62%) as red prisms, m.p. 288° (direct crystallization from DMF).

Anal. Calcd. for $C_{19}H_{12}N_4O_5$: C, 60.64; H, 3.19; N, 14.89. Found: C, 60.56; H, 3.31; N, 14.73.

Compound **9***a* (4.91 g), sodium hydroxide (0.4 g), DMF (25 ml), and NEt_3 (5 ml) gave **14** (1.1 g, 27%) as red needles, m.p. 163° (from benzene–hexane).

Anal. Calcd. for $C_{19}H_{12}BrN_3O_3$: C, 55.61; H, 2.93; Br, 19.51. Found: C, 55.49; H, 2.84; Br, 19.58.

Compound **11** (3.09 g), sodium hydroxide (0.2 g), DMF (15 ml), and NEt_3 (5 ml) gave **15** (1.8 g, 62%) as yellow needles, m.p. 215–216° (from benzene–hexane).

Anal. Calcd. for $C_{19}H_8Br_2Cl_4N_2O$ (mol. wt. 582): C, 39.16; H, 1.37; N, 4.81. Found (577, vapour pressure, benzene): C, 39.45; H, 1.45; N, 4.82.

Alternative Syntheses of 13a and 14 from 5a (1)

Compound **5***a* (1) (0.3 g), *p*-fluoronitrobenzene (0.14 g), NEt_3 (5 ml), and MeCN (15 ml) were boiled together under reflux for 4 h. Solvents were removed *in vacuo* and the residue was washed with water and dried. Crystallization from benzene gave **13***a* (0.24 g, 60%), m.p. and mixture m.p. 221–222°.

An analogous experiment in which *o*-fluoronitrobenzene (0.14 g) replaced the *p*-isomer gave, after crystallization from hexane–toluene, **14** (0.20 g, 50%), m.p. and mixture m.p. 162–163°.

We thank the National Research Council of Canada for financial support and the Province of Ontario for award of a Graduate Fellowship (G.A.P.).

1. A. J. ELLIOTT and M. S. GIBSON. J. Chem. Soc. Perkin I, 2915 (1972).
2. R. HUISGEN and R. FLEISCHMANN. Liebigs Ann. Chem. **623**, 47 (1959); W. RIED and E. KAHR. Chem. Ber. **103**, 331 (1970).
3. J. F. BUNNETT and R. E. ZAHLER. Chem. Rev. **49**, 361 (1951); N. W. GILMAN, P. LEVITAN, and L. H. STERNBACH. J. Org. Chem. **38**, 373 (1973) and refs. cited therein.
4. (*a*) A. F. HEGARTY, J. A. KEARNEY, M. P. CASHMAN, and F. L. SCOTT. Chem. Commun. 689 (1971); (*b*) A. S. SHAWALI and H. M. HASSANEEN. Tetrahedron Lett. 1299 (1972); (*c*) A. F. HEGARTY, J. A. KEARNEY, and F. L. SCOTT. Tetrahedron Lett. 3211 (1972).
5. E. FISCHER. Liebigs Ann. Chem. **248**, 239 (1887).
6. I. T. BARNISH and M. S. GIBSON. J. Chem. Soc. C, 854 (1970); P. D. CALLAGHAN and M. S. GIBSON. J. Chem. Soc. C, 2106 (1970).
7. D. J. BERRY, I. COLLINS, S. M. ROBERTS, H. SUSCHITZKY, and B. J. WAKEFIELD. J. Chem. Soc. C, 1285 (1969).
8. R. HUISGEN, M. SEIDEL, G. WALLBILLICH, and H. KNUPFER. Tetrahedron, **17**, 3 (1962).
9. F. D. CHATTAWAY and A. J. WALKER. J. Chem. Soc. **127**, 975 (1925).
10. R. CIUSA and M. MEGA. Gazzetta, **58**, 836 (1928).
11. J. M. BURGESS and M. S. GIBSON. Tetrahedron, **18**, 1001 (1962).

Detection of Reversible Reactions in Solution Using Group Enthalpies of Transfer. Formation of Benzaldehyde Hemiacetals in Methanol[1]

RICHARD FUCHS, THOMAS M. YOUNG, AND RANDOLPH F. RODEWALD
Department of Chemistry, University of Houston, Houston, Texas 77004

Received July 23, 1973

The enthalpies of transfer from methanol to dimethylformamide for a wide variety of aromatic compounds are additive properties of the groups present within the molecules. Values of $\Delta\Delta H_s$ fail to be additive for benzaldehydes by an amount of energy which increases with increasing electron withdrawing power of the substituent. Nuclear magnetic resonance studies indicate that this results from hemiacetal formation in methanol, which varies from nil for *p*-dimethylamino-, *p*-hydroxy-, and *p*-methoxybenzaldehyde to 71% for the *p*-nitro compound. The non-additivity of group $\Delta\Delta H_s$ values can indicate that specific interactions are occurring with a solvent, even though no stable product can be isolated.

Les enthalpies de transfert du méthanol à la diméthylformamide pour un grand nombre de composés aromatiques sont des propriétés additives des groupes présents dans les molécules. Les valeurs de $\Delta\Delta H_s$ ne sont pas additives pour les benzaldéhydes à cause d'une quantité d'énergie qui augmente lorsque le pouvoir d'attraction des électrons par le substituant augmente. Des études r.m.n. ont montré que cette relation dépend de la formation d'hemiacétal dans le méthanol, dont le pourcentage varie de zéro pour le *p*-diméthylamino-, le *p*-hydroxy- et le *p*-méthoxybenzaldéhyde à 71% pour le dérivé *p*-nitro. La non-additivité des valeurs de $\Delta\Delta H_s$ pour un groupe peut alors montrer qu'il existe des interactions spécifiques avec un solvant même si aucun produit stable ne peut être isolé. [Traduit par le journal]

Can. J. Chem., **51**, 4122 (1973)

Recently the enthalpies of solution (ΔH_s) of a large number of aromatic compounds were measured in methanol (MeOH) and in *N*,*N*-dimethylformamide (DMF) (1, 2). From the ΔH_s values enthalpies of transfer ($\Delta\Delta H_s$) (MeOH → DMF) were determined. The important observation was made that values of $\Delta\Delta H_s$ are additive functions of the substituent groups present, regardless of the relative positions of each group on the aromatic ring. Small deviations from additivity exceeding the experimental error occurred in cases such as *o*-nitroaniline and *o*-nitrophenol, where intramolecular hydrogen bonding is known to occur. Some of the group enthalpies of transfer determined (in kcal/g group wt.) are C_6H_5, −0.3; Cl, −0.1; NO_2, −0.8; $COCH_3$, −1.0; OH, −1.7; $N(CH_3)_2$, −0.5; OCH_3, −0.6; and CH_3, +0.03. The individual group $\Delta\Delta H_s$ values were discussed (2) in terms of the greater dipole moment, hydrogen bond acceptor ability, and solvent–solvent association forces of DMF (relative to MeOH), and the resulting more exothermic dipole–dipole, dipole – induced dipole, and hydrogen bonding interactions with polar, polarizable, and hydrogen bond donating groups, respectively. The group $\Delta\Delta H_s$ values show some correlation with the changes in ^{19}F chemical shifts caused by the same groups in *m*-substituted fluorobenzenes, when the compounds are transferred from a "normal" aprotic solvent to a "weakly protonic" solvent such as methanol (3). Comparisons (2) of the $\Delta\Delta H_s$ values for aromatic and aliphatic compounds with the limited number of $\Delta\Delta G$ values available (4) suggest that, as in the case of ions (5), free energies of transfer among solvents other than water are largely determined by the enthalpy contribution. Thus the enthalpy of transfer is a meaningful indication of the change in solvation that a molecule, group, or ion undergoes upon transfer from one solvent to another. The observation of additivity of group $\Delta\Delta H_s$ values in many molecules permits the calculation of $\Delta\Delta H_s$ for other molecules, provided that the appropriate group values are known.

Results and Discussion

The enthalpies of solution of a series of *m*- and *p*-substituted benzaldehydes in methanol and in *N*,*N*-dimethylformamide, and the resulting enthalpies of transfer [$\Delta\Delta H_s = \Delta H_s(\text{DMF}) - \Delta H_s(\text{MeOH})$] are listed in Table 1. In the final column are apparent $\Delta\Delta H_s$ values for the aldehyde group, based on the observed $\Delta\Delta H_s$ for the compound less the group enthalpies of transfer

[1]The financial support of the Robert A. Welch Foundation (Grant E-136) is gratefully acknowledged.

Can. J. Chem. Downloaded from www.nrcresearchpress.com by 84.22.46.98 on 09/08/12
For personal use only.

TABLE 1. Enthalpies* of solution and of transfer of substituted benzaldehydes in methanol and dimethylformamide at 25°

	ΔH_s†		$\Delta\Delta H_s$	
Substituent	MeOH	DMF	M → D	—CHO‡
p-$N(CH_3)_2$§	6.3	4.6	−1.7	−0.9
p-OH§	4.0	1.2	−2.8	−0.8
p-OCH_3	1.53	−0.19	−1.72	−0.8
p-CH_3	0.88	−0.08	−0.96	−0.67
H	0.64	−0.25	−0.89	−0.57
p-Cl§	4.0	3.6	−0.4	0.0
m-Cl	−0.92	−0.17	0.75	1.15
m-NO_2§	2.1	4.2	2.1	3.2
p-NO_2§	2.2	4.7	2.5	3.6

*In kcal/mol.
†Calorimetric values ±0.1 kcal/mol (solids), ±0.05 (liquids). Concentration range 10^{-4} to 10^{-3} *M*.
‡Apparent group enthalpy of transfer for —CHO [= $\Delta\Delta H_s$(M → D) − calcd. $\Delta\Delta H_s$ for remainder of molecule].
§Solid compounds at 25°.

for the benzene ring and the substituent. Benzaldehyde has a dipole moment (2.78 D) only slightly less than that of acetophenone (2.96 D) (6). Since the exothermic enthalpy of transfer of the acetyl group (−1.0 kcal/g group wt.) has been attributed (2) mainly to the larger dipole–dipole interaction with DMF than with methanol, an aldehyde group $\Delta\Delta H_s$ of perhaps −0.7 to −1.0 might be anticipated. A value of −0.8 is, in fact, found (within experimental error) for the three benzaldehydes with strongly electron releasing substituents, *p*-$N(CH_3)_2$, *p*-OH, and *p*-OCH_3. Slightly less negative values are calculated for the *p*-CH_3 and unsubstituted members, and increasingly positive values are found as the electron withdrawing character of the substituents increases: *p*-Cl < *m*-Cl < *m*-NO_2 < *p*-NO_2. Rather similar values of ΔH_s(DMF) are observed for the liquid aldehydes, −0.25 to −0.08 kcal/mol, whereas the range is 1.53 to −0.92 in methanol, with the values becoming less endothermic with increasing electron withdrawal. A similar trend exists with the solid aldehydes, with the possible exception of the *p*-OH compound.

It therefore appears that enthalpies of solution of benzaldehydes possessing electron withdrawing substituents are more exothermic (or less endothermic) in methanol than might be expected. This thermal effect might be attributed to an exothermic reaction of the aldehydes occurring in methanol, such as uncatalyzed hemiacetal formation, and, possibly, to the greater solvation of the reaction product than of the reactants by methanol. We were surprised that the entire heat effect in the calorimetric measurements was released within 1–2 min, in view of the somewhat slower rates of hemiacetal formation reported for acetaldehyde (7).

The p.m.r. spectra of *p*-dimethylamino-, *p*-methoxy-, *m*-chloro-, and *p*-nitrobenzaldehyde in methanol and in dimethylformamide were examined. The first two aldehydes showed similar peaks in both solvents, including the aldehydic (formyl) proton about 9.9 p.p.m. downfield from TMS, but the second two had an additional singlet in methanol, absent in DMF, at 3.6 p.p.m. due to methoxy protons of the hemiacetal. The hemiacetal α-proton and presumably the hydroxyl proton are masked by the hydroxyl proton of neat methanol at 4.8 p.p.m. *p*-Nitrobenzaldehyde had peak areas in the formyl/methoxy proton ratio of 0.29/0.71 × 3, leading to the conclusion that 71% of the original aldehyde exists in methanol solution as the hemiacetal. This is confirmed by the formyl/aromatic proton ratio of 0.28/4, which indicates that over 70% of the aldehyde has been converted to another substance. The $(CH_3)_2N$— and CH_3O— compounds had formyl/substituent proton ratios of 1/5.9 and 1/2.9, respectively, indicating that no appreciable amount of aldehyde has been diverted in either case by reaction with methanol.

Using the reasonable assumption that the enthalpy of reaction for the formation of hemiacetal, and the difference in enthalpy of solvation of reactants and products are the same for all of the benzaldehydes, one may use the apparent —CHO

Can. J. Chem. Downloaded from www.nrcresearchpress.com by 84.22.46.98 on 09/08/12
For personal use only.

Can. J. Chem. Downloaded from www.nrcresearchpress.com by 84.22.46.98 on 09/08/12
For personal use only.

group enthalpies of transfer (Table 1, last column) to calculate the percentage of hemiacetal formed from the other benzaldehydes. The $\Delta\Delta H_s$ value for the aldehyde group (MeOH → DMF) is −0.8 kcal/g group wt. Apparent group $\Delta\Delta H_s$ values may differ from this in an amount directly dependent on the amount of hemiacetal formation. *p*-Nitrobenzaldehyde differs from this by 3.6 − (−0.8) = 4.4 kcal, due to a 71% conversion to hemiacetal. A 100% conversion would have led to a discrepancy of 4.4/0.71 = 6.2 kcal. From these considerations the following amounts of hemiacetal formation in methanol may be calculated: *m*-NO_2, 65%; *m*-Cl, 31.5%; *p*-Cl, 13%; H, 3.7%; and *p*-CH_3, 2.1%. Relative equilibrium constants may be calculated for the hemiacetal forming reactions, assuming a constant methanol concentration; $K = k$[hemiacetal]/[aldehyde]. From the equilibrium constants for the *p*-NO_2, *m*-NO_2, *m*-Cl, *p*-Cl, H, and *p*-CH_3 systems a satisfactory Hammett equation plot of log K *vs.* σ can be constructed. From the plot log K values for the *p*-OCH_3, *p*-OH, and *p*-$N(CH_3)_2$ systems can be estimated, and from these the percent of hemiacetal formation can be derived, even though the amount of hemiacetal formation (*p*-OCH_3, 1.1%; *p*-OH, 0.7%; *p*-$N(CH_3)_2$, 0.06%) is too small to affect, within experimental error, the enthalpies of solution of these aldehydes in methanol.

The average of two p.m.r. determinations of the formyl and hemiacetal peak areas for *m*-chlorobenzaldehyde indicates hemiacetal formation to the extent of 33%. Because the addition of methanol to aldehydes is an equilibrium, the reaction may proceed to a slightly greater extent in the dilute calorimetric solutions than in the relatively concentrated n.m.r. solutions.

The true enthalpy of transfer of *p*-nitrobenzaldehyde may be calculated from the following group values: —NO_2, −0.8; —C_6H_4—, −0.3; —CHO, −0.8 = −1.9 kcal/mol. The measured value of 3.6 kcal/mol corresponds with 71% formation of hemiacetal. The difference in the two values results from enthalpies of reaction, of desolvation of reacting aldehyde and methanol, and of solvation of hemiacetal. Group $\Delta\Delta H_s$ values are not available for the latter term, but it is believed that the enthalpies of desolvation of reactants and of solvation of the product approximately cancel, leaving the enthalpy of reaction as the principal contributing term.

Experimental

The calorimetric method used was that previously described (2, 8). Sample concentrations were in the range of 10^{-4} to 10^{-3} *M*. Liquid samples were introduced using a microliter syringe. The methanol and DMF were reagent grade materials which were dried with 3A and 4A molecular sieve, respectively. The aldehydes were commercial samples which were freshly purified via the bisulfite addition products, and recrystallized or distilled. Physical constants were in agreement with literature values.

N.m.r. spectra were obtained with a Varian T-60 spectrometer, using solutions which were about 5% aldehyde by weight, with tetramethylsilane added.

Conclusions

In a series of *m*- and *p*-substituted benzaldehydes the amount of hemiacetal formation increases with the electron withdrawing power of the substituent. This behavior was initially recognized by variations in the apparent enthalpy of transfer of the aldehyde group. Group $\Delta\Delta H_s$ values constitute a potentially general method for detecting reactions of solutes with solvents, even in systems such as the present one, where no isolable product is formed.

1. R. Fuchs, L. L. Cole, and R. F. Rodewald. J. Am. Chem. Soc. **94**, 8645 (1972).
2. R. Fuchs and R. F. Rodewald. J. Am. Chem. Soc. **95**, 5897 (1973).
3. R. W. Taft, E. Price, I. R. Fox, I. C. Lewis, K. K. Anderson, and G. T. Davis. J. Am. Chem. Soc. **85**, 709 (1963).
4. A. J. Parker. Chem. Rev. **69**, 1 (1969).
5. B. G. Cox and A. J. Parker. J. Am. Chem. Soc. **95**, 402 (1973).
6. A. L. McClellan. Tables of experimental dipole moments. W. H. Freeman and Co., San Francisco. 1963.
7. G. W. Meadows and B. DeB. Darwent. Can. J. Chem. **30**, 501 (1952); G. W. Meadows and B. DeB. Darwent. Trans. Faraday Soc. **48**, 1015 (1952).
8. R. F. Rodewald, K. Mahendran, J. L. Bear, and R. Fuchs. J. Am. Chem. Soc. **90**, 6698 (1968).

Influence of Lewis Acids on the Diels–Alder Reaction. V. The Reaction of Furan with Dimethyl Acetylenedicarboxylate[1,2]

A. W. McCulloch, D. G. Smith, and A. G. McInnes

Atlantic Regional Laboratory, National Research Council of Canada, Halifax, Nova Scotia

Received July 10, 1973

The Diels–Alder addition of furan to dimethyl acetylenedicarboxylate (DMAD) affords a monoadduct **1**. The position and steric course of further addition of furan to the latter are temperature dependent. At temperatures of 50° or below addition occurs mainly at the activated double bond to give *endo-endo* **4** and *endo-exo* **5** diadducts. At 100° addition occurs at the less substituted double bond of the monoadduct to give analogous *endo-endo* **7** and *endo-exo* **9** diadducts; further addition of furan to the latter at 100° affords four triadducts **12–15**. The configurations of all these products were determined by p.m.r. and assignments confirmed by simulation of the spectra.

$AlCl_3$ causes enormous rate enhancement of the Diels–Alder additions of furan to DMAD and to the activated double bond of the monoadduct. In the presence of the Lewis acid the predominant diadduct formed is the *endo-exo* isomer **5**.

L'addition du type Diels–Alder du furanne sur l'acétylènedicarboxylate de diméthyle (DMAD) conduit au produit de monoaddition **1**. La position et le mécanisme stérique d'additions supplémentaires du furanne sur le produit **1** dépendent de la température. A 50 °C ou en-dessous l'addition se produit principalement sur la double liaison activée pour donner des produits de double addition *endo-endo* **4** et *endo-exo* **5**. A 100 °C, l'addition se produit sur la double liaison la moins substituée du produit de monoaddition pour donner les produits de double addition analogues *endo-endo* **7** et *endo-exo* **9**; des additions supplémentaires du furanne sur ces derniers produits à 100 °C conduisent à quatre produits de triple addition **12–15**. Les configurations de tous ces produits ont été déterminées par r.m.n. et les attributions ont été confirmées par simulation des spectres.

Le $AlCl_3$ entraîne une augmentation enorme de la vitesse d'addition du type Diels–Alder du furanne sur le DMAD et sur la double liaison activée du produit de monoaddition. En présence de l'acide de Lewis, le produit majeur de double addition formé est l'isomère *endo-exo* **5**.

[Traduit par le journal]

Can. J. Chem., **51**, 4125 (1973)

Introduction

In the course of our studies of $AlCl_3$ acceleration of the Diels–Alder reactions of heterocyclic dienes with acetylenic dienophiles (1–3) we have investigated the reaction of furan with dimethyl acetylenedicarboxylate (DMAD). This communication details the results of our studies on both the thermal and $AlCl_3$-promoted reactions of these addends.

The reaction of furan with DMAD involves initial formation of a monoadduct **1** which can then function as a dienophile. Further addition of furan can occur at the more substituted double bond of **1** to give a diadduct of type **2** or at the less substituted double bond to give a diadduct of type **3**. There are three possible configurations of **2**, namely *endo-endo* **4**, *endo-exo* (or *exo-endo*) **5**, and *exo-exo* **6**, and four possible configurations of **3**, namely *endo-endo* **7**, *exo-endo* **8**, *endo-exo* **9**, and *exo-exo* **10**.[3]

The temperature dependence of the thermal reaction of furan and DMAD was the subject of a recent paper by Slee and LeGoff (4). These workers found that at room temperature the major product (90%) was **5** with only 6% **4**, while at 100° the chief products were **7** (4.3%) and **9** (27.0%). They also isolated a triadduct of type **11** (3.7%) from the reaction at higher temperature, but did not establish its stereochemistry.

As has been pointed out by Martin and Hill in their review of the stereochemistry of the

[1]NRCC No. 13459.

[2]Presented in part at the 55th Canadian Chemical Conference of the Chemical Institute of Canada, Quebec City, Quebec, June, 1972.

[3]The system which we have adopted to define stereochemistry in **2** is that originally used by Stockman (17), in which the relationship of the ring-juncture substituents to the two bridged rings are denoted, reading from left to right. We have used this system also to define the stereochemistry of **3** (and the triadducts **11**), where the ring-juncture substituents are hydrogen atoms. In these cases the most heavily substituted ring is placed to the left.

Can. J. Chem. Downloaded from www.nrcresearchpress.com by 210.87.254.105 on 09/05/12
For personal use only.

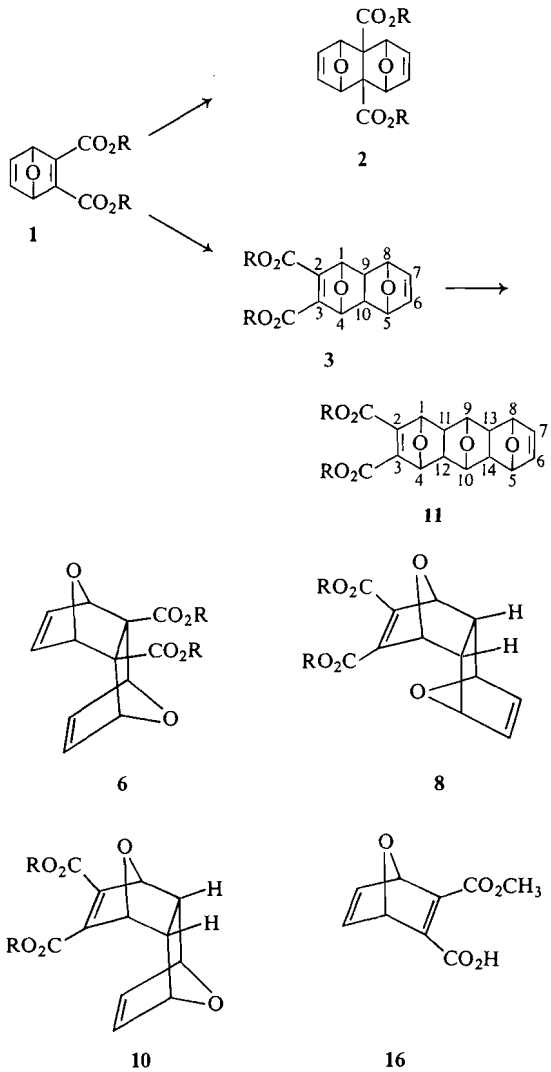

Diels–Alder reaction, in practically all additions using norbornene type dienophiles the diene is subject to "steric approach control" by the dienophile. A considerable body of experimental evidence indicates that, with the exception of systems having a heavily substituted bridge, approach of the diene is preferred at the bridged face of the dienophile (5). If this rule is applicable to the Diels–Alder additions of furan to the oxanorbornadiene **1**, formation of diadducts **6**, **8**, and **10** will be highly improbable; the observed formation of **4**, **5**, **7**, and **9**, on the other hand, is consistent.

Compounds **1** (6–8) and **4** (6, 9, 10) are well authenticated; both have also been reported as products of the photochemical reaction of furan with DMAD (11).[4] Slee and LeGoff were the first to report the isolation of **5**, **7**, and **9** (4).

Results and Discussion

Thermal Reaction

We have investigated the initial phases of the thermal reaction at three temperatures (25, 50, and 100°). At each temperature the reaction was carried out in a sealed tube and was monitored by p.m.r. Typical results are given in Table 1. These serve to illustrate the features noted below.

(*a*) Initially the reactants are converted to **1** and little diadduct is formed.

(*b*) At room temperature further addition of a second molecule of furan to the more substituted double bond of **1** occurs to give diadducts **4** and **5**; isomer **5** is formed faster than **4**.[5]

(*c*) At 50° or in the initial stages of reaction at 100° equilibration occurs, resulting in a gradual buildup of isomer **4** relative to **5**.[6]

(*d*) The combination of furan and **1** to give **7** and **9** is slow, and significant amounts of these products are observed only at higher reaction temperatures (> 50°) and longer reaction times. Isomer **9** is formed faster than **7**. It was not possible to monitor the reaction for a subsequent buildup of **7** relative to **9**, since addition of a third molecule of furan to these compounds was competitive.

We have repeated the preparative scale reaction at 100° (18 h), carried out by Slee and LeGoff (4), and have also isolated **1** (4.5%), **4**

[4]It seems probable that these compounds are actually products of the thermal reaction, and the yields of **1** and **4** reported are consistent with this. Formation of these compounds by a photoaddition process would be contrary to the Woodward–Hoffman rules (12).

[5]Our results from a series of reactions at room temperature (Table 1) indicate that after 25 days approximately 50% diadduct was formed with a **5** to **4** ratio of 3:1. These findings conflict with those of Slee and LeGoff who report 90% formation of **5** after 5 weeks, with only 6% **4** (a ratio of 15:1!). However they observed crystallization of the product while our reactions remained homogeneous. This suggests that an equilibrium exists between **1**, **4**, and **5**, and that removal of **5** from solution by precipitation drives the equilibrium in solution towards further formation of this isomer.

[6]We have also monitored the retrogression of **5**. Under the conditions used (50° in C_6D_6) we observed approximately 80% retro reaction during the first 5 days; with increasing time we again observed slow formation of **4** and as expected an increasing **4**:**5** product ratio. Independent experiments showed that at 50° retrogression of **5** occurs at least 10 times faster than that of **4**.

Can. J. Chem. Downloaded from www.nrcresearchpress.com by 210.87.254.105 on 09/05/12
For personal use only.

Can. J. Chem. Downloaded from www.nrcresearchpress.com by 210.87.254.105 on 09/05/12
For personal use only.

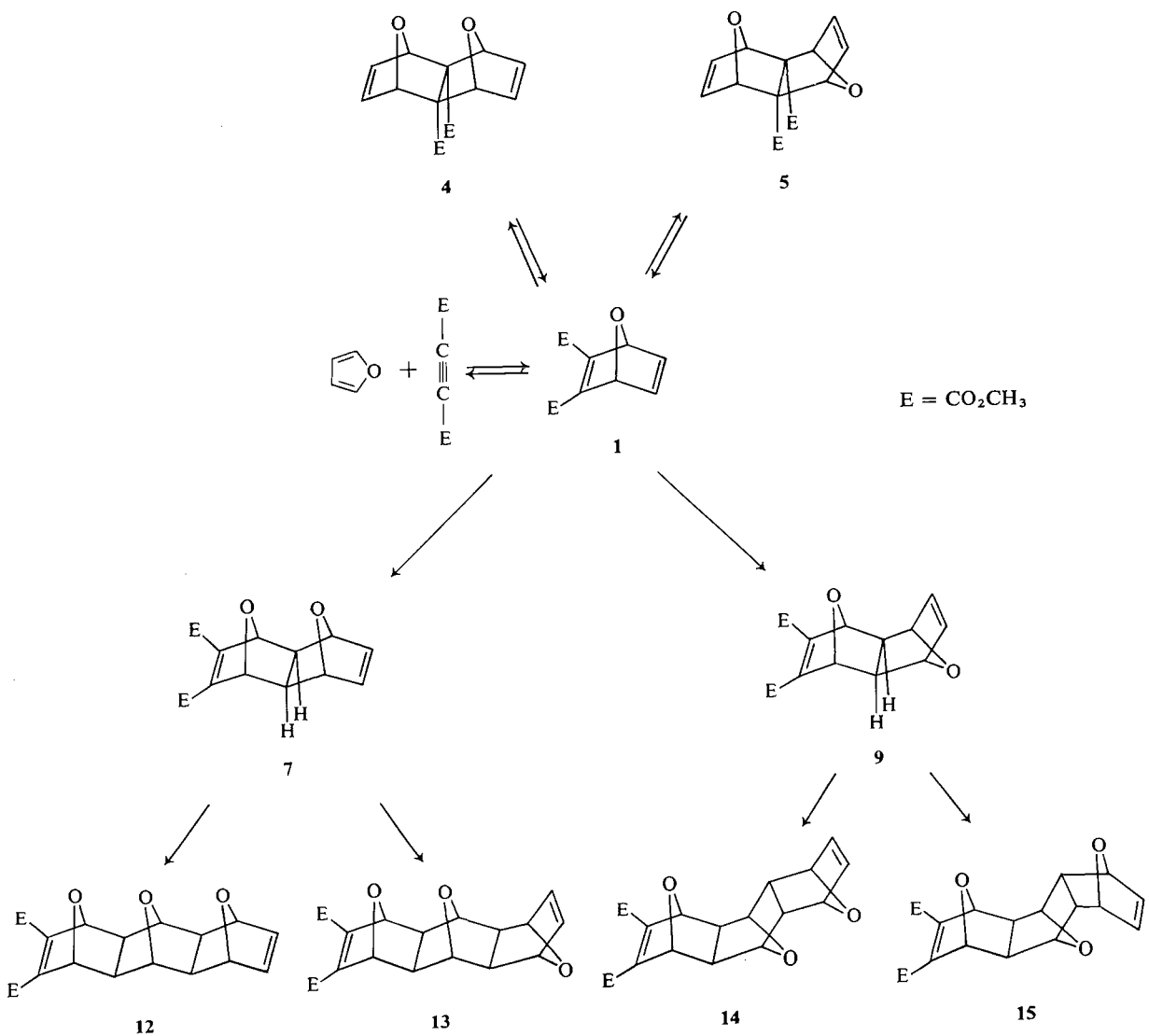

SCHEME 1

TABLE 1. Reaction of furan with DMAD (reactant ratio 2:1; no solvent)

Temperature (°C)	Time	Yields (%)* 1	4	5	7	9
25	2 days	25	—	—	—	—
	3 days	33	1	3	—	—
	4 days	39	2	7	—	—
	7 days	43	4	14	—	—
	8 days	44	5	17	—	—
	10 days	44	6	20	—	—
	15 days	43	8	28	—	—
	18 days	41	9	33	—	—
	25 days	37	12	39	—	—
50	0.67 h	7	—	—	—	—
	1.67 h	13	—	—	—	—
	5 h	26	1	3	—	—
	17 h	31	7	15	—	—
	24 h	29	10	19	—	—
	42 h	21	15	27	—	—
	48 h	20	17	27	—	—
	64 h	17	20	27	1	2
	136 h	12	31	22	2	6
100	25 min	35	4	6	—	—
	50 min	38	13	2	1	2
	125 min	31	23	2	2	5
	220 min	25	29	2	2	7

*The yields, based on furan, were calculated by integration of the appropriate olefinic and/or bridgehead proton signals in the p.m.r. spectra. Reactions were carried out in sealed p.m.r. tubes.

(3.0%), **7** (15.4%), and **9** (26.6%). In addition we obtained as products not one, but *four* triadducts of type **11**, the stereochemistry of which we have established, on the basis of p.m.r. spectral evidence (see below) as *endo-endo-endo-endo* **12**, *endo-endo-endo-exo* **13**, *endo-exo-endo-endo* **14**, and *endo-exo-endo-exo* **15**. It is noteworthy that the latter four products must be formed by addition of furan to the less substituted double bond of the *endo-endo* **7** and *endo-exo* **9** diadducts. In accord with the principles controlling addition described by Martin and Hill (5) only these 4 out of a possible 16 triadducts of type **11** would be expected. Thus **12** (1.5%) and **13** (2.7%) arise through addition of furan to **7**, while **14** (4.2%) and **15** (6.1%) are formed by addition of furan to **9**. The relative yields of the four triadducts reflect both the predominance of **9** over **7** (**14** + **15** > **12** + **13**) and the preferred initial formation of an *endo-exo* ring juncture (**15** and **13**) over one that has *endo-endo* stereochemistry (**14** and **12**).

Although detailed kinetic studies would be a necessary prerequisite for understanding the mechanisms of the Diels–Alder associations discussed above and summarized in Scheme 1 it is still possible to draw some conclusions.

At the outset it should be emphasized that equilibration between **1**, **4**, and **5** has been demonstrated experimentally. Since it is known that adducts of furan generally undergo relatively facile retrogression, it seems likely that under the reaction conditions used diadducts **7** and **9** or any of the four triadducts could undergo retrogression–equilibration. However, since this has not been proved, use of the terms "kinetic" and "thermodynamic" is inappropriate to a discussion of the present products.

Addition of furan to **1** can in theory take place in eight ways. Figure 1 illustrates the transition states for these additions, analogous to those envisaged by Herndon and Hall for the dimerization of cyclopentadiene (13). We shall limit our discussion to the observed additions, that is, those satisfying the rule of steric control, leading to products **4**, **5**, **7**, and **9**. These four reactions are homocompetitive. The preferred initial formation of diadducts **4** and **5**, arising by addition at the more substituted double bond of **1**, is to be expected due to the presence of electron-attracting substituents in the dienophile (14).

As we have seen the formation of **9** is preferred to that of **7** (Table 1). There are no carbonyl substituents at the site of addition in the dienophile so that no secondary orbital overlap is possible. Similarly, production of **5** is preferred over that of **4** (Table 1). This parallelism suggests that the role of secondary attractive forces in the latter case is negligible. While this would be contrary to the ideas of Woodward and Hoffmann (12), it is in accord with the suggestion of Herndon and Hall who have proposed that such interactions between centres which are not bonded in the product may be relatively unimportant and that the stabilities of *endo* and *exo* transition states are governed predominantly by geometrical overlap of the π-orbitals at the primary centers where bond formation is in process (13).

The additions of furan to **1** (to give **9** and **7**), **7** (to give **12** and **13**), and **9** (to give **14** and **15**) are analogous to the Diels–Alder addition of furan to maleic anhydride which yields *endo* (kinetic) and *exo* (thermodynamic) adducts (15). The primary product formed in each case (**9**, **13**, and **15**) corresponds to the *endo* adduct; its formation obeys the Alder *endo* rule. However,

Can. J. Chem. Downloaded from www.nrcresearchpress.com by 210.87.254.105 on 09/05/12
For personal use only.

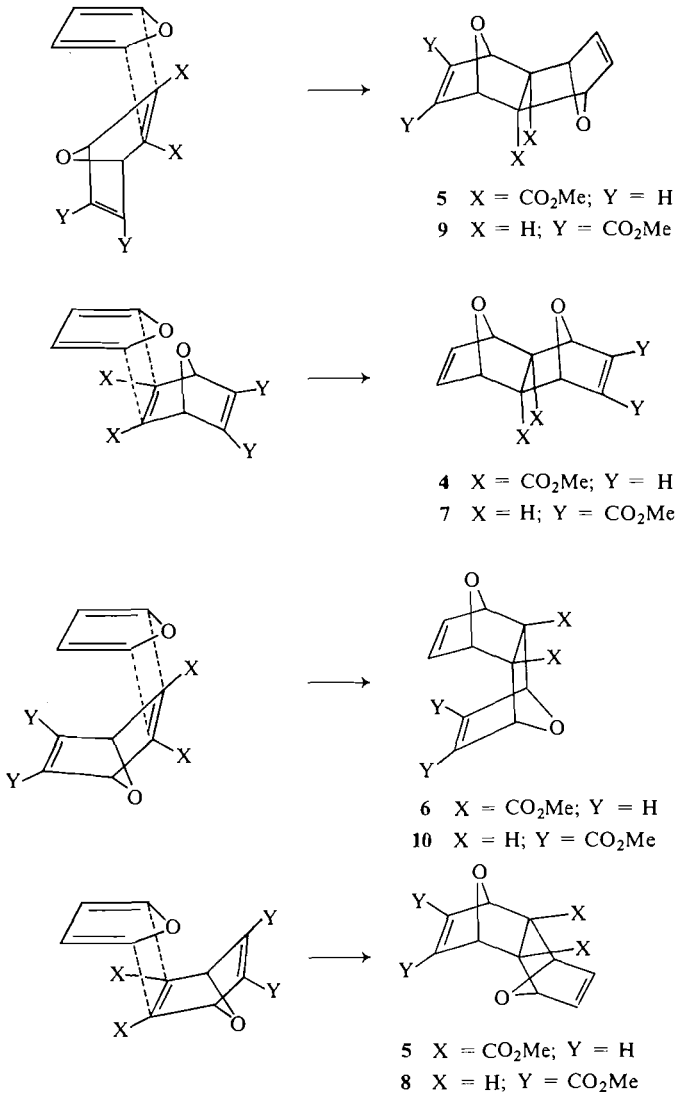

FIG. 1. Addition of furan to **1**.

addition to give **5** is contrary to the Alder *endo* rule,[7] which by definition requires maximum overlap involving the double bonds of activating substituents in the dienophile (14). The same conclusion was reached by Slee and LeGoff (4). In contrast, formation of diadduct **4** obeys the *endo* rule.

$AlCl_3$-promoted Reaction

Anhydrous $AlCl_3$ had a two-fold effect on the reaction of furan with DMAD at room temperature. In the first place it caused an enormous enhancement (approximately $\times 10^4$) in the rates of the Diels–Alder additions of furan to both DMAD and **1**, in common with our results on other Diels–Alder additions of furans to acetylenic esters (3). Secondly, the kinetically favored **5** was by far the major diadduct produced; only a trace of **4** could be detected and no addition occurred at the less substituted double bond of **1**. For example, a reaction mixture 0.4 *M* in furan and 0.2 *M* in DMAD and $AlCl_3$ (in CH_2Cl_2) showed at least 30% conversion of DMAD to

[7]Isomer **5** could in theory arise by an *endo* addition process (see Fig. 1), but this would involve invalidation of the rule of steric approach control (5).

Can. J. Chem. Downloaded from www.nrcresearchpress.com by 210.87.254.105 on 09/05/12
For personal use only.

Can. J. Chem. Downloaded from www.nrcresearchpress.com by 210.87.254.105 on 09/05/12
For personal use only.

TABLE 2. P.m.r. parameters for **1**, **16**, **4**, and **5**

No.	Compound structure	Chemical shifts (Hz)	System	Chemical shifts* (Hz)	Coupling constants (Hz)
1	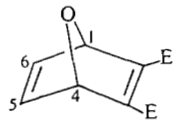	3.80 (OCH_3) 5.67 (H_1H_4)	$A(H_1)X(H_6)X'(H_5)A'(H_4)$	$\nu_1 = \nu_4 = 0$ $\nu_5 = \nu_6 = 93.6$	$J_{1,6} = J_{4,5} = 1.9$ $J_{1,5} = J_{4,6} = 0.2$ $J_{1,4} = 1.5; J_{5,6} = 5.5$
16†	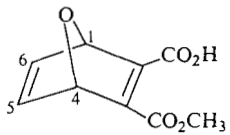	3.21 (OCH_3) 12.17 (OH) 5.39 (H_1)	$X(H_1)A(H_6)B(H_5)Y(H_4)$	$\nu_1 = 0; \nu_6 = 77.0$ $\nu_5 = 85.5; \nu_4 = 20.0$	$J_{1,6} = J_{4,5} = 1.9$ $J_{1,5} = J_{4,6} = 0.2$ $J_{1,4} = 1.6; J_{5,6} = 5.4$
4	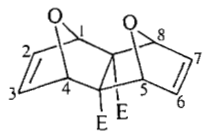	3.63 (OCH_3) 5.07 (H_1H_4 or H_5H_8)	$A(H_1$ or $H_8)X(H_2$ or $H_7)$ $X'(H_3$ or $H_6)A'(H_4$ or $H_5)$	$\nu_1 = \nu_4 = \nu_5 = \nu_8 = 0$ $\nu_2 = \nu_3 = \nu_6 = \nu_7 = 92.4$	$J_{1,2} = J_{3,4} = J_{5,6} = J_{7,8} = 1.7$ $J_{1,3} = J_{2,4} = J_{5,7} = J_{6,8} = 0.1$ $J_{1,4} = J_{5,8} = 1.1$ $J_{2,3} = J_{6,7} = 5.7$
5‡	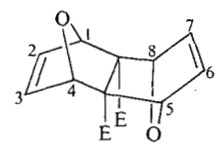	3.71 (OCH_3) 5.17 (H_1H_4)	$A(H_1)X(H_2)X'(H_3)A'(H_4)$	$\nu_1 = \nu_4 = 0$ $\nu_2 = \nu_3 = 128.0$	$J_{1,2} = J_{3,4} = 1.7$ $J_{1,3} = J_{2,4} = 0.1$ $J_{1,4} = 0.9; J_{2,3} = 5.7$
		4.52 (H_5H_8)	$A(H_5)X(H_6)X'(H_7)A'(H_8)$	$\nu_5 = \nu_8 = 0$ $\nu_6 = \nu_7 = 79.2$	$J_{5,6} = J_{7,8} = 1.8$ $J_{5,7} = J_{6,8} = 0.2$ $J_{5,8} = 1.3; J_{6,7} = 5.9$

*For computer purposes the chemical shift of the highest field proton (or protons when chemically equivalent) was empirically given a value of 0.0 Hz and all others were measured relative to it. These shifts are from the simulated spectra.

†Spectrum recorded in benzene-d_6.

‡The assignment of the four-spin systems to the hydrogens of the two bridged rings of 5 was based on comparison with the spectra of the corresponding diadduct of furan and ethyl propiolate. In the latter the presence of a ring-juncture hydrogen allowed unequivocal assignments to be made (23).

Can. J. Chem. Downloaded from www.nrcresearchpress.com by 210.87.254.105 on 09/05/12
For personal use only.

adduct (**1** and **5**) in only 1 min at room temperature, the molar ratio of **1** to **5** being *ca.* 4:1. Negligible reaction occurred at the same concentration level in 30 min in the absence of the Lewis acid. After 1 h at room temperature the isolated yields (based on DMAD) of **1** and **5** were 20 and 22%, respectively. As expected considerable diene polymerization occurred. The monoadduct acid **16** was obtained as a by-product (6.6%), presumably arising by work-up hydrolysis of **1**.

It was established independently that neither **4** nor **5** dissociate appreciably (> 10%) to **1** and furan in the presence of an equimolar amount (0.2 *M* in CH_2Cl_2) of $AlCl_3$ for 1 h at room temperature. Consequently **5** is isolated in the $AlCl_3$-promoted reaction as the predominant diadduct since this kinetically-controlled product forms a reasonably stable complex with the Lewis acid, thus inhibiting retrogression and subsequent equilibration. This behavior is similar to that which we have observed previously with monoadducts of pyrroles and other furans with DMAD which also form complexes with $AlCl_3$ (1, 2).

Previous work in this laboratory and by other workers (16) indicates that in $AlCl_3$-promoted Diels–Alder reactions the role of the Lewis acid is to lower the enthalpy of activation. Consequently, the fact that the reaction of the addends in the presence of $AlCl_3$ produces predominantly **5** would seem to imply that the activation energy for the formation of the latter is lowered to a greater extent than in the case of **4**.

Proton Magnetic Resonance Spectra

No systematic analysis of the p.m.r. spectra of **1**, **4**, **5**, **7**, and **9** has been carried out. We have therefore analyzed the 60 MHz spectra of these compounds, and also of the acid **16** and the four triadducts **12**–**15**. The parameters were checked by means of simulation of the spectra using a Varian Spectrosystem 100. In all cases the experimental and simulated spectra were superposable within experimental error. The relevant parameters are detailed in Tables 2–4.

Monoadducts 1 and 16 (Table 2)

The olefinic and bridgehead protons of **1** form an AXX′A′ system in which the signals appear as deceptively simple triplets (*cf.* ref. 11). Analysis necessitated observation of two outer low-intensity lines, symmetrically placed on each side of each "triplet", and was carried out in the same way as reported for the very similar spectrum for the four ring hydrogens of furan (18, 19). Values of $J_{5,6}$, $J_{1,4}$, and of $(J_{1,5} + J_{1,6})$ (the spacing between the apparent outer lines of each triplet) are obtainable directly from the spectrum.

The olefinic and bridgehead protons of the asymmetric compound **16** (in benzene-d_6) comprise an XABY system in which the X and Y parts appear as slightly broadened triplets. In this case it was possible to obtain independent values for $J_{1,6}$ (1.9 Hz) and $J_{1,5}$ (0.2 Hz) directly from the spectrum.

Diadducts 4 and 5 (Table 2)

The stereochemistry of **4** and **5** can be established from their spectra on the basis of symmetry arguments. Isomer **4** possesses C_{2v} symmetry and as a result its p.m.r. spectrum consists of two superposed equivalent AXX′A′ systems for the identical pairs of bridgehead and olefinic protons. In contrast, isomer **5** has only C_s symmetry and consequently the bridgehead and olefinic protons of one bridged ring are not equivalent to the corresponding protons of the other ring. The p.m.r. spectrum of **5** thus consists of two independent AXX′A′ systems. The AXX′A′ systems of **4** and **5** appear in each case, as in **1**, as pairs of deceptively simple triplets. The sub-spectra were analyzed in a manner similar to that of **1**.

Diadducts 7 and 9 (Table 3)

The differing ring-juncture stereochemistry of isomers **7** and **9** is readily established from the multiplicity of the signals in their spectra for the bridgehead (H_5H_8) and ring-juncture (H_9H_{10}) protons. In the case of **7** the *endo-endo* configuration requires that the dihedral angles between these protons be close to 90°, resulting in near absence of coupling (20–22).[8] In contrast, the *endo-exo* configuration of **9** requires a dihedral angle of approximately 45°, resulting in a significant $J_{5,10}$ (4.9 Hz). The four ring hydrogens ($H_5H_6H_7H_8$) of **7** give rise to an AXX′A′ system as before, with a pair of deceptively simple triplets. Analysis of this system was carried out in the same way as for **1**, **4**, and **5**.

In the case of **9** we observe a six-spin system

[8]Since the ring-juncture hydrogens in both **7** and **9** are *endo* to the ring carrying the ester groups, the signal for bridgehead hydrogens (H_1H_4) appears as a singlet in the spectrum of each isomer.

Can. J. Chem. Downloaded from www.nrcresearchpress.com by 210.87.254.105 on 09/05/12
For personal use only.

TABLE 3. P.m.r. parameters for **7** and **9**

Compound*	Chemical shifts(δ)				System	Chemical shifts† (Hz)			Coupling constants‡ J_{pq} (Hz)								
	OCH_3	H_1H_4	H_5H_8	H_9H_{10}		H_5H_8	H_6H_7	H_9H_{10}	5,6 7,8	5,7 6,8	5,8	5,9 8,10	5,10 8,9	6,7	6,9 7,10	6,10 7,9	9,10
7	3.80	5.11	4.92	2.21	$A(H_5)X(H_6)X'(H_7)A'(H_8)$	0	93.0		1.6	0.1	0.6			5.8			
9	3.82	4.76		2.85	$A(H_5)M(H_6)M'(H_7)$ $A'(H_8)X'(H_9)X(H_{10})$	121.0	209.5	0	1.8	0.2	0.7	−0.2	4.9	6.0	0.0	0.0	7.6

*For numbering see structure 3.
†For computer purposes the chemical shift of the highest field protons was empirically given a value of 0.0 Hz and others measured relative to it. These shifts are from the simulated spectra.
‡All other couplings with H_9 and $H_{10} \leq 0.2$ Hz.

Can. J. Chem. Downloaded from www.nrcresearchpress.com by 210.87.254.105 on 09/05/12
For personal use only.

TABLE 4. P.m.r. parameters for **12**, **13**, **14**, and **15**

	Compound					
Parameter*	**12**	**13**	**14**		**15**	
Chemical shifts (δ)						
OCH_3	3.79	3.79	3.80		3.79	
H_1H_4	5.16	5.09	4.93		5.00	
H_5H_8	4.88	4.82	4.83		4.84	
H_6H_7	6.34	6.20	6.36		6.26	
H_9H_{10}	4.52	4.13	4.49		4.12	
$H_{11}H_{12}$	1.83	2.05	2.69		2.60	
$H_{13}H_{14}$	2.08	2.43	2.02		2.68	
System	$A(H_5)X(H_6)$ $X'(H_7)A'(H_8)$	$A(H_5)M(H_6)M'(H_7)$ $A'(H_8)X'(H_{13})X(H_{14})$	$A(H_5)X(H_6)$ $X'(H_7)A'(H_8)$	$A(H_9)X(H_{11})$ $X'(H_{12})A'(H_{10})$	$A(H_5)M(H_6)M'(H_7)$ $A'(H_8)X'(H_{13})X(H_{14})$	$A(H_9)M(H_{13})M'(H_{14})$ $A'(H_{10})X'(H_{12})X(H_{11})$
Chemical shifts† (Hz)						
H_5H_8	293.0	289.5	290.0		291.0	
H_6H_7	380.5	372.0	381.5		376.0	
H_9H_{10}				269.5		247.0
$H_{11}H_{12}$				161.5		156.0
$H_{13}H_{14}$		146.0			161.0	161.0
Coupling‡						
Constants J_{pq} (Hz)						
5,6 = 7,8	1.6	1.7	1.6		1.8	
5,7 = 6,8	0.1	0.1	0.1		0.1	
5,8	0.6	0.6	0.6		0.6	
5,13 = 8,14		−0.2			−0.2	
5,14 = 8,13		4.9			4.9	
6,7	5.8	5.8	6.0		5.9	
9,10				0.6		0.6
9,11 = 10,12				5.4		5.6
9,12 = 10,11				0.2		0.2
11,12				8.7		8.7
13,14		7.7				7.3

*For numbering see structure **11**.
†Shifts are downfield from tetramethylsilane. These shifts are from the simulated spectra.
‡All other couplings with H_{11}, H_{12}, H_{13}, and $H_{14} \leq 0.2$ Hz.

Can. J. Chem. Downloaded from www.nrcresearchpress.com by 210.87.254.105 on 09/05/12
For personal use only.

for $H_5H_6H_7H_8H_9$ and H_{10}. Absence of coupling between the olefinic (H_6H_7) and ring-juncture (H_9H_{10}) hydrogens, however, allows the deceptively simple triplet observed for the former (due to their coupling with the bridgehead hydrogens) to be analyzed as before. The bridgehead and ring-juncture hydrogens ($H_5H_{10}H_9H_8$) comprise essentially a separate AXX'A' subsystem with the signal for H_9H_{10} appearing as a deceptively simple quartet. Once again, observation of low-intensity wings symmetrically disposed about the centroid of the "quartet" allows analysis of the system. The separation between the apparent outer lines of the "quartet" is equal to $J_{5,10} + J_{5,9}$ ($J_{AX} + J_{AX'}$).

Triadducts 12–15 (Table 4)

The p.m.r. spectra of all four compounds clearly establish the general structure **11**, as each compound shows a signal for only *two* olefinic hydrogens.

The elucidation of the configurations of the four isomers was based essentially on the arguments outlined above in confirming the ring-juncture stereochemistry of **7** and **9**. The signal for the bridgehead hydrogens (H_1H_4) on the ring carrying the ester groups was observed in all cases as a singlet, confirming (as in the cases of **7** and **9**) that the neighboring ring had been added from the bridged face of the dienophile. In addition, a similar mode of addition of the second furan molecule results in virtual absence of coupling between H_9H_{10} and $H_{13}H_{14}$ in the triadducts. The signal for the olefinic hydrogens (H_6H_7) always appeared as a deceptively simple triplet, allowing partial analysis of the AXX'A' sub-spectrum for $H_5H_6H_7H_8$. The neighboring bridgehead hydrogens (H_5H_8) appeared either as a "triplet" (if the C_{13-14} ring juncture was *endo–endo*) or as a very broad multiplet (if the C_{13-14} ring juncture was *endo-exo*, involving additional coupling of $H_5H_8$with H_{13} and H_{14}). In the latter case $H_{13}H_{14}$ appeared as a deceptively simple "quartet" (*cf.* H_9H_{10} in **9**). The remaining ring-juncture relationships were readily deduced on the basis of the multiplicity ("quartet" or singlet) of the signals for the ring-juncture ($H_{11}H_{12}$) and bridgehead (H_9H_{10}) hydrogens.

The spectrum of compound **14** can be interpreted on the basis of either *endo-exo-endo-endo* or *endo-endo-exo-endo* stereochemistry. However, although the latter could arise via the *endo-endo* diadduct **7**, its formation would be contrary to the principle of steric approach control which governs these additions. Hence, this triadduct is concluded to be the expected *endo-exo-endo-endo* isomer.

Infrared and Mass Spectra

Diadducts **4**, **5**, **7**, and **9**, and all four triadducts show in their i.r. spectra *two* strong absorptions (1716–1720 and 1737–1745 cm^{-1}) in the carbonyl region (see Experimental). This may be attributed to steric interaction between the two ester groups. This effect can be observed on the i.r. time scale, whereas averaging prevents observation of separate methoxyl resonances by p.m.r. There are only very slight differences in the spectra of isomers; for example, the absorptions of **12–15** at 1600–1750 cm^{-1} are essentially identical. A medium-intensity C=C stretching vibration absorption (1635–1639 cm^{-1}) is observed in the spectra of all compounds carrying carbomethoxyl substituents on a double bond. The base peak in the mass spectra of all the adducts was observed at *m/e* 68 ($C_4H_4O^+$), reflecting the tendency of these molecules to undergo retrogression with loss of furan.

Reaction of Furan with Acetylenedicarboxylic Acid

In view of our results it seemed pertinent to reexamine the corresponding reaction of furan and acetylenedicarboxylic acid. A diadduct was first isolated by Diels and Alder (10), but it was not until recently that Kallos and Deslongchamps (9) on chemical grounds established that it was the *endo-endo* isomer **18** and not the alternative *endo-exo* **19** as reported by Stockmann (17). However, in both of the latter studies the only material examined was that which crystallized from the ethereal reaction solution. No attempt was made to determine whether **18** was the product of kinetic or thermodynamic control, or for that matter to establish whether it was in fact the only diadduct formed. We repeated the reaction and confirmed that the material which crystallized from solution was **18** by converting it to **4** with diazomethane. Reaction solutions (solvent ether, furan 8 *M*, acetylenedicarboxylic acid 4 *M*) were then monitored by p.m.r. (temperature 36°). Characteristic signals were obtained for **17** ("triplets" at average δ 7.10 and 5.73), **18** ("triplets" at average δ 6.62 and 5.18), *and* **19** ("triplets" at average δ 6.68, 6.40, 5.06, and 4.60). After 1 h (≪10% addends reacted) the

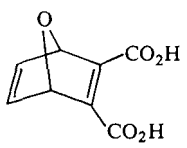

17

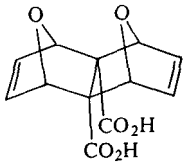

18

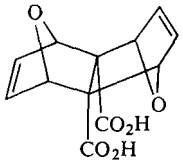

19

molar ratio of **19** to **18** was approximately 2:1, whereas at the end of 24 h (*ca.* 20% addends reacted) this ratio had changed to 1:4 and **18** had started to crystallize from solution, thus driving the equilibrium in solution towards its further formation.

Experimental

The p.m.r. spectra were obtained on a Varian A-60A spectrometer equipped with a V-6058 spin decoupler, using $CDCl_3$ as solvent (unless stated otherwise) and tetramethylsilane as internal standard. Spectral simulations were carried out using a Varian Spectrosystem 100. The i.r. spectra were recorded on a Perkin-Elmer 521 spectrometer and the mass spectra on a Dupont-CEC 21-491 spectrometer.

Reaction of Furan and DMAD

Monitoring of Reactions

Forward Reaction. Mixtures of furan (272 mg, 0.004 *M*) and DMAD (284 mg, 0.002 *M*) were sealed in p.m.r. tubes which were then immersed in constant temperature baths maintained at 25, 50, or 100°. The reactions were monitored by p.m.r. and the yields of products (based on furan) calculated from the integrated intensities of the signals for the ring hydrogens of the unreacted furan and the olefinic and bridgehead hydrogens of the products. The results are summarized in Table 1.

Retrogression of diadduct 5. A saturated solution of **5** in benzene-d_6 was sealed in a p.m.r. tube which was then immersed in a constant temperature bath maintained at 50°. The reaction was monitored by p.m.r. and the product composition measured on the basis of integrated intensities as above. A retrogression of 80% was observed in 5 days.

Diadduct **4** underwent only 25% retrogression to furan and **1** in 3 h at 100° (toluene solution).

Reaction of Furan and DMAD at 100°

Furan (22.7 g, 0.334 *M*) and DMAD (14.2 g, 0.100 *M*) were placed in a 100 ml stainless steel vessel of a "Baskerville" high pressure autoclave. The reaction temperature was maintained at approximately 100° for 20 h. The product was a highly viscous orange syrup (35.5 g), totally soluble in $CHCl_3$. This was chromatographed on Mallinckrodt silicic acid (100–150 mesh). Elution with chloroform afforded:

(*a*) The monoadduct **1** as a yellow oil (0.95 g, 4.5%). ν_{max} ($CHCl_3$) 1733, 1640, 1600 cm^{-1}.

(*b*) *Endo-exo* diadduct **9** as a colorless solid (7.40 g, 26.6%). Recrystallization from EtOH gave colorless rosettes, m.p. 118–120° (lit. 120–122° (4)). Highest molecular ion at *m/e* 246 (7%); base peak at *m/e* 68; prominent ions at *m/e* 217 (5%), 153 (8%), 150 (33%), and 119 (17%). ν_{max} ($CHCl_3$) 1739, 1717, 1639 cm^{-1}.

(*c*) *Endo-endo* diadduct **4** eluted with diadducts **9** and **7**. Estimated yield (from p.m.r.) 3%.

(*d*) *Endo-endo* diadduct **7** as a colorless solid (4.29 g, 15.4%). Recrystallization from EtOH gave colorless prisms, m.p. 158–160° (lit. 157–159° (4)). Highest molecular ion at *m/e* 246 (3%); base peak at *m/e* 68; prominent ions at *m/e* 217 (9%), 153 (26%), 150 (34%), and 119 (17%). ν_{max} ($CHCl_3$) 1737, 1716, 1637 cm^{-1}.

(*e*) *Endo-exo-endo-exo* triadduct **15** as a colorless solid (2.10 g, 6.1%).[9] Recrystallization from EtOH gave colorless needles, m.p. 188–192° (dec.) but dependent on rate of heating (lit. 213–215° (4)). Highest molecular ion at *m/e* 246 (3%); base peak at *m/e* 68; prominent ions at *m/e* 217 (8%), 153 (20%), 150 (33%), 119 (10%), and 94 (12%). ν_{max} ($CHCl_3$) 1740, 1718, 1639, 1603 cm^{-1}.

Elution was now continued with 2% MeOH–$CHCl_3$. Separation of the triadduct fractions so obtained was carried out by repeated preparative t.l.c. on silicic acid (2% MeOH–$CHCl_3$ as eluant). This afforded, in order of their elution:

(*a*) *Endo-endo-endo-exo* triadduct **13** as a colorless solid (0.94 g, 2.7%). Recrystallization from EtOH gave colorless prisms, m.p. 182–186° (dec.), dependent on rate of heating. Highest molecular ion at *m/e* 346 (1%); base peak at *m/e* 68; prominent ions at *m/e* 278 (7%), 249 (3%), 246 (6%), 217 (9%), 153 (27%), 150 (29%), 119 (7%), 95 (30%), and 94 (12%). ν_{max} ($CHCl_3$) 1739, 1719, 1636, 1602 cm^{-1}.

(*b*) *Endo-exo-endo-endo* triadduct **14** as a colorless solid (1.44 g, 4.2%). Recrystallization from EtOH gave colorless flakes, m.p. 227–229° (dec.). Highest molecular ion at *m/e* 246 (4%); base peak at *m/e* 68; prominent ions at *m/e* 217 (8%), 185 (5%), 153 (12%), 150 (46%), 119 (9%), and 94 (9%). ν_{max} ($CHCl_3$) 1740, 1718, 1639, 1602 cm^{-1}.

(*c*) *Endo-endo-endo-endo* triadduct **12** as a colorless solid (0.52 g, 1.5%). Recrystallization from EtOH gave colorless needles, m.p. 267–269° (dec.). Highest molecular ion at *m/e* 346 (2%); base peak at *m/e* 68; prominent ions at *m/e* 278 (1%), 249 (4%), 246 (6%), 218 (38%), 217 (10%), 185 (5%), 153 (28%), 150 (28%), 119 (6%), and 94 (15%). ν_{max} ($CHCl_3$) 1739, 1718, 1635, 1602 cm^{-1}.

Reaction of Furan and DMAD in the Presence of $AlCl_3$

A solution of DMAD (5.68 g, 0.04 *M*) in CH_2Cl_2 (50 ml) was added to a stirred suspension of anhydrous $AlCl_3$ (5.32 g, 0.04 *M*) in CH_2Cl_2 (100 ml) to give a yellow-green solution. To this was now added a solution of furan (5.44 g, 0.08 *M*) in CH_2Cl_2 (50 ml). During the initial stages of addition of the diene (external cooling by cold water bath) the temperature rose from 20 to 30° and a dark red gum was deposited. Stirring was continued for 1 h at room temperature. The dark red solution was

[9]This was the triadduct isolated, but not identified, by Slee and LeGoff (4).

Can. J. Chem. Downloaded from www.nrcresearchpress.com by 210.87.254.105 on 09/05/12
For personal use only.

poured into and shaken vigorously with cold water. The aqueous phase was separated and extracted with CH_2Cl_2 and the combined CH_2Cl_2 solutions dried (Na_2SO_4) and evaporated to give a viscous dark red oil (9.51 g). The product was chromatographed over silicic acid using $CHCl_3$ as eluant. This afforded, in order of their elution from the column:

(*a*) Unreacted DMAD (681 mg, 12.0%), identified by p.m.r.

(*b*) Monoadduct **1** (1.70 g, 20.2%) as a yellow oil.

(*c*) Monoadduct acid **16** (0.52 g, 6.6%), after extraction of the impure solid fractions with hot petroleum ether (b.p. 60–80°). Recrystallization from petroleum ether gave colorless needles, m.p. 86–87°. Highest molecular ion at *m/e* 196 (16%); base peak at *m/e* 68; prominent ions at *m/e* 150 (11%), 139 (18%), 136 (18%), 119 (28%), and 44 (29%). ν_{max} ($CHCl_3$) 1730, 1683, 1627 cm^{-1}.

(*d*) *Endo-exo* diadduct **5** as a colorless solid (2.4 g, 21.6%). Recrystallization from EtOH gave colorless prisms, m.p. 114–115° (dec.) (lit. 120–122° (4)). ν_{max} ($CHCl_3$) 1745, 1725, 1604 cm^{-1}.

(*e*) *Endo-endo* diadduct **4** was indicated by p.m.r. Estimated yield (from p.m.r.) 1.5%.

Compound **4** was isolated from the products of a thermal reaction, by fractional crystallization from EtOH, as colorless plates, m.p. (dec.) 147–149° (lit. 154–156° (9), 148° (10)); ν_{max} ($CHCl_3$) 1745, 1720, 1602 cm^{-1}.

We wish to thank Mrs. M. G. Flack and Mr. J. Van Ingen for valuable technical assistance. Thanks are also due to Mr. P. F. Seto for the i.r. spectra.

1. R. C. Bansal, A. W. McCulloch, and A. G. McInnes. Can. J. Chem. **47**, 2391 (1969); **48**, 1472 (1970).
2. A. W. McCulloch and A. G. McInnes. Can. J. Chem. **48**, 3152 (1971).
3. A. W. McCulloch, B. Stanovnik, D. G. Smith, and A. G. McInnes. Can. J. Chem. **47**, 4319 (1969).
4. J. D. Slee and E. LeGoff. J. Org. Chem. **35**, 3897 (1970).
5. J. G. Martin and R. K. Hill. Chem. Rev. **61**, 537 (1961).
6. O. Diels and S. Olsen. J. Prakt. Chem. 156, 285 (1940).
7. G. Stork, E. E. van Tamelen, L. J. Friedman, and A. W. Burgstahler. J. Am. Chem. Soc. **75**, 384 (1953).
8. H. Prinzbach, M. Arguelles, and E. Druckrey. Angew. Chem. Int. Ed. **5**, 1039 (1966).
9. J. Kallos and P. Deslongchamps. Can. J. Chem. **44**, 1239 (1966).
10. O. Diels and K. Alder. Justus Liebig's Ann. Chem. **490**, 243 (1931).
11. R. P. Gandhi and V. K. Chadha. Chem. Commun. 552 (1968).
12. R. B. Woodward and R. Hoffmann. The conservation of orbital symmetry. Verlag Chemie, Weinheim. 1970.
13. W. C. Herndon and L. H. Hall. Tetrahedron Lett. 3095 (1967). *cf.* W. C. Herndon. Chem. Rev. **72**, 157 (1972).
14. J. Sauer. Angew. Chem. Int. Ed. **6**, 16 (1967).
15. F. A. L. Anet. Tetrahedron Lett. **25**, 1219 (1962).
16. T. Inukai and T. Kojima. J. Org. Chem. **32**, 872 (1967).
17. H. Stockmann. J. Org. Chem. **26**, 2025 (1961).
18. R. J. Abraham and H. J. Bernstein. Can. J. Chem. **39**, 216 (1961).
19. D. M. Grant, R. C. Hirst, and H. S. Gutowsky. J. Chem. Phys. **38**, 470 (1963).
20. F. A. L. Anet. Can. J. Chem. **39**, 789 (1961).
21. J. Mantecon, L. Cortes, E. Payo, and A. Salazar. J. Org. Chem. **32**, 3796 (1967).
22. M. Karplus. J. Am. Chem. Soc. **85**, 2870 (1963).
23. A. W. McCulloch, D. G. Smith, and A. G. McInnes. Unpublished work.

Can. J. Chem. Downloaded from www.nrcresearchpress.com by 210.87.254.105 on 09/05/12
For personal use only.

Structure of the Second Coordination Sphere of Transition Metal Complexes. IV. Solvent Effects

D. R. EATON AND K. L. CHUA

Department of Chemistry, McMaster University, Hamilton, Ontario

Received May 3, 1973

The participation of various solvents in the second coordination sphere of Co(II) pyrazolylborate has been investigated. Equilibrium constants relative to carbon tetrachloride as a second sphere ligand have been obtained. The ability of a solvent to participate in the second sphere depends predominantly on its dipole moment and it is concluded that Van der Waals forces are responsible for outer sphere binding.

La participation de différents solvants à la seconde sphère de coordination du pyrazolylborate de Co(II) a été étudiée. Les constantes d'équilibres relatives au tétrachlorure de carbone en tant que coordinat de la seconde sphère ont été obtenues. La possibilité pour un solvant d'intervenir dans la seconde sphère dépend essentiellement de son moment dipolaire et il a été conclu que les forces de Van der Waals sont responsables des liaisons extérieures à la sphère. [Traduit par le journal]

Can. J. Chem., **51**, 4137 (1973)

Can. J. Chem. Downloaded from www.nrcresearchpress.com by 210.87.254.6 on 09/05/12
For personal use only.

We have previously reported n.m.r. structural studies of the weak second sphere complexes formed between coordinately saturated Co(II) trispyrazolylborate compounds and other ligands present in solution (1, 2). These studies have also been extended to include the structures of ion pairs formed by analogous trispyrazolylmethane complexes (3). The motivation underlying this research is the belief that the efficiency of ligand exchange processes depends intimately on the ability of a metal complex to hold incoming ligands in a second coordination sphere where they are readily available for further reaction (4). The efficiency of a sequence of such ligand exchange reactions determines the overall efficiency of homogeneous catalysis. The Co(II) trispyrazolylborates comprise a particularly favorable substrate system for studies of this kind since the strongly bound tridentate ligands cannot be replaced by the monodentate ligands added which, if they are going to interact at all, can therefore only occupy positions in the second coordination sphere. Further, the large magnetic anisotropy of these Co(II) complexes give rise to dipolar shifts in the n.m.r. spectra of surrounding molecules and hence provides a probe to investigate the structure of such a second sphere. Previous studies have demonstrated that anions tend to prefer to occupy positions close to the three-fold axis of the chelate whereas neutral molecules such as aniline and pyridine are located perpendicular to this axis and have preferred orientations which may or may not be favorable for a subsequent ligand exchange reaction. It is apparent that the solvent plays a part in determining the detailed structure of the second sphere. Thus it was argued previously (3) that anions occupy positions on the symmetry axis because the more favorable positions perpendicular to the axis are preferentially taken by the dipolar solvent molecules. Similarly the observed n.m.r. shifts of neutral molecules depend strongly on the solvent used, indicating competition between added ligands and solvent molecules for the limited number of places in the second sphere. The present note reports some further studies with Co(II) trispyrazolylborates aimed at clarifying solvent effects.

The crux of the method used for studying second sphere structure lies in the equation (5)

$$\Delta\nu_0 = -\text{constant}\frac{(3\cos^2\theta - 1)}{r^3}(\chi_{\parallel} - \chi_{\perp})$$

which relates the dipolar n.m.r. shift of a magnetic nucleus to its position in space relative to the cobalt chelate. Unfortunately this equation (the detailed form of which has been discussed recently (6)) cannot be used directly since it is impossible to disentangle $\Delta\nu_0$ from the equilibrium constant K of a reaction

$$X + L \rightleftharpoons XL$$

which determines the fraction of the ligand L complexed to the chelate X. Only the product $K\Delta\nu_0$ is experimentally accessible (1). This

Can. J. Chem. Downloaded from www.nrcresearchpress.com by 210.87.254.6 on 09/05/12
For personal use only.

limitation determined the strategy of the present experiments. We wish to determine the relative tendencies of different solvents to occupy positions in the second sphere, *i.e.* the relative values of K for the above equilibrium. The direct approach would be to observe the dipolar shifts of the solvent molecules. Unfortunately not all solvents contain hydrogen or other nuclei suitable for n.m.r. experiments and even if they do the observed shifts will depend on both K and $\Delta\nu_0$ which will both vary from solvent to solvent. We have therefore adopted the procedure of measuring the extent to which a given solvent will displace a common ligand from the second coordination sphere.

Aniline was chosen as the common ligand and carbon tetrachloride as the common solvent. Previous results have shown that the aniline shifts are larger in carbon tetrachloride than in other solvents indicating that carbon tetrachloride has the least tendency to displace aniline from the second coordination sphere. Aliquots of solvent were therefore added to a standard solution of aniline plus Co(II) trispyrazolylborate in carbon tetrachloride and the n.m.r. shifts of the aniline protons measured as a function of the concentration of added solvent. Plots of data obtained in this way are shown in Fig. 1. These plots refer to the ortho proton of aniline. Other positions behave similarly but the shifts are somewhat smaller. In order to determine the isotropic shift due to the second sphere interaction, which is defined as the difference between free ligand frequency and complexed ligand frequency it is necessary to determine the aniline chemical shifts in the various mixtures used. The data shown in Fig. 1 were therefore corrected appropriately, using as calibration curves plots of the chemical shifts of aniline in carbon tetrachloride plus added solvent. Consider the equilibria

[1] $$XS + L \rightleftharpoons XL + S \qquad K_1$$

and

[2] $$XS + S' \rightleftharpoons XS' + S \qquad K_2$$

in which X represents the Co(II) complex, L is aniline, S is carbon tetrachloride, and S′ the added solvent. The observed n.m.r. shift is the weighted average of the shift for complexed and that for free aniline, *i.e.*

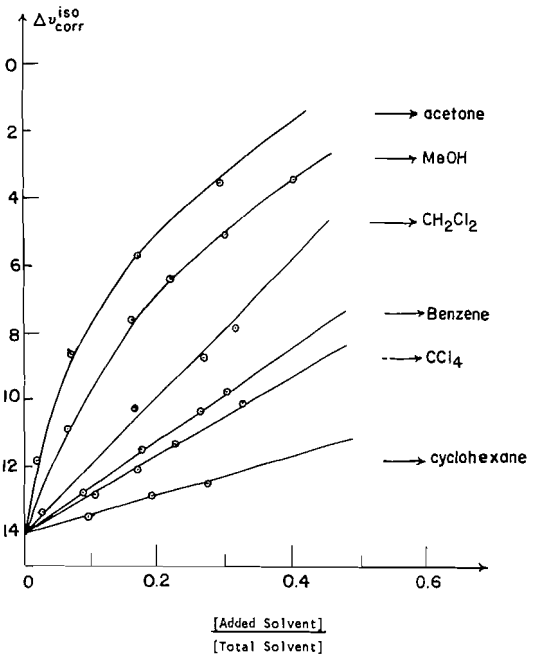

FIG. 1. Chemical shifts of the *ortho* protons of aniline in the presence of Co(II) pyrazolylborate and added solvents. Shifts in Hz at 100 MHz.

$$\Delta\nu = \frac{[XL]}{[XL] + [L]}\Delta\nu_0$$

where $\Delta\nu_0$ is the frequency of complexed aniline. Assuming the degrees of association of L and S′ in eqs. 1 and 2 are small it may be readily shown that

[3] $$\Delta\nu = \frac{K_1 x}{S + K_1 l}\Delta\nu_0$$

and

[4] $$\Delta\nu' = \frac{K_1 x}{S + K_1 l + K_2 S'}\Delta\nu_0$$

where $\Delta\nu$ is the aniline shift in the absence of a second solvent, $\Delta\nu'$ is the shift in the presence of the second solvent, x is the concentration of cobalt complex (assumed to be small), l is the concentration of aniline, S is the concentration of carbon tetrachloride, and S' that of the added solvent. Part of the difference between $\Delta\nu$ and $\Delta\nu'$ is due to the dilution of the solution on adding the second solvent. It is therefore appropriate to compare the shift produced by adding the second solvent ($\Delta\nu'$) with that produced by adding an equal amount of carbon tetrachloride

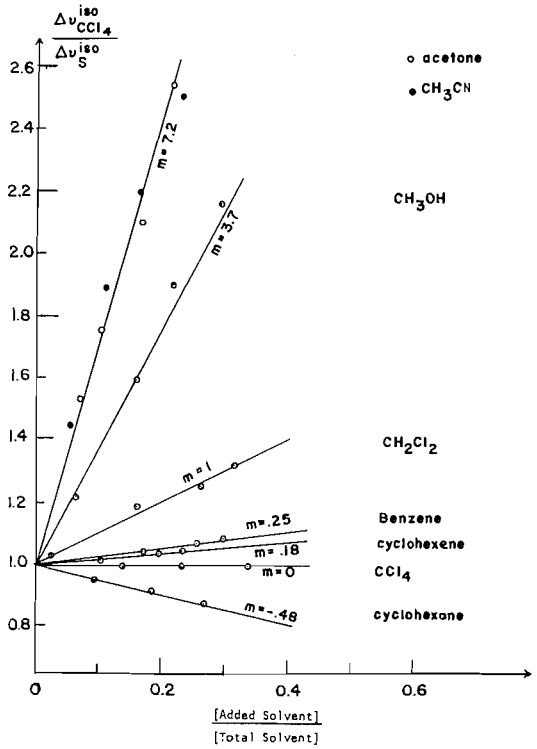

FIG. 2. Relative chemical shifts in carbon tetrachloride and different solvents. m is the slope of the line.

($\Delta\nu''$). Substitution in eq. 4 together with the approximation that $S \gg S'$, x, and l gives[1]

$$\frac{\Delta\nu''}{\Delta\nu'} = 1 + (K_2 - 1)\frac{S'}{S}$$

Plots of $\Delta\nu''/\Delta\nu'$ *vs.* the mole fraction of S' should therefore be linear with slopes equal to $(K_2 - 1)$. Such plots are shown in Fig. 2 for several solvents and the resulting values of (K_2) are collected in Table 1.

It is concluded from the data of Table 1 that the interactions responsible for binding in the second coordination sphere are essentially Van der Waals forces. The equilibrium constant clearly increases with the dipole moment of the ligand. Ligands for which hydrogen bonding with the nitrogen of the first sphere pyrazolyl ligands would be feasible do not appear to have anomalously high positions in the series. All of the non-polar molecules show a relatively small tendency to form second sphere complexes. Cyclohexane proves to be a somewhat worse second sphere ligand than carbon tetrachloride. The above conclusion is consistent with the values of 2–3 kcal previously obtained for the enthalpy of formation of the aniline second sphere complex (1). Perhaps the most significant point though is that the range of equilibrium constants obtained shows that there are very marked preferences for different molecules in the second coordination sphere, which must be reflected in the ease of substitution in the first sphere.

[1]A derivation of this expression for the relative chemical shifts is available at a nominal charge, from the Depository of Unpublished Data, National Science Library, National Research Council of Canada, Ottawa, Canada K1A 0S2.

TABLE 1. Relative equilibrium constants for second sphere coordination

Ligand	K_2	Dipole moment μ
CH_3CN	8.2	3.92
$(CH_3)_2CO$	8.2	2.88
CH_3OH	4.7	1.70
CH_2Cl_2	2.0	1.60
C_6H_6	1.25	0
C_6H_{10}	1.18	0
C_6H_{12}	0.52	0

Experimental

Proton n.m.r. spectra were obtained on a Varian HA 100 instrument. Chemical shifts were internally referred to TMS. Analytical grade solvents were used without further purification.

The authors are indebted to the National Research Council of Canada for financial support of this research and to Dr. S. Trofimenko of the E. I. Du Pont Co. for providing the sample of cobalt(II) trispyrazolylborate.

1. D. R. EATON. Can. J. Chem. 47, 2645 (1969).
2. D. R. EATON, H. O. OHORODNYK, and L. SEVILLE. Can. J. Chem. 49, 1218 (1971).
3. D. R. EATON, L. SEVILLE, and J. P. JESSON. Can. J. Chem. 49, 2751 (1971).
4. M. L. TOBE. Mechanisms of inorganic reactions. Adv. Chem. 49, 7 (1965).
5. H. M. MCCONNELL and R. E. ROBERTSON. J. Chem. Phys. 29, 1361 (1958).
6. R. J. KURLAND and B. R. MCGARVEY. J. Magn. Res. 2, 286 (1970).

Can. J. Chem. Downloaded from www.nrcresearchpress.com by 210.87.254.6 on 09/05/12
For personal use only.

Thermodynamic Properties of Cyclopentanol + *p*-Dioxane Mixtures at 25 °C[1]

S. C. ANAND,[2] J.-P. E. GROLIER,[3] OSAMU KIYOHARA,[4] and G. C. BENSON
Division of Chemistry, National Research Council of Canada, Ottawa, Canada K1A 0R6

Received July 19, 1973

Excess enthalpies, excess volumes, and total vapor pressures were measured for cyclopentanol + *p*-dioxane mixtures at 25 °C. The method of Barker was used to calculate vapor–liquid equilibria and excess Gibbs free energies from the vapor pressure results. A comparison with results (from the literature) for the systems cyclohexane + cyclopentanol and cyclohexane + *p*-dioxane indicates that the excess thermodynamic properties of cyclopentanol + *p*-dioxane mixtures arise primarily from the disruption of the structure of the *p*-dioxane solvent.

Les enthalpies d'excès, les volumes d'excès et les pressions de vapeur totales ont été mesurés à 25 °C pour des mélanges cyclopentanol + *p*-dioxane. La méthode de Barker a été utilisée pour calculer les équilibres liquide–vapeur et les énergies libres de Gibbs d'excès. Une comparaison de nos résultats avec ceux de la littérature, pour les mélanges cyclohexane + cyclopentanol et cyclohexane + *p*-dioxane, fait apparaître que les propriétés thermodynamiques d'excès des mélanges cyclopentanol + *p*-dioxane résultent principalement de la rupture de la structure du solvant *p*-dioxane, dans ces mélanges.

Can. J. Chem., 51, 4140 (1973)

Previous publications (1–4) from our laboratory have described the measurement of various thermodynamic properties for a number of binary systems formed by mixing cycloalkanols with other organic solvents. For the most part these have been nonpolar cycloalkanes, but some systems have involved the polar solvent acetone. From the point of view of thermodynamic behavior and theories of mixtures, the system cyclopentanol + *p*-dioxane is an interesting subject for study, since, although the dipole moment of *p*-dioxane is relatively small, the *p*-dioxane molecule has high local electric fields which lead to strong proton accepting character.

Experimental

Materials

Both of the components were purified in an F & M preparative gas chromatograph (Model 775). Care was taken to avoid exposure of the purified materials to moist air. Before the *p*-dioxane was used in the vapor–liquid equilibrium studies, it was vacuum distilled over anhydrous ferrous sulfate and stored under its own vapor in a dark flask to inhibit its decomposition to peroxide. The usual chemical methods (5) failed to show the presence of peroxide in freshly prepared samples. The vapor pressures of samples from separate preparations agreed within ±0.01 Torr; however after a period of 3 or 4 days the vapor pressure at 25 °C increased by about 0.1 Torr and remained constant for a number of days thereafter. Chemical analysis of these older samples revealed traces of peroxide, thus it appears that a slight conversion to peroxide occurred even in the absence of light. Only freshly prepared samples of *p*-dioxane were used for the vapor–liquid studies.

Physical properties of the purified components are compared with values from the literature (6–10) in Table 1. In most cases the agreement is good.

Apparatus and Techniques

A modified form of Van Ness dilution calorimeter (11) was used to determine the enthalpies of mixing. The error of the enthalpy results is estimated to be less than ±0.5% over most of the concentration range. Volumes of mixing were determined in a dilution dilatometer which has been described previously (12); the uncertainty in the value for an equimolar mixture is estimated to be less than ±0.002 $cm^3\ mol^{-1}$.

Equilibrium vapor pressures of mixtures of known total composition were determined by the static method in a cell similar to that used by Singh and Benson (13). The pressure at 25.000 ± 0.001 °C was measured to ±0.005 Torr with a quartz spiral gauge which was calibrated by comparison with a mercury manometer. The distribution of material between the vapor and liquid phases was computed by a modified form of Barker's analysis (1, 14). The empirical expression

$$[1] \qquad X^E = x_1(1 - x_1) \sum_{j=1}^{n} a_j(1 - 2x_1)^{j-1}$$

was used to represent the concentration dependence of the molar excess Gibbs free energy G^E at constant temperature. The values of the n coefficients a_j in eq. 1 were determined by an iterative calculation which minimized the sum of the squares of the deviations between calculated and observed values of the pressure. The analysis

[1]NRCC No. 13483.

[2]National Research Council of Canada Postdoctorate Fellow 1971–1973.

[3]Visiting French Scientist 1972–1973, attached to C.N.R.S. (Paris) from the University of Clermont-Ferrand, Clermont-Ferrand, France.

[4]National Research Council of Canada Postdoctorate Fellow 1971–1973. Present address: Department of Chemistry, Université de Sherbrooke, Sherbrooke, Québec.

Can. J. Chem. Downloaded from www.nrcresearchpress.com by 210.87.254.5 on 09/05/12
For personal use only.

TABLE 1. Physical constants of component liquids at 25 °C

Compound	Refractive index n_D		Density d (g cm^{-3})		Vapor pressure p^0 (Torr)	
	Measured	Literature	Measured	Literature	Measured	Literature
Cyclopentanol	1.45159	1.4505*	0.94291	0.94298†	2.20	—
p-Dioxane	1.41998	1.41973‡	1.02821	1.02800†	35.74	37.4§ 36.18‖ 36.61¶

*Extrapolated from ref. 6.
†Interpolated from ref. 6.
‡Reference 7.
§Reference 8.
‖Reference 9.
¶Reference 10.

was repeated with increasing values of n and the minimum number of coefficients needed to give an adequate representation of the results was determined. Since only total compositions were known directly, it was necessary at each iteration to calculate the mole fraction of cyclopentanol x_1 in the liquid by allowing for the material present in the vapor phase (1). The vapor pressure of *p*-dioxane is much larger than that of cyclopentanol, hence only the second virial coefficient for *p*-dioxane ($B_{22} = -1720$ cm^3 mol^{-1}, estimated from the correlation of O'Connell and Prausnitz (15)) was used in correcting for imperfection of the vapor phase. The validity of this approximation was confirmed by further calculations employing rough estimates of the virial coefficients B_{11} and B_{12}. These led to values of G^E which did not differ significantly from those reported in this paper.

Results

Vapor pressures of *p*-dioxane, measured at temperatures in the range 14–51 °C, are listed in Table 2. These values are represented by the Antoine form

$$[2]\quad \log_{10}(p/\text{Torr}) = 7.50915 - 1559.92/[236.88 + (t/°\text{C})]$$

with a standard error of estimate equal to 0.10 Torr. At 30 °C this equation leads to a pressure of 46.14 Torr, in excellent agreement with the lower of the two values observed most recently by Byer *et al.* (16). It has been reported that some of the physical properties of *p*-dioxane (viscosity (17), dielectric constant (18)) show an anomaly at about 26 °C in their temperature dependence curves, and this has been attributed to the existence of a boat form for *p*-dioxane at higher temperatures. A plot of $\log_{10} p$ against the reciprocal of the absolute temperature, for the present results shows no evidence of a change in slope around 26 °C.

The results of the vapor–liquid studies of cyclopentanol (1) + *p*-dioxane (2) mixtures are summarized in Table 3, where p is the observed pressure, x_1 and y_1 are the mole fractions of cyclopentanol in the liquid and vapor phases, and G^E is the molar excess Gibbs free energy of the liquid phase. The experimental values of the molar excess enthalpies H^E and of the molar excess volumes V^E are given in Tables 4 and 5.

TABLE 2. Experimental values of the vapor pressure of *p*-dioxane

t (°C)	p (Torr)	Δp (Torr)*
14.598	20.24	−0.007
18.469	25.10	0.024
25.000	35.74	−0.058
30.011	46.17	−0.007
35.015	59.09	0.048
39.503	73.17	0.117
44.178	91.14	−0.167
50.093	118.34	0.049

*$\Delta p = p$(eq. 2) − p(experimental).

TABLE 3. Vapor–liquid equilibria for cyclopentanol (1) + *p*-dioxane (2) at 25 °C

x_1	y_1	p (Torr)	G^E (J mol^{-1})
0.1215	0.0159	32.20	220.5
0.1859	0.0235	30.54	314.0
0.2707	0.0331	28.49	412.5
0.2824	0.0344	28.25	427.0
0.3705	0.0441	26.22	494.3
0.3946	0.0468	25.68	508.1
0.4558	0.0540	24.32	534.9
0.4899	0.0582	23.48	535.8
0.4982	0.0592	23.27	534.9
0.5351	0.0642	22.42	538.0
0.5687	0.0690	21.57	530.6
0.5738	0.0698	21.47	532.8
0.6724	0.0875	18.71	478.6
0.7801	0.1194	15.08	380.4
0.8176	0.1374	13.54	333.3
0.8959	0.2073	9.64	217.0
0.9228	0.2555	8.00	163.9

Can. J. Chem. Downloaded from www.nrcresearchpress.com by 210.87.254.5 on 09/05/12
For personal use only.

Can. J. Chem. Downloaded from www.nrcresearchpress.com by 210.87.254.5 on 09/05/12
For personal use only.

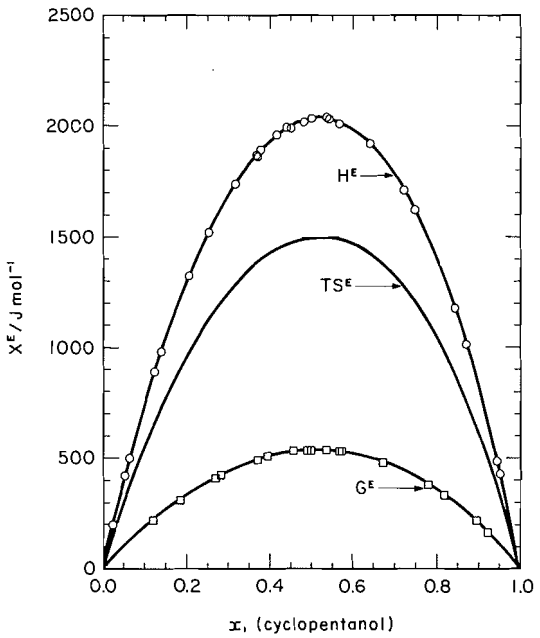

FIG. 1. Excess thermodynamic properties H^E, G^E, and TS^E for cyclopentanol (1) + *p*-dioxane (2) mixtures at 25 °C. Experimental results: ○, H^E; □, G^E. The curves for H^E and G^E are calculated from eq. 1 with coefficients from Table 6; the curve for TS^E is the difference of the H^E and G^E curves.

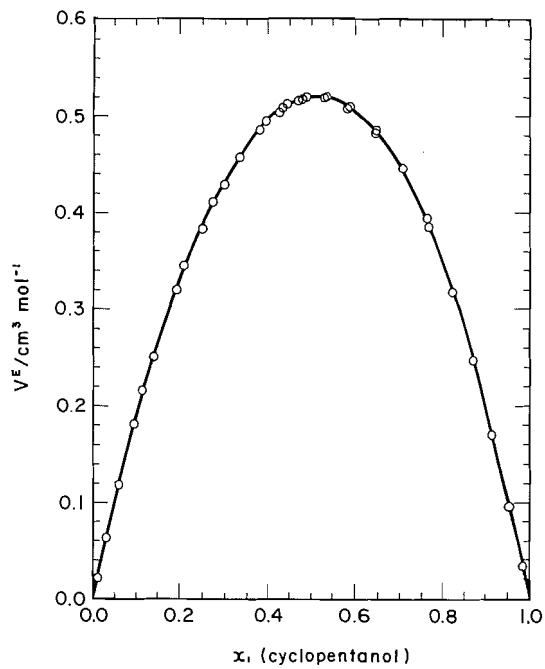

FIG. 2. Excess volume V^E for cyclopentanol (1) + *p*-dioxane (2) mixtures at 25 °C. Experimental results: ○. The curve is calculated from eq. 1 with coefficients from Table 6.

Figures 1 and 2 provide graphical presentations of these results.

The same functional form (eq. 1), which represented G^E satisfactorily, was also found to be suitable for smoothing the results for H^E and V^E. The coefficients were determined for each set by the method of least squares. These values are listed in Table 6, along with the coefficients for G^E obtained from the Barker analysis. The last column of the table gives values of the standard error of estimate σ calculated from the equation

$$[3] \quad \sigma = [\textstyle\sum_1^{n_{obs}} (X_{obs}{}^E - X_{calcd}{}^E)^2/(n_{obs} - n)]^{1/2}$$

where n_{obs} is the number of experimental results and n is the number of coefficients in the rep-

TABLE 4. Experimental values of the molar excess enthalpy of cyclopentanol (1) + *p*-dioxane (2) at 25 °C

x_1	H^E (J mol^{-1})	x_1	H^E (J mol^{-1})
0.0247	197.8	0.4490	1994.2
0.0549	422.8	0.4805	2021.6
0.0656	501.1	0.4990	2036.2
0.1256	893.8	0.5353	2040.9
0.1411	983.3	0.5408	2034.1
0.2066	1325.8	0.5661	2012.1
0.2530	1521.9	0.6419	1924.6
0.3158	1742.3	0.7203	1711.5
0.3656	1867.5	0.7482	1625.1
0.3690	1866.0	0.8423	1177.3
0.3765	1896.7	0.8708	1015.6
0.4156	1963.8	0.9444	486.4
0.4382	1996.6	0.9517	429.4

TABLE 5. Experimental values of the molar excess volume of cyclopentanol (1) + *p*-dioxane (2) at 25 °C

x_1	V^E (cm^3 mol^{-1})	x_1	V^E (cm^3 mol^{-1})
0.0110	0.0225	0.4701	0.5164
0.0316	0.0640	0.4793	0.5176
0.0603	0.1189	0.4894	0.5200
0.0965	0.1818	0.5305	0.5182
0.1154	0.2161	0.5369	0.5195
0.1414	0.2512	0.5850	0.5075
0.1932	0.3204	0.5894	0.5090
0.2095	0.3456	0.6444	0.4823
0.2496	0.3834	0.6469	0.4850
0.2736	0.4117	0.7061	0.4456
0.2992	0.4292	0.7634	0.3937
0.3318	0.4574	0.7660	0.3850
0.3808	0.4860	0.8231	0.3168
0.3961	0.4951	0.8716	0.2461
0.4260	0.5040	0.9166	0.1691
0.4343	0.5089	0.9548	0.0953
0.4451	0.5128	0.9843	0.0332

TABLE 6. Values of coefficients for eq. 1 determined by the method of least squares

X^E	a_1	a_2	a_3	a_4	σ
H^E (J mol^{-1})	8138.49	−513.51	771.40	−133.69	4.8
V^E (cm^3 mol^{-1})	2.0792	−0.0883	0.1140		0.0019
G^E (J mol^{-1})	2147.98	−119.68	41.84		2.5

resentation. The curves for G^E, H^E, and V^E, in Figs. 1 and 2, were calculated from eq. 1 using the coefficients from Table 6. A curve for the excess entropy term TS^E, obtained from the relation

$$[4] \qquad TS^E = H^E - G^E$$

is also shown in Fig. 1.

Discussion

Cyclopentanol + p-dioxane mixtures show positive deviations from Raoult's law. In Fig. 1, the curves for H^E, G^E, and TS^E are positive throughout the whole concentration range and are nearly symmetrical about $x_1 = 0.5$. The values of H^E are relatively large compared to those for mixtures of p-dioxane with other polar solvents. Negative excess enthalpies have been reported for p-dioxane + chloroform (19) and a sigmoid-shaped curve was found for p-dioxane + water (20). Negative excess enthalpies have also been reported for mixtures of p-dioxane with carbon tetrachloride (21) and benzene (22) but positive values were observed with cyclohexane (20, 23). The excess Gibbs free energy is negative for mixtures of p-dioxane with chloroform (19) and positive for mixtures with water (20), carbon tetrachloride (24), benzene (24), and cyclohexane (20). It appears from these findings that the tendency for p-dioxane to form a complex with other molecular species depends very much on the nature of the other species.

Chemical association theories have been fairly successful in explaining the thermodynamic behavior of mixtures of p-dioxane with chloroform (19), benzene (24), and carbon tetrachloride (24). In all of these systems there is a strong interaction between unlike species in the mixture and the excess entropy is negative; in some cases the existence of a stable compound has been confirmed by solid–liquid phase diagrams (25, 26). However, in view of the large positive values found for the excess entropy of the present system, it is very unlikely that a chemical association theory could be used to explain and correlate its thermodynamic properties.

It is instructive to compare the thermodynamic properties of cyclopentanol + p-dioxane mixtures with those of cyclohexane + cyclopentanol (3) and of cyclohexane + p-dioxane (20, 23, 24, 27, 28). Considering equimolar mixtures, the excess enthalpy of cyclopentanol + p-dioxane is of similar magnitude to the sum of the H^E values for the other two systems. The excess enthalpy of cyclohexane + cyclopentanol comprises contributions from dispersion forces and the disruption of hydrogen bonds; that for cyclohexane + p-dioxane comprises contributions from dispersion forces and the breakup of electrostatic interactions (mainly quadrupole) between p-dioxane molecules. Rather surprisingly the excess enthalpy of cyclohexane + p-dioxane is roughly twice as large as that for cyclohexane + cyclopentanol. Thus it may be inferred that the breakup of structure in p-dioxane makes a very important contribution to H^E when mixtures are formed with other solvents. The fact that the H^E and TS^E curves for cyclopentanol + p-dioxane are slightly skewed towards mixtures rich in cyclopentanol suggests that the positional and orientational disorder resulting from the breakup of the p-dioxane structure is somewhat greater than that resulting from the disruption of the hydrogen-bonded alcohol structure.

The excess volume of a mixture is also the resultant of a number of competing effects (29, 30). For the present system, the breakup of the structures of both cyclopentanol and p-dioxane will contribute positive terms to V^E; heterogeneous complex formation and the fitting of one solvent into the structure of the other will make negative contributions. The value of V^E for an equimolar cyclopentanol + p-dioxane mixture is roughly twice as large as that for cyclohexane + cyclopentanol but only about one half of the value for cyclohexane + p-dioxane. These results again point to the important role played by the breakup of the p-dioxane structure in

Can. J. Chem. Downloaded from www.nrcresearchpress.com by 210.87.254.5 on 09/05/12
For personal use only.

determining the excess thermodynamic properties of the present system. It appears that the contribution to V^E from this effect is more important than the contribution from the disruption of hydrogen bonds and that contributions from complex formation and interstitial solution are relatively of much less significance.

We are indebted to Mr. C. J. Halpin and Mr. P. J. D'Arcy for their capable assistance in all phases of the experimental work.

1. G. C. BENSON, S. MURAKAMI, and D. E. G. JONES. J. Chem. Thermodyn. **3**, 719 (1971).
2. D. E. G. JONES, I. A. WEEKS, S. C. ANAND, R. W. WETMORE, and G. C. BENSON. J. Chem. Eng. Data, **17**, 501 (1972).
3. G. C. BENSON, S. C. ANAND, and O. KIYOHARA. Presented at Third International Conference on Chemical Thermodynamics 1, Baden, Austria, September 3–7, 1973.
4. O. KIYOHARA, S. C. ANAND, and G. C. BENSON. J. Chem. Thermodyn. In press.
5. J. ROSIN. Reagent chemicals and standards. 5th ed. D. van Nostrand, Toronto. 1967.
6. J. TIMMERMANS. Physico-chemical constants of pure organic compounds. Vol. 1. Elsevier, New York. 1950.
7. T. D. LING and M. VAN WINKLE. J. Chem. Eng. Data, **3**, 88 (1958).
8. J. L. CRENSHAW, A. C. COPE, N. FINKELSTEIN, and R. ROGAN. J. Am. Chem. Soc. **60**, 2308 (1938).
9. A. L. BACARELLA, A. FINCH, and E. GRUNWALD. J. Phys. Chem. **60**, 573 (1956).
10. S. CABANI, G. CONTI, and L. LEPORI. Trans. Faraday Soc. **67**, 1943 (1971).
11. S. MURAKAMI and G. C. BENSON. J. Chem. Thermodyn. **1**, 599 (1969).
12. H. D. PFLUG and G. C. BENSON. Can. J. Chem. **46**, 287 (1968).
13. J. SINGH and G. C. BENSON. Can. J. Chem. **46**, 1249 (1968).
14. J. A. BARKER. Aust. J. Chem. **6**, 207 (1953).
15. J. P. O'CONNELL and J. M. PRAUSNITZ. Ind. Eng. Chem. Process Des. Dev. **6**, 245 (1967).
16. S. M. BYER, R. E. GIBBS, and H. C. VAN NESS. AIChE J. **19**, 245 (1973).
17. S. S. URAZOVSKII and P. A. CHERNYAVSKII. Tr. Khar'k. Politekh. Inst. im V.I. Lenina **26** Ser Khim-Tekhnol No. 6, 29 (1959); Chem. Abstr. **56**, 10930 (1962).
18. S. S. URAZOVSKII and I. I. EZHIK. Russ. J. Phys. Chem. (Eng. Transl.) **36**, 500 (1962).
19. M. L. MCGLASHAN and R. P. RASTOGI. Trans. Faraday Soc. **54**, 496 (1958).
20. A-L. VIERK. Z. Anorg. Chem. **261**, 283 (1950).
21. I. R. MCKINNON and A. G. WILLIAMSON. Aust. J. Chem. **17**, 1374 (1964).
22. V. H. KHAN and S. V. SUBRAHMANYAM. Trans. Faraday Soc. **67**, 2282 (1971).
23. H. W. PRENGLE JR., F. L. WORLEY JR., and C. E. MAUK. J. Chem. Eng. Data, **6**, 395 (1961).
24. D. D. DESHPANDE and S. L. OSWAL. J. Chem. Soc. Faraday Trans. I, **68**, 1059 (1972).
25. S. M. S. KENNARD and P. A. MCCUSKER. J. Am. Chem. Soc. **70**, 3375 (1948).
26. J. B. OTT, J. R. GOATES, and N. F. MANGELSON. J. Chem. Eng. Data, **9**, 203 (1964).
27. H. W. PRENGLE JR., E. G. FELTON, and M. A. PIKE, JR. J. Chem. Eng. Data, **12**, 193 (1967).
28. J. ROVEILLO and M. GOMEL. C.R. Acad. Sci. Ser. C, **266**, 845 (1968).
29. G. C. PARASKEVOPOULOS and R. W. MISSEN. Trans. Faraday Soc. **58**, 869 (1962).
30. K. NAKANISHI and H. SHIRAI. Bull. Chem. Soc. Jap. **43**, 1634 (1970).

Can. J. Chem. Downloaded from www.nrcresearchpress.com by 210.87.254.5 on 09/05/12
For personal use only.

Oxidative Addition of 3,5-Dinitrobenzoyl Chloride to *trans*-Chlorocarbonylbis(dimethylphenylphosphine)iridium(I)

ALBERT RICHARD NORRIS AND JOHANNES ANTONIUS VAN KESSEL

Department of Chemistry, Queen's University, Kingston, Ontario

Received July 18, 1973

Trans-[IrClCO{$(CH_3)_2C_6H_5P$}$_2$] undergoes oxidative addition with 3,5-dinitrobenzoyl chloride in benzene, ether, and benzene–ether mixtures to yield two isomeric Ir(III) complexes containing the 3,5-dinitrobenzoyl group σ-bonded to the metal via the acyl carbon atom. The structures and properties of these two complexes are described.

Le composé [IrClCO{$(CH_3)_2C_6H_5P$}$_2$]-*trans*, subit une addition oxydative en présence du chlorure de dinitro-3,5 benzoyle dans le benzène, l'éther et des mélanges benzène–éther, pour conduire à deux complexes isomériques de Ir(III) contenant le groupe dinitro-3,5 benzoyle lié au métal par un lien σ via l'atome de carbone du groupe acyle. On décrit les structures et les propriétés de ces deux complexes.

[Traduit par le journal]

Can. J. Chem., **51**, 4145 (1973)

Can. J. Chem. Downloaded from www.nrcresearchpress.com by 210.87.254.42 on 09/05/12
For personal use only.

Introduction

Many metals are known to form complexes containing σ-bonded alkyl and aryl groups (1), but relatively few complexes are known which contain a metal center σ-bonded either directly, or through one or more atoms, to an aromatic ring containing one or more nitro groups (2–9).

Metal complexes containing σ-bonded nitroaromatic compounds with nitro groups on the ring in 2,4-, 3,5-, and 2,4,6-positions are of particular interest to us in connection with studies of the reactions of bases and nitroaromatic compounds (10, 11). Of prime interest is the effect of the metal center (plus ligands) on both the modes of reaction (12) and the rates of reaction of the base and the nitroaromatic compound. In addition, valuable information on the characteristics of metal ligand bonds could, in principle, be obtained from proton magnetic resonance studies of such complexes since the chemical shifts of the hydrogens in the nitroaromatic compounds are very sensitive to the electron density in the ring (12, 13).

As an extension of earlier studies involving the oxidative addition of picryl chloride to Pt{$(C_6H_5)_3P$}$_3$ and Pt{$(C_6H_5)_3As$}$_3$ (5), we have investigated the oxidative addition reactions (14) of a number of 1-X-2,4-dinitro-, 1-X-3,5-dinitro-, and 1-X-2,4,6-trinitrobenzenes (X = Cl, CO_2H, SO_2Cl, COCl, CN, and $CONH_2$) with *trans*-$IrClCOL_2$ (L = $(C_6H_5)_3P$ and $(CH_3)_2C_6H_5P$). The preparation and properties of two isomeric Ir(III) complexes resulting from the oxidative addition of 3,5-dinitrobenzoyl chloride to *trans*-[IrClCO{$(CH_3)_2C_6H_5P$}$_2$] are reported here.

Experimental

Reagents

Eastman 3,5-dinitrobenzoyl chloride was purified by sublimation under vacuum at 40–50 °C. The melting point, determined in a sealed glass capillary on a Gallenkamp melting point apparatus, was 68.0–68.5 °C. Literature melting point, 69.5 °C (15).

Dimethylphenylphosphine (Maybridge Research Chemicals) was purified by vacuum distillation at 12.5 mm mercury and 70 °C. The compound was stored and handled under an atmosphere of dry nitrogen.

Chloroiridic acid ($H_2IrCl_6{\cdot}xH_2O$, Alfa Inorganics and Johnson, Matthey and Mallory Ltd.) was used without purification.

Thiophene-free benzene (Fisher Certified or "Baker Analyzed" Spectrophotometric Reagent) was refluxed over sodium wire, then distilled and stored under a dry nitrogen atmosphere. Fisher certified methanol and ethanol were purified by the Grignard method described by Vogel (16), then distilled and stored under dry nitrogen. All other solvents were A.R. grade or better and were usually stored over Linde 4A Molecular Sieve. For operations under nitrogen solvents were thoroughly degassed with dry nitrogen immediately prior to use.

All other reagents used were A.R. grade or better and were used without further purification.

Equipment

Ultraviolet–visible absorption spectra were recorded on Unicam SP 800 and Cary 14 spectrophotometers using matched optical glass cells of 1.0 cm pathlength. Spectra were recorded at approximately 25.0 °C. When a spectrum was required on a solution containing an oxygen- or water-sensitive compound, one of the cells was stoppered with a serum cap or a plug of silicone rubber and alternately evacuated and filled with dry nitrogen several times. Transfer of the solution, itself prepared in an atmosphere of dry nitrogen, was accomplished by means of a hypodermic syringe.

Infrared spectra were recorded on Beckman IR-10 and Perkin–Elmer 180 double beam grating spectrophotometers. Samples were run as Nujol or hexachlorobutadiene mulls or in solution using matched solution cells

Can. J. Chem. Downloaded from www.nrcresearchpress.com by 210.87.254.42 on 09/05/12
For personal use only.

equipped with either KBr or CaF_2 windows. A polystyrene film was used to calibrate the spectra recorded on the IR-10. All frequencies reported are believed to be accurate to $\pm 5\ cm^{-1}$.

Nuclear magnetic resonance spectra were recorded on a Bruker HX-60 spectrometer. The proton resonance absorbance of tetramethylsilane (TMS) was used as an internal lock and all proton chemical shifts are quoted relative to internal TMS. Phosphorus-31 peak positions were determined by an INDOR technique. Trimethylphosphite (−141 p.p.m. from 85% H_3PO_4) was used as a standard and all phosphorus-31 chemical shifts are quoted relative to 85% H_3PO_4. Concentrations of the solutions were of the order of 5–10% by weight. In those cases in which spectra were recorded on solutions containing oxygen- or water-sensitive compounds, an n.m.r. tube fitted with a serum cap was alternately evacuated and filled with dry nitrogen prior to introduction of the solution via a hypodermic syringe. Chemical shifts and coupling constants are believed accurate to $\pm 0.01\ \tau$ and 0.5 Hz, respectively.

Except as noted, melting points were determined between glass plates on a Nalge melting point apparatus. The melting points are uncorrected.

All operations involving the handling of 3,5-dinitrobenzoyl chloride and chloroiridic acid were carried out as much as possible in a dry box constructed of Plexiglass. A dry atmosphere was maintained in the box by using a Fisher pressure-vacuum air pump to circulate air from the box through tubes filled with silica gel and Linde 4A Molecular Sieve. Trays of phosphorus(V) pentoxide were kept inside the box and changed as required.

Analyses of the new compounds were carried out by Galbraith Laboratories, Inc. (Knoxville, Tenn.) and by the Analytical Services Section, Department of Chemistry, Stanford University.

Preparations

Preparation of Hydridodichlorocarbonylbis(dimethylphenylphosphine)iridium(III) (Configuration I)

The procedure followed was essentially that reported by Deeming and Shaw (17) though our yields were highly variable if their procedure was followed exactly. We obtained the highest yield of product if the chloroiridic acid was used as soon as possible after receipt of a new shipment, the reaction solution was made 1.5 to 2 times more dilute than reported (17), was filtered before starting the reaction, and the reaction was carried out until the color of the solution had changed to a light yellow and the dark brown precipitate on the tube, used to bubble carbon monoxide through the solution, was starting to form at an appreciable rate.

Since the water content of the starting chloroiridic acid was unknown. percentage yields based on iridium or a comparison with the literature yields is not possible. A typical procedure starting with 1.2 g $H_2IrCl_6 \cdot XH_2O$ yielded 0.9 g of product.

Preparation of trans-Chlorocarbonylbis(dimethylphenylphosphine)iridium(I) {trans-[IrClCO-{$(CH_3)_2C_6H_5P$}$_2$]}

This complex was prepared by the dehydrohalogenation of hydridodichlorocarbonylbis(dimethylphenylphosphine)iridium(III) according to the method reported by Deeming and Shaw (17). Recrystallization of the crude product from methanol under a nitrogen atmosphere yielded fine yellow needles with a melting point 116–123 °C (decomposition) and molar extinction coefficient (ε) at 432 nm in benzene at 25.0 °C, of 610 $M^{-1}\ cm^{-1}$. The reported melting point and ε_{432} in benzene for this compound are 116–122 °C (decomposition) (17) and 598 $M^{-1}\ cm^{-1}$ (18), respectively.

Dichloro-3,5-dinitrobenzoylcarbonylbis(dimethylphenylphosphine)iridium(III) (Compound A)

3,5-Dinitrobenzoyl chloride (0.17 g, 7.5×10^{-4} mol) in benzene (1.0 ml) was added under nitrogen with continuous stirring to a solution of *trans*-[IrClCO{$(CH_3)_2C_6H_5P$}$_2$] (0.20 g, 3.76×10^{-4} mol) in benzene (1.0 ml).

Within a few minutes a yellow solid precipitated out of solution. The solid was stirred with the solution for about an hour then collected by filtration under nitrogen and washed with cold dry benzene. Yield of dry product: 0.12 g (67%). Recrystallization from a benzene–petroleum ether (90–120 °C) mixture yielded bright yellow needles, melting point 125–131 °C (decomposition).

Anal. Calcd. for $C_{27}H_{28}N_2O_6Cl_2P_2Ir$ (compound with 0.50 mol benzene of solution per mole of Ir complex); C, 40.45; H, 3.53; N, 3.50; Cl, 8.87. Found: C, 40.22; H, 3.59; N, 3.43; Cl, 9.21.

Recrystallization of the yellow solid from a chloroform–ethanol mixture also yielded bright yellow needles, melting point, 121–125 °C (decomposition).

Anal. Calcd. for compound with 0.50 mol chloroform of solution per mole of Ir complex: C, 35.80; H, 3.10; N, 3.31; Cl, 15.10. Found: C, 35.92; H, 3.16; N, 3.52; Cl, 15.64.

Dichloro-3,5-dinitrobenzoylcarbonylbis(dimethylphenylphosphine)iridium(III) (Compound B)

A solution of 3,5-dinitrobenzoyl chloride (0.11 g, 4.7×10^{-4} mol) in ether (5 ml) was added under nitrogen with stirring to a solution of *trans*-[IrClCO{$(CH_3)_2C_6H_5P$}$_2$] (0.25 g, 4.7×10^{-4} mol) in 25 ml of ether. A yellow solid precipitated almost immediately and was collected by filtration under nitrogen. Chromatography of the yellow solid on neutral activated alumina with chloroform as eluent, followed by precipitation of the solid by addition of ethanol to the chloroform solution, yielded the product as pale yellow plates, melting point 197–200 °C (decomposition with gas evolution).

Anal. Calcd. for $C_{24}H_{25}N_2O_6Cl_2P_2Ir$: C, 37.80; H, 3.31; N, 3.67; Cl, 9.30. Found: C, 37.46; H, 3.20; N, 3.59; Cl, 9.28.

Results and Discussion

On mixing benzene solutions of *trans*-[IrClCO{$(CH_3)_2C_6H_5P$}$_2$] and 3,5-dinitrobenzoyl chloride under nitrogen the absorbance at 432 nm, the absorption maximum of the Ir(I) complex, decreased with time and eventually a colorless solution resulted. Kinetic studies in benzene at 25.0 °C indicated that the reaction was first order in both reactants and had a specific rate constant in the forward direction of approximately 3 $M^{-1}\ s^{-1}$. Infrared (i.r.) spectra of benzene solutions at various stages of the re-

TABLE 1. Pertinent infrared data* for *trans*-[IrClCO{$(CH_3)_2C_6H_5P$}$_2$], 3,5-dinitro benzoyl chloride and the reaction products, compounds A and B

Compound	ν(C≡O) (cm^{-1})	ν(>C=O) (cm^{-1})	ν_{asy} (NO_2) (cm^{-1})	ν_s(NO_2) (cm^{-1})	ν(Ir—Cl) (cm^{-1})
trans-[IrClCO{$(CH_3)_2C_6H_5P$}$_2$]	1960	—	—	—	311
3,5-Dinitrobenzoyl chloride	—	1760	1535	1340	—
A	2065	1602	1529	1338	307 m 271
B	2055	1600	1525	1334	304 m 224 m

*Nujol and hexachlorobutadiene mulls; values in cm^{-1}; all bands are strong unless otherwise stated, m = medium.

action showed that as the intensities of the Ir(I) carbonyl and 3,5-dinitrobenzoyl chloride acyl stretching frequencies (at 1960 and 1760 cm^{-1}, respectively) decreased, new bands which appeared at approximately 2060 and 1600 cm^{-1} simultaneously increased in intensity. Proton magnetic resonance (p.m.r.) spectra in the 8 τ region of reaction mixtures at different times showed, in addition to resonances attributable to the Ir(I) complex, eight well-separated lines of approximately equal intensity plus a pair of overlapping triplets. The integration ratio of the eight single lines to the pair of overlapping triplets was approximately 3:1 and was apparently constant throughout the course of the reaction. When reaction of the Ir(I) complex was complete, the number of resonance absorbances in the 0 to 10 τ region and the relative intensities of these absorbances remained constant. The results indicate therefore the fairly rapid formation in benzene of at least two Ir(III) complexes (A and B) in the approximate ratio 3:1 with negligible interconversion between the two complexes under the conditions used to study the i.r. and p.m.r. spectra.

Preparative reactions in either benzene or ether gave mixtures of A and B. For reactions carried out in benzene, conditions could be chosen such that A preferentially crystallized from the reaction mixture. The solution which remained contained both A and B. Both products were precipitated from solution by adding the reaction mixture to 40–50 ml of boiling *n*-hexane. Recovery of pure A could be achieved by recrystallizing this mixture from a benzene – petroleum ether (90–120 °C) mixture. Recovery of pure B resulted when the mixture of solids was recrystallized from a chloroform–ethanol mixture. Compound A in benzene underwent no changes but in chloroform was converted, over a period of several days at room temperature, to compound B. Both the bright yellow, needle-like crystals of compound A and the pale yellow, plate-like crystals of compound B were found to be light sensitive and to darken after several days of exposure to light. The nature of the decomposition products was not ascertained.

Pertinent infrared absorption data for the starting reactants and the two products A and B are listed in Table 1. The most dramatic change in the frequencies attributable to the 3,5-dinitrobenzoyl group occur in the acyl (C=O) stretching frequency. The shift from 1760 cm^{-1} to about 1600 cm^{-1} is similar to changes observed in the oxidative addition of other acyl halides (7, 19, 20). The shift of the C≡O stretching frequency from 1960 cm^{-1} in the Ir(I) complex to 2065 and 2055 cm^{-1} in the two Ir(III) complexes is a characteristic feature of oxidative addition reactions of this type (17, 20, 21). This increase in CO frequency is diagnostic of decreased backbonding to CO as a result of the oxidation.

The stereochemical arrangements of chlorine atoms about Ir(III) can be readily determined by far i.r. data since the Ir—Cl stretching frequency is quite dependent on the ligand *trans* to the chlorine and is insensitive to the *cis* ligands (22). For example, compounds with Cl *trans* to Cl absorb in the region 315–335 cm^{-1}; Cl *trans* to CO, in the region 297–315 cm^{-1}; Cl *trans* to a trialkyl- or triarylphosphine, in the 270–290 cm^{-1} region; and Cl *trans* to an acyl group, in the 215–247 cm^{-1} region.

On the basis of the far i.r. data compound A contains a Cl *trans* to a CO (307 cm^{-1}) and a Cl *trans* to a dimethylphenylphosphine (271 cm^{-1}) and no Cl *trans* to an acyl group. Compound B, on the other hand, contains a Cl *trans* to CO (304 cm^{-1}) and a Cl *trans* to an acyl group (224 cm^{-1}). The lack of any strong absorption

Can. J. Chem. Downloaded from www.nrcresearchpress.com by 210.87.254.42 on 09/05/12
For personal use only.

TABLE 2. Proton magnetic resonance data* for *trans*-[IrClCO{$(CH_3)_2C_6H_5P$}$_2$], 3,5-dinitrobenzoyl chloride and the two reaction products, compounds A and B

Compound	Peaks† (τ)	Coupling constants (Hz)	Assignment‖
trans-[IrClCO{$(CH_3)_2C_6H_5P$}$_2$]	8.07 t	3.5‡	P—CH_3
3,5-Dinitrobenzoyl chloride	0.75 d	1.8	H_A
	0.68 t	1.8	H_B
A	8.44 d	12.0	P_1—CH_3
	8.34 d	11.5	
	8.19 d	10.5	P_2—CH_3
	8.08 d	10.0	
	1.07 s		H_A + H_B
B	7.80 ovt	12.0§	P—CH_3
	2.19 d	2.1	H_A
	1.31 t	2.0	H_B

*$CDCl_3$ solution; internal TMS lock. All chemical shifts relative to internal TMS except as noted.
†s = singlet; d = doublet; t = triplet; ovt = overlapping triplets.
‡Apparent coupling constant.
§Separation of outermost peaks.
‖H_A and H_B refer to the two *ortho* protons and the one *para* proton respectively on the nitroaromatic ring. P_1 and P_2 refer to the two non-equivalent phosphorus nuclei at 32 and 43 p.p.m. respectively from 85% H_3PO_4.

for either compound in the region 315 to 335 cm^{-1} rules out a Cl *trans* to a Cl in either compound.

The relative positions of methyl-substituted phosphine ligands in octahedral iridium(III) complexes can be determined by p.m.r. spectroscopy using the method of Jenkins and Shaw (23). Complexes with mutually *trans* phosphines exhibit a triplet for the methyl proton resonances because of strong coupling between the *trans* phosphorus nuclei. With the phosphorus atoms in a mutually *cis* position the resonance of the methyl protons is split into a doublet since the two phosphorus atoms do not couple strongly in this case.

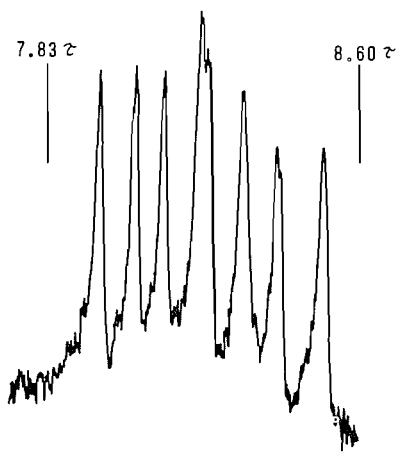

FIG. 1. Proton magnetic resonance spectrum of compound A in the methylphosphine resonance region.

The p.m.r. spectrum of compound A showed eight distinct sharp resonances in the methyl hydrogen region of the spectrum (Fig. 1, Table 2). By using INDOR techniques (24) it was shown that the eight lines were due to magnetically non-equivalent methyl groups coupled with two non-equivalent phosphorus nuclei at 32 and 43 p.p.m. upfield from 85% H_3PO_4. On irradiating at one phosphorus resonance four of the eight lines collapsed to a doublet leaving the position of the other four lines unaltered. Irradiation at the

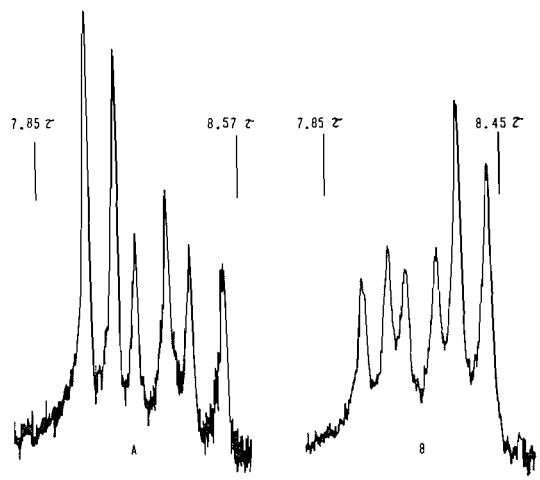

FIG. 2. Proton magnetic resonance spectrum of compound A in the methylphosphine resonance region when (*A*) the phosphorus nucleus 43 p.p.m. upfield from 85% H_3PO_4 is decoupled and (*B*) the phosphorus nucleus 32 p.p.m. upfield from 85% H_3PO_4 is decoupled.

Can. J. Chem. Downloaded from www.nrcresearchpress.com by 210.87.254.42 on 09/05/12
For personal use only.

Can. J. Chem. Downloaded from www.nrcresearchpress.com by 210.87.254.42 on 09/05/12
For personal use only.

second phosphorus resonance had the opposite effect (Fig. 2). These observations can only be consistent with a molecule containing mutually *cis*, non-equivalent dimethylphenylphosphines with no plane of symmetry through the Ir—P bonds. Of the two structures **1** and **2** which satisfy these requirements, only structure **2** is also

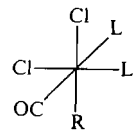

1

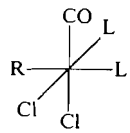

2

R = $(O_2N)_2C_6H_3C(=O)$—
L = $(CH_3)_2C_6H_5P$

R = $(O_2N)_2C_6H_3C(=O)$—
L = $(CH_3)_2C_6H_5P$

consistent with the far i.r. data which shows that compound A contains a Cl *trans* to a CO and a Cl *trans* to a dimethylphenylphosphine. Compound A is therefore assigned Structure **2**. By virtue of the disposition of the dimethylphenylphosphine ligands in this compound it is hereafter referred to as the *cis* isomer.

The p.m.r. spectrum of compound B in the methyl hydrogen region showed a pair of overlapping triplets which collapsed to a sharp narrow doublet as a result of phosphorus-31 decoupling. Thus a *trans* arrangement of phosphines must exist in the molecule. Of the two possible structures **3** and **4** containing *trans* phosphines, **3** must be excluded since it has a plane of symmetry through the Ir—P bonds and would be expected to give rise to a single triplet in the methyl hydrogen region. The assignment of structure **4** to compound B is fully in accord with

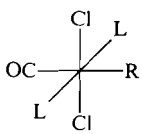

3

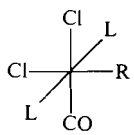

4

R = $(O_2N)_2C_6H_3C(=O)$—
L = $(CH_3)_2C_6H_5P$

R = $(O_2N)_2C_6H_3C(=O)$—
L = $(CH_3)_2C_6H_5P$

the far i.r. results which indicate that this compound contains a Cl *trans* to a CO and a Cl *trans* to an acyl group. Since the dimethylphosphine ligands are *trans* in structure **4**, compound B is referred to as the *trans* isomer.

The experimental results indicate therefore that in benzene, ether and benzene–ether mixtures *trans*-$[IrClCO\{(CH_3)_2C_6H_5P\}_2]$ reacts with 3,5-dinitrobenzoyl chloride to yield an approximately 3:1 mixture of the *cis*- and *trans*-dichloro-3,5-dinitrobenzoylcarbonylbis(dimethylphenylphosphine)iridium(III) complexes.

Oxidative addition of acyl halides to square planar iridium(I) complexes of the type *trans*-$IrClCOL_2$ (where L = *tertiary* phosphine or arsine) are well known (7, 20, 25) and have been reported (20, 26) to give *trans*-adducts via the following mechanism (14)

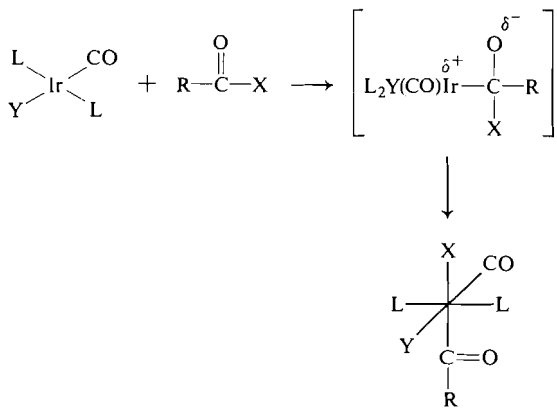

That the solvent can play an important role in determining the stereochemistry of the addition and possible isomerization of the initial product has been the subject of several reports (26–28). Our experimental results indicate that both **2** and **4** are being produced in the same ratio throughout the reaction and that conversion between the two forms is very slow. Whereas the *cis* isomer (**2**) can only arise from a *cis* addition of the acyl halide, the *trans* isomer (**4**) could be the result of either a *cis*- or a *trans*-addition. Our results cannot tell us whether these two addition reactions are proceeding simultaneously to yield the observed mixture of isomers or whether there is an initial formation of a third species which rapidly rearranges to give a mixture of the isomers. It is clear however, that oxidative addition of 3,5-dinitrobenzoyl chloride to *trans*-$[IrCOCl\{(CH_3)_2C_6H_5P\}_2]$ proceeds via a mechanism quite different to that proposed by Halpern (14). Steric factors may be very important in this system in determining both the mode of addition and the stereochemistry of the final products.

Can. J. Chem. Downloaded from www.nrcresearchpress.com by 210.87.254.42 on 09/05/12
For personal use only.

The resonance absorbance patterns of the ring protons in 3,5-dinitrobenzoyl chloride and in the 3,5-dinitrobenzoyl groups in the *cis* and *trans* isomers are not identical. In both 3,5-dinitrobenzoyl chloride and the *trans* isomer, the magnetically non-equivalent H_A and H_B protons in **5** gave the expected doublet and triplet in the ratio

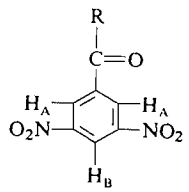

5

R = Cl, $IrCl_2CO\{(CH_3)_2C_6H_5P\}_2$

of 2:1. In the *cis* isomer a sharp singlet was found at 1.07 τ which integrated to three protons relative to the twelve protons associated with the methyl hydrogens of the two dimethylphenylphosphines. The two protons H_A and H_B seem therefore to be magnetically equivalent in the *cis* isomer. The p.m.r. spectra of aromatic compounds are known to be markedly affected by solvents (29),[1] and a highly specific solvent nitroaromatic ring interaction may be the source of the differences noted above. A study of the p.m.r. spectra of 3,5-dinitrobenzoyl chloride and the *cis* and *trans* isomers in a variety of solvents and over a range of temperatures is planned in an effort to ascertain the factors which give rise to these differences in resonance absorbance patterns.

The i.r. and p.m.r. spectra of the two isomers show some interesting differences (Tables 1 and 2). The N—O stretching modes in the *cis* isomer are only slightly lower (2 and 6 cm^{-1}) than the corresponding vibrations in 3,5-dinitrobenzoyl chloride. This suggests that in the *cis* isomer the electron density in the ring is not significantly altered compared to the electron density in 3,5-dinitrobenzoyl chloride. The observation that in the *cis* isomer the resonance absorbance of the nitroaromatic ring protons is only 20 Hz upfield from the mean position of the resonance absorbances of the protons in 3,5-dinitrobenzoyl chloride is consistent with this suggestion. In the *trans* isomer the resonance absorbances of the H_A and H_B protons are shifted further upfield (38 and 87 Hz, respectively) and there is a somewhat larger decrease (6 and 10 cm^{-1}) in the frequencies of the N—O stretching modes. Both observations imply that there is a more extensive delocalization of the electron density from the metal center into the ring in the case of the *trans* isomer (5).

An attempted decarbonylation of the *cis* isomer by refluxing in toluene for 24 h under nitrogen resulted in no decarbonylation but a complete conversion to the *trans* isomer. Refluxing a *p*-xylene solution of the *trans* isomer under nitrogen for 24 h did not result in decarbonylation and the starting material was recovered unchanged. The evolution of a gas on melting of the *trans* isomer at 197–200 °C may imply loss of CO from the compound but the nature of the resulting product has not yet been established. Kubota *et al.* (7–9) have noted that decarbonylation reactions of Ir(III) complexes containing

O
‖
RC—

are not as facile when R = *p*-$NO_2C_6H_4$— as when R = *p*-$CH_3OC_6H_4$— or $C_6H_5CH_2$—. Therefore it may prove to be very difficult to decarbonylate or decarboxylate iridium(III) complexes in which the R group contains two or more nitro groups on the ring. If this is indeed the case, oxidative additions of an appropriately substituted acyl halide or benzoic acid followed by decarbonylation or decarboxylation may not offer a simple general route to the preparation of complexes containing a metal center directly σ-bonded to an aromatic ring containing one or more nitro groups.

Both *cis* and *trans* isomers and 3,5-dinitrobenzoyl chloride react with tetraphenylarsonium cyanide in chloroform to give the characteristically deep red colored solutions associated with the formation of σ complexes (12, 13, 30). The results of equilibrium and kinetic studies of these interactions will be published separately.

[1]In hexadeuteroacetone the p.m.r. spectrum of 3,5-dinitrobenzoyl chloride shows a sharp singlet for the three nitroaromatic ring protons.

A portion of this work was carried out while one of the authors (A.R.N.) was on a sabbatical leave at Stanford University. Thanks are extended to Professor H. Taube for making research space and equipment available during that time. The authors are indebted to Drs. M. C. Baird and B. K. Hunter for numerous valuable discussions concerning the p.m.r. spectra. Financial support by the National Research Council of Canada is gratefully acknowledged.

1. G. W. PARSHALL and J. J. MROWCA. Adv. Organomet. Chem. **1**, 157 (1968).
2. J. P. COLLMAN and W. R. ROPER. J. Am. Chem. Soc. **88**, 180 (1966).
3. J. P. COLLMAN, M. KUBOTA, F. D. VASTINE, J. Y. SUN, and J. W. KANG. J. Am. Chem. Soc. **90**, 5430 (1968).
4. M. C. BAIRD. J. Organomet. Chem. **16**, p. 16 (1969).
5. A. R. NORRIS and M. C. BAIRD. Can. J. Chem. **47**, 3003 (1969).
6. C. V. SENOFF. Can. J. Chem. **48**, 2444 (1970).
7. M. KUBOTA and D. M. BLAKE. J. Am. Chem. Soc. **93**, 1368 (1971).
8. M. KUBOTA, D. M. BLAKE, and S. A. SMITH. Inorg. Chem. **10**, 1430 (1971).
9. M. KUBOTA and B. M. LOEFFLER. Inorg. Chem. **11**, 469 (1972).
10. L. H. GAN and A. R. NORRIS. Can. J. Chem. **42**, 4290 (1971).
11. E. BUNCEL, A. R. NORRIS, K. E. RUSSELL, and R. TUCKER. J. Am. Chem. Soc. **94**, 1646 (1972).
12. E. BUNCEL, A. R. NORRIS, and K. E. RUSSELL. Q. Rev. London, **22**, 123 (1968).
13. M. J. STRAUSS. Chem. Rev. **70**, 667 (1970).
14. J. HALPERN. Acc. Chem. Res. **3**, 386 (1970).
15. D. D. PERRIN, W. L. F. ARMAUGO, and D. R. PERRIN. Purification of laboratory chemicals. Pergamon Press Ltd., London. 1966. p. 147.
16. A. VOGEL. Practical organic chemistry. Longmans, Green and Co. Ltd., London. 1966. p. 163.
17. A. J. DEEMING and B. L. SHAW. J. Chem. Soc. A, 1887 (1968).
18. A. J. DEEMING and B. L. SHAW. J. Chem. Soc. A, 1802 (1969).
19. D. M. ADAMS and G. BOOTH. J. Chem. Soc. 1112 (1962).
20. A. J. DEEMING and B. L. SHAW. J. Chem. Soc. A, 1128 (1969).
21. L. VASKA. Acc. Chem. Res. **1**, 335 (1968).
22. M. JENKINS and B. L. SHAW. J. Chem. Soc. 6789 (1965).
23. M. JENKINS and B. L. SHAW. Proc. Chem. Soc. 279 (1963).
24. E. B. BAKER. J. Chem. Phys. **37**, 911 (1962).
25. J. CHATT, N. P. JOHNSON, and B. L. SHAW. J. Chem. Soc. A, 604 (1967).
26. J. P. COLLMAN and C. T. SEARS, JR. Inorg. Chem. **7**, 27 (1968).
27. D. M. BLAKE and M. KUBOTA. Inorg. Chem. **9**, 989 (1970).
28. A. J. DEEMING and B. L. SHAW. Chem. Commun. 751 (1968).
29. R. FOSTER and C. A. FYFE. *In* Progress in nuclear magnetic resonance spectroscopy. Vol. 4. *Edited by* J. Emsley, J. Feeney, and J. Sutcliffe. Pergamon Press, Oxford. 1969.
30. A. R. NORRIS. Can. J. Chem. **45**, 2703 (1967).

Can. J. Chem. Downloaded from www.nrcresearchpress.com by 210.87.254.42 on 09/05/12
For personal use only.

Hydrogen Peroxide Oxidation of Coordinated Thiocyanate Ion in *cis*- and *trans*-$[Coen_2NH_3NCS]^{2+}$: The Preparation and Properties of *trans*-$[Coen_2NH_3CN]^{2+}$

ALBERT RICHARD NORRIS AND JAMES WILLIAM LENNOX WILSON

Department of Chemistry, Queen's University, Kingston, Ontario

Received July 19, 1973

The hydrogen peroxide oxidation of thiocyanate ion in *cis*- and *trans*-$[Coen_2NH_3NCS]^{2+}$ leads to the formation of the corresponding *cis*- and *trans*-cyanoammine- and diamminebis(ethylenediamine)cobalt-(III) complexes. The spectral properties of the previously unreported *trans*-$[Coen_2NH_3CN]^{2+}$ are reported and compared to the spectral properties of the *cis*-isomer.

Observations are made concerning the reaction conditions which favor a high percent conversion of *trans*-$[Coen_2NH_3NCS]^{2+}$ to *trans*-$[Coen_2NH_3CN]^{2+}$.

L'oxydation par le peroxyde d'hydrogène de l'ion thiocyanate dans le $[Coen_2NH_3NCS]^{2+}$-*cis* et -*trans* conduit à la formation des complexes *cis* et *trans* cyanoamine et diamine bis(éthylenediamine) cobalt (III). Les propriétés spectrales du composé, pas encore décrit, $[Coen_2NH_3CN]^{2+}$-*trans* sont rapportées et comparées à celles de l'isomère-*cis*.

On fait certaines observations concernant les conditions de réaction qui favorisent une conversion complète du $[Coen_2NH_3NCS]^{2+}$-*trans* en $[Coen_2NH_3CN]^{2+}$-*trans*. [Traduit par le journal]

Can. J. Chem., **51**, 4152 (1973)

Introduction

We have previously reported (1) that oxidation of coordinated thiocyanate ion in $[Co(NH_3)_5NCS]^{2+}$ by hydrogen peroxide in an acid medium leads to the formation of both $[Co(NH_3)_5CN]^{2+}$ and $[Co(NH_3)_6]^{3+}$. Other oxidizing agents such as IO_3^-, IO_4^-, MnO_4^-, $S_2O_8^{2-}$, ClO_2^-, BrO_3^-, and Ce^{4+} are also capable of oxidizing the coordinated thiocyanate ion but none appears to be as effective as hydrogen peroxide in producing the cyanide-substituted product (2–4).

As part of kinetic studies[1] of the hydrogen peroxide oxidation of thiocyanate ion in *cis*- and *trans*-$[Coen_2NH_3NCS]^{2+}$ we have established that the starting complexes give rise exclusively to the corresponding *cis* and *trans*-cyanoammine- and diamminebis(ethylenediamine)cobalt-(III) complexes. Infrared, ultraviolet–visible, and proton magnetic resonance spectra have been recorded for the previously unreported *trans*-$[Coen_2NH_3CN]Cl_2$. These are compared to the corresponding spectra of the *cis*-isomer. Observations are also presented concerning the dependence of the percent conversion of *trans*-$[Coen_2NH_3NCS]^{2+}$ to *trans*-$[Coen_2NH_3CN]^{2+}$ on various reaction parameters.

[1]A. R. Norris and J. W. L. Wilson. Results to be published.

Experimental

Reagents

trans-$[Coen_2Cl_2]Cl$, *trans*-$[Coen_2ClNCS]NCS$, *trans*-$[Coen_2NH_3NCS](NCS)_2$, *cis*-$[Coen_2NH_3NCS]S_2O_6$, *cis*-$[Coen_2NH_3CN]Cl_2$, *trans*-$[Coen_2(NH_3)_2]Br_3$, and *cis*-$[Coen_2(NH_3)_2]Cl_3$ were prepared and recrystallized following published procedures (5–7).

trans-$[Coen_2NH_3NCS]Cl_2$ was prepared as follows. A solution containing about 400 mg of the twice-recrystallized thiocyanate salt was dissolved in approximately 30 ml of dilute aqueous acetic acid and the solution passed through a column (1 × 12 cm) of Dowex 50W-X2 ion-exchange resin (200–400 mesh) in the acid form. When all the complex was absorbed the column was washed with 50 to 100 ml of 0.01 *M* HCl in order to completely remove any thiocyanate ion. On passage of 1.0 *M* HCl through the column a small amount of *trans*-$[Coen_2(NCS)_2]^+$ was eluted from the column. Elution with 2.0 *M* HCl brought down an orange-colored solution which was filtered and freeze-dried. The solid obtained in the freeze-drying procedure was recrystallized from an ethanol–water mixture containing added tetra-*n*-butylammonium chloride. The crystals which formed were collected by filtration and dried to constant weight in vacuo over phosphorus(V) pentoxide. In a typical procedure 400 mg of thiocyanate salt yielded approximately 300 mg of freeze-dried solid and 200 mg of recrystallized *trans*-$[Coen_2NH_3NCS]Cl_2$. In spite of repeated recrystallizations, *trans*-$[Coen_2NH_3NCS](NCS)_2$ always contained small amounts of *trans*-$[Coen_2(NCS)_2]NCS$ as an impurity. This impurity could only be removed by employing the chromatographic procedure described above.

Values of absorption maxima (λ_1 and λ_2) and molar extinction coefficients at the absorption maxima (ε_1 and ε_2) for each of the complexes prepared in this study are given in Table 1.

Can. J. Chem. Downloaded from www.nrcresearchpress.com by 210.87.254.40 on 09/05/12
For personal use only.

TABLE 1. Absorption maxima (λ_1 and λ_2) and molar extinction coefficients at the absorption maxima (ε_1 and ε_2) of some cobalt(III) complexes*

Compound	λ_1(nm)	$\varepsilon_1(M^{-1}\ cm^{-1})$	λ_2(nm)	$\varepsilon_2(M^{-1}\ cm^{-1})$	Reference
trans-$[Coen_2Cl_2]Cl$	617	36.1	—	—	This work
trans-$[Coen_2ClNCS]NCS$	557	137.3	324	2013	This work
trans-$[Coen_2NH_3NCS](NCS)_2$	488	177	304	1591	This work
trans-$[Coen_2NH_3NCS]Cl_2$	488	167	303	1530	This work
trans-$[Coen_2(NH_3)_2]Br_3$	464	62.9	336	56.3	This work
cis-$[Coen_2NH_3NCS]S_2O_6$	489	207	300	1660	This work
cis-$[Coen_2NH_3CN]Cl_2$	436	71.5	322	78.6	This work
"	436	77.6	322	85.1	7
cis-$[Coen_2(NH_3)_2]Cl_3$	470	73.0	341	62.0	10
A	436	74.3	322	82.3	This work
B	470	—	341	—	This work
C	434	56.0	322	59.9	This work
D (chloride salt)	464	61.4	336	54.8	This work
(bromide salt)	464	62.0	336	56.0	This work

*Values were measured on a Cary 14 recording spectrophotometer employing solutions of approximately 10^{-3} *M* concentration and matched cells of path lengths 1.0, 2.0, and 5.0 cm. The cell compartment was thermostatted at 25.0 °C in all cases.

Stock solutions of hydrogen peroxide (~10 *M*) were prepared using Baker hydrogen peroxide (30 vol%) containing 0.05% $Na_4P_2O_7 \cdot 10H_2O$ as a preservative. The peroxide content was determined iodimetrically following Vogel's procedure (8). The stock solutions were stored in the refrigerator when not in use and were re-standardized periodically.

Stock solutions, 2.50 *M* in perchloric acid, were prepared by diluting 207 ml of G. F. Smith double-distilled, lead-free, 70% perchloric acid to 1000 ml total volume with distilled water. The stock solutions were standardized by titration of 1.0 ml aliquots with 0.100 *N* sodium hydroxide to the phenolphthalein end-point.

Stock solutions, 2.50 *M* in sodium perchlorate, were prepared by dissolving 153.055 g (1.250 mol) of sodium perchlorate (G. F. Smith reagent grade, anhydrous, dried at 100 °C for 24 h) in distilled water and diluting to 500 ml total volume. The concentration of sodium perchlorate was checked by pipetting 5.0 ml aliquots of stock solution into tared evaporating dishes, evaporating the solvent and drying the resulting solids to constant weight at 100 °C.

Stock solutions containing *cis*- and *trans*-$[Coen_2NH_3NCS]^{2+}$ were prepared by dissolving an accurately weighed amount of *cis*-$[Coen_2NH_3NCS]S_2O_6$ or *trans*-$[Coen_2NH_3NCS]Cl_2$ in a known volume of distilled water. To inhibit base hydrolysis solutions were acidified to p*H* 3.00 with dilute hydrochloric acid and stored in the refrigerator when not in use. No detectable changes in the ultraviolet–visible absorption spectrum of either stock solution were noticed after 10 days storage under these conditions.

All other reagents used were A.R. grade or better and were used without further purification.

Instruments

Ultraviolet–visible absorption spectra were recorded on a Cary 14 recording spectrophotometer using matched silica cells of 1.0 and 5.0 cm path lengths. The temperature in the cells was maintained constant to ±0.1 °C by circulating water from a constant temperature bath through a specially designed cell holder in the spectrophotometer.

Infrared spectra were recorded on Beckman IR-10 and Perkin–Elmer 180 recording spectrophotometers operating in the double-beam mode. Samples were prepared in potassium bromide or cesium iodide discs (1% w/w concentration) and spectra recorded versus air or an attenuator in the reference beam path. Spectra were calibrated using a polystyrene film and all frequencies are believed to be accurate to within ±5 cm^{-1}.

Proton magnetic resonance spectra of the *cis*- and *trans*-series of complexes were recorded on Varian HA-100 and Bruker HX-60 spectrometers respectively. For spectra recorded on the HX-60, the sodium salt of 3-(trimethylsilyl)-propane sulfonic acid (DSS) was used as an internal standard with the proton signal of the methyl groups being used as the "lock" signal. For spectra recorded on the HA-100, external tetramethylsilane (TMS) was used as a reference and a "lock" signal. Chemical shift values (τ) are given relative to the standard (τ = 10.00 p.p.m.). Samples normally contained about 20 mg of complex dissolved in 0.50 ml 1.8 *M* D_2SO_4. Spectra were always recorded immediately after preparation of the solutions and again after intervals of 12 and 24 h to check for signs of possible decomposition of the complex.

Product Distribution Studies and Recovery of Reaction Products

One hundred ml of solution containing from 1.0×10^{-4} to 1.2×10^{-3} mol of complex and known amounts of H_2O_2, $HClO_4$, and $NaClO_4$ was allowed to stand in the dark at 25.0 °C until the reaction had gone to completion (> 10 half-lives). The ultraviolet–visible absorption spectrum of a portion of the solution was recorded, the solution diluted by a factor of about two and passed through an ion-exchange column (1 × 12 cm) containing Dowex 50W-X2 (200–400 mesh) in the H^+ form. When all the complex was absorbed the column was washed with 100 ml of distilled water to ensure the removal of all counter-anions. With 0.50 *M* HCl as eluent no colored species were removed from the column though there was some slight separation of the band at the top of the column into a lower yellow band and an upper orange band. The yellow band could be completely removed from the column by using 1 *M* HCl as eluent while 3 *M* HCl was

Can. J. Chem. Downloaded from www.nrcresearchpress.com by 210.87.254.40 on 09/05/12
For personal use only.

TABLE 2. Analytical results for compounds A, C, and D

Compound	Preparation	Elemental analysis (%) C	H	N	Cl
A*	(*i*)	20.15	6.26	28.93	24.31
	(*ii*)	20.17	6.76	26.98	24.32
	(*iii*)	19.64	6.57	27.46	23.82
C†	(*i*)	19.38	6.83	26.79	23.04
	(*ii*)	19.50	6.52	26.74	22.66
D‡	(*i*)	14.16	7.02	25.36	31.51

*Anal. Calcd. for $[Coen_2NH_3CN]Cl_2$: C, 20.49; H, 6.53; N, 28.67; Cl, 24.19.
†Anal. Calcd. for $[Coen_2NH_3CN]Cl_2 \cdot H_2O$: C, 19.34; H, 6.82; N, 27.04; Cl, 22.80.
‡Anal. Calcd. for $[Coen_2(NH_3)_2]Cl_3 \cdot H_2O$: C, 14.23; H, 7.17; N, 24.90; Cl, 31.79.

required to remove the material contained in the orange band. No evidence was ever obtained for other species, such as $[Co(H_2O)_6]^{2+}$, being present on the resin. The ultraviolet–visible spectra of the filtered 1 and the 3 *M* HCl fractions were recorded and the solids in these fractions recovered by freeze-drying of the solutions.

Two methods of determining product distribution were employed. For the reaction mixtures, absorbances at the known positions of maximum absorption of each complex were used in conjunction with the known molar extinction coefficients of each product at those wavelengths to calculate the amount of each complex present in solution. Alternatively, for each fraction from the ion-exchange column, the absorbances at the absorption maxima could be used together with the known molar extinction coefficients of the complex at the absorption maxima and the volume of eluent to calculate the amount of complex in that particular fraction. The two methods of determining the amount of each product usually agreed to better than ±5 %.

The following procedure was used to recrystallize the solid recovered from the freeze-drying of the 1 *M* HCl fractions. Fifty to one hundred mg of the yellow solid was dissolved in 0.50 ml of warm (~60 °C) distilled water containing 0.5 g tetra-*n*-butylammonium chloride. Enough warm absolute ethanol was added to the solution to cause a slight turbidity (~1 ml) and the solution then allowed to cool in an ice-salt bath. The yellow crystals which formed were collected by filtration, washed thoroughly with absolute ethanol, acetone, and ether and dried to constant weight *in vacuo* over phosphorus(V) pentoxide. A second crop of crystals could usually be obtained by adding further ethanol and tetra-*n*-butylammonium chloride to the filtrate obtained in the first filtration. The recrystallized yellow salts recovered from the 1 *M* HCl fractions obtained in the oxidations of *cis*- and *trans*-$[Coen_2NH_3NCS]^{2+}$ are hereafter referred to as compounds A and C, respectively.

In studies of the oxidation of *cis*-$[Coen_2NH_3NCS]^{2+}$ the orange solid recovered by freeze-drying of the 3 *M* HCl fractions was very hygroscopic and could not be precipitated from solution as a chloride or bromide salt. For this reason the freeze-dried solid was simply dried to constant weight *in vacuo* over phosphorus(V) pentoxide before its spectral properties were determined. This salt is referred to hereafter as compound B.

In studies of the oxidation of *trans*-$[Coen_2NH_3NCS]^{2+}$ the orange solid recovered by freeze-drying of the 3 *M* HCl fractions was recrystallized both as a chloride salt from ethanol–water (using the procedure described above) and as a bromide salt from an aqueous solution containing added sodium bromide. The recovered crystals were washed with ethanol, acetone, and ether and dried to constant weight *in vacuo* over phosphorus(V) pentoxide. Both the chloride and the bromide salt are hereafter referred to as compound D.

Elemental analyses were carried out by Galbraith Laboratories, Inc. (Knoxville, Tenn.) and by the Analytical Services Section, Department of Chemistry, Stanford University.

Results and Discussion

By analogy with the results obtained in the oxidation of $[Co(NH_3)_5NCS]^{2+}$ (1), the oxidation of *cis*- and *trans*-$[Coen_2NH_3NCS]^{2+}$ by hydrogen peroxide in an acid medium might be expected to lead to cyanoammine- and diamminebis(ethylenediamine)cobalt(III) species. The results of the chromatographic separation indicated that this was almost certainly the case: for both starting complexes the only products eluted from the column came off with 1 and 3 *M* HCl indicating charges of +1 and +3 respectively for the complexes formed (9).

The results of elemental analysis on three separate sample preparations of compound A and the calculated percentages of carbon, hydrogen, nitrogen, and chlorine in $[Coen_2NH_3CN]Cl_2$ are given in Table 2. The results of elemental analysis are completely consistent with the formulation of the +1-charged complex recovered from the 1 *M* HCl fraction as a cyanoamminebis(ethylenediamine)cobalt(III) chloride.

Values of λ_1, λ_2, ε_1, and ε_2 for compound A and for a sample of *cis*-$[Coen_2NH_3CN]Cl_2$, prepared according to the method of Ohkawa, Hidaka, and Shimura (7), are listed in Table 1. Both of the compounds have values of absorp-

Can. J. Chem. Downloaded from www.nrcresearchpress.com by 210.87.254.40 on 09/05/12
For personal use only.

TABLE 3. Infrared spectral characteristics of the isomeric $[Co(en)_2NH_3CN]Cl_2$ complexes*

Region (cm^{-1})	Nature of peaks		Assignments†
	cis-$[Coen_2NH_3CN]Cl_2$	*trans*-$[Coen_2NH_3CN]Cl_2 \cdot H_2O$	
3300–3500		3460 cm^{-1} (broad, strong)	ν(OH) (due to lattice H_2O)
3100–3200	Very broad doublet 3060, 3150 cm^{-1}	Very broad doublet 3100, 3190 cm^{-1}	$\nu(NH_3)$, $\nu(NH_2)$
2000–2500	Sharp, strong singlet 2130 cm^{-1}	Sharp, strong singlet 2130 cm^{-1}	$\nu(C\equiv N)$
1500–1700	1570 (broad, strong), shoulder at 1615 cm^{-1}	Broad peak, split, very strong, 1600, 1610 cm^{-1}	$\delta(NH_2)_d$
1400–1500	Strong, single peak 1445 cm^{-1}	Doublet, 1435, 1445 cm^{-1} (medium), shoulder at 1445 cm^{-1}	CH_2 bend
1350–1400	Doublet, 1338 and 1360 (medium), shoulders at 1370 cm^{-1}	Doublet, 1360 and 1375 cm^{-1} (medium), shoulder at 1350 cm^{-1}	
1310–1320	Doublet, 1310 and 1320 cm^{-1} (weak)	Doublet, 1310 and 1320 cm^{-1} (weak)	CH_2 wag
1280–1300	Doublet, 1295 (medium) and 1275 cm^{-1} (weak)	Doublet, 1300 (weak), 1280 cm^{-1} (medium)	$\delta(NH_3)_s$
1200–1250	Singlet, broad, weak 1225 cm^{-1}, shoulder 1210 cm^{-1}	Singlet, sharp, weak 1240 cm^{-1}	
1200–1100	Three peaks, 1165 cm^{-1} (medium), 1145 cm^{-1} (strong), 1110 cm^{-1} (weak, broad)	Quartet 1120, 1138, 1152, 1170 cm^{-1} (weak, medium, medium, weak)	NH vib $\delta(NH_2)_s$
1000–1060	Three peaks, 1055 cm^{-1} (sharp, strong), 1000 and 1015 cm^{-1} (medium)	Two peaks, 1055 cm^{-1} (strong), 1005 cm^{-1} (medium)	ν(C—C) or ν(C—N) in the en ring
860–890	One peak, weak 890 cm^{-1}, shoulder at 878 cm^{-1}	Singlet, weak 885 cm^{-1} shoulder (very weak) 897 cm^{-1}	CH_2 rock
800–850	Four definite bands, 845, 828, 808, 783 cm^{-1} (medium, medium, medium, weak, respectively)	Very broad, strong slightly split 817 cm^{-1}, 835 cm^{-1}	
720–750	One peak, very weak split 710, 715 cm^{-1}	Two peaks, weak 730 cm^{-1}, 750 cm^{-1}	
610–500	Two bands, four peaks, 560, 580 cm^{-1} (strong), 500 cm^{-1} (medium), shoulder 510 cm^{-1}	Very broad single peak 615 cm^{-1}, weak single peaks 505, 548 cm^{-1}	ν(Co—N) and NH_2 rock
450–350	Eight bands, 465 cm^{-1} ,445 cm^{-1}, 435 cm^{-1} medium; 410, 402, 490, 478, 468 cm^{-1} all weak	Six bands, 465, 435, 410 cm^{-1}, medium; 390, 375, 365 cm^{-1}, weak.	Chelate ring deformation (Co—N)

*Readings are accurate to ±5 cm^{-1}.
†References 15–18 and 22.

tion maxima and molar extinction coefficients in reasonable agreement with those reported for *cis*-$[Coen_2NH_3CN]Cl_2$ (7). Compound A possessed absorption minima at 371 ($\varepsilon = 19.5\ M^{-1}\ cm^{-1}$) and 282 nm ($\varepsilon = 22.0\ M^{-1}\ cm^{-1}$) while the prepared sample of *cis*-$[Coen_2NH_3CN]Cl_2$ possessed absorption minima at 371 ($\varepsilon = 17.2\ M^{-1}\ cm^{-1}$) and 282 nm ($\varepsilon = 15.6\ M^{-1}\ cm^{-1}$). Ohkawa, Hidaka, and Shimura's resolution of the *cis*-compound into its enantiomers (7) leaves little doubt that the complex has a *cis*-geometry.

The infrared (i.r.) spectrum of compound A was identical in all respects to the i.r. spectrum of an authentic sample of *cis*-$[Coen_2NH_3CN]Cl_2$.

Can. J. Chem. Downloaded from www.nrcresearchpress.com by 210.87.254.40 on 09/05/12
For personal use only.

Can. J. Chem. Downloaded from www.nrcresearchpress.com by 210.87.254.40 on 09/05/12
For personal use only.

Pertinent details of the spectrum are given in Table 3.

The proton magnetic resonance (p.m.r.) spectra of compound A and an authentic sample of *cis*-$[Coen_2NH_3CN]Cl_2$ were also identical. Resonance absorbances were noted at 4.96, 5.42, 6.16, and 7.20 τ. The first two resonance absorbances were rather broad and were not of equal intensity. The third resonance absorbance was very broad and of low intensity but always present in the spectra of the samples. The last absorbance was broad, had a shoulder on the downfield side and, at the maximum, showed some indication of splitting (peak separation ~3 Hz). The ratio of the sum of the areas of the peaks at 4.96, 5.42, and 6.16 τ to the area of the peak at 7.20 τ was 1:1.35. If the resonances at 4.96, 5.42, and 6.16 τ are assigned to the NH_2 protons of ethylenediamine, and the resonances in the 7.20 τ region assigned to the NH_3 protons and the CH_2 protons of ethylenediamine, the expected ratio of areas is 1:1.37. When either compound A or authentic *cis*-$[Coen_2NH_3CN]Cl_2$ was dissolved in D_2O there was a rapid disappearance of the resonances at 4.96, 5.42, and 6.16 τ and the shoulder on the downfield side of 7.20 τ resonance, and a considerable narrowing of the band width of the 7.20 τ resonance absorbance. These observations are fully consistent with the proposed assignments.

The starting *cis*-$[Coen_2NH_3NCS]^{2+}$ complex ion in 1.8 *M* D_2SO_4 possessed resonance absorbances at 4.72, 5.54, 6.50, and 7.17 τ. Integration ratios were 2.50(4.72 + 5.54 τ):1(6.50 τ):2.70-(7.17 τ). Assignments of the resonance absorbances at 4.72 and 5.54 τ to NH_2 protons, the resonance at 6.50 τ to the NH_3 protons and the resonance at 7.17 τ to the CH_2 protons of ethylenediamine would require the integration ratios to be 2.66:1:2.66.

Compound B and an authentic sample of *cis*-$[Coen_2(NH_3)_2]Cl_2$ were found to have identical ultraviolet–visible, i.r., and p.m.r. spectra. Ultraviolet–visible absorption maxima occurred at 470 and 341 nm in good agreement with published values (10). Proton resonance absorbances occurred at 5.04, 5.42, 6.72, and 7.22 τ. The 5.04 τ resonance absorbance was very broad compared to the three remaining resonances. Integration ratios were 1.32(5.04 + 5.42 τ):1(6.72 τ):1.35-(7.22 τ). Assignment of the 5.04 and 5.42 τ resonances to the NH_2 protons, the 6.72 τ resonance to the NH_3 protons and the 7.22 τ resonances to the CH_2 protons of ethylenediamine would require the integration ratios to be 1.33:1:1.33. Buckingham, Durham, and Sargeson (11) have reported a similar p.m.r. spectrum for *cis*-$[Coen_2(NH_3)_2](ClO_4)_3$ in 1.8 *M* D_2SO_4 though with possibly more splitting of the band at 5.04 τ than we observed.

All the available evidence indicates therefore that oxidation of *cis*-$[Coen_2NH_3NCS]^{2+}$ by hydrogen peroxide in an acid medium leads to the formation of *cis*-$[Coen_2NH_3CN]^{2+}$ and *cis*-$[Coen_2(NH_3)_2]^{3+}$ as the only products.

The results of elemental analysis for two different sample preparations of compound C and the calculated percentages of carbon, hydrogen, nitrogen, and chlorine in $[Coen_2NH_3CN]Cl_2 \cdot H_2O$ are given in Table 2. The analytical results support the formulation of compound C as a cyanoamminebis(ethylenediamine)cobalt(III) complex.

Values of λ_1, λ_2, ε_1, and ε_2 for compound C are given in Table 1. Minima in the absorption curve occurred at 368 (ε = 14.0 M^{-1} cm^{-1}) and 287 nm (ε = 24.9 M^{-1} cm^{-1}). The positions of the absorption maxima and minima and the values of $\varepsilon_{(\lambda_{max})}$ and $\varepsilon_{(\lambda_{min})}$ which characterize compound C clearly distinguish it from *cis*-$[Coen_2NH_3CN]Cl_2$. The lower values of $\varepsilon_{(\lambda_{max})}$ for compound C, as compared to the $\varepsilon_{(\lambda_{max})}$ values for compound A, are completely compatible with the formulation of compound C as the *trans*-isomer of cyanoammine bis(ethylenediamine)-cobalt(III) chloride (12–14).

The i.r. spectrum of compound C possesses a strong, sharp C≡N stretch at 2030 cm^{-1} as does the i.r. spectrum of compound A. Otherwise the i.r. spectra of the two compounds are markedly different. A tabulation of the i.r. absorption bands of the two compounds together with tentative assignments of the various bands are given in Table 3. Given that both compounds A and C are cyanoamminebis(ethylenediamine)cobalt(III) salts, a comparison of the spectra of the two compounds in the 1580–1620, 870–900 and 610–500 cm^{-1} regions would lead to the prediction that compound A had the *cis*-configuration and compound C had the *trans*-configuration (15–17).

The proton magnetic resonance spectrum of compound C in 1.8 *M* D_2SO_4 showed resonance absorbances at 5.25, 5.65, 6.43, and 7.18 τ. The 5.25 and 5.65 τ resonances were broad and of equal intensity and the third and fourth resonances were fairly sharp. The resonances at

Can. J. Chem. Downloaded from www.nrcresearchpress.com by 210.87.254.40 on 09/05/12
For personal use only.

5.25 and 5.65 τ are assigned to the NH_3 protons,[2] the resonance at 6.43 is assigned to the protons on NH_3 and the resonance at 7.18 τ is assigned to the CH_2 protons of ethylenediamine. On this basis the expected ratios of peak areas are 2.67:1:2.67. The observed ratios were 2.91:1:2.71. *trans*-$[Coen_2NH_3NCS]Cl_2$ possessed a broad resonance absorbance centered at 4.89 τ and a sharp resonance centered at 7.10 τ. The ratio of the integrated areas was 1:1.41.

The analytical data for compound D (as the chloride salt) and the calculated percentages of carbon, hydrogen, nitrogen, and chlorine in $[Coen_2(NH_3)_2]Cl_3 \cdot H_2O$ are shown in Table 2.

The absorption maxima of the chloride and bromide salts of compound D were identical to those of an authentic sample of *trans*-$[Coen_2(NH_3)_2]Br_3$ and the molar extinction coefficients of all three species were nearly identical (Table 1).

The i.r. spectra of D, recrystallized as the bromide salt, and an authentic sample of *trans*-$[Coen_2(NH_3)_2]Br_3$ were essentially identical and agreed in all respects with the spectrum reported by Rigg and Sherwin (18).

Proton magnetic resonance spectra of D and an authentic sample of *trans*-$[Coen_2(NH_3)_2]Br_3$ were also identical. Resonance absorbances were noted at 4.97 τ and 7.11 τ with a shoulder on the 7.11 τ resonance at approximately 6.93 τ. The ratio of the integrated areas was 1:1.76. If the resonance at 4.97 τ is assigned to the NH_2 protons, that at 6.93 τ to the NH_3 protons and that at 7.11 τ to the CH_2 protons of ethylenediamine, the expected integration ratio is 1:1.75.

Thus, on the basis of the available evidence, oxidation of *trans*-$[Coen_2NH_3NCS]^{2+}$ by H_2O_2 in acid media leads to *trans*-$[Coen_2NH_3CN]^{2+}$ and *trans*-$[Coen_2(NH_3)_2]^{3+}$ as the only products.

As no cleavage of a cobalt–nitrogen bond is required in the conversion of a coordinated thiocyanate ion to a coordinated ammonia, ammine-containing products of the same geometry as the starting complex are not unexpected. Garbett and Gillard have shown that periodate oxidation of a number of optically active thiocyanate-containing cobalt(III) complexes yielded the corresponding ammine-containing product in which the optical activity was preserved (19). The oxidation of a coordinated thiocyanate ion to yield a coordinated cyanide ion must at some point, however, involve a linkage isomerization in order to yield the resulting C-bonded cyanide-containing complex. It is of interest that for both our *cis*- and *trans*- starting complexes and for (−) *cis*-$[Coen_2(NCS)_2]^+$ (20) this presumably intramolecular isomerization leads to no geometrical isomerization. To determine how general this behavior is we plan to investigate the reactions of other suitable *cis*–*trans* pairs.

Since other methods of preparing *trans*-$[Coen_2NH_3CN]^{2+}$ have not been reported an effort was made to determine reaction conditions which would lead to the highest percent conversion of *trans*-$[Coen_2NH_3NCS]^{2+}$ to *trans*-$[Coen_2NH_3CN]^{2+}$. Experimentally the hydrogen peroxide concentration range covered was from 0.5 to 7.0 *M*, the $[H^+]$ was varied from 0.05 to 0.50 *M* and the initial concentration of complex was varied from 1.0×10^{-4} to 1.0×10^{-3} *M*. All studies were carried out at 25.0 °C.

At fixed concentrations of hydrogen peroxide, hydrogen ion, and initial complex, variations in the ionic strength of the medium over the range 0.1 to 0.50 *M* had no apparent effect on the percent conversion of the starting complex to *trans*-cyanoamminebis(ethylenediamine)cobalt(III).

At a fixed ionic strength and fixed concentrations of hydrogen peroxide and hydrogen ion, the percent conversion depended markedly on the initial concentration of complex. As indicated in Fig. 1, highest percent conversions were obtained at the lowest initial concentrations of *trans*-$[Coen_2NH_3NCS]^{2+}$. Perhaps Werner's failure to isolate a cyanide ion-containing product in any of his studies (6, 21) lies with this result as he used solutions containing very high concentrations of the starting complex and, under these conditions, we would expect an almost 100% conversion of the starting complex to the ammine-containing product.

The addition of *trans*-$[Coen_2NH_3CN]^{2+}$ to the reaction mixtures had no apparent effect on the percent conversion of starting complex to *trans*-$[Coen_2NH_3CN]^{2+}$. In solutions to which *trans*-$[Coen_2(NH_3)_2]^{3+}$ was added, the percent conversion of starting complex to *trans*-$[Coen_2NH_3CN]^{2+}$ decreased slightly as the initial concentra-

[2]For a series of *trans*-$[Coen_2NH_3X]^{n+}$ complexes (X = Cl^-, Br^-, NCS^-, NH_3, H_2O, and CN^-), only for X = CN^- did the NH_2 protons show a distinct splitting into two resonances. However, it has been observed that the higher X is in the spectrochemical series the greater is the half-width at half-height of the band associated with the NH_2 resonances. This phenomenon is under further investigation.

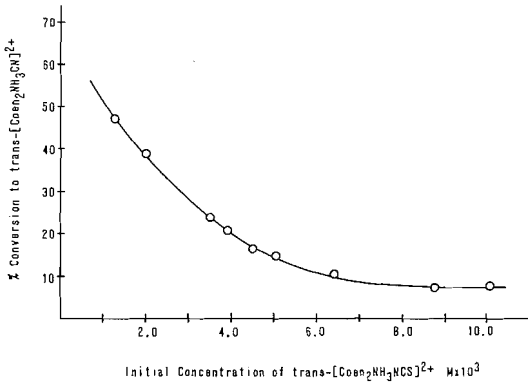

FIG. 1. % conversion of *trans*-$[Coen_2NH_3NCS]^{2+}$ to *trans*-$[Coen_2NH_3CN]^{2+}$ as a function of the initial concentration of *trans*-$[Coen_2NH_3NCS]^{2+}$; $[H_2O_2] = 2.00$ M; $[H^+] = 0.50$ M; $\mu = 0.50$ M; $T = 25.0$ °C.

tion of *trans*-$[Coen_2(NH_3)_2]^{3+}$ was increased. Separate studies showed that neither of the reaction products undergoes further reaction under the conditions employed in these studies. It is somewhat surprising therefore to find that the addition of *trans*-$[Coen_2(NH_3)_2]^{3+}$ should affect the percent conversion.

At a fixed ionic strength and fixed concentration of starting complex and hydrogen ion the percent conversion showed a maximum as the concentration of hydrogen peroxide was increased from 0.50 to 7.0 M. This point of maximum conversion moved to lower concentration of hydrogen peroxide as the concentration of hydrogen ion was increased. Over the range 0.10 to 0.50 M in hydrogen ion, the maximum occurred in the 3.5 to 1.5 M range of hydrogen peroxide concentrations. As the concentration of hydrogen ion was increased from 0.10 to 0.50 M, there was only a slight increase in the percent conversion at all concentrations of hydrogen peroxide.

In summary, the highest percent conversions of *trans*-$[Coen_2NH_3NCS]^{2+}$ to *trans*-$[Coen_2NH_3CN]^{2+}$ at 25.0 °C were found for solutions whose initial concentration of complex was $< 1 \times 10^{-4}$ M, whose concentration of hydrogen ion was about 0.50 M and whose concentration of hydrogen peroxide was in the range 1.5 to 2.5 M. The implications of these observations regarding the mechanism of conversion of *trans*-$[Coen_2NH_3NCS]^{2+}$ to *trans*-$[Coen_2NH_3CN]^{2+}$ are under investigation.

A portion of the work described was carried out while one of the authors (A.R.N.) was on a sabbatical leave at Stanford University. Thanks are extended to Professor H. Taube for several valuable discussions concerning the results of this work and for making research space and equipment available during that time. Financial support by the National Research Council of Canada is acknowledged.

1. S. M. CALDWELL and A. R. NORRIS. Inorg. Chem. **7**, 1667 (1968).
2. K. SCHUG, B. O. MINIATAS, A. J. SADOWSKI, T. YANO, and K. UENO. Inorg. Chem. **7**, 1669 (1968).
3. A. R. NORRIS and D. PATTERSON. J. Inorg. Nucl. Chem. **31**, 3680 (1969).
4. B. O. MINIATAS. Ph.D. Thesis. Illinois Institute of Technology, 1970.
5. J. C. BAILAR, JR. Inorganic synthesis. Vol. II. *Edited by* W. C. Fernelius. McGraw–Hill, New York. 1946. p. 223.
6. A. WERNER. Liebig's Ann. der Chim. **386**, 1 (1912).
7. K. OHKAWA, J. HIDAKA, and Y. SHIMURA. Bull. Chem. Soc. Jap. **40**, 2830 (1967).
8. A. VOGEL. A textbook of quantitative inorganic analysis. 3rd ed. Longmans, Green, and Co., London. 1962. p. 363.
9. D. A. BUCKINGHAM, I. I. OLSEN, A. M. SARGESON, and H. SATRAPA. Inorg. Chem. **6**, 1027 (1967).
10. A. J. MCCAFFERY, S. F. MASON, and B. J. NORMAN. J. Chem. Soc. 5094 (1965).
11. D. A. BUCKINGHAM, L. DURHAM, and A. M. SARGESON. Aust. J. Chem. **20**, 257 (1967).
12. Y. SHIMURA and R. TSUCHIDA. Bull. Chem. Soc. Jap. **29**, 311 (1956).
13. B. N. FIGGIS. Introduction to ligand fields. Interscience Publishers, New York. 1966. pp. 234–237.
14. W. L. JOLLY. The synthesis and characterization of inorganic compounds. Prentice–Hall, Inc., Englewood Cliffs, N.J. 1970. p. 333.
15. P. E. MERRIT and S. E. WIBERLY. J. Phys. Chem. **59**, 55 (1959).
16. M. E. BALDWIN. J. Chem. Soc. 4369 (1960).
17. M. N. HUGHES and W. R. MCWHINNIE. J. Inorg. Nucl. Chem. **28**, 1659 (1966).
18. J. M. RIGG and E. SHERWIN. J. Inorg. Nucl. Chem. **27**, 653 (1965).
19. K. GARBETT and R. D. GILLARD. J. Chem. Soc. 6084 (1965).
20. R. D. GILLARD and R. MASKILL. J. Chem. Soc. (A), 2813 (1971).
21. A. WERNER. Zeit. fur Anorg. Chem. **22**, 91 (1900).
22. K. KRISHNAN and R. A. PLANE. Inorg. Chem. **5**, 582 (1966).

Can. J. Chem. Downloaded from www.nrcresearchpress.com by 210.87.254.40 on 09/05/12
For personal use only.

An Ionization Chamber Study of Electron and Ion Decay in Irradiated Ammonia

D. R. McCracken and D. A. Armstrong

Department of Chemistry, University of Calgary, Calgary, Alberta T2N 1N4

Received July 9, 1973

Ionization chambers with plane parallel and coaxial electrodes have been used to study the ion and electron concentrations in ammonia subjected to 120 kvp X-ray pulses of 17 and 30 ms duration. Differences in the numbers of positive and negative ions collected on the application of pulses of high voltage imply that free diffusion of electrons to the cell walls occurs in the early part of the X-ray pulse until it is inhibited by the positive ion space charge. Thereafter, positive and negative ions decay at equal rates.

The rate constant for the neutralization reaction

$$e + NH_4^+.nNH_3 \rightarrow \text{Neutral products}$$

at 1200 Torr of ammonia and 297 °K was calculated to be $4.2 \pm 1.0 \times 10^{-5}$ cm^3 ion^{-1} s^{-1}. However, unless extensive precautions are taken to remove electron-attaching impurities reactions between $NH_4^+.nNH_3$ ions and impurity negative ions are dominant. The results are discussed and compared to other work on electron–ion neutralization reactions.

On a utilisé des chambres d'ionisation possédant des électrodes planes parallèles et coaxiales afin d'étudier les concentrations d'ions et d'électrons dans de l'ammoniaque soumis à des expositions de rayons-X (120 kvp) d'une durée de 17 et de 30 ms. Les différences dans le nombre des ions positifs et négatifs recueilli lors d'application d'impulsions de haut voltage impliquent qu'une diffusion libre des électrons vers les parois de la cellule se produit au début de l'exposition de rayons-X jusqu'à ce qu'elle soit arrêtée par la charge des ions positifs dans l'espace.

La constante de vitesse pour la réaction de neutralisation

$$e + NH_4^+.nNH_3 \rightarrow \text{produits neutres}$$

à 1200 Torr en ammoniaque et à 297 °K est égale à $4.2 \pm 1.0 \times 10^{-5}$ cm^3 ion^{-1} s^{-1}. Cependant, à moins de prendre de sérieuses précautions afin d'enlever les impuretés susceptibles de fixer des électrons, les réactions dominantes sont celles entre les ions $NH_4^+.nNH_3$ et les impuretés ioniques négatives. On discute les résultats et on les compare aux autres travaux sur les réactions de neutralisation ion-électron.

[Traduit par le journal]

Can. J. Chem., 51, 4159 (1973)

Introduction

Ion neutralization reactions are an essential component of the mechanism of any gas phase radiolysis and a knowledge of their nature is therefore necessary for a complete understanding of such systems. For example, it is important to know whether ion neutralization is predominantly homogeneous or whether it occurs at the walls of the radiation cell (1). Also, when homogeneous processes *are* involved it is desirable to determine whether these are two- or three-body in nature, since the energetics and dynamics are different.

Rate coefficients for the neutralization reactions of various pairs of negative and positive ions have already been reported (2). Also, measurements of ion decay in ionization chambers have been used to determine the three-body neutralization coefficient α for the ions formed by pulse-radiolysis in several electron-attaching gases such as air (3), oxygen (4), the hydrogen halides, and nitrous oxide (5). However, apart from studies in high temperature flames (6) and recent work on the neutralization of positive ions of aromatic hydrocarbons in nitrogen (7), there is a lack of information on electron–ion neutralization processes in systems where electrons may remain free at the temperatures and pressures typically employed in radiation chemistry. The purpose of this investigation was to study ion recombination in ammonia utilizing the pulsed-X-ray ion decay technique. Drift tube experiments (8) have shown electrons to remain free up to at least 170 Torr in this gas and from high

Can. J. Chem. Downloaded from www.nrcresearchpress.com by 210.87.254.5 on 09/05/12
For personal use only.

Can. J. Chem. Downloaded from www.nrcresearchpress.com by 210.87.254.5 on 09/05/12
For personal use only.

pressure mass spectrometric studies (9) the positive ions formed by radiation are known to be $NH_4^+.nNH_3$.

Experimental

Materials

Research grade ammonia from the Matheson Company was purified and stored in a mercury-free high vacuum system fitted with an oil diffusion pump and a Wallace–Tiernan pressure gauge. It was thoroughly degassed by pumping on it during sublimation from one trap to a second which was held at liquid nitrogen temperature. After this, except in a few initial experiments (see below), it was sublimed into a tube containing metallic sodium and liquified until the characteristic blue color of sodium solutions in ammonia had appeared. This procedure served to remove water and electron-attaching impurities. Any gases evolved were pumped off, and if deemed necessary the ammonia was subjected to a second set of sublimations. Finally, it was stored at liquid nitrogen temperature in a tube containing sodium.

Irradiation Cells

Some experiments were carried out in a cyclindrical Pyrex cell with plain parallel ends serving as electrodes. This cell, with length 2 cm and diameter 10 cm, had a continuous aluminized electrode at one end and a 4 cm diameter collecting electrode circumscribed by an insulating space of 2 mm and a 10 cm diameter guard ring at the other end. However, most experiments were conducted in coaxial cells of the type shown in Fig. 1. The electrodes were constructed by coating the Pyrex surface with graphite. Prior to use all cells were baked under vacuum at a temperature of 400 °C for a period of at least 10 h. In most experiments a small side arm containing a sodium mirror was attached to the ionization chamber.

Lifetime Apparatus

The X-ray unit and rotating sector have already been described (5). The pulse widths used here were 17.6 or 30 ms, each being followed by an identical decay period.

Apart from a few minor modifications the design of the electronic system and bridge circuit were essentially the same as those used by McGowan (3). At a set delay time after each ionizing pulse a high voltage was applied to an electrode within the cell for a period of about 4 ms and the charge due to ions remaining in the calibrated volume of the cell was collected on a second electrode connected through the bridge to the input of a dynamic capacitor electrometer (Victoreen 475A). The time constant of the electrometer was long relative to the time of revolution of the sector, so that a steady electrometer current was recorded. The number of ions collected per revolution is equal to the magnitude of this current divided by the frequency of rotation of the sector and the electron charge (3).

Procedures

The ionization chambers were attached to the vacuum line and after evacuation and baking were filled with freshly degassed ammonia to the desired pressure. The ammonia was then condensed in the side-arm of the cell and the cell sealed off under vacuum. Subsequently, the ammonia was liquified, allowing any remaining electron-attaching impurities to react with electrons produced by dissolution of the sodium mirror in those cases where one was present. Following this treatment the ammonia was slowly evaporated into the cell leaving any solid reaction products in the sidearm. The cell was then placed in position in the ion lifetime apparatus. All experiments reported here were performed at 297 ± 2 °K.

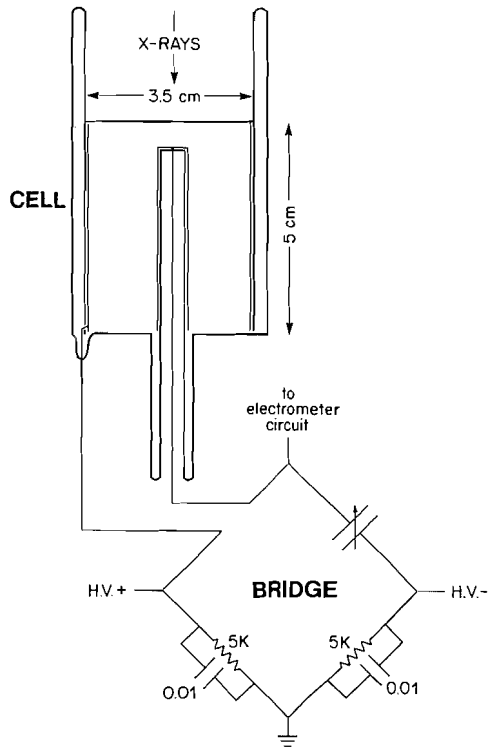

FIG. 1. Diagram of cylindrical cell with graphite coated coaxial electrodes. Cell is shown connected to bridge for (+,i) collection (see text).

Results and Interpretation

Effect of Oxygen and Electron-attaching Impurities

Typical behavior for an ammonia sample which was thoroughly degassed but had not been treated with sodium is illustrated in Fig. 2*a*. Assuming that the negative and positive ions have equal concentrations the value of α for homogeneous recombination is given by the slope of second-order plots of $1/n$ *vs.* decay time, where n is the ion concentration. Figure 2*a* gives such plots for n equal to the negative ion concentration for a 500 Torr sample of ammonia in the cylindrical cell with aluminum electrodes and guard ring. The line with closed circles was obtained

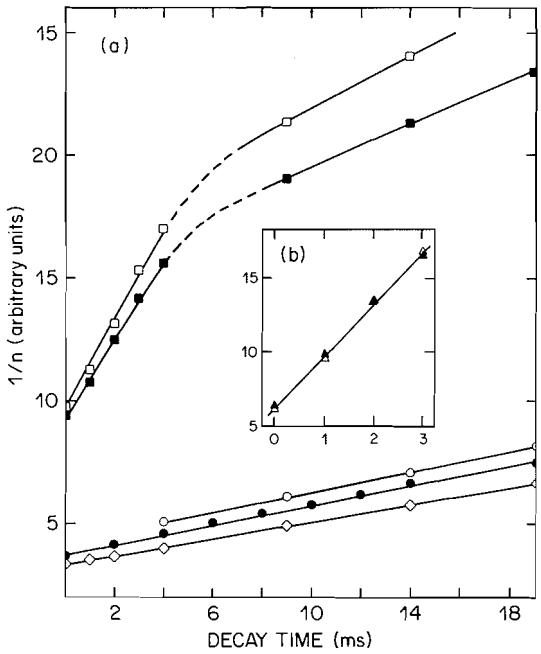

FIG. 2. Plots of $1/n$ *vs.* time: (*a*) Showing the effects of "radiation cleanup" and addition of oxygen for 500 Torr of NH_3 at 297 ± 2 °K in a cell with plane parallel aluminum electrodes. Accumulated doses in eV g^{-1} × 10^{-16} are: ●, ≃3; ○, ≃10; ■, ≃54; □, ≃100; and ◇, ≃100 after addition of ≃0.02 Torr of oxygen. (*b*) For 1200 Torr of "cleaned up" NH_3 at 297 ± 2 °K in a cell with coaxial graphite electrodes. △, after preirradiation to 10^{18} eV g^{-1}; ▲, same sample after treatment with sodium mirror.

immediately after preparation of the sample and gives $\alpha = 2.0 \times 10^{-6}$ cm^3 ion^{-1} s^{-1}. The other lines were observed after the doses stated in the figure caption had been absorbed by the sample. The increase in initial slope of the plots shows that α increases markedly with dose. The same type of behavior was observed in the cylindrical cells with graphite coated coaxial electrodes and in either cell at other pressures.

Using the G values for nitrogen and hydrogen production taken from the recent literature (10–12) it can be shown that the decomposition of 500 Torr of ammonia at a dose of 100×10^{16} eV per g would have been approximately 1.5×10^{-4}%. Since the products of irradiation, nitrogen and hydrogen, are non-polar and inert to electrons, at such small concentrations they should not influence the electron or positive ion reactions in the system. Furthermore, as has been previously reported (13) and further illustrated in Fig. 2*a*, the addition of minute traces of oxygen reduces the magnitude of α to 1.72×10^{-6} cm^3 ion^{-1} s^{-1}, which is typical of three-body ion neutralization coefficients in gases where the electrons are attached (5). We therefore attribute the change in α with initial irradiation in Fig. 2*a* to radiation removal of electron-attaching impurities. These are most likely to be oxygen and/or oxides of nitrogen, and they are probably converted to water and nitrogen in the reducing atmosphere of irradiated ammonia. The fact that the $1/n$ *vs.* time plots for irradiated ammonia in Fig. 2*a* bend over at decay times above 6 ms suggests that some long-lived ions are still present and that complete clean-up of electron-attaching impurities was not achieved at the doses given in Fig. 2*a*. However, as we shall see below the simple second order rate expression is not strictlyvalid under the present conditions and the curvature is due in part to this feature.

When the ammonia was liquified over sodium and thoroughly degassed prior to admission to the irradiation cell, values of α greater than 10^{-5} cm^3 s^{-1} were obtained without any previous irradiation treatment. When sodium was also present in the small side-arm attached to the ionization chamber and the ammonia was condensed on it after sealing off the cell, then very little pre-irradiation was required before the α value became independent of dose. At that point further treatment with sodium in the side-arm of the cell was also without effect. Figure 2*b* illustrates this for an ammonia sample at a pressure of 1150 Torr in a cell of the design shown in Fig. 1 with negative ions collected. The sample was irradiated to a total absorbed dose of about 10^{18} eV g^{-1} before the measurements plotted as open triangles were taken. It was then condensed on the sodium mirror and liquified. As shown in Fig. 2*b* this produced no change in the ion concentrations or the value of α.

The remainder of the experiments with ammonia were performed with samples which had been treated with sodium both prior to and after admission to the ionization chamber. They were also irradiated until no further change was observed in the ion concentrations before determinations of α were made.

Positive and Negative Ion Concentrations

For cells with coaxial geometry having a small axial electrode and a larger outer electrode four different collection arrangements are possible. First, the inner electrode can be attached

Can. J. Chem. Downloaded from www.nrcresearchpress.com by 210.87.254.5 on 09/05/12
For personal use only.

Can. J. Chem. Downloaded from www.nrcresearchpress.com by 210.87.254.5 on 09/05/12
For personal use only.

to the point on the bridge at which the electrometer is connected (see Fig. 1) and the outer electrode to the same bridge terminal as the positive lead from the high voltage pulser. This causes positive ions to be collected on the inner electrode and is henceforth signified by (+,i). Reversal of the polarity of the voltage pulser causes negative ions to be collected on the inner electrode and is referred to as (−,i). The electrometer can also be made to receive current from the outer electrode by simply reversing the leads to the cell. The collection modes (+,o) and (−,o) can then be achieved by appropriate choice of polarity of the voltage pulser.

Because of the novel character of the results with ammonia some preliminary observations with air are presented first. As well as providing a useful check on the apparatus, they permit direct comparison between the behavior in ammonia and a typical electron-attaching gas in the same cell. Figures 3*a* and *b* show plots of $1/n$ and n *vs.* time for 660 Torr of air in the cell with coaxial electrodes. The points at negative times in Fig. 3*b* are for runs in which the collection of ions was pushed back into the period of irradiation. In these cases the number of ions collected per sector revolution exceeds the number present at the instant the voltage was applied by an amount equal to the product of the period of overlap of the high voltage with the radiation and the rate of ion production. The latter quantity can be determined by measuring the rate of ionization with the sector stopped. The ion concentrations at negative times in Fig. 3*b* were all corrected in this way. The concentrations of negative ions observed for (−,i) collection are seen to be identical for collection times of 1.5 and 4 ms and to be the same within experimental error as the positive ion concentrations for (+,i) collection.

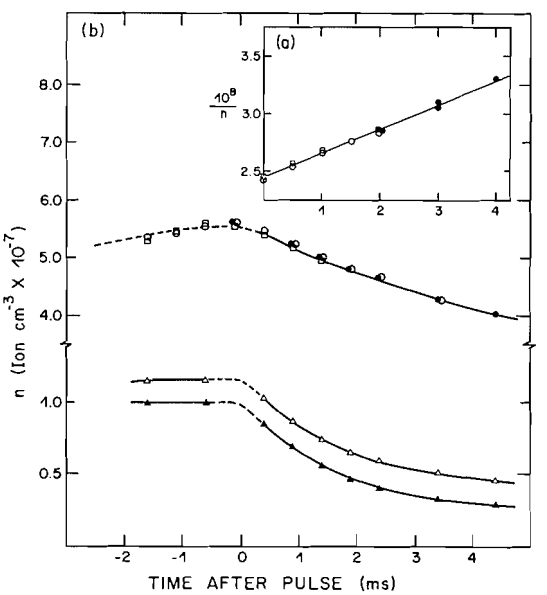

FIG. 3. Plots of $1/n$ and n *vs.* time after radiation pulse for air and ammonia in the cell with coaxial electrodes. Points on the line in Fig. 3*a* and upper curves in 3*b* are for 660 Torr of air with: ●, 1.4 ms (−,i) collection; ○, 4 ms (−,i) collection; and □, 4 ms (+,i) collection. Points on the two lower curves in Fig. 3*b* are for 1200 Torr of ammonia with: ▲, 4 ms (−,i) collection; and △, 4 ms (+,i) collection, respectively.

The slope of the single line through the second order plots in Fig. 3*a* gives $\alpha = 1.57 \times 10^{-6}$ cm^3 ion^{-1} s^{-1}, in good agreement with 1.63×10^{-6} observed by McGowan (3) for untreated laboratory air at a similar ion density and ion age. The line drawn through the data in Fig. 3*b* was calculated from this value of α and the steady ionization rate (6.12×10^9 ion pairs cm^{-3} s^{-1}).

The two lower lines in Fig. 3*b* are respectively the electron and positive ion concentrations calculated from the (−,i) and (+,i) ion currents for 1200 Torr of ammonia with a 4 ms collection period. The end of pulse concentrations are close to a steady state situation and when taken in conjunction with the rate of ionization during the radiation pulse (3.44×10^9 ion pairs cm^{-3} s^{-1}) they require $\alpha > 3 \times 10^{-5}$ cm^3 ion^{-1} s^{-1}, which is to be compared with similar high values from plots such as Fig. 2*b* and with $2.5 \pm 0.5 \times 10^{-5}$ cm^3 ion^{-1} s^{-1} previously reported (13) for ammonia at 500 Torr.

Of special interest is the significant difference between the positive ion and electron concentrations, which clearly exists before the end of the radiation pulse and continues through the decay period. Its occurrence is in complete contrast to the straightforward behavior discussed above for air and previously observed in other electron-attaching gases studied in this laboratory. Furthermore, there was no difference between the positive and negative ion concentrations for ammonia to which traces of oxygen had been added or from which the electron-attaching impurities had not been removed. For these reasons and because electrons have much higher diffusion coefficients and mobilities than molecular ions the present behavior in purified am-

Can. J. Chem. Downloaded from www.nrcresearchpress.com by 210.87.254.5 on 09/05/12
For personal use only.

monia is attributed to losses of electrons which occur prior to the application of the collecting field. Mechanisms for this are considered below.

From experiments on the drift velocity of electrons in gaseous ammonia (8, 14) it can be shown that the diffusion coefficient of electrons at 297 °K and 1200 Torr should be 3 ± 1 cm^2 s^{-1}. By contrast the ammonium positive ions which would be clustered at our pressure by 5 or more ammonia molecules (9) will have a diffusion coefficient of about 0.015 cm^2 per s. (This has been calculated from expression (9–3–14) of ref. 15.[1]) Theoretical (17) and experimental studies (15) on plasmas have shown that when such a disparity in diffusion coefficients exists a significant fraction of the electrons produced during the ionization period may diffuse to the walls of the cell before their movement becomes controlled by the space charge resulting from the excess of positive ions which builds up in the body of the cell and the growing wall potential. At this point the effective diffusion coefficient of the electrons, D_s, falls appreciably below the free diffusion coefficient, D_e, while that of the positive ions rises above D_+, causing the wall currents of electrons and positive ions to become equal (17, 18). Assuming no stray potentials or imbalance of the bridge, the number of electrons diffusing to the inner and outer electrode in the cells with coaxial geometry should be in the first approximation proportional to their areas.[2] Since the inner one has one quarter of the area of the outer, 80% of the electrons which diffuse to the two electrodes during the period of free diffusion will be lost for (−,i) collection, whereas only 20% will be lost for (−,o) collection. Thus, the difference between the apparent electron concentrations derived from (−,o) and (−,i) collection should correspond to approximately 60% of the wall loss of electrons during the period of free diffusion.

Wall diffusion of electrons will also effect the apparent concentration of positive ions. When positive charge is collected the net current recorded by the electrometer is the difference between the number of positive ions arriving at the electrode during the period of collection and the number of electrons which reached it during the period of free diffusion. There should therefore be correspondence between the apparent ion concentrations derived from (+,i) and (−,o) ion currents and between those from (−,i) and (+,o). This correspondence is established in Fig. 4*a* in which plots of apparent ion concentration *vs.* time for all four methods of collection are presented. The 1200 Torr sample of ammonia was irradiated with the same X-ray intensity for each collection mode and the pulse widths were 17.0 ms.

The high mobility of electrons in ammonia (~ 150 cm^2 s^{-1} V^{-1} calculated from data in ref.

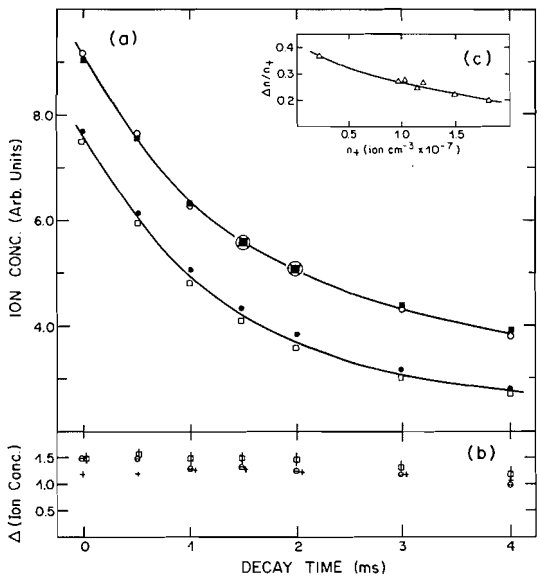

FIG. 4. Apparent ion concentrations *vs.* time for a 1200 Torr sample of ammonia in the cell with coaxial electrodes. (*a*) Apparent ion concentrations for □, (+,o); ●, (−,i); ■, (+,i); and ○, (−,o) plotted as a function of decay time. (*b*) For the same sample as in (*a*) above: ⊞, difference between n_+ from (+,i) and (+,o) collection; ⊖, difference between n_- from (−,o) and (−,i) collection; For a duplicate sample: +, difference between n_+ from (+,i) and (+,o). (*c*) $\Delta n/n_+$ (see text) plotted as a function of n_+.

[1]This expression actually gives the ion mobility K_+. However for our conditions the identity $D = KkT/e$ should hold (15). It should also be noted that the calculated value of K_+ (and hence D_+) for $NH_4^+.nNH_3$ does not change drastically with n, 0.82 and 0.60 cm^2 V^{-1} s^{-1} for $n = 4$ and 8, respectively (*cf.* 0.74 and 0.67 for positive ion clusters of $n = 2$ and 4 in H_2O (16)).

[2]The above analysis is approximate since the ends which constitute some 20% of the total area of the cell walls are neglected. However, electron loss to these insulating surfaces should be much less than to the electrodes, for while the former will build up a wall potential negative charge arriving at the electrodes will leak away through the electrometer or bridge circuit. Thus the positive ion space charge will be the single important factor controlling electron diffusion to the electrode surfaces. By the same token one may expect somewhat larger electron deficits in our cells than in systems without only insulating walls.

Can. J. Chem. Downloaded from www.nrcresearchpress.com by 210.87.254.5 on 09/05/12
For personal use only.

14 as opposed to 0.5 to 3 for molecular ions, *cf.* ~2.2 for O_2^- in oxygen from ref. 19) means that stray potentials arising from minor imbalances in the bridge circuit or contact potentials in the cell electrodes could also cause a preferential electron current to the outer electrode. The complete reversibility of the system as exemplified in Fig. 4*a* eliminates any possibility of a large contribution from circuit imbalance. The effect of contact potentials is harder to assess. However, when subjected to continuous irradiation and connected to the electrometer with no applied potential, the cells used here usually gave only small ionization currents,[3] and in some instances, as for example the cell with the ammonia used for the experiments in Fig. 4*a*, the ionization current corresponded to electron transport to *the inner* electrode, not the outer. Also the electron deficit was reproducible from one coaxial cell to another and was observed in the 10 cm diameter cell with plane parallel aluminum electrodes. These observations lead to the conclusion that it is primarily caused by free diffusion of the electrons and not by fortuitous contact potentials.

To determine whether the electrons continued to diffuse independently of the positive ions during the period of decay, the differences between the (−,o) and (−,i) concentrations and between the (+,i) and (+,o) concentrations were plotted as a function of time after the irradiation pulse in Fig. 4*b*. A similar plot of the difference between (+,i) and (+,o) for a different run under similar conditions is given for comparison. In all three instances the magnitude of the difference is seen to remain reasonably constant and perhaps to decrease slightly at longer times. This confirms that free diffusion of electrons has ceased at the end of the pulse, if not before. The magnitude of the fractional electron deficit $\Delta n/n_+$ $(=(n_+ - n_-)/n_+)$ calculated from the ion concentrations is shown as a function of the positive ion concentration n_+ in Fig. 4*c*.

Kinetics of the Ion and Electron Decay

The electron deficiencies noted above have quite far-reaching kinetic consequences. First, although the initial slopes of $1/n_+$ or $1/n_e$ *vs.* time plots are linear and provide an estimate of α and a useful measure of the purity of the ammonia samples, the simple rate expression.

$$[1] \qquad \alpha t = \frac{1}{n} - \frac{1}{n_0}$$

does not apply. Secondly, the spatial distributions of the electrons and positive ions at the end of the pulse differ. Thirdly, as the ion concentrations decrease during the decay period the rate of diffusion of both electrons and positive ions to the wall will increase. This is shown both by the theoretical analysis of Allis and Rose (17) and recent experiments (18). In the light of these facts we chose to avoid the use of integrated rate expressions, and calculated the neutralization coefficient from the slopes of ion decay plots and the concentrations of electrons and positive ions at 1 ms after the irradiation pulse. These values are referred to as α_{app}, since they require correction for spatial inhomogeneity and the wall diffusion contribution to decay.

Both the present experimental data in Fig. 4*c* and theoretical work (17, 18) show that $(n_+ - n_-)/n_+$ becomes smaller as n_+ increases. Furthermore, it is well known that the contribution of wall diffusion to α_{app} decreases with ion density (20). Therefore to minimize the uncertainty from these two sources values of α_{app} were plotted against $1/n_+$ in Fig. 5 and extrapolated to $1/n_+ = 0$. The intercept gave $\alpha = 4.2 \times 10^{-5}$ cm^3 ion^{-1} s^{-1} for ammonia at 298 °K and 1200 Torr. The remaining uncertainty should not exceed ±25%, which is the magnitude of $(n_+ - n_-)/n_+$ at $n_+ = 1.5 \times 10^7$ (see Fig. 3*c*).

Discussion

The effects illustrated in Fig. 2*a* demonstrate the need for extreme care in ensuring the removal of electron-attaching impurities from gases which

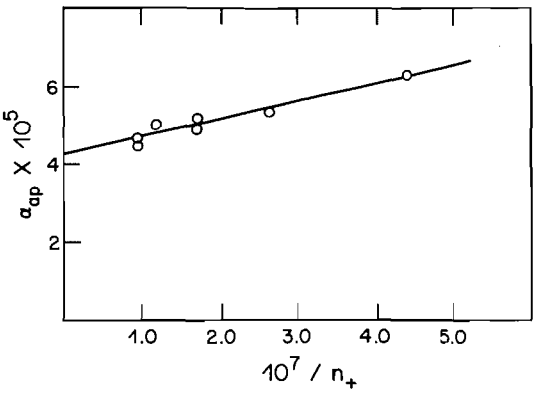

FIG. 5. Plot of α_{app} *vs.* $1/n_+$.

[3]Approximately 0.1% of the saturation ionization current with applied voltage.

Can. J. Chem. Downloaded from www.nrcresearchpress.com by 210.87.254.5 on 09/05/12
For personal use only.

are themselves unreactive toward electrons.[4] This is particularly serious in low dose-rate studies with Co^{60} sources which produce steady state ion concentrations of $n_+ \lesssim 10^8$ ion cm^{-3}. Here as little as $4 \times 10^{-4}\%$ of an impurity with a three-body attachment coefficient of $\sim 4 \times 10^{-30}$ cm^6 $molecule^{-2}$ s^{-1} (*cf.* oxygen, Table 6.7 of ref. 14) in a non-attaching gas at normal pressure will scavenge all electrons, altering the nature of the ion neutralization reactions until cleanup has been achieved. For other impurities with two-body electron capture reactions even lower levels of impurity may be required. The present experience with ammonia shows that pumping during sublimation does not remove all attaching components. Thus, impurities other than oxygen may be present.

Electron deficits do not appear to have been recognized previously in gases under conditions relevant to radiation chemistry. However, as indicated above the present observations are qualitatively in accord with theoretical and experimental studies of low pressure plasmas. Furthermore the mathematical analysis of Kregel (21) for Frieberg and Weaver's data (22) on isothermal helium plasmas leads to electron deficits of $1–2 \times 10^6$ cm^3. These are in the same range as the deficiencies that can be calculated from our data (*cf.* Figs. 3*b* and 4*c*), and they give comparable electrical fields of 0.5–1.5 V at the cell perimeters (21).

Ion–ion neutralization reactions in gases at normal pressure typically have neutralization coefficients of 3×10^{-6} ion cm^{-3} s^{-1} or less (5, 15) and the present value of α is some ten to twenty times larger. In a preliminary note (13) this was attributed to the approximately hundred-fold larger relative velocity for electron–ion collisions, and it should be noted that the three other neutralization reactions reported to have $\alpha \gtrsim 10^{-5}$ cm^3 ion^{-1} s^{-1} involve collisions of this type. Thus, the room temperature rate constant for hydronium neutralization

[2] $e + H_3O^+ \rightarrow$ Neutral products

calculated from the flame ionization data of Kelly and Padley (6) is 8×10^{-6} cm^3 ion^{-1} s^{-1}, and Lawrence and Firestone (23) have reported $k_3 = 7.6 \times 10^{-4}$ cm^3 ion^{-1}

[3] $e + CH_5^+ \rightarrow$ Neutral products

from a competition kinetic study. More recently Sauer and Mulac (7) have observed a value in excess of 10^{-5} cm^3 ion^{-1} s^{-1} for k_4

[4] $e +$ naphthalene$^+ \rightarrow$ Neutral products

in a pulse radiolysis study.

In addition to the high relative velocity of approach large neutralization coefficients require an efficient mechanism for stabilization of the electron–ion pair. In this connection it should be noted that the positive NH_4^+ ions would have been heavily clustered in ammonia at the temperatures and pressures used here. Indeed from the results of high pressure mass spectrometry (9) we conclude that the proportion of ions with n less than 5 taking part in reaction 5

[5] $e + NH_4^+.nNH_3 \rightarrow$ Neutral products

would have been negligible. Furthermore, n may be as large as twenty, and ionic radii of 8 Å and higher may be expected. Since the electron may approach to within 13 Å or less of the positive ion,[5] the chances of its exciting vibrations in the cluster are relatively high and clustering may greatly enhance the cross section for stabilization in two body encounters. Further work will be required before the relative importance of this and other possible mechanisms of stabilization, such as radiation emission and collision with a neutral molecule, can be established. Continued investigations of the present kind should yield information concerning the temperature and pressure dependence of α in ammonia. It is also expected that the work will be extended to hydrocarbons and other gases of common interest to radiation chemists.

The authors are indebted to Dr. D. E. Wilson for many helpful discussions and for contributing to experimental data during the early part of this work. They also

[4]It is worth noting that a 60% increase in the electron drift velocity in ammonia was observed under conditions which caused a 20% decomposition (8). Since no special precautions to remove electron-attaching impurities were reported it would seem that these effects could have been due to the slowing of the electron drift by attachment–detachment reactions with impurities, which were cleaned up on long exposure to electrons as in the present instance. The value of D_e in NH_3 at 1200 Torr may therefore be larger than 3 cm^2 s^{-1} calculated above.

[5]From collision theory it can be shown (*cf.* ref. 2) that the cross section derived from $\alpha = 4.2 \times 10^{-5}$ cm^3 ion^{-1} s^{-1} effectively corresponds to approach of the electron to a distance of 13 Å or less from the positive charge. Strong interactions with the clustered molecules should therefore occur.

acknowledge the financial assistance of the National Research Council of Canada and the University of Calgary, and a helpful discussion with Dr. G. R. Freeman.

1. T. W. WOODWARD and R. A. BACK. Can. J. Chem. **41**, 1463 (1963).
2. B. H. MAHAN and J. C. PERSON. J. Chem. Phys. **40**, 392 (1964); G. H. FISH, B. H. MAHAN, and E. K. PARKS. J. Chem. Phys. **48**, 2649 (1967).
3. S. MCGOWAN. Phys. Med. Biol. **10**, 25 (1965).
4. S. MCGOWAN. Can. J. Phys. **45**, 439 (1967).
5. D. E. WILSON and D. A. ARMSTRONG. Can. J. Chem. **48**, 598 (1970).
6. R. KELLY and P. J. PADLEY. Trans. Faraday Soc. **66**, 1127 (1970).
7. M. C. SAUER, JR. and W. A. MULAC. J. Chem. Phys. **55**, 1982 (1971).
8. J. L. PACK, R. E. VOSHALL, and A. V. PHELPS. Phys. Rev. **127**, 2084 (1962).
9. A. M. HOGG and P. KEBARLE. J. Chem. Phys. **43**, 449 (1965); A. M. HOGG, R. M. HAYNES, and P. KEBARLE. J. Am. Chem. Soc. **88**, 28 (1966).
10. G. R. A. JOHNSON and M. SIMIC. Adv. Chem. **82**, 197 (1968).
11. J. A. EYRE and D. SMITHIES. Trans. Faraday Soc. **63**, 241 (1970).
12. A. W. BOYD, C. WILLIS, and A. O. MILLER. Can. J. Chem. **49**, 2283 (1971).
13. D. E. WILSON and D. A. ARMSTRONG. J. Phys. Chem. **75**, 444 (1971).
14. L. G. CHRISTOPHOROU. Atomic and molecular radiation physics. Wiley, New York. 1971.
15. E. W. MCDANIEL. Collision phenomena in ionized gases. Wiley, New York, N.Y. 1964.
16. H. EIBER. Z. Angew. Phys. **15**, 103 (1962).
17. W. P. ALLIS and D. J. ROSE. Phys. Rev. **93**, 84 (1954).
18. R. A. GERBER, M. A. GUSINOW, and J. B. GERARDO. Phys. Rev. A**3**, 1703 (1971).
19. L. HARRISON and J. L. MORUZZI. J. Phys. D: Appl. Phys. **5**, 1239 (1972).
20. E. P. GRAY and D. E. KERR. Ann. Phys. **17**, 276 (1959).
21. M. D. KREGEL. J. Appl. Phys. **41**, 1978 (1970).
22. R. J. FREIBERG and L. A. WEAVER. Phys. Rev. **170**, 336 (1968).
23. R. H. LAWRENCE and R. F. FIRESTONE. Adv. Chem. **58**, 278 (1966).

Can. J. Chem. Downloaded from www.nrcresearchpress.com by 210.87.254.5 on 09/05/12
For personal use only.

Ring C Functionalized Diterpenoids. Part II.[1] Cleavage of the Cyclopropane Ring in Methyl *ent*-Trachyloban-19-oate with Thallic Acetate

HELEN MARGARET CAMPBELL, PATRICK ALISTAIR GUNN, ALAN JAMES MCALEES, AND ROBERT MCCRINDLE[2]

Chemistry Department, University of Guelph, Guelph, Ontario N1G 2W1

Received July 26, 1973

Reaction of methyl *ent*-trachyloban-19-oate (**1***a*) with thallic acetate gave four major products including the *ent*-atisane derivatives, **2–4**. Since the substrate is readily obtainable from the common sunflower, this reaction provides a valuable route to these and related compounds. The fourth compound, **5**, may derive from an *ent*-atisane intermediate by contraction of ring D.

La réaction de l'*ent*-trachylobanoate-19 de méthyle avec l'acétate thallique a conduit à quatre produits majeurs dont les dérivés **2–4** de l'*ent*-atisane. Puisque le substrat est facile à isoler du tournesol commun, cette réaction permet donc d'obtenir aisément ces différents produits. Le quatrième composé, **5**, peut provenir d'un intermédiaire *ent*-atisane par contraction du cycle D. [Traduit par le journal]

Can. J. Chem., **51**, 4167 (1973)

As indicated in the preceding paper, we have been interested in synthesizing ring C oxygenated diterpenoids, among them 13-substituted *ent*-atisanes. Consideration of short yet potentially efficient routes to the latter led us to investigate the reaction of methyl *ent*-trachyloban-19-oate (**1***a*) with thallic acetate in acetic acid. It was anticipated that this oxidative cleavage would lead to functionalized derivatives of the type required since **1***b* is known to give predominantly isoatisirene (**6**) when exposed to electrophilic reagents such as protonic (2, 3) or Lewis (4) acids. The present paper deals with the four major products obtained by oxidative cleavage of **1***a* with thallic acetate and indicates that this reaction does indeed provide a useful route to 13-substituted *ent*-atisanes.

Extraction (1) of sunflower (*Helianthus annuus*) heads, depleted of seeds, afforded *ent*-trachylobanic acid, the methyl ester (**1***a*) of which was then treated with thallic acetate in acetic acid at 75° for 4 days. The fractions obtained by chromatography of the product over alumina fell, on t.l.c. analysis, into four main groups. The first of these consisted of substrate (20%). The second group (38%, based on substrate consumed) obviously contained several compounds and indeed subsequent investigations of these fractions have revealed the presence of at least 12 components, olefinic monoacetates and ketones. The next group (26%) comprised three diacetates while the ultimate fractions (*ca.* 7%) contained more polar compounds which have not yet been examined further. Four of the reaction products were present in major amount, two olefinic monoacetates and two diacetates. The former pair were contained in several of the more polar fractions in the second group. Since these could not be resolved readily by preparative t.l.c. they were combined and subjected to mild hydrolysis with sodium hydroxide in aqueous methanol, conditions which did not affect the carbomethoxy group. The two major components of the resulting mixture were separated and purified by preparative t.l.c., first on silica gel and then silica gel – silver nitrate (12%). The less polar of the two was an allylic alcohol (**7***a*; 8%),[3] m.p. 163–164°. Multiplets at τ 4.11 (d, 1 H-14), 4.48 (q), and 6.57 (d) and singlets at τ 9.54 (3 H-20), 8.89 (3 H-17), and 8.83 (3 H-18) show the presence of an isolated allylic system (*cf.* ref. 5) and of three quaternary methyl groups respectively. The high-field position of the C-20 methyl resonance results from shielding by the Δ^{13} olefinic bond (5, 6). The hydroxyl group is placed at C-12 rather than at C-14 since a very large downfield shift of the C-17 methyl group resonance is observed upon addition of tris(dipivaloylmethanato)europium ($Eu(dpm)_3$), the normalized (7) ratio of the shifts induced in the methyl resonances being 10:2.7:1.4 for C-17,

[1]For Part I see ref. 1.

[2]To whom correspondence should be addressed.

[3]The numbering system used for formulae **5** and **7** is not systematic but rather a consequence of mechanistic considerations.

Can. J. Chem. Downloaded from www.nrcresearchpress.com by 210.87.254.5 on 09/05/12
For personal use only.

C-20, and C-18, respectively. Use of the shift reagent also resolves the two doublets ($J = 11$ Hz) expected for the isolated C-15 methylene group. The observation that the magnitude of the lanthanide induced shift of the resonance of one of these protons (the α proton) is even greater than that of the C-17 methyl resonance (normalized ratio 10:7.7, respectively) allows assignment of the β configuration to the hydroxyl function. Conversion of the allylic alcohol (**7***a*) into the corresponding acetate (**5**) and ketone (**7***b*) and a study of their spectroscopic properties reinforced our conclusions concerning the structure of **7***a*. Further support for this structural assignment comes from the plausible nature of the mechanism one may write (see below) to explain the formation of **5** from **1***a*. It was shown by analytical t.l.c. on silica gel and silver nitrate – silica gel that the acetate (**5**) prepared from **7***a* was indeed a major product in the original monoacetate fraction.

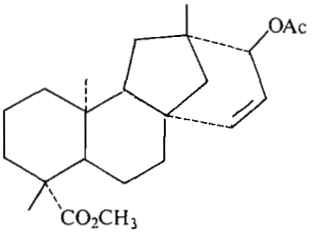

5

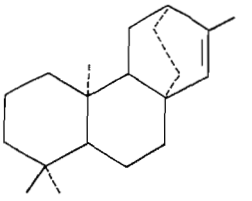

6

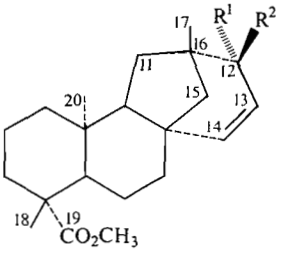

7

a $R^1 = H; R^2 = OH$
b $R^1 + R^2 = O$

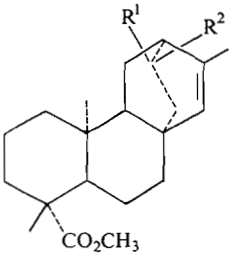

8

a $R^1 = H; R^2 = OH$
b $R^1 + R^2 = O$
c $R^1 = R^2 = H$
d $R^1 = H; R^2 = OTs$
e $R^1 + R^2 = SCH_2CH_2S$

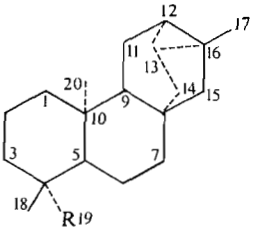

1

a $R = CO_2CH_3$
b $R = CH_3$

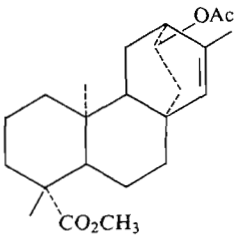

2

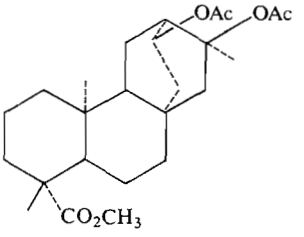

3

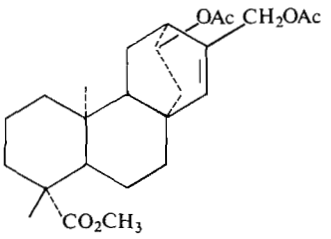

4

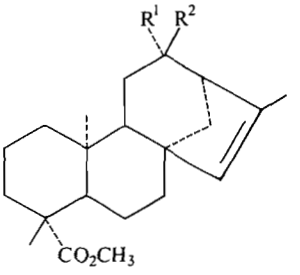

9

a $R^1 = H; R^2 = OAc$
b $R^1 + R^2 = O$
c $R^1 = R^2 = H$
d $R^1 = H; R^2 = OTs$

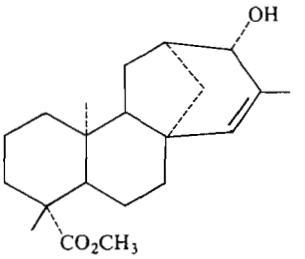

10

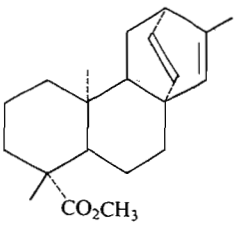

11

Can. J. Chem. Downloaded from www.nrcresearchpress.com by 210.87.254.5 on 09/05/12
For personal use only.

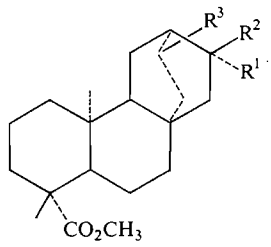

12

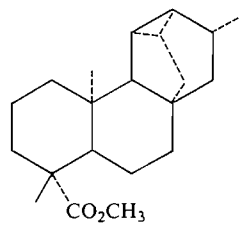

13

a $R^1 = CH_3$; $R^2 = H$; $R^3 = OH$
b $R^1 = H$; $R^2 = CH_3$; $R^3 = OH$
c $R^1 = CH_3$; $R^2 = H$; $R^3 = OTs$
d $R^1 = CH_3$; $R^2 = H$; $R^3 = OAc$

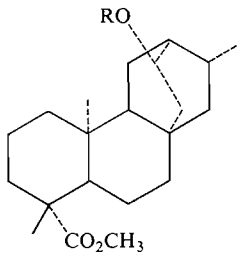

14

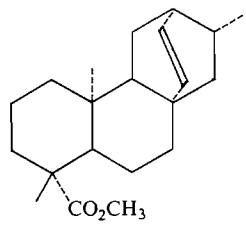

15

R = $-C(CH_3)_2CH_2CH_3$

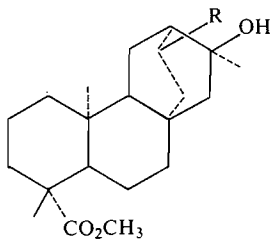

16

a R = OH
b R = OAc

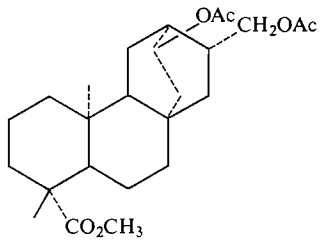

17

The second component isolated from the hydrolysis mixture was the hydroxy ester **8***a* (10%), m.p. 124°, acetylation of which yielded **2**, m.p. 130–132°, the major constituent of the entire monoacetate fractions (t.l.c. evidence). Easily identified in the n.m.r. spectra of **2** and **8***a* are resonances attributable to two tertiary methyl groups, a carbinyl like proton, and a proton and a methyl group attached to an olefinic bond. The presence of these structural features and of —OH···π hydrogen bonding in the i.r. spectrum of **8***a* led us to consider two structures **2** and **9***a*, obtainable from **1***a* by scission of the C_{13}—C_{16} or C_{12}—C_{16} bonds, respectively, for the acetate. The former alternative was soon judged as more acceptable for three reasons. First, on mechanistic grounds, it was anticipated by analogy with the reaction of trachylobane (**1***b*) with acids (see above) that the C_{13}—C_{16} bond would be more susceptible to electrophilic attack. Second, the values of the chemical shift of the olefinic proton for the alcohol (τ 4.35) and the acetate (τ 4.27) accord more closely with those expected (8, 9) for isoatisirene (*ca.* τ 4.2–4.5) rather than isokaurene (*ca.* τ 5) derivatives. Third, in the n.m.r. spectrum of the derived ketone, m.p. 176–179°, if the structure were **8***b*, 2 H-14 should give rise to an AB quartet while in **9***b* the equivalent geminal pair of protons α to the ketonic carbonyl should show additional coupling to H-9. In fact the ketone shows a clean doublet (τ 7.39) with a spin–spin coupling (J_{AB} = 19 Hz) of the magnitude predicted (10) for a methylene group α to a carbonyl. This resonance is ascribed to the α-oriented hydrogen[4] at C-14. Unfortunately, the resonance due to the β-hydrogen, which is shielded by the double bond, is obscured by other resonances at higher field, even when the spectrum is recorded in benzene or in the presence of $Eu(dpm)_3$.

Since none of these arguments is compelling, more convincing proof of the structure of these compounds was sought. An obvious possibility would be to remove the oxygen function from ring C, thus forming **8***c* or **9***c*, both known (9) compounds, and two attempts were made to accomplish this. In the first, the possibility of forming the *p*-toluenesulfonate **8***d* or **9***d* and then removing this group reductively with lithium aluminum hydride was explored. However, as feared (*cf.* ref. 11), although the ester formed, it decomposed on work-up and gave[5] the alcohol **10**. It should be noted that the production of **10** does not serve to distinguish be-

[4]In this paper substituents designated α or β on the α-bridge of rings C–D refer to orientations *syn* and *anti* to C-20, respectively.

[5]To be published; A. J. McAlees and R. McCrindle.

Can. J. Chem. Downloaded from www.nrcresearchpress.com by 210.87.254.5 on 09/05/12
For personal use only.

Can. J. Chem. Downloaded from www.nrcresearchpress.com by 210.87.254.5 on 09/05/12
For personal use only.

tween the possible structures of the tosylate, **8***d* or **9***d*, since *both* could readily rearrange to this alcohol. In the second attempt, the thioketal of the ketone (**8***b* or **9***b*) was prepared and treated with freshly prepared Raney nickel in acetone. The only pure product isolated by preparative t.l.c., in small yield, was an unstable diene, m.p. 132–136°, *m/e* 314, of probable structure **11**. It has n.m.r. resonances attributable to three olefinic protons at about τ 4, a methyl attached to a double bond, and two tertiary methyls, one of which (C-20) is strongly shielded by the new double bond and resonates at τ 9.58. A minute fraction, which appeared to be the expected isoatisirene **8***c* from its t.l.c. and g.l.c. behavior, was also isolated. There was no detectable amount of the isokaurene derivative **9***c* in the product. It seems likely that two major effects combine to reduce very severely the yield of the desired product, namely, the steric hindrance experienced by C-13 from the C-20 methyl group and the ease with which the system rearranges. Thus intermediate radicals at C-13 rather than attaching hydrogen atoms might form **11** or rearrangement products. In any event the reaction did not provide unambiguous proof of the structure of the substrate and therefore one further attempt was made to achieve this.

Catalytic hydrogenation of **8***a* afforded two alcohols the structures of which were readily assigned. The major, m.p. 134–135°, is the less polar on t.l.c. as would be expected if the hydroxyl and the C-17 methyl group interact sterically as in **12***a*. This conclusion gained strong support from the observation that $Eu(dpm)_3$ induces a much larger chemical shift change for the C-17 methyl in **12***a* (normalized ratio, C-17: C-20:C-18, 10:2.8:1.3) than in the minor alcohol **12***b*, m.p. 121–123° (corresponding ratio, 10:7.3:3.1). The tosylate (**12***c*) of the major alcohol when exposed to sodium *t*-amylate in *t*-amyl alcohol at 85° for 15 h formed three products (*cf.* ref. 12) which were separated by preparative t.l.c. on silver nitrate–silica gel. Structures were assigned to the two less polar, minor, products on chromatographic and spectral evidence only. The least polar of the three has *m/e* 316 (M) and an identical t.l.c. mobility to that of **1***a* on silver nitrate – silica gel but a slightly longer g.l.c. retention time on SE-30. Since its n.m.r. spectrum is devoid of resonances attributable to an olefinic proton but does indicate the presence of one secondary and two tertiary methyl groups in the molecule it may be formulated as **13**. The compound of intermediate polarity was readily recognized as a *t*-amyl ether from the complexity of the methyl region in its n.m.r. spectrum and the molecular ion peak at *m/e* 404 and the expected fragmentation pattern in its mass spectrum. Bearing in mind its genesis it may be assigned the tentative structure **14**. The most polar, major product, m.p. 89–93°, had n.m.r. signals from two olefinic protons (τ 4.05, d, J_{obs} = 4 Hz) and one secondary and two tertiary methyl groups. Two distinct pieces of evidence allowed a firm assignment of structure (**15**) to the compound. First, one of the tertiary methyl groups resonates at τ 9.61. This reveals that the double bond is exerting a marked shielding effect on the C-20 methyl group as is found in isoneoatisirene derivatives (6) but not in Δ^{11}-kaurenes (1, 13). Second, one of the most intense peaks in its mass spectrum appears at *m/e* 274(M − 42) and results from a retro-Diels–Alder reaction, a mode of cleavage which is unavailable to Δ^{11}-kaurenes. Thus the major component in the monoacetate fraction from the oxidative cleavage could be formulated as **2** rather than **9***a*.

The diacetate fraction, which contained three components, was subjected to preparative t.l.c. This yielded very major portions of both the most and the least polar of these in an essentially pure state. The remaining, minor, component has not been obtained free of the former. The n.m.r. spectrum of the least polar diacetate **3**, m.p. 162–163°, has a broad multiplet at τ 5.14 arising from a proton of the type C*H*OAc but no other low-field signals. Also present are singlets attributable to three methyl groups at τ 9.24 (C-20), 8.87 (C-18), and 8.42 (C-17), the chemical shift of the last reflecting its attachment to a carbon atom which in addition bears an acetate group. The similarity of several aspects of this n.m.r. spectrum to that of **2**, bearing in mind the expected (14) *trans* addition involved in the opening of the cyclopropane ring, led to a tentative assignment of structure **3** to this compound. The following transformations fully endorsed this conclusion. Pyrolysis of the diacetate at 200°/15 mm gave **2** while hydrolysis afforded the diol **16***a*, m.p. 220–221°. Significantly, i.r. spectra of dilute solutions of the derived diol monoacetate **16***b*, ν_{OH} 3612 cm^{-1}, show no evidence of intramolecular hydrogen bonding and thus the configuration at C-16 must

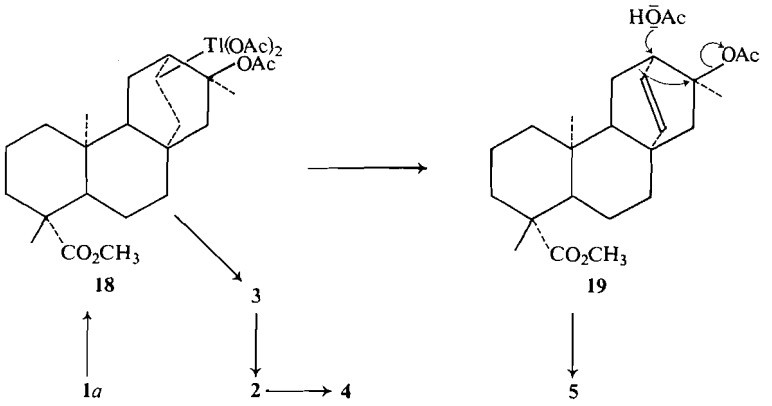

SCHEME 1

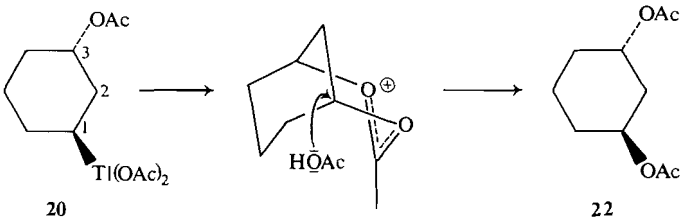

SCHEME 2

be as shown in **16** and **3**. A plausible structure (**4**) for the most polar diacetate was readily deduced by comparing its n.m.r. spectrum with that of **2**, the only outstanding difference being that the resonance at τ 8.24 (3 H-17) in the latter is replaced by one at τ 5.52 (2 H-17) in the former. Evincive evidence for this structure was obtained by subjecting the diacetate to hydrogenation in ethanol–triethylamine over palladized charcoal. One of the two products was simply the oily dihydro derivative **17**; however the other product was **2**, formed by hydrogenolysis of the allylic acetate group. It is noteworthy that **12***d* was not detected in the product.

The production, in reasonable yield, of **2** (10%), **3** (18%), and **4** (6%) by oxidative cleavage of methyl *ent*-trachyloban-19-oate represents an effective route to synthetically versatile *ent*-atisane intermediates. Especially attractive are the following aspects. The substrate is readily obtained from the common sunflower. The yield of monoacetate **2** can be bolstered, if desired, by its formation from **3** (*ca.* 90%) and **4** (*ca.* 55%). Finally, the axial substituent at C-4 provides a handle for the introduction of substituents into rings A and B.

Work is progressing on the minor products from the oxidative cleavage of **1***a* and the results will be presented later along with a detailed discussion of the mechanistic pathways to the various products. However, a provisional scheme which satisfactorily explains the production of compounds **2–5** is outlined (see Scheme 1, **18** and **19**). The formation of **18** involves a *trans* opening of the cyclopropane ring on reaction with thallic acetate as postulated (14). In the simple systems (*e.g.* **20**) upon which mechanistic conclusions have been based, solvolysis of the thallic substituent has been suggested to involve participation of the C-3 acetate group. Attack of acetate anion on this bridged acetoxonium ion (**21**) then leads to the observed product, the *trans* diacetate (**22**) (Scheme 2). In the present case (**18**), bridging of this nature is sterically impossible and retention of configuration at C-13 would appear to be most reasonably explained by internal nucleophilic substitution.

Experimental

Melting points are uncorrected and were determined on a Kofler hot-stage apparatus. For normal analytical and preparative t.l.c., chromatoplates were spread with

Can. J. Chem. Downloaded from www.nrcresearchpress.com by 210.87.254.5 on 09/05/12
For personal use only.

Can. J. Chem. Downloaded from www.nrcresearchpress.com by 210.87.254.5 on 09/05/12
For personal use only.

Kieselgel G. (Merck), while silver nitrate – silica gel chromatoplates in addition contained 12% of the former. Gas liquid chromatography was carried out with a Varian Aerograph 1200 gas chromatograph using a stainless steel column ($\frac{1}{8}$ in. × 10 ft packed with 5% SE-30) and nitrogen as carrier gas with a flow rate of 25 ml/min. Light petroleum was of b.p. 60–80°. Microanalyses were by Mr. H. S. McKinnon, Guelph. Infrared solution spectra were recorded in carbon tetrachloride on a Beckmann I.R. 12 spectrophotometer and u.v. spectra in ethanol on a Unicam S.P. 800 spectrophotometer. Proton magnetic resonance spectra were run on a Varian Associates A-60A or HA 100 spectrometer in carbon tetrachloride, unless otherwise stated, using approximately 0.3 *M* solutions and tetramethylsilane as internal standard. Mass spectra were run on a Varian Associates CH 7 instrument.

The Oxidative Cleavage

The ester **1***a* (3.40 g) was treated with thallic oxide (1.5 g) in glacial acetic acid (65 ml) for 2 days at 75° with stirring. More thallic oxide (1 g) was then added and the reaction allowed to proceed for a further 2 days. The solvent was removed *in vacuo* and the residue extracted with ether. This extract was washed carefully with saturated aqueous sodium bicarbonate (twice) and brine. The resulting solution was dried and the solvent evaporated to afford an oil (3.60 g). This oil was chromatographed over alumina (Fisher; 80–200 mesh; 120 g) in light petroleum. Elution with light petroleum – ethyl acetate (49:1) afforded starting material (690 mg) and with light petroleum – ethyl acetate (24:1) seven fractions (1.227 g total) containing several compounds of very similar mobility on t.l.c. The last three of these were combined (556 mg) and hydrolyzed with excess sodium hydroxide in refluxing methanol for 1 h (see below). Fractions (966 mg total) eluted with light petroleum – ethyl acetate (23:2) contained compounds giving three poorly resolved spots on t.l.c. (ethyl acetate – light petroleum, 1:4). These fractions were combined and subjected to preparative t.l.c. (ethyl acetate – light petroleum, 1:9, run thrice) (see below). Further elution of the column with light petroleum – ethyl acetate (9:1, 1:1, and 1:9) gave complex mixtures (289 mg) of more polar materials (t.l.c. evidence).

The hydrolysis products (see above) were separated by preparative t.l.c. (ethyl acetate – light petroleum, 1:9, run twice) and afforded the two major components. The least polar was the hydroxy ester *7a* (212 mg) which was further purified by preparative t.l.c. on silver nitrate – silica gel (ethyl acetate – light petroleum, 3:7) and then crystallization from a mixture of these two solvents. It had m.p. 163–164°; ν_{max} 3620 and 1730 cm^{-1}; τ 4.11 (d, 1 H-14, J = 9.5 Hz), 4.48 (q, 1 H-13, J = 3.5 and 9.5 Hz), 6.57 (d, 1 H-12, J = 3.5 Hz; s on irradiation at 4.48), 8.83 (s, 3 H-18), 8.89 (s, 3 H-17), and 9.54 (s, 3 H-20); in presence of 0.4*M* Eu(dpm)$_3$ τ 2.25 (d, 1 H-14, J = 9.5 Hz), 3.62 (d, 1 H-15, J = 11 Hz), 5.02 (s, 3 H-17), 6.46 (d, 1 H-15, J = 11 Hz), 8.27 (s, 3 H-18), and 8.48 (s, 3 H-20); *m/e* 332 (M).

Anal. Calcd. for $C_{21}H_{32}O_3$: C, 75.86; H, 9.70. Found: C, 75.76; H, 10.00.

The derived (acetic anhydride – pyridine) acetate (**5**) had a mobility on t.l.c. on silica gel (ethyl acetate – light petroleum, 1:9) and silver nitrate – silica gel (ethyl acetate – light petroleum, 3:7) identical with that of one component of the fractions which had been hydrolyzed (see above). After crystallization from methanol it had m.p. 130–132°; τ ($CDCl_3$) 3.94 (d, 1 H-14, J = 9.5 Hz), 4.46 (q, 1 H-13, J = 3.5, 9.5 Hz), 5.14 (d, 1 H-12, J = 3.5 Hz), 7.96 (s, 3H, —OCO*CH*$_3$), 8.81 (s, 3H, —*CH*$_3$), 8.92 (*s*, 3H, —*CH*$_3$), and 9.49 (s, 3 H-20).

Anal. Calcd. for $C_{23}H_{34}O_4$: C, 73.76; H, 9.15. Found: C, 73.97; H, 9.16.

The more polar, major, component obtained by preparative t.l.c. of the hydrolysis products was the hydroxy ester **8***a* (287 mg). It also was further purified by preparative t.l.c. on silver nitrate – silica gel (ethyl acetate – light petroleum, 3:7) and then crystallization from a mixture of these two solvents. It had m.p. 124°; ν_{max} 3620 (free OH), 3603 (bonded OH), and 1728 cm^{-1}; τ 4.35 (br s, 1 H-15), 6.23 (m, 1 H-13), 8.24 (d, 3 H-17, J = 1.5 Hz), 8.86 (s, 3 H-18), and 9.32 (s, 3 H-20); *m/e* 332 (M).

Anal. Calcd. for $C_{21}H_{32}O_3$: C, 75.86; H, 9.70. Found: C, 76.10; H, 9.72.

The derived acetate (**2**) was identical (same criteria as for **5** above) with the major component of the fractions which had been hydrolyzed and had m.p. 130–132° (from methanol); τ ($CDCl_3$) 4.27 (broad s, 1 H-15), 5.16 (m, 1 H-13), 8.03 (s, 3H, —OCO*CH*$_3$), 8.24 (d, 3 H-17, J = 1.5 Hz), 8.82 (s, 3 H-18), and 9.23 (s, 3 H-20).

Anal. Calcd. for $C_{23}H_{34}O_4$: C, 73.76; H, 9.15. Found: C, 73.89; H, 9.02.

The fractions from the alumina column which were submitted directly to preparative t.l.c. (see above) yielded three components, the one (109 mg) of intermediate polarity being contaminated with a small amount of the most polar. The least polar, major, constituent was the diacetate **3** (652 mg) which crystallized readily from hexane and had m.p. 162–163°; τ 5.14 (m, 1 H-13), 8.05 (s, 3H, —OCO*CH*$_3$), 8.11 (s, 3H, —OCO*CH*$_3$), 8.42 (s, 3 H-17), 8.87 (s, 3 H-18), and 9.24 (s, 3 H-20).

Anal. Calcd. for $C_{25}H_{38}O_6$: C, 69.10; H, 8.81. Found: C, 69.38; H, 8.70.

This diacetate **3** (48 mg) on distillation (twice) at 200°/15 mm afforded essentially pure monoacetate **2** (37 mg), identified by m.p., m.m.p., n.m.r., and t.l.c.

The most polar component from preparative t.l.c. of the diacetate fractions was **4** (215 mg). This was obtained as an oil which failed to crystallize. It was purified by distillation at 165°/0.2 mm and had τ 4.05 (broad s, 1 H-15), 5.24 (m, 1 H-13), 5.52 (broad s, 2 H-17), 8.00 (s, 3H, —OCO*CH*$_3$), 8.11 (s, 3H, —OCO*CH*$_3$), 8.85 (s, 3 H-18), and 9.23 (s, 3 H-20), *m/e* 430 (M).

Anal. Calcd. for $C_{25}H_{36}O_6$: C, 69.42; H, 8.39. Found: C, 69.54; H, 8.53.

Enone 7b

Alcohol *7a* (52 mg) in methylene chloride (5 ml) was treated with a solution of chromium trioxide (150 mg) and pyridine (0.25 ml) in the same solvent (5 ml) at 20° for 30 min. Ethyl acetate (50 ml) was then added and the resulting mixture washed with water (twice). The recovered product, an oil (55 mg), by preparative t.l.c. (ethyl acetate – light petroleum, 1:4, run twice) afforded the enone *7b* (39 mg), which crystallized from light petroleum and had m.p. 152–155°; ν_{max} 1735 and 1695 cm^{-1}; λ_{max} 236 nm (ε 8700); τ ($CDCl_3$) 2.98 (q, 1 H-14, J = 2, 9.5 Hz, former long range to 1 H-15, see ref. 5), 4.14 (d, 1 H-13, J = 9.5 Hz), 8.81 (s, 3 H-17 and 3 H-18), and 9.53 (s, 3 H-20).

Can. J. Chem. Downloaded from www.nrcresearchpress.com by 210.87.254.5 on 09/05/12
For personal use only.

Anal. Calcd. for $C_{21}H_{30}O_3$: C, 76.33; H, 9.15. Found: C, 76.45; H, 9.22.

Ketone 8b

Oxidation of alcohol **8***a* (55 mg) as above afforded the ketone **8***b* (44 mg) which had m.p. 176–179° (from light petroleum); ν_{max} 1738 and 1705(sh) cm^{-1}; τ ($CDCl_3$) 4.17 (broad s, 1 H-15), 7.39 (d, 1 H-14, J = 19 Hz), 8.32 (d, 3 H-17, J = 1.5 Hz), 8.80 (s, 3 H-18), and 9.27 (s, 3 H-20).

Anal. Calcd. for $C_{21}H_{30}O_3$: C, 76.33; H, 9.15. Found: C, 76.28; H, 9.06.

Formation of the Thioketal 8e and its Treatment with Raney Nickel

A solution of the ketone **8***b* (42 mg) in dry ether was treated with freshly distilled boron trifluoride etherate (0.5 ml) and ethane dithiol (0.3 ml) at 20° for 6 days. Ether (20 ml) was then added and the resulting solution washed with aqueous potassium hydroxide (4 *N*, 10 ml, twice) and water, dried, and the solvent evaporated. Preparative t.l.c. of the product (55 mg) afforded as the least polar, major constituent, the oily thioketal **8***e* (48 mg); τ ($CDCl_3$) 4.36 (broad s, 1 H-15), 6.75 (m, 4H, thioketal), 8.15 (d, 3 H-17, J = 1.5 Hz), 8.82 (s, 3 H-18), and 9.10 (s, 3 H-20).

Freshly prepared Raney nickel (1 g) was deactivated by stirring in refluxing acetone for 3 h. The thioketal **8***e* (48 mg) was then added in acetone and the heating continued for a further 15 h. Removal of the Raney nickel and acetone left a residue, shown to be a complex mixture by t.l.c. A fraction (12 mg) of similar polarity to **8***c* was recovered by preparative t.l.c. (ethyl acetate – light petroleum, 1:19). This ran as seven spots, none of which had an R_f corresponding to that of **9***c* on silver nitrate – silica gel (ethyl acetate – light petroleum, 3:97). Separation of these by preparative t.l.c., using these conditions furnished a very small amount of an oil (< 1 mg) having identical t.l.c. ($AgNO_3$–SiO_2), g.l.c. (retention time at 200°, 265 s) and mass spectral behavior with that of an authentic sample of **8***c*.[6] The major, much more polar component (**11**) of the mixture was also recovered as an oil (6 mg) which slowly decomposed at 20° (t.l.c. evidence). Crystallization from moist methanol gave plates, m.p. 132–136°; τ ($CDCl_3$) 3.80 (m, 1 H-13 and 1 H-14), 4.43 (broad s, 1 H-15), 8.25 (d, 3 H-17, J = 1.5 Hz), 8.80 (s, 3 H-18), and 9.58 (s, 3 H-20); *m/e* 314 (M).

Catalytic Hydrogenation of the Hydroxy Ester 8a

Hydrogenation of **8***a* (175 mg) in ethyl acetate over palladized charcoal (180 mg) for 0.5 h yielded two products which were separated by preparative t.l.c. (ethyl acetate – light petroleum, 1:9, run twice). The less polar was the alcohol **12***a* (118 mg) which crystallized from ethyl acetate – light petroleum and had m.p. 134–135°; τ 6.10 (broad s, 1H-13), 8.83 (d, 3 H-17, J = 7 Hz), 8.88 (s, 3 H-18), and 9.32 (s, 3 H-20); with 0.4 *M* Eu(dpm)$_3$ τ 2.47 (d, 3 H-17, J = 7 Hz), 7.53 (s, 3 H-20) and 8.02 (s, 3 H-18).

Anal. Calcd. for $C_{21}H_{34}O_3$: C, 75.41; H, 10.25. Found: C, 75.58; H, 10.05.

The more polar was the isomeric alcohol **12***b* (50 mg) which, when crystallized from ethyl acetate – light petroleum had m.p. 121–123°; τ 6.12 (broad s, 1 H-13), 8.83 (s, 3 H-18), 9.02 (d, 3 H-17, J = 6.5 Hz), and 9.30 (s, 3 H-20); with 0.4 *M* Eu(dpm)$_3$ τ 6.58 (d, 3 H-17, J = 6.5 Hz), 7.52 (s, 3 H-20), and 8.08 (s, 3 H-18).

Anal. Calcd. for $C_{21}H_{34}O_3$: C, 75.41; H, 10.25. Found: C, 75.55; H, 10.49.

Formation of the Olefin 15

Alcohol **12***a* (88 mg) was treated with excess *p*-toluenesulfonyl chloride in pyridine (3 ml) for 14 h. Ether (50 ml) was added and the resulting mixture extracted with aqueous sodium hydroxide (20 ml, 2 *N*, twice) and water. The ether layer was then dried and the solvent evaporated *in vacuo*, residual pyridine being removed by azeotropic distillation with benzene. Thin layer chromatography of the oily residue showed one clean spot, the tosylate **8***d*, less polar than substrate. This tosylate was heated with a large excess of sodium *t*-amylate in *t*-amyl alcohol at 85° for 18 h. Work-up with ether–water furnished an oil (73 mg) which gave three major fractions, of very similar polarity, by preparative t.l.c. over silver nitrate – silica gel (ethyl acetate – light petroleum, 1:199, run five times). The least polar was the pentacyclic ester **13** (11 mg) which solidified and had m.p. 71–74°; τ 8.84 (s, 3 H-18), 8.98 (d, 3 H-17, J = 6.5 Hz), and 9.28 (s, 3 H-20); *m/e* 316 (M). It had an identical R_f with that of **1***a* on silver nitrate – silica gel (ethyl acetate – light petroleum, 3:97) but a slightly longer retention time (555 s) on g.l.c. at 182° than that (516 s) of **1***a*. The component of intermediate polarity (**14**) was also obtained as an oil (8 mg). It had a very complex n.m.r. spectrum at about τ 9 and *m/e* 404 (M), 375, 334, 333, 317, and 316. The most polar component was the olefin **15** (31 mg) which after crystallization from methanol had m.p. 89–93°; τ 4.05 (d, 1 H-13 and 1 H-14, J_{obs} = 4 Hz), 8.85 (s, 3 H-18), 9.26 (d, 3 H-17, J = 6 Hz), and 9.61 (s, 3 H-20); *m/e* 316 (M) and 274 (M – C_3H_6).

Anal. Calcd. for $C_{21}H_{32}O_2$: C, 79.70; H, 10.19. Found: C, 79.83; H, 10.27.

The Diol 16a and Monoacetate 16b

Diacetate **3** (34 mg) was hydrolyzed by treatment with potassium hydroxide in refluxing methanol for 3 h. Work-up with ether–water gave an oil, consisting essentially (t.l.c.) of one polar compound (**16***a*). This was purified by preparative t.l.c. (ethyl acetate – light petroleum, 3:7, run twice) and crystallization from a mixture of these two solvents. It (22 mg) had m.p. 220–221°; τ ($CDCl_3$) 6.00 (octet, 1 H-13), 8.55 (s, 3 H-17), 8.83 (s, 3 H-18), and 9.28 (s, 3 H-20).

Anal. Calcd. for $C_{21}H_{34}O_4$: C, 71.96; H, 9.78. Found: C, 72.03; H, 9.80.

Acetylation with acetic anhydride – pyridine furnished the monoacetate **16***b* which was purified by preparative t.l.c. (ethyl acetate – light petroleum, 1:5). The resulting oil had ν_{max} 3612 and 1735 cm^{-1}; τ 5.20 (m, 1 H-13), 8.10 (s, 3H, —OCOCH_3), 8.72 (s, 3 H-17), 8.88 (s, 3 H-18), and 9.27 (s, 1 H-20).

Catalytic Hydrogenation of the Diacetate 4

Hydrogenation of diacetate **4** (137 mg) in ethanol (60 ml) and triethylamine (10 ml) over 5% palladized charcoal (100 mg) yielded an oil giving only two spots on t.l.c. on both silica gel (ethyl acetate – light petroleum, 1:9) and silver nitrate – silica gel (ethyl acetate – light petroleum, 3:7). The two components were separated by preparative t.l.c. The less polar (68 mg) was the acetate **2**, m.p. 130–

[6]Professor R. M. Coates kindly supplied this sample.

132°, identified by m.m.p., t.l.c., and n.m.r. The more polar component, the oily diacetate **17** (54 mg), was purified by distillation at 165°/0.2 mm and had τ 5.15 (m, 1 H-13), 8.04 (s, 6H, 2 —OCOCH_3), 8.45 (s, 3 H-17), 8.83 (s, 3 H-18), and 9.23 (s, 3 H-20).

Anal. Calcd. for $C_{25}H_{38}O_6$: C, 69.10; H, 8.81. Found: C, 69.32, H, 8.88.

We thank the National Research Council of Canada for an operating grant.

1. A. J. McAlees and R. McCrindle. Can. J. Chem. This issue.
2. R. A. Appleton, A. J. McAlees, A. McCormick, R. McCrindle, and R. D. H. Murray. J. Chem. Soc. 2319 (1966).
3. G. Hugel, L. Lods, J. M. Mellor, and G. Ourisson. Bull. Soc. Chim. France, 2394 (1965).
4. J. St. Pyrek. Tetrahedron, **26**, 5029 (1970).
5. M. Laing, P. Sommerville, D. Hanouskova, K. H. Pegel, and L. P. L. Piacenza. Chem. Commun. 196 (1972).
6. N. N. Girotra and L. H. Zalkow. Tetrahedron, **21**, 101 (1965).
7. D. G. Buckley, G. H. Green, E. Ritchie, and W. C. Taylor. Chem. Ind. (London), 298 (1971).
8. W. Herz, R. N. Mirrington, H. Young, and Y. Y. Lin. J. Org. Chem. **33**, 4210 (1968). A. H. Kapadi and S. Dev. Tetrahedron Lett. 2751 (1964). G. Hugel, L. Lods, J. M. Mellor, D. W. Theobald, and G. Ourisson. Bull. Soc. Chim. France, 2882 (1965). A. H. Kapadi and S. Dev. Tetrahedron Lett. 1255 (1965).
9. R. M. Coates and E. F. Bertram. J. Org. Chem. **36**, 2625, 3722 (1971).
10. L. M. Jackman and S. Sternhell. Applications of nuclear magnetic resonance spectroscopy in organic chemistry. Pergamon Press, Oxford. 1969. p. 274.
11. W. A. Ayer and P. D. Deshpande. Can. J. Chem. **51**, 77 (1973).
12. A. Nickon and N. H. Werstiuk. J. Am. Chem. Soc. **89**, 3915 (1967).
13. J. D. Connolly and I. M. S. Thornton. J. Chem. Soc. Perkin Trans. **1**, 732 (1973).
14. R. J. Ouellette, A. South, and D. L. Shaw. J. Am. Chem. Soc. **87**, 2602 (1965).

Can. J. Chem. Downloaded from www.nrcresearchpress.com by 210.87.254.5 on 09/05/12
For personal use only.